

361-55

SCI

PAMPHLET BOX

Physics Abstracts

Science Abstracts Series A
January - June 1987

Subject Index (A-L)

U.I.C.

SEP 16 1987
LIBRARY

inspec

The Institution of Electrical Engineers

SIX-MONTHLY INDEXES TO PHYSICS ABSTRACTS

Twice a year as part of their subscription to Physics Abstracts, subscribers receive cumulative indexes for the periods January-June and July-December. Each index is in two parts—a Subject Index, and an Author Index which comprises personal and corporate author indexes, and indexes to conferences, book titles, and bibliographies. The List of Journals abstracted by INSPEC is also included with the July-December issue of the Author Index, while the supplement to that List is included with the January-June issue.

Cumulative indexes for earlier years are also available: for details please see the inside back cover.

Subject index

The Subject index provides an alphabetical subject key to the articles included in the abstracts journal. Some general guidance on its use is given below:

1. Look in the index for the name of the specific subject in which you are interested. In most cases this name will be a heading in the index and you will find relevant articles listed under it. The majority of the subject headings fall into the following categories: property, phenomenon, substance or named objects, instrument, device, theory, method, process, application, event.
2. Occasionally you will be directed from the subject heading chosen to a different heading under which the relevant or additional articles are listed.
3. If you do not find the subject heading you first chose, try a more general heading.
4. Each entry under the heading relates to an article appearing in the abstracts journal and gives the serial number of that article in the journal preceded by the last digit of the current year, e.g. 7-12345; i.e. Abstract number 12345 in the abstracts journal for 1987.

The language of the article, if it is not English, is also indicated, e.g. light-pulse wave form monitoring with 500ps resoln. (Japanese) 7-49850.

Each entry starts with a Keyword or Keyphrase considered to be most relevant to the heading. On sorting these Keywords, the qualifying prefixes are usually ignored, (e.g. α -brass, 5-sulphosalicylic, 31 Cygni, n-Ge are sorted under brass, sulphosalicylic, Cygni, respectively).

There are three main Keyword lists: alphabetical A-Z, elementary particles, and chemical symbols (organic substances are written and not given as chemical formula). More than one Keyword list may be present under each subject heading.

For document on, say, 'photoemission of germanium' at least two access points 'photoemission' and 'germanium' are provided. Under the heading 'photoemission' the Keyword will be 'Ge' and under 'germanium' the Keyword will be 'photoemission'.

In a case like this, it is advisable and quicker to use the heading 'photoemission' and go straight to the chemical symbol list for 'Ge'.

Intermetallic compounds are indexed under the appropriate alloy headings. The chemical formula is used as Keyword. However, it is important to realise in searching the chemical symbol list that, at present, alloys and intermetallic compounds are sorted separately. For example FeCo is sorted at the end of the Fe- list e.g. Fe-Al,... Fe-Co,... Fe-Si,... Fe-Si-B,... FeCo,... FeSi and so on in this order.

PHYSICS ABSTRACTS is published twice monthly by the Institution of Electrical Engineers in association with the Institute of Electrical and Electronics Engineers Inc. 2nd Class postage paid at Piscataway, N.J. 08854-4150, USA. POSTMASTER: Send address changes to INSPEC/IEEE SERVICE CENTRE, 445 Hoes Lane, Piscataway, N.J. 08854-4150.

Printed by Unwin Brothers Limited, The Gresham Press, Old Woking, Surrey.

© 1987, THE INSTITUTION OF ELECTRICAL ENGINEERS. All rights reserved. No part of this publication may be reproduced, stored in a retrieval system, or transmitted, in any form or by any means, electronic, mechanical, photocopying, recording or otherwise without the prior permission of the Institution of Electrical Engineers.

Abbreviations and Acronyms

Abbreviations and acronyms are used in the modifiers in all INSPEC Compendex Subject Indexes. Individual terms should be readily understood in the context of the subject headings. Inorganic substances are usually given by their chemical formulae, iron and aluminium compounds appear in the formulae less as MIG and MAG (where M is metal element, e.g. YIG and MAG), (Pb, Sn, TiO₂ and Pb, Sn, TiO₂) appear as PLET and PZT. Organic substances including liquid crystals are not given by their chemical formulae. Abbreviations are used.

Physics Abstracts

Science Abstracts Series A

January – June 1987

Subject Index (A – L)

CONTENTS

Abbreviations and Acronyms
Subject index (A – L)

S1

Abbreviations and Acronyms

Abbreviations and acronyms are used in the modifiers in all INSPEC Cumulative Subject Indexes. Individual terms should be readily understood in the context of the subject headings. **Inorganic substances** are usually given by their chemical formulae. Iron and aluminium garnets appear in the formulae lists as MIG and MAG (where M is metal element, e.g. YIG and YAG); $(\text{Pb},\text{La})(\text{Zr},\text{Ti})\text{O}_3$ and $\text{Pb}(\text{Zr},\text{Ti})\text{O}_3$ appear as PLZT and PZT. **Organic substances** including **liquid crystals** are not given as formulae but common abbreviations are used.

1D	one-dimensional	ASCII	American standard code for information interchange
2D	two-dimensional	ASIC	application specific integrated circuit
3D	three-dimensional	ASK	amplitude shift keying
A/D	analogue-to-digital	ATC	air traffic control
ABS resin	acrylonitrile-butadiene-styrene resin	ATE	automatic test equipment
AC	alternating current	ATF	Advanced Toroidal Facility
ACSR	aluminium conductor steel reinforced	ATM	automatic teller machine or Axilrod-Teller-Moto
ACV	air cushion vehicle		
ADC	analogue-to-digital conversion	ATR	attenuated total reflection
ADM	adaptive delta modulation	ATWS	anticipated transients without scram
ADP	administrative data processing	AVC	automatic volume control
ADPCM	adaptive differential pulse code modulation	AWGN	additive white Gaussian noise
ADS	automatic depressurisation system		
AE	acoustic emission	BARITT	barrier injection transit time
AEC	atomic electron correlation(s)	BBD	bucket-brigade device
AES	Auger electron spectra(oscopy)	BBGKY	Bogoliubov-Born-Green-Kirkwood-Yvon
AF	audio frequency	BCC	body centred cubic
AFC	automatic frequency control	BCD	binary-coded decimal
AFL	abstract family of languages	BCH	Bose-Chadhuri-Hocquenghem
AFMR	antiferromagnetic resonance	BCS	Bardeen-Cooper-Schrieffer
AFR	away from reactor (spent fuel storage)	BCT	body centred tetragonal
AGB	asymptotic giant branch	BEBC	Big European Bubble Chamber
AGC	automatic gain control	BEDT-TTF	bio(ethylenedithio)-tetrathiofulvalene (-inium)
AGR	advanced gas-cooled reactor	BEM	boundary element method
AGS	alternating gradient synchrotron	BEPC	Beijing Electron Positron Collider
AGV	automatic guided vehicle	BER	bit error rate
AI	artificial intelligence	BFL	buffered FET logic
AKR	auroral kilometric radiation	BFO	beat-frequency oscillator
ALARA	as low as reasonably achievable	BH	buried heterostructure
ALU	arithmetic logic unit	BIL	buried injection logic
AM	amplitude modulation or air mass number	BIMOS	bipolar/metal-oxide-semiconductor
ANOVA	analysis of variance	BIS	bremsstrahlung isochromat spectroscopy
ANSI	American National Standards Institute	BIST	built in self test
APACHE	Accelerator for Physics and Chemistry of Heavy Elements	BPSG	borophosphosilicate glass
APC	adaptive predictive coding	BPSK	binary phase shift keying
APCM	adaptive pulse code modulation	BRD	W Germany
APCVD	atmospheric pressure chemical vapour deposition	BRET	Breeder Reprocessing Engineering Test
APD	avalanche photodiode	BSG	borosilicate glass
APFIM	atom probe field in microscopy	BTSC	Broadcast Television Systems Committee
APR	acoustic paramagnetic resonance		
APRFR	Army Pulsed Radiation Facility Reactor	BVP	boundary value problem
APS	appearance potential spectra(oscopy)	BWIP	Basalt Waste Isolation Project
APW	augmented plane wave	BWO	backward wave oscillator
APWR	advanced pressurised water reactor	BWR	boiling water reactor
ARMA	autoregressive moving average	BWT	backward wave tube
ARPES	angle resolved photoemission spectra (oscopy)		
ARQ	automatic repeat request	C-V	capacitance-voltage
ARUPS	angular resolved ultraviolet photoelectron spectra	C ²	command and control
		C ³	command control communications or cleaved coupled cavity

C ³ I	command control communications and intelligence	CIDEP	chemically induced dynamical electron polarisation
C ³ L	complementary constant current logic	CIDNP	chemically induced dynamical nuclear polarisation
CAAB/AM	companded single sideband amplitude modulation	CIEH	charge iterated extended Huckel
CAD	computer aided design	CIHY	configuration interaction Hylleras
CADAT	computer aided design and testing	CIM	computer integrated manufacturing or constituent interchange model
CADD	computer aided draughting and design	CMI	computer managed instruction
CAE	computer aided engineering	CML	current-mode logic
CAI	computer assisted instruction	CMOS	complementary metal oxide semiconductor
CAL	computer aided learning	CNC	computerised numerical control
CAM	computer aided manufacturing	CNDO	complete neglect of differential overlap
CANDU	Canadian deuterium uranium	COM	computer output to microform (fiche or film)
CAR	computer aided retrieval	COMFET	conductivity-modulated field effect transistor
CARS	coherent antiStokes Raman scattering (spectra)	COVA	computer code validation
CATT	controlled avalanche transit transistor	CP	charge, parity
CATV	community antenna television or cable television	CPA	coherent potential approximation or critical path analysis
CB	citizens' band	CPC	compound parabolic concentrator
CBI	computer based instruction	CPFSK	continuous phase frequency shift keying
CBOOA	cyanobenzylidene octyloxylaniline	CPM	continuous phase modulation or critical path method
CBT	computer based training	CPSK	coherent phase shift keying
CCBA	coupled channel Born approximation	CPT	charge, parity, time
CCCS	current controlled current source	CPU	central processing unit
CCFL	counter current flow limiting (LOCA phenomenon)	CRBR	Clinch River Breeder Reactor project
CCD	charge-coupled device	CRDA	control rod drop accident
CCIR	International Radio Consultative Committee	CRO	cathode ray oscilloscope
CCITT	International Telephone & Telegraph Consultative Committee	CRSR	coherent resonant Stokes rotation
CCL	capacitor-coupled logic	CRT	cathode ray tube
CCTF	Cylindrical Core Test Facility	CS	coupled states
CCTR	Culham Conceptual Tokamak Reactor	CSM	continuous slowing down models
CCTV	closed circuit television	CSMA	carrier sense multiple access
CCVS	current controlled voltage source	CSMA/CD	carrier sense multiple access with collision detection
CD	compact disc	CSP	channel substrate planar
CD-ROM	compact disc ROM	CSRS	coherent Stokes-Raman spectra(oscropy)
CDFR	Commercial Demonstration Fast Reactor	CSSB/AM	companded single sideband amplitude modulation
CDI	collector diffusion isolation	CT	computerised tomography
CDLC	cellular data link control	CTD	charge transfer device
CDM	code division multiplexing	CTL	complementary-transistor logic
CDMA	code division multiple access	CTR	controlled thermonuclear reactor
CDW	charge-density wave	CVD	chemical vapour deposition
CECL	cascode-emitter coupled logic	CVSDM	continuously variable slope delta modulation
CEGB	Central Electricity Generating Board	CW	continuous wave
CEM	channel electron multiplier	D/A	digital-to-analogue
CEPA	coupled electron pair approximation	DAC	digital-to-analogue conversion
CERN	European Council for Nuclear Research	DAD	digital audio disc
CESR	conduction electron spin resonance	DAMA	demand assigned multiple access
CFAR	constant false alarm rate	DASD	direct access storage device
CFG	context free grammar	DAT	digital audio tape
CFL	context free language	DAW	dry active waste
CFSK	coherent frequency shift keying	DBMS	database management system
CGTO	contracted Gaussian-type orbital	DBR	distributed Bragg reflector
CHF	coupled Hartree-Fock		
CHP	combined heat and power		
CI	configuration interaction		
CID	charge injection device		

DBS	direct broadcasting by satellite	E1,E2	electric dipole, quadrupole
DC	direct current	E ² PROM	electrically erasable programmable read-only-memory
DCFL	direct-coupled FET logic	EAROM	electrically alterable read-only-memory
DCLC	drift cyclotron loss cone (instability)	EAS	extensive air shower
DCT	discrete cosine transform	EAX	electronic automatic exchange
DCTL	direct-coupled transistor logic	EB	exponential Born
DDC	direct digital control	EBBA	4-ethoxybenzylidene-4'-n-butylaniline
DDL	diode-diode logic	EBIC	electron beam induced current(s)
DDR	E Germany	EBR	experimental breeder reactor
DECENT	distribution of exact classical energy transfer	EBT	Elmo Bumpy Torus
DES	data encryption standard	ECC	emergency core cooling
DESY	Deutsches Electron Synchrotron	ECCM	electronic counter-counter measures
DF	Dirac-Fock	ECCS	emergency core cooling system
DFB	distributed feedback	ECELR	Epithermal Critical Experiment Laboratory Reactor
DFF	decision feedback equaliser	ECG	electrocardiography (-gram)
DFT	discrete Fourier transform	ECL	emitter coupled logic
DH	double heterostructure	ECM	electronic countermeasures
DHF	Dirac-Hartree-Fock	ECRH	electron cyclotron resonance heating
DIL	dual-in-line	EDA	ethylene diamine
DIP	dual in-line package	EDAX	energy dispersive X-ray analysis
DITE	Divertor in Torus Experiment	EDIF	electronic data interchange format
DLTS	deep level transient spectra(oscopy)	EDP	electronic data processing
DM	delta modulation	EDTA	ethylene diamine tetra-acetic acid
DMA	direct memory access	EDTV	extended definition television
DMM	digital multimeter	EDW	electron density wave
DMOS	double-diffused metal-oxide-semiconductor	EDX	energy dispersive X-ray
DMSO	dimethylsulphoxide	EEG	electroencephalography (-gram)
DNA	digital network architecture or deoxyribonucleic acid	EELS	electron energy loss spectra(oscopy)
DNMR	double nuclear magnetic resonance	EEPROM	electrically erasable programmable read-only-memory
DOBAMBC	p-decyloxybenzylidene p'-amino 2-methyl butyl cinnamate	EFG	edge-defined film fed growth
DoD	Department of Defense (USA)	EFL	emitter-follower logic or emitter-function logic
DOPSK	differential offset phase shift keying	EFM	extended Flygare method
DORIS	Dopple-Ring-Speicher	EFT	electronic funds transfer
DOS	disc operating system	EHD	electrohydrodynamics
DOVETT	double velocity transit time	EHDTV	enhanced high definition television
DP	data processing	EHF	extremely high frequency
DPCM	differential pulse code modulation	EHP	electron-hole potential method
DPDA	deterministic pushdown automaton	EHT	extra high tension or extended Huckel theory
DPPH	diphenylpicrylhydrazyl	EHV	extra high voltage
DPSPK	differential phase shift keying	EIRP	equivalent isotropically radiated power
DQPSK	differential quadrature phase shift keying	ELDOR	electron electron double resonance
DRAM	dynamic random access memory	ELF	extremely low frequency
DS-SSMA	direct sequence-spread spectrum multiple access	EM	electromagnetic
DSAM	Doppler shift attenuation method	EMC	electromagnetic compatibility or European Muon Collaboration
DSB	double sideband	EMF	electromotive force
DSC	differential scanning calorimetry	EMG	electromyography (-gram)
DSI	digital speech interpolation	EMI	electromagnetic interference
DSP	digital signal processor	EMP	electromagnetic pulse
DSS	decision support system	EMS	energy management system
DTA	differential thermal analysis	ENDOR	electron nuclear double resonance
DTL	diode transistor logic	ENG	electronic newsgathering
DTTP	Demonstration Tokamak Power Plant	EOF	end of file
DTU	dual topological unitarisation	EOG	electrooculography (-gram)
DV-X α	discrete variational X α method	EPMA	electron probe microanalysis
DVM	digital voltmeter	EPR	electron paramagnetic resonance
DWBA	distorted wave Born approximation	EPRI	Electric Power Research Institute
DWIA	distorted wave impulse approximation		
DWPF	Defence Waste Processing Facility		

EPROM	erasable programmable read-only-memory	FSDE	fission suppressed direct enrichment (breeder blanket)
ERG	electroretinography (-gram)	FSK	frequency-shift keying
ESA	European Space Agency	FSGO	floating spherical Gaussian orbitals
ESCA	electron spectroscopy for chemical analysis	FTR	Fast Test Reactor
ESCAR	Experimental Superconducting Accelerating Ring	FWHM	full width half maximum
ESD	electrostatic discharge or electron stimulated desorption	GAMBIT	gate modulated bipolar transistor
ESF	engineering safety features	GANIL	Grand Accelérateur National a Ions Lourds
ESP	electrostatic precipitators	GCFR	gas-cooled fast breeder reactor
ESPRIT	European Strategic Programme for Research in Information Technology	GCHWR	gas cooled heavy water moderated reactor
ESS	electronic switching system	GCM	generator coordinate method
EUV	extreme ultraviolet	GDR	giant dipole resonance
EW	electronic warfare	GETR	General Electric Test Reactor
EX-OR	exclusive-OR (logic)	GHF-NO-CI	generalised Hartree-Fock/natural orbital/configuration interactions
EXAFS	extended X-ray absorption fine structure	GIAO	gauge-invariant atomic orbitals
FAMOS	floating gate avalanche metal-oxide-semiconductor	GIS	gas insulated switchgear (or system)
FBC	fluidised bed combustion	GKS	Graphical Kernel System
FBR	fast breeder reactor	GMDH	group method of data handling
FCC	face centred cubic	GMR	giant monopole resonance
FCI	fuel-cladding interaction	GMSK	Gaussian filtered minimum shift keying
FDM	frequency division multiplex(ing)	GO	Gaussian orbitals
FDMA	frequency division multiple access	GPED	gas phase electron diffraction
FDNC	frequency dependent negative conductance	GPIB	general purpose interface bus
FDNR	frequency dependent negative resistance	GPM	ground potential model
FEA	finite element analysis	GPS	Global Positioning System
FECL	feedback ECL	GQR	giant quadrupole resonance
FED	Fusion Engineering Device (USA)	GRIN	graded (gradient) refractive index
FEDC	Fusion Engineering Device Centre	GSPC	gas scintillation proportional chamber (or counter)
FEL	free electron laser	GTHTGR	gas turbine HTGR
FEM	field emission microscopy or finite element method	GTO	gate turn-off or Gaussian-type orbitals
FER	Fusion Experimental Reactor (Japan)	GUT	grand unified theory
FET	field effect transistor	GVB	generalised valence bond
FFHR	fusion-fission hybrid reactor	HAM	hydrogenic atoms in molecules
FFT	fast Fourier transform	HBT	heterojunction bipolar transistor or N-(p-hexyloxybenzylidene)-p-toluidene
FFTF	Fast Flux Test Facility	HCDA	hypothetical core disruptive accident
FGD	flue gas desulphurisation	HCMOS	high speed complementary metal oxide semiconductor
FHNC	Fermi hypernetted chain	HCP	hexagonal close packed
FIFO	first in first out	HDLC	high level data link control
FIM	field ion microscopy	HDTV	high definition television
FIMOS	floating gate ionisation injection metal-oxide-semiconductor	HEED	high energy electron diffraction
FIR	far infrared or finite impulse response	HEMP	high altitude electromagnetic pulse
FLIR	forward looking infra-red	HEMT	high electron mobility transistor
FLOPS	floating point operation per second	HEU	highly enriched uranium (93% U235)
FM	frequency modulation	HEU/Th	highly enriched U/Th fuel
FMIT	Fusion Materials Irradiation Test Facility	HEXFET	hexagonal MOSFET
FMR	ferromagnetic resonance	HF	high frequency or Hartree-Fock
FMS	flexible manufacturing systems	HFB	Hartree-Fock-Bogoliubov
FMSR	Fast Mixed Spectrum Reactor	HFEF	Hot Fuel Examination Facility
FPC	fusion power core	HFET	heterojunction field effect transistor
FPLA	field programmable logic array	HFIR	high flux isotope reactor
FPT	finite perturbation theory	HFITR	High Field Ignition Test Reactor
FRMR	field reversed mirror reactor	HFO	Hartree-Fock-Overhauser
		HFS	Hartree-Fock-Slater or hyperfine structure

HGMS	high gradient magnetic separation	IGFET	insulated gate field effect transistor
HIXE	heavy ion induced X-ray emission	IGT	insulated gate transistor
HJBT	heterojunction bipolar transistor	IHEP	Institute of High Energy Physics
HJFET	heterojunction field effect transistor	IIR	infinite impulse response
HLL	high level language	IKBS	intelligent knowledge-based system
HLLW	high level liquid waste	IKO	Institute v. Kernph. Ouder Amsterdam
HLW	high level waste	ILS	instrument landing system
HMO	Huckel molecular orbitals	ILW	intermediate level (radioactive) waste
HMOS	high-performance metal-oxide-semiconductor	IMPATT	impact avalanche transit time
HMTSeF	hexamethylenetetraselenafulvalene (-inium)	INDO	intermediate neglect of differential overlap
HMTTF	hexamethyltetraathiofulvalene (-inium)	INDOR	internuclear double resonance
HOAB	heptyloxyazoxybenzene	INEPT	insensitive nuclei enhanced by polarisation transfer
HOMO	highest occupied molecular orbitals	ING	intense neutron generator
HPCS	high-pressure core sprays	INO	iterative natural orbital
HREELS	high resolution electron energy loss spectra (oscopy)	INST	Information Network System or inertial navigation system
HREM	high resolution electron microscopy	INTELSAT	international telecommunications satellite consortium
HSLA	high strength low alloy (steel)	INTOR	International Tokamak Reactor
HT	high tension	IOC- ω	inclusion of the overlap charges in the omega
HTGR	high temperature gas-cooled reactor	IPSE	integrated programming support environment or project support environment
HTGR SC/C	HTGR steam cycle cogeneration	IPSS	international PSS
HV	high voltage	IR	infrared
HVAC	heating, ventilation and air conditioning	IRDO	intermediate retention of differential overlap
HVDC	high voltage direct current	IREB	intense relativistic electron beam
HVEM	high voltage electron microscopy	IRED	infrared emitting diode
HVIC	high voltage integrated circuit	IRS	information retrieval system
HWLWR	heavy water moderated light water cooled reactor	ISABELLE	intersecting storage and acceleration
HWR	heavy water reactor	ISDN	integrated services digital network
HZP	Hot Zero Power	ISFET	ion-sensitive field effect transistor
I-V	current-voltage	ISI	intersymbol interference
I/O	input/output	ISL	integrated Schottky logic
I ² L	integrated injection logic	ISO	International Standards Organization
I ³ L	isoplanar I ² L	ISR	intersecting storage ring
IAEA	International Atomic Energy Agency	ISS	ion scattering spectroscopy
IAR	isobaric analogue resonance	ISX	impurity study experiment
IAS	isobaric analogue state	IT	information technology
IBA	interacting boson approximation	ITC	ionic thermocurrents
IBFA	interacting boson-fermion approximation	ITEP	Institute of Theoretical and Experimental Physics
IBM	interacting boson model	ITO	indium tin oxide
IBPBAC	isobutyl-4-(4'-phenylbenzylideneamino) cinnamate	ITR	Ignition Test Reactor
IC	integrated circuit	IU	Indiana University
ICDF	intermediate coupling Dirac-Fock	IVO	improved virtual orbitals
ICF	inertial confinement fusion	IVP	initial value problem
ICP	inductively coupled plasma		
ICPP	Idaho Chemical Processing Plant	JAERI	Japan Atomic Energy Research Institute
ICRF	ion cyclotron range of frequencies	JCL	job control language
ICRH	ion cyclotron resonance heating	JET	Joint European Torus
IDT	interdigital transducer	JFET	junction field effect transistor
IEPA	independent electron pair approximation	JINR	Joint Institute for Nuclear Research
IETS	inelastic electron tunnelling spectra (oscopy)	JIT	just-in-time
IF	intermediate frequency	JT-60	Japanese Tokamak-60
IFA	ionisation front accelerator		
IFE	intelligent front end	KBS	knowledge based system
IGES	initial graphics exchange specification	KdVS	Korteweg-de Vries

KEK	Japan National Laboratory for High Energy Physics	LSPB	Large Scale Prototype Breeder
KKR	Korringa-Kohn-Rostoker	LSSD	level sensitive scan design
LAMPF	Los Alamos Meson Physics Facility	LSTF	Large Scale Test Facility
LAN	local area network	LTE	local thermodynamic equilibrium
LC	inductance-capacitance	LUMO	lowest unoccupied molecular orbitals
LCAO	linear combination of atomic orbitals	LV	low voltage
LCBO	linear combinations of (semi-localised) band orbitals	LWBR	light water breeder reactor
LCD	liquid crystal display/device	LWHCR	light water high convertor reactor
LCGO	linear combination of Gaussian orbitals	LWR	light water reactor
LCP	Large Coil Program	M1,M2	magnetic dipole, quadrupole
LCRO	linear combination of Rydberg orbitals	MAC	multiplexed analogue component
LCTF	Large Coil Test Facility	MADO	Mulliken approximation for differential overlap
LD	laser diode	MAGFET	magnetic field sensitive field effect transistor
LDD	lightly doped drain	MAN	metropolitan area network
LDPE	low density polyethylene	MAP	manufacturing automation protocol
LEAR	Low Energy Antiproton Ring	MARS	Mirror Advanced Reactor Study
LEC	liquid encapsulated Czochralski	MBBA	4-methoxybenzylidene-4'-n-butylaniline
LED	light emitting diode	MBE	molecular beam epitaxy
LEED	low energy electron diffraction	MBPT	many body perturbation theory
LEFD	Large Experimental Fusion Device	MCD	magnetic circular dichroism
LEP	Large Electron Positron (CERN)	MCFR	magnetic confinement fusion reactor
LET	linear energy transfer	MCP	microchannel plate
LEU	low enrichment uranium (10% U235)	MCPESCF	multiconfiguration paired excitation SCF
LEU/Th	low enrichment U/Th fuel	MCSCF	multiconfiguration self-consistent field
LF	low frequency	MCVD	modified chemical vapour deposition
LHRH	lower hybrid resonance heating	MCX α	multiconfiguration X α
LIFO	last in first out	MCZDO	multi-centre zero differential overlap
LIM	linear induction motor	MEC	molecular electron correlation(s)
LIME	laser induced magnetically enhanced	MEDO	multipole expansion of diatomic overlap
LLTR	Large Leak Test Rig	MEG	magnetoencephalography (-gram)
LLW	low level (radioactive) waste	MESFET	metal-semiconductor field effect transistor
LMC	Large Magellanic Cloud	MEU	Medium Enrichment Uranium (20% U235)
LMFBR	liquid metal fast breeder reactor	MEU/Th	Medium Enrichment U/Th fuel
LMIS	liquid metal ion source	MF	medium frequency
LMS	least mean square	MFP	mean free path
LMTO	linear combination of muffin tin orbitals	MFR	mirror fusion reactor
LNG	liquified natural gas	MFSK	multiple frequency shift keying
LOCA	loss of coolant accident	MFTF	Mirror Fusion Test Facility
LOCE	loss of coolant experiment	MHD	magnetohydrodynamics
LOCOS	local oxidation of silicon	MIC	microwave integrated circuit
LOF	loss of flow	MID	magnetically insulated diode
LOFT	Loss of Flow Test Facility	MIDP	microwave induced delayed phosphorescence
LOFW	loss of feed water	MIEHM	modified iterative extended Huckel method
LOG	linear quadratic Gaussian	MIM	metal-insulator-metal
LONA	low noise amplifier	MIMD	multiple input multiple data
LOOSP	loss of onsite power	MIMO	multiple input multiple output
LP	linear programming	MIND	mass impregnated non-draining
LPC	linear predictive coding	MINDO	modified incomplete neglect of differential overlap
LPCS	low pressure core spray	MIPS	million instructions per second
LPCVD	low pressure chemical vapour deposition	MIS	metal-insulator-semiconductor or management information system
LPE	liquid phase epitaxy		
LPFL	low pinchoff-voltage FET logic		
LPI	low probability of intercept		
LQG	linear quadratic Gaussian		
LSA	limited space charge accumulation		
LSD	local spin density or loop shut-down		
LSI	large-scale integration		

MISFET	metal-insulator-semiconductor field effect transistor	NBETF	Neutral Beam Engineering Test Facility
MIT	Massachusetts Institute of Technology	NBI	neutral beam injection
MITATT	mixed tunnelling avalanche transit time	NBPS	neutral beam power systems
MLB	multilayer board	NBS	National Bureau of Standards
MLC	multilayer ceramic	NC	numerical control
MLE	maximum likelihood estimation	NCBR	nitride cooled breeder reactor
MLS	microwave landing system	NCMET	non-closed shell many electron theory
MLW	medium level (radioactive) waste	NDDO	neglect of diatomic differential overlap
MM	millimetre	NDE	nondestructive evaluation
MMF	magnetomotive force	NDRO	nondestructive readout
MMI	man machine interface	NDT	nondestructive testing
MMIC	monolithic microwave integrated circuit	NEA	negative electron affinity
MNOS	metal-nitride-oxide-semiconductor	NEMO	non-empirical molecular orbitals
MO	molecular orbitals	NET	Next European Tokamak
MOCIC	molecular orbital constraint of interaction coordinates	NEVE	non-empirical valence-electron
MOCVD	metal-organic chemical vapour deposition	NHS	National Health Service
MODFET	modulation doped field effect transistor	NIC	negative impedance convertor
MODPOT	modulator potential	NLP	natural language processing
MOS	metal-oxide-semiconductor	NMOS	N-channel metal-oxide-semiconductor
MOSFET	metal-oxide-semiconductor field effect transistor	NMR	nuclear magnetic resonance
MOST	metal-oxide-semiconductor transistor	NMR-ON	NMR on oriented nuclei
MOV	metal oxide varistor	NNDO	neglect of non-neighbour differential overlap
MOVPE	metal-organic vapour phase epitaxy	NOR	not-or(logic)
MOX	mixed oxide fuel	NPL	National Physical Laboratory
MPH	moving plasmoid heater	NQR	nuclear quadrupole resonance
MPSK	multiple phase shift keying	NRC	Nuclear Regulatory Committee
MPU	microprocessing unit	NRM	natural remanent magnetisation
MQORC	modified quadrature overlapped raised cosine	NRZ	non-return to zero
MQW	multiple quantum well	NSRR	Nuclear Safety Research Reactor
MRAC	model reference adaptive control	NSSS	nuclear steam supply system
MRD	multiple-reference double excitation	NTL	nonthreshold logic
MRINDO	modified Rydberg INDO	NTO	natural transition orbitals
MRP	materials requirements planning	NTSC	National TV Standards Committee
MRP II	manufacturing resources planning	NWPA	Nuclear Waste Policy Act
MS	management science	OA	office automation
MSI	medium scale integration	OCR	optical character recognition
MSK	minimum shift keying	ODE	ordinary differential equation
MSR	molten salt reactor	ODMR	optical detection of magnetic resonance
MSSW	magnetostatic surface wave	OEIC	optoelectronic integrated circuit
MSU	Michigan State University	OEM	original equipment manufacture
MSW	magnetostatic waves	OER	oxygen enhancement ratio
MSX α	multiple scattering X alpha	OH	ohmic heating
MTBF	mean-time between failures	OHTE	Ohmically Heated Toroidal Experiment
MTF	modulation transfer function	OPHF	orbital polarised Hartree-Fock
MTI	moving target indicator	OPW	orthogonal plane wave
MTL	merged-transistor logic	OQPSK	offset quadrature phase shift keying
MTTF	mean time to failure	OR	operations research
MTX α	muffin-tin X α	ORELA	Oak Ridge Electron Linear Accelerator
MUF	material unaccounted for or maximum usable frequency	ORNL	Oak Ridge National Laboratory
MWPC	multiwire proportional chamber	OS	operating system
NAL	National Accelerator Laboratory	OSI	open systems interconnection
NAND	not-and(logic)	OTDR	optical time domain reflectometry
		OTEC	ocean thermal energy conversion
		OTF	optical transfer function
		OTS	Orbital Test Satellite

OTSG	once-through steam generator	PMDR	phosphorescence microwave double resonance
OZI	Okubo-Zweig-lizuha (quark model)	PMOS	P-channel metal-oxide-semiconductor
PAA	paraazoxyanisole	PMR	proton magnetic resonance
PABX	private automatic branch exchange	PMS	pre-main-sequence
PAC	perturbed angular correlation	PN	planetary nebula(e)
PAHR	post accident heat removal	PNDO	partial neglect of differential overlap
PAL	phase alternate line or programmable array logic	PNO-CI	pair natural orbital configuration interaction
PAM	pulse amplitude modulation	PNS	Pulsed Neutron Source
PAP	paraazoxyphenetole	POL	pair orthogonalised Lowdin
PBF	power bursts facility	POPAE	protons on protons and electrons
PBFA	Particle Beam Fusion Accelerator	POPOP	phenyl-oxazoly-phenyl-oxazoly-phenyl
PBL	planetary boundary layer	PORV	power operated relief valve
PBR	pebble bed reactor	POS	point of sale
PBT	permeable base transistor	PPB	parts per billion
PBX	private branch exchange	PPDP/S	Pariser-Parr-Del Bene-Pople/Segal calculations
PC	printed circuit or personal computer or programmable controller	PPI	plan position indicator
PCAC	partially conserved axial currents	PPM	pulse position modulation or parts per million
PCB	polychlorinated biphenol or printed circuit boards	PPP	Pariser-Parr-Pople
PCES	phase change energy storage	PRA	probabilistic risk assessment
PCI	pellet-cladding interaction	PRDDO	partial retention of diatomic differential overlap
PCILOCC	perturbative configuration interaction using localised orbitals for crystal calculation	PREPP	Process Experimental Pilot Plant
PCM	pulse code modulation	PRF	pulse recurrence (repetition) frequency
PCRV	prestressed concrete reactor vessel	PROM	programmable read-only-memory or Pockels readout optical modulator
PCV	primary containment vessel	PS	proton synchrotron (CERN)
PCX	plasma confinement experiment	PSD	power shut-down or power spectral density
PD	partial discharge	PSDN	packet switched data network
PDE	partial differential equation	PSG	phosphosilicate glass
PDF	probability density function	PSK	phase shift keying
PDX	Poloidal Divertor Experiment	PSS	packet switching service or Packet SwitchStream
PEC	photoelectrochemical cell	PSTN	public switched telephone network
PEM	photoelectromagnetic	PSU	power supply unit
PEP	Positron Electron Photon (Stanford)	PTFE	polytetrafluoroethylene
PES	photoelectron spectra (spectroscopy)	PTH	plated through hole
PET	polyethylene terephthalate or positron emission tomography	PTM	pulse time modulation
PETRA	Positron Electron Tandem Ringbeschleuniger Anlage	PV	photovoltaic
PF	poloidal field or power factor	PVC	polyvinyl chloride
PFM	pulse frequency modulation	PVD	physical vapour deposition
PFR	Prototype Fast Reactor	PWA	partial wave analysis
PHWR	pressurised heavy water reactor	PWB	printed wiring board
PID(PI,PD)	proportional+integral+differential (derivative)	PWBA	plane wave Born approximation
PIPECO	photoion photoelectron coincidence	PWIA	plane wave impulse approximation
PIUS	process inherent ultimately safe	PWM	pulse width modulation
PIXE	photon induced X-ray emission	PWR	pressurised water reactor
PLA	phase locked arrays or programmable logic array	QA	quality assurance
PLBR	Prototype Large Breeder Reactor	QAM	quadrature amplitude modulation
PLC	programmable logic control	QASK	quadrature amplitude shift keying
PLCC	plastic leadless chip carrier	QC	quality control
PLD	programmable logic device	QCD	quantum chromodynamics
PLL	phase locked loops	QDMBPT	quasi-degenerate many-body perturbation theory
PLT	Princeton Large Torus	QED	quantum electrodynamics
PM	pulse modulation or phase modulation	QFSK	quadrature frequency shift keying
PMMA	polymethylmethacrylate		

QORC	quadrature overlapped raised cosine	SAR	synthetic aperture radar
QOSRC	quadrature overlapped squared raised cosine	SARSAT	search and rescue satellite aided tracking
QPM	quark-parton model	SAW	surface acoustic waves
QPR	quadrature partial response	SAXS	small-angle X-ray scattering
QPSK	quaternary phase shift keying	SC	switched capacitor
		SCADA	supervisory control and data acquisition
R & D	research and development	SCC	stress corrosion cracking
RAD	ribbon-against-drop	SCF	self-consistent field
RAM	random access memory	SCFL	source-coupled FET logic
RBE	relative biological effectiveness	SCH	separate confinement heterostructure
RBMK	light water cooled, graphite moderated reactor	SCL	space charge limited
RBS	Rutherford backscattering	SCPC	single channel per carrier
RC	resistance-capacitance	SCPT	self-consistent perturbation theory
RCIC	reactor core isolation cooling	SCR	silicon controlled rectifier
RCNDO	Rydberg CNDO	SCSI	small computer system interface
RCS	rapid cycling synchrotron or reactor coolant systems	SCTF	Slab Core Test Facility
RCTL	resistor-capacitor-transistor logic	SDFL	Schottky-diode FET logic
RDBMS	relational database management system	SDI	selective dissemination of information or Strategic Defense Initiative
REA	rod ejection accident	SDLC	synchronous data link control
RF	radio frequency	SDM	space division multiplexing
RFI	radio frequency interference	SDMA	space division multiple access
RFPR	reversed field pinch reactor	SDO	shielded diatomic orbitals
RFX	Reversed Field (Pinch) Experiment	SED	stochastic electrodynamics
RG	renormalisation group	SEHF	spin extended Hartree-Fock
RGB	red green blue	SEM	scanning electron microscopy
RHEED	reflection high energy electron diffraction	SERS	surface enhanced Raman scattering
RHF	restricted Hartree-Fock	SEXAFS	surface extended X-ray absorption fine structure
RIA	reactivity initiated accident	SFE	solar-flare effect
RIE	reactive ion etching	SFL	substrate fed logic
RINDO	Rydberg INDO	SGEMP	system generated electromagnetic pulse
RISC	reduced instruction set computer	SGHWR	steam generating heavy water reactor
RKKY	Rudermann-Kittel-Kasuya-Yosida	SHF	superhigh frequency
RLC	resistance-inductance-capacitance	SHG	second harmonic generation
RMS	root-mean-square	SICOS	sidewall base contact structure
RNA	ribonucleic acid	SIL	single-in-line
RNS	residue number system	SIMD	single instruction multiple data
ROM	read-only memory	SIMOS	stacked-gate injection metal-oxide-semiconductor
RPA	random phase approximation	SIMOX	separation by implantation of oxygen
RPAE	random phase approximation with exchange	SIMS	secondary ion mass spectroscopy
RPM	relaxation potential model or revolutions per minute	SIN	Swiss Institute of Nuclear Research
RPV	reactor pressure vessel	SINDO	scaled INDO
RTA	rapid thermal annealing	SIPOS	semi-insulating polycrystalline silicon
RTG	radioisotope thermoelectric generators	SIS	semiconductor-insulator-semiconductor
RTL	resistor-transistor logic	SISAM	spectrometer with interference selective amplitude modulation
RTP	rapid thermal processing	SISO	single input single output
RTTY	radio teletypewriter	SIT	static induction transistor
		SLC	Stanford Linear Collider
S/N	signal-to-noise	SLIC	subscriber line interface circuit
SACCI	symmetry adapted cluster configuration interaction	SLSF	Sodium Loop Safety Facility
SAINT	self-aligned implantation for N ⁺ -layer technology	SMA	surface mount(ed) assembly
SAMO	simulated ab initio molecular orbitals	SMATV	satellite master antenna television
SAMOS	stacked gate avalanche injection metal-oxide-semiconductor	SMC	Small Magellanic Cloud or surface mount(ed) component
SAN	small area network	SMD	surface mount(ed) device
		SMES	superconductive magnetic energy storage

SMPS	switched mode power supply	SURMAC	surface magnetic confinement
SMQORC	staggered modified quadrature overlapped raised cosine	SUSY GUT	supersymmetric grand unified theory
SMT	surface mount(ed) technology	SVC	static VAR compensator
SN	supernova(e)	SW	short wave
SNA	Systems Network Architecture	SWEPP	Stored Waste Examination Pilot Plant
SNM	special nuclear material	SWR	sodium water reactor or standing wave ratio
SNR	signal to noise ratio or supernova remnant	SXAPS	soft X-ray appearance potential spectra(oscopy)
SNS	superconducting normal superconducting or Spallation Neutron Source	TAB	tape automated bonding
SOG	strongly orthogonal geminal	TASI	time assignment speech interpolation
SOI	silicon on insulator	TAT	transatlantic telephone cable
SOS	silicon on sapphire	TBBA	terephthal-butylaniline
SPA	separated pair approximation	TCNE	tetracyanoethylene
SPC	stored program control	TCNQ	tetracyanoquinodimethane
SPCP	single parity check product (code)	TCR	temperature coefficient of resistance
SPEAR	Stanford Positron Electron Asymmetric Ring	TCXO	temperature compensated crystal oscillator
SPECT	single photon emission computerised tomography	TDHF	time-dependent Hartree-Fock
SPHF	spin polarised Hartree-Fock	TDF	Technology Demonstration Facility or transborder data flow
SPLEED	spin polarised low energy electron diffraction	TDM	time division multiplex(ing)
SPS	Super Proton Synchrotron (CERN)	TDMA	time division multiple access
SQAM	superposed quadrature amplitude modulation	TDMF	time dependent mean field theory
SQL	standard query language	TDPAC	time differential perturbed angular correlation
SQPR	staggered quadrature partial response	TDS	thermal desorption spectra(oscopy)
SQPSK	staggered quadrature phase shift keying	TE	transverse electric
SQUID	superconducting quantum interference device	TEA	transversely excited atmosphere
SRAM	static random access memory	TED	transferred electron device
SREMP	source region electromagnetic pulse	TEGFET	two-dimensional electron gas field effect transistor
SRMCASE	symmetry-restricted-multiconfiguration annihilation of single excitations	TEM	transverse electromagnetic or transmission electron microscopy
SRV	safety release valve	TEXT	Texas Experimental Tokamak
SS-TDMA	satellite switched time division multiple access	TF	toroidal field
SSB	single sideband	TFCX	Toroidal Fusion Core Experiment
SSBW	surface skimming bulk wave	TFT	thin film transistor
SSC	sudden storm commencement or Superconducting Super Collider	TFTR	Tokamak Fusion Test Reactor
SSCR	spectrum shift controlled reactor	TGA	thermogravimetric analysis
SSFL	Schottky-barrier coupled Schottky-barrier gate FET logic	TGFB	triglycine fluoroberyllate
SSI	small scale integration	TGS	triglycine sulphate
SSMA	spread spectrum multiple access	TGSe	triglycine selenate
SST	sea surface temperature or supersonic transport	THF	tremendously high frequency
STD	salinity-temperature-depth or subscriber trunk dialling	THORS	Thermal-Hydraulic Out-of-Reactor Safety Facility
STEC	solar thermal energy conversion	THTF	Thermal Hydraulic Test Facility
STEM	scanning transmission electron microscopy	TIL	two interdigitation level
STI	scientific and technical information	TJS	transverse junction stripe
STL	Schottky transistor logic	TLD	thermoluminescent dosimeter(-ry)
STM	scanning tunnelling microscopy	TM	transverse magnetic
STO	Slater-type orbitals	TMC	Test Module Coil
STOL	short take-off and landing	TMHR	tandem mirror hybrid reactor
STP	Slater-transfer Preuss	TMI	Three Mile Island
		TMMC	tetramethylammonium manganese chloride
		TMR	tandem mirror reactor
		TMTSeF	tetramethyltetraselenafulvalene (-inium)
		TMTTF	tetramethyltetrathiofulvalene(-inium)
		TMX-U	Tandem Mirror Experiment-Upgrade
		TNS	The Next Step
		TOF	time-of-flight

TOP	technical office protocol or transient overpower accident	VDM	vector dominance model
TPC	time projection chamber	VDT	visual display terminal
TPD	temperature programmed desorption	VDU	visual display unit
TPTF	Two Phase Flow Test Facility	VDW	van der Waals
TRAPATT	trapped plasma avalanche triggered transit	VFO	variable frequency oscillator
		VHF	very high frequency
TREAT	Transient Reactor Test Facility	VHPIC	very high performance integrated circuit
TRM	thermoremanent magnetisation	VHSIC	very high speed integrated circuit
TRRR(TR ₃)	time resolved resonant Raman (spectra (-oscopy))	VHV	very high voltage
TRU	transuranic (waste)	VJFET	vertical junction field effect transistor
TSC	thermally stimulated currents	VLBI	very long base line interferometry
TSD	thermally stimulated desorption	VLF	very low frequency
TSEE	thermally stimulated exo-electron emission	VLSI	very large scale integration
TSIC	thermally stimulated ionic currents	VM	virtual machine
TSeF	tetraselenafulvalene(-inium)	VMOS	vertical channel metal-oxide-semiconductor
TSeT	tetraselenatetracene	VOR	VHF omnidirectional range
TSTA	Tritium Systems Test Facility	VPE	vapour phase epitaxy
TTL	transistor transistor logic	VRC	visual record computer
TTMP	transit time magnetic pumping	VRDDO	variable retention of diatomic differential
TTT	tetrathiotetracene	VS	virtual storage
TTY	teletype terminal	VSAT	very small antenna terminals
TUCA	transient undercooling accident	VSF	vestigial sideband
TUCOP	transient undercooled overpower accident	VSEPR	valence shell electron pair repulsion
TV	television	VSWR	voltage standing wave ratio
TVRO	TV receive only	VTOL	vertical take-off and landing
TW	travelling wave	VTR	voltage transformation ratio or video tape recorder
TWT	travelling wave tube	VUV	vacuum ultraviolet
		VVER	water moderated water cooled reactors
UART	universal asynchronous receiver transmitter	VVVF	variable voltage variable frequency
UCHF	uncoupled Hartree-Fock		
UCN	ultra cold neutrons	WAN	wide area network
UHF	ultra high frequency or unrestricted Hartree-Fock	WARC	World Administrative Radio Conference
UHPS	underground hydroelectric pumped storage	WAXS	wide-angle X-ray scattering
UHV	ultra high voltage	WDF	wave digital filter
UJT	unijunction transistor	WDM	wavelength division multiplex(ing)
UKAEA	United Kingdom Atomic Energy Authority	WIPP	Waste Isolation Pilot Plant
ULA	Uncommitted logic array	WKB	Wentzel-Kramers-Brillouin
ULF	ultra low frequency	WORM	write once read many times
ULSI	ultra-large scale integration	WP	word processing
UMD	unitised microwave devices	WR	Wolf-Rayet
UPS	ultraviolet photoelectron spectra(oscopy) or uninterruptible power supply	WSI	wafer scale integration
US	ultrasonic	WWER	water moderated water cooled reactors
USART	universal synchronous/asynchronous receiver transmitter	XANES	X-ray absorption near edge structure
UUT	unit under test	XLPE	cross-linked polyethylene
UV	ultraviolet	XOR	exclusive-OR
		XPD	cross-polarisation discrimination
VAD	vapour phase axial deposition	XPS	X-ray photoelectron spectra
VAN(S)	value added network (services)	XUV	X-ray-ultraviolet
VB	valence bond		
VCCS	voltage controlled current source	ZEBRA	Zero Energy Breeder Reactor Assembly
VCO	voltage controlled oscillator	ZGS	zero gradient synchrotron
VCR	video cassette recorder	ZPPR	zero power plutonium reactor
VCVS	voltage controlled voltage source	ZTP	Z toroidal pinch

Subject Index

1/f noise *see random noise*

2-6 semiconductors *see II-VI semiconductors*

3-5 semiconductors *see III-V semiconductors*

3-6 semiconductors *see III-VI semiconductors*

4-6 semiconductors *see IV-VI semiconductors*

A-centre lasers *see colour centre lasers*

A-centres

Si, O-vacancy pair deep level carrier capture and emission press. depend.

meas., lattice relax. determ. 7-21862

CaF₂:Li⁺(Na⁺), EPR of colour centres 7-17222

GaSe:Mn single crystals, optical props. 7-27777

Ge:Zn deep impurity, shallow positive acceptor, far IR photocond. meas. 7-7157

KCl, cryst. F_A (Li)-centres exposed to radiation, bleaching rate 7-37060

KCl crystals with F_A(Li)-centres, double beam clarification kinetics (*Russian*) 7-53253

KCl:Li, F_A-centre crystals, diffraction efficiency of photoinduced gratings 7-62818

KCl:Li, self-induced light polarisation oscills., stochastic field effects (*Russian*) 7-43208

KCl:Li crystals, F_A-centres self-induced resonant radiation polarisation changes study (*Russian*) 7-33358

KCl:Ti, photoionisation of Ti³⁺, intense excitation in A-absorption band (*Russian*) 7-16554

KCl_{1-x}Bi_xLi mixed crystals, F_A centre absorpt. and emission spectra studies 7-12064

KI:Li (F₂⁺)_A centre, selective two-step photoionisation using 1.06 μm radiation 7-38053

NaCl:Ti, photoionisation of Ti³⁺, intense excitation in A-absorption band (*Russian*) 7-16554

p-Si, gamma-ray irradi., recombination centres, p-n junction meas. 7-37985

Si, radiation defect thermal ionisation, effect of dislocations on activation energy 7-6680

SrF₂:Na⁺, EPR of colour centres 7-17222

ZnS:Al, Cr, Fe crystals, recomb. luminesc., EPR and photocond. meas. 7-3076

A/D conversion *see analogue-digital conversion*

ab initio calculations

3d metal compounds, equilibr. geometry, pot. surface, ab initio calcs. 7-15511

acetamide, rotational barriers, polarisation functions, ab initio SCF calcs. 7-15496

acetic acid, unimol. pyrolysis mechanisms, ab initio quantum-chem. study 7-46805

acetylacetone enolate anions, collision-induced losses of ketene, mass spectra 7-13839

acetyldimethylphosphine, geometries and rotation barriers, structures, ab initio calcs. 7-15501

acetylene, binding energies, ab initio HF calcs. 7-49894

acetylene, elec. polarisabilities, ab initio calcs. 7-5585

acetylene, protonated, d₀(d₃), struct., vibr. freqs., IR intensities 7-5677

acrolein, cycloaddition intermediate, semiempirical MINDO/3 SCF and CI calcs. 7-56983

alkali halides, refractive index, Szigeti charge, dielec. parameters ab initio calcs. 7-13082

alkali metal monohydroxides, high temp. photoelectron spectroscopy, ab initio MO calcs. 7-50251

alkali metals, structural properties, ab initio calc. 7-21156

alkali metals ionic clusters, stability and struct. Xα and ab initio methods 7-10421

alkali-metal atoms, photoionisation cross sections, ab initio RRPA calcs. 7-36462

alkane molecules, T beta-decay, molecular effects, neutrino mass determ. 7-49310

alkane molecules, T beta-decay, molecular final-state interactions 7-49311

allenes, monosubstitution, stabilisation energies, isodemic methyl exchange reaction study, ab initio LCAO SCF calcs. 7-25389

anion-water complexes, struct. and binding energy, ab initio study 7-15483

atomic diabatic states, nonadiabatic interactions, CI wave fns. expansion, ab initio LCAO SCF CI calcs. 7-49945

atomic micro-clusters, electronic struct., ab initio studies 7-31203

atomic transition and ionisation energies, g-Hartree ab initio calcs. 7-15488

azoles, protonation energies and tautomerism, basis set effects 7-25374

azoles, UV photoelectron spectral assignment, ab initio. MRD CI calcs. 7-50239

benzene, valence and Rydberg states, CASSCF-contracted CI calcs. 7-56997

benzene+NO⁺, struct. and energetics, calc. by ab initio MO computations 7-8267

p-benzoquinone, struct. and vibr. anal., ab initio HF calcs. 7-25372

p-benzosemiquinone radical anion, struct. and vibr. anal. ab initio HF calcs. 7-25372

bibliography, Quantum Chemistry Literature Database, 1985 7-41031

bicyclic compounds, valence force field and vibr. wavenumber calcs., IR and Raman data comparison 7-50079

bicyclo (1.1.1) pentane, bonding and geometry, quasi ab-initio PRDDO method, GVB-type correl. 7-25404

bipyridine, dications and cation radicals, conformational struct. ab initio calc. 7-15497

1,1'-bipyrrrole, rot. isomerism, mol. conformation, electronic struct. ab initio STO calcs. 7-15478

ab initio calculations continued

bis(π-allyl) nickel, photoelectron spectrum, semi-empirical and ab initio Green's Function methods 7-30950

bond order and valence indices, rels. to Mulliken's population anal. and covalent chemical reactivity 7-56948

butane, rot. pot. functions, ab initio and MM2 calcs. 7-10404

butatrienone-do(d₃), struct., vibr. anal. ab initio MO calcs., microwave spectroanal. 7-25491

carbamic acid derivatives, torsional changes, ab initio structural studies 7-15502

carbonyl imines, relative stability, ab initio SCF MO study 7-57003

carboranes, optimised struct. and relative stabilities, ab initio calcs. 7-30930

chlorin free base, UV absorpt. spectra intensities, ab initio SCF-CI calcs. 7-10447

chlorobenzenes, temporary anion states, electron transmission spectroscopy 7-42597

chlorophyll-H₂O system, ab initio LCAO SCF MO calcs., ionisation pot., electron affinity, intermol. mechanics 7-8520

compound metal clusters, struct. and electronic structs. calcs. 7-15783

conjugated hydrocarbon ions, stability ab initio calcs. 7-42462

correlation energy, scaling in perturbation theory calcs. of bond energies and barrier heights 7-10391

crown ethers, simulated ab initio MO calc. 7-49908

1-cyanoaziridine, internal rot. and nitrogen inversion, ab initio and MNDO calcs. 7-15516

cyclen mols. in water, Monte Carlo simulation, pot. function, ab initio calcs. 7-21071

cyclic ketones, α-bond rupture, photochem. reaction, ab initio SCF CI calcs. 7-56998

cyclopentene, struct., ab initio MO calcs. 7-49895

cyclopropene, low-lying excited states, UV spectrum, ab initio study 7-62393

cyclopropenes, structs. and strain energies, substituent effects, ab initio MO calcs. 7-56950

cyclopropylamine, substituent effect, struct., ab initio calcs., microwave spectra 7-62354

cytosine and thio derivatives, tautomerism, ab initio study 7-837

deltic acid, crystal struct., vibr. anal., monoanion props., ab initio SCF calcs. 7-25387

di-t-butyl silylene, triplet ground-state, electronic and steric effects, ab initio calcs. 7-25419

diacetylene, elec. polarisabilities, ab initio calcs. 7-5585

diamond, interstitial H or muonium, Hartree-Fock analysis 7-32947

diamond, muonium, anomalous, model as body-centered interstitial muonium, HF calc. 7-45899

diamond, optical phonons and elasticity at megabar stresses 7-21375

diamond (111) surface reconstruction, energy minimisation calculations 7-12434

diarylphosphonyl radical, kinetic and spectrosc. characterisation 7-62419

diamonic molecules, photoemission processes, ab initio calcs. 7-19676

1,2-dichlorobenzene-d₃(d₄), isotopic species, r₀ structure calcs., microwave spectra 7-19834

1,2-dichloroethane, rot. isomerism, energy levels and struct., vib. anal. ab initio SCF MO calcs. 7-19690

dielectronic recombination, electric field enhancement over Rydberg spectrum 7-5618

1,2-difluoroethane, gauche and trans conformers, stability, ab initio calcs. 7-15500

trans-difluoroethylene ozonide, struct. dipole moment, ab initio HF calcs., microwave spectra 7-10557

dimethyl ether-sulphur dioxide complex, photoelectron spectra 7-15646

dimethyl silylene, triplet ground-state, electronic and steric effects, ab initio calcs. 7-25419

dimethylamine radical cation, hyperfine coupling tensors, ab initio UHF calcs. 7-25373

dimethyldioxirane, electronic struct. and geometry, NMR chem. shifts 7-62406

4,4-dioxy-4-thia-1-acetyl-1,4-dihydropyridine, heteroaromaticity, p-d bonding, NMR, crystallography and calcs. 7-15623

disulphide bond, S-S dihedral angle, ab initio SCF MO calcs. and 7-15504

electron and two-photon momentum distrib., ab initio calc. using LMTO formation 7-46182

electronic struct. and dynamics, conf., Snowbird, UT, USA (April 1986) 7-55877

ethane, ground state, thermal decomp. pathways, ab initio electronic struct. calcs. 7-15476

ethanediazonium ions, unimol. dissoc., ab initio and semiempirical MNDOC calcs. 7-15513

ethyl, ethenyl and ethynyl anions, structs. and rearrangement processes, ab initio MO calcs. 7-59757

ethylene, bending force const. attenuation, ab initio CI calcs. 7-49939

bidentate ethylene diamine complexes with ions Na⁺, Li⁺ and H⁺, ab initio MO calcs., binding energy 7-10383

ethylene dications, F-substituted, geometries and energies, ab initio calcs. 7-10401

ethylenes, fluorinated, photoelectron spectrosc. 7-42682

ethylenes, monosubstituted, struct., ab initio calcs. 7-850

ethylmethysilane, rot. pot. functions, ab initio and MM2 calcs. 7-10404

fluoromethanes, protonated, structs., energetics, ab initio MO calcs. 7-56956

1-fluoropropane, nuclear spin-spin coupling consts., calcs. using IPPP method 7-36644

fluorosilanes, protonated, structs., energetics, ab initio MO calcs. 7-56956

formaldehyde, protonated, rot. const., ab initio MO calcs. 7-25349

ab initio calculations continued

formamide, rot. barriers, polarisation functions, ab. initio SCF calcs. 7-15496

formic acid dimer, symm. stretching modes in gas phase 7-25475

formic acid radical cation and its isomers, pot. energy surface, ab initio quantum chemical methods appl. 7-42521

formyl cyanide, vibr. freqs. and geometry, ab initio electron correl. calcs. 7-49938

formyl radical pair, anharmonic vibr. effects, ab initio SCF-CI calcs. 7-10444

1-formylaziridine, internal rot. and nitrogen inversion, ab initio and MNDO calcs. 7-15516

formylcyclopropane, internal rot. and nitrogen inversion, ab initio and MNDO calcs. 7-15516

formylphosphine, geometries and rotation barriers, structures, HF-calcs. 7-15501

glycine, zwitterion, electronic excitation spectrum, aq. solvation effects, CI calcs. 7-50160

glycolic acid, rot. isomerisation, ab initio SCF calcs., IR Ar matrix spectra 7-19851

guanine-metabolite adducts, ab initio and CNDO/2 and MINDO/3 calcs. 7-49928

halogen thiocyanates (isothiocyanates), ionis. pots., photoelectron spectrosc. and ab initio calcs. 7-25601

hydrides, relative energy characts., electronic correl. in ab initio calcs. 7-15528

hydrocarbon peroxy radicals, ab initio MO and electron correl. calcs. 7-49951

hydroxyethylene, cycloaddition intermediate, semiempirical MINDO/3 SCF and CI calcs. 7-56983

8-hydroxyquinoline, intramol. H bonding, UV photoelectron spectra and MO calcs. 7-25367

8-hydroxyquinoline-N-oxide, intramol. H bonding, UV photoelectron spectra and MO calcs. 7-25367

iminoborane, and derivatives, electronic struct. ab initio calcs. 7-847

ion-neutral mol. interactions, intermolecular potential functions, additivity 7-10699

ionic solids, interaction energies, relativistic ab initio calc., review 7-52109

ionic solids, relativistic ab initio calcs., review 7-52110

ionic solids, stabilisation of CsCl versus NaCl struct., ab initio pseudopotential calcs. 7-58199

ionisation phenomena, ab initio wave functions 7-36444

ions, in cryst., dipole-quadrupole dispersion coefficients, ab initio coupled HF calcs. 7-11986

isocytosine, and thio derivatives, tautomerism, ab initio study 7-837

isoformyl cation, force field, equilbr. geometry, ab initio determ. 7-62293

isoformyl cation, rot.-vibr. energies, ab initio pot. surfaces 7-62264

lysophosphatidyl ethanolamine, energetics, hydration struct., ab initio pots. 7-65300

(M-OH₂)⁺ complexes, charge transfer and electric mobility, ab initio SCF calcs. 7-62253

magnetism and electronic struct. at surfaces and interfaces, ab initio calcs. 7-58854

metal clusters, ionisation phenomena, ab initio wave functions 7-36444

metals, twin-boundary energies and entropies, const. press. Monte Carlo calc. 7-2028

metals and alloys, phase diagrams, ab initio calc. using electronic and thermodynamic perturbation theory 7-17516

methane, binding energies, ab initio HF calcs. 7-49894

methane, electron scatt. cross section calc., parameter-free model interaction 7-62535

methane, proton-proton spin-spin coupling surface 7-42645

methane ion, photoelectron spectrum, Jahn-Teller effect, ab initio SCF and CI calcs. 7-42683

methanediazonium ions, unimol. dissoci., ab initio and semiempirical MNDOC calcs. 7-15513

methanimine, fluorination effect on double bonds, SCF HF and MP2 ab initio calcs. 7-10384

methoxycarbene, energies, struct., vibr. freqs. and unimol. reactivities 7-10398

methyl carbons, chemical shielding, struct. effects, ¹³C NMR spectra anal., ab initio IGLO calcs. 7-25358

methyl ether, mol. charge similarity index study, appl. to isosteric cpds. 7-56978

methyl fluoride, pot. surface studied using ab initio MO theory with electron correl. energy 7-42494

methyl imino sulphur difluoride, ab initio calcs. at SCF level, equilbr. geometries and population anal. 7-10382

2-methyl oxetan, vibr. circular dichroism spectra, expt. and theoretical results 7-50208

methyl sulphide, mol. charge similarity index study, appl. to isosteric cpds. 7-56978

s-cis methyl vinyl ether, coupled torsional and bending motions, microwave Fourier transform spectra 7-62355

N-methyl-N'-nitro-N-nitrosoguanidine, conform. struct. and stability, ab initio MNDO calcs. 7-25406

N-methylacetamide-formamide, varying H bond geometry, N-H bond vibr. properties, ab initio calcs. 7-10407

1-methylallyl cation, photoionisation mass spectrometry, heat of form., ionisation energies, ab initio MO calcs. 7-13798

methylamine, N-methyl substitution, bond dissoci. energies, SCF calcs. 7-15503

methylamine radical cation, hyperfine coupling tensors, ab initio UHF calcs. 7-25373

methylidiazohydroxide, dissoci., ab initio calcs., rel. to carcinogenesis 7-56962

methylene, low-lying singlet and triplet states, substituent effects 7-10429

methylene radical, ¹A₁ state and ¹A₁-³B₃ coupling, visible absorpt. and mag.-rot. spectra 7-49903

methyleneamino compounds, electronic struct. calcs. 7-56964

methyleneonium ylide, pot. surface studied using ab initio MO theory with electron correl. energy 7-42494

methylhydroxycarbene, energies, struct., vibr. freqs. and unimol. reactivities 7-10398

N-methylhydroxylamine, N-methyl substitution, bond dissoci. energies, SCF calcs. 7-15503

methylimine, protonation, C=N bond rehybridisation rel. to stretching force const. 7-30925

methylthiirane, vibr. spectra and ab initio calcs. 7-50147

ab initio calculations continued

1-methyluracil, isotopic derivatives vibr. spectra, ab initio Hartree-Fock SCF calcs. 7-15589

molecular excited states, decay via radiative and dissoci. mechanisms, ab initio MRD-CI calcs. 7-57001

molecular nucl. mag. shielding consts. ab initio wave function calcs. 7-5594

molecules, clusters, solids and crystals, ab initio calcs. 7-56930

molecules, macroscopic solvation, electron distrib. ab initio INDO SCF calcs. 7-54099

molecules, neutral and anionic, proton affinities, ab initio calcs., role in ion-mol. reactions 7-5590

monohalomethane, harmonic force fields and vibr. spectra, ab initio HF calc. 7-50064

nitromethane, isomers, struct., quantum mech. harmonic force field calcs. 7-56952

N-nitrosamine metabolites, alkylating species, role in carcinogenesis 7-49889

nitrosomethanol, rotamers, struct., ab initio calcs. 7-56955

organic molecules, photochemical processes, ab initio quantum chemical calcs. 7-59772

organic ring systems, edge inversion at trivalent phosphorus centre, NMR spectra anal., ab initio SCF calcs. 7-25362

n-pentane, bond distances and angles, ab initio gradient geometry refinement 7-852

periodic polypeptides, band struct. ab initio HF cryst. orbital calcs. 7-23298

pharmacologically active cpds., similarity meas. calcs. 7-49890

phosphamethane, fluorination effect on double bonds, SCF HF and MP2 ab initio calcs. 7-10384

phospholipids, interaction with H₂O and Na⁺, ab initio SCF calcs. 7-59919

phosphonium ylides, fluorine-substituted, struct., energetics, ab initio SCF calcs. 7-30923

polyacetylene, alkaline metal doped, ab initio SCF MO calc. of electronic struct. 7-64048

polyacetylene, N-containing analogues, electronic struct., conduction props., ab initio study 7-32911

polyacetylene, Raman scatt. from CDW, ab initio calcs. 7-46015

polyacetylene, solitons, electronic props., local space approx. 7-52506

polyalanine fragment, solvent struct. hydration, Monte Carlo simulation 7-23299

polyfuran and copolymers, electronic struct., cond. props., ab initio cryst. orbital calcs. 7-52410

polyisothianaphene, electronic struct. and conduction properties 7-45119

polypyrrole and copolymers, electronic struct., cond. props., ab initio cryst. orbital calcs. 7-52410

polythiophene and copolymers, electronic struct., cond. props., ab initio cryst. orbital calcs. 7-52410

porphyrin free base, UV absorpt. spectra intensities, ab initio SCF-CI calcs. 7-10447

position annihilation, electron-positron interactions, review 7-46179

propane, mol. charge similarity index study, appl. to isosteric cpds. 7-56978

propanediazonium ions, unimol. dissoci., ab initio and semiempirical MNDOC calcs. 7-15513

I(1,1,1) propellane, bonding and geometry, quasi ab-initio PRDDO method, GVB-type correl. 7-25404

propene, electronic states, electron impact spectrosc. and ab initio CI calcs. 7-25417

propylamine, fragmentation, electron impact mass spectrometry, ab initio MO calcs. 7-50387

propylene, bending force const. attenuation, ab initio CI calcs. 7-49939

propylsilane, rot. pot. functions, ab initio and MM2 calcs. 7-10404

proteins, aperiodic, electronic struct., ab initio calcs. 7-23273

pure liq. metals, ab initio variational thermodynamic calcs., hard-sphere Yukawa model 7-26606

pyrazine, successive protonation, ab initio quantum chem. calcs. 7-56957

radical anions, single cryst., dissoci., struct. investig. 7-33275

semiconductor heterojunction discontinuities, self-consistent density functional calcs. 7-7364

semiconductor heterojunctions, self-consistent density functional calcs. 7-17097

silathylene, harmonic vibr. freqs., IR spectra, ab initio SCF CI calcs. 7-15600

spin-spin coupling consts., ab initio diamagnetic spin-orbital contrib. 7-927

squaric acid, crystal struct., vibr. anal., monoanion props., ab initio SCF calcs. 7-25387

struct., stability and bonding 7-10392

tetrachloromethane dication, isomers, mass spectrometry and ab initio calc. investig. 7-36513

1,2,4,5-tetramethylenebenzene, geometry optimisation, ab initio CI calcs. 7-15524

tetramethyleneethane, singlet ground state, ab initio calcs. 7-62259

tetramethyltin, vac. UV spectra, interpretation 7-50171

transition elements, first row, energy-adjusted ab initio pseudopots. 7-49898

transition metal aluminides (TAI, T=Fe, Co, Ni, V), electronic struct. of vacancies 7-16975

transition metals, ab initio interatomic potentials 7-21395

transition metals and their alloys, mag. atoms, quantum statistical ab initio theory 7-58969

triatomic molecules, bending vibrs., Schrodinger eqn. calcs. 7-36581

triatomic molecules, partition function calcs., ab initio and sums of states methods 7-56966

s-triazine, gas phase, mol. struct., GPED anal., ab initio force field calcs. 7-36457

tribromoacetamide, ¹⁵N isotope effects, Raman spectra, ab initio calcs. 7-19871

tribromomethyl radical, geometry and electronic struct., SWXα calcs., ab initio UHF calcs. 7-19703

trichloromethyl radical, struct. and electronic states, ab initio UHF SWXα calcs. 7-30949

trifluoromethyl imino sulphur difluoride, ab initio calcs. at SCF level, equilbr. geometries and population anal. 7-10382

trimethylamine radical cation, hyperfine coupling tensors, ab initio UHF calcs. 7-25373

troloxone, antiepileptic drug, electrostatic pot., ab initio SCF-MO-LCA. study 7-855

ab initio calculations continued

- uracil and thio derivatives, tautomerism, ab initio study 7-837
 vibr., semiclassical calc. from ab initio pots. using 2D spline fn. 7-30936
 vinyl alcohol, aq. soln., ketonization, ab initio STO-3G calcs. 7-22988
 vinyl formate, gas phase structure anal., ab initio calcs., molecular mechanics calcs., IR spectra 7-19691
 vinylene carbonate, struct. and vibr. spectra, ab initio CNDO/2 and INDO calcs. 7-49930
 water, liq., three-body forces and single-molecule dynamics 7-11880
 Ag-Pd, random alloys, residual electrical resistivity, first-principles calc. 7-2569
 Ag(CO)_n, (n=1,3) electronic struct. 7-36445
 Al, grain boundaries, Na and H impurities, small cluster quantum chemical calcs. 7-38017
 Al_n clusters, (n=5,9,13), electronic struct. and bonding 7-15775
 AlF₃, pot. energy curves for excited states, ab initio CI calcs. 7-49948
 Ar, 2s and 2p shake-up energy, X α theory, X-ray transition energies 7-10422
 Ar, K suprathreshold struct., ab initio calcs. 7-36466
 Ar-HCl, energy levels, ab initio close coupling calcs. 7-50292
 Ar+Ar⁺, total differential scatt. cross section, 15-400 keV 7-62489
 Ar+NO, rot. inelastic cross section determ. sudden approx. 7-25637
 (ArH)⁺, short-range pot. curves, Lyman- α line blue wing (*French*) 7-10463
 ArHe⁺, doublet states, ab initio CI calcs. 7-56989
 As₂Se₃, cryst., optical props., ab initio total energy calcs. 7-45965
 As₂Se₃, crystalline, electronic and geometric struct., ab initio total-energy calcs. 7-12607
 AuH bonding, ab initio fully relativistic calcs. 7-15531
 BF⁺, radical cations in Ne matrix, generated by laser sputtering and high temp. sources, EPR, CI calcs. 7-25604
 BF₃, electric-field gradients, NMR shielding tensors, NQR coupling const., ab initio HF calcs. 7-19693
 BF₃.H₂O, electronic struct., EEL and UV photoelectron spectra, ab initio MO STO calcs. 7-36449
 B₄H₄, polyboranes, nucl. coupling const. HF calcs. 7-19688
 B(OH)₃, electron density, X-ray diffr. determ. at 105 K, ab initio calcs. 7-44458
 Be⁺, electron impact-excitation, reson. transition, ab initio treatment 7-42768
 Be²⁺-H₂O, geometry and vibr. freqs., ab initio HF calcs. 7-49881
 Br plasma, laser produced, oscillator strengths, X-ray transitions, ab initio calcs. 7-16334
 Br₃⁻, electrical cond. mechanism, tight-binding and ab initio pseudopot. calc. 7-52546
 C-containing mols., X-ray emission spectra, ab initio MO HF calcs. 7-36642
 C_s, geometric isomers, ab initio calc. of equilb. struct. 7-62291
 C₆, cyclic ground state, struct., ab initio calcs. 7-42819
 CBe₂ struct., stability and bonding 7-10392
 CCH, X² Σ^+ state, rot.-vibr. energies, ab initio calc. using nonrigid bender Hamiltonian 7-25422
 CH₃N²⁺, pot. energy surface, ab initio MO calcs. 7-10390
 CH₃NO₂, potential energy surface, rearrangements, ab initio calcs. 7-10465
 C₂H₂O⁺, x=3 to 5, struct. isomers, gas-phase ion mobility study, ab initio calcs. 7-36456
 CO, chemisorbed, ionisation phenomena, ab initio wave functions 7-36444
 CO monolayer on Si (111), electronic props., pseudofunction method calcs. 7-2659
 CO, short range interactions 7-19999
 Ca III, allowed transactions, oscill. strengths and excitation energies 7-5631
 Ca⁺, 4p-3d triplet, broadening by He 7-62323
 Ca₃(PO₄)₂OH, EXAFS spectrum anal., spherical wave theory 7-33485
 Cl isoelectronic sequence, allowed 3-3 transitions, Slater parameter optimisation, HF CI calcs. 7-48205
 Cl₂ third-harmonic generation, nonadiabatic effects, coupled eqns. calcs. 7-1222
 Cl₃, electronic struct., ab initio SCF and CI study 7-5605
 CoAl, electronic struct. of antistructure Co atoms and Co-vacancies 7-7165
 CoGa(Al), electronic struct. of vacancies 7-16975
 Cr(CO)₆, SCF-SW-X α ab initio XANES calcs. 7-64776
 CsI, press. induced structural instability, ab initio pseudopotential techniques 7-52042
 Cu (100), field induced vibr. freq. shifts of chemisorbed CO and CN 7-45991
 Cu cluster surface, Na atom adsorpt. SCF ab initio and CI calcs. 7-52259
 Cu, shock Hugoniot, ab initio interatomic pot. calcs. 7-21395
 Cu surface, Raman intensity of adsorbate vibr., cluster-model calc. 7-27089
 Cu-Zn (Ga)(Ge), random alloys, residual electrical resistivity, first-principles calc. 7-2569
 Cu₃, ground state surface, ab initio calcs. 7-42467
 Cu(CO)_n, (n=1,3) electronic struct. 7-36445
 CuH(CuF)(CuCl) and their cations, ab initio calcs. chemical reactivity 7-10400
 Er II, hyperfine struct. meas. by collinear fast beam laser and RF laser double reson. spectra 7-49957
 Er, low-lying states electronic density, ab initio multiconfiguration DF calcs. 7-15486
 FCP and higher-lying isomer, struct., stabilities, ab initio study 7-864
 FDF⁻, IR spectrum, ab initio calcs. 7-25506
 FHF⁻, IR spectrum, ab initio calcs. 7-25506
 Fe II, electron impact excitation, collision strengths, R matrix method, CI calcs. 7-25424
 FeAl, X-ray emission and absorpt., ab initio self-consistent band struct. calcs., LMTO method 7-64826
 Fe(H₂O)₆²⁺ clusters, intermol. pot. fn. and pot. energy surface, ab initio UHF calcs. 7-25354
 FeRh, X-ray emission and absorpt., ab initio self-consistent band struct. calcs., LMTO method 7-64826
 Ge (111), chemisorption of atomic H, nonempirical cluster-model study 7-38332
 Ge, structural props., ab initio pseudopotential calcs. 7-44797
 GeH₄⁺, Jahn-Teller, struct. and energy distortions ab initio CI calcs., HF calcs. 7-15523
 H atoms, finite chains, intermediate one-particle states 7-7145

ab initio calculations continued

- H+HO₂, abstraction reaction, saddle point geometries and barrier heights, ab initio SDCI calcs. 7-46806
 H⁺+HF, charge transfer processes, ab initio calcs. 7-5744
 H₂ and isotopes, nonadiabatic eigenvalues and adiabatic matrix elements 7-62381
 H₂ and isotopomers, rot. transition, Raman line position 7-62380
 H₂, b² Σ^+ , excited states, mag. effects, ab initio calcs. 7-10413
 H₂ double photoionisation cross sections and electron energies, ab initio calcs. 7-15654
 H₂, E,F¹ Σ_g^+ state, REMPI, ab initio calcs. 7-62470
 H₂ formulation of ab initio optical potential for electron elastic scatt. 7-15714
 H₂, low energy elastic positron collisions, R-matrix method 7-50361
 H₂, short range interactions 7-19999
 H₂-Ar pairs collision-induced rototranslational spectra, ab initio dipole-moment surface 7-15493
 H₂-H₂, energy levels, ab initio close coupling calcs. 7-50292
 H₂-HF complex, struct., bonding, vibr. freq. shift 7-19817
 H₂+H, collision-induced dissociation at interstellar densities 7-55448
 H₃⁺ and isotopomers, IR spectra, ab initio calcs. 7-30929
 HCN, elec. polarisabilities, ab initio calcs. 7-5585
 HCN, vibr. energy levels calc. using ab initio pot. energy function, CI calcs. 7-25484
 HCP and higher-lying isomer, struct., stabilities, ab initio study 7-864
 HCl⁻, bound electronic states, ab initio Born-Oppenheimer calcs. 7-42469
 HF, macroscopic solvation, electron distrib. ab initio INDO SCF calcs. 7-54099
 H₃GeX (X=F, Cl, Br, I), harmonic force fields and vibr. spectra, ab initio HF calc. 7-50064
 H₃N-HF-HF, H bond cooperativity, structural and energetic props., ab initio calcs. 7-19697
 H₂NC⁺, interstellar mol., pot. energy surfaces, ab initio MO theory 7-19687
 H⁻(NH₃) cluster, struct., stability, ab initio MO calcs. 7-56965
 H⁻(NH₃)₂ cluster, struct., stability, ab initio MO calcs. 7-56965
 H₂O dimer, transition from trapped to solvated electrons, ab initio calcs. 7-19700
 H₂O, excited state pot., photodissoc. ab initio calcs. 7-19978
 H₂O₂, overtone excited states, torsion-vibr. interactions 7-50072
 (H₂O)_n, n=4 to 8, geometries and relative energies, Monte Carlo energy minimisation study, ab initio SCF calcs. 7-30921
 H₂O⁺ (H₂O)₂, SCF interaction energies, nonadditivity 7-57143
 (H₂O)_nO₂⁻ clusters, charge transfer interaction investigated using ab initio MO theory, binding energy calc. 7-5809
 H₂P₂ isomers, electronic states, ab initio mol. electronic struct. theory 7-56934
 H₂P₂, unimol. rearrangement, ab initio investig. 7-25342
 H₂P₂⁺, unimol. rearrangement, ab initio investig. 7-25342
 H₃P-HF-HF, H bond cooperativity, structural and energetic props., ab initio calcs. 7-19697
 H₂POOH, bonding, ab initio calcs., proton exchange reactions 7-5589
 H₂POSH, bonding, ab initio calcs., proton exchange reactions 7-5589
 H₂PSSH, bonding, ab initio calcs., proton exchange reactions 7-5589
 H₂S, pot. energy surfaces, spectroscopic props., ab initio CEPA calcs. 7-19686
 H₂S⁺, pot. energy surfaces, spectroscopic props., ab initio CEPA calcs. 7-19686
 HSCN (HNCS), ionis. pots., photoelectron spectrosc. and ab initio calcs. 7-25601
 H₃Si-B₂H₅, form., geometry, ab initio calcs. 7-25376
 H₄SiO₄, force fields, ab initio MO calcs. 7-25375
 H₂SiX (X=F, Cl, Br, I), harmonic force fields and vibr. spectra, ab initio HF calc. 7-50064
 H₂SNX (X=F, Cl, Br, I), harmonic force fields and vibr. spectra, ab initio HF calc. 7-50064
 HX-HCP complexes (X=F, Cl, Br) H bonding ab initio calcs. 7-56960
 HX-HNC complexes (X=F, Cl, Br) H bonding ab initio calcs. 7-56960
 HX-XCN complexes (X=F, Cl, Br) H bonding ab initio calcs. 7-56960
 He I triplets, collisional excitation cross sections and implications for primordial He abundance 7-55446
 He⁺ low energy ion-surface scatt., reionisation process theory 7-22413
 He+H₂⁺→HeH⁺+H, endothermic reaction on ab initio pot. energy surface, dynamics 7-54103
 He+H⁺(H⁺), double ionisation, ab initio calcs. 7-42737
 He+NO, rot. inelastic cross section determ. sudden approx. 7-25637
 HeH⁺(HeD⁺), rot.-vibr. states calcs. 7-36576
 HeLi₂ van der Waals system, pot. energy surface 7-62261
 I₃⁻, electrical cond. mechanism, tight-binding and ab initio pseudopot. calc. 7-52546
 K⁺, electron affinity and photodetachment cross sections, ab initio multi-channel calcs. 7-36463
 Li, ²S ground state, specific mass shift, isotope shift, ab initio calcs. 7-36495
 Li cpds., energy stability, struct., vibr. spectra, MO LCAO SCF calcs. 7-15512
 Li, crystal and electronic struct., ab initio HF cluster method 7-44443
 Li first row compounds, solvation energies calc. 7-8269
 Li like ion plasma, population inversion collisional-radiative model 7-25463
 Li surface, CO chemisorption, molecule-cluster interaction ab initio SCF-CI calcs. 7-45013
 Li-H₂ system, second derivative nonadiabatic coupling matrix elements determ. pot. energy surfaces 7-42501
 Li-vinylidene complex, struct., bonding, ab initio CI calcs. 7-49935
 Li+HCl quenching reaction, electronic struct., ab initio SCF CI calcs. 7-56995
 Li₂+H₂, ab initio study 7-8257
 LiH⁺, ground and first excited state electron affinities, extended-Koopman's-theorem, ab initio calcs. 7-25352
 (LiH)_n linear infinite chains study, pseudo-lattice method, ab initio SCF calcs. 7-36470
 Li₂S, triplet ground-state, electronic and steric effects, ab initio calcs. 7-25419
 methanol, protonated, rot. const., ab initio MO calcs. 7-25349
 methyl+H→methane, ab initio pot. energy surfaces, channel model calcs. 7-28276
 MgO (001), ab initio Hartree-Fock calcs. 7-27378
 Mn²⁺-F⁻, ligand field correl. effects ab initio MBPT calcs. 7-21874

ab initio calculations continued

- N at. and mol. chemisorption on graphite finite cluster models, HF calcs. 7-16689
- N IV, spontaneous radiative transition probabilities, ab initio CI calcs. 7-50261
- N₂, elec. polarisabilities, ab initio calcs. 7-5585
- N₂, Hopfield series, autoionisation, perturbation effects 7-10408
- N₂, liq. and fluid press., intermol. pots. comparison, mol. dynamics simulation 7-63419
- N₂, low energy elastic positron collisions, R-matrix method 7-50361
- N₂, short range interactions 7-19999
- N₂, transition moments and pot. energy curves, ab initio calcs. 7-42472
- N₂⁺, spectroscopic props. ab initio GTO CEPA study 7-15525
- N₃BH₃, struct., ab initio calcs. 7-49887
- NF₃, integrated intensities and IR absorpt. bands, ab initio (3.1) calcs. 7-56953
- NH₃ dimer, geometry and energy calcs. SCF calcs. 7-15499
- NH₃ dimer, ionis., proton transfer, ab initio pot. energy surface calc. 7-42518
- NH₃, integrated intensities and IR absorpt. bands, ab initio (3.1) calcs. 7-56953
- NH₃⁺ radical cation, hyperfine coupling tensors, ab initio UHF calcs. 7-25373
- NH₃+H₂, ab initio potential-energy surface, HF, SCF calcs. 7-10716
- NH₄⁺, stability against dissociation and NH₃H⁺ form., pot. energy surfaces, ab initio CI calcs. 7-30955
- NH₃H⁺, stability, pot. energy surfaces, ab initio CI calcs. 7-30955
- NO dimer, ionisation phenomena, ab initio wave functions 7-36444
- NO²⁺, ²Σ⁺ and ⁴Π states, ab initio MC SCF CI calcs. 7-49937
- NO₂ and ions, deform. densities, d function role in ab initio calcs. 7-62260
- NO₂⁻, electron deform. density, basis set depend. 7-62252
- N₂O, protonated, struct. determ. by ab initio MP2 gradient method 7-25343
- N₂O, protonation site and energies, N₂OH⁺ struct. ab initio MO calcs., SCF calcs., CI calcs. 7-15480
- N₂OH⁺ isomers, struct. and energy levels, ab initio MO, SCF and CI calcs. 7-15481
- NSCl₃, NSOF and NSF₃ and their isomers, ab initio calcs. at SCF level, equilib. geometries and population anal. 7-10382
- NaCN, ab initio coupled HF calcs. of multipole moments and dipole polarisability of CN⁻ 7-5587
- Ne, is shake-up energy, Xα theory, X-ray transition energies 7-10422
- Ne VII, spontaneous radiative transition probabilities, ab initio CI calcs. 7-50261
- Ne-He van der Waals mol. pot., ab initio HF SCF calcs. 7-36459
- Ne-like ion plasma, laser produced, reson. transitions, X-ray diagnostics 7-20932
- Ne-like ions, Ca XI to Mn XVI, laser plasma, spectra 7-49989
- Ne-N₂ interaction, intermol. pot. fns., ab initio calc. 7-57146
- Ne⁹⁺+Ne(0), low Z ion-atom collisions, relativistic SCF calcs. 7-10409
- Ni-like ion plasma, laser produced, reson. transitions, X-ray diagnostics 7-20932
- Ni-Mo, random alloys, residual electrical resistivity, first-principles calc. 7-2569
- Ni_n (n=1 to 6) clusters, electronic struct., ab initio SCF and CI calcs. 7-10446
- O V, spontaneous radiative transition probabilities, ab initio CI calcs. 7-50261
- O+HD reaction probabilities and rate consts. ab initio pot. energy surface 7-65295
- O+HD reaction rates, variational transition state theory 7-59749
- OH+cytosine, ab initio SCF MO calcs. 7-8478
- PF₃, integrated intensities and IR absorpt. bands, ab initio (3.1) calcs. 7-56953
- PH₃, integrated intensities and IR absorpt. bands, ab initio (3.1) calcs. 7-56953
- PX, PX⁺ and PX⁻ where X = H, F and Cl, low-lying electronic states, ab initio calcs. 7-30937
- Pd(001), H adsorption, coverage depend. props., ab initio calcs. 7-38340
- PdGe, bonding, electronic states, ab initio HF-CI calcs. 7-42497
- PrCl₃ cryst. field correlation effects in Pr³⁺-Cl⁻, ab initio calcs. 7-7177
- Pt(111) with adsorbed CO, He-adsorbate scatt., potentials and total scatt. cross-sections 7-59363
- PuF₆, low lying 5f to 5f excitations, ab initio study, electron correl. effects 7-42502
- RbCn, SCF pot. energy and dipole surface calc. 7-42579
- Rb₂ZnCl₄, incommensurate transition, pot. energy and mol. dynamics ab initio calcs. 7-21435
- Ru, electronic, structural and cohesive props., theoretical study 7-37922
- S isoelectronic series, transition probabilities and wavelengths 7-15550
- S-compounds, bond order and valence indices for use with ab initio wave functions 7-56947
- SC⁺+H₂ endothermic reaction ab initio pot. energy surfaces 7-13746
- SF₃ radicals, electronic struct., ab initio SCF CI calcs. 7-19716
- SH₃ radicals, electronic struct., ab initio SCF CI calcs. 7-19716
- S₂N₂, excited states, ab initio CI calcs. 7-42491
- SO₂ and ions, deform. densities, d function role in ab initio calcs. 7-62260
- SPCl₂F⁻, radical, ESR and ab initio quantum chem. study 7-42654
- Si(111), chemisorption of atomic H, nonempirical cluster-model study 7-38332
- Si clusters, in presence of O, Si-Si bond breaking, total energy calcs. 7-50438
- Si isoelectronic sequence, allowed 3-3 transitions, Slater parameter optimisation, HF CI calcs. 7-48206
- Si, muonium, anomalous, model as body-centered interstitial muonium, HF calc. 7-45899
- Si, off-centre impurities and defects, local electronic struct. valence-bond theory calcs. 7-2532
- a-Si:H, defect structure, ab initio theory 7-32298
- Si-O, cluster computations related to thermal donors 7-16990
- Si-O₂B, ab initio MO electronic struct. calcs. 7-38499
- Si-Ge heterojunction, structural and electronic props. 7-21997
- SiC, cubic, ab initio calc. of ground state props. 7-6751
- SiC₂, protonated isomers, struct. and proton affinity, ab initio HF MO calcs. 7-25384
- SiCl, spectral and struct. props., MO calcs. 7-25418
- SiF₄, electric-field gradients, NMR shielding tensors, NQR coupling consts. ab initio HF calcs. 7-19693
- SiF₄, force fields, ab initio MO calcs. 7-25375

ab initio calculations continued

- Si₂Ge_{1-x} coherently strained bulk alloys on Ge (001) substrate, indirect band gap and band alignment calcs. 7-2481
- SiH₄, electron impact cross sections, spherical-complex-optical pot., ab initio HF calcs. 7-49904
- SiH₄⁺, Jahn-Teller, struct. and energy distortions ab initio CI calcs., HF calcs. 7-15523
- Si₂H₆, struct. and stability, ab initio calcs., heat of form. 7-10441
- SiH₃F_b (a+b=4), NMR shielding consts., ab initio coupled HF calcs. 7-42646
- Si₂H₂O, polarisation functions, ab initio MO calcs. 7-62263
- SiO₄-Li, crystalline quartz with Li-associated electron trap, electronic struct. 7-21860
- SnCl₄ vac. UV spectra, interpretation 7-50171
- SnH₄⁺, Jahn-Teller, struct. and energy distortions ab initio CI calcs., HF calcs. 7-15523
- Sr+Ar, ¹P fluoresc. line broadening, ab initio close-coupled scatt. calcs. 7-36494
- TeF₆, electron affinity calcs. 7-36453

abacs see nomograms**aberrations**

- aberrations in optics and particle optics only*
see also lenses: optical instrument testing; particle optics
- 35mm camera lenses used for photogrammetry, lens distortions and calibration 7-40393
- aberration-corrected systems, design principles 7-50687
- achromatic mirror lens with corrected opening aberration (Czech) 7-62810
- achromatic single-component kinoform objective, with circular aberration coeff. 7-25737
- annular aperture diffraction patterns, aberration analysis 7-62639
- beam cleanup with stimulated Raman scattering in the intensity-averaging regime 7-20340
- biocular magnifiers and design methods 7-50695
- chromatic aberration, longitudinal, pseudocolour effects, metrology appl. 7-42953
- combined electric-magnetic focusing-deflection system, relativistic fifth order geom. aberration eqn. 7-10838
- combined electrostatic focusing-deflection systems, asymptotic aberrations 7-10835
- compensated spherical surfaces in optical systems 7-25924
- conic constant and paraxial radius of curvature measurements for conic surfaces 7-20474
- converter for marine quartz gravimeter 7-29262
- crossed-field analyzer, aberration anal., elec. and mag. field expressions 7-10841
- Czerny-Turner monochromator: astigmatism in the classical and in the crossed beam dispositions 7-20396
- deflection magnets, set of independent aberration coeffs. 7-1019
- diffraction grating, anaplanic grazing incidence, theory 7-11101
- electron beam in combined electromagnetic focusing-deflection system with spherical cathode, relativistic aberration theory 7-62613
- electron beams, aberrations in combined electromagnetic focusing spherical cathode lens, theory (Chinese) 7-36868
- electron beams, relativistic aberrations in combined electromagnetic focusing-deflection system, theory (Chinese) 7-36869
- electron beams combined in focusing system with spherical cathode, aberration theory 7-62612
- electron guns, spherical aberration elimination using aspherical mesh lenses 7-20121
- electron lens, probe forming, axial geometrical aberrations meas. by means of shadow image of fine particles 7-42882
- electron matrix lens, aberrations reduction using offset apertures 7-20122
- electron optical system, aberration shift relations, matrix derivation 7-18938
- electron optics aberration corrector 7-20124
- electron probe design, miniature variable energy, for nanometric analysis, electron opt. parameters 7-18939
- electron-optical cathode systems; aberration coefficients anal. 7-57263
- electrostatic cathode lenses, design, Pontryagin's max. principle 7-42884
- electrostatic lenses, geometrical aberrations, comment and reply 7-62611
- electrostatic lenses, spherical aberration reduction 7-10836
- electrostatic membrane mirror, configuring by least-squares fitting 7-31422
- electrostatic round lenses, multipole lenses and deflectors, aberration theory 7-1021
- express method of measuring aberrations in objectives (Russian) 7-5842
- focusing heliostats in solar electric station, angular and linear aberrations 7-54268
- focusing mirrors, thermooptic aberrations, heat transfer study 7-57509
- Gaussian beams, generally astigmatic, propag. along skew ray paths 7-62623
- grating element for the entry and focusing of radiation in a planar waveguide 7-37126
- GRIN-rod lenses used in single-mode optical devices, aberration anal. 7-31421
- high contrast phase electron microscopy, improved method 7-35643
- high performance two-electrode electron gun lens, microscopy appls. 7-5827
- holographic elements, curved, aberration coeffs. 7-36887
- holographic gratings, aberration-corrected, design for use with Seya-Namioka monochromators 7-25947
- holographic lens using polyvinyl carbazole material, aberration correction 7-25745
- holographic wavelength demultiplexer for optical fiber communications 7-25774
- Hopkins variance formula extended to low relativemodulations 7-10879
- IR imaging system design, critical issues 7-50673
- IR objective, use of proustite crystal in performance meas. 7-57511
- laser aberration reversal using phase conjugation 7-50653
- laser resonator, frequency pulling and anomalous dispersion, aberration and perturbation effect 7-11004
- lens design, aberration theory and the meaning of life 7-50678
- lens design, aspheres use 7-50690
- lens design, automatic, use of multi-image plane merit function 7-43310
- lens design, Brixner optimisation procedure 7-50683
- lens design, conf., Cherry Hill, USA (June 1985) 7-48161
- lens design, glass combinations selection method for aberration correction 7-50684
- lens design, interactive computer program 7-50693

aberrations continued

- lens design, merit function construction with possible achievement of global min. 7-50682
- lenses, geodetic, short-focus, spherical aberration 7-43295
- lenses, planar geodesic, anisotropic aberrations, definition 7-15818
- long focus objective, holographic method of testing, optimum conditions calc. 7-57512
- magnetic focusing and deflection systems of camera tubes (*Chinese*) 7-10837
- microcomputer-based image processing aids in optical analysis and simulation 7-36891
- mirrors, thermo-optic aberrations with central holes 7-43303
- monochromator, off-plane constant-deviation, using holographic concave gratings 7-43336
- multicomponent lens system, design of individual components, singlet use 7-20379
- multivariate aberration series, acceleration of convergence 7-5846
- multivariate Lagrangian aberration functions, singularities 7-5844
- multivariate Lagrangian aberration series, extension of convergence 7-5845
- nematic liq. crystals., orientational self-focusing, aberration pattern polarisation asymmetry 7-11077
- nematic liquid crystal, orientational aberrational self-focusing, temperature effects 7-62804
- nonaxially symmetric optical systems, aberration field props. 7-50691
- nonlinear distortion compensation of light beams with restricted deform. of control mirror 7-50622
- nonsymmetric systems, aberration characts. 7-50689
- optical system, wave spherical aberration approximate eval. 7-42992
- phase conjugators, passive, abilities to perform aberration correction on laser beam 7-20362
- phase contrast objective, point spread function in spherical aberration presence 7-37084
- phase measurements with image holography 7-25782
- phase retrieval, practical appl. for the space telescope 7-62638
- phase-contrast objectives, calc. of allowable aberrations 7-57510
- photolithographic scale dividing, optical problems (*German*) 7-30106
- polarisation aberrations of lenses 7-50686
- projection system with electrostatic lenses, aberrations calc. 7-57517
- projector image aberrations, illumination system collimator effect 7-57516
- projector with electrostatic lenses, chromatic aberrations anal. 7-57518
- rainbow holography, one-step using spherical mirror 7-10881
- reflection gratings, grazing incidence, in high resolution scanning spectrometers 7-20401
- relativistic fifth order geometrical aberration eqn. of combined focusing-deflection system (*Chinese*) 7-36867
- retinal optical intensity profile model for computer-aided visual acuity assessment 7-59976
- scaling method for optical systems 7-50669
- solenoidal magnetic lens, space-charge correction of spherical aberration 7-5825
- spherical aberration, diffraction intensities 7-57259
- spherical aberration, intermediate, geometric and diffractive parameters, comparison 7-42983
- spherical gradient-index sphere lens, spherical aberration minimisation 7-31527
- stimulated Raman scattering production of high quality laser beams 7-15930
- Strehl ratio phase-space representation, ambiguity function 7-57257
- surface fabrication errors of optical systems, wavefront deformations calcs. 7-57262
- telescope, three-mirror, third-order aberrations formulae and design program 7-55466
- TEM lens shape with min. spherical aberration coeff., computation method 7-18936
- thermally induced and coherent phasing of beams, stimulated Brillouin scatt. 7-37045
- third order aberration coefficients, target values 7-50688
- tube lenses, finite length, geometrical aberrations 7-31234
- TV projection lens, wide-angle, design 7-50699
- uniform and Gaussian beam diff. comparison, aberration balancing 7-62621
- unstable cavity, aberration sensitivity, second-order theory 7-31256
- unstable-cavity sensitivity to spatially localized intracavity phase aberrations 7-25717
- vector aberration theory and the design of off-axis systems 7-50685
- visual instrument testing, wavefront aberration effects 7-57610
- Wood and GRIN rod lenses, third- and fifth-order aberrations 7-31419
- GaAs Fresnel waveguide grating lenses, aberration corrected, simulation 7-26036
- H₂ Raman amplifier, Stokes phase preservation 7-20342

aberrations (visual) *see vision defects*

abrasion

- see also hardness; wear*
- 3D shape effect on abrasive wear 7-17652
- binary carbide tool coatings, wear resistance, mechanistic model calcs. 7-53915
- ceramics, abrasive wear, fine-scale, by plastic cutting process 7-3458
- ceramics and cemented carbides, sliding and abrasive wear mechanisms, comparison 7-3463
- conference, tribology and lubrication, Tokyo, Japan (July 1985) 7-4631
- cordierite glass and glass-ceramic, comparative single-point diamond scratching behaviour 7-46654
- cutting tool materials, mech. props., wear-resist. relations 7-3443
- diamond, abrasion by plasma deposited SiO₂ films 7-13608
- glass fibre reinforced PTFE composites, sliding and abrasive wear rel. to fibre content 7-28144
- hard materials, frictional behavior of diamond and cubic BN abrasives 7-3461
- hard materials, wear resist., comparative study 7-3457
- magnetic tapes, friction reduction by acoustic excitation 7-65148
- metallic materials, surface refinement by ion implantation, friction, abrasive and corrosion resist. (*German*) 7-53949
- optical coatings and surfaces, abrasion resistance 7-50661
- polydiphenylborosiloxane/aminimide-cured epoxy resin composites, friction and abrasion props. 7-39677
- resinoid bonded abrasive materials, cyclic fatigue and reliability 7-17630
- rubber vulcanizates, natural and styrene butadiene, environment effect on friction and wear 7-8131

abrasion continued

- steel, abrasion resistance after heat treatment 7-17697
- steel, gouging abrasive near mechanism, investig. with aid of pendulum single-pass grooving 7-22846
- steel, high speed, wear mechanisms and tool life rel. to microstruct. 7-8128
- steel, low-alloy, abrasive wear correl. with alloy additions 7-65151
- steel, Ni, abrasive wear rel. to anisotropic ferrite-martensite microstruct. 7-13607
- steel, sliding lubricated contact, wear and crit. failure load, effect of solid contamination 7-33803
- steel, wear resist. under wet-abrasive erosion conditions 7-22848
- wear mechanism, wear process successive obs. in SEM 7-8229
- wear mechanism clarification, contact surface deform. effect on wear and friction 7-8134
- C steel-cast Fe-Cr bimetal, interface bonding strength (*Korean*) 7-17618
- Fe, cast, white, Cr-Mo, unidirectionally solidified, sclerometric study 7-3455
- Fe-Cr-C-B hard surfacing weld deposits, abrasive wear resist. and microstruct. 7-22847
- Fe-Mn-Al, processing and props., effect of Si and C additions 7-17707
- SiO₂ films, plasma deposited, diamond abrasion props. 7-13608
- TiC-steel hard alloys, wear resist. in abrasive jet, methods of improvement 7-3448
- TiC-steel hard alloys, abrasive and hydroabrasive wear 7-17656
- TiN-C(BN), hard composite coatings, deposition and props. 7-46623
- WC-Co, cemented carbides, abrasion, controlling mechanism 7-3460
- WC-FeNi cemented carbides, abrasion, controlling mechanism 7-3460
- Zn-based alloys, mechanical props., alloying addition effects (*Japanese*) 7-8090

abrasive wear *see abrasion*

absolute gravity *see gravity*

absolute pressure measurement *see pressure measurement*

absolute temperature *see temperature*

absorbers (surge) *see surge protection*

absorption

- for absorption of substances see sorption*
- see also acoustic wave absorption; electromagnetic wave absorption*
- seismic waves, absorption effects on plane waves in layered media 7-28868
- seismic waves, nonuniform waves propag. in space divided by thin fluid-filled fracture 7-28891

absorption coefficients (optical) *see optical constants*

absorption spectra *see spectra*

absorption wavemeters *see wavemeters*

abstract data types *see data structures*

abundance ratio *see element relative abundance; isotope relative abundance*

AC machines

- see also AC motors; synchronous machines*
- recrystallised dielectromagnetics for AC machine magnetic circuits 7-22725

AC motors

- see also induction motors*
- submerged driving motor for liquid He flow rate meas., IMGC calibration facilities 7-63234

AC network analysers *see network analysers*

accelerated testing *see life testing*

acceleration

- see also acceleration control; acceleration measurement; accelerometers*
- ablative macroparticle accelerator using electron beam diodes for accelerating projectiles 7-36266
- automobile deceleration force by the coast-down method 7-18541
- coal dust flame acceleration, feedback control model for unsteady flow 7-65326
- free-fall acceleration values, reduction 7-29278
- gravitational acceleration, meas. using bouncing rubber ball 7-48237
- molecular dynamics, noninertial accelerations, statistical correlations study, electromagnetic field effect 7-62344

acceleration control

- see also acceleration measurement*
- space vehicles, inertial navigation algorithms, for high life-to-drag vehicle during atmospheric entry 7-4289

acceleration measurement

- see also acceleration control*
- fibre optic sensors, development, configs., and appls., review 7-31485
- flow acceleration measurements using laser Doppler anemometry 7-31904
- free-fall acceleration values, reduction 7-29278
- optical measurement of velocity and acceleration with colour coding 7-11568
- photoelastic fibre optic sensor, force, pressure, acceleration and sound meas. (*German*) 7-11159
- piezoelectric accelerometers, dynamic matching for differential acceleration measurement 7-56229
- US identification system for coded moving objects 7-1361
- vibration characterisation by force and acceleration meas. 7-9812

accelerators (particle) *see particle accelerators*

accelerometers

- see also acceleration measurement*
- bubble-tube accelerometer for elementary mechanics teaching 7-14739
- double-ended tuning fork quartz accelerometer, design and characts. 7-56230
- force-balance linear standard accelerometer, low-frequency 7-41358
- geological targets, penetration expts. 7-14271
- high sensitivity, for modal analysis 7-24643
- nuclear power stations, diagnostic subsystems in Czechoslovakia (*Czech*) 7-19386
- piezoelectric accelerometers, dynamic matching for differential acceleration measurement 7-56229
- quartz tuning fork resonator transducers 7-35512
- SAW accelerometers using integrated thick and thin film technologies 7-301
- test and calibration facilities, for frequency range 20 to 600 Hz 7-4820

acceptor levels *see impurity electron states*

access control (buildings) *see safety systems*

- accidents**
see also electric shocks; explosions; safety
 AEROSIM-S code for dry aerosols, FBR containment appls., user manual 7-56723
 aerosol source terms in nuclear reactor accidents, ex-vessel fission product releases 7-36219
 airborne radioactive gases inside a nuclear reactor containment building, Monte Carlo program to calc. exposure rate 7-54766
 artificially perforated Zr barrier fuel rods, fission product release in test loop 7-783
 boiling heat transfer, anal. using hot ball quenching method (*Chinese*) 7-49596
 bubbling flow, local volume gas fraction, time history meas. (*German*) 7-25108
 BWR, MSIV-ATWS events, power level and pressure suppression pool temp. 7-42155
 BWR, new scenario for intersystem LOCAs 7-42162
 BWR, TRACB04 study on suppression pool swelling during containment venting 7-42156
 BWR core meltdown accident, estimate of fission product release 7-777
 BWR LOCA, two bundle loop tests, SAFER03 and TRAC-BD1 anal. 7-36210
 BWR suction line break LOCA, ROSA III RUNs 942 and 943, initial fluid condition effects 7-19416
 BWR-4 Mark I containment, severe accident, survivability of electrical equipment 7-42180
 BWR/6 DBA analysis with limited ECC 7-42154
 CANDU 600 MW(e) reactor, defective fuel detection in operating plant 7-784
 CANDU LOCA, radial heat transfer from fuel to moderator, RAMA and CHAN II codes 7-15297
 Chernobyl, lessons for Western Europe 7-30628
 Chernobyl, Soviet information evaluation 7-30627
 Chernobyl, technical appraisal 7-62015
 Chernobyl accident, causes and consequences (*French*) 7-62035
 Chernobyl accident, causes and effect in Spain/Italy (*Spanish*) 7-5373
 Chernobyl accident, event sequence, consequences, anal. (*German*) 7-25147
 Chernobyl accident, first evaluation of Soviet report (*German*) 7-25125
 Chernobyl accident, RBMK construction and operational features, accident causes (*German*) 7-56803
 Chernobyl accident, thermal hydraulic characteristics and follow up calcs. (*Japanese*) 7-62021
 Chernobyl fallout, detecting and meas. in Nordic countries 7-30715
 Chernobyl fallout, monitoring and impact on UK 7-42229
 Chernobyl nuclear reactor accident, individual dose assessment at Berkeley, UK 7-3880
 Chernobyl power station, nuclear accident and comparison with Daya Bay power station design 7-15277
 Chernobyl RBMK-1000 reactor, computer simulation of accident initiation (*German*) 7-62019
 Chernobyl reactor accident, UK aquatic environment, fisheries viewpoint 7-42230
 Chernobyl reactor surface temp. analysis using Landsat TM images 7-49585
 Chernobyl safety design comparisons with Ontario Hydro reactors 7-10270
 conf., Dresden, Germany (March 1985) 7-24266
 conf., Toronto, Ont., Canada (1986) 7-9587
 conference on fission product behaviour and source term research, Snowbird, UT, USA (July 1984) 7-10
 conference on iodine chemistry in reactor safety, Harwell, England (Sept. 1985) 7-48176
 conference on the safety and reliability of reactor pressure components, Stuttgart, Germany, (Oct. 1985) 7-9583
 conference on two-phase flow dynamics, Lake Placid, NY, USA (Aug. 1984) 7-4627
 criticality accident detection at nuclear reprocessing plants, CEA developments 7-36174
 dryout heat flux for core debris bed, particle size mixing and coolant flow effects 7-30623
 EBR-II, LOF transients without scram, primary pump coastdown characteristics, effects 7-15278
 EFWS, bus configurations, four-train versus two-train support 7-42161
 fast gas-cooled reactors, accident analysis methods (*Russian*) 7-5403
 fast reactor HCDA anal., two phase flow aspects, ANEXDI code 7-15302
 fault identification systems, model-based, development, nuclear reactor appl. 7-19412
 FBR irradiated MOX fuel, transient fission gas release during direct heating expts. 7-778
 FBRs, safety assessment of severe accidents 7-62029
 FFTF, GEM shutdown device appl., use in unprotected LOF events 7-36227
 fissile material, critical soln., heating-up, nucleation and boiling 7-19368
 fission product neutron capture transformation effects on decay power after reactor LOCA 7-49587
 fission product reduced source terms for ex-plant consequence modeling and emergency planning 7-62031
 fusion reactor accident, tritium cleanup predictions after atmospheric release, TMAP code anal. 7-36258
 HTGR fuel behaviour at very high temps., TRISO coated LEU particles 7-19364
 HTGR severe air ingress accident, graphite/O₂ reaction kinetics for various graphites 7-19415
 improbable nuclear reactor accidents, source-term containment anal. recent progress review 7-36218
 inherently safe power plant designs 7-792
 large size LMFBRs, designs for inherent safety capability, accident anal. 7-36223
 large steam-line break LOCAs, similarity study for ROSA-III, FIST and BWR-6 7-49593
 learning curve estimation techniques for nuclear industry 7-15296
 LMFBR, accelerated two-phase flow through perforated plates during core-disruptive accident 7-30609
 LMFBR, hypothetical core meltdown accident, pressure depend. of particle bed dryout heat flux 7-5393
- accidents continued**
 LMFBR, reactivity effects of hydrocarbon, effect of group constant generation method 7-56808
 LMFBR, smoke-release behaviour of burning liquid Na pools, safety anal. 7-49592
 LMFBR, voided cores, fuel vapour pressure buildup dynamics during transient heating 7-36215
 LMFBR HCDA, particle phase size effects in disassembly accident transient 7-25142
 LMFBR steam generator large leak accident, heat transfer into module shell tube 7-62016
 LMFBR sub-assemblies, mech. response under local accident conditions, state-of-the-art review 7-25129
 LMR, ATWS and LOF events, reactivity feedback uncertainties effects on inherent shutdown 7-36224
 LMR, ATWS calc. using SASSYS/SAS4A, effects of radial core expansion reactivity feedback model 7-36222
 LNG vapour plume, interaction with storage tanks, simulation 7-1593
 LOCA, air-water two-phase cross flow resistance in rod bundle 7-5356
 LOCA, peak cladding temp. calcs., LOFT anal. 7-42158
 LOCA, uncertainty anal. using Fourier amplitude sensitivity test 7-42160
 LOCA, very small cold-leg break, RELAP5/MOD1 predictions, ROSA IV expt. 7-19410
 LOCA with severe fuel damage, radiation heat transfer model for SCDAP code 7-36216
 LWR, coarse-mesh method for 1-D reactor kinetics, accident anal. 7-42140
 LWR, core damage frequency from internal initiators, PRA at Peach Bottom 7-42146
 LWR, core damage frequency from internal initiators, PRA level-1 study 7-42145
 LWR, core damage frequency from internal initiators in Grand Gulf 7-42148
 LWR, core damage frequency from internal initiators of Sequoyah 7-42147
 LWR, fuel rod performance during fission product release into coolant, validity limits of calcs. 7-56757
 LWR, heat transfer model for volumetrically heated nuclear debris beds 7-49591
 LWR, hypothetical core meltdown accident, pressure depend. of particle bed dryout heat flux 7-5393
 LWR, severe core damage, PRA methodology 7-42149
 LWR accidents, empirical aerosol correlations using MAAP 2.0 and 3.0 7-56722
 LWR degraded core coolability, two-phase flow through porous media 7-5394
 LWR degraded cores, fission product release and retention phenomena 7-776
 LWR fuel rods, simple model for predicting fission gas release 7-789
 LWR fuel under degraded core conditions, fission gas release prediction, FASTGRASS-VFP model 7-790
 LWR irradiated fuel under accident conditions, fission product release 7-773
 LWR LOCA, jets formed by high pressure subcooled water and steam-water mixtures 7-5391
 LWR LOCA, phase separation mechanisms in branching conduits, review 7-5384
 LWR LOCA, pressure transient and two-phase swelling due to small top break 7-5389
 LWR LOCA, reflood simulation, numerical anal. based on KREWET code 7-15299
 LWR LOCA, two-phase flow in unbounded two-phase critical flows 7-25131
 LWR meltdown accident, fuel-coolant mixing, unsteady 1D 2-fluid model, PHOENICS code 7-5395
 LWR safety, main contributions to the KfK Nuclear Safety Project, review 7-36221
 LWR severe core damage accident, uncovered core thermal-hydraulics, model dev. 7-30624
 LWR severe fuel damage events, burnup effects on fission product release 7-787
 LWR small break LOCA expts. at LOFT, RETRAN-03 anal. of LP-SB-1 and LP-SB-2 7-36237
 LWR structured sensitivity anal. for severe accidents using MAAP 2.0 code 7-42189
 LWR thermal-hydraulics after a severe accident, Power Burst Facility anal. with SEFDAN code 7-49586
 MAEROS model for multicomponent aerosol dynamics, uncertainty and sensitivity anal. 7-19411
 magnetic fusion reactors, melting and evaporation during disruptions, approx. analytical soln. 7-56839
 Magnox reactors, ingestion dose study from postulated releases 7-42231
 MHTGR confinement radiation releases, aerosol removal rates 7-42172
 molten reactor core/concrete interactions in HCDA, mass and heat transfer simulation 7-25138
 MPA thermoshock expt. anal. using TRAC PF 1 code, PTS in reactor ECC conditions 7-13588
 multicomponent aerosol modelling, numerical implementation for reactor accident mitigation 7-56800
 nonequilibrium film boiling in rod bundle geometries, post-CHF test 7-42151
 nuclear power plant accident management expert system, AMES 7-62055
 nuclear power plant advanced concepts reviews, Chernobyl accident implications 7-62049
 nuclear power plants, fire detection and suppression anal. 7-36213
 nuclear power plants, risk studies of accidents (*German*) 7-62018
 nuclear reactor accidents, fission product release expts. overview 7-772
 nuclear reactors, safety principles during operation and accidents (*Dutch*) 7-10263
 nuclear research, summary of recent papers (*Dutch*) 7-54670
 nuclear safety after Chernobyl 7-34000
 organic iodides formation under reactor accident conditions 7-49604
 Oyster Creek emergency off-site dose assessment, ocean breeze inclusion 7-30725
 PNP-500 HTGR, Cs release during a heat-up accident, fission product transport 7-15286
 PNP-500 pebble bed reactor, massive water ingress accidents, computer anal., graphite corrosion (*German*) 7-5371
 PRA, continuous Bayes theorem updating 7-42159
 PRA, level-1, smart approach 7-42144

accidents continued

- preventive safety at nuclear facilities, criticality accident prevention 7-36175
 PUFF-PLUME emergency response atmospheric dispersion model, field eval. at SRL 7-34292
 PWR, characteristics of releases from TREAT source-term experiment STEP-1 7-42170
 PWR, key radionuclide calcs. for failed fuel analysis 7-42176
 PWR, large break LOCA, dispersed flow heat transfer during reflood 7-42150
 PWR, LOCA, simulation using TREAT source term expt. 7-42169
 PWR, multi-loop, power plant accident anal., digital simulator for transients and accidents 7-15301
 PWR accident, source term determ. and expt. verification methods (*German*) 7-56801
 PWR containment, postaccident conditions, airborne dose rates/skyshine radiation calcs. 7-19554
 PWR hot leg, two-phase flow during natural circulation in once through steam generators 7-49579
 PWR hot leg, two-phase natural circulation flows, literature survey for SBLOCA 7-49580
 PWR LOCA, FLECHT and FLECHT-SEASET reflood tests anal. with RELAP5/MOD2 7-25025
 PWR LOCA, two-phase flow during bottom reflooding, computer modelling 7-49599
 PWR LOCA fuel deformation and rupture simulation, PYTHONS code 7-56720
 PWR pressurizer, accident and transient anal., nonequilibrium three-region model 7-36195
 PWR prestressed containments, response to earthquakes, gas cloud explosions and aircraft impact 7-10264
 PWR source term inventory and decay power, sensitivity to core management parameters 7-30630
 PWR steam generator tube rupture transients, thermal-hydraulics in simulated 4-loop facility 7-49571
 radiation impact of Chernobyl in Western Europe 7-30714
 radioactivity, contamination, damage and risks (*Italian*) 7-47262
 radiological emergencies, mobilisation of robotic and teleoperated mobile vehicles at accidents 7-30633
 RBMK-1000 reactors, heat transfer during accidental emissions, numerical anal. (*Russian*) 7-5402
 RBMK-1000/LWR comparison, differences in fuel coolant and moderator, Chernobyl accident (*Dutch*) 7-10213
 reactor accident consequences, effects of rain and snow on contamination 7-42143
 Reactor Analysis Support Package, guidelines for LWR thermohydraulic safety anal. 7-42190
 reactor containment integrity and radionuclide behaviour during severe accidents, review of R&D 7-779
 reactor containment thermohydraulics in major accidents (*German*) 7-56802
 reactor core debris bed, dryout heat flux, effects of system pressure and particle size 7-19406
 reactor LOCA, critical flow of initially subcooled flashing liquids, homogeneous equilib. model 7-5388
 reactor LOCA, ECCS, operation, active cavity model for flashing 7-5387
 reactor LOCA, pressure surge prediction in one-component two-phase bubbly flow 7-5398
 reactor LOCA, transition boiling heat transfer studies using the hot cylinder quenching method 7-25112
 reactor severe core damage accidents, containment response, integrated phenomenological anal., CONTAIN code 7-36220
 reactor trips involving balance of plant failures 7-42163
 Rheinsberg reactor, coolant flow rate determ. during coolant pump failures (*German*) 7-25106
 road accidents rel. to drivers' vision, 3 South African studies 7-65743
 Rossendorf research reactor, coolant boiling expts. (*German*) 7-56786
 San Onofre Unit 1, problems of material aging and reliability 7-42177
 Santa Maria de Garona BWR, upgrade modifications to safety equipment 7-30625
 SASCHA programme on fission product release under reactor core melting conditions, review 7-774
 SIPA, French simulator for PWR post-accident training and anal. 7-42110
 sizewell B PWR, degraded core anal., accident risks 7-62033
 source term composition effects on offsite doses after reactor accidents 7-782
 source term research implications for ex-plant reactor accident consequences modelling 7-780
 Space Shuttle Challenger, wind conditions on day of launch failure 7-60314
 spent fuel transportation, safety criteria and accident anal. 7-42241
 steam generator tubing, primary side stress corrosion cracking, remedial measures 7-30613
 steel, austenitic stainless, fusion reactor blanket material, oxidation and volatilisation rates in air 7-53957
 TMI-2, accident and recovery, defuelling and reactor inspection 7-42191
 TMI-2 reactor cavity, neutron dosimetry using solid-state track detectors 7-30717
 TMI-2 reactor vessel, gamma scanning of primary shield cavity, results 7-42238
 Tsjernobyl accident, appl. of two-dimensional trajectory model to radioactivity transport 7-59894
 TWOLAY program for heat transfer in stratified molten pools after PWR or LMFBR accidents 7-30501
 vapour explosions with a mass of grains, fuel-coolant interaction in reactor accident 7-19405
 VVER-1000 reactor, heat transfer during accidental emissions, numerical anal. (*Russian*) 7-5402
 worst case reactor accidents, fission product source term methodology 7-781
 WWER-440, cold leg break LOCA, fuel rod thermomech. eval. under blowdown conditions (*Russian*) 7-49598
 Zarnowiec nuclear power station, safety system eval. (*Polish*) 7-19413
 Zircaloy oxidation and embrittlement criteria for emergency core cooling system acceptance, safety margins 7-36154
 Zircaloy-4, oxidation under limited steam supply from 1000-1400°C, LWR accident anal. 7-53968
 Zircaloy-4 PWR fuel cladding, deformation, embrittlement and oxidation during LOCA 7-25036

accidents continued

- ⁶⁰Co γ -source, accidental irradiation of technician, long-term follow-up: eye, skin and blood effects 7-34195
 Cs and I source terms of irradiated UO₂ reactor fuel 7-775
 CsI solution radiolysis in conditions related to a PWR severe accident 7-49600
 Fe surface, I retention modelling, role in source term reduction, reactor accident anal. 7-33961
 HTO, accidental intake: report of 2 cases 7-40316
 HTO and T, accidental release: models and in situ expts. on various plant species 7-60095
³H, accidental releases from fusion reactors 7-54777
 I₂ gas phase radiation chemistry in reactor post-accident environments 7-49601
 I₂ volatility from evaporating PWR primary coolant films in accidents 7-49603
 I₂-H₂O vapour partitioning under severe reactor accident conditions 7-49602
 T release in fusion reactor test cell, modelling, operation of atmospheric cleanup system 7-36259
 U acute accidental inhalation by 3 men: 38 yr. follow-up 7-34289
 UO₂ debris beds in pressurised water pools, coolability, DCC-1 and DCC-2 results 7-15279
 UO₂ irradiated fuel, ¹³⁷Cs and ¹²⁹I leaching, rel. with fuel element power 7-786
 UO₂ operating fuel elements, short-lived fission product release under oxidising conditions 7-785
 UO₂ trace irradiated pellets, volatile fission product release 7-788
 UO₂-Na fuel-coolant interaction, thermodynamic bounds, LMFBR appl. 7-42138

accommodation coefficient see sorption

accretion disks

- A0355+26, temporary disk model for hard X-ray pulse profile and period evolution 7-55712
 active galactic nuclei, new accretion disk models rel. to optical and UV spectra 7-60813
 EG And, symbiotic star, mag. field 7-18424
 V1343 Aql (SS 433), models 7-14590
 Aql X-1, irradiated accretion disk model from persistent X-ray emission and bursts obs. 7-66661
 R Aqr, accretion disk model for UV variability and mass expulsion 7-55651
 R Aqr, thick accretion disk model rel. to jet obs. at UV and radio wavelengths 7-55686
 V1343 Aquilae (SS 433), Doppler-shifted X-ray line emission obs. rel. to accretion disk obscuration 7-9493
 baroclinic waves in a vertically stratified thin accretion disk 7-14477
 black holes, neutrino and γ -Ray emission due to nucl. reactions of accreting matter (*Russian*) 7-24160
 black holes accretion disks, adiabatic jets from funnels of thick disks 7-34844
 OY Car, SU UMa-type dwarf nova, accretion disk struct. from IUE obs. in superoutburst 7-55689
 cataclysmic binaries, accretion disk boundary layer, 2D numerical models 7-60667
 cataclysmic binaries, accretion disk inclination and limb darkening rel. to mass spectrum of white dwarfs 7-29476
 cataclysmic variable stars, ang. momentum transport in accretion disks magnetospheres 7-47918
 cataclysmic variables, accretion disk parameters rel. to inclination and orbital phase dependent resonance line profile calcs. 7-60692
 cataclysmic variables, effect of scatt. cloud on hot spots flickering 7-55667
 U Cep, classical Algol binary system, photometry rel. to accretion structs. 7-4512
 U Cep, photometric asymmetry of disturbed eclipses rel. to distrib. of circumstellar matter 7-47991
 close binary systems, particles ejection owing to sudden increase in initial vels. (*Chinese*) 7-4502
 comoving-frame radiative transfer equation 7-55441
 compact objects accretion disks in bimetric gravit. theory as test for general relativity 7-9365
 T CrB, recurrent nova, accretion disk struct. from UV obs. (1978 to 1986) 7-47941
 SS Cyg, dwarf nova, accretion disk behaviour in quiescence and in outburst from IUE obs. 7-55688
 CH Cyg, eclipsing symbiotic star, photometry, spectra and radio flux var. origin (*Russian*) 7-40846
 Cyg X-2, spectral variability, circumstellar structure 7-66660
 formation in binary systems (*Japanese*) 7-4508
 giant planets, protosatellite accretion disks, global characts. 7-34914
 GX 339-4, vel. var. and accretion disk evidence 7-47974
 HD 164270, variable WC9 star, model of close binary with precessing disk 7-47925
 hydromagnetic turbulence in differentially rotating disks, implications for α -value in accretion disks 7-18354
 interacting binary stars, mass transfer and accretion disks rel. to evolution 7-47997
 IRS 16 NW+object A in Sgr A* direction, interpretation 7-40959
 LMC X-3, X-ray binary containing black hole, search for far-UV emission from accretion disk 7-55733
 luminous accretion disk systems, IUE-Voyager observations 7-66623
 magnetic loops in accretion disk corona, struct. and stability 7-4431
 magnetised accretion disk system, magnetodynamic mechanism for jets form. 7-55460
 Markarian 335, soft X-ray excess in Seyfert 1, accretion disk 7-60804
 massive protostars, temp. struct. in accretion flows rel. to emergent IR radiation field 7-29471
 meridional flow in self-gravitating body, mechanical flow in barotropic star with const. ang. momentum 7-29464
 MXB 1730-335, X-ray burster, accretion disc behaviour and neutron star size 7-60709
 neutron stars, disk-magnetosphere boundary struct. rel. to free precession in quasi-periodic oscillators 7-55713
 nonmagnetised low-mass X-ray binary stars, X-ray spectra from accretion disk 7-60719
 numerical method for models of double white dwarf binaries and central white dwarf-heavy disk systems 7-60573
 V2051 Oph, possible low-field polar, intermittent accretion model 7-60694

accretion disks continued

- IP Ori stars, evidence for disk accretion, IR spectral obs. 7-66581
- FU Peg, eclipsing dwarf nova, dimensions of white dwarf and accretion disk from high-speed photometry 7-14595
- AG Peg, symbiotic star, mag. field 7-18424
- planetary satellites accretion models 7-34862
- polarization and beaming of accretion disk radiation 7-47688
- BV Pup, dwarf nova, disk struct. from X-ray, UV and optical obs. 7-47922
- quasars, new accretion disk models rel. to optical and UV spectra 7-60813
- rapidly rotating gas disks, struct. determ. via versatile two-dimensional method 7-9457
- semi-detached close binary star, mass transfer and accretion disk model 7-60727
- U Sge, classical Algol binary system, photometry rel. to accretion structs. 7-4512
- spiral structure development in gaseous disks, due to nonlinear convective instability 7-66766
- stellar wind accretion models, general case of accretion from inhomogeneous medium 7-9460
- thin disk model for UV excess of quasars and Seyfert 1 galaxies 7-40956
- transient X-ray source model involving neutron star accretion disk 7-29513
- twisted accretion disks, density distrib., appl. to X-ray binary stars 7-34969
- X-ray binaries, QPO power spectra as signatures of ang. position and radial vel. of boundary layer clumps 7-47986
- X-ray binary stars, twisted accretion disks, density distrib., appl. to X-ray binary stars 7-34969
- X-ray burster radiation, angular distrib. and polarization 7-4506
- young stars, accretion-driven jets modelling, role of mag. fields and accretion disks 7-60643
- D, synthesis in stellar atm. in binary systems with accretion disks (*Russian*) 7-24218

accumulation layers

- 2D electron systems, width effect on magnetoconductivity 7-27353
- n-GaAs, depletion and accumulation layer profiles, self-consistent Hartree approx. calcs. 7-27375
- n⁻-GaAs/Al_xGa_{1-x}As/n⁺-GaAs capacitors, accumulation layers magneto-tunnelling obs. 7-12880
- n-Hg_{0.8}Cd_{0.2}Te accumulation layer electrons, tilted field cyclotron resonance 7-7591
- InP/native oxide MIS structures, interface elec. props. 7-33851
- Si, accumulation layers, quasi-1D transport, strong localisation 7-64359
- p-Si wafer, minority-carrier diffusion length determ., photocurrent generation method 7-38579
- a-Si:H/a-SiN_x/H multilayer films, coplanar conductance, voltage-induced anomalies study 7-2729
- SiO₂/SiC interface. elec. characts., MOS conductance technique meas. 7-12873
- Te (0001), conductivity of size-quantised holes, hydrostatic pressure effects 7-45428
- ZnO:H, quantised accumulation layers on ZnO surfaces, photoenhancement 7-7304

accumulators *see secondary cells***acidity** *see pH***acids, organic** *see organic compounds***acoustic analysis**

- glottal explosive of Ryukyuan dialect of Japanese, acoustic analysis (*Japanese*) 7-11226
- slab-heating square inductor vibration and acoustic analysis (*Russian*) 7-62905

acoustic applications

- see also ultrasonic applications*
- atmosphere temperature profile meas. in troposphere and stratosphere, radio acoustic technique 7-14360
- ceramic tubes, acoustic anal., nondestructive examination method 7-13705
- Coastal Ocean Dynamics Experiment, shipboard Doppler current profiling 7-9260
- corona discharge, bridged-over, control using high-intensity sound 7-20581
- dust extraction in industrial plants (*German*) 7-57664
- gas analyser for binary mixtures 7-39939
- high intensity low frequency sound used for cleaning purposes 7-26115
- nuclear radiation detection using acoustic technique 7-36427
- ocean current sensing, space-time analysis of acoustic scintillations 7-9258
- oceanographic acoustic Doppler current profiler, intercomparison with conventional instruments and tidal flow model 7-9266
- oceanographic acoustic Doppler current profiling, form volunteer commercial ship 7-9261
- oceanographic acoustic Doppler profile current meter, field evaluations 7-9264
- oceanographic acoustic Doppler profiler intercomparison expt., Delaware Bay (1984) 7-9263
- oceanographic acoustic Doppler profiles, surface wave kinetic energy influence 7-9274
- oceanographic current meters standardisation problems and solutions 7-9272
- oceanographic shallow water tomography, acoustic reciprocal transmission expts. 7-9259
- oceanographic surface current meas., CODAR intercomparison, Delaware Bay (1984) 7-9254
- piezoelectric materials, acoustic resonance techniques for temp., stress and impurity characterization 7-45938
- pulse combustion, characts., appls., and research needs 7-65594
- remote sensing of atmosphere and oceans, symposium, Paris (October 1985) 7-48133
- smart acoustic current meters, experiences in Lake St. Clair, Canada/USA 7-9255
- snow, modelling as acoustically porous material 7-55120
- sonic logging, 2D spectrum anal. 7-55332
- sound freq. in resonant pipe, displacement meas. 7-24622
- space, containerless technology appls. 7-11245
- underwater acoustic exploration, appl. of array processing for parallel linear recursive Kalman filtering 7-65986
- vessel-mounted acoustic Doppler current profiler, for use in rivers and estuaries 7-9262

acoustic applications continued

- wave theoretical approach to acoustic current profiling 7-4821
 - Au, acoustic-jet plating of 7.5 MHz 7-59462
 - Cu, acoustic-jet plating of 7.5 MHz 7-59462
- acoustic arrays**
- acoustic helical antenna for submerged end-fire array appls. (*Japanese*) 7-31560
 - annular array transducers for ultrasound imaging systems 7-31620
 - atmospheric sounding, switched-beam planar arrays suitable for high-resolution acoustic sounders 7-9209
 - beam deflector of SAW formed by an IDT array of 'flash grating' type (*Chinese*) 7-20514
 - beamforming output, high resolution deconvolution algorithms 7-31575
 - biomedical US probe and array using PZT-polymer 1:3 composite 7-3848
 - biomedical US transducer array performance with PZT-polymer composite piezoceramic 7-3850
 - biomedical US transducer array two-dimensional displacement analysis 7-1364
 - biomedical US transducers, pressure field distrib. evaluation in attenuating media 7-3852
 - circular infrasound array for improving signal-to-noise ratio (*Chinese*) 7-20513
 - cylindrical, effect of surrounding shell on directivity pattern 7-16037
 - directional array approach for the measurement of rotor noise source distributions with controlled spatial resolution 7-50879
 - directivity synthesis test bed using Lamb waves 7-50869
 - dynamically-focussed US array for cancer therapy 7-54683
 - high spatial resolution digital system for ultrasonic imaging 7-31597
 - high-quality loudspeaking system development with acoustic signal processing (*Japanese*) 7-57661
 - horizontal array in a shallow sea, calcs. 7-62894
 - Jacobi arrays and circle relationships 7-26096
 - Jacobi sensor arrangement for maximum array directivity 7-26095
 - parametric arrays, applications to shallow water (*Chinese*) 7-37240
 - parametric receiving array as a practical sound receiver 7-20522
 - phase synthesis of a sector directivity pattern for an array consisting of a small number of elements 7-50870
 - polyvinylidene fluoride sheet evaluation for large sonar arrays 7-2986
 - postbeamformer interference canceller, effect of bandwidth on performance 7-6055
 - sonar beamformer, sampled phase-delay, high resolution 7-31606
 - sonic microwave-antenna simulator 7-43582
 - US phased arrays, mechanical, electric and piezoelectric interaction 7-1365
 - US transducer construction with screen-printed matching layers 7-1370
 - wide angle electronic sector scanning with curved arrays 7-31605
- acoustic delay lines**
- see also ultrasonic delay lines*
 - SAW dispersive delay line using dispersive interdigital transducer with periodic electrodes 7-6053
 - transit time of pressure propagation prediction and obs. 7-50880
- acoustic detectors** *see acoustic transducers*
- acoustic devices**
- see also acoustic delay lines; acoustic generators; acoustic microscopes; acoustic microwave devices; acoustic parametric devices; acoustic radiators; acoustic receivers; acoustic resonators; acoustic transducers; bells; surface acoustic wave devices; ultrasonic devices*
 - AlPO₄, berlinite, hydrothermal cryst., growth, X-ray topography, bulk acoustic wave device characts. 7-59391
- acoustic dispersion**
- see also ultrasonic dispersion*
 - energy relations for acoustic waveguides 7-43468
 - Lennard-Jones fluid, repulsive, sound dispersion, density depend. 7-12212
 - SAW dispersive delay line using dispersive interdigital transducer with periodic electrodes 7-6053
 - spherical acoustic waves in a medium with spatial dispersion 7-50799
 - water, liq., collective dynamics, sound dispersion 7-26613
 - Al, dislocation kinks, tunneling, acoustic study 7-2023
 - SiO₂-YX-SiO₂, anisotropic layered systems subject to static deformation, SAWs 7-43495
- acoustic echoes** *see echo*
- acoustic emission**
- andesite, acoustic emissions for triaxial compression (*Japanese*) 7-66111
 - andesite acoustic emission, for rock under triaxial compression 7-18322
 - ceramics, crack propagation by double-torsion method (*Japanese*) 7-59614
 - coherent fracture, acoustic emission 7-53834
 - dielectrics, electrical breakdown, physics, acoustic theory appl. 7-33329
 - glass, microdefect accumulation kinetics during optical irradiation 7-38050
 - glass fibre reinforced PVC matrix, acoustic emission during irreversible deform. 7-3380
 - graphite, AGR fuel sleeves, irradi., bending, AE obs. 7-723
 - graphite, fracture criterion, acoustic emission studies (*Japanese*) 7-8088
 - head-on collision of two vortex rings 7-31622
 - ice deformation and breaking 7-16053
 - metal tritides, disorder induced by aging 7-21199
 - PMMA, microdefect accumulation kinetics during optical irradiation 7-38050
 - polymer crystallisation, assoc. acoustic emission due to stress release 7-44704
 - quartz glass, microdefect accumulation kinetics during optical irradiation 7-38050
 - rock failure, rupture length and propag. speed determ. from seismic and acoustic data 7-8855
 - signal amplitude correlation with material deform. rate 7-33895
 - steel, martensitic, intergranular crack nucleation, fractographic and acoustic emission meas. (*Russian*) 7-33766
 - stick-slip friction, acoustic output 7-50905
 - vortex motions, acoustic emissions 7-51171
 - Al, acoustic emission during deform. of high-purity single crystals. 7-59588
 - Al, deformed, acoustic emission on heating 7-51958
 - Al-Sn, bearing alloys, run-in kinetics, friction, contact resist., AE signals 7-17655
 - Al-(Mg), AE during deform., effect of struct. state (*Russian*) 7-38127
 - Be, AE as function of grain size during plastic deform. (*Russian*) 7-59582
 - Cr films, acoustic emission during electrodeposition 7-52329

acoustic emission continued

- Cu-Co, age hardened, tensile deform., acoustic emission characts. 7-13536
- Fe₇Si₃, magnetoelastic acoustic emission 7-33257
- GeTe, α - γ phase transformation kinetics, effect of heat treatment 7-63795
- LiF, fracture, mag. field effects 7-16675
- NbT_{0.59}, acoustic emission and swelling, ageing effects 7-33708
- SiC fibre reinforced Al alloys, whisker or particulate hybrids, mech. props. 7-13537
- TaT_x ($x = 0.12, 0.103, 0.42$), acoustic emission and swelling, ageing effects 7-33708
- Zr alloys, hydride cracking, acoustic emission studies 7-59637

acoustic emission testing

- aircraft, structural crack detection studies 7-33906
- brittle materials, detecting damage surfaces 7-46779
- conference on water reactor safety, Gaithersburg, MD, USA, (Oct. 1985) 7-48152
- crack initiation sites, determ. using digital NDE workstation 7-65277
- defect characterisation in three dimensions 7-3563
- fatigue crack unstable development, regularities investig. using acoustic emission 7-22962
- glass, AE source characteristics from thermal crack 7-21341
- glass fibre reinforced polyester, aligned, AE stress corrosion cracks 7-59722
- glass fibre reinforced polyester resin composite, fracture toughness and microfractures, AE obs. (*Japanese*) 7-33779
- high temp. crystallisation, flaw form., AE detection, automatic system 7-3557
- noise emission analysis for determining crackinitiation during instrumental notched bar impact testing (*German*) 7-8216
- nuclear power stations, diagnostic subsystems in Czechoslovakia (*Czech*) 7-19386
- online acoustic emission monitoring of cracks in nuclear systems, review 7-54066
- optical fibre cut-end inspection method using acoustic emission sensor (*Japanese*) 7-11189
- piezoelectric receiving transducer, reciprocity calibration 7-62937
- plywood, interior adhesion inspection 7-20542
- polyester resin, glass-reinforced, stress corrosion cracks, acoustic emission monitoring 7-53926
- polystyrene, slow crack propag., crazing and fracture, acoustic emission study 7-32555
- pulsed photoacoustic materials characterization 7-46755
- PVC, rubber modified or filled, damage kinetics, AE analysis 7-54063
- scratch adhesion testing, critical load for coating loss, acoustic emission 7-3549
- shape memory alloy, intrinsic stresses evaluation by AE 7-39829
- signal amplitude correlation with material deform. rate 7-33895
- steel, C, inverse magnetostrictive effect and electromagnetic non-destructive testing methods 7-13714
- steel, corrosion monitoring by AE 7-22956
- steel, Cr-Mo, breakaway oxidation and internal cracking at 900°C, freq. anal. of AE signal 7-17718
- steel, mild, acoustic emission during corrosion in FeCl₃ soln. 7-39814
- steel, Ni-Mo, wide plate crack arrest testing using acoustic emission, reactor pressure vessel appl. 7-53886
- steel, rotor type, deformed, microcrack dimens. rel. to acoustic emission parameters and struct. 7-65258
- structural testing applications, metallic and composite structures 7-33883
- surface crack initiation and growth, determ. using pot. drop method (*German*) 7-8241
- technique for friction and wear obs. and seizure prediction (*Japanese*) 7-59721
- wood defect inspection using impact excitation method 7-20541
- Al, acoustic emission during corrosion in FeCl₃ soln. 7-39814
- Al, acoustic emission during deform. of high-purity single crystals. 7-59588
- Al-Cu-Mg, Al-Mg, plastic deform., AE, X-ray obs. (*Russian*) 7-46579
- Al-Cu-Mg, deformed, dislocation struct., AE obs., electron microscopy (*Russian*) 7-39832
- Al-Mg, deformed, dislocation struct., AE obs., electron microscopy (*Russian*) 7-39832
- β -Al₂O₃-Na₂O, ZrO₂ toughened solid electrolyte, failure initiation, critical current density, AE obs. 7-38252
- C fibre reinforced plastic, damage states, US and acoustic emission study (*German*) 7-22828
- Cu, acoustic emission during corrosion in FeCl₃ soln. 7-39814
- Cu, brittle oxide formed during oxidation, AE technique, alternative to thermogravimetry 7-65274
- Cu, electrotech. grade, acoustic emission characts. in elastoplastic deform. 7-39816
- SiC, stress intensity factor meas. using notched and surface flaw specimens 7-65251

acoustic equipment

- see also acoustic arrays; acoustic wave interferometers; ultrasonic equipment*
- array directivity synthesis test bed using Lamb waves 7-50869
- ocean acoustic inhomogeneities remote recording instrumentation 7-29299
- parametric sonar use for oceanographic research 7-29298
- sound level meters, Japanese testing and calibration methods 7-1334
- vertical SODAR for planetary boundary layer acoustic sounding (*German*) 7-9246

acoustic field

- 3D acoustic radiation with flow, BEM 7-16202
- aeroacoustic high intensity field meas. using cooling power anemometer 7-16039
- aerofoil cascades, acoustic effects due to turbulence 7-16016
- atmospheric waveguide propagation near impedance boundary with stratification (*Russian*) 7-20492
- attenuating media, US field theory 7-31546
- axisymmetric sources of complex shape, sound radiation 7-62873
- axisymmetric vortex sound, acoustic wave field determ. 7-51182
- biomedical US transducers, pressure field distrib. evaluation in attenuating media 7-3852
- computer-aided sound propagation anal. method (*Japanese*) 7-20483
- convergence type aerial ultrasonic source with a stripes mode vibration plate and formation of high intensity ultrasonic field (*Japanese*) 7-31611

acoustic field continued

- corona discharge, bridged-over, control using high-intensity sound 7-20581
- deep-sea sound field, effect of vel. profile near surface 7-43502
- discrete spectrum of the sound field of a point source in a stratified moving medium 7-62889
- elastodynamic spectral energy density, time and geometry independence 7-43487
- energy flux in a cylindrical duct with compliant walls in the presence of air flow 7-62859
- extensional-wave and flexural-wave contributions to the sound field radiated by a fluid-loaded infinite plate 7-6036
- factories, acoustic scale modelling 7-62916
- farfield radiation patterns of a circular piston in a soft baffle with nonfinite extent 7-43485
- frequency filtering in model acoustic waveguides 7-43465
- high frequency sound field in a duct for a line source at an arbitrary position (*Japanese*) 7-31547
- hybrid type infinite element, finite element approach to unbounded Poisson and Helmholtz problems 7-1003
- impingement on wedge, edge-tone flowfield 7-11483
- inhomogeneous media, asymptotic methods for solving wave diffraction problems 7-26055
- intensity fields of continuous-wave axisymmetric transducers 7-62939
- lecture halls, large, scale model expts. 7-6048
- liquid-solid interfaces, refl. acoustic field distrib., nondestructive evaluation (*Japanese*) 7-57651
- low Mach number flows, acoustic radiation, 3-D boundary element scheme 7-11402
- magnetised compressible media, spatial mapping and time reversal 7-20097
- mean path length in random acoustic fields in solids 7-6047
- noise fields radiated by random sources on a plane 7-50836
- nonlinear response in evaluating the subjectivediffusiveness of sound fields 7-6050
- numerically efficient full wavefield approach to synthetic seismogram computation 7-26117
- oblique scanning acoustic microscope confocal beam formation 7-1340
- ocean acoustic noise field, long-period hydrodynamic perturbations 7-62893
- ocean sound field sensing method 7-66308
- oscillations, thermally induced, stability boundary, num. method 7-26074
- piston, rectangular, diffracted transient field 7-31567
- plane circular sound source, nonlinear radiation (*French*) 7-1300
- plane-layered waveguide, effect of motion of acoustic source on sound field 7-50801
- point source, sound field calcs. 7-43466
- potential flows, linear and nonlinear acoustic wave eqns. 7-16015
- radiation of a sound field by a slender body of revolution 7-16007
- rectangular concave source, radiation field calcs. (*Japanese*) 7-43488
- SAW filters, acoustic field investig. using fibre optic homodyne laser probe 7-1358
- SAW reflection/transmission at boundary between metallized and free surfaces (*Japanese*) 7-11204
- shallow sea, amplitude fluctuations of a sound field along a stationary acoustic test range 7-50826
- slender elastic bodies of revolution, plane wave scattering 7-62860
- sound freq. in resonant pipe, displacement meas. 7-24622
- synchronized Schlieren method for vortex shedding in cascade during acoustic resonance 7-20572
- time harmonic cylindrical SAW excitation 7-43470
- ultrasonic field radiation force calculations 7-62877
- underwater, frequency spectra of a noise field in a plane-layered waveguide 7-16026
- underwater low-frequency noise fields 7-43508
- US hyperthermia simulation using finite element model 7-47181
- US piezoelectric transducer pressure field calc. and expt. 7-1367
- US transducers with curved surface for improved lateral resolution 7-43618
- vibrating circular piston in infinite baffle, acoustic field anal. using BEM (*Japanese*) 7-43491
- waveguides, irregular, investigation of mode conversion 7-16004

acoustic generators

- see also earphones; loudspeakers; photoacoustic effect*
- shallow prospecting on land by means of a novel electroacoustical P-Wave pulse generator 7-34751
- ultrasonic power generator using voltage-vector controlled resonant inverter 7-20535
- versatile melody generator, DIY (*German*) 7-16049
- X-ray generated US signals, characts. and imaging appls. 7-43624

acoustic holography

- backpropagated scattered wave inversion for arbitrary receiver geometry 7-26092
- cylindrical components, US testing, tomographical evaluation of multifrequency-holography data (*German*) 7-8238
- elastodynamic wave holographic imaging 7-31582
- generalized nearfield acoustical holography for cylindrical geometry: theory and experiment 7-62920
- HOLOSAPT holography/synthetic aperture imaging technique 7-26104
- image processing using liquid crystal convertor 7-1319
- industrial noise analysis appls. 7-31580
- inverse filter design for holographic imaging systems with small apertures 7-31583
- near-field acoustic holography 7-11222
- root-mean-square optimal solutions of selective holography 7-57272
- SAR image holography using acoustic lens for 3D underwater imaging 7-43513
- scanning laser acoustic microscope for holographic and tomographic imaging 7-26094
- short-wave, sound source reconstruction (*German*) 7-43545
- tomographic image reconstruction from holographic B-scan signal 7-31584
- underwater acoustics, pattern recognition appls. 7-31581
- US 3D C-scan imaging using holographic reconstruction 7-43546
- US holography with liquid crystal convertor and image processing system 7-43547

acoustic imaging

- see also acoustic holography; acoustic microscopy*
- ambiguity functions for diffraction tomography using back-and-forth propagation 7-26106

acoustic imaging continued

- annular array transducers for ultrasound imaging systems 7-31620
- attenuation correction using Mellin transform 7-26090
- B-mode echogram texture analysis 7-28637
- B-scan image reconstruction, influence of point spread function 7-31576
- B-scan imaging, fast Kalman filter derivation 7-31578
- backward propag., spatial freq., sampling window effects (*Chinese*) 7-11220
- bat sonar perception systems 7-47131
- biomedical US probe and array using PZT-polymer 1:3 composite 7-3848
- biomedical US transducer array performance with PZT-polymer composite piezoceramic 7-3850
- biomedical US transducer array two-dimensional displacement analysis 7-1364
- biopsy studies using ultrasound 7-34206
- blood, ageing, effect of motion on sonographic and NMR patterns 7-54684
- cardiac tissue imaged with US sector scanning, spectral anal. method 7-34214
- cardiac wall motion during exercise, computerised quantitative segmental anal. from 2D echocardiograms 7-34321
- combined shear-compression ultrasound reflection tomography 7-26112
- conference, The Hague, Netherlands (Apr. 1985) 7-24293
- cylinder, isotropic and homogeneous, theor. and numerical results 7-31555
- defect detection using ultrasonic B-scan, transducer beam divergence effects 7-31617
- diffraction correction method for backscatter coefficient using echoes scattered by a thin line (*Japanese*) 7-43592
- diffraction tomography, quantitative, with pulsed acoustic fields 7-50877
- echo diagnostic ultrasound: history, transducers, artefacts and new applications 7-28633
- echocardiograms, 2D, automatic and intelligent left ventricular contour detect. 7-34212
- echocardiographic scan images, cine, spatial and temporal processing: automated myocardial border tracking 7-28638
- echocardiographic visualisation of acute myocardial ischaemia 7-28631
- echocardiography, 2D., microcomputerised image processor and 3D reconstruction of left ventricle 7-34213
- echocardiography, 2D, in infants and children, book 7-60061
- echocardiography, attenuation correction 7-23417
- echocardiography, computer assisted anal. of left ventricular function 7-34211
- echographic imaging, 2-D Wiener inverse filtering 7-26091
- echography, geometric and intensity distortion 7-47189
- elastodynamic wave holographic imaging 7-31582
- hand-held ultrasonic medical image scanner, design 7-54688
- high resolution ultrasonic tissue characterization 7-34208
- high resolution ultrasound computerised tomography 7-34207
- high spatial resolution digital system for ultrasonic imaging 7-31597
- HOLSAFT holography/synthetic aperture imaging technique 7-26104
- hydrothermal plumes at seafloor spreading centres, acoustic imaging 7-6032
- image contrast processes in thermal and thermoacoustic imaging 7-43587
- image reconstruction fidelity using the Born and Rytov approximations 7-26087
- impedance tomography, reconstruction procedures 7-31607
- interactive processing system for ultrasonic compound imaging, real-time image processing and texture analysis 7-23419
- inverse filter design for holographic imaging systems with small apertures 7-31583
- lightweight US data acquisition and graphic display system 7-1335
- limited angle reflection mode computerized tomography 7-28635
- medical B-mode imaging data sampling, US beamwidth effect on attenuation 7-47191
- medical diagnosis, US imaging 7-60059
- medical images, deterministic approach towards speckle reduction 7-60060
- myocardial signature: absolute backscatter, cyclical variation, frequency variation, and statistics 7-23418
- nonlinear parameter imaging CT system using parametric acoustic array 7-34204
- ocean acoustic tomographic mapping (*Japanese*) 7-47560
- ophthalmology, ultrasonic therapy and imaging 7-28632
- optical-digital joint Fourier transform classification of liver echotexture 7-34209
- passive, through inhomogeneous media, appl. of phase closure technique 7-26102
- phase tomography, velocity and temperature measurement 7-34205
- photothermal imaging, spatial resolution of subsurface structure 7-26110
- planar acoustic tomography, image reconstruction using hexagonal arrays 7-26088
- prior inverse filtering for high-resolution pulse-echo images 7-26089
- Q-profiling for inverse sand scattering 7-31551
- range resolution improvement with a new signal processor implementing a fast Kalman estimator 7-31574
- ray tracing on a grid using sound vel., error evaluation 7-20520
- reconstruction for synthetic aperture diffraction tomography (*Chinese*) 7-57638
- recovery of ultrasonic impulse response by spectral extrapolation 7-26085
- reflection acoustic microscopic response model for specimen structural variation 7-1339
- resolution limits in inversion by parameter estimation 7-26083
- resolution limits of acoustical echo systems 7-26100
- scanning laser acoustic microscope for holographic and tomographic imaging 7-26094
- scanning laser acoustic microscope high-resolution imaging with digital processing 7-1318
- scanning laser acoustic microscope image reconstruction theory 7-1338
- sea floor imaging long-range, low-freq., spatial resolution aspects 7-28999
- seismic imaging, spectral resolution aspects 7-26116
- soft tissue movement information in ultrasonic M-mode images 7-34210
- sound-beam topography, cryst. defect imaging in quartz 7-11237
- spatial resolution in ultrasonic pulse echo texture analysis 7-28636
- speckle reduction in pulse-echo images by using phase insensitive summation and multiplicative techniques 7-28634
- submarine topographical information based on seabed bathymetric system (*Japanese*) 7-43595

acoustic imaging continued

- subsurface defect acoustic imaging in composites and roughened samples 7-3568
 - subsurface imaging by scanning acoustic microscopy 7-3569
 - thermal wave imaging with thermoacoustic detection 7-43586
 - thermoacoustic wave imaging and depth profiling cell 7-1337
 - thin hard coatings, adhesion test methods, review 7-46741
 - time domain diffraction tomography 7-26105
 - time domain formulation of pulse-Doppler ultrasound and blood velocity estimation by cross correlation 7-23416
 - tissue US attenuation meas. using scanned B-mode tomogram 7-23477
 - tomographic image reconstruction from holographic B-scan signals 7-31584
 - transient fields from focused acoustic waves 7-31599
 - transmission acoustic microscopy with focal planedetection 7-1343
 - transmission thermoacoustic imaging without contact 7-31601
 - two-dimensional ultrasonic scanning method using a circular-array transducer 7-20523
 - ultrasonic, digital scan converter design 7-31603
 - ultrasonic, inverse scattering image reconstruction 7-20519
 - ultrasonic backscatter meas., effect of transducer focusing 7-20545
 - ultrasonic echography, acousto-optic deconvolution 7-26113
 - ultrasonic imaging systems for robot object recognition 7-26097
 - ultrasonic pulse-echo imaging using instantaneous freq. information 7-31596
 - ultrasonic tissue characterization imaging research program 7-34203
 - ultrasonic transmission image restoration theory 7-31598
 - ultrasonic underwater imaging of cracks in concrete 7-33908
 - ultrasonics conference, San Francisco, USA (Oct. 1985) 7-11
 - ultrasonogram displays on liq. crystal TV and fluorescent vacuum tube 7-31602
 - undersea ultrasonic imaging system with electronic scan (*Japanese*) 7-43594
 - underwater, cross-fan beam scanning (*Japanese*) 7-43593
 - US B-scans, speckle reduction using weighted averaging in spatial compounding 7-43539
 - US cross sectional images, Fourier domain reconstruction 7-43609
 - US imaging of layered structures using nondestructive subnanosecond photoacoustic pulse generation 7-43581
 - US inverse scattering perturbation theories, reconstruction algorithms 7-43474
 - US kidney images recognition by 2D dynamic programming method 7-18034
 - US tomography, resolution improvement using adaptive filtering (*Japanese*) 7-34202
 - US wave field meas. using light beam CT system (*Japanese*) 7-57652
 - wide angle electronic sector scanning with curved arrays 7-31605
 - X-ray generated US signals, characts. and imaging appls. 7-43624
 - Si, polycrystalline columnar crystals, acoustic visualisation 7-8242
- acoustic impedance** *see also acoustic wave velocity*
- 1D random lattices, Anderson localisation of waves (*French*) 7-16013
 - cylindrical cavities, acoustical admittance calcs. 7-57620
 - flow resistance meas., theory 7-11234
 - flow resistance meas. technique 7-11233
 - glottal opening and flow, measurement of effects on glottal impedance 7-47128
 - grass-covered ground, acoustic impedance meas. at low freqs. using phase difference technique 7-50876
 - middle-ear input admittance, changes during postnatal auditory development in chicks 7-40165
 - mutual radiation impedance of double-disk source, radiated power effect 7-31613
 - orifices, effect of grazing turbulent pipe flow 7-43463
 - phase gradient method of measuring the acoustic impedance of materials 7-50875
 - plate before an enclosed air volume 7-16001
 - resonators, multilayer, low freq., specific characts. of mass reactance 7-16038
 - Riccati equations describing impedance relations for forward and backward excitation in the one-dimensional cochlea model 7-65765
 - rigid frame model of porous media for the acoustic impedance of snow 7-31548
 - seismic 1D inverse problem and impedance determ. 7-47369
 - thickness-mode piezoelectric transducer constants, automatic meas. and calibration system 7-1369
 - tube muffler, nonlinear acoustic resistance effects (*Chinese*) 7-20486
 - US transducer construction with screen-printed matching layers 7-1370
 - vertical seismic profiling 1D inverse problem, soln. 7-34390
 - PZT-epoxy composites, thinning, ceramic width, acoustic impedance study 7-51954
- acoustic insulating materials** *see noise abatement*
- acoustic intensity** *see also acoustic noise; loudness*
- air ducts, cylindrical, radial sound level variations and cross modes 7-50847
 - circular vibrating membrane, acoustic pressure analysis 7-11211
 - frequency weighted sound pressure of a movingpoint source in a nondissipative medium 7-1301
 - infinite plate, vibrational/acoustical intensity relationship 7-31563
 - measurement without error caused by phase difference between meas. instruments (*Japanese*) 7-11236
 - plate turbulent boundary layer acoustic pressure spectrum 7-43496
 - program for combining sound pressure levels in noise, BASIC 7-62909
 - thin elastic plates, point-forces, acoustic power radiated 7-50834
 - tube muffler, nonlinear acoustic resistance effects (*Chinese*) 7-20486
 - vocal tract shapes, power spectra, Doppler degradation, bat and dolphin waveforms 7-8604
- acoustic intensity measurement**
- A-weighting response rule-of-thumb 7-31594
 - acoustic power measurements of focused waves: radiation force and Raman-Nath methods 7-11203
 - aeroacoustic high intensity field meas. using cooling power anemometer 7-16039
 - diffraction correction for radiation force measurement on an ideal plane reflector 7-11228
 - impact forming machine, sound power det. 7-50871
 - microphone screens for acoustic measurement in turbulent flows 7-31593
 - piston Radiation Investigations using two-microphone sound intensity method 7-57649

acoustic intensity measurement continued

- rotating microphones method, phase mismatch and position error cancellation 7-62932
- sound power measurements in a rectangular reverberation room (*Japanese*) 7-62928
- US diagnostic devices, USA Food and Drug Administration guidelines 7-3851

acoustic magnetic resonance

- see also *acoustic nuclear magnetic resonance; acoustic paramagnetic resonance*
- No entries

acoustic measurements see *acoustic variables measurement***acoustic microscopes**

- 160 MHz gas-medium scanning acoustic microscope 7-1342
- elastic wave propag., accurate field anal. 7-43472
- elastic wave propag. focusing props. of small-aperture lenses 7-43473
- microprocessor-controlled, 50-2000 MHz range 7-20544
- oblique scanning acoustic microscope confocal beam formation 7-1340
- off-centre concave transducer for acoustic microscopy 7-20566
- planar focusing lens design and operation 7-1341
- reflection acoustic microscopic response model for specimen structural variation 7-1339
- scanning, for subsurface sample imaging, spatial resolution 7-31604
- scanning acoustic microscope, state of development 7-11238
- scanning acoustic microscopy, NDT appl. 7-3564
- scanning laser acoustic microscope for holographic and tomographic imaging 7-26094
- scanning laser acoustic microscope image reconstruction theory 7-1338
- scanning laser acoustic microscope with digital data acquisition 7-50882
- semiconductor device inspection using Leitz ELSAM acoustic microscope (*German*) 7-31591
- spherical focusing transducers, ray-optical analysis 7-1371

acoustic microscopy

- alumina surface crack characterisation by scanning acoustic microscopy 7-3567
- broad-band electrical matching of transducers for acoustic microscopy 7-62940
- ceramics NDT by acoustic microscopy with single zoom lens 7-3570
- coal, thermal charactn., piezoelectric photoacoustic microscopy 7-44643
- electron-acoustic microscopic study on dislocation lines in the base region of α - β Si-Tr 7-20538
- imaging mode, quantitative results 7-26111
- industrial applications of large-scale 10-100 MHz system 7-43598
- integrated circuit subsurface features, detect. by photoacoustic microscopy 7-50873
- ion beam excited acoustic image and specific element image of teeth 7-20536
- Lamb wave velocity meas. in thin plates 7-2332
- multilayered plate, acoustic material signature calc. 7-37300
- NDT appls. of scanning acoustic microscopy, NPL developments 7-22959
- nondestructive evaluation of materials by photoacoustic microscope and photothermal beam deflection 7-20585
- photoacoustic microscopy, real-time theory 7-50872
- physical acoustics, conf., Varenna, Italy (July 1984) 7-9599
- polycrystalline materials, evolution of scatt. loss by line-focus-beam acoustic microscope 7-2331
- Powercore strip, amorphous metal ribbon layers, bonding study 7-22975
- quartz, dopphine twinning, acoustic microscopy obs. 7-21233
- Rayleigh wave theory and appls., conf., London, England (July 1985) 7-22
- sapphire, sub-surface, defect obs., by Rayleigh wave reflection in scanning acoustic microscope 7-13710
- scanned microscopy techniques 7-26103
- scanning acoustic microscopy, appls. of Rayleigh waves 7-1353
- scanning acoustic microscopy, NDT appl. 7-3564
- scanning acoustic microscopy 7-26098
- scanning acoustic microscopy 7-37299
- scanning electron acoustic microscopy, signal generation and contrast mechanisms 7-24726
- scanning electron acoustic microscopy and its applications 7-43599
- scanning electron microscopy, thermal- and acoustic-wave techniques 7-48917
- scanning laser acoustic microscope high-resolution imaging with digital processing 7-1318
- scanning laser photoacoustic microscopy, phase transition studies 7-20582
- scanning mode, practical resolution limits 7-31600
- scanning tomographic mode, optimal observation angles 7-26107
- subsurface crack analysis 7-20537
- subsurface defect acoustic imaging in composites and roughened samples 7-3568
- subsurface imaging by scanning acoustic microscopy 7-3569
- surface cracks, acoustic microscopy 7-46768
- thermal wave microscopy techniques 7-26108
- thermal wave/thermoacoustic microscopy, spatial resolution 7-26109
- transmission acoustic microscopy with focal planedetection 7-1343
- transmission mode US microscopy for low temp. work 7-20518
- ultrasonic microspectroscopy using Rayleigh waves 7-1354
- ultrasonics conference, San Francisco, USA (Oct. 1985) 7-11
- Al, mechanically deformed, thermoacoustic imaging 7-46757
- Al_2O_3 , crack imaging using scanning acoustic microscopy 7-28257
- Al_2O_3 , reflection scanning acoustic microscopy of partly embedded cracks 7-46769
- $\text{Al}_2\text{O}_3\text{-N}_2^+$, ion implantation, ion-acoustic microscopy 7-51792
- GaAs, substrates, multi-technique approach to defect microstructure characterisation 7-52215
- LiNbO_3 , proton-exchanged, acoustic microscopic studies 7-21597
- Mn-Zn ferrite US scatt. loss evaluation by line-focus-beam acoustic microscope 7-2331
- Nb, supercond., nondestructive inspection by scanning laser acoustic microscopy 7-3566
- $\text{ZrO}_2\text{-N}_2^+$, ion implantation, ion-acoustic microscopy 7-51792

acoustic microwave devices

- see also *acoustic transducers; surface acoustic wave devices*
- LiNbO_3 bulk wave acousto-optic deflector beam steering by interdigital transducer 7-1255

acoustic mode of crystals see *lattice dynamics***acoustic noise**

- 1150 kV power lines, acoustic noise due to corona (*Russian*) 7-1314
- active cancellation system 7-37259

acoustic noise continued

- active suppression of flow-excited cavity oscillations (*French, English*) 7-31774
- aerodynamic noise principles (*Chinese*) 7-11208
- air ducts, cylindrical, radial sound level variations and cross modes 7-50847
- axisymmetric vortex sound, acoustic wave field determ. 7-51182
- broadband sock-associated noise and screech tones 7-20502
- burner nozzle combustion noise expts. 7-50843
- cavitation damage and noise spectra in a polymer soln. 7-62887
- choice reaction time and paired associates learning tasks, effects of noise and vibration 7-54677
- cold heading workshop noise 7-20505
- community and individual response to changes in traffic noise exposure 7-46986
- computer simulation of noise processes (*Chinese*) 7-57639
- contribution factors of sound source, estimation method 7-11213
- correlation of vehicular noise to various trafficand geometrical characteristics in Thessaloniki/Greece 7-8469
- crack initiation during instrumented notched bar impact testing, noise analysis (*German*) 7-8216
- critical masking interval meas. for click in wideband noise 7-57634
- cross-cultural study on noise problems 7-34088
- deafness due to exposure to music, Japanese study (*Japanese*) 7-47113
- diving helmet noise, instrumentation methods for meas., diver hearing appl. 7-60146
- Dutch two-obstruent sequences, voicing perception, voice and noise parameters effect 7-37273
- entertainment noise levels 7-46988
- environmental noise and vibration data (*Japanese*) 7-46985
- exposure level calcs. for constant slope patterns 7-50838
- factory building environmental noise 7-17932
- falling liq. film, vapour generation nucleate boiling, acoustic diagnostic technique 7-11502
- fields radiated by random sources on a plane 7-50836
- film loop noise levels in cameras and projectors (*Russian*) 7-62913
- frequency domain acoustic noise canceller, frequency bin adaptive filtering 7-37247
- friction and contact noise, conf., Delft, Netherlands (June 1985) 7-48168
- Gaussian-Gaussian mixture, underwater noises modelling, detection 7-43512
- hand-held tools, sound power levels (*French*) 7-43525
- hearing damage in military service, noise-induced HF losses, study on 38, 294 conscripts 7-54613
- hearing impairment caused by loud music (*Japanese*) 7-47109
- hearing loss development during long-term exposure to occupational noise 7-54615
- helicopter impulsive noise, theory and expt. 7-11214
- helmet noise and divers' hearing 7-60019
- HF travelling-bubble cavitation noise generation 7-16221
- Hong Kong, ambient traffic noise levels 7-59898
- industrial noise analysis appls. of acoustic holography 7-31580
- infrasound, human perception levels 7-50841
- intermittent flow, 2-fluid model 7-11212
- intrusive sounds, noise ratings 7-57632
- Japanese music, effect on performers' hearing (*Japanese*) 7-47111
- jet noise, effect of upstream disturbance (*Chinese*) 7-57630
- laminated composite plates, sound transmission characts. 7-57633
- linear correlation function for random noise or vibration 7-11218
- listening levels of reproduced stereo sound in a house (*Japanese*) 7-43521
- loud music, effect on hearing (*Japanese*) 7-47112
- muff-type hearing protectors, effects on speech intelligibility in noise 7-40172
- multiple scattering noise in 1D, universality through localisation length scaling 7-1315
- ocean acoustic noise field, long-period hydrodynamic perturbations 7-62893
- parameter identification in noise, statistical evaluation 7-62912
- perceptual space for repetitive impulses and environmental noises (*Japanese*) 7-47114
- personal Hi-Fi, hearing impairment effects (*Japanese*) 7-47110
- physical origins of acoustical noise 7-11216
- physiological effects of low frequency noise, Japanese study 7-28598
- piezoelectric semiconductors, amplified acoustic noise anal., Bragg light diffr. method 7-43625
- program for combining sound pressure levels in noise, BASIC 7-62909
- psychophysiological acoustics of indoor sound due to traffic noise during sleep 7-18014
- recognition of speech under stress and in noise 7-37287
- residential noise, extraordinary statistical samples (*Japanese*) 7-20500
- road traffic, kerbside L_{10} level prediction 7-50837
- road traffic noise, effects on daily life, Japanese survey (*Japanese*) 7-46984
- road traffic noise annoyance assessment 7-50844
- road traffic noise level distribution, probabilistic evaluation 7-46987
- short-base acoustic ranging systems, source location accuracy, receivers comparison 7-43511
- speech, acoustic noise reduction by two dimensional spectral smoothing and spectral amplitude transformation 7-37246
- speech kinematics, effects of white noise masking and low pass filtering 7-47125
- steam power station gas duct bends, noise reduction calc. (*Russian*) 7-26078
- stick-slip friction, acoustic output 7-50905
- tinnitus as a source of internal noise 7-8594
- trachea noise biofeedback device to help reduce bronchospasm in asthmatics 7-8754
- underground, noise and vibration sources 7-43524
- underwater low-frequency noise fields 7-43508
- urban noise surveys 7-54405
- urban traffic noise, cannon and facade effects 7-46989
- verbal communication in noise 7-6057
- vertebrate hearing, evolution rel. to noise 7-54588
- vocal tract shapes, power spectra, Doppler degradation, bat and dolphin waveforms 7-8604
- wall response evaluation, effect of signal processing operations 7-16032
- word recognition using multisensor speech input in high ambient noise 7-37288

acoustic noise control *see noise abatement*

acoustic noise measurement

directional array approach for the measurement of rotor noise source distributions with controlled spatial resolution 7-50879
induction motor driven by PWM inverter with 20 kHz switching freq. using Bi-MOS power transistors, acoustic noise 7-62934
marine sediment transport, acoustic detection 7-6033
PGN-200M loop steam generators, noise level measurements 7-61982
pump cavitation monitoring by single fluid-borne noise meas. 7-37502
RAS III, modular noise diagnostics system for reactor primary circuit monitoring (*German*) 7-56787
speech recognition, Rasti method of acoustic meas. (*Swedish*) 7-1333
tyred wheels, noise investigation, array processor use (*German*) 7-6041

acoustic nuclear magnetic resonance

biological tissue acoustic NMR, clinical diagnosis appl. 7-23414
CsI, cryst., γ -irrad., acoustic nucl. reson. (*Russian*) 7-22152
NaCl:Cu, nuclear quadrupole spin-phonon interaction 7-22155
NaF:Cu, nuclear quadrupole spin-phonon interaction 7-22155

acoustic paramagnetic resonance

$\text{Al}_2\text{O}_3\text{:C}^{4+}\text{V}^{3+}$, electron-phonon interaction and impurity energy levels, APR and EPR studies (*Russian*) 7-45814

acoustic parametric amplifiers

modulation of the sound velocity in a colloid by an external electromagnetic field 7-43622

acoustic parametric devices

see also acoustic parametric amplifiers; acoustic parametric oscillators
arrays, applications to shallow water (*Chinese*) 7-37240
parametric receiving array as a practical sound receiver 7-20522

acoustic parametric oscillators

No entries

acoustic power measurement *see acoustic intensity measurement*

acoustic pressure measurement *see acoustic intensity measurement*

acoustic radiators

see also acoustic generators; Doppler effect
axisymmetric bodies, theoretical analysis (*German*) 7-16000
axisymmetric sources of complex shape, sound radiation 7-62873
convex panels with time-harmonic transverse oscil., acoustic radiation efficiency 7-1308
cylindrical cavities, sound generation due to flow excitation 7-43500
hydrodynamic losses in the radiation of sound 7-50891
nonlinear parameter eqns. 7-62884
oscillations, thermally induced, stability boundary, num. method 7-26074
plane circular sound source, nonlinear radiation (*French*) 7-1300
plate of variable thickness, sound radiation 7-16029
rectangular concave source, radiation field calcs. (*Japanese*) 7-43488
rectangular panels coupled in an L shape, acoustic radiation 7-62875
slow-disc waveguide radiators (*Japanese*) 7-20555
time-delay spectrometry for ultrasonic transducer characterisation 7-16041
variable subsonic velocity source, radiating domain sound field 7-43469
vibrating circular piston in infinite baffle, acoustic field anal. using BEM (*Japanese*) 7-43491
 LiNbO_3 bulk wave acousto-optic deflector beam steering by interdigital transducer 7-1255

acoustic reactance *see acoustic impedance*

acoustic receivers

see also microphones
parametric receiving array as a practical sound receiver 7-20522
time-delay spectrometry for ultrasonic transducer characterisation 7-16041

acoustic resistance *see acoustic impedance*

acoustic resonators

acoustic finite elements and their industrial applications 7-16014
Helmholtz resonators, nonlinear tuning curves 7-43497
liquid-filled resonator tube, influence of gas bubbles 7-62880
multilayer, low freq., specific characts. of mass reactance 7-16038
SAW resonators, acceleration and vibration effects 7-57644
scattering of flexural waves by a resonator mounted on a plate 7-62904
speed of sound to speed of light ratio, meas. 7-20543
US resonator, plano-concave, for velocity dispersion meas. 7-16042
Al plate US backscatter and resonance expts. 7-2108
 LiNbO_3 strip-type resonator 7-57657
 LiTaO_3 strip-type resonator 7-57657

acoustic signal processing

active noise cancellation system 7-37259
adaptive array with binaural processor 7-31579
adaptive lattice noise canceller and optimal step size 7-43528
adaptive noise cancellation, variable length lattice filter use 7-43527
angular spectrum decomposition: improving the resolution 7-26081
array beamforming output, high resolution deconvolution algorithms 7-31575
audio teleconferencing, adaptive summing technique 7-37264
audioconference rooms and reverberators, modelling 7-37253
B-scan image reconstruction, influence of point spread function 7-31576
B-scan imaging, fast Kalman filter derivation 7-31578
bat echolocation calls, non-stationary signal modelling 7-16034
bioacoustic signal spectral analysis in noise 7-16035
coarticulation models of syllabic nuclei, multi-speaker validation 7-43564
combined Fourier/shock spectra for improved test specification 7-20498
comparison of optical and acoustical signal processing techniques 7-1317
complex wave fields propagation, reconstruction using Hilbert-Hankel transform 7-43514
computer simulation of noise processes (*Chinese*) 7-57639
continuous speech signals, automatic segmentation, new statistical approach 7-11221
contribution factors of sound source, estimation method 7-11213
digital methods 7-14743
Doppler flowmetry, perturbation meas. using power spectrum analysis 7-50852
Doppler ultrasonic flowmetry, signal analysis using PLL 7-50851
Doppler US signals, CW, statistical props. and speckle, simulation model 7-43538
echo canceller based on subjective assessment, echo return loss 7-37262
echo canceller for teleconference systems 7-37263
echographic imaging, 2-D Wiener inverse filtering 7-26091
enclosures, acoustic evaluation using dig. signal processing 7-6042
energy acoustic system, functional method of parameter estimation 7-37236
French nasal vowels, anal., synthesis and perception 7-37292

acoustic signal processing continued

frequency domain acoustic noise canceller, frequency bin adaptive filtering 7-37247
gas flow velocity distribution meas. based on nonlinear effect of ultrasonics (*Japanese*) 7-31905
geosound signal detection, appl. of adaptive dig. filtering (*Chinese*) 7-20508
high temp. crystallisation, flaw form., AE detection, automatic system 7-3557
high-quality loudspeaking system development (*Japanese*) 7-57661
holographic matched filtering, membrane modulator appl. 7-43541
holography, image processing using liquid crystal converter 7-1319
image reconstruction fidelity using the Born and Rytov approximations 7-26087
imaging, attenuation correction using Melling transform 7-26090
imaging, backward propag., spatial freq., sampling window effects (*Chinese*) 7-11220
imaging range resolution improvement with a new signal processor implementing a fast Kalman estimator 7-31574
impulse response estimation, time window effects 7-31573
impulse response measurement using Golay codes 7-37304
impulse response of system to rectangular pulse 7-31572
integral equations in diagnosis problems (*Russian*) 7-34234
interactive processing system for ultrasonic compound imaging, real-time image processing and texture analysis 7-23419
inverse filter design for holographic imaging systems with small apertures 7-31583
Japanese stop consonant recognition using local spectral peaks 7-50861
knowledge engineering appls. (*Japanese*) 7-20511
linear correlation function for random noise or vibration 7-11218
liver acoustic attenuation estimation using zero-crossings technique 7-23397
medical tomography, real-time analysis of Doppler waveforms 7-62918
microcomputer based system for acoustic analysis of voice characteristics 7-37286
moving sound source, compensation of Doppler effect 7-37265
noise emission analysis for determining crackinitiation during instrumental notched bar impact testing (*German*) 7-8216
ocean bottom loss, wide angle, estimation by normal incident acoustic pulse 7-43542
passive underwater tracking with nonlinear feedback, convergence anal. 7-31557
pathological voice acoustic anal., adaptive comb filtering method 7-37283
phonetic labeling methodology for speech recognition research 7-43572
phonetically based semivowel recognition system 7-43571
pictorial information transmission using point sound image, study for visually handicapped sensory aids appl. (*Japanese*) 7-34341
planar acoustic tomography, image reconstruction using hexagonal arrays 7-26088
postbeamformer interference canceller, effect of bandwidth on performance 7-6055
prehollowing howlback detection method 7-37260
prior inverse filtering for high-resolution pulse-echo images 7-26089
probabilistic inverse scattering, resolution theory 7-31577
quadratic effects in the scattering of Rayleigh waves by a rectangular projection 7-43537
reconstruction for synthetic aperture diffraction tomography (*Chinese*) 7-57638
recovery of ultrasonic impulse response by spectral extrapolation 7-26085
reflection coefficients determ. for dispersive systems, cepstral methods 7-43543
resolution enhancement of processed seismic data using prior weighting functions 7-26084
resolution limits in inversion by parameter estimation 7-26083
reverberation time meas. using signal averaging 7-16036
room acoustics, inverse control using multiple loudspeakers and/or microphones 7-37252
room reverberation time meas. using cross-correlation of two relatively prime pseudorandom sequences 7-62914
sample matrix adaptive beam former implemented in beam space, output statistics 7-50853
SAR image holography using acoustic lens for 3D underwater imaging 7-43513
SAW filters, method for false signal level reduction 7-57640
Schur algorithm for seismic inversion and continuous-time prediction 7-26086
seismogram synthesis for use in acoustic well-logging 7-47364
SETI, time and space acousto-optic folded spectrum processing 7-26080
shock spectra, use of signal envelopes to describe bandlimited response 7-31565
snoring signals, anal. and classification 7-37256
sonar system simulation design technique (*Chinese*) 7-11219
sonic logging, 2D spectrum anal. 7-55332
sound field in room, grasp and development of spatial information by closely located four-point microphone 7-37258
sound program signals, stochastic process model 7-37267
sound sources location by searching the minimum value of error function 7-37305
source detection using cross spectra between pairs of sensors distributed in space 7-43608
source separation and note identification in polyphonic music 7-37261
spatial resolution of migration algorithms 7-26082
speech recognition, knowledge-based acoustic-phonetic processing techniques 7-37290
speech spectrum analysis using coherent optics (*Chinese*) 7-20510
stereo reproduction, relationship between cross-correlation function and sound image width (*Japanese*) 7-47108
stochastic sound system, digital filter design for state estimation 7-6056
stratigraphic filter theory, effects of parallel bedding and random inhomogeneities 7-28877
thermoacoustic wave imaging and depth profiling cell 7-1337
time discrimination of impulsive overlapping echos (*French*) 7-37255
time series modelling by generalized adaptive function, appl. to random noise data 7-37268
time varied gain functions for pulsed sonars 7-20496
transformation technique as practical tool 7-37257
ultrasonic materials testing, flow-to-grain echo ratio enhancement 7-62919
ultrasonic materials testing resolution upgrade using deconvolution inverse filter 7-22952
ultrasonic NDT, autoregressive spectral analysis (*French*) 7-20509

acoustic signal processing continued

- underwater, likelihood ratio calcs. 7-6054
- underwater acoustics, reconstruction of complex-valued propagating wave fields by Hilbert-Hankel transforms 7-42975
- underwater tracking, 3D, that considers acoustic medium effects 7-43544
- US 3D C-scan imaging using holographic reconstruction 7-43546
- US B-scans, speckle reduction using weighted averaging in spatial compounding 7-43539
- US cross sectional images, Fourier domain reconstruction 7-43609
- US materials charactn. 7-33892
- US pulse echo signals, processing for electro-acoustic conversion distortion removal (*Japanese*) 7-43540
- US signal processing for near surface defect detect. and thickness meas. 7-39830
- visual characterization of speech spectrograms 7-43566
- wall response evaluation, effect of signal processing operations 7-16032
- wave theoretical approach to acoustic current profiling 7-4821
- waveform complexity, Fourier transform formulated, theory and expt. 7-37266
- LiNbO₃ degenerate acoustic elastic convolver, crystal orientation dependencies of figure of merit 7-62917

acoustic sources *see acoustic radiators***acoustic streaming**

No entries

acoustic superradiance

No entries

acoustic surface wave devices *see surface acoustic wave devices***acoustic surface waves** *see surface acoustic waves***acoustic transducers**

- see also acoustoelectric transducers; ultrasonic transducers*
- diffraction correction for radiation force measurement on an ideal plane reflector 7-11228
- EM acoustic transducer and laser acoustic source for noncontact detection of surface-breaking cracks 7-3551
- fibre optic acoustic sensors, state of the art 7-11243
- multifrequency SAW waveguide resonators, amplitude-freq. characts. anal. 7-16050
- physical acoustics, conf., Varenna, Italy (July 1984) 7-9599
- piezoelectric transducer, mechanical impulse response, optical probing 7-20551
- planar phased array acousto-optic Bragg cell transducer 7-37303
- pyroelectric detection of radiation-induced thermal wave phenomena 7-43615
- RF discharge as low press. contactless sonic wave sensor 7-43585
- SAW interdigital transducers, anal., validity of model of Tancrrell and Holland 7-6068
- terminal selection using acoustic triangulation technique 7-1355
- PZT ceramic SAW interdigital transducers, anal., validity of model of Tancrrell and Holland 7-6068

acoustic variables measurement

- see also acoustic intensity measurement; acoustic noise measurement; acoustic wave velocity measurement; ultrasonic measurement*
- cepstral technique for reflection coeff. det., accuracy considerations 7-20516
- Coir, rubberized wideband acoustic absorption meas. 7-20548
- concert halls, transient distortion, sound differences anal. (*German*) 7-62929
- ear canal meas. of eardrum sound pressure level in simulators 7-8592
- flow resistance meas., theory 7-11234
- flow resistance meas. technique 7-11233
- grass-covered ground, acoustic impedance meas. at low freqs. using phase difference technique 7-50876
- intensity measurement without error caused by phase difference between meas. instruments (*Japanese*) 7-11236
- nonlinearity parameter meas. using nonlinear interaction of sound waves (*Japanese*) 7-50883
- pathological voice qualities meas. for medical purposes 7-37285
- phase gradient method of measuring the acoustic impedance of materials 7-50875
- photoelastic fibre optic sensor, force, pressure, acceleration and sound meas. (*German*) 7-11159
- polyurethane foam, acoustic reflection coeff. det. using cepstral techniques 7-20515
- reverberation time meas. 7-43606
- reverberation time meas. using signal averaging 7-16036
- signal freq. meas. techniques (*Japanese*) 7-31592
- sound level meters, Japanese testing and calibration methods 7-1334
- sound system, % Al_{cons} meas. 7-43596
- speaker identification, acoustic speech feature parameters effects (*Japanese*) 7-1321
- statistical spatial acoustics, reverberation time meas. for low density of eigenfrequencies (*German*) 7-57637
- underwater sound absorption coeff. meas. using reverberation method 7-20527
- US attenuation in suspensions meas., coherent scattering contribution 7-16040
- wave-flow index, vocal efficiency measure 7-37301

acoustic velocity *see acoustic wave velocity***acoustic wave absorption**

- see also noise abatement; ultrasonic absorption*
- Coir, rubberized wideband acoustic absorption meas. 7-20548
- conductors, sound absorption and velocity under weak localisation conditions 7-38646
- epoxy resin, viscoelastic behaviour 7-21348
- fluids, acoustic wave propag. 7-6351
- glass, nonlinear relaxational acoustic attenuation, perturbation theory calcs. 7-32578
- insulators with spiral mag. struct., sound absorption 7-38918
- layer-periodic materials, stimulated Brillouin scatt. threshold, light and sound attenuation calcs. 7-3060
- liver acoustic attenuation estimation using zero-crossings technique 7-23397
- low-ceilinged room acoustics (*German*) 7-43530
- metals, ferromagnetic, elastic moduli anomalies, thermodynamic theory (*Russian*) 7-2080
- metals, ferromagnetic, sound propagation, velocity and absorption 7-38919
- metals, longitudinal sound absorpt. oscills. orientation anomalies under magnetic breakdown (*Russian*) 7-51955

acoustic wave absorption continued

- metals, sound attenuation by electrons 7-63747
- mode conversion at biological media interface 7-18012
- noise propag., effect of sound absorption by air 7-50839
- nonequilibrium solid, SAW attenuation, gas-induced high freq. anomalies 7-52218
- ocean, layered bottom, resonance absorption effects 7-16027
- p-wave pair states, spin-orbit interaction and crystal field effects 7-38806
- piezoceramic-polymer-composites, damping props. 7-64575
- porous composites, transport props., pore-size parameter studies 7-38657
- porous-walled duct flow with gas injection, acoustic boundary layer 7-20793
- RF absorber horn test system 7-43605
- RF anechoic room absorbers eval. in 30 to 1000 MHz range 7-43604
- sea surface loss in surface ducts and shallow water 7-66160
- sound absorbing panel calcs. 7-50840
- sound attenuation in water fog 7-37239
- surface acoustic solitons, attenuation due to surface roughness 7-21599
- suspensions, HF acoustic perturbation propag. singularities 7-13832
- underwater sound absorption coeff. meas. using reverberation method 7-20527
- wave equation, inhomogeneous ID, in lossy medium, soln. using inverse scatt. method 7-62885
- Al-Zn dilute alloys, stress-induced mixed dumbbell tunnelling, sound propag. meas. (*Russian*) 7-51674
- Bi₂Ge₂O₁₂ single cryst. growth, characterisation and appls. 7-33550
- (CoF₂)_{0.5}(BaF₂)_{0.2}(NaPO₃)_{0.3}, AC magnetic susceptibility and acoustic wave attenuation meas. 7-59020
- Ga, sound attenuation oscillatory deviation in weak mag. field, Fermi surface cross section and electron rel. determ. 7-2106
- a-H₂O films, low temp. elastic props. 7-45099
- ⁴He, liq. films, first and second sound 7-32734
- Kr gas, acousto-optic interaction in FIR 7-37623
- LaMgAl₁₁O₁₉, elastic and anharmonic props., acoustic meas. 7-44706
- SF₆, liq., acousto-optic interaction in FIR 7-37623
- SiO₂, fused, frequency dependent equation of state 7-51987
- SiO₂-CaO-MgO-Na₂O glass, frequency dependent equation of state 7-51987
- Xe gas, acousto-optic interaction in FIR 7-37623
- YAl₃(BO₃)₄, pure and Nd doped crystals, acoustic wave absorpt. meas., temp. and freq. depend. 7-16697
- ZnO thin film layered struct., SAW rapid attenuation 7-44983

acoustic wave amplification*see also acoustoelectric effects*

- astrophysical plasma environment, cosmic ray effects and sound waves amplification 7-34861
- CdS, Brillouin spectra of acoustoelectronic interaction 7-7292
- Ni, thermoelectric amplification of acoustic waves, CO₂ laser irradiation 7-33055

acoustic wave attenuation *see acoustic wave absorption***acoustic wave diffraction***see also ultrasonic diffraction*

- axisymmetrical system with two separated spherical caps, scalar wave diffr. (*Ukrainian*) 7-11197
- elastic waves, in layered-inhomogeneous solid media 7-16028
- experiment, rel. to geometrical theory 7-35179
- fast computation of SAW diffraction by asymptotic techniques 7-57623
- Fresnel approx., validity and physical explanation 7-55935
- grating with finite-transmissivity strips 7-50798
- inhomogeneous media, asymptotic methods for solving wave diffraction problems 7-26055
- loudspeaker baffles, edge diffraction, geometric theory of diffraction appl. 7-31612
- piston, rectangular, diffracted transient field 7-31567
- planar wave diffraction at inclined semiplane in stratified fluid (*Russian*) 7-20485
- plane wave scattering by pointed body of revolution 7-16002
- Rayleigh diffraction transfer function calcs. 7-50813
- refracting cylindrical barrier calcs. 7-62865
- seismic data, diffraction separation, Karhunen-Loeve, transform appl. 7-57618
- seismic pulses, diffraction effects 7-28908
- semi-infinite membrane in presence of a vertical barrier 7-43489
- slender elastic bodies of revolution, plane wave scattering 7-62860
- surface-breaking discontinuities, Rayleigh wave diffr. 7-27084
- time-domain analysis of acoustic wave propagation, diffraction and radiation 7-31553
- transverse cusp diffraction catastrophes: some pertinent wave fronts and a Pearcey approximation to the wave field 7-62866
- underwater acoustics, finite element analysis appl. (*French*) 7-11209
- US cross sectional images, Fourier domain reconstruction 7-43609
- variable thickness fluid layer 7-50809
- wedges, cylindrical acoustic pulse diffraction 7-11196

acoustic wave diffusion *see acoustic wave scattering***acoustic wave effects***see also acoustic magnetic resonance; acousto-optical effects; acoustoelectric effects; biological effects of acoustic radiation; sonoluminescence; ultrasonic effects*

- acoustic-to-seismic transfer function for outdoor ground surfaces 7-26070
- Boussinesq and Cauchy radiation stresses in solids 7-51960
- ceramic materials, nondestructive evaluation, converging-surface-acoustic-wave technique investig. 7-54049
- coherent combination-frequency reflection of electromagnetic waves from a rough interface exposed to acoustic radiation 7-43494
- fluid-filled cylindrical shell, plane acoustic pressure wave 7-43516
- gas-vapour bubble oscillations in acoustic field, num. investig. 7-52022
- heated plate, acoustically perturbed 2D separated flow 7-16195
- intrinsically irreversible or natural engines, thermoacoustic aspects 7-13927
- jets, turbulent, 2D, acoustic enhancement of widening rate and turbulence intensity 7-51261
- jets, turbulent, influence of mode composition of acoustic perturbations 7-62945
- magnetic tapes, friction reduction by acoustic excitation 7-65148
- oscillation excitation is supersonic boundary layer by external acoustic field 7-51046
- porous-walled duct flow with gas injection, acoustic boundary layer 7-20793

acoustic wave effects continued

As_2S_3 , amorphous, characts. control using acoustic domain 7-20576
 $\text{Ni}_{1-x}\text{Co}_x\text{Fe}_2\text{O}_4$ polycryst. magnetostrictive ferrite, long-term bulk acoustic wave memory 7-59099

acoustic wave interference

see also *acoustic wave interferometers*; *acoustic wave interferometry*
 No entries

acoustic wave interferometers

see also *acoustic wave interferometry*
 No entries

acoustic wave interferometry

see also *acoustic wave interferometers*
 laser-generated ultrasound, detect. using confocal Fabry-Perot interferometer 7-50893
 US mode conversion, pulsed photoacoustic investig. 7-50894

acoustic wave propagation

see also *acoustic dispersion*; *atmospheric acoustics*; *Doppler effect*; *liquid helium sound propagation*; *seismic waves*; *shock waves*; *surface acoustic waves*; *ultrasonic propagation*; *underwater sound*
 1D random lattices, Anderson localisation of waves (French) 7-16013
 acoustic surface waves on an impenetrable cylinder with periodically varying circular cross section 7-43475
 acoustic wave collapse in nonequilib. mol. gas, effect of second viscosity coeff. 7-44093

acoustoelastic effects caused by plastic anisotropy growth 7-62991
 air-filled granular media, acoustic slow wave propag. 7-50822
 alkali metal-alkali halide mixtures, liq., longitudinal collective modes 7-6744

alloy film, magnetostrictive, on glass substrate, magneto-SAW propag. 7-22127

atmospheric effects on close-to-ground propag. 7-43499

atmospheric waveguide propagation near impedance boundary with stratification (Russian) 7-20492

average velocity of propagation of modulated oscillations along a plane waveguide 7-16008

axisymmetric bodies with boundary conditions 7-26060

axisymmetric sources of complex shape, sound radiation 7-62873

boundary layer effect on scale model simulation 7-20493

chemically reacting ideal gas, calcs. 7-62867

columnar-jointed rock mass, cross-hole acoustic meas. 7-47367

complex wave fields propagation, reconstruction using Hilbert-Hankel transform 7-43514

concert halls transient distortion, sound differences anal. (German) 7-62929

convex panels with time-harmonic transverse oscills., acoustic radiation efficiency 7-1308

cubic piezoelec. crystals., acoustic props. changes in elec. field 7-64295

cylindrical duct with wall corrugations 7-50816

cylindrical elastic shell excited by internal monopole source, sound radiation 7-1307

decorrelation of acoustic energy propagated over disjoint paths in a turbulent ocean 7-62900

dielectrics, electrical breakdown, physics, acoustic theory appl. 7-33329

disordered medium, acoustic wave propag., crossover in Anderson transition, acoustic localisation with flow 7-63748

downslope propag. loss over a continental slope 7-62896

downslope propagation of normal modes in a shallow water wedge 7-62898

ducts, parallel shear flow 7-62871

edge waves, use in waveguide fabrication (French) 7-62876

elastic waves propagation in media with thin rigid inclusions 7-50832

energy flux in a cylindrical duct with compliant walls in the presence of air flow 7-62859

ferroelectric ceramics, elec. field-excited acoustic waves parametric instability, wave eqn. calcs. 7-6727

fibre acoustic waveguide, weakly guiding, leaky modes anal. 7-43471

fluids, acoustic wave propag. 7-6351

gas mixtures, acoustical oscillations 7-63242

geometrical strong discontinuity formulas for computational wave motions 7-50814

glass, shock wave propagation phenomena 7-51941

guided SAWs in surface acoustic $\Delta v/v$ waveguides on anisotropic piezoelec. substrates, approx., anal. (Japanese) 7-43603

heavy fermion systems, Gruneisen parameter electron-phonon coupling 7-2138

helical surface waves on an elastic cylinder 7-50800

HF acoustic propagation, range dependent ocean channel transition 7-47465

ID random medium, minimum wave-localisation length 7-15805

inhomogeneous media, Helmholtz eqns. 7-43486

inhomogeneous media, pseudo-spectral Chebyshev scheme, modelling 7-41115

leafy foliage sound propag. simulation 7-50824

linear inviscid wave propag. in waveguide with right angle bend, acoustic pressure calcs. 7-26061

linear inviscid wave propag. in waveguide with right angle bend, transmission coeff. calcs. 7-26062

linear longitudinal waves in isotropic media with shear and volume viscosity, propagation 7-31549

linear sound propag. for 1-component, 2-phase bubbly medium 7-57617

long range nonlinear acoustic propagation, geometrical and diffusive effects 7-26068

low-ceilinged room acoustics (German) 7-43530

magnets-acoustic-gravity waves propag., solar appl. (Chinese) 7-4306

metals, ferromagnetic, sound, propagation, velocity, and absorption 7-38919

microscope, elastic wave propag., accurate field anal. 7-43472

microscope, elastic wave propag. focusing props. of small-aperture lenses 7-43473

mode conversion in layered structures with magnetic inhomogeneities 7-62878

mode propag. in western North Atlantic Ocean 7-31558

moving sound source analysis, orbit determ. using linear sensor array 7-43492

multiple scattering noise in 1D, universality through localisation length scaling 7-1315

near-grazing propag. over rough surfaces, inversion of data 7-43479

network of wave guides, strong localisation 7-61115

noble gas mixtures, anomalous sound propagation and mode degeneracy 7-31550

acoustic wave propagation continued

nonisentropic propag. in uniform ducts using Euler eqns. 7-6314

nonlinear damping in liq. with gas bubbles 7-20491

nonlinear viscoelastic body, unidimensional acoustic wave propagation (Russian) 7-20490

normal mode filtering for downslope propagation in a shallow water wedge 7-62899

numerically efficient full wavefield approach to synthetic seismogram computation 7-26117

ocean, stepwise coupled modes, decoupling algorithm 7-43506

ocean, underwater sound propag. 7-18203

ocean bottom loss, wide angle, estimation by normal incident acoustic pulse 7-43542

ocean bottom-limited sound channel, propag. meas. 7-62895

ocean current sensing, space-time analysis of acoustic scintillations 7-9258

ocean transmission characts. (Japanese) 7-43509

oceanographic shallow water tomography, acoustic reciprocal transmission expts. 7-9259

one-dimensional acoustic pulse propagation in linear layered hereditary medium (Russian) 7-20644

outdoor ground impedance at grazing incidence, FFT-based meas. 7-57650

parametric waveforms and spectra of the primary pulses with two kinds of envelopes 7-26066

physical acoustics, conf., Varenna, Italy (July 1984) 7-9599

plane-wave propagation in a uniform pipe in the presence of a mean flow and a temperature gradient 7-43483

plate, porous, vibr. under action of acoustic disturbances 7-43520

PMMA, shock wave propagation phenomena 7-51941

point source near field propag. 7-20487

polyatomic gas, sound wave propagation 7-44092

polypropylene film, fibrillation, sonic pulse propag., stress-strain meas. 7-26669

porous layered media, Biot waves propagation 7-6028

porous media acoustic props., recent developments 7-11200

potential flows, linear and nonlinear acoustic wave eqns. 7-16015

pressure wave propagation in fluid flowing through porous medium 7-6310

quantum liq.-quantum cryst. phase interface, hydrodynamic eqns., sound transmission calcs. 7-32746

quartz, leaky surface wave propag. characts. and new cut with small temp. coeff. 7-12453

quartz, surface wave propag. characts. and influence on device performance 7-12451

radiation of a sound field by a slender body of revolution 7-16007

Rayleigh wave propag. theory developed by Lord Rayleigh 7-1309

Rayleigh waves and associated acoustic wave mode propag. 7-1311

rectangular panels coupled in an L shape, acoustic radiation 7-62875

reflection coefficients determ. for dispersive systems, cepstral methods 7-43543

resonant phase matching of surface waves on impenetrable spheroids 7-50805

rough surface scattering characts., equivalent impedance for smooth surface 7-50802

sea ice, laboratory-grown, acoustical reflection and scattering from underside 7-43507

seafloor geoacoustic properties determ., appl. of three related reson. methods 7-66097

semi-infinite fluid adjacent to damped elastic infinite plate, impulsive force effect study 7-63052

SH wave propag. in piezoelectric ceramic plates 7-21603

SH-wave line source radiation characts. 7-50815

shear subsurface wave propag., viscous loading effects 7-16021

shear wave effects on propagation to near-bottom and sub-bottom receivers 7-62897

short-base acoustic ranging systems, source location accuracy, receivers comparison 7-43511

singular dispersive medium, wave propag., absorpt. theorem 7-56056

solar atmosphere, time dependent acoustic wave calc. 7-34959

sound beams in a nonlinear isotropic solid 7-62879

sound perturbation propagation in gas-liquid systems 7-26054

sound propagation in a plane wave guide with an elastic wall section 7-20482

spatial autocorrelation functions for calculations of effective propagation constants in polycrystalline materials 7-43481

spatially inhomogeneous pulsed volume source characts. 7-16019

sphere in 2-layer half-space, acoustic response 7-26064

spherical acoustic waves in a medium with spatial dispersion 7-50799

stochastic multipath transmission calcs. 7-62862

superfluid film, third sound rel. to crossover in Anderson transition 7-63748

suspensions, HF acoustic perturbation propag. singularities 7-13832

thermo-optical sound generation in a metal 7-16052

time-domain analysis of acoustic wave propagation, diffraction and radiation 7-31553

transient wave propagation in a viscoelastic layered composite—an approximate theory 7-62872

transient waves in lossy and lossless media 7-31552

two co-planar half-plane plates, acoustic properties 7-50823

underwater acoustic exploration, appl. of array processing for parallel linear recursive Kalman filtering 7-65986

underwater acoustics, finite element analysis appl. (French) 7-11209

underwater tracking, 3D, that considers acoustic medium effects 7-43544

uniform asymptotic solution for the Green's function for the two-dimensional acoustic equation 7-62868

vibration propagation and sound radiation in structures, meas. by impulsive excitation (Japanese) 7-16698

vortices, compact, sand radiation theory 7-16020

wave eqn. soln. using Lax-Wendroff method 7-43476

in ZZ (Russian) 7-61129

$\text{Bi}_{12}\text{GeO}_{20}(\text{SiO}_{20})$, acoustical activity, inelastic neutron scattering study 7-32577

CdS photosensitive cryst., 3D light diffraction from acoustic instability 7-33362

$\text{Li}_2\text{B}_2\text{O}_7$, temp. compensated piezoelectric cryst. SAW study 7-12452

LiNbO_3 , proton exchanged, SAW props. study 7-12454

LiNbO_3 , shallow gratings, leaky surface waves, trapping and temp. compensation 7-12449

Li_2TiO_3 , shallow gratings, leaky surface waves, trapping and temp. compensation 7-12449

acoustic wave propagation continued

- PZT-adhesive-PZT (glass), acoustic boundary waves propag. along thin layer between two bonded substrates 7-21602
 SF₆, optoacoustic signal generated by pulsed IR radiation 7-41480
 TeO₂, small-divergence acoustic beams formation 7-58418
 ZnO-SiO₂ multilayer structures, SAW propag. characts. 7-21601

acoustic wave reflection

- see also echo; reverberation; ultrasonic reflection*
 angular variation of reflection coeff. 7-11198
 anomalous sound reflection from a rough liquid-solid interface 7-16011
 cepstral technique for reflection coeff. det., accuracy considerations 7-20516
 concert hall acoustics, image model 7-1316
 discharge-tube walls, expt. obs. 7-26411
 Earth subsurface, wave reflectors and sources detection 7-23562
 elastic wave scattering at dislocation edges at low angles (*Russian*) 7-51959
 liquid-solid interface, at near-Rayleigh angles of incidence 7-16006
 liquids, effect of plane electrolyte layer 7-50803
 live-end-dead-end type recording studio control rooms, rear-wall reflection patterns 7-31571
 longitudinal energy flux in the reflection of a transverse wave at the boundary of a piezoelectric crystal with vacuum 7-50804
 material acoustic properties, modelling by use of equivalent multilayer systems 7-16693
 polyurethane foam, acoustic reflection coeff. det. using cepstral techniques 7-20515
 quartz, rotated Y-cut, reflected bulk acoustic wave characts. 7-44702
 reflection coefficients determ. for dispersive systems, cepstral methods cepstral methods for the determination of reflection coefficients for dispersive systems 7-43543
 SAW reflection/transmission at boundary between metallized and free surfaces (*Japanese*) 7-11204
 SAW reflections, two-component, from surface breaking slots 7-50819
 shallow water, low freq. sound reflection coeff. of bottom 7-43505
 snow, modelling as acoustically porous material 7-55120
 spectral characteristics of pulse signals in multiple reflection from the layered bottom and surface of the ocean 7-62891
 spherical cavity periodic array theory 7-26056
 transverse-wave reflection at a piezoelectric-semiconductor interface under acoustic bonding conditions 7-16005
 tired wheels, noise investigation, array processor use (*German*) 7-6041
 viscoelastic coating for reducing sound wave reflection, gradient techniques 7-62874
⁴He solid-liquid interface, acoustic wave-transmission, second sound effects 7-21568

acoustic wave refraction

- see also acoustic dispersion; ultrasonic refraction*
 No entries

acoustic wave scattering

- see also ultrasonic scattering*
 3 semi-infinite screens, theory 7-50817
 active synthesis of a scattered sound field 7-62863
 Anderson localisation in random array of scatterers, pseudosphere approx. calcs. 7-43490
 anomalous sound reflection from a rough liquid-solid interface 7-16011
 axisymmetric bodies with boundary conditions 7-26060
 backpropagated scattered wave inversion for arbitrary receiver geometry 7-26092
 backscattered response of sedimentary particles 7-57626
 bounded sound wave scattering by a periodically ribbed plate 7-1297
 circular cylindrical shell, influence of free modes of vibration on sound scattering 7-26057
 complex-frequency poles of the acoustic scattering amplitude, and their ringing 7-57619
 cylinder, isotropic and homogeneous, theor. and numerical results 7-31555
 cylindrical shells in water (*French*) 7-50825
 cylindrical wire, Rayleigh and breathing modes 7-11195
 diffraction correction method for backscatter coefficient using echoes scattered by a thin line (*Japanese*) 7-43592
 Earth surface, inverse scattering, asymptotic anal. 7-40420
 edge wave at infinitesimal edge element 7-62858
 elastic prolate spheroids, axisymmetric characts. 7-16009
 elastic targets, time-freq. analysis 7-57616
 elastic wave scattering at dislocation edges at low angles (*Russian*) 7-51959
 energy characteristics of the backscattering of sound by a rough ocean surface 7-43503
 energy streamlines for a spherical shell scattering plane waves 7-43480
 exact boundary conditions for scattering problems 7-50811
 finite cylindrical shells, amplitude of resonance sound scattering 7-62861
 fluid cylinder, inverse scattering problem, spectral analysis 7-1295
 fluid cylinder with denser fluid inside, spectral analysis 7-1294
 fluid cylinder with denser fluid loading, spectral analysis 7-1293
 focussed wave beam superposition calcs. 7-62881
 forward scattered waves in random media—the probability distribution of intensity 7-50828
 gratings of densely packed compliant tubes 7-50808
 Helmholtz integral eqn. method 7-50812
 high-frequency bottom backscatter measurements in shallow water 7-26073
 inhomogeneous waveguide, sand scattering theory 7-43478
 inverse scattering problems in acoustic (review) 7-62857
 layer of spheres simulating ocean bottom 7-43504
 long-wavelength acoustic scatter from rough surfaces 7-11199
 lossy media, 1-D inverse acoustic scattering 7-31554
 low freq. sound penetration through arbitrarily shaped aperture in rigid screen 7-43477
 low freq. sound waves, multiple scattering by wind waves 7-62890
 multiple scattering noise in 1D, universality through localisation length scaling 7-1315
 multiple scattering of low-frequency sound waves by surface roughness 7-16003
 weakly nonlinear acoustic instabilities 7-57624
 nonlinear sound scattering by vibrating surface 7-43498
 ocean, horizontal coherence function calcs. 7-50829
 ocean gas bubble sensing using acoustic pulses 7-43501
 ocean waveguides, low freq. sound attenuation 7-62892
 oceans, acoustic scatt. and total internal reflection 7-6035

acoustic wave scattering continued

- particle/turbulence scattering coexistence theory 7-43482
 period slotted waveguide scattering characts. 7-62864
 plane wave scattering by pointed body of revolution 7-16002
 plate with rough surfaces, sound wave scatt. 7-16017
 polar plots of intensity of scattered acoustic waves from a rigid cylinder 7-50797
 probabilistic inverse scattering, resolution theory 7-31577
 Q-profiling for inverse sand scattering 7-31551
 quadratic effects in the scattering of Rayleigh waves by a rectangular projection 7-43537
 Rayleigh wave scattering by wedge, boundary method approach 7-26196
 reactive silencers, analytical model based on Bragg scattering 7-50845
 resonance acoustic scattering from stacks of bonded elastic plates 7-50806
 resonance scattering by viscoelastic objects 7-62869
 resonance spectra of elongated elastic objects 7-62870
 rough surface scattering characts., equivalent impedance for smooth surface 7-50802
 rough surfaces, Kirchhoff approx. 7-26063
 sea ice, laboratory-grown, acoustical reflection and scattering from underside 7-43507
 semi-infinite membrane in presence of a vertical barrier 7-43489
 shells, circular, cylindrical, sound wave scatt. 7-57621
 shells, submerged elastic, proper background choice in resonance scattering 7-37241
 slender body scattering theory 7-50807
 small-slope approximation in the problem of sound scattering by a rough rigid surface 7-16010
 spatial autocorrelation functions for calculations of effective propagation constants in polycrystalline materials 7-43481
 spherical shells, internal loss calcs. 7-16012
 suspensions, highly concentrated (*Chinese*) 7-11193
 target responses and echo formation process (*French*) 7-43464
 time-domain farfield scattering of plane acoustic waves by a penetrable object in the Born approximation 7-26058
 time-harmonic waves in reson. region, inverse scatt. problem 7-6030
 tissue characterization, freq. dependence of backscattering coeff. 7-34191
 transient fields from focused acoustic waves 7-31599
 underwater, by elastic cylindrical shells 7-20484
 underwater scattering, hybrid modelling scheme 7-20497
 underwater sound, scatt. and absorpt. contribs. to sea surface loss in surface ducts and shallow water 7-66160
 US cross sectional images, Fourier domain reconstruction 7-43609
 viscoelastic bodies forced time-harmonic vibr. propag., acoustic scatt. inverse problem 7-62901
 water surface covered by oil layers, statistical analysis 7-43462
 wave equation, inhomogeneous ID, in lossy medium, soln. using inverse scatt. method 7-62885
 Ba_{0.5}Sr_{0.5}TiO₃ polycryst. films, SAW scatt. and ferroelec. transitions 7-44984
 p-CdGeAs₂ semicond., hole mobility and scatt., temp. depend. study 7-52609
- acoustic wave transmission**
see also ultrasonic transmission
 circular reversing chamber mufflers, transmission loss calcs. 7-50842
 double doors, sound transmission charact. 7-43531
 elastic wave scattering at dislocation edges at low angles (*Russian*) 7-51959
 energy acoustic system, functional method of parameter estimation 7-37236
 holes and slits, effect of absorber fillings (*German*) 7-11194
 laminated composite plates, sound transmission characts. 7-57633
 liquids, effect of plane electrolyte layer 7-50803
 low freq. sound penetration through arbitrarily shaped aperture in rigid screen 7-43477
 material acoustic properties, modelling by use of equivalent multilayer systems 7-16693
 plate, porous, vibrs. under action of acoustic disturbances 7-43520
 rigid screen with arbitrarily-shaped aperture, analytical, approach 7-37235
 SAW reflection/transmission at boundary between metallized and free surfaces (*Japanese*) 7-11204
 spherical cavity periodic array theory 7-26056
 spurious resonances in adaptations of elastic layer model to simulate liquid layers 7-26059
 wall response evaluation, effect of signal processing operations 7-16032
 wall transmission loss, evaluation using statistical energy analysis 7-11217
 walls, acoustic sealing of holes and slits 7-43536
⁴He solid-liquid interface, acoustic wave transmission, second sound effects 7-21568
- acoustic wave velocity**
see also acoustic dispersion; liquid helium sound propagation; shock waves; ultrasonic velocity
 average velocity of propagation of modulated oscillations along a plane waveguide 7-16008
 benzene, acoustic and thermodynamic props., press. and temp. depend. 7-63745
 conductors, sound absorption and velocity under weak localisation conditions 7-38646
 cyclohexane, acoustic and thermodynamic props., press. and temp. depend. 7-63745
 epoxy resin, viscoelastic behaviour 7-21348
 gas, spherically symmetric pair-pot. energy fn., second acoustic virial coeff. method calc. 7-62481
 granular structures, phonon density of states and inverse decay length 7-6743
 humid air, characteristic impedance 7-26071
 marine sediment, sound vel. provinces in Cape Basin from multichannel seismic refl. profiles 7-55008
 metals, ferromagnetic, sound propagation, velocity and absorption 7-38919
 mode conversion at biological media interface 7-18012
 modulation of the sound velocity in a colloid by an external electromagnetic field 7-43622
 one-dimens. gas, strong interaction, one-particle density matrix 7-48547
 paramagnets, tetragonal, magnetoelastic excitations and struct. phase transitions 7-27489
 point source, sound field calcs. 7-43466

acoustic wave velocity continued

- polypropylene film, fibrillation, sonic pulse propag., stress-strain meas. 7-26669
 quartz crystal, low temp. sound velocity, fast neutron irradiation effects study 7-12160
 ray tracing on a grid using sound vel., error evaluation 7-20520
 rock samples containing tetrahydrofuran hydrates, acoustic and resistivity meas. 7-55026
 shock waves, equation of state calcs. 7-21393
 sodium p-n octylbenzenesulphonate, aq. solns., micelle form., acoustic and rheological props. 7-13823
 supercritical water, vel. of sound meas. at high temp. and press. 7-16691
 time of flight neutron diffr. meas. 7-32575
 two-phase medium, gas content and speed of sound, calc. with surface tension forces 7-51279
 vapour-gas-liquid systems, adiabatic compression and sound vel. 7-31873
 wave equation, inhomogeneous ID, in lossy medium, soln. using inverse scatt. method 7-62885
 (Cr_{1-x}Al_x)₂Mo₃, antiferromagnetism disappearance, comp. depend., elec. resist. and sound rel. meas. 7-2843
 CsI, Hugoniot overtake sound-rel. meas. 7-44705
 CsI, shock wave overtake meas. 7-21353
 D, spin-polarized, ground state props. 7-27055
³He, liquid, magnetic properties, density functional anal. 7-21559
⁴He, liq. films, first and second sound 7-32734
 K₂(MoO₄)₂, elastic characts. near structural phase transition, sound vel. meas. (Russian) 7-26872
 Li_{0.5}Pb_{0.2} liq. mixture, fast sound computer simulation, Mori-Zwanzig formalism 7-44696
 LaMgAl₁₁O₁₉, elastic and anharmonic props., acoustic meas. 7-44706
 Mn_{0.61}Zn_{0.35}Fe_{2.04}O₄ single cryst., low temp. acoustic props. anomalies, spin-reorientation transitions 7-51957
 Pd₄₀Ni₆₀P₂₀ metallic glass, structural relax., shear and longitudinal sound. vel. meas. 7-51655
 ZnO-AlN-glass, SAW characts. study 7-12448

acoustic wave velocity measurement

- see also *ultrasonic velocity measurement*
 graphite, velocity of sound meas. by pulsed neutron diffraction 7-38125
 rarefaction wave velocities determ. 7-48713
 sonic logging, 2D spectrum anal. 7-4203
 speed of sound to speed of light ratio, meas. 7-20543

acoustic waveguides

- atmospheric waveguide propagation near impedance boundary with stratification (Russian) 7-20492
 average velocity of propagation of modulated oscillations along a plane waveguide 7-16008
 edge waves, use in waveguide fabrication (French) 7-62876
 elastic wave, periodic waveguides, finite element anal. (Japanese) 7-6148
 energy relations for acoustic waveguides 7-43468
 fibre acoustic and optical waveguides, similarities and differences 7-1298
 fibre acoustic waveguide, weakly guiding, leaky modes anal. 7-43471
 finite amplitude distortion and dispersion of anoplanar mode in a waveguide 7-6029
 frequency filtering in model acoustic waveguides 7-43465
 horns, discrete section synthesis (French) 7-43602
 impedance method of calculating the characteristics of normal modes in layered-inhomogeneous liquid-elastic waveguides 7-43467
 inhomogeneous waveguide, sand scattering theory 7-43478
 irregular, investigation of mode conversion 7-16004
 linear inviscid wave propag. in waveguide with right angle bend, acoustic pressure calcs. 7-26061
 linear inviscid wave propag. in waveguide with right angle bend, transmission coeff. calcs. 7-26062
 multifrequency SAW waveguide resonators, amplitude-freq. characts. anal. 7-16050
 normal modes in a rough waveguide: theory and experiment 7-43484
 ocean waveguide explosive source energy determ. 7-50827
 ocean waveguides, inhomogeneous, layered, dispersion characts. 7-16025
 period slotted waveguide scattering characts. 7-62864
 plane-layered waveguide, effect of motion of acoustic source on sound field 7-50801
 slow-disc waveguide radiators (Japanese) 7-20555
 surface acoustic $\Delta\rho/\nu$ waveguides on anisotropic piezoelec. substrates, approx. anal. (Japanese) 7-43603
 underwater, frequency spectra of a noise field in a plane-layered waveguide 7-16026
 underwater sound, historical perspective on sea surface loss in surface ducts and shallow water 7-66160
 weakly guiding acoustic fibre longitudinal modes 7-1299
 LiNbO₃, proton exchanged, SAW props. study 7-12454
 Ta₂O₅ strip waveguides, SAW propag. and acousto-optic interaction efficiency 7-20583

acoustic waves

- see also *acoustic emission; magnetoacoustic effects; shock waves; surface acoustic waves; ultrasonic waves*
 coupled acoustic and vortical instability interactions 7-31809
 inverse problems using penalised likelihood method 7-37233
 Navier-Stokes mean flows interacting with vortex and acoustic oscillations 7-43958
 neutrino beam generation in stressed medium 7-14397
 nonlinear hyperbolic systems, resonantly interacting high freq. waves, asymptotic theory 7-56058
 nonlinear singular integral eqns. arising in physical problems 7-36859
 picosecond interferometric technique for study of phonons in Brillouin frequency range 7-14998
 plane layered media, global matrix formulation of wave phenomena 7-61125

acoustical laboratories

- see also *anechoic chambers; reverberation chambers*
 No entries

acoustics

- see also *acoustic applications; acoustic devices; acoustic equipment; acoustic noise; anechoic chambers; architectural acoustics; atmospheric acoustics; audio acoustics; hearing; musical acoustics; photoacoustic effect; sound reproduction; ultrasonics; underwater sound; vibrations*
 Acoustical Society of America, 112th meeting, conf., Anaheim, Calif., USA (Dec. 1986) 7-35085
 branched gas circuits, acoustical charact. anal. using signal graphs 7-63219

acoustics continued

- quadratic parametric processes, Lie algebraic approach, quantum optics, quantum acoustics 7-36923
 speech, acoustics and signal processing, conf., Tokyo, Japan (April '86) 7-35100
 vocal tract shapes, power spectra, Doppler degradation, bat and dolphin waveforms 7-8604
- acousto-optical devices**
 see also *acousto-optical effects*
 800 MHz bandwidth acousto-optical spectrometer at Helsinki Observatory 7-60561
 acoustic holography, image processing using liquid crystal convertor 7-1319
 acoustoelectrooptic multichannel spectrum analyzer 7-50714
 Bragg cell, large time aperture, materials selection 7-37136
 Bragg cell, wideband, materials selection 7-37137
 Bragg diffraction, devices and appls. 7-45983
 Bragg diffraction by deep bulk acoustic waves, appl. in optic spectrum analyzer 7-20584
 Cologne 3m radiotelescope acousto-optical spectrometers 7-34878
 correlator, multichannel space-integrating, general I and Q data processing 7-10870
 correlators possible appls. in radiointerferometry 7-60569
 deflector used in real-time scanning laser microscope for biological research 7-47292
 delay line for optical distrib. processing 7-42977
 developments in integrated optical components (German) 7-50789
 fibre optic acoustic sensors, state of the art 7-11243
 fibre-optic acousto-optic tunable filter 7-5979
 filters, tunable, applications 7-37119
 frequency modulation of optical beam using ultrasonic diffraction grating 7-20405
 glass series, active material selection for acousto-optic mode-lockers 7-57493
 holographic filtering use 7-20409
 image information transmission, storage, and acquisition using an acousto-optic cell and optical matched filters 7-20143
 integrated acousto-optic device modules for communication, signal processing, and computing 7-31526
 integrated acousto-optic mode locker, appl. to Ar ion laser 7-37005
 interferometer using Koster's prisms for RF direction of arrival meas. 7-41445
 LiNbO₃ proton-exchange 128° Y-cut optical waveguides, acousto-optic interaction effects 7-62824
 loss modulators for laser mode-locking characts. 7-37129
 modulator, for I photodissociation laser, active mode locking (Korean) 7-25852
 modulators, deflectors and Q-switches, basics 7-50605
 optical cellular array processors 7-25720
 optical waveguides, acousto-optic cell appls. 7-1264
 planar acoustooptic 2×2 commutator switch 7-50741
 planar phased array acousto-optic Bragg cell transducer 7-37303
 polarisation state control of optical instruments, using fibre optics or Bragg cells 7-14992
 polarisation state control using fibre optic techniques 7-43421
 SAW acousto-electron-optic device, Raman-Nath regime meas. and calcs. 7-20550
 scanning laser acoustic microscope with digital data acquisition 7-50882
 signal processing system intermodulation products 7-1041
 signal processors, incoherent-light space-integrating 7-50499
 signal processors, polarisation effects 7-25723
 spectrographs for ground and space submm astronomy 7-34877
 spectrometer for RATAN-600 radio telescope, design and performance 7-66463
 thin-film travelling-wave light modulator, diffraction efficiency 7-5987
 tunable filter, rotating linearly polarised light source appl. 7-18850
 two-dimensional light scanning by waveguide acoustic modes of a plate 7-25944
 ultrasonic sensor using optical fibres (French) 7-62935
 ultrasonics conference, San Francisco, USA (Oct. 1985) 7-11
 waveguide-type optical separators using acousto-optical effects 7-62825
 CdS_{1-x}Se_x crystal waveguide Bragg light modulators 7-1288
 LiNbO₃:Ti waveguide collinear Bragg diff. cell, acousto-optic interaction efficiency anal. 7-37234
 LiNbO₃ bulk wave acousto-optic deflector beam steering by interdigital transducer 7-1255
 Ta₂O₅ strip waveguides, SAW propag. and acousto-optic interaction efficiency 7-20583
- acousto-optical effects**
 see also *acousto-optical devices*
 anthracene thin crystal wafers, high freq. acoustic phonons and deformation waves, optical detection 7-22218
 Bragg diffraction, devices and appls. 7-45983
 Bragg diffraction by deep bulk acoustic waves, appl. in optic spectrum analyzer 7-20584
 Bragg regime extension through Hamming apodisation of sound field 7-25712
 brass diffraction, phase characteristics 7-13127
 crystal internal strains, acousto-optical study (French) 7-7671
 Gaussian beam divergence meas. using SAW modulation 7-20297
 glass series, active material selection for acousto-optic mode-lockers 7-57493
 inverse scattering and three-wave interaction in nonlinear optics appl. to sound wave generation 7-11030
 leaky wave spatial spectrum generated by guided wave scatt. from acoustic wave 7-31460
 light diffraction by ultrasonic beams, multiple plane-wave anal. 7-5833
 LiNbO₃ proton-exchange 128° Y-cut optical waveguides, acousto-optic interaction effects 7-62824
 MBBA-EBBA nematic liq. cryst., acoustooptic effects 7-45984
 multiple plane wave approach to acousto-optic interactions anal. 7-17305
 optical detection of nanosecond acoustic pulses 7-43584
 optical detection of ultrasound 7-43583
 piezoelectric semiconductors, amplified acoustic noise anal., Bragg light diff. method 7-43625
 Rayleigh wave generation using acousto-optical interactions 7-1376
 Rayleigh wave theory and appls., conf., London, England (July 1985) 7-22
 Rayleigh waves, laser interferometry meas. 7-1345
 SAW, laser probing using proximity reference gratings 7-1211

acousto-optical effects continued

- solitons, acoustoelectromagnetic, motion control 7-39082
- stationary part of the Fresnel diffraction field of two antiparallel sound beams separated in space 7-57665
- three-wave acoustooptic interaction 7-39081
- transient atomic concentrations, spatial mapping using acousto-optic deflection 7-39931
- ultrasonic echography, acousto-optic deconvolution 7-26113
- ultrasonic light diffraction effects 7-37307
- ultrasonic light diffraction phenomena 7-20575
- ultrasonic pulse characterization using acousto-optic method 7-62948
- waveguide, single-mode, stimulated Brillouin scattering, influence of sound diffraction 7-1225
- weakly nonlinear dispersive media, three-wave interaction including frequency doubling effects 7-43215
- a-As₂Te(se)₃, surface phonon generation and picosecond light pulse detection 7-12456
- Cd₃Ge₃O₁₂, single cryst. growth, characterisation and appls. 7-33550
- Bi₂S₃ photosensitive cryst., 3D light diffr. from acoustic instability 7-33362
- a-Ge, surface phonon generation and picosecond light pulse detection 7-12456
- H₂-F₂-HF gaseous mixture, light initiated chain reaction, stimulated light scatt. study 7-62778
- KAl(SO₄)₂·12H₂O, cubic, second order electroelastic tensor studies 7-27668
- KD₂PO₄, impulsive stimulated Brillouin scattering near structural phase transition 7-13126
- Kr gas, acousto-optic interaction in FIR 7-37623
- LiNbO₃, uniaxial crystal anisotropic acousto-optic interactions 7-3021
- LiNbO₃:T surface, acousto-optic interaction, photoelastic and electro-optic contrbs. 7-45982
- LiNbO₃:Ti, acousto-optical diffr. elastic strain and electric field effects 7-45985
- LiTaO₃, extremal directions of anisotropic diffraction and collinear acousto-optic interaction 7-17304
- NaBi(MoO₄)₂, elastic and elastooptic props. 7-7672
- Ni surface phonon generation and picosecond light pulse detection 7-12456
- PbMoO₄, optical radiation modulation by coherent ultrasonic excitation 7-27692
- SF₆, liq., acousto-optic interaction in FIR 7-37623
- α-SiO₂, extremal directions of anisotropic diffraction and collinear acousto-optic interaction 7-17304
- Te, off-optical axis anisotropic acousto-optical diffraction 7-59177
- Xe gas, acousto-optic interaction in FIR 7-37623
- ZnS:Mn electrolum. thin film-based structs., native memory formation, supersonic effects study (Russian) 7-3020

acoustoelasticity *see elasticity***acoustoelectric devices**

- see also acoustoelectric transducers*
- centrosymmetrical dielectric, Rayleigh waves on surface excited by external periodic electric field 7-31614

acoustoelectric effects

- acoustoelectronic interaction of surface acoustic waves in structures with a piezoelectric insulator layer 7-63932
- cubic piezoelec. crystals, acoustic props. changes in elec. field 7-64295
- ferroelectric ceramics, elec. field-excited acoustic waves parametric instability, wave eqn. calcs. 7-6727
- ferroelectric crystals, domain memory studies, sound generation method 7-39053
- impulse response measurement using Golay codes 7-37304
- longitudinal energy flux in the reflection of a transverse wave at the boundary of a piezoelectric crystal with vacuum 7-50804
- piezoelectric semiconductors, acoustoelectric effects, interaction of ultrasound with Mössbauer gamma rays, effect of conduction electrons 7-33056
- piezoelectric semiconductors, small-signal conductivity, diffusion of electrons, system with nonequilib. phonons 7-45313
- PMMA, charge motion and self-relaxation, pulsed electro-acoustic meas. 7-27655
- semiconductors, acoustical Hall effect 7-58823
- sound sources location by searching the minimum value of error function 7-37305
- Ag₃AsS₃, incommensurate phase, electroacoustic echo obs. 7-45400
- Ag₃SbS₃, pyrragrite single crystals, electroacoustic echo 7-7293
- Au, discontinuous films, charge carrier mobility, temp. depend. 7-22035
- Bi, filamentous single crystals, static skin effect and acoustoelectric instability 7-38644
- Bi plates, magnetoacoustoelectronic instabilities, joint action of two strong electric fields 7-52694
- Bi, solid-state plasma, microwave harmonics, parametric excitation of hypersound 7-38609
- CdS, acoustoelectronic system, solitons obs. 7-45401
- CdS, Brillouin spectra of acoustoelectronic interaction 7-7292
- CdS, single crystal, US wave absorption, impurity distrib. effect., electron-probe X-ray anal. 7-53241
- CdS single crystals, acoustoelectronic interaction, ultrasonic attenuation and amplification, dislocation motion effects (Russian) 7-21953
- CdSe, single crystal, US wave absorption, impurity distrib. effect., electron-probe X-ray anal. 7-53241
- GaAs/LiNbO₃ struct., SAW parametric generation with light pumping 7-63934
- α-GaSe, acoustoelectronic interaction, piezoelectric effect 7-45399
- In, single-crystal plate, acoustohelicon resons. 7-52695
- LiIO₃, acoustoionic interaction 7-39041
- α-LiIO₃ crystals (Chinese) 7-20568
- LiNbO₃/CdSe multilayer structs. with ohmic contacts, electroacoustic conversion, SAW excitation 7-58839
- LiNbO₃-Si, acoustoelectronic storage, effects of illumination, temp. change, electric fields 7-7405
- Pb₂Ge₂O₁₁, acoustic devices, appl. of regular domain structs. 7-20567
- Pr/H₂(PMo₁₂Mo₄)₂·22H₂O-polyethylene oxide interface, audiofrequency behaviour 7-52693
- Si MOS struct., phonon emission spectroscopy of 2D electron gas 7-27435
- Si, slow surface state determ. by SAW technique 7-21959
- W, electromagnetic absorption of ultrasound near Doppler-shifted cyclotron resonance 7-45402

acoustoelectric effects continued

- ZnO, on LiNbO₃(Bi₁₂SiO₂₀), growth, acoustoelectric props. 7-38645
 - ZnO-Si structures, transverse acoustoelectric effect 7-45398
- acoustoelectric transducers**
- see also earphones; headphones; hydrophones; loudspeakers; microphones*
 - boiler tube NDT inspection systems 7-20549
 - bond graph modelling of transducers for sound-powered telephone 7-57660
 - piezoelectric, bimorph diaphragm design (Japanese) 7-43620
 - room acoustics alteration using electro-acoustic systems (German) 7-16033
 - surface magnetoelastic wave excitation by meander-line transducer 7-62936
 - wooden plates, vibration mode meas. using TV-holographic and electroacoustical methods 7-31716
 - Pb₂Ge₂O₁₁, acoustic devices, appl. of regular domain structs. 7-20567
 - PbLaZrO₃TiO₃, electrostrictive ceramics, SAW transduction, electronic control 7-12450
 - PbMgO₃NbO₃, electrostrictive ceramics, SAW transduction, electronic control 7-12450
- acoustoluminescence** *see sonoluminescence*
- acoustomagnetic effects** *see magnetoacoustic effects*
- acoustooptics** *see acousto-optical effects*
- actinide alloys**
- see also actinide compounds; neptunium alloys; plutonium alloys; thorium alloys; uranium alloys*
 - actinide-noble metal alloys, thermodynamic props., coupled reduction meas. 7-13752
 - actinide-transition metal alloys, AM₂, A=U-Np, M=Fe-Ni, magnetism and electronic props. 7-27505
 - conference, Aix en Provence, France (Sept. 1985) 7-9579
 - physics and chemistry of actinides, handbook 7-24317
- actinide compounds**
- see also compounds of individual actinides, e.g. uranium compounds*
 - see also actinide alloys*
 - conference, Aix en Provence, France (Sept. 1985) 7-9579
 - glasses, leaching (French) 7-19353
 - ions in aq. soln., thermodynamic props., oxidation states, coordination number and struct., review 7-12322
 - moderately delocalised, mag. behaviour, anisotropy of crit. correlations 7-7474
 - oxidic, systematic props., oxidation states, fluorite lattice and thermodynamic props., review 7-12013
 - photoelectron spectroscopy, review of present status 7-39348
 - photoemission, final state multiplet, screening effects 7-39349
 - physics and chemistry of actinides handbook 7-24317
 - Van Vleck paramagnetic susceptibility, cryst. field effect, temp. depend., approximate formulae, review 7-12935
- actinide metal compounds** *see actinide compounds*
- actinide metals** *see actinides*
- actinides**
- see also individual actinides, e.g. uranium*
 - biological behaviour, consequence for radiation protection (French) 7-40223
 - bulk magnetic and transport props. 7-12953
 - conference, Aix en Provence, France (Sept. 1985) 7-9579
 - coordination chemistry, ligand site matching 7-19366
 - elastic neutron scatt. and diffr. studies, review 7-12945
 - giant resonance absorption spectra of 4d electrons 7-10471
 - isotopes in the marine environment 7-40314
 - Mössbauer spectroscopy 7-22172
 - optical absorption spectra 7-27730
 - photoemission, final state multiplet, screening effects 7-39349
 - physics and chemistry of actinides, handbook 7-24317
 - preparation and physical props. 7-17778
 - solid state and thermodynamic props., f-electron bonding and struct., review 7-12321
 - superconductivity, simple transition metal-type and heavy fermion behaviour 7-12897
 - ThO₂, prep. and EPR study of actinide and rare earth ions 7-27598
- actinium**
- see also nuclei with*
 - solid state and thermodynamic props., f-electron bonding and struct., review 7-12321
 - ²²⁷Ac, α-particle source, absolute energy meas. 7-42276
 - ²²⁸Ac in natural background γ-radiation spectrum 7-19550
- actinium compounds**
- No entries
- actinometers** *see radiometers*
- actinometry** *see radiometry*
- activation analysis** *see chemical analysis by nuclear reactions and scattering*
- active nitrogen** *see nitrogen*
- active oxygen** *see oxygen*
- activity (thermodynamics)** *see thermodynamic properties*
- actuators**
- see also electric actuators*
 - servo hydraulic materials testing machines, Instron 1340 Series 7-8209
 - solar cell arrays, vibration and attitude control, reaction wheel actuator 7-28400
 - stiffness calculations for superlight industrial robots 7-22743
- adaptive antenna arrays** *see antenna phased arrays*
- adaptive control**
- see also adaptive systems; model reference adaptive control systems*
 - arterial pressure, mean, computer control with Na nitroprusside: adaptive model-based system 7-40359
 - heart, artificial, adaptive control technique, rel. to blood press. and flow 7-3933
 - magnetic hysteresis, low freq. meas., well-defined time depend. of flux density, meas. system 7-29985
 - solar central receiver, adaptive control, modelling and simulation 7-59877
- adaptive delta modulation** *see delta modulation*
- adaptive optics**
- see also optical phase conjugation*
 - dynamic characteristics of optical adaptive systems 7-43285
 - electromechanical compensators of optical-image displacement 7-20387
 - extended inhomogeneous paths, two-freq. phase conjugation 7-43249

adaptive optics continued

- FIRST telescope, active optics and spectral range extension in IR 7-60553
- flexible mirror in astronomical telescope, IR background speckle noise 7-55467
- IR imaging system performance assessment, improved minimum resolvable temp. difference system 7-34154
- laser beam in medium containing droplets, nonlinear refraction phase compensation 7-4183
- laser resonator Q-factor modulation using methods of adaptive nonlinear optics (*Russian*) 7-50604
- multilayered deformable mirrors with monomorph and bimorph actuators 7-43283
- nonlinear distortion compensation of light beams with restricted deform. of control mirror 7-50622
- phase front reconstruction of light wave by Fourier optics method 7-36893
- sharpness function maximisation problem, object obs. in coherent light through randomly inhomogeneous medium 7-25714
- Hg reflector geometry variation by immersed-electrode current (*Spanish*) 7-11095

adaptive systems

- see also *adaptive control; adaptive optics; cognitive systems; learning systems; model reference adaptive control systems; pattern recognition; self-adjusting systems*
- conf., Los Alamos, New Mexico, USA (May 1985) 7-48157
- frequency domain acoustic noise canceller, frequency bin adaptive filtering 7-37247
- high-quality loudspeaking system development with acoustic signal processing (*Japanese*) 7-57661
- vibration transducer with multichannel adaptive system for dynamic parameters meas. 7-61326

adders

- electro-optic Bragg gratings for integrated optical combinatorial logic, full-adder 7-26040
- optical adder based on spatial filtering 7-11099
- optical computing using hybrid encoded shadow casting, binary full- and ternary half-adder 7-1032

adding machines see *calculating apparatus***adherence** see *adhesion***adhesion**

- 7-28112
- abrasive wear mechanism clarification, contact surface deform. effect on wear and friction 7-8134
- beam, two-layer cpd., damping characts., influence of quality of adhesion 7-50972
- cell deposition on inclined plate, effect of gravity 7-34120
- ceramic coatings, plasma sprayed on stainless steel, hot isostatic pressing, hardness, bond strength 7-13624
- ceramic-metal interfaces, grain boundaries, bonding and interfacial structure 7-26765
- ceramic/metal jointed interface, strain distrib. determ., laser speckle photography (*Japanese*) 7-54037
- coatings, friction and adhesion meas. using microtribometer 7-46742
- coatings, liquid droplet spraying, adhesion to substrate 7-3165
- cracked-lap shear specimen thickness for interlaminar fracture toughness determ., delamination vs. adherend failure 7-1510
- α -cyanoacrylate cements for biomed. equipment, opt. parameters 7-25910
- debonding equation in fracture mechanics, derivation 7-20656
- durable optical adhesives for optical components (*Japanese*) 7-62850
- elastomers, adherence, study by cyclic unloading expt. 7-33909
- elastomers, sliding friction mechanics, asperities adhesion fracture 7-53922
- epoxide adhesive interfaces, props. and regulation (*Russian*) 7-37400
- film adhesion, sliding wear appls. 7-28145
- film properties, magnetron sputtering apparatus performance 7-59420
- formocorundums abrasive, simulation of polymer binders using organic liqs., bond strength investig. 7-38301
- graphite fibre reinforced Mg matrix composites, fabrication, fibre coatings, wetting, adhesion 7-46374
- interfacial bonding and adhesion, conf., Aspen, CO, USA (Aug. 1985) 7-24269
- ion beam enhanced adhesion 7-65279
- joints, adhesive, defect detection, NDT techniques 7-28248
- joints, adhesive, engineering failure envelope 7-33763
- joints, nondestructive evaluation 7-13717
- joints of dissimilar metals, adhesively bonded strength evaluation 7-46791
- lap joints, yield strength in tension, compression and torsion, Poisson ratio 7-39591
- leucosapphire, simulation of polymer binders using organic liqs., bond strength investig. 7-38301
- liquid metal-alumina systems, nonreactive, thermodynamic adhesion (*French*) 7-54073
- materials selection for hard coatings, multicomponent refractory material systems 7-46668
- metal matrix composites, liq. metal infiltration prep., wetting 7-46372
- metal wear resistance, ion implantation and ion assisted coatings 7-3513
- metal-ceramic dental prostheses, strength rel. to surface roughness of metal frames 7-40365
- metal-ceramic interfacial props., thermodynamics 7-12506
- metal-metal and metal-dielectric systems, adhesion calc. 7-7023
- metallic and compound films, mech. props., relation between different quantities 7-8041
- metals, internal interfaces, grain boundary struct., intergranular fracture 7-26766
- nitride and carbide thin films, high-rate reactive sputtering processes and props. study (*Polish*) 7-33559
- noble metal film adhesion on sapphire, ion beam induced enhancement 7-21292
- optical coating, improvements from deposition using cryopumps 7-3185
- particle impact on cylinder at high Reynolds number, adhesion efficiency 7-31710
- peeling-pressure sensitive adhesive, photon and radiowave bursts, time and size correl. 7-28262
- platelet adhesion to fibrinogen-coated glass at an abrupt tubular expansion viewed with fluorescent video-microscopy 7-40183
- poly-p-phenylene benzobisthiazole-epoxy composite, adhesive behaviour 7-65278

adhesion continued

- polyethylene coatings, oxidation effect on adhesional strength (*Russian*) 7-8151
- polyethylene-metal, adhesion of metal films, effects of Ar^+ bombardment 7-28267
- polyimide films, prep. and adhesion to Ag surface, XPS 7-65314
- polymer films, radiation-induced implantation in metallic substrates 7-8163
- polymer interfaces, bonding and adhesion 7-28265
- polymers, friction, electrophysical phenomena 7-17654
- polyphenylene sulphide coatings, internal struct., curing effect 7-28861
- polypropylene sheets, highly oriented, adhesion in laminates 7-8245
- Powercore strip, amorphous metal ribbon layers, bonding study 7-22975
- pressure sensitive adhesives, ball rolling motion, friction coefficient, viscoelastic props. 7-28234
- PTFE surface chemical struct. and adhesive props., effects of low-energy electron bombardment 7-44963
- rubber-glass interfaces, form. and rupture (*French*) 7-54072
- scale adhesion and growth mechanisms, S effect 7-65206
- scratch adhesion testing, critical load for coating loss, acoustic emission 7-3549
- semiconductor interfaces, bonding and adhesion, characterisation techniques, electronic struct. 7-27418
- sheet, orthotropic, adhesively bonded to a stringer, crack tip stress intensity factors 7-1497
- single fibre composites, stress transfer, critical fibre length, Young's modulus ratio 7-59558
- solids in contact, interfacial bonding 7-27148
- solvent welded joints, struct. and strength rel. to bonding solvent 7-28263
- steel, Cr-Mo, friction pair, surface layer structural modifications (*Russian*) 7-39678
- steel, high speed, wear mechanisms and tool life rel. to microstruct. 7-8128
- steel, stainless, ion implanted with N, fretting wear resist. 7-13636
- steel, stainless SUS304, fretting props. in vac. environment, oxidative and adhesive wear 7-8122
- steel sheet, hot-dipping into Al-Zn eutectoid base superplastic alloy (*Japanese*) 7-59664
- steel sheet, PET and PVC coated, corrosion resist. and adhesion strength (*Japanese*) 7-8165
- steel-rubber, adhesive bond strength quality assurance using acousto-US technique 7-33881
- steel/composite, double-lap joints, stress anal. and failure props. 7-33769
- strength of cemented joints in polymer materials, device for meas. 7-54036
- surface and interface analysis, appls. conf., Veldhoven, Netherlands, (Oct. 1985) 7-24289
- thin films, adhesion measurement by indentation 7-45093
- thin hard coatings, adhesion test methods, review 7-46741
- thin metallic films, adhesion to substrate 7-46788
- vacuum symposium, Tokyo, Japan (1985) (*Japanese*) 7-14698
- wedge test for adhesive joints, mechanics 7-33872
- Ag interfacial surface energy atomistic estimation and adhesion meas. (*Japanese*) 7-58657
- Al, anodising by chromic acid, surface struct., abrasion resist., hardness, adhesion props. 7-13646
- Al film on Si, wire bondability 7-21710
- Al-Mg, adhesive-adherend interface under load, stresses in adhesive bond 7-28260
- Al_2O_3 film-stainless steel adhesion, improvement using surface precipitates (*Japanese*) 7-22880
- Au interfacial surface energy atomistic estimation and adhesion meas. (*Japanese*) 7-58657
- Au mechanical resonance spectra 7-21712
- Be, adhesive-adherend interface under load, stresses in adhesive bond 7-28260
- Bi-Sb, effect of additions of Bi and Sn in solder 7-12399
- C diamondlike films, deposition with C^+ and hydrocarbon ion beams, mechanical props., comparison 7-59417
- C fibre reinforced plastic, cemented lap joint, stress-strain state and strength 7-33794
- C thin surface layers on steel substrates, anticorrosion props., ion bombardment effects study 7-27202
- C-ZnX (X=S, Se), adherence of diamondlike C films, use of intermediate layers 7-46624
- Cr, electrodeposited, groove adhesion tests 7-46789
- Cr evaporated and ion assisted deposited coatings, microstruct., electron microscope obs. 7-52335
- CrCo-porcelain and CrNi-porcelain dental prostheses, strength rel. to surface roughness of metal frames 7-40365
- Cu interfacial surface energy atomistic estimation and adhesion meas. (*Japanese*) 7-58657
- CuO and magnesia ceramic, direct bonding region, thermal resistance 7-37395
- Fe films on insulators, H^+ bombardment, Mossbauer and adhesion study 7-32517
- Fe/Fe- $\text{FeO}/\text{Al}_2\text{O}_3$ systems, diffusion bonded, interface chemistry, bonding strength 7-28079
- FeCrAlY, Al_2O_3 adhesion mechanism 7-33843
- HfN(C) reactively sputtered wear resistant coatings, struct., hardness and adhesion props. study 7-52330
- In-glass, glow discharge induced changes 7-12577
- In-glass vacuum seal, adhesion strength, meas. method 7-59715
- MgF_2 films deposited on fused SiO_2 with ion beam assistance, adhesion, internal stresses 7-21749
- MgO sputtered coatings on metal substrates, adhesion and structural props. 7-52337
- MoN_x sputtered coatings, tribological props. in contact with Cu 7-53911
- MoS_2 sputtered films, tribological props., ion beam mixing effects 7-3441
- Nb-Ti-O ceramic coatings, synthesis by reactive ion plating and sputter deposition, struct., electrophysical props. 7-64031
- Ni film on sapphire substrate, adhesion, mechanical resonance spectra 7-21712
- Ni/NiO/ZrO₂, partially stabilised, bonding, stresses, shear strength 7-39845
- Ni-Co-Cr-Al-Y coatings, electron beam deposition, oxidation rel. to pretreatment 7-46702
- Ni-Cr, bonding to dental glass 7-39844
- Ni-P-B electrodeless coatings, prep. and deposit characts. 7-59671
- $\text{Ni}_{60}\text{Cr}_{34}$ alloy, plastic strain rate difference with Cr_2O_3 oxide (*French*) 7-17682

adhesion continued

- NiCrAlY, Al_2O_3 adhesion mechanism 7-33843
 Pt film adhesion on thermally grown alumina, O enhancement 7-46790
 Ru-Ti-O ceramic coatings, synthesis by reactive ion plating, struct., electrophysical props. 7-64031
 Si, wettability and adhesion with Sn-Si(Sb)(As) melts 7-21576
 Si-pyrex, irreversibility of anodic bonding 7-33910
 Si-Si surfaces, direct bonding, silanol group reactions and O diffusion mechanisms 7-21791
 Si- SiO_2 -Cu(Ni), light induced deposition of metal films on SOI substrates 7-46354
 Si_3N_4 ceramic, bonding to stainless steel, using Cr and Mn prediffusion (Japanese) 7-8147
 Si_3N_4 , wear properties in rolling contact 7-8126
 SiO_2 evaporated and ion assisted deposited coatings, microstruct., electron microscope obs. 7-52335
 SiO_2 in aqs. solns. of cetylpyridinium bromide and inorganic salts, coagulation, thermodynamic stability 7-8326
 SiO_2 -polyimide interface, locus of failure, XPS study 7-28261
 Ta_2O_5 evaporated and ion assisted deposited coatings, microstruct., electron microscope obs. 7-52335
 TiC film ion plated on austenitic stainless steel, adherence rel. to ionisation (Japanese) 7-53636
 TiC/Fe multicomponent films on steel, sputter deposition and characteris. (Japanese) 7-3167
 TiC-WC-TaC-Co three-phase sintered carbides, Ta content influence on struct. and props. 7-65097
 TiN coatings, internal stress and adherence 7-52374
 TiN coatings on steel substrates, growth, struct., props. 7-33799
 TiN films on tool steel, plasma-assisted CVD deposited, interfacial composition 7-52303
 TiN ion plated films, tempering effects 7-59461
 TiN protective coatings on cemented carbides, adhesion and toughness 7-65159
 TiN thin film, adhesion on PBI plastic produced by large-current ion implantation machine (Japanese) 7-8149
 TiN-C(BN), hard composite coatings, deposition and props. 7-46623
 TiN-coated gear cutting hobs, wear characteristics, mechanical and structural props. 7-53980
 TiN-coated high-speed steel cutting tools, coating quality and surface finish., tool metallurgy and design 7-53979
 TiN-Fe sputtered binary coatings on steel substrates (Japanese) 7-59419
 TiN(C) 7-52330
 TiO_2 evaporated and ion assisted deposited coatings, microstruct., electron microscope obs. 7-52335
 W LPCVD films by WF_6/Si reduction method, influence of deposition variables 7-17461
 W nonselective CVD films, adhesion to SiO_2 7-17760
 W-C coatings on stainless steel, sputter deposited, mechanical props., effect of interlayers 7-53983
 Zn alloy films on Al, growth and adhesion rel. to application technique 7-13396
 ZnS thin films, radiation enhanced adhesion to SiO_2 substrates 7-32504
 ZrN(C) reactively sputtered wear resistant coatings, struct., hardness and adhesion props. study 7-52330
 ZrO_2 (partially stabilised)/steel system, solid state bonding with Ti interlayer 7-28264
 ZrO_2 ceramics, wettability of metals 7-52191
 ZrO_2 , Y_2O_3 stabilised thermal barrier coatings, ionisation assisted physical vapour deposition 7-46349

adiabatic compression, plasma see plasma heating

adiabatic demagnetisation see magnetic cooling

adion see adsorption

ADM see delta modulation

administrative data processing

see also management information systems; medical administrative data processing; spreadsheet programs; word processing
 environmental information software, waste management case study 7-8472
 resources management master planning, GIS and remote sensing role 7-4072

admittance see electric admittance

admittance measurement see electric admittance measurement

ADP see administrative data processing

ADP (ammonium dihydrogen phosphate) see ammonium compounds

adsorbed layers

see also monolayers

- 5d dimers on W (211) and (110) and Ta (211), stability 7-52285
 acetylene, on Cu (100), XANES fluoresc. yield meas. 7-64751
 acridine, adsorbed on Al_2O_3 , tunnelling spectra study 7-52264
 adenine series adsorbed on aqueous Ag sol, SERS study 7-17947
 ad molecular processes, laser induced, energy and phase relax. 7-21610
 ad molecules on metal particles, giant Raman scatt. effect 7-52255
 adsorbate covered metal surfaces, electronic states 7-52719
 adsorbate resonances, fractional occupation and van der Waals interactions 7-27376
 adsorbate-induced initial states, angle-resolved photoemission cross section 7-17062
 alkali metal, adsorbed layers on Si (100) 2×1 , anisotropic plasmons (Japanese) 7-21967
 alkali metal adsorbed layers on solid surfaces (Japanese) 7-21966
 alkali metal overlayers on graphite, electronic struct. initial stages of intercalation 7-53503
 anharmonic adspecies, transient excitation by pulsed laser radiation 7-21611
 ANNNI model, two-dimensional, wetting phenomena 7-27064
 apparent atom size w.r.t. density of states in scanning tunnelling microscope, bias voltage depend. 7-44321
 Ar, on graphite, fluid-solid monolayer transition, simulation 7-32796
 arachidic acid, adsorbed layer on Ag, form. and struct., IR spectra, optical ellipsometry 7-44992
 aromatic adsorbed on SiO_2 and Al_2O_3 - SiO_2 , IR spectra 7-10573
 atom-surface interaction, dipole and quadrupole contributions 7-52282
 azide, cyanate and thiocyanate adsorbed on Ag electrodes, pot. difference IR spectra, coverage depend. orientation 7-22522
 benzene, adsorbed on graphite (BN), rot. dynamics and orientation, NMR spectra 7-53161
 benzene, adsorbed on Os (0001), mol. struct., angle-resolved UV photoemission spectral study 7-53492

adsorbed layers continued

- benzene, chemisorbed on Pt {110}, influence of orientation on H-D exchange reactions 7-59781
 benzene, on Cu and Ag single cryst. surfaces, mol. orientation, XANES determ. 7-64769
 benzene and azabenzene adsorbed on Cu(111) and Au(110), electron affinity levels studied by inverse photoemission 7-44991
 benzenethiolate adsorbed on Ag surface, SERS study 7-62385
 biological macromolecules adsorbed on surfaces, struct., optical studies 7-28458
 1,3-butadiene adsorbed on Ag films, SERS 7-22251
 1-butene adsorbed on Ag films, SERS 7-22251
 butylamine, adsorbed on SiO_2 , Al_2O_3 and CaO, thermal desorption and IR study 7-39110
 cadmium arachidate, Langmuir-Blodgett multilayers, order-disorder transitions, Raman spectra 7-53309
 cadmium stearate Langmuir-Blodgett films on sapphire, thermal disordering, optoacoustic IR spectra anal. 7-52236
 carbon tetrafluoride adsorbed on graphite, nonwetting growth and cluster formation 7-2359
 cellulose substrate, room-temp. phosphoresc., H-bonding props. 7-31102
 chemisorbed atoms, electronic struct. and tunnelling current 7-6962
 chemisorbed atoms, vibration, electron-hole friction mechanism 7-38317
 coated transparent crystal, laser heating 7-63654
 colloidal grains with adsorbed polymer layers, neutron scattering anal. 7-21621
 crystal violet, adsorpt. on Ag island films, surface-enhanced reson. Raman scatt. 7-46022
 cyanobiphenyls, monolayer on H_2O , optical SHG meas. 7-17288
 desorption, electron and photon-stimulated, probes of surface struct. and bonding 7-32817
 diatomic mol. on substrate, reson. laser induced desorption, classical and quantum models 7-58618
 dichlorodimethylsilane, coated reson. cells, alkali metal interaction wall relax. 7-59317
 diffraction methods for struct. determ. of surfaces and overlayers 7-2324
 diffusion on hexagonal lattice 7-21636
 diphilic polyelectrolytes, conc. effect on wetting of Teflon 7-38302
 disordered surface, atom scatt. randomly corrugated hard wall and sudden approx. 7-53489
 dye laser molecules adsorbed on optical surface, SHG and THG (Chinese) 7-57457
 dye molecules adsorbed on silicate matrix, UV electronic spectra 7-42639
 EELS studies of surfaces and adsorbates 7-3128
 electroactive species, Fourier transform IR reflectron absorpt. spectra 7-23093
 enhanced IR absorption of adsorbed molecules on thin metal films, electromagnetic effect 7-27805
 ethane, adsorbed on graphite, phase transitions, thermodynamics and struct. anal., LEED obs. 7-32797
 ethane, on Cu (100), XANES fluoresc. yield meas. 7-64751
 ethane, on graphite, phase transitions, thermodynamics and struct. anal., LEED obs. 7-32797
 ethene, on Cu (100), XANES fluoresc. yield meas. 7-64751
 ethylene adsorbed on graphite, layering and layer-critical-point transitions 7-12471
 ethylene on Cu, Ag and Au films, adsorbate-substrate bonding 7-52292
 ethylene on Cu (100), C K-edge structure of chemisorbed molecules 7-27824
 ethynidyne, adsorbed on Pd/ Al_2O_3 , CO adsorpt., IR spectra studies 7-2371
 ethyne adsorbed on zeolite, time resolved FTIR obs. 7-54182
 excited states near a small metal particle, nonradiative lifetime 7-45422
 fatty acids, monolayer on H_2O , optical SHG meas. 7-17288
 fibrinogen saturated adsorbed layer, variable angle reflectometry (French) 7-28459
 flavin derivatives, adsorbed on oxide layers, photophysics study 7-7738
 flavins on Ag colloids, SERS 7-64626
 formate ion incorporated into tunnel junction, quantitative analysis of inelastic tunnelling spectrum 7-38769
 formate on Cu surfaces, adsorpt. site symm. and bond lengths, SEXAFS data, multishell simulation anal. 7-63947
 FTIR characterisation of high surface materials and adsorbed species 7-46042
 gas-solid interface, photon-phonon conversion, laser-linewidth effects 7-58599
 gases, adsorbed, surface diffusion, connectivity effects 7-46864
 graphite incommensurate overlayer on Pt (111), LEED 7-63930
 graphite on Pt (110), nucleation and orientation 7-21664
 halide and pseudohalides at Au surface, SERS, metal-adsorbate vibr. freqs., surface bonding 7-12468
 heteroepitaxial systems, domain size determ. from LEED angular profiles 7-7075
 high energy ion scatt., struct. anal. of surfaces and interfaces 7-22410
 hindered rotations of adsorbed molecules, energy levels and thermodynamic props. 7-27130
 hydrocarbons adsorbed on transition metal surfaces, EELS studies of bonding 7-3128
 imidazole, on microlithographically prepared Cu, SERS obs. 7-27712
 imperfect surfaces and adsorbates, short range order and correlations 7-6953
 impurities adsorbed on Si during plasma etching in a CF_4 discharge 7-6940
 indigo dyes adsorbed on Ag hydrosol particles, SERS spectra 7-46870
 inert gas atoms, physisorbed, induced dipole moment 7-52243
 interactions on transition metal surfaces, self-consistent calcs., tight binding formalism 7-2382
 interface response theory of discrete composite systems 7-38424
 interface wandering in pure and impure and bulk phases 7-32791
 inverse photoemission spectra of adsorbates on metals, model Hamiltonian study 7-33478
 ketene adsorbed on Pt(III), surface chemistry, substrate temp. influence, EELS 7-46867
 Kr on graphite, 2-D system with competing interactions, phase transitions 7-6791
 laser-induced photodesorption 7-52281
 laser-stimulated desorption of adsorbed molecules via electronic excitation 7-59309
 laser/surface-enhanced isotope separation of species adsorbed on solid surfaces 7-20070

adsorbed layers continued

- long-chain amphiphile on solid substrate, thermally induced disorder, Fourier transform IR spectra 7-12467
- macromolecules adsorbed on single surface, generating function methods 7-21622
- metal films, etching, kinetic model, electron flux activation 7-3492
- metal particles, quantum size effects 7-7597
- metal surfaces, EELS studies of dynamics 7-3127
- metal/electrolyte interface, electrodynamics, surface soliton form. 7-21958
- methane, on graphite, multilayer growth mode 7-32795
- methane, on graphite, multilayers, adsorpt. isotherms and heat of adsorpt. 7-32794
- methane, physisorbed on NaCl (100), EELS spectra 7-13289
- methane adsorbed on graphite, bilayer and trilayer 7-2363
- methane adsorbed on graphite, multilayer melting transition 7-6992
- methane on graphite, heat capacity calcs., quantum cell model 7-52076
- methane on graphite, LEED 7-27129
- methanol monolayers, stretch vibr. obs., optical sum-freq. generation 7-58610
- 1-methyl-1'-octadecyl-2,2'-cyanine perchlorate dye, Langmuir-Blodgett multilayers, Ag/glass substrate, distance depend of SERS 7-32801
- N-methyl-thioacetamide on Cu and Ag surfaces, enhanced Raman spectroscopic obs. on rot. isomers 7-46037
- methylviologen, radical cation dimers, adsorbed on colloidal CdS surface, relax. 7-27095
- mismatched overlayers, dislocation depinning, mol. dynamics investig. 7-7011
- molecular adsorbates, structure determ. using dynamic LEED and HREELS 7-12493
- molecules on Ag sol, adsorpt. forces in SERS 7-52254
- molecules photodesorption by IR laser-adsorbate coupling 7-58616
- monolayer, Ising model, 2D random field, correlations 7-6754
- monolayers, pulsed laser induced desorption from metal surfaces 7-58617
- near edge X-ray adsorption fine structure spectroscopy 7-27822
- News-Anderson model, time-depend., for moving particles on metal surfaces 7-52263
- O-nitrobenzoic acid and pyridine coadsorbed on Ag sol, SERS excitation profiles 7-33373
- noble gas mixtures on graphite and Ag, ordering and phase separation 7-21651
- noble gases adsorbed on metals, interatom interactions, LEED studies 7-7014
- nonmagnetic, elastic spin-polarised LEED studies, book contrib. 7-32233
- nonmagnetic, spin-resolved photoemission, book contrib. 7-33521
- optical absorption spectra of adsorbates on metal surfaces 7-27741
- order-disorder phase transition, effect on rate of elementary processes 7-6976
- ordered structures, quantitative description 7-32831
- organic adsorbates, structure from elastic diffuse LEED 7-12494
- orientation, electronic excitation by electron beam, differential cross-section meas. 7-27101
- overlayer, specularly reflected X-rays, surface EXAFS meas. 7-3117
- overlayers on metal surfaces, atomic struct. and composition 7-7013
- pentadecanoic acid monolayers, stretch vibr. obs., optical sum-freq. generation 7-58610
- phase transformations in adsorbed layers, conf., Oxford, England, (17-18 Dec. 1985) 7-29575
- phase transitions in adsorbed films, monolayer adsorption, perturbational approach 7-21665
- phenazine, adsorbed on Al₂O₃, tunnelling spectra study 7-52264
- phenol adsorbed on ZnO surface, surface CARS spectroscopy 7-46036
- photodesorption, laser-induced, effect of resonant vibrational energy transfer 7-52293
- photostimulated phase transitions on semicond. surface, reson. conditions calcs. (Russian) 7-45016
- physisorbed atoms on anisotropic rectangular lattice, struct. factor of incommensurate phases 7-52250
- physisorbed film-substrate many-body interaction energy, non-pair-additive contrib. calcs. 7-2383
- poly(α -methylstyrene) adsorbed monolayer on mica, intermolecular force meas. 7-21623
- polyelectrolyte, adsorbed in charged surface, mean spans calcs. 7-44995
- positronium on jellium surface, positron states model anal. 7-38347
- pyrazine, on Ag (111), affinity level, EELS, inverse and direct photoemission spectra studies 7-52724
- pyrazine, on Cu and Ag single cryst. surfaces, mol. orientation, XANES determ. 7-64769
- pyridine, adsorbed on Ag, electrode pot. and Raman line intensities 7-19865
- pyridine, chemisorbed on Pt {110}, influence of orientation on H-D exchange reactions 7-59781
- pyridine, on Ag (111) and Ag polycrystalline substrates, struct., electron bands, LEED, UPS 7-53506
- pyridine, on Ag surface, IR laser stimulated desorption mol. spectroscopy 7-58614
- pyridine, on Cu and Ag single cryst. surfaces, mol. orientation, XANES determ. 7-64769
- pyridine adsorbed on ZnO surface, surface CARS spectroscopy 7-46036
- pyridine on Cu and Ag surfaces, resonance Raman contrib. to SERS in aq. media 7-3055
- quinoxaline on Ag colloid particles, SERS, adsorbate orientations 7-22265
- rare earth adsorbates on metal surfaces, EPR line shapes 7-53129
- reentrant wetting phenomena and crit. behaviour near bulk critical points 7-44956
- resorufin adsorbed on γ -Al₂O₃, fluoresc. line narrowing and site-selection expt. 7-10655
- rhodamine 6G, aq. solns., conc. distrib. near adsorbing surface, UV-visible spectra 7-42640
- rhodamine B in submono-, mono- and multilayer systems, fluoresc. decays and spectral props. 7-19938
- scanning tunnelling microscopy appl. 7-18920
- semiconductor and metal adatom overlayers, diffusion and interactions 7-7012
- solid surface, physics, conf., Smolenice, Czechoslovakia (Sept. 1984) 7-48170
- solid-liq. interface, Fourier-transform IR spectroscopy with photothermal beam deflection appl. 7-52234
- spectroscopy of single atoms in the scanning tunneling microscope 7-33060

adsorbed layers continued

- structure-dependent optical phenomena 7-45953
- submonolayer coatings on W plates, transverse magnetoresist. under static skin effect conditions (Russian) 7-45369
- submonolayer film, phase diagram, intrinsic and extrinsic ordering forces, diffusive functional theory calcs. 7-63952
- succinonitrile on Cu and Ag surfaces, enhanced Raman spectroscopic obs. on rot. isomers 7-46037
- superlattices, surfaces and interfaces, structural, electronic and mag. props. 7-16849
- surface analysis in far IR, triple modulation FTIR spectrometry 7-54223
- surface analysis using grazing incidence X-ray scatt. 7-26592
- surface coherent antiStokes Raman spectroscopy as analytical tool 7-1233
- surface EM wave FTIR spectroscopy of very thin films 7-41506
- surface EXAFS, Debye-Waller factor, influence of adsorbed monolayer 7-39316
- surface FTIR-ATR spectroscopy, lower limit of thickness of measurable surface layer 7-41508
- surface induced dipole moments, face specificity 7-21618
- surface lattice dynamics of ordered overlayers on metals 7-2342
- surface migration 7-2368
- surface science, conference, Julich, Germany (April 1986) 7-55890
- surface science techniques, book 7-60888
- surface topography meas. using scanning tunnelling microscopy 7-37814
- tetrafluoromethane on graphite, phase diagram, phase transitions 7-38338
- tetraphenylporphine on Ag surface, fluoresc. quenching and interference effects 7-36675
- thermal desorption spectra, effect of adsorbate diffusion into the solid 7-52283
- thermal relaxation of adsorbed atoms in an intense laser field 7-38330
- thin overlayers, struct. determ. by AES or XPS 7-33490
- toluene adsorbed on activated C, IR spectra 7-10573
- transition metal oxides, catalysts, laser Raman spectra 7-53295
- s-triazine, on Cu and Ag single cryst. surfaces, mol. orientation, XANES determ. 7-64769
- 1,2,4-triazole, on microlithographically prepared Cu, SERS obs. 7-27712
- trimethylsilyl groups adsorbed on SiO₂, ²H NMR spectra investig. 7-2375
- tunnel diffusion, effect of lateral interactions 7-27125
- two-level atoms on conventional and phase conjugated surfaces, laser induced phenomena 7-57025
- vibrational spectroscopy, lineshapes and dissipative processes 7-45956
- water vapour, electron stimulated adsorption on Pt 7-63955
- water-in-oil emulsions, adsorbed-solvated layers, optical obs. 7-59798
- X-ray photoelectron diff. studies of surface and epitaxial overlayer structures, review 7-27862
- XANES spectra, multiple scattering effects 7-13260
- Ag adsorbate geometry determ. on Si (111), X-ray photoelectron diff. study (Japanese) 7-11852
- Ag clusters, vibrational characteristics, SERS studies 7-22255
- Ag on Si (111), geometric struct. and density of states, cluster model and charge self-consistent extended Huckel method calcs. 7-21619
- Ag on Si (111), geometry and local electron states 7-58626
- Ag on Si (111), inverse photoemission spectroscopy 7-59280
- Ag on Si (111), struct. anal. by impact collision ion scatt. spectroscopy 7-6999
- Ag on Si (111), structure, scanning tunnelling microscopy studies 7-58625
- Ag on W (110), thermal desorption spectroscopy 7-27119
- Ag ordered overlayer on Si (111), surface states, inverse photoemission studies 7-2660
- Ag particles, adsorbate light scatt., energy transfer induced interfacial optical processes 7-39109
- Ag-AgCl surface system, adsorpt.-enhanced Raman scatt. and optical absorpt. 7-53301
- AgCl, adsorbed, Ag cluster SHG enhancement by transient resonances 7-20325
- Al coadsorbed with N₂ on Ni, N(1s) spectrum 7-21968
- Al on Ni and Cu surfaces, electronic struct. and oxidation of surface 7-22443
- Al on plasma passivated Si, subsurface H barrier layer obs. 7-17745
- Ar adsorbed films, surface melting and roughening 7-38342
- Ar on Au (111), He atom-surface scatt. 7-27851
- Ar on graphite, positronium formation 7-33483
- Ar physisorbed monolayers on graphite, melting transition, high resolution synchrotron X-ray diff. study 7-63780
- Ar, physisorbed on Cu, laser-induced thermal desorption 7-17817
- Ar-CO mixtures on graphite, ordering and phase separation 7-21651
- Ar-N₂ mixtures on graphite, ordering and phase separation 7-21651
- As overlayer on Si (111), removal of surface reconstruction 7-21587
- Au adsorbate layer struct. on Mo (110), Auger electron peak shape study 7-46254
- Au, epitaxial growth on W (100); adsorbate props. 7-38329
- Au on Ni, partial sputtering cross sections 7-59331
- Au on Si (111), inverse photoemission spectroscopy 7-59280
- Au on Si (111), SEM, LEED and scanning Auger microscopy obs. 7-21056
- Au on W (110), thermal desorption spectroscopy 7-27119
- Au ordered overlayer on Si (111), surface states, inverse photoemission studies 7-2660
- Au underpotential deposit on SnO₂:F electrode 7-44998
- Ba coadsorbed with N₂ on Ni, N(1s) spectrum 7-21968
- Ba, on polycrystalline W and W-Os thermionic cathode surfaces, SEXAFS studies 7-64774
- Br on Ag (110), normal exit XPS studies 7-2380
- C on Fe (100), gasification by O, CO desorption 7-6993
- C on Ni (100), electronic struct. 7-7315
- CN chemisorbed on Cu (100), field induced vibr. freq. shifts 7-45991
- C₂N₂ on Pt (111), reaction with coadsorbed H₂ 7-54186
- CO, adsorbed, integral absorpt. coeff., IR vibr. spectroscopy 7-53323
- CO adsorbed on graphite, pinwheel and herringbone structs. 7-7015
- CO, adsorbed on highly dispersed Pd and Pt, vibr. spectra 7-12475
- CO, adsorbed on Ni (001), 7-52235
- CO adsorbed on Pt (111), vibr., site conversion, IR spectra 7-58613
- CO, adsorbed on Pt (111), He thermal beam scattering 7-53475
- CO and K coadsorbed on Ni (111), adsorbates electrostatic interaction, IR reflection-absorption spectra, TPD, LEED obs. 7-32824
- CO and Pt (111), LEED structural anal. 7-2376
- CO, chemisorbed, bonding, comment and reply 7-12472

adsorbed layers continued

- CO, chemisorbed, ionisation phenomena, ab initio wave functions 7-36444
 CO chemisorbed on Cr (110), electron stimulated desorption 7-63965
 CO chemisorbed on Cu (100), field induced vibr. freq. shifts 7-45991
 CO, chemisorbed on Ni (111), mol. orientation, effect of adsorbed K, ESDIAD study 7-32825
 CO chemisorbed on Ni (110), mag. props. investigated by spin-polarised electron beams 7-58994
 CO, chemisorbed on Pt (111), adsorbate vibr. modes, inelastic He atom scatt. obs. 7-32782
 CO coadsorbed with K on Ru (001), angle resolved Auger lineshapes 7-2372
 CO coadsorbed with K on Pt (111), inverse photoemission 7-52726
 CO, free and adsorbed mol., valence wavefunctions, deexcitation electron spectroscopy 7-36756
 CO on Cu, Raman intensity of adsorbate vibr., cluster-model calc. 7-27089
 CO on Fe (100), adsorbate tilted dissociation precursor 7-58642
 CO on Fe (100), UPS characterisation of a and b adsorption states 7-27126
 CO on Ni, bremsstrahlung isochromat spectroscopy 7-27379
 CO on Ni clusters, surface electronic and mag. struct. 7-21969
 CO, on Pt (111), molecule-substrate vibr. mode, IR emission spectra study 7-57126
 CO on stepped Pt surfaces, coupled harmonic oscillator models 7-52230
 CO, physisorbed multilayer, near-threshold electronic excitation, EELS spectra anal. 7-45001
 CO, terminally bonded on Ru (001), vibr. dephasing 7-17318
 CO, A=12, 13 on Ni (100), surface charact. by Raman spectroscopy 7-42625
 Cl on Ag (111), weakly ordered and disordered, struct. studies 7-2365
 Cl, on Ag single crystals, adsorbate-substrate bond lengths, coverage depend., SEXAFS 7-63948
 Cl⁻ on Ag, surface enhanced Raman spectrum pot. depend., surface coverage and mutual depolarisation effects 7-7686
 Co, adsorbed on Cu (111), surface EXAFS investig. (French) 7-6957
 Co, on Ag film, surface enhanced Raman scattering study 7-3037
 Cs adsorbed on Si, migration and equilibrium in strong elec. field 7-2351
 Cs, on Ag single crystals, adsorbate-substrate bond lengths, coverage depend., SEXAFS 7-63948
 Cs on Si (111), effect on surface oxidation 7-54025
 Cu deposition, initial stages, on MgO (001) and ZnO (10 $\bar{1}$ 0) 7-63959
 Cu on Si (111), inverse photoemission spectroscopy 7-59280
 Cu on W (110), thermal desorption spectroscopy 7-27119
 Cu ordered overlayer on Si (111), surface states, inverse photoemission studies 7-2660
 D on Ni (100), vibr. motion, high resolution EELS 7-12458
 D on Rh (111), delocalised quantum behaviour, EELS study 7-38666
 D₂ on Si, phonon scatt. 7-21609
 Fe-tetrasulphonated phthalocyanines, photography, SERS and electrochemical studies 7-13155
 Ga on Si (111), X-ray photoelectron and Auger electron diff. 7-27116
 Ge on Si (111), X-ray standing wave studies 7-58629
 H, adsorbed on Ni(Pd) surfaces, order-disorder transitions, theory 7-12492
 H adsorption sites on Ru (001) at saturation coverage, LEED 7-58645
 H, chemisorbed on metal clusters, ionisation threshold, photoionisation TOF mass spectra 7-20085
 H, chemisorbed on Ni (110), induced (1 \times 2) reconstruction 7-58851
 H on Ni (100), vibr. motion, high resolution EELS 7-12458
 H on Ni (110), competing surface reconstruction mechanisms 7-7004
 H on Ni (110), struct. determ., LEED studies 7-45004
 H on Ni (111), phase diagrams based on model interactions 7-21650
 H, on Pd (100) and (111), surface resonances in vibr. spectroscopy 7-52229
 H on Pd (110), row pairing model 7-2370
 H on Rh (111), delocalised quantum behaviour, EELS study 7-38666
 H on Ru (0001), adsorbate bonding and vibr. 7-52291
 H on Si (001), RHEED intensities 7-27123
 H on Si (110), atomic configuration, LEED studies 7-2314
 H, on W (001), disclivive surface reconstructions, incommensurate sandwiches 7-52223
 H on W (100), long and short range fluctuations, lattice dynamical model 7-7002
 H on Zn (0001), thermal desorption spectra 7-21646
 H overlayer ordering on Ni and Pd (110) surfaces, embedded-cluster model anal. 7-52256
 H, spin polarised, adsorbed on He, sticking coeff. and 2D superfluidity 7-6912
 H-permeation and recycling, molecular chemisorption model 7-8302
 H₂, adsorbed by metals, kinetics, oxide layer effects at room temp. 7-33965
 H₂, adsorbed on metals, kinetics model of chemisorption layer (Korean) 7-32813
 H₂, adsorbed on Nb, kinetic model (Korean) 7-32814
 H₂ chemisorbed on Si (100), transition from the dihydride to the monohydride phase 7-58631
 H₂, chemisorption on Ru (001), effect of coadsorbed O₂ 7-33959
 H₂, in metallic glasses, prep., struct. and props. 7-26663
 H₂ on graphite, rotational states of physisorbed molecules 7-52278
 H₂ on Pt (111), reaction with coadsorbed C₂N₂ 7-54186
 H₂ on Si, phonon scatt. 7-21609
 H₂ on W, Mo, Re, high-field corrosion, field-ion microscopy studies 7-33830
 H₂-D₂ mixtures adsorbed on graphite, phase diagrams 7-52180
 H₂O, struct., role in disperse system filtration prop. form. 7-51297
 He, binding energies on simple metal surfaces, van der Waals energy 7-38663
 HeRh²⁺ adsorbed compound ion, field dissociation by atomic tunneling 7-33919
 He, adsorbed on Grafoil, nuclear ferromagnetism and surface ferromagnetic effect 7-2296
 He, adsorbed on solid surface, magnetism (Japanese) 7-21564
 He-H₂ mixtures adsorbed on graphite, phase diagrams 7-52180
 He, adsorbed on graphite order-disorder transition, sp. ht. anal. 7-58563
 He, on Vycor, superfluid transition, constrained randomness, Harris criterion 7-44935
 In adatom on Si (100), bonding coordination number, synchrotron photoemission studies 7-45071
 K adatoms on W (112), density fluctuation simulation 7-32806

adsorbed layers continued

- K adsorbed on Cu (001), valence-electronic struct., work function changes and EELS 7-45002
 K coadsorbed with CO on Pt (111), inverse photoemission 7-52726
 K on Co foil, CO adsorption, XPS and AES studies 7-8296
 K, on Cu (001), two-dimensional condensation, LEED obs. 7-12478
 K on Fe (III) surface precovrage, promotion of surface reactions with N₂ 7-13807
 K-graphite (0001)-(2 \times 2) surface intercalated structure, LEED calcs. 7-6952
 K-Ni coadsorbed layer on W (110), field emission flicker noise 7-32807
 Kr, adsorbate, excited states assignment 7-52725
 Kr adsorbed on graphite, adsorption isotherm meas. near commensurate-incommensurate transition 7-38337
 Kr coadsorbed with NO₂ on Ag (110), magnetic resonance 7-59113
 Kr on Au (111), He atom-surface scatt. 7-27851
 Kr on graphite, incommensurate phase, computer simulation studies 7-7009
 Kr on Pt (111), adsorbate-substrate vibr. coupling 7-52221
 Kr, physisorbed films on Pt (111), impurity-quenched orientational epitaxy 7-45003
 LaNi₅ oxide surface layers, H₂ adsorpt. kinetics 7-32833
 Li adatoms on W (110) nuclear quadrupole interactions, NMR study 7-2937
 γ -methacryloxypropyltrimethoxysilane, chem. reaction on PbO surface, Fourier transform IR spectra 7-53308
 N c(2 \times 2) on Cu(100), surface phonon dispersion, LEED, AES and EELS studies 7-12459
 N, on Ni (100), surface phonon dispersion, adsorbate induced reconstruction 7-52225
 N₂ adsorpt. on Zr cathode, material and structural changes during arc operation 7-46866
 N₂, chemisorbed on Fe (111) surface, adsorbate geometry, angle resolved XPS anal. 7-45009
 N₂ chemisorbed on Pd (110), EELS, LEED and AES 7-63960
 N₂ on clean or Ba- or Al-promoted Ni, N(1s) spectrum 7-21968
 N₂, on graphite, mol. zero-point energies, out-of-plane orientation, nucl. reson. photon scatt. study 7-32819
 N₂ on graphite, pinwheel and herringbone structs. 7-7015
 N₂ on graphite, positronium formation 7-33483
 N₂ on graphite, second surface virial coefficient 7-6970
 N₂ on graphite basal plane, computer simulation 7-52297
 N₂ on W, Mo, Re, high-field corrosion, field-ion microscopy studies 7-33830
 N₂, physisorbed multilayer, near-threshold electronic excitation, EELS spectra anal. 7-45001
 N₂, surface layer on graphite, motion investig. 7-32792
 NO adsorbed on Pt, high-speed ramped field desorption spectra 7-32810
 NO, coadsorbed on Rh (111) with CO and O, EELS 7-16860
 NO, coadsorbed with Kr on Ag (110), magnetic resonance 7-59113
 NO₂, on Ag (110) with physisorbed Kr, EPR, LEED AES studies 7-53116
 Na adatoms on W (110), nuclear quadrupole interactions, NMR study 7-2937
 Na on Si (111), effect on surface oxidation 7-54025
 Ne film on Ag, triple-point wetting 7-32760
 Ne on Si, phonon scatt. 7-21609
 Ni (001), adsorbed Na, photoelectron diffraction spectrum calc. and Fourier transform anal. (Chinese) 7-13326
 Ni (100), adsorbed ethylene, hybridisation, Auger lineshape determ. 7-15576
 Ni on Cu (111), CO adsorption studies 7-21658
 Ni on Si (001)-(2 \times 8), surface structure 7-21586
 Ni on W (110), thermal desorption spectroscopy 7-27119
 NiCO, single-and multi-photon ionisation process dynamics 7-36701
 Ni(OH), model for OH chemisorption on Ni surface, bonding study 7-52240
 O (2 \times 1) on Cu (110), surface reconstruction, mean free path and Debye-Waller factor, SEXAFS study 7-46238
 O, chemisorbed on Cu (110), synchrotron X-ray scatt. study 7-7003
 O, chemisorbed on oxides, elec. Props., role in gas sensing mechanism 7-7250
 O films adsorbed on graphite, triple point wetting and surface melting 7-45007
 O monolayer surface on exfoliated graphite, positron annihilation study at low temps. 7-38346
 O on Ba covered Cu, XPS and UPS studies 7-2373
 O, on Cu (110), adsorbate induced reconstruction, XANES 7-53447
 O, on different Cu surfaces, reaction with CO and H₂ 7-59784
 O on Ni, clean and Ba covered, XPS and UPS studies 7-2373
 O on Ni (001), self-consistent field He scatt. cluster model calcs. 7-53471
 O on Ni (001) and (110) surfaces, He diff. results 7-7809
 O on Ni (110), struct. anal., low energy ion recoil spectra study 7-2384
 O, on Pt (111), surface phonon dispersion, inelastic atom scatt. meas., lattice dynamical calcs. 7-52226
 O on Rh (111), ion bombarded, desorbed atoms distributions 7-22420
 O₂ 7-3608
 O₂, adsorbed on MgO, atomic and mol. beams, induced luminesc. 7-13231
 O₂, adsorbed on Pt (111) and Ni (100), p(2 \times 2) structures, surface phonons, bond-stretching interactions 7-21607
 O₂, chemisorbed on MgO, photostimulated desorption 7-27107
 O₂ chemisorbed on Ni (110), mag. props. investigated by spin-polarised electron beams 7-58994
 O₂, effect on secondary ion emission 7-64859
 O₂, on Cu (110) and polycrystalline surfaces, UPS, XPS, AES, EELS, LEED studies 7-32820
 O₂ on Fe, Ni and Cr, effect on surface magnetism 7-58973
 O₂ on graphite, positronium formation 7-33483
 O₂ on W (100), diffuse LEED intensity meas. 7-1823
 O₂ overlayers on Ni (100), elastic diffuse and inelastic electron scatt. 7-22402
 O₂, physisorbed on Cu, laser-induced thermal desorption 7-17817
 OH, adsorbed on transition metal surface, vibr. modes anal. 7-45008
 OH, on SiO₂, FTIR characteris. 7-46042
 O(2 \times 1) on Ni (110), SAXAFS study 7-64768
 Os clusters and complexes, Al₂O₃ supported, structs., EXAFS 7-62560
 Pb on Cu (110), struct. and melting, X-ray scatt. studies 7-7016
 Pb on Ge (111), photoelectron scatt., temp. depend. 7-13328

adsorbed layers continued

- Pb overlayer of Cu (100), growth, phase transitions and struct., thermal energy He atom scatt. study 7-63943
 Pb overlayer on Pt (100), underpotential deposited 7-58646
 Pb, overlayers on Cu (111), spot profile anal. of LEED 7-51586
 Pd underpotential deposit on SnO_2 :F electrode 7-44998
 Pt overlayer on $\text{Hg}_{1-x}\text{Cd}_x\text{Te}$, overlayer-cation reaction, XPS, UPS and LEED studies 7-65349
 Pt thin films on TiO_2 (110), XPS and depth profile data 7-22437
 Pt underpotential deposit on SnO_2 :F electrode 7-44998
 Rh clusters, on Rh (100), diffusion, classically exact overlayer dynamics 7-38328
 Rh overlayers on Si surfaces, FIM 7-52284
 Rh underpotential deposit on SnO_2 :F electrode 7-44998
 Ru underpotential deposit on SnO_2 :F electrode 7-44998
 Ru(100) surface, CO adsorbed monolayers, surface spectroscopy 7-15931
 S c(2×2) adsorbate geometry on Ni (001), angle-resolved-photoemission extended-fine struct. studies 7-27111
 S on Ni, field electron emission props. 7-33529
 S on Ni (011), struct., angle-resolved-photoemission extended fine struct. studies 7-63950
 S on Ni (100), angle-resolved photoemission extended fine-structure oscillations 7-64873
 S on Ni (100), segregation kinetics, AES and LEED studies (*Chinese*) 7-58607
 S, on Ni (110), azimuthally depend. XANES 7-64773
 S, on Ni (110) and (111), surface struct., SEXAFS, XANES studies 7-64770
 S, on Ni-Mo (6 at.%), oxidation, ESCA study 7-22897
 S on Pd(111), adsorbate oxidation kinetics (*German*) 7-33953
 S on Pt (111), surface crystallography using LEED and R factor analysis 7-27120
 SCN ions, adsorbed on evaporated Ag films, SERS 7-32838
 SF_6 monolayer on graphite, X-ray diffraction studies 7-6965
 SF_6 on graphite, Kr physisorption studies (*French*) 7-32799
 SF_6 , physisorbed on Cr target, coverage effect on sputtering behaviour 7-64845
 Sb overlayer on GaAs (110) p(1 × 1), domain size, LEED profile anal. 7-7075
 Sb overlayers on GaAs (110), electronic band bending at interface 7-58895
 Sb p(1 × 1) overlayer on III-V semiconductors, atomic and electronic struct. 7-7007
 Si and oxidised Si on Pt (111), effect on water adsorption and dissociation 7-27134
 a-Si:H, plasma enhanced CVD, integrated model 7-39423
 SiH_4 , pyrolysis on hydrogenated a-Si surface, reaction mechanism and kinetics 7-13739
 SiO deposited on CaF_2 , surface separation and vol. absorpt. in photothermal spectroscopy 7-53297
 SiO_2 , kinetics of growth on Si, optical props. 7-17740
 SiO_2 native oxide, ion and electron bombardment induced surface modifications studies 7-12175
 Sm overlayers on Al (111), homogeneous intermediate valence, photoemission 7-39351
 Sn adsorbate geometry determ. on Ge (111), X-ray photoelectron diffr. study (*Japanese*) 7-11852
 Te, adsorbed on GaAs, surface structure 7-12460
 W (110), adsorbed Si, struct. and composition 7-7013
 Xe, adsorbate, excited states assignment 7-52725
 Xe, adsorbed multilayers on Ru (001), inverse photoemission spectra, final-state screening effects 7-13251
 Xe adsorbed on graphite, thermodynamics of first-order and continuous melting 7-2358
 Xe on Au (110), final state screening in inverse photoemission spectra 7-3104
 Xe on Au (111), He atom-surface scatt. 7-27851
 Xe on graphite, incommensurate-commensurate phase transition, X-ray diffr. obs. 7-32793
 Xe on graphite, low temp. struct. and incommensurate-commensurate transition, electron diffr. study 7-38335
 Xe, on InP-Au interface, Fermi level pinning, growth charact., photoemission spectra 7-22009
 Xe, on Pt (111), He gas-surface interaction studies 7-33503
 Xe overlayer raft orientation on Pt (111), mol. dynamics study 7-38334
 Xe, physisorbed on Cu, laser-induced thermal desorption 7-17817
 X-ray ethylene coadsorbed films on graphite, layering and mixing transitions 7-58624
 Xe-Kr mixtures adsorbed on graphite, X-ray diffraction studies 7-6966

adsorption

- see also heat of adsorption
 active C, organic compounds adsorption, intradiffusional kinetics model 7-32830
 adatom, neighbour effects on permanent electric dipole, Feynman propag. anal. 7-27110
 adatom clusters, formation under coadsorption of reactants 7-6974
 adsorption-desorption phenomena, macroscopic meas. and microscopic interpretation 7-27136
 alkali metal chloride melts, anodic Cl evolution, galvanostatic transient anal. 7-33938
 amphiphilic molecules, adsorpt. and orientation, liq.-liq. interface 7-12403
 angular scan-attenuated total reflection spectra, appl. to study of molecular adsorption and desorption 7-4901
 atomic electronic charge density near solid body, appl. to physisorption 7-42448
 atoms, on fractal surface, crit. temps., van der Waals eqn. calcs. 7-2352
 binary metal alloy clusters, generation and reactivity 7-15784
 biporous spherical particles, restricted vol., isothermal adsorpt., finite difference method investig. 7-27097
 bombardment-induced segregation and redistribution 7-58381
 bond making and breaking at surfaces 7-28335
 bulk gas separation by pressure swing adsorption 7-54258
 n-butane, adsorpt. on Ir (110), activation with translational energy 7-39336
 catalyst surface, fractal clustering of reactants 7-3605
 catalytic particles, structure, TEM charact. studies 7-32241
 closed type adsorption cooling system utilising solar heat, simultaneous transport of heat and adsorbate 7-8440
 conference, Oconomowoc, WI, USA (April-May 1985) 7-18468

adsorption continued

- coumarin, at dropping Hg-electrode, $\text{Cd}^{2+}(\text{In}^{3+})$ reduction retardation 7-58609
 critical adsorpt. of fluid 7-21626
 cryocoolers with multi-stage compression and reduced void volume 7-315
 crystal growth, surface coarsening by macrostep formation 7-26683
 crystalline substrates, disordered adsorpt., diffuse LEED intensity meas. 7-1823
 4-cyanopyridine, adsorpt. on Ag electrode, electrochem. reduction, SERS 7-54165
 diatomic molecule-metal surface interaction, multidimensional potential energy surface 7-53490
 dynamics of adsorption, exchange reactions and defect form. at solid surfaces, computer simulations 7-32823
 electropositive adsorbate induced work function changes, semi-empirical mathematical relationships 7-7333
 energetic heterogeneity of solids, determ. from adsorption data, review 7-2387
 equilibria for binary gaseous mixtures on heterogeneous surface 7-6959
 extruded adsorbent pellets, N_2 meas transfer, skin resistance 7-16836
 field emission, conference, Berlin, Germany (July 1986) 7-29577
 flexible polymers, in limited volumes, behavior (*Russian*) 7-25694
 freezing and interfaces, appl. of density functional theories in 2D and 3D 7-32621
 FTIR characterisation of high surface materials and adsorbed species 7-46042
 graphite, adsorption of N_2 , second surface virial coefficient 7-6970
 graphite, $\text{Ar} + \text{N}_2 + \text{CO}$ submonolayer mixtures physisorbed on graphite, LEED study 7-2364
 graphite (0001), of Cs, induced work function changes, LEED obs. 7-33064
 graphite physisorbed surfaces, positron lifetime studies 7-39269
 graphite surface, methane adsorption, incomplete wetting at low temps. 7-32798
 graphite surface (0001), SF_6 covered, Kr physisorption studies (*French*) 7-32799
 graphite-Cs interaction compound, H_2 adsorpt., domain mobility and rot. tunnelling spectrum 7-63525
 heterogeneous adsorption behaviour in soil, effect on ion transport 7-29104
 heterogeneous catalysts, adsorpt. complexes with NH_3 , vibr. study, IR spectra anal. 7-36607
 HTGR, adsorpt. removal of CO_2 from He coolant 7-30514
 III-V semiconductor surfaces, virtual gap states and Fermi level pinning by adsorbates 7-2654
 incomplete crystals, surfaces, defects, interfaces and layered structures, theory 7-16926
 initial stages, He scatt. study 7-59365
 ionic, 2 parallel capacitors model 7-32786
 kaolinite, of alkali metal ions, free energy, additivity rules (*German*) 7-2233
 kinetics and energetics studies at surface and interfaces 7-2422
 linear chain of adsorption sites, desorption, kinetic ising model 7-21649
 liquid films, adsorption on porous substrates, thermodynamic stabilities 7-12408
 metal films, work functions, coverage dependence 7-38676
 metal substrates, adsorption of alkali metals, influence of adsorbate coverage on work function 7-2669
 metal substrates, interaction of H 7-21670
 metal surface, field adsorbed He and Ne, atom-probe spectroscopy studies 7-32803
 metal surface, interaction with dipole, electronic struct. calcs. 7-2663
 metal surfaces, adsorbate binding 7-12491
 metal surfaces, field adsorption of rare gases 7-21648
 metal surfaces, inverse photoemission studies, review 7-59279
 metals, adsorbed H_2 , kinetics model of chemisorption layer (*Korean*) 7-32813
 metals, chemisorbed CO, affinity levels, energy and composition 7-59780
 nuclear fuel reprocessing, dissolver off-gas treatment, use of mineral zeolite as nitrogen oxides adsorbent 7-30575
 organic materials, crystal growth kinetics, tailor-made additives influence 7-58171
 organic substance adsorption on Hg electrode, electromag.-radiation study 7-13805
 overlayer formation, Auger peak-to-peak height corrections 7-27832
 particles adsorbed on spherical surface, statistical thermodynamics, canonical ensemble 7-41231
 photoelectron spin-polarisation spectroscopy, appl. in adsorbate physics 7-3145
 phthalocyanine thin films, gas-surface reactions, elec. cond. meas., ESCA 7-52262
 polyacetylene- I_2 complexes, monosubstituted, isomerism, elec. cond., UV spectra 7-45289
 polyarylate-polydimethylsiloxane rigid block copolymers, domain struct., electron microscopy (*Russian*) 7-63520
 polycrystalline materials, intercrystalline internal adsorption, terminology (*Russian*) 7-58611
 polyethylene glycols, adsorpt.-exclusion behaviour during chromatography (*Russian*) 7-23095
 polymer chain adsorption on small particles investig. (*Russian*) 7-36832
 porous catalysts, temp.-programmed desorpt., modeling and expt. verifications 7-13799
 porous minerals, N_2 adsorption, isotherm calcs. 7-6969
 PTFE surface chemical struct. and adhesive props., effects of low-energy electron bombardment 7-44963
 pyridine, Ni(II) and Fe(III) individual and binary hydroxides and oxides, gas chromatography and IR spectra study 7-39917
 random sequential adsorption in one and two dimens., geometry 7-9762
 random sequential adsorption onto the surface of small spheres 7-44994
 rhodamine 6G solns., adsorpt. effect on UV absorpt. spectra 7-39142
 rubber solutions, inverse sedimentation of glass-phenol formaldehyde resin hollow microspheres 7-38325
 sapphire surface, long range interaction between rare gas atoms/molecules and surfaces, calc. 7-3135
 self-induced adsorption, surface vacancy generation 7-44993
 semiconductor electrodes, adsorption, review 7-16867
 semiconductor film growth kinetics under simultaneous doping conditions 7-45052
 semiconductor surface chemistry, adsorption and desorption kinetic meas. combined with Auger spectroscopy 7-65348
 semiconductor surfaces, interaction with H_2 7-58632

adsorption continued

- semiconductor-fluid interfaces, illum., adsorption, competition for photogenerated charge carriers 7-27105
 silica gel, of O_2 , photoform., rot. dynamics, ESR obs. 7-25566
 simple cubic lattice, inelastic scatt. and trapping of an atom 7-27122
 simple fluids in cylindrical and slit-like pores, capillary condensation and adsorption 7-32756
 simple metals, physisorption interaction of H_2 7-12480
 soil, adsorption of sulphate, role in long-term sulphate dynamics 7-29102
 solid solutions, surface composition, multilayer adsorption 7-6938
 solid surfaces, chemistry and physics, book 7-60891
 steel, stainless, SO_2 and CO adsorpt. kinetics and laser-stimulated surface oxidation 7-63958
 submonolayer ordering and multilayer adsorption, simple lattice gas models 7-12490
 substrate size, effect on adsorption binding energy 7-38339
 surface struct. determ. using angle-resolved photoemission extended fine struct. 7-7822
 surfactant mixtures, immiscible ideal solns., ideal interfacial layer 7-6921
 transition metal surfaces, dissociative adsorption of H_2 , effect of impurities 7-16876
 trifluoromethanesulphonic acid electrolyte in fuel cells, O solubility, diffusion coeff., reduction rate, adsorption on Pt surface 7-28395
 two-phase three component solns., interfacial tension 7-6923
 ultrafiltration, membrane-solute interactions effects on pure solvent transfer 7-54177
 vacuum microbalance, automated, for adsorption isotherm meas. 7-41397
 vacuum symposium, Tokyo, Japan (1985) (*Japanese*) 7-14698
 vapour-pressure isotherms, high-precision, apparatus errors and results 7-56252
 water adsorpt. on SiO_2 gels, viscosity determ. by pulse NMR method 7-7604
 weak ferromagnet surface, ground state, influence of adsorbed gas molecules 7-45596
 zeolites, conf., Burgas, Bulgaria (June 1985) 7-60885
²² NaCl, aq. soln., adsorpt. and diffusion at low concs. 7-27106
 {100}, of I, surface phases, SEXAFS, multishell simulation anal. 7-59303
 Ag (100), of Cl, Auger, LEED, XPS, thermal desorption studies 7-58635
 Ag (110), adsorption of ethylene and ethylene oxide, work function, LEED, UPS, TDS meas. 7-52270
 Ag (110), clean and O_2 covered, adsorption and reaction of acetonitrile 7-28344
 Ag (110), He selective adsorpt., bound-state reson. meas., interaction pot. electron density depend. 7-21631
 Ag (110), O and O_2 adsorption, dispersion, bonding and precursor state 7-6991
 Ag (110), of ethylene oxide, surface interactions, XPS, TDS, AES, EELS studies 7-33963
 Ag (111), Frank-Van der Merwe growth of Pd, AES, surface reflectance spectra studies 7-32829
 Ag electrode, competitive adsorption of pyridine and monosubstituted pyridine, SERS study 7-22267
 Ag film, of lauric acid, reflectivity and laser excited surface plasmon spectroscopy meas. 7-45011
 Ag, of cyclopentene, on stepped (221) surface, mol. orientation 7-27099
 Ag, of pyridine, on (110) surface, coverage-depend, phase transition, SHG obs. 7-37029
 Ag thin film, resist. increase during O_2 adsorpt., surface roughness effects calcs. 7-45519
 Ag-Au, external surface adsorption isotherm 7-6978
 AgCl, of 3,3'-dimethyl-9-ethylthiacarbocyanine dyes, XPS study 7-33964
 Al surface, plasma oxidised, adsorption of benzoic acid and benzaldehyde, SIMS and XPS 7-65351
 Al- AlO_3 -Pb tunnel diode, $NiCl_2 \cdot 6H_2O$ soln. phase adsorpt., inelastic electron tunnelling spectra 7-12877
 Al_2O_3 , adsorpt. of acridine and phenazine, tunnelling spectra study 7-52264
 Al_2O_3 , methanol adsorpt. Fourier transform IR spectra 7-38345
 Ar small clusters, sticking coeff. of Ar 7-64861
 As_2S_3 thin films, dissolution investig., surfactant effects 7-6802
 Au (110), clean and oxidised, adsorption and oxidation of CO and CO_2 , surface reactions 7-59782
 Au (110), clean and oxidised, adsorption of formic acid and formaldehyde, acid-base and nucleophilic reactions 7-59783
 Au ion beam, residual ranges in various media, time of flight spectra and adsorption meas. 7-25333
 Au, smooth surface with adsorbed crystal-violet molecules, resonant Raman scatt., charge-transfer excitation 7-17320
 BN surface, long range interaction between rare gas atoms/molecules and surfaces, calc. 7-3135
 Bi electrode, single cryst., of butyl acetate 7-52239
 Bi, electrodes, polycrystalline, adsorpt. of cyclohexanol 7-32785
 Bi of K, in alcohol solvents 7-52238
 Bi, single cryst., adsorpt. of tertiary butyl alcohol 7-32784
 C, activated, adsorption of Ag, mathematical model 7-44999
 C, activated, heterogeneity, benzene adsorption 7-28342
 C electrodes, of Cl, theory 7-12462
 C-K, NO adsorpt. and reduction 7-63946
 CO adsorption on Cu (111)-Fe cryst. 7-21616
 CO_2 wall, Ar wetting transitions, density functional theory and modified hypernetted chain calcs. 7-63913
 CaF_2 surface, long range interaction between rare gas atoms/molecules and surfaces, calc. 7-3135
 CdS surface, of rhodamine B mol., kinetic and binding energy determ. (*Russian*) 7-21667
 CdTe, electrodeposition from acidic aq. solns., voltammetry 7-27188
 Ce (001), H_2 adsorption, initial stages of hydride form., UPS, LEED and EELS studies 7-21629
 Co catalyst, O_2 adsorpt. and oxidation of Si at $CoSi$ (100) surfaces 7-46865
 Co foil surface, preadsorbed K, CO adsorption, XPS and AES studies 7-8296
 Co surface, metal atom catalysed oxidation, UPS and AES studies 7-46865
 Cs-Sb-based photocathodes, stability and O adsorption energies 7-38344
 Cu (10,10) and (510), of Pb, faceting, LEED, AES studies 7-32828
 Cu (100), of S, (2 \times 2) surface struct., LEED anal. 7-32827
 Cu (100), Pb epitaxial growth, thermal He atom scattering 7-52351

adsorption continued

- Cu (100) and (110), formate adsorption, bonding, EXAFS studies 7-38341
 Cu (110), of H, adsorbate movement-induced subsurface reconstruction, LEED and atom diff. meas. 7-27114
 Cu (110) stepped Faces, O_2 adsorption 7-27132
 Cu (110) surface, K doped, CO adsorption, EELS study 7-7006
 Cu (111), of Cl, surface struct., SEXAFS, photoelectron diff. studies 7-64775
 Cu (111), of TCNQ, vibr. spectra, EELS, work function meas. 7-52228
 Cu (111) and (110), atomic adsorption of O, inverse photoemission study 7-7783
 Cu (111) surface electronic struct., perturbations induced by adsorption of K 7-52720
 Cu (111) with Ni overlayers, CO adsorption studies 7-21658
 Cu (111)-Fe surface alloys, prep. and oxidation 7-22870
 Cu bright plating electrodeposition kinetics, adsorption on cathode surface (*Russian*) 7-33942
 Cu cluster surface, of Na atom, SCF ab initio and Cl calcs. 7-52259
 Cu electrode, of halide ions, electroreflectance obs. 7-13132
 Cu particles, ZnO-supported, of CO, ethylene, and $CO-N_2O$ mixtures, vibr. spectra, operation of metal surface selection rule 7-53350
 Cu plates, monomer films form. and polymerisation 7-65347
 Cu-Ni, external surface adsorption isotherm 7-6978
 Fe (110), (111) and stepped (110), of CO_2 , UPS, work function meas. 7-12484
 Fe (111), CO_2 adsorption and dissociation, ARUPS 7-63961
 Fe films, ethane and ethylene adsorpt. and reaction, mass spectra, XPS, UPS, electrical resistance and work function meas. 7-32837
 Fe microcrystals on SiO_2 , adsorption of H_2 , positron annihilation studies 7-39311
 Fe, passive, adsorption and absorpt. of Cl^- ions 7-28340
 Fe, pitting corrosion, role of Cl^- ions (*Japanese*) 7-33829
 Fe, surface, H_2 and N_2 interactions, pulsed laser atom probe studies 7-32811
 Fe surface, polycryst., interaction with $O_2(N_2)$, electron spectrosc. obs. 7-7794
 Fe surface oxide layer, reduction by H adsorption, AES and LEED studies 7-8297
 Fe-base alloys, grain boundary internal adsorption of C and P, segregation study (*Russian*) 7-6961
 Fe-based amorphous alloys, O_2 adsorption, ion bombardment effects 7-21637
 Fe-Mn(S), surface comp. and surface tension, effect of S and Mn (*Chinese*) 7-6916
 $Fe_{14}Nd(Y)(Ce)_2B$, or H, fine particles prep., mag. props., recording appls. 7-53660
 GaAs (110), oxidation, photoemission spectra studies 7-3147
 GaAs (100), ambient induced surface effects, O adsorption, photolum., conductivity 7-45429
 GaAs (110), adsorption of Al, soft X-ray photoemission spectra study 7-53494
 GaAs (110), O_2 adsorption, electronic props., contact pot. meas. 7-2353
 GaAs (110), of O_2 , confirmation of two-step uptake model 7-2355
 GaAs (111), alkali metal covered, adsorption of O_2 7-63957
 GaAs molecular layer epitaxy, UV light effects, photo-assisted reactions and adsorpt. phenomena (*Japanese*) 7-7048
 GaAs surface, H_2S adsorption, orientation and temp. depend. 7-58634
 GaP-electrolyte interfaces, Fourier transform IR spectroscopy 7-27124
 Ge (100), H adsorption, high resolution energy loss spectra study 7-38331
 Ge surface, H_2S adsorption, orientation and temp. depend. 7-58634
 H adsorption and desorption on milligram samples 7-6981
 H, adsorpt. on La-Mg alloy, H storage investig. 7-52241
 H_2 , adsorbed by metals, kinetics, oxide layer effects at room temp. 7-33965
 H_2 , adsorption on $LaNi_5$ oxide surface layers, kinetics 7-32833
 H_2 , adsorption rate at H_2 - $LaNi_5$ interphase, diffusion coeff. eval. 7-32696
 H_3PO_4 electrolyte in fuel cells, O solubility, diffusion coeff., reduction rate, adsorption on Pt surface 7-28395
³He-He surfaces, adsorption energy of spin polarised at. H, relax. and recomb. processes 7-44949
⁴He superfluid saturated film, spin polarised H thermal accommodation meas. 7-38299
⁴He-³He binary liquid mixtures, complete wetting 7-27049
 Hg electrode-soln. interface, 2-anion simultaneous adsorpt., elec. double layer parameters algorithm 7-54132
 Hg_2Cl_2 , photocatalytic props., O_2 photogeneration from water 7-54151
 InAs (110), oxidation, correlated changes of electronic surface props. 7-2354
 InP (100), ambient induced surface effects, O adsorption, photolum., conductivity 7-45429
 InP (110), oxidation, photoemission spectra studies 7-3147
 Ir (111) with graphite monolayer, adsorbed Cs atoms, photo- and electron-stimulated deformation of monolayer 7-58627
 K films, of H_2O , XPS, UPS, work function meas. 7-12485
 KCl, films CO adsorpt., IR investig. 7-63945
 KH_2PO_4 , crystal growth spiral morphology on {100} surfaces; impurity effects, step kinetics 7-16459
 $KMnO_4$, thermal stability changes upon adsorption of water vapour in an electric field 7-8262
 LaB_6 (001), adsorption of Cs, surface structure and work function 7-6977
 LaB_6 (001), field evaporation in the presence of H_2 , atom probe FIM 7-21652
 $LiAlO_2$ surface adsorpt. isotherms, T inventory appl. 7-52246
 LiF surface, long range interaction between rare gas atoms/molecules and surfaces, calc. 7-3135
 Lil impinging Re surface, surface ionisation in high vacuum, work function increases due to adsorpt. 7-46264
 MgO , adsorption induced luminescence, O atomic and mol. beams 7-13231
 Mo (100), adsorption of Ba and O, electron spectroscopy for quantitative anal. 7-13278
 Mo (100), chemically modified, chemisorption bond energies of Lewis acids and bases 7-23056
 Mo (100), chemically modified by adsorption of B, C, O, CO, surface atom oxidation states, ESCA meas. 7-28333
 Mo (110), O_2 adsorption, temperature-related aspects 7-12464

adsorption continued

- Mo, adsorption of Ba and Cs, bonding energies, thermionic emission studies 7-12463
 Mo, sticking coeffs. of O₂ and N₂, meas. by cathode sputtering 7-12476
 Mo surface, struct. phase transitions 7-2327
 MoO₃, adsorption of methanol, influence of photoinjected H on adsorptivity 7-63942
 MoS₂(0001), Ar⁺-sputtered, adsorption props., LEED, AES, EELS, and work function studies 7-52275
 N₂ on Fe and Re crystals, adsorpt. and dissoc., EHT calcs. 7-56988
 Na surface, of O₂, photoemission and Auger studies 7-17063
 Na₂CaAl₂Si₂O₁₂·6H₂O, zeolite, adsorption and desorption of ethylene, TPD study 7-32826
 NaCl surface, nucleation and growth of Au-Cu alloys from vapour phase 7-39391
 Na₂O-11Al₂O₃, β -alumina, effect of NO₂ sorption on electrical conductivity 7-21511
 Nb, adsorbed H₂, kinetic model (*Korean*) 7-32814
 Nb, adsorption of Ba and Cs, bonding energies, thermionic emission studies 7-12463
 Ni (100), adsorpt. of CO and D, diffusion, investig. 7-6960
 Ni (100), adsorption of CO, C₂H₄, O₂ or H₂, X-ray induced secondary electron emission 7-27866
 Ni (100), clean and O covered, adsorption and decomposition of N₂O 7-58644
 Ni (100), coadsorption of H₂ and CO 7-27117
 Ni (100), Cu overlayer growth, X-ray induced secondary electron emission meas. 7-27865
 Ni (100), H₂ dissociation dynamics, quantum mechanical study 7-54168
 Ni (100), K treated, rare gas physisorption, wetting, photoemission spectra 7-32822
 Ni (100), of CO, poisoning in heterogeneous catalysis, role of electronegativity 7-13818
 Ni (100), of ethylene, determ. of adatom abundance using elastic recoil detect. anal. 7-33984
 Ni (100), S-covered, adsorption of NO 7-6990
 Ni (110), adsorption and reaction of CO₂ and CO₂/O co-adsorption 7-52289
 Ni (110), adsorption and thermal decomposition of NH₃, isolation and identification of NH₂ and NH 7-6986
 Ni (110), coadsorption of O and water, EELS study 7-32821
 Ni (110), of D₂, LEED, TDS, RBS, nucl. reaction anal., work function meas. 7-58638
 Ni (110), of H, overlayer ordering, embedded-cluster model anal. 7-52256
 Ni (110), of O, electron stimulated ion desorption O⁺ yield meas. 7-12487
 Ni (110), of O, surface phases, absolute coverages 7-12486
 Ni (111), adsorption and reactions of methyl thiocyanate 7-21640
 Ni (111), CO adsorption, well defined gas-solid interphase, statistical rate theory approach 7-21655
 Ni (111), coadsorption of NH₃ and CO, multilayer formation studied by metastable quenching spectroscopy 7-21639
 Ni (111), H₂ and D₂ adsorpt. isotope effects, kinetic investig. 7-21624
 Ni (111), N₂ adsorption, XPS, UPS, work function and TPD studies 7-52272
 Ni (111), of Te, adsorbate induced C segregation and dissolution 7-12477
 Ni (111), ordering of acetylene and ethylene, LEED, EELS 7-52269
 Ni (115), of H₂, surface corrugation effects, He diff. study 7-2381
 Ni {100}, of I, surface phases, SEXAFS, breakdown of Fourier filtering single shell anal. 7-59304
 Ni films, adsorption of benzonitrile and alkyl cyanides, XPS 7-52288
 Ni, films, ethane and ethylene adsorpt. and reaction, mass spectra, XPS, UPS, electrical resistance and work function meas. 7-32837
 Ni, H permeation, diffusion and surface rate coeff., press.-modulated adsorpt.-desorpt. 7-58612
 Ni, of ¹²CO(¹³CO), surface charactn. by Raman spectroscopy 7-42625
 Ni, of N₂, on (110) surface, FT IR refl.-absorpt. spectrosc. obs. 7-27100
 Ni, of S, surface geometry, low energy ion scatt. determ. 7-53474
 Ni, polycryst., adsorption-desorption of CO, kinetics 7-16873
 Ni₃B, amorphous, surface electronic struct. during crystallisation and O₂ and CO adsorption 7-7308
 Ni₅₀Fe₅₀ (100) alloy, segregation and adsorption of S 7-21617
 Ni₆₀Fe₄₀ (100), initial oxidation and sulphidation, LEED study 7-58641
 NiO (100), of CO, ethylene and H₂O, surface reactions 7-23055
 NiO, of NO, IR transmission spectra, calorimetry studies 7-58640
 Np migration in salt brine aquifers 7-40056
 O adsorption and desorption on Sn-Sb₂O₃ catalyst kinetics 7-63944
 O₂ adsorpt. on GaAs, UPS 7-59371
 Pb electrodeposition from aq. HCl soln. onto Pt (111) 7-27954
 Pd (001), H adsorption, coverage depend. props., ab initio calcs. 7-38340
 Pd (100), adsorption of cyanogen, Penning ionisation electron spectroscopy, UPS, TPD studies 7-52268
 Pd (100), clean and S covered, adsorption and desorption of NO, surface reactions, TPD, EELS, LEED 7-58639
 Pd (100), of cyanogen, Penning ionisation electron spectroscopy, UPS, TPD studies 7-52268
 Pd (100) with Na (NaO) overlayers, adsorption of methanol, formaldehyde and formic acid 7-21657
 Pd (110), adsorbed states of O, EELS and LEED study 7-27115
 Pd (110), O₂ adsorption 7-52274
 Pd (110), of H, overlayer ordering, embedded-cluster model anal. 7-52256
 Pd (110), of O₂ at 300K, LEED and EELS studies 7-27093
 Pd (111), CO and O co-adsorption, SIMS and TPD studies 7-27137
 Pd (111) and (100), hydrogenation of adsorbed CN 7-6985
 Pd, adsorbed CO, vibr. spectra 7-12475
 Pd films, adsorption of benzonitrile and alkyl cyanides, XPS 7-52288
 Pd, H permeation, diffusion and surface rate coeff., press.-modulated adsorpt.-desorpt. 7-58612
 Pd, small crystallites, effect of particle size on stoichiometry of CO adsorption 7-6984
 Pt (110), catalytic CO oxidation, kinetic oscillations 7-28346
 Pt (110), water adsorption 7-21644
 Pt (111), coadsorption of K and CO, structural and vibrational studies 7-52266
 Pt (111), contaminated with Si or oxidised Si, interaction with water 7-27134
 Pt (111), O adsorbate-induced surface-phonon softening 7-58600

adsorption continued

- Pt (111), of ethylene oxide, surface interactions, XPS, TDS, AES, EELS studies 7-33963
 Pt (111), Xe adsorption, thermodynamic meas. 7-6982
 Pt, adsorbed CO, vibr. spectra 7-12475
 Pt anode in fuel cell, performance in presence of CO and CO₂, CO poisoning adsorption parameters calc. 7-13855
 Pt anode in phosphoric acid fuel cell electrolyte, H₂S poisoning 7-46933
 Pt, catalyst particles, adsorbed S-induced faceting, TEM study 7-27109
 Pt electrode, in anhydrous methanol solns., added water effects 7-33936
 Pt electrodes, of CO, vibr. spectrum, electrochemical pot., stark tuning rate 7-10570
 Pt, electron stimulated adsorption, of vapour 7-63955
 Pt, of Bi, on (111) surface, growth modes, spectrosc., LEED and work function investig. 7-27102
 Pt, of CO, reaction with O, surface catalysed reaction, surprisal anal. 7-3601
 Pt surface, graphite island form., FEM, SEM and AES studies 7-32805
 Pt, surface (110), deuteration of adsorbed pyridine, EELS study 7-7006
 Pt, surface structure and adsorbate bonding, NMR studies 7-13050
 Pt/TiO₂ thermally treated model catalysts, CO adsorption 7-54184
 Pt-Rh surfaces, N₂ and CO adsorption, temp. depend. and work function studies 7-33960
 Pt-S surface, effect of S-induced surface reconstruction on CO adsorption 7-6987
 Ra adsorptive uptake by waste inactive microbial biomass 7-40313
 Rh (100), coadsorption of CO and H₂, adsorbate-adsorbate interactions effects 7-44997
 Rh (111), coadsorbed of CO, O and NO, EELS 7-16860
 Rh (111), NO adsorpt. and dissoc., EELS and LEED study 7-16859
 Rh surfaces, adsorption and desorption of NO, effect of surface structure 7-6994
 Rh surfaces, clean and B contaminated, adsorption and dissociation of H₂O 7-27135
 Rh(110), adsorpt. of H(D), form. of high density chemisorbed phase, LEED investigations 7-27094
 Ru (001), alkali modified, adsorption of O, TDS, AES, EELS, work function meas. 7-58637
 Ru (001), chemisorption and rot. epitaxy of Li, LEED, TDS obs. 7-12479
 Ru (001), clean and O covered, of NO₂, EELS, thermal desorption mass spectrometry 7-52267
 Ru (001), coadsorption of H₂O and Li 7-21645
 Ru (001), H₂ chemisorption, effect of coadsorbed O₂, LEED spectra anal. 7-33959
 Ru, of ethylene, on (001) surface, H₂(CO₂) coadsorpt. effects 7-32789
 SO₂ removal by injected limestone sorbents, graphite element drop-tube reactor design 7-22978
 Si (100), adsorption of H₂O, photon stimulated ion desorption surface EXAFS 7-58633
 Si (100), exposed to CO, CO₂, O₂, NO and SO₂, photodesorption 7-52290
 Si (100), of H₂O, surface struct., photon stimulated ion desorption SEXAFS determ. 7-64752
 Si (100), reaction with propylene, adsorption and desorption kinetic meas. combined with Auger spectroscopy 7-65348
 Si (100) and (111), of K, AES, work function meas. 7-32818
 Si (100)-(2×1), adsorption kinetics of propylene, propane and methane, chemical activity of C=C double bond 7-27127
 Si (100)2×1, adsorbed H, surface structure, high resolution, IR spectroscopy 7-13169
 Si (111), acetylene adsorpt., rehybridisation, vibr. investig., EELS 7-17816
 Si (111), adsorbed Mo(CO)₆, laser induced electronic excitation followed by CO desorption 7-12470
 Si (111), Ge adsorption, $\sqrt{3} \times \sqrt{3}$ adatom models 7-7008
 Si (111), metal atom catalysed oxidation, UPS and AES studies 7-46865
 Si (111), of H, electronic struct. calcs. 7-27377
 Si (111)7×7 surface, total-energy calcs. for Takayanagi model 7-2345
 Si, CVD, adsorption on Si (111) of Si-H system species, rel. to temp., supersaturation, bond strength and press. 7-33583
 Si cleaved surface, of ethylene, high resolution EELS study 7-63951
 Si, kinetics of growth of SiO₂ layer, optical props. 7-17740
 Si, plasma passivated, subsurface H barrier layer obs. after surface adsorption of Al 7-17745
 Si surface, etching by HCl/H₂ mixtures, low pressure gas composition 7-65221
 Si surface, of benzene and pyridine, temp. depend., annealing effects on sorption states 7-2360
 Si surface, of O, orientation depend., AES and photoelectron spectra 7-52237
 Si surface, reaction with propylene, effect of addition of H 7-54187
 Si surface etching by HCl/H₂ gas mixtures 7-65220
 Si surface layers characterisation after annealing in an RF H plasma 7-58630
 Si surfaces, (100) and (111), XeF₂ exposure, F coverage, XPS studies 7-2379
 Si surfaces, adsorbed C, annealing behaviour, XPS and AES studies 7-27108
 a-Si:H/a-SiO₂:H superlattice micropores, pyrene molecules adsorption and confinement 7-27112
 SiO₂, deposition from SiH₄-N₂O, role of adsorption stages 7-17447
 Si-electrolyte interface, Fourier transform IR spectroscopy 7-27124
 Si-SiO₂ interface formation by catalytic oxidation using adsorbed alkali metals 7-54017
 a-Si_{1-x}C_x-x:H films, adsorbates influence on conductance, surface state 7-33115
 SiO₂, deposition from SiH₄-N₂O, role of adsorption shapes 7-17447
 SiO₂ in aqs. solns. of cetylpyridinium bromide and inorganic salts, coagulation, thermodynamic stability 7-8326
 SiO₂ in NaCl solns., surface pot., polyoxyethylene soln. influence 7-6968
 SiO₂, vitreous, surface, adsorption and thermal accommodation of Pt single atoms 7-27133
 SiO₂, with adsorbed OH, FTIR characteris. 7-46042
 SiO₂:Na with adsorbed SO₂ and H₂S, FTIR and Raman spectra obs., Na promotion of Claus process 7-46869
 Si(111), adsorption of ethylene, vibr. study 7-45012
 SnO₂-Pd-Sb H₂ gas sensor insensitive to alcohol (*Japanese*) 7-56242
 SrTiO₃ (100), of H₂O, surface struct., photon stimulated ion desorption SEXAFS determ. 7-64752
 TiFe, of O, AES study 7-59312

adsorption continued

- Ti₄Fe₂O₇, of O, AES study 7-59312
 TiNi, of O, AES study 7-59312
 UO₂(SO₄)₃ solution, adsorption equilibrium study 7-25084
 V, sticking coeffs. of O₂ and N₂, meas. by cathode sputtering 7-12476
 V₂O₅, adsorption of methanol, influence of photoinjected H on adsorptivity 7-63942
 (VO)₂P₂O₇, adsorpt. of H₂O and pyridine, IR spectra 7-17818
 W (001), H adsorption, commensurate-incommensurate phase transitions 7-7010
 W (001) clean surface, reconstruction transition, effect of surface steps and adsorbate-induced perturbations 7-6935
 W (100), C and Si coadsorption, Auger spectra studies 7-63954
 W (100) and (110), of H, very low electron energy refl. study 7-12488
 W (100) and (110), of O₂, low temp. adsorpt. kinetics and weakly-bound states, molecular beam technique studies (*Russian*) 7-16871
 W (110), adsorption of Eu, Gd and Tb 7-27118
 W (110), field adsorption and desorption of H, atom probe FIM 7-21647
 W (110), MBE growth of BaO films 7-16886
 W (110), of Cu, Ag and Au, calcs. based on nonadditive effective binding pot. 7-12483
 W (112) face, arrangement and thermal stability of O adsorption states 7-6975
 W, He field adsorption and evaporation 7-32802
 W point single crystal, Lu and Ba adsorption, field emission characteristics 7-12466
 W, sticking coeffs. of O₂ and N₂, meas. by cathode sputtering 7-12476
 W surface, field adsorption of He 7-32816
 W surface, He fluid adsorption and diffusion, atom-probe field ion microscopy studies 7-32808
 W surface, Hg absorption, field emission microscopy studies 7-32804
 W surface, struct. phase transitions 7-2327
 WO₃, adsorption of methanol, influence of photoinjected H on adsorptivity 7-63942
¹³⁵Xe adsorption on activated charcoal, effects of water vapour 7-40076
 (YEuTmCa)₃(FeGe)₂O₁₂, epitaxial films, O ion adsorpt. bubble diameter variation effect 7-22125
 ZnO, of vibr. excited O₂, interaction 7-15692
 ZnO-Na₂O-Al₂O₃-SiO₂, zeolite, partially exchanged, IR and neutron scatt. studies of adsorbed ethene 7-7001
 Zr cathode, material and structural changes during arc operation in N₂ 7-46866
 ZrSiO₄, burnt zircon with alkali hardeners, humidity sensitivity 7-18793

aerials see antennas

aerodynamics

- see also compressible flow; flow; hypersonic flow; jets; shock waves; supersonic flow; transonic flow; turbulence; wind tunnels
 3D hypersonic rarefied gas flow around rotating bodies 7-20761
 actuator disc analysis of unsteady subsonic cascade flow 7-1464
 aeroacoustic high intensity field meas. using cooling power anemometer 7-16039
 airfoil cascades, hybrid aerodynamic problems, variational principles 7-43963
 airfoil with oscillating flap, unsteady wake meas. at transonic speed 7-51208
 airfoils, intersection of jets 7-37238
 algebraic multigrid method (AMG) applied to fluid flow problems 7-37487
 annular cascade oscill. in transonic flow, unsteady aerodynamic characts. 7-37490
 atmospheric gliding entry, heating, scaling relations 7-51200
 automobile deceleration force by the coast-down method 7-18541
 axial-turbine cascade, subsonic profile shape optimisation 7-11453
 axisymmetric vortex sound, acoustic wave field determ. 7-51182
 bird flight, calc. of lift, thrust and drag 7-18011
 Burger's eqn., convergence to steady-state of solns. 7-26234
 circular structures, aerodynamic forces, turbulence and 3D effects 7-11450
 coefficient, determ. using aerodynamic equivalence method 7-1586
 complex dependences approximation in averaging eqns., appls. 7-20758
 computational fluid dynamics in aeronautics, conf., Aix-en-Provence, France, (April 1986) 7-48191
 cylinder, circular, sectional aerodynamic calcs., free-stream turbulence scale effects (*Japanese*) 7-51206
 delta wing, ascent of Ferri point on upwind side 7-51213
 detached flow around profiles with ang. points, computer modelling 7-43924
 detonation shock waves, transonic flow behind wave front, stationarity conditions 7-63174
 drag, transient, induced 7-6235
 dust particles, deposition, interaction with shock wave 7-1610
 entropy layer absorption effect on supersonic flow heat transfer of sub-merged circular cone 7-43975
 Euler eqn. calcs., zonal-boundary scheme 7-20676
 finite state modelling 7-51199
 flycasting mechanics, flyline investig. 7-50
 force exerted by loop vortex motion, aerodynamic sound theory 7-1577
 gas distributor plate of fluidised and bubbled beds, aerodynamical modelling 7-57916
 gas dynamics, quasi-equilibrium, thermodynamic theory 7-51204
 gas-dynamics equations, invariant difference schemes (*Russian*) 7-63173
 gasdynamic flow form. for colliding plates at sharp angle 7-63169
 high temperature gases in annular channel with cold walls, heat transfer in turbulent flow (*Russian*) 7-1557
 horizontal axis wind turbines anal. using vortex lifting line method 7-63171
 industrial and building aerodynamics, conf., Aachen, Germany (June 1985) 7-14699
 internal flow, Navier-Stokes eqn. num. soln. (*French*) 7-57872
 inviscid axial flow in compressor rotor, leading-edge effects, flowfield meas. 7-11562
 inviscid incompressible flow, wake rollup behind wing, vortex panel calc. 7-20732
 isentropic gas dynamic eqns., simplified Godunov schemes for 2X2 systems of conservation laws 7-51229
 isentropic gas dynamics, rarefaction waves, vacuum state 7-57871
 isentropic gas flows, 2D, of double-wave type, classification 7-1581
 jets, turbulent, influence of mode composition of acoustic perturbations 7-62945

aerodynamics continued

- laminar incompressible separated flows, iterative boundary-layer-type solver 7-11380
 lifting force on aerofoil, companion of explanations 7-48234
 lifting surface theory, singular functions, integration 7-6237
 local interaction theory, aerodynamic calc. 7-43971
 mesh generation by a sequence of transformations 7-51201
 meteoroids ablation, radiative heat exchange determ. using radiant heat conduction approximation 7-34948
 minimum entropy principle in the gas dynamics equations 7-26235
 multi-element aerofoils, hybrid subcritical and supercritical flow method 7-16203
 multielement aerofoils, linearised theory, thickness, camber and stagger effects 7-37484
 nonconservative dynamical systems, stability criteria, appl. to wing flutter 7-18590
 oscillating airfoil, stall process, method for computing flow fields around moving bodies 7-65789
 oscillating cascades, unsteady flow, asymptotic solns. 7-37437
 polytropic ideal gas, nonfixed on the boundary, 1D motion 7-11449
 radiative heat fluxes in supersonic flow of inviscid gas over 3D bodies 7-43972
 rotary-wing aeroelasticity, time-domain unsteady aerodynamics appls. 7-20686
 separation structures on cylindrical wings (*French*) 7-11451
 shock wave propagation, in tube, boundary disturbance form. 7-31838
 shock-free transonic airfoils with a given pressure distribution 7-26312
 solid bodies, motion in atmosphere, numerical study (*Russian*) 7-63172
 spinning baseball, lateral force study 7-48231
 stream suction problem, singular integral eqn. of singular function type, numerical soln. (*Russian*) 7-26305
 subsonic bluff-body flows, wake periodicity 7-31807
 supersonic flow around semi-infinite plate, Navier-Stokes eqns. 7-11456
 swirled working fluid flow, aerodynamic calc. 7-6219
 time-dependent aerodynamics, transonic speeds on an aerofoil 7-6241
 trailing-edge mesh influence on skin friction, Navier-Stokes calcs. 7-20740
 transonic, book 7-14717
 tube banks, staggered, heat transfer characts. in crossflow of air with varying temp. differences (*Russian*) 7-1556
 turbulent afterburning jets, temp. and conc. fluctuations, num. investig. 7-26362
 turbulent boundary layers, surface roughness effects and transition modelling 7-31769
 turbulent flow over nonrotating cylinder, press. distrib. and fluctuations meas. 7-43868
 turbulent flowfield visualisation, computer generated, for flow around cubic model 7-37447
 unsteady compressible viscous flow over airfoils, integro-differential and finite-difference methods 7-31821
 upstream cylinder vibr. effect on stationary downstream cylinder 7-16201
 viscous incompressible laminar flow, drag reduction, optimal control 7-57794
 vortex breakdown over delta wing (*French*) 7-11433
 wave propagation in a weakly dispersive medium, 1D wave eqn. 7-31825
 weak disturbance velocity measurement, bulk density in porous media 7-31826
 weakly swirled turbulent jet 7-20771
 wind turbines, multiple actuator disc theory 7-20743
 wing, potential flow, aerodynamic props., discrete vortex method anal. 7-11448
 wing, rotating, laminar boundary layer eqns. 7-11381
 wing, stationary turbulent boundary layer anal. 7-11397
 wing, symmetrical, thin, ground effect, lifting-line solution 7-6234
 wing profile, flow separation, aerodynamic hysteresis 7-57870
 CO₂ laser, TE CW, influence of electrical discharge homogeneity 7-50537
 H flame-out in air flow, gas dynamic struct., interaction effect 7-26315
 H₂-He mixture, radiant heat transfer body shape influence 7-20715
 SF₆ puffer-type circuit breakers, effects of aerodynamic shocks on performance 7-51223

aeroelasticity see elasticity

aeronomy see upper atmosphere

Aerosols see aerosols

aerosols

- see also foams
 2D blunt body sampling, mathematical theory, flow calcs. 7-31867
 AEROSIM-S code for dry aerosols, FBR containment appls., user manual 7-56723
 aerosol source terms in nuclear reactor accidents, ex-vessel fission product releases 7-36219
 Aerosol-OT, stabilised microemulsion, X-ray scatt. data, fractal anal. 7-54190
 aggregation phenomena and fractal aggregates (*French*) 7-9757
 airborne particles, ICP emission spectrometry investig. 7-54233
 airborne particles scavenging by collision with water drops, combined effects of microdynamic mechanisms 7-55200
 Antarctic, radiative heating due to stratospheric aerosols, implications for O₃ depletion 7-55175
 Antarctic polar stratospheric clouds and aerosols, SAM II meas. 7-55160
 Antarctic spring stratosphere; aerosol and temp. var., lidar obs. 7-60325
 Antarctic troposphere and stratosphere, balloon obs. 7-55225
 Arctic anthropogenic aerosols, climatic effects 7-55193
 Arctic polar stratospheric clouds, airborne lidar meas. 7-60334
 Athens, Greece, turbidity meas. and components 7-9174
 Atlantic Ocean, atm. aerosols temporal and spatial var. anal. 7-4085
 atmosphere, aerosol conc. changes in drops due to particle scavenging and redistribution by coagulation 7-55201
 atmosphere, aerosol extinction at Cerro Tololo Inter-American Observatory 7-47542
 atmosphere, aerosol inhomogeneities, lidar data anal. (*Russian*) 7-29132
 atmosphere, aerosol light extinction efficiency theory 7-14375
 atmosphere, aerosol profile in stratosphere between 1977 and 1984 AD 7-4136
 atmosphere, aerosol scavenging rate 7-55188
 atmosphere, As and Sb in aerosols over English Channel and N Atlantic 7-29075
 atmosphere, beam propagation through slab scattering media, small angle approx. 7-57237

aerosols continued

- atmosphere, coastal environment standard radiation atm. aerosol models 7-55259
- atmosphere, diurnal and annual vars. of water vapour and aerosols at Cagliari Astronomical Observatory 7-40547
- atmosphere, effect on climate (*Italian*) 7-60372
- atmosphere, El Chichon and "mystery cloud" aerosols in stratosphere and mesosphere 7-23803
- atmosphere, entry characts. of dust samplers used in British nuclear industry 7-40079
- atmosphere, hazy, radiative characts. 7-4182
- atmosphere, ice-forming nuclei concentrations (*Russian*) 7-18278
- atmosphere, late Quaternary aerosol concs: from Antarctic ice core record 7-55208
- atmosphere, lidar equation taking account of polarization, second order scattering and travelling time effects 7-60380
- atmosphere, measurement method for aerosol light absorpt. (*Russian*) 7-9221
- atmosphere, model evaluation with Brownian diffusion technique 7-4086
- atmosphere, observations of fine-disperse fraction of aerosol (*Russian*) 7-9083
- atmosphere, optical absorption coeff., meas. technique (*Chinese*) 7-18305
- atmosphere, optical props. and humidity effects (*Russian*) 7-29241
- atmosphere, particles photoelectric charging, implications for ion comp. and chem. reactions 7-28326
- atmosphere, polar organic compounds in particulates 7-14327
- atmosphere, polarisation-scatt. phase functions, one-parametric model (*Russian*) 7-29240
- atmosphere, pollutant aerosols, long-range transport anal. by particle-induced X-ray emission 7-4192
- atmosphere, Se and Te composition of aerosols of Missouri, USA 7-18273
- atmosphere, seasonal var. of methylarsenic compounds in airborne particulate matter 7-34638
- atmosphere, sulphate aerosol scavenging, 3D mesoscale model use 7-40059
- atmosphere, volcanic aerosol from El Chichon and lidar depolarization observations 7-29243
- atmosphere, volcanic eruption aerosol, horizontal transport and evolution modelling 7-23819
- atmosphere by Brazil, particulates in natural and urban atmosphere 7-34081
- atmosphere of Beijing, China, particulate dry deposition velocity (*Chinese*) 7-29219
- atmosphere of India, aerosol characts. at Pune and Srinagar 7-29180
- atmosphere of Tyohu, Japan, SO_4^{2-} and NO_3^- content in aqueous aerosols (*Japanese*) 7-47511
- atmospheric, multiwave laser sounding, review 7-34678
- atmospheric correlation-time measurements and effects on coherent Doppler lidar 7-60385
- atomiser electrostatic spray nozzle, aerodynamically shaped for insecticide selective deposition 7-51262
- black aerosol found in winter Atlantic coastal snow storms, NY 7-14318
- Brownian diffusion and particle coagulation 7-48564
- S California, vertical pollutant distrib. and boundary layer struct., airborne lidar obs. 7-3734
- Cenozoic temperature variations, stratospheric aerosol effects 7-34666
- charged particles, spatial correl., turbulence influence 7-8324
- cloud condensation nuclei, conc., obs. and prediction discrepancies 7-4088
- cloud condensation nuclei chem., anal. technique 7-3589
- coal fly ash radionuclides chemical anal. using alpha, gamma and X-ray fluorescence spectroscopy 7-23266
- collection of airborne pollution particles for analytical electron microscopy 7-17935
- conference, aerosols in science, medicine and technology, Garmisch, Germany (Sept. 1985) 7-9577
- conference on fission product behaviour and source term research, Snowbird, UT, USA (July 1984) 7-10
- corona field, charged aerosol particle motion 7-32156
- Cumbria, England, characts. of airflow, aerosols, precipitation and clouds in boundary layer 7-4096
- Denver, USA, winter haze modelling 7-34673
- drops, explosive vaporization under CO_2 laser beam irradiation 7-57388
- dry deposition of 4-50 μm dolomite particles on vegetation, flat surfaces and deposition gauges 7-4083
- dusty weak ionised gas, phys. and physicochem. props. 7-20841
- electric generator overheating, early diagnostics using data for release of aerosols in insulation (*Russian*) 7-59787
- electrodynamic thermogravimetric analyzer for aerosol particle kinetics obs. 7-3620
- electrohydrodynamic equations with dispersed phase particles with diffusion charging 7-1642
- electrostatic charging of solid particles and liquid droplets 7-26586
- environmental problems, mathematical models, book 7-60890
- exchange in remote troposphere 7-55224
- extinction properties of visible-, IR- and mm radiation (94 GHz) 7-9176
- fibre array polar nephelometer, scattered light phase functions meas. for atmospheric particles 7-23896
- flow and vapour characterisation by photothermal methods 7-51345
- fluorescence spectrometer for a single electrostatically levitated micro-particle 7-9905
- FOG-82, cooperative field study of radiation fog, exptl. design and results 7-9068
- fractal aggregates, imaging, in-line holograms, digital decoding 7-10884
- gravitational settling, turbulent flow field 7-51284
- gravitational settling in randomly orientated cellular flow fields 7-1616
- Great Dun Fell, England, meteorological conditions 7-34661
- haze, air quality and meteorologic conditions anal. w.r.t. aerosol conc. in USA 7-18303
- Helsinki, Finland, atm. radioactive aerosols size distrib. following Chernobyl accident 7-46978
- hydrodynamically interacting particles, thermophoretic motion calcs. 7-46874
- ice, microscopic filament form. in elec. field 7-14362
- ice nucleation studies of AgI-AgCl solid solns., X-ray diffr. obs. 7-58179
- ice-nucleating bacteria and delayed effects of cloud seeding with NaI 7-66239
- Indian monsoon radiative forcing model, role of stratospheric aerosols 7-55196
- irradiated atmospheric air, aerosol formation 7-11515

aerosols continued

- laser beam in medium containing droplets, nonlinear refraction phase compensation 7-4183
- laser Doppler anemometer, two-colour four-beam system, two-phase mist flow meas. 7-37581
- lidar system for atmospheric aerosol meas., design aspects 7-18320
- light scattering, 10.6- μm extinction coeff., forward-scatter meter 7-57238
- liquid aerosols, laser-induced breakdown, droplet size effects 7-44272
- liquid droplet aerosols in APS 3300, behaviour 7-59789
- liquid jets, breakup and atomisation, transient behaviour 7-51249
- LWR accidents, empirical aerosol correlations using MAAP 2.0 and 3.0 7-56722
- marine aerosols, actinide enrichment 7-3742
- Martian dust, MECA workshop, Tempe, Arizona (February 1986) 7-29603
- Martian limb hazes, vertical struct. from scattered light profiles 7-55513
- meteosat IR meas., surface and cloud-top temp. determ. atmospheric correction scheme 7-18310
- mica nuclear track microfilter cascade fractionator, industrial appl. 7-36408
- mica nuclear track microfilter props. for industrial aerosol meas. instrument 7-36407
- microparticles from Antarctic Dome C ice core samples, TEM study 7-55228
- Miyazaki Prefecture, effect of typhoons on sea salt deposition on insulators (*Japanese*) 7-66248
- monofuel, combustion, num. investig. 7-8283
- multicomponent aerosol modelling, numerical implementation for reactor accident mitigation 7-56800
- New Zealand, sea salt wind-borne transport and deposition, implications for corrosion 7-14361
- ocean water, synthetic, AES study using solution nebulisation 7-13835
- optical bistability of aerosol particle 7-43199
- optical stratification in turbid atmosphere, airborne meas. 7-47536
- organic neutral molecules, solubilisation in AOT inverse micelles in n-heptane, distrib. eval., fluoresc. quenching data 7-54191
- particle, transverse motion in a laser radiation field 7-46881
- particle agglomeration under action of high intensity acoustic field 7-20573
- particle charging process, electric field depend. 7-20786
- particle identification and classification by STEM 7-32242
- particles, spherical, thermophoresis at arbitrary Knudsen nos. 7-63185
- photochemical mist formation in Ob River valley, correl. with meteorological characts. 7-9136
- photoelectric aerosol sensor, chemical response to different aerosol systems 7-11514
- polar stratospheric clouds, characts. during form. of Antarctic O_3 hole 7-55163
- polycyclic organic matter in atm., evidence for transformation 7-3735
- radioactive, cryogenic sampling device 7-59902
- radioactive, IZV-3 radiation meters checking, Rn daughter products meas. 7-9220
- radioactive areas ventilation, filter testing, aerosol mixing 7-30727
- reactor accident, MAEROS model for multicomponent aerosol dynamics, uncertainty and sensitivity anal. 7-19411
- reactor aerosol behaviour, effect of hygroscopicity 7-42166
- Ross Island, Antarctica, aerosol, physical props. 7-60333
- sampler for atmos. aerosols, inlet sampling efficiency 7-65671
- sampling device for atmos. aerosols, tubular thin-walled inlet 7-65670
- sampling into vertical cylindrical sonde from immobile medium 7-34732
- SASCHA programme on fission product release under reactor core melting conditions, review 7-774
- sea-salt aerosols, lidar obs. rel. to struct. of unstable marine boundary layer 7-29133
- smoke injection into atmosphere during nuclear war, protracted climatic effects 7-66297
- solid aerosol particles, ideal and nonideal, use of aerodynamic particle sizer as real time monitor 7-59790
- solid particulates and aerosol droplets at entrance of pore, hydrodynamic and mol. wall interaction effects 7-51270
- soluble aerosols and gases, rainout lifetimes 7-55189
- South Pole, aerosol meas. at Amundsen-Scott Station 7-55226
- spherical particles at arbitrary Knudsen no., thermophoresis, gas-kinetic eqn. 7-44030
- St. Louis, summer aerosol, $(\text{NH}_4)_2\text{SO}_4$ contrib. to light scatt. 7-47538
- stratosphere, aerosol obs., balloon-borne polarimetric expt. 7-14373
- stratosphere, Antarctic springtime meas. of O_3 , NO_2 and aerosol extinction by SAM II, SAGE and SAGE II 7-55161
- stratosphere, condensation of HNO_3 and HCl in winter polar stratospheres 7-55162
- stratosphere, O_3 and aerosol measurements in springtime Antarctic stratosphere (November 1985) 7-55155
- stratosphere, reaction rate for $\text{HCl} + \text{ClONO}_2$ on surfaces 7-54091
- sunlight spectral attenuation for 8-13 μm range (*Russian*) 7-29239
- thermophoresis at arbitrary Knudsen numbers 7-44014
- thermophoretic forces acting on a spheroid 7-1666
- Trivandrum, India, aerosol altitude vertical profiles, monsoon effects, lidar obs. 7-66213
- troposphere, seasonally variable background (1972-85) 7-14374
- turbogenerator insulation heating monitoring by aerosol detection (*Russian*) 7-13822
- unitary fuel aerosol, burning in closed region, planar problem 7-13833
- volcanic aerosols, effects on atmospheric extinction at McDonald Observatory 7-47541
- water aerosol, light scattering, evaporation effect study 7-62626
- water in atmospheric aerosol drops, activity calcs. 7-9110
- Western Ghats, India, crepuscular rays form. 7-9173
- Ag aerosols, enhanced photoyield 7-33518
- C particulates in marine atmosphere, long-range transport from continents 7-55221
- CSl aerosol particles growth in steam environment, effects on removal 7-15281
- HNO_3 cloud formation in cold Antarctic stratosphere, role in form. of springtime O_3 hole 7-47508
- KCl, solute trapped from air-acetylene flame, morphological investig. 7-28362

- aerospace**
 see also *aerospace computing; aerospace control; aerospace instrumentation; aerospace propulsion; aerospace simulation; aerospace test facilities; aircraft; space research; space vehicles*
 conference, Washington, DC, USA (Sept. 1986) 7-48171
 material advances 7-27875
- aerospace applications of computers** see *aerospace computing*
- aerospace biophysics**
 anise, induction of somatic embryogenesis in microgravity 7-8719
 Antibio experiment on *E. coli* on Spacelab D1 mission, preliminary results 7-8709
Bacillus subtilis, growth and differentiation under microgravity 7-8710
 Biorack experiments on Spacelab D-1, results 7-8704
Chlamydomonas reinhardtii, circadian rhythm in a Zeitgeber-free environment, space flight obs. 7-8708
 cognitive processes of spatial coordinate assignment, perceptual cues weighting, Spacelab expt. 7-8724
 cress roots, development and gravity sensing under microgravity 7-8718
E. coli, effects of microgravity on genetic recombination 7-8711
 embryogenesis and aging of *Drosophila melanogaster* flown in Space Shuttle 7-8715
 embryogenesis and organogenesis of stick insects under spaceflight conditions 7-8716
 erythrocytes, aggregation under zero gravity 7-3889
 flight hardware for chemical fixation of living material in the microgravity environment 7-8717
 holographic optical elements, industrial appls. in display systems 7-25753
 impact load effect on spinal cord, full-scale and computational expts. 7-34294
 intraocular pressure, monitoring under μG conditions (German) 7-8722
 lentil root, gravity perception, Biorack expt. 7-8720
 life sciences experimentation, autonomous, in space stations, visual monitoring 7-23467
 lymphocytes, human, sensitivity to gravity obs. (German) 7-8705
 mammalian cell polarisation at the ultrastruct. level, effect of microgravity, Spacelab D1 mission obs. 7-8707
 mammalian tissues, particulate radiation damage, electron microscopy appls. 7-28623
 mass discrimination in weightlessness, improvement with arm movements of higher acceleration 7-8723
 organic crystals growth in a microgravity environment 7-22456
 Paramecium experiment on D1 mission of Spacelab 7-8706
 Physarum polycephalum, steady compensation of gravity effects 7-8712
 pilots and cosmonauts, visual stress model—a psycho-physiological method for operational reliability evaluation 7-60106
 protein crystal growth, preliminary investigations using the Space Shuttle 7-23286
 protein single crystal growth under microgravity 7-23285
 space motion sickness preflight adaptation training: preliminary studies with prototype trainers 7-60105
 spaceflight heavy-ion dosimetry data comparison with CREME model LET spectra 7-60107
 Spacelab D1 mission, dosimetric mapping inside Biorack 7-8713
 spacelab experiments on space motion sickness 7-60104
 venous pressure in microgravity 7-8721
 vertebrate gravity receptors, embryonic development, frog obs. 7-8714
 AgCl-detectors in space biophysics, biological effects of cosmic ray HZE particles, evaluation methods 7-34295
- aerospace computer control**
 see also *aerospace computing*
 ERS-1 active microwave instrumentation, operational control 7-47550
- aerospace computing**
 see also *aerospace computer control*
 3D flow obs. by interferometry and image processing 7-37576
 aerodynamics, mesh generation by a sequence of transformations 7-51201
 human factors, conf., Dayton, OH, USA (Sept.-Oct. 1986) 7-35114
 life sciences experimentation, autonomous, in space stations, visual monitoring 7-23467
 SIAM, microcomputer aided crack detection system (French) 7-13713
 space engineering, conf., Sydney, Australia (March 1986) 7-26
 Space Station solar dynamic power system, simulation 7-65494
 star camera and aspect determ. system for balloon-borne payloads 7-55418
 wings, transonic flow calc. using higher-order approximation method 7-51211
- aerospace control**
 see also *aerospace computer control; attitude control*
 inertial positioning problem in Hamiltonian mechanics 7-4195
 optimisation of power supply and temp. control system of space vehicle, static determinate formulation 7-4290
 planetary spacecraft automation development trends 7-55426
 Prognoz-10, instrumentation control 7-55417
 Salyut-6/Kosmos 1267 and Salyut-7/Kosmos-1443 orbital complexes, generalised gravit. orientation regime 7-34832
 Space Infrared Telescope Facility, Space Shuttle-based, active image stabilization 7-9377
 space vehicles, inertial navigation algorithms, for high life-to-drag vehicle during atmospheric entry 7-4289
- aerospace engines**
 Stirling engine for model aircraft propulsion, design and test 7-65543
- aerospace instrumentation**
 see also *aircraft instrumentation; Langmuir probes*
 airborne reconnaissance, conf., Diego, CA, USA (Aug. 1985) 7-18491
 airborne reconnaissance, operational cartography appl. 7-23517
 electric field double probe sensors on GEOS-2, long-term behaviour of photo-electron emission 7-66426
 ERS-1 active microwave instrumentation, operational control 7-47550
 fiber-optic gyro for space applications 7-30005
 image resolution limits resulting from mechanical vibrations 7-20158
 large-acceptance space spectrometer for cosmic ray research, toroidal coil configurations 7-40699
 mechanical and fountain-effect pumps for liq. He in-orbit transfer 7-61339
 Michelson interferometer, hand-held, design and sensitivity for Space Shuttle glow obs. 7-55421
 modulated grid Faraday cup. plasma instruments, response function 7-23972
 Space Telescope Imaging Spectrograph, preliminary performance goals 7-60550
- aerospace instrumentation continued**
 space-borne detector materials, formation of disintegration products 7-66425
 spaceborne imaging radars, Earth and planetary obs. 7-55334
 speckle, interferometer, imaging, in space, image reconstruction by speckle masking 7-31258
 SPOT satellite series, characts. 7-47551
 technology breakout in energy conversion, conf., San Diego, CA, USA (Aug. 1986) 7-60875
 UV radiometers, detector elec. characteristics 7-41417
 UV radiometers, detector optical characteristics 7-41418
 GaAs monolithic integrated optics, performance in space environment 7-26028
- aerospace propulsion**
 see also *aerospace engines*
 interstellar space flight, 36th International Astronautical Congress, Stockholm, Sweden (October 1985) 7-2
 optimisation of power supply and temp. control system of space vehicle, static determinate formulation 7-4290
 Stirling engine for model aircraft propulsion, design and test 7-65543
- aerospace simulation**
 see also *aerospace test facilities*
 artificial satellites, electric charge build-up in magnetospheric environment, secondary electron yields 7-55415
 human spinal cord effects of impact loads, full-scale and computational expts. 7-34294
 inverse integral equation method, turbomachine cascades 7-6244
 vestibular and visual perception cues, coordination 7-14011
- aerospace test facilities**
 see also *wind tunnels*
 batteries for spacecraft, testing facilities at the European Space Battery Test Centre 7-55412
 ERM thermal anal., heat radiation case study using finite element method 7-20588
 ground testing of fighter aircraft, p-static discharge effects 7-50452
 spacecraft analysis, bidirectional scattering distrib. function meas. using computer controlled facility 7-41414
 temperature-controlled chamber for IR mirrors testing 7-57519
- AFC** see *automatic frequency control*
- AFMR** see *antiferromagnetic resonance*
- afterglows**
 electron distribution function, metastable atom+atom collision effects 7-21030
 inert gas afterglow, step by step excitation electron distrib. 7-26572
 microwave-afterglow studies, electron heating, dissociation, recombination, electron temp. and density 7-11813
 Ar, flowing afterglow, metastable influence, expt. apparatus description 7-58073
 Ar+NH₃, dissociation, excitation, nascent vibr. and rot. distrib. 7-46824
 GeH⁺(GeD⁺) in He afterglow, a³P₀₊₁-X¹Σ⁺ visible band system 7-50152
 He+Ar, 2³P₁ state quenching 7-62319
 He+N₂⁺, rot. transfer coeff. determ. (French) 7-10708
 He+Rb, afterglow, inelastic collisions quenching cross sections 7-42746
 Kr, electron impact, low energy, in afterglow 7-20060
 N₂ afterglow, U cpd. interaction appl. to laser isotope separation 7-39898
 Ne²⁺ in Ar plasma afterglow, ambipolar diffusion coeff. meas. 7-20949
 Ne₂⁺ glow discharge, time depend. of spectral line intensities from afterglow plasma 7-32142
 O₂-Ar afterglow, rotationally-resolved bands obs. at 373 to 474 nm 7-29326
- age (Earth)** see *geochronology*
- age determination, radioactive** see *radioactive dating*
- age hardening** see *precipitation hardening*
- ageing**
 see also *precipitation hardening; strain ageing*
 alloys, dislocation glide during ageing, hardening phase particle interaction modelling (Russian) 7-38010
 alloys, heterophase structures, nonequilibrium state diagrams (Russian) 7-17555
 amorphous polymers, yield stress rel. to ageing, nonequilibrium glassy state 7-46562
 bisphenol-A-based epoxy resins, physical props. rel. to curing 7-46539
 conducting polymer films produced by Ar⁺ irradiation of HPR-204, physical and elec. props. 7-26808
 CR-39, time dependence of track response, ageing effects 7-42364
 cycloaliphatic epoxy resin, ageing, irradiation environmental conditions effect 7-33707
 garnet bubble films, H₂⁺-implanted, thermal stability and ageing 7-22124
 glass fibre reinforced polyester laminate, hydrothermal ageing, degradation, US obs. 7-13708
 glass fibre reinforced polymers, hydrothermal behaviour, mech. props. rel. to water absorpt. 7-46665
 insulators, electric and mechanical breakdown, space environment effects simulation 7-39013
 macrocrack growth kinetics in aging viscoelastic bodies under variable loads 7-63071
 metal tritides, disorder induced by aging 7-21199
 metals, segregation during exponential cooling to an aging temperature 7-53744
 Monel K-500, precip. of intermetallic γ' phase and carbide phases 7-33678
 natural versus artificial aging of nuclear power plant components 7-56765
 Nimonic 105, Ni-base superalloys, precip. and tensile deform. behaviour 7-65078
 optical fibres, silicone-coated, influence of pH solns. on strength and dynamic fatigue 7-6006
 p-n junction, glass passivated, polarisation induced instability 7-2680
 pineapple leaf fibre reinforced rubber, phys. and mech. props. 7-3378
 plastic materials, thermal ageing, reaction kinetics (German) 7-46529
 polyamides, aliphatic, nonhomogeneous thermooxidative degradation during heat ageing (Russian) 7-28060
 polydecane amide films, thermal ageing in wet atmos., anal. (Russian) 7-7073
 polyetheretherketone, phys. ageing characts. 7-65110

ageing continued

polyethylene dielec. thin films, hot-electron-induced damage and charge storage, electron spectra studies 7-27662
 polyethylene/ionomer blends, insulating material, aging characteristics 7-39025
 polymeric dielectric, in partial discharge, depression rel. to elec. ageing (Russian) 7-26577
 polyoxymethylene, ageing, residual stress, crystallinity, WAXS 7-39550
 polystyrene, ageing after quenching, positron lifetime distributions 7-39566
 polystyrene blends, secondary relax. dielec. props., memory effect 7-53221
 polysulphide rubber-butadiene-acrylonitrile copolymer/PVC blend, mech. props., ageing and solvent resist. 7-39593
 polyurethane insulation, thermal and elec. aging, prebreakdown phenomena, FTIR spectra study 7-39568
 polyvinyl methyl ether, ageing, enthalpy relax. meas. 7-8029
 PTFE and PVDF, aging, irradiation by X-rays, electron and ion beams, XPS study 7-32498
 rod, nonuniformly ageing viscoelastic, with small deform., thermal stability 7-11317
 rods of non-homogeneously ageing anisotropic viscoelastic material, stability 7-26184
 SAW resonators, 600 MHz band, driving current dependence of ageing drift 7-20553
 semiconductor laser aging, electronic apparatus (Czech) 7-57317
 semiconductor laser phase-locked array, five-stripe, junction down mounting, high power CW operation 7-57364
 semiconductor lasers, power control (German) 7-50578
 shape memory alloys, ageing and thermal cycling effects 7-3336
 solid dielectrics, breakdown and prebreakdown phenomena, charge transport and dielectric aging 7-39014
 spinodal decomposition, nonlinear effects 7-39479
 steel, austenitic, bombarded with Ar ions, ageing temp. effects on structure, microhardness and sputtering 7-65120
 steel, austenitic, Mn-Cr, hardening characts. and hydroextrusion parameters (Russian) 7-59540
 steel, austenitic stainless, creep cavitation rel. to S and P impurity segregation 7-39587
 steel, austenitic stainless, long term creep, transient strain induced strengthening 7-28090
 steel, austenitic stainless, microstructure rel. to cathodic H charging 7-28039
 steel, austenitic stainless, surface phase transform. rel. to H charging and ageing 7-17530
 steel, cast duplex stainless, spinodal reaction and G-phase precipitation, FIM atom probe anal. 7-33670
 steel, Cr-Mo, normalised, tempered, neutron irradi., 390-550°C, tensile props. 7-17621
 steel, Cr-Mo, sintered, ageing and steam oxidation, effect of P 7-7930
 steel, Cr-Mo type, ageing effect on heat resist. props. after cold deform. and tempering 7-22813
 steel, Cr-Mo type, deformed, struct. and mech. props. after long ageing 7-8106
 steel, Cr-Ni-Mo, maraging, mech.-props. rel. to heat treatment (Japanese) 7-53792
 steel, Cr-Ni-Mo-Nb, precipitates formation, effect of He 7-13460
 steel, CrMoV, cold rolled, effects of ageing on mechanical properties (Russian) 7-13478
 steel, dual-phase, Bauschinger effect and coercivity, effect of ageing (Chinese) 7-8045
 steel, ferritic, unirradiated, low activation, microstructure and mechanical props. 7-53863
 steel, low C, Al killed sheet, overaging, continuous annealing, carbide precip., hardness (Korean) 7-46474
 steel, low C, H diffusion and trapping by TiC precipitates (Chinese) 7-7998
 steel, maraging, hydraulically pressed, struct., texture and hardening (Russian) 7-3323
 steel, maraging, sintered, ageing process, precip. phases investig. 7-3322
 steel, Nb-V microalloyed, matrix and grain boundary precipitation, effect of heat treatment 7-46493
 steel, Ni-Co-W, maraging, martensite isothermal aging, hardness, struct. and elec. resist. kinetic behaviour study 7-17553
 steel, secondary hardening, alloy carbide precipitation, FIM atom probe studies 7-33671
 steel, stainless, austenitic, valve type, heat treatment schedule effect on failure nature 7-3423
 steel, stainless, duplex, corrosion imaged and welded conditions, microstruct. effect 7-39698
 steel, stainless, microstruct., aging effects, atom probe FIM, optical and analytic electron microscopy studies 7-33700
 steel, stainless, Ni-Cr precision alloy, spread of local overloads in microstruct. of aged and nonaged specimens 7-8061
 superalloys, stress rupture notch sensitivity, grain boundary precip. (Chinese) 7-13541
 Teflon-FEP electrets, stability, stretching effects 7-27650
 thin metal films, polycryst., specular reflection coeff., effect of ageing 7-12884
 triglycerides, obs. of physical ageing by positron lifetime meas. 7-39229
 viscoelastic ageing medium, stability of lining of horizontal opening 7-1454
 viscoelastic ageing solid, build-up with solid-liq. transition 7-43711
 vision and aging 7-17970
 Ag thin films, discontinuous, post-deposition resist., ageing studies 7-58909
 Ag-As-Se glasses, electrical conductivity studies 7-27369
 AgBr-AgI crystals, strain-ageing 7-6627
 Al alloy, ageing, positron annihilation study 7-39295
 Al quenched, tensile flow stress, effect of grain size and strain 7-22756
 Al-Ag, steady-state creep, effect of isochronal ageing 7-17598
 Al-Ag (5.9 at.%), precip., positron study 7-46485
 Al-Ag alloys, isothermal ageing, hardness and creep behaviour 7-8068
 Al-Co, melt spinning, microstruct., precip., microhardness (Korean) 7-46444
 Al-Cu (2.5 wt.%), electrical resistivity, effect of precipitation 7-12697
 Al-Cu (3.76 wt.%), rheocast, partially homogenised, ageing response, microhardness 7-46499
 Al-Cu-In alloy, deformed, θ -phase precipitation 7-22691
 Al-GaSb interfacial chem. reactions, surface refl. Raman Scatt. study 7-2275

ageing continued

Al-Hf dilute quenched cold-worked alloys, vacancy migration recovery processes, PAC and positron annihilation studies 7-39545
 Al-Li, coarsening of δ' precipitates 7-33663
 Al-Li, grain boundary precipitate free zone growth kinetics 7-33662
 Al-Li, quenched, ageing, light ion irradi., δ phase form. and particle growth 7-26807
 Al-Li (9.5 at.%), coarsening of δ -Al₃Li precipitates, var. of average Li content in Al matrix 7-3313
 Al-Li-Cu-Mg-Zr, yield stress, temp. and strain rate depend. (Japanese) 7-33734
 Al-Li-Cu-Mg-Zr powder alloy, superplastic, high modulus and hardness 7-53816
 Al-Li-Cu-Zr, fracture, ageing and comp. depend. 7-22784
 Al-Li-Cu-Zr, nucleation of precipitates 7-46476
 Al-Li-Cu-(Mg), fracture, effect of subgrain struct. and ageing practice 7-13563
 Al-Li-Sc, cast, decomp., mech. props., struct. (Russian) 7-59532
 Al-Li-Zr rapidly solidified alloy, plastic deform. characts. 7-22777
 Al-Mn-Fe alloy, aging characteristics, pre-cold working effects 7-53758
 Al-Ti-Gd, rapidly solidified ribbons, aged, ternary phase precipitate identification 7-3311
 Al-Zn, ageing, effect of specimen thickness, SAXS study (Japanese) 7-22731
 Al-Zn (12 at.%) alloy, size-shape relation of Guinier-Preston zones, SAXS study 7-13455
 Al-Zn (15 at.%), precip. during ageing, interaction of continuous and cellular mechanism 7-13454
 Al-Zn alloy, positron lifetime and ang. correlation study 7-45860
 Al-Zn alloys, quenching effect on growth of Guinier-Preston zones, resistivity 7-22733
 Al-Zn-Mg, serrated flow, second phase precip., dislocation ageing 7-22755
 Al-Zn-Mg (4.5, 1.75 at.%), ageing, specific surface energy of Guinier-Preston zones 7-28046
 Al-Zn-Mg alloy, precipitation hardening, plastic flow instability 7-22757
 Al-Zr-V, rapid solidification, age hardening, solid soln. form. (Korean) 7-46475
 Au thin films, on Au (111), surface-diffusion-induced ageing processes 7-45080
 B fibre reinforced Al matrix composites, transverse mech. props., isothermal exposure effect 7-39688
 C fibre reinforced plastics, strength, thermomech. props. thermal spiking and moisture absorpt. effect 7-28085
 Ce(Co,Cu,Fe)₆, magnetically hard, heat treatment effects on struct. and mag. characts. 7-27564
 Co-Al, ageing kinetics, precipitation studies (Russian) 7-3332
 Co-Al, precipitation product dissolution (Russian) 7-58479
 Co-Al (10.9 at.%), cellular prep. from supersaturated solid soln. (Russian) 7-65045
 Co-Al alloys, magnetic hardening 7-33209
 Co-Cr-N, surgical implant alloy, mech. props., microstruct. rel. to N addition 7-60125
 Co-W, ageing, polymorphism, cellular mechanism (Russian) 7-59514
 Cr, electrodeposits from Cr₂(SO₄)₃-potassium formate baths, hardness (Japanese) 7-59471
 Cr, electroplated deposits, hardness rel. to C content, heat treatment, bath comp. (Japanese) 7-17480
 Cr-Ta-C, ageing, hardening processes, carbide separation and dissolving (Russian) 7-59541
 Cu and alloys, neutron irradi. effects, elec. cond., fusion reactor appl. 7-51835
 Cu and Cu/Ag composite discontinuous thin films, aging and field effect studies 7-7413
 Cu, anodic oxidation in KOH soln., in situ spectroelectrochemical anal. 7-28192
 Cu discontinuous films, aging, elec. field and temp. effects 7-64364
 Cu thin film, surface electromag. waves damping, deposition technique study 7-59274
 Cu thin films, discontinuous, post-deposition resist., ageing studies 7-58909
 Cu-Al-Ag (5.4, 5.2 wt.%), ageing, hardness, precip. energy 7-65127
 Cu-Al-Mn, thermoelastic martensite form., effect of thermal and stress cycling 7-22680
 Cu-Be (2 wt.%), ageing, lattice rearrangement (Russian) 7-39553
 Cu-Co, dynamic fracture characts., void nucleation at incoherent precipitates 7-17628
 Cu-Co (2 at.%), age-hardened, fatigue behaviour 7-33786
 Cu-Co (2 at.%), underaged, fatigue props., comparison of single crystals and polycrystals. (German) 7-46648
 Cu-Cr bronze, decomp. kinetics of supersaturated solid solns. 7-3320
 Cu-Ni-Al, two-step ageing, microstruct., mech. props. 7-39565
 Cu-Ni-Al (7.5, 2.5 at.%), thermomech. treatment (Japanese) 7-8013
 Cu-Ni-Cr, spinodal decomp., X-ray diffr. and TEM study 7-22732
 (CuAu)-Co single crystals, under- and over-aged, additivity of precip. and solid soln. hardening 7-65051
 CuZnAl, isothermal growth of thermoelastic martensite, quenching and ageing effects 7-53730
 (Fe,Ni)₃V, LRO alloys, mech. props., effects of strain rate and long-term ageing 7-53796
 Fe, pure, diffusion of H, dislocation trapping, interstitial impurities effect (Japanese) 7-52140
 Fe-Al-Mn, fatigue crack growth 7-65130
 Fe-Cr-Co permanent magnetic alloys, casting 7-53051
 Fe-Cr-Co-Si-Ti, permanent mag. alloy, ductile, effect of heat treatment on mag. props. (Korean) 7-8137
 Fe-Cr-Mo-Mn-C-P, sintered, ageing and steam oxidation, effect of P 7-7930
 Fe-Cu-P, sintered, ageing and steam oxidation, effect of P 7-7930
 Fe-Mn, FCC alloys, H-induced martensitic transform. (Japanese) 7-33655
 Fe-Mo (14.5 wt.%), ageing, discontinuous dislocational transform., coercivity obs. 7-3305
 Fe-Ni-Al, sintered, ageing, precip. strengthening, tensile strength 7-39536
 Fe-Pt (36 at.%), cryst. struct., permanent mag. props. (Japanese) 7-53036
 Fe-Si-Al, carbide precip. kinetics, core loss 7-8001
 Fe-Si-B alloy glass, crystn., effect of solid-liq. interfacial energy 7-16437
 Fe₇₃B₁₃Si₁₄, amorphous alloys, mag. losses, aging kinetics 7-59056
 FeOOH sols, crystallisation, Mossbauer study 7-38970

ageing continued

- GaAs_{0.5}P_{0.5} degraded LEDs, origin of nonradiative centres, photocapacitance, electrolum. spectra 7-53413
 a-HgSe films, elec. conductivity, thermoelectric power, optical absorpt. 7-22050
 Mg-Gd supersaturated solid soln., precipitate cryst. struct. (*Russian*) 7-33665
 Mg-Zn metallic glasses, room temp. stability, crystallisation and precipitation 7-11931
 Na circuit materials corrosion, electrochemical potentiokinetic reactivation method (*Czech*) 7-61966
 Nb single crystals, reverse lattice nodes form rel. to N diffusion (*Russian*) 7-58201
 Nb-Al alloys, struct. and supercond. props. (*Russian*) 7-1945
 NbT_{0.59}, acoustic emission and swelling, ageing effects 7-33708
 Nd-Fe-B system, temp. depend. of coercive force, effect of annealing, aging and sintering 7-27560
 Ni superalloy, MAR M002, borides analysis using convergent beam electron diffr. 7-22699
 Ni, Young's modulus, H₂ effects (*Chinese*) 7-39569
 Ni-Al-Mo, precip. in Ni-base superalloys 7-53745
 Ni-Al(Si), aged γ/γ' alloys, He²⁺ implantation studies 7-22690
 Ni-B-C-based alloys, γ phase, prolonged ageing effects (*Russian*) 7-59551
 Ni-base superalloys, stability of lamellar $\gamma-\gamma'$ struct. 7-46566
 Ni-Be (2 wt.%), ageing, lattice rearrangement (*Russian*) 7-39553
 Ni-Cr-W superalloy, experimental, tensile props., effect of carburisation and aging 7-59576
 Ni-Fe-Cr, age hardenable, SCC in PWR coolant water, heat treatment and Zr additions effect 7-39708
 Ni-Mo (20 at.%), ageing, yield strength rel. to prior α grain size 7-39507
 Ni-Sn, ageing, discontinuous coarsening of cellular precipitate at grain boundary 7-39528
 Ni₂Cr, order-disorder transform. kinetics, P content effect 7-13446
 PbMg_{1/3}Nb_{2/3}O₃-PbTiO₃, MnO doped, relaxor ferroelec. ceramics, dielec. ageing effects 7-22195
 Si-O₂ ion implanted, octahedral oxide particle nucleation and growth 7-16776
 Sm₂(Co, Fe, Cu, Zr)₁₇ sintered compact permanent magnet, mag. props., comp. and heat treatment effects (*Korean*) 7-2894
 SnO₂-Sb spray deposited coatings, comp., elec. props. thermal treatments, AES study 7-22393
 Ta wire, cold worked, internal friction, hydride precip. (*Chinese*) 7-8034
 TaT_x ($x = 0.12, 0.103, 0.42$), acoustic emission and swelling, ageing effects 7-33708
 TaT_x, evolution of lattice spacing and damage 7-16582
 Te-Ge alloy glass, isothermal surface crystallisation 7-58576
 Ti alloys, ordered structure form. during decomp. of metastable β -phase (*Russian*) 7-53725
 Ti, heat treated, softening, in situ HVEM obs. 7-17548
 Ti-Al (6 to 16 wt.%), ordered DO₁₉ phase form., DTA study 7-39484
 Ti-Ni (51 at.%), aged shape memory alloy, precip. morphology, comp., cryst. struct. 7-28049
 TiN films, colour, aging and tempering effects 7-46159
 U-Ti (4 at.%), quenching, decomp., TEM obs. 7-39527
 W, LPCVD on Si-Ge alloy for interconnect appls. 7-17472
 W-Ni-Fe system, matrix and interfacial precip. 7-46478
 Y-Fe-B system alloys, mag. props. 7-27563
 Zn-based alloys, mechanical props., alloying addition effects (*Japanese*) 7-8090
 ZnO ceramics ageing under AC voltage (*French*) 7-39564
 ZnS:Cu, electrophosphors, aging phenomena 7-27791
 Zr-Nb (20 wt.%), ageing behaviour, effect of H 7-46527
 ZrO₂, CeO₂ containing tetragonal polycrystals, thermal stability, mech. props. 7-28101
 ZrO₂, MgO partially stabilised ceramics, thermal treatment, mech. props., microstruct. 7-65067
 ZrO₂, Y₂O₃ partially stabilised, hot isostatic pressing, high temp. mech. props. 7-28082
 ZrO₂, Y₂O₃ partially stabilised, microstruct. after ageing at high temp. 7-65061
 ZrT, ZrT_{1.6}, ageing, TEM study 7-51773

aggregates (materials) *see composite materials*

aging *see ageing*

agriculture

- see also farming*
 E Africa, climate prediction for averting drought-caused famines 7-9158
 N America, climate change influences on future grain corn yields 7-55047
 China, agricultural yields rel. to circulation and weather (*Chinese*) 7-29224
 cotton crops, irrigation, evapotranspiration, soil moisture etc. 7-29032
 drainage pipes under field, finite-element drainage problem with boundary conditions 7-29119
 ethanol fuel production from wheat, technico-economic aspect (*French*) 7-28385
 fruit quality measurement by microwave impedance tomography (*Japanese*) 7-28800
 Joint Agricultural Weather Facility, operational assessment programme 7-29126
 remote sensing, Space Remote Sensing Center projects and commercial prospects 7-60258
 remote sensing, vector soln. for mean EM fields in layer of random particles 7-14365
 remote sensing of Earth resources, database design (hardware and software) 7-60410
 remote sensing techniques for state of crops and soil 7-23651
 rice paddy fields, methane release to atmosphere in atmosphere 7-40073
 soil, water downward percolation rate for intermittent flood irrigation conditions 7-29110
 soil erosion by wind, measurement apparatus, book 7-35136
 soil moisture estimation and forecasting for irrigated fields, stochastic method 7-23732
 solar kiln dryers for timber and agricultural produce 7-39965
 solar thermal conversion technology for European agriculture, book 7-28415
 E USA, agriculture impact on soil erosion in Chesapeake Bay area 7-23707

agriculture continued

- USA and Canada Interior Plains, anomalous moisture conditions persistence 7-23835
 zeolites use, conf., Burgas, Bulgaria (June 1985) 7-60885
Aharonov-Bohm effect *see quantum theory*
air
see also terrestrial atmosphere
 air-CO (propane) mixtures, flame front propag. convective vertex form. 7-13777
 air-H₂O interface, fatty alcohol monolayers, spin model 7-27104
 air-water (hexadecane), natural convection in complex enclosed space, heat transfer 7-11421
 air-water countercurrent flow in horizontal tubes, flooding study 7-57902
 air-water jets, confined two phase, analytical entrainment model (*Chinese*) 7-1596
 air-water transient flow, pressure drop and void fraction 7-6288
 air-water two-phase flow in annuli, phase distrib. 7-44009
 air-water upflow in vertical annular channels, true gas content expt. 7-16265
 arc, free burning with Li or I, plasma comp., Gibbs free energy calcs. 7-37795
 arc discharge, current conducting channel in near electrode zones 7-1795
 atmospheric, fast response Langmuir probe for diffusion studies 7-34724
 atmospheric, optical breakdown during axicon laser focusing 7-44288
 atmospheric, optical discharge plasma sustained by Nd laser radiation, diagnostics 7-63355
 breakdown by laser radiation, mechanism modelling 7-20996
 breakdown in discharges, emission study 7-26574
 cross flow over heated cylinder, heat transfer coeff. investig. 7-43892
 crossflow, tube surface press. fluctuations, statistical anal. 7-44048
 density meas., using variable-volume aerometric body 7-4818
 discharge inception voltage from free cond. particles in air 7-51544
 flow, confined turbulent, over asymm. roughened surfaces, mean flow parameters (*Chinese*) 7-11399
 flow in pipes, local heat transfer coeffs. meas. 7-11412
 flow with fine droplets, evaporative cooling heat transfer 7-11508
 gaseous charge explosion, blast wave propag. 7-57881
 hot wire air flow meter for automobile engine intake mass air flow rate meas. 7-37587
 ice-air composite materials, melting process study 7-26335
 ignition voltage of spark gaps in technically important gases (*Czech*) 7-32144
 impulse breakdown voltage for nonuniform field gaps with different wavefronts 7-51546
 impulse breakdown voltage of slightly nonuniform field gaps, wavefront effect 7-32145
 impulse surface discharge in compressed air in nonuniform field, characts. 7-51550
 ionisation by fast electron pulse, nonequilibrium conductivity 7-6364
 ionisation currents in cylindrical chambers 7-37778
 ionisation is viscous shock layer 7-11466
 isentropic charge eqns. 7-31919
 jet, development and breakaway, coanda effect, interferometric, Schlieren and shadowgraph investigs. 7-51358
 laminar flow and heat transfer in tube bank, finite element calcs. 7-51313
 laser beam, kinetic self-focusing in air 7-20299
 laser plasma, secondary spark-over under microsecond pulses 7-11665
 methane-air laminar counterflow diffusion flames, struct., CARS meas. 7-57939
 methane-air laminar diffusion flames, struct. 7-65327
 methane-air turbulent diffusion flames laminar-flamelet modelling 7-57938
 negative corona, neutral densities and temps., optical interferometric and thermocouple studies 7-26569
 negative corona discharge current, halobenzene admixture influence 7-32176
 optical breakdown near solid rough surface, time of appearance 7-26386
 plasma, laser, decaying, shock wave interaction mechanism 7-44175
 positive corona discharge, influence of water mols., mass spectra anal. 7-32180
 propane-air flames, explosion venting, 2D Navier-Stokes eqns. 7-51340
 refractive index, integral, in precision rangefinding, error of point approx. method 7-66342
 sound wave propagation 7-44092
 spark breakdown time-lag, negative ion effects 7-29233
 spark propagation at surface of charged dielectric, expt. 7-58077
 spark propagation at surface of charged dielectric, theory 7-58078
 CO₂ in air of W Europe and British Isles, 19th-century vars. 7-9144
 H flame-out in air flow, gas dynamic struct., interaction effect 7-26315
 H₂-air turbulent mixing in coaxial jets 7-37505
 O₃, admixture in air influence on Trichel pulse characts., electron attachment rate determ. 7-20034
 Zn-air button type battery for hearing aids (*Japanese*) 7-65890
air bubbles *see bubbles*
air clutches *see clutches*
air compressors *see compressors*
air conditioning
see also ventilation
 aquifer thermal energy storage for Canada Centre 12-storey office building 7-65607
 closed type adsorption cooling system utilising solar heat, simultaneous transport of heat and adsorbate 7-8440
 heat-actuated air conditioner/heat pump, new concept 7-65526
 humidity measuring devices and controllers (*Japanese*) 7-56296
 ice slurry system for low temperature thermal energy storage 7-65622
 Nevada desert test site heat pump strategy 7-8429
 porous-bed solar air heater, functional aspects 7-28412
 quality-degrading substances and conditioning equipment (*German*) 7-40069
 solar active cooling systems, comparison using fuzzy decision analysis package 7-59876
air permeability *see permeability*
air pollution
see also air pollution detection and control; smoke
 seasonal variations in atmosphere caused by bomb tests 7-23256
 acid deposition and lake, acidification, role of groundwater 7-23247
 acid deposition data from New Jersey Pine Barrens, air parcel trajectory anal. 7-40061

air pollution continued

- acid rain in India, model of monsoon effects near coal-fired power plants 7-65663
- acid rain in urban and rural areas, environmental effects 7-3743
- acid rain modelling, turbulent spiral boundary layer and thermal wind simulator 7-14370
- acidic precipitation, conf., Muskoka, Ontario, Canada (Sept. 1985) 7-48167
- aerosol, observations of fine-disperse fraction (*Russian*) 7-9083
- aerosol, polar organic compound composition of particulates 7-14327
- aerosol characts. at Pune and Srinagar, India 7-29180
- aerosol concentration in drops, changes due to particle scavenging and redistrib. by coagulation 7-55201
- aerosol light extinction efficiency theory 7-14375
- aerosol source terms in nuclear reactor accidents, ex-vessel fission product releases 7-36219
- aerosols, effect on climate (*Italian*) 7-60372
- aerosols, long-range transport anal. by particle-induced X-ray emission 7-4192
- air quality modelling using kernel method for advection-diffusion eqn. 7-14332
- airborne particles scavenging by collision with water drops, combined effects of microdynamic mechanisms 7-55200
- North America, long-range N oxide pollutant transport model 7-60306
- Antarctic O₃ stratospheric depletion, effects of Cl and Br pollution 7-55173
- Arctic anthropogenic aerosols, climatic effects 7-55193
- Arctic precipitation, sulphate content over last 90 years from glacier ice 7-23252
- Athens, Greece, air temp. and climatic change, anthropogenic effects 7-66287
- Athens basin, simulation of sea and land breezes for pollution studies 7-60342
- Atlantic Ocean, atm. aerosols temporal and spatial var. anal. 7-4085
- Atmospheric Release Advisory Capability for radioactive materials, contour-to-grid methods 7-40078
- Beijing, China, sulphate and carbonaceous aerosols due to coal burning 7-34082
- Beijing, China, suspended particulate dry deposition velocity (*Chinese*) 7-29219
- Brazil, particulates in natural and urban atmosphere 7-34081
- S California, vertical pollutant distrib. and boundary layer struct., airborne lidar obs. 7-3734
- chemical deposition, stochastic modelling of space-time struct. 7-23239
- chloromethane in upper troposphere and stratosphere, spectroscopic detection 7-9076
- climatic changes, anthropogenic factors (*Russian*) 7-9163
- cloud acidification, chemical and microphysical observations of clouds over Ontario, Canada 7-40530
- cloud acidification process, numerical model calculation (*Chinese*) 7-9063
- cloud formed by artificial heat source, microphysics study 7-18286
- coal-fired power plants, atmospheric pollution caused by metal and halogen elements, SO_x and NO_x (*Dutch*) 7-40070
- computer simulation of air pollution chemistry 7-54393
- conference, Santa Clara, USA (Jan. 1986) 7-41018
- conference, Seoul, South Korea (May 1985) 7-40982
- conifers exposed to environmental pollutants, time-resolved fluoresc. rel. to photosynthetic system 7-47156
- Delhi, India, urban diffusion model 7-8466
- Denver, USA, winter haze modelling 7-34673
- dicarboxylic acids in air of Los Angeles, USA, due to motor vehicles 7-54387
- dichlorofluoromethane, atmospheric lifetime and annual release estimates 7-29150
- diesel emissions in Vienna, Austria, tracer study using Dy cpds. added to fuel 7-59899
- diffusion from elevated and ground point sources in neutral boundary layers, turbulent energy model 7-34580
- diffusion over complex terrain, Gaussian trajectory model 7-14369
- dispersion, climatology of convective boundary layer parameters over Ontario, Canada 7-40512
- dispersion in building wakes, wind tunnel expts. 7-1573
- dispersion modeling using partial differential eqn. and generalised laws (*German*) 7-54392
- dispersion studies, use of negative ion generator and collector system 7-29314
- district heating for domestic heating emissions reduction (*German*) 7-46979
- dry deposition of 4-50 μm dolomite particles on vegetation, flat surfaces and deposition gauges 7-4083
- Edmonton, Canada, urban visibility rel. to H₂O vapour from industry 7-14376
- electric field disturbances 7-29231
- electrostatic charging of solid particles and liquid droplets 7-26586
- NW Europe, acidic nitrogen species as pollutants, long-range transport and deposition in rain 7-34085
- fly ash from coal- and oil-fired power stations, shape, size and composition 7-34080
- forest decline, acid rain and other contributory factors, report 7-28419
- W Germany, O₃, NO₂, and SO₂ concentration observations 7-54389
- Geysers geothermal area, California, dispersion model for complex terrain 7-60313
- Great Dun Fell, England, meteorological conditions 7-34661
- Greenland snow-ice core, record of air pollution changes 7-18292
- Hamburg, W Germany, atmos. radiative heating due intense pollution 7-4101
- Helsinki, Finland, atm. radioactive aerosols size distrib. following Chernobyl accident 7-46978
- isolated hill, short-range dispersion experiments on windward slope 7-34572
- homogeneous gas phase mechanism for regional acid deposition model 7-3737
- IFDM computer model, CPU-time reduction 7-54399
- India, acidity of rainfall affected by basic soil dust in atmosphere 7-29184
- Indianapolis, USA, fog chemistry at urban Midwest site 7-55187
- indoor air chemically reactive pollutants modelling 7-8464
- insulator contamination from industrial plant precipitated pollution (*Russian*) 7-59891
- International Association for Great Lakes Research, 29th conference, Scarborough, Ontario (May 1986) 7-18507

air pollution continued

- ionosphere, vibr. relax. of CO₂ during injection from spacecraft 7-34087
- ions from high-voltage equipment 7-29234
- Irish Sea, Sellafield plant waste, actinides enrichment in marine aerosols 7-3742
- Kuwait, modelling of Shuaiba Industrial Area 7-54400
- Lake Powell area, Utah-Arizona, USA, mesoscale air quality for stagnant conditions 7-14330
- lateral dispersion from tall stacks 7-66242
- Laurel Mountains peat bog, USA, atm. chemicals deposition chronology 7-9075
- licensed radioactivity release levels from French nuclear facilities (*German*) 7-56873
- long-range transport and acid deposition, chemical mechanism for model 7-29156
- long-range transport by Eulerian model, for cumulus cloud ensemble 7-34576
- long-range transport in remote regions, symposium, Honolulu, Hawaii (August 1985) 7-48166
- long-range transport of continental particulate C in marine atmosphere 7-55221
- Los Angeles, USA, identification of dimethyl sulphate and monomethyl hydrogen sulphate 7-8463
- Lucknow, India, 1982 rainfall comp. 7-9129
- marble tombstone weathering due to air pollution, Philadelphia, USA 7-59886
- Masaya volcano, Nicaragua, comp., distrib. and neutralisation of volcanic 'acid rain' 7-9145
- methane and aerosol, in atmosphere of Kislovodsk, USSR (*Russian*) 7-54388
- methane in atmosphere, IR radiation models 7-18302
- methane release from rice paddy fields in Italy 7-40073
- methyl peroxide, photochemical formation in boundary layer of atmosphere 7-29155
- modelling, num. method and computer simulation 7-54394
- modelling of air pollutant conc. distrib., statistical models 7-14333
- modelling of air pollution and applications, conference, St. Louis, Missouri (April 1985) 7-48181
- multicomponent aerosol modelling, numerical implementation for reactor accident mitigation 7-56800
- municipal waste incinerator plants, polynuclear aromatic cpd. pollution 7-34083
- New Hampshire, USA, acid rain trends between AD 1900 and 1980 at Hubbard Brook 7-13943
- nitrate scavenging by rain and snow, for Long Island, New York, USA 7-40531
- non-Gaussian climatological model for air quality simulations 7-55243
- nuclear facilities, prod. of air pollutants leeward (*German*) 7-65664
- nuclear war climate perturbations, indirect effects due to smoke from fires 7-14323
- nuclear winter, smoke scavenging by atmospheric ozone 7-9109
- numerical model of urban area pollution concentrations 7-59888
- oil-rig at sea, downwind pollution dispersion, wind tunnel expts. 7-55185
- Oyster Creek emergency off-site dose assessment, ocean breeze inclusion 7-30725
- Palmer Station, Antarctica, atmospheric trace gas trends (1982-1985) 7-55159
- particulate dry deposition velocity for suburbs of Beijing, China (*Chinese*) 7-29219
- passive scalar diffusion, second order modelling 7-8468
- peroxyacetyl nitrate in ambient air of Sidney, Australia 7-59890
- peroxynitrate formation rate in stratosphere, CFC₂O₂ + NO₂ reaction kinetics 7-23802
- pesticides in fog droplets in USA, at high concentrations 7-60365
- Philadelphia, USA, SO₂ pollution and marble tombstone weathering 7-59886
- Pinjara alumina refinery, Australia, SO₂ pollution 7-59901
- plume, visual perception by humans 7-54390
- plume chemical evolution, model of turbulence reacting plume 7-14334
- plume chemistry model, application to NO-NO₂-O₃ system 7-14335
- plume concentration fluctuation models in one- and two-dimensions 7-23794
- plume dispersion in convective conditions, horizontal dispersion meas. 7-40062
- plume dispersion in turbulence, Monte Carlo simulation 7-54396
- nonbuoyant plume dispersion modelling, based on meteorological scaling parameters 7-60308
- plume dispersion over elevated terrain, model performance 7-3733
- plume downwind dispersion, exponential eqn. theory 7-55186
- plume from electric power station, lidar obs. of concentration fluctuations 7-17930
- plume from point source, diffusion model of convective boundary layer 7-66244
- plume of chemically active cpds., expanding box model for long-range transport 7-60312
- plume rise and dispersion, Salford software model 7-54398
- plume visibility and radiative transfer budgets 7-34671
- pollutant concentrations distrib., modelling estimation of one and two-parameter statistical distrib. 7-40067
- polycyclic aromatic hydrocarbons, characterisation from reference air particulate samples 7-54385
- polycyclic aromatic hydrocarbons (PAH), in soil and air in Norway, effect of Al plant 7-54374
- polycyclic organic matter in atm., evidence for transformation 7-3735
- precipitation acidity, determ. of decrease resulting from decreased SO₄²⁻ conc. 7-54391
- PUFF-PLUME emergency response atmospheric dispersion model, field eval. at SRL 7-34292
- pulverised coal combustors, NO emissions, swirling flow effect 7-51155
- Pune, India, aerosol characts., of natural and industrial origin 7-29180
- radioactive fallout from Chernobyl nucl. reactor, influence on atmos. elec. fields 7-40536
- radioactive fallout on west Algerian coast, early 1985 (*French*) 7-59895
- radioactive gases inside a nuclear reactor containment building, Monte Carlo program to calc. exposure rate 7-54766
- Raman spectroscopy, role in study of energy sources, literature review since 1977 7-59827
- Rio de Janeiro, Brazil, aerosol characterization study 7-65661
- rocket exhaust gas diffusion in exponential atmosphere 7-14400
- Sao Paulo (American), washout ratios of nitrate, non-sea-salt sulphate and sea-salt 7-60309

air pollution continued

- screening model, development of MICROGAUSS-I 7-54401
 slope winds and pollutant transport, influence of atmospheric stability 7-60305
 smoke injection into atmosphere during nuclear war, protracted climatic effects 7-66297
 smoke plumes above large-scale fires, nuclear winter simulations 7-65662
 smoke source term for nuclear winter studies, effects of uncertainties on climatic predictions 7-34668
 South Pole, aerosol meas. at Amundsen-Scott Station 7-55226
 spreadsheet sulfur deposition model 7-54397
 Srinagar, India, aerosol charact., of natural and industrial origin 7-29180
 St. Louis, Missouri, USA, O₃ ground level concs. at rural site 7-34573
 street canyon pollution dispersion model 7-34571
 sulphate atmospheric aerosol, scavenging 7-40059
 sulphate deposition from atm., adsorption by soil, implications for dynamics in hydrological systems 7-29102
 sulphate deposition from atm., conc. in streams 7-28426
 sulphate production in hill cap clouds and subsequent deposition to hill 7-14331
 sulphates, scavenging coeff. estimates from sequential precip. samples on Long Island 7-8467
 summertime O₃ and SO₂ climatology in E United States (1977 to 1981) 7-40066
 thermal power stations, SO₂ pollution forecasting 7-55244
 Topographic Air Pollution Analysis System 7-54395
 toxaphene, pollutant transport to Lake Michigan 7-34084
 toxaphene deposition to E North America, determ. from peat accumulation 7-40064
 transport by trajectory model, using synoptic vertical wind data 7-60304
 transport eqns., multistep/multigrad implicit technique 7-54402
 trees, in Europe, disease and death 7-54376
 trichlorofluoromethane, atmospheric lifetime and annual release estimates 7-29150
 troposphere, one-dimensional photochemical model with trade-wind boundary-layer parameterisation 7-9146
 Tsjernobyl radioactive fallout, appl. of two-dimensional trajectory model to radioactivity transport 7-59894
 turbulence classification, computer program 7-55247
 two-particle relative diffusion by Monte Carlo simulation 7-34574
 Tyohu, Japan, SO₄²⁻ and NO₃⁻ content in aqueous aerosols (*Japanese*) 7-47511
 United States E and Gulf coasts, conc. and sources of CO and H₂ 7-55197
 urban area pollution, numerical model for SO₂ and sulphate concs. 7-59889
 urban areas traffic pollution, O₃ form. simulation 7-3736
 urban boundary layer, mixing depth. rel. to wind speed and heat island formation 7-14336
 urban heat island influence on low-level winds 7-18282
 urban warming in North America, average warming rate (1941 to 1980) 7-29146
 URFOR, urban-scale computer model for short-term prediction of air pollution (*Polish*) 7-66205
 NE USA, MAP3S network precipitation chemistry results 7-60310
 E USA, particulates of natural and anthropogenic origin at rural site 7-4119
 NE USA, sulphate and nitrate in wintertime precipitation 7-60311
 USA and Canada, dry deposition of S and N oxides 7-34570
 vehicle exhaust emission control equipment, to limit NO₂ 7-59905
 Venice, statistical study of pollutant concs. via generalised gamma distrib. 7-34090
 Virginia Key, Florida, washout ratios of nitrate, non-sea-salt sulphate and sea-salt 7-60309
 Washington, DC, USA, tracer dispersion expts. 7-60307
 Whiteface Mt., New York, USA, pollution wet deposition, trajectory analysis 7-14325
 Yala Glacier, Nepal, tritium vertical profile in glacier ice 7-40082
 CO in Antarctic atmosphere, concentration in AD 1977 to 1985 period (*Russian*) 7-18276
 CO, in atmosphere of Kislovodsk, USSR (*Russian*) 7-54388
 CO in streets of Thessaloniki, Greece, prediction models based on meas. 7-59897
 CO in troposphere, November 1981, concentration observations 7-29154
 CO, methane and OH concentrations in AD 1980 to 2035 period, model 7-29153
 CO₂, 19th-century vars. in W Europe and British Isles from anal. of contemporary air masses 7-9144
 CO₂ air pollution on global scale, rel. to global fossil fuel consumption scenarios 7-40071
 CO₂ concentration in lower troposphere, simultaneous meas. at neighbouring mountain stations 7-55199
 CO₂, geochemical C cycle disturbance and impact on biosphere 7-40546
 CO₂, greenhouse effect with CO₂ enhanced biological methanogenesis 7-29152
 CO₂, ice core record of ¹³C/¹²C ratio in past two centuries 7-34637
 CO₂ increase and climate change, review 7-55253
 CO₂ problem and increase in global temperatures (*French*) 7-40515
 CO₂, total world production due to wood fuel burning 7-54386
¹⁴C activity of atmosphere, response of hydrological systems 7-23253
¹³⁷Cs in air and soil, use to meas. aerosol scavenging rate and vertical profile 7-55188
 HNO₃, air pollution due to nuclear explosions in atmos., glacier ice core record 7-46982
 HNO₃ cloud formation in cold Antarctic stratosphere, role in form. of springtime O₃ hole 7-47508
 H₂O₂ and CH₃OOH, photochemical formation in boundary layer of atmosphere 7-29155
 HOCl, gaseous, UV absorpt. spectrum, rel. to atm. modelling 7-25534
 H₂S atmospheric pollution from geothermal power plants (*Polish*) 7-23120
 H₂S, release from natural gas well blowout in Alberta, Canada 7-40072
 HTO and T, accidental release: models and in situ expts. on various plant species 7-60095
³H atmospheric release rel. to precipitation contamination 7-54382
³H fallout detection in tree ring records, short term precipitation 7-23255
 Hg emissions from cement factory, influence on environment 7-40060
⁸⁵Kr, atmospheric activity monitoring 7-23259

air pollution continued

- ⁸⁵Kr, ground air mesoscale transport from European reprocessing plants 7-23260
 N pollution in hydrosphere and atmosphere, appls. of isotopic studies 7-28422
 NH₃, effect of precip. on vertical profiles 7-40513
 NO concentration prediction, appl. of regression model 7-40063
 NO₂, air pollution in W Germany 7-54389
 N₂O in troposphere near to Florida, day and night vertical profiles 7-40537
 O₃ in eastern USA, O₃ diurnal variations at rural mountain 7-40620
 O₃, surface concs. at rural sites in Latrobe Valley and Cape Grim, Australia 7-40065
 Pb concentration changes in Antarctic ice during Wisconsin/Holocene transition 7-40074
 Rn, indoor, seasonal variation in houses, southwestern USA 7-28722
²²²Rn concentrations in USA homes, statistical distrib. and health hazards 7-65666
 SO₂, air pollution in W Germany 7-54389
 SO₂, air pollution near to oil refinery at Mathura, India 7-28433
 SO₂ concentrations in Venice area, probability model 7-17929
 SO₂ emissions and acid deposition in USA, monthly data (1980-4) 7-40075
 SO₂ in Valladolid urban area, Spain, spatial and temporal distrib. 7-3738
 SO₂ oxidation over Ljubljana, Yugoslavia, in wintertime atmosphere 7-34575
 SO₂ pollution in Cracow area, Poland, short-term concs. modelling 7-40068
 SO₂ removal by 2D frontal rain system 7-34577
 Se and Te content of aerosols in Missouri, USA 7-18273
 U, fallout from nuclear powered satellites and volcanic eruptions, detect. in rain 7-3740
 U refinery in Canada, U dust distrib. and radiation dose to public 7-59887
- air pollution detection and control**
 acid rain deposition modelling for policy anal. 7-13944
 acidic deposition meas. standardisation 7-23265
 aerometric database for field experiment, real-time display and development 7-54407
 aerosol analysis methods for chem. comp., particle sizes and conc. determ. 7-4085
 aerosol sampler, efficiency of tubular thin-walled inlet 7-65670
 aerosol sampler inlet (non-isoaxial), sampling efficiency study 7-65671
 apparatus for ⁸⁵Kr and ¹³³Xe meas. in fission reactor emergency situations 7-28439
 aqueous foam to reduce radioactive material dispersed in sabotage incidents 7-30518
 atmospheric deposition of inorganic contaminants, anal. using nuclear techniques 7-34092
 atmospheric trace element detection by differential absorption spectroscopy (*German*) 7-46991
 automatic station for O₃ pollution monitoring and data telemetry 7-59900
 cellulose nitrate as Rn and daughter detectors for indoor meas. 7-49824
 cellulose nitrate films for miners personal dosimetry 7-49822
 Chernobyl accident, radiation measurements in Hungary 7-5492
 coal fly ash radionuclides chemical anal. using alpha, gamma and X-ray fluorescence spectroscopy 7-23266
 coal-fired power stations, radioactivity, review 7-59893
 collection of airborne pollution particles for analytical electron microscopy 7-17935
 Commodore 64 home computers for air pollution monitoring 7-54418
 conference, aerosols in science, medicine and technology, Garmisch, Germany (Sept. 1985) 7-9577
 cryogenic sampler for collecting radioactive gases and aerosols 7-59902
 diesel emissions, use of Dy as tracer to study aerosol sources 7-59899
 dry additive process for flue gas desulphurisation in power plants, use of Ca(OH)₂ and CaCO₃ (*German*) 7-46980
 dry sorbent injection technologies for SO₂ and simultaneous NO_x control 7-65667
 dust samplers used in British nuclear industry, entry charact. investigation 7-40079
 environmental problems, mathematical models, book 7-60890
 environmental protection, meas. technology (*German*) 7-3745
 filters, industrial, for particle sizes in submicron range, retention efficiency 7-59903
 flue gas, continuous emission monitoring and meas. procedures (*German*) 7-28436
 flue gas desulphurisation, NOXSO, SOXAL and limestone process evaluation 7-46983
 flue gas purification develop. in coal-fired heat power plants (*German*) 7-46981
 flue gas scrubber corrosion rel. to pH and trace element concentrations 7-40077
 ground level air radionuclide conc. 1984-1986, N. Germany and N. Norway 7-59896
 hazardous gas monitoring system in chem. manufacturing facility, open path FTIR air monitor 7-54416
 heat and power generation from coal, SO₂, SO₃, NO, NO₂ and CO removal from flue gases (*German*) 7-65653
 hydroxymethanesulfonate, determination in wet deposition by chromatography method 7-54406
 IR-laser spectroscopy for measurement applications in the industrial environment 7-23267
 irradiated atmospheric air, aerosol formation 7-11515
 laser beam remote sensing of tropospheric gases (*German*) 7-40081
 laser photoacoustic spectroscopy of humid and polluted air 7-20569
 LR-115-11 Kodak track film indoor Rn meas. 7-49738
 mica nuclear track microfilter cascade fractionator, industrial appl. 7-36408
 mica track filters for Rn meas. 7-49734
 microprocessor coating thickness and air dust pollution gauges 7-61317
 modelling of air pollution and applications, conference, St. Louis, Missouri (April 1985) 7-48181
 monitoring equipment, components, materials and operating principles 7-23263
 natural Rn daughter exposure meas. in French houses 7-54414
 nuclear track microfilters, recent developments and appls. 7-65659
 open track films for ²²²Rn-meas. in dwellings 7-49825

air pollution detection and control continued

- organic compounds, thermal desorpt./gas chromatographic anal. using hollow tube collectors 7-17928
- organic vapours, detection with active and passive sensors, comparison 7-46990
- particle emission from gasoline powered vehicles, emission, deposition and re-emission 7-59892
- particle-induced X-ray emission for aerosols long-range transport anal. 7-4192
- particulate control technology transfer and utilisation, 6th symposium, New Orleans, LA, USA (Feb. 1986) 7-65668
- photoelectric aerosol sensor, chemical response to different aerosol systems 7-11514
- plants used for detect. of SO₂ pollution 7-59901
- plastic detectors/Ilford emulsion comparison for Rn and daughter activity 7-49821
- plastic-bag sampler for passive radon monitoring 7-42423
- polar ice air bubbles for pollution monitoring and bubble age 7-4068
- pollutant concentrations distrib. modelling estimation of one and two-parameter statistical distrib. 7-40067
- polycyclic aromatic hydrocarbons, diesel particulate matter identification, chromatography 7-34079
- quality-degrading substances and conditioning equipment (German) 7-40069
- radioactive areas ventilation, filter testing, aerosol mixing 7-30727
- radioactive environmental monitoring around nuclear plant 7-28432
- radioactive Kr and Xe gases, double filter method for meas. 7-40317
- radioactive pollution, low-level gamma-ray study 7-23236
- radioiodine adsorption on silica gel 7-28434
- radioisotope gauge apple. and development 7-61311
- radiological dispersion patterns following explosive sabotage incidents 7-36300
- radionuclide concentration meas. in atm. around nuclear power reactors 7-23257
- reactive intermediates determination by matrix isolation FTIR spectroscopy 7-54417
- regional acid deposition calculations with the IBM PC Lotus 1-2-3 system 7-54408
- regional radiation environment monitoring systems near nuclear plants 7-8462
- remote sensing data processing by group method of data handling, environmental management appl. (Japanese) 7-65673
- screening model, development of MICROGAUSS-1 7-54401
- simulation models for air quality, computerized system for evaluation 7-54409
- software for real-time acoustic remote sensing instrumentation and atmospheric pollution control 7-54403
- SSNTD technique for Rn and thoron meas. in the environment 7-42430
- statistical modelling of pollutant concentrations, appl. of generalised gamma distrib. 7-34090
- survey data of radionuclides in environmental materials 7-17931
- techniques for spatial data display 7-54404
- trace elements in atmosphere of Ankara, neutron activation anal. 7-3739
- trace-element concentration meas. in air masses, neutron activation appl. 7-34086
- track element dosimeter for Rn meas. in air 7-42424
- track etch detectors for Rn meas. 7-49735
- vehicle exhaust emission control equipment, to limit NO₂ 7-59905
- vertical cylindrical sonde for aerosol sampling 7-34732
- CO, personal exposure monitor with automatic data-logging 7-3943
- CO₂, reducing build-up in Earth atmosphere 7-65669
- HCl detection in atm. by laser-induced fluorescence of CO₂ 7-46993
- ⁸⁵Kr, sampling unit for air sample 7-23258
- N pollution in hydrosphere and atmosphere, appls. of isotopic studies 7-28422
- NO concentration prediction, appl. of regression model 7-40063
- O₂ as environmental poison 7-65660
- Pb, particulate and gaseous, in exhaust gas determ., plasma emission and atomic absorpt. spectrometry 7-59803
- Pu, isotopes, radiochem. determ. in atmospheric samples 7-3616
- Rn concentration in Danish dwellings, CR-39 track detector meas. 7-49826
- Rn daughters automatic meas. instrument for atm. precipitation 7-49847
- Rn daughters in indoor air, Swedish limitation schemes 7-34286
- Rn dosimetry, rectangular geometry effects 7-42426
- Rn exhalation and diffusion parameters in solids, plastic track meas. 7-54411
- Rn permeability through plastics by track techniques 7-42427
- Rn personal dosimeter for miners 7-49736
- SO₂ concentrations prediction in Venice area, appl. of probability model 7-17929
- SO₂, in humid air, level meas. by chromatography 7-34078
- SO₂ pollution in Cracow area, Poland, short-term concs. modelling 7-40068
- T release in fusion reactor test cell, modelling, operation of atmospheric cleanup system 7-36259
- Th isotopes, radiochem. determ. in atmospheric samples 7-3616
- U isotopes, radiochem. determ. in atmospheric samples 7-3616
- ¹³³Xe adsorption on activated charcoal, effects of water vapour 7-40076
- ZnO-SiO₂-Si SAW chemosensor for NO₂ gas concentration meas. 7-3621

air pumps *see compressors*

air tightness detection *see leak detection*

aircraft

- see also aerospace control; aerospace instrumentation; helicopters*
- advanced turbo propeller, active control of interior noise 7-50846
- automatic ultrasonic materials testing system, US-1000 for C-fibre composite aircraft components 7-22965
- Boeing 727 series, response to microburst winds 7-66241
- ground testing of fighter aircraft, p-static discharge effects 7-50452
- icing conditions detection method, by ground-based microwave radiometry 7-23871
- KS-147A LOROP camera integration into RF-5E aircraft 7-18898
- KS-147A LOROP camera system for RF-5E aircraft 7-18899
- lightning strike events, rel. to thunderstorm struct. 7-29172
- plastic and advanced plastic composites, design methods and applcs., book 7-4642
- remotely piloted aircraft for remote sensing 7-55289
- static charging by collisions with ice crystals 7-55212

aircraft continued

- structural crack detection studies using acoustic emission testing 7-33906
- weather forecasts for reduction in fuel consumption 7-66249

aircraft instrumentation

- displays, direct-view and collimated under display, visual perception 7-54575
- ERASME airborne side-looking C-band radar, data processing and calibration 7-9205
- forestry and range applications of high altitude reconnaissance technology 7-23905
- KS-147A LOROP camera integration into RF-5E aircraft 7-18898
- KS-147A LOROP camera system for RF-5E aircraft 7-18899
- oblique CCD reconnaissance camera operation, atmospheric effects 7-18900

airglow

- see also atmospheric spectra; nightglow; sky brightness*
- comet impacts responsible for UV dayglow holes, rel. to lunar seismicity 7-40727
- small comet influx to Earth rel. to airglow holes and H₂O conc. in mesosphere 7-40622
- dayglow transients caused by small comet influx, comments and reply 7-60601
- geocorona, Dynamics Explorer observations from 1981 to 1985 AD 7-55337
- imaging system for OH airglow, using image intensifier and solid state sensor 7-29288
- near-Earth space environment, spaceglow and material erosion 7-60506
- polar mesopause, large-amplitude semidiurnal temp. var, airglow, meas. 7-34754
- Shuttle glow, chemilum. processes 7-47602
- Shuttle glow, rammed surface temp. dependence 7-9284
- Shuttle glow and critical ionization velocity phenomena 7-55377
- Space Shuttle glow optical emissions during mission STS 41-G 7-34834
- spacecraft glows, surface-catalysed reactions role 7-14401
- H α emission, intensity meas. rel. to H dissipation flux and thermosphere temp. 7-23922
- NO, dayglow UV emissions in γ , δ , ϵ bands 7-29324
- O airglow at 630 nm and O(¹D) quenching by O(³P) 7-34761
- O, UV intercombination emissions in dayglow 7-60438
- O₂ dayglow, due to Σ state band system 7-34760
- OH near-IR airglow vibrational state populations 7-23926
- SF₆ release expt. at F-region altitudes, excitation of O permitted lines 7-9282

alarm systems

- nuclear plant alarms, handling and presentation 7-62030
- nuclear power plant alarm-filtering system for advanced test reactor 7-62054
- nuclear power plant availability improvement by reactor trip prediction software 7-10275
- radiation survey meter calibration tardiness alarm 7-8695

albedo

- Arctic Ocean, snow melt, sea ice and surface albedo 7-23658
- arid rangeland, New Mexico, Landsat albedo meas. 7-14286
- atmospheric optics, inverse problems 7-47537
- Charon, radius and albedo from occultation by Pluto (1986 December 29) 7-55530
- climate simulations to BP 18000 years, surface condition effects 7-29236
- close binary stars, monochromatic albedos and temp. distrib. on distorted surfaces 7-18439
- comet dirty ice grains, albedos evol. 7-24067
- P/Comet Halley (1982i), nucleus albedo from Vega mission obs. 7-9438
- P/Comet Halley (1982i), nucleus albedo rel. to total cometary mass in solar system 7-24077
- cometary nuclei albedos rel. to nature of P/Comet Halley (1982i) 7-34936
- concrete shield, fast neutron albedo calcs. 7-30622
- 511 Davida, speckle interferometry and photometry rel. to dimensions, rot. pole and albedo 7-24045
- Earth, albedo meas. during Earth Radiation Budget Experiment (ERBE) 7-9067
- Earth atmosphere, bispectral satellite measurements rel. to cloud cover estimation 7-29148
- Earth surface, correl. of spectral radiance parameters measured from multiband space images 7-66339
- giant planets, relations between spherical albedo and observable characs. of planetary atmosphere 7-24031
- interstellar grains, albedo and scatt. props. from CCD surface photometry of refl. nebulae 7-55773
- interstellar grains in Orion Molecular Cloud 2, near-IR albedo from refl. nebulae obs. 7-55765
- LDN 1642, high-latitude cloud, grain characs. 7-48062
- Neptune, albedo variations, modulation by solar cycle 7-66502
- Neptune, geometric albedo between 2100 and 3350 Å 7-24062
- plane-parallel media, radiation transfer, natural eigenfunctions anal. 7-6081
- Pluto, albedo and radius from occultation of Charon (1986 December 29) 7-55530
- surface albedo of Sahel, climatic effects of change 7-66290
- surface albedo vars. in Africa, Meteosat image meas. method 7-55272
- Trifid reflection nebulae, dust grain characs. 7-35024
- Uranus, geometric albedo between 2100 and 3350 Å 7-24062
- wind-roughened sea surface, albedos and glitter patterns generation 7-9006

alclad *see aluminium alloys*

Alfvén waves *see magnetohydrodynamic waves; solid-state plasma*

algebra

- see also Boolean algebra; linear algebra; matrix algebra*
- AKNS system, integrable equations, Lie algebra and nonisospectral evolution equations 7-35209
- algebraic function fields of genus one over real closed fields, isomorphism theorem 7-60994
- algebraic groups as products to two subgroups, one of which is solvable 7-18555
- Ashkin-Teller model, 2D conformal symmetry and critical 4-spin correl. fns. 7-48999
- automorphic forms and number theory, conference, Sendai, Japan (Nov. 1983) 7-48196
- Banach algebra, algebraic and topological props. 7-55957
- Banach algebras produced by 2D integral operators 7-60938

algebra continued

- Banach spaces, bounded compact approx. property and noncompactness measures 7-55950
 Banach spaces, complex anal., book 7-14725
 Bogolyubov generating functions, quantum method, current Lie algebra, representations, functional eqns. 7-41240
 book, foundations for classical mechanics 7-14723
 bosonic string compactification, conformal subalgebras of Kac-Moody algebras 7-35826
 bounded analytic functions, Banach algebra, closed and prime ideals 7-24349
 C* algebra approach to analyticity in quantum statistical mechanical models 7-56148
 canonical commutation relations on bounded interval in Hilbert space 7-48538
 Cartan-type graded Lie algebras positive and negative graded modules 7-35196
 classical dynamical systems, geometric description 7-24407
 Clifford algebra, conf. Canterbury, England (Sept. 1985) 7-4639
 cohomology and deformations of Lie superalgebras 7-48272
 commutants and bicommutants of unbounded operator algebras 7-48271
 complex fuzzy events in classical and quantum information systems, algebraic props. 7-61152
 contraction of Lie algebras 7-35194
 cosine families in Banach spaces, perturbation 7-18563
 Demazure-Weyl formulas, and generalization of the Borel-Weil-Bott theorem 7-9645
 dimensional regularization and non-associative Dirac-Clifford algebra 7-35714
 Dirac formalism, mathematical introduction, book 7-60896
 distributive lattices, equivalence systems and congruence systems 7-29916
 Euclidean Kac-Moody algebras spanned by principal subalgebra action, highest weight representations 7-48273
 fermion theories, causal phase-space approach, Clifford algebras 7-9752
 filtered Lie algebras, intrinsic nilpotent approx. (French) 7-24368
 finite dimensional Lie algebra, structure of PI-envelope 7-29676
 foliation topology, symposium, Tokyo, Japan (July 1983) 7-48197
 free modules over algebras of finite groups, characterisation 7-60971
 functions similar to Lie functions, algebras 7-60941
 generalized superspaces, anal. over σ -commutative algebras 7-4653
 geometrical objects, transformation laws, algebraic approach 7-48270
 geometrical objects, transformation laws, supersymm., no. system of octonions 7-49009
 graded calculus of variations, algebraic model 7-29672
 hermitean oscillator-like realisations of classical algebras and superalgebras in Hilbert space 7-41655
 Hilbert space, invariant subspace problem for contractions (French) 7-55948
 imbeddings of non-commutative separable extensions in Galois extensions 7-60936
 infinite symplectic group, Riesz ring approach 7-55962
 interacting vector boson model, boson representations of symplectic algebras 7-41912
 Iwasawa and triangle decomp. eval. for Lie algebra real forms 7-18552
 Kac-Moody algebras, Harish-Chandra modules of complex semisimple Lie groups (French) 7-55947
 L-kernel approach to quantisation of phase space polynomials 7-61147
 left approximate identities in algebra of compact operators on Banach spaces 7-60966
 Lie $gl(n+1, R)$ algebra, boson realisations 7-29871
 Lie superalgebras, Casimir operators for infinite-dimens. representations 7-9647
 Lie superalgebras, polynomial identities 7-60942
 Lie superalgebras, principal five-dimensional subalgebras 7-41056
 Lie superalgebras $B(0, n)$, irreducible \ast -representations 7-41054
 Liouville series, Masser's conjecture on algebraic independence of values 7-48290
 many-electron systems, symmetric group approach, spin-depend. operators 7-15475
 many-particle operator algebras, statistical physics conf., Koszeg, Hungary, Aug.-Sept. 1984 7-48194
 many-particle operators, algebraic aspects 7-48292
 massless higher-spin fields, coupling and gauge algebra, rel. to string theories 7-177
 mathematical models in mechanics, book 7-55906
 minimal polynomial of a resolvent 7-60951
 momentum operators for large systems, W* algebra description 7-29791
 multi-valued functional construction, general method 7-61033
 multiplicity-free 6j symbols, algebraic expressions, G_2 isoscalar factors 7-29796
 n-dimensional Kepler problem, spinor regularisation, Clifford algebraic construction 7-61089
 n-angelian Lie algebras (Russian) 7-60934
 nilpotent subalgebra of Zassenhaus algebra, 2-cohomologies 7-60939
 nonexistence of hidden variables in the algebraic approach 7-29787
 nonlinear Schrodinger eqn., local and nonlocal conserved quantities 7-56063
 number of terms in transmittance corresponding to a two-port cascade 7-55946
 octonions in gauge theories, soln. using composition algebras 7-35713
 point projection onto a linear manifold, computing algorithm error anal. 7-24405
 Poisson Lie algebra C^∞ , deformations of subalgebras 7-48435
 predictor-solver continuation methods, convergence cones near bifurcation 7-35203
 prespectrality of generalised derivations 7-60965
 prolongation theory, non-Archimedean approach 7-29679
 q-state Potts model operator algebra representations, transfer matrix spectrum 7-35436
 quadratic parametric processes, Lie algebraic approach, quantum optics, quantum acoustics 7-36923
 quantum fields, relations with local algebras of observables 7-41642
 rational identities of radical algebras 7-29657
 reaction-diffusion equations, stability of steady state solns. 7-29952
 relativistic wave equations, invariance algebras and superalgebras 7-61440
 Schrodinger non-relativistic conformal symmetries and invariant tensor fields 7-35674
 second-order perturbation algebra of invariant operators 7-60962
 semigroup algebras of commutative and cancellative semigroups, radicals 7-24364

algebra continued

- semigroups and lattices, independence of groups of automorphisms and retracts 7-60975
 $Sp(2)/T(2)$ Grassmann Euclidean group, extended BRST SUSY, pseudomass, pseudospin 7-61491
 $sp(4, R)$ symplectic algebra generators, matrix representation 7-60948
 spaces L_∞ with mixed norm in an infinite-dimensional torus 7-60940
 special embeddings, symmetry breaking scheme anal. 7-30232
 spinor and algebraic spinor structures, parallel spinor fields on space-time manifold 7-29834
 statistical physics and field theory conf., Groningen, Netherlands, Aug. 1985 7-55899
 stochastic equations, existence and uniqueness of soln. and semimartingales 7-29730
 string field algebra for gauge-invariant interaction of bosonic string 7-49109
 string field theory candidates from C* algebra cohomology 7-19036
 $SU(2) \times SU(2)$ 2D chiral Wess-Zumino model, operator algebra and correl. functions 7-19016
 superconformal algebras, relation to integrable nonlinear systems and quantum string theory 7-56463
 superconformal field theory with modular invariance on a torus 7-15080
 supergravity theories based on free differential algebras, factorisation and gauge transforms, in supergravity theories based on free differential algebras 7-187
 supermanifolds, topological structure, superprojective space 7-29662
 three-wave resonant interaction eqns. in (2+1) dims., group anal., Lie algebra 7-29769
 Toeplitz operators and quantum mechanics 7-14812
 topological algebras, selected topics, book 7-9608
 transformation laws of geometrical objects, algebraic approach 7-29656
 unitary positive energy representations of the gauge group 7-61441
 unitary representations induced from maximal parabolic subgroups 7-24369
 vector coherent state theory in a group with non-commuting raising generators 7-60977
 vertex operators for non-simply-laced algebras 7-24367
 Virasoro algebra, anomalous term derivation by topological method 7-19081
 Virasoro algebra, non-unitary proof for highest weight representations 7-48268
 Virasoro algebra, von Neumann Algebra and critical eight-vertex SOS models 7-24589
 Virasoro algebra in 2+1 dimensions and angular momentum fractionalization 7-61467
 Virasoro algebra in the solution space of the Ernst equation 7-60949
 von Neumann algebras associated to quantum-mechanical constants of motion 7-48399
 W*-algebra, metrics on sets of states 7-55958
 W*-algebras, convergences 7-29659
 XY model, C* algebra approach to ground states 7-48631
- algebraic manipulation** *see symbol manipulation*
- algorithm theory**
see also computability; computational complexity
 computability and physical theories 7-18589
 point projection onto a linear manifold, computing algorithm error anal. 7-24405
- algorithms (computer listings)** *see subroutines*
- aliphatic compounds** *see organic compounds*
- alkali metal alloys**
see also caesium alloys; lithium alloys; potassium alloys; rubidium alloys; sodium alloys
 binary alloys, low temp. phase diagram, compression effects 7-33641
- alkali metal compounds**
see also alkali metal alloys; alkali metal halides; caesium compounds; francium compounds; lithium compounds; potassium compounds; rubidium compounds; sodium compounds
 chlorate ion pairs, coord. structs., FT. IR matrix isolation spectra 7-62367
 cyanide halide mixed crystals, orientational glass state 7-21140
 cyanide-halide mixed crystals., orientational glass state dynamic props., microscopic model calcs. 7-63756
 cyanide-halide mixed crystals., orientational glass state static props., microscopic model calcs. 7-63591
 cyanides, multipole interaction effects on cohesive and anharmonic props. 7-1942
 graphite intercalation compounds, first stage, with heavy alkali metals, electronic props. 7-2463
 hydrides, ground state reduced pot. curves 7-10466
 hydrides, inter-ionic bonding and thermodynamic functions, microscopic theory (Russian) 7-58198
 hydroxide vapour, ion clustering struct., chem. equilib., mass spectra 7-17814
 hydroxides, electron affinity, mass spectrometric determ. 7-15740
 hydroxides, saturated vapours, composition, mass spectrometric determ. 7-33985
 iodides, Debye-Waller factors of ^{129}I , Mossbauer study 7-2135
 mixed alkali borate glasses, transform. range viscosity, thermal expansion 7-52103
 monohydroxides, high temp. photoelectron spectroscopy, ab initio MO calcs. 7-50251
 oxides, electron affinity, mass spectrometric determ. 7-15740
 oxides with antiferroite structure, F^+ -centre absorption energy calcs. 7-12658
 photodissociation, photofragment fluoresce. anal. 7-19974
 polyphosphides, passivation of III-V semiconductor surfaces 7-39778
 silicate glasses, internal friction, amplitude depend., cooperative movement parameter near the glass transition temp. 7-2099
 silicate glasses containing alkali and alkaline earth metals, alkali ion mobility (Japanese) 7-27007
 silicates, aq. solns., longit. ^{29}Si nucl. mag. relax. 7-33285
 tetrafluorotetracyanoquinodimethan(TCNFQ), charge transfer salts, comparative EPR studies 7-53114
 zeolite A ion source, emission characts. 7-49776
- alkali metal halides**
see also compounds of individual alkali metals, e.g. sodium compounds
 active media for tunable crystal lasers 7-25823
 aqueous solutions, ion hydration, dielec. props., microwave spectrosc. obs. (French) 7-54111

alkali metal halides continued

- binary common-anion mixtures, correl. of thermochem. and phase-diagram data 7-3286
 binary common-anion mixtures, phase diagrams, thermodynamic anal. 7-3287
 broad gap crystals, luminescence, synchrotron radiation studies 7-33432
 chloride melts, anodic Cl evolution, galvanostatic transient anal. 7-33938
 chlorides, electron-stimulated desorption, Coulombic ejection mechanism 7-59315
 chlorides, molten, ionic diffusion coeffs. calcs. 7-32689
 chlorides, particle bombardment-induced secondary photon emission 7-59264
 colour centres, Hartree-Fock cluster computations 7-16985
 crystal growth in stationary crucible 7-59413
 crystalline solids, electrostatic Madelung and cohesive energies 7-44442
 crystals, charge transfer excitons, perturbation method anal. (*Chinese*) 7-12611
 crystals, optical breakdown threshold, size depend. 7-44615
 crystals, positronium momentum distrib., effective mass determ., annihilation γ -rays ang. correl. meas. 7-45235
 crystals, self-trapped exciton recomb. luminesc.-recomb. induced F-centre form. anticorrel. calcs. 7-13201
 crystals, dislocation displacements distrib. characts., local dislocation density effects (*Russian*) 7-21214
 desorption, UV-photon-stimulated, laser-synchrotron studies of dynamics 7-21612
 electron and photon stimulated positive ion desorption dynamics calcs. 7-27141
 electron bombardment, excited-atom production 7-22400
 electron- and ion-induced sputtering, atomic excitation 7-59348
 eutectic composites, growth, struct., mech., elec. and optical props. 7-33648
 F-centre formation threshold by two-photon absorpt. 7-32437
 F-centre production, impurity aggregate effects 7-21202
 F-F' conversion, polaron theory 7-21201
 fused salts, nearest cation-anion distance, hard-sphere calcs. 7-21070
 Ge^{2+} impurity ion in alkali halide crystals, triplet excited relaxed states, ODMR study 7-2953
 halides with Ti^+ impurities, excitons, optical absorpt. D band study 7-64096
 hardening, effect of dislocation elec. charge 7-51816
 impurity ion off-centre dipoles 7-64163
 impurity local and gap mode freq. calcs. 7-26888
 interionic potentials based on charge transfer model 7-58197
 interionic pots. determ. 7-42720
 iodide crystals, luminesc. induced by photo-generated excitons, excitation spectra struct. 7-46103
 iodides, electron-stimulated desorption, Coulombic ejection mechanism 7-59315
 liquid mixtures of alkali metals and halides, longitudinal collective modes 7-6744
 luminescence, conference, Rovno, USSR (Nov. 1984) 7-24263
 microcrystalline powders, correl. between coloration stability and micro-hardness 7-32486
 mixed alkali halides, electronic dielectric const. and fractional ionic character of chemical bond 7-2966
 mixed crystals, phys. props., review 7-37943
 monium centres 7-45901
 neutral molecule incorporation, composite form. at room temp. 7-54101
 photon-surface interaction dynamics 7-27826
 polarised luminesc., model of Ga^+ , Ge^{2+} , In^+ , Sn^{2+} , Ti^+ , Pb^{2+} centres 7-27753
 positron states, hopping- and tunnelling-diffusion calcs. 7-44921
 powdered, electrophysical investigation during molding 7-7232
 radiation induced electrostatic instability on surface of ionic crystals 7-46816
 refractive index, Szegedi charge, dielec. parameters ab initio calcs. 7-13082
 Schottky defect energy, effect of three-body forces 7-21864
 Schottky defect form. enthalpy-Debye temp. correl. study 7-26742
 solid solns., thermodynamic props. calc. model 7-52086
 solutions, in water-acetamide mixtures, partial molal vol. meas. 7-58389
 trapped atomic H and muonium 7-45900
 UV laser beam profile monitor using alkali halide crystals 7-37011
 water-LiBr absorption cooling system thermodynamic design data 7-23208
 XANES K-spectra, cryst. pot. and size effects 7-64748
 XANES spectra, single site approx. via ideal crystal Green's functions 7-64747
 CsI dislocation study using US technique 7-21362
 Ga^+ impurity ion in alkali halide crystals, triplet excited relaxed states, ODMR study 7-2953

alkali metals

- see also caesium; francium; lithium; potassium; rubidium; sodium*
 adsorbed layers on Si (100) 2×1 , anisotropic plasmons (*Japanese*) 7-21967
 adsorbed layers on solid surfaces (*Japanese*) 7-21966
 adsorption on metal substrates, influence of adsorbate coverage on work function 7-2669
 alkali, atom-inert gas atom complexes, optical pumping, polaris. effects 7-15536
 alkali doped inert gas solids, matrix-bound systems, dipolar excitonic insulator transitions, mean field theory 7-45163
 alkali metal cation-halogen anion microclusters, structs. and energetics 7-8266
 alkali-inert gas pair diffusion cross sections, light-induced drift 7-51366
 alkali-metal- NH_3 sections, metal-nonmetal transitions 7-2486
 atom distrib. in boundary layers of combustion prod. plasma, nonequib. chemical reactions effect 7-57990
 atom-He system, Rydberg energy levels, Coulomb and Coulomb-Stark-Green fn. 7-42476
 atomic fluids, thermodynamic and electronic props. 7-45157
 atoms, collision induced amplified emission 7-10513
 atoms, core-polarisation effects, oscillator strength calcs. 7-25454
 atoms, interaction with dichlorodimethylsilane coated reson. cells wall relax. 7-59317
 atoms, light-induced drift, effect of hyperfine splitting 7-15557
 atoms, orientation, alignment and HFS 7-50278
 atoms, photoelectron spectra, correl. effects, CI study 7-62450
 atoms, population capture, optical-microwave pumping 7-25464

alkali metals continued

- atoms(ions), reson. line electron-impact broadening 7-20058
 atoms in ground state, polarisation ellipse rot., optical self-pumping in mag. field 7-50004
 atoms in mixture with mol. gases, cooling in supersonic nozzle, population inversion of electronic states 7-31304
 atoms in rare gas matrices, Rydberg states, model pot. 7-5737
 atoms in strong field, static Stark effect 7-50007
 BCC, thermodynamic props. 7-6828
 cations, half-wave pots., solvent effects 7-23029
 CDW instabilities and thermoelec. parameters 7-12707
 cluster beams, photoionis. mass spectra, abundance distrib. 7-15768
 clusters, structures, pseudopotential method, local density approx. 7-36840
 condensed phase, thermodynamic props. study 7-32684
 dimers, diffuse $1^3\Pi_g-x^3\Sigma_u^+$ bands, recombination in discharge plasma 7-19828
 impurities and defects, electronic structure 7-27299
 intracellular distribution, in ICRP Reference Man 7-65861
 ion-binding to poly(4-vinylbenzo-18-crown-6), charact. eval. 7-10469
 ions, adsorpt. on kaolinite, free energy, additivity rules (*German*) 7-2233
 ions in inert gases, energy distrib. 7-20839
 liquid, one-component plasma structure factors 7-32264
 liquid, struct., total partition function and thermal props. calcs. 7-6502
 liquid mixtures of alkali metals and halides, longitudinal collective modes 7-6744
 low temp. nonlocal electromagnetic ultrasound generation calcs. (*Russian*) 7-7294
 mixtures, collisional ionisation study (*French*) 7-10729
 multiple-cavity hollow cathode, arc discharge, gas containing alkali metal atom additions 7-32179
 photoionisation cross sections 7-50039
 plasma, phase diagram, eqn. of state study 7-37634
 plasma, ternary recombination coeffs., cumulative ionisation 7-44102
 polyacetylene, alkali metal doped, role of spin-orbit coupling in EPR spectra 7-64527
 polyacetylene, alkali metal doped, semiconductor-metal transition, EPR study 7-64528
 positron annihilation, high-momentum components and core enhancement effects 7-46195
 Ramsey resonance of alkali hyperfine doublet, frequency standard appl. 7-19733
 structural properties, ab initio calc. 7-21156
 surfaces, electron spectroscopy by deexcitation of metastable He atoms 7-59364
 tensile strength under (110) uniaxial stress (*Chinese*) 7-26825
 thermoelectric converter, role of O in porous Mo electrodes 7-13925
 vapour, optically pumped in RF field, spatial transport of population inversion 7-19782
 vapour number density, optical determ. using Faraday rotation 7-48696
alkaline earth alloys
see also barium alloys; beryllium alloys; calcium alloys; magnesium alloys; strontium alloys
 No entries
alkaline earth compounds
see also barium compounds; beryllium compounds; calcium compounds; magnesium compounds; radium compounds; strontium compounds
 halide eutectic composites, growth, struct., mech., elec. and optical props. 7-33648
 halides, aq. solns., ion hydration, dielec. props., microwave spectrosc. obs. (*French*) 7-54111
 laser and Fourier transform spectroscopy 7-19872
 silicate glasses, P_2O_5 added, struct., ^{31}P and ^{29}Si NMR 7-32302
 monohalides, electronic struct. from laser microwave double resonances spectra 7-10638
 orthovanadates, solid solns., defect struct. and electrochem. changes of O 7-32787
 orthovanadates, stoichiometry, stripping voltammetry studies 7-63836
 orthovanadates, surface electrochem. of O, cyclic voltammetric obs. 7-33957
 oxides, colour centres, Hartree-Fock cluster computations 7-16985
 silicate glasses containing alkali and alkaline earth metals, alkali ion mobility (*Japanese*) 7-27007
 sulphide phosphors, prep. and thermolum. review 7-17488
alkaline earth metals
see also barium; beryllium; calcium; magnesium; radium; strontium
 photoionisation cross sections 7-50039
alkalinity *see pH*
allotropism *see polymorphism*
alloy steel
see also tool steel
 austenite, hot working, transition from multiple- to single-peak recrystn. 7-65057
 bearing, fretting wear in seawater 7-8124
 bearing type, austenite transform. kinetics and internal stresses in bainitic hardening 7-39563
 boronised, boride-substrate interface morphology 7-53984
 boronizing and alloying elements influence 7-59661
 case hardened, struct. and contact endurance after plastic surface deform., tempering effect 7-46706
 constructional, struct. and props. after high-temp. thermomech. isothermal working 7-46522
 cost, nonmetallic inclusions influence on fracture character 7-3421
 Cr-Mo, rolling contact fatigue, asperity interacting frequency effect 7-39616
 Cr-MoVW ferritic steel, ductile-brittle transition temp., irradi. flux depend. 7-56825
 crack arrest toughness, moment modified compact tension specimen, PTS conditions 7-13695
 crack arrest toughness, proposed ASTM test method, European experience 7-13694
 cracking resistance, effect of strain rate and test temp. 7-13548
 creep-fatigue life, long-term, prediction and evaluation 7-39796
 cryogenic, Al alloying effect on mech. and mag. props. 7-39679
 die, heat-resistant, optimum hardening, temps., struct. and mech. props. 7-8022
 die, preliminary heat treatment schedule 7-8023
 dislocation struct. rel. to cyclic bending strain 7-22760
 dual phase, continuous cooling, transform. processes and products 7-28034

alloy steel continued

dual phase, effective grain size, cleavage crack propag. 7-28118
 dual phase, work hardening, accommodation strains in ferrite phase, finite element analysis 7-17550
 dual-phase, micro alloyed, mech. props. and struct., effect of process variables 7-65108
 electrical resistivity and magnetisation, temp. depend. 7-38535
 eutectoid, 1.3 wt.% Cr, specimen prep. technique influence on analytical TEM obs. of partitioning 7-22950
 eutectoid, microstruct. obs. of bainite stars 7-53695
 fatigue crack, closure behaviour, S-shaped unloading curve method (Japanese) 7-13684
 fatigue crack propagation, local crack-tip strain approach 7-63057
 fatigue crack propagation rate, effect of overloads 7-59623
 fatigue fracture surface at elevated temps., X-ray fractographic study (Japanese) 7-8098
 fatigue threshold, effective, influencing factors 7-46607
 ferrite-pearlite, fractographic characts. of fatigue crack development 7-46643
 ferritic, energy-dispersive X-ray analysis, contamination influence on P meas. in presence of Mo 7-23106
 ferritic, fusion reactor first wall, implantation-driven permeation characts. 7-49640
 ferritic, structural materials, welling after neutron and ion irradi., comparison 7-58357
 ferritic alloy claddings for LMFBR mixed oxide fuel pins 7-30562
 ferritic steel, fusion reactor first wall material, development and testing 7-53860
 ferritic-pearlitic, welded joints, hot embrittlement proneness 7-39658
 first wall candidate ferrite alloys, Ni doped, postirrad. tensile behaviour 7-56827
 foils, H charged, internal friction, quasi-molecular state (Russian) 7-59561
 forged powder, prod. from water-sprayed Astalloy powders, fracture toughness 7-13572
 frictional behavior of diamond and cubic BN abrasives 7-3461
 fusion reactor blanket material, oxidation and volatilisation rates in air 7-53957
 heat-resistant, N and V influence on mech. and service props. 7-8105
 high Ni, reactor irradi., dislocation struct. and steady-state creep (Russian) 7-2068
 high Si, rapid solidification in double roller method 7-22665
 high strength, H assisted cracking in aq. environment 7-3393
 high strength, H induced SCC rel. to galvanisation (German) 7-3521
 high strength, near threshold fatigue crack growth behaviour, effect of prior austenitic grain size 7-53906
 high strength structural, finishing monitoring by magnetic structurescope based on the Barkhausen effect 7-28241
 high-alloy, specimen dimens. effect on cracking resist. determ. accuracy 7-13549
 high-strength low-C weldable, C content effect on struct. and mech. props. 7-46583
 high-strength steels, corrosion-fatigue strength, notch effect 7-26842
 high-strength wire, prod. parameters influence on corrosion cracking tendency in H₂S media 7-17693
 hot rolled microalloyed, proeutectoid ferrite transform. kinetics, microstruct. modelling 7-17526
 HSLA, C/N ratio in (TiNb)(CN) precip., EELS obs. 7-22698
 HSLA, carbonitride particle response to weld thermal cycle 7-33661
 HSLA, corrosion in sea water, long term exposure tests, alloying elements effect 7-3482
 HSLA, electron channelling line width degradation, dependence on deform. mode 7-39613
 HSLA, gouging abrasive near mechanism, investig. with aid of pendulum single-pass grooving 7-22846
 HSLA, H-induced crack propag., method to evaluate crit. H conc. 7-65116
 HSLA, high strain-rate behaviour, Bodner-Partom viscoplastic constitutive model description 7-33754
 HSLA, mech. props. rel. to ferrite substruct. and grain size. 7-13531
 HSLA, microalloyed, precipitate size and comp., influence of reheating temp., investig. by electron microscopy 7-65054
 HSLA, Nb, ductile fracture, plastic deform. mechanisms 7-28115
 HSLA, partially coated, SCC, non-uniform H charging effect 7-3483
 HSLA, rolled sheets, residual surface stresses, corrosion pot., X-ray obs. 7-39704
 HSLA, submerged arc welds, acicular ferrite nucleation by inclusion phases 7-17525
 HSLA, TM-rolling, role of reverse temper embrittlement 7-8112
 HSLA steel, precip. anal., EDX and EELS 7-46495
 HY series, laser weldments, S and Ni effects on mech. props. 7-13602
 ion-beam-assisted deposited coatings, processing of metals for improved corrosion resist., surface modification program 7-65200
 linepipe weldments, ductility rel. to cathodic protection 7-39578
 low activation, tempering, toughness, ductile-brittle transition props. 7-53862
 low alloy, α/γ equil. phase boundary calc. (Chinese) 7-7959
 low alloy, arc weld deposits, austenite grain struct. 7-39494
 low alloy, B-containing, near-threshold fatigue cracks 7-46605
 low alloy, damaged surface, comp., displacement dislocations, Auger spectra (Russian) 7-59620
 low alloy, fatigue fracture in air and 3.5% NaCl soln., X-ray fractography (Japanese) 7-8099
 low alloy, fracture toughness assessment using elec. pot. method in comparison with standardized multiple specimen method 7-22932
 low alloy, hot dip aluminizing, alloy layer growth, influence of Si additions 7-3502
 low alloy, hot forming, transform. behaviour, struct. (German) 7-59518
 low alloy, low C, tempering investig., epitaxial ferrite stability studies (Russian) 7-13479
 low alloy, microstruct., mech. props. rel. to cooling rate 7-46514
 low alloy, pearlite free, fracture energy, effect of microstruct. parameters (Russian) 7-33787
 low alloy, retarded brittle fracture, crack nucleation stress and internal microstresses (Russian) 7-8084
 low alloy, structural transformations during continuous cooling and isotherms 7-22636
 low alloy, sulphide cracking, role of H 7-39726
 low alloy, surface crack growth under axisymm. cyclic bending 7-28130
 low alloy, trace element precipitation and segregation, hot brittleness effects (French) 7-17608

alloy steel continued

low alloy XC60, N implanted, grazing incidence X-ray diffraction 7-16591
 low C, alloying using high-intensity sources 7-28179
 low dose neutron irradiation, spectral effects on yield stress for A302B 7-51850
 low-alloy, abrasive wear correl. with alloy additions 7-65151
 low-alloy, bainitic transform., kinetics and mechanism 7-13447
 low-alloy, H-beams, controlled rolling effect on mech. props. 7-39562
 low-alloy, high-temp. drop in plasticity 7-46640
 low-alloy, nitriding temperature in glow discharge effect on nitride zone thickness and comp. 7-8176
 low-alloy, Te-containing, nonmetallic inclusions and austenite grains 7-39522
 low-alloy construction, nonmetallic inclusions influence on impact strength and fracture type 7-8085
 low-C, Ni influence on struct., fracture resist. and fractographic features 7-3420
 low-C, tempering temp. effect on mech. props. and crack resist. 7-39654
 low-pearlite, rules of austenite decomp. in continuous cooling 7-3339
 low-pearlite, subjected to controlled rolling, complex microalloying effect 7-46523
 LWR, pressure vessel materials, environmental sensitive cracking (German) 7-10214
 managing, 18 Ni, erosion, effect of microstruct. and mech. props. 7-22849
 managing, precip. and notch toughness, effect of Cr (Japanese) 7-22798
 managing, fatigue at low growth rates 7-39621
 managing, hydraulically pressed, struct., texture and hardening (Russian) 7-3323
 managing, low-temp. internal friction, H effects (Russian) 7-33710
 managing, sintered, ageing process, precip. phases investig. 7-3322
 managing, struct., mech. props. and cavitation-corrosion stability (Russian) 7-46684
 martensitic, tempering after surface plastic deform. effect on damageability in cyclic loading 7-46705
 martensitic transformation, residual stresses establishment 7-33657
 metastable, anomalous plasticity, slip, microtwinning and martensitic transformations (Russian) 7-8056
 micro-alloyed, low C, B containing, heat-affected zone props. 7-17543
 microalloyed, abnormal grain growth in austenite range (German) 7-7958
 microalloyed, carbonitride charactn. (German) 7-13461
 microalloyed, fatigue crack propag., effect of short-term static overload 7-13573
 microalloyed, high strength, phys. metallurgy and appls. 7-65066
 microalloyed, hot ductility rel. to grain size and precip. 7-28088
 microalloyed dynamic recrystn., transition of flow behaviour 7-53756
 Mn and Nb treated, high temp. ductility loss, grain boundary segregation 7-46573
 nitrided, prior heat treatment effect on mech. props. 7-46707
 nitrided layer, hardness distrib. prediction model 7-39746
 nitriding, carbonitride phase comp. in zone of inner nitriding 7-39747
 nuclear plant irradiated steel handbook 7-38069
 nuclear pressure vessel, dynamic fracture toughness, crack tip strain behaviour, EM force appl. 7-28126
 nuclear reactor pressure vessel, thermal transient, crack arrest in K-gradient 7-46617
 oxidation performance of Magnox and AGR boiler materials in high press. CO₂ 7-59676
 oxidation studies using EELS and EDX in the TEM 7-17734
 positron annihilation parameter and H behaviour in 4340 steel, effects of tempering temps. 7-46205
 power metallurgy coatings obtained by impact wave method, struct. form. 7-65211
 power plant components, remaining creep life assessment 7-8220
 pressure vessel, fatigue crack growth rates under various conditions of loading and environment 7-28203
 pressure vessel weld metal, cleavage fracturing stages at inclusion sites 7-8092
 quenched, high hardenability, thermal stress and strain generation 7-8071
 roll type, crack resist. as criterion of effectiveness, alloying and heat treatment parameters influence 7-53884
 sliding lubricated contact, wear and crit. failure load, effect of solid contamination 7-33803
 stress state nondestructive detect. with polarised US waves 7-3552
 structural, Cr surface alloyed layer, form. by CO₂ laser (Korean) 7-28196
 structural, flow stress, high temp. and strain rate (Chinese) 7-13504
 structural, heat treated, coercivity in various remanent magnetization states, NDT method development 7-65259
 structural, micromechanisms of near-threshold fatigue crack propag. 7-13551
 structural, powder, hardenability and hardness penetration, effect of comp. and porosity 7-22807
 structural, STEM-EDS X-ray microanalysis of grain boundary segregation 7-22702
 structural, struct. rel. to cold deformability, softening heat treatment methods development 7-39556
 structural, temper embrittlement, preferential segregation, Auger spectra 7-53737
 structure evolution during strong plastic deformation (Russian) 7-3358
 structure statistical parameter evaluation, image processing automation (Russian) 7-10877
 superhardenable treated, transform kinetics 7-39535
 surface layer repeated thermomechanical strengthening, mech. props. and failure character 7-53994
 tensile ductility limit calc. (Russian) 7-39597
 wear resistance under wet-abrasive erosion conditions 7-22848
 weld joint, austenitic surfacing-pearlitic transition zone, cyclic crack resist. 7-17691
 B-containing, H-embrittled grain boundaries, Auger anal. 7-59633
 C-Mn, Nb-modified, creep crack characts. at 360°C 7-46631
 CR-Mo-Ni, temper embrittlement, effect of V additions 7-13575
 CR-Mo-V, thermal fatigue resist., effect of initial struct. 7-28132
 Ca, inclusion globularising, Ba additions effect 7-21193
 Cr, austenitisation, recrystallisation, pearlite transform. rel. to hot deform. 7-28033
 Cr, coarsening behaviour of complex carbide particles, role of Si (Korean) 7-8000
 Cr, corrosion resist., influence of thermomech. treatment 7-22873

alloy steel continued

- Cr, Cr-Mo, fatigue, statistical anal. of pooled S-N data 7-65136
 Cr, ferritic, neutron irradi., isochronal annealing, elec. resist. recovery 7-58348
 Cr, heat-resisting, mech. props., effect of W (*Japanese*) 7-17617
 Cr, high C, notched rods, breaking by heating process, elastic-plastic stress analysis (*Japanese*) 7-33777
 Cr, reduced activation alloys, development, fusion material appl. 7-53664
 Cr, spring, residual stress meas., effect of decarburisation, shot peening and cyclic torsion loading (*German*) 7-22904
 Cr, surface saturation with B by laser radiation 7-8172
 Cr type, dislocation struct. after hydraulic pressing followed by austempering 7-3334
 Cr type, structural heredity in heat cycling 7-33703
 Cr type, with plasma and powdered Al coatings, SCC behaviour 7-17686
 Cr-Al, brittle failure rel. to overheating, fractography 7-22796
 Cr-Mg, deformed, struct. and mech. props. after long ageing 7-8106
 Cr-Mn, austenitic, corrosion in thermally convective Li 7-53960
 Cr-Mn, austenitic, thermal and mech. props., fusion reactor appl. 7-53795
 Cr-Mn, structurally free cementite form. rel. to Cr and Mn addition 7-22675
 Cr-Mn-Si-Ni, SCC in aq. NaCl soln., microstruct. effect 7-8196
 Cr-Mn(V), bainite transform. kinetics, austenitising and working conditions effect 7-22674
 Cr-Mo, breakaway oxidation and internal cracking at 900°C, freq. anal. of AE signal 7-17718
 Cr-Mo, chamber wall, Light Ion Beam Fusion Target Development Facilities, activation studies 7-49732
 Cr-Mo, corrosion in flowing Pb-Li environment 7-53959
 Cr-Mo, corrosion in flowing Li environment, temp. and purity depend. 7-53961
 Cr-Mo, corrosion in molten thermally convective Pb-Li 7-53962
 Cr-Mo, crack initiation under sustained load, effect of impurity segregation 7-65111
 Cr-Mo, creep fracture 7-33784
 Cr-Mo, creep-fatigue cracks, high temp., strain range partitioning anal. (*Japanese*) 7-33781
 Cr-Mo, cross-section precip. extraction replica technique 7-54042
 Cr-Mo, cyclic softening, creep and fatigue, fusion reactor appls. 7-53757
 Cr-Mo, cyclic stress-strain response at elevated temps. 7-39624
 Cr-Mo, cylindrical bar, fatigue crack propag. 7-21346
 Cr-Mo, dual-phase, as-rolled, corrosion fatigue behaviour 7-46710
 Cr-Mo, elevated temp. combined erosion-corrosion, particle impacts 7-3517
 Cr-Mo, elevated temp. erosion-corrosion 7-3518
 Cr-Mo, elevated temp. strength, H attack resistivity and stress relief cracking suscept. improvements 7-13583
 Cr-Mo, erosion-corrosion, effect of temp. 7-3519
 Cr-Mo, fatigue, criterion for omission of variable amplitude loading histories 7-22794
 Cr-Mo, fatigue crack growth, influence of ambient environment 7-28107
 Cr-Mo, ferritic, effective H permeability 7-44918
 Cr-Mo, ferritic, fatigue crack growth, transients due to change in ΔK or R 7-46646
 Cr-Mo, ferritic, HT-9, mech. props. as function of heat treatment 7-53858
 Cr-Mo, ferritic, reduced activation fusion reactor structural material, development 7-53665
 Cr-Mo, friction pair, contact zone surface struct. and mech. props. (*Russian*) 7-59640
 Cr-Mo, friction pair, surface layer structural modifications (*Russian*) 7-39678
 Cr-Mo, high C, bonded carbide, secondary temper hardening, microstruct. 7-17542
 Cr-Mo, ion nitriding, transform. of (Cr,M)₂C₃-type carbides 7-17701
 Cr-Mo, mech. stability of retained austenite, absence of H influence 7-28125
 Cr-Mo, non-equilib. grain-boundary segregation kinetics 7-59525
 Cr-Mo, normalised, tempered, neutron irradi., 390-550°C, tensile props. 7-17621
 Cr-Mo, normalised heavy section plate, weld cold cracking susceptibility (*Japanese*) 7-3425
 Cr-Mo, oxidation kinetics, breakaway oxidation and inversion phenomena 7-17714
 Cr-Mo, plate, directional solidification, rolling, strength, toughness, microstruct., weldability 7-59622
 Cr-Mo, sintered, ageing and steam oxidation, effect of P 7-7930
 Cr-Mo, solubility of S in presence of Mn and Si 7-39524
 Cr-Mo, surface degradation in elevated temp. gas-particle streams 7-3520
 Cr-Mo, thermodynamic props. of carbides, 985K 7-17536
 Cr-Mo, toughness, impurity element effects 7-53856
 Cr-Mo, tube, fatigue crack growth at high temp. 7-59632
 Cr-Mo, tube, high temp. press. fatigue testing 7-65246
 Cr-Mo, weld metal, creep crack growth 7-17623
 Cr-Mo ferritic steel, 14 MeV neutron irradi., mech. prop. changes 7-56821
 Cr-Mo ferritic steel, rust chemical reduction 7-30565
 Cr-Mo ferritic-martensitic, fracture toughness precip. of Laves phases 7-53849
 Cr-Mo type, ageing effect on heat resist. props. after cold deform. and tempering 7-22813
 Cr-Mo type, temp. and deform. rate conditions influence on mech. props. 7-33752
 Cr-Mo-Al, plasma-nitrided, fretting fatigue strength (*German*) 7-33848
 Cr-Mo-Fe-C, crack resist., temp. and comp. depend. study (*Russian*) 7-13553
 Cr-Mo-Nb, oxidation kinetics, breakaway oxidation and inversion phenomena 7-17714
 Cr-Mo-Ni ferritic-martensitic steel, irradi. in RTNS-II, TEM study 7-58345
 Cr-Mo-Ni-Mn, stress relief cracking, impurity effects 7-46635
 Cr-Mo-V, bainitic, high strain amplitude fatigue, cyclic stress and diametral strain response 7-39643
 Cr-Mo-V, Bauschinger effect in cyclic plasticity 7-3355
 Cr-Mo-V, creep crack growth at 838K, const. load behaviour 7-17625
 Cr-Mo-V, creep crack growth at 838 K, displacement-controlled loading behaviour 7-17626
 Cr-Mo-V, creep curves, exponential descriptions 7-65106
 Cr-Mo-V, creep ductility, impurity and microstruct. effects 7-46587

alloy steel continued

- Cr-Mo-V, cyclic creep accel. and retardation at room and elevated temp. 7-39581
 Cr-Mo-V, high temp. ductility, effects of B 7-46588
 Cr-Mo-V, ion nitriding characts. (*Korean*) 7-8162
 Cr-Mo-V, multistep cycling and cycling with compression hold at elevated temps. 7-13576
 Cr-Mo-V, nitrided, wear resist. rel. to preliminary thermomech. treatment 7-17659
 Cr-Mo-V, porosity assoc. with insoluble carbides, probable effect on rolling contact fatigue 7-17639
 Cr-Mo-V, rail, fatigue crack growth 7-8114
 Cr-Mo-V, rotor, high temp. creep, prior austenite grain size effect 7-53828
 Cr-Mo-V, structural, austenite form. during rapid continuous heating (*Russian*) 7-33702
 Cr-Mo-V creep eqns., parameter estimation methods 7-65107
 Cr-Mo-V type, heat treatment, impurities effect on temper embrittlement susceptibility 7-3419
 Cr-Mo-V type, service props. in different struct. conditions 7-8107
 Cr-Mo(-Ni), secondary-hardening, bainitic embrittlement 7-3405
 Cr-Ni, fatigue crack resistance, influence of stress conc. 7-33792
 Cr-Ni, low alloy, rare earth-containing, temper embrittlement susceptibility, effect of S 7-65131
 Cr-Ni, low-C, butterfly martensite, crystallographic characts. (*Russian*) 7-6580
 Cr-Ni, microsegregation phenomena in long-term holding at 400°C 7-13458
 Cr-Ni high-temp. type, N and heat treatment effect on struct. and mech. props. 7-33688
 Cr-Ni type, temper hardened, strain rate effect on plastic deform. resist. and energy characts. 7-39601
 Cr-Ni-Co VKS6, struct. and mech. characts., effects of Ni, Co and heat treatment 7-8108
 Cr-Ni-Cu, welded specimens, residual stress meas. mag. induced US vel. obs. 7-46761
 Cr-Ni-Mn (*Russian*) 7-59531
 Cr-Ni-Mo, fracture toughness rel. to austenitising temp. (*Japanese*) 7-33778
 Cr-Ni-Mo, Ge and melting, method influence on mech. props. at high temp. 7-8025
 Cr-Ni-Mo, H-induced delayed fracture under mode II loading (*Chinese*) 7-65119
 Cr-Ni-Mo, low alloy, SCC and corrosion fatigue in artificial seawater, effect of yield strength (*Chinese*) 7-8152
 Cr-Ni-Mo, maraging, mech.-props. rel. to heat treatment (*Japanese*) 7-53792
 Cr-Ni-Mo, structural elements, crit. stresses, theoretical-expt. determ. 7-31707
 Cr-Ni-Mo type, austenitisation conditions effect on austenite decomp. kinetics and mech. characts. 7-39557
 Cr-Ni-Mo-Fe-C, reversible temper brittleness kinetics investig. (*Russian*) 7-13554
 Cr-Ni-Mo-Nb, precipitates formation, effect of He 7-13460
 Cr-Ni-Mo-V, and weld metals for LWR press. vessels, brittle failure resist. 7-59636
 Cr-Ni-Ti-Al, cold-prestrained, length changes during annealing 7-65058
 Cr-Ni-W, fatigue striation, macrocrack propag. (*Chinese*) 7-8074
 Cr-Si type parts, mag. characts. after isothermal hardening, heat treatment quality inspection method 7-65261
 Cr-W, ferritic steel, unirradiated, low activation, microstructure and mechanical props. 7-53863
 Cr-W-V, ferrite, low activation, correl. of hot microhardness with elevated temp. tensile props. 7-53797
 CrMoV ferritic steels, He containing, fatigue behaviour in fusion reactor 7-56828
 CrMoV steel cold-rolled, effects of aging on mechanical properties (*Russian*) 7-13478
 CrMoVNbNi steel, Ni addition effect on void formation following irradi. 7-56822
 Fe-9Cr ferritic steel, 40 keV Cu⁺, Fe⁺ and fission neutron irradi. effects. 7-56823
 FeCrNiWMo alloys, sputtering effects on props 7-36240
 Mn, austenitic, friction induced martensitic transform., wear resist., work hardened surface layer 7-17531
 Mn, fatigue resist., effect of Mo and V alloying, carbide precip. 7-8109
 Mn, Hadfield, strain hardening, plastic flow 7-28055
 Mn, impact toughness depend. on Mn/C ratio 7-39657
 Mn, influence of S on failure mechanism in dual α/γ phase (*French*) 7-33760
 Mn, lath martensite, embrittlement in specimens containing 6 to 10% Mn (*Japanese*) 7-33774
 Mn, medium carbon, gas cylinder, fatigue behaviour (*Chinese*) 7-3411
 Mn, pipeline, magnetisation and magnetostriction, effect of stress 7-33256
 Mn, work hardening, martensite form. (*Russian*) 7-39510
 Mn-Al-Nb, cryogenic, low temp. tensile props., effect of Al content 7-46576
 Mn-Cr, case carburising, mech. props., influence of inclusion characts. 7-65135
 Mn-Cr, electron radiation damage in fusion reactor materials, voids 7-2064
 Mn-Mo-V, reactor piping material, strength, deformation and fracture behaviour 7-13578
 Mn-V, continuously cooled, hardness rel. to martensite vol. fraction 7-28121
 Mn-V, low-pearlitic, normalised, struct. and mech. props., sheet thickness depend. 7-8006
 Mn-V-Mo austenitic, struct. and precipitation hardening (*Russian*) 7-17541
 Mo-Ni-Mn, creep fracture mechanisms and rupture life 7-65137
 Nb, microalloyed, austenite-nonstoichiometric precip. equilib. 7-3303
 Nb-Al, impact behaviour, influence of grain boundary carbide density 7-13574
 Nb-V, linepipe, H-induced cracking 7-22881
 Nb-V, matrix and grain boundary precipitation, effect of heat treatment 7-46493
 Nb-V microalloyed, controlled rolled, yield strength rel. to microstruct. (*Chinese*) 7-13503
 Ni, abrasive wear rel. to anisotropic ferrite-martensite microstruct. 7-13607

alloy steel continued

- Ni, bainite transform. kinetics, influence of grain size 7-65030
 Ni, heat treatment method effect on struct. and mech. props. 7-39561
 Ni, laser-induced C atom directional motion 7-44894
 Ni, maraging, corrosion fatigue crack initiation and growth 7-3413
 Ni maraging steel, austenite form. characts. (*Russian*) 7-46466
 Ni, N29, crystallostruct. changes during reverse martensitic transform., effect of ultrasonic action (*Russian*) 7-53724
 Ni, p/m type, fracture struct. features 7-33789
 Ni, plate manufacture, direct quenching and tempering process 7-59556
 Ni, plates, direct quenching and tempering manufacturing process (*Japanese*) 7-3342
 Ni, reverse austenite transform., Mossbauer study (*Chinese*) 7-65028
 Ni, sulphide stress cracking susceptibility rel. to tempering 7-17712
 Ni-Co-Mo, managing, ultrahigh strength, delayed fracture in H environment 7-28135
 Ni-Co-Mo, maraging, fracture toughness rel. to heat treatment, precip., Auger spectra 7-65124
 Ni-Co-Mo, maraging, lath martensite boundary cracking near threshold stress intensity factor (*Japanese*) 7-53846
 Ni-Co-Mo, maraging, ultrahigh strength, H embrittlement rel. to coatings 7-28136
 Ni-Co-Mo, maraging, ultrahigh strength, H embrittlement rel. to Ni or Cu coating 7-28137
 Ni-Co-W, maraging, martensite-austenite reversible transforms. during tensile deform. and thermal cycling 7-17528
 Ni-Co-W, maraging, martensite isothermal aging, hardness, struct. and elec. resist. kinetic behaviour study 7-17553
 Ni-Cr, anelastic props. of grain boundaries and transition temp., effect of temper embrittlement 7-22815
 Ni-Cr, deform. dislocation struct., fracture 7-33740
 Ni-Cr, ductile-to-brittle transition temp. shift due to temper embrittlement and neutron irradiation. evaluation by small-punch test 7-28114
 Ni-Cr, duplex phase, plastic deform. modelling 7-28084
 Ni-Cr, fatigue resistance under combined effect of cyclic bending and cyclic torsion 7-28131
 Ni-Cr, tensile flake form., H damage, dislocation transportation (*Chinese*) 7-8077
 Ni-Cr-Mo, autofrettaged tubes, residual stress determ. by neutron and X-ray diffraction. 7-33743
 Ni-Cr-Mo, crack branching in H embrittlement (*Japanese*) 7-53847
 Ni-Cr-Mo, cylinder-on-disc lubricated sliding wear expts. (*Chinese*) 7-59639
 Ni-Cr-Mo, ΔK_{th} testing method for plastic zone size at fatigue crack tip 7-17748
 Ni-Cr-Mo, fracture toughness testing methods, comparison 7-37402
 Ni-Cr-Mo, H embrittlement in artificial seawater, effect of H content (*Japanese*) 7-53868
 Ni-Cr-Mo, high strength, fracture toughness, US meas. 7-28238
 Ni-Cr-Mo, high strength, modified HY 130, corrosion fatigue and electrochem. reactions 7-65201
 Ni-Cr-Mo, hydrogen embrittlement susceptibility, austenitising heat treatment prior-austenite grain size effect 7-3415
 Ni-Cr-Mo, phase transform., structural inheritance, dislocations effect (*Russian*) 7-39503
 Ni-Cr-Mo, pressure vessel, environmentally assisted fatigue crack growth 7-17638
 Ni-Cr-Mo, pressure vessel, crack tip opening displacement, stretch zone width correl. 7-39670
 Ni-Cr-Mo, rel. between crack tip opening displacement, J-integral and stress intensity factor 7-63073
 Ni-Cr-Mo, turbine disc, Ni electrodeposit, corrosion protection, pot.-pH diagrams 7-39699
 Ni-Cr-Mo, vacuum carburising with methane (*Japanese*) 7-13631
 Ni-Cr-Mo, weldments, dynamic fracture toughness, split Hopkinson bar technique 7-13685
 Ni-Cr-Mo-V, J-crack-opening displacement relationship depend. on work hardening exponent 7-16120
 Ni-Cr-Mo-V, low alloy, with 850 N/mm² yield strength, hydrogen-induced crack form. 7-3437
 Ni-Cr-Mo-V for turbine disc, fracture mechanics anal. 7-13589
 Ni-Cr-based, high temp. strength, modified ausforming effects (*Japanese*) 7-8089
 Ni-Mo, heavy section, elastodynamic fracture analysis of large crack-arrest experiments 7-53887
 Ni-Mo, LWR pressure vessel cladding, irradiation effects and flaw structs. 7-53888
 Ni-Mo, upper shelf fracture toughness rel. to prestrain 7-17622
 Ni-Mo, wide plate crack arrest testing using acoustic emission, reactor pressure vessel appl. 7-53886
 Ni-Mo-Mn, stable crack growth monitoring AC/DC pot. drop technique 7-33887
 Si, recrystallised grain growth, 650 to 850°C 7-46509
 Si-Al, core loss reducing effect of AP 7-33208
 Si-Al, Sb additions, effect on internal oxidation and mag. permeability 7-33206
 Si-Mn, sintered, mech. props. (*German*) 7-22831
 Si-Mn-Mo, austenitising, bainite transform., lump-like composite struct., mech. props. (*Chinese*) 7-13477
 Ti, microalloyed, austenite-nonstoichiometric precip. equilib. 7-3303
 Ti, nitrided, mech. props. rel. to cold working 7-28089
 Ti-N, ultra low C, precip./austenite equilib. 7-3302
 TiC-steel hard alloys, wear resist. in abrasive jet, methods of improvement 7-3448
 TiC-steel hard alloys, abrasive and hydroabrasive wear 7-17656
 V properties and uses in engineering alloys, review 7-39456
 V, thermal softening, carbide structural parameters rel. to alloying 7-22728
 W-Mo high-speed, nitrogen effect on stabilisation of austenite 7-8021
 WC-Co cermet particle reinforced low alloy steel composite, elastic constants., laser US technique 7-65268

alloying additions

- Bauschinger effect, influence of alloying elements and grain size (*German*) 7-17605
 ferrous laminated composite with unique microstruct., development by C diffusion control 7-17501
 first wall candidate ferrite alloys, Ni doped, postirrad. tensile behaviour 7-56827
 hard metal parts, sintered, local alloying 7-27997

alloying additions continued

- IN 100 superalloy, MC carbide props. rel. to transition element doping 7-13456
 Mo-Ni, activated sintered, sintering behaviour and mech. props. 7-7929
 oxidation resistant alloys, external scale form., third element control 7-39750
 silicide coatings on Mo alloy, scale resist., influence of Fe and Be additions 7-22875
 stainless steel films, amorphous and amorphous-crystalline with refractory metal additions, magnetron sputtering 7-39380
 steel, alloy type, boronizing and alloying elements influence 7-59661
 steel, austenitic stainless, intergranular SCC resist., influence of Si 7-46681
 steel, austenitic stainless, liq. phase sintering, effect of Si additions 7-53678
 steel, austenitic stainless, Ti addition effect on swelling under HVEM conditions 7-58343
 steel, Ca, inclusion globularising, Ba additions effect 7-21193
 steel, catalytic carbonitriding, thermogravimetric anal. of effect of rare earth addition (*Chinese*) 7-8153
 steel, Cr, coarsening behaviour of complex carbide particles, role of Si (*Korean*) 7-8000
 steel, Cr, heat-resisting, mech. props., effect of W (*Japanese*) 7-17617
 steel, Cr-Mo-Ni, temper embrittlement, effect of V additions 7-13575
 steel, Cr-Mo-V type, heat resistant, impurities effect on temper embrittlement susceptibility 7-3419
 steel, Cr-Ni-Co VKS6, struct. and mech. characts., effects of Ni, Co and heat treatment 7-8108
 steel, Cr-Ni-Mo, Ge and melting method influence on mech. props. at high temp. 7-8025
 steel, cryogenic, Al alloying effect on mech. and mag. props. 7-39679
 steel, duplex stainless, sintered, mech. props., corrosion resist. and high temp. oxidation resist. 7-7928
 steel, fine-grained, Zr effect on struct. and phase comp. 7-39525
 steel, heat-resistant, N and V influence on mech. and service props. 7-8105
 steel, high speed, service performance rel. to Ca and Zr microalloying 7-3366
 steel, high temp. ductility, effects of B 7-46588
 steel, high-speed, thermal stability improvement by laser alloying 7-8170
 steel, high-speed p/m tungstenless, Mo and V effect on microstruct. and operating props. 7-33788
 steel, HSLA, corrosion in sea water, long term exposure tests, alloying elements effect 7-3482
 steel, HSLA, microalloyed, precipitate size and comp., influence of reheating temp., investig. by electron microscopy 7-65054
 steel, HSLA, Ti and Nb additions effect on coarse grained heat affected zone 7-16765
 steel, HY series, laser weldments, S and Ni effects on mech. props. 7-13602
 steel, low alloy, rare earth-containing, temper embrittlement susceptibility, effect of S 7-65131
 steel, low C, alloying using high-intensity sources 7-28179
 steel, low-alloy, abrasive wear correl. with alloy additions 7-65151
 steel, low-alloy, Te-containing, nonmetallic inclusions and austenite grains 7-39522
 steel, low-C, Ni influence on struct., fracture resist. and fractographic features 7-3420
 steel, low-pearlite, subjected to controlled rolling, complex microalloying effect 7-46523
 steel, micro-alloyed, low C, B containing, heat-affected zone props. 7-17543
 steel, Mn, fatigue resist., effect of Mo and V alloying, carbide precip. 7-8109
 steel, roll type, crack resist. as criterion of effectiveness, alloying and heat treatment parameters influence 7-53884
 steel, stainless, corrosion resistance, Al and Si alloying effects (*French*) 7-17711
 steel, stainless, ferrite, high-Cr, solubility of Ti and Nb carbides, temp. depend. of internal friction obs. 7-53740
 steel, stainless, martensitic, low-activation, for first wall and blanket structures, development prospects 7-42194
 steel, tool, H-13 hot-work, partial substitution of Nb for V 7-13463
 Al alloy, binary, alloying capacity for solid soln. obtained by casting under press. 7-53716
 Al and alloys, dynamic restoration during hot rolling 7-22724
 Al-Cu-Mg, fracture behaviour, influence of fine transition-metal particles and grain struct. 7-3406
 Al-Ni-Pt, high temp. oxidation rel. to alloying additions, ion implantation, Rutherford backscatt. 7-53987
 Al-Si, hot dip aluminizing, alloy layer growth, influence of Si additions 7-3502
 Al-Si-Sb, directionally solidified eutectics, inter-Si flake spacing rel. to Sb addition 7-53717
 Al-Si-Zn-Mg-Ti-(Sr) system alloys, mech. props., Sr microalloying effect 7-3377
 Al-Zn-Mg, Al-Cu, superplasticity rel. to grain refining addition elements 7-46561
 Al-Zn-Mg-Cu alloy, microalloying effect on struct. and mech. props. 7-53755
 Co-Cr surgical implant alloy, mech. props., effects of N additions 7-59573
 Co-Cr-Al-Hf(Y), high temp. oxidation rel. to alloying additions, ion implantation, Rutherford backscatt. 7-53987
 Co-Ni evaporated recording media, improvement of mag. props. and corrosion resistance by Pr additions 7-33825
 Co₂Ti, alloying behaviour, phase equilib. 7-7968
 CrMoVNi steel, Ni addition effect on void formation following irradiation. 7-56822
 CrMoVNi steel, Ni addition effect on void formation following irradiation. 7-56822
 Cu-based binary alloys, Young's modulus, microalloying effects (*Russian*) 7-33711
 Cu-Ni-P, P addition effect on struct. and strength 7-53669
 Cu-Sn, ductility at elevated temps., effect of small amounts of B, P or Mg 7-53904
 Cu-Sn-B(Mg)(P), ductility at high temp., alloying additions effect (*Japanese*) 7-13515
 Cu-Zn-Al shape memory alloys, grain refinement 7-53774
 EuSe, mag. phases, press., alloying effects, NMR and mag. studies 7-2847

alloying additions continued

- Fe high temp. ductility, effects of B 7-46588
 Fe, porous, segregation of impurity elements, alloying elements selection and activated sintering 7-53742
 Fe-based metallic glasses, retardation of annealing embrittlement by Ce microadditions 7-65118
 Fe-C base ternary and multicomponent alloys, eutectic temp. and comp., theoretical calc. 7-59504
 Fe-C-based alloys, high C, rapidly solidified, mech. props. 7-22673
 Fe-Cr, high temp. oxidation, effect of various amounts of Ce and CeO₂ 7-53945
 Fe-Cr-Al, C solubility, influence of Ti and Nb, high-temp. oxidation resist. 7-22876
 Fe-Cr-Al-Ce, microstruct., high temp. corrosion rel. to Ce additions 7-13648
 Fe-Mn-Al, processing and props., effect of Si and C additions 7-17707
 Fe-Ni-Cr-Ti-B, constant elastic alloy, torsion reson. freq. temp. coeff. rel. to B content (Chinese) 7-13488
 Fe-Si alloy, high-Si, alloy elements influence on plasticity and mag. props. 7-8067
 Fe-Si alloy wires, rapidly solidified by in-rotating-water-spinning method, prod. and props. (Japanese) 7-22654
 Fe-Si-Al(Ga)(Al)(Ni)(Co)(Cr)(Mn)(Nb), atomic ordering and mechanical props. 7-11990
 Fe_{90-x}B_{10-x}Zr₁₀, amorphous, B addition effect on mag. props., elec. resistivity, crystallisation (Chinese) 7-7487
 FeCrNiWMo alloys, sputtering effects on props 7-36240
 Mo-Ag, pseudoballoys, Ni and Co effect on interphase interaction 7-27975
 Mo-V(Nb)(Ti)(Zr), solid soln. hardening, alloying element effects, Vickers hardness meas. (Korean) 7-3319
 Nb corrosion resist. in molten Li, alloying influence 7-17689
 Nb₂(Ge,Si), A15 phase, Si stabilisation, supercond. transition temp., sp. ht. meas. 7-45532
 Ni base superalloys, techniques for required props. prod. (Turkish) 7-59657
 Ni-base superalloys, cast, solidification behaviour w.r.t. Hf additions (Chinese) 7-7984
 Ni-base superalloys, creep resist. improvement, role of Re additions, APFIM study 7-22772
 Ni-base ternary alloys and superalloys, hot corrosion in SO₂/O₂ atm. 7-65175
 Ni-base ternary alloys and superalloys, hot corrosion mechanism in SO₂/O₂ atm. 7-65176
 Ni-Cr alloy, wrought, Hf effect on struct. and mech. props. 7-33689
 Ni-Fe-Cu, mag. props., hardness, elec. resist., V, Nb and Ta additions effect (Japanese) 7-12998
 Ni-Si-Mg, high temp. oxidation rel. to alloying additions, ion implantation, Rutherford backscatt. 7-53987
 Ni₃Al, solid soln. hardening with ternary additions, Young's modulus 7-13464
 Ni₃Al-Be, ductility, strength, grain boundary segregation, solid soln. strengthening, Be addition effect 7-39608
 Ni₃Al(B,Ti), rapidly solidified powders, struct. of consolidated products 7-3222
 Ni₃Al(Ga)(Ge), alloying addition lattice location, phenomenological description 7-32463
 NiTi, martensitic transform. rel. to d-transition element alloying (Russian) 7-59519
 Ti-Cr-Fe alloyed with Si, high-Cr, sinterability and mech. props. improvement 7-64986
 V-Mo-Zr-C, V-Nb-Zr-C and V-Zr-C, oxidation on heating in air, alloying elements influence 7-17687
 VCe formed by Ce ion implantation, lattice-location studies of Ce ions 7-2042
 V₂Ge solid solns. of Fe, Cr and Co, elec. resist. (Russian) 7-45273
 V₂Si solid solns. of Fe, Cr and Co, elec. resist. (Russian) 7-45273
 W-Ag pseudoballoys, Ni and Co effect on interphase interaction 7-27975
 W-Cu pseudoballoy, Si alloying effect on solute redistrib. and ductility characts. 7-53741
 WC-Ni hard metal parts, sintered, local alloying 7-27997
 Zn, electroplating in acidic bath, corrosion resist. improvement with Co and Cr additions 7-13640
 Zn-Al, bicrystals and polycrystals, creep grain boundary strengthening 7-22747

alloys

alloys such as Au-Cu, Au-Cu-Zn are indexed under components of the named elements i.e. gold alloys; copper alloys; zinc alloys in these examples

see also actinide alloys; alkali metal alloys; alkaline earth alloys; alloying additions; aluminium alloys; antimony alloys; arsenic alloys; bismuth alloys; boron alloys; cadmium alloys; dilute alloys; eutectic alloys; gallium alloys; germanium alloys; indium alloys; lead alloys; liquid alloys; mercury alloys; phosphorus alloys; rare earth alloys; selenium alloys; silicon alloys; solid solutions; superalloys; tellurium alloys; thallium alloys; tin alloys; transition metal alloys; zinc alloys

2D grain structures, topology, geometry, nucleation conditions 7-32853
 A₂B_{1-x} BCC alloys, low temp. props., spin fluctuations, alloying effects 7-52402

advanced metals developments 7-27978
 aerospace material advances 7-27875
 ageing, heterophase structures, nonequilib. state diagrams (Russian) 7-17555

amorphisation from melt, determ. 7-6516
 amorphous, hierarchical structs., SANS studies 7-51643
 amorphous, modified mag. Kondo theory 7-33000
 amorphous, partial pair distribution function determ. 7-51640
 amorphous, struct. features, HREM 7-1883
 amorphous, unresolved Mossbauer spectra with multiple convolutions, FFT-based processing 7-38972

amorphous alloys, magnetocaloric effect anomaly 7-38868
 amorphous alloys, radial distrib. fn., analytical determ. of area below first peak 7-32289

amorphous and crystalline, local atomic struct., computer simulation 7-58160

amorphous and liquid, internal press. kinetic component, eqn. of state calc. (Russian) 7-2139

atomic diffusion via vacancies, quasielastic coherent scatt. studies 7-58527

alloys continued

- BCC, polycrystalline, dislocation struct., strain hardening (Russian) 7-59545
 BCC ordered alloy, high temp. mag. states (Russian) 7-64466
 bend tests for stress corrosion testing 7-54040
 binary, directional solidification, morphological and thermosolutal instabilities, perturbation anal. 7-58446
 binary, freezing, convective and morphological instabilities 7-32615
 binary, low-melting, microhardness 7-22797
 binary, phase diagrams and short range order, Monte Carlo simulations 7-53704
 binary, self-diffusion in surface layer (Russian) 7-44898
 binary, short range order, coherent pot. approx. 7-7142
 binary, simultaneous external and internal oxidation, form. of two-phase regions in diffusion zone (Russian) 7-46704
 binary, unidirectional solidification, cell-dendrite transition criterion (Chinese) 7-65018
 binary alloy, freezing, morphological instability evolution, model cryst. growth system 7-1925
 binary alloy surface, atomic arrangements 7-32776
 binary alloys, geometrically non-equivalent nodes, ordering theory (Russian) 7-44744
 binary alloys, Monte Carlo calc. of configurational entropy and combinatory factor 7-63846
 binary alloys, TEM study of precipitate growth mechanisms 7-52064
 binary alloys of BCC metals, interdiffusion coeffs. 7-44896
 binary non-crystalline alloys, electronic density of states calc. 7-45112
 binary semiconductor alloys, directional solidification, convection, segregation, ampoule and furnace design 7-59501
 binary simple metal alloys, melting point trends and elemental variables corrls. 7-63775
 binary system components, estimating insolubility 7-44819
 binary systems, vacancy form. energy calcs., pair pot. theory 7-32429
 cellular precipitation and dissolution, model analysis 7-53743
 composites, laminated, struct.-performance maps 7-17574
 concentrated disordered alloys, positron annihilation in vacancies 7-39290
 creep activation energy 7-63732
 creep modelling for engineering design 7-22776
 d- and f-alloys anomalous props. due to charge density fluctuations 7-7132
 defects, stress- and fatigue-induced, small angle neutron scatt. studies 7-58273
 diamagnetic susceptibility of pure metals and binary alloys 7-45615
 diffusion layer at cathodes in ionic melts 7-52150
 dislocation annihilation and strain hardening (Russian) 7-46500
 dislocation glide during ageing, hardening phase particle interaction modelling (Russian) 7-38010
 disordered, density of states approx., overlapping Lorentzian functions calcs. 7-38435
 disordered, multi-site correlations, at. size effect 7-16347
 disordered alloy surfaces, density of states calc. 7-21961
 disordered alloys, positron annihilation studies of solids 7-64728
 dual-phase, simulation of growth process of minor phase grains 7-65050
 electrochemical deposition, cryst. growth modelling 7-59386
 electron diffraction analysis, appl. of theoretical diffr. patterns 7-11853
 electron irradi. induced transforms. 7-2065
 electronic structure, positron annihilation studies, review 7-45126
 electronic structure, positron studies 7-64730
 external scale form., third element control 7-39750
 fatigue non-damaging notches 7-38103
 FCC, binary, with nearest neighbour interactions, ordering 7-21403
 FCC, internal friction, interaction between dislocation kinks and substitutional solute atoms 7-51935
 flue gas scrubber corrosion rel. to pH and trace element concentrations 7-40077
 formulation of new materials 7-13341
 fracture, deform., porosity effect 7-22750
 French Metallurgy Society meeting, Paris, France (Oct. 1986) (French) 7-29579
 heat resistant gas turbine alloys, creep behaviour (German) 7-3389
 heavy fermion alloys, Kondo exponent, conc. depend. 7-27495
 heterogeneous, fusion kinetics 7-3280
 high-melting, fracture toughness (Polish) 7-44679
 icosahedral and amorphous structures, fractal coefficients 7-26646
 immiscible melts, separation under reduced gravity (German) 7-22972
 interatomic interaction pots., temp. depend. investig. (Russian) 7-12314
 intermetallic phases, appl. as high temp. materials, review 7-22775
 interstitial alloy vol. and phase diagram, order-order transition, conc. depend. calcs. (Russian) 7-32640
 interstitial alloys, order-order transitions (Russian) 7-39502
 ion beam mixing, metastable surface alloy form. and stability 7-16652
 ion bombardment-induced segregation and redistribution 7-58381
 ion projection ranges and their distrib., personal computer programs (Japanese) 7-6659
 irradiation damage, instantaneous processes 7-58314
 L₁₂ intermetallics, localised grain-boundary electronic states and intergranular fracture calcs. 7-45215
 laminated membranes consisting of alloy and oxide layers, non-steady-state H permeation 7-6889
 Laves phase, liquid quenching, transformations and phase diagrams 7-65059
 Laves phases, and struct. rel. cpds., interstitial site occupancy of H atoms 7-16549
 local and macroscopic viscosities in solid state 7-46555
 long-range order structs., diffusion of H 7-21508
 magnetic alloys, antiphase boundaries 7-12407
 magnetic alloys, phase breakdown model, Curie temp., magnetisation (Russian) 7-45677
 magnetisation coercive force for industrial alloys YuN14DK34T5, YuNDK15, YuN14DK24 and YuN14DK25BA 7-17202
 major element segregation in irradiated binary and ternary alloys 7-32661
 martensitic transformations, long-period 1-D struct. form. 7-13451
 materials science and processing, outline of trends 7-46282
 materials synthesis under high-pressure, shock loading 7-33934
 metal-ceramic particle composites, cast, solidification, struct. and props. 7-7932
 metal-H system, surface props. investig. 7-33487
 metal-H systems, statistical thermodynamic aspects of bonding 7-6576
 metallic binary alloy solid solns. with retrograde solidus, decomposition 7-21457

alloys continued

- molten salts, microscopic struct. and dynamics, review 7-44348
 morphological analysis of eutectic structures, automatic image analysis 7-7987
 nonuniformly distrib., internal friction rel. to diffusion (*Russian*) 7-65074
 order-disorder phenomena, Ising model calcs. allowing for atomic vibrations 7-21400
 ordered, L₂ and L₁, grain boundary structs., twist boundaries, geometrical models 7-63628
 ordered binary alloys of isovalent metals, superconducting transition temp., conc. depend. (*Russian*) 7-64386
 ordered L₁ superstruct., lattice state near stacking faults (*Russian*) 7-6642
 ordered substitution alloys, lattice parameters, elasticity modulus (*Russian*) 7-46542
 ordering binary alloy, FCC Ising, multiautom interactions, low temp. behaviour and Monte Carlo simulations 7-6755
 ordering effects in metallic alloys (*French*) 7-21151
 packing defect energy rel. to electron density (*Russian*) 7-45212
 particle dissolution kinetics, size determ., DSC obs. 7-3309
 phase diagrams, ab initio calc. using electronic and thermodynamic perturbation theory 7-17516
 phase separation, low Q SANS studies 7-52066
 phonon point contact spectroscopy, review (*Russian*) 7-12788
 Pirogov-Sinai theory and phase diagrams of alloys 7-58440
 plastic deformation in conditions of quasihydrostatics (*Russian*) 7-59586
 polycrystalline alloys, plastic deform., stress induced martensitic transform. (*Japanese*) 7-13514
 polymorphic transformations, composition-inhomogeneous states form. (*Russian*) 7-3296
 positron annihilation and vacancy-impurity binding in α -FCC alloys 7-39289
 positron localisation, affinity to solute clusters and size limitations 7-46200
 powder production by US gas atomisation 7-17499
 precipitation, atom probe field ion microscopy studies, statistical anal. 7-30124
 precipitation modelling under cascade damage 7-52059
 preferential sputtering, isotope enrichment 7-59328
 pseudobinary alloys, tetrahedrally coordinated, Coulomb energy calcs. 7-1941
 pseudoelasticity and shape memory effects, review 7-8060
 quasicrystalline alloys, unstable chemical struct. 7-44453
 quasicrystals, alloy quasiperiodic structures, diffraction pattern simulations 7-6585
 random alloy, phenomenological coeffs. for atom transport 7-38241
 random binary alloys, electronic props., max. entropy method 7-16929
 rapidly solidified, conf., Boston, MA, USA (Dec. 1985) 7-18496
 rapidly solidified alloys, developments and engng. design implications, review 7-27967
 segregation during exponential cooling to an aging temperature 7-53744
 self-diffusion and melting point 7-21507
 shape memory alloy, intrinsic stresses evaluation by AE 7-39829
 shape memory alloys, simulation of material behaviour 7-2088
 sheet, superplastic free bulging, mech. anal. 7-32552
 sheet metal forming limits under complex strain paths using void growth and coalescence model 7-13532
 short-range order investig. in alloys containing lattice vacancies, using Monte Carlo method (*Russian*) 7-51761
 solid solution alloys, FCC and BCC lattice structs., H diffusion models 7-21532
 solidification, differential thermal anal., modelling (*French*) 7-65024
 spectral emissivity, 2-13 μ m, 700-900K 7-44872
 spin-glass temperature, conc. depend. 7-45691
 square root diffusivity 7-12349
 steady state creep, strain response to complete unloading 7-59568
 strengthening diagram, relationship with dislocation kinetics (*Russian*) 7-53753
 structural, creep and stress relax. mechanism 7-46571
 structurally superplastic flow, texture, neutron and X-ray obs. 7-46589
 substitutionally random, electron localisation and metal-insulator transition, CPA calcs. 7-27302
 superplastic, necking, fracture, strain rate sensitivity, cavity growth 7-28087
 superplastic flow, void growth mechanism 7-28086
 superplastic plastic instabilities and uniaxial tensile ductilities, effect of grain growth 7-53820
 surface amorphisation by nanosecond ion beams 7-6517
 surfaces, ion beam and laser processing for improved corrosion resist., surface modification program 7-65200
 temperature-conc.-density phase diagram calcs. 7-3282
 ternary substitutional, electronic structure, KKR-CPA method 7-64074
 thermal conductivity theory, Lorenz ratio 7-45272
 ultrahigh-temperature thermionic conversion in space nuclear power, material considerations 7-65506
 undercooled, rapid dendrite growth 7-65014
 Y₂Fe₁₄B alloys, magnetic anisotropy and spin reorientations 7-38855

almanacs see *astronomical ephemerides*

alnic alloys see *iron alloys*

Al₂O₃ see *alumina*

Al₂O₃- α see *corundum*

α -Al₂O₃ see *corundum*

alpha-decay

- see also *alpha-decay theory; alpha-particle spectra*
 1/f fluctuations, evidence for nonexistence, expt. 7-35981
²⁶⁴108, decay and synthesis expts. 7-49347
 A=156, nuclear data sheets, levels J^π, transitions, decays 7-41025
 chemical effects of α decay in uranium minerals 7-19544
 heavy and superheavy nuclei, masses and decay properties 7-5149
 heavy nuclei, α -like superfluid phase 7-15192
 heavy rare-earth nuclei, alpha decay widths 7-602
 magnetic monopole induced α -particle tunnelling 7-5203
 nuclear data sheets, recent references May-August 1986 7-35131
 superheavy elements, nuclear properties and laboratory synthesis, review 7-61904
¹⁴⁷Sm α -decay, lifetime increase due to monopole field 7-5203
 Am separation and activity meas. in sea algae 7-54370
²⁴¹Am, α -decay, internal pair production and γ -ray intensities 7-19211
⁴⁰Ca, T=2 state alpha-particle decay width from ³⁶Ar(α,α)³⁶Ar 7-49434
²⁴³Cm, half-life determ. 7-30385

alpha-decay continued

- ¹⁵²Er, radioactivity study using mass-separated sources 7-41945
 As, A \leq 247, decay props. 7-35982
 As, A \leq 247, neutron deficient isotope decay props. 7-19212
²¹⁸Po, half-life determ., α -spectrometric method 7-30386
⁴⁰Sc decay, selected aspects in the structure of beta-delayed particle spectra 7-49346
²³⁵U, α value in thermal neutron energy point 7-56658
²³⁵U(n,f), international fission foil mass intercomparison, α -decay rates 7-42086

alpha-decay theory

- see also *alpha decay*
 decay mode predictions for spontaneous α -particle and heavy ion emission (*Rumanian*) 7-15207
 even-even nuclei with Z=104-110, theoretical spontaneous fission and α -decay half-lives 7-49485
 Fermi liquid model anal. of α -clustering and α -decay 7-41922
 spectra intensity, exciton model of precompound emission 7-24963
²⁹Ne, parity nonconserving alpha decay widths, Fermi liquid model and RPA model 7-15204

alpha-particle absorption

No entries

alpha-particle angular distribution

- see also *alpha-particle spectra*
²⁷Al(¹⁶O,X), coincidence meas. of light particles and evaporation residues 7-61906
²⁷Al(¹⁶O, α), 62, 84.5 MeV, α energy spectra and ang. distrib., direct emission mech. 7-30440
¹⁴⁴Nd(p, α)¹⁴¹Pr, 25 MeV, level excitation, α -particle distrib., knock-on contributions 7-10154
¹¹⁹Sn, nuclear shape study using γ - α angular correlations 7-41891
¹⁷⁰Yb, nuclear shape study using γ - α angular correlations 7-41891

alpha-particle attenuation see *alpha-particle absorption*

alpha-particle detection and measurement

- see also *alpha-particle spectrometers; radioactivity measurement*
 alpha particle spectroscopy using a magnetic spectrograph and a large SSNTD spark counter 7-19625
 alpha-particle corona streamer counter 7-55333
 BGO, energy resolutions for p and α 7-5557
 bioassay procedures for radionuclides for atomic radiation workers 7-8696
 calibration of radon detectors 7-49823
 calibration of radon detectors in simulated natural environment 7-54413
 cellulose nitrate as Rn and daughter detectors for indoor meas. 7-49824
 cellulose nitrate films for miners personal dosimetry 7-49822
 cellulose nitrate track detector, water effects on sensitivity and track regression 7-30866
 coal fly ash radionuclides chemical anal. using alpha, gamma and X-ray fluorescence spectroscopy 7-23266
 CR-39, α -spectrometry using chemical and electrochemical etching 7-30829
 CR-39, α -track registration energy range broadening using electrochemical etching 7-30870
 CR-39, automated image anal. of α and p etched tracks 7-30880
 CR-39, automatic α -track acquisition with Frascati PEPR 7-30882
 CR-39, response to α -particles, heat and humidity effects 7-30861
 CR-39, study of electrochemically etched α and p tracks as function of energy 7-30869
 energy meas. using cellulose acetate SSNTD 7-49855
 etched track Rn dosimeters, international intercomparisons 7-49737
 fast-neutron spectrometry using the triple- α reaction in the CR-39 detector 7-42408
 foil-type electret dosimeter for surface α -contamination monitor 7-36304
 Harwell solid state alpha detector, sources of series resistance 7-36418
 human bone, microdistribution of α -active nuclides, CR-39 autoradiography study 7-54733
 ion implanted semiconductor detectors, radiation resistance (*Russian*) 7-49836
 Josephson tunnelling junctions for α -particle detection 7-56910
 LR115 detector, radiotoxicology appl. for low-level α -activity meas. 7-54830
 LR-115 II, α -detection efficiency, effective volume 7-19657
 LR-115 Kodak SSNTD, α -counting efficiency and thermoluminescence dating appl. 7-36401
 LR-115-11 Kodak track film indoor Rn meas. 7-49738
 lung tissue, microdistribution of α -active nuclides, CR-39 autoradiography study 7-54732
 Makrofol E, particle registration studies and etching techniques 7-30875
 Makrofol E α -tracks, relationship between pre-etched track length and track spot size 7-30878
 mica track filters for Rn meas. 7-49734
 minerals, heavy ion track etching, implications for α -recoil track dating 7-36434
 multiwire position sensitive proportional chamber (*Rumanian*) 7-15457
 natural radioactivity in Mexican building material by SSNTD 7-49827
 natural Rn daughter exposure meas. in French houses 7-54414
 open track films for ²²²Rn-meas. in dwellings 7-49825
 parallel plate avalanche counter at moderate specific ionisation, timing props. 7-5541
 phantom microdosimetric spectrometer, ionising radiation quality meas. 7-8692
 photomultiplier-based track counting system for SSNTDs 7-19655
 plastic detectors/Ilford emulsion comparison for Rn and daughter activity 7-49821
 polycarbonate foil, electrochemically etched α -tracks 7-42425
 solid state α -sensitive floor monitor 7-36306
 solid state nuclear track detectors, conference, Rome, Italy (Sept. 1985) 7-40991
 SSNTD technique for Rn and thoron meas. in the environment 7-42430
 SSNTDs, advantages in alpha emitter and fissile material array 7-49828
 track etch detectors for Rn meas. 7-49735
 zircon sand, α -activity in airborne particulate, cellulose nitrate track detector study 7-49856
 Am alpha particle activity in sea sediment, detection with plastic foils 7-36431
 B detection in vegetable samples and solutions using (n, α) technique 7-33980
 CsI(Tl), energy resolutions for p and α 7-5557
 CsI(Tl) scintillator with photodiode readout, response to light particles and heavy ions 7-25312

alpha-particle detection and measurement continued

- ²³⁷Np, amount in environment (*French*) 7-40315
 Rn concentration in Danish dwellings, CR-39 track detector meas. 7-49826
 Rn dosimetry, rectangular geometry effects 7-42426
 Rn personal dosimeter for miners 7-49736
 Si surface barrier detector, annular transmission, fabrication and characts. 7-19661
¹⁴⁷Sm ion beam cross section meas. using SSNTD 7-19594
 U contamination in Al foils, CR-39 track detector study 7-54218
 U prospecting, soil survey using Rn α -detection 7-55311

alpha-particle effects

- Ag¹¹¹In, O agglomeration in presence of radiation defects 7-26791
 cyclohexane, α and γ induced solute fluoresc., single photon counting expts. 7-62448
 9,10-dichloroanthracene monocrystals, alpha scintillations, decay kinetics 7-7769
 fluorapatite, relative defect-production efficiency for fission fragments, alpha decay and electron irradiation 7-12167
 lung cancer after exposure to ²²²Rn daughters in mines and homes (*German*) 7-65816
 Melinex, energy straggling and stopping power of 4 and 5.486 MeV α -particles 7-34199
 radiobiological effect of α -emitting nuclides incorporated in the lungs microdistrib. of radioactive substance and radiation protection (*Russian*) 7-47172
 sphene, natural radiation damage, fission track and thermoluminescence props. 7-51889
 steels, stainless, α -particle irradiated, mech. props. and microstruct. 7-51872
 tissue equivalent materials, energy straggling and stopping power of 4 and 5.486 MeV α -particles 7-34199
 B₂O₃-SiO₂-M₂O (M = Na, K) glasses, ion implantation effects appl. for radioactive waste disposal 7-32519
 Bi₃Ni, α -irrad. and H implanted, elec. resist. and superconducting T_c 7-7202
 Ca₂Nd₆(SiO₄)₆O₂:Cm, radiation effects, appl. for nuclear waste disposal 7-32522
 Ca₂Nd₆(SiO₄)₆O₂:Cm ceramic simulated nuclear waste forms, radiation effects on microstruct. and fracture props. 7-58373
 CaPuTi₂O₇, substituted zirconolite, high level waste, self-irrad. effects, mech. props. 7-805
 CaZrTi₂O₇, zirconolite, alpha-recoil damage 7-6692
 CaZrTi₂O₇:Cm, radiation effects, appl. for nuclear waste disposal 7-32522
 Cu, ion irrad., sputtering and lattice damage, cryst. orientation effect 7-64843
 Cu-He system, closed swelling layer, internal stress distrib. (*Russian*) 7-59571
 Fe, alpha phase, high energy proton and alpha-particle irrad., radiation defects (*Russian*) 7-16645
 Fe, low energy ⁴He ion range and damage distrib. 7-63674
 Gd₂Ti₂O₇:Cm, radiation effects, appl. for nuclear waste disposal 7-32522
 KCl, heat treated, alpha particle dechannelling, range meas. by F-coloration depth determ. 7-32512
 Mo, alpha-particle-induced defects, annealing, positron annihilation studies 7-44633
 Mo, low energy ⁴He ion range and damage distrib. 7-63674
 Na₂O-SiO₂ glass, relative defect-production efficiency for fission fragments, alpha decay and electron irradiation 7-12167
 Nb film supercond. props., α particle bombardment and thermal cycling effects 7-33704
 Nb, radioactivation monitoring based on local activation by p,d, α 7-49726
 Nb-H system, alpha-particle irrad., defect annealing behaviour 7-44605
 Ni-Si, ductility, influence of rad.-induced segregation 7-53798
²³⁹Pu cancer risk, reduction by chelation therapy, mouse expts. 7-18029
 p-Si, alpha-particle irrad., defect form. and thermal stability 7-38073
 Si surface-barrier detector as source of slow protons 7-49777
 Si:B, ion implanted, defect and dopant depth profile studies 7-2045
 Si:B p-n⁺ junction, injection annealing of radiation defects 7-12161
 Ta, L-subshell ionis., proton deuteron and alpha impact induced, low-velocity effects 7-51879
 Ta, radioactivation monitoring based on local activation by p,d, α 7-49726
 W, L-subshell ionis., proton deuteron and alpha impact induced, low-velocity effects 7-51879
 Zr, radioactivation monitoring based on local activation by p,d, α 7-49726

alpha-particle interactions see alpha particle-nucleus reactions**alpha-particle model see nuclear cluster model****alpha particle-nucleus reactions**

- for inelastic alpha particle-nucleus scattering, see "alpha particle-nucleus scattering"
⁴He(α ,X), $\sqrt{S_{NN}}=31.2$ GeV, nuclear stopping power, Lund model comparisons 7-10161
 multistrut models, test of hadron-nucleus and nucleus-nucleus interactions 7-41771
 (α ,cny), c=charged particle, model description for particle- γ coincidences, inclusion of direct/compound phases 7-10162
 (α ,d), excitation of high-spin states in 2s-1d shell nuclei 7-19151
²¹Al(α ,X), A=⁴He,¹²C, 3.65 GeV/nucleon, cross-section meas. (*Russian*) 7-24987
²⁷Al(α ,X)¹⁸F, A=⁴He,¹²C, 3.65 GeV/nucleon, cross-section meas. (*Russian*) 7-24987
²⁷Al(α ,t)²⁸Si, proton threshold states in ²⁸Si*, astrophysical significance 7-19267
¹⁹⁷Au(α ,f), ang. anisotropy and critical ang. momentum 7-42094
²⁰⁹Bi(α ,f), ang. anisotropy and critical ang. momentum 7-42094
²⁰⁹Bi(α ,xn γ X), X=p,d,t, E_x=45,75,110 MeV, preequilibrium mechanism anal., particle- γ coincidence technique 7-19264
¹²C(α ,X)¹¹C, A=⁴He,¹²C, 3.65 GeV/nucleon, cross-section meas. (*Russian*) 7-24987
¹²C(α , γ)¹⁶O, 0.94-2.84 MeV, absolute cross sections, γ -ray distrib., excitation fn. meas. 7-42037
¹³C(α ,p), differential cross section meas. and DWBA calcs. 7-30343
⁴⁰Ca(α ,X), 10-27 MeV, fusion excitation fn. oscillations, optical model anal. 7-19268
⁴⁰Ca(α ,ap), quasifree knockout, DWIA calcs. and spectroscopic factors 7-42038

alpha particle-nucleus reactions continued

- ⁴⁰Ca(α ,p)⁴³Sc, 25.8 MeV, α -nucleus ALAS potential, diff. cross sections 7-30436
⁵²Cr(α ,X), total cross section meas. 7-42042
⁶⁹Cu(⁴He,X), 3.65 GeV/nucleon, hadron yields, angular distrib. meas. (*Russian*) 7-24987
^AFe(α ,X), A=54,58, total cross section meas. 7-42042
²H(α , γ)⁶Li stellar reaction rate, influence of ²H and ⁶Li quadrupole moments 7-24126
³H(α , γ), astrophysical energies, resonating group study 7-42033
^AH(α , γ)^{A+4}Li, A=2,3 microscopic potential model studies of light nuclearcapture reactions 7-697
³He(α , γ), astrophysical energies, resonating group study 7-42033
³He(α , γ)⁷Be, microscopic potential model studies of light nuclearcapture reactions 7-697
⁴He(α , π^0 X), $\sqrt{S_{NN}}=31$ GeV, invariant cross section meas. 7-61899
⁴He(α ,X), $\sqrt{S_{NN}}=31$ GeV, neutral energy spectra, obs. of KNO scaling 7-35897
⁴He(α ,X), many-particle rapidity correlations, cluster model framework 7-19220
⁴He(α ,X), multiplicity dependence of transverse momentum spectra at ISR energies 7-56581
⁴He(α , π^0 X), $\sqrt{S_{NN}}=31$ GeV, high p_T invariant cross section meas. 7-35907
⁶Li(α ,X), inelastic coupling potential, microscopic anal. based on coupled channel resonating group method 7-56688
⁷Li(α , Δ), 3.7 GeV/A, Δ polarization study 7-5253
⁷Li(α , π^0 Δ), 4.5 A GeV/c, reaction analysis 7-708
 Li(α ,X), exchange processes contrib., finite range distorted wave anal. 7-36017
²⁵Mg(α ,³He), 81 MeV, ²⁶Mg stretched states, spectroscopic factors and strength 7-35920
⁹⁴Mo(α ,n), 12-18 MeV, ⁹⁷Ru excited states, level schemes, spins and transitions 7-35921
¹⁰⁰Mo(α ,n), 12-18 MeV, ¹⁰³Ru excited states, level schemes, spins and transitions 7-35921
²³Na(α ,n), total cross section meas. 7-41998
¹⁴²Nd(α ,2n), ¹⁴⁴Sm lifetime meas. and particle core coupling calcs. 7-30438
^ANi(α ,X), A=58,64, total cross section meas. 7-42042
^ANi(α ,p), 25.4, 26 MeV, A=58, 60, 62, optical and ZR DWBA anal., optical pot. ambiguities (*Chinese*) 7-5250
¹⁶O(α , γ), forbidden E1 transitions, microscopic calcs. using generator coord. method 7-30373
¹⁶O(α ,X)¹⁶O, microscopic investigation of bremsstrahlung reaction 7-36016
¹⁶O(α ,ap), quasifree knockout, DWIA calcs. and spectroscopic factors 7-42038
¹⁶O(α , γ)²⁰Ne, resonant reaction rates, stellar appl. 7-695
²⁰⁶Pb(α ,4n), 51-55 MeV, ²⁰⁶Po yrast structure, transitions, T_{1/2} and isomer 7-41878
²⁰⁶Pb(α ,f), ang. anisotropy and critical ang. momentum 7-42094
²⁰⁶Pb(α ,He)²⁰⁹Pb, 183 MeV, neutron response fns., high-spin single particle strengths, DWBA anal. 7-19154
¹⁸²Re(α ,f), ang. anisotropy and critical ang. momentum 7-42094
²⁹Si(α ,d)³¹P, 25 MeV, microscopic DWBA anal. 7-19265
³¹Si(α ,d)³²P, 25 MeV, microscopic DWBA anal. 7-19265
¹⁵⁹Tb(α ,xn γ X), X=p,d,t, E_x=45,75,110 MeV, preequilibrium mechanism anal., particle- γ coincidence technique 7-19264
⁴⁸Ti(α ,p γ), particle-gamma angular correlation meas. 7-30370
⁵⁰Ti(α ,X), total cross section meas. 7-42042
⁵⁰Ti(α ,f), ang. anisotropy and critical ang. momentum 7-42094
 U(α ,X), 100 MeV, neutron cluster search (*Russian*) 7-42040
 U(α ,pf), 20, 40 MeV, backward angle proton emission in central collisions 7-5305
¹⁸²W(α ,f), ang. anisotropy and critical ang. momentum 7-42094
⁶⁵Zn* compound system, preequilibrium α -emission, angular momentum effects 7-56693

alpha particle-nucleus scattering

- (α , α'), giant resonance, RPA transition density 7-25007
 (α , α'), optical model description up to 200 MeV, review 7-42039
 (α , α'), coupled-channels formalism up to 200 MeV, review 7-42039
³⁶Ar(α , α')³⁶Ar, T=2 state in ⁴⁰Ca, alpha-particle decay width 7-49434
 (α , α'), isovector dipole mode duplication of monopole mode signature 7-5211
¹²C(α , α'), elastic scattering, hard core effect 7-42031
⁴⁰Ca(α , α'), 104 MeV, comparison of model indep. optical pot. anal. 7-699
⁴⁰Ca(α , α'), 12-18 MeV, excitation fn. calcs., optical model anal. 7-19268
⁴⁰Ca(α , α')⁴⁰Ca, resonating rays in ion-ion scattering from an optical potential 7-49435
⁴He(α , α'), high energy elastic scatt., Chou-Yang conjecture 7-61743
 Li(α , α'), exchange processes and spin-orbit pot. effects 7-30437
²⁰Ne(α , α')²⁰Ne, g-factor meas., critical assessment 7-10102
^APt(α , α'), A=194,196,198 electric quadrupole moments of first excited states 7-10103
²⁸Si(α , α'), 5-12 MeV, resonances and quasimolecular states, optical anal. 7-19224
^AZr(α , α'), A=92,94, spin assignments, ang. distrib. meas. 7-10160
⁹⁰Zr(α , α'), second 0⁺ state excitation, form factors and transitions, CC anal. 7-30369

alpha-particle scattering see alpha particle-nucleus scattering**alpha-particle spectra****see also alpha-particle angular distribution**

- alpha particle spectroscopy using a magnetic spectrograph and a large SSNTD spark counter 7-19625
 CR-39, α -spectrometry using chemical and electrochemical etching 7-30829
 heavy rare-earth nuclei, alpha decay widths 7-602
 intensity, exciton model of precompound emission 7-24963
²²⁷Ac, α -particle source, absolute energy meas. 7-42276
²⁷Al(¹⁶O, α), 62, 84.5 MeV, α energy spectra and ang. distrib., direct emission mech. 7-30440
^{242m}Am, spontaneous-fission half-life meas., α -spectra, fission fragment spectra 7-61927
²⁵²Cf, α -particle source, absolute energy meas. 7-42276
²⁴²Cm, spontaneous-fission half-life meas., α -spectra, fission fragment spectra 7-61927
⁴He(α ,X), $\sqrt{S_{NN}}=31$ GeV, neutral energy spectra, obs. of KNO scaling 7-35897

alpha-particle spectra continued
Pu content of Mururoa Atoll coral samples, alpha spectrometry study 7-54415
²³⁴U/²³⁸U activity ratios in geological materials, determ. by α spectrometry 7-60255

alpha-particle spectrometers
see also *alpha-particle spectra*
alpha particle spectroscopy using a magnetic spectrograph and a large SSNTD spark counter 7-19625
phantom microdosimetric spectrometer, ionising radiation quality meas. 7-8692
Ra and actinide samples for α -spectroscopy by electrodeposition (*Spanish*) 7-49782
Si pin photocells, high resolution α -particle detector 7-62201
Xe, liquid scintillation spectrometer 7-62199

alpha-particles
No entries

alpha-radiation see *alpha-particles*

alpha-rays see *alpha-particles*

alpha-rhythm see *bioelectric potentials*

alpha-rhythm measurement see *electroencephalography*

alternators
free-piston linear alternator solar Stirling engine concept 7-65539

altitude measurement see *height measurement*

alumina
see also *corundum*
 α -phase, X-ray diffr. whole-powder-pattern fitting without reference to a structural model 7-32214
adhesion mechanism on FeCrAlY and NiCrAlY 7-33843
adsorption of acridine and phenazine, tunnelling spectra study 7-52264
 β -Al₂O₃-Na₂O solid electrolyte for advanced high energy density battery 7-39981
amorphous, Pt particle covered, ethylene hydrogenation, intrinsic size effects 7-3607
amorphous layers, formation and annealing, ion irradiation 7-58385
amorphous matrix with small ferromag. Fe particles, mag. props., comparison with spin glasses 7-7557
anodic film, barrier layer, surface imaging using scanning tunneling microscope 7-17706
anodic films on Al, struct., magic spinning NMR study 7-22382
anodic oxidation coatings on Al, electrolytic colouring, mag. field effects (*Japanese*) 7-59662
anodised substrate, Pb borosilicate glass dielec. thin film props. study 7-17269
beta phase, diffusion of implanted ions (*Chinese*) 7-51798
bicrystals, high-purity, grain boundary structures 7-58668
birefringent, millimeter wave dielectric meas. 7-14978
capillary design for Ar milliwatt laser (*German*) 7-20274
cation solute segregation to surface of α -Al₂O₃ 7-21593
ceramic, casting by doctor-blade method, effect on props. of green tape (*Japanese*) 7-22620
ceramic, grain boundaries, microanal. 7-16577
ceramic degradation mechanisms, Na-S cell reliability models 7-59831
ceramic diaphragm differential-pressure transducer 7-61354
ceramics, friction and wear measured by a pin-on-disk method (*Japanese*) 7-22850
ceramics, green and sintered, elasticity calc. from US velocity meas. 7-2085
ceramics, grindability, effect of microstruct. 7-22862
ceramics, microstruct.-mech. prop. relationship 7-65147
ceramics, sintering, effect of TiO₂ (*Japanese*) 7-3248
ceramics and coated carbides for matching stainless steels, failure mechanisms 7-3432
clay suspensions, montmorillonite and kaolinite, viscosities and densities 7-23551
coating thickness meas. and control during thermal spraying 7-61315
coatings, ion beam and chemically etched, comparison 7-22868
coatings, plasma sprayed on stainless steel, hot isostatic pressing, hardness, bond strength 7-13624
coatings made by sol-gel process, mechanical props. 7-22867
crack imaging using scanning acoustic microscopy 7-28257
crack propagation by double-torsion method (*Japanese*) 7-59614
cracks, partly embedded, reflection scanning acoustic microscopy 7-46769
cubic γ -phase, form. during electron irradiation of MgAl₂O₄ spinel 7-26802
CVD, morphology rel. to growth conditions 7-17431
CVD coating morphology, trace impurity effects 7-3191
CVD coatings, high-temperature microhardness profiles 7-28181
CVD technologies, rate controlling mechanisms, growth morphology 7-33575
diffusion of ¹¹⁰Ag tracer, 627-1400°C 7-2270
discs, thermal shock reliability, Weibull parameters, bending and fracture testing 7-3408
dispersed in Cu, directional solidification in reduced gravity (*German*) 7-22658
dispersion of surface polaritons 7-2505
electrical ceramics, high-alumina, sintered state range widening, temp. depend. of melt apparent viscosity 7-46396
electrical props., radiation effects 7-52617
engineering ceramics, texture 7-28057
fibre reinforced Al, fatigue crack propag., effect of aq. environments 7-17624
fibre reinforced Al alloy matrix composites, fabrication process 7-46377
fibre reinforced Al composites, compressive failure modes, dead weight or machine loading 7-39663
fibre reinforced metal matrix composites, liq. metal infiltration prep., wetting 7-46372
fibres, strength distrib., multi-model Weibull distrib. 7-28081
filled poly(acrylic acid) composite, filler chem. influence on T_g behaviour, dynamic mech. spectroscopy 7-59559
film, prep. by pyrolysis of Al isopropylate 7-17448
film, transparent, growth from ultrafine alumina sol characteris. 7-13395
film adhesion to stainless steel, improvement using surface precipitates (*Japanese*) 7-22880
film preparation by isopropylate pyrolysis 7-17448
films, electron emission characts., continuous dynode appl. 7-17376
films, optical props., stoichiometry depend. 7-53421
films, RF sputtered, high intensity electron beam irradiation effects 7-44626

alumina continued
 α -foreign phase influence on RE-activated aluminate phosphors UV stability (*German*) 7-27779
formation by O₂⁺ implantation in Al foils, sheet resist. and XPS meas. 7-26780
fretting wear in seawater 7-8124
frictional behavior of diamond and cubic BN abrasives 7-3461
gamma irradiated, thermoluminescence from F and F⁺ centres (*Korean*) 7-27795
gel containing Li₂O, phase transitions, LiAlO₂ battery felt prep. 7-22601
glass, gel produced, optical transmission rel. to heat treatment 7-27733
grain boundary glassy phase, ion milling of TEM specimens 7-44327
high field dielec. relax. effects 7-7641
hot-pressed, friction and wear 7-59642
insulating thin films, normal press. CVD (*German*) 7-59453
internal friction, high temp., rel. to grain boundary diffusion 7-63743
ion beam sputtered protective coating for Kapton solar array blanket 7-3705
ion-rich β - and β'' -phases, superionic props., homogeneity ranges and conductivities 7-21520
ion-rich β - and β' -phases, superionic props., local and long-range order determ. 7-21519
joining by inducing localised reducing conditions 7-46787
kaolin-mullite, charactn. of spinel phase formed in thermal sequence 7-37937
laser ablation, laser-induced fluorescence study 7-46249
laser evaporation, luminescence of generated plasma 7-63354
lattice relaxation induced by electronic relax. 7-44622
liquid metal-alumina systems, nonreactive, thermodynamic adhesion (*French*) 7-54073
metal-Al₂O₃-InP struts., improved elec. props. with heat resist. interface 7-38753
metallised Al₂O₃ ceramic seal for combustion heated thermionic energy converter 7-65509
mixing of metal overlayers, ion beam irradiation, rapid thermal annealing, pulsed laser irradiation 7-58330
mullite, Al₂O₃ and ZrO₂ particle reinforced, prep. by reaction sintering, fractographic study 7-22800
mullite powders, props. and microstruct. of fired bodies (*Japanese*) 7-22626
mullite-alumina composites, sintering and charactn. 7-3252
neutron irradiation, microstruct., mech. props. 7-51843
neutron irradiation, permittivity and dielec. loss studies 7-33321
particle shape of plasma sprayed oxides, SEM obs. 7-2403
particles, sharp, erosion of 304 stainless steel 7-3453
particles, ultrafine, laser prod. 7-13406
phase transition temp. determ. in optical ovens for refractory materials 7-30014
polishing compound used on GdGG, with/without colloidal SiO₂ 7-37212
polycrystalline, fracture toughness, R-curve behaviour rel. to grain size 7-46615
polycrystalline, X-ray and proton irradiation, elec. cond. studies 7-33014
polycrystalline ceramics, shock fracture and recompaction, double impact technique study 7-33880
polycrystalline ceramics, spall strength, plate impact meas., spall zone model calcs. 7-33797
porous anodic films on Al, microstruct. 7-22882
porous ceramics, elec. cond. and fluid flow permeability correls. 7-38566
porous materials, strain hardening, compaction eqns. 7-64953
powder, metallised, heater appl. (*Japanese*) 7-23204
powder compacts, shock wave profiles 7-38118
powder densification by interface-reaction controlled grain boundary diffusion 7-64950
powders, fine high purity, props. and sinterability (*Japanese*) 7-22621
powders, high press. compaction, density, pore size, grain size of α -phase 7-13413
propylene-Al₂O₃ system, mixing and flow props. (*Japanese*) 7-44832
protective coatings, reactive magnetron sputtering, microelectronics appl. 7-33556
refractory ceramic, wettability and contact angle with Al melt, nitride additive effects (*Russian*) 7-12402
scale adhesion and growth mechanisms, S effect 7-65206
scale growth on Fe-Cr-Al alloys, diffusion and transport props. 7-65214
shock loaded, release behaviour, plate impact expts. 7-2101
sintered, erosion and strength degradation 7-17663
sintered, small-angle neutron scattering from porosity 7-39825
sintered, X-ray stress meas. (*Japanese*) 7-8169
small particles, HREM, single cryst. struct. anal. 7-1824
spinel growth, interface struct. investig. 7-16566
sputter deposited, characterisation, X-ray photoelectron loss spectroscopy 7-59382
strengthening, mech. props. and microstruct. (*Japanese*) 7-22820
strengthening by reactions with Si film, effect of ion irradiation, 7-28160
substrate for Si solar cells in high concentration photovoltaic module 7-17874
substrate on NiO, NiAl₂O₄ form. investig. 7-16877
subsurface layers formed by O₂⁺ ion implantation into Al, O₂ bubbles obs. 7-2035
supported Fe particles, low-rate growth 7-32779
supported Rh, CO-induced struct. changes, H₂ effect, IR study 7-23063
surface, adsorbed butylamine, thermal desorption and IR study 7-39110
surface, methanol adsorpt. Fourier transform IR spectra 7-38345
surface, Pt film adhesion, O enhancement 7-46790
surface crack characterisation by scanning acoustic microscopy 7-3567
surface electrocathodolum., defect state transitions under high voltage stress 7-39187
surface morphological changes induced by narrow beam bombardment 7-51868
surface passivation for thin Si solar cell 7-23191
surface structure and rearrangements, atomic imaging 7-27078
surfaces, catalytic reactions, studies by positron annihilation 7-39309
thermally activated muonium formation 7-53200
thin films, quantitative anal. by AES 7-59310
thin films, refr. index dispersion meas. using interf. method 7-18863
thin films, spectral ellipsometric TEM and electron spectra studies 7-27208
trigonal crystal, elastic constants, rectangular parallelepiped resonance study 7-38090
uniaxial, transverse bulk polaritons, IR refl. 7-17319
UV laser sputter etching effects, laser-induced fluoresc. and interferometry studies 7-26798

alumina continued

- vitreous bonded, crack nucleation and growth at elevated temps. 7-33770
waveguide, pump injection into FIR laser resonator 7-43356
wear behaviour, cathodolum. mode appl. in SEM 7-8228
wear mechanism in dry rolling friction 7-59643
wear mechanisms, sliding and abrasive comparison 7-3463
wear resistance, comparative study of hard materials 7-3457
X-ray microtomography with synchrotron radiation 7-47224
zeolite, ZSM-5, crystallisation kinetics from organic solvent-water mixture 7-22457
zeolite ZSM-5, hydrothermal synthesis, nucleation and growth 7-33537
Al₂O₃-SiO₂, surface centres, electronic and energy characts. 7-7323
Ag₂O-Al₂O₃ ceramics and single crystals, cond. fluctuations and contact noise meas. 7-58840
Ag₂S-Al₂O₃ composites, stoichiometry and homogeneity, interfacial effects 7-6815
Al/Al₂O₃/Au thin film struct., dielec. props. meas. and equivalent circuit anal. 7-17115
Al/Al₂O₃/Au tunnel junction, electromagnetic modes anal. 7-27439
Al-Al₂O₃ crystalline oxide tunnel barriers on superconductor surfaces, thermal oxidation 7-7448
Al-Al₂O₃-Ag MIM structs. biased near breakdown voltage, optical emission 7-52853
Al-Al₂O₃-Au MIM structs. biased near breakdown voltage, optical emission 7-52853
Al-Al₂O₃-Au sandwich struct., forming process in high elec. field (Japanese) 7-22028
Al-Al₂O₃-MgO, cast particulate composites, microstruct. and mech. props. 7-65086
Al₂O₃-stainless steel composite 7-3464
Al₂O₃ anodic films, thickness depend. of dielectric breakdown voltage 7-39007
Al₂O₃, catalysts, small angle X-ray scatt. anal. 7-16352
 γ -Al₂O₃, chemisorpt. of CO₂(ethene), thermal desorpt. spectrosc. obs. 7-16872
Al₂O₃ films, ion secondary electron emission 7-22416
Al₂O₃, minerals, shock induced radiation 7-27694
gamma-Al₂O₃, resorufin adsorbed layers, fluoresc. line narrowing and site-selection expt. 7-10655
Al₂O₃ SiO₂ gel, IR and ²⁷Al NMR.MAS spectra AlO₆, AlO₄ vibr. freq. (French) 7-64534
Al₂O₃-C₆₀ CVD layers, C and S distrib., SIMS anal. 7-6668
Al₂O₃-Cr³⁺, surface temp. meas., fluoresc. appl. 7-19947
Al₂O₃-Fe, single cryst., thermoluminesc. response 7-27794
Al₂O₃-Fe₂Y, high temp. DC elec. cond. rel. to superalloy oxide scale adherence 7-52615
Al₂O₃-Fe spheroids, Norton Masterbeads for solid particle solar receiver, optical props. 7-40043
Al₂O₃-Fe spheroids, Norton Masterbeads for solid particle solar receiver, optical props. 7-40044
Al₂O₃-Mg, microstruct. development during intermediate and final-stage sintering 7-64952
Al₂O₃-N₂⁺, ion implantation, ion-acoustic microscopy 7-51792
 β -Al₂O₃-Nd³⁺, solid state laser host, optical props. 7-57343
Al₂O₃-Ti³⁺, solid laser material, active ion distributions 7-57342
Al₂O₃/Al system, nondestructive depth profiling using secondary emission spectroscopy 7-27836
Al₂O₃/Fe interface, ion beam mixing, conversion electron Mossbauer spectra studies 7-63679
 β -(β -Al₂O₃-(Na_{0.6}K_{0.4})₂O, mixed-alkali-mixed phase cpds., acoustic study 7-63749
Al₂O₃-Al, ion plated coatings using pulsed O₂ process 7-22586
Al₂O₃-B₂O₃-SiO₂-Cu₂O glass, Cu activated, photoconductivity, lumin., influence of radiation defects 7-45381
Al₂O₃-CaO cement-glass microsphere composites, relative dielectric permittivity 7-33319
Al₂O₃-Co solar absorber coating, spectrally selective surfaces 7-23223
Al₂O₃-Cr₂O₃ ceramic coatings, thermo-sprayed, microstruct. studies (Japanese) 7-22628
Al₂O₃-Cr₂O₃-ZrO₂ system, subsolidus, high temp. phase relation 7-17519
Al₂O₃-Cu, effective thermal cond. determ. 7-27037
Al₂O₃-Fe particle dispersed system, cosputtered films, EXAFS study 7-64810
Al₂O₃-H₂O-based heterogeneous monotype systems, hardening and binding props. 7-65052
 β -Al₂O₃-K₂O-NaO, ionic conductivity, mixed alkali effect 7-52131
Al₂O₃-La₂O₃-NiO(CuO), phase transformations and solid soln. form. 7-2176
Al₂O₃-MgO, diphasic xerogels, densification, sintering, isostructural seed, epitaxy 7-27987
Al₂O₃-MgO-TiO₂-Na₂O system, sintering and creep, Na₂O influence, Cable and Reijnen-Readley models (German, English) 7-7933
Al₂O₃-Na₂O, beta-type ionic cond., mixed alkali effects, percolation model 7-12355
 β -Al₂O₃-Na₂O, cation-conductive ceramics examined by 1 MV HRTEM 7-2258
 β -Al₂O₃-Na₂O, ceramics, electrophoretic deposition 7-13390
 β -Al₂O₃-Na₂O, ion-exchange reaction with α -AgI, potentiometric study 7-54230
 β -Al₂O₃-Na₂O, solid electrolytes, Debye-Huckel-type relax. processes 7-17800
 β -Al₂O₃-Na₂O, ZrO₂ toughened solid electrolyte, failure initiation, critical current density, AE obs. 7-38252
 β -Al₂O₃-Na₂O ceramic electrolyte; electrophoretic deposition 7-13411
 β -Al₂O₃-Na₂O solid electrolytes, degradation in Na-S batteries 7-3466
 β -Al₂O₃-Na₂O solid electrolyte in alkali metal thermoelec. converter, ion cond. props. 7-13925
 β -Al₂O₃-Na₂O:Fe³⁺, luminesc. thermal effects 7-33444
 β -Al₂O₃-Na₂O-Ag₂O solid electrolyte, appl. in SO₂ sensor 7-326
 β -Al₂O₃-Na₂O-ZrO₂ ceramics, transform toughened, fabrication, mech. props. ionic resist. 7-65143
Al₂O₃-Nb, high temp. interactions, X-ray diffr., DTA studies 7-8259
Al₂O₃-Nb interface, grain boundary struct., elemental comp. determ., TEM obs. 7-21225
Al₂O₃-Nb₂O₅-rich material from Nb₂O₅-Al₂O₃-B₂O₃-Na₂O glass 7-51658
Al₂O₃-SiC composites, microstruct. and mech. props. (Japanese) 7-22821
Al₂O₃-SiO₂, adsorpt. of aromatics, IR spectra 7-10573
Al₂O₃-SiO₂, mullite ceramics, sol mixture prep., drying method effect (Japanese) 7-7944

alumina continued

- Al₂O₃-SiO₂ as fibrous insulator of solar receiver, temp. meas. using thermocouples 7-59872
Al₂O₃-SiO₂, mullite, prep. by sol-gel method, microstruct. and mech. props. 7-46386
Al₂O₃-Ta₂O₅ thin films, dielec. props. rel. to electrolum. display appls. 7-2975
Al₂O₃-Ti interface reactions studied by AES and UPS 7-21702
Al₂O₃-TiC, CVD coating on cemented carbides, diffusion of Co and W, TEM/AES study 7-27942
Al₂O₃-TiC-TiN composite ceramics, microstruct., hardness, tool appls. 7-65144
Al₂O₃-TiN composite, interfacial reaction and mass transport of components during sintering 7-3254
Al₂O₃-TiO₂, mech. props. and microstruct., influence of TiO₂ additions. (Japanese) 7-22706
Al₂O₃-TiO₂ composite powders, prep., transform. temp. 7-27985
Al₂O₃-TiO₂ system detonation coatings, struct. and phase characts., physico-mech. props. 7-65212
Al₂O₃-TiO₂-NaO_{1/2} system, elec. cond. meas. to detect suspected liq. phase 7-39467
Al₂O₃-TiO₂-SiO₂ composite, thermal shock resist. 7-33771
Al₂O₃-TiO₃ amorphous films, thermal expansion and coordination state of cations 7-44860
Al₂O₃-transition metal film interfaces, thermal reaction, backscattering spectra, X-ray diffr. studies 7-52304
Al₂O₃-ZrO₂, rapid solidification, alumina dendrite morphology 7-21424
Al₂O₃-ZrO₂, Zr environment, EXAFS studies 7-63465
Al₂O₃-ZrO₂ ceramics, densification kinetics 7-27992
Al₂O₃-ZrO₂ ceramics, hot forging characts., grain size 7-3370
Al₂O₃-ZrO₂ composite ceramics, microstruct., hardness, tool appls. 7-65144
Al₂O₃-ZrO₂ composites, high temp. behaviour and microstruct. study with HVEM (Japanese) 7-22819
Al₂O₃-ZrO₂ toughened ceramics, dry friction and wear against steel 7-8125
Al₂O₃-ZrO₂-Y₂O₃ system, synthesis and props. 7-22614
Al₂O₃-ZrO₂ composites, microstruct. charactn. by Raman spectroscopy (Japanese) 7-22684
Al₂O₃-mullite composites, thermal and mech. props., effect of comp. (Japanese) 7-26987
Au/Al₂O₃, wettability of single crystals, between metal melting point and 1673 K (French) 7-63902
B₂O₃-Li₂O-LiCl-Al₂O₃, amorphous ionic conductor, crystallisation, position annihilation study (Chinese) 7-37872
BaO-B₂O₃-Al₂O₃, aluminoborate glass, X-irrad., optical and thermal bleaching 7-45820
BaO-La₂O₃-Al₂O₃ system, synthesis, characterisation and spectroscopic investigations of mixed hexa-aluminates 7-63827
BaO-La₂O₃-Nd₂O₃-Al₂O₃ systems, synthesis, characterisation and spectroscopic investigations of mixed hexa-aluminates 7-63827
BaO-Nd₂O₃-Al₂O₃ system, synthesis, characterisation and spectroscopic investigations of mixed hexa-aluminates 7-63827
BaO-Al₂O₃-Eu²⁺, Mn²⁺ phosphor, luminesc. props. 7-46112
BaO-Al₂O₃-Eu²⁺ phosphor, luminesc. props. 7-46112
BaPb β (II)-alumina, superstructure, high resolution electron microscopy study 7-12021
CaF₂-Al₂O₃, dispersed solid electrolyte systems, enhanced ionic conduction 7-16801
CaF₂-Al₂O₃ (ZrO₂) dispersions, single and polycrystalline, elec. conductivity 7-27005
CaO-Al₂O₃ glass, 3-5 μ m transmission, rain erosion resist., surface crystallisation treatment 7-37070
CaO-Al₂O₃-SO₃-H₂O hydrated inorganic salts found in concrete, thermal energy storage appls. 7-17922
CaO-Al₂O₃-SiO₂ cement, macro-defect-free processing and low freq. dielec. response 7-13081
CdO-Al₂O₃-P₂O₅ glasses, EPR spectra, synthesis effects 7-64530
CoO-Al₂O₃ dispersed oxides, positron annihilation 7-39275
Cs₂O-Al₂O₃-SiO₂ thermionic cathode as efficient electron source 7-9923
Cu-Al₂O₃, dispersion strengthened powder alloys struct. and mech. props. 7-53667
Cu-Al₂O₃ films, dispersion strengthened, flow stress, temp. depend. (Russian) 7-53815
CuO-Al₂O₃ dispersed oxides, positron annihilation 7-39275
Cu₂O-Al₂O₃-Al moisture transducer, design and development 7-41395
Fe/Fe-FeO/Al₂O₃ systems, diffusion bonded, interface chemistry, bonding strength 7-28079
Fe-Al₂O₃ melt, steam explosion suppression by coolant viscosity increase 7-8284
Fe₂O₃-Al₂O₃, synthetic wustite, elec. cond., doping elements effect (Korean) 7-2609
GaAs-Al₂O₃, interface struct., dielectric film mol. beam epitaxial growth 7-38360
K₂O-Al₂O₃-B₂O₃-Fe₂O₃-Gd₂O₃ glasses, mag. props., composition dependences 7-2823
K₂O-Ga₂O₃-SiO₂-Al₂O₃-Fe₂O₃-FeO melts, struct. role of Fe³⁺, Ga³⁺, Al³⁺, Fe redox ratio 7-26635
Li-Al₂O₃-P₂O₅-Ag glasses, Ag⁰ centre thermal and photochemical conversion, spectroscopic consequences 7-39906
LiCl-Li₂O-B₂O₃-Al₂O₃, amorphous Li⁺ conductor, crystn. and phase separation, interface effect (Chinese) 7-38245
Li₂O-Al₂O₃-TiO₂, synthesis and props. 7-33643
 β -Mg₂O-Na₂O, study of Na⁺ motion by quasi-elastic neutron scatt. 7-63875
MgO-Al₂O₃ ceramic coatings, thermo-sprayed, microstruct. studies (Japanese) 7-22628
MgO-Al₂O₃-SiO₂, leucosapphirine, crystal growth by directional crystn., gas inclusions formation 7-33539
MgO-Al₂O₃-SiO₂-GeO₂ cordierite ceramics, sintering, microstruct., thermal props. 7-52088
MgO-Al₂O₃-SiO₂-ZrO₂, low thermal expansion dec. insulators 7-2237
MgO-M₂O₃-ZrO₂ (M = Al, Cr), subsolidus phase relations 7-17519
MgO(Al₂O₃)_n, electron beam irrad., point defect aggregation, screw dislocation climb 7-63662
MgO-Al₂O₃ epitaxial film substrate for Si solid phase epitaxy 7-38399
Na/ β -Na₂O-Al₂O₃/NiCl secondary cell, characterisation 7-65428
 β -Na₂Al₂Mg₂Al₂-xO₁₇ based multivalent β -aluminas, synthesis 7-33628
Na₂O-11Al₂O₃, β -alumina, effect of NO₂ sorption on electrical conductivity 7-21511

alumina continued

- $\text{Na}_2\text{O-Al}_2\text{O}_3$, ^1H , ^{27}Al and ^{23}Na NMR studies 7-22148
 β - $\text{Na}_2\text{O-Al}_2\text{O}_3$, struct. at 5K, ^{23}Na NMR 7-7595
 β - $\text{Na}_2\text{O-Al}_2\text{O}_3$, structure at 5K, ^{23}Na NMR 7-7594
 β - $\text{Na}_2\text{O-Al}_2\text{O}_3$ ionic conductors, mechanical and electrical relax. 7-44687
 β - $\text{Na}_2\text{O-Al}_2\text{O}_3$ - $\text{CdO}:\text{Cr}^{3+}$, luminescence spectra 7-33448
 $\text{Na}_2\text{O-Al}_2\text{O}_3$ - GeO_2 glasses, ionic transport meas., packing density depend. 7-32710
 $\text{Na}_2\text{O-Al}_2\text{O}_3$ - SiO_2 glass system, strength and struct. features 7-58150
 $\text{Na}_2\text{O-Al}_2\text{O}_3$ - SiO_2 - H_2O , zeolite ASM-5, framework site resolution and assignment by X-ray and NMR meas. correl. 7-25541
 $\text{Na}_2\text{O-B}_2\text{O}_3$ - Al_2O_3 glass struct., NMR and computer simulation 7-1898
 $\text{Na}_2\text{O-CaO-Al}_2\text{O}_3$ - SiO_2 system, synthesis of glasses by sol-gel process 7-64997
 $\text{Na}_2\text{O-Nd}_2\text{O}_3$ - Al_2O_3 system, struct. of single cryst. with magnetoplumbite struct. 7-6602
 $\text{Na}_2\text{O} \cdot n\text{Al}_2\text{O}_3$, mullite struct., form. by solid state reaction 7-7937
 $\text{Nb-Al}_2\text{O}_3$, diffusion processes and interphase boundary morphology 7-16817
 Nb_2O_5 - Al_2O_3 - B_2O_3 - Na_2O - SiO_2 , phase separable glass, heat treatment leaching, X-ray diffraction anal. 7-51658
 $\text{Ni-Al}_2\text{O}_3$, diffusion processes and interphase boundary morphology 7-16817
 $\text{Ni-Al}_2\text{O}_3$ composites, small metal particles, high resolution electron microscopy and X-ray diff. meas. 7-46376
 NiAl_2O_4 , spinel growth, thin film Al_2O_3 substrate, topotactic relationships 7-58717
 $\text{Pd/Al}_2\text{O}_3$ surfaces, ethylidyne covered, CO adsorpt., IR spectra studies 7-2371
 $\text{Pt-Al}_2\text{O}_3$ catalysts, small angle X-ray scatt. anal. 7-16352
 $\text{Pt-Al}_2\text{O}_3$ composites, small metal particles, high resolution electron microscopy and X-ray diff. meas. 7-46376
 SiC or Si_3N_4 whisker reinforced composites, microwave sintering, microstruct. 7-27995
 Si_3N_4 - Al_2O_3 - Y_2O_3 -(CeO_2)-(La_2O_3) ceramics, sintered, IR and Raman spectra 7-46000
 Si_3N_4 - Y_2O_3 - Al_2O_3 , pressureless sintering 7-17503
 SiO_2 - Al_2O_3 , mullite form. from xerogels, X-ray and IR obs. 7-46391
 SiO_2 - Al_2O_3 glass, roller-quenched, NMR evidence for 4-, 5- and 6-fold Al sites 7-44384
 SiO_2 - Al_2O_3 powders, prep. by spray pyrolysis, sinterability, effect of chem. comp. (Japanese) 7-3246
 SiO_2 - Al_2O_3 system, charact. of spinel phase from xerogels and form. process of mullite 7-39464
 SiO_2 - Al_2O_3 vitreous systems, low temp. sp. ht. and thermodynamic props. study 7-63842
 SiO_2 - Al_2O_3 - CaCO_3 - Na_2CO_3 glass system, Ar^+ ion beam effects 7-32521
 SiO_2 - Al_2O_3 - Li_2O - ZnO - TiO_2 - ZrO_2 - As_2O_3 - Cr_2O_3 :Cr, glass ceramic, time resolved spectra 7-63478
 $\text{Sn/Al}_2\text{O}_3$, wettability of single crystals. between metal melting point and 1673 K (French) 7-63902
 SrCl_2 - Al_2O_3 system, enhancement of ionic conductivity 7-2256
 TiCl_3 - Al_2O_3 , ionic transport investig. 7-16798
 $\text{W-Al}_2\text{O}_3$ - K_2O - SiO_2 , doped wire, effect of dopants on microstruct. (Korean) 7-17547
 Y_2O_3 , Al_2O_3 coatings on Ni-based superalloy, appl. as high temp. protective coatings for gas turbines 7-46695
 Y_2O_3 - Al_2O_3 system, prepared by sol-gel process, IR vibr. spectra study 7-33384
 Y_2O_3 - Al_2O_3 - B_2O_3 system, glass formation, props. and struct. 7-2205
 $\text{ZnO-Na}_2\text{O-Al}_2\text{O}_3$ - SiO_2 , zeolite, partially exchanged, IR and neutron scatt. studies of adsorbed ethene 7-7001
 ZrO_2 , Al_2O_3 stabilised thin films 7-45062
 $\text{ZrO}_2/\text{Al}_2\text{O}_3$ ceramic incoherent interface struct. 7-16430
 ZrO_2 - Al_2O_3 composite powder, thermal decomposition prep. for porous ceramics 7-13422
 ZrO_2 - Al_2O_3 composite, Y_2O_3 -stabilised, compressive deform. 7-28100
 ZrO_2 - Al_2O_3 films, composition and struct., X-ray emission and ESCA studies 7-22385
 ZrO_2 - Y_2O_3 partially stabilized, Al_2O_3 effect on retaining tetragonal particles, matrix toughening 7-59485

aluminium

- see also nuclei with
1.43 MeV γ -ray penetration of shields, benchmark data 7-5487
acoustic emission during corrosion in FeCl_3 soln. 7-39814
acoustic emission during deform. of high-purity single crystals. 7-59588
adlayer on plasma passivated Si, subsurface H barrier layer obs. 7-17745
adsorbed on Ni and Cu surfaces, electronic struct. and oxidation of surface 7-22443
AE during deform., effect of struct. state (Russian) 7-38127
Amazon River, continental shelf, clay mineral reactions effect on Al distrib. in sediments and waters 7-34551
angular dependent photoelectric yield and optical constants 7-45387
anodic films, double-refraction theory 7-39743
anodic oxidation coatings, electrolytic colouring, mag. field effects (Japanese) 7-59662
anodic oxide films, dissolution kinetics in KF solns. 7-39705
anodic polarisation in NaCl soln., instantaneous impedance study 7-23032
anodised, variation in polarised light intensity with grain orientation 7-54041
anodising by chromic acid, surface struct., abrasion resist., hardness, adhesion props. 7-13646
anodising in Na_2SO_4 and H_2SO_4 solns., AC impedance meas. (Japanese) 7-13632
aquatic organism acidification effects, data evaluation and compilation 7-40054
atom, electron inelastic scatt. cross-sections 7-5775
atom, g_f factors, many-body calcs. 7-62265
atom, hyperfine struct., magnetic-dipole- and electric quadrupole coupling consts., atomic fluoresc., MCHF method 7-30985
atom, level energies and oscillator strengths, coupled channel model calcs., energy depend. sensitivity 7-49906
atomic cluster, trapping regions around impurity atoms, charge density 7-53195
Auger electron emission by Ar bombardment, Monte Carlo simulations 7-53470
Auger electron spectra, deconvolution calcs. 7-24728
Auger emission, ion-induced, review 7-59360

aluminium continued

- Auger energy, Slater transition state calcs., metallic and atomic states, jellium model 7-38475
barrier film formation, anion incorporation and migration 7-53947
bicrystals, grain boundary rumpling during sliding 7-2030
bremsstrahlung isochromat spectra, electron-energy losses 7-22377
C fibre reinforced Al, segregation of doping elements, Si, Bi 7-65046
calorimetric study of laser-irradiated thin foil targets 7-32026
charge-induced effect on creep and hardness 7-21598
chemisorption, interaction of atoms and mols. with surfaces, cluster approx., total energy calcs. 7-52265
clusters, electron energy spectra, size effects 7-7103
coadsorbed with N_2 on Ni, N(1s) spectrum 7-21968
coated fibre, high-temp. effects 7-11146
coating, highly reflecting diffusers, middle-IR region, develop. status study 7-57615
coating, plasma and powdered, on Cr steel, SCC behaviour 7-17686
coating on expanded polystyrene, thermal flux meas., compensated heat flow meter appl. 7-4838
coating on Rene and pure Ni, high temp. oxidation, TEM obs. 7-28202
coatings, atmospheric corrosion products in industrial and marine environments 7-39716
cohesive props., effective medium approach 7-45201
conversion layers on Al, struct., TEM, LAMMA, AES, XPS, SIMS, ion scatt. spectra 7-23094
cooldown mass flow requirements for He or N cooling systems 7-56281
Corbino effect, thickness variations effects 7-38539
corrosion in carbon tetrachloride, inhibition 7-54010
corrosion in NaCl solns., influence of hydrostatic press. and salt conc. 7-39271
corrosion inhibition in HCl by thiosemicarbazide derivatives 7-3487
corrosion protection by Ce corrosion coatings 7-53988
corrosion resistant coating on GdTbFe, mag. props. 7-53952
cracking behaviour during liquid Hg embrittlement 7-22816
creep rate, role of grain boundary movements 7-44666
crystals with edge dislocations, 2D angular correlation of positron annihilation radiation 7-39242
cyclic deformation of single crystals. at low const. plastic strain amplitude 7-65114
cylinder in water, Franz and Stoneley SAW mode obs. 7-1303
cylindrical tank, water-filled, damping characteristic determ. from vibration meas. 7-16200
cylindro-inner cones, freezing point, radiant emission characts. 7-56254
defect struct. during plastic deformation, periodic variation 7-44656
defects in cultured quartz, IR and laser spectroscopic charactn. 7-59234
deformed, acoustic emission on heating 7-51958
deposition onto sputtered and cleaved $\text{Hg}_{1-x}\text{Cd}_x\text{Te}$ surfaces 7-33513
determination in gallium and aluminium oxinate mixtures, fluorimetry 7-54231
deuteron irradi., multiple fracture planes, bubble growth 7-58372
diagnostic radiology, Al equivalence of materials used, dependence on beam quality 7-34242
diffusion annealing effects on Mo plates magnetoresist. (Russian) 7-7408
diffusion into Fe, influence of mag. field, radioactive isotope study (Russian) 7-52157
direct conversion electrodes, material effects on energy conversion efficiency, neutral beam injection system appl. (Japanese) 7-10277
directionally solidified, rolling, recrystallisation texture 7-33646
discontinuous films, large scale coalescence, post-deposition DC resistance increase 7-45069
dislocation kinks, tunneling, acoustic study 7-2023
disordered films, density of states, electron-electron interactions, tunnel conductance meas. 7-52393
displacement cascade damage computer simulation using binary collision approx. code (Japanese) 7-32535
divacancy effect, annihilation radiation Doppler broadening meas. 7-37982
divacancy migration and small vacancy cluster form. 7-37977
dopant intercalation into InSe and GaSe layer cpds., Auger and IR spectra studies (Russian) 7-32476
ductile fracture, plane stress, essential work of fracture vs. energy dissipation rate 7-20649
ductile fracture rel. to heat treatment, vacancy conc. effect 7-8095
dynamic fracture of ductile solids, internal state variable description 7-26844
dynamic restoration during hot rolling 7-22724
electrodeposition from nonaq. solns. (Japanese) 7-64964
electron energy spectrum, temp. effects and mag. susceptibility (Russian) 7-7102
electron mean-free-path calculations using a model dielectric function 7-52583
electron pair correl. functions, real space variational calcs. 7-52479
electron scatt. by Al atoms in solids, polarisation and exchange 7-22401
equilibrium vacancy ensemble, study using angular correlation of positron annihilation-radiation 7-39233
evaporated films, O contaminated, recrystn., after annealing 7-38412
explosively launched expanding ring test, computer simulation and anal. 7-33878
fatigue, dislocation mobility (French) 7-13539
fatigue cycling, oscillatory variation of half-width of X-ray diff. line profiles 7-46645
FCC crystal structure, secondary ion emission, current density effects 7-59318
ferrofluid-Al particle composite, microwave absorption studies 7-59306
film, laser deposition for metallisation 7-53631
film, low energy electron transmission, inelastic and elastic scattering cross section calcs. 7-63698
film, quantum size effects and dimensionality 7-45521
film, reactively evap., morphology and opt. props. 7-59272
film, surface roughness characterisation, spectroscopic ellipsometry method 7-9819
film deposition from partially ionised vapour flux, fast ion interactions 7-12531
film deposition on amorphous substrates 7-21770
film deposition using magnetron-plasma CVD system 7-64931
film growth by UV laser photolysis of trimethylaluminium 7-54153
film on Si, wire bondability 7-21710
film resistivity depend. on thickness and annealing time 7-11242
films, chemisorption of O, Al-O bond lengths, photoemission EXAFS meas. 7-64871
films, magnetron sputtering, target profile changes 7-7853

aluminium continued

films, vapour deposited, effect of O partial press. 7-52339
 films and wires, fluctuation and localisation effects 7-64176
 films on InP, wet anodisation, compositional profiles 7-65216
 films on Si, Auger depth profiles using a dual ion gun system 7-22429
 finite compression of solids, second order thermoelastic anal. 7-43708
 foil, anodic etching, influence of activators and passivators in electrolyte on surface area increase (*Polish*) 7-22889
 foil, H^+ induced ridge electrons emission 7-46270
 foils, alumina form. by O_2^+ implantation, sheet resistance and XPS meas. 7-26780
 foils, electron absorpt. and scatt. energy spectra, Monte Carlo calcs. 7-22399
 foils, U contamination study using CR-39 track detectors 7-54218
 fourth-order thermal expansion coeff. fn. 7-44868
 fracture, size effect tests 7-59595
 freely burning arc discharge, self-reversed reson. spectral lines 7-32157
 freezing point, thermodynamic temp. meas. between 683K and 933K using IR pyrometer 7-18788
 Frenkel pair formation energy, pseudopot. theory anal. (*Russian*) 7-6617
 fusion reactor first wall, plasma disruption damage calc. 7-791
 fusion reactor first wall behaviour after plasma disruption, electron beam expt. 7-62068
 gamma-ray attenuation coeff. obs. incorporating detector resolution 7-63656
 Gibbs free energy at melting nonstructural contribution estimation 7-2156
 grain boundaries, Na and H impurities, small cluster quantum chemical calcs. 7-38017
 grain boundary energies from local-electron-density distributions 7-6634
 grain refinement by horizontal circular vibration 7-22650
 graphite fibre reinforced Al, fatigue crack propag., effect of aq. environments 7-17624
 graphite fibre reinforced Al composite, corrosion protection to NaCl soln. exposure 7-3488
 hardness, effect of thermomech. history 7-53873
 heavy ion impact, secondary electron energy spectra 7-46265
 heliostat reflectant surfaces optical properties (*Rumanian*) 7-28388
 heterogeneous shock wave response, holographic interferometry studies 7-32571
 high press. strength, shock wave expts. 7-22782
 high purity, elec. cond., low-temp. plastic deform. effects (*Russian*) 7-17009
 high purity macrocrystalline, internal friction peak, contrib. of bamboo boundaries 7-8037
 high purity samples, cryoconductivity investig. (*Russian*) 7-12695
 hornblende, Al content as empirical igneous barometer 7-55029
 hot dense plasma, at. props. and transition probabilities 7-57032
 Hugoniot meas. to 420 GPa using a two-stage light-gas gun 7-21397
 hysteresis behaviour of medium temp. peaks (*French*) 7-63742
 implanted, FCC solid Ar bubbles, X-ray diff. 7-2043
 impurity diffusion, with form. of segregation phases at dislocations (*Russian*) 7-52146
 induction-heated conductor, relax. temp.-electric self-oscillations (*Russian*) 7-52665
 internal friction peak obs., dislocation configurations 7-38115
 ion implantation of O_2^+ , Al_2O_3 subsurface layers formation, O_2 bubbles obs. 7-2035
 ion implanted, inert gas solid bubbles, high resolution electron microscopy studies 7-32424
 ion trapping of D^+ , mechanisms 7-64857
 ion-implanted, processing of metals for improved corrosion resist., surface modification program 7-65200
 IR spectrum, intraband and interband processes 7-22256
 island films, optical props., Maxwell Garnett and Hampe-Shklyarevskii theories 7-3102
 laser irr. planar target, simultaneous meas. shock breakout and X-ray transmission 7-44207
 laser plasma, population inversion X-ray spectra 7-26506
 laser-produced line plasmas, soft X-ray spectroscopy techniques 7-11701
 late-type giant stars, abundance anal. rel to departures from LTE in Na and Al 7-60662
 lattice dynamics and three-body forces, phonon freq. Debye-Waller factor calcs. 7-63760
 lattice sparing of interstitial solid solns. of B and C, deform. interaction, pseudopotential method (*Russian*) 7-58271
 light interstitial motion, recent expts. 7-52114
 liquid, dielectric function, neutron and X-ray scatt. methods 7-52481
 liquid, struct., X-ray, 800-1600°C (*Russian*) 7-58128
 long-range oscillatory surface relaxations simulation 7-2317
 magnetron sputtered ion plating on A3 steel (*Chinese*) 7-22473
 masks for Si or SiO_2 etching in CF_4/O_2 plasmas 7-65222
 mechanically deformed, thermoacoustic imaging 7-46757
 mesh IR diffractive filters fabricated by electron beam lithography, spectral and polarising characters. 7-62816
 metal films, mech. props., relation between different quantities 7-8041
 metallic electron charge density to electron momentum density transformations 7-27249
 metallic glass reinforced Al composite fabrication by multi-lamina explosive compaction 7-59482
 metallisation on semi-insulating GaAs, electromigration failure anal. 7-44927
 mirror, absorptance meas. at glancing incidence, photoacoustic calorimetry 7-20380
 mirror coatings, UV reflectivity loss, in space 7-25938
 mirrors, LaF_3 and $LiYF_4$ broadband VUV reflectance coatings 7-57520
 molten, soln. kinetics of stainless steel 7-16753
 monocrystalline, Harper-Dorn creep, dislocation network theory 7-22749
 monocrystals, 6N purity, thermal cond. minimum 7-17011
 muon trapping and diffusion after electron irradiation, μSR study 7-45864
 NDT, computed tomography appl. 7-28254
 NDT appls. of computed tomography, basic principles 7-28253
 neutron irr., positron trapping rates, temp. depend. 7-46218
 nonmagnetic samples, ferromag. behaviour 7-53040
 nuclear quadrupole interactions in the presence of muons 7-53192
 overlayer an amorphous W-Si thin films, interfacial reactions 7-21763
 overlayers interaction with amorphous alloy diffusion barriers 7-21761
 overlayers on Si, Schottky barrier formation, local electronic struct., EELS study 7-21975

aluminium continued

oxide anodic films, struct., surface EXAFS, magic angle spinning NMR studies 7-22382
 oxidised surface, adsorption of benzoic acid and benzaldehyde, SIMS and XPS 7-65351
 particles, ignition behind detonation and shock waves 7-8287
 particles, ultrafine, laser prod. 7-13406
 phonon density of states from heat capacity temp. depend., inverse problem 7-6736
 phonon spectra, dynamical pseudopot. shell model calcs. 7-51965
 plasma, heavy ion plasma double layers, particle-in-cell simulations 7-31993
 plasma, high density, high temp. at. pot., comparison with bremsstrahlung Gaunt factors, density functional theory 7-63254
 plasma, K-shell reson. lines, spot spectroscopy diagnostics 7-37742
 plasma, KrF laser produced, ablation parameters 7-44206
 plasma, laser-supported detonation waves in obliquely incident beam 7-11648
 plasma created by laser at 1.05, 0.53 and 0.26 μm , soft X-ray imaging to study thermal transport 7-1735
 plasma etching, solutions for 'pump damaging' etch and CVD processes 7-35528
 plastic deform. and supercond. props., 0.5 to 4.2K (*Russian*) 7-8055
 plastic deformation under impact loading, metallography, SEM and TEM studies (*Russian*) 7-3361
 plate US backscatter and resonance expts. 7-2108
 polycrystalline, deformed, positron trapping and annihilation 7-39258
 polycrystalline, high temp. creep, strain hardening rates during primary stage 7-65104
 polycrystalline, near surface struct., simultaneous He^+ and H^+ implantation effects 7-58302
 polycrystalline target, sputtering by 40 keV Ar^+ ions, computer simulation 7-64848
 positive muon diffusion and hopping rate 7-52111
 positron annihilation at surface 7-39308
 positron lifetime spectroscopy, determ. of source correction and backscattering 7-39284
 positronium work function, temp. depend. 7-58859
 powder production from melts by centrifugal atomisation 7-7924
 powders, cold sintering 7-64972
 powders, dynamic consolidation 7-39457
 proton irradiation, 800 MeV, gas accumulation at grain boundaries 7-58361
 pure, 7-65182
 quartz:Al, static magnetisation of $Al-O^-$ centres, electric field effects 7-38900
 quenched, secondary defect form., isochronal annealing, positron lifetime study 7-39298
 quenched, tensile flow stress, effect of grain size and strain 7-22756
 recrystallisation, cryst. boundary stresses, synchrotron X-ray topography study 7-26684
 recrystallisation, repeated cold rolling effect, Vickers hardness obs. 7-59543
 reflectivity meas. on shock-unloading solids 7-27693
 relaxation process studied by positron annihilation 7-6698
 in river water in Cumbria 7-13933
 rolling contact deformation of 1100 disks 7-17594
 SAW generation by thermoelasticity for nondestructive testing appl. 7-44981
 selective CVD technology 7-53629
 shearing properties, axial compressive stress effects 7-8063
 sheet, anisotropic, work hardening and limit strain assessment in biaxial stretching 7-13534
 sheet, dislocation relax. contrib. to deform., internal friction and dynamic modulus meas. during creep 7-63626
 sheet, press formability and anisotropic yield, Bassani-type criteria 7-28068
 sheets, rolled, US SH wave vel., ang. depend. 7-38126
 shielding slabs, penetration of 2.75 MeV γ -rays 7-30712
 shock adiabats, shell effects 7-2104
 shock loading, constitutive relation 7-26865
 shocked, polycryst. positron annihilation ang. correlation studies 7-46197
 Si-Al Schottky barriers, Ar ion implantation damage, thermal anneal recovery 7-17101
 single cryst., transverse conduction electron focusing and specular reflection 7-52407
 single cryst. and bicrystal, polygonisation substruct., grain boundary effects (*Russian*) 7-58287
 single crystals, helical dislocations with low dislocation density 7-51774
 single-layer metallic structures obs. in EUV and VUV 7-22215
 small particles in amorphous materials, far-IR absorpt. spectra 7-64623
 soft X-ray laser research at Palaiseau 7-20205
 soft X-ray spectra, using photon excitation from synchrotron light source 7-30150
 solid, thermal diffusivity, mirage-effect meas. 7-45271
 sputtered thin films, struct. props. 7-21758
 steady-wave shock compression, thermoplastic shear 7-51937
 structural elements, corrosion in contact with building materials (*German*) 7-3522
 structures, corrosion damage depth meas., eddy current method (*German*) 7-13711
 submicrosecond elastic loading, material relax. phenomena 7-12186
 substrate, two step pot. model of Na overlayer, nonlocal corrections to Fresnel optics calc. 7-64716
 superconducting, penetration-depth anisotropy, quasiparticle magnetospectroscopy 7-12910
 Superconducting, positron annihilation 7-45556
 superconducting microbridges, phase slip centres 7-38819
 superconducting transition temperature, press. depend. 7-22058
 surface, (100), CO adsorption, EELS and thermal desorp. 7-17815
 surface, (110), Ar^+ sputtered, vacancy-type defect distrib., variable energy positrons study, mol. dynamics simulations 7-12429
 surface, (110), atomic arrangements 7-32776
 surface, (110), H_2^+ scatt., charge exchange 7-3133
 surface, (110), scatt. of H_2^+ ions, resonant transition rates for charge transfer 7-3134
 surface, (111), Pd and Ag films, growth and electronic struct., UPS, LEED and AES studies 7-52350
 surface, clean and oxidised, secondary ion emission. 7-64851
 surface, glazing-angle scattering and neutralization of positron beam 7-46178

aluminium continued

- surface, H^+ Auger and resonant neutralisation, charge capture probability, parameter-free perturbation theory calcs. 7-3141
- surface, H^+ Auger neutralisation, transition rate calcs. 7-3140
- surface, impulse coupling coeff. and Nd:glass laser irradi.-induced material removal study 7-64828
- surface, investigation using surface behaviour diagrams 7-27077
- surface, ion induced secondary electrons, surface topography effects 7-13280
- surface, ion irradiated, flaking, orientation dependence 7-38074
- surface, low energy positron interactions, elastic and inelastic scatt. calcs. 7-39330
- surface, Mo low temp. growth, electron spectra studies 7-12540
- surface, O_2 adsorption, electron beam effects, AES and secondary electron emission studies 7-27835
- surface, polycryst., single cryst. and amorphous, ballistic collision cascade anisotropies 7-58379
- surface (100), positron surface states, 2D ang. correl. of annihilation radiation, momentum density study 7-39305
- surface (110), Ar ion damage production, mol. dynamics simulation 7-58378
- surface (110), Ar-induced Auger electron emission, Doppler broadening 7-59345
- surface (110), sputtered defect profile, variable-energy positron beam meas. 7-38077
- surface (111), energy distrib. of reemitted nonthermalised positrons 7-16662
- surface analysis using XPS and electrochemistry 7-28370
- surface damage, dislocation struct., TEM anal. 7-16564
- surface homogeneous intermediate valence of Sm overlayers, photoemission 7-39351
- surface oxidation, diffusion of Au atoms through oxide layers 7-8200
- surface plasmon excitation of small supported particles, EELS study 7-45197
- surface plasmons, electron energy loss peaks 7-7305
- surface roughness parameter measurement, diamond turned, light scattering technique 7-61318
- surfaces, (100) and (110), electronic props. calc. using layer method 7-45105
- surfaces, low energy positron diffr. pattern calcs., scatt. processes anal. 7-39331
- surfaces (111) and (110), surface tensile stress tensor calcs. 7-44982
- target, He^{+} electron capture and stripping cross sections 7-10753
- target in Ar plasma, CW laser materials interaction, spectroscopic studies 7-63313
- textured substrate for a-Si solar cell fabrication 7-23156
- thermal expansion of solids, three-terminal capacitance cell construction and calibration 7-29966
- thermodynamics during high-pressure shock 7-21352
- thin films, corrective trimming by laser controlled wet chem. etching 7-28195
- thin films, elec. cond. quantum size effect, Kubo formalism study 7-22034
- thin films, pulsed laser melting, transient elec. resist. and reflectance meas. 7-12141
- thin films, spin-orbit scatt., localisation and superconductive tunnelling studies 7-45242
- thin films, stress relax. mechanisms 7-21784
- thin films, vacancy redistrib. kinetics, machine modelling study (Russian) 7-6860
- thin films on Si substrates, plastic props., meas. by submicron indentation hardness, substrate curvature techniques 7-58720
- thin supercond. film, nonlinear RF props., vortex pair creation, critical effects 7-17137
- tricrystals, grain boundary sliding, triple point fold form. mechanism 7-65101
- ultra-high pressure shock generation using UV high power lasers 7-30028
- ultrasonic attenuation in a transverse mag. field, electron mean free path 7-64296
- unstable plastic deformation at low temp., superconducting transition effects (Russian) 7-6709
- US deformation, modelling of reduced bandwidth distortion to wide-area electron channelling mapping 7-16694
- vacuum-deposited films, topography charactn. by ellipsometry 7-9817
- vacuum-deposited films, topography charactn. by light scattering 7-9816
- wettability against ZrO_2 ceramics 7-52191
- wettability of SiC 7-58569
- wire connections, contact resist., effect of fretting 7-21980
- work fn., temp. depend., anal. 7-52737
- X-ray $L_{2,3}$ emission satellites, one electron contrib. 7-22388
- yield loci, expt. investig. 7-51923
- Ag-Al layered structures, backscattering spectra, aqal. by computer program 7-64840
- Al and Al alloys, appearance potential spectroscopy, matrix elements 7-59305
- Al based composite, rheocasting, microstruct., fracture, worn surface (Chinese) 7-13407
- Al, high purity samples, Doppler-broadened positron annihilation spectra, fast Fourier transform/power spectra deconvolution method 7-33481
- Al III, relative emission-line strengths in Sun 7-47799
- Al III line strengths in early type stars, non-LTE calcs. 7-18405
- Al, photothermal-optical-beam-deflection imaging, nonlin. effects 7-48722
- Al powder-steel composite coatings, prod. by compacting electrophoretic and electrostatic deposits protective props. 7-3491
- Al^+ , electron impact ionisation, absolute cross-section meas. 7-25667
- Al^+ ion source, RF, with metal discharge chamber 7-30114
- Al^{10+} recombining laser plasma, soft X-ray amplification 7-63321
- Al^{10+} , recombining laser produced plasma, population inversion 7-26509
- Al:Ar, solid Ar bubble, diffraction anal. 7-16547
- Al:Bi-KCl:Bi, bilayer cpd., Bi ion implantation, thermal annealing 7-32474
- Al:Eu $^{3+}$, ion implanted, anodization, electroluminesc. obs. 7-7761
- Al:F, electron-stimulated desorption, Coulombic ejection mechanism 7-59315
- Al/a-SiC films, RF sputtered, interfacial struct. and reactions, 573-773K (Japanese) 7-53583
- Al/Ga layers, surface plasmon dispersion, plasma wave effects, reflectivity meas. 7-58848
- Al/ Al_2O_3 /Au thin film struct., dielec. props. meas. and equivalent circuit anal. 7-17115
- Al/ Al_2O_3 /Au tunnel junction, electromagnetic modes anal. 7-27439

aluminium continued

- Al/ Al_2O_3 films, ion plated in Ar- O_2 gas mixture, structure anal. 7-7899
- Al/Cu friction welds, microstruct. and mech. props. (German) 7-46792
- Al/GaAs epitaxial contacts, MBE growth 7-22488
- Al/GaAs(InP) interfaces, interactions, XPS and elec. transport studies 7-7384
- Al/ $Hg_{1-x}Cd_xTe$ interfaces, morphology, Hg bonding effects 7-7021
- Al/III-V semiconductor interfaces, laser-induced chem. reactions 7-7017
- Al/InP UHV-cleaved and laser annealed interface, acceptor-like electron traps 7-7310
- Al/Nb sputter deposited multilayer VUV mirrors, design and fabrication 7-31424
- Al/NNb/Al sputtered thin film system, tunnelling charactn., comment 7-58575
- Al/Pt/Si structures, PtSi formation 7-63972
- Al/Si contacts, diffusion at room temp. (German) 7-32724
- Al/ $SiO_2/Si_3N_4/Si$ illuminated struct., nonlinear capacitance props. study 7-38731
- Al/ SiO_2/Si MIS contacts in inversion layer solar cells 7-3680
- Al/TiN/Si contacts for VLSI, analytical electron microscopy 7-58651
- Al-a-Nb $_2O_5$, heterostructure, morphology, electrophysical parameters 7-13394
- Al-air alkaline batteries, thermodynamic framework for efficiency estimation 7-3636
- Al-air battery with crystallizer to extend electrolyte lifetime, traction appls. 7-65441
- Al- Al_2O_3 , ion plated coatings using pulsed O_2 process 7-22586
- Al- Al_2O_3 crystalline oxide tunnel barriers on superconductor surfaces, thermal oxidation 7-7448
- Al- Al_2O_3 -Ag MIM struts. biased near breakdown voltage, optical emission 7-52853
- Al- Al_2O_3 -Au MIM struts. biased near breakdown voltage, optical emission 7-52853
- Al- Al_2O_3 -Au sandwich struct., forming process in high elec. field (Japanese) 7-22028
- Al- Al_2O_3 -MgO, cast particulate composites, microstruct. and mech. props. 7-65086
- Al- AlO_x -Pb tunnel diode, $NiCl_2 \cdot 6H_2O$ soln. phase adsorpt., inelastic electron tunnelling spectra 7-12877
- Al-An-Si MIM structures, electroreflectance, props. 7-38773
- Al-As $_2S_3$ -n-Si, I-V characteristics 7-7390
- Al-Au interfaces, dose profiles for 100 to 1250 keV photons, ONETRAN calcs. 7-56874
- Al-Cu, thin interface regions, EXAFS studies 7-59285
- Al-Cu interface, grazing incidence X-ray study of interfacial reactions 7-21543
- Al-Cu interfacial interaction, struct., synchrotron radiation photoemission study 7-22444
- Al-Dy $_2O_3$ -Al thin-film sandwiches, dielec. polarisation props. 7-38772
- Al-ethyl alcohol interface, surface polaritons, four-wave mixing 7-43244
- Al-FeS $_2$, secondary cell, positive electrode reaction kinetics, AC impedance study 7-8372
- Al-FeS $_2$, secondary cell, charactn. of $AlCl_3/1$ -butylpyridinium chloride electrolyte (Japanese) 7-8371
- Al-FeS $_2$, secondary cell performance develop. using $AlCl_3/1$ -butylpyridinium chloride electrolyte 7-8370
- Al-FeS $_2$, secondary cell with basic $AlCl_3$ -NaCl melt, cell performance and positive electrode reaction (Japanese) 7-13852
- Al-GaAs, pure and Si or Zn doped interfaces, composition depth profile, pulsed laser atom probe study 7-32842
- Al-GaAs (100) interface, Schottky barrier form. 7-2717
- Al-GaAs interfaces, convergent beam electron diffr. patterns 7-27156
- Al-GaAs Schottky barrier contacts, MBE grown, interface reactions, vacuum annealing effects 7-45022
- Al-GaAsO-GaAs structures, energy diagram 7-33096
- Al-GaAsb interfacial chem. reactions, surface refl. Raman Scatt. study 7-2275
- Al-Ge-Si, heterojunction ohmic contacts 7-27432
- Al-He system, He bubbles, mol. dynamics simulations and positron states 7-58778
- Al-InP Schottky barriers, defects introduced by mech. polishing 7-39768
- Al-InP Schottky diodes formed on cleaved surfaces 7-58850
- Al-insulator-Si, optical and elec. charact. of $(Al_2O_3)_{1-x}(AlN)_x$ 7-38766
- Al-Langmuir film-SnO $_2$, photovoltage spectra 7-64354
- Al-Mo multilayered films, struct., elec. props. 7-58863
- Al-Ni multilayered films, struct., elec. props. 7-58863
- Al-Pb disordered 3D normal metal-superconductor composite, elec. transport, magnetisation meas. 7-64383
- Al-PbTe electrical contacts, photothermal deflection meas. 7-38784
- Al-polyacrylic acid interface, reactivity, comp., XPS 7-28334
- Al-polyethylene, adhesion of metal films, effects of Ar $^+$ bombardment 7-28267
- Al-polyethylene interface, reactivity, comp., XPS 7-28334
- Al-polyethylene-Al thin film structures, anomalous Poole-Frenkel effect obs. 7-52851
- Al-Sb, Xe ion irradiated, intermixing rates, backscattering spectra, anal. by computer program 7-64840
- Al-semiconductor interfaces, form. of active electronic barrier, novel approach in corrosion prevention 7-65178
- Al-Si interface, amorphous W-Zr films on diffusion barriers 7-21504
- Al-Si struct., cond., transverse elec. field depend. 7-27417
- Al-Si:Ar,H, ion implanted ultrahigh Schottky barriers, interfacial traps, DLTS study 7-45489
- Al-Si $_3$ N $_4$ -GaAs struts., interface state density profile determ., DLTS spectra interpretation 7-38733
- Al-SiO $_2$: N interface traps and effective barrier height, nitriding effects obs. 7-38790
- Al-SiO $_2$ -Si MOS capacitors, optical and thermal cross-section of interface states, photocapitance meas. 7-38742
- Al-SiO $_2$ -Si system, contact pot. difference, effect of processing conditions 7-38746
- Al-stainless steel powder compacts, liq. phase sintering 7-7916
- Al-Ti (CoSi $_2$)-Si contacts, four-terminal resistor struts. for contact resist. determ. from end resist. meas. 7-73730
- Al-Ti-Cu multilayer films, thickness and composition anal. using X-ray fluorescence 7-46898
- Al-Xe, implanted, form. of solid precipitates and fluid bubbles, TEM obs. 7-38032
- Al $^{3+}$ -chymotrypsinogen (poly-L-aspartate), interactions, Raman spectra investig. of conform. changes 7-57071
- Al+Be $^+$, K-shell X-ray prod. cross section meas. 7-15680

aluminium continued

- Al+SO₂-AlO+SO, pulsed crossed supersonic beam expt., energy threshold determ. (*French*) 7-33915
 Al+U⁶⁸⁺(U⁸³⁺)(Xe⁴⁵⁺), electron stripping, cross section meas. 7-64849
 Al⁺+H⁺, charge transfer and ions. 7-31162
 Al_n clusters, (n=5,9,13), electronic struct. and bonding 7-15775
 Al_n⁺ (n=1 to 4), cluster ions, mass selected, prod., continuous source 7-10805
 Al_n⁺ (n=2,3)+O₂(H₂O)(ethylene), absolute cross sections, meas. 7-5743
 Al₃⁺+O₂ mass selected ions, reaction study 7-22993
 Al₃⁺+H, charge-transfer reaction, mol. representation, CI calcs. 7-36485
 Al₂O₃ anodic porous film on Al, microstruct. 7-22882
 Al₂O₃ fibre reinforced Al, fatigue crack propag., effect of aq. environments 7-17624
 Al₂O₃ fibre reinforced Al composites, compressive failure modes, dead weight or machine loading 7-39663
 Al₂O₃/Al system, nondestructive depth profiling using secondary emission spectroscopy 7-27836
²⁶Al in the interstellar medium, review 7-48050
 Ap-Xe-Kr(Ar), ion implanted, bubble growth, lattice parameters, TEM obs. 7-51803
 B fibre reinforced Al, strength characts. 7-33768
 B fibre reinforced Al matrix composite, TiB₂ coated, prep. using liq. phase infiltration 7-3229
 B fibre reinforced Al matrix composites, transverse mech. props., isothermal exposure effect 7-39688
 B fibre reinforced Al tube under multi-axial loadings, elastic-plastic deformation 7-46548
 Co-Al system, diffusion markers in thin films Co₂Al₃ formation 7-58549
 Cr-Al system, diffusion markers in thin, film CrAl₃ formation 7-58549
 Cu-Al bilayers, EXAFS and X-ray reflectivity meas. 7-27821
 Cu₂O-Al₂O₃-Al moisture transducer, design and development 7-41395
 Fe-Al bilayered samples, ion beam induced atomic mixing 7-6689
 GaAs (110), adsorption of Al, soft X-ray photoemission spectra study 7-53494
 GaAs with Al honeycomb substrate, flat-plate space solar panels interconnector design 7-13879
 GaAs:Al, surface layer, degree of disordering, effect of dopant 7-63929
 GaAs:Al⁺, ion implantation damage 7-38024
 GaAs-Al junction, interface states, DLTS study 7-58892
 GaAs(110)-Al, Schottky barrier form., effect of surface and interface kinetics 7-2668
 p-Ge:Al, annealing kinetics of radiation defects, influence of impurity binding energy 7-39547
 Ge:Sb(Al)(Ga)(In), heavily doped, charge carrier scatt., elec. cond., Hall effect meas. 7-7228
 He ion implanted Al disks, He re-emission ratios and surface obs. (*Japanese*) 7-12089
 In₂O₃:Sn-ZnS:Cu,Cl,Mn-Al, surface electrical conductivity in ZnS:Cu,Cl,Mn thin films 7-38672
 LiH:Al single crystals, secondary emission, exciton luminesc. and reson. Raman scatt. studies 7-3038
 MgF₂-Al Schottky detectors, frequency and polarisation-selective 7-41470
 MgO:Al, positron lifetime spectra, impurity effects 7-39278
 MgO:Al crystals, cathodolum., effect of heat treatment 7-7767
 Mn²⁺Mn³⁺SiO₂:Fe(Ca)(Al), antiferromagnetism and spin glass order, mag. meas. 7-27518
 Mo-Al system, diffusion markers in thin film MoAl₁₂ formation 7-58549
 Na-like ions, steady-state population inversion 7-19780
 Nb-Al thin film diffusion couples, Nb₃Al Al₅ phase form. during annealing, XPS and Auger studies 7-58548
 Ni reinforced Al, matrix crystn. and sintering, role of reinforcing phase 7-33625
 Ni/Al multilayers, RBS spectra, automatic iterative fitting 7-22428
 Ni/Al thin film interactions, phase formation sequence 7-21701
 Ni/Al/Si system, contact structure formation by rapid thermal melting 7-45019
 Ni-Al system, diffusion markers in thin film Ni₃Al formation 7-58549
 Pd/Al composite film MOS structure, H₂ sensitivity 7-52842
 Si:Al, atom and acceptor depth distributions of channelled Al as a function of ion energy and crystal orientation 7-21247
 Si:Al, depth profiles, redistrib. of annealed Al implants 7-63640
 Si:Al, hydrogenation and annealing kinetics 7-2527
 Si:Al, ion implanted and annealed, Al precipitation, TEM studies 7-21238
 Si:Al, Mg transmutation doping by proton irradi. 7-38027
 Si:Al, random and channelled implantation profiles and range parameters of dopants 7-21246
 Si:Al films, LPE in a temperature-gradient field 7-64936
 Si:Al implanted crystals, amorphous surface regions with crystalline impurity grains, TEM study 7-58579
 Si:Al surfaces, SIMS anal. of contaminants 7-33989
 Si:Al thermal donor props., impurity effects, DLTS, Hall effect, and admittance spectra meas. 7-21851
 Si:Al(In), recrystallisation by pulsed electron beam, impurity profiles 7-16605
 Si/Al, oxidation by microwave excited O₂+N₂ mixture plasma (*Japanese*) 7-65198
 a-Si/Al films, laser-induced phase transitions, time resolved TEM study 7-38056
 p-Si/Al Schottky barriers, Ar⁺ implantation damage, oxidation, etching and elec. props. 7-21290
 n-Si/SiO₂/Al struct., inductive admittance meas. 7-17108
 Si-Al, P, defect struct. and dynamics 7-16552
 Si-Al optically excited diaphragms, reson. freq., temp. depend. 7-18971
 Si-Al Schottky barrier diodes, ion implant modification 7-45498
 Si-Al structures, ion mixing, effect of interfacial oxide 7-21537
 Si-Cos₂Ta₅₀-Al, amorphous Cos₂Ta₅₀ alloys as diffusion barriers 7-44923
 Si-SiO₂-xN₂-xN₂/3-Al structures, interface states, DLTS study 7-45513
 SiC fibre reinforced Al composite, corrosion protection to NaCl soln. exposure 7-3488
 SiC fibre reinforced Al, fatigue crack propag., effect of aq. environments 7-17624
 SiC fibre reinforced Al composite wires, neutron irradi., mech. props., fusion reactor appl. 7-49628
 SiC fibre reinforced Al wires, neutron irradi., mech. props., fusion reactor appl. 7-53794
 SiC whisker or particle reinforced Al composites, deform. thermal expansion, strengthening mechanisms 7-3373

aluminium continued

- SiC whisker reinforced Al matrix composites, interaction, with eutectic brazing alloys 7-46689
 SiC whisker reinforced Al, flame spraying fabrication and forging, whisker distrib. and strengths 7-59483
 α-Si:Al,B,O crystals, photolum. and electrolum. studies (*Russian*) 7-22344
 β-Si:Al,N films, ion implanted, rapid thermal annealing and p-n junction formation 7-17569
 SiC:Al thin films, impurity 7-27192
 Si:Al⁺, stoichiometric disturbances due to ion implantation 7-6651
 β-Si:Al⁺ epitaxial films, ion implanted, rapid thermal annealing 7-16905
 SiC-Al composites, heat treatment and neutron irradi. effects on mech. props. 7-65081
 a-Si_{1-x}Ge_x:H/Al Schottky barrier form. and characts. 7-12787
 a-Si_{1-x}Ge_x:H/a-Si:H/Al Schottky barrier form. and characts. 7-12787
 Si₃N₄/Al/Invar ceramic/metal joints, rel. between tensile and three-point bending strengths 7-39583
 SiO₂-Al Schottky detectors, frequency and polarisation-selective 7-41470
 SnO₂-n-Sb₂S₃-Al structures, polarization current relaxation and space charge 7-33090
 α-TeO₂:Al single crystals, electron irradi., colour centre ESR obs. 7-33271
 TiO₂:Al, absorption and photolysis spectra 7-22290
 U₃Si, U₃Si₂ powders dispersed in Al matrix, heat of reaction, DTA 7-719
 V-Al system, diffusion markers in thin film VAl₃ formation 7-58549
 ZnO:Al films, RF reactive sputter deposition, struct., elec. and optical props. (*Japanese*) 7-27900
 ZnS:Al, Cr, Fe crystals, recomb. luminesc., EPR and photocond. meas. 7-3076
 ZnS:Al, electron capture processes, role of donors, transient ESR meas. 7-45347
 ZnS:Al, low resistivity, grown by MOVPE 7-27921
 ZnS:Al, temp. depend. of visible photolum., ESR studies 7-46099
 ZnSe:Al, impurity diffusion coefficients, cathodoluminesc. study 7-27017
 ZnSe:Al, MOCVD growth, deep level characterisation 7-52519
 ZnSe:Al, single crystals, growth, exciton luminesc. 7-22453
 ZnSe:Cu,Al,Fe crystals, melt-grown, absorpt. coeff., impurity effects 7-3070
 ZnTe:Al, crystals, vacancy-impurity complexes, ODMR studies 7-2530

aluminium alloys

see also aluminium compounds

- ΔK_{th} testing method for plastic zone size at fatigue crack tip for A5083-0 alloy 7-17748
 ageing, positron annihilation study 7-39295
 Al-Li-Mg powders, mech. alloying 7-64968
 Al-Mn quasicrystal, struct. model with m35 symm. 7-6570
 Al-Zn-Mg-Cu, impact toughness improvement by intermediate thermomech. treatment 7-53907
 Alnico 5, Fe-Co-Ni-Al-Cu, microstruct. and mag. props., effects of heat treatment (*Korean*) 7-8138
 binary, alloying capacity for solid soln. obtained by casting under press. 7-53716
 binary, liq., thermodynamic props. (*Korean*) 7-26978
 bronze BRAZh, elec. discharge sintering of powder from swarf, electrophys. and mech. props., microstruct. 7-27974
 corrosion, cathodic polarisation in mortar (*Japanese*) 7-53969
 corrosion of alloys buried in mortar and concrete, effect of NaCl (*Japanese*) 7-46692
 corrosion of alloys in mortar, effect of Na⁺ and Ca²⁺ ions (*Japanese*) 7-46693
 cracking resistance, effect of strain rate and test temp. 7-13548
 creep, high temp., role of surface layer in power law breakdown 7-65089
 creep behaviour, uniaxial transient, under varying stress states (*Chinese*) 7-13513
 crystal structure and microstructure, metallography studies 7-58204
 dilute disordered alloys, vacancy form. energy, comp. and temp. depend. calcs. 7-37983
 dry etching using image reversal photoresists. (*Japanese*) 7-65199
 ductile, expt. simulation of intercryst. sliding and fracture 7-2095
 Duralumin type, stability of struts in compression in elastoplastic range 7-22771
 dynamic restoration during hot rolling 7-22724
 fatigue crack growth rate dispersion rules 7-17615
 fatigue life predictions under complex loading (*Chinese*) 7-46594
 fatigue macrocrack initiation at stress raisers 7-13547
 FeCrAlloy, interaction with Na₂O.2SiO₂ glass 7-3501
 fibre reinforced Ti-base alloy, development of creep-resisting composites 7-3228
 fibre-reinforced Al alloy-matrix composites fabrication process 7-46377
 fracture toughness determination from thin side-grooved specimens 7-59706
 fretting, fatigue crack growth, spherical particle form. 7-3445
 graphite fibre reinforced Al-Mg-Fe, unidirectional and angle-ply, strength and fracture anal. 7-59605
 graphite particle dispersed Al-Si alloys, powder extruded, wear characts. (*Japanese*) 7-53909
 heat exchanger materials for OTEC 7-65571
 heat treatment, prediction of start of exposure phase 7-33698
 high press. strength, shock wave expts. 7-22782
 high-strength, damage process, thermometric investig. (*German*) 7-3439
 hot workability, determ. of high temp. flow stress (*Korean*) 7-28076
 icosahedral quasicrystals, high resolution electron microscopy 7-16497
 IN 100 superalloy, MC carbide props. rel. to transition element doping 7-13456
 Inconel MA 6000, oxide dispersion strengthened superalloy, cyclic creep, HF effect, anelastic mod. 7-53827
 joints of dissimilar metals, adhesively bonded strength evaluation 7-46791
 life prediction for corrosion fatigue 7-39629
 liquid dynamic compaction, microstruct. and precipitation, TEM study 7-59529
 mechanical alloying, development of strong alloys 7-39534
 medium strength, formability rel. to microstruct. 7-17592
 Mg-Al alloys, precipitation and recrystallisation rates under small external stress 7-17532
 microhardness correction procedures evaluation, 7075 Al alloy 7-3550
 molten, resistance of tool steels 7-33835

aluminium alloys continued

Monel K-500, precip. of intermetallic γ' phase and carbide phases 7-33678
Ni₃Al₈O₈-based alloys, magnetic and structural props. studies 7-45635
Nimonic 80, coupled plastic and creep damage at finite deform. (Japanese) 7-33736
Nimonic 80A, crack growth under sulphidising conditions, metallography 7-59680
oxidation studies using EELS and EDX in the TEM 7-17734
plates, crack opening after discontinuous growth, laser interferometry studies (Russian) 7-46604
position diffusion towards spheroidal inclusions (Russian) 7-39216
positron traps, classification in age-hardenable alloys 7-38517
powder from high press. gas atomisation, TEM study 7-17493
pressure testing at elevated temps., portable equipment 7-13689
quasicrystals, electron diffraction structure anal. (German) 7-37930
R-curve, effect of initial fatigue crack applic. conditions and crack length meas. method 7-22945
rapidly solidified, pitting corrosion 7-17678
rare earth alloys, R₂(Fe,Al,Co)₁₄B, mag. props., composition depend. 7-53030
rare earth aluminium RAl₂ layered structural sintered composite, mag. entropy 7-59016
rare earth-Al alloys, RAl₂, paramagnetic fluctuations, muon spin rotation studies 7-12941
Rene 80, first stage aluminised coating microstruct., STEM obs. 7-17709
sheets, LY12CZ, fracture resist. characts., crack initiation, stable and unstable propag. (Chinese) 7-46592
surface, UV laser pulse irradi., microscopic crater form. 7-12124
surface analysis using XPS and electrochemistry 7-28370
tensile flow stress beyond necking, determ. at very high strain rate 7-63726
TRISTAN e⁺e⁻ colliding beam ring, Al alloys, corrosion resistance to cooling water (Japanese) 7-42248
two phase alloys, high temp. deformation, microtexture 7-16563
ultrahigh vacuum system for MBE 7-53595
US nonlinearity dependence on second phase precipitates, obs. 7-2111
vacuum chamber for MBE 7-61345
vacuum chamber for MBE growth (Japanese) 7-33569
wear of materials prepared by ingot techniques, squeeze casting and rapid solidification, comparative investig. 7-13605
weldability, pulsed laser 7-13702
X-ray mirror substrates, grazing incidence, precision machining/metrology facility 7-37222
Ag-Ag, thin film system, phase growth, electron microscope obs. 7-58488
 α -Ag-Al, thermal expansion, X-ray determ. 7-32685
Ag-Al alloy, superconductor film structs., fabrication and appls. (Spanish) 7-27483
Ag-Al film couples, interfacial phase form., in situ annealing X-ray diffr. obs. 7-21705
Ag-Ge-Ga-Al FCC alloys, faulted structure, X-ray diffr. studies 7-58292
Ag-Mn-Al, beta to zeta reversible transformation, elec. resist. meas. (Russian) 7-16728
AgAl concentrated alloys, vacancy activation enthalpies 7-32431
AgAl, short-range order-induced equilib. resist. conc. depend. meas. 7-26700
Al alloy, corrosion effects on fatigue crack propagation 7-39628
Al alloys, photothermal-optical-beam-deflection imaging, nonlin. effects 7-48722
Al alloys containing Li, rapid solidification, bibliography 7-41029
Al and Al alloys, appearance potential spectroscopy, matrix elements 7-59305
Al base alloys, fusion reactor first wall, plasma disruption damage calc. 7-791
Al base alloys, positron localisation, affinity to solute clusters and size limitations 7-46200
Al base alloys, rapid solidification technology 7-39493
Al brass, corrosion inhibition by Schiff bases in acid media 7-22892
Al brass, SCC in acidic sulphate solns, Cl⁻ conc. effect 7-17679
Al dilute alloys, deviation from Matthiessen's Rule, three group model 7-12601
Al Zn alloy, positron localisation, affinity to solute clusters and size limitations 7-46200
Al/V.PtSi/Si Schottky barrier diode metallisation system 7-2666
Al-Ag, anelastic effects due to precip. and dissoln. 7-13487
Al-Ag, decay and short-range ordering (Russian) 7-44795
Al-Ag, γ' precip. growth, TEM studies at atomic level 7-46491
Al-Ag, ledge interphase boundaries, growth kinetics, computer modelling 7-65041
Al-Ag, steady-state creep, effect of isochronal ageing 7-17598
Al-Ag (5 wt.%), anelastic effects, quench sensitivity, precip. and dissolution 7-53784
Al-Ag (5.9 at.%), precip., positron study 7-46485
Al-Ag alloys, γ' precipitates, convergent-beam electron diffr. studies, space-group anal. 7-11854
Al-Ag alloys, isothermal ageing, hardness and creep behaviour 7-8068
Al-Al₂Cu eutectic alloys, chill cast, directionally solidified, hot rolling microstruct. 7-46447
Al-Al₂Ni eutectic alloys, chill cast, directionally solidified, hot rolling microstruct. 7-46447
Al-Am, quasicrystalline and crystalline alloys, temp. dependence of elec. resistivity 7-2574
Al-Ba-La system, phase equilib. study 7-3279
Al-base alloy, IN-9021, fatigue morphology 7-39653
Al-base alloys, IN-9021, SCC fracture behaviour 7-39744
Al-base bearing alloyed, leaded, wear characts. 7-33808
Al-base icosahedral alloys, elec. resist. and Hall coeff. studies 7-27316
Al-Cd single crystals, Cd-vacancy complex disassociation under ion irradiation 7-26741
Al-Co, melt spinning, microstruct., precip., microhardness (Korean) 7-46444
Al-Co icosahedral alloys, struct., elec. and mag. props. 7-6583
Al-Cr, quasicrystalline and crystalline alloys, temp. dependence of elec. resistivity 7-2574
Al-Cr(Mn)(Fe) amorphous films, quasicrystalline transformation by ion irradiation 7-2071
Al-Cu, Al-Cu-Si, superplastic strain rate sensitivity index 7-3387
Al-Cu, corrosion protection by Ce corrosion coatings 7-53988
Al-Cu, creep rupture under tri-axial tension 7-53839
Al-Cu, dendritic growth models, comparison of theory with expt. 7-22649

aluminium alloys continued

Al-Cu, directionally crystallised, crystallographic texture transform. during wear 7-17660
Al-Cu, microsegregation, effect of solidification rate 7-46480
Al-Cu, solidification, microsegregation in coarsened dendritic microstruct. 7-28048
Al-Cu (1.87 wt.%), stability of metastable defects at elevated temps. 7-38207
Al-Cu (2 wt.%) single crystals, rolled, shear band form. rel. to θ' precipitates 7-3385
Al-Cu (2 wt.%) single crystals, rolled, shear band form., θ precip. 7-28099
Al-Cu (2.5 wt.%), creep deform., effect of θ precipitates 7-65088
Al-Cu (2.5 wt.%), electrical resistivity, effect of precipitation 7-12697
Al-Cu (3 at.%) precip. growth kinetics of θ' - and θ -phases 7-39519
Al-Cu (3.76 wt.%), rheocast, partially homogenised, ageing response, microhardness 7-46499
Al-Cu (4.5 wt.%), laser treated, surface solidification with moving heat source 7-22648
Al-Cu compact, struct. form. during sintering 7-53675
Al-Cu films, characterisation by SIMS, Auger spectroscopy and TEM 7-12550
Al-Cu-Be (3, 0.1 wt.%), precip. reactions 7-53738
Al-Cu-In alloy, deformed, θ' -phase precipitation 7-22691
Al-Cu-Li, 2020, low-cycle fatigue, effect of environment and temp. 7-28117
Al-Cu-Li, cryogenic toughness, orientation effects 7-39669
Al-Cu-Li, plastic deform. in conditions of quasihydrostatics (Russian) 7-59586
Al-Cu-Li alloys, cyclic fracture, mechanisms 7-46634
Al-Cu-Li-Mn-Cd, 2020, micromechanisms governing elevated temp. fracture resist. 7-22803
Al-Cu-Mg, annealed, creep, 623-723 K 7-53802
Al-Cu-Mg, 2024, averaged, yield loci, expt. investig. 7-51923
Al-Cu-Mg, 2024, TEM specimen prep. parallel and perpendicular to machined surfaces 7-39808
Al-Cu-Mg, 7090, powder metallurgy, fatigue crack growth, influence of load ratio 7-28124
Al-Cu-Mg, Al-Mg, plastic deform., AE, X-ray obs. (Russian) 7-46579
Al-Cu-Mg, cast composite, mica particle distrib. 7-46375
Al-Cu-Mg, crack propagation resist., in connection with limiting crack resist. 7-59629
Al-Cu-Mg, D16T, endurance over wide range of stress variation 7-22811
Al-Cu-Mg, deformed, dislocation struct., AE obs., electron microscopy (Russian) 7-39832
Al-Cu-Mg, fatigue crack propagation rate, effect of overloads 7-59623
Al-Cu-Mg, fracture behaviour, influence of fine transition-metal particles and grain struct. 7-3406
Al-Cu-Mg, growth by Stepanov's method, macro- and microstructure, strength, plasticity meas. 7-33546
Al-Cu-Mg, hot workability, recrystallisation during torsional deform. (Korean) 7-46559
Al-Cu-Mg, IN 9021, corrosion behavior 7-39733
Al-Cu-Mg, IN 9021, creep crack growth fracture morphology 7-53881
Al-Cu-Mg, stability of struts in compression in elastoplastic range 7-22771
Al-Cu-Mg, strip with hole, fatigue resist., effect of multiple local plastic deform. 7-59625
Al-Cu-Mg r-curve behaviour of double edge notched tensionspecimens in plane stress 7-13701
Al-Cu-Mg system, D16 alloy, struct. changes during electron bombardment 7-8005
Al-Cu-Mg-Al₂O₃-Al₄C₃, IN 9021, mechanically alloyed precip. hardened, tensile behaviour 7-13525
Al-Cu-Mn, fracture toughness, all modes 7-65121
Al-Cu(Mg)(Ag) system, trapping and diffusion mechanism, μ SR study 7-45863
Al-Fe, ion induced metastable phases 7-63673
Al-Fe, rapidly cooled, Al₃Fe₄ tenfold twins, TEM obs. 7-63631
Al-Fe system, phase diagram, DTA obs. 7-39485
Al-Fe-Ce, quasicrystalline decagonal phase, TEM 7-46492
Al-Fe-Ce-La-Nd-Rr alloys rapidly quenched, positron annihilation studies 7-46184
Al-Fe-Mg, solidified from liq. phase, struct. (Russian) 7-39498
Al-Fe-Mischmetal, wear, comparative investigations, and prep. method role 7-13605
Al-Fe-Mn icosahedral alloys, elec. resist. and Hall coeff. studies 7-27316
Al-Fe-Mn powder, rapidly solidified, microstruct. 7-46445
Al-Fe-R, R=Ce, Er, Nd or Gd, rapidly solidified microstruct. 7-59502
Al-Fe-Si, 1060 alloy, corrosion in p-quinone and acetic acid 7-28170
Al-Fe-Si, dil., solidification, intermetallic cpd. form. 7-13442
Al-Fe-Si, quasicrystalline phases and amorphous structure 7-51637
Al-Fe-Si, TEM geometric projection of crystal struct. 7-16501
Al-Fe-Si system, intermetallic phases, electron probe microanalysis, X-ray diffr. 7-59491
Al-Fe-Si-TiO₂, dispersion hardened, strength props., effect of matrix particle size and oxide vol. fraction 7-17544
Al-Fe-V rapidly solidified sheets, mech. props., hot rolling effects 7-22838
Al-Fe-Zr, wear, comparative investigations, and prep. method role 7-13605
Al-G brazing alloys with active Ti additive, bonding of Syalon 7-39846
Al-Ge, dilute alloys, quenched, formation and growth of vacancy type clusters, positron annihilation study 7-39294
Al-Ge, TEM anal. of Ge precip. morphology 7-46489
Al-Ge (12 at.%), alloy ribbons, prep. by centrifuge melt spinning, effect of process variables on characts. 7-46366
Al-Ge alloys, obs. of Ge pentagonally twinned precipitate needles 7-12297
Al-Ge eutectic alloy interaction with SiC whisker reinforced Al matrix composites 7-46689
Al-Ge mixture, H implanted, evidence for metal-insulator transition in Al 7-2483
Al-Ge-X, amorphous ductile, with two separate phases, form. range and props. for X=Mn, Fe, Co or Ni 7-59493
Al-H, H-point defect interactions, extended Huckel mol. orbital calcs. 7-44533
Al-H system, vibr. spectrum of isolated H impurity, isotope effects (Russian) 7-32593
Al-H(He) systems, vacancy-impurity centres, positron lifetime meas. 7-39254
Al-He ion irradi. system, bubble form., positron lifetime meas. 7-37966

aluminum alloys continued

- Al-He system; He bubble form. by proton irradi., positron studies 7-44526
- Al-Hf dilute quenched cold-worked alloys, vacancy migration recovery processes, PAC and positron annihilation studies 7-39545
- Al-In, monotectic alloy, section prep., micromilling, polishing (*German, English*) 7-22937
- Al-La, oxidation kinetics 7-65190
- Al-Li, coarsening of δ' precipitates 7-33663
- Al-Li, grain boundary precipitate free zone growth kinetics 7-33662
- Al-Li, quenched, ageing, light ion irradi., δ' phase form. and particle growth 7-26807
- Al-Li (9.5 at.%), coarsening of δ' -Al₃Li precipitates, var. of average Li content in Al matrix 7-3313
- Al-Li alloys, grain boundary fracture 7-39644
- Al-Li base alloys, deform. and fracture 7-39594
- Al-Li base system, solid-state phase transform. 7-46456
- Al-Li-Be alloys, arc-melted, microstruct. evaluation 7-22655
- Al-Li-Be alloys, rapidly solidified, microstruct. eval. 7-22656
- Al-Li-Cu, T₂ phase, icosahedral struct. 7-16425
- Al-Li-Cu-Mg quaternary alloy, initiation of voiding at second-phase particles 7-39645
- Al-Li-Cu-Mg-Zr, wear, comparative investigs. and prep. method role 7-13605
- Al-Li-Cu-Mg-Zr, yield stress, temp. and strain rate depend. (*Japanese*) 7-33734
- Al-Li-Cu-Mg-Zr die forgings, mech. props., microstruct. 7-46636
- Al-Li-Cu-Mg-Zr powder alloy, superplastic, high modulus and hardness 7-53816
- Al-Li-Cu-Zr, 2090, small fatigue crack growth 7-22817
- Al-Li-Cu-Zr, Al-Li-Zr, nucleation of δ' and β' precipitates 7-59527
- Al-Li-Cu-Zr, fracture, ageing and comp. depend. 7-22784
- Al-Li-Cu-Zr, nucleation of precipitates 7-46476
- Al-Li(Mg)(Mg), fracture, effect of subgrain struct. and ageing practice 7-13563
- Al-Li-Cu(Mg), stress corrosion resist. and mech. props. 7-33833
- Al-Li-Ge, corrosion rel. to Ge content 7-39715
- Al-Li-Mn (Cu), precip.-hardened, cyclic stress response and deform. behaviour 7-22791
- Al-Li-Sc, cast, decomp., mech. props., struct. (*Russian*) 7-59532
- Al-Li-Zn (Cu) icosahedral quasicrystals, solid state reaction and rapid solidification prep. comparison 7-37864
- Al-Li-Zn-Mg-Cu alloys, microstruct. evolution 7-53739
- Al-Li-Zr rapidly solidified alloy, plastic deform. characts. 7-22777
- Al-Li(Mg)(Na)(Be), thermal surface oxide layers, SIMS characterisation 7-13650
- Al-Mg, 5052, oxide thin surface films, AES anal. (*Japanese*) 7-17723
- Al-Mg, AE during deform., effect of struct. state (*Russian*) 7-38127
- Al-Mg, adhesive-adherend interface under load, stresses in adhesive bond 7-28260
- Al-Mg, creep, stress exponent, dynamic strain ageing, dislocation struct. 7-17591
- Al-Mg, deformed, dislocation struct., AE obs., electron microscopy (*Russian*) 7-39832
- Al-Mg, liq., excess entropy of mixing, resist. calcs. 7-2571
- Al-Mg, plasma-coated, heat treatment effect on fine struct. and failure mechanism 7-3496
- Al-Mg, rapidly solidified powders, effect of extrusion parameters on props. 7-39595
- Al-Mg, strengthening diagram, relationship with dislocation kinetics (*Russian*) 7-53753
- Al-Mg (Mn), plastic deform. and supercond. props., 0.5 to 4.2K (*Russian*) 7-8055
- Al-Mg (0.2 wt.%), subgrain growth rel. to prior cold work and annealing temp. 7-17551
- Al-Mg (5 at.%), creep, interpretation of internal stress determ. from dip tests 7-65091
- Al-Mg (5 at.%), Portevin-Le Chatelier band kinetics, video recording 7-65103
- Al-Mg (5 wt.%) polycrystals, high temp. deform., microstruct. 7-13501
- Al-Mg (6.5 wt.%), grain boundary segregation, STEM-EDX analysis 7-39518
- Al-Mg (9.8 wt.%), AlMgSi, AlZnCuMgZr, directional solidification, microstruct. (*German*) 7-46452
- Al-Mg alloy, charge transfer, X-ray emission and UPS studies 7-3118
- Al-Mg alloys, spall strength, impact stress and strain-rate depend. studies 7-33796
- Al-Mg alloys, steady-state creep, microstruct. development 7-53817
- Al-Mg alloys 5056 and 5083, recrystn. kinetics after hot deform. 7-3328
- Al-Mg surface layers, electronic and atomic structs., heat treatment effects (*Russian*) 7-58575
- Al-Mg-Bi-Cr, low activation alloy development for reacting plasma experiment 7-15384
- Al-Mg-Ce system, liquidus, intermetallic compound (*Chinese*) 7-7960
- Al-Mg-Cu-Zr, low activation alloy development for reacting plasma experiment 7-15384
- Al-Mg-Li, 14 MeV neutron irradi., mech. props. microscopic struct. 7-56820
- Al-Mg-Mn, fatigue, criterion for omission of variable amplitude loading histories 7-22794
- Al-Mg-Mn, fracture toughness, all modes 7-65121
- Al-Mg-Si, Al-Mg, cast, mica particle dispersed composites, struct., strength, hardness 7-59574
- Al-Mg-Si, annealed, plastic flow under multiaxial cyclic loading 7-33725
- Al-Mg-Si, chamber wall, Light Ion Beam Fusion Target Development Facilities, activation studies 7-49732
- Al-Mg-Si, compression test, high speed, microcomputer system, split Hopkinson bar technique 7-13686
- Al-Mg-Si, high-purity, nucleation and growth of precipitates and the bubbles, effect of 600 MeV protons 7-58364
- Al-Mg-Si, squarely extruded, texture and mech. props. (*Japanese*) 7-33694
- Al-Mg-Si/TiC composites, implantation modified, friction, surface chemistry 7-46660
- Al-Mg-Zn system, fracture viscosity rel. to surplus phase morphology 7-46610
- Al-Mg-Zn(Cu) icosahedral quasicrystals, solid state reaction and rapid solidification prep. comparison 7-37864
- Al-Mg-mica particle composites, prep. and props. 7-22613
- Al-Mg-(Si), 800 MeV proton irradi., gas accumulation at grain boundaries 7-58361

aluminum alloys continued

- Al-Mg-(Si), response to single and multistage compression 7-53830
- Al-Mg-(Si), solidification, continuous and interrupted, development of microstruct. and homogenisation (*German*) 7-53719
- Al-Mg(Ca)(Zn)(Si)(Ge) dilute alloys, divacancy effect, annihilation radiation Doppler broadening meas. 7-37982
- Al-Mn, Al-rich alloy, rapidly solidified, crystn. of quasicryst. icosahedral phase 7-63472
- Al-Mn, electron wind-induced muon drift 7-52115
- Al-Mn, icosahedral-glass and icosahedral quasicrystal models distinguished via high-resolution lattice imaging 7-32295
- Al-Mn, lattice model of quasicrystalline phase, high resolution electron microscope images 7-37866
- Al-Mn, periodic and quasiperiodic crystals 7-1928
- Al-Mn, pressure induced quasi-crystal to crystal transition for melt span alloys 7-16726
- Al-Mn, quasicrystal diffraction patterns, distortion and peak broadening 7-11981
- Al-Mn, rapid solidification, extended solid soln. and eutectic growth 7-33647
- Al-Mn, rapidly quenched, icosahedral phase, comp. analysis 7-26699
- Al-Mn, rapidly solidified, decagonal phase morphology 7-39499
- Al-Mn (14 at.%), solidification, icosahedral and T-phase form. temp. rel. to cooling rates 7-53718
- Al-Mn (15 wt.%), melt spun ribbons, icosahedral struct., decomp. rel. to annealing 7-28030
- Al-Mn alloy, decagonal phase, struct. model 7-63552
- Al-Mn alloy icosahedral quasicryst., mag. and elec. props. studies 7-2858
- Al-Mn alloys, cryst. and amorphous phases, mag. props. 7-17163
- Al-Mn alloys, icosahedral, amorphous and cryst. local struct., EXAFS study 7-63466
- Al-Mn alloys, icosahedral symmetry versus local icosahedral environments, NMR spectra meas. 7-63536
- Al-Mn icosahedral alloy form. by pulsed electron beam and laser beam surface melting 7-26924
- Al-Mn icosahedral alloys, elec. resist. and Hall coeff. studies 7-27316
- Al-Mn periodic and aperiodic alloys, local atomic environments 7-44454
- Al-Mn quasicrystal, two-dimensional Patterson synthesis, optical method 7-11993
- Al-Mn quasicrystalline and metastable phases, phase form. and thermal stability 7-26644
- Al-Mn quasicrystals, 1D translational periodicity and ten-fold rotation axis 7-26643
- Al-Mn quasicrystals, field ion images, computer simulation studies 7-32368
- Al-Mn quasicrystals, local struct., EXAFS and XANES studies 7-6582
- Al-Mn quasicrystals, nonuniform local magnetism, NMR spin echo studies 7-22090
- Al-Mn surface icosahedral phase form., ion beam mixing and interdiffusion 7-16653
- Al-Mn system, G-phase form. and stability range 7-22663
- Al-Mn system, quasicrystal form., metallurgy 7-3295
- Al-Mn-Cr-Si quasicryst. atomic struct., pulsed neutron scatt. meas. 7-5139
- Al-Mn-Fe, wear, comparative investigs. and prep. method role 7-13605
- Al-Mn-Fe alloy, aging characteristics, pre-cold working effects 7-53758
- Al-Mn-Ru-Si icosahedral alloys, EXAFS study 7-39317
- Al-Mn-Si, quasicryst., X-ray diffr., TEM and SEM study 7-12299
- Al-Mn-Si, quasicrystalline phases and amorphous structure 7-51637
- Al-Mn-Zr (7.1 wt.%), rapidly solidified, quasicrystalline phase precip. 7-3310
- Al-Mn-(Si) rapidly solidified alloys, quasicrystal form. by electron beam melting 7-26915
- Al-Mn(Fe)(Cr), quasicrystals, diffraction pattern simulations 7-6585
- Al-Mo, rapid solidification processed, diffusion-induced dislocation migration 7-65047
- Al-Mo (11 at.%), rapidly solidified, equilib. phase development 7-46436
- Al-Nb amorphous films, elec. props. and charactn. (*Japanese*) 7-32977
- Al-Ni binary system., solid soln. types study by positron annihilation 7-46207
- Al-Ni powder mixtures, shock-induced chemical reactions, optical meas. 7-39463
- Al-Ni-Fe-(Co) powders, cold sintering 7-64972
- Al-Ni-Pt, high temp. oxidation rel. to alloying additions, ion implantation, Rutherford backscatt. 7-53987
- Al-Pb, monotectic alloy, section prep., micromilling, polishing (*German, English*) 7-22937
- Al-Pd, ion induced metastable phases 7-63673
- Al-Pd, rapidly solidified, decagonal phase morphology 7-39499
- Al-R (R=Er,Nd,Gd) rapidly solidified alloys, microstruct. and thermal props. 7-26667
- Al-R (R=Gd, Ho, Er, Y) alloys, intermediate phase metastable extensions, DSC and X-ray diffr. studies 7-21413
- Al-Sc, oxidation kinetics 7-65190
- Al-Si, brittle failure rel. to overheating, fractography 7-22796
- Al-Si, chill-cast, heat flow and dendritic arm spacing during solidification 7-53714
- Al-Si, cold worked, damping characts. 7-28064
- Al-Si, dilute alloys, quenched, formation and growth of vacancy type clusters, positron annihilation study 7-39294
- Al-Si, grain refinement, effect of solute content 7-59503
- Al-Si, graphitic, hot extruded powders, sintering, antifriction props. 7-13409
- Al-Si, hot dip aluminizing, alloy layer growth, influence of Si additions 7-3502
- Al-Si, hypereutectic alloys, primary Si particles 7-33649
- Al-Si, microsegregation, effect of solidification rate 7-46480
- Al-Si, protective coatings, reactive magnetron sputtering, microelectronics appl. 7-33556
- Al-Si, talc particle reinforced composites, prep., wear and mech. props. 7-13408
- Al-Si, wear, comparative investigs. and prep. method role 7-13605
- Al-Si, wettability of SiC 7-58569
- Al-Si (12.7 wt.%), eutectic microstruct., twinning and branching mechanisms 7-17521
- Al-Si (1.14 at.%), supersaturated, anomalous solute conc. fluctuation under elec. current influence 7-13457
- Al-Si alloy high efficiency solar cells 7-3682
- Al-Si eutectic, Sr-modified, fibrous Si cryst. morphology, TEM study 7-28015
- Al-Si eutectic, unmodified, Al grain struct. 7-65012

aluminium alloys continued

Al-Si eutectic alloy interaction with SiC whisker reinforced Al matrix composites 7-46689
Al-Si eutectic alloys, partial modification mechanism 7-59498
Al-Si LM 13 alloy with graphite particles, gravity die cast, dispersed graphite effect on freezing rate 7-59506
Al-Si melts, sorption degassing, struct. 7-3290
Al-Si thin film metallisations, Hall-Petch relation 7-2442
Al-Si/MoSi₂ stable contacts to shallow junctions 7-52847
Al-Si/Ti/Al-Si VLSI metallisation, electromigration and microstruct. props. 7-21550
Al-Si-Cu castings, fatigue strength improvement by shot peening (Japanese) 7-8100
Al-Si-Cu sputtered electrode for VLSI, Cu distributions meas. by RBS 7-2415
Al-Si-Fe, RR 58, electroslag refined, creep 7-39582
Al-Si-Mg (7, 0.3 wt.%), strength and ductility, effect of macroporosity 7-3386
Al-Si-Mn alloys, cryst. and amorphous phases, mag. props. 7-17163
Al-Si-Mn-Fe, intermetallic phases, TEM obs., extraction replica technique 7-39807
Al-Si-Pb-Bi, duplex alloys, melt quenching, microstruct. supercond. props. 7-45593
Al-Si-Sb, directionally solidified eutectics, inter-Si flake spacing rel. to Sb addition 7-53717
Al-Si-SiC(Si₃N₄), composites, thermal props. (Japanese) 7-52164
Al-Si-SiO₂ sand composites, prep. and mech. props. 7-17500
Al-Si-X, amorphous ductile, with two separate phases, form. range and props. for X=Mn, Fe, Co or Ni 7-59493
Al-Si-Zn-Mg-Ti-(Sr) system alloys, mech. props., Sr microalloying effect 7-3377
Al-Si-graphite particle reinforced composite, solidification, microstruct. 7-28028
Al-Si(Ge)(Ga), low temp. diffusion and trapping of muons 7-45865
Al-Sm, oxidation kinetics 7-65190
Al-Sn, bearing alloys, run-in kinetics, friction, contact resist., AE signals 7-17655
Al-Ti, powder metallurgy alloys, mech. and thermal stability 7-64973
Al-Ti, rapid solidification processed/mechanically alloyed, high temp. deform. 7-65100
Al-Ti alloys, 1D antiphase domain structures 7-63557
Al-Ti brazing alloys with active Ti additive, bonding of Syalon 7-39846
Al-Ti-Gd, rapidly solidified ribbons, aged, ternary phase precipitate identification 7-3311
Al-Ti-based homogeneous alloy films, elec. resist., microstruct., electromigration, comp. effects 7-21765
Al-transition metal alloys, vacancy-ordered phase and 1D quasiperiodicity 7-63551
Al-transition metal quasicrystalline alloys, isomorphism, neutron diffr. meas. 7-51638
Al-V, rapidly quenched, icosahedral phase, comp. analysis 7-26699
Al-V alloy, amorphous and quasicrystalline state, electron diffr. study 7-63562
Al-V alloys, phase transitions between amorphous, quasicrystalline and crystalline phases 7-63807
Al-V films, precip. from metastable solid solns. 7-65048
Al-V icosahedral alloys, elec. resist. and Hall coeff. studies 7-27316
Al-W/Ti(Ni) thin film reactions, W diffusion marker studies 7-2277
Al-Zn, 7075, fatigue life, size effect in randomly loaded specimens 7-22795
Al-Zn, ageing, effect of specimen thickness, SAXS study (Japanese) 7-22731
Al-Zn, disintegration kinetics, hardening temp. effects 7-52055
Al-Zn, fatigue particle coarsening, vacancy creation 7-53895
Al-Zn, Guinier-Preston zones, size distrib., small angle X-ray scatt. studies 7-28043
Al-Zn, homogeneous nucleation of precipitates 7-53733
Al-Zn, ion induced metastable phases 7-63673
Al-Zn (11 wt.%), dislocation density in high temp. creep 7-39611
Al-Zn (12 at.%) alloy, size-shape relation of Guinier-Preston zones, SAXS study 7-13455
Al-Zn (15 at.%), precip. during ageing, interaction of continuous and cellular mechanism 7-13454
Al-Zn (1.95 wt.%), X-ray microanal. in medium voltage electron microscope, radiation effects 7-46902
Al-Zn alloy, positron lifetime and ang. correlation study 7-45860
Al-Zn alloys, quenching effect on growth of Guinier-Preston zones, resistivity 7-22733
Al-Zn dilute alloy, mixed dumbbells orientational ordering transition (Russian) 7-51688
Al-Zn dilute alloys, stress-induced mixed dumbbell tunnelling, sound prop. meas. (Russian) 7-51674
Al-Zn eutectic, oriented crystallisation, buoyancy-driven convection effects 7-27887
Al-Zn eutectoid-base superplastic alloy for hot-dipping of steel sheet (Japanese) 7-59664
Al-Zn-Ag, phase diagram tie-lines, anomalous SAXS studies 7-53705
Al-Zn-Mg, 7020, thin welded joints, ductile crack growth of surface cracks 7-59594
Al-Zn-Mg, 7075, grain boundary precip., crystallographic orientation depend. 7-22686
Al-Zn-Mg, 7090, fracture, stress intensity rel. to notch root radius 7-17635
Al-Zn-Mg, Al-Cu, superplasticity rel. to grain refining addition elements 7-46561
Al-Zn-Mg, corrosion protection by Ce corrosion coatings 7-53988
Al-Zn-Mg, environmentally assisted cracking at high vel. 7-65213
Al-Zn-Mg, IN9021, powder metallurgy, fatigue crack growth, influence of load ratio 7-28124
Al-Zn-Mg, plasma-coated, heat treatment effect on fine struct. and failure mechanism 7-3496
Al-Zn-Mg, serrated flow, second phase precip., dislocation ageing 7-22755
Al-Zn-Mg, small fatigue crack growth from a keyhole notch 7-65133
Al-Zn-Mg, small surface crack prop. 7-65142
Al-Zn-Mg, TEM specimen prep. parallel and perpendicular to machined surfaces 7-39808
Al-Zn-Mg (4.5, 1.75 at.%), ageing, specific surface energy of Guinier-Preston zones 7-28046
Al-Zn-Mg alloy, precipitation hardening, plastic flow instability 7-22757

aluminium alloys continued

Al-Zn-Mg-Cu, 7475, environment sensitive fracture using shadow optical method of caustics 7-39647
Al-Zn-Mg-Cu, 7475, superplasticity, constitutive eqn., evaluation of parameters 7-65085
Al-Zn-Mg-Cu, fatigue crack prop., influence of microstruct. (German) 7-22833
Al-Zn-Mg-Cu, high-energy rate powder metallurgy processed, microstruct. evaluation 7-22607
Al-Zn-Mg-Cu, high-strength alloys, long-term marine atm. stress corrosion tests 7-46679
Al-Zn-Mg-Cu, microalloying effect on struct. and mech. props. 7-53755
Al-Zn-Mg-Cu, notched and unnotched bars, macroscopic shear localisation and fracture 7-46633
Al-Zn-Mg-Cu, strain distrib. within crack tip plastic zones 7-3396
Al-Zn-Mg-Cu-Ni-Zr, modified 7075, prod. by liq. dynamic compaction, struct. and props. 7-46437
Al-Zn-Mg-Mn-Si, rapid solidification, superplasticity 7-53826
Al-Zn-(Cu), solidification, continuous and interrupted, development of microstruct. and homogenisation (German) 7-53719
Al-Zr-Mg (Cu), grain boundary struct. and superplasticity, electron microscopy studies (Russian) 7-6630
Al-Zr-V, rapid solidification, age hardening, solid soln. form. (Korean) 7-46475
Al-Zr(Nb)(Mo), molten, thermodynamic props. 7-21450
AlCo powders, dynamic consolidation 7-39457
AlCuLi alloys, large quasicrystalline dendrites, triacontahedral solidification morphology 7-32345
AlCuLi quasicrystalline struct., construction 7-37929
AlCuSiC composite, shock response 7-26867
Al₃Fe tenfold twins in rapidly cooled Al-Fe alloy, TEM obs. 7-63631
AlH₃, isolated H impurity vibr. spectrum, isotope depend. (Russian) 7-16703
Al₈₆M₁₄ (M=Mn,Cr), quasicrystals, EXAFS studies 7-64804
Al₄M chem. reaction, M=refractory metal, for Si LPE layer form. 7-7043
AlMgSc first wall materials, sputtering and radiation induced segregation 7-38072
AlMn films, ion irradiation-induced amorphous to quasicryst. transform., comp. depend. study 7-16654
AlMn icosahedral phase, atomic struct., electron diffr., studies 7-32366
AlMn, icosahedral struct., EXAFS 7-26701
AlMn, quasicrystalline phases, plasmon electron energy loss spectroscopy and electrical resistivity 7-3123
AlMn quasiperiodic material, disorder systematics, X-ray scatt. studies 7-11995
Al₈₉Mn₁₁, icosahedral and crystalline phases, vibr. density of states, neutron scatt. study 7-44726
Al_{1-x}Mn_x cryst. and quasicryst. alloys, struct. and mag. props. 7-1949
Al₄Mn alloy, decagonal and icosahedral phase coexistence, electron diffr. studies 7-11991
Al₄Mn, diffraction approach to the structure of decagonalquasi-crystals 7-6586
Al₆Mn, icosahedral, fine line struct. in convergent beam electron diffr. 7-63560
Al₈₀Mn₂₀, quasicrystalline icosahedral phase, sp. ht., mag. props. 7-52955
Al₈₆Mn₁₄, atomic level interpretation of quasicrystal microstructure 7-16498
Al₈₅Mn₁₅Cr₈, quasicrystals, EXAFS studies 7-64804
Al₄Mn_{1-x}Fe_x, rapidly quenched, crystn. process, high temp. X-ray studies 7-1922
Al₈₆Mn₇Fe₇, Al₈₆Mn₁₄, icosahedral alloys, obs. of mirror-related grains 7-37867
AlMnSi, icosahedral and α-phase structs., EXAFS anal. 7-63554
AlMnSi, icosahedral struct., EXAFS 7-26701
AlMnSi, quasicrystalline phases, plasmon electron energy loss spectroscopy and electrical resistivity 7-3123
(Al₈Mn)_{1-x}Si_x, icosahedral phase transform., electron microscope study 7-2187
Al₁₂Mo precipitate microstruct. and orientation, implantation and annealing effects, electron microscopy study 7-16782
AlNi-Si, interfacial interactions, Rutherford backscattering spectrometry, TEM 7-12505
Al₃Ni-Al eutectic alloy, Bauschinger effect, influence of Al₃Ni dispersion state (Japanese) 7-22761
AlNiFe_{0.5}, reactor fuel cladding, corrosion resistance, rupture strength, neutron irradiation effects testing 7-59670
AlPt-Si, interfacial interactions, Rutherford backscattering spectrometry, TEM 7-12505
AlSi-Ti bilayer structs., effect of Si on reaction kinetics 7-58546
AlSi-Ti multilayer interconnects on oxidised Si substrates, electromigration resistance 7-21713
AlSi-Ti(Ta) layered films, compound formation and Si behavior 7-21762
Al₈₀Si₂₀ melt spun ribbons, microstructures and superconducting transition temperatures 7-38222
AlSi₃Ni, reactor fuel cladding, corrosion resistance, rupture strength, neutron irradiation effects testing 7-59670
AlZn alloys, precipitates, small angle X-ray scatt. study 7-46473
AlZn coatings, atmospheric corrosion products in industrial and marine environments 7-39716
AlZn dilute alloys, electron irradiation induced interstitial defects, EXAFS study 7-63661
Au-Al alloy, superconductor film structs., fabrication and appls. (Spanish) 7-27483
AuAl alloys, Al diffusion, NMR study 7-33287
AuAl₂ intermetallic cpds., charge redistrib., L-edge XANES study 7-64816
B fibre reinforced Al alloy, corrosive media influence on crack resist. 7-17668
BaAl₄, structural relationship to CaRh₂B₂ 7-16496
C fibre reinforced Al-Cu(Mg) composites, tensile strength, fracture, interfacial bond strength 7-33744
C fibre reinforced Al-Zn-Mg alloy, linear thermal expansion coeff., 25 to 400°C 7-52093
Ca-Al-Ga metallic glasses, electron transport 7-45264
Cd(Cu_{1-x}Al_x)₂, mag. and cryst. props. 7-27506
Cd(Fe_{1-x}Al_x)₂, Fe-rich intermetallics, mag. and elec. props. 7-45621
CeAl, electronic structure, spectroscopic and thermodynamic props., impurity Anderson Hamiltonian 7-32900
CeAl₂, electronic structure, spectroscopic and thermodynamic props., impurity Anderson Hamiltonian 7-32900

aluminium alloys continued

- CeAl₃, electronic struct. determ. 7-52417
 CeAl₃, low-temp. high-field magnetoresist. meas. 7-38541
 CeAl₃-Mo point contacts, low temp. I-V charact., thermoelec. effects obs. 7-27382
 CeAl₃ heavy fermion system, muon Knight shift study 7-45886
 CeAl₃ heavy fermion system, fluctuating bands 7-58736
 CeAl₃ Kondo lattice, coherent regime, Hall effect temp. depend. study 7-52581
 CeAl₃ nonmagnetic Kondo lattices, coherent regime, Hall effect temp. depend. meas. 7-52582
 CeAl₃, properties of heavy electron metals 7-45535
 CeAl₃, quasiparticle band struct., local-density approx. anal. 7-27250
 Ce_{0.8}La_{0.2}Al₃ nonmagnetic Kondo lattices, coherent regime, Hall effect temp. depend. meas. 7-52582
 Ce_xLa_{1-x}Al₃ solid solns., magnetic and thermoelectric props. 7-7212
 Co-Al, ID disordered structural states, form., quenching, X-ray diffr. study 7-44784
 Co-Al, ageing kinetics, precipitation studies (*Russian*) 7-3332
 Co-Al, precipitation product dissolution (*Russian*) 7-58479
 Co-Al (10.9 at.%), cellular prep. from supersaturated solid soln. (*Russian*) 7-65045
 Co-Al alloys, magnetic hardening 7-33209
 Co-Al solid solutions, porous decay, temp. conc. existence limits (*Russian*) 7-33680
 Co-Al-Fe(Ni), B2, slow plastic flow props. between 1100 and 1400 K 7-46565
 Co-Cr-Al-Hf(Y), high temp. oxidation rel. to alloying additions, ion implantation, Rutherford backscatt. 7-53987
 CoAl, combustive synthesis, physicochemical props. 7-7918
 CoAl, electronic struct. of antistructure Co atoms and Co-vacancies 7-7165
 CoAl, electronic struct. of vacancies 7-16975
 CoAl, ordered B2 polycryst., Young's modulus, temp. and comp. depend. 7-33716
 CoAl₃ phases, binding anal. 7-44445
 CoCrAl alloys, microstruct., atom probe FIM and TEM studies 7-33636
 CoCrAlY electron beam physical vapour deposition coating microstruct., TEM characterisation 7-52334
 CoCrAlY, hot corrosion, ZnSO₄-Na₂SO₄ reactions 7-28188
 CoCrAlY, sputter ion plated coatings for gas turbines 7-53971
 Cr-Al dilute alloys, mag. phase diagram, mag. susceptibility studies (*Russian*) 7-2840
 (Cr_{1-x}Al_x)₂Mo₅, antiferromagnetism disappearance, comp. depend., elec. resist. and sound rel. meas. 7-2843
 Cu-Al, diffusion coefficients, composition depend. (*Russian*) 7-32701
 Cu-Al, dynamic recrystallisation, grain boundary bulging 7-39540
 Cu-Al, H trapping, positron annihilation spectra 7-33482
 α-Cu-Al, ordered domain charactn. from dissoln. kinetics study 7-22693
 Cu-Al, rel. between phase comp. and electron conc. (*Russian*) 7-53700
 Cu-Al (111), S segregation, LEED and AES studies 7-2321
 Cu-Al (25 wt.%), diffusion coeff., segregation, high temp. creep of β-phases (*French*) 7-32658
 Cu-Al (6 wt.%), erosion by spherical non-friable steel shot, impact angle effect 7-8136
 Cu-Al bronze, hot deform. and annealing, mechanical props. and softening kinetics 7-17552
 Cu-Al bronzes, microstruct., corrosion 7-39697
 Cu-Al film couples, interfacial phase form., in situ annealing X-ray diffr. obs. 7-21705
 Cu-Al film resistivity depend. on thickness and annealing time 7-11242
 Cu-Al long-period superlattice, interface struct., TEM and HREM study 7-16499
 Cu-Al-Ag (5.4, 5.2 wt.%), ageing, hardness, precip. energy 7-65127
 Cu-Al-Co(Mn)(Fe)(Ni), stacking fault energy determ. (*Russian*) 7-12082
 Cu-Al-Fe, Al bronze, superplasticity, effect of Fe content 7-65109
 Cu-Al-Mg alloys, complex oxide form. and precipitate morphology (*Russian*) 7-33664
 Cu-Al-Mn, surface layers, change in chem. state during annealing investig. using Auger spectroscopy (*Russian*) 7-33834
 Cu-Al-Mn, thermoelastic martensite form., effect of thermal and stress cycling 7-22680
 Cu-Al-Ni, β-phase alloys, fracture rel. to grain boundary precip. and Ni content 7-59604
 Cu-Al-Ni, cryst. struct. of α' martensite formed during deform. (*Russian*) 7-53814
 Cu-Al-Ni, shape memory alloys, polycrystalline, cyclic deform., fatigue above transform temp. 7-3434
 Cu-Al-Ni shape memory alloys, polycrystalline, cyclic deform. and fatigue above transform. temp. 7-3433
 Cu-Al-Ni-Fe bronze, laser glazing, microstruct. 7-52197
 Cu-Al-Ni-Fe-Mn bronze, cast, laser surfacing, improved corrosion resist., microstruct. characteris. 7-13651
 Cu-Al-Ni-Ti-Zr, shape memory alloy, grain refinement, fracture mode, Ti and Zr additions effect 7-3301
 Cu-Al-Si, rel. between phase comp. and electron conc. (*Russian*) 7-53700
 Cu-Al-Zn, β-phase stability, mech. props. rel. to quenching rate 7-33659
 Cu-Al-Zn, rel. between phase comp. and electron conc. (*Russian*) 7-53700
 Cu-Al-Zn-Mn-Ni shape memory alloy, positron annihilation study 7-46206
 Cu-Fe-Al, cold rolled, γ to α transform. of fine α-Fe precipitates, mag. props. 7-3300
 Cu-Fe-Al alloys, thermoelec. power temp. depend. (*Russian*) 7-12706
 Cu-Fe-Mg-Ni-Al alloy, stress relaxation in tension and creep in torsion 7-44667
 Cu-Ge-Ga-Al FCC alloys, faulted structure, X-ray diffr. studies 7-58292
 Cu-Mn-Al alloys, mag. and structural props. study 7-2895
 Cu-Ni-Al, two-step ageing, microstruct., mech. props. 7-39565
 Cu-Ni-Al (7.5, 2.5 at.%), thermomech. treatment (*Japanese*) 7-8013
 Cu-Ti-Al single crystals, strain hardening due to multiple twinning (*Russian*) 7-46501
 Cu-Za-Al ribbons, rapidly, quenched, martensitic transform., stabilisation 7-22678
 Cu-Zn-Al, dislocation density and mobility during reversible martensitic transforms. 7-26759
 Cu-Zn-Al, quenched sheets, shape change rel. to thermal cycle (*Japanese*) 7-53790
 Cu-Zn-Al, shape memory alloy, type II twins in self-accommodating martensite plate variants 7-22752

aluminium alloys continued

- Cu-Zn-Al, thermoelastic, two way memory effect, dislocation form. model 7-22741
 Cu-Zn-Al, thermoelastic, two-way memory effect, dislocations origin 7-22754
 Cu-Zn-Al (26.4 wt.%), shape memory alloy, martensitic transform: crystallography (*Chinese*) 7-7994
 Cu-Zn-Al (26.4 wt.%), shape memory alloy, crystallography of martensitic transform. (*Chinese*) 7-7995
 β-Cu-Zn-Al alloys, elastic constants and lattice stability 7-13492
 Cu-Zn-Al shape memory alloys, rapidly solidified, microstruct. and props. (*Chinese*) 7-8043
 Cu-Zn-Al shape memory alloys, grain refinement 7-53774
 Cu-Zn-Al-Zr, shape memory alloys, grain-refined, effect of grain size on transform. temp. 7-39512
 Cu-Zu-Al, liq. alloys, activity of Zn (*Japanese*) 7-53698
 CuAl random alloys, positron state, rel. to 2D ang. correlation 7-45230
 CuAl, short-range order-induced equilib. resist. conc. depend. meas. 7-26700
 CuAl-quartz, SAW resonators, annealing behaviour and phase noise performance 7-11242
 Cu_{1-x}Al_x, α-phase, specific heat 7-12312
 CuAlNi deformed single cryst., internal friction amplitude depend. (*Russian*) 7-13491
 Cu₂MnAl, Heusler alloy, heat and press. processed, changes in phys. props. during heating (*Russian*) 7-59645
 Cu₂MnAl, high press. phase transition, elec. resist., saturation magnetisation, lattice parameters (*Russian*) 7-46457
 CuZnAl alloys, β-phase, defects study by positron annihilation 7-39297
 CuZnAl, isothermal growth of thermoelastic martensite, quenching and ageing effects 7-53730
 DyAl₂, monocrystalline, longitudinal μSR studies, ferromag. and paramag. phases 7-45876
 DyAl₂, muon spin relax. in paramag. and ferromag. regimes 7-45879
 DyAl₂, paramag. fluctuations, μSR study 7-45878
 DyAl₂ single crystals, low temp. heat capacity meas. in mag. field, mean field approx. calcs. 7-27530
 Dy_{1-x}Al_x, intrinsic coercive field 7-45728
 Dy₂Y_{1-x}Al_x, intrinsic low field susceptibility studies 7-45633
 Dy₂Y_{1-x}Al_x, intrinsic coercive field 7-45728
 ErAl₂, intrinsic coercive field 7-45729
 ErAl₂ single crystals, low temp. heat capacity meas. in mag. field, mean field approx. calcs. 7-27530
 Fe-Al, ²⁶Al diffusion, radioactive isotope meas. (*Russian*) 7-32700
 Fe-Al, alloying for oxidation resist. improvement, comparison between ion implantation and laser irradi. 7-22883
 Fe-Al, atomic radial distrib. function, close order sorting parameter (*Russian*) 7-58206
 Fe-Al, B2-ordered alloys, dislocation energies and mobilities 7-58283
 Fe-Al, coercive field meas. 7-64491
 Fe-Al, disordered, phonon dispersion curves 7-2124
 Fe-Al, thin foil, interfacial migration, velocity-driving force relations 7-46411
 Fe-Al (40 at.%), electron irradi., Huang scatt. from interstitials 7-58272
 Fe-Al cold-rolled nonbrittle powder strip prep., texture and mag. props. 7-46370
 Fe-Al disordered alloys, electronic struct., mag. props. and Mossbauer spectra 7-64073
 Fe-Al disordered alloys, mag. props., site-diluted Ising model calcs. 7-2873
 Fe-Al metastable alloy sputtered film, mag. props., comp. depend., X-ray diffr. and Mossbauer meas. 7-7559
 Fe-Al-C (3.8, 1.8 wt.%), martensite crystallostruct. changes, effect of temp. and heating/cooling rates (*Russian*) 7-53727
 Fe-Al-Co ordering alloys, phase separations 7-33634
 Fe-Al-Mn, austenitic, SCC in NaCl soln. 7-8195
 Fe-Al-Mn, fatigue crack growth 7-65130
 Fe-Al-N, nitriding, surface layer struct., Mossbauer spectra (*Russian*) 7-59672
 Fe-Al-Si, Sendust, magnetocrystalline anisotropy 7-33165
 Fe-Al-Si system, electronic struct. interatomic bonding, X-ray emission spectra analysis (*Russian*) 7-39320
 Fe-Co-Ni-Al-Cu metallic alloy ordering and spinodal decomposition, atom probe FIM study 7-33676
 Fe-Cr-Al, C solubility, influence of Ti and Nb, high-temp. oxidation resist. 7-22876
 Fe-Cr-Al alloys, Al₂O₃ scale growth 7-65214
 Fe-Cr-Al-Ce, microstruct., high temp. corrosion rel. to Ce additions 7-13648
 Fe-Cr-Ni-Al-Si-Mn, oxidation from 700 to 1000°C 7-65207
 Fe-Mn-Al, mag. props., struct. and deform. texture 7-2892
 Fe-Mn-Al, plasma nitriding, sputtering and redeposition of cathode material 7-39752
 Fe-Mn-Al, processing and props., effect of Si and C additions 7-17707
 Fe-Mn-Al-Cr system, rel. between γ-ε transform. temp. and comp. of metastable austenite region (*Chinese*) 7-7993
 Fe-Nd-B-Al sintered magnets, TEM studies 7-51999
 Fe-Ni-Al, sintered, ageing, precip. strengthening, tensile strength 7-39536
 Fe-Ni-Al-C (22, 8, 2.4 wt.%), rapidly quenched, metastable modulated struct., analytical STEM study 7-46450
 Fe-Ni-Al-Co system, miscibility gap, phase decomp. in Alnico mag. alloys 7-17537
 Fe-Si (3 wt.%), high-Al, denitriding in solid state on heating in vac. 7-8159
 Fe-Si-Al, atomic ordering and mechanical props. 7-11990
 Fe-Si-Al, carbide precip. kinetics, core loss 7-8001
 Fe-Si-Al, electrical steel sheet, rollability, core losses (*German*) 7-59549
 Fe-Si-Al, high-Si, alloy elements influence on plasticity and mag. props. 7-8067
 Fe-Si-Al, Sendust films, DC opposite sputtered, mag. and crystallographic characteristics 7-7847
 Fe-Si-Al alloy single crystals, mag. props. (*Japanese*) 7-22104
 Fe-Si-Al films, magnetoelectric effect and anisotropy fields 7-59071
 Fe₇₀Al₃₀, reentrant spin glass, field induced modulated spin structure 7-38882
 FeAl, B2-structured, annealed and slow cooled, occurrence of displacement fringes 7-6808
 FeAl, electronic struct. of vacancies 7-16975
 FeAl, ordered B2 polycryst., Young's modulus, temp. and comp. depend. 7-33716

aluminium alloys continued

FeAl, short-range order-induced equilib. resist. conc. depend. meas. 7-26700
FeAl, X-ray emission and absorpt., ab initio self-consistent band struct. calcs., LMTO method 7-64826
FeAl₃, Fe₂Al₃, combustive synthesis, physicochemical props. 7-7918
FeAl₃ phases, binding anal. 7-44445
Fe₃Al, near surface atomic correlations depth profiling, total reflection of synchrotron radiation 7-52214
FeAlNiCoCu permanent magnetic material, phase decomposition kinetics, atom probe FIM study 7-33669
FeCrAlY, Al₂O₃ adhesion mechanism 7-33843
FeCrAlY coatings, ion-implanted, oxidation behaviour 7-53974
FeMnAl, low temperature specific heat (Chinese) 7-12306
(Fe_{0.15}Ni_{0.85})₇₅P₁₆B₆Al₃, static scaling in an amorphous metallic spin glass 7-38871
FeNiAlCoTiCuS permanent magnetic material, phase comp. and ordering, atom probe FIM and TEM studies 7-33635
(Fe_{0.15}Ni_{0.85})₇₅P₁₆B₆Al₃, amorphous spin glasses, relaxation 7-53000
(Fe_{0.15}Ni_{0.85})₇₅P₁₆B₆Al₃, magnetic susceptibility appl. of dynamic scaling 7-59019
(Fe_{0.15}Ni_{0.85})₇₅P₁₆B₆Al₃, metallic spin glass, time decay of saturated remanent magnetisation 7-59058
(Fe_{0.15}Ni_{0.85})₇₅P₁₆B₆Al₃, metallic glass, struct. relax., theory (Russian) 7-44397
GdAl₃, paramag. fluctuations, μ SR study 7-45878
Gd(Al_{1-x}Ga_x)₂, cryst. struct., paramag. susceptibility, elec. resist. meas. 7-16492
Gd_{2-x}La_xAl₃, pseudobinary cpd., mag. props., disorder effects 7-7523
La-Al, glass, short-range struct., pulsed neutron and X-ray diffraction 7-1912
LaAl nonmagnetic metallic glasses, negative TCR and electronic struct. studies 7-52562
La_{100-x}Al_x metallic glasses, electron transport 7-45265
La(Fe_{0.9}Al_{0.1})₁₃, mag. props. determined via neutron scatt. and Mossbauer spectroscopy 7-2820
LaNi_{4.77}Al_{0.22}-LaNi₅, hydride chem. heat pump, thermodynamics 7-13926
LaNi_{4.7}Al_{0.3}H_x-n-undecane suspension, H₂ absorpt. kinetics 7-33966
Li-Al/FeS₂ cell with LiCl-LiBr-KBr molten electrolyte 7-65439
LiAl B32-type Zintl phases, mag. props., exchange enhancement, APW calcs. 7-27504
Mn-Al icosahedral quasicrystals, local structure 7-11997
Mn-Al-C, anisotropic permanent magnet, rotational hysteresis 7-53050
Mn-Al-C ferromag. alloys, phase, transformations. and struct. defects, positron annihilation study 7-46461
Mn-Al-C system, mag. and struct. transform. (Russian) 7-59014
MnAlSi and MnAl icosahedral crystals, structure, EXAFS studies 7-11996
Mo/Al-Si interdiffusion kinetics and contact resistance study for VLSI appls. 7-21714
Nb-Al, fig. quenched, supercond. transition temp., cooling rate depend. 7-45537
Nb-Al alloys, struct. and supercond. props. (Russian) 7-1945
Nb-Al-Ge superconductors, pinning force, mech. meas. 7-64417
Nb₃Al, supercond. transition and mag. fields, muon spin resonance studies 7-52878
Nb₃Al superconducting state, zero-field muon spin relax. rate 7-53203
Nb₃Al superconducting tape prepared by CO₂ laser beam irradiation 7-17145
Nb₃Al/Pb magnetron sputtered Josephson tunnel junction props., film deposition conditions dependence 7-58955
Nb₃(Al-Ge), high T_c supercond., Raman spectra studies 7-7699
Nb₃Al₂Si₁₄B_{0.5}, A-15 superconducting tapes for high mag. fields, fabrication 7-33133
Nd-Fe-B-Co-Al based permanent magnets, mag. props. and temp. characts. 7-53045
NdAl₂, electronic structure, spectroscopic and thermodynamic props., impurity Anderson Hamiltonian 7-32900
Nd₂(Fe_{0.7}Al_{0.3})₁₄B, reduction of mag. hyperfine fields and Curie temp. on Al substitution, Mossbauer spectra 7-38859
Nd₂Fe_{14-x}Al_xB, crystallographic and mag. props. 7-27522
NdFeBCoAl magnets, Curie temp., coercive force and magnetisation 7-52982
Nd₂Fe_{14-x-y}Co_yAl_xB alloys, permanent mag. props. 7-45755
Nd₂(Y_{1/2}Fe_{1-x}Al_x)₁₄B, intrinsic and permanent mag. props. (Chinese) 7-13003
Ni base superalloys, pressure vessel performance, strength, ductility, comp., struct. 7-3365
Ni-Al, aged γ/γ' alloys, He²⁺ implantation studies 7-22690
Ni-Al, heterophase structures, nonequilib. state diagrams (Russian) 7-17555
Ni-Al (20 wt.%), planar flow cast, cooling rates and microstruct. 7-59505
Ni-Al alloy phase transforms. during ion beam mixing, electron diffr. and microscopy studies 7-16655
Ni-Al alloys, premartensitic behaviour, neutron scatt. study 7-44717
Ni-Al alloys, rapidly solidified, mech. props. 7-22839
Ni-Al dilute alloys, oxide growth and microstruct. at high temp. 7-17735
Ni-Al intermetallic cpds., charge redistrib., L-edge XANES study 7-64816
Ni-Al liq. alloys, enthalpies of mixing 7-46487
Ni-Al ordered alloys, long-range oscillatory surface relaxations simulation 7-2317
Ni-Al powder system, cpd. formation during shock wave loading 7-39460
Ni-Al powders, gasless combustion synthesis, particle size 7-46368
Ni-Al synthesis by shock compression of composite particles 7-39462
Ni-Al system, diffusion interaction of the β and γ' phases 7-38242
Ni-Al-B based alloys, site occupations, APFIM and channelling studies 7-32367
Ni-Al-Co-Cr-Ta, polycrystalline superalloys, microstruct. rel. to Ta content 7-46446
Ni-Al-Co-Nb superalloy, interphase boundary, FIM atom probe study 7-33683
Ni-Al-Cr, melt spun ribbons, microstruct., mech. props., Cr conc. effect 7-28031
Ni-Al-Cr based alloy plasma-sprayed thermal barrier coatings, sp. ht. and thermal cond. meas. and 2D computer simulation 7-7076
Ni-Al-Fe system, phase equilibria in the Ni-rich region 7-39487
Ni-Al-La, defect form., disordering, strengthening effect of La addition 7-22708

aluminium alloys continued

Ni-Al-Mo, precip. in Ni-base superalloys 7-53745
Ni-Al-Mo eutectic high temp. alloy, directional solidification within ZrO₂ supporting skin (German) 7-22660
Ni-Al-Mo-W system, constitution of Ni₃Al-Ni₃Mo-Ni₃W section 7-13434
Ni-base superalloy, cast, high Al-Ti, eutectic form. and σ -phase control (Chinese) 7-7983
Ni-base superalloy, oxidation in steam at 800°C, role of Al and Ti 7-65203
Ni-base superalloy, single cystal., SRR99, creep behaviour 7-17587
Ni-base superalloys, creep resist. improvement, role of Re additions, APFIM study 7-22772
Ni-base superalloys, γ' strengthened, creep and microstruct. rel. to refractory elements 7-3364
Ni-Co-Cr-Al-Y, plasma sprayed, high temp. tensile and creep behaviour 7-28083
Ni-Co-Cr-Al-Y coatings, electron beam deposition, oxidation rel. to pretreatment 7-46702
Ni-Co-Cr-Mo-Al-Ti prealloyed powder, parts prod. by hot pressing (French) 7-13400
Ni-Cr-Al (20, 12.5 wt.%), coatings containing dispersed oxides, high temp. oxidation 7-33842
Ni-Cr-Al films, thin film resistor appl., struct., temp. coeff. of resist. props. 7-58912
Ni-Cr-Co-Mo-Nb-Ti-Al superalloy, microstruct. and mech. props. with high-temp. heating 7-3341
Ni-Cr-Co-Mo-Ti-Nb-Al, heat-resisting, supersaturated solid soln., isothermal decomp. kinetics 7-33682
Ni-Cr-Co-Mo-Ti-Nb-Al, heat-resisting, hot strain rate effect on microstruct. and mech. props. 7-39559
Ni-Cr-W-Si-Al-C, heat resistant coatings on Ni alloys 7-3498
Ni-Mn-Al, martensitic transform. (German) 7-46471
Ni-NiAl, formation of NiAl coatings by CVD, kinetics 7-59451
Ni-Si-Mg, high temp. oxidation rel. to alloying additions, ion implantation, Rutherford backscatt. 7-53987
 β -NiAl alloys, structural vacancies and T-antistruct. atoms, positron trapping study 7-39300
 β' -NiAl, electron charge distrib., HEED meas. 7-16502
NiAl, electronic struct. of vacancies 7-16975
NiAl, high temp. oxidation, alumina scales, markers and tracer anal. 7-17724
NiAl, Ni₂Al₃, combustive synthesis, physicochemical props. 7-7918
NiAl single crystal, surface oxide softening 7-39751
NiAl, slow plastic creep props. between 1200 and 1400 K, effect of comp. and grain size 7-65084
NiAl thin films, ion irradi. induced amorphisation studies rel. to cascade parameters 7-63671
NiAl/Ni thin film interactions, phase formation sequence 7-21701
NiAl₃ phases, binding anal. 7-44445
Ni₃Al, molten, wetting of TiC-WC, compact (Ti,W)C-Ni₃Al, composites prep. 7-64987
Ni₃Al, alloying addition lattice location, phenomenological description 7-32463
Ni₃Al and NiAl, positron annihilation and DSC studies of diffusion mechanisms 7-46204
Ni₃Al, atomic struct. of alloy surface, LEED study 7-38306
Ni₃Al, computer simulation of grain boundaries, effect of comp. 7-21228
Ni₃Al, dislocation bowing and partial separation during in situ straining, TEM obs. 7-63617
Ni₃Al, dislocation line stability 7-21212
Ni₃Al, L₁₂ ordered alloys, grain boundary strength and fracture, electronic and struct. studies 7-33756
Ni₃Al, L₁₂ ordered intermetallic cpds., symm. tilt boundaries, geometrical models 7-32454
Ni₃Al, L₁₂ struct., grain boundary ordering configs. 7-32456
Ni₃Al, polycrystalline, grain boundary fracture model 7-53896
Ni₃Al produced by shock compaction, TEM 7-39480
Ni₃Al, rapidly solidified, B segregation to grain boundaries, atom probe FIM 7-22688
Ni₃Al, rapidly solidified, C segregation to grain boundaries 7-46483
Ni₃Al, solid soln. hardening with ternary additions, Young's modulus 7-13464
Ni₃Al, stiffness const., dislocation line energy and tension, ultrasonic vel. meas. 7-63719
Ni₃Al surface, atomic struct., LEED study 7-38307
Ni₃Al, thermal and elec. cond., temp. and comp. depends. 7-64200
Ni₃Al-B, elevated temp. ductility, effect of testing environment 7-39614
Ni₃Al-B, grain boundary adhesion 7-16350
Ni₃Al-B, with and without Hf additions, dynamic embrittlement at 600°C 7-65112
Ni₃Al-B rapidly solidified alloy, B distrib. at grain and antiphase boundaries, atom probe FIM and TEM studies 7-33637
Ni₃Al-B-Hf alloys, B and Hf grain boundary segregation, ductility, atom probe FIM study 7-33675
Ni₃Al-Be, ductility, strength, grain boundary segregation, solid soln. strengthening, Be addition effect 7-39608
Ni₃Al(B,Ti), rapidly solidified powders, struct. of consolidated products 7-3222
NiAlCrY, high temp. oxidation, alumina scales, markers and tracer anal. 7-17724
Ni₃AlHfB/Ni couples, up-hill Hf interdiffusion studies 7-12378
Ni₃(Al_{0.52}Mn_{0.48}), L₁₂ ordered alloys, grain boundary strength and fracture, electronic and struct. studies 7-33756
NiAlTi, decomposition kinetics, TEM, FIM and SANS studies 7-53748
NiAlTi alloys, alumina scale growth mechanism, ¹⁸O tracer study 7-33840
NiCoCrAlY, plasma sprayed coatings, low cycle fatigue behaviour 7-22793
NiCrAlTi, sputter ion plated coatings for gas turbines 7-53971
NiCrAlY, Al₂O₃ adhesion mechanism 7-33843
Ni₂MnAl, Heusler alloys, Curie temp., effect of hydrostatic press. 7-64455
Ni₆₀Nb_{40-x}Al_x metallic glasses, form. and stability, X-ray diffr., DSC obs. 7-58155
NpAl₂, high press. studies 7-16689
NpCr₂Al_{8-x}, mag. props., Mossbauer effect and neutron diffr. 7-59127
NpCu₂Al_{8-x}, mag. props., Mossbauer effect and neutron diffr. 7-59127
NpFe₂Al_{8-x}, mag. props., Mossbauer effect and neutron diffr. 7-59127
Pb-Al-Mg-Sn-Li, strength and microstruct. 7-8047
Pd-Al liq. alloys, enthalpies of mixing 7-46487

aluminium alloys continued

- PrAl₂, electronic structure, spectroscopic and thermodynamic props., impurity Anderson Hamiltonian 7-32900
 PrAl₃, Cryst. pot. model for description of cryst. elec. field effects 7-45599
 Pr₇Co₆Al₇, crystal struct., determ. 7-16494
 Pr-Al liq. alloys, enthalpies of mixing 7-46487
 Pt-Al-Cr coatings, structure and 700°C hot corrosion behaviour 7-53973
 R₂Al₃Si (R=Pr,Gd,Tb,Dy,Ho,Er,Tm,Lu), electronic struct., X-ray emission bands *(Russian)* 7-45138
 Sc(CO_{1-x}Al_x)₂, pseudobinary system, weak itinerant ferromagnetism 7-2825
 Sc(Co_{1-x}Al_x)₂, anomalous high field magnetisation 7-64438
 SiC fibre reinforced Al alloys, whisker or particulate hybrids, mech. props. 7-13537
 SiC fibre reinforced Al-Mg, thermal residual stress 7-63848
 SiC particle reinforced Al-Cu-Mg composite, failure mechanism, SEM obs. 7-65132
 SiC whisker reinforced Al alloy, fabrication and props. 7-53680
 TbAl₃ single crystals, low temp. heat capacity meas. in mag. field, mean field approx. calcs. 7-27530
 Tb_{0.95}Gd_{0.05}Al₂, NMR of ¹⁵⁹Tb *(Russian)* 7-45832
 Tb₂Gd_{1-x}Al₃, intrinsic low field susceptibility studies 7-45633
 Tb₂Gd_{1-x}Al₃, intrinsic coercive field 7-45729
 TbAl₃, press. induced AlB₂ to MgCu₂-type struct. transition 7-12263
 (Ti,W)C-Ni₃Al, composite prep. by liq. phase sintering, wettability of carbide by molten Ni₃Al, 7-64987
 Ti-6Al-4V, electron beam welded, neutron irradi. effects 7-56832
 Ti-Al, brittle failure rel. to overheating, fractography 7-22796
 Ti-Al (6 to 16 wt.%), ordered DO₁₉ phase form., DTA study 7-39484
 Ti-Al powder mixture subject to explosive shock-wave loading, compound formation 7-39461
 Ti-Al system, oxidation behaviour, role of N 7-28198
 Ti-Al-Cr-FeSi, AT3 alloy, corrosion resist. and hydrogenation susceptibility in dil. H₂SO₄ soln. 7-17685
 Ti-Al-Cr-Mo, VT3-1 mech. props. depend. on decomp. product morphology for metastable phases 7-39655
 Ti-Al-Fe, mech. props., investig. as implant material *(German)* 7-46647
 Ti-Al-Mo-Cr, VT3-1, struct. changes during US case hardening *(Russian)* 7-53991
 Ti-Al-Mo-Cr, VT3-1, vac. annealing of blanks after isothermal deform., hydrogen plasticising effect 7-8027
 Ti-Al-Mo-Cr and Ti-Al-Mo-Zr, VT3-1 and VT9, two-phase, microstruct. and failure nature correl. 7-8110
 Ti-Al-Mo-Cr VT3-1, cooling regimes in heat treatment effect on mech. props. 7-8026
 Ti-Al-Mo-Fe, struct. changes during phase transitions *(Russian)* 7-53721
 Ti-Al-Mo-V, fatigue failure resist., appl. of high-freq. loading methods 7-59627
 Ti-Al-Mo-V-Cr, VT22, metallographic study of β -solid soln. decomp. 7-39523
 Ti-Al-Mo-Zr(Si) alloys, superplastic characts., H alloying effect 7-8049
 Ti-Al-Nb, rapidly solidified, microstructural studies 7-22668
 Ti-Al-Nb (6.2 wt.%), fusion weld, defect regions, cracking, porosity, interstitial analysis 7-28109
 Ti-Al-Nb-Zr, plastic deform., elect. resist. oscils. 7-20605
 Ti-Al-Sn, silicide precipitates struct. 7-63561
 Ti-Al-Sn, specific heat capacities *(German)* 7-2228
 Ti-Al-Sn, weld metal, cryogenic toughness *(Japanese)* 7-46620
 Ti-Al-Sn-Zr, high-cycle fatigue damage, predicting onset, engng. appl. for long crack fatigue threshold data 7-22789
 Ti-Al-Sn-Zr-Mo (6.2,4.2 wt.%) superplastic deform., temp. depend. 7-39588
 Ti-Al-V, environmentally assisted cracking at high vel. 7-65213
 Ti-Al-V, high-cycle fatigue damage, predicting onset, engng. appl. for long crack fatigue threshold data 7-22789
 Ti-Al-V, in power generation industry 7-46283
 Ti-Al-V, pseudo-alpha alloys, BCC lattice hydrides *(Russian)* 7-53751
 Ti-Al-V, spall strength and fracture mechanism 7-46627
 Ti-Al-V, struct., martensitic transform., cooling rate depend. *(Russian)* 7-46469
 Ti-Al-V, ternary phase diagram 7-28017
 Ti-Al-V, VT20 and VT6, annealing temp. effect on mech. props. of semi-finished products 7-39558
 Ti-Al-V, VT23, α and β phases, temp. relationship of chem. comp. *(Russian)* 7-39520
 Ti-Al-V (6, 4 wt.%), hardness and alpha/beta ratio, effect of O 7-3430
 Ti-Al-V (6, 4 wt.%), powder metallurgy, fatigue props. rel. to microstruct. 7-8096
 Ti-Al-V (6, 4 wt.%) plates, rolling, heat treatment, microstruct., mech. props., turbine blade appl. 7-17644
 Ti-Al-V (6, 4 wt.%) texture stability during rolling in two-phase field 7-46508
 Ti-Al-V (6.4 wt. %) superplastic deform., temp. depend. 7-39588
 Ti-Al-V (6.4 wt. %), annealed fatigue crack growth in water, SEM fractography *(Chinese)* 7-8076
 Ti-Al-V (6.4 wt. %), α morphology rel. to thermomech. treatment 7-46520
 Ti-Al-V (6.4 wt. %), fracture, deform., porosity effect 7-22750
 Ti-Al-V (6.4 wt. %), machined sheet test pieces, superplastic deform. 7-22763
 Ti-Al-V (6.4 wt. %), powder metallurgy, thermomechanically treated, deform. behaviour 7-53908
 Ti-Al-V (6.4 wt. %), strain distrib. within crack tip plastic zones 7-3396
 Ti-Al-V (6.4 wt. %) r-values after superplastic strain 7-53806
 Ti-Al-V (6.4 wt. %)/Ti(CWC) composites, implantation modified, friction, surface chemistry 7-46660
 Ti-Al-V cast strip, prep. by melt overflow rapid solidification 7-22609
 Ti-Al-V PT3V pseudo- α -alloy, fatigue resist. at increased temps. 7-17611
 Ti-Al-V-Mo-Cr, VT23, gas impregnation influence in heat treatment, rapid heating effect 7-17696
 Ti-Al-Zr, IMI 829, low cycle fatigue 7-22792
 Ti-Al-Zr-Mo-Si, creep resistance, silicides obs., effect on mechanical props. and fracture 7-8051
 Ti-Al-base alloys, fatigue failure resist., appl. of high-freq. loading methods 7-59628
 Ti-Cr-Mo-Al, textured sheets, Young's modulus anisotropy, elastic consts. calc. 7-46535
 Ti-Ni-Al rapidly quenched amorphous alloys, thermal stability studies 7-21123
 TiAl, aluminide layers on Ti, high temp. cyclic oxidation 7-17719

aluminium alloys continued

- TiAl, deform. at high temp., flow and brittle fracture stress *(Japanese)* 7-13516
 Ti_{1-x}Al_x, long period struct. 7-16500
 Ti₃Al, struct., phase comp. rel. to crystallisation rate and heat treatment 7-46442
 Ti₃Al-Nb alloys, ductility and fracture toughness, dispersoid modification effects 7-22779
 Ti₃Al-Nb-Er rapidly solidified alloy, microstruct. effects and dispersoid stability 7-22669
 Ti₃Al-Zr, rapidly solidified, microstructural studies 7-22668
 TmAl₃ polycrystals, low temp. heat capacity meas. in mag. field, mean field approx. calcs. 7-27530
 UAl₂, μ SR meas. 7-45874
 UAl₃, spin-fluctuation material, magnetoresistivity 7-45278
 UAlNi(Co)(Ru) ternary alloys, magnetic behaviour, elec. resist. and sp. ht. meas., 5f electron effects 7-12999
 UCu_{4.5}Al_{7.5}, antiferromagnetic suscept. meas. 7-12954
 UFe₂Al_{12-x}, ferromagnetic suscept. meas. 7-12954
 U(Mn_{1-x}Al_x), paramagnetic props. meas., temp. depend. study 7-27494
 UNiAl, surface segregation behaviour 7-33519
 VAl, electronic struct. of vacancies 7-16975
 W fibre reinforced Fe-Cr-Al superalloy, surface cladding and matrix deform., thermomech. loading 7-46568
 YAl nonmagnetic metallic glasses, negative TCR and electronic struct. studies 7-52562
 Y₂(Fe,Al,Co)₁₄B, mag. props., composition depend. 7-53030
 Y(Mn_{1-x}Al_x)₂, spin glass behaviour 7-52996
 YNiAl, surface segregation behaviour 7-33519
 Zn-Al, bicrystals. and polycrystals., creep grain boundary strengthening 7-22747
 Zn-Al, solidification, segregation, foundry procedure appl. 7-53712
 Zn-Al (22 wt.%), sheet, superplastic bulging, technological anal. 7-65093
 Zn-Al (5 wt.%) coating on low C sheet steel, Zn quenching technique 7-33847
 Zn-Al alloys, corrosion behaviour, effect of Al content and cooling conditions 7-54008
 Zn-Al alloys, transient creep, structural transformation effect 7-22758
 Zn-Al coated steel, corrosion behaviour, effect of matrix struct. *(Japanese)* 7-33826
 Zn-Al eutectic alloy interaction with SiC whisker reinforced Al matrix composites 7-46689
 Zn-Al-Cu, superplastic, cavitation damage 7-65080
 Zn-Al-Cu (Z₂O.5%), superplastic behaviour 7-28093
 Zn-Al-Mg alloy, defect and grain boundary diffusion-controlled positron trapping study 7-39301
 ZrF₄-BaF₂-NaF-AlF₃ glass, crystn. *(Japanese)* 7-26659
 ZrNiAl, surface segregation behaviour 7-33519

aluminium compounds

- see also *alumina; aluminium alloys; aluminosilicate glasses*
 p-AlGaAs/GaAs modulation-doped heterostruct., liq. phase epitaxy and carrier props. 7-33074
 aluminosilicates, at. charges, SCF and semiempirical calcs. 7-2942
 alumite disc prep. using anodic oxidation *(Japanese)* 7-46672
 carborundum refractory provisions with aluminium-chromium phosphate binder 7-46395
 III-V heterostructures, tunnelling, relevance to electronic devices 7-58885
 oxide, nitride and element, L₂₃VV valence Auger transitions 7-27828
 α -quartz: AlO₄, hyperfine and quadrupole interactions, ENDOR study 7-2951
 sialon, abrasive polishing problems 7-53939
 sialon, commercial, static fatigue and creep resist. 7-59601
 β -sialon, composite ceramics, microstruct., hardness, tool appls. 7-65144
 sialon ceramics, processing, Al ion redistrib., crystallisation EDX analysis 7-3237
 topaz, radiation damage, rel. to trace water 7-32489
 zeolite 13X, hydrophobic, generation by exchange with octadecylammonium ion 7-13809
 zeolite theta-1, structural TEM studies 7-16534
 (Al,Ga)As films, doped, Si migration during MBE growth 7-27171
 (Al,Ga)As/(Ca,Sr)F₂ multilayer structures, MBE grown, broadband high-reflectivity mirrors fabrication 7-11091
 (Al,Ga)As/GaAs undoped quantum wells, Al and Ga interdiffusion, photoluminesc. study 7-2271
 Al complexes, Al (III)-amino acid complexes, stability const. determ., ionophoretic technique investig. 7-28381
 Al/Al₂O₃ films, ion plated in Ar-O₂ gas mixture, structure anal. 7-7899
 Al-Al₂O₃-Pb tunnel diode, NiCl₂·6H₂O soln. phase adsorpt., inelastic electron tunnelling spectra 7-12877
 Al-based sputtered hard compound films, struct. and props. 7-46318
 Al-C-O/Al sputtered solar selective absorbing surfaces *(Chinese)* 7-40025
 Al-Mg spinel, substrate, resonance Raman scattering of Si film 7-64017
 Al-N, sputter deposited, characterisation, X-ray photoelectron loss spectroscopy 7-59382
 Al-O, sputter deposited, characterisation, X-ray photoelectron loss spectroscopy 7-59382
 Al_{0.5}Ag_{0.7}As, femtosecond carrier dynamics 7-58829
 Al₂(Al_{1-x}Si_{2-x})O_{10-x}, mullite, cryst. struct., X-ray diff. data refinement 7-55030
 AlAs, atomic layer epitaxy, review 7-13362
 AlAs, energy bands, cohesive energy, form. energy, self-consistent calcs. 7-21995
 AlAs optical props., pseudodielec. function, spectroscopic ellipsometry meas. 7-52487
 AlAs, VPE growth by chloride transport method 7-64930
 AlAs:Si films and AlAs:Si-GaAs:Si superlattices, MBE growth and electrical props. 7-22052
 AlAs:Si MBE layers, photoluminesc. 7-39160
 AlAs/GaAs modulated struct., high resolution double-cryst. X-ray diff. studies 7-7029
 AlAs/GaAs superlattices, X-point excitons 7-33069
 AlAs/GaAs superlattice/GaAs interface, inversion holes, long term storage 7-45442
 AlAs/GaAs superlattice mixing induced by Si⁺ implantation 7-58649
 AlAs/GaAs:Si super-doped structs., short-period superlattice electrical and defect props. *(Japanese)* 7-7353
 AlAs/GaAs/AlAs quantum wells, eigenvalues calcs. 7-12820
 AlAs-GaAs double-barrier structures, resonant tunnelling, room temp. effects 7-21985

aluminium compounds continued

- AlAs-GaAs Fibonacci superlattice, quasiperiodic ordering, X-ray scatt. study 7-2692
- AlAs-GaAs MIS capacitors, dynamic storage of holes 7-33071
- AlAs-GaAs quantum-wells, low temp. growth by modified MBE 7-39386
- AlAs-GaAs superlattices, Si ion implantation, dose-dependent mixing 7-12500
- AlAs-GaAs superlattice waveguides in separate confinement heterostructure laser diodes, threshold current density 7-20267
- AlAs-GaAs superlattice, Si⁺ implantation, depth dependent mixing 7-27032
- AlAs-GaAs superlattices, Si migration during MBE growth 7-27171
- AlAs-GaAs superlattices, disordering by Si and S implantation 7-45024
- AlAs-GaAs superlattice, compositional disordering control by Ar ion implantation 7-51806
- AlAs-GaAs superlattices, lattice dynamics 7-52220
- AlAs-GaAs superlattices, lattice vibration, Raman spectra 7-63937
- AlAs-GaAs superlattices, phase transitions under high press. 7-64016
- Al₂Be₃(SiO₃)₆, beryl, crystal X-ray dispersing devices, comparison with multilayers 7-9929
- AlBr₃, RF ion source with metal discharge chamber 7-30114
- AlBr₃NH₃, vapour phase, vibr. anal., high temp. IR spectra 7-31050
- AlCl+CO₂, rate coefficient meas., HT FFR kinetics study 7-46793
- AlCl₃ layer struct., IR vibr. spectra 7-13151
- AlCl₃ solns., complexing, mol. dynamics studies 7-6496
- AlCl₃/1-butylpyridinium chloride electrolyte for Al-FeS₂ secondary cell, phys. and elec. characts. (Japanese) 7-8371
- AlCl₃-graphite intercalation cpd., phases and phase transform., X-ray crystallography (French) 7-44783
- AlCl₃·6H₂O single cryst., polarised IR reflection spectra 7-3054
- AlF, photoionis., laser sputtering and high-temp. vapourisation reactions 7-15629
- AlF, pot. energy curves for excited states, ab initio CI calcs. 7-49948
- AlF⁺, radical, matrix ESR and CI investig. 7-15629
- AlF₃ glass, optical dispersion, reflection spectra in vacuum and extreme UV region 7-27734
- AlF₃-based glasses, IR fibres, prep. and props. 7-37182
- AlF₃-CaF₂-BaF₂ glasses, Raman spectroscopic study 7-7692
- Al_{0.8}Ga_{1-x}As-GaAs multiple quantum wells, photoluminescence studies, press. depend. (Chinese) 7-13194
- Al_{0.8}Ga_{1-x}Te, low press. OMVPE, Te doping, Hall effect, carrier conc., photolum. 7-21242
- AlGaAs BH laser with flared waveguides, high power operation 7-57352
- AlGaAs, chemical beam epitaxial growth investig. 7-7878
- AlGaAs, DX centres, DLTS signature anal. 7-45204
- AlGaAs epitaxial layers and superlattices, X-ray diff. analysis 7-21047
- AlGaAs epitaxial layers, large scale MOVPE growth 7-22552
- AlGaAs epitaxial layers, MOCVD, compositionally graded growth technique for device structs. 7-22553
- AlGaAs epitaxial wafers, highly uniform growth by large capacity MOCVD reactor 7-22551
- AlGaAs heterostructs., low temp. LPE growth 7-64939
- AlGaAs high-power pulsed laser 7-10997
- AlGaAs high-power ridge-waveguide GRIN-SCH laser diode 7-10988
- AlGaAs injection heterolasers and integrated laser-photodetector pairs, prepared by microcleaving 7-31343
- AlGaAs integrated-hybrid Bragg heterostruct. laser thermal stability of distributed-refl. spectral bands 7-57393
- AlGaAs intraband relaxation dynamics of photo-excited carriers 7-52691
- AlGaAs laser, mode hopping suppression by saturable absorber 7-62696
- AlGaAs laser, tunability and mode-transition characteristics 7-20293
- AlGaAs laser, tunability, appl. to Cd⁺ ion drift velocity meas. (Japanese) 7-20294
- AlGaAs laser arrays with Si disordered facet windows, high power operation 7-43140
- AlGaAs laser diode, HF stabilisation 7-15864
- AlGaAs laser diode array travelling-wave amplifier, high peak power, gateable picosec. optical pulses 7-20252
- AlGaAs laser diodes, MOCVD grown, struct. fabrication and characts. (Japanese) 7-20272
- AlGaAs laser diodes, MBE grown, fabrication and characts. (Japanese) 7-20273
- AlGaAs laser rib-waveguide, gain- to index-guiding transition 7-31315
- AlGaAs, laser-assisted MOVPE growth 7-64928
- (AlGa)As lasers, separately pumped, continuous control 7-20287
- AlGaAs layer, separating on GaAs surface, growth mechanism, Auger depth profiling 7-44434
- AlGaAs layers MOCVD using dimethyl aluminium hydride, C acceptors, photolum. 7-22517
- AlGaAs low current threshold visible laser diodes, (AlGaAs)_m(GaAs)_n superlattice quantum well 7-10926
- AlGaAs, low press. MOCVD grown, surface morphology and defects 7-64023
- AlGaAs, MOCVD, design of safe facility 7-22529
- AlGaAs, MOCVD growth on Ge substrates for high efficiency tandem solar cell appl. 7-3671
- AlGaAs, MOCVD growth, refractive indices meas. by in situ reflectometry 7-59270
- AlGaAs, MOVPE, laser assisted, selective area irradi., carrier conc. 7-22545
- AlGaAs MQW lasers, index-guided, fabrication by selective disordering using Be focused ion beam implantation 7-20269
- AlGaAs monolithic three-junction solar-cells, computer modelling 7-3672
- AlGaAs multiquantum well-buried optical guide lasers, fabrication by Si-induced disordering 7-10995
- AlGaAs superlattice for visible laser diode, energy band structure (Japanese) 7-12823
- AlGaAs superlattices, donor state instability, DLTS and Hall meas. 7-12663
- AlGaAs surface cleaning using ECR radical beam gun 7-54028
- AlGaAs terrestrial solar cells, high-efficiency concepts 7-8390
- AlGaAs, triethylgallium pyrolysis temp. in presence of AsH₃ or trimethylaluminium 7-22541
- AlGaAs:Mg LPE layers, Mg doping and injection laser threshold current 7-12092
- AlGaAs:Mg-GaAs:Se concentrator solar cells, 26 percent efficient 7-3699
- AlGaAs:Sb, MBE growth, Sb doping 7-2038
- AlGaAs:Si-GaAs 2D electron gas structure, scatt. mechanisms 7-38718
- AlGaAs:Si(Zn), MOCVD, impurity induced disordering, quantum well laser fabrication and characts. 7-27934

aluminium compounds continued

- AlGaAs/AlAs multiquantum-well structs., staggered band alignments 7-7361
- AlGaAs/GaAs, abrupt heterojunction structures, large area uniformity, MOVPE reactor design 7-22524
- AlGaAs/GaAs DBR laser with multiquantum well active/passive waveguides 7-57350
- AlGaAs/GaAs DFB laser diodes, MOCVD growth, CW operating characts. 7-25836
- AlGaAs/GaAs heterointerface solid-state far IR emitter utilising 2D plasmon 7-53414
- AlGaAs/GaAs heterojunction bipolar transistor, self-aligned with InGaAs emitter cap 7-45492
- AlGaAs/GaAs heterostruct., quasiautomatic system, electronic struct. studies 7-38699
- AlGaAs/GaAs laser diodes, advanced optoelectronic technology 7-1187
- AlGaAs/GaAs long cavity ridge waveguide DFB lasers, spectral linewidth reduction 7-1179
- AlGaAs/GaAs modulation-doped heterojunctions, 2D electron gas, DX centres 7-38694
- AlGaAs/GaAs ridge waveguide quantum well lasers with high quantum efficiency 7-15905
- AlGaAs/GaAs selectively doped heterointerface under high elec. field appl., 2D plasmon 7-52637
- AlGaAs/GaAs solar cells, proton irradiated, defect production 7-46936
- AlGaAs/GaAs superlattice 7-64324
- AlGaAs/GaAs two-junction monolithic cascade solar cell in lattice-matched system 7-13862
- AlGaAs/GaAs waveguide phase modulators, wavelength depend. 7-43361
- AlGaAs/GaAs:Si heterostruct., MBE growth on polar surfaces 7-7863
- AlGaAs/GaAs/AlGaAs selectively doped double heterojunction FET system, high mobility electron subband struct. studies 7-12838
- AlGaAs/GaAs/AlGaAs selectively doped double heterostructs., electron conc. and mobility 7-12839
- AlGaAs/GaAs/AlGaAs single quantum well, negative differential mobility and drift vel. overshoot 7-52803
- AlGaAs/GaAs/Ge multijunction solar cell, model for calc. of displacement damage by radiation 7-13878
- AlGaAs/GaAs/InGaAs multijunction solar cell, model for calc. of displacement damage by radiation 7-13878
- AlGaAs/GaInAs two-junction monolithic cascade solar cell in lattice-mismatched system 7-13862
- AlGaAs/GaInAs two-terminal multijunction solar cell spectral response meas. 7-13871
- AlGaAs-GaAs, band-gap discontinuity, determ. by quantum oscillations of photolum. intensity 7-13217
- AlGaAs-GaAs, DFB lasers, low threshold, 0.88 μ m emission, MOCVD fabricated with ridge waveguide struct. 7-5906
- AlGaAs-GaAs, heterostructures, density of states of Landau levels 7-52822
- AlGaAs-GaAs, modulation doped heterostructs., high field transient transport 7-12836
- AlGaAs-GaAs, selectively doped heterojunctions, energy relax. of 2D electrons, deformation potential constant 7-12801
- AlGaAs-GaAs 2D electron gas structs., scatt. mechanisms 7-52783
- AlGaAs-GaAs cascade solar cells, efficient two-junction monolithic, grown by MOCVD 7-65483
- AlGaAs-GaAs concentrator solar cells with high efficiency, design and fabrication 7-3669
- AlGaAs-GaAs DFB struct. with multiquantum well for surface emitting laser 7-10939
- AlGaAs-GaAs DFB-TJS external-cavity laser with optical phase control loop, spectral linewidth 7-20222
- AlGaAs-GaAs DH injection laser, optical and transport props., emission energy shift, threshold current meas. 7-1101
- AlGaAs-GaAs DH injection lasers, MOCVD growth on Si substrates 7-57356
- (AlGa)As-GaAs DQW-SCH lasers grown by MOCVD, design, fabrication and characterisation 7-36990
- AlGaAs-GaAs extended state superlattices, shallow donor state transition energies 7-33082
- AlGaAs-GaAs GRIN-SCH SQW laser, wide-stripe, injection locking 7-20290
- AlGaAs-GaAs graded barrier quantum well heterostructure laser diodes with compositionally graded and superlattice buffer layers 7-57353
- AlGaAs-GaAs heteroepitaxial wafer for solar cell appls., uniform growth by MOCVD 7-64929
- AlGaAs-GaAs heteroface space solar cells with 21 percent conversion efficiency 7-3694
- AlGaAs-GaAs heteroface solar cells, role of window layer 7-3695
- AlGaAs-GaAs heterointerface, ballistic transport of quasi-2D electron gas 7-52788
- AlGaAs-GaAs heterojunctions, Be⁺, O⁺ ion implantation, impurity profiles, elec. characts. meas., SIMS, annealing 7-12813
- AlGaAs-GaAs heterostructures, organometallic VPE grown, galvanomagnetic effect 7-12800
- AlGaAs-GaAs heterostructures, zero mag. field thermopower meas., temp. var. 7-33075
- AlGaAs-GaAs heterostructures, dissipationless quantum Hall effect, size-depend, quantised breakdown 7-45469
- AlGaAs-GaAs heterostructure travelling-wave amplifier based on injection laser diode 7-62694
- AlGaAs-GaAs index-guided lasers with mode filter, props. study 7-5905
- AlGaAs-GaAs laser diodes, elec. field depend. of photoconductivity spectra 7-20227
- AlGaAs-GaAs MQW CCD spatial light modulators using electroabsorption effects 7-20407
- AlGaAs-GaAs MQW waveguides, nonlinear propag. 7-26033
- AlGaAs-GaAs narrow spectral linewidth semiconductor optical-fiber ring laser 7-25817
- AlGaAs-GaAs pair-groove-substrate MQW laser with self-aligned stripe geometry 7-20260
- AlGaAs-GaAs quantum wells in waveguides, physics and appls. 7-26034
- AlGaAs-GaAs selectively doped heterostructures, orientation effect on contact resistance 7-38680
- AlGaAs-GaAs self-pulsing lasers, quasiperiodic route to chaos under large signal current modulation 7-62706
- AlGaAs-GaAs single quantum well, MBE growth interruption, well width fluctuations 7-7865
- AlGaAs-GaAs single quantum wells with growth interrupted heterointerfaces, photoluminesc. 7-39168

aluminium compounds continued

- AlGaAs-GaAs solar cells, MOCVD on GaAs, Ge and Ge-Si substrates 7-3650
- AlGaAs-GaAs solar cells, high efficiency DH cells fabrication using MOCVD 7-3693
- AlGaAs-GaAs solar cells, fabrication on Si substrates 7-46937
- AlGaAs-GaAs solar cell fabrication, elec. characts. and space appl. 7-54307
- AlGaAs-GaAs space solar cells, LPE production and characterisation 7-3666
- AlGaAs-GaAs split gate heterojunction FET, elec. resist., Hall effect, influence of electronic subband mag. depopulation 7-38740
- AlGaAs-GaAs superlattices, impurity electron states (*Japanese*) 7-12662
- AlGaAs-GaAs superlattices, Si-Be co-doping, compositional disordering suppression, SIMS study 7-16878
- AlGaAs-GaAs superlattices, Se (Si)(Mg)(Be) ion implantation, intermixing, residual damage 7-26782
- AlGaAs-GaAs-AlGaAs single quantum well heterostruct., negative differential mobility and drift velocity overshoot 7-52787
- AlGaAs-GaAs-Si, Be superlattices, correlation between Si diffusion and Si-induced disordering 7-38034
- AlGaAs-GaInAs cascade solar cells, efficient two-junction monolithic, grown by MOCVD 7-65483
- AlGaAs-GeAs n-n heterojunction, thermionic current and capacitance, effect of subband quantisation in 2D electron gas 7-17090
- AlGaAs-Si mechanically stacked multijunction solar cells, optical effects of thin film adhesives 7-3670
- Al_{0.23}Ga_{0.77}As multilayer structures, vertical transport 7-38719
- Al_{0.26}Ga_{0.74}As, instability of electron-nuclear spin system in strong mag. field, luminesc. study 7-7729
- Al_{0.26}Ga_{0.74}As/GaAs heterojunction, high mobility 2-D hole gas 7-2679
- Al_{0.28}Ga_{0.72}As, photoluminescence half-width and intensity, temp. depend. 7-39179
- Al_{0.3}Ga_{0.7}As, thermal and ion-assisted reactions with Cl₂ 7-28349
- Al_{0.3}Ga_{0.7}As/GaAs quantum wells, photocond. of confined donors 7-7282
- Al_{0.3}Ga_{0.7}As-GaAs optically-pumped multiple quantum well laser 7-5922
- Al_{0.3}Ga_{0.7}As-GaAs quantum well structure, electric-field-induced optical modulation, theory using Monte Carlo approach 7-17077
- Al_{0.4}Ga_{0.6}As-GaAs, intraband recomb., luminesc. spectra anal. 7-53387
- Al_{0.4}Ga_{0.56}As-GaAs quantum wells, MBE grown, tunnelling assisted photon emission, photoluminescence meas. 7-46120
- Al_{0.55}Ga_{0.45}As:Te edge region photocapacitance at constant bias, anal. 7-7287
- AlGa_{1-x}As, hot-electron capture at DX centres 7-45344
- AlGa_{1-x}As layers, form. by regrowth on surface of GaAs during contact with undersaturated liq. containing Al 7-46311
- AlGa_{1-x}As, AlAs and GaAs epitaxial multilayers as optical interferometric elements 7-342
- AlGa_{1-x}As bandgap determ. by Schottky barrier spectral response meas. 7-2667
- AlGa_{1-x}As cascade solar cells, OM-VPE growth, in-situ-grown tunnel junction 7-8387
- AlGa_{1-x}As crystals, DX centre props. 7-2534
- AlGa_{1-x}As, DX centre, theory 7-12654
- n-AlGa_{1-x}As epitaxial layers, graded-gap, resistance, press. dependence 7-33113
- AlGa_{1-x}As film formation by laser beam interaction with AlAs/GaAs multilayer structure 7-12570
- AlGa_{1-x}As films and multilayer structures, MOCVD growth and characterisation, review 7-33586
- AlGa_{1-x}As, Ga interstitial identification by ODMR 7-33302
- AlGa_{1-x}As heteroepitaxial layers formed by metalloorganic chem. hydride method, electrophys. props., comp. effect 7-64370
- AlGa_{1-x}As heterojunction, tunnelling current modulation by optical phonons 7-27394
- AlGa_{1-x}As homojunctions, minority-carrier diffusion, TOF studies 7-12797
- AlGa_{1-x}As layers and quantum well struct., MOVPE growth chemistry 7-22550
- AlGa_{1-x}As, low press. OMVPE, selective growth embedding in etched grooves on GaAs 7-22554
- AlGa_{1-x}As MBE layers, deep electron traps, flux ratio effects 7-12641
- AlGa_{1-x}As, MOCVD, equil. gas phase species 7-22542
- AlGa_{1-x}As p-n junction solar cell radiation-induced defects obs. using DLTS 7-13875
- AlGa_{1-x}As solar cells, MOCVD growth and characterisation, review 7-34043
- AlGa_{1-x}As surface, protection by As and GaAs ultrathin layers, AES sputter depth profiles 7-54022
- AlGa_{1-x}As, thin films, Raman spectroscopy, characterisation 7-53354
- AlGa_{1-x}As:Be epitaxial layers, ion implanted, rapid thermal annealing 7-21257
- AlGa_{1-x}As:Mg/GaAs:Se quantum well heterostruct., photopumped laser operation 7-25818
- AlGa_{1-x}As:Si, deep donor centres 7-45217
- AlGa_{1-x}As:Si, LEDs, luminesc. props. (*Korean*) 7-27786
- AlGa_{1-x}As:Si, Si diffusion from sputtered Si film 7-58537
- AlGa_{1-x}As/GaAs, multilayer and superlattice structs., electronic subbands 7-58877
- AlGa_{1-x}As/GaAs multi-quantum-well Zn-diffused mesa BH lasers, submilliwatt lasing 7-10991
- AlGa_{1-x}As/GaAs photoexcited heterojunction, charge transfer calcs. 7-12688
- AlGa_{1-x}As/GaAs quantum wells, photolum., periodic variation investig. 7-2688
- AlGa_{1-x}As-AlAs quantum well, magneto-optical absorpt. study 7-7681
- AlGa_{1-x}As-GaAs BH quantum well edge-injection laser array 7-57355
- AlGa_{1-x}As-GaAs broad area quantum well lasers, single-mode single-lobe operation 7-10930
- AlGa_{1-x}As-GaAs double heterostruct. injection laser, power-current characteristics study 7-62704
- AlGa_{1-x}As-GaAs heterostructures, 2D electron space charge layers, plasmon and magnetoplasmon excitation 7-38696
- AlGa_{1-x}As-GaAs heterointerface, 2D electron gas density 7-45448
- AlGa_{1-x}As-GaAs heterostruct. injection laser with coupled cavity, dynamic stability 7-62705
- AlGa_{1-x}As-GaAs heteroface solar concentrator cells, space and terrestrial appls. 7-65486
- AlGa_{1-x}As-GaAs LOC lasers for high power low threshold current density operation, optimisation 7-10934

aluminium compounds continued

- AlGa_{1-x}As-GaAs layered structures, metal organic VPE grown, depth profiles, SIMS anal. 7-21684
- AlGa_{1-x}As-GaAs mesa BH MQW lasers with 880 μ A threshold current at 77 K 7-50595
- AlGa_{1-x}As-GaAs quantum wells, doubly reson. LO phonon Raman scatt., photoluminescence spectra 7-53327
- AlGa_{1-x}As-GaAs stripe-geometry quantum well heterostructure lasers defined by defect diffusion 7-1181
- AlGa_{1-x}As-GaAs superlattices, ion implanted, defect struct. 7-26783
- AlGa_{1-x}As-GaAs superlattices, integer quantum Hall effect at microwave frequencies 7-52820
- AlGa_{1-x}As-GaAs-GaAs heterostructures, photosensitivity spectra 7-64319
- AlGa_{1-x}As-AlAs heterojunctions, band discontinuities meas. 7-27407
- AlGaInP layers on InP, LPE growth 7-33608
- AlGaInP, MOCVD, photolum., quantum wells, double heterostruct. laser appl. 7-39405
- AlGaInP visible semicond. lasers, mesa stripe struct., MOVPE grown, 621 nm CW operation at 0°C 7-20262
- AlGaInP visible semiconductor lasers grown by metalorganic vapor phase epitaxy 7-50590
- AlGa_{1-x}N epitaxial layers, MOCVD, growth mechanism, Ga incorporation rate 7-39411
- AlGa_{1-x}N MOVPE growth, struct. and elec. props. 7-21729
- AlGa_{1-x}N, photoluminescence in the edge emission region 7-27778
- Al_{0.4}Ga_{0.6}Sb-GaSb-Al_{0.4}Ga_{0.6}Sb MBE strained layer DH, optically pumped laser oscill. 1.6 to 1.8 μ m 7-5888
- AlH₃, ¹H and ²⁷Al NMR investig. 7-27615
- AlH₃, cryst. imperfection obs., TEM 7-32445
- AlInAs-GaInAs superlattices, electronic transport and depletion by tunnelling 7-27395
- AlInAs-GaInAs heterostruct., alloyed NiGeAuAgAu ohmic contacts, charact. 7-22016
- AlInAs-GaInAs selectively doped heterostructs., MOCVD growth, HIFET fabrication appl. 7-17429
- AlInAs-GaInAs superlattices, quantum photoconductivity, effective mass filtering 7-12847
- Al_{0.25}In_{0.75}As, transient transport in central-valley-dominated ternary III-V alloys 7-7253
- Al_{0.48}In_{0.52}As:Si, MBE grown, crystalline and optical props. 7-52322
- Al_{0.48}In_{0.52}As-Ga_{0.47}In_{0.53}As SQW, electron temp. depend. on well width, photolum. obs. 7-12810
- Al_{1-x}In_xAs-GaAs strained layer superlattices, X-ray diffraction and excitation spectroscopy studies 7-12853
- (Al_{0.02}In_{0.98})₂Se₃, metastable complex defects, ESR studies 7-33270
- AlN amorphous film, plasma CVD from metal organic Al source 7-52368
- AlN corrosion protective coating for TbFe₂ magneto-optical media 7-53953
- AlN crystal, phonon energy calcs. 7-2119
- AlN, electronic struct., first principles LCAO calc. 7-21813
- AlN, film, RF reactive sputtering, effects of N content 7-39383
- AlN films, OMVPE, Hall mobilities, impurity band 7-39410
- AlN formed by N ion implantation of Al, electronic struct. 7-58926
- AlN, fusion reactor first wall, thermal shock behavior 7-25189
- AlN, hot pressed, elec. cond. rel. to CaO addition 7-38559
- AlN, hot pressed ceramic, porosity effect on elec. cond. 7-7223
- AlN, protective coatings, reactive magnetron sputtering, microelectronics appl. 7-33556
- AlN reactively evaporated encapsulating films, annealing, RBS and RHEED studies 7-21744
- AlN sputtered film, Kerr effect enhancement 7-64610
- AlN thin crystalline stoichiometric film, electronic struct., electron spectra studies 7-58916
- AlN, undoped and control doped films, luminesc. studies 7-27790
- AlN-sapphire, low temp. epitaxial film growth 7-13387
- AlN_x nonstoichiometric sputtered films, electron localisation, transport props. 7-58929
- AlNH₄(SO₄)₂ multicharged electrolyte soln. in water-tert butyl alcohol, viscosity and density studies 7-52104
- AlNbO₄:Cr³⁺ tunable IR laser crystals, fluorescent spectra 7-43110
- AlO (B²⁺-X²⁺) system, Franck-Condon factors, isotope effect 7-10671
- AlO, B-X system vibr. bands in sunspot spectra 7-60525
- Al₂O₃, He I photoelectron spectra, relativistic DVM SCC X α calcs. 7-50252
- (Al₂O₃)_{1-x}(AlN)_x, optical and elec. charact. in MIS struct. 7-38766
- (Al₂O₃)_{1-x}(AlN)_x film, optical and elec. props., comp. depend. 7-38766
- AlOH, enthalpy of form., mass spectrometric determ., equil. const., ionisation pot. 7-59777
- Al(OH)₃ sols, gelation, pH, temp., ageing time 7-46875
- Al(OH)₃ aggregate fractal structs., X-ray scatt. functions 7-32381
- AION, neutron irradi., permittivity and dielec. loss studies 7-33321
- AlOOH, stacking fault and size effects on X-ray diffr. line profile calc. 7-2032
- AlP(As)(Sb), elastic coefficients, pressure effects 7-63720
- α -AlPO₄, berlinite, elastic const., thermal behaviour (*Chinese*) 7-6699
- AlPO₄, berlinite, growth defects and incommensurate phase obs. by high temp. X-ray topography 7-32423
- AlPO₄, berlinite, high-temp. X-ray diffr. studies 7-12015
- AlPO₄, berlinite, hydrothermal cryst., growth, X-ray topography, bulk acoustic wave device characts. 7-59391
- α -AlPO₄, berlinite, piezoelec. and elastic props., effect off defects on phys. props. 7-51909
- AlPO₄, berlinite, synthesis and charactn. of new polymorphic modification 7-53534
- AlPO₄, berlinite: characterization of crystals with a low water concentrations and design of bulk wave resonators 7-59396
- AlPO₄, cryst., prep. by reaction using BPO₄ 7-46388
- AlPO₄ dielectric films for Ge MIS structures, inversion layers obs. 7-45502
- AlPO₄, glass, dielectric, charge buildup, influence on charging electron beam motion 7-44294
- AlPO₄, heat treated, IR meas., temp. coeff. of delay and insertion loss 7-13486
- AlPO₄, modulated phase, electron microscopy study 7-26937
- Al₂P₂O₇, synthesis and struct. 7-1969
- AlPO₄·1.5 H₂O, crystal struct., X-ray⁴ studies 7-12003
- AlSb, hot electron luminesc. 7-46119
- AlSb:Se, donor studies, incoherent laser saturation method 7-27298

aluminium compounds continued

- AlSb-GaSb superlattices, low-temp. growth by plasma process (*Japanese*) 7-7061
- AlSb-GaSb superlattices, X-ray diffr. analysis 7-21047
- Al₂SiO₅ polymorphs, dislocation strain energy 7-16555
- Al₂Si₂O₇H₁₂ cluster, electronic struct. and state densities, MINDO/3 and CNDO/2 calcs. 7-57201
- Al₂Si₂O₇H₁₆ cluster, electronic struct. and state densities, MINDO/3 and CNDO/2 calcs. 7-57201
- Al₂Si₂O₅(OH)₄ kaolinite, FTIR photoacoustic spectra 7-48881
- Al₂Si₂O₅(OH)₄Co₃O₄, X-ray anomalous scatt. difference patterns in powder diffr. anal. 7-16356
- AlTiO₄:Cr³⁺ tunable IR laser crystals, fluorescent spectra 7-43110
- Al₂(TiO₃)₃ ceramics, sintering, microstruct., bending strength, additives effect (*Japanese*) 7-17601
- Al₂TiO₃ ceramics, form. by solid state reaction of Al₂O₃ and TiO₂ powders 7-46385
- Al₂TiO₃-mullite composites, thermal and mech. props., effect of comp. (*Japanese*) 7-26987
- Al₂(WO₄)₃:Cr³⁺, tunable IR laser crystals, fluorescent spectra 7-43110
- AlXO₄(S₄)(X=P,As), dielec. const. meas. w.r.t. bond ionicity (*French*) 7-38988
- BaMnAlF₄, exchange interactions, mag. susceptibility meas. 7-45654
- Ba(PnO₃)₂:AlF₃-NaF system, glass form. and props. 7-11929
- BeAl₂O₄:Cr³⁺ alexandrite, emission spectrum conc. of broad-band solid-state lasers 7-43114
- Be₃Al₂(SiO₃)₆:Cr³⁺ emerald, spectral energy transfer, fluorescence line narrowing 7-33441
- Be₃Al₂Si₂O₁₀, beryl, electron-irradiation induced amorphism 7-32505
- Ca-SiAlON ceramic system, A'=B' transition study 7-16738
- Ca₃Al₂Ge₂-Si₃O₁₂:Tb, cathodoluminescence, photoluminescence props. 7-53404
- CaF₂-BaF₂-AlF₃ glasses, struct., transition metal ion EPR studies 7-6545
- CdF₂-LiF-AlF₃-PbF₂ glasses, potential as a practical glass 7-37074
- CoAlFeO₄, cubic spinel, Mossbauer anal. 7-33304
- CuAl_{1-x}Ga_xSe₂, chem. transport reactions, growth and morphology 7-7830
- Fe_{3-x}Al_xO₄, substituted magnetite, reactivity in O₂, relation with cation distrib. (*French*) 7-46829
- Fe_{2-x}Al_xO₃-1.8 H₂O substituted ferrihydride, Mossbauer, X-ray diffr. and electron microscopy studies 7-7617
- Ga-As-AlGaAs superlattice, laser induced disordering and Si impurity incorporation 7-45018
- GaAlAs channelled-substrate-planar laser, measuring modulus and phase of chirp/modulated power ratio 7-57391
- GaAlAs DH laser amplifier, Fabry-Perot type, gain and frequency bandwidth 7-20228
- GaAlAs diode laser, frequency shift in magnetic field 7-5885
- GaAlAs diode laser, gain compression, picosecond transmission meas. 7-20289
- GaAlAs heterostructures with an insulating layer 7-12866
- GaAlAs injection lasers, single-frequency, linewidth investig. 7-25819
- GaAlAs, LIMA anal., effect of alloy composition on secondary ion yields 7-28376
- GaAlAs laser, collinear nearly degenerate four-wave mixing in amplifying media 7-11071
- GaAlAs laser, LPE grown, effect of crystal defects on reliability 7-36960
- GaAlAs laser amplifier, high sensitivity picosecond optical pulse detection 7-50565
- GaAlAs laser diode, extremely weak feedback, lasing wavelength shift anal. 7-31325
- GaAlAs laser diodes, stripe geometry, directly modulated in microwave range, freq. response study 7-11017
- GaAlAs laser diodes, self-coupling effects and appls. 7-57386
- GaAlAs laser diodes under microwave intensity modulation, linearity charactn. 7-10944
- GaAlAs laser struts., double crystal X-ray rocking curves, interference peaks 7-44303
- GaAlAs laser-diode array, high-speed electronic beam steering 7-43185
- GaAlAs lasers, injection, photodetection props. 7-31379
- GaAlAs lasers, polarisation-resolved low-frequency noise 7-15863
- GaAlAs MOCVD layers, stoichiometry variation determ., pulsed laser atom probe anal. 7-12305
- GaAlAs, MOVPE growth rate, orientation depend. 7-22556
- (GaAl)As monolithic composite-cavity laser, chem. etching technique 7-50579
- GaAlAs morphological stability in epitaxy, appl. to optoelectronic monolithically integrated structures 7-27172
- GaAlAs passive waveguide, intrinsic optical bistability obs. 7-57425
- GaAlAs, semiconductor laser coupled with short external cavity, stable single longitudinal mode operation 7-62737
- GaAlAs single freq. heterostruct. injection lasers, LPE and VPE growth 7-62699
- GaAlAs strip waveguides, optical transistor effects, expt. study 7-37026
- GaAlAs substrate, GaAs ultrathin layers, liquid phase epitaxial growth 7-53645
- GaAlAs wideband free-space lasercom transmitter, design 7-31354
- GaAlAs wideband lasercom transmitter, performance 7-31355
- GaAlAs:Si, DX centres, nonexponential thermal emission kinetics 7-12640
- GaAlAs/GaAs, junction isolated LED structures, MOCVD, characts. 7-27935
- GaAlAs/GaAs, semicond. superlattice heterojunction interface, SIMS anal. (*Japanese*) 7-2396
- GaAlAs/GaAs circular BH surface emitting lasers, fabrication using selective meltback method 7-5911
- GaAlAs/GaAs heterostructure, absorption coeff. and thermal conductivity meas. by photothermal spectroscopy 7-41474
- GaAlAs/GaAs MOCVD growth for surface emitting lasers 7-53630
- GaAlAs/GaAs single quantum well laser, current pumped, second quantised state lasing 7-50559
- GaAlAs/GaAs surface-emitting linear laser arrays with etched mirrors 7-20255
- GaAlAs/GaAs TJS lasers on Si substrates, MOCVD growth 7-62691
- GaAlAs/GaAs:C quantum wells interface struct. and luminesc. efficiency 7-7735
- GaAlAs-GaAs DFB lasers with double channel planar buried heterostructure, low threshold operation 7-20256
- GaAlAs-GaAs DFB laser with double-channel planar BH 7-50594
- GaAlAs-GaAs epitaxial superlattice, X-ray double crystal characterisation, rocking curves calc., computer simulation technique 7-58105

aluminium compounds continued

- GaAlAs-GaAs heterojunctions, fractional quantum Hall effect obs. 7-52821
- GaAlAs-GaAs heterostructures grown by MOCVD, transition region, ellipsometric anal. 7-2388
- GaAlAs-GaAs heterostructures, dissipationless quantum Hall effect, crit. current density meas. 7-2696
- GaAlAs-GaAs heterostructure solar cells, multijunction with bulk graded bandgap/p-n junction 7-3676
- GaAlAs-GaAs heterostructure, LPE grown, interface photoluminescence spectra 7-53390
- GaAlAs-GaAs laser, light-activated, negative resistance, characts. (*Chinese*) 7-5901
- GaAlAs-GaAs laser diodes, catastrophic optical damage, electrolum., cathodolum., EBIC and TEM obs. 7-57329
- GaAlAs-GaAs laser failure causes and distrib., laboratory service life tests 7-62692
- GaAlAs-GaAs MOCVD solar cells on Ge and Ge/Si substrates 7-23182
- GaAlAs-GaAs MQW, optical bistability due to induced absorpt., model 7-5943
- GaAlAs-GaAs MQW structure, compositional fluctuations, STEM/EDX microanal. 7-45077
- GaAlAs-GaAs microcavity surface-emitting laser 7-57361
- GaAlAs-GaAs modulation doped quantum wells, hot carrier energy relax., time resolved photoluminescence spectra 7-52828
- GaAlAs-GaAs monolithic laser amplifier, C³, with bistable characts. 7-25842
- GaAlAs-GaAs multi-heterostructures, MOCVD growth for surface emitting lasers 7-59440
- GaAlAs-GaAs pnnp laser, carrier transport in heterostructure base region, carrier confinement factor in lasing region 7-43094
- GaAlAs-GaAs quantum well superlattices, applied electric field, quasi-eigenstates and eigenenergies, determ. 7-33072
- GaAlAs-GaAs quantum well heterostructures, grown by MOCVD, props. 7-45479
- GaAlAs-GaAs ridge waveguide DFB lasers, lateral anal. 7-62686
- GaAlAs-GaAs solar cells grown by MBE, material props. and device parameters 7-23164
- GaAlAs-GaAs superlattice, electronic struct., envelope function approx., phonon limited mobility, Boltzmann eqn. 7-2698
- GaAlAs-GaAs superlattice, Auger sputter depth profiling 7-21254
- GaAlAs-GaAs superlattice struct., dynamic SIMS profiles 7-22417
- GaAlAs-GaAs superlattices, density of states of Landau levels, sp. ht., magnetisation meas. 7-52823
- GaAlAs-GaAs surface-emitting laser diodes, lateral pumping struct. 7-57359
- GaAlAs-GaAs surface-emitting laser with TiO₂-SiO₂ dielec. multilayer reflector 7-59427
- GaAlAs-Mo junctions, Schottky barrier height, electrical props. 7-64346
- (Ga_{0.5}Al_{0.5})As, MBE grown, elastic consts., diffuse X-ray scatt. study 7-16918
- Ga_{0.60}Al_{0.40}As, electron-hole plasma diffusion, spatially resolved gain and luminesc. spectra 7-12747
- Ga_{0.65}Al_{0.35}As-GaAs quantum wells, elect. field-induced decrease of exciton lifetimes 7-45481
- Ga_{0.8}Al_{0.2}As-GaAs-Ga_{0.8}Al_{0.2}As quantum well struts., electroluminescence spectra, model 7-33365
- Ga_{1-x}Al_xAs, indirect-gap crystals, hot photolum., polarisation characts. 7-46092
- Ga_{1-x}Al_xAs, ion-implanted, defect creation 7-21240
- Ga_{1-x}Al_xAs-GaAs-Ga_{1-x}Al_xAs heterostructures, tunneling through indirect-gap barriers 7-21999
- Ga_{1-x}Al_xAs, Al concentration profiling using nucl. resonances 7-6811
- Ga_{1-x}Al_xAs and GaAs multilayer structures, metalorganic MBE growth 7-7860
- Ga_{1-x}Al_xAs, DX centres, inner and outer crossing lattice relax. 7-45218
- Ga_{1-x}Al_xAs, disorder effects of Raman scatt. 7-7704
- Ga_{1-x}Al_xAs MIS and SIS structures, prep. by metallorganic chem. hydride method, electrophysical props. 7-22018
- Ga_{1-x}Al_xAs, quantitative anal. by SIMS (*Chinese*) 7-54239
- Ga_{1-x}Al_xAs quantum-well wires, Wannier excitons, binding energies 7-64092
- Ga_{1-x}Al_xAs solid soln. epitaxial layer composition, Raman determ. 7-64628
- Ga_{1-x}Al_xAs:Si(Se), MBE growth, dopant incorporation 7-12533
- Ga_{1-x}Al_xAs:Si, electrical current induced liq. phase epitaxy 7-27955
- Ga_{1-x}Al_xAs/Ga_{1-x}Al_xAs/GaAs double barrier tunnelling struct., negative resist. calcs. 7-45451
- Ga_{1-x}Al_xAs-GaAs, thickness and conc. of thin Ga_{1-x}Al_xAs epitaxial films, determ. by photoemission jumps method (*French*) 7-38381
- Ga_{1-x}Al_xAs-GaAs 2D quantum well heterostructures, magneto-impurities, mag. field and press. effects 7-52728
- Ga_{1-x}Al_xAs-GaAs heterojunctions, impurities, optical props. 7-27396
- Ga_{1-x}Al_xAs-GaAs multiple well heterostructures, far IR absorpt. by shallow donors 7-45458
- Ga_{1-x}Al_xAs-GaAs quantum wells, diamag. shift of exciton energy levels 7-21824
- Ga_{1-x}Al_xAs-GaAs quantum well structures, energy spectra of donors and acceptors, spatially dependent screening effects 7-45459
- Ga_{1-x}Al_xAs-GaAs quantum well, hydrogenic donor low-lying excited states, reson. states, positions and widths 7-45460
- Ga_{1-x}Al_xAs-GaAs quantum wells, with indirect gas semicond. barriers, electron tunnelling 7-64340
- Ga_{1-x}Al_xAs-GaAs superlattices, shallow impurity state binding energies 7-45416
- Ga_{1-x}Al_xAs-GaAs superlattices, in appl. elec. field, interband optical transitions 7-53274
- Ga_{1-x}Al_xAs-GaAs-Ga_{1-x}Al_xAs quantum well, donor ion dielec. response 7-45417
- GaAlAsSb/GaSb/GaInAsSb injection double heterostructure laser, room temp. operation 7-62697
- GaAlSb/GaSb (111) heterostructures, signs of misfit dislocations, X-ray topographic determ. 7-38349
- Ga_{0.94}Al_{0.06}Sb/GaSb epitaxial struct., misfit dislocations anomalous visibility, Bragg geometry X-ray topograms 7-2019
- Ga_{0.96}Al_{0.04}Sb layers, liq. phase epitaxial growth, elec. and photoelec. characterisation 7-39443
- Ga_{1-x}Al_xSb epitaxial layers, MOCVD, morphology rel. to growth conditions 7-39408
- GaAs:Si/Al_xGa_{1-x}As quantum wells, photolum. studies 7-39178

aluminium compounds continued

- GaAs/Si/AlAs multiquantum well structs., band struct. and photolum. studies 7-12843
- GaAs/Si(B)-Ga_{0.25}Al_{0.75}As:Si(B) quantum wells, ion implanted, TEM and photolum. studies 7-58865
- GaAs/(GaAl)As LOC lasers, MOCVD growth and characts. 7-25835
- GaAs/Al quantum wells, MBE growth, photoluminescence and absorption linewidth studies 7-7749
- GaAs/Al_{0.38}Ga_{0.62}As lattice-matched superlattice photoelectrochem. electrodes, photocurrent spectra 7-45377
- GaAs/Al_{1-x}Ga_xAs modulation-doped heterostructs., 2D electron gas mobility meas. and calcs. 7-12840
- GaAs/Al_{1-x}Ga_xAs superlattices, layered electron gas plasmons, Raman scatt., Green's functions calcs. 7-17131
- GaAs/Al_{1-x}Ga_xAs 3D ICs, selection rule for epitaxial growth techniques, LPE, MOVPE and MBE 7-46326
- GaAs/Al_{1-x}Ga_xAs heterostruct., 2-D density of states in extreme quantum limit 7-2455
- GaAs/Al_{1-x}Ga_xAs heterostructs., 2D electron gas, polaron screening effects, optical absorpt. calcs. 7-2511
- GaAs/Al_{1-x}Ga_xAs heterostructure interfaces, band discontinuities, electrical meas. 7-52814
- GaAs/Al_{1-x}Ga_xAs heterojunction photodiodes, band discontinuities 7-58871
- GaAs/Al_{1-x}Ga_xAs heterostruct. localisation and interaction in a strong mag. field 7-64343
- n-GaAs/Al_{1-x}Ga_xAs multilayer heterostructs., nonlinear high-freq. effects during vertical transport 7-2694
- GaAs/Al_{1-x}Ga_xAs multi-quantum well structs., photoluminescence studies 7-3078
- GaAs/Al_{1-x}Ga_xAs modulated structs., MBE growth kinetics, RHEED studies 7-7066
- GaAs/Al_{1-x}Ga_xAs modulation doped heterostruct., high temp. annealing effects (*Chinese*) 7-12805
- GaAs/Al_{1-x}Ga_xAs MBE grown superlattices, effect of barrier config. and interface quality on props. 7-52790
- GaAs/Al_{1-x}Ga_xAs quantum-well bound states, valence-band offsets 7-7313
- GaAs/Al_{1-x}Ga_xAs quantum wells, excitonic transitions, photocurrent spectra studies 7-7816
- GaAs/Al_{1-x}Ga_xAs RIE using CCl₂F₂, selectivity 7-22920
- GaAs/Al_{1-x}Ga_xAs superlattices, magnetophonon oscills. damping, polar-optical phonon contrib. calcs. 7-27391
- GaAs/Al_{1-x}Ga_xAs superstructure, TEM images, composition anal. by thickness fringes, simulation 7-38353
- GaAs/Al_{1-x}Ga_xAs superlattices, optical transitions involving unconfined states, barrier width depend., photolum. spectra 7-52773
- n-GaAs/Al_{1-x}Ga_xAs/n⁺-GaAs capacitors, accumulation layers magnetotunnelling obs. 7-12880
- GaAs/Al_{1-x}Ga_xAs, tunnelling through III-V low-barrier heterostructures 7-52799
- GaAs/AlAs, short period superlattices, MOCVD growth, Raman scatt., AES, X-ray diffr. 7-27386
- GaAs/AlAs 1-D MBE superlattice, struct. parameters, X-ray double cryst. diffr. studies (*Chinese*) 7-12503
- GaAs/AlAs doped quantum well waveguides, IR intersubband absorpt. 7-59192
- GaAs/AlAs double barrier struct., electron transport, scatt. matrix theory 7-12822
- GaAs/AlAs heterostruct., transition layer form. during LPE 7-45074
- GaAs/AlAs MBE superlattice, interface struct., HREM study 7-17096
- GaAs/AlAs MQW structures, life-time-free switching of luminescence by elec. fields 7-52791
- GaAs/AlAs MQW structure, exciton-induced dispersion of electroreflectance at room temp. 7-53277
- GaAs/AlAs quantum wells, photoexcited transport 7-2674
- GaAs/AlAs quantum well structures, electroreflectance spectra and field-induced refractive index modulation 7-13135
- GaAs/AlAs single quantum well heterostructures confined by short-period superlattices, photoluminesc. 7-22296
- GaAs/AlAs superlattice, optical phonons and interface thickness, Raman scatt. studies 7-7705
- GaAs/AlAs superlattices, electronic band structure, pseudopot. method calc. 7-17084
- GaAs/AlAs superlattices, folded acoustical Raman line intensities 7-46050
- GaAs/AlAs:Mg/GaAs tunnel structs., current transport mechanisms 7-7357
- GaAs/AlAs/GaAs:Se heterojunctions, elec. behaviour, DLTS studies 7-7360
- p⁺-GaAs/AlGaAs, double barrier, hot electron energy distrib. study using resonant tunnelling electron spectroscopy 7-45447
- GaAs/AlGaAs 2D electron gas MBE structures, carrier mobility and density meas. 7-64321
- GaAs/AlGaAs heterostructs. on Si substrate, MOCVD and MBE growth 7-7883
- GaAs/AlGaAs modulation doped heterostructs., transport props. studies 7-52752
- GaAs/AlGaAs multi-quantum well heterostructures, optical gain, well width depend 7-46130
- GaAs/AlGaAs multiple quantum well structures, hot-carrier relaxation, femtosecond optical meas. 7-52750
- GaAs/AlGaAs multiple-quantum-well structures, shallow donors, far infrared spectroscopy 7-39121
- GaAs/AlGaAs quantum wells, MBE growth, interface disorder studies 7-7026
- GaAs/AlGaAs quantum wells, MBE growth and energy levels, photoluminescence meas. 7-7067
- GaAs/AlGaAs quantum wells and double heterostruct. lasers, chemical beam epitaxy, photolum. 7-22523
- GaAs/AlGaAs quantum well structures, MOCVD growth, photolum., TEM obs. 7-27929
- GaAs/AlGaAs quantum wells, Monte Carlo study of hot electron transport 7-52804
- GaAs/AlGaAs separate confinement heterostructure lasers, LPE prep. 7-10940
- GaAs/AlGaAs single and coupled double wells, energy depend. light hole mass. photolum. spectra anal. 7-38691
- GaAs/AlGaAs single heterojunction quantum well structs., photolum. characts. 7-46085

aluminium compounds continued

- GaAs/AlGaAs single quantum wells, interrupted MBE growth and temperature-dependent optical spectra 7-46082
- GaAs/AlGaAs superlattice, compositional disordering by focused ion beams 7-6695
- GaAs/AlGaAs superlattices, Si implanted, compositional disordering, SIMS studies 7-12091
- GaAs/AlGaAs superlattices, hydrogenic impurity ground level wave function calcs., variational procedure 7-12664
- GaAs/AlGaAs superlattice heterostructures, MBE on nonplanar substrates 7-59425
- GaAs/AlGaAs superlattices, valence band electronic struct., pseudopot. calcs. 7-64339
- GaAs/Ga_{1-x}Al_xAs, short period superlattices, MOCVD growth, Raman scatt., AES, X-ray diffr. 7-27386
- GaAs/Ga_{1-x}Al_xAs graded interface superlattice band struct. calcs. 7-58879
- GaAs/Ga_{1-x}Al_xAs multilayered structures, polariton dispersion relations 7-7125
- GaAs/Ga_{1-x}Al_xAs quantum well struct., exciton linewidth calcs., polar optical phonon scatt. 7-2491
- GaAs/Ga_{1-x}Al_xAs heterojunctions, anomalous quantum Hall effects 7-17085
- GaAs/GaAlAs 2D electron gas, cyclotron resonance study 7-2676
- GaAs/GaAlAs disordered superlattices, carrier localisation obs. 7-12818
- GaAs/GaAlAs double quantum well structures, ambipolar carrier transport, optical TOF study 7-12802
- GaAs/GaAlAs double-well superlattice, ultra-fast optical modulator 7-52801
- GaAs/GaAlAs graded gap superlattices, high velocity vertical transport 7-52802
- GaAs/GaAlAs HJFET and HJBT 7-52811
- GaAs/GaAlAs heterostruct. laser with monolayer superlattice, threshold currents 7-62698
- GaAs/GaAlAs planar MQW structure, nonlinear coupling of guided waves 7-11106
- GaAs/GaAlAs quantum-well structures, optical time-of-flight investigation 7-52800
- GaAs/GaAlAs single quantum wells, steady-state photoluminescence studies 7-7750
- GaAs/GaAlAs single quantum well laser, threshold current density 7-25816
- GaAs/GaAlAs superlattice, optical phonons and interface thickness, Raman scatt. studies 7-7705
- GaAs/GaAlAs superlattice structs., metalorganic MBE growth 7-7864
- GaAs/GaAlAs TEGFET, resistance laboratory unit determ., using quantum Hall effect 7-18812
- GaAs/GaAlAs ultrathin layer systems, MOCVD growth and struct. props. 7-7063
- GaAs/GaAlAs/GaAs heterostructure barriers, tunnel current and electron tunnelling times with mag. field 7-52810
- GaAs/n-AlGaAs MBE-grown selectively doped heterostructs., 2D electron gas, transport props. 7-21988
- GaAs-(Al,Ga)As double heterojunction lasers, dislocation control, electroluminescence 7-7046
- GaAs-(Al,Ga)As-GaAs heterojunction barrier, tunneling current, probe pressure effect 7-45441
- GaAs-(Al,Ga)As heterostructure, modulation-doped, valence band mixing, and optical emission 7-7344
- GaAs-(Al,Ga)As heterojunctions, low temp. elec. transport props. 7-33084
- GaAs-(Al,Ga)As inelastic light scattering by electronic excitations in semiconductor heterostructures 7-13171
- GaAs-Al_{0.37}Ga_{0.63}As quantum wells, photolum. studies, MBE growth, effect of interruption 7-39150
- GaAs-Al_{0.3}Ga_{0.7}As, thin single quantum well, MBE growth kinetics, normal and inverted interfaces 7-45045
- GaAs-Al_{0.65}Ga_{0.35}As, transverse junction stripe laser, lateral heterobarrier by diffusion enhanced alloy disordering 7-10929
- GaAs-Al_{0.7}Ga_{0.3}As single quantum well, photolum., transient response to electric field, carrier lifetime 7-7757
- GaAs-Al_{0.7}Ga_{0.3}As SQW structure, photolum. switching by pulsed elec. field 7-13197
- GaAs-Al_{1-x}Ga_xAs, multiple quantum well structs., expansion of electron-hole plasma, time-resolved Raman studies 7-22258
- GaAs-Al_{1-x}Ga_xAs-AlAs, p-type quantum wells, resonant Raman scatt. 7-22259
- GaAs-Al_{1-x}Ga_xAs, internal photoemission method for determ. of band offsets 7-12832
- GaAs-Al_{1-x}Ga_xAs, heterojunction form. anal. 7-39436
- GaAs-Al_{1-x}Ga_xAs, superlattices, carrier behaviour, mag. field effect 7-45449
- GaAs-Al_{1-x}Ga_xAs, p-n junction waveguide, phase modulation, orientation depend. 7-57536
- GaAs-Al_{1-x}Ga_xAs, modulation-doped quantum wells, photoabsorpt., electronic props. 7-64330
- GaAs-Al_{1-x}Ga_xAs (001) superlattices, periodicity, charge density and zone folding effects 7-2685
- GaAs-Al_{1-x}Ga_xAs heterojunctions, subband Landau-level spectroscopy 7-21996
- GaAs-Al_{1-x}Ga_xAs heterostructures, voltage-controlled dissipation in the quantum Hall effect 7-27393
- GaAs-Al_{1-x}Ga_xAs heterojunction, chemical pot. of electrons, effect of mag. field 7-38682
- GaAs-Al_{1-x}Ga_xAs heterostructures, selectively doped, electron transport in strong electric fields 7-38687
- GaAs-Al_{1-x}Ga_xAs junction, 2D electron gas, plasmons, radiation absorpt. and emission 7-2686
- GaAs-Al_{1-x}Ga_xAs lattice-mismatched heterojunctions, misfit strain relaxation, X-ray study 7-21718
- GaAs-Al_{1-x}Ga_xAs multiple quantum well, electron-phonon interaction 7-2684
- GaAs-Al_{1-x}Ga_xAs multiple quantum well structs., nonequilib. LO phonons 7-12457
- GaAs-Al_{1-x}Ga_xAs modulation-doped structure, parallel cond. in quantum limit 7-12808
- GaAs-Al_{1-x}Ga_xAs multiple-quantum-well struct., electron heating below 1K 7-12817
- GaAs-Al_{1-x}Ga_xAs MBE superlattices, low temp. photoluminesc. spectra 7-22340

aluminium compounds continued

- GaAs-Al_xGa_{1-x}As MQW and superlattice structures, far-IR reflectivity 7-27724
- GaAs-Al_xGa_{1-x}As multiple heterostructures, variable angle of incidence spectroscopic ellipsometry 7-39055
- GaAs-Al_xGa_{1-x}As MOCVD quantum well structures, time-resolved photolum. 7-53410
- GaAs-Al_xGa_{1-x}As quantum well structure, recomb. dynamics, photolum. obs. 7-12809
- GaAs-Al_xGa_{1-x}As quantum wells, doubly resonant LO-phonon Raman scatt. obs. 7-27722
- GaAs-Al_xGa_{1-x}As quantum wells, homogeneously broadened 2D excitonic transitions, optical dephasing 7-45461
- GaAs-Al_xGa_{1-x}As quantum wells, photoreflectance spectra, hydrostatic press. 7-52784
- GaAs-Al_xGa_{1-x}As quantum wells, parabolic, light scatt. studies 7-64651
- GaAs-Al_xGa_{1-x}As superlattice, composition anal., electron microscopy studies 7-7028
- GaAs-Al_xGa_{1-x}As semicond. superlattice, exciton transitions study 7-52432
- GaAs-Al_xGa_{1-x}As superlattice, dimensionality of subbands, plasmon dispersion 7-52765
- GaAs-Al_xGa_{1-x}As solar cell, operation with band-gap gradient in space charge region 7-54295
- GaAs-Al_xGa_{1-x}As superlattice, hole subbands (*Chinese*) 7-58873
- GaAs-Al_xGa_{1-x}As superlattices, electronic and optical props., alloying and press. effects 7-64327
- GaAs-Al_xGa_{1-x}As type I superlattices, electronic struct., tight binding calcs. 7-45475
- GaAs-Al_xGa_{1-x}As-GaAs, multilayer struct., variable angle of incidence spectroscopic ellipsometric study 7-48830
- GaAs-Al_xGa_{1-x}As-GaAs, perpendicular transport, tunnelling, thermionic emission studies 7-52781
- GaAs-Al_xGa_{1-x}As-GaAs transverse magnetic field effects on tunnelling 7-58874
- GaAs-AlAs, Al_xGa_{1-x}As-AlAs, multi quantum well structs., picosecond spectra. 2D excitons 7-13215
- GaAs-AlAs, solid soln., temp.- and current-controlled LPE, theoretical model 7-39447
- GaAs-AlAs, superlattices, mixing, ion implantation, rapid thermal annealing, Raman scattering 7-53355
- GaAs-AlAs alternate monolayer compounds structures, MBE growth 7-21716
- GaAs-AlAs device structs., MBE prep. using In-free mounting techniques 7-3183
- GaAs-AlAs double barrier heterostructures, resonant tunnelling through quantum well states 7-58870
- GaAs-AlAs heterojunctions, asymmetrically doped, photoresponse under external bias 7-38692
- GaAs-AlAs MBE MQW struct., photoluminesc. spectra (*Chinese*) 7-59240
- GaAs-AlAs MQW structures, Ga⁺ ion implantation defects 7-44585
- GaAs-AlAs multiple quantum wells, photoconductivity, photoreflectance and photolum. meas. 7-27368
- GaAs-AlAs short period superlattice, photoexcited carriers, dynamics 7-53402
- GaAs-AlAs superlattice struct., lithographic fabrication of TEM cross-sections 7-370
- GaAs-AlAs superlattices, acoustic and electronic props. 7-6730
- GaAs-AlAs superlattices, 2D excitons, magneto-optical study (*Japanese*) 7-13139
- GaAs-AlAs superlattice, energy bands, cohesive energy, form. energy, self-consistent calcs. 7-21995
- GaAs-AlAs superlattices, Se implantation, effect on compositional disordering 7-26784
- GaAs-AlAs superlattices, folded acoustic branches, leakage-induced and disorder-activated modes 7-33389
- GaAs-AlAs superlattices, confined longitudinal and transverse phonons, phonon spectrum calc. 7-38142
- GaAs-AlAs superlattices, Raman scattering finite size effects 7-39105
- GaAs-AlAs superlattices and AlAs, energy band gap calc., self-interaction correction to local density approx. 7-45144
- GaAs-AlAs ultra-thin layer semicond. superlattices, energy band and stable structs. study 7-52789
- GaAs-AlAs-GaAs heterostructure, tunnelling transmission probability, many-band pseudopotential model 7-38701
- GaAs-AlAs(InAs) superlattices, lattice distortions 7-12510
- GaAs-AlGaAs, high quality MOVPE quantum wells, optical props. 7-53406
- GaAs-AlGaAs, hot carriers in quasi-2-D polar semiconductors 7-12807
- GaAs-AlGaAs, MBE materials for high-speed digital heterostructure devices 7-45480
- GaAs-AlGaAs, multiple quantum well structs., 2s state, excitons, luminesc. study 7-22337
- GaAs-AlGaAs, noise, localised states, quantum Hall effect 7-45413
- GaAs-AlGaAs and GaAs-AlAs quantum well structs., resonant Raman scatt., depend. on electric field 7-7707
- GaAs-AlGaAs as IR sensor material, characts. (*Japanese*) 7-56339
- GaAs-AlGaAs heterointerface, band offsets, overview 7-12831
- GaAs-AlGaAs heterojunctions, fractional quantum Hall effect of 2D electrons (*Japanese*) 7-12827
- GaAs-AlGaAs heterojunctions, energy band discontinuities, internal photoemission meas. 7-13331
- GaAs-AlGaAs heterojunction, narrow 2D electron gas, mag. depopulation of 1D subband 7-17080
- GaAs-AlGaAs heterojunctions, scanning tunnelling microscopy, potentiometry 7-52780
- GaAs-AlGaAs heterostructures, 2D electron system, collective excitations, light scatt. (*Japanese*) 7-12633
- GaAs-AlGaAs heterostruct., band discontinuity determ., DLTS, interface charge density, trap conc. 7-12833
- GaAs-AlGaAs heterostructures, energy band alignment, thermionic emission of holes 7-13319
- GaAs-AlGaAs heterostructures, equipotential distrib. in quantum Hall effect 7-21994
- GaAs-AlGaAs heterostructures, transport props. of 2D electron and hole gases 7-52812
- GaAs-AlGaAs high-power laser array of phase-locking free struct. 7-62725
- GaAs-AlGaAs large optical cavity semicond. laser arrays 7-10989

aluminium compounds continued

- GaAs-AlGaAs MQW, intraband relaxation dynamics of photo-excited carriers 7-52691
- GaAs-AlGaAs MQW electroabsorpt. modulator for non-resonant optoelectronic logic gate 7-37139
- GaAs-AlGaAs MQW optical NOR gate, exciton and carrier dynamics, time resolved obs. 7-50628
- GaAs-AlGaAs MQW structures, MBE grown, material parameters meas. 7-38721
- GaAs-AlGaAs modulation-doped quantum wells, photolum., giant oscillations, influence of mag. fields 7-7751
- GaAs-AlGaAs modulation-doped heterointerface, photoluminescence spectra studies 7-46137
- GaAs-AlGaAs multiple quantum well lasers, voltage-controlled optical bistability, 2D exciton 7-5883
- GaAs-AlGaAs multiple quantum wells, temp. depend. of photoreflectance 7-7753
- GaAs-AlGaAs multiple quantum well structs., photolum. under high laser excitation 7-13213
- GaAs-AlGaAs quantum wells, high electric field, interband transitions, photocurrent spectra obs. 7-7289
- GaAs-AlGaAs quantum well heterostructures, spectroscopy of excitons and phonons 7-7706
- GaAs-AlGaAs quantum wells, Stark shifts for heavy- and light-hole levels, well size depend. 7-12794
- GaAs-AlGaAs quantum wells, picosecond photolum. photocurrent spectra 7-13214
- GaAs-AlGaAs quantum wells, etched ultrasmall structs., photolum. excitation spectra meas. 7-22293
- GaAs-AlGaAs quantum well structs., luminesc. from 2s heavy hole exciton, low temp. 7-22338
- GaAs-AlGaAs quantum well heterostruct. devices, atm. press. MOVPE growth 7-22574
- GaAs-AlGaAs quantum well heterostructures, electronic props. 7-27405
- GaAs-AlGaAs quantum wells, MBE grown, photolum. study 7-27758
- GaAs-AlGaAs quantum wells, hot electrons, Monte Carlo study 7-38708
- GaAs-AlGaAs quantum wells, field-induced lifetime enhancements, ionisation of excitons 7-39181
- GaAs-AlGaAs quantum wells, electron-phonon scatt. rate reduction by total spatial quantisation 7-45482
- GaAs-AlGaAs quantum wells, FIR studies of shallow donors 7-52819
- GaAs-AlGaAs SCH lasers, lasing gain and threshold current 7-31327
- GaAs-AlGaAs short cavity multimode quantum well lasers, dry etching, threshold current and single mode operation 7-20253
- GaAs-AlGaAs superlattice, surface and interface optical phonons, EELS studies 7-6955
- GaAs-AlGaAs superlattice, lattice images, high contrast TEM obs. 7-7027
- GaAs-AlGaAs superlattices, band structure of holes (*Japanese*) 7-12825
- GaAs-AlGaAs superlattices and superstructures, growth by metal organic CVD (*Japanese*) 7-13386
- GaAs-AlGaAs superlattice defects, DLTS study 7-21854
- GaAs-AlGaAs superlattices, electronic props., calc. methods 7-27406
- GaAs-AlGaAs superlattice, hot electrons, real space transfer effect, photolum. studies 7-39180
- GaAs-AlGaAs superlattices, magnetotransport 7-45471
- GaAs-AlGaAs three-terminal cascade solar cells with selective electrodes 7-23184
- GaAs-AlGaAs-GaAs heterostructure barriers, quantum tunnelling 7-52816
- GaAs-AlGaAs-GaAs large area graded gap diodes, discrete resistance levels obs. at low temps. 7-52749
- GaAs-AlGaAs-InGaAs strained-layer quantum well heterostructures, negative differential resistance 7-45443
- GaAs-Ga_{0.3}Al_{0.7}As quantum wells, uniaxial stress depend. of spatially confined excitons 7-33078
- GaAs-Ga_{0.7}Al_{0.3}As heterojunction, donor-acceptor radiative recomb. mechanism, photolum. spectra study 7-17083
- GaAs-Ga_xAl_{1-x}As superlattices and heterojunctions, electronic struct. 7-12821
- GaAs-Ga_{1-x}Al_xAs semiconductor superlattice, effective mass, mag. quantisation influence 7-52754
- GaAs-Ga_{1-x}Al_xAs heterojunction, 2D electron and hole mobilities 7-7350
- GaAs-Ga_{1-x}Al_xAs heterojunctions, electron energy levels 7-17082
- GaAs-Ga_{1-x}Al_xAs heterostruct., light interf. meas. of thickness and comp. during epitaxial growth 7-64026
- GaAs-Ga_{1-x}Al_xAs modulation-doped quantum well, photoluminesc. studies 7-2687
- GaAs-Ga_{1-x}Al_xAs multiple quantum wells, intrinsic and extrinsic photolum. 7-39183
- GaAs-Ga_{1-x}Al_xAs quantum well, electronic states in semiconductor heterostructures 7-7307
- GaAs-Ga_{1-x}Al_xAs quantum wells, interband photocond. and excitonic Landau level transitions in mag. field 7-27390
- GaAs-Ga_{1-x}Al_xAs quantum well structures, electronic props. 7-52817
- GaAs-Ga_{1-x}Al_xAs superlattices, optical props. 7-3007
- GaAs-Ga_{1-x}Al_xAs superlattices, Brillouin scatt. 7-3063
- GaAs-Ga_{1-x}Al_xAs superlattice, phonons, acoustic and optic modes 7-12455
- GaAs-Ga_{1-x}Al_xAs superlattice localised states in barrier 7-17079
- GaAs-Ga_{1-x}Al_xAs superlattice, plasmon propagation across layers 7-27276
- GaAs-Ga_{1-x}Al_xAs undoped quantum wells, excitonic spectrum, valence band coupling and Fano resonance effects calcs. 7-27256
- GaAs-Ga_{1-x}Al_xAs heterojunction, nonequilibrium electron-phonon scatt. 7-45457
- GaAs-GaAlAs, modulation doped heterostructures, spectroscopy of 2D plasmas 7-2702
- GaAs-GaAlAs, multiple quantum well struct., transient photoconductivity characterisation 7-52692
- GaAs-GaAlAs, quantum well lasers, characts., comparison with GaInAs-InP 7-5891
- GaAs-GaAlAs, quantum well wires and boxes, optically detected carrier confinement, cathodolum 7-39188
- GaAs-GaAlAs, structures, 2D localisation and interaction effects 7-52531
- GaAs-GaAlAs diode laser array, diffraction-limited emission, aperture graded-index lens external cavity 7-11005
- GaAs-GaAlAs fast MQW absorber for mode locking of semicond. lasers. 7-50655

aluminium compounds continued

- GaAs-GaAlAs heterojunction, 2D system, high order fractional quantisation obs. 7-27397
- GaAs-GaAlAs heterojunctions, cyclotron resonance, screening effects 7-38706
- GaAs-GaAlAs heterojunction bipolar transistors, ^{24}Mg and ^{64}Zn implanted profiles 7-44591
- GaAs-GaAlAs heterojunctions, electron-phonon interactions, cyclotron and magnetophonon reson. meas. 7-45463
- GaAs-GaAlAs interface dislocations, stereographic obs. by IR light scatt. 7-32235
- GaAs-GaAlAs MQW optical waveguides, nonlinear props. 7-37027
- GaAs-GaAlAs MQW structures, exciton-exciton interaction 7-52439
- GaAs-GaAlAs MQW ultrafast all-optical gate with subpicosecond ON and OFF response time 7-11026
- GaAs-GaAlAs multilayer structures, Auger depth profiles using a dual ion gun system 7-22429
- GaAs-GaAlAs multiple quantum well structs., quasi-2D electron-hole plasma, band-filling effects, band gap renormalisation 7-7754
- GaAs-GaAlAs multiple quantum well structs., band-gap renormalisation 7-58888
- GaAs-GaAlAs passive MQW waveguide resonators, all-optical switching effects, expt. study 7-15967
- GaAs-GaAlAs pnnp laser diode, optical bistability and switching characs. 7-62752
- GaAs-GaAlAs quantum wells, exciton binding energy, magneto-optical determ. 7-7752
- GaAs-GaAlAs quantum wells, extrinsic photolum. 7-7755
- GaAs-GaAlAs quantum well structs., recomb. dynamics of carriers 7-12830
- GaAs-GaAlAs quantum well excitons, interface disorder and mobility 7-52808
- GaAs-GaAlAs quantum wells, nonlinear optics and electro-optics 7-52809
- GaAs-GaAlAs quantum wells, excitonic coupling in elec. field, photolum. spectra 7-64094
- GaAs-GaAlAs quantum-box lasers, 3D, gain and threshold current density 7-10937
- GaAs-GaAlAs resonant injection quantum well diodes and lasers 7-43104
- GaAs-GaAlAs superlattice, mag. levels 7-52476
- GaAs-GaAlAs superlattice structs., impact ionisation coeff., lucky drift model 7-52793
- GaAs-GaAlAs superlattices, electron states in microstructs. 7-52807
- GaAs-GaAlAs:Si modulation doped quantum wells, electron mobility, temp. depend. 7-45473
- GaAs-GaAlAs-GaAs heterojunction barriers, single particle tunnelling, five level k.p. theory 7-64341
- GaAs $_{1-x}$ Al $_x$ As MQW, MOCVD grown, excitons, photoluminescence spectra 7-38702
- (GaAs) $_{28}$ (AlAs) $_{24}$ superlattices, lattice distortion, X-ray diffr. studies 7-63974
- GaInAs-AlInAs heterojunctions, parallel conduction, quantum Hall effect, hydrostatic press. 7-52764
- GaInAs-AlInAs(InP) and GaAs-AlGaAs superlattice avalanche photodiodes, impact ionisation theory appl. 7-58886
- Ga $_{0.28}$ In $_{0.72}$ As/Al $_{0.28}$ In $_{0.72}$ As photodiode heterostructures, atm. press. MOCVD, 2 μm , sensitivity, structural charactn. 7-27933
- Ga $_{0.47}$ In $_{0.53}$ As/Al $_{0.48}$ In $_{0.52}$ As modulated struct., high resolution double-cryst. X-ray diffr. studies 7-7029
- Ga $_{0.47}$ In $_{0.53}$ As/Al $_{0.7}$ In $_{0.3}$ As superlattices, electronic struct., strain-induced elec. field effects 7-7358
- Ga $_{0.47}$ In $_{0.53}$ As/Al $_{0.48}$ In $_{0.52}$ As quantum well, interband magnetoabsorpt. meas., effective mass determ. 7-17088
- Ga $_{0.47}$ In $_{0.53}$ As/Al $_{0.48}$ In $_{0.52}$ As superlattices grown by MBE, structural charactn. 7-52792
- Ga $_{1-x}$ In $_x$ As-Al $_{1-y}$ In $_y$ As superlattices, electronic struct., depend. on growth axis 7-64329
- GaInAsSb/AlGaAsSb injection lasers, threshold current density reduction 7-5886
- Ga $_{0.85}$ In $_{0.15}$ As $_{0.13}$ Sb $_{0.87}$ /Al $_{0.4}$ Ga $_{0.6}$ As $_{0.035}$ Sb $_{0.965}$ DH lasers, MBE grown, 2.07 μm laser oscillation 7-43096
- GaInP-AlGaInP-GaAs heterostructures, MOVPE, Hall effect, photolum. 7-39401
- Ga $_x$ In $_{1-x}$ P/Al $_x$ Ga $_x$ As heterostructs., OMVPE, photolum., lattice matching 7-39402
- GaSb/AlGa $_{1-x}$ Sb MBE grown superlattices, effect of barrier config. and interface quality on props. 7-52790
- GaSb/AlSb single quantum wells, electroreflectance and photoluminescence studies 7-46136
- GaSb/AlSb strained-layer heterojunction valence band discontinuity, XPS core level meas. 7-21984
- GaSb-AlGa $_{1-x}$ Sb multi quantum wells, excitons, electric field effect, photocurrent spectra obs. 7-7288
- GaSb-AlSb multiple quantum well structs., size-induced direct to indirect gap transition 7-7373
- GaSb-AlSb quantum well lasers, reduction of Auger effect, 1.5 μm wavelength region 7-5893
- GaSb-AlSb quantum wells, optical transitions, obs. 7-46086
- GaSb-AlSb quantum-well structures, 2E $_g$ transitions 7-46128
- GaSb-AlSb strained quantum well, electronic states in semiconductor heterostructures 7-7307
- GaSb-AlSb strained-layer superlattices, electronic props. 7-52817
- GaSb $_0$ -AlSb quantum wells, nonparabolic behaviour under hydrostatic press. 7-64328
- Gd $_2$ [Al $_2$ (Ga $_{1-x}$ Fe $_x$) $_2$]O $_{12}$ mag. solid soln. systems for regenerator materials 7-59015
- InAlAs, growth by MBE, alloy clustering, surface quality, role of kinetics and thermodynamics 7-32866
- InAlAs/InGaAs modulation-doped heterostructs., 2D electron gas mobility meas. 7-12842
- InAlAs-InGaAs resonant tunnelling barrier struct., MBE grown, NDR characs. 7-52796
- In $_{0.18}$ Al $_{0.82}$ As-GaAs strained layer superlattices, Raman studies 7-12854
- In $_{0.52}$ Al $_{0.48}$ As optical waveguides, MBE growth on InP 7-11107
- In $_x$ Al $_{1-x}$ As, MBE growth rates, temp. dependence 7-17426
- In $_x$ Al $_{1-x}$ As/Au Schottky barrier heights, composition dependence 7-45431
- In $_x$ Al $_{1-x}$ As/GaAs strained-layer superlattices, effective mass reversal 7-17078

aluminium compounds continued

- InF $_2$ -PbF $_2$ -BaF $_2$ -SrF $_2$ -YF $_3$ -AlF $_3$ -UO $_2$ F $_2$, luminesc., lifetime meas. 7-27750
- InGaAlAs, props. for integrated optics/optoelectronics in optical fibre communication systems, review 7-11178
- InGaAlP epilayers, MOCVD, laser appl. 7-39404
- InGaAlP transverse mode stabilized visible laser diodes fabricated by MOCVD selective growth 7-50591
- InGaAs/InAlAs MQW pin diodes, room temp. current oscillations 7-45454
- InGaAs/InAlAs multiple quantum well structs., nonlinear spectroscopy 7-1236
- n $^+$ -InGaAs/InAlAs/n $^-$ -InGaAs, conduction band discontinuity determ. by current-voltage meas. 7-7352
- InGaAs-InAlAs MQW structure, anisotropic electroabsorpt. and optical modulation 7-13134
- InGaAs-InAlAs multiple quantum wells, long wavelength optical modulation, electro-optical effects 7-7677
- InGaAs-InAlAs strained-layer superlattices, MBE grown, optical characterisation 7-13142
- In $_{0.53}$ Ga $_{0.48}$ As/In $_{0.52}$ (Ga $_{1-x}$ Al $_x$) $_{0.48}$ As heterostructures, conduction band edge discontinuity 7-12815
- In $_{0.53}$ Ga $_{0.47}$ As/In $_{0.52}$ Al $_{0.48}$ As quantum wells, lamp annealing interdiffusion and optical props. 7-12502
- In $_{0.53}$ Ga $_{0.47}$ As-In $_{0.52}$ Al $_{0.48}$ As modulation-doped heterostructs., interface roughness scatt. 7-2678
- In $_x$ Ga $_{1-x}$ As-In $_x$ Al $_{1-x}$ As superlattices, lattice-matched and lattice-mismatched, dislocation filtering 7-21671
- In $_x$ Ga $_{1-x}$ As-In $_x$ Al $_{1-x}$ As heterojunction, cyclotron resonance linewidth due to alloy scatt. 7-27399
- InGaAsSb/AlGaSb DH lasers, MBE grown, room-temperature 2.2 μm operation 7-20219
- InGaP/InGaAlP double heterostructure and multiquantum-well laser diodes, MBE growth and characterisation 7-62689
- InGaP-InGaAlP MQW structs., room temp. excitons 7-58745
- KAl(MoO $_4$) $_2$:Cr $^{3+}$ tunable IR laser crystals, fluorescent spectra 7-43110
- KAl(SO $_4$) $_2$ multicharged electrolyte soln. in water-tert butyl alcohol, viscosity and density studies 7-52104
- KAl(SO $_4$) $_2$ solutions, effect of impurities on props. 7-6495
- KAl(SO $_4$) $_2$ ·12H $_2$ O, alum. crystals, habit changes by novel additives to nutrient 7-44439
- KAl(SO $_4$) $_2$ ·12H $_2$ O:Cr $^{3+}$, optical absorpt. spectrum study, cryst. field and site symm. determ. 7-59232
- K(AlSi $_2$ O $_6$), synthetic pollicite, high temp. X-ray diffr. study 7-21176
- KAlSi $_2$ O $_6$, thermally stimulated luminesc. at low temps. 7-13238
- K $_{1.50}$ Al $_{1.50}$ Ti $_{6.50}$ O $_{16}$ hollandite-type struct. refinement, cation substitution effects study 7-58232
- LaNi $_4$ AlH $_x$ and LaNi $_4$ As $_x$ H $_x$, dynamical disorder of H, quasi-elastic neutron scatt. study 7-21535
- LiAlF $_4$ ion conducting layer in WO $_3$ based electrochromic windows, recent R&D 7-37122
- LiAlO $_2$ ceramic breeder material, fabrication for NET programme 7-798
- LiAlO $_2$, fusion blanket material, effects of sweep gas, extraction vessel material and ceramic props 7-49664
- MgAl $_2$ O $_4$, particle shape of plasma sprayed oxides, SEM obs. 7-2403
- Mg $_2$ Al $_2$ Si $_2$ O $_{18}$, cordierite, electron-irradiation induced amorphism 7-32505
- Mg $_2$ Al $_2$ Si $_2$ O $_{18}$ and solid solutions, thermal expansion (*Japanese*) 7-21496
- MgO(Al $_2$ O $_3$) $_2$ spinel, first-order twin boundaries struct., TEM obs. and computer simulation studies 7-51782
- MgO(Al $_2$ O $_3$) $_2$ spinel, lateral twin boundaries struct., electron microscopy obs. and computer simulation studies 7-51783
- Mn $_2$ Al $_2$ Si $_2$ O $_7$ spin glass, dynamic and static scaling exponents 7-38879
- NH $_4$ Al(SO $_4$) $_2$ ·12H $_2$ O secondary nucleation from soln., effect of insoluble additives 7-26681
- NH $_4$ AlPO $_4$ ·F $_2$ O $_2$ ·H $_2$ O system, phase relations, AlPO $_4$ stability 7-65009
- NH $_4$ Al(SO $_4$) $_2$ ·12H $_2$ O:Cr $^{3+}$, X-ray radiation damage, EPR and optical absorption studies 7-26799
- NaAlCl $_4$ molten salt for new advanced high energy density battery 7-39981
- NaAlSi $_3$ O $_8$, thermally stimulated lumin., spectral anal. 7-46154
- Na $_2$ Al $_2$ Si $_2$ O $_{10}$, tetranatrolite, cryst. struct., X-ray diffr. studies 7-44481
- NaF-AlF $_3$, cryolite melt, struct., computer simulation (*Chinese*) 7-6494
- (PBr $_4$) $_2$ (AlBr $_4$) $_2$ complex, mol. vibr., Raman and IR spectra anal. 7-46021
- PbF $_2$ -MnF $_2$ -Al(PO $_3$) $_3$ glasses, conductivity and mechanical relax 7-16803
- Rb(AlSi $_2$ O $_6$), synthetic leucite, high temp. X-ray diffr. study 7-21176
- Rb $_{1.47}$ Al $_{1.47}$ Ti $_{6.53}$ O $_{16}$ hollandite-type struct. refinement, cation substitution effects study 7-58232
- Rb $_2$ KAlF $_6$, structural phase transitions 7-52044
- SbBr $_2$ -AlBr $_4$ complex, struct. Raman spectra study 7-46020
- ScAl $_2$ C $_3$, cryst. struct. determ. 7-58242
- Si-Al-O-N sialon, bonding investig., active Ti additive role, fracture strength and microstruct. 7-39846
- SiAlON composites, interfacial microstruct. 7-16429
- SiAlON-YAG ceramics, Auger electron microscopic quantification of phase comp. 7-22951
- SiC-AlN ceramics, elevated temp. creep, role of grain size 7-39584
- Si $_3$ N $_4$:AlN, grain boundary phases, EM anal. 7-16569
- Si $_3$ N $_4$:Y $_2$ Al $_2$ O $_{12}$, grain boundary phases, EM anal. 7-16569
- Si $_3$ N $_4$ -AlN-rare earth oxide systems, subsolidus phase relationships 7-39489
- Sialon, static-fatigue limit of materials containing small flaws 7-39620
- SrAlF $_6$:Cr $^{3+}$, laser material, EPR study 7-45807
- (Ti,Al)N layers on high speed steel, morphology and props., deposition temp. and sputtering atmosphere depend. 7-53975
- Ti-Al-N coatings on high-speed steel substrates, characterisation by Auger electron spectroscopy and X-ray photoelectron spectroscopy 7-53982
- TiAlN coatings, sputter ion plating, struct. and protective props. 7-53976
- TiAlOC coatings, CVD, composition, struct. and wear resistance 7-53929
- Y-Si-Al-O-N ceramics, phase relationships 7-65011
- Y-Si-Al-O-N glasses, Si coordination, NMR studies 7-1906
- YAG:Nd $^{3+}$, impurity two-photon absorpt. cross section meas. 7-53375
- YAG:Pr $^{3+}$, up-conversion, stepwise photon absorpt. process 7-13193
- ZnO-AlN-glass, SAW characs. study 7-12448
- ZrF $_2$ -BaF $_2$ -AlF $_3$ glass, viscous flow vs. phase separation, DSC study 7-44383
- ZrF $_4$ -BaF $_2$ -GdF $_3$ -AlF $_3$ -NaF-FeF $_3$, optical fibre glasses, trace amounts of Fe, characterisation 7-2956
- ZrF $_4$ -BaF $_2$ -LaF $_3$ -AlF $_3$ glass, etching method for prep. of IR fibres with high tensile strength 7-1243

aluminium compounds continued

- ZrF₄-BaF₂-LaF₃-AlF₃-NaF glass, crystal growth and microstruct. 7-1896
 ZrF₄-BaF₂-LaF₃-AlF₃ optical fibres, gamma irradiation, EPR and IR studies 7-37183
 ZrF₄-BaF₂-LaF₃-AlF₃, heavy metal fluoride glass system, viscosity and crystallisation 7-37883
 ZrF₄-BaF₂-NaF-AlF₃-LaF₃ glasses, crystallisation study 7-63491
 ZrF₄-PbF₂-AlF₃-LiF-NaF glasses, mixed alkali effect, DC cond. 7-63873
 ZrF₄-PbF₂-AlF₃-NaF-KF glasses, mixed alkali effect, DC cond. 7-63873

aluminosilicate glasses

- bonding of dental glass to Ni-Cr alloys 7-39844
 cordierite glass and glass-ceramic, comparative single-point diamond scratching behaviour 7-46654
 E-glass, coord. of iron, ESR and mag. meas. 7-13021
 GRIN glass, delta-n control by additives in AgCl diffusion baths 7-31528
 magic-angle spinning NMR, review 7-64536
 oxynitride glasses, dielectric studies 7-55917
 porcelain, sintering kinetics, struct. evolution 7-28004
 powders, calcia-aluminosilicate, sintering and crystn., kinetic processes 7-37877
 thermodynamics, miscibility and phase separation 7-63498
 Al₂O₃-SiO₂-Cr mullite transparent glass ceramics, Cr³⁺ luminesc. 7-46102
 Al₂O₃-SiO₂-CaO glasses containing rare alkali oxides, struct. and elec. props. 7-6528
 Al₂O₃-SiO₂-Fe₂O₃-CaO-MgO-Na₂O-K₂O glass batch melting, interaction between solid, liq. and gas 7-7946
 Cu-ruby glasses, optical props., transmission and attenuation spectra 7-13177
 Li₂O-Al₂O₃-SiO₂ glass, sputtering, SIMS depth profiling 7-13314
 Li₂O-Al₂O₃-SiO₂ glass., cryst. phase nucleation, DTA, X-ray diff. 7-58156
 Li₂O-MgO(CaO)-Al₂O₃-SiO₂, multicomponent glasses, sequence of cryst. phases 7-26648
 Li₂O-SiO₂ based photosensitive glass, machining without photoresist 7-22865
 MgO-Al₂O₃-SiO₂ glass-ceramics, nucleation crystallisation, modulus of rupture, acousto-US obs. 7-59723
 Na₂O-Al₂O₃-SiO₂ glasses, elastic props., annealing and Al substitution effects 7-8035
 Na₂O-Al₂O₃-SiO₂:Eu³⁺ glass, impurity laser-excited site-selective fluorescence line-narrowing spectra 7-13200
 Na₂O-CaO-Al₂O₃-SiO₂ glass ceramic system, spherulitic growth, mech. props. 7-46405
 Na₂O-CaO-Al₂O₃-SiO₂ system, synthesis of glasses by sol-gel process 7-64997
 Na₂O-CaO-Al₂O₃-TiO₂-SiO₂:Eu³⁺ glass ceramic, impurity laser-excited site-selective fluorescence line-narrowing spectra 7-13200
 Na₂O-Fe₂O₃-Al₂O₃-SiO₂, Fe³⁺ ESR spectra, valence-coord. state 7-45813
 Na₂O-SiO₂-Al₂O₃, glass, longitudinal electrostriction tensor component 7-2982
 Na₂O-ZrO₂-Al₂O₃-SiO₂ glasses, ionic cond., glass transition temp. meas. 7-26998
 Nb₂O₅-Al₂O₃-B₂O₃-Na₂O-SiO₂, phase separable glass, heat treatment leaching, X-ray diffraction anal. 7-51658
 PbTiO₃ based glass ceramics piezoelectricity, pyroelectricity and ferroelectricity 7-7654
 SiC fibre reinforced Li₂O-Al₂O₃-SiO₂ glass ceramics, tensile and flexural strength 7-13520
 SiC fibre reinforced Li₂O-Al₂O₃-SiO₂ glass ceramic composite, thermomech. mismatch 7-46538
 SiO₂-Al₂O₃, thermal capacity, thermodynamic props. 7-12307
 SiO₂-Al₂O₃ vitreous systems, low temp. sp. ht. and thermodynamic props. study 7-63842
 SiO₂-Al₂O₃-CaCO₃-Na₂CO₃ glass system, Ar⁺ ion beam effects 7-32521
 SiO₂-Al₂O₃-MgO-Cr₂O₃ glass, magnetism of spinel microcrystals, ESR study 7-27594
 SiO₂-Al₂O₃-MgO-TiO₂-Cr₂O₃ based glass ceramics, Cr³⁺ laser emission and excitation spectra 7-22299
 SiO₂-Al₂O₃-ZnO-Li₂O:Cr³⁺ garnite type glass ceramics, laser excited emission spectra 7-22288
 SiO₂-Na₂O-Al₂O₃-ZnO-Fe₂O₄-Si glass system, Fe behaviour at various compositions and reducing conditions 7-1899
 SiO₂-Na₂O-CaO-Al₂O₃-MgO glasses, heavy ion irradiation, enhanced diffusion, preferential sputtering 7-32523
 SiO₂-Na₂O-CaO-MgO-Al₂O₃-BaO-FeO₃ glass, elec. field stimulated Na depletion 7-6897
 SrTiO₃-Al₂O₃-SiO₂ glass-ceramics, low temp. dielec. props. 7-7636
 SrTiO₃-SiO₂-Al₂O₃ glass-ceramics, anomalous crystn. behaviour obs. 7-44395
 Y₂O₃-ZnO-Al₂O₃-SiO₂, glass form. and crystn., effect of ZnO additions 7-44382

AM (modulation) *see* amplitude modulation

amateur radio *see* radiocommunication

ambient temperature *see* temperature

amblyopia *see* vision defects

americium

see also nuclei with

- alpha particle activity in sea sediment, detection with plastic foils 7-36431
 aqueous soln., reaction rate consts. of radiation-produced transients 7-60903
 behaviour in aqueous solns. containing Fe, radwaste treatment appl., colloids 7-19529
 diffusion and distrib. in CaCO₃ deep ocean sediment samples 7-36273
 enrichment in marine aerosols 7-3742
 neutron-activation detectors with fissionable nuclides 7-56907
 nuclear waste, leaching by salt solns. 7-36272
 pseudocolloids, formation and transport in aqueous systems 7-5476
 radioassay of Pu or Am in biological samples, low-energy photon detector 7-54819
 separation and activity meas. in sea algae 7-54370
 solid state and thermodynamic props., f-electron bonding and struct., review 7-12321
 solubility, influence for nuclear waste repositories 7-36271
 superconductivity, simple transition metal-type and heavy fermion behaviour 7-12897
 valence-band photoelectron spectrum interpretation 7-64875

americium continued

- ²⁴¹Am electrodeposition geometry in the assay of environmental samples 7-28718
²⁴¹Am, hyperfine struct. of 2 eV level, laser inducer fluorescence study 7-25680
²⁴¹Am, lakes, seasonal anoxia, actinide release 7-60286
²⁴¹Am, processing chemistry 7-19375
- americium compounds**
 Am_{0.25}Np_{0.25}U_{0.5}O_{2-x}, thermal conductivity at elevated temperatures 7-21551
 AmO₂, photoacoustic-spectroscopy 7-27731
 Am₂O₃, photoacoustic-spectroscopy 7-27731
 Am_{0.5}U_{0.5}O_{2-x}, thermal conductivity at elevated temperatures 7-21551
- ammeters**
 clamp-type ammeter with the magnetic sensor using parametric oscillation 7-4864
 high-frequency ammeters with wideband current transformers for measurements in high-voltage circuits 7-48770
 portable instrument for noncontacting DC current measurements 7-56303
- ammonia**
 absorption into water in packed tower, mass transfer coeffs. meas 7-266
 adsorption and thermal decomposition on Ni (110), isolation and identification of NH₂ and NH 7-6986
 adsorption complexes with heterogeneous catalysts, vibr. study, IR spectra anal. 7-36607
 alkali-metal-NH₃ sections, metal-nonmetal transitions 7-2486
 analytical microwave spectrometer employing a Gunn oscillator locked to the rotational absorption line 7-15008
 anthracene-NH₃, jet-cooled clusters, van der Waals complexes, exciplexes, visible fluoresc. spectra 7-19936
 in atmosphere, effect of precip. on vertical profiles 7-40513
 chemical storage of energy, kinetics of heterogeneous reactions 7-23229
 chemisorption bond energies on chemically modified Mo (100) surface 7-23056
 chemisorption on Al, interaction with surface, cluster approx., total energy calcs. 7-52265
 coadsorption with CO on Ni (111), multilayer formation studied by metastable quenching spectroscopy 7-21639
 cryogenic, high press. shock temp. meas. 7-32566
 dimer, ionis., proton transfer, ab initio pot. energy surface calc. 7-42518
 dimer struct., electron spectra anal., HF calcs. 7-36686
 dimers, geometry and energy calcs. SCF calcs. 7-15499
 dipolar couplings in liq. crystals, anisotropic forces, NMR study 7-62413
 dissociation on Si (100) surface, rate-limiting steps at low-temp. 7-2366
 Egg Nebula (CRL 2688), NH₃ and cyanodiacetylene mapping 7-4540
 electron impact excited, Balmer line emission cross sections 7-20065
 formaldehyde+NH₃, molecular collisions, rotational cross sections, ΔJ=0 transitions, elec. field effects (French) 7-5754
 formation of carbamic acid, urea and carbonic acid from CO₂, H₂O and NH₃ 7-8268
 gas mixture-laser interaction model, appl. to thermally activated laser-induced CVD 7-46333
 high temperature absorpt. of laser radiation 7-51385
 inert gas-NH₃ ion form. by electron ionisation, mass anal. ion kinetic energy spectra 7-13736
 interstellar, hot NH₃ obs. towards H₂O masers near W3(OH) 7-9525
 interstellar, inversion line obs., molecular cloud kinetic temps. 7-66700
 interstellar, maser and thermal emission obs. toward star-forming region (W51 IRS 2) 7-66702
 Jupiter, NH₃ abundance and cloud opacities determ. from Voyager IRIS data 7-24051
 Jupiter, upper troposphere, zonal mean characts., Voyager IR obs. anal. 7-24052
 kinetics of H₂SO₄ and NH₃ reactions for chemical storage of solar energy 7-40048
 laser, compact high-power finite-impulse-response, pumped in CO₂ laser cavity 7-5907
 laser, CW MIR, intensity and half-widths, absorpt. meas. 7-36941
 laser, isotopically substituted ¹⁵NH₃, with two-photon optical pumping 7-43069
 lasers, FIR, instabilities and chaotic emission 7-15849
 lasers, line-tunable operating at wavelengths of 11 to 14 μm 7-5872
 lasers, optically pumped, CW operation in mid-IR 7-36950
 LiKSO₄:NH₃ single crystals, low temp. phase transitions, EPR study 7-27599
 liquid, normal potentials of metals 7-39903
 liquid charged dielectric sphere, electron bound states 7-21960
 low-cost solar-energy stimulated absorption refrigerator for vaccine storage 7-65576
 matrix isolated, orientation-inversion motions, inertial model 7-42580
 metal-NH₃ generator as pulsed and continuous power source 7-63362
 molecular jets, Raman scatt., Franck-Condon and double reson. study 7-31082
 molecular outflow sources, NH₃ obs. anal. 7-66576
 molecule, 193 nm photolysis NH and ND generation, fluoresc. 7-62442
 molecule, ν₂ band, vibr.-rot. transitions, press. broadening coeffs., IR spectra anal. 7-50121
 molecule, Å state, rot. depend. lifetimes and excitation profiles, Raman spectra 7-62378
 molecule, double photoionisation and fragmentation, PIPICO method anal. 7-19985
 molecule, electron impact, excited fragment absolute emission cross sections 7-5776
 molecule, electron impact, excited NH radical form. 7-36800
 molecule, electron impact excitation cross-sections, correction for excited fragment escape 7-25671
 molecule, excited vibr. state, rot.-inversion levels, collisional relax., visible obs. 7-62392
 molecule, integrated intensities and IR absorpt. bands, ab initio (3.1) calcs. 7-56953
 molecule, mag. suscept. theory in atomic quantities terms 7-25366
 molecule, mol. beam laser Stark spectroscopy, ν₂ band, transition dipole moment meas. 7-50209
 molecule, nucl. mag. shielding consts. ab initio wave function calcs. 7-5594
 molecule, nuclear quadrupole coupling consts., solvent effects (French) 7-25558
 molecule, optimised geometries and harmonic freqs., MP2 calcs. 7-62255
 molecule, photoionisation cross section, ground state inversion pot. method/diff. theory 7-945

ammonia continued

- molecule, point charge models and FSGO-wave fn., mol. electrostatic pot. and fields (*German*) 7-25632
- molecule, radical emission cross sections for plasma diagnostics (*Japanese*) 7-20934
- molecule, S₂ bands, isotope shift, diode laser spectra 7-19845
- molecule, stretching force consts. inner-shell polarisation effect, HF calcs. 7-15588
- molecule, two photon bound-bound electronic transition calcs. 7-31136
- molecule, vibr., inversion doubling, vibrational calcs., use of intramol. pair pots. 7-31014
- molecule and clusters, UPS using pulsed gaseous free jets 7-36685
- molecule unimolecular dissociation, pot. energy surface, classical trajectory study 7-13745
- MOSFET, Pt-gate, ammonia sensitivity, dependence on gate electrode morphology 7-61330
- NGC 2071, refl. nebula, nearby bipolar flow source NH₃ obs. 7-24181
- nitrobenzenes para-substituted, solvated anion radicals reaction kinetics in liq. NH₃, ESR spectra anal. 7-19907
- OMC-1, NH₃ line emission, search for linear polarisation 7-48011
- Perseus globules, physical and chem. conditions, NH₃ and cyanoacetylene obs. 7-35021
- perylene-NH₃, jet-cooled clusters, van der Waals complexes, exciplexes, visible fluoresce. spectra 7-19936
- phase II, orientationally disordered, Raman spectra 7-22239
- pre-melting second-order transform., isothermal compressibility and expansivity meas. 7-32631
- quantum resolved molecular-beam scattering from W(100) 7-15695
- Raman laser, single-mode homogeneously broadened, self-pulsing instabilities 7-10922
- reactant in RF plasma CVD reactor, flow, temp., conc. fields, num. simulation 7-26501
- reaction with SiO₂ films 7-13763
- scattering from W(100), two-photon reson. three photon laser ionisation spectra 7-10768
- solar production system, conceptual design 7-65588
- solvated electron, visible absorption. spectrum short-wavelength wing 7-42631
- solvation energies of Li first row compounds with H₂O and NH₃ 7-8269
- stability, form. from NH₄⁺, pot. energy surfaces, ab initio CI calcs. 7-30955
- superradiant Raman FIR laser with nonlinear reson. four-wave mixing generation of medium IR emission 7-50657
- water electrolyzers and the use in electrolytic H₂ and NH₃ production 7-23231
- C₂MnCl₂.2.4NH₃+4.8NH₃, thermochemical energy storage, kinetic study (*French*) 7-17782
- CO-NH₃ mixtures, photoionisation discharge, energy characts. 7-21027
- CO₂-NH₃ mixtures, photoionisation discharge, energy characts. 7-21027
- H₂N-HCl, H-bonded dimer charactn., rot. FT microwave spectrum 7-25490
- H₂N-HF-HF, H bond cooperativity, structural and energetic props., ab initio calcs. 7-19697
- H₂O-NH₃ ice mixtures, optical consts. determ. 7-23993
- LiKSO₄.NH₃⁺, EPR spectra, ⁷Li spin-flip satellites 7-64525
- ND₃, elastic consts. and elasto-optic coeffs., Brillouin spectra anal. 7-53359
- (NH₃)₂⁺, multiply charged clusters, decomp. channels 7-15790
- (NH₃)₂, quasispherical dimer, vibr.-rot. struct. 7-15670
- NH₃⁺ radical cation, hyperfine coupling tensors, ab initio UHF calcs. 7-25373
- NH₃/Na matrix, Na⁺ identification, absorption and MCD spectra anal. 7-30973
- NH₃-H₂O system for solar refrigeration in Egypt 7-40041
- NH₃-N₂(methane), excess molar enthalpy and heat capacity 7-44825
- NH₃+Ar, dissociation, excitation, nascent vibr. and rot. distrib. 7-46824
- NH₃+Fe clusters, reaction kinetics, cluster binding sites and adsorbate binding energies 7-54106
- NH₃+formaldehyde, rotationally inelastic scatt. cross sections, modified Anderson theory calcs., 7-50321
- NH₃+H₂, ab initio potential-energy surface, HF, SCF calcs. 7-10716
- NH₃+HX where X=Cl, Br, I, gas phase charge transfer complexes, pot. curves 7-13733
- NH₃+He, Rydberg atom ionisation, rot. deexcitation 7-36737
- NH₃+Hg, photosensitised reaction, complex form., luminesc. spectra 7-8256
- NH₃+NO⁺, cross section as a fn. of ion vibr. level, REMPI time of flight spectra, mass spectra 7-20028
- NH₃⁺+H₂, ion-molecule reaction rate at low-temp. conditions of interstellar space 7-23007
- NH₃⁺+NO, cross section as a fn. of ion vibr. level, REMPI time of flight spectra, mass spectra 7-20028
- (NH₃)_n (n=2 to 5), clusters, electronically excited Å states, two-photon ionisation, mass spectroscopy 7-15761
- NH₄⁺, Fourier transform ion cyclotron reson. mass spectrometry 7-13734
- NH₂D and ND₂H, IR spectra, vibr.-rot. band, inversion doubling 7-25517
- NH₂D, IR and microwave spectra, rot. anal. 7-25518
- NH₂D in Orion KL, detect. and abundance 7-60754
- NH₃(ND₃), adsorbed on Ag film, IR laser photodesorption spectroscopy 7-17825
- NH₃(ND₃) band intensity and symmetry effect on absorpt. spectrum 7-57049
- NH₃(ND₃), predissociation, dissociation, attachment cross section 7-50279
- ¹⁴NH₃ laser pumped transversely by CO₂ laser 7-1085
- ¹⁵NH₃ laser, optical pumping, spectroscopic schemes 7-43073
- ¹⁵NH₃ laser pumped transversely by CO₂ laser 7-1085
- TiCl₄+NH₃, RF glow discharge, plasma enhanced CVD of TiN 7-39427

ammonia clocks see atomic clocks

ammonium compounds

- bis(tetramethylammonium)AgI₃I₁₅:NH₄I, O probe, electrical conductivity and struct. 7-52147
- bromides as electrolyte of Zn-Br cells 7-39986
- chalcogenide intercalation compounds with NH₃ guest species, NMR 7-53160
- hexafluorometallates, phase transitions 7-6787
- hydrogen bis(trichloroacetate) single cryst., internal modes, IR and Raman spectra studies 7-26877

ammonium compounds continued

- hydrogen tartrate, dislocation etch pits 7-37999
- hydrogen tartrate, ferroelectric, crystal growth and dislocation etching kinetics 7-51770
- intercalation cpd. struct., enthalpy of reaction 7-46841
- monosubstituted ammonium compounds, ¹H NMR chemical shifts of solvent water 7-36648
- (NH₄)₃PCl₄O₁₆, polycrystn., internal vibr., IR and Raman spectra 7-22263
- susceptibility meas., PMR, X-ray and neutron diff. 7-45244
- trioxalato-chromate (III) trihydrate, crystallochemical study (*French*) 7-26738
- AlNH₄(SO₄)₂, multicharged electrolyte soln. in water-tert butyl alcohol, viscosity and density studies 7-52104
- CrNH₄P₂O₇ and α- and β-CrNH₄HP₃O₁₀, preparation and characts. 7-3161
- Fe(NH₄)₂(SO₄)₂.6H₂O, EPR of Mn²⁺, Mn²⁺-Fe²⁺ exchange interaction 7-2924
- Hg(NH₄)₂Na₂(P₃O₉)₂, cryst. struct. determ. 7-1956
- LiND₃SO₄, ferroelastic and ferroelectric domain struct., SEM obs. 7-27675
- LiN(H₂D)₂SO₄ crystals, vibr. spectra and ferroelec. transition, Raman scatt. study 7-53304
- Li⁺(NH₄)₂(NH₃)₂TiS₂(^{x+y})⁻ intercalation cpd., NH₃ oxidation, charge compensation 7-32354
- LiNH₄SO₄, ferroelastic and ferroelectric domain struct., SEM obs. 7-27675
- Mg(NH₄)₂(SO₄)₂.6H₂O, EPR of Mn²⁺, Mn²⁺-Fe²⁺ exchange interaction 7-2924
- Mn-NH₄ solutions, electrolysis, pH rise at cathode 7-33937
- ND₃DSeO₄, deuterated ASe, crystals, dielectric relax. 7-45930
- ND₄ReO₄, heat capacity anal. 7-26984
- ND₄SCN, phase transitions, spin lattice relax. study 7-33286
- NH₄⁺, stability against dissociation and NH₃.H⁺ form., pot. energy surfaces, ab initio CI calcs. 7-30955
- NH₄⁺, atomic multipoles, molecular potentials, interaction energies SCF MO calcs., atomic multipole expansion 7-19696
- NH₄Al(SO₄)₂.12H₂O secondary nucleation from soln., effect of insoluble additives 7-26681
- NH₄AlPO₄.P₂O₇.H₂O system, phase relations, AlPO₄ stability 7-65009
- NH₄Al(SO₄)₂.12H₂O:Cr³⁺, X-ray radiation damage, EPR and optical absorption studies 7-26799
- NH₃CdF₃, heat capacities determ. in temp. range 5 to 350K 7-44842
- NH₄Cl aq. soln. finite sink for atmospheric heat engine 7-40022
- NH₄Cl, irregular fractal-like crystal growth, diffusion-limited aggregation model 7-2445
- NH₄Cl, phase transitions, elec. props. study 7-17257
- NH₄Cl, spontaneous and field induced current peaks at order-disorder phase transition 7-45948
- NH₄Cl, undoped and Ni doped, TSC, polarisation meas., 150-500K 7-52645
- NH₄ClO₄, rotational diffusion of rare spin ¹⁷O, NMR (*Japanese*) 7-58535
- NH₄D⁺, ν₄ fundamental band, IR difference-freq. laser spectra 7-50096
- NH₄(D₂Cl):Cu²⁺ crystals, impurity optical absorpt. spectrum temp. depend. study 7-53374
- NH₄F in dioxane-methanol mixtures, assoc. constant, from cond. meas. 7-33939
- NH₄Fe₂F₆, topotactic oxidation for FeF₃ synthesis 7-17396
- NH₄H₂(IO₃)₃, proton cond. and cryst. struct., X-ray and neutron diff. studies 7-12026
- NH₄H₂PO₄, antiferroelectricity, role of H bonds 7-64582
- NH₄H₂PO₄ crystals, kinetics of dislocation growth of dipyrmaid and prism faces 7-58578
- NH₄H₂PO₄, temp. depend. IR active lattice modes in para- and antiferro-electric phase 7-46012
- NH₄H₂PO₄:Co²⁺, optical absorption spectrum 7-46077
- NH₄H₂PO₄:SeO₄²⁻, partially deuterated, D concentrations in H₂PO₄⁻ and NH₄⁺ radicals, ESR spectra 7-27671
- NH₄HSO₄ single crystals, surface layer phase transitions, surface cond. anomalies obs. 7-63925
- (NH₄)₂H(SO₄)₂:Cu²⁺ single crystals, EPR study 7-53118
- NH₄HSeO₄ crystals, deuterated, pyroelectric props. 7-13098
- NH₄HSeO₄, X-ray irradiation, existence of incommensurate phase, permitt. meas. 7-33338
- (NH₄)_{0.32}H_{0.16}WO₃, intercalation cpd. struct., enthalpy of reaction 7-46841
- (NH₄)₂HfF₆, thermally activated α-β transition 7-12258
- (NH₄)₂Hf₂(O₄OH)(SO₄)₁₀(H₂O)₇, struct. X-ray diff. 7-6613
- β-NH₄LiSO₄, elastic stiffness constants, ultrasonic pulse echo overlap meas. 7-12188
- NH₄MgF₃, heat capacities determ. in temp. range 5 to 350K 7-44842
- NH₄MnX₃ (X=Cl, F), absorpt. spectra 7-33410
- (NH₄)₂Mo₂Br₈, press. tuning IR spectral shifts 7-22242
- (NH₄)₂MoO₄.Ni(NO₃)₂, interaction, effect of mechanical activation on NiO:MoO₃ ratio 7-8261
- NH₄NO₃ aq. soln. finite sink for atmospheric heat engine 7-40022
- (NH₄)₂NaFeF₆, low-temperature phase transitions characterisation by Fourier transform IR spectroscopy 7-52046
- NH₄Np(OH)₅, cryst. struct. determ. (*French*) 7-16511
- (NH₄)₂Pb(Cu(NO₃)₂)₂ struct. phase transform., ESR study 7-13026
- (NH₄)₂PdCl₄, NH₄⁺ rot. pot., inelastic neutron scatt. study 7-26676
- (NH₄)₂PtCl₄, NH₄⁺ rot. pot., inelastic neutron scatt. study 7-26676
- (NH₄)₂SO₄, contrib. to light scatt. in St. Louis summer aerosol 7-47538
- (NH₄)₂SO₄ crystal, cryst. fields calc., Madelung energies and cryst. pots. 7-64180
- (NH₄)₂SO₄, crystal growth, contact nucleation rel. to Cr ion conc. 7-16462
- (NH₄)₂SO₄, partially deuterated, phase transition, heat of transition 7-53246
- (NH₄)₂SO₄, phase transitions, appl. of NH₃⁺ paramag. probe to mol. motion 7-27604
- (NH₄)₂SO₄:Ti, mol. orbitals, EHT calc., rel. to absorption spectra 7-64181
- (NH₄)₂SO₄:Ti crystal, temp. depend. of optical absorption bands 7-64671
- (NH₄)₂SO₄.Al₂(SO₄)₃.24H₂O crystals, growth rate dispersion from aq. soln. 7-59392
- (NH₄)₂SeCl₄, crystal struct. investig. 7-12001
- (NH₄)₂SeO₄.2NH₄HSeO₄, single cryst., superionic phase transition at 378 K 7-52125

ammonium compounds continued

- $\text{NH}_4\text{Sn}_2\text{F}_5$, F^- motion, NMR and electrical conduction 7-52132
 $(\text{NH}_4)_3\text{Sn}_2\text{F}_{11}$, high temperature form, crystal structure (French) 7-26727
 $(\text{NH}_4)\text{TeF}_6(\text{HCl})_{0.25}(\text{H}_2\text{O})_{0.25}$, tunnel-type cryst. struct., single cryst. X-ray diff. meas. 7-44495
 $\text{NH}_4\text{UO}_2(\text{NO}_3)_3$, charge transfer bands position, ionisation pot. effects, luminesc. spectra anal. 7-46146
 $(\text{NH}_4)_{1.84}\text{V}_3\text{O}_8$, intercalation cpd. struct., enthalpy of reaction 7-46841
 $(\text{NH}_4)_3\text{VO}_2\text{F}_4$, cryst. struct., struct. of $\text{VO}_2\text{F}_4^{3-}$ ion 7-32400
 $(\text{NH}_4)_2\text{ZnBr}_4$, thermosensitive photo-selective phenomenon in single crystals, Raman scatt. obs 7-46038
 $(\text{NH}_4)_2\text{ZnCl}_4$, internal motions and phase transitions, PMR studies 7-2993
 $(\text{NH}_4)_3(\text{ZnCl}_4)\text{Cl}$ crystals, electron-density distrib. at 120 K 7-58219
 NH_4ZnF_3 , heat capacity, thermodynamic functions 7-52071
 $\text{Rb}_{1-x}(\text{ND}_4)_x\text{D}_2\text{PO}_4$, structural glass phase, X-ray scatt. meas. 7-26660
 $\text{Rb}_{1-x}(\text{ND}_4)_x\text{D}_2\text{PO}_4$, NMR in random fields, cluster formation and local dynamics of D glass 7-38959
 $\text{Rb}_x(\text{NH}_4)_{1-x}\text{AlF}_4$, ESR study of orientational order with Fe^{3+} probe 7-53119
 $\text{Rb}_{1-x}(\text{NH}_4)_x\text{H}_2\text{AsO}_4$, proton glassy state, dielec. props. 7-13075
 $\text{Rb}_{1-x}(\text{NH}_4)_x\text{H}_2(\text{P,As})\text{O}_4$, mixed system, proton localisation, obs. by incoherent neutron scatt. 7-12224
 $\text{Rb}_{0.61}(\text{NH}_4)_{0.39}\text{H}_2\text{PO}_4$, mixed crystal, dielec. study of ferroelec. transition 7-53248
 $\text{Rb}_{1-x}(\text{NH}_4)_x\text{H}_2\text{PO}_4$, lattice constants, temp. and concentration dependence, X-ray diffraction anal. 7-1976
 $\text{Rb}_{1-x}(\text{NH}_4)_x\text{H}_2\text{PO}_4$, press. depend. of proton glass freezing, dielec. props. 7-2209
 $\text{Yb}_{0.06}(\text{NH}_3)_{0.32}\text{TiS}_2$ intercalation compounds, structural and magnetic studies 7-63593
 $\text{Zn}(\text{NH}_4)_2(\text{SO}_4)_2 \cdot 6\text{H}_2\text{O}$, EPR of Mn^{2+} , Mn^{2+} - Fe^{2+} exchange interaction 7-2924

amorphisation

- alloy surfaces, amorphisation during nanosecond ion beam irradiation 7-6517
 alloys, electron irradi. induced transforms. 7-2065
 binary alloys, crystal-amorphous transformation, thermodynamics and kinetics 7-21108
 ceramics, electron irradi. induced transforms. 7-2065
 diamond, type IIa, ion implanted, volume expansion 7-58298
 direct impact induced amorphisation, effect of ion beam annealing 7-58383
 dislocation core, molecular dynamics method study 7-6624
 disordering transitions, nucleation mechanism, review 7-44743
 electron microscopy, high resolution, in intermetallic compounds 7-44377
 inorganic crystals, atomic coordination numbers and defects, geometric estimate 7-63571
 ion beam modification of materials, conf., Catania, Italy (9-13 June 1986) 7-60865
 metal alloys, amorphisation from melt, determ. 7-6516
 metallic glasses, one-component, amorphisation and crystallisation (Russian) 7-32301
 metallic thin films, amorphisation and film anal., ion beam techniques 7-37868
 Nb_3Ir films, supercond. transition temp., effect of radiation induced disordering 7-45540
 rare earth alloys, RNi_2 Laves phase ($\text{R}=\text{Y}, \text{La}, \text{Ce}, \text{Pr}, \text{Sm}, \text{Gd}, \text{Tb}, \text{Dy}, \text{Ho}, \text{Er}$), H induced amorphisation 7-51641
 sapphire, ion implantation, mechanical surface property modifications 7-32473
 Te elemental and alloy thin films, laser irradi. effects, refl. meas., optical data storage appl. 7-12144
 TEM, conference, Boston, MA, USA (Dec. 1985) 7-35119
 Ag-Cu(Ni) systems, amorphisation induced by ion mixing 7-21300
 Al-V alloys, phase transitions between amorphous, quasicrystalline and crystalline phases 7-63807
 Al_2O_3 , amorphous layers, formation and annealing, ion irradiation 7-58385
 B-Fe, ion beam mixing, effects of Xe^+ implantation (Chinese) 7-51886
 B-Ni, ion beam mixing, effects of Xe^+ implantation (Chinese) 7-51886
 $\text{BaFe}_{12}\text{O}_{19}$, defects created by Kr ion bombardment, HREM study 7-12168
 $\text{Be}_3\text{Al}_2\text{Si}_6\text{O}_{18}$, beryl, electron-irradiation induced amorphism 7-32505
 $\text{Ca}_2\text{Nd}_4(\text{SiO}_4)_6\text{O}_2\text{:Cm}$, radiation effects, appl. for nuclear waste disposal 7-32522
 $\text{Ca}_2\text{Nd}_4(\text{SiO}_4)_6\text{O}_2\text{:Cm}$ ceramic simulated nuclear waste forms, radiation effects on microstruct. and fracture props. 7-58373
 $\text{CaZrTi}_2\text{O}_7\text{:Cm}$, radiation effects, appl. for nuclear waste disposal 7-32522
 $\text{Cd}_{1-x}\text{Mn}_x\text{Se}$, powder, stress effects, amorphisation (Korean) 7-27960
 Co-Sn multilayers, amorphisation and interdiffusion, EXAFS and XANES studies 7-64812
 Cu-Ti, high resolution electron microscopy 7-44377
 Cu-Ti alloy system, electron irradi.-induced amorphisation, chemical disordering effects study 7-16640
 Cu-Zr, amorphisation under action of high press. and shear deform. (Russian) 7-58163
 Cu_2Ti_3 , electron irradiation induced amorphisation, high resolution electron microscopy 7-44373
 Fe-B-Si and Fe-B-Si-Cr-Mo-W alloys, finely cryst. and amorphous structs. on surface by laser treatment 7-8175
 Fe-Ni-P-C, amorphisation under action of high press. and shear deform. (Russian) 7-58163
 Fe-Te sputtered films, CsCl-type ordering and amorphisation 7-64021
 Ga crystalline film amorphisation by pulsed excimer laser irradi., residual resist. and T_c meas. 7-12140
 $\text{Ga}_{1-x}\text{Al}_x\text{As}$, ion-implanted, defect creation 7-21240
 GaAs:P , ion implanted and pulse laser annealed, Raman study 7-6653
 GaAs:Si , ion implanted, amorphisation and epitaxial regrowth, defect depth profiles 7-12088
 GaAs:Zn , ion damage and recrystn. annealing, conversion electron EXAFS meas. 7-64821
 $\text{Gd}_2\text{Ti}_2\text{O}_7\text{:Cm}$, radiation effects, appl. for nuclear waste disposal 7-32522
 Hf-Ni, amorphous phase form. by solid-state reaction, dominant moving species 7-21706
 MgAl_2O_4 , Ar^+ ion irradi., XPS and RBS characterisation 7-32514
 $\text{Mg}_2\text{Al}_2\text{Si}_2\text{O}_{10}$, cordierite, electron-irradiation induced amorphism 7-32505

amorphisation continued

- MoSi_3 , amorphous layer form. on ion beam mixing of Mo films on Si 7-21301
 Ni ion implantation and pulsed laser melt quenching, metastable phase and defect struct. form. studies 7-16625
 Ni single crystal, amorphisation by Zr polycrystal bilayers 7-63463
 Ni/Nb alternating layers, ion beam mixing 7-21303
 Ni/Zr thin film diffusion couples, amorphisation, DSC studies 7-26639
 Ni-B, implanted, mech. props., disorder and amorphicity 7-53819
 Ni-P, implanted, mech. props., disorder and amorphicity 7-53819
 Ni-Zr, amorphous phase formation by solid state reaction, evidence for nucleation barrier 7-58146
 NiAl thin films, ion irradi. induced amorphisation studies rel. to cascade parameters 7-63671
 Ni_3B , amorphisation by ion implantation, RBS/channelling studies 7-11912
 PbO-SiO_2 mixtures, thermohomogenised layers, UV photoelectron spectra study 7-59370
 a-Se, structural disorder model 7-26641
 Si, amorphisation and crystallisation 7-11914
 Si, amorphised and rapidly thermally annealed, extended defects 7-16660
 Si, defect diagnostics for submicrometer VLSI, book contrib. 7-44562
 Si, electron and ion irradiation induced amorphisation, point defect dispersion and mobility 7-11916
 Si homogeneous amorphisation, ion implantation energy depend. study 7-63638
 Si, ion implantation, damage profile studies, multilayer model (Chinese) 7-6648
 Si, ion implantation-induced amorphous layer, temp. and dose depend. model calcs. 7-16594
 Si Schottky diodes, H_2^+ bombarded, elec. props. 7-38677
 Si, self-implantation, damage production kinetics 7-21239
 Si, self-implantation-induced temp. depend. amorphisation, TEM and Monte Carlo simulation studies 7-16595
 Si, self-implanted, defects and amorphisation 7-2041
 Si, self-implanted, strain 7-51918
 Si:Al implanted crystals., amorphous surface regions with crystalline impurity grains, TEM study 7-58579
 Si:As, ion implantation-induced defects 7-32433
 Si:As:P, double diffused shallow junctions, rapid thermal annealing 7-22006
 Si:As $^+(As_2^+)$, ion implanted, phys. props., spreading resist., TEM, Rutherford backscattering, SIMS 7-26775
 Si:B, amorphisation by ion implantation 7-38080
 Si:B, ion implanted, amorphous layer thickness, SIMS profiling 7-51794
 Si:BF $_3^+$ (001), ion implanted, residual defects, cross-sectional TEM study 7-32471
 Si:Ge, Ge $^+$ preamorphisation implants, effect on extended defect formation during subsequent solid phase epitaxy 7-16599
 Si:Ge $^+$, ion implanted and annealed, crystalline to amorphous transformation, TEM study 7-32643
 a-Si:H, amorphous to microcrystalline structure transformation, phase stabilisation 7-63475
 Si:P, ion implanted, dynamic annealing, dose rate effects 7-12093
 Si:Sn:B, shallow junction formation, preamorphisation by Sn implantation 7-7338
 β -SiC monocryst. thin films, ion implantation and annealing, amorphisation and recrystn. processes study 7-16596
 Ti-Ni, crystalline to amorphous transitions, struct. anal. 7-44375
 TiNi alloy, amorphisation by high press. shear deform. (Russian) 7-8053
- amorphous-crystalline transformations** see crystallisation
- amorphous magnetic materials** see magnetic properties of amorphous substances
- amorphous semiconductors**
 see also chalcogenide glasses; electrical conductivity of amorphous semiconductors and insulators; insulators
 As-S, amorphous semicond. films, laser action on light sensitivity (Russian) 7-64713
 bremsstrahlung isochromat spectroscopy for electronic struct. of semiconductors and heterojunctions 7-52795
 channelling contrast microscopy, He $^+$ microbeam, semiconductor impurity profiles 7-51587
 compositionally modulated superlattices, growth and struct. 7-27168
 conference, Palo Alto, CA, USA (April 1986) 7-29602
 doped semiconductors, prep. and thermal cond., review 7-38279
 electronic and transport props., coherent potential approx. 7-27241
 electronic states, transport, theory 7-27239
 films, laser-induced explosive crystallisation, Raman microprobe analysis 7-12430
 glasses, semicond. doped, integrated nonlinear optical device fabrication 7-25873
 glassy, delocalised charge carrier mobility, temp. depend. 7-52613
 heterostructures in amorphous semiconductor devices, characts. and appls. (Japanese) 7-52770
 hierarchical lattices, phase transition universality sputtered, photoelec. props. 7-35486
 hydrogenated, NMR studies, rel. to growth process 7-38405
 II-VI cpds., electronic struct. of bulk and defect sites, tight-binding recursion method 7-45222
 III-V cpds., electronic struct. of bulk and defect sites, tight-binding recursion method 7-45222
 localised states in amorphous semiconductors prepared by fast glass transition 7-63818
 microelectronics appls., conf., Los Angeles, CA, USA (Jan. 1986) 7-24282
 multijunctions, charge carrier transport, theoretical anal. 7-38690
 multiple trapping, effect of defect level 7-27237
 optical absorpt., tight-binding model 7-45961
 photoconductivity behaviour during the approach to steady state 7-38637
 polymers, conducting, nonlinear optical processes 7-62781
 Poole-Frenkel effect, field-dependent behaviour 7-12727
 a-Si:H, structural characterisation, hyperfine interaction, ESR, ENDOR 7-53135
 Si:H solar cells, i-layer stability thickness dependency 7-17880
 Si photovoltaic module performance 7-3684
 Si solar cells, conversion efficiency improvement 7-17879
 solar cells, amorphous, with specified optical, elec. and recomb. props., optimisation model 7-54300
 solar cells, quantum efficiency meas. techniques 7-8425

amorphous semiconductors continued

- SOS, double solid phase epitaxial regrowth, amorphous layer, self-implantation, ion energy, defect density 7-58691
 superlattices, amorphous, carrier relax. processes (*Chinese*) 7-58864
 superlattices, mean free path and size quantisation 7-22003
 superlattices, stochastic carrier transport props. (*Chinese*) 7-12791
 tetrahedrally bonded, long-range disorder and local order 7-63473
 tetrahedrally bonded, dangling-bond and void-like structs., microscopic structural model 7-21803
 transient photoconductivity measurements of amorphous semiconductors by subnanosecond nitrogen lasers 7-18806
 x-ray absorption studies of amorphous semiconductors, review 7-64756
 AlN amorphous film, plasma CVD from metal organic Al source 7-52368
 As-S, amorphous semicond. films, laser action on light sensitivity (*Russian*) 7-64713
 BaO-V₂O₅-Fe₂O₃ semiconducting glasses, elec. props., Mossbauer, EPR and X-ray diffr. studies 7-7236
 Bi₂O₃-V₂O₅-CaO system, vitreous oxide semiconductor, polarisation processes 7-59139
 Cd₃As₂ amorphous films, structure and growth morphology 7-45078
 CdGeAs₂, glassy, optoelectronic props., photoelectrochemical investigation 7-45382
 CdGeAs₂/Ni amorphous films, elec. cond., low temp. impurity breakdown, high field effects 7-52625
 Cd₂GeAs₄ semiconducting glass, electrolytic dissolution in HCl and water 7-12289
 CdGeP₂, glassy, optoelectronic props., photoelectrochemical investigation 7-45382
 Cd_{1-x}Mn_xSe, powder, stress effects, amorphisation (*Korean*) 7-27960
 a-CdS/n-Si heterojunctions, elec. props. 7-64342
 CdTe amorphous thin films, electrical and optical props. 7-22045
 Co₂In₂S_{3+x} thin films, spray pyrolysis deposited, structural and optical props. 7-22468
 Cr-Ge thin film interface, interdiffusion, reaction and intermixing, soft X-ray photoemission study 7-27028
 p-crystalline Si/n-amorphous Si heterojunction, electrostatic pot. barrier distrib. calcs. 7-58881
 CuInSe₂ thin film, electron beam evaporation optical props. (*Korean*) 7-27801
 CuInTe₂ film, flash evap., DC cond. mechanisms, density of states 7-22041
 Fe₈₀C₂₀-Si compositionally modulated amorphous struct., mag. and diffusional props. study 7-7564
 Fe₂Se₃ and As₂Se₃-Fe₂ films, electronic props. 7-58922
 a-Ga_{1-x}As_x-x:H, plasma deposition in RF capacitively coupled system 7-64927
 GaAs, L near-edge structure, X-ray photoabsorpt. spectra 7-64766
 a-GaAs, optical absorpt. and refractive index spectra 7-27735
 GaAs:H amorphous sputtered films, AC cond. studies 7-21947
 a-GaAs:H:F, electronic struct., dangling bonds, cluster-Bethe lattice method calcs. 7-12592
 GaAs-AlAs, superlattices, mixing, ion implantation, rapid thermal annealing, Raman scattering 7-53355
 a-GaAs-Si (100), epitaxial regrowth by excimer laser annealing, FET fabrication 7-32875
 GaAs(P)(Sb):H, vibrational excitations, impurity-host atom complexes, IR absorpt. data interpretation 7-44724
 Ge, amorphous and partially crystallised, X-ray absorpt. investig. of struct. (*German*) 7-46241
 Ge, amorphous films, laser induced image storage 7-11078
 Ge, amorphous films, struct. and crystn., EXAFS study 7-64005
 Ge, amorphous layers on GaAs, solid phase epitaxial Growth during annealing 7-21777
 a-Ge films, dynamics of laser annealing by transient grating method 7-12122
 a-Ge films, laser-induced phase transitions, time resolved TEM study 7-38056
 a-Ge, molecular dynamics simulation, struct. of solid phases 7-32293
 a-Ge, surface phonon generation and picosecond light pulse detection 7-12456
 Ge, thermodynamic interrelation between amorphous, diamond cubic and liquid states 7-12245
 a-Ge:D,H, plasma deposited, deuteron magnetic resonance 7-27626
 a-Ge:H, B, P, As, dopant incorporation and doping efficiency 7-44587
 a-Ge:H, elec. props., effect of H plasma press. (*Korean*) 7-27332
 Ge:H, H composition at surfaces and interfaces 7-27083
 Ge:H films, post-deposition hydrogenated, electrical props. 7-32296
 a-Ge:H glow discharge deposited thin films, H content determ., spectroscopic ellipsometry study 7-38365
 a-Ge:H/Si:H superlattice struct., light absorption and photocond. studies 7-38715
 Ge:H-Si:H amorphous superlattices, electrical transport 7-7336
 Ge:Si, ion-implanted amorphous surface layers, EXAFS 7-27823
 a-Ge/au interfaces, atomic intermixing, asymmetries 7-21682
 a-Ge/Pb/a-Ge trilayers, melting transition of Pb 7-32884
 Ge-Pb multilayers, cumulative disorder and X-ray line broadening 7-32847
 a-Ge-Si:H:F, multijunction solar cells, performance data 7-40011
 GeN_x-H, amorphous, reactively sputtered, optical and electronic props. 7-58830
 GeO₂-PrCl₃ glasses, elec. props., effect of PrCl₃ content 7-21907
 GeS₂AgAu films prep. by simultaneous vacuum evaporation, Au effect on metal-photosurface deposition (*Japanese*) 7-3177
 a-Ge₂Se₆Bi₁₀ thin film, photoconductivity 7-17052
 a-Ge₂S₃:D,F, D NMR lineshapes and spin-lattice relax. studies 7-45836
 a-GeSi:H, deposition kinetics and structural control 7-45087
 GeSi:H:F double Schottky barrier structures, surface photovoltage meas. and calc. 7-17093
 a-GeSi:H,F/a-Si:H,F superlattices, elec. transport studies 7-38716
 a-GeSi:H alloy tandem-type solar cells, conversion efficiency 7-40014
 a-GeSi-films, photochemical vapour deposition, review 7-46345
 Ge_{1-x}Sn_x amorphous films, structural changes on annealing 7-16422
 a-HgSe films, elec. conductivity, thermoelectric power, optical absorpt. 7-22050
 In₂O₃:Sn films, prep. by thermal decomposition of organometallic cpds., optical and electrical props. 7-17483
 InSb amorphous films, metal-semicond. transitions, superconductivity 7-64085
 InSb metalorganic magnetron sputtered films, structural and compositional characts. 7-21725

amorphous semiconductors continued

- MoSe₃S cathode for secondary Li batteries, prep. and characterisation 7-64948
 Na₂B₄O₇-Pb₂O₄-CuO glasses, elec. props., effect of added CuO 7-2605
 Nb/a-Si/Nb structures, AC Josephson effect 7-12919
 Nb-a-Si-Nb Josephson junctions, for IR laser radiation response near plasma reson. freq. 7-58958
 P, radiative recomb., time-resolved photolum. study 7-13212
 a-P, sputtered, response to intense ion bombardment 7-27447
 PbV₂O₆, vitreous and crystalline, mag. props. 7-7473
 SbS₃, amorphous thin films, electrical resistivity 7-45523
 a-Sb₂S₃ films, thermally induced relax. of mechanical stresses 7-8032
 Se, amorphous, vitrification and crystallisation, thermal prehistory effects (*Russian*) 7-63479
 Se, amorphous films, crystn., kinetic study 7-21101
 Se, amorphous-crystalline mixture, electrical conductivity formula, anal. 7-58804
 Se, elec. resist. and Hugoniot shock wave vel. meas. 7-32567
 a-Se, residual potential, dark discharge 7-27360
 a-Se, structural disorder model 7-26641
 Se, thin films, amorphous, crystn. 7-44371
 Se vitreous chalcogenide semicond. layers, deep trapping levels, photostimulated effects (*Russian*) 7-2754
 Se_{1-x}Te_x-Se photoreceptors, xerographic time of flight technique for drift mobility determ. 7-58807
 Si : BF₂ preamorphised implanted samples, defects and leakage currents abs. 7-38514
 Si alloy development for photovoltaic power devices 7-34045
 a-Si alloy monolithic solar cells, ultralight modules and appls. 7-3663
 a-Si alloy tandem solar cells, spectral response and I-V characts. 7-54315
 a-Si alloy ultralight photovoltaic modules consisting of solar cells, space and terrestrial appls. 7-65485
 Si, amorphisation and crystallisation 7-11914
 Si, amorphised films, solid phase epitaxial regrowth, TEM characterisation 7-32883
 Si, amorphous, ion implanted, picosecond laser induced crystn. 7-16621
 Si, amorphous, p-n solar cells, light-induced defects influence on performance 7-17910
 Si, amorphous, pulsed laser irradi., time-resolved X-ray absorption studies 7-3115
 Si, amorphous, single-junction and multijunction solar cells, US DOE/SERI research project 7-8392
 Si, amorphous and crystalline, light reflection, optical third-harmonic generation 7-11059
 Si, amorphous and single cryst., etching rate, ion backscatt. and channelling meas. 7-28231
 Si, amorphous film, density-of-gap-states distrib. field effect meas. analytic determ. 7-52391
 Si, amorphous film, Rutherford backscattering, depth resolution, modelling of noise sources 7-53487
 Si, amorphous foil, time-resolved X-ray absorption during pulsed laser irradiation 7-12128
 Si, amorphous layer radiation detector development 7-30858
 Si, amorphous thin film solar modules, excitation intensity effects on photocurrent response 7-40000
 Si, amorphous to crystalline transformation, TEM in situ technique 7-44376
 a-Si based integrated type X-ray sensor (*Japanese*) 7-15456
 Si, bibliography, 1985 update 7-24331
 Si, Bragg diffraction of crystalline clusters 7-44374
 Si CVD thin film, struct. and elec. props. 7-21730
 Si, crystalline, ion-implanted and amorphous, light diffraction by transient gratings 7-11034
 Si, crystalline and amorphous, Monte Carlo growth simulation models 7-16470
 a-Si, density of states, spectral function, calcs. using eqn. of motion method in k-space 7-27236
 Si, deposition system, Si₂H₆ generation device 7-22501
 a-Si, doped, thermal equilibration struct. 7-1887
 Si, EPR-active centres, floating bond defects 7-38506
 Si, electron and hole concentration modelling 7-64269
 Si, electron and ion irradiation induced amorphisation, point defect dispersion and mobility 7-11916
 a-Si, epitaxial growth using laser heating 7-53566
 Si film, deposition by photolytic or pyrolytic disoc. of SiH₄ under laser irradi. 7-13388
 Si film, small-angle scatt. of electrons in STEM obs. of defects and voids 7-21754
 Si films, amorphous-crystalline mixtures, annealing effect on optical props. 7-59273
 a-Si films, density measurement using quartz oscillator 7-7079
 a-Si films, ion implanted device structures, solid phase epitaxy, elec. props. 7-12564
 a-Si films, preparation in separated ultra-high vacuum reaction chamber 7-59434
 a-Si films, surface passivation, study by photothermal deflection spectroscopy 7-59689
 a-Si foils, pulsed laser irradi., clusters and plasmas, time resolved X-ray absorpt. meas. 7-64755
 a-Si, generation-recombination rate 7-33032
 a-Si high quality films and superlattice solar cells, prep. method 7-46346
 a-Si hybrid photovoltaic and thermal solar collector 7-59856
 Si, IR absorpt., local phonon-induced bond angle distortion model 7-26642
 a-Si, IR spectra calcs., static charge effects 7-3040
 Si, ion implantation-induced amorphous layer, temp. and dose depend. model calcs. 7-16594
 a-Si, ion implanted, 2D model of nucleation and regrowth 7-38408
 Si, ion implanted, amorphous phase transformation during rapid thermal annealing 7-16435
 Si, ion implanted, laser beam melting and resolidification 7-12126
 Si, lamellate structure 7-21740
 a-Si, large area uniform thin films, production by scanning plasma method (*Japanese*) 7-17449
 a-Si, low temp. electron transport near mobility edge 7-38562
 a-Si, metallic state, prep., characts., appl. in devices (*Japanese*) 7-52697
 Si, monocrystalline, polycrystalline and amorphous solar cells, circulation meas. and spectral error reduction 7-13903
 Si monolithically interconnected photovoltaic panels, single chamber glow discharge manufacturing process 7-13892

amorphous semiconductors continued

- a-Si, obliquely deposited film, elec. and optical props. 7-12529
 Si p-amorphous/n-cryst. anisotype heterojunction characts., acceptor doping level depend. 7-7355
 a-Si, p-i-n solar cells, CVD deposition from Si_2H_6 7-59841
 a-Si p-i-n solar cells with graded interface 7-23133
 a-Si photoconductor for liquid crystal spatial light modulator 7-43350
 a-Si photovoltaic modules, electrochemical degradation 7-17870
 Si porous amorphous sputtered films, oxidation, IR spectra studies 7-3532
 a-Si position sensitive photodetector (*Japanese*) 7-30093
 Si, positive ion yields of impurities in amorphous and crystalline samples 7-17381
 a-Si, prep. by low press. CVD, characts. 7-7884
 a-Si protection layer on the surface of V/Si during silicide formation 7-58662
 a-Si pure and H doped films, defects and microvoids, positron annihilation study 7-45086
 a-Si, pure and H-doped, structural props., EXAFS study 7-64760
 a-Si, recomb. via dangling bonds, occupation statistics 7-38515
 a-Si, SERI Amorphous Silicon Measurements Task Force results 7-54308
 Si, self-implantation-induced temp. depend. amorphisation, TEM and Monte Carlo simulation studies 7-16595
 a-Si solar cell, light induced degradation, quantitative anal. 7-17911
 a-Si solar cell characteristics improvement for indoor consumer electronics (*Japanese*) 7-65471
 a-Si solar cell modules fabricated with single-chamber load-lock deposition system 7-59860
 Si solar cell perform. under global irradiance, atmospheric parameters effect 7-59850
 a-Si solar cell submodules, integrated type, laser patterning method 7-65470
 a-Si solar cells, dynamic inner collection efficiency 7-39992
 Si solar cells, fabrication and characts. 7-13891
 a-Si solar cells, fabrication methods using UHV reaction chamber system, high conversion efficiency 7-54293
 a-Si solar cells, insulator-semiconductor interface properties 7-13901
 a-Si solar cells, open circuit voltage 7-46935
 a-Si solar cells, vidicon mode characterisation 7-8421
 a-Si solar cells on textured Al substrate, prep. by chemical etching 7-23156
 a-Si solar cells prepared by thermal evap. 7-23140
 a-Si solar cells with spectral response shift, applicability of reference cell method to perform. meas. 7-59858
 a-Si technology, review of developments 7-38551
 a-Si, tetrahedrally bonded, bond angle disorder 7-32297
 Si, thermodynamic interrelation between amorphous, diamond cubic and liquid states 7-12245
 Si thin film, bulk trap spectroscopy by temp.-modulated space-charge-limited current meas. 7-45338
 Si, thin film, Raman spectroscopy, characterisation 7-53354
 Si:Ag, implantation damage regrowth studied via Ag depth profiling 7-22730
 Si:As⁺, epitaxial regrowth, CW Ar laser annealing (*Korean*) 7-27197
 Si:As⁺(As⁺), ion implanted, phys. props., spreading resist., TEM, Rutherford backscattering, SIMS 7-26775
 Si:B, amorphous, solar cell, roll-to-roll mass prod. process 7-17902
 Si:B, F implanted amorphous layers, struct. and elec. props., ESR and Hall effect meas. 7-26634
 Si:B, preamorphised, B diffusion during rapid thermal annealing 7-32717
 Si:B layers, preamorphised and-ion implanted, structural and elec. characterisation 7-52347
 Si:BF₃⁺, ion implanted, solid phase epitaxial growth, cross-sectional TEM study 7-38364
 a-Si:B(P)(As), implanted ion distrib., lateral spreading, theoretical predictions and computer simulation 7-16604
 Si:Cu, amorphous, explosive crystn., RBS and time-resolved reflectivity studies 7-21265
 Si:Cu, ion implantation-amorphised, direct imaging of pulsed laser-induced buried molten layers 7-12130
 a-Si:D,F, D NMR lineshapes and spin-lattice relax. studies 7-45836
 a-Si:D,F, plasma deposited, deuteron magnetic resonance 7-27626
 a-Si:D(D,H), deuteron mag. resonance, annealing effects 7-33292
 Si:F,H, amorphous, high efficiency solar cells fabrication and props. 7-17901
 a-Si:F,H films, glow discharge deposition, B doping efficiency 7-17436
 a-Si:H, ²⁹Si and ¹H NMR spectra, peak position and line shape 7-2934
 a-Si:H, ambipolar drift length meas. using steady-state photocarrier grating technique 7-45390
 α-Si:H, amorphous, coherent potential approx., potential well analogy 7-27240
 Si:H, amorphous, dendritic web, Czochralski flat plate modules and concentrator module, price comparison 7-17904
 Si:H, amorphous, p-i-n solar cells, stability behaviour, impurities and doping residues effect 7-17912
 Si:H, amorphous, solar cells, current-induced and light-induced degradation, non-equivalence 7-17908
 Si:H, amorphous film, optical absorption and bandgap rel. to temp. (*Korean*) 7-59228
 a-Si:H, amorphous to microcrystalline structure transformation, phase stabilisation 7-63475
 a-Si:H, B, P, As, dopant incorporation and doping efficiency 7-44587
 a-Si:H, B, P-type, increased elec. cond. studies 7-45337
 a-Si:H, B₂H₆(PH₃), localised density of states, electrophotography study 7-32957
 a-Si:H, broken bond local environment relax., g-factor, cluster calcs. 7-37876
 a-Si:H, bulk, surface state densities, Bethe lattice method, CPA calcs. 7-32898
 a-Si:H, C superlattice struct., solar cell performance 7-46945
 a-Si:H, carrier trapping and recombination, IR enhancement spectra of photoconductivity 7-33052
 a-Si:H, charge transport and relax., luminesc. long-time tail distribns. anal. 7-39185
 a-Si:H, conductivity, fundamental pre-exponential factor, Meyer-Neldel rule 7-7249
 a-Si:H, configurational models and adiabatic potentials of H 7-51632
 a-Si:H, contact resist. meas. technique 7-24658
 α-Si:H, cross-polarisation dynamics, NMR 7-53151
 a-Si:H, deep trapping, transient photocurrent saturation 7-21952

amorphous semiconductors continued

- a-Si:H, defect structure, ab initio theory 7-32298
 a-Si:H, density of states, SCLC meas., effect of injection electrodes 7-64265
 a-Si:H, deposition rates in diode and triode discharges 7-3193
 a-Si:H, distrib. of states study by capacitance-voltage method 7-7089
 a-Si:H, divacancy electron struct., semiempirical CNDO/2 cluster calcs. 7-38495
 a-Si:H, doped, electronic transport 7-21916
 a-Si:H, EXAFS, spherical wave anal. and multiple scatt. effects 7-64740
 a-Si:H, elastic properties 7-21323
 a-Si:H, electron traps, telegraph noise spectroscopy 7-21928
 a-Si:H, electronic density of states, DLTS and capacitance transient spectra anal. 7-45134
 a-Si:H, electronic struct., inadequacy of the conventional view 7-32961
 a-Si:H, electronic struct. modelling with small clusters 7-64057
 a-Si:H, electronic transport 7-33004
 a-Si:H, evaporated samples, post-hydrogenation, characts. 7-59103
 a-Si:H, extended state mobility and tail-state distrib. 7-2617
 a-Si:H, fluctuation induced gap states 7-27242
 a-Si:H, form. by ion flux control under toroidal mag. field (*Japanese*) 7-17446
 a-Si:H, gas-phase and ion-implantation doped, doping efficiencies 7-51790
 a-Si:H, glow discharge deposited, nucleation, substrate temp. effects 7-22504
 a-Si:H, glow discharge deposited, light soaking effects 7-52872
 a-Si:H, glow discharge deposition, surface roughness evolution 7-64933
 a-Si:H, glow discharge prepared, steady-state photoconductivity 7-38632
 a-Si:H, glow discharge thin films, deposition rate, optical props., influence of substrate temp. 7-59460
 a-Si:H, glow-discharge deposition, growth kinetics, radical separation technique 7-22513
 a-Si:H, H clustering, multiple quantum NMR 7-32671
 Si:H, H composition at surfaces and interfaces 7-27083
 a-Si:H, H₂ distrib., exodiffusion spectra 7-27026
 a-Si:H, influence of H on defects and instabilities 7-26647
 a-Si:H, intrinsic glow-discharge, elec. noise meas. 7-64297
 a-Si:H, laser-assisted CVD growth, optical props. 7-22210
 a-Si:H, light induced degradation at high illum., inverse Staebler-Wronski effect 7-23195
 a-Si:H, light soaked, dangling bond creation 7-12150
 a-Si:H, light-induced dangling bonds, annealing behaviour 7-12119
 a-Si:H, light-induced degradation 7-2047
 a-Si:H, light-induced electron spin resonance 7-33274
 a-Si:H, light-induced metastable dangling bonds, annealing 7-12118
 a-Si:H, localised electronic state, light soaking and current injection 7-16994
 a-Si:H, metastable defect states, capacitance studies 7-45225
 a-Si:H, mobility gap state transitions, transient photocapacitance studies 7-12669
 a-Si:H, NMR props. of ortho-H₂ centres 7-2935
 a-Si:H, neutral dangling bond defect, photocarrier processes 7-32962
 a-Si:H, non-exponential photocurrent decay, anal. 7-38633
 a-Si:H, optical dispersion relations, determ. 7-33353
 a-Si:H, photo-CVD deposition, initial processes (*Japanese*) 7-7053
 a-Si:H, photocond. response, light soaking effects 7-45396
 a-Si:H, photoconductivity and light-induced changes 7-2640
 a-Si:H, photoconductivity exponent for recombination at dangling bonds 7-33054
 a-Si:H, photocurrent, surface recombination effects 7-33048
 a-Si:H, photoinduced absorpt., ps decay 7-27684
 a-Si:H, photolum. and photoconductivity studies 7-33456
 a-Si:H, photoluminescence, high temp. annealing effects 7-7745
 a-Si:H, photoluminescence, thermal quenching 7-53389
 a-Si:H, picosecond photoinduced absorption and transmission 7-3006
 a-Si:H, picosecond photoinduced absorption decays, interference effects 7-3012
 a-Si:H, plasma deposited NMR, Pake doublet 7-27617
 a-Si:H, plasma enhanced CVD, integrated model 7-39423
 a-Si:H, prep. in rotary plasma isolated reactor and props. 7-7891
 a-Si:H, RF glow discharge prod., high deposition rate study 7-7889
 a-Si:H, RF sputtered, dangling bond electron spin-lattice relaxation 7-22141
 a-Si:H, RF sputtered, dangling bond energies, ESR studies 7-45818
 a-Si:H, recomb. at dangling bonds and steady-state photocond. Fermi level depend. calcs. 7-12734
 a-Si:H, SCL currents, step-by-step anal. 7-2623
 a-Si:H, Si-H-Si three centre bonds IR spectra, LCAO-MO-SCF-STO-3G calcs. 7-6741
 a-Si:H, Staebler-Wronski effect and metastable light-induced defect creation kinetics model 7-64284
 a-Si:H, surface deep hole trap, photocurrent studies 7-45424
 a-Si:H, surface structure, inert gas plasma exposure effects 7-21584
 a-Si:H, thermal-equilib. processes, electronic transport 7-64167
 Si:H, transient photoconductivity characterisation 7-52692
 a-Si:H, triplet exciton recomb., ODMR studies 7-2490
 a-Si:H,B, effective p⁺ doping by plasma-assisted B diffusion 7-38036
 a-Si:H,B, thin films, thermoelectric power 7-58826
 a-Si:H,B films, hole transport, time-of-flight meas. 7-45320
 a-Si:H,B p-i-n and n-i-p solar cells, doping profile effects 7-46947
 a-Si:H,B/a-Si:H,P doping modulated superlattice, photo-induced excess conductivity 7-17051
 a-Si:H,B(As) RF sputtered coatings, gas-phase doping efficiency 7-63471
 a-Si:H,B(P) films, dopant conc. meas. and depth profiling by means of (p,γ) resonant reactions 7-12555
 a-Si:H,B(P) films, optical props. 7-64720
 a-Si:H,Cl glow discharge films, Raman scatt. 7-39116
 a-Si:H,D, H abstraction from surface, HD formation 7-39914
 Si:H,F by thermal CVD, photosensitivity, spin density, conductivity and p-n type 7-17454
 a-Si:H,F films, dark discharge mechanism of surface potential (*Japanese*) 7-17034
 a-Si:H,F films, glow discharge decomposition from Si₂F₆ 7-64924
 a-Si:H,F films, H-radical-assisted CVD, hole transport 7-64264
 a-Si:H,F films, initial carrier trapping stages observed by femtosecond spectroscopy 7-27301
 a-Si:H,F films, prep. using H radical assisted CVD (*Japanese*) 7-17430
 a-Si:H,F multijunction solar cells, performance data 7-40011
 a-Si:H,F solar cells, radiation hardness to 1 MeV protons 7-23180
 a-Si:H,F/a-Si,Ge,H,F superlattices, elec. transport studies 7-38716

amorphous semiconductors continued

- Si:H,F/a-Si:H,F,Ge multiple junction solar cells on stainless steel substrates 7-13902
- a-Si:H,F/a-SiGe₂H,F multiple layered films for enhancement in photoreponse in near IR spectrum 7-52668
- a-Si:H,F-Si_{0.4}Ge_{0.6}H,F superlattices, carrier scatt., optical absorpt. study 7-38711
- Si:H,Ge single junction and tandem solar cells, thin film properties and corollary plasma diagnostics 7-13893
- a-Si:H,N thin films, activated reactive evaporation 7-13355
- a-Si:H,O films, RF sputtered, photoelec. props. 7-38627
- a-Si:H,P, electron lifetime, excitation energy depend. 7-45349
- a-Si:H,P multilayer films, plasma CVD and elec. cond. studies 7-39428
- a-Si:H,P(B) films, ion implanted, photoelectric and optical props. 7-38615
- a-Si:H,P(B) p-i-n solar cells, open-circuit volt., wavelength depend. 7-46948
- a-Si:H (C,H) (O,H) (N,H), annealing of metastable defects 7-3343
- Si:H amorphous, recombination-enhanced defect reactions, reversibility 7-45343
- a-Si:H and a-Si films, electrical conductivity and struct. 7-52866
- a-Si:H and a-Si:H, B films, photoinduced changes in elec. props. 7-38634
- a-Si:H and a-Si:H,P, electron nuclear double resonance expts. 7-2950
- Si:H based alloy thin films, optical constants determ., device modelling appl. 7-7666
- a-Si:H based alloys for solar cells, elec. props. and degradation behaviour 7-52642
- a-Si:H biased activated reactive layer evaporation and charactn. 7-59428
- Si:H binary alloys, crystallisation of polysilane 7-21105
- a-Si:H CVD coating, high temp. elec. cond. meas. 7-45336
- a-Si:H CVD films, density of states distrib., I-V characts. meas. 7-45113
- a-Si:H doping modulated films, photocond., carrier separation effects 7-38641
- a-Si:H doping modulated multilayers, light-induced excess conductivity 7-38643
- a-Si:H doping modulated superlattices, light-induced excess cond., deposition effects 7-27410
- a-Si:H doping superlattice interface struct. charactn. 7-58652
- a-Si:H evaporated layer production from RF discharge, growth mechanism and props. 7-64898
- a-Si:H film, photo-assisted plasma CVD 7-33593
- a-Si:H film, photoenhanced deposition and characts. 7-53635
- a-Si:H film prep. by compressed mag. field magnetron sputtering (Japanese) 7-46323
- a-Si:H films, annealed, structural changes, PMR studies 7-7596
- a-Si:H films, annealing, compressive stress, H evolution 7-28059
- a-Si:H films, bond angle distortions, substrate temp. effects, Raman study 7-7882
- a-Si:H films, CVD, electrical and optical props. 7-33596
- a-Si:H films, CVD, optical and electronic props. 7-33597
- a-Si:H films, CVD using microwave excited Ar plasma stream 7-64918
- a-Si:H films, carrier transport 7-17023
- a-Si:H films, charge carrier dynamics, influence of preparation conditions 7-33053
- a-Si:H films, columnar morphology, evolution of vibr. spectra 7-64646
- a-Si:H films, contact potential difference, surface photovoltage and conductivity 7-58855
- a-Si:H films, deep levels in the mobility gap 7-12670
- a-Si:H films, density of states and photoconductivity 7-45392
- a-Si:H films, depth profiling of constituents and impurities, elastic proton scatt. 7-45044
- a-Si:H films, discharge and CVD deposition, surface reactions 7-33601
- a-Si:H films, electron irradi., photocond., absorpt. coeff. spectral depend. 7-64279
- a-Si:H films, electronic props., effects of γ -irradiation 7-38584
- a-Si:H films, glow discharge deposited, persistent photoconductivity 7-58835
- a-Si:H films, glow discharge deposition 7-65325
- a-Si:H films, glow-discharge-deposition, initial nucleation and growth 7-63997
- a-Si:H films, growth and photovoltaic appls. 7-64236
- a-Si:H films, growth habit, influence of substrate struct., ellipsometry, study 7-45055
- a-Si:H films, high rate deposition and impurity doping effects (Japanese) 7-13385
- a-Si:H films, high rate deposition by RF planar magnetron sputtering (Japanese) 7-39373
- a-Si:H films, laser induced CVD using SiH₄ photodecomposition 7-13376
- a-Si:H films, light-induced bond breaking 7-12517
- a-Si:H films, light-induced defects and internal stresses 7-12751
- a-Si:H films, metal-semiconductor contacts, characterisation 7-38724
- a-Si:H films, metastable optically induced ESR, time depend. 7-45800
- a-Si:H films, photo-CVD from SiH₄-H₂ 7-39394
- a-Si:H films, photo-enhanced CVD 7-33594
- a-Si:H films, photochemical vapour deposition from SiH₄-H₂ 7-64916
- a-Si:H films, photocond. characts. stabilisation (Japanese) 7-45393
- a-Si:H films, photoconductivity, thermal quenching obs. 7-52686
- a-Si:H films, plasma CVD, deposition kinetics (Japanese) 7-17450
- a-Si:H films, RF glow discharge deposition, optical and electrical props. 7-33598
- a-Si:H films, reactive deposition 7-33592
- a-Si:H films, sputter deposition, optical and ESR props. 7-33565
- a-Si:H films, thermal-equilibrium defect processes 7-26640
- a-Si:H films and p-i-n solar cells, photo-assisted CVD and opto-electronic characterisation 7-33595
- a-Si:H films and solar cells, light induced effects 7-46954
- a-Si:H films deposited by dual ion beam sputtering, characterisation 7-32882
- a-Si:H films deposited in He atmosphere, characts. 7-45056
- a-Si:H films high-rate deposition by RF planar magnetron sputtering (Japanese) 7-1419
- a-Si:H films photo-CVD, photoelectric and structural props. 7-7869
- Si:H films preparation by CVD 7-17453
- a-Si:H films with columnar morphology, Raman scatt. study 7-64644
- Si:H heterojunction solar cell modules, fabrication by laser scribing 7-13900
- a-Si:H high efficiency p-i-n solar cells using superlattice p-layers 7-23177
- a-Si:H junction position sensitive photodetector 7-56343
- a-Si:H large area integrated solar cells, fabrication 7-40013

amorphous semiconductors continued

- a-Si:H material and p-i-n cell, light-induced charge 7-17055
- a-Si:H material and solar cells, light induced effects 7-23139
- Si:H microcrystalline films, glow discharge prep., elec. and optical props. 7-7415
- a-Si:H modulation doped multilayers, persistent photocond. studies 7-38642
- a-Si:H modulation doped multilayers, planar and perpendicular cond. meas. 7-38717
- a-Si:H multilayer films, charge transfer doping, cond., photocond. meas. 7-38735
- a-Si:H p^+-i-n^+ struct., freq.-depend. noise studies 7-45484
- Si:H p^+-n-i structs., memory switching, transient current instability study 7-52762
- a-Si:H p-i-n solar cells, behaviour after light soaks through p-layer and n-layer 7-8398
- a-Si:H p-i-n solar cells, light induced degradation, effects of impurities and temp. 7-17886
- a-Si:H photo-CVD coatings, characterisation using TFT structure 7-38561
- a-Si:H pin solar cells, open-circuit volt., temp. and light intensity depend. 7-46949
- a-Si:H pin solar cells, photocurrent, transient behaviour 7-46950
- a-Si:H semiconductor-metal system, field effect problems, I-V meas. 7-38728
- a-Si:H short range order, impurity distrib. effects, EXAFS study 7-64761
- aSi:H solar cell characts. change due to long term temp. stresses 7-8393
- a-Si:H solar cell on polymer substrate, roll-to-roll prep. 7-59861
- a-Si:H solar cell prep. by laser-induced CVD of SiH₄ 7-7890
- a-Si:H solar cell technology in Japan, recent advances 7-40009
- a-Si:H solar cells, density of states asymmetry effects 7-46946
- Si:H solar cells, dynamic equilibrium dangling bond density 7-17878
- a-Si:H solar cells, hydrogenated microvoids and light-induced degradation 7-54294
- a-Si:H solar cells, impurities and metastable centres 7-40010
- a-Si:H solar cells, integrated series connection 7-40015
- a-Si:H solar cells, kinetics of light-induced degradation and thermal annealing 7-17909
- a-Si:H solar cells, leakage currents, electrochem. treatment effects 7-65467
- a-Si:H solar cells, optically induced degradation 7-59848
- Si:H solar cells, p-layer doping by plasma assisted B diffusion 7-13898
- a-Si:H solar cells, photo-CVD prep. 7-17885
- a-Si:H solar cells, photoconductivity-open cct. voltage relation 7-8396
- Si:H solar cells, radiation damage by 12 MeV protons and annealing 7-13895
- a-Si:H solar cells, turn-off character, wavelength depend. 7-46951
- a-Si:H solar cells, uses of transparent conducting oxides 7-46953
- Si:H solar cells deposited from disilane, blue response and efficiency improvement 7-17877
- a-Si:H solar cells eval., quantum efficiency meas. techniques 7-54314
- Si:H solar cells on textured glass substrate with SiO₂ film 7-13899
- a-Si:H solar cells prod. by positive-column glow-discharge method 7-8397
- Si:H solar cells stability, role of Si-H bonds studied by Fourier transform infrared spectroscopy 7-13896
- a-Si:H sputtered film, low-temp. optical props. 7-3101
- a-Si:H sputtered films, intrinsic stress, H effects 7-7078
- a-Si:H stable heterojunction solar cells develop., thermal degradation phenomenon 7-65477
- a-Si:H surfaces and interfaces, microstruct., ellipsometry studies 7-38362
- Si:H thin film photovoltaic production, safety and industrial engineering 7-13894
- Si:H thin film solar cells, device properties 7-13897
- a-Si:H thin film solar cells, repeatable meas. system for accelerated stress testing 7-23174
- a-Si:H thin film solar cells, light soaking condition effects 7-46956
- a-Si:H thin films, bulk and interface struct., in situ ellipsometry study 7-27200
- a-Si:H thin films, elec. and optical props., thickness depend. 7-46168
- a-Si:H thin films, ohmic and quasi-ohmic contacts 7-38729
- a-Si:H two-junction, two-terminal tandem solar cells, stability and efficiency 7-46957
- a-Si:H ultrathin layers, CW photoluminescence, layer thickness depend. 7-13202
- a-Si:H ultrathin layers, photoluminescence characts., layer thickness depend. in variety of sample configurations 7-46123
- a-Si:H/CdTe heterojunction, X-ray image sensor fabrication 7-41557
- a-Si:H/CuInS₂ heterojunctions, photovoltaic behaviour, c-v meas. 7-7340
- a-Si:H/Ge:H superlattice struct., light absorption and photocond. studies 7-38715
- a-Si:H/Pd system, silicide form., struct. and electronic props. 7-38363
- a-Si:H/SiC tandem solar cell, thermal and light-induced degradation 7-46955
- a-Si:H/SiN_x interface, slow states, transient photoconductivity studies 7-38670
- a-Si:H/SiN_x:H (a-SiC:H) double-barrier structs., resonant tunnelling coeffs. 7-45467
- a-Si:H/SiO₂:N,H heterostruct., transport props 7-38768
- a-Si:H/SiO₂/metallic gate struct., capacitance-volt. characts. 7-45515
- a-Si:H/Ti/Al system, solid state reactions, TEM and SAD studies 7-3602
- a-Si:H/a-Ge:H multilayer films, photoconductivity enhancement 7-27443
- $n^+-a-Si:H/a-Si:H/a-SiC:H$ heterostructures, electrophotographic props. 7-45485
- a-Si:H/a-Si_{0.2}C_{0.8}H superstructures, hot electron conduction 7-45453
- a-Si:H/a-Si_{1-x}C_xH solar cells, light trapping on SnO₂:F 7-46952
- a-Si:H/a-Si_{1-x}C_xH superlattices, glow-discharge deposition 7-7879
- a-Si:H/a-Si₃N₄H superlattices, plasma deposition methods 7-39439
- a-Si:H/a-SiC:H heterojunction, valence-band discontinuity, photocurrent-voltage measurements 7-58868
- a-Si:H/a-SiGe:H multilayers, reactive deposition 7-33592
- a-Si:H/a-SiN_x:H, amorphous multilayer structures, optical props. 7-3014
- a-Si:H/a-SiN_x:H heterostructures, interface formation and microstructural evolution 7-2389
- a-Si:H/a-SiN_x:H interface system, struct. and electronic props. 7-38361
- a-Si:H/a-SiN_x:H interface, deep states and photoluminescence spectra, transistor characts. 7-39186
- a-Si:H/a-SiN_x:H multilayer films, coplanar conductance, voltage-induced anomalies study 7-2729

amorphous semiconductors continued

- a-Si:H/a-SiN_x:H superlattices, interface struct., optical reflectance determ. 7-12497
- a-Si:H/a-SiN_x:H superlattices, interface defects and disorder 7-52306
- a-Si:H/a-SiN_x:H superlattice interface struct. charactn. 7-58652
- a-Si:H/a-SiN_x:H superlattice films, prep., struct., and optical props. (Chinese) 7-58676
- a-Si:H/a-SiO₂:H superlattice micropores, pyrene molecules adsorption and confinement 7-27112
- a-Si:H/a-SiO(N)_x:H multilayer films, interface electroabsorpt. meas. 7-2689
- a-Si:H/c-Si heterojunctions, energy-band discontinuities, internal photoemission studies 7-58869
- a-Si:H/c-Si heterojunctions, reverse current characteristics 7-58887
- a-Si:H/crystalline Si heterojunction, photosensitivity studies 7-38714
- a-Si:H/metal junction, pot. profile determ. 7-2715
- Si:H-CuInSe₂ thin film tandem solar cells, energy based perform. and eval. 7-13890
- a-Si:H-Pt Schottky barrier contact, photocurrent excitation nonadditivity effects 7-17099
- Si:H-Si_{1-x}C_x:H amorphous super struct., hot electron generation 7-52794
- a-Si:H-Si₃N₄:H double barrier structures, resonant tunnelling 7-52848
- Si:H-SiC:H heterojunction, amorphous solar cell anal. (Chinese) 7-34029
- a-Si:H-SiN_x:H, multilayer struct. study using HREM 7-16879
- a-Si:H-SiN_x:H interface, compositional profile, Rutherford backscatt. study 7-13292
- a-Si:H-SiN_x:H layered structures, effect of a-SiN_x:H composition on band bending near interface 7-45510
- a-Si:H-based films, photochemical vapour deposition, review 7-46345
- a-Si:H-based heterojunction stacked solar cells, design and fabrication 7-40012
- a-Si:H(F), mobility edge, density of states and carrier activation energy calcs., random Bethe lattice approach 7-16937
- Si:H(F)-SiGe:H(F) amorphous multilayer struct., fabrication and near IR photoconductivity characts. 7-52797
- Si:H(Sn,H)(C,H), amorphous alloy fabrication and characterisation 7-8389
- Si:Hg⁺, ion implant range distributions, Rutherford backscatt. studies 7-2073
- Si:In, amorphous, low temp. annealing, impurity diffusion, phase separation and crystn. studies 7-16808
- a-Si:P, selective doping and solid phase epitaxial growth, MOSFET appls. 7-27893
- Si:P(Al), random and channelled implantation profiles and range parameters of dopants 7-21246
- Si:P(B) LPCVD films, amorphous and polycrystalline, struct., elec. resist. meas. 7-52870
- Si:Sb,As, cryst. aid amorphous, impurity band form., X-ray spectra studies 7-12650
- a-Si:Se(Te) thermally evaporated films, photoelectronic props. 7-38640
- Si:Zn, amorphous-crystalline interface, backscattering and channelling study 7-6663
- a-Si/Al films, laser-induced phase transitions, time resolved TEM study 7-38056
- a-Si/Au thin film bilayers, Si crystallisation study 7-21699
- a-Si/c-Si interface, microcrystallites and orientational proximity effect, HREM image interpretation, comment and reply 7-45028
- Si/Ge amorphous layered system, implanted ion depth distribns. 7-21250
- Si/Ge amorphous multilayer films, interdiffusion, neutron scatt. meas. 7-32722
- Si/metal interfaces, silicide form. kinetics during thermal annealing 7-16897
- a-Si/Si(111) interface ordering, X-ray diffr. 7-32848
- Si/Ti amorphous superlattices, high resolution photovoltaic position sensing 7-48847
- a-Si-Ge multilayer films, interdiffusion, modulation wavelength depend. 7-27033
- a-Si-Ge multilayer interfaces, Raman scatt., X-ray diffr. characterisation 7-27167
- a-Si-metal-Si structures, rapid thermal sintering and annealing 7-21700
- Si-polyethersulphone, amorphous, solar cell development 7-8394
- Si-SiC superlattice structures, prep. by photo-CVD, solar cell appl. 7-54326
- a-Si-SnO₂ interface, solid state reaction, XPS study 7-22449
- Si-Ti amorphous superlattices, electronic and photoelectronic props. 7-12795
- Si-Ti amorphous superlattice films, lateral photoeffect 7-45487
- Si-Ti amorphous superlattice films, lateral photovoltage, wavelength dependence 7-45488
- Si-Ti thin-film superlattices, structure 7-38350
- a-Si_{1-x}C_x:H films prepared by plasma CVD method, props. (Japanese) 7-12543
- a-(Si-Ge)_xH, prep. in rotary plasma isolated reactor and props. 7-7891
- a-SiC films, glow discharge deposition from tetramethyldisilane 7-64919
- a-SiC films, photo-assisted CVD and opto-electronic characterisation 7-33595
- a-SiC films, photochemical vapour deposition, review 7-46345
- SiC:H, amorphous CVD film, electron optical characterisation 7-52372
- a-SiC:H, elec., optical and local structure props. 7-45089
- a-SiC:H, RF sputtered, dangling bond electron spin-lattice relaxation 7-22141
- a-SiC:H,B, effective p⁺ doping by plasma-assisted B diffusion 7-38036
- a-SiC:H,B, thin films, thermoelectric power 7-58826
- SiC:H,F amorphous films, struct., elec. and optical props. 7-22360
- SiC(H,F), amorphous, electronic and structural props. 7-17054
- SiC:H amorphous films, glow discharge deposited, photoconductivity, microstructure effects 7-58831
- a-SiC:H film prepared by magnetron sputtering, elec. and optical props. (Japanese) 7-12887
- a-SiC:H films, CVD, electrical and optical props. 7-33596
- a-SiC:H glow discharge films, IR vibr. spectra 7-53434
- a-SiC:H glow-discharge plasma deposition, photosensitivity, prep. conditions depend. 7-46338
- a-SiC:H thin films, glow discharge deposition, energy gap and activation energy 7-46352
- a-SiC:H/a-Si:H double-barrier structs., resonant tunnelling coeffs. 7-45467
- a-SiC:H/a-Si:H/n⁺-a-Si:H heterostruct., electrophotographic props. 7-45485
- SiC:H-Si:H heterojunction, amorphous solar cell anal. (Chinese) 7-34029
- a-SiC:H-a-Si:H, solar cell, fabricated by plasma deposition (Korean) 7-33585

amorphous semiconductors continued

- a-SiC:H(B), thin film, solar cells fabricated by plasma deposition (Korean) 7-33585
- a-SiC-a-Si:H stable heterojunction solar cell 7-23178
- a-Si_{1-x}C_x:H films, glow discharge deposition, optical emission spectroscopic diagnostics 7-39412
- a-Si_{1-x}C_x:H/a-Si:H solar cells, light trapping on SnO₂:F 7-46952
- a-Si_{1-x}C_x:H, B(P) films, valence band localised holes, light-induced ESR spectra studies 7-53110
- a-Si_{1-x}C_x:H, Si-K β spectra, soft X-ray emission spectra (Japanese) 7-13268
- a-Si_{1-x}C_x:H, valence band, UPS studies (Chinese) 7-38443
- a-Si_{1-x}C_x:H,B(P) thin films, H bonding and H content, IR spectra studies (Chinese) 7-12524
- Si_{1-x}C_x:H films, amorphous, bond lengths, comp. depend., EXAFS study 7-64757
- a-Si_{1-x}C_x:H thin films, struct. investig., electron diffr. studies 7-2430
- Si₂C_{1-x}:H, local atomic arrangement, EELS and electron diffraction 7-44378
- a-Si_xC_{1-x}:H films, adsorbates influence on conductance, surface state 7-33115
- a-SiGe:D, F, vibr. modes, Fourier transform IR spectra studies 7-46053
- a-SiGe:D,F, plasma deposited, deuteron magnetic resonance 7-27626
- SiGe:F,H, amorphous, high efficiency solar cells fabrication and props. 7-17901
- SiGe:F solar cells, chemical basis for high efficiency 7-17884
- SiGe:H, amorphous, electronic and structural props. 7-17054
- SiGe:H, amorphous, p-i-n solar cells, stability behaviour, impurities and doping residues effect 7-17912
- SiGe:H, amorphous, solar cell efficiency improvement using graded band-gap layer at i/n interface 7-54327
- a-SiGe:H, F glow discharge films, elec. and optical props. 7-46169
- a-SiGe:H,F alloy films, F incorporation and annealing props. 7-44588
- a-SiGe:H,F alloys for solar cells, prep. by DC and RF discharge deposition 7-17900
- a-SiGe:H,F films, glow discharge deposition and elec. props. 7-64917
- a-SiGe:H,F glow discharge films, microcrystallinity studies 7-45088
- a-SiGe:H,F glow discharge films, electronic transport and density of states 7-45114
- a-SiGe:H,F solar cells, radiation hardness to 1 MeV protons 7-23180
- a-SiGe:H,F/Pd(Au)(Ni), Schottky barrier height, internal photoemission meas. 7-45501
- a-SiGe:H alloys for solar cells, electronic and optical props. 7-17899
- SiGe:H amorphous films, glow discharge deposited, photoconductivity, microstructure effects 7-58831
- a-SiGe:H films, CVD, electrical and optical props. 7-33596
- a-SiGe:H films, NMR, ESR and IR studies 7-45833
- a-SiGe:H films, photo-assisted CVD and opto-electronic characterisation 7-33595
- a-SiGe:H glow discharge films, field effect density of states determ. 7-21796
- SiGe:H solar cells preparation by photo-CVD 7-17885
- a-SiGe:H thin films for solar cells, electrical and structural properties relationship 7-17898
- a-SiGe:H/a-Si:H multilayers, reactive deposition 7-33592
- a-SiGe_xH_{1-x}/a-Si:H,F multiple layered films for enhancement in photoreponse in near IR spectrum 7-52668
- a-Si_{1-x}Ge_x:H/Al Schottky barrier form. and characts. 7-12787
- a-Si_{1-x}Ge_x:H/a-Si:H/Al Schottky barrier form. and characts. 7-12787
- Si_{1-x}Ge_x:H films, optical band gap, photocond. props. 7-52672
- a-Si_{1-x}Ge_x:H, electron and hole transport 7-7259
- a-Si_{1-x}Ge_x:H, F, light-induced degradation meas. 7-45397
- a-Si_{1-x}Ge_x:H,F alloy films, RF glow discharge deposition in ultrahigh vacuum reactor 7-53619
- Si_{1-x}Ge_x:H amorphous alloys, electronic struct., soft X-ray and photoelectron spectra studies 7-27857
- Si_{1-x}Ge_x:H films, amorphous, bond lengths, comp. depend., EXAFS study 7-64757
- Si₂Ge_{1-x}:H,F amorphous films, struct., elec. and optical props. 7-22360
- α -SiGeH, electronic and transport props., coherent potential approx. 7-27241
- α -SiH, electronic and transport props., coherent potential approx. 7-27241
- Si₂H₄, amorphous alloy films, microstructure, XPS study 7-22436
- a-SiN:H, electrical behaviour 7-2627
- a-SiN:H films, optical absorption const. evaluation by photothermal deflection spectroscopy 7-22361
- a-SiN_x amorphous glow discharge films, gap state distrib., photocurrent phase shift anal. 7-7421
- a-SiN_x:H CVD film, IR and ²⁹Si NMR studies 7-38952
- SiN_x:H films, amorphous, bond lengths, comp. depend., EXAFS study 7-64757
- a-SiN_x:H plasma-enhanced CVD film props. rel. to SiH₄-N₂ gas vol. ratio, RF power and substrate temp. (Korean) 7-3201
- a-SiN_x:H/a-Si:H double-barrier structs., resonant tunnelling coeffs. 7-45467
- a-SiN_x:H/a-Si:H interface system, struct. and electronic props. 7-38361
- a-SiN_x:H/a-Si:H interface, deep states and photoluminescence spectra 7-39186
- a-SiN_x:H/a-Si:H superlattice films, prep., struct., and optical props. (Chinese) 7-58676
- a-Si_{1-x}N_x:H,B films, ESR and IR spectra studies 7-7780
- a-Si_{1-x}N_x:H films, H₂ evolution 7-17445
- a-Si₂N_{1-x}:H,B films, DC sputtered, photoelectronic and optical props. 7-27361
- a-SiO₂:H films, local struct. EXAFS study 7-59291
- a-SiSn:Cl,H glow discharge films, elec. and optical props. (Chinese) 7-58805
- a-Si_{1-x}Sn_x:H films, electronic structure of divalent defects 7-32960
- a-Si_{1-x}Te_x amorphous alloys, electronic and optical props. 7-7234
- Si_{1-x}(ZnS)_x:H amorphous films, synthesis and characterisation 7-17420
- a-Si solar cells, transparent Ag contacts and ITO antireflection coating 7-65478
- V₂O₅ and Li₂V₂O₅, amorphous thin films, electrical conductivity 7-58921
- V₂O₅-P₂O₅-Bi₂O₃(Sb₂O₃) glasses, DC conductivity 7-45316
- V₂O₅-TeO₂ glasses, memory switching 7-27370
- V₂O₅-TeO₂-PbO, elec. and optical props. (Korean) 7-27330
- ZnO-V₂O₅ glasses, DC conductivity 7-27327
- Zn₃P₂ amorphous films, preparation and optical props. 7-13360
- Zn₃P₂ thin films, amorphous-crystalline transitions, elec. cond., 100-300K 7-38560

amorphous state

- see also electrical conductivity of amorphous metals and alloys; electrical conductivity of amorphous semiconductors and insulators; electron energy states of amorphous solids; magnetic properties of amorphous substances; vitreous state
- alloy thin films, thermal stability 7-21761
- alloys, amorphous, partial pair distribution function determ. 7-51640
- alloys, amorphous, struct. features, HREM 7-1883
- alloys, amorphous and liquid, internal press. kinetic component, eqn. of state calc. (Russian) 7-2139
- alloys, cold shortness (Russian) 7-39649
- alloys, double-layer struct. unit model 7-16423
- alloys, icosahedral and amorphous structures, fractal coefficients 7-26646
- alloys, isothermal compressibility, theoretical analysis (Russian) 7-58391
- alloys, Laves phase, liquid quenching, transformations and phase diagrams 7-65059
- alloys, rapidly solidified, conf., Boston, MA, USA (Dec. 1985) 7-18496
- alloys with immiscible metallic particles, superconducting props. 7-2791
- crystallisation, cubic crystalline precipitate morphology, strain energy effects 7-26963
- diffusion-controlled interfacial growth, dense branching morphology form. 7-21147
- disordered solids, hydrogen absorption, model 7-26970
- ethyl cellulose, sintering, activation energy 7-64998
- film, crystallisation kinetics, statistical model 7-16426
- gas transport, structural implications 7-63870
- heat capacity of two-level systems, kinetic theory (Russian) 7-58502
- heat capacity theory for amorphous media (Russian) 7-52074
- ice, amorphous high-density struct. by neutron diffr. 7-37865
- ice, cryst. and amorphous, positronium formation at low positron energy 7-27815
- Lennard-Jones solid, shear deform.-induced orientational ordering, computer simulation 7-38155
- magnetic resonance lineshapes, computation for EPR and NMR 7-2922
- metal alloy hydrides, disordered, theory of electronic states 7-27243
- metallic glasses-H₂, mechanical relaxation behavior 7-26859
- metals, interstitial diffusion and trapping, Monte Carlo simulations 7-32721
- metals, multiple scattering effects, cluster calcs. 7-7100
- molecular glasses, β -processes anal. 7-20074
- optical data storage, phase-change properties, transition metal elements effects 7-50662
- pentacene, vacuum deposited amorphous films, X-ray diffr. and photoelectron spectra anal. 7-22434
- polyarylates, amorphous, glassy, plastic deform. in stress relax. and creep regimes (Russian) 7-63730
- polyesters, aromatic, conformational reorganisation viewed by Raman spectra 7-32311
- polymeric liquids and glasses, equations of state, multiple hole energy model 7-21388
- polymers, secondary relax. processes, thermal history effect 7-63819
- polystyrene, tensile strength, effects of temp. and mol. wt. (Japanese) 7-33737
- positron lifetime spectrum in amorphous materials, annealing effects (Chinese) 7-27814
- PTFE, amorphous and cryst., irradiated, thermal characts. (Russian) 7-6681
- stainless steel films, amorphous and amorphous-crystalline with refractory metal additions, magnetron sputtering 7-39380
- STEM technique for quantifying ang. correl. 7-21057
- superconductors, disordered and amorphous nontransition metals and alloys, electron-phonon coupling strength and phonon spectrum calcs. 7-52889
- surface modification by ion beam methods, review 7-27081
- targets, sputtered particles, angular distrib. 7-59342
- thermal cond. w.r.t. phonon-fracton anharmonic interactions 7-2283
- thermal conductivity, temp. dependence 7-21553
- thin films, conference, India (Jan. 1985) 7-4619
- thin films, stress meas. during deposition, review 7-52380
- thin targets, mean scatt. angle, first moments of longit. distrib., elastic losses of ion energy 7-26806
- transition metal alloys, amorphous, short-range order, approx. to coherent locator (Russian) 7-58731
- transition metal alloys, disordered; electron struct. and positron annihilation (Russian) 7-45133
- transition metal alloys, liquid and amorphous, chemical short-range order, electronic theory 7-44349
- transition metal amorphous alloy coatings, microindentation response, microstruct. and composition effects 7-46625
- transition metal silicide layers, electron microscope exam. (German) 7-45081
- X-ray diffraction analysis of amorphous materials, features and rel. between methods (Japanese) 7-21119
- zirconia transparent gel-monolith from Zr alkoxide, controlled hydrolysis prep. 7-8313
- Al (100), polycryst., single cryst. and amorphous, ballistic collision cascade anisotropies 7-58379
- Al-a-Nb₂O₃, heterostructure, morphology, electrophysical parameters 7-13394
- Al-Mn alloys, local struct., EXAFS study 7-63466
- Al-V alloys, phase transitions between amorphous, quasicrystalline and crystalline phases 7-63807
- Al₂O₃, film, prep. by pyrolysis of Al isopropylate 7-17448
- Al₂O₃ film, transparent, growth from ultrafine alumina sol characteris. 7-13395
- Al₂O₃, formation and annealing, ion irradiation 7-58385
- α -Al₂O₃, ion implantation, crystallisation of amorphous surface layers 7-58304
- Al₂O₃-TiO₂ amorphous films, thermal expansion and coordination state of cations 7-44860
- As, amorphous, vibr. density of states, EXAFS, Debye-Waller factors 7-64820
- As₂S₃, amorphous, low freq. light scatt. 7-27714
- BN, film, optical and compositional props. 7-39206
- BN, ion-plated, prep. and charact. 7-17477
- Bi-Ag, struct. of 10 mole % Ag alloy, liq. and amorphous states 7-6512
- C, amorphous film, modification by inert gas ion irradiation 7-64018
- C, extinction spectra of submicron grains in UV-visible range 7-35023
- a-C films, crystallisation, influence of residual stresses and density fluctuations 7-21750
- C layers, arc plasma deposition, struct., mech. props. (Russian) 7-22581

amorphous state continued

- a-C thin films, bonding core-EELS and ¹³C NMR studies 7-21099
- a-C:H, diamondlike, dielectric film, props. rel. to deposition parameters 7-39419
- a-C:H, film, optical and compositional props. 7-39206
- a-C:H, film, optical and electronic props. rel. to deposition parameters 7-38406
- a-C:H, film, optical energy gap, density, hardness 7-39204
- a-C:H, film, plasma emission spectroscopy, chem. anal. 7-38407
- a-C:H, films, plasma deposition characterisation of hydrocarbons used 7-39422
- a-C:H, props., review 7-51630
- C:H amorphous film's, plasma deposition, discharge elec. characteristics 7-46344
- C:H amorphous films, glow discharge deposited from CH₄+H₂, annealing behaviour 7-64922
- a-C:H films, glow discharge deposited, valence electron props., electron energy loss spectra study 7-13288
- a-C:H plasma grown films, struct., physical props. 7-58713
- a-C:H polymeric layers, plasma-activated CVD produced, spectroscopic investigations 7-22572
- CO₂, amorphous solid, mol. vibr., IR spectra anal. 7-53307
- Co₇₀Si₃₀ amorphous films, coercive force rel. to crystallisation (Russian) 7-59078
- CaTiO₃, ion implantation, crystallisation of amorphous surface layers 7-58304
- Ce-Si(Ni)(Co), amorphous, electronic configuration of Ce 7-7191
- Co-P, amorphous, pulse plated, electrochemical props., corrosion resist. (Japanese) 7-53954
- Co-Y alloys, low temp. sp. ht. study, crystalline and amorphous phases 7-52995
- CoFeMoB amorphous thin films, prep. and high-freq. impedance studies 7-53585
- (Co_{0.85}Fe_{0.06}Ni_{0.08}Nb_{0.01})₇₅Si₁₀B₁₅ amorphous alloys, structural relax. and crystn., positron annihilation studies 7-37869
- Co₈₅Fe₂Si₁₂B₂ amorphous alloys, annealing, positron annihilation parameters anal. 7-39303
- Co₇₅Si₁₀B₁₅, amorphous powder, static consolidation, mechanical and mag. props. 7-3217
- Co₇₇Si₁₀B₁₃, structural anal. (Korean) 7-26637
- Co₂₅Ti₇₅, amorphous struct., neutron and X-ray diffr. 7-58149
- Cr-Ni (45 wt.%) amorphous free-standing thin films, struct. transformations, pulse laser irradiation 7-38382
- Cr₇₅Si₂₅ thin films, microstruct. and resist., room temp. to 950°C 7-38410
- Cu-Ti alloys, amorphous and crystalline, H absorption 7-2369
- Cu-Zr amorphous alloy, induced recrystallisation by electron and laser beam irradiation 7-12152
- Cu_{0.85}Sn_{0.15}, amorphous melt-quenched alloys, crystn. (Russian) 7-37881
- Cu₄₈Ti₅₂, amorphous, crystallisation, intermediate long period superlattice phase form. 7-21098
- CuTiH_x, amorphous hydrides, quasi elastic and inelastic neutron scatt. 7-21382
- Cu₁₀Zr₇, cryst. and amorphous, muon spin resonance studies 7-53196
- e⁻ scavenging, generalized master eqn. theory 7-21884
- Eu, Pd_{1-x}, amorphous mixed valent alloys, X-ray absorpt. spectra 7-64802
- (Fe, Co, Ni)-P layers, electrochemical deposition, struct. (Chinese) 7-7037
- Fe, with Cr-C, Cr-Mo double layer films, Ar and Xe ion bombardment (Chinese) 7-51885
- Fe-B, amorphous alloys, crystallisation, morphology rel. to sample thickness (Russian) 7-37861
- Fe-B (15 at.%), amorphous powder and strip, struct., mag. props., thermal stability (Russian) 7-63470
- Fe-B amorphous alloys, interference functions, X-ray diffr. study and cluster calcs. 7-26656
- Fe-Co-B films, phase transition, microstruct. 7-33568
- Fe-Cr, P implanted amorphous alloys, corrosion, passivation, microstruct. 7-65180
- Fe-Cr-B, amorphous, Cr redistribution between phases during crystallisation, Mossbauer spectroscopy 7-21100
- Fe-Cr-Mo-Zr amorphous alloys, corrosion resistance (Japanese) 7-65194
- Fe-Cu-Ag amorphous alloys produced by vapor quenching 7-7849
- Fe-Ni-B, amorphous, shock loading, inclusions dissolving, domain struct. (Russian) 7-63487
- Fe-P amorphous alloy preparation by electroplating 7-17489
- Fe-Si-B, amorphous alloys, crystallisation, morphology rel. to sample thickness (Russian) 7-37861
- Fe-Ti-C ion-implanted amorphous alloys, precipitate microstruct. studies, conc. depend. 7-16434
- Fe-V, amorphous and metastable cryst. alloys prod. by vap. quenching 7-46420
- Fe₈₀B₂₀ amorphous alloys, EXAFS meas. at B k-edge 7-64807
- Fe₈₄B₁₆ amorphous alloy, heterogeneous surface struct., Mossbauer differential conversion electron spectra anal. 7-2319
- (Fe_{1-x}Co_x)₈₀B₂₀, crystallisation kinetics (Korean) 7-26638
- (Fe_{1-x}Mn_x)₇₈B₂₂, amorphous alloys, lattice parameters, annealing, X-ray diffr., elec. resist. 7-37878
- (Fe_{1-x}Ni_x)₈₀B₂₀, contribution of Ni to hyperfine fields (Korean) 7-27636
- Fe₄₀Ni₄₀B₂₀, amorphous alloys, domain wall motion, SEM obs. 7-52978
- Fe₄₀Ni₄₀B₂₀, amorphous alloy, Barkhausen noise, neutron irradiation effect 7-53029
- Fe₄₅Ni_{44.5}B_{10.5}, amorphous, internal friction, thermo-EMF struct., annealing effect (Russian) 7-59560
- Fe₅₀Ni₃₀B₂₀, amorphous alloys, domain wall motion, SEM obs. 7-52978
- Fe₈₁Ni₁₈B₁Si₂, glassy alloys, variation of mag. inhomogeneity 7-45634
- Fe₃₀Ni₃₆Cr₁₂Mo₂Si₃B₁₅, amorphous alloy, Curie temp., press. effect 7-52976
- Fe₄₀Ni₄₀P₁₄B₆ amorphous alloys, annealing, positron annihilation parameters anal. 7-39303
- Fe₇₀Ni₁₀P₁₃C₇, amorphous powder, crystallisation (Russian) 7-58162
- Fe₇₀Ni₁₀S₁₀B₁₀, amorphous and cryst. states., oxidation (Russian) 7-53993
- (Fe_{0.6}Ni_{0.4})₈₂Si₁₈B₁₀ amorphous alloys, structural relax. and crystn., positron annihilation studies 7-37869
- Fe_{0.44}Ni_{0.76}Si_{0.78}B_{1.45}C_{0.25}, amorphous filler metal, struct. props. (Korean) 7-32292
- Fe₂O₃ amorphous film deposition by laser CVD 7-39416
- Fe₂Sb_{100-x}, amorphous, metal-insulator transition and effects of localisation and correlation 7-45407
- Fe₆₇Si₃₃ amorphous films, coercive force rel. to crystallisation (Russian) 7-59078

amorphous state continued

- Fe₇₅Si₂₅ thin amorphous films, plastic deform. (*Russian*) 7-59585
 FeSiB amorphous alloy, double-layer struct. unit model 7-16423
 Fe₇₅Si₂₅B₁₃, structural anal. (*Korean*) 7-26637
 (Fe_{1-x}V_x)₈₄B₁₆, amorphous, low temp. resistivity anomaly (*Chinese*) 7-64198
 Fe_{84-x}V_xB₁₆, amorphous alloys, crystn., products and kinetics 7-51677
 Ga film, vac. condensates, struct. and opt. characts. 7-2404
 Ga ultrathin amorphous films, superconductivity threshold studies 7-22059
 Gd-Fe sputtered amorphous films, structural relax., positron lifetime meas. 7-37870
 GdCo-based glasses, double transition behaviour induced by anisotropy 7-22109
 GdFe and GdCo amorphous thin films, electrical conductivity, influence of mag. order 7-7409
 H impurities, conference, Rhodes, Greece (Sept. 1985) 7-24302
 H-metal disordered systems, neutron vibr. spectroscopy, review 7-21381
 a-H₂O films, low temp. elastic props. 7-45099
 La₂O₃ film, DC cond. mechanism 7-22055
 Mg-based amorphous alloys, elec. resist., press. depend. 7-7199
 Mn-Ga, film, prep. by ionised cluster beam deposition 7-3205
 Mo/Si, amorphous multilayers, annealing, diffusion, structural relax. 7-52309
 Mo-Ni thin films, struct., composition and homogeneity 7-2436
 Mo-Si amorphous alloys, cluster formation and percolation 7-27455
 Nb-a-Nb₂O₅, heterostructure, morphology, electrophysical parameters 7-13394
 NbC, amorphous films, prep. and characts. 7-7885
 a-Nb₂O₅, film, by alkoxide method on Nb and Al substrates 7-13394
 Ni-Ag amorphous thin films, crystallisation and internal constraints (*French*) 7-2433
 Ni-B amorphous alloys, crystallisation produced by ion implantation, TDPA study 7-32288
 Ni-Nb amorphous films, early stages of reaction with cryst. Au films 7-21703
 Ni-P, amorphous electrodeposited alloys, short-range order (*Russian*) 7-32291
 Ni-P amorphous alloy electrodeposition and corrosion obs. 7-27953
 Ni-P electrodeposited amorphous alloy, prep. and characterisation 7-22598
 Ni-Ti films, sputter deposition and ion beam mixing, microstruct. 7-44630
 Ni-Ti(Ta)(Cr), amorphous and cryst. reaction with Si studied by RBS and TEM 7-21704
 Ni-Zr amorphous alloy, Ni and Zr mobilities 7-32698
 Ni-Zr amorphous powder, prep. by mechanical alloying 7-33623
 Ni₄Ag_{1-x}, amorphous thin film, RF sputtered, real-time crystallization kinetics (*French*) 7-52349
 Ni₇₇Si₁₀B₁₃, structural anal. (*Korean*) 7-26637
 NiZr-H₂, metallic glass, pressure-concentration isotherms 7-26665
 Ni₄₂Zr₅₈, amorphous alloy, local struct., EXAFS and neutron diff. studies 7-64813
 P, passivation of III-V semiconductor surfaces 7-39778
 Pb_{0.67}Bi_{0.33}, prep. by low temp. ion beam mixing (*Chinese*) 7-51887
 Pb₈₀Si₂₀, amorphous, thermal stability, Auger study 7-58577
 Pd-H₂, Pd-based ternary system, hydrogen absorption, model 7-26970
 Pd₈₈U₂₀cSi₂₀c, alloys, glassy to icosahedral quasicrystalline phase transition, elec. and mag. props. 7-37863
 Pt alloys, fast-quenched, struct. and props. (*Russian*) 7-59555
 Rb, Voronoi polyhedra statistics, changes during rapid quenching, computer simulation 7-32263
 Sb layers, amorphous phase stability rel. to metal overdeposits 7-52324
 Sb₂S₃ amorphous condensers, electroelectret state and local levels studies (*Russian*) 7-45923
 a-Si:H, broken bond local environment relax., g-factor, cluster calcs. 7-37876
 a-Si_{1-x}C_x films, RF sputtered, IR absorpt., X-ray diff., RHEED (*Japanese*) 7-53584
 a-SiN₃H dielectric films with low defect density 7-39036
 Si₃N₄, CVD from Si₂Cl₆-NH₃-H₂ gas mixture 7-22560
 a-Si₃N₄H films deposited by plasma enhanced CVD, optical and elec. props. 7-39205
 Si₃N₄-SiC film, hybrid material prepared by plasma CVD, microhardness and internal stress 7-13616
 Si₃N₄-SiC film, hybridisation by plasma CVD 7-13379
 SiO₂, amorphous, annealing and relax. in high-press. phase 7-17329
 SiO₂, amorphous, densified, O diffusion kinetics, annealing, gamma-ray effects 7-52127
 SiO₂, amorphous, neutron diff. meas., inelastic scatt. corrections 7-11850
 SiO₂ amorphous optical fibers, material dispersion study over IR region 7-7663
 SiO₂ amorphous substrates, fabrication for TEM studies of ultrathin polycrystalline films 7-35504
 SiO₂, γ-ray induced defect centres, thermal bleaching 7-63659
 SiO₂, microporous thin films, thermochemical nitridation in NH₃ 7-46726
 SiO₂, stoichiometric and sub-stoichiometric, defect creation, photoablation, pulsed UV irradiat. 7-58315
 a-SiO₂, with high surface area, local order 7-52201
 Si_{1-x}Sn_xO_{1+x} amorphous thin films, optical and structural studies 7-64714
 SnO₂, amorphous film, vacuum prep., struct., crystallisation 7-53594
 Ta-ir alloy, amorphous, rapidly solidified, high temp. oxidation 7-33841
 Ta₅₅Ir₄₅ amorphous alloy, crystallisation study 7-58145
 Ta₂Cu_{1-x} amorphous thin-film diffusion barriers on GaAs, thermal and structural stabilities 7-52321
 Tb₃Fe₇₀ amorphous films, radial distribution function 7-37860
 Ti-Ni(Co)(Fe), amorphous phases, mechanical alloying 7-27972
 Ti-Pd, formation by mechanical alloying methods 7-59479
 TiC amorphous films, organic molecules detection by static SIMS 7-64838
 TiC, amorphous films, prep. and characts. 7-7885
 TiCu-H₂, thermal stability of hydrides 7-26664
 TiO₂ films, phase transitions, Raman spectra 7-12556
 TiO₂ films, pulse laser irradiated, Raman studies of phase transformations 7-12569
 TiO₂, reactive ion beam deposition, crystallisation 7-45091
 Ti₂Cu(SO₄)₂, glassy γ-modification, structural and electronic props. studies 7-58161

amorphous state continued

- U based intermetallic compounds, fission gas swelling, cryst. struct. stabil. 7-42115
 V₂O₅-P₂O₅ amorphous cathode Li secondary batteries, ethylene carbonate/2-methyltetrahydrofuran electrolyte 7-3635
 V₇₅Si₂₅ amorphous films, crystallisation and elec. props. 7-21102
 W-Si amorphous thin films, interfacial reactions with polycryst. metal overlayers 7-21763
 W-Ti-Si system, metallisation materials, amorphous phase form. and stability 7-22640
 W-Zr amorphous films as diffusion barriers between Al and Si 7-21504
 WO₃ amorphous films as high-contrast inorganic ion resists 7-63672
 WO₃ thin films, transparent, amorphous, prep. by dip-coating method 7-53644
 WSi₂ amorphous films, crystallisation, stacking faults and resistivity 7-21759
 W-Si, reactively sputtered films, metastable phase form. 7-52340
 Y₂Pd_{1-x}, amorphous mixed valent alloys, X-ray absorpt. spectra 7-64802
 Yb amorphous films, stability, effect of mag. field (*Russian*) 7-52319
 Zr_{1-x}Cu_x amorphous sputtered alloys, low energy excitations, sp. ht. meas., structural relax. effects 7-11913
 ZrO₂ films, pulse laser irradiated, Raman studies of phase transformations 7-12569
 ZrO₂, Y₂O₃ stabilised, amorphous second phase, sintering, grain morphology, fracture roughness, surface degradation 7-46612
 Zr₂Pd-H₂, thermal stability of hydrides 7-26664
 Zr₃Rh-H₂, amorphous alloy formation, solid state reactions 7-27982
 Zr₃Rh-H₂, thermal stability of hydrides 7-26664
amorphous state structure see noncrystalline state structure
amplification
 see also acoustic wave amplification; amplifiers
 optical analog signal amplification by backward Raman scattering 7-37042
 profoundly deaf persons' hearing aid with bandwidth-compression-limited amplification 7-34161
 superheterodyne amplification and generation of electromagnetic waves in electron beams 7-36855
 Ba₂NaNb₅O₁₅ cryst., elec. cond. small signal amplification 7-27333
 Nd:YAG, regenerative amplification of temporarily compressed picosecond pulses at 2 kHz 7-43108
amplification measurement see gain measurement
amplifiers
 see also amplification; differential amplifiers; fluidic amplifiers; parametric amplifiers; power amplifiers; preamplifiers; radiofrequency amplifiers; ring lasers; wideband amplifiers
 DFB semiconductor optical amplifiers, adjustable gain and bandwidth 7-57365
 excimer laser amplifiers, scalability, double-pass and expanding beam geometries calcs. 7-43143
 MOSFET chopper amplifier based signal source, brain voltage changes meas. appl. 7-23480
 myoelectric control, amplifier input impedances 7-3937
 nonlinear optical amplifier, resolution method for moment eqns. 7-43254
 toroid-amplifier system for mag. meas. of current in biological tissue, capabilities 7-23493
 CO₂ laser amplifier, multiatmosphere high gain, characts. and gain at 9.294 μm 7-57366
amplifying see amplification
amplitrons see microwave tubes
amplitude limiting circuits see limiters
amplitude modulation
 see also pulse amplitude modulation
 acousto-optic modulators, deflectors and Q-switches, basics 7-50605
 fibre interferometer/amplitude modulator, two-mode 7-50750
 fibre optic temperature sensor based on light amplitude modulation 7-50767
 semiconductor lasers field spectra computing asymmetry due to noise obs. (*Japanese*) 7-15862
 unified standard for RF signal shape and spectrum parameter meas., design 7-48773
 He-Ne laser at 0.633 μm, frequency stabilisation, using polarisation modulation 7-20295
amplitude modulation, optical see amplitude modulation; optical modulation
amplitude selectors see limiters
analogue computer applications see analogue simulation
analogue computer methods see analogue simulation
analogue-digital conversion
 see also digital-analogue conversion
 acoustical communication in animals, digital signal processing 7-50854
 angle digitisers, precision accuracy-checking method based on multifaced prisms 7-41335
 beam current integrator using a single chip A/D converter 7-15461
 bioacoustic, digital signal acquisition, analysis and synthesis, microcomputer based system, PAL 7-54817
 electrode, multiplexed implantable, for monitoring evoked responses in cerebral cortex, design 7-47305
 event sampling by particle-number difference, using high-speed A/D processor 7-10365
 fibre-optic sensors, developments and signal conversion problems (*German*) 7-26019
 field ion micrographs, image processing, video digitiser and frame memory system 7-30122
 film digitisation, low cost solutions implementation 7-18893
 Fourier transform spectrometer, Los Alamos design with microprocessor control 7-48860
 FTIR spectroscopy, quantitative, ADC errors 7-48877
 interferogram fringe analysis by photodiode array digitizer 7-30073
 length measuring systems with CCD arrays, resolution improvement (*German*) 7-61312
 multilayer holographic functional element in an analog-digital converter 7-62647
 NMR spectrometer, computer control of magnetic field homogeneity 7-48795
 optical analysis and simulation, microcomputer-based image processing aids 7-36891
 portable continuous blood pressure monitor utilizing an M68705 microcomputer 7-28755
 pulse height spectra, ADC histogram effects, improved fitting formula 7-62237

analogue-digital conversion continued

- Raman spectra obtained with optical multichannel spectrometer, digitisation and processing 7-15010
- solar pond geometric mean temp. meas., digital meter design 7-54356
- turbulence measurement with inclined hot wire probe, 3D angle calibration method (*Japanese*) 7-6338
- two-parameter data-acquisition system for slit-scan chromosome analysis 7-35501
- UA2 vertex detector, FASTBUS based 100 MHz FADC system for drift chambers 7-42306
- US velocity and attenuation meas., microcomputer-controlled phase-sensitive detection 7-50881
- VLBI correlators, signal loss due to imperfect fringe rot. 7-47722

analogue integrated circuits *see* **linear integrated circuits****analogue simulation**

- pyroelectric detector signals analysis 7-348

analysing power *see* **polarisation in nuclear reactions and scattering****analytical chemistry** *see* **chemical analysis****anaphoresis** *see* **electrophoresis****AND gates** *see* **logic gates****Anderson model**

- 1D, anomalous scaling and generalised Lyapunov exponents 7-45108
- d-wave superconductivity in the large-degeneracy limit of the Anderson lattice 7-45551
- acoustical 1D random lattices, Anderson localisation of waves (*French*) 7-16013
- alloys, substitutionally random, electron localisation and metal-insulator transition, CPA calcs. 7-27302
- Anderson localisation, upper critical dimens., wave function anomalous scaling behaviour 7-38428
- Anderson localization, one-dimensional, supersymmetric replica trick 7-12580
- Anderson-Hubbard model, real-space renormalisation group method 7-38842
- Bethe ansatz soln., cryst. field and spin-orbit coupling effects 7-2449
- Bethe ansatz soln. and thermodynamic props. 7-2448
- chalcogenide glasses, field dependent negative U-model and switching 7-7252
- conductivity, metal-insulator transition 7-52696
- Coulomb repulsion between localised and extended states 7-17157
- Curie temp. calcs. long range magnetic order and intermediate valence, Anderson model 7-45247
- degenerate Kondo lattice, magnetic instability and sp. ht. calcs. 7-58977
- dirty superconductors, conductivity and diamag. susceptibility fluctuations near Anderson localisation 7-45563
- disordered medium, acoustic wave propag., crossover in Anderson transition, acoustic localisation with flow 7-63748
- disordered surfaces, electrons and 1/f noise 7-38669
- disordered systems, finite-size scaling and correlation lengths 7-35464
- dynamic susceptibility, freq. depend., $1/N_f$ expansion studies 7-2816
- exponential localisation under very weak assumptions on potential distrib. 7-52381
- f-electron and conduction electron superconductivity, periodic Anderson model, self-consistent calcs. 7-12908
- generalised Anderson model, mixed valence system modelling 7-2562
- heavy electron Fermi liquids, Hubbard model anal., similarities to ^3He 7-2522
- heavy electron systems, Fermi liquid theory anal. of specific heat and magnetic susceptibility 7-38484
- heavy electrons, Gutzwiller method 7-27228
- heavy fermion alloys, Kondo exponent, conc. depend. 7-27495
- heavy fermion alloys, Kondo exponent, conc. depend. 7-27497
- heavy fermion metals, supercond. upper crit. field, temp. depend. 7-45587
- heavy fermion superconductivity, conduction band and virtual bound states, Kondo-like interaction, periodic Anderson Hamiltonian calcs. 7-27460
- heavy-fermion metals, electronic spectral density, periodic Anderson model 7-7087
- impurity model, finite U, ground state and spectroscopic props. 7-2817
- inelastic scattering in Anderson localization, detailed meas. 7-52527
- intermediate valence and heavy fermion model systems 7-33122
- Kondo lattices, heavy-fermion superconductivity 7-2775
- large dimensionality spaces, Bethe lattice, localisation length and dielec. const. calcs. 7-52384
- lattice, low temp. sp. ht., functional integral approach, boson representation 7-16788
- local Fermi liquid theory of Anderson impurity model 7-52507
- localization, Anderson model dynamics, anal. using Schrodinger eqn. soln. algorithms 7-56066
- low temp. lattice, large-orbital-degeneracy expansion in the Kondo limit 7-64037
- magnetically dilute spin systems, mag. reson. freq. shift at low temps. 7-45793
- metal-insulator transition, conductivity exponent calc., σ -model anal. 7-12610
- mixed valent compounds, electronic properties, theory 7-21880
- mixed valent compounds, static susceptibility of the periodic Anderson hamiltonian 7-22096
- nonlinear σ model, Anderson transition 7-64089
- one-dimensional periodic Anderson Hamiltonian, effect of disordered conc. nonmagnetic impurities 7-27517
- one-dimensional periodic Anderson model, quantum Monte Carlo simulation 7-52938
- periodic, ground state props. 7-58972
- periodic, interatomic hybridisation, singular density of states, narrow band limit anal. 7-16927
- periodic Anderson Hamiltonian, paramagnetic ground state 7-2809
- periodic Anderson model, extended and localised states 7-38504
- periodic model, appl. of Gutzwiller method 7-45109
- random Hubbard alloys, localisation-affected conductivity, numerical studies 7-45223
- random systems with off-diagonal disorder, localisation studies 7-32959
- rare earth alloys, X-ray absorpt. L_{III} spectra, Anderson impurity model 7-64819
- rare earth semiconductors, valence changes, many-impurity Anderson model 7-7186
- single particle excitation spectra, scatt. eqns., S-matrix approach 7-52385
- strongly correlated Fermi systems, Gutzwiller saddle-point approx., functional integral approach 7-207

Anderson model continued

- superconductivity and random disorder in the zero-bandwidth limit 7-58945
- transition metal alloys, disordered, localised and extended state coexistence 7-7175
- transport props. at low temps. 7-27311
- two-band Anderson-type model in 1D, mag. susceptibility and other ground-state props. 7-22092
- valence fluctuating lattice systems, self-consistent perturbation theory 7-2561
- variational ground state for the periodic Anderson model 7-7083
- wave functions in smooth aperiodic pots., Anderson localisation 7-2446
- Ce alloys, electronic structure, spectroscopic and thermodynamic props., impurity Anderson Hamiltonian 7-32900
- Ce compounds, heavy-fermion state in the Anderson lattice 7-7476
- Ce cpds., X-ray absorpt. edges, many body effects, determ. 7-64789
- Ce impurity system, degenerate Anderson model, Bethe-ansatz soln. 7-2559
- Ce mixed valence cpds., many body theory for spectroscopies 7-64790
- CeCu₈ heavy fermion system, photoemission and inverse photoemission studies 7-3148
- CeN, narrow band material, high resolution photoemission 7-33512
- Fe₂ZrSe₂, intercalated layered cpd., thermopower and low DC field magnetisation study 7-17199
- InSb, impurity bands and their conductivity in strong mag. fields 7-45152
- La cpds., X-ray absorpt. edges, many body effects, determ. 7-64789
- NdAl₂, electronic structure, spectroscopic and thermodynamic props., impurity Anderson Hamiltonian 7-32900
- Ni₂Fe₃O₄, elec. cond., thermolec. power meas., 10-300K 7-38648
- n-nP, Anderson transition in a mag. field 7-16944
- PrAl₂, electronic structure, spectroscopic and thermodynamic props., impurity Anderson Hamiltonian 7-32900
- TaS₂, 1T polytype, CDW transition obs. by positron annihilation 7-39267
- TaSe₂, 2H polytype, CDW transition obs. by positron annihilation 7-39267
- U compounds, heavy-fermion state in the Anderson lattice 7-7476
- U-based heavy Fermion systems, final-state effects in inverse photoemission 7-53437
- UBe₁₃ coherent Kondo state, upper critical field calcs. 7-2793
- Yb impurity system, degenerate Anderson model, Bethe-ansatz soln. 7-2559

Anderson transition *see* **Anderson model; metal-insulator transition****anechoic chambers**

- RF absorber horn test system 7-43605
- RF anechoic room absorbers eval. in 30 to 1000 MHz range 7-43604

anelastic relaxation

- see also Bordoni effect; creep; elastic aftereffect; internal friction; Snoek effect; stress relaxation; Zener relaxation*
- BCC metals, Snoek-Koster relax. model investig. (*Russian*) 7-12115
- capron, relax. and phase transitions, spectrosc. investig. (*Russian*) 7-63811
- disordered systems, nonexponential relaxations 7-64566
- Earth, viscoelastic static displacements generation by localised seismic source 7-28887
- epoxide resins, spiro type, acid anhydride cured, mech. relax. props. 7-21349
- fibre-reinforced polymer composites, relaxation property anisotropy 7-46534
- glass, low temperature properties, below transition temp., relaxation 7-1910
- Inconel MA 6000, oxide-dispersion hardened superalloy, cyclic creep and anelastic relax anal. 7-17596
- metallic glasses-H₂, mechanical relaxation behavior 7-26859
- PEEK, cryst., mech. relax., electron beam irradi. effects 7-16686
- polyaryl-ether-ether-ketone, semicryst., mech. relax., electron beam irradi. effects 7-12204
- polyethylene, dielec. and mechanical relaxations, rate theory eqn. calcs. 7-26983
- polypropylene films, glass isotactic, crystallisation, struct., dynamic mech. props. 7-16445
- viscoelastic materials, dynamic parameters meas., vibr. transducer design 7-61326
- Zircaloy-4, cold worked, anelastic contrib. to high temp. stress relax., model 7-65072
- AgI-Ag₂MoO₄ glasses, ionic conductors, mechanical and electrical relax. 7-44687
- Fe-base alloys, interstitial impurity-dislocation binding energy (*Russian*) 7-58310
- Fe-N, Snoek-Koster relax., dislocation effects (*Russian*) 7-44686
- Mn-Cu alloy, nonlinear anelasticity and temp. depend. lattice const., nonlinear resonance curve meas. 7-63741
- β -Na₂O-Al₂O₃ ionic conductors, mechanical and electrical relax. 7-44687
- Nb, tunnelling of H and D trapped by O(N), anelastic relax. meas. 7-39572
- Nb-Ti-H(D), anomalous anelastic relax., statistical model 7-28065
- Nb-Ti-H(D), substitutional alloys, intermediate temp. relax., Fermi-Dirac model 7-26858
- Nb-Ti-H(D) alloys, anomalous anelastic relax., statistical model anal. 7-8036
- Si:Pd, inelastic relax., neutron irradi. effects 7-44689
- V-Ti-H(D), substitutional alloys, intermediate temp. relax., Fermi-Dirac model 7-26858

anelasticity*see also anelastic relaxation*

- Inconel MA 6000, oxide dispersion strengthened superalloy, cyclic creep, HF effect, anelastic model 7-53827
- mechanics of damage and fatigue, conf., Haifa, Israel (Jul. 1985) 7-48139
- metal-H, systems, anelastic props. 7-26856
- steel, austenitic stainless, creep and anelasticity at const. homogeneous dislocation struct. 7-17586
- steel, Ni-Cr, anelastic props. of grain boundaries and transition temp., effect of temper embrittlement 7-22815
- Al-Ag, anelastic effects due to precip. and dissoln. 7-13487
- Al-Ag (5 wt.%), anelastic effects, quench sensitivity, precip. and dissolution 7-53784

anelasticity continued

- Au mechanical resonance spectra 7-21712
- Ni film on sapphire substrate, adhesion, mechanical resonance spectra 7-21712

anemometers

see also laser velocimeters

- aeroacoustic high intensity field meas. using cooling power anemometer 7-16039
- bubble diameter meas. by fringe method, using laser Doppler anemometer 7-16278
- calibration accuracy (*Rumanian*) 7-26368
- calibration of mechanical anemometers in wind tunnels (*Rumanian*) 7-6337
- electronic gonioanemometer (*Italian*) 7-18309
- fibre laser Doppler anemometer and boundary-layer meas. appl. 7-37609
- hot wire, oscillating, response 7-37588
- hot wire air flow meter for automobile engine intake mass air flow rate meas. 7-37587
- hot wire anemometry, book 7-51357
- hot-film anemometer meas., correction for ambient temperature changes 7-57946
- hot-film anemometers, const. temp., calibration in water 7-11567
- hot-wire anemometer compensated for ambient temperature variations 7-16275
- hot-wire techniques for Reynolds stress tensor determ. for 3D flows 7-57945
- laser Doppler anemometer, two-colour four-beam system, two-phase mist flow meas. 7-37581
- laser Doppler anemometer arrangement measurements (*Polish*) 7-57965
- laser Doppler anemometer for measuring superlow velocities 7-43812
- laser Doppler anemometer for vel. meas. in enclosed flames (*German*) 7-18765
- microanemometers for meas. at very low air velocities, calibration 7-44069
- scanning three-velocity-component laser Doppler anemometer 7-16277
- thermogrammetry and thermal engineering conf., Budapest, Hungary (April 1987) (*Hungarian*) 7-56258
- turbulence measurement with Gill propeller anemometers, directional response study 7-55276
- turbulent flow and mass transfer of unstabilised stream in channel with obstacle 7-11391
- twin-propeller, low-friction design with wind vane, performance testing 7-34723
- velocity meas. in stirred tanks, hot-film const. temp anemometer probes 7-16273
- wind turbine test data correl. optimisation using frequency response matching 7-8357

anemometry

- drag anemometry for measuring velocities in electromagnetically driven flows 7-44076
- flow acceleration measurements using laser Doppler anemometry 7-31904
- flowing two-phase dispersed particles, metrology using optical diffusion (*French*) 7-31895
- fluidised beds, freeboard, vel. meas. using laser Doppler anemometer 7-11527
- gas jet impacting a cavity, temp. and velocity meas., flow anal. 7-43999
- grid mixing tank, turbulence meas. using laser-Doppler anemometer 7-1656
- hot wire anemometry, book 7-51357
- hot-wire anemometry, turbulent flow meas., evaluation of analytical systems 7-16274
- hot-wire data corrections for high intensity turbulence 7-37448
- inviscid axial flow in compressor rotor, leading-edge effects, flowfield meas. 7-11562
- laser Doppler anemometer meas. corrections for curved channel flow 7-37608
- laser Doppler anemometry, counter based in wet steam flow 7-57969
- laser-Doppler anemometer, pipe flow, laminar to turbulent flow transition, sinusoidal flow modulation 7-16262
- thermal plume, turbulent struct., vel. field (*French*) 7-31762
- turbulent boundary layer, heated, hot-wire meas. of velocity and temp. fluctuations 7-63236
- turbulent boundary layers external factors effect with directional injection and suction 7-6199
- turbulent flow characts. in wake of circular cylinder (*Russian*) 7-1574
- turbulent flow meas. in ribbed-wall flow channel and comparison with model 7-57947
- underwater optical probe for laser Doppler anemometry 7-16279
- unsymmetrical 2-D diffuser characts. in steady and unsteady flows (*Japanese*) 7-6203

angiography *see diagnostic radiography*

angle measurement *see angular measurement*

angular correlation techniques

- $\text{KAl}_2(\text{AlSi}_3\text{O}_{10})(\text{OH})_2$, cryst. struct. anisotropy, positron annihilation method 7-13255
- $\text{KMg}_3(\text{AlSi}_3\text{O}_{10})(\text{OH})_2$, cryst., struct. anisotropy, positron annihilation method 7-13255

angular measurement

see also angular velocity measurement

- base quantity vs derived quantity 7-18746
- Cartesian oval fibre-optic lens as linear to angular position converter 7-43407
- circular gauge, systematic errors correction, computerised calibration procedure 7-56244
- digitisers, precision accuracy-checking method based on multifaced prisms 7-41335
- encoder automatic calibration system (*Japanese*) 7-56213
- fibre optic sensors for rotation rate meas. (*German*) 7-11161
- fibre-optic liquid film sensor for 2-phase annular and stratified flow 7-37611
- goniometers, interference, operating reliability, effect of lateral beam displacement 7-41452
- multireflected autocollimation approach 7-35495
- NPL role in standardisation and calibration 7-18747
- null detector, interference-type, for ang. position of object meas. 7-56327
- optical angle-measuring instrument using three-dimensional linkage 7-41415
- optical method of angular displacement when the rotation axis steeply inclines 7-41333

angular measurement continued

- optical system having concentric objective use in angle-measuring instrument 7-50671
- optron displacement sensor [geophysical application], geophysical equipment appl. 7-4809
- prisms certification for standard angular meas. 7-294
- quartz crystal resonator blanks, X-ray machine 7-37806
- speckle photography fringes, 2D digital processing, angular determ. accuracy 7-41441
- transducer for angular and linear displacements with separated gratings 7-4829
- turbulence measurement with inclined hot wire probe, 3D angle calibration method (*Japanese*) 7-6338
- wavefront sensor, integrated optical, lens focusing onto detector array 7-26041
- wind direction meas., electronic gonioanemometer (*Italian*) 7-18309
- zenith angle transducers in deviation recorders, accuracy (*Russian*) 7-34707

angular momentum

- accreting compact stars, ang. momentum accretion from inhomogeneous medium 7-9460
- astronomical systems, ang. momentum-mass relation rel. to characteristic actions $\hbar^{(6)}$ in struct. of Universe 7-4602
- cataclysmic variable stars, ang. momentum transport in accretion disks magnetospheres 7-47918
- conservation laws 7-14483
- inverse sprinklers, conservation principle 7-40
- operators, spherical coords. obs. 7-41041
- self-similar scaling in stellar and atomic systems 7-14683
- stars in visual binary, angular momentum-mass relation and mass ratio distrib. 7-18432
- zero turns, explanation 7-54
- $\text{He}+\text{H}_2$, angular momentum collisional alignment Born approx. calcs. 7-964
- ^3He , superfluid B-phase, orbital ang. momentum in mag. field 7-38289
- $^{15}\text{Sm}^{(16)\text{O,X}}$, linear and angular momentum transfer in incomplete fusion reactions 7-42054

angular momentum theory

see also quantum theory; Regge poles and trajectories

- Aharonov-Bohm scatt., ang. momentum nonconservation 7-29808
- angular momentum traces, generating functions 7-120
- Clebsch-Gordan coefficient for nonspecial Gel'fand basis of $\text{SU}(m/n)$ for 5-particle system 7-35312
- electrostatic exchange interaction and characteristics of X-ray spectra 7-25337
- generalized Langer corrections 7-9692
- harmonic oscillator, two-dimensional, isotropic, coherent angular momentum states 7-56077
- Jucys-Bandzaitis diagrammatic technique in angular momentum theory and second quantization 7-24463
- multiplicity-free 6j symbols, algebraic expressions, G_2 isoscalar factors 7-29796
- Racah coefficients, degree one polynomial zero calcs. 7-48432
- Racah coefficients, nontrivial zeros, nonlinear solns. 7-48421
- rigid body undergoing motion, constancy of angular momentum vector 7-41096
- weight-1 6j coefficients, complete determ. of zeros 7-29795

angular velocity measurement

No entries

anharmonic oscillators *see harmonic oscillators*

animal communication *see biocommunications*

anisotropy, magnetic *see magnetic anisotropy*

anisotropy, magnetocrystalline *see magnetic anisotropy*

annealing

- see also electron beam annealing; graphitising; incoherent light annealing; laser beam annealing; magnetic annealing; recrystallisation annealing; solution annealing; stress relaxation*
- alkaline earth orthovanadates, stoichiometry, stripping voltammetry studies 7-63836
- alloy, nonuniformly distrib., internal friction rel. to diffusion (*Russian*) 7-65074
- alloys, heat resistant gas turbine, creep behaviour (*German*) 7-3389
- amorphous polymers, yield stress rel. to ageing, nonequilib. glassy state 7-46562
- anthracene single crystals., structural imperfections as triplet exciton traps, defect recovery 7-64160
- apatite, fission tracks thermal annealing, chem. comp. effects 7-60252
- austenitic stainless steel, defects study by positron annihilation 7-39296
- bimetallic film couples, interfacial phase form., in situ annealing X-ray diffr. obs. 7-21705
- bisphenol A polycarbonate crystals, melting point rel. to vapour induced crystallisation and annealing treatment 7-32312
- borosilicate glasses, ultrasonic velocity, variation during annealing (*Russian*) 7-26099
- CdS-CuInSe_2 solar cells fabricated by DC magnetron sputtering of Cu_2Se and In_2Se_3 7-23170
- defects, annealing and creation kinetics, ESR transient spectroscopy 7-2928
- diamond, radiation damage prod. of 5RL centres, phonons, absorpt. spectra, cathodoluminescence studies 7-33461
- dielectric films, on compound semiconductors, conf., Las Vegas, USA (Oct. 1985) 7-35108
- diffusion-controlled interfacial growth, dense branching morphology form. 7-21147
- 14,4'-diphenylmethane diisocyanate 1,4-butanediol, thermal degradation 7-8272
- direct impact induced amorphisation, effect of ion beam annealing 7-58383
- discontinuous metallic thin films, on amorphous and crystalline substrates, electron irradiation stimulated coalescence 7-2437
- epidote, radiation damage study using fission track and thermoluminescence methods 7-51818
- epoxy-epoxyester polymers, relax. and specific orientation in surface layers (*Russian*) 7-63918
- FCC pure metals, neutron irradiated, thermal stability of cascade defects, annealing expt. 7-51856
- fission track closure temperatures, numerical calcs. 7-36435
- fluorophosphate glass, type OK1, interrelationship of refr. index, viscosity and F content 7-57492

annealing continued

- garnet bubble films, H_2^+ -implanted, H out-diffusion suppression of over-layers 7-38259
- glass transition, memory effects 7-2204
- grain growth during isothermal annealing, Monte Carlo simulation 7-17561
- heavy ion track annealing in plastic track detectors 7-19628
- III-V semiconductor-Au system, heat treatment, gaseous species evolution, mass spectra studies 7-39881
- Inconel 600 and 690, SCC under high temp. NaOH, comp. and annealing effect 7-39710
- ion beam modification of materials, conf., Catania, Italy (9-13 June 1986) 7-60865
- irradiated metals, isochronal annealing PAC monitored defect reactions anal. 7-44623
- metal films, characterisation by SIMS, Auger spectroscopy and TEM 7-12550
- metal tubes, ductile, no. of cracks in axial splitting 7-59597
- metallic-based layered struct., depth profile anal. using multilayer, anodisation 7-27170
- metals, neutron irradiation damage (*Japanese*) 7-32508
- micaceous minerals, track annealing studies 7-36402
- microelectronic materials processing, appl. of neutron depth profiling, book contrib. 7-44595
- MOS structure, X-ray irradiation, trapped hole spatial depend., tunnelling anal. and annealing meas. 7-58902
- MOS structures, interface and bulk traps, effect of processing steps 7-38758
- optical glass filter manufacturing, spectral characts. 7-5961
- PEEK film, unit cell parameters, annealing temp. depend., WAXS obs. 7-64008
- PET fibres, heat treatment kinetics 7-44407
- PET films, crystallisation under strain, annealing, morphology, mech. props. 7-44415
- PMMA, two-stage deform. recovery, annealing study under dimensional constraint 7-32554
- pMOS dosimeters, long-term annealing and neutron response 7-56880
- poly ether ether ketone film, zone annealing prep., dynamic modulus, tensile strength 7-8038
- polybutylene, crystallisation, electron microsc. obs. 7-32309
- polybutylene terephthalate fibres, heat treatment kinetics 7-44408
- polybutylene terephthalate fibres, phase transitions, surface characterisation, spectrosc. methods 7-63505
- polycarbonate, two-stage deform. recovery, annealing study under dimensional constraint 7-32554
- polyesters, aromatic, conformational reorganisation viewed by Raman spectra 7-32311
- polyethylene, low density, environmental stress cracking in methanol, heat treatment effect 7-8146
- polyimide surface, in situ anal. of H, C, N and O using direct recoil time-of-flight technique 7-54242
- polypropylene, isotactic, position annihilation lifetime investig. 7-32501
- polypropylene, oriented, thermal expansion behaviour 7-6839
- polypropylene films, glass isotactic, crystallisation, struct., dynamic mech. props. 7-16445
- polystyrene, two-stage deform. recovery, annealing study under dimensional constraint 7-32554
- polytrimellitimide film, molecular aggregation, SAXS obs. 7-51665
- positron lifetime spectrum in amorphous materials, annealing effects (*Chinese*) 7-27814
- potential energy surfaces, simulated annealing study 7-31211
- powder plastically worked articles, annealing effect on behaviour in temp. jump and substruct. 7-27961
- PTFE, oriented, annealing, crystn. lattice temp. behaviour (*Russian*) 7-6840
- PVC, rigid, stabilised, crystallinity detection by hardness testing 7-8223
- PVC-polycaprolactone interface, diffusion, temp. and time depend. 7-32723
- pyrographite, highly irradiated, property change on thermal annealing 7-63665
- quartz: Cu^+ (Fe^+) (Nb^+), ion implanted, coloration and transparency (*Japanese*) 7-7656
- quartz: Al, static magnetisation of $Al-O^-$ centres, electric field effects 7-38900
- quartz, as-grown or Li^+ , Na^+ , Cu^+ electrodiffused, radiation-induced conductivity 7-6691
- α -quartz, neutron irradiated and annealed, positron annihilation and mag. susceptibility meas. 7-39274
- quartz crystal irradiation effects study using low-temp. dielec. relax. 7-58334
- rapid thermal processing, conf., Boston, MA, USA (Dec. 1985) 7-14713
- sapphire: Ti^{3+} laser material, scattering centre formation mechanism 7-10960
- semiconducting materials, cryst., and device appls., book 7-60894
- semiconductor wafer, ion implanted dopant profile evolution during annealing, diffusion eqn., anal. 7-58536
- semiconductors, processing and charactn. techniques, conf., Los Angeles, CA, USA (Jan. 1986) 7-18489
- Si-Al Schottky barriers, Ar ion implantation damage, thermal anneal recovery 7-17101
- silicide formation on Si, epitaxial nature, initial nucleation processes and effect 7-21767
- silicides, rapid thermal annealing 7-21545
- SIPOS, AES and XPS studies (*Chinese*) 7-33511
- SOI buried layer form. by high dose implantation, mass transport studies 7-32479
- SOI struct., implanted buried oxide elec. props., high temp. annealing effects 7-58904
- SOI structures, ion implanted, defect EPR spectra studies 7-27603
- SOI wafers, O implantation prep., background doping effects 7-32478
- sphene, natural radiation damage, fission track and thermoluminescence props. 7-51889
- steel, alloyed structural, struct. rel. to cold deformability, softening heat treatment methods development 7-39556
- steel, austenitic stainless, bright annealed, selectively absorbing surface, oxidation prep. 7-8186
- steel, austenitic stainless, rapidly solidified, microstruct. characterisation 7-22672
- steel, Cr, ferritic, neutron irradiation, isochronal annealing, elec. resist. recovery 7-58348
- steel, Cr-Mo-V, ion nitriding characts. (*Korean*) 7-8162

annealing continued

- steel, Cr-Ni, microsegregation phenomena in long-term holding at $400^\circ C$ 7-13458
- steel, Cr-Ni-Mo, maraging, mech. props. rel. to heat treatment (*Japanese*) 7-53792
- steel, Cr-Ni-Mo-Nb, precipitates formation, effect of He 7-13460
- steel, Cr-Ni-Ti-Al, cold-prestrained, length changes during annealing 7-65058
- steel, dual phase, effective grain size, cleavage crack propag. 7-28118
- steel, dual-phase, micro alloyed, mech. props. and struct., effect of process variables 7-65108
- steel, dual-phase, Mn-partitioning, austenite form. 7-39552
- steel, ferritic, reactor material, neutron irradiation, positron annihilation studies 7-46215
- steel, Hadfield, cold-deformed, fine struct. anal., brittle fracture (*Russian*) 7-59570
- steel, high speed, powders, transform., struct. and props., prior annealing effect 7-13452
- steel, high-speed p/m tungstenless, Mo and V effect on microstruct. and operating props. 7-33788
- steel, low C, Al killed sheet, overaging, continuous annealing, carbide precip., hardness (*Korean*) 7-46474
- steel, low C, capped, grain growth during subcritical annealing 7-46519
- steel, low C, mech. props., effect of cold working and annealing (*Chinese*) 7-13473
- steel, low C lamination, decarburization, grain size, carbide morphology 7-8016
- steel, mild, brittle fracture, microcracks effect (*Russian*) 7-59618
- steel, p/m, heat treatment effect on strength and yield parameters 7-53775
- steel, pressure vessel, neutron irradiation, defect microstruct., SANS and TEM studies 7-58351
- steel, stainless, austenitic, valve type, heat treatment schedule effect on failure nature 7-3423
- steel, stainless, FCC structure, multiple grain-boundary contacts (*Russian*) 7-12079
- steel, stainless, films, sputter deposited, vacuum annealing-induced solute depletion 7-64012
- steel, stainless, martensitic and austenitic, amplitude depend. damping rel. to annealing and tempering (*German*) 7-13498
- steel, stainless, oxidation and descaling behaviour, influence of annealing (*Japanese*) 7-59665
- steel, structural, austenite form. during rapid continuous heating (*Russian*) 7-33702
- steel, V, W₂, laser surface melting, effects of prior heat treatment 7-65195
- steel bimetallic plate, cold-clad, diffusion processes in preboundary zone 7-46708
- steel sheet, low C, Al-killed, cold-rolled, batch-annealed, recrystn. model for controlling mech. props. 7-13474
- steel structural, powder, hardenability and hardness penetration, effect of comp. and porosity 7-22807
- steels, C and austenite welded joint, microhardness, effect of C redistrib. 7-13571
- superalloy Li_2 structures, high temp. deform. mechanisms (*French*) 7-22766
- system, silicide form., struct. and electronic props. 7-38363
- TEM, solid state phase transformations, atomic mechanisms, in situ technique 7-44376
- TLD electron trap level determ. by two temperature annealing 7-16970
- triglycerides, obs. of physical ageing by positron lifetime meas. 7-39229
- triglycine sulphate, single cryst., neutron irradiation, elec. cond. 7-7227
- ZnO:Bi (Sb) (transition metal), Schottky-like barriers, ion implantation, annealing 7-58860
- Ag, proton and ion irradiation, self-interstitial atom interactions with defect clusters, elec. resist. meas. 7-58384
- Ag/In thin film couples, interface $AgIn_2$ cpd. form. and props., gamma ray spectra 7-21688
- Ag-Au bilayers, EXAFS and X-ray reflectivity meas. 7-27821
- Ag-Cu (12 at.%), supersaturated solid soln., decomp. kinetics, effect of creep (*Russian*) 7-33748
- α -Ag-Mg, annealed, twin like domain boundary, high resolution electron microscopy 7-26763
- Ag-Mg, commensuration and discommensuration characteristics, modulation periods 7-46463
- Ag-O solid solutions, annealing, grain boundary segregation of O 7-33679
- AgGaSe₂ crystals, light scatt. and transparency, annealing expts. 7-3338
- Al (110), Ar^+ sputtered, vacancy-type defect distribs., variable energy positrons study, mol. dynamics simulations 7-12429
- Al, ductile fracture rel. to heat treatment, vacancy conc. effect 7-8095
- Al, polycrystalline, deformed, positron trapping and annihilation 7-39258
- Al, quenched, secondary defect form., isochronal annealing, positron lifetime study 7-39298
- Al:Bi-KCl:Bi, bilayer cpd., Bi ion implantation, thermal annealing 7-32474
- Al/Pt/Si structures, PtSi formation 7-63972
- Al-Ag, decay and short-range ordering (*Russian*) 7-44795
- Al-Ag (5 wt.%), anelastic effects, quench sensitivity, precip. and dissolution 7-53784
- Al-Co, melt spinning, microstruct., precip., microhardness (*Korean*) 7-46444
- Al-coated fibre, high-temp. effects 7-11146
- Al-Cr(Mn)(Fe) amorphous films, quasicrystalline transformation by ion irradiation 7-2071
- Al-Cu-MG, annealed, creep, 623-723 K 7-53802
- Al-Fe, ion induced metastable phases 7-63673
- Al-Fe-Mg, solidified from liq. phase, struct. (*Russian*) 7-39498
- Al-GaAs Schottky barrier contacts, MBE grown, interface reactions, vacuum annealing effects 7-45022
- Al-Ge mixture, H implanted, evidence for metal-insulator transition in Al 7-2483
- Al-He ion irradiation, system, bubble form., positron lifetime meas. 7-37966
- Al-Li-Zn (Cu) icosahedral quasicrystals, solid state reaction and rapid solidification prep. comparison 7-37864
- Al-Mg (0.2 wt.%), subgrain growth rel. to prior cold work and annealing temp. 7-17551
- Al-Mg (6.5 wt.%), grain boundary segregation, STEM-EDX analysis 7-39518
- Al-Mg-Si, annealed, plastic flow under multiaxial cyclic loading 7-33725

annealing continued

- Al-Mg-Zn system, fracture viscosity rel. to surplus phase morphology 7-46610
- Al-Mg-Zn(Cu) icosahedral quasicrystals, solid state reaction and rapid solidification prep. comparison 7-37864
- Al-Mn (15 wt.%), melt spun ribbons, icosahedral struct., decomp. rel. to annealing 7-28030
- Al-Mo, rapid solidification processed, diffusion-induced dislocation migration 7-65047
- Al-Si-Cu sputtered electrode for VLSI, Cu distributions meas. by RBS 7-2415
- Al-V films, precip. from metastable solid solns. 7-65048
- Al-W/Ti(Ni) thin film reactions, W diffusion marker studies 7-2277
- Al-Xe, implanted, form. of solid precipitates and fluid bubbles, TEM obs. 7-38032
- Al-Zn, ion induced metastable phases 7-63673
- Al-Zn-Mg-Mn-Si, rapid solidification, superplasticity 7-53826
- Al-(Mg), AE during deform., effect of struct. state (*Russian*) 7-38127
- AlAs/GaAs superlattice mixing induced by Si⁺ implantation 7-58649
- AlAs-GaAs superlattices, Si ion implantation, dose-dependent mixing 7-12500
- AlAs-GaAs superlattice, Si⁺ implantation, depth dependent mixing 7-27032
- AlGaAs-GaAs superlattices, Se (Si)(Mg)(Be) ion implantation, intermixing, residual damage 7-26782
- AlGaAs-GaAs-Si, Be superlattices, correlation between Si diffusion and Si-induced disordering 7-38034
- Al₂Mo precipitate microstruct. and orientation, implantation and annealing effects, electron microscopy study 7-16782
- AlN, hot pressed, elec. cond. rel. to CaO addition 7-38559
- AlN reactively evaporated encapsulating films, annealing, RBS and RHEED studies 7-21744
- α -Al₂O₃, corundum, single crystals, wear rate, influence of annealing 7-53920
- α -Al₂O₃, ion implantation, crystallisation of amorphous surface layers 7-58304
- Al₂O₃, mixing of metal overlayers, ion beam irradi., rapid thermal annealing, pulsed laser irradi. 7-58330
- Al₂O₃, profiled, plastic flow in surface layers during diffusion welding 7-33730
- α -Al₂O₃:Br, ion implanted, RBS and annealing studies 7-32515
- Al₂O₃/Fe interface, ion beam mixing, conversion electron Mossbauer spectra studies 7-63679
- β -Al₂O₃-Na₂O:Fe³⁺, luminesc. thermal effects 7-33444
- Al₂O₃-Ti interface reactions studied by AES and UPS 7-21702
- As-Se, amorphous, short range structures, EXAFS studies (*Chinese*) 7-37871
- a-As₂S₃ vapour deposited films, thermostructural and photostructural changes, EXAFS study 7-64003
- Au crystallites, annealing, grain boundary untwisting and untilting, dislocation climb and glide 7-12076
- Au crystals, small, surface twin form., high resolution electron microscopy 7-44566
- Au films, surface plasmon modes 7-7316
- Au, quenched, vacancy clustering, positron annihilation 7-44534
- Au thin films, on Au (111), surface-diffusion-induced ageing processes 7-45080
- Au/In thin film couples, interface AuIn₂ cpd. form. and props., gamma-ray spectra 7-21688
- Au-GaAs, annealed, interface erosion 7-21683
- Au-GaAs, contact, structural and elec. props. 7-27424
- Au-Ge-GaAs, interfacial reactions, struct. after annealing 7-27154
- Au-InP, solid-state reactions, Au₂P₃ formation 7-58550
- Au₂Cr, atomic ordering, X-ray struct. anal. (*Russian*) 7-1933
- Au₇₅Cu₂₅ and Au₇₀Cu₃₀, local order, X-ray diffuse scatt. meas. 7-26972
- BN, ion-plated, prep. and charact. 7-17477
- BN MIS structures, form. by reactive pulse plasma method, on Si or SiO₂ substrates, phys. props., annealing effects 7-22023
- BN polycrystals, heat treatment conditions effect on mech. and service props. 7-53894
- Ba-La-Cu-O system, possible high T_c superconductivity 7-2770
- BaCuFe₁₁O₂₇ W-type hexagonal ferrite, intermediate valency, oxidation annealing, magnetisation and neutron diff. studies 7-7187
- Bi, positron trapping in deformation induced defects 7-39257
- C, amorphous film, modification by inert gas ion irradiation 7-64018
- C fibres, Celion, elec. resist., temp. depend. 7-65073
- C fibres, Celion, mechanical and fracture behaviour 7-22786
- C fibres, pretorsional deform., annealing, acid treatment, struct., mech. props 7-22768
- C, glass-like, heat treatment, pore growth kinetics 7-58147
- C MIS structures, form. by reactive pulse plasma method, on Si or SiO₂ substrates, phys. props., annealing effects 7-22023
- C:H amorphous films, glow discharge deposited from CH₄+H₂, annealing behaviour 7-64922
- CaF₂, cryst., defect struct., high temp. (*German*) 7-32449
- CaF₂-CoSi₂-Si, MBE growth of epitaxial insulator-metal-semicond. struct. 7-22496
- CaF₂-Si, MBE of CaF₂ on Si and overgrowth with Si or Ge characts. 7-22495
- CaF₂-Si interface, with epitaxially grown insulator, post-growth annealing treatments 7-7074
- CaFe₂Mn_{1-x}O_{3-y} ferrites, microdomains, role in oxidation, reduction and annealing 7-46830
- CaMoO₄, microhardness anisotropy meas., quenching and annealing temp. effect 7-63738
- CaSO₄:Dy, gamma radiation damage on thermolum. 7-38059
- CaTiO₃, ion implantation, crystallisation of amorphous surface layers 7-58304
- Cd,Hg_{1-x}Te, LPE and MOVPE grown, elec. props. and annealing 7-53512
- CdIn₂S₄, optical props., annealing and γ -ray irradiation effects 7-13211
- Cd₃Nb₂O₇ ceramic, high press. phase transition and dielec. props. 7-2177
- CdS, electron beam irradiated, red flash-like luminescent centres, annealing 7-7740
- CdS evaporated films, cathodolum., effect of thermal annealing 7-22353
- CdS photoconductive thin films, optimum spray pyrolysis preparation conditions 7-17418
- CdS single crystals, nonequilib. high-temp. vacuum annealing effects, intrinsic defect transform. 7-58764
- CdSb thin films, preparation and thermolec. props. 7-64374

annealing continued

- CdSe, optimally annealed in molten Cd, DC galvanomagnetic props. 7-27352
- CdSe thin film liquid-junction photovoltaic cell, photoelectrochem. charactn. 7-54331
- CdSe thin films, electrodeposited from SeSO₃²⁻ soln., comp. performance, polarography, RBS, cyclic voltammetry, power meas. 7-2411
- CdSe:Cu films, radiative recomb. centres form., photolum. spectra studies (*Russian*) 7-33453
- CdSe(S) thin films, electrophys. props., electron irradiation effects study, solar cell appl. 7-16894
- CdTe: B⁺ (Cu⁺) ion implantation damage, rapid thermal annealing, photolum. anal. 7-39162
- CdTe, annealing in Cd or Hg vapour, defect concentrations 7-65064
- CdTe layers, electrochemical deposition, struct. and elec. props. 7-12526
- p-CdTe, single crystal and thin film, chemical etching study 7-46724
- Ce (001), H₂ adsorption, initial stages of hydride form., UPS, LEED and EELS studies 7-21629
- Ce-(Fe,Co)-(B,Si) system alloys, melt spun ribbons, mag. props. (*Japanese*) 7-53052
- CeCo_{1-x}Si_{2+x}, cryst. struct., homogeneity range, X-ray diff., electron probe anal. 7-37939
- Co-Al, precipitation product dissolution (*Russian*) 7-58479
- Co-based metallic glasses, flash annealing under stress 7-52971
- Co-Fe bilayer thin films, annealing behaviour, mag. props. 7-59079
- Co-Fe-V-Si-B metallic glass, Co-rich, temp. and annealing dependences of magnetostriction const. 7-33255
- Co-Pt bilayer thin films, annealing behaviour, mag. props. 7-59079
- Co-Sb system, α -solid soln., interdiffusion (*Japanese*) 7-6861
- Co-Si, direct solidification, on Si:B(As)(P), rapid thermal annealing 7-21546
- Co-Si bilayered films, chem., elec., and struct. charges upon annealing 7-22037
- Co-Sn multilayers, amorphisation and interdiffusion, EXAFS and XANES studies 7-64812
- CoCr evaporated films, mag. props. 7-33225
- (Co_{0.85}Fe_{0.06}Ni_{0.08}Nb_{0.01})₇₅Si₁₀B₁₅ amorphous alloys, structural relax. and crystn., positron annihilation studies 7-37869
- Co₇₁Fe₂₄Si₁₅B₁₀ and Co₇₅Si₁₅B₁₀ amorphous alloys, mag. props., stress and annealing depend. 7-33250
- Co₈₅Fe₅Si₁₀B₂ amorphous alloys, annealing, positron annihilation parameters 7-39303
- CoO_x sputtered thin, annealing effects on mag. props. and structure, Co-CoO layer separation 7-27180
- CoP amorphous films, FMR spectra during crystallisation 7-53142
- Co₈₀P₂₀, amorphous films, electrodeposited, optical and NMR spectra, annealing effect (*Russian*) 7-45831
- CoSi₂-Si, solid phase epitaxial growth of CoSi₂, nonultrahigh vacuum method 7-45043
- Co₇₅Si₁₀B₁₅, amorphous powder, static consolidation, mechanical and mag. props. 7-3217
- Cr-Si system, thin film silicide phases, formation and microstructure 7-2435
- CrSi₂,Ar⁺ ion beam induced surface and subsurface modifications, AES study 7-64846
- Cr₂Si, Ar⁺ ion beam induced surface and subsurface modifications, AES study 7-64846
- Cu (115), low temp. behaviour of surface roughness 7-6941
- Cu alloys, high-strength, rad.-enhanced recrystn. 7-51871
- Cu, electrodeposits, ductility, effect of inclusions 7-58719
- Cu, FCC structure, multiple grain-boundary contacts (*Russian*) 7-12079
- Cu, fatigue near surface indentations and pits, deform. 7-46628
- Cu, polycrystalline, annealed, large deform., combined tension-torsion, incremental plasticity theory 7-46554
- Cu, recrystallisation texture, deformation temp. effects (*Russian*) 7-8007
- Cu:Ar(Ne)(C), single crystal, ion implantation, damage profile anal. using Auger electron spectroscopy 7-51802
- Cu/In thin film couples, interface CuIn₂ cpd. form. and props., gamma ray spectra 7-21688
- Cu-Al, diffusion coefficients, composition depend. (*Russian*) 7-32701
- α -Cu-Al, ordered domain charactn. from dissoln. kinetics study 7-22693
- Cu-Al bilayers, EXAFS and X-ray reflectivity meas. 7-27821
- Cu-Al bronze, hot deform. and annealing, mechanical props. and softening kinetics 7-17552
- Cu-Al-Mn, surface layers, change in chem. state during annealing investig. using Auger spectroscopy (*Russian*) 7-33834
- Cu-Al-Zn-Mn-Ni shape memory alloy, positron annihilation study 7-46206
- Cu-Fe, implanted solid solns., Mossbauer study on thermal dynamics of Fe atoms 7-45855
- Cu-Fe host-impurity system, O ion bombarded, internal oxidation, Mossbauer spectra studies 7-59131
- Cu-He system, closed swelling layer, internal stress distrib. (*Russian*) 7-59571
- Cu-Kr system, Kr bubble growth, positron annihilation studies 7-39247
- Cu-Mn-Al alloys, mag. and structural props. study 7-2895
- Cu-Nb, supercond. composites, low temp. plasticity, annealing hardening, strength (*Russian*) 7-59579
- Cu-Ni alloys, chemisorpt.-induced surface segregation, time-of-flight atom probe and AES studies 7-32657
- Cu-Si interface, surface struct., angle resolved Auger electron emission determ. 7-21672
- Cu-Sn, diffusion coefficients, composition depend. (*Russian*) 7-32701
- Cu-Zn-Al shape memory alloys, grain refinement 7-53774
- Cu-Zr metallic glass, elec. cond., annealing effects 7-7198
- CuAl-quartz, SAW resonators, annealing behaviour and phase noise performance 7-11242
- CuAu I and II, initial ordering stages, twinning, periodic antiphase boundaries, electron microscopy 7-28032
- CuAu, ordering and recrystallisation, TEM studies (*Russian*) 7-16479
- Cu₃Au, electron irradiation, long range ordering, recovery, vacancy migration and clustering, positron lifetime study 7-39543
- Cu₃Au, quenched, vacancies, ordering and annealing, positron lifetime and elec. resist. meas. 7-39544
- CuB:He, neutron irradiated, annealing behaviour of defects, positron annihilation study 7-39291
- CuInSe thin films, flash evaporation prep. and characterisation 7-7893
- CuInSe₂ polycryst. semicond. growth from melt, surface props., ion bombardment and annealing effects 7-46304
- CuNiFe, electron irradi., decomposition kinetics and morphology 7-58491

annealing continued

- Cu₂O films, annealing of Cu and O vacancies, cathodoluminescence study 7-59263
 Cu_{1-x}S-Cd_{1-x}Zn_xS thin film solar cells perform., depend. on annealing temp. 7-17861
 Cu_{0.85}Sn_{0.15}, amorphous melt-quenched alloys, crystn. (*Russian*) 7-37881
 Cu₄₈Ti₅₂, amorphous, crystallisation, intermediate long period superlattice phase form. 7-21098
 Cu₂Ti_{100-x}, x=50-66, metallic glasses, crystn., DTA, X-ray diffr., hardness meas. 7-63489
 DyIG:Ga,Bi, RF sputtered films for magneto-optical memory, mag. props. 7-64613
 Eu₂PCl(Br)(I), prep., mag. props. and cryst. struct. (*German*) 7-32379
 Fe (100) 7-8154
 Fe, amorphous, elastic constants, relax. effects 7-51910
 Fe, Armco, annealed and cold worked, neutron irradiation damage 7-2067
 Fe based eutectic alloy powder, plasma coatings with interstitial phases, tribotechnical props. 7-17731
 Fe films on Ni substrates, magnetism and interface processes, in-situ conversion electron Mossbauer study 7-7571
 α -Fe single crystals, activation energy of S diffusion, surface segregation, AES obs. 7-39529
 Fe single crystals, Bi ion implantation, high substitutional fractions 7-58299
 Fe sputtered films, mag. perpendicular anisotropy, Mossbauer studies 7-59076
 Fe/Ni Reed blades, Au coated, AES/SEM study 7-44972
 Fe-Ag sputtered films, thermal stability, X-ray diffr. and Mossbauer studies 7-58679
 Fe-Al, ²⁶Al diffusion, radioactive isotope meas. (*Russian*) 7-32700
 Fe-Al (40 at.%), electron irradiation, Huang scatt. from interstitials 7-58272
 Fe-Al(Si) cold-rolled nonbrittle powder strip prep., texture and mag. props. 7-46370
 Fe-B (15 at.%), amorphous powder and strip, struct., mag. props., thermal stability (*Russian*) 7-63470
 Fe-B based metallic glasses, embrittlement, formation of B-rich zones 7-59598
 Fe-B metallic glasses, struct. relax., Curie temp. meas. 7-21124
 Fe-B-Ce-based metallic glasses, mag. domain structs. and annealing embrittlement 7-27586
 Fe-B-based amorphous alloys, struct. evolution during heating (*Russian*) 7-16418
 Fe-based metallic glasses, retardation of annealing embrittlement by Ce microadditions 7-65118
 Fe-Co-B films, phase transition, microstruct. 7-33568
 Fe-Cr-B-Si, amorphous, annealing effects on Curie temp. 7-45675
 Fe-Cr-Si-B metallic glass wires, corrosion rel. to crystallinity and comp. 7-46701
 Fe-Cu, neutron irradiation, defect microstruct., SANS and TEM studies 7-58351
 Fe-Cu sputtered films, thermal stability, X-ray diffr. and Mossbauer studies 7-58679
 Fe-N, Snoek-Koster relax., dislocation effects (*Russian*) 7-44686
 Fe-N martensite, transform. kinetics, anal. by nonisothermal dilatometry 7-8004
 Fe-Ni, martensitic transform., defect form., positron annihilation study (*Chinese*) 7-39213
 Fe-Ni (36 at.%), Invar, oxidation, effect of annealing conditions 7-28167
 Fe-Ni alloys, martensitic transform., positron annihilation study of defects 7-39266
 Fe-Ni films, γ -phase low temp. precipitation investig. (*Russian*) 7-33666
 Fe-Ni thin films, α to γ transform, redistrib. of atoms in submicrostruct. (*Russian*) 7-53722
 Fe-Ni-B metallic glasses, crystallisation, microhardness (*Russian*) 7-59617
 Fe-R-B (R=rare earth) metallic glass permanent magnets, TEM studies 7-26661
 Fe-Si, grain oriented, hot rolling texture, thickness variations 7-8009
 Fe-Si, rapidly quenched ribbons, grain growth, mag. props. 7-8017
 Fe-Si (3 wt.%), continuously cast slabs, high temp. grain growth during reheating 7-8019
 Fe-Si (3 wt.%), grain oriented, desulphurisation kinetics, 899-1171°C 7-8002
 Fe-Si-B amorphous alloys, hypoeutectic, thermal stability and soft mag. props. 7-11928
 Fe-Ti-N, mech. props. rel. to cold working 7-28089
 Fe-TiB₂ eutectic system, microhardness, modulus of elasticity (*Russian*) 7-39648
 FeAl, B2-structured, annealed and slow cooled, occurrence of displacement fringes 7-6808
 Fe₈₁B₁₉ amorphous alloy, thermally activated time fluctuations of nucl. spin orientation 7-7622
 Fe₈₃B₁₇, metallic glass, struct. relax. X-ray and neutron diffr. study 7-6521
 Fe₇₈B₁₃Si₉, amorphous alloys, mag. losses, aging kinetics 7-59056
 Fe₇₈B₁₃Si₉ amorphous ribbons, ferromag. resonance 7-27606
 Fe₈₀B₁₄Si₆ amorphous ribbons, anisotropy of losses 7-45658
 Fe₇₇B₁₆Si₇Cr₂ metallic glass, crystallisation, DSC and X-ray diffr. studies 7-11932
 FeCo alloy, electronic struct., effect of ordering, positron annihilation and Mossbauer effect study 7-45142
 Fe₆₇Co₁₈B₁₄Si₁ amorphous mag. alloy, crystallisation, elec. resist., TEM obs. 7-11927
 Fe₄₃Cr₂₅Ni₂₀B₁₂ glass, devitrification, mag. meas. and X-ray diffr. studies 7-21128
 (Fe_{1-x}Mn_x)₇₈B₂₂, amorphous alloys, lattice parameters, annealing, X-ray diffr., elec. resist. 7-37878
 Fe₇₅Mo₅Si₉B₁₃, amorphous, structural relax. and quasi-texture 7-11925
 Fe₄₀Ni₄₀B₂₀ amorphous thin films, coercive field, annealing effects 7-7553
 Fe₄₀Ni₄₀B₂₀ amorphous alloy, effect of plastic deform. on mech. and mag. props. (*Russian*) 7-53810
 Fe_{45.5}Ni_{44.5}B_{10.3}, amorphous, internal friction, thermo-EMF struct., annealing effect (*Russian*) 7-59560
 Fe₄₀Ni₄₀P₂₀ amorphous alloy, electron struct. and surface struct., XPS and UPS studies 7-27238
 Fe₄₀Ni₄₀P₁₄B₆ amorphous alloys, annealing, positron annihilation parameters anal. 7-39303
 Fe₄₀Ni₄₀P₁₄B₆, Metglass 2826, crystn. behaviour, influence of annealing atm. 7-53768

annealing continued

- (Fe_{0.8}Ni_{0.4})₈₂Si₁₈B₁₀ amorphous alloys, structural relax. and crystn., positron annihilation studies 7-37869
 Fe₇₅Ni₅Si₉B₁₃, amorphous, structural relax. and quasi-texture 7-11925
 FeO, fine particles, magnetic and morphological props., annealing effects study 7-53766
 Fe₂O₃:Ti(Sn,Nb), γ -ray damage, impurity effects on annealing 7-6679
 Fe₈₀P₂₀, amorphous ribbons, structural relax., crystallisation, Mossbauer spectra (*Chinese*) 7-11918
 FePGA, amorphous, magnetoelastic props. 7-27591
 FePd, annealed, transport and thermal expansion props. 7-46512
 Fe₇₈Si₁₂B₁₀ amorphous alloys, surface crystallisation and mag. props. 7-51649
 Fe₃(1- δ)O₄, magnetite, synthesis, crystal growth and characterisation 7-2647
 GaAs, decomposition during rapid thermal annealing 7-13657
 GaAs, defects, positron lifetime spectra 7-37979
 GaAs, electron-irradiated, relative density of levels of radiation defects 7-52500
 GaAs, high temp. annealing, prevention of thermal surface damage 7-39546
 GaAs, ion implanted, rapid thermal annealing, review 7-58296
 GaAs LEC substrates, EL2 deep donor kinetics under annealing, IR absorpt., DLTS, Hall effect meas. 7-32955
 GaAs LEC wafers, cathodolum. mapping, IR absorpt., X-ray topography obs. 7-33462
 GaAs MBE layers on Si (100), crystalline quality, rapid thermal annealing effects 7-12519
 GaAs, metastable state annealing 7-27297
 GaAs molecular beam epitaxial layers, defect density reduction by thermal annealing, TEM study 7-45041
 GaAs, n-type, proton irradiated, effects of annealing on optical properties 7-28155
 GaAs, neutron transmutation doped, thermal annealing effects, channelling anal. (*Chinese*) 7-12178
 GaAs, neutron-irradiated, vacancy annealing, positron-lifetime study 7-64727
 GaAs, ohmic contact, form. using ion beam mixing 7-21299
 GaAs, proton bombarded, H platelets, TEM obs. 7-12164
 GaAs pure and Si, Mn or Cu doped crysts., impurity and defect props., heat treatment, photolum. studies 7-39163
 GaAs, Schottky barrier formation, effect of surface annealing 7-12785
 GaAs, semi-insulating LEC crystals, thermal conversion, DLTS studies 7-7150
 GaAs, surface region, heat-treated, photoluminescence, antisite defect obs. 7-39167
 GaAs: Si(Se)(Zn)(Be), ion implanted, rapidly annealed, damage removal process 7-17043
 GaAs:B, ion implanted, near-intrinsic and extrinsic photocapacitance due to the EL2 level 7-7147
 GaAs:Be⁺, ion implanted, residual microstruct., TEM studies 7-32675
 GaAs:Ge, Se, diffused contact regions, rapid thermal annealing 7-17103
 GaAs:In, LEC growth, annealing, solid soln. hardening, dislocation density, elec. props. 7-17404
 GaAs:In annealed substrates, In distribution in surface region 7-44959
 GaAs:Mg⁺, formation of p-type layers using ion implantation and rapid thermal annealing 7-45311
 GaAs:Se, ion implanted, annealing mechanism 7-26777
 GaAs:Si, annealing behaviour of impurities in presence of stress 7-65060
 GaAs:Si, ion implanted, amorphisation and epitaxial regrowth, defect depth profiles 7-12088
 GaAs:Si, ion implanted and rapid thermal annealed, activation efficiency, crystal stoichiometry effects 7-51791
 GaAs:Si(Be)(Mg), rapid annealing, temp. depend. of damage removal and carrier activation 7-17032
 GaAs:Sn(Te)(Zn) surface layers, luminesc., electrophys. parameters, effect of annealing 7-64680
 GaAs:Te, annealing encapsulation props. of SiO₂, Si₃N₄ and Si_xN_yO₂ films 7-8030
 GaAs:Te films, flash evaporation, annealing, elec. props. 7-64373
 GaAs/AlGa_{1-x}As modulation doped heterostruct., high temp. annealing effects (*Chinese*) 7-12805
 GaAs/Au contacts, interface morphology 7-45020
 GaAs/Ge heterojunction interfaces, cyclic behaviour of band discontinuities 7-7365
 GaAs-AlAs MQW structures, Ga⁺ ion implantation defects 7-44585
 GaAs-AlGaAs heterojunctions, Be⁺, O⁺ ion implantation, impurity profiles, elec. characts. meas., SIMS, annealing 7-12813
 GaAs-anodic oxide interfaces, annealing, As enrichment, photoluminescence, Rutherford backscattering anal. 7-21687
 GaAs-Nb(NbN) Schottky barriers 7-58856
 GaAs-thermal oxide interfacial chem. reactions, Raman spectra, AES 7-27145
 GaAs_{1-x}P_x:Be⁺-GaP:Be⁺ strained-layer superlattices, ion implantation doping, structural study 7-38030
 GaAs_{1-x}P_x:Be⁺-GaP:Be⁺ strained layer superlattices, ion implantation doping, optical and elec. props., device appls. 7-44583
 GaInAs, pn junction formation by simultaneous implantation and diffusion annealing 7-38028
 GaInAs-SiO₂ system, annealing behaviour, SIMS and elec. meas. 7-38270
 GaP epitaxial layers, MOCVD growth on Si, TEM and SEM 7-38416
 GaP, neutron irradiated and as-grown, vacancy defects, positron studies 7-2012
 GaP:He⁺, implanted, swelling, strain and radiation damage 7-6694
 Gd-Fe sputtered amorphous films, structural relax., positron lifetime meas. 7-37870
 Ge, amorphous layers on GaAs, solid phase epitaxial Growth during annealing 7-21777
 Ge, electron irradiation, annealing kinetics, impurity effects 7-16630
 Ge, ionisation-stimulated annealing of Frenkel pairs under electron or gamma irradiation 7-38061
 Ge microcrystals, gas-evaporated, thermal annealing, Raman and electron microscopic study 7-64635
 Ge sputtered (100) textured film, TEM grain growth obs. 7-45040
 Ge surface state characts., surface struct. and low temp. annealing effects 7-45426
 p-Ge, undoped, deep level defects produced by electron irradiation, annealing 7-12660
 Ge:As(Sb)(Te)(Bi), implanted, heavy ion damage, TEM, annealing studies 7-63676

annealing continued

p-Ge:B(Al)(Ga)(In), annealing kinetics of radiation defects, influence of impurity binding energy 7-39547
a-Ge:H, elec. props., effect of H plasma press. (*Korean*) 7-27332
Ge:O, thermal donor binding energies 7-16989
Ge:Si, ion-implanted amorphous surface layers, EXAFS 7-27823
Ge-Mo-GaAs ohmic contact, fabrication and characts. study 7-45490
Ge₂Se_{6-x}Te_x amorphous chalcogenide, elec. cond., bulk and thin film effects 7-7238
Ge₂Si_{1-x}-Si multilayers, MBE grown, thermally annealed, Ge diffusion, strain relax., ion channelling, backscattering anal. 7-6896
Ge_{1-x}Sn_x amorphous films, structural changes on annealing 7-16422
GeTe, α - γ phase transformation kinetics, effect of heat treatment 7-63795
GeTe₂ amorphous films, struct. changes by annealing 7-63467
a-Ge_{1-x}Te_x films, crystallisation behaviour and local order 7-44386
Ge₂₀Te₈₀ glasses, heat capacity, relax. and thermodynamic kinetics during annealing 7-44843
a-H₂O films, low temp. elastic props. 7-45099
HgCdTe epitaxial layers, Hall effect and elec. resist. characterisation 7-64375
HgCdTe: In, ion implanted, damage and rapid thermal annealing 7-63637
HgCdTe:B⁺, ion implanted n⁺p junction, lifetime and carrier conc. profile 7-45450
Hg_{1-x}Cd_xTe, electron-irradiated, positron annihilation 7-38060
Hg_{1-x}Cd_xTe films, LPE using a semiclosed rotational boat 7-64937
Hg_{1-x}Cd_xTe:B, ion implanted, annealing, nature oxide encapsulation 7-2036
HgCr₂Se₄, magnetisation, temp. depend. 7-45629
HgGa₂Se₄, photocond., photoluminescence spectra, annealing and ion implantation effects 7-39152
HgGa₂Se₄, single cryst., deep levels, photocond. and photolum. spectra 7-7159
a-HgSe films, elec. conductivity, thermoelectric power, optical absorpt. 7-22050
HgTe, electron-irradiated, positron annihilation 7-38060
HOH₂ films, H annealing, elec. resist 7-64000
In film, irreversible resistivities during annealing process 7-64365
In, impurity-induced vacancy clustering, positron studies 7-38044
In, monovacancy formation enthalpy, positron annihilation Doppler broadening studies 7-37976
InAs, nuclear transmutation doping 7-38025
InAs surface on InP, epitaxial regrowth 7-2431
InAs_{0.9}Sb_{0.1} IR detector, photoresponsivity meas. 7-7274
In_{0.5}Ga_{0.5}As:Be, high dose implants, rapid thermal annealing 7-16602
InGaP/InGaAlP multiquantum-well laser diodes, MBE growth and characterisation 7-62689
In_{0.3}Sn films, prep. by thermal decomposition of organometallic cpds., optical and electrical props. 7-17483
InP (100), prep. by P deposition and annealing, surface reconstruction, LEED, EELS studies 7-38311
InP crystals and solar cells, radiation-induced defects, room-temperature annealing 7-39993
InP, electron irradiation, damage, impurity effects 7-12154
InP, high resistivity layer form. by ion implantation, ohmic contact characterisation 7-38035
InP MIS structures, prep. by RF plasma oxidation, interface elec. props. 7-2731
InP:Be(Si), isothermal anneal techniques, comparison 7-16603
InP:Hg ion implanted at 200°C, rapid thermal annealing, carrier conc. and mobility 7-32469
InP:Si, substrate, encapsulated annealing, using SiN encapsulant 7-39779
InP:Zn, ion implantation and annealing, Raman studies 7-6652
InP-Au interface, Fermi level pinning, growth characts., photoemission spectra 7-22009
InSb (1-1-1) (3 × 3) reconstructed, X-ray diffr. studies 7-6951
InSb MOS interfaces, annealing, O diffusion and reaction 7-58665
Ir single crystals, bulk self-diffusion, radiometric anal. (*Russian*) 7-58530
Ir-Pt (2 at.%), surface segregation, AES study 7-27066
KBr microcrystalline powders, interstitial cluster stability 7-32485
KBr:Eu²⁺, impurity precipitates, Raman spectra meas. during annealing 7-64634
KCl:Eu²⁺, impurity precipitates, Raman spectra meas. during annealing 7-64634
Kl:Eu²⁺, impurity precipitates, Raman spectra meas. during annealing 7-64634
La_{1-x}Sr_xMO₃ (M=Cr, Mn, Fe, Co), electrodes for high temp. oxide fuel cells 7-54291
Li based oxide ceramics, fusion breeders, chemical compatibility with stainless steels 7-49646
LiAlO₂, ceramic breeder material, post irradi. T recovery 7-49647
LiF, cryst., defect struct., high-temp. annealing effects (*German*) 7-32448
LiMnFe₂O₄ ferrite, solid solution form. in contact diffusion pairs 7-2273
LiNbO₃, optoelectronic material, radiation effects 7-26811
LiNbO₃, planar waveguides, He⁺ ion implantation, transient annealing 7-25965
LiNbO₃ polycrystalline films, prep. by hydrolytic decomp. of metal alkoxide alcoholic solns., SEM obs. 7-7044
LiNbO₃:Fe, and undoped crystals, decay of γ -centres 7-7658
LiNbO₃:He⁺ implanted waveguide stability 7-43364
LiNbO₃:He⁺ optical waveguides, thermal annealing 7-15983
LiNbO₃:Mg, incorporation of H⁺, IR spectra of OH⁻ ions 7-7724
Li₂O, ceramic breeder material, post irradi. T recovery 7-49647
Li₂O, neutron and ion irradi. damage, ESR and optical absorption studies 7-32509
MgO, deformed and annealed, red cathodoluminescence spectrum 7-27792
MgO, electron irradi., stored energy, differential thermal anal. studies 7-32503
Mg₇Zn₂₄, amorphous, crystn., X-ray small angle scatt. 7-11935
Mn-Al-C ferromag. alloys, phase, transformations, and struct. defects, positron annihilation study 7-46461
Mn-Ni alloys, γ -phase decomposition, annealing and quenching, X-ray phase anal. 7-17510
MnO₂, crystallite size, strain, X-ray diff. study 7-2221
Mn_{0.97}Ti_{0.03}As, mag. phase transitions, effect of Ti additions 7-27519
Mo, alpha-particle-induced defects, annealing, positron annihilation studies 7-44633
Mo, cold worked, defect annealing behaviour, positron annihilation studies 7-37975

annealing continued

Mo, radiation annealing hardening low temp. peak 7-22739
Mo, single cryst., recrystallised after hydraulic extrusion, wide-angle boundaries of anomalous grain 7-44563
Mo thin monocryst. plates magnetoresist., Al atoms diffusion annealing effects (*Russian*) 7-7408
Mo/Al-Si interdiffusion kinetics and contact resistance study for VLSI appls. 7-21714
Mo/Si, amorphous multilayers, annealing, diffusion, structural relax. 7-52309
Mo-H proton irradiated system, defect annealing, positron lifetime studies 7-38043
Mo-N system, neutron irradi., isochronal annealing, positron annihilation studies 7-46531
Mo-Re (27 wt.%), rolling, reorientation, annealing effect (*Russian*) 7-39598
MoN B1 phase sputtered films, mag. susceptibility and defect struct. 7-53087
MoS₂ films, RF magnetron sputtered, elec. and optical props. 7-2747
MoSi₂:As-poly Si struct., redistribution of As by silicidation tempering 7-51812
(NH₄)₂MoO₄-Ni(NO₃)₂, interaction, effect of mechanical activation on NiO:MoO₃ ratio 7-8261
Na₂B₄O₇-NiO, tetraborate glass, optical absorpt. effects of NiO additions and annealing 7-22851
NaCl:Eu single cryst., EuCl₂ phase precipitation, fluoresc. and X-ray diffr. studies 7-46108
NaNbO₃ polycrystalline films, prep. by hydrolytic decomp. of metal alkoxide alcoholic solns., SEM obs. 7-7044
Na₂O-Al₂O₃-SiO₂ glasses, elastic props., annealing and Al substitution effects 7-8035
Na₂O-CaO-SiO₂ glass, cracktip blunting kinetics, annealing, corrugated surface 7-46611
(Nb,Ti)₃ Sn, supercond. mag. material, fusion reactor conditions simulation 7-52922
Nb alloys, borosilicide coatings, X-ray obs. (*Russian*) 7-45066
Nb thin whiskers, struct., heat treatment effects, SEM study 7-12579
Nb:He⁺(H⁺) films, radiation defects produced by ion implantation 7-7059
Nb-Al thin film diffusion couples, Nb₃Al A15 phase form. during annealing, XPS and Auger studies 7-58548
Nb-H system, alpha-particle irradi., defect annealing behaviour 7-44605
Nb-H system, electron irradi., vacancy recovery, positron lifetime studies 7-37972
Nb-N, internal friction rel. to quenching temp. (*Russian*) 7-46543
Nb-Ti, supercond. mag. material, fusion reactor conditions simulation 7-52922
Nb₃(Ge,Si), A15 phase, Si stabilisation, supercond. transition temp., sp. ht. meas. 7-45532
Nb₃Sn multifilamentary composite superconductor, bronze processed, global pinning force, critical mag. field, grain size 7-22078
Nd-Dy-Fe-B-based sintered magnet, microstruct., heat treatment effects 7-53767
Nd-Fe-B system, temp. depend. of coercive force, effect of annealing, aging and sintering 7-27560
Ni (110), adsorption of O, surface phases, absolute coverages 7-12486
Ni (110), defects developed by epitaxial growth of Ni film or ion bombardment 7-63924
Ni epitaxial growth on Fe (001), LEED and AES studies 7-64022
Ni, fatigue cycling, lattice defect characterisation 7-37978
Ni finite films, sputtered, struct. and compositional studies 7-64024
Ni, He implanted, defects study by monoenergetic positron beam 7-39293
Ni, irradi. with energetic ions, defect prod. and recovery 7-58370
Ni powder plastically worked articles, annealing effect on behaviour in temp. jump and substruct. 7-27961
Ni, quenched and deformed, vacancy clustering, positron annihilation 7-44534
Ni/Al-Si system, contact structure formation by rapid thermal melting 7-45019
Ni-B, implanted, mech. props., disorder and amorphicity 7-53819
Ni-base superalloys, stability of lamellar γ - γ' struct. 7-46566
Ni-based consolidated rapidly solidified alloys, strengthening mechanisms 7-22712
Ni-Cr-Si thin films, influence of Si on props. 7-22493
Ni-Fe-Cu, mag. props., hardness, elec. resist., V, Nb and Ta additions effect (*Japanese*) 7-12998
Ni-Fe-In ternary Permalloy electroplated films, mag. props. and thermal stability 7-33236
Ni-Fe-Mn system, coexistence of Ni₃(FeMn) and Ni(MnFe) superstructures (*Russian*) 7-1946
Ni-GaAs, metallurgical reactions, heavy ion Rutherford backscattering spectrometry 7-53488
Ni-GaAs interfacial reactions, contact elec. props. 7-12504
Ni-H proton irradiated system, defect annealing, positron lifetime studies 7-38043
Ni-Kr system, Kr bubble growth, positron annihilation studies 7-39247
Ni-Mo (6 at.%), oxidation, ESCA study 7-22897
Ni-Mo-Cr-B powders, amorphous and microcrystalline, shock consolidated, wear props. 7-46655
Ni-Mo-Cu-Fe-Mg, coarse-grained PC permalloys, annealing-twin density (*Japanese*) 7-3330
Ni-Mo-Fe-Cr alloy, transient phase obs during long range ordering to Ni₃Mo, electron diffr. study 7-63806
Ni-P, implanted, mech. props., disorder and amorphicity 7-53819
Ni-P electrodeless deposited amorphous coatings, wear resistance, crystallisation effects 7-53913
Ni-rich alloys, vacancy swelling suppression mechanism 7-46511
Ni-Si bilayered films, chem., elec., and struct. charges upon annealing 7-22037
Ni-Si-B, nonferromagnetic amorphous wide ribbons, Young's modulus anisotropy 7-3354
Ni-Te, vapour deposited thin films, annealing behaviour 7-3345
Ni-Ti(Ta)(Cr), amorphous and cryst. reaction with Si studied by RBS and TEM 7-21704
(Ni-Pd)₈₂Si₁₈ amorphous alloys, corrosion behaviour, struct. relax. effects. 7-8166
Ni₃Al-Be, ductility, strength, grain boundary segregation, solid soln. strengthening, Be addition effect 7-39608
Ni₆₄B₃₆, metallic glass, struct. relax. X-ray and neutron diffr. study 7-6521

annealing continued

- Ni₇₂B₁₇Si₃, ultrafine fine-grained, prep. from amorphous ribbon, creep deform. 7-22748
- Ni₈₃Cr₇Fe₃Si₃B₃, amorphous alloy, crystallisation (*Chinese*) 7-6518
- Ni_{69.2}Cr_{6.6}Si_{13.7}B_{7.9}Fe_{2.6}, amorphous alloy, 70 MeV Ni¹⁶ ion irradi., surface swelling 7-16646
- Ni₃Fe, ordered and disordered, mag. permeability studies 7-59053
- (Ni₃Fe)_xCr_x alloys, ordering study, comp. depend., electron diff. and Mossbauer meas. 7-51690
- Ni₃Mn-NiCr tie line, disordering kinetics, neutron diff. investig. (*Russian*) 7-32347
- Ni₄Mo-Cr, isothermal annealing, structural changes 7-46462
- NiO, substoichiometric, positron annihilation meas. 7-37981
- NiSi₂, epitaxial growth on Si (111) inside miniature size oxide openings 7-58673
- NiSi₂ formation by reaction of filament evaporated Ni with Si substrate 7-38268
- NiSi₂-Si, interface states, barrier height, Fermi level 7-27430
- NiTi alloy powder, shock compaction 7-59480
- a-P, sputtered, response to intense ion bombardment 7-27447
- PLZT ceramics, mechanical strength, composition and polarisation depend., microindentation meas. 7-6697
- Pb, superconducting transition, deform. strengthening, dislocation density (*Russian*) 7-58939
- Pb-Tl, Bridgman growth, pattern generation at solidification front, forbidden cells 7-22651
- Pb₃Ge₃O₁₁:Gd³⁺, impurity ion reorientation kinetics 7-45940
- PbIn_{1/2}Nb_{1/2}O₃, antiferroelec., phase transition, B-site cation order effects 7-7651
- PbO-K₂O-Sb₂O₃-As₂O₃ flint type glasses, viscosity near annealing temp., depend. on PbO conc. 7-58151
- PbSe films, photosensitivity mechanism 7-58923
- Pb_{0.88}Sn_{0.12} Te cryst., annealing characts. and laser fabrication (*Chinese*) 7-10933
- PbTi_xZr_{1-x}O₃ piezoceramic, annealing in gaseous media with controllable comp., effect on electrophysical props. 7-8012
- Pd film, vapour quenched, resistivity meas., indirect obs. of amorphous to crystalline transition 7-52864
- Pd silicide formation, in situ ellipsometric studies 7-21694
- Pd/Si:B,As/Si:B, As ion implant redistribution during Pd₂Si formation using rapid thermal annealing 7-16816
- Pd-Ag-Fe (1 and 2 at.%), plastically deformed, elec. resist., short range order effects 7-27318
- Pd-GaAs, metallurgical reactions, heavy ion Rutherford backscattering spectrometry 7-53488
- Pd-GaAs, phase formation sequence, morphology 7-27153
- Pd-Si, nonferromagnetic amorphous wide ribbons, Young's modulus anisotropy 7-3354
- Pd-U-Si glassy state, quasicrystalline phase form., X-ray and electron diff. studies 7-26645
- Pd_{100-x}Ag_x, plastically deformed, elec. resist., short range order effects 7-27318
- PdCuSi, amorphous, reversible and irreversible changes in the thermal conductivity 7-45267
- PdFe ordered alloy, discontinuous domain coalescence (*Russian*) 7-2025
- Pd₄₀Ni₄₀P₂₀ metallic glass, structural relax., shear and longitudinal sound vel. meas. 7-51655
- PdSi, phase transform. to Pd₂Si, kinetics 7-16795
- PdSi₂-Si, interface states, barrier height, Fermi level 7-27430
- PdSiCu, amorphous, ultrasonic vel., mechanical props. (*Korean*) 7-26874
- Pd_{58.8}U_{20.6}Si_{20.6} alloys, glassy to icosahedral quasicrystalline phase transition, elec. and mag. props. 7-37863
- PrCo₅, microstructure and coercivity, effect of annealing, 650-850°C 7-38905
- Pt/SiN/Si structure, nucleation kinetics and spatial distribution of spherulitic PtSi clusters 7-21675
- Pt-GaAs, metallurgical reactions, heavy ion Rutherford backscattering spectrometry 7-53488
- Pt-group metal silicides epitaxial growth on Si (111) 7-21760
- Pt-Rh surfaces, N₂ and CO adsorption, temp. depend. and work function studies 7-33960
- Pt₃Si_{1-x}/n-GaAs contacts, elec. and metallurgical characts. 7-64345
- δl-Pu-Ga (1.5 wt.%) foils, cold rolling, annealing, microstruct., TEM obs. 7-59544
- RSi_{2-x}Si (R=Sc, Y, Gd, Ho, Tb, Dy, Er, Tm, Yb, Lu), silicide thin films, phase composition, conductance, surface morphology 7-7072
- Rh/GaAs Schottky contact, correlation between solid-state reaction and electrical props. 7-58655
- Ru-Cu₂S system, annealing, phase comp., DTA 7-46412
- Sb films, amorphous, vacuum-deposited, growth of hexagonal plate cryst. 7-51634
- Sb-S, thin films, amorphous and thermally annealed, optical props. (*Russian*) 7-17352
- Sb-Se, thin films, amorphous and thermally annealed, optical props. (*Russian*) 7-17352
- a-Sb₂Si₃ films, thermally induced relax. of mechanical stresses 7-8032
- Se, amorphous films, crystn., kinetic study 7-21101
- Se, thin films, amorphous, crystn. 7-44371
- Si (001), scanning tunnelling microscopy 7-27072
- Si (001)-(2×8), clean and Ni contaminated, ordered-defect model 7-21586
- Si (111) with ordered Cu, Ag and Au overlayers, inverse photoemission spectroscopy 7-59280
- Si (111) with oxidised Cr overlayer, CrSi₂ formation and reduction of Cr₂O₃ during annealing 7-58660
- Si (111)/Au interfaces, structural and electronic props., annealing effects 7-21679
- Si (111)-(7×7), interface formation during W deposition 7-58710
- p-Si, alpha-particle irradi., defect form. and thermal stability 7-38073
- Si, amorphisation and crystallisation 7-11914
- Si, amorphised films, solid phase epitaxial regrowth, TEM characterisation 7-32883
- Si, amorphous to crystalline transformation, TEM in situ technique 7-44376
- Si, broken dislocation bonds, annealing effects, optical polarisation of nuclear moments study 7-38008
- Si buried oxide form. mechanisms by ion implantation 7-44580
- Si, charged defect states at grain boundaries 7-44564
- Si crystals, radiation defect stabilisation and annealing kinetics study (*Russian*) 7-44608

annealing continued

- Si, Czochralski, electron-irradiated, DLTS and photoluminesc. studies 7-7149
- Si, Czochralski grown, electron irradi., thermal donor form. 7-21868
- Si defect annealing and impurity activation during high-intensity As⁺ implantation doping 7-58295
- Si dendritic web ribbon, electrical and struct. props. 7-16922
- Si, dislocation density reduction by thermal cyclic annealing 7-12072
- Si, dislocation loops, generated by ion implantation and furnace annealing, depth profiles, RBS, X-ray diff., TEM anal. 7-51882
- Si dislocation-free single crystals, microdefect recomb. activity, electron irradi. and annealing effects, SEM study (*Russian*) 7-21287
- Si, electron irradi., obs. of IR bands during annealing, kinetic study 7-45214
- Si film growth for MOS-VLSI, Ti and Pt silicide form. 7-7870
- Si films, amorphous-crystalline mixtures, annealing effect on optical props. 7-59273
- Si, grain boundary pot. barrier and role of distorted bonds 7-46080
- Si, implantation damaged, transient enhanced dopant diffusion 7-44910
- Si, indentation dislocation rosettes length, influence of Vickers indenter edge orientation rel. to slip directions 7-58284
- Si, interstitial-based intrinsic gettering process appl. to multilevel defects structs. 7-38048
- a-Si, ion implanted, 2D model of nucleation and regrowth 7-38408
- Si ion-implanted with MeV energy B⁺, P⁺ and As⁺ ions, annealing behaviour 7-51776
- Si, ionisation-stimulated annealing of Frenkel pairs under electron or gamma irradiation 7-38061
- Si, laser induced defects, rapid and classical thermal processing, annealing kinetics 7-44609
- Si layers, electron irradiation-induced defect levels, annealing behaviour, DLTS studies 7-52493
- Si MBE layers, defect characterisation, luminesc., TEM studies 7-13227
- Si, mag.-field Czochralski-grown neutron transmutation doped, thermal behaviour 7-53574
- Si materials science issues in IC processing 7-35115
- Si, neutron irradi. induced IR absorpt. bands 7-46004
- Si, neutron irradiated, recovery 7-39567
- Si, neutron-irradiated, photoluminescence study of annealing process 7-51833
- Si, neutron-transmutation doped, spatially resolved carrier lifetime meas. 7-7257
- Si, oxidative packing defect form. during high temp. annealing 7-44522
- Si polycrystalline films, sheet resistance, rapid thermal annealing prior to and post As ion implantation 7-12886
- Si, polycrystalline layers, TEM meas. of grain size 7-32672
- Si, positron diffusion 7-39281
- Si, quantum well controlled conductivity, new donors 7-38491
- Si, rapid thermal annealing of ion implanted layers, role of trapped interstitials 7-17568
- Si, reactive sputter etching, damage removal methods 7-17742
- Si, recoil implantation of O₂, characterisation by double-crystal X-ray diffraction, TEM, Monte Carlo simulation 7-51807
- Si SOI structure, O⁺ implantation and high temp. annealing 7-44579
- Si SOI structures, implanted buried oxide, high-temp. annealing 7-6654
- Si, single crystal wafer, oxidation, rapid thermal processing 7-22928
- Si single crystals, insulating cpd. form. by ion beam synthesis, RBS, SIMS and cross-sectional TEM studies 7-26779
- Si solar cells, multicrystalline, thermal annealing for fabrication 7-17865
- Si, solid-phase amorphous to crystalline transformation for shallow junction processing 7-32642
- Si substrate for W CVD, effect of dopants and crystal perfection 7-22576
- Si surface, 100, in situ anal. of H, C, N and O using direct recoil time-of-flight technique 7-54242
- Si surface, effect of preoxidation annealing, ion implantation and sputtering on oxide film decomposition 7-63999
- Si surface, temp. depend. absorpt. of benzene and pyridine, annealing effects on sorption states 7-2360
- Si surface layers characterisation after annealing in an RF H plasma 7-58630
- Si, surface nitridation, current status 7-33866
- Si surface studies with a high resolution transmission electron microscope 7-21595
- Si surfaces, adsorbed C, annealing behaviour, XPS and AES studies 7-27108
- Si, transmutation doped, carrier lifetime and hall effect, high temp. processing effects 7-33027
- Si wafer substrates, oxide removal, transient mass spectrometry, XPS studies 7-13670
- Si wafers, doped by neutron transmutation, minority carrier lifetime, photocond., annealing 7-38785
- Si, with transition metal impurities, detect. using rapid thermal annealing 7-2044
- Si¹¹¹Cd, hyperfine interactions, temp. depend., gamma-ray spectra studies 7-64553
- Si:Ag, implantation damage regrowth studied via Ag depth profiling 7-22730
- Si:Al, depth profiles, redistrib. of annealed Al implants 7-63640
- Si:Al, ion implanted and annealed, Al precipitation, TEM studies 7-21238
- Si:Ar, high dose implanted, thermal regrowth, RHEED studies 7-21734
- Si:As, ion implantation-induced defects 7-32433
- Si:As, ion implanted polycrystalline films, electrical activation by rapid thermal annealing 7-58914
- Si:As, precipitation and cluster form., elec. resist., backscatt. and TEM studies (*Chinese*) 7-12285
- Si:As, Rutherford backscattering-particle induced X-ray emission analysis 7-54251
- Si:As₂P, double diffused shallow junctions, rapid thermal annealing 7-22006
- Si:As (B)(BF₃⁺), p-n junction diode, rapid thermal annealing 7-22005
- Si:As films, preannealed and As ion implanted, structural changes during transient pot-annealing 7-16904
- Si:As ion implanted, defect structs. generated by buried amorphous layer regrowth 7-38078
- Si:As ion implanted films, defects charactn. by AC Hall effect meas. 7-38601
- Si:As⁺, heavily doped, ion implant deactivation 7-17567
- Si:As⁺(As₂⁺), ion implanted, phys. props., spreading resist., TEM, Rutherford backscattering, SIMS 7-26775

annealing continued

Si:As(B), ion implant redistribution, diffusion modelling 7-16814
 Si:As(Sb)(Bi), implanted, heavy ion damage, TEM, annealing studies 7-63676
 Si:Au, laser radiation effects on impurity levels 7-12645
 Si:Au, supersaturated low-temp. substitutional impurities, annealing 7-6665
 Si:B, BF_3^+ ion implantation and rapid thermal annealing 7-21241
 Si:B, electron-irradiated, AC hopping conductivity and DLTS 7-44624
 Si:B, ion implanted, B diffusion, rapid thermal annealing 7-58538
 Si:B, ion implanted, defect and dopant depth profile studies 7-2045
 Si:B, ion implanted, transient annealing and residual defect DLTS study (Chinese) 7-12642
 Si:B, O, heavily doped, O precipitation, diffuse X-ray scatt. studies 7-32669
 Si:B, O epitaxial wafers, effect of pre- and postdeposition annealing on O precipitation 7-45060
 Si:B,C,O, O clustering and thermal donor formation kinetics 7-17566
 Si:B,O(Sb,O), heavily doped Czochralski wafers, O precipitation, 450°C thermal annealing 7-58477
 Si:B plastically deformed crystals, dislocation struct. and elec. activity, annealing effects study 7-37998
 Si:B $^+$ (BF_3^+), ion implanted, characterisation by IR attenuated total reflection spectroscopy 7-17327
 Si:B(Al), hydrogenation and annealing kinetics 7-2527
 Si:B(As)-Ti(Co), silicide formation using rapid thermal processing, defect behaviour 7-32726
 Si:B(P)(As)(Sb), retarded and enhanced dopant diffusion related to implantation-induced excess vacancies and interstitials 7-63881
 Si:C,O, luminescence props. of shallow donor centre 7-17347
 Si:C(P), C diffusion during annealing and P in-diffusion 7-16812
 Si:Co, supersaturated solid solution, annealing 7-63642
 Si:D, ion implanted, channelling meas. 7-16597
 a-Si:D(D,H), deuteron mag. resonance, annealing effects 7-33292
 Si:Ga, electron irradiated and annealed, photoluminescence spectra 7-13206
 Si:Ga, highly cond. shallow junction layer form. by ion implantation 7-38037
 Si:Ge, Ge^+ preamorphisation implants, effect on extended defect formation during subsequent solid phase epitaxy 7-16599
 Si:Ge $^+$, ion implanted and annealed, crystalline to amorphous transformation, TEM study 7-32643
 Si:H, ion implanted and annealed, H depth distrib. 7-26785
 a-Si:H, light-induced dangling bonds, annealing behaviour 7-12119
 a-Si:H, light-induced metastable dangling bonds, annealing 7-12118
 a-Si:H, photoluminescence, high temp. annealing effects 7-7745
 a-Si:H, thermal-equilib. processes, electronic transport 7-64167
 a-Si:H evaporated layer production from RF discharge, growth mechanism and props. 7-64898
 a-Si:H films, annealed, structural changes, PMR studies 7-7596
 a-Si:H films, annealing, compressive stress, H evolution 7-28059
 a-Si:H films, electron irradi., photocond., absorpt. coeff. spectral depend. 7-64279
 Si:H films, ion implant redistribution 7-16921
 a-Si:H films, light-induced bond breaking 7-12517
 a-Si:H films and solar cells, light induced effects 7-46954
 Si:H floating zone single crystals, neutron irradi., isochronal annealing behaviour, positron annihilation studies 7-21288
 a-Si:H solar cells, dynamic equilibrium dangling bond density 7-17878
 a-Si:H solar cells, kinetics of light-induced degradation and thermal annealing 7-17909
 a-Si:H solar cells, radiation damage by 12 MeV protons and annealing 7-13895
 Si:In, substitutional ion implanted dopants, electron and positron channelling studies 7-26778
 Si:N, deep level generation and annihilation 7-16612
 Si:N, N incorporation and behaviour 7-16598
 Si:O, C, thermal donor form., T<800K 7-27294
 Si:O, Czochralski crystals, O precipitates, small-angle neutron scattering 7-58484
 Si:O, Czochralski grown, O-related defects after annealing, IR TEM and resistivity meas. 7-32466
 Si:O, defects created by electron irradiation and subsequent thermal treatments, review 7-16642
 Si:O, energy levels and capture cross-sections of thermal donors 7-16988
 Si:O, IR absorption spectra of thermal donors 7-17326
 Si:O, low thermal donor conc. layer formation during annealing 7-17564
 Si:O, low thermal donor conc. layer formation during annealing 7-17565
 Si:O, magnetic resonance of O-related defects 7-17223
 Si:O, oxide precipitate nucleation, thermal donor formation kinetics 7-32667
 Si:O, precipitation phenomena, growth law for disc precipitates 7-16770
 Si:O, thermal donor binding energies 7-16989
 Si:O, thermal donor formation, kinetics 7-6664
 Si:O, thermal donors, photothermal ionisation spectroscopy and IR transmission meas. 7-16987
 Si:O,B $^+$, ion implanted, reverse annealing 7-16617
 Si:O,C, O precipitation, thermal donor generation and annihilation effects 7-16773
 Si:O,C, yield stress, impurities and O precipitate morphology effects 7-16674
 Si:O,C,N, precipitation phenomena, TEM studies 7-16768
 Si:O/Si interfaces, MBE grown, O trapping effects 7-16881
 Si:P, transient enhanced dopant diffusion 7-52136
 n-Si:P,C, electron-irradiated and injection-annealed, vacancies, dislocations and C interstitials 7-51815
 Si:P,O,D, donor passivation and reactivation 7-17031
 Si:P,Sb, mixing of P and Sb ions by recoil implantation, sheet resist., annealing temp. depend. 7-21291
 Si:P thin films, surface energy-driven grain growth during rapid thermal annealing 7-63994
 Si:P $^+$ (PF_3^+), ion implanted, rapid thermal annealing, solar cell appls. 7-23193
 Si:P(Al), random and channelled implantation profiles and range parameters of dopants 7-21246
 Si:P(As)(P,B)(As,B) films, surface energy driven secondary grain growth 7-22740
 Si:P(B) LPCVD films, amorphous and polycrystalline, struct., elec. resist. meas. 7-52870
 Si:Sb,As, cryst. aid amorphous, impurity band form., X-ray spectra studies 7-12650

annealing continued

Si:Sn, ion implanted, annealing behaviour, channelling and conversion electron Mössbauer spectroscopy 7-13485
 Si:Sn,B, shallow junction formation, preamorphisation by Sn implantation 7-7338
 Si:Ti ion implanted layers, defect form. and precipitation, electron microscopy studies 7-12097
 Si:transition metals, anomalous diffusion and gettering 7-2264
 Si:W $^+$ layers, implanted and annealed, struct., TEM, electron diffr. studies 7-32858
 Si/Ge amorphous multilayer films, interdiffusion, neutron scatt. meas. 7-32722
 Si/metal interfaces, silicide form. kinetics during thermal annealing 7-16897
 Si/Ni system, silicide formation, ion beam induced, embedded markers and moving species 7-21298
 Si/PtSi/V/Al Schottky barrier diode metallisation system 7-2666
 Si/SiO $_2$ system, two-step oxidation and interface structs. 7-3542
 Si-Au interface, atomic bonding 7-58663
 Si-B $^+$, Ge^+ , preamorphised shallow junctions, end-of-range and mask edge lateral damage 7-38071
 Si-binary alloy interfacial interactions, Rutherford backscattering spectrometry, TEM 7-12505
 Si-Cu interface, atomic bonding 7-58663
 Si-Fe, ion implanted, channeling/RBS studies 7-2039
 Si-Ge interface, solid phase epitaxy, intermixing, EXAFS, AES, LEED obs. 7-63973
 Si-Ge:O, single crystal, thermodynamic rel. to solubility of O 7-12648
 a-Si-metal-Si structures, rapid thermal sintering and annealing 7-21700
 Si-Si interfaces, MBE grown, sputter cleaned, microstructure, electron microscopy obs. 7-12512
 Si-Si $_3\text{N}_4$, SOI, N $^+$ implanted, microstructural characterisation 7-52300
 Si-Si $_3\text{N}_4$, SOI structs. formed by N $^+$ implantation EPR of defects 7-33273
 Si-Si $_3\text{N}_4$ SOI structs., formation by N $^+$ implantation 7-32532
 Si-SiO $_2$, buried layer SOI structs., elevated temp. high dose O $^+$ implantation, effect of annealing 7-32530
 Si-SiO $_2$, buried oxide formation by O $^+$ implantation, donor creation, enhanced conductivity 7-32529
 Si-SiO $_2$, buried oxide SOI struct., effects of annealing temp. on characts. 7-33099
 Si-SiO $_2$, E' centre in thermally grown SiO $_2$, bias depend. annealing 7-45503
 Si-SiO $_2$, interface trap annealing, rapid thermal processing 7-22027
 Si-SiO $_2$, new donors effect, interface effect due to internal oxidation 7-33093
 Si-SiO $_2$, SOI struct., deep O $^+$ implantation, strain and damage in Si 7-32531
 Si-SiO $_2$, SOI structs. formed by O $^+$ implantation, EPR of defects 7-33272
 Si-SiO $_2$ interface, wet oxidised, RF plasma annealing effects 7-54026
 Si-SiO $_2$ SOI struct. formed by high dose ion implantation, high resolution TEM study 7-59690
 Si-TiSi $_2$, TiSi $_2$ local epitaxial growth on Si (111), rapid thermal annealing, annealing ambient 7-33856
 Si-W CVD film interaction, annealing, silicide formation 7-2390
 Si-Yb interfaces, mixed valence of Yb, synchrotron radiation photoemission spectra, metal coverage and annealing temp. depend. 7-32966
 SiC (0001) and (000 $\bar{1}$) surface segregation, electron spectroscopy 7-21459
 SiC, mixing of metal overlayers, ion beam irradi., rapid thermal annealing, pulsed laser irradi. 7-58330
 α -SiC, sintered, occurrence and distrib. of B-containing phases 7-39466
 β -SiC:Al $^+$ (P $^+$) epitaxial films, ion implanted, rapid thermal annealing 7-16905
 β -SiC:B(N) films, ion implanted, rapid thermal annealing 7-17569
 a-Si:C,H, elec., optical and local structure props. 7-45089
 6H-SiC:P, impurity paramagnetic and elec. props. study 7-53130
 a-Si $_2$ -C $_x$ H $_y$, Si-K β spectra, soft X-ray emission spectra (Japanese) 7-13268
 a-SiGe:H,F alloy films, F incorporation and annealing props. 7-44588
 Si $_1$ -Ge $_x$ films, optical band gap, photocond. props. 7-52672
 SiN $_x$:H films, amorphous, glow discharge deposited, IR absorpt. and Raman scatt. spectra 7-46003
 Si $_3\text{N}_4$ CVD layers, etch rate modification by ion bombard. and annealing 7-28217
 Si $_3\text{N}_4$ ceramics, hot pressed, fatigue test with Knoop indentation, residual stress effects (Japanese) 7-17640
 Si $_3\text{N}_4$ films, plasma deposited, bonds and defects 7-17437
 Si $_3\text{N}_4$ MNOS structures, degradation, thermoactivation spectroscopic study 7-12872
 Si $_3\text{N}_4$, mixing of metal overlayers, ion beam irradi., rapid thermal annealing, pulsed laser irradi. 7-58330
 Si $_3\text{N}_4$ -Ti, reaction under rapid thermal annealing 7-39334
 SiO $_2$, amorphous, annealing and relax. in high-pressure phase 7-17329
 SiO $_2$, amorphous, densified, O diffusion kinetics, annealing, gamma-ray effects 7-52127
 SiO $_2$ films, effects of nitridation press. on props. 7-33818
 SiO $_2$ films, low temp. CVD, dielec. const., dissipation factor 7-59149
 SiO $_2$, γ -ray induced defect centres, thermal bleaching 7-63659
 SiO $_2$, hot carrier trapping characts., effect of post-oxidation annealing 7-64268
 SiO $_2$ low temp.-CVD films, DC dielec. breakdown studies 7-22188
 SiO $_2$, mixing of metal overlayers, ion beam irradi., rapid thermal annealing, pulsed laser irradi. 7-58330
 SiO $_2$, optoelectronic material, radiation effects 7-26811
 SiO $_2$, surface nitridation, current status 7-33866
 SiO $_2$, thermal films, defect formation by high temp. annealing 7-45035
 SiO $_2$ thermal films, nitridation 7-58680
 SiO $_2$ thin films in MOS capacitors, wear-out charactn., processing depend. 7-38756
 SiO $_2$ ultrathin gate oxide films, breakdown props., post-oxidation annealing effects 7-22187
 SiO $_2$, vitreous, aluminium-oxygen hole centre, chemical annealing 7-51646
 SiO $_2$:B(P), thermally grown, diffusion of ion-implanted dopants 7-38041
 SiO $_2$:Cl, ion implanted, Cl ion redistrib., SIMS studies 7-21249
 SiO $_2$:Sb, ion-implanted, diffusion 7-58542
 SiO $_2$:P $_2$ O $_5$ glass, reflow characts, rapid thermal annealing 7-59553
 SiO $_2$ -Si interface, insulator props. after exposure to H $_2$ +N $_2$ and NH $_3$. 7-59693

annealing continued

- SiO₂-P films, pure and doped, low press. CVD growth, structural, optical, elec. props. 7-27186
 SiO₂-N₂ films, plasma-enhanced CVD deposited, annealing 7-32861
 Si_{1-x}Sn_xO_{1+x} amorphous thin films, optical and structural studies 7-64714
 Si(001), biatomic steps 7-38309
 Sn, phase transitions, Doppler broadened positron annihilation studies 7-38190
 SnO₂/Sb thin films, doped and undoped, prep. by photolysis, phys. props. 7-22368
 SnTe, low temp. iodide method synthesis, X-ray reaction product studies 7-64945
 SrO.5.6Fe₂O₃, doped with kaolin and BaB₂O₄, sintering temp., effect on structural and mag. parameters 7-7543
 Ta, Ne implanted, annealing behaviour of H traps 7-46506
 Ta-H system, electron irradi., vacancy recovery, positron lifetime studies 7-37972
 Ta-Nb bimetal, accelerated mutual diffusion during thermal cycling (*Russian*) 7-44926
 Ta₂O₃ crystalline films, sputter deposited, phys. and elec. props. 7-2412
 Te-As-S chalcogenide system, annealing, crystalline precipitate phase form., X-ray diffr. anal. 7-16751
 TeO₂-Ge₂Sn films, optical props., thermal stability 7-39207
 Ti alloy sheet, vac. annealing temp. influence on surface relief 7-17688
 Ti binary alloys, reduced technological plasticity and struct. (*Russian*) 7-17583
 Ti, oxidation, Rutherford backscattering spectrometry, AES, X-ray diffr., elec. resist. meas. 7-22894
 Ti Si₂ epitaxial growth kinetics on (111)Si, TEM study 7-58683
 Ti thin films, dissolution and diffusion of O, resist., X-ray diffr., particle backscatt. and AES studies 7-58913
 α-Ti:Si, ion implanted, diffusion profiles, annealing behaviour 7-12369
 Ti-Al-Mo-Cr alloy, VT3-1, vac. annealing of blanks after isothermal deform., hydrogen plasticising effect 7-8027
 Ti-Al-Mo-Fe, struct. changes during phase transitions (*Russian*) 7-53721
 Ti-Al-V, ternary phase diagram 7-28017
 Ti-Al-V (6.4 wt.%), annealed fatigue crack growth in water, SEM fractography (*Chinese*) 7-8076
 Ti-Al-V (6.4 wt.%), α morphology rel. to thermomech. treatment 7-46520
 Ti-Al-V alloys, VT20 and VT6, annealing temp. effect on mech. props. of semifinished products 7-39558
 Ti-Cu-Ni-Si amorphous alloys, structural relax. annealing, X-ray diffr. studies 7-6537
 Ti-Cu-Ti thin films, reaction kinetics, stress, and microstruct. 7-21764
 Ti-N ion deposited film, struct., phase comp. and mechanical props., comp. depend., X-ray diffr. study 7-12573
 Ti-Si interface, nucleation and growth of TiSi₂, influence of O₂ 7-21541
 Ti-Si interface, self-aligned Ti silicide formed by rapid thermal annealing 7-2391
 Ti-Si thin films, silicide phase formation 7-21695
 Ti-Si:As⁺(P⁺)(BF₂⁺), TiSi₂ formation, ion implantation doping and masking oxide film effects 7-21708
 TiB₂, plasma-enhanced CVD films on Si, furnace annealing, metallisation appls. 7-38411
 TiC, ultrafine powder behaviour during annealing and sintering 7-3244
 TiFe, adsorption of O, AES study 7-59312
 TiFe, oxidised, bulk and surface phase composition 7-46700
 Ti₄Fe₂O, adsorption of O, AES study 7-59312
 TiN films, ion plated, stability anal. 7-2400
 TiN thin films, activated reactive evaporation deposited, vacuum annealing, struct., mech. props. 7-8010
 TiN-TiSi₂ bilayers and selectivity doped thin films, material characterisation 7-33817
 TiN_{0.1-x}-TiSi_x bilayer, formation by rapid thermal anneal in N₂ 7-21547
 TiNi, adsorption of O, AES study 7-59312
 TiO_x, amorphous reactive ion beam deposition, crystallisation 7-45091
 TiSi₂ formation on Si by rapid thermal annealing 7-21707
 TiSi₂, oxidation, Rutherford backscattering spectrometry, AES, X-ray diffr., elec. resist. meas. 7-22894
 TiSi₂ vacuum electron beam evaporation, annealing effects, Auger and electron diffr. anal. 7-22492
 TiSi₂:As(Sb) layers, dopant redistribution during silicidation by rapid thermal annealing, ion scatt. spectra study 7-21253
 Tm₃Fe₂O₁₂, double phase transition, EXAFS studies 7-63799
 U_{0.85}Gd_{0.15}O_{2+x} pellets, reaction with Cs fission product, annealing, diametral expansion 7-56756
 UO_{2+x} pellets, reaction with Cs fission product, annealing, diametral expansion 7-56756
 US, magnetic character, effects of fission damage, neutrons 7-13000
 V polycrystalline films, struct. defect disappearance, activation energy, elec. resist. meas. 7-26740
 V/Si, silicide formation, comparison of SiO₂ and a-Si surface protection layers 7-58662
 V-CR-Ti (15, 15 wt.%), mech. props., effect of heat treatment and impurity conc. 7-53857
 V-N system, metastable ordered phases, cryst. struct. (*Russian*) 7-44447
 W (011) plane, edge atoms surface migration activation energy, emission current meas. 7-32887
 W, electron and proton irradi., thermal annealing, positron annihilation studies 7-46214
 W films on GaAs substrates, electrical resistivity after high temp. annealing 7-64366
 W films prep. by various deposition methods, effects on elec. resist. 7-52860
 W reactively sputtered films, elec. resist., microstructure, effects of N or O partial press. 7-52861
 W wire, grain boundary struct. annealing above 1800K 7-6636
 W wire doped with K, morphology and behaviour of K bubbles at varied temps. 7-2223
 W/C multilayer films, thermal stability, X-ray diffr. studies 7-27169
 W/C multilayer films for X-ray reflectors, thermal stability 7-32871
 W-Cu-Ti(Zr), saturation rate of porous W with Cu, effect of Ti and Zr 7-3220
 W-GaAs, Schottky contact, electrical and metallurgical studies 7-27422
 W-GaAs diode system, Schottky barrier degradation after high temp. annealing 7-33089
 W-H system, H-defect interactions, positron annihilation studies 7-38045

annealing continued

- W-Re alloys, annealed and sintered, elevated temp. softening, appl. for thermionic energy conversion 7-28077
 W-Ti-Si interface, WSi₂ form. by rapid thermal annealing, growth kinetics, Ti film effects 7-63969
 WSi₂ films, electrical transport props. 7-58908
 WSi₂, silicide formation by rapid thermal annealing, Raman scatt. study 7-59193
 WSi₂-TiSi₂ bilayer, on Si, rapid thermal annealing 7-21549
 WSi₂ CVD films on Si and Si₃N₄ coated Si, excess Si redistribution upon annealing 7-21723
 WSi₂ films, CVD, resistivity and composition changes by annealing 7-2738
 WSi₂ films, sputter deposited from cold pressed, vacuum sintered composite target, annealing, comp., resist. meas. 7-21719
 W₂Si₃-GaAs, Schottky contact, electrical and metallurgical studies 7-27422
 W₂Si₃, reactively sputtered films, metastable phase form. 7-52340
 Y-Fe-B system alloys, mag. props. 7-27563
 YAlO₃:Pr³⁺ single crystals, colour centres, optical absorption spectra studies 7-63610
 YIG films, H₂ annealed, Mossbauer study 7-45847
 YIG:Ga, Bi, RF sputtered films for magneto-optical memory, mag. props. 7-64613
 YIG:H, sp. ht. and annealing behaviour, conversion-electron Mossbauer spectroscopy study 7-17253
 Zn, deformation recovery, positron annihilation spectroscopy 7-21329
 Zn, neutron irradiated, yield-stress recovery 7-22720
 ZnO varistor, grain-boundary pot. barrier, effects of annealing 7-16568
 ZnO:Al films, RF reactive sputter deposition, struct., elec. and optical props. (*Japanese*) 7-27900
 ZnO-Bi₂O₃ mixtures, lattice parameters, depend. on Bi₂O₃ conc. 7-1974
 ZnS, rare earth impurities, electrolum. of Schottky barriers, photolum., charge compensation, and impurity electron states 7-64700
 ZnS, single crystal, annealed in O, intrinsic defects rel. to elec. and luminesc. props. 7-12649
 Zr, doped with O, mech. props. and elec. resist. at 4.2 K influence of annealing (*French*) 7-59554
 Zr, neutron irradiated, solute effects on damage production and recovery 7-51861
 Zr-Co, amorphous alloys, microhardness and struct. relax. (*Chinese*) 7-65069
 Zr-Fe amorphous alloys, chemical short range order, thermal relaxation and ion irradiation effects 7-44385
 Zr-Ir, hardening by dispersed ω-phase particles, annealing effect (*Russian*) 7-65053
 Zr-Ni, amorphous alloys, microhardness and struct. relax. (*Chinese*) 7-65069
 Zr-Os, hardening by dispersed ω-phase particles, annealing effect (*Russian*) 7-65053
 Zr-Ti(Sn)(Dy)(Au), neutron irradiated, solute effects on damage production and recovery 7-51861
 Zr-Ti(Sn)(Au), low temp. damage prod. and recovery after fusion neutron irradiation 7-51862
 Zr_{1-x}Cu_x amorphous sputtered alloys, low energy excitations, sp. ht. meas., structural relax. effects 7-11913
 ZrF₄-BaF₂-LaF₃-AlF₃-LiF glass, X-ray radiation damage, EPR studies 7-21278
 e-ZrH₂, shape memory effect (*Russian*) 7-59577
 ZrN films, ion plated, stability anal. 7-2400
 ZrO₂-Y₂O₃, rapidly quenched, microstruct. evolution by annealing 7-22737
 Zr₂Pb₃, fusion blanket neutron multiplier, fabrication and props. 7-49656

annealing, magnetic *see magnetic annealing*

anodes

- arc current distrib. meas. at anode for pressure 10⁻⁶ to 10 torr 7-32165
 bipolar batteries with common electrolyte paths, leakage currents 7-28392
 ceramic oxides, cond., for use as molten carbonate fuel cell electrodes 7-13854
 electron distribution fn. in anode sheath of glow discharge, kinetic problem soln. 7-37627
 liquid metal anodes, dissolution during low freq. current interruptions 7-12287
 magnetically insulated transmission line in PROTO II accelerator, anode and cathode joints, gap closure 7-30756
 molten carbonate fuel cells, fabrication of bubble press. barriers 7-13856
 plasma anode glow oscillations, mechanism 7-20892
 spot formation, time determ., photoelec. method 7-11789
 vacuum prebreakdown currents, anode oxidation effects 7-37780
 X-ray tube anode, evolution 7-18066
 Al-air battery with crystallizer to extend electrolyte lifetime, traction appls. 7-65441
 C electrode, glassy, anodic process in LiF-NaF-KF eutectic, Cl⁻ effect 7-23028
 nCdS-n-GaAs photoanode, flux anal. of multiple junction solar cells 7-23162
 He glow discharge, electron conc. meas. in anode region 7-11788
 IrO₂ coated anode for V redox cell, eval. of electrode materials 7-54286
 Ni anodes for molten carbonate fuel cells, stabilisation 7-39988
 Pt anode in fuel cell, performance in presence of CO and CO₂, CO poisoning adsorption parameters calc. 7-13855
 Ti-Ru oxide anodes, durability in Cl cells with Hg anodes 7-32562
 TiO₂ photoanode thickness effect on quantum yield of photoelectrolytical cells 7-40018

anodes, electrochemical *see electrochemical electrodes*anodic machining *see electrolytic machining*

anodisation

- Al films on InP, wet anodisation, compositional profiles 7-65216
 alumite disc prep. using anodic oxidation (*Japanese*) 7-46672
 dielectric films, on compound semiconductors, conf., Las Vegas, USA (Oct. 1985) 7-35108
 metallic-based layered structs., depth profile anal. using multilayer anodisation 7-27170
 oxide growth by plasma anodisation, ionic transport processes 7-65162
 spark discharge anodic oxidation layers and composites, appl. fields 7-65189
 Al, anodic films, double-refraction theory 7-39743
 Al, anodic oxidation coatings, electrolytic colouring, mag. field effects (*Japanese*) 7-59662

anodisation continued

- Al, anodic polarisation in NaCl soln., instantaneous impedance study 7-23032
- Al, anodised, variation in polarised light intensity with grain orientation 7-54041
- Al, anodising by chromic acid, surface struct., abrasion resist., hardness, adhesion props. 7-13646
- Al, anodising in Na_2SO_4 and H_2SO_4 solns., AC impedance meas. (Japanese) 7-13632
- Al, barrier film formation, anion incorporation and migration 7-53947
- Al:Eu^{3+} , ion implanted, anodization, electroluminesc. obs. 7-7761
- Al_2O_3 anodic porous film on Al, microstruct. 7-22882
- C, glassy, anodic oxidation of surfaces 7-46850
- CdS anodic film growth, initial stages, voltammetry and computer simulation studies 7-28216
- Cu, anodic oxidation in KOH soln., in situ spectroelectrochemical anal. 7-28192
- Fe, passive anodic oxide form., surface anal., XPS, ion scatt. spectra 7-22895
- Fe-Cr, passive anodic oxide form., surface anal., XPS, ion scatt. spectra 7-22895
- GaAs, surface oxidation, effect of anodizing conditions 7-13669
- GaInAs, anodic oxides, growth and composition 7-39781
- GaInAs epitaxial layer on InP, depth profiling and interface detection using anodic oxidation 7-45057
- HgCdTe anodic oxide surface analysis by laser ionisation 7-13275
- $\text{Hg}_{0.78}\text{Cd}_{0.22}\text{Te}$, stoichiometry of anodic oxides, quantitative meas. 7-39782
- InP/native oxide MIS structures, interface elec. props. 7-33851
- InSb, anodic native oxide, interface width, AES profiles 7-22911
- InSb surface, oxidation at room temp. 7-46734
- Ni, anodic polarisation, film identification by Raman spectra 7-28194
- Ni-P, glassy, dissolution in H_2SO_4 and HCl electrolytes 7-28189
- PdRhPSi(SiNi), amorphous laser processed surface alloy on cryst. Ni in NaOH soln., anodic characts. 7-28317
- Pt anode in phosphoric acid fuel cell electrolyte, H_2S poisoning 7-46933
- Si, anodic oxidation in pure water, appl. to MOS structs. 7-39776
- Si MOS structures, anodically and thermally grown, breakdown field strengths 7-17113
- Si, oxidation 7-65227
- Si, oxide growth by plasma anodisation, current efficiency and temp. depend. 7-39777
- Si SOI structures using buried layers of oxidised porous Si 7-13660
- Si-pyrex, irreversibility of anodic bonding 7-33910
- Ti alloys, hot salt SCC rel. to surface conditions (Chinese) 7-13623

anodised coatings *see anodised layers***anodised layers**

- oxide anodic films on Al, struct., surface EXAFS, magic angle spinning NMR studies 7-22382
- Al, anodic oxide films, dissolution kinetics in KF solns. 7-39705
- Al, anodising by chromic acid, surface struct., abrasion resist., hardness, adhesion props. 7-13646
- Al, investigation using surface behaviour diagrams 7-27077
- Al-GaAsO-GaAs structures, energy diagram 7-33096
- Al_2O_3 anodic film, barrier layer, surface imaging using scanning tunneling microscope 7-17706
- Al_2O_3 anodic films on Al, struct., magic angle spinning NMR study 7-22382
- GaAs-anodic oxide interfaces, annealing, As enrichment, photoluminescence, Rutherford backscattering anal. 7-21687
- $\text{Hg}_{0.78}\text{Cd}_{0.22}\text{Te}$, stoichiometry of anodic oxides, quantitative meas. 7-39782
- $\text{Hg}_{1-x}\text{Cd}_x\text{Te}$ crystals, anodic oxide capped, thermal stability 7-65225
- Nb_2O_5 , anodic amorphous oxide films, short-range order 7-28200
- Ni, anodic polarisation, film identification by Raman spectra 7-28194
- Si-aqueous electrolyte interfaces, impedance spectra, freq. dispersion 7-27414
- Si_3N_4 films prep. by plasma anodisation, XPS depth profiling 7-58667
- SiO_2 anodic native oxide interfaces on InSb for passivation 7-22917
- Ta_2O_5 , anodic amorphous oxide films, short-range order 7-28200
- Ti anodic oxide film, Raman spectra 7-46688
- ZrO_2 anodic films, charge storage props. study 7-58930

anodised thin films *see anodised layers***anolytes** *see electrolytes***anomalous skin effect**

- alkali metals, low temp. nonlocal electromagnetic ultrasound generation calcs. (Russian) 7-7294
- metals, anomalous skin effect, Fermi surface curvature effects (Russian) 7-58827
- metals, EM generation of acoustic waves, theory 7-51945

antenna accessories

- see also antenna feeders; directional couplers*
- 1.5K cryogenerator for use with SIS detectors 7-30023
- antennas and propagation, conf. Philadelphia, PA, USA (June 1986) 7-41011

antenna arrays

- see also antenna phased arrays; directional couplers; microwave antenna arrays*
- ERS-1 wind scatterometer antenna, mechanical aspects 7-23975
- low-cost satellite image reception and analysis facility 7-66305

antenna components *see antenna accessories***antenna feeders**

- Cassegrain large antennas, quasioptical coupling of Gaussian beam systems, radiotelescope performance 7-40698
- multiple reflector antennas, diffraction losses calc., asymptotic transition region theory 7-50471

antenna lobe patterns *see antenna radiation patterns***antenna patterns** *see antenna radiation patterns***antenna phased arrays**

- 405 MHz phased array antenna for atmospheric wind measurement 7-34752
- adaptive array with binaural processor 7-31579
- planar phased array acousto-optic Bragg cell transducer 7-37303
- radioastronomical images, very large array phase data modelling by Box-Jenkins method 7-14504

antenna radiation patterns

- aperture antenna radiation, arbitrary scatterers presence, excited field calc. 7-50468

antenna radiation patterns continued

- Effelsberg 100 m radiotelescope, surface meas. by microwave holography 7-24005
- energy characts., directional props. of antenna in turbulent atmosphere 7-23825
- ERASME airborne side-looking C-band radar, data processing and calibration 7-9205
- far field pattern, reflector support boom effect 7-50472
- field patterns of microstrip antenna in two component plasma 7-6397
- gravitational wave detectors, antenna patterns of interferometric detectors for linearly polarised waves 7-55453
- Hertzian dipole radiation in stratified uniaxial anisotropic media, computation 7-36860
- horn antenna with low sidelobe response for observations of diffuse celestial radiation 7-47701
- measurement using extended radio sources 7-56234

antenna reflectors

- dihedral corner reflector, physical theory of diffraction, double reflections anal. 7-42863
- Effelsberg 100 m radiotelescope, surface meas. by microwave holography 7-24005
- far field pattern, reflector support boom effect 7-50472
- GIOTTO spacecraft high gain antenna mechanical design and development 7-23974
- HF field expression, reflector caustic region, Maslov method appl. 7-36852
- RATAN-600 radio telescope, improvement of surface precision of primary mirror reflecting elements 7-60537
- space antennas, high precision composite sandwich antennas anal. 7-24012
- spaceborne radiometer antenna reflector, MM wave, development 7-23920
- strained radiotelescope reflectors, phase distortions compensation, automatic control 7-60541

antenna theory

- antennas and propagation, conf. Philadelphia, PA, USA (June 1986) 7-41011
- aperture antenna radiation, arbitrary scatterers presence, excited field calc. 7-50468
- Cassegrain antennas, phase and frequency stability, appls. 7-60547
- dipole EM radiation, in chiral media using dyadic Green's function 7-1005
- E polarisation, thin wire loop, backscattered field anal. 7-36861
- HF field expression, reflector caustic region, Maslov method appl. 7-36852
- multiple reflector antennas, diffraction losses calc., asymptotic transition region theory 7-50471
- optical lens systems, antennas explanation (German) 7-20381
- planar meshes with discrete loads, circuit modelling, equiv. mesh impedances 7-62600
- radiation pattern energy characts., directional props. of antenna in turbulent atmosphere 7-23825
- radioastronomy principles (book) 7-35140
- spherically symmetric inhomogeneous isotropic media, fields of sources calcs. 7-37696

antennas

- see also antenna radiation patterns; broadcast antennas; dipole antennas; directive antennas; microwave antennas; radar antennas; receiving antennas; reflector antennas*
- antennas and propagation, conf. Philadelphia, PA, USA (June 1986) 7-41011
- brain tumors, interstitial microwave hyperthermia, swept freq. meas of antennas 7-14106
- dielectrically-loaded conducting spheres, FEM for scattering 7-15808
- lightning discharge, current induced in aerial on buried telecom. line (French) 7-10817
- space antennas, high precision composite sandwich antennas anal. 7-24012
- wind scatterometer antenna release shock loads 7-23976

anthropology

- standardization in anthropometry and biomechanics 7-54665

anti-transmit-receive tubes *see gas-discharge tubes; radar equipment***antibaryons** *see baryons***anticorrosion coatings** *see corrosion protective coatings***anticrossing spectroscopy** *see energy level crossing***antiferromagnetism**

- No entries

antiferroelectric materials

- see also antiferroelectricity; ferroelectric materials*
- vibr. spectroscopic study 7-39115
- $\text{K}_2\text{Ba}(\text{NO}_2)_4$, successive phase transitions, dipolar frustration 7-53247
- $\text{NH}_4\text{H}_2\text{PO}_4$, antiferroelectricity, role of H bonds 7-64582
- $\text{NH}_4\text{H}_2\text{PO}_4$, temp. depend. IR active lattice modes in para- and antiferro-electric phase 7-46012
- $\text{NH}_4\text{H}_2\text{PO}_4\cdot\text{SeO}_3$, partially deuterated, D concentrations in H_2PO_4^- and NH_4^+ radicals, ESR spectra 7-27671
- NaOD, low temp. phase transform., heat capacity, calorimetric study 7-16785
- $\text{PbIn}_{1/2}\text{Nb}_{1/2}\text{O}_3$, antiferroelec., phase transition, B-site cation order effects 7-7651
- $\text{Pb}(\text{M}_{1/2}\text{Sb}_{1/2})\text{O}_3$, perovskite type antiferroelectrics, (M=Sc, Ho-Lu), X-ray and dielec. characts. 7-7649
- $\text{PbMn}_{2/3}\text{MO}_3$, perovskite-type cpds., (M=Mo, Te, Re), dielec. and mag. props. 7-7650
- PbZrO_3 -based piezoelectric ceramics containing $\text{Pb}(\text{Zn}_{1/3}\text{Nb}_{2/3})\text{O}_3$ 7-2984
- $\text{Rb}_{0.61}(\text{NH}_4)_{0.39}\text{H}_2\text{PO}_4$, mixed crystal, dielec. study of ferroelec. transition 7-53248
- TiHf_2 , non-polar crystals, antiferroelectric ordering, 1D mechanism 7-33344

antiferroelectricity

- see also antiferroelectric materials*
- alumina, ion-rich β - and β'' -phases, superionic props., homogeneity ranges and conductivities 7-21520
- antiferroelectric nematic, singlet orientational distrib. fn., Monte Carlo anal. 7-2989
- non-polar crystals, antiferroelectric ordering, 1D mechanism 7-33344
- packed antiferroelectric chains, thermodynamic features 7-53244
- CdTiO_3 , nonlinear props. in high electric fields 7-7668

antiferroelectricity continued

- NaOD, ^{23}Na critical longitudinal relax. time near antiferroelec. transition 7-17235
 PZT ceramic, pressure induced ferroelectric-antiferroelectric transition 7-22201
 PZT, paraelectric phase transition broadening due to coexistence of ferroelectric and antiferroelectric phases 7-45942

antiferromagnetic Curie temperature *see* Curie temperature**antiferromagnetic-ferromagnetic** *transitions* *see* ferromagnetic-antiferromagnetic transitions**antiferromagnetic-paramagnetic** *transitions* *see* paramagnetic-antiferromagnetic transitions**antiferromagnetic properties of substances**

see also antiferromagnetism; magnetic semiconductors

- 7-45845
 BCC ordered alloy, high temp. mag. states (Russian) 7-64466
 (BEDT-TTF)₂, superconducting and mag. instabilities 7-45697
 (BEDTTF)₂AuCl₂, antiferromag. ground state, AFMR meas. 7-27608
 (BEDTTF)₂Cl₂, antiferromag. ground state, AFMR meas. 7-27608
 bis(ethylammonium)copper tetrachloride, spin-flop transition, temp. depend. of critical angle (Russian) 7-33171
 bis(methyl ammonium) iron tetrachloride, mag. susceptibility rel. to thermal and mag. history 7-22095
 bisethylammonium copper tetrachloride rhombic antiferromagnet, magnetic phase diagram, press. effects study (Russian) 7-52981
 braunites, Mn²⁺Mn³⁺SiO₂Fe(Ca)(Al), antiferromagnetism and spin glass order, mag. meas. 7-27518
 dimethylammonium manganese chloride, 1D antiferromagnet, nuclear spin-lattice relax., effect of nonlinear excitations 7-59122
 ethyl ammonium tetrachlorocuprate, antiferromagnet, domain-wall spin reorientation study 7-53026
 ethylamine platinum trichloride, Wolfram's red salt, bound domain wall pairs 7-27545
 Fermi surface, 2D angular correlation studies 7-39236
 hemerythrin, binuclear Fe cluster, PMR probe investig. 7-50184
 magnetic insulators, light absorpt. by intersublattice charge transfer 7-46065
 manganese formate, Mn(HCOO)₂·2H₂O, magnetic transitions, compression and mag. dilution effects 7-52986
 bis-methylammonium tetrachloro manganese antiferromag. crystals, struct. deform. by exciton self-localisation, luminesc. spectra fine struct. study (Russian) 7-27752
 orthoferrites, mag. and dielec. props. at submillimetre wavelengths 7-38990
 photoinduced magnetism, effects on magnetisation in antiferromagnetic materials 7-52931
 positive muon diffusion in helicoidally-ordered antiferromagnets 7-45870
 rare earth alloys, RMn₂, R=heavy rare earth, mag. state, spin echo NMR spectra 7-27629
 rare earth dihydrides, Fermi surface nesting 7-52398
 superconductors, upper crit. mag. field (Russian) 7-58963
 tetrachlorobis(ethylammonium)copper(II), antiferromag. spin wave freqs., parallel pumping 7-58997
 tetramethylammonium manganese (III) trichloride 1D antiferromagnet, exciton trapping, luminesc. investig. 7-52434
 (TMTSF)₂PF₆, metal-insulator transition, lattice expansion 7-64086
 (TMTSF)₂X, superconducting and mag. instabilities 7-45697
 transition metal dimers, antiferromagnetic coupling, ligand spin polarisation, broken symmetry UHF calcs. 7-22084
 transition metal phosphorous trisulphides, electronic, structural and mag. props., intercalation cpds. and chemical props. 7-44499
 [α-]Mn₂S antiferromag. semicond., elec. and mag. props. 7-7244
 AgO, tetragonal, struct. and mag. props. 7-32399
 Ag_{0.5}V_{0.5}PS₃, struct., metal ordering and mag. props. 7-16517
 Al₃₀Mn₃₀, quasicrystalline icosahedral phase, sp. ht., mag. props. 7-52955
 AuCr, competing antiferromagnet, mag. phase diagram 7-59023
 Ba₂CaCuFe₂F₁₄, heteronuclear trimers with ferrimag. behavior (French) 7-64448
 Ba₂CaCu₂Fe₂F₁₄, exchange interactions, mag. susceptibility meas. 7-45654
 BaCa_{1/2}Sr_{1/2}Fe₄O₈, mag. ordering 7-45624
 BaLaFeO₄, layered cpds., bidimensional mag. coupling, Mossbauer spectra 7-27637
 BaMnAlF₄, exchange interactions, mag. susceptibility meas. 7-45654
 BaMnF₄, 2D Heisenberg magnet, spin dynamics and EPR linewidth 7-38932
 BaMnF₄, magnon polaritons, wave propagation in mag. systems with spontaneous electric polarisation 7-12961
 BaMnGaF₇, exchange interactions, mag. susceptibility meas. 7-45654
 CaLaFeO₄, layered cpds., bidimensional mag. coupling, Mossbauer spectra 7-27637
 Cd(Cu_{1-x}Al_x)₂, mag. and cryst. props. 7-27506
 Cd(Cu_{1-x}Ni_x)₂, mag. and cryst. props. 7-27506
 Cd_{1-x}Mn_xS, antiferromag. exchange constants between nearest-neighbour Mn²⁺ ions 7-64449
 Cd_{1-x}Mn_xTe dilute antiferromagnet, high field magnetisation meas. 7-64486
 Cd_{1-x}Mn_xTe, interband Faraday rot. meas. 7-39093
 Cd_{1-x}Mn_xTe_{1-y}Se_y, magnetic suscept. and ESR meas., temp. depend. study 7-45636
 Cd_{1-x}Mn_xTe_{1-y}Se_y pseudoternary semimag. semicond., mag. suscept. and exchange interaction data anal. 7-7501
 Cd₂Zn₂Mn₂Te(Se) pseudoternary semimag. semicond., mag. suscept. and exchange interaction data anal. 7-7501
 CeIn₃ antiferromagnetic alloys, thermoelec. power meas., band gap form. 7-38543
 (Ce_{1-x}La_x)In₃ antiferromagnetic alloys, thermoelec. power meas., band gap form. 7-38543
 CePb₃ heavy fermion material, magnetism and superconductivity 7-52880
 CePb₃, possible superconductivity in nearly antiferromagnetic itinerant fermion systems 7-38802
 CeRu₂Si₂, heavy fermion, magnetism and spin fluctuation effects induced by partial substitution 7-38850
 Cf oxides, Cf₂O₃, Cf₂O₁₂, CfO₂, BaCfO₃, mag. susceptibility meas. 7-12937
 Co-CoO multilayered films, exchange anisotropy 7-27579
 CoCl₂-graphite intercalation cpds., mag. susceptibility meas. 7-45638
 CoF₂, antiferromag. insulator, H-odd linear dichroism of exciton-magnon transitions 7-53282
 CoGaInS₄ layer cpds., struct. and mag. props., XPS studies 7-44498

antiferromagnetic properties of substances continued

- Co₂Mg_{1-x}O, Neel temp., var. with mag. dilution 7-27516
 γ-CoNiMn alloys, mag. phase diagram, neutron diff. methods (Russian) 7-45667
 CoO, heat capacity in vicinity of strong fluctuations, nonpower-law behaviour 7-2865
 Cr (001), near-surface antiferromagnetism and surface ferromagnetism, photoelectron spectroscopy 7-59381
 Cr, cryst. and mag. states, effect of neutron irradi. in reactor (Russian) 7-51866
 Cr, magnetovolume, thermal expansion and Gruneisen parameters 7-33260
 Cr, single crystals, single modulating mag. state form., neutron obs. (Russian) 7-58982
 Cr single crystals, thermoelec. power near the Neel temp., precursor behaviour 7-64209
 Cr, surface EM wave absorpt., 4-350K 7-33354
 Cr, zero field muon spin rotation study 7-45871
 Cr-Mo dilute alloys, magnetoelasticity, antiferromagnetism disappearance effects 7-45789
 Cr-Ru, BCC alloys, supercond. and mag. props. 7-7443
 Cr-V alloy, magnetovolume, thermal expansion and Gruneisen parameters 7-33260
 (Cr_{1-x}Al_x)₉₅Mo₅, antiferromagnetism disappearance, comp. depend., elec. resist. and sound rel. meas. 7-2843
 Cr₂BeO₄ multi-sublattice antiferromag., elec. polarisation, magnetoelc. effect calcs. (Russian) 7-7577
 Cr₂BeO₄ orthorhombic antiferromagnet, double exchange long-period magnetic struct. calcs. 7-2818
 CrVO₄, magnetic phase transitions, mag. suscept. and sp. ht. meas. 7-2842
 CsCoCl₂·2H₂O, 1D antiferromagnet, exciton transfer, absorpt. spectra 7-27254
 Cs₂FeCl₄·H₂O, antiferromagnet, mag. phase diagram, spin wave excitations, Mossbauer spectra 7-45676
 CsMnCl₃ antiferromag. crystals, struct. deform. by exciton self-localisation, luminesc. spectra fine struct. study (Russian) 7-27752
 CsMnCl₃·2H₂O, 1D Heisenberg magnet, spin dynamics and EPR linewidth 7-38932
 CsMnF₃ antiferromagnet, parametrically excited magnon redistrib. and chaos 7-17167
 CsNiF₃, dynamical critical slowing down, spin fluctuation relax. time, mag. suscept. meas. 7-38897
 CsVCl₃, one-dimens. Heisenberg antiferromag., mag. excitations, neutron scatt. study 7-7482
 Cu complex, CuBr₂·2DMSO, linear chain antiferromag., optical birefringence 7-7679
 Cu II carboxylate dimers, antiferromagnetism, nonempirical valence bond calcs. 7-10436
 Cu-based binary dilute alloys, electron struct., X-ray Lα emission spectra studies 7-12598
 CuCl₂·2DMSO, paramagnetic susceptibility of antiferromagnetic quantum chain 7-52997
 Cu₉₈Fe₂, antiferromagnetic interactions, EXAFS and XANES anal. of Fe atom environment and clustering 7-64808
 CuSO₄·5D₂O, indirect nucl. spin-spin interaction above chain crit. field 7-2948
 CuSO₄·5H₂O, indirect nucl. spin-spin interaction above chain crit. field 7-2948
 Dy thin films, influence of thickness on mag. phase transitions 7-38860
 DyAg, antiferromag. crystalline and ferromag. amorphous alloys, spin dynamics, μSR study 7-45873
 Dy₃Al₅O₁₂, refrigerant characts. for Carnot mag. refrigerator 7-56286
 Er-H solid soln., mag. props., H addition effects 7-7510
 ErFeO₃, antiferromag. domain struct., spin reorientation region 7-45723
 Eu(As_{1-x}P_x)₂, mag. phase transitions, strip line transmission spectra studies 7-64438
 EuRh₁₄Sn₄₂, anomalous mag. and elec. props. 7-64440
 Eu₂S, mag. ordered and paramag. phases, Raman scatt. 7-22246
 Eu₂Sr_{1-x}Te, dilute antiferromag., phase diagram, spin glass props. (German) 7-12981
 EuTe, bound magnetic polarons, spin dynamics 7-7502
 Fe, BCC, mag. ordering and electronic struct. (Russian) 7-33170
 Fe overlayers or sandwiches with Cu (001), electronic and mag. props. 7-64499
 Fe ultrathin films on Pd (111), photoemission, LEED and AES studies 7-45068
 Fe-Au-Fe double layers, exchange coupling 7-27510
 Fe-Cr-Fe double layers, exchange coupling 7-27510
 Fe-Ni Invar, high-field hysteresis and ferromag.-antiferromag. coexistence 7-22122
 FeBO₃, antiferromagnet, parametric excitation of magnons with a decay spectrum 7-52966
 FeCO₃, antiferromag., magneto-optical determ. of exchange parameters (Russian) 7-53283
 FeCl₃, magnetostriction, X-ray diff. meas. 7-33258
 FeClMoO₄ layered compound, struct. and mag. props., Mossbauer effect, mag. suscept., and neutron diff. studies 7-58981
 Fe_{1-x}Co_xCl₂, Fe²⁺ localised excitation and spin orientation, ESR studies 7-64524
 Fe_{1-x}Co_xCl₂, random-field and competing-anisotropy effects, sp. ht. study 7-2872
 FeNiCr disordered FCC alloys, paramagnetic-antiferromagnetic-spin glass reentrant transition obs. 7-17175
 Fe₂Ni_{85-x}Mn₁₅, low temp. sp. ht. near ferromag.-antiferromag. transition (Russian) 7-7512
 Fe_{1-x}O, double electron exchange, Mossbauer spectroscopy 7-17168
 α-Fe₂O₃, hematite, magnetoelastic wave, parametric amplification in reversal of wavefront 7-7578
 Fe₂O₃, hematite, magnetoelastic wave propagation, polarisation effects 7-7581
 α-Fe₂O₃, reduction-sintering prep., mag. props. 7-59054
 α-Fe₂O₃ single crystal, backward surface wave, parametric instability and amplification 7-22128
 Fe₂O₄, magnetite, cryst. struct. under press., rel. to Neel temp. 7-16524
 FePO₄-II, high press. phase, mag. props. 7-45852
 FeRh, X-ray emission and absorpt., ab initio self-consistent band struct. calcs., LMTO method 7-64826
 Fe₇SiO₂₂(OH)₂, grunerite, mag. order, quasi-one dimensional antiferromag. with spin canting transition 7-58983
 FeTiO₃, mag. struct. 7-7484

antiferromagnetic properties of substances continued
FeTiO₃, oblique easy-axis antiferromag. neutron scatt. study of mag. excitations 7-45643
FeVO₄, magnetic phase transitions, mag. suscept. and sp. ht. meas. 7-2842
Fe_{1-x}Zn_xF₂ diluted Ising antiferromagnet, magnetisation critical exponent crossover, Mossbauer meas. 7-7529
Fe₂Zr₆, mag. susceptibility, elec. resist., magnetoresistance meas. 7-52954
Fe₂ZrSe₂, intercalated layered cpd., thermopower and low DC field magnetisation study 7-17199
Gd(Cu_{1-x}Co_x)₂, mag. and crystallographic props. 7-38903
GdIn₃, antiferromagnetic alloys, thermoelec. power meas., band gap form. 7-38543
He³, solid, spin-wave region reson. freq., magnon corrections calcs. 7-52185
³He, BCC solid, nuclear magnetism, molar volume depend. 7-58565
HoVO₄, enhanced nucl. order, nucl. orientation study 7-64550
KCoF₃ antiferromagnetic cryst., electronic Raman scatt. by high-energy magnetic excitons 7-46016
K₂Co₂Fe_{1-x}F₄, oblique antiferromag. phase, spin waves, inelastic neutron scatt. study 7-64443
K₂Cu₂Mn_{1-x}F₄, quasi-two-dimensional mixed ferromagnetic-antiferromag. system, mag. phase transitions, intermediate spin glass phase 7-27525
KFeSe₂, hydrogenated, ESR meas. in 100 to 320K range 7-13016
K₂MAF₄, optical dichroism, spin forbidden *d-d* transitions, intensity prod. mechanisms 7-33360
La(Fe_{1-x}Al_x)₁₃, mag. props. determined via neutron scatt. and Mossbauer spectroscopy 7-2820
La₂NiO₄, quasi-2D, canted antiferromag. order studies 7-33153
LiFeClMoO₄, synthesis, struct. and low temp. magnetism 7-21172
Mn-Sn, homogenised, mag. props., thermal expansion 7-2900
MnCl₂-graphite intercalation cpds., mag. susceptibility meas. 7-45638
MnF₂ and site-diluted (Mn_{0.5}Zn_{0.5})F₂, μ SR studies above and below Neel temp. 7-45875
MnF₂, antiferromag., muon level crossing resonance 7-53186
MnF₂, antiferromag., muon level-crossing reson. 7-59133
MnF₂ antiferromagnetic superlattices with magnetisation perpendicular to surface, collective excitations, magnetostatic theory 7-45647
MnF₂ films, antiferromagnetic, dipole-exchange spin-wave modes 7-45771
MnF₂, light scatt. from magnons 7-45996
MnF₂, thermal behaviour of two-exciton bands 7-2497
Mn_{1-x}Fe_x, sputtered films, mag. props. 7-38915
Mn₁₁Ge₈, intermetallic compound, mag. props. 7-52985
MnHg_{1-x}Au_x, cubic to orthorhombic transition and mag. suscept. meas. 7-52037
Mn_{1-x}Ni_xAs, structural and magnetic phase diagrams 7-6784
MnO, band struct., optical props. 7-32912
Mn₂P, electronic struct., mag. props., KKR, LMTO methods, LSD approx. 7-64070
MnPS₃, layered cpd., mag. props. 7-52951
 α -Mn₂S, antiferromag. semiconductors, elec. conductivity 7-64240
MnTe, electronic struct. in magnetically ordered and disordered phases, tight-binding calcs. 7-45145
MnTe₂, mag. phase transition, neutron powder diff. study 7-64456
MnTiO₃, quasi-2D antiferromag., spin dynamics 7-52987
(Mn_{0.5}Zn_{0.5})F₂ diluted antiferromag. spin-wave-quasilocalised excitation crossover 7-22101
Mn_{0.5}Zn_{0.5}F₂, sp. ht. meas. in random fields 7-33178
Mn₂Zn_{1-x}F₂, 3D site-random Ising magnet, crit. behaviour 7-17186
N(CH₃)₄VOF₃H₂O, V⁴⁺-V⁴⁺ pair, mag. interaction (*French*) 7-58987
NaMnCl₃ quasi 2D antiferromagnet, deforming magnetic exciton and light absorpt. characts. 7-53284
NdFeSi₂, struct. and mag. props. studies (*French*) 7-37950
NdIn₃ antiferromagnetic alloys, thermoelec. power meas., band gap form. 7-38543
NdZn, antiferromag. skew scatt. Hall effect 7-52578
NiFeAlO₄, cation distrib. and canted spin alignment, Mossbauer obs. 7-22169
NiS_{1-x}Se_x, effect of Se substitution on mag. and electrical transition 7-2846
NiWO₄, monoclinic biaxial antiferromagnet, antiferromag. reson. study near spin-flop transition 7-53138
NpAs₂, single crystals, Hall resistivity 7-12739
O, solid, α - β phase transition, magnetoelastic coupling and antiferromag. order effects 7-58193
 β -O₂ solid, rhombohedral Heisenberg antiferromag., neutron scatt. 7-7480
Pb_{0.35}Gd_{0.05}Te, antiferromag. exchange constant between nearest-neighbour Gd³⁺ ions 7-59002
PbMn_{2/3}MO₃, perovskite-type cpds., (M=Mo, Te, Re), dielec. and mag. props. 7-7650
Pb_{1-x}Mn_xTe, indirect exchange interaction between Mn²⁺ ions 7-27509
PbTe:Gd, mag. props. EPR study 7-53126
Pd₃Fe hydrated ordered alloy, mag. behaviour, Mossbauer studies (*Russian*) 7-2890
Pd₃Y_{1-x}Dy_xSn, Heusler alloy system, field-induced reentrant superconductivity 7-2765
Pr, longitudinally polarised antiferromagnetic phase, magnetic excitations, neutron scatt. interpretation 7-64445
Pr, paramagnetic-antiferromagnetic transition, spin ordering model 7-52988
PrMnSi₂, struct. and mag. props. studies (*French*) 7-37950
Pt₃MnFe_{1-x}, mag. state near critical composition (*Russian*) 7-17170
Rb_{1-x}Cs_xFeCl₃, random singlet-magnetic ground state system, mag. ordering effects 7-33167
RbCuCl₃ single crystals, mag. suscept. meas., exchange interactions, magnetic and crystallographic transitions studies 7-52950
RbFeCl₃, hexagonal antiferromagnet, singlet-ground-state system, mag. excitations (*Japanese*) 7-22112
Rb₂MnCl₄, optical dichroism, spin forbidden *d-d* transitions, intensity prod. mechanisms 7-33360
Rb₂MnCl₄, quasi-2D uniaxial antiferromagnet, mag. phase diagram 7-7517
RbMnF₃, thermal behaviour of two-exciton bands 7-2497
SiO₂-Al₂O₃-MgO-Cr₂O₃ glass, magnetism of spinel microcrystals, ESR study 7-27594
Smln₃ antiferromagnetic alloys, thermoelec. power meas., band gap form. 7-38543
SmRh₄B₄, magnetic transition temps., RKKY interaction studies 7-22107

antiferromagnetic properties of substances continued
SrLaFeO₄, layered cpds., bidimensional mag. coupling, Mossbauer spectra 7-27637
 α -Ti, mag. suscept. and elec. resist. meas., itinerant antiferromagnetism, comment 7-33151
TiU₂S₅, mag. props. 7-22120
TiFe_{2-x}Se₂ layered cpd. single cryst., magnetic and structural props., Mossbauer and X-ray diff. studies 7-2848
U-Ni-As(P), ternary particles, cryst. struct. and mag. props. 7-12955
U_{0.95}Th_{0.05}Pt₃, ground state antiferromag. order, neutron diff. meas. 7-38847
UAs muon spin rot., relax. rate, freq. shift, and magnetic transitions 7-45891
UAs_{0.95}Se_{0.05}, disappearance of type-I antiferromag. struct., neutron diff. study 7-45620
UAs_{1-x}Se_x system, mag. phase diagram, neutron diff. study 7-12971
UAuCu₄, magnetic props., X-ray diff., NMR and mag. suscept. meas. 7-52948
UBr(Cl)(I)₃, magnetic transitions, antiferromag. order and cryst. field splitting, neutron scatt. study 7-12974
UCu₄Al_{7.5}, antiferromagnetic suscept. meas. 7-12954
URuSi₃, mag. and elec. props. 7-45674
U_{1-x}Np_xO₂, x=0.25, 0.75, magnetic structure, neutron diffraction study 7-58978
UPT₃, doped, strain-dependent mag. anomalies 7-12978
UPT₃, heavy-fermion system, development of antiferromag. correlations 7-64435
UPT₃, possible superconductivity in nearly antiferromagnetic itinerant fermion systems 7-38802
URu₂Si₂, monocrystalline, thermal expansion and sp.ht. 7-44866
UX₃ (XLL=S,Se,Te), trichalcogenides, mag. susceptibility study 7-12958
U₂Zn₁₇, point contact spectroscopy meas. 7-52748
(VO)₂P₂O₇, 1D spin 1/2 Heisenberg antiferromagnet, mag. susceptibility meas. 7-45639
Y_{1-x}Dy_x, dilute alloys, spin density wave antiferromagnetism 7-52947
ZnCr_{1-x}Ga_{0.4}O₄, antiferromagnetic frustrated spinel, noncritical behaviour near its freezing temp. 7-38875
Zn_{1-x}Mn_xTe, antiferromag. exchange constants between nearest-neighbour Mn²⁺ ions 7-64449
Zn_{0.95}Mn_{0.05}Te, antiferromag. exchange const. determ., free exciton Zeeman splitting meas. 7-22229
Zn_{1-x}Mn_xTe, interband Faraday rot. meas. 7-39093

antiferromagnetic resonance
(BEDTTF)₂AuCl₂, antiferromag. ground state, AFMR meas. 7-27608
(BEDTTF)₂Cl₂, antiferromag. ground state, AFMR meas. 7-27608
four-lattice rhombic antiferromagnet, reson. props., exchange, and high freq. suscept. calcs. (*Russian*) 7-13037
organic conductors, low temp. ground state, antiferromagnetic resonance probes 7-45827
orthoferrites, mag. and dielec. props. at submillimetre wavelengths 7-38990
quasi-one-dimensional conductors, anisotropic SDW and triplet supercond. state properties 7-45706
tetramethyltetraselenafulvalene salts, organic superconductors, antiferromag. anisotropy, SDW amplitude, nesting vector 7-22146
EuCrO₃, coexistence of mag. and electric dipole ordering after optical pumping 7-17171
FeBO₃, antiferromagnet, parametric excitation of magnons with a decay spectrum 7-52966
GdFeO₃ orthoferrite crystals, RF mag. props. and frozen rare earth sublattice 7-17225
MnPS₃, layered cpd., mag. props. 7-52951
NiWO₄, monoclinic biaxial antiferromagnet, antiferromag. reson. study near spin-flop transition 7-53138
tetramethyltetrafulvalene salts, organic superconductors, antiferromag. anisotropy, SDW amplitude, nesting vector 7-22146

antiferromagnetism
see also antiferromagnetic properties of substances; exchange interactions (electron); metamagnetism
anisotropic electron fluid, magnon spectrum and attenuation 7-59000
anisotropic Heisenberg chain, Monte Carlo study of crossover behaviour and solitons 7-7532
Blume-Capel model, ferromag. and antiferromag. props. 7-2867
bond-diluted Heisenberg antiferromagnet, spin damping near percolation threshold 7-17194
charge transfer compounds, thermodynamic and dynamic props. 7-59048
coexistence of superconductivity and antiferromagnetism (*Chinese*) 7-12895
coexistent phase in antiferromagnet. Kondo lattice (*Chinese*) 7-64431
conducting antiferromagnets, collective excitations (*Russian*) 7-58998
crystals, toroidal ordering and impurity scattering 7-38838
dilute antiferromagnet, random-field Ising model 7-7528
dislocation-generated domain walls at spin-reorientation phase transitions (*Russian*) 7-53023
double sublattice, metamagnetic soft mode, spin dynamics, suscept. and thermodynamics 7-59012
easy-axis antiferromagnet, magnetoelastic domain wall oscillations 7-38917
easy-axis antiferromagnets, nuclear spin relax. 7-17233
elastic Ising antiferromagnets on a triangular lattice 7-33185
ferroelectric antiferromagnet, resonance interaction of spin waves with polarisation waves 7-7579
ferromagnet-antiferromagnet superlattice struct., mag. props. 7-2831
films, dipole-exchange spin-wave modes 7-45771
four-lattice rhombic antiferromagnet, reson. props., exchange, and high freq. suscept. calcs. (*Russian*) 7-13037
ground state, possible description without introducing anomalous means 7-45604
Gutzwiller-Hubbard-Kanamori model, crystallization props. 7-58974
Heisenberg antiferromagnet, corrections to power-law behaviour 7-33137
Heisenberg antiferromagnetic chain, S=1/2 random-exchange, correlation effects 7-52928
Heisenberg antiferromagnetic rings, finite lattice extrapolations for ground state energies 7-38896
Heisenberg antiferromagnets, multicritical points 7-27541
Heisenberg ferromagnet, easy-axis, phase transitions, mech. model 7-41034
Heisenberg model, 1-D, ground state struct. 7-45721

antiferromagnetism continued

- Heisenberg models with competing interactions, quantum fluctuations and phase diagram 7-38895
 hexagonal perovskites, antiferromag., magnetoelastic interaction (*Russian*) 7-33248
 high freq. phonon generation in antiferromagnets, nonresonant parallel pumping (*Russian*) 7-33157
 Hubbard model, temperature-induced metal insulator transitions (*Russian*) 7-45153
 Hubbard model, three-dimensional half-filled band sector, magnetic props., Monte Carlo simulation 7-58971
 incommensurate antiferromagnetic struct., equilb. states and precession excitation spectra, phase diagram study (*Russian*) 7-27521
 incommensurate crystals and mag. crystals, 2D topological vortex-type defects 7-7462
 Ising antiferromagnet, ground-state entropies in two and three dimensions 7-45717
 Ising antiferromagnet with site-diluted free surface, surface phase diagram 7-45718
 Ising antiferromagnets in maximum critical fields 7-17185
 Ising model with general spin S, ground state props. 7-58968
 Ising random-field model, multicritical points 7-17187
 Ising square lattice, antiferromagnetic susceptibility and short-range correlation function 7-38893
 Ising-like Heisenberg antiferromagnets on a triangular lattice, mag. props. 7-27540
 longitudinal weak ferromagnetism, disproportionate magnetic struct. and the Dzyaloshinski inhomogeneous interaction (*Russian*) 7-45627
 low symm. magnets, domain boundaries struct. and energy calcs. (*Russian*) 7-33200
 magnetic phase diagram, Ising model on 2D triangular lattice, antiferromag. interactions 7-53012
 magnetic struct. phase transitions in antiferromagnets, exchange magnetostriiction 7-38863
 magnetic superconductor, coexistent states of ferro- and antiferromagnetism 7-58950
 magnon dynamic and kinematic interactions 7-64447
 metals and alloys, 4f-local moments, SDW instability 7-58970
 nearly antiferromagnetic itinerant fermion systems, possible superconductivity 7-38802
 NMR enhancement effects in antiferromagnets with two nuclear spin systems 7-38947
 noncollinear mag. material, antiferromag. mode relax., magnon damping (*Russian*) 7-7498
 numerical simulations with a special purpose computer 7-17182
 one-dimensional Heisenberg antiferromagnet, soft modes 7-2832
 one-dimensional spin-1-bilinear-biquadratic exchange Hamiltonian, crossover effects 7-7464
 parametric magnons, effect on spectra of other quasi-particles 7-52967
 parametric spin wave systems in antiferromagnets 7-33159
 planar-rotator model under h_a fields 7-2799
 polycrystalline orthorhombic antiferromagnet, spin flop field in high field magnetisation 7-7481
 Potts model, simple cubic lattice, critical fluctuations and phase transitions, Monte Carlo simulations 7-35457
 quantum spin chains, random exchange effects, Monte Carlo study 7-64475
 quantum spin chains of arbitrary spin quantum number, phase diagrams and correlation exponents 7-33191
 quasi-one-dimensional systems, spin-Peierls transition 7-59047
 s-f model with antiferromag. s-f exchange 7-45653
 semiconductor, bound magnetic polarons, spin dynamics 7-7502
 singlet superconductivity, mean field theories in extended Hubbard models 7-27461
 soliton dynamics in antiferromagnetic chain 7-52998
 solitons in antiferromag. chains, dyon analogs 7-2798
 spin 1/2 triangular antiferromagnet, thermodynamic props. 7-59046
 spin-1/2 Heisenberg antiferromagnet, triangular lattice, Ising-like exchange anisotropy, magnetisation process 7-53021
 strongly correlated Fermi systems, Gutzwiller saddle-point approx., functional integral approach 7-207
 superconductor, antiferromag., spin wave spectrum 7-38852
 superconductors, anomalous behavior 7-58964
 superlattices with magnetisation perpendicular to surface, collective excitations, magnetostatic theory 7-45647
 toroidal collective excitations and the optical properties of crystals 7-39059
 two-dimensional antiferromag. Heisenberg model, correl. fns. 7-2880
 two-dimensional antiferromagnetic Blume-Capel model, Monte Carlo simulation 7-64471
 two-dimensional Hubbard model, mag. props., mean-field phase diagram and spin-spin correls. 7-64429
 uniaxial antiferromagnet, two-dimens. mag. vortices, dynamical props. 7-53005
 wiggler magnet, antiferromag. cryst., used in synchrotron radiation and FEL 7-57223
 X-ray emission spectra, hyperfine effects 7-13264
 X-Y model, spin-1/2 antiferromagnetic rings, ground state finite-size scaling calcs. 7-56179
 X-Y model, triangular lattice in mag. field, phase diagram, spin wave free energy calcs. 7-17178
 XY antiferromagnetic rings, finite lattice extrapolations for ground state energies 7-38896

antihyperons *see hyperons***antimony**

- see also nuclei with*
 Auger electron spectra, main and satellite structures 7-7795
 Auger energy, Slater transition state calcs., metallic and atomic states, jellium model 7-38475
 film, etching by methyl radicals in discharges 7-3507
 films, amorphous, vacuum-deposited, growth of hexagonal plate cryst. 7-51634
 halophosphate:Sb phosphors, Sb location, Mossbauer spectra studies 7-63634
 layers, amorphous phase stability rel. to metal overdeposits 7-52324
 LiH:Sb³⁺ single crystals, nuclear spin-lattice relax. time anisotropy anomaly studies (*Russian*) 7-33290
 liquid droplets, undercooling and crystallisation 7-39496
 muon Knight shift press. depend. meas. and mol. cluster calcs. 7-45890

antimony continued

- overlayer on GaAs (110) p(1 × 1), domain size, LEED profile anal. 7-7075
 overlayers on GaAs (110), electronic band bending at interface 7-58895
 overlayers on GaAs (110) and GaP (110), ARUPS 7-59378
 p(1 × 1) overlayer on III-V semiconductors, atomic and electronic struct. 7-7007
 refining by continuous zone melting 7-3163
 seawater and atmos. aerosol of English Channel and N Atlantic, As and Sb contents 7-29075
 single crystals, dislocation thermoactivated amplitude-dependent internal friction (*Russian*) 7-51934
 surface, (111), LEED studies using automatized high-speed data acquisition system 7-21589
 ultrathin films on Si, electromigration, scanning AES study 7-63891
 Al-Sb, Xe ion irradiated, intermixing rates, backscattering spectra, anal. by computer program 7-64840
 AlGaAs:Sb, MBE growth, Sb doping 7-2038
 Ba_{0.9}Sr_{0.1}TiO₃:Sb, positive temp. coeff. of resist., synthesis method depend. 7-45324
 Bi:Sb, magnetocond. in 13 T mag. field at low temp. 7-7209
 pCdTe:Sb epilayers, photoassisted MBE growth 7-53607
 Co-Sb superlattices, NMR study (*Japanese*) 7-13046
 FeNiCr:Sb,P, grain boundary segregation, Auger and energy dispersive X-ray mapping 7-16571
 GaAs:Sb, deep level formed by Sb doping 7-52496
 GaN:Sb, antise dopant incorporation, Mossbauer spectra study 7-12086
 Ge:Sb, Cu, impurity photoconductivity, field and spectrum dependences, exclusion effect 7-38635
 n-Ge:Sb, electron heating, photocond., photo-Hall effect 7-12765
 Ge:Sb, implanted, heavy ion damage, TEM, annealing studies 7-63676
 Ge:Sb, mobility anisotropy coeff. determ. 7-12715
 Ge:Sb single cryst., extended defects, X-ray topography meas. 7-38020
 Ge:Sb(Al)(Ga)(In), heavily doped, charge carrier scatt., elec. cond., Hall effect meas. 7-7228
 GeTe:Sb, solution mechanism of impurities, effect of heat treatment 7-21455
 p-Hg_{0.78}Cd_{0.22}Te:Sb LPE films, elec. props. 7-7426
 InAs:Sb(Ga)(Mn), single crystal, elec. inhomogeneity, effects of isovalent impurities 7-7229
 InP:Fe,Ga,Sb, LEC growth, dislocation density, resistivity, SIMS obs. 7-53552
 InP:Ga,As,Sb single crystals, LEC growth, isoelectronic doping, dislocation density, X-ray topography 7-33549
 InP:S,Ga,Sb, LEC growth, appl. mag. field method, dislocation etching 7-53553
 Mo/Sb multilayer film, superconductivity and structural characterisation 7-17128
 Pb-acid cells, dissolution and immobilisation of Sb, cell design 7-54289
 Sb³⁺ in RBO₃ (R=Sc, Y, La, Gd, Lu), luminesc. 7-33442
 Sb-Cd(Zn), thermodynamic functions are modelled by chemical-physical theory, Gibbs energy 7-52051
 Sb+He⁺, L-subshell ionisation, X-ray prod. 7-50303
 Sb₂ cluster, laser vaporisation and photoionis., TOF mass spectrometry 7-31201
 Si:As, Sb, Sb diffusion 7-44915
 Si:B(Ga)(As)(Sb) 7-2040
 Si:O, P, Sb wafers, O precipitation during simulated CMOS cycles 7-38218
 Si:P,Sb, mixing of P and Sb ions by recoil implantation, sheet resist., annealing temp. depend. 7-21291
 Si:P,Sb, Sb diffusion 7-44915
 Si:Sb, dry oxidation retarded impurity diffusion, SIMS meas. and numerical simulations 7-27014
 Si:Sb, heavily doped, laser induced oxidation 7-13672
 Si:Sb, implanted, heavy ion damage, TEM, annealing studies 7-63676
 Si:Sb, local lattice relax. around impurity, K-edge EXAFS study 7-64159
 Si:Sb, pot. enhanced doping during MBE growth, elec., optical props., cryst. quality 7-12112
 n-Si:Sb, resistivity at low temp. appl. to bolometers 7-41471
 Si:Sb, retarded and enhanced dopant diffusion related to implantation-induced excess vacancies and interstitials 7-63881
 Si:Sb,As, cryst. aid amorphous, impurity band form., X-ray spectra studies 7-12650
 Si:Sb,O, heavily doped crystals, behaviour of O and dopants 7-32483
 Si:Sb,O, heavily doped Czochralski wafers, O precipitation, 450°C thermal annealing 7-58477
 Si:Sb MBE, electron irradi. effect on doping levels and profiles 7-63660
 Si:Sb MBE film, doped by electron impact ion source, improved doping characts. 7-12101
 Si:Sb MBE layers, doping by secondary implantation 7-12102
 Si:Sb substrate for W CVD, effect of dopants and crystal perfection 7-22576
 Si:Sb thermal donor props., impurity effects, DLTS, Hall effect, and admittance spectra meas. 7-21851
 Si:Sb(As)(P)(B) epitaxial films, low temp. deposited by low press. CVD, autoping 7-27182
 SiGe superlattice structures, Sb doped, MBE grown, comp., doping profiles, SIMS, Rutherford backscattering spectra 7-7035
 SiO₂:Sb, ion-implanted, diffusion 7-58542
 SnO₂:Sb spray deposited coatings, comp., elec. props. thermal treatments, AES study 7-22393
 SnO₂:Sb thin films, doped and undoped, prep. by photolysis, phys. props. 7-22368
 SnO₂-Pd-Sb H₂ gas sensor insensitive to alcohol (*Japanese*) 7-56242
 SnTe:Sb, solution mechanism of impurities, effect of heat treatment 7-21455
 Ti/Si:As,Sb interface, dopant redistrib. during silicide form. by rapid thermal processing 7-63641
 TiSi₂:As(Sb) layers, dopant redistribution during silicidation by rapid thermal annealing, ion scatt. spectra study 7-21253
 ZnO:Sb, Schottky-like barriers, ion implantation, annealing 7-58860

antimony alloys

- see also antimony compounds*
 intermetallic cpds., charge redistrib., L-edge XANES study 7-64816
 polycrystalline, elastic constns. meas. 7-21319
 stainless steel-Sb, X-ray microanalysis, of equilibrium and nonequilibrium segregation 7-46488

antimony alloys continued

- Ag-Mn-Sb, dilute metallic spin glasses, response time, temp. depend. study 7-2896
- Ag-Sb, liq., activity coeffs. of O 7-3284
- AgSb, impurity-vacancy and impurity-impurity interactions calc. from diffusion enhancement 7-6672
- Al-Si-Sb, directionally solidified eutectics, inter-Si flake spacing rel. to Sb addition 7-53717
- As-Sb alloys, magnetoresist., thermomag. power and Fermi surface quantum oscils. meas. 7-2578
- Bi-Sb alloys, magnetic suscept. field depend., electron band struct. effects (*Russian*) 7-12936
- Bi-Sb high temp. kinetic coeffs. oscills., band struct. and magnetoresist. temp. depend. studies (*Russian*) 7-12738
- Bi-Sb:Te(Sn) thin films, elec. props 7-64376
- Bi-Sb(-Te), single cryst. alloys, component distrib., stratified heterogeneity 7-46302
- Bi_{1-x}Sb_x, anomalous magnetoresistance, quantum limit 7-58795
- Bi_{1-x}Sb_x narrow-gap semicond., intraband breakdown, current-voltage characts., size effect conditions 7-52624
- Cd-Sb melts, crystallisation and structural state, phase equilib. diagrams 7-46441
- CdSb, optical energy gap and light emission (*Japanese*) 7-53264
- CdSb-In crystal, In atom electrodiffusion study 7-63890
- Co-Sb system, α -solid soln., interdiffusion (*Japanese*) 7-6861
- Cs-Sb-based photocathodes, stability and O adsorption energies 7-38344
- Cs₃Sb surface film, detection on multialkali photocathodes 7-46912
- Cu-Sb (1 wt.%), creep crack growth, 450-650°C 7-33758
- CuSb vacancy formation enthalpy, positron annihilation studies 7-7787
- Fe-Ni-Sb, grain boundary segregation of Ni and Sb 7-22689
- Fe-Sb, dilute alloys, electron irradiated, vacancy-solute interaction, positron lifetime, muon spin rotation studies 7-39288
- Fe₂Sb_{100-x}, amorphous, metal-insulator transition and effects of localisation and correlation 7-45407
- FeSnSb dilute alloys, local lattice relax. around impurity, K-edge EXAFS study 7-64159
- Gd-Sb, phase diagram, peritectic reactions, congruent melting, DTA, microstructural and X-ray anal. 7-39481
- InSb-NiSb eutectic composite, rel. between metal fibre morphology and elec. props. 7-59644
- Li-In-Sb, ternary phase diagram, electrochem. investig. 7-58441
- MnSb, epitaxial growth of ferromagnetic monolayers 7-2909
- Na₃Sb, NA vapour sensor based on conductivity variation 7-18774
- Nb-Sb alloys, B8 phase, diffusion studies 7-12354
- Nb₂Sb Al₁₅ material, displacement correl. functions temp. depend. calcs. 7-51962
- Nb₂Sb_{1-x}Sb_x Al₁₅ pseudobinary alloy, structural transitions and related anomalies 7-38182
- Ni_{1-x}Fe_xMnSb, half-metallic ferrimag., mag. and crystallographic props. 7-45672
- NiMnSb, half-metallic ferromagnet, positron-annihilation study 7-21802
- NiMnSb Heusler alloys, positron annihilation studies of solids 7-64728
- Ni₂MnSb Heusler alloys, galvanomag. props. and magnetisation meas., fermi level shift effects 7-7207
- Ni₂MnSb, Heusler alloys, Curie temp., effect of hydrostatic press. 7-64455
- Ni_{93.35}Sb_{6.65} and Ni_{78.5}Sb_{21.5} alloys, characterisation studies (*French*) 7-28010
- NiSnInSb dilute alloys, local lattice relax. around impurity, K-edge EXAFS study 7-64159
- Pb-Sb, grain refinement, effect of solute content 7-59503
- PuSb, heat capacity meas. 7-12975
- PuSb, hybridisation-mediated anisotropic mag. behaviour 7-2850
- Sb-Ge-Zn system, thermodynamic investig. (*German*) 7-53703
- Sb-Sn alloy, maximum microsegregation from peritectic phase systems 7-12286
- Sb-Sn system, phase diagram, thermodynamics 7-3283
- Sb-Zn melts, crystallisation and structural state, phase equilib. diagrams 7-46441
- Sb₂Bi, cluster, laser vaporisation and photoionis., TOF mass spectrometry 7-31201
- SbSn dilute alloys, muon Knight shift and trapping, comp. and temp. depend. 7-45889
- Sc-Ga(In)(Sb), alloy form, thermodynamics 7-22637
- Sn-Ag-Sb thermal fatigue-resistant solder alloys, equilibrium solidification 7-46443
- Sn-Sb, dil., planar solid-liq. interface, morphological development and stability (*Korean*) 7-7985
- Sn-Sb (2 at.%), morphological development of planar solid-liq. interface (*Korean*) 7-17523
- Sn-Sb melts, short-range order 7-63438
- Sn-Sb system, high press. phase transitions, X-ray diffr. study 7-6779
- Ti₇₅Sb₂₅, with Cr and Fe impurities, supercond. transition temp., impurity conc. depend. 7-2768
- Ti₇Sb₂, giant cells, polyhedral packing 7-11992
- U₃Sb₂Cu₂, cryst. struct., mag. props. 7-38864
- YbSb₂, superconductivity study 7-58962
- Zn-Sb melt, ordering models 7-44351

antimony compoundssee also *antimony alloys*

- free-resistant material, Sb₂O₃ influence on effectiveness, chem. anal. (*Russian*) 7-65378
- Mossbauer isomer shifts, first-principles scalar-relativistic linear muffin-tin orbital method calcs. 7-2957
- polyacetylene:SbF₅, identification of dopant species, X-ray absorpt. and Mossbauer spectra 7-65377
- Sb₂O₄, thermodynamic stability, EMF obs. 7-46828
- Ag₃SbS₃, pyrragrite single crystals, electroacoustic echo 7-7293
- Ag₃SbS₃, pyrragrite, incommensurate phase, NQR study 7-45837
- As-Sb-Se glasses, calorimetric meas. 7-26652
- Ba(Li_{0.25}Sb_{0.75})O₃, cubic perovskite, prep. and struct. 7-63589
- Ba(Na_{0.25}Sb_{0.75})O₃, cubic perovskite, prep. and struct. 7-63589
- (Bi_{1-x}Sb_x)₂Te₃ single crystal, optical constants, IR spectra study 7-46030
- Bi_{2-x}Sb_xTe₃ polycryst. semicond. films, laser annealing effects 7-58317
- Bi_{2-x}Sb_xTe_{3-y}Se_y, carrier density, depend. of anisotropy parameter 7-7226
- Bi₂Te₃-Bi₂Se₃-Sb₂Te₃ system, solid solns., layered cpd. formation 7-21454
- Cu-Sb-S compounds, valence bands and semiconducting gaps, nonstoichiometry and phase separation 7-16941

antimony compounds continued

- Eu-Sb-S, synthesis and props. 7-44471
- Eu-Sb-Se(Te), synthesis and props. 7-44471
- Ge-Sb-S glasses, bulk and thin film samples, optical and photo-acoustic props. study 7-22211
- Ge-Sb-Te system, diffusion of Fe, Cr and Ni impurities 7-21527
- (GeSe₂)₇₀(GeTe)₁₅(Sb₂Te₃)₁₅, glass transition, thermodynamic and thermokinetic characts. 7-26953
- K₂SbPO₆, solid-state reaction prep. and cryst. struct. determ., X-ray diffr. study 7-1980
- Mn₂Sb₂O₃, synthesis and cryst. struct., X-ray powder diffr. meas. 7-58240
- PbCl₂-Sb₂O₃ glass system, structural aspects 7-44389
- PbO-K₂O-Sb₂O₃-As₂O₃ flint type glasses, viscosity near annealing temp., depend. on PbO conc. 7-58151
- 5PbS₂Sb₂S₃, boulangerite, elec. cond. (*Korean*) 7-27331
- Sb-Ge-Se-Mn, effect of Mn impurity on comp. and physicochemical props. 7-11922
- Sb-S, thin films, amorphous and thermally annealed, optical props. (*Russian*) 7-17352
- Sb-Sb₂Se₃-SbI₃ system, phase diagrams investig. 7-2212
- Sb-Se, thin films, amorphous and thermally annealed, optical props. (*Russian*) 7-17352
- Sb_{1-x}Bi_x crystals, elec. props. at ferroelec. Curie point 7-2991
- SbBr₂-AlBr₃ complex, struct. Raman spectra study 7-46020
- SbBr₃ single crystal growth in gel 7-22458
- SbCl₃, struct., GPED automatic background subtraction 7-15710
- SbCl₃ intercalated graphite, stage 2, basal plane resistivity and phase diagram 7-45258
- SbCl_mF_{3-m} graphite intercalation cpds., struct., X-ray diffr. studies 7-12008
- SbF₃ single crystal growth in gel 7-22458
- SbH₃, isotopic species, mol. vibrs., inversion splitting calcs. 7-19997
- SbI₃ film, photosensitive, heating effect on elec. cond., switching behaviour 7-58920
- SbI₃ single crystal growth in gel 7-22458
- SbNbO₄ and (Sb_{1-x}Bi_x)NbO₄, vibr. spectroscopic study 7-39115
- β -Sb₂O₄V(Mo), struct. characterisation, X-ray, neutron, and electron microscopy studies 7-32383
- SbP(As)O(S)₄, dielec. const. meas. w.r.t. bond ionicity (*French*) 7-38988
- SbS₃, amorphous thin films, electrical resistivity 7-45523
- SbS₃ amorphous condensers, electroelectret state and local levels studies (*Russian*) 7-45923
- a-SbS₃ films, thermally induced relax. of mechanical stresses 7-8032
- Sb₂S₃, nonstoichiometric forms in PbSb₂S₄-Sb₂S₃ region of Pb-Sb-S phase diagram 7-6812
- Sb₂S₃ single crystal optical absorption and luminescence obs., 2 to 367K (*Japanese*) 7-39151
- SbS₃ thin films, vacuum deposited, elec. and photoconductive props. (*Korean*) 7-52682
- SbS₃-electrolyte interfaces, electrochemical photovoltaic cell fabrication appl. 7-40016
- SbS₃-I₂ system, SbSI form. and melting diagram 7-26919
- Sb₂S₃-PbS systems, non-stoichiometric phases close to Sb₂S₃, structure 7-32674
- SbS₃-Sb₂Se₃, hollow mixed crystals vapour growth, morphology and whisker growth 7-7831
- SbSBr, ferroelec. semicond., band struct., X-ray spectral studies 7-58739
- SbSI cryst., dielec. const. determ., chem. bond approach, MWH band struct. calcs. 7-17260
- SbSI, crystals, grown from melt, microhardness study 7-12196
- SbSI, elec. charactn. of crystals, grown from melt by temp. fluctuation technique 7-13104
- SbSI, elec. cond., ferroelec., phase transition temp. 7-45326
- SbSI, ferroelectric semiconductor, photoacoustic spectroscopy 7-16696
- SbSI, hollow cryst. growth from vap. 7-53520
- SbSI, SbSOI, cryst. growth and elec. charactn. 7-53564
- SbSI, single cryst., nonlin. electromechanical parameter meas. 7-13094
- SbSI single crystals, vapour growth, morphology rel. to temp. gradients 7-46287
- SbSeI, crystals, grown from melt, microhardness study 7-12196
- Sb₂Te₃ crystal, semimetallic, semicond. behaviour at low temps. 7-12716
- Sb₂Te₃ doped crystals, energy formation of antisite defects 7-21204
- Sb₂Te₃:Sn, TI, single crystals, X-ray spectral microanalysis 7-44590
- Sb₂Te₃ crystals, pure and Cd-doped, point defects, reflectivity and elec. props. room temp. meas. 7-33008
- SbX₂-GaX₃ complex; X=Cl, Br; struct. Raman spectra study 7-46020
- Sn-Sb₂O₃ catalyst, O absorb. and desorp. kinetics 7-63944
- SnO₂-n-Sb₂Al structures, polarization current relaxation and space charge 7-33090
- Tl-SbTiSe₃, liq., semicond., elec., mag. and thermoelec. props. 7-58825
- Tl-SbTiTe₃, liq., semicond., elec., mag. and thermoelec. props. 7-58825
- TlBi_{1-x}Sb_xVI, solid solns., band spectrum double inversion to semimetallic state 7-38452
- V₂O₅-P₂O₅-Sb₂O₃ glasses, DC conductivity 7-45316
- Yb-Sb-S(Se), synthesis and props. 7-44471
- Yb-Sb-Te ternary system, phase diagram investigs. 7-2174
- YbBiS(Te), synthesis and props. 7-44471

antineutrinos see *neutrinos***antineutrons** see *neutrons***antinucleons** see *nucleons***antiphase boundaries**

- alloys, dislocation annihilation and strain hardening (*Russian*) 7-46500
- alloys, ordered, L₂₀ and L₁₂, grain boundary structs., twist boundaries, geometrical models 7-63628
- alloys with periodic antiphase boundary struct., dislocation motion 7-63620
- B2 ordered alloy, edge dislocation, computation of core struct. 7-37991
- binary crystals, FCC, ordering, Monte Carlo simulation 7-38154
- disordering transitions, nucleation mechanism, review 7-44743
- magnetic alloys, antiphase boundaries 7-12407
- semiconductors, polycrystalline, extended interfacial defects, geometrical character 7-6640
- transition metal alloys, binary, substitutional, segregation and order 7-22685
- Au-Mn (15 at.%), disordered phase, high resolution electron microscopy study 7-63834
- AuCu₃, ordered alloy, antiphase boundary form. energy, atomic config., Morse pot. approx. (*Russian*) 7-46419
- Au₂Zn, non-periodic antiphase boundaries, obs. by HREM 7-63550

antiphase boundaries continued

- Co₃Ti, effect of plastic deformation on mag. props. 7-33259
 Cu-Au quenched alloys, diffuse X-ray scatt., microdomain model anal. 7-6814
 CuAu I and II, initial ordering stages, twinning, periodic antiphase boundaries, electron microscopy 7-28032
 Cu₃Au ordered alloys, twin boundary structure, TEM anal. 7-2027
 Cu₃₁Pd, long-period superstructures 7-21430
 Cu₄₈Ti₅₂, amorphous, crystallisation, intermediate long period superlattice phase form. 7-21098
 Fe-Al, thin foil, interfacial migration, velocity-driving force relations 7-46411
 Fe-Co-V, ordered alloy, plastic deform., antiphase boundaries (Russian) 7-39596
 γ-Fe₂O₃ particles, pure and Co-modified, microstructural defects 7-58497
 GaAs epilayers grown on Ge or Ge/Si substrates, defects 7-21778
 GaAs, nucleation and growth on Ge, antiphase boundary struct. 7-2420
 NaNbO₃-Nb₂O₅-WO₃ system, crystal struct., twinning, fouling and antiphase boundary operations 7-63567
 Ni-Al-Cr, melt spun ribbons, microstruct., mech. props., Cr conc. effect 7-28031
 Ni₃Al, rapidly solidified, B segregation to grain boundaries, atom probe FIM 7-22688
 Ni₃Al-B rapidly solidified alloy, B distrib. at grain and antiphase boundaries, atom probe FIM and TEM studies 7-33637
 Ni₃Fe, ordered alloy, antiphase boundary form. energy, atomic config., Morse pot. approx. (Russian) 7-46419
 Ni₃Ga, atomic ordering, strain disruption (Russian) 7-53808
 PbTe-type narrow gap semicond., with antiphase boundary, physical realisation of parity anomaly 7-38432
 β-SiC, epitaxially grown, antiphase boundaries 7-46722
 SiC(100), cubic, grown on Si(100) by CVD, surface morphology 7-46339
 Ti-Ni (51 at.%), aged shape memory alloy, precip. morphology, comp., cryst. struct. 7-28049
 W (100) with adsorbed H, long and short range fluctuations, lattice dynamical model 7-7002
 ZrO₂-Y₂O₃, displacive cubic to tetragonal phase transform. 7-65027
 ZrO₂-Y₂O₃ system, microstruct. resulting from diffusionless cubic to tetragonal phase transform. 7-39501

antiphase domains

- see also antiphase boundaries*
 semiconductors, polycrystalline, extended interfacial defects, geometrical character 7-6640
 Al-Ti alloys, 1D antiphase domain structures 7-63557
 Cu (100), dense Pb monolayer, LEED anal. 7-6989
 Cu₃Pt ordering kinetics, comp. depend., X-ray and DTA studies 7-26940
 Fe-Al, interfacial migration, velocity-driving force relations 7-46411
 GaAs epitaxial layers and heterostructures grown on Si substrates, material props. 7-7046
 GaAs MOCVD growth on Ge (100) and Si (100) substrates, antiphase and single domains 7-27925
 GaAs/Ca₃Sr_{1-x}F₂ (100) SOI structures, epitaxial GaAs films, antiphase disorder 7-52315
 GaAs-Si p-n heterojunctions, interface charge polarity 7-38686
 GaP films, MBE grown on Si, antiphase domain structures 7-64014
 PdFe ordered alloy, discontinuous domain coalescence (Russian) 7-2025
 SiC(100), cubic, grown on Si(100) by CVD, surface morphology 7-46339
 Ti-Al-Nb, rapidly solidified, microstructural studies 7-22668
 Ti₃Al-Zr, rapidly solidified, microstructural studies 7-22668
 ZrO₂-Y₂O₃ system, microstruct. resulting from diffusionless cubic to tetragonal phase transform. 7-39501

antiprotons *see* protons**antireflection coatings**

- achromatic, graded-index, for broad spectral region 7-43323
 antiscattering single layer theory, antiscatt. antirefl. coatings 7-1029
 Chebyshev and Butterworth spectral responses 7-43321
 design for fibre optic communication equipment, production run simulation 7-25937
 dielectric coatings for laser mirrors, fabrication 7-15965
 dielectric surface-relief gratings as antireflection coatings 7-43320
 diffraction gratings, soft X-ray, efficiency enhancement by multilayer coating 7-25946
 Fabry-Perot etalons, antireflection coating stress 7-30064
 IR components with diamond-like coatings development, appl. and testing 7-31434
 IR optics advances 7-11079
 lens design, antirefl. coating parameters introduction in design phase 7-50680
 microchannel spatial light modulator with improved resolution and contrast ratio 7-25954
 multilayer coatings, for excimer laser, reflectivity calcs. 7-57521
 multilayer systems, effect of breakdown in periodicity 7-20391
 preparation and testing for high power lasers at 1.06 μm 7-1249
 protective coatings, reactive magnetron sputtering, microelectronics appl. 7-33556
 quality, reliability and process parameter optimisation 7-5973
 scatter from fluid patches in optical thin-film-coatings 7-1028
 sol-gel thin films used in solar energy appls. 7-37106
 solar cell coverglass thermal characts., improvements by thin film coatings 7-13884
 three-layer, layer thickness meas. technique 7-43324
 a-C:H diamond-like coating on Ge, rain erosion resistance improvement obs. 7-31435
 Co₂O₃-FeO_x selective coatings, spray pyrolysis for high temp. appls. 7-5974
 CuInSe₂-ZnCdS thin film polycryst. solar cell efficiency improvement using antireflection coatings 7-23186
 ITO antireflection coating for a-Si solar cells with transparent Ag contacts 7-65478
 PbF₂ environmentally nonpolluting antireflective coating of ZnSe optics 7-11097
 PbO-SiO₂ glass sputtered antireflection coatings on semiconductor laser facets 7-15964
 Si solar cell, planar, antireflection coatings effects 7-54303
 Si solar cells, polycrystalline, efficiency improvement using plasma treatments 7-13909
 a-Si_{1-x}N_x films, plasma CVD deposited, as antireflective coatings for solar cells (Japanese) 7-23141

antireflection coatings continued

- Si₃N₄ antireflection coating, sputter deposition and optical props., laser appls. 7-59421
 Si₃N₄ film synthesis by ion-assisted deposition, antireflection coating use 7-37213
 SiO₂ film synthesis by ion-assisted deposition, antireflection coating use 7-37213
 TiO_x antireflection coatings, appl. in Si alloyed inversion layer solar cells 7-17864
antislit defects *see* point defects
APD *see* avalanche photodiodes
API gravity *see* density
APL listings
 pyroxene, structural formulae and end member calculation, APL program 7-66313
 sea bed contour map construction from random data by interpolation 7-34727
apodisation *see* acoustic imaging; optical images
apparatus *see* instrumentation; instruments
apparent porosity *see* porosity
appearance potential *see* ionisation potential
appearance potential spectra
 appearance potential spectra, scanning Auger microprobe for meas. of work fn. 7-64824
 metals, appearance pot. spectra, many-body effects, single-particle excitation contrib. calcs. 7-22387
 solids, mean free paths of electrons, determ. by soft X-ray excitation pot. spectroscopy 7-46242
 Al and Al alloys, appearance potential spectroscopy, matrix elements 7-59305
 Cr, extended appearance potential fine structure anal. 7-27825
 LaB₆, orientational effects of interactions of electrons in APS spectra 7-46243
 Ti, inner-shell excitations, energy-calibrated APS, correlation effects obs. 7-46247
 Ti, SXAPS spectra, L₃ line shape 7-39322
 Ti-Si interface, silicide form., Auger and appearance pot. spectra studies 7-45031
 V, inner-shell excitations, energy-calibrated APS, correlation effects obs. 7-46247
 V, orientational effects of interactions of electrons in APS spectra 7-46243
appearance potential spectroscopy
 surface physics appl. of Auger and appearance potential spectroscopy (Rumanian) 7-17368
appliances, domestic *see* domestic appliances
applied mechanics *see* mechanics
approximation theory
see also function approximation; interpolation; least squares approximations
 aeroplane wings, transonic flow calc. using higher-order approximation method 7-51211
 beam, shock-loaded, large plastic strains eval. 7-43752
 boundary integral equation on polygonal domains, superconvergent approxs. to soln. 7-48323
 creep strength characteristics extrapolation, parametric methods suitability 7-22942
 creep strength rapid prediction, thermoactivation analysis basis, residual life eval. after TMT 7-22941
 cylinder, hollow, with nonplanar end-faces, stressed state, approx. method 7-16067
 deformable bodies, three-dimens. stability theory, construction elements, approx. approach 7-16086
 dynamical systems, simultaneous rational approximations 7-18587
 lens design program using simultaneous linear inequalities, improved version 7-50681
 monotonic operator problems, regularisation using discrete approximation (Russian) 7-61058
 piecewise-Chebyshev approximation of exptl. data (Russian) 7-56206
 plane wave diffraction, impedance cylinder with arbitrary cross section, quasiwave asymptotic form 7-50467
 ranging by optical method, precision, for long baseline meas., error of point approx. method for air integral refr. index 7-66342
 seismology, reciprocity principle rel. to approx. soln. of wave eqn. 7-54896
 shell, spherical, thick-walled, under short pulse loading max. stresses eval. 7-20640
APR *see* acoustic paramagnetic resonance
APS *see* appearance potential spectra; appearance potential spectroscopy
APW calculations
 alkali halides, XANES K-spectra, cryst. pot. and size effects 7-64748
 crystal lattice, spiral mag. struct., band struct. calcs. 7-7096
 diamond, energy band gap calc., self-interaction correction to local density approx. 7-45144
 metal alloy hydrides, disordered, theory of electronic states 7-27243
 self-consistent linearized, accelerating the convergence of calcs. 7-45122
 superlattices, surfaces and interfaces, structural, electronic and mag. props. 7-18649
 Ag-based dilute alloys, low temp. elec. resist. 7-52565
 Al, nuclear quadrupole interactions in the presence of muons 7-53192
 Ar, solid, band struct., classical nonrelativistic nonselfconsistent APW calcs. 7-64076
 As, structural calcs. 7-7143
 Be, charge density distrib., local density approx. calcs. 7-6577
 Ce alloy cubic Laves phases, electronic struct., self-consistent APW calcs. 7-12599
 Ce alloys, electronic struct., pseudopotential method 7-27245
 Cr, band structure 7-7105
 Cr, positron annihilation radiation, 2D angular correlation distrib. 7-53440
 Cr₂TiS₂, intercalated dichalcogenide, electronic struct. 7-52387
 CsI, high press. metallisation, relativistic self-consistent APW calcs. 7-21812
 Cu, nuclear quadrupole interactions in the presence of muons 7-53192
 Cu-based dilute alloys, low temp. elec. resist. 7-52565
 Cu₂O, electronic struct. and binding mech. 7-2482
 Dy, band struct., effect of nonspherical pot., warped muffin-tin approx., APW method 7-27246

APW calculations continued

- Fe₂TiS₂, intercalated dichalcogenide, electronic struct. 7-52387
 GaAs-AlAs superlattices, GaAs and AlAs, energy band gap calc., self-interaction correction to local density approx. 7-45144
 LiAl(Ga)(In)(Zn)(Cd) B32-type Zintl phases, mag. props., exchange enhancement, APW calcs. 7-27504
 NaIn B32-type Zintl phases, mag. props., exchange enhancement, APW calcs. 7-27504
 Nb and its dihydride, Compton profiles 7-59281
 NiAs-type compounds, electronic band struct., magnetism and structural phase transitions (*Japanese*) 7-21815
 Ni₂Ge, momentum density distrib., Compton scatt., positron annihilation, symmetrised APW method 7-64069
 Pb, self-consistent relativistic band struct., normal and high press. 7-52413
 Pd, angular correlation of positron annihilation radiation, calc. 7-39244
 PdH, angular correlation of positron annihilation radiation, calc. 7-39244
 Ru (0001) with adsorbed H monolayer, adsorbate bonding and vibr. 7-52291
 SeGa₃, band struct., coupling energy (*Russian*) 7-58732
 Si, energy band gap calc., self-interaction correction to local density approx. 7-45144
 Sr, relativistic band struct., self-consistent calcs. under normal and high press. 7-64068
 Ta (001), struct., instability, and reconstruction model energetics, general-pot. LAPW calcs. 7-44969
 Ta, Compton profiles, APW calcs. 7-27809
 Ti, Compton profiles due to valence electrons, self-consistent calcs. 7-13250
 Ti, SXAPS spectra, L₃ line shape 7-39322
 TiH₂, Compton profiles due to valence electrons, self-consistent calcs. 7-13250
 UO₂, band struct., angle resolved and reson. photoemission study 7-27856
 UPt₃, heavy fermion superconductivity and normal state props. 7-52412
 V and its dihydride, Compton profiles 7-59281
 V, positron annihilation radiation, 2D angular correlation distrib. 7-53440
 W (001), struct., instability, and reconstruction model energetics, general-pot. LAPW calcs. 7-44969
 W, Compton profiles, APW calcs. 7-27809
 Yb, relativistic band struct., self-consistent calcs. under normal and high press. 7-64068

arbiters (computers) *see* **computer interfaces**

arc discharges *see* **arcs (electric)**

arc furnaces

- metallurgical furnaces with arc plasmatrons, AC appls. to feeding plants (*Polish*) 7-11799
 Xe arc image furnace, appl. to LaB₆ cryst. growth by floating zone method 7-33552

arc heaters *see* **arc furnaces**

arc lamp annealing *see* **incoherent light annealing**

arc lamps

No entries

arc welding

- FCAW weld metal, self-shielded, nitride and N contents estimation method 7-59710
 steel, C-Mn, arc welds, as-deposited strength, toughness, microstruct. 7-13555
 steel, ferritic stainless, Mo, welding, heat affected zones, microstruct., thermal history 7-53769
 steel, HSLA, submerged arc welds, acicular ferrite nucleation by inclusion phases 7-17525
 steel, low alloy, arc weld deposits, austenite grain struct. 7-39494

archaeoastronomy *see* **astroarchaeology**

archaeology

see also **astroarchaeology**

- Dead Sea area during Neolithic period, implications of high lake level at 6700 yr BP 7-55087
 fossil bone U content, SSNTD anal. 7-49831
 Kodayama tumulus, fault displacement caused by 1510 earthquake 7-8863
 roof-tiles used as floor of kitchen oven in Italy, polyphase magnetization 7-47336
 shallow prospecting on land by means of a novel electroacoustical P-Wave pulse generator 7-34751
 Sopron, Hungary, archaeological baked clay, archaeomagnetic ages (*Hungarian*) 7-18113
 Au archaeological artifacts, light element determ. by nuclear reactions 7-59814

archaeomagnetism *see* **paleomagnetism**

archeomagnetism *see* **paleomagnetism**

architectural acoustics

see also **anechoic chambers**; **echo**; **noise abatement**; **reverberation**

- audioconference rooms and reverberators, modelling 7-37253
 broadcast and recording studio, electronic architecture 7-6063
 building partitions, study of sound transmission class system 7-43533
 Canadian homes, typical meas. 7-43532
 cinema and lecture hall acoustic design by computer (*Hungarian*) 7-50850
 classroom speech intelligibility studies 7-6052
 concert hall acoustics, image model 7-1316
 concert halls, multichannel reverberation system design 7-6043
 concert halls transient distortion, sound differences anal. (*German*) 7-62929
 double doors, sound transmission charact. 7-43531
 dynamical state estimation method based on the nonlinear mixed stochastic model in room acoustics 7-37248
 electro-acoustic techniques in the boardroom 7-6046
 electro-acoustics in architecture 7-6044
 electronic architecture applications 7-6045
 enclosures, acoustic evaluation using dig. signal processing 7-6042
 factories, acoustic scale modelling 7-62916
 floating floors for impact and airborne noise control 7-37245
 lecture halls, large, scale model expts. 7-6048
 live-end-dead-end type recording studio control rooms, rear-wall reflection patterns 7-31571
 low-ceilinged room acoustics (*German*) 7-43530
 mean path length in random acoustic fields in solids 7-6047

architectural acoustics continued

- Monastery of 'Santo Domingo de Silos', church acoustics 7-57636
 nonlinear response in evaluating the subjectivediffusiveness of sound fields 7-6050
 Olympic main coliseum, acoustic simulation (*Japanese*) 7-62915
 Palais Acropolis in Nice, France (*French*) 7-43529
 predictors of speech intelligibility in rooms 7-6051
 radio outside broadcast vehicles, acoustical considerations 7-26079
 reverberant room, response of multiple microplanes to single acoustic source 7-43534
 reverberation time difference limens for artificial reverberation signals under monophonic listening condition (*Japanese*) 7-31569
 reverberation time meas. 7-43606
 room acoustics, inverse control using multiple loudspeakers and/or microphones 7-37252
 room acoustics alteration using electro-acoustic systems (*German*) 7-16033
 room reverberation time in an almost-two-dimensional diffuse field 7-37250
 room reverberation time meas. using cross-correlation of two relatively prime pseudorandom sequences 7-62914
 rooms, localization of sound, onset and duration effects 7-47106
 rooms, probabilistic response of sound insulation systems 7-31568
 silencer joints, acoustical insulation props. (*German*) 7-57631
 single wall insulation, statistical energy analysis (*Japanese*) 7-43535
 sound field, fundamental physical parameters extraction by multidimensional anal. 7-37254
 sound field in room, grasp and development of spatial information by closely located four-point microphone 7-37258
 sound insulation system, dynamical identification method, conditioned obs. based 7-43526
 sound recording control room design incorporating RFZ, LFD and RPG diffusors 7-37249
 space variances in the mean-square pressure at the boundaries of a rectangular reverberation room 7-6049
 speech recognition, room acoustics effects (*German*) 7-1322
 statistical spatial acoustics, reverberation time meas. for low density of eigenfrequencies (*German*) 7-57637
 studio control room design, psychoacoustic considerations 7-31570
 trapezoid-terraced hall (*German*) 7-50848
 TV, radio, post production studios, modular construction 7-20507
 TV studios, slideway type sound absorbers use (*Russian*) 7-37251
 two probabilistic evaluation methods for single and double wall type sound insulation systems with arbitrary random noise excitation 7-50849
 wall response evaluation, effect of signal processing operations 7-16032
 wall transmission loss, evaluation using statistical energy analysis 7-11217
 walls, acoustic sealing of holes and slits 7-43536
- architectural CAD**
 cinema and lecture hall acoustic design by computer (*Hungarian*) 7-50850
 hybrid solar house design and control using microcomputers 7-3627
- architectural computer aided design** *see* **architectural CAD**
- architecture**
see also **building**; **civil engineering**
 earthquakes, analysis of damage to buildings by OR techniques 7-60169
 nuclear power station design and seismic ground motion is Central Europe (*German*) 7-19404
- architecture, computer** *see* **computer architecture**
- arcing** *see* **arcs (electric)**
- arcing, switches** *see* **circuit-breaking arcs**
- arcs (electric)**
see also **arc furnaces**; **arc lamps**; **arc welding**; **circuit-breaking arcs**
 air-blown electric arc, gas dynamics 7-11817
 alloy ingot preparation, thermal plasma arc melting 7-27968
 cathode arc plasma flow in a Knudsen layer 7-58088
 cathode crater formation, in metal-vapor vac. arcs, time-depend. description 7-26560
 collective drifting motion of cathode spots in an axial magnetic field 7-32162
 conducting plate in two-temp. plasma, pot. distrib. in Debye discontinuity 7-58025
 conductivity, characts. asymptotic calcs. 7-32154
 conf., Saskatoon, Canada, May 1986 7-29595
 critical current density, V-I characts. 7-26553
 cross flow effects 7-26550
 current conducting channel in near electrode zones 7-1795
 current distrib. meas. at anode for pressure 10⁻⁶ to 10 torr 7-32165
 DC arc, atomic space-time distrib. 7-20993
 DC arcs, equivalent circuits synthesis, math. modelling based on MHD description of plasma (*Russian*) 7-57986
 deflected wall-stabilised relax. process, thermodynamics soln. 7-44273
 dense gas, high-current arc development, hydrodynamic effects study 7-51529
 dense plasma, H α line Stark-broadened profile meas. 7-20935
 EM projectile accelerators, arc-driven, 3D plasma model 7-32117
 epoxy spacers exposed to sparks and SF₆ arcing byproducts, surface characterisation 7-39692
 escalating arcing ground fault phenomenon, effect of preventative solns. on equipment specifications 7-51530
 extinguishing devices for protecting anode wall in MHD channel 7-44291
 flow phenomena in high-power repetitively-pulsed gas-flow spark gaps 7-32192
 free-burning, powder anal, multielement spectrographic method 7-8345
 free-burning arcs with molten anodes, temp. distrib. meas. 7-1801
 high pressure arc plasmas, variational and transport props. 7-31941
 high-current vacuum arc near Cu cathode, spectroscopic meas. and anal. 7-26558
 hollow cathode arc, beam electron relax. 7-21005
 hollow cathode arc, plasma turbulence, effect on plasma viscosity and ion transport 7-44169
 hollow cathode arc discharges, electron distrib. functions 7-21003
 interaction with turbulent gas flow, semiempirical model 7-32155
 interelectrode flashover in the presence of a weakly ionised plasma channel created by laser irradiation 7-44281
 jet energy dissipation in gaseous target 7-1791
 magnetically confined vacuum arcs, plasma parameter meas. 7-32163
 magnetoelectrostatic confinement, limitations 7-51484
 metal cathode, hot, evaporating, in stationary vacuum arc with diffuse cathode emission, thermal conditions 7-58087

arcs (electric) continued

- miniature high current metal ion source 7-19593
- multiple-cavity hollow cathode, arc discharge, gas containing alkali metal atom additions 7-32179
- plasma-wall contact, arcing 7-37698
- plasmatron, two-jet, electric arc characteristics in transverse mag. field 7-63360
- post-arc cond., circuit breaker arc, plasma parameters meas. 7-32183
- pulsed plasma, Balmer beta core, electron density meas. 7-6477
- railgun arcs, interchange instability 7-11814
- rotated arc, non-LTE studies, spectroscopic diagnostics 7-1805
- solar cells, biased concentrator, plasma interactions 7-59840
- supersonic arc jet, expansion 7-21016
- thermal plasmas, high press., radiation emission coeffs. 7-26551
- tokamak interior wall, elec. arc form. 7-51457
- turbulent flow segment, investig. in electric arc 7-26566
- turbulent gas flow in cylindrical channel, interactions of electric arc 7-44056
- two-jet plasmatron, elec. arc interaction with solid body 7-44280
- vacuum arc, gas ion effect on plasma instabilities 7-1797
- vacuum arc, turbulence, particle acceleration, Buneman instability 7-1796
- vacuum arcs, high current, anode discharge mode and cathode plasma state 7-44284
- vacuum arcs, transient electron shield currents 7-37777
- vacuum-arc centrifuge, rotational props. 7-56253
- vaporization and breakdown of thin columns of water 7-59145
- Ag, resonant-like reabsorption in AC arc plasma 7-13842
- Al freely burning arc discharge, self-reversed reson. spectral lines 7-32157
- β -Al₂O₃-Na₂O, solid electrolytes, Debye-Huckel-type relax. processes 7-17800
- Ar arc plasmatron, natural gas high temp. pyrolysis 7-39886
- Ar electric arc initial section of plasmatron channel, calc. based on MHD eqns. 7-63395
- Ar, gas pressure effect on arc cathode erosion and cathodic plasma expansion 7-32164
- Ar, high-pressure plasma, elec. and optical props. 7-26552
- Ar, hollow cathode arc, steady-state low-press., diagnostics 7-26561
- C, cathode erosion and power flow in vac.-arc centrifuge 7-26562
- C III vacuum arc discharge, reson. photoexcitation, fluoresc., X-ray laser prototype 7-20987
- Cl I, arc plasma, Stark broadening of spectral lines study 7-36536
- Cs, arc, low-voltage, ionisation instability appearance 7-44289
- Cs plasma in hollow-cathode arc 7-16344
- Cu, resonant-like reabsorption in AC arc plasma 7-13842
- F, low current arc, spectroscopic study 7-26581
- H discharge, atmospheric pressure, transition region, static V-I characteristics 7-51536
- H duoplasmatron arc, plasma emission mechanism 7-26532
- H, lines in arc plasma, shift meas. 7-11709
- He, gas pressure effect on arc cathode erosion and cathodic plasma expansion 7-32164
- Hg, high pressure decaying arc., spectroscopic temp. meas. 7-11809
- Hg high-pressure discharge with NaI additives, model and diagnostics 7-1800
- Hg low press. plasma, elec. double layers 7-1705
- Hg-Tl high press. lamp arcs, partial press. determ. 7-26554
- I, arc in air, plasma comp., Gibbs free energy calcs. 7-37795
- InI-Hg arc, high-press., spectroscopic studies 7-44278
- Li, arc in air, plasma comp., Gibbs free energy calcs. 7-37795
- Mg, cathode erosion and power flow in vac.-arc centrifuge 7-26562
- Mn(II), modified wall stabilised arc, hook measurements study 7-37755
- N II pulsed arc, Stark broadened lines 7-36534
- Na, freely burning arc discharge, self-reversed reson. spectral lines 7-32157
- SF₆ double nozzle arcs, flow field determ., spectroscopic temp. meas. 7-26583
- SF₆, gas pressure effect on arc cathode erosion and cathodic plasma expansion 7-32164
- SF₆, high-current discharges, optical diagnostics 7-37775
- β -SiC, ultrafine powder synthesis in thermal arc plasmas 7-27916
- Ti vacuum arc characterisation and struct. of deposited Ti and TiN films 7-63392
- V II, in arcs, transition probabilities, IR emission spectroscopy 7-5633

area measurement

- digital radiographic assessment of coronary arterial geometric diameter and videodensitometric cross-sectional area 7-28675
- urethra, female, probe for meas. of cross-sectional area and press. 7-3910

argon

see also nuclei with

- 3s-subshell excitation, photoabsorption spectra anal., HF calcs., config. interaction calcs. 7-30947
- 160 MHz gas-medium scanning acoustic microscope 7-1342
- adsorbed films, surface melting and roughening 7-38342
- adsorbed monolayers on MgO (100), LEED anal. (French) 7-21620
- adsorbed on Au (111), He atom-surface scatt. 7-27851
- adsorbed on graphite, positronium formation 7-33483
- adsorbed on graphite surface, positron lifetime studies 7-39269
- adsorption on graphite, fluid-solid monolayer transition, simulation 7-32796
- Allende meteorite, cosmogenic Ar components identification by laser microprobe 7-55584
- N Apennines, deformation phases dating using K-Ar and ⁴⁰Ar/³⁹Ar techniques 7-40459
- Ar, elastic scatt. of electrons, phaseshifts and differential cross sections, local-density approx. 7-19695
- arc, current conducting channel in near electrode zones 7-1795
- arc plasmatron, natural gas high temp. pyrolysis 7-39886
- atom, Auger emission, electron-electron coincidence investig. 7-30996
- atom, dipole (e,2e) cross sections, plane-wave Born calcs. 7-30935
- atom, dipole-quadrupole dispersion coefficients, ab initio coupled HF calcs. 7-11986
- atom, double ionisation by single electron impact 7-62526
- atom, electron (positron) elastic scatt., calcs. 7-977
- atom, electron (positron) elastic scatt. 7-36768
- atom, electron impact ionisation, cross sections, fast-neutral beam method, TOF spectra 7-42769
- atom, electron scatt., cross section meas. 7-31171
- atom, electron scattering length 7-20049

argon continued

- atom, electron stepwise excitation effective cross section of 2p_y level from metastable states 7-31174
- atom, excitation energies, coupled cluster method calcs. 7-49893
- atom, fast electron bremsstrahlung cross sections 7-36780
- atom, ionis. behind normal plasma shock waves, conservation eqns. 7-31980
- atom, K suprathreshold struct., ab initio calcs. 7-36466
- atom, kinetic energy density, nonlocal correl. fn., CI wave fns. and HF calcs. 7-42496
- atom, metastable number density, ICP-AAS eval. 7-54237
- atom, metastable population meas. and flow instability due to shock wave, comparison with models 7-16207
- atom, multivacancy effects in X-ray emission spectra 7-36522
- atom, photoionis. with synchrotron radiation, angle-resolved electron spectra 7-905
- atom, photoionisation, photoelectron and electron momentum spectroscopy 7-36560
- atom, positron differential elastic scattering cross-section meas. 7-25656
- atom, self-consistent exchange parameters, radial depend. anal. 7-49920
- atom, small angle differential cross sections for electron elastic scatt. 7-15713
- atom, spectral line press. broadening and shift 7-42553
- atom, spectral lines, determ. of transition probabilities using 27.12 MHz inductively-coupled plasma 7-50023
- atom, spectral lines, neutral broadening 7-5733
- atom, subvalent electron participation in X-ray and X-ray electron spectra 7-10478
- atom, thermal cond. coeffs. based on interatomic pot. 7-51370
- atomic beam source, metastable, for time-of-flight appls. 7-41533
- atomic impurities in Ne, optogalvanic effect 7-30970
- atoms, multiple ionisation by intense laser pulse 7-62332
- atoms, positron scattering, cross-section meas. 7-20054
- atoms, transition energies, X-ray spectra, X α theory, X-ray transition energies 7-10422
- basalts of mid-ocean ridges, inert gas abundances 7-60198
- benzene, Ar matrix isolated, vac. UV and MCD absorpt. spectra 7-15635
- breakdown, ruby laser induced 7-11579
- chemical reaction and charge-transfer processes, RIOSA quantum-mechanical study. 7-31159
- clusters, mass distrib. meas. and struct. model 7-15762
- cryogenic crystals, exciton diffusion and energy transport studies 7-52438
- crystal, dielec. const., density depend., in-cryst. polarisability calc. 7-22175
- dense plasma, elec. cond. determ. 7-37642
- dense plasmas, continuum ξ -factor determ. 7-20865
- diacetylene-HF complexes in solid Ar, IR spectra, H-bonding 7-10574
- dielectronic satellite spectra, transition rates and energies 7-51512
- dimer, interaction pot. calc. 7-5733
- dimer, spectroscopic consts., coherent VUV and XUV radiation sources 7-10472
- discharge, homogeneous longit. mag. field effects 7-21026
- discharge, nonequilib. behaviour of electrons 7-21039
- discharge, thermionic cathode double sheath-plasma interaction 7-1707
- doped with Cl₂, ArCl* and Cl*₂ formation and excited states anal., mol. fluoresc. study 7-19946
- electric arc initial section of plasmatron channel, calc. based on MHD eqns. 7-63395
- electron collisions, cross section meas. for scatt. length determ. 7-20055
- electron swarms, collision cross sections 7-37619
- England, Ar isotope geochemistry of W mineralisation 7-8876
- excimer laser, tunable intense coherent radiation generation around 126 nm, stimulated Raman scatt. in H₂ 7-20328
- excimer states, photoionisation cross sections 7-57137
- fibre laser, stimulated Brillouin scattering, single-mode and multimode pumped, spontaneous mode locking 7-1079
- fluid, collective modes 7-1833
- fluid, viscosity and thermal cond. 7-60900
- gas, crit. behaviour, modified hypernetted chain eqns., nonuniversal quantities 7-44090
- gas, diffusion coeff. of Hg interaction pot. determ. 7-6348
- gas, discharge, pulsed electron beam injection, potential profile, temporal evolution 7-51534
- gas, doubly-ionised by electron impact, spectral line Stark broadening meas. 7-62320
- gas, electron beam deposition 7-5771
- gas, intense light ion beams, current neutralisation 7-36363
- gas, optical breakdown threshold, press. dependence (Korean) 7-31923
- gas, Rayleigh-Brillouin gain spectra 7-10473
- gas, supercontinuum generation with femtosecond pulses 7-25908
- gas, surface-wave discharges, wave propagation and diagnostics 7-63390
- gas, surface-wave produced microwave discharges 7-63389
- gas, thermalised free positron annihilation rate studies 7-50390
- gas pressure effect on arc cathode erosion and cathodic plasma expansion 7-32164
- gas puff Z-pinch implosions, X-ray emission, appl. to X-ray lasers 7-26483
- glow discharge, shock wave acceleration 7-6478
- high press. discharge, X-ray initiated, laser appls., anal. 7-63385
- high-pressure plasma, elec. and optical props. 7-26552
- hollow cathode arc, steady-state low-press., diagnostics 7-26561
- hollow cathode glow discharge, Fe, I-line excitation processes, investig. 7-19775
- hollow cathode glow discharge, UV radiation and positive ions, investig. 7-21000
- inductively coupled plasma torch, gas flow dynamics, light scatt. technique 7-11795
- ion average equilib. charge state determ., H⁺ secondary ion yield meas. on Au and C target surfaces 7-42757
- ion bombardment, of Cr-C, Cr-Mo deposited on Fe, surface amorphous alloys (Chinese) 7-51885
- ion bombardment of thin films, secondary emission yield, incident charge state depend. 7-59319
- ion bombardment on Al, Auger electron emission, Monte Carlo simulation 7-53470
- ion extraction using radial field discharge 7-41534
- ion implantation, of glass, effect on mechanical and optical props. (Chinese) 7-51796
- ion laser, high-power, with extended functional capabilities 7-25839
- ion laser integrated acousto-optic mode locker design 7-37005

argon continued

- ion lasers excited by low-energy electron beams 7-20186
 ion mixing, effect on oxidation of Zr (*Chinese*) 7-53997
 ions, multiple scatt. at TaC (001) surfaces 7-22426
 ions, target sputtering, surface analysis, glow discharge optical spectroscopy (*French*) 7-20998
 iron laser, wideband power regulation system 7-31347
 laser annealing, a-Si:As⁺ epitaxial regrowth (*Korean*) 7-27197
 laser coagulator, LAK, for ophthalmic therapy 7-8673
 laser coagulator, use in ophthalmic therapy 7-8674
 laser power standard, automatic calibration system, expt. (*Japanese*) 7-11019
 laser with modern capillary design for milliwatt operation (*German*) 7-20274
 laser-induced discharges, electron distribution function, collision frequency effects 7-63387
 laser-sustained plasma, power absorpt. 7-32024
 laser-sustained plasma in axisymmetric flowfields, 2D model 7-11661
 latt. dynamics, phonon line shapes at high temp. 7-2122
 Lennard-Jones cryst. struct., mol. dynamics method 7-16487
 liquid, dil. soln. of CO, linear biased correlated walk, general soln. 7-61237
 liquid, effective momentum transfer cross section for excess electrons 7-21956
 liquid, Kr diffusion coeff. determ., cryogenic temp. controller 7-30020
 liquid, sound dispersion in repulsive Lennard-Jones fluids, density depend. 7-12212
 liquid, thermodynamic stability and viscosity behaviour or melting curve 7-12247
 liquid charged dielectric sphere, electron bound states 7-21960
 matrix isolation of NH(ND), radiative decay and radiationless relax., lifetime meas. 7-10653
 metastable ions, optical pumping in hollow cathode discharge 7-30990
 molecule, radiative lifetimes, time-resolved fluorescence study 7-5619
 monolayers adsorbed on ionic crystals, critical temps. 7-21666
 Mont Saint Hilaire plutonic complex, Quebec, Canada, Ar isotopes and emplacement history 7-4007
 Moon, solar cosmic ray inert gases in regolith minerals 7-14507
 multilayer, physisorbed on Cu, laser-induced thermal desorption 7-17817
 non-neutral ion plasma generation and diagnostics 7-51513
 nonpolar fluid, electron mobility near crit. point 7-7243
 p- 7-21010
 physisorbed monolayers on graphite, melting transition, high resolution synchrotron X-ray diff. study 7-63780
 physisorption on K treated Ni (100), wetting, photoemission spectra 7-32822
 plasma, collisional drift instability in a variable radial electric field 7-16303
 plasma, CW laser materials interaction, spectroscopic studies 7-63313
 plasma, DC pulse generation creation and stabilisation processes study 7-32098
 plasma, electron mobility and conductivity, numerical solns. 7-31944
 plasma, flowing afterglow, metastable influence, expt. apparatus description 7-58073
 plasma, heavy ion plasma double layers, particle-in-cell simulations 7-31993
 plasma, inductively coupled, two-temperature model 7-63361
 plasma, laser-sustained, theory 7-20911
 plasma, multidipole confinement 7-44229
 plasma, non-isothermal, excited level populations 7-11588
 plasma, relativistic electron beam gas puff Z pinch, spectroscopic studies 7-58044
 plasma characts., study of high current discharges appl. to pulsed-power devices 7-32188
 plasma column prod. by EM surface wave, recomb. controlled regime 7-20908
 plasma etching reactors, energy distrib. of ions 7-37759
 plasma with Al target, CW laser materials interaction, spectroscopic studies 7-63313
 positive column, spectrosc. investig. 7-21010
 positron annihilation and diffusion, computer-based anal. 7-50378
 positron annihilation and elastic scatt. cross sections 7-42763
 positron drift and diffusion in crossed elec. and mag. fields, simulation 7-36760
 rapidly quenched, Voronoi polyhedron distrib. calc., mol. dynamics method 7-26636
 rare gas floating monolayers, dynamics in self-consistent phonon theory 7-2362
 refractive index meas. in diamond anvil cell 7-35534
 RF discharge plasma, electron and ion transport meas. 7-20874
 RF discharge plasma, electron swarm, time-resolved spectroscopy 7-20959
 RF glow discharges, low-pressure, large-signal time domain modeling 7-58076
 RF ion source, with metal discharge chamber 7-30114
 rhodamine 6G dye laser, Ar flashlamp pumping (*Korean*) 7-25813
 rot. resolved fluoresc. excitation spectra 7-25597
 small clusters, sticking coeff. of Ar 7-64861
 solid, band struct., classical nonrelativistic nonselfconsistent APW calcs. 7-64076
 solid, Brillouin scatt. intensities evaluation 7-33403
 solid, electronic sputtering by keV H ions 7-59353
 solid, energy transfer during ion bombard. 7-64842
 solid, high press. eqn. of state, interatomic pots. 7-58431
 solid, high press. eqn. of state 7-21396
 solid, pair potential, effective medium approach 7-45201
 solid, phonons, close to melting 7-63757
 solid, sputtering mechanism by keV ions 7-59354
 solid bubbles in implanted Al 7-2043
 solid crystalline films, electron stimulated desorption, exciton mechanism calcs. (*Russian*) 7-27096
 solid matrix with methyl radical, ENDOR/TRIPLE spectra of matrix-isolated molecules 7-30058
 spin-orbit splitting, determ. from ab initio pseudopotential 7-2547
 surface (111), desorp. of HCl, internal state depend. 7-6963
 surface wave discharges, influence of excitation frequency 7-63386
 sustained plasmas, continuous wave laser gas heating 7-32023
 w for 150 MeV protons, dosimetry appl. 7-14133
 water vapour, Ar sensitised, pulse radiolysis, OH radical dynamics 7-8292

argon continued

- weakly ionised plasma, high frequency instability, inelastic collisions study 7-31975
³⁺, ground state pot. energy surface, MRD-CI calcs. 7-30959
 Ar II lines, laser generation in water cooled helical hollow cathode discharge 7-57299
⁴⁰Ar/³⁹Ar dating of minerals, errors due to ³⁹Ar loss during neutron activation 7-60390
 Al:Ar, solid Ar bubble, diffraction anal. 7-16547
 Al-Si:Ar,H, ion implanted ultrahigh Schottky barriers, interfacial traps, DLTS study 7-45489
 Al-Xe-Ar, ion implanted, bubble growth, lattice parameters, TEM obs. 7-51803
 AlAs-GaAs superlattice, compositional disordering control by Ar ion implantation 7-51806
 Ar + Ti, Ti excited state total ang. momentum charge, radiation quenching 7-42735
 Ar + Ti, triplet state quenching and excitation transfer processes 7-19761
 Ar + vinylidene radical, collisional quenching, rate consts., time resolved spectra 7-31104
 Ar, elastic electron scatt., multiple scattering method cross section calcs., anal. of method 7-25370
 Ar fluid, positronium bubble and positron induced clusters, positron lifetime meas. 7-39246
 Ar II, dense plasma, spectral line study 7-36552
 Ar II, multiplet and supermultiplet Stark broadening 7-10491
 Ar III, energy levels, optical spectra anal. 7-62308
 Ar ion clusters, unimol. decomp., average kinetic energy meas. 7-28301
 Ar VII, electron impact excitation, LS coupling, distorted wave approx. 7-42767
 Ar XII, N I-like ion, forbidden lines identification in solar EUV spectrum 7-66441
 Ar⁺, pseudopotentials, path integral simulations 7-5736
 Ar⁺, 3p⁴4p configuration, multielectron photoionisation, relativistic HF calcs. 7-36567
 Ar⁺ beam, microwave ion source, beam extraction expts. 7-363
 Ar⁺ bombardments of metal-polyethylene, effects on adhesion 7-28267
 Ar⁺ CW laser beam, central dark-space form. (*Chinese*) 7-57390
 Ar⁺ collision with surface, direct recoil ion fractions, kinetic energy depend. 7-13302
 Ar⁺ laser, 514 and 458 nm, for use in holography 7-62721
 Ar⁺ laser, He-Ne laser, performance assessment of laser wavemeter (*Korean*) 7-24692
 Ar⁺ laser light, SHG in urea crystal (*Chinese*) 7-57458
 Ar⁺ photoionisation pumping via two-electron shakeup 7-20195
 Ar⁺, transition probabilities and radiative lifetimes, saturated fluoresc. spectra anal. 7-42543
 Ar²⁺, energy level radiation lifetime calcs. 7-25455
 Ar²⁺, (n=9, 13), metastable ion beams, forbidden lines, visible spectrum 7-57022
 Ar²⁺, heavy ion impact on gas target, long-lived states form., K X-ray spectra anal. 7-30980
 Ar:Co₂, electronic energy transfer investig. 7-31149
 Ar/C₂F₆ mixtures, Penning ionisation for diffuse discharge switching appls. 7-37622
 Ar/Ne mixtures, electron swarm, Penning ionisation effects, Boltzmann eqn. anal. 7-1802
 Ar/Ne mixtures, Townsend first ionisation coeff. Penning ionisation effects 7-37776
 Ar-CF₄ mixtures in corona discharges in diffuse discharge switch appls., decomposition 7-37799
 Ar-CO₂ interface, wetting, model 7-2303
 Ar-CO₂ interface, wetting transitions, density functional theory and modified hypernetted chain calcs. 7-63913
 Ar-H₂, low-press. plasma, form. and vanishing charact. times 7-32097
 Ar-H₂ mixture, plasma jet, 941.04 Å emission 7-11704
 Ar-H₂ mixtures, transport and relax. cross-sections, close-coupling calcs. 7-51363
 Ar-H₂O, two-phase mixture, voids fraction meas. 7-44072
 Ar-H₂O plasmas, dissoc. processes, macroscopic kinetics 7-32173
 Ar-HCl, energy levels; ab initio close coupling calcs. 7-50292
 Ar-HCl gas mixtures, electron irradi., negative differential conductivity 7-63243
 Ar-HCl van der Waals complexes, IR spectra, secular eqn. calc. 7-31031
 Ar-HF binary complex, long-lived metastable systems 7-36515
 Ar-halide excimers, interaction with simple cryogenic liquids 7-42776
 Ar-He mixture, density meas. up to 8000 bar, Lennard-Jones comparison 7-1669
 Ar-hexamethyldisiloxane glow discharge, charge carrier prod. 7-32172
 Ar-Hg complex, electronic states struct., pot. energy curves, visible fluoresc. spectra anal. 7-36631
 Ar-Kr liquid mixtures, diffusion coeffs., simulation 7-44344
 Ar-N₂, rot. inelastic scatt., forward and inverse functional var. 7-5753
 Ar-N₂ laser, energy and efficiency, effect of Ne and He impurities 7-50545
 Ar-N₂ laser, proton beams angle and energy characts. determ. appl. 7-36368
 Ar-N₂ laser pumping by plasma focus generated charged particle beams, num. calcs. 7-63367
 Ar-N₂ solid mixtures, orientational ordering, collective versus noncollective behaviour 7-21103
 Ar-N₂ solid mixtures, sp. ht. due to N₂ mol. rot. 7-32680
 Ar-N₂O van der Waals complex, mol. beam IR spectra 7-31030
 Ar-N₂(CO) molecular beams, shock heated, vibrational relaxation 7-10717
 Ar-NO₂ system, muon spin relax. in transverse and longit. mag. fields 7-50413
 Ar-Ne discharge, steady-state cataphoretic density profile, collapse 7-44287
 Ar-Ne mixture, density meas. up to 8000 bar, Lennard-Jones comparison 7-1669
 Ar-PF₃ complex, rot. and distortion consts., microwave spectrum 7-62353
 Ar-perfluorocarbon systems, time-dependent electron mobilities calcs. 7-20835
 Ar-SF₆ plasma, negative ion detect., wall probe method appl. 7-20960
 Ar-TEA gas mixtures, emission spectra in proportional counter 7-62226
 Ar-tetrachloromethane, RF discharge, GaAs etching study 7-32167
 Ar-tetrachloromethane(benzene); intermol. pot., sphericalisation 7-10701
 Ar-tetrafluoromethane glow discharge etching of Si 7-32170

argon continued

- Ar-trifluorochloromethane discharges, for plasma etching of Si:P, parametric modelling and impedance anal. 7-28221
 Ar-trifluorochloromethane discharges, for plasma etching of Si:P, modelling of ion bombard. energy distrib. 7-28222
 Ar-Xe laser at 1.73 μm , electron beam and electric field pumped 7-1077
 Ar-Xe pulse-periodic large-volume electron beam-controlled laser, IR transitions in Xe atom 7-43059
 Ar+¹⁷⁴Yb, collisional velocity thermalisation, echo techniques 7-36732
 Ar+Ar⁺, total differential scatt. cross section, 15-400 keV 7-62489
 Ar+Ba, collisional redistrib., laser-induced fluoresc. 7-62492
 Ar+CO₂(N₂), vacuum UV lines, Stark broadening 7-891
 Ar+Cn, rot. levels, collisional energy transfer, state-resolved study 7-10713
 Ar+Cs⁺, low-energy collisions, absolute total cross section meas., curve-crossing model anal. 7-36749
 Ar+H, electron capture cross sections 7-10747
 Ar+H, Rydberg atom depopulation, scattering cross section, 7-10732
 Ar+H₂, pot. energy surfaces calcs. 7-50301
 Ar+H₂⁺ collisions, dissociation and electron capture cross section meas. 7-31156
 Ar+H₂O, rot.-vibr. lines, collisional broadening 7-42743
 Ar+H⁺, capture theory, first-order Born approx. Coulomb boundary conditions 7-10745
 Ar+H⁺, electron capture, K-shell cross sections 7-10752
 Ar+H⁺, p state ionisation, density matrix parameters meas., DWBA calcs. 7-36743
 Ar+H⁺, recoil ion prod. from zero-impact-parameter 7-50310
 Ar+H⁺ two-electron charge exchange mol. states, nonorthogonal CI calcs. 7-50339
 Ar+H⁺(He²⁺), electron emission, impact parameter depend., TOF, coincidence spectra anal. 7-42747
 Ar+H-like ion projectile ionisation cross section 7-969
 Ar+He, 2¹P₁ state quenching 7-62319
 Ar+He, bimolecular and termolecular, deexcitation reactions (French) 7-10724
 Ar+He, electronically excited atoms, beam sources 7-20008
 Ar+He⁺(H₂⁺), electron loss to the continuum, absolute cross sections 7-50304
 Ar+He⁺(Ne⁺), charge exchange into excited states in collisions 7-31155
 Ar+Hg, excitation transfer between fine struct. states, fluoresc. spectroscopy 7-62504
 Ar+I₂⁺, collision, rotational energy transfer 7-36734
 Ar+K, fine-struct. transitions, differential cross section meas. 7-62493
 Ar+methane (methane-d₄)(SiH₄)(tetrafluoromethane), energy transfer, simulation 7-15690
 Ar+N₂⁺, absolute state to state total cross sections meas. 7-46825
 Ar+N₂⁺, charge transfer collision, Franck-Condon principle at low collision energies study 7-62511
 Ar+N₂+CO, submonolayer mixtures physisorbed on graphite, LEED study 7-2364
 Ar+N⁺, transfer ionization, differential cross section meas. 7-50325
 Ar+NH₃, dissoci. excitation, nascent vibr. and rot. distrib. 7-46824
 Ar+NO, rot. inelastic cross section determ. sudden approx. 7-25637
 Ar+Na, fine-struct. branching ratios, meas. 7-15676
 Ar+Na₂, state selected rot. transitions, scatt. induced ang. momentum alignment 7-20005
 Ar+Ne*(3s³P₂, 3¹P₀), ionis., fine struct. depend. product branching 7-15673
 Ar+O, 557.7 nm line profile, collision complex spectroscopy (French) 7-5751
 Ar+O⁶⁺(C⁴⁺), one-step double electron capture 7-50344
 Ar+OCS semiclassical press. broadening calcs. 7-965
 Ar+OH, A² Σ^+ -X² Π band pressure broadening 7-50305
 Ar+Rb oscillator strength, pot. curves (French) 7-10728
 Ar+SO₂, intermol. energy transfer, trajectory study, rovibrational mol. energy depend. 7-31151
 Ar+SO₂, intermol. energy transfer, trajectory calcs., rate coeffs. for rovibrational states 7-31152
 Ar+Sr, Sr ¹P fluoresc. line broadening, ab initio close-coupled scatt. calcs. 7-36494
 Ar+Sr⁺, collisional broadening of Sr⁺ reson. line, visible spectra 7-49988
 Ar+Sr⁺(Ca⁺)(Mg⁺), reson. line broadening and shift rates, pot. calc. 7-15683
 Ar+Ti, quenching and excitation transfer processes, fluoresc. 7-10725
 Ar+trifluoromethane, crossed beam reaction giving trifluoromethyl group 7-33935
 Ar+Yb, collisional dephasing suppression investig. 7-15684
 Ar⁺+Ar(N₂), absolute spin-orbit state excitation cross sections, fine-struct. 7-42730
 Ar⁺+H₂, chemical reaction and charge-transfer processes, RIOSA quantum-mechanical study. 7-31159
 Ar⁺+H₂(N₂) collisions, ion energy-loss spectroscopy 7-50324
 Ar⁺+Kr (CO)(CO₂), charge exchange cross-sections meas. 7-62519
 Ar⁺+N₂, charge exchange reactions, TEPCO method anal. 7-20076
 Ar⁺+N₂, charge transfer, crossed mol. beam study 7-57166
 Ar⁺+N₂, charge transfer collision, Franck-Condon principle at low collision energies study 7-62511
 Ar⁺+N₂, electron transfer, state-to-state study 7-10714
 Ar⁺+N₂ collisions, low energy charge transfer reactions, time-of-flight spectra studies 7-31163
 Ar⁺+Na, Rydberg electrons removal, cross section meas. 7-36742
 Ar⁺+Na₂MoO₄(NaNbO₃)(MoO₃)(Nb₂O₅), ion-induced decomp., metalisation channels, XPS anal. 7-57149
 Ar⁺+Ne, time of flight energy spectra, long lived excited Ar⁺ state 7-62486
 Ar⁺+O₂ collisions, low energy charge transfer reactions, time-of-flight spectra studies 7-31163
 Ar⁺+tetrafluoromethane, excitation cross sections 7-62501
 Ar¹⁷⁺+H⁺, fine-struct. excitation, plasma screening effects, ion-sphere and Debye-Huckel models 7-62509
 Ar⁴⁺+D₂(D), collision parameters, energy-gain spectra meas., multichannel Landau-Zener model anal. 7-36752
 Ar⁴⁺+He(H₂), total one-electron capture cross sections 7-10754
 Ar₂ laser induced fluorescence 7-19916
 Ar₂, radiative lifetime of A₁ states, time-resolved fluoresc. 7-19952
 Ar₂⁺, mobility, temp. and field depend. 7-51380
 Ar₂+Xe(Kr), van der Waals bond exchange, mol. beam study, ang. and vel. distrib. 7-23000

argon continued

- Ar₂⁺+N₂, charge-transfer, mol. dynamics study 7-50335
 Ar₇, melting transition and nonrigid dynamics onset, mol. dynamics simulation study 7-26920
 Ar⁺He(Ne), charge exchange into excited states in collisions 7-31155
 Ar₁, 4p-3s transition array, IR lines transition probabilities 7-36547
 C₂N₂-Ar gaseous mixture, collision-induced absorpt., quadrupole moments, IR and microwave spectra 7-50098
 CO-Ar system phase diagram, critical point determ., X-ray diff. study (Russian) 7-6776
 CO₂-Ar gaseous mixture, collision-induced absorpt., quadrupole moments, IR and microwave spectra 7-50098
 CdS:Ar⁺, ion implantation damage 7-26812
 Cu-Ar, single crystal, ion implantation, damage profile anal. using Auger electron spectroscopy 7-51802
 D₂-Ar spectrophotometric lamp, construction and material influence 7-41422
 H₂-Ar, externally sustained discharge, instability mechanism 7-63381
 H₂-Ar, rot. line broadening calc., projection operator algebra and linked cluster theorem 7-42687
 H₂-Ar mixture, frequency conversion by stimulated Raman scattering 7-43233
 H₂-O₂-Ar mixture, reflected-shock flowfield calcs., random choice method appl. 7-20812
 He-Ar lasers, pumping by CO₂-laser induced optical break-down 7-62668
 Hg-Ar, low press. electrical discharge, isotope effects, hyperfine struct. 7-37786
 Hg-Ar discharge, degenerate four-wave mixing 7-5958
 Hg-Ar discharge, Hg 6³P₁ and 6¹P₁ reson. level population study 7-57011
 Hg-Ar mixture, pulsed-periodic discharge plasma, optical characts. time depend. 7-37782
 Hg-Ar mixtures, electron energy distrib. functions meas. 7-21028
 Hg-Ar mixtures, in discharge, current variations and plasma parameters 7-21011
 Hg-Ar mixtures, in positive column, radius and plasma parameter variation 7-20956
 LiF:Ar⁺, defect and colloid production by ion implantation 7-26746
 Mg/Ar ionisation chambers used as γ -ray dosimeters in mixed neutron-photon fields, characts. 7-34282
 N₂-Ar mixture, depolarized Rayleigh light scattering, temp. dependence 7-31053
 N₂O-CO-Ar, superequilibrium pumping, Ar dilution effects 7-25611
 N₂O-CO-H₂-Ar, superequilibrium pumping, Ar dilution effects 7-25611
 Na+Rg optical collisions, (Rg = He, Ne, Ar, Kr, Xe), fine struct. branching ratio determ. 7-10704
 Ne-Ar, solid, local phase transition near impurity center 7-26945
 Ne-Ar mixtures, transient cathoporetic segregation in a discharge tube 7-20988
 No-Ar, van der Waals species, multiphoton ionis. 7-10694
 O₂-Ar etching plasmas, spatially resolved detection of O atoms by two-photon laser-induced fluorescence 7-20917
 SF₆-Ar, photorefractive deflection technique using parallel and overlapping probe and pump beams appl. 7-51377
 SF₆-Ar mixtures vibr. relax. time resolved IR multiphoton absorpt. 7-5752
 SF₆-Ar₂ clusters, spectroscopic obs. of phase coexistence 7-36842
 SF₆+O₂+Ar, plasma etching of Si, kinetic model 7-39784
 Si-Ar, ground state one-electron energies, SCF MS X_a calcs. 7-44582
 Si-Ar laminated structure formed by Ar ion doping, electoreflectance 7-7676
 Si-Ar surface barriers, ion implantation damage, thermal anneal recovery 7-17101
 Si-Ar⁺, ion implanted thin film, defect form., dose depend. study 7-51793
 SiH₄-Ar plasma, particle number densities, masses and size distrib. meas. 7-37761
 SiH₄-Ar-N₂, gas mixture, DC discharge plasma creation, spectroscopic meas. 7-20946
 SiH₄+Si₂H₆+Ar+H₂, plasma enhanced CVD of a-Si:H, integrated model 7-39423
 Xe-Ar, laser-induced collisional energy transfer, multiphoton ionisation study 7-57152
 Xe-Ar:H, plasma, comp. eval. 7-1733

argon compounds

- AF discharge excimer laser, capacitor-transfer-type with automatic preionisation, efficiency 7-20201
 Ar-benzene(tetrazine), van der Waals rovibr. states, intermolecular pot. 7-5735
 Ar-NH₃, microwave spectrum of K=0 states 7-25493
 Ar-NO van der Waals mols., microwave and RF spectra, hyperfine parameters 7-31026
 Ar₂-HF(DF) trimers, mol. rot., hyperfine struct., spectra anal. and calcs. 7-50060
 ArCl, formation in Cl₂ doped Ar, excited states anal., mol. fluoresc. study 7-19946
 ArF excimer laser, electron-beam pumped, using low-pressure Ar-Rich mixture 7-36945
 ArF, excimer laser amplifiers VUV anti-Stokes Raman line generation 7-57450
 ArF laser, electron-beam-excited, investig. 7-43074
 ArF, photodissoc., CARS 7-11062
 ArH⁺, low-lying mol. states nonorthogonal CI calcs. 7-50339
 ArHCl, intracavity for IR laser spectroscopy, van der Waals bonds, vibr. motions 7-10589
 ArHF van der Waals complexes in supersonic jets, IR laser spectra 7-19842
 (ArH)⁺, short-range pot. curves, Lyman- α line blue wing (French) 7-10463
 ArH⁺ exciplex laser, active medium modelling 7-62672
 (ArH)⁺, pot. energy curves, semi-diabatic model (French) 7-10464
 ArHe⁺, doublet states, ab initio CI calcs. 7-56989
 ArHe²⁺, mol. states, MRD-CI calcs. 7-36492
 ArHe²⁺, mol. states, MRD-CI calcs. 7-36492
 ArN₂⁺, charge transfer dynamics, vibronic approach 7-50333
 ArXe, excited states, photoionisation and predissoc. 7-19959
 ArXe⁺, DC discharge in supersonic jet, UV-visible emission spectra anal. 7-19874

argon compounds continued

- (SF₆)_n(Ar)_m clusters, supersonic jet, Fourier transform IR spectra 7-15598
 Si-Ar:Hg⁺, ion implant range distributions, Rutherford backscatt. studies 7-2073

arithmetic (digital) see digital arithmetic**Armco iron see iron****armouring (cables) see cable sheathing****aromatic compounds see organic compounds****ARPES see photoemission****array processors see parallel processing****arrays (antenna) see antenna arrays****arsenic**

see also nuclei with

- amorphous, vibr. density of states, EXAFS, Debye-Waller factors 7-64820
 amorphous and crystalline, bond strength anal., EXAFS temp. depend. study 7-64763
 atom, fluoresc., SRS eval. as excitation source 7-30981
 atomic fine structure analysis 7-15529
 geochemistry, seasonal var. of methylarsenic compounds in airborne particulate matter 7-34638
 ion implantation doping of Si, defect annealing and impurity activation 7-58295
 ion implantation in Si polycrystalline films, annealing, sheet resistance 7-12886
 ion implementation, formation of WSi₂ (Chinese) 7-51797
 magnetothermoelectric power meas. in quantising mag. fields 7-45362
 overlayer on Si (iii), removal of surface reconstruction 7-21587
 polyphenylenesulphide:As conducting polymers, ion implantation techniques 7-21923
 seawater and atmos. aerosol of English Channel and N Atlantic, As and Sb contents 7-29075
 speciation in natural waters and sediments 7-23250
 structural calcs. 7-7143
 surface (0001), laser pulsed oxidation modification 7-58320
 ultrathin layers, protection for Al_xGa_{1-x}As, AES sputter depth profiles 7-54022
 As + He⁺, L shell X-ray prod. cross sections meas., first Born approx. and ECPSR theory anal. 7-36526
 As, Fermi surface characs., hydrostatic press. depends. (Russian) 7-32896
 As₂, electronic states, spectroscopic props., SCF CI calcs. 7-62294
 p-Ge:As, Hall effect and electrical conductivity, temp. corrections 7-38592
 Ge:As, implanted, heavy ion damage, TEM, annealing studies 7-63676
 Ge:As (111), surface electronic struct., photoemission studies 7-2658
 a-Ge:H, B, P, As, dopant incorporation and doping efficiency 7-44587
 InP surface, stabilisation for MIS devices 7-38767
 InP:Ga,As,Sb single crystals, LEC growth, isoelectronic doping, dislocation density, X-ray topography 7-33549
 InP-InP:As epitaxial layers, dislocation reduction, device performance effects 7-7354
 MoSi₂:As-poly Si struct., redistribution of As by silicidation tempering 7-51812
 p-Si:As oxidation in HCl ambient, impurity pile-up, bubble pattern form. and local oxide bowing 7-13675
 Si:Ar, high dose implanted, thermal regrowth, RHEED studies 7-21734
 Si:As, deep level spectra, ion implanted defects, laser annealing 7-21869
 Si:As, dopant diffusion, finite element based simulation, quasilinear formulation with remeshing scheme 7-21526
 Si:As, heavily doped, laser induced oxidation 7-13672
 Si:As, high dose implanted, defect density reduction by low temp. oxidation 7-58297
 Si:As, highly doped, spinodal decomposition and clustering 7-52063
 Si:As, implanted, heavy ion damage, TEM, annealing studies 7-63676
 Si:As, implanted, supersaturated soln., defect struct., TEM obs. 7-58483
 Si:As, implanted ion distrib., lateral spreading, theoretical predictions and computer simulation 7-16604
 Si:As, impurities at dislocations and grain boundaries, high-resolution TEM imaging 7-37815
 Si:As, ion implant redistribution, diffusion modelling 7-16814
 Si:As, ion implantation, damage profiles determ. by spectroscopic ellipsometry and stripping (Chinese) 7-32468
 Si:As, ion implantation-induced defects 7-32433
 Si:As, ion implanted, diffusion and defects, transient scanning electron beam annealing 7-38065
 Si:As, ion implanted, electronic transport props. 7-7233
 Si:As, ion implanted, pulsed laser annealing, optical reflection kinetics 7-58323
 Si:As, ion implanted, rapid thermal annealing 7-16615
 Si:As, ion implanted, rapid thermal annealing, metastable activation 7-16616
 Si:As, ion implanted polycrystalline films, electrical activation by rapid thermal annealing 7-58914
 Si:As, laser annealed, Raman scatt. study 7-53325
 Si:As, p-n junction diode, rapid thermal annealing 7-22005
 Si:As, precipitation and cluster form., elec. resist., backscatt. and TEM studies (Chinese) 7-12285
 Si:As, retarded and enhanced dopant diffusion related to implantation-induced excess vacancies and interstitials 7-63881
 Si:As, Rutherford backscattering-particle-induced X-ray emission analysis 7-54251
 Si:As, Sb, Sb diffusion 7-44915
 Si:As,In, formation of In-As complexes, perturbed angular correlation technique obs. 7-17254
 Si:As,P, double diffused shallow junctions, rapid thermal annealing 7-22006
 Si:As diffusion source, diffusion into single crystal Si 7-32727
 Si:As doped layers, IR transmission spectra 7-59208
 Si:As films, heavily doped, grown by partially ionised MBE, phys. and elec. characts. 7-12561
 Si:As films, preannealed and As ion implanted, structural changes during transient pot-annealing 7-16904
 Si:As ion implanted, defect structs. generated by buried amorphous layer regrowth 7-38078
 Si:As ion implanted films, defects charactn. by AC Hall effect meas. 7-38601

arsenic continued

- Si:As on sapphire, ion beam recrystallised and laser annealed, elec. props. 7-16649
 Si:As polycrystalline films, rapid thermal processing before and after ion implantation, effect on cond. 7-22046
 Si:As porous layer, impurity diffusion under incoherent light exposure 7-38258
 Si:As single-domain reconstructed (100) surface state dispersion and struct., LEED and photoemission studies 7-38667
 Si:As substrate, dopant effects on formation kinetics of Pt silicides 7-21697
 Si:As substrate, dopant redistrib. during silicide formation 7-21255
 Si:As substrate for W CVD, effect of dopants and crystal perfection 7-22576
 Si:As surface, TiSi₂ formation 7-12551
 Si:As/SiO₂ interface, oxidation rates and oxide props., dopant effects determ. 7-12514
 Si:As-Ti(Co), silicide formation using rapid thermal processing, defect behaviour 7-32726
 Si:As⁺, epitaxial regrowth, CW Ar laser annealing (Korean) 7-27197
 Si:As⁺, heavily doped, ion implant deactivation 7-17567
 Si:As⁺(As₂⁺), ion implanted, phys. props., spreading resist., TEM, Rutherford backscattering, SIMS 7-26775
 Si:As(As₂B) films, surface energy driven secondary grain growth 7-22740
 Si:As(P)(B)-SiO₂ interface, segregation, transport coeffs. of impurities 7-63880
 Si:B(Ga)(As)(Sb) 7-2040
 a-Si:H, B, P, As, dopant incorporation and doping efficiency 7-44587
 a-Si:H,As RF sputtered coatings, gas-phase doping efficiency 7-63471
 Si:P,As polycrystalline CVD film, etch rate free carrier depend., doping level and grain size depend. meas. 7-28219
 Si:Sb,As, cryst. aid amorphous, impurity band form., X-ray spectra studies 7-12650
 Si:Sb(As)(P)(B) epitaxial films, low temp. deposited by low press. CVD, autoping 7-27182
 Ti/Si:B,As,Sb interface, dopant redistrib. during silicide form. by rapid thermal processing 7-63641
 TiSi₂:As films on Si, impurity diffusion 7-7077
 TiSi₂:As(Sb) layers, dopant redistribution during silicidation by rapid thermal annealing, ion scatt. spectra study 7-21253
 ZnSe:As, MOCVD growth, exciton and deep emission bands 7-52367

arsenic alloys

see also arsenic compounds

- As-Sb alloys, magnetoresist., thermomag. power and Fermi surface quantum oscils. meas. 7-2578
 As₂Se_{100-x}, vitreous chalcogenide semicond. layers, deep trapping levels, photostimulated effects (Russian) 7-2754
 Co-Ni-As mixtures, phase diagram isothermal sections, binding 7-46418
 Fe-Co-As mixtures, phase diagram isothermal sections, binding 7-46418
 Te₈₀Si₂₀As overcoated trilayer struct., laser writing mechanism, microscopy studies 7-20149
 UAs muon spin rot., relax. rate, freq. shift, and magnetic transitions 7-45891

arsenic compounds

see also arsenic alloys

- As-S, amorphous semicond. films, laser action on light sensitivity (Russian) 7-64713
 chalcogenide-metal contacts, interdiffusion, struct., comp., electron irradi. effects 7-21686
 polyacetylene:AsF₆, identification of dopant species, X-ray absorpt. and Mossbauer spectra 7-65377
 polyacetylene:AsF₆⁻ (CISO₃⁻) (FeCl₄⁻) metallic elec. cond. studies 7-64231
 polyacetylene:I (AsF₆) films, synthesis, elec. and optical props. 7-63513
 Ag-As-Se glasses, electrical conductivity studies 7-27369
 Ag₃As₂S₃ undoped proustite crystals, photolum. obs. 7-33445
 Ag_{0.15}As_{0.425}Se_{0.425-x}Te_x chalcogenide glasses, ionic and electronic cond., comp. depend. study 7-12768
 As-Ge-Se-Te chalcogenide glass fibres for thermal IR transmission 7-37193
 As-S, amorphous semicond. films, laser action on light sensitivity (Russian) 7-64713
 As-S (Se) chalcogenide glasses, far-IR absorption spectra and spatial charge fluctuation 7-7696
 As-S glass IR fibre, Teflon clad, optical loss due to water diffusion 7-57556
 As-S:Ag photodoping, energy expenditure determ. (Russian) 7-21261
 As-S-I semicond. glass system, IR and Raman spectra studies 7-3058
 As-Sb-Se glasses, calorimetric meas. 7-26652
 As-Se, amorphous, short range structures, EXAFS studies (Chinese) 7-37871
 As-Se and As-Se-Te IR chalcogenide tube waveguides 7-37195
 As-Se glass, IR optical materials, production 7-37075
 As-Se glasses, defect levels and photoconductivities 7-12673
 As-Se:Ag amorphous films, Ag doping profiles, ellipsometric studies 7-7779
 As-Te-based glasses, small polaron hopping and transport props. 7-21911
 AsF₃-graphite, intercalation compounds, staging phenomenon studied using Ising model 7-58464
 AsF₃-graphite intercalation cpd., stage 1, nonresonant intercalant modes, Raman scatt. studies 7-38136
 AsF₃-graphite intercalation cpd., galvanomag. props. 7-58822
 AsGeSe, IR transmitting fibre optics, spectral props. 7-37179
 As₁₀Ge_{22.5}Se_{67.5} glass grating couplers, fabrication using electron beam induced Ag doping (Japanese) 7-62817
 As₂Ge_{20-x}Se₈₀, amorphous struct. study, positron lifetime spectra meas. 7-37886
 As₄₀Ge₁₀Se₂₅S₂₅ glass grating couplers, fabrication using electron beam induced Ag doping (Japanese) 7-62817
 AsH₃ gas, hazard characterisation in large scale manufacture of GaAs photovoltaic cells 7-39998
 AsH₃ gas source for MBE, mass spectrometry 7-53592
 AsH₃, isotopic species, mol. vibrs., inversion splitting calcs. 7-19997
 AsH₃, thermal decomp. rates, relevance to GaAs growth by MOCVD 7-22540
 AsO₄³⁻, electronic struct., ionisation pot. MS-Xa calcs. (French) 7-856
 As₂O₅, structural phase transition, Raman scatt. 7-6785
 As₂S₃, realger, X-ray chemical shift, K absorpt. spectra anal. 7-46239
 AsS₃, glassy, viscosity, rel. to intensity and spectral comp. of light 7-12342

arsenic compounds continued

- As_{1-x}S_x:Ag film, coordination distance determ., EXAFS study 7-64004
 As₂S₃, amorphous, bulk glass and thin films, photostructural changes, EXAFS meas. 7-39314
 As₂S₃, amorphous, characts. control using acoustic domain 7-20576
 As₂S₃, amorphous, low freq. light scatt. 7-27714
 As₂S₃, amorphous chalcogenide optical grid, submicron resolution, VLSI appls. 7-48899
 As₂S₃, amorphous films, persistent photocurrent 7-45389
 As₂S₃, chalcogenide glass, photoinduced gradient waveguide form. (*Russian*) 7-43374
 As₂S₃ films, prep. by spin coating or melt quenching, optical props. 7-39208
 As₂S₃ films photorefractive effect investig. using optical filtering 7-45990
 As₂S₃ glass, photostructural effects, EXAFS study 7-64758
 As₂S₃, glassy photodeformation 7-44654
 As₂S₃, orpiment, X-ray chemical shift, K absorpt. spectra anal. 7-46239
 As₂S₃ thin films, dissolution investig., surfactant effects 7-6802
 As₂S₃ thin films, natural paramagnetic centres obs. (*Russian*) 7-45799
 As₂S₃ thin films, photodarkened, reversible recording and erasure of holograms 7-50511
 a-As₂S₃ vapour deposited films, thermostructural and photostructural changes, EXAFS study 7-64003
 As₂S₃, vitreous, γ -irradiated, EPR of radiation-stimulated paramag. centres (*Russian*) 7-2929
 As₂S₃:Ag, amorphous, charge fluctuation, Ag doping effects 7-7700
 As₂S₃, crystalline and glassy, bond strength anal., EXAFS temp. depend. study 7-64763
 As₄₀S₃₀Se₃₀ glasses, surface pot. relax., TSC meas. 7-64261
 As₂S₃, amorphous films, persistent photocurrent 7-45389
 As₂S₃, amorphous thin film, bulk trap spectroscopy by temp.-modulated space-charge-limited current meas. 7-45338
 As₂Se₃, cryst., optical props., ab initio total energy calcs. 7-45965
 As₂Se₃, cryst. struct., X-ray meas., MULTAN anal. 7-2000
 As₂Se₃, crystalline, electronic and geometric struct., ab initio total-energy calcs. 7-12607
 As₂Se₃, non-exponential photocurrent decay, anal. 7-38633
 As₂Se₃ single cryst. growth from vapour phase, crucible diameter and sealing press. depend. 7-27877
 As₂Se₃ single crystals, geminate pair recomb., photocond., photoluminescence meas. 7-38581
 As₂Se₃:Ni films, electronic struct. and transport props. 7-12595
 As₅₀Se₅₀ amorphous films used for optical recording, structural transformation mechanisms (*Russian*) 7-51823
 As₂Se_{100-x}, chalcogenide glass, Vickers microhardness indentation and fracture mechanics 7-21342
 (As₂Se₃)_{1-x}(As₂Te₃)_x glasses, molecular struct., chemical equivalence of Te absorpt. and ¹²⁹I emission Mossbauer spectroscopy 7-59129
 As₂Se_{3-x}Fe_x films, electronic props. 7-58922
 As_{0.5}Se_{0.5}Te_{0.3} chalcogenide glass, struct. models, X-ray diffr. and Monte Carlo calcs. 7-6548
 As_{0.45}Se_{0.10}Te_{0.45} glassy alloy, struct. model and switching props. 7-1904
 (As₂Se₃)_{1-x}TL_x, elec. and thermal transport props., effect of TL addition 7-38200
 α -As₂Te₃ films, hole transport investigation by transient field-effect and time-of-flight methods 7-22040
 As₂Te₃, metastable state, rhombohedral struct. study (*French*) 7-44496
 As_{2-x}Te_{3-x}In_{2x} and As_{20-x}Te_{80-x}In_{2x} systems, chalcogenides, thin films, optical and electrical props. 7-27446
 a-As₂Te(se₃)₂ surface phonon generation and picosecond light pulse detection 7-12456
 As₂V₄O₁₃, cryst. struct., X-ray diffr. study 7-26702
 As₂X₃, X=S,Se,Te, thin film, electron irradi. effect 7-16636
 Bi_{2-x}As₂S₃ thin films, solution-gas interface deposition technique 7-7901
 C-AsF₆ intercalation cpd., Raman scatt., coupled electron-phonon excitation 7-46045
 CoAs₃, smaltite, X-ray chemical shift, K absorpt. spectra anal. 7-46239
 FeAsS, arsenopyrite, X-ray chemical shift, K absorpt. spectra anal. 7-46239
 Ge-As-Se and As-Se chalcogenide optical glass fibres, prep. and characterisation 7-37194
 Ge-As-Se chalcogenide glasses, structural models, medium range order and interference functions, first sharp diffr. peak calcs. 7-6540
 Ge-As-Se-Te chalcogenide glass fibres for transmission in the 8 to 12 μ m range 7-37192
 Ge-Se-As glasses, elastic constants, rigidity percolation 7-44648
 Ge₁₀As₄₀Se₂₅S₂₅ and Ge_{22.5}As₁₀Se_{67.5} glass films, photodarkening effect, exposure characts. (*Japanese*) 7-64706
 P₂As₂S₃, occupationally disordered cryst., struct. 7-58218
 PbO-K₂O-Sb₂O₃-As₂O₃ flint type glasses, viscosity near annealing temp., depend. on PbO conc. 7-58151
 Si-Te-As-Ge chalcogenide glass film, electronic processes in strong elec. field 7-45524
 SiO₂-Al₂O₃-Li₂O-ZnO-TiO₂-ZrO₂-As₂O₃-Cr₂O₃:Cr, glass ceramic, time resolved spectra 7-63478
 Te-As-S chalcogenide system, annealing, crystalline precipitate phase form., X-ray diffr. anal. 7-16751
 Tl₃AsSe₃ crystals, Bridgman growth, dislocation etching, thermal stress distrib. 7-21208
 V₂O₅-As₂O₃-B₂O₃, vitreous, elec. cond., semiconducting props. 7-2620

art

- practical holography, conf., Los Angeles, CA, USA (Jan. 1986) 7-24281
 pulsed holographic art practice 7-25777
 sandwich holography appl. to stress anal. of paintings on canvas 7-31284

articulation (speech) see speech**artificial hearts see artificial organs****artificial intelligence**

- see also adaptive systems; automata theory; biocybernetics; brain models; expert systems; knowledge engineering; learning systems; neural nets; self-adjusting systems*
 conf., Los Alamos, New Mexico, USA (May 1985) 7-48157
 fusion reactor neutral beam source conditioning with AI techniques 7-19462
 lens design program, intelligent, development 7-50676
 lens design program by microcomputer with artificial intelligence 7-50677
 lens design software, human dimension 7-50675
 myocardial scintigrams, symbolic reasoning in PROLOG 7-40253
 nuclear power plant availability improvement by reactor trip prediction software 7-10275

artificial intelligence continued

- nuclear power plant disturbance analysis using artificial intelligence, SAAP-2 system 7-19338
 system theory, conf., Knoxville, TN, USA (Apr. 1986) 7-14714
 upper arm prosthesis, intelligent control system (*Chinese*) 7-60127
- artificial kidneys see artificial organs**
- artificial limbs**
 above-knee prostheses, stance phase control; knee control vs. SACH foot design 7-54812
 amputee's stump, shape measuring probe-type system for prosthetics CAD 7-34349
 bond graph simulation of a mobile two-legged mechanism 7-8771
 DC motors in wheelchairs and prostheses, switching converters for efficient control 7-34355
 feedback in design of artificial limbs 7-34345
 myoelectric elbows proportional control mode selection, cocontraction approach 7-28776
 natural and artificial control of movements 7-65895
 Rehabilitation R&D Progress Reports 7-28774
 self-adaptive myoelectric processor, automatic calibration to amputee's muscle movements 7-47291
 sensory feedback in upper limb prostheses, robotics perspective 7-34347
 upper arm prosthesis, intelligent control system (*Chinese*) 7-60127
- artificial organs**
see also prosthetics
 biological/medical engineering, Fort Worth, Texas, USA (Nov. 1986) 7-65870
 cardiovascular devices—past, present and future direction 7-65674
 critical and emerging issues in artificial organs 7-65807
 heart, adaptive control technique, rel. to blood press. and flow 7-3933
 kidney, press. losses in apparatus with capillary channels made of semipermeable film 7-28772
 left ventricular assist device, computerised 7-40369
 left ventricular assist device, pulsed US Doppler rel. obs. 7-8667
 mass transfer in fluids flowing through rot. nonaligned straight tubes, medical device appl. 7-65803
 membrane lung performance during low blood flow CO₂ removal, model 7-8772
 pneumatic portable artificial heart drive system, design based on efficiency anal. 7-65893
 ventricular assist device, elec., power consumption minimisation by design of optimal controller 7-8769
- artificial satellites**
see also solar power satellites
 1971-30B (Touresol rocket) at 15th-order resonance, orbit analysis 7-55420
 activation products, production on satellite components by protons in low earth orbit 7-44631
 altimetric satellites, global nondynamic orbit improvement 7-14392
 Arabsat telecom. spacecraft, solar generator and telemetry of orbit performance 7-65488
 Ariel satellites, contrib. to British X-ray astronomy 7-24019
 ASTRO-C X-ray astronomy satellite, microprocessor-based attitude control system, development 7-55465
 Australia satellite data, meteorological appls. 7-4291
 autonomous satellite navigation using observations of starlight atmospheric refraction 7-60418
 axisymmetric satellite on elliptical orbit, resonant periodic motion 7-34830
 batteries for spacecraft, testing facilities at the European Space Battery Test Centre 7-55412
 BRASA-1, Brazilian satellite for environmental data collection (*Spanish*) 7-66354
 Bulgarian-1300, attitude determ. from mag. field meas. 7-29376
 circular orbit, autonomous Hamiltonian systems, explicit formula for stability study 7-34841
 collisions with and degradation of orbiting space telescopes 7-9361
 COS-B, telescope in-flight calibration of sensitivity and background behaviour of instrument 7-60539
 Cosmos 1402, U fallout in rain following satellite decay 7-3740
 Cosmos 58 orbit, 15th-order resonance and geopotential harmonics 7-54852
 Cosmos-1500, digital processing of side-looking radar imagery 7-66340
 cosmos-1500, effect of meteorological conditions on radar images of Earth's surface 7-66217
 Cosmos-1500 satellite, radar system design and appls. 7-66424
 dynamical system parameters estimation from obs. appl. of local polynomials 7-34887
 electric charge build-up in magnetospheric environment, secondary electron yields 7-55415
 electron-irradiated dielectric discharges, statistical behaviour 7-55423
 equatorial satellites, librational motion in gravit. field of rot. nonspherical planet 7-34831
 ERM thermal anal., heat radiation case study using finite element method 7-20588
 ERS-1, wind scatterometer antenna release shock loads 7-23976
 ERS-1 active microwave instrumentation, operational control 7-47550
 ERS-1 European remote sensing satellite, ground reception facilities for Australia 7-4292
 ERS-1 satellite, Australian involvement 7-4294
 ERS-1 wind scatterometer antenna, mechanical aspects 7-23975
 Estec sun simulator for researching the thermal behaviour of satellites (*Dutch*) 7-55422
 Exosat, X-ray astronomy satellite, review of mission 7-55464
 explosions and space debris, mass distrib. 7-66420
 Far Infrared Submillimetre Space Telescope mission 7-34866
 Far Ultraviolet Spectroscopic Explorer telescope technology 7-29398
 FIRST, instrumentation considerations 7-47890
 FIRST mission, general outline 7-60508
 FIRST telescope, active optics and spectral range extension in IR 7-60553
 FIRST use for giant planets atm. studies 7-47743
 Fuse/Lyman satellite telescope, photon-counting array detectors 7-47714
 geodynamic twin satellite, relative motion anal. 7-4285
 GEOS-2, long-term behaviour of photoelectron emission from elec. field double probe sensors 7-66426
 geostationary satellite, position meas. using ground radiobeacons 7-60503
 geosynchronous debris in Earth orbit, CCD search 7-55413
 geosynchronous satellite motion under gravitational effects 7-55414
 global satellite laser ranging use for tectonic deform. anal. 7-55287

artificial satellites continued

- GPS radionavigation satellite, orbit determ. by regional network double difference carrier phase obs. 7-34684
- GPS use for NBS calibration service, time and frequency transfer, appl. 7-14926
- Hipparcos mission (*French*) 7-47669
- Hubble Space Telescope calibration, IUE spectra of UV standard stars 7-60735
- Hubble Space Telescope performance, prediction using optical surface anal. code 7-25930
- Hubble Space Telescope Satellite, config. and technological aspects 7-55473
- Intercosmos 13 rocket (1975-22B), inclination var. analysis 7-55419
- IR satellite image processing, kinetic temp. image modelling 7-23899
- ISEE-3, energetic ion results (EPAS) in deep geomag. tail 7-29367
- ISEE-3, plasma meas. rel. to distant magnetotail struct. and dynamics 7-29366
- ISEE-3 Geotail Mission, mag. field meas. 7-29369
- ISEE-3 Geotail Mission, suprathermal ion and electron results 7-29368
- ISIS-II spacecraft, discharge of RF-induced DC potential by positive ions 7-66427
- Japan, satellites and space science 7-60507
- Japanese scientific satellites and space probes, design and communication aspects (*Japanese*) 7-47665
- JEOS, JANUS Earth Observation Satellite 7-34824
- LAGEOS, sensitivity to changes in Earth's (2,2) gravity coeffs. 7-34825
- Large Deployable Reflector, characts. 7-60555
- Large Deployable Reflector System concept 7-29399
- large space antenna assembly feasibility at space station 7-60540
- laser ranging, chord and relative height estimation from single data passes (*Chinese*) 7-3961
- laser ranging, observations smoothing via correction of orbital parameters and station coordinates 7-54844
- launches during 1984, annual schedule (*French*) 7-14474
- low-earth-orbit satellite tracking and data acquisition, use of microcomputer systems 7-55425
- Lyman UV astronomy mission, instrumentation and objectives 7-66430
- Lyman UV astronomy mission and instrumentation 7-66429
- meteorological, GOES-I, J, K instruments developed by Kodak 7-23971
- meteorological, solar radiator for cooling IR detectors in geostationary orbit 7-18878
- meteorological, radiometers, IR detectors and their calibration 7-23898
- meteorological IR satellite, optical design of imaging system 7-55321
- meteorological satellite data access in Australia, requirements and technical infrastructure 7-4293
- meteorological satellite proposal, low equatorial orbiter in 3-hour orbit 7-55329
- Meteosat for obtaining weather pictures from space (*German*) 7-23970
- Microwave Limb Sounder 183 GHz radiometer 7-60433
- Mirabooka X-ray astronomy experiment 7-4339
- motion, problem of critical inclination and commensurability (*Chinese*) 7-4284
- motion about mass centre in circular orbit 7-66438
- near-Earth space environment, spaceglow and material erosion 7-60506
- NOAA data processing system (*Japanese*) 7-4287
- occluding disk in high orbit, use for X-ray sources meas. 7-60567
- optical observations and fundamental catalogue corrections 7-29415
- optical remote sensing from space, conf., Cannes, France (Nov. 1985) 7-35094
- orbital data, appl. to determ. of semi-annual var. of upper atmosphere density 7-4245
- orbital inclination function, trigonometric series representations 7-4299
- orbital motion, reduction of magnitude of correl. coeffs. between orbital elements 7-29384
- orbital perturbations, Henon mapping with Pascal 7-34836
- orbital perturbations, implications for lunar secular accel. and tidal energy and dissipation 7-14301
- orbital resonances, determ. of geopotential harmonics of order 15 and 30 from anal. of 25 satellites 7-65923
- orbital theory, connection between Tisserand's polynomials and inclination functions 7-47664
- orbits, perturbation by Earth zonal harmonics 7-23984
- orbits with periodic flights around Moon, use in very long baseline radio interferometry 7-34833
- P78-2 (SCATHA), boom potential in sunlight at geosynchronous altitudes 7-34827
- periodic solutions of Hamiltonian systems, appl. in satellite dynamics 7-66435
- perturbed Keplerian motions, linearisation of 3D problems in non-centered force fields 7-34837
- Prognoz-10, algorithms for satellite crossing times of solar wind shocks determ. 7-55417
- Prognoz-10, BIFRAM instruments for solar wind meas. 7-55409
- Prognoz-10, dynamics and bowshock meas. in Intershock project 7-55416
- Prognoz-10, EPSW expts. in Intershock project 7-55408
- QUASAT, scientific and industrial appls. for Australia 7-4340
- Quasat role in VLBI, appl. for interstellar refr. meas. 7-60576
- relativistic equations of motion, determ. for satellite in orbit about finite-size rotating Earth 7-34826
- remote sensing, orbit selection to ensure round-the-clock coverage 7-55298
- remote sensing satellites, appls. in Pakistan 7-4206
- remote sensing satellites, Doppler props. of radars in circular orbits 7-4288
- remote sensing satellites, simultaneous Earth obs. from two satellites 7-4204
- remote sensing using polar orbiting platform, conf., Avignon, France (June 1986) 7-48190
- rotation in plane of elliptical orbit, struct. of higher-order reson. zones 7-34829
- Salyut-6/Kosmos 1267 and Salyut-7/Kosmos-1443 orbital complexes, generalised gravit. orientation regime 7-34832
- satellite launches during 1984, annual schedule (*French*) 7-14474
- satellite remote sensing, Doppler props. of radars in circular orbits 7-4288
- second order trajectory predictor derivation in terms of geometrical variables 7-23969
- Shuttle glow and critical ionization velocity phenomena 7-55377
- Solar Max samples, erosion studies 7-46743
- Solar Maximum Mission, surface impact craters anal. 7-4386

artificial satellites continued

- Space Remote Sensing Center projects and commercial prospects 7-60258
- Space Shuttle bay area, ion species observations 7-60462
- Space Shuttle glow optical emissions during mission STS 41-G 7-34834
- Spot (satellite probe for Earth observation), large market for space imaging (*French*) 7-60505
- SPOT and Landsat imaging and equipment, conf., Innsbruck, Austria (April 1986) 7-55887
- SPOT satellite series, characts. 7-47551
- stability at triangular libration point in restricted elliptical three-body problem 7-66436
- Sun sensor for high precision attitude control of astronomical satellite (*Chinese*) 7-4286
- symmetric satellite with viscoelastic antenna in circular orbit, evolution of spin about mass centre 7-34828
- synchronous orbits, Extended Semianalytical Kalman Filter appl. 7-29386
- Szebehely's problem extended to holonomicsystems with a given integral of motion 7-4303
- tethered satellite (on end of cable from larger satellite), electric current behaviour 7-9360
- Tethered Satellite System, Langmuir probe meas. in plasma sheath of charged satellite 7-37744
- tethered satellite system (*German*) 7-47668
- Viking, satellite characts. and orbit determ. 7-9359
- X-ray instrumentation, conf., Cannes, France (December 1985) 7-24279
- AlGaAs-GaAs heteroface space solar cells with 21 percent conversion efficiency 7-3694
- Si solar arrays for low Earth orbit space stations, advanced module concept 7-3659
- Si solar cell array, 30 kW, for space appls. 7-3660
- Si solar cell arrays for EURECA space vehicle 7-3661

artificial vision *see computer vision*

asbestos

- asbestos-brucite-polyphenylene sulphide composites 7-53925
- fibres, Fourier transform photoacoustic spectroscopy 7-51952
- lung tissue, autopsied, from asbestos workers, Mossbauer effect study 7-65849

asdic *see sonar*

aspherical lenses

- see also aberrations*
- aberration field properties of simple non-axially symmetric optical systems 7-50691
- design, aspheres use 7-50690
- fabrication, diamond turning with MOORE machine 7-31539
- focusing lenses for high-power multi-wavelength laser systems 7-62808
- large optics, aspherical component grinding 7-26046
- planar geodesic, anisotropic aberrations, definition 7-15818
- planoconvex graded-index rod lens for coupling laser diode to single-mode fibre 7-15973
- plastic aspherical lens design and fabrication in Japan 7-43459
- precision molded, for camera or compact disk systems 7-43318
- TV projection lens, wide-angle having aspherical surfaces 7-50698
- wide-aperture objectives for radiation concentration 7-43302

assembling

- see also microassembling*
- automated single-mode optical coupler manufacturing 7-26049
- holographic microscope, projection type, for microcircuits assembly and QC 7-62650
- large space antenna assembly feasibility at space station 7-60540
- solar cell high throughput automated fabrication line with ion implantation and halogen lamp annealing 7-8417

assembly lines *see assembling*assembly methods *see assembling*

association

- see also association of liquids; associative ionisation*
- aggregation models, transitions in large-scale struct. 7-29907
- alkali halides, neutral molecule incorporation, composite form. at room temp. 7-54101
- alkylamines, surface ionis. mass spectra 7-10763
- alkylamines intercalation into $\text{HfCa}_2\text{Nb}_3\text{O}_{12}$, structural studies 7-65306
- allyl chloride, dissociation attachment cross sections 7-28290
- aminoalcohols, surface ionis. mass spectra 7-10763
- anion-water complexes, struct. and binding energy, ab initio study 7-15483
- anthracene crystal monolayer, photodimer disorder effects, UV reflection spectra anal. 7-53362
- ascorbic acid radical, strong perchloric acid soln., free radical protonation equilib., ESR study 7-33918
- azoles, protonation energies and tautomerism, basis set effects 7-25374
- benzenes monosubstituted, H-bonded complexes with fluoroalkanol and fluoroalkyl ethers, ^1H NMR study 7-42651
- benzyl chloride, dissociation attachment cross sections 7-28290
- 1,4-bis(β -pyrazinyl-2-vinyl)-benzene, solns. and solid state, irr. and solvent effects, visible fluoresc. anal. 7-36674
- 1,3-butadiene + HCl, addition, internal excitation effect, rate const. meas. 7-17761
- carbazole + 4-cyanopyridine (benzonitrile), H bonding interaction 7-17784
- 5-chloro-2-hydroxypyridine, tautomerism, IR and UV spectra 7-31047
- chlorobenzene, dissociation attachment cross sections 7-28290
- complex molecule production in dense interstellar clouds 7-14640
- compound formation in cluster beams, mass spectrosc. obs. 7-15782
- 2-dicyanomethylene-1,3-indanedione-methylated [2,2]paracyclophanes charge transfer complexes, IR and mass spectroscopy 7-25523
- diffuromethyl diradical, form. obs., dimerisation rate const. determ. 7-28291
- ethylenediamine ligands, vibr. circular dichroism, ion assoc., ring conform. and ring currents 7-31084
- geminate pair recombination, interaction pot., anisotropic reactivity 7-22986
- hydrazines, surface ionis. mass spectra 7-10763
- hydrophobic effects in soln. chem., integral eqn., Monte Carlo study 7-59751
- imidazole, vibr. spectrum, solvent, protonation and metal ion coord. effects, UV Raman spectra 7-25526
- iminoborane, and derivatives, electronic struct. ab initio calcs. 7-847

association continued

- indolecarboxylic acids, proton transfer reactions in excited singlet state, fluoresc. spectra study 7-22318
 inert gas-NH₃ ion form. by electron ionisation, mass anal. ion kinetic energy spectra 7-13736
 interstellar clouds, reactions at low temps. 7-13764
 ion-molecule association and clustering form., thermochemical data 7-18514
 lithium biphenylide-biphenyl association in methyltetrahydrofuran soln., comment 7-28293
 lumiflavin vibr., isotope freq. shift, IR spectra 7-918
 mean spherical approximation, chem. ion assoc. and dipolar dumbbells 7-54141
 merocyanine dyes, J aggregate form. in mixed monolayers, visible spectra and surface pressure-area isotherms anal. 7-31059
 methanol, associates, H bonding, struct. CNDO/BW calcs. 7-56985
 methanol, vapour, homogeneous nucleation rates, heat of assoc. effects 7-26926
 methanol-n-hexane, equilibr. assoc. const., NMR 7-932
 methanol-trimethylamine, associates, H bonding, struct. CNDO/BW calcs. 7-56985
 methyl cation+H₂ radiative assoc. rate 7-3585
 methyl ion+ethylene (acetylene) reaction, collision complexes form. 7-39867
 5-methylcytosine, incorporation in nucleic acids 7-54441
 methylation, protonation, C=N bond rehybridisation rel. to stretching force const. 7-30925
 multicomponent systems, association, thermodynamic functions (*German*) 7-21411
 nickel (II) tetra(p-vinylphenyl) porphyrin, benzene soln., aggregation and luminesc. props., visible spectra anal. 7-42635
 nitrobenzenes para-substituted, solvated anion radicals reaction kinetics in liq. NH₃, ESR spectra anal. 7-19907
 organometallic adduct formation during MOCVD growth of InGaAs films 7-33588
 perylene, protonation, X-ray diffr., NMR, EPR and gas phase mass spectra anal. 7-46843
 pivalic acid in dil. solution, dimerisation, IR spectroscopy 7-65313
 poly(2-vinylpyridine), protonated, dil. soln. with trifluoroacetic acid, excimer emission, fluoresc. anal. 7-31196
 poly(4'-vinylbenzo-18-crown-6), ion-binding characts., eval. 7-10469
 poly(4-vinylpyridine), protonated, dil. soln. with trifluoroacetic acid, excimer emission, fluoresc. anal. 7-31196
 poly(γ-benzyl L-glutamate) aggregation with rhodamine B, fluoresc. depolarisation 7-31096
 polystyrene latex spheres, aggregation kinetics, laser light scatt. 7-13827
 polystyrene-divinylbenzene, 2,2'-dipyridylamine binding, transition metal complexes form. 7-23014
 pyrazine, successive protonation, ab initio quantum chem. calcs. 7-56957
 quarternary ammonium salts, surface ionis. mass spectra 7-10763
 radiative association, role of electronic transitions from rate of CH₃⁺+H₂=CH₃⁺+hν 7-66714
 trans-retinylidene Schiff base, protonation on crystal surfaces, attenuated total refl. IR study 7-50102
 rhodamine dyes, polar and nonpolar solvent mixtures, aggregation, luminesc. meas. 7-7758
 riboflavin, and derivatives, vibr., isotope freq. shift, IR spectra 7-918
 tetracyanoethylene-methylated [2.2]paracyclophanes charge transfer complexes, IR and mass spectroscopy 7-25523
 thiosemicarbide, bonding and struct., effect of protonation, ¹⁴N quadrupole reson. spectra anal. 7-33295
 thiosemicarbide hydrochloride, bonding and struct., effect of protonation, ¹⁴N quadrupole reson. spectra anal. 7-33295
 tracer diffusion in dense ethanol, correl. for nonpolar and H-bonded solvents 7-32688
 trifluoromethyl radical+O₂, rate const. meas., laser photolysis and time-resolved mass spectrometry 7-8249
 trimethylsilyl+O₂(aromatic bases), assoc. binding energies meas., mass spectra 7-54096
 urethane form. reaction, H bonding, CNDO/BW calcs. 7-56985
 vinyl chloride, dissoc. attachment cross sections 7-28290
 weak molecular complexes, isomerism, molar heat capacity at const. press. investig. 7-28305
 zinc (II) tetra (p-vinylphenyl) porphyrin, benzene soln., aggregation and luminesc. props., visible spectra anal. 7-42635
 C₆₀ and similar substances, inert gas trapping, possible occurrence in meteorites 7-50436
 C₆₀MnCl₂.2.4NH₃+4.8NH₃, thermochemical energy storage, kinetic study (*French*) 7-17782
 CO⁺+CO+M, where M=CO, Ne and He, association reactions, third-order kinetics, temp. depend. 7-46817
 Ca²⁺+D-ribose (D-arabinose), enthalpies, sp. heat and molal vols. at 25°C 7-8253
 Co complexes and related cpds., aq. soln., densities, viscosities and electrolytic cond. (*Japanese*) 7-12347
 D₂O, H- and D-bonded dimers, relative stabilities, IR spectra 7-62364
 Fe complexes, Fe(II)-neutral N bases, reactivity, basket-handle super-struct. effects 7-54100
 FeH_x, prep. under high press., Mossbauer obs. 7-33313
 H, atomic, electron- and nuclear-spin polarised, in liq. He covered cells 7-32748
 H, spin-polarised, inverse predissociation at low temps. 7-21571
 H, spin-polarised atomic, three-body recombination 7-32749
 H_n⁺, even cluster ions, form., reactivity collision-induced dissoc., isotope effects, mass spectra anal. 7-50434
 HCN cluster form. in carbon tetrachloride matrix, IR spectra 7-19841
 HDO, H- and D-bonded dimers, relative stabilities, IR spectra 7-62364
 H₂O, associated species, stretching force const., mol. interaction effects, CNDO calcs. 7-25396
 H₂O, H- and D-bonded dimers, relative stabilities, IR spectra 7-62364
 HPO₃ radical, strong perchloric acid soln., free radical protonation equilib., ESR study 7-33918
 Hg+Xe, complex form., equilibr. const. 7-19752
 KC₈/D₂O intercalation cpd., X-ray diffr., NMR, EPR and gas phase mass spectra anal. 7-46843
 Li⁺+dimethyl ether, assoc., rate const., pot. energy surface, canonical variational transition states theory 7-54108
 N-HO bond complexes, association equilib. const. using dielectric relax. data 7-65291
 2N₂+N₂⁺(NO⁺), assoc., temp. depend. 7-13742
 N₂⁺+2N₂, assoc., temp. depend. 7-13742

association continued

- NO⁺+NO, association reactions, third-order kinetics, temp. depend. 7-46817
 NO+NO₂=N₂O₃, kinetic meas., time-resolved IR laser absorpt. 7-17771
 NO₂ adsorption on Ag (110), surface nitrate formation 7-52286
 Na+Na assoc. ionisation, at. alignment, effect vel. depend. 7-28306
 NaO+O₂(CO₂), assoc. reactions with third body He, N₂ or N₂O, kinetics, atm. appl. 7-59748
 Na₂O-CaO-SiO₂ glass, hydration, fluid flow effects 7-13758
 NaXe, spin-rotation coupling, spin relaxation rate 7-25542
 No⁺+2N₂, assoc., temp. depend. 7-13742
 O₂⁺+2O₂(2N₂) assoc., temp. depend. 7-13742
 Pd electrodes, surface hydride formation 7-23067
 SO₃ radical, strong perchloric acid soln., free radical protonation equilib., ESR study 7-33918
 Zn ferrite, shock-synthesised or furnace-reacted, mag. props. 7-38904
association factor (liquids) see *association of liquids*
association of gases see *association*
association of liquids
 see also *colloids*
 n-alcohols, IR intensities in liq. phase, OH vibrs., assoc. model 7-53336
 4-n-alkylbicyclo (2,2,2)-octan-1-carboxylic acids, spin-spin relax. 7-59121
 muonium+benzoic acid derivatives, addition reaction in aq. solns., Hammett free energy 7-15744
 nematic liq. crystals, molecular association, influence on dielectric and electro-optic props. 7-16407
 pentanol isomers, n-heptane solvent, mol. assoc., optical Kerr effect study 7-62429
 Mu+hydrocarbons, chem. dynamics in liq. phase 7-54093
 NH₄F in dioxane-methanol mixtures, assoc. constant from cond. meas. 7-33939
associative ionisation
 He+He, associative ionisation in glow discharges 7-62506
 Na+Na, associative ionis. cross section meas., spin-selected velocity depend. 7-42736
 Na+Na assoc. ionisation, at. alignment, effect vel. depend. 7-28306
 Na+Na(3p), assoc. ionis., Na₂⁺ form., alignment anal. 7-960
associative storage see *content-addressable storage*
astatine
 see also *nuclei with*
 ²¹¹At, possible applications to human cancer therapy, review 7-28657
astatine compounds
 No entries
ASTERISK spectroscopy see *Raman spectroscopy*
asteroid satellites see *planetary satellites*
asteroids
 336 Lacadiera, occultation of SAO 185428 7-66494
 1977 DV3=Periodic Comet Skiff-Kosai (1976 XVI), precise positions and orbital elements 7-9435
 1985 CQ1, astrometric obs. and orbital elements from La Silla, Chile (*French*) 7-60593
 1986 ephemerides of minor planets, book 7-9603
 1986 RA, discovery positions, orbital elements and ephemeris of Amor object 7-4360
 1986 RA, ephemeris (1986 September 7 to 1987 January 25) and orbital characts. 7-4361
 1986 TN, 1986 TO, 1986 TP, new fast-moving asteroids, discoveries and precise and approx. positions 7-18366
 1986 TN, time correction for astrometric obs. (1986 October 6) 7-24044
 1986 TO, Aten-type asteroid, astrometric obs. correction, orbital elements, and ephemeris 7-24044
 1986 UD=Comet Urata-Nijima (1986o), precise positions, parabolic orbital elements, and ephemeris 7-29431
 1986 UD, fast-moving asteroidal object, discovery, astrometric positions and magnitude estimate 7-29421
 1986 WA, astrometric positions, orbital elements and ephemeris (1986 December to 1987 February) 7-47751
 1986 WA, fast-moving asteroidal object discovery 7-34905
 1986 WA, positions, orbital elements, and ephemeris of Apollo object 7-40739
 1987 AB, discovery positions of fast-moving object 7-55519
 1987 ephemerides of minor planets, book 7-9604
 259 Aletheia, occultation of SAO 160139 on 1986 May 10, Australian obs. 7-14516
 American Astronomical Society, 18th annual meeting of Division for Planetary Sciences, conf., Paris, France (November 1986) 7-24255
 29 Amphitrite, obs. data and model 7-40745
 apocentric librators and the reducing transform. 7-23981
 bidirectional reflectance spectroscopy, extinction coeff. and opposition effect in particulate medium 7-24033
 binary asteroids and satellites of asteroids, implications for occultation obs. 7-18367
 1 Ceres, thermal emission model based on IR and diameter observations 7-40741
 Ceres; visual magnitude estimates (1986 April) 7-14516
 Ceres (asteroid no.1), occultation of BD+8°471 star on 13 Nov 1984, photoelectric obs. 7-55432
 511 David, speckle interferometry and photometry rel. to dimensions, rot. pole and albedo 7-24045
 Eccentricid system, asteroids and meteoroids inside Earth's orbit 7-24085
 Germinid meteors parent body, orbital elements, mass and size from spatial struct. of meteor swarm 7-66519
 Henon mapping with Pascal, asteroid simulation 7-34836
 1026 Ingrid, lost minor planet, identification with 1986 ES₂, 1957 UC, 1981 WL₆, and 1963 GD 7-40740
 Juno, surface comp. and visible spectral characts. (*Russian*) 7-24047
 22 Kalliope, photoelectric photometry and pole orientation from magnitude-aspect' relations 7-47749
 Kirkwood gaps origins (*French*) 7-4359
 1179 Mally, recovery of lost object and additional images 7-40738
 Marian surface impacts, effect of impact-generated gas cloud on solid ejecta accel. 7-55585
 Meteoritical Society, 49th annual meeting, New York (September 1986) 7-18506
 micropolar planetary asteroids, orbital dynamics (*French*) 7-40744
 minerals remote diagnostics, photometric system from spectral props. of achondrites and ordinary chondrites 7-66521

asteroids continued

- Minor Planet Circulars, piecewise positions, elements, ephemerides, and new numbers 7-24046
- Minor Planet Circulars, precise positions, elements, ephemerides, and new numbers, and names 7-40743
- Minor Planet Circulars 10781-10884, precise posns., elements, ephemerides, new nos. and names 7-9399
- Minor Planet Circulars 10885-10988, precise posns., elements, ephemerides and new nos. 7-9400
- Minor Planet Circulars 10989-11094, precise posns., elements, ephemerides, and new nos. 7-9401
- Minor Planet Circulars 11095-11198, precise posns., elements, ephemerides, new nos. and names 7-9402
- Minor Planet Circulars 11275-11374, precise positions, elements, ephemerides, and new numbers 7-40742
- Minor Planet Circulars 11465-11560, precise positions, elements, ephemerides, and new numbers 7-55520
- Minor Planet Circulars 11561-11680, precise positions, elements, ephemerides, new numbers, and names 7-66495
- 473 Noll, relocation of lost asteroid 7-47752
- oblique planetary impacts, process for obtaining meteorite samples from other impacts 7-34957
- orbital motion, effects of subtle planetary perturbations by Earth-Moon system 7-4297
- orbits, effects of secular resonances ν_6 and ν_5 7-47748
- orbits near 3:1 resonance, hyperbolic twist mapping model 7-34909
- origin of small bodies, explosion of Asteron 7-29417
- 2 Pallas, thermal emission model based on IR and diameter observations 7-40741
- proper orbital elements characts. 7-34908
- rotation axes determ. via amplitude-magnitude method 7-34907
- rotation characteristics of large asteroids 7-34906
- secular resonance ν_6 , orbital evolution 7-14515
- size distribution 7-47750
- surface materials characts. 7-40729
- Vesta mission to Venus, comet and asteroids for 1990s 7-40667
- zodiacal dust cloud source, implications of solar flare track densities in interplanetary dust particles 7-55531

astigmatism *see vision defects*

astroarchaeology

- archaeoastronomy and roots of science, conference San Francisco (January 1980) 7-41019
- Jutland stone circles (*Danish*) 7-40725
- New and Old World astroarchaeology 7-24023
- stellar alignments, atmospheric extinction effects 7-55255

astrobiology *see extraterrestrial life*astroblesmes *see meteorite craters*

astrometry

- 1934-638, galaxy, red CCD image characts. 7-35056
- 1985 CQ1, astrometric obs. and orbital elements from La Silla, Chile (*French*) 7-60593
- 1986 RA, discovery positions, orbital elements and ephemeris of Amor object 7-4360
- 1986 TN, 1986 TO, 1986 TP, new fast-moving asteroids, discoveries and precise and approx. positions 7-18366
- 1986 TN, time correction for astrometric obs. (1986 October 6) 7-24044
- 1986 TO, Aten-type asteroid, astrometric obs. correction, orbital elements, and ephemeris 7-24044
- 1986 UD, fast-moving asteroidal object, discovery, astrometric positions and magnitude estimate 7-29421
- 1986 WA, astrometric positions, orbital elements and ephemeris (1986 December to 1987 February) 7-47751
- 1986 WA, positions, orbital elements, and ephemeris of Apollo object asteroid 7-40739
- 1987 AB, discovery positions of fast-moving object 7-55519
- A and F-type dwarf stars in C0318+484 (α Per cluster), space vels. 7-4531
- astrolabe obs., light deflection, corrected Li expression 7-66431
- astrolabe observations, statistical analysis (*French*) 7-66473
- atmospheric limitations to Earth rot. parameters determ. 7-60412
- C0318+484 (α Per cluster), internal kinematics of A and F-type dwarf stars 7-4531
- 3C 119, compact steep spectrum source, peculiar morphology 7-40949
- 3C 263, double-lobed quasar, superluminal motion, SHF obs. 7-48095
- cataclysmic binary stars, positions for 20 previously poorly located objects 7-18345
- P/Comet Boethin (1985n), TA report (1986 January 3-19) 7-14532
- P/Comet Bus (1987f), recovery, astrometry, orbital elements and ephemeris (1987 January to May) 7-55558
- P/Comet Du Toit-Hartley (1986q), recovery, astrometry and total visual magnitude estimate 7-47775
- PI Comet Giacobini-Zinner (1985 XIII), astrometric positions (June to October 1985) 7-66504
- P/Comet Halley, (1982i), optimum orbit determ. via ground-based astrometry and Vega spacecraft obs. 7-14525
- P/Comet Halley (1910 II), astrometric obs. by J. Tebbutt 7-55943
- P/Comet Halley (1982i), accurate positions (*Chinese*) 7-29425
- P/Comet Halley (1982i), TA positions (1985 November-December) 7-14533
- Comet Levy (1987a), obs., orbital elements and ephemeris (1987 January 5 to February 4) 7-47779
- Comet Levy (1987a), positions and magnitudes (1987 January) 7-47780
- P/Comet Lovas 2 (1986p), astrometric positions, orbital elements and ephemeris 7-47778
- P/Comet Lovas 2 (1986p), positions, orbital elements and ephemeris 7-47774
- Comet Lovas (1986p), positions, elements, and ephemeris (1986 Nov.-Dec.) 7-40780
- P/Comet Skiff-Kosai (1976 XVI)=1977 DV3, precise positions: (1977 February 13 to March 12) 7-9435
- Comet Sorrells (1986n), discovery, total visual magnitude estimates and positions 7-29428
- Comet Sorrells (1986n), precise positions, 1986 November 2 to 4, orbital elements, and ephemeris 7-29430
- P/Comet Tempel 2 (1987g), recovery positions and ephemeris 7-55561
- Comet Terasako (1987d), positions, elements, ephemeris, and magnitude (1987 Jan.-Feb.) 7-55553
- comet Urata-Nijijima (1986o) (=1986 UD), precise positions (1986 October 30 to November 4) 7-29431
- astrometry continued
- P/Comet Wild 3 (1987e), recovery positions (1987 January-February) 7-55557
- Comet Wilson (1986l), visual obs. and positions (1986 Aug.-Sep.) 7-34932
- P/Comet Wiseman-Skiff (1987b), astrometry, elements and ephemeris 7-55548
- comets, TA reports (1986 Aug.-Nov.) 7-55533
- compact extragalactic radiosources, VLBI astrometry 7-35055
- Earth rotation parameters determ., appl. of lunar laser ranging data (*Chinese*) 7-3959
- Earth rotation parameters determ. estimation of accuracy in different freq. bands 7-54843
- Earth rotation parameters determ. optimal conditions (*Chinese*) 7-3960
- 40 Eri A, proper motion meas. rel. to gravit. lens effect on background star 7-47861
- extragalactic radiosources, milliarcsecond VLBI nuclei positions 7-14671
- galaxies in Corona Borealis region, redshift survey rel. to large-scale struct. 7-40922
- Galilean satellites, anal. of occultation obs. and comparison with theories 7-47754
- HD 97950, central object of giant H II region NGC 3603, speckle masking obs. 7-29502
- Hipparcos mission (*French*) 7-47669
- Hyades stars, positions and 60 mm obs. 7-4535
- interferometer, POINTS design 7-40712
- IRAS 03134+5958, possible Herbig-Haro object, proper motion meas. 7-66720
- Jupiter, satellite positions and flux density meas. by VLA in SHF 7-40746
- BL Lac objects, updated precise positions and relation to galaxies and quasistellar objects 7-47732
- LHS 288, LHS 1070, new nearby faint red stars, parallaxes and photometry 7-4455
- M22, globular cluster, stellar proper motions, membership, and photometry 7-4530
- Minor Planet Circulars, precise positions for asteroids and ten comets 7-24046
- Minor Planet Circulars, precise positions for asteroids and ten comets 7-40743
- Minor Planet Circulars 10781-10884, precise posns. for asteroids and eight comets 7-9399
- Minor Planet Circulars 10885-10988, precise posns. for asteroids and 17 comets 7-9400
- Minor Planet Circulars 10989-11094, precise posns. for asteroids and nine comets 7-9401
- Minor Planet Circulars 11095-11198, precise posns. for asteroids and 16 comets 7-9402
- Minor Planet Circulars 11275-11374, precise positions for asteroids and 18 comets 7-40742
- Minor Planet Circulars 11465-11560, precise positions for asteroids and 22 comets 7-55520
- Minor Planet Circulars 11561-11680, precise positions for asteroids and 22 comets 7-66495
- NGC 6611, very young open cluster, stellar proper motions and membership 7-40882
- Nova And 1986, astrometric position and Dec. 1986 magnitudes 7-40843
- Nova And 1986, precise position and pre-nova candidate identification 7-47907
- Nova Cen 1986, discovery, position, magnitudes, photometry, prenova identifications 7-24146
- Nova Lac 1986, object at $\alpha=22^h22^m07^s$, $\delta=+48^\circ12'41''$ which is not a nova 7-34993
- NSV 6708, magnitude range, finder chart, and position 7-18416
- open clusters, photographic relative proper motions of member stars (*Chinese*) 7-4526
- Paris Observatory APP 1985 meas. and time and latitude (*French*) 7-60509
- Phoebe, astrometric positions 7-34918
- photoelectric meridian circle, annual and diurnal vars. of graduation error 7-47702
- planet right ascension determ. using photoelectric transit instrument, correction method (*Chinese*) 7-4343
- planetary systems, search methods 7-55722
- point sets, subsets, bijection, and quadratic system 7-40672
- polarissima method for absolute azimuth determ. with transit circle 7-4346
- Potsdam PZT star catalogue, comparison with four NPZT catalogues 7-4355
- proper motion stars in field SE of 45 Oph, photometric study and catalogue 7-60577
- proper-motion stars, parallaxes from photographic astrometry 7-4296
- PSR 1855+09, white dwarf companion star of binary millisecond pulsar 7-29500
- radio sources near 3C 84 and 3C 273, right ascensions and 7.6 cm flux densities 7-66774
- radio stars, finding charts for Hipparcos mission 7-9385
- α Sco, optical and radio positions comparison (*French*) 7-24131
- Selected Area 57 quasar candidates catalogue of multicolour photometry, variability and astrometry 7-4591
- V503 Sgr (=G154-12), variability and proper motion of star 7-47831
- Simeiz-Pushchino interferometer obs. 7-4334
- SMC, Nova 1986, discovery, position and visual magnitude estimates 7-47910
- SN 1986K, in anonymous galaxy in Cetus, discovery, precise position, and magnitude estimate 7-9502
- SN 1986L in NGC 1559, precise position and magnitudes 7-18427
- SN 1986N, type Ia supernova in NGC 1667, spectroscopic obs. and precise positions 7-47956
- SN 1987A, in LMC, discovery, precise position, possible progenitor, photometry, and spectrum 7-66628
- SN 1987A in LMC, precise position rel. to progenitor identification 7-66642
- SN 1987A in LMC, progenitor position, photometry, and polarization 7-66631
- SN 1987A in LMC, Type II SN, astrometry, spectral and photometric obs. and progenitor characts. 7-66629
- SN 1987B in NGC 5850, Feb. 1987 supernova observations 7-66635
- solar system objects, CDS Scientific Council Meeting, Bordeaux, France (May 1985) 7-4618

astrometry continued

- stars of South Galactic Cap, astrometry, trigonometric parallaxes, proper motions and photometry 7-47734
 stars of South Galactic Cap, parallaxes and proper motions rel. to stellar populations, density functions, and luminosity distribs. 7-47832
 Tautenburg Schmidt plates, astrometric model 7-66432
 Tokyo Astronomical Obs., Time and Latitude Bulletins (April to June 1986) 7-23977
 Tokyo Astronomical Obs., Time and Latitude Bulletins (July-September 1986) 7-55433
 Tokyo Photoelectric Meridian Circle, diurnal var. of instrumental const. 7-4332
 triple stars north of +70°, micrometric meas. (*German*) 7-60717
 Ursa Minor dwarf galaxy, star proper motions and bright-star photometry 7-14653
 USNO Halley watch astrometric catalogue 7-34888
 USNO meridian circle, internal refr. errors 7-4333
 Van Biesbroeck 8, IR speckle interferometry rel. to binary nature 7-66587
 variable star catalogues and the Hipparcos astrometric satellite (*French*) 7-9384
 visual binary stars, mass ratios from photographic astrometry 7-4296
 visual binary stars, orbital elements for 20 systems 7-4507
 visual double stars, orbital elements for six pairs (*French*) 7-18430
 visual double stars, orbital elements for twenty-one pairs 7-18431
 VLBI station location determination in terrestrial reference frame (*French*) 7-66314
 VLBI use for Earth rot. parameters determ. (*Chinese*) 7-29248
 X-ray sources, occultation techniques for ultra-high ang. resolution meas. 7-60567

astronautics see *space research***astronomical catalogues**

- Be stars, $H\alpha$ profiles atlas and shell struct. 7-14577
 5C20 deep survey of Abell 2218 at 408 and 1407 MHz 7-18456
 cometary orbits, calcs. from 1982-3 obs. 7-66505
 common proper motion stars in the AGK 3 catalogue, list 7-29413
 database for public use, CDS Scientific Council Meeting, Bordeaux, France (May 1985) 7-4618
 early-type galaxies with emission lines 7-60578
 early-type stars, spectral energy distribs. from 0.15 to 4.8 μm 7-29466
 emission-line stars in Canis Major star formation region, spectroscopic and photometric survey 7-18360
 faint galaxies, photometric catalogues and cosmological implications 7-60915
 fundamental catalogue corrections using artificial satellite obs. 7-29415
 G5 to M-type stars at South Galactic Pole, catalogue rel. to density distribs. 7-4448
 galaxies, nearby, effect of Virgocentric flow model on observed rels. 7-40723
 outer Galaxy H I layer, volume densities atlas in cuts through composite data cube 7-18358
 General Catalogue of Variable Stars, search for optically variable objects in Texas radio source survey 7-4580
 globular clusters in M31, cluster candidates in $3^\circ \times 3^\circ$ field 7-66478
 interstellar 217 nm band, catalogue of equivalent widths 7-66479
 IRAS data, formats and availability 7-47733
 IRAS low resolution spectra atlas 7-24021
 IUE Atlas of Planetary Nebulae and related objects, status report 7-48056
 IUE low-dispersion spectra reference atlas, UV classification of peculiar stars 7-60636
 IUE-observed objects, bibliographical index (1978-85) 7-60579
 BL Lac objects, updated list and relation to galaxies and quasistellar objects 7-47732
 M31, interstellar H I holes list 7-35036
 Markarian galaxies, catalogue 7-55496
 massive stars in M31, obs. in OB associations 7-40926
 meteorite collection of Museo Nacional de Ciencias Naturales, Madrid, Spain, inventory 7-9386
 meteoroid bodies inside Earth's orbit (Eccentricid system), catalogue and characts. 7-24085
 nebulous objects in outer Galaxy, catalogue for vel. field in Southern Hemisphere 7-18359
 NGC 346, young open cluster in SMC, stellar identification charts and VRI photometry 7-48002
 NGC 6946, spiral galaxy, catalogue and characts. of 643 H II regions 7-29414
 Palomar Sky Survey II 7-24022
 Palomar-Westerbork survey of northern spiral galaxies 7-40724
 planetary nebulae, identification of misclassified objects from red and near-IR photometry 7-4542
 Potsdam PZT star catalogue, comparison with four NPZT catalogues 7-4355
 proper motion stars in field SE of 45 Oph 7-60577
 quasar fields surveys, catalogue and background galaxy counts near intermediate-redshift QSOs 7-55495
 radio patrol of northern Milky Way, catalogue of sources 7-4356
 radio sources, extragalactic, 5-GHz survey 7-4353
 radio sources in galactic plane near $l=54^\circ$, WSRT radio continuum obs. 7-35057
 SAO catalogue, luminosity classes of M-type stars 7-4435
 SBS, Byurakan second spectral sky survey in UMa field 7-4352
 Selected Area 57 quasar candidates catalogue of multicolour photometry, variability and astrometry 7-4591
 SMC globular clusters stars, identification charts and spectral classification catalogues 7-29412
 SMC globular clusters stars, spectral classification of bright stars 7-4354
 solar spectral lines in 430 to 670 nm wavelength range with large Stokes V-amplitudes outside sunspots, catalogue 7-66554
 standard stars revised MK spectral types for G0 and later 7-9467
 star clusters in SMC, catalogue of 213 new clusters 7-47735
 stars of South Galactic Cap, astrometry, trigonometric parallaxes, proper motions and photometry 7-47734
 stars with possible planetary systems, catalogue 7-66480
 Sun, photosphere and corona mag. fields (1976 to 1985) 7-4428
 Texas radio source survey, search for optically variable objects 7-4580
 USNO Halley watch astrometric catalogue 7-34888
 UV-excess galaxies, Kiso survey 7-4351

astronomical catalogues continued

- UV-excess objects in Galactic plane, KPD survey for white dwarfs and subdwarfs 7-9383
 variable star catalogues and the Hipparcos astrometric satellite (*French*) 7-9384

astronomical ephemerides

- 1986 ephemerides of minor planets, book 7-9603
 1986 RA, discovery positions, orbital elements and ephemeris of Amor object 7-4360
 1986 RA, ephemeris (1986 September 7 to 1987 January 25) and orbital characts. 7-4361
 1986 TO, Aten-type asteroid, orbital elements and ephemeris (1986 October 27 to December 26) 7-24044
 1986 WA, astrometric positions, orbital elements and ephemeris (1986 December to 1987 February) 7-47751
 1986 WA, positions, orbital elements, and ephemeris of Apollo object asteroid 7-40739
 1987, ephemerides and event calendar for Belgium (*French*) 7-41022
 1987 British Astronomical Association Handbook 7-24318
 1987 Bureau des Longitudes ephemerides (*French*) 7-29380
 1987 ephemerides of minor planets, book 7-9604
 1987 Observer's Handbook of RAS Canada 7-35128
 P/Comet Bus (1987f), recovery, astrometry, orbital elements and ephemeris (1987 January to May) 7-55558
 P/Comet Grigg-Skjellerup, 1987 predictions, orbit improvement and ephemeris 7-40761
 P/Comet Halley, (1982i), optimum orbit determ. via ground-based astrometry and Vega spacecraft obs. 7-14525
 P/Comet Halley (1982i), a priori position prediction error from terrestrial and space-probe meas. 7-4370
 Comet Levy (1987a), obs., orbital elements and ephemeris (1987 January 5 to February 4) 7-47779
 Comet Levy (1987a), position in January 1987 and ephemerides 7-60602
 Comet Levy (1987a) discovery, orbital elements, magnitude eqn. and ephemeris (1987 January 25 to March 6) 7-55539
 P/Comet Lovas 2 (1986p), astrometric positions, orbital elements and ephemeris 7-47778
 P/Comet Lovas 2 (1986p), positions, orbital elements and ephemeris 7-47774
 Comet Lovas (1986p), positions, elements, and ephemeris (1986 Nov.-Dec.) 7-40780
 Comet Nishikawa-Takamizawa-Tago (1987c), discovery, elements and ephemeris (1987 January 25 to March 1) 7-55538
 Comet Nishikawa-Takamizawa-Tago (1987c), positional observations, orbit and ephemeris 7-55549
 Comet Nishikawa-Takamizawa-Tago (1987c), positional observations and improved orbit and ephemeris 7-55552
 P/Comet Skiff-Kosai (1976 XVI)=1977 DV3, precise positions and orbital elements 7-9435
 Comet Sorrells (1986n), ephemeris (1986 November 26 to 1987 January 10) in 5-day steps 7-47769
 Comet Sorrells (1986n), Nov. 1986 discovery and ephemeris 7-40776
 Comet Sorrells (1986n), orbital elements, magnitude eqn. and ephemeris (1987 January 25 to March 1) 7-55541
 comet Sorrells (1986n), orbital elements and ephemeris 7-29432
 P/Comet Tempel 2 (1987g), recovery positions and ephemeris 7-55561
 Comet Terasako (1987d), ephemeris (1987 January-March) 7-55542
 Comet Terasako (1987d), orbital elements, ephemeris and visual observations 7-60603
 Comet Terasako (1987d), positions, elements, ephemeris, and magnitude (1987 Jan.-Feb.) 7-55553
 P/Comet Urata-Nijijima (1986o), independent discovery and ephemeris (1986 November 16 to 1987 January 15) 7-40779
 comet Urata-Nijijima (1986o) (=1986 UD), parabolic orbital elements and ephemeris (1986 October 22 to November 26) 7-29431
 P/Comet Urata-Nijijima (1986o) ephemeris (1986 December 1 to 16) in 5-day steps 7-47770
 P/Comet Wild 3 (1987e), orbital elements and ephemerides 7-55559
 Comet Wilson (1986l), ephemeris (1986 October 17-December 26) 7-24074
 Comet Wilson (1986l), ephemeris for 17 Sept. to 16 Dec. 1986 period 7-4369
 Comet Wilson (1986l), orbital elements, magnitude eqn. and ephemeris (1987 January 25 to March 31) 7-55540
 P/Comet Wilson (1986l), orbital elements and ephemeris 7-47776
 P/Comet Wiseman-Skiff (1987b), astrometry, elements and ephemeris 7-55548
 cometary orbits, calcs. from 1982-3 obs. 7-66505
 P/Comets Tsuchinshan 1 and 2, improved orbits and ephemerides 7-40762
 AA Dor (LB 3459), sdOB-type eclipsing binary ephemeris from primary minima obs. 7-24167
 Draconid meteors, possibility of strong shower (1986 October 8 to 9) 7-4385
 Dynamical Astronomy Division, 17th regular meeting, Santa Barbara, California (April 1986) 7-29571
 Galilean satellites, compact ephemerides (August 1987 to February 1988) 7-4295
 Galilean satellites, heliometer obs. (1891 to 1906) comparison with modern ephemerides 7-24048
 lunar calendars, missing date-lines determ. 7-66433
 Minor Planet Circulars, ephemerides for 65 asteroids and three comets 7-40743
 Minor Planet Circulars, ephemerides for 97 asteroids and two comets 7-24046
 Minor Planet Circulars 10781-10884, ephemerides for 108 asteroids and one comet 7-9399
 Minor Planet Circulars 10885-10988, ephemerides for 89 asteroids and four comets 7-9400
 Minor Planet Circulars 10989-11094, ephemerides for 109 asteroids and five comets 7-9401
 Minor Planet Circulars 11095-11198, ephemerides for 108 asteroids and one comet 7-9402
 Minor Planet Circulars 11275-11374, ephemerides for 64 asteroids and 6 comets 7-40742
 Minor Planet Circulars 11465-11560, ephemerides for 102 asteroids and 9 comets 7-55520
 Minor Planet Circulars 11561-11680, ephemerides for 100 asteroids and 13 comets 7-66495

astronomical ephemerides continued

- NSV 12040, W UMa star, first ephemeris from photoelectric and visual obs. 7-66669
 planetary satellites, cartographic coordinates and rotational coordinates (1985) 7-34893
 planets, cartographic coordinates and rotational coordinates (1985) 7-34893
 proper, dynamical and coordinate time scales (*Rumanian*) 7-18347
 Saturnian satellites, compact ephemerides (April to October 1987) 7-4295
 Uranian satellites, compact ephemerides (April to October 1987) 7-4295
 Venus, recurrent phenomena assoc. with Venus/Earth orbital resonance 7-66489
 visual double stars, orbital elements and ephemerides for twenty-one pairs 7-18431
 BW Vul, β Cep star, photometric ephemeris for 1982 from coordinated photoelectric obs. 7-29485
 Comet Sorrells (1986n), parabolic orbital elements and ephemeris (1986 October 17 to November 26) 7-29430

astronomical instruments

- see also *astronomical observations; astronomical techniques; astronomical telescopes; planetaria; radiotelescopes*
 21-cm spectrometer of RATAN-600 radio telescope, receiving unit 7-60559
 800 MHz bandwidth acousto-optical spectrometer at Helsinki Observatory 7-60561
 acousto-optical spectrographs for ground and space submm astronomy 7-34877
 acousto-optical spectrometer for RATAN-600 radio telescope, design and performance 7-66463
 astrometric interferometer, POINTS design 7-40712
 British long-baseline gravit. wave observatory, feasibility study 7-29408
 Cassini mission for Saturn 7-40754
 Cassini mission to Saturn, reflection spectrometer 7-40755
 cavity-type absolute radiometer on Spacelab 1, appl. to solar const. determ. 7-66549
 CCD for time-resolved stellar photometry 7-9381
 CCD sensor X-ray performance enhancement, X-ray astronomy appl. 7-30149
 CCDs for ROSAT star sensors, testing and characterisation 7-29401
 Cologne 3m radiotelescope acousto-optical spectrometers 7-34878
 Cologne 3m radiotelescope mm and submm spectrometer 7-34871
 comparison and calibration lamp illumination system for Multiple Mirror Telescope, fibre optical system 7-4342
 conference, Tucson, AZ, USA (March 1986) 7-48162
 correlation (balanced) polarimeter for RATAN-600 radio telescope, polarisation chars. 7-66465
 coude spectrograph at Calar Alto Observatory, zero-point and accuracy of radial rel. obs. 7-29409
 CR-39 detector foil meas., cosmic ray LET spectra, automatic scanning technique 7-34809
 cryogenic gravitational wave antenna with resonant capacitive transducer and d.c. SQUID amplifier 7-34881
 cryogenic optical systems and instruments, conference, Los Angeles, California, (January 1986) 7-24283
 Cuffey Iris Astrophotometer, partial automation 7-14494
 diffraction gratings and Henry Rowland, conference, Baltimore, Maryland (June 1984) 7-18493
 Durham Polaris seeing monitor, design and testing 7-66461
 echelle spectrographs, scattered light background correction method 7-34874
 electro-optical meteor observation systems, appls. and results 7-47716
 energetic particle detector on Giotto spacecraft, particle obs. in Comet Halley environment 7-14529
 equator projector sundials 7-47715
 ESA Photon Counting Detector, nonlinearity meas. 7-34875
 Exosat, X-ray astronomy satellite, review of mission 7-55464
 Extreme Ultraviolet Explorer Satellite, calibration of thin film filters, 68 to 912 Å 7-24015
 Fabry-Perot multichannel spectrometer for infrared astronomy 7-55474
 faint object spectroscopy instrumentation 7-55493
 Far Ultraviolet Spectroscopic Explorer telescope technology 7-29398
 FIR photometer, improved design 7-14492
 FIRST, instrumentation considerations 7-47890
 GIOTTO spacecraft high gain antenna mechanical design and development 7-23974
 grating calibration facilities for Extreme Ultraviolet Explorer 7-24712
 gravitational wave detectors, antenna patterns of interferometric detectors for linearly polarised waves 7-55453
 gravitational wave detectors, influence of time-depend. gravit. fields on superconducting oscillatory ccts. 7-41181
 Halley Multicolour Camera, vibration effects in flat mirror, analysis and reduction 7-18355
 high resolution instrumentation for solar studies, meeting, Toulouse, France (September 1984) 7-18498
 high-resolution submillimetre heterodyne spectrometer 7-353
 Hipparcos astrometry mission, diffraction grid fabrication by electron beam lithography 7-24014
 Hipparcos mission (*French*) 7-47669
 Hipparcos project, grid pattern calibration by e-beam 7-29403
 ideal bolometer, background power effect on performance 7-56344
 IKAR-16 automated solar spectral-polarisation complex of RATAN-600 radio telescope, configuration and software 7-66460
 IR 1D speckle interferometry system 7-55488
 far-IR blackbody source of variable temperature, for use in IR astronomical radiometry 7-40713
 IR camera with hybrid 32x32 HgCdTe CCD array 7-60560
 IR low-background bolometers, calibration system 7-9899
 IUE SWP camera, technique for short-period temporal studies of X-ray pulsars 7-55494
 Joint European Amateur Photometer (JEAP) 7-47712
 Kamioka solar neutrino search 7-40694
 large optics technology, conf., San Diego, USA (Aug. 85) 7-35089
 large-acceptance space spectrometer for cosmic ray research, toroidal coil configurations 7-40699
 laser gravitational wave detector, light wave interference, quantum fluctuations effects 7-43039
 laser level for adjustment of RATAN-600 radio telescope, design and performance 7-66468
 Lyman UV astronomy mission, instrumentation and objectives 7-66430

astronomical instruments continued

- Lyman UV astronomy mission and instrumentation 7-66429
 Magellan, Venus mission, SAR instrumentation 7-55468
 Magellan SAR, system test and calibration 7-48681
 Magellan SAR system 7-55469
 Mirrabooka X-ray astronomy experiment 7-4339
 multilayer optics for solar soft X-ray/XUV obs. 7-41562
 observing techniques and instrumentation, book 7-60910
 optical filters, the IPF-6 interference-polarisation filter 7-50722
 parallel shear interferometer for stellar interferometry 7-29402
 PEPSIOS, Polytetralon Pressure Scanned Interferometric Optical Spectrometer 7-18377
 PEPSIOS system, modifications and Periodic Comet Halley (1982i) imaging 7-18356
 photometers, 1/f noise 7-40716
 photometric near-IR spectrometer using Si:Bi hybrid array 7-30103
 photon counting detectors for space astronomy, wedge and strip image readout systems 7-47713
 photon counting imaging microchannel plate detectors calibration, for EUV astronomy 7-29404
 photon-counting array detectors for Fuse/Lyman satellite telescope, development and performance 7-47714
 photon-counting system, appl. to registration of light flashes from image-tube screen 7-60558
 polarimeter spectrometer for radio astronomy 7-14495
 polarisation systems, props. of Muller matrices 7-66464
 prime-focus spectrographs with holographic gratings, design and performance 7-4341
 Prognoz-10, BIFRAM instruments for solar wind meas. 7-55409
 Prognoz-10, EPSW expts. in Intershock project 7-55408
 radio receiver for K-band, using cryogenically cooled amplifier 7-60548
 retrograde motion demonstration model machine 7-18531
 ROSAT position sensitive proportional counter, radiation entrance window development 7-29405
 SETI, ultranarrowband searches with dedicated signal processing hardware 7-24013
 solar EUV instrumentation, calibration in space 7-24009
 Solar Magnetic Field Telescope, principle of vector mag. field meas. (*Chinese*) 7-4330
 solar radiance meter for circumsolar radiation meas. 7-35566
 solid state image sensors and their appls., conf., Cannes, France (Nov. 1985) 7-24288
 solid state submm radiometer, chars., astron. appl. 7-60552
 solid-state imaging arrays, conf., San Diego, CA, USA (Aug. 1985) 7-29582
 space antennas, high precision composite sandwich antennas anal. 7-24012
 space craft plasma diagnostics equipment 7-14510
 Space Telescope Imaging Spectrograph, preliminary performance goals 7-60550
 spaceborne camera using TI TC-104 linear CCD array 7-29406
 speckle, interferometer, imaging, in space, image reconstruction by speckle masking 7-31258
 spectral receiver (1.35 cm wavelength) for RATAN-600 radio telescope, design 7-66466
 spectrograph of 1-m Yale telescope at Cerro Tololo, stability 7-24016
 spectrographs two-dimensional detectors, optimal extraction of single-object spectra 7-47729
 spectrophotometer, three-channel, on Vega spacecraft, appl. to P/Halley investigation 7-14472
 Stable Solar Analyzer instrument for solar oscillations obs. 7-9375
 submillimetre astronomy, conf., Segovia, Spain (June 1986) 7-41013
 submm detectors chars. 7-47711
 submm heterodyne spectrometer for astron. and atm. meas. 7-60562
 Sun sensor for high precision attitude control of astronomical satellite (*Chinese*) 7-4286
 telescope mounting for shipborne obs. of solar corona during eclipse (*French*) 7-40696
 Tokyo Photoelectric Meridian Circle, diurnal var. of instrumental consts. 7-4332
 UC Berkeley submm heterodyne receiver for spectroscopy 7-34879
 UK/NL EHF telescope spectrometer system 7-34876
 USNO meridian circle, internal refr. errors 7-4333
 UV imaging photon detector, large format for astronomical spectroscopy 7-56342
 VEGA space probes, TV real-time software (*Hungarian*) 7-29379
 Vega-1 and 2 at Periodic Comet Halley (1982i), instrumentation and results (*Russian*) 7-4373
 White Cliffs Solar Power Station VHE γ -ray instruments 7-60566
 X-ray and EUV calibration techniques, sources and detectors, conf., San Diego, CA, USA (Aug. 1986) 7-24286
 X-ray detectors, role in British X-ray astronomy 7-24019
 X-ray instrumentation, conf., Cannes, France (December 1985) 7-24279
 Zeeman analyser of CASPEC at ESO, appl. to spectropolarimetry of mag. stars 7-29484
 AgCl-detectors in space biophysics, biological effects of cosmic ray HZE particles, evaluation methods 7-34295
 D₂O Cherenkov detector for solar neutrinos 7-40695

astronomical masers

- electron-cyclotron maser instability as a source of plasma radiation, solar appl. 7-66449
 HH 6, H₂O maser emission detect. 7-4539
 IC 4553, megamaser galaxy, 5 cm OH absorption 7-40911
 interstellar H₂O masers in star form. regions 7-4539
 IRAS sources in mol. clouds, search for H₂O masers 7-35066
 IRC +10420, post AGB star, mass-loss region, circumstellar environment and atm. chars. 7-66583
 Mira variables of short period, search for OH and SiO maser lines 7-14580
 OH-IR stars at Galactic Centre, showing SiO maser emission 7-60666
 Orion 8 km s⁻¹ H₂O maser source, time behaviour 7-24233
 S235B region, evidence for methanol maser emission from young stellar object 7-24188
 semi-regular variables of short period, search for OH and SiO maser lines 7-14580
 VX Sgr, VLBI obs. of SiO masers rel. to physical conditions in circumstellar envelope 7-55619
 solar type V continuum bursts, electron-cyclotron maser instability 7-47805
 stars, radio burst mechanism, fully relativistic electron maser 7-4317

astronomical masers continued

- H₂O maser emission from OH-IR stars, obs. in 23 objects 7-24140
 H₂O masers in nearby galaxies, luminosities and line profiles 7-14661
 H₂O masers near W3(OH), obs. of assoc. hot NH₃ emission 7-9525
 NH₃ maser and thermal emission obs. toward star-forming region (W51 IRS 2) 7-66702
 OH circumstellar masers assoc. with IRAS sources, Nancay radiotelescope obs. 7-34978
 OH IIa sources, nonthermal emission lines (*Chinese*) 7-66690
 OH maser emission from galaxies IR 1017+08 and Zw 475.056, 1667 MHz obs. 7-29539
 OH-IR stars near galactic centre, luminosities and progenitor characts. 7-14584
 SiO emission from evolved stars 7-47951
 SiO maser emission from OH-IR stars at Galactic Centre 7-60666
 SiO maser sources, monitoring obs. at 7 mm wavelength (1977 to 1979) 7-4449

astronomical observations

see also *gamma-ray astronomical observations*; *infrared astronomical observations*; *radioastronomical observations*; *ultraviolet astronomical observations*; *visible astronomical observations*; *X-ray astronomical observations*

- A0535+26/HDE 245770, X-ray/Be transient system, X-ray, UV and optical monitoring 7-55734
 Boulder 4201 active region, mag. field obs. (*Chinese*) 7-4396
 cold dark matter, ultralow background solar search 7-55393
 P/Comet Giacobini-Zinner, solar wind flow past comet 7-9426
 P/Comet Giacobini-Zinner (1984e), ion comp. and upstream solar wind obs. 7-60604
 P/Comet Halley, (1982i), energetic particles obs. by Giotto spacecraft 7-14529
 P/Comet Halley (1982i), bow shock position and struct. during Vega encounters 7-9423
 P/Comet Halley (1982i), coma mag. field characts., Vega obs. (*Russian*) 7-4381
 P/Comet Halley (1982i), cometary ion obs. at and within cometopause region 7-14530
 P/Comet Halley (1982i), dust coma meas. by Vega (*Russian*) 7-4380
 P/Comet Halley (1982i), dust environment, Vega SP-2 expt. obs. (*Russian*) 7-4378
 P/Comet Halley (1982i), dust particles, Vega spacecraft Puma obs. (*Russian*) 7-4375
 P/Comet Halley (1982i), hydromagnetic waves near O⁺ or H₂O⁺ ion cyclotron freq. 7-9419
 P/Comet Halley (1982i), inner coma critical ionization velocity effects 7-9424
 P/Comet Halley (1982i), ion dynamics and distrib., Suipei spacecraft observations 7-9420
 P/Comet Halley (1982i), ion tail disturbance, 31 Dec. 1985 event 7-9418
 P/Comet Halley (1982i), plasma and neutral gas meas. from Vega 1 and 2 spacecraft 7-14523
 P/Comet Halley (1982i), solar wind interaction meas. by Vega spacecraft 7-14522
 P/Comet Halley (1982i), Suipei spacecraft observations of pickup ions 7-9422
 P/Comet Halley (1982i), upstream cometary pick-up ion observations 7-9428
 P/Comet Halley (1982i), Vega SP-1 obs. of dust coma (*Russian*) 7-4379
 P/Comet Halley (1982i), Vega-1 meas. of secondary electron currents induced by impacts 7-14521
 P/Comet Halley (1982i), Vega-1 neutral gas obs. (*Russian*) 7-4382
 P/Comet Halley (1982i), wave and plasma meas. on Vega-1 and Vega-2 spacecraft 7-14524
 cosmic ray He nuclei, rigidity spectrum rel. to ³He/⁴He ratio at high energies 7-66410
 cosmic ray positron observations from 10 to 20 GeV, balloon-borne meas. using geomag. east-west asymmetry 7-66411
 cosmic rays, anomalous correl. between hadrons and electromagnetic particles 7-34816
 cosmic rays, Cerenkov pulse width of extensive air-showers with energies above 10¹⁵ eV 7-14459
 cosmic rays, diurnal anisotropy vars. rel. to heliospheric transport parameters 7-66408
 cosmic rays, penetrative high-energy showers obs. in Chacaltaya emulsion chamber 7-34815
 cosmic rays, temporal fluctuations at rigidities 4 to 180 GV 7-14427
 cosmic rays in outer heliosphere, spacecraft obs. of H⁺ and He²⁺ 7-9342
 cosmic rays solar diurnal anisotropy, secular changes in upper cut-off rigidity 7-66407
 Crab Nebula, EAS, composition anal., distrib. functions 7-14461
 Cyg X-3, EAS, composition anal., distrib. functions 7-14461
 Cyg X-3, Oct. 1985 RF burst and gamma-ray event, cosmic ray shower observations 7-66790
 Cygnus X-3, underground muons, new evidence from Soudan 1 7-40863
 early-type stars, spectral energy distrib. from 0.15 to 4.8 μm 7-29466
 galactic cosmic radiation, H and He isotopes rel. to source abundances and interstellar propag. 7-55394
 gravitational wave detection experiments, correl. of geophys. factors 7-47697
 IC 443, supernova remnant, multiwavelength investigation 7-40896
 Kamioka solar neutrino search 7-40694
 M87, effect of radio jets on X-ray emission from galactic halo 7-66752
 M87, relation of jet to nearby Virgo cluster galaxies 7-35047
 Markarian galaxies, catalogue 7-55496
 MKN 739, multiple nucleus galaxy, interstellar characts. 7-55790
 neutrinoless double beta-decay, ultralow background solar search 7-55393
 BV Pup, dwarf nova, X-ray, UV and optical obs. 7-47922
 Seyfert galaxies, narrow-line, with permitted Fe II emission (Mrk 507, 5C 3.100, I Zw 1), optical, X-ray, and IR props. 7-66751
 SN 1987A in LMC, neutrino signal obs. (1987 February 23) 7-66637
 solar axions, ultralow background search 7-55393
 solar constant, meas. by Earth Radiation Budget Experiment (ERBE) (1984 October 25 to 26) 7-9067
 solar constant, vars. during 1978-9 and 1981 from Nimbus-7 and SMM meas. 7-4409
 solar flare electrons exciting type III radio bursts, electron speeds determ. 7-66533

astronomical observations continued

- solar flare particles, element abundances rel. to temp. of energetic particle emission regions 7-66532
 solar flares with cosmic ray emissions, time behaviour of EM radiation 7-29453
 solar particle events, pitch angle distrib. obs. rel. to local scatt. props. of interplanetary medium 7-55392
 solar wind, ion composition meas. using Prognostic-10 BIFRAM instrumentation 7-55409
 solar wind, loop structure behind travelling shock event, props. 7-60501
 solar wind, near-Earth shock, ions distrib. function dynamics 7-55406
 solar wind, near-Earth shocks, plasma waves characts., BUDVAR complex obs. 7-55407
 solar wind, shock-associated energetic particles, Intershock project EPSW expts. obs. 7-55408
 solar wind, shocks fine struct., BIFRAM plasma spectrometer meas. 7-55405
 solar wind, vel. waves rel. to cometary flares 7-4371
 Venus, gravity studies of Aphrodite Terra 7-34899
 Venus, lightning evidence 7-47746
 Virgo cluster galaxies, relation to M87 jet 7-35047

astronomical observatories

- advanced technology optical telescopes, conf., Tucson, United States (March 1986) 7-55886
 British long-baseline gravit. wave observatory, feasibility study 7-29408
 Cagliari Astronomical Observatory, Sardinia, diurnal and annual vars. in water vapour contents 7-40547
 Cerro Tololo Inter-American Observatory, atmospheric extinction meas. 7-47542
 Keck Observatory 10m telescope, design and development work status, fabrication plans 7-40693
 Large Deployable Reflector, development of lightweight glass mirror segments 7-37226
 McDonald Observatory, Texas, 20 years of atmospheric extinction meas. (1960 to 1980) 7-47541
 Mount Graham Submillimetre Telescope project 7-60554
 Mount Wilson star 7-48264
 Northern Hemisphere Observatory, results from Isaac Newton Telescope 7-24011
 site testing, conf., La Silla, Chile (Oct. 1983) 7-35117
 D₂O Cherenkov detector for solar neutrinos 7-40695

astronomical spectra

- see also *stellar spectra*
 0133+476, 0235+164, 1749+096, 2131-021, variable quasars, spectral evolution from multifreq. radio obs. 7-40955
 1146+111 B,C, quasar, evidence against gravit. lens nature, spectral obs. 7-29553
 1701+610, QSO with tidal tail, CCD imaging and spectroscopic obs. 7-4589
 Abell galaxy clusters, radio spectral indices from obs. at 11.1, 6.3 and 2.8 cm 7-18454
 acousto-optical spectrographs for ground and space submm astronomy 7-34877
 active galactic nuclei, computational methods for emission-line spectrum 7-9534
 active galactic nuclei, emission spectrum of high-density photoionisation models and low-ionisation lines 7-9535
 active galactic nuclei, IUE meas. rel. to X-ray characts. 7-66770
 active galactic nuclei, narrow emission line region o III 500.7 nm forbidden line 7-40933
 active galactic nuclei, new accretion disk models rel. to optical and UV spectra 7-60813
 active galactic nuclei, spectroscopic obs. and red shifts 7-4566
 active galaxies, H I 21-cm emission obs. 7-48066
 anomalous Zeeman effect, moments and expansion coeffs. 7-66443
 anomalous Zeeman effect and its influence on the line absorption and dispersion coefficients 7-60513
 B2 1225+317, QSO, high-resolution spectroscopy of z=1.79 absorpt. line system 7-66782
 B2 1225+317, quasar, Lyman-alpha forest from 3140 Å to 3940 Å 7-48097
 B2 1320-299, quasar with asymmetric radio struct., spectral indices and morphology 7-35065
 B335, Bok globule, cyanoacetylene obs. 7-18448
 B 335, compact bipolar outflow source, EHF obs. 7-47893
 bidirectional reflectance spectroscopy, extinction coeff. and opposition effect in particulate medium 7-24033
 blazars, spectral properties of blazars in for UV, IUE obs. 7-48074
 blazars, spectral properties of X-ray selected objects 7-48075
 blue compact galaxies, spectrophotometric anal. 7-40920
 blue irregular galaxies, massive star content determ. from IUE obs. 7-48088
 3C 120, Seyfert galaxy, UV and optical obs. in two different states 7-55832
 3C 273, quasar, particle accel. in jet hotspot rel. to radio to IR spectrum 7-14676
 4C 29.30, extended optical line and radio emission, galaxy merger 7-55805
 3C 371, N-galaxy/BL Lac object, X-ray energy spectrum obs. 7-55802
 3C 428, neglected 3C radio source, spectral index and polarisation distrib. from VLA obs. 7-14672
 Cas A, appl. of H I lines broad wings obs. to tenuous gas expansion vel. determ. 7-66691
 Cas A, fast moving knot, IR spectral and photometric meas. 7-66708
 Cas A, supernova remnant, 1.2-mm map rel. to synchrotron and IR spectra 7-24176
 Case emission-line galaxies in direction of Bootes void, spectroscopic survey 7-29534
 Cen A (NGC 5128), X-ray intensity and spectrum obs. from Tenma 7-55828
 Cen Z (NGC 5128), hard X-ray/soft gamma-ray spectrum from obs. at MeV energies 7-66754
 central galaxies in southern clusters, optical spectra rel. to evidence for star form. 7-55821
 Clump 1, unusual mol. cloud complex near galactic centre, ¹²CO and ¹³CO obs. 7-48044
 clusters of galaxies, components red shifts determ. 7-60817
 Cn1-1, planetary nebula, dust and central star characts. 7-35019
 Cologne 3m radiotelescope acousto-optical spectrometers 7-34878
 Cologne 3m radiotelescope mm and submm spectrometer 7-34871

astronomical spectra continued

- P/Comet Crommelin (1984 IV), scanner spectral obs. 7-34934
P/Comet Giacobini-Zinner (1984e), column densities, prod. rates and spectral obs. 7-47767
P/Comet Giacobini-Zinner (1984e), H₂O prod., CO₂⁺ and plasma concentrations, spectrophotometric obs. 7-47793
P/Comet Giacobini-Zinner (1984e), high dispersion spectral obs. 7-47792
P/Comet Giacobini-Zinner (1984e), spectral obs. during ICE encounter 7-18380
P/Comet Giacobini-Zinner (1984e) spectral obs. 7-60604
P/Comet Halley, (1982i), bacterial grain model for 2 to 4 μ m spectrum 7-34937
P/Comet Halley, (1982i), in situ photopolarimetric meas. of dust and gas in coma 7-14527
P/Comet Halley (1982i), 1986 March spectral characts. (Chinese) 7-29426
P/Comet Halley (1982i), 3 μ m spectroscopy and photometry 7-24070
P/Comet Halley (1982i), 52-hour periodicity in emission-line fluxes 7-55563
P/Comet Halley (1982i), Fabry-Perot ground-based obs. 7-18377
P/Comet Halley (1982i), far UV spectral images from sounding rockets 7-47785
P/Comet Halley (1982i), ground-based obs. of 3.2-3.6 μ m emission features 7-24071
P/Comet Halley (1982i), H α and 630 nm meas. 7-18378
P/Comet Halley (1982i), HCN detect. 7-60598
P/Comet Halley (1982i), HCN production 7-24072
P/Comet Halley (1982i), high dispersion spectral obs. 7-47792
P/Comet Halley (1982i), line profiles and images 7-18356
P/Comet Halley (1982i), MMT spectroscopic obs. (1986 Nov.) 7-47771
P/Comet Halley (1982i), near IR obs. from Vega-2 spacecraft 7-14520
P/Comet Halley (1982i), O, C and CO prod. rates determ., UV spectra anal. 7-18379
P/Comet Halley (1982i), OH emission and absorption meas. at 18 cm 7-55572
P/Comet Halley (1982i), polarimetry of visible and UV molecular bands 7-66503
P/Comet Halley (1982i), post-perihelion obs. of H₂O from KAO 7-47786
P/Comet Halley (1982i), rocket-borne UV spectroscopy, CO and C abundances 7-47784
P/Comet Halley (1982i), role of CO₂ in outbursts 7-47783
P/Comet Halley (1982i), search for CO⁺ MM-wave transitions 7-24081
P/Comet Halley (1982i), spectral and visible magnitude obs. 7-55554
P/Comet Halley (1982i), spectroscopy of 3.4 μ m emission feature 7-55537
P/Comet Halley (1982i), UV spectrum evol. (1985 September to 1986 June) 7-47794
P/Comet Halley (1982i), Vega IKS IR spectrum 7-40775
P/Comet Halley (1982i), Vega IR spectral obs. (Russian) 7-4376
P/Comet Halley (1982i), Vega three-channel spectroscopy in visible and near-UV ranges 7-14519
P/Comet Halley (1982i), Vega-2 TKS expt. obs. (Russian) 7-4377
P/Comet Halley (1982i) 7-40777
P/Comet Halley (1982i) search for H₃O⁺ emission 7-9524
Comet Hartley-Good (1985 XVII), polarimetry of visible and UV molecular bands 7-66503
Comet Sorrells (1986n), MMT spectroscopic obs. (1986 Nov.) 7-47771
P/Comet Urata-Nijima (1986o), MMT spectroscopic obs. (1986 Nov.) 7-47771
Comet Wilson (1986l), MMT spectroscopic obs. (1986 Nov.) 7-47771
Comet Wilson (1986l), OH line emission obs. 7-66511
Comet Wilson (1986l), total visual magnitude estimates, spectra and CCD imaging 7-4367
cometary nebulae, thin jets, pinch effect mechanism and spectral characts. 7-29473
comets, ³²S₂ photodissoc. lifetime rel. to near-IR [S I] emission 7-24075
comets, IUE observations and UV characts. 7-47791
comets, optical and near-IR obs. rel. to wavelength depend. of grain scatt. 7-55535
comets, submm spectroscopy 7-47795
comets, UV spectra, S compounds identification 7-55574
compact blue dwarf galaxies, stellar populations and evol. 7-48078
compact H II regions, IRAS meas. 7-66695
cosmic microwave background, entropy of perturbed background radiation 7-66791
cosmic microwave background, temp. fluctuations induced by gravitational lensing 7-4595
cosmic microwave background radiation, temp. meas. at 3.3 mm wavelength 7-29556
Crab Nebula, 1.2 mm map rel. to synchrotron and IR spectra 7-24176
Crab Nebula, γ -ray spectral obs. 7-55857
CRL 618, proto-planetary nebula, H₂S(1) line profile 7-35031
V645 Cyg-Duck Nebula complex, characts. and obs. 7-60655
Cygnus Loop, high-resolution X-ray spectroscopic evidence of nonequilibrium conditions 7-48037
DDDM-1, C-poor halo planetary nebula, element abundances from optical and UV obs. 7-60766
dense molecular cloud cores, formyl radical and formyl ion obs. 7-48064
diffuse interstellar bands, C molecules as possible carriers 7-48020
diffuse interstellar bands, charge transfer model 7-55787
diffuse interstellar bands, constraints on dust grain hypothesis 7-55762
diffuse interstellar bands in LMC, obs. at 637.6 and 637.9 nm 7-55758
diffuse interstellar lines, astrophysical influences on line strengths 7-48021
diffuse microwave background radiation, temp. at 12 cm wavelength 7-55859
distant radiogalaxies, evidence for intervening lensing objects 7-35035
30 Dor, area spectroscopy of northern part of core 7-66698
dwarf galaxies, 21-cm line widths rel. to luminosity classification extension 7-60794
dwarf irregular galaxies, CNO abundances determ. 7-40939
dwarf irregular galaxies, search for ¹²CO emission from twelve objects 7-35033
1E 0104.2+3153, identification with BAL QSO, visible and X-ray obs. anal. 7-66787
early-type galaxies, H I content versus star form. and ionised gas 7-29528
early-type galaxies, X-ray surface brightness distrib. and spectral props. 7-55799

astronomical spectra continued

- early-type galaxies with emission lines, catalogue 7-60578
echelle spectrograph, camera lens system design 7-55475
echelle/CCD spectrograph obs. of extended objects at high dispersion 7-66474
EGG Nebula (CRL 2688), NH₃ and cyanotriacetylene mapping 7-4540
emission nebulae, implications of atomic data for astrophysics for element abundances 7-40689
emission-line galaxies showing WR emission features 7-35039
ESO 428-G14, new Seyfert 2 galaxy, photometric and spectroscopic study 7-9538
ESO-223-PN 10 and ESO-095-PN 12, planetary nebulae, abundance determ., spectrophotometric obs. anal. 7-66722
ESO-390-G 05, galaxy, abundance determ., spectrophotometric obs. anal. 7-66722
extragalactic H II regions, abundances and spectra 7-66742
extragalactic H II regions, collisional effects in He I triplets rel. to primordial He abundance 7-55446
extragalactic H II regions, He abundance and dY/dZ meas. 7-40937
faint galaxies as probes for distant Universe 7-4610
faint H α emission-line galaxies, spectral obs. 7-35032
faint object spectroscopy 7-55493
Fairall 9, Seyfert 1 galaxy, simultaneous EXOSAT and IUE obs. 7-66747
Far Infrared Submillimetre Space Telescope mission 7-34866
FIRST observational potential 7-48093
Fornax dwarf spheroidal galaxy, globular clusters radial vel. 7-14649
G1200-2038, dwarf galaxy with Seyfert characts., spectroscopy and imaging obs. 7-48069
G34.3+0.2, compact H II region, NH₃ obs. of warm molecular core 7-24173
G54.73+0.61, compact radio source, spectral index determ. from WSRT obs. 7-35057
G7.7-3.7, highly-polarised radio supernova remnant, spectral index and polarisation meas. 7-48045
galactic 511 keV line and positronium beams 7-62547
galactic centre, radio spectral indices from 43-GHz continuum obs. 7-24219
galactic centre neutral disk, CO and CS obs. 7-35040
galactic corona, IUE obs. rel. to kinematics, ionisation, and abundances 7-48054
galactic disk, obs. from l=-150° to l=82° in sub-millimetre range 7-4558
galactic halo study using γ -rays from WIMP annihilation 7-9542
galactic nuclei, 3.28 μ m feature and continuum emission obs. 7-9533
galactic nuclei, spectroscopic obs. for complete sample of galaxies 7-40921
galactic ridge radio recombination lines, origin from H272 α lines survey 7-66718
galaxies, C IV emission line behaviour in active nuclei, IUE spectra 7-60790
galaxies, large-scale distrib. determ. from wide-angle samples of objective-prism spectra 7-66771
galaxies, narrow emission line active objects, UV to IR continuum 7-40912
galaxies active nuclei, distrib. function description of cloud props. 7-29535
galaxies from Einstein Observatory sample, radio and X-ray props. of elliptical and SO galaxies 7-66753
galaxies near groups of galaxies, radial vel. meas. 7-4550
galaxy pairs and small groups, H I spectral characts. 7-14669
gamma-ray burst sources, spectra and thermal synchrotron radiation 7-48103
gamma-ray emission lines at 0.51 and 1.81 MeV from galactic centre, model for common origin 7-24238
gamma-ray line emission, constraint on origin of mass 22 nuclei in astrophysical environments 7-35069
GC 1556+335, quasar, ejected or intervening material model for absorpt.-line spectrum 7-29552
P/Giacobini-Zinner (1985 XIII), periodic emission-line flux vars. in near-nucleus zone 7-55564
giant extragalactic H II regions in nearby galaxies, integrated H α profiles 7-14624
giant planets, atm. study in submm range with FIRST 7-47743
globular clusters in M87, spectroscopic obs. 7-48001
Gum Nebula region, cometary globules and dark clouds obs. 7-55750
HD 50896, WR star, line of sight high-vel. interstellar gas detect., possible SNR 7-14627
Herbig-Haro objects exciting stars, evolutionary characts. determ. from spectral and lumin. meas. 7-40898
high-resolution submillimetre heterodyne spectrometer 7-353
Hydra I cluster of galaxies, red shifts determ. 7-60816
IC 1297, double-ring planetary nebula, spectrum and chemical analysis 7-60759
IC 351, high-resolution obs., fluxes and electron temp. of small planetary nebula 7-14629
IC 443, supernova remnant, multiwavelength investigation 7-40896
IC 443, supernova remnant, obs. in coronal [Fe X] 6374 Å line 7-48051
In torus, O I and S I densities from UV spectra 7-55522
instrumentation and techniques, conf., Tucson, AZ, USA (March 1986) 7-48162
intermediate Seyferts, emission line spectra, composite models 7-40913
interstellar 217 nm band, catalogue of equivalent widths 7-66479
interstellar 220 nm extinction feature, charge transfer model 7-55787
interstellar 220 nm feature, interpretation 7-48018
interstellar 443-nm diffuse absorption band, equivalent width obs. 7-24187
interstellar absorption lines towards SN 1987A in LMC, radial vel. systems identification 7-66637
interstellar bubbles, wind driven, soft X-ray spectra 7-4545
interstellar C₂, (3,0) Phillips band detect. towards ζ Oph 7-48043
interstellar C I, 809 GHz fine-structure line obs. in dense mol. clouds 7-66717
interstellar C II 232.5 nm line, appl. to C abundance determ. toward ρ Oph and β Sco. 7-9531
interstellar C IV and Si IV in local ISM, evidence from IUE obs. of late B-type stars 7-60771
interstellar CH, search for abundance vars. towards L134 dark cloud 7-66701
interstellar chemistry and submm astron. 7-48060

astronomical spectra continued

- interstellar clouds, dust IR spectra rel. to chemical evolution of molecules 7-48014
- interstellar CO, J=2-1 obs. of three southern star form. regions 7-18441
- interstellar cold clouds, CO radio-line profiles interpretation 7-4544
- interstellar cyanoacetylene, nonequib. excitation of rot. levels 7-60743
- interstellar cyclopropenylidene (C_3H_2), $2_{20}-2_{11}$ absorpt. line obs. in cold dark clouds 7-66716
- interstellar diffuse bands in reddened OB stars, molecular origins 7-66697
- interstellar dust, appl. of EXAFS studies 7-24185
- interstellar dust, submm characts. 7-48059
- interstellar dust, UV-visible extinction spectra of submicron amorphous C grains 7-35023
- interstellar extinction curves shapes, IUE anal. of 2175 Å bump 7-48039
- interstellar grains emission, radiative transfer rel. to grain models 7-48013
- interstellar H_2 line emission from centre of Galaxy, spatial distrib. and vel. field 7-9528
- interstellar H I in halo and LMC 7-60768
- interstellar IR silicate bands, exptl. investigations rel. to silicate dusts identification 7-48017
- interstellar matter, characts. 7-66725
- interstellar medium, IUE evidence for diffuse collisionally ionised C IV and Si IV below $Z=1$ kpc 7-55783
- interstellar medium, submm obs. 7-48058
- interstellar Mg I absorption line, IUE obs. rel. to limits on 'local fluff' 7-55782
- interstellar mm and sub-mm spectroscopy 7-14644
- interstellar molecular clouds, submillimeter spectral lines obs. in very dense regions 7-66711
- interstellar molecules, IR spectroscopy 7-14638
- interstellar Na I line strength versus reddening relation, influence on stellar population synthesis 7-9526
- interstellar nearby gas, IUE and optical spectral meas. 7-66729
- interstellar NH_3 , maser and thermal emission obs. toward star-forming region (W51 IRS 2) 7-66702
- interstellar OH 1667 MHz absorpt. towards Cas A, VLA obs. 7-55761
- interstellar PO, upper limits to abundances in dense clouds from microwave obs. 7-66713
- interstellar polycyclic aromatic hydrocarbon cations, doubly-charged 7-55774
- interstellar radiative shocks, dynamical models and line spectra of steady shocks 7-55454
- interstellar S and Zn in high density sight-lines abundances 7-66730
- interstellar submm mol. transitions 7-47698
- interstellar UV absorption lines, equivalent width data statistics and new oscillator strengths for Si II, Fe II and Mn II 7-55444
- interstellar UV absorption lines towards A0 V star HD 119921, C IV and Si IV lines obs. 7-48057
- interstellar UV extinction curves towards OB associations, statistical anal. of IUE obs. 7-55785
- interstellar UV extinctions towards OB associations and star-forming regions, IUE obs. 7-55786
- interstellar very broad-band extinction structure, obs. by combined uvby and UBv photometry 7-48019
- interstellar [Fe X] 637.5 nm absorpt. in galactic halo and LMC, implications for million degree gas 7-55758
- Io, ground-based IR obs. anal. 7-34916
- IR fine-structure transitions in gaseous nebulae, new collisional data 7-40689
- IR reflection nebulae in Orion Molecular Cloud 2, photometry, polarimetry and spectrophotometry 7-55765
- IRAS 00275-2859, identification as quasar, spectral characts. 7-18462
- IRAS 1912+172P09, new binary planetary nebula, spectroscopy and JHKL photometry 7-48046
- IRAS galaxies, sub-millimetre obs. 7-9532
- IRAS low resolution spectra atlas 7-24021
- IRAS low-temp. unidentified print sources, ^{13}CO and ^{12}CO obs. 7-48006
- IRAS sources in mol. clouds, search for H_2O masers 7-35066
- Jovian radio emission, S-burst spectra rel. to localisation of S-component sources 7-24049
- Juno, surface comp. and visible spectral characts. (*Russian*) 7-24047
- Jupiter, magnetosphere-Io torus system characts. 7-47758
- Jupiter, NH_3 abundance and cloud opacities determ. from Voyager IRIS data 7-24051
- Jupiter, origin of Io-phase-dependent S-bursts in decametric radio spectra 7-47753
- Jupiter, water vapour abundance and distrib. in atmosphere, IR obs. 7-60594
- L1551 molecular cloud, VLA obs. of 4.8 GHz H_2CO transition 7-60765
- BL Lac candidates, X-ray selected, optical spectroscopy of six objects 7-48085
- large interstellar molecules, thermal props., absorpt. bands, and chemical stability 7-24189
- LDN 1551-IRS 5, circumstellar CO abundance characts. 7-47893
- LDN 1641, second mol. cloud core discovery, EHF obs., HCN and H_2 mapping 7-14622
- line formation theory, statistical description of radiation fields on basis of invariance principle 7-23986
- LkHα 101, small-scale vel. struct. in nearby H I 7-48038
- local interstellar medium, multi-component vel. struct. 7-35018
- luminous axion clusters, photon decay, measurable luminosities 7-47694
- M175SW, molecular cloud, CO submm mapping 7-60748
- M17 (Omega Nebula), Hα vel. field 7-66704
- M17 molecular cloud, vel. struct. anal., CO mapping 7-60745
- M17 SW molecular cloud, submillimetre molecular spectroscopy with Texas MWO radio telescope 7-55763
- M31, NE spiral arm mol. complex, CO mapping 7-66734
- M33, H I survey Ing Westerbrook Synthesis Radio Telescope 7-66739
- M81, O and N abundance gradients from spectrophotometry of H II regions 7-40941
- M82, CO absorpt. line obs. rel. to large mol. halo or intergalactic mol. gas 7-24223
- M82, interstellar medium in central 1 kpc of active galaxy 7-55816
- M87 close companions, photometric and spectral characts. 7-66735
- Markarian 231, Seyfert 1 galaxy, morphology and nuclear spectroscopy 7-48067
- Markarian 231, Seyfert galaxy/QSO, CO (J=1-0) emission detect. and optical imaging 7-66757

astronomical spectra continued

- Markarian 306, double nucleus galaxy, spectroscopic investigation 7-24199
- Markarian 35 (=NGC 3353), spectrophotometric characts. 7-40910
- Markarian 380 as $z=0.475$ Seyfert galaxy, spectrophotometry 7-40915
- Markarian 3, Seyfert 2 galaxy, dust in emission-line gas 7-66746
- Markarian 490, high ionisation starburst galaxy, spectroscopic and imaging obs. 7-4574
- Markarian galaxies, catalogue 7-55496
- MC 1331+170, QSO, limit on surface brightness of Lyman alpha disk absorber 7-4587
- Mercury, K discovery in planetary atmosphere 7-24036
- merged galaxies remnants, vel. dispersions and evol., spectral obs. 7-55797
- metal rich globular clusters, spectral characts. 7-14614
- meteorites optical spectra, comparative anal. of spectral props. of achondrites and ordinary chondrites 7-66521
- methanol, torsionally excited, in hot mol. cloud cores, centimetre-wave lines obs. 7-48005
- MKN 739, multiple nucleus galaxy, interstellar characts. and obs. 7-55790
- molecular clouds, plasma characts. and Cherenkov microwave emission-line mechanism (*Chinese*) 7-66690
- molecular observations with Cologne University 3-m radio telescope, obs. 7-24004
- molecular outflow sources, NH_3 obs. anal. 7-66576
- molecular spectra, program for symmetry-adapted rotational eigenfunctions and energy levels of asymmetric top molecules 7-4324
- molecular spectra of the outer planets and satellites 7-14511
- molecular time-resolved spectroscopy 7-14491
- MR 2251-178, quasar, spectral obs. of knots detected in O III 495.9+500.7 m forbidden lines emission 7-35060
- MSH 05-22(0503-286), giant radiogalaxy characts. 7-40918
- N44C1, LMC H II region, exciting star characts. 7-40892
- narrow absorption lines from cooling flows in intracluster gas 7-66761
- nebulae, O and N abundances determ. from far-IR emission-lines 7-40722
- Neptune, geometric albedo between 2100 and 3350 Å 7-24062
- NGC 1023-1023A as interacting galaxies, spectral and photometric characts. 7-35037
- NGC 1068, high-excitation extranuclear gas, spectrophotometry of Seyfert galaxy 7-24211
- NGC 1068, Seyfert galaxy, detect. of broad UV Fe II lines in spectrum of nucleus 7-14663
- NGC 1566, barred spiral galaxy, imaging spectroscopy of spiral arm 7-24214
- NGC 2024, H II region, VLA maps of formaldehyde absorpt. 7-48041
- NGC 2071, refl. nebula, nearby bipolar flow source NH_3 obs. 7-24181
- NGC 2403, spiral galaxy, chemical comp. gradient and stellar mass limit 7-40940
- NGC 2798, interacting galaxy, evidence from UV spectroscopy from starburst in galactic nucleus 7-55830
- NGC 3256, galaxy, evidence from UV spectroscopy from starburst in galactic nucleus 7-55830
- NGC 3448, amorphous galaxy, photometry and H I dynamics 7-35041
- NGC 3923 and 3051, shell galaxies, shell lumin. characts., spectrophotometric obs. 7-55796
- NGC 4151, Seyfert 1 galaxy, C IV 155 nm line profile obs. (1978 to 1983) 7-60814
- NGC 4151, Seyfert 1 galaxy, obs. of new outflowing absorpt. component in Mg II line profile 7-55834
- NGC 4151, Seyfert galaxy, detect. of intense Fe line emission at 6.4 keV 7-18452
- NGC 4214, 4449, blue irregular, galaxies, kinematics of H II regions 7-40925
- NGC 4922, binary galaxy, spectrophotometric investigation 7-24200
- NGC 5023, edge-on dwarf galaxy, H I layer thickness 7-24208
- NGC 5383, barred spiral galaxy, CO obs. 7-55827
- NGC 5506, Seyfert galaxy, EXOSAT obs. of fractal X-ray time variability and spectral invariance 7-66764
- NGC 5548, Seyfert 1 galaxy, double broad-line emitting regions as evidence for supermassive binary system 7-66756
- NGC 5548, Seyfert 1 galaxy, evidence for black hole accretion event, He II obs. 7-35052
- NGC 5548, Seyfert 1 galaxy, optical spectrum vars. rel. to multiple-component broad-line region 7-66750
- NGC 55, magellanic-type galaxy, H I and radio continuum obs. 7-9539
- NGC 7023, outflow source, CO mapping 7-60772
- NGC 7293 (Helix Nebula), outer filament high radial vel. 7-60767
- NGC 7469, Seyfert 1 galaxy, EXOSAT obs. of rapid hard X-ray variability and soft X-ray excess 7-48077
- NGC 7469, type 1 Seyfert galaxy, emission lines mapping rel. to circumnuclear starburst 7-29536
- non-cosmological redshifts of spectral lines 7-66459
- nonlinear problem of incoherent anisotropic scatt., soln. 7-4309
- OH 5 cm absorption towards IC 4553, megamaser galaxy 7-40911
- OMC-1, NH_3 line emission, search for linear polarisation 7-48011
- OMC-1, obs. of P(2,1) line of H_2O^+ 7-9524
- OMC-1, submillimetre molecular spectroscopy with Texas MWO radio telescope 7-55763
- optical H II regions, possible connection with mol. clouds, CO obs. 7-40887
- Ori A, monitoring obs. of SiO maser emission at 7 mm wavelength (1977 to 1979) 7-4449
- Orion A, He abundance, spectral obs. (*Russian*) 7-40951
- Orion KL, NH_2D detect. and abundance 7-60754
- Orion Molecular Cloud 1, H_2 line polarisation obs. rel. to discovery of H_2 refl. nebula 7-14633
- Orion Nebula, element abundance determ. from IUE lines 7-55784
- Orion Nebula, ionization structure, IR line obs. and models 7-60757
- Orion Nebula intense 6.7-keV Fe X-ray emission line detect. from high-temp. plasma 7-55780
- Orion region, extinction and dust characts. 7-66728
- Orion-KL region, maps of high-vel. CO outflow 7-29522
- pentynylidene radical (C_5H), detect. of $^{13}C_{3/2}$ state (in IRC+102.16) 7-23988
- Perseus dark clouds, visual extinction and CO emission 7-14623
- Perseus globules, physical and chem. conditions, NH_3 and cyanoacetylene obs. 7-35021
- PG 0946+301, broad absorption line QSO, spectrum from 550 to 4250 Å 7-55852

astronomical spectra continued

- PG 1351+64, low-luminosity quasar, UV and optical variability obs. 7-55851
- PHL 61, identifications of quasar radio absorption lines 7-29551
- PHL 61, quasar, search for CO (*Russian*) 7-40957
- PHL 61, quasar, spectral obs. (*Russian*) 7-40958
- PHL 957, QSO, limit on surface brightness of Lyman alpha disk absorber 7-4587
- PHL 957, quasar, absorpt. line systems nature 7-35061
- Pisces-Perseus supercluster galaxies, 21-cm survey in declination zone +21.5° to +27.5° 7-4576
- PKS 1912-54 and 2135-14, QSO absorption line systems 7-40953
- PKS 2005-489, BL Lac object, spectral characts. 7-18450
- PKS 2152-69, detached nuclear-like activity, CCD obs. of radiogalaxy 7-55824
- PKS 2155-304, BL Lac object, IUE obs. (1979 to 1985) 7-55833
- planet thermal emission, model spectrum reconstruction 7-66484
- planetary nebulae, abundances of C III and N IV, C II and N III recomb. lines anal. 7-4538
- planetary nebulae, internal motions in 32 genuine PNe and misclassified object 7-4541
- planetary nebulae, line and continuum spectra of rarefied cosmic plasma (*German*) 7-55776
- planetary nebulae, spectroscopic obs. of 21 genuine and misclassified objects 7-66703
- planetary nebulae, UV spectra interpretation, dissertation 7-66724
- compact planetary nebulae, wind-shell model for radio continuum spectra 7-55751
- planetary nebulae and related objects, IUE Atlas 7-48056
- planetary nebulae in LMC and SMC, IUE survey 7-48055
- planetary spectra, Gaussian anal. of temp. effects on 1-μm refl. spectra of mafic minerals 7-29006
- Population III, heating of dust and radiative spectrum (*Chinese*) 7-66680
- Population III stars, evidence in isotropic background radiation 7-47998
- propyne, 2₀ band study, Fourier transform IR spectra anal. rel. to Titan atmosphere 7-50119
- protogalaxies and protocluster pancakes, IR line emission 7-4600
- protostar formation regions, submm astronomy with FIRST 7-47890
- Q0118-031B, optimal extraction of spectra from obs. with two-dimensional detectors 7-47729
- Q1100+772, Q2201+315, intermediate-redshift quasars, line profiles from high signal-to-noise UV spectra 7-55850
- QSO absorption lines origin 7-60828
- QSOs, C IV absorpt. systems characts. 7-66780
- QSOs, emission line profiles from Keplerian cloud ensembles 7-4586
- QSOs, high-redshift, from UK Schmidt Telescope objective prism plates, spectroscopic obs. 7-24236
- QSOs in PC survey, obs. of low-z broad absorption line objects 7-24234
- quasar candidates, objective-prism survey rel. to quasar distrib. clustering (*Chinese*) 7-4581
- quasar candidates among flat-spectrum radio sources, optical spectra and redshifts (*Chinese*) 7-4582
- quasar candidates in SA 94 field, objective-prism classification of US objects 7-66779
- quasar in direction of LMC (0557-672), V-magnitude and redshift 7-4592
- quasar pairs, absorpt. line spectra rel. to galaxy correls. and quasars environment 7-24216
- quasars, absorption line systems characts. 7-35058
- quasars, effects on spectrum and brightness of gravit. micro-lensing 7-9364
- quasars, energy puzzle of broad line region 7-9553
- quasars, H I 21-cm emission obs. 7-48066
- quasars, low-redshift, archival study of IUE obs. 7-60835
- quasars, Lyman α and 21 cm lines form., role of dwarf galaxies and globular star clusters 7-40952
- quasars, new accretion disk models rel. to optical and UV spectra 7-60813
- quasars, nonspherical clouds model for Lyman-alpha absorpt. lines 7-60805
- quasars, UV continuum shape from IUE obs. 7-55849
- quasars damped Ly α absorption, implications for disk galaxies form. 7-55794
- quasars from PG survey, X-ray spectra, X-ray to IR continuum 7-48094
- quasars L α absorption systems, constraints on intergalactic voids at high redshifts 7-55823
- quasars of large redshift, CCD survey and spectral obs. 7-55846
- quasars UV spectra, evidence for redshift evolution of intergalactic absorpt. clouds number density 7-55829
- radio galaxies, spectral index distrib. for edge-brightened double sources from 0.6 GHz mapping 7-66737
- radio recombination line emission towards galactic centre, constraints on ionised gas props. 7-66719
- radio sources, extragalactic, spectral index-flux density relation at 408 MHz rel. to cosmological evolution 7-4578
- radioastronomical spectra (book) 7-35140
- RCW 103, young supernova remnant, obs. of expanding shells in filamentary edge of remnant 7-14632
- Red Rectangle (HD 44179), role of visible luminesc. from polycyclic aromatic hydrocarbons 7-48008
- reduction of spectra, summary of available programs 7-4350
- reflectance spectra, absorption band positions extraction 7-14503
- reflection nebulae, IUE obs. review 7-66726
- resonance scattering spectra appl. to very weak mag. fields diagnostics in diffuse media 7-23991
- S140 IRS 1, CO obs. of assoc. bipolar outflow 7-66710
- S235B region, mol. line obs. of young stellar object 7-24188
- Saturn rings, IUE spectral obs. 7-47759
- Saturn satellites, telescopic obs. 7-34919
- Selected Area 57 quasar candidates catalogue of multicolour photometry, variability and astrometry 7-4591
- Seyfert 1 galaxies, emission line profiles and profile ratios 7-55818
- Seyfert galaxies, absolute spectrophotometry 7-24228
- Seyfert galaxies, CO emission, spatial distrib. and central source 7-55808
- Seyfert galaxies, emission-line variability 7-14648
- Seyfert galaxies, IUE obs. and comparison with low-redshift quasars 7-60835
- Seyfert galaxies, narrow-line, with permitted Fe II emission (Mrk 507, 5C 3.100, I Zw 1), optical, X-ray, and IR props. 7-66751
- Seyfert galaxy nuclei, near-UV spectroscopy rel. to reddening and Bowen fluoresc. 7-55801

astronomical spectra continued

- Seyfert-1 galaxies, UV spectra rel. to nature of broad-line region 7-55831
- Sgr B2, obs. of P(2,1) line of H₃O⁺ 7-9524
- Sh2-155, emission region, blue refl. nebula detect., emission-line characts. 7-66723
- Sh2-235, mol. cloud-ionised emission nebula interface modelling, C recomb. lines obs. anal. 7-48012
- SMC N2, planetary nebula, speckle obs. and spectrum rel. to expansion rel. and age 7-24183
- SN 1987A in LMC, line of sight interstellar spectral features 7-66629
- SN 1987A in LMC, line-of-sight interstellar-intergalactic material 7-66632
- southern spiral galaxies, BV photometry and radial vel. 7-66768
- spherical stellar systems, line profiles for completely analytical family of anisotropic Plummer models 7-55741
- spiral galaxies, star form characts., far-IR lumin. and CO line obs. anal. 7-4563
- spiral galaxies in Virgo Cluster, radio continuum spectra 7-9540
- star clusters, grid of properties, use for population synthesis 7-29518
- star formation regions, far IR, submm and mm dust emission spectra 7-24180
- starburst galaxies, spectroscopic study 7-24222
- submillimetre molecular spectroscopy with Texas MWO radio telescope, results from OMC-1 and M17 SW mol. clouds 7-55763
- submm heterodyne spectroscopy 7-31041
- supercritical winds, Comptonisation and spectral evol. 7-55437
- supergiant elliptical galaxies, spectroscopic studies, dissertation 7-66769
- supernova remnants, colliding, oblique shock refls. rel. to anomalous H I vel. features 7-24175
- supernova remnants, H I 21-cm emission during radiative expansion stage 7-60744
- supernova remnants, nonsteady shock model for permitted O I line emission from O-rich nebulosity 7-55779
- synchrotron radiation, corrections in derivation of formulae 7-55442
- thin disk model for UV excess of quasars and Seyfert 1 galaxies 7-40956
- Titan, Voyager IRIS spectra rel. to N₂+N₂ collisions 7-60521
- Titan (Saturn VI), HCN detect. at 88 GHz 7-9410
- Tully-Fisher relation, type effect and Malmquist bias 7-14646
- Uranus, geometric albedo between 2100 and 3350 Å 7-24062
- Uranus, methane-d, detect. at 1.6 μm wavelength 7-55529
- urea, rot. transition, appl. to interstellar studies 7-10559
- Ursa Major I(S) group galaxies, ¹²CO and far-IR obs. 7-29548
- UV imaging photon detector, large format for astronomical spectroscopy 7-56342
- UV lines of highly ionized atoms in cooling gas 7-23992
- UV standard stars for calibration of Hubble Space Telescope, IUE spectra 7-60735
- Vela supernova remnant, spectral index distrib. rel. to radio emission from Vela X 7-24174
- Venus, UV balloon obs. 7-14512
- Venus, Venera 11 and 12 meas. of He I 58.4 nm emission rel. to outgassing history 7-9396
- very local interstellar medium, IUE study 7-66727
- Virgo Cluster spiral galaxies, CO obs. 7-55800
- VIRIS-VAX interactive reduction of IUE spectra 7-40720
- W3(OH), hot NH₃ obs. towards H₂O masers near W3(OH) 7-9525
- wideband spectrometer backends, review 7-34876
- X-ray continuum emission from optically thin plasmas, approximation formulae for nonrelativistic average Gaunt factors 7-18349
- X-ray sources, effects of one-generation pair production in synchrotron self-Compton sources 7-55452
- YM 29 (Sharpless 274) spectrograms and emission-line study of planetary nebula 7-55756
- ^{e+}^{e-} annihilation in interstellar H₂ gas, laboratory simulation 7-14426
- ²⁶Al, interstellar, gamma-ray line emissivity from Wolf-Rayet star prod. 7-47830
- C₂ spectra in comets, synthetic Swan band profiles of ¹²C¹²C and ¹²C¹³C 7-60532
- CN, oscillator strengths and dissociation energies 7-4327
- CO line formation in bipolar flows, line profiles in accelerated outflows 7-48042
- CO measurements with submm heterodyne spectrometer 7-60562
- CS⁺, upper limits in diffuse interstellar clouds 7-35020
- Fe II, UV doubly-excited lines obs. in laboratory and in A-type star 21 Peg 7-66585
- H I, recombination line intensities, Case B calcs. 7-57023
- H I absorpt. line profile in microwave background, effects of gas heating in presence of H₂ 7-24205
- H I line profiles from Southern Milky Way, results from fully-sampled survey 7-40894
- H II regions, dust characts. 7-40901
- H II regions, extragalactic, line ratios modelling rel. to element abundances 7-40903
- H II regions, H radio recombination line emission 7-60746
- H II regions, photoionisation models rel. to abundances and ionising star temp. determ. 7-40907
- HC₃N, interstellar, J=4-3 line obs. in TMC-1, DR-21 and M17 rel. to mol. clouds struct. (*Russian*) 7-55777
- H₂NC⁺, interstellar mol., pot. energy surfaces, ab initio MO theory 7-19687
- HN₂O⁺, millimetre-wave spectrum and mol. consts. 7-29387
- H₂O masers in nearby galaxies, luminosities and line profiles 7-14661
- H₂O-NH₃ ice mixtures, optical consts. determ. 7-23993
- H₃O⁺, P(2,1) line obs. in interstellar medium and Periodic Comet Halley (1982i) 7-9524
- He II, recombination line intensities Case B calcs. 7-57023
- Li differential depletion in diffuse interstellar clouds 7-66706
- Mg IV forbidden lines, electron impact excitation rate coeffs. for Mg³⁺ 7-55455
- Mg V forbidden lines, electron impact excitation rate coeffs. for Mg⁴⁺ 7-55455
- NH radical, rot.-vibr. anal. for X³Σ⁻ state, IR Fourier transform spectra 7-19847
- Na-like ions, relative emission-line strengths for Al III and Si IV in Sun 7-47799
- O II forbidden lines, improved radiative transition probabilities 7-66442
- OH absorption in extragalactic sources, Arecibo survey 7-40895
- OH, interstellar, obs. of highly excited states towards galactic H II regions 7-24177

astronomical spectra continued

- OH interstellar clouds vel., use for Sun-galactic centre distance determ. 7-4554
- OH, laboratory meas. of rot. spectrum with tunable far-IR radiation 7-47691
- OH maser emission from galaxies IR 1017+08 and Zw 475.056, 1667 MHz obs. 7-29539
- OH radical, Cherenkov microwave line emission mechanism for mol. clouds spectra (*Chinese*) 7-66690
- Si II, interstellar, UV equivalent width data statistics and new oscillator strengths 7-55444

astronomical spectroscopy *see astronomical spectra; spectroscopy***astronomical techniques**

see also astrometry; radioastronomical techniques

- N-body hierarchical force calc. algorithm with N log N growth 7-47673
- active galactic nuclei modelling, computational methods for emission-line spectrum 7-9534
- advanced image processing and planetological appl., conference, Vulcano, Italy (September 1985) 7-24270
- asteroid rotation characteristics determ. methods 7-34906
- asteroids photometry, system from spectral props. of achondrites and ordinary chondrites 7-66521
- astrometry, statistical model for Tautenburg Schmidt plates 7-66432
- atmospheric Cerenkov technique, appl. to obs. of very-high-energy gamma rays from astronomical objects 7-60916
- automatic spectrogram reading on SAO AS USSR photometric complex 7-66472
- Be stars, rot. determ. method (*Chinese*) 7-66467
- CCD imaging at low-light-levels 7-47703
- Chandrasekhar perturbation methods for rotating polytropic stars, error-removing techniques 7-14559
- P/Comet Halley, dust impacts and detectors on space probes 7-34946
- cometary coma morphology and dust emission pattern modelling, appl. to P/Halley (1982i) 7-14526
- cometary dust studies using ground-based near-IR obs. (*Chinese*) 7-18357
- complete linearisation method appl. to solar prominences emission lines anal. (*Chinese*) 7-4391
- computerised image detection system for Kiso Schmidt plates, appl. to Orion Association 7-55477
- coronal magnetic fields analysis, struct. and stability determ. via dynamic relaxation technique 7-55592
- cosmic ray research, toroidal coil configurations 7-40699
- cosmic ray track analysis by expert system using distributed problem solving 7-55388
- cosmic-background neutrino detection using acoustic phonon scattering technique 7-55476
- coude radial velocity obs. at Calar Alto Observatory, zero-point and accuracy 7-29409
- data decomposition into sum of nonlinear functions, appl. to astronomical obs. 7-4347
- deconvolution method for photometric and spectroscopic obs., theory and appl. 7-4348
- delta-S method for RR Lyr type stars metal abundance determ. 7-66476
- differential speckle imaging with the cophased Multiple Mirror Telescope 7-55490
- digital image processing techniques used in astronomy, appl. to diff. data 7-11828
- distance calibration, mean absolute magnitudes and trigonometric parallaxes 7-60624
- distance calibration, proper motion effects of stars 7-60625
- dynamical system parameters estimation from obs. appl. of local polynomials 7-34887
- Earth rotation parameters determ., appl. of lunar laser ranging data (*Chinese*) 7-3959
- Earth rotation parameters determ. estimation of accuracy in different freq. bands 7-54843
- Earth rotation parameters determ. optimal conditions (*Chinese*) 7-3960
- echelle spectroscopy, scattered light background correction method 7-34874
- electro-optical meteor observation, techniques and results 7-47716
- element abundances determ. in gaseous nebulae, results from IUE lines anal. 7-55784
- external potentials expansions of ellipsoidal bodies, analytical continuation 7-47719
- extrasolar planets, search methods 7-55722
- faint object spectroscopy 7-55493
- far-IR emission-lines from nebulae, use for O and N abundances determ. 7-40722
- Finson-Probstein method of comet dust tails anal. 7-60563
- Fourier optics methods, appl. to imaging props. of large reflecting telescopes 7-66461
- Fourier transform spectrometry, OH radical study of Sun at National Solar Observatory 7-55482
- fourth-order Henyey method for stellar models 7-66469
- frequency variations detect. in variable stars, new method and appl. to β Cep star δ Cet 7-29477
- g-modes of nonradially pulsating relativistic stars, slow-motion formalism 7-9463
- galactic chemical evolution models construction technique 7-40721
- galaxies automated surface photometry, calibration and validation of photometric technique 7-60575
- galaxies bulge-to-disk ratios determination, χ^2 minimisation scheme for spiral galaxies 7-48071
- galaxies distance measurement, appl. of more precise L- σ distance indicator 7-9541
- galaxies luminosity function determination, non-parametric method for magnitude-limited samples 7-24212
- galaxies luminosity index as distance indicators 7-14668
- galaxy photometry, improved formulae for transformation of CGCG magnitudes to B_1 system 7-48086
- gamma-ray light curves analysis, appl. of kernel density estimators 7-47718
- U Gem stars, period lengths estimation methods (*German*) 7-9378
- grating spectroscopy and Henry Rowland, conference, Baltimore, Maryland (June 1984) 7-18493
- gravitational potential determ. for arbitrary mass distrib. Poisson integral expansion method 7-66447
- gravitational potential determ. for axisymmetric mass distrib., hydrodynamic test results 7-66446

astronomical techniques continued

- gravity determination for pole-on binary systems, appl. to 31 Aql 7-4434
- half-range moment methods for radiative transfer in spherical geometry 7-60520
- high resolution techniques in solar physics, meeting, Toulouse, France (September 1984) 7-18498
- Hubble constant determ. method involving observation of gravitational waves 7-9559
- image construction of astronomical objects using coherency functions, atm. distortion compensation 7-55481
- image processing methods used in E Germany for analysis of planetary probe data (*German*) 7-66477
- image processing technique for Halley Multicolor Camera system 7-9380
- image reconstruction, weighted shift-and-add technique, statistical analysis 7-55489
- image restoration via the shift-and-add algorithm, appl. to extended chromosphere of Betelgeuse 7-40719
- imaging spectroscopy, preliminary performance goals for Space Telescope Imaging Spectrograph 7-60550
- indirect imaging methods, conf., Sydney, Australia (Aug.-Sept. 1983) 7-41016
- initial value problems, simple adaptive grids in 1D 7-66457
- interstellar molecules, study method involving laboratory photofragment spectroscopy 7-24017
- interstellar scintillation use for meas. of pulsar space vel. 7-60698
- far-IR blackbody source of variable temperature, for use in IR astronomical radiometry 7-40713
- IR speckle interferometry 7-55488
- IR spectroscopy, Ottawa, Ont., Canada (June 1985) 7-48160
- IUE spectra, VIRIS-VAX interactive reduction 7-40720
- Kepler's equation solution, procedures using FORTRAN 7-24018
- laser microprobe use for cosmogenic Ar components identification in Allende meteorite 7-55584
- line coincidence statistics appl. to stellar comp. anal. 7-55684
- long-baseline optical interferometry and refr. index struct. function saturation 7-60574
- weak magnetic fields meas. in diffuse media, appl. of reson. scatt. spectra 7-23991
- maximum entropy method deconvolution 7-14500
- maximum entropy method use for cosmic rays transport equation approx. soins. 7-60564
- Michelson stellar interferometry, pupil plane and image plane imaging 7-47727
- multi-image analysis for surface features recognition on planetary satellites 7-34917
- nebencharacteristics method use for stellar atm. 2D flow calcs. 7-14478
- nuclear methods for lunar soil sample analysis (*Rumanian*) 7-18363
- numerical method for models of double white dwarf binaries and central white dwarf-heavy disk systems 7-60573
- objective prism spectra wide-angle samples use for large-scale galaxy distrib. anal. 7-66771
- observing techniques and instrumentation, book 7-60910
- occultation techniques for ultra-high ang. resolution meas. of X-ray sources 7-60567
- optical filters, the IPF-6 interference-polarisation filter 7-50722
- optical reflection from planetary surfaces, operator-eigenvalue theory 7-24032
- optimization algorithms, simulated annealing and neural network processing 7-47724
- orbiting object location, calcs. 7-52
- phase recovery with dual nonredundant arrays 7-42956
- phase retrieval from a dichromatic analysis of speckles 7-31261
- photoelectric photometry for amateurs 7-47725
- photoelectric radial velocities measurement, appl. to pulsation anal. of Cepheid variables 7-9500
- photographic hypersensitisation techniques applied to photography, Kodak 2415 film 7-56363
- photographic photometry, characteristic curves empirical expression 7-55480
- photographic technique for studying Mars in violet light 7-18364
- photometric method for determ. of characts. of companions of classical Cepheids 7-55665
- photometry, 1/f noise 7-40716
- photometry, appl. of photon-counting system to photon flux statistics 7-60558
- photometry, Johnson U passband characts. 7-4349
- planet right ascension determ. using photoelectric transit instrument, correction method (*Chinese*) 7-4343
- planetary gravitational potential expansion, convergence improvement methods 7-47742
- planetary radarclinometry, mathematical theory and algorithm 7-34372
- plasma, numerical methods for MHD calcs. 7-55449
- plasma computational physics conference, Eibsee, Germany (May 1986) 7-48137
- polarimetry of hard γ -ray sources 7-4593
- polarissima method for absolute azimuth determ. with transit circle 7-4346
- pupil and image plane interferometry at optical wavelengths: visibility and phase analysis 7-55491
- quasars selection using slitless technique 7-18460
- radial velocity of giant stars in globular clusters, spectroscopic meas. method 7-40718
- radiation fields at line freq., calc. method 7-4345
- reduction of spectra, summary of available programs 7-4350
- reflectance spectra information extraction, absorption band positions determ. 7-14503
- remote sensing data inversion 7-47723
- RI photometric systems photographic and photometric 7-66475
- rich clusters of galaxies 7-14502
- rocky surface mineralogy, by optical and IR reflectance spectroscopy 7-29291
- secondary spectrum search in β Lyr, line identification method 7-55714
- SETI, laser signals search from nearby stars 7-34889
- SETI, time and space acousto-optic folded spectrum processing 7-26080
- shearing spectroscopy and interferometry, high angular resolution 7-47717
- shift-and-add imaging 7-55486
- short-period temporal studies with IUE, pulse-phased spectroscopy technique for X-ray pulsars 7-55494
- Sobolev resonant function approx. use for the Ambartsumian-Chandrasekhar and Hopf functions determ. 7-40717

astronomical techniques continued

- solar chromosphere modelling, appl. of submillimetre limb brightness profile 7-55590
- solar constant measurement from snow melting from barn roof 7-48256
- solar Doppler measurements, spatial smearing errors rel. to limb effect and large-scale vel. fields 7-66551
- solar electrons in interplanetary space due to type III radiobursts, trajectory determ. by radio method 7-47649
- solar magnetic fluxtubes modelling, numerical method 7-47804
- solar neutrino detection, workshop, Tsukuba-gun, Japan (August 1986) 7-48193
- solar photosphere turbulence, determ. by observation of spectra, 'crossing' method 7-47731
- solar proton flares forecasting, appl. of fuzzy clustering theory to short-term forecasts (*Chinese*) 7-4389
- solar radiation measurement, comparison of NBS SURF and W UV irradiance standards 7-11086
- solar rotation observing methods 7-55589
- solar spectra of He I resonance line in EUV, curve-of-growth measurement technique 7-9373
- solar temperature, 4 GHz, undergraduate expt. 7-53
- solar vector magnetic field measurement, principle of Solar Magnetic Field Telescope (*Chinese*) 7-4330
- solar wind corotating interaction region determ. method, using solar wind velocity data 7-55402
- solar X-ray spectra multi-temp. anal. methods 7-24020
- speckle imaging by filtered weighted-shift-and-add technique 7-47726
- speckle interferogram inverse filtering for HST roll deconvolution 7-55487
- speckle interferometric data analysis, weighted shift-and-add algorithm 7-55485
- speckle interferometry, cross-spectrum techniques appl. 7-55492
- speckle interferometry, image reconstruction by speckle masking, speckle spectroscopy, multiple-mirror interferometry 7-55484
- speckle interferometry, potential accuracy of stellar ang. dias. and limb darkening meas. 7-47720
- spectroscopy, optimal extraction of single-object spectra from obs. with two-dimensional detectors 7-47729
- spectroscopy, prime-focus spectrographs with holographic gratings 7-4341
- squeezed states use in general relativity interferometric tests 7-4329
- star formation rates determ. in late-type galaxies, surface photometric technique (*German*) 7-24207
- stars automated 2D classification, use of Vilnius system multicolour photometry 7-29410
- statistical detection of observational errors (*French*) 7-66473
- stellar amplitude interferometry, first angular diameter determ. 7-40811
- stellar composite-spectra analysis, digital subtraction technique and appl. to HR 6902 (G9 II+B8 V) 7-66674
- stellar granulation detect. methods 7-60572
- stellar interferometry, real-time fringe contrast meas. 7-29402
- stellar Lyman alpha profiles anal., observed profiles correction for interstellar absorpt. and geocoronal emission 7-60637
- stellar photometry, partial automation of Cuffey Iris Astrophotometer 7-14494
- stellar population synthesis in galaxies, implications of interstellar Na I line strength-reddening relation 7-9526
- stellar pulsation mode identification from line profile vars., effects of temp. var. and toroidal modes 7-55613
- stellar spectroscopy, image processing by FFT (*French*) 7-14499
- stellar structure determ., two-dimensional method for rapidly rotating stars 7-9457
- stellar turbulent flow calc. method 7-18403
- step-focus photographic technique for recording stellar colour 7-14505
- submm coherent and incoherent detect. techniques for FIRST mission 7-47711
- submm heterodyne spectroscopy 7-31041
- submm spectroscopy for comets 7-47795
- subsonic flows analysis, consistent approximation of viscous terms 7-34845
- Sun, active regions mag. field determ. (*Chinese*) 7-4344
- supercluster probing using marginal gravitational lenses 7-55456
- time series analysis methods 7-55629
- Ulysses spacecraft mission for exploration of high solar latitude solar wind 7-55472
- variable stars modelling, phase-space reconstruction and dimension computation 7-29463
- Wilson-Devinney method for light curves anal., soln.-convergence chars. 7-14501
- X-ray imaging, rotational aperture synthesis 7-47728
- Zanstra temperature method for planetary nebular central stars 7-60653

astronomical telescopes

- see also *radiotelescopes*
- 690 GHz InSb bolometer, 2I-He hybrid cryostat 7-30024
- adaptive flexible mirror, IR background speckle noise 7-55467
- advanced technology optical telescopes, conf., Tucson, United States (March 1986) 7-55886
- balloon-borne UV telescope (*Spanish*) 7-55742
- Cassegrain telescope with spherical lens corrector, image quality improvement (*Chinese*) 7-4331
- common-user submm receiver for UKIRT and UK-NL telescopes 7-34883
- compact quasi-optical dual LO receiver for 300-500 GHz 7-34882
- computer-aided control system, for 90 cm Schmidt-Cassegrain type telescope 7-4337
- conference, Tucson, AZ, USA (March 1986) 7-48162
- COS-B, telescope in-flight calibration of sensitivity and background behaviour of instrument 7-60539
- Exosat, X-ray astronomy satellite, review of mission 7-55464
- eye-piece holder on mag. runners (*French*) 7-29395
- Far Infrared Space Telescope (FIRST), high precision composite sandwich antennas anal. 7-24012
- Far Infrared Submillimetre Space Telescope mission 7-34866
- Far Ultraviolet Spectroscopic Explorer telescope technology 7-29398
- Far Ultraviolet Spectroscopic Explorer telescope technology 7-40709
- FIRST telescope, active optics and spectral range extension in IR 7-60553
- four-mirror, performance and complexity comparison of aspheric and spherical primaries 7-37092
- Fourier transform telescope for subarcsecond imaging of solar flare X-rays and γ -rays 7-40706

astronomical telescopes continued

- Fuse/Lyman satellite telescope, photon-counting array detectors 7-47714
- gamma-ray telescope, 1TeV, design and evaluation 7-34884
- graphite fibre reinforced glass sandwich reflectors for far-IR astronomy, thermal stability 7-37093
- high energy gamma-ray telescopes, source location capability 7-9376
- historical development, rationale for design changes, cost drivers 7-37087
- Hubble Space Telescope, collisions with and degradation by artificial satellites 7-9361
- Hubble Space Telescope, performance prediction using OSAC code 7-40707
- Hubble Space Telescope, using Tektronix CCD array 7-29407
- Hubble Space Telescope calibration, IUE spectra of UV standard stars 7-60735
- Hubble Space Telescope inverse filtering of degraded images using speckle interferogram 7-55487
- Hubble Space Telescope performance, prediction using optical surface anal. code 7-25930
- Hubble Space Telescope primary mirror, test and eval. 7-40708
- Hubble Space Telescope Satellite, config. and technological aspects 7-55473
- image processing technique for Halley Multicolor Camera system 7-9380
- IR instruments and chars. (*Japanese*) 7-60546
- Isaac Newton Telescope, history and results 7-24011
- Itek optical technology in manufacturing and metrology 7-37227
- IUE telescope, light scatt. profile determ. 7-60551
- Keck Observatory 10m telescope, design and development work status, fabrication plans 7-40693
- LAMAR protoflight X-ray mirror assembly, design, fabrication and testing 7-47705
- large aperture telescopes with parabolic and spherical primaries, comparison 7-25931
- large aspheric optics, rapid fabrication using computer-controlled opt. surfacing unit 7-37224
- Large Deployable Reflector, chars. 7-60555
- Large Deployable Reflector, development of lightweight glass mirror segments 7-37226
- Large Deployable Reflector, IR to sub-mm, upgrading by active pupil wavefront correction 7-47707
- Large Deployable Reflector, moderate cost, system concept 7-40711
- Large Deployable Reflector System concept 7-29399
- large optics assembly and testing in space 7-40704
- large optics technology, conf., San Diego, USA (Aug. 85) 7-35089
- large reflecting telescopes, imaging props. 7-66461
- layered synthetic microstructures for solar EUV telescopes 7-40703
- lightweight composite mirrors for IR astronomy 7-57519
- liquid-mirror telescope, history of concept 7-9374
- Lyman UV astronomy mission, instrumentation and objectives 7-66430
- Lyman UV astronomy mission and instrumentation 7-66429
- mirror, honeycomb sandwich, borosilicate, blank prep. by spin casting 7-37225
- mirror, honeycomb sandwich, thermal design 7-37089
- mirror, large multicomponent, image parameters 7-37090
- MMT, differential speckle interferometry 7-55490
- Mount Graham Submillimetre Telescope project 7-60554
- mounting for shipborne obs. of solar corona during eclipse (*French*) 7-40696
- multilayer X-ray imaging systems for solar telescopes 7-41568
- multilayered mirrors for EUV solar imaging telescopes, space qualification 7-34864
- multilayered X-ray rocket-borne telescope for solar corona studies 7-40700
- Multiple Mirror Telescope, comparison and calibration lamp illumination system 7-4342
- observing techniques and instrumentation, book 7-60910
- optical test methods used in HIPPARCOS telescope performance evaluation 7-31537
- orbiting space telescopes, collisions with and degradation by artificial satellites 7-9361
- Palomar 60 in. camera lens system design for echelle spectroscopy 7-55475
- phase retrieval, practical appl. for the space telescope 7-62638
- photoelectric meridian circle, annual and diurnal vars. of graduation error 7-47702
- photoelectric transit instrument use for planet right ascension determ. (*Chinese*) 7-4343
- Ritchey-Chretien solar telescope for 30.4 nm, aspherisation and multilayer coating 7-39388
- Robus, telescope carrying platform based on Rosat experience (*German*) 7-47667
- SIRTF, a cryogenically cooled IR telescope 7-34873
- SIRTF, dynamic optical deformations of chopping secondary mirror 7-24008
- Solar Magnetic Field Telescope, principle of vector mag. field meas. (*Chinese*) 7-4330
- Solar Optical Telescope, irregular surface simulation using spline fitting 7-43311
- Space Infrared Telescope Facility, Space Shuttle-based, active image stabilization 7-9377
- Space Telescope, preliminary performance goals for Imaging Spectrograph 7-60550
- spectral slicing X-ray telescope systems, design and anal. 7-40701
- spectral slicing X-ray telescope using layered synthetic microstructure X-ray optics 7-4335
- star camera and aspect determ. system for balloon-borne payloads 7-55418
- submillimetre astronomy, conf., Segovia, Spain (June 1986) 7-41013
- submillimetre spectroscopy and appls. conf., Cannes, France (Dec. 1985) 7-29585
- submm telescope, laser system for local oscillator use in heterodyne receiver 7-34869
- Texas University 7.6m. telescope design progress report 7-40710
- three-mirror, third-order aberrations formulae and design program 7-55466
- transformation of scientific objectives into spacecraft activities 7-66462
- transit circle for absolute azimuth determ. with polarissima method 7-4346
- two-telescope, Michelson interferometry, phase reconstruction 7-55491
- UC Berkeley submm heterodyne receiver for spectroscopy 7-34879
- UKIRT mm and submm receivers 7-34880

astronomical telescopes continued

- UV, with normal incidence concave diffraction grating spectrometer, calibration 7-29400
- Vega project, three-channel spectrophotometer for P/Comet Halley investigation 7-14472
- Wolter I X-ray telescopes, point spread function meridional section formula 7-40702
- X-ray telescope, grazing incidence relay optics for solar astronomy, performance 7-47706
- X-ray telescope for use in spectrometer for astronomy 7-47704
- X-ray telescope mirrors, surface scatt. meas. by triple axis spectrometer 7-37104
- Yunnan Observatory .1 m telescope, optical quality test (*Chinese*) 7-29394
- Be mirror for large optics, fabrication by hot isostatic pressing 7-37228
- C fibre reinforced sandwich panels for far-IR telescope mirrors, thermal stability tests 7-40705
- ⁴He, superfluid, props. and appls. for cooling IR space telescopes 7-48751
- InSb array IR imaging camera, for astronomical appls. 7-34865
- InSb charge injection device arrays, IR camera for astronomical imaging 7-34872

astronomy *see astronomy and astrophysics***astronomy and astrophysics**

- see also astroarchaeology; astronomical instruments; astronomical observations; astronomical observatories; astronomical spectra; astrophysical fluid dynamics; clusters of galaxies; cosmology; extraterrestrial life; galaxies; gamma-ray astronomy; infrared astronomy; intergalactic matter; occultations; planetaria; radioastronomy; solar system; ultraviolet astronomy; X-ray astronomy*
- 1986 annual review, book 7-24315
- 1987 British Astronomical Association Handbook 7-24318
- AAVSO 74th Annual Meeting, conf., South Hadley, MA, USA (November 1985) 7-4623
- Alfven waves of finite amplitude, modulational instability theory 7-34855
- American astronomers, evolving demographics 7-35191
- American Astronomical Society, 169th meeting, Pasadena, California (January 1987) 7-48135
- ancient comets and meteor showers, temporal correlations and genetic associations 7-55543
- angular momentum versus mass, conservation laws 7-14483
- anomalous Zeeman effect, moments and expansion coeffs. 7-66443
- archaeoastronomy and roots of science, conference San Francisco (January 1980) 7-41019
- Astronomical Society of Pacific summer scientific meeting, Boulder, Colorado (July 1986) 7-41002
- Astronomische Gesellschaft assembly, Hamburg, Germany (September 1986) 7-48151
- atomic data for astrophysics, recent developments 7-40689
- baryon and lepton number violation in astrophysics 7-55866
- black hole accretion MHD, entropy accretion rate and moving black hole accretion 7-14599
- black hole electrodynamics (*Russian*) 7-9507
- black holes, energy extraction by Penrose process 7-40683
- Boltzmann gas, semi-relativistic, fitting formulae for eqn. of state 7-40685
- bosonic instability of charged black holes, particle creation and accumulation processes (*Russian*) 7-55702
- Cartan's contortion, relation to Eotvos torsion expt. 7-4326
- CASCA 1986 annual meeting, conf., Penticton, Canada (June 1986) 7-48148
- CDS Scientific Council Meeting, Bordeaux, France (May 1985) 7-4618
- charged particles motion in superposed dipole and uniform mag. fields, allowed region 7-14482
- chemistry, organic cpd. and biomolecular precursor form., hot atom chemistry appls. 7-26813
- comets, history of research, book 7-24330
- conducting body moving through magnetoplasma, plasma wave generation 7-9369
- conference of Astronomical Science Group of Ireland, Dublin, Ireland (September 1985) 7-24262
- cosmions, effects in Sun and in globular cluster stars 7-55436
- cosmology, characteristic actions $\hbar^{(4)}$ in struct. of Universe 7-4602
- cosmos, space education, conf., Copenhagen, Denmark (Aug. 1986) 7-48182
- creation of Universe, from before Big Bang to end of Planck era 7-66795
- data networks, CDS meeting, Strasbourg, France (1985 November) 7-4617
- Dynamical Astronomy Division, 17th regular meeting, Santa Barbara, California (April 1986) 7-29571
- Einstein equations with fourth-order derivative terms, appl. to Bianchi-type I space times 7-48111
- Einstein-Born-Infeld theory, duality rotations and type-D solns. 7-47683
- electron and positron emission spectra for relativistic plasmas 7-40684
- force-free EM oscillations, cylindrical oscills. spectrum 7-34857
- fourth-order gravitation, Newtonian limit 7-47684
- gamma-ray emission from relativistic plasma 7-40684
- gas-phase synthesis of organophosphorus compounds, implications for atmospheres of giant planets 7-24058
- general relativity, generalised harmonic gauge conditions as field eqns. for lapse and shift 7-47678
- gravitational lensing by low mass objects (stars and planets), diffraction effects 7-40682
- gravitons in general relativity, implications of photon hypothesis in electrodynamics 7-41164
- Green's function in curved space-time, Hadamard construction (*German*) 7-66444
- Henry Rowland and astronomical spectroscopy, conference, Baltimore, Maryland (June 1984) 7-18493
- induced causality in astrophysics, alternatives to general relativity 7-47676
- interacting quantum field theory in curved space-time, S-matrix approach 7-47675
- interstellar molecular clouds chemistry, grain surface reactions anal. from matrix isolation study 7-24179
- Kaluza-Klein gravitational theory, astrophysical data and cosmological solns. 7-9363
- large interstellar molecules, thermal props., absorpt. bands, and chemical stability 7-24189

astronomy and astrophysics continued

- liquid-mirror telescope, history of concept 7-9374
- magnetism blowup of force-free bipolar magnetic field in infinite region of space 7-40687
- material content of Universe, conference, London, England (October 1985) 7-55884
- modified gravitation theories, alternatives to dark matter models 7-47692
- molecular astrophysics, NATO conf., Bad Windsheim, Germany (1984 July) 7-9589
- molecular astrophysics 7-14488
- molecular ions 7-14489
- molecular spectra, program for symmetry-adapted rotational eigenfunctions and energy levels of asymmetric top molecules 7-4324
- molecular time-resolved spectroscopy 7-14491
- non-Euclideanism in general relativity and cosmology, mathematical formalism 7-34851
- observational physics and astrophysics, book 7-55916
- opacity of gases containing no metals at astrophysical conditions 7-24003
- orbiting object location, calcs. 7-52
- oscillating free-connection flow past infinite porous vertical limiting surface, effects of mass transfer 7-14479
- partially open magnetospheres with and without magnetodisks, analytical models 7-55443
- Planck length as cosmological constraint, derivation 7-34852
- planetary magnetospheres, similarity model illustrating effects of toroidal mag. field and rotation 7-9407
- plasma conf., Sukhumi, USSR (May 1986) 7-48174
- plasma convection in horizontal magnetic field with periodic boundary conditions 7-4328
- plasma physics, role of Planck-Larkin partition function in occupation numbers for reacting plasmas 7-55440
- plasma universe model, cosmogony, X-ray and X-ray spectra, Saturnian rings 7-14486
- polarised electron-positron pairs annihilation in strong mag. fields, one-quantum annihilation cross-section 7-47674
- polytropic configurations within homogeneous background matter, equilibria and instabilities 7-4316
- Q-nuclei, binding energies and effects on stellar H burning 7-55445
- quark-hadron transition in cosmology, effects on primaeval nucleosynthesis 7-47677
- radiative transfer, statistical description of radiation fields on basis of invariance principle 7-23986
- radiative transfer eqn. soln. 7-55910
- radiative-transfer problems with reflective boundary conditions, modified spherical-harmonic method 7-34853
- Reginald Purdon de Koch (1902-80), extraordinary variable star observer, biography 7-60926
- relativistic astrophysics, conformal potential of stationary axisymmetric vacuum 7-47682
- relativistic astrophysics, eqns. of motion for test particles with internal struct. 7-41165
- relativistic astrophysics, linear problem for five-dimensional projective field theory 7-47681
- relativistic astrophysics and gravitation, conference, Potsdam, Germany (October 1985) 7-40980
- resonance scattering spectra appl. to very weak mag. fields diagnostics in diffuse media 7-23991
- resonant fast dynamo in chaotic shear flows, theory 7-20808
- rigidly rotating perfect fluids in general relativity, Wahlquist soln. 7-47680
- self-citation rates in astron. papers 7-60853
- solar calendar, appl. of shifting date line 7-9362
- solar photosphere, force free mag. fields in spherical coordinates (*German*) 7-14549
- space-time structure, relation to quantum mechanics 7-47679
- spectral theory and stability in astrophysics, appl. to ideal MHD eqns. 7-34854
- strange matter, physics and astrophysics 7-49050
- strong shock wave propag. in medium with exponentially varying density, similarity soln. 7-14481
- synchrotron radiation, corrections in derivation of formulae 7-55442
- thermonuclear reaction rates, determ. from (p,n) reactions (on targets with A=92 to 122) 7-34859
- tidal energy dissipation, comparison between astronomical and geophysical estimates 7-14301
- viscous jets dynamics, numerical calcs. 7-4565
- Mg³⁺, electron impact excitation rate coeffs. 7-55455
- Mg⁴⁺, electron impact excitation rate coeffs. 7-55455

astronomy computing*see also computerised instrumentation*

- N-body hierarchical force calc. algorithm with N log N growth 7-47673
- common-user submm receiver for UKIRT and UK-NL telescopes 7-34883
- compact quasi-optical dual LO receiver for 300-500 GHz 7-34882
- cosmic ray track analysis by expert system using distributed problem solving 7-55388
- data networks, CDS meeting, Strasbourg, France (1985 November) 7-4617
- data processing, conf., Tucson, AZ, USA (March 1986) 7-48162
- digital image processing techniques used in astronomy, appl. to diffraction 7-11828
- galactic luminosity profile analysis by curve matching 7-55825
- Halley's comet and planets, graphical orbit display in UCSD Pascal 7-55479
- Hubble Space Telescope, performance prediction using OSAC code 7-40707
- image detection system for Kiso Schmidt plates, appl. to Orion Association 7-55477
- image processing methods used in E Germany for analysis of planetary probe data (*German*) 7-66477
- image processing technique for Halley Multicolor Camera system 7-9380
- IR 2D detector array, microcomputer-based data acquisition 7-9382
- IUE spectra, VIRIS-VAX interactive reduction 7-40720
- Kepler's equation solution, procedures using FORTRAN 7-24018
- large aspheric optics, rapid fabrication using computer-controlled opt. surfacing unit 7-37224
- maximum entropy method deconvolution 7-14500
- optimization algorithms, simulated annealing and neural network processing 7-47724

astronomy computing continued

- Prognost-10, algorithms for satellite crossing times of solar wind shocks determ. 7-55417
 radiotelescope calibration, automated system (*French*) 7-60542
 reduction of spectra, summary of available programs 7-4350
 SETI, ultranarrowband searches with dedicated signal processing hardware 7-24013
 transformation of scientific objectives into spacecraft activities 7-66462
 VEGA space probes, TV real-time software (*Hungarian*) 7-29379
 VLA, radiotelescope and its DEC computers 7-24006

astrophysical fluid dynamics

- see also *astrophysical jets*
 2D flows in stellar atm., use of nebencharacteristics method 7-14478
 1759+211, nearby radio galaxy, hydrodynamic models for oscillating radio jet 7-55820
 anisotropic fluid distributions in bimetric general relativity 7-34846
 barotropic fluids, angular vel. for general steady states 7-60531
 blast waves, energy content in stellar model 7-34856
 Boltzmann gas, semi-relativistic, fitting formulae for eqn. of state 7-40685
 Cas A, tenuous gas expansion vel. determ. via H I lines broad wings obs. 7-66691
 cellular convection theory, nonlinear bifurcation 7-55459
 classical novae, Lagrangian hydrodynamic code for evolution through complete cycle 7-29493
 collimated outflows in interstellar mol. clouds, model for Herbig-Haro objects (HH 7-11) 7-55775
 collisionless gravitating systems, spherical collapse stability 7-40678
 cometary dust halo formation, time-dependent numerical modelling 7-55536
 comoving-frame radiative transfer equation, general Eulerian formulation 7-55441
 convection columns in rotating, heated cylindrical annulus 7-51128
 convection in planetary atmospheres and stars, zero-gravity expts. 7-29393
 convection in rotating hemispherical shell with radial gravity, Spacelab simulation expts. 7-55450
 convective turbulence with rot. and mag. fields, mixing length theory 7-29388
 converging magnetogasdynamic cylindrical shock waves in a uniform atmosphere 7-37552
 core dynamo, for Couette-Poiseuille flow 7-65941
 cosmological large-scale density perturbations evolution, triggering of early star form. and galaxy form. 7-66794
 cylindrical-symmetric relativistic shock wave with azimuthal mag. field, nonexistence 7-4325
 cylindrical-symmetrical relativistic shock wave, motion in presence of axial mag. field 7-4322
 cylindrically-symmetrical relativistic shock waves 7-47685
 density waves in satellite precursor disks 7-34862
 differentially rotating perfect fluid stars, stability 7-40796
 differentially rotating self-gravitating gas cloud, stability of isothermal configurations 7-40679
 disk galaxies, gas flow simulation, tilts and corrugation waves evol. 7-60806
 galactic disks collisions with high-velocity clouds, 2D hydrodynamic simulations 7-48065
 galaxies radio trails, bending by galactic winds and rot. 7-35045
 galaxies spiral density waves, effects of cloud collisional damping 7-66755
 galaxy satellite orbits decay by dynamical friction, 3D modelling 7-60801
 giant planets, protosatellite accretion disks, global characts. 7-34914
 gravitational potential determ. for axisymmetric mass distrib., hydrodynamic test results 7-66446
 heat transfer in unsteady MHD Couette flow of electrically conducting viscous incompressible rarefied gas, theory 7-66448
 homocentric rotating torus, dynamical instability and growth rate upper limit 7-47693
 homogeneous uniformly rot. McLaurin spheroid in mag. field, equilib. and stability, stellar appl. 7-47686
 hydromagnetic turbulence in differentially rotating disks, implications for α -value in accretion disks 7-18354
 induction equation in spherical region with boundary, Green's function determ. 7-66445
 initial value problems, simple adaptive grids in 1D 7-66457
 interstellar bubbles, structure and evolution is multiphase interstellar medium 7-60764
 interstellar gas clouds orbits in galactic bulges, cloud stability anal. 7-66707
 interstellar giant molecular clouds, turbulence theory rel. to star form. 7-29525
 interstellar molecular clouds, mass-radius-vel. dispersion relations rel. to cloud fragmentation 7-55753
 interstellar neutral gas shell surrounding H II region, dynamical evolution 7-66692
 interstellar shock waves, limits of validity of isothermal approximation 7-60742
 interstellar superbubbles, evolution through sequential supernova explosions in plane-stratified gas distrib. 7-55778
 isotropic stellar systems, linear oscills., non-radial modes 7-35014
 Jupiter, Great Red Spot, simulation (*Russian*) 7-47695
 Jupiter magnetosphere, centrifugal field line breaking and upper limit to Io mass injection 7-66496
 large-amplitude wave in gas disk, stationary periodic wave theory 7-23987
 low-frequency oscillations of uniformly rotating stars, freqs. of gravity modes and rot. modes 7-60635
 mass transfer effects on transient behaviour of asymptotic laminar boundary layer 7-4323
 meridional flow in self-gravitating body, mechanical flow in barotropic star with const. ang. momentum 7-29464
 MHD shock waves in interstellar mol. clouds, theory for oblique mag. fields for oblique mag. fields 7-66454
 MHD theory, system of eqns. on special Riemann manifold 7-65939
 MHD theory, system of eqns. using Riemann theta functions 7-65940
 modal analysis of rotating polytropic cylinders, gravitationally unstable mode and relation to r-mode 7-18453
 nonlinear compressible convection penetrating into stable layers and producing internal gravity waves 7-60631

astrophysical fluid dynamics continued

- nonlinear convection of compressible fluid in rot. spherical shell, theory 7-9459
 Per, lawn-sprinkling shock model for nonradial oscills. 7-47849
 planetary atmospheres, mass fractionation during transonic escape of gases rel. to loss of water from Mars and Venus 7-55508
 planetary rings, nonlinear density waves struct. 7-55506
 planetary surfaces, vapour jets from oblique impacts rel. to planetary meteorites ejection 7-34957
 plasma interchange instabilities driven by magnetic buoyancy, for solar interior 7-66456
 plasma shock waves stability modification by cosmic rays accel. 7-34861
 radiative convection in stratified atmosphere, anelastic eqns. soln. 7-29389
 radiative shocks, dynamical models and line spectra of steady shocks 7-55454
 rocket effect on gravitating mass-losing object, axisymmetric hydrodynamic theory 7-23995
 Saturn ring systems, large-amplitude stationary periodic wave theory rel. to rings fine struct. 7-23987
 self similar cylindrical shock wave in radiating magnetogasdynamics 7-34847
 self-similar flow behind a spherical shock with varying strength in an inhomogeneous self-gravitating medium 7-60516
 semi-detached close binary star, mass transfer 2D modelling 7-60727
 shallow water flow incident upon slender orography, semi-geostrophic response to elongated ridge 7-29122
 shock waves from point-sources in a heat-conducting gas 7-34849
 shock waves propagation in gas with cosmic rays, instability (*Russian*) 7-40652
 skin friction in unsteady free-convection flow past accelerated plate 7-4321
 solar atmosphere, current sheets form model 7-66539
 solar atmosphere, time dependent acoustic wave calc. 7-34959
 solar coronal loops, quasi-steady mass flows model 7-47808
 solar faculae, hillock and cloud model 7-55593
 solar magnetic fluxtubes, numerical magnetostatic solns. 7-47804
 solar nebula, nonlinear tidal interaction with protoplanets 7-47737
 solar p-mode oscillations, compressive waves propag. through fibril mag. fields 7-66541
 solar quiescent prominences, static current-sheet models 7-66540
 solar transition region, cool loops flow model for fast downflows 7-66537
 spiral galaxies form., gravitating rotating gaseous disk, nonlinear convective instability development calcs. 7-66766
 stellar core collapse, electron capture effects 7-55614
 subsonic flows, consistent approximation of viscous terms 7-34845
 supernova remnants, nonsteady shock model for permitted O I line emission from O-rich nebulosity 7-55779
 topological stability of finite-length mag. flux tubes, theory 7-66556
 turbulent Alfvén waves, contrib. to origin of bipolar galactic and extragalactic jets 7-60523
 turbulent compressible convection in deep atmosphere, validity of numerical approach 7-47690
 vertically stratified thin accretion disks, baroclinic waves 7-14477
 C stars, coupled hydrodynamic-radiative transfer models for dust-driven stellar winds 7-55641
 H II regions internal motions, ordered and random components 7-40902

astrophysical jets

- 1759+211, nearby radio galaxy, VLA obs. of oscillating jets 7-55820
 1919+479 radiogalaxy, observational constraints on bending of radio jets 7-40929
 V1343 Aql (=SS 433), extended radio struct. obs. with European VLBI Network 7-29478
 V1343 Aql (SS 433), jet funnel vertex angle from absence of high-speed light vars. 7-66596
 V1343 Aql (SS 433), model of expanding sources in jets 7-60519
 R Aqr, UV variability and mass expulsion from IUE obs. 7-55651
 R Aqr jet, obs. at UV and radio wavelengths 7-55686
 bipolar galactic and extragalactic jets, prod by turbulent Alfvén waves 7-60523
 bipolar molecular flows, CO line form. in accelerated outflows 7-48042
 bipolar nebular and jets from young stars Calar Alto obs. 7-48027
 blazars, beaming model 7-60799
 braided jets in galaxies with compact radio nuclei 7-55810
 3C 119, compact steep spectrum source, peculiar morphology, models involving jets 7-40949
 3C 219, radiogalaxy, jets collimation and polarisation 7-14647
 3C 273, quasar, particle accel. in jet hotspot rel. to radio to IR spectrum 7-14676
 3C 273 jet, swinging relativistic plasma beam model 7-66783
 3C 2, compact steep-spectrum quasars, lobes characts. 7-60833
 collimated outflows in interstellar mol. clouds, model for Herbig-Haro objects (HH 7-11) 7-55775
 P/ Comet Halley (1982), CN jets obs. 7-47788
 V645 Cyg-Duck Nebula complex, characts. and obs. 7-60655
 expanding sources, synchrotron and inverse Compton emission 7-60519
 extragalactic jets, appl. as probes of surrounding medium 7-55822
 galactic centre lobe, twin-jet model rel. to former Seyfert galaxy stage 7-66740
 galaxies radio trails, bending by galactic winds and rot. 7-35045
 general relativistic decollimation of jets, effects of defocusing by spacetime curvature 7-60522
 Haro 6-5 complex, struct., polarisation obs. 7-48049
 interstellar bipolar sources formation in dense mol. clouds, isotropic wind collimation models 7-24182
 interstellar shock waves and jets in star-forming clouds, implications of H₂ 2 μ m obs. 7-55760
 IRC 1 in M17, bipolar outflow source and nebulosity, spectral characts. 7-60748
 L 1551 bipolar flow, extended IR radiation 7-40890
 LDN 1551, bipolar nebula IR emission characts. 7-48061
 M87, relation of jet to nearby Virgo cluster galaxies 7-35047
 magnetic energy dissipation in force-free jets, implications for radio galaxies 7-29391
 magnetically confined jet, 2D axisymmetric numerical simulations 7-55447
 magnetodynamic formation mechanism, dynamics of rotating magnetised mass accretion 7-55460
 Markarian 231, Seyfert 1 galaxy, optical imaging of nuclear jet 7-48067
 mass entrainment into astrophysical jets 7-40686

astrophysical jets continued

- molecular outflow sources, NH_3 obs. anal. 7-66576
- NGC 613, barred spiral galaxy with collimated outflow from nucleus 7-60779
- NGC 7023, outflow source, CO mapping 7-60772
- PKS 0521-36, radiogalaxy, optical jet and nucleus photometric characts. 7-55789
- PKS 2155-304, BL Lac object, IUE obs. (1979 to 1985) rel. to jet models 7-55833
- planetary surfaces, vapour jets from oblique impacts rel. to planetary meteorites ejection 7-34957
- radiogalaxy jet interaction with ambient gas 7-29532
- Sco X-1, lobe characts. determ., VLA obs. 7-60721
- superluminal radio sources, flows, EVN and MERLIN obs. 7-66775
- DG Tau B knot system, CCD spectra, jet obs. 7-55767
- transonic motion of adiabatic jets from funnels of thick disks 7-34844
- young stars, accretion-driven jets modelling 7-60643
- young stars, CCD obs. of assoc. optical jets 7-55617
- He peculiar stars, IUE obs. of magnetically controlled jet-like stellar winds 7-47949

astrophysics computing

- see also computerised instrumentation*
- Henon mapping with Pascal, dynamic systems simulation 7-34836
- Jupiter, physical and visual simulation 7-34910
- reduction of spectra, summary of available programs 7-4350

asynchronous motors *see induction motors***ATM forces *see intermolecular forces*****atmosphere, solar *see solar atmosphere*****atmosphere, terrestrial *see terrestrial atmosphere*****atmosphere, upper *see upper atmosphere*****atmospheric acoustics**

- acoustic-to-seismic transfer function for outdoor ground surfaces 7-26070
- aerodynamic noise principles (*Chinese*) 7-11208
- boundary layer effect on scale model simulation 7-20493
- discrete spectrum of the sound field of a point source in a stratified moving medium 7-62889
- grass-covered ground, acoustic impedance meas. at low freqs. using phase difference technique 7-50876
- humid air, characteristic impedance 7-26071
- leafy foliage sound propag. simulation 7-50824
- low freq. sound waves, multiple scattering by wind waves 7-62890
- noise propag., effect of sound absorption by air 7-50839
- outdoor ground impedance at grazing incidence, FFT-based meas. 7-57650
- planetary boundary layer meas. by vertical SODAR (*German*) 7-9148
- propagation close to ground, atmospheric effects 7-43499
- radio acoustic meas. of temp. profile in troposphere and stratosphere, exptl. results 7-14360
- soil, porous, acoustic coupling calcs. 7-26072
- upper stratosphere, acoustic pulse incomplete reflection, model (*Russian*) 7-4118
- switched-beam planar arrays suitable for high-resolution acoustic sounders 7-9209
- turbulence intermittence and acoustic signal reflection (*Russian*) 7-60330
- typhoons, infrasonic signals and eye pressure 7-29176
- vertical SODAR for planetary boundary layer acoustic sounding (*German*) 7-9246
- waveguide propagation near impedance boundary with stratification (*Russian*) 7-20492

atmospheric boundary layer

- 3D model of mesoscale processes of oceanic energy-active zones (*Russian*) 7-23808
- acid rain modelling, turbulent spiral boundary layer and thermal wind simulator 7-14370
- air-water interface, turbulent heat and water vapour transfer 7-23679
- air-water interface wave-induced press., fluctuations, wave generation by wind 7-16198
- S Alberta, Canada, chinooks distinguishing nocturnal features 7-47493
- E Antarctica, low-level katabatic winds 7-55129
- Arabian Sea, air-sea interface, sensible and latent heat fluxes 7-14292
- Arabian Sea, boundary layer turbulence during Indian SW monsoon 7-23793
- Arenal Reservoir, Cost Rica, air flow modification due to reservoir construction 7-14346
- Argentina continental shelf, temp. and humidity profiles, planetary boundary layer modelling 7-34579
- Athens basin, simulation of sea and land breezes for pollution studies 7-60342
- atmosphere, tracer transport model, particle dry-deposition parameterization scheme 7-18289
- atmospheric tide differences in surface layers and ground level 7-60341
- Attica, Greece, sea breeze characts. 7-4092
- Baikal-Amur Mainline area of USSR, surface heat balance study 7-23816
- Bangladesh, evaporation rates, water pan observations 7-29092
- baroclinicity effects on neutral planetary boundary layer struct. 7-23792
- Bay of Bengal, atmospheric struct. during suppressed and active convective periods 7-55211
- Bay of Bengal, turbulence struct. of boundary layer 7-60356
- Brush Creek Valley, Colorado, mass transport by along-valley wind systems 7-29143
- S California, vertical pollutant distrib. and boundary layer struct., airborne lidar obs. 7-3734
- Canterbury Plains, New Zealand, contrib. of orographic effect to interacting multi-scale wind systems 7-55203
- South China Sea, cold surge event influence on boundary layer struct. 7-60345
- closure parameter determ. in higher-order closure models 7-55128
- convective boundary layer, closures for pressure-scalar covariances 7-66233
- convective boundary layer length scales 7-9085
- convective boundary layer simulation, efficiency of different higher-order turbulence models 7-57819
- convective boundary-layer parameters, climatology over Ontario, Canada 7-40512
- convective layer, diffusion model, numerical simulation 7-66243
- convective layer, diffusion model of plume released from point source 7-66244

atmospheric boundary layer continued

- Cumbria, England, characts. of airflow, aerosols, precipitation and clouds in boundary layer 7-4096
- cumulus, intermittent convection 7-66254
- daytime boundary layer evolution over mountainous terrain, upslope flow 7-4153
- diabatic wind and temp. profiles obtained from a 100 metre tower 7-23790
- diffusion from elevated and ground point sources in neutral boundary layers, turbulent energy model 7-34580
- diffusion in marine boundary layer, SF_6 tracer expts. and parameterization 7-18285
- dispersion studies, use of negative ion generator and collector system 7-29314
- dissipative waves excited by gravity-wave encounters with stratified boundary layer 7-34598
- dry deposition in surface layer, accuracy of current meas. techniques 7-18281
- Eagle Valley, Colorado, temp. inversion buildup and wind struct. 7-55202
- East African topographic effect on flow driven by zonally symmetric forcing 7-34593
- Ekman layers and surface wind/current differences 7-60327
- El Nino, simple model involving atm. convergence feedback 7-34536
- energetics in low-resolution general circulation model, effects of topography 7-9099
- entrainment instability and cloud break up for marine boundary layer 7-23798
- evaporation at catchment-scale, parameterization method involving atmospheric boundary layer 7-18231
- evaporation from water surface in humid tropical area of India 7-29090
- flow over nearly 2D hill 7-9137
- FOG-82, cooperative field study of radiation fog, exptl. design and results 7-9068
- Frankfurt, Germany, surface layer wind field, characts. estimation, use of three-layer mesoscale model 7-60320
- frictional convergence at coastlines 7-47516
- general circulation, comparison of filters for high latits. using shallow water eqns. 7-9133
- geostrophic momentum approx. 7-55136
- Geyers geothermal area, California, dispersion model for complex terrain 7-60313
- global oceans, monthly mean precipitable water and surface level humidity 7-29202
- Hamburg, W Germany, atmos. radiative heating due intense pollution 7-4101
- height of internal boundary layer for offshore winds with 10 m to 100 km fetches (*German*) 7-55237
- hill, flow over isolated hill summit in Somerset, England 7-55132
- isolated hill, short-range dispersion experiments on windward slope 7-34572
- Indian Ocean, evaporation from equatorial regions 7-23791
- inversion layer acoustic sounder obs. at Athabasca, Alberta, Canada 7-23800
- irregular terrain airflow, model formulation 7-4100
- irregular terrain influence on boundary layer struct., model calcs. 7-23795
- Judean Hills, Israel, valley and mountain winds interaction with sea and land breezes 7-23811
- Kakinada sand spit, India, atm. elec. meas. 7-23806
- lake-land breeze anal. (*Chinese*) 7-55209
- land surface heat balance and atmos. surface layer (*Russian*) 7-60328
- large water droplets dispersion model 7-34583
- lateral dispersion from tall stacks 7-66242
- lateral dispersion measurement method involving aircraft oblique photography 7-23918
- marine, surface temperature, ship observations 7-4217
- marine boundary layer, dynamic struct. of vortices formation over ocean surface heat anomalies 7-9134
- marine boundary layer, effect of wind speed on thermal structure of upper ocean 7-14302
- marine boundary layer, effects on seasonal evolution of ocean upper layer circulation; 7-9020
- marine boundary layer above waves, momentum and energy fluxes (*Russian*) 7-55184
- marine boundary layer at Tarapur, India, acoustic sounder observations 7-55131
- mesoscale variability of atmos. of N Atlantic off Scotland 7-23797
- mesoscale wind variability, meas. near Point Conception, California (spring 1983) 7-29144
- methyl peroxide, photochemical formation in boundary layer of atmosphere 7-29155
- microwave line-of-sight links, elevated atmospheric duct, multipart fading anal. 7-47482
- Monsoon depression baroclinic growth, effect of Ekman boundary layer friction 7-9122
- mountain valley, thermal asymmetry and cross-valley circulation 7-4099
- neutrally stable atmospheric boundary layer flow, drag coeff. theory 7-14357
- nocturnal boundary layer over sloping terrain, numerical simulation (*Chinese*) 7-4080
- nocturnal drainage flow interaction with ambient winds, model 7-23799
- nocturnal temperature inversion evol. 7-4095
- nocturnal wind shear 7-34578
- numerical models of stable boundary layer (*Chinese*) 7-29218
- ocean surface wind measurement, Seasat scatterometer studies of effect of wave height and environmental conditions 7-66159
- ocean waves and simultaneous atmos. press. micropulsations (*Russian*) 7-8965
- ocean-atmosphere boundary layers interaction, effects of surface wave layer 7-8989
- equatorial Pacific, boundary layer struct. during FGGE 7-60359
- parameterization, FORTRAN programs 7-55246
- particulate dry deposition velocity for suburbs of Beijing, China (*Chinese*) 7-29219
- Pasquill stability class estimation from windspeed and sensible heat flux data 7-55130
- Pasquill stability classes at coastal station, diurnal and seasonal var. 7-9124
- planetary boundary layer eqns. soln. by finite element technique 7-9232
- planetary boundary layer meas. by vertical SODAR (*German*) 7-9148

atmospheric boundary layer continued
 planetary boundary layer wind profiles 7-14340
 plume dispersion in convective conditions, horizontal dispersion meas. 7-40062
 nonbuoyant plume dispersion modelling, based on meteorological scaling parameters 7-60308
 plume from electric power station, lidar obs. of concentration fluctuations 7-17930
 pollutant dispersion, wind tunnel expts. 7-1573
 pollutant transport by slope winds, influence of atmos. stability 7-60305
 pollution, plume concentration fluctuation models in one- and two-dimensions 7-23794
 pollution dispersion model for urban street canyons 7-34571
 pollution plume chemical evolution, model of turbulent reacting plume 7-14334
 pollution plume chemistry model, application to NO-NO₂-O₃ system 7-14335
 Priestley-Taylor evaporation formula performance, effect of synoptic-scale advection 7-4093
 radiative cooling in valleys and hollows 7-55134
 radiowave propagation and acoustic sounding developments 7-34607
 remote sensing method for surface pressure, using satellite sensed wind data 7-60417
 reservoir causing modification of air flow 7-14346
 roughness of land surface 7-55239
 sea and land breeze interaction with valley and mountain winds 7-23811
 sea breeze on a steep coast, mountains causing calm zone 7-4102
 sea ice influence on boundary layer, for marginal ice zone 7-34605
 semi-geostrophic flow over synoptic-scale topography 7-66260
 shallow water flow incident upon slender orography, semi-geostrophic response to elongated ridge 7-29122
 simple model of boundary layer involving sensitivity to surface evaporation 7-23796
 snow-covered surface, evaporated water vapour flux driving convection 7-4089
 space charge of metallic ground points beneath thunderstorm, due to corona discharge (*Chinese*) 7-29222
 stratified surface layer, similarity scales evaluation using wind speed and temp gradient 7-40514
 stratumcumulus-topped layer, third-order turbulence closure model stability 7-9102
 subsidence in nocturnal boundary layer 7-18280
 supercooled fogs artificial dispersal, anal. by lidar 7-34733
 surface heat flux and afternoon unstable temperature gradients 7-9066
 surface layer temperature profiles determ., use of three-parameter inferior mirage model 7-23804
 temperature inversion formation by numerical model (*Russian*) 7-55183
 temperature profile in marine surface layer, below 10 metres altitude (*Russian*) 7-18275
 temperature profiles in a thin layer over the sea 7-14368
 trade-wind boundary-layer, parameterisation for one-dimensional photochemical model of troposphere 7-9146
 turbulence characts. at 80 m level, influence of terrain type (*German*) 7-55236
 turbulence classification, computer program 7-55247
 turbulence closure model using Schumann's method 7-55133
 turbulence in flow over 2D hills 7-66256
 turbulence intermittence and acoustic signal reflection (*Russian*) 7-60330
 turbulence intermittency, airborne observational study (*Russian*) 7-4113
 turbulent diffusion in stratified surface layer, stochastic model (*Russian*) 7-9082
 turbulent dispersion from elevated source, nondimens. character and integral scale 7-6202
 two layer model for the barotropic stationary turbulent planetary boundary layer 7-40519
 unstable marine boundary layer, struct. determ. from lidar and aircraft obs. 7-29133
 urban boundary layer, mixing depth. rel. to wind speed and heat island formation 7-14336
 urban turbulence parameters, roughness effects 7-34582
 urban warming in North America, average warming rate (1941 to 1980) 7-29146
 Vancouver, BC, Canada, energy balances in rural and suburban areas 7-4098
 vegetation canopy, model of sunlight penetration involving leaf distribution 7-4097
 vertical SODAR for planetary boundary layer acoustic sounding (*German*) 7-9246
 vertical temp. gradient estimation using near-surface obs. 7-66343
 Washington, DC, USA, tracer dispersion expts. 7-60307
 water vapour measurement, satellite remote sensing technique 7-4112
 wind, environmental conditions in passages between buildings 7-14353
 wind, turbulence length scales in wind engineering 7-14354
 wind environment assessment at ground level, acceptable criteria determ. 7-14352
 wind field at nighttime, influence of city urban heat island 7-18282
 wind field of surface layer, spatial correlation function observations (*Russian*) 7-18277
 wind measurement in planetary boundary layer, lidar method accuracy 7-14347
 wind profile determ. method, using Doppler radar and lidar (*Russian*) 7-4210
 wind vector profiles 7-34614
 wind-wave relationships, Seasat radar altimeter meas. 7-34581
 CO₂, air-sea exchange in coastal areas 7-55083
 CO₂, gas exchange between air and sea, effect of breaking ocean waves 7-23704
 CO₂, ocean-atmosphere gas transfer in tropical Atlantic 7-29076
 H₂O₂ and CH₃OOH, photochemical formation in boundary layer of atmosphere 7-29155
 O₃ in equatorial Pacific boundary layer 7-29157
 O₃, surface concs. at rural sites in Latrobe Valley and Cape Grim, Australia 7-40065

atmospheric chemistry

acetonitrile-water mixtures, stratosphere-related aspects of gas phase ion chemistry 7-13775
 Antarctic atmosphere, O₃ var. modelling, chem. and dynamical effects 7-55172
 Antarctic O₃ depletion, chemical mechanisms for spring O₃ decrease 7-55165

atmospheric chemistry continued

Antarctic O₃ hole, effects of HNO₃ and HCl condensation in winter polar stratospheres 7-55162
 Antarctic O₃ hole formation, relation to characts. of polar stratospheric clouds 7-55163
 Antarctic O₃ stratospheric depletion, effects of Cl and Br pollution 7-55173
 Antarctic stratosphere, dynamics and photochemistry rel. to NO₂ and O₃ vars. 7-55158
 auroral zone mesosphere, radar obs. of negative-ion photodetachment at sunrise 7-66376
 carbonyl cpd. chemistry, review 7-34569
 cloud acidification, chemical and microphysical observations of clouds over Ontario, Canada 7-40530
 cloud condensation nuclei chem., anal. technique 7-3589
 clouds 7-55198
 conference, Seoul, South Korea (May 1985) 7-40982
 D-region, ion reaction scheme and cluster form. 7-60435
 dichlorofluoromethane, atmospheric lifetime and annual release estimates 7-29150
 dichlorofluoromethylperoxy radical + NO₂ forming peroxyxynitrate, rate const. at stratosphere conditions 7-23802
 F₂-layer peak electron density reduction due to N₂ vibrational excitation in summer 7-29355
 formic acid, atmospheric chemistry model for clouds 7-18290
 homogeneous gas phase mechanism for regional acid deposition model 7-3737
 hydrocarbon (nonmethane) chemistry of troposphere, 1D model 7-29168
 lower ionosphere, scale times and scale lengths assoc. with charged particle fluctuations 7-29359
 ions, hydration processes 7-29230
 long-range transport and acid deposition, chemical mechanism for model 7-29156
 mesosphere, auroral-zone, ion chemistry rel. to radar obs. of negative-ion photodetachment at sunrise 7-66376
 mesosphere Na chemistry, applicability of steady-state model 7-9281
 methyl peroxide, photochemical formation in boundary layer of atmosphere 7-29155
 mid-latitude mesosphere and thermosphere, comp. modelling 7-14402
 narrow cold-frontal rainbands, N and S scavenging 7-55191
 near-Earth space environment, spaceglow and material erosion 7-60506
 nighttime chemistry for offshore oceanic environment and dry environment 7-34584
 nitrate flux on Ross Ice Shelf, Antarctica, relation to solar cosmic rays 7-55091
 O₃ depletion in polar upper stratosphere, effects of meteoric material 7-55166
 organic acids in precipitation of Wisconsin, USA 7-14326
 organosulphur compounds, atm. photooxidation mechanisms anal. 7-54113
 particles photoelectric charging, implications for ion comp. and chem. reactions 7-28326
 peroxyxynitrate formation rate in stratosphere, CFCl₂O₂ + NO₂ reaction kinetics 7-23802
 photochemical mist formation in Ob River valley, correl. with meteorological characts. 7-9136
 photochemistry of terrestrial atmosphere, book 7-48210
 pollution plume chemical evolution, model of turbulent reacting plume 7-14334
 pollution plume chemistry model, application to NO-NO₂-O₃ system 7-14335
 pollution plume of chemically active cpds., expanding box model for long-range transport 7-60312
 polycyclic organic matter in atm., evidence for transformation 7-3735
 positive ion clustering with acetonitrile 7-999
 precipitation acidity, determ. of decrease resulting from decreased SO₄²⁻ conc. 7-54391
 scavenging of N and S, assoc. chem. processes 7-55192
 scavenging of S and N from rainbands and clouds, assoc. chem. processes 7-55191
 Shuttle glow, chemilum. processes 7-47602
 Shuttle glow, rammed surface temp. dependence 7-9284
 spacecraft glows, surface-catalysed reactions role 7-14401
 stratosphere, dynamically and chemically controlled vars. of NO₂ and O₃ in Antarctica 7-55157
 stratosphere, O₃ and NO₂ var. (1979 to 1984) 7-29205
 stratosphere, photochemical model rel. to LIMS obs. 7-66269
 stratosphere, photolysis rate calc. method with molecular scattering 7-29162
 stratosphere O₃ comp., implications of ClONO₂ + HCl(H₂O) reaction kinetics 7-54089
 stratospheric NO₂ amounts, transport and photochemical effects 7-47487
 sulphate production in hill cap clouds and subsequent deposition to hill 7-14331
 sulphate scavenging coefficient, estimates from sequential precip. samples on Long Island 7-8467
 thermosphere, NO energetics and IR radiation in disturbed heated thermosphere 7-4247
 trace gas measurements using matrix isolation-FTIR spectroscopy 7-55316
 trichlorofluoromethane, atmospheric lifetime and annual release estimates 7-29150
 troposphere, one-dimensional photochemical model with trade-wind boundary-layer parameterisation 7-9146
 volcanic plume from Etna, geochemistry and chemical reactions 7-34428
 As methylation, seasonal var. of methylarsenic compounds in airborne particulate matter 7-34638
 CO, methane and OH concentrations in AD 1980 to 2035 period, model 7-29153
 Cl chemistry in Antarctic stratosphere, impact of OClO and Cl₂O₂ on O₃ concs. 7-55164
 ClO + ClO reaction kinetics, implications for Antarctic O₃ 7-54090
 ClONO₂ + HCl, homogeneous and heterogeneous components, kinetics, implications for stratosphere chem. 7-54091
 HCl in middle stratosphere, obs. and modelling 7-14363
 HNO₃ cloud formation in cold Antarctic stratosphere, role in form. of springtime O₃ hole 7-47508
 H₂O in stratosphere, importance of methane oxidation source 7-34650
 H₂O₂ and CH₃OOH, photochemical formation in boundary layer of atmosphere 7-29155
 H₂O₂ + S(IV), reaction kinetics in rainwater samples 7-29170

atmospheric chemistry continued

- HOCl, gaseous, UV absorpt. spectrum, rel. to atm. modelling 7-25534
 HSO_5^- , formation in atmospheric clouds, model 7-18290
 N cpd. chemistry in troposphere of Colorado, USA 7-18288
 NH_3 , effect of precip. on vertical profiles 7-40513
 $\text{NaO} + \text{O}_2(\text{CO}_2)$, assoc. reactions with third body He, N_2 or N_2O , kinetics, atm. appl. 7-59748
 O^+ S state production by O_2^+ dissociative recombination in thermosphere 7-34759
 O airglow at 630 nm and $\text{O}(^1\text{D})$ quenching by $\text{O}(^3\text{P})$ 7-34761
 $\text{O} + \text{NO}_2$ (ClO) stratospheric reactions, rate const. meas. 7-8265
 O_2 electron impact dissociative excitation of $\text{OI}(2p^4\text{D}-3s^3\text{D}^\circ)$, λ 1172.6 Å multiplet transition 7-31179
 O_2 molecular photodissociation and Herzberg continuum 7-34757
 O_2 nightglow, excited states populations from rotationally-resolved afterglow spectrum 7-29326
 O_2 , potential energy curve, photodissociation and adsorp. spectra 7-5624
 O_2^+ in dayside ionosphere 7-55363
 O_3 2D monthly average balance with Chapman chemistry 7-47488
 O_3 , electronically excited state, radiative lifetime and quenching mechanism 7-31110
 O_3 form. in atm. effect of urban areas traffic pollution 7-3736
 O_3 formation, implications of surface concs. at rural sites in Latrobe Valley and Cape Grim, Australia 7-40065
 O_3 in middle atmosphere, physicochemical theory for latitudinal-seasonal vars. of O_3 conc. and mixing ratio 7-9280
 O_3 , metastable, occurrence and assoc. chem. reactions 7-55340
 O_3 minimum in Antarctic during springtime, photochem. model and 11-year solar cycle 7-29149
 O_3 , photochemical behavior near to 1 mbar level 7-29160
 O_3 seasonal variations at high latita. in Southern Hemisphere, general circulation model simulation 7-55167
 OH in tropical clouds, cloud chemistry model 7-18290
 $\text{OH} + \text{CO}$, reaction kinetics at atmospheric conditions 7-40529
 SO_2 , air pollution removal by 2D frontal rain system 7-34577
 SO_2 in atmosphere over Ljubljana, Yugoslavia, oxidation in wintertime conditions 7-34575
 SO_2 , O_3 -induced oxidation to aqueous sulphate in warm cloud conditions 7-54114

atmospheric composition

- see also atmospheric chemistry
acetic acid in rainfall of Wisconsin, USA 7-14326
acetic acid source determ. 7-55195
acid rain from Masaya volcanic, Nicaragua, comp., distrib. and neutralisation 7-9145
aerosol, laser backscattering study of aerosol struct. (Russian) 7-9169
aerosol, observations of fine-disperse fraction (Russian) 7-9083
aerosol, optical coeff., meas. technique (Chinese) 7-18305
aerosol, polar organic compound composition of particulates 7-14327
aerosol characts. at Pune and Srinagar, India 7-29180
aerosol concentration in drops, changes due to particle scavenging and redistrib. by coagulation 7-55201
aerosol in Late Quaternary atmosphere, Antarctic ice core record 7-55208
aerosol light absorpt. coeff., measurement method (Russian) 7-9221
aerosol profile in stratosphere between 1977 and 1984 AD 7-4136
aerosols, atmospheric, multiwave laser sounding, review 7-34678
aerosols, long-range transport anal. by particle-induced X-ray emission 7-4192
n-alkanes in atmosphere of Wisconsin, USA, in particulates and as vapour 7-14328
Antarctic, stratosphere temperature, effects of O_3 depletion 7-55174
Antarctic atmosphere, O_3 losses, role of heating perturbations 7-55171
Antarctic atmosphere, O_3 seasonal distrib. and thermal struct. 7-55168
Antarctic atmosphere, O_3 var. modelling, chem. and dynamical effects 7-55172
Antarctic O_3 comp., implications of ClO+ClO reaction kinetics 7-54090
Antarctic O_3 decreases, possible dynamic cause 7-55170
Antarctic O_3 depletion, chemical mechanisms for spring O_3 decrease 7-55165
Antarctic O_3 depletion, implications of nitrate flux on Ross Ice Shelf rel. to solar cosmic rays 7-55091
Antarctic O_3 depletion, implications of SAM II meas. of polar stratospheric clouds and aerosols 7-55160
Antarctic O_3 depletion, implications of stratospheric NO_2 meas. at Syowa station 7-55158
Antarctic O_3 hole, effects of HNO_3 and HCl condensation in winter polar stratospheres 7-55162
Antarctic O_3 hole, impact of OCIO and Cl_2O_2 on O_3 concs. in stratosphere 7-55164
Antarctic O_3 hole, implications of satellite obs. of polar stratospheric clouds 7-55156
Antarctic O_3 hole formation, relation to characts. of polar stratospheric clouds 7-55163
Antarctic O_3 stratospheric depletion, effects of Cl and Br pollution 7-55173
Antarctic spring, stratospheric heating rates and diabatic circulation, implications for O_3 depletion 7-55176
Antarctic stratosphere, O_3 density rel. to regional atm. circulation 7-55169
Antarctic stratosphere upwelling causing O_3 depletion 7-55175
anthropogenic radionuclides meas. around nuclear power reactors, method for ^3H , ^{14}C , ^{85}Kr and ^{133}Xe 7-23257
Arctic precipitation, sulphate content over last 90 years from glacier ice 7-23252
Atlantic Ocean, atm. aerosols temporal and spatial var. anal. 7-4085
azelaic acid, in atmospheric particulates of Japan 7-14327
Brazil, particulates in natural and urban atmosphere 7-34081
chemical deposition, stochastic modelling of space-time struct. 7-23239
Chinese energy consumption growth forecast and implications for atmospheric CO_2 increase 7-28418
chloromethane in upper troposphere and stratosphere, spectroscopic detection 7-9076
cloudwater at Scandinavian clear air site 7-55223
conference on natural and man-made ions in atm., London, England (October 1985) 7-24304
D-region, ion composition use for mesosphere H_2O estimation 7-60435
dichlorofluoromethane, atmospheric lifetime and annual release estimates 7-29150
diffusion studies in atmospheric air, using Langmuir probe 7-34724

atmospheric composition continued

- El Chichon and "mystery cloud" aerosols in stratosphere and mesosphere 7-23803
ethane, identification from 1951 IR solar spectrum 7-55124
W Europe, climate simulation and CO_2 -induced climate change 7-66285
fluoride in precipitation, natural background levels in India 7-14329
formic acid, atmospheric chemistry model for clouds 7-18290
formic acid in rainfall of Wisconsin, USA 7-14326
formic acid source determ. 7-55195
glutaric acid, in atmospheric particulates of Japan 7-14327
Greenland snow-ice core, record of air pollution changes 7-18292
hydroxymethanesulphonate in atm. precipitation 7-60326
ice-forming nuclei concentration, dependence on temperature and supersaturation (Russian) 7-18278
India, acidity of rainfall affected by basic soil dust in atmosphere 7-29184
Indian sea areas, rainwater comp. during monsoon season 7-9123
inert gases isotopic compositions, effects of mass fractionation during transonic gas escape 7-55508
outer ionosphere, D^+ concs. rel. to charact. freqs. of deuteron whistlers 7-18335
ions, hydration processes 7-29230
Laurel Mountains peat bog, USA, atm. chemicals deposition chronology 7-9075
Lucknow, India, 1982 rainfall comp. 7-9129
magnetotail plasma sheet, comp and plasma props. 7-34789
melanin content of human skin, evidence for past climates? 7-66289
mesosphere, Antarctic springtime meas. of O_3 , NO_2 and aerosol extinction by SAM II, SAGE and SAGE II 7-55161
mesosphere, auroral-zone, NO conc. from radar obs. of negative-ion photodetachment at sunrise 7-66376
mesosphere H_2O estimation determ. from D-region ion comp. data 7-60435
mesosphere Na chemistry, applicability of steady-state model 7-9281
mesosphere Na layer, lidar obs. 7-34753
methane, emission from tropical forest soils 7-40528
methane and aerosol, in atmosphere of Kislovodsk, USSR (Russian) 7-54388
methane release from rice paddy fields in Italy 7-40073
methylarsenic compounds in airborne particulate matter, seasonal var. 7-34638
microwave plasma emission characteristics in near IR 7-55318
mid-latitude mesosphere and thermosphere, comp. modelling 7-14402
middle atmosphere, EHF sounding from Space Shuttle 7-40568
middle atmosphere, minor constituents diurnal var. rel. to thermal structs. in Eastern and Western Hemispheres 7-66375
midlatitude stratosphere BrO and ClO comp. 7-60324
Millimetre Atmospheric Sounder on Shuttle for passive sounding (German) 7-40617
N compounds, scavenging in narrow cold-frontal rainbands, numerical model 7-55191
negative ion composition in troposphere, chemical model 7-55210
nitrate flux on Ross Ice Shelf, Antarctica, relation to solar cosmic rays 7-55091
nitrate scavenging by rain and snow, for Long Island, New York, USA 7-40531
nuclear winter, smoke scavenging by atmospheric ozone 7-9109
 O_3 data from Nimbus-7 SBUV instrument 7-55178
 O_3 depletion in polar upper stratosphere, effects of meteoric material 7-55166
organic acids in precipitation of Wisconsin, USA 7-14326
peroxyacetyl nitrate and N cpds. in troposphere of Colorado, USA 7-18288
photochemical mist formation in Ob River valley, correl. with meteorological characts. 7-9136
pollutant concentrations distrib. modelling estimation of one and two-parameter statistical distrib. 7-40067
Precambrian atmosphere, O_2 and CO_2 concs. from palaeosols chemistry and mineralogy 7-29018
Precambrian atmosphere, transition to O_2 -rich state, geological evidence 7-18304
primordial atmosphere, climatic consequences of high CO_2 levels 7-66271
propionic acid in rainfall of Wisconsin, USA 7-14326
radiation absorbers in atmosphere, distrib. estimation using infrared 3-band images (Japanese) 7-47577
rare gases rel. to formation of atmosphere 7-60386
Rio de Janeiro, Brazil, aerosol characterization study 7-65661
Saharan dust transport by atmosphere, observations and model 7-14343
Saharan dust transport by atmosphere, review 7-9073
Samoa (American), washout ratios of nitrate, non-sea-salt sulphate and sea-salt 7-60309
scavenging of N and S, assoc. chem. processes 7-55192
SCRIBE interferometer atmospheric emission spectra 7-55319
Central Sierra Nevada, United States Winter storms ice-phase water capture regions identification, use of snow O isotopic comp. 7-4084
soluble gas removal by warm precipitating stratiform clouds 7-55230
soluble gases, rainout lifetimes 7-55189
storm acid precipitation and stream water geochemistry 7-23777
stratosphere, Antarctic springtime meas. of O_3 , NO_2 and aerosol extinction by SAM II, SAGE and SAGE II 7-55161
stratosphere, climate modelling, band strengths temp. depend., low temp. meas. using Freons 7-55252
stratosphere, condensation of HNO_3 and HCl in winter polar stratospheres 7-55162
stratosphere, contrib. of gas constituents to radiative balance 7-9098
stratosphere, far-IR spectrum, high resolution meas. with Fourier transform spectrometer 7-55262
stratosphere, IR spectroscopy with balloon-borne cryogenic Fourier spectrometer 7-60377
stratosphere, mixing ratio gradients during simulation of winter polar vortex 7-47489
stratosphere, O_3 and NO_2 var. (1979 to 1984) 7-29205
stratosphere, trace gas transport by planetary waves during major warming event in winter 7-29161
stratosphere, tracer transport on isentropic surface as function of polar vortex area 7-29134
stratosphere NO_2 and O_3 in Antarctica, dynamically and chemically controlled vars. 7-55157
stratosphere O_3 comp., implications of $\text{ClONO}_2 + \text{HCl}(\text{H}_2\text{O})$ reaction kinetics 7-54089
stratosphere O_3 profiles meas. by ROCOZ-A 7-55308

atmospheric composition continued

- stratosphere trace constituents, meridional distrib. 7-9087
 stratospheric far-IR emission analysis, synthetic spectra and FTIR meas. comparison 7-55315
 succinic acid, in atmospheric particulates of Japan 7-14327
 sulphates, scavenging coeff. estimates from sequential precip. samples on Long Island 7-8467
 summertime O₃ and SO₂ climatology in E United States (1977 to 1981) 7-40066
 thermosphere, evidence for metastable O₃, assoc. chem. reactions 7-55340
 thermosphere, ion composition, rocket-borne mass spectrometer meas. 7-66373
 thermosphere, neutral mass density calc. 7-47585
 thermosphere, NO energetics and IR radiation in disturbed heated thermosphere 7-4247
 thermosphere O and nightglow 7-47603
 Thumba, India, atm. O₃ meas. 7-66214
 toxaphene deposition to E North America, determ. from peat accumulation 7-40064
 trace element detection by differential absorption spectroscopy (German) 7-46991
 trace gas measurements using matrix isolation-FTIR spectroscopy 7-55316
 trace gas trends at Palmer Station, Antarctica (1982-1985) 7-55159
 trichlorofluoromethane, atmospheric lifetime and annual release estimates 7-29150
 troposphere, one-dimensional photochemical model with trade-wind boundary-layer parameterisation 7-9146
 Tyohu, Japan, SO₄²⁻ and NO₃⁻ content in aqueous aerosols (Japanese) 7-47511
 United States E and Gulf coasts, conc. and sources of CO and H₂ 7-55197
 upper atmosphere, EISCAT obs. of neutral mass 7-29316
 NE USA, MAP3S network precipitation chemistry results 7-60310
 E USA, particulates of natural and anthropogenic origin at rural site 7-4119
 NE USA, sulphate and nitrate in wintertime precipitation 7-60311
 Virginia Key, Florida, washout ratios of nitrate, non-sea-salt sulphate and sea-salt 7-60309
 volcanic aerosol from El Chichon and lidar depolarization observations 7-29243
 volcanic eruption aerosol; horizontal transport and evolution modelling 7-23819
 volcanic plume from Etna, geochemistry and chemical reactions 7-34428
 volcanic plumes from Etna and Mt. St. Helens, particle geochemistry 7-34427
 As and Sb in aerosols over English Channel and N Atlantic 7-29075
¹⁰Be cosmogenic radionuclide production during Pleistocene 7-23842
 C isotope composition of methane in atmosphere 7-29167
 C particulates in marine atmosphere, long-range transport from continents 7-55221
 CO and O₃ in global stratosphere and troposphere, tracer horizontal spectra 7-29164
 CO in Antarctic atmosphere, concentration in AD 1977 to 1985 period (Russian) 7-18276
 CO, in atmosphere of Kislovodsk, USSR (Russian) 7-54388
 CO in troposphere, November 1981, concentration observations 7-29154
 CO in troposphere of Saudi Arabia, India, Arabian Sea, conc. obs. 7-18291
 CO measurements with submm heterodyne spectrometer 7-60562
 CO, methane and OH concentrations in AD 1980 to 2035 period, model 7-29153
 CO₂, 19th-century vars. in W Europe and British Isles from anal. of contemporary air masses 7-9144
 CO₂, air-sea exchange in coastal areas 7-55083
 CO₂ and land biota destructivity 7-34640
 CO₂ atmosphere conc. in Cenozoic, effect on climate 7-34666
 CO₂ climate sensitivity and model dependence of results 7-66298
 CO₂ concentration in lower troposphere, simultaneous meas. at neighbouring mountain stations 7-55199
 CO₂ concentrations during preindustrial times (Russian) 7-9081
 CO₂, emission from tropical forest soils 7-40528
 CO₂, exchange rate between atmos. and ocean, isotopic meas. techniques 7-23884
 CO₂, gas exchange between air and sea, effect of breaking ocean waves 7-23704
 CO₂, geochemical C cycle disturbance and impact on biosphere 7-40546
 CO₂, ice core record of ¹³C/¹²C ratio in past two centuries 7-34637
 CO₂ increase, response of ocean-atmosphere system (Russian) 7-23834
 CO₂, ocean-atmosphere gas transfer in tropical Atlantic 7-29076
 CO₂, total world production due to wood fuel burning 7-54386
 COF₂ in stratosphere, concentration determined by IR solar absorpt. observations 7-9077
 ACO, A=12,13 in upper atm., detect. with submillimetre heterodyne spectrometer 7-353
¹⁴C, activity meas. in atmosphere, anal. methods 7-54214
¹⁴C concentrations, seasonal vars. 7-23256
 ClONO₂, stratosphere conc. profile from IR spectral observation 7-9167
 D and H concentrations in daytime thermosphere 7-60437
 H in exosphere, Monte Carlo model of solar cycle influences 7-55338
 H₂¹⁸O, hot band, IR spectral line positions and intensities 7-36623
 HCl detection in atm. by laser-induced fluorescence of CO₂ 7-46993
 HCl in atm., ground-based IR solar spectra anal. 7-40538
 HCl in middle stratosphere, obs. and modelling 7-14363
 HCl in stratosphere, near-IR satellite remote sensing and interference from OH airglow 7-23926
 HNO₃, air pollution due to nuclear explosions in atmos., glacier ice core record 7-46982
 HNO₃, cloud formation in cold Antarctic stratosphere, role in form. of springtime O₃ hole 7-47508
 H₂O conc. in mesosphere, airglow holes and small comet influx 7-40622
 H₂O in middle atmos., vertical profile observations 7-34758
 H₂O₂ in polar ice cores, long-term record 7-55229
 HO₂NO₂, IR spectra of stratosphere at 802 cm⁻¹ and conc. profile 7-9168
 HSO₅⁻, formation in atmospheric clouds, model 7-18290
 Hg emissions from cement factory, influence on environment 7-40060
 I₂, detect. in atmospheric, differential reson. technique 7-40552
⁸⁵Kr, sampling unit for air sample 7-23258

atmospheric composition continued

- N pollution in hydrosphere and atmosphere, appls. of isotopic studies 7-28422
 NH₃, effect of precip. on vertical profiles 7-40513
 NO concentration prediction, appl. of regression model 7-40063
 NO concentrations in thermosphere and nightglow continuum 7-47605
 NO, dayglow UV emissions and vertical profile 7-29324
 NO in upper atmosphere, geomagnetic latitudinal conc. distrib. 7-9278
 NO in upper atmosphere, near-midnight nightglow and vertical profile 7-9283
 NO, NO₂ and other N cpds., troposphere conc. observations in Colorado, USA 7-18288
 NO, Zeeman modulated radiometer for remote detection 7-55313
 NO₂ in stratosphere, obs. by ground-based and balloon-borne techniques at Syowa Station (69.0°S, 39.6°E) 7-55158
 NO₂ in stratosphere above USSR, concentration variations (Russian) 7-60331
 N₂O, emission from tropical forest soils 7-40528
 N₂O in troposphere near to Florida, day and night vertical profiles 7-40537
 Na layer at nighttime, seasonal and nocturnal variations 7-55339
 Na layer in upper atmos., formation from dust particles 7-66372
 Na layer near to 80 km altitude, Na density variations during twilight 7-29322
 O isotope composition above 100 km altitude, deep-sea spherule evidence 7-9441
 O₂ nightglow, excited states populations from rotationally-resolved afterglow spectrum 7-29326
 O₂, UV cross sections and photodissociation rate consts. for stratosphere 7-55260
 O₂, 2D monthly average balance with Chapman chemistry 7-47488
 O₃ and aerosol measurements in springtime Antarctic stratosphere (November 1985) 7-55155
 O₃ conc. in S Hemisphere, influence of medium-scale waves 7-29151
 O₃ content and sources for tropical atmosphere 7-55194
 O₃ content determination via mutual covariation links between temp. and O₃ content, accuracy of determ. 7-9135
 O₃ decrease in Antarctic stratosphere, role of planetary waves 7-55148
 O₃ decrease of Antarctica and southern mid-latitudes, TOM observations 7-55146
 O₃ density variations, meas. by Nimbus-7 and SME 7-60323
 O₃ depletion above Antarctica, recent observations 7-55141
 O₃ determination, balloon borne instrumentation, BOIC intercomparison expt. 7-29159
 O₃ distribution in atmosphere (Russian) 7-40521
 O₃, Dobson data, statistical anal. methods 7-55307
 O₃, global minima in historical record 7-55153
 O₃ in Antarctic stratosphere, decreases in springtime rel. to circulation 7-55151
 O₃ in boundary layer of equatorial Pacific 7-29157
 O₃ in eastern USA, O₃ diurnal variations at rural mountain 7-66220
 O₃ in middle atmosphere, latitudinal-seasonal vars. of O₃ conc. and mixing ratio 7-9280
 O₃ in stratosphere, DIAL meas. from Shuttle, error analysis 7-40560
 O₃ in stratosphere, O₃ isotope measurements at Texas, USA, ⁴⁹O and ⁵⁰O observations 7-66209
 O₃ in stratosphere above Antarctica, conc. changes correl. to temperature and circulation 7-55142
 O₃ in stratosphere above Antarctica, conc. rel. to temperature changes 7-55152
 O₃ in stratosphere above Antarctica, AD 1985 vertical distrib. 7-66210
 O₃ in stratosphere above Antarctica, O₃ depletion in AD 1971 to 1984 period 7-66211
 O₃ in stratosphere of Antarctica and southern mid-latitudes 7-55144
 O₃ in troposphere of Colorado, USA 7-18288
 O₃ measurement by M-124 filter ozonometer 7-34734
 O₃ measurement device using HARTLEY band (German) 7-9247
 O₃ measurement with Nimbus-7 TOMS instrument 7-55177
 O₃ minimum in Antarctic during springtime, photochem. model and 11-year solar cycle 7-29149
 O₃ nighttime increase, ground-based EHF radiometry of mesosphere 7-47593
 O₃ over Antarctica, interannual variability during circumpolar vortex breakdown 7-55139
 O₃ over Antarctica, ozonosphere conc. decrease in AD 1961 to 1985 period 7-55140
 O₃ remote sensing, information content of upward directed IR radiation 7-23865
 O₃ remote sensing, SBUV satellite meas. technique for Antarctic O₃ vertical profiles 7-55145
 O₃ seasonal variations at high latits. in Southern Hemisphere, general circulation model simulation 7-55167
 O₃, statistical trend analysis for troposphere and stratosphere 7-29158
 O₃, surface concs. at rural sites in Latrobe Valley and Cape Grim, Australia 7-40065
 O₃ total content, decrease at South Pole, Antarctica (1964-1985) 7-55154
 O₃ total content, determ. from remotely-sensed data 7-66216
 O₃ vertical distrib. influenced by stratospheric intrusions 7-23820
 O₃ vertical distrib. over Dakshin Gangotri, Antarctica 7-66215
²¹⁰Pb in air and soil, use to meas. aerosol scavenging rate and vertical profile 7-55188
 Rn daughters automatic meas. instrument for atm. precipitation 7-49847
²²²Rn concentrations in USA homes, statistical distrib. and health hazards 7-65666
²²²Rn in Subantarctic and Antarctic, long-range transport from remote continents 7-55222
 S compounds, scavenging in narrow cold-frontal rainbands, numerical model 7-55191
 SO₂, air pollution near to oil refinery at Mathura, India 7-28433
 SO₂ concentrations in Venice area, probability model 7-17929
 SO₂ in Venice, statistical study of pollutant concs. via generalised gamma distrib. 7-34090
 SO₂ pollution in Cracow area, Poland, short-term concs. modelling 7-40068
 SO₄²⁻, contrib. of decreased concs. to decrease in precip. acidity 7-54391
 Se and Te content of aerosols in Missouri, USA 7-18273

atmospheric density *see* atmospheric pressure and density

atmospheric duct *see* atmospheric electromagnetic wave propagation

atmospheric dynamics *see* atmospheric movements

atmospheric electricity

see also atmospheric electromagnetic wave propagation; atmospheric ionisation; electrojets; ionosphere; lightning; thunderstorms
 airborne meas. of fields prod. by convective clouds 7-55213
 auroral arc electrodynamics correlation with neutral winds 7-47609
 biological significance of air ions 7-28496
 Birkeland currents correlated with d.c. elec. fields 7-55347
 breakdown due to rock fracture, light emission (*Chinese*) 7-29000
 clouds undergoing precipitation, elec. props. 7-29212
 conference on natural and man-made ions in atm., London, England (October 1985) 7-24304
 dayside auroral ionosphere, ion convection and elec. fields 7-55348
 E-region, equatorial irregularities, phase vel. depend. on polarisation elec. field 7-47628
 ELF fields in Earth-ionosphere resonator, day-night inhomogeneity effect 7-66219
 field diffusion in three-dimensional conductor, air-subsoil coupling (*French*) 7-28843
 field disturbances, man-made 7-29231
 ground coronae effects during lightning flashes 7-55122
 high-latitude ionosphere, elec. fields and pot. patterns for different interplanetary conditions 7-14421
 ice, microscopic filament form. in elec. field 7-14362
 ionosphere, characts. of longit. currents in cusp as function of interplanetary mag. field orientation 7-4261
 ionosphere, collisional ion cyclotron instability, effect of finite current channel width 7-47630
 ionosphere, cond. var. effect on VLF waves in Earth-ionosphere waveguide 7-47626
 ionosphere, conductivity distrib. rel. to duct propag. of short-period MHD wave 7-66392
 ionosphere, conductivity models generation method 7-14395
 ionosphere, contrib. of By-component of IMF to north-south asymmetry of geomag. activity 7-9336
 ionosphere, current systems, mag. field contribution to crust meas. 7-14191
 ionosphere, discharge of RF-induced spacecraft DC potential by positive ions 7-66427
 ionosphere, effect of electron temp. on electron number density and dynamics of equatorial E-region 7-66390
 ionosphere, elec. dipole field in inhomogeneous plasma 7-29330
 ionosphere, electrical and electrothermal conductivities compared with Mars and Venus 7-34781
 ionosphere, Langmuir probe measurements in sheath of highly charged body 7-37744
 ionosphere, near-field radiation from pulsed electron beams in space 7-66391
 ionosphere, relationship between EM drift components at mid and low latitudes 7-9315
 ionosphere, resonant phenomena accompanying seismic-ionospheric electrical interaction 7-28890
 ionosphere, storm sudden commencement elec. fields 7-60492
 Kakinada sand spit, India, atm. elec. meas. 7-23806
 lightning, charge deposition to ground for cloud-to-ground discharges 7-29171
 magnetosphere, Birkeland currents rel. to damping of Pi 2 pulsations 7-47631
 magnetosphere, current-driven double layers, field-aligned current density and pot. difference 7-34802
 magnetosphere, electron energy spectra and electrostatic cyclotron waves during diffuse auroras 7-34763
 magnetosphere, electrostatic wave trapping near magnetospheric equator 7-34788
 magnetosphere, geosynchronous region, bounce-phase bunched ion distrib. model, elec. field effects 7-47639
 magnetosphere, polar parabolic heavy ion flow, elec. field effects 7-60455
 magnetosphere, standing waves struct., elec. and mag. field obs. 7-9326
 magnetosphere, storm-time reconfiguration as cause of strong precip. of energetic protons 7-9316
 magnetosphere electric field measurement, effects of photoelectron emission from GEOS-2 double probe sensors 7-66426
 measurement method for conduction current, using balloon-borne wire antenna 7-29289
 metallic ground points beneath thunderstorm, calc. of space charge due to corona discharge (*Chinese*) 7-29222
 north polar currents in winter, geomag. activity effects 7-60450
 plasmopause, elec. field and convection characts. at midnight 7-34770
 radiation belts, elec. fields rel. to protons spatial distrib. at high and low latitudes 7-4274
 radioactive fallout from Chernobyl nucl. reactor, influence on atmos. elec. fields 7-40536
 spark breakdown time-lag, negative ion effects 7-29233
 Sq day-to-day var. in geomag. conjugate areas, current effects 7-60452
 stratosphere above Arctic storm system, elec. field observations 7-18293
 stratospheric electrical conductivity variations above thunderstorms 7-29169
 isolated thundercloud over mountains, microphysics, kinematics and electrification 7-34602
 thunderclouds, elec. field and precip. growth in finite cloud 7-29206
 thunderclouds of abnormal polarity, for clouds grown from negatively charged air 7-29227
 thunderstorm anvil clouds, elec. characts. and dynamics (*Chinese*) 7-29121
 thunderstorm electric field measurement method using a corona probe 7-18318

atmospheric electromagnetic wave propagation

see also atmospheric light propagation; ionospheric electromagnetic wave propagation; magnetospheric electromagnetic wave propagation; tropospheric electromagnetic wave propagation
 Antarctic ice cap influence on VLF propagation, diffraction round ice cap 7-47491
 North Atlantic anomalous microwave propagation, long-range expt. 7-47481
 atmospheric radio noise, MF and HF, bandwidth expansion effects on voltage deviation parameters 7-60366
 cm and mm wave propagation, tropical raindrop size characts. and effects 7-66280

atmospheric electromagnetic wave propagation continued

Earth's atmosphere radio transillumination, signal parameters, ionosphere effect 7-55367
 ELF fields in Earth-ionosphere resonator, day-night inhomogeneity effect 7-66219
 estimation of partitioned set of parameters 7-40554
 HF groundwave and skywave propagation 7-40643
 mesosphere, auroral zone, radar echoes rel. to obs. of negative-ion photodetachment at sunrise 7-66376
 meteor burst propagation and system design 7-40644
 microwave communication, equatorial and tropical regions, rain effects 7-66281
 microwave line-of-sight links, elevated atmospheric duct, multipart fading anal. 7-47482
 microwave propagation of short bursts 7-34664
 MM wave propagation through sand and dust storms, effect of particle size 7-47480
 mm-wave propag. characts. of atmosphere (*German*) 7-66207
 near-mm wave propag., instrumentation for study 7-4219
 radar refractive index fluctuations appl. to turbulence obs. in middle and lower atmosphere 7-47598
 radio acoustic meas. of temp. profile in troposphere and stratosphere, expl. results 7-14360
 radio waves scattering from underdense meteor trains, electron volume density formulae 7-4383
 radiowave propagation and acoustic sounding developments 7-34607
 randomly oriented particle layer, vector solution for mean EM fields 7-14365
 sandstorm effect on radiowave propag., system design for Riyadh, Saudi Arabia 7-4111
 spatial correlation coefficients of rainfall intensity inferred from statistics of rainfall intensity and rain attenuation 7-47474
 UHF/SHF SATCOM propagation and system design 7-40555
 VHF radar echoes, appl. to obs. and meas. of middle atmosphere turbulence 7-4246
 Vostok station, Antarctica, humidity and subMM transparency (*Russian*) 7-23822

atmospheric electron precipitation

auroral electron precip., relation to LHR noise obs. by S-310JA-6 sounding rocket 7-66393
 burst precipitation induced perturbations on multiple VLF propagation paths in Antarctica 7-66379
 conjugate polar cusp electron precipitation obs. by DE 1 and DE 2 satellites 7-29347
 D-region disturbance signatures during substorm growth phase and onset 7-29335
 dayside aurora, assoc. electron precipitation and ionosphere convection morphology characts. 7-55352
 electron distributions of north and south polar cap regions, electron precipitation processes 7-9300
 induced ionisation enhancement in ionosphere, effect on VLF waves in Earth-ionosphere waveguide 7-47626
 inner radiation belt, electron distribution function and radial diffusion coeff. (at $L=1.2$ to 1.4) 7-34805
 ionosphere, contrib. of By-component of IMF to north-south asymmetry of geomag. activity 7-9336
 ionosphere, electron energy spectra and electrostatic cyclotron waves during diffuse auroras 7-34763
 midday auroral oval, rocket meas. of electron influx 7-55349
 morningside aurora electron precipitation characts. 7-29349
 narrow electron beam precipitation associated with narrow auroral arc 7-47607
 intense polar rain, polar cap and magnetotail obs. and acceleration processes 7-23940
 intense polar rain occurring symmetrically in both hemispheres and solar wind interaction 7-29356
 poleward edge of mid-latitude trough, formation orientation and dynamics 7-23938
 pulsating aurora and absence of hydromagnetic waves in conjugate equatorial magnetosphere 7-55358
 quiet-time precipitation, correlated electron and X-ray meas. 7-47624
 radiation belts, slot region electron precipitation, triggering mechanism 7-9325
 storm-time precipitation flux variations, for 2 Dec. 1977 storm 7-9289
 variations at $L\sim 4$, depend. on local time, substorms and season 7-34771
 wave-particle interactions in outer trapping and morningside auroral regions, model 7-55373

atmospheric elementary particle precipitation

see also atmospheric electron precipitation; atmospheric proton precipitation
 auroral precipitation, contrib. to mesospheric radar echoes and obs. of negative-ion photodetachment 7-66376
 F-region, heating rates due to auroral precipitation 7-34772
 flux due to gyroresonant pitch angle scatt. by whistler mode waves 7-60490
 ion conics formation, laboratory obs. by vel.-space tomography of plasma 7-44250
 ionosphere dayside cusp, particle fluxes and longit. currents as function of IMF orientation 7-4261
 proton precipitation due to proton interaction with electrostatic VLF waves 7-34807
 South Atlantic mag. anomaly, charged particle fluxes in inner magnetosphere 7-4275
 stochastic instability of charged particles in geomag. trap, theory 7-34804

atmospheric humidity

see also hygrometers
 3D trajectories, wind and humidity characts. determ. 7-55190
 aerosols optical props. and humidity effects (*Russian*) 7-29241
 S Africa, summer rainfall distrib., effects of circulation and humidity 7-47492
 W Africa-E Atlantic region, simulated rainfall, effects of enhanced initial moisture fields 7-47499
 S Alberta, Canada, chinooks distinguishing nocturnal features 7-47493
 Arabian Sea, low-level inversion synoptic characts. (during MONEX-79) 7-9120
 Argentina continental shelf, temp. and humidity profiles, planetary boundary layer modelling 7-34579
 Athens, Greece, turbidity meas. and components 7-9174
 Bangladesh, evaporation rates, water pan observations 7-29092

atmospheric humidity continued

- Belgium, meteorological observations, AD 1981-5 at Uccle (*French, Flemish*) 7-47484
 Cagliari Astronomical Observatory, Sardinia, diurnal and annual vars. in water vapour contents 7-40547
 convective systems of 100 km scale during GATE, heat and moisture transport 7-29189
 cumulus moisture transport effect on GCM climate simulation 7-66291
 DIAL monitoring, H₂O absorption line parameters 7-47535
 East Germany, evaporation height rel. to air temp., global radiation and saturation deficit (*German*) 7-9055
 El Nino, simple model involving atm. convergence feedback 7-34536
 FOG-82, cooperative field study of radiation fog, exptl. design and results 7-9068
 global oceans, monthly mean precipitable water and surface level humidity 7-29202
 Gulf of Carpentaria, 1984 October 25-6 morning glory wind surges, temp. and humidity meas. 7-4091
 Ireland, high absolute humidities episode (1983 July 12 to 13) 7-40541
 lidar in inhomogeneous atm., backscatter/extinction ratio humidity effects 7-40562
 Local AFOS MOS programme appl. to wind prediction 7-34679
 mesosphere, H₂O conc., airglow holes and small comet influx 7-40622
 mesosphere and stratosphere, vertical profile observations by Spacelab One 7-34758
 Millimetre Atmospheric Sounder on Shuttle for passive sounding (*German*) 7-40617
 near-mm wave propag., instrumentation for study 7-4219
 relative humidity measurement using alpha-particle corona streamer counter 7-55333
 remote sensing of precipitable water by ground based 1.35 cm radiometry (*Chinese*) 7-29311
 satellite remote sensing of atmospheric water vapour, appl. of IR meas. 7-4112
 satellite retrievals, systematic errors 7-66266
 snow-covered surface, evaporated water vapour flux driving convection 7-4089
 stratified atmosphere heating is model for moist convection 7-4127
 stratosphere, H₂O budget, satellite observations and importance of methane oxidation 7-34650
 stratosphere, satellite temp. and humidity meas. rel. to polar stratospheric clouds 7-55156
 stratosphere, tracer transport on isentropic surface as function of polar vortex area 7-29134
 stratus clouds, numerical modelling of water content and dew point deficit 7-9132
 supercooled liquid water in clouds at mountaintop sites, meas. in Colorado Rockies 7-29147
 supersaturation field around growing graupel in supercooled clouds 7-34591
 total vertical water vapour determ., methods comparison 7-4087
 tracer horizontal spectra in global stratosphere and troposphere 7-29164
 tropical squall line, cloud water and water vapour content retrieval 7-4212
 tropical squall line, diagnostic modelling study of stratiform cloud region 7-29136
 troposphere, water vapour effect on VLBI meas. of vertical crust motion 7-9227
 troposphere radiowave propagation, water vapour correction in GPS baseline determ. 7-9228
 SW United States, summer precipitation singularity, moisture transport 7-47494
 vapour condensation heating, contrib. to seasonal movements of subtropical high ridge line 7-40508
 vertical crust motion meas. by mobile VLBI and GPS, effects of atm. water vapour 7-9226
 Vostok station, Antarctica, humidity and subMM transparency (*Russian*) 7-23822
 water in atmospheric aerosol drops, activity calcs. 7-9110
 water vapor vertical profile structures retrieved from satellite data via classification and discrimination 7-4218
 water vapour content, microwave radiometric meas. at NPL 7-34606
 LiNbO₃ SAW oscillator for humidity and temp. meas. 7-4232

atmospheric ionisation

- auroral zone mesosphere, radar obs. of negative-ion photodetachment at sunrise 7-66376
 conference on natural and man-made ions in atm., London, England (October 1985) 7-24304
 cosmic ray induced ionisation intensity meas. 7-40308
 cosmic-ray induced ionization intensities near Kaohsiung, Taiwan, ground, sea-level meas. (*Chinese*) 7-55399
 D-region, winter-time, electron densities and wind vels. from partial refl. radar obs. 7-47612
 F₂-layer, ionisation response to solar 10.7 cm flux 7-14408
 F₂-layer visualisation, eleven years of ionospheric chromatograms 7-23848
 high voltage transmission lines, corona discharges and ion prod. 7-29232
 ionosphere, critical velocity phenomena, anomalous ionization 7-66388
 outer ionosphere, D⁺ concs. rel. to charact. freqs. of deuteron whistlers 7-18335
 ionosphere, discharge of RF-induced spacecraft DC potential by positive ions 7-66427
 ionosphere, effect of electron temp. on electron number density and dynamics of equatorial E-region 7-66390
 lower ionosphere, effect of negative ions on use of whistlers as diagnostic technique 7-66381
 ionosphere, effects of lower atm. nucl. explosion (*Chinese*) 7-29257
 lower ionosphere, electron density determ. via radio waves resonance scattering method 7-47613
 ionosphere, enhancements, effect on VLF waves in Earth-ionosphere waveguide 7-47626
 ionosphere, ionisation vars. rel. to radio waves absorpt. during solar eclipse 7-29361
 low ionosphere, local and long-distance effects of meteor showers 7-4256
 ionosphere, plasma concentration vars. in main ionospheric trough during mag. storm (1978 December 18 to 19) 7-34780
 ionosphere, plasma instabilities rel. to nonlinear wave structs. generation 7-66386
 ionosphere, plasma parameters meas. in vicinity of Space Shuttle 7-29360

atmospheric ionisation continued

- ionosphere, reson. ionisation accompanying seismic-ionospheric electrical interaction 7-28890
 lower ionosphere, scale times and scale lengths assoc. with charged particle fluctuations 7-29359
 ionosphere irregularities, relation to VHF scintillations increase during mag. activity 7-34762
 ionosphere winter anomaly, effects on propag. of LF (40 kHz) radio waves 7-47611
 ions from high-voltage equipment 7-29234
 magnetosphere, ISEE-3 energetic ion results (EPAS) in deep geomag. tail 7-29367
 magnetosphere, suprathermal ion and electron results from ISEE-3 Geotail Mission 7-29368
 meteor ionisation, radio propag. mechanism and system design 7-40644
 meteor ionisation, radio waves scattering from underdense meteor trains 7-4383
 meteoric ionisation, possible causal relation between fireballs and noctilucent clouds 7-29437
 negative ion composition in troposphere, chemical model 7-55210
 negative ion effects on spark breakdown time-lag in air 7-29233
 particles photoelectric charging, implications for ion comp. and chem. reactions 7-28326
 thermosphere, ion composition, rocket-borne mass spectrometer meas. 7-66373
 water in atmospheric aerosol drops, activity calcs. 7-9110
 X-ray and UV induced ionisation of molecules 7-24001
 NO⁺ rel. to ionospheric E-layer height vars. and daytime valley 7-40625

atmospheric light propagation

- aerosol inhomogeneities, lidar data anal. (*Russian*) 7-29132
 aerosol light extinction efficiency theory 7-14375
 S California, levelling refr. 7-8791
 clouds, reflectivity meas. during Earth Radiation Budget Experiment (ERBE) 7-9067
 coherent Doppler lidar, atm. correlation time meas. 7-60385
 extinction at Cerro Tololo Inter-American Observatory, (January to July 1984) 7-47542
 extinction measurements at McDonald Observatory, UVB results (1960 to 1980) 7-47541
 extinction properties of visible-, IR- and mm radiation (94 GHz) 7-9176
 fog, optical attenuation coeffs. 7-34672
 FOG-82, cooperative field study of radiation fog, exptl. design and results 7-9068
 free-space laser communications system design, SNR impact 7-34676
 geometric optics ray eqns., integral representation 7-14378
 heterodyne lidar with laser receiver for remote sounding of atm. 7-4214
 internal refraction in USNO meridian circle, theory and obs. 7-4333
 IR absorption by water vapour, diurnal and annual vars. at Cagliari Astronomical Observatory, Sardinia 7-40547
 IR laser radiation propag. in weak atmosphere, phase fluctuations 7-40565
 IR propagation, effect on two-angle viewing method for ocean surface temp. determ. 7-66338
 laser beam in medium containing droplets, nonlinear refraction phase compensation 7-4183
 laser radar, coherent FM CW, signal amplitude distrib. meas. 7-40570
 lidar equation, noise proof inversion 7-47540
 lidar equation taking account of polarization, second order scattering and travelling time effects 7-60380
 lidar in inhomogeneous atm., backscatter/extinction ratio humidity effects 7-40562
 light pollution, mathematical model for predicting night-sky glow 7-9172
 light wave time-dependent characts., fluctuating wind effect, expt. investig. 7-55263
 mode correction for turbulent distortions of optical waves 7-42914
 nonlinear and random phase distortions, compensation 7-66302
 optical beams propag. and turbulent rainfall characts. (*Russian*) 7-29131
 outgoing longwave irradiance estimation, appl. of column weighting model 7-29242
 phase fluctuations of optical wave through atm. turbulence, probability density function 7-57246
 polar stratosphere clouds, extinction meas. rel. to Antarctic O₃ hole form. 7-55163
 radiative transfer, atmospheric correction to sea surface temp. determ. by remote sensing 7-40485
 radiative transfer, relation to atmospheric vertical temp. distrib. (*French*) 7-14338
 radiative transfer theory, small-angle approx. and numerical soln. 7-36878
 random medium with Kolmogorov spectrum and inner scale of turbulence, intensity covariance of point source 7-57245
 Rayleigh backscatter lidar signals, temp. retrievals 7-9165
 Saugus-Palmdale, California, atm. refr. error in historical levelling surveys 7-8790
 scintillation effects on centroid anisoplanatism 7-57243
 scintillations in turbulent atmosphere, two-colour correlation 7-14372
 smoke optical depth determ. in nuclear winter studies, uncertainties in smoke source term 7-34668
 stratosphere, Antarctic springtime meas. of O₃, NO₂ and aerosol extinction by SAM II, SAGE and SAGE II 7-55161
 stratosphere, radiative transfer rel. to radiative balance determ. 7-9098
 stratosphere aerosol extinction in Antarctica, SAM II meas. 7-55160
 sunlight spectral attenuation for 8-13 μ m range (*Russian*) 7-29239
 turbid stratified anisotropically scattering media, light transmission theory (*Russian*) 7-4178
 turbulent atmosphere, high-resolution image form. of coherently illuminated objects 7-55261
 turbulent atmosphere, image form., isoplanatism problem of optical systems 7-50502
 turbulent atmosphere, thermal self-interaction of partially coherent laser beam 7-31376
 turbulent medium, I-K distrib. for random optical fields 7-34674
 water vapour refr. index in IR windows, 19 to 7.8 μ m 7-39066
 CO₂ laser radar performance, target and atmospheric influence 7-40571

atmospheric measuring apparatus

- see also air pollution detection and control; ionospheric measuring apparatus; meteorological instruments
 active cavity radiometers in unshuttered appls. performance characts. 7-14381
 aerosol sampler, efficiency of tubular thin-walled inlet 7-65670

atmospheric measuring apparatus continued

- aerosol sampler inlet (non-isooxial), sampling efficiency study 7-65671
 airborne microwave rain scatterometer/radiometer, DP software system (Japanese) 7-23908
 airborne microwave rain scatterometer/radiometer, hardware system development (Japanese) 7-23907
 airborne microwave rain scatterometer/radiometer, satelliteborne weather radar system (Japanese) 7-23911
 airglow (OH) imaging system, using image intensifier and solid state sensor 7-29288
 anemometer with twin-propeller, low-friction design, performance testing 7-34723
 aureolemeter, airborne meas. of optical stratification of aerosols in turbid atmosphere 7-47536
 aurora CCD-image intensifier camera, for all-sky observation 7-40603
 balloon borne remote sensing, single-axis platform performance 7-23913
 balloon-borne remote sensing, single-axis platform design 7-23912
 camera for cloud drop size meas. 7-55277
 Campbell-Stokes sun radiation recorder with photocells (Italian) 7-29265
 cloud physics instrumentation calibration, using holographic imaging 7-23897
 cloud-to-ground Lightning Position and Tracking System for electric utility weather problems 7-14371
 cryogenic sampler for collecting radioactive gases and aerosols 7-59902
 dust samplers used in British nuclear industry, entry characts. investigation 7-40079
 East Coast Lightning Detection Network with computer-based display system 7-47556
 electric field double probe sensors on GEOS-2, long-term behaviour of photo-electron emission 7-66426
 electrical fields prod. by convective clouds, airborne meas. using field mill sensors 7-55213
 Eppley pyrgeometer calibration for airborne meas. 7-60393
 ERS-1 wind scatterometer antenna, mechanical aspects 7-23975
 EUV instrumentation, calibration in space 7-24009
 fibre array polar nephelometer, scattered light phase functions meas. for atmospheric particles 7-23896
 FIR photometer, improved design 7-14492
 FOG-82, cooperative field study of radiation fog, exptl. design and results 7-9068
 GOES-I, J, K instruments developed by Kodak 7-23971
 grating spectrometer with imaging photon detector, for auroral and airglow obs. 7-34722
 Great Dun Fell, England, field station instruments 7-34661
 Halogen Occultation experiment, Si photodiode array for solar edge tracking 7-23900
 heterodyne lidar with laser receiver for remote sounding of atm. 7-4214
 high-resolution submillimetre heterodyne spectrometer 7-353
 ion analyser for use beneath high voltage transmission lines, corona discharges and ion prod. 7-29232
 IR satellite, optical design of imaging system 7-55321
 IZV-3 radiation meters checking 7-9220
 Langmuir probe for diffusion studies in atmospheric air 7-34724
 lidar system for atmospheric aerosol meas., design aspects 7-18320
 lidar telescope overlap function and effects of misalignment for unstable resonator transmitter and coherent receiver 7-9183
 M-124 filter ozonometer 7-34734
 magnetosphere plasma diagnostics instrumentation 7-14510
 meteorological satellite IR detectors, cooling by passive radiation 7-18878
 meteorological station with automatic data transmission, software and test results (German) 7-55266
 Michelson interferometer, slightly-cooled high-resolution, for limb emission meas. from space 7-55317
 microcomputer-based solar and meteorological data acquisition and control system 7-4186
 Microwave Limb Sounder 183 GHz radiometer 7-60433
 microwave radiometers, effects of rain on surface 7-9213
 middle and upper atmosphere radar at Shigaraki, Japan, first results 7-47561
 Millimetre Atmospheric Sounder on Shuttle for passive sounding (German) 7-40617
 Millimetre Wave Atmospheric Sounder for Space Shuttle 7-40568
 near-mm wave propag., instrumentation for study 7-4219
 negative ion generator and collector system for dispersion studies 7-29314
 photothermal radiometer for concentrated sunlight intensity measurements 7-23919
 pollution monitoring, automatic station and data telemetry system 7-59900
 precipitable water remote sensing method, by ground-based 1.35 cm radiometry (Chinese) 7-29311
 PROUST radar for UHF stratosphere-troposphere meas. 7-60421
 radiometers, absolute cavity (PMO6), and expt. charactn. 7-35562
 radiosondes, thermistors characts. var., implications for air temp. meas. 7-9233
 remote sensing, satellite automatic picture transmission, design of grey scale test pattern generator 7-29292
 ROCOZ-A use for stratosphere O₃ profiles meas. 7-55308
 satellite-borne, radiometers, IR detectors and their calibration 7-23898
 SCRIBE interferometer atmospheric emission spectra 7-55319
 soil erosion by wind, measurement apparatus, book 7-35136
 solar radiance meter for circumsolar radiation meas. 7-35566
 solar radiation meas., network meas. characts. 7-55218
 solar radiometry instrumentation, calibration techniques, and standards 7-55326
 spectral solar irradiance instrumentation and measurement techniques, spectroradiometers 7-55327
 submm heterodyne spectrometer for astron. and atm. meas. 7-60562
 switched-beam planar arrays suitable for high-resolution acoustic sounders 7-9209
 thunderstorm electric field measurement method using a corona probe 7-18318
 turbulence measurement with Gill propeller anemometers, directional response study 7-55276
 vertical cylindrical sonde for aerosol sampling 7-34732
 vertical SODAR for planetary boundary layer acoustic sounding (German) 7-9246
 whistler at low latitudes, automatic obs. of polarisation, meas. and tracking equipment (Japanese) 7-34749

atmospheric measuring apparatus continued

- wind scatterometer antenna (WSA), on ERS-1, release shock loads calc. 7-23976
 CO, personal exposure monitor with automatic data-logging 7-3943
 CO remote sensing by gas filter radiometry, instrumentation and data reduction 7-18317
 CO₂ laser radar, coherent FM CW, signal amplitude distrib. meas. 7-40570
 LiNbO₃ SAW oscillator for humidity and temp. meas. 7-4232
 NO, Zeeman modulated radiometer for remote detection 7-55313
 O₃ determination, balloon borne instrumentation, BOIC intercomparison expt. 7-29159
 O₃ measurement device using HARTLEY band (German) 7-9247
 Rn daughters automatic meas. instrument for atm. precipitation 7-49847
- atmospheric movements**
see also atmospheric turbulence; wind
 aerosols, model evaluation with Brownian diffusion technique 7-4086
 air parcel trajectory analysis, appl. to acid deposition data from New Jersey Pine Barrens 7-40061
 air pollution modelling and applications, conference, St. Louis, Missouri (April 1985) 7-48181
 air quality simulations, nonGaussian climatological model 7-55243
 air-sea interactions role in mesoscale devel., conf., Honolulu, USA (August 1985) 7-60858
 N America and adjacent ocean sectors, flour patterns 7-34624
 AMPTE artificial comet release, solar wind-Ba ions collisionless coupling 7-60483
 Antarctic, circulation quasi-geostrophic flow soln. 7-60319
 Antarctic, lee-vortices 7-60322
 Antarctic atmosphere, O₃ var. modelling, chem. and dynamical effects 7-55172
 Antarctic general circulation model for winter, effect of sea-ice extent 7-34643
 Antarctic spring, stratospheric heating rates and diabatic circulation, implications for O₃ depletion 7-55176
 Antarctic stratosphere, dynamics and photochemistry rel. to NO₂ and O₃ vars. 7-55158
 Antarctic stratosphere upwelling causing O₃ depletion 7-55175
 anticyclonic turning, assoc. with prolonged clear air turbulence over British Isles (1985 September 4) 7-14359
 E Arctic Ocean, sea ice form., synoptic conditions 7-34535
 N Atlantic depression passing over British Isles, Christmas 1985 depression 7-55234
 Atlantic Ocean, atm. aerosols temporal and spatial var. anal. 7-4085
 N Atlantic Ocean, west-central region, explosive cyclogenesis 7-47497
 atmospheric tide differences in surface layers and ground level 7-60341
 S Australia, obs. of internal atmospheric bores and cold front 7-55127
 axisymmetric flow in rot. spherical shell, numerical expts. 7-20733
 baroclinic and barotropic instability spectra as functions of N in N -level models 7-34590
 baroclinic limited area forecast model, appl. of nonlinear normal mode initialisation expt. 7-29190
 baroclinic planetary modes in deep and shallowspherical atmospheric models (Chinese) 7-4077
 baroclinic unstable wave, growth rate and phase vel. 7-9115
 baroclinically unstable waves at large supercriticality, nonlinear dynamics 7-9088
 barotropic jet with slow streamwise var., instability 7-66230
 barotropic models using bounded derivative and normal mode initialization methods 7-60351
 barotropic modon propagation over slowly varying topography, perturbation theory 7-4108
 barotropic motion, effects of orography (Russian) 7-29130
 barotropic study of free and forced planetary waves 7-60335
 Bay of Bengal, atmospheric struct. during suppressed and active convective periods 7-55211
 Bernoulli function behaviour for case of non-negative absolute vorticity 7-34656
 blocking events in S Hemisphere general circulation over Pacific 7-34599
 blocking of general circulation, perturbation theory 7-4108
 blocking over N Atlantic, adiabatic invariants and FGGE data (Russian) 7-23807
 boundary layer flow over irregular terrain, model formulation 7-4100
 Brush Creek Valley, Colorado, mass transport by along-valley wind systems 7-29143
 S California, vertical pollutant distrib. and boundary layer struct., airborne lidar obs. 7-3734
 Charney baroclinic-instability with Rossby wavetrains 7-18287
 circulation classification, objective typing procedures comparison 7-4131
 compressible gas dynamical eqns., rapidly oscill. solns. (Russian) 7-55181
 convection, comparison of GR FEM models 7-18298
 convection in cumulus, JASIN meas. 7-66254
 convection over snow-covered surface 7-4089
 convective boundary layer, diffusion model, numerical simulation 7-66243
 convective boundary layer, diffusion model of plume released from point source 7-66244
 convective boundary layer length scales 7-9085
 convective boundary layer simulation, efficiency of different higher order turbulence models 7-57819
 convective boundary-layer parameters, climatology over Ontario, Canada 7-40512
 convective instability effect on ocean surface wind algorithm, Seasat scatterometer studies 7-66159
 convective scaling, numerical anal. 7-9084
 convective systems of 100 km scale during GATE, heat and moisture transport 7-29189
 cumulonimbus clouds, role of convectively available potential energy 7-4142
 cumulus convection, heating of vortices, nonlinear response 7-9101
 cumulus ensemble effects on GATE large-scale vorticity and momentum 7-9105
 cumulus moisture transport effect on GCM climate simulation 7-66291
 dayside auroral ionosphere, ion convection and elec. fields 7-55348
 deep tropical convection assoc. with large-scale convergence, numerical simulation 7-34589
 Delhi, India, urban diffusion model 7-8466
 Denver hailstorm, 1984 June 13, wind vels. and storm dynamics 7-29127
 depression over Bay of Bengal, latent heat distrib. study (Chinese) 7-18265

atmospheric movements continued

- diffusion from elevated and ground point sources in neutral boundary layers, turbulent energy model 7-34580
 diffusion in marine boundary layer, SF₆ tracer expts. and parameterization 7-18285
 diffusion of Gaussian puffs 7-66257
 diffusion over complex terrain, Gaussian trajectory model 7-14369
 diffusion studies in atmospheric air, using Langmuir probe 7-34724
 dispersion studies, use of negative ion generator and collector system 7-29314
 dissipative waves excited by gravity-wave encounters with stratified boundary layer 7-34598
 divergent flow, derivation from rotational flow using vel. potential 7-66268
 dominant frequency-dependent 3D atm. modes, struct., energetics and evol. 7-9086
 downraught from convective clouds, vel. and temp. 7-9131
 dry deposition of 4-50 μ m dolomite particles on vegetation, flat surfaces and deposition gauges 7-4083
 dynamical systems arising in Galerkin approximation problems (*Russian*) 7-4116
 dynamics of atmosphere, absorbing upper boundary conditions for numerical models 7-34653
 E-region, semi-diurnal tide, EISCAT obs. 7-34782
 E-region, vertical velocity structures from SABRE obs. 7-4254
 eddy kinetic energy of S Hemisphere during January and July (FGGE) 7-47518
 El Nino-Southern Oscillation events in AD 1531 to 1841 period 7-60315
 Eliassen-Palm flux divergence interpretation 7-66267
 environmental problems, mathematical models, book 7-60890
 equatorial electrojet, drift speeds of irregularities of kilometre and metre sizes 7-4257
 equatorial electrojets, small scale plasma motions, HF Doppler obs. 7-55361
 NW Europe, acidic nitrogen species as pollutants, long-range transport and deposition in rain 7-34085
 W Europe, climate simulation and CO₂ induced climate change, general circulation model anal. 7-66285
 explosive mid-latitude, synoptic-scale storms dynamics, effects of intense cumulus convection 7-4164
 extratropical geopotential height and tropical convection, coherent fluctuations on intraseasonal time scales 7-4129
 f-plane models, radiative upper boundary condition capable of transmitting gravity waves 7-29200
 F-region, equatorial American sector, vertical plasma drifts 7-34773
 FGGE general circulation statistics, satellite data effects 7-66265
 finite amplitude Charney and Green waves, dynamic regimes 7-9090
 Fram Strait, ice transport, atm. forcing 7-34539
 frictional convergence at coastlines 7-47516
 Mesoscale Frontal Dynamics Project, for W Europe 7-66304
 frontogenesis, variable resolution finite-element model 7-34622
 moist frontogenesis by analytic model 7-34596
 gas diffusion in exponential atmosphere 7-14400
 GATE waterspouts, interacting cumulus processes 7-4120
 general circulation, comparison of filters for high latits. using shallow water eqns. 7-9133
 general circulation, Hough harmonics for nonlinear shallow-water models 7-60357
 general circulation, influence of large-scale topography on subtropical high formation (*Chinese*) 7-29217
 general circulation, linearised barotropic and baroclinic equations, Arnoldi's method 7-61078
 general circulation, transient cyclone-scale vorticity forcing of blocking highs 7-9094
 general circulation energetics, 3D normal mode expansions 7-47517
 general circulation model, appl. to anal. of protracted climatic effects of massive smoke injection 7-66297
 general circulation model, dependence on wet or dry initial conditions for Sahara 7-34644
 general circulation model, difference scheme test (*Chinese*) 7-4078
 general circulation model, dynamic and thermodynamic influences of Tibetan Plateau 7-29135
 general circulation model, effects of topography on atmospheric energetics 7-9099
 general circulation model, month-to-month persistence of anomalies compared with Earth's atmosphere 7-9093
 general circulation model, simulation of O₃ seasonal variations at high latits. in Southern Hemisphere 7-55167
 general circulation model, thermal balance sensitivity 7-66221
 general circulation model of climate, with improved parameterizations 7-40558
 general circulation models, influence of surface and vegetation 7-9152
 general circulation models, systematic westerly bias due to orographic gravity wave drag 7-34645
 general circulation multiple equilibria, and role of topography and circulation (*Russian*) 7-4115
 general circulation of baroclinic planetary atmosphere, effect of surface drag 7-34655
 general circulation stationary regime, model including orography (*Russian*) 7-9080
 geostrophic adjustment process, numerical simulation and gravity-inertia waves (*Chinese*) 7-18257
 Geysers geothermal area, California, dispersion model for complex terrain 7-60313
 Global Weather Experiment Special Observing Period I, wind field vertical struct. 7-34610
 gravity waves, effects of Doppler shifts on wave spectra observed by MST radar 7-47490
 gravity waves in ionosphere, radiointerferometric obs. 7-4253
 internal gravity waves in troposphere, 2D model of convectively forced waves 7-34641
 gravity waves in upper atmos., EISCAT observations 7-29317
 Great Dun Fell, England, meteorological conditions 7-34661
 Hadley circulations on a nonuniformly heated rotating plate 7-63159
 heat-induced tropical circulation with mean wind 7-66263
 hurricanes, ice distribution and convection 7-4121
 hydrostatic atmospheric gravity waves, influence of Coriolis force due to Earth's rot. (*French*) 7-18271
 India, monsoonal fields sequential evol. 7-29203
 Indian seas, 1984 cyclones and depressions 7-9112
 Indian Summer monsoon, 30-50 day activity interannual var. 7-34611

atmospheric movements continued

- inertia-gravity waves trapped against a vertical barrier, theory 7-4109
 internal waves and turbulence in troposphere and lower stratosphere 7-23814
 internal waves in mesosphere, stratosphere and troposphere 7-40517
 intraseasonal oscillations appearing in GFDL general circulation model 7-34597
 ionosphere, convection morphology and particle precipitation assoc. with dayside aurora 7-55352
 ionosphere, interhemispheric plasma transport 7-14409
 ionosphere, midday polar cusp and polar cap plasma convection rel. to auroral emissions 7-34777
 ionosphere, relationship between EM drift components at mid and low latits. 7-9315
 ionosphere D-region, dynamical regime over E Siberia during quiet and disturbed conditions 7-47614
 January climate simulation, general circulation model, removal of zonally-uniform sea surface temp. 7-47526
 Johnston convective complex, PA, USA, vertical motion, vorticity and precipitation 7-9091
 Kansas, USA, downbursts, visual obs. and rel. to aviation weather obs. 7-29204
 large scale motion chaotic forms (*Chinese*) 7-4074
 large-scale atmospheric motion and dissipative structs. (*Chinese*) 7-9057
 large-scale circulation anal., appl. of cloud cover estimation using bispectral satellite measurements 7-29148
 large-scale horizontal motion in atmos., stability study (*Chinese*) 7-29216
 large-scale motion, dynamic effects of orography 7-9116
 large-scale quasi-stationary patterns extended-range predictability 7-4163
 lateral dispersion from tall stacks 7-66242
 lateral dispersion measurement method involving aircraft oblique photography 7-23918
 lee cyclogenesis, initial stage development 7-60347
 lee waves, 2D time-depend. quasi-geostrophic theory 7-9103
 limited-area initialisation expts. using normal mode approach 7-4168
 linear baroclinic waves, structural determinism and simple nonlinear equilibration 7-9095
 linearly stratified, rotating flow over long ridges in a channel 7-6224
 long-range transport in remote regions, symposium, Honolulu, Hawaii (August 1985) 7-48166
 long-range transport of continental ²²²Rn in Subantarctic and Antarctic 7-55222
 long-range transport of continental particulate C in marine atmosphere 7-55221
 low-latitude middle atm., diurnal propagating tides 7-60436
 low-order intermediate modes, bifurcations 7-66226
 macrocirculation classification indices using objective method 7-23815
 magnetosphere, charged particle motion in magnetotail 7-9335
 magnetosphere, ISEE-3 energetic ion results (EPAS) in deep geomag. tail 7-29367
 magnetosphere, plasmasheet boundary, field-aligned plasma flow generation 7-60488
 magnetosphere, polar parabolic heavy ion flow 7-60455
 magnetosphere, small plasma beams and clouds transverse deflection and dissipation 7-60484
 magnetosphere, suprathermal ion and electron results from ISEE-3 Geotail Mission 7-29368
 magnetosphere convective flows and spatial gradients determ. methods 7-9230
 distant magnetotail, structural and dynamical aspects from ISEE-3 plasma meas. 7-29366
 E Mediterranean, penetration of early winter polar air mass 7-34627
 meso-alpha-scale convective complexes, study of meso-beta-scale characts. 7-34635
 mesopause, wind vels. rel. to characts. of noctilucent clouds 7-23925
 mesoscale circulation due to mesoscale melting snow temperature perturbation 7-29173
 mesoscale meteorological fields, spatial fitness implications 7-47509
 mesosphere, gravity waves indicated by density fluctuations 7-40621
 mesosphere, temp. and circulation vars. in middle and high latitudes 7-47590
 mesosphere, wind and tide meas. determ. from meteors radar obs. 7-55341
 mesosphere and lower thermosphere internal waves, vertical propagation characts. 7-47601
 microdynamic mechanisms for airborne particles scavenging by collision with water drops, model studies 7-55200
 mid-latitude medium scale travelling ionospheric disturbances, source regions characts. 7-60446
 middle atmosphere, gravity wave effects under solstice conditions with 3-D circulation model 7-47597
 middle atmosphere, zonally averaged dynamical model vel. to regions of polar mesospheric clouds 7-47596
 middle atmosphere dynamics and remote sensing, symposium, Prague (Aug. 1985) 7-40986
 middle atmosphere dynamics measurements, first results from middle and upper atmosphere radar 7-47561
 middle atmosphere dynamics over Saskatoon, 1981-2 spectral study 7-47586
 middle atmosphere var. due to solar activity oscills. (of period 27 and 13 days) 7-66369
 midlatitude circulation influenced by El Nino SST anomalies 7-40543
 midlatitude cyclones, subsynoptic vertical energy fluxes 7-40544
 modal amplitudes in interacting triads, probability distrib. with arbitrary random forcing 7-9097
 moist convection, low-order spectral model 7-47515
 monsoon 30-50 day oscill. theory 7-60317
 Monsoon depression baroclinic growth, effect of Ekman boundary layer friction 7-9122
 monsoon depression scale waves baroclinic growth, influence of low level wind shear 7-4135
 monsoon depressions, energy aspects 7-9113
 monsoon depressions, WNW movement and precipitation characts. mechanism 7-66253
 monsoon energetics, for strong and break monsoons 7-29181
 SW monsoon of 1979 AD, short-range prediction of onset phase 7-29178
 Montana thunderstorm, precipitation particles growth trajectories 7-4124
 mountain passage, homogeneous rotating fluid flow 7-18189
 mountain ridge, airflow and orographic wave clouds, theory (*Russian*) 7-4114
 New England, USA, 1982 December 11 storm, band form. 7-29199

atmospheric movements continued

- non-cancellation instability in horizontal advection schemes for momentum schemes 7-4137
 nonlinear balance and gravity-inertial wave saturation in a simple atmospheric model 7-1582
 nonlinear waves on a coupled density front 7-63163
 normal mode oscillations of atmos. of short-period, theory and obs. 7-40533
 Northern Hemisphere, 1986 spring meteorological conditions 7-4166
 Northern Hemisphere standing eddies in winter, NCAR and GLA models 7-60348
 Northern Hemisphere winter troposphere, circulation anomalies due to low latitude heating anomalies (*Chinese*) 7-4076
 S Norway, circulation rel. to avalanche winters (1855-1985) 7-4172
 numerical prediction, use of physico-mathematical models 7-9074
 numerical weather prediction models, implicit versus explicit convective heating 7-47500
 omega diagnostic computations, accuracy 7-34631
 orographic cyclones in extratropical region 7-34642
 orography influence on zonal circulation, 3-level nonlinear model (*Russian*) 7-55182
 oscillation of zonal mean characts. of motion on a spherical Earth (*Chinese*) 7-9058
 equatorial Pacific, meteorological parameters during AD 1982-3 El Nino 7-29166
 NE Pacific Ocean, 1985 cyclones 7-47507
 Pasquill stability classes at coastal station, diurnal and seasonal var. 7-9124
 passive scalar diffusion, second order modelling 7-8468
 N Peru, convection, in clouds and rain in coastal areas, AD 1983 obs. 7-60350
 planetary scale flow interactions with gravity waves, SKYHI general circulation model simulation 7-34592
 planetary wave breaking in stratosphere 7-4158
 planetary wave response to stationary tropical heating, for atmos. with vertical and meridional shear 7-40523
 planetary-scale flow, objective anal. 7-47505
 plasmapause, elec. field and convection characts. at midnight 7-34770
 plasmasphere, flux tube refilling after mag. storm, temporal features 7-47623
 plasmosphere, H^+ and He^+ flow along mag. field lines 7-9299
 plume dispersion in convective conditions, horizontal dispersion meas. 7-40062
 nonbuoyant plume dispersion modelling, based on meteorological scaling parameters 7-60308
 polar air stream baroclinic disturbances, diagnostic study 7-60343
 polar cap F-region, plasma patches dynamics 7-34779
 polar high stability, theoretical dynamic analysis (*Chinese*) 7-29223
 polar mesopause, large-amplitude semidiurnal temp. var. due to pseudotide generated by gravity waves 7-34754
 pollutant aerosols, long-range transport anal. by particle-induced X-ray emission 7-4192
 pollutant dispersion, wind tunnel expts. 7-1573
 pollutant long-range transport by Eulerian model, for cumulus cloud ensemble 7-34576
 pollutant transport by slope winds, influence of atmos. stability 7-60305
 pollution plume dispersion over elevated terrain, model performance 7-3733
 pollution transport by trajectory model, using synoptic vertical wind data 7-60304
 post-noon auroral oval dynamics 7-55350
 precipitating convection, dynamical aspects. 7-60336
 Pyrenees, 1982 March 23 lee wave event anal. 7-4156
 QE II storm, 1978 September 9-11, develop., influence of upstream upper-level baroclinic processes 7-4149
 Qinghai-Xizang (Tibet) plateau, vortex development and maintenance, numerical model 7-4139
 quasi-biennial oscillation in equatorial stratosphere 7-60363
 quasi-geostrophic baroclinic disturbances with condensational heating, linear devel. 7-60340
 quasigeostrophic vortices, Lyapunov-stable solns. 7-43925
 radiation belts, protons diffusion and scatt. rel. to spatial distrib. at high and low latits. 7-4274
 regional atmospheric modeling system 7-55248
 regional finite-element model of circulation, using semi-implicit semi-Lagrangian integration schemes 7-60349
 Ross Island, Antarctica, aerosol, physical props. 7-60333
 Rossby - gravity wave model, slow manifold of primitive eqn. system 7-9100
 Rossby and gravity wave breaking, definition of concept 7-29213
 Rossby wave (normal mode) interference with quasi-stationary waves 7-34601
 Rossby wave energy, energy flux and Lagrangian (*Chinese*) 7-9059
 Rossby wave stability in shear flow, influence of orography (*Chinese*) 7-29225
 Rossby wave stability influenced by large-scale orography (*Chinese*) 7-18256
 Rossby-Haurwitz waves weak nonlinear coupling 7-60318
 rotating barotropic atmosphere, finite amplitude disturbance wave ensemble-zonal mean flow nonlinear reson. interaction (*Chinese*) 7-4079
 rotating cylindrical annulus, imposed temp. gradient, flow regimes study, appl. to atm. dynamics 7-43933
 rotating differentially heated annulus with unstable stratification, convection characts. (*Russian*) 7-29129
 sandstorms of Arabian Gulf, due to anomalous anticyclones? 7-55233
 sea-breeze circulations over Cape York Peninsula and the generation of Gulf of Carpentaria cloud line disturbances 7-29140
 seasonal movements of subtropical high ridge line, contrib. of vapour condensation heating 7-40508
 semi-implicit version of grid point model of shallow water eqns., without Helmholtz eqns. 7-60354
 severe rainband, flow dynamics and stability 7-9096
 shallow water flow incident upon slender orography, semi-geostrophic response to elongated ridge 7-29122
 smooth atmospheric motions, scaling and computation 7-4161
 SOUSY VHF radar measurements in the lower and middle atmosphere 7-23870
 Southern Hemisphere, wintertime tropospheric planetary scale activity reduction, effect on Antarctic O_3 7-55170
 Southern Hemisphere blocking episode and transient eddy influence on zonal flow 7-34600

atmospheric movements continued

- Southern Hemisphere circulation, zonal teleconnections and longitude-time lag correl. 7-34603
 Southern Hemisphere lower stratosphere, trajectories anal. 7-55169
 Southern Hemisphere zonal wind variations, AD 1979 index cycles 7-34630
 spectral general circulation model, blocking events climatology in perpetual January simulation 7-29137
 spectral general circulation model, local vorticity and heat balances for blocking anticyclones 7-29138
 stratified atmosphere heating is model for moist convection 7-4127
 stratocumulus model with an internal circulation 7-66227
 stratosphere, area of polar vortex as diagnostic for tracer transport on isentropic surface 7-29134
 stratosphere, dynamically and chemically controlled vars. of NO_2 and O_3 in Antarctica 7-55157
 stratosphere, equatorial waves in wind field 7-66212
 stratosphere, temp. and circulation vars. in middle and high latitudes 7-47590
 stratosphere, trace gas transport by planetary waves during major warming event in winter 7-29161
 stratosphere, winter polar vortex simulated as material entity 7-47489
 stratosphere and lower mesosphere, zonal winds and temperature 7-4248
 stratosphere O_3 transport, relation to total O_3 decrease at South Pole, Antarctica (1964-1985) 7-55154
 stratosphere of S Hemisphere, circulation changes including polar vortex and warming events 7-55149
 stratosphere polar vortex, O_3 and aerosol meas. rel. to vortex motion (November 1985) 7-55155
 stratosphere trace constituents, meridional distrib. 7-9087
 stratospheric NO_2 amounts, transport and photochemical effects 7-47487
 supercritical dynamics of baroclinic disturbances in the presence of asymmetric Ekman dissipation 7-34588
 surface tension driven convection subjected to rotation and non-uniform temperature gradient 7-6213
 synoptic scale disturbances with circular symmetry 7-34625
 synoptic-scale advection, effect on Priestley-Taylor evaporation formula performance 7-4093
 synoptic-scale cyclones, effects of sea ice and snow cover 7-47498
 terrain following coordinate models, press. gradient force and calc. of initial temp. 7-4138
 thermosphere, circulation models and wind regime from meteor radar obs. 7-47589
 lower thermosphere, momentum flux vars. from mid-latitude meteor wind obs. 7-55343
 lower thermosphere, role of tides in thermodynamics for solstice conditions 7-47595
 thermosphere, tides in 80 to 100 km height region 7-47594
 thermosphere, wave-associated density disturbances 7-55342
 thermosphere dynamics influenced by ion drag in winter 7-55336
 thermosphere wind measurements by EISCAT, ionosphere effects 7-29319
 thermosphere wind pattern at high-latitude, general circulation model calc. 7-29320
 thunderstorm anvil clouds, elec. characts. and dynamics (*Chinese*) 7-29121
 Tibetan Plateau, summer weather systems develop., sensible heating effects on vortices 7-60339
 tidal oscillations in stratosphere, general circulation model calcs. 7-40534
 tides for solstice conditions, numerical simulations 7-9277
 tides in atmosphere, theory in geometric height and log-press. coords. 7-29323
 tides in atmosphere, theory of treatment of IR radiative damping 7-29208
 tides in upper atmosphere, EISCAT obs. of tidal motions 7-29317
 tornado simulation, momentum diffusion effects in axisymmetric vortices 7-57850
 toxaphene, pollutant transport to Lake Michigan 7-34084
 tracer transport of the diabatic circulation deduced from satellite observations 7-9104
 traditional cyclone freq. maps, biases anal. 7-29193
 trajectories in stratosphere, photochemical model rel. to LIMS obs. 7-66269
 transient medium-scale wave activity in the summer stratosphere 7-9069
 transient quasi-geostrophic eddies, 3D propagation 7-29139
 travelling ionospheric disturbances and daylight mid-latitude spread-1 7-60451
 tropical atmosphere model with circulation depend. heating and specific humidity 7-34595
 tropical convection during northern summer, 40-50 day oscill., outgoing longwave radiation anal. 7-34623
 tropical cyclone, mature struct. and motion 7-4146
 tropical cyclones, future direction of motion, upper flow asymmetry effects 7-47503
 tropical easterly flow, interaction between meridional and zonal disturbances 7-40509
 tropical squall line, diagnostic modelling study of stratiform cloud region 7-29136
 tropical synoptic-scale diagnosis, test of ECMWF model 7-29196
 troposphere, one-dimensional photochemical model with trade-wind boundary-layer parameterisation 7-9146
 Tsjernobyl radioactive fallout, appl. of two-dimensional trajectory model to radioactivity transport 7-59894
 two-particle relative diffusion by Monte Carlo simulation 7-34574
 two-way interactive nesting procedure with variable terrain resolution, appl. to jet streak 7-34621
 Typhoon No. 7507, kinematical fields from upper air obs. (1975 August 17 to 23) 7-40510
 typhoon trade, random dynamic prediction model 7-18295
 ultra-long wave activity, by 3-layer baroclinic model (*Chinese*) 7-18269
 ultra-long waves forced by topography, propag. (*Chinese*) 7-4075
 unit Kingdom, real-time long-range forecasting using ensemble of numerical integrations 7-29294
 E United States, anticyclones paths rel. to climatology of summertime O_3 and SO_2 7-40066
 United States, Florida and Colorado, lightning activity, topographic convection effects 7-34620
 unstable marine boundary layer, struct. determ. from lidar and aircraft obs. 7-29133
 upper atmosphere, gyres and jets, viscous pumping and spin-down 7-9279

atmospheric movements continued
 upper atmosphere, seasonal and tidal variations of temperature and density 7-29315
 upper atmosphere neutral temperature and winds from EISCAT obs. 7-29318
 upper level frontogenesis 2D primitive eqn. model, role of vertical deform. 7-4122
 urban areas traffic pollution, transport and role in O₃ form. 7-3736
 W USA, synoptic classification of 10 years of 500 mb weather maps 7-4140
 vertical displacements due to quasi-horizontal atmospheric motions 7-29165
 vertical normal modes of a mesoscale model using ascaled height coordinate 7-9107
 vertical velocity in atmosphere, periodic solns. of non-stationary eqn. 7-18296
 vertical velocity spectrum for troposphere and stratosphere 7-14341
 vortices formation over ocean surface heat anomalies, dynamic struct. 7-9134
 vorticity equation, exact time depend. solns. 7-1578
 Washington, DC, USA, tracer dispersion expts. 7-60307
 wave-mean flow in general circulation model 7-29141
 weakly nonlinear dynamics of a planetary Greenmode and atmospheric vacillation 7-9089
 weather prediction, primitive equations, energy conserving Galerkin finite element schemes 7-66346
 westerlies in equatorial region, variations and relation to low-latitude circulation (Chinese) 7-9060
 Winter. MONEX area, tropopause height short term var. rel. to deep convection 7-4128
 winter stratosphere, enstrophy transfer to planetary waves 7-4125
 zonal available potential energy and kinetic energy (Chinese) 7-18262
 zonal circulation, corpuscular-tropospheric effect of solar wind streams 7-47475
 zonal circulation affected by heating anomalies 7-9065
 zonal current, eddy effects, conventional and transformed Eulerian diagnostics 7-66264
 zonal flow at surface, predicted by eddy flux parametrization scheme 7-34646
 zonal shear flow in circular geometry, laboratory expt. study of instability (Russian) 7-60329
 zonal tides, influence on Earth's rot. rate (Chinese) 7-4073
 zonal wind minimum in stratosphere, due to mesoscale mountain wave breaking 7-40522
 S pollutant, trajectory and deposition 7-54397

atmospheric noise *see* **atmospherics**

atmospheric optics
see also **atmospheric light propagation; sky brightness; sunlight**
 advanced technology optical telescopes, conf., Tucson, United States (March 1986) 7-55886
 aerosol, optical and microphysical properties (Russian) 7-4179
 aerosol, optical coeff., meas. technique (Chinese) 7-18305
 aerosol light extinction efficiency theory 7-14375
 aerosol optical characts., laser backscattering study (Russian) 7-9169
 aerosols in turbid atmosphere, airborne meas. of optical stratification 7-47536
 aerosols optical props. and humidity effects (Russian) 7-29241
 air pollution plume, visibility and radiative transfer budgets 7-34671
 Angstrom's turbidity coeff., determ. from direct total solar irradiance meas. 7-66355
 artificial night sky illumination 7-3746
 astrometry, use for Earth rot. parameters determ., atm. limitations 7-60412
 astronomical observatories, seeing conditions, conf., La Silla, Chile (Oct. 1983) 7-35117
 astronomical optical image, atmosphere and spatial spectrum distortion, statistical model 7-57255
 astronomical seeing, anal. of imaging props. of large reflecting telescopes 7-66461
 Athens, Greece, turbidity meas. and components 7-9174
 autonomous satellite navigation using observations of starlight atmospheric refraction 7-60418
 cloud extinction profile measurements by lidar using Klett's inversion method 7-9184
 clouds, optical radiation intensity for horizontally inhomogeneous clouds (Russian) 7-40564
 complex solar halo over Arnhem, Netherlands (1985 February 26) 7-23841
 Denver, USA, winter haze modelling 7-34673
 diffraction rings, demonstration using a Tensor lamp 7-48245
 duststorm detection by satellite remote sensing 7-66329
 Edmonton, Canada, urban visibility rel. to H₂O vapour from industry 7-14376
 extinction, ordinary and volcanically induced vars. (1972-85) 7-14374
 extinction effects on stellar alignments 7-55255
 fog, optical attenuation coeffs. 7-34672
 geometric optics ray eqns., integral representation 7-14378
 image quality; influenced by fluctuation of atmos. parameters (Russian) 7-60383
 imaging of Earth surface from satellite, effect of atmos. horizontal inhomogeneities 7-66301
 inverse problems of atmospheric optics 7-47537
 far IR, extinction and scatt. due to circular ice cylinders (Russian) 7-55258
 IR astronomy, atm. effects (Japanese) 7-60546
 IR cooling rate calculation, for cooling due to H₂O vapour (Chinese) 7-29221
 IR radiation transfer, transmission of the CO₂ 15 μ m band 7-40688
 IR remote sensing of atmos. temperature, thermal radiation transfer model (Japanese) 7-18316
 La Silla, Chile, extinction evol. 7-4177
 laser beam remote sensing methods 7-40605
 lidar optical extinction coeff. profiling method (Russian) 7-18315
 Linke turbidity factor, optical thickness of clean dry atmosphere 7-47512
 melanin content of human skin, evidence for past climates? 7-66289
 methane in atmosphere, IR radiation models 7-18302
 mirage effect, 3D calcs. using personal computer 7-50484
 oblique CCD reconnaissance camera operation; atmospheric effects 7-18900
 ocean-atmos. system, visible region spatial radiance field 7-55180

atmospheric optics continued
 Oelsnitz, East Germany, halo obs. (German) 7-9175
 polarisation-scatt. phase functions, one-parametric model (Russian) 7-29240
 polarised light scattering from nonspherical particles of a particular orientation (Russian) 7-55257
 polluted atmosphere radiative heating, influence of soot 7-4101
 pollution plume, visual perception by humans 7-54390
 radiative transfer eqn. solution with improved algorithm (Chinese) 7-29244
 radiative transfer in plane-parallel medium with space-depend. albedo, Fourier transform soln. 7-34850
 reflection in turbulent atmosphere under induced temperature nonuniformity of refractive index 7-60384
 refractive index profile determ. method, astronomical refraction technique (Russian) 7-18314
 refractive index structure function for turbulence ranges, saturation and long-baseline optical interferometry 7-60574
 remote sensing, multispectral scanner surveying, specular-spot and hotspot regions 7-60403
 remote sensing, terrain illumination influence on imaging from space 7-60402
 remote sensing (book) 7-35139
 remote sensing of atmos. optical parameters from space, method involving imaging of land 7-55296
 sea surface, dye patches used for remote sensing observation, spectral radiance and visibility 7-60405
 sea surface, light reflection coefficients for slant path lidar (Russian) 7-4180
 sea surface light scattering (Russian) 7-8966
 sea surface temperature, algorithms from AVHRR data 7-4241
 seeing forecasting 7-4184
 shortwave and longwave radiation, STREX 1980 measurements 7-29174
 Spain, atmospheric transmission for cloudless skies from daily global radiation 7-9141
 St. Louis, summer aerosol, (NH₄)₂SO₄ contrib. to light scatt. 7-47538
 stars, image refraction in atm., use for press. and temp. vertical profiles retrieval (Russian) 7-29277
 surface layer three-parameter inferior mirage model use for temp. profiles determ. 7-23804
 temperature remote sensing for cloudy atmosphere, IRT radiation transfer model 7-60399
 optical transfer operator construction, using multiple refl. and spatial freq. methods 7-60381
 turbid stratified anisotropically scattering media, light transmission theory (Russian) 7-4178
 turbulent medium, I-K distrib. for random optical fields 7-34674
 USSR, statistical characts. of optical thickness 7-55256
 vegetation canopy, model of sunlight penetration involving leaf distribution 7-4097
 Western Ghats, India, crepuscular rays form: 7-9173
 CO₂ absorption bands, thermal radiation flux calcs. (Russian) 7-60382

atmospheric pollution *see* **air pollution**

atmospheric precipitation
see also **ice; rain; snow**
 acetic acid source determ. 7-55195
 acid deposition data from New Jersey Pine Barrens, air parcel trajectory anal. 7-40061
 acid precipitation, stochastic modelling of space-time struct. of chemical deposition 7-23239
 acidity of precipitation, determ. of decrease resulting from decreased SO₄²⁻ conc. 7-54391
 aerosol concentration in drops, changes due to particle scavenging and redistrib. by coagulation 7-55201
 airborne particles scavenging by collision with water drops, combined effects of microdynamic mechanisms 7-55200
 aircraft, static charging by collisions with ice crystals 7-55212
 E Asia, dynamic and thermodynamic influences of Tibetan Plateau on general circulation model 7-29135
 Australia, diagnostic study of first year of operational Model Output Statistics forecasts 7-55125
 Brazil, estimation of global solar radiation and evap. from precip. data 7-66272
 Brazil coast, mean sea-level var. with atm. temp., press., precipitation and evaporation 7-18194
 Bremen, West Germany, summer temp., precipitation and sunshine characts. 7-9162
 cloud seeding with NaI, delayed effects 7-66239
 convection, dynamical aspects and assoc. precipitation 7-60336
 corrosion-related aspects of the chemistry and freq. of occurrence of atmospheric precipitation 7-46664
 Cumbria, England, characts. of airflow, aerosols, precipitation and clouds in boundary layer 7-4096
 cumulonimbus clouds, introductory review 7-4142
 Denver hailstorm, 1984 June 13, meteorological obs. 7-29127
 El Nino-Southern Oscillation, 1877-8 event rel. to 1982-3 event 7-4051
 W. Europe, climate simulation and CO₂ induced climate change, general circulation model anal. 7-66285
 formic acid source determ. 7-55195
 hail, remote sensing with S-band dual linear polarization radar 7-66344
 hail cell radar reflectivity profiles in Switzerland 7-14348
 hail embryo definition, morphology and growth in clouds (Chinese) 7-18260
 hail growth in 3D storm cloud model (Chinese) 7-4081
 hail suppression by cloud seeding, Grossversuch IV expt. in Switzerland 7-14344
 hailstone embryo types rel. to hailstorm cell form (Chinese) 7-18266
 hailstone two-stage growth and accreted ice props. 7-34647
 hailstones, density of accreted ice, laboratory expts. 7-34648
 homogeneity test applied to precipitation data 7-47565
 hydroxymethanesulphonate precipitation 7-60326
 India, droughts incidence, seasonal aridity index anal. 7-9049
 Indian monsoon radiative forcing model, role of stratospheric aerosols 7-55196
 Indian summer monsoon precipitation, relation to global sea-level press. distrib. in April and July 7-29207
 Integrated Lake-Watershed Acidification Study database documentation 7-46976
 ion precipitation in isolated and latitudinally narrow regions, for ions up to 1 keV 7-23941

atmospheric precipitation continued

- Johnston convective complex, PA, USA, vertical motion, vorticity and precipitation 7-9091
 Lagrangian time scales 7-55190
 Local AFOS MOS programme appl. to wind prediction 7-34679
 luni-solar periodic components in precipitation data 7-66208
 mapping of precip. fields, appl. of empirical orthogonal functions 7-29142
 McCloud Lake, soft water acidic lake in Florida, ion fluxes in precip. 7-23763
 measurement networks characts. (*German*) 7-4229
 measuring systems comparison (*German*) 7-4230
 microwave absorption measurements of melting spherical and nonspherical hydrometeors 7-9106
 monsoon depressions, WNW movement and precipitation characts. mechanism 7-66253
 Montana thunderstorm, precipitation particles growth trajectories 7-4124
 multiyear drought durations, freq. anal. technique 7-23758
 neutral particle precipitation from ring current and equatorial EUV O I nightglow 7-29325
 NE Nevada, precip. reconstruction, 1600 to 1982, using tree ring indices 7-29145
 nitrate flux on Ross Ice Shelf, Antarctica, relation to solar cosmic rays 7-55091
 tropical S Pacific during FGGE, precipitation estimates 7-66262
 polarization diversity radar interpretation 7-66232
 preferred orientation relationship with dual polarisation radar echo characts. 7-60367
 Qinghai-Xizang (Tibet) Plateau, Quaternary lakes retreat and climatic significance (*Chinese*) 7-55104
 radar, meteorological appls. 7-47548
 radar signature in thunderstorms, 3-body scattering 7-60369
 radioisotope distribution in precipitation, surface and groundwaters in NW Yugoslavia 7-23254
 radiowave scattering, effect of meteorological conditions on satellite radar images of Earth's surface 7-66217
 river flood modelling and forecasting, empirical relationship 7-40504
 scalar dynamic precipitation model, state estimation from time-aggregate obs. 7-23830
 scavenging of N and S, assoc. chem. processes 7-55192
 Central Sierra Nevada, United States Winter storms ice-phase water capture regions identification, use of snow O isotopic comp. 7-4084
 South Dakota, USA, stochastic daily precipitation models, parameters seasonal and regional var. 7-23781
 storm acid precipitation and stream water geochemistry 7-23777
 sulphate deposition from atm., adsorption by soil, implications for dynamics in hydrological systems 7-29102
 sulphate deposition from atm., conc. in streams 7-28426
 sulphate scavenging coefficient, estimates from sequential precip. samples on Long Island 7-8467
 surplus or deficit precipitation analysis using index method 7-23715
 thunderclouds, elec. field and precip. growth in finite cloud 7-29206
 toxaphene deposition to E North America, determ. from peat accumulation 7-40064
 tropical squall line, diagnostic modelling study of stratiform cloud region 7-29136
 SW United States, summer precipitation singularity, bursts and breaks synoptic-dynamic characts. 7-47494
 United States, warm-season precipitation, mesoscale convective system contrib. 7-66237
 United States and Canada, 1986 June, water conditions 7-9053
 variations, correl. with ground self pot. var. 7-29275
 H+He(H₂)(N₂)(O₂), differential scatt. cross-sections for neutral particle precipitation 7-5739
 H₂O₂ in polar ice cores, long-term record 7-55229
³H fallout detection in tree ring records, short term precipitation 7-23255
 NH₃ washout, effect of precip. on vertical profiles 7-40513
 Rn concentration in precipitation, automatic measuring apparatus 7-49847

atmospheric pressure *see atmospheric pressure and density***atmospheric pressure and density**

- 500 mb geopotential height eigenfunctions, comparison 7-47520
 absorption in longwave radiation parameterisations, press. and temp. depend. 7-60379
 S Alberta, Canada, chinooks distinguishing nocturnal features 7-47493
 E Asia, dynamic and thermodynamic influences of Tibetan Plateau on general circulation model 7-29135
 S Asia, local rainfall rel. to southern Oscillation Warm Events 7-34628
 N Atlantic, low pressure record for centre of active depression 7-66278
 S Australia, obs. of internal atmospheric bores and cold front 7-55127
 Belgium, meteorological observations, AD 1981-5 at Uccle (*French, Flemish*) 7-47484
 blocking anticyclones, local vorticity and heat balances in spectral general circulation model 7-29138
 blocking events, climatology in perpetual January simulation of spectral general circulation model 7-29137
 blocking highs, forcing by transient cyclone-scale vorticity transfer 7-9094
 Brazil coast, mean sea-level var. with atm. temp., press., precipitation and evaporation 7-18194
 convective boundary layer, closures for pressure-scalar covariances 7-66233
 cosmic ray muon intensities at deep underground facilities, atm. effects 7-34811
 El Nino-Southern Oscillation, 1877-8 event rel. to 1982-3 event 7-4051
 European temperature and precipitation rel. to N Atlantic atmos. pressure characts. 7-66246
 global sea-level press. distrib. in April and July, relation to Indian summer monsoon precip. 7-29207
 Gulf of Carpentaria, Australia, southerly nocturnal wind surges and bores, assoc. press. patterns 7-29195
 height fields anomalies, month-to-month persistence in general circulation model and Earth's atmosphere 7-9093
 hemispheric forecast error correlations for geopotential and temp., horizontal struct. 7-4150
 India, monsoonal fields sequential evol. 7-29203
 interpolation methods for press. vertical profiles reconstruction 7-34730
 Local AFOS MOS programme appl. to wind prediction 7-34679
 magnetotail plasma sheet, comp and plasma props. 7-34789

atmospheric pressure and density continued

- W Mediterranean Sea, press. and wind fields obs. 7-34609
 mesosphere, gravity waves indicated by density fluctuations 7-40621
 middle atmosphere 1984 spring processes 7-34616
 midlatitude low, pressure field, shape fitting appl. 7-4148
 Millimetre Atmospheric Sounder on Shuttle for passive sounding (*German*) 7-40617
 monthly long-range forecasts for United Kingdom, exptl. forecasting system 7-14358
 Northern Hemisphere, press. var. 7-4171
 Northern Hemisphere surface press. and temp. 7-34665
 ocean, quasi-steady shelf circulation driven by along-shelf wind stress and open-ocean pressure gradients 7-47456
 ocean continental shelf edge waves forcing, numerical model studies of long-period waves 7-8993
 pressure gradient force in sigma coord. models, error reduction method 7-34729
 profiling method for press. and temp., astronomical refraction technique (*Russian*) 7-18314
 remote sensing of N Hemisphere pressure field, data acquisition scheme 7-66328
 remotely sensed winds used to calculate ocean surface pressure field 7-60417
 solar cycle in air press. records 7-14339
 Southern Hemisphere subtropical highs location model 7-47526
 squall line pressure and temp. from dual-Doppler obs. 7-66223
 subtropical high ridge line, contrib. of vapour condensation heating to seasonal movements 7-40508
 surface pressure remote meas. using O₂ A-band absorption 7-14380
 thermosphere, geopotential mean height fields in southern hemisphere 7-47592
 thermosphere, H dissipation flux density rel. to temp. 7-23922
 thermosphere, neutral mass density calc. 7-47585
 thermosphere, wave-associated density disturbances 7-55342
 typhoons, infrasonic signals and eye pressure 7-29176
 United Kingdom, skill of exptl. monthly long-range mean sea level press. forecasts 7-40539
 E United States, anticyclones paths rel. to climatology of summertime O₃ and SO₂ 7-40066
 SW United States, summer precipitation singularity, bursts and breaks synoptic-dynamic characts. 7-47494
 upper atmosphere, seasonal and tidal variations of temperature and density 7-29315
 upper atmosphere, semi-annual density var. 7-4245
 vertical profiles retrieval from refr. meas. (*Russian*) 7-29277
 weather analysis procedure for surface pressure determination from wind data (*German*) 7-55238
 zonal circulation, corpuscular-tropospheric effect of solar wind streams 7-47475
 zonal tides, influence on Earth's rot. rate (*Chinese*) 7-4073

atmospheric proton precipitation

- magnetosphere protons precip., effects of storm-time reconfiguration of magnetosphere mag. field 7-9316

atmospheric radiation

- absorbers of radiation in atmosphere, distrib. estimation using infrared 3-band images (*Japanese*) 7-47577
 absorption in longwave radiation parameterisations, press. and temp. depend. 7-60379
 AKR and maser synchrotron instability 7-47641
 AKR emissions from magnetosphere, satellite interferometric measurements 7-40650
 Antarctic, radiative heating due to stratospheric aerosols, implications for O₃ depletion 7-55175
 N Atlantic, radiation budget of ocean-atmos. system, interannual variation 7-55179
 Atlantic region, visible and near IR solar radiation for cloudy days (*Russian*) 7-60332
 auroral kilometer radiation, cyclotron maser radiation from localized source 7-55372
 auroral kilometer radiation, Prognost-10 obs. 7-55378
 auroral LHR noise, obs. by S-310JA-6 sounding rocket (1978 August 27) 7-66393
 Baikal-Amur Mainline area of USSR, surface heat balance study 7-23816
 bispectral satellite measurements, appl. to cloud cover estimation 7-29148
 cirrus cloud, influence on climate and weather processes, global perspective 7-4157
 cloud shading, implications for mesoscale circulations generation and modification 7-34617
 cloud-radiation interaction in 3D model of mesoscale processes of oceanic energy-active zones (*Russian*) 7-23808
 clouds, optical radiation intensity for horizontally inhomogeneous clouds (*Russian*) 7-40564
 coastal environment standard radiation atm. aerosol models 7-55259
 cumulus cloud influence on solar radiation intensity 7-4105
 daylight availability data generation from existing solar radiation data bases 7-60428
 Dhahran, Saudi Arabia, insolation meas., diffuse fraction estimation 7-3625
 diffuse irradiance meas. under clear skies, shade ring correction 7-47543
 diffuse solar radiation model applicability to Huntsville, Alabama 7-60370
 diffusivity factor methods for atmospheric thermal radiation modeling 7-47496
 Earth radiation budget, differences for oceanic and continental regions 7-14345
 Earth Radiation Budget Experiment (ERBE), meas. data (1984 November 15) 7-9067
 Earth-emitted radiation, variability from one year of Nimbus-6 ERB data 7-9092
 East Germany, evaporation height rel. to air temp., global radiation and saturation deficit (*German*) 7-9055
 ELF hiss propagation inside and outside plasmasphere, statistical study from GEOS-1 obs 7-34787
 Eppley pyrgometer calibration for airborne meas. 7-60393
 f-plane models, radiative upper boundary condition capable of transmitting gravity waves 7-29200
 Greece, sunshine duration rel. to altitude, latitude and longitude 7-66296
 hazy atmosphere radiative characts. 7-4182

atmospheric radiation continued

high-altitude auroral zone, ray tracing of Z-mode emissions from source regions, assoc. plasma characs. 7-47642
 impulsive atmospheric noise, hourly APDs, semitropical location and evening transition period 7-47483
 Indian monsoon radiative forcing model, role of stratospheric aerosols 7-55196
 internal polarised radiation in multilayered atmospheres, computation 7-14377
 ionosphere, near-field radiation from pulsed electron beams in space 7-66391
 ionospheric noise, ELF wave generation in lower ionosphere 7-9307
 ionospheric plasma, stimulated radio emission at second harmonic of pump wave freq. 7-29331
 IR cooling rate calculation, for cooling due to H₂O vapour (*Chinese*) 7-29221
 IR downward radiation flux at Earth's surface, satellite remote sensing technique 7-14390
 IR radiance, near horizon, rel. to sea surface temp., model for 8 to 12 μ m band 7-60374
 IR radiation, H₂O absorpt. rel. to satellite remote sensing of atmospheric water vapour 7-4112
 IR radiation, procedure for remote sensing of atmospheric temp. with high vertical resolution 7-66218
 IR radiation transfer, transmission of the CO₂ 15 μ m band 7-40688
 far IR radiative transfer, non-LTE model for far IR bands 7-23923
 far IR radiative transfer model for mesosphere, for CO₂, H₂O, N₂ and O₂ bands 7-23924
 IR remote sensing of atmos. temperature, thermal radiation transfer model (*Japanese*) 7-18316
 IR satellite image processing, kinetic temp. image modelling 7-23899
 IR upward directed radiation information content for O₃ remote sensing 7-23865
 Italy, global irradiation estimation, Angstrom equation fitted using least squares method 7-55215
 longwave downward radiation, thermal emissivity model, angular dependence 7-18283
 longwave radiation in mountainous areas, influence on energy balance of alpine snowfields 7-23727
 low latitude discrete chorus emissions and VLF hiss 7-55355
 magnetosphere, LF electrostatic waves assoc. with auroral kilometeric radiation 7-47640
 magnetosphere, quasi-electrostatic half-electron-gyrofrequency VLF emissions 7-4272
 magnetospheric AKR showing harmonic struct., DE 1 observations 7-55376
 magnetotail, broadband noise generation by beam acoustic instability 7-34801
 non-stationary Markov chains for modelling of daily radiation data 7-34654
 mesosphere, radiance/temperature vars., Nimbus 6 PMR expt. meas. 7-47588
 methane in atmosphere, IR radiation models 7-18302
 microwave brightness temperature of stratosphere, zonal wave number variance 7-29163
 Microwave Limb Sounder 183 GHz radiometer 7-60433
 northern summer outgoing longwave radiation anal., determ. of tropical convection 7-34623
 ocean-atmos. system, visible region spatial radiance field 7-55180
 outgoing longwave irradiance estimation, appl. of column weighting model 7-29242
 outgoing longwave radiation var. 7-29191
 Pakistan, daily solar radiation incident on flat tilted surface 7-55216
 planetary radiation budget, diurnal var., geostationary satellite obs. 7-4185
 plasmasphere hiss and VLF chorus initiating radiation belts slot region electron precipitation 7-9325
 polluted atmosphere radiative heating, influence of soot 7-4101
 Pune, India, daylight illumination studies 7-9118
 radiance variance from heterogeneous scenes in optical and IR 7-47533
 radiative cooling in valleys and hollows 7-55134
 radiative transfer eqn. solution with improved algorithm (*Chinese*) 7-29244
 radiatively interactive clouds in cumulus convection Kuo parameterization 7-66221
 radioactive fallout on west Algerian coast, early 1985 (*French*) 7-59895
 radiometric measurements, appl. to determ. of atmosphere total O₃ content 7-66216
 remote sensing (book) 7-35139
 RF radiation from lightning return strokes, influence of Earth conductivity 7-40535
 SHF emission, effect on meas. of cosmic background radiation 7-55463
 shortwave and longwave radiation, STREX 1980 measurements 7-29174
 solar eclipse sky brightness, contrib. of K-corona scattered light 7-66535
 solar UV-B and visible radiation under cloudless skies 7-66270
 stratosphere, radiance/temperature vars., Nimbus 6 PMR expt. meas. 7-47588
 stratosphere, radiative balance determ. from Nimbus-7 LIMS meas. 7-9098
 stratosphere, satellite IR radiances rel. to polar stratospheric clouds 7-55156
 sunshine duration at Weißenstephan, Germany, modelling using non-stationary Markov chains 7-34654
 surface, wind roughened, albedos and glitter patterns generation 7-9006
 surface emissivity near Lake Eyre, NOAA-7 AVHRR meas. 7-14287
 temperature remote sensing for cloudy atmosphere, IRT radiation transfer model 7-60399
 terrestrial atm., radiative transfer problem 7-9171
 thermal IR reflection, angular emissivity meas. of soils rel. to remote sensing (*French*) 7-55291
 thermal radiation flux, line-by-line calcs. accounting for CO₂ absorpt. bands (*Russian*) 7-60382
 thermosphere, NO energetics and IR radiation in disturbed heated thermosphere 7-4247
 tropical synoptic-scale diagnosis, test of ECMWF model 7-29196
 UV-B daily totals from routine meteorological obs. 7-4132
 vegetation canopy, model of sunlight penetration involving leaf distribution 7-4097
 VLF emissions at mid-latitude, statistical characs. 7-55387
 VLF quiet band phenomena observed during conjugate VLF signal propagation study 7-34797

atmospheric radiation continued

VLF wave generation upon appearance of anomalous resistance 7-34791
 volcanic dust from El Chichon in stratosphere, solar radiation anomalies 7-34677
 X-rays due to quiet-time electron precipitation 7-47624
 O₃ in mesosphere, ν_3 vibrationally excited mode showing nonlocal thermodynamic equilibrium 7-18328

atmospheric radioactivity
see also fallout
 aerosol radiation meters checking, Rn daughter products meas. 7-9220
 Tjernobyl radioactive fallout, appl. of two-dimensional trajectory model to radioactivity transport 7-59894
²²²Rn concentrations in USA homes, statistical distrib. and health hazards 7-65666

atmospheric spectra
see also atmospheric optics
 absorption by H₂O vapour and O₂ 7-60375
 auroral and airglow obs., using grating spectrometer with imaging photon detector 7-34722
 bispectral satellite measurements, appl. to cloud cover estimation 7-29148
 chloromethane in upper troposphere and stratosphere, spectroscopic detection 7-9076
 D-region, winter-time scattered signals freq. spectra from partial refl. radar meas. 7-47612
 dayside aurora, EUV-near IR O mission features obs. 7-55345
 deuterium whistlers in outer ionosphere, charact. freqs. in five-component plasma 7-18335
 ethane, identification from 1951 IR solar spectrum 7-55124
 ethane, Q branches of ν_7 fundamental band, intensities rel. to atmospheric meas. 7-5672
 extinction at Cerro Tololo Inter-American Observatory, mol. absorpt. parameters 7-47542
 Fourier transform spectral analysis of far IR emission 7-14379
 geocoronal H I emission, correction for effects on observed stellar Lyman alpha profiles 7-60637
 high-resolution submillimetre heterodyne spectrometer 7-353
 intracavity laser spectroscopy of atm. 7-43189
 ionosphere, absorption of cosmic radio noise at high latitudes, spectrum 7-14405
 IR absorption, LOWTRAN computer model 7-60378
 IR radiance, near horizon, rel. to sea surface temp., model for 8 to 12 μ m band 7-60374
 far IR radiative transfer model for mesosphere, for CO₂, H₂O, N₂ and O₂ bands 7-23924
 far IR spectral absorption in 1700 to 2100 cm⁻¹ band region (*Russian*) 7-9170
 IR spectroscopy, math. representation, resolution and role of model in anal. 7-48875
 IR spectroscopy from space, ATMOS expt. on Spacelab-3 7-55314
 methane, absolute strengths and self-broadened widths in IR spectra 7-36622
 Michelson interferometer, slightly-cooled high-resolution, for limb emission meas. from space 7-55317
 microwave plasma emission characteristics in near IR 7-55318
 nightglow, O and O₂ quenching parameters for precursors 7-47604
 nightglow O₂ (A² Σ_u^+) vibrational populations, altitude dependence 7-47606
 radiation absorbers in atmosphere, distrib. estimation using infrared 3-band images (*Japanese*) 7-47577
 remote sensing (book) 7-35139
 SCRIBE interferometer atmospheric emission spectra 7-55319
 stratosphere, climate modelling, band strengths temp. depend., low temp. meas. using Freons 7-55252
 stratosphere, far-IR spectrum, high resolution meas. with Fourier transform spectrometer 7-55262
 stratosphere, IR spectroscopy with balloon-borne cryogenic Fourier spectrometer 7-60377
 stratospheric far-IR emission analysis, synthetic spectra and FTIR meas. comparison 7-55315
 sunlight spectral absorpt. and total vertical water vapour determ. 7-4087
 temperature meas. by molecular rotational band obs. with Fabry-perot interferometer 7-47546
 trace gas measurements using matrix isolation-FTIR spectroscopy 7-55316
 CO IR atmospheric transmittance, band model 7-40563
 CO measurements with submm heterodyne spectrometer 7-60562
 CO₂ in middle and upper atmosphere, 15 microns band in IR spectra 7-23923
 COF₂ in stratosphere, concentration determined by IR solar absorpt. observations 7-9077
 ClONO₂, stratosphere conc. profile from IR spectral observation 7-9167
 H₂¹⁸O, hot band, IR spectral line positions and intensities 7-36623
 HCl in atm., ground-based IR solar spectra anal. 7-40538
 H₂O, absorpt. of 2.3 μ m radiation 7-57060
 H₂O absorption line parameters rel. to DIAL monitoring of atmosphere 7-47535
 H₂O dimer, far IR absorpt. spectra 7-47539
 H₂O, IR spectrum rel. to satellite remote sensing of atmospheric water vapour 7-4112
 H₂O, IR spectrum rel. to diurnal and annual vars. of water vapour at Cagliari Astronomical Observatory 7-40547
 H₂O vapor absorption at 1.3 μ m 7-60376
 HOCl, gaseous, UV absorpt. spectrum, rel. to atm. modelling 7-25534
 HO₂NO₂, IR spectra of stratosphere at .802 cm⁻¹ and conc. profile 7-9168
 NO, Zeeman modulated radiometer for remote detection 7-55313
 N₂O IR transmittance, band models comparison 7-19860
 O nightglow, energy transfer characs. 7-47603
 O₂ absorption line parameters rel. to DIAL monitoring of atmosphere 7-47534
 O₂ nightglow, rotationally-resolved bands obs. at 373 to 474 nm in O₂-Ar afterglow 7-29326
 O₂, photoabsorpt. cross section, Herzberg continuum, UV obs. 7-36639
 O₂, potential energy curve, photodissociation and adsorp. spectra 7-5624
 O₂, UV absorpt. cross-sections, 195-241 nm, Herzberg continuum 7-34675
 O₂, UV cross sections and photodissociation rate consts. for stratosphere 7-55260

atmospheric spectra continued

- O₂, UV molecular absorption continua and radiative lifetimes UV molecular absorption continua and radiative lifetimes 7-15620
- O₃ density variations, meas. by Nimbus-7 and SME 7-60323
- O₃, electronically excited state, radiative lifetime and quenching mechanism 7-31110
- O₃ in mesosphere, ν_3 vibrationally excited mode showing nonlocal thermodynamic equilibrium 7-18328
- O₃ measurement device using HARTLEY band (*German*) 7-9247
- O₃, UV absolute absorpt. cross sections 7-50161

atmospheric structure

- Arabian heat low, surface energy budget and struct. 7-4151
- Arabian heat low structure, bulk tropospheric heat budget 7-4152
- Bay of Bengal, atmospheric struct. during suppressed and active convective periods 7-55211
- boundary layer, temp., stratification and wind vector profiles 7-34614
- Charney baroclinic-instability with Rossby wavetrains 7-18287
- D-region, winter-time, scatt. irregularities scale from partial refl. radar meas. 7-47612
- extratropical geopotential height and tropical convection, coherent fluctuations on intraseasonal time scales 7-4129
- hemispheric forecast error correlations for geopotential and temp., horizontal struct. 7-4150
- ionosphere, plasma instabilities rel. to nonlinear wave structs. generation 7-66386
- ionosphere irregularities, relation to VHF scintillations increase during mag. activity 7-34762
- magnetosphere, suprathermal ion and electron results from ISEE-3 Geotail Mission 7-29368
- distant magnetotail, structural and dynamical aspects from ISEE-3 plasma meas. 7-29366
- mesosphere Na layer, lidar obs. 7-34753
- middle atmosphere 1984 spring processes 7-34616
- nocturnal boundary layer over sloping terrain, numerical simulation (*Chinese*) 7-4080
- nocturnal temperature inversion evol. 7-4095
- radiation belts, spatial distrib. of protons at high and low latits. 7-4274
- stratified surface layer, similarity scales evaluation using wind speed and temp gradient 7-40514
- synoptic scale disturbances with circular symmetry 7-34625
- United States, summer monthly mean surface temp. field rel. to 700 mb height field 7-34667
- SW United States, summer precipitation singularity, intensity intraseasonal var., press. and 500 mbar data anal. 7-47494
- unstable marine boundary layer, struct. determ. from lidar and aircraft obs. 7-29133
- vertical profiles reconstruction by interpolation methods 7-34730

atmospheric techniques

- see also air pollution detection and control; ionospheric measuring apparatus; ionospheric techniques; meteorological instruments; weather forecasting*
- acoustic remote sensing of atmosphere and oceans, symposium, Paris (October 1985) 7-48133
- aerometric database for field experiment, real-time display and development 7-54407
- aerosol, optical coeff., meas. technique (*Chinese*) 7-18305
- aerosol analysis methods for chem. comp., particle sizes and conc. determ. 7-4085
- aerosol light absorpt. coeff., measurement method (*Russian*) 7-9221
- aerosol radiation meters checking, Rn daughter products meas. 7-9220
- aerosol remote sensing using lidar system, design aspects 7-18320
- aerosol sampler, efficiency of tubular thin-walled inlet 7-65670
- aerosol sampler inlet (non-isoaxial), sampling efficiency study 7-65671
- aerosol sampling into vertical cylindrical sonde from immobile medium 7-34732
- air parcel trajectory analysis, appl. to acid deposition data from New Jersey Pine Barrens 7-40061
- air pollution modelling and applications, conference, St. Louis, Missouri (April 1985) 7-48181
- air pollution screening model, development of MICROGAUSS-I 7-54401
- airborne microwave rain scatterometer/radiometer system, microwave backscatter expt. of ocean surface (*Japanese*) 7-23910
- airborne microwave rain scatterometer/radiometer system, rain meas. and data anal. (*Japanese*) 7-23909
- aircraft icing conditions detection method, by ground-based microwave radiometry 7-23871
- Angstrom's turbidity coeff., determ. from direct total solar irradiance meas. 7-66355
- anthropogenic radionuclides meas. around nuclear power reactors, method for ³H, ¹⁴C, ⁸⁵Kr and ¹³⁵Xe 7-23257
- areal quality control of min. temp. and sunshine duration, principal component and near neighbour methods 7-4141
- ARMA stochastic processes for daily average temp. anal. 7-34639
- autonomous satellite navigation using observations of starlight atmospheric refraction 7-60418
- boundary layer characts. meas. by acoustic sounder 7-4096
- boundary layer parameterization, FORTRAN programs 7-55246
- chemical deposition, stochastic modelling of space-time struct. 7-23239
- circulation classification, objective typing procedures comparison 7-4131
- cloud amount determ., comparison of surface and satellite meas. methods 7-9079
- cloud base height estimation, use of condensation levels calc. from ground instruments 7-4144
- cloud condensation nuclei chem., anal. technique 7-3589
- cloud cover estimation, appl. of bispectral satellite measurements 7-29148
- cloud extinction profile measurements by lidar using Klett's inversion method 7-9184
- cloud imaging from satellites, structural-stochastic model for imaging 7-14391
- cloud systems imaged by satellites, synoptic analysis and diagnosis methods (*German*) 7-40542
- clouds radar echo characteristics over Black, Kara and E Siberian seas 7-34615
- cloudtop height remote sensing method using Meteor satellite 7-60400
- computer algorithms for checking weather data (*German*) 7-55330
- computer graphics, stereo display terminals for McIDAS system 7-60389
- data banks for climatological data, design and use for monthly data records 7-9178

atmospheric techniques continued

- daylight availability data generation: from existing solar radiation data bases 7-60428
- differential reflectivity technique for rainfall meas. 7-23869
- diffuse irradiance meas. under clear skies, shade ring correction 7-47543
- Doppler radar data for cloud water and water-vapour contents determ. 7-4212
- Doppler weather radar, spectral moments recovery from overlaid echoes 7-9210
- Doppler wind velocity measurements with radar or lidar, use of discrete spectral peak freq. estimator 7-9212
- dust storm detection, satellite remote sensing-image processing methods 7-66329
- Earth's atmosphere radio transillumination, signal parameters, ionosphere effect 7-55367
- eddy correlation technique for determination of turbulent fluxes 7-23848
- electric conduction current measurement method using balloon-borne wire antenna 7-29289
- electro-optic phase modulation gas correlation spectroscopy 7-9182
- electron precipitation fluxes determ., use of bremsstrahlung and riometer meas. 7-47624
- ERS-1 wind and wave calibration workshop, Schliersee, Germany (June 1986) 7-24305
- flash flood warning systems for real-time operation 7-60388
- fog cover remote sensing at night satellite IR radiometry method (AVHRR) 7-4216
- Fourier transform spectral analysis of far IR emission 7-14379
- frequency response functions gain and phase, estimation of confidence intervals 7-23857
- FRONTIERS radar and satellite method, study of split cold fronts 7-55207
- global horizontal borrowing appl. to correction of negative mixing ratios in spectral models 7-34738
- GPS carrier phase for centimeter-level surveys, initial results 7-60419
- gravity waves measurement, effects of Doppler shifts on wave spectra observed by MST radar 7-47490
- hail remote sensing with S-band dual linear polarization radar 7-66344
- heterodyne lidar with laser receiver for remote sounding of atm. 7-4214
- hot wire anemometry, book 7-51357
- hydroxymethanesulfonate, determination in wet deposition by chromatography method 7-54406
- image processing, phase closure with rotational shear interferometers 7-36895
- incoherent scatter radar probing of GP-100 km atm. and ionosphere 7-9211
- interpolation methods for press. and temp. profiles reconstruction in atm. 7-34730
- intracavity laser spectroscopy 7-43189
- IR downward radiation flux at Earth's surface, satellite remote sensing technique 7-14390
- IR satellite image processing, kinetic temp. image modelling 7-23899
- IR spectroscopy, math. representation, resolution and role of model in anal. 7-48875
- IR spectroscopy from space, ATMOS expt. on Spacelab-3 7-55314
- Israel Meteorological Service numerical forecasts, use of satellite sounding 7-34736
- jackknife regression scheme with intraseasonal var. index for seasonal temp. prediction 7-47567
- laboratory experimental models, optical method for measuring interface wave amplitudes 7-4201
- land surface albedo, regional value determ. by satellite method 7-66345
- land surface remote sensing and climate, conf., Rome, Italy (Dec. 1985) 7-23921
- laser beam remote sensing methods 7-40605
- laser beam remote sensing of tropospheric gases (*German*) 7-40081
- laser remote sensing, nonlinear refr. phase compensation of light beam in droplet medium 7-4183
- lateral dispersion measurement method involving aircraft oblique photography 7-23918
- least mean square algorithm for prediction and freq. tracking of nonstationary data 7-34737
- lidar for supercooled fogs artificial dispersal anal. 7-34733
- lidar investigation of clouds 7-55135
- lidar technique appl. to laboratory meas. of atmospheric temp. and backscatter ratio 7-9238
- light refraction at low elevation angles; use for press. and temp. vertical profiles retrieval (*Russian*) 7-29277
- light wave time-dependent characts., fluctuating wind effect, expt. investigation 7-55263
- lightning holographic apparatus for studying simulated lightning in laboratory 7-26575
- lightning storms intensity determ. using centimetre and metre-wave radar (*Russian*) 7-47549
- Limb Infrared Monitor of the Stratosphere, influence of O₃ ν_3 band in mesosphere 7-18328
- limb sounding from Space Shuttle, use for middle atm. studies 7-40568
- longwave radiation estimation in mountainous areas, appl. to energy balance of alpine snowfields 7-23727
- magnetosphere, resonance frequency of magnetic force lines, measurement using gradient method 7-55369
- magnetosphere convective flows and spatial gradients determ. method 7-9230
- magnetosphere inductive electric fields, determ. method using whistler and ionospheric data 7-4270
- magnetospheric VLF radio waves spectral estimation, one-bit correlation method 7-9337
- meteorological fields mapping, developments in use of empirical orthogonal functions 7-29142
- meteorological observational network global analysis errors 7-34739
- meteorological station with automatic data transmission, software and test results (*German*) 7-55266
- meteosat IR meas., surface and cloud-top temp. determ. atmospheric correction scheme 7-18310
- micropulsations in magnetosphere, magnetogram deconvolution method for P₂ pulsations 7-4271
- microwave plasma emission characteristics in near IR 7-55318
- middle atmosphere dynamics measurements, first results from middle and upper atmosphere radar 7-47561
- middle atmosphere oblique vel. radar obs. 7-60338
- multiyear drought durations, freq. anal. technique 7-23758
- night-sky glow prediction, mathematical model 7-9172

atmospheric techniques continued

- numerical integrations ensemble use for real-time long-range forecasting 7-29294
- observing system sensitivity experiments for objective analysis and weather forecasting models 7-60353
- ocean surface evaporation, estimation method using remote sensing data 7-23791
- ocean surface wind measurement, Seasat scatterometer studies of effect of wave height and environmental conditions 7-66159
- optical extinction coeff. profiling method using lidar (*Russian*) 7-18315
- optical parameters of atmos., satellite remote sensing method involving imaging of land 7-55296
- outgoing longwave irradiance estimation, appl. of column weighting model 7-29242
- particle-induced X-ray emission for aerosols long-range transport anal. 7-4192
- periods of normals appl. in climatology (*German*) 7-9164
- planetary boundary layer eqns. soln. by finite element technique 7-9232
- planetary boundary layer meas. by vertical SODAR (*German*) 7-9148
- polar ice air bubbles for pollution monitoring and bubble age 7-4068
- pollutant concentrations distribns. modelling estimation of one and two-parameter statistical distribns. 7-40067
- pollution from diesel vehicles, use of Dy as tracer to study aerosol sources 7-59899
- pollution modelling, short-term SO₂ concs. calc. in Cracow area, Poland 7-40068
- pollution modelling, statistical study of pollutant concs. via generalised gamma distrib. 7-34090
- precipitable water remote sensing method, by ground-based 1.35 cm radiometry (*Chinese*) 7-29311
- precipitation measurement networks characts. (*German*) 7-4229
- pressure and density profiling method, astronomical refractive technique (*Russian*) 7-18314
- pressure at ocean surface, determination using remotely sensed wind data 7-60417
- surface pressure field determination using wind data, iterative procedure (*German*) 7-55238
- pressure field of N Hemisphere, remote sensing data acquisition system 7-66328
- pressure gradient force in sigma coord. models, error reduction methods 7-34729
- radar, meteorological appls. 7-47548
- radar Doppler spectral width and thunderstorm turbulence 7-60415
- radar use for areal precipitation estimation over Oklahoma 7-9234
- radiation absorbers in atmosphere, distrib. estimation using infrared 3-band images (*Japanese*) 7-47577
- radioactive dust sampling, entry characts. of dust samplers used in British nuclear industry 7-40079
- rain cell size statistics derived from radar obs. 7-23805
- rain measurement by radar, importance of droplet size distrib. 7-14351
- rain remote sensing, satellite passive microwave imagery methods 7-47563
- rain remote sensing by microwave radiometry method using classification algorithm 7-23874
- rain remote sensing from space, by passive microwave methods 7-60387
- rainfall and cloud remote sensing by satellite, monitoring methods used by Bristol University 7-47562
- refractive index profile determ. method, astronomical refraction technique (*Russian*) 7-18314
- relative humidity measurement using alpha-particle corona streamer counter 7-55333
- remote sensing, satellite automatic picture transmission, design of grey scale test pattern generator 7-29292
- remote sensing methods for arid and semiarid regions 7-9186
- satellite proposal, low equatorial orbiter in 3-hour orbit 7-55329
- satellite remote sensing for global weather prediction, review 7-55324
- satellite water vapour imagery for weather anal. and forecasting, research developments 7-55335
- scalar dynamic precipitation model, state estimation from time-aggregate obs. 7-23830
- sea surface temperature imaging, appl. of Advanced Very High Resolution Radiometer (AVHRR) data 7-14297
- sediment chemical analysis for Cd, Ag, Pd, Tl, atomic absorpt. method 7-40601
- shape fitting appl. to press. low 7-4148
- ship observations use for interdecadal climate changes anal. 7-4217
- signal processing, use of communications techniques 7-29411
- similarity scales evaluation in stratified surface layer, appl. of wind speed and temp gradient 7-40514
- solar angle derivation for design of solar energy system using vector algebra 7-46970
- solar energy fluctuation determ. in lower atmospheric using spectral anal. techniques 7-14364
- solar insolation data analysis by means of Allan variance and Fourier transform 7-60371
- solar irradiance measurement comparison of NBS SURF and W UV irradiance standards 7-11086
- SOUSY VHF radar measurements in the lower and middle atmosphere 7-23870
- static wind load measurement, appl. of six-component high-freq. piezoelectric balance 7-14356
- statistical methods for Dobson total O₃ data anal. 7-55307
- stratosphere, far-IR spectrum, high resolution meas. with Fourier transform spectrometer 7-55262
- stratospheric far-IR emission analysis, synthetic spectra and FTIR meas. comparison 7-55315
- stratus clouds evolution modelling, numerical method 7-9132
- superposed epoch analysis method 7-34743
- surface layer three-parameter inferior mirage model use for temp. profiles determ. 7-23804
- surface pressure remote meas. using O₂ A-band absorption 7-14380
- temperature meas. by molecular rotational band obs. with Fabry-perot interferometer 7-47546
- temperature meas. using remote sensing IR data (*Japanese*) 7-34750
- temperature measurement, remote sensing procedure with high vertical resolution 7-66218
- temperature profile meas. in troposphere and stratosphere, radio acoustic technique 7-14360
- temperature remote sensing by satellite IR radiometry, constrained inversion technique 7-29293

atmospheric techniques continued

- temperature remote sensing for cloudy atmosphere, IRT radiation transfer model 7-60399
- temperature remote sensing using IR data (*Japanese*) 7-18316
- total vertical water vapour determ., methods comparison 7-4087
- trace element detection by differential absorption spectroscopy (*German*) 7-46991
- trace gas measurements using matrix isolation-FTIR spectroscopy 7-55316
- turbulence, numerical synthesis of trivariate velocity realisations 7-9078
- turbulence classification, computer program 7-55247
- turbulence measurement in middle atmosphere, VHF radar technique 7-4246
- turbulence measurement with Gill propeller anemometers, directional response study 7-55276
- vertical temp. gradient estimation using near-surface obs. 7-66343
- water vapor vertical profile structures retrieved from satellite data via classification and discrimination 7-4218
- water vapour content, microwave radiometric meas. at NPL 7-34606
- water vapour measurement, satellite remote sensing technique 7-4112
- weather forecasting, design and appls. of generalised Australian Model Output Statistics system 7-55126
- weather forecasting, diagnostic study of first year of Model Output Statistics forecasts in Australia 7-55125
- weather forecasting, exptl. monthly long-range forecasting system for United Kingdom 7-14358
- weather forecasting initialisation techniques 7-66358
- weather prediction, forecasts for community by students at Lowell University Massachusetts 7-29128
- weather prediction, primitive equations, energy conserving Galerkin finite element schemes 7-66346
- wind at sea-surface, remote sensing method involving whitecaps 7-9216
- wind determination by sodar method (*Chinese*) 7-9180
- wind direction mean and standard deviation, single-pass estimation 7-66240
- wind environment assessment at ground level, acceptable criteria determ. 7-14352
- wind field analysis using upper air observing network data, optimum grid length 7-29177
- wind meas., 405 MHz phased array antenna design 7-34752
- wind meas. using airborne IR Doppler lidar 7-40561
- wind measurement in planetary boundary layer, lidar method accuracy 7-14347
- wind profile determ. method, using Doppler radar and lidar (*Russian*) 7-4210
- wind speed extraction with pulse-limited radar altimeter, effect of whitecaps and foam 7-29306
- winds over ocean, improved radar altimeter wind speed algorithm 7-66347
- CO remote sensing by gas filter radiometry, instrumentation and data reduction 7-18317
- CO₂, exchange rate between atmos. and ocean, isotopic meas. techniques 7-23884
- HCl detection in atm. by laser-induced fluorescence of CO₂ 7-46993
- HCl in stratosphere, near-IR satellite remote sensing and interference from OH airglow 7-23926
- I₂, detect. in atmospheric, differential reson. technique 7-40552
- ⁸⁵Kr, sampling unit for air sample 7-23258
- NO concentration prediction, appl. of regression model 7-40063
- O₃ content determination via mutual covariation links between temp. and O₃ content, accuracy of determ. 7-9135
- O₃ determination, balloon borne instrumentation, BOIC intercomparison expt. 7-29159
- O₃ remote sensing, information content of upward directed IR radiation 7-23865
- O₃ remote sensing, SBUV satellite meas. technique for Antarctic O₃ vertical profiles 7-55145
- O₃ total content determ. from remotely-sensed data 7-66216
- SO₂ concentrations prediction in Venice area, appl. of probability model 7-17929

atmospheric temperature

- absorption in longwave radiation parameterisations, press. and temp. depend. 7-60379
- air-sea temperature difference rel. to wind algorithm, Seasat scatterometer studies 7-66159
- Alaska, permafrost temp. profile, evidence for climate change 7-66299
- S Alberta, Canada, chinooks distinguishing nocturnal features 7-47493
- Alberta, Canada, Holocene vegetation and climate changes 7-23840
- Antarctic, circulation features determ. from temp. field anal. 7-60319
- Antarctic, stratosphere temperature, effects of O₃ depletion 7-55174
- Antarctic atmosphere, O₃ seasonal distrib. and thermal struct. 7-55168
- Antarctic spring stratosphere; aerosol and temp. var., lidar obs. 7-60325
- Antarctica, cooling of stratosphere at Syowa 7-55147
- Antarctica stratosphere, temperature decrease in AD 1979 to 1985 period 7-55143
- Arabian heat low, surface energy budget and struct. 7-4151
- Arabian Sea, low-level inversion synoptic characts. (during MONEX-79) 7-9120
- Arctic anthropogenic aerosols, climatic effects 7-55193
- E Arctic Ocean, sea ice form., synoptic conditions 7-34535
- Arctic polar stratospheric clouds, airborne lidar meas. 7-60334
- Argentina continental shelf, temp. and humidity profiles, planetary boundary layer modelling 7-34579
- E Asia, dynamic and thermodynamic influences of Tibetan Plateau on general circulation model 7-29135
- Athens, Greece, air temp. and climatic change 7-66287
- Atlantic Ocean tropical cyclones, cloud canopy tops temp. and future max. winds 7-29197
- Australia, diagnostic study of first year of operational Model Output Statistics forecasts 7-55125
- Australia, major droughts prediction from temp. anal. 7-4170
- Australia, max. and min temps prediction via generalised Model Output Statistics forecasting system 7-55126
- Baikal-Amur Mainline area of USSR, surface heat balance study 7-23816
- Belgium, meteorological observations, AD 1981-5 at Uccle (*French, Flemish*) 7-47484
- Berlin, Germany, stratosphere temperature-height standard-profile 7-4103

atmospheric temperature continued

- Birmingham, England, occurrences of very warm and very cold spells 7-55232
- boundary layer, diabatic wind and temp. profiles obtained from a 100 metre tower 7-23790
- boundary layer, temp., stratification and wind vector profiles 7-34614
- boundary layer, temperature inversion formation by numerical model (*Russian*) 7-55183
- boundary layer above marginal ice zone of ocean 7-34605
- boundary layer radiative heating for heavily polluted atmos. 7-4101
- boundary layer wind and temp. mesoscale variations of N Atlantic off Scotland 7-23797
- Brazil coast, mean sea-level var. with atm. temp., press., precipitation and evaporation 7-18194
- Bremen, West Germany, summer temp., precipitation and sunshine char. acts. 7-9162
- Britain, temperature changes since 22000 years BP, beetle remains record 7-60373
- W Canada, temperatures existing 42000 and 34000 years BP 7-23833
- Canterbury Plains, New Zealand, topographic effects rel. to interacting multi-scale wind systems 7-55203
- Cenozoic temperature variations, stratospheric aerosol effects 7-34666
- climatological temperatures on different time scales, scale invariance 7-9155
- cosmic ray muon intensities at deep underground facilities, atm. effects 7-34811
- DIAL monitoring, O₂ absorption line parameters 7-47534
- downdraught from convective clouds, vel. and temp. 7-9131
- Eagle Valley, Colorado, temp. inversion buildup and wind struct. 7-55202
- earthquakes, atmospheric temperature anomaly for prediction 7-28897
- East Germany, evaporation height rel. to air temp., global radiation and saturation deficit (*German*) 7-9055
- El Nino-Southern Oscillation, 1877-8 event rel. to 1982-3 event 7-4051
- English Channel, wind and temp. characts. for 1066 September, chroniclers' records anal. 7-29650
- equatorial thermosphere, excess heating during storm sudden commencement 7-47584
- Eurasia, snow-ice cover, correlation with rainfall and temp. in E China 7-29238
- W Europe, climate simulation and CO₂ induced climate change, general circulation model anal. 7-66285
- European temperature and precipitation rel. to N Atlantic atmos. pressure characts. 7-66246
- extratropical cyclones 7-60346
- F-region, high-latitude, electron temp. during solar max. and winter conditions 7-34772
- Finland, lake ice freeze-up and break-up dates rel. to air temp. climate 7-14342
- geostationary satellite temperature retrievals, assimilation into numerical prediction model 7-34618
- global temperature changes, annual and seasonal (1960 to 1985) 7-47527
- global trends in AD 1957 to 1979 period, for 850 to 30 mbar altitudes 7-40532
- greenhouse effect, radiation absorption in Earth's atmosphere causing heating 7-40556
- Gulf of Carpentaria, 1984 October 25-6 morning glory wind surges, temp. and humidity meas. 7-4091
- Hamburg, W Germany, atmos. radiative heating due intense pollution 7-4101
- hemispheric forecast error correlations for geopotential and temp., horizontal struct. 7-4150
- Himalaya mountains, glaciation upper limit and assoc. characts. 7-55090
- India, SW monsoon, rainfall distrib. and assoc. thermodynamic parameters anal. 7-9121
- N Indian Ocean, 1972-3 air-sea interactions in monsoon conditions 7-9014
- ionosphere, effect of electron temp. on electron number density and dynamics of equatorial E-region 7-66390
- ionosphere, electron and ion temperatures model 7-9314
- ionosphere, plasma parameters meas. in vicinity of Space Shuttle 7-29360
- ionosphere, reson. heating accompanying seismic-ionospheric electrical interaction 7-28890
- IR cooling rate calculation, for cooling due to H₂O vapour (*Chinese*) 7-29221
- Ireland, dew-print temps. during high absolute humidities episode (1983 July 12 to 13) 7-40541
- Kuhlungsborn Observatory, East Germany, 27 kHz noise temporal var. rel. to temp. 7-9149
- land surface heat balance and atmos. surface layer (*Russian*) 7-60328
- lidar technique appl. to laboratory meas. of atmospheric temp. and backscatter ratio 7-9238
- magnetotail plasma sheet, comp and plasma props. 7-34789
- marine, use of ship observations 7-4217
- marine atmosphere, temp. stratification rel. to vortices formation over ocean surface heat anomalies 7-9134
- measurement by radiosondes, implications of change in thermistor characts. 7-9233
- mesopause, summer temps. rel. to form. of noctilucent clouds 7-23925
- mesopause and lower thermosphere in winter, N polar region temps. 7-34755
- mesoscale meteorological fields, spatial fitness implications 7-47509
- mesosphere, radiance/temperature vars., Nimbus 6 PMR expt. meas. 7-47588
- mesosphere, temp. and circulation vars. in middle and high latitudes 7-47590
- mesosphere, temperature struct. changes due to solar cycle, at 44 to 77°E 7-34756
- mesosphere and stratosphere over Volgograd, search for solar cycle relationship 7-47599
- meteosat IR meas., surface and cloud-top temp. determ. atmospheric correction scheme 7-18310
- middle atmosphere, EHF sounding from Space Shuttle 7-40568
- middle atmosphere, gravity wave effects under solstice conditions with 3-D circulation model 7-47597
- middle atmosphere, thermal structs. in Eastern and Western Hemispheres over solar cycle 7-66375
- middle atmosphere, winds and temps. vars. rel. to regions of polar mesospheric clouds 7-47596
- middle atmosphere 1984 spring processes 7-34616

atmospheric temperature continued

- Millimetre Atmospheric Sounder on Shuttle for passive sounding (*German*) 7-40617
- minimum temp. surveys 7-4133
- minimum temperature, principal component and near neighbour methods for areal quality control 7-4141
- molecular rotational band obs. with Fabry-Perot interferometer for temp. determ. 7-47546
- monthly long-range forecasts for United Kingdom, exptl. forecasting system 7-14358
- monthly mean anomalies, month-to-month persistence in general circulation model and Earth's atmosphere 7-9093
- monthly mean surface temperature anomaly specification for Europe and Asia 7-23809
- mountain valley, thermal asymmetry and cross-valley circulation 7-4099
- multichannel autoregressive spectral estimators, performance 7-40553
- near-surface air temp. meas. for min. temp. surveys 7-4133
- New Mexico, USA, Pleistocene climate indicated by groundwater isotopes 7-23838
- nocturnal temperature inversion evol. 7-4095
- Northern Hemisphere, 1986 spring meteorological conditions 7-4166
- Northern Hemisphere, volcanic activity and climate since 1500 AD (*German*) 7-9161
- Northern Hemisphere surface press. and temp. 7-34665
- nuclear winter, protracted climatic effects of massive smoke injection into atmosphere 7-66297
- equatorial Pacific, boundary layer struct. during FGGE 7-60359
- tropical Pacific, temperature of tropopause during El Nino 7-29175
- plasmasphere, electron temp. vars. along geomag. field lines rel. to electron density profiles and VLF paths 7-4258
- Pleistocene climate and vegetation of S central British Columbia, Canada 7-23833
- Point Conception, California, temp-vars. rel. to mesoscale wind variability (spring 1983) 7-29144
- polar mesopause, large-amplitude semidiurnal temp. var. as evidence for pseudotides 7-34754
- polar stratosphere, winter cooling rel. to chemical mechanisms for spring decrease in Antarctic O₃ 7-55165
- profiling method for press. and temp., astronomical refraction technique (*Russian*) 7-18314
- Puerto Rico airport site at San Juan, temp. trends between 1956 and 1983 AD 7-60316
- Qi-Lian mountain area, Nanshan, China, air temperature climate (*Chinese*) 7-18299
- radio acoustic meas. of temp. profile in troposphere and stratosphere, exptl. results 7-14360
- Rayleigh backscatter lidar signals, temp. retrievals 7-9165
- remote sensing, satellite sensing procedure with high vertical resolution 7-66218
- remote sensing, temp. estimation model (*Japanese*) 7-34750
- remote sensing of temp. by IR radiometry, constrained inversion technique 7-29293
- remote sensing of temperature of cloudy atmosphere, IR radiation transfer model 7-60399
- remote sensing of temperature using IR data (*Japanese*) 7-18316
- satellite retrievals, systematic errors 7-66266
- seasonal temperature prediction, use of jackknife regression scheme with intraseasonal var. index 7-47567
- S Sierra Nevada, California, Late Holocene upper timberline var. rel. to temp. changes 7-55251
- Central Sierra Nevada, United States, winter storms ice-phase water capture regions identification, temp. characts. 7-4084
- Snake River Plain, United States, contrasting climatic histories resulting from multiple thermal maxima 7-47530
- South China Sea, palaeoclimate and palaeoceanography during Holocene, sediment O isotopic anal. (*Chinese*) 7-55264
- Southern Hemisphere, global temperature struct., seasonal changes 7-23817
- Southern Hemisphere, observational study of stratosphere warming event 7-55150
- Southern Hemisphere, surface air temp. vars. (1851 to 1984) 7-29237
- squall line pressure and temp. from dual-Doppler obs. 7-66223
- stratified surface layer, similarity scales evaluation using wind speed and temp. gradient 7-40514
- stratosphere, quasiperiodic perturbations due to solar activity, 3D simulation 7-66371
- stratosphere, radiance/temperature vars., Nimbus 6 PMR expt. meas. 7-47588
- stratosphere, satellite temp. and humidity meas. rel. to polar stratospheric clouds 7-55156
- stratosphere, temp. and circulation vars. in middle and high latitudes 7-47590
- stratosphere, temp. meas. rel. to radiative balance 7-9098
- stratosphere, temperature-height standard profile for Central Europe (Berlin) 7-4103
- stratosphere above Antarctica, O₃ conc. rel. to temperature changes 7-55152
- stratosphere and lower mesosphere, zonal winds and temperature 7-4248
- stratosphere and troposphere, horizontal spectra of potential temperature 7-29164
- stratosphere warming, GCM simulation rel. to high-latit. O₃ seasonal vars. in Southern Hemisphere 7-55167
- stratosphere warmings, relation to total O₃ decrease at South Pole, Antarctica (1964-1985) 7-55154
- stratus clouds, numerical modelling of temp. and water content 7-9132
- structure coefficient, appl. for astronomical seeing 7-4184
- summer stratosphere, transient wave activity from LIMS temp. data 7-9069
- surface layer over ocean, temp. profile below 19 metres altitude (*Russian*) 7-18275
- surface layer temperature profiles determ., use of three-parameter inferior mirage model 7-23804
- synoptic scale disturbances with circular symmetry, sensitivity to pot. temp. var. 7-34625
- temperature profiles in a thin layer over the sea 7-14368
- thermosphere, NO energetics and IR radiation in disturbed heated thermosphere 7-4247
- thermosphere, temp. meas. rel. to H dissipation flux 7-23922
- turbulence classification, computer program 7-55247
- Udine and Lignano Sabbiadoro, Italy, daily average temp. anal. by ARMA stochastic processes 7-34639

atmospheric temperature continued

- United Kingdom, skill of exptl. monthly long-range forecasts 7-40539
- United Kingdom, temp. extremes (for 1984 and 1985) 7-66279
- United States, summer monthly mean surface temp. field rel. to 700 mb height field 7-34667
- upper atmosphere, seasonal and tidal variations of temperature and density 7-29315
- upper atmosphere, winter temperature from EISCAT observations 7-29316
- upper atmosphere neutral temperature and winds from EISCAT obs. 7-29318
- upper level frontogenesis 2D primitive eqn. model, role of vertical deform. 7-4122
- urban boundary layer, mixing depth. rel. to wind speed and heat island formation 7-14336
- urban warming in North America, average warming rate (1941 to 1980) 7-29146
- USA, temperature anomalies correl. to Pacific SST of Kuroshio region 7-4134
- E USA, tree-ring record of past climate 7-23839
- Venetian Lagoon, freezing since 9th century AD rel. to climate of W Europe and England 7-66286
- vertical profiles reconstruction by interpolation methods 7-34730
- vertical profiles retrieval from refr. meas. (*Russian*) 7-29277
- vertical temp. gradient estimation using near-surface obs. 7-66343
- vertical temperature distrib., relation to solar and atmospheric radiation propag. (*French*) 7-14338
- VISSR Atmospheric Sounder data, effect on Limited-Area Finemesh Model 7-47501
- wind-chill indices 7-55204
- CO₂, greenhouse effect with CO₂ enhanced biological methanogenesis 7-29152
- LiNbO₃ SAW oscillator for humidity and temp. meas. 7-4232
- O₃ content-temperature mutual covariation, appl. to atmospheric O₃ content determ. 7-9135

atmospheric thermodynamics

- see also *atmospheric temperature*
- S Alberta, Canada, chinooks distinguishing nocturnal features 7-47493
- Antarctic, radiative heating due to stratospheric aerosols, implications for O₃ depletion 7-55175
- Antarctic atmosphere, O₃ losses, role of heating perturbations 7-55171
- Antarctic spring, stratospheric heating rates and diabatic circulation, implications for O₃ depletion 7-55176
- Arabian heat low, surface energy budget and struct. 7-4151
- Arabian heat low structure, bulk tropospheric heat budget 7-4152
- S Asia, local rainfall rel. to southern Oscillation Warm Events 7-34628
- blocking anticyclones, local vorticity and heat balances in spectral general circulation model 7-29138
- Canterbury Plains, New Zealand, thermotopographic effects rel. to interacting multi-scale wind systems 7-55203
- compressible gas dynamical eqns., rapidly oscill. solns. (*Russian*) 7-55181
- convective boundary-layer parameters, climatology over Ontario, Canada 7-40512
- convective heating in tropical South Pacific during FGGE 7-66262
- convective systems of 100 km scale during GATE, heat and moisture transport 7-29189
- cumulonimbus clouds, role of convectively available potential energy 7-4142
- diffusion from elevated and ground point sources in neutral boundary layers, turbulent energy model 7-34580
- diffusivity factor methods for atmospheric thermal radiation modeling 7-47496
- Eagle Valley, Colorado, temp. inversion buildup and wind struct. 7-55202
- Earth Radiation Budget Experiment (ERBE), meas. data (1984 November 15) 7-9067
- El Nino, simple model involving atm. convergence feedback 7-34536
- energetics in low-resolution general circulation model, effects of topography 7-9099
- energy balance model climate, effects of altered exchange coeffs. 7-4176
- F-region, heating rates 7-34772
- general circulation model, dynamic and thermodynamic influences of Tibetan Plateau 7-29135
- general circulation model, thermal balance sensitivity 7-66221
- global oceans, monthly mean precipitable water and surface level humidity 7-29202
- gravity wave effects under solstice conditions 7-47597
- Greece, air enthalpy rel. to bioclimatological types grouping. and geographic distrib. 7-9150
- India, SW monsoon, rainfall distrib. and assoc. thermodynamic parameters anal. 7-9121
- India, SW monsoon active and break phases, sensible heat fluxes 7-4094
- N Indian Ocean, Bowen ratio distrib. 7-9117
- ionosphere, dissipation of energy of powerful SHF radiation 7-4262
- ionosphere, electrical and electrothermal conductivities compared with Mars and Venus 7-34781
- ionosphere, thermal electron quenching of N^{(2)D}, implications for photoelectron flux and thermal electron temp. 7-14412
- ionosphere, vibr. relax. of CO₂ during injection from spacecraft 7-34087
- land surface heat balance and atmos. surface layer (*Russian*) 7-60328
- large-scale energy flux divergence 7-47506
- latent heat fluxes over spruce forest and Priestley-Taylor evaporation formula, effects of synoptic-scale advection 7-4093
- magnetosphere, contrib. of non-adiabatic effects to charged particle motion in magnetotail 7-9335
- magnetosphere, evidence for large bulk ion conic heating region 7-47632
- marine boundary layer, effects of surface wave layer on atmosphere-ocean boundary layers interaction 7-8989
- middle atmosphere, radiative heating and cooling rates 7-60337
- monsoon 30-50 day oscill. theory, role of heat 7-60317
- monsoon depressions, energy aspects 7-9113
- monsoon depressions, WNW movement, role of heat sources 7-66253
- Northern Hemisphere winter troposphere, circulation anomalies due to low latitude heating anomalies (*Chinese*) 7-4076
- nuclear winter studies, effects of uncertainties in smoke source term 7-34668
- numerical weather prediction models, implicit versus explicit convective heating 7-47500
- quasi-geostrophic baroclinic disturbances with condensational heating, linear devel. 7-60340

atmospheric thermodynamics continued

- radiation budget, variability of Earth-emitted radiation from one year of Nimbus-6 ERB data 7-9092
- SOUSY VHF radar measurements in the lower and middle atmosphere 7-23870
- stratified atmosphere heating is model for moist convection 7-4127
- stratosphere, area of polar vortex as diagnostic for tracer transport on isentropic surface 7-29134
- stratosphere, radiative balance determ. from Nimbus-7 LIMS meas. 7-9098
- stratus clouds evolution, numerical modelling 7-9132
- surface energy flux anomalies, month-to-month persistence in general circulation model and Earth's atmosphere 7-9093
- thermosphere, NO energetics and IR radiation in disturbed heated thermosphere 7-4247
- lower thermosphere, role of tides in thermodynamics for solstice conditions 7-47595
- Tibetan Plateau, summer weather systems develop., sensible heating effects on vortices 7-60339
- tropical cyclone, mature struct. and motion 7-4146
- tropical squall line, wind and thermodynamic data rel. to stratiform cloud region modelling 7-29136
- SW United States, summer precipitation singularity, bursts and breaks synoptic-dynamic characts. 7-47494
- vapour condensation heating, contrib. to seasonal movements of subtropical high ridge line 7-40508
- vertical temperature distrib., relation to solar and atmospheric radiation propag. (*French*) 7-14338
- vortices, nonlinear response to heating by cumulus convection 7-9101
- vortices formation over ocean surface heat anomalies, dynamic struct. 7-9134
- winter stratosphere, integrated enstrophy budget determ. from Nimbus-7 LIMS data 7-4125
- CO₂ liq. finite sink for atmospheric heat engine 7-40022
- NH₄Cl aq. soln. finite sink for atmospheric heat engine 7-40022
- NH₄NO₃ aq. soln. finite sink for atmospheric heat engine 7-40022

atmospheric turbulence

- acid rain modelling, turbulent spiral boundary layer and thermal wind simulator 7-14370
- acoustic return intensity and intermittence of turbulence (*Russian*) 7-60330
- antenna radiation pattern energy characts., directional props. of antenna in turbulent atmosphere 7-23825
- Arabian Sea, boundary layer turbulence during Indian SW monsoon 7-23793
- astronomical object image construction using coherency functions, atm. distortion compensation 7-55481
- atmosphere-telescope system, image form. through turbulent atm., isoplanatism problem 7-50502
- balance equations in periodic domain, numerical model, balanced turbulence 7-34604
- Bay of Bengal, turbulence struct. of boundary layer 7-60356
- boundary layer, closure parameter determ. in higher-order closure models 7-55128
- boundary layer flow over nearly 2D hill 7-9137
- boundary layer parameterization, FORTRAN programs 7-55246
- neutral boundary layer struct., influence of baroclinicity 7-23792
- boundary layer struct. over irregular terrain, model calcs. 7-23795
- boundary layer turbulence intermittency (*Russian*) 7-4113
- chaos motions in velocity shear flow, Lorenz eqn. theory (*Chinese*) 7-18258
- Charney baroclinic-instability with Rossby wavetrains 7-18287
- classification, computer program 7-55247
- clear air turbulence over British Isles, 1985 September 4, obs. of extensive prolonged CAT event 7-14359
- clear-air turbulence forecasting by automated method 7-4143
- closure model for turbulence, theory using Schumann's method 7-55133
- coherent Doppler lidar, atm. correlation time meas. 7-60385
- coherently illuminated objects in turbulent atm., high-resolution image form. 7-55261
- convective boundary layer, effects of turbulence on horizontal plume dispersion; 7-40062
- convective boundary layer simulation, efficiency of different higher order turbulence models 7-57819
- diffusion from elevated and ground point sources in neutral boundary layers, turbulent energy model 7-34580
- dispersion studies, use of negative ion generator and collector system 7-29314
- energetics in low-resolution general circulation model, effects of topography on eddy components 7-9099
- entrainment into turbulent flows 7-55064
- flow over 2D hills, modification of turbulence 7-66256
- flow over progressive water wave, eddy viscosity model 7-51193
- free-space laser communications system design, SNR impact 7-34676
- hill, flow over isolated hill summit in Somerset, England 7-55132
- isolated hill, short-range dispersion experiments on windward slope 7-34572
- internal waves and turbulence in troposphere and lower stratosphere 7-23814
- ionosphere, perturbed reflection layer, electric field calc. 7-40637
- ionosphere, plasma parametric turbulence in mag. field 7-1697
- ionosphere, plasma turbulence meas. in vicinity of Space Shuttle 7-29360
- ionosphere, reson. turbulence accompanying seismic-ionospheric electrical interaction 7-28890
- ionosphere, turbulence associated with 2D magnetised Rayleigh-Taylor instability, spectral characts. 7-44170
- IR laser radiation propag. in weak atmosphere, phase fluctuations 7-40565
- Kakinada sand spit, India, atm. elec. meas. 7-23806
- large water droplets dispersion model 7-34583
- laser beam, partially coherent, in turbulent atm., thermal self-interaction 7-31376
- light propagation through thin turbulent layer, compensation of nonlinear random phase distortions 7-66302
- light reflection in turbulent atmosphere under induced temperature nonuniformity of refractive index 7-60384
- light scattering, turbulent medium, I-K distrib. for random optical fields 7-34674
- light wave time-dependent characts., fluctuating wind effect, expt. investig. 7-55263

atmospheric turbulence continued

- lower atmosphere high-resolution turbulence obs. by middle and upper atmosphere radar 7-47598
 magnetosheath, MHD turbulence obs. 7-34786
 magnetosphere, turbulence evolution during substorms rel. to damping of Pi 2 pulsations 7-47631
 magnetotail, broadband turbulence obs. 7-34801
 marine atmosphere, turbulent viscosity rel. to vortices formation over ocean surface heat anomalies 7-9134
 marine boundary layer, effects of surface wave layer on atmosphere-ocean boundary layers interaction 7-8989
 measurement with Gill propeller anemometers, directional response study 7-55276
 middle atmosphere high-resolution turbulence obs. by middle and upper atmosphere radar 7-47598
 middle atmosphere turbulence, obs. and meas. by VHF radar 7-4246
 mode correction for turbulent distortions of optical waves 7-42914
 numerical synthesis of trivariate velocity realisations 7-9078
 optical wave phase fluctuations through atm. turbulence, probability density function 7-57246
 peninsula convection over S British Isles, 13 May 1986 case 7-4145
 phase retrieval from a dichromatic analysis of speckles 7-31261
 radar, meteorological appls. 7-47548
 rain characteristics in turbulent atm., determ. from optical beams propag. characts. (Russian) 7-29131
 random medium with Kolmogorov spectrum and inner scale of turbulence, intensity covariance of point source 7-57245
 refractive index structure function for turbulence ranges, saturation and long-baseline optical interferometry 7-60574
 scidar/lidar ground-based study of gravity-wave assoc. turbulence 7-9166
 scintillation effects on centroid anisoplanatism 7-57243
 stratocumulus-topped boundary layer, third-order turbulence closure model stability 7-9102
 surface layer of atmos. (stratified), stochastic model of turbulent diffusion (Russian) 7-9082
 terrain type influence on surface layer turbulence characts. (German) 7-55236
 thunderstorm turbulence and radar Doppler spectral width 7-60415
 turbulence characteristics from microwave amplitudescintillations 7-9108
 two layer model for the barotropic stationary turbulent planetary boundary layer 7-40519
 two-particle relative diffusion by Monte Carlo simulation 7-34574
 upper atmosphere, two-dimensional second-order model for turbulent flow 7-9111
 urban turbulence parameters, roughness effects 7-34582
 wind, environmental conditions in passages between buildings 7-14353
 wind, turbulence length scales in wind engineering 7-14354

atmospheric wind see wind**atmospherics**

- see also atmospheric electromagnetic wave propagation; whistlers
 auroral LHR noise, obs. by S-310JA-6 sounding rocket (1978 August 27) 7-66393
 dry deposition in surface layer, accuracy of current meas. techniques 7-18281
 ELF fields in Earth-ionosphere resonator, day-night inhomogeneity effect 7-66219
 ELF hiss propagation inside and outside plasmasphere, statistical study from GEOS-1 obs 7-34787
 EM emission during seismic activity, crustal mechanical-electric convertors model 7-8856
 EM field horizontal and vertical fields for lightning above finitely conducting ground 7-34586
 ground electric field due to intracloud lightning 7-34587
 impulsive atmospheric noise, hourly APDs, semitropical location and evening transition period 7-47483
 interference pulses in VLF band, statistical props. of time intervals 7-34659
 ionosphere, near-field radiation from pulsed electron beams in space 7-66391
 ionosphere, reson. RF emission accompanying seismic-ionospheric electrical interaction 7-28890
 Kuhlungsborn Observatory, East Germany, 27 kHz noise temporal var. rel. to temp. 7-9149
 magnetosphere, electron energy spectra and electrostatic cyclotron waves during diffuse auroras 7-34763
 magnetosphere, electrostatic wave trapping near magnetospheric equator 7-34788
 magnetosphere, quasi-electrostatic half-electron-gyrofrequency VLF emissions 7-4272
 MF and HF atmospheric radio noise, bandwidth expansion effects on voltage deviation parameter 7-60366
 radiation belts slot region electron precipitation, lightning as trigger mechanism 7-9325
 RF radiation from lightning return strokes, influence of Earth conductivity 7-40535
 VLF propagation at high southern latitudes, from sferic observations 7-47617

atom-atom collisions*includes reactive collisions*

- alkali metal atoms, collision induced amplified emission 7-10513
 angular momentum coupling 7-10706
 atoms in a low field, review 7-898
 binary model for collisional redistrib. of light 7-10705
 collision kernels, use of classical transport theory 7-36725
 dense plasma, atomic species description model 7-63255
 dynamics, laser effects, overview 7-20002
 hyperfine struct., collisional transform. of alignment into orientation 7-30961
 inert gas atoms, anisotropic collisions with atoms and ions, intermultiplet mixing 7-57154
 ion-pair formation collisions, model simulation of differential cross sections 7-10737
 light negative ion formation using Rydberg atoms 7-10707
 metal atoms and ions, lasing mechanism and energy characts., relax. processes of metastable states 7-62673
 rainbow scatt. study in mol. and nucl. physics, and surface science 7-62482
 resonant processes, production of three charged particles, reaction cross-section calcs. 7-42752

atom-atom collisions continued

- scattering differential cross. section, depolarisation interference struct. 7-5740
 solar convective zone outer layer, spectral lines pressure shift diagnostic study 7-40793
 vapours, highly polarised, laser optical pumping with velocity-changing collisions, theoretical anal. 7-36556
 Ar, metastable population meas. and flow instability due to shock wave, comparison with models 7-16207
 Ar+He, bimolecular and termolecular, deexcitation reactions (French) 7-10724
 Ar+Ne(³s²P₂, ³P₀), ionis., fine struct. depend. product branching 7-15673
 Ar+O, 557.7 nm line profile, collision complex spectroscopy (French) 7-5751
 Ar⁺+Kr (CO)(CO₂), charge exchange cross-sections meas. 7-62519
 Ba vapour laser, mechanism limiting pulse repetition freq. 7-43071
 Ba+Ar, collisional redistrib., laser-induced fluoresc. 7-62492
 C+H(H⁺), methane form. kinetics model 7-5745
 Ca⁺+He(Ne), collisional lasers, high specific output energy 7-43078
 Ca+He, saturated two-photon absorpt. in perturber bath 7-888
 Ca+He, spin-changing collision cross section 7-25641
 Cs, optically pumped, hyperfine relax. with Ar collisions 7-10511
 D+D reaction, detection of occurrence during shock fracture of D₂O ice 7-39874
 Eu⁺+He (Ne), collisional lasers, high specific output energy 7-43078
 H⁺+muonic H, low energy collisions, isotopic derivatives, cross sections, electron screening effect 7-31143
 H+Ar, Rydberg atom depopulation, scattering cross section, 7-10732
 H+H, 1s-2s excitation, cross sections, Born approx. 7-10730
 H+H, ion-pair form. reaction, mol. treatment 7-50340
 H+H₂(He)(N₂)(Ne)(Ar), 20-100 keV, charge exchange cross section meas. (Chinese) 7-5765
 H+He(Ar)(Ne)(Kr)(Xe), electron capture cross sections 7-10747
 He collisional depopulation rate by Rb thermal collisions (German) 7-15694
 He-Ne mixtures collision induced far IR translational absorpt. 7-10563
 He+Ar, 2¹P₁ state quenching 7-62319
 He+Cs(Rb), He2²P₁ and 2²S₀ state quenching 7-57153
 He+He, associative ionisation in glow discharges 7-62506
 He+He, ionis. cross section meas. 7-62494
 He+He⁺, time-depend. HF wave functions, variationally improved transition amplitude 7-36739
 He+Li(Na)(K)(Rb)(Cs), Penning ionisation, pot. well depth calcs., electron energy spectra anal. 7-62510
 He+Na(K)(Pb)(Cs), inelastic collisions at thermal energies 7-983
 He+Ne excitation transfer processes, quasimolecule form. 7-5758
 He+positronium, annihilation spectrum 7-62547
 He+Rb, afterglow, inelastic collisions quenching cross sections 7-42746
³He-³He(He), elastic scatt. cross section ratio, nucl. spin lattice relax. time anal. 7-42652
 Hg, diffusion coeff. in Ar gas, interaction pot. determ. 7-6348
 Hg+Hg(Ar), excitation transfer between fine struct. states, fluoresc. spectroscopy 7-62504
 Hg+Hg(Ar)(N₂), 6s6d and 6s7d states, collisional quenching 7-36730
 Hg+Xe collisions, Hg radiative lifetimes and deactivation rate consts., mol. fluoresc. study 7-19752
 K+Ar(He), fine-struct. transitions, differential cross section meas. 7-62493
 K+inert gas, 5d²P_{1/2}-5²P_{3/2} fine struct. mixing 7-50306
 K+K(Rb), Doppler free two-photon spectra, freq. shift, line broadenings 7-57155
 Li+He(Ne), electric field effect, fluoresc. and radiative decay rate determ. 7-20009
 Li Rydberg states, collisional line broadening, trilevel photo. echo meas. 7-19772
 Li+Cs, ion pair prod. cross sections, beam-gas study 7-39871
 Li+Na, ion-pair production, laser excitation effect 7-62502
 NH, collision-induced intersystem crossing investigated using ArF laser photolysis 7-42692
 Na, collisionally aided coherent atomic optical emission 7-42561
 Na-He(Ne)(Ar), optical collisions, fine struct. branching cross-sections, nonadiabatic theory 7-959
 Na+He, Na D line broadening and shift (French) 7-10501
 Na+He(Ne)(Ar)(Kr)(Xe), fine-struct. branching ratios, meas. 7-15676
 Na+Na, associative ionis. cross section meas., spin-selected velocity depend. 7-42736
 Na+Na assoc. ionisation, at. alignment, effect vel. depend. 7-28306
 Na+Na collisions, Rydberg state forbidden transitions in laser-assisted processes 7-5617
 Na+Na(Na⁺), ion pair prod., laser excitation effect 7-62507
 Na+Na(3p), assoc. ionis., Na₂⁺ form., alignment anal. 7-960
 Na+Rg optical collisions, (Rg = He, Ne, Ar, Kr, Xe), fine struct. branching ratio determ. 7-10704
 Na+Xe, Na D lines, collisional broadening, fine-struct. mixing, depolarisation 7-62503
 Na+Xe (Ne), Na D lines, far wings obs. using fluoresc. excitation method 7-62317
 Ne+He* collisions, nonadiabatic transitions 7-62487
 Ne+He(Ar), electronically excited atoms, beam sources 7-20008
 Ne⁺+He, collisions, nonadiabatic transitions 7-62487
 Ne⁺⁺+He, polarization effects in collision-induced intramultiplet mixing 7-5749
 O+He, van der Waals interaction, mol. beam study 7-20001
 Rb+Ar(He), oscillator strength, pot. curves (French) 7-10728
 Rb+Rb, collisional ion-pair form., Coulomb pot. 7-15698
 Rb+Rb(K), Doppler free two-photon spectra, freq. shift, line broadenings 7-57155
 SR + inert gases, collisional energy transfer, time resolved fluoresc. meas., quenching cross sections 7-62497
 Sm, four-wave light mixing, collision-and stochastic-fluctuation induced Hanle reson. 7-15559
 Sm vapour, vel. diffusion effects, RF-laser double reson., Raman heterodyne investig. 7-882
 Sr+Ar, ¹P fluoresc. line broadening, ab initio close-coupled scatt. calcs. 7-36494
 Ti+Ar(He)(Ne), Ti excited state total ang. momentum charge, radiation quenching 7-42735
 Ti+Ar(Ne)(He), triplet state quenching and excitation transfer processes 7-19761

atom-atom collisions continued

- Ti+Ar (Ne) quenching and excitation transfer processes, fluoresc. 7-10725
 Ti+inert gas, $6P_{1/2}7P_{1/2}$, $3/2$ two-photon line broadening and shift 7-49983
 Tm+Ne, optical pumping of Tm ground-state sublevels 7-50027
 Tm+Ne(Xe), excited state transition cross sections, nonreson. fluoresc. 7-42540
 Xe, radiative collisions, curve crossing, two-photon laser excitation 7-19810
 Xe+Ar(Kr), Xe long-wavelength continuum in VUV spectral region 7-49986
 Yb+Ar, collisional dephasing suppression investig. 7-15684
¹⁷⁴Yb+He(Ar), collisional velocity thermalisation, echo techniques 7-36732
 Zn+He⁺(He*), Penning and charge transfer reactions, Zn⁺ levels excitation 7-5746
 Zn+Ne 307.6 nm line absorpt. and collision cross section 7-30975

atom-electron collisions see atomic electron impact excitation; atomic electron impact ionisation; elastic scattering of electrons by atoms and molecules

atom-ion collisions

- includes reactive collisions
 see also charge exchange
 A+H⁺, (A=Sm, Tm, Ta, Ho, Au, Pb, W, Lu), $K_{\alpha 2}$ to $K_{\alpha 1}$ intensity ratio meas. 7-963
 atom+molecular ion, vibr. relax. 7-62499
 atom-ion collisions, K shell charge transfer cross sections, symmetric eikonal theory 7-50328
 atomic collision processes, resonant transfer excitation and dielectronic recomb. review 7-50366
 atomic negative ions, electron detachment, overview 7-15563
 charge exchange, reaction dynamics, crossed mol. beam collisions 7-57167
 continuum emission, wave fn. calcs. 7-15681
 electron capture, first order Born perturbation theory 7-10746
 electron capture, off-shell Coulomb radial wavefunctions soln. 7-62520
 electron capture, symmetric eikonal theory 7-31144
 electron transfer, bibliography of investigs. 7-20007
 emission-angle depend. post collision interaction 7-25644
 excited state prod. by negative ion detachment 7-15686
 heavy ion+atom (ion), strongly asymmetric, K-L vacancy sharing 7-20011
 high resolution Auger spectroscopy in energetic ion atom collisions, review 7-62490
 highly charged ions, multiple-electron capture, classical over-barrier model 7-10744
 hyperfine struct., collisional transform. of alignment into orientation 7-30961
 inert gas+H⁺, electron transfer and ionis., δ -electron spectrosc. 7-42685
 inert gas atoms, anisotropic collisions with atoms and ions, intermultiplet mixing 7-57154
 inert gas atoms+H₂⁺ (D₂⁺), (N₂⁺), (C₂⁺), high Rydberg fragments, kinetic energy spectra 7-42745
 inner-shell ionisation by H⁺ collisions 7-42750
 ion chemistry, gaseous, hybrid BEQQ mass spectrometer appls. 7-48904
 L subshell ionisation probabilities vacancy sharing 7-15697
 laser assisted charge exchange reactions, theoretical and expt. investig. (French) 7-5759
 Ni+Ni collisions, quasimol. form., X-ray spectra study 7-31157
 potential curves, modified Tang-Toennies model 7-36722
 symmetric heavy ion collisions, K X-ray prod., target thickness fn., X-ray spectra anal. 7-30978
 Al+Be⁺, K-shell X-ray prod. cross section meas. 7-15680
 Al⁺+O₂(H₂O)(ethylene), absolute cross sections, meas. 7-5743
 Al³⁺+H⁺, charge-transfer reaction, mol. representation, CI calcs. 7-36485
 Ar⁴⁺, heavy ion impact on gas target, long-lived states form., K X-ray spectra anal. 7-30980
 Ar+Ar⁺, total differential scatt. cross section, 15-400 keV 7-62489
 Ar+Ar⁺, 3p³d config. mixing, spectrum anal. 7-62308
 Ar+H₂⁺, chemical reaction and charge-transfer processes, RIOSA quantum-mechanical study. 7-31159
 Ar+H₂⁺ collisions, dissociation and electron capture cross section meas. 7-31156
 Ar+H⁺ two-electron charge exchange mol. states, nonorthogonal CI calcs. 7-50339
 Ar+H⁺(He²⁺), electron emission, impact parameter depend., TOF, coincidence spectra anal. 7-42747
 Ar+H-like ion projectile ionisation cross section 7-969
 Ar+N₂⁺→Ar⁺+N₂, electron transfer reaction, state-to-state study 7-36746
 Ar+Sr⁺, collisional broadening of Sr⁺ reson. line, visible spectra 7-49988
 Ar+Sr⁺(Ca⁺)(Mg⁺), reson. line broadening and shift rates, pot. calc. 7-15683
 Ar⁺+Ar, absolute spin-orbit state excitation cross sections, fine-struct. 7-42730
 Ar⁺+N₂, charge transfer collision, Franck-Condon principle at low collision energies study 7-62511
 Ar⁺+D, collision parameters, energy-gain spectra meas., multichannel Landau-Zener model anal. 7-36752
 Ar⁺He(Ne), charge exchange into excited states in collisions 7-31155
¹³⁸Ba+H⁺, elastic backscatt., K-shell ionis. probability, reson. effect 7-42748
 Be⁴⁺+He, charge exchange cross sections, quasimolecule Feshbach method calcs. 7-36754
 C+H(H⁺), methane form. kinetics model 7-5745
 C³⁺+He, transfer excitation, electron emission, forward-backward asymmetries 7-973
 C⁴⁺+He, double charge transfer process, differential cross sections, quantal study 7-62512
 C⁴⁺+He, two-electron capture cross sections, comparison of calc. methods 7-15703
 C⁴⁺+He(H₂)(Ar)(Xe), one-step double electron capture 7-50344
 C⁶⁺+He, (quasi)-two-electron collision systems 7-5764
 CS₂⁺+atom(molecule), (q=2, 3), electron capture 7-5763
 Ca⁺+He(Ne), collisional lasers, high specific output energy 7-43078
 Cl+Be⁺, K-shell X-ray prod. cross section meas. 7-15680
 Cs⁺, low-energy collisions with atoms and mols., absolute total cross section meas., curve-crossing model anal. 7-36749

atom-ion collisions continued

- Cs+HeH⁺, HeH bound excited state form., predissoc. and radiative dis-
 soc. 7-20033
 Eu⁺+He (Ne), collisional lasers, high specific output energy 7-43078
 F+Au, X-ray emission from multiply ionized atoms (Rumanian) 7-15699
 F+Be⁺, K-shell X-ray prod. cross section meas. 7-15680
 Fe+D(He)(C)(N)(O), thick target bombardment, X-ray production cross sections 7-20025
 Ge+Ge⁺, L-shell ionisation, X-ray yield, threshold behaviour 7-10734
 H atoms, proton collisions, higher-order electron capture processes 7-25647
 H, electron capture by bare ions, coupled-state calcs., convergence 7-31166
 H plasma, ion collisions, low-energy charge exchange, XUV spectra 7-20032
 H+C³⁺, pot. energy curves, spin-coupled VB theory 7-957
 H+fully stripped ion collision, electron capture, travelling MO expansion study 7-50341
 H+H⁻, charge transfer processes, H₂⁻ autodetaching states 7-15705
 H+H⁺, atomic data relevant to edge plasmas 7-20063
 H+H⁺, electron capture, strong pot. Born approx. calcs. 7-972
 H+H⁺, reson. electron capture from excited 2 s states, cross section calcs. 7-36747
 H+H⁺ collisions, H₂⁺ system emission and absorpt. processes (French) 7-10552
 H+H-like ions, 1s-2s excitation, cross sections, Born approx. 7-10730
 H⁺+He, collisional detachment neutralization at high energy 7-15685
 H⁺+He, single-electron detachment, time correlated electron spectrum study. 7-36741
 H⁺+Xe, collisional excitation and decay of ¹P shape resonance 7-5616
 H⁺+Ar, p state ionisation, density matrix parameters meas., DWBA calcs. 7-36743
 H⁺+Ar(Kr) recoil ion prod. from zero-impact-parameter 7-50310
 H⁺+Cs charge transfer collisions, laser radiation influence 7-25646
 H⁺+Dy(Yb), L-subshell ionisation cross section, X-ray emission 7-50327
 H⁺+H, electron capture at intermediate energies from 1 to 200 keV 7-62515
 H⁺+H, symmetric resonant charge transfer collisions in ultralow collision energy range 7-31164
 H⁺+H₂(He)(N₂)(Ne)(Ar), 20-100 keV, charge exchange cross section meas. (Chinese) 7-5765
 H⁺+H(Ar), capture theory, first-order Born approx. Coulomb boundary conditions 7-10745
 H⁺+H(Ar), electron capture, K-shell cross sections 7-10752
 H⁺+H(He), 2l-electron capture, first-Born-type approximation, cross sections 7-10743
 H⁺+He collisions, secondary electron spectra, Wannier ridge obs. 7-10736
 H⁺+He⁺(Ne⁹⁺)(Ar¹⁷⁺)(Fe²⁵⁺), Fine-struct. excitation, plasma screening effects, ion-sphere and Debye-Huckel models 7-62509
 H⁺+K, ionisation and charge transfer collisions, cross section meas. 7-20031
 H⁺+K charge transfer collisions, laser radiation influence 7-25646
 H⁺+Na charge transfer collisions, laser radiation influence 7-25646
 H⁺+Nd(Sm)(Tm), K-shell ionisation cross sections 7-50326
 H⁺+Ne(Na)(Mg), multiple ionisation, charge transfer cross sections 7-15706
 H⁺+Ru charge transfer collisions, laser radiation influence 7-25646
 H₂+fully stripped ion collision, electron capture, travelling MO expansion study 7-50341
 H₂+He, elastic and inelastic scatt. mechanisms, energy loss spectra 7-15671
 H₂+He(Ne)(Ar), electron loss to the continuum, absolute cross sections 7-50304
 H₂+He→H⁺+H+He, degenerate product electronic state distrib. determ. 7-50299
 H⁺L(Cr,Fe,Co,Zn), k-shell ionization cross sections and theoretical models 7-5627
 He⁺+Ne(Ar), charge exchange into excited states in collisions 7-31155
 He+H⁺(H⁺), single and double ionisation by fast antiproton and proton impact 7-20027
 He, collisions with fast, highly charged ions, electron capture to the continuum meas. 7-20026
 He, multiply charged ions collisions, semiclassical model, double electron transitions 7-10733
 He plasma, ion collisions, low-energy charge exchange, XUV spectra 7-20032
 He⁺+light target atoms (28≤Z≤46), L shell X-ray prod. cross sections meas., first Born approx. and ECPSSR theory anal. 7-36526
 He⁺ bombard. of target atoms, shadow cone form. calc. 7-36731
 He²⁺, charge exchange collisions, multiply charged closed K shell targets, exponential model study 7-25426
 He+(He²⁺)(C⁶⁺)(O⁸⁺), electron capture cross section calc. by distorted-wave perturbation theory 7-50336
 He+Ar⁴⁺(I⁴⁺), total one-electron capture cross sections 7-10754
 He+B⁵⁺(O⁸⁺)(Si¹⁴⁺), double- and single-electron capture and loss cross section meas., OBK scaling calcs. 7-42756
 He+C⁶⁺(Ne¹⁰⁺) electron capture, bound and continuum states, impulse approx. 7-50329
 He+C⁶⁺(O⁸⁺), intermediate energy collisions, electron capture cross sections, AO expansion method calcs. 7-25381
 He+Ca⁺(Mg⁺), pot. curves reson. line broadening and shift parameters 7-50302
 He+H₂⁺ collisions, dissociation and electron capture cross section meas. 7-31156
 He+H₂⁺ reaction, expt. and quantum mech. results 7-3584
 He+H₂⁺→HeH⁺+H, endothermic reaction on ab initio pot. energy surface, dynamics 7-54103
 He+H⁻, electron detachment, energy and ang. distrib. 7-20013
 He+H⁺, charge transfer, second-order Born and Faddeev-Watson approx. 7-62516
 He+H⁺, electron ejection, double differential cross section meas. 7-20024
 He+H⁺, simultaneous single-electron capture, H²⁺ production, existence of critical scatt. angle 7-10750
 He+H⁺, united atom rot. coupling collisions 7-958
 He+H⁺(H⁺), double ionisation, ab initio calcs. 7-42737

atom-ion collisions continued

- He+He⁺, excitation fns., transition moment and pot. energy curves (Japanese) 7-50307
 He+He⁺, single and double ionis., cross section meas. 7-31148
 He+He⁺(He²⁺), ejected electron distrib. shape, series expansion and fitting anal. 7-15675
 He+Kr⁴⁺, state-selective electron capture, translational energy spectra 7-50337
 He+Li³⁺(C⁶⁺)(O⁸⁺), electron capture, Coulomb integral eval. 7-15679
 He+Ne²⁺, collisional transition probabilities, avoided crossing, nonadiabatic effects (French) 7-10727
 He+O⁵⁺, resonant transfer excitation, Auger spectra obs. 7-50309
 He+Sr⁺(Ca⁺)(Mg⁺), reson. line broadening and shift rates, pot. calc. 7-15683
 He⁺+Ca(Cr)(Cu), target K-shell ionis., cross-sections and probabilities 7-50343
 He⁺+Cd(2n), exothermic charge exchange with excitation cross sections 7-42755
 He⁺+He collisions, projectile ionization, doubly differential cross section study 7-971
 He⁺+He⁺, electron capture cross sections, SCF-CI calcs. 7-15526
 He⁺+He(Ne)(Ar), electron loss to the continuum, absolute cross sections 7-50304
 He⁺+Ne(Na)(Mg), multiple ionisation, charge transfer cross sections 7-15706
 He²⁺+He, symmetric resonant charge transfer collisions in ultralow collision energy range 7-31164
 He²⁺+K, ionisation and charge transfer collisions, cross section meas. 7-20031
 He⁴⁺+Ag(Cd)(In)(Sn)(Sb)(Te)(I), L-subshell ionisation, X-ray prod. 7-50303
 HeH⁺+Cs, dissociative charge exchange 7-5766
 He²⁺ electron capture and stripping cross section in Al, Ni, Ag and Au targets 7-10753
 In+In⁴⁺, L-shell ionisation, X-ray yield, threshold behaviour 7-10734
 K+Be⁺, K-shell X-ray prod. cross section meas. 7-15680
 K+H⁺(Ar⁺), line shifts and widths, Stark broadening study (French) 7-10500
 Kr+He⁺, analytic repulsive pot. calc. 7-50308
 Kr+Kr ions, quasimolecular Auger emission, impact energy depend. 7-25645
 Kr+Kr⁴⁺, L-shell ionisation, X-ray yield, threshold behaviour 7-10734
 Li⁺ bombard. of target atoms, shadow cone form. calc. 7-36731
 Li+He²⁺, electron capture, Coulomb integral eval. 7-15679
 Li⁺+He, n=Z levels, alignment and orientation (French) 7-10723
 Mg+H₂⁺, direct dissociative charge exchange investig. 7-50332
 Mg⁺+He(Ar), charge cloud orientation, excitation, propensity rule 7-62498
 Mo+Mo⁴⁺, L-shell ionisation, X-ray yield, threshold behaviour 7-10734
 N²⁺+Kr(Xe), energy loss spectra 7-50334
 N⁷⁺+Ar, transfer ionization, differential cross section meas. 7-50325
 N²⁺+Au, impact ionisation, L₃ subshell alignment, coupled states anal. 7-25643
 N²⁺+Ar, absolute state to state total cross sections meas. 7-46825
 Na⁺ bombard. of target atoms, shadow cone form. calc. 7-36731
 Na+Be⁺, K-shell X-ray prod. cross section meas. 7-15680
 Na+H⁺, excitation cross sections, travelling at orbital calcs. 7-62505
 Na+He⁺, charge transfer, excitation processes coupled state impact parameter model 7-62518
 Na+Ne⁺, impact excitation, spin exchange, fluoresc. spectra anal. 7-25450
 Na+Ne⁺(Ar⁺)(Xe⁺), Rydberg electrons removal, cross section meas. 7-36742
 Ne⁺+Au, impact ionisation, L₃ subshell alignment, coupled states anal. 7-25643
 Ne⁺ bombard. of target atoms, shadow cone form. calc. 7-36731
 Ne+Ar⁺, time of flight energy spectra, long lived excited Ar⁺ state 7-62486
 Ne+Fe⁸⁺(F⁹⁺), k-k charge transfer, excitation patterns, Auger spectra 7-15682
 Ne+H₂⁺ collisions, dissociation and electron capture cross section meas. 7-31156
 Ne+H⁺, electron capture probabilities at large scatt. angles 7-62517
 Ne+H-like ions projectile ionisation cross section 7-969
 Ne+He²⁺, charge transfer reaction rate constants 7-22983
 Ne+He⁺, analytic repulsive pot. calc. 7-50308
 Ne+Kr⁴⁺, state-selective electron capture, translational energy spectra 7-50337
 Ne⁺+He(Ar), charge exchange into excited states in collisions 7-31155
 Ne⁷⁺+H₂ charge exchange collisions, Ne⁶⁺ excited states, VUV spectra anal. 7-20030
 Ne⁷⁺+He, transfer excitation in low-energy collisions, spectroscopic meas. 7-15696
 Ne⁴⁺+D, collision parameters, energy-gain spectra meas., multichannel Landau-Zener model anal. 7-36752
 Ne⁴⁺+Ne(O), low-Z collisions, relativistic SCF calculations 7-10409
 O, collisions with wide range of targets, K-shell ionisation, polarisation and binding effects 7-31165
 O⁺+H-H⁺+O, ion reaction at interstellar cloud conditions 7-23008
 O⁵⁺+He collisions, reson. transfer and excitation to specific LS-coupled state, O⁶⁺ AES 7-36744
 O⁶⁺+He, (quasi-)two-electron collision systems 7-5764
 O⁶⁺+He(H₂)(Ar)(Xe), one-step double electron capture 7-50344
 O₂+K, O₂⁻ ion form., rate consts. 7-33926
 P+Be⁺, K-shell X-ray prod. cross section meas. 7-15680
 Pb²⁶⁺+Sn(Xe), impact parameter depend. target K X-ray emission, XES spectra anal. 7-62314
 Pb⁵⁺+Ag, electron capture, K X-ray emission spectra study 7-36524
 S, collisions with wide range of targets, K-shell ionisation, polarisation and binding effects 7-31165
 S+Au, X-ray emission from multiply ionized atoms (Rumanian) 7-15699
 Si+Be⁺, K-shell X-ray prod. cross section meas. 7-15680
 Sm+H⁺, 4 MeV collisions, L-subshell ionisation probabilities, impact parameter depend. 7-42749
 Sm⁸⁺+Xe collisions, q=34 to 52, resonant electron transfer and L-shell excitation, X-ray spectra study 7-30979
 Ti+D(He)(C)(N)(O), thick target bombardment, X-ray production cross sections 7-20025
 Ti+He⁺(Li⁺)(H⁺), inner-shell ionis. polarisation effect, variational wave fn. calc. 7-62491

atom-ion collisions continued

- U⁹⁺+Sn, electron capture, K X-ray emission spectra study 7-36524
 VO⁴⁺+inert gases, collision-induced dissociation studied by ion beam tandem mass spectrometer 7-23001
 Xe+He⁺, analytic repulsive pot. calc. 7-50308
 Xe+N⁷⁺, transfer ionization, differential cross section meas. 7-50325
 Xe+Xe⁺, L-shell ionisation, X-ray yield, threshold behaviour 7-10734
 Zn+He⁺(He²⁺), Penning and charge transfer reactions, Zn²⁺ levels excitation 7-5746
- atom-molecule collisions
 see also atom-molecule reactions; molecular rotational-vibrational energy transfer
 alkali metal-mol. gas mixture, cooling in supersonic nozzle, population inversion of electronic states 7-31304
 atom+molecular ion, vibr. relax. 7-62499
 atom-chain energy transfer, lattice chain length depend. 7-57159
 collisional time-correlation functions for molecular interactions 7-36719
 gas flows, low density collisional stimulation, intramol. motion and relax., macroscopic quantum effects 7-15693
 light negative ion formation using Rydberg atoms 7-10707
 polarised rot. transfer rates, vel. depend., close-coupled calcs. 7-42741
 rainbow scatt. study in mol. and nucl. physics, and surface science 7-62482
 reactivity, reactant rot. effect, classical and quantum effects in model system 7-15672
 vinylidene + He(Ar)(N₂)(H₂)(CO)(methane), collisional quenching, rate consts., time resolved spectra 7-31104
 Ar+Cn, rot. levels, collisional energy transfer, state-resolved study 7-10713
 Ar+I₂^{*}, collision, rotational energy transfer 7-36734
 Ar+methane (methane-d₄)(SiH₄)(tetrafluoromethane), energy transfer, simulation 7-15690
 Ar+NH₃, dissociation, nascent vibr. and rot. distrib. 7-46824
 Ar+N₂, rot. inelastic cross section determ. sudden approx. 7-25637
 Ar+Kr, CO(CO₂), charge exchange cross-sections meas. 7-62519
 CdH+He(Ar), collisional rot. transitions, scaling rules (French) 7-10709
 D+H₂, HD+H, quantum mech. reactive scatt. problem, L² soln. 7-62485
 D₂CO + inert gas, Coriolis enhanced vibr. energy transfer theory and its appls. 7-31153
 F+H₂, reactive scattering, hybrid solution to coupled equations 7-57164
 H + H₂, deactivation rate consts., low and high temp. 7-20020
 H+CO, rot. distrib. from reson. and direct scatt., coupled channel scatt. calcs. 7-46826
 H+CO, scatt., rot. distrib. and collision lifetimes calcs. 7-25638
 H+CO₂, rot. resolved hot atom collisional excitation by time-resolved diode laser spectra 7-10731
 H+D₂, HD+D, product rot.-state distrib., information-theoretic anal. using perturbation method 7-62495
 H+H₂, atomic data relevant to edge plasmas 7-20063
 H+H₂, electron capture cross sections 7-10747
 H+H₂, reactive scattering, hybrid solution to coupled equations 7-57164
 H+H₂, resonant scatt., rot. distrib. 7-39858
 H+H₂ reactive scatt., quantum mech. 3-D calcs. 7-50293
 H+H₂ reactive scattering in hyperspherical coordinates 7-57151
 H+N₂(CO₂)(SF₆), Rydberg atom depopulation, scattering cross section, 7-10732
 H₂-Ar pairs collision-induced rototranslational spectra, ab initio dipole-moment surface 7-15493
 H₂+Ar(Kr)(Xe), pot. energy surfaces calcs. 7-50301
 H₂+H₂, deactivation of vibrationally excited H₂ by collisional transfer 7-10722
 H₂+MuH, low energy scatt. 7-15674
 H₂⁺+He-H⁺+H+He, degenerate product electronic state distrib. determ. 7-50299
 H₂⁺, n=5-23, cluster, dissociation in Ar gas target 7-36844
 He + H₂, V - T rate consts., numerical and anal. calcs. 7-20022
 He, ground state, one-electron loss cross section in H₂ gas 7-50338
 He para-difluorobenzene, vibr. energy transfer 7-50318
 He+CO(CO₂), vibr. relax., coupled states calcs. 7-50317
 He+ferrocene (Fe(CO)₅), dissociation, excitation, mol. orbital correls. 7-10735
 He+H₂, collision-induced rototranslational spectra 7-15677
 He+H₂, collisional excitation, translational-vibr. transition probability computation 7-42732
 He+H₂, vibr. transition probabilities, semiclassical algebraic description 7-25636
 He+H₂ autoionising systems, Born-Oppenheimer approx., diatomics-in-molecules calcs. 7-5742
 He+H₂(O₂), vibr.-translation energy transfer determ. 7-57160
 He+H₂, angular momentum collisional alignment Born approx. calcs. 7-964
 He+N₂, potential energy surface, multiproperty obs. 7-25633
 He+N₂(O₂), bimolecular and termolecular, deexcitation reactions (French) 7-10724
 He+N₂⁺, rot. transfer coeff. determ. (French) 7-10708
 He+NH₃, Rydberg atom ionis., rot. deexcitation 7-36737
 He+N₂, rot. inelastic cross section determ. sudden approx. 7-25637
 He+O₂, rot. inelastic collision, polaris.-preserving propensities 7-36736
 He⁺+monohalobenzenes, mol. electronic struct. and relativities determ., Penning ionisation spectra anal. 7-25642
 Hg+Hg(Ar)(N₂), 6s6d and 6s7d states, collisional quenching 7-36730
 Hg+N₂, excitation transfer between fine struct. states, fluoresc. spectroscopy 7-62504
 I+HI, 3D trajectory study 7-42729
 I₂⁺+He, collision, rotational energy transfer 7-36734
 I₂⁺+I₂, collision, rotational energy transfer 7-36734
 K + N₂, electronic and vibr. excitation, cross section meas. 7-36735
 K+NaCl, cross section estimation 7-20004
 KH+Ar(He), mol. A²Σ⁺ state, collision induced transitions (French) 7-10726
 Li₂+He (Xe), rot. energy transfer cross sections, studied using polarisation ratio vel. depend. 7-42740
 Li₂+He(Kr), total integral scatt. cross-sections 7-36728
 Li₂⁺, excitation and rot. transfer, rate const. determ. (French) 7-5750
 Mg+H₂, reactive collision dynamics by far using laser scatt. 7-28296
 NH, collision-induced intersystem crossing investigated using ArF laser photolysis 7-42692
 Na impurity in vibrationally nonequilibrium N₂ jet, excited state population and deactivation 7-42744

atom-molecule collisions continued

Na + electronegative molecule, thermal collisions, laser-induced ionis. mechanism 7-62488
Na + H₂, energy transfer expts., CARS 7-10719
Na₂ + Ar(He)(Ne), state selected rot. transitions, scatt. induced ang. momentum alignment 7-20005
Na₂ + He, collisional depolarisation, fluoresc. spectra anal. 7-19924
Na₂ + He scatt. precession induced fluoresc. modulation 7-19928
NaH + Ar(He), mol. A¹Σ⁺ state, collision induced transitions (*French*) 7-10726
Na* + N₂, quenching, classical trajectory calcs. 7-50300
O + H₂, cross section estimation 7-20004
O + H₂ → OH + H, reagent translational energy effect, pot. energy surface calc. 7-42739
OCS + Ar semiclassical press. broadening calcs. 7-965
OH + N, state specific collision dynamics 7-20014
Rb + H₂(D₂), fine-structure transition cross-sections, quantum-mechanical calcs., importance of perturber rotational levels 7-57161
SO₂ + Ar, intermol. energy transfer, trajectory study, rovibrational mol. energy depend. 7-31151
SO₂ + Ar, intermol. energy transfer, trajectory calcs., rate coeffs. for rovibrational states 7-31152
Ti + N₂(H₂), triplet state quenching and excitation transfer processes 7-19761
Ti + N₂, quenching and excitation transfer processes, fluoresc. 7-10725
Xe + Cl₂(Br₂)(I₂), atom and excitation transfer, energy disposal, product rot. alignment 7-31158

atom-molecule reactions

see also atom-molecule collisions
collinear reactive collisions, transition state calcs. 7-59746
diacetylene + O, rate const. meas., flash photolysis-reson. fluoresc. method 7-8263
excited atom reaction dynamics, charactn. by laser induced fluoresc. 7-46836
methylidyne ion + H, ion reaction at interstellar cloud conditions 7-23008
muonium + aromatic cpds., reaction rate const. 7-50415
muonium + diatomic molecule, gas-phase reaction dynamics 7-54092
muonium + ethylene, reaction, on amorphous SiO₂ 7-54166
oriented symmetric top mols., reactivity, rot. state depend. 7-46809
reactive scattering, quantum mechanical, via exchange kernels, exchange interaction calcs. 7-28284
Al + SO₂ → AlO + SO, pulsed crossed supersonic beam expt., energy thresh. determ. (*French*) 7-33915
Ar + trifluoromethane, crossed beam reaction giving trifluoromethyl group 7-33935
Ar₂ + Xe(Kr), van der Waals bond exchange, mol. beam study, ang. and vel. distrib. 7-23000
B + O₂, gas-phase oxidation, rate const., fluoresc. and chemiluminesc. study 7-22985
Ba + N₂O, chemiluminescence, vibr. and rot. modes, translational energy and internal state influence 7-13780
Ba + Cl₂(Br₂)(N₂O)(NO₂) (carbon tetrachloride) 7-13781
Ba + Cl₂ → BaCl₂, mechanism, chemiluminesc. 7-28292
Ba + N₂O, oriented reactants, product polarised emission, chemiluminesc. 7-22992
Ba + trifluoriodomethane, BaI product state distrib. 7-25595
CO + O → CO₂ in dense interstellar mol. clouds, role of grain surface reactions 7-24179
CO⁺ + H, ion reaction at interstellar cloud conditions 7-23008
Cl + methyl iodide, excitation function, microcanonical variational transition state theory 7-22995
Cl + HCl, prod. rot. distrib., centrifugal sudden distorted wave study 7-46808
Cs + H₂, CsH form. kinetics, rot. distrib. (*French*) 7-13728
Cs + trichlorotrifluoroethane, vapor phase reactions, chemiluminesc. obs. 7-59767
Cu + N₂O, collisional quenching, time-resolved emission and chemiluminescence 7-28285
D + H₂, mol. beam scatt. study, differential cross sections meas. 7-39860
DCO⁺ + H → HCO⁺ + D, ion reaction at interstellar cloud conditions 7-23008
F + H₂, bond angle-bond distance coordinate system, energy conserving trajectories 7-28287
F + H₂(HD)(D₂), quantum reaction probabilities, hyperspherical coordinates 7-13754
F + H₂ → HF + H, collinear transition state, CI calcs. 7-54105
F + I₂, reaction dynamics, quasiclassical trajectory studies 7-22998
F + I₂, reactive collision, IF laser induced fluoresc. (*French*) 7-13727
Fe-H₂O reaction under high pressure, implications for evolution of Earth 7-8887
H + F₂(Cl₂), kinetic isotope effects, dynamics calcs. 7-54098
H + H₂, and isotropic analogs, reactive scatt. 7-17776
H + H₂, collision theory thermal rate const., on SLTH pot. surface 7-54085
H + H₂, hemiquantal reaction dynamics with ingoing half-trajectory matching 7-28271
H + H₂, reactive scatt., infinite order sudden approx., discrete variable representation 7-65297
H + H₂, resonant scatt., rot. distrib. 7-39858
H + H₂ collinear exchange reaction, time depend. arrangement channel quantum mechs. eqns. 7-17780
H + H₂ reactive scattering in hyperspherical coordinates 7-57151
H + HO₂, abstraction reaction, saddle point geometries and barrier heights, ab initio SDCl calcs. 7-46806
H + methyl- methane, ab initio pot. energy surfaces, channel model calcs. 7-28276
H + N₂O, hot atom reaction, chem. laser, nonequilib. processes 7-1092
H₂-F₂-HF gaseous mixture, light initiated chain reaction, stimulated light scatt. study 7-62778
He + Br₂(I₂)(ICl)(IBr), bound and continuum states, excitation transfer, optical and electron spectroscopy investig. 7-36689
He + ferrocene (Fe(CO)₅), dissoc. excitations, mol. orbital correls. 7-10735
He + H₂⁺ → HeH⁺ + H, endothermic reaction on ab initio pot. energy surface, dynamics 7-54103
He + H₂ → HeH + H, quasiclassical trajectory calcs. 7-39876
He + N₂, reaction kinetics at atm. press., three-body processes 7-22984
He + O₂(N₂)(NO), scatt., total differential cross-sections 7-39865
Hg + NH₃, photosensitised reaction, complex form., luminesc. spectra 7-8256

atom-molecule reactions continued

K + methyl iodide (ethyl iodide) (n-propyl iodide), reactive collision, medical group effect, mol. beam study, cross section meas. 7-39900
K + iodomethane → KI + Methyl radical, orientation depend., classical trajectory calcs. 7-39866
K + NaCl reaction complex form., blue shifted emission in visible spectra 7-22981
K + NaCl → Na* + kCl, laser-assisted reaction obs. 7-33925
K + RbCl, crossed mol. beam expts. involving long-lived collision complexes 7-22999
K + tetrachloroethene (tetrafluoroethene), vapor phase reactions, chemiluminesc. obs. 7-59767
KrF* and Kr₂F*, formation kinetics in He/Ar/Kr/F₂ mixtures (*Chinese*) 7-39892
Li + XF (where X = Mu, ¹H, ³H, ¹⁰H), quasiclassical trajectory calcs., isotopic and orientational study 7-33923
Li + HCl, laser catalysed reaction, pot. surfaces and transition dipoles 7-39861
Li + HCl quenching reaction, electronic struct., ab initio SCF CI calcs. 7-56995
Li + HF, 3D reaction, differential cross section calc. 7-59739
Mg + H₂, reactive collision complex form., far wing laser light scatt. 7-22982
Mg + H₂, reactive collision dynamics by far using laser scatt. 7-28296
Mg + N₂O, reaction dynamics, high resolution laser fluoresc. spectra 7-8252
Mu + F₂(Cl₂), kinetic isotope effects, dynamics calcs. 7-54098
Mu + H₂(D₂) reaction, rate const., 480 to 675K 7-50412
Mu + hydrocarbons, chem. dynamics in liq. phase 7-54093
N₂O + Ba reaction, chemiluminesc. study, N₂O electric dipole moment sign meas. 7-54116
Na + N₂O, gas phase kinetics, rate const. determ. 7-28272
Na + O₃, gas phase kinetics, rate const. determ. 7-28272
O + CH₃, exothermic reactions, rate const., classical trajectory study 7-17783
O + CO, recomb. chemiluminesc. spectrum calc. 7-46807
O + ethylene reaction intermediates microwave kinetic spectroscopy 7-13748
O + H₂, crossed mol. beam expts. involving long-lived collision complexes 7-22999
O + H₂(HD)(D₂), trajectory isotope effects. pot. energy surfaces 7-65296
O + HCl, steric requirements, reagent rot. effect 7-57150
O + HD reaction probabilities and rate const. ab initio pot. energy surface 7-65295
O + HD reaction rates, variational transition state theory 7-59749
O + N₂ → N + NO, reaction rate const., vibr. excitation effect, information theory approx. 7-46832
O + NO₂ (ClO) stratospheric reactions, rate const. meas. 7-8265
O + SF₂(SF₂)(SOF), gas-phase reaction rel. to plasma processing 7-3586
O₂ + O → O₃, in dense interstellar mol. clouds, role of grain surface reactions 7-24179
OH + O₂, isotope exchange reactions, LMR detection, rate const. meas. 7-39882
Rb + perfluoroheptene, vapor phase reactions, chemiluminesc. obs. 7-59767
Si_n-WF₆ (n=2 to 6), Fourier transform ion cyclotron reson. mass spectrometry 7-31200
SiH₄ + Hg, SiH₄ decomposition by Hg(6³P₁) photosensitisation 7-54149
Xe + Cl₂(Br₂)(I₂), atom and excitation transfer, energy disposal, product rot. alignment 7-31158
Xe + ICl, form. of XeCl and XeI, fluoresc. 7-17773
Xe₂ + Kr, van der Waals bond exchange, mol. beam study, ang. and vel. distrib. 7-23000

atom probe field ion microscopy

calibration of flight-time-focused time-of-flight atom probe 7-18906
finely dispersed systems, microstruct. parameters, atom-probe anal. 7-33677
image processing, video digitiser and frame memory system 7-30122
mass analysis with a signal height discriminating timer 7-30127
metal surface, field adsorbed He and Ne, atom-probe spectroscopy studies 7-32803
overlayers on metal surfaces, atomic struct. and composition 7-7013
polypyrrole:BF₄⁻O, dopant distrib., atom probe anal. 7-32480
polypyrrole, oxidation, atom-probe study 7-46822
Poschenrieder-type energy compensator with large acceptance angle 7-30123
software package for on-line anal. 7-30128
statistical data anal., appl. to alloy decomposition 7-30124
statistical data anal., confidence limits 7-30125
steel, austenitic stainless, precipitation and B grain boundary segregation studies 7-33673
steel, cast duplex stainless, spinodal reaction and G-phase precipitation, FIM atom probe anal. 7-33670
steel, secondary hardening, alloy carbide precipitation, FIM atom probe studies 7-33671
steel, stainless, microstruct., aging effects, atom probe FIM, optical and analytic electron microscopy studies 7-33700
steel, stainless, surface segregation and grain boundary precipitation during heating, atom probe study 7-33672
surface analysis using pulsed-laser TOF atom probe field ion microscopy 7-23080
time of flight anal., flared-type micro channelplate detection efficiency 7-30126
Al-GaAs, pure and Si or Zn doped interfaces, composition depth profile, pulsed laser atom probe study 7-32842
CoCrAl alloys, microstruct., atom probe FIM and TEM studies 7-33636
Cu-Co (2.7 at.%), decomp., atom probe FIM 7-3268
Cu-Ni alloys, chemisorpt.-induced surface segregation, time-of-flight atom probe and AES studies 7-32657
Fe oxide passive film composition and growth, atom probe depth profiling anal. 7-32869
Fe, surface, H₂ and N₂ interactions, pulsed laser atom probe studies 7-32811
Fe-Co-Ni-Al-Cu metallic alloy ordering and spinodal decomposition, atom probe FIM study 7-33676
Fe-Ni-Al-Co system, miscibility gap, phase decomp. in Alnico mag. alloys 7-17537
FeAlNiCoCu permanent magnetic material, phase decomposition kinetics, atom probe FIM study 7-33669

atom probe field ion microscopy continued

- FeNiAlCoTiCuS permanent magnetic material, phase comp. and ordering, atom probe FIM and TEM studies 7-33635
- Fe₄₀Ni₄₀B₂₀ metallic glass ribbon, failure mechanics and atom probe study correlations 7-28139
- GaAlAs MOCVD layers, stoichiometry variation determ., pulsed laser atom probe anal. 7-12305
- LaB₆ (001), field evaporation in the presence of H₂, atom probe FIM 7-21652
- Ni base superalloys, interphase boundaries, FIM atom probe study 7-33683
- Ni-Al-B-based alloys, site occupations, APFIM and channelling studies 7-32367
- Ni-B, precipitation and B grain boundary segregation studies 7-33673
- Ni-base superalloys, creep resist. improvement, role of Re additions, APFIM study 7-22772
- Ni-Cu binary alloys, surface segregation (*Japanese*) 7-12422
- Ni-Cu binary alloys, surface segregation studied by atom-probe 7-44966
- Ni-Ti metallic alloy ordering and spinodal decomposition, atom probe FIM study 7-33676
- Ni₃Al, rapidly solidified, B segregation to grain boundaries, atom probe FIM 7-22688
- Ni₃Al-B rapidly solidified alloy, B distrib. at grain and antiphase boundaries, atom probe FIM and TEM studies 7-33637
- Ni₃Al-B-Hf alloys, B and Hf grain boundary segregation, ductility, atom probe FIM study 7-33675
- Ni₄₅Pd₃₅P₂₀ metallic glass, decomposition, crystallisation and embrittlement, atom-probe FIM study 7-33639
- Pd/Si interface composition and silicide form., atom probe FIM study 7-32845
- Pd-SiC interface, compositional depth profiles and intermixing, atom probe FIM study 7-32843
- Si oxides, native and thermal films and Si/oxide interfaces, stoichiometry and interface transition layer, atom probe FIM study 7-32844
- Ti-Cu alloys, Guinier-Preston zones, multi-layer struct., atom probe FIM study 7-33674
- Ti-SiC interface, compositional depth profiles and intermixing, atom probe FIM study 7-32843
- TiN planar magnetron sputtering, thin coating deposition on high speed steel substrate, TEM and atom probe FIM studies 7-33561
- W (110), field adsorption and desorption of H, atom probe FIM 7-21647
- W surface, field adsorption of He 7-32816
- W surface, He fluid adsorption and diffusion, atom-probe field ion microscopy studies 7-32808
- W-Ni dilute alloy, Ni enrichment at screw dislocations, atomistic calcs. and atom probe FIM meas. 7-33638

atom-surface impact

- see also sputtering
- adsorbate resonances, fractional occupation and van der Waals interactions 7-27376
- adsorption dynamics, exchange reactions and defect form. at solid surfaces, computer simulations 7-32823
- alkali metal adsorbed layers on solid surfaces, metastable He deexcitation spectroscopy (*Japanese*) 7-21966
- alkali metal atoms, interaction with dichlorodimethylsilane coated reson. cells wall relax. 7-59317
- alkali metal surfaces, electron spectroscopy by deexcitation of metastable He atoms 7-59364
- atom passing through thin film, radiation excitation 7-42738
- atomic beam diffr., use in surface struct. anal. 7-6944
- bound state existence confirmation for atomic and mol. projectiles inside solid targets, expt. investig. (*French*) 7-22427
- charged particle, interaction with solid surface, general formalism, spherical geometry 7-2652
- continuum model of solid with free surface 7-64866
- disordered surface, atom scatt. randomly corrugated hard wall and sudden approx. 7-53489
- general theory of scattering 7-59359
- glass surface, He atom scatt. 7-64863
- glass surface, polished, thermal Cs atom reflection 7-22411
- graphite (001), surface phonon dispersion, inelastic atom scatt. study 7-52227
- graphite surface with Xe monolayer, H atom scatt. resonances 7-64864
- hybridisation interaction between He and metal surface 7-38664
- imperfect surfaces and adsorbates, short range order and correlations 7-6953
- inelastic energy loss and electron emission 7-17384
- inelastic scattering and trapping of an atom on a cold, simple-cubic lattice 7-27122
- low temp. solids, low energy atom and ion bombardment, sputtering and radiation damage mechanisms study 7-27844
- low-energy atom scattering from surfaces, appl. in struct. anal. 7-33504
- metal surface quasi-stationary spectrum of nearby Rydberg atoms 7-49984
- molecule sputtering, atom- and ion-induced, collision mechanisms 7-59349
- neutral beam incident ion-scattering spectroscopy, shadowing and focusing effects 7-53491
- noble metal surfaces, high resolution inelastic He-atom scatt., surface phonon dispersion relations 7-3144
- one-dimensional atom-surface energy transfer, consistent quantum treatment 7-27840
- oriented atom scatt., anisotropic charge transfer rates 7-59366
- quantum sticking theory, simplified model 7-22424
- rainbow scatt. study in mol. and nucl. physics, and surface science 7-62482
- resonance states, complex rot. method appl. 7-50391
- sapphire surface, long range interaction between rare gas atoms/molecules and surfaces, calc. 7-3135
- secondary-electron emission, beam-foil experiments with molecular ions, anal. 7-39326
- sputtering and atomic collisions, computer simulations 7-59323
- surface science, modern techniques, book 7-60911
- thermal attenuation, multiphonon contrib. 7-39338
- transition metal surfaces, He atom scattering potential energy surfaces, vibr. substrate relax. effects 7-53478
- transition metal surfaces, metastable noble-gas atom interactions 7-64852
- Ag (110), ion bombardment, He atom scatt. 7-64863
- Ag surface, (111), one-phonon scatt. of He atoms 7-3143

atom-surface impact continued

- Ar small clusters, sticking coeff. of Ar 7-64861
- Au (111) with adsorbed layers of inert gases, He atom-surface scatt. 7-27851
- Au, energy spectrum, scattering trajectories, of light atoms H, D and He 7-64854
- BN surface, long range interaction between rare gas atoms/molecules and surfaces, calc. 7-3135
- CaF₂ surface, long range interaction between rare gas atoms/molecules and surfaces, calc. 7-3135
- Cu (100), Pb epitaxial growth, thermal He atom scattering 7-52351
- Cu (100), surface characterisation by In probe atoms, electric field gradient 7-2553
- Cu (110), H adsorpt., adsorbate movement-induced subsurface reconstruction, LEED and atom diffr. meas. 7-27114
- Cu, energy spectrum, scattering trajectories, of light atoms H, D and He 7-64854
- Cu single cryst. target, atomic and mol. ion surface semichannelling, Lindhard atomic string model calcs. 7-63697
- Cu surface, Cu atom sticking and penetration, computer simulation studies 7-59326
- Cu, surface roughening transition, He beam diffr. study 7-52202
- He atoms, scattering from rare-gas-plated graphite 7-3136
- He scatt. study of the initial stages of adsorption and 2D phase transitions 7-59365
- He scattering apparatus for gas-surface interaction studies 7-33503
- He scattering from O chemisorbed layer on Ni (001), cluster model calcs. 7-53471
- He-metal impact, density functional approach, dynamic response at metal surfaces, van der Waals interaction, excitation of electron-hole pairs 7-3129
- He-NaCl (001) system, interaction potentials for diffraction 7-22425
- InP single crystal (100) surface, atomic scatt., electron-hole pair creation 7-27841
- In₂₋₃Sn₃O_{3-γ} protective coatings for Galileo spacecraft, radiation testing 7-59647
- Ir foil sample, Cs diffusion and surface ionisation studies 7-3138
- LiF surface, long range interaction between rare gas atoms/molecules and surfaces, calc. 7-3135
- LiF(001), surface optical phonons, obs. by inelastic He scatt. 7-44987
- MgO, adsorption induced luminescence, O atomic and mol. beams 7-13231
- Mo surface, Ta deposition, short range bonding interaction, RBS meas. 7-3142
- MoS₂-based double layer solid lubricant, friction-reducing coatings 7-46669
- Ni (001) and (110) surfaces, adsorbed O, He diffr. results 7-7809
- Ni (115), H₂ adsorpt., surface corrugation effects, He diffr. study 7-2381
- Ni, energy distrib. surface peak of scattered He ions and atoms 7-64855
- Ni, energy spectrum, scattering trajectories, of light atoms H, D and He 7-64854
- Ni surface, reflected D charge state fractions study 7-46268
- Ni, surface roughening transition, He beam diffr. study 7-52202
- Pb overlayer of Cu (100), growth, phase transitions and struct., thermal energy He atom scatt. study 7-63943
- Pt (111), adsorbed CO, He thermal beam scattering 7-53475
- Pt (111), clean and O covered, surface phonon dispersion, inelastic atom scatt. meas., lattice dynamical calcs. 7-52226
- Pt (111), Xe adsorption, thermodynamic meas. 7-6982
- Pt (111) with adsorbed CO, He-adsorbate scatt., potentials and total scatt. cross-sections 7-59363
- Pt (111) with adsorbed Kr, adsorbate-substrate vibr. coupling 7-52221
- Pt surface, clean and H-covered, He atom diffr. intensity calcs. 7-3139
- Rb, vapor, wall-induced velocity changing collisions, laser optical pumping, complete Doppler coverage 7-962
- Si surface, (111)(2×1), obs. of 10 meV Einstein oscillator mode 7-38320
- Si surface, atomic and mol. F reactions, XPS studies 7-28350
- Te (1010), He atom scatt. 7-64863
- W surfaces, chemisorbed ²³Na, nuclear-spin-polarized thermal atom scattering 7-53476
- Xe monolayer on Pt (111), thermal He scatt. data anal., comment 7-21633
- atomic absorption spectroscopy**
- characteristic mass, in graphite furnace atomic absorpt. spectrometry, calc. 7-8346
- high-quality quartz crystals impurities assessment, production developmental results 7-59823
- pipetting device, microvolume, for atomic absorpt. spectrometry 7-4900
- surfactants, anionic, in wastewater, indirect at. absorpt. determ. using liquid-liquid extraction 7-17925
- trace elements in biological materials determ., new techniques in X-ray fluoresc. and atomic absorpt. spectrometries 7-18101
- ultrasonic nebulization of liquid samples for analytical inductively coupled plasma-atomic spectroscopy: anupdate 7-8350
- Voigt effect coherent forward scattering atomic spectrometer eval. 7-64608
- Zeeman atomic absorption spectrometry, extended range, using 3-field AC magnet 7-30098
- Ar, metastable number density, ICP-AAS eval. 7-54237
- Fe, I-line excitation processes, investig. 7-19775
- Fe₃O₄, magnetite-laced microspheres, mag. moment meas. 7-53064
- KCl, solute trapped from air-acetylene flame, morphological investig. 7-28362
- Ni(CO)₄, shock pyrolysis; homogeneous nucleation, spectroscopic investig. 7-46823
- Pb, particulate and gaseous, in exhaust gas determ., plasma emission and atomic absorpt. spectrometry 7-59803
- Se, specific column and atomic absorpt. spectroscopic determ. 7-33976
- Te, specific column and atomic absorpt. spectroscopic determ. 7-33976
- Tl, determ. by atomic absorption spectrometry for river sediment, coal, coal fly ash 7-59801
- atomic beam electric resonance**
- No entries
- atomic beam magnetic resonance**
- alkali metal isotopes, radioactive, ground state hyperfine struct. determ. by RF mag. reson. and laser optical pumping 7-25681
- ampere reproduction from proton gyromag. ratio and quantum magneto resonance phenomena 7-61309

atomic beams

- see also atom-molecule reactions; atom-surface impact; atomic beam electric resonance; atomic beam magnetic resonance; particle velocity analysis; plasma-beam interactions 7-30985
- atomic cooling, stopping and trapping 7-10504
- clusters in beams, review 7-31204
- coincidence laser spectroscopy, ultrasensitive technique for fast ionic or atomic beams 7-30100
- collimation and decollimation by laser radiation 7-42782
- collimation and decollimation by laser radiation pressure 7-42785
- collinear laser-fast-beam spectroscopy, collisional ionisation detection scheme 7-18882
- deflection and focusing by reson. light field 7-42786
- fast atom bombardment mass spectrometry, industrial appls. 7-54206
- heavy atoms, hyperfine struct., isotope shift nucl. struct. effects optical spectra 7-19768
- high current heavy atom beam system for plasma diagnostics 7-1758
- laser beam-zz for photon statistics test 7-10902
- laser coding and EM trapping 7-19777
- laser cooling, reson. radiation press., simulation approach 7-15555
- plasma diagnostics, Kalman filters for signal processing and beam modulation 7-1761
- plasma Zeeman spectroscopy using high-intensity Li beam 7-6460
- Rabi and Ramsey interrogations of metastable beams 7-25459
- radioactive atoms, laser spectroscopy photon correl. technique 7-19769
- resonance ionisation spectroscopy, coincidence detection 7-57188
- stopping with laser light, entropy prod. 7-42556
- TFTR diagnostic neutral beam for ion temp. meas. 7-6468
- two-level atoms, beam compression by laser radiation press. 7-42555
- Ag, frequency standard, optically pumped 7-18763
- Ba, double Rydberg states, ionisation, two-photon and TOF mass spectra 7-19809
- Ba, fast atomic beam laser fluoresc., g-factor 7-10483
- Ba I, 1P_1 level branching, reson. fluoresc. intensity depend. 7-50000
- Ba, superelastic collisions with electrons (*French*) 7-10758
- Ba, three-level system, dynamic Stark effect 7-42548
- Ca, optical frequency standard based on Ramsey excitation 7-14925
- Ca, two-photon Hanle effect in Ramsey interrogation 7-15560
- Cs atomic beam, cooling using laser 7-10897
- Cs atomic clock, velocity distrib. determ. 7-18755
- Cs beam primary frequency standard, C-field setting, transitions and disturbances 7-18757
- Cs, frequency reference, metrological analysis 7-41351
- Cs, frequency standard with narrow atomic velocity distrib. ranges, Ramsey patterns 7-18758
- Cs, parity violation, crossed beam interference technique 7-10497
- D+H₂, mol. beam scatt. study, differential cross sections meas. 7-39860
- Fe, atomic beam, atom density meas., laser induced fluoresc. 7-19762
- Ga, hyperfine struct., magnetic-dipole- and electric quadrupole coupling consts., atomic fluoresc., MCHF method 7-30985
- Ga, radiative lifetimes, fluoresc., MCHF calcs. 7-30946
- H beam production using electron coding technique, future expts. 7-50401
- H excited state, laser spectroscopy in mag. field 7-10460
- H, laser spectroscopy with relativistic beams 7-19778
- H⁺, laser spectroscopy with relativistic beams 7-19778
- He beam hyperfine struct. evolution and tensor polarisability determ. in elec. field. 7-57028
- Hg, $6^1S_0-6^3P_1$ transition isotope shift in UV absorpt. spectra 7-19770
- In, hyperfine struct., magnetic-dipole- and electric quadrupole coupling consts., atomic fluoresc., MCHF method 7-30985
- Li beam, mag. field meas., Zeeman and motional-Stark effect 7-19766
- ^{24}Mg fine structure transition via linear Ramsey interrogation 7-884
- Na, atomic beam absolute intensity, reson. fluoresc. obs. 7-36530
- Na atomic neutral beam, laser technique for collimating and focusing 7-62610
- Na, degenerate resonant parametric interaction in spatially separated optical fields 7-43220
- Na+Na assoc. ionisation, at. alignment, effect vel. depend. 7-28306
- ^{23}Na beam, polarisation components meas. 7-61875
- Ne+He(Ar), electronically excited atoms, beam sources 7-20008
- U, production by hollow-cathode discharge and characterisation by fluorescence spectroscopy 7-365
- ^{174}Yb , 2-level system, resonant excitation response 7-15544
- Zr, ionis. pot. determ., two laser field-ionis. spectroscopy 7-5650
- Zr, metal beam, laser prod. and diagnostics, rel. to isotope separation 7-42783
- Zr surface, N₂ laser irr., at. beam prod. 7-21276

atomic clocks

- see also frequency measurement; time measurement
- frequency standards (*French*) 7-9822
- Laboratoire Primaire du Temps et des Frequences, metrological activities in 1986 (*French*) 7-9821
- laser frequency standards, review 7-36977
- servo-controlled lasers progress and appls. 7-20307
- time and frequency meas., fundamentals (*French*) 7-9820
- VLBI appls. (*French*) 7-30068
- Cs, atomic beam frequency standard, NRLM-II, atomic vel. distrib. and second-order Doppler shift 7-14910
- Cs clocks charact. in perturbed environment (*French*) 7-29984
- Cs primary atomic clock, PTB design, preliminary results 7-18756
- Cs, velocity distrib. determ. 7-18755
- H maser built at Johns Hopkins University, long term performance 7-18759
- H maser miniature passive clock, NBS design, characts. and performance 7-18760

atomic clusters

- alkali metal clusters, structures, pseudopotential method, local density approx. 7-36840
- beams, refractory laser spectroscopy 7-15794
- C_n⁺ and C_n⁺ abundance distrib., magic nos. 7-42815
- charged metallic particles, charging energy and stability 7-57200
- classical pot. energy surfaces investigated using simulated annealing method 7-62556
- clustering in solids, time-resolved multiple-quantum NMR investig. 7-59115
- electron attachment to van der Waals clusters 7-20090
- electronic characteristics of small metal particles (*Dutch*) 7-52396
- electronic structure of micro-clusters, ab initio studies 7-31203

atomic clusters continued

- generation and detection, size distrib., review 7-31204
- ground states, Hubbard models 7-10809
- heavy clusters, ionis. dynamics, cluster ion-photoelectron coincidence 7-15791
- inert gases, condensation in free jets, scaling laws, similarity relations 7-42825
- ionised cluster beam technique for thin film deposition 7-17478
- laser excitation dynamics of at. and mol. clusters in free jets 7-42823
- metal atom cluster cpds., electronic struct., rel. to atoms and solids 7-15785
- metal clusters, ionisation threshold, photoionisation TOF mass spectra 7-20085
- metal particles, quantum size effects 7-7597
- metal trimer clusters photodissoc., bound-free transitions fluoresc. study 7-23045
- metallic clusters, produced by liq. metal ion source, stability and struct. 7-31205
- metals, condensation in free jets, scaling laws, similarity relations 7-42825
- multiple-scatt. theory, appl. of a non-muffin-tin pot. general pot. develop. 7-36839
- N-atom polar deltahedra, tensor surface harmonic theory, pairing principle 7-50439
- polyatomic mols. Rydberg states, cryst. field theory 7-10804
- polynuclear metal cluster bonds, chemical sub-micron structure (*Dutch*) 7-50437
- 3^+ , ground state pot. energy surface, MRD-CI calcs. 7-30959
- Ag clusters, small, photolytic, oscill. of photoionisation thresholds on AgBr grain surface 7-36841
- Ag dimers and clusters, matrix isolated, guest-host interaction and photochem. transform. 7-15786
- Ag₃ clusters isolated in solid Xe matrices, reson. Raman scatt. and photoionisation process 7-25696
- Ag₃⁺, electronic struct., Dirac scattered wave study 7-42818
- Ag_n clusters, multiply charged, stability 7-50440
- Al⁺+O₂(H₂O)(ethylene), absolute cross sections, meas. 7-5743
- Al_n⁺+O₂ mass selected ions, reaction study 7-22993
- Ar ion clusters, unimol. decomp., average kinetic energy meas. 7-28301
- Ar small clusters, sticking coeff. of Ar 7-64861
- B clusters, magnetic properties, Heisenberg Hamiltonian 7-57199
- Bi_n⁺ ions, (n/p≤14, p≤4), mass spectrum from liquid metal ion source study (*French*) 7-5807
- C cage molecules of icosahedral symmetry, stability anal. 7-20088
- C₂ cluster, Swan band emission obs. 7-62558
- C₂, Coulomb and exchange-correlation energies, local density functional calcs. 7-20087
- C₄, struct., energies, single reference CI calcs. 7-19720
- C₆, cyclic ground state, struct., ab initio calcs. 7-42819
- C₆₀ and similar substances, inert gas trapping, possible occurrence in meteorites 7-50436
- C₆₀, cage-like struct., HMO calcs. 7-15520
- C₆₀ cluster, electronic structure, LMTO calcs. 7-19682
- C₆₀ cluster, spherical, DV-Xα electronic struct. 7-10806
- C_n⁺ cluster, (n=1 to 25), form. in laser vaporisation source, kinetics 7-5808
- C_n clusters, spheroidal clusters, rehybridisation and π-orbital alignment 7-25695
- C_n icosahedral clusters, struct. anal. and magic numbers 7-31202
- C_n⁺, (n=1 to 110), laser vaporisation prod., TOF mass spectrometric detect. 7-15760
- C_n⁺, mass resolved cluster ions, photofragmentation 7-15789
- C_n⁺, (a=+or-), clusters, mass resolution, photofragmentation and photodetachment spectroscopy 7-15795
- C_n⁺+D₂(O₂) cluster ions, ion+mol. reactions 7-50432
- C_n⁺(a=+or-), abundance distrib., magic numbers, photoionis. mass spectroscopic investig. 7-15759
- Cs vapour, comp. study, reson. doublet absorpt. meas. 7-36518
- Cu cluster surface, Na atom adsorpt. SCF ab initio and CI calcs. 7-52259
- Cu ionic clusters, evaporation, evaporation ensemble approach, unimol. rate consts. effects 7-62562
- Ge clusters, TOF mass spectra 7-20084
- Ge_n⁺ microcluster, pulsed conc. spectra, bonding and growth kinetics 7-19740
- Ge_n⁻ semicond. cluster anions, photodetachment and photofragmentation 7-36837
- H_n⁺, even cluster ions, form., reactivity collision-induced dissoc., isotope effects, mass spectra anal. 7-50434
- H⁺(NH₃) cluster, struct., stability, ab initio MO calcs. 7-56965
- H⁺(NH₃)₂ cluster, struct., stability, ab initio MO calcs. 7-56965
- Hg clusters, form., atomic photon and electron impact ionisation, mass spectra study 7-50430
- Kn, laser photoionisation of clusters containing up to 101 atoms 7-42822
- Li microclusters, fragmentation channels rel. to magic number studies 7-5811
- Li_n clusters, n=2 to 13, electronic struct. and magic numbers, LCAO-Xα calcs. 7-31206
- Na clusters, at. desorpt. energies determ. 7-15787
- Na microclusters, fragmentation channels rel. to magic number studies 7-5811
- Na₃ excitation spectrum, excited states 7-15770
- Nb₂, metal cluster in solid Kr and Xe matrices, absorption and reson. Raman spectroscopy 7-31055
- Ni₆ cluster, metal-metal bonding (*German*) 7-1002
- Pb and PbS ionised atomic clusters, fragmentation, TOF mass spectroscopic study 7-10807
- S_n clusters, fragmentation investig. 7-15792
- Si clusters, in presence of O, Si-Si bond breaking, total energy calcs. 7-50438
- Si clusters, TOF mass spectra 7-20084
- Si, laser ablation, cluster and plasma formation, time-resolved X-ray monitoring 7-37710
- Si_n (n=10 to 32), clusters, growth and struct., solid-liq. transform., mol. dynamics simulation 7-26682
- Si_n⁻, semicond. cluster anions, photodetachment and photofragmentation 7-36837
- Si_n⁺, clusters, mass resolution, photofragmentation and photodetachment spectroscopy 7-15795
- Si_n-WF₆ (n=2 to 6), Fourier transform ion cyclotron reson. mass spectrometry 7-31200

atomic clusters continued

- Sm small clusters, matrix isolated, mixed valence, critical cluster size 7-64186
 Sn₃, electronic states, pot. energy surface, relativistic calcs. 7-5613

atomic collision processes *see atomic inelastic collisions; elastic scattering of atoms and molecules***atomic electric moment**

- 7-30985
 adatom, neighbour effects on permanent electric dipole, Feynman propag. anal. 7-27110
 inert gas atoms, physisorbed, induced dipole moment 7-52243
 inert-gas atoms, hyperpolarizabilities, local-density approx. method 7-25630
 parity and time-reversal violation in nuclei and atoms 7-30325
 photoionisation, threshold effects in strong-field, non-perturbative realistic model 7-36563
 Rydberg atoms, props. and quantum optics 7-1064
 time reversal invariance, elec. dipole moments 7-19779
 two-level atoms, intrinsic optical bistability, quantum-electrodynamical many-body treatment. 7-37019
 Ga, hyperfine struct., magnetic-dipole- and electric quadrupole coupling consts., atomic fluoresc., MCHF method 7-30985
 H, external electric field, first-order perturbed wave fn. 7-36465
 H-like ions, nucl. quadrupole moment, HFS 7-49914
 He, Kohn-Sham time-depend. orbital density functional theory, hydrodynamic formulation 7-25678
 In, hyperfine struct., magnetic-dipole- and electric quadrupole coupling consts., atomic fluoresc., MCHF method 7-30985
 Na atoms, nonlinear parametrical EM wave interaction, saturation, stark shift and multipole radiation effects calcs. (Russian) 7-19767
 Na, nonlinear parametrical EM wave interaction, saturation, stark shift and multipole radiation effects calcs. (Russian) 7-19767
¹²⁹Xe, time reversal invariance, elec. dipole moments 7-19779

atomic electron configuration interactions *see atomic electron correlations***atomic electron correlations**

- collective and planetary motion in atoms 7-49955
 diabatic states, nonadiabatic interactions, CI wave fns. expansion, ab initio LCAO SCF CI calcs. 7-49945
 diagrammatic VB method for CI calcs. 7-19711
 first-row atoms, exchange correlation energies, \bar{E}_a method calcs. 7-56993
 generalised exchange local-spin-density-functional theory, 7-36499
 ionisation energy and electron affinity, correl. energy estimation by local approx. 7-56991
 ions and atoms, closed shell, polarisability, local density approximation 7-56999
 lanthanides, hyperfine struct. in low-lying configs. 7-49954
 negative ions, autodetaching states, electron correl. effects 7-19789
 oscillator strengths, transition energies and probabilities, CI STO calcs. 7-25423
 rare earth ions in crystals, electron correl. contribs. to elec. dipole transition amplitudes 7-36549
 two-electron atoms, rigid body solns., electron equilb. constellations derived 7-30958
 valence electron correlation energy calculation 7-42493
 Ar, 3s-subshell excitation, photoabsorption spectra anal., HF calcs., config. interaction calcs. 7-30947
 Ar, kinetic energy density, nonlocal correl. fn., CI wave fns. and HF calcs. 7-42496
 Ba, doubly excited states, electron correl., laser spectra 7-10459
 Be, electronic energy, Green's fn. calc. 7-10445
 Be, excitation energies, multiconfig. linear response and full CI calcs. 7-36487
 Be, isoelectronic series, dielectronic recomb. rates calcs. 7-50352
 Be, kinetic energy density, nonlocal correl. fn., CI wave fns. and HF calcs. 7-42496
 C isoelectronic series, intercombination transition probabilities, CI calcs. 7-36489
 C V, electron impact excitation of inelastic transitions 7-979
 Ca III, allowed transitions, oscill. strengths and excitation energies 7-5631
 Cd, oscillator strengths and excitation energies, relativistic CI and MCRHF calcs. 7-50260
 Cl isoelectronic sequence, allowed 3-3 transitions, Slater parameter optimisation, HF CI calcs. 7-48205
 Cl VI, forbidden and allowed transition, electron impact excitation 7-62529
 Cr²³⁺, dielectronic satellite spectra CI HFS calcs. 7-42506
 Cs, 5s ionisation, PES satellite struct., CI approach 7-62296
 Cu cluster surface, Na atom adsorpt. SCF ab initio and CI calcs. 7-52259
 Fe II, contrib. of configuration interaction to UV doubly excited lines 7-66585
 Fe II, electron impact excitation, collision strengths, R matrix method, CI calcs. 7-25424
 Fe, multiply charged ions, electron-impact ionisation, excitation energies and cross section calcs. 7-25425
 Fe XV, oscillator strengths, transition energies and probabilities, CI STO calcs. 7-25423
 Fⁿ (n=0 or 1), MBPT and coupled cluster calc., comparison with CI 7-49899
 H⁻, ground state energy calcs. using hyperspherical coords. 7-49880
 He, correlated wavefunctions, dynamical anal. 7-49941
 He, correlation energy, Fulde's local approach studies 7-30957
 He, electron impact ionisation, distorted-wave impulse approx. 7-31175
 He, exchange correlation energies, \bar{E}_a method calcs. 7-56993
 He, ground state energy calcs. using hyperspherical coords. 7-49880
 He isoelectronic series, correl. effects, local level, CI partitions 7-49940
 He, photoionisation, partial cross-sections and Rydberg series resons. 7-903
 He, ²S resonant state, projection-operator formalism, CI calcs. 7-36498
 He²⁺, charge exchange collisions, multiply charged closed K shell targets, exponential model study 7-25426
 He-like ions, double-excited, electron correl. 7-19722
 He-like ions, electron excitation, distorted-wave polarised orbital approach 7-62531
 He⁺+He⁺, electron capture cross sections, SCF-CI calcs. 7-15526
 Hg, oscillator strengths and excitation energies, relativistic CI and MCRHF calcs. 7-50260
 Kr, kinetic energy density, nonlocal correl. fn., CI wave fns. and HF calcs. 7-42496

atomic electron correlations continued

- Kr²⁸⁺, electron impact excitation cross sections, CI calcs. 7-36493
 Li, ²S ground state, specific mass shift, isotope shift, ab initio calcs. 7-36495
 Li, ⁴P₁ levels, relativistic autoionisation, threshold phenomena, CI mechs. 7-49950
 Li, ⁴P₁ level, relativistic autoionisation, CI mechs. 7-49949
 Li, excited states, electron correlation calc. (Chinese) 7-10438
 Li, spin density, cusped gaussian wave functions 7-42504
 Li-like ions, first excited state, intra- and inter-shell correl. effects 7-62295
 Li+HCl quenching reaction, electronic struct., ab initio SCF CI calcs. 7-56995
 Mg, ¹P doubly excited autoionisation states, CI calcs. 7-36497
 Mg, 3snl excited series, CI HF calcs. 7-36496
 Mg, exchange correlation energies, \bar{E}_a method calcs. 7-56993
 Mg isoelectronic series, energy levels, multiconfig. optimised pot. model calcs. 7-19723
 Mo V, HF calcs. and spectra 7-10477
 N IV, spontaneous radiative transition probabilities, ab initio CI calcs. 7-50261
 Ne, correl. energy calc. using basis set of explicitly correl. Gaussian geminals 7-5609
 Ne diatomic coupled cluster method, MBPT 7-56996
 Ne, kinetic energy density, nonlocal correl. fn., CI wave fns. and HF calcs. 7-42496
 Ne, MBPT and coupled cluster calc., comparison with CI 7-49899
 Ne VII, spontaneous radiative transition probabilities, ab initio CI calcs. 7-50261
 Ne^{**}, He-like, X-ray and Auger transition rates 7-36507
 Ni_n (n=1 to 6) clusters, electronic struct., ab initio SCF and CI calcs. 7-10446
 O, electron affinity, CI STO calcs. 7-5606
 O V, spontaneous radiative transition probabilities, ab initio CI calcs. 7-50261
 Pb, electron momentum spectra, multiconfiguration DF wavefunction 7-50351
 Ra atom, relativistic splittings of Cooper minima, RRPA study 7-862
 Si isoelectronic sequence, allowed 3-3 transitions, Slater parameter optimisation, HF CI calcs. 7-48206
 Sr+Ar, ¹P fluoresc. line broadening, ab initio close-coupled scatt. calcs. 7-36494
 Yb, photoionisation, relativistic RPA calcs. 7-42567
 Zn I, subvalence d-shell absorpt. spectrum 7-49953
 Zn, L_{2,3}-MM Auger electron spectrum, correl. effects influence 7-57037

atomic electron impact excitation*see also electron spectra*

- alignment and orientation in collisional excitation 7-42764
 alkali metal atoms(ions), reson. line electron-impact broadening 7-20058
 atom-electron (positron) interactions, semiempirical polaris. pots. calcs. 7-974
 atomic collision processes, resonant transfer excitation and dielectronic recomb. review 7-50366
 atomic impurities in Ne, optogalvanic effect 7-30970
 atoms, electron bremsstrahlung energy spectra 7-24319
 atoms in a low field, review 7-898
 Born partial wave integrals, numerical evaluation 7-48462
 charged particles, heavy, inelastic scatt., quasiclassical statistical model 7-15728
 dielectronic recombination in elec. fields, quantum defect theory 7-62527
 distorted-wave methods in electron-impact excitation of atoms and ions 7-10759
 Doppler profile analysis, optical instrument design and construction (Japanese) 7-31172
 electron scatt. in a laser field, modified perturbation theory 7-36572
 electron-ion resonance scatt., WKB calcs. and multichannel quantum-defect theory, effect of electric field 7-15546
 fermionium production in electron-atom collisions 7-36811
 gas causing inelastic backscattering of electrons, analytical calculation 7-50350
 ion beam apparatus for meas. 7-57190
 ionised gas physics, conf., Sibenik, Yugoslavia, (Sept. 1986) 7-24307
 ions, lines electron impact shifts, modified semiempirical approach 7-892
 Kroll-Watson formula, electron-atom collisions in presence of strong laser field 7-5638
 laser assisted atomic physics studies at Griffith University 7-20073
 metal atoms and ions, lasing mechanism and energy characts., relax. processes of metastable states 7-62673
 monoenergetic positronium, creation in gas 7-36784
 polyatomic mols., reson. electron impact, vibr. energy loss selection rules 7-15725
 positron and positronium atomic physics 7-36783
 positron-atom scatt., partial cross sections 7-36788
 positron-gas collisions, charge exchange, ortho-positronium form. 7-62513
 positrons in gases 7-36782
 light rare earths, Ly_{2,3} satellite, X-ray emission spectra anal. 7-36523
 Rydberg series, electron scatt., Stark broadening reson. struct. 7-50009
 shock excitation of internal shells of light atoms 7-31173
 stimulated collective inelastic stopping effect 7-36781
 two-photon bremsstrahlung in the Coulomb field 7-42766
 Ar, electron collisions, cross section meas. for scatt. length determ. 7-20055
 Ar, electron scatt., cross section meas. 7-31171
 Ar, electron stepwise excitation effective cross section of 2p₃ level from metastable states 7-31174
 Ar, electron swarms, collision cross sections 7-37619
 Ar gas, electron beam deposition 7-5771
 Ar, metastable population meas. and flow instability due to shock wave, comparison with models 7-16207
 Ar, positron scattering, cross-section meas. 7-20054
 B²⁺, electron-impact ionisation, excitation-autoionisation contrib. 7-978
 Ba, superelastic collisions with electrons (French) 7-10758
 Be, double electron excitation cross section, distorted wave approach 7-50379
 Be I isoelectronic series, atomic and spectral data for typical tokamak plasma conditions 7-24322
 Be⁺, electron impact-excitation, reson. transition, ab initio treatment 7-42768
 Be-like ions, electron impact excitation rates 7-10760
 Be-like ions, excitation cross sections, Coulomb-Born approx. 7-25658

atomic electron impact excitation continued

- Bi, electron scatt., relativistic effects, Kohn-Sham theory 7-42765
 C⁻ V, electron impact excitation of inelastic transitions 7-979
 C³⁺, ion beam apparatus for meas. 7-57190
 Cl⁻ VI, forbidden and allowed transition, electron impact excitation 7-62529
 Cr³⁺ dielectronic recombination, photon/ion coincidence meas. 7-10756
 Cs⁺, effective electron inelastic excitation cross section, resonance effects study 7-42772
 Fe II, electron impact excitation, collision strengths, R matrix method, CI calcs. 7-25424
 H, effects in flaring solar chromosphere 7-34843
 H, electron and positron scatt., exact eikonal approx. 7-50360
 H, electron impact excitation, excited state polarisation and ang. correls. 7-36772
 H, electron impact excited, polarisation and ang. correl. relations 7-31170
 H, inelastic electron scatt., eikonal Born series study (*Spanish*) 7-15727
 H ions, Stark-broadening effect, simulation technique applied to models for Lyman α line 7-15721
 H, mesic 2 s state, elastic and inelastic slow electron scatt. 7-10781
 H, metastable 2s state, electron impact ionis., triple differential cross-sections 7-25665
 H plasma, computer simulated binary collision hypotheses, Stark broadening 7-10492
 H, positron scattering, inelastic and superelastic, calcs. 7-36790
 H⁺, positron impact electron detachment, with excitation, threshold law calcs. 7-25668
 H₂, electron impact, in laser field, one-photon free-free transitions 7-980
 H₂S, electron scatt., low energy, absolute total cross-sections meas. 7-25650
 He, 3 ³P state lifetime, electron-photon delayed coincidence technique meas. 7-62533
 He, 3¹D state electron impact excitation, electron-polarised photon coincidence study 7-36774
 He, 3¹P state, electron polarised photon coincidence expts. 7-5772
 He, alignment and orientation, electron impact excitation 7-50373
 He doubly excited states, electron impact excitation, generalised oscillator strengths 7-873
 He electron impact excitation, electron-photon polarisation correls. 7-10761
 He, electron impact excitation, orientation parameter anal., exam. of Steph-Golden model 7-20053
 He, electron impact excitation, excited state polarisation and ang. correls. 7-36772
 He, electron impact excitation, metastable state, laser induced fluoresc. 7-50372
 He, electron impact excitation, fine-struct. effect, electron spin polarisation fn. 7-50374
 He, electron impact excitation, Stokes' parameters, electron-photon coincidence spectra anal. 7-50377
 He electron scatt. below excitation threshold, phase shift anal. 7-15715
 He, forbidden lines intensities, diagnostics 7-51516
 He I triplets, collisional excitation cross sections and implications for primordial He abundance 7-55446
 He isoelectronic series, electron scatt., plasma screening effect, distorted wave approach study 7-62532
 He, positron impact excitation of 2¹S and 2¹P states, distorted wave approximation. calcs. 7-36795
 He, positron impact triplet-triplet excitation 7-36789
 He, positron mobility edge, Monte Carlo simulation 7-44086
 He, positron scattering, cross-section meas. 7-20054
 He, positron scattering, inelastic and superelastic, calcs. 7-36790
 He-Kr bicomponent system, electron thermalisation processes obs. by pulse-radiolysis microwave cond. method 7-20051
 He-like ions, electron excitation, distorted-wave polarised orbital approach 7-62531
 He-N₂ mixtures, metastable the electron impact excitation coeffs. 7-20059
 He-Zn metal vapor mixture, laser excitation by electron guns 7-26534
 He+Na(K)(Pb)(Cs), inelastic collisions at thermal energies 7-983
 Hg, discharge, low-pressure, excited state pop. mechanisms determ. using pulsed optical pumping 7-26557
 Hg, electron scatt., relativistic effects, Kohn-Sham theory 7-42765
 Hg⁺, Beutler spectral lines, electron impact excitation fn. 7-20056
 Hg⁺, electron impact cross sections of spectral lines and excited states 7-25659
 Hg²⁺, Beutler spectral lines, electron impact excitation fn. 7-20056
 Hg²⁺, electron impact cross sections of spectral lines and excited states 7-25659
 K, 4 ²P impact excitation by polarised electrons, fluoresc. polarisation study 7-31177
 k, electron scatt., relativistic effects, Kohn-Sham theory 7-42765
 K, plasma, electron collisions, momentum transfer cross sections, expt. data fit 7-20845
 K⁺, effective electron inelastic excitation cross section, resonance effects study 7-42772
 KI, electron impact, line shifts and widths, Stark broadening study (*French*) 7-10500
 Kr, electron impact, low energy, in afterglow 7-20060
 Kr, electron impact excitation into metastable states effective cross sections 7-36775
 Kr, electron scatt., cross section meas. 7-31171
 Kr, electron scatt., intermediate energy, elastic and inelastic, differential cross-sections 7-25648
 Kr gas, electron beam deposition 7-5771
 Kr ion, O-like, electron impact excitation, coupling effects 7-982
 Kr²⁸⁺, electron impact excitation cross sections, CI calcs. 7-36493
 Li, double electron excitation cross section, distorted wave approach 7-50379
 Li, positron inelastic scatt., calc. of angular correlation parameters 7-15723
 Liq. Ar, effective momentum transfer cross section for excess electrons 7-21956
 Mg³⁺, electron impact excitation rate coeffs. 7-55455
 Mg⁴⁺, electron impact excitation rate coeffs. 7-55455
 Mg-like ions, electron impact excitation, LS coupling, distorted wave approx. 7-42767
 Na, 3²P state, electron impact excitation, differential cross section and alignment parameter meas. 7-20052
 Na, electron scatt., relativistic effects, Kohn-Sham theory 7-42765

atomic electron impact excitation continued

- Na, optically pumped, spin-polarised electron scatt., state selection 7-25663
 Na-like ions, electron excitation rates rel. to relative emission-line strengths for Al III and Si IV in Sun 7-47799
 Ne, electron impact excitation, metastable state, laser induced fluoresc. 7-50372
 Ne, electron impact induced post-collisional KL_{2,3}L_{2,3} Auger decay 7-5773
 Ne, electron scatt., cross section meas. 7-31171
 Ne, electron thermalisation processes obs. by pulse-radiolysis microwave cond. method 7-20051
 Ne gas, electron beam deposition 7-5771
 Ne⁺, excess electron localisation, QUPID calcs. 7-20029
 O, atomic excitation by electron impact, the ³P-¹S transition 7-50368
 O, atomic excitation by electron impact, the ³P-³S^o transition 7-50369
 O⁺, electron impact excitation cross sections, R-matrix method calcs. 7-50375
 O³⁺, electron-impact ionisation, excitation-autoionisation contrib. 7-978
 Pb, electron scatt., relativistic effects, Kohn-Sham theory 7-42765
 Rb⁺, effective electron inelastic excitation cross section, resonance effects study 7-42772
 SO₂, electron scatt., low energy, absolute total cross-sections meas. 7-25650
 Se XXV plasma, laser produced, electron impact, laser transitions 7-26508
 Si plasma, laser prod., electron density sensitive emission line ratios 7-32081
 Ti II, electron impact, 6¹S₀-6³P₁ intercombination transition excitation resonance obs. 7-36778
 Xe, 90° scatt. angle excitation functions 7-25662
 Xe, electron impact excitation cross-sections 7-25661

atomic electron impact ionisation

- see also *electron spectra*
 Ar, gas, doubly-ionised by electron impact, spectral line Stark broadening meas. 7-62320
 atoms and ions, electron impact total and partial ionisation cross sections 7-60897
 binary ionisation processes, correl. effects, semiclassical description 7-36779
 charged particles, heavy, inelastic scatt., quasiclassical statistical model 7-15728
 cross sections and rate coeffs. determ. 7-57180
 dipolar reactions, triple differential cross sections Born approx. 7-50370
 electron-atom collisions in external laser field, n-phonon processes 7-50038
 energy partitioning deviations, electron motion eqns. 7-15720
 heavy target, boundary layers arising when intermediate energy beam is stopped 7-16292
 intensity ratio and ionis. cross section meas. 7-57178
 ionising collisions, electron vel. distrib., energy partition effect 7-989
 laser assisted atomic physics studies at Griffith University 7-20073
 light elements, electron impact K-shell ionisation cross-sections, anal. appls. 7-25666
 medium and heavy elements, L-subshell ionisation cross sections, X-ray spectra anal. 7-30977
 momentum spectroscopy, differential cross section 7-36771
 positron and positronium atomic physics 7-36783
 positron-atom scatt., partial cross sections 7-36788
 positron-gas collisions, charge exchange, ortho-positronium form. 7-62513
 positron-gas system, EM wave irr., positron distrib. 7-36761
 positronium, in ethane gas, cavities rel. to orthopositronium annihilation rates 7-36824
 positrons in gases 7-36782
 Rydberg series, electron scatt., Stark broadening reson. struct. 7-50009
 Ag, electron inelastic scatt. cross-sections 7-5775
 Al, electron inelastic scatt. cross-sections 7-5775
 Al⁺, electron impact ionisation, absolute cross-section meas. 7-25667
 Ar, double ionisation by single electron impact 7-62526
 Ar, electron impact ionisation, cross sections, fast-neutral beam method, TOF spectra 7-42769
 Ar, fast electron bremsstrahlung cross sections 7-36780
 Ar gas, thermalised free positron annihilation rate studies 7-50390
 Ar, metastable ions, optical pumping in hollow cathode discharge 7-30990
 Ar, metastable population meas. and flow instability due to shock wave, comparison with models 7-16207
 Ar, positron annihilation and diffusion, computer-based anal. 7-50378
 Ar, positron drift and diffusion in crossed elec. and mag. fields, simulation 7-36760
 B²⁺, electron-impact ionisation, excitation-autoionisation contrib. 7-978
¹³⁸Ba, laser-excited, electron impact ionisation cross section, hyperfine levels 7-36776
 Br, electron impact ionisation cross sections meas., TOF spectra 7-42770
 C, electron inelastic scatt. cross-sections 7-5775
 Cd⁺, electron impact ionisation, absolute cross-section meas. 7-25667
 Cl, electron impact ionisation cross sections meas., TOF spectra 7-42770
 Cs⁺, electron impact s-ionisation, ultrasoft X-ray spectroscopy study (*Russian*) 7-984
 F, electron impact ionisation cross sections meas., TOF spectra 7-42770
 Fe, multiply charged ions, electron-impact ionisation, excitation energies and cross section calcs. 7-25425
 Fe, multiply-charged ions, electron-impact ionisation cross sections, crossed-beam meas., rate coefficient calcs. 7-25660
 Ga, electron impact ionisation function meas. 7-50367
 H, effects in flaring solar chromosphere 7-34843
 H, fast electron impact ionisation, higher-order effects 7-50371
 H, ionisation by electron and positron collisions, cross. section calc. 7-15726
 H, positron annihilation, computer expt. 7-36791
 H, positron impact ionis. cross section 7-36793
 H, positron impact ionisation, Faddeev formalism calcs. 7-36794
 H, second Born triple-differential cross section meas. 7-57179
 H, triple differential cross sections, coupled pseudostate calcs. 7-50376
 H, triple differential cross section at intermediate energies 7-62528
 He atom, positron impact ionisation 7-36786
 He, autoionising states, use of virial theorem in wavefunction calcs. 7-25465
 He, electron impact autoionisation, triple differential cross sections, first-order model calcs. 7-25466

atomic electron impact ionisation continued

- He, electron impact ionisation, intermediate energy 7-25664
 He, electron impact ionisation, distorted-wave impulse approx. 7-31175
 He, electron impact ionisation, cross sections, fast-neutral beam method, TOF spectra 7-42769
 He, electron impact ionisation cross section, modified-Glauber-approx. study, higher-order effects 7-42771
 He, electron impact triple differential ionisation cross-section calcs. 7-36773
 He, fast electron impact ionisation, triple differential cross section calcs. 7-25657
 He, fast electron impact ionisation, triple differential cross sections, Coulomb wave fns. calcs. 7-50365
 He, ionisation by positron impact, partial cross-section meas. 7-36777
 He, ionisation by positron impact 7-36785
 He, low energy triply differential electron impact ionisation cross sections 7-15722
 He, metastable state, positive column, ionis. process investig. 7-20057
 He, positron collisions, positronium form. cross sections 7-15724
 He, positron thermalisation and annihilation 7-63245
 He, positronium form. by positron scatt., cross-section calcs. 7-36796
 He, total ionisation cross sections for positrons 7-36787
 He⁺, ionisation by electron and positron collisions, cross. section calc. 7-15726
 He-H mixtures, positron annihilation, simulation 7-36792
 Hg, clusters form., mass spectra study 7-50430
 Hg, electron impact ionisation efficiency curves, reson. struct. 7-5774
 Hg⁺, electron impact ionisation, absolute cross-section meas. 7-25667
 I, electron impact ionisation cross sections meas., TOF spectra 7-42770
 In, electron impact ionisation function meas. 7-50367
 K⁺, electron impact s-ionisation, ultrasoft X-ray spectroscopy study (*Russian*) 7-984
 Kr, electron impact ionisation, cross sections, fast-neutral beam method, TOF spectra 7-42769
 Kr, gas, doubly-ionised by electron impact, spectral line Stark broadening meas. 7-62320
 La, fast electron bremsstrahlung cross sections 7-36780
 Li, electron impact ionisation, positronium form. 7-31176
 Li, positron impact, positronium form. cross-sections 7-36797
 N³⁺, intrashell autoionis. levels, electron scatt. 7-50030
 N⁶⁺, intrashell autoionis. levels, electron scatt. 7-50030
 Ne, electron impact ionisation, cross sections, fast-neutral beam method, TOF spectra 7-42769
 Ne, gas, doubly-ionised by electron impact, spectral line Stark broadening meas. 7-62320
 Ne gas, thermalised free positron annihilation rate studies 7-50390
 Ne, positron thermalisation and annihilation 7-63245
 O⁵⁺, electron impact ionisation, excitation-autoionisation contrib. 7-978
 Pd isoelectronic series, 4¹⁰ subshell, photoionis. and electron impact ionis. 7-902
 Rb⁺, electron impact s-ionisation, ultrasoft X-ray spectroscopy study (*Russian*) 7-984
 S_n clusters, fragmentation investig. 7-15792
 V, electron inelastic scatt. cross-sections 7-5775
 Xe, electron impact ionis., partial cross section meas. 7-62530
 Xe, fast electron bremsstrahlung cross sections 7-36780
 Xe, gas, doubly-ionised by electron impact, spectral line Stark broadening meas. 7-62320

atomic electron scattering *see* **atomic electron impact excitation**; **atomic electron impact ionisation**; **elastic scattering of electrons by atoms and molecules**

atomic emission spectroscopy

- (201) plane study using LEED, AES and angle-resolved UPS, Fermi wave vector determ. 7-58846
 airborne particles, ICP emission spectrometry investig. 7-54233
 atmospheric deposition of inorganic contaminants, anal. using nuclear techniques 7-34092
 atmospheric microwave plasma emission characteristics in near IR 7-55318
 free-resistant material, Sb₂O₃ influence on effectiveness, chem. anal. (*Russian*) 7-65378
 ICP-AES, microcomputer-controlled dual-channel monochromator 7-54236
 ICP-AES, weighted lin. regression, review 7-8347
 internal standard element selection and evaluation, plasma emission spectrometric anal. 7-28363
 modulated sample introduction system for ICP atomic emission spectrometry 7-61384
 ocean water, synthetic, AES study using solution nebulisation 7-13835
 scattered radiation, theory 7-33987
 selective line modulation atomic spectrometry, noise sources 7-61383
 selective spectral line modulation, sample modulation appls. 7-61382
 solution spectrochemistry, at. emission sources 7-15004
 spectral analysis, computer calcs. 7-46910
 spectrometer design for atomic emission spectrosc., spectral characts. 7-35601
 ultrasonic nebulization of liquid samples for analytical inductively coupled plasma-atomic spectroscopy: anupdate 7-8350
 AgCl films deposited by evaporation and RF sputtering, compositional and morphological anal. 7-16892
 Ca, ground state, ICP atomic fluoresc. spectrometry 7-54234
 Ca, spatial distrib. profiles, ICP atomic emission and fluoresc. 7-54235
 Fe, inductively coupled plasma, emission, computer simulation 7-8348
 KCl, solute trapped from air-acetylene flame, morphological investig. 7-28362
 Li, isotopic anal., SES-ICP investig. 7-46908
 Pb, particulate and gaseous, in exhaust gas determ., plasma emission and atomic absorpt. spectrometry 7-59803
 Rb_{0.3}MoO₃, (201) plane study using LEED, AES and angle-resolved UPS, Fermi wave vector determ. 7-58846
 Sr, ground state, ICP atomic fluoresc. spectrometry 7-54234

atomic energy *see* **nuclear power**

atomic excited states

- see also* **atomic metastable states**; **atomic resonant states**
 alkali metal atom-He system, Rydberg energy levels, Coulomb and Coulomb-Stark-Green fn. 7-42476
 alkali metal atoms in rare gas matrices, Rydberg states, model pot. 7-5737
 atom passing through thin film, radiation excitation 7-42738

atomic excited states continued

- atom-ion collisions, excited state prod. by negative ion detachment 7-15686
 atomic impurities in Ne, optogalvanic effect 7-30970
 atomic lineshape, convergent anal. of radiative matrix elements 7-19774
 atomic multipole transitions, positions of minima in multipole matrix elements 7-36550
 cascade Zeeman quantum beats, stepwise pulsed-laser excitation, four-level model 7-50014
 coherent three-level J-C model, analytic solns. 7-49964
 cooperative radiation from three identical two-level atoms, near-field and super-radiance effects 7-15579
 dense plasma, atomic species description model 7-63255
 dielectronic recombination in elec. fields, quantum defect theory 7-62527
 dipole polarisability of atoms and ions, ionis. pot. correl. 7-42529
 discrete states in the continuum, generation by coupling of bound states 7-36509
 excited atom reaction dynamics, charactn. by laser induced fluoresc. 7-46836
 four-level atoms, multiphoton processes, fluoresc. spectra calcs. 7-62318
 four-level velocity-selective atomic model, nonstationary effects, time-dependent anal. 7-36555
 highly charged ions, excited-state stability and X-ray lasers 7-31305
 hydrogenic Zeeman effect, second-order perturbation calc. 7-50012
 K, 4²P impact excitation by polarised electrons, fluoresc. polarisation study 7-31177
 laser excitation dynamics of at. and mol. clusters in free jets 7-42823
 laser spectroscopy, conf., Maui, HI, USA, June 1985 7-9586
 light negative ion formation using Rydberg atoms 7-10707
 local frequency redistribution in reson. line photons, elastic collisions effects 7-10757
 magnetic substates for radiative transition with arbitrary polarisation 7-5639
 metals, sputtering by ion bombardment, excited states of sputtered atoms 7-7807
 mixed states, spatial separation into coherent components in field of traveling radio wave 7-49967
 molecule-ion collisions, excited state prod. by negative ion detachment 7-15686
 multi-level atom, randomly modulated, second order optical process 7-50522
 nonidentical two-level atoms, retarded and nonretarded interactions 7-31142
 one-atom maser, quantum collapse and revival, observation 7-43041
 open-shell atoms, ions and excited states, photoionisation 7-36562
 optical susceptibility saturation in strong amplitude-modulated fields, matrix continued fractions anal. 7-20371
 oscillator strengths, transition energies and probabilities, CI STO calcs. 7-25423
 perturbation-theory method of calculating the energies and excitation energies of atomic, molecular, and solid-state systems 7-5596
 photoionisation, threshold effects in strong-field, non-perturbative realistic model 7-36563
 polarised light, radiative transfer, obs. 7-1382
 positive ions, Z=2 to 50, quantum defect values 7-24323
 light rare earths, L_{γ23} satellite, X-ray emission spectra anal. 7-36523
 reaction channel with attractive Coulomb force, threshold continuity theorems 7-10697
 Rydberg atom, QED model testing 7-10458
 Rydberg atom circular, stability in vanishing elec. field. 7-49966
 Rydberg atom in gas discharge, optogalvanic diagnostics 7-32187
 Rydberg atom two-photon micromaser theory 7-50526
 Rydberg atoms, props. and quantum optics 7-1064
 Rydberg atoms, QED approach to energy level calcs. 7-62302
 Rydberg atoms, Stark effect, electron-ion resonance scatt., WKB calcs. and multichannel quantum-defect theory 7-15546
 Rydberg atoms in elec. polarised states 7-24475
 Rydberg atoms near metal surface, quasi-stationary spectrum 7-49984
 Rydberg formula, revised for two-electron [core]n² systems, binding energy calcs. 7-25435
 Rydberg masers, at. and field fluctuations, squeezed radiation source 7-10905
 Rydberg series, electron scatt., Stark broadening reson. struct. 7-50009
 Rydberg state prod. classical limit 7-876
 Rydberg states, dipolar and quadrupolar elec. transition, radial integrals (*French*) 7-10455
 Rydberg states, high-lying, generation and decay in beam-foil encounters 7-49965
 Rydberg states with high quantum numbers in external fields (*German*) 7-19732
 screened Coulomb potential, energy levels and oscillator strengths calcs. 7-25628
 single-quantum transition, spectral line contour, QED theory 7-50020
 small-sample superradiance, dipole-dipole interaction, statistical anal. 7-57282
 spatially nonuniform excitation, effective lifetimes, approx. calcs. 7-30964
 spin-dependent interactions, I^N configs., matrix elements identities 7-42515
 super-dense hollow cathode discharge, plasma light amplification (*Japanese*) 7-6476
 three-level atoms, chaos and interaction with self-consistent fields 7-15556
 transition and ionisation energies, g-Hartree ab initio calcs. 7-15488
 two-electron atoms, excited states interdimensional degeneracies and near degeneracies 7-14808
 two-electron atoms, rigid body solns., electron equilib. constellations derived 7-30958
 two-level atom density matrix eqns., frictional force and hysteretic effects in a standing light wave field 7-42563
 two-level atoms, excited, microscopic maser theory 7-15837
 two-level atoms, quantum evol., state selective reservoir effect 7-15835
 two-step excitation alignment factors 7-62305
 vacuum UV light polarisation, freq. conversion and fluorescence studies 7-10849
 Al, level energies and oscillator strengths, coupled channel model calcs., energy depend. sensitivity 7-49906
 Ar, 3s-subshell excitation, photoabsorption spectra anal., HF calcs., config. interaction calcs. 7-30947
 Ar, excitation energies, coupled cluster method calcs. 7-49893
 Ar, H-like and doubly excited He-like, dielectronic satellite spectra, transition rates and energies 7-51512

atomic excited states continued

- Ar⁺+Ne, time of flight energy spectra, long lived excited Ar⁺ state 7-62486
- Ar⁺He(Ne), charge exchange into excited states in collisions 7-31155
- As I, fine structure analysis 7-15529
- Au + Ne⁺(N₂⁺), impact ionisation, L₃ subshell alignment, coupled states anal. 7-25643
- B III, core excited quartet and doublet state, beam-foil study 7-42514
- Ba autoionising states, internal conversion and fluoresc. two-step process 7-25467
- Ba, double Rydberg states, ionisation, two-photon and TOF mass spectra 7-19809
- Ba, doubly excited states, electron correl., laser spectra 7-10459
- Ba, doubly excited states, two-photon laser excitation spectra (French) 7-10474
- Ba neutral atoms, high-lying states, laser pumped, two-photon spectra 7-19811
- ¹³⁸Ba, laser-excited, electron impact ionisation cross section, hyperfine levels 7-36776
- Ba+Ar, collisional redistrib., laser-induced fluoresc. 7-62492
- BaI, highly excited levels, two-channel quantum defect method 7-57010
- Be, ³P^o and ¹P^o Rydberg series, autoionising states, complex eigenvalue Schrödinger eqn. soln. 7-62329
- Be, electronic energy, Green's fn. calc. 7-10445
- Be I isoelectronic series, atomic and spectral data for typical tokamak plasma conditions 7-24322
- Be III, transition wavelengths among doubly excited states 7-49980
- Br, photodissoc., initiated by laser emission 7-65339
- Br, photodissoc. prod. electronic states, Raman spectra anal. 7-42530
- C, double excitation and ionisation by strong pulsed laser 7-42571
- Ca atomic beam, optical frequency standard based on Ramsey excitation 7-14925
- Ca, laser-XUV excited state spectroscopy 7-19746
- Cl isoelectronic sequence, allowed 3-3 transitions, Slater parameter optimisation, HF CI calcs. 7-48205
- Cl, Rydberg states transition, 6.7 μm, obs. 7-42538
- Co, level energies and oscillator strengths, coupled channel model calcs., energy depend. sensitivity 7-49906
- Cr²³⁺, dielectronic satellite spectra CI HFS calcs. 7-42506
- Cs, 5s ionisation, PES satellite struct., CI approach 7-62296
- Cs highly excited atoms as coherent radiations source, superradiative transitions 7-57027
- Cs, highly forbidden 6S_{1/2}-7S_{1/2} transition atomic parity violation meas. 7-31184
- Cu, resonant photoemission, atomic correl. effect 7-907
- D, resonant IR two-photon ionisation 7-15573
- F I, excited levels, photoionisation cross-sections, Thomas-Fermi calcs. 7-10423
- F VI, 2nd Rydberg series correl., HF-term energy separation 7-30939
- Fe I, cascade Zeeman quantum beats, stepwise pulsed-laser excitation, fluoresc. anal. 7-49997
- Fe I, II, excited state level populations in ICP discharge 7-30963
- Fe II, electron impact excitation, collision strengths, R matrix method, CI calcs. 7-25424
- Fe II, energy levels for UV doubly excited lines in laboratory and in A-type star 21 Peg 7-66585
- Fe XV, oscillator strengths, transition energies and probabilities, CI STO calcs. 7-25423
- Fe⁺, excited state selected, one-colour UV multiphoton ionis. 7-36506
- Ga, radiative lifetimes, fluoresc., MCHF calcs. 7-30946
- Gd, autoionising states, electric field effects, UV spectra anal. 7-42531
- Ge I, odd parity energy levels, precise spectroscopic assignments 7-846
- H degenerate Rydberg states spectrum in crossed fields 7-25437
- H, diamagnetic Rydberg states, meas. and calcs. 7-5615
- H, electric field effects, Feynman path-integral formalism 7-42547
- H, electron impact excitation, excited state polarisation and ang. correl. 7-36772
- H, electron impact excited, polarisation and ang. correl. relations 7-31170
- H, electronic states in uniform mag. field, cylindrical adiabatic approx. calcs. 7-42479
- H excited state, laser spectroscopy in mag. field 7-10460
- H, excited state, translational energy distrib. in DC discharge, spectroscopic meas. 7-20946
- H excited states, 1D atom construction using external electric fields 7-19730
- H excited states, photoionisation in strong elec. fields 7-10526
- H, ion recomb. and level pops., role of charge exchange 7-31925
- H ions, Stark-broadening effect, simulation technique applied to models for Lyman α line 7-15721
- H, mesic 2 s state, elastic and inelastic slow electron scatt. 7-10781
- H, microwave ionisation of highly excited states, stochastic effects 7-15562
- H Rydberg atom, Lamb shift in waveguides 7-10458
- H, Rydberg atoms, low-velocity charge transfer, classical scaling failure 7-15707
- H Rydberg states, Doppler-free two-photon spectra 7-10533
- H Rydberg states, Rydberg constant determ. by two-photon spectroscopy 7-25433
- H, Stark effect and field ionis. 7-5628
- H, Stark effect in strong field 7-50008
- H⁺, ¹P^o symmetry, Wannier two-electron ionis. ladder, wave fn. calc. 7-62274
- H⁺, two-electron doubly excited states, quantum number classification 7-49886
- H-like ions, spontaneous emission spectral line, natural broadening shape 7-42541
- H+Ar(N₂)(CO₂)(SF₆), Rydberg atom depopulation, scattering cross section. 7-10732
- H₂⁺+He, elastic and inelastic scatt. mechanisms, energy loss spectra 7-15671
- H*, excited fragment from mol. dissoci., effect on electron impact excitation cross-sections 7-25671
- He⁺ + Ne(Ar), charge exchange into excited states in collisions 7-31155
- He, ¹P^o symmetry, Wannier two-electron ionis. ladder, wave fn. calc. 7-62274
- He, 3 ³P state lifetime, electron-photon delayed coincidence technique meas. 7-62533
- He, 3D state electron impact excitation, electron-polarised photon coincidence study 7-36774

atomic excited states continued

- He collisional depopulation rate by Rb thermal collisions (German) 7-15694
- He, collisions with fast, highly charged ions, electron capture to the continuum meas. 7-20026
- He, double excited states, correl. wavefunction calcs. (French) 7-10454
- He doubly excited states, electron impact excitation, generalised oscillator strengths 7-873
- He, electron impact excitation, excited state polarisation and ang. correl. 7-36772
- He, electron impact excitation, fine-struct. effect, electron spin polarisation fn. 7-50374
- He, electron impact excitation, Stokes' parameters, electron-photon coincidence spectra anal. 7-50377
- He I, transition wavelengths among doubly excited states 7-49980
- He I excited states in He-Se laser discharge, population density ratios determ. from Kirchhoff's law 7-58072
- He isoelectronic sequence, relativistic second-order many-body corrections 7-870
- He isoelectronic series, electron scatt., plasma screening effect, distorted wave approach study 7-62532
- He, photoelectron satellites at threshold, photoelectron spectra anal. 7-36564
- He, photoelectron satellite branching ratios, asymmetry parameters, UV PES anal. 7-62333
- He, plasma, collision induced transitions between singlet and triplet levels, laser fluoresc. 7-20846
- He, plasma, excited state lifetimes determ. 7-20947
- He Rydberg state, absolute photoionisation cross section 7-62331
- He, transition probabilities and oscillator strengths, for singly excited states 7-48207
- He, two-electron doubly excited states, quantum number classification 7-49886
- He-like ions, double-excited, electron correl. 7-19722
- He-like ions, energy level population autoionisation states (French) 7-10518
- He+C⁶⁺(Ne¹⁰⁺) electron capture, bound and continuum states, impulse approx. 7-50329
- He+NH₃, Rydberg atom ionis., rot. deexcitation 7-36737
- He+Na(K)(Pb)(Cs), inelastic collisions at thermal energies 7-983
- He+Rb, afterglow, inelastic collisions quenching cross sections 7-42746
- ⁴He, three atoms interacting through intermol. pot., Efimov state 7-5738
- ⁴He⁺, odd-parity coherence in beam-foil excitation 7-909
- He*+Ne, collisions, nonadiabatic transitions 7-62487
- Hg, discharge, low-pressure, excited state pop. mechanisms determ. using pulsed optical pumping 7-26557
- Hg discharge, low-pressure, laser diagnostics 7-58085
- Hg, excited atoms, superelastic electron collisions, plasma prop. meas., plasma electron spectroscopy 7-20852
- Hg, in N₂-Kr matrix, electronic-to-vibr. energy transfer and relax., fluoresc. spectrum 7-49985
- Hg⁺, electron impact cross sections of spectral lines and excited states 7-25659
- Hg²⁺, electron impact cross sections of spectral lines and excited states 7-25659
- Hg+Hg(Ar)(N₂), 6s6d and 6s7d states, collisional quenching 7-36730
- Ho, ionic bombardment, continuous spectrum form. 7-42528
- I, (²P_{1/2}) state, absolute yield from I₂ photodissoc., optoacoustic spectrosc. meas. 7-49963
- I, photodissoc., initiated by laser emission 7-65339
- In sputtered excited neutral atoms vel. distrib. meas. and deexcitation model calcs. 7-875
- K, Rydberg state, avoided crossings in elec. field using blackbody radiation 7-15558
- K+K(Rb), Doppler free two-photon spectra, freq. shift, line broadenings 7-57155
- Kr, 3p excitation, multiple photoionisation cross sections, TOF mass spectrometer anal. 7-19802
- Kr, atom, multielectron photoelectron meas. 7-5643
- Kr, photoionization cross sections of excited states, UPES anal. 7-50241
- Kr, Rydberg states, four-photon excitation 7-62328
- Kr²⁸⁺, electron impact excitation cross sections, CI calcs. 7-36493
- Kr⁴⁺+He(Ne), state-selective electron capture, translational energy spectra 7-50337
- Li + He(Ne), electric field effect, fluoresc. and radiative decay rate determ. 7-20009
- Li, excited states, electron correlation calc. (Chinese) 7-10438
- Li, excited states, quantum defect and isotopic shift meas., millimeter wave ODR spectroscopy 7-15538
- Li, high-freq. Stark effect, laser-induced fluoresc. anal. 7-36529
- Li II, transition wavelengths among doubly excited states 7-49980
- Li Rydberg states, collisional line broadening, trilevel photo. echo meas. 7-19772
- Li⁺, ¹P^o symmetry, Wannier two-electron ionis. ladder, wave fn. calc. 7-62274
- Li-like ions, first excited state, intra- and inter-shell correl. effects 7-62295
- Mg, ¹P doubly excited autoionisation states, CI calcs. 7-36497
- Mg, 3snl excited series, CI HF calcs. 7-36496
- Mg, autoionising Rydberg states, reson. ionisation mass spectrometry 7-19785
- Mg, excitation energies, coupled cluster method calcs. 7-49893
- Mg II, core-excited states, energy levels and lifetimes, HF calcs. 7-867
- Mg, spectra struct. and isotope shifts, many-body perturbation theory calcs. 7-50019
- Mg-like ions, energy levels, model-pot. relativistic perturbation calcs. 7-24320
- Mo I, lifetimes, branching ratios and transition probabilities 7-36692
- Na, 3²P state, electron impact excitation, differential cross section and alignment parameter meas. 7-20052
- Na, 3P state, photoionization polarization and correlation characteristics, energy dependence 7-5648
- Na, collisionally aided coherent atomic optical emission 7-42561
- Na, excited atom, quenching and time resolved fluoresc. 7-30983
- Na, excited state, collisional repop. upon laser-pumping in H₂-O₂-Ar flame 7-62325
- Na highly excited atoms as coherent radiations source, superradiative transitions 7-57027
- Na impurity in vibrationally nonequilibrium N₂ jet, excited state population and deactivation 7-42744

atomic excited states continued

- Na ion beam generation, field ionisation of laser-excited Rydberg atoms 7-57186
 Na ion formation in vapour containing laser selected Rydberg atoms 7-10462
 Na, laser excitation, competition between photoionization and two-photon Raman coupling 7-10529
 Na, optical piston dynamics using light-induced drift 7-10508
 Na, two-photon-excited state trilevel echo 7-19808
 Na vapour, laser-excited, anomalous blue shifted emission near D_1 transition 7-49996
 Na, vapour, light-induced current calcs. and meas. 7-44096
 Na-like ions, Rydberg states, dynamic polarisability, HF calcs. 7-62273
 Na+Na collisions, Rydberg state forbidden transitions in laser-assisted processes 7-5617
 Na+Ne⁺, impact excitation, spin exchange, fluoresc. spectra anal. 7-25450
 Na+Ne⁺(Ar⁺)(Xe⁺), Rydberg electrons removal, cross section meas. 7-36742
 NaI core-excited states, energy levels and lifetimes, HF calcs. 7-867
 Ne, 2p³3d level population in Hf discharge afterglow, press. depend. 7-20853
 Ne, high-frequency discharge, dissoc. recomb. of excited atoms in afterglow 7-10456
 Ne, optical saturable absorpt. in difference magnetooptic reson., relax. const. calc. 7-62793
 Ne, photoelectron satellites at threshold, photoelectron spectra anal. 7-36564
 Ne, plasma, Stark broadening and shift parameters, visible spectra anal. 7-62310
 Ne pulsed transverse discharge, population inversion, secondary process influence 7-58084
 Ne⁺+He(Ar), charge exchange into excited states in collisions 7-31155
 Ne⁺+He, transfer excitation in low-energy collisions, spectroscopic meas. 7-15696
 Ne*+He, collisions, nonadiabatic transitions 7-62487
 Ne** He-like, X-ray and Auger transition rates 7-36507
 Ne**+He, polarization effects in collision-induced intramultiplet mixing 7-5749
 O⁺, electron impact excitation cross sections, R-matrix method calcs. 7-50375
 Pr³⁺, excited state, NMR meas. by indirect optical detect. 7-15545
 Ra, photoionisation, 20-channel relativistic random phase calcs., interchannel coupling 7-36566
 Rb excited states, radiative lifetimes, depopulation cross sections, fluoresc. 7-10502
 Rb, vap., optically pumped, reson. quality factor optimisation 7-42564
 Rb-Xe laser-enhanced spin-exchange collisions 7-10453
 Rb+Rb(K), Doppler free two-photon spectra, freq. shift, line broadenings 7-57155
 Si isoelectronic sequence, allowed 3-3 transitions, Slater parameter optimisation, HF CI calcs. 7-48206
 Si, level energies and oscillator strengths, coupled channel model calcs., energy depend. sensitivity 7-49906
 Sm³⁺+Xe collisions, q=34 to 52, resonant electron transfer and L-shell excitation, X-ray spectra study 7-30979
 Sr, autoionising series, multichannel quantum-defect theory model data fit, UV PES study 7-62334
 Sr, Rydberg states with n/100, laser spectroscopy 7-10461
 Sr+Ar, ¹P fluoresc. line broadening, ab initio close-coupled scatt. calcs. 7-36494
 T, spin-polarised hypernuclear-atom systems, Efimov effect 7-31189
 Ti⁺ excited state selected, one-colour UV multiphoton ionis. 7-36506
 Ti, interaction pot. diffusion coeffs. in inert gases 7-31913
 Tm+Ne(Xe), excited state transition cross sections, nonreson. fluoresc. 7-42540
 V⁺, excited state selected, one-colour UV multiphoton ionis. 7-36506
 Xe, 4p excitation, multiple photoionisation cross sections, TOF mass spectrometer anal. 7-19802
 Xe, 90° scatt. angle excitation functions 7-25662
 Xe, J=0 autoionisation, multichannel-quantum-defect theory anal. 7-36559
 Xe, Rydberg states, four-photon excitation 7-62328
 Y I, II excited levels, lifetimes meas. 7-50021
 Yb, ³P₁-¹S₀ transition, oscillator strength, lifetime, coherent optical techniques and fluoresc. spectra 7-42542
¹⁷⁴Yb+He(Ar), collisional velocity thermalisation, echo techniques 7-36732
 Zn XII to XX, wavelength and energy levels 7-49981

atomic explosions see *nuclear explosions***atomic fine structure**

- coherent transients meas. with ultrashort light pulses 7-31187
 hot laser-produced plasmas, Stark-broadened Lyman line asymmetry 7-63356
 model atom, radiative properties, external magnetic field and monochromatic radiation field 7-19694
 Rydberg atoms, QED approach to energy level calcs. 7-62302
 Ar+Ne*(3s³P₂, ³P₀), ionis., fine struct. depend. product branching 7-15673
 Ar⁺+Ar, absolute spin-orbit state excitation cross sections, fine-struct. 7-42730
 Ar⁺+N₂, absolute spin-orbit state excitation cross sections, fine-struct. 7-42730
 As I, fine structure analysis 7-15529
 Be isoelectronic series, fine struct. multiconfigurational DF calcs. 7-62266
 Bi, low-energy electron elastic scatt. calcs. 7-50362
 Ca⁺, 4p-3d triplet, broadening by He 7-62323
 Cs atoms laser spectroscopy of 109.1 nm transition 7-19745
 Fe II, electron impact excitation, collision strengths, R matrix method, CI calcs. 7-25424
 Fr, second resonance doublet, wavelength meas. fine-, hyperfine structure, isotope shifts 7-57020
 Ge I, odd parity energy levels, precise spectroscopic assignments 7-846
 H⁺+He⁺(Ne⁺)(Ar⁺)(Fe²³⁺), Fine-struct. excitation, plasma screening effects, ion-sphere and Debye-Huckel models 7-62509
 He, 1 s4d config. fine struct., Zeeman sublevels crossing fields 7-50015
 He, electron impact excitation, fine-struct. effect, electron spin polarisation fn. 7-50374

atomic fine structure continued

- He-like ions, radiative corrections, multiconfigurational DF study 7-62299
 He+Ca⁺(Mg⁺), pot. curves reson. line broadening and shift parameters 7-50302
 Hg, low-energy electron elastic scatt. calcs. 7-50362
 Hg+Hg(Ar)(N₂), excitation transfer between fine struct. states, fluoresc. spectroscopy 7-62504
 K⁺, electron affinity and photodetachment cross sections, ab initio multichannel calcs. 7-36463
 K+Ar(He), fine-struct. transitions, differential cross section meas. 7-62493
 K+inert gas, 5²P_{1/2}-5²P_{3/2} fine struct. mixing 7-50306
 Kr XXIX 2s²2pⁿ-2s2pⁿ⁺¹ transition meas. 7-880
 Kr XXVIII 2s²2pⁿ-2s2pⁿ⁺¹ transition meas. 7-880
⁷Li II, absolute wavelength determination, fine struct. determ. 7-10771
 Mg, config., fine struct. parameters Zeeman sublevel energies 7-36543
 Mg isoelectronic series, energy levels, multiconfig. optimised pot. model calcs. 7-19723
 Mg, spectra struct. and isotope shifts, many-body perturbation theory calcs. 7-50019
²⁴Mg fine structure transition via linear Ramsey interrogation 7-884
 Na-He(Ne)(Ar), optical collisions, fine struct. branching cross-sections, nonadiabatic theory 7-959
 Na+He(Ne)(Ar)(Kr)(Xe), fine-struct. branching ratios, meas. 7-15676
 Na+Rg optical collisions, (RG = He, Ne, Ar, Kr, Xe), fine struct. branching ratio determ. 7-10704
 Na+Xe, Na D lines, collisional broadening, fine-struct. mixing, depolarisation 7-62503
 Pb, low-energy electron elastic scatt. calcs. 7-50362
 Rb+H₂(D₂), fine-structure transition cross-sections, quantum-mechanical calcs., importance of perturber rotational levels 7-57161
 Tl, low-energy electron elastic scatt. calcs. 7-50362
 ZnSe:Mn, ⁴F states, spin-orbit interactions and dynamical Jahn-Teller effect 7-21875
- atomic fluorescence**
 7-30985
 atomic vapour, lifetime determ., fluoresc. study 7-36546
 Autler-Townes doublet, transient suppression under resonant driving field 7-10495
 cascade Zeeman quantum beats, stepwise pulsed-laser excitation, four-level model 7-50014
 coherent population trapping, non-Markovian character relaxation processes study, Raman spectra 7-19755
 composite system, two-photon transition amplitude, relativistic invariance 7-36531
 diacetylene +O, rate const. meas., flash photolysis-reson. fluoresc. method 7-8263
 energy measurements in vac.-UV region, use of reson. fluorescence 7-57502
 excited atom, radiative process fluctuations 7-889
 excited atom reaction dynamics, charactn. by laser induced fluoresc. 7-46836
 four-level atoms, multiphoton processes, fluoresc. spectra calcs. 7-62318
 gas-phase alkali compound photodissociation, photofragment fluoresc. anal. 7-19974
 graphite furnace produced atoms, laser excited, fluoresc. 7-30982
 high-Z elements, Li, La, Lb and Ly X-ray prod. cross sections, meas. 7-19801
 intermittent atomic fluorescence 7-10484
 ion trapped in Lamb-Dicke limit, laser-cooled, reson. fluoresc. 7-10481
 K, 4 ²P impact excitation by polarised electrons, fluoresc. polarisation study 7-31177
 laser-blow-off plasmas, velocity distrib. meas. 7-20879
 light amplification coefficient and intensity, spasmodic increase during metastable atom and mol. condensation (Russian) 7-50523
 light elements, electron impact K-shell ionisation cross-sections, anal. appls. 7-25666
 magneto-optic resonances in fluorescence induced by the wind effect 7-25453
 many-atom system, reson. fluoresc. 7-36532
 model atom, radiative properties, external magnetic field and monochromatic radiation field 7-19694
 multiphoton excitation techniques for combustion diagnostics 7-17789
 noise spectrum in mag. field, polarisation moments 7-42546
 optical susceptibility saturation in strong amplitude-modulated fields, matrix continued fractions anal. 7-20371
 quantised atom, spontaneous emission phenomenon 7-1045
 quantum fluctuations and squeezing in quantised field mode interaction 7-1049
 quantum optics, absorber theory 7-1046
 light rare earths, Ly_{2,3} satellite, X-ray emission spectra anal. 7-36523
 Rayleigh scatt., redistrib. function 7-19758
 single atom fluorescence, random telegraph signal with dark periods from laser excitation 7-15540
 spontaneous emission and absorpt., quantum state interference 7-25449
 three-level atoms, macroscopic quantum jumps 7-15833
 three-level system, quantum jumps, fluoresc. anal. 7-50001
 two level atom, pulse-induced reson. fluoresc. spectrum, temporal diff. and eigenvalue interpretation 7-15543
 two-level atom, reson. fluoresc. spectrum, atomic recoil influence 7-42544
 two-level atom, resonance fluorescence, time-resolved correlation spectroscopy 7-10482
 two-level atom, two-photon resonance fluoresc. distrib. calcs. 7-50043
 two-level atomic laser, spontaneous emission, laser line broadening 7-50573
 two-level atoms, laser driven, time depend. spectra, additional sidebands 7-19757
 two-level atoms, redistribution of radiation, Rayleigh scatt., atomic fluoresc., stochastic process calcs. 7-19754
 two-level atoms in damped cavity, spontaneous emission 7-25452
 two-level atoms on conventional and phase conjugated surfaces, laser induced phenomena 7-57025
 two-level one and two atoms, reson. fluoresc., nonlinear and stimulated effects 7-25448
 two-level system, laser-driven, coupled to metastable state, photon count statistics 7-1051
 two-level system, reson. fluorescence, photon statistics 7-49995
 two-photon resonance fluorescence 7-10488

atomic fluorescence continued

- vacuum UV light polarisation, freq. conversion and fluorescence studies 7-10849
 $\text{Al}_2\text{O}_3\text{:Cr}^{3+}$, surface temp. meas., fluoresc. appl. 7-19947
 ^{241}Am , hyperfine struct. of 2 eV level, laser induced fluorescence study 7-25680
 Ar electron stepwise excitation effective cross section of $2p_3$ level from metastable states 7-31174
 Ar, metastable ions, optical pumping in hollow cathode discharge 7-30990
 Ar^+ , transition probabilities and radiative lifetimes, saturated fluoresc. spectra anal. 7-42543
 As, fluoresc., SRS eval. as excitation source 7-30981
 Ba autoionising states, internal conversion and fluoresc. two-step process 7-25467
 Ba, fast atomic beam laser fluoresc., g-factor 7-10483
 Ba I, $^1\text{P}_1$ level branching, reson. fluoresc. intensity depend. 7-50000
 Ba, three-level system, dynamic Stark effect 7-42548
 Ba $^+$, fluoresc. obs. using cross-saturating sideband absorpt. 7-19751
 Ba $^+$, laser excited resonance fluorescence, obs. of quantum jumps 7-10512
 Ba $^+$ single ion, laser excited reson. fluoresc., quantum jumps obs. 7-30984
 ^{138}Ba I, three-level system, fluoresc., evidence for quantum jumps 7-19756
 Ba+Ar, collisional redistrib., laser-induced fluoresc. 7-62492
 Ba-Sr $^+$, laser-induced charge exchange, quasi-mol. model, fluores. anal. 7-36748
 ^{138}Ba , dynamic Stark effect in three level system 7-10498
 C III vacuum arc discharge, reson. photoexcitation, fluoresc., X-ray laser prototype 7-20987
 Ca, 422.7 nm resonance line, lineshape anal., rare gas perturbation, fluoresc. spectra study 7-19753
 Ca, reson. photon emission quantum interference effect, fluoresc. 7-10486
 Ca, spatial distrib. profiles, ICP atomic emission and fluoresc. 7-54235
 Ca $^+$ + He(Ne), collisional lasers, high specific output energy 7-43078
 Ca+He, saturated two-photon absorpt. in perturber bath 7-888
 Cd $^+$, alignment after photoionis., fluoresc. radiation polarisation meas. 7-890
 Cl atom, $\text{Ka}_{1,2}$ X-ray emission lines, many electron effects 7-887
 Cr $^{23+}$, dielectronic satellite spectra CI HFS calcs. 7-42506
 Cs, atom, spontaneous decay suppression at optical frequencies, test of vac.-field anisotropy in confined space 7-57026
 D+methyl radical, rate const. determ., laser photolysis and reson. fluoresc. 7-8250
 Eu $^+$ + He (Ne), collisional lasers, high specific output energy 7-43078
 atomic beam, atom density meas., laser induced fluoresc. 7-19762
 Fe I, cascade Zeeman quantum beats, stepwise pulsed-laser excitation, fluoresc. anal. 7-49997
 Fe, I-line excitation processes, investig. 7-19775
 Ga, hyperfine struct., magnetic-dipole- and electric quadrupole coupling consts., atomic fluoresc., MCHF method 7-30985
 Ga, photofragment from trimethylgallium fluoresc. study 7-23046
 Ga, radiative lifetimes, fluoresc., MCHF calcs. 7-30946
 H, flames, two-step saturated fluoresc. detect. 7-19759
 H, multiphoton excitation techniques for combustion diagnostics 7-17789
 H-like ions, spontaneous emission spectral line, natural broadening shape 7-42541
 H+methyl radical, rate const. determ., laser photolysis and reson. fluoresc. 7-8250
 H $^+ \text{L}(\text{Cr, Fe, Co, Zn})$, k-shell ionization cross sections and theoretical models 7-5627
 He, 3^1D state electron impact excitation, electron-polarised photon coincidence study 7-36774
 He, electron impact excitation, metastable state, laser induced fluoresc. 7-50372
 He, plasma, collision induced transitions between singlet and triplet levels, laser fluoresc. 7-20846
 He $^+$, photoionisation production and fluorescence angular distrib. 7-25451
 He-Ne laser, mode-crossing reson., intracavity distance and mode-locking quality anal. 7-31373
 He(2^3S), metastable state, reactivity, rate coeff. determ., fluoresc. 7-19760
 Hg, discharge, low-press., excited state pop. mechanisms determ. using pulsed optical pumping 7-26557
 Hg discharge, low-press., laser diagnostics 7-58085
 Hg, in N_2 matrix, electronic-to-vibr. energy transfer and relax., fluoresc. 7-49992
 Hg, in N_2 -Kr matrix, electronic-to-vibr. energy transfer and relax., fluoresc. spectrum 7-49985
 Hg $^{2+}$, resonance fluorescence study, obs. of quantum jumps 7-10485
 Hg+Hg(Ar)(N_2), excitation transfer between fine struct. states, fluoresc. spectroscopy 7-62504
 Hg+Xe collisions, Hg radiative lifetimes and deactivation rate consts., mol. fluoresc. study 7-19752
 I, 1315 nm forbidden emission satellite spectra 7-49999
 In, hyperfine struct., magnetic-dipole- and electric quadrupole coupling consts., atomic fluoresc., MCHF method 7-30985
 K+inert gas, $5d^2\text{P}_{1/2-5/2}\text{P}_{3/2}$ fine struct. mixing 7-50306
 LaF $_3$:Dy $^{3+}$ (Ho $^{3+}$)(Er $^{3+}$), surface temp. meas., fluoresc. appl. 7-19947
 Li + He(Ne), electric field effect, fluoresc. and radiative decay rate determ. 7-20009
 Li beam, mag. field meas., Zeeman and motional-Stark effect 7-19766
 Li, high-freq. Stark effect, laser-induced fluoresc. anal. 7-36529
 ^{24}Mg single stored ion, nonclassical resonance fluorescence radiation obs. 7-42545
 Mo I, lifetimes, branching ratios and transition probabilities 7-36692
 $\text{N}^+(\text{S})$ metastable state produced by electron impact on N_2 and UV aurora 7-29328
 Na, atomic beam absolute intensity, reson. fluoresc. obs. 7-36530
 Na, D lines, collision-induced fluoresc., Rayleigh components 7-49998
 Na diffusion coeffs. in He, Ne, N_2 and CO_2 , fluoresc. detection 7-6346
 Na, excited atom, quenching and time resolved fluoresc. 7-30983
 Na, excited state, collisional repop. upon laser-pumping in $\text{H}_2\text{-O}_2\text{-Ar}$ flame 7-62325
 Na, fluorescence spectra, spontaneous emission, excited state Raman and resonance enhanced three-photon scattering 7-10487
 Na vapour, laser-excited, anomalous blue shifted emission near D $_1$ transition 7-49996

atomic fluorescence continued

- Na+He(Ne)(Ar)(Kr)(Xe), fine-struct. branching ratios, meas. 7-15676
 Na+Ne $^+$, impact excitation, spin exchange, fluoresc. spectra anal. 7-25450
 Na+Xe, Na D lines, collisional broadening, fine-struct. mixing, depolarisation 7-62503
 Na+Xe (Ne), Na D lines, far wings obs. using fluoresc. excitation method 7-62317
 Na * , fluoresc. meas. 7-33925
 Ne, electron impact excitation, metastable state, laser induced fluoresc. 7-50372
 Ne, σ and π fluoresc. profiles, population trapping and Zeeman coherences study 7-25447
 Ne ** , He-like, X-ray and Auger transition rates 7-36507
 O atom, flame diagnostics by two-photon fluoresc., UV laser appl. 7-23015
 O III 313.3 nm in Seyfert galaxy nuclei, Bowen fluoresc. efficiency from near-UV spectroscopy 7-55801
 O $_2$ -Ar etching plasmas, spatially resolved detection of O atoms by two-photon laser-induced fluorescence 7-20917
 Pr $^{3+}$, excited state, NMR meas. by indirect optical detect. 7-15545
 Rb excited states, radiative lifetimes, depopulation cross sections, fluoresc. 7-10502
 SR + inert gases, collisional energy transfer, time resolved fluoresc. meas., quenching cross sections 7-62497
 Se, fluoresc., SRS eval. as excitation source 7-30981
 SiH $_4$, Si $_2\text{H}_6$ and SiH $_2\text{Cl}_2$ plasmas, optical emission spectroscopy, mass spectrometry and laser-induced fluorescence 7-37764
 Sr ions, in air-acetylene flame, time decay, laser-induced ionis. detect. 7-62316
 Sr, isotope shift and hyperfine struct., atomic fluoresc. anal. 7-30987
 Sr, laser beam excited, collisional and radiative relax. 7-5637
 Sr+Ar, ^1P fluoresc. line broadening, ab initio close-coupled scatt. calcs. 7-36494
 Te, fluoresc., SRS eval. as excitation source 7-30981
 Ti + Ar(He)(Ne), Ti excited state total ang. momentum charge, radiation quenching 7-42735
 Ti I, N_2 laser induced fluoresc. in vapour cloud, quenching 7-19763
 Ti+Ar(Ne)(He)(N_2)(H_2), triplet state quenching and excitation transfer processes 7-19761
 Ti+Ar(Ne)(N_2) quenching and excitation transfer processes, fluoresc. 7-10725
 Ti, hyperfine struct., quantum beat spectra anal. 7-31000
 Tm+Ne(Xe), excited state transition cross sections, nonreson. fluoresc. 7-42540
 U, hyperfine structure of 2 and 4 eV levels, laser induced fluorescence study 7-25679
 U, production by hollow-cathode discharge and characterisation by fluorescence spectroscopy 7-365
 ^{235}U atoms, hyperfine structure, laser fluorescence spectroscopy 7-49993
 Va, singly ionised, lifetimes and oscillator strengths meas., fluoresc. and Fourier-transform spectra anal. 7-30986
 Xe amplified spontaneous emission studies 7-15830
 Xe, two-photon excitation, IR decay, press. effect 7-50041
 Xe, two-photon excitation and fluorescence 7-15541
 Yb, $^3\text{P}_1\text{-}^1\text{S}_0$ transition, oscillator strength, lifetime, coherent optical techniques and fluoresc. spectra 7-42542
 ^{174}Yb , 2-level system, resonant excitation response 7-15544
 Zn, fluoresc., SRS eval. as excitation source 7-30981
 Zn $^+$, alignment after photoionis., fluoresc. radiation polarisation meas. 7-890
 Zn $_n$ ($n \leq 6$) matrix isolated cluster, optical spectra investig. 7-50433
 Zr, metal beam, laser prod. and diagnostics, rel. to isotope separation 7-42783

atomic fluorescence spectroscopy *see atomic emission spectroscopy*

atomic forces

- alkali halides, interionic pots. determ. 7-42720
 anilinium, long range interactions, near UV spectra, MNDO and CNDO calcs. 7-19879
 bis (trihalomethyl) ether, conformer struct. and stability, rot. barriers, torsional force consts., mol. mechanics calcs. 7-19998
 bis (trihalomethyl) thioether, conformer struct. and stability, rot. barriers, torsional force consts., mol. mechanics calcs. 7-19998
 closed-shell atoms, s-state and total electron density, convolution relation, HF calcs. 7-42475
 cooperative atomic interactions in a single-mode laser 7-43049
 cooperative radiation from three identical two-level atoms, near-field and super-radiance effects 7-15579
 cooperative spontaneous radiation from two different atoms (*German*) 7-31002
 cyclopropane, electron density, electrostatic pot. and bare nucl. pot. scalar field similarities 7-19736
 diabatic states, nonadiabatic interactions, CI wave fns. expansion, ab initio LCAO SCF CI calcs. 7-49945
 diazine, electron density, electrostatic pot. and bare nucl. pot. scalar field similarities 7-19736
 high-Z ion, partially ionized, effective potential 7-955
 intramolecular dynamics calculations, effective Hamiltonians 7-19995
 intramolecular nuclear magnetic relaxation, correlation time 7-31070
 ion-pair formation collisions, model simulation of differential cross sections 7-10737
 isoelectronic atoms, total energy, nucl. attraction energy and interelectron interaction 7-50287
 magnetic lattice gas of molecules in transverse field, molecular field approx. 7-2802
 metal vapours and vapour-gas mixtures, atomic interactions and transport coeffs. 7-11575
 methyl group motion, rotation barrier and spin-lattice relax. time meas. 7-50291
 nonidentical two-level atoms, retarded and nonretarded interactions 7-31142
 oxirane, electron density, electrostatic pot. and bare nucl. pot. scalar field similarities 7-19736
 photoionisation, relativistic Cooper minima for ground-state atoms, independent-particle approx. calcs. 7-62275
 photoionisation of ions, ionic and point-Coulomb relativistic Cooper minima, independent particle approx. calcs. 7-62276
 three particle loosely bound states, adiabatic hyperspherical approx. 7-10702

atomic forces continued

- Al plasma, high density, high temp. at. pot., comparison with bremsstrahlung Gaunt factors, density functional theory 7-63254
 Be, ground state, exact density-pot. relation 7-42726
 H, external electric field, first-order perturbed wave fn. 7-36465
 H₂, interat. interactions in van der Waals region, Epstein Nesbet calc. 7-36491
 H₂⁺, interat. interactions in van der Waals region, Epstein Nesbet calc. 7-36491
 H₂O-Cu(Ni), complexes, bonding, intermolecular, electron, correl. 7-10449
 He₂, dispersion energy, partial wave expansion and damping phenomenon 7-50283
 He₂, interat. interactions in van der Waals region, Epstein Nesbet calc. 7-36491
⁴He, three atoms interacting through intermol. pot., Efimov state 7-5738
 I+Na, ion-pair formation collisions, model simulation of differential cross sections 7-10737
 N₂⁺ + Au, impact ionisation, L₃ subshell alignment, coupled states anal. 7-25643
 Ne⁺ + Au, impact ionisation, L₃ subshell alignment, coupled states anal. 7-25643

atomic hyperfine structure

- see also Lamb shift*
 alkali metal atoms, orientation, alignment and HFS 7-50278
 alkali metal atoms, population capture, optical-microwave pumping 7-25464
 alkali metal isotopes, radioactive, ground state hyperfine struct. determ. by RF mag. reson. and laser optical pumping 7-25681
 coherent transients meas. with ultrashort light pulses 7-31187
 collisional transform. of alignment into orientation 7-30961
 conf., Leningrad, USSR, April 1985 7-29574
 heavy atoms, hyperfine struct., isotope shift nucl. struct. effects optical spectra 7-19768
 highly ionized atoms, hyperfine splitting, Hartree-Fock-Dirac calcs. 7-30974
 inductivity coupled plasma, emitted lines, widths and shapes 7-54232
 lanthanides, hyperfine struct. in low-lying configs. 7-49954
 laser ultrasensitive high-resolution spectroscopy of short-lived radioactive atoms 7-10522
 light-induced drift, effect of hyperfine splitting 7-15557
 muonic T, hot atom thermalisation, Monte Carlo simulation 7-17805
 muonium, hyperfine splitting, electron-line radiative recoil correction calcs. 7-5792
 photon echo form. on reson. levels with HFS 7-43257
 radioactive atoms, HFS, isotope shift using computer controlled dye laser 7-20249
 radioactive atoms, laser spectroscopy photon correl. technique 7-19769
 Ramsey resonance of alkali hyperfine doublet, frequency standard appl. 7-19733
 spin-dependent interactions, ¹⁹F configs., matrix elements identities 7-42515
 three-level atoms, optical free induction decay quantum beat 7-57482
 tilted-multifold hyperfine interaction in nuclear spectroscopy 7-56604
 Al, hyperfine struct., magnetic-dipole- and electric quadrupole coupling consts., atomic fluoresc., MCHF method 7-30985
²⁴¹Am, hyperfine struct. of 2 eV level, laser induced fluorescence study 7-25680
 Ba II, isotope shift, hyperfine struct., fast ion beam spectra 7-19743
¹³⁸Ba, laser-excited, electron impact ionisation cross section, hyperfine levels 7-36776
 Cd isotopes, hyperfine structure splitting, isotope shift meas. 7-41885
 Cs, 6S and 7S states, off-diagonal hyperfine interaction 7-19726
 Cs atoms laser spectroscopy of 109.1 nm transition 7-19745
 Cs, optically pumped, hyperfine relax. with Ar collisions 7-10511
 Cs, parity-violating 6S→7S amplitude evaluation 7-10457
¹³³Cs, ⁷²P_{3/2} state, level crossing in elec. and mag. fields 7-50003
 Er II, hyperfine struct. meas. by collinear fast beam laser and RF laser double reson. spectra 7-49957
¹⁹F nuclei in single-electron ions, Coulomb excited, γ -angular correls. 7-49292
 Fr, second resonance doublet, wavelength meas. fine-, hyperfine structure, isotope shifts 7-57020
²²¹Fr, radioactive isotope detection, laser resonant photoionisation method 7-42572
 Ga, hyperfine struct., magnetic-dipole- and electric quadrupole coupling consts., atomic fluoresc., MCHF method 7-30985
 H atom, Dirac equation, separation and eigenvalue anal., hyperfine splitting in IS state, 2S state shift 7-36807
 H-like ions, nucl. quadrupole moment, HFS 7-49914
 He beam hyperfine struct. evolution and tensor polarisability determ. in elec. field. 7-57028
³He, hyperfine struct., relativistic contribs. contribs. 7-42509
 Hg UV spectra, isotopic shifts and hyperfine splittings 7-49987
 Hg-Ar, low press. electrical discharge, isotope effects, hyperfine struct. 7-37786
 In, hyperfine struct., magnetic-dipole- and electric quadrupole coupling consts., atomic fluoresc., MCHF method 7-30985
 Li, ultrafine structure, nonrelativistic approx. 7-5612
 Li-like ions, hyperfine structure, relativistic corrections, nucl. struct. effects 7-57007
¹⁶³Lu, A-173-6, resonance ionization mass spectrometry for high resolution optical spectra 7-19744
 Mg, spectra struct. and isotope shifts, many-body perturbation theory calcs. 7-50019
 Mn, in Ar solid, ENDOR/ESR spectra 7-5710
 Mn vapour laser, emission spectrum and its time evolution 7-1088
 MnH, in Ar solid, ENDOR/ESR spectra 7-5710
 Na D₂ line determ. in elec. field 7-10772
 Na, hyperfine population relax. in wall collisions 7-62326
^{20,22}Ne, specific mass isotope shift, laser optogalvanic spectra 7-19771
 Pr³⁺, excited state, NMR meas. by indirect optical detect. 7-15545
 Rb I and II, HFS, isotope shift fast-beam laser spectroscopy 7-42534
⁸⁷Rb vapour, multiphoton reson. under hyperfine optical pumping 7-36568
 Si²⁺ transverse Fe and Gd foils transient mag. fields 7-10537
 Sr, isotope shift and hyperfine struct., atomic fluoresc. anal. 7-30987
 Tl, hyperfine struct., quantum beat spectra anal. 7-31000
 Tm ground-state sublevels, optical pumping, depolarisation cross section meas. 7-50027

atomic hyperfine structure continued

- U, hyperfine structure of 2 and 4 eV levels, laser induced fluorescence study 7-25679
²³⁵U atoms, hyperfine structure, laser fluorescence spectroscopy 7-49993
 ZnI 307.6 nm line absorpt. and collision cross section 7-30975
- atomic inelastic collisions**
see also atom-atom collisions; atom-ion collisions; atom-molecule collisions; atom-molecule reactions; atomic electron impact excitation; atomic electron impact ionisation; beam foil spectra; ionisation of atoms atom+structureless charged particle, second-order optical potentials and R-matrix theory 7-18640
 atomic excitation probability in optical collisions 7-31146
 atomic lineshape, convergent anal. of radiative matrix elements 7-19774
 binary atomic collisions, inelastic energy loss and electron emission 7-17384
 collinear laser-fast-beam spectroscopy, collisional ionisation detection scheme 7-18882
 delta electron spectrum, semiclassical impact parameter expansion 7-50298
 interspecies transfer of momentum and energy in disparate-mass gas mixtures 7-42734
 isolated spectral lines, quasistatic ion broadening 7-36548
 j=1 state atoms, collisional polaris. cross-sections 7-42733
 lanthanide ions, exchange collisions with positronium 7-50405
 light-induced drift, effect of hyperfine splitting 7-15557
 linear absorpt. magneto-optical reson. by anisotropic collisions 7-36533
 log derivative method, piecewise constant diagonal reference pot. addition 7-36726
 long-range terms in atomic collisions 7-961
 nonlinear optics, collision-induced processes effects (French) 7-11025
 plasma, phase shift in impact approx., trajectory effects 7-51388
 post collision interaction, Auger line shift 7-50040
 slow heavy particle collisions, nonadiabatic coupling, generalised anti-Demkov model 7-20012
 three-body rearrangement and break-up, critical angle second-order scattering 7-5747
 time-dependent line transport calcs., Monte Carlo scheme 7-20897
 two-level atoms, redistribution of radiation, Rayleigh scatt., atomic fluoresc., stochastic process calcs. 7-19754
 Ba, vapour, laser-pumped, collisional and radiative processes 7-5642
 C III vacuum arc discharge, reson. photexcitation, fluoresc., X-ray laser prototype 7-20987
 Cu²⁺, effective charge, around 4 MeV per nucleon 7-50297
 H plasma, collisions, Stark broadening calcs. 7-10493
 H+He(H₂)(N₂)(O₂), differential scatt. cross-sections for neutral particle precipitation 7-5739
 H₂ collisional effect on broadening and shift coeff. in vibr.-rot. spectra 7-15584
 He II, Stark broadening calcs. 7-10494
 K²⁺, effective charge, around 4 MeV per nucleon 7-50297
 Na, D lines, collision-induced fluoresc., Rayleigh components 7-49998
 Na, hyperfine population relax. in wall collisions 7-62326
 Na, two-photon-excited state trilevel echo 7-19808
 Si, multiply ionised atom, heavy ion induced X-ray emission, post collision and processes 7-65365
 Sml, 12.76 μ m forbidden line broadening 7-36517
 Xe-Ar, laser-induced collisional energy transfer, multiphoton ionisation study 7-57152

atomic interaction potential *see atomic forces***atomic magnetic moment**

- see also gyromagnetic ratio*
 7-30985
 fluorescence noise spectrum in mag. field, polarisation moments 7-42546
 gases, RF wave-induced population inversion and magnetisation transport calcs. 7-51384
 inert gas atoms, physisorbed, induced dipole moment 7-52243
 rare earth metals, total angular momentum, atomic mag. moments, calc. 7-62540
 total angular momentum, atomic mag. moments, calc. 7-62540
 Ba, fast atomic beam laser fluoresc. 7-10483
 Br XXV to XXI, spectra and energy levels 7-25444
 Co, total angular momentum, atomic mag. moments, calc. 7-62540
 Cr cpds, total angular momentum, atomic mag. moments, calc. 7-62540
 F-like ions, Zr³¹⁺ to Sn⁴¹⁺, X-ray transitions 7-25445
 Fe, total angular momentum, atomic mag. moments, calc. 7-62540
 Ga, hyperfine struct., magnetic-dipole- and electric quadrupole coupling consts., atomic fluoresc., MCHF method 7-30985
 H-like ions, nucl. quadrupole moment, HFS 7-49914
 In, hyperfine struct., magnetic-dipole- and electric quadrupole coupling consts., atomic fluoresc., MCHF method 7-30985
²⁴Mg fine structure transition via linear Ramsey interrogation 7-884
 Na, nonlinear parametrical EM wave interaction, saturation, Stark shift and multipole radiation effects calcs. (Russian) 7-19767
 Ni, total angular momentum, atomic mag. moments, calc. 7-62540

atomic mass

- see also isotopes; mass spectra; nuclear mass*
 Hugoniot values, calc. from atomic props. 7-74475
²³⁸Fm, Z, A and half-life meas. 7-19159
 Ga, reference sample, absolute isotropic abundance ratio and at. weight 7-42779
³H-³He atomic mass difference, effects of ³He⁺ metastable 2²S_{1/2} state, mass spectrometric anal. 7-5782

atomic metastable states

- afterglows, electron distribution function, metastable atom+atom collision effects 7-21030
 coherent population trapping, non-Markovian character relaxation processes study, Raman spectra 7-19755
 cooperative self-diffraction in resonator, Maxwell eqn. solns. 7-42558
 electronic excitation cross sections, freq. depend. 7-25436
 inert gas afterglow, step by step excitation electron distrib. 7-26572
 j to j' transition between degenerate levels, superradiance theory, polarisation properties 7-10536
 light amplification coefficient and intensity, spasmodic increase during metastable atom and mol. condensation (Russian) 7-50523
 metal atoms and ions, lasing mechanism and energy characts., relax. processes of metastable states 7-62673
 Rabi and Ramsey interrogations of metastable beams 7-25459
 three-level atoms, macroscopic quantum jumps 7-15833
 three-level system, quantum jumps, fluoresc. anal. 7-50001

atomic metastable states continued

- two-level system, laser driven, coupled to metastable state, photon count statistics 7-1051
 7-36519
 Al, Na-like ions, steady-state population inversion 7-19780
 Ar electron stepwise excitation effective cross section of $2p_9$ level from metastable states 7-31174
 Ar, flowing afterglow, metastable influence, expt. apparatus description 7-58073
 Ar, metastable ions, optical pumping in hollow cathode discharge 7-30990
 Ar, metastable number density, ICP-AAS eval. 7-54237
 Ar, metastable population meas. and flow instability due to shock wave, comparison with models 7-16207
 Ar, pulsed metastable atomic beam source for time-of-flight applications 7-41533
 Arⁿ⁺, (n=9, 13), metastable ion beams, forbidden lines, visible spectrum 7-57022
 Ar^{q+}, heavy ion impact on gas target, long-lived states form., K X-ray spectra anal. 7-30980
 Ar⁺+Kr (CO)(CO₂), charge exchange cross-sections meas. 7-62519
 Ba I, ¹P₁ level branching, reson. fluoresc. intensity depend. 7-50000
 Ba vapour laser, mechanism limiting pulse repetition freq. 7-43071
 Ba⁺, laser excited resonance fluorescence, obs. of quantum jumps 7-10512
 Ba⁺, metastable autoionising state, lifetime meas. 7-19788
 Ba⁺ single ion, laser excited reson. fluoresc., quantum jumps obs. 7-30984
 Ba+Cl₂(Br₂)(N₂O)(NO₂) (carbon tetrachloride) 7-13781
 Be⁺, metastable ion, shape resons. scaled local density calcs. 7-42464
 C isoelectronic series, intercombination transition probabilities, CI calcs. 7-36489
 Ca, atomic beam, two-photon Hanle effect in Ramsey interrogation 7-15560
 Ca⁺+He(Ne), collisional lasers, high specific output energy 7-43078
 Caⁿ⁺, (n=11, 12), metastable ion beams, forbidden lines, visible spectrum 7-57022
 Ca+H₂(D₂), collisional quenching, time-resolved emission spectra anal. 7-36528
 Cs, quasimetastable energy levels, appl., XUV emission studies 7-10480
 Cu+N₂O, collisional quenching, time-resolved emission and chemiluminescence 7-28285
 Eu⁺+He(Ne), collisional lasers, high specific output energy 7-43078
 Fe, multiply charged ions, electron-impact ionisation, excitation energies and cross section calcs. 7-25425
 Fe, multiply-charged ions, electron-impact ionisation cross sections, crossed-beam meas., rate coefficient calcs. 7-25660
 H, metastable 2s state, electron impact ionis., triple differential cross-sections 7-25665
 H, reson. electron capture from excited 2 s states, cross section calcs. 7-36747
 H⁺, charge transfer into 2S state, differential cross sections meas. 7-36750
 H+He(Ar)(Ne)(Kr)(Ne)(H₂), electron capture cross sections 7-10747
 H+Br₂(I₂)(ICl)(IBr), bound and continuum states, excitation transfer, optical and electron spectroscopy investig. 7-36689
 He, atom, with turbulent flow, two electron group model for RF ionisation 7-31921
 He discharge, atomic and molecular metastables, population transient behaviour 7-37783
 He, electron impact excitation, metastable state, laser induced fluoresc. 7-50372
 He, ground state, gas discharge, longit. nucl. relax. time, temp. depend. 7-20997
 He, metastable state, positive column, ionis. process investig. 7-20057
 He, pulsed metastable atomic beam source for time-of-flight applications 7-41533
 He-N₂ mixtures, metastable the electron impact excitation coeffs. 7-20059
 He+Ar(N₂)(O₂), bimolecular and termolecular, deexcitation reactions (French) 7-10724
 He+ferrocene (Fe(CO)₅), dissoci. excitations, mol. orbital correls. 7-10735
 He+Li(Na)(K)(Rb)(Cs), Penning ionisation, pot. well depth calcs., electron energy spectra anal. 7-62510
 He⁺+H₂(N₂)(O₂)(CO)(NO), metastable state, collisional quenching cross section 7-62315
³He⁺, metastable 2S_{1/2} state, effect on ³H-³He mass difference 7-5782
 He⁺+Zn, Penning and charge transfer reactions, Zn⁺ levels excitation 7-5746
 He(2³S), metastable state, reactivity, rate coeff. determ., fluoresc. 7-19760
 He⁺(2S), muonic, binding in He gas, quenching mechanism study 7-36812
 Hg²⁺, resonance fluorescence study, obs. of quantum jumps 7-10485
 K^{q+}, (n=10, 11, 14), metastable ion beams, forbidden lines, visible spectrum 7-57022
 Kr, electron impact excitation into metastable states effective cross sections 7-36775
 Kr³⁺, spontaneous two-photon decay rates 7-15530
 Li, ⁴P₁ level, relativistic autoionisation, CI mechs. 7-49949
 Mg, metastable ion, shape resons. scaled local density calcs. 7-42464
²⁴Mg fine structure transition via linear Ramsey interrogation 7-884
 N²⁺+Kr(Xe), energy loss spectra 7-50334
 Nb^{q+}, (n=14, 15, 16), metastable ion beams, forbidden lines, visible spectrum 7-57022
 Ne atoms, 1S₂ metastable states, non-radiative lifetimes 7-37772
 Ne discharges, optogalvanic spectra using tunable laser radiation 7-61389
 Ne, electron impact excitation, metastable state, laser induced fluoresc. 7-50372
 Ne metastable atoms, spectral condensation in dye laser intracavity spectroscopy 7-50551
 Ne+Ar, ionis., fine struct. depend. product branching 7-15673
 Ne+He(Ar), electronically excited atoms, beam sources 7-20008
 O, photoproduction cross sections, mass spectrometry, photoionisation and photodissociation 7-10681
 O₂, glow discharge, metastable at. and mol. processes 7-16342
 Ti, 6³P_{3/2} metastable and 6¹P_{1/2} ground state relax. 7-36505
 Xe atoms, J=1 even-parity autoionisation 7-50029

atomic metastable states continued

- Xe, autoionising Rydberg series, two-photon spectra anal. 7-36570
 Xe, radial distrib. in He-Xe pulsed discharge 7-26573
atomic orbitals *see atomic structure*
atomic orbitals calculations
see also GO calculations; GTO calculations; STO calculations
 3d transition metal atoms and ions, approx. atomic orbitals, basis set reduction, maximum overlap method, mol. and solid state calc. appls. 7-840
 alkali metal atom-He system, Rydberg energy levels, Coulomb and Coulomb-Stark-Green fn. 7-42476
 alkaline-earth atoms, two-electron interaction study 7-15491
 atom in molecule, effective state calcs., orbital population anal. (Russian) 7-62278
 atomic lineshape, convergent anal. of radiative matrix elements 7-19774
 atoms and ions, H to Ne, relativistic Gaussian basis sets 7-36468
 conference, Marineland, Florida, USA (March 1986) 7-40985
 disordered alternate structures, electron energy spectrum 7-42458
 electrostatic exchange interaction and characteristics of X-ray spectra 7-25337
 elementary algebraic method for average radii approxs. 7-839
 group theoretical treatment 7-836
 hydrides, first and second row, NMR chem. shift bond length derivatives 7-42644
 localised internal orbitals, fourth-order Moller-Plesset perturbation theory 7-49900
 methane C atom modified atomic orbital basis set calcs. 7-19681
 model atom, radiative properties, external magnetic field and monochromatic radiation field 7-19694
 reduction of orbital sets, computer program OFMO 7-49865
 s-orbitals, quality determ. by least squares and constrained var. methods 7-49866
 two-level atom density matrix eqns., frictional force and hysteretic effects in a standing light wave field 7-42563
 valence state energies molecular orbital wave functions; interaction parameters, GTO calcs. 7-15506
 X α method, ab initio exchange-correlation parameter study 7-56972
 Al, level energies and oscillator strengths, coupled channel model calcs., energy depend. sensitivity 7-49906
 Ar²⁺ energy level radiation lifetime calcs. 7-25455
 Be, modified HF SCF equation 7-56970
 Co, level energies and oscillator strengths, coupled channel model calcs., energy depend. sensitivity 7-49906
 H, electronic states in uniform mag. field, cylindrical adiabatic approx. calcs. 7-42479
 H, Griffin-Hill-Wheeler eqn., discretisation, Gaussian type orbitals calcs. 7-30945
 H, Kepler-Coulomb problem, coherent states and propagators time variables 7-62277
 H, periodic orbits, quantisation in mag. field 7-30932
 H-like systems in arbitrary mag. fields, ground and excited states wave functions expansion calcs. 7-2519
 H-like systems in arbitrary mag. fields, expansion-variational calcs. 7-36467
 He, modified HF SCF equation 7-56970
 He+C⁶⁺(O⁸⁺), intermediate energy collisions, electron capture cross sections, AO expansion method calcs. 7-25381
 Kr²⁺ energy level radiation lifetime calcs. 7-25455
 Mg, ¹P states, two-electron interaction study 7-15491
 Mn, reduced basis set, Adamowicz's and max. overlap methods 7-56932
 Na+H⁺, excitation cross sections, travelling at. orbital calcs. 7-62505
 Na+Li⁺, charge exchange collisions, cross sections calcs., atomic-orbital expansions method 7-36460
 Na⁺+Li, charge exchange collisions, cross sections calcs., atomic-orbital expansions method 7-36460
 Ne diatomic coupled cluster method, MBPT 7-56996
 Ne VII, transitions between n=2 and n=3 levels 7-19747
 O, orbital energies, UHF calcs. phys. interpretation 7-56931
 Si, level energies and oscillator strengths, coupled channel model calcs., energy depend. sensitivity 7-49906
atomic polarisability
 alkali metal clusters, structures, pseudopotential method, local density approx. 7-36840
 atom-atom potentials via electron gas theory 7-36720
 atom-surface interaction, dipole and quadrupolar contributions 7-52282
 dipole polarisability of atoms and ions, ionis. pot. correl. 7-42529
 electronic polarisability, Schrödinger eqn., numerical soln. method anal. 7-24457
 inert-gas atoms, hyperpolarizabilities, local-density approx. method 7-25630
 ions and atoms, closed shell, polarisability, local density approximation 7-56999
 K, 4 ²P impact excitation by polarised electrons, fluoresc. polarisation study 7-31177
 reduced electronegativities and atomicpolarizabilities of certain elements 7-5784
 transition metal atoms, first series, atomic polarisability eval. by variational perturbation approach 7-49911
 van der Waals interaction between atom and metal surface, response function approach 7-21964
 vapours, highly polarised, laser optical pumping with velocity-changing collisions, theoretical anal. 7-36556
 Au, valence energy and polarisability, semiempirical pseudopot. calcs. 7-56926
 Ba, valence energy and polarisability, semiempirical pseudopot. calcs. 7-56926
 Be, excitation energies, oscillator strengths, polarisabilities, HF calcs. 7-56929
 Cs, scalar Stark polarizability for 6s-7s transition 7-62322
 Cs vapour, comp. study, reson. doublet absorpt. meas. 7-36518
 H atom in molecule, polarisability change calcs. (Russian) 7-62279
 H, ground state, 2⁻-pole Cauchy moment computation 7-5629
 He beam hyperfine struct. evolution and tensor polarisability determ. in elec. field. 7-57028
 He, Kohn-Sham time-depend. orbital density functional theory, hydrodynamic formulation 7-25678
 He²⁺, charge exchange collisions, multiply charged closed K shell targets, exponential model study 7-25426
 Hg, valence energy and polarisability, semiempirical pseudopot. calcs. 7-56926

atomic polarisability continued

- I, four-photon ionisation, three-photon resons., AC Stark broadening 7-57036
- N, high freq. excitation, vac. UV spectra 7-10476
- Na-like ions, Rydberg states, dynamic polarisability, HF calcs. 7-62273
- ¹⁶O, collisions with wide range of targets, K-shell ionisation, polarisation and binding effects 7-31165
- Pb, valence energy and polarisability, semiempirical pseudopot. calcs. 7-56926
- ³²S, collisions with wide range of targets, K-shell ionisation, polarisation and binding effects 7-31165
- Sr+Ar, ¹P fluoresc. line broadening, ab initio close-coupled scatt. calcs. 7-36494
- Tl, valence energy and polarisability, semiempirical pseudopot. calcs. 7-56926

atomic positron scattering *see* **atomic electron impact excitation; atomic electron impact ionisation; elastic scattering of electrons by atoms and molecules**

atomic potentials *see* **atomic forces**

atomic power *see* **nuclear power**

atomic reactors *see* **fission reactors**

atomic resonant states

- collisional energy transfer, time resolved fluoresc. meas., quenching cross sections 7-62497
- dielectronic recombination, electric field enhancement over Rydberg spectrum 7-5618
- negative ions, autodetaching states, electron correl. effects 7-19789
- nonlinear susceptibility, radiation pressure effects 7-1219
- photon echo form. on reson. levels with HFS 7-43257
- photon-dressed discrete states in the continuum 7-19813
- Ramsey resonance of alkali hyperfine doublet, frequency standard appl. 7-19733
- stimulated photon echo, information storage duration dependences calcs. 7-62798
- sum-rules in resonance calculations with complex coordinates 7-42527
- surface, corrugated, scatt. of atoms, resonance states, complex rot. method appl. 7-50391
- two level atom, pulse-induced reson. fluoresc. spectrum, temporal diffr. and eigenvalue interpretation 7-15543
- two-level atom, two-photon resonance fluoresc. distrib. calcs. 7-50043
- two-level atomic gaseous medium, light beam reson. interaction, radiation trapping effect 7-42559
- two-level atoms in nonlinear Fabry-Perot system, output-input characts. 7-15923
- two-level one and two atoms, reson. fluoresc., nonlinear and stimulated effects 7-25448
- As, fluoresc., SRS eval. as excitation source 7-30981
- Ba⁺ single ion, laser excited reson. fluoresc., quantum jumps obs. 7-30984
- Be⁻ shape reson., complex-rotated HF method 7-842
- Cd-Cd(Kr) mixture, reson. line broadening, interaction pot., anal. 7-36520
- Ga, resonant state, autoionis., electron spectra 7-900
- H, elastic electron scatt., reson. struct. study 7-20045
- H, highly excited, quasi-Landau struct. 7-36510
- H⁺, photoionisation and photodissociation, six photon ionisation, vibrational levels 7-10682
- H⁺+Xe, collisional excitation and decay of ¹P shape resonance 7-5616
- He, doubly excited autoionising resonance states, Hylleraas-type wave fn. calcs. 7-30940
- He, electron impact excitation, metastable state, laser induced fluoresc. 7-50372
- He⁻, ²S resonant state, projection-operator formalism, CI calcs. 7-36498
- He-like systems, energies and widths of singlet and triplet S resonances 7-36508
- Hg 6³P₁ and 6¹P₁ reson. level population study in Hg-Ar discharge 7-57011
- I, four-photon ionisation, three-photon resons., AC Stark broadening 7-57036
- I, photoemission cross-section and ang. distrib. parameters, inner and outer shell ionisation 7-15565
- In, resonant state, autoionis., electron spectra 7-900
- Li, positron inelastic scatt., calc. of angular correlation parameters 7-15723
- Na, atomic beam absolute intensity, reson. fluoresc. obs. 7-36530
- Na⁺+N₂, quenching, classical trajectory calcs. 7-50300
- Ne, atom, dielectric satellite lines of X resonance line, calcs. 7-5621
- Ne discharges, optogalvanic spectra using tunable laser radiation 7-61389
- Ne, electron impact excitation, metastable state, laser induced fluoresc. 7-50372
- Pb, autoionis., electron spectra 7-900
- ⁸⁷Rb vapour, multiphoton reson. under hyperfine optical pumping 7-36568
- Se, fluoresc., SRS eval. as excitation source 7-30981
- Sm, four-wave light mixing, collision- and stochastic-fluctuation induced Hanle reson. 7-15559
- Sm vapour, collision-induced Ramsey resons. obs. oscillating zeeman sublevel coherence detection 7-874
- ⁸⁷Sr, optical isotope shift in 6s²-6s6p resonance transition 7-5635
- Te, fluoresc., SRS eval. as excitation source 7-30981
- Th, giant dipole resonance absorption, two-laser technique 7-5620
- Xe, autoionisation under two- and three-photon excitation 7-15561
- Zn, fluoresc., SRS eval. as excitation source 7-30981

atomic scattering factors *see* **crystal atomic structure; crystallography; lattice dynamics**

atomic spectra

see also **atomic fluorescence; atomic hyperfine structure; atomic spectral line breadth; atomic structure; beam-foil spectra; conversion electron spectra; radiative corrections; Russell-Saunders coupling; Stark effect; Zeeman effect**

- Alentsev-Fock method, statistical anal. 7-36583
- anomalous Zeeman effect, moments and expansion coeffs. 7-66443
- atom-ion collisions, Z=32 to 54, L-shell ionisation, X-ray yield, threshold behaviour 7-10734
- atomic systems, collision-free multiple photon processes 7-62342
- atomic vapour collision kernels, use of classical transport theory 7-36725
- atoms, transition energies, X-ray spectra, X α theory, X-ray transition energies 7-10422
- atoms in a low field, review 7-898

atomic spectra continued

- Auger transitions, relative intensities for KMX and KXY groups 7-25442
- cascade transition spectrum correlations during perturbation by strong monochromatic field 7-50006
- coincidence laser spectroscopy, ultrasensitive technique for fast ionic or atomic beams 7-30100
- conference, Marineland, Florida, USA (March 1986) 7-40985
- cooperative radiation from three identical two-level atoms, near-field and super-radiance effects 7-15579
- cooperative spontaneous radiation from two different atoms (German) 7-31002
- dipole polarisability of atoms and ions, ionis. pot. correl. 7-42529
- disequilibrium and self-organisation, book 7-24328
- dressed-atoms, stimulated pair transition in strong light fields 7-62327
- emission and photoexcitation spectra, mean energies calc. 7-30969
- energy levels, radiation effects and corrections 7-49960
- FTIR spectrometer, high resolution, for atomic, mol. and cryst. spectroscopy 7-41505
- generalised quasienergy states, at. spectrum in intense multimode radiation field 7-36535
- giant resonance absorption spectra of 4d electrons 7-10471
- heavy atom spectra sources for use with high resolution Fourier transform spectrometer 7-50403
- heavy atoms, hyperfine struct., isotope shift nucl. struct. effects optical spectra 7-19768
- heavy Ni-like ions, X-ray transition energies 7-19749
- high resolution synchrotron spectroscopy appl. 7-19742
- highly ionized atoms, hyperfine splitting, Hartree-Fock-Dirac calcs. 7-30974
- inert gases multiphoton ionization in intense ultraviolet laser fields 7-19797
- IR fine-structure transitions in gaseous nebulae, new collisional data 7-40689
- JET spectroscopic diagnostics in VUV region 7-6451
- laser assisted atomic physics studies at Griffith University 7-20073
- laser excitation, pulse-shape effects 7-43026
- line radiation transfer (book) 7-55910
- local frequency redistribution in reson. line photons, elastic collisions effects 7-10757
- Lyman-alpha profiles, ion dynamics effects, computer simulated study 7-10470
- magnetic substrates for radiative transition with arbitrary polarisation 7-5639
- medium-Z elements, K α satellite, transition assignment, nonrelativistic single configuration HF calcs. 7-30941
- metal atoms, core excitation reson., decay channels 7-906
- multi-photon absorption processes, atom and molecule excitation (Japanese) 7-10530
- multilevel atoms, generalised at. redistrib. functions, three-photon process 7-49978
- multivacancy effects in X-ray emission spectra 7-36522
- negative ions, autodetaching states, electron correl. effects 7-19789
- nonlinear problem of incoherent anisotropic scatt., soln. 7-4309
- one-electron and inner-shell energy levels in high Z atoms, X-ray spectra 7-19750
- PLT tokamak plasma, time-resolved spectra in 80-330 Å region 7-6466
- positronium, yield and emission spectra, in perfluorobenzene-cyclohexane mixtures, excited states effects 7-15741
- PS-3.5 spheromak, flow field study by C⁺ impurity spectral line shifts 7-26403
- radioactive atoms, laser spectroscopy photon correl. technique 7-19769
- rare earth atoms, 4d shell vacancies, radiational decay of states, X-ray spectra studies 7-10479
- resonance scattering spectra appl. to very weak mag. fields diagnostics in diffuse media 7-23991
- Rydberg atoms near metal surface, quasi-stationary spectrum 7-49984
- Rydberg states, dipolar and quadrupolar elec. transition, radial integrals (French) 7-10455
- satellite bands in Fourier integral approach 7-50024
- single atom fluorescence, random telegraph signal with dark periods from laser excitation 7-15540
- solar spectral lines in 430 to 670 nm wavelength range with large Stokes V-amplitudes outside sunspots, catalogue 7-66554
- spatially resolved plasma spectroscopy using multifiber commutator 7-6454
- spontaneous emission and absorpt., quantum state interference 7-25449
- spontaneous emission by single atom in ideal cavity 7-31001
- SPRED multichannel VUV spectrograph upgrade for TFTR and PBX tokamaks 7-6463
- subpicosecond transient excitation of atomic vapor and the measurement of optical phase 7-18851
- sum-rules in resonance calculations with complex coordinates 7-42527
- super-dense hollow cathode discharge, plasma light amplification (Japanese) 7-6476
- Thomson scatt. diagnostics, deconvolution of H- α profiles 7-6457
- three-level atoms, chaos and interaction with self-consistent fields 7-15556
- two-level atom, global critical instability in atom-field interaction 7-894
- two-level atom, resonance fluorescence, time-resolved correlation spectroscopy 7-10482
- two-level atoms, statistical, spectral and dynamical props., comment 7-896
- two-level atoms, two-photon absorpt. process 7-57039
- two-level atoms in damped cavity, spontaneous emission 7-25452
- two-photon two-level interactions, ionisation and cascade decay' effects 7-15574
- UV lines of highly ionized atoms in cooling gas 7-23992
- X-ray and electron spectroscopy, conf., Irkutsk, USSR (Sept. 1984) 7-9574
- Zeeman spectral struct. in strong reson. EM field 7-57029
- Al freely burning arc discharge, self-reversed reson. spectral lines 7-32157
- Al III, relative emission-line strengths in Sun 7-47799
- Al III line strengths in early type stars, non-LTE calcs. 7-18405
- Al isoelectronic series highly ionised atoms injected into PLT and TFTR discharges, spectra 7-19748
- Al₂, spectroscopic consts., coherent VUV and XUV radiation sources 7-10472
- Ar, 3s-subshell excitation, photoabsorption spectra anal., HF calcs., config. interaction calcs. 7-30947

atomic spectra continued

- Ar III, energy levels, optical spectra anal. 7-62308
 Ar, K suprathreshold struct., ab initio calcs. 7-36466
 Ar, multivacancy effects in X-ray emission spectra 7-36522
 Ar, Rayleigh-Brillouin gain spectra 7-10473
 Ar, subvalent electron participation in X-ray and X-ray electron spectra 7-10478
 Ar XII, N I-like ion, forbidden lines identification in solar EUV spectrum 7-66441
 Arⁿ⁺, (n=9, 13), metastable ion beams, forbidden lines, visible spectrum 7-57022
 ArI, 4p-3s transition array, IR lines transition probabilities 7-36547
 Au, photon cross section meas. 7-57016
 Au³⁺, Ni-like, population inversion, ionisation model 7-25462
 B II, beam-foil spectra, identification 7-49982
 B III, beam-foil spectra, identification 7-49982
 B IV, beam-foil spectra, identification 7-49982
 Ba, doubly excited states, electron correl., laser spectra 7-10459
 Ba, doubly excited states, two-photon laser excitation spectra (French) 7-10474
 Ba II, isotope shift, hyperfine struct., fast ion beam spectra 7-19743
 Ba, vapour, laser-pumped, collisional and radiative processes 7-5642
 Ba⁺, optical Lamb-Dicke confinement 7-19807
 BaI, highly excited levels, two-channel quantum defect method 7-57010
 Be III, transition wavelengths among doubly excited states 7-49980
 Bi, K_α/K_β X-ray intensity ratios 7-42537
 Br, photodissoc. prod. electronic states, Raman spectra anal. 7-42530
 Br plasma, laser produced, oscillator strengths, X-ray transitions, ab initio calcs. 7-16334
 Br XXV to XXI, spectra and energy levels 7-25444
 C I 538 nm line in solar spectrum, appl. as temp. diagnostics for photospheric inhomogeneities 7-66553
 C IV emission line behaviour in active galactic nuclei, IUE spectra 7-60790
 C IV in OB-type stars, ionisation fraction determ. from UV line profiles and IR excesses 7-47884
 C IV resonance line investig. using gas-liner pinch 7-9868
 C VI 182 Å line in C-Fe plasma radiation cooling and gain calc. 7-6360
 Ca, 422.7 nm resonance line, lineshape anal., rare gas perturbation, fluorescence, spectra study 7-19753
 Ca III, allowed transitions, oscill. strengths and excitation energies 7-5631
 Ca, laser-XUV excited state spectroscopy 7-19746
 Ca, metastable states energy pooling time-resolved emission spectra anal. 7-36519
 Ca XIX, laser plasma, dielectronic satellites intensities 7-44244
 Caⁿ⁺, (n=11, 12), metastable ion beams, forbidden lines, visible spectrum 7-57022
 Cd, autoionisation widths, calcs. and optogalvanic spectra 7-36521
 Cd-Cd(Kr) mixture, reson. line broadening, interaction pot., anal. 7-36520
 CdCr₂Se₄, Cd vapour pressure determ. by atomic absorption method 7-63790
 CdSe, Cd vapour pressure determ. by atomic absorption method 7-63790
 C I atom, K_{α1,2} X-ray emission lines, many electron effects 7-887
 C, L_{2,3}M_{4,5}M_{4,5} Auger process, meas. 7-57038
 Cs atoms laser spectroscopy of 109.1 nm transition 7-19745
 Cs, D₂ line, saturated absorpt. spectra anal. 7-19781
 Cs, gas phase atoms, detect. by 2-photon resonant ionisation spectroscopy 7-42533
 Cs, IR stimulated Raman scatt. 7-30972
 Cs, isotope shifts, relativistic DF contrib., reson. doublet, UV laser spectroscopy 7-10475
 Cs, photoionisation in 650 to 760 Å UV spectra 7-50033
 Cs plasma, first reson. doublet absorpt. 7-37753
 Cs vapour, comp. study, reson. doublet absorpt. meas. 7-36518
 Cu I plasma, at. quantities, diagnostic determ., capillary discharge technique 7-11787
 Cu, photon cross section meas. 7-57016
 Cu plasma, Ne-like, gain expt. 7-20876
 Cu XIII and XVII, excitation rate coeff. meas. in TEXT 7-44223
 D, Rydberg const. meas. via Balmer-α wavelength single-photon determ. 7-36516
 Er, low-lying states electronic density, ab initio multiconfiguration DF calcs. 7-15486
 F, low current arc, spectroscopic study 7-26581
 F-like ions, energy level distances, relativistic perturbation theory calcs. 7-866
 F-like ions, Zr³¹⁺ to Sn⁴¹⁺, X-ray transitions 7-25445
 Fe II, UV doubly-excited lines obs. in laboratory and in A-type star 21 Peg 7-66585
 Fe II oscillator strengths and lifetimes 7-57019
 Fe III forbidden emission lines, identification in UV spectrum of Sun 7-47813
 Fe, L_{2,3}M_{4,5}M_{4,5} Auger process, meas. 7-57038
 Fe XV, allowed transitions, Hartree-Fock and Dirac-Fock calcs. 7-15494
 Fr, isotope shifts, relativistic DF contrib., reson. doublet, UV laser spectroscopy 7-10475
 Ga II and Ga III lines in HD 25823 and HD 17081, UV spectrum synthesis compared with IUE obs. 7-47943
 Ga VII, optical spectrum, 3d-3d^{4p} transitions, Hartree-Fock calcs. 7-57018
 Gd, autoionising states, electric field effects, UV spectra anal. 7-42531
 Ge I, odd parity energy levels, precise spectroscopic assignments 7-846
 Geⁿ⁺ microcluster, pulsed conc. spectra, bonding and growth kinetics 7-19740
 H degenerate Rydberg states spectrum in crossed fields 7-25437
 H, diamagnetic Rydberg states, meas. and calcs. 7-5615
 H excited state, laser spectroscopy in mag. field 7-10460
 H I, recombination line intensities, Case B calcs. 7-57023
 H, laser spectroscopy with relativistic beams 7-19778
 H, line number to line intensity, logarithmic relationship 7-49977
 H, Lyman-α line Stark struct. using VUV laser system 7-62321
 H plasma, low n Balmer line intensities, T-tube glass-to-plasma boundary layer study 7-37701
 H plasma, T-tube boundary layer effects on spectral intensities ratios, temp. determ. 7-37635
 H, Rydberg const. meas. via Balmer-α wavelength single-photon determ. 7-36516
 H spectra, spatially resolved, resulting from explosion of water droplet in air 7-42632

atomic spectra continued

- H, two-photon spectra of 1s-2s transition 7-10532
 H⁻, free-free absorpt. coeff., R-matrix method 7-62524
 H⁻, laser spectroscopy with relativistic beams 7-19778
 H-like systems in arbitrary mag. fields, expansion-variational calc. 7-36467
 H⁺L(Cr, Fe, Co, Zn), k-shell ionization cross sections and theoretical models 7-5627
 He, 3¹P state, electron polarised photon coincidence expts. 7-5772
 He I, transition wavelengths among doubly excited states 7-49980
 He I excited states in He-Se laser discharge, population density ratios determ. from Kirchhoff's law 7-58072
 He I triplets, collisional excitation cross sections and implications for primordial He abundance 7-55446
 He II, recombination line intensities Case B calcs. 7-57023
 He plasma, spatially resolved line-intensity meas., electron density determ. 7-36641
 He+C⁶⁺(Ne¹⁰⁺) electron capture, bound and continuum states, impulse approx. 7-50329
 Hg, 6¹S₀-6³P₁ transition isotope shift in UV absorpt. spectra 7-19770
 Hg atom, two-photon excitation cross section, Hartree-Slater self-consistent calcs. 7-50042
 Hg, in N₂ matrix, electronic-to-vibr. energy transfer and relax., fluoresc. 7-49992
 Hg, in N₂-Kr matrix, electronic-to-vibr. energy transfer and relax., fluorescence spectrum 7-49985
 Hg, transitions, relativistic SCF calcs. 7-49979
 Hg UV spectra, isotopic shifts and hyperfine splittings 7-49987
 Ho, ionic bombardment, continuous spectrum form. 7-42528
 Ho surface, ion sputtering, emission spectra studies 7-64853
 I, 1315 nm forbidden emission satellite spectra 7-49999
 K, Rydberg states, microwave multiphoton transitions obs. 7-25474
 Kⁿ⁺, (n=10, 11, 14), metastable ion beams, forbidden lines, visible spectrum 7-57022
 Kr XXIX 2s²2pⁿ-2s2pⁿ⁺¹ transition meas. 7-880
 Kr XXVIII 2s²2pⁿ-2s2pⁿ⁺¹ transition meas. 7-880
 Kr₂, spectroscopic consts., coherent VUV and XUV radiation sources 7-10472
 Li II, transition wavelengths among doubly excited states 7-49980
 Li II, absolute wavelength determination, fine struct. determ. 7-10771
 Lu, A-173-6, resonance ionization mass spectrometry for high resolution optical spectra 7-19744
 Mg atoms, ultrasoft X-ray emission spectra studies 7-10615
 Mg I, non-LTE study of solar IR emission lines near 12 microns 7-66334
 Mg I and Mg II, IR spectrum 7-50135
 Mg IV forbidden lines, electron impact excitation rate coeffs. for Mg³⁺ 7-55455
 Mg IX, 1s²21l'-1s²21l' transition, correl. and relativistic effects 7-42552
 Mg, satellite and hypersatellite lines in K-L Auger spectrum 7-30999
 Mg V forbidden lines, electron impact excitation rate coeffs. for Mg⁴⁺ 7-55455
 Mg fine structure transition via linear Ramsey interrogation 7-884
 Mn, forbidden transitions probabilities, intracavity laser, visible spectra anal. 7-42535
 Mn I lines in solar spectrum, appl. as temp. diagnostics for photospheric inhomogeneities 7-66553
 Mo V, HF calcs. and spectra 7-10477
 N, high freq. excitation, vac. UV spectra 7-10476
 N I like ions, identification of forbidden lines of Si VIII, S X and Ar XII in solar spectrum 7-66441
 N IV, spontaneous radiative transition probabilities, ab initio CI calcs. 7-50261
 N spectra, spatially resolved, resulting from explosion of water droplet in air 7-42632
 N⁺(S) metastable state produced by electron impact on N₂ and UV aurora 7-29328
¹⁴N, antiprotonic atom, 4f strong interaction level width 7-31191
 Na, 3¹P state, electron impact excitation, differential cross section and alignment parameter meas. 7-20052
 Na atoms, degenerate resonant four-wave parametric scatt. of CW emission during optical pumping 7-75033
 Na atoms in flame, laser-probed resonant Voigt effect, analytical detection sensitivity 7-19764
 Na D₂ line determ. in elec. field 7-10772
 Na, freely burning arc discharge, self-reversed reson. spectral lines 7-32157
 Na, pionic atom, 2p-1s transition width and energy 7-62544
 Na, violet bands, electronic assignments 7-883
 Na⁺ identification, Na/NH₃ matrix, absorption and MCD spectra anal. 7-30973
²³Na, antiprotonic atom, 4f strong interaction level width 7-31191
 Nbⁿ⁺, (n=14, 15, 16), metastable ion beams, forbidden lines, visible spectrum 7-57022
 Ne, 3s₂-2p₄ transition, linear absorpt. coeff., mag. field effect 7-57030
 Ne, atom, dielectric satellite lines of X resonance line, calcs. 7-5621
 Ne atoms dressed by optical photons, spectra meas., nearly degenerate four-wave mixing 7-10517
 Ne discharges, optogalvanic spectra using tunable laser radiation 7-61389
 Ne impurity immersed in liq. metallic H, polarisation effects on core levels 7-64158
 Ne metastable atoms, spectral condensation in dye laser intracavity spectroscopy 7-50551
 Ne, plasma, Stark broadening and shift parameters, visible spectra anal. 7-62310
 Ne V, theoretical emission line ratios and solar obs. 7-886
 Ne VII, spontaneous radiative transition probabilities, ab initio CI calcs. 7-50261
 Ne VII, transitions between n=2 and n=3 levels 7-19747
 Ne-like ion plasma, laser produced, reson. transitions, X-ray diagnostics 7-20932
 Ne-like ions, Ca XI to Mn XVI, laser plasma, spectra 7-49989
 Ne-like ions, energy level distances, relativistic perturbation theory calcs. 7-866
 Ne-like ions, precision wavelength meas. in X-ray spectra 7-36525
 Ne⁷⁺+H₂ charge exchange collisions, Ne⁶⁺ excited states, VUV spectra anal. 7-20030
 Ni, L_{2,3}M_{4,5}M_{4,5} Auger process, meas. 7-57038
 Ni XXVII plasma, X-ray spectral diagnostics 7-20931

atomic spectra continued

- Ni-like ion plasma, laser produced, reson. transitions, X-ray diagnostics 7-20932
 O, antiprotonic atom, 4f strong interaction level width 7-31191
 O I line emission from O-rich nebulosities in supernova remnants, non-steady shock model 7-55779
 O II, $3p^2D_{1/2,3/2,5/2,7/2}$ energy levels, beam-foil lifetimes 7-15551
 O forbidden lines, improved radiative transition probabilities 7-66442
 O III, $3p^2P$ and $3p^2D$ energy levels, beam-foil meas. 7-30976
 O, Rydberg transitions, IR laser absorpt. spectra 7-57017
 O spectra, spatially resolved, resulting from explosion of water droplet in air 7-42632
 O V, spontaneous radiative transition probabilities, ab initio CI calcs. 7-50261
 P VI-XIII, in plasmas, spectra, 22-92 Å 7-15537
 Pd V, fifth spectrum anal. 7-42532
 Pt, photon cross section meas. 7-57016
 Ra I and II, HFS, isotope shift fast-beam laser spectroscopy 7-42534
 Rb, IR stimulated Raman scatt. 7-30972
 Rb XXIX 7-5626
 S isoelectronic series, transition probabilities and wavelengths 7-15550
 S, UV photoionisation and autoionisation 7-10523
 S X, N I-like ion, forbidden lines identification in solar EUV spectrum 7-66441
 Se I, spectral lines, transition probability meas. by emission method 7-50022
 Se, photoionisation and autoionisation, UV spectra 7-10524
 Si II, autoionizing levels and identification of 1400 Å feature in Ap-Si stars 7-40821
 Si II, III and IV line strengths in B-type stars, non-LTE calcs. 7-18406
 Si II, interstellar, UV equivalent width data statistics and new oscillator strengths 7-55444
 Si IV, relative emission-line strengths in Sun 7-47799
 Si VIII, N I-like ion, forbidden lines identification in solar EUV spectrum 7-66441
 Si XIII and XIV, laser-heated plasma, 2l-3l' and 2l-4l' transitions 7-57021
 Sr, (7s)(5s²)S transition, two-photon absorpt., quantum interference 7-881
 Sr ions, coincidence laser spectroscopy, ultrasensitive technique for fast ionic or atomic beams 7-30100
 Sr, Rydberg states with n/100, laser spectroscopy 7-10461
 Sr, scattered light obs. with laser excitation 7-30968
 Sr XXX X-ray lines, wavelengths and identifications 7-5626
 Ta I, absolute transition probabilities 7-57031
 Th, K_{α}/K_{β} X-ray intensity ratios 7-42537
 Th, plasma, XUV spectra, isotope line identification, HF and DF calcs. 7-15487
 Ti, H-like, dielectronic satellite spectra 7-19741
 Ti I, absorpt. spectrum between 1900 Å to 2315 Å 7-49990
 Ti XXI, laser plasma, dielectronic satellites intensities 7-44244
 Ti+inert gas, $6P_{1/2}7P_{1/2}$, $3/2$ two-photon line broadening and shift 7-49983
 U, K_{β}/K_{α} X-ray intensity ratios 7-42537
 U, spectral line classification, isotope shifts, Lande g factors, pattern-recognition technique 7-62309
 V II, in arcs, transition probabilities, IR emission spectroscopy 7-5633
 V, fifth spectrum, 2300-450 Å 7-885
 W I, absolute transition probabilities 7-57031
 XVIII, Mg-like spectrum 7-25443
 Xe, long-wavelength continuum in VUV spectral region 7-49986
 Xe, subvalent electron participation in X-ray and X-ray electron spectra 7-10478
 Xe₂, spectroscopic consts., coherent VUV and XUV radiation sources 7-10472
 Y XXXI X-ray lines, wavelengths and identifications 7-5626
 Yb vapour, stimulated photon echo theory 7-31406
 Zn I, subvalence d-shell absorpt. spectrum 7-49953
 Zn XII to XX, wavelength and energy levels 7-49981
 ZnI 307.6 nm line absorpt. and collision cross section 7-30975
 Zr XIV XUV spectra, identification of $3d^3-3d^4f$ transition 7-5625

atomic spectral line breadth

- alkali metal atoms(ions), reson. line electron-impact broadening 7-20058
 Ar, gas, doubly-ionised by electron impact, spectral line Stark broadening meas. 7-62320
 atomic lineshape, convergent anal. of radiative matrix elements 7-19774
 atomic systems, transient temporally modulated laser radiation interaction 7-20296
 atoms and ions, Stark width and shift regularities 7-36539
 Cherenkov radiation effect 7-15549
 coherent population trapping, non-Markovian character relaxation processes study, Raman spectra 7-19755
 excited fragment, Doppler profile analysis, optical instrument design and construction (Japanese) 7-31172
 highly charged ions, excited-state stability and X-ray lasers 7-31305
 inductivity coupled plasma, emitted lines, widths and shapes 7-54232
 inert gas dense plasmas, temp. and density profiles, Stark linewidth and shift 7-37752
 isolated spectral lines, quasistatic ion broadening 7-36548
 line profiles influenced by selective ionization in low pressure discharges 7-21002
 multiply charged ions in hot dense plasma, line shapes, simulation (French) 7-11696
 multiwave mixing Doppler broadening effects 7-15578
 n-photon absorption, excitation transition probability calc. 7-42714
 neutral atoms, Stark broadening parameter estimation 7-10490
 plasma, phase shift in impact approx., trajectory effects 7-51388
 plasma, Stark parameters meas. of 447.15 nm line electron density determ. 7-36540
 plasma, Stark parameters meas. of 492.2 nm line, electron density determ. 7-36541
 RF optical resonance line; effect of elastic collisions 7-57148
 Rydberg series, electron scatt., Stark broadening reson. struct. 7-50009
 satellite excitation, complementary branching ratios 7-10519
 single-quantum transition, spectral line contour, QED theory 7-50020
 two-level atom, pulse compression by spectral hole 7-57483
 two-level atomic system, double optical reson. with homogeneous broadening 7-62341
 two-level atoms, quantum evol., state selective reservoir effect 7-15835

atomic spectral line breadth continued

- two-level atoms, redistribution of radiation, Rayleigh scatt., atomic fluctuations, stochastic process calcs. 7-19754
 two-level atoms variable transition freq., optical radiation modulation 7-42554
 two-photon absorption from a phase-diffusing field, effect of random frequency fluctuations 7-10535
 ultra-high-resolution echo spectroscopy in a strong magnetic field 7-43264
 vapour, multiplet, spectral broadening, temp. depend. 7-42551
 Ag, resonant-like reabsorption in AC arc plasma 7-13842
 Ar II, dense plasma, spectral line study 7-36552
 Ar II, multiplet and supermultiplet Stark broadening 7-10491
 Ar, spectral line press. broadening and shift 7-42553
 Ar, spectral lines, neutral broadening 7-5733
 Ar+CO₂(N₂), vacuum UV lines, Stark broadening 7-891
 Ar+Sr⁺(Ca⁺)(Mg⁺), reson. line broadening and shift rates, pot. calc. 7-15683
 C III, Z-pinch plasma, Stark broadening of spectral lines 7-36537
 C⁵⁺, plasma, Balmer line Stark broadened profiles 7-26513
 Ca, 422.7 nm resonance line, lineshape anal., rare gas perturbation, fluorescence, spectra study 7-19753
 Ca, atomic beam, two-photon Hanle effect in Ramsey interrogation 7-15560
 Cd⁺, 4p-3d triplet, broadening by He 7-62323
 Cd-Cd(Kr) mixture, reson. line broadening, interaction pot., anal. 7-36520
 Cs vapour, comp. study, reson. doublet absorpt. meas. 7-36518
¹³³Cs atoms, optically polarised spin system, mag. reson. characts. in wide-band noise RF field 7-42539
 Cu, resonant-like reabsorption in AC arc plasma 7-13842
 Fe I 1564.854 nm line diagnostics of solar magnetic flux tubes 7-66531
 Fe I lines in solar facular areas, shifts and asymmetries 7-66529
 Fe I solar photospheric lines, 5-min. oscills. in wings and bisectors 7-66530
 Ga I and II, stellar line Stark broadening 7-55690
 Ge I, line profiles, Stark widths meas. 7-10489
 H, elastic electron scatt., reson. struct. study 7-20045
 H, excited state, translational energy distrib. in DC discharge, spectroscopic meas. 7-20946
 H in solar photosphere models 7-29454
 H ions, Stark-broadening effect, simulation technique applied to models for Lyman α line 7-15721
 H, line width, isotope shift and Rydberg constant determ. 7-25433
 H plasma, α line shift and profile 7-44243
 H plasma, Balmer- α line Stark broadening, simulation 7-11697
 H plasma, β spectral line peak asymmetry 7-51518
 H plasma, collisions, Stark broadening calcs. 7-10493
 H plasma, computer simulated binary collision hypotheses, Stark broadening 7-10492
 H plasma diagnostics using ion impact Stark broadening 7-51517
 H radio recombination line broadening in plasma 7-29390
 H, Stark effect in strong field 7-50008
 H, two-photon 1s-2s transition, high resol. laser spectroscopy 7-19806
 H, two-photon spectra of 1s-2s transition 7-10532
 H-like atoms, spectral restructuring in magnetised plasma in quasimonochromatic elec. field 7-19776
 H-like ion plasma, laser interaction, X-ray line emission self absorpt. and escape factors 7-37689
 H-like ions, spontaneous emission spectral line, natural broadening shape 7-42541
 H β line broadening in solar chromosphere (Chinese) 7-29441
 He autoionising states, laser-induced transition 7-42566
 He, electron impact excitation, Stokes' parameters, electron-photon coincidence spectra anal. 7-50377
 He, forbidden lines intensities, diagnostics 7-51516
 He II, Stark broadening calcs. 7-10494
 He plasma, spectral line Stark broadening for theta-pinch turbulent plasma parameter meas. 7-44255
 He-like ions, plasma, laser interaction, X-ray line emission self absorpt. and escape factors 7-37689
 He+Ca⁺(Mg⁺), pot. curves reson. line broadening and shift parameters 7-50302
 He+Sr⁺(Ca⁺)(Mg⁺), reson. line broadening and shift rates, pot. calc. 7-15683
 Hg arc plasmas, diagnostics of excitation nonequilibrium using self-reversed emission lines 7-51511
 Hg, Stark broadening, line shift and width 7-50010
 Hg⁺, Beutler spectral lines, electron impact excitation fn. 7-20056
 Hg²⁺, Beutler spectral lines, electron impact excitation fn. 7-20056
 I, four-photon ionisation, three-photon reson., AC Stark broadening 7-57036
 In, L X-ray spectra study 7-42536
 K self-broadened reson. line, heat-pipe oven, superheating effect study 7-36553
 K+K(Rb), Doppler free two-photon spectra, freq. shift, line broadenings 7-57155
 KI, H⁺, Ar⁺ and electron impact, line shifts and widths, Stark broadening study (French) 7-10500
 Kr, gas, doubly-ionised by electron impact, spectral line Stark broadening meas. 7-62320
 Kr, visible transitions, autoionis. obs., optogalvanic spectra 7-57035
 Li Rydberg states, collisional line broadening, trilevel photo. echo meas. 7-19772
 Mg, ¹P doubly excited autoionisation states, CI calcs. 7-36497
 Mg, $3p^2$ ¹S state, autoionis., multiphoton excitation, line shape obs. 7-899
²⁴Mg fine structure transition via linear Ramsey-interrogation 7-884
 Mn vapour laser, emission spectrum and its time evolution 7-1088
 N II pulsed arc, Stark broadened lines 7-36534
 Na, D line broadening and shift by the perturbation (French) 7-10501
 Na+Xe, Na D lines, collisional broadening, fine-struct. mixing, depolarisation 7-62503
 Ne, gas, doubly-ionised by electron impact, spectral line Stark broadening meas. 7-62320
 Ne II, Stark parameters meas. 7-36538
 Ne, optical saturable absorpt. in difference magneto-optic reson., relax. const. calc. 7-62793
 Ne, plasma, Stark broadening and shift parameters, visible spectra anal. 7-62310

atomic spectral line breadth continued

- Ne, σ and π fluoresc. profiles, population trapping and Zeeman coherences study 7-25447
 Rb+Rb(K), Doppler free two-photon spectra, freq. shift, line broadenings 7-57155
 Se I, spectral lines, transition probability meas. by emission method 7-50022
 Sml, 12.76 μ m forbidden line broadening 7-36517
 Sr, autoionising series, multichannel quantum-defect theory model data fit, UV PES study 7-62334
 Sr⁺ reson. line, collisional broadening by Ar, visible spectra 7-49988
 Sr+Ar, ¹P fluoresc. line broadening, ab initio close-coupled scatt. calcs. 7-36494
 Th, plasma, XUV spectra, isotope line identification, HF and DF calcs. 7-15487
 Ti I, absorpt. spectrum between 1900 Å to 2315 Å 7-49990
 Ti IV, plasma-induced atomic level broadening 7-63262
 Ti, Stark broadening, line shift and width 7-50010
 Ti+inert gas, 6P_{1/2}-7P_{1/2}, _{3/2} two-photon line broadening and shift 7-49983
 Tm ground-state sublevels, optical pumping, depolarisation cross section meas. 7-50027
 V V, plasma-induced atomic level broadening 7-63262
 Xe amplified spontaneous emission studies 7-15830
 Xe atoms, J=1 even-parity autoionisation 7-50029
 Xe, gas, doubly-ionised by electron impact, spectral line Stark broadening meas. 7-62320
 Zn XII to XX, wavelength and energy levels 7-49981

atomic structure

- see also atomic electron correlations; atomic excited states; atomic fine structure; atomic orbitals calculations; atomic polarisability; atomic spectra; nuclear screening; Russell-Saunders coupling; triplet state atom, Thomas-Fermi kinetic energy functional, Weizsacker-type gradient corrections 7-36475
 atomic kinetic energy density, approx. functionals study, HF calcs. 7-36476
 atomic states, radiative prod. and destruction 7-19673
 atoms, Zeeman spectra struct. in strong reson. EM field 7-57029
 aufbau principle, chessboard model 7-14738
 Buttle corrections to R matrix 7-62248
 closed-shell atoms, s-state and total electron density, convolution relation, HF calcs. 7-42475
 collective and planetary motion in atoms 7-49955
 complex resonance eigenvalues by the Lanczos recursion method 7-10375
 conference, Marineland, Florida, USA (March 1986) 7-40985
 Dirac operators, consistency of use in basis set, variational solns. with Dirac hole theory 7-19692
 EI transition arrays, simulation by collective vector method 7-15472
 electronic charge density near solid body, appl. to physisorption 7-42448
 electronic chemical potential calc. 7-25336
 electronic struct. and dynamics study by electron spectroscopy 7-36755
 energy levels, radiation effects and corrections 7-49960
 exchange energy from approx. density pot. rel., gradient expansion 7-10371
 exchange energy functional based on Dirac and Fermi-Amaldi approximations 7-36455
 exchange energy functionals, rational fn. representation, HF calcs. 7-49905
 exponential approximation for the density matrix and the Wigner's distribution 7-5582
 fourth-row atoms, core electron Coulomb and exchange operators calcs. 7-30944
 general coupled-cluster methods, MBPT, analytic energy gradients 7-19674
 graphical unitary group approach to arbitrary spin representations 7-49867
 graphite, ultrasmall scanning tunnelling microscope for use in a liquid-helium storage Dewar 7-20075
 ground state energies, var. calcs. with trial binomial functions (Russian) 7-62251
 heavy positive ions, energy, dimensionality depend., 1/Z expansion 7-36441
 hydrogenic atoms in potential $V(r)=gr+\lambda r^2$, exact solns., ground-state eigenvalue bounds, moment calcs. 7-49910
 hydrogenic multipole sum rules, closed-form results 7-62249
 hydrogenic species, relativistic atomic struct. calcs., momentum space approach 7-42461
 inert gas, hollow cathode discharge, at. energy level excitation; laser lines 7-1804
 intermediate states, Pauli principle and Green function technique 7-5578
 ions, ground state electronic struct., Dirac-Slater method anal. (Chinese) 7-56925
 isoelectronic series, application of a variational fn. to ground-state energies 7-15485
 j=1 state atoms, collisional polaris. cross-sections 7-42733
 Jaynes-Cummings type model with multiphoton transitions, population dynamics 7-35778
 kinetic-energy functionals via Pade approximations 7-42523
 lanthanide and scandinide contractions 7-9633
 long-range pots., quantum-defect theory implementation 7-834
 many-electron atoms, quantum-mechanical model 7-25338
 many-electron systems, symmetric group approach, spin-depend. operators 7-15475
 matter, electronic struct., atomic physics models 7-5575
 mechanical atom model, Zeeman effect during liberating phase (Danish) 7-42520
 medium-Z elements, Kaⁿ satellite, transition assignment, nonrelativistic single configuration HF calcs. 7-30941
 micro-clusters, ab initio studies of electronic struct. 7-31203
 microscopic quantum stress tensors calc. 7-42481
 momentum expectation value ratios upper bounds Drescher's inequality 7-15473
 monatomic gases, large angle neutron scatt., collisions effect on dynamical form factor 7-50296
 multiconfigurational SCF electronic energy domain struct. 7-19683
 multidimensional equation, ground state energy; upper and lower bounds, construction 7-41124
 multiple core holes, electronic system response and spectra prod., many-body theory 7-42477
 negative ions, Yukawa pots., bound-state and scatt. props. calcs. 7-30927

atomic structure continued

- neutral atoms, energy investig. using statistical formulas 7-57004
 orbital systems, fractionally occupied, density functional theory, appl. to ionisation and transition energies 7-42451
 perturbation-theory method of calculating the energies and excitation energies of atomic, molecular, and solid-state systems 7-5596
 photoionisation, relativistic Cooper minima for ground-state atoms, independent-particle approx. calcs. 7-62275
 product tensor operators action between pure and mixed configurations 7-5167
 prolate spheroidal coordinates, variational approach, soln. to Poisson's eqn. 7-5579
 quadrupole solvation energy calcs. atomic charges 7-13751
 quasirelativistic theory, Dirac second-order eqn. 7-49958
 R matrix theory, rel. to Titchmarsh-Weyl theory and its complex rotated analogue 7-42450
 relativistic bound-state energies determ. extremum principles 7-868
 relativistic many-fermion systems, vacuum-induced Friedel-type oscillations 7-29887
 relativistic quantum mechanics 7-36503
 resonance state determ. using complex scaling method 7-36443
 s-orbitals, quality determ. by least squares and constrained var. methods 7-49866
 second-row atoms, g_J factors, many-body calcs. 7-62265
 semiclassical self-consistent field 7-42484
 shifted 1/N expansion for energy eigenvalues of the exponential cosine screened Coulomb potential 7-36442
 spectral line radiation transfer (book) 7-55910
 spin and charge densities, HF and UHF calcs. 7-19684
 spin-dependent interactions, 1N¹ configs., matrix elements identities 7-42515
 static electronic props., bivariational coupled-cluster approach 7-15471
 stationary perturbation theory 7-30919
 structure calcs., relativistic effects 7-36504
 Thomas-Fermi eqn., constructive method 7-36478
 Thomas-Fermi theory, rel. to electron subshell filling 7-49870
 transition metal atoms, first series, atomic polarisability eval. by variational perturbation approach 7-49911
 two-electron atomic states with conserved angular momentum and parity, Schrodinger eqn. 7-5593
 two-electron atoms, mol. description 7-845
 two-level atom, global critical instability in atom-field interaction 7-894
 two-level atoms, statistical, spectral and dynamical props., comment 7-896
 U(p,q) and U(n) Lie groups, complementarity relation, atomic physics appls. 7-10380
 valence state energies molecular orbital wave functions; interaction parameters, GTO calcs. 7-15506
 valency, density matrix definition 7-15474
 van der Waal's radii, electron density and solvent effects study 7-62300
 wave functions, graphical method 7-49864
 Al plasma, high density, high temp. at. pot., comparison with bremsstrahlung Gaunt factors, density functional theory 7-63254
 Ar III, energy levels, optical spectra anal. 7-62308
 Ar, K suprathreshold struct., ab initio calcs. 7-36466
 Ar, kinetic energy density, nonlocal correl. fn., CI wave fns. and HF calcs. 7-42496
 Ba, 6s5d states, optical pumping, rel. to radiative lifetimes 7-42560
 Ba, energy struct., HF-Dirac method 7-30938
 Be, excitation energies, multiconfig. linear response and full CI calcs. 7-36487
 Be, ground state, exact density-pot. relation 7-42726
 Be, isoelectronic series, dielectronic recomb. rates calcs. 7-50352
 Be, kinetic energy density, nonlocal correl. fn., CI wave fns. and HF calcs. 7-42496
 Be, multi-config. HF and many-body perturbation theory calcs. 7-19699
 Be, second-order energy calcs. using Gaussian-type geminals, Monte Carlo quadrature formulas 7-25363
 C₂ clusters, spheroidal clusters, rehybridisation and π -orbital alignment 7-25695
 Ca, electronic struct. calcs., relativistic effects 7-36504
 Ca II, model atom with four levels plus continuum use for solar calcs. (Chinese) 7-29442
 Ca+He, saturated two-photon absorpt. in perturber bath 7-888
 Cd, oscillator strengths and excitation energies, relativistic CI and MCRHF calcs. 7-50260
 Cs, 6S and 7S states, off-diagonal hyperfine interaction 7-19726
 Cu^{II}, effective charge, around 4 MeV per nucleon 7-50297
 D, Rydberg const. meas. via Balmer- α wavelength single-photon determ. 7-36516
 Eu, photoemission, orbital-collapse effects 7-15572
 F-like ions, energy level distances, relativistic perturbation theory calcs. 7-866
 Fe XV, allowed transitions, Hartree-Fock and Dirac-Fock calcs. 7-15494
 Ga to Kr, Coulomb and exchange operators, valence electron only SCF calcs. 7-15507
 Ge I, mpnd and mssp³ configs., J=3⁰ energy level calcs. 7-36451
 H atom, compressed, energy shift calcs. 7-35175
 H, ionised gas-laser interaction, dynamic Stark effect (French) 7-6395
 H, model atom with four levels plus continuum use for solar calcs. (Chinese) 7-29442
 H, Rydberg const. meas. via Balmer- α wavelength single-photon determ. 7-36516
 H, stretched, microwave-driven, level mixing 7-42524
 H⁺, ground state energy calcs. using hyperspherical coords. 7-49880
 H⁺, ground states, Rayleigh-Schrodinger perturbation expansions 7-844
 H⁺, ground-state energy, comparison of a variational fn. with previous calcs. 7-15485
 H-like atom, spectrum in high-frequency EM field analytic solution 7-42483
 H-like atom, transition-matrix elements determ. 7-56944
 H-like atoms, stability, particle in a spherical box theory 7-9629
 H-like systems in arbitrary mag. fields, ground and excited states wave functions expansion calcs. 7-2519
 He, 3¹P state, electron polarised photon coincidence expts. 7-5772
 He energy levels, relativistic correction, variational calcs. 7-869
 He, ground state, correl. energy eval., correl. fn. influence 7-36447
 He, ground state energy calcs. using hyperspherical coords. 7-49880
 He, ground states, Rayleigh-Schrodinger perturbation expansions 7-844
 He, ionised gas-laser interaction, dynamic Stark effect (French) 7-6395
 He, n ¹D₂ levels, alignment and orientation in elec. field 7-865

atomic structure continued

- He, N-electron atom, electronic energy in a space of constant curvature (French) 7-36500
 He, positron impact excitation of 2S and 2P states, distorted wave approximation. calcs. 7-36795
 He to U, electron-nucl. cusp. SCF wave functions 7-49879
 He-like ions, multiconfiguration DF study 7-62298
 Hg, oscillator strengths and excitation energies, relativistic CI and MCRHF calcs. 7-50260
 Hg⁺, Beutler spectral lines, electron impact excitation fn. 7-20056
 Hg²⁺, Beutler spectral lines, electron impact excitation fn. 7-20056
 Kr, kinetic energy density, nonlocal correl. fn., CI wave fns. and HF calcs. 7-42496
 Kr XXIX 2s²pⁿ-2s2pⁿ⁺¹ transition meas. 7-880
 Kr XXVIII 2s²pⁿ-2s2pⁿ⁺¹ transition meas. 7-880
 Krⁿ⁺, effective charge, around 4 MeV per nucleon 7-50297
 Li microclusters, fragmentation channels rel. to magic number studies 7-5811
 Li, N-electron atom, electronic energy in a space of constant curvature (French) 7-36500
⁷Li II, absolute wavelength determination, fine struct. determ. 7-10771
 Mg, 3p² S state, autoionis., multiphoton excitation, line shape obs. 7-899
 Mn, vapour, photoelectron ang. distrib. and drag current, nondipole part 7-15575
 Mo V, HF calcs. and spectra 7-10477
 Na microclusters, fragmentation channels rel. to magic number studies 7-5811
 Ne, electronic kinetic energy, energy-density functional calcs. 7-42465
 Ne, kinetic energy density, nonlocal correl. fn., CI wave fns. and HF calcs. 7-42496
 Ne-like ions, Ca XI to Mn XVI, laser plasma, spectra 7-49989
 Ne-like ions, energy level distances, relativistic perturbation theory calcs. 7-866
 Ni, low-lying states, MBPT/CC calcs. 7-10388
 Ni_n (n=1 to 6) clusters, electronic struct., ab initio SCF and CI calcs. 7-10446
 O II, 3p²D<sub>1/2,3/2,5/2,7/2 energy levels, beam-foil lifetimes 7-15551
 P, II levels, hollow cathode discharge, self-alignment and radiative lifetime meas. 7-10678
 S₄N₂²⁺ dication, HF instabilities 7-15508
 Si I, mpnd and mmp³ configs., J=3⁰ energy level calcs. 7-36451
 Si I, mmp³, mpnd J=3⁰ levels, 3-limit 4-channel representations 7-36452
 Si, multiply ionised atom, heavy ion induced X-ray emission, post collision and processes 7-65365
 Sn I, mpnd and mmp³ configs., J=3⁰ energy level calcs. 7-36451
 Sn I, mmp³, mpnd J=3⁰ levels, 3-limit 4-channel representations 7-36452
 Sr, quadratic Zeeman effect for nonhydrogenic systems 7-36544
 Th III, doubly ionised, 5f²-config. 7-19738
 Tl, 6²P_{3/2} metastable and 6²P_{1/2} ground state relax. 7-36505
²³⁵U, spectral line classification, isotope shifts, Lande g factors, pattern-recognition technique 7-62309
 XVIII, Mg-like spectrum 7-25443
 Zn XII to XX, wavelength and energy levels 7-49981
 Zn XIV XUV spectra, identification of 3d⁹-3d⁸4f transition 7-5625</sub>

atomic structure, crystals *see crystal atomic structure*

atomic weight *see atomic mass*

atoms

- see also exotic atoms; helium atoms; hydrogen neutral atoms; positronium*
 No entries

ATR tubes *see gas-discharge tubes; radar equipment*

attaching *see joining processes*

attenuation *see absorption; dispersion (wave); scattering; transmission*

attenuation measurement

- free space permittivity meas. of lossy dielectrics 7-14979
 gradient optical fibres, splice attenuation (German) 7-1277
 integrated optical waveguide attenuation meas. by prism coupling and scattered light techniques 7-43363
 IR optical fibres, meas. system for dispersion, attenuation, numerical aperture, optical time-domain reflectometry 7-37229
 microprocessor meter of radiation attenuationcoefficient in solutions 7-4876
 microwave link during dust storms, attenuation at 2 and 7.5 GHz, obs. 7-55137
 microwave rain attenuation and water vapour radiometric meas. at NPL 7-34606
 optical fibre connectors, meas. (German) 7-43391
 optical fibres testing, single-mode, standard meas. procedures 7-26018
 US velocity and attenuation meas., microcomputer-controlled phase-sensitive detection 7-50881
 waveguide below cutoff attenuation standard calibration, using repeatable attenuation step 7-14972

attenuators

- indirect detection experiments, computer-controlled attenuator 7-24679

attitude control

- ASTRO-C X-ray astronomy satellite, microprocessor-based attitude control system, development 7-55465
 astronomical satellite, Sun sensor for high precision attitude control (Chinese) 7-4286
 conference on space exploitation and utilisation, Honolulu, HI, USA (1985 December) 7-24297
 large space antenna assembly feasibility at space station 7-60540
 Sakigake and Susei Japanese Halley's Comet explorers, attitude and orbit control system 7-55568
 Salyut-6/Kosmos 1267 and Salyut-7/Kosmos-1443 orbital complexes, generalised gravit. orientation regime 7-34832
 solar cell arrays, vibration and attitude control, reaction wheel actuator 7-28400
 solar cell arrays, vibration and attitude control using differential sensors 7-28399
 stereometric camera, parallel orientation of camera base to datum plane in close-range photogrammetry 7-3970
 telescope mirror, Keck Observatory 10m, design and development work status, fabrication plans 7-40693

attitude control continued

- turbulence measurement with inclined hot wire probe, 3D angle calibration method (Japanese) 7-6338
 X-ray set, diagnostic, optical centering unit adjustment device 7-28664

audio acoustics

- see also audio recording; audio systems; hearing; speech*
 critical masking interval meas. for click in wideband noise 7-57634
 live-end-dead-end type recording studio control rooms, rear-wall reflection patterns 7-31571
 partition-stereophony to reproduce spatial hearing events (Japanese) 7-20571
 psychoacoustic tests on the audibility of aliasing components (German) 7-1332
 studio control room design, psychoacoustic considerations 7-31570

audio discs *see video and audio discs*

audio equipment

- see also gramophones; loudspeakers; microphones; pick-ups; video and audio discs*
 acoustics, speech and signal processing, conf., Tokyo, Japan (April '86) 7-35100
 versatile melody generator, DIY (German) 7-16049

audio recording

- see also video and audio discs*
 broadcast and recording studio, electronic architecture 7-6063
 computer controlled sound negative processing 7-4904
 control room design incorporating RFZ, LFD and RPG diffusers 7-37249
 dichotic stimulation for central auditory testing, audio tape production, computer programs 7-47084
 live-end-dead-end type recording studio control rooms, rear-wall reflection patterns 7-31571
 studio control room design, psychoacoustic considerations 7-31570
 AG content reduction, colour positive motion-picture films, photographic indices effect (Russian) 7-4905

audio systems

- see also acoustic devices; acoustic equipment*
 electro-acoustic techniques in the boardroom 7-6046
 electro-acoustics in architecture 7-6044
 electronic architecture applications 7-6045
 high-quality loudspeaking system development with acoustic signal processing (Japanese) 7-57661
 sound system, %AL_{cont} meas. 7-43596
 stereophonic system improvement of 70 mm cinematography (Russian) 7-9914

audio-visual aids *see audio systems; educational aids; technical presentation*

auditory activity *see hearing*

auditory evoked potentials *see bioelectric potentials; hearing*

auditory perception *see hearing*

Auger deexcitation *see Penning ionisation*

Auger effect

- AES, sputter depth profile analysis, hybrid-electron-ion gun and CMA spectrometer 7-39941
 alkali metal surfaces, electron spectroscopy by deexcitation of metastable He atoms 7-59364
 alloys, preferential sputtering, segregation, mixing and diffusion 7-59337
 analytical electron microscopy of thin films, review (Czech) 7-59261
 angular distribution and polarisation of Auger electrons 7-30997
 applied materials charact., conf., San Francisco, CA, USA (April 1985) 7-18495
 Auger transitions, relative intensities for KMX and KXY groups 7-25442
 automatic spectrum recognition, software package 7-24733
 backscattering factors, prediction from meas. of spectral backgrounds 7-28378
 chalcogenide-metal contacts, interdiffusion, struct., comp., electron irradiation effects 7-21686
 chemical analysis of mineral grain surfaces, Auger spectroscopy method 7-60426
 cleaved surface, struct. and comp. 7-12426
 conference, Oconomowoc, WI, USA (April-May 1985) 7-18468
 conversion layers on Al, struct., TEM, LAMMA, AES, XPS, SIMS, ion scatt. spectra 7-23094
 corrosion science, role of electron spectroscopy, review 7-22860
 crystal orientation effects in X-ray and Auger electron microanalysis 7-23109
 depth profiling, interface resolution 7-54246
 depth profiling, preferential sputtering of Te-based alloy thin films 7-54247
 depth profiling by lineshape anal. 7-28380
 diamond, KVV Auger electron spectra calcs., band and cluster approx. methods 7-46252
 diatomic mol., orbital stress and transition stress calc., bond lengths, rot. const. photoelectron spectra 7-42503
 dimethyl methylphosphonate, Auger and photoelectron spectra 7-57132
 double-pass cylindrical-mirror analyzer, imaging props. charact. 7-24731
 electron spectrometer calibration and quantitative Auger anal. 7-24729
 electronics and vacuum physics, conf., Bratislava, Czechoslovakia (Sept. 1985) 7-24292
 ethylene, adsorpt. on Ni (100), hybridisation, Auger lineshape determ. 7-15576
 fatigue apparatus for testing in UHV and controlled environments, computer-controlled 7-39811
 film characterisation and microanalysis, sputtering, AES and XPS destructive depth profiling methods 7-53454
 Fourier smoothing of scanning Auger microscope images using an optimal Wiener filter technique 7-16368
 glass, electromigration and charging effects during Auger and XPS analysis of insulators 7-17393
 graphite monolayer, on Re surface, struct. and props., AES, TDS and thermionic emission anal. 7-45017
 high resolution Auger spectroscopy in energetic ion atom collisions, review 7-62490
 III-V semiconductor-metal interface, reaction and interdiffusion, review 7-21544
 instrumentation, data reduction, depth profiles 7-22390
 ion implantation induced nonequilibrium surface layers, electron emission props. 7-12090
 ion-induced Auger emission from solid targets, review 7-59360
 ionic desorption, Auger-induced, nonadiabatic effects 7-38326

Auger effect continued

KLM group transitions, intensity distrib., intermediate coupling effect 7-5649
 L subshell ionisation probabilities vacancy sharing 7-15697
 laser interactions with condensed matter, review 7-12125
 light elements, electron impact K-shell ionisation cross-sections, anal. appls. 7-25666
 light rare earths, $L_{2,3}$ satellite, X-ray emission spectra anal. 7-36523
 low energy SEM combined with LEED 7-21056
 luminescent centres in crystals, impact excitation and Auger quenching, appl. to ZnS:Mn 7-27827
 magnetic surfaces, polarised electron probes 7-33264
 materials microanalysis, techniques, review 7-54244
 medium and heavy elements, L-subshell ionisation cross sections, X-ray spectra anal. 7-30977
 metal clusters, dispersed in polymeric matrices, synthesis and props. 7-17370
 metal films, characterisation by SIMS, Auger spectroscopy and TEM 7-12550
 metal reflectors in EUV, surface contamination, AES study 7-41563
 metal surfaces, ionic slow collisions, Auger neutralisation 7-53482
 metal surfaces, oxidation, Ar^+ ion bombardment effects, AES study 7-39755
 metal surfaces, quantitative analysis using XPS or AES, data reduction techniques 7-28371
 metal-carbide composites, implantation, modified, friction, surface chemistry 7-46660
 metal-H system, surface props. investig. 7-33487
 metal-metal superlattices, prep. by sputtering, struct. charact. 7-3172
 metallic films, growth by laser photolysis of carbonyls, C and O incorporation mechanisms 7-58685
 methane, fine struct. near C-K edge region in photon W-value 7-19962
 microelectronic devices and materials, characterisation methods, book 7-41028
 MONOS structures, shaped Auger anal. 7-63980
 Mossbauer radiation, resonant detection, conversion- and Auger-electron spectra 7-42657
 multilayer structures, Auger depth profiles using a dual ion gun system 7-22429
 multilayered structures for soft X-ray mirrors, physical charactn. 7-37098
 multispectral scanning Auger imaging technique 7-23110
 multivalent traps, capture to emission ratios 7-7260
 nitride coatings on high-speed steel substrates, characterisation by Auger electron spectroscopy and X-ray photoelectron spectroscopy 7-53982
 overlayer formation, Auger peak-to-peak height corrections 7-27832
 oxide layer on chemically polished and etched InP (111), ion scatt. spectra, AES, ESCA 7-22925
 p-n diode structures, low gap, Auger suppression and negative resist. 7-12812
 trans-polyacetylene chain, bipolaron form. and desorpt., Su-Schrieffer-Heeger model calcs. 7-52454
 post collision interaction, Auger line shift 7-50040
 Powercore strip, amorphous metal ribbon layers, bonding study 7-22975
 PVC surface, sputtered, AES, electron beam induced dissociation 7-20077
 quantitative Auger anal., backscattering factors (Chinese) 7-7793
 rare earth metals, partial photoionisation cross sections at 3d thresholds 7-57138
 rare earths, 4f levels, appearance pot. spectrosc. 7-39324
 reaction layers, AES depth profile anal., under different wear test conditions 7-28147
 reactive ion etching, AES, photoluminescence, SEM obs. 7-65241
 recombination of dislocation excitons 7-38578
 resolution function of CMA systems used for Auger signal measurements 7-30119
 sample manipulator for Auger angular dependence studies 7-35626
 scanning Auger electron microprobe, spatial resolution improvement to ultimate values 7-30131
 scanning Auger microscopy, quantitative multi-element analysis 7-23112
 scanning Auger microscopy and AES, effects of peak to background ratios 7-23111
 scanning Auger microscopy as a high-resolution microprobe for geologic materials 7-34683
 scanning tunnelling microscopy, current saturation through image surface states 7-7320
 secondary ion emission, oxygen pressure dependence 7-64859
 semiconductor device structures, Auger sputter depth profiling 7-21254
 semiconductor face-pumped laser, bimolecular recombination, bistability theory 7-57336
 semiconductor industry, appl. of SIMS, SAES, XPS 7-16847
 semiconductor materials characterisation, electron, ion, X-ray and optical probe methods 7-27203
 semiconductor materials examination, methods and problems in quantitative AES profiling 7-53458
 semiconductor microelectronic structures, depth profiling by SIMS and AES 7-26790
 semiconductor surface chemistry, adsorption and desorption kinetic meas. combined with Auger spectroscopy 7-65348
 semiconductor surfaces, interaction with H_2 7-58632
 semiconductors, Auger recombination via deep double-charged centres (Ukrainian) 7-12732
 silicide formation on Si, initial nucleation processes 7-21767
 silicides, quantitative Auger anal., correction factors 7-27831
 simple metals Auger energy, Slater transition state calcs., metallic and atomic states, jellium model 7-38475
 SIPOS, AES and XPS studies (Chinese) 7-33511
 small molecules, multiple photoionisation and photodissociation, mass spectrometer and coincidence studies 7-19965
 SOL films lamp zone melting recrystallisation, effect of plasma nitrided SiO_2 encapsulant 7-38391
 SOL films, zone-melting recrystallisation, capping techniques 7-38390
 SOS films, pulsed laser beam excitation, femtosecond dynamics 7-13249
 spectroscopy, data processing, extended computer program 7-33983
 spectroscopy, deconvolution calcs. 7-24728
 sputter depth profiling, factor anal., appl. to elemental detect. limits 7-23081
 sputtered particles, ang. distrib., effect of target environment, AES study 7-64028
 stainless steel electrode surface damage anal. in high energy spark gaps 7-33991

Auger effect continued

steel, B-containing, H-embrittled grain boundaries, Auger anal. 7-59633
 steel, C-Mn and Nb treated, high temp. ductility loss, grain boundary segregation 7-46573
 steel, ion implantation and thermal oxidation treatments for wear reduction 7-3481
 steel, low alloy, damaged surface, comp., displacement dislocations, Auger spectra (Russian) 7-59620
 steel, martensitic stainless, precipitation hardened, impact toughness rel. to Mo content, AES obs. 7-39666
 steel, Ni-Co-Mo, maraging, fracture toughness rel. to heat treatment, precip., Auger spectra 7-65124
 steel, stainless, passivity, bipolar model 7-46687
 steel, structural, temper embrittlement, preferential segregation, Auger spectra 7-53737
 sulphide minerals, interpretation of AES 7-22391
 surface anal. methods (Japanese) 7-63921
 surface analysis, AES, XPS, ISS and SIMS, review 7-28372
 surface analysis by AES and XPS, appl. of data compilations to improve meas. uncertainty 7-28377
 surface and interface anal. for electronic devices and circuits 7-17373
 surface behaviour diagrams, for surface and interfacial reactions 7-27077
 surface friction layers, study by AES method (Russian) 7-59674
 surface physics appl. of Auger and appearance potential spectroscopy (Rumanian) 7-17368
 surfaces, high-resolution mag. meas. with spin polarised electrons 7-3119
 SVV spectra of crystals, Auger transitions, calc. of probabilities (Russian) 7-33488
 techniques for surface and thin film analysis 7-33992
 thin overlayers, quantitative AES depth profiling studies 7-7796
 thin overlayers, struct. determ. by AES or XPS 7-33490
 TiC, high-resolution Auger spectra, discrete variational $X\alpha$ method 7-16942
 transition metal amorphous alloy coatings, microindentation response, microstruct. and composition effects 7-46625
 transition metal disilicide films, electrical transport props. 7-58908
 transition metal nitrides and carbides, hard wear-resistant coatings, microstructural and microchemical characterisation 7-52328
 transition metals, Auger spectroscopy, edge effects 7-3121
 trimethyl phosphite, Auger and photoelectron spectra 7-57132
 work function meas., appearance potential spectra, scanning Auger microprobe 7-64824
 X-ray photoelectron and Auger electron spectroscopy in surface anal. 7-24732
 (110), O_2 dissociative chemisorpt. studies 7-2377
 Ag (100), adsorption of Cl, Auger, LEED, XPS, thermal desorption studies 7-58635
 Ag (110), adsorption of ethylene oxide, surface interactions, XPS, TDS, AES, EELS studies 7-33963
 Ag (110), with physisorbed Kr, adsorption of NO_2 , EPR, LEED AES studies 7-53116
 Ag film on Cu substrate, depth profile shape, AES, influence of crystallographic orientation 7-27205
 Ag, XPS, background removal 7-39355
 Ag-Si interfaces, micro-quantitative AES anal. using SEM-SAM apparatus 7-27147
 Ag-Zn, corrosion in H_2S , surface analysis, AES, XPS (Japanese) 7-53955
 AgCu thin epitaxial films, struct. investig. (Russian) 7-12528
 Ag(Ni, S) ternary alloys, surface cosegregation props. 7-52206
 Ag, Auger electron spectra, main and satellite structures 7-7795
 Al (110), Ar-induced Auger electron emission, Doppler broadening 7-59345
 Al (111), Pd and Ag films, growth and electronic struct., UPS, LEED and AES studies 7-52350
 Al Auger electron emission by Ar bombardment, Monte Carlo simulations 7-53470
 Al film growth by UV laser photolysis of trimethylaluminium 7-54153
 Al oxide, nitride and element, $L_{2,3}VV$ valence Auger transitions 7-27828
 Al surface, H^+ Auger and resonant neutralisation, charge capture probability, parameter-free perturbation theory calcs. 7-3141
 Al surface, H^+ Auger neutralisation, transition rate calcs. 7-3140
 Al surface, ion induced secondary electrons, surface topography effects 7-13280
 Al surface, O_2 adsorption, electron beam effects, AES and secondary electron emission studies 7-27835
 Al_{1-x}Si_xC films, RF sputtered, interfacial struct. and reactions, 573-773K (Japanese) 7-53583
 Al/III-V semiconductor interfaces, laser-induced chem. reactions 7-7017
 Al/Pt/Si structures, PtSi formation 7-63972
 Al-GaAs Schottky barrier contacts, MBE grown, interface reactions, vacuum annealing effects 7-45022
 Al-Mg, 5052, oxide thin surface films, AES anal. (Japanese) 7-17723
 AlGaAs layer, separating on GaAs surface, growth mechanism, Auger depth profiling 7-44434
 AlGaAs surface cleaning using ECR radical beam gun 7-54028
 AlGaAs-GaAs superlattices, Se (Si)(Mg)(Be) ion implantation, intermixing, residual damage 7-26782
 Al₂Ga_{1-x}As film formation by laser beam interaction with AlAs/GaAs multilayer structure 7-12570
 AlGa_{1-x}As surface, protection by As and GaAs ultrathin layers, AES sputter depth profiles 7-54022
 $\alpha-Al_2O_3$, cation solute segregation to surface 7-21593
 Al₂O₃ films, optical props., stoichiometry depend. 7-53421
 Al₂O₃ thin films, quantitative anal. by AES 7-59310
 Al₂O₃-Co solar absorber coating, spectrally selective surfaces 7-23223
 Al₂O₃-Ti interface reactions studied by AES and UPS 7-21702
 AlSb-GaSb superlattices, low-temp. growth by plasma process (Japanese) 7-7061
 Ar, Auger emission, electron-electron coincidence investig. 7-30996
 Ar III, energy levels, optical spectra anal. 7-62308
 Au (110), electron emission, interaction of multiply charged ions with surface 7-53473
 Au adsorbate layer struct. on Mo (110), Auger electron peak shape study 7-46254
 Au epitaxial ultra-thin films, X-ray diffr. studies 7-27204
 Au surface, H^+ Auger neutralisation, transition rate calcs. 7-3140
 Au, surface layer comp., Auger spectra (Russian) 7-58703
 Au thin films, on Au (111), surface-diffusion-induced ageing processes 7-45080
 Au, XPS, background removal 7-39355

Auger effect continued

- Au-Cu alloys, surface composition, sequential ion scatt. spectroscopy-Auger electron spectroscopy meas. 7-22394
 Au-Cu sputtered alloys, segregation, surface compositional changes 7-58585
 Au-SiO₂-Si MIS structures, Au-SiO₂ boundary anal. 7-12867
 AuGa₂-GaAs (001), chemically unreactive interfaces formation 7-7050
 AuGe-GaAs, ion beam induced phenomena 7-12166
 AuNiGe-GaAs ohmic contacts, microstruct. anal. and contact resist. meas. 7-2393
 BF₃ (BCl₃) (BBR₃), electron impact, Auger and Coster-Kronig spectra 7-15719
 BN pyrolytic crucibles for MBE, AES, XPS, SIMS, and bulk anal. after vac. baking 7-53596
 Ba autoionising states, internal conversion and fluorenc. two-step process 7-25467
 BaO MBE on W (110) 7-16886
 Be, ^{3p} and ^{1p} Rydberg series, autoionising states, complex eigenvalue Schrodinger eqn. soln. 7-62329
 Bi, adsorpt. and growth modes on Pt (111), spectrosc., LEED and work function investig. 7-27102
 C, dielectric film growth, on GaAs and InP substrates 7-39420
 a-C:H films, plasma deposited, optical props. 7-27799
 C⁺ + He(H₂)(Ar)(Xe), one-step double electron capture 7-50344
 CO, soft X-ray induced fragmentation, Auger electron-ion coincidence study 7-36700
 CaF₂-Si (111) interface, electronic struct. 7-38737
 Cd, main and satellite structures 7-7795
 Cd₉₉Ag₃, Ag density of states, Auger and photoelectron spectra, Clogston-Wolff model calcs. 7-2451
 Cd_{0.9}Hg_{0.1}Te surface, electron-stimulated processes 7-13279
 CdS single crystals, subsurface region comp., laser radiation effects, AES study (Russian) 7-58329
 CdS-Cu₂S, solar cells, SEM and Auger microanalysis 7-23189
 CdSe_{0.65}Te_{0.35}/aqueous polysulphide interface, photoelectrochemical props. 7-52829
 CdTe, crystallographic polarity, determ. from Auger electron spectra 7-64830
 CdTe films, electrochemically deposited, comp., struct., AES, electron probe anal., X-ray diff. spectroscopy 7-58694
 CdTe films on InSb, interface struct. and band offsets 7-58664
 Co, Auger spectra, extended fine structures 7-64831
 Co foil surface, preadsorbed K, CO adsorption, XPS and AES studies 7-8296
 Co, L_{2,3}M_{4,5}M_{4,5} Auger process, meas. 7-57038
 Co surface, metal atom catalysed oxidation, UPS and AES studies 7-46865
 Co, X-ray emission K_{α1,2} spectra 7-64825
 Co-Ni-P electroless plated thin films, microstructure, mag. props., mag. recording appl. 7-27581
 Co-P electroless plated thin films, microstructure, mag. props., mag. recording appl. 7-27581
 CoCr films, corrosion in H₂SO₄, AES study 7-33824
 CoGa₂O₄, crystal growth, chemical vapour transport, struct., mag. and electronic props. 7-53517
 Co₈₀Ni₂₀ magnetic thin films, obliquely deposited, oxidation behaviour 7-65217
 CoSi (100), metal atom catalysed oxidation, UPS and AES studies 7-46865
 CoSi₂ self-aligned silicide technology using rapid thermal processing 7-52154
 Cr (110), chemisorption of O₂ 7-21662
 Cr and Cr-compounds, Auger and absorpt. spectra involving M_{2,3} levels, atomic effects 7-59311
 Cr carbonaceous films, prod. in situ in Tokamak TEXTOR, depth profiling 7-22893
 Cr, X-ray emission K_{α1,2} spectra 7-64825
 Cr²³⁺, dielectronic satellite spectra CI HFS calcs. 7-42506
 Cr/Cu multilayer structs., scanning Auger microprobe depth profiling, sputtering effects 7-58659
 Cr/Ni interface broadening and topography of Auger sputtered profiles 7-53485
 Cr-Ni multilayer thin film structures, AES depth profiling during sample rotation 7-27829
 Cr₂₃C₆, high-resolution Auger spectra, discrete variational Xα method 7-16942
 CrSi₂Ar⁺ ion beam induced surface and subsurface modifications, AES study 7-64846
 Cr₃Si, Ar⁺ ion beam induced surface and subsurface modifications, AES study 7-64846
 Cs, oxidation, quantum size effect of conduction electrons 7-13643
 CsI, surface stoichiometry, changes under electron and laser radiation 7-44961
 Cu (10,10) and (510), adsorption of Pb, faceting, LEED, AES studies 7-32828
 Cu (100), c(2X2)N overlayer, surface phonon dispersion, LEED, AES and EELS studies 7-12459
 Cu (100), XANES fluorenc. yield meas. of submonolayer linear hydrocarbon mols. 7-64751
 Cu (110), surface energy anisotropy, surface reconstruction 7-2346
 Cu (110) stepped faces, O₂ adsorption 7-27132
 Cu (111) with Ni overlayers, CO adsorption studies 7-21658
 Cu (111)-Fe crystal, CO adsorption 7-21616
 Cu (111)-Fe surface alloys, prep. and oxidation 7-22870
 Cu, Auger spectra, extended fine structures 7-64831
 Cu clusters on graphite, Auger spectra, size effect on linewidths 7-53455
 Cu deposited 7-65361
 Cu epitaxial film struct. and surface purity on MgO single cryst. substrates 7-16896
 Cu films, interaction with Cl₂, bulk diffusion processes 7-21783
 Cu films on MgO, epitaxial and electronic structures, LEED, AES, and EELS studies 7-52352
 Cu, resonant photoemission, atomic correl. effect 7-907
 Cu surface, interaction with Cl₂ 7-21642
 Cu surface modified by Al, electronic struct. and oxidation of surface 7-22443
 Cu, X-ray emission K_{α1,2} spectra 7-64825
 Cu, XPS, background removal 7-39355
 Cu:Ar(Ne)(C), single crystal, ion implantation, damage profile anal. using Auger electron spectroscopy 7-51802
 Cu/Pd metallic superlattices, UPS, LEED, AES and ISS studies 7-3153

Auger effect continued

- Cu-Al (111), S segregation, LEED and AES studies 7-2321
 Cu-Al₂O₃, interaction, X-ray photoelectron spectroscopy, Auger electron spectroscopy 7-58669
 Cu-Al-Ni-Ti-Zr, shape memory alloy, grain refinement, fracture mode, Ti and Zr additions effect 7-3301
 Cu-Fe host-impurity system, O ion bombarded, internal oxidation, Mossbauer spectra studies 7-59131
 Cu-Mn dilute alloys, oxidized formation, Auger lines' relative intensities 7-17726
 Cu-Ni alloys, chemisorpt.-induced surface segregation, time-of-flight atom probe and AES studies 7-32657
 Cu-Ni electrodeposition, comp. modulated alloy form. 7-59468
 Cu-Pd alloy, surface segregation, scanning Auger electron microscopy study 7-21578
 Cu-Rh, dilute alloy, surface composition, Auger electron spectroscopy 7-16845
 Cu-Si interface, surface struct., angle resolved Auger electron emission determ. 7-21672
 Cu-Ti alloys, amorphous and crystalline, H absorption 7-2369
 Cu-Zn, preferential sputtering, AES and SIMS studies 7-53467
 CuBe, oxidised, secondary electron emitters, AES and ESCA studies (Chinese) 7-54238
 Cu₂S-CdS solar cells, comp. of differing junction types, AES, SIMS determ. 7-23167
 Cu₂Si, oxidation, XPS and Auger spectra 7-22899
 CuSnBe bronze sheets, lamination investig., Auger and photoelectron studies (Russian) 7-13628
 ErSi₂, behaviour under ion bombard. and O exposure, AES, EELS 7-33506
 EuO (100), cleaved surface, struct. and comp. 7-12426
 EuS (100), cleaved surface, struct. and comp. 7-12426
 EuTe (100), cleaved surface, struct. and comp. 7-12426
 FE-Cr coatings for gun bores, morphology and erosive wear 7-46697
 Fe (100), resonant photoemission near 3p-electron excitation threshold 7-64876
 Fe (100) 7-8154
 Fe (100) with surface C, gasification by O, CO desorption 7-6993
 Fe, Auger spectra, extended fine structures 7-64831
 Fe, epitaxial growth on Cu (100) 7-52353
 Fe films, particulate, vapour deposition on Al₂O₃ growth and props. 7-17427
 Fe, L_{2,3}M_{4,5}M_{4,5} Auger process, meas. 7-57038
 Fe, magnetic surfaces, spin polarised Auger electrons 7-53456
 Fe particles on planar Al₂O₃ supports, low rate growth 7-32779
 α-Fe single crystals, activation energy of S diffusion, surface segregation, AES obs. 7-39529
 Fe surface, polycryst., interaction with O₂(N₂), electron spectrosc. obs. 7-7794
 Fe surface oxide layer, reduction by H adsorption, AES and LEED studies 7-8297
 α-Fe surfaces, segregated elements, bonding state 7-16763
 Fe thin films, stress development during oxidation 7-45096
 Fe ultrathin films on Pd (111), photoemission, LEED and AES studies 7-45068
 Fe, X-ray emission K_{α1,2} spectra 7-64825
 Fe/Fe-FeO/Al₂O₃ systems, diffusion bonded, interface chemistry, bonding strength 7-28079
 Fe/Ni Reed blades, Au coated, AES/SEM study 7-44972
 Fe-B amorphous sandwich films, concentration-dependent diffusion 7-45027
 Fe-based amorphous alloys, O₂ adsorption, ion bombardment effects 7-21637
 Fe-C-N, ion implanted, C surface contamination, AES and XPS studies 7-38312
 Fe-Cr-Mo, surface segregation, Auger anal. 7-16844
 Fe-Cu, epitaxially grown Fe films, electronic and crystallographic struct. 7-27214
 Fe-GaAs(001)-c(8X2) interface, simultaneous epitaxy and substrate out-diffusion 7-38355
 Fe-N, implantation at 77 K, surface comp., microstructure, AES, HVEM, transmission HEED studies 7-38033
 Fe-Si thin films, silicide formation, AES and EELS studies 7-32862
 Fe-Si-C single cryst., surface segregation and interactions 7-2322
 Fe-Sn (100), surface structural transitions during Sn surface segregation 7-52210
 Fe₈₀B₂₀ ribbons, amorphous and crystallised, surface comp., electronic props., topography, AES, XPS, ion scatt. studies 7-27065
 γ-Fe₂N, Auger spectra, electronic struct. (Russian) 7-64832
 FeNiCr, grain boundary solute segregation 7-56833
 FeNiCr:Sn, grain boundary segregation, Auger and energy dispersive X-ray mapping 7-16571
 Fe₄₀Ni₄₀P₁₆B₄, amorphous and crystallised alloys, surface oxidation behaviour 7-59666
 α-Fe₂O₃, photoemission satellites, electronic struct. 7-39358
 FeSi oxidised interface system, XPS, XAES and Auger parameter studies 7-7025
 Fe_{0.74}Tb_{0.26}, amorphous, oxidation 7-65192
 GaAlAs-GaAs heterostructures grown by MOCVD, transition region, ellipsometric anal. 7-2388
 GaAs (100)-Ni interface, effect of O on diffusion and compounding 7-21539
 GaAs (111), sorption of O, surface struct., AES anal. 7-53457
 GaAs (511) and (711) surfaces, struct. studies using LEED AES, and EELS 7-2312
 GaAs excimer-laser-stimulated CVD, polycryst. thin film growth and props. 7-64912
 GaAs films on amorphous insulating substrates, laser recrystallisation 7-38397
 GaAs films on oxidised Si, zone melting recrystallisation 7-38396
 GaAs, laser-enhanced oxidation, X-ray photoelectron and Auger electron spectroscopy 7-17739
 GaAs, laser-induced melting and nonlinear optical studies 7-12432
 GaAs, MBE initial growth stage on (100) Si substrate, RHEED, AES and TEM 7-52356
 GaAs MBE layer growth and surface anal. (Korean) 7-2417
 GaAs surface, H₂S adsorption, orientation and temp. depend. 7-58634
 GaAs surface cleaning using ECR radical beam gun 7-54028
 GaAs surface oxidation, AES, XPS and ellipsometry studies 7-22927
 GaAs, surface oxide desorption, temp. meas., Auger anal. 7-58608

Auger effect continued

- GaAs, surface potential barrier in ion-etched (100) surface, electron-voltaic effect 7-7819
- GaAs:In annealed substrates, In distribution in surface region 7-44959
- GaAs:Sn epilayers, MOCVD using triethylgallium and tetraethyltin, characterisation 7-22515
- GaAs/Au contacts, growth modes, AES, UPS, XPS and RHEED studies 7-21753
- GaAs/Ga_{1-x}Al_xAs (AlAs), short period superlattices, MOCVD growth, Raman scatt., AES, X-ray diff. 7-27386
- GaAs-Mo Schottky diodes, elec. characts. and microstruct. study 7-22015
- GaAs-thermal oxide interfacial chem. reactions, Raman spectra, AES 7-27145
- Ga_xIn_{1-x}As/GaAs heterostructures, low press. MOVPE, photolum., Auger profiling 7-27389
- GaP, ion-induced Auger electron emission under shadowing conditions 7-64841
- n-GaSb impurity Auger hole recomb. via deep acceptor, electron density depend. calcs. 7-38573
- GaSb-AlSb quantum well lasers, reduction of Auger effect, 1-5 μ m wavelength region 7-5893
- GaSe layer cpd., Al dopant intercalation, Auger and IR spectra studies (Russian) 7-32476
- Gd, spin-polarised Auger electron spectroscopy 7-33489
- Ge, amorphous films, laser induced image storage 7-11078
- Ge surface, GeO stabilisation on laser irradi., X-ray photoelectron spectra anal. 7-46723
- Ge surface, H₂S adsorption, orientation and temp. depend. 7-58634
- Ge-Sn heterostructure, MBE growth in ultra-high vac. system 7-2423
- GeMo-GaAs ohmic contact, fabrication and characts. study 7-45490
- GeSi thermally evaporated epitaxial heterolayers on GaAs substrate, Si distrib. (Russian) 7-63988
- GeSi-Si strained layer superlattices, growth using limited reaction processing 7-39430
- Ges_{0.5}Te_{0.5}, Auger elemental depth profiling, preferential sputtering 7-54247
- HBr, electron impact, Auger and Coster-Kronig spectra 7-15719
- H₂O, vap., mol. Auger transition rates, appl. to Auger spectrum, Stieltjes imaging method 7-62458
- He⁺(2S), muonic, binding in He gas, quenching mechanism study 7-36812
- HgCdTe, electronic struct., alloying effects, ETBM calc. method 7-64080
- Hg_{1-x}Cd_xTe MBE layers, plasma oxidation, oxide growth, comp. and surface struct. 7-54018
- I, X-ray photoelectron and Auger electron spectrosc. 7-5647
- In, main and satellite structures 7-7795
- In monolayer and multilayer surface diffusion, growth mode and thermal stability on W (100), LEED, TDS and scanning AES studies 7-2386
- In-Sn alloy, diffusion coeffs. of In and Sn determ. by AES using Xe ion bombardment 7-22405
- In-Sn alloys, solid and liquid, surface composition, Auger electron spectra study 7-12421
- InAs (110), oxidation, correlated changes of electronic surface props. 7-2354
- InGaAsP BH lasers, radiative, Auger and nonradiative currents 7-57312
- InGaAsP/InP heterostructures, carrier lifetimes and quantum efficiencies, photoluminesc. studies 7-64675
- InP (110) cleaved surface and Schottky diodes 7-58850
- InP, reactive ion etching, AES, photoluminescence, SEM obs. 7-65241
- InP:Sn substrate/epilayer interface, Sn depth profiling, AES and SIMS studies 7-27146
- n-InP:Zn, Zn diffusion 7-63882
- n-InP/Au Schottky contacts, surface treatment by plasma-induced O radicals, AES study 7-38674
- InP/Pd (110) interface, chem. reactions, overlayer morphology and Fermi level pinning 7-7020
- InSb, anodic native oxide, interface width, AES profiles 7-22911
- InSb, carrier lifetime, pressure depend. 7-52644
- InSb MOS interfaces, annealing, O diffusion and reaction 7-58665
- InSb surface, oxidation at room temp. 7-46734
- InSb-SiO₂ MIS structures, photo-CVD fabrication 7-38739
- InSe layer cpd., Al dopant intercalation, Auger and IR spectra studies (Russian) 7-32476
- Ir-Pt (2 at.%), surface segregation, AES study 7-27066
- Kr, 3p excitation, multiple photoionisation cross sections, TOF mass spectrometer anal. 7-19802
- Kr+Kr ions, quasimolecular Auger emission, impact energy depend. 7-25645
- La₂O₃ cryst., Auger spectra, electron polarisation effect 7-59313
- La₂O₃ dielectric system, Auger and photoelectron spectra, fine structures 7-13322
- Li₂, photoionisation and Auger electron emission, HF calcs. 7-36703
- Mg, local density of states region, determ. by core-core-valence Auger transitions 7-39325
- Mg, satellite and hypersatellite lines in K-LI Auger spectrum 7-30999
- MgO, cation solute segregation to surface 7-21593
- MgO, ion-induced Auger electron emission under shadowing conditions 7-64841
- Mn_{1-x}Zn_xFe₂O₄ substrates, Auger microprobe temperature profiles of contamination residue 7-59822
- Mo (100), adsorption of Ba and O, electron spectroscopy for quantitative anal. 7-13278
- Mo (110) chemically modified surface, Au thin film form. study 7-12489
- Mo, arc melting, impurity content, mech. props. 7-27980
- Mo/Si superlattice, sputtered, struct. anal. 7-45030
- Mo/Sb multilayer film, superconductivity and structural characterisation 7-17128
- Mo-Pd-Si, thin film metallisation system, interdiffusion, cpd. formation 7-21538
- Mo-Si(111)(2 \times 1) interface, early formation stage 7-27150
- MoS₂, intercalated with Fe, Ni and Pd, AES, sputtering studies 7-63867
- MoS₂(0001), Ar⁺-sputtered, adsorption props., LEED, AES, EELS, and work function studies 7-52275
- Mo(100), pulsed laser irradiated, use of LEED for surface damage charact. 7-21592
- N₂ soft X-ray-induced fragmentation, Auger electron-ion coincidence studies 7-42697
- N₂O, fragmentation by monochromatic soft X-rays, time-of-flight mass spectra 7-25610

Auger effect continued

- Na surface, interaction with O₂, photoemission and Auger studies 7-17063
- Nb/Si multilayered thin films, supercond. props. (Japanese) 7-64405
- Nb-Al thin film diffusion couples, Nb₃Al A15 phase form. during annealing, XPS and Auger studies 7-58548
- Nb-Si films, sputtered, superconducting props. 7-17126
- NbC, amorphous films, prep. and characts. 7-7885
- NbN(C) sputtered films on Nb substrates, surface props. 7-64833
- NbSe single crystals, vapour transport growth, superficial charact., AES 7-46253
- Ne, Auger process, relativistic close-coupling approach 7-62340
- Ne, electron impact induced post-collisional KL_{2,3}L_{2,3} Auger decay 7-5773
- Ne+F⁸⁺(P⁹⁺), k-k charge transfer, excitation patterns, Auger spectra 7-15682
- Ne**, He-like, X-ray and Auger transition rates 7-36507
- Ni (100), adsorbed S, segregation kinetics, AES and LEED studies (Chinese) 7-58607
- Ni (100), clean and O covered, adsorption and decomposition of N₂O 7-58644
- Ni (110) and (111), adsorbed S, surface struct., SEXAFS, XANES studies 7-64770
- Ni, Auger spectra, extended fine structures 7-64831
- Ni carbonaceous films, prod. in situ in Tokamak TEXTOR, depth profiling 7-22893
- Ni, D permeation rel. to surface impurities and Ar sputtering 7-52141
- Ni epitaxial growth on Fe (001), LEED and AES studies 7-64022
- Ni films on Mo or Cu surfaces, out-diffusion through Au overlayers 7-12511
- Ni finite films, sputtered, struct. and compositional studies 7-64024
- Ni, L_{2,3}M_{4,5}M_{4,5} Auger process, meas. 7-57038
- Ni, magnetic surfaces, spin polarised Auger electrons 7-53456
- Ni, oxidation, oxide epitaxy depend. on growth temp., LEED, AES, ellipsometry studies 7-22869
- Ni silicides, oxidation, catalytic effect of near-noble metal on Si oxidation 7-3545
- Ni surface modified by Al, electronic struct. and oxidation of surface 7-22443
- Ni, X-ray emission K $\alpha_{1,2}$ spectra 7-64825
- Ni/Cr multilayer films, AES sputter profiling, depth resolution 7-59358
- Ni-Cr alloy, surface segregation, scanning Auger microprobe study 7-22703
- Ni-Cr multilayers, interface resolution in Auger depth profiles 7-27830
- Ni-Fe (100) surface, break-up of oxide films by S₂ impingement, LEED and AES meas. 7-46260
- Ni-Pt, surface segregation, composition anal., AES studies 7-7999
- Ni-Si interface reactions induced by pulsed incoherent light, silicide formation 7-32725
- Ni₇₅B₁₅Si₁₀ amorphous alloy, metalloid redistribution, scanning Auger microprobe study 7-32655
- Ni₅₀Fe₅₀ (100) alloy, segregation and adsorption of S 7-21617
- NiFe₂O₄ sputtered films, struct., comp., AES study 7-22478
- NiFe₂O₄-MgO sputtered films, struct., comp., AES study 7-22478
- NiGeAuAgAu alloyed ohmic contacts to AlInAs-GaInAs heterostruct., charact. 7-22016
- NiO thin films, electrochromic switching props. determ. 7-39089
- Ni₂Si growth kinetics from Ni and Ni-V films on Si surfaces, TEM, AES, X-ray diff. and backscatt. studies 7-45032
- NiTi sputtered films on glass substrates, interfacial reaction, Auger study 7-22395
- O⁵⁺+He, resonant transfer excitation, Auger spectra obs. 7-50309
- O⁵⁺+He collisions, reson. transfer and excitation to specific LS-coupled state, 0° AES 7-36744
- O⁶⁺+He(H₂)(Ar)(Xe), one-step double electron capture 7-50344
- O₂, adsorbed on Cu (110) and polycrystalline surfaces, UPS, XPS, AES, EELS, LEED studies 7-32820
- P-containing compounds, Auger parameters and relativistic Dirac-Fock atomic calcs. 7-15651
- Pb electrodeposition from aq. HCl soln. onto Pt (111) 7-27954
- Pb-In-Au fine-grained codeposited alloy films, RF plasma oxidation 7-53970
- Pb₂Ge₂O₇, surface segregation of Pb upon heating to the melting pt. 7-6931
- Pb₈₀Si₂₀, amorphous, thermal stability, Auger study 7-58577
- Pb₉₇Sn₃ alloy surface, sputtering related phenomena (Chinese) 7-59316
- PbSnEuTe, superlattices, prep. by hot wall epitaxy, props. (Japanese) 7-12546
- Pb_{1-x}Sn_xTe surfaces, AES, LEED and Kikuchi pattern obs. 7-52200
- Pd (001), angle-resolved Auger electron spectroscopy, incident beam effects 7-3122
- Pd (100) with Na (NaO) overlayers, adsorption of methanol, formaldehyde and formic acid 7-21657
- Pd (110) with chemisorbed N₂, EELS, LEED and AES 7-63960
- Pd Frank-Van der Merwe growth on Ag (111), AES, surface reflectance spectra studies 7-32829
- Pd monolayers on Ta(110), morphology and struct. phase transitions 7-38374
- Pd-Rh, high temp. air oxidation, surface comp., AES 7-22891
- PdSi, phase transform. to Pd₃Si, kinetics 7-16795
- Pd(111), with adsorbed S, Auger electron spectroscopy study of adsorbate oxidation kinetics (German) 7-33953
- Pt (100) with underpotential deposited Pb 7-58646
- Pt (110), surface energy anisotropy, surface reconstruction 7-2346
- Pt (111), adsorption of ethylene oxide, surface interactions, XPS, TDS, AES, EELS studies 7-33963
- Pt on Si, struct. and comp. of silicides formed in photon annealing, Auger obs. 7-2402
- Pt surface, graphite island form., FEM, SEM and AES studies 7-32805
- Pt surfaces, impurity segregation, high resolution AES studies 7-33668
- Pt-group metal silicides epitaxial growth on Si (111) 7-21760
- Pt-Rh alloys, surface composition, lattice vibrational entropy 7-52207
- Pt_{1-x}Si_x/n-GaAs contacts, elec. and metallurgical characts. 7-64345
- Pt₃Sn oxidation at low pressure, AES, ESCA, ISS study 7-17725
- Pt₃Ti (111), chemisorption of CO and O₂ 7-27131
- Rh epitaxial film struct. and surface purity on clean and Cu-covered MgO single cryst. substrates 7-16896
- Rh surfaces, clean and B contaminated, adsorption and dissociation of H₂O 7-27135
- Ru (001), alkali modified, adsorption of O, TDS, AES, EELS, work function meas. 7-58637

Auger effect continued

- Ru (001), CO and K coadsorpt., angle resolved Auger lineshapes 7-2372
 Ru (001), coadsorption of H₂O and Li 7-21645
 Ru (001), H₂ chemisorption, effect of coadsorbed O₂, LEED spectra anal. 7-33959
 Ru (1010) with K overlayers, struct. and energetics, chemisorption and desorption studies 7-21659
 S-containing compounds, KLL Auger and core level photoelectron shifts, binding energy 7-15647
 Sb, main and satellite structures 7-7795
 Se, Auger spectroscopy, edge effects 7-3121
 Se₃₀Te₇₀, Auger elemental depth profiling, preferential sputtering 7-54247
 Si (III) surface, Cu deposition, Auger electron spectrosc. obs. (*Russian*) 7-27833
 Si (100), nitridation kinetics in NH₃ by thermal activation or electron bombard., LEED, AES, and TDS study 7-39770
 Si (100), reaction with propylene, adsorption and desorption kinetic meas. combined with Auger spectroscopy 7-65348
 Si (100), reactivity, thermal desorption of propylene, defect- and electron-enhanced chemistry 7-21660
 Si (100) and (111), adsorption of K, AES, work function meas. 7-32818
 Si (100)-(2×1), adsorption kinetics of propylene, propane and methane, chemical activity of C=C double bond 7-27127
 Si (100)2×1, interaction with O₂ and N₂O 7-63962
 Si (111), metal atom catalysed oxidation, UPS and AES studies 7-46865
 Si (111), thermal oxidation, initial stages, AES, LEED and photoelectron spectra studies 7-3543
 Si (111) with adsorbed Ga, X-ray photoelectron and Auger electron diffraction 7-27116
 Si (111)/Au interfaces, structural and electronic props., annealing effects 7-21679
 Si (111)-(7×7), interface formation during W deposition 7-58710
 Si buried oxide structure formed by O ion implantation 7-12099
 Si carbonaceous films, prod. in situ in Tokamak TEXTOR, depth profiling 7-2893
 Si, contamination levels, sensitivity of meas. 7-54245
 Si, diffusion length depend. on cooling rates and bulk resistivity 7-7266
 Si ion implanted surface dopant cross-contamination, enhanced diffusion effects 7-32719
 Si, oxidation, catalytic effect of near-noble metal 7-3545
 Si oxide, nitride and element, L₂₃VV valence Auger transitions 7-27828
 SiO₂ structures, implanted buried oxide, high-temp. annealing 7-6654
 Si, semi-insulating polycrystalline films, electrical conduction mechanism 7-52869
 Si solar cell performance, influence of heavy doping 7-23147
 Si solar cells, heavy doping effects 7-3653
 Si surface, Ar⁺ ion impact, LMM and LVV Auger electron emission 7-59320
 Si surface, electromigration of Ag, In, Sb, and Sn ultrathin films, scanning AES study 7-63891
 Si surface, O adsorpt., orientation depend., AES and photoelectron spectra 7-52237
 Si surface, reaction with propylene, effect of addition of H 7-54187
 Si, surface contamination during reactive ion beam etching with Cl₂ 7-3539
 Si surface layers characterisation after annealing in an RF H plasma 7-58630
 Si surface roughening by reactive ion etching, mech. 7-65240
 Si surface state after plasma etching in a diode type system 7-6940
 Si surfaces, adsorbed C, annealing behaviour, XPS and AES studies 7-27108
 Si:B(P), microcrystalline, LPCVD production, anal and solar cell appls. 7-17452
 Si:C,N, ion implanted, C surface contamination, AES and XPS studies 7-38312
 Si:H, polycrystalline, grain boundary interactions 7-12117
 Si:(Ti)(Ge)(P)/Pt system, impurity migration during silicide form. 7-6895
 Si/a-SiO₂/ZrO₂-Y₂O₃, SOI system fabrication, charact. 7-22025
 Si/Au buried interface struct. determ., optical second harmonic generation studies 7-63982
 Si/PtSi(CrSi₂) Schottky diodes, surface imperfection induced elec. leakage paths 7-2719
 Si/Ti selectively sputter deposited interface, Auger and Rutherford backscatt. studies 7-21690
 Si-Au interface, atomic bonding 7-58663
 Si-B₂O₃ interaction during Si MBE, Auger spectra study 7-13277
 Si-Cu, interface, Auger electron emission (*Russian*) 7-17100
 Si-Cu interface, atomic bonding 7-58663
 Si-Ge interface, solid phase epitaxy, intermixing, EXAFS, AES, LEED obs. 7-63973
 Si-InP (110) heterojunction, characterisation 7-33079
 Si-metal-Si multilayers, backscattering contribution to Auger line intensity 7-28379
 Si-SiO₂, interface props., ellipsometry (*Russian*) 7-17293
 Si-SiO₂, MBE SOI formation, Auger study 7-32876
 Si-SiO₂, Si oxidation kinetics, interface width determ. 7-39764
 Si-SiO₂ interface, AES depth profiling during sample rotation 7-27829
 Si-silicide interfaces, electronic struct. 7-21972
 Si-Ta interface, depth profile, Ar⁺ ion bombard., Auger electron spectra anal. 7-46261
 Si-Ti(TiSi₂), Schottky barrier height investig. 7-2716
 SiAlON-YAG ceramics, Auger electron microscopic quantification of phase comp. 7-22951
 SiC (0001) and (0001) surface segregation, electron spectroscopy 7-21459
 SiC (0001) surface, slip lines, AES studies 7-44559
 SiC corroded, scanning Auger microscopy study 7-13617
 SiC-based ceramics, sintered and hot isostatically pressed, microanalytical investigation 7-27991
 SiH₄, 2p threshold, reson. relax. processes, XPS 7-42684
 SiH₄, core-excited state, Auger decay 7-42689
 SiH₄, mol. orbitals dynamic polarisation in Auger emission 7-5724
 SiN films, Auger line, influence of Ar⁺ ion bombardment 7-39339
 Si₃N₄, surface structure and chemisorption, XPS, AES and direct recoil studies 7-32790
 Si₃N₄-Ti, reaction under rapid thermal annealing 7-39334
 Si₃N₄-x amorphous thin films grown by ion beam assisted deposition, IR and ion beam anal. 7-39209

Auger effect continued

- Si₃N₄ film form. and charact., ion and vapour deposition method 7-13370
 SiO₂, electron induced dissoc., AES study 7-22392
 SiO₂ films, effects of nitridation press. on props. 7-33818
 SiO₂ films, hydrogenation during thermal nitridation in NH₃ 7-13763
 SiO₂, gate dielectric films, growth by rapid thermal processing, material and electrical props. 7-16906
 SiO₂ native oxide, ion and electron bombardment induced surface modifications studies 7-12175
 SiO₂ optical waveguides, low-loss planar, fabrication using thermal nitridation and charact. 7-26032
 SiO₂ surface interaction with CF₃⁺ and CH₄⁺, mol. sputtering model calcs., AES meas. 7-27854
 SiO₂-Si interface, roughening induced during AES depth profiling 7-21685
 SiO₂, amorphous, photoassisted oxidation 7-46662
 SiO₂ films deposited by reactive evaporation, characterisation 7-64013
 SiO₂ thin films, plasma enhanced CVD deposited, Si chem. states, IR spectra, XPS, AES 7-21721
 SiON-GaAs interface, plasma enhanced CVD deposited SiON, NH₃ plasma pretreatment effects 7-7874
 SiO₂N_y films, deposited by plasma-enhanced CVD, charact. 7-2413
 SiO₂N_y, high press. NH₃-nitrided, elec. characts. 7-39039
 SiO₂N_y LPCVD layers, phys. and elec. charact. 7-38792
 Sm⁴⁺+Xe collisions, q=34 to 52, resonant electron transfer and L-shell excitation, X-ray spectra study 7-30979
 Sn, main and satellite structures 7-7795
 Sn-Ge interface form., growth mode, AES, RBS studies 7-58666
 SnO₂/Sb spray deposited coatings, comp., elec. props. thermal treatments, AES study 7-22393
 Ta films, maskless ion beam assisted deposition 7-46342
 TaH_c foils, H desorpt., Auger electron and thermal desorpt. spectra studies 7-32800
 Ta₂O₅/H films, NPL standard, distrib. of H, AES and SIMS 7-26789
 TbFeCo/dielectric interface, chemical stability, interdiffusion and oxidation, AES, XPS and RBS depth profile studies 7-12513
 (Te₉₀Ge₁₀)_{100-x}O, Auger elemental depth profiling, preferential sputtering 7-54247
 (Ti,Al)N layers on high speed steel, morphology and props., deposition temp. and sputtering atmosphere depend. 7-53975
 Ti, Auger spectroscopy, edge effects 7-3121
 Ti, inner-shell excitations, correlation effects, XPS, AES and APS 7-46247
 Ti, oxidation, Rutherford backscattering spectrometry, AES, X-ray diffraction, elec. resist. meas. 7-22894
 Ti thin films, dissolution and diffusion of O, resist., X-ray diffraction, particle backscatt. and AES studies 7-58913
 Ti-Si interface, silicide form., Auger and appearance pot. spectra studies 7-45031
 Ti-Si MIS Schottky barriers, influence of silicide formation on barrier height, Auger meas. 7-45499
 TiC, amorphous films, prep. and characts. 7-7885
 TiC film ion plated on austenitic stainless steel, adherence rel. to ionisation (*Japanese*) 7-53636
 TiC_x, KVV Auger electron spectra and band struct. (*Russian*) 7-17371
 TiFe, adsorption of O, AES study 7-59312
 Ti₂Fe₂O, adsorption of O, AES study 7-59312
 TiN films on tool steel, plasma-assisted CVD deposited, interfacial composition 7-52303
 TiN, plasma enhanced CVD, rel. to reactive sputtering 7-39427
 TiN, sputter-deposited thin films, AES, XPS and RBS studies 7-52327
 TiN(C) hard reactively sputtered and evaporated coatings, composition and microstruct. studies 7-52331
 TiN(C) sputtered films on Nb substrates, surface props. 7-64833
 TiNi, adsorption of O, AES study 7-59312
 TiO₂(110), stoichiometric and defective surfaces, chemisorption of H₂ and CO 7-6983
 TiSi₂ formation kinetics on Si (100) and Si (111) 7-38273
 TiSi₂, oxidation, Rutherford backscattering spectrometry, AES, X-ray diffraction, elec. resist. meas. 7-22894
 TiSi₂ vacuum electron beam evaporation, annealing effects, Auger and electron diffraction anal. 7-22492
 TIL, X-ray photoelectron and Auger electron spectrosc. 7-5647
¹⁶⁹Tm, KLL group Auger electron spectrum meas. 7-30995
 U surface oxidation, substoichiometric oxide form., AES and XPS studies 7-46714
 UO₂ thin films form by oxidation, luminesc. studies 7-22351
 V, inner-shell excitations, correlation effects, XPS, AES and APS 7-46247
 V surface, S segregation, effect on H permeation, AES anal. 7-32660
 VC, high-resolution Auger spectra, discrete variational X α method 7-16942
 VC_x, KVV Auger electron spectra and band struct. (*Russian*) 7-17371
 W (100), C and Si coadsorption, Auger spectra studies 7-63954
 W (110), adsorption of Eu, Gd and Tb 7-27118
 W CVD films, chem. charact. 7-16915
 W films, maskless ion beam assisted deposition 7-46342
 W LPCVD film thickness depend. on native oxide thickness 7-17473
 W, polycryst. foils and single crystals, chemical etching, ion bombardment effects, AES study 7-28212
 W selective LPCVD films on Si substrate, characts. 7-38409
 W selective low press. CVD growth on Ti, TiSi₂ and PtNiSi, surface reactions, struct. 7-27183
 W, surface, interaction of He molecules, Auger anal. 7-64858
 W thin films, plasma-assisted etching, ion bombardment effects, quartz cryst. microbalance studies 7-28211
 W-Si amorphous thin films, interfacial reactions with polycryst. metal overlayers, AES study 7-21763
 W-Ti-Si interface, WSi₂ form. by rapid thermal annealing, growth kinetics, Ti film effects 7-63969
 WSi_x CVD films on Si and Si₃N₄ coated Si, excess Si redistribution upon annealing 7-21723
 Xe, 4p excitation, multiple photoionisation cross sections, TOF mass spectrometer anal. 7-19802
 Xe, charge referencing during XPS sputter profiles 7-15566
 Xe ion laser, short-wavelength, pumped by Auger decay, obs. 7-36938
 Xe vacancy cascade following inner-shell ionisation, Monte Carlo simulation 7-30998
 Y₂O₃-ZrO₂/Fe, high dose ion implanted, profile shapes and electronic cond. 7-32472

Auger effect continued

- Zn, $L_{2,3}$ -MM Auger electron spectrum, correl. effects influence 7-57037
 $ZnCr_2O_4$, crystal growth, chemical vapour transport, struct., mag. and electronic props. 7-53517
 Zn_3P_2 valence band struct., XPS and Auger lineshape studies 7-45150
 $ZnSe-In_{1-x}Sn_xO_{3-y}$ junctions, microstruct. optical props., influence of deposition method 7-21689
 $ZnTeSeS$, superlattices, prep. by hot wall epitaxy, props. (*Japanese*) 7-12546
Zr (0001) HCP to BCC phase transition He^+ capture effects, AES, TDS and SIMS studies 7-58590
Zr-Ni dil. alloy, Auger electron anal. of oxides 7-22907
 ZrC_x , reactively sputtered films, optical props. 7-39202
 $ZrN(C)$ hard reactively sputtered and evaporated coatings, composition and microstruct. studies 7-52331

Auger electrons *see Auger effect***Auger recombination** *see Auger effect; electron-hole recombination***Auger showers** *see cosmic ray showers and bursts***Auger spectra** *see Auger effect***Auger spectroscopy** *see Auger effect***augmented plane wave calculations** *see APW calculations***aural null direction finders** *see radio direction-finding***aurora**

see also atmospheric elementary particle precipitation; atmospheric spectra

- arc electrodynamics correlation with neutral winds 7-47609
aurora borealis and aurora australis, relation to solar wind-magnetosphere interaction (*French*) 7-60439
CCD-image intensifier camera, for all-sky observation 7-40603
conjugacy of electron and proton auroras (near $L=6.1$) 7-60440
dayside aurora, assoc. electron precipitation and ionosphere convection morphology characts 7-55352
dayside aurora, EUV-near IR O mission features obs. 7-55345
electron energy spectra and electrostatic cyclotron waves during diffuse auroras, coordinated obs. 7-34763
emissions and interplanetary mag. field B_z component 7-34777
F-layer irregularity obs. of SAR arc event 7-60470
faint auroral arc, study of elec. field configuration and plasma parameters 7-29337
flare activity during magnetically quiet periods 7-55379
LHR noise, obs. by S-310JA-6 sounding rocket (1978 August 27) 7-66393
low-latitude aurora and storm time current systems 7-29327
magnetosheath plasma transfer signatures in dayside aurora 7-9285
narrow auroral arc, EISCAT and optical observations 7-47607
night sky obs. using grating spectrometer with imaging photon detector 7-34722
plasma, electrostatic potential due to high-speed plasma flow 7-14403
post-noon auroral oval dynamics 7-55350
pulsating aurora, resonant phenomena accompanying seismic-ionospheric electrical interaction 7-28890
pulsating aurora and concurrent geomagnetic pulsations 7-47634
stable auroral red arc conditions, bi-Maxwellian transport eqns. 7-55365
visibility in NE America and W Europe 7-47608
 N_2^+ , electron impact on N_2 , A $^2\Pi_u$ state excitation rate meas. 7-19934
NO aurora, IR radiation and energetics in disturbed heated thermosphere 7-4247
 $N^+(^4S)$ metastable state produced by electron impact on N_2 and UV aurora 7-29328

austempering *see heat treatment***austenitic stainless steel**

- α -particle irradiated, mech. props. and microstruct. 7-51872
abrasive wear mechanism, wear process successive obs. in SEM 7-8229
accelerated fretting wear testing using ultrasonics 7-22967
age hardenable, SCC in PWR coolant water, heat treatment and Zr additions effect 7-39708
air exposure effects, mixed Fe-Cr oxide/hydroxide film form., XPS study 7-22878
Alloy 800, pitting corrosion in chloride-sulphate media, potentiodynamic polarisation 7-65184
Alloy 800 H, high temp. fatigue, damage mechanism (*German*) 7-17604
amplitude depend. damping rel. to annealing and tempering (*German*) 7-13498
austenite ordering struct., X-ray diffr. studies (*Russian*) 7-6579
austenitic-pearlitic, N effect on phase comp. and props. 7-53754
bars, cylindrical, with deviations from ideal form, creep behaviour (*German*) 7-3390
biaxial loading, high temp. intergranular crack growth 7-53902
boronizing and alloying elements influence 7-59661
bright annealed, selectively absorbing surface, oxidation prep. 7-8186
BWR pipe welds, toughness and tensile props. 7-46650
cavitation erosion tests (*German*) 7-33809
ceramic coatings, plasma sprayed, hot isostatic pressing, hardness, bond strength 7-13624
cold-worked, irradi. and unirradi., liq. Cs, Te-induced fatigue embrittlement 7-46637
cold-worked, SCC and hydrogen embrittlement 7-13637
compatibility with liq. and solid T breeding materials 7-53966
corrosion, γ -radiation effect 7-28173
corrosion, high temp., by oxidising gases (*Korean*) 7-8161
corrosion and grain boundary Cr depletion, comparison in modified Strauss test 7-39728
corrosion fatigue, crack initiation determ. (*German*) 7-3527
corrosion in flowing Li environment, temp. and purity depend. 7-53961
corrosion in flowing Pb-Li environment 7-53959
corrosion in flowing PbLi eutectic 7-53958
corrosion in high temp. water containing both dissolved H and O 7-65177
corrosion in molten thermally convective Pb-Li 7-53962
corrosion in Na loop system, downstream effects 7-3504
corrosion in thermally convective Li 7-53960
corrosion product release in lithiated high temp. water, mechanism and kinetics 7-65172
corrosion rate, pitting, meas. by means of 60 Hz Lissajous figure (*Japanese*) 7-8212
corrosion resist. in Cl^- containing water at high temp. (*German*) 7-3525
corrosive wear in NaCl soln. 7-8191
crack propagation resist., in connection with limiting crack resist. 7-59629
austenitic stainless steel continued
crack tip cyclic plastic work, load ratio, frictional work 7-53897
creep, effect of hydrogen charging (*Chinese*) 7-8042
creep and anelasticity at const. homogeneous dislocation struct. 7-17586
creep cavitation rel. to S and P impurity segregation 7-39587
creep rupture, fatigue cracking in flowing liq. Na 7-53843
creep rupture, in-beam, 873K 7-53851
creep rupture properties of heavy section Type 304 forgings for LMFBRS 7-13582
creep strain, resulting changes in subboundary mesh size 7-46575
creep study, 773 to 1073 K, of EP 838 7-59567
creep-fatigue cracks, high temp., strain range partitioning anal. (*Japanese*) 7-33781
crevice corrosion NaCl soln., electrochemical kinetics 7-39701
defects study by positron annihilation 7-39296
disc bend test, parameterize anal. 7-54039
dislocation structure and secondary cyclic hardening at 600°C 7-33783
dual phase, phase transform. obs. using thermomag. analysis 7-53696
ductile failure under biaxial loading, thermal transients, analytical model 7-59609
elastic moduli at 4 K, C and N effects 7-46541
electrical resistivity and magnetisation, temp. depend. 7-38535
electron beam welded, void swelling under electron irradi. 7-51830
electron irradi., cold working, vacancy swelling, void form., carbide precip., electron microscopy 7-21282
extrinsic grain boundary dislocations, spreading kinetics 7-44569
fatigue, low cycle, 350 to 550°C, microstruct. developments, effect on cyclic strength and life 7-39646
fatigue, low-cycle, notch effect at elevated temps., life prediction 7-53899
fatigue crack development, fractographic characts. 7-46643
fatigue crack growth and crack closure under creep conditions (*Japanese*) 7-59616
fatigue crack growth at notch root in elastic-plastic region (*Japanese*) 7-58404
fatigue crack growth in FBR castings and weldments, fast neutron irradiation effects 7-28127
fatigue in simulated fast reactor environments, type 316L 7-39759
fatigue props., time-depend modes, dislocation concepts appl. 7-28128
FBR material, crack propag. under creep-fatigue interaction condition 7-22837
FCC lattice, stacking fault energy calcs. (*Russian*) 7-12081
foil, air oxidation, Cr depletion, Mossbauer spectra 7-39702
Frascati Tokamak limiters, struct. and chem. modifications compared with disruption simulation damage 7-51521
fusion reactor blanket material, oxidation and volatilisation rates in air 7-53957
fusion reactor first wall, fast neutron irradi., microstruct. evolution model 7-51846
fusion reactor first wall behaviour after plasma disruption, electron beam expt. 7-62068
fusion reactor first wall material, H permeability study 7-62058
fusion reactor material, low-activation, constitution, struct. and mech. props. 7-42195
grain boundary microstruct., He embrittlement resistance 7-56829
heat-resistant, carburisation, effect of scale constitution 7-33844
heavy ion bombarded, η -phase precipitate form., electron microscopy studies 7-13459
heterogeneities, small angle neutron scatt. studies 7-51580
high cycle fatigue props., age hardening 7-13598
high press. deform., twinned struct., TEM obs. (*Russian*) 7-46578
high temp. ductility, H and He effects 7-5406
ignition of bulk type 302, by laser heating 7-3516
in-reactor deform. 7-56826
Inconel welds joining dissimilar metals, radiographic evaluation 7-39828
intercrystalline corrosion causes and countermeasures (*German*) 7-17729
intercrystalline corrosion rel. to chromium carbide precip. 7-53986
ion-nitrided, struct. and props. 7-22884
Kh12N23 precipitation hardened steel, Ar ion bombardment, ageing temp. effects on structure, microhardness and sputtering 7-65120
laser surface melted, residual stresses 7-3506
laser welded, pulsed and continuous, solidification behaviour and microstruct. characts. 7-13444
liquid phase sintering, effect of Si additions 7-53678
long term creep, transient strain induced strengthening 7-28090
low activation, development, mechanical props., fusion reactor structural material 7-53799
low cycle fatigue damage, crack initiation (*Japanese*) 7-33780
low dose neutron irradiation, spectral effects on yield stress for AISI 316 7-51850
LWR, pressure vessel materials, environmental sensitive cracking (*German*) 7-10214
LWR cladding, oxidation in high temp. steam, LOCA appl. 7-727
LWR piping, ASME code for flaw eval. 7-13601
machining of stainless steels, failure mechanisms of ceramics and coated carbides 7-3432
materials erosion and redeposition studies at PISCES facility, net erosion under redeposition 7-49637
mechanical properties, H effects (*Russian*) 7-46603
microbial pitting mechanism 7-39724
microstructure rel. to cathodic H charging 7-28039
neutron irradiation effects on mech. props., damage and yield stress 7-51865
nitrided, ion milling 7-59660
nonequilibrium grain-boundary segregation kinetics 7-59525
nuclear grade, SCC in simulated BWR environments 7-46682
nuclear plant irradiated steel handbook 7-38069
on-site oxidation monitoring in AGRs 7-59677
oxidation and descaling behaviour, influence of annealing (*Japanese*) 7-59665
oxidation performance of Magnox and AGR boiler materials in high press. CO_2 7-59676
oxidation state in divertor of Heliotron E plasma device, XPS obs. 7-17704
oxide scales formed in CO_2 at 825°C, microstruct., influence of ion implantation 7-65196
passivation and pitting corrosion rel. to Ti stabilisation and Mn content (*German*) 7-39756
passivation pot., Cr content depend., percolation model 7-22879
passive films, photoelectrochemical charactn. 7-28171
passive layers, elec. cond. rel. to W alloying 7-17676
PCA, tritium permeation props. 7-38239

austenitic stainless steel continued

- pipe, subjected to bending deform., fracture instability, effect of multiple circumferential through-wall cracks 7-65122
- pipe weldments, toughness at LWR operating temps. 7-13599
- pitting corrosion behaviour in NaCl solns. under heat transfer conditions (Japanese) 7-33832
- pitting corrosion in NaCl soln., electrochemical obs. 7-39700
- plastic creep, laws of high temp. behaviour (French) 7-13523
- polarization effects in galvanic corrosion 7-39706
- powder compacts, props., influence of sintering conditions (Korean) 7-17496
- pre-precipitation phenomena associated with γ form. 7-22696
- precipitate stability, during heavy ion irradiation 7-58367
- precipitation and B grain boundary segregation studies 7-33673
- precipitation of σ -phase, equivalent Cr concept 7-59528
- precipitation strengthened, creep fracture, 875-975K 7-8046
- pure, solid/liquid interface, pulse echo US study of location during solidification and melting 7-52006
- PVC-stainless steel powder mixtures, shock consolidation, densification, industrial appls. 7-39473
- quenching from liq. state, cooling rate calc. 7-22726
- radiation damage process obs. using high voltage electron microscopy 7-51831
- rapidly solidified, microstruct. characterisation 7-22672
- rapidly solidified by melt spinning, photocalorimetric cooling rate meas. 7-46438
- reactor pipe fracture safety analysis using limit load and J-integral techniques 7-13585
- reduced activation alloys, development, fusion material appl. 7-53664
- residual stress meas. SEM/ASTM round robin study 7-13680
- rolled, characts. of α - γ transform. in different texture components. (Russian) 7-59516
- SCC, chloride, O and corrosion pot. effects 7-39719
- SCC, delayed fractures under mode III loading, H induced cracking 7-53898
- SCC at const. load in molten NaCl-CaCl₂ at 570°C 7-53944
- SCC resistance, intergranular, influence of Si 7-46681
- SCC susceptibility in polythionic acids 7-65183
- sensitisation resistance improvement, application of analytical electron microscopy 7-39762
- sensitised, corrosion in sulphidising atmosphere 7-17710
- sensitised, SCC, re-anal. of results from constant extension rate tests 7-39723
- sensitised, SCC in high temp. Na₂SO₄ soln. 7-39735
- sensitized, intergranular corrosion, inhibition mechanism of S-containing additives 7-53946
- single crystal, SCC and pot. depend. in MgCl₂ soln. (Japanese) 7-33831
- single crystals, rolling texture and elastic consts. (Russian) 7-51912
- sliding wear, high temp., in CO₂ atm., effect of low conc. additions of O₂ 7-33806
- sliding wear, unlubricated, reciprocating, in CO₂ at 20 to 600°C 7-17662
- slow strain rate SCC in NaCl soln., cathodic protection 7-39709
- softening mechanism in hot working 7-3333
- strain ageing and load relax. behaviour at room temp. 7-28092
- strain distrib. within crack tip plastic zones 7-3396
- strain hardening in powder metallurgy alloys 7-22721
- strain martensite determ., eddy current method 7-3559
- strain rate sensitivity, strain hardening and yield behaviour 7-53829
- streaking effects of H induced ϵ martensite phase, TEM obs. 7-28038
- strength and toughness at 4K, fusion energy magnets appl. 7-53793
- stress corrosion cracking susceptibility, cathodic reduction treatment effects 7-8185
- structural materials, swelling after neutron and ion irradiation, comparison 7-58357
- surface, S containing corrosion inhibitor removal 7-39717
- surface degradation in elevated temp. gas-particle streams 7-3520
- surface phase transform. relat. to H charging and ageing 7-17530
- SUS316, 40 keV Cu⁺, Fe⁺ and fission neutron irradiation effects. 7-56823
- swelling by electron irradiation, influence of appl. stress (Japanese) 7-16632
- swelling under dual ion beam irradiation. 7-44629
- tensile, creep and low-cycle fatigue props., effect of prestrain (Japanese) 7-46621
- tensile and impact props., effect of grain boundary carbides 7-33785
- thermal and mech. props., fusion reactor appl. 7-53795
- threshold behaviour of small fatigue cracks at notch root 7-3395
- Ti modified, void swelling and precipitation, aging effects 7-33685
- transition class, deform. method effect on microstruct. 7-3299
- type 304, tubes, surface stress meas. using blind-hole strain gauge method, calibration 7-65249
- Type 316, microstruct. exam. around weldments 7-22697
- uniaxial straining, sensitisation developments, STEM/EDS and electrochemical potentiokinetic reactivation methods 7-54014
- unlubricated wear at room temp., environment influence, type 316 steel 7-8121
- US response from artificial defects 7-46762
- valve type, heat treatment schedule effect on failure nature 7-3423
- void stability, effect of O 7-58262
- weld joint, austenitic surfacing-pearlitic transition zone, cyclic crack resist. 7-17691
- weld metal, tensile and fracture props. at 4K 7-53901
- Al base alloys, fusion reactor first wall, plasma disruption damage calc. 7-791
- Al-stainless steel powder compacts, liq. phase sintering 7-7916
- Al₂O₃ film adhesion, improvement using surface precipitates (Japanese) 7-22880
- Cr-Mn and Cr-Mn-Ni types, corrosion and SCC behaviour 7-17683
- Cr-Mo, weld metal, creep crack growth 7-17623
- Cr₂₃C₆ precipitation kinetics (German) 7-46486
- D permeability, He irradiation effects 7-2267
- Fe-Ti/AISI 304 stainless steel system, ion beam mixed, wear and friction studies 7-46657
- H plasma, pulsed, surface blistering, formation mechanism 7-63667
- He production and long-term activation by protons and deuterons, fusion reactor appl. 7-58371
- He-induced creep ductility loss, prediction and anal. 7-53854
- Mo and/or N alloyed, recrystn. after hot working 7-3326
- Mo ion plated, corrosion resist. in flowing Na environment 7-59667
- Mo-N alloyed, static recrystn. and hot ductility 7-3327
- N alloyed, mech. prop.-struct. relationship 7-3316
- N segregation to grain boundaries 7-59537
- N-bearing, Nitronic 60, fretting wear at temps. up to 600°C 7-17653

austenitic stainless steel continued

- N-containing, thermochemically produced, wear 7-17651
- N-rich alloys, vacancy swelling suppression mechanism 7-46511
- Ti addition effect on swelling under HVEM conditions 7-58343
- Ti-stabilised, high temp. embrittlement modification of rad. induced He distrib. by thermo mech. pretreatment (German) 7-17643
- TiN dispersion hardened, creep below transition stress 7-65079
- Zn_{0.25}Cd_{0.75}Se mixed crystals., electron and hole deep level traps 7-16980
- austenitic steel**
- see also austenitic stainless steel
- carbide nucleation, precipitation growth in nonoxidable austenitic steel (Spanish) 7-53732
- cold deformed, mag. props. (Russian) 7-45734
- corrosion product layers in PWRs at pH 7 (German) 7-19356
- crack initiation at grain-boundary triple points in high-temp. deform., continuum mech. model 7-28104
- fusion reactor first wall, gas thermal desorption by plasma streams 7-49616
- fusion reactor first wall, implantation-driven permeation characts. 7-49640
- fusion reactor first wall material, development and testing 7-53860
- Hadfield, cold-deformed, fine struct. anal., brittle fracture (Russian) 7-59570
- martensite transformation start temperature increase in electrolytic H impregnation, internal microstresses role 7-17690
- martensitic transformation, residual stresses establishment 7-33657
- martensitic transformation, strain-induced, strain rate effect 7-7996
- metastable, anomalous plasticity, slip, microtwinning and martensitic transformations (Russian) 7-8056
- microstructure and mechanical props. after low-temp. TMT, tempering temp. influence 7-17554
- precipitates, small, moire imaging in TEM 7-46490
- slip processes in intersecting planes, α martensite form. (Russian) 7-33728
- thermal desorption after high-energy d implantation 7-52232
- ultrasonic measurement of internal temperature distribution 7-46776
- V-butt weld, US beam propag. theory 7-22966
- welded joint with C steel, microhardness, effect of C redistrib. 7-13571
- welded joints with ferritic steel, thermally loaded, struct. and mech. props. 7-8102
- weldments, C redistrib., general soln. 7-21506
- Al-Mn, mech. props., oxidation and corrosion behaviour 7-65218
- Cr-Mn, thermal and mech. props., fusion reactor appl. 7-53795
- Mn, friction induced martensitic transform., wear resist., work hardened surface layer 7-17531
- Mn-Al, Al atom short range ordering, Mossbauer studies (Russian) 7-16480
- Mn-Cr, fatigue crack growth behaviour 7-59593
- Mn-Cr, hardening characts. and hydroextrusion parameters (Russian) 7-59540
- Mn-V-Mo, struct. and precipitation hardening (Russian) 7-17541
- Nb-V, matrix and grain boundary precipitation, effect of heat treatment 7-46493
- ⁵⁹Ni doped, design of single variable He effects expt. for FFTF irradiation expts. 7-49666
- austenitising** see heat treatment
- Autler-Townes effect** see Stark effect
- autoalignment model** see Hanle effect
- autoionisation**
- see also Auger effect
- alkali earth metals, photoionisation cross sections 7-50039
- atom-ion collisions, emission-angle depend. post collision interaction 7-25644
- atomic multiphoton autoionisation by smooth laser pulses 7-15577
- atoms, laser-induced autoionization from a double Fano system 7-57034
- complementary branching ratios by satellite excitation 7-19786
- complex scaling method appl. 7-42565
- continuum states, photoexcitation, dressed-reson. representation, appl. to laser-enhanced autoionis. 7-15655
- continuum-continuum coupling and the pole approximation 7-36558
- diatomic molecules, dissociative single and double photoionisation, photoion spectra anal. 7-19984
- electric fields effect on autoionising resonances 7-10520
- electron-ion resonance scatt., WKB calcs. and multichannel quantum-defect theory, effect of electric field 7-15546
- highly charged ions, multiple-electron capture, classical over-barrier model 7-10744
- methyl fluoride, dissociative ionis., methylene and methyl ions, form., photoelectron spectra 7-10662
- molecular ions, electron capture, rot.-vibr. transitions in autoionisation, CF method anal. 7-20036
- molecular photoionisation, autoionisation struct. described using projector-operator formalism 7-42696
- molecules, autoionising states, avoided crossings 7-950
- population trapping in nonstationary conditions 7-31291
- positronium molecule, autoionisation state, complex coordinate rot. 7-994
- Rydberg series, electron scatt., Stark broadening reson. struct. 7-50009
- satellite excitation, complementary branching ratios 7-10519
- Si II, autoionizing levels and identification of 1400 Å feature in Ap-Si stars 7-40821
- stimulated Raman scattering, off-resonant enhancement investig. 7-50148
- B III, core excited quartet and doublet state, beam-foil study 7-42514
- B²⁺, excitation-impact ionisation, excitation-autoionisation contrib. 7-978
- B-like ion plasma, dielectronic satellites 7-58054
- Ba atoms, multistep photoionisation, total angular momenta of autoionisation steps 7-50031
- Ba autoionising states, internal conversion and fluoresc. two-step process 7-25467
- Ba⁺, metastable autoionising state, lifetime meas. 7-19788
- Ba⁺, photoionisation absolute cross section meas. 7-50034
- Be, ³P⁰ and ¹P⁰ Rydberg series, autoionising states, complex eigenvalue Schrödinger eqn. soln. 7-62329
- Be III, transition wavelengths among doubly excited states 7-49980
- Be⁺⁺+He, charge exchange cross sections, quasimolecule Feshbach method calcs. 7-36754
- C³⁺+He, transfer excitation, electron emission, forward-backward asymmetries 7-973
- CO, B²⁺ state, electronic autoionis., cross section calc. 7-15656
- CO electron impact ionisation efficiency curves, reson. struct. 7-5774
- CO, electrostatic autoionis., review 7-951

autoionisation continued

- CO₂, autoionisation and isotope effect in threshold UPS 7-19948
 Cd, autoionisation widths, calcs. and optogalvanic spectra 7-36521
 Cd⁺, autoionising states, picosecond soft-X-ray ionis. spectroscopy 7-10521
 Cr and Cr-compounds, Auger and absorpt. spectra involving M_{2,3} levels, atomic effects 7-59311
 F⁵⁺, quintet transitions, beam-foil spectra anal. 7-31004
 Fe, multiply charged ions, electron-impact ionisation, excitation energies and cross section calcs. 7-25425
 Fe, multiply-charged ions, electron-impact ionisation cross sections, crossed-beam meas., rate coefficient calcs. 7-25660
 Fe²¹⁺, dielectronic recomb., rate coeff. calc. 7-30991
 Fe²²⁺, dielectronic recomb., rate coeff. calc. 7-30991
 Ga, resonant state, autoionis., electron spectra 7-900
 Gd, autoionising states, electric field effects, UV spectra anal. 7-42531
 H₂, autoionising Σ_u^+ and Π_u states, theory 7-5646
 H₂, photodissociation of doubly excited states, Lyman- α fluoresc. spectra anal. 7-19945
 H₂, Rydberg states, nonpenetrating, autoionis., energy-level struct. calcs. 7-15492
 H₂⁺, electron impact, autoionising states, avoided crossings 7-950
 H₂Se, photoionisation, ionisation pot. and bond energies 7-19979
 H₂Se, photoionisation and autoionisation, UV spectra 7-10524
 He, autoionising states, laser-induced transition 7-42566
 He, autoionising states, use of virial theorem in wavefunction calcs. 7-25465
 He, double excited states, correl. wavefunction calcs. (French) 7-10454
 He, doubly excited autoionising resonance states, Hylleraas-type wave fn. calcs. 7-30940
 He, electron impact autoionisation, triple differential cross sections, first-order model calcs. 7-25466
 He I, transition wavelengths among doubly excited states 7-49980
 He-like ions, energy level population autoionisation states (French) 7-10518
 He+H₂, autoionising systems, Born-Oppenheimer approx., diatomic-molecules calcs. 7-5742
 HeN⁷⁺ quasi-molecule, autoionisation 7-62459
 Hg, electron impact ionisation efficiency curves, reson. struct. 7-5774
 In, resonant state, autoionis., electron spectra 7-900
 Kr, 3p excitation, multiple photoionisation cross sections, TOF mass spectrometer anal. 7-19802
 Kr autoionising region, multiphoton ionisation study 7-62336
 Kr, Rydberg states, four-photon excitation 7-62328
 Kr, visible transitions, autoionis. obs., optogalvanic spectra 7-57035
 Li, ⁴P_{1/2} levels, relativistic autoionisation, threshold phenomena, CI mechs. 7-49950
 Li, ⁴P_{1/2} level, relativistic autoionisation, CI mechs. 7-49949
 Li II, transition wavelengths among doubly excited states 7-49980
 Mg, ¹P doubly excited autoionisation states, CI calcs. 7-36497
 Mg, 3p² ¹S state, autoionis., multiphoton excitation, line shape obs. 7-899
 Mg, autoionising Rydberg states, reson. ionisation mass spectrometry 7-19785
 Mg II, core-excited states, energy levels and lifetimes, HF calcs. 7-867
 Mg-like ions, electron impact excitation, LS coupling, distorted wave approx. 7-42767
 Mn, vapour, photoelectron ang. distrib. and drag current, nondipole part 7-15575
 N⁵⁺, intrashell autoionis. levels, electron scatt. 7-50030
 N⁶⁺, intrashell autoionis. levels, electron scatt. 7-50030
 N₂, electron impact ionisation efficiency curves, reson. struct. 7-5774
 N₂, electron-impact ionisation, double differential cross section, TOF spectra anal. 7-42774
 N₂, Hopfield series, ab initio theory 7-10408
 N₂, triplet Rydberg state, autoionis., TOF mass spectra 7-19963
 N₂, autoionisation decay, reson. charact. 7-50389
 NO, A(² Σ^+) state, two-photon ionis., non-Franck-Condon behaviour 7-25615
 NO, autoionisation of $\nu=3$ Rydberg states, branching ratios, multiphoton spectra anal. 7-36718
 NO, autoionising levels, two-photon spectra 7-10688
 NO, rot. resolved autoionising levels, wavelength depend. photoelectron spectra 7-25605
 N₂O, electronic autoionisation studies using vibr. resolved const. ionic spectroscopy, dispersed fluoresc. 7-25592
 NaI core-excited states, energy levels and lifetimes, HF calcs. 7-867
 Ne, electron impact induced post-collisional KL_{2,3}L_{2,3} Auger decay 7-5773
 Ne⁷⁺+H₂ charge exchange collisions, Ne⁶⁺ excited states, VUV spectra anal. 7-20030
 O³⁺, electron-impact ionisation, excitation-autoionisation contrib. 7-978
 O₂, autoionisation states, vibr. assignments 7-50073
 O₂, electron impact ionisation efficiency curves, reson. struct. 7-5774
 O₂, photoproduction cross sections, mass spectrometry, photoionisation and photodissociation 7-10681
 O₂⁺, X² Π_g vibr. branching ratios, 905-1000 Å, autoionis. effect 7-50272
 Pb, resonant state, autoionis., electron spectra 7-900
 SF₆, UV photoionisation and autoionisation 7-10523
 SF₆, S 1s core-level photoionis. spectra 7-941
 Se, photoionisation and autoionisation, UV spectra 7-10524
 Se XXIV and XXV plasma, dielectronic recombination calcs. 7-26510
 SeH, photoionisation, ionisation pot. and bond energies 7-19979
 SiH₄, 2p threshold, reson. relax. processes, XPS 7-42684
 Sm⁴⁺+Xe collisions, q=34 to 52, resonant electron transfer and L-shell excitation, X-ray spectra study 7-30979
 Sr, autoionising series, multichannel quantum-defect theory model data fit, UV PES study 7-62334
 Sr, autoionizing levels meas. (Chinese) 7-5645
 Ti II, electron impact, 6¹S₀-6³P₁ intercombination transition excitation resonance obs. 7-36778
 Xe, 4p excitation, multiple photoionisation cross sections, TOF mass spectrometer anal. 7-19802
 Xe, 5p photoionis., angle- and spin-resolved photoelectron spectroscopy, expt. charact. 7-904
 Xe atoms, J=1 even-parity autoionisation 7-50029
 Xe, autoionisation under two- and three-photon excitation 7-15561
 Xe, autoionising region, multiphoton ionisation study 7-62336
 Xe, autoionising Rydberg series, two-photon spectra anal. 7-36570

autoionisation continued

- Xe, J=0 autoionisation, multichannel-quantum-defect theory anal. 7-36559
 Xe, Rydberg states, four-photon excitation 7-62328
automata theory
see also finite automata; switching theory
 cellular automata local connectivity and quantum field tessellation 7-35686
automatic frequency control
 electromechanical laser-beam modulator with high-frequency stability 7-31372
 ultrasound technical processes, automatic output parameter regulation 7-11232
 X-band time-domain EPR spectrometer, computer-controlled 7-30054
automatic guided vehicles *see computerised materials handling; vehicles*
automatic programming
 FORTRAN code automatic generation, in LISP, for finite difference method appl. to flow 7-37468
automatic test equipment
 bidirectional scattering distrib. function meas. using computer controlled facility 7-41414
 biotissues, automatic tensile test system 7-23489
 computerized test system for thermal-mechanical fatigue crack growth 7-39801
 demagnetisation system for NDT 7-65260
 ellipsometer for birefringent components and systems meas. (German) 7-24687
 fatigue apparatus for testing in UHV and controlled environments 7-39811
 fault detection procedure for faulty sensors, implementation 7-5368
 flexible US scanner using industrial robot for NDT 7-22970
 flowmeter calibration, computer-aided test system 7-37591
 III-V semiconductors, carrier concentration and mobility profiling 7-45315
 impact testing, computer-assisted 7-59707
 integrated dynamic test/modelling system 7-26232
 laser wavemeter, compact, automatic, for tunable IR diode lasers 7-43181
 liquid meter checking system 7-57957
 materials testing machine, microprocessor-aided process meas. and control technology (German) 7-65265
 metal fatigue testing system, microcomputer based 7-46749
 microcomputer-based equipment for infralow-frequency vibration parameters meas., seismometers testing appl. 7-4208
 MOS device, microcomputer-based instrumentation system for carrier transport study 7-64350
 optical components microscopic inclusions location, automatic inspection device using Q-switched YAG laser 7-31544
 optical fibre loss, automatic meas. of spectral depend., cutback method and system (Czech) 7-26052
 piezoelectric solids elastoelectric response to cyclic stresses obs., using computerised system 7-39810
 primary cells testing, MnO₂ and Li, using microcomputer-based test station (Czech) 7-23128
 prosthetic heart valve test apparatus, microcomputer-based data acquisition system 7-40364
 remote weighing of irradiated fuel pins at FFTF 7-49546
 reverberation time meas. 7-43606
 robotic US scanning system for NDT of composites 7-22969
 robotics in US NDT, conf., London, England, 1986 7-18505
 SEM image analysis, fully automated system 7-56385
 solar cell optical and electrical charact., meas. systems 7-13906
 spectral analyser for meas. of thermomechanical response of solids to low-frequency dynamic loads 7-43814
 stereo real-time metrology with CCD cameras 7-47314
 tensile testing machine modification to perform simultaneous tensile and torsion tests 7-22948
 ultrasonic materials testing system, US-1000 for C-fibre composite aircraft components 7-22965
 vibration transducer for dynamic parameters meas. of viscoelastic materials 7-61326
 Al-Mg-Si, compression test, high speed, microcomputer system, split Hopkinson bar technique 7-13686
 He-Ne laser beam meas. using direct looking apparatus for light intensity distribution (Japanese) 7-56314
 Si junction detector, characterisation by automatic system 7-19663
automatic testing
 ceramics, brittle, non-oxide, flaw charactn., computer-aided US testing 7-54064
 composite panel, whole-field strain determ. using coherent opt. processing 7-57779
 demagnetisation system for NDT 7-65260
 ellipsometer for birefringent components and systems meas. (German) 7-24687
 IR imager performance meas., objective meas. of minimum resolvable temp. difference 7-30092
 metal-insulator-metal (semiconductor) structs., circuit anal., automated 7-27438
 optical asymmetrical elliptical preforms or fibres, index profile meas. 7-50760
 optical fibre loss, automatic meas. of spectral depend., cutback method and system (Czech) 7-26052
 optical filtering, noncoherent, for automating testing of semiconductor structures 7-20153
 thermocouples under field conditions, using online identification 7-4848
automation, social aspects *see social aspects of automation*
automobile electronics *see automobiles*
automobile industry
 photovoltaic power system for car battery manufacturing plant 7-3692
 Si IC sensor technology and applications (German) 7-24644
automobiles
 car battery sealing and rechargeability improvement (Japanese) 7-65430
 exhaust emission control equipment, to limit NO₂ 7-59905
 hot wire air flow meter for automobile engine intake mass air flow rate meas. 7-37587
 magnetic flux-gate compass for automobile navigation 7-330
 plastic and advanced plastic composites, design methods and appls., book 7-4642
 vibration isolation, optimal charact., jerk vs. acceleration 7-50980

automobiles continued

voltage amplification in dense plasma focus, appl. to car spark plugs 7-63374

H₂ vehicle fuel appls. in USSR (*French*) 7-54368

autoradiography *see radioisotope scanning and imaging***autoresonant accelerators** *see collective accelerators***avalanche diodes**

see also avalanche photodiodes; IMPATT diodes

Raman spectroscopy, interferometric observation, photomultiplier and avalanche diode detectors appls. 7-61379

semiconductor detector for single optical photons, 60 ps time resolution 7-42335

avalanche photodiodes

long-wavelength components by VPE 7-46343

superlattice APDs, impact ionisation, theory 7-12850

superlattice avalanche photodiodes, impact ionisation theory appl. 7-58886

Ge, avalanche photomultiplication in the far infrared 7-45375

Ge_{0.6}Si_{0.4} rib waveguide avalanche photodetectors for 1.3 μ m optical fibre communication 7-9896

Ge_xSi_{1-x}-Si strained-layer heterostructure, transport, optical props. and appls. 7-7349

InGaAs layers on InP, LPE growth 7-33608

InGaAs/InP photodiodes, MOCVD growth and characts. 7-27932

InGaAs-InP 1.5 μ m photodetectors, optical communication appls. 7-37202

In_{1-x}Ga_xAs-InP heterostructure APD for 1.55 μ m optical fibre communication system (*Japanese*) 7-62843

InP-Ga_{0.4}In_{0.53}As superlattice, electron and hole impact ionisation rates 7-17076

Si avalanche photodiode for photon correlation meas., passive quenching 7-41463

avalanches, carrier *see impact ionisation***avalanches, electron** *see electron avalanches***avalanches, electron-hole** *see impact ionisation***avionic systems** *see aircraft instrumentation***Avogadro's number** *see constants***avoided crossing** *see energy level crossing***axicons** *see lenses***Axilrod-Teller-Moto dispersion forces** *see intermolecular forces***axiomatic field theory**

3D Abelian gauge model, simplicial pseudorandom lattice study, lattice as extremum of action 7-4975

$\lambda\phi^4$ Gaussian effective action, comparison with free vacuum energy, confinement 7-15065

$\lambda\phi^4$ theory, nonhomogeneous boson condensation, vacuum structure and temp. effects 7-397

$\lambda\phi^4$ theory, two-, three-dimensional, finite temp. props., Monte Carlo anal. 7-24798

$\lambda\phi^4$ theory in N dimensions 7-400

$\lambda\phi^4$ theory triviality problem in time-dependent space-time 7-18998

$(\lambda\phi)_{3+1}$, gaussian effective potential, nontrivial positive λ_B soln. 7-409

σ models, minimal R operation in the 1/N expansion 7-35719

ϕ_4^4 theory with negative coupling 7-49005

ϕ_4^4 quantum field theory, coupling constant bound violation 7-9980

$(\phi^{2N})_2$ field theory, mass gap and mass renormalisation using finite elements method 7-35702

ϕ^4 field theory, critical behaviour and random walk representations 7-48532

ϕ^4 field theory in (1+1) dimens., post-Gaussian approx. approaching the critical region 7-41615

Φ^4 field theory on square lattice, finite size scaling anal. 7-9945

ϕ^4 theory, conformal anomalies, path integral formulation 7-423

ϕ^4 theory, statistical physics conf., Kozeg, Hungary, Aug.-Sept. 1984 7-48194

ϕ^4 theory, stochastic quantization simulation with slave eqns. 7-48960

ϕ^6 model in 3+1 dimensions, exact solns. 7-41598

abelian gauge field dynamics, acceleration 7-405

abelian lattice gauge theories, large Wilson loop averages from the Schwinger-Dyson equation 7-61456

Abelian lattice gauge theories, mean field methods for strings and monopoles 7-24772

Abelian U(1) lattice gauge theory, mag. monopoles and charged states 7-24760

Abrikosov lattice in the theory of electroweak interactions 7-19051

Adler-Bell-Jackiw anomaly in lattice gauge theory (*Chinese*) 7-48978

automorphisms of algebraic varieties and Yang-Baxter equations 7-35425

axial model in curved space-time 7-61453

bosonic knotted strings, Liouville equation, Fuchsian Groups 7-30165

chiral fermion propagation on 2D fractal structs. 7-48981

chiral SU(2) \times SU(2) lattice theory with spin 3/2 action in 2D, Monte Carlo anal. 7-15067

closed-time-path functional formalism in curved spacetime, cosmological back-reaction problems 7-41215

Coleman-Weinberg transition on a lattice, mean field anal. 7-35705

conference, strong interactions and gauge theories, Les Arcs, Savoie, France (March 1986) 7-60876

confined Yang-Mills field, prop. props. and condensate form. 7-48991

conformally invariant scalar field, anisotropy damping and particle prod. at finite temp. 7-56132

critical phenomena, field theory applications 7-41578

dimensional phase transitions, interacting spinors, gauge fields, background gravity, cell complex 7-35697

Dirac fermion prop. on hypercubic lattice with random hopping parameters 7-4967

discretization effects on classical Klein-Gordon lattice 7-35668

effective coupling constant, finite temp., one-loop approximation calcs. 7-41577

effective gauge action on a finite-size lattice, SU(2) theory simulations 7-41620

Eguchi-Kawai model, triangle-lattice quenched, Monte Carlo study 7-30156

Eguchi-Kawai models, stochastic quantisation 7-56450

electroweak SU(2) \times U(1) lattice gauge theory with variable-length Higgs fields 7-24791

elementary scalar particle existence, U(1) Higgs model and scalar electrodynamics 7-10017

Euclidean boson quantum field theory, existence and props. 7-4948

axiomatic field theory continued

Euclidean field theory, Gibbs measures, local aspects and partial differential eqns. 7-35662

Euclidean lattice, unified treatment of Poincare, de Sitter and conformal gravity 7-56131

Euclidean lattice quantum gravity, functional integration and diffeomorphism group 7-176

Euclidean SU(2) gauge theory, elliptic solns. 7-4974

Federbush model, infinite number of infinite hierarchies of conserved quantities, Lie-Backlund transforms. 7-35671

fermion field on a random lattice 7-35716

fermionic fields, species doubling and transfer matrices 7-56431

finite temperature phase transition in chiral limit of lattice QCD 7-61561

finite temperature quantum field theory in curved spacetime, quasilocal effective Lagrangians 7-41216

finite temperature SU(2) gauge theory, correlation length temp. depend., screening, deconfinement 7-41606

gauge fields, factorisation condition for bidimensional and pseudo-Euclidean groups 7-48946

gauge hierarchy problem, mass generation by nonperturbative quantum effects 7-19007

glueball (0^{++}), mass scaling, SU(N) Hamiltonian lattice calcs., Monte Carlo anal. 7-35807

glueball wave functional calcs. using lattice technique 7-61580

glueballs, tensor and scalar, mass calcs., in lattice gauge theory 7-61587

gluon mass, gluon propagator calcs. in Landau gauge, SU(3) lattice anal. 7-61588

gluon thermodynamics with an extended plaquette action, deconfinement in lattice QCD 7-41723

Gross-Neveu model, Gaussian anal., ground and bound states, analogy with $\lambda\phi^4$ 7-35698

Gross-Neveu model, generalisation for several coupling constants 7-30201

Gross-Neveu model, lattice actions, effects of one-loop improvement on scaling behaviour 7-410

hadron-hadron interactions, orthogonal lattice gauge field configurations, nucleon-nucleon system 7-41842

Hamiltonian lattice SU(N)_cQCD, mechanism to lift the Goldstone degeneracy 7-49081

heavy quark forces and potentials in SU(2) lattice gauge theory (*Chinese*) 7-35657

hierarchical scalar lattice field theories, non-Gaussian renormalisation group fixed point 7-9938

Higgs boson masses, perturbative calcs. 7-61452

hybrid stochastic algorithms, generalised Fokker-Planck eqn., lattice gauge theory appl. 7-24770

infrared divergences in the ϕ^4 and Wess-Zumino models 7-30198

instantons on a space-time lattice 7-4985

Kaluza-Klein theory for SU(2) particle scatt. off Euclidean instanton 7-35750

Lagrangian field theories defined on jet bundles of fibred manifold, Cartan form construction 7-56415

lattice action sum rules, appl. to glueballs and static quark pots. 7-48959

lattice fermion, incomplete LDU decomposition, appl. to conjugate residual methods 7-41082

lattice fermion derivative formulation, locality and chirality without spectrum doubling 7-41632

lattice fermions in odd dimensions 7-61430

lattice field theories with fermion degrees of freedom, near algorithm for numerical simulation 7-41602

lattice gauge theories, analytical approach based on dynamical eqns. 7-15066

lattice gauge theories with matter fields, order parameter 7-61486

lattice gauge theory, baryon mass calc., quark mass renormalization 7-30155

lattice gauge theory, boundary condition effects on interior plaquettes 7-41582

lattice gauge theory, continuum limit and renormalized trajectory, weak coupling expansions 7-19009

lattice gauge theory, disordered fermion couplings and fermion doubling problem 7-9964

lattice gauge theory, geometric anal. of lattice actions 7-56414

lattice gauge theory, global symmetry restoration in high temperature Higgs theories 7-61423

lattice gauge theory, H dibaryon mass using bag model parameters 7-61485

lattice gauge theory, heat bath method for vectorized processing 7-18974

lattice gauge theory, high-temperature QCD and quark matter 7-56416

lattice gauge theory, microcanonical ensemble techniques 7-48934

lattice gauge theory, Monte Carlo renormalization group methods 7-61476

lattice gauge theory, Monte Carlo renormalization group transformation, β -fn. anal. 7-9957

lattice gauge theory, propagator of Susskind fermions 7-35683

lattice gauge theory, static screening lengths in finite-temperature pure gluon plasma 7-19003

lattice gauge theory, stochastic quantization using Langevin and Fokker-Planck eqns. 7-24792

lattice gauge theory, surface representations of Wilson loop expectations, confinement 7-24771

lattice gauge theory, topology and instanton struct., Monte Carlo simulation 7-61482

lattice gauge theory simulation using the APE computer 7-61488

lattice gauge theory simulations, conf., Wuppertal, Germany, Nov. 1985 7-60883

lattice gauge theory with Wilson fermions, hadron mass calcs. 7-61483

lattice gauge-Higgs theories with local \times global symmetry groups including exact solutions 7-18992

lattice Gross-Neveu model, recovery of chiral symm. 7-19010

lattice Higgs model, analytic and Monte Carlo methods 7-61480

lattice Monte Carlo simulation with Wilson fermions, current algebra, quark masses 7-15069

lattice Monte Carlo simulations of QCD at finite baryonic density 7-49082

lattice N=2 Wess-Zumino model, local Hamiltonian Monte Carlo study 7-15052

lattice QCD, $\beta=5.7$, evidence for scaling, SU(3) deconfinement temp. anal. 7-19072

lattice QCD, chiral symm. breaking in strong coupling limit 7-56514

lattice QCD, connection with nuclear many-body problem 7-35802

axiomatic field theory continued

lattice QCD, deconfining phase transition and continuum limit 7-61568
 lattice QCD, deconfining transition 7-56508
 lattice QCD, finite temperature, phase transitions 7-35804
 lattice QCD, improved actions, redundant operators and scaling 7-56513
 lattice QCD, large N with Susskind fermions, continuous flavour symmetries 7-15123
 lattice QCD, large scale computing aspects 7-49068
 lattice QCD, light hadron and quark masses, large lattice results 7-15139
 lattice QCD, numerical simulation of interacting fields and static interquark pot. 7-61575
 lattice QCD, problems with finite density simulations 7-5058
 lattice QCD, quenched SU(2) simulation with staggered fermions, chiral limit 7-61602
 lattice QCD, strongly coupled, fermions in Euclidean formulation 7-30247
 lattice QCD, t-expansion method 7-61573
 lattice QCD, weak Hamiltonian, eye diagrams, calculational technique 7-477
 lattice QCD, with Wilson fermion action, finite temp. behaviour, implication on spectroscopic studies 7-19066
 lattice QCD at finite density 7-56509
 lattice QCD sum rules and spontaneous chiral symm. breaking, Monte Carlo simulation 7-61603
 lattice QCD with quark loops, Lanczos algorithm simulation 7-61571
 lattice QCD with staggered fermions, chiral props. 7-61576
 lattice QCD with Susskind fermions, current algebra relation 7-41730
 lattice QCD with Wilson fermions, fast fermionic algorithms 7-61572
 lattice QED, parity-violating fermionic vacuum currents, numerical study 7-19058
 lattice Schrodinger operators with exponential disorder, cut discontinuity, large order behaviour 7-9937
 lattice SU(2) chiral model, complex Langevin simulation on non Abelian group 7-61479
 lattice SU(2) Yang-Mills theory, anal. as nuclear many-body problem 7-35802
 lattice SU(3) gauge theory, deconfined phase, gluon plasma thermodynamic props. 7-41741
 lattice SU(3) gauge theory, finite size results 7-35704
 lattice SU(N)×SU(N) chiral models, two-loop coupling constant renormalization 7-424
 lattice SU(N) QCD study at finite chem. pot. and baryon density 7-474
 lattice theory, Hamiltonian formulation for gauged nonanomalous chiral theories 7-19001
 lattice theory, weak matrix element calcs., chiral behaviour and multipoint Green's fns. 7-61484
 lattice U(1) gauge Higgs model, free charge in confining phase 7-48966
 lattice U(1) gauge Higgs model, Monte Carlo study of confinement 7-468
 lattice U(1) Higgs gauge theory, phase structure 7-4983
 lattice Yang-Mills theory, phase cell approach 7-24758
 lightest glueball mass in SU(2) and SU(3) gauge theories, lattice size depend. 7-41722
 local scalar fields, canonical quantisation over quantum space-time 7-48942
 low-dimensional lattice fermion field theories, finite element methods 7-4956
 massive ϕ^4 theory, dimensional regularisation, mass independence of minimal subtraction scheme 7-41626
 massive scalar field, renormalized vacuum expectation value of stress tensor, Hadamard function 7-18996
 massless $\lambda\phi^4$ model, infrared dimensional singularities 7-56400
 massless scalar field with gravity, Einstein's field eqns. in 3D space-time 7-41209
 mean fields and self consistent normal ordering of lattice spin and gauge field theories 7-9978
 mesons, micrononcausal Euclidean wave functions assuming Yukawa type couplings 7-41596
 metric space-time as renormalisation group eqn. fixed point on fractal structs. 7-48505
 N=2 harmonic superspace with central charges, appl. to self-interacting massive hypermultiplets 7-19020
 non-perturbative QCD, algorithm for transport coeffs. using lattice Monte Carlo methods 7-49071
 nonAbelian chiral anomaly from lattice regularization 7-15072
 nonAbelian O(N)-invariant σ models, origin of asymptotic freedom 7-41634
 nonperturbative BRS invariance and the Gribov problem 7-61454
 nonperturbative method in field theory, gauge technique, infrared region solns. 7-41616
 numerical simulation using Cray supercomputers 7-61557
 O_N invariant self-interacting theory, Gaussian quantisation and symmetry breaking, Goldstone theorem 7-24775
 O(2) and O(3) nonlinear σ -models on 2D lattice at large β 7-61457
 O(3) nonlinear σ model, numerical simulation by Parisi-Wu stochastic quantization 7-19008
 O(N) σ model, 1/N expansion, essential singularity in analytic regularization 7-56445
 O(N) σ -model, lattice actions, effects of one-loop improvement on scaling behaviour 7-410
 O(n) (0^2)₂₋₄ model, 1/N expansion, essential singularity in analytic regularization 7-56445
 O(N) model, composite operator formalism, finite temperature anal. 7-24778
 one-loop operator matrix elements in the Unruh vacuum 7-14845
 one-plaquette U(N) gauge model with fermions, leading order topological expansion 7-35721
 orthogonal lattice-gauge field configurations for hadron-hadron interactions 7-41841
 parallel computing in lattice theory 7-61487
 phase structure of finite temperature lattice gauge theories 7-49002
 phase-space formalism for quantized fields in complex space-time 7-61420
 Polyakov string theory from Φ^3 theory 7-61631
 propagation of boundary effects in large systems on vectorprocessors 7-4989
 pseudoscalar lattice mesons, relative charge distrib. for qq pair 7-49072
 pseudoscalar meson electric form factor calcs. lattice QCD anal. 7-35801
 QCD, lattice quantum field theory (Czech) 7-5042

axiomatic field theory continued

QCD, nonperturbative hadron phase, chromoelectric flux and action quantisation 7-41736
 QCD, quenched lattice approximation, hadron mass calcs. 7-61581
 QCD and the lattice, introductory remarks 7-56507
 QCD lattice gauge theory, updating fermions with Lanczos method 7-49052
 QCD scale fixing, lattice Monte Carlo calcs. 7-30239
 QCD spin-depend. static pots., SPINSUB vectorised code for Monte Carlo computation 7-41721
 QED₂, discretized light-cone quantization and lattice gauge calcs. 7-56497
 quantum fields, relations with local algebras of observables 7-41642
 quark matter, conference, Pacific Grove, CA, USA (April 1986) 7-55881
 quark propagators on large lattices, extension in time by distant source method, quenched QCD 7-61559
 quark-gluon plasma, perturbative and nonperturbative theory, review 7-56510
 quarkless QCD, transport coeffs., lattice estimates 7-35798
 quenched QCD hadron mass calcs. on 16⁴ spacetime lattice 7-61604
 random lattice, doubling problem and chiral symm. breaking 7-394
 random lattice gauge systems and interacting gaussian surfaces, strong coupling expansion 7-48958
 random lattices versus regular lattices, Ising model, fermions on random lattices 7-35466
 real 0^3+0^4 field in (1+1) dims. at finite temp., soliton solns. 7-9944
 real- and imaginary-time field theory at finite temperature and density 7-48983
 Savvidy model, absence of deconfining phase transition at one-loop order 7-41735
 scalar field theory with matrix fields, renormalisability in 1/N expansion 7-61470
 scalar glueball mass estimate, pure gauge lattice QCD calcs., four-parameter improved action 7-487
 scalar lattice QCD, hadron static props., form factors, charge radii, lepton widths 7-49080
 scaling limits and DLR equations in the Euclidean field theory 7-49003
 Schrodinger field on a Galileo lattice, explicit finite difference schemes 7-41609
 Schwarzschild black holes, nucleation of vacuum phase transitions, Euclidean action 7-56102
 sine-lattice eqn., nearly integrable soliton props. of kink solns. 7-392
 solvable lattice models with broken Z_N symmetry and Hecke's indefinite modular forms 7-24773
 spin and lattice gauge models, topological excitations, mean field methods 7-9973
 staggered fermion symmetry group, irreducible representations 7-19024
 standard SU(2) Higgs model, Monte Carlo study on lattices 7-9949
 static potentials from bosonic string models, lattice Monte Carlo calcs. 7-61612
 statistical QCD, deconfinement and chiral symm. restoration, Monte Carlo anal. 7-61569
 string theory, lower critical dims. and curved backgrounds 7-41763
 SU₂ lattice gauge theory, strong-coupling anal. of space-time critical dimensionality 7-56430
 SU(2)₃ noncompact lattice gauge simulations 7-35690
 SU(2)×U(1) lattice gauge theory, phase transitions, Monte Carlo anal. 7-406
 SU(2) deconfining phase transition, correlation length and susceptibility, Monte Carlo methods 7-56515
 SU(2) lattice gauge Higgs theory, Monte Carlo anal. at finite temp. 7-24796
 SU(2) lattice gauge theory, evidence against asymptotic freedom 7-41631
 SU(2) lattice gauge theory, finite temperature, Migdal renormalization group anal. 7-9966
 SU(2) lattice gauge theory, instanton density calcs. 7-4985
 SU(2) lattice gauge theory, Monte Carlo renormalization group study 7-19002
 SU(2) lattice gauge theory, phase structure, Schwinger-Dyson eqn. of a Wilson loop, deconfinement 7-24780
 SU(2) lattice gauge theory, quark and gluon string tensions 7-417
 SU(2) lattice gauge theory, renormalisation and continuum limit of composite operators 7-19017
 SU(2) lattice gauge theory, spontaneously broken, chiral symmetry realization 7-9958
 SU(2) lattice gauge theory with dynamical fermions, glueball mass calcs. 7-9959
 SU(2) lattice gauge theory with dynamical fermions, static quark pot. 7-61478
 SU(2) lattice gauge theory with mixed action, Z(2) monopoles and specific heat 7-48962
 SU(2) Yang-Mills lattice theory, correlation lengths and finite size effects 7-56426
 SU(3) lattice gauge theory, $\Delta\beta$ and asymptotic scaling 7-4955
 SU(3) lattice gauge theory, Hamiltonian connected movements, expectation values 7-41605
 SU(3) lattice gauge theory, Monte Carlo calcs. of gluon propagator 7-61474
 SU(3) lattice gauge theory, Monte Carlo simulation of fermionic fields 7-48964
 SU(3) lattice gauge theory, scaling behaviour of heavy-quark potential 7-486
 SU(3) lattice gauge theory, sweep-sweep correlations of Polyakov loops 7-413
 SU(3) lattice gauge theory, topological susceptibility Monte Carlo calcs. 7-61455
 SU(3) lattice gauge theory, topology for $\beta>5.6$ 7-56453
 SU(3) lattice gauge theory on 32³ lattices, sweep to sweep corrs. of Polyakov loops 7-15075
 SU(3) lattice QCD, β -function at large β , Monte Carlo renormalisation group anal. scaling deviations 7-24781
 SU(N) lattice gauge theories, topological charge in Monte Carlo simulation 7-48938
 SU(N) lattice gauge theory, Langevin eqns. and stochastic quantization 7-35691
 SU(N) Yang-Mills theory, d=4, lattice actions, effects of one-loop improvement on scaling behaviour 7-410
 superconformal field theory with modular invariance on a torus 7-15080
 SUSY σ -models in 4D as quantum theories, vacua and effective lagrangians 7-48967

axiomatic field theory continued

- SUSY O(N) model, coupling constant behavior at high temp. 7-41664
- symmetric ϕ^4 model, saddle-point config. 7-421
- ten-dimensional heterotic strings from Niemeier lattices 7-30255
- tessellation and cellular automata local connectivity 7-35686
- Thirring model, derivative coupling model equivalence and fermionic Green's fns. 7-48993
- Thirring model at non-zero temp., family of exact solns. 7-48980
- three-dimensional field theory, construction from ϕ^6 Lagrangian 7-9972
- topological charge of lattice gauge fields 7-35663
- toroidal compactification of heterotic superstrings 7-41679
- twisted Eguchi-Kawai model, complete set of twists 7-41648
- two-particle potential in: $\lambda(\phi^6 - \phi^4)$: field theory 7-49120
- U(1) and SU(2) average plaquette energies up to third order approx. in cumulant expansion 7-41579
- U(1) lattice gauge theory, 3D, meson mass calcs. in quenched approx. 7-15068
- U(1) lattice gauge theory, analytical results for average plaquette energy 7-61426
- U(1) lattice gauge theory, iterative approach, $d=4$ β -function and free energy 7-30189
- U(1) lattice gauge theory, mass gap, variational calcs. 7-30157
- U(1) lattice gauge theory, renormalisation group transformations (Chinese) 7-35658
- U(1) lattice gauge theory with Higgs fields, 4 dimens., monopoles, matter representations role 7-41603
- U(1) lattice gauge-Higgs model, zero temperature, phase diagram anal. 7-56401
- U(1) problem on a lattice, massless π^0 and massive η 7-48996
- U(1) varied-modular Higgs model, phase struct. simulation 7-18973
- vacuum polarization in curved backgrounds deduced from Hadamard kernels 7-48503
- vector meson radiative decay in lattice QCD 7-35879
- Ward identities on the lattice for Wilson fermions 7-56419
- Wightman fields, weakly local massive, weak asymptotic Abelianess with respect to space-like directions 7-41640
- Yang-Mills theory, nonperturbative approach to strong-coupling confinement 7-56433
- Yang-Mills theory, nonperturbative calcs. away from strong coupling 7-56434
- Z₂ gauge theory, finite lattice effects 7-389
- Z(2) lattice gauge theory, critical exponents, finite temp. calcs. 7-49054
- Z(2) lattice gauge theory, Polyakov loop effective couplings, Monte Carlo calc. 7-41619
- Z(3) lattice gauge model, entropy and free energy, Monte Carlo calcs. 7-9956
- zero-point field in a circular-motion frame 7-41610
- η^+ mass and topology in SU(3) lattice gauge theory 7-24783
- η^+ mass in SU(3) lattice gauge theory, topology 7-429
- $\pi \rightarrow \pi^0 e^+ \nu$, lattice QCD Monte Carlo simulations 7-35763
- π - η mass difference in lattice QCD, U(1) problem, strong coupling expansion 7-41810
- V- $\pi\gamma$, decay amplitude calcs., lattice QCD anal. 7-35801

axions *see intermediate bosons***backscatter**

- see also particle backscattering*
- acoustic backscatter from ocean bubble clouds, meas. by automatically recording inverted echo sounder (ARIES) 7-8991
- airborne microwave rain scatterometer/radiometer system, microwave backscatter expt. of ocean surface (Japanese) 7-23910
- airborne microwave rain scatterometer/radiometer system, rain meas. and data anal. (Japanese) 7-23909
- atmospheric correlation-time measurements and effects on coherent Doppler lidar 7-60385
- auroral E-region, radar irregularities due to plasma instability types 7-60447
- complex structure backscatter, flat-plate physical optics approximation 7-57217
- dielectric targets composed of continuous assembly of circular discs, light scatt. 7-50482
- E polarisation, thin wire loop, backscattered field anal. 7-36861
- electron beam bombarded plate, backscatter, transmission and energy, release 7-36872
- equivalent current method, backscattering from triangular cylinder and hexahedron calc. 7-42865
- fibre optic gyroscope, phase modulated, coherent backscatter analysis 7-43427
- gamma-source backscatter density gauges modelling 7-34716
- Gaussian random surface, light scatt. backscattering enhancement and depolarisation 7-62627
- Io surface materials, phase curves interpretation in terms of Hapke's function 7-55523
- ionosphere, SABRE backscatter meas. rel. to E-region vertical velocity structures 7-4254
- lidar technique appl. to laboratory meas. of atmospheric temp. and backscatter ratio 7-9238
- light, weak localization in finite slab, anisotropy effects and light-path classification 7-42925
- light backscattering, statistical soln. 7-50486
- microwave radar sensing, modelling interactions between ocean and environment 7-60423
- MU radar obs. of troposphere and lower stratosphere, backscattered VHF echo power, aspect sensitivity 7-40550
- multipoint fibre optic refractive index sensors 7-43419
- nondestructive coating thickness meas. 7-13703
- nonlinear three-wave stimulated Brillouin scatt., implications for optical fibres 7-37036
- ocean backscatter depression in C and Ku bands due to surface oil 7-8460
- ocean surface, whitecap and foam effects on wind speed extraction with pulse-limited radar altimeter 7-29306
- optical fibre OTDR, range and accuracy in backscatter measurements 7-15999
- optical passive ring resonator gyro, reson. characts. of backscatt. 7-50753
- optical waveguide, single-mode, stimulated Brillouin scattering, influence of sound diffraction 7-1225
- optically thick medium exposed to laser beam, anisotropic back scatt. 7-62629
- phase-insensitive detection for measurement of backscattered ultrasound 7-43590

backscatter continued

- polyethylene, medium-density, noncontact monitoring of cyclic loading and stress relax. by US backscatter 7-59724
- pulse narrowing by backward stimulated Brillouin scattering 7-15936
- radar backscatter from Earth's surface, digital processing of satellite side-looking radar images 7-66340
- radar backscatter from troposphere and stratosphere, appl. in radio acoustic meas. of temp. profile 7-14360
- radar cross-sections, higher order diffractions from a circular disk 7-42866
- Rayleigh backscatter lidar signals, atmospheric temp. retrievals 7-9165
- ring laser, two-mode, with backscatter, freq. depend. 7-37000
- scalar fields, Born and Rytov approx. equivalence 7-24485
- single-mode optical fibres, charactn. using spontaneous Brillouin backscattering technique 7-6026
- swift ion total backscattering from solid targets at grazing incidence 7-53483
- two parallel conducting strips, arbitrarily oriented, EM plane wave scattering study (Japanese) 7-42859
- X-ray refl., half-degree ang. interval obs. in backscatter from high-quality cryst. 7-64723
- Al plate US backscatter and resonance expts. 7-2108
- CaCO₃ crystal, formation of picosecond pulses by stimulated Raman backscattering 7-1226

backward wave oscillations *see backward wave tubes; electromagnetic oscillations***backward wave tubes**

- see also carcinotrons*
- No entries

bacteriorhodopsin *see proteins***Badgers rule** *see bond lengths; molecular force constants***bag models** *see quark confinement***bagging** *see packaging***bainitic steel** *see steel***bainitic transformations** *see solid-state phase transformations***balance (physiological)** *see mechanoreception***balanced amplifiers** *see differential amplifiers***balanced input amplifiers** *see differential amplifiers***balances**

- see also weighing*
- attraction force meas., using torsion balance and capacitive position transducer 7-41407
- Cavendish balance, Leybold version elec. and mech. modification 7-18538
- comparator using flexure-strip suspensions 7-48699
- high frequency piezoelectric balance, static wind load meas. 7-14356
- metrological characts. of precision balances, with automatic readout 7-41346
- quartz microbalance for thickness meas. of metallic glass films (French) 7-29982
- standard balances with upper scale limits up to 10 kg 7-41347
- vacuum microbalance, automated, for adsorption isotherm meas. 7-41397
- C fluorination, thermobalance for investig. 7-41349

Balescu-Lennard theory *see plasma collision processes***ball lightning** *see lightning***ballistic electronic conduction** *see high field effects***ballistics**

- see also impact (mechanical); military equipment*
- fly ball trajectory, analytical soln. 7-48230
- vortex flows, ballistics of objects in system 7-11427

balloons

- see also aircraft*
- hot air, flight duration, surface characts. effects 7-50906
- hydraulic pump driven by low-level temp. difference 7-54335
- Mark I single-axis platform performance, for balloon borne remote sensing 7-23913
- SCRIBE interferometer atmospheric emission spectra 7-55319
- single-axis platform design for balloon-borne remote sensing 7-23912
- star camera and aspect determ. system for balloon-borne payloads 7-55418
- stratospheric balloons use for geomag. anomalies meas. 7-47574
- UV telescope characts. (Spanish) 7-55742

banana regime *see plasma collision processes***band gap** *see energy gap***band model of magnetism**

- see also Hubbard model*
- actinides bulk magnetic and transport props. 7-12953
- antiferromagnetic metals and alloys, 4f-local moments, SDW instability 7-58970
- crystal lattice, spiral mag. struct., band struct. calcs. 7-7096
- energy bands, effective hamiltonians 7-2805
- extended s-f model, elec. cond. calc. 7-64194
- field theoretical approach to solid state physics 7-12934
- Gutzwiller-Hubbard-Kanamori model, crystallization props. 7-58974
- Hubbard model, degeneracy and quantum effects 7-7469
- itinerant electron ferromagnetism, mag. susceptibility, Curie-Weiss law 7-27501
- itinerant electron model with crystalline or mag. long-range order 7-17152
- itinerant ferromagnets, electron and magnon spectra, spin fluctuation effects, dynamical suscept. calcs. (Russian) 7-12960
- itinerant ferromagnets, heavy fermion superconductivity (Chinese) 7-38805
- nearly antiferromagnetic itinerant fermion systems, possible superconductivity 7-38802
- one-dimensional degenerate Hubbard model, Monte Carlo simulations 7-45609
- segregated-stack organic charge transfer solids, mag. props. 7-17151
- tight-binding itinerant ferromagnet, spin wave anal. 7-2833
- toroidal collective excitations and the optical properties of crystals 7-39059
- transition metal systems, induced magnetic form factors, neutron scatt. calcs. 7-7470
- transition metal thin films, ferromagnetic, surface spin waves, multiband model 7-2834
- weakly itinerant ferromagnetic systems, magnetoelastic anomalies due to spin fluctuations 7-53106

band model of magnetism continued

- CdCr₂Se₄ thin films, ferromagnetic semicond., multielectron energy struct., absorpt. spectrum, temp. and doping depend. 7-38488
 Co, BCC and FCC forms, ferromag. phases investig. 7-2851
 Cr surface magnetism, effect of adsorbed O 7-58973
 Cr-Mo dilute alloys, magnetoelectricity, antiferromagnetism disappearance effects 7-45789
 Fe, BCC and FCC forms, ferromag. phases investig. 7-2851
 Fe, ferromagnetic, band struct. and optical props. 7-2476
 Fe, static paramag. spin susceptibility at finite temps. 7-33138
 Fe surface magnetism, effect of adsorbed O 7-58973
 MnTe, electronic struct. in magnetically ordered and disordered phases, tight-binding calcs. 7-45145
 Ni, BCC and FCC forms, ferromag. phases investig. 7-2851
 Ni, static paramag. spin susceptibility at finite temps. 7-33138
 Ni surface magnetism, effect of adsorbed O 7-58973
 PdNi alloys, magnetic clusters interaction energy calcs. 7-45652
 Sc(Co_{1-x}Al_x)₂, anomalous high field magnetisation 7-64438
 α-Ti, mag. suscept. and elec. resist. meas., itinerant antiferromagnetism, comment 7-33151
 U_xY_{1-x}B₄ system, mag. props., XPS and bremsstrahlung-isochromat spectroscopy studies 7-17172
 Y₃Fe₅O₁₂/Si, band model of photoinduced magnetic effects 7-17214
 Zr_{1-x}Ni_x amorphous alloys, itinerant electron magnetism, AC susceptibility meas. (Chinese) 7-27490

band-pass filters

- see also crystal filters; vocoders
 imaging bandpass electron energy analyser 7-375
 narrow band-pass interference filter for fibre optic thin film temperature sensor 7-25992

band structure

- see also band structure of crystalline metals and alloys; band structure of crystalline semiconductors and insulators; band structure of semimetals; band theory models and calculation methods; Brillouin zones; conduction bands; degenerate semiconductors; electron energy states of amorphous solids; electron energy states of liquid metals; electron energy states of liquid semiconductors; energy gap; Fermi surface; many-valley semiconductors; valence bands
 (BEDT-TTF)₂I₃, alpha and beta phases, electronic struct., EELS studies 7-45118
 (BEDT-TTF)₂ReO₄, band electronic struct. 7-7094
 (BEDT-TTF) BrO₄, band electronic struct. 7-7094
 α-(BPDT-TTF)(Ni(dmit)₂)₂, struct. phase transition accompanied by change of electronic struct. 7-52704
 conference, Marineland, Florida, USA (March 1986) 7-40985
 Curie temp. calcs. long range magnetic order and intermediate valence, Anderson model 7-45247
 electron-lattice coupled quarter filled band systems, 1D, solitons 7-45181
 electronic characteristics of small metal particles (Dutch) 7-52396
 electronic wave functions, localisation due to local topology 7-21847
 ferromagnets, electronic struct. determ. by spin- and angle-resolved photoemission, book contrib. 7-33522
 Fourier-transformed Compton profile for band occupancy determ. 7-21801
 graphite, electronic band struct., unoccupied, angle-resolved inverse photoemission study 7-64725
 graphite, secondary-electron emission and electron-energy loss spectra 7-33491
 graphite, single cryst., synchrotron radiation-excited angle-resolved photoemission 7-17391
 graphite intercalated with alkali metals, electron struct., soft X-ray emission spectroscopy 7-45117
 graphite intercalation compound with H₂SO₄, optical study of K-point π-band dispersion 7-17317
 graphite-K intercalation cpd., C₆K, electronic band struct., angle resolved UPS study 7-27232
 hydrides, amorphous and crystalline, comparative studies via incoherent scatt. 7-21798
 incommensurate systems, fractal spectra, Aubry model energy spectrum 7-12581
 luminescent centres in crystals, impact excitation and Auger quenching, appl. to ZnS:Mn 7-27827
 metals, collective excitations and interband transitions 7-2459
 one-dimensional CDW states, self-similar band structure and electron-phonon coupling 7-21833
 one-dimensional quasicrystals, electronic struct., tight-binding model 7-32892
 organic conductors, IR absorption spectra and electron-electron interactions 7-46032
 organic linear chain conductors, IR and near IR props. 7-22247
 periodic Anderson model, interatomic hybridisation, singular density of states, narrow band limit anal. 7-16927
 poly(N,N'-bis(phenoxyphenyl)-pyromellatitimide), valence electronic struct., UPS spectrum 7-42806
 polyaniline, conducting polymer, electronic and electrochem. props., MNDO calc. 7-2462
 polyaniline, in situ optical and ESR studies during electrochemical doping 7-26670
 polydiacetylenes, electronic struct., substituent-induced strain effect, MNDO calcs. 7-10427
 polyisothianaphthene, electronic struct. and conduction properties 7-45119
 polymer, direct space exchange lattice sums, convergence props. 7-21797
 polymers, electronic structures, self-consistent, first principles calcs. 7-7090
 positron annihilation wavefunction effects 7-7092
 quasi-1D wire, thermopower, effect of subband struct., determ. 7-7213
 quasi-lattices, two-dimensional, tight binding electron props. 7-27233
 quasi-one-dimensional density-wave systems, electronic struct., high mag. field effects 7-58754
 quasicrystal, one-dimensional, electronic states, Fibonacci sequence 7-52394
 rare earth light, insulating cpds., core hole screening, X-ray absorpt. studies 7-64796
 semiconductor superlattices with ultrathin layers (Japanese) 7-12824
 semiconductors, collective excitations and interband transitions 7-2459
 semimetals, collective excitations and interband transitions 7-2459
 singularity of formfactor of pseudopot. assoc. with resonance scatt. of electrons (Russian) 7-58727

band structure continued

- surface and solid state physics based on spin polarised electrons (German) 7-64045
 (TMTCF)₂X salts (C=S,Se), crystal struct., press. and temp. depend. 7-44520
 two dimensional quasi-periodic Penrose lattice, electronic and vibr. modes, localised states and band struct. 7-27300
 zero-gap type I state, spontaneous destruction in quantising mag. field 7-2460
 C₆CS, first stage intercalation cpd., self-consistent band struct. calc. 7-52395
 C₆K first stage intercalation cpd., self-consistent band struct. calc. 7-52395
 C₆K, intercalation cpd., density of states, interlayer band occurrence 7-2454
 C₆Rb, first stage intercalation cpd., self-consistent band struct. calc. 7-52395
 CrO₂, half-metallic ferromagnet, band struct. calcs. 7-7091
 Cr₂TiS₂, intercalated dichalcogenide, electronic struct. 7-52387
 Fe₈₀B₂₀ amorphous alloys, EXAFS meas. at B k-edge 7-64807
 Fe₂TiS₂, intercalated dichalcogenide, electronic struct. 7-52387
 GaAs-Al_xGa_{1-x}As, internal photoemission method for determ. of band offsets 7-12832
 GaAs-Al_xGa_{1-x}As, modulation-doped quantum wells, photoabsorpt., electronic props. 7-64330
 GaAs-AlAs superlattices, 2D excitons, magneto-optical study (Japanese) 7-13139
 GaAs-AlGaAs heterointerface, band offsets, overview 7-12831
 GaAs-AlGaAs heterojunctions, energy band discontinuities, internal photoemission meas. 7-13331
 GaAs-AlGaAs heterostruct., band discontinuity determ., DLTS, interface charge density, trap conc. 7-12833
 GaAs-AlGaAs heterostructures, energy band alignment, thermionic emission of holes 7-13319
 GaAs-AlGaAs superlattices, band structure of holes (Japanese) 7-12825
 Ga_{1-x}In_xAs-Al_{1-y}In_yAs superlattices, electronic struct., depend. on growth axis 7-64329
 KC₈ intercalation cpd., polarisation depend. XANES study 7-59298
 KH₂ graphite intercalation cpd., struct. and electronic props. 7-27234
 KH_{0.8}C_x, polarisation depend. XANES study 7-59298
 (LiH)_x linear infinite chains study, pseudo-lattice method, ab initio SCF calcs. 7-36470
 Li_{0.9}Mo_{0.9-x}W_{0.1}, W substitutional effects on elec. resistivity and transport props. 7-45260
 (Na_{1-x}Li_x)_{0.9}Mo_{0.9}O₁₇, Na substitutional effects on elec. resistivity and transport props. 7-45260
 NbH, β- and γ-phases, electronic struct. and phonon anharmonicity 7-45199
 NbSe₂, CDW conductor, magnetothermopower studies 7-64226
 Ni-ZnSe-SiO₂-Si struct., energy barriers for photocharging of trapping sites in ZnSe layer 7-52844
 S₂N₂, photoelectron spectrum, valence ionic state calc. by many-body Green's function method 7-10667

band structure of crystalline metals and alloys

- for band structure of semiconductor alloys see band structure of crystalline semiconductors and insulators or electron energy states of amorphous solids
 Al₁₅ compounds, martensitic and supercond. phase transitions 7-58942
 actinide metals, solid state and thermodynamic props., f-electron bonding and struct., review 7-12321
 actinide-transition metal alloys, AM₂, A=U-Np, M=Fe-Ni, magnetism and electronic props. 7-27505
 alkali metal clusters, structures, pseudopotential method, local density approx. 7-36840
 alloys, ternary substitutional, electronic structure, KKR-CPA method 7-64074
 DC transport in metals 7-17010
 electronic structure, positron annihilation studies, review 7-45126
 Fermi surface, 2D angular correlation studies 7-39236
 ferromagnetic, electronic quasiparticle struct., temp. depend. 7-32908
 films, electron states calc., allowance for transition layer in construction of pot. (Russian) 7-58733
 intermetallic cpds., charge redistrib., L-edge XANES study 7-64816
 metal, soft X-ray absorpt., numerical anal. 7-17361
 metals, EM generation of acoustic waves, theory 7-51945
 metals, metallic electron charge density to electron momentum density transformations 7-27249
 Ni, electron core states overlap at very high compressions 7-21849
 positron annihilation, 2D angular correlation studies 7-39237
 positron annihilation studies of solids 7-64728
 positron studies of electronic struct. of metals and alloys 7-64730
 surface (001), metastable BCC phase, electronic struct. and magnetism 7-45418
 transition metal borides, AlB₂ type, electronic struct. study, heats of formation anal., HMO calcs. 7-25409
 transition metal magnetism, singular volume dependence, spin-polarised band structure calcs. 7-22108
 transition metal systems, induced magnetic form factors, neutron scatt. calcs. 7-7470
 transition metals, Slater-Koster parameters, transferability and scaling 7-64072
 two-dimensional angular correlation of positron annihilation radiation 7-39239
 Ag-Au, valence level splitting 7-45139
 AgCd, electronic structure, disordering effects (Russian) 7-32901
 Al clusters, electron energy spectra, size effects 7-7103
 Au₂Ag intermetallic cpds., charge redistrib., L-edge XANES study 7-64816
 AuAl₃ intermetallic cpds., charge redistrib., L-edge XANES study 7-64816
 AuGa₂ intermetallic cpds., charge redistrib., L-edge XANES study 7-64816
 Bi, dielectric function, temp. depend. of band struct. parameters 7-7138
 Cd₉Ag₃, Ag density of states, Auger and photoelectron spectra, Clogston-Wolff model calcs. 7-2451
 Cd_{1-x}Hg_x alloys, electronic structure dependence on crystal lattice parameters 7-45141
 Ce alloy cubic Laves phases, electronic struct., self-consistent APW calcs. 7-12599
 Ce alloys, electronic struct., pseudopotential method 7-27245

band structure of crystalline metals and alloys continued

- Ce alloys, electronic structure, spectroscopic and thermodynamic props., impurity Anderson Hamiltonian 7-32900
 Ce, core and valence photoemission, calc. 7-33516
 Ce, electronic struct. and superconducting transition temp. calcs. (*Chinese*) 7-27244
 CeAl₂, electronic struct. determ. 7-52417
 CeAl₃, heavy fermion system, fluctuating bands 7-58736
 CeAl₃, quasiparticle band struct., local-density approx. anal. 7-27250
 CeBe₁₃, band struct. calc. 7-32905
 CeCu₂Si₂, quasiparticle band struct., local-density approx. anal. 7-27250
 Ce₂La_{1-x}Cu₈, electronic states, resonant photoemission study 7-53496
 CeO₂, electronic struct. determ. 7-52417
 CePb₃, heavy fermion material, magnetism and superconductivity 7-52880
 CePd₃, electronic structure and intrinsically selective absorption 7-38444
 Co, optical props., electronic struct. depend. (*Russian*) 7-33356
 Co₉₂Fe_{0.08}, FCC, Fermi surface, de Haas-van Alphen studies 7-52406
 Cr, band structure 7-7105
 Cr, paramagnetic, two-photon momentum distrib. 7-45128
 Cr₂Si, Al₁₅ cpds., 2D angular correlation of positron annihilation radiation 7-39238
 Cs, positron annihilation and pressure-induced electronic s-d transition 7-22378
 Cu (001), adsorbed K, valence-electronic struct., work function changes and EELS 7-45002
 Cu dilute alloys with 3d elements, electronic struct., K-edge XAS study 7-64066
 Cu, electronic props., spectrosc. investig. 7-59216
 Cu-Fe alloys, electronic structure and impurity states, optical investigations (*Russian*) 7-32943
 Cu₁₃, fragmental cluster model and electronic struct. (*Ukrainian*) 7-12597
 CuNi, substitutionally disordered, electronic struct., LCAO-CPA calcs. 7-64067
 Dy, band struct., effect of nonspherical pot., warped muffin-tin approx., APW method 7-27246
 Er-H solid soln., mag. props., H addition effects 7-7510
 Fe, BCC, mag. ordering and electronic struct. (*Russian*) 7-33170
 Fe dilute alloys with 3d elements, electronic struct., K-edge XAS study 7-64066
 Fe, Fermi surface change near the mag. transition 7-16935
 Fe, ferromagnetic, band struct. and optical props. 7-2476
 α -Fe, H-H binding energy, lattice location and heat of formation 7-32361
 Fe, Hall effect, anomalous, and energy band struct. (*Russian*) 7-52414
 Fe itinerant ferromagnets, electronic struct. determ., spin depend. inverse photoemission studies, book contrib. 7-33479
 Fe-Al disordered alloys, electronic struct., mag. props. and Mossbauer spectra 7-64073
 Fe-Al-Si system, electronic struct. interatomic bonding, X-ray emission spectra analysis (*Russian*) 7-39320
 Fe-Co-Cr-Mo alloys, electronic struct. and mag. props., X-ray spectra studies (*Russian*) 7-32902
 Fe-Ge amorphous and cryst. layers, short range order and valence bands 7-13266
 FeAl, X-ray emission and absorpt., ab initio self-consistent band struct. calcs., LMTO method 7-64826
 FeCo alloy, electronic struct., effect of ordering, positron annihilation and Mossbauer effect study 7-45142
 Fe₂P, electronic struct., mag. props., KKR, LMTO methods, LSD approx. 7-64070
 FeRh, X-ray emission and absorpt., ab initio self-consistent band struct. calcs., LMTO method 7-64826
 Fe₂Si, electronic struct. and X-ray spectra, disorder effects (*Russian*) 7-32903
 Fe₂Si, transition metal impurities, electronic struct. and site preference 7-12653
 Gd₂ (Co_{1-x}Mn_x)₁₇, Co contribution to magnetocrystalline anisotropy, point charge model 7-45665
 GdCu, optical props. and electronic struct. investigs. (*Russian*) 7-13174
 GdPd₃, electronic structure and intrinsically selective absorption 7-38444
 Hf-Os, electronic, mag., supercond. and glass forming ability rel. to stability 7-38846
 HfFe₂, electronic struct. and mag. props., tight-binding approx. calcs. 7-2475
 In_{1-x}Sn_x alloys, electronic structure dependence on crystal lattice parameters 7-45141
 Ir (111), spin-resolved photoemission meas. of transitions to secondary unoccupied bands 7-53501
 K, electronic band struct., interatomic distance, role of p-orbitals, EHT tight-binding calcs. 7-32906
 LaAg, nonmag. cpds., transport props. and electronic struct. 7-2575
 LaBe₁₃, band struct. calc. 7-32905
 LaPd₃, electronic structure and intrinsically selective absorption 7-38444
 Li alloys, Zintl phases, binary and ternary, electron densities, sp³-bonding character, calc. 7-32907
 Li, crystal and electronic struct., ab initio HF cluster method 7-44443
 Li, electron-electron scatt., elec. resistivity meas. 7-32981
 Li, electronic band struct., interatomic distance, role of p-orbitals, EHT tight-binding calcs. 7-32906
 Li, simple local pseudopotential 7-32888
 LuAg, nonmag. cpds., transport props. and electronic struct. 7-2575
 LuFe₂, electronic struct. and mag. props., tight-binding approx. calcs. 7-2475
 Mn, band occupancy determ. using Fourier-transformed Compton profile 7-21801
 Mn₂P, electronic struct., mag. props., KKR, LMTO methods, LSD approx. 7-64070
 Mo-Re alloys, electron struct., X-ray spectra studies (*Russian*) 7-45135
 Mo_{1-x}Re_x system, thermal EMF and topological electronic transition 7-45286
 MoSi₂, band structure 7-27248
 Na, electronic band struct., interatomic distance, role of p-orbitals, EHT tight-binding calcs. 7-32906
 Nb and its dihydride, Compton profiles 7-59281
 Nb, electronic structure, positron annihilation wavefunction effects 7-7092
 Nb, Fourier transform of 2D angular correlation 7-38439
 NbC_xN_y, nonstoichiometric, supercond. transition temp. and band struct. (*Russian*) 7-58935

band structure of crystalline metals and alloys continued

- Nb₃Ir, Al₁₅ cpds., 2D angular correlation of positron annihilation radiation 7-39238
 Nb₃Mb_{1-x} alloys and elemental metals, 2D angular correlation spectra studies, band struct. 7-39235
 Ni alloys, core-level shifts anal., LMTO energy band calcs. 7-38487
 Ni, band occupancy determ. using Fourier-transformed Compton profile 7-21801
 Ni dilute alloys with 3d elements, electronic struct., K-edge XAS study 7-64066
 Ni, Fermi surface change near the mag. transition 7-16935
 Ni, ferromag., magneto optical effects and band struct. (*Russian*) 7-59188
 Ni, Hall effect, anomalous, and energy band struct. (*Russian*) 7-52414
 Ni itinerant ferromagnets, electronic struct. determ., spin depend. inverse photoemission studies, book contrib. 7-33479
 Ni, quasi-particle and band-calc. spectra, w.r.t. valence band photoemission meas. 7-2474
 Ni, spin polarised electronic struct., mag. and bonding props. 7-32904
 Ni, spin polarised positron annihilation 7-46187
 Ni-Al intermetallic cpds., charge redistrib., L-edge XANES study 7-64816
 Ni-based alloys, magnetic props. under high press., effects on s and d band electrons 7-7542
 Ni-Ge amorphous and cryst. layers, short range order and valence bands 7-13266
 Ni-H system, band structure calcs. 7-45140
 Ni₆₄Fe_{0.36} intermetallic cpds., charge redistrib., L-edge XANES study 7-64816
 Ni_{1-x}Fe_xMnSb, half-metallic ferrimag., mag. and crystallographic props. 7-45672
 Ni₃Ga, momentum density distrib., Compton scatt., positron annihilation, symmetrised APW method 7-64069
 NiH, spin polarised electronic struct., mag. and bonding props. 7-32904
 NiH clusters, charge distrib., Hartree-Fock SCF INDO calcs. 7-52411
 NiMnSb, half-metallic ferromagnet, positron-annihilation study 7-21802
 Ni₂P, electronic struct., mag. props., KKR, LMTO methods, LSD approx. 7-64070
 NiTi, electronic phase diagram for B2-R transition 7-52388
 Os single cryst., energy band struct. and optical absorpt. studies 7-16938
 Pb, self-consistent relativistic band struct., normal and high press. 7-52413
 Pd, angular correlation of positron annihilation radiation, calc. 7-39244
 Pd monolayers on Ta(110), morphology and struct. phase transitions 7-38374
 Pd, reflectivity and electronic struct. studies 7-17298
 Pd₂Fe, disordered phase, electronic struct. anal. 7-58735
 Pd₂Fe, electronic struct. 7-52415
 PdH, angular correlation of positron annihilation radiation, calc. 7-39244
 PdH_x, electronic density of states, recursion method 7-64043
 PdH_x, H-induced lattice expansion and effective H-H interaction 7-52247
 Pt (110), hybridisation of electronic bands, spin-polarised UV photoemission spectra 7-45421
 Pt (111), spin polarised photoemission, relativistic energy bands obs. by vector anal., parity- and spin-mixing 7-7820
 RAl₂Si (R=Pr,Gd,Tb,Dy,Ho,Er,Tm,Lu), electronic struct., X-ray emission bands (*Russian*) 7-45138
 Rb, electronic band struct., interatomic distance, role of p-orbitals, EHT tight-binding calcs. 7-32906
 Re, Fermi surface, 2D angular correlation of positron annihilation radiation 7-39240
 Ru, electronic, structural and cohesive props., theoretical study 7-37922
 Ru, Fermi surface, 2D angular correlation of positron annihilation radiation 7-39240
 SbSn dilute alloys, muon Knight shift and trapping, comp. and temp. depend. 7-45889
 ScGa₃, band struct., coupling energy (*Russian*) 7-58732
 Sn, valence band struct., angle resolved photoelectron spectra 7-52416
 Sr, relativistic band struct., self-consistent calcs. under normal and high press. 7-64068
 Ta, Compton profiles, APW calcs. 7-27809
 ThBe₁₃, band struct. calc. 7-32905
 Ti clusters, electronic props., CNDO method 7-27247
 Ti, Fermi surface, 2D angular correlation of positron annihilation radiation 7-39240
 Ti-Cr alloys, cryst. and electronic struct., decomposition of β -solid soln. 7-37931
 Ti-Fe, electronic, mag., supercond. and glass forming ability rel. to stability 7-38846
 TiC_x, KVV Auger electron spectra and band struct. (*Russian*) 7-17371
 TiH_{1.98} and Ti, Compton profiles meas. 7-7785
 TiH₂, electronic struct., cluster method (*Russian*) 7-64071
 TiP₃, electronic structure and intrinsically selective absorption 7-38444
 U alloys, optical and elec. transport props., review 7-13119
 UAu₃, band struct., theoretical XPS intensities 7-39353
 UBe₁₃, band struct. calc. 7-32905
 UFe₂, spin-polarised energy bands, density of states and eqn. of state 7-58734
 UIr₃, band struct., theoretical XPS intensities 7-39353
 UPt₃, band struct., theoretical XPS intensities 7-39353
 UPt₃, heavy fermion superconductivity and normal state props. 7-52412
 UPt₃ single crystals, electronic structure, low energy reflectivity study 7-45137
 URh₃, 5f band narrowing, evidence from resonant photoemission 7-27855
 URh₂B, 5f band narrowing, evidence from resonant photoemission 7-27855
 URu₃, 5f band narrowing, evidence from resonant photoemission 7-27855
 URu₃ (Rh₃) (Pd₃) (Ir₃) (Pt₃), hybridisation, electronic struct. and props. 7-45136
 URu₂B, 5f band narrowing, evidence from resonant photoemission 7-27855
 USi₃(Sn₃)(Ru₃), electronic struct. and f hybridisation 7-12600
 U_{1-x}Th_xRe₂, polymorphic transform., supercond. crit. temp., low temp. sp. ht. meas. 7-17125
 V and its dihydride, Compton profiles 7-59281
 V, Fourier transform of 2D angular correlation 7-38439
 V-Fe-H alloys, positron annihilation near crit. electron conc. 7-46199
 V₁₃, fragmental cluster model and electronic struct. (*Ukrainian*) 7-12597
 VC_x, KVV Auger electron spectra and band struct. (*Russian*) 7-17371
 W, Compton profiles, APW calcs. 7-27809

band structure of crystalline metals and alloys continued

- W, valence bands, angle resolved XPS spectra 7-22441
 Y, electronic struct., electron-phonon matrix and superconductivity, high press. effects, KKR calcs. 7-21805
 Y, electronic structure, electron-phonon matrix, supercond. transition temp. (*Chinese*) 7-12596
 Y, pressure-induced superconductivity, band struct. and sp. ht. press. depend. calcs. 7-7431
 Y₂(Co_{1-x}Mn_x)₁₇, Co contribution to magnetocrystalline anisotropy, point charge model 7-45665
 YAg, nonmag. cpds., transport props. and electronic struct. 7-2575
 Y₂Co₃, electronic struct. and mag. props. 7-7104
 Y₂Fe₁₄B, electronic struct. and mag. props. recursion method calcs. 7-2452
 YH_x system, mag. susceptibility and electronic struct. (*Russian*) 7-58988
 YPd₃, electronic structure and intrinsically selective absorption 7-38444
 Yb, relativistic band struct., self-consistent calcs. under normal and high press. 7-64068
 Zn, phonon spectrum fine structure 7-16702
 Zr, momentum density distrib. in α and ω phases by position annihilation meas. 7-46183
 Zr-Co, electronic struct., supercond. and magnetism 7-64398
 Zr-Ru, electronic, mag., supercond. and glass forming ability rel. to stability 7-38846
 ZrFe₂, electronic struct. and mag. props., tight-binding approx. calcs. 7-2475

band structure of crystalline semiconductors and insulators

- see also conduction bands; energy gap; valence bands*
 7-33352
 (*Chinese*) 7-38446
 activity coeffs. of electrons and holes in semicond. with parabolic density of states 7-27324
 BAS, structural and electronic props., pseudopotential method, local density approx. 7-32353
 α -(BEDT-TTF)₂I₃, struct. charact. and band electronic struct. below metal-insulator transition 7-2007
 binary compound polar semiconductors with nonparabolic energy bands, electronic struct. 7-2478
 compositionally graded semiconductors and device appls., book contrib. 7-73233
 diamond, electron correlation, band gaps and quasiparticle energies 7-27278
 diamond, electronic structure, STEM study 7-16939
 diamond, large unit cell CNDO calculations 7-7106
 diamond, ultradisperse, obtained from C plasma, energy spectrum 7-22384
 diamond crystals, band structure, LMTO calcs. 7-2477
 electron irradi., hole effective mass parameters, cyclotron reson. 7-58730
 graphite, degeneracy lifting, perturbational approach 7-52399
 heterojunction band lineups and interface dipoles, tight binding theory 7-7368
 heterojunction discontinuities, self-consistent density functional calcs. 7-7364
 hole subbands, 4X4 Luttinger-Kohn Hamiltonian, numerical soln. 7-38783
 II-V semiconds., cryst. growth, characterisation and appls., review 7-26685
 II-VI semiconductor lattice matched heterojunctions, common anion rule failure 7-7367
 III-V semicond. alloys, vel.-field characts., band struct. effects, CPA calcs. 7-64243
 III-V semiconds., electronic struct. calcs. 7-12608
 III-V semiconductors, hot-electron photoluminescence, polarisation 7-46118
 layer crystals dynamics, long wavelength vibrs. factor group anal. 7-58424
 local density band structure, self-energy corrections 7-7097
 narrow-gap cpd. semiconds., weak-coupling polarons, band nonparabolicity effects, comment 7-21830
 periodic polypeptides, band struct. ab initio HF cryst. orbital calcs. 7-23298
 quantum crystals, energy spectrum, quasi-averaged value calcs. (*Russian*) 7-21570
 rare earth molybdates, improper ferroelectrics, energy spectrum and vacuum UV spectra 7-33413
 rare earth silicides, R₂Co₃Si₅ X-ray spectra and valence band electronic struct. 7-33484
 resonant states, strong mag. field, Coulombic impurity pot. 7-32925
 scanning electron microscope cathodoluminescence technique for anal. of band structure in solids 7-51595
 semiconducting materials, cryst., and device appls., book 7-60894
 semiconductor alloys, band struct. and reduced local symm., virtual-cryst. approx. calcs. 7-38451
 semiconductor solid solutions, electron struct., X-ray and XPS spectra studies 7-12605
 semiconductor superlattice, bulk and surface plasma modes, band dispersion 7-33085
 semiconductor superlattices, dynamical screening, quasi-2D electron gas, electron-phonon interactions 7-45464
 semiconductors, cryst. and amorphous, and heterojunctions, electronic struct. using bremsstrahlung isochromat spectroscopy 7-52795
 semiconductors, cubic, photoionisation of deep acceptors, drag of holes by light 7-12754
 superlattice band structures of group IV and III-V semicond., axial strain effects 7-2697
 TCNQ, valence band density-of-states 7-38434
 tetrakis(alkylthio)tetrathiafulvalenes, valence electronic struct., UPS, EHT calcs. 7-21810
 transition metal carbides, discrete X_α calcs. and high resolution Auger spectra 7-16942
 transition metal phosphorous trisulphides, electronic, structural and mag. props., intercalation cpds. and chemical props. 7-44499
 [Ag₂Ge₂P₁₂]Ge(Si)₆, bonding relationships and electronic struct. calcs. 7-16941
 [Ag₂Sn₂P₁₂]Ge(Si)₆, bonding relationships and electronic struct. calcs. 7-16941
 AgNO₂ crystal, room temp. electronic energy band calcs. 7-7113
 AgNO₂ crystals, band structure calc. 7-21807
 β -Ag₂Se, high temp. phase, band parameters, energy struct. 7-12603

band structure of crystalline semiconductors and insulators continued

- Al, electron energy spectrum, temp. effects and mag. susceptibility (*Russian*) 7-7102
 AlAs, energy bands, cohesive energy, form. energy, self-consistent calcs. 7-21995
 AlGaAs superlattice for visible laser diode, energy band structure (*Japanese*) 7-12823
 AlGaAs/GaAs heterostruct., quasiaatomic system, electronic struct. studies 7-38699
 AlGaAs-GaAs-AlGaAs single quantum well heterostruct., negative differential mobility and drift velocity overshoot 7-52787
 Al_{1-x}Ga_xN, photoluminescence in the edge emission region 7-27778
 AlN, electronic struct., first principles LCAO calc. 7-21813
 Ar, solid, band struct., classical nonrelativistic nonselfconsistent APW calcs. 7-64076
 As₂Se₃, crystalline, electronic and geometric struct., ab initio total-energy calcs. 7-12607
 (BN)_n, degeneracy lifting, perturbational approach 7-52399
 BaO, self-consistent electronic struct. 7-32910
 BaPb_{1-x}Bi_xO₃, electron-phonon interaction and superconductivity 7-27463
 BaTiO₃, electronic struct., special features (*Russian*) 7-45146
 BaZrO₃, valence band struct., X-ray-electron spectra studies 7-12604
 Bi, effective electron mass, quasi-1D systems, theoretical investig. 7-2468
 Bi magnetic suscept. field depend., electron band struct. effects (*Russian*) 7-12936
 Bi-Sb alloys, magnetic suscept. field depend., electron band struct. effects (*Russian*) 7-12936
 C cubic crystals, electron struct., cluster approx., X α calcs. 7-38445
 CaF₂, directional gamma ray Compton profile meas. and LCAO calcs. 7-2063
 CaO, self-consistent electronic struct. 7-32910
 CaO, XANES spectra, band struct. calcs. 7-64738
 CdZrO₃, valence band struct., X-ray-electron spectra studies 7-12604
 CdCr₂Se₄, band structure characteristics and props. of nonequilibrium carriers, cathodoabsorption 7-46064
 CdCr₂Se₄ thin films, ferromagnetic semicond., multielectron energy struct., absorpt. spectrum, temp. and doping depend. 7-38488
 CdCr₂Se₄-Ga, lightly doped, ferromag., photoconductivity, band struct. 7-7278
 CdGa₂S(Se)₄ defect chalcopyrite struct. crystals, linear optical response, atomic core electron contrib. calcs. 7-39061
 Cd_{1-x}Hg_xTe, band gap collapse, effects of Hg 5d electrons 7-64075
 CdSO₄·8H₂O·CrO₄²⁻, optical absorption spectra, electronic transitions 7-27740
 CdSb crystals, band struct., LCAO calcs. 7-58737
 CdSe, dielectric fn. and interband crit. points. 7-2480
 CdSe_{1-x}Te_x, bowing parameter of direct band gap, press. depend. 7-38453
 CeB₆, optical props. and band struct., spectroscopic ellipsometry meas. 7-13157
 CeN, narrow band material, high resolution photoemission 7-33512
 CoO, band structure and optical absorption edge 7-45147
 CsI, high press. metalisation, relativistic self-consistent APW calcs. 7-21812
 Cu complex, Cu(II) saccharinate, electronic struct. and cryst. struct. 7-27251
 Cu-based binary dilute alloys, electron struct., X-ray L α emission spectra studies 7-12598
 CuFeS₂, electronic struct., K-edge EXAFS study 7-64079
 Cu₂O, electronic struct. and binding mech. 7-2482
 Cu_{2-x}Se, electrical resistivity, temp. and carrier density dependences 7-38556
 Cu₃SnP₁₀, bonding and electronic struct. studies 7-26694
 ErSi₃, electronic struct., X-ray emission spectra studies 7-52419
 EuSi₃, electronic struct., X-ray emission spectra studies 7-52419
 γ -Fe₄N, Auger spectra, electronic struct. (*Russian*) 7-64832
 Fe_{1-x}O, wustite, electronic struct. and X-ray absorption spectra 7-2479
 α -Fe₂O₃, photoemission satellites, electronic struct. 7-39358
 FeS₂-electrolyte photoactive interface, electronic props. 7-33086
 GaAs, band-gap shifts 7-22333
 GaAs, covalent cryst., electronic struct., cluster approx. 7-52403
 GaAs, energy bands, cohesive energy, form. energy, self-consistent calcs. 7-21995
 GaAs, heavily doped, carrier-carrier and carrier-dopant interactions 7-21903
 n-GaAs impurity bands and band tailing 7-21809
 GaAs, L near-edge structure, X-ray photoabsorpt. spectra 7-64766
 GaAs, laser material, intervalence band absorpt. coeff. calc. 7-3015
 GaAs quantum wells, band offsets, inelastic light scatt. studies 7-7362
 GaAs, valence charge density, X-ray diffr. study, comparison with calculated results (*French*) 7-16940
 GaAs/AlAs superlattices, electronic band structure, pseudopot. method calc. 7-17084
 GaAs/Ga_{1-x}Al_xAs graded interface superlattice band struct. calcs. 7-58879
 GaAs-Al_{1-x}Ga_xAs quantum wells, parabolic, light scatt. studies 7-64651
 GaAs-Al_{1-x}Ga_xAs superlattice, hole subbands (*Chinese*) 7-58873
 GaAs-AlAs ultra-thin layer semicond. superlattices, energy band and stable structs. study 7-52789
 GaAs-GaAlAs superlattice, electronic struct., envelope function approx., phonon limited mobility, Boltzmann eqn. 7-2698
 GaAs_{1-x}P_xN, bound excitons, energy spectrum, optical absorpt. cross section, two-band model 7-16945
 Ga_{0.47}In_{0.53}As, laser material, intervalence band absorpt. coeff. calc. 7-3015
 Ga_{0.38}In_{0.72}As_{0.6}P_{0.4}, laser material, intervalence band absorpt. coeff. calc. 7-3015
 Ga_{1-x}In_xP_{1-y}As_{1-y}InP heterojunction interfaces, electron energy band structure (*Chinese*) 7-33070
 GaN, band struct., pseudopotential method anal. 7-52421
 GaP, energy band calculations (*Chinese*) 7-38446
 GaP(As)(Sb), band structure, polarisation-dependent angle-resolved photoemission spectroscopy 7-21814
 Ge crystals, band structure, LMTO calcs. 7-2477
 Ge cubic crystals, electron struct., cluster approx., X α calcs. 7-38445
 Ge, electron correlation, band gaps and quasiparticle energies 7-27278
 Ge, holes optical effective mass, determ. by interf. method 7-17290
 Ge, n-type and ultrapure samples, electron transport and press. coeffs. 7-2615

band structure of crystalline semiconductors and insulators continued

- Ge, pure and heavily doped, dielec. function, impurity conc. depend., spectroellipsometric meas. 7-2525
- GeO₂ rutile crystals, electronic struct., scalar-relativistic muffin-tin-orbital calcs. 7-64077
- GeTe, energy bands, relativistic empirical tight binding theory 7-45149
- GeTe, valence and energy spectrum, supercond. state 7-45534
- HfB, electronic struct., chem. bonding, Green's function methods 7-58741
- HgCdTe, electronic struct., alloying effects, ETBM calc. method 7-64080
- Hg_{1-x}Mn_xSe, zero gap semimag. semiconductor, inversion asymmetry spin level splitting 7-58784
- HgTe-CdTe superlattice, IR magneto-optics and band struct. 7-13138
- HgTe-CdTe superlattices, band struct., optical and magneto-optical studies 7-64337
- In-Ga-As-P films highly excited, ps band filling 7-43261
- InAs/GaAs strained-layer superlattices, band struct., TEM, X-ray and photolum. spectra 7-38722
- InAs-GaSb superlattice, band offset press. depend., magneto-optical studies 7-38698
- InAs-GaSb thin film heterostruct., superlattice, electron transverse effective mass 7-21990
- InAsSb/GaSb n-n heterojunctions, band discontinuities, C-V and I-V meas. 7-7366
- In_{0.9}Ga_{0.1}As, photoluminescence determ. of effects due to In alloying 7-46096
- InGaAsP, optical gain spectra, effects of energy band struct. (Chinese) 7-59239
- InN, band struct., pseudopotential method anal. 7-52421
- InP(As)(Sb), band structure, polarisation-dependent angle-resolved photoemission spectroscopy 7-21814
- In₂Te₃Fe, Fe²⁺ elec. inactivity study, mag. suscept., Mossbauer spectra and XPS anal. 7-52494
- K_{0.9}Mo_{0.1}O₁₇ electronic struct., room temp. UV photoemission spectra study 7-46272
- LaB₆, optical props. and band struct., spectroscopic ellipsometry meas. 7-13157
- La₂Li_{0.5}Co_{0.5}O₄, ⁵⁷Co, Ti, ⁵⁷Fe⁴⁺ anomalous charge state obs., ⁵⁷Co³⁺ nuclear decay studies 7-21881
- Li-TaS₂ intercalation cpds., room temp. optical transmission spectra, charge transfer and band struct. modification 7-45962
- LiCl, electron correlation, band gaps and quasiparticle energies 7-27278
- LiF crystal, X-ray spectra rel. to electronic struct. (Russian) 7-39319
- LiH, electronic struct., mol. cluster calcs. 7-7110
- Mg₂Si antiferroelectric semicond., electronic struct. calcs. 7-12608
- Mn oxides, oxides, Ni- and Co-containing, structural chemistry, EXAFS studies 7-63578
- MnO, band struct., optical props. 7-32912
- MnTe, electronic struct. in magnetically ordered and disordered phases, tight-binding calcs. 7-45145
- Mo₆L₆L'₆ (L, L' = S, Se, Cl, Br), cluster compounds, electronic struct., 3-band model, tight-binding and extended Huckel method calcs. 7-32913
- NbH₄, mag. spin susceptibility and Knight shift 7-33141
- NiAs-type compounds, electronic band struct., magnetism and structural phase transitions (Japanese) 7-21815
- NiTe₂, electronic struct. determ. by self-consistent LMTO-ASA method 7-7111
- P, black, interplanar forces caused by electron-lattice interaction 7-63547
- Pb_{1-x}Mn_xTe, indirect exchange interaction between Mn²⁺ ions 7-27509
- PbSe, energy band structure, thermoreflectance study 7-3028
- Pb_{1-x}Sn_xTe narrow-gap semicond., electron-electron interaction, effect on permitt., two-band model 7-52420
- PbTe-Pb_{1-x}Sn_xTe superlattice, electronic structs., envelope pn. approx. 7-45465
- PbTe(Se)(S), energy bands, relativistic empirical tight binding theory 7-45149
- PbZrO₃, valence band struct., X-ray-electron spectra studies 7-12604
- Pd₃Si, reflectivity and electronic struct. studies 7-17298
- PdTe₂, electronic struct. determ. by self-consistent LMTO-ASA method 7-7111
- PtTe₂, electronic struct. determ. by self-consistent LMTO-ASA method 7-7111
- Re₄L₆L'₆ (L, L' = S, Se, Cl, Br), cluster compounds, electronic struct., 3-band model, tight-binding and extended Huckel method calcs. 7-32913
- SbSBr, ferroelec. semicond., band struct., X-ray spectral studies 7-58739
- SbSI cryst., dielec. const. determ., chem. bond approach, MWH band struct. calcs. 7-17260
- SbSI, ferroelectric semiconductor, photoacoustic spectroscopy 7-16696
- Si, charge density, compact orbitals, LMTO tight binding representation 7-21806
- Si crystals, band structure, LMTO calcs. 7-2477
- Si cubic crystals, electron struct., cluster approx., X_α calcs. 7-38445
- Si, electron correlation, band gaps and quasiparticle energies 7-27278
- Si, large unit cell CNDO calculations 7-7106
- n-Si, piezoresistance associated with bending of the energy relief at the bottom of the conduction band 7-13095
- Si-SiGe strained layer superlattices, electric subbands 7-2700
- Si-SiGe strained-layer superlattices, optical and electronic props. 7-53353
- SiC, covalent cryst., electronic struct., cluster approx. 7-52403
- Si₃Ge_{1-x} coherently strained bulk alloys on Ge (001) substrate, indirect band gap and band alignment calcs. 7-2481
- SiO₂ cryst. and amorphous, point defects and electronic props. 7-64082
- SiO₂, electronic structure, direct and inverse photoemission and soft X-ray emission spectra (French) 7-59374
- SiO₂-related materials, cryst. and amorphous, electronic struct. calcs. 7-64081
- SnO₂ rutile crystals, electronic struct., scalar-relativistic muffin-tin-orbital calcs. 7-64077
- SnS(Se)(Te), electronic props., ionicity and isomeric shift correl. 7-7114
- SnSe, IR absorpt. edge, transition temp. coeffs. 7-27721
- SnTe, energy bands, relativistic empirical tight binding theory 7-45149
- SrZrO₃, valence band struct., X-ray-electron spectra studies 7-12604
- TeO₂ rutile crystals, electronic struct., scalar-relativistic muffin-tin-orbital calcs. 7-64077
- TiB, electronic struct., chem. bonding, Green's function methods 7-58741
- TiC, energy band struct., Fermi energy and density of states, vacancy states effects, LMTO-ASA calcs. 7-64078

band structure of crystalline semiconductors and insulators continued

- TiN_x epitaxial layers, atomic and electronic struct., growth, physical props. 7-32854
- TiO₂ clusters, electronic props., determ. using Ti CNDO parameters 7-27247
- TiX₂B (X=C, N, O) electronic struct., chem. bonding, Green's function methods 7-58741
- TiB_{1-x}Sb_xVI₂ solid solns., band spectrum double inversion to semimetallic state 7-38452
- TiCl crystal, electronic struct. 7-38449
- TiInSe₂, electronic struct., synchrotron radiation photoelectron spectra 7-52422
- Ti₃MS₄ (M=P, As, Ta), electronic energy struct. and bonds, X-ray spectra studies 7-45148
- U glasses, unoccupied 5f states, XANES study 7-39318
- UO₂, band struct., angle resolved and reson. photoemission study 7-27856
- VC_x energy band struct., Fermi energy and density of states, vacancy states effects, LMTO-ASA calcs. 7-64078
- WC electronic struct. and magnetic suscept., UV and X-ray photoelectron spectra 7-53493
- Y₂Fe₂O₁₂Si, band model of photoinduced magnetic effects 7-17214
- Zn_{0.9}Hg_{0.1}Se, electrophysical props. and carrier scatt. mechanisms 7-17024
- Zn₃P₂ valence band struct., XPS and Auger lineshape studies 7-45150
- ZnS, covalent cryst., electronic struct., cluster approx. 7-52403
- ZnS, cryst., p-type cond., luminesc. 7-13226
- ZnS:Fe electronic struct., K-edge EXAFS study 7-64079
- ZnS:Mn, impact excitation and Auger quenching 7-27827
- ZnS₂Te_{1-x} semicond., optical bowing 7-33352
- ZrB, electronic struct., chem. bonding, Green's function methods 7-58741
- ZrN, electronic struct., metal vacancy effects, KKR-CPA method anal. 7-12606
- band structure of semimetals**
- high temp. kinetic coeffs. oscills., band struct. and magnetoresist. temp. depend. studies (Russian) 7-12738
- As, Fermi surface characts., hydrostatic press. depends. (Russian) 7-32896
- Bi band parameter temp. depend. galvanomag. coeffs. and mobility, L-hole effect calcs. 7-2461
- Bi, electronic structure, effect of ion implantation 7-45143
- HfTe₃, Fermi surface, effective masses, energy bands, determ. from Schubnikov-de Haas effect 7-64051
- SCN compensated semimetal single crystals, electronic struct., reflectivity and elec. props. meas. 7-27253
- TiB_{1-x}Sb_xVI₂ solid solns., band spectrum double inversion to semimetallic state 7-38452
- band theory models and calculation methods**
- see also APW calculations; band model of magnetism; band structure; cellular method; free-electron approximation; Hubbard model; KKR calculations; k-p calculations; Kronig-Penney model; muffin-tin potential; nearly-free-electron approximation; OPW calculations; pseudopotential methods; relativistic band structure calculations; tight-binding calculations
- 2D periodic spatial structures, electronic props. calc. using layer method 7-45105
- 3d transition metal atoms and ions, approx. atomic orbitals, basis set reduction, maximum overlap method, mol. and solid state calc. appls. 7-840
- crystalline solids, allowed and forbidden bands in a periodic potential and an electric field 7-12586
- electron closed shells, bare Coulomb pot., density matrices 7-27226
- electron clouds at different sites, overlap integral calcs. 7-16925
- energy differences between structurally different crystals 7-7144
- Green's function band theory, convergence props. 7-27235
- heavy fermion systems, itinerant f-electron model 7-38808
- Hohenberg-Kohn-Sham theory, formulation 7-38427
- iterative transfer perturbation method, appl. to interaction between polymer and small molecules 7-64049
- linked cluster expansion in MBPT and coupled-cluster theory 7-49871
- metallic electrons, pair correl. functions, real space variational calcs. 7-52479
- molecular crystals, electronic energy bands, perturbation theory calcs. 7-16934
- momentum Bloch functions, closure property 7-45123
- one-electron energy band eigenvalue interpolation, integration scheme 7-32894
- trans-polyacetylene, equivalent orbital theory, electronic struct. study 7-64062
- rare earth metals, ground and excited state props., local density total energy calcs. 7-7141
- semiconductor alloys, band struct. and reduced local symm., virtual-cryst. approx. calcs. 7-38451
- semiconductor superlattices, electronic props., calc. methods 7-27406
- semiconductors, neutral vacancy electron states, orbital removal method 7-64047
- semiconductors and insulators, local density band structure, self-energy corrections 7-7097
- superlattices, band theory 7-45124
- transition metal borides, AlB₂ type, electronic struct. study, heats of formation anal., HMO calcs. 7-25409
- transition metal cpds., charge and magnetisation densities, mol. cluster studies 7-27224
- AlN, electronic struct., first principles LCAO calc. 7-21813
- Ce compounds, band description with localising orbitals 7-45121
- CuNi, substitutionally disordered, electronic struct., LCAO-CPA calcs. 7-64067
- FeAl, X-ray emission and absorpt., ab initio self-consistent band struct. calcs., LMTO method 7-64826
- FeRh, X-ray emission and absorpt., ab initio self-consistent band struct. calcs., LMTO method 7-64826
- Li, simple local pseudopotential 7-32888
- PbTe-Pb_{1-x}Sn_xTe superlattice, electronic structs., envelope pn. approx. 7-45465
- a-Si:H(F), mobility edge, density of states and carrier activation energy calcs., random Bethe lattice approach 7-16937
- Ti clusters, electronic props., CNDO method 7-27247
- TiO₂ clusters, electronic props., determ. using Ti CNDO parameters 7-27247

bands (kink) *see kink bands*

bandwidth compression

see also vocoders

profoundly deaf persons' hearing aid with bandwidth-compression-limited amplification 7-34161

bang-bang control

solar energy system, cycling rate effect on energy collection for bang-bang controllers 7-8438
viscoelastic coating for reducing sound wave reflection, gradient techniques 7-62874

bar code readers *see mark scanning equipment*

Bardeen-Cooper-Schrieffer theory *see BCS theory*

barium

see also nuclei with

¹³⁷Ba tracer for flow meas. by transit time method (Finnish) 7-57970
adsorbed on Cu, O adsorpt., XPS and UPS studies 7-2373
adsorbed on Ni, O adsorpt., XPS and UPS studies 7-2373
adsorption with Cs on Mo(Nb), bonding energies, thermionic emission studies 7-12463
adsorption with Lu on W, field emission characteristics 7-12466
adsorption with O on Mo (100), electron spectroscopy for quantitative anal. 7-13278
AMPTE artificial comet release, solar wind-Ba ions collisionless coupling 7-60483
atom, 6s5d states, optical pumping, rel. to radiative lifetimes 7-42560
atom, autoionising states, complementary branching ratios by satellite excitation 7-19786
atom, doubly excited states, electron correl., laser spectra 7-10459
atom, energy struct., HF-Dirac method 7-30938
atom, fast atomic beam laser fluoresc., g-factor 7-10483
atom, quadratic Zeeman effect for nonhydrogenic systems 7-36544
atom, superelastic collisions with electrons (French) 7-10758
atom, valence energy and polarisability, semiempirical pseudopot. calcs. 7-56926
atom doubly excited states, two-photon laser excitation spectra (French) 7-10474
atomic vapour, lifetime determ., fluoresc. study 7-36546
atoms, double Rydberg states, ionisation, two-photon and TOF mass spectra 7-19809
atoms, multistep photoionisation, total angular momenta of autoionisation steps 7-50031
atoms, three-level system, dynamic Stark effect 7-42548
autoionising states, internal conversion and fluoresc. two-step process 7-25467
BCC, first-principles phonon spectrum, three-ion forces and transition-metal behaviour 7-38135
bonding on thermionic emission cathode surface, EXAFS study 7-44970
coadsorbed with N₂ on Ni, N(1s) spectrum 7-21968
column density meter, high precision technique for line-of-sight vapour densities meas. 7-48695
giant resonance absorption spectra of 4d electrons 7-10471
ion beam magnetic field and space pot. diagnostic for STM plasma 7-1764
ions, Ne-like, precision wavelength meas. in X-ray spectra 7-36525
Knudsen ultrahigh-temperature thermionic energy conversion for space nuclear power 7-65507
liquid phase, density and surface tension 7-44957
monovalent ion, metastable autoionising state, lifetime meas. 7-19788
neutral atoms, high-lying states, laser pumped, two-photon spectra 7-19811
phonon spectra, dynamical pseudopot. shell model calcs. 7-51965
singly and doubly charged ion form. by nonlinear laser induced ionisation 7-42573
thermoelectric power meas. up to 8 GPa 7-64208
vapour, laser-pumped, collisional and radiative processes 7-5642
vapour IR source for subpicosecond photography 7-41502
vapour laser, mechanism limiting pulse repetition freq. 7-43071
Ba + N₂O, chemiluminescence, vibr. and rot. modes, translational energy and internal state influence 7-13780
Ba I, ¹P₁ level branching, reson. fluoresc. intensity depend. 7-50000
Ba II, isotope shift, hyperfine struct., fast ion beam spectra 7-19743
Ba⁺, Ba, laser mechanism and energy characts., relax. processes of metastable states 7-62673
Ba⁺, fluoresc. obs. using cross-saturating sideband absorpt. 7-19751
Ba⁺, laser excited resonance fluorescence, obs. of quantum jumps 7-10512
Ba⁺, optical Lamb-Dicke confinement 7-19807
Ba⁺, photoionisation absolute cross section meas. 7-50034
Ba⁺ single ion, laser excited reson. fluoresc., quantum jumps obs. 7-30984
¹³⁸Ba, laser-excited, electron impact ionisation cross section, hyperfine levels 7-36776
Ba²⁺ and Ca²⁺, single-channel currents in rabbit skeletal muscle sarcoplasmic reticulum 7-28476
Ba + Ar, collisional redistrib., laser-induced fluoresc. 7-62492
Ba + Cl₂(Br₂)(N₂O)(NO₂) (carbon tetrachloride) 7-13781
Ba + Cl₂-BaCl₂, mechanism, chemiluminesc. 7-28292
Ba + N₂O, oriented reactants, product polarised emission, chemiluminesc. 7-22992
Ba + N₂O reaction, chemiluminesc. study, N₂O electric dipole moment sign meas. 7-54116
Ba + Sr⁺, laser-induced charge exchange, quasi-mol. model, fluores. anal. 7-36748
Ba + trifluoriodomethane, BaI product state distrib. 7-25595
BaI, highly excited levels, two-channel quantum defect method 7-57010
¹³⁸Ba, dynamic Stark effect in three level system 7-10498
¹³⁸Ba I, three-level system, fluoresc., evidence for quantum jumps 7-19756
¹³⁸Ba + H⁺, elastic backscatt., K-shell ionis. probability, reson. effect 7-42748
KNO₃:Ba²⁺, radiation decomp., impurity particle size effect 7-63682
Na₂O-SnO₂-SiO₂:Ba²⁺, glass diffusion of cations, 500-800°C 7-12371
RbBr:Ba²⁺, Z₂ colour centres, picosecond relax., nonstationary spectra 7-59233

barium alloys

see also barium compounds

Al-Ba-La system, phase equilib. study 7-3279
BaAl₄, structural relationship to CaRh₂B₂ 7-16496
Ba₂CaCuFe₂F₁₄, heteronuclear trimers with ferrimag. behavior (French) 7-64448

barium alloys continued

Ge-Ba, liq. alloys, enthalpy of form. 7-23050

PdBa, ion implantation induced nonequilibrium surface layers, electron emission props. 7-12090

barium compounds

see also barium alloys

BaTiO₃ photorefractive crystals 7-42991
β-Ba₂Bo₂O₄, crystal vibr. assignment, Raman and IR spectra anal. 7-53346
fluorizirconate glass, chem. durability, reaction with water 7-39682
hollandites, modelling tunnel-cation displacements using struct.-energy calcs. 7-32374
oxalate dihydrate single crystals, Vickers microhardness meas. 7-63736
oxides, AM₂O₃(M₂O₄)_n, derived from the rutile structure by chemical twinning, structural evolution and stability 7-16757
[Ba₂Cs₂]⁺[(Ti,Al)_{2x+y}⁺Ti_{8-2x-y}⁴⁺]₁₆ hollandites, structural chemistry 7-51726
AlF₃-CaF₂-BaF₂ glasses, Raman spectroscopic study 7-7692
(Ba,Ca)F₂ layers, MBE growth on non-lattice-matched Si substrates 7-27216
(Ba,Sr)TiO₃ film metal-dielectric-metal system, polarisation switching 7-52849
Ba ferrite filled styrene-isoprene-styrene composite, dynamic mech., elec. and mag. props. 7-13001
Ba-La-Cu-O system, possible high T_c superconductivity 7-2770
Ba-Zn ferrite carriers for electrophotography, charactn. 7-4903
Ba₂Al₂Ti_{8-2x}O₁₆, with K, Rb and Cs substitution, cryst. struct., neutron diff. study 7-63563
BaAr, excitation spectra in supersonic jet, spectroscopic const. determ. 7-25591
β-Ba₂Bo₂O₄ crystals, efficient UV generation by frequency doubling 7-43231
β-Ba₂Bo₂O₄ single crystals, flux growth, SHG appl. 7-59390
Ba(Bi,Pb)O₃, semiconducting props., X-ray powder diff. and transport meas. (Japanese) 7-64237
BaBr₂H₂O, cryst. struct., comparative study with isotopic halides, bifurcated H bonds 7-63543
Ba₂CaCu₂Fe₂F₁₄, exchange interactions, mag. susceptibility meas. 7-45654
Ba(Ca_{1/3}Nb_{2/3})O₃-PbZrO₃-PbTiO₃ ceramics, hot-pressed, ferroelectric phase transitions 7-7652
BaCa_{1/2}Sr_{1/2}Fe₄O₈, mag. ordering 7-45624
BaCrO₃, mag. susceptibility meas. 7-12937
BaCl, B²Σ⁺-X²Σ⁺ transition, rot. anal., FTS and diode laser spectra 7-10581
BaCl₂-HCl, cond. meas. at 298.15 K, anal. using Lee and Wheaton eqn. 7-16792
BaCl₂H₂O, cryst. struct., comparative study with isotopic halides, bifurcated H bonds 7-63543
Ba(ClO₃)₂H₂O, polycryst., librational motions, zero-field NMR 7-15622
Ba(ClO₃)₂H₂O single crystal, Fourier transform IR spectroscopy, quantitative intensity meas. 7-48869
BaCo₂Fe₁₆O₂₇, Curie temp., magnetization, susceptibility, mag. anisotropy meas. (French) 7-27507
BaCo₂Fe₁₆O₂₇, hexagonal ferrites, neutron diff. studies 7-45622
BaCo₂Fe₁₆O₂₇, W-type hexagonal ferrite, cryst. struct. and Co location 7-6605
Ba(Cr,Si)O₄, barite struct. type hashemite, cryst. struct. determ. 7-32375
BaCs₄(PO₃)₆, cryst. struct. determ. 7-1954
α-Ba₂Cu₅F₁₄, crystalline structure (French) 7-26730
BaCoFe₇O₂₇, W-type hexagonal ferrite, intermediate valency, oxidation annealing, magnetisation and neutron diff. studies 7-7187
BaF₂ (111), laser sputtering, layer-dependent 7-13274
BaF₂ (111) surface, laser-induced sputtering, wavelength dependence 7-13273
BaF₂, Bridgman-Stockbarger growth and scintillation props. 7-59408
BaF₂ crystals, γ-irrad., optical absorpt. 7-58275
BaF₂ crystals for time resolution improvement in TOF positron emission tomography system 7-47222
BaF₂ epitaxial buffer layers for semiconductor heteroepitaxy 7-12522
BaF₂, linear thermal expansion meas. 7-44863
BaF₂, low temp. thermal expansion, calc. 7-44867
BaF₂, phase transitions, influence of shear deformation 7-21429
BaF₂, phys. props., effective pot. calcs. 7-26692
BaF₂, precip. from aq. soln., orthorhombic to cubic transform. 7-17502
BaF₂ scintillators, positron lifetime meas., Ag thermal vacancy form. data 7-42434
BaF₂ scintillators, pulse height response in charged particle detection 7-42321
BaF₂, substrate, periodic microrelief, laser irradiation, of nitrocellulose film 7-63927
BaF₂, thermal expansion from 296 to 1173 K 7-12327
BaF₂, thermally activated muonium formation 7-53200
BaF₂, UV attenuation 7-51944
BaF₂-based solid solns., ionic conductors with fluorite struct., thermal conductivity study 7-38275
BaF₂-Si structures, heteroepitaxial growth, struct., elec. props. 7-12567
BaF₂-ThF₄-YbF₄ glass, electron irradiation effects, Yb³⁺ optical transitions 7-27764
BaF₂-ZrF₄ glass, Zr local environment, EXAFS studies 7-63485
BaF₂-ZrF₄-FeF₂ glasses, Raman scatt. study 7-27713
BaFCl, IR lattice vibr., dielectric dispersion and lattice dynamics 7-3044
BaFCl:Dy(Cu), thermolum., X-irradiated at room temp. 7-53419
BaFCl:Sm³⁺(Eu³⁺)(Gd³⁺)(Ho³⁺)(Er³⁺)(Yb³⁺), charge transfer excitation and emission spectra 7-64688
BaFe_{12-2x}Co_xTi₂O₁₉, superfine particles, coercivity conc. and aspect ratio depend. meas. 7-53054
Ba₂Fe₂²⁺Fe₁₂³⁺O₂₂ hexagonal ferrite, hydrothermal synthesis, elec., magnetic and structural characterisation 7-45637
BaFe₁₂-Mn₂O₁₉, magnetoplumbite system, transport props., influence of internal electric field 7-52662
BaFe₁₂-Mn₂O₁₉, Mn substitution effects on mag. props. (Chinese) 7-7486
Ba_{1.06}Fe_{10.92}Mn_{1.02}O₁₉ and Ba_{1.03}Fe_{11.97}O₁₉ single crystals, white synchrotron radiation topography 7-6606
BaFe₂O₉ acicular media for perp. mag. recording, dynamic props. 7-59061
BaFe₂O₉, Bloch domain boundary, Neel boundary transition in mag. field, NMR study (Russian) 7-33195
BaFe₂O₉, defects created by Kr ion bombardment, HREM study 7-12168

barium compounds continued

- BaFe₂O₇, dispersion and particle packing of mag. oxide powders 7-3233
 BaFe₂O₇, FMR linewidth, temp. and freq. dependence 7-53140
 BaFe₂O₇ films, RF diode sputtering prep. and mag. props. (*Japanese*) 7-7852
 BaFe₂O₇, fine powder for particulate perp. mag. recording media, coercivity meas. method 7-59062
 BaFe₂O₇, hexaferrite, cryst. struct. formation and transformations 7-44489
 BaFe₂O₇, hexagonal ferrites, neutron diffr. studies 7-45622
 BaFe₂O₇, microcrystalline powders, prep. by glass synthesis method (*French*) 7-46394
 BaFe₂O₇, particulate media, magnetisation props, temp. effects study 7-53055
 BaFe₂O₇, particulate coatings, pigment-to-binder loading effects 7-53056
 BaFe₂O₇, powders, coprecipitated, magnetisation reversal, mag. dilution effects 7-53062
 BaFe₂O₇, synthesis by hydrolysis of barium acetate and tris (acetylacetonate) iron (*Japanese*) 7-46392
 BaFe₂S₄ and Ba₁₃(Fe₂S₄)₁₂, vernier struct. series, high resolution electron microscope study 7-6603
 Ba_{0.65}Ga_{10.8}O_{16.84}, cryst. struct., single cryst. X-ray reflection studies 7-6608
 Ba_{1-x}Gd_xF_{2+x}, defect struct., ionic thermocurrents, dielec. meas., EPR obs. 7-44907
 BaGeO₃-Ga₂O₃-CaO-CaF glasses, IR transmission spectra, depend. on composition 7-3031
 Ba₉Ge₂₃O₅₃(OH)₄, high press. phase, cryst. struct., X-ray diffr. study 7-32412
 BaI, X₂S⁺ and C^{II} states, hyperfine struct. MODOR 7-10637
 BaI, X₂S⁺ product, distrib., fluoresc. detect. 7-25595
 BaI₂H₂O, cryst. struct., comparative study with isotypic halides, bifurcated H bonds 7-63543
 BaIn₂Fe₁₀O₁₉, single crystals, magnetocrystalline anisotropy consts., anomalous temp. depend. 7-45664
 BaLaCuO, magnetic susceptibility meas., indication of high-T_c superconductivity 7-58953
 Ba_{1-x}La_xF_{2+x} solid solutions, thermally stimulated depolarisation currents 7-53226
 BaLaFeO₄, layered cpds., bidimensional mag. coupling, Mossbauer spectra 7-27637
 BaLaFeO₄, prep. and characterisation 7-1987
 BaLaGaO₇, luminescence props. 7-27768
 Ba₁LaNb₃Nd³⁺(Eu³⁺) single crystals, spectral-luminesc. props. 7-39169
 (Ba_{1-x}La_x)TiO₃ semiconducting ceramic props., grain boundary and dopant effects (*Japanese*) 7-6631
 (Ba_{1-x}La_x)(Ti_{1-y}Zr_y)_{1-x/4}O₃ ceramics, electrostrictive effect 7-53240
 Ba(Li_{0.25}Sb_{0.75})O₃, cubic perovskite, prep. and struct. 7-63589
 BaLn₂O₇-TiO₂, (Ln=La,Nd), phase props., X-ray and elec. meas. 7-2220
 BaMg₂Fe₁₆O₂₇, Curie temp., magnetization, susceptibility, mag. anisotropy meas. (*French*) 7-27507
 BaMg₂Fe₁₆O₂₇, hexagonal ferrites, neutron diffr. studies 7-45622
 BaMnAlF₄, exchange interactions, mag. susceptibility meas. 7-45654
 BaMnF₄, 2D Heisenberg magnet, spin dynamics and EPR linewidth 7-38932
 BaMnF₄, incommensurate modulated phase, struct. study 7-1993
 BaMnF₄ magnetic system with linear magneto-elec. coupling, electromag. mode calcs. 7-45791
 BaMnF₄, magnon polaritons, wave propagation in mag. systems with spontaneous electric polarisation 7-12961
 BaMnGaF₇, exchange interactions, mag. susceptibility meas. 7-45654
 Ba₂Mn₈O₁₈, synthetic hollandite, thermal behaviour (*Japanese*) 7-28026
 BaMn_{1-x}Ta_x(Zn)₃O₃ phase struct. and transforms., high resolution electron microscopy obs. 7-58237
 Ba(NO₂)₂, cryst. struct., X-ray diffr. study 7-32411
 Ba(NO₃)₂, phys. props., effective pot. calcs. 7-26692
 Ba(NO₃)₂, radiation generation in resonator under stimulated Raman scatt. conditions 7-43222
 Ba(NO₂)₂D₂O, lattice vibrs., mol. contrib., Raman spectra 7-46007
 Ba(NO₂)₂· $\frac{1}{2}$ H₂O, cryst. phase transition at 211K, DTA and dielec. meas. 7-32633
 Ba₂NaNb₅O₁₅, parametric light scattering, nonlinear diffraction 7-37044
 Ba₂NaNb₅O₁₅, threshold conditions for oscillation which the aid of shifted and unshifted dynamic gratings 7-1228
 Ba₂NaNb₅O₁₅, atom sublattices, selective high resolution electron microscopy 7-6486
 Ba₂NaNb₅O₁₅ cryst., elec. cond. small signal amplification 7-27333
 Ba₂NaNb₅O₁₅ incommensurate ferroelec. thin films, disinclinations, textures, four-state clock model description 7-257
 Ba₂NaNb₅O₁₅, Rayleigh scattering, intensity oscillations 7-7711
 Ba₂NaNb₅O₁₅ single crystals, spatio-temporal electrical instabilities 7-52632
 Ba₂NaNb₅O₁₅, X-ray irradiated ferroelectrics, radioluminesc. and thermolum. 7-27797
 Ba(Na_{0.25}Sb_{0.75})O₃, cubic perovskite, prep. and struct. 7-63589
 BaNi₂Sc₃O₁₅, metastable, cryst. struct., X-ray diffr. study (*German*) 7-16514
 BaNpO₄, oxo-neptunates, Mossbauer and mag. studies 7-13063
 BaO films on W, field emission spectroscopy 7-13334
 BaO MBE on W (110) 7-16886
 BaO, reflection spectra, 4d ionisation threshold 7-46234
 BaO, self-consistent electronic struts. 7-32910
 BaO-Al₂O₃-B₂O₃ glass, constitution 7-21120
 BaO-B₂O₃ glass, containing Fe₂O₃, heat treatment and γ -irrad., IR study 7-16627
 BaO-B₂O₃-Al₂O₃, aluminoborate glass, X-irrad., optical and thermal bleaching 7-45820
 BaO-B₂O₃-Fe₂O₃ glasses, γ -irradiated and heat treated, elec. conductivity and crystn. 7-21510
 BaO-CeO₂, phase relations, thermodynamic parameters 7-6829
 BaO-Fe₂O₃-B₂O₃-based glasses, crystallisation behaviour, nucleating agent effects 7-51650
 BaO-La₂O₃-Al₂O₃ system, synthesis, characterisation and spectroscopic investigations of mixed hexa-aluminates 7-63827
 BaO-La₂O₃-Nd₂O₃-Al₂O₃ systems, synthesis, characterisation and spectroscopic investigations of mixed hexa-aluminates 7-63827
 BaO-Mg(Zn)O-P₂O₅ glasses, internal friction investig. 7-6721

barium compounds continued

- BaO-Nd₂O₃-Al₂O₃ system, synthesis, characterisation and spectroscopic investigations of mixed hexa-aluminates 7-63827
 BaO-RuO₂-Fe₂O₃ system, equilibria description 7-65340
 BaO-TiO₂-B₂O₃(V₂O₅)(MoO₃), phase equilib. 7-46430
 BaO-V₂O₅-Fe₂O₃ semiconducting glasses, elec. props., Mossbauer, EPR and X-ray diffr. studies 7-7236
 Ba(OH)₂·8H₂O latent heat storage unit, power range 2-6 kW, 25 kWh 7-8446
 BaO.Nd₂O₃·5TiO₂, ceramics, matrix phase struct. 7-39488
 BaO.Al₂O₃·Eu²⁺·Mn²⁺ phosphor, luminesc. props. 7-46112
 BaO.Al₂O₃·Eu²⁺ phosphor, luminesc. props. 7-46112
 BaO·4B₂O₃ glasses, crystallisation 7-63490
 Ba(PO₃)₂-AlF₃-NaF system, glass form. and props. 7-11929
 Ba(PO₃)₂-LiBa(Mg)AlF₆ glasses, Raman spectra and network struct. studies 7-7695
 Ba(PO₃)₂-LiF gamma irradiated activated glasses, optical absorpt. and ESR spectra correls. 7-13030
 BaPO₃, polycryst., chem. shielding and dipolar coupling, NMR investig. 7-57089
 Ba₃(PO₄)₃OH, synthetic, cryst. struct. determ. 7-21173
 Ba₃(PO₄)₂·4H₂O, cryst. struct. 7-6610
 Ba(Pb, Bi)O₃ superconducting ceramics, surface resistance 7-38829
 BaPb β (II)-alumina, superstructure, high resolution electron microscopy study 7-12021
 BaPb_{0.75}Bi_{0.25}O₃ ceramic granular superconductor, infinite cluster detection, local heating method 7-2797
 BaPb_{1-x}Bi_xO₃, 0 $\leq x \leq 0.30$, hydrothermal cryst. growth 7-46290
 BaPb_{1-x}Bi_xO₃ bicrystals, nature of Josephson tunnel barrier 7-45568
 BaPb_{1-x}Bi_xO₃, electron-phonon interaction and superconductivity 7-27463
 BaPb_{1-x}Bi_xO₃, electronic struct., photoemission studies 7-59375
 BaPb_{1-x}Bi_xO₃, semicond. phase, CDW gap, optical meas. 7-53328
 BaPb_{1-x}Bi_xO₃ soln.-grown single crystals, crystallographic symmetries, effect on supercond. props. 7-37916
 BaPb_{1-x}Bi_xO₃, supercond. props., press. effects 7-45533
 BaPb_{1-x}Bi_xO₃, supercond. crystals, hydrothermal synthesis and props. 7-53532
 BaPb_{1-x}Bi_xO₃, supercond., struct. and elec. props. 7-58247
 BaPb_{1-x}Bi_xO₃, superconductivity and metal-semicond. transition 7-58940
 BaPb_{1-x}Bi_xO₃, supercond. characts., press. effect versus composition effect 7-58941
 Ba_{0.73}Pb_{0.27}F_{2.27} nonstoichiometric phase struct., neutron diffr. study 7-63587
 Ba₂Ti₄O₁₂ (R=La, Pr, Nd, Sm), dielectric props. at low temps. 7-45909
 BaS:Sm³⁺, photolum. of Sm³⁺ ions 7-59246
 BaSO₄, barite, IR and far IR optical props. 7-13116
 BaSO₄, barite, X-irrad., thermally stimulated luminesc., trap distrib. 7-59266
 BaSO₄ disordered diffuse solid scatterer, light scatt., weak localisation effects 7-22276
 BaSO₄ powder, solubility in water containing strong acidic ion exchange resin 7-21468
 BaSO₄, precip. growth, nucleation process, light scatt. obs. 7-16465
 BaSO₄, precipitation membranes, current-voltage curves 7-33967
 BaSO₄-culture medium interface, phys. and biological dosimetry 7-28703
 BaSe, pressure-induced metallisation 7-52698
 Ba₂Sn₂Mn(Ni)(Co)Fe_{10-x}Ga_xO₂₂ hexagonal ferrites, cryst. and magnetic struct. studies 7-44474
 Ba_{0.1}Sr_{1.1}Ca_{0.8}Fe_{1.0}La₂O₃, hexagonal ferrites, influence of electric field on struct. and props., Mossbauer study 7-7616
 Ba_{0.4}Sr_{0.4}Ca_{0.2}Fe_{1.0}O₁₉, hexagonal ferrites, influence of electric field on struct. and props., Mossbauer study 7-7616
 Ba_{2-x}Sr_xK_{1-y}Na_yNb₅O₁₅, ferroelectric tungsten bronzes, crystal growth and optical appl. 7-39085
 BaSrNb₂O₆, ferroelectric thin films, pyroelec. props. 7-59154
 BaSrNb₄O₁₂, chaotic states, high resolution electron microscope study 7-3001
 Ba₂Sr_{1-x}Nb₂O₆ optical phase conjugator, absolute phase shift 7-20364
 Ba₂Sr_{1-x}Nb₂O₆ paraelec. phase, polarisation distrib. studies 7-38993
 Ba₂Sr_{1-x}Nb₂O₆, poly- and single-domain samples, integrated light scatt. and polarisation 7-53361
 Ba_{0.03}Sr_{0.97}TiO₃, single crystal, electronic transport behaviour 7-33011
 Ba_{0.5}Sr_{0.5}TiO₃ polycryst. films, SAW scatt. and ferroelec. transitions 7-44984
 Ba_{0.9}Sr_{0.1}TiO₃:Sb, positive temp. coeff. of resist., synthesis method depend. 7-45324
 Ba_{1-x}Sr_xTiO₃ system, ferroelectric, weakly broadened phase transition 7-45944
 (Ba_{1-x}Sr_x)₂Zn₂Fe₁₂O₂₂ helimagnet single cryst., neutron diffr. study 7-52942
 BaTe, vaporisation thermodynamics and formation enthalpies (*German*) 7-26930
 Ba(Ti, Zr)O₃ powders, hydrothermal prep. 7-64957
 BaTiO₃ 0°-cut and 45°-cut crystals, hybrid phase conjugator/modulator props. 7-20357
 BaTiO₃, acceptor state behaviour, influence of impurities and lattice defects 7-2539
 BaTiO₃ based ceramics for multilayer ceramic capacitors, chemical processing 7-46399
 BaTiO₃ capacitor material, elec. field distrib. around flaws, finite difference modelling 7-64574
 BaTiO₃ ceramics, grain struct. and phase anal. (*German*) 7-58496
 BaTiO₃ ceramics, Maxwell-Wagner relax. and degradation 7-2970
 BaTiO₃ ceramics, sintering, liq. phase enhanced discontinuous grain growth control 7-46384
 BaTiO₃ ceramics, zone sintering, dielec. props. rel. to microstruct. 7-13078
 BaTiO₃ composites, dielec. and elec. props., rel. to prep. and microstruct. 7-64559
 BaTiO₃, cryst. dynamics near T_c, Mossbauer diffr. study 7-6733
 BaTiO₃ crystal, signal correlation with phase conjugate holographic reconstruction 7-20155
 BaTiO₃ crystal self-pumping for large aperture interferometer with phase-conjugate self-reference beam 7-9884
 BaTiO₃, crystalline samples, low temp. sp. ht. meas. 7-2225
 BaTiO₃, defect behaviour, computer-based atomistic simulation studies 7-16548
 BaTiO₃, dielectric, electrical and acoustic props. 7-53224

barium compounds continued

- BaTiO₃ double phase conjugation mirror, anal., demonstration and laser struct. 7-43252
 BaTiO₃, elec. cond. rel. to point defects 7-6619
 BaTiO₃, electro-optic props. 7-39088
 BaTiO₃, electronic struct., special features (*Russian*) 7-45146
 BaTiO₃, ferroelectric transition dynamics 7-26904
 BaTiO₃, ferroelectric, optical switching 7-37020
 BaTiO₃, ferroelectric solid, microwave absorpt., Curie temp. and ultrasonic attenuation 7-39049
 BaTiO₃, fine-grained superplastic creep in reducing environment 7-28075
 BaTiO₃, form. from metallo-organic precursors, kinetics 7-39465
 BaTiO₃, forward- and backward-stimulated photorefractive scatt. 7-57461
 BaTiO₃, grain boundary inhomogeneity phenomena, microcontact meas. (*German*) 7-58893
 BaTiO₃, hexagonal, optical props. around 222K struct. phase transition 7-27685
 BaTiO₃ imaging threshold detector using phase-conjugate resonator 7-6019
 BaTiO₃, Nd₂O₃-modified, defect struct. and dielec. props 7-37968
 BaTiO₃, PTCR ceramics, SIMS 7-9919
 BaTiO₃, perovskite, TEM study of dislocations 7-38003
 BaTiO₃ phase conjugator, absolute phase shift 7-20364
 BaTiO₃ phase conjugator, coherent image subtraction using phase conjugate interferometry 7-25727
 BaTiO₃ phase-conjugate mirror, partial cancellation of specular reflection 7-5956
 BaTiO₃, photo-excited holes, photorefractive meas. of mobility anisotropy 7-21918
 BaTiO₃, photorefractive conical diffraction 7-7655
 BaTiO₃ photorefractive crystals, image amplification by two- and four-wave mixing 7-11042
 BaTiO₃ photorefractive devices, effect of temp. variation 7-20368
 BaTiO₃ photorefractive props. 7-22205
 BaTiO₃ photorefractive element in laser cavity, mode selection 7-43167
 BaTiO₃ piezoelectric ceramics, studies for appl. in electromechanical filters 7-20558
 BaTiO₃, polycryst., glasslike behaviour at very low temp. 7-27647
 BaTiO₃, polycrystalline, dielec. breakdown, microstructural effects 7-39021
 BaTiO₃ rigid dielectric with polarisation inertia, wave propag. 7-7634
 BaTiO₃, self-pulsing and self-pumping, bistability and noncommutative behaviour 7-43201
 BaTiO₃ self-pumped phase conjugate mirror, instabilities 7-62790
 BaTiO₃ single cryst., elastic and piezoelec. coeffs. 7-2979
 BaTiO₃, submillimetre dispersion of permittivity 7-64556
 BaTiO₃, vibronic ferroelec., correl. length estimate (*Russian*) 7-17277
 BaTiO₃:⁵⁷Fe, multiphonon transitions from modulated hyperfine electric field gradients 7-27633
 BaTiO₃:Ce, Mg, Ga(Cr)(Cu), double doping study 7-2037
 BaTiO₃:Fe³⁺, ferroelectric transition, EPR 7-33343
 BaTiO₃:Mn, Mn oxidation state change near phase transitions 7-16974
 BaTiO₃:Mn⁴⁺, EPR spectra, spin-Hamiltonian consts. 7-45812
 BaTiO₃:Mn(Cr), impurity electronic struct., molecular-orbital calcs. 7-45213
 BaTiO₃:Nb(Ca), ferroelec. domains, SEM and TEM obs. 7-2998
 BaTiO₃:Nd, ceramics, diffuse phase transform 7-16731
 BaTiO₃:Ni ceramic, H defect diffusion 7-58545
 BaTiO₃:Y₂O₃(La₂O₃)(Ce₂O₃), semiconductor props., influence of dopant oxides 7-6650
 BaTiO₃-based ceramic, nonlin. electromechanical parameter meas. 7-13094
 BaZn₁₁O₁₉ graphite-rubber composites, varistors fabrication 7-58841
 BaTiO₃-TiO₂, heterogeneous ceramics, processing for dielectric appls. 7-64984
 BaTi₄O₉ single crystals, growth by floating zone method 7-17415
 BaTi_{2-x}Sn_xFe₄O₁₁, crystal structures and mag. props. 7-12024
 Ba₂Ti_{5-x}Zr_xO₁₂, synthesis, stability, cryst. chem. 7-53681
 Ba_{1-x}U_xF_{2+x} solid solutions, thermally stimulated depolarisation currents 7-53226
 Ba₃(VO₄)₂ substrates for hexaferrite film growth 7-52320
 BaVS₃, low temp. phase transitions, powder neutron diff. 7-38181
 BaY₂F₈:Pr³⁺, stimulated emission spectra, laser action excitation 7-27745
 BaYb₂F₈:Er active medium optimisation, lasing parameters at 1.96 μ m 7-31330
 BaYb₂F₈:Er(Tm), energy levels Stark struct., crystn. field interactions 7-58782
 BaZn₁₁Cu₉Fe₁₆O₂₇ hexaferrite, competing anisotropies, first order magnetisation processes and spin transitions obs. 7-38856
 BaZnGeO₄, phase transitions, X-ray study 7-52036
 BaZrO₃, valence band struct., X-ray-electron spectra studies 7-12604
 Ca_{1-x}Ba_xF₂ epitaxial layer growth and struct., electron microscopy studies 7-27174
 CaF₂-BaF₂ epitaxial bilayers on Si (111), characterisation 7-12521
 CaF₂-BaF₂-AlF₃ glasses, struct., transition metal ion EPR studies 7-6545
 CaO-BaO-P₂O₅ glasses, internal friction investig. 7-6721
 CaO-BaO-P₂O₅ glass fibres, stress optical studies 7-7673
 (CaO)₂₅(BaO)₂₅(P₂O₅)₅₀ glass fibres, struct., birefringence, density and thermal shrinkage, drawing parameters depend. 7-6536
 Co-Ba-Ni-O₂ thermal resistance thermometer study (*Chinese*) 7-24650
 (CoF₂)_{0.5}(BaF₂)_{0.2}(NaPO₃)_{0.3}, AC magnetic susceptibility and acoustic wave attenuation meas. 7-59020
 FeO₂-CaO-MgO-BaO-Na₂O, wustite solid solns., interdiffusion coeffs., 1073-1473K (*Japanese*) 7-12357
 Fe₂O₃-BaO-B₂O₃-V₂O₅ glasses, Fe³⁺ site occupancy, Mossbauer studies 7-6541
 GaF₃:Mn cubic cryst., local lattice instability near impurity, ESR study 7-53123
 GeO-BaO thin films between metallic electrodes, elec. props. 7-22054
 InF₂-PbF₂-BaF₂-SrF₂-YF₃-AlF₃-UO₂F₂, luminesc., lifetime meas. 7-27750
 K₂Ba(NO₂)₄, successive phase transitions, dipolar frustration 7-53247
 La-Ba-Cu-O system, superconducting transition above 40 K, high press. 7-58946
 La_{1-x}Ca_{0.55x}Ba_{0.45x}FeO_{3- δ} , elec. cond. props. rel. to struct. 7-63871
 Li₂O-BaO-B₂O₃:VO²⁺, borate glasses, ESR of VO²⁺ ion 7-59110
 MgF₂-BaF₂ mixtures, films, prep., physicochemical and optical props. 7-3178

barium compounds continued

- Mg₂SiO₄, fosterite-based ceramic with BaO addition, synthesis, sintering, struct. and props. 7-46397
 MnO₂-BaMnO₃ system, pseudo-binary, phase relation and thermal behaviour of synthetic hollandite, Ba_xMn₈O₁₈ (*Japanese*) 7-28026
 Pb₄Ba_{0.3}Ge₃O₁₁, rhombohedral, acoustic symmetry and vibr. anharmonicity 7-16695
 (Pb₂Ba_{1-x})TiO₃, ferroelec. solid solns., dielectric and hysteresis props. 7-64588
 SiO₂-Na₂O-CaO-MgO-Al₂O₃-BaO-FeO₃ glass, elec. field stimulated Na depletion 7-6897
 SrBaNb₂O₆ as self-pumped phase conjugator 7-5957
 SrBaNb₂O₆:Ce as self-pumped phase conjugator 7-5957
 SrBaNb₂O₆:Ce crystal optical oscillator based on frequency-degenerate pumping 7-25887
 Sr_{0.5}Ba_{0.5}Nb₂O₆, incommensurate superstructures, phase transition, electron diff. study 7-63792
 Sr_{0.6}Ba_{0.4}Nb₂O₆, doped and undoped, photorefractive props. 7-39057
 Sr_{0.6}Ba_{0.4}Nb₂O₆, photorefractive props. 7-22205
 Sr_{0.6}Ba_{0.4}Nb₂O₆ photorefractive props. 7-45955
 Sr_{0.6}Ba_{0.4}Nb₂O₆:Ce, photorefractive props. 7-22205
 Sr_{0.6}Ba_{0.4}Nb₂O₆:Ce(Fe), photorefractive props. 7-45955
 Sr_{0.6}Ba_{0.3}Nb₂O₆:Ce crystals, light emission obs. during freq.-degenerate laser pumping 7-15947
 Sr_{0.75}Ba_{0.25}Nb₂O₆:Ce self-starting passive phase conjugate. mirror 7-43243
 Sr_{1-x}Ba_xNb₂O₆ bronze piezoelectric for SAW device applications 7-17271
 Sr_{1-x}Ba_xNb₂O₆, ferroelectric tungsten bronzes, crystal growth and optical appl. 7-39085
 Sr₂Ba_{1-x}Nb₂O₆ photorefractive crystal, wavefront-reversing mirror characteristics 7-43247
 SrFe₂O₉, dispersion and particle packing of mag. oxide powders 7-3233
 SrO-BaO-P₂O₅ glasses, internal friction investig. 7-6721
 Y_{1-x}Ba_xCrO₃, electrical and thermal transport props 7-45319
 ZrF₄-BaF₂-AlF₃ glass, viscous flow vs. phase separation, DSC study 7-44383
 ZrF₄-BaF₂-CsF glasses, ionic conductivity 7-52129
 ZrF₄-BaF₂-GdF₃-AlF₃-NaF-FeF₃, optical fibre glasses, trace amounts of Fe, characterisation 7-2956
 ZrF₄-BaF₂-LaF₃, mid-IR glass and optical fibres, dispersion characts. 7-37178
 ZrF₄-BaF₂-LaF₃-AlF₃ glass, etching method for prep. of IR fibres with high tensile strength 7-1243
 ZrF₄-BaF₂-LaF₃-AlF₃-NaF glass, crystal growth and microstruct. 7-1896
 ZrF₄-BaF₂-LaF₃-AlF₃ fluoride glasses, lanthanide J-levels high yield luminesc. study 7-22309
 ZrF₄-BaF₂-LaF₃-AlF₃ optical fibres, gamma irradiation, EPR and IR studies 7-37183
 ZrF₄-BaF₂-LaF₃-AlF₃, heavy metal fluoride glass system, viscosity and crystallisation 7-37883
 ZrF₄-BaF₂-NaF glasses, crystallisation study 7-11933
 ZrF₄-BaF₂-NaF-AlF₃ glass, crystn. (*Japanese*) 7-26659
 ZrF₄-BaF₂-NaF-AlF₃-LaF₃ glasses, crystallisation study 7-63491
 ZrF₄-BaF₂-ThF₄-LiF quaternary glasses, ionic cond. and NMR studies 7-6865
 ZrF₄-LaF₃-BaF₂-NaF glasses, EPR of Cu²⁺ ions 7-27593

Barkhausen effect

- ferromagnetic materials, magnetoacoustic and Barkhausen emission study NDT appl. 7-45749
 losses induced by irreversible Barkhausen jumps of sinusoidally moving 180° domain wall, multidomain wall motion 7-27555
 magnetic structurescope based on the Barkhausen effect 7-28241
 magnetoresistive elements, Barkhausen noise meas., magnetoresistive suscept. method 7-48785
 NDT, induction transducers for magnetic. jump detection, design and computation problems 7-39823
 PVDF films, thermal Barkhausen effect, spontaneous polarisation 7-59142
 steel, low C, magnetoacoustic emission, magnetisation, Barkhausen effect in decarburised steel 7-33207
 structural steels, coercivity and Barkhausen noise power spectrum, stress depend. meas. 7-7548
 Cu_{1-x}Cd_xFe₂O₄, irreversible magnetisation. depend. on magnetising field 7-64487
 Fe₄₀Ni₄₀B₂₀, amorphous alloy, Barkhausen noise, neutron irradiation effect 7-53029
 Fe_{77-x}Si_{7+x}B₁₅ amorphous wires, Barkhausen and Matteucci effects, influence of tensile and compressive stress 7-33254
 Mg_{81-x}Cr_xFe₂O₄, Barkhausen noise parameters correl. with strength 7-22963
 Ni-Cr wire, irreversible magnetisation, effect of plastic deformation 7-53041
 SiFe, grain oriented, Barkhausen noise behaviour, effect of local strain 7-33205

Barnett effect see gyromagnetic effect; magnetisation

barometers

No entries

barometric pressure see atmospheric pressure and density

barrages see dams

barrel distortion see aberrations

barretters see thermistors

baryon-baryon interactions

see also baryon-baryon scattering; hyperon-nucleon interactions; nucleon-nucleon interactions
 forces, review of present status 7-49165

baryon-baryon scattering

see also baryon-baryon interactions; hyperon-nucleon scattering; nucleon-nucleon scattering
 multiple scattering matrix elements, color parts, SU(3) group 7-41827

baryon decay

see also baryon hadronic decay; baryon leptonic decay; hyperon decay; proton decay
 dibaryon resonance decay mechanism, diquark-cluster model anal. 7-61671
 experimental review of nucleon decay 7-56546
 monopole-induced baryon decay, role of Abelian and nonAbelian anomalies 7-9996

baryon decay continued

- nonstrange baryon resonances, pion decay amplitudes, semirelativistic quark model 7-35868
- nucleon decay, KAMIOKA experiment, atmospheric neutrino background and pion nuclear effect 7-49140
- nucleon decay, mag. monopole catalytic reaction, appl. to galactic nuclei (Chinese) 7-66439
- particle and nucl. physics intersections conf., Lake Louise, Canada, May 1986 7-29569
- weakly decaying charmed baryon lifetime differences due to preasymptotic bound state effects 7-41801
- Δ^{++} decay props., $\nu_d d \rightarrow \pi X$ reaction anal. 7-19117
- $\Lambda_c^+ \rightarrow \Delta e \nu$, chiral lagrangian method, partial widths and branching ratio 7-35867
- n beta-decay, mag. field effects, spin effects and ν mass 7-41800
- N decay search, atmospheric ν -induced backgrounds 7-19109
- $n \rightarrow p e \bar{\nu}$, g_A/g_V meas. from beta-asymmetry meas. 7-35866
- $n \rightarrow p e \bar{\nu}$, neutron lifetime meas. techniques 7-56544
- $n \rightarrow p e \bar{\nu}$, recent expt. developments 7-56543

baryon electric moment

- see also hyperon electric moment; nucleon electric moment
- No entries

baryon hadronic decay

- constituent quark model picture for non-leptonic hyperon decays 7-49139
- $B_c \rightarrow B_c \pi$ (B =baryon), anal. using effective chiral Lagrangian method 7-49084
- $\Delta(1232) \alpha N \pi$, in nuclei, no. of nucleons involved in decay 7-61842
- H dibaryon, weak decays, decay rates and branching fractions 7-35869
- H dibaryon, weak decays, wave function 7-41799
- Δ nonmesonic decay in hypernuclei, hybrid quark hadron model anal. 7-41798
- $\Lambda_c \rightarrow p K^+ \pi^+$, lifetime meas. 7-61669
- $\Lambda_c \rightarrow 1/2^+ +$ mesons, generalised chiral lagrangian method 7-24883
- Λ_c^+ hadronic decay, statistical model anal. 7-15148
- $\Lambda_c \rightarrow K^0 p \pi^+ \pi^-$, Λ_c^+ polarization meas. from $^{12}C(n, \Lambda_c^+)$, 40-70 GeV/c 7-5088
- $\Lambda_c \rightarrow \Delta^+ \pi^+ \pi^-$, Λ_c^+ polarization meas. from $^{12}C(n, \Lambda_c^+)$, 40-70 GeV/c 7-5088
- $\Lambda_c \rightarrow \Sigma^+ \pi^- \pi^+$, charmed baryon decay, nuclear emulsion obs. 7-15150
- $N(1535) \rightarrow N \eta$, anal. using effective Lagrangian method 7-49084
- $\Sigma^+ \rightarrow \pi^+ n$, charmed baryon decay, nuclear emulsion obs. 7-15150
- $\Sigma_c^0 \rightarrow \Lambda_c^+ \pi^-$, charmed baryon decay, nuclear emulsion obs. 7-15150

baryon interactions see baryon-baryon interactions**baryon leptonic decay**

- No entries

baryon magnetic moment

- see also hyperon magnetic moment; nucleon magnetic moment
- constituent quark model calcs. 7-56552
- d, magnetic moments of multiquark systems, chiral bag model 7-41816

baryon mass

- see also hyperon mass
- dibaryons, $B=2$ states, colour singlet dynamics 7-35810
- heavy hadrons, explicit mass formulas 7-35789
- lattice gauge theory, baryon mass calc., quark mass renormalization 7-30155
- lattice gauge theory, H dibaryon mass using bag model parameters 7-61485
- multibaryon reson., mass formula 7-504
- multiflavour QCD, nonAbelian bosonization and baryon mass formulae 7-61579
- QCD sum rules and the Skyrme model at large N_c 7-61583
- Skyrme model, baryon masses 7-418
- \bar{f} mass determ. from $pp \rightarrow \bar{f} n$ interactions 7-542
- p, diquark model calcs. 7-49101

baryon photoproduction

- see also hyperon production; neutron production; proton production
- No entries

baryon production

- see also baryon photoproduction; hyperon production; neutron production; proton production
- (d,X), X-mesons, baryons, quark-gluon phase transition and strangeness anal. 7-49390
- $\delta d \rightarrow pp \pi^+$, pp invariant mass distrib., obs. of narrow resonance structure 7-24893
- $e^+ e^- \rightarrow$ heavy baryons, perturbative QCD anal. 7-35887
- $e^+ e^- \rightarrow \Delta X$, inclusive production, angular distribution asymmetry 7-35885
- $e N \rightarrow e \Delta$, high Q^2 , N- Δ form factors, perturbative QCD anal. 7-19119
- $\gamma d \rightarrow pp \pi^+$, dibaryon resonance search, 2.16-2.32 GeV/c² mass region 7-24892
- $\gamma \gamma \rightarrow BB$, baryon production, Q^2 dependence, QCD anal. 7-19148
- (K, π Y), hypernuclear formation, pole graph method anal. 7-42074
- (p,X), X-mesons, baryons, quark-gluon phase transition and strangeness anal. 7-49390
- pp , 32 GeV/c, inclusive baryonic reson. prod., constitutive model 7-5127
- $pp \rightarrow n \Delta^{++}$, one-pion exchange model anal. of $^1H(^3He, \Delta^{++})$ 7-24988
- $^4_0 p \rightarrow (\eta^0, \omega) \Delta^{++}$, 16 GeV/c, helicity amplitude anal. 7-15173
- $^4_0 Ar(p, 2px)$, 1 GeV, cross section meas., obs. of low-lying dibaryon resonances 7-56680

baryon resonances

- see also hyperon resonances
- baryon resonances and bound states in NN system 7-30277
- baryonium, influence of relativistic effects on level widths 7-10064
- baryonium, strange, standard model anal. of strange $B = O$ states 7-41676
- cumulative dibaryon resonance obs. in pion-nucleus interactions 7-36060
- dibaryon, strangeness-1, future search at AGS 7-36056
- dibaryon, strangeness-2, future search at AGS 7-36056
- dibaryon resonance decay mechanism, diquark-cluster model anal. 7-61671
- dibaryons, $B=2$ states, colour singlet dynamics 7-35810
- dibaryons, positive parity, strangeness -1 potential model anal. 7-24846
- electromagnetic transitions and deformations in nucleons and deltas 7-41812
- hedgehog baryon state, soliton bag model with scalar mesons 7-18990
- kink-bag system in (1+1) dimens., breathing motion, inertia of confined vacuum 7-19070
- lattice gauge theory, H dibaryon mass using bag model parameters 7-61485

baryon resonances continued

- multi-pion multi-nucleon hadronically stable states 7-5135
- multibaryon reson., mass formula 7-504
- nonstrange baryon resonances, pion decay amplitudes, semirelativistic quark model 7-35868
- photoproduction, helicity amplitudes in Skyrme model 7-19118
- Roper resonance and πN phase shift in the Skyrme model with defect 7-18988
- strange dibaryons, mass spectrum and level density 7-61635
- $\Delta(1232) \alpha N \pi$, in nuclei, no. of nucleons involved in decay 7-61842
- Δ^{++} production props. in $\nu_d d \rightarrow \pi X$, 1.6 GeV 7-19117
- $\delta d \rightarrow pp \pi^+$, pp invariant mass distrib., obs. of narrow resonance structure 7-24893
- $\gamma d \rightarrow pp \pi^+$, dibaryon resonance search, 2.16-2.32 GeV/c² mass region 7-24892
- H dibaryon, weak decays, decay rates and branching fractions 7-35869
- H dibaryon, weak decays, wave function 7-41799
- $K^- p \rightarrow \Delta \pi$, quark contribution to nuclear force 7-551
- $\Delta(1405)$, $K(K)N$ scattering anal. in cloud bag model 7-35905
- $\Delta_c \rightarrow p K^- \pi^+$, lifetime meas. 7-61669
- Λ_c^+ , semi-leptonic branching ratio calcs., statistical model anal. 7-15148
- $\Lambda_c \rightarrow 1/2^+ +$ mesons, generalised chiral lagrangian method 7-24883
- Λ_c^+ hadronic decay, statistical model anal. 7-15148
- $N(1535) \rightarrow N \eta$, anal. using effective Lagrangian method 7-49084
- N and Δ , electromagnetic mass differences in the Skyrme model 7-5092
- N^* isobars, excitation in $pp \rightarrow d \pi^+ 725$ MeV-2.3 GeV 7-5123
- NN-mesons, LEAR experiments 7-49166
- (p, π^-), relativistic stripping model anal. in Δ resonance region 7-49400
- $pp \rightarrow d \pi^+$, excitation functions and high resolution search for narrow dibaryons 7-5209
- $pp \rightarrow \Delta^{++} n$, partial wave anal. in dibaryon resonance region 7-35895
- $pp \rightarrow Y X$, 300, 460 MeV/c, gamma-spectra meas., baryonium state search 7-49172
- $pp \rightarrow pn \pi^+$, partial wave anal. in dibaryon resonance region 7-35895
- $pp \rightarrow pp$, excitation functions and high resolution search for narrow dibaryons 7-5209
- $\pi d \rightarrow \pi pn$, dibaryon state search in kinematically complete meas. 7-5120
- NN bound state problem, appl. to deuteron and 4,4 resonance 7-19033
- $\pi^- p \rightarrow \eta \Delta^0(1232)$, 3.3 GeV/c, differential cross section and total cross section 7-35904
- $\pi^- p \rightarrow \gamma n$, $p_\pi = 301-625$ MeV/c analyzing power meas. near Δ and Roper resonances 7-5121
- $^4_0(1480)$, quasinuclear NN bound state study 7-5061
- $^4_0 Ar(p, 2px)$, 1 GeV, cross section meas., obs. of low-lying dibaryon resonances 7-56680
- $^{12}C(\pi, \pi' \gamma)$, 116-226 MeV, $\pi^- \gamma$ angular correlation meas., Δ -hole model predictions 7-19307
- $^2H(\pi, \pi)$, tensor analyzing power meas., resolution of dibaryon resonance production problem 7-30451
- Λ_c^+ , polarisation determination from cascade decays 7-41865
- $\pi^- p \rightarrow \pi^0 n$, left-right asymm. in Roper resonances region, partial wave anal. comparison 7-35903

baryon scattering see baryon-baryon scattering**baryon spin and parity**

- see also hyperon spin and parity
- hedgehog chiral soliton bags, spin-isospin projection using collective coordinates, nucleons 7-19074
- QCD, nucleon spin conservation at short distances 7-490
- SUSY QCD, nucleon spin conservation at short distances 7-490
- n beta-decay, mag. field effects, spin effects and ν mass 7-41800
- NN annihilation, dynamical selection rules, quark-gluon model 7-5126
- NN scattering, radial excitations, RGM and constituent quark model calcs. 7-19125
- NN symmetric Lorentz invariant scatt. amplitude, Yukawa representation 7-41830
- $\bar{n} p$, low energy scatt., anal. power, spin depend. 7-24904
- $n p$ scattering, spin and isospin nonconservation by a colour force 7-30285
- $p N$ scattering, parity violation tests at high energy 7-30207
- pp scattering, parity violation tests at low and intermediate energies 7-30207
- $\pi p \rightarrow \pi p$, spin rotation parameter meas. 7-61734

baryons

- see also baryon resonances; hyperons; nucleons
- $1/2^+$ baryons, EM mass differences in quark and Skyrme models 7-41811
- baryon-number nonconservation in superstring models 7-453
- chiral soliton model, baryons as rotating excitations 7-5066
- consistent quark model with chromodynamics, baryon spectrum calcs. 7-30249
- cosmological baryon diffusion and inhomogeneities in big-bang plasma 7-60848
- cosmological baryon number in homogeneities, effects of quark-hadron transition 7-47677
- early Universe, baryon concentration in string wakes at $z \geq 200$ rel. to galaxy form. 7-14687
- early Universe, baryon-entropy ratio 7-4598
- effective chiral Lagrangian with $U(3) \times U(3)$ symmetry for baryons 7-49084
- effective Lagrangians for the chiral quark phase and the Skyrmin parameters 7-19069
- electroweak properties in QCD 7-56522
- mass spectrum, convexity props. in pot. models with flavour independence 7-503
- model independent exchange current determ. in e^- scatt. and baryons as topological solitons 7-35743
- monopole-induced baryon decay, role of Abelian and nonAbelian anomalies 7-9996
- multiquark states, constituent quark models 7-41703
- nonrelativistic quark model, baryons, N-body quantum problem in configuration space 7-10141
- observables in chiral bag model 7-61606
- relativistic quark model with chromodynamics, anal. of baryons 7-19075
- Skyrme model for baryons, hybrid model and Wess-Zumino-Witten action 7-30197
- spontaneous CP-violating models without strong CP problem, cosmological baryon prod. 7-49037
- strangeness induced baryon size 7-19067
- structure, hyperfine interactions 7-56518
- technibaryon missing mass bounds 7-19042

baryons continued

- Universe baryon asymmetry, depend. on eqn. of state 7-24243
- $B \rightarrow B_1\pi$ (B =baryon), anal. using effective chiral Lagrangian method 7-49084

BASIC listings

- Beaufort wind scale—measured speed conversion program 7-55235
- computer graphics for water-quality investigations, Tickell diagram plotting, BASIC listing 7-9030
- geomagnetism, total magnetic field of two-dimens. body of arbitrary shape, calc. program 7-34718
- magnetic anomaly over structurally complex bodies, use of subtended solid angle, DEC-BASIC-PLUS-2 program 7-9192
- multichannel scaling with a VIC-20 or Commodore 64 7-49841
- nuclear weapons, Microsoft BASIC programs showing local effects 7-30676
- optical design program for Apple Macintosh 7-50692
- program for combining sound pressure levels in noise 7-62909
- sea bed contour map construction from random data, spline method 7-34728
- soil testing, BASIC program 7-34735
- stress, FEA using microcomputer 7-48357
- WSU-MAP: a microcomputer-based reconnaissance mapping system for Kansas subsurface data 7-40584

basicity *see pH***batch processing (industrial)**

- binary batch distillation in tray or packed columns, optimal control 7-58450

bathymetry

- Amazon River continental shelf, bedforms 7-34460
- arc-continent collision zones, vertical movements rel. to sedimentary sequences 7-28966
- Arcachon Basin (French W coast), drainage channel network chart (*French*) 7-55058
- Astrid Ridge off Queen Maud Land, Antarctica, fracture zone nature, bathymetric obs. 7-66035
- NE Atlantic continental margin, seafloor canyon directions and tectonic implications 7-55005
- N Atlantic Ocean, residual geoid anomalies rel. to lithosphere thermal evolution 7-28814
- S Atlantic Ridge, geology in 20 to 30 degrees South area 7-34410
- Bali Basin, tectonic origin, anal. of gravity, bathymetry and earthquake data 7-66073
- Cape depression, SE Atlantic, bathymetry and dredged rocks 7-40465
- Chile Ridge-Chile Trench interaction, mag., thermal and bathymetric characts. 7-66074
- data acquisition and processing system (SDS III) 7-66361
- digital sonar imaging, processing techniques for images from GLORIA 7-4220
- Galapagos spreading centre, 3D gravity study of 95-5°W propagating rift 7-60196
- global seafloor depth rel. to oceanic geoid 7-65919
- GLORIA, long-range sidescan sonar for deep ocean mapping 7-47583
- W Gulf of Mexico, bathymetry interaction with Loop Current eddy 7-9003
- hydrographic data, digital, requirements 7-47422
- hydrographic survey information processing system 7-47421
- Middle America Trench, Guatemala, subduction erosion versus sediment offscraping at toe of trench 7-14248
- midocean ridge subsidence rates, for fast and intermediate spreading centres 7-23625
- Narmada-Son lineament on W India continental margin, magnetic anomalies and tectonics 7-54991
- nautical charting system II for National Ocean Service 7-47423
- central North Sea, valley asymmetry as evidence for periglacial activity 7-14285
- ocean floor bathymetry, implications for Earth tectonics (*Russian*) 7-66076
- S Pacific, Eltanin fault system, tectonic and magmatic ridges 7-23610
- NE Pacific, spreading centre with episodic volcanicity and nonsteady state rift valley 7-54974
- Red Sea rift, basin morphology rel. to mineral comp. of surface sediments 7-14261
- Sea Beam multibeam sonar system for study of seafloor 7-66363
- sea bed contour map construction from random data, iterative method 7-34725
- sea bed contour map construction from random data, spline method 7-34726
- sea bed contour map construction from random data, spline method 7-34728
- sea bed contour map construction from random data by interpolation 7-34727
- sea floor imaging long-range, low-freq., spatial resolution aspects 7-28999
- seabed topography meas. by multibeam sonar using complex fast Fourier transform 7-66327
- ship-board echo location system accuracy and system for East-Scheldt storm barrier construction 7-47558
- Shirshov Ridge, Bering Sea, topography and struct. of seafloor 7-34473
- side scan sonar records, use of image processing 7-66368
- sonar digital swath method for bathymetric sounding 7-66360
- sonar method, bathyscan precision swath sounder 7-66362
- Sovanco Fracture Zone, rotated crustal blocks, bathymetric obs. 7-47415
- submarine accretionary wedges, evidence from Barbados for origin of convex wedges 7-28992
- submarine canyons, seismic vel. replacement by wave-eqn. datuming before stack 7-29269
- submarine topographical information based on seabeam bathymetric system (*Japanese*) 7-43595
- tidal current ridges, form. mechanism and developmental conditions 7-40461
- Tonga Trench axis and intersection with Louisville guyot chain 7-54955
- undersea features name file for personal computer, database description 7-65927
- Var ridge, Western Mediterranean, submarine sedimentary dunes built by turbidity currents (*French*) 7-34466

batteries *see cells (electric); primary cells; secondary cells; solar cells***battery testers**

- spacecraft batteries, testing facilities at the European Space Battery Test Centre 7-55412

battery testers continued

- Ni-Cd cell containing Pellon 2536 separator, life testing, satellite appl. 7-65446
- Ni-Cd secondary cell performance effect of Cd electrode sinter, cell testing 7-65448

Bauschinger effect

- β -brass bicrystals, Bauschinger effect, grain boundary contrib. 7-46574
- hundred years of Bauschinger effect (*German*) 7-41046
- metals, plastic forming operations, Bauschinger effect 7-46557
- steel, Cr-Mo-V, Bauschinger effect in cyclic plasticity 7-3355
- steel, dual-phase, Bauschinger effect and coercivity, effect of ageing (*Chinese*) 7-8045
- steel, low C, strain ageing, internal stress, Bauschinger effect 7-39612
- Al thin films, stress relax. mechanisms 7-21784
- Al_3Ni -Al eutectic alloy, Bauschinger effect, influence of Al_3Ni dispersion state (*Japanese*) 7-22761
- Cu and alloys, Bauschinger effect, influence of alloying elements and grain size (*German*) 7-17605
- Ti-Mn, alpha and beta phases, yield and tensile strength, ductility, Bauschinger behaviour, fatigue life, crack propag. 7-8052

Bayard-Alpert gauges *see ionisation gauges***Bayes methods**

- glasses, Rayleigh and Brillouin scattering spectra, Bayesian deconvolution 7-13173
- reliability estimate for multiparameter NDT 7-3562

bays (magnetic) *see geomagnetic variations***BBGKY equation** *see integro differential equations***BCS theory***see also many-body problems*

- 154 cpds., supercond. rel. to martensitic transition, microscopic theoretical model 7-2767
- clean superconductor, linear response to EM radiation 7-52888
- heavy electron superconductors, normal impurity effects, excitation spectrum 7-27462
- heavy fermion systems, BCS supercond. theory 7-7441
- macroscopic quantum systems, weakly coupled, limiting Gibbs state calcs., appl. to Josephson oscillator 7-45582
- many-valley superconductors, phase oscills., Fermi liq. effects 7-33124
- metallic films, weakly localised regime, interaction effects 7-64173
- nonequilibrium supercond. thin films, multigap state density instability, kinetic eqns. 7-52891
- nucleon system interacting through pairing force, specific heat, finite-temperature BCS plus RPA anal. 7-56619
- p-wave superconductors, ultrasound attenuation 7-27468
- parity dependent NBCS formalism at finite nuclear temp. using NUCPAR program 7-49256
- polyacenic skeletons, low temp. ordered states, superconductivity 7-64396
- quasi-one-dimensional conductors, quantised density wave ordering induced by mag. field 7-45702
- rare-earth nuclei, multipole moments, generator coordinate method anal. 7-41895
- strongly coupled electron-phonon systems, 1D and 2D, BCS pairing versus bipolaron crystallisation 7-45552
- superconducting Hamiltonian for f electron systems 7-45549
- superconductivity and random disorder in the zero-bandwidth limit 7-58945
- superconductors, disordered and amorphous nontransition metals and alloys, electron-phonon coupling strength and phonon spectrum calcs. 7-52889
- superconductors in strong mag. field, Fermi liquid interaction influence 7-52896
- thin supercond. films, parallel nucleation field determ., quasiclassical BCS theory calcs. 7-7458
- TTF(Ni(dmit)₂), molecular supercond., BCS and small supercond., lattice parameters (*French*) 7-2759
- Dy isotopes, proton-pair energies, neutron-number dependence 7-30349
- Gd isotopes, proton-pair energies, neutron-number dependence 7-30349
- Hg₃-AsF₆, 1D BCS Hamiltonian 7-45558
- Sm isotopes, proton-pair energies, neutron-number dependence 7-30349

beam choppers

- pulsed positron beam production for slow positron lifetime studies 7-35630

beam-foil spectra

- bound state existence confirmation for atomic and mol. projectiles inside solid targets, expt. investg. (*French*) 7-22427
- Rydberg states, high-lying, generation and decay in beam-foil encounters 7-49965
- secondary-electron emission, beam-foil experiments with molecular ions, anal. 7-39326
- soft X-ray source, coherent, using transition radiation 7-18948
- ultrathin foils for Coulomb-explosion experiments 7-57184
- B II, beam-foil spectra, identification 7-49982
- B III, beam-foil spectra, identification 7-49982
- B III, core excited quartet and doublet state, beam-foil study 7-42514
- B IV, beam-foil spectra, identification 7-49982
- Be-like ions, transition probabilities, line strength 7-15548
- C foils, beam-foil convoy electron double differential distrib. for proton irradi. 7-22408
- C foils, charge equil. of swift H beams 7-22409
- F^{3+} , quintet transitions, beam-foil spectra anal. 7-31004
- He, n D_2 levels, alignment and orientation in elec. field 7-865
- $^4He^+$, odd-parity coherence in beam-foil excitation 7-909
- In II and III, cascade corrected lifetime meas. 7-50016
- Kr³⁶⁺, emerging from solid foils, anomalous population of deep capture states 7-42758
- O II, $3p^4D_{1/2,3/2,5/2,7/2}$ energy levels, beam-foil lifetimes 7-15551
- O III, $3p^3P$ and $3p^3D$ energy levels, beam-foil meas. 7-30976
- O III, $3p^3S_1$ energy level, radiative lifetime meas. 7-10676
- Si^{2+} transverse Fe and Gd foils transient mag. fields 7-10537
- U^{90+} , He-like, Lamb shift from beam-foil time of flight meas. 7-36551

beam-foil spectroscopy

- anamorphic Doppler-matched condensing system, improved light collection from fast atomic beams 7-15739

beam handling equipment*see also particle beam diagnostics*

- 150 MW klystron, design and test results (*Japanese*) 7-19606
- accelerating-storage unit superconducting magnet testing using cryogenic equipment 7-48754
- aplanatic objective in mirror microscope for ultracold neutrons 7-18912

beam handling equipment continued

- beam chopper development at LAMPF 7-49759
 beam current integrator using a single chip A/D converter 7-15461
 BESSY multipole magnet, electron opt. props. and electron trajectories 7-42254
 betatron magnetic circuit temp. distrib. calc. (*Russian*) 7-42247
 betatron magnetically-switched electron injector, operating characts. 7-30794
 CEBAF cavity cryostat 7-62183
 CEBAF cryogenic system 7-62184
 centrifugal electrostatic focusing system, bunching mechanism and kinetic anal. of relativistic electron beam 7-36871
 collimated synchrotron radiation, Z-shaped wire profile and position monitor 7-35625
 conference, linear accelerators, Stanford, CA, USA (June 1986) 7-60878
 constant impedance structures, raising the beam blow up threshold current (*Chinese*) 7-5496
 CW injector linac for 35 MeV double sided microtron (*Japanese*) 7-19557
 cyclotron electrostatic deflector, transmission matrix calcs. (*Chinese*) 7-5522
 DC EM wigglers, performance limitations for FEL 7-1125
 disk-and-washer cavities for an accelerator 7-15433
 electron accelerator, wake field acceleration by proton bunches 7-62140
 electron beam excitation using glass foils 7-35627
 electron emitter stabilised by grid 7-16341
 electron matrix lens, aberrations reduction using offset apertures 7-20122
 electron storage rings using superconducting magnets 7-49778
 Electron Test Accelerator, beam injector, chopper and buncher system 7-25271
 electrostatic electron-beam deflectors, comparison of electron optics 7-18910
 ENEA free electron laser, linearly polarized EM undulator, design parameters 7-1137
 external electrostatic deflector pulse selection techniques 7-62165
 focusing of multiply charged energetic ions using solenoidal B and radial E lenses 7-56899
 free electron laser EUV, three-dims. simulation 7-43131
 free electron lasers, conference, Tahoe City, CA, USA (Sept. 1985) 7-6
 gas beam source, electromagnetically driven 7-48915
 grid pulse generator for KEK PF linac (*Japanese*) 7-56903
 grid pulser for short pulse e^- gun, design and simulation (*Japanese*) 7-19610
 grid shutter in a vacuum photorecorder 7-18914
 HERA magnet measurement facility, cryogenic system 7-49781
 HIRF tandem accelerator energy analysing magnet, calibration 7-49765
 high brightness electron injector for FEL driven by RF linacs 7-1117
 high intensity neutrino beam prod. at meson factories, focusing device, magnets 7-5517
 high intensity positron beam and ang. correl. expt. techniques and apparatus, Cu single cryst. data 7-42274
 high performance avalanche pulse generator for e^- gun appl. (*Japanese*) 7-19612
 high power characteristic measurements of resonant ring (*Japanese*) 7-19605
 high resolution analysing magnet with aberration correction, 2D field mapping and field correction 7-25283
 high voltage pulser for beam pulsing of e^+ linac (*Japanese*) 7-19611
 hybrid undulator design considerations for FEL 7-1123
 induction linac accelerators, current pulse shortening 7-49750
 inhomogeneous magnetic fields with axial symmetry, 5th order ang. aberrations, corrections (*Chinese*) 7-5508
 insertion device beam line optics, review 7-43305
 insertion device Beam Line Wunder design at SSRL 7-42256
 insertion device performance in ESRF 7-42251
 insertion devices, future developments, limitations 7-42257
 insertion devices, variational theory 7-42879
 intense slow positron beams from electron accelerators 7-35635
 ion focused transport experiments 7-62189
 ion implanter, ion beam transport system, ion-optical characteristics (*Korean*) 7-24723
 ionic impact processing machines develop. (*Japanese*) 7-53637
 KEK e^+ injection system, beam characts. (*Japanese*) 7-19613
 KEK technology for future linacs, RF sources and structures 7-62124
 L-band amplifier for Osaka Univ., linac (*Japanese*) 7-19575
 lasertron spent beam collector material desorption tests 7-62116
 LEP collider, refrigeration system of superconducting accelerating cavities 7-49780
 linear acceleration, conf., Tsukuba, Japan, (Sept. 1986) 7-18504
 linear accelerators, RF cavity design and codes 7-62128
 linear accelerators, Wake Field calculations using the MAFIA 3D BCI code 7-62138
 linear periodic magnets using permanent magnet segments, wigglers and undulators 7-5514
 linearly polarized undulator for UCSB free electron laser, laser gain depression 7-1126
 low energy positron beam for surface studies, design 7-35631
 low- β ion acceleration with a MEQALAC 7-15448
 MAFIA, 3D EM CAD system for magnets, RF structs., and transient wake-field calcs. 7-62136
 magnetic modulator for proton storage ring, design and anal. 7-30817
 magnetic quadrupole multiplet microbeam forming systems (*Chinese*) 7-10325
 magnetically confined slow positron beam in ultra-high vacuum 7-35632
 Marx bank, low jitter, for cold cathode electron beam sources (*Chinese*) 7-4912
 maximum efficiency of a conventional klystron output cavity 7-62186
 microwave undulator utilising a plane rectangular waveguide 7-62187
 multilayer monochromators and supermirrors, X-ray and neutron, controlled sputter deposition 7-33563
 multipole field generation using permanent magnets 7-49763
 multipole wiggler design producing circularly polarized synchrotron radiation 7-49772
 muon spin resonance facility at TRIUMF 7-49760
 nanosecond electron injector 7-36367
 negative ion injector extension for JAERI tandem accelerator 7-56898
 NERL 35 MeV linac, twin linac pulse radiolysis system (*Japanese*) 7-19566
 neutron beam spatial condensation by asymmetric diff. in thermal neutron monochromatisation 7-16363

beam handling equipment continued

- on-demand beam pulsing system for thick sample PIXE anal. 7-56374
 optical klystron, theory 7-360
 optical klystron, XXUV laser harmonic generation, effects of wiggler errors 7-1127
 permanent magnet helical wiggler model for FEL off-axis orbit anal. 7-1124
 permanent steering magnets, analytical expressions (*Chinese*) 7-10324
 PF linac, high power klystron, permanent focusing magnets (*Japanese*) 7-19604
 plasma erosion switch, reflecting system 7-44268
 positive ion sources and injectors for linacs 7-62126
 positron beams, low-energy, field-assisted moderator 7-62152
 power supplies to magneto-optical elements of particle channels, digital remote control system 7-42268
 precision alignment of permanent magnet drift tubes 7-62177
 predisperser electron gun for an electron monochromator 7-15034
 proton window for a spallation breeder with 300 MW beam power 7-19527
 pulse width selecting system for e^+ beam transport line (*Japanese*) 7-19609
 pulsed positron beam production for slow positron lifetime studies 7-35630
 pulsed power systems for modified betatron accelerator 7-30793
 pulsed slow positron beams, production using 35 MeV electron Linac 7-35634
 pulsed transmission line linear accelerator, beam generation, acceleration, transport and extraction 7-62188
 Pulselac induction accelerator, post-acceleration gap operation 7-30810
 recoil separator, adaptable computer control system 7-5520
 RF accelerating cavities, 3D calcs. using the URMEL-3D code 7-62137
 RF ion source, focusing system, expt. and theoretical investigations. 7-10840
 RF power amplifier with dedicated interlock and feedback controller 7-62114
 RF structs. for excitation of electrooptic transducer by beam in picosecond electron linac 7-15428
 RF superconducting linac structures for heavy ions and electrons 7-62119
 RF system for prebuncher for nanosec. beam accelerator (*Japanese*) 7-19570
 RF tuning of the KEK 40 MeV proton linac (*Japanese*) 7-19602
 RF window breakdown (*Japanese*) 7-19603
 RFQ linear accelerators in research and industry 7-62125
 sample manipulator for Auger angular dependence studies 7-35626
 short pulse grid pulser for positron generator gun (*Japanese*) 7-19607
 single bunch compressor system, design and operation (*Japanese*) 7-19614
 single gap debuncher cavity for the 40 MeV proton linac (*Japanese*) 7-19615
 SLAC Linear Collider, linac developments 7-62123
 slow positron beam, tagged, gated, high intensity, highly polarised 7-35633
 slow positron production by the use of the ETL linac (*Japanese*) 7-19569
 solenoidal magnetic lens, space-charge correction of spherical aberration 7-5825
 solid yoke bending magnetic, eddy current effects during slow acceleration (*Chinese*) 7-25284
 SSC2, efficiency function of trim coils (*Chinese*) 7-10326
 storage ring magnet for muon g-2 meas., design 7-36349
 super HILAC upgrade project, MEVVA ion source, beam transport line 7-62133
 superconducting post accelerator linac for JAERI tandem 7-36371
 synchrotron beam line critical elements, heat transfer studies 7-42255
 synchrotron radiation mirror, lacquer-coated, irradi. with undulator light, surface heating 7-43307
 synchrotron radiation mirror, thermal distortion prediction with finite element analysis 7-43306
 tapered wiggler for FEL, desirable excitation patterns 7-1122
 thermal design of drift tubes for high-gradient linacs 7-62113
 transverse field focusing 180 keV negative ion accelerator, design and fabrication 7-15439
 transverse field focusing matching/pumping system for beam injection 7-15440
 trim coils power supplies, for the Milan Superconducting Cyclotron 7-25272
 TRIUMF, muon facilities 7-49761
 undulator, linear, variable gap permanent magnet, for ENEA free electron laser expt 7-43151
 undulator, long, evolution of radiation beam system 7-42880
 undulator, microwave, theory construct, and expt. results 7-42878
 undulator, short period, design and performance 7-42252
 undulator, soft X-ray, performance predictions 7-42876
 vacuum interface to a soft X-ray synchrotron beam line 7-18967
 vacuum system for multipurpose 14 MeV neutron source 7-35529
 variable gap permanent magnet linear undulator for ENEA-FEL expt. 7-1191
 variable-angle invert-rotator for beam transport 7-62169
 wiggler, NdFe-steel hybrid permanent magnet, development for insertion in SPEAR ring 7-42250
 wiggler and alternating-gradient quadrupole field for free electron laser, electron beam envelopes and matching conditions 7-1128
 wiggler beam monochromator, distortion from synchrotron radiation thermal loading, finite element analysis 7-42269
 wiggler design, 3 Tesla, with supercond. windings, for ESRF 7-42253
 C stripper foils, long lived, development 7-15436
 H⁻ beamline, pressure in transverse field focusing, matching/pumping system 7-15441
 NbTi-Cu Al stabilised superconducting detector magnet technology for high energy accelerators, review 7-49779
 NbTi-Cu dipole superconducting magnet for accelerators, develop. 7-5510
 U ion acceleration in split coaxial RFQ (*Japanese*) 7-19573

beam handling techniques

- see also mass spectroscopy; particle beam diagnostics; particle optics
 Advanced Test Accelerator, electron beams, laser guiding 7-10327
 Applied-B ion diode expts. on Particle Beam Fusion Accelerator-I 7-10310
 atmosphere negative ion generator and collector system for dispersion studies 7-29314
 atomic beam, deflection and focusing by reson. light field 7-42786

beam handling techniques continued

- atomic beam laser cooling, reson. radiation press., simulation approach 7-15555
- atomic beams, collimation and decollimation by laser radiation 7-42782
- atomic beams, collimation and decollimation by laser radiation pressure 7-42785
- beam phase spaces with noncentrosymmetric configs., transport through linear fields (*Chinese*) 7-5509
- betatron-synchrotron resonances and misalignment in free electron laser oscillators with quadrupole focusing 7-1172
- charged particle acceleration by transverse EM wave in static mag. field (*Japanese*) 7-20119
- charged-particle beams in cylindrical waveguide, ponderomotive confinement 7-35624
- conference, linear accelerators, Stanford, CA, USA (June 1986) 7-60878
- control of beam dynamics in high energy induction linacs 7-62176
- cooling methods for stored ion beams 7-30795
- Delft ion beam pattern generator project progress 7-41532
- electromagnet systems, optimum mathematical design 7-49758
- electron acceleration in vacuum by two laser beams 7-50480
- electron accelerator, wake field acceleration by proton bunches 7-62140
- electron beam, nonrelativistic high-current, vacuum dielectric channel, external mag. field 7-62175
- electron beam guiding from RF accelerator by laser-ionized channel 7-56891
- electron beam trapping into gyro-magnetic autoresonance, Coulomb field effects 7-42887
- electron beams, electrostatic blanking system (*Slovak*) 7-61399
- electron cooling, multi-GeV, anal. 7-36357
- electron emitter stabilised by grid 7-16341
- electrons, radial focusing in bi-periodic slow-wave struct. with high accel. rate 7-41550
- emittance growth in high-current linacs, field energy calcs. 7-62118
- focusing mechanism in the pulselac CU accelerator 7-62112
- free electron laser EUV, three-dimens. simulation 7-43131
- free electron lasers, conference, Tahoe City, CA, USA (Sept. 1985) 7-6
- frequency control of KEK-PS new 40 MeV linac (*Japanese*) 7-19574
- frequency standards based on stored ions 7-14924
- HERMES III, passive control of high-energy high-current beam 7-30809
- high intensity positron beam and ang. correl. expt. techniques and apparatus, Cu single cryst. data 7-42274
- high-current electron beams, Buneman instability in neutral gas, ion collective acceleration 7-49749
- imaging bandpass electron energy analyser 7-375
- in-flight capture of ions into a Penning trap 7-5513
- insertion devices, future developments, limitations 7-42257
- insertion devices, variational theory 7-42879
- intense slow positron beams from electron accelerators 7-35635
- ion beams, intense, propagation across plasma-filled magnetic cusp 7-42261
- ion focused transport experiments 7-62189
- ion-focused transport of relativistic electron beams 7-30813
- large superconducting accelerators (*French*) 7-10321
- light negative ion sources, beam extraction and acceleration, conf., Palaiseau, France, March 1986 7-9601
- linear acceleration, conf., Tsukuba, Japan, (Sept. 1986) 7-18504
- Los Alamos FEL, status 7-1106
- low energy positron beam for surface studies, design 7-35631
- magnetically confined slow positron beam in ultra-high vacuum 7-35632
- multiple-beam collimation of X-rays 7-18958
- negative ion beam acceleration and transport experiments 7-15032
- negative ion beam extraction and acceleration from low field surface produced sources 7-15445
- negative ion beam extraction and acceleration from volume prod. sources 7-15446
- plasma channels for light ion beam propag. in target development facility 7-15357
- plasma diagnostics, Kalman filters for signal processing and beam modulation 7-1761
- ponderomotive confinement of particle beam in cylindrical waveguide 7-31235
- positron reemission enhancement, secondary moderation 7-35636
- production of an ion beam from a beam focus 7-57228
- proton beam deflection phenomena in a Pulselac post-acceleration gap 7-56892
- proton beam focusing by z-discharged plasma channel, expt. and theoretical results 7-11804
- proton bombardment elemental analysis, reliability using air mounted sample 7-59815
- pulsed positron beam production for slow positron lifetime studies 7-35630
- pulsed slow positron beams, production using 35 MeV electron Linac 7-35634
- pulsed transmission line linear accelerator, beam generation, acceleration, transport and extraction 7-62188
- quadrupole triplet employed in beam design 7-10322
- radiation sources for IR to γ -rays, development 7-42877
- relativistic electron beam, high-intensity, bending in circular dielectric structs. 7-18909
- relativistic electron beam generation in laser-based foilless diode 7-42267
- relativistic electron beams, periodic permanent magnet field-transport 7-57226
- relativistic heavy ion collector, magnet system status 7-36347
- slow positron beam, tagged, gated, high intensity, highly polarised 7-35633
- stochastic momentum cooling, helical type kicker 7-62157
- synchrotron, vertical electron oscillations, dynamics control 7-56889
- TRISTAN positron generator beam transport system (*Japanese*) 7-19568
- variable-angle invert-rotator for beam transport 7-62169
- β polarization technique for low energy storage rings, anal. for LEAR 7-30911
- Ar^+ beam, microwave ion source, beam extraction expts. 7-363
- Cs atomic beam, cooling using laser 7-10897
- H beam production using electron coding technique, future expts. 7-50401
- H beam from pulsed magnetically insulated diodes 7-10343
- H extraction, effect of weak mag. field in front of plasma electrode 7-10341
- H extraction and electron control in multipole ion source 7-18915
- H extraction from volume sources 7-15447
- H ion extraction from mirror ECR source 7-10334

beam handling techniques continued

- H ion high current density accelerator, design and diagnostics 7-15429
- H⁰ variable beam extraction from the Univ. of Manitoba Cyclotron 7-49764
- H⁺ beam, space charge compensation by pregenerated plasma 7-44200
- Na atomic neutral beam, laser technique for collimating and focusing 7-62610
- Na ion beam generation, field ionisation of laser-excited Rydberg atoms 7-57186
- beam splitters (optical)** *see optical elements*
- beam-trapping** *see self-focusing*
- bearings (machine)** *see machine bearings*
- BEBO method** *see bonds (chemical)*
- behavioural sciences**
 - see also psychology*
 - pattern recognition in rabbits, oscillating network model 7-54618
 - rabbit nictitating membrane response to piezoceramic vibrotactile CS, classical conditioning 7-8775
- behavioural sciences computing**
 - see also behavioural sciences*
 - apparent movement of short-range process and pattern perception, theoretical and methodological approaches 7-60003
 - bending motions, computer-controlled displays 7-59999
 - cinematic space, shape and psychophysics 7-60004
 - computer graphics and surface perception 7-60001
 - digital image-processing techniques for the display of images and modeling of visual perception 7-59997
 - dynamic stereo displays for research on the recovery of three-dimensional structure 7-60000
 - human colour-discrimination, Stiles's anal. 7-8562
 - motion perception research, use of computer graphics animation 7-59996
 - perception laboratory, problems encountered 7-60008
 - pure orientation filtering, scale invariant image processing tool for perception research and data compression 7-60005
 - sensory thresholds, efficient estimation 7-59986
 - spatial vision research, use of computers 7-59971
 - visual stimuli on Commodore Amiga, use of DeLuxePaint package 7-60002
- bells**
 - see also musical instruments*
 - No entries
- Belousov-Zhabotinski reaction** *see chemical equilibrium; chemical reactions; reaction kinetics theory*
- bending**
 - see also bending strength; buckling; stress analysis; torsion*
 - annular membranes, large deformations under vertical edge loads 7-6107
 - Aramid fibre reinforced composite beams, viscoelastic-plastic anal. in flexure 7-33717
 - arches, shallow, optimal forms rel. to deflection 7-6114
 - bar, bending vibrs., amplitude-dependent internal friction, influence of non-uniformly stressed condition (*Russian*) 7-58410
 - bar, hyperstatic nonlinear bending 7-6091
 - bars, initially curved, dynamic elastoplastic buckling 7-63024
 - beam, infinite periodic, bending wave propag. 7-57722
 - beam, shock-loaded, large plastic strains eval. 7-43752
 - beam deflection meas. by phase shifting holographic interferometry 7-31288
 - beams, cold-bent, flowchart for overbend prediction 7-6103
 - beams, elastoplastic, biaxial dynamic bending 7-62999
 - beams, finitely deformed 3-D, tangent-stiffness expression, use in space frame analysis 7-6104
 - beams, symmetric laminated, optimal design considering damping 7-31639
 - beams, symmetrical bending, precision test equipment, loading system 7-63091
 - beams, thin-walled open, elastic nonlinear static analysis 7-62984
 - beams and rods, small strain deformations including large deflections 7-1423
 - bow-tie fibres, microbending losses 7-57572
 - bow-tie fibres with const. curvature, macrobends 7-57573
 - cantilever beam, large deflections with vertical load at free end (*Japanese*) 7-11294
 - cements, bending stress determ. from density of localised cracks (*German*) 7-22935
 - ceramics, bending fatigue, room temp. (*Japanese*) 7-13597
 - ceramics, fracture toughness evaluation using chevron-notched specimens (*Japanese*) 7-59613
 - circular plate, symmetrically loaded, variable thickness, bending problem 7-57709
 - column, simply supported, under tangential follower force, self-adjoint system 7-6125
 - columns, inelastic post-buckling 7-37359
 - composite column, Euler load determ. by direct computation 7-62976
 - composite material shallow sandwich shells, finite deflection eqns. and linear stability problem (*Chinese*) 7-43721
 - $\text{Cu}_2\text{Mo}_6\text{S}_8$, shape memory effect and rhombohedral-triclinic transition (*Russian*) 7-8058
 - curved beam elements with penalty relaxation 7-37335
 - cylindrical, asymmetrically loaded, stability and large deformation behaviour 7-11306
 - disc bend test, parameterize anal. 7-54039
 - ductile-brittle transition temp. determ. from miniature disc bend tests 7-54038
 - dynamic stress intensity factors, meas. using FFT analyser, appl. to drop weight impact three-point bend testing (*Japanese*) 7-59712
 - dynamic three-point bending test, finite element anal. considering contact and frictional effects (*Japanese*) 7-57776
 - dynamically loaded pipes with circumferential flaws, behaviour under internal pressure and external loads 7-13577
 - elasticity theory, variational problems, with small parameter 7-24428
 - end-notch flexure specimen, mode II interlaminar fracture toughness, finite element anal. 7-1509
 - epoxy resins, effects of epoxy number and hardener on properties (*German*) 7-22973
 - fibre reinforced composite, energy dissipation properties, anisotropy 7-6143
 - fibre-reinforced beam with step, finite three point bending 7-43689
 - flexure specimen, end-notched, for mode II testing, design and anal. 7-51005

bending continued

- fluid surfaces, effective bending rigidity calcs., integration meas. 7-58571
four-point bending, large deflections, fundamental theory (*Japanese*) 7-11293
frame response to a harmonic excitation, taking into account the effects of shear deformation and rotary inertia, Timoshenko beam theory 7-6132
glass fibre reinforced polymers, hydrothermal behaviour, mech. props. rel. to water absorpt. 7-46665
glass fibre reinforced polypropylene, damping characts. 7-59565
glass fibre reinforced polypropylene, short-fibre, struct. and mech. props., effects of moulding geometry 7-3348
glass fibre reinforced polypropylene, subjected to pure bending, dynamic tensile props. 7-46545
graphite, AGR fuel sleeves, irradiation, bending, AE obs. 7-723
Hexsyrn rubber, high-flex ozone resistant, prep. and appl. 7-13767
ice, single crystal, fracture toughness and macrofractography (*Japanese*) 7-16676
inextensible cloth or cable networks with bending stiffness, continuum theory 7-1400
kinking of crack emanating from free surface of beam under pure bending 7-43783
Kirchhoff plate bending, C^1 finite element family 7-24418
Kirchhoff-plate bending using C^1 finite elements (*Spanish*) 7-18598
laminated composite plate theory, with improved in-plane response 7-37354
laminated plates, non-classical approx. bending theory (*Chinese*) 7-43692
large deflection behaviour, four-point bending test, estimation by simple reduction method (*Japanese*) 7-51006
ligament, plastic, ahead of edge-crack, combined loading 7-11349
linear elastic beam elements of MODULEF library (*French*) 7-31655
martensitic transformations, stress-induced, anal. of inelastic bending 7-65032
membrane, transversely loaded, geometrically nonlinear analysis 7-6095
metal-polymer two-layer plates under bending load, strength and stiffness calc. 7-57713
metals, bend tests for stress corrosion testing 7-54040
microbend-induced birefringence in optical fibres, temp. dependence 7-43425
microbending losses analysis in single-mode fibres 7-11115
optical bent birefringent fibre, compensated sensing based on retardation characts. 7-50752
optical cable, losses resulting from excess fibre length (*Japanese*) 7-50782
optical fibre single-mode, step-index, microbending losses, anal. 7-20452
optical fibres, Gaussian-profile dispersion-shifted, VAD manufactured, design and performance 7-11128
optical fibres, single-mode, curvature depend. of effective cutoff wavelength 7-57586
optical single mode fibres, microbending loss eval. 7-57565
pipelines, initiation and propag. of buckles 7-26180
plastic film covered steel plates, thermoelastic props. meas. 7-33713
plate, bending anal. using fourth order eqn. finite element algorithm 7-29759
plate, cracked, bending, stress intensity factor computation via path-independent integral 7-37380
plate, elastoplastic, bending anal. by BEM 7-43705
plate, large-amplitude deflected, free vibration 7-43757
plate, rectangular, uniformly compressed, post-critical state (*Polish*) 7-43727
plate, thick, bimodulus, post-buckling behaviour (*Chinese*) 7-11318
plate, thick rectangular, buckling, high-order deform. theory (*Chinese*) 7-11320
plate analysis using initial-value method 7-20600
plate bending, direct boundary element method 7-24419
plate bending, stability regions 7-16080
plate bending element, bilinear, force evaluation 7-57707
plate bending elements, nonconforming shape functions (*Chinese*) 7-50958
plate bending using new hybrid element method 7-16070
plate element, transverse shear deformation (*Chinese*) 7-26153
plate flexure with creep, inverse problems 7-11303
plates, anisotropic laminated elastic, finite deflections 7-37336
plates, bent, strain energy upper and lower bounds 7-26138
plates, bimodulus thick circular, axisymmetric buckling analysis using FEM 7-57716
plates, circular, elasto-plastic deflection analysis, full system vs. layered yield criteria prediction 7-1450
plates, circular incompressible, variational principle for large axisymmetric strain 7-31660
plates, first-ply failure analysis of composite laminates 7-63053
plates, flexible, rectangular, on nonlinearly elastic base, optimal design 7-62995
plates, inelastic, bending problems, influence functions use (*German*) 7-20606
plates, laminated, boundary layer approach to free-edge stress concentration 7-26158
plates, multilayered shear-deformable, finite elements 7-43667
plates, orthogonally stiffened, under lateral and axial loads, nonlinear anal. 7-37360
plates, orthotropic, linear bending and buckling, eigenvalue problems 7-37352
plates, orthotropic folded, elasticity versus finite strip analysis 7-1427
plates, orthotropic rectangular linear elastic under biaxial loads, post-buckling stability 7-50966
plates, polygon-shaped bent, strain energy inequalities 7-26139
plates, prismatic, folding, instability by finite strip method (*Spanish*) 7-20611
plates, rectangular on linear elastic foundation, nonlinear dynamic response 7-20599
plates, rectangular thin laminated composites, bending analysis using FEM 7-57708
plates, sandwich with unidirectional thickness variation, stress anal. 7-43718
plates, sectorial, laminar, orthotropic, flexure anal. on basis of finite-shear theory 7-63014
plates, sheardeformable elastic, small finite deflections 7-26144
polymer films, stress development during thermal cycling, bending beam technique 7-28063
prismatic guyed mast, bending and torsional freqs. 7-57711
pulley belt in steady motion, influence of bending stiffness on shape 7-11312

bending continued

- PVC-styrene-butadiene rubber blends, bending in elastic range 7-39606
ring stiffened circular plates, asymm. buckling 7-6126
rod, curved elastic, vibr. in plane of curvature during heating 7-43751
rod, curvilinear sectional stability of planar bending mode with allowance for initial defects 7-31661
rod-type vibr.-freq. transducers, resonator shape optimisation 7-1482
second order correction formula for the eigenfrequencies of a bending plate (*French*) 7-6120
sheet metals with complex strain bending histories, elastic-plastic spring-back 7-37348
shell, stresses under local loads, calc. using Timoshenko method 7-57696
shell analysis using a simple flat hybrid stress element 7-16081
shell element, curved C^0 , based on assumed natural-coordinate strains 7-11313
shells, spherical, and circular membranes, flexure theory, stochastic bifurcation 7-26151
shells, thin elastic, variational formulation for large deflections 7-43671
shells of revolution, rubber-like, undergoing torsionless axisymmetric deformation, strain-energy density 7-43687
slabs, frequencies and modes of bending vibrations with allowance for propagating modes; 7-11338
steel, dislocation struct. rel. to cyclic bending strain 7-22760
steel, fatigue resistance under combined effect of cyclic bending and cyclic torsion 7-28131
steel, mild, cold-form-rolled, rotary bending fatigue behaviour (*Japanese*) 7-53866
steel, secondary-hardening, bainitic embrittlement 7-3405
steel, stainless, pipe, subjected to bending deform., fracture instability, effect of multiple circumferential through-wall cracks 7-65122
strain gauge sensitivity in plastic range 7-6168
stress functions in a problem of elasticity theory (*French*) 7-62986
thin diaphragm capacitive pressure sensor simulator 7-61328
thin flat-walled structures, buckling, spline finite strip method 7-1459
thin-walled sections under combined bending and torsion, nonlinear theory 7-57698
thin-walled structures under combined loading, elastic buckling anal. using finite strip method 7-20612
waveguide bend configuration with low-loss characteristics 7-37147
Ce plate, isostructural $\gamma \rightarrow \alpha$ transformation, shape changes (*Russian*) 7-46464
Cu dislocated single cryst., sub-grain misorientation, de Haas-van Alphen meas. 7-12300
Cu-Zn-Al, quenched sheets, shape change rel. to thermal cycle (*Japanese*) 7-53790
GaSe single crystal, surface bending, radius of curvature determ., Berg-Barret method (*Russian*) 7-38305
Ge single crystal, microstruct. of fragments (*Russian*) 7-38107
Mo single crystals, struct. changes during annealing after bending deform. (*Russian*) 7-44446
Nb₃Sn tape, Cu-coated, effect on crit. bending diameter (*Russian*) 7-33747
Ni-Al-Cr, melt spun ribbons, microstruct., mech. props., Cr conc. effect 7-28031
Si 7-26753
Si₃B₂O₇, thermal donor formation, bending stress effects 7-17563
SiC, instrumented impact testing, absorbed energy 7-28237
Si₃N₄, sintering, under rotary bending, mirrorlike region of fractured surface (*Japanese*) 7-3436
Zn-based alloys, mechanical props., alloying addition effects (*Japanese*) 7-8090
ZrO₂, partially stabilised, instrumented impact testing, absorbed energy 7-28237
- bending of light** see gravitation; light
- bending strength**
bone, mech. props. and morphology, effects of Ca deficient diet, goose obs. 7-3822
effect of ion irradiation, 7-28160
epoxide resins, particulate filled, parameters determining strength and toughness 7-65071
epoxy composites, Fe powder reinforced, flexural props., water condition temp. depend. 7-59587
epoxy resin, aminimide-cured, mica reinforced, improved mech. props. 7-59489
fibre reinforced composites, compressive-flexural/shear failure mode transition, interface strength 7-39586
fibre reinforced plastics, hybrid, tensile, compressive, flexural and shear props., review 7-39532
fused quartz particulate composite, fracture behaviour (*Chinese*) 7-8079
glass, number of cracks at fracture rel. to ultimate stress 7-22809
glass fibre reinforced epoxy and polyester composites, flexural failure mechanisms, global stress plane 7-8082
graphite, bend strength and fracture strain under press. 7-46595
graphite, nucl. grade, fracture processes and oxidation effects 7-28157
graphite, nucl. grade, pitchcoke, irradiation, mech. props., radiolytic oxidation effect 7-25032
graphite fibre reinforced epoxy laminates, holographic interferometry analysis of bending rigidity loss 7-59733
graphite fibre reinforced epoxy resin composites, multidimensionally braided, tensile, compressive and flexural props. 7-33726
I-section members with flexible webs, inelastic flexural-torsional buckling strength (*Japanese*) 7-20610
Kevlar 29 fibre reinforced bone and dental cements, mech. props. 7-28080
Kevlar 49-285 style fabric for space structures use, thermoelastic behaviour 7-37329
metal-polymer two-layer plates under bending load, strength and stiffness calc. 7-57713
Mo-Ni, activated sintered, sintering behaviour and mech. props. 7-7929
optical fibres, strength meas. by bending 7-43384
optical glasses bending strength meas. 7-50665
PEEK and C fibre reinforced PEEK materials potential as bioimplants 7-60126
plate bending, finite element model with limit analysis capacity 7-63013
polyamide 6-polyethylene blends, miscibility, mech. props. 7-59535
polymer honeycomb filter, strength and stiffness in shearing determ. 7-17634
polypropylene, hot isostatic pressing, mech. strength improvement 7-7955
polypropylene mica filled composites, struct.-mech. props. relations 7-1919

bending strength continued

- quartz, SC cut, compression and flexure stress effects (*French*) 7-65098
 sialon, commercial, static fatigue and creep resist. 7-59601
 steel, CrMoV, cold rolled, effects of ageing on mechanical properties (*Russian*) 7-13478
 steel, high-speed p/m tungstenless, Mo and V effect on microstruct. and operating props. 7-33788
 steel, low-tensile, crack resist. in elastoplastic region under static loading 7-33793
 steel, tool, heat treatment cycles, original struct. and deform. influence on mech. props. 7-39560
 Al₂O₃ discs, thermal shock reliability, Weibull parameters, bending and fracture testing 7-3408
 Al₂O₃, joining by inducing localised reducing conditions 7-46787
 Al₂O₃, strengthening, mech. props. and microstruct. (*Japanese*) 7-22820
 Al₂O₃-SiC composites, microstruct. and mech. props. (*Japanese*) 7-22821
 Al₂O₃-SiO₂, mullite, prep. by sol-gel method, microstruct. and mech. props. 7-46386
 Al₂O₃-TiO₂, mech. props. and microstruct., influence of TiO₂ additions. (*Japanese*) 7-22706
 Al₂O₃-TiO₂-SiO₂ composite, thermal shock resist. 7-33771
 Al₂O₃-ZrO₂ composites, microstruct. charactn. by Raman spectroscopy (*Japanese*) 7-22684
 Al₂(TiO₃)₃ ceramics, sintering, microstruct., bending strength, additives effect (*Japanese*) 7-17601
 Al₂TiO₃-mullite composites, thermal and mech. props., effect of comp. (*Japanese*) 7-26987
 Bi alloy impregnated Ti, composite pseudoalloy, mech. props., Bi alloy content depend. 7-28095
 C, carbonisation chem. of phenol formaldehyde resin and product mech. props. 7-46802
 C fibre reinforced epoxy, unidirectional, fracture strength, role of matrix resin 7-53845
 C fibre reinforced plastic, thermal fatigue, flexure strength (*Japanese*) 7-13568
 CeO₂-ZrO₂-Y₂O₃ thermal barrier coating, plasma-sprayed, thermal and mech. props. (*Japanese*) 7-27899
 LaCrO₃-Cr cermets, mech. props., interparticle welding 7-39630
 Mg_{1-x}Cr_xFe₂O₄, Barkhausen noise parameters correl. with strength 7-22963
 Mg₂SiO₄, fosterite-based ceramic with BaO addition, synthesis, sintering, and props. 7-46397
 Mo, arc melting, impurity content, mech. props. 7-27980
 Mo-ZrO₂, sintered composites, mech. props, microstruct. (*Japanese*) 7-13558
 Na₂O-CaO-Al₂O₃-SiO₂ glass ceramic system, spherulitic growth, mech. props. 7-46405
 Nb₃Sn filamentary superconductor with high bending strength, fabrication (*Slovak*) 7-58965
 PZT ceramics, ordered void struct., dielec. const., flexure strength 7-63607
 Si, single cryst., ultimate strength, surface treatment effect 7-2090
 SiC ceramics, hot pressed, grinding, surface damage, bending strength (*Japanese*) 7-17602
 SiC fibre reinforced Al alloys, whisker or particulate hybrids, mech. props. 7-13537
 SiC fibre reinforced Al composite wires, neutron irradi., mech. props., fusion reactor appl. 7-49628
 SiC fibre reinforced Li₂O-Al₂O₃-SiO₂ glass ceramics, tensile and flexural strength 7-13520
 SiC, sintered, fracture after Li exposure 7-28103
 SiC, sintered, microstruct. and props., influence of fabrication method (*Japanese*) 7-22622
 SiC whisker reinforced Si₃N₄, microstruct. and props. 7-22824
 SiC-Al composites, heat treatment and neutron irradi. effects on mech. props. 7-65081
 Si₃N₄ based powder materials with SiC component, comp. effect on mech. props. 7-27998
 Si₃N₄ ceramics, hot pressed, fatigue test with Knoop indentation, residual stress effects (*Japanese*) 7-17640
 Si₃N₄, hot-pressed, tensile strength at room and elevated temp. (*Japanese*) 7-65139
 Si₃N₄, nitridation of Si powder compacts in N₂-H₂ gas mixture (*Japanese*) 7-3247
 Si₃N₄, sintered, fatigue strength under rotary bending 7-65128
 Si₃N₄, sintered, microstruct., mech. props., Pr₆O₁₁ additive effect 7-17506
 Si₃N₄, surface flaws effect on strength 7-59638
 Si₃N₄/Al/Invar ceramic/metal joints, rel. between tensile and three-point bending strengths 7-39583
 Si₃N₄-SiC reaction sintered ceramics, oxidation effect on strength 7-65163
 Si₃N₄-Y₂O₃, hot pressed, fracture, flexural strength, temp. degradation 7-13546
 Si₃N₄-Y₂O₃-Al₂O₃, pressureless sintering 7-17503
 Ti-Al-Mo-Cr alloy, VT3-1, vac. annealing of blanks after isothermal deformation, hydrogen plasticising effect 7-8027
 TiC-Fe-Cr alloyed with Si, high-Cr, sinterability and mech. props. improvement 7-64986
 TiC-Ni-Mo sintered carbides, struct. and physicomech. props. 7-3256
 TiC-WC-Ta-Cr hard metals, Ta conc. effect on comp. and physicomech. of carbide and Co phases 7-53708
 TiC-WC-Ta-Cr three-phase sintered carbides, Ta content influence on struct. and props. 7-65097
 TiN-Ni heterophase materials, strength rel. to sintering characts. and components conc. 7-53822
 ZrO₂ advanced ceramics, props. and appl. 7-13416
 ZrO₂, CeO₂ containing tetragonal polycrystals, thermal stability, mech. props. 7-28101
 ZrO₂ ceramics, strength, effect of freeze-drying of Zr(OH)₂ 7-13415
 ZrO₂, Y₂O₃ partially stabilised, hot isostatic pressing, high temp. mech. props. 7-28082
 ZrO₂, Y₂O₃ stabilised, phase transform., mech. props., surface struct. rel. to polishing (*Japanese*) 7-53791
 ZrO₂, Y₂O₃-doped, powders, sinterable, chemically coprecipitated in non-aq. medium 7-64982
 ZrO₂-CaO-P₂O₅-SiO₂ glass ceramics, prep. and mech. props. (*Japanese*) 7-7942
 ZrO₂-Y₂O₃ ceramics, toughened, prep., microstruct., mech. props. 7-3409
 (ZrO₂)_{0.9}(Y₂O₃)_{0.1} fliantite crystals, bending and compressive strength temp. depend. meas. 7-44653

berkelium

- see also nuclei with
 solid state and thermodynamic props., f-electron bonding and struct., review 7-12321

berkelium compounds

No entries

beryllium

- see also nuclei with
 adhesive-adherend interface under load, stresses in adhesive bond 7-28260
 AE as function of grain size during plastic deform. (*Russian*) 7-59582
 atmosphere, ¹⁰Be cosmogenic radionuclide production during Pleistocene 7-23842
 atom, ³Po and ¹Po Rydberg series, autoionising states, complex eigenvalue Schrodinger eqn. soln. 7-62329
 atom, electronic energy, Green's fn. calc. 7-10445
 atom, excitation energies, multiconfig. linear response and full CI calcs. 7-36487
 atom, excitation energies, oscillator strengths, polarisabilities, HF calcs. 7-56929
 atom, g-Hartree ab initio calcs. 7-15488
 atom, ground state, exact density-pot. relation 7-42726
 atom, HF eqns., Griffin-Hill-Wheeler version 7-42459
 atom, kinetic energy density, nonlocal correl. fn., CI wave fns. and HF calcs. 7-42496
 atom, modified HF SCF equation 7-56970
 atom, multi-config. HF and many-body perturbation theory calcs. 7-19699
 atom, second-order energy calcs. using Gaussian-type geminals, Monte Carlo quadrature formulas 7-25363
 atoms, double electron excitation cross section, distorted wave approach 7-50379
 charge density distrib., local density approx. calcs. 7-6577
 cool CP stars, search for Be, IUE spectral obs. 7-47930
 cooldown mass flow requirements for He or N cooling systems 7-56281
 determination in natural water, by electron capture detect. gas chromatography 7-13932
 electronic surface states investig. 7-17061
 energy multiplier in fusion reactor blanket, costs and benefits 7-49625
 fusion machine wall material erosion and impurity prod. 7-62074
 ion 4f to 5g transition generation obs. in recombining laser plasma 7-57303
 isoelectronic series, dielectronic recomb. rates calcs. 7-50352
 limiter material for ISX-B tokamak 7-19422
 liquid, pseudoclassical approach to electron and ion density correlations 7-6503
 mirror for large optics, fabrication by hot isostatic pressing 7-37228
 mirrors for large optics, preparation by hot isostatic pressing 7-26045
 negative metastable ion, shape resons. scaled local density calcs. 7-42464
 polycrystalline. plasmon dispersion, EELS meas. 7-27283
 porous materials, strain hardening, compaction eqns. 7-64953
 prototype limiter for JET, thermal fatigue tests, microcracking 7-5415
 SNC meteorites, ¹⁰Be contents determ. 7-40785
 sputter deposition using high rate confined ion beam cylinder technique 7-53586
 superplastic flow, electron microscopy studies (*Russian*) 7-3360
 surface passivation, angular dependent X-ray photoelectron spectroscopy 7-27864
 technical grade, size instability during low temp. thermal cycling (*Russian*) 7-33699
 AlGaAs MQW lasers, index-guided, fabrication by selective disordering using Be focused ion beam implantation 7-20269
 AlGaAs-GaAs superlattices, Si-Be co-doping, compositional disordering suppression, SIMS study 7-16878
 AlGaAs-GaAs-Si, Be superlattices, correlation between Si diffusion and Si-induced disordering 7-38034
 Al_{0.9}Ga_{0.1}As:Be epitaxial layers, ion implanted, rapid thermal annealing 7-21257
 AuBe-Cr-Au-InP, improved ohmic contact 7-64310
 Be I isoelectronic sequence, short wavelength laser calcs. 7-20214
 Be III, transition wavelengths among doubly excited states 7-49980
 Be⁺ shape reson., complex-rotated HF method 7-842
 Be⁺, electron impact-excitation, reson. transition, ab initio treatment 7-42768
 Be⁺ ion implantation in GaAs-AlGaAs heterojunctions 7-12813
 Be-Ti multilayer interference system, struct. and phase composition, electron microscopy, X-ray and neutron diff. meas. 7-63984
 Be⁺+U⁶⁺(U⁸⁺)(Xe⁴⁵⁺), electron stripping, cross section meas. 7-64849
 Be⁺+F(Na)(Al)(Si)(P)(Cl)(K), K-shell X-ray prod. cross section meas. 7-15680
 Be⁴⁺+He, charge exchange cross sections, quasimolecule Feshbach method calcs. 7-36754
 Be₁₃ and Be₅₅, stability and struct., binding energy, ionisation pot. 7-11988
 Be₂, bonding, appl. of local spin density approx., comparison with other studies 7-25371
 Be₂, chem. bonding, kinetic energy anisotropy investig. 7-10396
 Be₂⁺-H₂O, geometry and vibr. freqs., ab initio HF calcs. 7-49881
¹⁰Be, conc. in meteorite, AMS meas. 7-66524
 GaAs:Be, MOVPE, diethylberyllium dopant source, elec. characts. 7-22521
 GaAs:Be, ion implanted, rapidly annealed, damage removal process 7-17043
 GaAs:Be, rapid annealing, temp. depend. of damage removal and carrier activation 7-17032
 GaAs:Si,Be, MBE, dopant interaction 7-52362
 GaAs_{1-x}P_x:Be⁺-GaP:Be⁺ strained-layer superlattices, ion implantation doping, structural study 7-38030
 GaAs_{1-x}P_x:Be⁺-GaP:Be⁺ strained layer superlattices, ion implantation doping, optical and elec. props., device appls. 7-44583
 Ga_{0.47}In_{0.53}As:Be epitaxial films, ion implanted, rapid thermal and furnace annealing 7-22729
 Ge:Be extrinsic photoconductor material, cryst. growth and characterisation 7-64893
 Ge:H,Be, shallow acceptor complexes 7-45219
 In_{0.53}Ga_{0.47}As:Be, high dose implants, rapid thermal annealing 7-16602
 InP:Be, doping using thermal atomic beams in chemical beam epitaxy 7-44584
 InP:Be, isothermal anneal techniques, comparison 7-16603
 Na₂O-SnO₂-SiO₂:Be²⁺, glass, diffusion of cations, 500-800°C 7-12371

beryllium continued

- Si-B, metastable impurity levels, self-consistent local-density total-energy calcs. 7-38503
Ti-coated Be substrates, bond failure, thin film fracture 7-59600

beryllium alloys

see also *beryllium compounds*

- Al-Be, thermal surface oxide layers, SIMS characterisation 7-13650
Al-Cu-Be (3, 0.1 wt.%), precip. reactions 7-53738
Al-Li-Be alloys, arc-melted, microstruct. evaluation 7-22655
Al-Li-Be alloys, rapidly solidified, microstruct. eval. 7-22656
CeBe₁₃, band struct. calc. 7-32905
Cu-Be, explosive cladding, martensitic transform., electron diff. 7-46468
Cu-Be, serrated flow, disappearance 7-17588
Cu-Be (2 wt.%), ageing, lattice rearrangement (*Russian*) 7-39553
Cu-Be (30 at.%), eutectoid decomp., spatial distrib. of α -phase (*Russian*) 7-53694
Cu-Be-Co, elec. resist., decomposition and coarsening effects 7-2573
CuBe, oxidised, secondary electron emitters, AES and ESCA studies (*Chinese*) 7-54238
CuBe, scatt. anisotropy of conduction electrons 7-38536
CuSnBe bronze sheets, lamination investig., Auger and photoelectron studies (*Russian*) 7-13628
Fe₈₁Be₁₃Si₃C₂ soft ferromag. metallic glasses, domain wall motion and energy dissipation studies 7-64478
LaBe₁₃, band struct. calc. 7-32905
Ni-Be (2 wt.%), ageing, lattice rearrangement (*Russian*) 7-39553
Ni₃Al-Be, ductility, strength, grain boundary segregation, solid soln. strengthening, Be addition effect 7-39608
ThBe₁₃, band struct. calc. 7-32905
TiBe₂, spin-fluctuation material, magnetoresistivity 7-45278
UBe₁₃, band struct. calc. 7-32905
UBe₁₃ coherent Kondo state, upper critical field calcs. 7-2793
UBe₁₃, elec. resist., Press. and mag. field effects 7-45562
UBe₁₃, heavy electron supercond., anomalous temp. depend. of mag. field penetration depth 7-2780
UBe₁₃, heavy fermion superconductors, Fermi surface and cooperative phenomena 7-2771
UBe₁₃, heavy fermion system, unusual low temp. Hall voltage behaviour obs. 7-38540
UBe₁₃, heavy-fermion superconductors, induced moment mag. form factors 7-12909
UBe₁₃, heavy-fermion superconductors, Landau-Khalatnikov US damping 7-12912
UBe₁₃, lattice gas heavy fermion-boson model anal. of specific heat, entropy and magnetic susceptibility 7-58505
UBe₁₃, obs. of antiferromag. correlations 7-22093
UBe₁₃ single crystals, normal and supercond. states, thermal cond. temp. depend. meas. 7-52166
UBe₁₃ superconducting thin films, mag. field studies 7-12928
UBe₁₃, superconductivity, simple transition metal-type and heavy fermion behaviour 7-12897
UBe₁₃, superconductivity 7-45535
UBe₁₃, U_{0.97}Th_{0.03}Be₁₃ and UBe_{12.94}Cu_{0.06}, low temp. high mag. field study 7-12911
U_{0.97}Th_{0.03}Be₁₃, heavy-fermion superconductor, muon Knight shift study 7-7628
U_{1-x}Th_xBe₁₃, anisotropic supercond. and ultrasound attenuation study 7-22067
U_{1-x}Th_xBe₁₃ heavy fermion superconds., muon Knight shift and zero-field relax. meas. 7-45887
(U_{1-x}Th_x)Be₁₃, superconductivity under pressure 7-12903
YbBe₁₃, low temp. Mossbauer study 7-33309
YbBe₁₃ single cryst., sp. ht. meas. 7-2227
(Zr₇Rh₂₅)₉₃Be₇, metallic glasses, impurity vibr. states, influence on thermodynamic and superconducting props. 7-38148

beryllium compounds

see also *beryllium alloys*

- beryl, high press. cryst. struct. and compressibilities 7-16505
birefringent ceramics, millimeter wave dielectric meas. 7-14978
cordierite, cryst. struct. refinement and thermal expansion, 100-550K 7-6609
BeAl₂O₄:Cr³⁺, alexandrite, nonradiative transition dynamics 7-1102
BeAl₂O₄:Cr³⁺, alexandrite, excited, absorpt. spectra, 220-900 nm 7-46075
BeAl₂O₄:Cr³⁺, solid laser material, active ion distributions 7-57342
BeAl₂O₄:Cr³⁺, alexandrite, emission spectrum conc. of broad-band solid-state lasers 7-43114
BeAl₂O₄:Cr³⁺, tunable laser output pulse kinetics, spectral condensation characts. 7-50570
BeAl₂O₄:Ni²⁺, chrysoberyl, laser induced fluoresc. and decay lifetime 7-46135
BeAl₂O₄:Ti³⁺, chrysoberyl crystal tunable laser, 0.7 to 0.9 μ m 7-25826
BeAl₂O₄-MgAl₂O₄ pseudo-binary system, phase relations (*Japanese*) 7-16721
Be₃Al₂(SiO₃)₆:Cr³⁺, emerald, spectral energy transfer, fluorescence line narrowing 7-33441
Be₃Al₂Si₂O₁₀, beryl, electron-irradiation induced amorphism 7-32505
Be₃AlSi₂O₁₀OH, euclase, high press. cryst. struct. and compressibilities 7-16505
BeBH₄⁺, relative energy characts., electronic correl. in ab initio calcs. 7-15528
BeCl₂, aq. soln., mol. dynamics, X-ray diff. study 7-21075
BeF₂-based glasses, thermal conductivity meas. 7-12382
BeH⁺, orbital energies, multipole moments and electric field gradients, HF calcs. 7-62270
BeH₂, closed shell configs. SINDO method calcs. 7-19705
BeO, beryllia, polycrystalline ceramics, spall strength, plate impact meas., spall zone model calcs. 7-33797
BeO, complex dielec. const. meas. at 245 GHz using double-beam interferometer 7-7632
BeO, neutron multiplication study by shift register coincidence technique 7-30467
BeO, optical props. of F⁺ centres 7-7717
BeO, orbital energies, multipole moments and electric field gradients, HF calcs. 7-62270
BeO powder prop., porous struct. changes during heating of powdered hydroxide and basic carbonate 7-22617
BeO, TSEE, pyroelectric properties influence 7-13340
BeO thermoluminescent phosphor, γ and in dosimetry using electrical conductivity 7-62095

beryllium compounds continued

- BeO/Li ceramic, sphere-pac forms, T breeder materials, thermal cond. 7-52163
BeO/LiAlO₂ blanket, neutron activation calcs. in Cascade 7-15380
Cr³⁺:BeAl₂O₄, alexandrite, laser material, nonradiative relaxation, picosecond time resolved studies 7-10956
Cr³⁺:BeAl₂O₄, alexandrite, lasers using low-magnification unstable resonators 7-36997
Cr³⁺:BeAl₂O₄ crystals, growth and laser performance 7-15870
Cr³⁺:BeAl₂O₄ laser, tunable, characts. (*Chinese*) 7-5902
LiBeH₃ and Li₂BeH₄, cryst. struct. and IR absorption 7-51720
UBe₁₃, electron-phonon coupling calcs., unconventional superconductivity mechanism 7-38811

Bessel differential equation see *Bessel functions***Bessel functions**

- beam-columns, tapered, exact Bernoulli-Euler static stiffness matrix 7-6122
cylindrical Bessel functions of complex argument, computation 7-41083
phase integral formulae and their relation to existing asymptotic formulae 7-35228
product with Gaussian, integral evaluation 7-48304
radial functions of non-self adjoint Laplace operator, inequalities (*Russian*) 7-48303
simultaneous integro-differential eqns., soln. using Kontorovich-Lebedev transform 7-55968
zeros of miscellaneous Bessel functions, ordering relations 7-29687

beta-decay

see also *beta-decay theory*; *beta-ray spectra*; *nuclear electron capture*; *radioactive decay periods*; *radioactive decay schemes*

- A=122, nuclear data sheets, levels, J^π, transitions, decays 7-41024
A=133, nuclear data sheets, levels, J^π, transitions, decays 7-60906
A=143, nuclear data sheets, levels, J^π, transitions, decays 7-14720
A=145, nuclear data sheets, levels, J^π, transitions, decays 7-29604
A=156, nuclear data sheets, levels, J^π, transitions, decays 7-41025
A=201, nuclear data sheets, levels, J^π, transitions, decays 7-60907
A=216, nuclear data sheets, levels, J^π, transitions, decays 7-29605
A=220, nuclear data sheets, levels, J^π, transitions, decays 7-29605
A=224, nuclear data sheets, levels, J^π, transitions, decays 7-29605
A=228, nuclear data sheets, levels, J^π, transitions, decays 7-29605
A=237, nuclear data sheets, levels, J^π, transitions, decays 7-29606
A=244, nuclear data sheets, levels, J^π, transitions, decays 7-60908
A=46, nuclear data sheets, levels, J^π, transitions, decays 7-41023
A=49, nuclear data sheets, levels, J^π, transitions, decays 7-14718
A=83, nuclear data sheets, levels, J^π, transitions, decays 7-60905
A=99, nuclear data sheets, levels, J^π, transitions, decays 7-14719
decay energies for fission products in JNDC FP Decay Data File 7-15236
double β -decay and ν props., review 7-30218
double beta-decay detector using high purity ⁷⁶Ge inside Si(Li) shielding, background test 7-49840
Fermi and Gamow-Teller transitions, comparison of beta-ray polarization with SU(2)_L × SU(2)_R × U(1) models 7-35977
Gamow-Teller β -decay of even nuclei near ¹⁰⁰Sn, struct. model calcs. 7-49330
half-lives, RPA and perturbation theory calcs. 7-49326
heavy nuclei, Gamow-Teller resonance in β^+ decay and delayed proton emission 7-49327
K X-ray fluorescence yield ratio meas. for 55 ≤ Z ≤ 82 7-10128
light neutron-rich isotopes, β -decay half life determ. 7-49325
low background scintillation installation for double beta decay experiments 7-19630
multielement proportional chamber for double beta-decay expt. 7-25315
neutrinoless double β -decay and lepton flavor violation 7-56468
neutrinoless double β -decay without Majorana neutrinos in supersymmetric theories 7-61839
neutrinoless double beta and 2 ν decays, nuclear structure effects on matrix elements 7-49335
neutrinoless double beta decay, exptl. results and techniques 7-49338
neutrinoless double beta-decay, neutrino mass, interaction properties 7-41947
neutrinoless double beta-decay, ultralow background solar search 7-55393
neutrinoless double- β decay and its relation to piondouble charge exchange 7-600
neutrinoless double-beta decay in supersymmetric theories; R-parity violation 7-35765
neutron-rich transuranic nuclei, beta-decay study 7-49323
nuclear beta-strength and neutrino mass, cosmological and astrophysical consequences 7-48129
nuclear data sheets, recent references May-August 1986 7-35131
nuclear data sheets, recent refs. Jan. to April 1986 7-31
particle and nucl. physics intersections conf., Lake Louise, Canada, May 1986 7-29569
proton-rich and neutron-rich nuclei, β -decay study 7-49324
proton-rich nuclei, superallowed β -decay and axial-vector strength renormalisation 7-49329
pulse ionisation chamber for ¹³⁶Xe double β -decay expt. 7-19631
space electric charge distrib. in surface layer of β -radioactive dielectrics 7-33326
superallowed 0⁺ → 0⁺ decays, electron and heavy neutrino mixing 7-35979
weak and EM interactions, conference, Heidelberg, Germany (July 1986) 7-48172
¹¹⁰Ag → ¹¹⁰Cd, gamma-transitions, multipole mixing ratio anal. 7-49314
¹²³Ag, half life meas. for neutron-rich nuclei 7-5200
²⁶Al, interstellar, near galactic centre, common origin for gamma-ray lines at 0.51 and 1.81 MeV 7-24238
^AAr β^+ decay, A=34, 35, Gamow-Teller resonance calcs. using shell-model wave fns. 7-49334
⁴⁰Ar, inverse β^+ decay for neutrino detection 7-15203
⁴¹Ar, beta-decay, half-life determ. 7-49308
¹²B, aligned nucleus, beta-ray angular distribution anal. 7-5195
⁴⁵Ca beta-decay, longitudinal electron polarization meas., relevance to deviations from parity violation 7-56650
^ACd, A=123,125,127 β -decay level schemes, search for intruder states in ^{123,125,127}In 7-19152
^ACd, A=123-130, strongly neutron rich fusion products, decay props 7-19210
^ACd, A=123-5,127,128, half life meas. for neutron-rich nuclei 7-5200
¹³⁰Cd, β -decay half-life and importance for r-process 7-49319

beta-decay continued

- ¹⁴¹Ce, decay rate meas., in standard solution (*Chinese*) 7-5196
³⁸Cl, β -decay and shell crossing, expt. study and shell model calcs. 7-5199
¹³⁷Cs decays, X- and γ -ray intensity meas. 7-61838
¹⁴⁰Cs, β -decay, ¹⁴⁰Ba levels and transitions, spin assignments, multipole mixing ratios 7-595
¹⁴⁵Cs, β -decay study for intrinsic reflection asymmetry search 7-5198
^ACu, A=74-78, strongly neutron rich fusion products, decay props 7-19210
¹⁴⁸Dy, giant Gamow-Teller excitations populated in β^+ decay 7-49364
¹⁵⁰Er, giant Gamow-Teller excitations populated in β^+ decay 7-49364
¹⁵²Er, radioactivity study using mass-separated sources 7-41945
^AEu, A=152, 154 half-life determ. 7-56642
¹⁷F, beta-ray asymmetry meas., sin θ_v , C_A/C_V limits 7-56647
^AGa, A=77-81, strongly neutron rich fusion products, decay props 7-19210
⁶¹Ge, beta-delayed proton decay 7-41946
⁷⁶Ge double beta decay experiments, review 7-41942
⁷⁶Ge neutrinoless double beta decay, ν mass limits and right handed current calcs. 7-49340
⁷⁶Ge, neutrinoless double β -decay 7-41949
⁷⁶Ge neutrinoless double β -decay, lepton number nonconservation, Milano expt. 7-56644
⁷⁶Ge $0\nu\beta\beta$ -decay, data anal., half-life determ. 7-61841
⁷⁶Ge-⁷⁶Se, neutrinoless, double beta-decay, $0^+ \rightarrow 0^+$ study, prelim. meas. 7-49342
⁷⁶Ge-⁷⁶Se, neutrinoless double beta-decay, limits on lepton number non-conservation 7-49339
³H, atomic effects in low energy β -decay 7-599
³H, beta decay, $\bar{\nu}_e$ mass upper limit 7-56651
³H, beta decay, $\bar{\nu}_e$ mass limit meas. 7-56652
³H beta spectra meas., exclusion of electron energy loss uncertainty in ν rest mass meas. 7-5201
³H beta-decay, molecular effects, neutrino mass determ. 7-49310
³H beta-decay, molecular final-state interactions 7-49311
³H, bound-state β -decay and ν mass meas. 7-56643
³H-¹²⁵I, dual isotope liquid scintillation counting (*Chinese*) 7-5197
⁸He, β -delayed triton emission 7-41950
²⁰³Hg decays, X- and γ -ray intensity meas. 7-61838
^AIn, A=105-108, beta⁺-decay energies determ., Q_{EC} values 7-19209
^AIn, A=123,131, strongly neutron rich fusion products, decay props 7-19210
¹¹¹In, beta-decay, half-life determ. 7-49308
⁸⁵Kr, neutron capture and β -decay, s-process abundances 7-55461
¹³⁸La, beta-decay half-life and dating of gneiss rocks from Scotland 7-49312
⁶Li-⁶He, on A=7-90, 210 MeV, spin-transfer strength probe, Gamow-Teller transitions 7-25003
¹⁵²Lu, identification and radioactivity study using mass-separated sources 7-41945
¹⁸⁰Lu, β -decay, ¹⁸⁰Hf^m fractional population, astrophysical consequences 7-49315
²⁴Mg, charge dependent matrix element between $4^+ T=1$ level and $4^+ T=0$ level 7-601
²⁹Mg, level struct. study, β and gamma decays, shell model comparison 7-49328
⁹⁹Mo beta decay, chemical effects 7-49309
¹⁰⁰Mo double beta-decay meas. 7-49343
¹⁰⁰Mo, neutrinoless double beta-decay, limits on lepton number nonconservation 7-49339
¹²N, aligned nucleus, beta-ray angular distribution anal. 7-5195
¹⁶N-¹⁶O, $0^+ \rightarrow 0^-$ transitions, exchange currents and configuration mixing effects 7-56649
²⁹Na, Gamow-Teller β -decay, shell model comparison 7-49328
¹⁵⁰Nd double beta-decay meas. 7-49343
³²P, induced beta activity determ. (*Czech*) 7-61837
³⁵P, β -decay and shell crossing, expt. study and shell model calcs. 7-5199
²³³Pa, β -decay using HPGe detectors 7-24962
¹⁴⁷Pm beta-decay, longitudinal electron polarization meas., relevance to deviations from parity violation 7-56650
²⁴¹Pu, half-life determ. 7-30380
^ARb, A=94,95, P_n values measured by β - γ spectroscopic method 7-5194
¹⁷Re, half-life determ., relevance to fine-structure const. 7-49345
¹⁰⁷Rh, level scheme study via γ -ray spectrum following β -decay, IBM comparison 7-41944
^AS, A=37, 38, β -decay and shell crossing, expt. study and shell model calcs. 7-5199
³⁰S β^+ decay strength calcs. 7-19198
⁷²Se beta decay energy anal. from ⁴²Ca(p,n) threshold determ. 7-49332
⁷⁹Se^m, stellar β -decay rate 7-49344
⁸²Se double beta decay meas. 7-41941
⁸²Se double beta-decay, 2ν , 0ν , half-life limits 7-49341
⁸²Se, double β -decay, half-life determ. from mineral isotopic composition 7-598
¹⁵¹Sm, neutron capture and β -decay, s-process abundances 7-55461
¹⁰⁰Sr, β -decay, strength function determ. (*Chinese*) 7-10127
^{T₂}, β -decay energy spectra, HeT⁺ electronic reson., and neutrino mass depend. 7-61840
¹⁶⁰Tb-¹⁶⁰Dy, decay investig. 7-49307
¹²⁸Te double beta decay meas. 7-41941
¹³⁰Te double beta decay meas. 7-41941
¹³⁰Te, double β -decay, half-life determ. from mineral isotopic composition 7-598
⁴³Ti, β -decay, expt. and shell model study 7-49331
²⁰⁴Tl beta-decay, longitudinal electron polarization meas., relevance to deviations from parity violation 7-56650
²⁰⁵Tl, forbidden β -decays 7-49320
¹⁵²Tm, low-spin isomer, radioactivity study using mass-separated sources 7-41945
¹⁵¹Yb, β -delayed proton spectrum structure, peaks from N=81 precursors 7-15202
¹⁵²Yb, giant Gamow-Teller excitations populated in β^+ decay 7-49364
¹⁵²Yb, radioactivity study using mass-separated sources 7-41945
¹⁶⁵Yb, β -decay, natural widths meas., neutrino mass determ. 7-49322
¹⁷⁵Yb-¹⁷⁵Lu, gamma-spectra, ¹⁷⁵Lu level anal. 7-49313
^AZn, A=75-80, decay props. and Q_{β} values 7-49318
^AZn, A=75-80, strongly neutron rich fusion products, decay props 7-19210
⁶⁰Zn, β^+ decay Q-value determ. 7-30382

beta-decay theory

- see also beta-decay; beta-ray spectra
 deformed nuclei, Gamow-Teller resonance anal. using quasiparticle-phonon model 7-49333
 double β -decay rates and ν mass calcs. 7-41943
 Fermi decays, verification of conserved vector current and standard model predictions 7-19208
 first-forbidden β -decays, constraints on parity mixing matrix elements from hard pion exchange 7-61836
 Gamow-Teller l-forbidden β -transitions in 2p-1f shell nuclei, lifetimes effects of NN interaction 7-5202
 mixing matrix and CP-violating phenomena 7-476
 neutrinoless double β -decay and lepton flavor violation 7-35728
 r-process, role of delayed neutrons in element production 7-60534
 superallowed β -decay, isospin-mixing corrections to Fermi matrix element 7-56648
 two-neutrino double beta decay, suppression by nuclear struct. effects, matrix elements 7-49316
 Z=56 to 66 neutron-deficient nuclei, nucleon stability, Hartree-Fock method calcs. (*Russian*) 7-30384
 n beta-decay, mag. field effects, spin effects and ν mass 7-41800
 $\pi^+(\Delta^-, \Delta^+) \pi^-$, reaction mechanism anal., selection rule, connection with 2β -decay on $J^P=0^+$ nuclei 7-30454
 $\pi^+(\Delta^0, \Delta^+) \pi^-$, reaction mechanism anal., selection rule, connection with 2β -decay on $J^P=0^+$ nuclei 7-30454
 SU(2)_L×SU(2)_R×U(1) electroweak models, constraints from nuclear beta-decay 7-56489
⁴⁸Ca(O_1^+)-⁴⁸Ti(O_1^+) $0\nu\beta\beta$ decay, uncertainties in nuclear matrix elements 7-49337
⁷⁶Ge, neutrinoless double beta decay calcs. comparison with decay half-life meas. 7-49336

beta-particles see beta-rays

beta-radiation see beta-rays

beta-ray absorption

- see also electron absorption
 No entries

beta-ray angular distribution

- see also beta-ray spectra

- $n \rightarrow p e \bar{\nu}_e$, g_A/g_V meas. from beta-asymmetry meas. 7-35866
¹²B, aligned nucleus, beta-ray angular distribution anal. 7-5195
¹⁷F, beta-ray asymmetry meas., sin θ_v , C_A/C_V limits 7-56647
¹²N, aligned nucleus, beta-ray angular distribution anal. 7-5195

beta-ray detection and measurement

- see also beta-ray spectrometers; radioactivity measurement

- β -emitter coloured samples, liq. scintillation counting, integral counting techniques 7-49783
 anticoincidence counting system, absolute activity meas. (*Korean*) 7-25329
 bioassay procedures for radionuclides for atomic radiation workers 7-8696
 continual scanning record of radioactivity distrib., corrections, smoothing 7-5571
 continual scanning record of radioactivity distrib., corrections, deconvolution 7-5572
 extrapolation chamber for β -ray detect., performance characts. 7-25302
 high resolution β^- digital autoradiography using a single step parallel plate chamber 7-5573
 low-energy β -imaging system for T distrib. meas. 7-42441
 medical beta source radiation charact. meas. 7-54748
 microchannel plate chevron as position sensitive detector for β -spectrometers 7-25313
 multilayer composite material for X-, γ - and β -ray detector windows 7-5570
 MWPC based system for digitizing electrophoretic gels 7-47296
 nondestructive coating thickness meas. 7-13703
 Opti-Fluor and Aqual-2 liquid scintillation cocktails, comparison of counting characts. 7-30835
 proportional chamber, multielement, for ¹³⁶Xe $\beta\beta$ decay 7-42287
 superconducting tunnel junction, β -particle detection by DC Josephson effect 7-30832
 unit of absorbed dose rate to tissue for beta radiation, PTB National Primary Standard 7-28717
 Si microstrip particle detector, low leakage current 7-19667
 Sr concentration determ. in environment, beta-ray counting flow cell 7-30896

beta-ray effects

- see also electron beam effects

- alanines, D- and L-, ⁹⁰Sr-⁹⁰Y- β -irrad., asymmetrical induced yields 7-59929
 carcinogenicity in mice rel. to acute and chronic effects of HTO 7-60053
 DNA repair kinetics after exposure to X-irrad. and to internal β -rays in CHO cells 7-28619
 DNA strand breaks induced by X-irrad. and internal β -rays, 3 classes 7-23408
 embryo, pre-implantation, mouse, radiotoxicity of ³H-thymidine and ³H-arginine 7-60051
 intestinal cell death induced by HTO in mice, obs. using a new ³H safety clean cabinet 7-60054
 mammalian cells, cultured, induction of cell killing, mutation and oncogenic transformation following exposure to tritiated water 7-60049
 myeloid leukaemia induction in animals, expt. designed to meas. RBE of ³H rel. to X-rays 7-60052
 neoplastic transformation, induction by low-dose-rate exposure to tritiated water 7-8664
 quartz, as-grown or Li-, Na-, Cu- electrodiffused, radiation-induced conductivity 7-6691
 somatic mutations induction in Tradescantia, effects of low dose tritiated water and tritium labelled compounds 7-60048
 HTO β -rays, RBE measured by effects on cultured mouse embryos at pre-implantation stage 7-60050
 NaCl positron annihilation parameters, irrad. effects determ. 7-46224
 NaCl, positron annihilation parameters, beta irrad. effects determ. 7-46225

beta-ray polarisation

- beta-decay, Fermi and Gamow-Teller transitions, comparison of beta-ray polarization with SU(2)_L×SU(2)_R×U(1) models 7-35977

beta-ray scattering *see* *beta-ray effects; collision processes; energy loss of particles; particle backscattering; potential scattering; transport processes*

beta-ray spectra

see also *beta-decay theory*

Σ^- -new, electron energy spectrum calcs. with radiative corrections 7-61670

^3H beta spectra meas., exclusion of electron energy loss uncertainty in ν rest mass meas. 7-5201

^3H beta spectra meas., ν_e mass, upper limit determ. (German) 7-35978

^3H beta spectrum, endpoint meas., $\bar{\nu}_e$ mass, upper limit determ. 7-35976

^3H beta spectrum meas., $\bar{\nu}_e$ mass, upper limit determ. 7-35975

T_2 , β -decay energy spectra, HeT^+ electronic reson., and neutrino mass depend. 7-61840

^{60}Zn , β^+ decay Q-value determ. 7-30382

beta-ray spectrometers

see also *beta-ray spectra; electron spectrometers*

β -emitter coloured samples, liq. scintillation counting, integral counting techniques 7-49783

microchannel plate chevron as position sensitive detector for β -spectrometers 7-25313

positron-annihilation apparatus for layerwise analysis of defects in solids 7-39219

Si:Li electron spectrometer for in-beam internal pair spectroscopy 7-49788

Xe, liquid scintillation spectrometer 7-62199

beta-rays

see also *electrons*

No entries

beta spectrometers *see* *beta-ray spectrometers*

betatrons

magnetic circuit temp. distrib. calc. (Russian) 7-42247

magnetically-switched electron injector, operating characts. 7-30794

pulsed power systems for modified betatron accelerator 7-30793

Bethe-Salpeter equation

electromagnetic bound system, Bethe-Salpeter eqn. and approx. soln. (Chinese) 7-24776

few-nucleon systems, relativistic calcs. 7-61843

heavy quarkonia, relativistic corrections to mass spectra 7-19092

many-electron atoms, relativistic HF and RPA calcs. 7-19675

photon dispersion in strong mag. field with positronium formation 7-41690

quarkonia spectra, solving momentum-space integral equations with confining potentials 7-35703

relativistic bound-state problems, running coupling constant 7-399

renormalized forms for connected N-point Green fns. 7-15048

Schrodinger equation, local equivalent, with relativistic kinematics, WKB approximation 7-56406

semiclassical approximation for relativistic potentials for massless particles 7-56441

tensor meson (2^{++}), quasi-free Bethe-Salpeter wave fn. calc. 7-48977

wave function, single-time reduction using causality and spectral props. 7-41639

$\bar{\nu}\bar{\nu}$ system with $J^{PC}=0^{+-}$, 1^{--} , 1^{+-} , 0^{++} , 1^{++} , Bethe-Salpeter wave fn. calcs. 7-48976

$q\bar{q}$ realistic pot. with running coupling constant, fine and hyperfine splitting 7-19068

$^2\text{H}(\mu, ^2\text{H})$, approx. Bethe-Salpeter wavefunctions 7-654

Bethe-Uhlenbeck equations *see* *quantum statistical mechanics*

bevatrons *see* *synchrotrons*

BGO detector *see* *scintillation counters*

BH lasers *see* *semiconductor junction lasers*

Bi-FET integrated circuits *see* *monolithic integrated circuits*

Bi-MOS integrated circuits *see* *monolithic integrated circuits*

bibliographic systems

IAEA/INIS online database 7-42446

Infrared and Raman Spectroscopy Literature Data Base, bibliography 1 October 1984 to 31 May 1986 7-41030

physical sciences databases, new developments 7-24325

bicrystals

β -brass bicrystals, Bauschinger effect, grain boundary contrib. 7-46574

epitaxial metal bicrystals containing grain boundaries, UHV deposition apparatus 7-39390

FCC bicrystals, computer simulation of non-uniform multiple slip (Japanese) 7-51780

grain boundary migration, diffusion induced misorientation depend. 7-21229

grain-boundary melting transitions, mol. dynamics simulations 7-21419

metallic filaments strongly anisotropic 2D system, weak localisation in magnetoresistance 7-45282

metals, grain boundary structure (German) 7-44571

semiconductor bicrystal, diffusion length and grain boundary recomb. vel. determ. by laser excitation 7-41402

shear incompatible, approx. evaluation method for elastic stresses by virtual array of dislocations (Japanese) 7-32841

structurally inhomogeneous boundaries, grain boundary atom diffusion (Russian) 7-16796

TEM, use of symmetry props. for precip. morphology anal. 7-46489

X-ray interferometer, wedge-shaped gap, spherical X-ray wave diffr., interference effects calcs. 7-63398

Al, grain boundary rumpling during sliding 7-2030

Al single cryst. and bicrystal, polygonisation substruct., grain boundary effects (Russian) 7-58287

Al-Ge, TEM anal. of Ge precip. morphology 7-46489

Al_2O_3 , high-purity, grain boundary structures 7-58668

Au, twin boundary struct. determ. of twinned bicrystals, convergent-beam electron diffraction study 7-51786

$\text{BaPb}_{1-x}\text{Bi}_x\text{O}_3$ bicrystals, nature of Josephson tunnel barrier 7-45568

CdTe, polycrystalline, grain boundaries elec. and optical characts. 7-38012

Cu, fatigued at high temp., microstruct. obs. in vicinity of cavitated grain boundaries 7-38019

Cu, isoaxial, with (001) tilt boundaries, dynamic recrystn., effect of grain boundaries 7-17549

Fe-Si (3 wt.%) bicrystals, domain struct. and magnetisation 7-12992

Fe-Si (5.8 at.%) bicrystals, plastic deform., coincident twin boundaries 7-13502

GaP bicrystals, potential barriers of grain boundaries 7-21976

Ge, bicrystal boundaries, transient spectra of dislocation levels 7-52497

bicrystals continued

InSb bicrystals, n-inversion layers, pressure dependence electron states 7-45468

LiF, pore-grain boundary configs., fracture surface, SEM obs. 7-32458

MgO:Fe , small angle [001] twist boundaries, Fe solute effect 7-32459

Nb superconducting bicrystals, flux pinning by symmetrical grain boundaries 7-64419

Nb, superconducting bicrystal, flux pinning by special grain boundary 7-64420

Ru-Ir bicrystal superlattice, stacking struct. and superconductivity 7-2432

Ru-Ir bicrystal superlattices, X-ray and transport studies 7-27159

Si, as-grown and annealed bicrystals, conductance of grain boundaries 7-64245

Si bicrystals, Czochralski growth, tilt boundaries 7-53558

Si bicrystals, grain boundaries, electronic states, transient capacitance spectroscopy meas. 7-7173

Si bicrystals, grain boundary carrier recombination, chemical origin 7-17039

Si bicrystals and thin films, grain boundaries, electronic props. 7-7172

Si bicrystals obtained by solid-phase intergrowth, interface region struct., electron microscopy 7-45023

Si, twin boundary struct. determ. of twinned bicrystals, convergent-beam electron diffraction study 7-51786

B-Ti-Mo, age and quench hardening, effects of cryst. orientation and surface condition (Japanese) 7-22709

Zn-Al, bicrystals and polycrystals, creep grain boundary strengthening 7-22747

biexcitons *see* *excitonic molecules*

big-bang theory *see* *cosmology*

bilinear systems *see* *linear systems; nonlinear systems*

bimetallic strips *see* *bimetals*

bimetallic wire *see* *bimetals*

bimetals

cylinder, temp. fields and residual stresses in cooling 7-33705

film couples, interfacial phase form., in situ annealing X-ray diffr. obs. 7-21705

steel bimetallic plate, cold-clad, diffusion processes in preboundary zone 7-46708

thermostats, stresses 7-35515

Ag-Al film couples, interfacial phase form., in situ annealing X-ray diffr. obs. 7-21705

C steel-cast Fe-Cr bimetal, interface bonding strength (Korean) 7-17618

Cu-Al film couples, interfacial phase form., in situ annealing X-ray diffr. obs. 7-21705

Mo/Inconel 601 bimetallic strips, explosively welded, thermal effects (German) 7-27144

Nb-Pb and Nb-Sn film couples, interfacial phase form., in situ annealing X-ray diffr. obs. 7-21705

binaries (stellar) *see* *binary stars*

binary adders *see* *adders*

binary stars

see also *cataclysmic binary stars; eclipsing binary stars; X-ray binary stars*

accreting binary stars, magnetodynamic jets form. through accretion of rotating magnetised mass 7-55460

active-chromosphere stars, UVB photometry of ten southern objects 7-40830

λ And, RS CVn star, simultaneous IUE and VLA obs. 7-47931

EG And, symbiotic star, mag. field 7-18424

λ And, two-component coronal model for EXOSAT obs. 7-40800

31 Aql, possible pole-on binary system, spectroscopic gravity determ. method 7-4434

UX Ari, RS CVn star, autumn 1981 photoelectric obs. of starspot activity 7-9513

UX Ari, RS CVn star, UHF and SHF obs. 7-66662

BD+13°3683, cool subdwarf, spectroscopic orbit and companion mass 7-40806

BD+37°444, double-lined binary in open cluster NGC 752, orbital elements and mass characts. determ. 7-66677

CK Boo, W UMa star, photoelectric obs. rel. to light curve vars. 7-40870

bright star binaries, statistical props. of systems with evolved primary components 7-29505

ν Car, close visual binary star, spectral and radial vel. study 7-24164

μ Cas, halo binary resolved at 850 nm wavelength 7-14570

V641 Cas, photometry of VV Cep type star 7-18414

α Cen binary system, non-resonance Ca I lines obs. in optical spectrum 7-4444

Cen X-4 (V822 Cen), optical behaviour of X-ray binary star 7-18411

DH Cep, BV light curves of massive close binary 7-18436

Cepheids, classical, companion stars characts. determ. 7-55665

δ Cet, β Cma star, photometric obs. rel. to binary star model 7-4468

5 Cet, ellipsoidal variable star, rot. vel. and mass ratio determ. 7-40878

close binary systems, monochromatic refl. effect and temp. distrib. on distorted surfaces 7-18439

coalescence of two white dwarfs in close binary systems (Japanese) 7-4508

collision probabilities in globular clusters, determ. for head-on binary collisions 7-60739

common proper motion stars in the AGK 3 catalogue, list 7-29413

RS CVn binaries, Ca II H and K emission line analysis 7-40865

RS CVn detached short-period stars, EXOSAT and IUE obs. 7-60723

RS CVn regular-period binaries, Mg II h and k line emission 7-40866

RS CVn stars, H α and Li I obs. of σ Gem, α Aur, HR 6469, and 93 Leo 7-18437

RS CVn stars, photometry and spot models rel. to rot. modulation and flares 7-4467

RS CVn stars, rot. characts., spectral obs. (Chinese) 7-66654

RS CVn stars, rot. vel., spectral obs. 7-60710

RS CVn stars, rot. vels. meas. (Chinese) 7-4503

RS CVn stars, rot.-chromospheric activity relations 7-47993

RS CVn stars, search for 843 MHz radio emission from active stars 7-55671

RS CVn stars, X-ray emission and coronal activities 7-66671

SU Cyg, binary Cepheid, lumin. determ. from IUE spectra 7-55682

SU Cyg, classical Cepheid, possible triple system, components masses and motion, IUE spectral characts. 7-55683

binary stars continued

- 16 Cyg A and B, solar analogue candidates, absolute magnitudes and luminosity-related parameters 7-24162
degenerate dwarfs produced by interacting binaries; number-mass distrib. 7-60652
double degenerate C-O dwarfs, evolution rel. to type I supernova rates in solar neighbourhood 7-24155
double stars, lunar occultations, photoelectric observations, final list 7-35003
BY Dra stars, photometry and spot models rel. to rot. modulation and flares 7-4467
ε Eri, age determ., implications of possible binary nature 7-66579
formation, two-body tidal capture of main sequence stars and white dwarfs 7-4500
formation by tidal capture, cross-sections for binary form- and stellar merger 7-29519
σ Gem, X-ray spectrum of RS CVn type binary 7-60728
general relativistic eqns. of motion for extended bodies 7-4510
Gliese 268, M dwarf double-lined binary, Digicon obs. 7-40875
gravitational wave emission from 2-neutron star binary coalescence, and Hubble const. determ. 7-9559
gravitational wave radiation, enhanced emission from perturbed wide binary stars 7-60730
hard binary, scatt. of third body, approx. 7-48000
HD 1383, massive double-lined spectroscopic binary star, spectroscopic orbits determ. 7-4523
HD 149162 system, orbit and props. from radial vels. and photometry 7-47978
HD 17198A, spectroscopic binary, orbital characts. and mass ratio, radial vel. anal. 7-55723
HD 1826, single-lined spectroscopic binary, photometric variability detect. 7-40871
HD 191765, Wolf-Rayet star, precessing neutron star companion model for light vars. 7-66615
HD 45166 (qWR+B8 V), obs. of gross UV spectral variability 7-47945
HD 50896, WR star, spectrophotometry and binary nature 7-55663
HD 55510, double-lined spectroscopic binary, orbital elements from photoelectric radial vels. 7-4518
HD 96008, close binary or pulsating star, nature uncertainty, photometric obs. 7-60715
hot H-deficient binaries as Type Ib supernovae progenitors 7-24154
HR 3562, HR 3600, short period B-type variables, photometric obs. and identification as ellipsoidal variables 7-47854
HR 5110, RS CVn star, UHF and SHF obs. 7-66662
HR 6902, composite-spectrum star, spectral types, orbital elements and mass ratio determ. 7-66674
HR 8107, new bright Be star, H α and UVB obs. 7-24152
interacting binary stars, IUE obs. rel. to evolution and models 7-47997
IRAS 1912+172P09, new binary planetary nebula, spectroscopy and JHK photometry 7-48046
HK Lac, RS CVn star, long-term light vars. obs. rel. to starspots distrib. 7-60724
late-type dwarfs, radial vel. meas. rel. to binary nature 7-9516
low-mass close binary stars, evolution with orbital ang. momentum losses 7-24121
mass anomalies of close binaries, due to metallicity and evolution and not to observational errors 7-40877
mass ratios distrib. 7-55721
mass transfer in close binary systems, particles ejection owing to sudden increase in initial vels. (*Chinese*) 7-4502
mass transfer in eccentric orbit binary systems, numerical simulations 7-14609
massive close binaries evolution with mass loss and overshooting, mass transfer in very massive system 7-29465
AT Mic, dMe star, UV and visible obs. 7-47934
MS-type stars, search for white dwarf companions, UV spectral obs. 7-47935
nearby wide binary systems, catalogue rel. to search for planetary systems 7-66480
in NGC 346, young open cluster in SMC, radial vel. study 7-48002
NS 105-67, massive double-lined O-type binary in LMC, spectroscopic obs. 7-55711
numerical method for models of double white dwarf binaries and central white dwarf-heavy disk systems 7-60573
observational characts. (*French*) 7-29510
in open clusters, influence on dynamical evolution of N-body clusters 7-55748
open clusters, RS CVn stars and blue stragglers 7-60741
α Ori, long-term spectroscopic monitoring by IUE rel. to close stellar companion 7-47877
4=σ Ori, MS star, white dwarf companion detect. and characts., UV spectra anal. 7-55681
II Peg, RS CVn binary, photometric study (1980 to 1985) 7-4513
II Peg, RS CVn star, 1986 JK photometry and light curves 7-4515
II Peg, RS CVn star, large amplitude spot var. 7-47984
II Peg, RS CVn star, UHF and SHF obs. 7-66662
AG Peg, symbiotic star, mag. field 7-18424
EZ Peg, UVB photometry of RS CVn star 7-9517
II Peg (=HD 224085), light curve of active chromosphere star 7-66612
ks Per and hot H-deficient binaries as Type Ib supernovae progenitors 7-24154
planetary motion about nearby binary stars, restricted elliptical three-body problem 7-29517
planetary nebulae binary nucleus, influence on structure 7-55757
pole-on binary systems, spectroscopic gravity determ. method and appl. to 31 Aql 7-4434
proper-motion stars, binary fraction from radial vel. obs. 7-47844
PSR 1855+09, white dwarf companion star of binary millisecond pulsar 7-29500
PSR 1855+09 discovery 7-60702
PSR 1913+16, binary pulsar, proper motion determ. from periastron times 7-55696
PSR 1937+214, 1.5 ms pulsar, evolution in precursor binary system 7-29499
pulsars, origin in binary systems 7-47963
Sanduleak -69°202 (SN 1987A progenitor), possible double nature 7-66634
semi-detached close binary star, mass transfer and accretion disk model 7-60727
16 Ser, binary Ba star, heavy element abundances 7-60680

binary stars continued

- CV Ser, WC8 star, wind modelling, C III UV and visible spectra anal. 7-66625
W Sgr, binary Cepheid, lumin. determ. from IUE spectra 7-55682
V4046 Sgr, T Tau star, UV and visible obs. 7-47869
ν Sgr and hot H-deficient binaries as Type Ib supernovae progenitors 7-24154
SN 1987A in LMC, multiple nature of progenitor star, (Sanduleak -69°202) 7-66636
SN 1987A in LMC, optical spectra, radiobrightness and double nature of progenitor 7-66634
spectroscopic binaries and blue stragglers in open cluster M67, spatial distrib. 7-40872
spectroscopic binary stars, vel. amplitude vars. rel. to freq. of triple and multiple systems 7-55708
spectroscopic binary stars of spectral types B0 to B9, search for H α emission 7-35005
stability of a hypothetical binary at the galactic center 7-55793
Sun, limiting orbital radius set by Galaxy from King-Innanen formula 7-4357
supermassive binary system in Seyfert galaxy NGC 5548, evidence from double broad-line emitting regions 7-66756
supernovae origin (book) 7-60914
V711 Tan (HR 1099), radio emission from starspots on RS CVn binary 7-55725
V711 Tau, RS CVn star, UHF and SHF obs. 7-66662
V711 Tau, RS CVn system, long-term vars. of chromospheric, transition-region and starspot activity 7-47995
V711 Tau (HR 1099), H α line obs. of bright RS CVn system 7-40873
three-body problem, elliptic restricted case, critical orbits, appl. to planets in binary systems 7-23979
ultrashort period binary stars in globular clusters, form. mechanism 7-66667
DM UMa (BD+61°1211), H α line obs. of single-lined RS CVn system 7-40873
RR UMi, semiregular variable in binary system, revised spectroscopic orbit 7-4520
Van Biesbroeck 8, IR speckle interferometry rel. to binary nature 7-66587
VB 8, comparison discovery and nature 7-55722
α Vir (Spica), uvby photometry 7-40823
visual binaries, angular momentum-mass relation and mass ratio distrib. 7-18432
visual binary stars, mass ratios from photographic astrometry 7-4296
visual binary stars, orbital elements for 20 systems 7-4507
visual double stars, obs. by 'old generation' observers, errors statistical anal. 7-14602
visual double stars, orbital elements for six pairs (*French*) 7-18430
visual double stars, orbital elements for twenty-one pairs 7-18431
PU Vul, peculiar symbiotic star, binary characts. and spectral obs. (*Chinese*) 7-4460
white dwarf in wide binaries, physical props., from multichannel spectro-photometry 7-14566
white dwarf star collapse in binary star systems, to form neutron stars 7-60704
white dwarfs in wide binaries, double degenerates and composite spectra 7-14567
wide binary radio pulsar systems, white dwarf masses determ. 7-60733
wide binary stars, theoretical implications of observational data 7-66664
wide binary stars in solar neighbourhood, dynamical fate 7-66663
Yale Bright Star Catalogue, duplicity search, ICCD speckle obs. 7-47973
CN-strong stars, origin due to binary coalescence 7-66601
D, synthesis in stellar atm. in binary systems with accretion disks (*Russian*) 7-24218
Fe and s-process isotopes from binary stars 7-47835
HD 96342, spectroscopic binary orbit from photoelectric radial vels. 7-24166
He degenerate dwarf form. in close binary system 7-60633
He stars, evolution of single and binary stars of 2.5 M $_{\odot}$ up to Ne ignition 7-4430

binding energy

- see also *lattice energy; nuclear binding energy*
N- acetylacrylate complexes with lanthanide cations, struct., ¹³C NMR and PMR (*French*) 7-19883
acetylene, binding energies, ab initio HF calcs. 7-49894
actinide metals, solid state and thermodynamic props., f-electron bonding and struct., review 7-12321
alkali cyanides, multipole interaction effects on cohesive and anharmonic props. 7-1942
alkali halides, interionic potentials based on charge transfer model 7-58197
alkali metals, structural properties, ab initio calc. 7-21156
alloys, binary, short range order, coherent pot. approx. 7-7142
anion-water complexes, struct. and binding energy, ab initio study 7-15483
atomic relativistic bound-state energies determ. extremum principles 7-868
bacteriochlorophyll a, config. for photosynthesis, SCF HF INDO calcs. 7-858
BAs, structural and electronic props., pseudopotential method, local density approx. 7-32353
chloroferrocenes, ionisation pot., electron impact study 7-20062
cohesion of solids under very high electronic excitation 7-51696
cohesive props., effective medium approach 7-45201
collisional sputtering theory 7-64847
crystalline solids, electrostatic Madelung and cohesive energies 7-44442
cyanogen, adsorption on Pd (100), Penning ionisation electron spectroscopy, UPS, TPD studies 7-52268
d-band metals, binding force, effective interatomic pots., strong scatt. open shell metals 7-32262
diatomic mols., mass-vel. corrections, relativistic kinetic energies 7-10452
dimethyl methylphosphonate, Auger and photoelectron spectra 7-57132
disaccharide maltose monohydrate, water binding modes, TSC meas. 7-38997
double core vacancies, energy calcs. 7-36450
effective medium approach 7-45201
electrostatic lattice energy, crystal lattice of point charges 7-51697
ethane-Ar, vibr. predissoc. IR spectra 7-19971

binding energy continued

- bidentate ethylene diamine complexes with ions Na^+ , Li^+ and H^+ , ab initio MO calcs., binding energy 7-10383
- exciton-phonon interactions, integral operator method, anal. (*Chinese*) 7-12612
- excitonic molecules, binding energies 7-16947
- ferromagnetic semicond., donor state, thermally induced abrupt shrinking 7-52510
- fluorite struct. crystals, phys. props., effective pot. calcs. 7-26692
- fluorite-type AB_2 crystals, cohesive energy and thermodynamical props. 7-51692
- graphite, single cryst., synchrotron radiation-excited angle-resolved photoemission 7-17391
- heavy electron Fermi liquids, Hubbard model anal., similarities to ^3He 7-2522
- ionic solids, overlap interactions and bonding 7-1940
- ionic solids, stabilisation of CsCl versus NaCl struct., ab initio pseudopotential calcs. 7-58199
- ionisation phenomena, ab initio wave functions 7-36444
- metal clusters, ionisation phenomena, ab initio wave functions 7-36444
- metal surfaces, field adsorption of rare gases 7-21648
- metal surfaces, plasmon effects on image states 7-7309
- methane, binding energies, ab initio HF calcs. 7-49894
- muonic complexes with atoms and molecules, chem. stability calcs. 7-36827
- muonic mols., three-body problem, generalised exponential expansion, binding energy calcs. 7-15747
- oxides, rutile-type, dipole polarisabilities, cohesive energies and press. derivatives of bulk moduli 7-2967
- perfluorobenzene, electron transfer reaction kinetics, binding energy role 7-22989
- perfluoromethylcyclohexane, electron transfer reaction kinetics, binding energy role 7-22989
- polarons, small radius, effective mass studies 7-38465
- positronic complexes with atoms and molecules, chem. stability calcs. 7-36827
- positronium, in ethane gas, cavities rel. to orthopositronium annihilation rates 7-36824
- pyridine chemisorption on oxidised Fe surface, XPS 7-27128
- pyrrole chemisorption on oxidised Fe surface, XPS 7-27128
- quasi-one-dimensional electron gas, screened hydrogenic impurity, binding energy 7-52508
- rare earth metals, ground and excited state props., local density total energy calcs. 7-7141
- Rydberg formula, revised for two-electron $[\text{core}]n\text{s}^2$ systems, binding energy calcs. 7-25435
- selenides, binding energy, XPS investig. 7-5720
- slurries, clay-rich, cohesion energy 7-66105
- solid surfaces, chemisorpt. of atoms binding energy, sum rules 7-16868
- sp-bonded nonmetal solids, cryst. stability and structural transition press., total-energy minimisation, tight-binding calcs. 7-2190
- sputtering, slow collisional, surface binding energy 7-59329
- sputtering yield meas., role of surface binding energy 7-59361
- substrate size, effect on adsorption binding energy 7-38339
- tetrahedral molecules, hybrid orbitals with d-character 7-56940
- transition metal surface, chemisorpt. of H, binding energy, sum rules 7-16868
- transition metals and their alloys, mag. atoms, quantum statistical ab initio theory 7-58969
- trimethyl phosphite, Auger and photoelectron spectra 7-57132
- trimethylsilylium + O_2 (aromatic bases), assoc. binding energies meas., mass spectra 7-54096
- vacancy-impurity atom binding energy; solidus condition 7-44602
- XPS, UPS, work function meas. 7-12485
- Ag (110), adsorption of ethylene and ethylene oxide, work function, LEED, UPS, TDS meas. 7-52270
- Ag alloys, dil., EFG, asymmetry parameter calcs. 7-2545
- Ag, binding energies and elastic constants, one-parameter model pseudopotential calc. 7-44650
- Ag monolayers, electronic struct. and binding energy, substrate effects, photoemission studies 7-39359
- Ag surface, binding energy of image-potential states 7-64303
- Al, chemisorption, interaction of atoms and mols. with surfaces, cluster approx., total energy calcs. 7-52265
- Al, hot dense plasma, at. props. and transition probabilities 7-57032
- Al-polyacrylic acid interface, reactivity, comp., XPS 7-28334
- Al-polyethylene interface, reactivity, comp., XPS 7-28334
- AlAs, energy bands, cohesive energy, form. energy, self-consistent calcs. 7-21995
- AlN, electronic struct., first principles LCAO calc. 7-21813
- AlSb, hot electron luminesc. 7-46119
- Ar, photoionisation, photoelectron and electron momentum spectroscopy 7-36560
- As_2Se_3 , crystalline, electronic and geometric struct., ab initio total-energy calcs. 7-12607
- As_2Se_3 single crystals, geminate pair recomb., photocond., photoluminescence meas. 7-38581
- Au alloys, dil., EFG, asymmetry parameter calcs. 7-2545
- Au, binding energies and elastic constants, one-parameter model pseudopotential calc. 7-44650
- Au core holes, final-state screening, total energy calcs. 7-2526
- Au, epitaxial growth on W (100), adsorbate props. 7-38329
- BaO , self-consistent electronic structures. 7-32910
- $\text{BaPb}_{1-x}\text{Bi}_x\text{O}_3$, electronic struct., photoemission studies 7-59375
- Be_{13} and Be_{55} , stability and struct., binding energy, ionisation pot. 7-11988
- Bi chalcogenides, binding energies, chem. shifts XPS and diffuse refl. spectra (*German*) 7-1943
- CO adsorbed on Pt, vibr. spectrum, electrochemical pot., stark tuning rate 7-10570
- CO, chemisorbed, bonding, comment and reply 7-12472
- CO, chemisorbed, ionisation phenomena, ab initio wave functions 7-36444
- CO monolayer on Si (111), electronic props., pseudofunction method calcs. 7-2659
- CaO , self-consistent electronic structs. 7-32910
- $\text{Cd}_{1-x}\text{Hg}_x\text{Te}$, band gap collapse, effects of Hg 5d electrons 7-64075
- CdS surface rhodamine B mol. adsorpt. kinetics, binding energy determ. (*Russian*) 7-21667
- CdSe , $\text{Te}_{1-x}\text{Se}_x$, bound excitons, thermal dissoc., photoluminescence, reflectivity meas. 7-46122

binding energy continued

- Ce, core and valence photoemission, calc. 7-33516
- $\text{Ce}_2\text{La}_{1-x}\text{Cu}_x$, electronic states, resonant photoemission study 7-53496
- Co (II) dithiocarbamates, X-ray photoelectron spectra 7-50256
- Cs surface, adsorbed Xe, core-electron binding energies, photoemission studies 7-3146
- Cu (001), surface electronic struct., relativistic effects, high resolution angle-resolved photoemission study 7-52723
- Cu (111) surface electronic struct., perturbations induced by adsorption of K 7-52720
- Cu, binding energies and elastic constants, one-parameter model pseudopotential calc. 7-44650
- Cu II complexes, dibenzylidithiocarbamate copper, bonding, XPS 7-19950
- Cu surface, binding energy of image-potential states 7-64303
- Cu, vacancy formation enthalpy, positron annihilation studies 7-7787
- Cu-like heavy positive ions, binding energy and electron density, relativistic Thomas-Fermi theory 7-49923
- Cu_n^- ($n=1-10$), cluster, photoelectron spectra 7-62561
- D_2 , solid, ground state energy in LOCW method 7-52181
- Fe (111), CO_2 adsorption and dissociation, ARUPS 7-63961
- α -Fe, dislocation pair jog, energy characts., mol. dynamics method anal. (*Russian*) 7-32440
- α -Fe, H-H binding energy, lattice location and heat of formation 7-32361
- Fe-base alloys, interstitial impurity-dislocation binding energy (*Russian*) 7-58310
- Fe-H system, electron and neutron irradi., positron lifetime meas. 7-44603
- Fe-H system, H-defect interactions study by positron annihilation 7-38046
- Fe-W (110), spin-resolved photoemission spectra of epitaxial Fe layers 7-46276
- Fe_{13} clusters, icosahedral and cubo-octahedral coordination, electronic struct., first-principles method calcs. 7-45132
- $\text{Fe}_{80}\text{B}_{20}$ ribbons, amorphous and crystallised, surface comp., electronic props., topography, AES, XPS, ion scatt. studies 7-27065
- $(\text{Fe}_{1-x}\text{Co}_x)_{78}\text{Si}_{12}\text{B}_{10}$ amorphous alloys, density of states, XPS studies (*Chinese*) 7-13320
- $\text{Ga}_{0.8}\text{Al}_{0.2}\text{As}$ - GaAs - $\text{Ga}_{0.8}\text{Al}_{0.2}\text{As}$ quantum well structs., electroluminescence spectra, model 7-33365
- $\text{Ga}_{1-x}\text{Al}_x\text{As}$ - GaAs - $\text{Ga}_{1-x}\text{Al}_x\text{As}$ quantum well, donor ion dielec. response 7-45417
- GaAs, energy bands, cohesive energy, form. energy, self-consistent calcs. 7-21995
- GaAs quantum-well wire hydrogenic impurity state binding energy and lowest exciton state lum. efficiency calc. 7-2683
- GaAs/AlGaAs superlattices, hydrogenic impurity ground level wave function calcs., variational procedure 7-12664
- GaAs-AlAs superlattices, 2D excitons, magneto-optical study (*Japanese*) 7-13139
- GaAs-AlAs superlattice, energy bands, cohesive energy, form. energy, self-consistent calcs. 7-21995
- GaAs- $\text{Ga}_{1-x}\text{Al}_x$ multiple well heterostructures, far IR absorpt. by shallow donors 7-45458
- GaAs- $\text{Ga}_{1-x}\text{Al}_x$ quantum wells, interband photocond. and excitonic Landau level transitions in mag. field 7-27390
- GaAs- $\text{Ga}_{1-x}\text{Al}_x$ quantum well structures, energy spectra of donors and acceptors, spatially dependent screening effects 7-45459
- GaAs- $\text{Ga}_{1-x}\text{Al}_x$ quantum well, hydrogenic donor low-lying excited states, reson. states, positions and widths 7-45460
- GaAs- $\text{Ga}_{1-x}\text{Al}_x$ undoped quantum wells, excitonic spectrum, valence band coupling and Fano resonance effects calcs. 7-27256
- $\text{GaAs}_{1-x}\text{Al}_x$ MQW, MOCVD grown, excitons, photoluminescence spectra 7-38702
- p-Ge:B(Al)(Ga)(In), annealing kinetics of radiation defects, influence of impurity binding energy 7-39547
- GeO, thermal donor binding energies 7-16989
- H_2 , solid, ground state energy in LOCW method 7-52181
- $(\text{HF})_3$, vibr. predissoc. IR spectra 7-19971
- $(\text{H}_2\text{O})_n$, clusters, charge transfer interaction investigated using ab initio MO theory, binding energy calc. 7-5809
- He, binding energies on simple metal surfaces, van der Waals energy 7-38663
- ^3He , liq., Fermi hypernetted chain calcs. 7-52174
- ^3He , liquid, binding energy, many-body correlations 7-6910
- HfPt, electronic struct. calcs. 7-45200
- Hg-Au, core holes, final-state screening, total energy calcs. 7-2526
- p- $\text{Hg}_{1-x}\text{Mn}_x\text{Te}$, highly doped, ground state of shallow acceptor 7-7167
- I, X-ray photoelectron and Auger electron spectrosc. 7-5647
- ICI-Ne, A, E and X states, binding energies, optical-optical double reson. 7-62425
- KCl-KBr mixed crystals, cohesion, harmonic and anharmonic props. calcs. 7-51907
- $\text{K}_{0.3}\text{MoO}_3$, electronic struct., UPS study 7-53499
- $\text{K}_{0.9}\text{MoO}_{17}$, electronic struct., room temp. UV photoemission spectra study 7-46272
- Li_n clusters, $n=2$ to 13, electronic struct. and magic numbers, LCAO-Xa calcs. 7-31206
- $\text{LiW}_2\text{O}_6\text{F}$, ordered O-F distrib., NMR, Raman spectra, electrostatic energy, site pot. calcs. (*French*) 7-32390
- Mo-H system, neutron irradi., H-void interactions 7-44604
- N_2^+ , Rydberg electron binding energy, UPS 7-872
- NO dimer, ionisation phenomena, ab initio wave functions 7-36444
- NO_2 amorphous insulator, Ar^+ sputtering, ang. distrib. and energy spectra study 7-27848
- Na, BCC, cohesive energies of solids, soft-core Thomas-Fermi pseudopot. 7-21845
- Na clusters, at. desorpt. energies determ. 7-15787
- NaF, thermal hopping of μ^+ between $\text{F}_\text{u}\text{F}$ centres 7-45903
- NaMoO_3F , ordered O-F distrib., NMR, Raman spectra, electrostatic energy, site pot. calcs. (*French*) 7-32390
- $\text{Na}_2\text{WO}_4\text{F}$, ordered O-F distrib., NMR, Raman spectra, electrostatic energy, site pot. calcs. (*French*) 7-32390
- Ni (100), (111) and (110), N_2 chemisorption, molecular cluster calcs. 7-52280
- Ni (100), S-covered, adsorption of NO 7-6990
- Ni (110), valence band satellite, obs. in photoelectron spectra 7-59377
- Ni films, adsorption of benzonitrile and alkyl cyanides, XPS 7-52288
- Ni, single and multiple defect props., mol. dynamics simulations 7-12060
- Ni:B(s), grain-boundary cohesion, impurity segregation effects, density-functional cluster model calcs. 7-44835

binding energy continued

- Ni-GeCl₄, binding energy rel. to Ni chem. state, XPS 7-17820
 Ni-P metallic glasses, electronic struct., XPS study 7-39357
 Ni_{100-x}Zr_x metallic glasses, H storage, press.-conc. isotherms, site occupation, binding energies 7-58153
 P-containing compounds, Auger parameters and relativistic Dirac-Fock atomic calcs. 7-15651
 Pd (111), high resolution inverse-photoemission study 7-17357
 Pd clusters in C matrix, electronic and struct. studies by EXAFS and XANES 7-17363
 Pd clusters on substrates, core-electron binding energy, photoemission initial and final state effects studies 7-27859
 Pd, evaporated on CdTe, core level electron binding energy shifts, photoemission spectra 7-22451
 Pd films, adsorption of benzonitrile and alkyl cyanides, XPS 7-52288
 Pd surface, adsorbed Xe, core-electron binding energies, photoemission studies 7-3146
 S-containing compounds, KLL Auger and core level photoelectron shifts, binding energy 7-15647
 SF₆, electron transfer reaction kinetics, binding energy role 7-22989
 SeGa₃, band struct., coupling energy (*Russian*) 7-58732
 Se film grown by hot wall epitaxy, XPS 7-7821
 SeO₂, binding energy, XPS investig. 7-5720
 Si (111) with adsorbed Ge, X-ray standing wave studies 7-58629
 Si, energy calcs. using four-centre integrals 7-27227
 Si, self-consistent band struct. and total energy, Shaw pot. calcs. 7-32909
 Si surfaces, (111) and (100), chemisorption of halogen atoms 7-6979
 Si:O, thermal donor binding energies 7-16989
 Sn complexes, ESCA, Mossbauer and IR spectrosc. investig. 7-5678
 TaC_x, defect states, core level binding energy and valence band struct., XPS meas. 7-27291
 TaC_x, substoichiometric, core-level binding energies and valence-band struct., XPS 7-22450
 TaIr, electronic struct. calcs. 7-45200
 (TaSe₄)₂I, electronic struct., positron annihilation and UPS study 7-53500
 (Ti,Ta)₂O₃ solid solns., chem. shift and cryst. field splitting rel. to valence charge, EXAFS 7-27818
 Ti+He⁺(Li⁺)(H⁺), inner-shell ionis. polarisation effect, variational wave fn. calc. 7-62491
 TiN compound layer prepared by ion implantation, XPS and FTIR obs., depth profile analysis of ion etched samples 7-59373
 TlI, excitons, band struct., polarised refl. spectra 7-27738
 TlI, X-ray photoelectron and Auger electron spectrosc. 7-5647
 W (110), adsorption of Cu, Ag and Au, calcs. based on nonadditive effective binding pot. 7-12483
 W surface, He fluid adsorption and diffusion, atom-probe field ion microscopy studies 7-32808
 WOs, electronic struct. calcs. 7-45200
 Xe photoionisation, photoelectron and electron momentum spectroscopy 7-36560
 Zn II complexes, dibenzylthiocarbamate zinc, bonding, XPS 7-19950
 ZnSiP₂ cryst., exciton absorpt. spectrum, energy gap and exciton binding energy determ. 7-2500

Bingham plastics and solids *see rheology***bioacoustics**

- see also biological effects of acoustic radiation; biomedical ultrasonics; hearing; sonar*
 attenuation and speed of ultrasound in lung: dependence upon frequency and inflation 7-28596
 attenuation measurement uncertainties caused by speckle statistics 7-8647
 bat acoustic signal analysis 7-18001
 bat echolocation calls, non-stationary signal modelling 7-16034
 bat sonar perception systems 7-47131
 bat-like sonar signals, sensitivity of Doppler tolerance 7-47130
 bats, sonar evaluation in natural environment 7-18002
 beluga whale, target detection using surface-reflected path 7-54621
 bioprosthetic heart valves, computer simulations of closing sounds 7-34343
 body fluid bubble oscillations 7-65780
 bovine tissue, variation of US backscatter with pathology 7-54675
 cardiac isovolumetric contraction, 1st heart sound 7-54424
 chest auscultation, reduction of heart sounds from lung sounds by adaptive filtering 7-54685
 digital signal acquisition, analysis and synthesis, microcomputer based system, PAL 7-54817
 digital signal processing in studies of animal acoustical communication, including human speech 7-50854
 echo delay discrimination by bats, phase evaluation in hypothetical receivers 7-47133
 egg white, freq. dependence of US absorption 7-54674
 femur, dose dependent lathritic, variation of sonic plesio-vel., rabbit obs. 7-65810
 fish swimbladder, nearfield acoustics 7-65779
 frog muscle, US vel. fluctuation meas. 7-23395
 liver, acoustic nonlinearity and sound speed, use for composition estimation 7-47157
 liver, pulsed finite-amplitude US passing through, harmonic distortion development 7-34190
 liver acoustic attenuation estimation using zero-crossings technique 7-23397
 mode conversion at biological media interface 7-18012
 muscular contraction, healthy and diseased human, sounds prod. 7-23508
 nonlinearity parameter meas. using nonlinear interaction of sound waves (*Japanese*) 7-50883
 pipistrelle bat, detection of normal and reversed replicas of its sonar pulses 7-3804
 prosthetic heart valves, Ionescu-Shiley, freq. anal. of closing sounds 7-28770
 Riccati equations describing impedance relations for forward and backward excitation in the one-dimensional cochlea model 7-65765
 serum albumin solutions, bovine, US absorption in freq. range 60 to 160 kHz 7-47154
 signal spectral analysis in noise 7-16035
 soft tissues, human, US attenuation meas. device (*Chinese*) 7-28783
 sounds, source levels, and associated behavior of humpback whales, Southeast Alaska 7-8608
 speech, traveling waves in the vocal tract 7-62921
 third heart sound in children, spectral anal., comparative study of max. entropy method and FFT 7-65818

bioacoustics continued

- tibia state alteration during antiorthostatic hypokinesia 7-34181
 tissue characterization, freq. dependence of backscattering coeff. 7-34191
 tissue composition prediction from in vitro US meas., expt. apparatus 7-14173
 tissue ultrasonic reflection simulation model 7-8648
 trachea noise biofeedback device to help reduce bronchospasm in asthmatics 7-8754
 UHF field exposed biological systems, acoustic effects, phys. modelling 7-40211
 ultrasound image texture via generalised Rician statistics, tissue signatures 7-47184
 US backscatter in the presence of phase distortion, method for quantitative estimates 7-60033
 wind instruments, aerodynamic analysis of playing methods 7-54645

biocommunications

- see also biocybernetics; hearing; learning systems; speech*
 brain, mouse, left hemisphere advantage for recognising US communication calls 7-54607
 digital signal processing in studies of animal acoustical communication, including human speech 7-50854
 vocal tract resonances in oscine bird sound prod.: evidence from birdsongs in a He atm. 7-47126

biocontrol

- see also biocommunications; biocybernetics*
 antagonist muscles, elec. stimulated, control algorithms testing, cat model, neural prosthesis appl. 7-8770
 arterial pressure, mean, computer control with Na nitroprusside: adaptive model-based system 7-40359
 conference on bioengineering, New Haven, CT, USA (March 1986) 7-16
 dynamics of the transcappillary fluid and plasma protein exchange 7-65729
 electrical stimulation open-loop control of human knee during swing 7-28763
 electrooculographic control system. discrete, for severely handicapped persons 7-8736
 EMG feedback and motor control restoration, controlled group study of 12 hemiparetic patients 7-13984
 eye: convergence insufficiency, fixation disparity, and control systems anal. 7-8567
 functional elec. stimulation hand grasp orthoses, tracking performance 7-28777
 functional neuromuscular control schemes for the upper limb 7-3748
 grasp control during functional neuromuscular stimulation, force/position feedback 7-28764
 haemodynamic control systems, closed loop identification 7-60027
 heart, artificial, adaptive control technique, rel. to blood press. and flow 7-3933
 heart rate and blood press., closed-loop identification of beat-to-beat interactions 7-8640
 interstitial microwave antenna hyperthermia system, power deposition pattern control 7-8677
 joint angle control of human arm, constraint. anal., model 7-23375
 joint angle sensors for closed-loop control of movements in paraplegics 7-28766
 locomotor movements, human, aspects of regulation 7-40181
 microvessels, flow control coordination by intercellular cond. 7-65797
 multi-jointed limb movement and posture control, simulation studies 7-65784
 myoelectric control, amplifier input impedances 7-3937
 myoelectric elbows proportional control mode selection, cocontraction approach 7-28776
 myoelectric signal of elec. stimulated muscle during recruitment, rel. to closed-loop control 7-3777
 neuromuscular motor control system (*Japanese*) 7-13982
 paralysed limbs, joint angle control by using functional electrical stimulation with digital PID control system (*Japanese*) 7-60128
 planar musculoskeletal model for studying posture induced by functional neuromuscular stimulation 7-28574
 posture control system, max. likelihood identification 7-60022
 posture-control system, selection of perturbation parameters for identification 7-28561
 renal filter control, system dynamics model 7-40201
 saccadic eye movements, time-optimal control 7-59978
 shoulder position evaluation for quadriplegics using neural prosthetic devices 7-28779
 smooth pursuit eye movement, control characts., model (*Japanese*) 7-47040
 stance phase control of above-knee prostheses: knee control vs. SACH foot design 7-54812
 systems analysis of respiratory control (*Japanese*) 7-14033

biocybernetics

- see also artificial intelligence; brain models; learning systems; man-machine systems; neural nets*
 genetic information encoding, cybernetics and genetic engineering 7-60924
 instrumentation prospects and problems 7-18087
 neocognitron, biocybernetic approach to visual pattern recognition 7-57258

biodiffusion

- electron transport, role of phys. parameters in regulation: diffusion, collision and complex form. 7-17964
 haemorheology, effect of couple stresses on unsteady convective diffusion in fluid flow through a channel 7-3811
 lens, rabbit, ageing, in vivo quasielastic light scatt. obs. 7-28500
 mitochondrial electron transport, diffusion and collision rel. to random collision model 7-17963
 nerve cell, membrane pot. clamping, cyclic nucleotide injection, intraneurone information processing 7-8527
 palmitic acid methyl ester, spin probe in adipose tissue, field gradient EPR 7-13962
 perforated membranes, diffusion 7-65717
 phospholipid monolayers, translational molecular diffusion, substrate coupling and phase transitions 7-8509
 plant cell membranes, water movement, cell wall deform., cooling effect 7-8525
 platelet diffusivity in flowing blood, fluid shear as a possible mechanism 7-28552
 platelets, human, lateral diffusion of lipid probes in surface membrane, ELDOR obs. 7-8526

biodiffusion continued

- protein crystal growth, convective diffusion in parent soln. 7-23287
 quaternary gas diffusion between alveolar and blood compartments, simulation 7-54508
 stratum corneum, lipophilic pathway, Fourier transform IR spectroscopy studies 7-54510
 structured media, diffusion, theory 7-17965
 O₂, myoglobin-facilitated diffusion, anoxia reduction 7-28484
 Rn, diffusion effects on tissue microdistribution, CR-39 autoradiography study 7-54731

bioelectric phenomena

see also *bioelectric potentials; biomagnetism*

- agar phantom electrically adaptable for tissue simulation in 5-40 MHz range, hyperthermia cancer treatment 7-65713
 air ions, biological significance 7-28496
 airway smooth muscle responsiveness to elec. field stimulation, K⁺-induced alterations 7-8548
 alternating electric field, model for action on a human 7-34187
 anaesthesia for surgery, prod. by elec. simulation of brain, generator 7-8759
 ankle movement prediction and evaluation with implantable peroneal stimulators 7-28778
 antagonist muscles, elec. stimulated, control algorithms testing, cat model, neural prosthesis appl. 7-8770
 atrial heart cell aggregates, embryonic chick, repolarisation currents 7-28491
 auditory frequency coding in the inferior colliculus, gerbil obs. 7-54596
 auditory system, in vivo elec. stimulation using multichannel photolithographic electrode arrays, cat obs. 7-3799
 axon, squid, modulation of aminopyridine block of K⁺ currents 7-23324
 axons, anal. of models or external stimulation 7-23329
 bacteriorhodopsin model membranes, kinetic anal. of displacement currents 7-28475
 bean sprout growth, effects of elec. or mag. fields (*Japanese*) 7-47151
 bed, static charge sensitive, for automatic anal. of sleep records 7-3896
 bilayer lipid membranes, simultaneous intracavity laser absorpt. spectroscopic and electrical meas. 7-13972
 biomembrane excitation, pulse and const. current stimulation, electrical circuit simulation 7-28479
 black bilayers of egg phosphatidyl ethanolamine, thermotropic changes in cond. 7-54489
 cable theory applied to blowfly receptor cells and large monopolar cells 7-47038
 cardiac, bioelectrical sources localisation, accuracy, magnetocardiography appl. 7-54542
 cardiac electrophysiological stimulation and online processing, automated system 7-34324
 cardiac gap junctions, single channel currents, embryonic heart obs. 7-8550
 cardiac impedance differential loop and its clinical significance (*Chinese*) 7-18088
 cardiac myocytes, Na⁺/Ca²⁺ exchange, effect of ouabain on voltage dependence 7-59958
 cardiac output monitoring by impedance cardiography during treadmill exercise 7-28733
 cardiac Purkinje fibres, rabbit, voltage-dependent block by tetrodotoxin of Na⁺ channel 7-54527
 cardiac Purkinje strands, K⁺-activated electrogenic Na⁺ pumping 7-28490
 cardiac sino-atrial node cells, charactn. of single pacemaker channels 7-47024
 cardiac tissue, impedance meas., tissue struct. model 7-13985
 cell electrofusion and other electrophysiological treatments, versatile low-cost apparatus 7-14164
 cell physiology and instrumentation (*Japanese*) 7-14171
 circular conducting cylinder, infinite- and finite-length, pots. prod. by arbitrary current sources 7-59969
 closed-loop electrical stimulation orthoses for restoration of quiet standing in paraplegia 7-28769
 conference on bioengineering, New Haven, CT, USA (March 1986) 7-16
 current dipole implanted in dogs, mag. localisation 7-54632
 currents induced in a human being for plane-wave exposure conditions 0-50 MHz and for RF sealers 7-3839
 DNA, aperiodic, electronic structure and cond. props. 7-23297
 DNA, elec. cond., possible mechanisms of action of an external electrostatic field 7-54668
 DNA, electric charge transfer phenomena, TSC investig. (*Czech*) 7-13948
 DNA, electronic structure and cond. props., calcs. 7-23296
 dorsal root ganglion cells, chick, activation of a transient inward current by step reductions in extracellular Ca²⁺ 7-23326
 dot matrix characters, perception through skin sensation by elec. stimulation 7-28546
 egg lecithin, bilayer lipid membranes, base conductance and electric breakdown, static mag. field effect 7-14030
 electric shock effects on the human body 7-24337
 electric shocks, injury by electric current passing through acupuncture points (*Russian*) 7-28493
 electrical safety limits for medical equipment 7-54794
 electrical shock safety criteria, conf., Toronto, Ontario, Canada (Sept. 1983) 7-18500
 electrical stimulation open-loop control of human knee during swing 7-28763
 electrocardiology, inverse soln. in 1D using a membrane model 7-8554
 electrodes, optimal design for electrosurgery, defibrillation, and external cardiac pacing: finite-element computer model 7-3928
 electrogoniometric gait recording, 3D 7-3823
 electrophysiological systems—a quantitative description 7-65739
 electroreceptors in the platypus 7-65911
 electrosensitivity in rays, spatial mechanisms analysis 7-47030
 electrostatic discharges from human body 7-34125
 electrostatic stimulation, human tracking of electrocutaneous signals, training effects 7-14025
 ELF electric fields, effects on neuronal activity in rat brain 7-28583
 ELF-LF electric fields, quantification of interaction with human bodies 7-3836
 EM hyperthermia, hot spot form. by locally induced currents 7-8753
 EMG study of side step for development of elec. stimulation patterns 7-28570
 ESD testing, rising slope reproducibility 7-42843

bioelectric phenomena continued

- functional elec. stimulation hand grasp orthoses, tracking performance 7-28777
 functional neuromuscular stimulation, parameter selection and upper limb characterisation 7-3764
 functional neuromuscular stimulation to augment walking; develop. stages 7-34333
 gap junction channel, its aq. nature as indicated by D₂O effects, temp. coeff. obs. on earthworm 7-28492
 gap junctional cond., linear relationship with permeability, frog blastomere obs. 7-40127
 gating current harmonics, dynamic props. of secondary activation kinetics in Na⁺ channel gating 7-59967
 gating current harmonics, dynamic transients and steady states with Na⁺ inactivation gating 7-8528
 grasp control during functional neuromuscular stimulation, force/position feedback 7-28764
 heart, danger of electricity (*German*) 7-3776
 heart, programmed stimulation, real time data collection 7-34329
 heart and respiratory activity monitoring by impedance change using neck electrodes 7-65869
 heart rate and arterial blood press. variability signals, auto-spectral and cross-spectral anal. 7-47270
 hippocampal slice prep., current source density estimation using microelectrode array data 7-54538
 human ESD: the phenomena, their reproduction and some associated problems 7-42842
 impedance cardiography, motion artifact from spot and band electrodes 7-28732
 implantable gait simulation using microprocessor-controlled trigger switches 7-34353
 implants for nerve stimulation in paraplegic patients, gate array appls. 7-34339
 injury currents, elec. and math. props. in wound healing 7-8552
 intracellular long-term measurements on contracting isolated hearts, expt. set-up 7-65902
 joint angle sensors for closed-loop control of movements in paraplegics 7-28766
 lateral prehension-release grasp charact. using functional neuromuscular stimulation 7-28576
 lipid membrane, ion transport, effects of double-layer polarisation 7-54490
 lipoproteins, surface charge determ. and its changes on peroxidation of lipids 7-40087
 lung, feline, dielec. polarisation at radio freqs. 7-59968
 lymphocytes, T, abnormal, from mice with lpr gene mutation, altered K⁺ channel expression 7-28487
 mitochondria from bovine heart, electrophoretic behaviour of H⁺ + AT-Pase proteolipid 7-59946
 multichannel portable functional electrical stimulation system for spinal cord injured persons 7-28765
 multipoint signal averager for repetitive bioelectric signals, microprocessor-based 7-18091
 muscle, elec. stimulated, discrete-time model 7-3779
 muscle fibre membrane, K cond., gramicidin A interaction, heating effect 7-8496
 muscles, electrically stimulated, effect of muscle nonlinearities on control 7-8644
 musculotendon actuator models for neuromuscular stimulation system CAD 7-28573
 myocardial electrical propag., 3D anisotropic model 7-40131
 natural walking with an electrical stimulator (*Swedish*) 7-40358
 nerve activity measurement and analysis, conf., London, England (Nov. 86) 7-41014
 neuromuscular electrical stimulation of quadriceps, effect of duty cycle on fatigue 7-34332
 neuromuscular electrical stimulation of quadriceps, patient preferences as to pulse freq. 7-34331
 neurons, polarisation by extrinsically applied elec. fields, model 7-40132
 Nitellopsis obtusa and Nitella translucens cells, membrane between chloroplast layer and moving cytoplasm, elec. obs. 7-40117
 ohmic conductance through the inwardly rectifying K channel and blocking by internal Mg²⁺ 7-47026
 organ of Corti, elec. coupling differences in vitro and in vivo 7-54593
 pancreatic β -cell, bursting, effect of intracellular Ca²⁺-sensitive K⁺ channel 7-28483
 pancreatic β -cells, elec. activity rel. to glucose 7-54504
 perception threshold to current pulses, comparison of Lapicque and exponential strength-duration curves 7-65910
 periodic polypeptides, band struct. ab initio HF cryst. orbital calcs. 7-23298
 phosphatidic acid bilayer lipid membranes, induction of capacitance and ionic currents by Ca²⁺ 7-54488
 photoinitiated ion movements in bilayer membranes containing Mg-octaethylporphyrin 7-8503
 photoreceptor membrane currents, inositol trisphosphate regulation, Hermisenda obs. 7-28518
 physiological effects of elec. currents (*German*) 7-3782
 plant protoplasts, cell fusion by elec. stimulation (*Japanese*) 7-47022
 pressure sore prevention by functional electrical stimulation of gluteus maximus muscle 7-34335
 propagation through electrically coupled cells, how a small SA node drives a large atrium 7-40128
 proteins, aperiodic, electronic struct., ab initio calcs. 7-23273
 proteins, electronic structure and cond. props., calcs. 7-23296
 purple membrane, electric polarisability, electrooptic scatt. spectra anal. 7-54530
 purple membrane suspensions, large transient nonproton ion movements 7-8502
 retinal electrical activity imbalance rel. to ocular dominance shift in kitten visual cortex 7-28517
 review of electrical impedance imaging 7-60116
 rotating electric fields, cell behaviour rel. to surface charges and cell structs. 7-28584
 sarcoplasmic reticulum from rabbit skeletal muscle, single-channel Ca²⁺ and Ba²⁺ currents 7-28476
 sensory receptors of cat's hindlimb, response to a transient, step-function DC elec. field 7-28581
 skeletal muscle, cultured, rat, single apamin-blocked Ca-activated K⁺ channels 7-23317

bioelectric phenomena continued

- skeletal muscle, developing rat, functional differences between 2 classes of Na^+ channels 7-3759
- skeletal muscle, frog, external $[\text{K}^+]$ and the block of the K^+ inward rectifier by external Cs^+ 7-23325
- skeletal muscle, multi-ion cond. and selectivity in the high-cond. Ca^{2+} -activated K^+ channel 7-40126
- skeletal muscle fibres, frog, quick-freezing following electrical stimulation 7-28798
- squid axons, voltage clamped, Na^+ current rel. to physico-chem. props. and struct. changes, disopyramide effects obs. 7-54529
- surface electrical stimulation of quadriceps in patients with spinal injury, response 7-34334
- T lymphocytes, human cloned helper, single-channel and whole-cell recordings of mitogen-regulated inward currents 7-40134
- thylakoid membrane, light scatt., photo-induced changes, surface charge effect 7-59934
- tinnitus, treatment by external elec. therapy 7-28762
- toroid-amplifier system for mag. meas. of current in biological tissue, capabilities 7-23493
- torso, human, automated system for elec. props. modelling 7-40137
- transmembrane ionic channels, permeability rel. to pore mouth charge distrib. 7-59941
- tumours, solid., dielec. props. during normothermia and hyperthermia 7-3778
- UHF local hyperthermia, electrode device and methodological problems of thermoradiotherapy (*Russian*) 7-23484
- vascular muscle cells, spontaneously contracting, Ca^{2+} and Na^+ channels 7-3760
- ventricular fibrillation, 60 Hz, thresholds for large-surface-area electrodes, animal expts. 7-3931
- volume measurements with an impedancimetric catheter, rel. to cond. and geometrical factors 7-3909
- walking using long leg braces or functional neuromuscular electrodes, relative energy cost 7-34336
- wheat seeds, germinating, dielec. response meas. using resonant cavity 7-34127
- Wolff-Parkinson-White preexcitation syndrome, computer simulation with a modified Miller-Geselowitz heart model 7-3765
- yeast, elec. impedance charge during growth and fermentation (*Japanese*) 7-47021
- yeast, voltage-dependent ion channel obs. 7-28486
- zwitterionic lipid bilayers, dielec. props. of polar head group region 7-8504
- Ca^{2+} channels, occult, in *Drosophila*, rel. to twinning of Ca^{2+} and voltage-activated K^+ 7-17966
- Ca^{2+} current in single heart cells, opposite effects of cyclic GMP and cyclic AMP 7-40135
- K^+ permeability of resting membrane, rel. to excitable K^+ channel 7-40112
- Na^+ translocation by Na^+/K^+ pump, voltage dependence 7-17957

bioelectric potentials

- see also *contact potential; electrocardiography; electroencephalography*
- achromatopsia, light induced oscills. of standing pot. 7-28505
- action potential elimination for blocking of struct. development of retinogeniculate synapses 7-3767
- action potential in lobster giant axon, effect of time-varying mag. fields 7-3766
- action potential propag. in septated nerve fibres, computerised numerical simulation 7-59960
- action potential propagation in demyelinated frog nerve, optical recordings 7-59962
- action potentials, unidirectionally propagating, generation using a monopolar electrode cuff 7-54514
- active fibres, line source models 7-54526
- adaptive filtering of evoked pots. 7-59907
- adaptive techniques for signal enhancement, human EEG and visually evoked responses 7-34319
- articulatory function assessment, handicapped aid 7-40136
- auditory brainstem evoked pots., finite impulse response digital filters appl. 7-23491
- auditory brainstem responses, effects of presbycusis and other types of hearing loss 7-54609
- auditory brainstem responses, freq. specificity 7-28543
- auditory brainstem responses from human adults and infants: restriction of freq. contrib. by notched-noise masking 7-34159
- auditory electric responses, individual differences, absolute latencies of brainstem vertex-positive peaks 7-28544
- auditory evoked responses, apparent response incompatibility effects rel. to task 7-65764
- auditory evoked responses, midlatency: differential recovery cycle charact. 7-65763
- auditory evoked responses during NREM sleep stage 2 in man, late component variants 7-23370
- auditory nerve-brainstem evoked response, depression in hypoxaemia: mechanism and site of effect 7-54584
- auditory offset tuning curves rel. to simultaneous and forward masking in mouse and gerbil 7-8587
- auditory tuning curves, whole nerve action pot. and auditory brainstem response, comparison in guinea pigs 7-54591
- autoassociative neural network, influence of noise on behaviour 7-54525
- body surface pot. mapping, recursive computation of LF baseline drifts 7-40338
- brain, single evoked pots., classification and detect. using time-freq. amplitude features 7-54534
- brain electrical and magnetic activity monitoring 7-8743
- brain event-related potentials, principal components anal., spectral methods 7-47031
- brain potentials, performance and measures of performance for estimators 7-23328
- brain voltage changes meas., signal source with MOSFET chopper amplifier 7-23480
- brainstem auditory evoked pots. in rhesus monkey, neural generators 7-8581
- brainstem auditory evoked responses in the hamster 7-54595
- cardiac action potential in beating heart cells, regulation of Na^+ -conducting Ca channel 7-54528
- cardiac action potentials and twitches, real time acquisition and analysis 7-65737
- cardiac tissue, anisotropic, electronic interactions 7-13989

bioelectric potentials continued

- carpal tunnel syndrome, electrophysiological aspects of 639 symptomatic extremities 7-3761
- central nervous system connections determ. by physiological methods 7-47037
- cerebral cortical contrs. to sensory evoked pots., hydranencephaly obs. 7-23342
- cerebral responses evoked by stimulation of the vesico-urethral junction in normal subjects 7-34124
- continuous evoked pots., visual and auditory, MTF obs. 7-8556
- cutaneous galvanic reaction parameters, automated recording system 7-40353
- EEG evokes pots., max. likelihood method for estimating 7-54421
- electrode, multiplexed implantable, for monitoring evoked responses in cerebral cortex, design 7-47305
- electrodes, recording and stimulating, for biological research 7-47306
- electroencephalographic signals, running spectrum anal. as an aid in representation and interpretation 7-65868
- electroglottograph signals, noisy speech anal. appl. 7-28545
- electroglottographic observations of young stutterers' fluency 7-8602
- electromyogram, singular value decomposition, locally quasi-stationary processing 7-47036
- electrooculogram and colour vision, effects of ethyl alcohol 7-28501
- electrophysiological diagnostics based on electrically active point responses 7-8749
- electroretinogram, single flash, electronic simulation model (*Japanese*) 7-59979
- EMG, clinical, basic problems of automatic analysis 7-8737
- EMG, computer based method for automated meas. of muscular activity periods 7-54818
- EMG, computerised, conf., New York, USA (April 1981) 7-4621
- EMG, pre- and postoperative comparison in children with cerebral palsy 7-3774
- EMG, quantitative, diagnostic yield of automated method 7-8742
- EMG, real-time FFT to monitor muscle fatigue 7-28734
- EMG, short time Fourier anal.: fast movements and constant contraction 7-54537
- EMG, surface and intramuscular, from the temporalis muscle, study of methods 7-3899
- EMG activity recording technique for lumbar multifidus in man 7-3772
- EMG automatic analysis with ANOPS computer, monopolar electrode use 7-8738
- EMG feedback and motor control restoration, controlled group study of 12 hemiparetic patients 7-13984
- EMG fine wire connections technique 7-23468
- EMG from human first dorsal interosseous muscles, Fourier and factor analysis 7-8545
- EMG measurements during bicycle pedalling, anal. 7-23380
- EMG of marine animals in situ, US biotelemetry system to obtain 7-3955
- EMG signal numerical analysis; three parameters for functional muscular values 7-3775
- EMG signal on-line analysis, microcomputer based neurophysiological measurements system 7-8739
- EMG-force model of elbow's antagonistic muscle pair 7-59966
- envelope EMG spectral analysis in the studies of physiological and pathological tremor 7-3897
- epilepsia partialis continua, distinction between myoclonus-related pot. and epileptic spike 7-54532
- ERG, local macular, in patients with Best's disease 7-28504
- ERG, oscill. pots. (*Italian*) 7-23337
- ERG, progress over 25 yrs. 7-17980
- ERG and visual evoked pot. abnormalities in myotonic dystrophy 7-23341
- ERG b-wave, rel. to outer segment disc shedding in rabbit retina 7-59982
- ERG components: a reappraisal 7-28506
- ERG of intact cat eye, mechanisms of azide induced increases in c-wave and standing pot. 7-40144
- ERGs of albino rabbits, simultaneously recorded, effects of intraocular perfusion with 2 alternating irrigation solns. 7-28507
- event related potentials, component and interval detection algorithms 7-34139
- event related pots., enhancement by iterative restoration algorithms 7-54535
- event-related potentials to speech sounds and tones, habituation 7-34155
- event-related pots., principal component anal., misallocation of variance 7-8537
- event-related pots. estimation improvement using statistical pattern classification, visuo-motor appl. 7-14002
- evoked dipole source potentials of the human auditory cortex 7-8580
- evoked muscle potential amplitude ratio at distal/proximal stimulation, subclinical neuropathy diagnosis 7-8539
- evoked potential analysis using crosscorrelation and dynamic time-warping 7-8551
- evoked potential components, mid and long latency, law of 3.5 c/sec 7-3771
- evoked potential maps in learning disabled children 7-8558
- evoked potentials characterization study (*Japanese*) 7-47033
- evoked potentials from passive elbow movements, modification by motor intent 7-14026
- evoked potentials in vision research 1961-86 7-17981
- evoked potentials processing with tactile and thermal stimulation; prototype system (*Spanish*) 7-34318
- extracellular neural recording with multichannel microelectrodes 7-8780
- extracellular potentials around active excitable structures with short geometric inhomogeneities 7-8538
- extracellular potentials of single muscle fibres, fibre end influence 7-8540
- F-response parameters in upper extremity, ulnar and median nerves, height influence 7-3762
- flash visual evoked response testing, effect of pupillary dilation 7-28503
- heart membrane pot., evaluation by positron-emission tomography, use of ^{11}C -triphenylmethylphosphonium 7-14113
- hippocampal slices from noncold-acclimated, cold-acclimated and hibernating hamsters, temp. effects on evoked pots. 7-54484
- ignorance-based signal estimation given multiple noisy realizations 7-47264
- implantable multielectrode array with on-chip signal processing, microprobe for biopotentials recording 7-28495
- implantable multielectrode array with on-chip signal processing, neural prostheses/biopotential recording appls. 7-34338

bioelectric potentials continued

- integrated EMG for different isometric tension levels, digital and manual surface spike counting 7-8543
- interference pattern analysis, clinical uses, effect of load, dynamic studies 7-8740
- intracellular microelectrode measurements in small cells evaluated with the patch clamp technique 7-40371
- intramuscular EMG signal estimation from surface EMG signal anal. 7-47035
- macular ERGs and contrast sensitivity as sensitive detectors of early maculopathy 7-28511
- magnetoencephalogram topography and source model of abnormal neural activities associated with lesions 7-47032
- man-operator psychophysiological state estimation (*Russian*) 7-8547
- median nerve, graduated pots. rel. to diagnosis of type of lesion in peripheral nervous system 7-3925
- midlatency auditory evoked responses: differential effects of sleep in the cat 7-8582
- midlatency auditory evoked responses: differential effects of sleep in the human 7-8583
- midmotoraxonal reexcitation in human peripheral nerve 7-8530
- mirror projection visual evoked pot. stimulator for presenting patterns in different orientations 7-3895
- motor unit action pot., model for decomposition, algorithm 7-3780
- motor unit action pot., model for decomposition, simulated pots. 7-3781
- motor unit action pots., reliable myoelec. signal detector based on propagation chars. 7-3902
- motor unit potentials with varying loads, automatic analysis 7-8741
- mouse liver cells, membrane pot. stability rel. to damaging agents exposure 7-8535
- movement-related brain pots., synchronisation rel. to computer detect of EMG edges 7-14027
- multi-modality evoked potentials in hypoxaemia, cat obs. 7-54583
- multi-modality evoked responses vs. temp. and thermal dose with whole-body hyperthermia in water bath 7-8500
- multichannel, single trial event related pot. classification 7-54533
- muscle fibre, frog, action potential parameter changes at different temps., math. modelling 7-3773
- muscle fibre conduction velocity calc. from EMG power spectra analysis 7-8546
- muscle fibre conduction velocity meas. with surface EMG, cross-correlation method 7-3763
- myoelectric control, amplifier input impedances 7-3937
- myoelectric elbows proportional control mode selection, cocontraction approach 7-28776
- myoelectric signal of elec. stimulated muscle during recruitment, rel. to closed-loop control 7-3777
- myoelectric signal processing effect on muscle force-EMG relation 7-8544
- myoelectric signals of neck and head, speech information 7-34164
- myotonia, recessive congenital, electrophysiological evaluation 7-8531
- nerve cell, membrane pot. clamping, cyclic nucleotide injection, intraneurone information processing 7-8527
- neuromuscular diseases, computerised electromyographic signal processing 7-54541
- noisy signals, anal. by nonparametric smoothing and differentiation, brain pots, appl. 7-54422
- nonlinear biological oscillator, periodic pulsatile stimulation 7-34093
- nonlinear selective filter for electrocardiograph 7-60108
- nystagmus induced by off vertical axis rotation, three-dimensional model 7-47047
- online spike form discriminator for extracellular recordings based on an analog correlation technique 7-3952
- P300 potential complex to auditory stimuli, subcortical correlates in man 7-23369
- paraplegics, EMG-controlled stimulation limb function discrimination using Karhunen-Loeve expansions 7-54540
- passive biotelemetry by freq. keying, low-level bioelec. data appl. 7-23492
- periodontal mechanoreceptor mediation of short latency excitatory reflex in human masseter muscle 7-3808
- potential depend. Na channels regulation, spectroscopy of combination scatter 7-8524
- presaccadic spike pot., rel. to eye movement direction 7-23340
- pulse blood flow of limbs, quantitative eval. using rheography 7-40352
- quantitative EMG rel. to noise 7-3898
- red blood cells suspended in carbohydrate-saline solns., deformability, effect of transmembrane pot. 7-34118
- remote physiological sensing: historical perspective, theories and preliminary developments 7-34298
- retinal pigment epithelial cells, acetazolamide-induced changes of membrane pots. 7-28509
- self-adaptive myoelectric processor, automatic calibration to amputee's muscle movements 7-47291
- short latency averaged evoked pots. recorded in thalamic and scalp zones of representation, comparison 7-34123
- short-latency auditory evoked pots. in the monkey, intracranial generators 7-3798
- short-latency auditory evoked pots. in the monkey, wave shape and surface topography 7-3797
- sleep EEG and EMG, computer program for automatic anal. 7-54783
- somatosensory evoked cortical pots. to median nerve stimulation, scalp topography and distrib. 7-34167
- somatosensory evoked pot. and sensory action pot. phenomena, simulation by 2D pot. field modelling 7-34166
- somatosensory evoked pot. ipsilateral and contralateral components following median nerve stimulation 7-23372
- somatosensory evoked potentials after stimulation of digital nerves in upper limbs: normative data 7-34168
- somatosensory evoked potentials in a brain-dead patient, unexpected myogenic contaminants 7-3893
- somatosensory evoked potentials recording, short latency, with median nerve stimulation 7-3807
- somatosensory evoked pots., short latency, in infants and children: developmental changes and maturational index 7-8606
- somatosensory evoked pots. to finger stimulation, N20 and P22 obs. 7-8605
- somatosensory evoked responses, short latency, increased latencies used for defining abnormality 7-8607
- somatosensory potentials in hemiplegics, intrahemispheric cond. delay 7-3806

bioelectric potentials continued

- somesthetic primary cortex evoked pots. elicited by central afferent stimulation 7-34169
- spatio-temporal elec. pot. patterns, rel. to biological growth 7-3783
- spectrally selective flash early receptor pot. in dichromats 7-28510
- spinal somatosensory evoked pots. monitoring during surgery, microprocessor-based system 7-23482
- stomach, human, noninvasive technique to monitor elec. and mech. activity 7-60110
- stria vascularis, DC pots. in different cells, in vitro obs. 7-54586
- stria vascularis potentials, in vivo electrophysiological obs. 7-54587
- surface EMG quantification, use of digital discriminators 7-8542
- surface myoelectric power spectral density as function of biceps brachii static load 7-8541
- task difficulty effects on steady state visual evoked response 7-54544
- trunk muscle and moments, relationship in sagittal and frontal planes 7-3784
- uterine electrohysteroogram processing for obstetrical monitoring 7-54791
- utricular afferents response to sinusoidal vibrations, simulation using spike generator mechanism model 7-47132
- venturi suction electrode array for clinical bodysurface mapping 7-3904
- vision, log-complex transforms of stimuli rel. to cortical responses they evoke 7-54558
- visual average evoked pots., usefulness of filtering and smoothing, statistical comparison 7-65749
- visual event-related pots. to coloured patterns and colour names 7-23349
- visual evoked pot. study of optic pathway conduction in insulin-dependent diabetics 7-28502
- visual evoked potential, source geometry and dynamics 7-54555
- visual evoked potential abnormalities in multiple sclerosis 7-14001
- visual evoked potential activity after induction of afterimages 7-47055
- visual evoked potential stimulation based on Commodore VIC 20 computer 7-3950
- visual evoked potentials, anal. through Wiener filtering applied to a small no. of sweeps 7-40142
- visual evoked potentials, comparison of fibre optical and video monitor stimulators in normals and multiple sclerosis patients 7-65865
- visual evoked potentials, source localisation man by principal components anal. 7-47052
- visual evoked potentials to dynamic random dot stimuli with varying dot density ratios of disparity to background 7-28512
- visual evoked potentials to luminance and chromatic contrast in rhesus monkeys 7-54557
- visual evoked pots., single-response, optimum multielectrode a posteriori estimates 7-60109

bioenergy conversion

- anaerobic digestion of $\text{Ca}(\text{OH})_2$ sludge for water treatment 7-46963
- anaerobic fermentation of organic waste for energy and fertiliser, efficiency 7-34052
- biogas daily production enhancement 7-40020
- biomass, alternate supply systems, cost anal. 7-65395
- biomass thermochemical liquefaction research sponsored by US Department of Energy, overview 7-65511
- biomass-to-methane conversion using batch system, optimal residence times 7-23205
- cyanobacterial heterocysts, photosystem I, energy conversion monitoring, photoacoustic spectra 7-47016
- electrical power generation using biogas and biomass (*Italian*) 7-46961
- energy harvest efficiency of energy crop, photosynthetic energy storage rate 7-46962
- ethanol fuel production from wheat, technico-economic aspect (*French*) 7-28385
- landfill gas recovery, natural and induced gas migration through cover materials 7-65396
- methane enrichment in anaerobic digestion, advanced concepts 7-65397
- organic waste value enhancement through biometanization 7-17919
- recovery from wastewater treatment sludge 7-8355
- renewable resources, microbiological conversion into liquid fuels 7-65512
- sludge treatment, advanced anaerobic process 7-65595
- technology breakout in energy conversion, conf., San Diego, CA, USA (Aug. 1986) 7-60875
- willow biomass production and utilisation 7-28406
- H_2 photoevolution by *Rhodospseudomonas palustris* in light-dark cycles 7-3722
- H_2 production efficiency from light energy conversion by photosynthetic bacterium *Rhodobacter sphaeroides* 8703 7-65644

biographical dictionaries *see biographies***biographies**

- Bauschinger effect, hundred years (*German*) 7-41046
- Carl Wilhelm Scheele (1742-1786) 7-60925
- founding fathers of physics, Christian beliefs 7-60931
- G.D. Cassini (1625-1712) and Saturn 7-29651
- Niels Bohr at 100: his life and work 7-29649
- Reginald Purdon de Koch (1902-80), extraordinary variable star observer, biography 7-60926
- vibrating string controversy of mid-1700s, classical wave eqn. 7-48262

biological cybernetics *see biocybernetics***biological effects of acoustic radiation**

- see also biomolecular effects of radiation; cellular effects of radiation*
- annoyance and skin conductance response to natural sounds 7-3838
- cancer, mutation theory, effects of EM and ultrasonic radiation on H_2 bonds in DNA (*Spanish*) 7-47152
- cats, effect on hearing of intense low freq. acoustic impulses 7-34160
- choice reaction time and paired associates learning tasks, effects of noise and vibration 7-54677
- dissolved gases, influence on biological and chem. effects of US 7-14044
- free radical production in aqueous solns. due to diagnostic US 7-50900
- hair cell damage produced by acoustic trauma in the chick cochlea 7-54597
- hearing damage effects of noise 7-28541
- hearing damage in military service, noise-induced HF losses, study on 38, 294 conscripts 7-54613
- hearing loss development during long-term exposure to occupational noise 7-54615
- hyperthermic cell killing, enhancement by nonthermal effect of US 7-60035
- interaural correlations in normal and traumatized cochleas: length and sensory cell loss 7-47158
- kidney stones elimination, focusing of acoustic pulses by an elliptical reflector 7-65811

biological effects of acoustic radiation continued

- liposomal membrane, US radiation induced lipid peroxidation 7-47159
- liver, therapeutic US effects in vivo: action and possible mechanisms 7-47160
- mononuclear phagocyte system, effects of therapeutic US on activity in vivo 7-14043
- physiological effects of low frequency noise, Japanese study 7-28598
- psychophysiological acoustics of indoor sound due to traffic noise during sleep 7-18014
- rabbit liver, histochemical effects of US (*Chinese*) 7-60034
- retinal rod outer segment suspensions, effect of sonication on nucleotide-dependent light scatt. changes 7-23398
- stereocilia, tip links, vulnerability to acoustic trauma in the guinea pig 7-54590
- testes, murine, low-kH-water-borne US effects 7-28599
- tibia state alteration during antithrostatic hypokinesia 7-34181
- US damage on biological targets obs. 7-3953

biological effects of alpha-particles *see alpha-particle effects; biological effects of ionising particles***biological effects of beta-rays** *see beta-ray effects; biological effects of ionising particles***biological effects of electric fields** *see bioelectric phenomena; biological effects of fields***biological effects of electrons** *see biological effects of ionising particles; electron beam effects***biological effects of fields**

- airway smooth muscle responsiveness to elec. field stimulation, K⁺-induced alterations 7-8548
- alternating electric field, model for action on a human 7-34187
- bacterial photosynthetic reaction centres, charge recombination, ultrafine interaction, mag. field effect 7-8516
- bean sprout growth, effects of elec. or mag. fields (*Japanese*) 7-47151
- blood, hypercoagulation syndrome in mobility-restricted rats, effect of a weak variable mag. field 7-54669
- cancer, mutation theory, effects of EM and ultrasonic radiation on H₂ bonds in DNA (*Spanish*) 7-47152
- chemical electric field effects in biological macromols., review 7-54444
- combustion processes under intense mag. fields, living organisms appl. 7-8285
- differential heating of tissues by UHF field, decrease of effect of ionising radiation (*Russian*) 7-28610
- DNA, elec. cond., possible mechanisms of action of an external electrostatic field 7-54668
- ELF electric fields, effects on neuronal activity in rat brain 7-28583
- ELF-LF electric fields, quantification of interaction with human bodies 7-3836
- erythrocytes, human, ferricyanide reduction in the presence of methylene blue, influence of a UHF EM field 7-40217
- haemopoietic tissue, ²⁵²Cf RBE and PLD-like effect of mag. fields, CFU-S assay 7-28590
- Lewis tumour graft, effect of a static nonuniform mag. field, mouse obs. 7-28595
- liposome vesicles, mag. field-induced drug permeability 7-40213
- living cell model for electric field and overvoltage effects (*Polish*) 7-60031
- lymphocytes, peripheral, human, effect of low-level 60 Hz EM fields 7-28582
- maintenance and operations personnel at 750 kV installations, effects of intense electric fields (*Rumanian*) 7-28585
- mammalian cells, irradi. with ²⁵²Cf and ⁶⁰Co, effects of alternating mag. fields on survival 7-28594
- mitogenic response of peripheral blood mononuclear cells, effect of ELF pulsed mag. fields 7-28580
- neurons, polarisation by extrinsically applied elec. fields, model 7-40132
- operant behaviour of rats, alteration by low-intensity mag. fields 7-28578
- rat tissue, mag. field effects, phase-contrast microscopy obs. 7-8645
- rotating electric fields, cell behaviour rel. to surface charges and cell structs. 7-28584
- sensory receptors of cat's hindlimb, response to a transient, step-function DC elec. field 7-28581
- static electricity, effects on human body (*German*) 7-54671
- strong static mag. field effects on living organisms and chem. reactions 7-8611
- thin film solar cells manufacture, elec. and EM hazards 7-59849
- thrombolytic process dynamics under conditions of a constant mag. field 7-3835
- UHF field exposed biological systems, acoustic effects, phys. modelling 7-40211

biological effects of gamma-rays

- see also biomolecular effects of radiation; cellular effects of radiation*
- aortic endothelial cells, bovine, cell cycle changes and cytotoxicity in irradi. cultures 7-40230
- biochemical change in rat tissues induced by combined effect of ²³⁹Pu and external γ -radiation (*Russian*) 7-47175
- bone marrow cells of BALB/c mice irradi. with ²⁵²Cf or ⁶⁰Co, micronuclei prod. 7-28615
- chromosome aberrations induced in human lymphocytes by acute X- and γ -radiation in vitro 7-3843
- clonogenic cells of Lewis lung carcinoma, survival after γ - and γ -neutron irradi. (*Russian*) 7-14055
- comparative biological effects of low dose, low dose-rate exposures to fission neutrons or ⁶⁰Co γ -rays 7-28588
- cotton plants, combined effect of γ -radiation and microelements (*Russian*) 7-47177
- D-amino Acid in irradiated and aged mouse, skin and lens obs. 7-18021
- differential heating of tissues by UHF field, decrease of effect of ionising radiation (*Russian*) 7-28610
- DNA, ϕ X174, radiation damage and biological effects 7-28617
- DNA injury in continuous long term low-dose irradi., fluorometric obs. in rats, mice and men (*Russian*) 7-54506
- E. coli, L-arabinose isomerase induction by γ -irrad. 7-40229
- E. coli cells, thermoinduced radioresistance and heat shock proteins (*Russian*) 7-13969
- Ehrlich ascites clonogenic tumour cells exposed to ⁶⁰Co γ -rays in hypoxic conditions, radiosensitivity (*Russian*) 7-47180
- Ehrlich ascites tumour clonogenic cells forming colonies in agar cultures in diffuse chambers, radiosensitivity (*Russian*) 7-47176
- emesis induced by ⁶⁰Co γ -rays in dogs, effects of lesions and drugs, neurophysiological aspects 7-60055

biological effects of gamma-rays continued

- epidemiological investigation of mutational diseases in the high background radiation area of Yangjiang, China 7-18019
- erythrocyte membrane, effects of γ -irrad. as shown by ESR, NMR and biochem. studies 7-60041
- fish cells, primary cultured with different ploidy, radiosensitivity obs. 7-60044
- hepatoma cells, change in initiation of DNA synthesis at a nuclear matrix and its DNA-protein content (*Russian*) 7-47174
- influenza viruses inactivated by γ -rays, physicochem. characts. (*Russian*) 7-46997
- intestinal uptake of nutrients, late effects of abdominal irradi. obs. 7-18030
- jejunal crypt cells, mouse, response to ¹³⁷Cs γ -rays and ²⁵²Cf neutron irradi. 7-28613
- Jejunal crypt stem-cell survival after fractionated γ -irrad. performed at different dose rates 7-60042
- keratinocytes, cultured, human and mouse, radiosensitivity obs. 7-8656
- lecithin, aq. soln., bilayer liposomes, radiation damage PMR relax. time determ. 7-34200
- life shortening in mice exposed to fission neutrons and γ -rays 7-40214
- LSA lymphoma, OER by survival time for ²⁵²Cs, low dose rate ¹³⁷Cs and acute ⁶⁰Co irradi. 7-28614
- lung, mouse, long term radiation effects and combined modalities 7-28622
- lymphocytes, human, chromosome aberrations yield rel. to dose (*Russian*) 7-18027
- lymphocytes, low-dose-irrad., decreased nucleic acid synthesis, effect of TCGF addition 7-8661
- lymphoid cells, rat, effect of ionising radiation on lipid metabolism 7-60040
- lymphoid organs, response to low dose rate ²⁵²Cf, ¹³⁷Cs and acute ⁶⁰Co irradi. 7-28591
- mammalian cells, irradi. with ²⁵²Cf and ⁶⁰Co, effects of alternating mag. fields on survival 7-28594
- meiotic abnormalities induced in tetraploid and hexaploid wheat by γ -rays and ethyl methanesulphonate 7-65719
- mitochondria, isolated, rat liver, effects of up to 475 Gy γ -rays 7-60043
- model membranes, modification of lipid domains by low levels of irradi. 7-8512
- pea, genetic anal. of continuous variation following hybridisation and irradi. 7-34194
- pearls, cultured, endurance on γ -irrad. 7-23411
- plant tissues exposed to γ -rays, dose distrib. patterns 7-34275
- plant tumours induction in Kalanchoe daigremontiana and potato (*Russian*) 7-14058
- potentially lethal damage in plateau-phase V790 cells after exposure to neutrons or γ -rays 7-40212
- protozoan reproduction, promotion by ionising radiation 7-40231
- sensorimotor cortex and caudate nucleus of rat brain, cholinergic process status after γ -irrad. (*Russian*) 7-47178
- skin, irradi. of previously irradi. mouse skin: early skin reaction and skin shrinkage 7-34198
- sublysin-72 in water solns., radiation inactivation (*Russian*) 7-13965
- synergistic effect of γ -radiation and quinoxalindioxins on mice and lymphoid cells in culture (*Russian*) 7-14062
- T-1 cells, human, inverse γ -ray dose rate effect in ²⁵²Cf RBE expt. 7-28616
- teratogenic effects in rats, potentiation by association of microwaves and ionising radiation 7-60039
- testis weight loss following ²⁵²Cf, ⁶⁰Co or ¹³⁷Cs irradi. in mice 7-28592
- testosterone, hydrated, EPR study of monoclinic and orthorhombic single crystals, γ -irrad. at 295K 7-23307
- vascular permeability, changes following thorax irradi. in rats 7-8665
- whole-body γ -irrad., changes in ECG and haemodynamics (*Russian*) 7-8659
- ²⁵²Cf brachytherapy treatment of localised tumours, B neutron capture enhancement, Chinese hamster cell obs. 7-28589
- ²⁵²Cf γ -neutron radiation biological effects, USSR studies 7-28611
- ²⁵²Cf-exposed human cells, pot. lethal damage and radioprotection 7-28612
- ⁶⁰Co γ -source, accidental irradi. of technician, long-term follow-up: eye, skin and blood effects 7-34195

biological effects of ionising particles

- see also biomolecular effects of radiation; cellular effects of radiation*
- alanines, D- and L-, ⁹⁰Sr-⁹⁰Y- β -irrad., asymmetrical induced yields 7-59929
- alpha-emitting nuclides incorporated in the lungs microdistrib. of radioactive substance and radiation protection (*Russian*) 7-47172
- beta-rays from HTO, acute and chronic effects in mice, rel. to carcinogenicity 7-60053
- bladder urothelium, mouse, electron irradi. effects, SEM obs. 7-60058
- Chinese hamster cells, modification by mesoporphyrin-IX derivatives of damage by He ions and protons (*Russian*) 7-14064
- Chinese hamster cells survival rel. to biological effectiveness of low energy protons 7-40221
- cosmic ray HZE particles, biological effects 7-34295
- DNA repair kinetics after exposure to X-irrad. and to internal β -rays in CHO cells 7-28619
- DNA strand breaks induced by X-irrad. and internal β -rays, 3 classes 7-23408
- embryo, pre-implantation, mouse, radiotoxicity of ³H-thymidine and ³H-arginine 7-60051
- intestinal cell death induced by HTO in mice, obs. using a new ³H safety clean cabinet 7-60054
- Japanese Tritium Programme: the University Programme on biological effects and environmental tritium 7-54773
- lung cancer after exposure to ²²²Rn daughters in mines and homes (*German*) 7-65816
- mammalian cells, cultured, induction of cell killing, mutation and oncogenic transformation following exposure to tritiated water 7-60049
- mammalian tissues, particulate radiation damage, electron microscopy appls. 7-28623
- model of ion track struct. based on classical collision dynamics 7-23410
- mutation induction in spores of Bacillus subtilis by accelerated very heavy ions 7-28618
- myeloid leukaemia induction in animals, expt. designed to meas. RBE of ³H rel. to X-rays 7-60052
- neoplastic transformation, induction by low-dose-rate exposure to tritiated water 7-8664

biological effects of ionising particles continued

- radiotherapy, dose distrib. of high-energy electron beam, chromosome aberration freqs. 7-14131
 rhabdomyosarcoma tumor cells, rat, pot. lethal damage repair after X-ray or Ne ions 7-18031
 somatic mutations induction in *Tradescantia*, effects of low dose tritiated water and tritium labelled compounds 7-60048
 tissue equivalent materials, energy straggling and stopping power of 4 and 5.486 MeV α -particles 7-34199
 whole-body uniform irradiation, with 1000 MeV protons, dose-rate contrib. to effect (Russian) 7-14067
 yeast cells, photoreactive damage rel. to O₂ effect in radio- and UV-sensitive mutants (Russian) 7-14053
 21. At, possible applications to human cancer therapy, review 7-28657
 HTO β -rays, RBE measured by effects on cultured mouse embryos at pre-implantation stage 7-60050
 HTO, RBE on cultured mammalian cells at mol. and cellular level 7-60047
³H, environmental aspects, toxicity, metabolism and dosimetry: research at CRNL 7-54774
 239Pu cancer risk, reduction by chelation therapy, mouse expts. 7-18029

biological effects of ionising radiation

- see also *biological effects of gamma-rays; biological effects of ionising particles; biological effects of X-rays; biomolecular effects of radiation; cellular effects of radiation*
 actinides, biological behaviour, consequence for radiation protection (French) 7-40223
 acute localized irradiation, use for X-ray and NMR tomography for diagnosis, pig expts. (French) 7-3869
 autoregulatory mechanisms in irradiated biosystems, reliability (Russian) 7-47171
 blood-brain, late effects of radiation, rat obs. 7-65814
 breast cancer, late radiation injuries of the lungs after combined treatment (Russian) 7-28609
 breast cancer risk in women rel. to ionising radiation (Russian) 7-54682
 cancer induction and nonstochastic effects 7-54679
 cancer mortality, correl. with natural radiation exposure in Japan 7-18022
 cellular adaptive response induction (Russian) 7-14052
 Chernobyl accident, radiation effects on humans in Switzerland (German) 7-8652
 chromosome aberrations and reproductive death of mammalian cells: quantitative correl. between these effects (Russian) 7-14054
 clonogenic capacity of irradiated cells, factors influencing, computer simulation study (Russian) 7-14061
 computer simulation of radiation-induced late effects by system dynamics 7-18024
 DNA, range of high LET effects from ¹²⁵I decays 7-8660
 DNA base damage induced by ionising radiation, review of current aspects 7-47169
 embryo and foetus, irradiation effect review 7-54680
 endotoxin, bacterial, detoxification by ionising radiation rel. to conc., phys. state, and purity 7-40228
 epidemiological evaluation of radiation risk using populations exposed at high doses 7-8687
 fibroblasts, human, mutation induction, evaluation of a specific quality function 7-3842
 Hodgkin's disease patients in prolonged clinical remission, radiation injuries (Russian) 7-8684
 hypoxic cells, radiosensitisation at low doses 7-23409
 image recognition methods, appl. to estimate radiation damage severity (Russian) 7-13946
 immune response, functional activity of involved cell systems at long times following sublethal irradiation (Russian) 7-14057
 inhaled particles, dosimetry, model for risk assessment, factors to be considered 7-54756
 isotopes in the marine environment 7-40314
 lipoxigenase systems after ionising irradiation, as a mediatory function of mol. factors (Russian) 7-14051
 logistic estimate of the final incidence of later radiation effects 7-8653
 lymphocyte subclasses and immunoglobulins, in adults receiving radiation treatment in infancy for thymic enlargement 7-18032
 macromolecules, radiation sensitivity, temp. depend. 7-15668
 malignant tumour development following irradiation, for preexisting tumors, double cancer autopsy cases study 7-18020
 membrane reception of prostaglandin E₂ in mouse tissues, effect of various doses of ionising radiation (Russian) 7-47173
 microdosimetric approach in radiation biology, correctness (Russian) 7-14063
 nuclear medicine workshop, Chalk River, Ont., Canada (Aug. 1985) 7-24308
 oncogenic transformation of cells in culture: pragmatic comparisons of oncogenicity, cellular and mol. mechanisms 7-60855
 peripheral blood lymphocytes of atomic bomb survivors, anal. using monoclonal antibodies 7-59947
 perspective on radiation risks 7-54681
 pulmonary changes, acute, assessment by CRT 7-14117
 radiation carcinogenesis, cumulative empirical distrib. functions, risk projection models 7-28705
 radioactivity, effects on human beings (Dutch) 7-14050
 risk assessment and biological basis of radiological protection, conf., Bristol, England (April 1986) 7-48134
 skeletal muscle and thyroid gland of rats injected with ¹³¹I, postirradiation changes (Russian) 7-14059
 thyroid gland, chick embryo, effect of low-level radiation on cAMP system (Russian) 7-14060
¹²⁵I decay rel. to amplification of oncogenes and integrated SV40 sequences in mammalian cells 7-40224
 4Ra, A=226,228, intake by early Ra dial workers in Illinois, health risks 7-8700
 Rn daughter exposure and cigarette smoking, lung cancer in Navajo men, U mining relationship 7-8703
 4Rn, A=220, 222, progeny inhalation, lung cancer risk at low doses of α particles 7-28608
 222Rn concentrations in USA homes, contrib. to lung cancer risk 7-65666

biological effects of ions see *biological effects of ionising particles; ion beam effects***biological effects of laser radiation**

- see also *biomolecular effects of radiation; cellular effects of radiation*
 π -laser, biomedical experiences 7-47208

biological effects of laser radiation continued

- biliary calculi, gallstones, pulsed-laser fragmentation, optical study 7-60036
 bovine serum albumin, photoinduced ionisation by holographic relax. method 7-14046
 corneal incisions induced by pulsed UV or IR lasers, comparative study on dogs 7-34193
 DNA, laser induced interstrand covalent crosslink, fluoresc. obs. 7-8490
 egg production and fertilisation of copepod *Tisbe Holothuria*, laser irradiation effects 7-8650
 enzymes of glutamic acid metabolism in rat liver and brain, influence of continuous and modulated laser radiation (Russian) 7-47164
 erythrocytes, effects of He-Ne laser light 7-3840
 hazard analysis, nominal hazard zone 7-60094
 health hazards, controls 7-65812
 intensity and temp. distrib. created by light emitted from an optical fibre embedded in tissue 7-47013
 macular laser lesions, image anal. 7-34229
 oesophageal carcinoma, human, selective vapourisation by Nd glass laser (Chinese) 7-18015
 pigmented biological tissues with granular struct., selective interaction of short laser pulses 7-54678
 surgical pulsed CO₂ lasers, asymptotic and dimensionless anal. of living tissue response 7-65813
 teeth, nuclear microprobe analysis (French) 7-46890
 therapeutic laser, CO₂ scanning, thermal effect on tissues 7-47162
 tissue morphological anal. and ablation rates in the UV and visible for laser angioplasty 7-23399
 tissue-laser interaction, thermal and biological aspects of medical laser appl. 7-60037
 wound healing stimulation by lasers, mouse obs. 7-34224

biological effects of magnetic fields see *biological effects of fields; biomagnetism***biological effects of microwaves**

- see also *biomolecular effects of radiation; cellular effects of radiation*
 2.45 GHz CW microwave radiation, effects of foraging behavior of white-throated sparrow 7-28606
 adrenal cortex, rat obs. 7-8651
 autoimmune reactions, expt. simulation by nonionising microwave radiation (Russian) 7-47163
 blood-brain barrier of rats, interaction of ethanol and microwaves 7-28601
 boundary element method for elastostatics with internal constraints 7-29758
 brain tissue and animal behaviour, effects of low-level RF and microwave radiation 7-23403
 broadcast transmitting station radiation hazards 7-14045
 contractile rate of isolated frog hearts, effects of pulsed microwave radiation 7-34192
 cytogenetic effects of microwave irradiation of male mouse germ cells 7-23404
 electric activity of isolated chick embryo hearts 7-28600
 erythroleukemic cells, murine, differentiation during exposure to microwave radiation 7-40218
 foot, rat, effect of local microwave irradiation on n. tibialis muscle activity (Russian) 7-47165
 groundwater contaminant transport, variable BEM soln. 7-55115
 human head internal heating by pulsed microwave irradiation, thermal stress calc. (Japanese) 7-47166
 hydromass behaviour, time-depend., boundary element method appl. 7-55118
 limb models heated with miniature annular phased applicator, energy deposition patterns 7-13970
 lining organisms, use of MM range EM radiation for studying specific processes 7-60144
 liposomes, conformational state, millimeter wave irradiation, Raman spectra study 7-23405
 low level of exposure, danger or not? 7-3841
 perfused phantom models of microwave irradiated tissue 7-8784
 radar workers at civilian airports, exposure survey of microwave radiation, Australia 7-47161
 RF radiation regulations 7-28605
Saccharomyces cerevisiae cells, effect of mm-wave irradiation on growth 7-28604
 serve vitality, elimination of microwave effects after blockage of active transport 7-60038
 shore wave field, numerical modelling by boundary element method 7-55079
 teratogenic effects in rats, potentiation by association of microwaves and ionising radiation 7-60039
 thymidine synchronised bovine lymphocytes exposed to 7.25 GHz microwaves, cytogenetic obs. 7-14048
 wheat seeds, germinating, dielec. response meas. using resonant cavity 7-34127

biological effects of neutrons

- see also *biomolecular effects of radiation; cellular effects of radiation*
 alanine system sensitivity, fast neutron irradiation effects 7-34188
 bone marrow cells of BALB/c mice irradiated with ²⁵²Cf or ⁶⁰Co, micronuclei prod. 7-28615
 brain, adult rabbit, late effects of fast neutrons and X-rays 7-60029
 clonogenic cells of Lewis lung carcinoma, survival after γ - and γ -neutron irradiation (Russian) 7-14055
 comparative biological effects of low dose, low dose-rate exposures to fission neutrons or ⁶⁰Co γ -rays 7-28588
 cytogenetic effectiveness of the therapeutic fast neutron beam emitted by cyclotron U-120 (Russian) 7-13976
 DNA, oriented, neutron-induced free radicals 7-23391
 erythroid units in canine bone marrow cells, survival on neutron or γ -irradiation 7-60056
 haemopoietic tissue, ²⁵²Cf RBE and PLD-like effect of mag. fields, CFU-S assay 7-28590
 hyperglycemia, short-term induced, influence on effectiveness of X- and neutron-radiation on HeLa cells (Russian) 7-14065
 induced activities in human body by thermal neutrons, calc. 7-54672
 jejunal crypt cells, mouse, response to ¹³⁷Cs γ -rays and ²⁵²Cf neutron irradiation 7-28613
 lethal and mutagenic effects of fast neutrons of different energy of *Streptomyces griseus* spores (Russian) 7-14041
 life shortening in mice exposed to fission neutrons and γ -rays 7-40214
 low dose effects, design and interpretation of 'top-up' expts. 7-60135

biological effects of neutrons continued

- LSA lymphoma, OER by survival time for ^{252}Cs , low dose rate ^{137}Cs and acute ^{60}Co irradi. 7-28614
 lymphoid organs, response to low dose rate ^{252}Cf , ^{137}Cs and acute ^{60}Co irradi. 7-28591
 mammalian cell culture, DNA single- and double-strand breaks by thermal neutrons 7-23392
 mammalian cells, irradi. with ^{252}Cf and ^{60}Co , effects of alternating mag. fields on survival 7-28594
 melanoma cells, cultured, RBE of thermal neutron beam and the $^{10}\text{B}(n, \alpha)^7\text{Li}$ reaction 7-60028
 neutron quality factor for dosimetry and biological damage 7-25258
 normal tissues, radiobiology of neutron effects, therapy appl. 7-28586
 nuclear research, summary of recent papers (*Dutch*) 7-54670
 potentially lethal damage in plateau-phase V790 cells after exposure to neutrons or γ -rays 7-40212
 protection considerations rel. to neutron effects in humans 7-28720
 RBE of fast neutrons rel. to dose for normal human skin and connective tissue (*Russian*) 7-47150
 spermatogonial stem cell population, mouse, variation in sensitivity to fission neutron irradi. 7-60032
 T-1 cells, human, inverse γ -ray dose rate effect in ^{252}Cf RBE expt. 7-28616
 testis weight loss following ^{252}Cf , ^{60}Co or ^{137}Cs irradi. in mice 7-28592
 tumour cell reproductive capability rel. to neutron RBE of cyclotron Y-120 (*Russian*) 7-54673
 yeast, wild-type and repair-deficient strain, fast neutron RBE for lethality and genotoxicity 7-23393
 ^{252}Cf brachytherapy, fast neutron beam therapy and radiobiology, conf., Lexington, KY, USA (April 1985) 7-24273
 ^{252}Cf brachytherapy treatment of localised tumours, B neutron capture enhancement, Chinese hamster cell obs. 7-28589
 ^{252}Cf γ -neutron radiation biological effects, USSR studies 7-28611
 ^{252}Cf implant neutron effects on dog brain 7-28593
 ^{252}Cf , tumour and normal tissue effects and therapeutic gain ratio 7-28587
 ^{252}Cf -exposed human cells, pot. lethal damage and radioprotection 7-28612

biological effects of protons see *biological effects of ionising particles; proton effects*

biological effects of radiation

- see also *biological effects of acoustic radiation; biological effects of fields; biological effects of ionising radiation; biological effects of laser radiation; biological effects of microwaves; biological effects of neutrons; biological effects of ultraviolet radiation; biomolecular effects of radiation; cellular effects of radiation; dosimetry; radiation therapy*
 bacteriorhodopsin model membranes, kinetic anal. of displacement currents 7-28475
 behavioural effects of exposure to NMR imaging, rat open-field behaviour and learning obs. 7-18016
 behavioural effects of exposure to NMR imaging, spatial memory tests on rats 7-18017
 brain tissue and animal behaviour, effects of low-level RF and microwave radiation 7-23403
 circadian pacemaker, human, resetting by bright light independently of sleep-wake cycle timing 7-14047
 corneal iridescence in fish, light-induced changes 7-47044
 currents induced in a human being for plane-wave exposure conditions 0-50 MHz and for RF sealers 7-3839
 fluorescent light, lack of effects on human muscle strength by kinesiology testing 7-23406
 intrauterine development in rats, low level RF radiation exposure effects 7-28603
 low radiation doses, effects and mechanisms, possible beneficial effects (*German*) 7-28577
 photoinitiated ion movements in bilayer membranes containing, Mg-octaethylporphyrin 7-8503
 Phycomyces, system anal. of light-growth response, wavelength 7-23401
 Phycomyces, system anal. of light-growth response with sum-of-sinusoids test stimuli 7-23400
 Phycomyces light-growth response, system anal., photoreceptor and hypertropic mutants 7-23402
 satellite transmit earth station, RF radiation hazards, menace or myth 7-18018
 solar radiation and the eye, review of knowledge relevant to eye care 7-8649
 temperature and nerve conduction velocity, warming-up cold extremity with IR radiation 7-3752
 thermogrammetry and thermal engineering conf., Budapest, Hungary (April 1987) (*Hungarian*) 7-56258
 tracing the thermic sum of radiation injuries by infrared image forming (*Hungarian*) 7-60030

biological effects of ultraviolet laser radiation see *biological effects of laser radiation; biological effects of ultraviolet radiation*

biological effects of ultraviolet radiation

- see also *biomolecular effects of radiation; cellular effects of radiation*
 C3H10T1/2 cells, transformation by UV irradi. to a unique, suppressible phenotype 7-65817
 DNA, laser induced interstrand covalent crosslink, fluoresc. obs. 7-8490
 DNA, UV induced thymine dimers, bound serotonin effect 7-8489
 DNA cleavage after UV-irradi., block by restriction endonucleases 7-18026
 DNA repair characts. of hybrid cell clone between xeroderma pigmentosum and Potorous tridactylis 7-60045
 HeLa cells, changes in UV-fluoresc. intensity in irradi. cells (*Russian*) 7-14056
 peptides, photoform. of radicals, 330-390 nm, 77K 7-8488
 plasmid damaged at a specific region by UV light, mutational DNA base sequence changes 7-59948
 proteins, photoform. of $\dot{\text{N}}=\text{CH}_2$ and HCO radicals after UV irradi. at 77K 7-28461
 visual acuity, UV effects in pseudophakia 7-34142
 yeast cells, photoreactivable damage rel. to O_2 effect in radio- and UV-sensitive mutants (*Russian*) 7-14053

biological effects of X-rays

- see also *biomolecular effects of radiation; cellular effects of radiation*
 binucleate cell form. in X-irradi. cultured mammalian cells, correl. to loss of colony-form. ability 7-60057
 blood serum and its components, comparative study of chemiluminesc. and resistance on ionising irradi. (*Russian*) 7-14066

biological effects of X-rays continued

- bone marrow granulocyte-macrophage progenitor cells and stromal colony-forming cells, human, effect of dose rate 7-8662
 brain, adult rabbit, late effects of fast neutrons and X-rays 7-60029
 cell contact effects absence in irradi. EMT6-Rw tumours 7-18033
 cell X-ray sensitivity in different regions of the sandwich, a diffusion-limited system for cell growth 7-40226
 cerebellum, developing rat, long-term neuropathological consequences of low-dose X-irradi. 7-18025
 chromosome aberrations induced in human lymphocytes by acute X- and γ -radiation in vitro 7-3843
 d-amino Acid in irradiated and aged mouse, skin and lens obs. 7-18021
 DNA repair kinetics after exposure to X-irradi. and to internal β -rays in CHO cells 7-28619
 DNA strand breaks induced by X-irradi. and internal β -rays, 3 classes 7-23408
 duodenal lesions by thoracic irradi., surface SEM studies 7-28621
 erythroid units in canine bone marrow cells, survival on neutron or γ -irradi 7-60056
 eye lens, mouse, X-ray acute radiation injury quantitative assessment, cataract development (*Russian*) 7-8658
 fading times required for apparently complete repair in irradi. tissues. 7-8654
 haematopoiesis and radiation in Harwell steel mice 7-40222
 heat and radiation interaction anal., CHO cells expts. 7-18028
 HeLa cells, X-irradiated, action of caffeine, recovery from pot. lethal damage 7-8666
 hyperglycemia, short-term induced, influence on effectiveness of X- and neutron-radiation on HeLa cells (*Russian*) 7-14065
 insular apparatus and adrenal cortex of rats, function at early times after irradi. (*Russian*) 7-47179
 jejunum, murine, method for localised hyperthermia and X-irradi. in situ 7-13966
 large bowel of rats, pathogenesis of chronic radiation ulcer, expt. obs. 7-34197
 low dose effects, design and interpretation of 'top-up' expts. 7-60135
 lung, CT assessment of X-ray-induced damage in mice 7-65815
 lymphocytes, human, cell survival and radiation induced chromosome aberrations 7-47168
 lymphocytes, human, lower limits of dose detect. after X-irradi. 7-34196
 mammalian cells, heat-induced cell killing rel. to heat radiosensitization 7-8521
 mammary carcinoma cells, murine, thermal radiosensitisation and thermotolerance 7-59937
 micronuclei induced during interphase of 4-cell mouse embryos in vitro after X-irradi. 7-28620
 model membranes, modification of lipid domains by low levels of irradi. 7-8512
 multicellular spheroids initiated from human melanoma xenograft lines 7-14049
 mutational extinction induced by sequential X-irradi. and actinomycin D treatments in CHO cells 7-8663
 myeloid leukaemia induction in animals, expt. designed to meas. RBE of ^3H rel. to X-rays 7-60052
 nuclear protein content and cell progression kinetics following X-irradi. 7-40225
 patient doses and risks from diagnostic radiology in north-east Italy 7-60089
 peripheral blood, lymphocytes from ageing donors, sensitivity to X-irradi. 7-8655
 population kinetic parameters for acute epidermal reactions in man 7-40227
 predictive models of cell death by exposure in vitro to X-rays and 1,3-bis(2-chloroethyl)-1-nitrosourea 7-60046
 prenatal low level irradi. effects on postnatal growth and adult behaviour in Wistar rats 7-40220
 prenatal obstetric X-ray exam., unborn child cancer risk, Oxford survey analysis 7-8694
 radiosensitisation of Chinese hamster cells by O_2 and misonidazole at low X-ray doses 7-40219
 rhabdomyosarcoma tumor cells, rat, pot. lethal damage repair after X-ray or Ne ions 7-18031
 serum T_4 level and response of thyroid gland to exogenous TSH in rats, 8 Gy X-irradi. effect 7-18023
 single-dose RBE and toxicity studies under conditions of hypothermia and hyperbaric O_2 7-28607
 skin, differential response in young and old rats to a combination of X-rays and wet or dry hyperthermia 7-23407
 stromal tissue, mouse, influence of prior heat treatment on effects of heat alone or combined with X-rays 7-59938
 yeast cells, X-ray induction of DNA double-strand breaks 7-8657

biological fluid dynamics

- see also *bioreology; haemodynamics*
 airlift-loop bioreactor with external loop, hydrodynamic model 7-40179
 burns patients, dynamic analysis of reanimation treatment effects 7-40202
 cerebrospinal fluid shunt flow meas., reproducible radionuclide procedure 7-65836
 foetal lungs, liq. flow to and from, influence of upper respiratory tract, sheep obs. 7-8617
 hollow-fibre modules, flow distrib. study 7-65783
 peristaltic pumping, effect of peripheral layer viscosity 7-54661
 perspectives in nontraditional biofluid mechs. 7-54652
 pleural liquid exchanges in anaesthetised rabbits, contrib. of Starling and lymphatic flows 7-8627
 renal filter control, system dynamics model 7-40201
 renal tubules, fluid waves 7-28547
 slow flow system in long permeable tubule, one- and two-dimensional models 7-47142
 steady flow in collapsible tube, flow limitation, oscills. of tube and flow velocity 7-51196
 syringe, slow viscous flow 7-65802
 urodynamic data-acquisition and anal. system, microcomputer-aided 7-3914
 vascular and urethral parameters meas., microprocessor-based signal processing system 7-54686

biological macromolecules *see macromolecules; molecular biophysics*

biological membranes *see biomembranes*

biological sciences *see biology*

biological specimen preparation

aminoplastic thin standards prep. method for X-ray microanalysis 7-60142

analytical ion microscopy for cell biology and tissue studies 7-40386

cryo-electron microscopy, cryst. size and cooling rate 7-3949

cryomicroscopy, specimen visualisation by cryoHVEM 7-40380

cryopreservation of biological specimens, possibility of using exponential cooling regimes 7-54815

deinococcus radiodurans, surface protein projected struct. determ. by cryomicroscopy 7-47003

embedding at low temp., new Lowicryl resins 7-3948

flight hardware for chemical fixation of living material in the microgravity environment 7-8717

ion beam etching using saddle field source, SEM studies 7-28797

light and electron microscopy of identical sites in semi-thin tissue sections under 200 kV TEM 7-3946

propane-jet freezing of fresh tissues without ice form. 7-40379

retina, whole mount method for sequential anal. of photoreceptor and ganglion cell topography 7-40382

SEM, TEM and light microscopy of fixed tissues in Epon blocks, correl. technique 7-40378

skeletal muscle fibres, frog, quick-freezing following electrical stimulation 7-28798

tissue culture cells, imaging intracellular elemental distrib. and ion fluxes using ion microscopy, freeze-fracture 7-60139

biological techniques and instruments

see also biological specimen preparation; biomedical equipment; biomedical measurement; microelectrodes; specimen preparation

action potentials, unidirectionally propagating, generation using a monopolar electrode cuff 7-54514

analytical ion microscopy for cell biology and tissue studies 7-40386

arterial blood-flow waveform meas. in intact animals: digital radiographic technique 7-54837

arteriovenous O₂ difference, spectrophotometric meas., role of light scatt. 7-3942

automatic manipulation of microlitre volumes of liquid reagents 7-41362

autoradiographic images, digital cluster anal. system to locate labelled cell regions 7-3958

autoradiographs, grain counting using pattern recognition 7-23490

bacteria, pathogenic, ultrarapid differentiation and identification using FTIR techniques 7-54835

bacteria, tethered, computerised video analysis 7-59957

bacterial motion; speed-distribution measurement of crowded particles by dynamic image processing utilizing pixel-based temporal-correlation analysis (Japanese) 7-47301

bacterial size distrib. change meas. under drugs by laser light scatt. (Japanese) 7-60145

bacteriorhodopsin, cryst., radiation-sensitive specimens, high resolution image quality achieved in electron diff. pattern 7-47302

biaxially tested soft tissues, strain quantification technique 7-54824

bioacoustic, digital signal acquisition, analysis and synthesis, microcomputer based system, PAL 7-54817

biological and technological appls. in air at atm. press. 7-4917

biological electron probe X-ray microanal., current status, history 7-8782

biopolymer components, UV resonance Raman spectroscopy appl. 7-23488

biotechnical measuring systems, raising interference immunity 7-54822

blood component platelet activating factor, IR spectroscopic characterisation 7-54499

bone, elemental concentrations, determ. using X-ray fluoresc. anal. 7-40381

bone marrow pressure chamber, permanently inserted Ti implant for intramedullary press. meas. 7-8779

bone microstructure quantification, semi-automatic image anal. 7-8776

bone Pb anal., comparison of 2 in vitro methods 7-23499

book, annual review of biophysics and biophysical chemistry 7-30

brain, regional cerebral blood flow, meas. method for freely moving, unstressed rats 7-28790

bronchial mucociliary clearance in unsedated dogs, meas. using radioaerosol technique 7-60137

cardiac action potentials and twitches, real time acquisition and analysis 7-65737

cardiac myocytes, single isolated, simple technique to meas. rate and magnitude of shortening 7-23494

CCD line-scan image sensor for meas. of red cell vel. in microvessels 7-8777

cell analysis, high resolution particle sizing using the combination of time-of-flight and light-scattering measurements 7-48684

cell automated classification techniques, imaging flow cytometer 7-8774

cell electrofusion and other electrophysiological treatments, versatile low-cost apparatus 7-14164

cell structure imagery, defocus and partially coherent illumination influence (German) 7-10845

cells, dynamic studies using laser-projection microscopy 7-14172

central nervous system connections determ. by physiological methods 7-47037

cerebral blood flow measurement, indicator elution curves analysis by microcomputer 7-40389

chlorophyll fluorescence, appl. in ecophysiology 7-47299

chlorophyll pigment concentration using low-altitude airborne ocean colour data 7-14163

classifier-directed signal processing in brain research, EEG and magnetencephalogram appl. 7-54820

coal beneficiation micro-organisms 7-65387

collagen alignment in normal ligaments, directional filtering for quantification 7-8786

computer assisted scanning laser monitor for optical quality meas. of excised crystalline lens 7-23507

conf., Vienna, Austria, February 1986 7-40989

contour-clamped homogeneous elec. fields, method for large DNA mols. separation 7-65906

cortex functional architecture, determ. by optical imaging of intrinsic signals 7-34362

cryobiology, status and outlook, review 7-54838

cryomicroscopy, specimen visualisation by cryoHVEM 7-40380

cultured endothelium, apparatus to study response to shear stress 7-65907

biological techniques and instruments continued

cutaneous galvanic reaction parameters, automated recording system 7-40353

cytoarchitectonics, nervous tissue struct. inhomogeneities, software and hardware aspects of evaluation and anal. system 7-34360

dark field electron microscopy for biological struct. determ., scattered electrons 7-40387

dentin, human and supporting bone, elastic modulus meas. by laser speckle photography 7-34183

diamond knife edges, megavolt and cryo electron microscopy 7-41547

differential cell design for in vivo photoacoustic meas. of skin absorbance 7-47293

digital microscopy for cellular/subcellular features identification 7-54821

diving helmet noise, instrumentation methods for meas., diver hearing appl. 7-60146

DNA distributions with abnormal stemlines determined by flow cytometry, automatic analysis 7-59949

dynamics in bio-mathematical perspective 7-56030

electrode, multiplexed implantable, for monitoring evoked responses in cerebral cortex, design 7-47305

electrodes, recording and stimulating, for biological research 7-47306

electrogoniometer for thoracolumbar rot. meas. 7-28786

electron microscope autoradiography, quantitative, multiple linear regression analysis application 7-60141

electron microscopic autoradiography intensification by enhancer ENLIGHTNING 7-368

electron microscopic images, contrast enhancement by optical shadow method 7-48916

electron microscopic molecule images reconstitution, correspondence analysis, struct. interpret. tool 7-60138

electron microscopy, beam damage, contrast, noise 7-8783

electron microscopy, surface relief of thin sections rel. to image quality 7-65904

EM hyperthermia, temp. distrib., 27-2450 MHz (Czech) 7-65714

EMG, computer based method for automated meas. of muscular activity periods 7-54818

EMG activity recording technique for lumbar multifidus in man 7-3772

EXAFS and XANES, conference, Abbaye Royale de Fontevraud, France, (July 1986) 7-60862

EXAFS characterisation of poorly cryst. deposits from biological systems in the presence of highly cryst. mineral 7-65900

extracellular neural recording with multichannel microelectrodes 7-8780

extracellular water vols. in tissue, meas. by Gd modification of ¹H-NMR spin lattice relax. 7-18100

facial skin features, image processing algorithms and photographic techniques 7-23501

film analysis, 3D, accuracy of direct linear transformation extrapolation 7-23495

finite impulse response digital filters, appl. to brainstem evoked pots. 7-23491

flow cytometric DNA data analysis 7-47303

flow modelling for a biological cell sorter using design optimisation 7-8475

flow system for the study of shear forces upon cultured endothelial cells 7-65908

fluorescence correlation spectroscopy, theory of sample translation 7-60132

fluorescence quenching data analysis program 7-62438

fluorescence tomography using synchrotron radiation 7-59806

fluorescent microscopy enhancement using imaging 7-28795

Fourier and computerised IR spectroscopy, Ottawa, Ont., Canada (June 1985) 7-48160

Fourier transform IR difference spectroscopy for elucidating biomolecular mechanisms 7-54832

Fourier transform IR spectroscopy, biological and biomedical appl. 7-54831

Fourier transform IR spectroscopy of live cells 7-54507

fruit quality measurement by microwave impedance tomography (Japanese) 7-28800

generalized median filters for biological signal processing 7-8785

glass microelectrodes, open tip: cond. through wall at tip 7-60134

halothane, anaesthetic, in green pepper, ¹⁹F NMR imaging 7-28468

head-mounted device for meas. of pointing to visual targets without seeing the pointing arm 7-47279

Hofkessel: an artificial afterload for cardiovascular research 7-18096

hormonal steroids, physiological levels detection by Fourier transform IR spectroscopy 7-54833

IBM PC/AT-based image acquisition and processing system for quantitative image anal. 7-28796

image anal., automatic classification of zooplankton 7-40385

industrial audiometric procedures 7-28542

instrumentation and cell physiology (Japanese) 7-14171

intracellular long-term measurements on contracting isolated hearts, expt. set-up 7-65902

intracellular microelectrode measurements in small cells evaluated with the patch clamp technique 7-40371

ion beam excited acoustic image and specific element image of teeth 7-20536

ion-selective electrodes for ion conc. measurement, operation in nonlinear suboptimal response range 7-56246

jejunum, murine, method for localised hyperthermia and X-irrad. in situ 7-13966

laser Doppler flowmetry, appl. to quantification of heat-induced changes in skin and RIF-1 tumour of mice 7-65711

laser microprobe mass analyzer, LAMMA 1000 7-8341

life sciences experimentation, autonomous, in space stations, visual monitoring 7-23467

ligaments, methodology to determ. mech. props. at high strain rates 7-65909

light and electron microscopy of identical sites in semi-thin tissue sections under 200 kV TEM 7-3946

linacs for medical and industrial applications 7-62110

lingual articulation, effect of palate shape, electro-palatography appl. 7-3802

lining organisms, use of MM range EM radiation for studying specific processes 7-60144

lipid/protein interaction, Fourier transform IR studies 7-54498

lipids, phase diagram construction, temp. gradient method using time-resolved X-ray diff. 7-54816

liver acoustic attenuation estimation using zero-crossings technique 7-23397

biological techniques and instruments continued

LR115 detector, radiotoxicology appl. for low-level α -activity meas. 7-54830
 lysozyme crystals, X-ray diffr. data collection and processing, high press. study 7-3944
 macromolecules, anomalous member identification of noisy image set 7-13957
 magnetic resonance in medicine and biology, conf., Montreux, Switzerland (Oct. 1985) 7-17
 magnetically ordered biological materials, Mossbauer spectroscopy 7-60133
 measurement methods, conf., Prague, Czechoslovakia (April 1985) 7-48169
 median eminence microvascular, 3D reconstruction 7-34356
 microbiological objects dielectric props. monitoring, use of microwave bridge (*Slovak*) 7-65896
 microelectrode resistance meter, improved, neuroscience appl. 7-28791
 microscope, soft X-ray, undulator based, design 7-47298
 microscope, soft X-ray at national synchrotron light source 7-18951
 microscopy with synchrotron radiation 7-18949
 monkey visual training using a microcomputer and a bicoloured LED 7-40383
 mother-of-pearl, fracture surfaces, analytical techniques appl. 7-8781
 multimicroelectrode fabrication by Si dry etching (*Japanese*) 7-23504
 multiwire coordinate detectors, uses in molecular biology and crystallography 7-47297
 muscle contractility, computerised experimental set-up 7-54649
 muscle fibre conduction velocity meas. with surface EMG, cross-correlation method 7-3763
 MWPC based system for digitizing electrophoretic gels 7-47296
 neuron tracing system, CARTOS-ACE, 3D reconstruction of electron micrographs 7-23502
 neuronal activity in human brain, feasibility of developing a method, theoretical review 7-65901
 neutron sources, dosimetric characteristics for biology and medicine 7-56894
 NMR, in vivo, spatially localised surface-coil method using Fourier series window function and two coils 7-24674
 NMR, rot. frame imaging rel. to animal tissue metabolic heterogeneity 7-13963
 NMR microscopy, 3D, signal to noise ratio, limited angle excitation 7-54826
 NMR spatially localised spectroscopy, selected vol. excitation using stimulated echoes 7-48806
 NMR spectroscopy oversampling technique improvement of dynamic range 7-24667
 nuclear microprobe analysis, compounds in laser irradiated teeth (*French*) 7-46890
 nucleoli, extraction from images of leucocytes by computerised image analysis 7-23505
 oil crops, oil and water content meas., standard specimens for checking NMR analysers 7-54823
 online spike form discriminator for extracellular recordings based on an analog correlation technique 7-3952
 optical fringe projection for study of deformations and projection 7-41438
 optical laser techniques, initial tooth and bone displacements meas. on dry skull 7-65796
 optical microscopic tomography 7-61373
 optical microscopic type, constrained resolution enhancement 7-47304
 orcein dye treatment, fluoresc. reactions and appls. 7-60140
 organ of Corti, computer-assisted morphometric anal. system 7-40373
 oscillation camera data processing, synchrotron radiation data in macro-molecular crystallography 7-18098
 palmitic acid methyl ester, spin probe in adipose tissue, field gradient EPR 7-13962
 papillary muscle, method for generation of rapid step in temp. 7-3753
 parallel electrode position sensitive detector system for high counting rates 7-47295
 passive biotelemetry by freq. keying, low-level bioelec. data appl. 7-23492
 pathological voice analysis and its appl. to laryngeal pathology 7-1323
 pearls, fluorescence spectra, mother oyster distinction 7-28793
 perfused phantom models of microwave irradiated tissue 7-8784
 pharmaceutical analysis using liquid chromatography 7-18099
 photoacoustic spectroscopy, biological sample anal. appl. 7-3941
 photoacoustics, appl. to biology 7-54463
 photodynamic treatment of tumours, optical monitoring of singlet O₂ generation 7-65897
 photoelectric plethysmography instrument for meas. of arterial elasticity in human fingers and rabbit forelegs 7-28794
 photoelectron microscopy, applications to biological surfaces 7-8773
 photogrammetric techniques using high-speed cineradiography, biomechanics research appl. 7-23500
 photogrammetry application for study of body movement and shape 7-28753
 photographic-based system for contrast sensitivity meas. 7-23498
 phototactic microorganism *Haematococcus pluvialis*, transient photore-sponses revealed by light scatt. 7-28481
 PIXE, determ. of trace elements in reproduction systems of rare animals 7-54828
 plant cells water transport props. determ., using automated pressure probe 7-23503
 plant stem diameter contactless measurement apparatus using LED and photodetector (*Japanese*) 7-23506
 plant stem water potential measurement and simulation (*Japanese*) 7-28799
 porous materials, boundary length and internal surface area meas. 7-40376
 pressure transducer for microcirculation, math. model (*Chinese*) 7-28784
 programmable, multifunction dual-channel waveform generator for visual psychophysics 7-60006
 prosthetics and orthotics, shape sensing by CAD/CAM techniques for fitting 7-34348
 prosthetics fitting, optical noncontact 3D body measurement 7-34350
 proteases, method for enhancing stability 7-47012
 protein crystallography, neutron, data-collection facility equipped with linear detector 7-14168
 protein crystallography, static and time-resolved, real-time reduction of area detector data by hardware 7-14170

biological techniques and instruments continued

protein crystallography with synchrotron X-radiation source, electronic area detector data reduction system 7-14167
 protein in aqueous solution, FTIR spectra, automatic water subtraction procedure 7-54836
 protein structure, restrained least-squares refinement, incorporation of fast Fourier transforms 7-54451
 protein structure by FTIR self-deconvolution 7-54476
 protein structure determination by FTIR 7-54471
 protein structure refinements, model-fitting procedure incorporating the double-null technique 7-54450
 protein structure-spectra correlations, nonaqueous solvent effects using FTIR and ATR flow cell 7-54472
 proteins and lipids, FTIR spectra, water subtraction procedure 7-54834
 proteins in membranes, powder samples, label positions, determ. by neutron and anomalous X-ray diffr. 7-3755
 pulse blood flow of limbs, quantitative eval. using rheography 7-40352
 pulse sequence for in vivo ¹H NMR with surface coil 7-14166
 quick-freeze differential scanning calorimetry, appl. to lipid domains in fluid membranes 7-65718
 rabbit nictitating membrane response to piezoceramic vibrotactile CS, classical conditioning 7-8775
 radioassay of Pu or Am in biological samples, low-energy photon detector 7-58419
 radiobiology, design and interpretation of 'top-up' expts. to investigate effects of low doses 7-60135
 radiolabelled pulse for the simultaneous study of anterograde and retrograde axonal transport 7-3951
 reflectometry, variable angle, fibrinogen saturated adsorbed layer appl. (*French*) 7-28459
 respiratory gas exchange calc. using mass spectrometer, correction for instrument time constant and transport delay 7-60143
 respiratory proprioceptor system in man, noninvasive technique for exam. 7-40374
 retina, digital image correlation methodology use for deform. quantification 7-59718
 ribosome particles, electron microscopical 3D reconstructions of individual particles 7-41546
 rotational viscometers, calibration, whole-blood, appl. 7-40372
 sandwich, a diffusion-limited system for cell growth, cell X-ray sensitivity in different regions 7-40226
 scanning fluorometer for rapid assessment of pyridine nucleotide and flavoprotein fluoresc. changes in vivo 7-8778
 scanning laser microscope, real-time, for biological research 7-47292
 selenoproteins in bovine kidneys, anal. using gel chromatography and neutron activation 7-34363
 SEM, TEM and light microscopy of fixed tissues in Epon blocks, correl. technique 7-40378
 SEM stereophotogrammetric method and system for three-dimens. eval. of features on flat substrates 7-40377
 skeletal maturity, fuzzy grammars for syntactic recognition from X-rays 7-34317
 skin colour measurement device based on photoelec. colorimeter 7-60136
 skin moisture assessment from meas. with a miniature resistance-type dew point sensor 7-3956
 solvent suppression pulse sequence for biomolecule ¹H NMR spectroscopy 7-28788
 spatial localization with surface coils using multiple-pulse chemical-shift scaling 7-24671
 spin-labelled proteins, meas. of rot. mol. motion by time-resolved saturation transfer EPR 7-40089
 spine, segmental motion meas., transducers mounting 7-3945
 stereocomputer, three axis, for SEM photogrammetry 7-4934
 stereological advances, recent, impact on quantitative studies of the nervous system 7-34357
 stereology for anisotropic cells, appl. to growth cartilage 7-3947
 strain of fresh human bones, meas. by strain gauge, method and obs. (*Chinese*) 7-28782
 stratum corneum, lipophilic pathway, Fourier transform IR spectroscopy studies 7-54510
 surgically implantable, crystal-controlled, temperature telemetry transmitter 7-65903
 synapses numerical density estimation, crit. evaluation of methods 7-34358
 technical information photocarrier appl. of biological light-sensitive carriers 7-40370
 temperature depth meas. using thermal microwave emission analysis 7-28785
 tendon stiffness: methods of meas. and significance for movement control, review 7-54825
 tensile test system, automatic, for biotissues 7-23489
 three-band microwave radiometer system for noninvasive measurement of the temperature at various depths 7-18102
 three-dimensional morphometric cytology, pictorial pattern recognition 7-28801
 time of flight small angle neutron scatt., resolution, calc., meas. on biological samples 7-18097
 time-resolved IR spectroscopy system, data acquisition and processing 7-48884
 tissue composition prediction from in vitro US meas., expt. apparatus 7-14173
 tissue low-temp. embedding, for electron microscopy 7-23496
 tissue optical absorpt. characts., microscope for studying 7-14174
 toroid-amplifier system for mag. meas. of current in biological tissue, capabilities 7-23493
 torso, human, automated system for elec. props. modelling 7-40137
 total body O, N, and C, meas. in vivo by photon activation anal. 7-54827
 trabeculae, bovine, tensile testing, device and obs. 7-3832
 trace elements in biological materials determ., new techniques in X-ray fluoresc. and atomic absorpt. spectrometries 7-18101
 transmitter binding sites, quantitative autoradiography with an image analyser 7-34359
 two-parameter data-acquisition system for slit-scan chromosome analysis 7-35501
 ultra-soft X-ray contact microscopy, plant and animal cytology appls. 7-40388
 ultrafast phenomena conf., Snowmass, CO, USA (June 1986) 7-24
 ultrasonic flow cytometer, tests using small particle suspensions 7-20529
 US attenuation meas. device for human soft tissues (*Chinese*) 7-28783

biological techniques and instruments continued

- US biotelemetry system to obtain EMGs from marine animals in situ 7-3955
- US damage on biological targets obs. 7-3953
- US transducers made from bone materials, charactn. 7-60130
- uterine myoma, human, quantitative PIXE anal. 7-23497
- vapour resistance of clothing, technique for in situ meas. 7-3957
- video images and computer graphics superimposition technique, human body biomechs. study appl. 7-34361
- violacein, thin layer chromatography and FTIR analysis 7-54469
- visual evoked potential stimulation based on Commodore VIC 20 computer 7-3950
- visual performance testing with stereoscopic TV displays, use of optical videodisk system 7-60129
- walking horse, technique to quantify skin displacement 7-28787
- wire chambers, use in structural biology 7-47294
- X-ray absorpt. spectroscopy, impact on biology, applications and development, review 7-65899
- X-ray camera using a 2D multiwire proportional chamber 7-51570
- X-ray contact microscopy, biology appls. 7-35655
- X-ray crystallography, real time digital display with adjustable persistence time for 2-D detectors 7-11849
- X-ray imaging of biological specimens 7-28792
- X-ray micro-CT scanner for biomedical appls. 7-47246
- X-ray microbeam method for articular dynamics analysis 7-3801
- X-ray monochromator for studying biological systems 7-65898
- X-ray time resolved expts., multiwire detector and data acquisition system, appl. to muscle 7-14169
- zooplankton population analysis, multiple microprocessor system using image processing 7-18103
- B detection in vegetable samples and solutions using (n, α) technique 7-33980
- CO, personal exposure monitor with automatic data-logging 7-3943
- Ca, near-trace-element concs. in organic matrix, electron energy loss anal. 7-46903
- I determination in biological materials by epithermal neutron activation analysis 7-34364
- ³⁹K NMR, in vivo tissue K meas., rat obs. 7-60131
- U content of vertebrate blood, SSNTD anal. 7-54829

biological transport *see* **biotransport****biology**

- see also biological fluid dynamics; biological techniques and instruments; biophysics; biotechnology; blood; cardiology; ecology; evolution (biological); medicine; physiology; zoology*
- Amazon River continental shelf, biological SiO₂ uptake and particle reactive elements fate 7-34550
- Antarctic Convergence, Atlantic Ocean, Pliocene var., radiolarian assemblages anal. 7-23697
- central Arctic Ocean, foraminifera dissolution intervals anal. 7-23696
- brachiopods, C and O isotopic anal., implications for Palaeozoic ocean 7-9029
- Cretaceous-Tertiary boundary extinctions, evidence at DSDP site 577, Shatsky Rise, Pacific Ocean 7-23706
- Cretaceous-Tertiary extinction event, palaeoceanography charactrs., isotopic and geochem. anal. 7-18104
- encyclopedia of beaches and coastal environments 7-35127
- Greece, air enthalpy rel. to bioclimatological types grouping and geographic distrib. 7-9150
- Indian Ocean, Quaternary temps. determ. and sediment planktic foraminifera chem. anal. 7-29074
- International Association for Great Lakes Research, 29th conference, Scarborough, Ontario (May 1986) 7-18507
- land biota destructivity and atm. CO₂ 7-34640
- Laurentian Trough sediments, Gulf of St. Lawrence, radionuclide profiles, sedimentation rates, and bioturbation 7-28995
- marine biology, effect of mining on commercial fisheries in USA exclusive economic zone 7-66096
- marine biology, environmental monitoring conference, Texel, Netherlands (June 1984) 7-18472
- marine biology, temp. regulation of bacterial activity during spring bloom off Newfoundland 7-4057
- micro-organisms, heat exposure expt. rel. to entry into planetary atmosphere 7-9275
- N Pacific Ocean-atm. system, Pliocene-Pleistocene evol., fossil diatoms anal. 7-23695
- phytoplankton cultures, non-Newtonian props. and oceanographic implications 7-14299
- Port Hope Harbour, Lake Ontario, sediment quality assessment and benthic community 7-28423
- Pripyat River forest and marsh landscapes, groundwater regime and balance on right bank 7-9050
- Reykjanes Ridge rift valley, Upper Quaternary sediments stratigraphy, foraminiferal anal. 7-29073
- S Sierra Nevada, California, Late Holocene upper timberline var. rel. to temp. changes 7-55251
- time course of the houseflies' landing response, leg movement evaluation 7-65785
- tree ring indices in NE Nevada, appl. to precip. reconstruction (1600 to 1982) 7-29145
- tree-ring widths rel. to solar activity, evidence for 7-year solar cycle during Miocene period 7-9456
- trees, in Europe, disease and death 7-54376
- C cycle in biosphere, impact of atmospheric disturbance of geochemical C cycle 7-40546

biology computing

- see also computerised instrumentation; computerised signal processing*
- action potential propag. in septated nerve fibres, computerised numerical simulation 7-59960
- autoradiographic images, digital cluster anal. system to locate labelled cell regions 7-3958
- bacteria, tethered, computerised video analysis 7-59957
- biomagnetic computational tools, trends: from procedural codes to intelligent scientific models 7-54634
- biopolymer conformation determination using NMR, CONFOR graphics program 7-54455
- blood gases, effect of ventilation and blood flow in lung 7-34173
- bone microstructure quantification, semi-automatic image anal. 7-8776
- cardiac action potentials and twitches, real time acquisition and analysis 7-65737
- cell automated classification techniques, imaging flow cytometer 7-8774

biology computing continued

- cerebral blood flow measurement, indicator elution curves analysis by microcomputer 7-40389
- clonogenic capacity of irradiated cells, factors influencing, computer simulation study (*Russian*) 7-14061
- Commodore VIC 20 based visual evoked pot. stimulator 7-3950
- cytoarchitectonics, nervous tissue struct. inhomogeneities, software and hardware aspects of evaluation and anal. system 7-34360
- DNA-ligand interactions, groove binding, computer simulations 7-54447
- electron microscopic molecule images reconstruction, correspondence analysis, struct. interpret. tool 7-60138
- electron microscopy of cell components, computer environment for 3D shaded perspective display 7-65905
- electrophoretic separation of macromolecules, two-dimensional multivariate data analysis 7-54440
- EMG, computer based method for automated meas. of muscular activity periods 7-54818
- evolutionary ecosystems, sources of diversity, EVOLVE III model anal. 7-54431
- expert systems and compiler techniques for intelligent implantable cardiac pacemakers 7-14162
- facial skin features, image processing algorithms and photographic techniques 7-23501
- fluorescent microscopy enhancement using imaging 7-28795
- human body biomechanics study, technique for superimposition of computer graphics and video images 7-34361
- IBM PC/AT-based image acquisition and processing system for quantitative image anal. 7-28796
- life sciences experimentation, autonomous, in space stations, visual monitoring 7-23467
- magnetic resonance imaging, computer model to optimize image contrast 7-54690
- manual materials handling task design using computerised biomechanical modelling 7-14040
- median eminence microvascular, 3D reconstruction 7-34356
- molecular design, computer-aided, conf., London, England (Oct. 1986) 7-50429
- monkey visual training using a microcomputer and a bicoloured LED 7-40383
- movement-related brain pots., synchronisation rel. to computer detect of EMG edges 7-14027
- muscle contractility, computerised experimental set-up 7-54649
- nerves and molecules 3D reconstruction and display using pattern recognition 7-65734
- neural circuit computing, model 7-13983
- neuron tracing system, CARTOS-ACE, 3D reconstruction of electron micrographs 7-23502
- neuron tracing through serial sections, use of shape knowledge to improve performance 7-3954
- nucleoli, extraction from images of leucocytes by computerised image analysis 7-23505
- organ of Corti, computer-assisted morphometric anal. system 7-40373
- paraplegics, EMG-controlled stimulation limb function discrimination using Karhunen-Loeve expansions 7-54540
- pattern generator, programmable, for visual evoked pot. anal. system 7-40384
- plasma renin assay calculation using Lotus 1-2-3 7-11585
- protein crystallography, restrained least-squares procedure using Numerix MARS-432 array processor 7-34105
- protein fluorescence quenching data analysis program 7-62438
- protein structure, restrained least-squares refinement, incorporation of fast Fourier transforms 7-54451
- protein structure prediction using databases 7-54456
- protein structure refinements, model-fitting procedure incorporating the double-null technique 7-54450
- proteins, conformational change mechanisms 7-54457
- radiation-induced late effects, computer simulation by system dynamics 7-18024
- retina display and reconstruction 7-14000
- thick specimens, computer-assisted video technique for preparing high resolution pictures and stereograms 7-28789
- three-dimensional morphometric cytology, pictorial pattern recognition 7-28801
- tissue ultrasonic reflection simulation model 7-8648
- torso, human, automated system for elec. props. modelling 7-40137
- transmitter binding sites, quantitative autoradiography with an image analyser 7-34359
- two-parameter data-acquisition system for slit-scan chromosome analysis 7-35501
- zooplankton population analysis, multiple microprocessor system using image processing 7-18103

biomagnetism

- action potential in lobster giant axon, effect of time-varying mag. fields 7-3766
- bacterial photosynthetic reaction centres, charge recombination, ultrafine interaction, mag. field effect 7-8516
- bean sprout growth, effects of elec. or mag. fields (*Japanese*) 7-47151
- blood, hypercoagulation syndrome in mobility-restricted rats, effect of a weak variable mag. field 7-54669
- blood and blood clots, paramag. effect of Fe on T₁ 7-17949
- brain electrical and magnetic activity monitoring 7-8743
- cardiac, bioelectrical sources localisation, accuracy, magnetocardiography appl. 7-54542
- cardiomagnetism, inverse problem soln. using a current multipole expansion of primary sources 7-54641
- cerebral magnetic fields, review 7-3809
- classifier-directed signal processing in brain research, EEG and magnetencephalogram appl. 7-54820
- combustion processes under intense mag. fields, living organisms appl. 7-8285
- computational tools, trends: from procedural codes to intelligent scientific models 7-54634
- cortical responses to painful CO₂ stimulation of nasal mucosa; a magnetencephalographic study in man 7-54620
- current dipole implanted in dogs, mag. localisation 7-54632
- eddy current magnetic shield with active compensation, improvement of props. 7-47192
- egg lecithin, bilayer lipid membranes, base conductance and electric breakdown, static mag. field effect 7-14030
- electrically silent magnetic fields 7-23373

biomagnetism continued

- extracellular water vols. in tissue, meas. by Gd modification of $^1\text{H-NMR}$ spin lattice relax. 7-18100
 eye movement, associated mag. field meas. (*Japanese*) 7-14031
 gallbladder bile, normal canine, alterations in NMR relax. during fasting 7-18004
 haemoglobin, inverse Faraday effect, mag. reson. Raman activity 7-65700
 haemopoietic tissue, ^{252}Cf RBE and PLD-like effect of mag. fields, CFU-S assay 7-28590
 intracellular motility and phagocytosis rate, mag.-particle probe behaviour 7-47139
 intracellular particles producing alterations in mag. characts. 7-65781
 intracranial dipoles, mag. localisation: simulation with a phys. model 7-14029
 inverse problem, basic math. and EM concepts 7-54626
 inverse problem, conf., Milton Keynes, England (Apr. 1986) 7-48155
 inverse problem, role of model and computational expts. 7-54628
 inverse problem and biomagnetism 7-54625
 inverse problem solution in magnetisation studies, dust in lungs of industrial workers appl. 7-54630
 inverse solutions based on magnetoencephalograms and EEGs, appl. to vol. cond. anal. 7-54637
 Lewis tumour graft, effect of a static nonuniform mag. field, mouse obs. 7-28595
 liposome vesicles, mag. field-induced drug permeability 7-40213
 lung tissue, autopsied, from asbestos workers, Mossbauer effect study 7-65849
 magnetic field effects on biological and chem. processes 7-47135
 magnetocardiographic data measurement and its movie display (*Japanese*) 7-14073
 magnetocardiographic isofield maps, torso geometry effect, computer model study 7-54640
 magnetocardiography based method for cardiac activity investig. 7-40351
 magnetoencephalogram and EEG, method for combining to determ. sources 7-54635
 magnetoencephalogram moving dipole inverse solns., effects of meas. errors and noise 7-3853
 magnetoencephalogram topography, simulation with sphere filled with saline soln. 7-8612
 magnetoencephalogram topography and source model of abnormal neural activities associated with lesions 7-47032
 magnetoencephalographic data anal. using homogeneous sphere model: empirical tests 7-54638
 magnetoencephalographic source models and physiology 7-54629
 magnetoencephalography, inverse problem, instrumental and analytical perspective 7-54627
 magnetoencephalography, inverse problem, medical perspective 7-54689
 magnetoreception pathways in a migratory salamander 7-18006
 magnetotactic bacteria, mag. props., SQUID obs. 7-8610
 mammalian cells, irradi. with ^{252}Cf and ^{60}Co , effects of alternating mag. fields on survival 7-28594
 mitogenic response of peripheral blood mononuclear cells, effect of ELF pulsed mag. fields 7-28580
 Mossbauer spectroscopy of magnetically ordered biological materials, Mossbauer spectroscopy 7-60133
 mouse liver, P containing metabolites, Zn powder injection; NMR obs. 7-8609
 myocardial proton spin-lattice relaxation time in vitro: effect of elapsed time after excision 7-47136
 neuromagnetic activity, synchronised spontaneous, data anal. technique 7-54633
 neuromagnetic fields interpretation, feasibility of homogeneous head model 7-54636
 neuromagnetic localisation, improved procedure 7-54639
 NMR imaging, optical detection of respiration and heart beats 7-47277
 operant behaviour of rats, alteration by low-intensity mag. fields 7-28578
 photosynthetic membranes suspended in cryoprotective glycerol- H_2O mixture, proton relax. time meas. 7-34170
 principles and clinical validity of biomag. method, review 7-47138
 rat tissue, mag. field effects, phase-contrast microscopy obs. 7-8645
 Roman crystalline lens, cataract development, water state, NMR spin echo obs. 7-8557
 skeletal muscle, NMR relax. times, dependence on fibre type and diet, rabbit obs. 7-18003
 strong static mag. field effects on living organisms and chem. reactions 7-8611
 temporal lobe epilepsy patients, mag. field, temporal region modelling 7-54631
 thrombolytic process dynamics under conditions of a constant mag. field 7-3835
 tissue T_2 transverse relax. rate, effect of interpulse delay 7-18005
 toroid-amplifier system for mag. meas. of current in biological tissue, capabilities 7-23493
 tumour models, expt., $^1\text{H-NMR}$ relax. times and water compartmentalisation 7-17950
 $^{45}\text{Ca}^{2+}$ efflux from isolated chick brains, lack of effect of static mag. field 7-28579

biomass conversion see *bioenergy conversion***biomechanics**

- see also *biological fluid dynamics; biorheology*
 3-axis goniometer for trunk range of motion meas. of worker in worksite 7-28567
 3D human body segmental motion meas. using laser scanning system 7-28568
 16-channel controller for implantable gait stimulation system, design 7-28781
 ankle joint dynamics, posn. depend., active mechs. 7-23385
 ankle joint dynamics, posn. depend., passive mechs. 7-23384
 ankle movement prediction and evaluation with implantable peroneal stimulators 7-28778
 aorta, circumferential variation in stiffness in large animals 7-8643
 aortic dissections, factors in propag. in canine thoracic aorta 7-54659
 aortic valve tissues, relative vols. of struct. components rel. to biochem. components 7-34182
 arterial anastomoses, laser-assisted and sutured, mech. props. under axial loading, rabbit obs. 7-23374
 arterial cast, compliant, wall motion and wall shear obs. 7-65804
 arterial elasticity in human fingers and rabbit forelegs, noninvasive automatic meas. using photoelec. plethysmography 7-28794

biomechanics continued

- arterial mechanics, strain energy density function and uniform strain hypothesis 7-54656
 articular cartilage in canine knee, indentation study of biomech. props. 7-54651
 astral mitotic spindles, phys. theory of orientation 7-65727
 automation range of motion meas. in cervical spine using video images 7-28747
 biaxially tested soft tissues, strain quantification technique 7-54824
 bicycle pedalling, EMG meas. anal. 7-23380
 biomedical engineering, conf., Shreveport, LA, USA (Oct. 1986) 7-18470
 bioprosthetic valves, closed, influence of stent height upon stresses on cusps, finite element model 7-23387
 bioprosthetic valves, porcine, leaflet stiffening effect on leaflet stresses 7-65889
 bird flight, calc. of lift, thrust and drag 7-18011
 blood vessels, nonlinear elasticity (*Chinese*) 7-18009
 bond graph simulation of a mobile two-legged mechanism 7-8771
 bone, fracture healing, assessment by spectral anal. 7-8730
 bone, mech. props. and morphology, effects of Ca deficient diet, goose obs. 7-3822
 bone marrow pressure chamber, permanently inserted Ti implant for intramedullary press. meas. 7-8779
 bones, fresh, human, strain, meas. by strain gauge, method and obs. (*Chinese*) 7-28782
 cancellous bone in canine proximal femur: elastic moduli, yield stress and ultimate stress 7-54657
 cardiac wall motion abnormalities detect., combined amplitude and phase anal. 7-28566
 cardiac wall motion abnormality visualised in the 30° RAO and 60° LAO projections, comparison of magnitude 7-28688
 cardiac wall motion during exercise, computerised quantitative segmental anal. from 2D echocardiograms 7-34321
 central mechanism of space sense, perception and movement control (*Japanese*) 7-14009
 cerebellum, role in visual guidance of movement, review 7-40143
 chinchilla cochlea, basilar membrane mechanics: low freq. responses and microphonics and spike initiation 7-47093
 closed-loop electrical stimulation orthoses for restoration of quiet standing in paraplegia 7-28769
 Cochlear hydromechanics modelling 7-65762
 cochlear mechanics and physiology, interrelationships (*French*) 7-47082
 collagen, tendon, specimen length rel. to tensile failure props. 7-34180
 collagenous tissues, repeated extensions, measured responses and medical implications 7-8641
 composite materials, columnar, subjected to impulsive loading, dynamic response testing 7-59708
 computer animation of human walking, real-time, for pathological gait evaluation 7-28569
 computerized biomedical models in manual work design 7-40209
 conference on bioengineering, New Haven, CT, USA (March 1986) 7-16
 conference on biomechanics, Mons, Belgium (Sept. 1986) (*French*) 7-9578
 consonant-vowel-consonant sequences production, effect of speaking rate on jaw and lip movements (*Japanese*) 7-34165
 coordinated biological motion, nonequilib. phase transitions, critical fluctuations 7-28564
 cornea, rabbit and human, mech. props. obs. 7-28556
 crescent-shaped wings and caudal fins, efficiency characts. 7-60024
 cultured endothelium, apparatus to study response to shear stress 7-65907
 cycling, analytical and experimental biomechanics 7-54666
 dental bridges, stress distrib. on alveolar bone surface, anal. using photoelastic coating technique (*Chinese*) 7-28767
 dentin, human and supporting bone, elastic modulus meas. by laser speckle photography 7-34183
 depressed elastic collapsible tube, expt. determ. of transversal Young's modulus, vein appl. (*French*) 7-3825
 Derby intramedullary nail, biomech. comparison 7-40362
 dynamic problems of biomechanics, deformable solid model with reaction 7-47140
 egg lecithin vesicles, pierced, elastic torques about membrane edges 7-23312
 elbow, stress anal. before and after radial head resection (*German*) 7-23376
 elbow, stresses after joint replacement, finite element method calcs. and expt. obs. (*German*) 7-54809
 electrical stimulation open-loop control of human knee during swing 7-28763
 electrogoniometer for thoracolumbar rot. meas. 7-28786
 electrogoniometric gait recording, 3D 7-3823
 EMG study of side step for development of elec. stimulation patterns 7-28570
 EMG-force model of elbow's antagonistic muscle pair 7-59966
 endoprosthetics, expt. results on mech. coupling 7-54811
 epiphyseal-based designs for tibial plateau components, stress anal. in frontal plane 7-3934
 epiphyseal-based designs for tibial plateau components, stress anal. in sagittal plane 7-3935
 equine ground reaction force data analysis 7-54650
 ergometric test methods and equipment 7-28752
 erythrocyte, live cell, shear elasticity, entropic nature 7-65725
 erythrocyte marginal bands, newt, extensional and flexural rigidity obs. 7-8631
 erythrocytes agglutinated by antibody, hydrodynamic force of breakup 7-40122
 erythrocytes agglutinated by antibody, interaction forces between 7-40121
 evoked potentials from passive elbow movements, modification by motor intent 7-14026
 expert system, LIFTAN, for analysis of manual lifting, risks of overexertion 7-40210
 eye movement, human, research review 7-17978
 fatigue in isometric contraction in a single muscle fibre: compartmental Ca^{2+} flow model 7-34179
 femoral stem of cemented total hip replacements, role of collar rel. to bone stresses and resorption 7-8760
 femoral stress anal., 3D, using CT scans and P-version FEM 7-8613
 femoropatellar joint, trajectory pattern and load-bearing capacity when diseased (*Japanese*) 7-8638

biomechanics continued

- finger arteries, noninvasive meas. of vol. elastic modulus using photoelec. plethysmography 7-3857
 fixation plate for tibia, anatomically contoured, biomech. testing 7-8762
 fluorescent light, lack of effects on human muscle strength by kinesiology testing 7-23406
 foetal movements recording, comparison of 3 methods 7-23389
 foetal proximal femoral chondroepiphysis, human, expt. determ. of linear biphasic constitutive coeffs. 7-3821
 foot, biomech. model 7-40191
 foot, human, spring in arch 7-47143
 foot pressure measurement: a review of clinical findings 7-8728
 force-interval relationship in heart muscle of mammals, Ca^{2+} compartment model 7-54648
 functional neuromuscular stimulation, parameter selection and upper limb characterisation 7-3764
 functional neuromuscular stimulation to augment walking, develop. stages 7-34333
 gait, temporal and spatial parameters meas. using a microcomputer system 7-40321
 gait analysis system, portable computerised, force distrib. meas. under foot in walking modes (*Japanese*) 7-14146
 gait correction two-channel orthotic stimulator (*Slovenian*) 7-23486
 grasp control during functional neuromuscular stimulation, force/position feedback 7-28764
 halo-vest on thorax, mobility: comparative biomechs. of 8 designs 7-8768
 hand-arm vibration syndrome in foundrymen and hard rock miners 7-28559
 handicapped person, determ. of 3D force and motion capability 7-8639
 head, human, mech. point impedance with and without skin penetration 7-34296
 heart, dynamic changes in regional vel. of shortening, anal. 7-40203
 heart, left ventricle over cardiac cycle, simulation model (*Japanese*) 7-47146
 heart valves, prosthetic, flexible support frame 7-3938
 hearts, local spatial phase analysis of left ventricular wall motion using Hilbert transform (*Japanese*) 7-47145
 hip endoprostheses, effects of stem design and material props. on stresses 7-40361
 hip joint motion during normal walking, state variable approach to function of muscular system 7-40200
 human body centre of gravity, statistical analysis of fluctuations in upright posture (*Japanese*) 7-14036
 human gait anal. math. model, quasi-linearisation technique 7-65791
 human gait data acquisition and processing using digital camera 7-65809
 impact load effect on spinal cord, full-scale and computational expts. 7-34294
 impact pressures delivered by oral water irrigation devices, expt. meas. 7-3929
 impedance characteristics, expt. modelling 7-3828
 implantable gait simulation using microprocessor-controlled trigger switches 7-34353
 implantable gait stimulation system, 16-channel microprocessor-based controller, features 7-28780
 impulsive force transmission along the lower skeletal extremity, in vitro simulation 7-40190
 inflation waves induced by axial accel. of the aorta 7-8637
 intervertebral discs, human, subjected to axial dynamic compression, biomech. props. 7-28553
 intracranial pressure: review of clinical problems, meas. techniques and monitoring methods 7-40323
 intraocular pressure, monitoring under μG conditions (*German*) 7-8722
 isovolumic contraction, left ventricular wall stresses determination using FEM 7-23378
 ivory, tensile props. and fracture rel. to comp. and struct. 7-14032
 jaw opening for vowels in vowel sequence words, effects of tempo and context 7-47148
 joint angle control of human arm, constraint. anal., model 7-23375
 joint angle sensors for closed-loop control of movements in paraplegics 7-28766
 jumping, estimation of power output and work done by human triceps surae muscle-tendon complex 7-34175
 knee, effect of muscular activity on valgus/varus laxity and stiffness 7-3819
 knee, human, passive resistance: effect of remobilisation 7-40199
 lateral prehension-release grasp charact. using functional neuromuscular stimulation 7-28576
 lattice shrinkage with increasing resting tension in stretched, single skinned fibres of frog muscle 7-8485
 left ventricle, spatial energy balance within a struct. model 7-54502
 left ventricular pressure decay in the myocardial wall 7-34186
 left ventricular regional wall motion, quantification using multiple-view radionuclide angiography and the centerline method 7-34268
 left-ventricular regional wall motion assessment, comparison of 2 nuclear cardiology techniques 7-3862
 leg power changes to vels. used in bicycle endurance training, specificity 7-8615
 lifting without spinal injury, safe loading 7-60026
 ligaments, methodology to determ. mech. props. at high strain rates 7-65909
 limb oscillations, rapid, role of intersegmental dynamics 7-28558
 lipid bilayers, charged, short range forces between, theoretical model 7-28478
 lips, upper and lower, movements during speech 7-8601
 loading myelography, functional exam. technique for lumbar spinal canal 7-18077
 locomotor movements, human, aspects of regulation 7-40181
 long jumpers, elite male, model of technique characts. 7-28557
 lower limb, quantitative functional anatomy with appl. to human gait 7-54658
 lumbar intervertebral segment study, nonlinear finite element model 7-65792
 lumbar nerve root lesions diagnosis, electronic comparison of toe strengths 7-3926
 lumbar vertebrae, human, dimensions in sagittal plane 7-23386
 lumbar vertebrae, progressive positions visualisation using CAT-scan data 7-3834
 lung parenchymal and airways recoil hysteresis, time dependence 7-8625
 lung tissue, human, mech. props. (*Chinese*) 7-28549
 lungs, elastic stability and surface tension 7-54662
 mammalian muscle fibres, rate constants for contractile cycle 7-60021

biomechanics continued

- mandibular kinesiographic meas., distorted, signal restoration 7-47149
 manual materials handling task design using computerised biomechanical modelling 7-14040
 mother-of-pearl, fracture surfaces, analytical techniques appl. 7-8781
 motor control performance tracking accuracy quantification system 7-28572
 motor cortex, primate, neuronal population coding of movement direction, arm appl. 7-28489
 movement-related brain pots., synchronisation rel. to computer detect of EMG edges 7-14027
 multi-jointed limb movement and posture control, simulation studies 7-65784
 multichannel portable functional electrical stimulation system for spinal cord injured persons 7-28765
 muscle, force enhancement phenomenon, simulation 7-34172
 muscle force predictions, sensitivity to changes in physiological cross-sectional area 7-3820
 muscle function anal., microcomputer system 7-40320
 muscle strength simulations using the articulated total body model 7-40207
 muscles, electrically stimulated, effect of muscle nonlinearities on control 7-8644
 musculoskeletal model of the human lower extremity 7-28575
 musculotendon actuator models for neuromuscular stimulation system CAD 7-28573
 myocardial contractility anal., computational method 7-14140
 nystagmus induced by off vertical axis rotation, three-dimensional model 7-47047
 ocular motility, excursion tests 7-65750
 osteoarthritic gait assessment, quantitative approach 7-54785
 osteosynthesis, l-sided external fixation, improved stability (*German*) 7-40182
 osteotomy gap, uniform, 3D strain fields 7-8636
 PEEK and C fibre reinforced PEEK materials potential as bioimplants 7-60126
 pelvic stress, concs. in acetabulum resulting from blow to right trochanter 7-40192
 pelvic stresses in vitro, efficacy of metal-backed acetabular prostheses 7-23383
 pelvic stresses in vitro, endoprostheses malising 7-23382
 pericardium, natural and chem. modified, relative extensibility rel. to gauge length standardisation 7-40194
 periodontal ligament, human, mech. props. of tooth and root sections 7-3824
 peristalsis, modelling and analysis considering intraluminal pressure (*Japanese*) 7-47147
 phase-locked modes, phase transitions and component oscillators in biological motion 7-60025
 phosphatidylglycerol bilayers in aq. electrolyte solns., forces between, obs. 7-28473
 phospholipid bilayers, solvent-mediated interaction, nonlocal electrostatic theory of hydration force 7-17958
 photogrammetric techniques using high-speed cineradiography, biomechanics research appl. 7-23500
 photogrammetry application for study of body movement and shape 7-28753
 planar musculoskeletal model for studying posture induced by functional neuromuscular stimulation 7-28574
 plant cell membranes, water movement, cell wall deform., cooling effect 7-8525
 porous-glassy-carbon/bone interface, loaded, shear strength, rabbit obs. 7-54643
 posture control system, max. likelihood identification 7-60022
 posture measurement in free space, precision increase, diseased/prosthetic knee clinical assessment 7-34300
 posture-control system, selection of perturbation parameters for identification 7-28561
 pressure distribution under the ischium of normalsubjects, meas. system 7-8729
 pressure sore prevention by functional electrical stimulation of gluteus maximus muscle 7-34335
 psoas fibres, skinned, rabbit, stiffness in MgATP and MgPPi soln. 7-23377
 red blood cells suspended in carbohydrate-saline solns., deformability, effect of transmembrane pot. 7-34118
 Rehabilitation R&D Progress Reports 7-28774
 respiratory mechanics, structural model of thorax and abdomen 7-54663
 rib response and breakage due to anteroposterior loads 7-28562
 right ventricular regional wall motion, meas. from biplane contrast angiograms using the centerline method 7-34262
 role of vision in producing motion sickness 7-54545
 saccadic eye movements, time-optimal control 7-59978
 seated human, response to vibr. and impact 7-3831
 semi circular canal, mech. model (*French*) 7-3800
 shock-absorbing properties of mammalian tissues and bones 7-3829
 shoulder complex, human, statistical database for biomech. props., kinematics 7-8632
 shoulder complex, human, statistical database for biomech. props., passive resistive props. 7-8633
 shoulder position evaluation for quadriplegics using neural prosthetic devices 7-28779
 single-leg swing-through gait using axillary crutches, biomech. study 7-14034
 skeletal muscle, effect of cross-bridge clustering and head-head competition on mech. response 7-28548
 skeletal muscle, frog, effect of a sub-ms temp. jump on the mech. tension of demembranised fibres 7-40180
 skeletal muscle sinusoidal oscills., energy stored and dissipated, frog obs. 7-40113
 skull, dry, initial tooth and bone displacements, optical laser techniques meas. 7-65796
 small vessel distensibility in man, noninvasive determ. 7-3908
 soft tissue, finite deform., anal. of mixture model in uni-axial compression 7-65806
 soft tissues, 2D, constitutive model and its appl. to expt. data 7-23381
 sphingomyelin bilayers, interactive forces 7-34115
 spinal motion segments, human, internal displacements from in vitro loading, expt. results and finite element model predictions 7-3833
 spine, method for identification of in vivo segmental stiffness props. 7-65801

biomechanics continued

- spine, segmental motion meas., transducers mounting 7-3945
- spinotrapezius muscle, rat, viscoelastic props. of microvessels 7-8630
- stance phase control of above-knee prostheses: knee control vs. SACH foot design 7-54812
- standardization in anthropometry and biomechanics 7-54665
- stomach, human, noninvasive technique to monitor elec. and mech. activity 7-60110
- stretch-induced delayed force development in guinea-pig taenia coli 7-3830
- surface electrical stimulation of quadriceps in patients with spinal injury, response 7-34334
- tendon stiffness: methods of meas. and significance for movement control, review 7-54825
- tendons and tendon sheaths, anal. of cumulative strain 7-54655
- tensile test system, automatic, for biotissues 7-23489
- thoraco-abdominal biomechs. research, use of quadruped models 7-40189
- tibia state alteration during antiothostatic hypokinesia 7-34181
- tibial bone, bovine, fracture props. 7-34177
- tibial components, bone stresses beneath, effect of interface, finite element modelling 7-40188
- tibial plateau, cement layer stresses, model obs., 3D strain rosettes 7-65798
- time course of the houseflies' landing response, leg movement evaluation 7-65785
- torso models for pushing and pulling, two and three dimensional 7-40206
- trabeculae, bovine, tensile testing, device and obs. 7-3832
- trabecular bone specimens, stiffness behaviour obs. 7-54660
- triceps surae muscle-tendon complex, human, model, jumping appl. 7-34174
- trunk loading, effect of unexpected loads 7-40208
- trunk muscle and moments, relationship in sagittal and frontal planes 7-3784
- turf grasses, physiological response to trampling pressure 7-34184
- urethra, female, probe for meas. of cross-sectional area and press. 7-3910
- urinary bladder, fibre strength assessment using expt. press. vol. curves: analytical method 7-65800
- vascular compliance of canine lung, longit. distrib. 7-8624
- ventricular mechs., model selection, sensitivity anal. approach 7-40196
- ventricular wall motion anal., tests of methods 7-40204
- video images and computer graphics superimposition technique, human body biomechs. study appl. 7-34361
- visceral pleura, excised canine, mech. behaviour obs. 7-54644
- visual feedback processing in positioning movements 7-8628
- vocal fold oscillation simulation using lumped mass-springs 7-60020
- vocal fold tissue, mech. props. 7-14039
- vocal fold vibration and speech signal, simultaneous high speed digital recording 7-47129
- walking, steady state gait movement induced from upright posture obs. 7-40195
- walking and ECG, computerised system for 24 hr simultaneous recording and anal. 7-40347
- walking horse, technique to quantify skin displacement 7-28787
- walking using long leg braces or functional neuromuscular electrodes, relative energy cost 7-34336
- weightbearing tissue contour and deformation by magnetic resonance imaging 7-28571

biomedical aids for handicapped *see handicapped aids*

biomedical applications of computers *see medical computing*

biomedical electronics

- see also electrocardiography; electroencephalography; microelectrodes; patient monitoring; patient treatment; prosthetics; sensory aids*
- active free-field equalizer for TDH-39 earphones 7-28768
- biofeedback system with interchangeable modules for applied research and clinical practice in underdeveloped countries 7-28761
- capacitive pressure sensor IC, micropower ccts. design for implantable device, biomedical appl. 7-34316
- Chorimac cochlear prosthesis, discrimination of elementary phonemes (French) 7-47288
- cochlear neuroprosthesis development, Czechoslovak project 7-8766
- critical and emerging issues in biosensors 7-65876
- cutaneous galvanic reaction parameters, automated recording system 7-40353
- developments, review (Italian) 7-18094
- digital subtraction radiography technology, equipment and techniques 7-40267
- ECG signal changes reconfiguration, using delta modulation (Czech) 7-60119
- EMG fine wire connections technique 7-23468
- heart rate monitor, design, operation and construction (Spanish) 7-40327
- IC realisation of a neuronal model 7-3919
- implantable electronic devices reliability, case studies 7-60122
- implantable gait simulation using microprocessor-controlled trigger switches 7-34353
- implantable multielectrode array with on-chip signal processing, micropore for biopotentials recording 7-28495
- implantable multielectrode array with on-chip signal processing, neural prostheses/biopotential recording appls. 7-34338
- implants for nerve stimulation in paraplegic patients, gate array appls. 7-34339
- intracranial pressure monitoring unit with computerised signal processing, improved design (Spanish) 7-34299
- Kent bypass pathway electronic simulator for cardiac arrhythmia study (Spanish) 7-8733
- lumbar nerve root lesions diagnosis, electronic comparison of toe strengths 7-3926
- modulation techniques for biotelemetry 7-34301
- multichannel digital temperature meter using transistor sensor, design for medical appls. (Spanish) 7-30010
- nerve activity measurement and analysis, conf., London, England (Nov. 86) 7-41014
- neurosurgical intensive care unit, computerised monitoring system 7-34320
- optical probe for on-line meas. of velopharyngeal valve opening 7-60071
- photoplethysmography: selecting optoelectronic components 7-28647
- radiotherapy, external beam, on-line electronic portal imaging system 7-14110
- RF-coupled phrenic nerve stimulator implant, temp. telemetry addition 7-28771

biomedical electronics continued

- scanning X-ray imaging system for quantitative arteriography and blood flow meas. 7-40266
- signal source with MOSFET chopper amplifier, brain voltage changes meas. appl. 7-23480
- some aspects of medical electronics for hospitals 7-14138
- techniques of recording motor unit action potentials 7-65877
- temperature, circuit for linear meas. 7-28739
- testing and safety of biomedical electronic instruments, Electrotechnical Testing Institute practices (Czech) 7-18090
- three channel cochlear neuroprosthesis for the deaf, implantable receiver/portable transmitter config. 7-8765
- tracheobronchial tree and pulmonary arteries, NMR imaging using electronic axial rot. 7-14102
- X-ray image intensifier, with large input aperture and high resolution (Czech) 7-35650
- O₂, singlet, optical monitoring of generation during photodynamic treatment of tumours 7-65897
- Si IC sensor technology and applications (German) 7-24644

biomedical engineering

- see also biomedical electronics; biomedical equipment; orthotics; patient treatment; prosthetics; sensory aids*
- anesthesia developments 7-65872
- Bioengineering Program of the Universidad Nacional de Tucuman (Argentina, 1974-85), cardiac fibrillation, defibrillation research 7-4650
- biological/medical engineering, Fort Worth, Texas, USA (Nov. 1986) 7-65870
- biomedical engineering education in the UK 7-65874
- conference, Shreveport, LA, USA (Oct. 1986) 7-18470
- critical and emergent issues in biosensors 7-65736
- critical and emerging issues in biomaterials 7-65871
- education, college-level programs in Indiana, Michigan, and Ohio 7-35144
- EEC research programme in biomedical engineering 7-4649
- human exercise and heat exchange in thermal environments 7-63154
- industry's perspective of critical issues in biomedical engineering education 7-65873
- muscle receptors and the regulation of muscle contractions 7-65808
- neuromuscular system bioengineering 7-65735
- new artificial devices, from laboratory to clinical use: The engineer's role in the ethics of experimentation 7-65875
- research, targeting to impact medical practice 7-3917

biomedical equipment

- see also biomedical electronics; biomedical measurement; handicapped aids; laser applications in medicine; orthotics; prosthetics; radioisotope scanning and imaging; sensory aids*
- 3-axis goniometer for trunk range of motion meas. of worker in worksite 7-28567
- 3D human body segmental motion meas. using laser scanning system 7-28568
- acceptance testing and hospital equipment management 7-54797
- alloy filter, effect on γ -camera images 7-65839
- anaesthesia for surgery, prod. by elec. stimulation of brain, generator 7-8759
- anatomical compensation filter for chest radiography, evaluation 7-28659
- anesthesia developments 7-65872
- APL Bioelectromagnetics Laboratory 7-47263
- arterial mean pressure, simple device for meas. and for calibration of arterial press. monitors. 7-8731
- audiobiofeedback system for sensory aid to handicapped persons 7-34344
- back and trunk musculature, devices for dynamic evaluation and rehabilitation, review 7-3923
- balloon dilation catheters for percutaneous transluminal angioplasty, technical characts. (German) 7-23481
- bed, static charge sensitive, for automatic anal. of sleep records 7-3896
- biological/medical engineering, Fort Worth, Texas, USA (Nov. 1986) 7-65870
- biplane multidirectional angiocardiology with a new X-ray system 7-14111
- blood pressure sensor for fibrillation detect. method, implantable defibrillator output circuit evaluation (Japanese) 7-14160
- blood velocity profile measurement by ultrasound Doppler shift method 7-37585
- capacitive pressure sensor IC, micropower ccts. design for implantable device, biomedical appl. 7-34316
- cerebral blood-flow meas. in ventilated premature babies, ¹³³Xe, inhalation system 7-23434
- coaxial TEM deep-body hyperthermia applicator, 3D model 7-14082
- complementary projector system for contrast sensitivity meas. 7-8748
- computed radiography system TCR 201 7-18067
- computed radiography system using an imaging plate as an X-ray sensor, TCR-201 7-40282
- computerised system for 24 hr simultaneous recording and anal. of walking and ECG 7-40347
- conference on bioengineering, New Haven, CT, USA (March 1986) 7-16
- conference on medical imaging and instrumentation, Boston, MA, USA (April 1985) 7-40996
- cutaneous galvanic reaction parameters, automated recording system 7-40353
- α -cyanoacrylate cements for biomed. equipment, opt. parameters 7-25910
- cybernetic instrumentation prospects and problems 7-18087
- data acquisition system for monitoring low birth weight neonates 7-3920
- diagnostic equipment type SDL-300 (Japanese) 7-16045
- digital diagnostic imaging, versatile image processor and its appl. in computed radiography 7-28673
- digital image store, 1024 \times 1024 pixel, with pulsed progressive readout camera, appl. to gastro-intestinal radiology 7-28680
- digital radiographic imaging system with multiple-slit scanning X-ray beam 7-54737
- digital radiographic units comparison 7-23448
- digital slot radiography system based on a linear X-ray image intensifier and 2D image sensors 7-23450
- digital subtraction angiographic units, quality assurance protocol 7-65824
- digital subtraction angiography system, high resolution 7-28679
- digital subtraction angiography systems, acceptance testing and calibration 7-47239
- digital subtraction radiography technology, equipment and techniques 7-40267
- dual-energy projection radiography using condenser X-ray generator and digital radiography apparatus 7-54739

biomedical equipment continued

- EEG, epileptogenic sharp transients detect., multichannel signal processor 7-54786
- electrical safety, conf., London, (Jan. 1987) 7-48195
- electrical safety limits for medical equipment 7-54794
- electrically powered biomedical equipment, safety standards 7-54795
- electrodes, recording and stimulating, for biological research 7-47306
- electrogoniometer, flexible, applying electroconductive rubber, clinical use (Japanese) 7-14139
- endoscopic micromanipulator for multiplanar transesophageal imaging 7-47190
- ergometric test methods and equipment 7-28752
- evoked potentials processing with tactile and thermal stimulation; prototype system (Spanish) 7-34318
- eye examination setup, OAP-311, rational refraction system 7-8747
- fibre optic beam delivery systems in high power laser surgery 7-47201
- fibre optic cable for CO₂ laser scalpel 7-14086
- fibre optic position verification device, radiation therapy appl. 7-47213
- fibre optic probes for ophthalmology 7-47206
- fibre optic thermometer for medical appl., using thermochromic transducer and TDM technique 7-47276
- fibre optical and video monitor stimulators, comparison in normals and multiple sclerosis patients 7-65865
- fibreoptic laser probe for treatment of occlusive vessel disease 7-34227
- filters for chest radiography, comparison 7-47229
- flexible waveguide for CO₂ laser surgery 7-34226
- Fourier and computerised IR spectroscopy, Ottawa, Ont., Canada (June 1985) 7-48160
- Fourier transform IR spectroscopy, biological and biomedical appl. 7-54831
- gait analysis system, portable computerised, force distrib. meas. under foot in walking modes (Japanese) 7-14146
- gamma camera, electronically collimated, gas scintillation utilisation 7-65845
- hand-held ultrasonic medical image scanner, design 7-54688
- head-mounted device for meas. of pointing to visual targets without seeing the pointing arm 7-47279
- heart rate monitor, design, operation and construction (Spanish) 7-40327
- heat delivery systems for hyperthermia treatment of psoriasis, comparison 7-14152
- heavy particle accelerator, design (Japanese) 7-54741
- hematoporphyrin derivative fluorescence detector 7-14148
- holographic endoscopy with gradient-index optical imaging systems and optical fibres 7-31271
- hyperthermia, localised: scanned, focused, multiple transducer US system 7-65819
- hyperthermia, Phase I regional device evaluation, microwave annular array vs. RF induction coil 7-47286
- hyperthermia applicator, completely implantable, with externalised temp. monitoring: tests in cond. gel 7-54703
- image intensifier digital imaging systems, struct. mottle obs. 7-54721
- image intensifier TV digital systems, accurate meas. of charact. curves by Al stepwedge technique 7-54726
- implantable multielectrode array with on-chip signal processing, neural prostheses/biopotential recording appls. 7-34338
- implantable telemetry systems finite element anal. of mag. fields 7-28754
- implanted cardiostimulators, polymeric insulation degradation (Czech) 7-23487
- inspired air conditioning equipment, hyperventilation challenge for asthmatics appl. 7-3911
- integrated voice analyzer for acoustic evaluation of pathological voice 7-40236
- interstitial microwave antenna array hyperthermia system, SAR patterns 7-8678
- interstitial microwave antenna hyperthermia system, power deposition pattern control 7-8677
- interstitial microwave antennas for thermal therapy 7-65825
- intracranial pressure monitoring unit with computerised signal processing, improved design (Spanish) 7-34299
- IR fibre optic device for cardiac cycle timing and photoplethysmography 7-3856
- IR vision systems, calibration from thermal emissivity standards 7-60117
- jet flowmeter, characts. (Bulgarian) 7-28740
- jet injector, some phys. aspects 7-65887
- joint angle sensors for closed-loop control of movements in paraplegics 7-28766
- kinesthetic charge detector for digital radiography, performance parameters 7-23449
- laser coagulator, argon type, use in ophthalmic therapy 7-8674
- laser coagulator, LAK argon type, for ophthalmic therapy 7-8673
- laser surgical instruments, surface treatment for improved safety 7-34328
- lead-off electrode systems, concept of local resolution 7-28738
- magnetic resonance imaging role in cardiovascular disease detection 7-54706
- magnetic-resonance imaging system using superconducting magnet (Japanese) 7-23478
- mammographic films and screens, comparative study 7-54716
- mammography, performance evaluation of a dedicated system 7-47235
- medical heavy particle accelerator, design (Japanese) 7-54741
- microcomputer system for muscle function anal. 7-40320
- microelectrodes, tip geometric area definition by plasma etching of Parylene, intracortical stimulation appl. 7-28760
- microprocessor based respirator digital simulation 7-14154
- microprocessor-based home monitor for sudden infantdeath syndrome 7-3921
- microprocessor-based time-of-flight respirometer 7-65866
- microscope, OPM-110, surgical experience in gen. practice 7-8757
- microscope, OPM-212F, use in ENT surgery 7-8755
- microscope use in microneurosurgery 7-8756
- microwave hyperthermia system, robot-operated, for testing large surface tumors 7-8675
- microwave interstitial applicators for hyperthermia, design with improved treatment vol. 7-65827
- microwave thermography system 7-60069
- mirror projection visual evoked pot. stimulator for presenting patterns in different orientations 7-3895
- multichannel digital temperature meter using transistor sensor, design for medical appls. (Spanish) 7-30010
- multichannel portable functional electrical stimulation system for spinal cord injured persons 7-28765
- multilayer mirrors as X-ray filters for slit scan radiography 7-34243

biomedical equipment continued

- muscle, time-resolved chambers, using multiwire proportional chambers 7-47144
- nerve activity measurement and analysis, conf., London, England (Nov. 86) 7-41014
- new artificial devices, from laboratory to clinical use: The engineer's role in the ethics of experimentation 7-65875
- NMR breast coil, design modification 7-14085
- NMR imager and spectrometer operating at similar freqs., relax. parameters comparison 7-18047
- NMR imaging, optical detection of respiration and heart beats 7-47277
- NMR imaging of breasts, receiver coil 7-65831
- NMR phantom, compact and high resolution, for multislice imaging 7-47209
- NMR whole-body machines, aspects of engng. design 7-60067
- nonlinear digital filter for separating nonstationary and stationary EEG waves 7-47267
- nuclear medicine acquisition station, microcomputer-based, low-cost 7-28681
- oesophageal electrodes for recording His-Purkinje activity based on signal variance, evaluation 7-23469
- ophthalmic applicators, B-particle, calibration of US National Bureau of Standards 7-47259
- ophthalmic combined Ar YAG-laser system 7-47197
- ophthalmological camera, wide-angle RCS-310 retinal camera, prototype experience 7-8745
- ophthalmological camera, wide-angle RCS-310 retinal camera design 7-8744
- ophthalmological laser slit lamp 7-47202
- optical fibre sensors chemical sensing, particularly in biomedical field, areas for use and techniques 7-31472
- optical fibres sensing in medicine 7-60072
- optical instrumentation for biomedical laser appls., conf., Innsbruck, Austria (April 1986) 7-40994
- optical self focusing operative microscope for microsurgery 7-54705
- optical storage technology for archiving digital medical images, review 7-28654
- oral water irrigation devices, impact press. delivered 7-3929
- permanent magnet structures for whole-body NMR diagnostics 7-54799
- phantom microdosimetric spectrometer, ionising radiation quality meas. 7-8692
- photoelectric plethysmography instrument for meas. of arterial elasticity in human fingers and rabbit forelegs 7-28794
- physiological pressure transducers, standard press. source for calibration 7-8732
- plethysmograph, granular strain gauge, for use as respiratory belt 7-14141
- plethysmograph for meas. of digital blood flow 7-40324
- plethysmography, whole-body, online real-time data processing system 7-3922
- polymer-based in vivo reference electrodes, functional mechanisms 7-40318
- position sensitive γ -ray detector for nuclear medicine, efficient design 7-14122
- Positome IIIp, a dynamic positron emission tomograph, imaging performance obs. 7-47215
- positron camera, multiwire proportional chamber, development of high-efficiency cathode converters 7-40271
- positron detection system for biochem. studies on living human brain 7-34240
- positron emission tomography, stationary high resolution, BGO detector unit 7-14119
- pressure distribution under the ischium of normalsubjects, meas. system 7-8729
- programmable visual display for diagnosing, assessing and rehabilitating unilateral neglect 7-65880
- pulmonary ventilation, simple low-resistance flap valve for expt. studies 7-3890
- pulsed US air flowmeter, design and construction 7-3845
- quadrature coil for NMR imaging 7-14087
- radiographic chest phantoms development 7-54725
- radiographic compensation filter made of Pb loaded acrylic, perceived advantages 7-65854
- radiographic digital imaging systems comparison: dedicated vs. add on 7-47237
- radiographic images, digital system for teletransmission 7-14108
- radiographic screen-film systems, MTF 7-60086
- radiotherapy, dosimetry of asymmetric X-ray collimators 7-54754
- rectilinear scanner, interfacing with a microcomputer 7-65858
- remote controlled X-ray television system Shimavision 900 (Japanese) 7-18093
- rotating phantom: evaluation of hard and software for gated gamma camera systems in nuclear medicine 7-23453
- safety, DHSS view 7-54796
- safety testing 7-54798
- scanning X-ray imaging system for quantitative arteriography and blood flow meas. 7-40266
- SEM stereophotogrammetric method and system for three-dimens. eval. of features on flat substrates 7-40377
- semi-automatic schistosome eggs detection system, image processing technique 7-47283
- single photon emission CT imaging with ¹²⁵I-labelled antibodies, comparison of low- and medium-energy collimators 7-40263
- single-photon-emission CT, high resolution, using 511 keV collimation 7-3871
- skin colour measurement device based on photoelec. colorimeter 7-60136
- skin in vivo meas. using dielectric time domain spectroscopy 7-14961
- Slitlamp Surgiscope, OPS-330, for microsurgery of eye 7-8758
- spectrophotometric measurements and instruments for medical analyses (Japanese) 7-337
- speculum surface finish effect on refl. of CO₂ laser beams 7-65830
- spherical tissue-equivalent proportional counter withcoaxial electric field 7-3868
- steel shield for NMR imaging, fabrication and performance 7-47274
- storage phosphor system for computed radiography: destructive scanning 7-23444
- storage phosphor system for computed radiography: screen optics 7-23445
- surface coil design for a vertical field MRI system, breast imaging appl. 7-18048
- surface electrode for high pO₂ values meas. (Chinese) 7-18083

biomedical equipment continued

surgical diathermy units, evaluation 7-23483
surgical instruments, diffuse laser light refl. from surfaces 7-47205
synchrotron beam line critical elements, heat transfer studies 7-42255
syringe, slow viscous flow 7-65802
testing and safety of biomedical electronic instruments, Electrotechnical Testing Institute practices (*Czech*) 7-18090
thromboelastograph, 2-channel, microprocessor-based 7-3903
tissue-equivalent phantom for diaphanography 7-54702
tomographic device providing information on chem. props. of body struct. 7-47217
toroidal rotary seal of IBM 2997 continuous flow cell separator, vels. and stress levels of axisymmetric azimuthal flow 7-3907
trachea noise biofeedback device to help reduce bronchospasm in asthmatics 7-8754
UHF local hyperthermia, electrode device and methodological problems of thermoradiotherapy (*Russian*) 7-23484
ultrasonic A-scan ophthalmoscope, eye abnormality diagnosis 7-40233
ultrasonic transducer design (*Turkish*) 7-28625
urethra, female, probe for meas. of cross-sectional area and press. 7-3910
urodynamic data-acquisition and anal. system, microcomputer-aided 7-3914
US diagnostic devices, USA Food and Drug Administration guidelines 7-3851
US Doppler flowmeter for use in theatre 7-47188
US scanner, high resolution, thyroid vol. determ. appl. 7-40235
US transmitter/receiver transducer, round-trip transfer function meas. (*Slovenian*) 7-23474
venturi suction electrode array for clinical bodysurface mapping 7-3904
whole body X-ray CT scanner SCT-2500T (*Japanese*) 7-18092
X-ray image intensifiers, detective quantum efficiency 7-23443
X-ray micro-CT scanner for biomedical appls. 7-47246
X-ray screen-film systems, logit model for MTF 7-54723
X-ray set, optical centering unit adjustment device 7-28664
X-ray tube, operating regime selection in radiodiagnostic investig., tissue heterogeneity effect 7-40278
X-ray tube anode, evolution 7-18066
X-ray tubes, half-value-layer increase owing to W buildup 7-14130
CO, personal exposure monitor with automatic data-logging 7-3943
Ge drift detector, tomographic device, for external analysis of tissue chemical props. 7-47273
Nd:YAG, CO₂ dual wavelength laser system for surgery 7-47198
Nd:YAG laser and sapphire contact probe, surgical appls. 7-34228

biomedical laser applications see laser applications in medicine

biomedical measurement

see also biological techniques and instruments; biomedical equipment; diagnostic radiography; electrocardiography; electroencephalography; laser applications in medicine; X-ray apparatus
3-axis goniometer for trunk range of motion meas. of worker in worksite 7-28567
3D human body segmental motion meas. using laser scanning system 7-28568
acoustic measurement of pathological voice qualities for medical purposes 7-37285
acute myocardial infarction, spectral anal. of heart rate fluctuations in evaluation of autonomous control 7-34313
aggregation of red cells expt. results., Space Shuttle Discovery appl. 7-3924
airways resistance, conversion between plethysmograph and perturbational meas. 7-3901
Alzheimer's disease, trace element imbalance meas. using sequential neutron activation anal. 7-34257
amputee's stump, shape measuring probe-type system for prosthetics CAD 7-34349
aorta, time domain resolution of forward and refl. waves 7-3900
APL Bioelectromagnetics Laboratory 7-47263
arterial blood pressure and heart rate variability signals, normal and pathological subjects evaluation appl. 7-34312
arterial elasticity in human fingers and rabbit forelegs, noninvasive automatic meas. using photoelec. plethysmography 7-28794
automation range of motion meas. in cervical spine using video images 7-28747
bacteria, pathogenic, ultrarapid differentiation and identification using FTIR techniques 7-54835
binocular fixation misalignment, objective meas. 7-8565
biofeedback system with interchangeable modules for applied research and clinical practice in underdeveloped countries 7-28761
biomagnetic method, principles and clinical validity, review 7-47138
blood, instantaneous flow, estimation from indicator-dilution curve after bolus injection of indicator 7-65867
blood, regional flow meas., theoretical anal. of transient clearance method 7-28736
blood, Se changes, cyclic activation anal. study 7-34100
blood, vol. flow in human common femoral artery. meas. using a duplex US system 7-28630
blood circulation measurement use in ophthalmic diagnosis 7-8746
blood flow velocity meas. in intraarterial digital subtraction angiography, pulsed-injection method 7-14128
blood O₂ saturation, in vivo meas. using quartz fibre optics and an optical multichannel analyser (*German*) 7-23423
blood pressure, diastolic, mean and systolic, numerical model of oscillometric determ. 7-65805
blood pressure measurement in postoperative hypertensive patients, comparison of intra-arterial and automated oscillometric methods 7-34297
blood pressure sensor for fibrillation detect. method, implantable defibrillator output circuit evaluation (*Japanese*) 7-14160
blood pressure signals, continuous long-term, decomposition into root components 7-34311
blood rate detector, one chip VLSI implementation using PPL 7-65881
blood velocity profile measurement by ultrasound Doppler shift method 7-37585
blood-rate detector, one-chip VLSI implementation using PPL 7-28756
body surface measurement and replication by photogrammetry and CAD 7-54695
bone, dual photon absorptiometry measurements, precision of dual photon absorptiometry measurements 7-40262
brain dopaminergic system, in vivo meas. using PET 7-18080
brain event-related potentials, principal components anal., spectral methods 7-47031

biomedical measurement continued

brain voltage changes meas., signal source with MOSFET chopper amplifier 7-23480
carcinoma of bladder and bronchus, in situ localisation, hematoporphyrin derivative fluorescence detector 7-14148
cardiac, bioelectrical sources localisation, accuracy, magnetocardiography appl. 7-54542
cerebral blood-flow meas. in ventilated premature babies, ¹³³Xe, inhalation system 7-23434
cerebrospinal fluid shunt flow meas., reproducible radionuclide procedure 7-65836
coronary blood flow, absolute, online computer meas. using a H₂ dilution catheter 7-28742
cross-modality matching of auditory and lingual vibrotactile sensations, magnitude estimation instrumentation 7-14028
cutaneous galvanic reaction parameters, automated recording system 7-40353
cybernetic instrumentation prospects and problems 7-18087
diastolic arterial press. in human fingers, meas. method using vol. oscillometry 7-3915
dichotic stimulation for central auditory testing, audio tape production, computer programs 7-47084
diffraction tomography in reconstructing marginal spatial frequency spectra for wave fields 7-3867
digital fluoroscopy, medical imaging 7-47271
DNA distributions with abnormal stemlines determined by flow cytometry, automatic analysis 7-59949
Doppler US 7-8672
drug effects detect. by EEG background activity stages identification 7-54781
EEG frequency analysis, filtering and aliasing of muscle activity 7-3894
effective airway resistance as determined by body plethysmography, meas. reliability 7-40187
electrodes, recording and stimulating, for biological research 7-47306
electrogastrographic signals, running spectrum anal. as an aid in representation and interpretation 7-65868
electrogoniometric gait recording, 3D 7-3823
ELF electric field meas., at human body surface 7-18840
EMG, surface and intramuscular, from the temporalis muscle, study of methods 7-3899
EMG activity recording technique for lumbar multifidus in man 7-3772
ergometric test methods and equipment 7-28752
eye, visual adaptation measurement using computer controlled device 7-34144
eye internal pressure meas., using electric sensors (*Slovak*) 7-60112
fibre optic chemical measurements in industry (*French*) 7-46894
fibre optic thermometer for medical appl., using thermochromic transducer and TDM technique 7-47276
finger arteries, noninvasive meas. of vol. elastic modulus using photoelec. plethysmography 7-3857
fingers, human, noninvasive method for estimating mean capillary press. and pre- and postcapillary resistance ratio 7-28735
fixation disparity, computerised meas. 7-8726
fixation disparity clinical meas., rel. to use of central fusion stimulus on the disparometer 7-8725
flash visual evoked response testing, effect of pupillary dilation 7-28503
flush-mounted hot film anemometer accuracy in pulsatile flow 7-8735
foetal movements recording, comparison of 3 methods 7-23389
foot pressure measurement: a review of clinical findings 7-8728
frog muscle, US vel. fluctuation meas. 7-23395
geometric illusions meas. using microcomputer (*Japanese*) 7-3788
haemodynamically compromised subjects, exercise test protocols, digital filtering and data processing 7-8727
hearing temporal resolution, expedient meas. method for speech intelligibility (*German, English*) 7-60017
hearing temporal resolution capacity for various hearing loss types, clinical investigation (*German, English*) 7-60018
heart rate and arterial blood press. variability signals, auto-spectral and cross-spectral anal. 7-47270
holographic testing appl. in medical device industry 7-40366
human chest measurement during respiration, using structured light 7-40326
human nails as trace-element monitor, neutron activation anal. study 7-34258
impact pressures delivered by oral water irrigation devices, expt. meas. 7-3929
impedance audiometry of children 7-28628
in vivo local US vel. meas. using crossed beam method 7-20525
infants, noisy ventilatory waveforms, robust computer algorithm for breaths. detect. 7-28737
intracranial pressure: review of clinical problems, meas. techniques and monitoring methods 7-40323
intraocular distances, system for continuous high-resolution meas. based on A-scan US 7-40234
intraocular pressure meas., noncontact tonometry through soft contact lenses 7-54780
IR vision systems, calibration from thermal emissivity standards 7-60117
lung permeability measurement in nonsteady state using tracers 7-54802
lung tissue, autopsied, from asbestos workers, Mossbauer effect study 7-65849
magnetocardiographic data measurement and its movie display (*Japanese*) 7-14073
magnetoencephalogram moving dipole inverse solns., effects of meas. errors and noise 7-3853
mandibular kinesiograph recorded signals, distorted, GMDH correction modelling 7-54790
mandibular kinesiographic meas., distorted, signal restoration 7-47149
mechanical point impedance of the human head, with and without skin penetration 7-34296
microscopy techniques (*Dutch*) 7-14143
microwave reflectometry, frequency-domain, image reconstruction, parameter identification, simulation tools appl. 7-65834
motor control performance tracking accuracy quantification system 7-28572
motor unit action pots., reliable myoelec. signal detector based on propag. characts 7-3902
multipoint signal averager for repetitive bioelectric signals, microprocessor-based 7-18091
muscle, time-resolved studies using multiwire proportional chambers 7-47144

biomedical measurement continued

- muscle fibre conduction velocity meas. with surface EMG, cross-correlation method 7-3763
- myocardial contractility anal., computational method 7-14140
- myotonia, recessive congenital, electrophysiological evaluation 7-8531
- nerve activity measurement and analysis, conf., London, England (Nov. 86) 7-41014
- neurofunction laboratory for quantitative assessment of movement disorders for spastic cerebral palsy patients 7-3918
- neurological disorders, meas. of sensory-motor integrated function, 3 computerised tracking tasks 7-3912
- NMR imaging, optical detection of respiration and heart beats 7-47277
- ocular lenses, human, in vivo meas. using quasielastic light scatt. 7-34231
- ophthalmic laser interferometry 7-47204
- optical fibre sensors chemical sensing, particularly in biomedical field, areas for use and techniques 7-31472
- optical fibres sensing in medicine 7-60072
- optical pachometry with contact lenses in situ, measurement artifact 7-40238
- optical probe for on-line meas. of velopharyngeal valve opening 7-60071
- os calicis, broadband US attenuation, and single photon absorptometry in the distal forearm: comparative study 7-40216
- osteoarthritic gait assessment, quantitative approach 7-54785
- photogrammetry application for study of body movement and shape 7-28753
- plethysmograph for meas. of digital blood flow 7-40324
- portable continuous blood pressure monitor utilizing an M68705 micro-computer 7-28755
- positron emission tomography meas. of regional lung density 7-14116
- posture measurement in free space, precision increase, diseased/prosthetic knee clinical assessment 7-34300
- pressure distribution under the ischium of normalsubjects, meas. system 7-8729
- prosthetics and orthotics, shape sensing by CAD/CAM techniques for fitting 7-34348
- prosthetics fitting, optical noncontact 3D body measurement 7-34350
- pulse blood flow of limbs, quantitative eval. using rheography 7-40352
- quantitative EMG rel. to noise 7-3898
- radioimmunoassay data processing software 7-40284
- remote physiological sensing: historical perspective, theories and preliminary developments 7-34298
- respiratory impedance, calcs. from forced random noise data, microcomputer-based system 7-3913
- retinal blood flow visualisation and meas. by laser speckle photography 7-47212
- rheumatic disease patients, seasonal variation in total body Ca, in vivo neutron activation anal. obs. 7-40251
- scanning X-ray imaging system for quantitative arteriography and blood flow meas. 7-40266
- SEM stereophotogrammetric method and system for three-dimens. eval. of features on flat substrates 7-40377
- skin, living human, thermo spectral anal. by Fourier transform IR spectroscopy 7-54707
- skin colour measurement device based on photoelec. colorimeter 7-60136
- skin in vivo meas. using dielectric time domain spectroscopy 7-14961
- skull, computer-aided tomogram, multiplex hologram 7-65883
- small vessel distensibility in man, noninvasive determ. 7-3908
- somatosensory evoked potentials in a brain-dead patient, unexpected myogenic contaminants 7-3893
- somatosensory evoked potentials recording, short latency, with median nerve stimulation 7-3807
- speckle metrology techniques, displacement and strain meas. 7-42936
- spectrophotometric measurements and instruments for medical analyses (Japanese) 7-337
- temperature, circuit for linear meas. 7-28739
- temperature retrieval by scanning radiometry 7-14104
- thermal pulse decay method for simultaneous meas. of local thermal cond. and blood perfusion 7-8734
- third heart sound in children, spectral anal., comparative study of max. entropy method and FFT 7-65818
- thyroid gland, vol. determ. by high resolution US scanner 7-40235
- tissue temperature profiles reconstruction, statistical-regularisation method 7-59939
- tourette syndrome patients, unmedicated and neurologically and intellectually intact, EEG findings 7-3892
- ultrasound diagnosis advances, conf., Dubrovnik, Yugoslavia (Sept. 1985) 7-25
- urethra, female, probe for meas. of cross-sectional area and press. 7-3910
- urine metabolites containing radioactive elements, determ. using molecular neutron activation anal. 7-34259
- US Doppler signals of blood vel. and adaptive filtering 7-8670
- US meas. of trunk muscle atrophy produced by lumbar spin orthoses 7-28639
- US transmitter/receiver transducer, round-trip transfer function meas. (Slovenian) 7-23474
- vascular prostheses, validity of some methods of estimating circumferential elastance 7-8761
- ventricular blood pressure meas. appl. of spline time varying digital filter 7-47268
- venturi suction electrode array for clinical bodysurface mapping 7-3904
- vertical fixation disparity, clinical evaluation, slope and adaptation to vertical prism 7-8568
- vessel sizing wire: accurate vessel measurement using digital subtraction arteriography 7-54740
- vision, contrast threshold measurement system 7-54563
- visual evoked potentials, anal. through Wiener filtering applied to a small no. of sweeps 7-40142
- visual evoked pots., single-response, optimum multielectrode a posteriori estimates 7-60109
- vocal fold vibration and speech signal, simultaneous high speed digital recording 7-47129
- volume measurements with an impedancimetric catheter, rel. to cond. and geometrical factors 7-3909
- weightbearing tissue contour and deformation by magnetic resonance imaging 7-28571
- Ca, total body meas. by neutron activation analysis, in vivo precision 7-65851
- Cl, total body, meas. by prompt γ in vivo neutron activation analysis 7-65848

biomedical measurement continued

- [¹²³I]iodoamphetamine, SPECT imaging and radiopharmaceutical prod., review 7-28656
- Na, total body meas. by neutron activation analysis, in vivo precision 7-65851
- O₂, singlet, optical monitoring of generation during photodynamic treatment of tumours 7-65897
- O₂, transcutaneous press. meas., reproducibility in normal volunteers 7-3891
- biomedical NMR**
- 3D display strategy based on 2D images 7-3860
- acoustic NMR of biological tissue, clinical diagnosis appl. 7-23414
- acute localized irradi., use for X-ray and NMR tomography for diagnosis, pig expts. (French) 7-3869
- angiography, methods that create projection images based on flowing blood 7-14080
- ankle: surface coil MR imaging at 1.5 T 7-28650
- astrocytic gliomas, ¹H NMR relax. times rel. to malignancy grade and tissue necrosis 7-18042
- behavioural effects of exposure to NMR imaging, rat open-field behaviour and learning obs. 7-18016
- behavioural effects of exposure to NMR imaging, spatial memory tests on rats 7-18017
- blood, ageing, effect of motion on sonographic and NMR patterns 7-54684
- blood flow imaging by cine magnetic resonance 7-14083
- blood flow meas. using NMR imaging technique, cardiovascular disease detection appl. 7-54694
- boundary effects from opposed magnetisation artifact in inversion recovery images 7-14093
- brain, cerebrospinal fluid signal enhancement in short TR gradient echo images 7-47194
- brain, high resolution Na NMR imaging, phys. 7-47210
- brain oedema, infarction and tumours, significance of proton relax. time meas. 7-18049
- brain tissue, healthy and diseased, T2 estimates, comparison using various NMR pulse sequences 7-14091
- breast and axillary tissue NMR imaging, correl. of signal intensities and relax times with pathological findings 7-14090
- breast coil, design modification 7-14085
- breast imaging, surface coil design for a vertical field MRI system 7-18048
- breast receiver coil for NMR imaging 7-65831
- breathing artifact in NMR imaging, mag. field dependence 7-18039
- cardiac gating in NMR imaging 7-40241
- cardiac imaging, pulse sequence generated oblique NMR imaging 7-40246
- cardiovascular disease detection role of mag. reson. imaging 7-54706
- cerebello-pontine angle, mag. resonance imaging 7-14074
- cerebral neoplasmas, clinical and expt., Na and ¹H NMR imaging 7-18060
- CNS tumours, contrast-enhanced NMR imaging, clinical review 7-3855
- colour display of quantitative blood flow and cardiac anatomy in a single NMR cine loop 7-60065
- complete localization of in vivo NMR spectra using two concentric surface coils and RF methods only 7-28751
- computer model to optimize image contrast 7-54690
- computerised NMR, clinical appls. (Italian) 7-47272
- computerised tomography, theoretical anal. (Chinese) 7-14144
- conference, magnetic resonance in medicine and biology, Montreux, Switzerland (Oct. 1985) 7-17
- conference on medical imaging and instrumentation, Boston, MA, USA (April 1985) 7-40996
- conference on medical imaging and PACS, Newport Beach, CA, USA (Feb. 1986) 7-18490
- contrast agents in magnetic resonance imaging, clinical experience 7-18059
- critical and emerging issues in diagnostic imaging: Dimensionality of the feature space 7-65782
- cryocooler design and use 7-54712
- cryogenic engineering conf., Berlin, Germany (April 1986) 7-48183
- cryogenics in NMR imaging 7-54710
- diffusion coefficient imaging method using an optimised pulse sequence 7-54698
- DIGGER, in vivo vol. selected NMR spectrosc. technique 7-35556
- direct Hankel transform system using rot. gradients 7-14078
- disease, understanding by use of NMR spectroscopy 7-14103
- dynamic digital subtraction imaging using fast low-angle shot NMR movie sequences 7-14092
- ENDOR imaging, in aq. solns. of nitroxides, viscosity or O₂ conc. 7-24673
- fibre optic strain gauge sensor, for detection of respiration and heart beats 7-47277
- Fourier imaging: appls. using modified Carr-Purcell-Meiboom-Gill sequence 7-28646
- Fourier transform NMR imaging, 2D, respiratory effects 7-14098
- grey level dynamic range in NMR imaging 7-23428
- haemorrhagic lesions, NMR imaging, evolution of intrinsic relax. parameters from time of onset of symptoms 7-54696
- head, adult human, NMR imaging using quadrature coil 7-14087
- head magnetic resonance imaging, choice of interpulse times 7-18056
- head magnetic resonance imaging, clinical optimisation 7-18057
- head trauma evaluation, mag. resonance rel. to CT 7-18061
- heart disease, diagnostic pots. of NMR 7-28655
- high-speed techniques for estimating T1 and T2 images 7-23429
- image nonuniformity: magnitude and methods for correction 7-54693
- image processing in cardiovascular radiology 7-65833
- image processing technology, medical radiography appl., review 7-65856
- image reconstruction, appl. of autoregressive moving average parametric modelling 7-14079
- image reconstruction from data acquired with imaging gradients having arbitrary time dependence 7-14081
- imager and spectrometer operating at similar freqs., relax. parameters comparison 7-18047
- imaging, patient loading simulation using inductive damping loops 7-14075
- imaging and in vivo spectroscopy, mag. suscept. var. effect 7-28749
- imaging computer simulation, implementation and preliminary results 7-23430
- imaging system using superconducting magnet (Japanese) 7-23478

biomedical NMR continued

- imaging systems, automated anal. of multiple performance characts. 7-54701
- imaging time halving by conjugation: demonstration at 3.5 kG 7-54708
- imaging using stimulated echoes 7-14096
- immunospecific NMR contrast agents 7-18053
- interactive proton MR image synthesis 7-65829
- intravascular signal in NMR imaging: differentiation of blood-flow signal from intraluminal disease 7-28652
- knee, 3N NMR imaging using surface coils 7-14084
- longitudinal relaxation time meas. with nonuniform tilt angles 7-23425
- lumbar spine imaging, comparison of circular and elliptical coils 7-3858
- magnetic window into bodily functions 7-14147
- Medicare's Prospective Payment System: paying for magnetic resonance imaging 7-4651
- 3D microscopy, signal to noise ratio, limited-angle excitation 7-54826
- mobile magnetic resonance scanning for improved health care at small centres 7-47278
- Monte Carlo simulation of spectrographic imaging data 7-54704
- motion artifacts reduction in 2D Fourier transform imaging 7-18054
- mouse liver, P containing metabolites, Zn powder injection, NMR obs. 7-8609
- MRI and CT images of human body, three dimensional reconstruction of surfaces 7-54804
- multi-echo NMR imaging, quantitative estimation of T2 7-3859
- multinuclear magnetic resonance imaging technique: simultaneous proton and Na imaging 7-18052
- multiple chemical shift selective NMR imaging using stimulated echoes 7-14097
- multiple-delay-multiple-echo NMR images, improved determ. of spin density, T_1 and T_2 from a 3-parameter fit 7-34218
- neuroradiology, conf., Amsterdam, Netherlands, (Sept. 1985) 7-14706
- nonionising radiation imaging, book 7-48202
- nonuniform magnetic field based mag. resonance imaging 7-14088
- nuclear medicine workshop. Chalk River, Ont., Canada (Aug. 1985) 7-24308
- osteopetrosis: NMR characts. at 1.5 T 7-28651
- parallel image acquisition from noninteracting local coils 7-54697
- passive screening of switched magnetic field gradients 7-14987
- pelvis, advances in NMR imaging at 0.15 T 7-54691
- permanent magnet structures for whole-body NMR diagnostics 7-54799
- phantom, compact and high resolution, for multislice imaging 7-47209
- phase contrast in NMR imaging, chemical shift imaging 7-18043
- phase-encoded NMR chem. shift imaging, generalisation 7-47193
- proton chemical-shift NMR imaging with nonuniform fields 7-14089
- pulse sequence for simultaneous determ. of T_1 and T_2 in NMR imaging 7-40245
- receiver coils in NMR imaging, phase and sensitivity 7-54700
- relaxation times meas. from NMR images, accuracy and precision 7-60066
- respiratory artifacts in NMR imaging, removal, comparison of respiratory triggering and gating techniques 7-14099
- respiratory motion artifacts suppression in NMR imaging 7-54699
- RF coils, importance for NMR tomography 7-3854
- RF technology for NMR imaging spectroscopy 7-34233
- Roman crystalline lens, cataract development, water state, NMR spin echo obs. 7-8557
- rotating-frame zeugmatography data, maximum entropy reconstruction 7-14165
- rotator cuff tears, preliminary appl. of high-resolution NMR imaging 7-14094
- signal-to-noise improvement in NMR imaging by B_1 homogeneity optimization 7-28649
- spatially localised spectroscopy, selected vol. excitation using stimulated echoes 7-48806
- state of the art and future of mag. resonance imaging 7-18055
- status and prospects 7-54711
- steel shield for NMR imaging, fabrication and performance 7-47274
- strong static mag. field effects on living organisms and chem. reactions 7-8611
- structure enhancement by subtraction in NMR imaging 7-54692
- superconducting mag. reson. imager, ferromag. screening 7-28748
- superconducting magnets, refrigerator coding systems 7-54713
- surface coil proton NMR imaging at 2T, coil design and appl. 7-28653
- surface-coil images, algorithm for compensation for sensitivity of surface coil 7-47195
- synthetic images, crit. evaluation of quality 7-18044
- T2 NMR imaging, use of ferromag. particles as a contrast agent 7-18045
- T2 NMR images, multi-exponential anal. 7-18046
- temporomandibular joints, high-resolution NMR imaging with particular emphasis on soft-tissue display 7-14077
- theoretical aspects, book 7-55915
- thermoregulatory consequences of NMR imaging 7-18051
- thorax and abdomen, 3D FLASH NMR imaging without triggering or gating 7-18038
- time-of-flight NMR flow imaging: selective saturation recovery with gradient refocusing 7-14095
- tissue characterisation using meas. relax. times in mag. resonance imaging 7-18058
- tissue discrimination optimisation method in NMR imaging 7-40244
- tissue T_1 , numerical computation from NMR intensity ratios 7-18050
- tomography, phase encoding method using a slice selection gradient for high speed flow vel. meas. 7-23426
- tomography using specially designed RF antennas 7-14076
- tracheobronchial tree and pulmonary arteries, NMR imaging using electronic axial rot. 7-14102
- tumour metabolism determ., pot. of NMR and PET 7-23424
- weightbearing tissue contour and deformation by magnetic resonance imaging 7-28571
- whole-body machines, aspects of engng. design 7-60067
- whole-body magnetic-resonance imaging, appl. of superconducting magnet (Japanese) 7-23479
- ^{13}C NMR imaging, phantom expts. 7-54624
- ^{19}F NMR appls. in medicine 7-23427
- H_2O , signal elimination in vivo, mistimed echo and repetitive gradient episode suppression 7-28750
- ^2H NMR spin-imaging of D_2O , pot. exogenous MRI label 7-18040
- ^{23}Na NMR in vivo imaging at 1.5 T in humans, methodology 7-14100
- ^{31}P NMR spectroscopy, in vivo, brain tumour photoradiation effects evaluation appl. 7-14101

biomedical phenomena see *biomedical engineering; medicine***biomedical radiography** see *diagnostic radiography***biomedical ultrasonics**

- A-scan ophthalmoscope, eye abnormality diagnosis 7-40233
- acoustic NMR of biological tissue, clinical diagnosis appl. 7-23414
- algorithms for fast computation of the intensity weighted mean Doppler freq. 7-65820
- angular spectrum propag. using max. entropy spectral estimation method 7-8669
- aorta, human foetus, interdependence of pulse wave variables, US obs. 7-40198
- arterial occlusive disease, US, diagnosis, some failings of pulsatility index and damping factor 7-47187
- B-mode echogram texture analysis 7-28637
- bibliography 7-9609
- bibliography 7-24332
- bibliography 7-41032
- bibliography 7-60918
- biopsy studies using ultrasound 7-34206
- blood, ageing, effect of motion on sonographic and NMR patterns 7-54684
- blood, vol. flow in human common femoral artery, meas. using a duplex US system 7-28630
- blood flow parameters estimation using pulse Doppler US with corrections for spectral broadening 7-8671
- blood flowmeter, pulsed Doppler system, serial data processing (Korean) 7-3846
- blood velocity, profile measurement by ultrasound Doppler shift method 7-37585
- blood velocity waveforms of superior mesenteric artery, pulsatility index, Doppler US obs. 7-28565
- bone, ultrasonic velocity meas. system 7-47182
- brachial artery, Doppler US vel. waveforms, vector based approach to age-related changes 7-65822
- breast tissue, freq. dependence of US attenuation and backscatt. 7-28597
- Canada, medical diagnostic US device output levels 7-47269
- cardiac Doppler diagnosis, book 7-29
- cardiac indices meas. from freq. transformed TAV Doppler US signals 7-28626
- cardiac stroke volume, in vivo meas. using multiple 2D echo views from 1 echo window 7-34215
- cardiac tissue imaged with US sector scanning, spectral anal. method 7-34214
- cardiac wall motion during exercise, computerised quantitative segmental anal. from 2D echocardiograms 7-34321
- carotid artery blood flow: single factor classification of Doppler waveforms 7-3844
- color coding medical ultrasound tissue images with frequency information 7-34201
- common carotid artery, vol. flow meas. with duplex scanning 7-18036
- conference, advances in ultrasound diagnosis, Dubrovnik, Yugoslavia (Sept. 1985) 7-25
- conference on bioengineering, New Haven, CT, USA (March 1986) 7-16
- CT by nonlinear interaction of sound waves (Japanese) 7-14069
- CW Doppler US spectra, comparison with spectra derived from a flow visualisation model 7-14071
- diagnostic devices, USA Food and Drug Administration guidelines 7-3851
- Doppler blood flow meas., error bounds 7-8672
- Doppler flowmeter for use in theatre 7-47188
- Doppler signals of blood vel. and adaptive filtering 7-8670
- Doppler US signals, CW, statistical props. and speckle, simulation model 7-43538
- dynamically-focussed US array for cancer therapy 7-54683
- echo diagnostic ultrasound: history, transducers, artefacts and new applications 7-28633
- echocardiograms, 2D, automatic and intelligent left ventricular contour detect. 7-34212
- echocardiographic assessment of ventricular volume microcomputer based method 7-40237
- echocardiographic scan images, cine, spatial and temporal processing: automated myocardial border tracking 7-28638
- echocardiographic visualisation of acute myocardial ischaemia 7-28631
- echocardiography, 2D, microcomputerised image processor and 3D reconstruction of left ventricle 7-34213
- echocardiography, 2D, in infants and children, book 7-60061
- echocardiography, attenuation correction 7-23417
- echocardiography, versatile digitisation and processing system 7-34216
- echography, geometric and intensity distortion 7-47189
- endoscopic micromanipulator for multipolar transesophageal imaging 7-47190
- expert diagnostic US system, statistical approach 7-23415
- free radical production in aqueous solns. due to diagnostic US 7-50900
- hand-held ultrasonic medical image scanner, design 7-54688
- high resolution ultrasonic tissue characterization 7-34208
- high resolution ultrasound computerised tomography 7-34207
- hydrophones for use in medical US fields, calibration 7-60063
- hyperthermia, localised: scanned, focused, multiple transducer US system 7-65819
- hyperthermia simulation using finite element model 7-47181
- image texture via generalised Rician statistics, tissue signatures 7-47184
- imaging, speckle artifact removal 7-65823
- in vivo local US vel. meas. using crossed beam method 7-20525
- interactive processing system for ultrasonic compound imaging, real-time image processing and texture analysis 7-23419
- intraocular distances, system for continuous high-resolution meas. based on A-scan US 7-40234
- kidney images recognition by 2D dynamic programming method 7-18034
- left ventricular assist device, pulsed US Doppler rel. obs. 7-8667
- limited angle reflection mode computerized tomography 7-28635
- medical B-mode imaging data sampling, US beamwidth effect on attenuation 7-47191
- myocardial signature: absolute backscatter, cyclical variation, frequency variation, and statistics 7-23418
- neonatal haemodynamics assessment, use of Doppler US 7-28629
- neuroradiology, conf., Amsterdam, Netherlands, (Sept. 1985) 7-14706
- neuroradiology, transcranial Doppler sonography rel. to angiography 7-18035

biomedical ultrasonics continued

- non-invasive ultrasonic method for blood flow and pressure measurements to evaluate the haemodynamic properties of the cerebro-vascular system 7-54646
- nonionising radiation imaging, book 7-48202
- nonlinear parameter imaging CT system using parametric acoustic array 7-34204
- ophthalmology, ultrasonic therapy and imaging 7-28632
- optical-digital joint Fourier transform classification of liver echotexture 7-34209
- os calcis, broadband US attenuation, and single photon absorptiometry in the distal forearm: comparative study 7-40216
- phase tomography, velocity and temperature measurement 7-34205
- physiotherapy transducers, performance of the NPL US beam calibrator 7-60062
- poststenotic flow disturbance in dog aorta as measured with Doppler US 7-8668
- probe and array using PZT-polymer 1:3 composite 7-3848
- pulse compression filter for ultrasonotomography utilizing $L(0,3)$ mode of the elastic waves in afused quartz rod (*Japanese*) 7-14068
- real-time analysis of Doppler waveforms 7-62918
- regurgitant flow through heart valves: hydraulic model applicable to US Doppler meas. 7-28563
- review of US imaging in medical diagnosis 7-60059
- soft tissue movement information in ultrasonic M-mode images 7-34210
- spatial resolution in ultrasonic pulse echo texture analysis 7-28636
- speckle reduction, deterministic approach 7-60060
- speckle reduction in medical US via spatial compounding 7-28627
- speckle reduction in pulse-echo images by using phase insensitive summation and multiplicative techniques 7-28634
- speckle texture in diagnostic ultrasound, detection and classification 7-47183
- stenosis and bulb induced spectral changes in CW Doppler US, in vitro obs. 7-65821
- superior vena caval blood flow vels. in adults, Doppler echocardiographic study 7-8623
- thyroid gland, vol. determ. by high resolution US scanner 7-40235
- time domain formulation of pulse-Doppler ultrasound and blood velocity estimation by cross correlation 7-23416
- tissue characterisation from US B-scan data, liver and spleen appl. 7-14072
- tissue characterization imaging research program 7-34203
- tissue US attenuation meas. using scanned B-mode tomogram 7-23477
- tomography, resolution improvement using adaptive filtering (*Japanese*) 7-34202
- transcranial Doppler sonography, exam. technique and normal reference values 7-14070
- transducer array performance with PZT-polymer composite piezoceramic 7-3850
- transducer array two-dimensional displacement analysis 7-1364
- transducer design for uniform insonation 7-3847
- transducers, multilayered, transmitting and receiving characts. time domain anal. 7-43616
- transducers, pressure field distrib. evaluation in attenuating media 7-3852
- transducers, PZT rod-polymer composite piezoelec. plate tailoring 7-3849
- transducers with curved surface for improved lateral resolution 7-43618
- transmitter/receiver transducer, round-trip transfer function meas. (*Slovenian*) 7-23474
- trunk muscle atrophy produced by lumbar spin orthoses, US meas. 7-28639
- ultrasonic transducer design (*Turkish*) 7-28625
- ultrasonics conference, San Francisco, USA (Oct. 1985) 7-11
- ultrasound Doppler velocimeter signals anal. using personal computers 7-54687
- umbilical artery, Doppler US indices derived from max. vel. waveforms 7-47185
- umbilical artery, Doppler US indices derived from mean vel. and first moment waveforms 7-47186
- vascular and urethral parameters meas., microprocessor-based signal processing system 7-54686

biomembrane transport

see also osmosis

- acetylcholine receptor channel, location of δ -subunit region determining ion transport 7-47025
- cardiac sarcoplasmic reticulum Ca channel, single-channel and $^{45}\text{Ca}^{2+}$ obs. 7-28477
- cell membrane permeability and cell inactivation of transformed mouse fibroblasts, heat-induced alterations 7-47023
- circular orifice, 3-D hydrodynamic interaction of a finite sphere, num. soln. 7-51303
- conductance heterogeneity in membrane channels formed by gramicidin A, cooperative study 7-54491
- diffusion through perforated membranes 7-65717
- Donnan equilibrium, effects of interionic forces 7-28474
- drug transport kinetics in membranes, simulation in organized assemblies 7-54511
- dynamics of the transcapillary fluid and plasma protein exchange 7-65729
- electron transfer at the membrane-soln. interface 7-59942
- extracellular potentials around active excitable structures with short geometric inhomogeneities 7-8538
- gap junctional cond., linear relationship with permeability, frog blastomere obs. 7-40127
- highly permeable contact membranes, role of microtubules in activity regulation 7-40125
- hollow-fibre modules, flow distrib. study 7-65783
- ion transport through lipid membrane, effects of double-layer polarisation 7-54490
- lateral transport of membrane components, effects of spatial variation in membrane diffusibility and solubility 7-8505
- liposome vesicles, mag. field-induced drug permeability 7-40213
- mixed-lipid membranes, electrokinetic effects, nonequilibrium thermodynamics 7-54495
- mu-opioid receptor in lipid bilayer, single-channel obs. 7-23313
- muscle fibre membrane, K cond., gramicidin A interaction, heating effect 7-8496
- nerve cell, membrane pot. clamping, cyclic nucleotide injection, intraneurone information processing 7-8527
- nonhomogeneous membrane, total mass transport 7-54180

biomembrane transport continued

- parametric resonance and amplification of periodic perturbations in membranes containing ionic channels with inactivation 7-40109
- photoinitiated ion movements in bilayer membranes containing Mg-octaethylporphyrin 7-8503
- photoreceptor membrane currents, inositol trisphosphate regulation, Hermisenda obs. 7-28518
- plant cell membranes, water movement, cell wall deform., cooling effect 7-8525
- platelets, human, lateral diffusion of lipid probes in surface membrane, ELDOR obs. 7-8526
- polyelectrolyte charge corrected mol. wt. and effective charge by sedimentation, transport through semipermeable membrane 7-59915
- potential depend. Na channels regulation, spectroscopy of combination scatter 7-8524
- purple membrane suspensions, large transient nonproton ion movements 7-8502
- skeletal muscle, cultured, rat, single apamin-blocked Ca-activated K^+ channels 7-23317
- skeletal muscle, developing rat, functional differences between 2 classes of Na^+ channels 7-3759
- skeletal muscle, multi-ion cond. and selectivity in the high-cond. Ca^{2+} -activated K^+ channel 7-40126
- stratum corneum, lipophilic pathway, Fourier transform IR spectroscopy studies 7-54510
- system cells, grapevine shoot, water crystallisation, nystatin treatment, plasma membrane pore size and hardening 7-8497
- transmembrane ionic channels, permeability rel. to pore mouth charge distrib. 7-59941
- Ca^{2+} channels, occult; in *Drosophila*, rel. to twinning of Ca^{2+} and voltage-activated K^+ 7-17966
- K^+ permeability of resting membrane, rel. to excitable K channel 7-40112

biomembranes

see also biomembrane transport; lipid bilayers

- autoregulatory mechanisms in irradiated biosystems, reliability (*Russian*) 7-47171
- bacteriorhodopsin model membranes, kinetic anal. of displacement currents 7-28475
- bilayers, hole-mediated stability and permeability 7-8507
- bile salt-lecithin vesicles mixed, formation, temp. depend., quasielastic light scatt. meas. 7-34114
- blood component platelet activating factor, IR spectroscopic characterisation 7-54499
- book, annual review of biophysics and biophysical chemistry 7-30
- cell membrane physiology and neutral connections (*Japanese*) 7-13975
- cellulose, bacterial, preferential orientation obs. 7-59943
- chinchilla cochlea, basilar membrane mechanics: low freq. responses and microphonics and spike initiation 7-47093
- chlorophyll a/b-protein complex II, light-harvesting, of higher plants, review 7-59951
- chlorophyll chloroplasts, temp. damage and acclimation mechanisms of photosynthetic apparatus 7-59955
- chlorophyll chloroplasts, temp. stress and prolonged darkening effect on photosynthetic apparatus 7-59956
- chlorophyll in vivo, exciton states and exciton interaction processes, nonlinear transmission effects 7-59931
- chlorophyll in vivo, large absorpt. unit reflected in fluoresc. enhancement effect 7-59932
- chlorophyll-protein complex II, light-harvesting, long-wavelength fluoresc. emission 7-59933
- chloroplast matrix, pea, protein-synthesising apparatus, light quality effect, sedimentary props. 7-59952
- chloroplast membranes, spectral effects of interaction with H^+ , absorpt. and fluoresc. spectra obs. 7-54503
- cochlea, chinchilla, basilar membrane mechanics: input-output functions, tuning curves and response phases 7-47092
- cochlear mechanics and physiology, interrelationships (*French*) 7-47082
- coherent excitation in polarisation wave band, Frohlich kinetic eqn., appl. to cellular membranes 7-54494
- dipalmitoylphosphatidylcholine vesicles, dynamic fluoresc. meas. on main phase transition 7-17954
- DL- α -dipalmitoylphosphatidylcholine, biomembrane, study by positronium annihilation 7-40116
- dye monolayers, short- and long-range interactions, light refl. and transmission 7-22206
- egg lecithin, bilayer lipid membranes, base conductance and electric breakdown, static mag. field effect 7-14030
- egg lecithin vesicles, pierced, elastic torques about membrane edges 7-23312
- electrocardiology, inverse soln. in 1D using a membrane model 7-8554
- energy conversion and storage using insertion materials 7-28391
- erythrocyte, live cell, shear elasticity, entropic nature 7-65725
- erythrocyte membrane, effects of γ -irrad. as shown by ESR, NMR and biochem. studies 7-60041
- erythrocyte membranes, viscosity and order, ns fluorometry obs. 7-40185
- erythrocyte receptors, human, adrenoreceptive function, fluoresc. probe 7-8501
- excitation, pulse and const. current stimulation, electrical circuit simulation 7-28479
- Fourier transform IR difference spectroscopy for elucidating biomolecular mechanisms 7-54832
- Fourier transform IR spectroscopy of live bacterium *A. laidlawii* cells 7-54507
- heart membrane pot., evaluation by positron-emission tomography, use of ^{11}C -triphenylmethylphosphonium 7-14113
- lipid domains in fluid membranes, appl. of quick-freeze differential scanning calorimetry 7-65718
- lipid/protein interaction, Fourier transform IR studies 7-54498
- liposomal membrane, US radiation induced lipid peroxidation 7-47159
- liposomes, conformational state, millimeter wave irrad., Raman spectra study 7-23405
- melittin in membranes, conformation, Raman spectra obs. 7-23294
- mesophyll chloroplasts from sugar cane, photosynthetic electron transport 7-59953
- mesophyll plastid, maize, greening under extreme low-light intensity 7-59954
- microwave effects, rel. to crit. phase transition 7-40114
- mitochondrial outer membrane channel arrays, binding of cytochrome c to lipid domains 7-59914

biomembranes continued

- model membranes, modification of lipid domains by low levels of irradiation 7-8512
- mouse liver cells, membrane potential stability rel. to damaging agents exposure 7-8535
- mucous membrane and cell components, absorptive spectrograms, rel. to optimum wavelength of laser cancer therapy (*Chinese*) 7-28641
- myotonia, recessive congenital, electrophysiological evaluation 7-8531
- neuronal membrane parameters, passive, comparison of optimisation and peeling methods 7-54517
- Nitellopsis obtusa and Nitella translucens cells, membrane between chloroplast layer and moving cytoplasm, elec. obs. 7-40117
- noise, spectral anal., variances 7-13971
- phospholipid membranes, model, complexes with poly(C) and poly(l).poly(C), IR spectroscopic obs. 7-40094
- phospholipid membranes, structural changes after peroxidation, spin probe study 7-28472
- photoreceptor membranes, light-depend. nucleotide exchange, catalysis by rhodopsin (*German*) 7-8495
- photosynthetic membranes suspended in cryoprotective glycerol-H₂O mixture, proton relax. time meas. 7-34170
- pink membrane prep. from deionised blue membrane of *H. halobium*, resonance Raman study 7-8506
- prostaglandin E₂ membrane reception in mouse tissues, effect of various doses of ionising radiation (*Russian*) 7-47173
- protein crystals, growth and character. 7-23288
- proteins, powder samples, label positions, determ. by neutron and anomalous X-ray diffraction 7-3755
- purple membrane, circular dichroic spectrum of L form and blue light product of M form 7-54492
- purple membrane, electric polarisability, electrooptic scatt. spectra anal. 7-54530
- rabbit nictitating membrane response to piezoceramic vibrotactile CS, classical conditioning 7-8775
- red blood cells suspended in carbohydrate-saline solns., deformability, effect of transmembrane potential 7-34118
- retinal pigment epithelial cells, acetazolamide-induced changes of membrane potentials 7-28509
- rhodopsin molecules in disc membrane of frog rod outer segments, 3D electron microscopical investigation 7-65690
- skeletal muscle sinusoidal oscills., energy stored and dissipated, frog obs. 7-40113
- stack structures, fluctuation pressure 7-47014
- thylakoid, light scatt., photo-induced changes, surface charge effect 7-59934
- thylakoid, light scatt., photo-induced changes, temp. treatment effect 7-59935
- thylakoid membranes and functional subunits, organisation, linear dichroism and fluorescence polarisation obs. 7-59944
- tympenic membrane, fibrous dynamic continuum model 7-47107
- vesicles of N-acyl sphingomyelins, X-ray scatt., bilayer thickness determ. 7-40111
- visceral pleura, excised canine, mech. behaviour obs. 7-54644

biomolecular effects of radiation

- see also biological effects of ... (type of radiation)*
- see also photosynthesis*
- alanine system sensitivity, fast neutron irradiation effects 7-34188
- alanines, D- and L-, ⁹⁰Sr-⁹⁰Y- β -irrad., asymmetrical induced yields 7-59929
- bacteriorhodopsin in polymer matrices, photochemical activity rel. to hydration 7-8518
- bovine serum albumin, photoinduced ionisation by holographic relax. method 7-14046
- chemical electric field effects in biological macromols., review 7-54444
- chlorophyll a, early form. of longwave aggregated forms 7-40095
- chlorophyll a/b-protein complex II, light-harvesting, of higher plants, review 7-59951
- chlorophyll chloroplasts, temp. damage and acclimation mechanisms of photosynthetic apparatus 7-59955
- chlorophyll chloroplasts, temp. stress and prolonged darkening effect on photosynthetic apparatus 7-59956
- chlorophyll in vivo, exciton states and exciton interaction processes, non-linear transmission effects 7-59931
- chlorophyll in vivo, large absorpt. unit reflected in fluoresc. enhancement effect 7-59932
- chlorophyll-protein complex II, light-harvesting, long-wavelength fluoresc. emission 7-59933
- chlorophylls a and b and aggregates, spectra in nematic liq. crystals and polyvinyl alcohol films 7-59930
- chloroplast matrix, pea, protein-synthesising apparatus, light quality effect, sedimentary props. 7-59952
- DNA, ϕ X174, radiation damage and biological effects 7-28617
- DNA, effect of combined treatment of ionising radiation and Pt complexes in vitro 7-40099
- DNA, laser induced interstrand covalent crosslink, fluoresc. obs. 7-8490
- DNA, oriented, neutron-induced free radicals 7-23391
- DNA, range of high LET effects from ¹²⁵I decays 7-8660
- DNA, UV induced thymine dimers, bound serotonin effect 7-8489
- DNA base damage induced by ionising radiation, review of current aspects 7-47169
- DNA cleavage after UV-irrad., block by restriction endonucleases 7-18026
- DNA luminescence, dependence on excitation energy (*Russian*) 7-28470
- endotoxin, bacterial, detoxification by ionising radiation rel. to concn., phys. state, and purity 7-40228
- fibroin, skin, photoform. of N=CH₂ and HCO radicals after mech. destruction at 77K 7-28460
- haemoglobin, rabbit, EM wave effects, Mossbauer spectra studies 7-13964
- influenza viruses inactivated by γ -rays, physicochem. characters. (*Russian*) 7-46997
- lecithin, aq. soln., bilayer liposomes, radiation damage PMR relax. time determ. 7-34200
- lipoygenase systems after ionising irradiation as a mediatory function of mol. factors (*Russian*) 7-14051
- macromolecules, radiation sensitivity, temp. depend. 7-15668
- mesophyll plastid, maize, greening under extreme low-light intensity 7-59954
- peptides, photoform. of radicals, 330-390 nm, 77K 7-8488

biomolecular effects of radiation continued

- photoreceptor membranes, light-depend. nucleotide exchange, catalysis by rhodopsin (*German*) 7-8495
 - proteins, photoform. of N=CH₂ and HCO radicals after UV irradiation at 77K 7-28461
 - protochlorophyll in model systems, photo-induced reversible changes in fluoresc. 7-54458
 - subtilysine-72 in water solns., radiation inactivation (*Russian*) 7-13965
 - testosterone, hydrated, EPR study of monoclinic and orthorhombic single crystals, γ -irrad. at 295K 7-23307
 - thylakoid membrane, light scatt., photo-induced changes, surface charge effect 7-59934
 - thylakoid membrane, light scatt., photo-induced changes, temp. treatment effect 7-59935
 - thylakoid membranes and functional subunits, organisation, linear dichroism and fluorescence polarisation obs. 7-59944
 - HTO, RBE on cultured mammalian cells at mol. and cellular level 7-60047
- biomolecules** *see macromolecules; molecular biophysics*
- bionics** *see biocybernetics*
- biophysical effects of radiation** *see biological effects of radiation*
- biophysical instrumentation** *see biological techniques and instruments*
- biophysical techniques** *see biological techniques and instruments*
- biophysics**
see also aerospace biophysics; biological fluid dynamics; biomechanics; cardiology; cellular biophysics; haemodynamics; hearing; molecular biophysics; speech; vision
 ants, foraging props., effects of random behaviour, amplification processes and participant numbers 7-54433
 biological matter, electromagnetic interactions and spontaneous symmetry breaking 7-8473
 book, annual review of biophysics and biophysical chemistry 7-30
 conference, 31st annual meeting of Biophysical Society, New Orleans, LA, USA (Feb. 1987) 7-55874
 connective tissue polarity: optical 2nd-harmonic microscopy, crossed-beam summation, and small-angle scatt. in rat-tail tendon 7-23394
 Dananians golden pupae, natural broad-band interference reflector microspectrophotometry 7-54676
 differential cell design for in vivo photoacoustic meas. of skin absorbance 7-47293
 light scattering from nucleated blood cells, numerical anal. 7-14042
 lung macroscopic model, material to simulate properties at RF and microwave frequency 7-47155
 Nitella alga, small-angle light scatt. subhertz anisotropy fluctuations detection 7-64662
 NMR, theoretical aspects, book 7-55915
 optical radar ranging through biological tissue 7-24640
 periodic competitive and cooperative systems, periodic solutions 7-40085
 science and health care—whence and whither, 1986 Assoc. Lecture of HPA 7-60852
 sunscreen penetration into human skin, photoacoustic in vivo study 7-47153
 thermoradiation characteristics of grapes 7-34189
 translucent materials, diode array spectrophotometric obs. 7-61386
- bioreology**
 actin system and the rheology of peripheral cytoplasm 7-65787
 adaptive thermal modelling, concept for meas. of local blood perfusion in heated tissues 7-65715
 alveolar flooding: a computer simulation 7-23379
 arterial flow at a 90° bifurcation, effects of non-Newtonian viscoelasticity and wall elasticity 7-3812
 blood, phase separation of erythrocytes, platelets and plasma at branches 7-54664
 blood, whole, calibration of rot. instruments for viscosity meas. 7-40372
 blood filtration rates, review 7-54654
 blood flow/haematocrit relationship in larger blood vessels, changes, rabbit obs. 7-3814
 blood rheology in myocardial infarction and hypertension 7-65788
 cartilage, instantaneous deform., effect of collagen fibre orientation and osmotic stress 7-3810
 Casson's fluid, pulsatile flow through stenosed arteries with appls. to blood flow 7-40186
 CCD line-scan image sensor for meas. of red cell vel. in microvessels 7-8777
 conference, Vancouver, BC, Canada, (July-Aug. 1986) 7-60857
 deformation free energy of bilayer membrane and its effect on gramicidin channel lifetime 7-40110
 erythrocyte membranes, viscosity and order, ns fluorometry obs. 7-40185
 erythrocytes, human, packing in centrifugal field 7-65721
 fingers, human, noninvasive method for estimating mean capillary pressure and pre- and postcapillary resistance ratio 7-28735
 haemoreology, effect of couple stresses on unsteady convective diffusion in fluid flow through a channel 7-3811
 human joint fluids, rheological characters. and lubrication props. 7-40178
 hydrated viscoelastic tissues, unconfined compression, biphasic poroviscoelastic anal. 7-3813
 macromolecular networks theory 7-65677
 microbial suspensions, rheological meas. (*German*) 7-14035
 microvessels, flow control coordination by intercellular cond. 7-65797
 muscle, force enhancement phenomenon, simulation 7-34172
 new trends, Poiseuille Award Lecture 7-60854
 plant vegetative tissue, cell wall elastic constitutive laws and stress-strain behaviour 7-40184
 platelet adhesion to fibrinogen-coated glass at an abrupt tubular expansion viewed with fluorescent video-microscopy 7-40183
 platelet aggregation, shear-induced, anal. with population balance maths. 7-8614
 platelet diffusivity in flowing blood, fluid shear as a possible mechanism 7-28552
 scleroglucan solns., low temp. sol-gel transition, rheological behaviour, optical rot. 7-51018
 spider web, phase changes during elongational flow rel. to spider suspension from freshly extruded thread 7-51237
 thromboelastograph, 2-channel, microprocessor-based 7-3903
 tissue blood perfusion, computer-based system for continuous on-line meas. using a thermal method 7-40319

bioionic generation *see* bioacoustics; mechanoreception

Biot-Savart law *see* electromagnetism

biotechnology

blood rate detector, one chip VLSI implementation using PPL 7-65881
genetic information encoding, cybernetics and genetic engineering 7-60924
new sensing materials (*Japanese*) 7-54142

biothermics

adaptive thermal modelling, concept for meas. of local blood perfusion in heated tissues 7-65715
agar phantom electrically adaptable for tissue simulation in 5-40 MHz range, hyperthermia cancer treatment 7-65713
Arrhenius analysis of the heat response of human melanoma xenografts 7-47011
bacterial activity during spring bloom off Newfoundland, temp. regulation 7-4057
bile salt-lecithin vesicles mixed, formation, temp. depend., quasielastic light scatt. meas. 7-34114
black bilayers of egg phosphatidyl ethanolamine, thermotropic changes in cond. 7-54489
blood, regional flow meas., theoretical anal. of transient clearance method 7-28736
blood-brain barrier of rats, interaction of ethanol and microwaves 7-28601
body temperature preference of cockroaches, effect of acclimation temp. and removal of peripheral temp. receptors 7-54483
bone, compact, thermophys. props. 7-17952
brain tumors, interstitial microwave hyperthermia, swept freq. meas. of antennas 7-14106
brain tumours, invasive and noninvasive microwave hyperthermia 7-14105
cancer treatment using RF techniques 7-47285
capacitive RF hyperthermia, skin toxicity minimisation using saline bolus 7-28640
cell membrane permeability and cell inactivation of transformed mouse fibroblasts, heat-induced alterations 7-47023
Chinese hamster ovary cells, temp.-dependent induction of thermotolerance 7-59940
chlorophyll chloroplasts, temp. damage and acclimation mechanisms of photosynthetic apparatus 7-59955
chlorophyll chloroplasts, temp. stress and prolonged darkening effect on photosynthetic apparatus 7-59956
CHO cells, thermal adaptation at 40°C, rel. to growth conditions and heat shock proteins 7-17953
circadian change of heat loss in response to change in core temp. in rats 7-54481
circuit for linear meas. of temp. 7-28739
cisplatin pharmacokinetics in normal dogs, effect of hyperthermia 7-47010
clinical hyperthermia, VLF induced heating 7-54806
coaxial TEM deep-body hyperthermia applicator, 3D model 7-14082
conference on bioengineering, New Haven, CT, USA (March 1986) 7-16
cryo-electron microscopy, cryst. size and cooling rate 7-3949
cryopreservation of biological specimens, possibility of using exponential cooling regimes 7-54815
dehydrated goats, selective sweat secretion and panting modulation 7-40104
differential heating of tissues by UHF field, decrease of effect of ionising radiation (*Russian*) 7-28610
dimyristoylphosphatidic acid/cholesterol bilayers, thermodynamic props. and phase transition kinetics 7-17955
DNA, conformational state in aq. solns., containing glycine, β -alanine and γ -aminobutyric acid 7-28446
Drosophila melanogaster populations, developmental temp. as a selective factor in balancing polymorphisms 7-40102
E. coli cells, thermoinduced radioresistance and heat shock proteins (*Russian*) 7-13969
EM hyperthermia, hot spot form. by locally induced currents 7-8753
EM hyperthermia, temp. distrib., 27-2450 MHz (*Czech*) 7-65714
EM techniques in hyperthermia, review 7-40240
environmental stress after atropine treatment 7-54482
evaporative cooling thresholds of lizards, effect of hypoxia 7-54486
evoked potentials processing with tactile and thermal stimulation; prototype system (*Spanish*) 7-34318
forearm, blood flow response to local temp., effect of nerve block 7-8532
gap junction channel, its aq. nature as indicated by D₂O effects, temp. coeff. obs. on earthworm 7-28492
Greece, air enthalpy rel. to climatological types grouping and geographic distrib. 7-9150
heartbeat rhythms of chick embryos, temp. effects 7-54479
hippocampal slices form noncold-acclimated, cold-acclimated and hibernating hamsters, temp. effects on evoked pots. 7-54484
human head internal heating by pulsed microwave irradiation, thermal stress calc. (*Japanese*) 7-47166
hyperthermia, book 7-55911
hyperthermia, chemotherapeutic agents and oncogenic transformation 7-13968
hyperthermia, local, small-scale temp. fluctuations in perfused tissue 7-8499
hyperthermia, localised: scanned, focused, multiple transducer US system 7-65819
hyperthermia, Phase I regional device evaluation, microwave annular array vs. RF induction coil 7-47286
hyperthermia, unbounded electromagnetic problems, hybrid element method 7-18037
hyperthermia and radiation in the treatment of superficial malignancy 7-65886
hyperthermia applicator, completely implantable, with externalised temp. monitoring: tests in cond. gel 7-54703
hyperthermia cell survival data, model-free way of representation 7-17960
hyperthermia treatment using 27 MHz waveguide applicator, relative heating patterns calc. 7-8676
hyperthermia using 13.56 MHz EM waves, specific absorpt. rate and tissue temp. 7-65826
hyperthermic cell killing, enhancement by nonthermal effect of US 7-60035
hyperthermic radiosensitisation of thermotolerant Chinese hamster ovary cells 7-17961

biothermics continued

interstitial microwave antenna array hyperthermia system, SAR patterns 7-8678
interstitial microwave antenna hyperthermia system, power deposition pattern control 7-8677
interstitial microwave antennas for thermal therapy 7-65825
interstitial microwave hyperthermia in a canine brain model 7-28645
IR thermogram processing system using a microcomputer (*Chinese*) 7-28643
IR vision systems, calibration from thermal emissivity standards 7-60117
jejunum, murine, method for localised hyperthermia and X-irrad. in situ 7-13966
larvae of *Salamandra salamandra*, development rate rel. to heat resistance 7-40107
laser-tissue interaction; thermal and biological aspects of medical laser appl. 7-60037
light intensity and temp. distrib. created by light emitted from an optical fibre embedded in tissue 7-47013
limb models heated with miniature annular phased applicator, energy deposition patterns 7-13970
lipids, phase diagram construction, temp. gradient method using time-resolved X-ray diff. 7-54816
lizard, *Lacerta vivipara*, selected body temps.: variation within and between populations 7-54485
lizards, thermal acclimation of metabolism and preferred body temp. 7-40105
macromolecules, radiation sensitivity, temp. depend. 7-15668
malic dehydrogenase, aspects of thermal inactivation 7-54478
mammalian cells, heat-induced cell killing rel. to heat radiosensitization 7-8521
mammalian cells, modification of thermal and thermochem. responses by adaptation to low pH 7-47018
mammary carcinoma, C3H, step-down heating effect development, factors of importance 7-65712
mammary carcinoma cells, murine, thermal radiosensitisation and thermotolerance 7-59937
melanin, sp. ht. below 3K 7-3754
microcalorimetric measurements on tissue cells attached to microcarriers in stirred suspension 7-23311
microwave hyperthermia, complications arising from spurious fields 7-28644
microwave hyperthermia, thermal dosimetry method using microwave radiometry for temp. control 7-65859
microwave hyperthermia system, robot-operated, for testing large surface tumors 7-8675
microwave interstitial applicators for hyperthermia, design with improved treatment vol. 7-65827
microwave thermography for medical apps. 7-60068
microwave thermography system 7-60069
mixed-lipid membranes, electrokinetic effects, nonequilibrium thermodynamics 7-54495
multi-modality evoked responses vs. temp. and thermal dose with whole-body hyperthermia in water bath 7-8500
muscle fibre, frog, action potential parameter changes at different temps., math. modelling 7-3773
muscle fibre membrane, K cond., gramicidin A interaction, heating effect 7-8496
muscle temperature and muscle metabolism during short-term exercise in the goat 7-54487
muscle tissue and contractile muscle models of *Salamandra salamandra* larvae, heat resistance changes 7-40106
myocardium, normothermic and hypothermic, meas. and spectral anal. of fibrillation 7-28494
myoglobin, thermal spin equil., high-resolution XANES study 7-65702
nerve conduction velocity and temp., time for warming-up cold extremity 7-3752
neural ganglia of cockroach, effect of temp. changes on spontaneous activity 7-54480
nuclear protein following heat shock: protein removal kinetics and cell cycle rearrangements 7-8522
nucleoids, restoration of hyperthermia-associated protein to DNA ratio 7-65720
oesophageal and tympanic temp. responses to core blood temp. changes during hyperthermia 7-8498
papillary muscle, method for generation of rapid step in temp. 7-3753
pelvic tumours, extensive, regional hyperthermia using an annular phased array applicator 7-40239
perfused phantom models of microwave irradiated tissue 7-8784
Phycomyces, system anal. of light-growth response, wavelength 7-23401
plant cell membranes, water movement, cell wall deform., cooling effect 7-8525
polysaturated hydrocarbon chains, natural, temp. dependence of conformational characts. 7-28453
proline, stabilising solute, calorimetric and IR spectroscopic study 7-8492
proteases, method for enhancing stability 7-47012
psoriasis, hyperthermia treatment, comparison of heat delivery systems 7-14152
quick-freeze differential scanning calorimetry, appl. to lipid domains in fluid membranes 7-65718
radiation and heat interaction anal., CHO cells expts. 7-18028
scrotal afferents, significance within the general thermoafferent system 7-40108
single-dose RBE and toxicity studies under conditions of hypothermia and hyperbaric O₂ 7-28607
skeletal muscle, frog, effect of a sub-ms temp. jump on the mech. tension of demembranised fibres 7-40180
skin, differential response in young and old rats to a combination of X-rays and wet or dry hyperthermia 7-23407
skin, living human, thermo spectral anal. by Fourier transform IR spectroscopy 7-54707
stromal tissue, mouse, influence of prior heat treatment on effects of heat alone or combined with X-rays 7-59938
surgical diathermy units, evaluation 7-23483
surgically implantable, crystal-controlled, temperature telemetry transmitter 7-65903
system cells, grapevine shoot, water crystallisation, nystatin treatment, plasma membrane pore size and hardening 7-8497
temperature depth meas. using thermal microwave emission analysis 7-28785
temperature retrieval by scanning radiometry 7-14104

biothermics continued

- temperature telemetry addition for an RF-coupled phrenic nerve stimulator implant 7-28771
- therapeutic laser, CO₂ scanning, thermal effect on tissues 7-47162
- thermal enhancement ratios for single and fractionated doseexternal beam radiation therapy combined with hyperthermia 7-14155
- thermal pulse decay method for simultaneous meas. of local thermal cond. and blood perfusion 7-8734
- thermography, review 7-60070
- thermoregulation, short-term adjustments involving opposite regional temp. changes 7-40103
- thermoregulatory consequences of NMR imaging 7-18051
- thermotolerance development in L1A2 tumour cells in vitro, evidence for an upper temp. limit 7-13967
- thermotolerance in CHO cells, development and modification by procaine 7-65710
- thermotolerance induction in mouse foot with prior hypoxic treatment 7-17951
- thylakoid membrane, light scatt., photo-induced changes, temp. treatment effect 7-59935
- thymidine synchronised bovine lymphocytes exposed to 7.25 GHz microwaves, cytogenetic obs. 7-14048
- time domain finite-difference modelling of biological systems in 3D, hyperthermia appl. 7-23269
- tissue blood perfusion, computer-based system for continuous on-line meas. using a thermal method 7-40319
- tissue temperature profiles reconstruction, statistical-regularisation method 7-59939
- tumour response in patients treated with a combination of radiotherapy and hyperthermia 7-47287
- tumours, solid., dielec. props. during normothermia and hyperthermia 7-3778
- UHF local hyperthermia, electrode device and methodological problems of thermoradiotherapy (*Russian*) 7-23484
- US hyperthermia simulation using finite element model 7-47181
- vascular tissues, heat transport mechanisms: model comparison 7-65716
- wind-chill indices 7-55204

biotite *see mica***biotransport**

- see also biodiffusion; biological fluid dynamics; biomembrane transport; cellular transport and dynamics; neurophysiology*
- ascending limb of Henle's loop, active transport and steady state distrib. of Na⁺ (*Chinese*) 7-28485
- cytochrome oxidase, redox-linked proton translocation: importance of gating electron flow 7-23316
- energy transport in biological systems, theoretical description (*Czech*) 7-13978
- living plants, transport processes review 7-65728
- muscle, compartmental Ca²⁺ flow model, fatigue in isometric contraction in a single fibre 7-34179
- nasal mucociliary transport in laryngectomees, ^{99m}Tc S colloid obs. 7-13979
- ⁴⁵Ca²⁺ efflux from isolated chick brains, lack of effect of static mag. field 7-28579
- N transport in tissues, phenomenological models 7-54509

bipolar integrated circuits

- capacitive pressure sensor IC, micropower ccts. design for implantable device, biomedical appl. 7-34316
- integrated magnetic field sensor based on magnetotransistors 7-48792
- solid-state devices and materials, conf., Tokyo, Japan (Aug. 1986) 7-48173
- SI bipolar transistors, impurity and carrier conc. profiles, electrochem. C-V method (*Chinese*) 7-12105

bipolar transistors

- see also bipolar integrated circuits*
- carrier-injected bipolar transistor optical modulators and switches 7-50732
- electron-acoustic microscopic study on dislocation lines in the base region of npn Si-Tr 7-20538
- HJBT 7-52811
- PBT picosecond electro-optic sampling 7-53278
- semiconductor device physics, conf., Madras, India (Nov.-Dec. 1985) 7-35102
- solid-state devices and materials, conf., Tokyo, Japan (Aug. 1986) 7-48173
- thermal sensors based on transistors and ICs review 7-48743
- AlGaAs/GaAs heterojunction bipolar transistor, self-aligned with InGaAs emitter cap 7-45492
- GaAs-GaAlAs heterojunction bipolar transistors, ²⁴Mg and ⁶⁴Zn implanted profiles 7-44591
- InGaAs/GaAs lattice-strained double heterojunction bipolar structs., comp., recomb. props. and device performance 7-64322
- InP/InGaAs heterojunction bipolar transistors, open-tube Zn diffusion 7-44914
- Si junctions very shallow, elec. field anal. 7-21989
- SiO epitaxial films for hetero-bipolar transistors 7-53599
- Si:P, meas. of heavy doping parameters 7-12855

bipoles *see network analysis; network synthesis***birefringence**

- see also flow birefringence; Kerr electro-optical effect; light polarisation; magneto-optical effects; mechanical birefringence; optical constants; optical rotation*
- beam splitters, fibre-optic polarising, anal. 7-15980
- α -(BEDT-TTF)₂(NO₃)₂, electronic excitations, optical study 7-53367
- bent birefringent fibre, compensated sensing based on retardation chars. 7-50752
- bicyclo(2.2.2)octane esters, mesogenic, transition temps., viscosity, birefr., electro-optical chars. 7-1863
- birefringent fibre waveguide with elliptic borosilicate cladding, polarisation chars. study 7-62835
- ceramic materials millimeter wave dielectric meas. 7-14978
- cholesteric blue phases, refractometric meas. 7-7664
- coil of single-mode fibre, birefringence and polarisation mode dispersion 7-31498
- components made from copolymer of styrene with acrylonitrile 7-43271
- Corning glass films, RF magnetron sputtered, optical props. 7-57552
- crosstalk meas. on high birefringence fibres 7-57566
- crystals, birefringence, Faraday effect, conversion of linear into circular light polarisation 7-59189

birefringence continued

- 1-cyclohexyl-phenyl-2-methyl ethylenes, synthesis and phys. props. 7-1870
- diamagnetic molecular system, magneto-chiral birefringence and dichroism at longitudinal elec. saturation 7-42661
- diamagnetic molecular system in DC electric field, magneto-spatial dispersive effect 7-31087
- diamagnetic molecules, magneto-chiral birefringence and dichroism, reorientational processes influence 7-15812
- dicubane, H bonding nature and vibr. structure, birefringence emission spectra anal. 7-19935
- dielectric cryst., linear magneto-optical effect anisotropy 7-39092
- diffraction, gyrotropic medium, half-plane, Wiener-Hopf eqns. soln. 7-50460
- dispersion curve pseudocrossing 7-39075
- Dralon fibres, gamma-irradiated, optical props. 7-39068
- dralon fibres of kidney cross-sectional shape, double refr. meas. 7-4882
- droplet clustering in microemulsions, electric birefringence study 7-28354
- ellipsometer for birefringent components and systems meas. (*German*) 7-24687
- ellipsometric characterisation of single mode fibres 7-43428
- Fabry-Perot cavity, nonlinear birefringent, polarisation bistability 7-37017
- ferrofluid, near mm wavelength studies of refr. indices by dispersive Fourier transform spectra 7-53289
- fibre, birefringent polarisation-maintaining, mode coupling distrib. meas. 7-31507
- fibre, polarisation maintaining with three layer elliptical cross section, transmission chars. 7-1268
- fibre birefringence determ. by normalised second-order factorial moment meas. 7-43376
- fibre chars. meas., rotating linearly polarised light source appl. 7-18850
- fibre optic couplers, single-mode polarisation maintaining 7-26011
- fibre optic current sensors using highly birefringent bow-tie fibres 7-15976
- fibre optic gyroscope, noise due to birefringence modulation 7-31479
- fibre optic magnetometer, polarimetric DC using composite metallic glass resonator 7-14981
- fibre optic stress location sensor 7-43420
- fibre polarisation components, birefringent, for sensor appls. 7-20450
- fibre-optic acousto-optic tunable filter 7-5979
- fibres, polarisation-maintaining birefringent, polarisation cross talk ultimate limit 7-25970
- fibres twisted birefringent, intensity discrimination 7-31503
- filter design for CW dye laser resonator, spectral tuning band 7-50720
- glass-CdSe-KS-19, light-induced anisotropy 7-43259
- graphite layers on diamond surfaces, optical anisotropy, effect of crystallographic orientation 7-53267
- GRIN lenses, optical performance assessment 7-31538
- gyroscopes, fibre optic, noise problems 7-20439
- n-heptane cryst., birefringence, compensation method meas. 7-45979
- high-birefringence fibres, dichroism eval. using crosstalk meas. 7-20421
- inhomogeneous crystals, optical props. as function of form. and obs. conditions 7-45980
- interference fringes in scattered beams in birefr. presence 7-50491
- layered inhomogeneous uniaxial media, light propag., pseudo-Stokes parameters, geometric optics approx. 7-57244
- liquid cryst. display, SBE type, fundamental characteristics (*Japanese*) 7-7670
- liquid cryst. display, SBE type, supertwisted nematic, display chars., effects of various parameters (*Japanese*) 7-7669
- liquid crystals, IR birefringent props. 7-39076
- lyotropic nematic with discotic micelles, orientation in mag. field 7-44357
- magnetic fluids, magneto-optical effects, birefringence 7-59186
- microbend-induced birefringence in optical fibres, temp. dependence 7-43425
- molecular Kerr relaxation theory for liquids in reorienting pulse fields 7-36663
- multiple beam interference for birefringence measurement in anisotropic crystals 7-41455
- (Na₂O)₂₅(Li₂O)₂₅(P₂O₅)₅₀ glass fibres, struct., birefringence, density and thermal shrinkage, drawing parameters depend. 7-6536
- nematic liq. cryst., localised deform. near surface defects, birefringence study 7-45978
- nematic liq. cryst., parallel-aligned, phase retardation depend. optical response time 7-3018
- nematic liq. crystals, light scatt. and. propag. chars. 7-39078
- nematic liq. crystals, relax. modes of order parameter fluctuations in vicinity of uniaxial-biaxial phase transition 7-26948
- nematic liquid crystals, torsional anchoring on substrates, birefringence study 7-1858
- nonlinear fibres, birefringent, nonperiodic power coupling 7-43379
- nonlinear media, polarisation instability and bistability 7-57443
- nonpolar fluid, ellipsoid mols., induced birefringence and dielectric polarisation 7-33363
- nonrigid molecules, elec. birefringence, field strength depend. 7-45989
- nylon bicomponent fibres, optical props., interf. determ. 7-45974
- octylcyanobiphenyl, liq. cryst., elastic consts., permitt., birefr. meas. 7-21314
- optical fibres, birefringent, anal. 7-57587
- optical fibres, polarisation-holding, internal rotation of birefringence axes 7-43400
- optical fibres, polarisation-maintaining and their appls., review 7-11136
- optical fibres, polarisation-maintaining with hollow circular pits 7-31494
- optical fibres, polished, D-shape, geometrical birefringence 7-62837
- optical fibres, refractive indices and birefringence meas., interferometric methods 7-29644
- PET film, trichroic IR absorpt. analysis, methods description 7-33380
- PET films, crystallisation under strain, annealing, morphology, mech. props. 7-44415
- phenyl 4-alkylcyclohexanecarboxylates, 4-alkoxymethylene and 4-alkoxy substituted, synthesis, phys. props. 7-1861
- photoelastic pressure sensor, using low-birefringence fibre 7-43429
- photorefractive anisotropic media, holographic beam coupling 7-57273
- polyacrylamide gels, spontaneous birefringence and photoelasticity 7-22217
- polymeric colloidal suspensions in polymeric suspending fluids, dichroism and birefringence meas. 7-11478

birefringence continued

- polyvinyl acetate film, trichroic IR absorpt. analysis, methods description 7-33380
 quartz, synthetic, edge dislocations, optical contrast, birefringence topography studies (*Chinese*) 7-59176
 quartz single-mode three-layer ring optical fibre, intrinsic birefringence and polarisation dispersion props. 7-50777
 readout system using reflecting discs, effect of birefringence of protective layer 7-57234
 Reusch's piles, selective light reflection, multiple domains (*French*) 7-36875
 rigid molecules, elec. birefringence, field strength depend. 7-45989
 rubber, gel and mol. wt. influence on mech. props. 7-37904
 single-mode fibres, birefr., chromatic and polarisation mode dispersion, interferometric meas. 7-57571
 single-mode single-polarisation fibre using resonant absorbing effect, theoretical study 7-43381
 Teflon-FEP electrets, stability, stretching effects 7-27650
 ternary microemulsion system, phase electric birefringence meas. 7-27699
 transparent biaxial crystals, nonlinear refr. in conical refr. region 7-31382
 22-tricosenoic acid Langmuir-Blodgett films, guided optical waves in ATR geometry 7-31462
 twisted birefringent media, characteristic directions 7-5834
 twisted nematic liquid cryst. cell, polarisation anal. using Poincare sphere (*Japanese*) 7-64603
 ultradisperse matrix mixture, optical props., struct. anisotropy effect 7-31250
 uniaxial crystal, anisotropic sum freq. generation with large angular aperture 7-57449
 unidirectional birefringent filter (*French*) 7-37118
 AlPO₄, modulated phase, electron microscopy study 7-26937
 BaTiO₃, hexagonal, optical props. around 222K struct. phase transition 7-27685
 Bi₁₂SiO₂ crystals, electrooptic consts. dispersion determ., linear approx. calcs. 7-53270
 Ca₃Mn₂Ge₃O₁₂ single domain crystals, birefringence and spontaneous phase transitions 7-17303
 CaO-BaO-P₂O₅ glass fibres, stress optical studies 7-7673
 (CaO)₂₅(BaO)₂₅(P₂O₅)₅₀ glass fibres, struct., birefringence, density and thermal shrinkage, drawing parameters depend. 7-6536
 CdTe, optical anisotropy due to spatial dispersion 7-53266
 CdTiO₃, nonlinear props. in high electric fields 7-7668
 CsLiCrO₄, ferroelectric phase transition 7-39047
 Cu complex, CuBr₂·2DMSO, linear chain antiferromag., optical birefringence 7-7679
 Cu(NO₃)₂·2.5 H₂O, EPR and magneto-microwave birefringence powder spectra 7-45810
 GdGG, paramag., mag. lin. birefr. meas. 7-53265
 K₂ZnCl₄ crystals, incommensurate phase, thermal memory effects, birefringence temp. depend. meas. (*Russian*) 7-17302
 LiKSO₄ phase transitions, domain form., optical birefr. meas. 7-3019
 NaBrO₃, X-ray birefringence and forbidden reflections 7-33475
 Na₂O-Li₂O-P₂O₅ glass fibres, stress optical studies 7-7673
 O₂ liquid, orientational dynamics 7-42717
 PLZT-PZN electro-optic ceramics, elec., opt. and switching props. 7-7646
 Pb₂Cr₂F₁₉, nonlinear optic, lattice consts., ferroelec. Curie temp., phase transition obs. at 555K 7-17275
 Pbln_{1/2}Nb_{1/2}O₃, antiferroelec., phase transition; B-site cation order effects 7-7651
 PbTiO₃, cryst. optical studies of precursor and spontaneous polarisation 7-45921
 RbHSeO₄, optical birefr. meas., temp. depend. 7-27689
 Rb₂ZnCl₄, cryst., incommensurate modulation, light propag. 7-22196
 a-Si, lamellate structure 7-21740
 SnTe, optical anisotropy due to spatial dispersion 7-53266
 YAlO₃:Ce, single cryst., birefringence spectra, 2-5 eV 7-13124
 YIG films, symmetrical single-mode magneto-optic waveguides, phase matching by stress appl. 7-45972
 YbAG, paramag., mag. lin. birefr. meas. 7-53265
 YbGG, paramag., mag. lin. birefr. meas. 7-53265
 ZnSe, optical anisotropy due to spatial dispersion 7-53266

bismuth

- see also nuclei with
 adsorption, of K, in alcohol solvents 7-52238
 adsorption and growth modes on Pt (111), spectrosc., LEED and work function investig. 7-27102
 adsorption of tertiary butyl alcohol on faces of single cryst. 7-32784
 atom, electron scatt., relativistic effects, Kohn-Sham theory 7-42765
 atoms, elastic scatt. of electrons, spin polarisation meas. 7-50364
 atoms, K_β/K_α X-ray intensity ratios 7-42537
 atoms, low-energy electron elastic scatt. calcs. 7-50362
 band parameter temp. depend. galvanomag. coeffs. and mobility, L-hole effect calcs. 7-2461
 effective electron mass, quasi-1D systems, theoretical investig. 7-2468
 electrode, single cryst., adsorpt. of butyl acetate 7-52239
 electrodes, polycrystalline, adsorpt. of cyclohexanol 7-32785
 electronic structure, effect of ion implantation 7-45143
 filamentous single crystals, static skin effect and acoustoelectric instability 7-38644
 film, etching by methyl radicals in discharges 7-3507
 films, elec. resistivity, 1600-4500 angstroms 7-2737
 films, IR and visible spectra, refractive index, extinction coeff. and dielectric const. 7-46156
 films, oxidation in air and superheated steam 7-46674
 films, size quantised, IR spectrum, optical cond., two-band model 7-27803
 high temp. kinetic coeffs. oscills., band struct. and magnetoresist. temp. depend. studies (*Russian*) 7-12738
 ions, laser produced spectra and QED effects 7-37747
 liquid, elec. resist. meas. 7-38532
 liquid metal ion source study 7-30799
 magnetic suscept. field depend., electron band struct. effects (*Russian*) 7-12936
 muon Knight shift anisotropy study 7-45893
 nonlinear cyclotron resonance, lineshape and mechanisms 7-32897
 nonlinear size cyclotron resonance, second harmonic generation calcs. (*Russian*) 7-13036
 phase diagrams, appl. for online press. and temp. calibration 7-4853

bismuth continued

- plates, magnetoacoustoelectronic instabilities, joint action of two strong electric fields 7-52694
 polycrystalline, internal friction temp. spectrum and microplasticity (*Russian*) 7-16684
 positron trapping in deformation induced defects 7-39257
 quasi-1D system, Einstein relation modification 7-33013
 rare earth iron garnets, Bi-doped, growth-induced anisotropy 7-22103
 refining by continuous zone melting 7-3163
 rhombohedral, lattice relax. and muon⁺ sites 7-53190
 segregation, at Al-carbon fibre interface 7-65046
 solid-state plasma, microwave harmonics, parametric excitation of hyper-sound 7-38609
 solidification of undercooled liquid, nucleation, pressure effects 7-38169
 superconducting phases, nonlinear I-V characts. struct., point contact obs. 7-2763
 surface, polycryst., simulated, elec. double-layer struct. anal. 7-52732
 thin films, lattice thermal cond. meas., modified Mayadas-Shatzkes model 7-21554
 thin films (111), melt growth, in-situ obs. by TEM 7-53573
 ultrasound absorption, amplitude and orientation dependences 7-26873
 ultrathin films, size quantization effect on effective electron mass 7-38778
 Al:Bi-KCl:Bi, bilayer cpd., Bi ion implantation, thermal annealing 7-32474
 Au-SiO₂-Bi, low temp. hot electron energy relaxation and inelastic collision times in thin metal films 7-27441
 Bi, dielectric function, temp. depend. of band struct. parameters 7-7138
 Bi, high press. phase transitions, EMF pulse study (*Russian*) 7-2166
 Bi II, 6s²6p² 3P₀-6s²6pnd ³D₁ series in photoabsorption 7-25469
 Bi:Si, magnetocond. in 13 T mag. field at low temp. 7-7209
 Bi-Cd, thermodynamic functions are modelled by chemical-physical theory, Gibbs energy 7-52051
 Bi-Ga two-layer film compositions, refl. and microstruct., temp. depend. 7-53428
 Bi-GaAs, distrib. coeff. of Bi, crystn. from molten solns. 7-46428
 Bi-In-Sn alloys system, phase relationships 7-13433
 Bi₂, two step polarisation spectroscopy 7-10609
 Bi³⁺ ions, (n/p ≤ 14, p ≤ 4), mass spectrum from liquid metal ion source study (*French*) 7-5807
 Bi, cluster, laser vaporisation and photoionis., TOF mass spectrometry 7-31201
 C:Bi films, ion implanted, projected ranges and range straggings, RBS anal. 7-63690
 CdS:Bi³⁺, ion implantation damage 7-26812
 DyIG:Ga, Bi, RF sputtered films for magneto-optical memory, mag. props. 7-64613
 GaAs:Bi, epitaxial layers, purification by Bi doping 7-58301
 GaAs-Al_xGa_{1-x}As heterojunction, chemical pot. of electrons, effect of mag. field 7-38682
 Ge:Bi, implanted, heavy ion damage, TEM, annealing studies 7-63676
 Ge₂₀Se₈₀:Bi chalcogenide glasses, doping, coordination number and cond. transition, EXAFS study 7-64764
 a-Ge₂₀Se₈₀:Bi films, n-type, electron transport props. studies 7-7422
 InP:Bi thin film, epitaxy, impurity distrib., photoluminesc. spectra anal. 7-53388
 PZT:Bi piezoelectric ceramics, vacancies, positron lifetimes 7-37980
 Pb_{1-x}Sn_xTe:Bi, free carrier density 7-38572
 Si:Bi, implanted, heavy ion damage, TEM, annealing studies 7-63676
 Si:Bi, solute trapping by lateral motion of {111} ledges 7-44592
 Si-Bi, metal implantation using pulsed electron beam 7-6882
 Si-Ge multilayered structures, Bi ion implanted, projected range distrib., glancing angle RBS anal. 7-63689
 SiO₂:Bi, ion implanted, projected ranges and range straggings, RBS anal. 7-63690
 YIG:Ga, Bi, RF sputtered films for magneto-optical memory, mag. props. 7-64613
 ZnO:Bi, Schottky-like barriers, ion implantation, annealing 7-58860
 ZnO:Cu(Bi), phosphor electroluminescence mechanism, spectral energy distrib. 7-7760

bismuth alloys

see also bismuth compounds

- Bi-Pb-Sn-Cd alloy negative electrode for secondary Li batteries (*Japanese*) 7-65435
 impregnated Ti, composite 'pseudoalloy', mech. props., Bi alloy content depend. 7-28095
 Al-Mg-Bi:Cr, low activation alloy development for reacting plasma experiment 7-15384
 Al-Si-Pb-Bi, duplex alloys, melt quenching, microstruct. supercond. props. 7-45593
 Bi-Ag, struct. of 10 mole % Ag alloy, liq. and amorphous states 7-6512
 Bi-based metallic glasses, thermal relax. processes 7-51653
 Bi-Ga, liq., elec. resist. meas. 7-38532
 Bi-MnBi eutectic, pure and modified, growth 7-59500
 Bi-Pb, superconducting transition temp., effect of plastic deform. 7-52879
 Bi-Pb alloys, supercond. and normal state, thermal cond., effect of plastic deform., 1.5-300K 7-17132
 Bi-Sb alloys, magnetic suscept. field depend., electron band struct. effects (*Russian*) 7-12936
 Bi-Sb high temp. kinetic coeffs. oscills., band struct. and magnetoresist. temp. depend. studies (*Russian*) 7-12738
 Bi-Sb:Te(Sn) thin films, elec. props 7-64376
 Bi-Sb-(Te), single cryst. alloys, component distrib., stratified heterogeneity 7-46302
 Bi-Sn, thermodynamic analysis of conc. fluctuations and homogeneous nucleation, glass form. 7-44852
 Bi-Te metastable solid soln., fine struct., X-ray diffr. studies 7-44449
 Bi-Tl, superconducting transition temp., effect of plastic deform. 7-52879
 Bi-Tl alloys, supercond. and normal state, thermal cond., effect of plastic deform., 1.5-300K 7-17132
 Bi-Zn liquid alloys with miscibility gaps, struct. 7-51611
 Bi₃Ni, α-irrad. and H implanted, elec. resist. and superconducting T_c 7-7202
 Bi_{1-x}Sb_x, anomalous magnetoresistance, quantum limit 7-58795
 Bi_{1-x}Sb_x, narrow-gap semicond., intraband breakdown, current-voltage characts., size effect conditions 7-52624
 Co-based amorphous alloys, anisotropic electrical magnetoresistivity at 295 K 7-58796
 Fe-Bi, ion implanted, high substitutional fractions 7-58299

bismuth alloys continued

- In-Bi, liq., heat of mixing, calorimetric study 7-12283
 In-Bi-Pb system, liq., thermodynamic props. (*Japanese*) 7-53699
 MnBi ferromag. thin films, reversed micro-domain growth, magneto-anisotropic dispersion 7-17205
 MnBi/Bi eutectic, freezing rates, convection effect on microstruct. 7-22652
 ($Mn_{1-x}Fe_x$)_{100-x}Bi_x films, evaporated, structure and mag. props. (*Japanese*) 7-59077
 Ni-SnPbBi system, crack form. in diffusion zone 7-3397
 Pb-Bi superconducting alloys with Bi precipitates, critical current density 7-17146
 Pb-Bi system, heat of fusion (*Russian*) 7-44766
 Pb-Bi system, peritectic crystallisation, cooling rate effect 7-46440
 Pb-Bi-Hg, liq., struct. microheterogeneity 7-11895
 Pb-Bi-Sn(In), alloy filaments, prod. by glass-coated melt spinning, enhancement of supercond. 7-58937
 Pt-Bi (22 wt.%), supercond. films, pinning in appl. mag. field (*Russian*) 7-64418
 Sb₂Bi₃ cluster, laser vaporisation and photoionis., TOF mass spectrometry 7-31201
 Se-Bi alloys, thermodynamic props. and phase equil. 7-3276
 Sn-Bi, heterogeneous, fusion kinetics 7-3280
 Sn-Bi system, heat of fusion (*Russian*) 7-44766
 Sn-Bi-Hg, liq., struct. microheterogeneity 7-11895

bismuth compounds

see also *bismuth alloys*

= 7-1986

- BGO, energy resolutions for p and α 7-5557
 chalcogenides, binding energies, chem. shifts XPS and diffuse refl. spectra (*German*) 7-1943
 (LuYBiPb)₃(FeGa)₅O₁₂, crystn. from soln. melt, component distrib. 7-21149
 oxides, small distortions, EXAFS transmission studies 7-63580
 Au-Bi₂GeO₂₀-Au MSMS, short-wave light illuminated, photocurrent kinetics 7-22029
 BaPb_{1-x}Bi_xO₃, semicond. phase, CDW gap, optical meas. 7-53328
 BaPb_{1-x}Bi_xO₃ soln.-grown single crystals, crystallographic symmetries, effect on supercond. props. 7-37916
 BaPb_{1-x}Bi_xO₃, supercond. props., press. effects 7-45533
 BaPb_{1-x}Bi_xO₃, supercond. crystals, hydrothermal synthesis and props. 7-53532
 (Bi,Tm)₃(Fe,Ga)₅O₁₂ garnet films, magnetisation reversal, pulsed mag. field nonuniformity effect 7-45783
 Bi complex, MBi(PO₄)₃, M=Cd, Pb, Co, Sr, Bo, structural and spectroscopic data correl., Raman and IR spectra anal. 7-53348
 Bi-Ge-S chalcogenide glasses doping mechanism and structural effects, EXAFS study 7-1909
 Bi-O, structural types, influence of Bi³⁺ lone pair electrons 7-1998
 Bi-Sb, adhesion, elec. phenomena, effect of additions of Bi and Sn in solder 7-12399
 Bi-Te-Ge, dissolution kinetics of Ge, diffusion controlled 7-44820
 Bi-Zn-Fe-O amorphous films, struct. and mag. props. 7-51645
 Bi_{2-x}As_xS₃ thin films, solution-gas interface deposition technique 7-7901
 Bi₂Se₃ and Bi₂Te₃, luminesc. studies, optical absorpt. edge 7-13209
 BiBr₃, NQR frequencies, electrical effects 7-17240
 Bi_{3-2x}Ca_{2x}Fe_{5-3x}In_xV_xO₁₂, single crystal, Mossbauer spectroscopy (*Chinese*) 7-17250
 Bi_{3-2x}Ca_{2x}Fe_{3-x}V_xO₁₂, sublattice magnetisation and Faraday rotation (*Chinese*) 7-17308
 Bi₂CdS₃ thin film photoelectrodes, electrochemical photovoltaic cell appls. 7-17918
 Bi₂Dy_{3-x}Fe_{3-x}Al₁₂O₁₂ garnet films, magneto-optical props. 7-64614
 (BiDySmLu)₃(FeAl)₅O₁₂ bubble garnet films, Bi-substituted, LPE growth rate reduction 7-45049
 (BiDySmLuGd)₃(FeGa)₅O₁₂ bubble garnet films, Bi-substituted, LPE growth rate reduction 7-45049
 Bi₂FeO₄₀, reflectivity spectra structure, thermorefectance 7-59207
 Bi₂(GaFe)₅O₁₂, epitaxial films, mag. and magnetooptical props. 7-53102
 (BiGdTm)₃(FeGa)₅O₁₂ single cryst. film, reverse-magnetisation domain nucleation studies 7-17208
 (BiGdTm)₃(FeGa)₅O₁₂ epitaxial films, microdomain nucleation near moving domain walls 7-45778
 Bi₂GeO₁₂:Cr, doped and undoped, three-phonon interactions 7-2127
 Bi₂GeO₂₀, acoustical activity, inelastic neutron scatt. study 7-32577
 Bi₂GeO₂₀ crystals, photorefractive parameters determ. using transient grating anal. 7-3004
 Bi₂GeO₂₀ crystals, elastooptical and elastogyratory coeffs. 7-59179
 Bi₂GeO₂₀ Czochralski-grown crystals., comp. anal., holographic storage props., stoichiometry depend. 7-63837
 Bi₂GeO₂₀, electrogyratory and electrooptic coupling 7-27701
 Bi₂GeO₂₀, photoelectric props., influence of deep trapping centres 7-7279
 Bi₂GeO₂₀ photorefractive crystals, degenerate four-wave mixing involving internal reflections 7-37047
 Bi₂GeO₂₀ piezoelec. semicond., photovoltaic displacement current, Hall component meas. 7-64286
 Bi₂GeO₂₀, pure and doped crystals phys. props. 7-7283
 Bi₂GeO₂₀, real time holographic image recording, diffraction efficiency (*Korean*) 7-25743
 Bi₂GeO₂₀, sillenites, IR transmission spectra 7-59194
 Bi₂GeO₁₂ crystals, imperfection nature, precipitates and bubbles 7-21463
 Bi₄Ge₂O₁₂ crystals., positron annihilation parameters determ., gamma irradiation effects 7-46223
 Bi₄Ge₂O₁₂, Czochralski growth, melt temp. fluctuations 7-53555
 Bi₄Ge₂O₁₂ detector 2D angular correlation apparatus for positron annihilation studies 7-36423
 Bi₄Ge₂O₁₂, high quality large cryst. growth, colour and precip. form., pulse height resolution 7-53554
 Bi₄Ge₂O₁₂, luminescence excitation and reflection spectra 7-46090
 Bi₄Ge₂O₁₂ scintillators, surface roughness and crystal shape effects 7-15452
 Bi₄Ge₂O₁₂ single crystals, shape, melt flow patterns, Czochralski growth conditions 7-16464
 Bi₄Ge₂O₁₂ single cryst. growth, characterisation and appls. 7-33550
 Bi₄Ge₂O₁₂, US wave absorpt., 0.5-9.4 GHz, 4.2-300K. 7-44701
 Bi₃ extrinsic semiconductor, reverse H-like series, light absorpt. study 7-53370

bismuth compounds continued

- BiI₃, layered semicond. with hexagonal end honeycombed structs., growth and optical props. 7-22277
 BiI₃, layered semiconductor clusters, degenerate four-wave mixing, quantum size effects 7-20358
 BiIG films, selected-area sputter epitaxy 7-7845
 Bi₂-In₂Te₃, carrier density, depend. of anisotropy parameter 7-7226
 BiLiF₄, lattice vibrs., Raman study 7-53329
 (BiLu)₃(FeGa)₅O₁₂ epitaxial films, microdomain nucleation near moving domain walls 7-45778
 (BiLu)₃(FeGa)₅O₁₂ film, magnetic bubble motion, Rayleigh surface wave effects 7-33245
 Bi₂MO₂₀:V, (M=Si,Ge,Ti), sillenite struct., local vibrs. of impurities, spectral study 7-7178
 Bi₂(MoO₄)₃, Czochralski growth, monoclinic unit cell (*Korean*) 7-27890
 Bi₃₈Mo₇O₇₈, cryst. struct. characterisation 7-1988
 BiNbO₄ and (Sb_{1-x}Bi_x)NbO₄, vibr. spectroscopic study 7-39115
 Bi₂O₃ dielectric films, activated reactive evaporation using resistively heated sources 7-13383
 Bi₂O₃ films from Bi oxidation in air and superheated steam 7-46674
 Bi₂O₃, ionic cond., w.r.t. lone pair separation and cryst. symm. 7-12361
 α -Bi₂O₃, local mag. fields, ²⁰⁹Bi NQR spectra 7-17241
 δ -Bi₂O₃ polycrystalline thin films, photoelectric props. 7-2638
 Bi₂O₃ thin films, traps, TSC meas. (*Japanese*) 7-7423
 Bi₂O₃-V₂O₅-CaO system, vitreous oxide semiconductor, polarisation processes 7-59139
 Bi₂O₃-ZrO₂-Y₂O₃ system, O ion conduction 7-44905
 BiOBr, cryst. struct. refinement 7-1964
 BiP(As)O(S)₄, dielec. const. meas. w.r.t. bond ionicity (*French*) 7-38988
 Bi₃₈PO₁₁₂:Nd³⁺, cryst. growth, spectroscopic props. of Nd³⁺ ions 7-46131
 (BiR)₃(FeGa)₅O₁₂, garnet films, pulsed magnetisation reversal, in-plane mag. field 7-45736
 Bi₂Ru₂O₇ thick film resistors with high TCR for temperature sensing 7-48735
 Bi₂S₃-PbBi₂S₄ system, chemically twinned phases, X-ray diffr., TEM obs. 7-32462
 Bi₂S₃-SnS, quasibinary section of Sn-Bi-S system 7-13437
 Bi₂SO₂₀, trapping levels, obs. using photorefractive effect 7-12639
 Bi_{1-x}Sb_x, photoconductivity in the FIR spectral range 7-12756
 Bi_{0.52}Sb_{0.48}Te₃, semiconducting solid soln., thermoelectric props 7-45365
 (Bi_{1-x}Sb_x)₂Te₃ single crystal, optical constants, IR spectra study 7-46030
 Bi_{2-x}Sb_xTe₃ polycryst. semicond. films, laser annealing effects 7-58317
 Bi_{2-x}Sb_xTe_{3-y}Se_y, carrier density, depend. of anisotropy parameter 7-7226
 BiSeI, dendritic, growth from vapour, characteris. 7-21788
 Bi₂Si(Ge)O₂₀ crystals., sillenite struct., dielec., elastic and piezoelec. props. calcs. 7-51714
 Bi₂Si(Ge)O₂₀, light-induced field redistrib., photocond. studies 7-38623
 Bi₂Si(Ge)_{1-x}O₂₀ solid solutions, IR spectra 7-7691
 Bi₂Si(Ge)(Ti)O₂₀, reflectivity spectra structure, thermorefectance 7-59207
 BiSi₂O₂₀ crystals, operative transformation of optical signals 7-36892
 Bi₂SiO₂₀ crystals., electrooptic consts. dispersion determ., linear approx. calcs. 7-53270
 Bi₂SiO₂₀, acoustical activity, inelastic neutron scatt. study 7-32577
 Bi₂SiO₂₀ crystal, phase conjugate signal at elevated temps. 7-43242
 Bi₂SiO₂₀ crystals, local vibrs. of Si isotopes, Raman spectra 7-7689
 Bi₂SiO₂₀ degenerate four-wave mixing, forward phase conjugate wave 7-50652
 Bi₂SiO₂₀, electrogyratory and electrooptic coupling 7-27701
 Bi₂SiO₂₀, holographic beam coupling in anisotropic photorefractive media 7-57273
 Bi₂SiO₂₀ MIS-liquid crystal structure, dynamic image processing 7-57532
 Bi₂SiO₂₀ monocrystals, holographic grating recording, improvement 7-10885
 Bi₂SiO₂₀, photo-induced impurity photoconductivity 7-7275
 Bi₂SiO₂₀ photoconductive addressing for liquid-crystal differentiating spatial light modulator 7-25956
 Bi₂SiO₂₀, photogalvanically active centres 7-45380
 Bi₂SiO₂₀ photorefr. crystals, moving grating erasure, expt. study 7-5940
 Bi₂SiO₂₀ photorefractive gratings, buildup and decay, effect of electric field 7-17306
 Bi₂SiO₂₀ photorefractive crystals, hologram fixing at room temp. 7-20160
 Bi₂SiO₂₀ photorefractive crystal, wave mixing with moving gratings, appl. to phase conjugation 7-20363
 Bi₂SiO₂₀, photorefractive, hologram recording, real-time defect enhancement using inversion props. 7-25771
 Bi₂SiO₂₀, photorefractive effect, simplified band transport model 7-27700
 Bi₂SiO₂₀, pure and doped crystals phys. props. 7-7283
 Bi₂SiO₂₀, sillenites, IR transmission spectra 7-59194
 Bi₂SiO₂₀, substrate for ZnO, acoustoelec. props. 7-38645
 Bi₂SiO₂₀:Mn,Cr single crystals, photoconductivity 7-33044
 Bi₂Te₃ and Bi₂Fe₃-derived solid solns., carrier density, depend. of anisotropy parameter 7-7226
 Bi₂Te₃ doped crystals, energy formation of antisite defects 7-21204
 Bi₂Te₃-based solid solns., CdCl₂ doped, thermal conductivity studies 7-45363
 Bi₂Te₃-Bi₂Se₃-Sb₂Te₃ system, solid solns., layered cpd. formation 7-21454
 Bi₂Te₃-S₂, carrier density, depend. of anisotropy parameter 7-7226
 Bi₂Te₃-Se₂, carrier density, depend. of anisotropy parameter 7-7226
 Bi₂Te₃-SeO₆, 7-45365
 Bi₂TiO₂₀, sillenites, IR transmission spectra 7-59194
 Bi₄Ti₃O₁₂ ceramic fabrication, grain-oriented, by normal sintering, sintering mechanisms (*Japanese*) 7-22619
 Bi₄Ti₃O₁₂, Raman spectroscopy and dielec. anomaly 7-39111
 (BiTm)₃(FeGa)₅O₁₂ epitaxial films, microdomain nucleation near moving domain walls 7-45778
 (BiTm)₃(FeGa)₅O₁₂, garnet films, pulsed magnetisation reversal, influence of temp. on integral characts. 7-45735
 BiVO₄, ferroelastic, optical soft mode, quantum nature, EPR and Raman spectra study 7-45795
 BiVO₄, pure and CaO doped polycryst. samples, sheelite struct., elec. cond., anion vacancy motion investigation 7-32712
 BiVO₄:Gd³⁺(Mn³⁺), ESR spectra, temp. depend. 7-22137
 Bi₃V₂IO₃₄, layered cpd., crystal-chemical and dielectric props. 7-6595
 BiX₂-GaX₄ complex; X=Cl, Br; struct. Raman spectra study 7-46020

bismuth compounds continued

- Bi₂XO₂₀ (X=Si,Ge,Ti), simultaneous anal. of vibr. spectra 7-46006
 (BiYLu)₃(FeGa)₅O₁₂, garnet films, pulsed magnetisation reversal, influence of temp. on integral characts. 7-45735
 (BiYLu)₃(FeGa)₅O₁₂ epitaxial films, microdomain nucleation near moving domain walls 7-45778
 Bi_{2-2x}Y_xO₃ solid soln., reversible cubic-hexagonal transform. obs. 7-32639
 Bi₂Zr₃O₁₂, sillenites, IR transmission spectra 7-59194
 (CdBi)(M_{1/2}Sb_{3/2})O₇, (M=Cr, Ga, V, Mn, Fe, Rh, Sc, In), pyrochlores, struct. and characterisation 7-1986
 CdO-Bi₂O₃, crystallographic state of CdO lattice during sintering with Bi₂O₃ addition 7-37944
 Ce_{1-x}Bi_xO₃F_{3-2x} solid solns., O substitution, influence on struct. and elec. props. (*French*) 7-12019
 Cs₃BiCl₆, cryst. struct., X-ray diffr. study 7-32389
 CsK₂BiCl₆, cryst. struct., X-ray diffr. study 7-32389
 Eu-Bi-S, synthesis and props. 7-44471
 Eu-Bi-Se(Te), synthesis and props. 7-44471
 Fe garnet films containing Bi, comp. study, and chemical etching anal. 7-45083
 (Gd,Bi)₃(FeGaAl)₅O₁₂ garnet films, selected area liq. phase epitaxy, local ion implantation effects 7-21726
 (GdBi)₃(FeAlGa)₅O₁₂ garnet films, LPE growth 7-59463
 Gd_{3-x}Bi_xFe₅O₁₂ crystal growth for 0.8 μ m optical isolator 7-57605
 Ge-S+bi chalcogenide glasses, struct., DTA and X-ray diffr. studies 7-6543
 GeO₂-Bi₂O₃-ZnO glass, coloration mechanism due to Bi₂O₃ and effects of ZnO addition 7-22291
 GeO₂-ZnO-Bi₂O₃ IR transmitting glasses 7-43276
 Ge₂₀S_{80-x}Bi_x, amorphous, electronic cond. props. under high press. 7-45328
 K₃BiCl₆·2KCl·KH₃F₄, improper ferroelectric phase transition, dielec. meas. 7-45943
 K₂Bi(MoO₄)₄, palmierite-type cpd., cryst. struct. determ. 7-21174
 K_{1.5}Bi_{1-x}Nd_xNb_{5.1}O₁₅, cryst. growth, spectral props. of Nd³⁺ ions 7-53405
 NaBi(MoO₄)₂, elastic and elastooptic props. 7-7672
 Na_{0.5}Bi_{0.5}TiO₃, Raman spectra study 7-53303
 Pb₃BiS₄ films, superconducting props. 7-22060
 PbBi₄Te₇, synthesis and physicochemical props. 7-13349
 PbNb₂O₆-BiTiMo₆ (M=Nb, Sb), solid soln. ceramics, piezoelec. const. studies 7-2980
 PbS-Bi₂S₃, chemically twinned phases, transformation to Galena struct. 7-12078
 Rb₂KBiFe₆, structural phase transitions 7-52044
 Sb_{1-x}Bi_xSi crystals, elec. props. at ferroelec. Curie point 7-2991
 α -SnBi₂S₄, congruently melting compound in Sn-Bi-S system, unit cell parameters 7-13437
 TlBi_{1-x}Sb_xVI₂ solid solns., band spectrum double inversion to semimetallic state 7-38452
 (TmBi)₃(FeGa)₅O₁₂ indicator film, visualisation of mag. field profile of thin-film magnetic heads 7-61359
 V₂O₅-P₂O₅-Bi₂O₃ glasses, DC conductivity 7-45316
 (YBi)₃(FeGa)₅O₁₂, epitaxial films, mag. bubble lattices, influence of external stresses 7-64503
 (YBi)₃Fe₅O₁₂, magnetooptic materials and their applications 7-27703
 (YLuBi)₃(FeGa)₅O₁₂, Ne⁺ implanted, CEMS study (*Chinese*) 7-7620
 (YLuBi)₃(FeGa)₅O₁₂:Ne⁺ films, stripe domain stabilisation by ion implantation 7-53100
 Y₂O₃-Bi₂O₃, local interactions and environments, EXAFS studies 7-63575
 (YTmBi)₃(FeGa)₅O₁₂ films, bubble wall states generation in rotating gradient expt. 7-53097
 YbBiS(Te), synthesis and props. 7-44471
 ZnO-Bi₂O₃ mixtures, lattice parameters, depend. on Bi₂O₃ conc. 7-1974
 ZnO-Bi₂O₃ system, sintering, role of Bi₂O₃ 7-64977

bistable multivibrators see flip-flops**bistable optical devices** see optical bistability**Bitter patterns** see magnetic domains**bitumen** see materials**BL Lac-type objects**

- 0133+476, 0235+164, 1749+096, 2131-021, variable quasars, multifreq. radio obs. 7-40955
 0754+101, V-magnitude obs. during new visual outburst (1986 September 30) 7-29540
 blazars, beaming model 7-60799
 3C 371, N-galaxy/BL Lac object, EXOSAT obs. 7-55802
 FIRST observational potential 7-48093
 IUE observational characts. rel. to X-ray characts. 7-66770
 Mrk 421, optical variability on short time scale 7-14660
 nuclei characts. (*French*) 7-66759
 OI 287, optical variation and outburst obs. (1980 to 1984) (*Chinese*) 7-4548
 OJ 287, BL Lac-type object, IR variability since 1983 outburst 7-48080
 OJ 287, V-photometric obs. 7-48076
 OJ 287, visual magnitude estimates (January 1987) 7-66760
 ON+325, optical variability on short time scale 7-14660
 PKS 0048-09, visible and IUE obs. 7-60798
 PKS 0537-441, multifreq. obs. in moderately active state 7-55811
 PKS 2005-489, spectral characts. 7-18450
 PKS 2155-304, IUE obs. (1979 to 1985) 7-55833
 S5 flat spectrum radio sources, analysis of complete sample 7-40947
 SHF and EHF obs. 7-48100
 short time-scale optical var. 7-14660
 spectral properties of blazars in for UV, IUE obs. 7-48074
 spectral properties of X-ray selected blazars 7-48075
 Texas radio source survey, search for optically variable objects 7-4580
 updated list of BL Lac objects, relation to galaxies and quasistellar objects 7-47732
 visible photometric obs. 7-66784
 X-ray luminosity-redshift relationship for extragalactic objects, observational data 7-14679
 X-ray selected BL Lac candidates, optical spectroscopy of six objects 7-48085

BL Lacertae-type objects see BL Lac-type objects**black holes**

see also gravitational collapse

- accreting model, two-temp. plasma cloud 7-40677
 accretion disk coronae, mag. loops struct. and stability 7-4431

black holes continued

- accretion disks, adiabatic jets from funnels of thick disks 7-34844
 accretion disks, general Eulerian formulation of comoving-frame radiative transfer equation 7-55441
 accretion disks in bimetric gravit. theory as test for general relativity 7-9365
 accretion MHD, entropy accretion rate and moving black hole accretion 7-14599
 active galactic nuclei, electron pair prod. rel. to bimodal spectral behaviour 7-9510
 active galactic nuclei, new accretion disk models rel. to optical and UV spectra 7-60813
 astrophysical jets formation, dynamics of rotating magnetised mass accretion 7-55460
 bosonic instability of charged black holes, particle creation and accumulation processes (*Russian*) 7-55702
 ω Cen, globular cluster, percentage of massive remnants from multimass dynamical model 7-9520
 charged collapsar, cross-section for test particles capture 7-4320
 Cyg X-1 and related sources, model for bimodal spectral behaviour 7-9510
 distorted Schwarzschild black holes, multipole moment formalism 7-48487
 Einstein equations, black hole solns. in asymptotically flat space-times 7-24486
 electrodynamics (*Russian*) 7-9507
 entropy, classical derivation 7-47969
 evaporating black holes, back reaction of quantum fields in presence of inflation 7-9506
 evaporation, closed superstring theories role, quantum coherence 7-66651
 event horizon, extended manifolds of general relativity, tachyon prod. 7-35348
 extreme Reissner-Nordstrom black holes, motion in low-vel. limit 7-14600
 formation and recoil in wide binary stars, contrib. to enhanced gravit. wave emission 7-60730
 galactic centre, implications of spatial distrib. and vel. field of H₂ line emission 7-9528
 galactic centre models and positron annihilation radiation 7-40943
 galactic nuclei Kerr black holes, optically-thick gas steady spherically-symm. accretion, outgoing radiative flux 7-35044
 Galaxy, black hole at galactic centre, observational evidence, review 7-29541
 gamma-ray emission from accretion onto a rotating black hole 7-55700
 general characteristics 7-24159
 Hawking radiation and quantum mechanical description, gravit. interaction 7-56106
 Hawking radiation of quantized black holes 7-55703
 HD 50896, Wolf-Rayet star, black hole model for X-ray emitting companion 7-55648
 higher-dimensional black holes in compactified space-times 7-47970
 horizon radiation, generalization to fermion fields 7-4499
 Kaluza-Klein blade hole, stationary, rotating, anal. of solns. for zero electric charge 7-60707
 Kaluza-Klein theory, classical, nonexistence of neutral black hole solns. with spacetime-internal space coupling 7-4742
 Kaluza-Klein theory, five dimensional, black holes coupled to time-dependent scalar fields 7-35370
 Kerr black hole, charged, structure of pseudo-Newtonian force 7-4498
 Kerr black hole, null geodesics in stationary Ernst-Wild space-time 7-61170
 Kerr black hole metrics, colinear, superposition, space-time structure (*Chinese*) 7-40861
 Kerr-Newman black hole in mag. field, surface geometry 7-56103
 LMC X-3, X-ray binary containing black hole, for-UV obs. by IUE 7-55733
 mass quantisation in string theory 7-61628
 massive Schwarzschild black hole, entropy in stable thermal equilib. 7-24502
 minihole evaporation dynamics, estimates and interpretation for high-energy physics 7-66653
 multiple black holes in asymptotically Euclidean static vacuum space-time, nonexistence 7-66652
 negative energy radiation from a charged black hole 7-4497
 neutrinos and γ -ray emission due nucl. reactions of accreting matter (*Russian*) 7-24160
 NGC 5548, Seyfert 1 galaxy, evidence for black hole accretion event, He II obs. 7-35052
 nonstationary central black hole in galaxy, possible effects on galactic struct. 7-60795
 nucleon-black hole interaction, Skyrme model anal. 7-9504
 origin (book) 7-60914
 Penrose process, energy extraction from black holes in EM fields 7-40683
 PKS 2155-304, BL Lac object, IUE obs. (1979 to 1985) rel. to accretion models 7-55833
 Population III stars forming black holes, origin for dark matter in Universe 7-47998
 primordial black holes as missing mass candidates in inflationary universe 7-4599
 quantised black hole, spectrum and entropy 7-55703
 quantum wave propagation near a black hole event horizon, QED scatt. 7-9505
 quasars, characts. review 7-48098
 quasars, new accretion disk models rel. to optical and UV spectra 7-60813
 radiated gravitational energy calc. using second-order Einstein tensor 7-35355
 radiating blackhole in a magnetic universe 7-60706
 radio galaxies, black holes ejection rel. to radio trails bending 7-35045
 relativistic collapse of cluster to black hole 7-66682
 rotating body gravitational field, motion of particles and photons 7-55704
 Schwarzschild, black hole, charged particle orbits in field of two charges 7-18653
 Schwarzschild black hole, dynamical stability of tori 7-9508
 Schwarzschild black hole, Ernst space-time representation, particle trajectory stability 7-55701
 Schwarzschild black hole, geodesic motion in globally regular space-time 7-47968
 Schwarzschild black hole, particle creation due to curvature 7-9509

black holes continued

- Schwarzschild black hole with cosmic string, thermodynamics and metric 7-18660
 Schwarzschild black holes, nucleation of vacuum phase transitions, Euclidean action 7-56102
 Schwarzschild metric, classical and quantum scattering theory for linear scalar fields 7-18684
 soft X-ray transients, relaxation to evolution of low-mass X-ray binaries 7-55707
 stability of a hypothetical binary at the galactic center 7-55793
 statistical physics and field theory conf., Groningen, Netherlands, Aug. 1985 7-55899
 supermassive black holes, general relativistic decollimation of radio jets 7-60522
 supermassive central black holes ejection from active galaxies and quasars 7-60797
 thin disk model for UV excess of quasars and Seyfert 1 galaxies 7-40956
 thin spherical matter shell, gravitational entropy, beyond black holes 7-4750
 47 Tuc, globular cluster, percentage of massive remnants from multimass dynamical model 7-9520
 vacuum expectation values of the energy-momentum tensor in two dimensions 7-41210

blast waves *see shock waves***blazars** *see BL Lac-type objects; quasars***bleaching, optical** *see optical saturable absorption***Bloch walls** *see magnetic domain walls***block polymers** *see polymer blends***blood***see also haemodynamics*

- activated platelets, human, soft X-ray microscopy studies 7-40124
 adaptive thermal modelling, concept for meas. of local blood perfusion in heated tissues 7-65715
 aggregation of red cells expt. results., Space Shuttle Discovery appl. 7-3924
 arterial flow at a 90° bifurcation, effects of nonNewtonian viscoelasticity and wall elasticity 7-3812
 arteriovenous O₂ difference, spectrophotometric meas., role of light scatt. 7-3942
 autoregulatory mechanisms in irradiated biosystems, reliability (Russian) 7-47171
 brain-blood, late effects of radiation, rat obs. 7-65814
 brain-blood barrier of rats, interaction of ethanol and microwaves 7-28601
 burns patients, dynamic analysis of reanimation treatment effects 7-40202
 carbonylhemoglobin, pH dependent XANES by fast dispersive spectroscopy 7-65708
 CCD line-scan image sensor for meas. of red cell vel. in microvessels 7-8777
 cell nuclei, erythrocytes and hepatocytes, small angle scatt. obs. 7-17959
 cells, mag. susceptibility investig. (Russian) 7-65790
 chromosome aberrations induced in human lymphocytes by acute X- and γ -radiation in vitro 7-3843
 core blood temp. changes during hyperthermia, oesophageal and tympanic temp. responses 7-8498
 cytogenetic effectiveness of the therapeutic fast neutron beam emitted by cyclotron U-120 (Russian) 7-13976
 deoxyhaemoglobin S, solns. and gels, quasi-elastic laser light scatt. 7-28464
 dynamics of the transcapillary fluid and plasma protein exchange 7-65729
 erythrocytes, aggregation under zero gravity 7-3889
 erythrocyte, live cell, shear elasticity, entropic nature 7-65725
 erythrocyte cells, dynamic studies using laser-projection microscopy 7-14172
 erythrocyte marginal bands, newt., extensional and flexural rigidity obs. 7-8631
 erythrocyte membrane, effects of γ -irrad. as shown by ESR, NMR and biochem. studies 7-60041
 erythrocyte membranes, viscosity and order, ns fluorometry obs. 7-40185
 erythrocyte receptors, human, adrenoceptive function, fluoresc. probe 7-8501
 erythrocytes, effects of He-Ne laser light 7-3840
 erythrocytes, human, ferricyanide reduction in the presence of methylene blue, influence of a UHF EM field 7-40217
 erythrocytes, human, packing in centrifugal field 7-65721
 erythrocytes agglutinated by antibody, hydrodynamic force of breakup 7-40122
 erythrocytes agglutinated by antibody, interaction forces between 7-40121
 erythroleukemic cells, murine, differentiation during exposure to microwave radiation 7-40218
 fibrin assembly, lateral aggregation and the role of the 2 pairs of fibrinopeptides 7-40091
 filtration rates, review 7-54654
 fingers, human, noninvasive method for estimating mean capillary press. and pre- and postcapillary resistance ratio 7-28735
 haematopoiesis and radiation in Harwell steel mice 7-40222
 haeme proteins, long-range electron transfer 7-8482
 haemoglobin, human, cooperative free energies for nested allosteric models 7-23272
 haemopoietic tissue, ²⁵²Cf RBE and PLD-like effect of mag. fields, CFU-S assay 7-28590
 haemoproteins and Fe porphyrins, ps relax. 7-34113
 haemorheology, effect of couple stresses on unsteady convective diffusion in fluid flow through a channel 7-3811
 haemorrhagic lesions, NMR imaging, evolution of intrinsic relax. parameters from time of onset of symptoms 7-54696
 hypercoagulation syndrome in mobility-restricted rats, effect of a weak variable mag. field 7-54669
 image processing in medical microscopy, blood smear analysis automation 7-65832
 immunoglobulin A from normal humans and myeloma patients, orientation and kinetics of surface denaturing 7-28442
 light scattering from nucleated blood cells, numerical anal. 7-14042
 lymphocyte, free energy of accumulation of a fluoresc. cation probe within the mitochondria 7-40118
 lymphocyte subclasses and immunoglobulins, in adults receiving radiation treatment in infancy for thymic enlargement 7-18032

blood continued

- lymphocytes, human, cell survival and radiation induced chromosome aberrations 7-47168
 lymphocytes, human, chromosome aberrations yield rel. to dose (Russian) 7-18027
 lymphocytes, human, lower limits of dose detect. after X-irrad. 7-34196
 lymphocytes, human, sensitivity to gravity obs. (German) 7-8705
 lymphocytes, low-dose-irrad., decreased nucleic acid synthesis, effect of TCGF addition 7-8661
 lymphocytes, peripheral, human, effect of low-level 60 Hz EM fields 7-28582
 methemoglobins, whole-blood, millimolar absorpt. parameter spectra, 660-1000 nm 7-40101
 microvessels, flow control coordination by intercellular cond. 7-65797
 mitogenic response of peripheral blood mononuclear cells, effect of ELF pulsed mag. fields 7-28580
 mononuclear phagocyte system, effects of therapeutic US on activity in vivo 7-14043
 neutrophil dynamics, normal, 1/f-like scaling, implications for haematological monitoring 7-3757
 nonlinear elasticity of blood vessels (Chinese) 7-18009
 nuclear techniques in diagnostic medicine, book 7-24312
 nucleoli, extraction from images of leucocytes by computerised image analysis 7-23505
 oligosaccharides, conformational statistics 7-13958
 oscillatory flow in viscoelastic tube, wave motions near instability limit 7-51316
 peripheral blood, lymphocytes from ageing donors, sensitivity to X-irrad. 7-8655
 peripheral blood lymphocytes of atomic bomb survivors, anal. using monoclonal antibodies 7-59947
 phase separation of erythrocytes, platelets and plasma at branches 7-54664
 platelet activating factor, IR spectroscopic characterisation 7-54499
 platelet adhesion to fibrinogen-coated glass at an abrupt tubular expansion viewed with fluorescent video-microscopy 7-40183
 platelet aggregation, shear-induced, anal. with population balance maths. 7-8614
 platelet diffusivity in flowing blood, fluid shear as a possible mechanism 7-28552
 platelet volume heterogeneity in acute thrombocytopenia, aperture impedance obs. on rats 7-3756
 platelets, human, lateral diffusion of lipid probes in surface membrane, ELDOR obs. 7-8526
 portable continuous blood pressure monitor utilizing an M68705 microcomputer 7-28755
 pressure regulation during surgery using self tuning controller 7-54805
 radiation dosimetry, picture-processing-based automated system 7-28713
 red blood cells suspended in carbohydrate-saline solns., deformability, effect of transmembrane pot. 7-34118
 rheology in myocardial infarction and hypertension 7-65788
 serum albumin, human, effect of hydration on mol.-dynamic props. in low temp. region 7-54436
 serum and its components, comparative study of chemiluminesc. and resistance on ionising irrad. (Russian) 7-14066
 serum T₄ level and response of thyroid gland to exogenous TSH in rats, 8 Gy X-irrad. effect 7-18023
 sickle cell haemoglobin aggregates, polymorphism: struct. basis for limited radial growth 7-65697
 sonographic and NMR patterns of ageing blood, effect of motion 7-54684
 steady-state macromolecular transport across a multilayered arterial wall, math. model 7-65793
 T₁ of blood and blood clots, paramag. effect of Fe 7-17949
 T lymphocytes, human cloned helper, single-channel and whole-cell recordings of mitogen-regulated inward currents 7-40134
 thromboelastograph, 2-channel, microprocessor-based 7-3903
 thrombolytic process dynamics under conditions of a constant mag. field 7-3835
 tissue blood perfusion, computer-based system for continuous on-line meas. using a thermal method 7-40319
 US flowmeter, pulsed Doppler system, serial data processing (Korean) 7-3846
 ventricular blood pressure meas. appl. of spline time varying digital filter 7-47268
 viscosity of whole-blood, calibration of rot. instruments for meas. 7-40372
⁶⁰Co γ -source, accidental irrad. of technician, long-term follow-up: eye, skin and blood effects 7-34195
 O₂ saturation, in vivo meas. using quartz fibre optics and an optical multichannel analyser (German) 7-23423
 Se changes in blood, cyclic activation anal. study 7-34100
 U content of vertebrate blood, SSNTD anal. 7-54829
 U distribution in blood samples, fission track study 7-54771

blood circulation *see haemodynamics***blood dynamics** *see haemodynamics***blood flow** *see haemodynamics***blood platelets** *see blood***blowing problem** *see boundary layers***blue brittleness** *see brittleness***board computers** *see microcomputers***Boide diagrams***see also frequency response*

unsteady aerodynamics, finite state modelling 7-51199

boilers

- AGR boilers, Heysham I and II and Hartlepool II modifications 7-15253
 AGR helically wound heat exchangers, vibration props. 7-56788
 alloy 600 nuclear steam generator tubes, local pitting conditions using Pourbaix diagrams 7-46716
 Alloy 600 PWR steam generator tubing, intergranular attack and SCC remedial methods 7-8199
 alloy 600 tubes, stress corrosion cracking in aggressive chemical environments 7-10230
 alloy 600 tubes in PWR steam generators, localised electrochem. corrosion 7-39760
 Alloy 690, thermally treated nuclear steam generator tubes 7-5334
 ASME Boiler and Pressure Vessel Code, design developments 7-49506

boilers continued

- CEGB single-phase erosion-corrosion research programme for AGR boilers 7-59679
 centrifugal separators for PWR power stations (*French*) 7-25102
 correlation for heat transfer between immersed surfaces and large-particle gas-fluidised beds 7-26127
 counterflow steam generator, water-sodium leaks, fault processes 7-5344
 dyeing, appl. of waste heat-recovery heat pumps (*Japanese*) 7-59867
 gas boilers, seasonal efficiency simulation and energy quality 7-65593
 Hartlepool/Heysham I AGRs, re-ferruling of pod boilers, boiler performance effects 7-56792
 hog fuel predrying by flue gas heat recovery 7-8356
 homogeneous flow model, validity for instability anal., steam generators 7-5379
 hydraulic pump driven by low-level temp. difference 7-54335
 LMFBR steam generator design and experience in the UK 7-56791
 LMFBR steam generator large leak accident, heat transfer into module shell tube 7-62016
 LMFBR steam generators, thermohydraulic instabilities, expt. results 7-5382
 LMFBR steam generators, thermohydraulic instabilities, nonlinear and linear anal. models 7-5381
 LWR steam generator U-tube rupture transient anal. using DRUFAN-02 code 7-49562
 modular HTGR plant, steam generator design considerations 7-62014
 Monju FBR, anal. and design for elevated temp. components 7-56717
 nuclear reactor U-tube steam generator, FAUST 3D 2-fluid code for thermal design anal. 7-36082
 nuclear steam generators, heat flux effects on concentration factor in crevices 7-19397
 PWR, steam generator tube bundle flow, turbulence force correlation 7-62003
 PWR boiler pipework, effect of feedwater conditioning on corrosion (*German*) 7-25115
 PWR feedwater, Cu oxides, acid chlorides, steam generator denting 7-5333
 PWR hot leg, two-phase flow during natural circulation in once through steam generators 7-49579
 PWR steam generator sludge piles, chemical cleaning 7-10227
 PWR steam generator thermohydraulic anal., ATHOS3 code 7-10244
 PWR steam generator tubing sampling, feasibility study 7-5364
 PWR steam generators, correlation of tube support struct. studies, corrosion 7-10246
 PWR steam generators, in-service cleaning (*German*) 7-15261
 PWR steam generators, tubesheet crevice-flushing effectiveness 7-56797
 PWR steam turbine secondary side SCC, remedial actions 7-61969
 PWR steam-generator simulation with non-equilibrium two-phase flow models 7-42122
 reactor construction codes and engineering mechanics conf., Paris, France, Aug. 1985 7-48153
 reactor steam generators, crevice hideout return testing, H_3BO_3 and $Ca(OH)_2$ effects 7-10247
 steel, mild, erosion-corrosion control using O_2 - NH_4 -hydrazine dosed feed-water in reactor boilers 7-59675
 steels, oxidation performance of Magnox and AGR boiler materials in high press. CO_2 7-59676
 stress corrosion cracking test of expanded steam generator tubes 7-56764
 submerged perforated screens, hydrodynamics in nuclear power station (*Russian*) 7-5352
 Surry steam generator, examination and eval., nondestructive testing 7-54065
 tube NDT inspection systems 7-20549
 VHTR steam generator, dryout and flow of gas-water flow in U and inverted U bends 7-5399
 water cooled reactors, steam generator tube performance during 1983 and 1984 7-25118
 NO_x in-furnace reduction, reburning, bench scale process evaluation 7-17798

boiling

see also boiling point

- boiling heat transfer, anal. using hot ball quenching method (*Chinese*) 7-49596
 bubble and transition-boiling regimes, heat transfer coeff. 7-11416
 bubble growth and collapse, transient boiling heat transfer in narrow channel 7-26346
 bubbles, maximum size during nucleate boiling in elec. field 7-50918
 chemical boiling, heat and mass transfer, gas liberation and free convection 7-43907
 critical heat flux of boiling Freon, correls. at high subcrit. press. 7-1389
 crossflow boiling heat transfer in tube bundles 7-11511
 cryogenic flow instability during adiabatic boiling 7-11385
 cryoturbogenerator rotors, heating and convection of boiling fluid 7-31796
 curves, calcs. from unsteady-state quenching tests 7-54257
 falling liq. film, vapour generation nucleate boiling, acoustic diagnostic technique 7-11502
 fibre optic probe for boilup heat transfer obs. 7-50778
 film, equilb. load calc. 7-52015
 first crisis, elementary hydrodynamic model, additive generalisation 7-31746
 fissile material, critical soln., heating-up, nucleation and boiling 7-19368
 flow boiling, critical heat flux prediction 7-43898
 flow systems, freq. response two-fluid model 7-1603
 forced convection boiling crisis in rod bundles, governing relationships investig. 7-26125
 forced convection boiling of R-12 under swirl flow, heat transfer 7-63162
 heat carriers in vertical pipes of low-head natural circulation systems, limiting thermal loads 7-43917
 heat transfer, to mixtures, capillary porous coating thickness effect 7-51101
 heat transfer coefficient, plasma-deposited coating particle size effect 7-50916
 hysteresis phenomena in boiling of trifluorotrchloroethane at porous surface 7-6770
 laminar film, pool boiling from curved surfaces, integral method calcs. 7-1568
 liquid, heat transfer in porous struct. 7-51102
 liquid boiling, heat and mass transfer 7-31627
 nucleate, equilb. load calc. 7-52015
 nucleate, onset on wick-covered wall 7-52016

boiling continued

- nucleate pool boiling, surface roughness and polymeric additive effect 7-11512
 OTEC shell and plate type evaporator, performance tests (*Japanese*) 7-54338
 point sink on plane with magnetic field, heat and mass transfer 7-1618
 polymer solutions, viscoelastic, boiling, rheological investig. 7-51015
 pool boiling, role of macrolayer evaporation at high heat flux 7-50927
 pool boiling, thermodynamic state of bulk-sat. liq. prediction 7-50928
 pool undergoing transient bulk boiling, pool height determ. 7-11261
 refrigerant R-142, boiling, heat flux in low press. natural circulation cooling system 7-11505
 steam-water two-phase flow, disturbance wave study 7-44022
 subcooled liquid, film boiling in channels, heat transfer and hydraulic resistance 7-51145
 subcooled water in narrow annuli low vel. flow, boiling crisis 7-11507
 toroidal loop, two-phase natural circulation 7-26280
 transient boiling, heat transfer mechanism 7-11253
 trichlorofluoromethane, down-flow shell-side forced convective boiling 7-63194
 two-phase thermosiphons, heat and mass transfer 7-11409
 underheated liquid, surface boiling, forced motion, Reynolds analogy appl. 7-31806
 vapour bubble, quasistatic growth on boiling liq. surface, contact angle var. 7-44951
 water, nucleate pool boiling during press. and power transients 7-1388
 He, film boiling, heat transfer, centrifugal forces effects 7-50920
 He II, pressurized, confined to channel, boiling phenomena 7-38280
 He, liquid, heat transfer with nucleate boiling in channels 7-11524
 K, liq., boiling, pressure effect on departing bubble 7-44774
 N_2 liq., forced flow in horizontal pipe, film boiling 7-51277
 O_2 , nucleate boiling at low gravity, microparameters 7-62962

boiling point

see also boiling; heat of vaporisation

- propane, liq., X-ray diffr. study near triple and boiling points 7-26611
 vapor composition calculations from bubble point temp. and liq. composition meas. 7-52026
 KH_2PO_4 crystals grown at boiling point, surface microtopography 7-21581

bolometers

- 2l-He hybrid cryostat for 690 GHz InSb bolometer 7-30024
 background power effect on ideal bolometer performance 7-56344
 IR low-background bolometers, calibration system 7-9899
 metal-film, bolometric measurements on high temp. plasma 7-1734
 multichannel bolometer for radiation measurements on the TCA tokamak 7-20943
 multichannel tangential bolometer on PBX, operation 7-1774
 photoconductor X/γ -ray detectors and X-ray bolometers 7-10361
 plasma radiation features, reconstruction from projections measured with two bolometer arrays 7-51514
 quartz bolometer for hot plasma diagnostics 7-11708
 radiation loss profiles in TFTR, high asymmetry 7-1770
 resistivity at low temp. appl. to bolometers 7-41471
 toroidal variation of power radiated from TFTR 7-1769
 Ge thin film bolometer with fast response 7-56261

Boltzmann equation

see also transport processes

- anisotropic cosmological model, Boltzmann and Vlasov kinetic eqns. 7-61189
 Boltzmann-Lorentz-Enskog equation, gas diffusion at moderate densities, anal. 7-37617
 boundedness of a bilinear operator derived from the Boltzmann collision term 7-4791
 cellular automaton fluid models, continuum eqns. for large-scale behaviour 7-35286
 charged particle transport calcs., finite element method, ICF appl. 7-36244
 charged particle transport in fully ionized plasma, flux-limited diffusion model 7-36246
 convective transport equation, finite element soln., determ. of optimal upstream weighting parameter 7-29764
 correlated exponential random walks, linear Boltzmann transport formulation 7-35407
 Coulomb systems, 2D self-consistent struct. formation, 2D Poisson-Boltzmann system 7-9751
 dilute dimple gas, equilibrium eigenmodes 7-16291
 discrete velocity Boltzmann equation, large-time behaviour 7-9803
 dynamical systems and statistical physics conf., Koszeg, Hungary, Aug.-Sept. 1984 7-48194
 electron distrib. function in gas discharge (*Russian*) 7-20995
 electron swarm in a model gas, diffusion coeffs., Monte Carlo simulation 7-1662
 electron swarm in a weakly ionized gas, numerical methods 7-61285
 energetic ions, flux and range distrib. calcs. appl. of Boltzmann transport eqn. 7-63692
 eulerian and Lagrangian particle transport with drag 7-48635
 exact bisoliton solns. for discrete models (*French*) 7-56188
 Fourier transform, for Maxwell model, transport coeffs. (*Korean*) 7-24605
 gas mixtures, acoustical oscillations 7-63242
 gas mixtures, dynamical self-struct. factor, matrix continued-fraction representation 7-63238
 gases, electron swarms, electron diffusion tensors, conservation inelastic collisions effects 7-37618
 gases, hard and Maxwellian mols., shock wave struct., local entropy balance, bimodel approach 7-26320
 gases, spin waves and quantum collective phenomena 7-48546
 graphite intercalation cpds., staging dislocation electronic struct., electron scatt. rates, residual resist. 7-52558
 Gross-Jackson kinetic model eqn., convergence 7-48642
 heat transfer between parallel plates at arbitrary Knudsen numbers 7-57883
 heated particle in rarefied gas, Brownian movement, kinetic description 7-51231
 heavy ion collisions, anisotropic hydrodynamics and isotropization of momentum 7-42053
 inhomogeneous similarity solns. for confining external forces 7-35476
 initial layer soln. for small Knudsen number 7-35475
 insulating crystals, weakly coupled electron-phonon systems, nonequilibrium phonons, quantum mech. Boltzmann eqn. 7-2128

Boltzmann equation continued

- integral transform of energy distrib. function 7-35477
 interaction round a face model, free energy expression 7-196
 kinetic gas theory formulation for Boltzmann-Fokker-Planck eqn. 7-63239
 linear particle transport theory, current density transients 7-56191
 Maxwellian gas, relax. to quasiequilibrium state 7-44085
 Maxwellian particle gas mixtures, coupled linearised Boltzmann eqn. 7-1664
 mechanics of continuous media, kinetic theory and material frame-indifference principle 7-24422
 methane, deposition plasma, homogeneous and heterogeneous chemistry, deposition of C:H 7-39424
 mineral waste dil. suspensions, interacting particles, kinetic theory 7-46880
 mixed problem for Boltzmann eqn. with Lorentz force term, global solns. 7-274
 monatomic gases, Chapman-Enskog approx. and Boltzmann eqn. calcs. 7-37615
 noble metals, near IR surface impedance, Maxwell-Boltzmann eqn. 7-7273
 nonisothermal gas mixture, transport coeff. calc. 7-11574
 nonlinear, soln. in unbounded domains 7-24601
 nonlinear Boltzmann eqn., nonisotropic solns. for relaxation process 7-35473
 nonlinear Boltzmann equations, integro-differential equations 7-56187
 nonlinear dynamics of multispecies Boltzmann equations 7-30483
 nonlinear homogeneous Boltzmann eqn., exact similarity solns. 7-61294
 nonlinear spatially homogeneous Boltzmann eqn. with external source, generating functions 7-48650
 osmotic coefficients for polyelectrolyte solutions with ionic mixtures from Poisson-Boltzmann eqn. 7-13806
 polarised Fermi gases, flow through narrow channels 7-32739
 polaron mobility, collision time calc. 7-21826
 polyelectrolytes, counterion condensation, Poisson-Boltzmann eqn. sol. 7-52029
 quantum transport equation for electric and magnetic fields 7-52550
 quasi-one-dimensional wire, cond., thermopower, effect of lifetime broadening 7-45252
 rarefied gas, high Mach number flow past almost specularly reflecting plate 7-63186
 semiconductor $n^+ - n - n^+$ submicron struct., ballistic electron transport 7-22004
 semiconductors, electron-phonon weak scatt. in high elec. fields, Boltzmann eqn. 7-2625
 singular perturbation method for normal solns., small Knudsen number example 7-35474
 slightly rarefied gas mixture, behaviour over plane boundaries 7-1592
 spatially homogeneous mixture of Maxwellian gases, Boltzmann eqn. solns. 7-29944
 Spencer-Lewis eqn. of electron transport theory, moment reconstruction technique 7-61290
 stars, photospheric plasmas, time-dependent radiative transfer, analytical methods 7-55451
 steady Boltzmann eqn., thermal layer solns. 7-51033
 subsystem interaction with boson field, kinetics 7-32591
 thermal relaxation, model problem 7-57974
 transport theory conf., Montecatini Terme, Italy, June 1985 7-60874
 transport theory connection with extended thermodynamics 7-29953
 weakly localised electrons, transport equation 7-7195
 Ag-based dilute alloys, low temp. elec. resist. 7-52565
 Ar, electron swarms, collision cross sections 7-37619
 Ar ion lasers excited by low-energy electron beams 7-20186
 Ar plasma, non-isothermal, excited level populations 7-11588
 Ar, plasma characts., study of high current discharges appl. to pulsed-power devices 7-32188
 Ar/Ne mixtures, electron swarm, Penning ionisation effects, Boltzmann eqn. anal. 7-1802
 Ar/Ne mixtures, Townsend first ionisation coeff. Penning ionisation effects 7-37776
 Bi: Sb: Te(Sn) thin films, elec. props 7-64376
 CO, RF molecular plasma, electron energy distrib. functions 7-37636
 CO, weakly ionised collision-dominated RF plasmas, electron kinetics 7-20856
 CO₂ waveguide laser, Cohen model 7-20183
 p-CdGeAs₂ semicond., hole mobility and scatt., temp. depend. study 7-52609
 CdS platelet, nonlinear optical and transport props. of many exciton system 7-32920
 Cu-based dilute alloys, low temp. elec. resist. 7-52565
 GaAs-GaAlAs superlattice, electronic struct., envelope function approx., phonon limited mobility, Boltzmann eqn. 7-2698
 H⁺ magnetic multicusp discharges, e^- energy distrib. function modelling 7-10337
³He, liquid, collision bracket of linearized quasiparticle Boltzmann equation 7-32740
⁴He, liq. films, first and second sound 7-32734
 N₂ gas breakdown by 13.56 MHz electric field 7-1806
 N₂ plasma, electron velocity distrib., self-consistent determ. 7-20859
 O₂ plasma, weakly ionised, electron heating and ionis. by RF fields 7-20862
 SF₆, electron swarm kinetics with attachment and ionis., higher-order Boltzmann eqn. calcs. 7-20854
 SF₆, RF molecular plasma, electron energy distrib. functions 7-37636

Boltzmann equation (gases) see kinetic theory of gases

Boltzmann-Vlasov equation see Vlasov equation

bond angles

- alkanes, prediction of ¹³C NMR spectra, rigid hydrocarbons geometrical parameters anal. 7-31068
 aluminosilicate glasses, magic-angle spinning NMR, review 7-64536
 2-azido-1,3-butadiene, vibr. spectra, mol. struct., conform., GPED anal., Raman and IR spectra anal. 7-36608
 1,1'-bipyrrrole, rot. isomerism, mol. conformation, electronic struct. ab initio STO calcs. 7-15478
 bis(dichlorophosphoryl)methane, struct., conformational equilb., GPED, Raman and IR spectra 7-57176
 bis (trihalomethyl) ether, conformer struct. and stability, rot. barriers, torsional force consts., mol. mechanics calcs. 7-19998
 bis (trihalomethyl) thioether, conformer struct. and stability, rot. barriers, torsional force consts., mol. mechanics calcs. 7-19998

bond angles continued

- borate glasses, structure and bonding, NMR studies 7-63503
 carbamic acid derivatives, torsional changes, ab initio structural studies 7-15502
 chain configs. in MX₅ cpds. with vertex sharing octahedra (German) 7-44460
 chlorophenoxyacetylpropylbenzenes, X-ray struct. investig. 7-12049
 α -cyanoacetohydrazide, crystal struct., neutron diff. anal., ab initio MO calcs. 7-36458
 P-cyanophosphathene, bond angles and length, rot. const., microwave obs. 7-62358
 di(2-pyridyl)dichalcogenides, conform. and rot. isomerism ¹³C NMR spin-lattice relaxation study 7-19888
 2,3-diazido-1,3-butadiene, vibr. spectra, mol. struct., conform., GPED anal., Raman and IR spectra anal. 7-36609
 1,2-dichlorobenzene-d₃(d₄), isotopic species, τ_0 structure calcs., microwave spectra 7-19834
 1,2-dichloroethene, isomeric mixtures, determ. of struct. and comp., GPED spectra anal. 7-36763
 diisopropylamine, mol. struct. and conform., GPED, Raman IR spectra, MO calcs. 7-20043
 dimethyl tin diacetate, solid-state and soln. struct., ²H and ³C NMR spectra study 7-25431
 dimethyl tin diacetate hydrolyzate, solid-state and soln. struct., ²H and ³C NMR spectra study 7-25431
 N,N'-dimethyl-4,4'-bipyridinium, oxidation states, electronic struct. and conform. anal. 7-25383
 disulphide bond, S-S dihedral angle, ab initio SCF MO calcs. 7-15504
 dithioformic acid, conform. struct. and stability, rot. barrier, SCF and HF calcs. 7-25427
 dodecafluorooctahydrothiophene, gas phase, geometric struct., GPED spectra anal. 7-36764
 ethanol, standard geometry functions 7-849
 ethylamine, geometrical structural parameters calcs. GPED 7-20042
 ethylamine standard geometry functions 7-849
 ethylenes, monosubstituted, struct., ab initio calcs. 7-850
 hexakis(dimethylsilyl)benzene, rot. isomerisation mechanism and barriers, ⁴H and ¹³C NMR spectra anal., EFF calcs. 7-25359
 hexakis(trimethylelementyl)benzenes, synthesis and crystal mol. struct., X-ray spectra anal., EFF calcs. 7-25360
 III-V ternary alloy semiconductors, short-range order 7-44821
 Lamellar cpds., X-ray absorpt. studies 7-59286
 methane, proton-proton spin-spin coupling surface 7-42645
 2-methoxy-2-oxo-1,3,2-oxazaphosphorinane, conformer struct. and populations, IR, NMR and X-ray spectra anal. 7-25509
 orthophosphates, ³¹P NMR chem. shift, anisotropies, struct. and cation effects 7-50187
 oxide crystals, TO₄ units, correl. of ang. and bond length distortions 7-32359
 n-pentane, bond distances and angles, ab initio gradient geometry refinement 7-852
 phenol, OH group rot., barrier height, MO study 7-848
 potassium dihydrogen triacetate, cryst. struct. study 7-44503
 propanol, standard geometry functions 7-849
 propyl fluoride, r_s struct., rot. isomerism, microwave spectra and moments of inertia meas. 7-10556
 propylamine, standard geometry functions 7-849
 silicate glasses, magic-angle spinning NMR, review 7-64536
 silicate glasses, structure and bonding, NMR studies 7-63503
 surface electron energy loss fine struct. spectroscopy, EXAFS-like anal. 7-64834
 surface struct. determ. using angle-resolved photoemission extended fine struct. 7-7822
 tetracloromethylenediphosphine struct., GPED 7-57175
 4,4,8,8-tetrafluorotricyclo(5.1.0.0^{3,5}) octane, syn isomer struct., X-ray anal. 7-21187
 2-thio-1,3,2-oxazaphosphorinane, conformer struct. and populations, IR, NMR and X-ray spectra anal. 7-25509
 (TMTCF)_x salts (C=S₂Se), crystal struct., press. and temp. depend. 7-44520
 transition metal borides, AIB₂ type, electronic struct. study, heats of formation anal., HMO calcs. 7-25409
 s-triazine, gas phase, mol. struct., GPED anal., ab initio force field calcs. 7-36457
 sym-tribromobenzene, struct., vibr., GPED 7-57177
 trichloromethyl radical, struct. and electronic states, ab initio UHF SWX₂ calcs. 7-30949
 1,6,12-trioxo-9-aza-9-butyl-5-germa-spiro[4,7]dodecane-2-one, cryst. and mol. struct. 7-12048
 As₂S₃, amorphous, bulk glass and thin films, photostructural changes, EXAFS meas. 7-39314
 Ba(NO₃)₂, cryst. struct., X-ray diff. study 7-32411
 Cu₂Cl(OH)₂, atacamite, struct. refinement, X-ray diff. study 7-32371
 Er complexes, (tricarbamidetriacetato)erbium(III) monocarbamide, cryst. struct. 7-12029
 F+H₂, bond angle-bond distance coordinate system, energy conserving trajectories 7-28287
 Fe complex [(ethyl)₄N]₆[Ti₆Fe₁₀(CO)₃₆], struct. and bonding study, HMO calcs. 7-25411
 GeBr₂, ground and triplet state, bond angle, density functional calc. 7-854
 GeCl₂, ground and triplet state, bond angle, density functional calc. 7-854
 H₂N-HF-HF, H bond cooperativity, structural and energetic props., ab initio calcs. 7-19697
 H₂O, mol. struct., density functional anal. 7-62272
 H₃P-HF-HF, H bond cooperativity, structural and energetic props., ab initio calcs. 7-19697
 H₂PO₄, n=1-3, tetrahedra distortion depend. on H bond length 7-63542
 Li₃BN₂, synthesis, polymorph struct., ionic cond. meas. 7-32388
 MnNa(H₂PO₃)₃·H₂O orthorhombic struct., bond lengths and angles, X-ray diff. study 7-32372
 Ni complex, bis(triphenylphosphine) adduct of Ni(NCS)₂, cryst. struct., X-ray study 7-12025
 O₃, photodetachment cross sections Franck-Condon anal. 7-57139
 PbTeO₃, tetragonal phase, cryst. struct., X-ray diff. study (French) 7-44466
 RbC₈, 2D graphite intercalation cpds., bond angle determ. EXAFS study, Debye-Waller anisotropy. 7-59293
 Si, amorphous, IR absorpt., local phonon-induced bond angle distortion model 7-26642

bond angles continued

- a-Si, tetrahedrally bonded, bond angle disorder 7-32297
 Si_n ($n=10$ to 32), clusters, growth and struct., solid-liq. transform., mol. dynamics simulation 7-26682
 $(\text{SiH}_3)_2\text{O}$ mol. struct., hydrolysis of Si-O bonds, density functional anal. 7-62272
 SiH_3OH , mol. struct., density functional anal. 7-62272
 SiO_2 , radial distrib. functions, glassy struct. and bond angles, Monte Carlo method 7-11924
Ti, oxides and silicates, Ti XANES study, site geometry, spectral features 7-59288
 UC_2 , gaseous molecular forms, discrete variational $X\alpha$ molecular orbital calcs. 7-10420

bond distance *see* **bond lengths****bond energy** *see* **ionisation potential****bond lengths**

- acetylacetone, mol. struct. determ. by gas phase electron diffr. 7-50358
acetyldimethyl phosphine, geometries and rotation barriers, structures, ab initio calcs. 7-15501
acetylene, chemisorption on Cu (100), σ -shape and π resonances, XANES 7-53448
adsorbates, near edge X-ray adsorption fine structure spectroscopy 7-27822
alkanes, prediction of ^{13}C NMR spectra, rigid hydrocarbons geometrical parameters anal. 7-31068
2-azido-1,3-butadiene, vibr. spectra, mol. struct., conform., GPED anal., Raman and IR spectra anal. 7-36608
azoles, protonation energies and tautomerism, basis set effects 7-25374
benzoic acid, crystn. state compression effect on struct. and proton transfer barrier height 7-12042
beryl, high press. cryst. struct. and compressibilities 7-16505
1,1'-bipyrrrole, rot. isomerism, mol. conformation, electronic struct. ab initio STO calcs. 7-15478
bis(dichlorophosphoryl)methane, struct., conformational equilb., GPED, Raman and IR spectra 7-57176
bis (trihalomethyl) ether, conformer struct. and stability, rot. barriers, torsional force consts., mol. mechanics calcs. 7-19998
bis (trihalomethyl) thioether, conformer struct. and stability, rot. barriers, torsional force consts., mol. mechanics calcs. 7-19998
borate glasses, basicity and geometry studies, MNDO calcs. 7-6529
carbamic acid derivatives, torsional changes, ab initio structural studies 7-15502
carboranes, optimised struct. and relative stabilities, ab initio calcs. 7-30930
trans- β -carotene, finite solid polyene, amorphous and cryst., visible absorpt. and wavelength-selective reson. Raman spectra 7-64641
charge transfer cpds., lattice geometry changes 7-6564
chlorophenoxyacetylpropylbenzenes, X-ray struct. investig. 7-12049
cordierite, cryst. struct. refinement and thermal expansion, 100-550K 7-6609
 γ -crystallin IIb, 3D model, construction from electron density maps using machine graphics 7-23301
 α -cyanoacetohydrazide, crystal struct., neutron diffr. anal., ab initio MO calcs. 7-36458
P-cyanophosphathene, bond angles and length, rot. const., microwave obs. 7-62358
cyclopropylamine, substituent effect, struct., ab initio calcs., microwave spectra 7-62354
diatomic mols., orbital stress and transition stress calc., bond lengths, rot. consts. photoelectron spectra 7-42503
2,3-diazido-1,3-butadiene, vibr. spectra, mol. struct., conform., GPED anal., Raman and IR spectra anal. 7-36609
1,2-dichlorobenzene- d_3 (d_4), isotopic species, r_0 structure calcs., microwave spectra 7-19834
1,2-dichloroethene, isomeric mixtures, determ. of struct. and comp., GPED spectra anal. 7-36763
diisopropylamine, mol. struct. and conform., GPED, Raman IR spectra, MO calcs. 7-20043
dimers, first row homonuclear, orbital forces and chemical bonding in density functional theory 7-5595
dimethyl tin diacetate, solid-state and soln. struct., ^2H and ^{13}C NMR spectra study 7-25431
dimethyl tin diacetate hydrolyzate, solid-state and soln. struct., ^2H and ^{13}C NMR spectra study 7-25431
N,N'-dimethyl-4,4'-bipyridinium, oxidation states, electronic struct. and conform. anal. 7-25383
dithioformic acid, conform. struct. and stability, rot. barrier, SCF and HF calcs. 7-25427
dodecafluorooctahydrothiophene, gas phase, geometric struct., GPED spectra anal. 7-36764
EPR and bonding parameter correlations, evidence for lattice relax. 7-45801
ethane, chemisorption on Cu (100), σ -shape and π resonances, XANES 7-53448
ethanol, standard geometry functions 7-849
 α -ethoxyacrolein semicarbazone, cryst. and mol. struct., X-ray diffr. 7-26734
ethylamine, geometrical structural parameters calcs. GPED 7-20042
ethylamine standard geometry functions 7-849
ethylene, chemisorption on C (100), σ -shape and π resonances, XANES 7-53448
fluorobenzenes, bond orders, MNDO evaluation 7-56981
formate on Cu surfaces, adsorpt. site symm. and bond lengths, SEXAFS data, multishell simulation anal. 7-63947
FT photoelectron spectroscopy, correl. fn. and harmonic oscillator approx. 7-10665
 HBF_4 , Γ_1 struct., bond lengths, microwave spectra 7-62357
heavy metal oxide germanate glasses, absolute Raman intensities, global criteria. 7-59201
hexakis(dimethylsilyl)benzene, rot. isomerisation mechanism and barriers, ^4H and ^{13}C NMR spectra anal., EFF calcs. 7-25359
hexakis(trimethylelementyl)benzenes, synthesis and crystal mol. struct., X-ray spectra anal., EFF calcs. 7-25360
hydrates, solid, mol. stretching freq. versus H bond distance correlation anal. 7-21370
hydrides, first and second row, NMR chem. shift bond length derivatives 7-42644
hydrocarbons, cyclic, k-shell excitation, EELS 7-20037
6-hydroxy-1,2-dihydroquinoline, 2,2,4-trimethyl substituted, cryst. and mol. struct., X-ray diffr. 7-16539

bond lengths continued

- III-V ternary alloy semiconductors, short-range order 7-44821
metal complexes, IR vibrational spectra, coordination bond length correlation 7-13161
metal surfaces, chemisorpt., surface bond length anal. 7-23057
methane, equilb. bond lengths, relativistic corrections 7-36477
methane, proton-proton spin-spin coupling surface 7-42645
methanol- d_4 , mol. struct., pulsed neutron diffr. study 7-63427
2-methoxy-2-oxo-1,3,2-oxazaphosphorinane, conformer struct. and populations, IR, NMR and X-ray spectra anal. 7-25509
(2-methylsulphanyl ethyl)trifluorosilane, Si-O bond length and cryst. struct. study 7-51734
molecular crystals, van der Waals at. radii 7-62301
multicomponent systems, bond length determ. from EXAFS data 7-63553
muonium energy profiles, unrestricted Hartree-Fock cluster calcs., comment and reply 7-45907
organic cpds. electron correl., SCF calcs. 7-19721
organic molecules, in soln., mixing time role in 2D heteronuclear NOE expt. 7-10634
orthophosphates, ^{31}P NMR chem. shift, anisotropies, struct. and cation effects 7-50187
oxide anodic films on Al, struct., surface EXAFS, magic angle spinning NMR studies 7-22382
oxide crystals, TO_4 units, correl. of ang. and bond length distortions 7-32359
oxides, near edge struct., local geometry and cation type effects 7-63576
6-oxo-2, 6-dihydroquinoline, 2,2,4-trimethyl substituted, cryst. and mol. struct., X-ray diffr. 7-16539
paraffins, cyclic, with long chain lengths, ^{13}C NMR chem. shift meas., cryst. structures 7-64537
n-pentane, bond distances and angles, ab initio gradient geometry refinement 7-852
polydicyanoacetylene, bond alternation, Huckel model anal. 7-5602
polysephenophene, electronic and struct. modifications during doping, EXAFS and XANES studies 7-63507
polythiophene derivatives, bandgaps, conductivities 7-64061
potassium dihydrogen triacetate, cryst. struct. study 7-44503
propanol, standard geometry functions 7-849
propyl fluoride, r_1 struct., rot. isomerism, microwave spectra and moments of inertia meas. 7-10556
propylamine, standard geometry functions 7-849
rare earth alloys, RMn_2 , R-heavy rare earth, mag. state, spin echo NMR spectra 7-27629
rare gases, field adsorption on metal surfaces 7-21648
semiconductor heterostructures, valence band discontinuity, modified Harrison model calcs. 7-27398
sp-bonded nonmetal solids, cryst. stability and structural transition press., total-energy minimisation, tight-binding calcs. 7-2190
superlattice band structures of group IV and III-V semicond., axial strain effects 7-2697
surface electron energy loss fine struct. spectroscopy, EXAFS-like anal. 7-64834
surface struct. determ. using angle-resolved photoemission extended fine struct. 7-7822
tetrachloromethylenediphosphine struct., GPED 7-57175
4,4,8,8-tetrafluorotricyclo(5.1.0.0^{3,5}) octane, syn isomer struct., X-ray anal. 7-21187
tetramethylammonium hexachloroplatinate, crystal struct. and theoretical symmetry analysis of phase transition sequence 7-51739
tetraphenylmethane, thermal motion, lattice dynamical model 7-44730
thermionic emission cathodes, surface struct., EXAFS study 7-44970
2-thio-1,3,2-oxazaphosphorinane, conformer struct. and populations, IR, NMR and X-ray spectra anal. 7-25509
thiouacil, tautomers, MNDO calcs. 7-56984
 $(\text{TMTCF})_2\text{X}$ salts (C=S,Se), crystal struct., press. and temp. depend. 7-44520
 $(\text{TMTSF})_2\text{PF}_6$, cryst. struct., neutron low temp. and X-ray high press. diffr. studies 7-44502
transition metal borides, AlB_2 type, electronic struct. study, heats of formation anal., HMO calcs. 7-25409
transition metal nitrides, organic polyenes, phosphazenes, struct. and orbital analogy 7-10389
s-triazine, gas phase, mol. struct., GPED anal., ab initio force field calcs. 7-36457
sym-tribromobenzene, struct., vibr., GPED 7-57177
trichloromethyl radical, struct. and electronic states, ab initio UHF SWX_α calcs. 7-30949
trifluoromethyl phosphorane, conform. and struct., GPED anal. 7-20044
trimethylsilylthiocyanate in gas phase, mol. struct. determ. by electron diffr. 7-50357
1,6,12-trioxo-9-aza-9-butyl-5-germa-spiro[4,7]dodecane-2-one, cryst. and mol. struct. 7-12048
Ag, with adsorbed Cl, adsorbate-substrate bond lengths, coverage depend., SEXAFS 7-63948
Ag, with adsorbed Cs, adsorbate-substrate bond lengths, coverage depend., SEXAFS 7-63948
Al films, chemisorption of O, Al-O bond lengths, photoemission EXAFS meas. 7-64871
Al-Mn-Ru-Si icosahedral alloys, EXAFS study 7-39317
 Al_2O_3 anodic films on Al, struct., magic angle spinning NMR study 7-22382
 $\text{Ar}_2\text{-HF}(\text{DF})$ trimers, mol. rot., hyperfine struct., spectra anal. and calcs. 7-50060
 $\text{As}_1\text{-S}_2\text{-Ag}$ film, coordination distance determ., EXAFS study 7-64004
AuH bonding, ab initio fully relativistic calcs. 7-15531
 $\text{B}(\text{OH})_3$, electron density, X-ray diffr. determ. at 105 K, ab initio calcs. 7-44458
 $\text{BaF}_2\text{-ZrF}_4$ glass, Zr local environment, EXAFS studies 7-63485
 $\text{Ba}(\text{NO}_3)_2$, cryst. struct., X-ray diffr. study 7-32411
Bi oxides, small distortions, EXAFS transmission studies 7-63580
 $\text{Bi}_{12}\text{FeO}_{40}$, reflectivity spectra structure, thermorefectance 7-59207
 BiOBr , cryst. struct. refinement 7-1964
 $\text{Bi}_2\text{Si}(\text{Ge})(\text{Ti})\text{O}_{20}$, reflectivity spectra structure, thermorefectance 7-59207
 Br_2 solid, high press. X-ray absorpt. study, energy dispersive mode 7-59299
 C_{60} cluster, electronic structure, LMTO calcs. 7-19682
CO monolayer on Si (111), electronic props., pseudofunction method calcs. 7-2659

bond lengths continued

- Ca₂, A^{1/2}+X^{1/2}+ red system, laser spectroscopy, rot. anal. and perturbation anal. 7-10652
 CaO-ZrO₂, defect struct., EXAFS studies 7-63608
 Ca₅(PO₄)₃OH, EXAFS spectrum anal., spherical wave theory 7-33485
 Ca(UO₂)₂(SiO₃OH)₂·5H₂O, β-uranophane, refined cryst. struct., thermal anal., IR spectra 7-55031
 CeO₂, bond lengths, Ce K-edge EXAFS meas. 7-64753
 CeSe₂O₆, cryst. struct., X-ray diffr. study (*French*) 7-26706
 Cl adsorbed on Ag (111), weakly ordered and disordered, struct. studies 7-2365
 ClO₂, struct., pot. functions, electron diffr. and spectroscopic data 7-15708
 Co (II) azelaic acid bis(phenylhydrazide), X-ray absorpt. near-edge struct. obs. 7-19881
 Co (II) sebatic acid bis(2,4-dinitrophenylhydrazide), X-ray absorpt. near-edge struct. obs. 7-19881
 Co²⁺, complexes, IR spectra, coordination bond length correlation 7-13160
 Cs₂, electronic states, laser induced fluoresc. 7-19912
 Cs_{1-x}Lu₃F_{10-x}, cryst. struct., space group, least-squares refinement 7-6604
 Cu (100), adsorption of S, (2×2) surface struct., LEED anal. 7-32827
 Cu (100) and (110), formate adsorption, bonding, EXAFS studies 7-38341
 Cu complex, CuCl₂·2-phenyl-4,4,5,5-tetramethylimidazoline-1-oxyl-3-oxide, mag. props. 7-51715
 Cu²⁺, complexes, IR spectra, coordination bond length correlation 7-13160
 Cu_n⁺ (n=1-10), cluster, photoelectron spectra 7-62561
 Cu₂Cl(OH)₃, atacamite, struct. refinement, X-ray diffr. study 7-32371
 CuCrO₄, cryst. struct. refinement from single-cryst. data 7-58211
 Cu₂Cr₂Sn_{2-2x}S₄ spinels, Cu-Cu distances, EXAFS studies 7-63585
 CuGa_{1-x}In_xSe₂ mixed chalcopyrite local struct., K-edge EXAFS meas. 7-63574
 Er complexes, (tricarbamidotriacetato)erbium(III) monocarbamide, cryst. struct. 7-12029
 F+H₂, bond angle-bond distance coordinate system, energy conserving trajectories 7-28287
 Fe (110), clean and O-covered, struct., surface extended energy loss fine struct., spectra obs. 7-12481
 Fe complex [(ethyl)₄N]₆[Fe₆(CO)₃₆], struct. and bonding study, HMO calcs. 7-25411
 Fe(II) tetraphenylporphyrin bis(tetrahydrofuran), electronic ground state, electron density meas. 7-51716
 FeOOH, poorly-ordered precursors, local struct., EXAFS studies 7-63577
 Fe₂SiO₄, spinels, cryst. struct. as function of temp. and heating duration 7-16522
 GaAs_{1-x}Sb_x, relaxed zinc-blende lattice, EXAFS study 7-64759
 GdFe₂B₄, cryst. struct. and interatomic distances 7-32380
 Ge amorphous films, struct. and crystn., EXAFS study 7-64005
 H₃N-HF-HF, H bond cooperativity, structural and energetic props., ab initio calcs. 7-19697
 H₂O, bond lengths and force consts., LR CI calcs. 7-56990
 H₂O, mol. struct., density functional anal. 7-62272
 H₂O-Cu(Ni), complexes, bonding, intermolecular electron correl. 7-10449
 H₃P-HF-HF, H bond cooperativity, structural and energetic props., ab initio calcs. 7-19697
 H₃PO₄, n=1-3, tetrahedra distortion depend. on H bond length 7-63542
 He₂²⁺, ground-state pot. curve, Moller-Plesset perturbation calcs., bond lengths 7-42455
 InGaAsP local struct., EXAFS and near-edge struct. studies 7-64006
 K, electronic band struct., interatomic distance, role of p-orbitals, EHT tight-binding calcs. 7-32906
 KD₃(WO₄)₂, vibr. characts. of O bonds, IR and Raman spectra 7-32587
 KZnF₃Mn²⁺, thermal expansion of the Mn²⁺-F⁻ bond 7-6836
 La complexes, (hexaquaquododecapropionate)tetralanthanum(III) dithiocarbamide dihydrate, cryst. struct. 7-12030
 La₂NiO₄, struct. characterisation of orthorhombic form 7-1990
 Li, electronic band struct., interatomic distance, role of p-orbitals, EHT tight-binding calcs. 7-32906
 Li₃BN₂, synthesis, polymorph struct., ionic cond. meas. 7-32388
 LiFeP₂O₇, cryst. synthesis, at. struct., DTA, X-ray diffr. study 7-26708
 Li₁₀Mo₆O₁₇ purple bronze, cryst. struct. determ. 7-58239
 Mg₂NiH₄ cryst. complexes, Madelung field effects, quantum chem. calcs. 7-11984
 MnNa(H₂PO₃)₃·H₂O orthorhombic struct., bond lengths and angles, X-ray diffr. study 7-32372
 Mn₂Sn_{1-x}Mo_xS₈, Mn dopant props., supercond. transition temp., EXAFS, XANES, photoemission studies 7-46236
 Mo-one-dimensional amorphous organic systems, EXAFS and X-ray scatt. studies 7-64779
 N substituted crystal structures, Pauling's second cryst. rule 7-37918
 N₂, bond lengths and force consts., LR CI calcs. 7-56990
 N₂ fluid, eqn. of state and vibron freq. thermodynamics, Monte Carlo, calcs. 7-12231
 NH₃D⁺, ν₄ fundamental band, IR difference-freq. laser spectra 7-50096
 NH₃NO₂, electronic ground and first triplet states' struct., SCF calcs. (*French*) 7-15498
 NO, γ(A²+X²Π_{1/2}) system, electronic transition moment variation 7-50257
 Na, electronic band struct., interatomic distance, role of p-orbitals, EHT tight-binding calcs. 7-32906
 NaCl:Cu⁺, lattice relax. around cuprous ion, EXAFS studies 7-64788
 Na₈Ti₃O₇(OH)₂[SiO₄]₄, polymorphous modification of natasite, cryst. struct., X-ray diffr. 7-26709
 NdCu₃Ru₄Ti_{4-x}O₁₂ and Nd_{2+x}/3Cu₃Ru₄Ti_{4-x}O₁₂, electrical conductivity and crystallographic characterisation (*French*) 7-17057
 NdFe₂B₄, cryst. struct. and interatomic distances 7-32380
 Nd₂MgTiO₆, cryst. struct., Rietveld refinement of neutron powder diffr. data 7-26705
 Ni (100) with adsorbed S, angle-resolved photoemission extended fine-structure oscillations 7-64873
 Ni {100}, adsorption of I, surface phases, SEXAFS, breakdown of Fourier filtering single shell anal. 7-59304
 Ni complex, bis(triphenylphosphine) adduct of Ni(NCS)₂, cryst. struct., X-ray study 7-12025
 Ni²⁺, complexes, IR spectra, coordination bond length correlation 7-13160

bond lengths continued

- Ni₂SiO₄, spinels, cryst. struct. as function of temp. and heating duration 7-16522
 O (2×1) chemisorbed layer on Ni (110), SAXAFS study 7-64768
 O adsorbed layer on Ni (110), struct. anal., low energy ion recoil spectra study 7-2384
 O₃, photodetachment cross sections Franck-Condon anal. 7-57139
 Pb glaze glass system, local coordination EXAFS studies 7-63484
 PbH₄, equilb. bond lengths, relativistic corrections 7-36477
 PbTeO₃, tetragonal phase, cryst. struct., X-ray diffr. study (*French*) 7-44466
 PbTiO₃, amorphous, with 10 mol.% B₂O₃, radial distrib. function determ., energy dispersive X-ray diffr. method 7-16420
 Pd (001), H adsorption, coverage depend. props., ab initio calcs. 7-38340
 Pt (111) with adsorbed S, surface crystallography using LEED and R factor analysis 7-27120
 PtMnGa, Curie temp., hydrostatic press. effect 7-27527
 Rb, electronic band struct., interatomic distance, role of p-orbitals, EHT tight-binding calcs. 7-32906
 Ru-one-dimensional amorphous organic systems, EXAFS and X-ray scatt. studies 7-64779
 S c(2×2) adsorbate geometry on Ni (001), angle-resolved-photoemission extended-fine struct. studies 7-27111
 SF₄, inner- and valence-shell excitation, X-ray and EELS study 7-57171
 SF₆, dimer dissoci., dimer conc., isotope effect, model and bolometer IR spectra anal. 7-19977
 SO₂, C¹B¹, electronic state, unequal bond lengths, two state vibronic model 7-25531
 SbCl_mF_{3-m} graphite intercalation cpds., struct., X-ray diffr. studies 7-12008
 SeO₂, struct., pot. functions, electron diffr. and spectroscopic data 7-15708
 Si:H, Si-H IR stretching bands, models, CNDO calc. 7-53314
 Si_{1-x}C_xH films, amorphous, bond lengths, comp. depend., EXAFS study 7-64757
 SiCl₄, spectral and struct. props., MO calcs. 7-25418
 SiF₄, dimer dissoci., dimer conc., isotope effect, model and bolometer IR spectra anal. 7-19977
 Si_{1-x}Ge_xH films, amorphous, bond lengths, comp. depend., EXAFS study 7-64757
 SiH₄, dimer dissoci., dimer conc., isotope effect, model and bolometer IR spectra anal. 7-19977
 (SiH₃)₂O mol. struct., hydrolysis of Si-O bonds, density functional anal. 7-62272
 SiH₃OH, mol. struct., density functional anal. 7-62272
 SiN_xH films, amorphous, bond lengths, comp. depend., EXAFS study 7-64757
 Si₂O(PO₄)₆, chem. shift meas., solid-state ²⁹Si MAS NMR 7-53163
 SmSe, high press. EXAFS studies at 77 K 7-64799
 Sr₂SiO₄, β to α' to β transition, modulated struct. 7-16724
 Sr₂UO₂(CO₃)₃·8H₂O, cryst. struct., X-ray diffr. study 7-44462
 Ti, oxides and silicates, Ti XANES study, site geometry, spectral features 7-59288
 Ti thin films, dissolution and diffusion of O, resist., X-ray diffr., particle backscat. and AES studies 7-58913
 Ti₈₄Si₁₆ metallic glass, total struct. factors, neutron and X-ray diffr. studies 7-6546
 Ti₃PO₄, optical SHG material, cryst. struct., X-ray diffr. study 7-44465
 Ti₄UO₂(CO₃)₃, cryst. struct., X-ray diffr. study 7-44463
 V₂O₅, cryst. struct. refinement 7-26703
 V₂TiO₅, valency distrib. determ., XANES 7-16509
 W (110), adsorption of Cu, Ag and Au, calcs. based on nonadditive effective binding pot. 7-12483
 WCl₃, struct. parameters, GPED statistical anal. 7-57174
 ZnO-SiO₂ amorphous system, structure, mol. dynamics computer simulation studies 7-21114
 ZnSe (110) surface atomic geometry and energy states, self-consistent pseudopot. calcs. 7-21582
 ZrF₄-BaF₂-CsF glasses, ionic conductivity 7-52129

bonds (adhesive) see adhesion

bonds (chemical)

- see also binding energy; bond angles; bond lengths; crystal binding; hydrogen bonds; intermolecular forces; lattice energy
 A15 compounds, cryst. struct. 7-6587
 acetonitrile, adsorption and reaction on clean and O covered Ag (110) 7-28344
 acetylene, chemisorbed state on noble metal surfaces 7-52261
 acetylenes, substituted, spin-spin coupling consts., 7-31074
 actinide metals, solid state and thermodynamic props., f-electron bonding and struct., review 7-12321
 actinides, optical absorption spectra, rel. to bonding 7-27730
 aliphatic systems, geminal H⁺¹³C coupling consts., Penney-Dirac calcs. 7-57095
 alkali borate glasses, M₂O-B₂O₃ (M=Li, Na, K, Rb, Cs), thermodynamic props. 7-2211
 alkali halide mixed crystals, electronic dielectric const. and fractional ionic character of chemical bond 7-2966
 alkali metal hydrides, inter-ionic bonding and thermodynamic functions, microscopic theory (*Russian*) 7-58198
 alkylamines, interaction with layered compounds 7-46838
 alkynyl(trimethyl)mercurials, synthesis, ¹³C, ²⁹Si and ¹⁹⁹Hg NMR 7-31071
 allenes, monosubstitution, stabilisation energies, isodemic methyl exchange reaction study, ab initio LCAO SCF calcs. 7-25389
 α-aminoalkyl radicals, electrochemical detection, bond dissoci. energies determ. using oxidation pots. 7-28286
 atomic orbital deformation in bond form., energy effects 7-25439
 benzene, π-electron SCF ground states, Kekule struct., VB and BORT calcs. 7-25414
 benzene, adsorbed on Os (0001), mol. struct., angle-resolved UV photoemission spectral study 7-53492
 benzenoid hydrocarbons, charge transfer spectra and struct. reson. theory 7-57165
 p-benzoquinone, struct. and vibr. anal., ab initio HF calcs. 7-25372
 p-benzoquinone radical anion, struct. and vibr. anal. ab initio HF calcs. 7-25372
 bicyclo (1.1.1) pentane, bonding and geometry, quasi ab-initio PRDDO method, GVB-type correl. 7-25404
 bond-order conservation, bond making and breaking on transition metal surfaces 7-21653

bonds (chemical) continued

- borate glasses, structure and bonding, NMR studies 7-63503
 borate minerals, unoccupied mol. orbitals of B-O bond mol. orbital calcs., XANES, NMR and electron transmission spectra 7-33281
 butadiene, π -electron SCF ground states, Kekule struct., VB and BORT calcs. 7-25414
 butane, multipole expansions 7-62256
 carbocations, atom and bond props., quantum theory 7-5576
 cellulose fibres, native and regenerated, chain modulus, intramolecular H bonding 7-17575
 ceramic-metal interfaces, grain boundaries, bonding and interfacial structure 7-26765
 charge, spin and momentum densities, conf., Sanga-Saby, Sweden (July, Aug 1985) 7-24258
 chemical bonding, validity of formal electron counting rules 7-63544
 composite system, design problems with allowance for interphase reactions 7-43661
 correlation energy, scaling in perturbation theory calcs. of bond energies and barrier heights 7-10391
 covalent bonds, electron density accumulation 7-15470
 covalent chemical bonding, MO anal. 7-49917
 cyclobutane, strain energies, bond energies, 1,3-interactions and σ -aromaticity 7-56933
 cyclobutene, IR spectra, vibr. struct. and C-H local mode dynamics 7-25510
 cyclopentadienyl metal cpds., struct., skeletal electron pair approach 7-10414
 cyclopropane, strain energies, bond energies, 1,3-interactions and σ -aromaticity 7-56933
 desorption, electron and photon-stimulated, probes of surface struct. and bonding 7-32817
 2,6-dichloroacetanilide, X-ray diffr. and NQR study, struct. and bond props. 7-12041
 dielectric coatings, mol. struct. and phys. props. Raman studies 7-45063
 difluoroacetylene, C-C triple bonds, bent bonds description 7-42482
 diheliumacetylene dication, metastable, C-He bond prediction 7-49888
 dimers, first row homonuclear, orbital forces and chemical bonding in density functional theory 7-5595
 4,4-dioxy-4-thia-1-acetyl-1,4-dihydropyridine, heteroaromaticity, p-d bonding, NMR, crystallography and calcs. 7-15623
 B-DNA model segment, binding of water 7-34099
 DNA-ligand interactions, groove binding, computer simulations 7-54447
 double bonds, through space interactions, UV photoelectron spectrosc. investig. 7-57130
 electron-lattice coupled quarter filled band systems, 1D, solitons 7-45181
 elements, monovalent, electron correlations and chemical bonds, Hubbard model 7-58755
 ethane, bond rupture surfaces, MC SCF calcs. 7-30922
 ethane chemisorbed state on noble metal surfaces 7-52261
 ethanes, substituted, NMR conformation studies, rot. energetics about C-C bond 7-31067
 ethylene, bending force const. attenuation, ab initio CI calcs. 7-49939
 ethylene, C-C bond description, HF and VB LCAO calcs. 7-25415
 ethylene, chemisorbed state on noble metal surfaces 7-52261
 ferrichromites, coordination and oxidation states, XPS and XANES studies 7-63583
 ferroelectric piezomaterials, thermal stability of the resonance freq. 7-64579
 fluorobenzenes, bond orders, MNDO evaluation 7-56981
 garnets, chemical bonds, ionicity, covalency (Russian) 7-16483
 germanium pentacoordinated compounds, structural correl. 7-10418
 glass, microdefect accumulation kinetics during optical irradiation 7-38050
 glass, oxide, bond strength and characteristic temp., three-band theory 7-63500
 glass, radiation-induced defects and ESR spectra 7-2050
 graphite- ClF_3 intercalation cpd., electrical conductivity 7-7295
 group VIII metal octahedral clusters, iterative extended Huckel calcs. 7-19689
 halide and pseudohalides at Au surface, SERs, metal-adsorbate vibr. freqs., surface bonding 7-12468
 heterojunction band offsets, two-level model anal. 7-7363
 4,7,13,16,23,26-hexaoxa-1,10,20,29-tetraazabicyclo [8.8.12]-tricontane-19,30-dithione, cryst. struct. 7-44508
 hexatriene, multipole expansions 7-62256
 HVEM, materials characterisation, critical voltage effect 7-37819
 hydrocarbons, heats of form., off-diagonal matrix elements, IOC- ω technique calcs. 7-39910
 hydrocarbons and fluorocarbons, plasma polymerised, cross-linking and average coordination 7-8276
 II-V semiconds., cryst. growth, characterisation and appls., review 7-26685
 III-V semiconductor-metal interface, reaction and interdiffusion, review 7-21544
 incoherent neutron scatt. cross-sections 7-990
 index, definition 7-877
 intermolecular interaction energies, SCF calcs., variation-perturbation procedure 7-15505
 ionic compounds, secondary ion emission, bond breaking model 7-59344
 ionic solids, overlap interactions and bonding 7-1940
 isobutyraldehyde, barriers to rotation adjacent to double bonds 7-10394
 isobutyric acid, barriers to rotation adjacent to double bonds 7-10394
 macromolecular systems, pressure equation generalisation 7-10784
 main group elements, electronegativities and hardnesses, bond hybridisation effects 7-36446
 materials design using a hierarchy of structural models 7-16350
 materials selection for hard coatings, multicomponent refractory material systems 7-46668
 metal complexes, charge density distribts. 7-25351
 metal-H systems, bonding, statistical thermodynamic aspects 7-21472
 metal-ligand complexes, nonvibronic d-d intensities, charge-transfer manifold props., simplified group function, MO calcs. 7-19698
 metal-metal multiple bonding, cluster electron count and geometries, HMO calcs. 7-25410
 metallic molecules and cpds., magnetic moment formation and mag. susceptibility 7-58995
 metalloporphyrin polystyrene covalent complex, electron transfer reaction 7-39879
 methane, bond rupture surfaces, MC SCF calcs. 7-30922
 methanimine, fluorination effect on double bonds, SCF HF and MP2 ab initio calcs. 7-10384

bonds (chemical) continued

- methyl ammonium boron trifluoride, nucl. quadrupole coupling, electronic struct. NMR 7-13043
 methyl isopropyl ketone, barriers to rotation adjacent to double bonds 7-10394
 methyl orange, and homologs, binding by copolymers, temp. depend 7-49975
 methylimine, protonation, C=N bond rehybridisation rel. to stretching force const. 7-30925
 molecular clusters, review, materials, architectures and uses (French) 7-15765
 molecules, charge distribution calculation, zero flux surface method 7-49876
 molten salts, microscopic struct. and dynamics, review 7-44348
 muonium-organic radical systems, struct., muon spin rot. studies 7-50410
 nitride coatings on high-speed steel substrates, characterisation by Auger electron spectroscopy and X-ray photoelectron spectroscopy 7-53982
 noncrystalline solids, bonding and struct., conf., Reston, VA, USA (May 1983) 7-60879
 nonergodic Thomas-Fermi theory, covalent bonding anal. 7-42452
 nucleic acids components, binding of water 7-34098
 octahalodiosmate(III) anions, struct. and bonding 7-16508
 organic molecular solids, violation of chloro-methyl exchange rule 7-2008
 organic mols., bond valency related to mol. strain, Coulson-Moffitt model anal. 7-25416
 oxidic actinide cpds., systematic props., oxidation states, fluorite lattice and thermodynamic props., review 7-12013
 Pb, tetrahedral bonding and crystal struct., first-principles theory 7-32355
 perfluorotrimethylgermyl anion, vibr., IR and Raman spectra (German) 7-31048
 Phillips and Van Vechten theory, Levin's modifications, d-electron effect on ionicity 7-16482
 phosphamethane, fluorination effect on double bonds, SCF HF and MP2 ab initio calcs. 7-10384
 platinum-cyanoalkene complexes, mol. vibr. study, Raman and IR spectra anal. 7-42626
 PMMA, environmental stress cracking in methanol, mol. props. effects 7-65153
 PMMA, microdefect accumulation kinetics during optical irradiation 7-38050
 poly(4'-vinylbenzo-18-crown-6), ion-binding characts., eval. 7-10469
 polycetylene:Br(I), polarised EXAFS and near edge spectra studies 7-64778
 polyatomic mols., localised highly excited anharmonic vibr. anal. 7-50075
 polycyclic benzenoid hydrocarbons, bond orders, MNDO study 7-10425
 polydihalogenoacetylene, band alternation and soliton excitations, Huckel model anal. 7-5601
 polydihalogenoacetylene, band alternation and solitons 7-63511
 polydimethylsiloxane, mech. induced sorption on SiO_2 , chain binding, collective and multiple aggregate processes 7-12474
 polyethylene oxide-melaminoformaldehyde coured copolymer, crystallisation and melting (Russian) 7-26923
 polyimide films, prep. and adhesion to Ag surface, XPS 7-65314
 polymer fracture, weak chem. bond effect (Russian) 7-42811
 polymer interfaces, bonding and adhesion 7-28265
 polymer resists, bonds, radiation effects and crosslinking 7-37907
 polymeric materials, stress relax., bond breaking, free vol. effects 7-22742
 polynuclear metal cluster bonds, chemical sub-micron structure (Dutch) 7-50437
 polystyrene, monodisperse, fracture, chain scission, mol. wt., temp. depend. 7-33776
 polyvinylidene fluoride, modifications under high energy heavy ion, X-ray and electron irradi., XPS study 7-38076
 powdered coating bonding during plasma deposition, diffusion kinetic mechanism 7-32874
 [1.1.1]propellane, bonding, generalised valence-bond calcs. 7-30954
 I(1.1.1) propellane, bonding and geometry, quasi ab-initio PRDDO method, GVB-type cor. 7-25404
 propylene, bending force const. attenuation, ab initio CI calcs. 7-49939
 PTFE, bonding and surface struct., ESCA investigation, electron beam interactions 7-51662
 PTFE and PVDF, aging, irradiation by X-rays, electron and ion beams, XPS study 7-32498
 quartz glass, microdefect accumulation kinetics during optical irradiation 7-38050
 rare earth silicides, $\text{R}_2\text{Co}_3\text{Si}_5$ X-ray spectra and valence band electronic struct. 7-33484
 rubber-epoxy materials exhibiting increased crack resistance, thermodynamic compatibility 7-17509
 Schiff's bases, neutral and protonated, C=N stretching freq. 7-31008
 semiconducting materials, cryst., and device appls., book 7-60894
 a-Si:H solar cells stability, role of Si-H bonds studied by Fourier transform infrared spectroscopy 7-13896
 silicate glasses, structure and bonding, NMR studies 7-63503
 silicates, bonding ^{17}O NMR, d-orbitals 7-13055
 simple molecules, charge density distribts. 7-25351
 solid materials, bonding, external electrostatic field effects 7-26693
 squaric acid, press. depend. of cryst. struct. 7-32417
 struct., stability and bonding 7-10392
 surface chemical bonds, electron spectroscopy methods 7-39364
 surface science techniques, book 7-60888
 surfaces, bond making and breaking 7-28335
 thiaryl compounds, struct. and bonding investigated at SCF level, electron correl. effects 7-10439
 thin film pulsed heating, thermal and plasma models 7-26946
 thiometalato complexes, mol. vibr., electronic struct., IR and Raman spectra study 7-57068
 transition metal complexes, spin and charge densities calcs. 7-27491
 transition metal crystal, BCC, metal-H bond investig. 7-32360
 transition metal hydrides, dipole moments, CASSCF/MRCI calcs. 7-10443
 transition metal mols., bonding, polyhedral hybrid approach 7-42490
 transition metal monocarbonyls, first row, electronic struct. and bonding 7-49897
 transition metal phosphorous trisulphides, electronic, structural and mag. props., intercalation cpds. and chemical props. 7-44499
 transition metal surface, bonding of adsorbed hydrocarbons, EELS studies 7-3128
 transition metal-H systems, bond weakening 7-63546

bonds (chemical) continued

- transition metals, second row hydrides, low-lying states, spectroscopic parameters determ. using large valence basis sets 7-42500
- tris(tetrahydroborato)titanium(II)-dimethoxyethane, cryst., X-ray structural investig. 7-51730
- two-sublattice crystals with spinel struct., crystal-chemical model of stability 7-16481
- vinyl pyrrolidone copolymers, highly swollen hydrogels preparation 7-21073
- zeolites, ion selectivity, appl. to chabazite 7-63874
- [Ag₆Ge₄P₁₂](Ge(Si)₆), bonding relationships and electronic struct. calcs. 7-16941
- [Ag₆Sn₄P₁₂](Ge(Si)₆), bonding relationships and electronic struct. calcs. 7-16941
- Ag (110), O and O₂ adsorption, dispersion, bonding and precursor state 7-6991
- Ag films, with surface adsorbed ethylene, adsorbate-substrate bonding 7-52292
- Ag interfacial surface energy atomistic estimation and adhesion meas. (Japanese) 7-58657
- Ag-brass, mixing layer, friction props., ion beam mixing (Chinese) 7-51888
- AgI-Ag₂O-B₂O₃ fast ion conducting glasses, struct., XANES studies 7-63483
- (AgO)_x complexes, (x=1,2), bonding and configuration, matrix isolation ESR spectra anal. 7-19905
- AgOH, metal-OH bonding study 7-52240
- AgSbS₃, ferroelectric transition, electric field perturbed NQR 7-17276
- Al, chemisorption, interaction of atoms and mols. with surfaces, cluster approx., total energy calcs. 7-52265
- Al_n clusters, (n=5,9,13), electronic struct. and bonding 7-15775
- α-Al₂O₃, muon spin relaxation, muon bonding versus muonium formation 7-45902
- AlP(As)(S)₄, dielec. const. meas. w.r.t. bond ionicity (French) 7-38988
- Ar₂+Xe(Kr), van der Waals bond exchange, mol. beam study, ang. and vel. distrib. 7-23000
- As, amorphous and crystalline, bond strength anal., EXAFS temp. depend. study 7-64763
- a-As₂S₃ vapour deposited films, thermostructural and photostructural changes, EXAFS study 7-64003
- As₂S₃, crystalline and glassy, bond strength anal., EXAFS temp. depend. study 7-64763
- As₂Se₃, crystalline, electronic and geometric struct., ab initio total-energy calcs. 7-12607
- (As₂Se₃)_x(As₂Te₃)_{1-x} glasses, molecular struct., chemical equivalence of ¹²⁵Te absorpt. and ¹²¹I emission Mossbauer spectroscopy 7-59129
- Au films, with surface adsorbed ethylene, adsorbate-substrate bonding 7-52292
- Au interfacial surface energy atomistic estimation and adhesion meas. (Japanese) 7-58657
- AuH bonding, ab initio fully relativistic calcs. 7-15531
- Au(O₂) complexes, bonding and configuration, matrix isolation ESR spectra anal. 7-19905
- closo-B₄H₄²⁻ clusters, bond indices, enthalpies, CNDO calcs. 7-10431
- B₄H₄, polyboranes, nucl. coupling const. HF calcs. 7-19688
- B₂O₃-SiO₂ glass, borosiloxane bond formation, sol-gel process, spectroscopic study 7-59117
- BP(As)(O)(S)₄, dielec. const. meas. w.r.t. bond ionicity (French) 7-38988
- Ba(PO₃)₂-LiBa(Mg)AlF₆ glasses, Raman spectra and network struct. studies 7-7695
- BaZrO₃, valence band struct., X-ray-electron spectra studies 7-12604
- Be₂, bonding, appl. of local spin density approx., comparison with other studies 7-25371
- Bi(O₂), ionic cond., w.r.t. lone pair separation and cryst. symm. 7-12361
- BiP(As)(O)(S)₄, dielec. const. meas. w.r.t. bond ionicity (French) 7-38988
- C containing compounds, chemisorbed on cold rolled steel sheets, XPS characterisation (French) 7-44965
- C, dielectric film growth, on GaAs and InP substrates 7-39420
- a-C thin films, bonding core-EELS and ¹³C NMR studies 7-21099
- a-C:H, film, plasma emission spectroscopy, chem. anal. 7-38407
- a-C:H, films, plasma deposition characterisation of hydrocarbons used 7-39422
- a-C:H plasma grown films, struct., physical props. 7-58713
- C_n clusters, spheroidal clusters, rehybridisation and π-orbital alignment 7-25695
- CBe₂ struct., stability and bonding 7-10392
- CO adsorbed on Pt, vibr. spectrum, electrochemical pot., Stark tuning rate 7-10570
- CO, chemisorbed, bonding, comment and reply 7-12472
- ¹³C shielding tensors, individual gauge for localised orbital contrib. 7-57005
- Ca²⁺, binding to bile salts, NMR investig. 7-54442
- CaF₂-Si, interface struct., high resolution TEM study 7-2394
- CaF₂-Si (111), interface form., photoemission study 7-2395
- Ca(SiO₃)₂, cryst. struct., vibr. spectra, force consts., Si-O bond charact. 7-37932
- CaZrO₃, valence band struct., X-ray-electron spectra studies 7-12604
- Ce₂Ni₄P₁₇, bonding relationships and electronic struct. calcs. 7-16941
- Co complexes, dimeric, bonding and struct. 7-56939
- Co_{0.55}Cu_{0.45}Cr₂S_{4-x}Se_x spinels, X-ray diffr. study 7-44475
- Co₂Ge, chemical bond, struct., short range order 7-32350
- CoSi₃, Mossbauer spectroscopy 7-59126
- Cr₂, bonding, appl. of local spin density approx., comparison with other studies 7-25371
- Cr(CO)₆, electronic struct., X-ray and photoelectron spectra 7-5699
- Cr₂TiS₂, intercalated dichalcogenide, electronic struct. 7-52387
- Cu (100), field induced vibr. freq. shifts of chemisorbed CO and CN 7-45991
- Cu complex, bis(dithiocarbamate) copper II, struct., NDDO calcs. 7-15515
- Cu complex, Cu II-acetylacetone-substituted 8-hydroxyquinolines, ESR obs. 7-19890
- Cu complexes, single and mixed ligand, bonding parameter, ESR obs. 7-50203
- Cu films, with surface adsorbed ethylene, adsorbate-substrate bonding 7-52292
- Cu II complexes, dibenzylidithiocarbamate copper, bonding, XPS 7-19950
- Cu interfacial surface energy atomistic estimation and adhesion meas. (Japanese) 7-58657
- Cu surface, Raman intensity of adsorbate vibr., cluster-model calc. 7-27089

bonds (chemical) continued

- Cu-CdTe interface form., effect of different cation-anion bond strengths 7-27149
- Cu-Hg_{0.75}Cd_{0.25}Te interface form., effect of different cation-anion bond strengths 7-27149
- (CuO)_x complexes, (x=1,2), bonding and configuration, matrix isolation ESR spectra anal. 7-19905
- Cu₂O, electronic struct. and binding mech. 7-2482
- CuOH, metal-OH bonding study 7-52240
- Cu₂SnP₁₀, bonding and electronic struct. studies 7-26694
- Eu chalcogenides, IR optical parameters, rel. to chemical bonds 7-53291
- FA (A=Li, Be, B, C, N, O, F), chem. bonding, kinetic energy anisotropy investig. 7-10396
- Fe complex (Fe(PH₃)₃(C₆H₁₃))⁺, localised INDO calcs. 7-49927
- Fe-Al-Si system, electronic struct., interatomic bonding, X-ray emission spectra analysis (Russian) 7-39320
- Fe-Te cluster, localised props., multiple scatt. Xα SCF method 7-21848
- FeCr₁₀P₁₃C₇ amorphous alloy, surface layer chemical bonds, XPS studies 7-12417
- Fe₂Ge, chemical bond, struct., short range order 7-32350
- Fe₇Nd₁₆B₈ plasma sprayed permanent magnets, charact. 7-45754
- (Fe_{1-x}Ni_x)TiH₃, critical study of β-region 7-27634
- FeP(As)(O)(S)₄, dielec. const. meas. w.r.t. bond ionicity (French) 7-38988
- Fe₂TiS₂, intercalated dichalcogenide, electronic struct. 7-52387
- Ga₂O, He I photoelectron spectra, relativistic DVM SCC Xα calcs. 7-50252
- GaP(As)(O)(S)₄, dielec. const. meas. w.r.t. bond ionicity (French) 7-38988
- Ge, mixed group III and group V ion implantation 7-21243
- Ge⁺ microcluster, pulsed conc. spectra, bonding and growth kinetics 7-19740
- GeO₂ rutile crystals, electronic struct., scalar-relativistic muffin-tin-orbital calcs. 7-64077
- GeSe₂, vitreous and crystalline states, energy difference, bond energy, calorimetry study 7-59775
- Ge₂Se_{6-x}Te_x amorphous chalcogenide, elec. cond., bulk and thin film effects 7-7238
- H₂, bond rupture surfaces, MC SCF calcs. 7-30922
- H₂-HF complex, struct., bonding, vibr. freq. shift 7-19817
- H₂O-Cu(Ni) complexes, binding, SCF CI calcs. 7-56958
- H₂SeO, geometry and energy, role of optimum supplementary d-orbitals 7-25344
- HfB, electronic struct., chem. bonding, Green's function methods 7-58741
- Hg_{1-x}Cd_xTe/Ag(Cu)(Al) interfaces, morphology, Hg bonding effects 7-7021
- In atom on Si (100), bonding coordination number, synchrotron photoemission studies 7-45071
- InO₂, He I photoelectron spectra, relativistic DVM SCC Xα calcs. 7-50252
- InP(As)(O)(S)₄, dielec. const. meas. w.r.t. bond ionicity (French) 7-38988
- Ir complexes, Vaska's cpd., ¹¹⁹Sn NMR study 7-10625
- K₂C₂O₄H₂O, deform. electron density study at 100 K 7-63565
- K₂O-P₂O₅-WO_{3-x} mixed valence glasses, local order, EXAFS and X-ray diffusion studies 7-1903
- La complex, Ln(NO₃)₃·1-bis(quinol-8-oxo)-3,5,9-trioxundecane, XPS 7-57133
- La-Al, glass, short-range struct., pulsed neutron and X-ray diffraction 7-1912
- La-Si, glass, short-range struct., pulsed neutron and X-ray diffraction 7-1912
- La₂Mo₂O₇, quasi-2D single cryst. struct. and electronic props. studies 7-58238
- La₂Ni₄P₁₇, bonding relationships and electronic struct. calcs. 7-16941
- Li bonds, existence and nature 7-48249
- Li-vinylidene complex, struct., bonding, ab initio CI calcs. 7-49935
- LiAlO₂, bond ionicities and structural props. calcs. 7-26691
- LiGaO₂, bond ionicities and structural props. calcs. 7-26691
- LiGaH₂, lattice vibr. spectrum, correlation method anal. 7-26881
- LiH, single cryst., electron momentum density and Compton profiles 7-3113
- LiInS₂, lattice vibr. and interatomic forces, IR reflectivity spectra anal. 7-26882
- LiInS(Se)(Te)₂, bond ionicities and structural props. calcs. 7-26691
- LiMo₅O₁₀, synthesis and struct., orthogonal nonintersecting octahedral cluster chains 7-32386
- LiNbO₃:Mg, incorporation of H⁺, IR spectra of OH⁻ ions 7-7724
- Li₂SO₄H₂O, charge density at 80 and 298 K, X-ray and neutron diff. 7-21166
- Li₂Si₇, chemical bonding, validity of formal electron counting rules 7-63544
- Li₂Si₈, electronic struct., INDO calcs. 7-38437
- LiV₂O₅, Li inserted, struct., neutron and X-ray powder diffr. anal. 7-32391
- γ-methacryloxypropyltrimethoxysilane, chem. reaction on PbO surface, Fourier transform IR spectra 7-53308
- Mg₂NiH₄, struct., thermal and elec. props., rel. to covalent bonding 7-21184
- Mo (110) chemically modified surface, Au thin film form. study 7-12489
- Mo complex, tetraacetomolybdenum, metal-metal quadruple bonds, normal coordinate anal. 7-42578
- Mo surface, Ta deposition, short range bonding interaction, RBS meas. 7-3142
- Mo₂Cl₈⁴⁻, metal-metal quadruple bonds, normal coordinate anal. 7-42578
- Mo₂Cl₈(PEt₃)₄, metal-metal multiple bonding, cluster electron count and geometries, HMO calcs. 7-25410
- Mo(Co)₆, electronic struct., X-ray and photoelectron spectra 7-5699
- MoSe₂S cathode for secondary Li batteries, prep. and characterisation 7-64948
- MoSi₂, band structure 7-27248
- NH₃, adsorp. complexes with heterogeneous catalysts, vibr. study, IR spectra anal. 7-36607
- NH₃ dipolar couplings in liq. crystals, anisotropic forces, NMR study 7-62413
- NH₃, vibr., inversion doubling, variational calcs., use of intramol. pair pots. 7-31014
- NO, coadsorbed on Rh (111) with CO and O, EELS 7-16860
- NO₂ and ions, deform. densities, d function role in ab initio calcs. 7-62260
- NO₂⁺, electron deform. density, basis set depend. 7-62252
- Na complex, NaI.diglyme, cryst. struct., bond bridging 7-51724

bonds (chemical) continued

- Na⁺, binding to bile salts, NMR investig. 7-54442
 Na₂O-Al₂O₃-SiO₂ glass system, strength and struct. features 7-58150
 NbCl₃, elastic constants meas. 7-6703
 NbCl₃(Br₃), vibr. anal., GF matrix method calcs. 7-42593
 Ni (110), adsorbed H; competing surface reconstruction mechanisms 7-7004
 Ni clusters with surface adsorbed CO, surface electronic and mag. struct. 7-21969
 Ni cobaltite, coordination and oxidation states, XPS and XANES studies 7-63583
 Ni complex, bis(dithiocarbamate) nickel II, struct., NDDO calcs. 7-15515
 Ni II complex, (salicylaldehyde)(acetylacetonate)ethylenediimine nickel(II), mixed and non-mixed complexes, PMR 7-31075
 Ni surface, with adsorbed N₂ or coadsorbed N₂ and Al or Ba, N(1s) spectrum 7-21968
 Ni₆ cluster, metal-metal bonding (*German*) 7-1002
 Ni(CO)₄, electronic struct., X-ray and photoelectron spectra 7-5699
 Ni₂Ge, chemical bond, struct., short range order 7-32350
 OA (A=Li, Be, B, C, N, O, F), chem. bonding, kinetic energy anisotropy investig. 7-10396
 OH groups, on basic oxide surfaces, stretching vibrs. and coordinating polyhedra props. 7-10551
 PH₃ dipolar couplings in liq. crystals, anisotropic forces, NMR study 7-62413
 PbO-SiO₂-K₂O coloured and colourless glasses, near IR absorpt. temp. depend. study 7-13146
 PbZrO₃, valence band struct., X-ray-electron spectra studies 7-12604
 Pd complexes, bivalent, mutual influence of ligands, vibr. spectrosc. investig. 7-10585
 PdGe, bonding, electronic states, ab initio HF-CI calcs. 7-42497
 Pr₆NiP₁₇, bonding relationships and electronic struct. calcs. 7-16941
 Pt (111) with coadsorbed CO and K, inverse photoemission 7-52726
 Pt complexes, ¹⁷O NMR study 7-10625
 Pt complexes, binuclear with bis(dimethylphosphino)methane ligands, NMR study 7-13045
 Pt(NH₃)₂Cl₂, relativistic and nonrelativistic electronic struct. and bonding, multiple scatt. wave study 7-36461
 Pt₂(P₂O₅H₂)₄²⁻, electronic struct., bonding and spectra SCF EHT calcs. 7-42489
 Re complex, tetraacetodichlororhenium, metal-metal quadruple bonds, normal coordinate anal. 7-42578
 Re(CO)₃(MO)(MOH)₂, (M=Mg,Al), evidence of metal-O bond, Raman and inelastic electron tunnelling spectra 7-7708
 Re₂Cl₆²⁺, metal-metal quadruple bonds, normal coordinate anal. 7-42578
 Rh surfaces, adsorption and desorption of NO, effect of surface structure 7-6994
 Rh_n(CO)_y, (x=4 to 7, y=12,15,16), metal cluster bonding topology, graph theory 7-42817
 Ru (0001) with adsorbed H monolayer, adsorbate bonding and vibr. 7-52291
 S-compounds, bond order and valence indices for use with ab initio wave functions 7-56947
 SO₂ and ions, deform. densities, d function role in ab initio calcs. 7-62260
 SBP(As)₂O(S)₄, dielec. const. meas. w.r.t. bond ionicity (*French*) 7-38988
 SbSBr, ferroelec. semicond., band struct., X-ray spectral studies 7-58739
 SBI crystal, dielec. const. determ., chem. bond approach, MWH band struct. calcs. 7-17260
 Se-CO, mol. bonding, pseudopot., and singles-and-doubles CI calcs. 7-10440
 SeO, low-lying states, SDCI calcs. 7-25421
 SeS, low-lying states, SDCI calcs. 7-25421
 Se, glassy state, phys. props., chem. bonds and defects 7-6530
 Si (100), static mode ion sputtering, bond breaking and atom ionisation 7-13306
 Si (100)-(2×1), adsorption kinetics of propylene, propane and methane, chemical activity of C=C double bond 7-27127
 Si (111), ordered Au, Ag, Cu overlayers, surface states, inverse photoemission studies 7-2660
 Si (111) with ordered Cu, Ag and Au overlayers, inverse photoemission spectroscopy 7-59280
 Si, broken dislocation bonds, annealing effects, optical polarisation of nuclear moments study 7-38008
 Si clusters, in presence of O, Si-Si bond breaking, total energy calcs. 7-50438
 Si, grain boundary pot. barrier and role of distorted bonds 7-46080
 Si, mixed group III and group V ion implantation 7-21243
 Si, X-ray structure factor, Pendellosung method meas. 7-32362
 a-Si:H, broken bond local environment relax., g-factor, cluster calcs. 7-37876
 a-Si:H, configurational models and adiabatic potentials of H 7-51632
 a-Si:H, divacancy electron struct., semiempirical CNDO/2 cluster calcs. 7-38495
 a-Si:H, plasma deposited NMR, Pake doublet 7-27617
 a-Si:H, plasma enhanced CVD, integrated model 7-39423
 a-Si:H, Si-H-Si three centre bonds IR spectra, LCAO-MO-SCF-STO-3G calcs. 7-6741
 a-Si:H films, light-induced bond breaking 7-12517
 a-Si:H solar cells, dynamic equilibrium dangling bond density 7-17878
 a-Si:H/a-Si₃N₄ heterostructures, interface defects and disorder 7-52306
 Si₂N(O), pseudo Jahn-Teller effect and chemical rebonding 7-16992
 Si-Au interface, atomic bonding 7-58663
 Si-Cu interface, atomic bonding 7-58663
 Si-Fe BCC alloy, struct. and mag. props., order-disorder transition effects (*Russian*) 7-32346
 a-Si-Ge multilayer interfaces, Raman scatt., X-ray diff. characterisation 7-27167
 Si-pyrex, irreversibility of anodic bonding 7-33910
 a-SiC:H, elec., optical and local structure props. 7-45089
 a-SiGe:H thin films for solar cells, electrical and structural properties relationship 7-17898
 SiH₂, ¹A₁, ³B₁ and ³B₂ states equilb. and stretched SiH bonds SCF CI calcs. 7-49944
 Si₃N₄ films, plasma deposited, bonds and defects 7-17437
 SiO₂ cluster, multipole expansions 7-62256
 SiO₂ cluster approx. of electron struct. 7-12591
 SiO₂ thin films, intrinsic bonding defects and impurities, EPR studies 7-13034

bonds (chemical) continued

- SiO₂ thin films, plasma enhanced CVD deposited, Si chem. states, IR spectra, XPS, AES 7-21721
 SiO₂N₂ films, deposited by plasma-enhanced CVD, charact. 7-2413
 Si-O, dielectric resin films, Fourier Transform Infrared spectra 7-53435
 Sm³⁺ complexes, UV and visible absorption spectra 7-13176
 SnF₂-SnF₄ system, Mossbauer reson. studies 7-7625
 SnO₂ rutile crystals, electronic struct., scalar-relativistic muffin-tin-orbital calcs. 7-64077
 SnYb(La-Gd)(Ca)(Sr)(Th)₃Rh₃Sn₁₂ crystals, structural distortion and chem. bonding, X-ray diff. studies 7-1947
 SrZrO₃, valence band struct., X-ray-electron spectra studies 7-12604
 Tc₂Br₁₂, metal-metal multiple bonding, cluster electron count and geometries, HMO calcs. 7-25410
 Te ctps., valence electron configs., X-ray chemical shift and Mossbauer isomer shift, SCF anal. 7-32893
 TeO₂ rutile crystals, electronic struct., scalar-relativistic muffin-tin-orbital calcs. 7-64077
 Th complex, bonding, Xα-SW MO calcs. 7-62283
 Ti-Cr alloys, cryst. and electronic struct., decomposition of β-solid soln. 7-37931
 TiB, electronic struct., chem. bonding, Green's function methods 7-58741
 Ti₆H₈He, interatomic bond rel. to He saturation (*Russian*) 7-38022
 TiN, deformation-induced stacking faults, synthesis by vibratory milling 7-44572
 TiN_x epitaxial layers, atomic and electronic struct., growth, physical props. 7-32854
 Ti₃MS₄ (M=P,As,Ta), electronic energy struct. and bonds, X-ray spectra studies 7-45148
 TiO₂, He I photoelectron spectra, relativistic DVM SCC Xalpha calcs. 7-50252
 U chalcogenides, ionicity and bond formation 7-32357
 UBe₁₃, heavy fermion cpd., lattice dynamics, EXAFS study 7-64792
 UIr, cryst. struct., X-ray diff. study 7-37927
 VN, deformation-induced stacking faults, synthesis by vibratory milling 7-44572
 VO, low-lying states, SDCI calcs. 7-25421
 V₂O₃, muon-O bonding, muon spin rot., site search calcs. 7-45897
 V₂O₅ gel, V site struct., polarised EXAFS and XANES studies 7-65355
 V₂O₃, metallic, electron state, electron diff. determ. 7-37921
 VS, low-lying states, SDCI calcs. 7-25421
 W (110), adsorption of Eu, Gd and Tb 7-27118
 W complexes, W (VI) isopropylidene, cryst. and mol. structs. 7-51722
 Xe₂+Kr, van der Waals bond exchange, mol. beam study, ang. and vel. distrib. 7-23000
 Zn II complexes, dibenzylthiocarbamate zinc, bonding, XPS 7-19950
 ZnMo₈O₁₀, synthesis and struct., orthogonal nonintersecting octahedral cluster chains 7-32386
 Zr complex, bonding, Xα-SW MO calcs. 7-62283
 ZrB, electronic struct., chem. bonding, Green's function methods 7-58741
- bone**
- alveolar cortical, elastic modulus meas. by laser speckle photography 7-34183
 bioactive glass ceramics, struct., phase relations 7-7982
 biomedical engineering, conf., Shreveport, LA, USA (Oct. 1986) 7-18470
 cancellous bone in canine proximal femur: elastic moduli, yield stress and ultimate stress 7-54657
 conduction microphone (*Japanese*) 7-43612
 conference on biomechanics, Mons, Belgium (Sept. 1986) (*French*) 7-9578
 contact gel as a source of error in X-ray films of the skull (*German*) 7-65855
 dental bridges, stress distrib. on alveolar bone surface, anal. using photoelastic coating technique (*Chinese*) 7-28767
 Derby intramedullary nail, biomech. comparison 7-40362
 digital radiography, dual energy subtraction, soft tissue and bone struct. images (*Japanese*) 7-14120
 doses of irradiation of patients during the use of ^{99m}Tc-pyrophosphate and ^{113m}In-indofur, bone tissue and red marrow (*Russian*) 7-3881
 dual photon absorptiometry measurements, precision 7-40262
 dynamic response testing of columnar composite materials subjected to impulsive loading 7-59708
 elbow, stress anal. before and after radial head resection (*German*) 7-23376
 elbow, stresses after joint replacement, finite element method calcs. and expt. obs. (*German*) 7-54809
 elemental concentrations, determ. using X-ray fluoresc. anal. 7-40381
 epiphyseal-based designs for tibial plateau components, stress anal. in frontal plane 7-3934
 epiphyseal-based designs for tibial plateau components, stress anal. in sagittal plane 7-3935
 erythroid units in canine bone marrow cells, survival on neutron or γ-irrad 7-60056
 femoral stem of cemented total hip replacements, role of collar rel. to bone stresses and resorption 7-8760
 femoral stress anal., 3D, using CT scans and P-version FEM 7-8613
 femoropatellar joint, trajectory pattern and load-bearing capacity when diseased (*Japanese*) 7-8638
 femur, dose dependent lathyrism, variation of sonic plesio-vel., rabbit obs. 7-65810
 femur samples, microdistribution of α-active nuclides, CR-39 autoradiography study 7-54733
 fixation plate for tibia, anatomically contoured, biomech. testing 7-8762
 foetal proximal femoral chondroepiphysis, human, expt. determ. of linear biphasic constitutive coeffs. 7-3821
 fracture healing, assessment by spectral anal. 7-8730
 hip endoprostheses, effects of stem design and material props. on stresses 7-40361
 implant orthopaedic surgery, conf., Marbella, Spain (July 1984)d 7-48188
 ivory, tensile props. and fracture rel. to comp. and struct. 7-14032
 joint endoprostheses, use of plastic materials (*German*) 7-34342
 Kevlar 29 fibre reinforced bone and dental cements, mech. props. 7-28080
 lumbar intervertebral segment study, nonlinear finite element model 7-65792
 lumbar vertebrae, human, dimensions in sagittal plane 7-23386

bone continued

- lumbar vertebrae, progressive positions visualisation using CAT-scan data 7-3834
- marrow cells of BALB/c mice irradiated with ^{252}Cf or ^{60}Co , micronuclei prod. 7-28615
- marrow granulocyte-macrophage progenitor cells and stromal colony-forming cells, human, effect of dose rate 7-8662
- marrow pressure chamber, permanently inserted Ti implant for intramedullary press. meas. 7-8779
- mechanical properties and morphology, effects of Ca deficient diet, goose obs. 7-3822
- microstructure quantification, semi-automatic image anal. 7-8776
- mineral assessment with dual energy CT scanning 7-47242
- nuclear techniques in diagnostic medicine, book 7-24312
- os calcis, broadband US attenuation, and single photon absorptiometry in the distal forearm: comparative study 7-40216
- osteoarthritic gait assessment, quantitative approach 7-54785
- osteopetrosis: NMR characts. at 1.5 T 7-28651
- osteosynthesis, 1-sided external fixation, improved stability (*German*) 7-40182
- osteosynthesis miniplate made of Ti, proposal for analytically-founded construction (*German*) 7-54810
- osteotomy gap, uniform, 3D strain fields 7-8636
- pelvic stress, concs. in acetabulum resulting from blow to right trochanter 7-40192
- pelvic stresses in vitro, efficacy of metal-backed acetabular prostheses 7-23383
- pelvic stresses in vitro, endoprostheses malsizing 7-23382
- peridental ligament, human, mech. props. of tooth and root sections 7-3824
- porous-glassy-carbon/bone interface, loaded, shear strength, rabbit obs. 7-54643
- pressure distribution under the ischium of normal subjects, meas. system 7-8729
- SEM stereophotogrammetric method and system for three-dimens. eval. of features on flat substrates 7-40377
- shock-absorbing properties of mammalian tissues and bones 7-3829
- skull, computer-aided tomogram, multiplex hologram 7-65883
- skull, dry, initial tooth and bone displacements, optical laser techniques meas. 7-65796
- spinal bone mineral determ. using automated contour detect.: appl. to single and dual energy CT 7-47243
- spinal fixation instrumentation, standardisation of testing procedures 7-8767
- spinal motion segments, human, internal displacements from in vitro loading, expt. results and finite element model predictions 7-3833
- spine, method for identification of in vivo segmental stiffness props. 7-65801
- spine, segmental motion meas., transducers mounting 7-3945
- strain of fresh human bones, meas. by strain gauge, method and obs. (*Chinese*) 7-28782
- temporomandibular joints, high-resolution NMR imaging with particular emphasis on soft-tissue display 7-14077
- thermophysical properties of compact bone 7-17952
- tibiae state alteration during antiothostatic hypokinesia 7-34181
- tibial bone, bovine, fracture props. 7-34177
- tibial components, bone stresses beneath, effect of interface, finite element modelling 7-40188
- tibial plate, cement layer stresses, model obs., 3D strain rosettes 7-65798
- tissue equivalent phantom materials for negative pions 7-65850
- tissue heterogeneity effect on operating regime selection of X-ray tube in radiodiagnostic investig. 7-40278
- trabeculae, bovine, tensile testing, device and obs. 7-3832
- trabecular bone density in proximal femur, quantitative CT assessment 7-14129
- trabecular bone specimens, stiffness behaviour obs. 7-54660
- ultrasonic velocity meas. system for thin solid samples 7-47182
- US transducers made from bone materials, charact. 7-60130
- X-ray microtomography with synchrotron radiation 7-47224
- ^{18}F , single-passage extraction in rabbit bone 7-40249
- Pb anal., comparison of 2 in vitro methods 7-23499
- ^{239}Pu , A=239,240, conc. in Japanese human tissues 7-18081
- ^{226}Ra , A=226,228, intake by early Ra dial workers in Illinois, health risks 7-8700
- ^{224}Ra in mouse bone, dosimetry calcs. 7-8690

Boolean algebra

- see also *Boolean functions; formal logic*
- cellular random nets, phase transitions 7-56171

Boolean functions

- Kauffman's random Boolean network, approach to the stationary state 7-56155
- symbolic substitution logic for digital optical computing 7-10859

Boolean lattices see *Boolean algebra***boosters (electric generators)** see *exciters***bootstrap models** see *bootstrapping***bootstrap theory** see *bootstrapping***bootstrapping**

- 2D conformal field theory, analytic geometry 7-48968
- chiral field, Bethe-ansatz soln., complete S-matrix and bootstrapping props. 7-48961
- d=2 conformally invariant SU(2) σ -model with Wess-Zumino term, primary operator 4-point correls. 7-56418
- demibootstrap approach to hadron-spectrum dynamics 7-19064
- RF current drive in tokamak devices, bootstrap effect 7-51400
- qq \rightarrow qq, (q=u,d,s), low-energy amplitudes, meson masses, N/D dispersion method anal. 7-61549

bootstraps see *bootstrapping***borate glasses**

- see also *borosilicate glasses*
- alkali borate glasses, $\text{M}_2\text{O}-\text{B}_2\text{O}_3$, (M=Li, Na, K, Rb, Cs), thermodynamic props. 7-2211
- basicity and geometry studies, MNDO calcs. 7-6529
- energy transfer in Cr^{3+} , Nd^{3+} codoped borate glass 7-33440
- mixed alkali borate glasses, transform. range viscosity, thermal expansion 7-52103
- optical dispersion, reflection spectra in vacuum and extreme UV region 7-27734
- oxynitride glass development, book contrib. 7-28003

borate glasses continued

- phase equilibria, thermodynamic model 7-2150
- reflection spectra in extreme UV region 7-22278
- structural groupings, NMR studies 7-11940
- structure and bonding, NMR studies 7-63503
- thermal expansion, sp. ht. meas. 7-44862
- thermodynamics, miscibility and phase separation 7-63498
- X-ray irradiat., ESR centres, review 7-7586
- $\text{AgI}-\text{Ag}_2\text{O}-\text{B}_2\text{O}_3$ fast ion conducting glasses, struct., XANES studies 7-63483
- $\text{AgI}-\text{Ag}_2\text{O}-\text{B}_2\text{O}_3$ glasses, superionic, crossover freq. between phonon and fraction regimes, scaling behaviour 7-44728
- $\text{Ag}_2\text{O}-\text{Ti}_2\text{O}_3-\text{B}_2\text{O}_3$ glasses, physical props. and tandem monovalent ions effect 7-3013
- $(\text{Ag}_2\text{O})_{0.1}(\text{B}_2\text{O}_3)_{0.9}$ glass network struct., mol. dynamics study 7-6539
- $(\text{Ag}_2\text{O})_x(\text{B}_2\text{O}_3)_{100-x}$ glasses, microstruct. and electronic cond. studies 7-6534
- $\text{B}_2\text{O}_3-\text{GeO}_2$ glass, vibrational spectra of structural units 7-3034
- $\text{B}_2\text{O}_3-\text{Li}_2\text{O}-\text{LiCl}-\text{Al}_2\text{O}_3$, amorphous ionic conductor, crystallisation, position annihilation study (*Chinese*) 7-37872
- $\text{B}_2\text{O}_3-\text{Na}_2\text{O}$ glasses, low temp. thermal cond. meas. 7-38277
- $\text{B}_2\text{O}_3-\text{PbO}-\text{Al}_2\text{O}_3$ glasses, phase separation, dynamical scaling 7-1908
- $\text{BaO}-\text{Al}_2\text{O}_3-\text{B}_2\text{O}_3$ glass, constitution 7-21120
- $\text{BaO}-\text{B}_2\text{O}_3$ glass, containing Fe_2O_3 , heat treatment and γ -irrad., IR study 7-16627
- $\text{BaO}-\text{B}_2\text{O}_3-\text{Al}_2\text{O}_3$, aluminoborate glass, X-irrad.; optical and thermal bleaching 7-45820
- $\text{BaO}-\text{B}_2\text{O}_3-\text{Fe}_2\text{O}_3$ glasses, γ -irradiated and heat treated, elec. conductivity and crystn. 7-21510
- $\text{BaO}-\text{Fe}_2\text{O}_3-\text{B}_2\text{O}_3$ -based glasses, crystallisation behaviour, nucleating agent effects 7-51650
- $\text{BaO} \cdot 4\text{B}_2\text{O}_3$ glasses, crystallisation 7-63490
- $\text{CaO}-\text{Al}_2\text{O}_3-\text{B}_2\text{O}_3$ glass, constitution 7-21120
- $\text{CdO}-\text{B}_2\text{O}_3-\text{Si}(\text{Ge})\text{O}_2$ network struct., coordination and bonding, comp. depend., NMR study 7-6535
- $(\text{CdO})_x(\text{B}_2\text{O}_3)_y(\text{GeO}_2)_z$ glasses, struct. and vibrational props., IR spectra study 7-7694
- $\text{Fe}_2\text{O}_3-\text{BaO}-\text{B}_2\text{O}_3-\text{V}_2\text{O}_5$ glasses, Fe^{3+} site occupancy, Mossbauer studies 7-6541
- $\text{Fe}_2\text{O}_3-\text{Na}_2\text{O}-\text{B}_2\text{O}_3$ glasses, Mossbauer study 7-7619
- $\text{K}_2\text{O}-\text{Al}_2\text{O}_3-\text{B}_2\text{O}_3-\text{Fe}_2\text{O}_3-\text{Gd}_2\text{O}_3$ glasses, mag. props., composition dependences 7-2823
- $\text{K}_2\text{O}-\text{B}_2\text{O}_3$, elec. cond., molar volume 7-58535
- $\text{K}_2\text{O} \cdot 2\text{B}_2\text{O}_3$ glasses, pulse irradiated, optical absorpt. spectra, temp. effects on the decay process (*Japanese*) 7-22281
- Li cpds., density w.r.t. atomic arrangements, comp. depend. 7-6533
- $\text{Li}_2\text{B}_4\text{O}_7/\text{CuCl}_2$ crystallised glasses, pure and doped, thermally stimulated exoelectron emission, thermolum. 7-27874
- $\text{Li}_2\text{B}_4\text{O}_7-\text{WO}_3$ glasses, dielec. behaviour, space charge effects 7-45917
- $\text{LiCl}-\text{Li}_2\text{O}-\text{B}_2\text{O}_3-\text{Al}_2\text{O}_3$, amorphous Li^+ conductor, crystn. and phase separation, interface effect (*Chinese*) 7-38245
- $\text{Li}_2\text{O}-\text{B}_2\text{O}_3$ ion conducting glass, effect of CaO substitutions on transport and physical props. 7-58535
- $\text{Li}_2\text{O}-\text{B}_2\text{O}_3$ glasses, rapidly quenched, struct. investig. by Raman spectra 7-1913
- $\text{Li}_2\text{O}-\text{B}_2\text{O}_3$ glasses, vibr. spectra and struct. 7-59196
- $\text{Li}_2\text{O}-\text{B}_2\text{O}_3-\text{WO}_3/\text{Co}(\text{Cr})$ glasses, optical props. 7-46079
- $\text{Li}_2\text{O}-\text{MO}-\text{B}_2\text{O}_3 \cdot \text{VO}^{2+}$ (M=Ba,Ca,Mg) borate glasses, ESR of VO^{2+} ion 7-59110
- $x\text{Li}_2\text{O} \cdot y\text{Li}_2\text{SO}_4 \cdot \text{B}_2\text{O}_3$, IR and Raman spectra, vibr. study and struct. 7-37879
- $\text{MgO}-\text{Na}_2\text{O}-\text{B}_2\text{O}_3$ glasses, FIR spectra 7-39123
- $\text{Na}_2\text{B}_4\text{O}_7-\text{NiO}$, tetraborate glass, optical absorpt. effects of NiO additions and annealing 7-22851
- $\text{Na}_2\text{B}_4\text{O}_7-\text{Pb}_3\text{O}_4-\text{CuO}$ glasses, elec. props., effect of added CuO 7-2605
- $\text{Na}_2\text{O}-\text{B}_2\text{O}_3$ glass, UV absorption spectra of Ag^+ ion 7-7721
- $\text{Na}_2\text{O}-\text{B}_2\text{O}_3$ glass struct., comparison with pyroborax 7-44391
- $\text{Na}_2\text{O}-\text{B}_2\text{O}_3$ glasses, effect of Na_2O addition, thermal expansion, sp. ht. meas. 7-44862
- $\text{Na}_2\text{O}-\text{B}_2\text{O}_3-\text{Al}_2\text{O}_3$ glass struct., NMR and computer simulation 7-1898
- $\text{Na}_2\text{O}-\text{B}_2\text{O}_3-\text{CuO}$ glasses, B ions coordination state studied by X-ray and Raman spectroscopy 7-1892
- $\text{Na}_2\text{O}-\text{B}_2\text{O}_3-\text{Fe}_2\text{O}_3$ glass, hyperfine parameter distrib., ^{57}Fe Mossbauer study 7-22170
- $\text{Na}_2\text{O}-\text{B}_2\text{O}_3-\text{Ga}_2\text{O}_3-\text{Y}_2\text{O}_3$ glass, porous, leaching and sintering 7-7953
- $\text{Na}_2\text{O}-\text{V}_2\text{O}_5-\text{B}_2\text{O}_3$ glasses, mixed ionic-electronic conduction 7-12769
- $\text{Na}_2\text{O}-\text{WO}_3-\text{B}_2\text{O}_3$ glass ceramics, containing W bronze, prep. and elec. props. (*Japanese*) 7-3261
- $\text{Na}_2\text{O} \cdot 2\text{B}_2\text{O}_3$ glasses, pulse irradiated, optical absorpt. spectra, temp. effects on the decay process (*Japanese*) 7-22281
- $\text{PbO}-\text{B}_2\text{O}_3$ glass form., crystallisation 7-37875
- $\text{PbO}-\text{B}_2\text{O}_3$ optical glass, props. and structure, effect of heat treatment 7-20377
- $\text{PbO}-\text{B}_2\text{O}_3-\text{Fe}_2\text{O}_3$ glass, ESCA study 7-26651
- $\text{PbO}-\text{Fe}_2\text{O}_3-\text{B}_2\text{O}_3$ glass ceramics, mag. props. and EPR spectra of precipitated mag. phases 7-45748
- $\text{PdO}-\text{CdO}-\text{B}_2\text{O}_3$ glasses, elec. cond. and density meas. 7-1895
- $\text{Y}_2\text{O}_3-\text{Al}_2\text{O}_3-\text{B}_2\text{O}_3$ system, glass formation, props. and struct. 7-2205

Bordoni effect

- No entries

boron

- see also *nuclei with*
- adsorption on Mo (100), surface atom oxidation states, ESCA meas. 7-28333
- amorphous, elec., optical and thermal cond. props. 7-21910
- atom, spin and charge densities, HF and UHF calcs. 7-19684
- atomic clusters, magnetic properties, Heisenberg Hamiltonian 7-57199
- crystal growth in solar furnace 7-33538
- crystalline, specific heat meas. using ^4He cryostats 7-35526
- defects produced by electron and X-ray irradiation, surface effects 7-6687
- detection in vegetable samples and solutions using (n, α) technique 7-33980
- diamond:B, hopping photoconductivity 7-38617
- diamond:B, VPE, physicochem. basis of doping (*Russian*) 7-16587
- dopant diffusion into Si, solar cell junction form. 7-28401
- doping in a-Si:H:F made by thermal CVD for conductivity and p-n type control 7-17454
- EELS analysis, inner shell excitation profiles visibility 7-22403
- electron probe microanalysis, quantitative 7-46886

boron continued

- fibre reinforced Al, bond form. between alitized B fibres and matrix in rolling 7-3331
 fibre reinforced Al, strength characts. 7-33768
 fibre reinforced Al alloy, corrosive media influence on crack resist. 7-17668
 fibre reinforced Al matrix composite, TiB₂ coated, prep. using liq. phase infiltration 7-3229
 fibre reinforced Al matrix composites, transverse mech. props., isothermal exposure effect 7-39688
 fibre reinforced Al tube under multi-axial loadings, elastic-plastic deformation 7-46548
 fibre reinforced Ti-base alloy, development of creep-resisting composites 7-3228
 graphite:B-Na intercalation cpd., Fermi level displacement, diamag. anisotropy and Hall effect meas. 7-16933
 ion implantation in V film, phase changes, electron microscopy study 7-12169
 molecule, ground state, excited vibr. levels struct., visible spectra anal. 7-50156
 powdered, O and H content eval. 7-27964
 semiconductor impurity concentration, microanalytical estimation 7-38040
 Si:B polycrystalline solar cell substrates, B conc. meas. using IR spectroscopy 7-23176
 sources and distrib. in geothermal fluids 7-23121
 thin film preparation, ion beam sputtering appl. 7-7850
 B I, isoelectronic sequence, short wavelength laser calcs. 7-20214
 B II, beam-foil spectra, identification 7-49982
 B III, beam-foil spectra, identification 7-49982
 B III, core excited quartet and doublet state, beam-foil study 7-42514
 B IV, beam-foil spectra, identification 7-49982
 B²⁺, electron-impact ionisation, excitation-autoionisation contrib. 7-978
 B/N coatings, ion plating, amorphous struct., wear resist. 7-22580
¹⁰B/¹¹B ratio, determ. in nucl. reactor moderator 7-56753
 B+O₂, gas-phase oxidation, rate consts., fluoresc. and chemiluminesc. study 7-22985
 B⁺+H⁺, pot. energy surfaces, diatomics-in-molecules calcs. 7-5748
 B³⁺+He, double- and single-electron capture and loss cross section meas., OBK scaling calcs. 7-42756
 B₂, chem. bonding, kinetic energy anisotropy investig. 7-10396
 Cd_{0.7}Hg_{0.3}Te:B⁺, ion implanted, photoreflection spectra in the edge absorption region 7-39099
 CdTe : B⁺ ion implantation damage, rapid thermal annealing, photolum. anal. 7-39162
 Fe:B polycrystalline films, amorphous alloy layer formation by ion implantation (Chinese) 7-6647
 GaAs:B, as-grown Czochralski crystals, EPR signal 7-38935
 GaAs:B, dislocation free crystals, microscopic defects, eutectic etching 7-16545
 GaAs:B, internal friction temp. depend. studies 7-38112
 GaAs:B, ion implanted, near-intrinsic and extrinsic photocapacitance due to the EL2 level 7-7147
 GaAs:B, ion implanted, struct. and damage distrib., TEM study 7-51893
 GaAs:B buried isolation layer form. by focused ion beam, FIBI-MBE system 7-51804
 GaAs:B-Ga_{0.25}Al_{0.75}As:B quantum wells, ion implanted, TEM and photolum. studies 7-58865
 GaAs:In, B, electrical props., role of residual B impurity, liquid encapsulated Czochralski growth 7-45312
 GaP:B, internal friction temp. depend. studies 7-38112
 p-Ge:B, annealing kinetics of radiation defects, influence of impurity binding energy 7-39547
 a-Ge:H, B, P, As, dopant incorporation and doping efficiency 7-44587
 HgCdTe:B, bulk and thin film, resonant impurity levels, magneto-transport studies 7-64162
 HgCdTe:B⁺, ion implanted n⁺p junction, lifetime and carrier conc. profile 7-45450
 Hg_{1-x}Cd_xTe:B, ion implanted, annealing, nature oxide encapsulation 7-2036
 InAs:B, internal friction temp. depend. studies 7-38112
 InP:B, internal friction temp. depend. studies 7-38112
 InP:B, multiphonon absorpt. 7-59211
 Ni:B, grain-boundary cohesion, impurity segregation effects, density-functional cluster model calcs. 7-44835
 Ni:B, ion implanted, high temp. oxidation, defect diffusion 7-33846
 NiSi₂-Si-B, epitaxial growth of NiSi₂, influence of dopant atoms 7-45039
 Si:As:B films, surface energy driven secondary grain growth 7-22740
 Si:As(P):B-SiO₂ interface, segregation, transport coeffs. of impurities 7-63880
 Si:B, amorphisation by ion implantation 7-38080
 Si:B, amorphous, solar cell, roll-to-roll mass prod. process 7-17902
 Si:B, B ion dose identification, HF C-U meas. 7-6661
 Si:B, B-vacancy complex, electronic and atomic struct., ENDOR studies 7-63649
 Si:B, BF₃⁺ ion implantation and rapid thermal annealing 7-21241
 Si:B, cold neutron irradiated, interaction cross sections 7-58349
 Si:B, critical supercond. current induced by proximity effect, mag. field depend. 7-22069
 Si:B, diffused through narrow windows, doping profiles 7-12113
 Si:B, diffusion and activation of implanted B during rapid thermal annealing 7-16643
 Si:B, doping by XeCl excimer laser irradi., ultra-shallow junction fabrication 7-58303
 Si:B, electron irradi. stimulated impurity diffusion 7-63878
 Si:B, electron-irradiated, AC hopping conductivity and DLTS 7-44624
 Si:B, excimer laser-induced shallow, diffusion, junction form. 7-38038
 Si:B, F implanted amorphous layers, struct. and elec. props., ESR and Hall effect meas. 7-26634
 Si:B, H, hydrogenation of B acceptor during electron injection by Fowler-Nordheim tunnelling 7-45504
 Si:B, hydrogenation and annealing kinetics 7-2527
 Si:B, implant redistribution during high pressure oxidation, SIMS and C-V meas. 7-27020
 Si:B, implanted ion distrib., lateral spreading, theoretical predictions and computer simulation 7-16604
 Si:B, impurities at dislocations and grain boundaries, high-resolution TEM imaging 7-37815
 Si:B, impurity diffusion from BN sources, non-Fickian model 7-27012
 Si:B, impurity transport in mag. Czochralski growth, computer simulation 7-58182

boron continued

- Si:B, ion implant redistribution, diffusion modelling 7-16814
 Si:B, ion implanted, amorphous layer thickness, SIMS profiling 7-51794
 Si:B, ion implanted, B diffusion, rapid thermal annealing 7-58538
 Si:B, ion implanted, defect and dopant depth profile studies 7-2045
 Si:B, ion implanted, dopant redistrib. during rapid thermal annealing 7-38042
 Si:B, ion implanted, pulsed laser annealing, optical reflection kinetics 7-58323
 Si:B, ion implanted, strain profile, double cryst. X-ray rocking curve simulation 7-2060
 Si:B, ion implanted, transient annealing and residual defect DLTS study (Chinese) 7-12642
 Si:B, laser microprobe mass analysis, quantitative 7-54250
 Si:B, low temp. epitaxial films, nonequilib. doping effects 7-58672
 Si:B, MBE grown, coevaporation doping 7-12562
 Si:B, mag. props. of the acceptor system 7-27496
 Si:B, magnetic Czochralski growth, computer simulation of B transport 7-32344
 Si:B, O, heavily doped, O precipitation, diffuse X-ray scatt. studies 7-32669
 Si:B, O epitaxial wafers, effect of pre- and postdeposition annealing on O precipitation 7-45060
 Si:B, p-n junction diode, rapid thermal annealing 7-22005
 Si:B, preamorphised, B diffusion during rapid thermal annealing 7-32717
 Si:B, retarded and enhanced dopant diffusion related to implantation-induced excess vacancies and interstitials 7-63881
 Si:B, SIMS depth profiles in the near-surface region, correction for ion yield transients 7-22430
 Si:B, SIMS depth profiles, characterisation and removal of ion yield transients in the near surface region 7-65368
 Si:B, Si₂O₃B, ab initio MO electronic struct. calcs. 7-38499
 Si:B, tail diffusion model 7-16815
 Si:B,C,O, O clustering and thermal donor formation kinetics 7-17566
 Si:B,Fe, EBIC and DLTS meas., comparisons 7-7265
 Si:B,H(D) Schottky and n⁺-p junction diodes, electrical transport of acceptor-compensating defect 7-16823
 Si:B,O, heavily doped crystals, behaviour of O and dopants 7-32483
 Si:B,O, heavily doped Czochralski wafers, O precipitation, 450°C thermal annealing 7-58477
 Si:B,O, thermal donor formation, bending stress effects 7-17563
 Si:B,O epitaxial wafers, internal gettering heat treatments and O precipitation 7-45059
 Si:B,P highly doped epitaxial layers, growth by low press. VPE 7-39432
 Si:B,P solar cells produced by pulsed excimer laser annealing of ion-implanted junctions 7-8419
 Si:B diffusion source, diffusion into single crystal Si 7-32727
 Si:B film deposition in Si₂H₆-B₂H₆-He gas system, doping effect 7-27184
 Si:B LPCVD films, amorphous and polycrystalline, struct., elec. resist. meas. 7-52870
 Si:B layers, preamorphised and ion implanted, structural and elec. characterisation 7-52347
 Si:B MBE layers, shallow states, photoluminescence spectra, doping level depend. 7-13228
 Si:B p⁺-n-n⁺ solar cells fabricated using masked ion implantation, electro-optical characts. 7-23143
 Si:B p⁺-n shallow junctions obtained by implantation into preamorphised Si, elec. charactn. 7-38703
 Si:B p-n⁺ junction, injection annealing of radiation defects 7-12161
 Si:B plastically deformed crystals, dislocation struct. and elec. activity, annealing effects study 7-37998
 Si:B polycrystalline films, rapid thermal processing before and after ion implantation, effect on cond. 7-22046
 Si:B solar cell emitter saturation current meas. by contactless photoconductivity decay method 7-13866
 Si:B thermal donor props., impurity effects, DLTS, Hall effect, and admittance spectra meas. 7-21851
 Si:B wafers, activated carrier density profile and scatt. rate meas., nondestructive IR attenuated total refl. technique 7-22207
 Si-Bi polycrystal-single cryst. interface, impurity diffusion across boundary 7-27013
 Si-B-Ti(Co), silicide formation using rapid thermal processing, defect behaviour 7-32726
 Si:B⁺, ion implanted, characterisation by IR attenuated total reflection spectroscopy 7-17327
 n-Si:B⁺, ion implanted, rapid thermal annealing, DLTS 7-16619
 Si:B⁺ submicron p-n junctions, ion implanted, dopant distrib., Raman study 7-21252
 Si:B(Ga)(As)(Sb) 7-2040
 Si:B(P), lateral diffusion, modeling LOCOS effects 7-33865
 Si:B(P), microcrystalline, LPCVD production, anal and solar cell appls. 7-17452
 a-Si:F,H films, glow discharge deposition, B doping efficiency 7-17436
 Si:Ge,B, IR absorpt. band broadening 7-64669
 a-Si:H, B, P, As, dopant incorporation and doping efficiency 7-44587
 a-Si:H, B, P-type, increased elec. cond. studies 7-45337
 a-Si:H, B films, ion implanted, photoelectric and optical props. 7-38615
 a-Si:H, B films, photoinduced changes in elec. props. 7-38634
 a-Si:H,B, effective p⁺ doping by plasma-assisted B diffusion 7-38036
 a-Si:H,B, RF sputtered films, optical and electrical props. 7-33470
 a-Si:H,B, thin films, thermoelectric power 7-58826
 a-Si:H,B films, dopant conc. meas. and depth profiling by means of (p,γ) resonant reactions 7-12555
 a-Si:H,B films, hole transport, time-of-flight meas. 7-45320
 a-Si:H,B p-i-n and n-i-p solar cells, doping profile effects 7-46947
 a-Si:H,B p-i-n solar cells, open-circuit volt., wavelength depend. 7-46948
 a-Si:H,B RF sputtered coatings, gas-phase doping efficiency 7-63471
 a-Si:H,B/a-Si:H,P doping modulated superlattice, photo-induced excess conductivity 7-17051
 a-Si:H solar cells, p-layer doping by plasma assisted B diffusion 7-13898
 Si:O,B⁺, ion implanted, reverse annealing 7-16617
 Si:P,B, SiO₂ coated cryst., floating zone growth under microgravity 7-53575
 Si:P,B films, surface energy driven secondary grain growth 7-22740
 Si:P,B polycrystalline CVD film, etch rate free carrier depend., doping level and grain size depend. meas. 7-28219
 Si:Sb(As)(P)(B) epitaxial films, low temp. deposited by low press. CVD, autodoping 7-27182
 Si:Sn,B, shallow junction formation, preamorphisation by Sn implantation 7-7338

boron continued

- Si-B⁺, Ge⁺, preamorphised shallow junctions, end-of-range and mask edge lateral damage 7-38071
 α -SiC:Al,B,O crystals, photolum. and electrolum. studies (Russian) 7-22344
 β -SiC:B films, ion implanted, rapid thermal annealing 7-17569
 SiC:B thin films, impurity 7-27192
 SiC:B⁺, stoichiometric disturbances due to ion implantation 7-6651
 α -SiC:H,B, effective p⁺ doping by plasma-assisted B diffusion 7-38036
 α -SiC:H,B, thin films, thermoelectric power 7-58826
 α -SiC:H(B), thin film, solar cells fabricated by plasma deposition (Korean) 7-33585
 α -Si_{1-x}C_xH_{1-x}B films, valence band localised holes; light-induced ESR spectra studies 7-53110
 α -Si_{1-x}C_xH_{1-x}B thin films, H bonding and H content, IR spectra studies (Chinese) 7-12524
 SiN_xH_{1-x}B, microcrystalline, wide-gap, RF glow discharge deposition 7-22503
 SiN_xH_{1-x}B microcrystalline films, B doping 7-44586
 α -Si_{1-x}N_xH_{1-x}B films, ESR and IR spectra studies 7-7780
 α -Si_{1-x}N_xH_{1-x}B films, DC sputtered, photoelectronic and optical props. 7-27361
 SiO₂:B, diffusion investig., H₂ annealing atmosphere effects 7-6876
 SiO₂:B, thermally grown, diffusion of ion-implanted dopants 7-38041
 Ti/Si:B,As,Sb interface, dopant redistrib. during silicide form. by rapid thermal processing 7-63641
 TiSi₂:B films on Si, impurity diffusion 7-7077
 TiX:B (X=C, N, O) electronic struct., chem. bonding, Green's function methods 7-58741

boron alloys

see also boron compounds

- brass, two-phase, Al-B Masteralloy addition, B redistrib. during solidification, grain refining effect 7-22664
 Fe-Ni-B metallic glasses, struct. and crystn. kinetics, DSC and X-ray diff. meas. 7-16436
 Fe-B, amorphous alloy, metallic glass ribbon, thermal diffusivity, photoacoustic study 7-45262
 misch metal-Fe-B melt-spun magnets, mag. and structural props. 7-53032
 rare earth alloys, R₂(Fe,Al,Co)₁₄B, mag. props., composition depend. 7-53030
 rare earth alloys, R₂Fe₁₄B, R=La-Nd, Sm, Gd-Tm, Lu and Y, ⁵⁷Fe Mossbauer spectra 7-64551
 rare earth-iron-boron permanent magnet materials, prep. and props., book contrib. 7-27981
 B-Si (18 wt.%), tribological coatings, low temp. sputter deposition 7-46322
 BW alloy fibre, torsional pendulum, shear modulus and internal friction meas. 7-48232
 CaIr₂B₃, structural relationship to BaAl₄ 7-16496
 CaRh₂B₃, structural relationship to BaAl₄ 7-16496
 Ce-(Fe,Co)-(B,Si) system alloys, melt spun ribbons, mag. props. (Japanese) 7-53052
 CeB₆, Fermi surface, 2D angular correlation of positron annihilation radiation 7-39241
 CeB₆ heavy fermion system, muon Knight shift study 7-45886
 CeB₆-Mo point contacts, low temp. I-V charact., thermoelec. effects obs. 7-27382
 Ce₂Fe₁₄B, anisotropy constants, temp. depend. (Chinese) 7-59003
 CeRh₃(Bi_{1-x}Si_x)₂, 4f shell dehybridisation, Curie temp. and mag. moments 7-45679
 Co-B, amorphous, thermodynamic, thermomag. and struct. studies (French) 7-16438
 Co-B amorphous alloys, ⁵⁹Co hyperfine field distrib., NMR spin echo studies 7-53174
 Co-based amorphous alloys, anisotropic electrical magnetoresistivity at 295 K 7-58796
 Co-Fe-V-Si-B metallic glass, Co-rich, temp. and annealing dependences of magnetostriction const. 7-33255
 Co-Si-B, change of elongation, rel. to conditions for hot working 7-3384
 Co-Si-B amorphous alloys, mag. props., annealing effects 7-27513
 Co_{100-x}B_x amorphous sputtered thin films, magnetic anisotropy origins 7-27583
 Co₇₀B₃₀ amorphous films, ferromag., induced mag. anisotropy (Russian) 7-52974
 Co₈₂B₁₈ amorphous alloy, reminiscent devitrification, X-ray diff. studies 7-6547
 Co₇₄Fe₆B₂₀ amorphous sputtered thin films, magnetic anisotropy origins 7-27583
 Co₆₉Fe_{4.5}Cr_{2.5}B₂₂ metallic glasses, long-time tunnelling heat relaxation meas. 7-38223
 CoFeMoB amorphous thin films, prep. and high-freq. impedance studies 7-53585
 (Co_{0.85}Fe_{0.06}Ni_{0.08}Nb_{0.01})₇₅Si₁₀B₁₅ amorphous alloys, structural relax. and crystn., positron annihilation studies 7-37869
 Co₅₇Fe₅Ni₁₀Si₁₁B₁₇, metallic glasses, superplastic deform. (Russian) 7-39599
 Co₅₈Fe₅Ni₁₀Si₁₁B₁₆, metallic glasses, multiplet splitting, XPS studies 7-27858
 Co₆₈Fe₇Ni₁₃Si₇B₃, amorphous alloy, superplasticity 7-3368
 CoFeSiB inhomogeneous magnetic alloys, anomalous Hall effect-magnetic polarisation correls. 7-7208
 (Co_{0.95}Fe_{0.05})₇₅Si₁₅B₁₀ amorphous alloy, mag. saturation 7-45632
 Co_{70.4}Fe_{4.6}Si₁₅B₁₀, amorphous alloy, mag. props. rel. to mag. coating 7-22123
 Co₇₁Fe₅Si₁₅B₁₀ and Co₇₅Si₁₅B₁₀ amorphous alloys, mag. props., stress and annealing depend. 7-33250
 Co₈₅Fe₅Si₈B₂ amorphous alloys, annealing, positron annihilation parameters 7-39303
 Co_{83.4}Fe₅Si_{7.5}Ge_{1.5}B_{2.5}, amorphous alloy, struct. changes after γ -irrad. (Russian) 7-58336
 (Co_{1-x}Mn_x)₂B, crystalline and amorphous, mag. and elec. props. 7-2827
 Co₈₄Nb₁₀B₆ fully crystallised metallic glass, fracture processes 7-22841
 Co₅₈Ni₁₀Fe₅B₁₆Si₁₁, metallic glass, reversible struct. transformation 7-1907
 Co₅₈Ni₁₀Fe₅B₁₆Si₁₁ amorphous ferromag. alloy struct., shock loading effects, mag. struct. anal. 7-2100
 Co₅₈Ni₁₀Fe₅B₁₆Si₁₁ amorphous ferromagnet, prep. and struct. 7-22605
 (Co_{0.6}Ni_{0.4})₇₈Si₁₄B₈ amorphous, itinerant electron charact., current induced reson. mag. field shift obs. 7-27590

boron alloys continued

- (Co_{1-x}Ni_x)₇₅Si₁₅B₁₀ amorphous alloys, magnetostriction and other mag. props. 7-45787
 Co₇₅Si₁₀B₁₅, amorphous powder, static consolidation, mechanical and mag. props. 7-3217
 Cr-BN amorphous films, supercond. transition temp. 7-27454
 Cu-B, cast struct., segregation, conc. undercooling 7-3291
 Cu-B, rapid solidified and ion implanted, struct. studies 7-21130
 Cu-Pt-B liquid metal ion source, B⁺ and P²⁺ ion emissions 7-41531
 Cu-Sn-B, ductility at high temp., alloying additions effect (Japanese) 7-13515
 CuB:He, neutron irradiated, annealing behaviour of defects, positron annihilation study 7-39291
 Er₂(Fe,Co)₁₄B, struct., composition depend. 7-51701
 Er₂(Fe,Mn)₁₄B, struct., composition depend. 7-51701
 Er_{0.135}Fe_{0.813}B_{0.052} melt spun ribbons, mag. and struct. props. 7-59059
 Er₂Fe₁₄B alloys, magnetic anisotropy and spin reorientations 7-38855
 Fe-B, amorphous, structural characterisation by laboratory EXAFS spectrometer 7-1911
 Fe-B, amorphous alloys, crystallisation, morphology rel. to sample thickness (Russian) 7-37861
 Fe-B, amorphous metallic films, SAX investig. (Russian) 7-51576
 Fe-B, atomic radial distrib. function, close order sorting parameter (Russian) 7-58206
 Fe-B, B solubility in Fe 7-7971
 Fe-B, metallic glasses, photoemission investig. (Slovak) 7-59369
 Fe-B (15 at.%), amorphous powder and strip, struct., mag. props., thermal stability (Russian) 7-63470
 Fe-B alloys, metastable crystalline, Mossbauer study of local atomic environments 7-17252
 Fe-B amorphous sandwich films, concentration-dependent diffusion 7-45027
 Fe-B based metallic glasses, corrosion in H₂SO₄, alloying effect 7-28201
 Fe-B based metallic glasses, embrittlement, formation of B-rich zones 7-59598
 Fe-B liq. and amorphous alloys, interference functions, X-ray diff. study and cluster calcs. 7-26656
 Fe-B metallic glasses, atomic radial distrib. functions, ultradispersed eutectic structural model 7-11923
 Fe-B metallic glasses, imperfection struct., positron annihilation studies 7-37885
 Fe-B metallic glasses, struct. relax., Curie temp. meas. 7-21124
 Fe-B rapidly quenched cryst. alloys, local atomic environments, spin echo NMR studies 7-7606
 Fe-B-Ce-based metallic glasses, mag. domain structs. and annealing embrittlement 7-27586
 Fe-B-Si and Fe-B-Si-Cr-Mo-W, finely cryst. and amorphous structs. on surface by laser treatment 7-8175
 Fe-B-based amorphous alloys, struct. evolution during heating (Russian) 7-16418
 Fe-Co-B films, phase transition, microstruct. 7-33568
 Fe-Co-B powders, amorphous mag. state, Mossbauer spectra study 7-45846
 Fe-Co-Si-B and Fe-Ni-Si-B glass, liq.-quenched, cooling condition depend. of saturated mag. flux density 7-58991
 Fe-Cr-B, amorphous, Cr redistribution between phases during crystallisation, Mossbauer spectroscopy 7-21100
 Fe-Cr-B metallic glasses, imperfection struct., positron annihilation studies 7-37885
 Fe-Cr-B-Si, amorphous, annealing effects on Curie temp. 7-45675
 Fe-Cr-C-B hard surfacing weld deposits, abrasive wear resist. and microstruct. 7-22847
 Fe-Cr-Si-B metallic glass wires, corrosion rel. to crystallinity and comp. 7-46701
 Fe-M-B metallic glasses (M=Ti,V,Cr,Mn,Co,Ni,Cu,Pd,C,Si,Ge,Sn), formation kinetics, thermal stability 7-58474
 Fe-Nd-B magnets, microstructure and mag. props. 7-53049
 Fe-Nd-B permanent magnets, prep. by liquid dynamic compaction 7-53661
 Fe-Nd-B system, phase relations 7-46422
 Fe-Nd-B-Al sintered magnets, TEM studies 7-51999
 Fe-Ni-B, amorphous, shock loading, inclusions dissolving, domain struct. (Russian) 7-63487
 Fe-Ni-B metallic glasses, crystallisation, microhardness (Russian) 7-59617
 Fe-Ni-Cr-Ti-B, constant elastic alloy, torsion reson. freq. temp. coeff. rel. to B content (Chinese) 7-13488
 Fe-Ni-Si-B glass alloy, liq. quenched, saturated mag. flux density, effect of peening 7-13611
 Fe-Ni-Si-B metallic glasses, imperfection struct., positron annihilation studies 7-37885
 Fe-R-B (R=rare earth) metallic glass permanent magnets, TEM studies 7-26661
 Fe-R-B (R=rare earth) metallic glass permanent magnets, struct. and mag. props. 7-27565
 Fe-Si-B, amorphous alloys, crystallisation, morphology rel. to sample thickness (Russian) 7-37861
 Fe-Si-B, normalising, decarburisation, secondary recrystallisation, mag. induction obs. 7-8020
 Fe-Si-B, solidification in mag. fields (Russian) 7-59508
 Fe-Si-B (10, 15 at.%), metallic glass, plastic deform. resist. 7-13521
 Fe-Si-B (10, 15 at.%) alloy glass, ion milling rate, cooling condition depend. 7-46690
 Fe-Si-B alloy glass, crystn., effect of solid-liq. interfacial energy 7-16437
 Fe-Si-B amorphous alloys, hypoeutectic, thermal stability and soft mag. props. 7-11928
 Fe-Si-B amorphous alloys, electron momentum distrib. and Fermi energy, Doppler broadening positron annihilation 7-39220
 Fe-Si-B mag. film, magnetoelastic wave generation and detection 7-59070
 Fe-Si-B metallic glasses, wear resist. 7-13604
 Fe-Si-B metallic glasses, struct. relax. (Chinese) 7-65070
 Fe-TiB₂ eutectic system, microhardness, modulus of elasticity (Russian) 7-39648
 Fe-W-B metallic glasses, imperfection struct., positron annihilation studies 7-37885
 Fe-Zr-B, amorphous, meas. of Curie temp. 7-2853
 (Fe-B)₈₅Nd₁₅ amorphous films, soft mag. props. 7-53077
 FeB amorphous magnetic thin films, spin wave mode linewidth meas. 7-45826

boron alloys continued

- Fe_{100-x}B_x amorphous alloy, temp. depend. of the resistivity (*Chinese*) 7-27314
- Fe_{100-x}B_x metallic glass system, elec. resist. under press. 7-7200
- Fe₅₀B₅₀ amorphous film, energy-dispersive X-ray diff. meas. 7-63401
- Fe₇₅B₂₅ polymorphous crystallisation into Fe₃B orthorhombic phase 7-37874
- Fe₈₀B₂₀ amorphous, partial pair distribution function determ. 7-51640
- Fe₈₀B₂₀ amorphous alloy, differential AC method of thermopower measurement 7-48776
- Fe₈₀B₂₀ amorphous alloys, EXAFS meas. at B k-edge 7-64807
- Fe₈₀B₂₀ amorphous surface layer produced laser irradiation, thickness meas. using X-ray diff. 7-44304
- Fe₈₀B₂₀ glass metals, temp. depend. of positron trapping effect 7-39292
- Fe₈₀B₂₀ metallic glasses, multiplet splitting, XPS study 7-27858
- Fe₈₀B₂₀ metallic glasses, retardation of annealing embrittlement by Ce microadditions 7-65118
- Fe₈₀B₂₀ ribbons, amorphous and crystallised, surface comp., electronic props., topography, AES, XPS, ion scatt. studies 7-27065
- Fe₈₁B₁₉ amorphous alloy, thermally activated time fluctuations of nucl. spin orientation 7-7622
- Fe₈₁B₁₉ amorphous ribbon, averaged spin orientation under uniaxial compression, Mossbauer spectra study 7-45792
- Fe₈₃B₁₇ amorphous powder, surface struct. rearrangement by pulverisation, CEMS obs. 7-13065
- Fe₈₃B₁₇ metallic glass, struct. relax. X-ray and neutron diff. study 7-6521
- Fe₈₃B₁₇ with V, Cr, Mn or Nb, amorphous, mag. contrib. to thermopower 7-45287
- Fe₈₄B₁₆ amorphous alloy, heterogeneous surface struct., Mossbauer differential conversion electron spectra anal. 7-2319
- Fe₈₄B₁₆ amorphous alloy, layer-by-layer phase anal., depth-selective conversion-electron Mossbauer spectroscopy 7-17255
- Fe₈₄B₁₆ amorphous alloy, interstitial element segregation during fracture (*Russian*) 7-53875
- Fe₈₅B₁₅ high energy heavy-ion irradiation, electrical resistance meas., evidence for electronic energy loss effect 7-58353
- Fe₇₅B₁₅Si₁₀ amorphous alloy powders, rapid quenching water atomisation process 7-46371
- Fe₇₈B₁₂Si₁₀ amorphous, very small angle neutron scatt. 7-44392
- Fe₇₈B₁₂Si₉ amorphous and partially crystalline alloy, high resolution TEM studies 7-21127
- Fe₇₈B₁₂Si₉ amorphous alloys, mag. losses, aging kinetics 7-59056
- Fe₇₈B₁₂Si₉ amorphous ribbons, ferromag. resonance 7-27606
- Fe₇₈B₁₂Si₉ glass reinforced Al composite, fabrication by multi-lamina explosive compaction 7-59482
- Fe₇₈B₁₂Si₉ magnetron sputtered amorphous alloys, thermal, mag. and magnetomechanical props. 7-33249
- Fe₇₈B₁₂Si₉ metallic glasses, retardation of annealing embrittlement by Ce microadditions 7-65118
- Fe₈₀B₁₂Si₈ amorphous alloy ribbons, processing conditions rel. to mag. prop. changes (*Korean*) 7-7919
- Fe₈₀B₁₄Si₆ amorphous ribbons, anisotropy of losses 7-45658
- Fe₈₀B₁₄Si₆ metallic glasses, long-time tunnelling heat relaxation meas. 7-38223
- Fe_{81.5}B_{14.5}Si₄ amorphous, mag. hyperfine fields under stress, Mossbauer study 7-22166
- Fe₈₂B₁₂Si₆ amorphous, initial crystallisation 7-44387
- Fe₈₃B₁₂Si₅ metallic glasses, crystn., magnetisation, scaling, mag. relax. meas. 7-63496
- Fe_{81.4}Si_{3.5}C₂ metallic glass, laser beam irradiation, high energy, shear band form. and cracking 7-59606
- Fe₈₀B₁₆Si₂C₂ metallic glasses, retardation of annealing embrittlement by Ce microadditions 7-65118
- Fe_{81.3}Si_{3.5}C₂ amorphous and cryst. alloy, Si diffusion and segregation 7-6859
- Fe_{81.3}Si_{3.5}C₂ Metglass 2605 SC, surface crystn. behaviour 7-58154
- Fe_{81.5}Si_{3.5}C₂ amorphous ferromag. alloy, acoustic waves, mag. field induced changes 7-2917
- Fe_{71.6}Si₆Cr₂ metallic glass, crystallisation, DSC and X-ray diff. studies 7-11932
- Fe_{90-x}B_xZr₁₀ amorphous, B addition effect on mag. props., elec. resistivity, crystallisation (*Chinese*) 7-7487
- Fe₇₀(CeNdPr)₂₀B₁₀ rapidly quenched ribbons, hard mag. props. 7-27562
- (FeCo)₈₀B₂₀ amorphous ultrafine particles, mag. props. 7-53063
- (Fe_{1-x}Co_x)₈₀B₂₀ amorphous alloy, crystallisation kinetics (*Korean*) 7-26638
- (Fe_{1-x}Co_x)₈₄B₁₆ amorphous alloy, temp. depend. of the resistivity (*Chinese*) 7-27314
- Fe₆₇Co₁₈B₁₅S metallic glass, magnetic aftereffect, thermal treatment, positron lifetime study 7-38907
- (Fe_{1-x}Co_x)₇₇B₁₃Si₁₀ amorphous alloys, Mossbauer study 7-7623
- Fe₆₇Co₁₈B₁₄Si₁ amorphous mag. alloy, crystallisation, elec. resist., TEM obs. 7-11927
- Fe₇₄Co_{10-x}Cr_xB₁₆ amorphous alloys, form. and crystn. 7-11930
- Fe₇₄Co_{10-x}Cr_xB₁₆ amorphous, prep. by melt spinning, X-ray diff., DSC, Mossbauer studies 7-46369
- Fe₂Co_{70-x}Cr_xSi₁₀B₁₅, x=0, 3, 6, 9, amorphous ferromagnet, 180° domain wall (*Korean*) 7-33198
- Fe_{5.85}Co_{72.15}Mo₂B₁₅Si₅ amorphous ribbons traversed by DC electric currents excess resistance, collective motion of ferromag. domain walls 7-32989
- (Fe_{1-x}Co_x)₇₈Si_{9.5}B_{12.5} amorphous alloys, density of states, XPS studies (*Chinese*) 7-13320
- Fe₆₇Co₁₈B₁₄Si₁ mean positron lifetimes after annealing (*Chinese*) 7-27814
- Fe_{90.5}Cr₂B₂₀ metallic glasses, electron transport props., disorder and mag. effects 7-52563
- Fe_{85.2}Cr_{7.5}B₁₅(Ni₄B₁₅) metallic glasses, mag. and elec. props. 7-13002
- Fe₄₃Cr₂₅Ni₂₀B₁₂ glass, devitrification, mag. meas. and X-ray diff. studies 7-21128
- Fe₇₀Cr₅Si₁₀B₁₅ metallic glass, field electron emission 7-33530
- Fe_{75-x}Cr_xSi₁₀B₁₅, x=0, 2, 4, 6, amorphous ferromagnet, 180° domain wall (*Korean*) 7-33198
- Fe_{90-x}Cr_x(SiB)₂₀ amorphous alloy, induced anisotropy, melt spinning effects (*Russian*) 7-59004
- (Fe_{1-x}M_x)₈₄B₁₆ (M=Co,Ni) thermoelectric power, influence of Ci(Ni) additives 7-32995
- (FeM)₈₀B₁₄Si₆, M=Mn, Mo, V, glass, magnetoresistance 7-64203
- (Fe_{1-x}Mn_x)₇₈B₂₂ amorphous alloys, lattice parameters, annealing, X-ray diff., elec. resist. 7-37878

boron alloys continued

- (Fe_{1-x}Mn_x)₈₄B₁₆ amorphous, Mn content effect on elec. resistivity (*Chinese*) 7-12692
- Fe₇₅Mo₅Si₁₀B₁₀ amorphous, structural relax. and quasi-texture 7-11925
- Fe₁₄Nd₂B magnets, high-field magnetostriction 7-53104
- Fe₁₄Nd₂B permanent magnet, Dy substituted positron annihilation studies 7-3108
- Fe₇₆Nd₁₆B₈ plasma sprayed permanent magnets, characts. 7-45754
- Fe₇₇Nd₁₅B₈ sintered permanent magnets, domain wall obs. 7-27544
- Fe₇₇Nd₁₅B₈-based melt spun ribbons, crystallisation and mag. props. 7-26662
- Fe₁₄Nd(Y)(Ce)₂B fine particles prep. by hydriding, mag. props., recording apps. 7-53660
- (Fe_{0.15}Ni_{0.85})₇₅P₁₆B₆Al₃ static scaling in an amorphous metallic spin glass 7-38871
- (Fe_{1-x}Ni_x)₈₀B₂₀ amorphous, contribution of Ni to hyperfine fields (*Korean*) 7-27636
- (Fe_{1-x}Ni_x)₈₄B₁₆ amorphous alloy, temp. depend. of the resistivity (*Chinese*) 7-27314
- Fe₄₀Ni₄₀B₁₀, Fe₃₀Cr₁₀Ni₄₀B₂₀ metallic glass, fracture toughness rel. to prep. and struct. 7-53870
- Fe₄₀Ni₄₀B₂₀ amorphous, positron annihilation studies 7-45859
- Fe₄₀Ni₄₀B₂₀ amorphous thin films, coercive field, annealing effects 7-7553
- Fe₄₀Ni₄₀B₂₀ amorphous and crystalline, elec. resistivity, temp. dependence 7-21892
- Fe₄₀Ni₄₀B₂₀ amorphous metallic films, SAX investig. (*Russian*) 7-51576
- Fe₄₀Ni₄₀B₂₀ amorphous alloys, domain wall motion, SEM obs. 7-52978
- Fe₄₀Ni₄₀B₂₀ amorphous alloy, Barkhausen noise, neutron irradiation effect 7-53029
- Fe₄₀Ni₄₀B₂₀ amorphous alloy, effect of plastic deform. on mech. and mag. props. (*Russian*) 7-53810
- Fe₄₀Ni₄₀B₂₀ concentration dependence of surface insulating coating, influence on magnetic props. 7-64479
- Fe₄₀Ni₄₀B₂₀ metallic glass ribbon, failure mechanics and atom probe study correlations 7-28139
- Fe₄₀Ni₄₀B₂₀ metallic glass, neutron diff. struct. factors determ. 7-51654
- Fe_{45.5}Ni_{44.5}B_{10.3} amorphous, internal friction, thermo-EMF struct., annealing effect (*Russian*) 7-59560
- Fe₅₀Ni₃₀B₂₀ amorphous alloys, domain wall motion, SEM obs. 7-52978
- Fe₅₁Ni_{49-x}B₂₀ amorphous ferromagnets, elec. resist. and thermopower meas., comp. and temp. depend. 7-45263
- Fe_xNi_{80-x}B₂₀ XRF and PIXE surface anal. 7-12411
- Fe₅₁Ni_{49-x}B₁₂Si₂ glassy alloys, variation of mag. inhomogeneity 7-45634
- Fe₃₀Ni₃₆Cr₁₂Mo₂Si₅B₁₅ amorphous alloy, Curie temp., press. effect 7-52976
- Fe₃₃Ni₄₀Mo₄B₁₈ metallic glass, positron annihilation (*Chinese*) 7-64726
- Fe₄₀Ni₃₈Mo₄B₁₈ amorphous, positron annihilation studies 7-45859
- Fe₄₀Ni₃₈Mo₄B₁₈ amorphous alloys, thermal devitrification kinetics 7-51651
- Fe₄₀Ni₃₈Mo₄B₁₈ metallic glass, conversion electron Mossbauer spectra 7-48926
- Fe₄₀Ni₃₈Mo₄B₁₈ soft ferromag. metallic glasses, domain wall motion and energy dissipation studies 7-64478
- Fe₄₀Ni₄₀Mo₄B₁₆ amorphous alloys, positron annihilation peakrate temp. depend. meas. 7-39302
- (FeNi)₇₈Mo₄B₁₇Si metallic glass, mag. shielding props., composition depend. 7-27558
- Fe₄₀Ni₃₈Mo₄B₁₆Si₂ ferromag. amorphous ribbons by field quenching technique, mag. anisotropy 7-33164
- Fe₄₀Ni₄₀P₁₄B₆ amorphous alloy, relax. struct. transforms., 80 to 300K 7-1890
- Fe₄₀Ni₄₀P₁₄B₆ amorphous alloys, annealing, positron annihilation parameters anal. 7-39303
- Fe₄₀Ni₄₀P₁₄B₆ amorphous ribbon, magnetoelastic, Matteucci effect meas. (*Spanish*) 7-53103
- Fe₄₀Ni₄₀P₁₄B₆ ferromag. amorphous alloy, struct. relax., effect of surface 7-28062
- Fe₄₀Ni₄₀P₁₄B₆ metallic glass, heterogeneous struct., EXAFS study 7-27816
- Fe₄₀Ni₄₀P₁₄B₆ metallic glasses, multiplet splitting, XPS study 7-27858
- Fe₄₀Ni₄₀P₁₄B₆ metallic glasses, superplastic deform. (*Russian*) 7-39599
- Fe₄₀Ni₄₀P₁₄B₆ Metglas 2826, magnetic ribbons, inverse Wiedemann effect for very low torsions 7-45786
- Fe₄₀Ni₄₀P₁₄B₆ Metglas 2826, crystn. behaviour, influence of annealing atm. 7-53768
- Fe₄₀Ni₄₀P₁₆B₄ amorphous and crystallised alloys, surface oxidation behaviour 7-59666
- (Fe_{0.15}Ni_{0.85})₇₅P₁₆B₆Al₃ amorphous spin glasses, relaxation 7-53000
- (Fe_{0.15}Ni_{0.85})₇₅P₁₆B₆Al₃ metallic spin glass, time decay of saturated remanent magnetisation 7-59058
- (Fe_{0.5}Ni_{0.5})₇₅P₁₆B₆Al₃ metallic glass, struct. relax., theory (*Russian*) 7-44397
- Fe₇₀Ni₅Si₁₀B₁₂ amorphous and cryst. states, oxidation (*Russian*) 7-53993
- Fe₂₀Ni₅₈Si_{10.08}B_{10.14} amorphous viscoelastic behaviour 7-21348
- (Fe_{0.6}Ni_{0.4})₈₂Si₁₀ amorphous alloys, structural relax. and crystn., positron annihilation studies 7-37869
- (Fe_{1-x}Ni_x)₇₇Si₁₀B₁₃ amorphous, structural anal. (*Korean*) 7-26655
- (Fe_{1-x}Ni_x)₇₇Si₁₀B₁₃ amorphous, effective mag. moment, Curie temp. (*Korean*) 7-27503
- Fe₁₀Ni₆₅Si₁₀B₁₅ spin glass, amorphous, effect of phase segregation during struct. relax. 7-39517
- Fe₄₀Ni₄₀Si₁₄B₄ metallic glass, positron trap depth distrib. determ., lifetime and Doppler effect meas. 7-39304
- Fe₇₀Ni₅Si₁₀B₁₂ amorphous alloys, thermal devitrification kinetics 7-51651
- Fe₇₅Ni₅Si₁₀B₁₃ amorphous, structural relax. and quasi-texture 7-11925
- (Fe₇₀Ni₃₀)₇₇Si₁₀B₁₃ amorphous spin glass, dynamic mag. susceptibility and critical phenomena (*Russian*) 7-7511
- Fe_{0.44}Ni_{0.76}Si_{0.78}B_{14.56}Co_{0.25} amorphous filler metal, struct. props. (*Korean*) 7-32292
- Fe₈₂P₁₁B₇ metallic glass, mag. anisotropy and correlated hyperfine interactions 7-7505
- FeSiB amorphous alloy, double-layer struct. unit model 7-16423
- Fe₇₇Si₁₀B₁₃ as-quenched and cold-rolled amorphous alloy, mag. props. 7-33219
- Fe₇₈Si₁₀B₁₂ amorphous ribbons, X-band ferromag. resonance, transmission of microwaves 7-27607
- Fe₇₈Si₁₀B₁₂ amorphous alloys, surface crystallisation and mag. props. 7-51649

boron alloys continued

Fe₇₈Si₂₁B₁₃, amorphous, tensile strength, elastic stiffness (Japanese) 7-3346
Fe₇₈Si₂₁B₁₃ amorphous ribbons, magnetoelastic effects on practical props. 7-33252
Fe_{90-x}Si₁₀B₁₀ amorphous alloys, multistep-micro-crystallisation studies 7-21129
(Fe_{1-x}W_x)_{84.5}B_{15.5} amorphous, low temp. resistivity anomaly (Chinese) 7-64198
Fe_{84-x}W_xB₁₆ amorphous alloys, crystn., products and kinetics 7-51677
(Fe_{1-x}W_x)_{84.5}B_{15.5} amorphous alloys, elec. and mag. props. (Chinese) 7-12969
Fe_{77-x}Si₇B₁₅ amorphous wires, Barkhausen and Matteucci effects, influence of tensile and compressive stress 7-33254
Gd₂Fe₁₄B alloys, magnetic anisotropy and spin reorientations 7-38855
Gd₂La_{0.5-x}Co_{2.5}B₁₀ mixed glasses, mag. props., phase transitions, microstruct. effects 7-64465
Ge_{80-x}Mn_xB₂₀ amorphous alloy, Curie point and crystallisation temp. 7-17173
Ho₂Fe₁₄B alloys, magnetic anisotropy and spin reorientations 7-38855
Ho₂Fe₁₄B single crystals, mag. anisotropy and magnetisation 7-27547
Ho₂Fe₁₄B spin reorientation, NQR meas. 7-52960
LaB₆, Fermi surface, 2D angular correlation of positron annihilation radiation 7-39241
La₂Ce_{1-x}B₆, Zeeman splitting, thermodynamics of Coqblin-Schrieffer model 7-58783
(La_{1-x}Ce_x)₂Fe₁₄B rapidly quenched ribbons, hard mag. props. 7-27549
Mn-P-B system, isothermal cross section at 1070K, lattice parameters of phases 7-53702
Mo-Bi-Si thermomdiffusion coating on Nb-Mo-Zr alloy, oxidation protection, heat resist. 7-8156
Nb-Hf-B system, phase equilib. in Nb corner 7-46415
Nb₇₃Al₂₇Si_{14.5}B_{0.5}, A-15 superconducting tapes for high mag. fields, fabrication 7-33133
Nb_{100-x}B_x alloy films, sputtered, elec. cond., hardness, amorphous and crystal struct. 7-13354
(Nd,Tb)₁₆₇Fe_{75.5}B_{7.8}, magnetisation meas., spin reorientation temp. 7-17161
Nd-Dy-Fe-B based sintered magnet, microstruct., heat treatment effects 7-53767
Nd-Fe-B, metastable amorphous alloys, crystn., thermal stability 7-39482
Nd-Fe-B, microstructure, scanning tunnelling microscopic studies 7-58494
Nd-Fe-B, permanent mag. alloy, Mossbauer spectroscopic study (Chinese) 7-7613
Nd-Fe-B, phase diagram, permanent mag. anal. 7-39486
Nd-Fe-B amorphous ribbons, effect of crystallisation conditions on hard mag. props. 7-27561
Nd-Fe-B based permanent magnets, hysteresis loop and mag. anisotropy 7-53031
Nd-Fe-B liquid-quenched alloys, mag. props. 7-27550
Nd-Fe-B permanent magnet, microstructure and coercivity 7-27559
Nd-Fe-B permanent magnets, prod. by hydrogen decrepitation/attritor milling route 7-22606
Nd-Fe-B permanent magnets, BCC phase mag. props. at grain boundaries 7-53044
Nd-Fe-B rapidly solidified permanent magnet materials, magnetisation processes and domain wall motion 7-38902
Nd-Fe-B rapidly solidified ribbons, magnetisation, quench rate depend. 7-53034
Nd-Fe-B sintered magnets, hysteresis loops, anal. 7-33215
Nd-Fe-B system, permanent magnet, mag. props (Korean) 7-7554
Nd-Fe-B system, temp. depend. of coercive force, effect of annealing, aging and sintering 7-27560
Nd-Fe-B-Co-Al based permanent magnets, mag. props. and temp. characts. 7-53045
NdB₆, Fermi surface, 2D angular correlation of positron annihilation radiation 7-39241
Nd₂Co₁₄B, NMR study 7-64544
Nd₂Co₁₄B, spin arrangements, 4.2-1100K 7-22094
Nd₂(Co₂Fe_{1-x})₁₄B alloys, mag. struct., preferential site occupation 7-45619
NdDyFe₁₄B spin orientation and preferential 4f site occupation, powder neutron diffr. study 7-22100
Nd₂(Fe_{0.67}Al_{0.33})₁₄B, reduction of mag. hyperfine fields and Curie temp. on Al substitution, Mossbauer spectra 7-38859
NdFeB, anisotropic permanent magnet, prep. and investig. 7-52969
Nd₂Fe₇B₈ based pseudobinary alloys, sintered permanent magnets, depend. of coercivity on anisotropy field 7-45744
Nd₁₅Fe₇B₈ permanent mag., rotational hysteresis energy and magnetisation reversal 7-64492
Nd₂Fe₁₄B alloys, magnetic anisotropy and spin reorientations 7-38855
Nd₂Fe₁₄B, cryst. field effects 7-45598
Nd₂Fe₁₄B, EFG tensor for interpretation of Mossbauer effect meas. near spin reorientation temp. 7-38968
Nd₂Fe₁₄B, elastic props. between 120 to 300K 7-27529
Nd₂Fe₁₄B, magnetic props., H₂ absorption effects 7-38906
Nd₂Fe₁₄B permanent magnet materials, prep. and props., book contrib. 7-27981
Nd₂Fe₁₄B permanent magnet, magnetic anisotropy const. determ. from unsaturated torque curves 7-52973
Nd₂Fe₁₄B single crystals, mag. anisotropy and magnetisation 7-27547
Nd₂Fe₁₄B sputtered films, perpendicular anisotropy 7-53073
Nd₂Fe₁₄B untextured polycryst., magnetic hyperfine fields, Mossbauer spectra anal. 7-12682
Nd₂Fe₂₃B₃, struct., Curie temp., X-ray diffraction anal. 7-11994
NdFeB-CoAl magnets, Curie temp., coercive force and magnetisation 7-52982
Nd₂Fe_{14-x-y}Co_xAl_yB alloys, permanent mag. props. 7-45755
Nd₂Fe_{14-x}Co_xB system, mag. phase transitions and anisotropy 7-27524
Nd₂Fe_{14-x}M_xB, (M=Co,Ni,Cu,V,Al,Cr,Mn), crystallographic and mag. props. 7-27522
Nd₂Fe_{12-x}Mn_xCo₂B, mag. props. 7-52946
Nd₂Fe_{14-x}Ru_xB alloys, mag. props., comp. depend. study 7-7547
Nd₂(Fe_{0.67}Si_{0.33})₁₄B, reduction of mag. hyperfine fields and Curie temp. on Si substitution, Mossbauer spectra 7-38859
NdHoDyFeB permanent magnets with zero temp. coeff. of induction 7-53047
Nd_{2-x}R_xFe₁₂Co₂B, mag. characts. 7-45670
Nd₂(Y₂)(Fe_{1-x}Al_x)₁₄B, intrinsic and permanent mag. props. (Chinese) 7-13003

boron alloys continued

Ni-Al-B, rapidly solidified, grain boundary segregation of B, atom probe FIM 7-22688
Ni-Al-B-based alloys, site occupations, APFIM and channelling studies 7-32367
Ni-B, electroless, heat induced struct. changes 7-13639
Ni-B, precipitation and B grain boundary segregation studies 7-33673
Ni-B, with transition metal additives, amorphous, mag. scatt. influence on transport props. 7-33001
Ni-B amorphous alloys, crystallisation produced by ion implantation, TDPA study 7-32288
Ni-B amorphous and crystalline alloys, vibr. density of states 7-38146
Ni-B amorphous films, ion implanted and sputtered, elec. props. 7-22032
Ni-B based electrochemical coatings, heat resistance, oxidation 7-3499
Ni-B-C-based alloys, γ phase, prolonged ageing effects (Russian) 7-59551
Ni-B-Si alloy liquid metal ion sources, ion formation 7-64878
Ni-B-Si ternary system, liq.-solid equilib. in Ni-rich region (French) 7-65004
Ni-Mo-B(P), metallic glasses, depth-composition profile, X-ray photoelectron study 7-63928
Ni-Mo-Cr-B powders, amorphous and microcrystalline, shock consolidated, wear props. 7-46655
Ni-P-B electroless coatings, prep. and deposit characts. 7-59671
Ni-Si-B, nonferromagnetic amorphous wide ribbons, Young's modulus anisotropy 7-3354
Ni-Si-B amorphous alloy films, electrical resistance and activation energy 7-27315
Ni-Si-B amorphous ribbons, surface charactn. 7-12420
Ni₃Al-B, elevated temp. ductility, effect of testing environment 7-39614
Ni₃Al-B, grain boundary adhesion 7-16350
Ni₃Al-B, with and without Hf additions, dynamic embrittlement at 600°C 7-65112
Ni₃Al-B rapidly solidified alloy, B distrib. at grain and antiphase boundaries, atom probe FIM and TEM studies 7-33637
Ni₃Al-B-Hf alloys, B and Hf grain boundary segregation, ductility, atom probe FIM study 7-33675
Ni₃Al(B,Ti), rapidly solidified powders, struct. of consolidated products 7-3222
Ni₃AlHfB/Ni couples, up-hill Hf interdiffusion studies 7-12378
Ni₃B, amorphisation by ion implantation, RBS/channelling studies 7-11912
Ni₃B, amorphous, surface electronic struct. during crystallisation and O₂ and CO adsorption 7-7308
Ni₃B/Ni eutectic, SEM and HREM struct. and chem. anal. 7-17515
Ni₄B₃₆ amorphous alloy, struct., boundary effects, computer simulation study (Chinese) 7-11920
Ni₆₄B₃₆, metallic glass, struct. relax. X-ray and neutron diffr. study 7-6521
Ni₃₀B₅₄C₁₆, B-rich amorphous alloy prep. by rapid quenching, crystn., hardness and elec. resist. 7-13441
Ni₇₅B₁₅Si₁₀ amorphous alloy, metalloid redistribution, scanning Auger microprobe study 7-32655
Ni₇₅B₁₇Si₈, ultrafine fine-grained, prep. from amorphous ribbon, creep deform. 7-22748
Ni₇₅B₁₇Si₈, ultrafine grained, creep deformation mechanisms 7-22781
Ni₈₃Cr₇Fe₂Si₄B₃, amorphous alloy, crystallisation (Chinese) 7-6518
NiCrSiB alloy coatings, sputter deposition, microstruct. variations 7-46351
Ni₆₉Cr₆Si_{13.7}B_{7.5}Fe_{2.6}, amorphous alloy, 70 MeV Ni⁶⁺ ion irradi., surface swelling 7-16646
(Ni_{1-x}Cu_x)₇₇B₁₃Si₁₀ pseudobinary metallic glass, low-temp. sp. ht. studies 7-12309
Ni_{52.5}Mo₃₉Cr₈B_{1.5} metallic glass, shock consolidated, wear props. 7-28154
Ni₇₇Si₈B₁₅, amorphous, tensile strength, elastic stiffness (Japanese) 7-3346
Ni₇₈Si₁₀B₁₂, metallic glass, shear crack propag. 7-65113
Ni₈₀Si₁₀B₁₀, Ni₈₀Si₁₅B₅ metallic glass, fracture toughness rel. to prep. and struct. 7-53870
Pd-B alloys, thermodynamic props. (German) 7-21486
Pd-B-H alloys, internal friction, elastic const. 7-26857
Pd-B-H dilute solutions, statistical mechanics 7-21669
Pd-Fe-B, mag. susceptibility, impurity effects 7-27520
Pd_{0.67}B_{0.33}, amorphous, prep. by low temp. ion beam mixing (Chinese) 7-51887
Pr-Co-B system, phase diagram over complete conc. range 7-3281
Pr₂Fe_{14-x}Co_xB system, struct. and magnetism 7-45631
PrB₆, Fermi surface, 2D angular correlation of positron annihilation radiation 7-39241
Pr₂Co₁₄B, spin arrangements, 4.2-1100K 7-22094
PrCo_{4-x}Fe_xB, crystallographic and mag. props. 7-45671
Pr₁₅Fe₇B₈, sintered permanent magnets, depend. of coercivity on anisotropy field 7-45744
Pr₂(Fe_{1-x}Co_x)₁₄B, mag. props. 7-64549
Pr_{2-x}R_xFe₁₂Co₂B, (R=Dy, Tb), mag. characts. 7-45670
Pu-Os-B system, phase equilibria and cryst. struct. 7-16781
Pu-Rh-B system, phase equilibria and cryst. struct. 7-16781
Pu-Ru-B system, phase equilibria and cryst. struct. 7-16781
R₂Co₁₄B, permanent magnet, props. and struct. 7-53053
R₂Fe₁₄B, cryst. field effects at rare-earth sites 7-45598
R₂Fe₁₄B, permanent magnet, props. and struct. 7-53053
R₂Fe_{14-x}Co_xB, spin reorientations 7-64484
R₂Fe_{14-x}Mn_xB (R= Y, Nd, Pr, Gd), mag. characts. 7-27523
R₂Fe_{12-x}Mn_xCo₂B (R= Pr, Gd), mag. props. 7-27500
Rh-B surface, effect of B surface segregation on adsorption and dissociation of H₂O 7-27135
Ru_xFe_{80-x}B₂₀ amorphous alloys, magnetic phase diagram, magnetisation and Mossbauer studies 7-53042
Sm-Co-B rapidly quenched ribbons, hard mag. props. and struct. 7-53048
Sm-Fe-Co-B-Si melt-spun alloys, mag. props. 7-27553
Tb₂Co₁₄B, spin arrangements, 4.2-1100K 7-22094
URh₃B, 5f band narrowing, evidence from resonant photoemission 7-27855
URu₃B, 5f band narrowing, evidence from resonant photoemission 7-27855
β-V-B, rhombohedral phase, struct. and solid solubility, X-ray single cryst. diffr. study 7-1948
W wire reinforced amorphous Ni₇₅B₁₇Si₈ matrix composite ribbons, melt spinning prep. 7-46373

boron alloys continued

- WC-Co-B system, formation mechanism of composite coating, electro-phoresis 7-3208
 Y-Fe-B system alloys, mag. props. 7-27563
 $Y_2Co_{14}B$ intermetallic cpd., electronic struct. and mag. props., tight-binding calcs. 7-2450
 $Y_2Co_{14}B$, NMR study 7-64544
 $Y(Dy)(Er)_{2-x}Th_3Fe_{14}B$ alloys, mag. props., comp. depend. study 7-7492
 $Y_2(Fe,Al,Co)_{14}B$, mag. props., composition depend. 7-53030
 $Y_7Fe_{14}B$, electronic struct. and mag. props. recursion method calcs. 7-2452
 $Y_2Fe_{14}B$, magnetic props., H_2 absorption effects 7-38906
 $Y_2Fe(Co)_{14}B$ alloys, magnetic anisotropy and spin reorientations 7-38855
 $Y_2Fe_{14-x}Si(Cu)B$ alloys, mag. props. 7-45681
 YRh_2B , supercond. and mag. props. 7-38800
 $YbCoB_4$, YCrB₄-type structure, formation in Yb-Co-B ternary systems 7-6581
 $YbFeB_4$, YCrB₄-type structure, formation in Yb-Fe-B ternary systems 7-6581
 $Yb_2Fe_{14}B$, exchange and cryst. field interactions 7-27512
 $YbNiB_4$, YCrB₄-type structure, formation in Yb-Ni-B ternary systems 7-6581

boron compounds

- see also borate glasses; boron alloys; borosilicate glasses
 B_2C , thermal stress fracture, grain size and porosity effects (Japanese) 7-8087
 BA, structural and electronic props., pseudopotential method, local density approx. 7-32353
 borate minerals, unoccupied mol. orbitals of B-O bond mol. orbital calcs., XANES, NMR and electron transmission spectra 7-33281
 $BS, X_2^{2+}, A^+ \pi, B^+ \Sigma^+$ states, potential energy curves, dissociation energy calcs. 7-50290
 P-carborane, plastic cryst. phases, mol. notions 7-63528
 icosahedral boron-rich solids 7-63537
 LWR spent control and absorber rods, T content for waste disposal 7-25245
 neutron capture therapy, boron containing nucleosides prep. 7-34249
 neutron capture therapy, novel boronated porphyrins 7-34250
 polypyrrole- BF_4^-O , dopant distrib., atom probe anal. 7-32480
 powdered B with acid and anhydride components, O and H content eval. 7-27964
 B/N coatings, ion plating, amorphous struct., wear resist. 7-22580
 BBr_3 , electron impact, Auger and Coster-Kronig spectra 7-15719
 B_2C , fast neutron irradiated, thermal cond. meas. 7-6900
 B_2C , neutron irradi., damage effect 7-36104
 B_2C ceramics, pressureless sintering with polycarbosilane addition 7-46389
 $B_{10}C_2H_{12}$, spin-lattice relax., $^{10}B, ^{11}B$ NMR 7-10623
 BCl_3 , 0-0 vibr. band, rot. constants, visible spectra anal. 7-50157
 BCl_3 , electron impact, Auger and Coster-Kronig spectra 7-15719
 BCl_3 , two-photon reson. spectroscopy of vibr. transitions, four-wave freq. mixing conditions 7-25882
 BF^+ radical cations in Ne matrix, generated by laser sputtering and high temp. sources, EPR, CI calcs. 7-25604
 BF_3 , electric-field gradients, NMR shielding tensors, NQR coupling const., ab initio HF calcs. 7-19693
 BF_3 , electron impact, Auger and Coster-Kronig spectra 7-15719
 BF_3 , mol. quadrupole moment and polarisability calcs. 7-10410
 $BF_3.H_2O$, electronic struct., EEL and UV photoelectron spectra, ab initio MO STO calcs. 7-36449
 $BH + H^+$, charge transfer dynamics 7-50331
 $B_{12}H_{12}^{2-}$, electronic struct., MS-Xalpha MO calcs. (French) 7-25390
 B_2H_6 , mol. vibr. coupling, dynamic electron transfers, variational method calcs. 7-36585
 $closo-B_{10}H_{10}^{2-}$ clusters, bond indices, enthalpies, CNDO calcs. 7-10431
 B_4H_4 , polyboranes, nucl. coupling const. HF calcs. 7-19688
 $BHF_2 (BDF_2)$, mol. consts., vibr. anal. 7-50058
 $B_2H_6X_2$, ^{11}B COSY NMR, substituent effects 7-19898
 B_2H_7X , ^{11}B COSY NMR, substituent effects 7-19898
 $^{11}B, a^1\Pi(0^+1) \rightarrow X^1\Sigma^+$ system, rot. anal. UV obs. 7-62397
 $Bl_3-CS_2(COS)$, vapour phase flash photolysis, electronic absorpt. spectra 7-23041
 $(BN)_n$, degeneracy lifting, perturbational approach 7-52399
 BN , complex dielec. const. meas. at 245 GHz using double-beam interferometer 7-7632
 BN , cubic, abrasives, frictional behavior on hard materials 7-3461
 BN , cubic, aggregate tools, microstruct. and wear 7-3462
 BN , cubic, polycryst., influence of sintering conditions on phys. props. 7-22618
 BN , EELS analysis, inner shell excitation profiles visibility 7-22403
 BN , engineering ceramics, prep., fabrication, appls. 7-53683
 BN , film, optical and compositional props. 7-39206
 BN , film, optical energy gap, density, hardness 7-39204
 BN film formation on InSb, plasmachemical methods 7-33584
 BN films, microwave plasma CVD process 7-17435
 BN , graphite-like powder particles, shock compression effects 7-39453
 $c-BN$, high press. sintering 7-22615
 BN , ion-plated, prep. and charact. 7-17477
 BN , laser-induced vaporization mass spectrometry of refractories 7-23079
 BN MIS structures, form. by reactive pulse plasma method, on Si or SiO_2 substrates, phys. props., annealing effects 7-22023
 $c-BN$, phase diagram, p,T,E 7-17517
 BN polycrystals, heat treatment conditions effect on mech. and service props. 7-53894
 BN , polymorphism studies, temp. and press. effects 7-1934
 BN protective coating on ZnS and ZnSe IR transmitting windows 7-46731
 BN , pyrolytic, macrodefects study 7-44523
 BN pyrolytic crucibles for MBE, AES, XPS, SIMS, and bulk anal. after vac. baking 7-53596
 BN samples, quantitative phase anal., elimination of texture effects 7-63771
 BN surface, adsorbed benzene, rot. dynamics and orientation, NMR spectra 7-53161
 BN surface, long range interaction between rare gas atoms/molecules and surfaces, calc. 7-3135
 BN ultrafine powder synthesis at -75 to 750°C 7-22629
 BN , wurtzite, sintered polycryst., texture form. during hot compacting at high press., sphalerite transition 7-53685

boron compounds continued

- BN , wurtzite-like, deformation and high-press. phase transitions 7-44804
 BN , wurtzite-type and zincblende-type, struct. changes by shock treatments 7-22676
 BN , wurtzitic compacts, sintered, particle size distrib., hardness, phase comp. 7-59603
 $BN:Cs(Br_2)$, intercalation cpd. formation 7-44574
 $B_n m^+$ cluster ions in laser plasma, laser ionisation mass spectrometry (German) 7-42816
 BO , electron affinities evaluation 7-5591
 BO , photolysis products, UV electronic absorpt. spectra 7-23041
 $BO + O_2$, gas-phase oxidation, rate consts., fluoresc. and chemiluminesc. study 7-22985
 BO_4^- anion clusters, hard basicity 7-25402
 B_2O_3 , melt, emissivity, nodal analysis (French) 7-63854
 $B_2O_3-SiO_2-M_2O$ ($M = Na, K$) glasses, ion implantation effects appl. for radioactive waste disposal 7-32519
 $B(OH)_3$, electron density, X-ray diffr. determ. at 105 K, ab initio calcs. 7-44458
 $BP(As)O(S)_4$, dielec. const. meas. w.r.t. bond ionicity (French) 7-38988
 BS , photolysis products, UV electronic absorpt. spectra 7-23041
 BS_2 , photolysis products, UV electronic absorpt. spectra 7-23041
 $B_{12}Y_{12}^{2-}$, ($Y = H, D, F, Cl, Br, I$) mol. vib., normal coordinate anal. 7-913
 $^{11}BF_3$, ground vibr. state, rot. transitions, microwave spectra anal. 7-50086
 $BaOTiO_2-B_2O_3$, phase equilib. 7-46430
 HBF_4 , rot. anal., microwave spectra 7-19832
 $Mg-B_{12}H_{12}$, stable conform., SCF-MO calcs. 7-15477
 N_2BH_3 , struct., ab initio calcs. 7-49887
 $Nb_2O_5-Al_2O_3-B_2O_3-Na_2O-SiO_2$, phase separable glass, heat treatment leaching, X-ray diffraction anal. 7-51658
 $NiSi_2-Si-BF_2$, epitaxial growth of $NiSi_2$, influence of dopant atoms 7-45039
 $(PBr_2)^+(BBr_4)^-$ complex, mol. vibr., Raman and IR spectra anal. 7-46021
 $PbO-B_2O_3$ flux, solubility of YIG, validity of anionic model 7-52062
 $PbO-B_2O_3$ optical glass, props. and structure, effect of heat treatment 7-20377
 $Si : BF_2$ preamorphised implanted samples, defects and leakage currents abs. 7-38514
 $Si:BF_2$, ion implanted, diffusion and defects, transient scanning electron beam annealing 7-38065
 $Si:BF_2$ wafers, activated carrier density profile and scatt. rate meas., non-destructive IR attenuated total refl. technique 7-22207
 $n-Si:BF_2^+$, ion implanted, rapid thermal annealing, DLTS 7-16619
 $Si:BF_2^+$, ion implanted, characterisation by IR attenuated total reflection spectroscopy 7-17327
 $Si:BF_2^+$, ion implanted, solid phase epitaxial growth, cross-sectional TEM study 7-38364
 $Si:BF_2^+$, p-n junction diode, rapid thermal annealing 7-22005
 $Si:BF_2^+(001)$, ion implanted, residual defects, cross-sectional TEM study 7-32471
 $Si:BF_2^+ p^-n$ diodes, BF_2^+ -implanted and rapid thermal annealed, junction leakage currents meas. 7-12814
 $Si:BF_2^+$ submicron p-n junctions, ion implanted, dopant distrib., Raman study 7-21252
 $a-Si:H, B_2H_6$, localised density of states, electrophotography study 7-32957
 $Si-B_2O_3$ interaction during Si MBE, Auger spectra study 7-13277
 $SiBF_3$, ion implantation damage, backscattering channelling meas. 7-63675
 $SiC-B_2C$, eutectic composites, microstruct. and mech. props. 7-64991
 $TiN-BN$, hard composite coatings, deposition and props. 7-46623
 $V_2O_5-As_2O_5-B_2O_3$, vitreous, elec. cond., semiconducting props. 7-2620
- boronising** see surface hardening
- borosilicate glasses**
 ATM-2 glass, Am-doped, Am concentration in solutions 7-32659
 birefringent fibre waveguide cladding, polarisation characts. study 7-62835
 borophosphosilicate glass, composition determ. by Rutherford backscatt. 7-17383
 borophosphosilicate glass film, rapid isothermal fusion 7-21425
 coating films, prep. by sol-gel method 7-46310
 corrosion studies, conventional and glancing angle EXAFS 7-59284
 devitrified simulated HLW glass, leaching, crystalline phases effects 7-49690
 dissolution method study using fission track method 7-53937
 durability, influence of $CS_2(O_2S)(U_3O_8)(ZnO)$ 7-8144
 E-glass, coord. of iron, ESR and mag. meas. 7-13021
 fission track etching using deionized water 7-53938
 HLW fixation in borosilicate glass, characts. in repository conditions 7-5458
 leaching behaviour, mol. struct. effects 7-21530
 low alkali borosilicate glasses, electrical resistivity, depend. on composition 7-58806
 mirror, replicated, appl. to large segmented opt. systems 7-37088
 mirror, telescope, Texas Univ. 7.6m design, progress report 7-40710
 mirror blank, honeycomb sandwich, prep. by spin casting 7-37225
 mirror segments, lightweight glass, development for Large Deployable Reflector 7-37226
 nuclear waste and vitrification chemistry 7-5446
 nuclear waste glass, leach behavior, devitrification 7-19532
 nuclear waste glass performance in geologic environment 7-5449
 nuclear waste glass suitability study, systems approach, preference to borosilicate glasses 7-5447
 nuclear waste glass vapourisation study 7-6774
 nuclear waste glasses, leached, containing U, EXAFS with grazing incidence 7-3116
 Pyrex, shock loading meas., impact failure modes determ. 7-33798
 simulated borosilicate radwaste glass, granite and water, geochemical interactions, repository appl. 7-807
 softening point determ., numerical method, calculator program (Czech) 7-6796
 solubility tests for HLW immobilisation 7-30705
 substrates with LiF:Mg,Ti layer, laser stimulated thermolum. 7-64703
 thermodynamics, miscibility and phase separation 7-63498
 ultrasonic velocity, variation during annealing (Russian) 7-26099
 uranyl borosilicate glass, excited states, fluoresc. 7-25588
 wetting by nitromethane- CS_2 liq. mixture 7-6927

borosilicate glasses continued

Al₂O₃-B₂O₃-SiO₂-Cu₂O glass, Cu activated, photoconductivity, lumin., influence of radiation defects 7-45381
B₂O₃-SiO₂:U(Np), doped glasses, optical spectroscopy study 7-39145
B₂O₃-SiO₂ glass, borosiloxane bond formation, sol-gel process, spectroscopic study 7-59117
B₂O₃-SiO₂-Li₂O-Na₂O-ZnO glasses, chemical durability 7-8143
B₂O₃-SiO₂-M₂O (M = Na, K) glasses, ion implantation effects appl. for radioactive waste disposal 7-32519
CdO-B₂O₃-SiO₂ glasses, photochromism, photocond. and ESR (*Japanese*) 7-22282
CsBSi₃O₆, glassy and crystalline, IR spectra 7-59199
Cu-ruby glasses, optical props., transmission and attenuation spectra 7-13177
KBSi₃O₆, glassy and crystalline, IR spectra 7-59199
Na₂O-B₂O₃-Nd₂O₃, SiO₂ substituted, leaching of Na₂O-B₂O₃, X-ray study of NdBO₃ 7-51657
Na₂O-B₂O₃-SiO₂, interaction with HNO₃, effect of volumes, radii of channels 7-13613
Na₂O-B₂O₃-SiO₂, Na desorption during X-ray microanalysis 7-23114
Na₂O-B₂O₃-SiO₂ glass, porous, sintering temp, glass transition temp. (*Japanese*) 7-7954
Na₂O-B₂O₃-SiO₂ glass ceramic, prep., SiO₂ replacement, phase separation, struct. 7-13428
Na₂O-B₂O₃-SiO₂ glass, Na⁺ self-diffusion and elec. cond. studies 7-21515
Na₂O-B₂O₃-SiO₂ glasses, liq. immiscibility rel. to trivalent oxide additions 7-39516
Na₂O-B₂O₃-SiO₂ ThO₂-rich porous glass ceramic, phase separation (*Afrikaans*) 7-13439
Nb₂O₅-Al₂O₃-B₂O₃-Na₂O-SiO₂, phase separable glass, heat treatment leaching, X-ray diffraction anal. 7-51658
²³⁷Np, diffusion in simulated high level waste glass 7-49684
P₂O₅-B₂O₃-SiO₂ CVD glass films, components characterization 7-45085
PbO-B₂O₃-SiO₂ glass dielec. thin films on anodised Al substrates 7-17269
RbBSi₃O₆, glassy and crystalline, IR spectra 7-59199
SiO₂-B₂O₃-K₂O-Na₂O-Al₂O₃-TiO₂-ZnO:Ti⁴⁺, diffusion 7-27022
SiO₂-B₂O₃-Na₂O-Al₂O₃ glasses, corroded, grazing incidence fluorescence EXAFS, near edge spectroscopy 7-59296
SiO₂-B₂O₃-ThO₂ based glasses, local struct. around actinide, EXAFS and optical spectral studies, appl. for nuclear waste glasses 7-59290
SiO₂-B₂O₃-UO_{2.66} based glasses, local struct. around actinide, EXAFS and optical spectral studies, appl. for nuclear waste glasses 7-59290

Borrmann effect see *X-ray crystallography; X-ray diffraction*

Bose-Einstein statistics see *quantum statistical mechanics*

Bose gas see *boson systems*

boson fluids see *boson systems*

boson systems

see also *liquid helium-4; quantum statistical mechanics*
2D, vortex pair dissociation kinetics calcs. (*Russian*) 7-58560
atoms, oscillatory exchange between traps containing Bose condensates 7-50028
Base-Einstein condensation, free boson gas in thermodynamic limit 7-29873
Bogolyubov generating functions, quantum method, current Lie algebra, representations, functional eqns. 7-41240
Bose condensation in random external potential 7-29883
Bose gases, nonideal binary mixture, collective variables study 7-6906
Bose-Einstein condensation, critical density and thermodynamic functions 7-29872
Bose-Einstein condensation, effect of repulsive interactions 7-29876
charged quantum fluids in 2D, ground state energy 7-29881
condensate, solitary wave solutions of nonlinear Schrodinger equation 7-18689
condensate fraction 7-32735
condensation in mean field and Huang-Yang-Luttinger models 7-56151
degenerate, many-time Green's functions kinetic asymptotics, variational determ. (*Russian*) 7-41245
elementary-excitation spectrum of a weakly interacting Bose system 7-29877
extended thermodynamics of ideal gases with 14 fields 7-56197
gas with Coulomb interaction, ground state energy 7-61217
identical boson systems, Monte Carlo simulations 7-24537
impenetrable bosons on a ring, Langevin simulations 7-48544
infinite systems, canonical commutation relations in Bose-Einstein statistics 7-56152
interacting Bose fluid, nonlinear quantum and classical renormalization-group trajectories 7-35396
interacting Bose system, microscopic study of ground state props. and excitation spectrum 7-32736
interacting boson-fermion systems, functional integrals, holomorphic representation 7-14860
lattice Bose gas in 1D, equilibrium thermodynamics 7-61276
Lie gl(n+1,R) algebra, boson realisations 7-29871
Marshall boson derivation, SU_c quantum case 7-387
molecular time scale generalised Langevin equation theory, second quantised version 7-56143
monoatomic Bose gas, heat conduction, thermo field dynamics methods 7-11251
nonideal Bose gas, chemical pot. and press., perturbation theory anal. 7-61222
one-dimensional Bose gas, current correlator asymptotics (*Russian*) 7-61224
photon gas, Bose-Einstein condensation in thermal equilibrium 7-29885
probability density for Bose-Einstein and Fermi-Dirac particles, Slater-Kahn functions 7-48537
quantum adiabatic approximation to interacting boson-fermion systems 7-41243
quantum ground state coupled to Bose gas, statistical mechanics models 7-56150
spin-boson systems, dilute-blip and Born approx. equivalence 7-29875
stars, gravitational equilibria of self-interacting scalar fields, maximum mass calcs. 7-24519
tunnelling particle coupled to boson system in double-well potential, ground state anal. 7-56146
two-level system coupled to a boson mode, large-*n* limit, chaos 7-35403
two-level system coupled to heat bath, noninteracting-blip approx. 7-56144

boson systems continued

wigner quantized operator and Bogolyubov's generating functional method in nonequilibrium statistical physics 7-41239
SrTi_{0.97}Zr_{0.03}O₃, superconductivity at low carrier conc. and indications of charged Bose gas 7-27453

bosons

see also *alpha particles; boson systems; deuterons; gravitons; intermediate bosons; meson resonances; mesons; photons*
 $\lambda\phi^4$ theory, nonhomogeneous boson condensation, vacuum structure and temp. effects 7-397
boson resonance decay width calcs., Reggeon anal. 7-5009
bosons and fermions, fundamental problems 7-14858
charged black holes, bosonic instability anal. (*Russian*) 7-55702
doubly charged pseudo-Goldstone bosons and dynamical SU(2)×U(1) breaking 7-41659
fermionic/scalar field theories on Riemann surfaces of arbitrary topology, equivalence 7-9954
metastable vacuum decay, presence of soliton localized soft fermionic and bosonic modes 7-4986
N=2 superconformal algebra, bosonic representation 7-19025
open bosonic strings in gravitational, tensor and Yang-Mills fields, renormalization props. 7-24826
quantum symmetries from quantum phases, fermions from bosons, a Z₂ anomaly and Galilean invariance 7-48970
sp(n,R), construction of boson realizations 7-431
hh→W(Z)+jet, QCD parton shower Monte Carlo model 7-41852
 ϕ production in heavy ion collisions (light pseudoscalar boson), QED calcs. 7-36022
Si:Cr,B, optically-induced spin orientation, EPR study 7-2927

boundaries see *boundary layers; boundary value problems; grain boundaries; metal-insulator boundaries; semiconductor-insulator boundaries; semiconductor-metal boundaries*

boundary-elements methods

2D elastostatics, stress computation by BEM 7-37330
2D magnetic field problems, boundary and finite element methods combined 7-62584
3D acoustic radiation with flow, BEM 7-16202
3D body, subjected to nonproportional loadings, non-uniform growth of plane crack 7-26209
boundary collocation method, boundary integral elements method, water flow in porous media 7-6311
broadband light modulators, quasi-matched-velocity travelling-wave type electrodes (*Japanese*) 7-43354
crack stress distribution, effect of holes 7-6154
elasticity theory problems, combined scheme using boundary-integral-eqn. and finite-element methods 7-56041
elastoplastic boundary value problem, Galerkin approach 7-50956
elastostatics, conforming versus nonconforming boundary elements 7-14760
electric field computation, finite-element and boundary-element methods combined (*Chinese*) 7-10822
electrostatic problems, integral eqns. for thin dielec or conducting layers 7-31209
fluid-structural vibration studies using boundary element method 7-99
groundwater movement modelling, boundary element technique 7-4059
hyperthermia, unbounded electromagnetic problems, hybrid element method 7-18037
inverse problem applications 7-1436
layered elastic systems, boundary element transfer matrix analysis 7-35281
linear stress analysis, comparison of boundary element and finite element methods 7-1390
multiple displacement discontinuities in 2D finite/infinite regions, indirect boundary element method 7-57748
Navier-Stokes eqns., arbitrarily convex quadrilateral elements (*Chinese*) 7-16144
nonstationary Stokes equation, boundary element spectral method 7-37421
numerical implementation of the boundary element method with point-source approximation of the potential 7-386
open boundary problems, differential and integral methods 7-50454
particle beam instabilities, wake field anal. by boundary element method (*Japanese*) 7-19616
particle beam position monitor, sensitivity calcs. using boundary elements method 7-49770
plate, elastoplastic, bending anal. by BEM 7-43705
plate, orthotropic, loaded hole, boundary element study 7-1402
plate bending, direct boundary element method 7-24419
reinforcement problems, formulation in terms of boundary integral equations 7-1410
semicircular core fibres, coupling characts. (*Japanese*) 7-20458
shallow water flow, boundary element soln. 7-40502
shells, shallow, boundary/interior element method for quasi-static and transient response analyses 7-6090
short magnetic cylinder in transverse time-harmonic mag. field, 7-62574
Stokes problem, stationary, boundary integral eqn. method (*Chinese*) 7-14779
thermal transport problem modelling using boundary element methods 7-51149
three-dimensional scalar potentials, hybrid finite-element/boundary-element solutions 7-50455
tokamak structural components, 3D analysis of eddy currents using boundary element method 7-25199
transient elastodynamic analysis of three-dimensional problems by boundary element method 7-34694
transient wave propagation, new applications of boundary element methods 7-35292
US levitation simulation, boundary- and finite-element approaches 7-1360
vibrating circular piston in infinite baffle, acoustic field anal. using BEM (*Japanese*) 7-43491
viscous flow boundary element analysis by penalty function formulation 7-37415
wave load on body with arbitrary shape, coupled element anal. (*Chinese*) 7-26298
Fe, cast/stainless steel couple, galvanic corrosion NaCl soln., boundary element prediction (*Japanese*) 7-13635

boundary layer flow *see* **boundary layers**

boundary layer turbulence

see also **atmospheric boundary layer**
 2-phase flow, spectral analysis of wall-pressure fluctuations 7-43881
 acid rain modelling, turbulent spiral boundary layer and thermal wind simulator 7-14370
 adverse press. gradient boundary layers, k - ϵ turbulence model 7-16172
 air flow confined turbulent, over asym. roughened surfaces, mean flow parameters (*Chinese*) 7-11399
 airborne optical telescope, boundary layer turbulence effects 7-57504
 arbitrary obstacle, 3-D boundary layer calc. (*French*) 7-11382
 atmospheric boundary layer parameterization, FORTRAN programs 7-55246
 atmospheric turbulence classification, computer program 7-55247
 blunt cone lateral surface heat exchange in boundary layer flow 7-1529
 boundary-layer transition, roughness trips influence 7-37449
 channel flow, ejections and bursts, struct. and timescales 7-51088
 channel flow, injection through porous wall, accel. and turbulence influence, investig. 7-26263
 circular cylinder in cross flow, tripping wire effect on boundary layer transition 7-43847
 circular cylinder in turbulent boundary layer, fluid forces 7-6200
 coherent structures in rear-wall part of boundary layer flow, k - ϵ model 7-57818
 compressible turbulent free shear layer interaction 7-51078
 concave surfaces, boundary layers, longit. vortical perturbations, stability diagram 7-63124
 convection turbulence near vertical heated plate, calc. 7-31793
 convective boundary layer simulation, efficiency of different higher order turbulence models atm. appl. 7-57819
 Coriolis force effects on turbulent boundary layer with pressure gradients 7-20695
 counter-rotating vortex pair induced flow at wall 7-31810
 customised shear layers on smooth and rough surfaces, development 7-51082
 cylinders subject to transverse streamline flow, turbulent boundary layer separation (*Russian*) 7-11400
 cylindrical surface modifications effect, H_2 bubble wire flow visualisation and anemometry meas. 7-6196
 diffusion, line-source near a surface, steady reversing shear flow, diffusion eqns. anal. 7-43884
 dispersion from elevated source, nondimens. character and integral scale 7-6202
 distributed roughness effect on transition enhancement 7-37433
 eddy viscosity in a turbulent boundary layer on a cylinder 7-51091
 ellipsoid of revolution, incompressible turbulent boundary layers, inverse mode calc. 7-31768
 entrainment flow paths, parallel and perpendicular relative efficiencies 7-20694
 entropy layer absorption effect on supersonic flow heat transfer of sub-merged circular cone 7-43975
 external factors effect with directional injection and suction 7-6199
 external turbulence effect on boundary layer flow in nozzle 7-1542
 fibre laser Doppler anemometer and boundary-layer meas. appl. 7-37609
 finite element anal. 7-31771
 flow and frictional resistance of uniformly accelerating or decelerating flat plate 7-1544
 flow-induced surface instabilities, Kramer-type compliant surfaces, irreversible processes effects 7-16159
 free convective heat transfer, temp. factor effect 7-63143
 free-convection boundary layer at heated vertical plate, heat transfer and temp. profiles 7-31795
 gas-liq. descending annular flow, phase boundary turbulence and heat exchange 7-63201
 hairpin vortices, generation in laminar boundary layers, obs. 7-57797
 heat and mass transfer, external turbulence effects 7-1541
 heat transfer, local coefficients from staggered bundles of rough tubes in crossflow, expt. 7-43894
 heat transfer in flow past turbulent boundary layer barriers 7-51100
 heated turbulent boundary layer, hot-wire meas. of velocity and temp. fluctuations 7-63236
 high-enthalpy gas flow, heat and mass transfer on catalytic wall 7-11510
 impermeable surface with injection, turbulent boundary layer, wall region struct. 7-11396
 incompressible fluid at technically rough surface, boundary layer parameter calc. 7-63125
 incompressible fluid between parallel plane walls, anisotropic turbulence 7-1545
 incompressible viscoelastic coatings, turbulent boundary layer, press. fluctuations 7-26264
 internal flow, Navier-Stokes eqn. num. soln. (*French*) 7-57872
 K - ϵ model, control vol. method soln. 7-11393
 laser interferometer skin-friction meter, numerical and expt. study 7-16276
 layer with longitudinal press. gradient and injection at different angles to wall 7-43879
 low Mach number flows, acoustic radiation, 3-D boundary element scheme 7-11402
 mean flow, drag reduction, review 7-16171
 microbubble skin friction reduction on an axisymmetric body in turbulent boundary layer 7-31772
 mixing across density interface in presence of rot. 7-1543
 nonequilibrium turbulent boundary layers with slit injection and suction, outer intermittent region 7-20696
 nonperturbing boundary-layer transition detector for hypersonic wind tunnel, based on laser interferometry 7-20821
 oblique shock waves and turbulent boundary layer interactions, meas. and model 7-16208
 orifices, effect of grazing turbulent pipe flow on acoustic impedance 7-43463
 oscillation excitation is supersonic boundary layer by external acoustic field 7-51046
 oscillatory turbulent flow in a cylindrical channel 7-57820
 plate, uniform and shear flows at high Reynolds numbers, boundary value technique appl. 7-63126
 plate turbulent boundary layer acoustic pressure spectrum 7-43496
 pulsating pipe flow, wall shear stress meas. 7-16264
 retarded turbulent boundary layer, Reynold's shear stress balance components 7-51085

boundary layer turbulence continued

ribbed wall channel, turbulent flow study using 2-component laser Doppler anemometry 7-37547
 rotating cylinder in quiescent fluid, turbulent shear flow, flow visualisation, eddies 7-16168
 roughness trips, effect on boundary layer transition 7-16167
 salt-stratified fluid, turbulent boundary layers, mixing, mean-circulation and transport rates 7-51086
 semielliptical afterbody near-wake, turbulence intensities 7-51150
 separation flow around a cylinder near a plane screen, num. modeling 7-63123
 separation layer, 2D, mean flow similarity 7-31767
 sharp-fin-induced shock wave-turbulent boundary layer interactions 7-20693
 shear flow, vorticity and vel. struct. function eqn. isotropic forms 7-51090
 sink-flow boundary layers, num. simulations 7-43882
 skin-friction drag reduction meas. 7-51081
 spin-down of a fluid in a low cylinder at large Reynolds numbers 7-51084
 spot dynamics, review 7-6194
 statistical characteristics of intermittent liquid film flow 7-20698
 steady and unsteady non-parallel boundary layers, 3D instabilities, cross flow 7-63117
 stratified flow, entrainment, sheared density interface study 7-51266
 streamline curvature effects on turbulence in shear layers 7-6201
 supersonic flow, investig. 7-57877
 supersonic turbulent flow, rapid expansion, bulk dilation role 7-51087
 surface compression elasticity modulus and Reynolds number, importance in interfacial turbulence and mass transfer 7-63128
 surface drag reduction by riblet modification, visualisation study 7-11394
 surface protrusion, desinent cavitation, press. gradient influence 7-16222
 surface renewal model for turbulent boundary-layer flow 7-6197
 surface roughness effects and transition modelling 7-31769
 third-order scalar transports, composite time scale model 7-51092
 transient layer, integral characts. 7-11395
 transition from laminar flow detection, using differential interferometer 7-20822
 transition mechanisms interchange 7-57795
 transition sensitivity, in flow around a circular cylinder, oil-flow photographs anal. 7-43848
 transonic speeds on an aerofoil, shock wave interference, shock/boundary-layer interactions 7-6241
 turbulence near a wall, limiting behaviour, Navier-Stokes computational models 7-16170
 two layer model for the barotropic stationary turbulent planetary boundary layer 7-40519
 unsteady incompressible turbulent boundary layer flow over a longitudinal cylinder 7-6195
 unsteady incompressible two-dimensional and axisymmetric turbulent boundary layer flows 7-1540
 vaporisation and dispersion from a surface to a turbulent boundary layer 7-52018
 vibrating tubes in air crossflow, heat transfer behaviour, temp. and velocity fluctuations 7-51094
 vibrations of cylindrical panels in a field of turbulent pressure fluctuations 7-63029
 viscoelastic fluid flow between rot. plates 7-43939
 viscous incompressible fluid, partial cavity form., cavitation flow calcs. 7-31846
 vortex ring, passive impurity loss 7-11426
 vortices, lock-on and shedding, circular cylinder, steady and oscillatory flow meas. 7-16192
 wall attachment device, turbulent flow field, control flow effects 7-20697
 wall function approach to boundary conditions in regions of adverse press. gradient 7-6198
 wall jet with turbulent boundary layer, 3D mixing 7-37503
 wall shear stress meas. in layer subject to strong press. gradients 7-26265
 wall-pressure peaks generation, flow struct. obs. 7-57821
 wave boundary layer, numerical model, ocean appl. 7-55053
 weakly swirled turbulent jet aerodynamics 7-20771
 wedges with leading edge sweep, heat transfer, premature transition 7-6211
 wing, stationary turbulent boundary layer anal. 7-11397
 I_2 , supersonic flow study by 3D visualization and laser-induced fluorescence 7-20751

boundary layer turbulent flow *see* **boundary layer turbulence**

boundary layers

see also **atmospheric boundary layer; boundary layer turbulence; plasma boundary layers**
 air boundary layer, active transition fixing and control 7-31740
 air-water interface, mass transfer in eddies 7-11493
 arbitrary obstacle, 3-D boundary layer calc. (*French*) 7-11382
 arch-type vortex, form. behind normal plate in laminar boundary layer 7-26288
 asymptotic laminar boundary layer, mass transfer effects on transient behaviour 7-4323
 axisymmetric free convection boundary layer flow of water at 4°C past slender bodies 7-20709
 axisymmetric laminar plume, asymptotic soln. for large Prandtl no. 7-26275
 axisymmetric wall jet on circular cylinder, boundary layer flows 7-57892
 Blasius flow, skin friction, heat transfer, variational soln. 7-20699
 CAD system with Denton scheme for flow program, comparison with expt. results 7-63177
 centrifuges, cylindrical, with compartments, sedimentation, Coriolis force reduction 7-20736
 circular cylinder in cross flow, tripping wire effect on boundary layer transition 7-43847
 circular jet with initially laminar boundary layers, turbulent interaction region 7-11486
 cold, transient and steady-state vertical natural convection flow, meas. and visualisations 7-43902
 complex shear flows, turbulence modelling 7-51077
 compressible boundary-layer transition, first and second role modes 7-11452
 compressible flow, boundary layer excitation by surface heating or cooling, numerical simulation 7-6181

boundary layers continued

compressible laminar boundary layer eqn's, stream function numerical soln. 7-6183

compressible laminar boundary layer flow with heat transfer, quasi-linearization technique 7-26247

computational fluid dynamics in aeronautics, conf., Aix-en-Provence, France, (April 1986) 7-48191

conducting viscous incompressible flow near an oscillating porous flat plate 7-6322

convection, finite-amplitude axisymmetric, between rigid rotating planes 7-26272

convection at high Rayleigh number in cubic cavity, inclination influence 7-16178

convection in viscous fluid, finite difference methods 7-14784

convective flow patterns in cylindrical layer, wave-vector field 7-51352

convergent air intake with plane walls, flow study 7-11465

converging condensing flows of steam, pulsation characts. 7-6239

corner flow, incompressible fluid with suction, heat transfer eval. 7-26277

cylinder, unsteady boundary layer eqns., frictional forces 7-1392

cylinder in cross flow of water with injection into boundary layer, heat transfer and drag 7-43888

detached flow problems, soln. using finite element method 7-18599

disperse streams, dynamics in presence of boundaries 7-43845

distributed roughness effect on transition enhancement 7-37433

drops, liquid, breakup, rarefaction waves 7-20785

duct blocking effect on crossflow and heat transfer in cylinder 7-1629

dust particles, deposition, interaction with shock wave 7-1610

electrodynamic effect on small perturbation development in the boundary layer on thin airfoil 7-1641

equations with power boundary layer, numerical soln. (Russian) 7-56023

equilibrium diffusion equation, mixed boundary condition, variational treatment 7-20684

film flow on a rotating disk 7-31749

flow visualisation using spark velocimetry 7-57968

forced oscillatory compressible flow past yawed cylinder, heat transfer 7-1585

free convection near continuously moving vertical plate, boundary layer eqns. solns 7-1569

free convective heat transfer, temp. factor effect 7-63143

free liquid film flow measurement by laser Doppler velocimeter 7-37606

free-convection, unsteady boundary-layer flow, semisimilar solns. 7-57834

front motion, metastability and subcritical bifurcations 7-51056

frontiers in fluid mechanics, book 7-4640

fuel spray ignition by hot surface 7-51337

Görtler vortices spacing on concave walls 7-31812

gravity influenced free surface flows, iteration method for integral equations (Chinese) 7-26246

hairpin vortices, generation in laminar boundary layer, obs. 7-57796

heat transfer, 1D problem solns. polynomial approx. 7-50907

heat transfer characteristics, of flat plate thermometers, effect of variable fluid property 7-43910

homogeneous fluid between rot. infinite disks, normal blowing effect 7-51161

horizontal flow past partially heat infinite vertical cylinder embedded in porous medium 7-6309

hydromagnetic Stokes flow in a rotating fluid with suspended small particles 7-44008

incompressible laminar boundary layer, MHD flow past non-isothermal cone 7-11554

incompressible laminar boundary layer flow, MHD with heat and mass transfer 7-20806

inviscid axial flow in compressor rotor, leading-edge effects, flowfield meas. 7-11562

laminar, boundary-layer flow past a cylinder with massive blowing 7-31742

laminar, transverse flow, num. solns. 7-57798

laminar boundary layer eqns. fast approx. soln. 7-16155

laminar boundary layer on cylinder, Dorodnitsyn's method calcs. (Russian) 7-20685

laminar boundary layers on continuous moving surface, momentum and heat transfer 7-63111

laminar compressible MHD boundary layer at wedge 7-6325

laminar end-wall vortex and boundary layer, numerical simulation 7-51181

laminar falling liquid film, heat transfer from horizontal smooth tube 7-63131

laminar film, pool boiling from curved surfaces, integral method calcs. 7-1568

laminar flow, active stabilisation, turbulence transition, drag reduction 7-20683

laminar flow, separation point determ. 7-31741

laminar flow, three-dimensional boundary layer eqns. in streamline coordinates, numerical soln. 7-51041

laminar flow past sudden expansions, Navier-Stokes solns. 7-43846

laminar incompressible 2D boundary layer eqns. similarity solns. 7-51042

laminar incompressible flow with large negative long. press. gradient, friction and heat transfer 7-51047

laminar incompressible separated flows, iterative boundary-layer-type solver 7-11380

laminar juncture flow, unsteady characteristics, visualisation 7-57799

laminar mixing layer in longit. mag. field 7-51048

laminar natural convective flow along isothermal vertical surface, stability 7-31744

laminar swirling flow on permeable surface 7-31815

laminar symmetric sudden expansion flow boundary layer eqn. limitation 7-16156

laminar to turbulent flow transition, boundary layer, wall vibr. effect 7-43880

laminar-turbulent boundary layers transition on cone 7-31745

Lennard-Jones fluids, thermoviscous coupling and nonlinear transport effects on plane Couette flow 7-57793

local separation zones in viscous jets, existence and nonuniqueness 7-1595

meridional sections of 3D boundary layer, heat transfer calcs. 7-51125

methane-air laminar counterflow diffusion flames, struct., CARS meas. 7-57939

MHD boundary layers, heat transfer, Joule heating and transpiration effects 7-37556

MHD flow in an infinite channel 7-6326

boundary layers continued

micropolar fluid over isothermal cone, natural convection boundary layer flow 7-43887

moving interface problems in slow viscous flows, FEM 7-16157

multilayer ideal incompressible heavy fluid flow past body 7-1601

natural convection, book 7-60909

natural convection, heated horizontal surface, numerical anal. 7-31777

natural convection in porous media, non-Darcian effects 7-31785

natural convection on downward-facing heated plate, average Nusselt number 7-31791

natural convection on plates with variable surface temp. or heat flux 7-31743

nematic flows, unit-sphere description 7-20688

non-Newtonian fluids, 3D boundary layer eqns., similarity solns. 7-37497

nonDarcy free convection boundary layer on axisymmetric and 2D bodies of arbitrary shape 7-43904

nonisothermal plane point jet, single-parameter self-similar problem 7-44002

oscillating boundary layers, mass transfer rates 7-6182

oscillating free-connection flow past infinite porous vertical limiting surface, effects of mass transfer 7-14479

particle deposition from gas-disperse flow in vicinity of stagnation point 7-63206

perturbation propag. in boundary layer on flat channel walls 7-51045

plane flows of smooth nearly elastic circular disks, boundary conditions 7-26374

plate, flat, with vectored surface mass transfer, heat transfer characts. (Chinese) 7-11398

plate, nonisothermal flat, free convection flow influenced by blowing or suction 7-11529

point sink on plane with magnetic field, heat and mass transfer 7-1618

polymeric granular solids on hot moving interface, melting, approx. soln., nonNewtonian boundary layers 7-32614

porous flat surface, movement in parallel free stream, boundary layer behaviour 7-43919

porous-walled duct flow with gas injection, acoustic boundary layer 7-20793

pouring liquid flow from container, free surface study 7-51258

rotating cone in external stream, boundary layer eqns., FORTRAN code 7-37468

rough annuli, heat transfer anal. 7-1548

rough tubes, in staggered bundles, local features of flow 7-1628

roughness trips, effect on boundary layer transition 7-16167

second-order boundary layers for steady, incompressible, three-dimensional stagnation point flows 7-51043

secondary flow in MHD generator channel with mag. field 7-1635

ships, flow around aft section, static pressure meas. 7-37594

spatial oscillations in confined rotating fluid, temporal development 7-16186

sphere, vibr. in spherical vol. of viscous fluid 7-50971

spherical particle surface, heat transfer investigated using mol. kinetic methods 7-63184

stationary states or flows in regions extended in one direction, stability conditions 7-1535

steady and unsteady non-parallel boundary layers, 3D instabilities, cross flow 7-63117

steady Boltzmann eqn., thermal layer solns. 7-51033

steady liquid compound jet flow, num. treatment 7-37506

steady-state flow in channels, heat transfer calcs., three-parameter model 7-51123

stratified fluid enclosed in cylinder through-flow, thermal adjustment 7-31856

supersonic dust-laden gas flow round blunt body, blowing effect 7-51217

supersonic viscous flow, parabolised Navier-Stokes eqn. 7-20753

surface pressure in 3D turbulent jet/boundary interaction 7-6262

surface-mounted obstacles, wakes, trailing vortices, channel-flow expts. and num. simulation 7-57844

thermal boundary layer on a plate 7-37451

thermally stratified fluid, vertical through-flow between flows, Navier-Stokes eqn. 7-31857

three-dimensional unsteady flow due to stretching surface 7-51044

Tollmien-Schlichting waves and flows governed by interactive boundary-layer eqns., Taylor-Görtler instabilities 7-26300

transition, roughness trips with rows of spherical elements 7-51050

turbulent developing flow at entrance to smooth pipe 7-51067

turbulent flow over nonrotating cylinder, press. distrib. and fluctuations meas. 7-43868

turbulent pulsating pipe flow, wall shear stress meas. 7-16264

two-dimensional gasdynamic calculations, modified boundary conditions 7-11373

two-dimensional magnetogasdynamic boundary layer flow in aligned mag. field, similarity solns. 7-57937

two-phase boundary layer, frictional stress meas. 7-44018

two-phase disperse boundary layer, condensate pulsation characts., effects on heat transfer and friction 7-51281

unsteady free-convection flow past accelerated plate, skin friction 7-4321

vertical cylinder embedded in saturated porous medium, free convection 7-63129

viscoelastic boundary layer flow past stretching plate with suction and heat transfer 7-6313

viscous flow, Stokes drag on falling hollow cylinders and conglomerates 7-51049

viscous incompressible flow, steady Navier-Stokes eqn. soln. 7-11425

viscous incompressible laminar flow, drag reduction, optimal control 7-57794

volume cycling in tapered pipe, dye streak meas., Eulerian and Lagrangian velocity profiles 7-44051

waves in wall layers by unsteady press. gradients, receptivity mechanism 7-26292

wedges with leading edge sweep, heat transfer, premature transition 7-6211

wing, rotating, laminar boundary layer eqns. 7-11381

wing profile, flow separation, aerodynamic hysteresis 7-57870

boundary-value problems

see also initial value problems

abstract time-dependent transport equations, initial-boundary value evolution problem 7-56190

anisotropic materials of different moduli, cylindrical shell theory 7-43684

asymmetric dynamic problems, higher-order boundary perturbation method 7-41098

boundary-value problems continued

- asymptotic behavior of solution to the Cahn-Hilliard equation 7-55966
 asymptotic expansions and boundary conditions for time-dependent problems 7-35247
 atmospheric optics, inverse problems 7-47537
 Babuska-Brezzi conditions for two kinds of rectangular elements (*Chinese*) 7-51029
 Banach spaces, bounded compact approx. property and noncompactness measures 7-55950
 bars, thin walled, torsion with annulus cross-section of variable size 7-26137
 Bass Strait, tidal and storm surge model 7-18206
 beams, elastic, positive deflections, fourth-order boundary value problems 7-37338
 bidimensional Vlasov stationary eqn., boundary value problem (*Russian*) 7-26392
 bifurcation for nonlinear boundary value problems, geometrical approach, pendulum eqn. appl. 7-48352
 biharmonic equation, reduction of boundary value problem to Stokes-type problem 7-18566
 biharmonic equations with complex boundary conditions, Pade approximants calcs. (*Russian*) 7-61064
 body with plane crack, elasticity theory three-dimens. problem, variational soln. method 7-63072
 boundary collocation methods, appl. in physics and engineering 7-29723
 boundary problems, solution using Vinner-Hopf system and inversion of integral transforms 7-4692
 Brownian motions, absorbing and reflecting, filtering problems 7-48579
 buckling in beam-column problem for anisotropic cylindrical shells 7-16082
 cavities, 2D of various shapes, compressibility 7-43716
 ceramic part, heat resistance under two-dimens. strain conditions 7-59630
 charged sphere, closed form solution to mixed boundary value problems 7-61002
 coating-solid interface, nonlinear mechano diffusion 7-17669
 coherent phase transformations, asymptotic form of small density differences 7-24615
 collocation for singular boundary value problems of second order 7-35252
 complex domain, behaviour of eigenfunction expansion, pointwise convergence 7-61040
 composite shell of revolution, flexible, weakened by notches, stress-strain state, num. method 7-16075
 composite slab, cooling 7-43645
 composite system, one dimens., with random parameters, dynamic processes 7-107
 composites 7-26218
 compressible materials, complex math. model of plastic flow 7-64959
 compressible Reynolds lubrication equation, existence and uniqueness of solns. 7-35288
 concrete, inelastic behaviour, damage mechanics constitutive theory, FEM model 7-35833
 convection in viscous fluid, finite difference methods 7-14784
 coupled stationary bifurcations in non-flux boundary value problems 7-29717
 crack at an interface in a uniform stress field 7-16125
 crack tip stress intensity factors, boundary integral method 7-16129
 criticality transport problems for spherical systems with specular boundary conditions 7-61292
 current distribution in conductors with arbitrary cross sections Binger, P.P. (Dept. of Electr. Eng., Toronto Univ., Ont., Canada) 7-62576
 cylinder, nonlinear elastic thick-walled, multi-parameter equations solution 7-26143
 cylindrical waveguides, aperiodic EM wave processes 7-50464
 cylindrical waveguides, resonance phenomena and aperiodic wave processes 7-50463
 difference boundary value problem, soln. for fourth-order elliptical operator (*Russian*) 7-56004
 difference boundary value problem, stability anal. using analytical calcs. 7-18568
 differential eigenproblems, error estimation 7-61007
 diffraction by gap between two breakwaters, long waves, matched asymptotic expansions soln. 7-47446
 Dirichlet problem, nonlinear, in semiinfinite cylinders, decay theorems 7-29688
 Dirichlet problem in crescent-shaped domain, solution 7-57670
 domain with cut, stress intensity coeffs. in quasistatic temp. problems, asymptotic form 7-26152
 Earth's temp. field, stationary heat eqn., temp. optimisation 7-8871
 eddy current inspection problems of weakly cond. weakly mag. media, EM field calcs. 7-39821
 eigenfunction methods and nonlinear hyperbolic boundary value problems at resonance, wave eqn. appl. 7-61121
 elastic body, three-dimens., asymptotics of stress-strain state in vicinity of pointed inclusion 7-6096
 elastic layer on rigid foundation with annular hole, torsion study 7-37332
 elasticity, unilateral boundary value problems, numerical approx. solutions 7-61105
 elasticity, unilateral BVPs, num. methods 7-24427
 elastoelectromagnetic Neumann boundary value problems, self-consistent theory 7-26145
 elastoplastic boundary value problem, Galerkin approach 7-50956
 elastostatics, linearised, existence and uniqueness theorems for boundary integral equations 7-61102
 elastostatics with generalised boundary conditions, Poisson ratio independence 7-14771
 electrode design for gas discharge laser using finite difference method 7-1178
 electrothermal processes, one-dimensional, boundary-value problems (*German*) 7-31623
 elliptic boundary value problems, Schwarz alternation method in a sub-space 7-18569
 elliptic boundary value problems 7-35240
 elliptic equations, degenerate, derivative estimates, existence theorems for Dirichlet and Neumann problems 7-24374
 elliptic problems on unbounded domains 7-35241
 elliptical equations, numerical procedures, capacitance matrix method (*Russian*) 7-56008
 EM field, open boundary problems solution using finite element method 7-31212

boundary-value problems continued

- EM fields, boundary Neumann's problem described by the integral equation—problems of analysis and synthesis (*Polish*) 7-20094
 EM wave absorpt. by conductors, comparison between exactly and approximated boundary conditions 7-42858
 fluids in porous medium, unsteady interface 7-14319
 fourth order elliptic boundary value problem, symmetries Green's theorem appl. 7-35239
 Fredholm alternative generalisation for nonlinear diff. operators, boundary value problem 7-9652
 glassy materials, fusion, boundary-value problem soln. 7-21416
 gravitation, nonlinear eqns., boundary-value problem solns. 7-24507
 heat conduction, boundary value problems, eigenvalues eval. 7-62949
 heat conduction, nonlinear, moving boundary problems, appl. of Backlund transformation 7-6074
 heat conduction equivalent transformations of grid models 7-11250
 heavily loaded semi-infinite cylindrical elastic shell, vibrs., boundary value problem 7-31690
 Helmholtz-type eqns., weak-element method 7-24484
 hollow conducting cylinder eddy current calc. 7-62585
 homogeneous fluid flow rate in porous media 7-51298
 hyperbolic differential equations, soln. of boundary-value problem, optimal control appl. 7-35220
 incompressible viscous fluid with density, initial boundary value problem, weak soln. 7-61112
 indefinite Sturm-Liouville problems, half-range solns. 7-55979
 initial-boundary value problems, pseudospectral method of soln. (*Russian*) 7-56006
 internal waves, nonstationary theory, existence theorems (*Russian*) 7-61130
 irregular saw-tooth shaped boundaries, normal mode analysis 7-6230
 jets, modulated, numerical modeling 7-63190
 Lamb's initial and boundary value problem, elastic medium with memory 7-41103
 laminar boundary layer on cylinder, Dorodnitsyn's method calcs. (*Russian*) 7-20685
 linear elastic fracture mechanics, computerised R-functions method 7-63066
 linear systems associated with discretised boundary value problems of ordinary diff. eqns. 7-35245
 linear thermo-microelasticity, first boundary initial value problem 7-57686
 Liouville equation, singular solutions on an interval 7-61057
 magnetic vortex field, 2D, with boundary conditions of 3rd kind, numerical determ. for tube drawing, inductive heating (*German*) 7-33811
 monotone iterative technique for boundary value problems (*German*) 7-14754
 monotone techniques for first order boundary value problem 7-55969
 multidimensional wave eqn., absorbing boundary conditions for difference approxs. 7-48384
 multilayer ideal incompressible heavy fluid flow past body 7-1601
 multiple and maximal periodicity in linear elastostatics 7-41105
 multiplicity results for nonlinear elliptic equations involving a critical Sobolev exponent 7-24397
 Navier-Stokes eqns., arbitrarily convex quadrilateral elements (*Chinese*) 7-16144
 Neumann boundary value problem, nonlinear, one-dimensional, multiplicity of solutions 7-35237
 nonhomogeneous boundary conditions, reduction method 7-4689
 nonlinear, numerical soln., ordinary differential eqns. (*Russian*) 7-56005
 nonlinear boundary value problems, difference schemes in L_2 net space 7-18565
 nonlinear boundary value problems, numerical soln. methods (*Russian*) 7-61063
 nonlinear electro-magneto-thermo-elasticity, steady-state problems 7-37331
 nonlinear higher order parabolic eqns. with absorption, finite speed of propagation and asymptotic rates 7-61038
 nonlinear initial-boundary value problems 7-55987
 nonlinear problems with finite number of solns. 7-55971
 nonlinear viscous fluid, stability of flow (*Russian*) 7-57803
 numerical solution of systems of 2nd order boundary value problems 7-35248
 operational calculus, application to initial and boundary value problems 7-55984
 optical fibres, birefringent, anal. 7-57587
 p-n junction, boundary conditions at high injection level in space charge region 7-17091
 parallel plates at arbitrary Knudsen numbers heat transfer study 7-57883
 periodic boundary value problem for differential equations with delay and monotone iterative method 7-61017
 piezoceramic shell, applied theory modification 7-43750
 plasma, lower hybrid heating, vacuum window device anal. 7-57995
 plate, elliptical, oscillation problem soln. with allowance for energy dissipation 7-20641
 plate, natural freqs. and forms of vibrs. in own plane, determ. method 7-20642
 plate, uniform and shear flows at high Reynolds numbers, boundary value technique appl. 7-63126
 plate bending using new hybrid element method 7-16070
 plates, elastic sandwich, use of boundary value problems solutions 7-26141
 plates, laminated, boundary layer approach to free-edge stress concentration 7-26158
 plates, rectangular, transversely loaded, upper and low bounds 7-43700
 plates and shells, finite strain large deformation, nonlinear theory 7-20602
 polarized light transfer, spectral props., existence and uniqueness of solns. 7-62624
 polyelectrolytes, counterion condensation, Poisson-Boltzmann eqn. sol. 7-52029
 polygonal topological networks in 2D, boundary value problems (*French*) 7-35211
 polytropic ideal gas, nonfixed on the boundary, 1D motion 7-11449
 pseudoparabolic equations, solution of boundary-value problems 7-35223
 quasi-linear hyperbolic eqns., conservative nonlinear operator difference scheme 7-18567
 quasilinear elliptic equation, numerical solution of first boundary value problem (*Russian*) 7-55975
 reaction-diffusion eqn., numerical solns. asymptotic behaviour 7-61284

boundary-value problems continued

- reaction-diffusion equations, pseudo-arclength continuation method for nonlinear eigenvalue problems 7-35481
- Riccati transformation in the solution of boundary value problems 7-35249
- rods, elastic, stationarity for non-selfadjoint problems 7-26178
- scattering matrices, bounds and norms 7-10811
- second order boundary value problems with nonlinear boundary conditions, upper and lower solns. 7-9650
- second order differential operator equations, boundary value problems 7-29712
- semilinear degenerate boundary value problems, existence and constructive enclosure of solutions 7-14755
- shell, cylindrical, axisymmetric dynamic problems soln. by num. methods 7-16105
- shell, cylindrical, hinged compressed, connected to elastic filler, axisymmetric stability, boundary conditions 7-43730
- shell, structural, initially stressed, vibr. and freq. characts. 7-16104
- shells, cylindrical, thick-walled, nonlinear cross section, stress state anal. 7-62993
- shells, linear thermoelastic, mech. contact, uniqueness theorem 7-37340
- shock layers in perturbed systems related to steady conservation laws 7-61113
- singular boundary value problems 7-55967
- singular perturbations for nonlinear hyperbolic-parabolic problems 7-61050
- singularly perturbed linear two-point boundary value problem analysis 7-35246
- solid solutions, phase equilibrium across coherent interface 7-38152
- solid-fluid mixtures, boundary conditions 7-6854
- Sommerfeld's half-plane problem type mixed boundary value problems 7-56001
- sorption-diffusion equations, singularly perturbed boundary-value problem, soln. asymptotics (*Russian*) 7-61297
- Stokes and Navier-Stokes eqns. with pressure boundary conditions (*French*) 7-56045
- Stokes equations, soln. for incompressible fluid in multiconnected domain 7-20797
- Stokes problem, stationary, boundary integral eqn. method (*Chinese*) 7-14779
- strain concentration in inhomogeneous boundless thin plate with circular opening 7-29754
- stratified media, current source in presence of insulating and conducting disks 7-25699
- streaming operator in bounded convex body, boundary conditions 7-61293
- Sturm-Liouville boundary value problems, sinc function computation of eigenvalues 7-61006
- Sturm-Liouville system, eigenvalues of boundary value problem from band matrix inverse 7-60959
- superlinear elliptic boundary value problems involving critical exponents, existence results 7-35227
- temperature discontinuities and infinite short-circuit diffusion phenomena 7-1377
- thermoelasticity problems, boundary integral methods 7-11296
- thin-walled structures under combined loading, elastic buckling anal. using finite strip method 7-20612
- three point boundary value problems, Liapunov theory appl. 7-29708
- three-dimensional exterior field problems, finite-element soln., inversion transformation 7-20096
- time evolution of spectral discretizations of hyperbolic systems 7-48322
- transonic full potential eqn., intermediate boundary condition in Holst AF2 scheme 7-26308
- two-beam problems, sixth-order multidervative method 7-24409
- two-dimensional slow viscous flows past obstacles in a half-plane 7-57788
- two-point boundary value problems, stability of finite difference schemes 7-35244
- vibrating string controversy of mid-1700s, classical wave eqn. 7-48262
- viscoelastic rectangular body excited by rectangular waveguide, vibr. and heating 7-16109
- viscoelastic solid growth under frontal hardening conditions, stressed state form. 7-43712
- viscous creeping motion equations, soln. using cartesian-tensors 7-14778
- viscous stratified flow, dynamics, initial boundary value problem soln. (*Russian*) 7-9675
- Volterra type integro-diff. eqns., periodic boundary value problems 7-29718
- water waves, large amplitude, num. computation 7-18326
- Webster's horn equation, solution, relation between coeff. and boundary values 7-35296
- well-posedness of one-way wave equations and absorbing boundary conditions 7-48383

bowing *see bending***brain**

- see also neurophysiology*
- anaesthesia for surgery, prod. by elec. simulation of brain, generator 7-8759
- auditory brainstem evoked pots., finite impulse response digital filters appl. 7-23491
- auditory brainstem response using excitatory and inhibitory neuron elements (*Japanese*) 7-8597
- auditory brainstem responses, effects of presbycusis and other types of hearing loss 7-54609
- auditory brainstem responses, freq. specificity 7-28543
- auditory brainstem responses from human adults and infants: restriction of freq. contrib. by notched-noise masking 7-34159
- auditory cortex, dog, role in discrimination of sound signals simulating sound source movement 7-40166
- auditory cortex, primary, ferret, representation of cochlea 7-8585
- auditory electric responses, individual differences, absolute latencies of brainstem vertex-positive peaks 7-28544
- auditory frequency coding in the inferior colliculus, gerbil obs. 7-54596
- auditory midbrain of grassfrog, sensitivity of neurons to temporal characts. of sound 7-40167
- auditory nerve-brainstem evoked response, depression in hypoxaemia: mechanism and site of effect 7-54584
- biplane fluorography: neuroangiographic appls. 7-18065
- blood flow measurement, indicator elution curves analysis by microcomputer 7-40389

brain continued

- blood flow measurement, multicompartiment analysis of trace clearance 7-18010
- blood-brain, late effects of radiation, rat obs. 7-65814
- blood-brain barrier of rats, interaction of ethanol and microwaves 7-28601
- blood-flow meas. in ventilated premature babies, ¹³³Xe, inhalation system 7-23434
- brainstem auditory evoked pots. in rhesus monkey, neural generators 7-8581
- brainstem auditory evoked responses in the hamster 7-54595
- central nervous system connections determ. by physiological methods 7-47037
- cerebello-pontine angle, mag. resonance imaging 7-14074
- cerebellum, developing rat, long-term neuropathological consequences of low-dose X-irrad. 7-18025
- cerebellum, role in visual guidance of movement, review 7-40143
- cerebral blood flow meas. using ¹³³Xe inhalation and dual detectors (*Chinese*) 7-8629
- cerebrospinal fluid shunt flow meas., reproducible radionuclide procedure 7-65836
- circulation in man, global math. model 7-40193
- classifier-directed signal processing in brain research, EEG and magnetoencephalogram appl. 7-54820
- CNS tumours, contrast-enhanced NMR imaging, clinical review 7-3855
- cortex functional architecture, determ. by optical imaging of intrinsic signals 7-34362
- cortical neurons in superior temporal sulcus of monkey, responses to band-pass spatial freq. filtered faces 7-59980
- cortical representation of gradient-adapted multiple-stimulus perimetry 7-23343
- cortical responses to painful CO₂ stimulation of nasal mucosa; a magnetoencephalographic study in man 7-54620
- CT image, 3-D shaded display, high-precision surface form. (*Japanese*) 7-47300
- cytoarchitectonics, nervous tissue struct. inhomogeneities, software and hardware aspects of evaluation and anal. system 7-34360
- dentate gyrus, long-term potentiation: induction by asynchronous volleys in separate afferents 7-65733
- dopaminergic system, in vivo meas. using PET 7-18080
- EEG power spectrum anal. of head-injured patients, computer assessment of neurological status 7-34128
- ELF electric fields, effects on neuronal activity in rat brain 7-28583
- enzymes of glutamic acid metabolism in rat liver and brain, influence of continuous and modulated laser radiation (*Russian*) 7-47164
- epilepsia partialis continua, distinction between myoclonus-related pot. and epileptic spike 7-54532
- event-related potentials, principal components anal., spectral methods 7-47031
- event-related potentials to speech sounds and tones, habituation 7-34155
- evoked dipole source potentials of the human auditory cortex 7-8580
- evoked potential maps in learning disabled children 7-8558
- evoked potentials, performance and measures of performance for estimators 7-23328
- evoked potentials, single, classification and detect. using time-freq. amplitude features 7-54534
- healthy and diseased tissues, T2 estimates, comparison using various NMR pulse sequences 7-14091
- hippocampal slice prep., current source density estimation using microelectrode array data 7-54538
- hippocampal slices from noncold-acclimated, cold-acclimated and hibernating hamsters, temp. effects on evoked pots. 7-54484
- inferior colliculus, guinea pig, spontaneous activity of single units, salicylate-induced changes 7-47120
- inferior colliculus, rat, dynamic props. of responses of single neurons 7-40163
- interstitial microwave hyperthermia in a canine brain model 7-28645
- intracranial dipoles, mag. localisation: simulation with a phys. model 7-14029
- intracranial pressure monitoring unit with computerised signal processing, improved design (*Spanish*) 7-34299
- large-scale neuron-glia network dynamics, rel. to brain functions 7-23327
- late effects of fast neutrons and X-rays on adult rabbit brain 7-60029
- lateral geniculate nucleus, reconstruction of equidistant colour space from responses of visual neurons of macaques 7-28514
- lateral geniculate nucleus chromatic data, macaque, principal component anal. 7-28515
- left hemisphere advantage for recognising US communication calls in mice 7-54607
- light penetration depth in normal and malignant human tissue, photodynamic therapy appl. 7-23396
- magnetic fields, review 7-3809
- magnetoencephalogram and EEG, method for combining to determ. sources 7-54635
- magnetoencephalogram moving dipole inverse solns., effects of meas. errors and noise 7-3853
- magnetoencephalogram topography, simulation with sphere filled with saline soln. 7-8612
- magnetoencephalogram topography and source model of abnormal neural activities associated with lesions 7-47032
- magnetoencephalographic source models and physiology 7-54629
- magnetoencephalography, inverse problem, instrumental and analytical perspective 7-54627
- magnetoencephalography, inverse problem, medical perspective 7-54689
- medial geniculate body, cat, functional props. and interactions of neuron pairs simultaneously recorded 7-54592
- median eminence microvascular, 3D reconstruction 7-34356
- membrane reception of prostaglandin E₂ in mouse tissues, effect of various doses of ionising radiation (*Russian*) 7-47173
- microwave and low-level RF radiation effects on brain tissue and animal behaviour 7-23403
- midlatency auditory evoked responses: differential effects of sleep in the cat 7-8582
- midlatency auditory evoked responses: differential effects of sleep in the human 7-8583
- monitoring brain electrical and magnetic activity 7-8743
- motor cortex, primate, neuronal population coding of movement direction, arm appl. 7-28489
- movement-related brain pots., synchronisation rel. to computer detect of EMG edges 7-14027

brain continued

- multi-modality evoked responses vs. temp. and thermal dose with whole-body hyperthermia in water bath 7-8500
- multiunitary activity anal. of cortical and subcortical structs. in photosensitive baboons 7-65748
- neoplasmas, clinical and expt., Na and ^1H NMR imaging 7-18060
- neuromagnetic localisation, improved procedure 7-54639
- neuromuscular motor control system (*Japanese*) 7-13982
- neuron and axon growth, connections between nerve cells and brain 7-17968
- neuron tracing through serial sections, use of shape knowledge to improve performance 7-3954
- neuronal activity in human brain, feasibility of developing a method, theoretical review 7-65901
- neuroradiology, conf., Amsterdam, Netherlands, (Sept. 1985) 7-14706
- neuroradiology, role of digital subtraction angiography, intra-venous and intra-arterial experiences 7-18078
- neuroradiology, transcranial Doppler sonography rel. to angiography 7-18035
- neurosurgical intensive care unit, computerised monitoring system 7-34320
- NMR imaging, cerebrospinal fluid signal enhancement in short TR gradient echo images 7-47194
- NMR imaging, Na, high resolution, phys. 7-47210
- NMR microscopy, 3D, signal to noise ratio, limited angle excitation 7-54826
- noisy signals, anal. by nonparametric smoothing and differentiation, brain pots, appl. 7-54422
- nuclear techniques in diagnostic medicine, book 7-24312
- oedema, infarction and tumours, significance of proton relax. time meas. 7-18049
- P300 potential complex to auditory stimuli, subcortical correlates in man 7-23369
- photoradiation therapy of brain tumours, effects evaluation with in vivo ^{31}P NMR spectroscopy 7-14101
- pion radiotherapy, use of positron emission tomography 7-28661
- pontine reticular neurons, mediation of firing pattern alterations by low threshold Ca^{2+} spike 7-65732
- positron detection system for biochem. studies on living human brain 7-34240
- positron emission tomography, human visual cortex mapping appl. 7-28516
- positron emission tomography in neuroradiology—integration of a research tool in clinical routine 7-18079
- positron emission tomography measurements of cerebral glucose metabolism, methodological factors affecting 7-40261
- posterior suprasylvian cortex of cat, visual receptive field props. 7-59981
- rabbit olfactory bulb, pattern formation/recognition, nonlinear dynamics 7-54543
- rat tissue, mag. field effects, phase-contrast microscopy obs. 7-8645
- regional cerebral blood flow, meas. method for freely moving, unstressed rats 7-28790
- regional cerebral blood flow meas. by ^{133}Xe , Alzheimer's disease diagnosis appl. 7-28676
- sensorimotor cortex and caudate nucleus of rat brain, cholinergic process status after γ -irrad. (*Russian*) 7-47178
- sensory evoked pots., cerebral cortical contribs., hydranencephaly obs. 7-23342
- short latency averaged evoked pots. recorded in thalamic and scalp zones of representation, comparison 7-34123
- short-latency auditory evoked pots. in the monkey, intracranial generators 7-3798
- short-latency auditory evoked pots. in the monkey, wave shape and surface topography 7-3797
- somatosensory evoked cortical pots. to median nerve stimulation, scalp topography and distrib. 7-34167
- somatosensory evoked pot. ipsilateral and contralateral components following median nerve stimulation 7-23372
- somatosensory system, cat, effect of cortical ablation on afferent activity 7-3805
- somesthetic primary cortex evoked pots. elicited by central afferent stimulation 7-34169
- steriological advances, recent, impact on quantitative studies of the nervous system 7-34357
- stereotactic radiosurgery of central nervous system disorders, He ion beam 7-40270
- striate cortex of cat, directional and orientational tuning for contrast and textured stimuli 7-34141
- subcortical dementia, EEG changes, Steele-Richardson-Olszewski syndrome patient obs. 7-54531
- surgery microscope use in microneurosurgery 7-8756
- temperature depth meas. using thermal microwave emission analysis 7-28785
- temporal lobe epilepsy patients, mag. field, temporal region modelling 7-54631
- tumors, interstitial microwave hyperthermia, swept freq. meas of antennas 7-14106
- tumors, regional cerebral blood flow meas. obs. 7-23390
- tumors, ^1H NMR spectra, human and rat obs. 7-47137
- tumours, invasive and noninvasive microwave hyperthermia 7-14105
- vesico-urethral junction stimulation evoked cerebral responses in normal subjects 7-34124
- vision, log-complex transforms of stimuli rel. to cortical responses they evoke 7-54558
- visual cortex, kitten, ocular dominance shift rel. to retinal elec. activity imbalance 7-28517
- visual cortex, review 7-23331
- visual evoked potentials, source localisation man by principal components anal. 7-47052
- voltage changes meas., signal source using MOSFET chopper amplifier 7-23480
- X-ray CT image, 3D display of cerebral ventricle 7-47280
- $^{45}\text{Ca}^{2+}$ efflux from isolated chick brains, lack of effect of static mag. field 7-28579
- ^{253}Cf brachytherapy of the brain, high LET, B enhancement 7-28670
- ^{252}Cf implant neutron effects on dog brain 7-28593
- ^{31}P NMR studies of human brain at 2 T 7-18041

brain models

- see also learning systems; neural nets
- associate recognition and storage in model network of physiological neurons 7-47028
- associative memory models, interaction asymmetry and pattern hierarchy 7-65730
- cognition, matrix and convolution models of brain organisation 7-47058
- computing with neural circuits: a model 7-13983
- content addressable memories, storage capacity increase by unlearning 7-54516
- cortico-cortical associations and EEG coherence, 2-compartmental model 7-13987
- dynamical Q-analysis of the structural variation influence on the central nervous system 7-13981
- evoked potentials characterization study (*Japanese*) 7-47033
- homogeneous head model, feasibility in interpretation of neuromag. fields 7-54636
- homogeneous sphere model magnetoencephalographic data anal. using homogeneous sphere model: empirical tests 7-54638
- Hopfield model, memory and learning props., numerical simulation 7-61215
- inverse solutions based on magnetoencephalograms and EEGs, appl. to vol. cond. anal. 7-54637
- layered neural network model applied to the auditory system 7-54581
- memories, working, solvable models 7-8533
- memory, hierarchical multilayer model 7-65731
- olfactory bulb of rabbits, oscillating network model of pattern recognition 7-54618
- physics, biological computation and complementarity 7-54524
- rapid-eye-movement brain state optimal monitor 7-23323
- sensorimotor hierarchies of gaze, tensor network modelling 7-54552
- texture discrimination, mathematical model based on human visual cortex functioning 7-54580
- vision research and image technology, human functions of information processing (*Japanese*) 7-28499
- brass**
- 63/37, electrochem. behaviour in binary mixtures of N_2N -dimethylformamide and water 7-46677
- α -phase, hot rolled, recrystallized microstruct., deform. processes 7-13500
- α -phase, Mossbauer spectroscopy 7-59125
- α -phase, rolling deform. texture, shear band angles 7-33724
- α -phase, SCC initiation after exposure to NaNO_2 soln. 7-65173
- α -phase, SCC propagation after exposure to NaNO_2 soln. 7-65174
- β -brass, elastic constants, phase stability, dynamic obs. 7-3347
- β -phase bicrystals, Bauschinger effect, grain boundary contrib. 7-46574
- abrasive wear mechanism, wear process successive obs. in SEM 7-8229
- corrosion inhibitors evaluation (*German*) 7-8197
- corrosion protective coating of Ag, props. 7-53950
- creep strain, anomalous instantaneous obs. after stress change 7-46585
- foil, L80, grain struct. form. after isothermal annealing 7-53761
- friction and wear characteristics of asbopolymer material 7-28153
- joints of dissimilar metals, adhesively bonded strength evaluation 7-46791
- Naval, transgranular SCC, dislocation distrib. 7-17708
- plated steel cords, mech. and cohesion props. in sulphurising environment 7-39740
- polycrystalline α -phase, low temp. solid-solution hardening, yield stress anal. 7-3321
- pressed component, strain distrib. 7-13530
- sheet formability, grain struct. and stress raisers influence 7-3376
- sputtering yield meas. with 3D stylus surface mapping system on α -brass 7-27850
- strength anomaly, effect of prestrain 7-38094
- stress assisted dezincification in NH_3 soln. 7-17675
- two-phase, Al-B Masteralloy addition, B redistrib. during solidification, grain refining effect 7-22664
- work function, influence of ordering 7-33062
- yield loci, expt. investig. 7-51923
- Ag-brass, mixing layer, friction props., ion beam mixing (*Chinese*) 7-51888
- Al brass, corrosion inhibition by Schiff bases in acid media 7-22892
- Al brass, SCC in acidic sulphate solns, Cl^- conc. effect 7-17679
- Sn alloyed 7-21157
- Bravais lattice** see crystal atomic structure
- brazing** see brazing
- brazing**
- see also soldering
- Si-Al-O-N Syalon, bonding investig., active Ti additive role, fracture strength and microstruct. 7-39846
- SiC whisker reinforced Al matrix composites, interaction, with eutectic brazing alloys 7-46689
- breakage** see fracture
- breakdown (electric)** see electric breakdown
- breakdown (mechanical)** see manufacturing processes
- breakdown diodes** see avalanche diodes; Zener diodes
- breeder reactors** see fission reactors
- bremstrahlung**
- see also electron radiation; gamma-ray spectra; gamma-rays; inverse photoemission spectroscopy; X-ray emission spectra; X-rays
- atmosphere, X-rays due to quiet-time electron precipitation 7-47624
- atom+ion, continuum emission, wave fn. calcs. 7-15681
- atoms, electron bremsstrahlung energy spectra 7-24319
- atoms, $Z=6$ to 92, bremsstrahlung double differential cross section, photon energy depend. 7-42569
- BLACKJACK 5, bremsstrahlung radiation source, for nuclear weapon simulation testing 7-30816
- charged particle bremsstrahlung by barrier penetration in 1D 7-29775
- classical bremsstrahlung ang. distrib. in Coulomb case 7-62606
- currents acting at finite length, electromagnetic and hadron radiation 7-10031
- depth-dose distributions, conversion from slab to spherical geometries for space-shielding appls. 7-56879
- EDX analysis in a 400 keV electron microscope 7-39945
- electron acceleration in a laser-irradiated plasma 7-11651
- electron storage rings, longitudinal ion motion, bremsstrahlung studies 7-10320
- excitation of atomic nuclei and of atoms in singlecrystals by charged particles 7-7784

bremsstrahlung continued

flash X-ray tubes, bremsstrahlung and K-series production efficiencies maximisation 7-380
flash X-ray tubes, bremsstrahlung maximisation and K-series production efficiencies 7-24747
free electron laser, induced magnetobremsstrahlung of electrons in an undulator field and an axial guide field 7-50574
free electron lasing by relativistic electron beam, quantum-kinetic theory 7-43124
graphite-K intercalation cpd., C_8K , anisotropic binding of K, nuclear resonance photon scatt. of bremsstrahlung 7-51695
heavy ion collisions, bremsstrahlung in the incoherent limit, simplified fireball model 7-61907
incomplete charge collection and X-ray microanalysis 7-23100
inverse bremsstrahlung absorption in the planar corona of a laser target 7-16335
inverse diode computations, using stationary particle codes 7-30812
inverse pinch diode research 7-30811
M87, bremsstrahlung model for X-ray emission from galactic halo 7-66752
methane, oscillator strength, X-ray and VUV absorpt. spectra 7-36643
PIXE, accurate anal. using INK computer program 7-54216
plasma, emission characteristics, soft X-ray region, plasma diagnostics, radiative-collisional model study 7-62312
plasma diagnostics, molecular origin of background light in Thomson scattering measurements 7-32089
polarised electrons in surface physics, book 7-29607
relativistic electrons, determ. in electron-ion ring using bremsstrahlung 7-19559
Rydberg-Bremsstrahlung maser emission, anal. 7-15836
Sco X-1, thermal bremsstrahlung model for UV continuum 7-55735
semiconductors, impurity doping by photonuclear reactions 7-16589
slow electrons, pot. scatt. in laser field 7-18639
solar flares, hard X-ray and gamma-ray bremsstrahlung prod by high-energy protons 7-55594
stimulated collective inelastic stopping effect 7-36781
strongly magnetised plasma, ordinary EM wave bremsstrahlung emission 7-51410
supernova remnants, bremsstrahlung radio emission during radiative expansion stage 7-60744
T-10 tokamak, large-scale perturbation, radial struct. 7-51427
tagged photon beams, intensity 7-56890
tetrafluoromethane, oscillator strength, X-ray and VUV absorpt. spectra 7-36643
thick-target bremsstrahlung spectra generated by the β particles of ^{90}Sr - ^{90}Y and ^{99}Tc 7-39212
thin crystals, electron irradi., Pendellosung radiation and coherent Bremsstrahlung 7-33476
two-photon, in Coulomb potential, cross-sections 7-42577
two-photon bremsstrahlung in the Coulomb field 7-42766
Wolf-Rayet stars, new evidence at X-ray and gamma-ray freqs., for non-thermal phenomena 7-55640
 $\bar{e}^+\bar{e}^- \rightarrow e^+e^- \gamma$, bremsstrahlung amplitude calcs. 7-61712
 $\bar{e}^+\bar{e}^- \rightarrow f\bar{f}\gamma$, bremsstrahlung amplitude calcs. 7-61712
hh \rightarrow hh, inelastic scatt., flux tube or bremsstrahlung 7-35893
pp \rightarrow pp γ , cross sections and analyzing power, pot. model calcs. 7-5115
Al plasma, high density, high temp. at. pot., comparison with bremsstrahlung Gaunt factors, density functional theory 7-63254
Ar, fast electron bremsstrahlung cross sections 7-36780
 $^{12}C(p,p)$, 1.7 MeV, $^{13}N^*$ compound nucleus, lifetime determ. from bremsstrahlung meas. 7-56679
CaF₂ TLDs, Al- or Ta-encapsulated, non-equilibrated bremsstrahlung dosimetry for 0.75 MeV electrons 7-56876
Fe ferromagnets, spin-resolved photoemission and bremsstrahlung calcs. and data anal., book contrib. 7-33523
 ^{163}Ho , electron capture decay, neutrino mass meas. using inner bremsstrahlung 7-56645
La, fast electron bremsstrahlung cross sections 7-36780
LiF TLDs, dose enhancement effects, comparison with 2D Monte Carlo calc. 7-56875
Ni ferromagnets, spin-resolved photoemission and bremsstrahlung calcs. and data anal., book contrib. 7-33523
 $^{54}Ni(^{14}N,\gamma X)$, 35 MeV/n, bremsstrahlung angular distrib. 7-5254
Si internal target of 1.3 GeV synchrotron, coherent bremsstrahlung generation and meas. 7-15434
 $U_xY_{1-x}B_4$ system, mag. props., XPS and bremsstrahlung-isochromat spectroscopy studies 7-17172
Xe, fast electron bremsstrahlung cross sections 7-36780

bremsstrahlung isochromat spectroscopy *see inverse photoemission spectroscopy*

bridge circuits

see also bridge instruments
absolute determ. of Farad, ohm and quantised Hall resistance at LCIE 7-14909
AC four-terminal bridge for low-resistance thermometry 7-9834
capacitance bridge for low-temperature, high-resolution dielectric measurements 7-48778
DC-AC hot-wire procedure for determining thermophysical properties under pressure 7-9830
diode-bridge temperature sensor 7-18783
eye internal pressure meas., using electric sensors (Slovak) 7-60112
four-terminal AC bridge, easy to build, for temp. down to 1K 7-14957
hot-wire anemometer compensated for ambient temperature variations 7-16275
IC microtransducer for air flow and differential pressure sensing 7-61329
inductance standard calibration method, using ratio transfer unbalanced bridge 7-18833
inverter, half-bridge HF variable voltage-fed, used for geophysical survey transmitter 7-23879
katharometer bridge circuit with linearising feedback 7-17840
microbridged objects dielectric props. monitoring, use of microwave bridge (Slovak) 7-65896
thermometer bridge circuit for precision meas. 7-48736
Wheatstone bridge with two thin film arms, dynamic balancing 7-22491
 3He melting curve thermometer, automated, pressure meas. appl. 7-14955

bridge instruments

see also bridge circuits
AC bridge apparatus for thermophysical props. of liquids meas. 7-4844
AC bridge for precision resistance meas., computer-controlled 7-18832

bridge instruments continued

AC four-terminal bridge for low-resistance thermometry 7-9834
AC mutual inductance bridge for magnetic susceptibility meas. 7-41408
automated cryogenic current comparator resistance bridge 7-18829
digital bridge for AC/DC transfer instruments comparison 7-18835
four-terminal AC bridge, easy to build, for temp. down to 1K 7-14957
HV capacitance meas. bridge, frequency dependent errors 7-18813
ionic conductors, solid, impedance studies, bridge balance conditions and error corrections (German) 7-30033
reference field strength meters with dipole antennas, appl. of thermistors 7-56232
solid ionic conductors, impedance meas. 7-9843
thermometer bridge circuit for precision meas. 7-48736
Wheatstone bridge with two thin film arms, dynamic balancing 7-22491

Bridgman method *see crystal growth from melt*

brightness

see also sky brightness
B2 radio quasars, magnitude distrib. rel. to optically-induced orientation bias 7-60832
black-body radiation, photon radiant and radiant exitance, analytic expression (Chinese) 7-50922
blackbody radiant source, low temp. large area, with heat pipe (Chinese) 7-50923
Cas A, supernova remnant, surface brightness map at 1.2 mm wavelength 7-24176
cinematography, brightness perception scaling, double-comparison method (Russian) 7-4906
P/Comet Halley (1982i), far-IR photometry obs. 7-18386
P/Comet Halley (1982i), JHK photometry and visual magnitude estimates (1987 January 28 to February 12) 7-66512
P/Comet Halley (1982i), total visual magnitude estimates (1986 November 3 to December 4) 7-40781
P/Comet Wilson (1986i), Feb. 1987 visual magnitudes 7-66513
Comet Wilson (1986i), total visual magnitude estimates (1986 October 17 to 23) 7-24079
comet Wilson (1986i), total visual magnitude estimates (1986 November 25 to December 7) 7-47772
Comet Wilson (1986i), total visual magnitude estimates (1986 December 20 to 27) 7-47781
P/Comet Wiseman-Skiff (1987b), total visual magnitude estimates (1987 January 22 and 26) 7-55551
cometary magnitude distribution, implications for fading of comets 7-55566
comets, brightness outbursts due to icy bodies fragmentation in solar wind high-speed streams 7-47768
comets, dust tails, density and brightness distrib. 7-60597
comets, flare activity rel. to velocity waves in solar wind 7-4371
Crab Nebula, surface brightness map at 1.2 mm wavelength 7-24176
dwarf galaxies, luminosity classification anal. 7-60794
dye laser, tunable with electro-optic Q-switching of coupled laser, characts. 7-1197
early-type galaxies, X-ray surface brightness distrib. and spectral props. 7-55799
Earth surface, correl. of spectral radiance parameters measured from multiband space images 7-66339
electron-optical image luminance amplifiers, resolution capability 7-50784
eye movement tracking, target brightness feedback (Japanese) 7-47049
galaxies, effects of gravit. amplification of brightest cluster galaxies by foreground clusters 7-24206
galaxies, redshift-magnitude formula for Universe with cosmological const. and radiation press. 7-40924
galaxies luminosity function determination, non-parametric method for magnitude-limited samples 7-24212
galaxies with box and peanut-shaped bulges, minor axis brightness profiles 7-29526
human face brightness level by semi-cylindrical illuminance (Japanese) 7-3790
ion beam generation and focusing from conical pinched electron beam diode 7-11806
irradiance calc. in D* determ., precision improvement (Chinese) 7-48825
LDN 1642, high-latitude cloud, IRAS mapping, visible surface brightness and extinction 7-48062
light diffusing materials, luminance factor meas. 7-41423
Lyman alpha disk absorbers towards QSOs, surface brightness limits 7-4587
M83, near-IR photometry characts. 7-60802
NGC 1381, edge-on S0 galaxy, components, surface photometry anal. 7-55792
physiological intensity transform function and lightness scale (Japanese) 7-3787
Pieron's law analysis of simple reaction time to light stimuli by the model considering threshold intensity (Japanese) 7-8561
quantum photometry, absolute spectral density meas. of energy brightness 7-62769
quasar luminosity evolution, flux-redshift relations in chronometric cosmology 7-24237
quasars, brightness scale length of outer regions rel. to active nuclei characts. (Russian) 7-55826
quasars, effects on spectrum and brightness of gravit. micro-lensing 7-9364
quasars luminosity function, flux conservation theory rel. to amplification by random gravit. lensing 7-23994
radiance theorem with partially coherent light 7-42900
radio galaxies, 0.6 GHz intensity and linear polarisation mapping of edge-brightened double sources 7-66737
radio sources, extragalactic, 5-GHz flux densities 7-4353
radio sources, spectral flux densities at 22 MHz 7-18457
radio sources near 3C 84 and 3C 273, right ascensions and 7.6 cm flux densities 7-66774
Seyfert galaxies, brightness scale length of outer regions rel. to active nuclei characts. (Russian) 7-55826
Seyfert galaxies, luminosity function and space density 7-24202
Seyfert galaxies, surface brightness distrib. 7-40909
SNRs, surface brightness-diameter relation 7-40889
SNRs, surface brightnesses and radio spectral indices 7-14621
soft X-rays from lasers, undulators and plasmas, coherence props. 7-18956
Sun, quiescent prominence, density and temp., EHF brightness temp. obs. 7-4407

brightness continued

- undisturbed background disk galaxies, surface brightnesses radial distrib. 7-66736
- undulator, soft X-ray, performance predictions 7-42876
- undulator sources, phase distribution of brilliance 7-31224
- vision, contrast threshold measurement system 7-54563
- vision, spectral luminous efficiency functions by heterochromatic brightness matching 7-47064
- X-ray sources, extragalactic, relation between X-ray luminosity and redshift 7-14679

Brillouin scattering *see Brillouin spectra***Brillouin spectra**

- see also stimulated Brillouin scattering*
- cadmium arachidate Langmuir-Blodgett films, elastic props., Brillouin scatt. study 7-32885
- glasses, Rayleigh and Brillouin scattering spectra, Bayesian deconvolution 7-13173
- laser harmonic spectroscopy use as plasma target diagnostic 7-26503
- metallic superlattices, elastic props., effect of strain 7-52376
- picosecond interferometric technique for study of phonons in Brillouin frequency range 7-14998
- plasma, double induced Mandelstam-Brillouin scatt., π states 7-11606
- plasma, Mandelstam-Brillouin scattering, modulation and self-focusing instabilities 7-58022
- poly(vinyl alcohol) hydrogels, elastodynamics, Brillouin scatt. meas. 7-39136
- PVC, gels, Brillouin light scatt. 7-42798
- quartz, incommensurate phase, temperature dependent low-frequency modes 7-6737
- Rayleigh-Brillouin gain spectroscopy in gases 7-10473
- silica aerogels, photon-fracton crossover, Brillouin scatt. meas. 7-46878
- single-mode optical fibres, charactn. using spontaneous Brillouin backscattering technique 7-6026
- TMMC, pure and Cu doped, struct. phase transitions, Brillouin scatt., study 7-46055
- two-phonon resonance light scatt., acoustic and optical phonons 7-64660
- whistler waves, stimulated Brillouin scattering in low-density collisionless plasmas 7-58019
- Ar, solid, Brillouin scatt. intensities evaluation 7-33403
- Au on NaCl, elastic surface wave anomalies near cluster to layer transition 7-21606
- C₆K and C₂₄K intercalation cpds., angle-depend. X-ray emission bands 7-46248
- CdS, bound-exciton states, resonant Brillouin scatt. 7-46062
- CdS, Brillouin spectra of acoustoelectronic interaction 7-7292
- Co-Cr films, mag. parameters, Brillouin light scattering study 7-53357
- Fe ultra thin films, Brillouin scatt. 7-27728
- Fe-Pd multilayer structs., localised phonon modes 7-46061
- Fe-Pd multilayer structures, collective spin waves 7-46060
- Fe-W, multilayer structures, collective spin waves 7-46060
- GaAs-Ga_{1-x}Al_xAs superlattices, Brillouin scatt. 7-3063
- HF solid, elastic and photoelastic anisotropy at high press. 7-2083
- ⁴H, liq. and solid, elastic props., and density up to 20 GPa 7-32733
- K₂O-PbO-SiO₂ glasses, chemically nonuniform struct., Rayleigh and Mandelstam-Brillouin scatt. 7-1891
- LaF₃, lattice phonons, high temp. Brillouin scatt. studies 7-46059
- LiKSO₄, Brillouin light scatt. between 20 and 80°C, elastic constants meas. 7-7712
- LiKSO₄, phase transition, low temp. Brillouin studies 7-44806
- ND₃, elastic consts. and elasto-optic coeffs., Brillouin spectra anal. 7-53359
- NaBi(MoO₄)₂, elastic and elasto-optic props. 7-7672
- NaN₃, trigonal-monoclinic phase transition, Brillouin scatt. studies 7-22275
- Nb₂Ir films, lattice-stiffness changes due to ion irradiation, Brillouin scatt. 7-52379
- P, black, surface acoustic props., Brillouin scatt. study 7-38316
- Pb₂Ge₂O₁₁, sound velocity discontinuities at the phase transition 7-17274
- RbI single cryst. high press. Brillouin scatt. meas. 7-3061
- n-Si, ultraheavily doped, Rayleigh surface waves, Brillouin scatt. study 7-21605
- SiO₂, amorphous, annealing and relax. in high-press. phase 7-17329
- Xe, solid, Brillouin scatt. intensities evaluation 7-33403

Brillouin zones

- see also band structure*
- [2D] Bravais lattices, Brillouin-zone integrations, geometric generation of special points 7-7082
- energy differences between structurally different crystals 7-7144
- N-isopropylcarbazole, phase transition, elastic props. 7-38087
- modulated structures, lattice dynamics, appl. to superlattices 7-52220
- momentum Bloch functions, closure property 7-45123
- quasicrystals, two-dimensional, acoustic phonon spectrum of Penrose tilings 7-26892
- superlattices, band theory 7-45124
- tetracyanobenzene-naphthalene (anthracene) complexes, charge-transfer crystals, orientational transitions, mean field approach 7-6783
- Cd_{1-x}Hg_x alloys, electronic structure dependence on crystal lattice parameters 7-45141
- Cu (001), variable temperature angle-resolved photoemission, non-direct transitions 7-64874
- Cu (100), Rayleigh phonon dispersion, stress-induced freq. shift, EELS studies 7-27090
- CuNi, substitutionally disordered, electronic struct., LCAO-CPA calcs. 7-64067
- Fe, Hall effect, anomalous, and energy band struct. (Russian) 7-52414
- GaAs (110) with ordered Sb overlayers, ARUPS 7-59378
- GaAs, laser material, intervalence band absorpt. coeff. calc. 7-3015
- GaAs-Al_xGa_{1-x}As type I superlattices, electronic struct., tight binding calcs. 7-45475
- GaAs-AlAs superlattices, lattice dynamics 7-52220
- Ga_{0.47}In_{0.53}As, laser material, intervalence band absorpt. coeff. calc. 7-3015
- Ga_{0.28}In_{0.72}As_{0.6}P_{0.4}, laser material, intervalence band absorpt. coeff. calc. 7-3015
- GaP (110), with ordered Sb overlayers, ARUPS 7-59378
- In_{1-x}Sn_x alloys, electronic structure dependence on crystal lattice parameters 7-45141
- Ni (100) with adsorbed C, electronic struct. 7-7315
- Ni, ferromag., magneto optical effects and band struct. (Russian) 7-59188

Brillouin zones continued

- Ni, Hall effect, anomalous, and energy band struct. (Russian) 7-52414
- Pt (111), clean and O covered, surface phonon dispersion, inelastic atom scatt. meas., lattice dynamical calcs. 7-52226
- Si surfaces, (111)7×7-Ge and (111)5×5-Ge, angle-resolved photoelectron spectra 7-3150
- Si/Si_{0.5}Ge_{0.5}-x strained layer superlattices, folded phonon dispersion 7-44718
- TiC (100), surface phonon dispersion curves, EELS determ. 7-52224
- TiH_x, X-ray diffr., lattice parameter change, density of states 7-44469
- W, valence bands, angle resolved XPS spectra 7-22441
- Zn, phonon spectrum fine structure 7-16702

Brinell testing *see hardness testing***bristles** *see fibres***brittle-ductile transitions** *see ductile-brittle transition***brittle fracture**

- see also ductile-brittle transition; notch brittleness*
- acoustic emission during coherent fracture 7-53834
- barrier puncture with brittle fracture by rigid cone 7-43786
- brass, Naval, transgranular SCC, dislocation distrib. 7-17708
- ceramic materials, wear mechanism in dry rolling friction 7-59643
- ceramics, static-fatigue limit of materials containing small flaws 7-39620
- cermets, structural materials, cyclic strength 7-59624
- contact flaws, strength, lateral crack growth effects 7-8091
- crack propagation in 3D, formulation 7-57739
- crack stability and toughness charact., book contrib. 7-26224
- crack tip opening displacement, ductile and brittle fracture anal. of surface flaws 7-63078
- disk, rotating, variable thickness, dynamic creep rupture 7-43781
- ductile-brittle transition in cleavage fracture 7-21339
- elastic body containing moving crack, dynamics 7-43788
- engineering materials, general yield criterion depend. on void growth 7-1444
- fatigue data statistical analysis 7-17636
- fibre reinforced composites, brittle, Weibull statistical distrib. of strength 7-3429
- glass specimens, brittle fracture threshold under effect of pulsed electron beam, effect of geometrical dimensions 7-3399
- glassy epoxy polymer V notched specimens, quasi brittle fracture (Polish) 7-46744
- graphite, nucl. grade, fracture processes and oxidation effects 7-28157
- high tensile steel electroplating, H₂ embrittlement fracture prevention (German) 7-33767
- ice, freshwater, crack resist. determ. 7-12195
- Li₂ intermetallics, localised grain-boundary electronic states and intergranular fracture calcs. 7-45215
- local approach of fracture, continuum damage mechanics 7-50988
- materials with defects, brittle compressive failure criterion 7-43762
- metallic glasses, ductile and brittle fracture at low temp. (Russian) 7-39650
- metals, internal interfaces, grain boundary struct., intergranular fracture 7-26766
- micromechanics of brittle failure in compression, splitting, faulting and brittle-ductile transition 7-13590
- Monel 400, embrittlement by Hg, effect of prestress 7-3431
- PMMA, brittle fracture, Rayleigh wave emissions 7-31699
- poly(1,4-dimethylene-trans-cyclohexyl suberate) mol. wt. blends, fracture energy and morphology 7-37899
- polycarbonate-polystyrene-acrylonitrile, coextruded multilayer composites, tensile props. 7-59572
- polymer fibre, discontinuous strength spectrum 7-17610
- solids, brittle, in nonuniform strain field, fracture 7-43784
- sphere, twisting, induced stress field 7-11314
- statistical analysis of cleavage fracture ahead of sharp cracks and rounded notches 7-13540
- steel, austenitic stainless, N-containing, thermochemically produced, wear 7-17651
- steel, B-containing, H-embrittled grain boundaries, Auger anal. 7-59633
- steel, brittle fracture induced photon emission (Russian) 7-33465
- steel, C, brittle fracture micromechanism in specimens containing intergranular cementite (Russian) 7-59621
- steel, C-Mn, hot ductility, influence of grain size 7-3374
- steel, C-Mn and Nb treated, high temp. ductility loss, grain boundary segregation 7-46573
- steel, Cr-Mo, crack initiation under sustained load, effect of impurity segregation 7-65111
- steel, Cr-Mo, toughness, impurity element effects 7-53856
- steel, Cr-Mo-V, rotor, high temp. creep, prior austenite grain size effect 7-53828
- steel, dual phase, effective grain size, cleavage crack propag. 7-28118
- steel, eutectoid, fully pearlitic, cleavage fracture stress, microstruct. effects 7-28123
- steel, ferritic-pearlitic, welded joints, hot embrittlement proneness 7-39658
- steel, fracture toughness of specimens with mixed microstruct., prediction using conc. model 7-13570
- steel, Hadfield, cold-deformed, fine struct. anal., brittle fracture (Russian) 7-59570
- steel, high strength, fatigue crack growth, slip localisation, intergranular fracture 7-28120
- steel, low alloy, retarded brittle fracture, crack nucleation stress and internal microstresses (Russian) 7-8084
- steel, low alloy, surface crack growth under axisymm. cyclic bending 7-28130
- steel, low-alloy construction, nonmetallic inclusions influence on impact strength and fracture type 7-8085
- steel, low-C, Ni influence on struct., fracture resist. and fractographic features 7-3420
- steel, maraging, fatigue at low growth rates 7-39621
- steel, martensitic stainless, brittle failure rel. to overheating, fractography 7-22796
- steel, martensitic stainless, precipitation hardened, impact toughness rel. to Mo content, AES obs. 7-39666
- steel, medium C, impact toughness and fracture, prolonged high tempering effects (Russian) 7-8083
- steel, mild, brittle fracture, microcracks effect (Russian) 7-59618
- steel, mild, fast fracture, crack arrest behaviour (Japanese) 7-59610
- steel, Mn-Cr, case carburising, mech. props., influence of inclusion characts. 7-65135
- steel, Mo-Ni-Mn, creep fracture mechanisms and rupture life 7-65137

brittle fracture continued

- steel, Ni, p/m type, fracture struct. features 7-33789
 steel, Ni-Cr, tensile flake form., H damage, dislocation transportation (*Chinese*) 7-8077
 steel, pressure vessel weld metal, cleavage fracturing stages at inclusion sites 7-8092
 steel, stainless, austenitic, valve type, heat treatment schedule effect on failure nature 7-3423
 steels, stainless, α -particle irradiated, mech. props. and microstruct. 7-51872
 steels and weld metals for LWR press. vessels, brittle failure resist. 7-59636
 structurally stress concentrated regions, brittle fracture strength eval. method 7-3424
 thickness effect in fracture toughness, probabilistic anal. 7-65123
 viscoelastic medium with microfractures, mechanical behaviour under extension and shear 7-29003
 Weibull parameters estimation using weight function 7-22934
 Zircaloy-2, low cycle corrosion fatigue in I_2 atmosphere 7-17705
 Al-Cu-Li alloys, cyclic fracture, mechanisms 7-46634
 Al-Cu-Mg, IN 9021, creep crack growth fracture morphology 7-53881
 Al-Li-Cu-Mg-Zr die forgings, mech. props., microstruct. 7-46636
 Al-Li-Cu-Zr, fracture, ageing and comp. depend. 7-22784
 Al-Mg and Al-Zn-Mg alloys, plasma-coated, heat treatment effect on fine struct. and failure mechanism 7-3496
 Al-Si, brittle failure rel. to overheating, fractography 7-22796
 C steel-cast Fe-Cr bimetal, interface bonding strength (*Korean*) 7-17618
 Co₈₄Nb₁₀B₆ fully crystallised metallic glass, fracture processes 7-22841
 Cr, low alloyed, elastobrittle failure under thermal loading stresses 7-33790
 Cu-Al₂O₃, dispersion strengthened powder alloys struct. and mech. props. 7-53667
 Cu-Al-Ni, β -phase alloys, fracture rel. to grain boundary precip. and Ni content 7-59604
 Cu-Al-Ni, shape memory alloys, polycrystalline, cyclic deform., fatigue above transform temp. 7-3434
 Cu-Al-Ni shape memory alloys, polycrystalline, cyclic deform. and fatigue above transform. temp. 7-3433
 Cu-Al-Ni-Ti-Zr, shape memory alloy, grain refinement, fracture mode, Ti and Zr additions effect 7-3301
 Cu-GeO₂, dispersion hardened polycryst., intermediate temp. embrittlement 7-53903
 Cu-Sn, ductility at elevated temps., effect of small amounts of B, P or Mg 7-53904
 Cu-Sn-B(Mg)(P), ductility at high temp., alloying additions effect (*Japanese*) 7-13515
 Fe, cast, nodular graphite, fatigue crack propag. rel. to microstruct., SEM obs. (*Chinese*) 7-13542
 Fe powders, hot pressing, fracture toughness, intergranular failure rel. to porosity 7-13596
 Fe-Ni-C and Fe-C, bainite reaction kinetics, austenitising temp. effect 7-13453
 Fe-Ni-Cr, reactor bolting material A-286, failure analysis 7-30536
 Fe-Ni-Cr (25.15 wt.%), MC stabilized, fatigue life, effects of implanted He 7-53852
 Ge single crystal, microstruct. of fragments (*Russian*) 7-38107
 Nb, pure, tensile deform., brittle fracture, H effect, SEM obs. (*Chinese*) 7-8078
 Ni 201 discs, H-induced rupture 7-3418
 Ni, intergranular H embrittlement kinetics 7-65134
 Ni-Si, ductility, influence of rad.-induced segregation 7-53798
 Ni₃Al-B, with and without Hf additions, dynamic embrittlement at 600°C 7-65112
 Ni₃Al-B, ductility, strength, grain boundary segregation, solid soln. strengthening, Be addition effect 7-39608
 Si single cryst., laser-driven shock induced damage study 7-64829
 Ti-Al, brittle failure rel. to overheating, fractography 7-22796
 TiAl, deform. at high temp., flow and brittle fracture stress (*Japanese*) 7-13516
 TiC-Ni-Mo sintered carbides, struct. and physicomech. props. 7-3256
 WC-TiC-Co hard alloy Ti5K6, heat treatment effect on failure mechanism 7-13550
 Zr alloys, hydride cracking, acoustic emission studies 7-59637

brittle materials *see* **brittleness****brittleness**

- see also brittle fracture; embrittlement; hydrogen embrittlement; liquid metal embrittlement; notch brittleness*
 ceramic, advanced, developments and research on cracking tendency 7-27989
 cutting tool materials, mech. props., wear-resist. relations 7-3443
 delayed damage in brittle solids 7-38111
 fracture mechanics and strength size effects, phys. evidence 7-57756
 fracture toughness, crack front irregularity effect 7-57740
 glass tubing, thermally induced crack propagation (*German*) 7-22805
 microcracked elastic solid, 1D constitutive model 7-1488
 polyethylene, chlorinated, prep., mech. and thermal props. 7-28006
 porous brittle solid, strength and elastic modulus, acousto-US study 7-21321
 porous brittle solids, Young's modulus 7-58396
 rocks, fracture anal. 7-66106
 steel, 4340, positron annihilation parameter and H behaviour, effects of tempering temps. 7-46205
 steel, alloy, trace element precipitation and segregation, hot brittleness effects (*French*) 7-17608
 steel, Cr-Ni-Mo-Fe-C, reversible temper brittleness kinetics investig. (*Russian*) 7-13554
 steel, ferritic-pearlitic, welded joints, hot embrittlement proneness 7-39658
 steel, medium C, impact toughness and fracture, prolonged high tempering effects (*Russian*) 7-8083
 steel, p/m, heat treatment effect on strength and yield parameters 7-53775
 steel, stainless, Cr type, chem. microinhomogeneity of solid solns. effect on brittleness 7-3422
 tensile fracture loci of brittle materials containing spherical voids 7-12200
 Fe-base alloys, grain boundary internal adsorption of C and P, segregation study (*Russian*) 7-6961
 LaNi₃, anisotropic H migration, deposition potentials, hardness, brittleness meas. 7-6873

brittleness continued

- Ni₃Al, computer simulation of grain boundaries, effect of comp. 7-21228
 TiC-WC-Ta-C-Co hard metals, Ta conc. effect on comp. and physicomech. of carbide and Co phases 7-53708
 W-Re, damage mechanisms, cold brittleness, dislocation motion (*Russian*) 7-59619
broadband amplifiers *see* **wideband amplifiers**
broadband networks
 fibre optic broadband networks, conf., Cannes, France (Nov. 1985) 7-35092
 single-mode connector for broadband network appls. 7-37155
broadcast antennas
see also broadcasting
 eLF/VLF/LF propagation and system design 7-40642
broadcasting
see also radio broadcasting; television broadcasting
 METSIS system for satellite broadcast of weather information; earth station config. 7-47522
 radio and TV announcers Japanese, intonation rules and acoustic characts. 7-43563
 recording and broadcast studio, electronic architecture 7-6063
broadside antennas *see* **antenna arrays**
bromine
see also nuclei with
 adsorbed on Ag (110), normal exit XPS studies 7-2380
 adsorpt. and reaction states on Ag (110), UV photoemission study 7-45014
 atmosphere pollutant, implications for Antarctic O₃ depletion 7-55173
 atom, electron impact ionisation cross sections meas., TOF spectra 7-42770
 atom, photodissoc., initiated by laser emission 7-65339
 atom, photodissoc. prod., electronic states, Raman spectra anal. 7-42530
 chemisorption on (111) and (100) surfaces of Si 7-6979
 chemisorption on Si (111), SCF HF cluster calculation 7-52251
 dopant in trans-polyacetylene, theoretical studies of polarised XANES 7-64823
 graphite-Br intercalation cpds., 2D stripe-domain system, melting transition 7-58449
 intercalation compounds with graphite, struct. and phase transitions, review 7-52041
 liquid, optical props. 7-17294
 molecule, B³II(0_u⁺), electronic self-quenching energy transfer rate consts. 7-20015
 molecule, EXAFS, inelastic processes, semiclassical treatment 7-64741
 molecule, inelastic scatt. from graphite surface, Monte Carlo classical trajectory calcs. 7-27837
 plasma, laser produced, oscillator strengths, X-ray transitions, ab initio calcs. 7-16334
 trans-polyacetylene: Br, polarised K edge XANES, short range order multiple scatt. calcs. 7-53445
 polyacetylene:Br(I), polarised EXAFS and near edge spectra studies 7-64778
 radioisotope production, anal. and appl., conf., Banff, Canada, Sept. 1985 7-24254
 tetrabromomethane:Br₂ dil. binary mixture, directional solidification, cellular instabilities 7-26921
 α -Al₂O₃:Br, ion implanted, RBS and annealing studies 7-32515
 BN:Br₂, intercalation cpd. formation 7-44574
 Br XXV to XXI, spectra and energy levels 7-25444
 Br⁻, in ethylene-glycol (ethylene glycol-water), primary medium effects 7-12313
 Br⁻, solns., positronium form. and hydrated positron reactions 7-17809
 Br⁻ solutions, anodic oxidation of anodic Cu 7-52052
 Br₂, recombination and relaxation dynamics of diatomic molecules in condensed phases 7-10684
 Br₂ solid, high press. X-ray absorpt. study, energy dispersive mode 7-59299
 Br₂⁺, excited state spin-orbit interaction 7-49962
 Br₂+Ba, chemiluminescent reactions; spin orbit state effect 7-13781
 Br₂+Xe, atom and excitation transfer, energy disposal, product rot. alignment 7-31158
 Br₃⁻, electrical cond. mechanism, tight-binding and ab initio pseudopot. calc. 7-52546
⁸¹Br, A=75-7, radioisotope prod. for medical appl., review 7-28693
 CdI₂:Br, indirect excitons, isoelectronic impurity effects, luminesc. spectra 7-27255
 Fe-Br, mag. hyperfine field of ⁸¹Br, NMR nuclear orientation study 7-13049
 I₂+He, bound and continuum states, excitation transfer, optical and electron spectroscopy investig. 7-36689
 KBr:Se²⁻, electronic spectroscopy 7-22319
 Zn-Br cells, selection of quaternary ammonium bromides as electrolyte 7-39986
bromine compounds
 bromide salt hydrates, H-bonded (H₂O.Br⁻)_∞ 7-51738
 intercalated with graphite, electromech. effect on heating 7-45414
 X-ray fluorescence anal. of K X-ray intensities 7-59805
 BrCN⁺, B²II state, radiationless transition, fluoresc.-photon coincidence study 7-31101
 BrF, FT IR spectra, rot. struct. 7-922
 BrO, RF discharge, optogalvanic detected IR spectra 7-20970
 BrO, stratospheric composition 7-60324
 C₂₈Br₂ intercalation cpd., 2-D system with competing interactions, phase transitions 7-6791
 HX-XCN complexes (X=F, Cl, Br) H bonding ab initio calcs. 7-56960
Brownian motion
see also colloids
 absorbing and reflecting motions, filtering problems 7-48579
 aerosol particles with fractal structure, effect of coagulation on diffusive spread 7-18728
 aerosols, Brownian diffusion and particle coagulation 7-48564
 aggregation, efficient algorithm for Brownian dynamics simulation 7-48552
 atmosphere aerosols, model evaluation with Brownian diffusion technique 7-4086
 bidispersion, dil., sedimentation and diffusion, Onsager symmetry, kinetic coeffs. 7-26322
 bimolecular reactions, diffusion influenced, kinetics study 7-65283

Brownian motion continued

- branching Brownian motion and KPP eqn., appl. to spatial trees (*French*) 7-56016
- charged particles motion, bounded systems with collisions 7-48521
- cosmic strings, fractal geometry and galaxy and cluster correlation functions 7-56115
- diffusion in bistable potential, general inverse friction expansion 7-29950
- diffusion limited kinetics 7-56167
- dynamical systems and statistical physics conf., Koszeg, Hungary, Aug.-Sept. 1984 7-48194
- electric field, obs. in laser 7-57293
- factorisations in fluctuating time change 7-56013
- fast variables elimination in Brownian motion problems 7-14871
- first-passage times for the Uhlenbeck-Ornstein process 7-35402
- fractional Brownian motion, max. likelihood estimation rel. to image texture, radiography appl. 7-13945
- gel-like sediment form., Brownian dynamics simulation, colloidal and hydrodynamic interaction effect 7-13825
- heated particle in rarefied gas, Brownian movement, kinetic description 7-51231
- Hookean dumbbells with anisotropic hydrodynamic drag and Brownian motion, Giesekus model 7-16216
- interacting Brownian particles in hydrodynamical limit, bulk diffusion and equilibrium fluctuations 7-48585
- interacting diffusions, fluctuation phenomena, tightness problem, stochastic evolution 7-211
- long-range interaction between Brownian particles 7-37616
- macromolecules, transport props. by Brownian dynamics 7-10789
- magnetic fluids, susceptibility calc. at low fields and low frequencies 7-13004
- Markov chain potentials, asymptotic behaviour, random walks and Brownian motion (*French*) 7-61228
- measure-valued critical branching Brownian motion, ergodic theory, local occupation time 7-9777
- particle diffusion in fluctuating fluid with creeping flow 7-20788
- particle in fixed dispersed layer, fluctuation hydrodynamics of Brownian motion 7-24560
- particles, interacting, stochastic descriptions 7-29900
- polymers, linear and ring, shapes, Brownian dynamics 7-42804
- polystyrene lattices, soln., salt-induced aggregation kinetics, quasielastic light scatt. 7-59796
- polystyrene submicron size sphere in aq. suspensions, multiple light scatt. 7-59220
- potential energy barrier, crossing by Brownian particles with curved reaction coords. 7-270
- quantum dynamical semigroups with Brownian motion, dilations 7-61216
- quantum mechanical stochastic differential equations, observables and multiple Wiener integrals 7-48543
- reaction-limited cluster aggregation kinetics, Smoluchowski eqns. modeling 7-41261
- reduced description of Brownian motion in a half-space with a partially absorbing boundary 7-41252
- RF traps, Brownian motion in a parametric oscillator model 7-29911
- sine-Gordon model, 1D, quantum Brownian motion of solitons, numerical simulation 7-24768
- sine-Gordon model with dissipation, quantum statistical mechanics 7-48575
- sols, shear flow, aggregative equilbr. 7-6291
- stochastic particle systems of interacting Brownian particles, equilibrium fluctuations 7-48586
- Stokes-Boussinesq-Langevin equation for time evolution with Alder-Wainwright effect 7-48565
- texture analysis by use of fractional Brownian motion, digital coronary angiograms, appl. 7-8474
- two-level atom, Brownian motion in light wave 7-897
- Wiener process, Brownian motion, Mobius' function and models (*Russian*) 7-24544

Brownian movement see *Brownian motion*

brush discharges see *discharges (electric)*

bubble chambers

- see also *position sensitive particle detectors*
- computerised photographs processing from bubble chambers 7-35498
- high spatial resolution track chambers, holographic data systems 7-36382
- holographic recording for bubble chamber, Q-switched ruby laser pulse stretching 7-43169
- neutrino detection, holographic recording techniques 7-25321
- photographs processing from large bubble chambers 7-36411
- practical holography, conf., Los Angeles, CA, USA (Jan. 1986) 7-24281

bubble memories, magnetic see *magnetic bubble memories*

bubble nuclei see *nuclear density*

bubble point see *boiling point*

bubble points see *bubbles*

bubbles

- see also *bubbles in solids; foams*
- acoustic turbulence, cavitation effects 7-11206
- acoustic wave, nonlinear damping in liq. with gas bubbles 7-20491
- air finger rise in cylindrical tube, rate determ. 7-57910
- air-water transient flow, pressure drop and void fraction 7-6288
- air-water two-phase flow in annuli, phase distrib. 7-44009
- axisymmetric headforms, cavitation inception, turbulence simulators effect 7-16223
- body fluid bubble oscillations 7-65780
- bubble columns, turbulent coalescing, gas holdup correl. 7-37516
- bubble-driven flow, fluid and bubble meas., numerical soln. 7-16237
- buoyant vapour bubbles modelling growth and collapse, rigid boundary, stagnation flow 7-16220
- cavitation nuclei meas. using optical system 7-51243
- circular fuel elements steam-generating bundles, voids fraction 7-6280
- column with draught tube and sieve plate, size of bubbles and liq. circulation 7-37517
- columns in liq. circulation regime, hydrodynamics 7-11499
- columns with low height to diameter ratio, optimum gas sparger design 7-44071
- conference, Cambridge, England (March 1986) 7-40987
- creeping flow around spherical gas-bubble in liquid, Oseen's eqn. soln. 7-37513
- cylinder, rotating horizontal, partially filled by viscous fluid, transient temp. distrib. 7-6215

bubbles continued

- diameter meas. by fringe method, using laser Doppler anemometer 7-16278
- excitation of surface waves by sound in a liquid containing gas bubbles 7-62883
- extended bubbles, velocities in inclined tubes 7-16231
- falling liq. film, vapour generation nucleate boiling, acoustic diagnostic technique 7-11502
- firm closure, lattice models, percolation on interstices of BCC lattice, bubble age 7-14320
- flow transition in inclined pipes 7-20782
- fluid phases, separation, and bubble dynamics in temp. gradient and microgravity conditions 7-20722
- fluid pressure measurement using bubbles insonified by two frequencies 7-20547
- formation at submerged orifice using boundary element method 7-6272
- free streamline model for a rising bubble 7-11520
- gas, in liq., press. pulse decay, num. study 7-6277
- gas absorption from single gas bubbles 7-6273
- gas bubble rise vel. in liq.-filled tube, surface tension and viscosity effects 7-57903
- gas phase in bubble columns in liq. circulation regime, residence time distrib. modelling 7-11500
- gas-bubble nucleation in supersaturated solns., gas diffusion into cavity 7-52095
- gas-bubble nucleation in supersaturated solns. during electrolysis, electrode surface effects 7-54139
- gas-liquid contact in Karr columns, press. drop, gas holdup and interfacial area 7-6284
- gas-liquid dispersions in bubble columns, flow instability 7-11498
- gas-liquid mixture, bubbly flow parameters, bubble breakup effect 7-44021
- gas-liquid mixture through nozzles, transient interphase energy transfer 7-6281
- gas-solid fluidised bed, freeboard region, two-phase flow behaviour 7-63209
- gas-vapour bubble oscillations in acoustic field, num. investig. 7-52022
- generating impact pressure, nonspherical collapse (*Chinese*) 7-20765
- glass melts, gas bubble dissolution and growth 7-2302
- growth and collapse, transient boiling heat transfer in narrow channel 7-26346
- heat transfer coeff. for bubble and transition-boiling regimes 7-11416
- Hele-Shaw cell bubble shape, surface tension effect 7-31869
- heterocoagulation by bubbles in a turbulent multiphase flow. 7-37529
- HF travelling-bubble cavitation noise generation 7-16221
- high pressure bubble growth in multicomponent liquid droplets in a flowing immiscible liquid stream 7-63785
- highly viscous pseudo-plastic non-Newtonian solns. in bubble columns, hydrodynamics, mixing 7-16234
- horizontal boiler tubes, dryout criteria for nonuniform heat flux 7-20713
- incompressible fluid with gas bubbles hydrodynamics eqns. soln. 7-11501
- insulating liquids, air bubbles attached to point electrodes 7-37779
- interactions and radiated pressure waves 7-16018
- interstellar bubbles, structure and evolution is multiphase interstellar medium 7-60764
- inviscid liquid shell surrounding incompressible gas bubble, axisymmetric oscillations 7-44027
- linear sound propag. for 1-component, 2-phase bubbly medium 7-57617
- liquid phase mixing in bubble columns with Newtonian and non-Newtonian fluids 7-6256
- liquid with vapour bubbles, finite duration pulses and shock wave evol. 7-6250
- liquid-filled resonator tube, influence of gas bubbles 7-62880
- low-velocity flow measurement by bubble/dye tracing technique 7-16283
- Marangoni convection, bubble motions induced by a temperature gradient 7-20717
- mass concentration waves dynamics in two-phase gas-liquid bubble mixture in pipe 7-6287
- mass transfer during bubbling in single and multi-orifice absorbers 7-6275
- maximum size during nucleate boiling in elec. field 7-50918
- molten carbonate fuel cells, fabrication of bubble press. barriers 7-13856
- motion in capillary tubes, wetting film thickness anal. 7-44952
- Newtonian liq., bubbly, translational drag force reduction 7-51293
- non-wetting melt in free fall, bubble-bridge config., contact angle 7-21572
- nonlinear wave propagation, gas-liquid media of bubble struct. 7-20787
- non-Newtonian flow, transient mass and heat transfer from drops or bubbles 7-11473
- ocean, bubble clouds meas. by automatically recording inverted echo sounder (ARIES) 7-8991
- ocean gas bubble sensing using acoustic pulses 7-43501
- organic liquid, multiple bubble collapse (*Chinese*) 7-11518
- organic liquids, bubble collapse (*Chinese*) 7-11516
- particles, drops and bubbles, velocity calcs. 7-57896
- physics of acoustic cavitation 7-11207
- point sink on plane with magnetic field, heat and mass transfer 7-1618
- polymer solutions, bubbles growth and collapse 7-37531
- power law fluid, multiple drop slow motion, drag and mass transfer 7-11472
- pressure pulse reflection at free surfaces of water 7-11480
- rise velocity of large bubbles in stagnant liquid in non-circular ducts, estimation 7-37524
- self-sustaining detonation 7-31839
- separation diameter, precooled volume effects 7-44024
- shock wave structure, liq. with bubbles, transient heat and mass transfer effect 7-6249
- single bubbles free rising in Newtonian liquids, gas desorption, mass transfer, drag coeffs. 7-16233
- size distribution in bubble beds 7-44012
- sizing using double freq. technique 7-31556
- soluble gas bubbles, dynamics in liq. 7-31866
- sphere, diffusion controlled growth from finite size, numerical solns. 7-44889
- spherical bubbles in turbulent flow, asymptotic diffusion coeffs. 7-6297
- steam condensation in pool water, press. oscill. threshold 7-26334
- superheated liq., flashing in glass capillaries 7-13797
- swirling flow, axisymmetric vortex breakdown in circular pipe 7-26286
- Taylor instability in streamer and bubble amplitude 7-11389
- toroidal bubble motion in unbounded incompressible fluid, velocity pot. determ. 7-31875
- toroidal loop, two-phase natural circulation 7-26280

bubbles continued

- transient dilation of bubbles and drops, theoretical basis for dynamic interfacial meas. 7-32757
 turbulence modelling of separation bubble 7-31756
 turbulent incompressible flow around aerofoils, separation bubbles 7-31761
 two component gas bubbles in fluid, diffusional driven oscillations 7-16235
 two-phase bubbly flow, simultaneous bubble and liquid vel. meas. using LDV 7-20777
 underheated liquid, surface boiling, forced motion, Reynolds analogy appl. 7-31806
 unidirectional solidification under microgravity, particles and bubbles behaviour (*German*) 7-44772
 unsteady compressible viscous flow over airfoils, integro-differential and finite-difference methods 7-31821
 vapor bubbles in liquid filled pipe, US imaging system 7-6333
 vapour bubble, quasistatic growth on boiling liq. surface, contact angle var. 7-44951
 vapour bubble dynamics in layer of underheated liquid 7-57909
 vapour bubble growth in superheated liquid vol., heat flux calc. 7-63204
 vapour bubble growth rate in turbulent flow, calc. 7-16239
 vapour bubbles, implosion and fragmentation, numerical solns. 7-51275
 vapour bubbles, simple model 7-51282
 vapour bubbling of moving underheated liquid, condensation and heat exchange 7-37525
 vapour filled bubbles, motion and development 7-6282
 vertical liquid jet system with downcomers, flow characts. 7-16226
 viscoelastic liquids, bubble velocity and coalescence 7-16232
 viscous fluid in Hele-Shaw cell, bubble form. motion and interaction 7-44026
 viscous Rayleigh-Plesset equation investigation, cavitation press. correl. to fluid viscosity 7-31847
 wave processes in liquid with gas bubbles, num. investig. 7-6248
 K, liq., boiling, pressure effect on departing bubble 7-44774
 N₂, liq., electrical breakdown in presence of thermally induced bubbles 7-63377
 O₂, nucleate boiling at low gravity, microparameters 7-62962
 O₃ solnolysis in aq. soln., reaction rate 7-13756
 o-*Ps*, in Ar, localisation 7-6684

bubbles in solids

- diamond, type Ia, voidites, evidence for crystalline phase containing nitrogen, cell constant determ. 7-2011
 first wall candidate alloys, HFIR irradi. microstruct. development 7-56824
 fusion materials, gas diffusion and temperature dependence of bubble nucleation during irradiation 7-51874
 gas bubble lattice form. and props. under light gas ion irradiation 7-63681
 glass, laser damage initial stage, luminesc. and microwave absorpt. obs. 7-31375
 glasses, calibration of dynamic small-sample analysis systems 7-65370
 inert gas bubble precipitate solid in Al, defects, high resolution electron microscopy studies 7-32424
 metal tritides, disorder induced by aging 7-21199
 metals, bubble nucleation and growth under neutron and proton irradi., nonequilib. statistics 7-51848
 metals, deuteron irradi., multiple fracture planes, bubble growth 7-58372
 steel, austenitic stainless, He-induced creep ductility loss, prediction and anal. 7-53854
 surface fracture during He⁺ ion bombardment 7-21294
 Al and Al alloys, 800 MeV proton irradi., gas accumulation at grain boundaries 7-58361
 Al, implanted, FCC solid Ar bubbles, X-ray diffr. 7-2043
 Al surface, ion irradiated, flaking, orientation dependence 7-38074
 Al:Ar, solid Ar bubble, diffraction anal. 7-16547
 Al-He ion irradi. system, bubble form., positron lifetime meas. 7-37966
 Al-He system, He bubble form. by proton irradi., positron studies 7-44526
 Al-He system, He bubbles, mol. dynamics simulations and positron states 7-58778
 Al-Mg-Si, high-purity, nucleation and growth of precipitates and the bubbles, effect of 600 MeV protons 7-58364
 Al-Xe, implanted, form. of solid precipitates and fluid bubbles, TEM obs. 7-38032
 Al₂O₃, profiled crystals, bubble distrib., cellular struct., residual stresses 7-32422
 Al₂O₃ subsurface layers formed by O₂⁺ ion implantation into Al, O₂ bubbles obs. 7-2035
 α-Al₂O₃:Br, ion implanted, RBS and annealing studies 7-32515
 Ap-Xe-Kr(Ar), ion implanted, bubble growth, lattice parameters, TEM obs. 7-51803
 Bi₄Ge₃O₁₂ crystals, imperfection nature, precipitates and bubbles 7-21463
 Bi₂Ni, α-irradi. and H implanted, elec. resist. and superconducting T_c 7-7202
 C thin surface layers on steel substrates, anticorrosion props., ion bombardment effects study 7-27202
 Cu-Kr system, Kr bubble growth, positron annihilation studies 7-39247
 Cu:Be, neutron irradiated, annealing behaviour of defects, positron annihilation study 7-39291
 Fe-C-H system, H charged, methane bubble form., positron studies 7-37967
 Fe-Cr (12 at.%), ferritic alloy, He⁺ implantation and Fe⁺ irradi., bubble nucleation and growth 7-58362
 He in Nb foil, magnetic flux pinning, temp. and field depend. studies 7-2794
 Mo:D, ion implanted, impurity trapping 7-38029
 Nb:Be⁺ films, radiation defects produced by ion implantation 7-7059
 Nb₂O₅, acoustic emission and swelling, ageing effects 7-33708
 Ni, creep, T charging, He bubble migration and coalescence 7-65102
 Ni, nucleation and growth of He platelets, computer simulation 7-58269
 Ni, T-induced He bubbles on grain boundaries migration and coalescence 7-58289
 Ni-He bubble system, He densities, SANS and TEM studies 7-58266
 Ni-Kr system, Kr bubble growth, positron annihilation studies 7-39247
 Si:BF₃⁻ (001), ion implanted, residual defects, cross-sectional TEM study 7-32471
 SiC, corrosion pitting by molten salts 7-59695

bubbles in solids continued

- TaT_x (x = 0.12, 0.103, 0.42), acoustic emission and swelling, ageing effects 7-33708
 TaT_x, evolution of lattice spacing and damage 7-16582
 UC, fission gas bubble destruction by radiation re-solution 7-42114
 UO₂, fission gas bubble destruction by radiation re-solution 7-42114
 W wire doped with K, morphology and behaviour of K bubbles at varied temps. 7-2223
 ZrT, ZrT_{1.6}, ageing, TEM study 7-51773
- bucket-brigade device arrays** *see charge-coupled device circuits*
- bucket-brigade devices** *see charge-coupled devices*
- buckling**
- annular plate, clamped, buckled states 7-6123
 bars, continuous, lying on elastic supports, nonlinear and buckling anal., theory of elastica (*German*) 7-20609
 bars, initially curved, dynamic elastoplastic buckling 7-63024
 beam theory, torsion, buckling and vibr. problems 7-1458
 beam-column problem for anisotropic cylindrical shells 7-16082
 beam-columns, tapered, exact Bernoulli-Euler static stiffness matrix 7-6122
 beamlike lattice trusses, anisotropic continuum models 7-6085
 beams/columns subjected to non-uniform axial loads, vibration and buckling 7-6140
 column, heavy compressed, with imperfections, buckling 7-1457
 column, simply supported, under tangential follower force, self-adjoint system 7-6125
 columns, inelastic post-buckling 7-37359
 columns, nonlinear viscoelastic, creep buckling 7-6102
 columns, thick-faced sandwich, buckling under distributed axial loads 7-26176
 columns, thin-faced sandwich, buckling under distributed normal loads 7-26175
 columns with elastic axial restraint, FEM-based stability analysis 7-50964
 composite cylindrical shells, buckling under external press. 7-37358
 composite material shallow sandwich shells, finite deflection eqns. and linear stability problem (*Chinese*) 7-43721
 composite shell, conical, stability calc. with allowance for cracking of binder in layers 7-16084
 cylinders, anisotropic, geometrically nonlinear pre-buckling state 7-1456
 cylinders, axially-loaded, elastic buckling, hidden symm. concepts 7-43724
 elastoplastic plate with incremental constitutive relation, buckling (*French*) 7-26179
 fibre reinforced composites, compressive-fluxural/shear failure mode transition, interface strength 7-39586
 films, decohesion from ceramic or semiconductor substrates 7-21711
 finite strain rod model, 3D, computational aspects 7-6119
 frame, two-bar, nonlinear stability anal., elastic type approach appl., buckling behaviour 7-43720
 heavy elastica, critical review 7-11286
 I-beams, inelastic distortional buckling analysis using FEM 7-43722
 I-section members with flexible webs, inelastic flexural-torsional buckling strength (*Japanese*) 7-20610
 laminated thick composite plates, buckling, hygrothermal effects 7-11321
 LMFBR materials, buckling anal. and design rules 7-49517
 metallic sheets, conductivity and surface buckling meas. by eddy current testing 7-54058
 one dimensional plastic buckling simulation of structural members (*Japanese*) 7-16083
 optical fibres, fusion-spliced, Zeiss-Linnik interferometric exam. 7-31531
 panels, cylindrical, instability, effect of centrally located midplane delamination 7-63022
 panels, rectangular, compression testing simply supported boundary conditions 7-33869
 paperboard, constitutive behaviour under uniaxial and biaxial loading 7-63019
 pipelines, initiation and propag. of buckles 7-26180
 plate, rectangular, uniformly compressed, post-critical state (*Polish*) 7-43727
 plate, thick, bimodulus, post-buckling behaviour (*Chinese*) 7-11318
 plate, thick rectangular, buckling, high-order deform. theory (*Chinese*) 7-11320
 plate, trapezoidal, on elastic base, vibration and buckling 7-48365
 plate elements, geometric stiffness matrix formulation 7-43723
 plates, bimodulus thick circular, axisymmetric buckling analysis using FEM 7-57716
 plates, elastic, flat, crit. linear buckling loads, dynamic meas. method 7-63023
 plates, multiannular, buckling analysis using power series numerical method 7-20607
 plates, orthogonally stiffened, under lateral and axial loads, nonlinear anal. 7-37360
 plates, orthotropic, linear bending and buckling, eigenvalue problems 7-37352
 plates, orthotropic rectangular linear elastic under biaxial loads, post-buckling stability 7-50966
 plates, prismatic, folding, instability by finite strip method (*Spanish*) 7-20611
 plates, rectangular laminated composite, dynamic stability analysis using finite strip method 7-6118
 plates, rectangular thin, bending vibr. study 7-57727
 plates, weakened by cracks, tensile and compressive buckling 7-6124
 plates and curved panels, fibre reinforced, post-buckling behaviour under compression and shear (*German*) 7-20615
 plates with partial edge loading, simplified buckling criterion appl. 7-31664
 plates/shells, two-dimensional FEM model for buckling analysis 7-57717
 polar orthotropic annular plates on elastic foundation subjected to hydrostatic loading 7-11329
 polymers, persistence length correlation with Euler buckling fluctuations 7-31668
 reactor construction codes and engineering mechanics conf., Paris, France, Aug. 1985 7-48153
 rectangular elastic plate problem, bifurcations near a multiple eigenvalue 7-6098
 ring stiffened circular plates, asymm. buckling 7-6126
 rod, curvilinear sectional stability of planar bending mode with allowance for initial defects 7-31661

buckling continued

- rods, completely supported, energylike functional for buckling load calc. 7-26183
- rods, elastic, stationarity for non-selfadjoint problems 7-26178
- rotating beam vibrations 7-11330
- rotating nonlinearly elastic rods, multiple steady state, buckled and unbuckled states 7-11291
- sandwich structures buckling strength study (*Chinese*) 7-11319
- shell, bifurcational stability problems soln. using finite element method 7-16087
- shell, cylindrical, buckling analysis on refined eqns. basis 7-43729
- shell, cylindrical, dynamic stability under nonaxisymmetry loading 7-57720
- shell, cylindrical, hinged compressed, connected to elastic filler, axisymmetric stability, boundary conditions 7-43730
- shell, cylindrical, long, confined, propagating buckles 7-43725
- shell, cylindrical, three-layer, spectrum of regions of dynamic instability 7-16085
- shell, multilayered, coiled, unidirectional buckling 7-16088
- shell, open sandwich conical, elastic-plastic, critical loads and stability loss (*Polish*) 7-43728
- shells, cylindrical, elastic-plastic buckling anal. 7-26181
- shells, cylindrical, stringer stiffened, buckling loads, multimode analysis, imperfections meas. 7-43726
- shells, cylindrical viscoelastic creep-stability anal. 7-26166
- shells, shallow saddle-shaped hyper, initial post-buckling behaviour 7-26177
- shells, spherical, orthotropic, shallow, on elastic foundation, nonlinear studies 7-37357
- shells laminated, buckling problems, nonlinear first order theory (*German*) 7-20614
- shells of revolution, cantilevered, pressure buckling 7-20613
- steel, carbon, thin walled square pipes subjected to compressive load, local buckling strength 7-17578
- steel nuclear containment building, buckling, expt. and anal. programme 7-53818
- thin elastic shells, general concept in rotation shell theory, to torus appl. 7-6101
- thin flat-walled structures, buckling, spline finite strip method 7-1459
- thin-walled structures under combined loading, elastic buckling anal. using finite strip method 7-20612
- tubes, curvilinear, under uniformly distributed load, nonlinear deformation and stability loss 7-6121
- tubes with rectangular cross-sections, local buckling 7-50967
- Al₂O₃ fibre reinforced Al composites, compressive failure modes, dead weight or machine loading 7-39663
- C fibre reinforced plastic post-buckling behaviour under compression and shear (*German*) 7-20615
- C fibre reinforced thermoplastic laminates, compressive strength 7-39580
- Cu current collecting grid on Si solar cells, oxidation and spalling 7-22910

buffers (chemical) see pH**building**

- see also architecture; civil engineering
- contactless measurement of wall insulations to prepare the reconstruction of old buildings (*Hungarian*) 7-56259
- earthquake-resistant raised floor systems, seismic support of electronic and computer equipment 7-4003
- industrial and building aerodynamics, conf., Aachen, Germany (June 1985) 7-14699
- radioactivity in building materials used in the Netherlands, proposed standard 7-34287
- thermogrammetry and thermal engineering conf., Budapest, Hungary (April 1987) (*Hungarian*) 7-56258

built-in testing see automatic testing**bulk density** see density**bulk diffusion** see diffusion in solids**bulk modulus** see elastic moduli**bundling** see packaging**buried heterostructure lasers** see semiconductor junction lasers**burning** see combustion**burnout** see combustion**burst noise** see random noise**buses (computers)** see computer interfaces**bushes** see bushings**bushings**

- high power RF cone bushings for PLT plasma heating 7-26460

business see commerce**business graphics**

- Atlas AMP, Map-Master, and Randmap, mapping packages for IBM PCs 7-28815

BWT see backward-wave tubes**C invariance**

- charge symmetry breaking and charge independence breaking, exptl. review 7-49017
- string theories, compactifications and θ -structures 7-18659
- n-p system, charge symmetry breaking 7-30434
- np scattering, $E_{\pi} = 189$ MeV, charge symmetry breaking search 7-5112
- $pd \rightarrow {}^3\text{He}^0$, 733 MeV, charge independence test 7-5113
- $pd \rightarrow \pi^+$, 733 MeV, charge independence test 7-5113

C³ lasers see semiconductor junction lasers**C listings**

- fractal dimensions of topographic surfaces, computation using C program 7-54845

C steel see carbon steel**cable insulation**

- see also insulating oils
- polyethylene films, high field dielectric loss meas. 7-17264
- polyethylene/ionomer blends, insulating material, aging characteristics 7-39025
- polymeric insulating material, dielec. breakdown strength rel. to lamella struct. 7-53237
- polymeric insulation, water treeing, failure and growth mechanisms 7-39034
- polymeric insulation, water treeing and morphology 7-39029
- pulsed power system, high voltage coaxial cable, polyethylene-insulated, breakdown properties (*Japanese*) 7-11797

cable insulation continued

- XLPE, cable insulation, water treeing, microstructural effects 7-39027
- XLPE insulation, water treeing 7-39026

cable jointing

- arc-fusion spliced fibres for improved reliability 7-11183
- optical fibre cable connection and loss meas. methods (*Japanese*) 7-43435
- optical fibre directional coupler splicing for duplex communication 7-50754
- single mode graded index optical fibre cables characts. 7-37204
- taper splice method for subscriber single-mode fibre cables 7-31530

cable laying

- JET nuclear fusion plant, gas-insulated HV cable for neutral injector (*German*) 7-62064
- optical fibre cable laying methods (*Japanese*) 7-43436

cable sheathing

- flame-retardant optical fibre cables, low smoke, halogen free, development 7-11164
- optical fibre cables, sheath retraction 7-11165

cable sheaths see cable sheathing**cables (electric)**

- see also coaxial cables; power cables; submarine cables; superconducting cables; telecommunication cables
- Cu, electrotech. grade, acoustic emission characts. in elastoplastic deform. 7-39816

CAD

- see also architectural CAD; circuit CAD; computer-aided analysis; control system CAD; interactive systems
- ADINA program use in nuclear plant CAD appls. 7-49505
- body surface measurement and replication by photogrammetry and CAD 7-54695
- computer mapping, minimal requirements for CAD 7-40402
- EELS spectrometer, magnetic shielding CAD 7-48923
- gas turbine CAD system with Denton scheme for flow program, comparison with expt. results 7-63177
- gas turbine computer-aided interactive design system, Denton scheme for flow program 7-63176
- glove boxes and enclosures, computer-aided design 7-30578
- hybrid solar house design and control using microcomputers 7-3627
- lens, EASE development and user friendliness 7-57514
- lens design, Brixner optimisation procedure 7-50683
- lens design, conf., Cherry Hill, USA (June 1985) 7-48161
- lens design, interactive computer program 7-50693
- lens design, merit function construction with possible achievement of global min. 7-50682
- lens design innovations 7-50674
- lens design program, intelligent, development 7-50676
- lens design program by microcomputer with artificial intelligence 7-50677
- lens design program using simultaneous linear inequalities, improved version 7-50681
- lens design software, human dimension 7-50675
- linear accelerators, RF cavity design and codes 7-62128
- linear accelerators, Wake Field calculations using the MAFIA 3D BCI code 7-62138
- MAD, accelerator, design tool kit 7-10315
- MAFIA, 3D EM CAD system for magnets, RF structs., and transient wake-field calcs. 7-62136
- manual materials handling task design using computerised biomechanical modelling 7-14040
- multivane expander simulation, design and operation optimisation 7-3713
- musculotendon actuator models for neuromuscular stimulation system CAD 7-28573
- optical design, aberration display technique 7-50689
- optical design program for Apple Macintosh 7-50692
- optical system design, 3D simulator appl. 7-62814
- optical system design, interactive ray-tracing program integrated with solid-modelling CAD system, Traz program 7-50679
- plastic and advanced plastic composites, design methods and applcs., book 7-4642
- plates structures, 3D, elastostatic anal., CAD, stress anal. 7-37334
- prosthetics and orthotics, shape sensing by CAD/CAM techniques for fitting 7-34348
- shadow moire topography equipment for skin diagnostics, using Sinclair Spectrum computer (*Czech*) 7-14145
- solar heating system CAD, flow diagram of design 7-46965
- Tandem Mirror Experiment Upgrade, computer aided design 7-15387
- TEM lens shape with min. spherical aberration coeff., computation method 7-18936
- tokamak fusion devices, superconducting poloidal field coils design, CAD program system development 7-5412
- two-lens cemented objective, struct. parameters automated calc. 7-37085

CAD/CAM

see also CAD

- amputee's stump, shape measuring probe-type system for prosthetics CAD 7-34349
- CAE, embedding of finite elements, prerequisites for software 7-15231
- CAE-nuclear engineering analysis on 32-bit work-station computers 7-36083
- structural dynamic models for nuclear plant design, CAE appl. 7-25023
- TFTR bumper limiter and protective plate graphite tile, computer aided design/manufacture 7-25196

cadmium

see also nuclei with

- atom, autoionisation widths, calcs. and optogalvanic spectra 7-36521
- atom, oscillator strengths and excitation energies, relativistic CI and MCRHF calcs. 7-50260
- atomic ion, autoionising states, picosecond soft-X-ray ionis. spectroscopy 7-10521
- Auger electron spectra, main and satellite structures 7-7795
- Auger energy, Slater transition state calcs., metallic and atomic states, jellium model 7-38475
- desorption from CdTe (001), surface stoichiometry and reaction kinetics, RHEED studies 7-21613
- electrodes, electrotechnological aspects and alkaline battery appls., review 7-3638
- films, laser-assisted oxidation 7-65208
- high pressure magnetoresist. near electronic topological transition (*Russian*) 7-7204

cadmium continued

isotopes, hyperfine structure splitting, isotope shift meas. 7-41885
monovalent ion, alignment after photoionis., fluoresc. radiation polarisation meas. 7-890
plates, Doppler-shifted cyclotron resonance and skin effect 7-17224
polycrystalline, internal friction temp. spectrum and microplasticity (*Russian*) 7-16684
polycrystalline, work-hardening and recovery during steady-state creep 7-63734
polycrystalline rolled sheets, flow stress, hydrostatic press. effect, 600 MPa (*Japanese*) 7-33735
positron detrapping at low temps., thermally activated mechanism 7-39252
positron lifetimes, prevacancy effect 7-37973
reactivity worth in MTR-fuel-type reactor 7-56772
refining by continuous zone melting 7-3163
single cryst., interatomic distance and thermal motion, K-shell EXAFS, temp. and orientation depend. 7-64814
single crystals, anisotropic thermal effect, first shell distance and thermal motion, EXAFS study 7-63753
surface resist. self-oscill. randomisation in the current-carrying state 7-45427
twin crossing during dynamic loading, dislocation interactions (*Russian*) 7-6629
vapour, coherent VUV generation by reson.-enhanced freq. mixing 7-50636
CaSO₄.1/2 H₂O:Cd, crystallisation from phosphoric acid 7-27882
Cd cathode sinter effects on Ni-Cd secondary cell performance 7-65448
Cd, polycrystalline, steady-state creep, internal and effective stresses 7-38100
Cd⁺, electron impact ionisation, absolute cross-section meas. 7-25667
Cd⁺, ion drift velocity in He glow discharge, meas. using AlGaAs laser (*Japanese*) 7-20294
Cd⁺ photoionisation pumping via two-electron shakeup 7-20195
Cd⁺ recombination laser oscillation, obs. 7-43075
Cd²⁺, reduction, rel. to coumarin adsorpt. on dropping Hg electrode 7-58609
Cd-Bi(Sb), thermodynamic functions are modelled by chemical-physical theory, Gibbs energy 7-52051
Cd-Cd(Kr) mixture, reson. line broadening, interaction pot., anal. 7-36520
Cd+He⁺, exothermic charge exchange with excitation cross sections 7-42755
Cd+He⁹⁺, L-subshell ionisation, X-ray prod. 7-50303
¹⁰⁹Cd, γ-ray emission rate meas. with well-type NaI(Tl) detector 7-25332
GaN:Cd, time-resolved photoluminesc. study 7-22347
Ga₂As₂O₁₂:Cd, photoelectret, photoconductivity 7-45919
GeTe-Cd, solution mechanism of impurities, effect of heat treatment 7-21455
He-Cd discharge in concentric hollow-cathode struct., spectrosc. obs. 7-20953
He-Cd hollow cathode laser, green line oscillations, lower levels population 7-43065
He-Cd laser, noise reduction by discharge current modulation 7-31348
He-Cd laser transitions, level width determ., double-mode lasing state 7-43080
He-Cd positive column discharge 441.6 nm laser level (*French*) 7-11811
He-Cd⁺ white light laser, hollow cathode, power stabilisation 7-57385
In_{1-x}Ga_xAs₂P_{1-x}, Cd on InP, activation energy of impurity 7-32942
In₂O₃:Cd films, optical and elec. props. 7-22365
InP:Cd, interstitial-substitutional diffusion, doping effects 7-6878
InP:Cd thin films, prep. and characts., appl. for solar cells 7-17895
InSb:Cd, heterogeneity study 7-21476
InSb:Te, Cd, Zn single crystals, Czochralski growth, solute distrib., mag. field effect on melt 7-3158
InSb:Te(Se)(S)(Cd)(Zn) thin films, doping, Hall effect meas. 7-21743
NaCl:OH⁻, Cd²⁺ single cryst., gamma irr., electronic and IR spectra 7-53320
Ni-Cd accumulators, examination of graphite additive to electrodes 7-39984
Ni-Cd advanced aerospace cell design 7-34014
Ni-Cd aerospace cells, 34 Ah, voltage-temperature charge verification testing 7-34019
Ni-Cd aerospace cells, flood starved design 7-34015
Ni-Cd aerospace cells, low Earth orbit life cycle characterisation testing 7-34020
Ni-Cd aerospace cells, separator qualification testing 7-34013
Ni-Cd aerospace cells, study of long term storage effects 7-34018
Ni-Cd alkaline accumulator develop. in Hungary (*Hungarian*) 7-17855
Ni-Cd batteries, design for consumer electronics appls. 7-59834
Ni-Cd batteries, Goddard model for aerospace appls., alterations using computer simulation 7-34017
Ni-Cd batteries for space appls., proceeding of NASA/Goddard workshop, Greenbelt, MD, USA (Nov. 1985) 7-29578
Ni-Cd cell, electrode kinetics and failure-mode prediction, internal short equiv. resist. estimation 7-54288
Ni-Cd cell containing Pellon 2536 separator, life testing, satellite appl. 7-65446
Ni-Cd cell failure mechanism and rate, reliability studies using Weibull statistics 7-65450
Ni-Cd cell separator with Pellon 2536, space qualification program 7-65445
Ni-Cd cells, additive effects on anodic behaviour of negative Cd electrode in KOH solutions 7-3637
Ni-Cd cells, General Electric 50 Ah, qualification testing of separator and positive plate processing 7-34012
Ni-Cd cells, O₂ recombination rate on plastic-bonded Cd electrode doped with Ni(OH)₂ 7-54287
Ni-Cd cells for spacecraft, self-discharge characts. at elevated temperatures 7-34016
Ni-Cd geosynchronous orbit satellite batteries, life prediction 7-65447
Ni-Cd high-capacity battery (*Japanese*) 7-65433
Ni-Cd high-performance battery (*Japanese*) 7-65434
Ni-Cd lightweight space battery, reliability and life testing 7-65449
Ni-Cd secondary cell performance effect of Cd electrode sinter, cell testing 7-65448
Ni-Cd secondary storage batteries, computerised management system for space vehicle appls. 7-34021
Ni-Cd storage batteries, structural features and additives effects on elec. props. of Ni active materials (*Hungarian*) 7-17857

cadmium continued

PdTe:Cd, free charge carrier conc., donor action and Te precipitates effects (*Russian*) 7-16592
Sb₂Te₃:Cd crystals, point defects, reflectivity and elec. props. room temp. meas. 7-33008
Si:¹¹¹Cd, hyperfine interactions, temp. depend., gamma-ray spectra studies 7-64553
SnTe:Cd, solution mechanism of impurities, effect of heat treatment 7-21455
TiO₂:Cd thin films, extension of optical absorpt. range by doping 7-39144

cadmium alloys
see also cadmium compounds
Bi-Pb-Sn-Cd alloy negative electrode for secondary Li batteries (*Japanese*) 7-65435
AgCd, electronic structure, disordering effects (*Russian*) 7-32901
AgCd, martensite transformation and shape memory effect, resistivity and thermoelectric power meas. 7-53729
Al-Cd single crystals, Cd-vacancy complex disassociation under ion irradiation 7-26741
Al-Cu-Li-Mn-Cd, 2020, micromechanisms governing elevated temp. fracture resist. 7-22803
Au-Cd (47.5 at.%), stress induced martensitic transform., pseudoelasticity 7-39610
Cd-Hg, ω-phase lattice parameters, influence of temp. and press. (*Russian*) 7-51704
Cd-In alloys, vacancy-induced elec. field gradient temp. depend., PAC meas. 7-52541
Cd-Sb melts, crystallisation and structural state, phase equilib. diagrams 7-46441
Cd-Sn-Pb, phase diagrams, thermodynamic formalism, computer calcs. 7-3269
Cd-Zn, alloys, two-phase, models of tensile behaviour from components 7-46570
Cd-Zn electroplated steel, extrusion, deform. force rel. to comp. and struct. 7-3367
Cd₇Ag₃, Ag density of states, Auger and photoelectron spectra, Clogston-Wolff model calcs. 7-2451
Cd_{1-x}Hg_x alloys, electronic structure dependence on crystal lattice parameters 7-45141
CdMg dilute alloys, muon Knight shift temp. depend. study 7-45892
CdMn, XY-type spin glass, uniaxially anisotropic, successive transitions 7-17188
CdSb, optical energy gap and light emission (*Japanese*) 7-53264
CdSb-In crystal, In atom electrodiffusion study 7-63890
CdTe, detector material, applications 7-45307
CdTe, single cryst., transmission region optical props., impurities effects 7-39128
In_{0.95}Ag_{0.05}Ga_{0.005}, ¹¹¹Cd quadrupole interaction, temp. dependence, lattice electric field gradients (*Chinese*) 7-7183
LiCd B32-type Zintl phases, mag. props., exchange enhancement, APW calcs. 7-27504
NaCd₂, cryst. struct., matrix algebra calcs. 7-63548
Ni-Mo-Cd electrocoated cathodes for water electrolysis, H₂ evolution kinetics 7-3728
Sm₁₁Cd₄₅, giant cells, polyhedral packing 7-11992
UCd₁₁ heavy electron system, antiferromag. phase transition, muon spin rot. and relax. meas. 7-45668
Zn-Cd monocystals, dislocation struct. as function of Cd content (*Russian*) 7-44556

cadmium compounds
see also cadmium alloys
arachidate, Langmuir-Blodgett films, angle-resolved photoemission with synchrotron radiation (*Japanese*) 7-3152
arachidate, Langmuir-Blodgett films, struct. disorder and polymerisation at elevated temp., IR spectra obs. 7-46163
arachidate, Langmuir-Blodgett multilayers, order-disorder transitions, Raman spectra 7-53309
calcium cadmium acetate hexahydrate single crystals, first order phase transition, thermal expansion meas. 7-26985
CdS-CuInSe₂ solar cells fabricated by DC magnetron sputtering of Cu₂Se and In₂Se₃ 7-23170
CdTe films, MBE growth, photoluminescence and TEM characterisation 7-22376
chalcogenides, cryst. growth by SSSR-zone melting method 7-64897
glass:CdSe gratings, darkening effect, optical phase conjugation 7-57476
glass-CdSe-KS-19, light-induced anisotropy 7-43259
surface, rhodamine B mol. adsorpt. kinetics, binding energy determ. (*Russian*) 7-21667
Au-CdIn₂S₂Se₂-In Schottky diodes, I-V charact. 7-33010
Bi₂CdS₄ thin film photoelectrodes, electrochemical photovoltaic cell appls. 7-17918
C CdCl₂, impurity local modes and secondary features, Raman spectra anal. 7-33372
(Cd,Mn)Te, atomic layer epitaxy, review 7-13362
(Cd,Mn)Te quantum well structure, wide-gap II-VI superlattices 7-7346
(Cd,Mn)Te/CdTe superlattice, optical props. heterointerface effects 7-7736
Cd complex, trans-bis(isothiocyanato)-tetrakis-4-methylpyridinecadmium (II), inclusion cpd., cryst. struct. 7-12031
Cd-Hg-Te phase diagram, numerical descriptions, review 7-26913
Cd₂As₂, amorphous films, structure and growth morphology 7-45078
(CdBi)₂(M_{1/2}Sb_{3/2})O₇, (M=Cr, Ga, V, Mn, Fe, Rh, Sc, In), pyrochlores, struct. and characterisation 7-1986
(CdBi)(MW)O₇, (M=Cr, Ga, V, Mn, Fe, Rh, Sc, In), pyrochlores, struct. and characterisation 7-1986
CdBr₂, impurity local modes and secondary features, Raman spectra anal. 7-33372
Cd(BrO₃)₂. 2H₂O(D₂O), H bonding, crystal struct., ¹H and ²D NMR anal. 7-22156
CdCl₂, aqs., cond. meas. at 298.15 K, anal. using Lee and Wheaton eqn. 7-16792
CdCl₂, cryst. struct., temp. var., determ. from CdCl₂Mn²⁺ EPR data 7-32382
CdCl₂ solns., aqs., dil., transport nos. determ. at 298.15 K 7-16793
CdCl₂(1-x)Br_{2x} layered mixed crystals., Raman-active phonon mode study 7-51970
Cd(CIO₄)₂.6H₂O, low-temperature phase transitions characterisation by Fourier transform IR spectroscopy 7-52046

cadmium compounds continued

- CdCr₂Se₄, band structure characteristics and props. of nonequilibrium carriers, cathodoabsorption 7-46064
 CdCr₂Se₄, Cd vapour pressure determ. by atomic absorption method 7-63790
 p-CdCr₂Se₄ ferromag. semicond., photocond. relax. time temp. depend. meas. 7-45383
 CdCr₂Se₄, ferromag. semiconducting thin films, influence of electric field on magnetisation 7-45738
 CdCr₂Se₄, photoferromagnetic effect, magnetic impurity effects, magnetisation reversal characts. meas. 7-17154
 CdCr₂Se₄ thin films, ferromagnetic semicond., multielectron energy struct., absorpt. spectrum, temp. and doping depend. 7-38488
 CdCr₂Se₄-Ga, lightly doped, ferromag., photoconductivity, band struct. 7-7278
 CdCr₂(Se_{1-x}S_x)₄ spinel, mag. prop. anomalies 7-64453
 Cd_{1-x}Cu_xFe₂O₄, canted spin arrangements 7-45618
 CdD, B²⁺-X²⁺ system study, near-UV spectra anal. 7-50164
 CdF₂, field enhanced electronic transport 7-45329
 CdF₂, US attenuation 7-51944
 CdF₂:Eu³⁺, electrolum. studies 7-27785
 CdF₂:Eu³⁺, hyperfine coupling in ⁷F₀ and ⁴D₀ states, ODMR meas., optical hole burning 7-45842
 CdF₂:Ga(Y)(Gd)(Eu) crystals, local field-enhanced electronic conduction, activation energy and Poole-Frenkel const. calcs. 7-38570
 CdF₂-LiF-AlF₃-PbF₂ glasses, potential as a practical glass 7-37074
 CdGa₂S₄, luminesc. associated with defect complexes 7-27757
 CdGa₂S₄ single crystals, chemical vapour transport growth, microhardness, crack patterns 7-7833
 CdGa₂S₄(Se)₄ defect chalcopyrite struct. crystals, linear optical response, atomic core electron contrib. calcs. 7-39061
 CdGeAs₂, amorphous, superimposed DSC crystn. peaks, nonlinear regression anal. 7-6514
 CdGeAs₂, glassy, optoelectronic props., photoelectrochemical investigation 7-45382
 CdGeAs₂, n-channel inversion layers, oscillatory diffusivity-mobility ratio, quantising mag. field 7-45419
 CdGeAs₂, SHG of single and multilongit. mode CO₂ laser emissions 7-43211
 p-CdGeAs₂ semicond., hole mobility and scatt., temp. depend. study 7-52609
 CdGeAs₂, ternary chalcopyrite semiconductor, gate capacitance in n-channel inversion layers, quantising mag. field 7-2733
 CdGeAs₂:Ni amorphous films, elec. cond., low temp. impurity breakdown, high field effects 7-52625
 Cd₂GeAs₄ semiconducting glass electrolytic dissolution in HCl and water 7-12289
 CdGeP₂, glassy, optoelectronic props., photoelectrochemical investigation 7-45382
 CdH + He(Ar), collisional rot. transitions, scaling rules (French) 7-10709
 CdHgTe detector, CO₂ laser detection appl. 7-5915
 CdHgTe focal plane arrays, sampling effects reduction 7-30090
 (CdHg)Te, LPE growth, use of in-situ wash melts 7-59466
 CdHgTe, optical nonlinearities and bistability 7-57435
 CdHgTe photodetectors for infrared measuring techniques (Russian) 7-4889
 Cd_{0.2}Hg_{0.8}Te, electron stimulated desorption of Hg 7-17378
 Cd_{0.2}Hg_{0.8}Te, galvanomagnetic props., effect of US treatment 7-38593
 Cd_{0.2}Hg_{0.8}Te surface, electron-stimulated processes 7-13279
 Cd_{0.23}Hg_{0.77}Te, time-resolved self-defocusing 7-43267
 Cd_{0.23}Hg_{0.77}Te:B⁺, ion implanted, photoreflection spectra in the edge absorption region 7-39099
 Cd_{1-x}Hg_xTe crystals, impurity band elec. conduction, Fermi glass model anal. 7-27328
 Cd_{1-x}Hg_xTe IR heterodyne detectors, intermediate temp. operation 7-35594
 n-Cd_{1-x}Hg_xTe, doped and undoped, minority-carrier lifetime 7-21932
 Cd_{1-x}Hg_xTe, abrupt interfaces using thermal and photo-MOVPE, Hall meas. 7-27917
 Cd_{1-x}Hg_xTe, band gap collapse, effects of Hg 5d electrons 7-64075
 Cd_{1-x}Hg_xTe, Bridgman growth using Accelerated Crucible Rotation Technique 7-46307
 p-Cd_{1-x}Hg_xTe, doped and undoped, minority carrier lifetime 7-45353
 Cd_{1-x}Hg_xTe, galvanomag. props. after metal-insulator transition 7-52655
 Cd_{1-x}Hg_xTe heterostructures, MOVPE, computer controlled reactor, charact. 7-59446
 Cd_{1-x}Hg_xTe IR photodiodes for 3 to 14 μm, comparison 7-41466
 Cd_{1-x}Hg_xTe, LPE and MOVPE grown, elec. props. and annealing 7-53512
 Cd_{1-x}Hg_xTe layers, MOVPE, CdTe substrate orientation effect, RHEED, SEM obs. 7-59447
 Cd_{1-x}Hg_xTe MOVPE growth on CdTe/sapphire substrate 7-27918
 Cd_{1-x}Hg_xTe MOVPE layers, elec. props. and Hall effect behaviour 7-27444
 Cd_{1-x}Hg_xTe, p-type, minority carrier exclusion 7-64242
 Cd_{1-x}Hg_xTe, photo-epitaxy, free radical mechanism 7-53612
 n-Cd_{1-x}Hg_xTe, single crystal, γ-irradiation, electrophysical props. in strong elec. field 7-7251
 CdI₂, interband two-photon absorpt., freq. depend. 7-33451
 CdI₂, layered cryst., Raman scatt. intensities and atomic bonding 7-22257
 CdI₂ single cryst., lux-ampere characts., temp. depend. 7-7285
 CdI₂, two-photon photocond. under double beam laser excitation 7-64285
 CdI₂:Br, indirect excitons, isoelectronic impurity effects, luminesc. spectra 7-27255
 CdI₂-Ag interface, absorpt. and luminesc. spectra studies (Russian) 7-59224
 CdIn_{0.3}Cr_{1.7}S₄ spin glass, equilibrium mag. fluctuations 7-64452
 CdInGaS₄ in MSM surface-barrier structs., photovoltaic effect and SCL currents 7-52687
 CdIn₂(Ga₂)S₄ single crystals, phase transforms., photoluminesc. studies 7-2171
 CdInGaSe₄, optical absorption spectra, hydrostatic pressure dependence 7-59222
 CdIn₂O₄ RF sputtered films, transparent heat mirror characts., elec. and optical meas. 7-39199
 CdIn₂O₄ thin films, DC reactive sputtered, elec. and optical props. 7-38788
 CdIn₂S₄, electron trap characts., TSC meas. 7-27340
 CdIn₂S₄ optical props., annealing and γ-ray irradiation effects 7-13211

cadmium compounds continued

- CdIn₂S₄ single cryst., chem. vapour transport growth and Vickers microhardness 7-21345
 CdIn₂S₂Se₂, semicond., optical and elec. props. 7-33010
 CdIn₂Se₄, energy spectra of local centres (Russian) 7-64150
 Cd_{1-x}Mn_xS, antiferromag. exchange constants between nearest-neighbour Mn²⁺ ions 7-64449
 Cd_{1-x}Mn_xS, crystal growth and charact. (Japanese) 7-7829
 Cd_{1-x}Mn_xSe, dil. mag. semicond., including long-range interactions, mag. props. anal. 7-7497
 n-Cd_{1-x}Mn_xSe, electric-dipole-induced spin resonance 7-27592
 n-Cd_{1-x}Mn_xSe, magnetoresist. and Hall effect meas. near metal-insulator transition 7-12741
 Cd_{1-x}Mn_xSe, powder, stress effects, amorphisation (Korean) 7-27960
 Cd_{0.6}Mn_{0.4}Te, spin-freezing process, time-depend. of thermoremanent magnetization 7-2863
 Cd_{0.8}Mn_{0.2}Te, dil. mag. semicond., low temp. mag. spectroscopy 7-64477
 Cd_{0.6}Mn_{0.2}Te/Cd_{0.7}Mn_{0.3}Te semimagnetic superlattices, electronic props., theory 7-45445
 Cd_{1-x}Mn_xTe, crit. dynamics, AC susceptibility meas. 7-33181
 Cd_{1-x}Mn_xTe, low-temperature magnetic spectroscopy with DC SQUID 7-48780
 Cd_{1-x}Mn_xTe, dil. mag. semicond., including long-range interactions, mag. props. anal. 7-7497
 Cd_{1-x}Mn_xTe dilute antiferromagnet, high field magnetisation meas. 7-64486
 Cd_{1-x}Mn_xTe exciton localisation, time resolved photolum. study 7-46106
 Cd_{1-x}Mn_xTe films, hot wall vacuum growth, twinned struct. 7-53593
 Cd_{1-x}Mn_xTe, frequency-dependent Faraday rotation 7-22225
 Cd_{1-x}Mn_xTe, interband Faraday rot. meas. 7-39093
 Cd_{1-x}Mn_xTe, low-temperature epitaxial growth, MBE and MOCVD 7-64906
 Cd_{1-x}Mn_xTe mixed cryst., far IR Fourier transform spectra, acoustic local mode and TA band mode 7-53378
 Cd_{1-x}Mn_xTe, muon spin precession freq. shift and relax. meas. 7-45881
 Cd_{1-x}Mn_xTe, photoluminescence position and lifetime 7-13205
 Cd_{1-x}Mn_xTe, refractive index dispersion and two-mode refl. spectra behaviour calc. model (Russian) 7-45971
 Cd_{1-x}Mn_xTe semimag. semicond., ESR line shape meas., comp. and temp. depend. 7-7584
 Cd_{1-x}Mn_xTe, semimagnetic semiconductor, optical absorpt. edge, press. dependence (Chinese) 7-39139
 Cd_{1-x}Mn_xTe sensing element for wideband optical fibre magnetic field sensor 7-25979
 Cd_{1-x}Mn_xTe-Cd_{1-y}Mn_yTe superlattices, electron diff. using partially coherent illumination 7-37807
 Cd_{1-x}Mn_xTe(Se), mag. field-induced exchange effects, photolum. meas. 7-27705
 Cd_{1-x}Mn_xTe_{1-y}Se_y, magnetic suscept. and ESR meas., temp. depend. study 7-45636
 Cd_{1-x}Mn_xTe_{1-y}Se_y pseudoternary semimag. semicond., mag. suscept. and exchange interaction data anal. 7-7501
 Cd(NO₃)₂·2H₂O, cryst. struct. 7-58220
 Cd(NO₃)₂·2KNO₃, cryst. struct. 7-58220
 Cd₂Nb₂O₇, ceramic, high press. phase transition and dielec. props. 7-2177
 Cd₂Nb₂O₇, Fe³⁺ ESR study 7-64516
 Cd₂Nb₂O₇, ferroelectric, electrooptic props. 7-59180
 Cd₂Nb₂O₇, soft mode damping in incommensurate phases, anomalous behaviour 7-38149
 CdO bent whiskers, three-dimens. reconstruction of electron microscope objects 7-56377
 CdO-Al₂O₃-P₂O₅ glasses, EPR spectra, synthesis effects 7-64530
 CdO-B₂O₃-SiO₂ glasses, photochromism, photocond. and ESR (Japanese) 7-27822
 CdO-B₂O₃-Si(Ge)O₂ network struct., coordination and bonding, comp. depend., NMR study 7-6535
 CdO-Bi₂O₃, crystallographic state of CdO lattice during sintering with Bi₂O₃ addition 7-37944
 CdO-Bi₂Ru₂O₇ thick film resistors with high TCR for temperature sensing 7-48735
 CdO-SiO₂-M₂O (M=Na,K,Li), glasses, thermal expansion, free volume 7-58152
 (CdO)₂(B₂O₃)₂(GeO₂)₂ glasses, struct. and vibrational props., IR spectra study 7-7694
 Cd(OH)₂ dendritic structures in agar gel 7-58723
 CdO, crystal structures and microphases, devil's staircase 7-11982
 Cd₂P₂S₆ intercalated with pyridine, D NMR study 7-33279
 Cd₂P₂S₆ intercalated with pyridine complexes of ferric ion, spectroscopic and ESR studies 7-64519
 CdS, A-exciton, normal-incidence exciton transmission and refl. spectra 7-39058
 CdS, absorpt. optical bistability, lattice heating study 7-43205
 CdS, absorption-induced optical bistability 7-57444
 CdS, acoustoelectronic system, solitons obs. 7-45401
 CdS, adsorbed methylviologen radical cation dimers, relax. 7-27095
 CdS and Zn_{1-x}Cd_xS, electron-pumped, high-efficiency semiconductor laser 7-5884
 CdS anodic film growth, initial stages, voltammetry and computer simulation studies 7-28216
 CdS based ceramics, radiative recomb. at high excitation levels (Russian) 7-3090
 CdS, bound-exciton states, resonant Brillouin scatt. 7-46062
 CdS, Brillouin spectra of acoustoelectronic interaction 7-7292
 CdS, carrier transport, defect effects, photoacoustic and photocurrent spectra 7-38626
 CdS composite logic gate element and multiplexer for optical computing and optical communications 7-57421
 CdS crystal growth and charact. (Japanese) 7-7829
 CdS crystals, surface polaritons, luminescence 7-64098
 CdS, electron beam irradiated, red flash-like luminescent centres, annealing 7-7740
 CdS, electron-hole exchange interaction for donor-acceptor pairs as a function of separation distance 7-52537
 CdS epitaxial films, initial oxidation stages, diffusion mass transport between CdO islands 7-8206
 CdS evaporated films, cathodolum., effect of thermal annealing 7-22353
 CdS excited state dynamics studied by transient grating techniques 7-12616
 CdS, excitonic polaritons, transmission and damping 7-58748
 CdS, exciton emission, phonon drag, inhomogeneous energy distrib. 7-39366

cadmium compounds continued

- CdS, film, charge transport, rel. to electrophysical props. 7-17121
 CdS films, formation by spray pyrolysis, characterisation of intermediate complexes 7-39372
 CdS films, spray deposited, laser annealing, struct., carrier mobility 7-58318
 CdS films, superlinearity of light-current characts. 7-64282
 CdS, fine activated, prep. and props. for electrophotographic appl. 7-41514
 CdS induced homojunction formation in p-CuInSe₂ 7-58867
 CdS, integral exciton absorpt. coeff., temp. depend. characts. 7-45959
 CdS inversion layers, carrier effective mass calcs. 7-64055
 CdS laser excited with several electron beams, light pulse formation 7-43098
 CdS, light emission under voltage pulses 7-7764
 CdS, luminesc. associated with defect complexes 7-27757
 CdS, nonradiative recombination, elec. transport, combined photoacoustic and photocurrent spectra 7-38582
 CdS, nonradiative recomb., elec. transport, combined photoacoustic and photoconductive spectra, theory 7-38583
 CdS on synthetic clay, luminesc. lifetimes, UV spectra 7-22297
 CdS, optical bistability 7-57432
 CdS, oxidised, SIMS/XPS characterisation 7-39934
 CdS particles deposited on porous vycor glass electron transfer and photoluminesc. dynamics 7-64678
 CdS photoconductive thin films, optimum spray pyrolysis preparation conditions 7-17418
 CdS, photoconductivity spectrum, surface excitons, localised hole in quantum inversion layer 7-12762
 CdS, photolum., exciton scatt. from defects and impurities, depend. on exciting light intensity 7-39156
 CdS photosensitive cryst., 3D light diffr. from acoustic instability 7-33362
 CdS plastically deformed cryst., reorientable defects, polarised luminesc. study 7-51749
 CdS platelet, nonlinear optical and transport props. of many exciton system 7-32920
 CdS platelets, fast all-optical switching 7-57430
 CdS polycryst. layers, photoelec. props. α -Cr₂O₃ regulator 7-45378
 CdS polycrystalline films, temp. variation in thermoelectric power 7-22048
 CdS, powder, metal-loaded, photoinduced electron-hole pair separation 7-59770
 CdS reaction with aq. CuCl, TEM 7-39920
 CdS, refractive index nonlinearity due to excitonic molecule resonance state 7-11044
 CdS resonant self-diffraction from dynamic laser-induced gratings 7-11036
 CdS, semicond. crystallite, quantum size effects, energy spectrum calc. 7-12613
 CdS, shallow donor problem, pseudopot. approach 7-45216
 CdS, single crystal, US wave absorption, impurity distrib. effect., electron-probe X-ray anal. 7-53241
 CdS single crystals, cathodoluminescence, memory effect 7-22352
 CdS single crystals, subsurface region comp., laser radiation effects, AES study (Russian) 7-58329
 CdS single crystals, acoustoelectronic interaction, ultrasonic attenuation and amplification, dislocation motion effects (Russian) 7-21953
 CdS single crystals, nonequilib. high-temp. vacuum annealing effects, intrinsic defect transform. 7-58764
 CdS skeletal and hollow crystals grown under time-increasing supersaturation 7-21144
 CdS small crystallites, zero-dimensional excitons 7-12615
 CdS surfaces, electron-beam-stimulated processes, real-time atomic-resolution electron microscopy 7-7798
 CdS, temperature-electric instability, spontaneous oscillation states 7-38616
 CdS thermally induced optical bistability study 7-11047
 CdS thin film MIS structs., band bending and interface state density 7-7402
 CdS thin films, deep trap depth, TSC meas. 7-58774
 CdS thin films, deposition by dip technique 7-3210
 CdS thin films, electrochem. bath deposition, photovoltaic cell props. 7-7900
 CdS, three types of electronic optical bistabilities 7-43262
 CdS, transmission and damping of excitonic polaritons 7-58747
 CdS waveplates for IR lasers, reproducible volume manufacture 7-37138
 CdS, wide-gap semiconductors, room-temperature optical nonlinearity 7-57440
 CdS, with compensated i-layer, photosimulated deep level transient spectroscopy 7-7765
 CdS, X-ray graphic elastic constants and lattice spectrum 7-32546
 CdS:Cu,Cl photoconducting films, photolum. spectra studies (Russian) 7-46140
 CdS:Gd, Cl film solar cells, gamma radiation effects on photoelectric properties 7-34032
 CdS:In-SnO₂ (glass), spray pyrolysed, photoelectrochemical studies 7-52830
 CdS:Ri⁺(Kr⁺)(Ar⁺)(Ne⁺), ion implantation damage 7-26812
 CdS/CdTe screen-printed thin-film solar cell for indoor consumer electronics (Japanese) 7-65472
 CdS/CdTe sintered solar cell photovoltaic props. rel. to CdS film sintering conditions (Korean) 7-65476
 CdS/CdTe solar cells, circulation meas. and spectral error reduction 7-13903
 CdS/CdTe solar cells, effects of CdS film thickness on photovoltaic props. 7-65468
 CdS/CuInSe₂ solar cells, modelling and anal. 7-17893
 CdS/CuInSe₂ thin film chalcopyrite solar cells, electroplating prep. 7-17894
 a-CdS/n-Si heterojunctions, elec. props. 7-64342
 CdS/polymer composites, degenerate four-wave mixing 7-62795
 CdS/ZnS, multilayer structures, MOCVD, wide band gap, interdiffusion characts. 7-53610
 CdS-Ag, size quantisation in CdS layer, surface plasma spectroscopy 7-32936
 CdS-CdSe-polysulphide-polysulphide multiple junction photoelectrochemical cells 7-59863
 CdS-CdTe heterostructure, closed-tube CVD and charactn. 7-59444
 CdS-CdTe screen printed solar cell modules, long term reliability tests 7-23158

cadmium compounds continued

- CdS-Cu₂S, solar cells, SEM and Auger microanalysis 7-23189
 CdS-Cu₂S heterojunction, form. by photoelectrochemical process, phys. props. under light irradi. 7-45456
 CdS-Cu₂S solar cells, comp. of differing junction types, AES, SIMS determ. 7-23167
 CdS-CuGaSe₂ solar cells, physical properties and photovoltaic potential of CuGaSe₂ thin films 7-12889
 CdS-CuGaSe₂ solar cell fabrication 7-22047
 CdS-CuInSe₂ Boeing solar cells, I-V characteristics meas. 7-8408
 CdS-CuInSe₂ solar cells, charge transport studies 7-12890
 CdS-CuInSe₂ solar cells, capacitance determ. of interfacial states 7-13916
 CdS-CuInSe₂ thin film solar cell, solid state photovoltaic research status at SERI 7-8389
 CdS-CuInSe₂ thin-film solar cells, junction formation and O role, EBIC studies 7-17915
 CdS-CuInSe₃ backwall solar cells, intrinsic loss mechanisms calc. 7-23187
 CdS-InP solar cells, high efficiency, with thermally evaporated window layers 7-3701
 nCdS-n-GaAs photoanode, flux anal. of multiple junction solar cells 7-23162
 CdS-Si and CdS-CuInSe₂ heterojunctions, struct., elec. and photoelectric props. 7-22001
 CdS+propanol-2 radical, photochemistry and radiation chemistry, non-linear optical effects 7-46858
 CdSO₄·8H₂O:CrO₄²⁻, optical absorption spectra, electronic transitions 7-27740
 3CdSO₄·8H₂O, site symm. of SO₄²⁻ ion, IR absorpt. spectra 7-33374
 CdS_{1-x} crystal waveguide Bragg light modulators 7-1288
 CdS_{1-x} doped, glass substrates for thin film waveguides 7-5941
 CdS_{1-x} doped filters, femtosecond nonlinearities using opt. Kerr effect 7-50660
 CdS_{1-x} doped glasses, optical nonlinearities 7-57431
 CdS_{1-x} mixed crystal, laser-induced probe-beam defocusing at band edge 7-7657
 CdS(Se)(Te):Mn, impurity EPR spin Hamiltonian parameter correl. calcs. 7-27597
 CdS_{1-x}Te_{1-x} single crystals, growth form CdCl₂-CdS-CdTe ternary system, liquidus surface anal. 7-33644
 CdSb, cryst. growth, characterisation and appls., review 7-26685
 CdSb crystals., band struct., LCAO calcs. 7-58737
 CdSb thin films, preparation and thermoelec. props. 7-64374
 CdSe, Cd vapour pressure determ. by atomic absorption method 7-63790
 CdSe cryst., low press. melt growth technique 7-33548
 CdSe crystals, laser beam defocusing, rel. to Hall mobility and carrier density 7-52652
 CdSe, dielectric fn. and interband crit. points. 7-2480
 CdSe electrodes, photoanodic dissolution in NaCl soln. (Japanese) 7-23026
 CdSe, exciton luminesc., polarisation depend. 7-59248
 CdSe heteroepitaxial layers, deposition on InAs 7-7045
 CdSe, highly excited, exciton dynamics, picosec. time-resolved gain-absorpt. spectra study 7-2494
 CdSe laser with microminiature cryogenic refrigerator 7-43153
 CdSe lattice defects, digital struct. anal. by ion beam thinning for high resolution electron microscopy 7-6616
 CdSe, optimally annealed in molten Cd, DC galvanomagnetic props. 7-27352
 CdSe, ordered structures, field ion microscopy studies 7-32768
 n-CdSe photoanode for H₂S photoelectrolysis, photoelectrochemical cell for H₂ production 7-54328
 CdSe, photogenerated high density electron-hole plasma, energy relax., rapid expansion 7-33039
 CdSe, single crystal, US wave absorption, impurity distrib. effect., electron-probe X-ray anal. 7-53241
 CdSe, stimulated photolum. 7-27776
 CdSe, strongly excited, electron-phonon interaction screening, luminesc. meas. 7-38606
 CdSe thin film liquid-junction photovoltaic cell, photoelectrochem. charactn. 7-54331
 CdSe thin films, electrodeposited from SeSO₃²⁻ soln., comp. performance, polarography, RBS, cyclic voltammetry, power meas. 7-2411
 n-CdSe thin films grown from low purity materials for solar cell appls. 7-65480
 CdSe thin films made by tarnishing 7-22587
 CdSe, wide-gap semiconductors, room-temperature optical nonlinearity 7-57440
 CdSe, X-ray graphic elastic constants and lattice spectrum 7-32546
 CdSe:Cu, deep levels investigated by photoconductivity and space-charge region capacitance techniques 7-7148
 CdSe:Cu, transient photocond. anal. 7-64288
 CdSe:Cu films, radiative recomb. centres form., photolum. spectra studies (Russian) 7-33453
 CdSe/ZnSe, multilayer structures, MOCVD, wide band gap, interdiffusion characts. 7-53610
 CdSe-CdTe-selenide-polyselenide multiple junction photoelectrochemical cells 7-59863
 CdSe-Cu₂S heterojunction solar cell, dry formation, electron microscope study 7-17916
 CdSe-polysulphide solar cells, nitrite reduction to ammonia 7-39999
 CdSe-polysulphide photoelectrochem. system. corrosion reactions, thermodynamic stability calcs. 7-28320
 (CdSe)_{1-x}(MnS)_x crystals, semimag. semiconductors, magneto-optic studies 7-64609
 CdSe(S) thin films, electrophys. props., electron irradiation effects study, solar cell appl. 7-16894
 CdSeTe-polysulphide solar cells, nitrite reduction to ammonia 7-39999
 CdSe_{0.65}Te_{0.35}/aqueous polysulphide interface, photoelectrochemical props. 7-52829
 CdSe_{1-x}Te_{1-x} and CdSe_xTe_{1-x}:Cu films, deep local states, photosensitivity, spectral study 7-22371
 CdSe_{1-x}Te_{1-x} bound excitons, thermal dissoc., photoluminescence, reflectivity meas. 7-46122
 CdSe_{1-x}Te_{1-x}, bowing parameter of direct band gap, press. depend. 7-38453
 CdSe_{1-x}Te_{1-x} inhomogeneous solid soln., semicond. films, Hall effect temp. depend. meas. 7-58915
 CdSe_xTe_{1-x} polycrystalline solid solutions in electrochemical solar cells, photosensitivity 7-54296

cadmium compounds continued

- CdSnAs₂ crystal growth from melt sealed by LiCl-KCl mixture 7-7839
 n-CdSnAs₂, photoluminescence 7-53393
 CdSnO₃, fundamental absorption edge, spectral dependence 7-45964
 CdSnO₃:PbO highly conducting films, characterisation 7-22049
 Cd₂SnO₄, CVD, struct., elec. and optical props. (Korean) 7-27940
 Cd₂SnO₄, sintering synthesis and props. 7-64954
 Cd₂SnO₄ transparent thin film electrodes prepared by DC reactive sputtering from Cd-Sn alloy targets 7-22477
 CdTe: B⁺(Cu⁺) ion implantation damage, rapid thermal annealing, photolum. anal. 7-39162
 CdTe (001), Cd and Te desorpt., surface stoichiometry and reaction kinetics, RHEED studies 7-21613
 CdTe (001) films, MBE grown on InSb substrates, low temp. photolum. studies 7-22317
 CdTe (100), photoemission studies, surface struct., growth behaviour, Schottky barrier and surface photovoltage 7-39352
 CdTe (100)-oriented single crystals, lattice dynamics temp. depend., X-ray studies 7-26880
 CdTe, acceptor higher excited states calcs. 7-52511
 CdTe amorphous thin films, electrical and optical props. 7-22045
 CdTe and CdZnTe, single-crystal substrates, struct. characterisation 7-32769
 CdTe, annealing in Cd or Hg vapour, defect concentrations 7-65064
 CdTe anomalous photovoltage films X-ray irradiation effects studies 7-58834
 CdTe, atomic layer epitaxy on CdTe (111) substrates, growth mech. 7-12525
 CdTe, atomic layer epitaxy, review 7-13362
 CdTe, cathode sputtering process statistical modelling, optical layer deposition 7-39375
 CdTe, cathodic electrochemical surface modifications, Cd layer form. 7-65239
 CdTe, closed tube CVD growth using NH₄Cl transport agent 7-27913
 p-CdTe, complex-formation processes at high concentrations of intrinsic defects 7-37963
 CdTe cryst., low press. melt growth technique 7-33548
 CdTe, crystallographic polarity, determ. from Auger electron spectra 7-64830
 CdTe crystals, resistive element defect electromigration, flicker noise enhancement 7-63889
 CdTe, D plasma etching, surface comp. 7-46730
 CdTe, d-core transitions, reflectivity spectra 7-53364
 CdTe electrochemical sensor, sensitivity 7-65363
 CdTe, electrodeposition from acidic aq. solns., voltammetry 7-27188
 CdTe, electron irradi., a (100) dislocation loops 7-6686
 CdTe, epitaxial growth on GaAs (100) 7-21779
 CdTe epitaxial layers, MBE growth on GaAs substrates, photoluminesc. 7-46083
 CdTe epitaxial layers on GaAs substrates, X-ray diff. 7-27201
 CdTe film, polycryst., grown by UV-enhanced OMCVD, picosecond photocond. 7-52873
 CdTe film in a photovoltaic cell, electrodeposition and props. 7-64938
 CdTe films, detachable oriented, VPE 7-33567
 CdTe films, electrochemically deposited, resistivity, carrier conc. and carrier mobility 7-7419
 CdTe films, electrochemically deposited, comp., struct., AES, electron probe anal., X-ray diff. spectroscopy 7-58694
 CdTe films, illum. with monochromatic light, anomalous photovoltaic effect 7-52684
 CdTe films, organometallic VPE growth mechanism 7-64914
 CdTe films on InSb, interface struct. and band offsets 7-58664
 CdTe filter for Cs vapour pumping (Russian) 7-31438
 CdTe grown on Si by LPMOCVD, physical props. 7-27181
 CdTe, heteroepitaxial growth on GaAs (100) substrates 7-45034
 CdTe heteroepitaxial layers, deposition on InAs 7-7045
 CdTe high-resistivity undoped crystals, defects, EBIC studies 7-21211
 CdTe homoepitaxy on CdTe (111) by laser MBE, nucleation kinetics 7-22499
 CdTe, IR optical materials, production 7-37075
 CdTe, ion milling, TEM 7-39344
 CdTe LPE layers, matrix atom diffusion, SIMS studies 7-21513
 CdTe layers, electrochemical deposition, struct. and elec. props. 7-12526
 CdTe, low-temperature epitaxial growth, MBE and MOCVD 7-64906
 CdTe, MBE growth, crystallographic orientations and condensation coeffs. 7-3180
 CdTe, MBE growth on GaAs substrates, struct. and optical props. 7-64907
 CdTe, MBE growth on Si using (Ca, Ba)F₂ buffer layer 7-46325
 CdTe MOVPE growth on InSb substrate, characts. 7-27920
 CdTe, MOVPE on {111}CdTe, twin nucleation 7-33579
 CdTe, metal, contacts, interfacial microstruct., elec. props., phase diagrams 7-45495
 CdTe, OMVPE growth on InSb substrates 7-33577
 CdTe, optical anisotropy due to spatial dispersion 7-53266
 CdTe, optical nonlinearities and bistability 7-57435
 CdTe photoelectrochemical solar cells, effects of Ru surface modification 7-40017
 CdTe, polycrystalline, grain boundaries elec. and optical characts. 7-38012
 CdTe polycrystalline thin film solar cells 7-17888
 CdTe, positron annihilation in defects at crystal surface, defect anal. 7-39306
 p-CdTe RF sputtered thin films, resistivity, forbidden gap, optical and X-ray diff. spectra studies 7-21747
 CdTe, Ru surface modified for solar cells XPS obs. 7-23202
 CdTe, Schottky-barrier height determ. including electron-hole recomb. and electron trapping effects 7-2720
 CdTe, segregation coeffs. of Ag, Co, I and In, recoil implanted radioactive tracer technique 7-21461
 CdTe, single crystal, structural perfection, X-ray topography 7-12070
 p-CdTe, single crystal and thin film, chemical etching study 7-46724
 CdTe single crystals, anisotropy of positron annihilation 7-39214
 CdTe strong-absorbing single crystals., Laue X-ray diff. thickness depend. anal. and interpretation (Russian) 7-44310
 CdTe tetrahedral cpds, mode Grüneisen parameters 7-44732
 CdTe thin film heterojunction solar cells 7-17914
 CdTe thin film solar cells, efficiency improvement 7-17883
 CdTe thin film solar cells fabricated by evaporation (Japanese) 7-34044
 CdTe, threshold conditions for oscillation which the aid of shifted and unshifted dynamic gratings 7-1228

cadmium compounds continued

- CdTe, very high conductivity films, formation and props. 7-45522
 CdTe:Co, Jahn-Teller interaction, influence of mag. field 7-16995
 CdTe:Fe²⁺, impurity vibronic coupling and near IR spectra characts. 7-26889
 n-CdTe:In, high mobility, growth by photoassisted MBE 7-22485
 CdTe:In, photocorrosion, vacancies, photoluminescence spectra 7-27948
 CdTe:P-CdS solar cells, control of open circuit voltage by carrier density variation 7-17887
 pCdTe:Sb epilayers, photoassisted MBE growth 7-53607
 CdTe:Sn, impurity compensation effect on elec. resist. and mobility 7-52614
 CdTe/(Cd,Mn)Te superlattice, optical props. heterointerface effects 7-7736
 CdTe/a-Si:H heterojunction, X-ray image sensor fabrication 7-41557
 CdTe/CdS-CuInSe₂/CdS tandem solar cells 7-17891
 CdTe/GaAs heterojunction, defect and impurity states, photovoltage meas. 7-17065
 CdTe/In₂O₃ solar cells, high efficiency 7-59838
 CdTe/InSb interface, quasi-2D electron gas obs. 7-21987
 CdTe/ZnTe superlattice, quasi-2D excitons in strongly localised regime 7-12617
 CdTe/(Ba,Ca)F₂ layers, MBE growth on non-lattice-matched Si substrates 7-27216
 CdTe-(Cd,Mn)Te MQW, optical and magneto-optical props. 7-13137
 CdTe-Ag interface, photoemission studies, surface struct., growth behaviour, Schottky barrier and surface photovoltage 7-39352
 CdTe-AuCu, AC contact impedance, influence on high freq., low temp. on fast transient junction meas. 7-64311
 CdTe-Cd_{0.6}Mn_{0.4}Te superlattices, high resolution electron microscope study 7-27162
 CdTe-CdMnTe, quantum wells, excitons and kinetics 7-12622
 CdTe-CdMnTe superlattices, photoluminesc. props. 7-13218
 CdTe-Cu interface form., effect of different cation-anion bond strengths 7-27149
 CdTe-Cu_{1.8} thin film polycrystalline solar transducers, photosensitivity spectra 7-34036
 CdTe-GaAs heteroepitaxial interface, at. resolution HVEM study 7-2392
 CdTe-HgTe superlattices, magnetotransport props. 7-33076
 CdTe-HgTe superlattices, IR material characterisation, transport phenomena anal. 7-64338
 CdTe-In₂-x-y-Sn₂O₃-y solar cells, spray deposited, elec. and photoelec. props. 7-54321
 CdTe-Se-Cu_{1.8} thin film polycrystalline solar transducers, photosensitivity spectra 7-34036
 CdTe-x-y-Se₂-y, mixed system, optical phonon frequencies 7-2123
 CdTiO₃, nonlinear props. in high electric fields 7-7668
 Cd₂Zn₃Mn₂Te(Se) pseudoternary semimag. semicond., mag. suscept. and exchange interaction data anal. 7-7501
 CdZnS/CuInSe₂ solar cells, spray pyrolysis prep. and characts. 7-8374
 CdZnS/CuInSe₂ solar cells, transient current studies of junction activity 7-8409
 n-CdZnS/p-CuInSe₂ polycrystalline solar cells, open circuit voltage 7-17889
 CdZnS-CuInSe₂ solar cell development for space appls. 7-13917
 CdZnS-InP heterojunction solar cell, numerical anal. 7-23155
 Cd_{0.8}Zn_{0.2}S films, solution-sprayed, photocurrent decay times 7-45525
 Cd_{1-x}Zn_xS-CuInSe₂ thin-film solar cells, voltage and light bias-dependent spectral response 7-8375
 CdZnTe, epitaxial growth via low press. CVD, IR detector appls. 7-64926
 CdZnTe, MBE growth on GaAs substrates, struct. and optical props. 7-64907
 Cd_{1-x}Zn_xTe mixed cpd. semicond., lattice consts. comp. depend., X-ray diff. study 7-58246
 Cd_{1-x}Zn_xTe, MBE growth 7-13358
 Cd_{1-x}Zn_xTe:Mn, hyperfine coupling constant, EPR study 7-22138
 Cd₂Zn_{1-x}Te, second-order optical process, transient behavior, luminesc., Raman scatt. 7-64689
 CsCdF₃:Gd³⁺, transferred hyperfine interactions, ¹⁹F ENDOR studies 7-53177
 Cs₂CdF₄:Cr³⁺, Li⁺, Cr³⁺ centres, EPR study 7-7589
 Cs₂Cd₂NO₃, synthesis and cryst. struct. (French) 7-32401
 Cu_{1-x}Cd_xFe₂O₄, irreversible magnetisation. depend. on magnetising field 7-64487
 Cu_{2-x}Cd_xTe-Zn_{39.5}Cd_{60.5}Te:I, heterojunction solar cells, fabrication and characterisation (Korean) 7-28402
 CuGaSe₂-ZnCdS wide bandgap solar cells for thin film tandem structs. 7-23172
 CuInSe₂-CdS heterojunctions deposition, in-line sputtering system 7-64900
 p-CuInSe₂-CdZnS-ZnO solar cells, device anal. 7-23171
 CuInSe₂-ZnCdS thin film polycryst. solar cell efficiency improvement using antireflection coatings 7-23186
 Cu₂S/CdS large-area solar cells, reactive sputtering 7-46943
 Cu₂S-CdS polycrystalline solar cell, freq. dispersion in admittance 7-65464
 Cu₂S-CdS solar cells, all-evaporation processed, characts. 7-8383
 Cu₂S-Cd_{1-x}Zn_xS thin film solar cells perform., depend. on annealing temp. 7-17861
 n-Hg_{1-x-y}Cd_xMn_yTe high field magnetoresist. and magnetisation, Mn-Mn exchange interaction effects 7-12964
 Hg_{1-x-y}Cd_xMn_yTe, Shubnikov-de Haas oscillations 7-21943
 Hg_{1-x}Cd_x(Mn_y)Te/CdTe superlattices, twin faults, X-ray obs. 7-45036
 Hg_{1-x}Cd_xSe, reson. Raman Scatt. meas. 7-7701
 HgCdTe, 0⁺ giant oscillation near semimetal-semiconductor transition 7-64053
 HgCdTe 32×32 CCD array for IR camera, for astronomy 7-60560
 n-HgCdTe, acceptor densities, photo-Hall determ. 7-58836
 HgCdTe and HgTe-CdTe superlattices, IR photolum. by Fourier transform spectroscopy 7-46134
 HgCdTe anodic oxide surface analysis by laser ionisation 7-13275
 HgCdTe as IR sensor material, characts. (Japanese) 7-56339
 HgCdTe, bulk melt growth and LPE, defect control 7-64940
 HgCdTe, cryst. growth by travelling heater method 7-64892
 HgCdTe, electrochemical and electrolyte electroreflectance studies 7-64607
 HgCdTe, electronic struct., alloying effects, ETBM calc. method 7-64080
 HgCdTe, epitaxial film, interdiffusion profiling, microreflection spectroscopy 7-53369

cadmium compounds continued

HgCdTe epitaxial layers and structures, characterisation of intentional dopants 7-12552
HgCdTe epitaxial layers, Hall effect and elec. resist. characterisation 7-64375
HgCdTe Fabry-Perot IR bistable devices, parameter optimisation 7-57396
HgCdTe focal plane array photodetectors, growth, performance and array fabrication 7-15001
HgCdTe, Hg-rich LPE growth using dipping furnace 7-64943
HgCdTe, high quality LPE on CdZnTe, IR detector anal. 7-64941
HgCdTe, homogenization, wetting elimination 7-38221
HgCdTe IR CCD coupling structure for space appls. 7-29309
HgCdTe IR detectors, epitaxial growth of CdZnTe substrate 7-64926
HgCdTe, IR nonlinear absorpt., dynamic Burstein-Moss effect (*Chinese*) 7-50615
HgCdTe IR photodetectors, magnetoresist. and cyclotron resonance characterisation 7-64054
HgCdTe in MIS struct., electroreflectance at 77K 7-13128
HgCdTe, LPE growth in multi-slice apparatus 7-64942
HgCdTe materials for infrared detectors, prep. techniques 7-64019
p-HgCdTe, minority carrier characterisation using light-modulated Hall effect 7-21934
HgCdTe, p-type, acceptor conc., IR reflectance studies 7-64600
HgCdTe photoconducting detector design for IR imaging 7-9900
HgCdTe, single cryst. growth by travelling heater method 7-64891
(HgCdTe) substrates for Ge overlayer growth, surface preparation effects 7-45037
HgCdTe: In, ion implanted, damage and rapid thermal annealing 7-63637
HgCdTe:B, bulk and thin film, resonant impurity levels, magneto-transport studies 7-64162
HgCdTe:B⁺, ion implanted n⁺p junction, lifetime and carrier conc. profile 7-45450
HgCdTe-CdZnTe heterojunctions, lattice matching 7-21717
Hg_{0.75}Cd_{0.25}Te-Cu interface form., effect of different cation-anion bond strengths 7-27149
Hg_{0.75}Cd_{0.22}Te, stoichiometry of anodic oxides, quantitative meas. 7-39782
p-Hg_{0.75}Cd_{0.22}Te:Sb LPE films, elec. props. 7-7426
Hg_{0.75}Cd_{0.21}Te, metal-insulator transition, mag. field induced, low temps. 7-45158
n-Hg_{0.8}Cd_{0.2}Te accumulation layer electrons, tilted field cyclotron resonance 7-7591
n-Hg_{0.8}Cd_{0.2}Te, condensed electron system, heat capacity, comment 7-58503
Hg_{0.8}Cd_{0.2}Te, Hg vacancies, heat of form. determ. 7-37969
Hg_{0.8}Cd_{0.2}Te, low temp. hot electron energy relax. time in extreme quantum limit mag. fields 7-33035
n-Hg_{0.8}Cd_{0.2}Te, magnetic field-induced metal-insulator transition, threshold field electron density depend. 7-52427
Hg_{0.8}Cd_{0.2}Te:Cu, activation energy of Cu shallow acceptors 7-64153
Hg_{1-x}Cd_xTe and related materials, far IR spectroscopy 7-39120
Hg_{1-x}Cd_xTe, pseudobinary melts, heat capacity, enthalpy of melting, thermal cond. 7-21477
Hg_{1-x}Cd_xTe crystals, anodic oxide capped, thermal stability 7-65225
Hg_{1-x}Cd_xTe crystals., lattice defect imaging, high resolution electron microscopy obs. 7-51769
Hg_{1-x}Cd_xTe, epitaxial growth by low temp. metalorganic CVD 7-27911
Hg_{1-x}Cd_xTe films, LPE using a semiclosed rotational boat 7-64937
Hg_{1-x}Cd_xTe films, organometallic epitaxial growth on CdTe and characterisation 7-22579
Hg_{1-x}Cd_xTe heterojunctions, supersymmetry, band-inverting contact 7-32717
Hg_{1-x}Cd_xTe, low frequency absorption bands (*Chinese*) 7-39095
Hg_{1-x}Cd_xTe, MBE growth, crystallographic orientations and condensation coeffs. 7-3180
Hg_{1-x}Cd_xTe MBE layers, plasma oxidation, oxide growth, comp. and surface struct. 7-54018
Hg_{1-x}Cd_xTe optical waveguides, high band gap, for 10.6 μm 7-37157
Hg_{1-x}Cd_xTe, photochemical organometallic vapour phase epitaxy 7-27946
Hg_{1-x}Cd_xTe resistors, Umklapp 1/f noise, Hooge parameter, relativistic correction 7-2649
Hg_{1-x}Cd_xTe surfaces, sputtered and cleaved, deposition of unreactive Au, UPS study 7-33514
Hg_{1-x}Cd_xTe with metallic donor clusters, anomalous Hall effect below mag. field induced metal insulator transition 7-2485
Hg_{1-x}Cd_xTe, zero gap, acceptor levels 7-27287
Hg_{1-x}Cd_xTe:B, ion implanted, annealing, nature oxide encapsulation 7-2036
Hg_{1-x}Cd_xTe/Ag(Cu)(Al) interfaces, morphology, Hg bonding effects 7-7021
Hg_{1-x}Cd_xTe/CdTe superlattices, MBE growth and props. 7-53602
Hg_{1-x}Cd_xTe/Pt interface, overlayer-cation reaction, XPS, UPS and LEED studies 7-65349
Hg_{1-x}Cd_xTe-CdTe superlattice, MBE growth and props. 7-7345
Hg_{1-x}Cd_xTe_{1-y}Se_y, existence region of wurzite struct. 7-53709
HgCdTe thin film solar cells fabrication 7-23188
HgTe-CdTe as IR sensor material, characts. (*Japanese*) 7-56339
HgTe-CdTe superlattices, cut-off wavelengths meas. 7-3030
HgTe-CdTe superlattice, MBE growth and props. 7-7345
HgTe-CdTe superlattices, growth of GaAs (100) substrates by MBE 7-12520
HgTe-CdTe superlattices, present status, props. and applications (*Japanese*) 7-12829
HgTe-CdTe superlattice, semimetallic, band structure calc. 7-12851
HgTe-CdTe superlattice, IR magnetooptics and band struct. 7-13138
HgTe-CdTe superlattice, alloying, far IR study 7-13143
HgTe-CdTe superlattices, IR optical props. 7-13166
HgTe-CdTe superlattices, IR photoluminesc. spectra 7-13219
HgTe-CdTe superlattices, struct. characterisation 7-27164
HgTe-CdTe superlattices, electronic props., calc. methods 7-27406
HgTe-CdTe superlattices grown on lattice-mismatched GaAs substrates 7-52341
HgTe-CdTe superlattices, band struct., optical and magneto-optical studies 7-64337
HgTe-Hg_{1-x}Cd_xTe double barrier, single quantum well heterostructures, resonant tunnelling 7-33068
HgTe-Hg_{1-x}Cd_xTe heterojunctions, hole Hall mobility enhancement 7-33077

cadmium compounds continued

HgZnTe, electrochemical and electrolyte electroreflectance studies 7-64607
K₂Cd₂(SO₄)₃:Sm, doped and undoped, thermoluminescence 7-39191
LiNbO₃/CdSe multilayer structs. with ohmic contacts, electroacoustic conversion, SAW excitation 7-58839
Mg₂Cd_{1-x}Se single cryst. solid solns., local centres parameters determ. (*Russian*) 7-32953
Mg₂Cd_{1-x}Se single crystals., impurity photocurrent temp. activation meas. and calcs. (*Russian*) 7-45394
β-Na₂O-Al₂O₃-CdO:Cr³⁺, luminescence spectra 7-33448
Ni₂Cd_{1-x}PS₃, IR, visible and UV spectra, dilution and intercalation effects 7-13175
Ni₂Cd_{1-x}Mn₂O₄ spinels, cation distrib., structural transitions and Jahn-Teller distortion 7-58227
Ni₂Cd_{1-x}PS₃, crystalline lamellar cpds. EXAFS studies of disorder 7-59295
Pb₂Cd_{1-x}F₂, phonon spectra, superionic props. 7-6735
Pb_{1-x}Cd_xSe films, laser deposition 7-59422
Pb_{1-x}Cd_xSe, inter-band transitions, thermoreflectance study 7-3029
PdO-CdO-B₂O₃ glasses, elec. cond. and density meas. 7-1895
RbCdF₃, struct. phase transition, ENDOR study 7-33298
RbCdF₃:Cr³⁺, tetragonal phase, ENDOR study 7-2952
Rb₂CdF₄:Cr³⁺, Li⁺, Cr³⁺ centres, EPR study 7-7589
Rb₂Cd₂(SO₄)₃:Mn²⁺, langbeinite, reversible phase transitions, EPR studies 7-63810
SiO-K₂O-CaO-MgO-CdO glass melts, evaporation 7-2160
SiO₂-CaO filled poly(acrylic acid) composite, filler chem. influence on T_g behaviour, dynamic mech. spectroscopy 7-59559
In-SnO₂-n-CdGeP₂:In heterojunction, elec. and photoelec. props. 7-45478
SnTe-CdS, phase diagram, in SnTe+CdS=SnS+CdTe ternary reciprocal system 7-13438
ZnCdS:Ag/Cd(S₂Se):Cu mixed photoconductor system for electrophotography 7-2636
Zn₂Cd_{1-x}S thin films, struct. and electrical props. 7-64372
Zn_{1-x}Cd_xSb solid soln., cryst. growth, characterisation and appls., review 7-26685
ZnCdSe, electron beam pumped, cathodolum., gain and stimulated emission 7-64701
Zn_{0.25}Cd_{0.75}Se mixed crystals., electron and hole deep level traps 7-16980
Zn₂Cd_{1-x}Te thin film heterojunction solar cells 7-17914
Zn₂Cd_{1-x}Te, crystals. grown from non-stoichiometric melts, Zn distrib. calc. 7-51678
Zn(PO₃)₂-CdCl₂-KCl glasses, electrical conductivity and IR spectra 7-2253
ZnS-CdS:Ag,Ni,Co phosphors, photolum., energy level model 7-59245
(ZnSe)₂(CdTe)_{1-x} films, CVD fabricated, phys. props. 7-7055
ZnTe-ZnCdS wide bandgap solar cells for thin film tandem structures. 7-23172

CAE see CAD/CAM

caesium
see also nuclei with
adatom, in graphite monolayer on Re surface, struct. and props., AES, TDS and thermionic emission anal. 7-45017
adsorbed atoms on graphite covered Ir (111), photo- and electron-stimulated deformation of graphite monolayer 7-58627
adsorbed on Ag single crystals, adsorbate-substrate bond lengths, coverage depend., SEXAFS 7-63948
adsorbed on Si, migration and equilibrium in strong elec. field 7-2351
adsorbed on Si (111), effect on surface oxidation 7-54025
adsorption on graphite (0001), induced work function changes, LEED obs. 7-33064
adsorption on LaB₆ (001), surface structure and work function 7-6977
adsorption with Ba on Mo(Nb), bonding energies, thermionic emission studies 7-12463
Amersham ¹³⁷Cs afterloading sources, associated X-ray spectra 7-60075
arc, low-voltage, ionisation instability appearance 7-44289
atom, 5s ionisation, PES satellite struct., CI approach 7-62296
atom, 6S and 7S states, off-diagonal hyperfine interaction 7-19726
atom, D₂ line, saturated absorpt. spectra anal. 7-19781
atom, IR stimulated Raman scatt. 7-30972
atom, isotope shifts, relativistic DF contrib., reson. doublet, UV laser spectroscopy 7-10475
atom, lasing action in Kr gas 7-15855
atom, optically pumped, spin-relax. rates 7-36557
atom, parity violation, crossed beam interference technique 7-10497
atom, photoionisation cross sections, ab initio RRPA calcs. 7-36462
atom, photoionisation in 650 to 760 Å UV spectra 7-50033
atom, quasimetastable energy levels, appl., XUV emission studies 7-10480
atom, resonance ionisation in presence of buffer gas collisions 7-10527
atom, scalar Stark polarizability for 6s-7s transition 7-62322
atom, spontaneous decay suppression at optical frequencies, test of vac.-field anisotropy in confined space 7-57026
atom, stopping with diode laser beam 7-10507
atomic beam, cooling using laser 7-10897
atomic beam, frequency reference, metrological analysis 7-41351
atomic beam, frequency standard appl., C-field setting, transitions and disturbances 7-18757
atomic beam clock, velocity distrib. determ. 7-18755
atomic beam freq. standards, distributed phase shift minimization 7-41356
atomic beam frequency standard, NRLM-II, atomic vel. distrib. and second-order Doppler shift 7-14910
atomic beam frequency standard with narrow atomic velocity distrib. ranges, Ramsey patterns 7-18758
atomic clock, PTB design, preliminary results 7-18756
atomic clocks charactn. in perturbed environment (*French*) 7-29984
atoms, diffusion through IR foil and surface ionisation 7-3138
atoms, elastic positron scatt., integral eqn. approach 7-42762
atoms, highly excited, as coherent radiations source, superradiative transitions 7-57027
atoms, optically polarised spin system, mag. reson. characts. in wide-band noise RF field 7-42539
atoms, reflection from polished glass surface 7-22411
atoms laser spectroscopy of 109.1 nm transition 7-19745
BCC single cryst., lattice dynamics, coherent inelastic neutron scatt. study 7-21376
beam freq. standards, atom transit time effect on stability 7-41355
beam frequency standard, optically pumped, progress 7-41354

caesium continued

- boiling liquid metal, critical heat flux (*German*) 7-49565
 covered GaAs (111), adsorption of O₂ 7-63957
 desorption from Pt, 1600-1900 K 7-58636
 electron pair correl. functions, real space variational calcs. 7-52479
 fallout, ¹³⁷Cs in soil of W Germany field, fallout spatial variability 7-65655
 gas phase atoms, detect. by 2-photon resonant ionisation spectroscopy 7-42533
 giant resonance absorption spectra of 4d electrons 7-10471
 high press. phase, β -Sn-type struct., pseudopot. perturbation calcs. 7-51938
 highly forbidden 6S_{1/2} - 7S_{1/2} transition atomic parity violation meas. 7-31184
 intercalation compound with graphite, C₂₄Cs(H₂)_x, domain mobility and rot. tunnelling spectrum 7-63525
 intracellular distribution, in ICRP Reference Man 7-65861
 ion, effective electron inelastic excitation cross section, resonance effects study 7-42772
 Knudsen ultrahigh-temperature thermionic energy conversion for space nuclear power 7-65507
 laser initiation of discharge channels for pulsed ion beam research 7-25291
 liquid alkali metals, temp. depend. of mag. susceptibility 7-33152
 liquid-vapour-interface, electron and ion distrib., self-consistent Monte Carlo simulation 7-32024
 metal-nonmetal transitions 7-2486
 molecule, electronic states, laser induced fluoresc. 7-19912
 molecule, photolysis, prompt and delayed, two photon technique 7-23043
 nonideal plasma, elec. cond. meas. 7-37643
 nonideal plasma, thermopower study 7-37645
 outer-core emission spectra, many-body effects and spin-orbit partner behaviour obs. 7-53436
 overlayers on graphite, electronic struct., initial stages of intercalation 7-53503
 oxidation, quantum size effect of conduction electrons 7-13643
 parity-violating 6S-7S amplitude evaluation 7-10457
 plasma, elec. cond., linear response theory 7-37646
 plasma, first reson. doublet absorpt. 7-37753
 plasma in hollow-cathode arc 7-16344
 plasma recombination lasers similar to thermionic converters 7-10915
 PNP-500 HTGR, Cs release during a heat-up accident, fission product transport 7-15286
 polyacetylene:Cs, elec. cond. temp. depend. meas. 7-17030
 positron annihilation, high-momentum components and core enhancement effects 7-46195
 positron annihilation and pressure-induced electronic s-d transition 7-22378
 strongly coupled cluster plasma, elec. cond. 7-37649
 surface, adsorbed Xe, core-electron binding energies, photoemission studies 7-3146
 surface-ionised plasma in hot cavity, power-shifted microwave reson. 7-58020
 tensile strength under (110) uniaxial stress (*Chinese*) 7-26825
 vapour, atomic vel. sampling stimulated photo echo 7-11073
 vapour, comp. study, reson. doublet absorpt. meas. 7-36518
 vapour, dimer spectral line shape, nonadiabatic effects study 7-36696
 vapour, generation of tunable IR ultrashort light pulses by nonlinear frequency conversion 7-1227
 vapour, optically pumped, hyperfine relax. with Ar collisions 7-10511
 vapour, two-photon reson. four-wave mixing and multiphoton ionis. in heat pipe oven 7-901
 vapour in heat pipe oven, two-photon resonant four-wave mixing obs. 7-43239
 BN:Cs, intercalation cpd. formation 7-44574
 C₂Cs, first stage intercalation cpd., self-consistent band struct. calc. 7-52395
¹³⁷Co irradiation rel. to testis wt. loss in mice 7-28592
 Cs + H₂⁺, dissociative charge exchange, H₂ predissociation, fragment spectra anal. 7-36753
 Cs III Auger laser, XUV at 63.8 nm, proposal 7-25801
 Cs⁻, low-energy collisions with atoms and mols., absolute total cross section meas., curve-crossing model anal. 7-36749
 Cs⁺, electron impact s-ionisation, ultrasoft X-ray spectroscopy study (*Russian*) 7-984
 Cs + H₂, CsH form. kinetics, rot. distrib. (*French*) 7-13728
 Cs + H⁺, charge transfer collisions, laser radiation influence 7-25646
 Cs + He, He2⁺P₁ and 2¹S₀ state quenching 7-57153
 Cs + He, inelastic collisions at thermal energies 7-983
 Cs + He, Penning ionisation, pot. well depth calcs., electron energy spectra anal. 7-62510
 Cs + HeH⁺, dissociative charge exchange 7-5766
 Cs + HeH⁺, HeH bound excited state form., predissoc. and radiative disoc. 7-20033
 Cs + Li, ion pair prod. cross sections, beam-gas study 7-39871
 Cs + trichlorotrifluoroethane, vapor phase reactions, chemiluminesc. obs. 7-59767
 Cs₂ reference for freq. stabilisation of 1.06 μ m Nd:YAG laser 7-57403
¹³⁷Cs, A=134,137, comparative pathway analysis in Hudson River estuary, dose assessment 7-8699
¹³³Cs, 7²P_{3/2} state, level crossing in elec. and mag. fields 7-50003
¹³³Cs alkali gas cell atomic freq. standards 7-41357
¹³³Cs, in Ba cpds., nucl. quadrupole interaction 7-10628
¹³⁴Cs removal from radioactive process waste water by coprecipitate flotation 7-36293
¹³⁵Cs alkali gas cell atomic freq. standards 7-41357
¹³⁷Cs alkali gas cell atomic freq. standards 7-41357
¹³⁷Cs, immobilization using hydrous TiO₂ and zeolite 7-10295
¹³⁷Cs in air and soil, use to meas. aerosol scavenging rate and vertical profile 7-55188
¹³⁷Cs irradiation of lymphoid organs 7-28591
¹³⁷Cs leaching from epoxide resin 7-19536
¹³⁷Cs, removal from reactor coolant by TiFe(CN)₆ 7-30679
¹³⁷Cs tracer for flow meas. by transit time method (*Finnish*) 7-57970
¹⁴⁰Cs, ground state hyperfine struct. determ. by RF mag. reson. and laser optical pumping 7-25681
 GaAs:Cs, impurity ion beam effects, SIMS depth profiling 7-22419
 Na₂O-SnO₂-SiO₂:Cs⁺, glass diffusion of cations, 500-800°C 7-12371
 Nd:YAG laser, 1.06 μ m Cs₂ reference for freq. stabilisation 7-57403
 SiO₂:Cs-Si MOS, semicond. flatband voltage depend. on impurity distrib. 7-27433

caesium alloys

- Cs-Sb-based photocathodes, stability and O adsorption energies 7-38344
 Cs-Se system, phase diagram 7-6759
 Cs_{1-x}K_x, low temp. phase diagram, compression effects 7-33641
 Cs_{1-x}Rb_x, low temp. phase diagram, compression effects 7-33641
 Cs₂Sb surface film, detection on multialkali photocathodes 7-46912
 Hg-Cs, liq. alloy, molar mag. susceptibility, temp. depend 7-7494
 K-Cs, liq., triplet conc. fluctuations in long wavelength limit 7-63439
 K-Cs, saturation vapour press. meas. 7-44780
 Na-Cs, liq., triplet conc. fluctuations in long wavelength limit 7-63439

caesium clocks see atomic clocks

caesium compounds

see also caesium alloys

- 4-trifluoromethyl-6-phenyl-3-cyano-2-pyridone X-ray struct. study 7-21192
 halides, low energy electron collisions, cross section-electronegativity relation 7-20061
 mixed halides, electronic dielectric const. and fractional ionic character of chemical bond 7-2966
 pentadecafluorooctanoate-water discoid micelle solns., order-disorder transitions, X-ray scatt., elec. cond., NMR meas. 7-26949
 poly(styrenesulphonate)s, enthalpy of dilution, large dielectric constant solvent 7-21483
 silicate phases, Cs₂MSi₂O₁₂, M=Be, Mg, Fe-Ni, Zn, Cd, with pollucite struct., cryst. struct., X-ray powder diff. 7-32409
 single-crystal two-layer fibres for visible and infra-red transmission 7-57569
 [Ba₂Cs₂][{(Ti₂Al)_{2x+y}³⁺ Ti_{8-2x-y}⁴⁺}] O₁₆ hollandites, structural chemistry 7-51726
 BaCs₂(PO₃)₆, cryst. struct. determ. 7-1954
 Cs₂AgAu^{III}X₆ (X=Cl,Br), valence study by X-ray absorption spectra at Au L₃ edge 7-7791
 CsAlF₄, struct., GPED automatic background subtraction 7-15710
 Cs_{1.32}Al_{1.32}Ti_{6.68}O₁₆, solid soln. with Ba_{1.11}Al_{2.22}Ti_{5.78}O₁₆, cryst. struct., neutron diff. study 7-63563
 Cs₂Au^{III}Cl₆, valence study by X-ray absorption spectra at Au L₃ edge 7-7791
 CsBSi₂O₆, glassy and crystalline, IR spectra 7-59199
 CsBi₂ graphite intercalation cpds., stage 1, α and β phases, X-ray diff. study 7-58226
 Cs₂BiCl₆, cryst. struct., X-ray diff. study 7-32389
 CsBr, luminescence quenching in F centers under pressure 7-22334
 CsBr, luminescing solids, nonradiative decay channels of electronic excitations 7-27760
 CsBr, two-halogen self-trapped excitons, metastable optical absorpt. 7-53365
 CsBr:Hg²⁺, Hg²⁺ centres, electronic absorpt. spectrum 7-59229
 CsBr-AgBr fibres, growth by Stepanov's method 7-31533
 Cs₂BrN₃, layered struct., X-ray diff. and Raman spectra study (*German*) 7-26715
 Cs₈ intercalation cpd., electron struct., soft X-ray emission spectroscopy 7-45117
 Cs_x (x=8,24), intercalation cpds., XANES studies, polarisation effects 7-59294
 CsCaCl₃, cubic to tetragonal phase transition, space group determ., X-ray studies 7-16736
 CsCaF₃, fluoroperovskites, IR refl. spectra, temp. depend. 7-22248
 CsCaF₃:Gd³⁺, transferred hyperfine interaction of impurity centres, ENDOR, EPR meas. 7-32946
 CsCaH₃, ternary hydride, crystal struct. 7-26729
 Cs₂CaF₄:Cr³⁺, Li⁺, Cr³⁺ centres, EPR study 7-7589
 CsCl aq. soln., water self-diffusion coeff. neutron scatt. time-of-flight meas. (*Russian*) 7-32692
 CsCl, F_H(OH⁻)-centre absorpt. bands, pseudopotential calc. 7-52512
 CsCl, luminescence quenching in F centers under pressure 7-22334
 CsCl:CN⁻, F_H(CN⁻)-centre absorption bands, pseudopotential method calcs. 7-22292
 CsCl-AgCl, binary molten mixtures, elec. cond. 7-12340
 CsCl-CsBr solid solutions, lattice parameter meas. by X-ray diffraction 7-58249
 CsCoCl₂·2H₂O, 1D antiferromagnet, exciton transfer, absorpt. spectra 7-27254
 Cs₃Cr₂I₉, critical singlet ground-state magnet, dimer excitations, inelastic neutron scatt. study 7-7477
 CsCrO₃Cl, CrO₃Cl⁻ vibronic anal., phosphorescence and Raman spectra 7-15605
 Cs₃Cr₂X₉ (X=Cl,Br,I), synthesis, struct., mag. props. 7-6601
 CsCuCl₃, dynamic Jahn-Teller effects, mag. susceptibility study 7-45613
 CsCuCl₃, Jahn-Teller induced helical deformations 7-7178
 CsDSO₄, cryst. struct. and III-II phase transition 7-44484
 CsDSO₄, superionic transition, NMR 7-38951
 CsFeCl₃, quasi-one-dimensional ferromag., mag. field effects on optical spectrum 7-3026
 Cs₂FeCl₅·H₂O, antiferromagnet, mag. phase diagram, spin wave excitations, Mossbauer spectra 7-45676
 Cs₃Fe₂F₉, precise struct. determ. and ferromag. props. anal. 7-1981
 Cs₂Fe(SO₄)₃, columnar cpds., vibr. spectra and phase transitions 7-17314
 CsH form. kinetics, rot. distrib. (*French*) 7-13728
 CsH, ground and excited states long range pot. curves calcs. 7-19994
 CsH, X¹ Σ ⁺ state, HF quality Slater basis sets 7-19719
 CsH₂AsO₄ and CsH₂D_{2(1-x)}AsO₄, ferroelectric, optical props., radiation effects 7-33406
 CsH₂AsO₄ crystals, electrogyration effects investig. 7-3022
 CsH₂AsO₄ ferroelec. cryst., EPR studies of AsO₄³⁻ centres 7-45816
 CsH_{0.1}D_{0.9}AsO₄, melting pt., phase diagram 7-21417
 CsH₂(D₂)PO₄, ferroelectrics, electrostrictive corrections to pseudo ID Ising model 7-59158
 CsH(D)SO₄ 7-63925
 CsH(D)SO₄ struct. and phase transitions, X-ray diff. studies 7-2170
 (Cs⁺(H₂O)_n)₂MoO₄^{x-}, composition and struct. 7-16518
 CsH₂PO₄ ferroelec., dielec. relax. meas. in paraelec. and ferroelec. phases, time domain spectroscopy method (*Japanese*) 7-4862
 CsH₂PO₄:Cu²⁺ pseudo-ID ferroelectric, 3D correls., EPR meas. 7-38931
 Cs₂HPO₄:Te(OH)₆, vibr. anal., IR and Raman spectra 7-39104
 CsH₂PO₄(d₂), polarised IR and Raman spectra, internal vibrs. 7-50125
 CsH₂PO₄(d₁), polarised IR and Raman spectra, transition dipole moments, orientation calcs. 7-50124
 CsHSO₄ cryst. struct. IR spectra study 7-63588
 Cs₄H₂V₁₀O₂₈·4H₂O, pseudo-orthorhombic cryst. struct. 7-58222
 Cs₂HgBr₄, phase transitions, microwave permitt. meas. 7-2184

caesium compounds continued

CsI aerosol particles growth in steam environment, effects on removal 7-15281
CsI, cryst., γ -irrad., acoustic nucl. reson. (*Russian*) 7-22152
CsI, Debye-Waller factors of ^{129}I , Mossbauer study 7-2135
CsI dislocation study using US technique 7-21362
CsI, excitons, three-photon magnetoabsorpt. meas., g-value determ. 7-2498
CsI, H_n^+ cluster ion impact-induced Cs^+ desorption, TOFS study 7-27843
CsI, high press. metallisation, relativistic self-consistent APW calcs. 7-21812
CsI, Hugoniot overtake sound-rel. meas. 7-44705
CsI, internal friction, plastic deformation, crystallographic orientation 7-12205
CsI, luminescence quenching in F centers under pressure 7-22334
CsI, press. induced structural instability, ab initio pseudopotential techniques 7-52042
CsI, shock wave overtake meas. 7-21353
CsI single crystals, dislocation internal friction mechanisms study 7-63625
CsI solution radiolysis in conditions related to a PWR severe accident 7-49600
CsI, submicrosecond elastic loading, material relax. phenomena 7-12186
CsI, surface stoichiometry, changes under electron and laser radiation 7-44961
CsI, two-photon induced luminesc. 7-64696
CsI: Hg^{2+} , Hg^{2+} centres, electronic absorpt. spectrum 7-59229
CsI:Na, exoelectron emission, phonon drag, inhomogeneous energy distrib. 7-39366
CsI:TL, energy resolutions for p and α 7-5557
CsI:TL, γ -ray radiation damage, recovery 7-63657
CsI-AgI, binary molten mixtures, elec. cond. 7-12340
Cs $_2$ IN $_3$, layered struct., X-ray diffr. and Raman spectra study (*German*) 7-26715
CsI(Na) inorganic scintillators, role of activators 7-33459
CsI(Na) scintillation detector, single-coordinate, position-sensitive, space resolution determ. 7-10359
CsI(Tl) scintillator response to light particles and heavy ions (*Italian*) 7-25327
Cs $_2$ K $_2$ (TeO $_3$), coordination, cryst. structs., lattice energy (*German*) 7-26714
CsK $_2$ BiCl $_6$, cryst. struct., X-ray diffr. study 7-32389
CsLiCrO $_4$, ferroelectric phase transition 7-39047
Cs $_{1-x}$ Lu $_x$ F $_{10-x}$, cryst. struct., space group, least-squares refinement 7-6604
CsMCl $_3$ (M=Cu, Cr), hexagonal Jahn-Teller crystals, struct. phase transitions, face-sharing coupling, ground-state configuration 7-2180
CsMCl $_3$ (M=Cu, Cr), hexagonal Jahn-Teller crystals, struct. phase transitions, mean-field approx. 7-2181
CsMF $_3$:Gd $^{3+}$ (M=Cd,Ca), transferred hyperfine interactions, ^{19}F ENDOR studies 7-53177
Cs $_2$ MI $_4$ NO $_3$, (M=Zn, Co, Cd), synthesis and cryst. struct. (*French*) 7-32401
CsMnBr $_3$, photoexcited crystals, exciton annihilation, luminesc. decay curves 7-53385
CsMnCl $_3$ antiferromag. crystals, struct. deform. by exciton self-localisation, luminesc. spectra fine struct. study (*Russian*) 7-27752
CsMnCl $_3$, photoexcited crystals, exciton annihilation, luminesc. decay curves 7-53385
CsMnCl $_3$ 2H $_2$ O, 1D Heisenberg magnet, spin dynamics and EPR linewidth 7-38932
CsMnF $_3$ antiferromagnet, parametrically excited magnon redistrib. and chaos 7-17167
Cs $_2$ Mo $_6$ Se $_6$, thermal expansion of ternary chalcogenides containing infinite (Mo $_6$ /Se $_6$) $_2$ chains 7-16791
CsNO $_3$, polycryst., IR absorpt. spectra 7-33396
CsNO $_3$ -NaNO $_3$ system, molten, refractive indices 7-64598
Cs $_2$ NaAlF $_7$:Cr $^{3+}$ (Fe $^{3+}$), impurity ion spin Hamiltonian parameters, EPR determ. 7-64523
Cs $_2$ Na $_2$ (FeO $_4$) $_2$, single cryst. prep. and structural characterisation (*German*) 7-37951
Cs $_2$ NaHoBr $_6$, excitation, electronic absorpt. and luminesc. spectra, crystal field splittings 7-46088
Cs $_2$ NaInCl $_6$:Cr $^{3+}$, elpasolite lattice, broadband near-IR luminesc. 7-17338
Cs $_2$ NaYBr $_6$:Cr $^{3+}$, elpasolite lattice, broadband near-IR luminesc. 7-17338
Cs $_2$ NaYCl $_6$:Cr, impurity photolum. spectra and lifetimes, thermal quenching and temp. depend. studies 7-3084
Cs $_2$ NaYCl $_6$:Cr $^{3+}$, elpasolite lattice, broadband near-IR luminesc. 7-17338
CsNiF $_3$, 1D easy plane ferromag., quantum Monte Carlo and transfer matrix calcs. 7-7468
CsNiF $_3$, dynamical critical slowing down, spin fluctuation relax. time, mag. suscept. meas. 7-38897
CsNiF $_3$, easy-plane ferromag. chain, quantum sp. ht. 7-7522
CsNiF $_3$, easy-plane ferromagnetic chains, sp. ht. and spin Hamiltonians, quantum statistics calcs. 7-64469
CsNiFeF $_6$ spin glass, equilibrium mag. fluctuations 7-64452
CsO-Nb $_2$ O $_5$ -Ga $_2$ O $_3$ glass structure, Raman spectroscopy 7-1902
Cs $_2$ O, influence on durability of borosilicate glass 7-8144
Cs $_2$ O-Al $_2$ O $_3$ -SiO $_2$ thermionic cathode as efficient electron source 7-9923
Cs $_2$ O-B $_2$ O $_3$ glasses, thermodynamic props. 7-2211
Cs $_2$ O-SiO $_2$ glasses, intrinsic and recomb. luminesc. and fundamental absorpt. spectra 7-13195
Cs $_2$ O-SiO $_2$ -based glasses, Cs $^+$ ion distrib., energy dispersive X-ray diffr. studies 7-21113
CsPbBr $_3$ and CsPbCl $_3$, ionic cond. and phase transforms., 30 to 380°C 7-58457
CsPbBr $_3$, lattice thermal expansion, 140-400°C, X-ray obs. 7-44859
Cs $_2$ Rb $_{1-x}$ UO $_2$ (NO $_3$) $_3$, solid soln., spectral luminesc. 7-13224
Cs $_2$ ReBr $_6$ (Cl $_6$), solid, IR and Raman spectra, vibr. anal. 7-53292
CsSCN, thermal vibrs. below structural phase transition at 470 K, neutron diffr. 7-63759
CsSD, mol. reorientation, elec. field gradient ^2H NMR 7-13052
CsSbF $_6$, high press. cryst. struct., Raman spectra studies 7-26860
CsSbTeO $_6$, ionic conductivity and powder X-ray diffr. characterisation 7-12362
CsSn $_2$ F $_5$, F $^-$ motion, NMR and electrical conduction 7-52132
Cs $_2$ TcBr $_6$ (Cl $_6$), solid, IR and Raman spectra, vibr. anal. 7-53292

caesium compounds continued

Cs $_2$ Ti $_{2-x/4}$ O $_4$ phase struct. and stability, composition depend., X-ray studies 7-58229
CsUO $_2$ (NO $_3$) $_3$, charge transfer bands position, ionisation pot. effects, luminesc. spectra anal. 7-46146
CsUO $_2$ (NO $_3$) $_3$, excited states, fluoresc. 7-25588
CsVCl $_3$, one-dimens. Heisenberg antiferromag., mag. excitations, neutron scatt. study 7-7482
CsVF $_4$, layer cpd., struct. phase transitions 7-6788
Cs $_2$ O $_2$, crystals, struct., cathodic reduction from melt, and elec. props. studies 7-58236
CsX (X=Cl,Br,I), low temp. thermal expansion, calc. 7-44867
Cs $_2$ Zn $_2$ (MoO $_4$) $_3$, cryst. struct. 7-58217
CsZnPO $_4$, crystal struct. of three phases 7-1967
 β -Cs $_2$ ZrF $_6$, ionic conductivity 7-52129
CsZr $_2$ P $_2$ O $_{12}$, thermal expansion, structural model 7-44858
Cs $_2$ [Fe(CN) $_5$ NO] $_2$ H $_2$ O, thermal behaviour and vibr. spectra 7-64632
Cs[Pd(S $_2$ C $_2$ (CN) $_2$) $_2$] $_2$ 0.5 H $_2$ O, low-dimensional metal at low-temp. and high-press. 7-45290
Rb $_{1-x}$ Cs $_x$ FeCl $_3$, random singlet-magnetic ground state system, mag. ordering effects 7-33167
ZrF $_4$ -BaF $_2$ -CsF glasses, ionic conductivity 7-52129

caesium generators see plasma diodes

caesium plasma diodes see plasma diodes

calcination see heat treatment

calcium

see also nuclei with
aquatic organism acidification effects, data evaluation and compilation 7-40054
atom, 422.7 nm resonance line, lineshape anal., rare gas perturbation, fluores. spectra study 7-19753
atom, electronic struct. calcs., relativistic effects 7-36504
atom, ground state, ICP atomic fluoresc. spectrometry 7-54234
atom, laser-XUV excited state spectroscopy 7-19746
atom, level energies and oscillator strengths, coupled channel model calcs., energy depend. sensitivity 7-49906
atom, metastable states energy pooling time-resolved emission spectra anal. 7-36519
atom, reson. photon emission quantum interference effect, fluoresc. 7-10486
atom, spatial distrib. profiles, ICP atomic emission and fluoresc. 7-54235
atomic beam, two-photon Hanle effect in Ramsey interrogation 7-15560
atoms, transition energies, X-ray spectra, X α theory, X-ray transition energies 7-10422
Ca II and K wings in solar spectra, existence of Fe II 396.94 nm line in wings 7-4398
column density meter, high precision technique for line-of-sight vapour densities meas. 7-48695
crystal, FCC, generalised Morse pot. and mech. stability 7-6575
dimer, $A^1\Sigma_u^+ - X^1\Sigma_g^+$ red system, laser spectroscopy, rot. anal. and perturbation anal. 7-10652
electron energy loss anal., near-trace-element concs. in organic matrix 7-46903
FCC and BCC, lattice dynamics 7-38134
ions, dielectronic recomb. with K-shell excitation 7-42761
late-type main sequence stars, Ca II and Mg II obs. 7-47839
liquid phase, density and surface tension 7-44957
low energy X-ray fluorescence anal. using annular ^{55}Fe source, Monte Carlo approach 7-8335
open clusters, subgiants and lower giant branch Ca II emission 7-60741
optical frequency standard based on Ramsey excitation in Ca atomic beam 7-14925
phonon density of states from heat capacity temp. depend., inverse problem 7-6736
phonon spectra, dynamical pseudopot. shell model calcs. 7-51965
 β Pic, circumstellar gas cloud, Ca II and Na I obs. anal. 7-24130
rheumatic disease patients, seasonal variation in total body Ca, in vivo neutron activation anal. obs. 7-40251
seawater K and Ca concentrations, potentiometric determ. over wide salinity range via admixture technique 7-14311
segregation to surface of MgO and α -Al $_2$ O $_3$ 7-21593
Sun, Ca phases rot. (1967-70) 7-4427
total body meas. by neutron activation analysis, in vivo precision 7-65851
YIG:Ca films, magneto-optical props., reducing treatment effects 7-64617
BaTiO $_3$:Ca, ferroelec. domains, SEM and TEM obs. 7-2998
Bi $_{1-x}$ Ca $_x$ Fe $_{1-x}$ V $_x$ O $_{12}$, sublattice magnetisation and Faraday rotation (*Chinese*) 7-17308
Ca II K-line, non-LTE calcs. for solar flares (*Chinese*) 7-29442
Ca III, allowed transitions, oscill. strengths and excitation energies 7-5631
Ca IX, electron impact excitation, LS coupling, distorted wave approx. 7-42767
Ca V, transition probabilities and wavelengths 7-15550
Ca XIX, laser plasma, dielectronic satellites intensities 7-44244
Ca $^+$ + He(Ne), collisional lasers, high specific output energy 7-43078
Ca $^+$, 4p-3d triplet, broadening by He 7-62323
Ca $^+$, lasing mechanism and energy charact., relax. processes of metastable states 7-62673
Ca $^{2+}$ and Ba $^{2+}$, single-channel currents in rabbit skeletal muscle sarco-plasmic reticulum 7-28476
Ca $^{2+}$, binding to bile salts, NMR investig. 7-54442
Ca $^{2+}$ channels, occult, in Drosophila, rel. to twinning of Ca $^{2+}$ and voltage-activated K $^+$ 7-17966
Ca $^{2+}$ current in single heart cells, opposite effects of cyclic GMP and cyclic AMP 7-40135
Ca $^{2+}$, induction of capacitance and ionic currents in phosphatidic acid bilayer lipid membranes 7-54488
Ca $^{2+}$, ion-selective electrode, subnanomolar range detection limit 7-17833
Ca $^{n+}$ (n=11, 12), metastable ion beams, forbidden lines, visible spectrum 7-57022
Ca $^{n+}$, reson. transfer and excitation, charge state and electron momentum distrib. depend. 7-970
Ca-SOCl $_2$ cells with Ca(AlCl $_4$) $_2$ -SOCl $_2$ electrolytes, performance improvement using C cathodes 7-65444
Ca-SiAlON ceramic system, A' \rightleftharpoons B' transition study 7-16738
Ca $^{2+}$ -ATPase interactions in sarcoplasmic reticulum, fluoresc. energy transfer as an indicator 7-59913

calcium continued

- Ca²⁺-sensitive cross-bridge dissociation of rabbit psoas fibres in the presence of Mg₂P₂O₇·3H₂O 7-40088
 Ca+H₂(D₂), collisional quenching, time-resolved emission spectra anal. 7-36528
 Ca+He, saturated two-photon absorpt. in perturber bath 7-888
 Ca+He, spin-changing collision cross section 7-25641
 Ca⁺He⁺, target K-shell ionis., cross-sections and probabilities 7-50343
 Ca⁺+Ar(He), reson. line broadening and shift rates, pot. calc. 7-15683
 Ca⁺+He, pot. curves reson. line broadening and shift parameters 7-50302
 Ca²⁺+D-ribose (D-arabinose), enthalpies, sp. heat and molal vols. at 25°C 7-8253
⁴⁵Ca²⁺ efflux from isolated chick brains, lack of effect of static mag. field 7-28579
⁴⁸Ca anomalies in carbonaceous chondrite hibonites 7-55579
 Cu+N₂O, collisional quenching, time-resolved emission and chemiluminescence 7-28285
 KCl:Ca, γ -irrad., Z₁-centre growth, effect of dislocations, thermolum. study 7-32487
 KCl:Ca, γ -irrad. Z₁ colour centres, mech. bleaching form. 7-6620
 KCl:Ca²⁺, Z₂⁺-centres, axial config., pseudopotential perturbation calc. 7-32952
 KCl:Br_{1-x}Ca, doped crystals, elastic constants, meas. using US pulse superposition method 7-26827
 LiH:Ca²⁺, elec. props., X-irradiation effects, DC cond., dielec. loss and ionic thermocurrent meas. 7-27341
 MgO:Ca²⁺ (100), entropy of segregation calcs. 7-2323
 Mn²⁺Mn₄³⁺SiO₁₂:Fe(Ca)(Al), antiferromagnetism and spin glass order, mag. meas. 7-27518
 NaCl:Ca, impurity dipoles, aggregation with dislocations under alternating elec. field 7-44598
 Na₂O-SnO₂-SiO₂:Ca²⁺, glass diffusion of cations, 500-800°C 7-12371
 RbBr:Ca²⁺, Z₂ colour centres, picosecond relax., nonstationary spectra 7-59233
 Si:Ca MOS capacitor elec. parameters, effects of process chemical purity 7-33103
 Ti XXI, laser plasma, dielectronic satellites intensities 7-44244

calcium alloys

see also calcium compounds

- Al-Ca dilute alloys, divacancy effect, annihilation radiation Doppler broadening meas. 7-37982
 Ba₂CaCuFe₂F₁₄, heteronuclear trimers with ferrimag. behavior (French) 7-64448
 Ca-Al-Ga metallic glasses, electron transport 7-45264
 Ca₃Ag₈, giant cells, polyhedral packing 7-11992
 CaIr₂B₂, structural relationship to BaAl₄ 7-16496
 CaRh₂B₂, structural relationship to BaAl₄ 7-16496
 La_{2-x}Ca_xMg₁₇, H₂ storage appl. 7-40052
 PbCaSn, rolling deform. texture, shear band angles 7-33724
 SnCa₃Rh₄Sn₁₂ crystals, structural distortion and chem. bonding, X-ray diff. studies 7-1947

calcium compounds

see also calcium alloys

- apatite, Ising crit. temp. of connected nets and morphological importance of F faces 7-16476
 apatite ceramics, with microstruct. controlled by Y³⁺ substitution, elec. props. 7-21523
 bis(oxalato)platinate, Ca_{0.756}[Pt(C₂O₄)₂].3H₂O, ID conductor, preparation and props. 7-52599
 calcium cadmium acetate hexahydrate single crystals, first order phase transition, thermal expansion meas. 7-26985
 calcium copper acetate hexahydrate single crystals, thermal expansion meas. 7-26985
 fluorapatite, relative defect-production efficiency for fission fragments, alpha decay and electron irradiation 7-12167
 glass powders, calcia-aluminosilicate, sintering and crystn., kinetic processes 7-37877
 gypsum, initial hardening with cement, pulse rheometry investig. 7-37411
 gypsum systems, Young's modulus rel. to porosity 7-46533
 kaersutite, cation distrib. and proton location, neutron diff. studies 7-63569
 marble, temp. effect on dielec. behaviour at 1 kHz 7-47434
 MgO-monticellite ceramic, high resol. TEM and STEM study 7-22738
 oxalate, crystal growth and aggregation, computer model, partial size distribution 7-16463
 oxalate, crystallization processes using reverse osmosis 7-53538
 oxalate crystals, precip. by reverse osmosis system, habit modifiers 7-16460
 oxalates, precip. from high ionic strength solns., nucleating phase, additives effect 7-59774
 salts, ion-molecule interactions in DMF, IR spectrosc. obs. 7-10584
 soda lime glass detectors, chemical etching characts. 7-30868
 tartrate single crystals, dielectric props. rel. to X-ray on γ -ray irradi. 7-59161
 wollastonite reinforced polyamide 6, strength props., depend. on humidity and temp. 7-39636
 (YSmLuCa₃)(FeGe)₂O₁₂, bubble lattice, magnetisation curves 7-53094
 (AlGa)As/(CaSr)F₂ multilayer structures, MBE grown, broadband high-reflectivity mirrors fabrication 7-11091
 AlF₃-CaF₂-BaF₂ glasses, Raman spectroscopic study 7-7692
 Al₂O₃-CaO cement-glass microsphere composites, relative dielectric permittivity 7-33319
 Al₂O₃-SiO₂-CaO glasses containing rare alkali oxides, struct. and elec. props. 7-6528
 Al₂O₃-SiO₂-Fe₂O₃-CaO-MgO-Na₂O-K₂O glass batch melting, interaction between solid, liq. and gas 7-7946
 (Ba,Ca)F₂ layers, MBE growth on non-lattice-matched Si substrates 7-27216
 Ba₂CaCu₂Fe₂F₁₄, exchange interactions, mag. susceptibility meas. 7-45654
 BaCa_{1/2}Sr_{1/2}Fe₄O₈, mag. ordering 7-45624
 BaGeO₃-Ga₂O₃-CaO-CaF glasses, IR transmission spectra, depend. on composition 7-3031
 Ba_{0.1}Sr_{1.1}Ca_{0.8}Fe₁₂O₁₉-La₂O₃, hexagonal ferrites, influence of electric field on struct. and props., Mossbauer study 7-7616
 Ba_{0.8}Sr_{0.4}Ca_{0.2}Fe₁₂O₁₉, hexagonal ferrites, influence of electric field on struct. and props., Mossbauer study 7-7616
 Bi_{3-2x}Ca_{2x}Fe_{5-x-y}In_yV₂O₁₂ single crystal, Mossbauer spectroscopy (Chinese) 7-17250

calcium compounds continued

- Bi₂O₃-V₂O₅-CaO system, vitreous oxide semiconductor, polarisation processes 7-59139
 BiVO₄:CaO polycryst. samples, sheelite struct., elec. cond., anion vacancy motion investigation 7-32712
 (Ca,Sr)F₂-GaAs heterostructure interfaces, twinning, Raman spectra 7-13148
 Ca(AlCl₄)₂-SOCl₂ cells, cond., C cathode performance improvement 7-13851
 Ca(AlCl₄)₂-SOCl₂ electrolytes in Ca-SOCl₂ cells, performance improvement using C cathodes 7-65444
 Ca₃Al₂Ge_{3-x}Si_xO₁₂:Tb, cathodoluminescence, photoluminescence props. 7-53404
 Ca(Al₂Si₂)O₇·28H₂O, natural stellerite, cryst. struct. refinement 7-12007
 CaAr, excitation spectra in supersonic jet, spectroscopic const. determ. 7-25591
 Ca_{1-x}Ba_xF₂ epitaxial layer growth and struct., electron microscopy studies 7-27174
 CaBr, pot. energy curves and dissociation energy, curve fitting procedure 7-36511
 CaCO₃, calcite, grain growth, effect of second-phase particles 7-39476
 CaCO₃, calcite, hydrothermal cryst. of growth and solubility in nitrate solns. 7-53533
 CaCO₃, calcite, polycrystals, elastic props. 7-44646
 CaCO₃ crystal, formation of picosecond pulses by stimulated Raman backscattering 7-1226
 CaCO₃ crystal symmetry elements determ. by SEM 7-58107
 CaCO₃ deep ocean sediment samples, distrib. and diffusion meas. of Np and Am radioisotopes 7-36273
 CaCO₃ filled multicomponent polypropylene blends, mech. and rheological props. 7-3381
 CaCO₃ filled polyethylene, light scattering, struct. aspects of dichromatic laser speckle patterns 7-42931
 CaCO₃ filled polypropylene melt, on-line pH monitoring of extrusion 7-59725
 CaCO₃, formation in cooling water, critical pH depend. 7-54158
 CaCO₃ marble rock, laser treatment 7-51821
 CaCO₃ porous minerals, dynamic shock-loaded response 7-26863
 CaCO₃, radiation generation in resonator under stimulated Raman scatt. conditions 7-43222
 CaCO₃, X-ray diff. whole-powder-pattern fitting without reference to a structural model 7-32214
 CaCO₃-CaSO₄·2H₂O-NaCl-CO₂-H₂O, solubility in 4-phase systems, thermodynamics 7-2210
 CaCO₃-MnCO₃ mixed cryst., metastable formation range and morphology 7-26910
 CaCl, E² Σ state, time-resolved optical double-reson. study 7-25590
 CaCl, ultraviolet C²H-X² Σ band system, rot. anal. 7-50168
 CaCl₂ absorbent for solar refrigeration, binding materials for structural improvement 7-23222
 Ca₂Co_{1-x}Fe₂O₄ substituted ferrite system, mag. props., comp. depend., Mossbauer study 7-7618
 CaCrO₄, spin-triplet state, luminescence and QDMR 7-64686
 Ca₂ErF₇ fluorites, superlattice structs. 7-44485
 CaF₂ (111), surface at struct. anal., impact-collision ion scatt. spectroscopy 7-63931
 CaF₂ coated Si waver, influence of metal films on optical scatter and microroughness 7-13242
 CaF₂, crack-free epitaxial film, on GaAs (100), surface morphology, elec. props. 7-39392
 CaF₂, cryst., defect struct., high temp. (German) 7-32449
 CaF₂ cryst., defect-induced hyper-Raman spectra obs. 7-53324
 CaF₂, directional gamma ray Compton profile meas. and LCAO calcs. 7-2063
 CaF₂ epitaxial films on Si, structural and electrical props. improvement by rapid thermal annealing 7-38400
 CaF₂, epitaxial growth, conf., Toronto, Ont., Canada (May 1985) 7-9588
 CaF₂, epitaxial growth on GaAs (100)(111), photoluminescence, Raman scattering Rutherford backscattering/channeling 7-59437
 CaF₂ film, on GaAs films, optical parameters 7-39204
 CaF₂, fluorite residual stress fields in cylindrical Bridgman-Stockbarger crystals 7-11976
 CaF₂ insulating layers on Si, epitaxial growth and charact. 7-39393
 CaF₂, lattice constant, force calc. in molecular dynamics simulations 7-51710
 CaF₂, linear thermal expansion meas. 7-44863
 CaF₂, low temp. thermal expansion, calc. 7-44867
 CaF₂, MBE growth of epitaxial insulator-metal-semicond. struct., CaF₂-CoSi₂-Si 7-22496
 CaF₂, MBE on Si and overgrowth with Si or Ge, characts. 7-22495
 CaF₂, microhardness study 7-51928
 CaF₂, multiphoton transitions between nuclear spin Zeeman levels obs. by rotary sat. method 7-38948
 CaF₂, optical damage, laser mass spectrometric study 7-58319
 CaF₂, phys. props., effective pot. calcs. 7-26692
 CaF₂, powder compacts, shock wave effects 7-51936
 CaF₂, profiled crystals, growth by Stepanov's method, appl. for optical components 7-31409
 CaF₂, SiO₂ adsorbed layers, surface separation and vol. absorpt. in photothermal spectroscopy 7-53297
 CaF₂ surface, long range interaction between rare gas atoms/molecules and surfaces, calc. 7-3135
 CaF₂ TLDs, Al- or Ta-encapsulated, non-equilibrated bremsstrahlung dosimetry for 0.75 MeV electrons 7-56876
 CaF₂, UV attenuation 7-51944
 CaF₂:⁵⁷Fe, Mossbauer absorption and emission expts., relax. and after-effect study 7-27635
 CaF₂:Ce, Mn crystals, energy transfer, optical absorpt. and luminesc. studies, X-ray irradi. effects 7-27773
 CaF₂:Ce,Mn, optically active sites, optical spectra 7-22305
 CaF₂:Ce³⁺, impurity ion-ligand nuclei interactions, ENDOR meas. and operator method calcs. 7-52538
 CaF₂:Ce³⁺, two-photon absorpt. cross section, anal. of lowest 4f-5d transition 7-46081
 CaF₂:Er³⁺, H⁻(D⁻), IR excitation and absorpt. spectra anal. of sites 7-53306
 CaF₂:Er³⁺ IR laser, Q-switched, CW operation 7-43107
 CaF₂:Er³⁺ IR lasers, upconversion pumping 7-43111
 CaF₂:Eu, X-ray luminesc., spectral-kinetic props. 7-39184

calcium compounds continued

CaF₂:Eu²⁺, ¹⁵³Eu-¹⁵¹Eu quadrupole moment ratio, optically detected NMR studies 7-22164
CaF₂:Eu³⁺, hyperfine coupling in ⁷F₀ and ⁵D₀ states, ODMR meas., optical hole burning 7-45842
CaF₂:Eu³⁺, O²⁻, quadrupole coupling and crystal-field shielding under hydrostatic press. 7-2551
CaF₂:Li⁺ (Na⁺), EPR of colour centres 7-17222
CaF₂:Mn, gamma irradiation-induced defects, absorpt. and excitation spectra studies 7-26801
CaF₂:Mn thermoluminescent phosphor, γ and in dosimetry using electrical conductivity 7-62095
CaF₂:Nd single cryst., thermoluminescence and X-ray fluorescence studies 7-33463
CaF₂:Nd single crystals, ionic conductivity study 7-21521
CaF₂:O crystals, O-vacancy centres, optical props. 7-7722
CaF₂:Sm²⁺, electronic Raman transitions study 7-46017
CaF₂:Sm²⁺,Nd³⁺ energy transfer efficiency 7-7734
CaF₂:Tm TLD discs of different thicknesses, fast neutron responses 7-54757
CaF₂:Tm²⁺ crystal, dynamic nuclear polarisation, strong hyperfine interaction, ENDOR study 7-45840
CaF₂:Tm³⁺, absorption spectra of optically excited Tm³⁺ 7-33418
CaF₂/GaAs (100) 7-64902
CaF₂-Al₂O₃, dispersed solid electrolyte systems, enhanced ionic conduction 7-16801
CaF₂-Al₂O₃ (ZrO₂) dispersions, single and polycrystalline, elec. conductivity 7-27005
CaF₂-BaF₂ epitaxial bilayers on Si (111), characterisation 7-12521
CaF₂-BaF₂-AlF₃ glasses, struct., transition metal ion EPR studies 7-6545
CaF₂-based solid solns., ionic conductors with fluorite struct., thermal conductivity study 7-38275
CaF₂-CeO₂, dispersed solid electrolyte systems, enhanced ionic conduction 7-16801
CaF₂-Nd single crystals, thermolum., spectra and X-ray luminesc. spectra 7-64704
CaF₂-Si, heteroepitaxy of Si and Ge 7-22497
CaF₂-Si, interface struct., high resolution TEM study 7-2394
CaF₂-Si (111), interface form., photoemission study 7-2395
CaF₂-Si (111), MBE grown, electronic struct. 7-2725
CaF₂-Si (111), UV irradiation-induced ordered struct., photoelectron spectroscopy study 7-7396
CaF₂-Si (111) interface, electronic struct. 7-38737
CaF₂-Si interface, strains in MBE grown insulator films, MeV ion channelling meas. 7-7080
CaF₂-Si interface, with epitaxially grown insulator, post-growth annealing treatments 7-7074
CaF₂-Si interface, with MBE grown insulator, trap states, I-V, C-V meas. 7-7407
CaF₂-Si SOI technology by heteroepitaxial growth 7-22022
CaF₂-Si structures, Ge heteroepitaxial planarised growth by electron beam exposure to predeposited layers 7-52855
CaF₂-Si structures, heteroepitaxial growth, struct., elec. props. 7-12567
CaF₂-Si(111), tensile strain, interfacial disorder, reordering 7-27163
Ca₂F(PO₄), twinned bicrystals, theoretical detect. of a dark contrast line, rel. to chem. props. of human dentin and enamel 7-40097
Ca₂F(PO₄), struct., spin dynamics, NMR study 7-59124
CaFe_{1-x}Mn_xO_{3-y}, ferrites, microdomains, role in oxidation, reduction and annealing 7-46830
CaFeO₇, crystal struct. (French) 7-16519
Ca₃Fe₂TiO_{8+x}, perovskites, microdomains, electron microscopy 7-16533
Ca₃Ga₂Ge₂O₁₂:Cr³⁺ garnet, ESR and ultrasonically modulated ESR studies 7-22139
Ca₃Ga₂Ge_{3-x}Si_xO₁₂:Tb, cathodoluminescence, photoluminescence props. 7-53404
Ca₃Ga₄O₉:Nd³⁺, luminescence and absorption spectra and stimulated emission 7-7732
CaH₂, ²Σ⁺ states, rot.-vibr. levels, pot. curves 7-62345
Ca(HSeO₃)₂.H₂O, cryst. struct., IR spectra, thermal behaviour 7-44479
Ca₂(HSeO₃)₂(Se₂O₃), cryst. struct., IR spectra, thermal behaviour 7-44479
CaLaFeO₄, layered cpds., bidimensional mag. coupling, Mossbauer spectra 7-27637
CaLa₂S₄ optical ceramic, powder synthesis 7-37067
CaMg(B₃O₆(OH)₃)₂.3H₂O, hydroboracite, thermal expansion 7-63850
(Ca_{1-x}Mg_xFe_{0.3}Mn_{0.1})(CO₃)₂, ankerite, ⁵⁷Mossbauer spectra relax. rates 7-27640
Ca₁₈Mg₂H₂(PO₄)₁₄, whitlockite, cryst. growth 7-53528
CaMgSi₂O₆ - CaFeSi₂O₆, solid solns. short range order parameters, determ. from EXAFS pair distrib. fns. 7-59289
CaMgSi₂O₆, diopside, thermal expansion and glass transition, quenched defects 7-12333
Ca₃Mn_{1.8}Fe_{1.2}O_{3+y}, perovskites, microdomains, electron microscopy 7-16533
CaMnGe₂O₆-Ca_{0.5}Mn_{0.5}SiO₃ cross section of CaSiO₃-MnSiO₃-MnGeO₃-CaGeO₃ system 7-2213
Ca₃Mn₂Ge₂O₁₂ single domain crystals, birefringence and spontaneous phase transitions 7-17303
CaMoO₄, cryst., photo-excited triplet state, EPR 7-13027
CaMoO₄, microhardness anisotropy meas., quenching and annealing temp. effect 7-63738
Ca₂Na₄K₂Si₂O₁₀F₄, chain-silicate canasite glass-ceramic, thermal shock behaviour, effect of crystn. 7-46613
Ca₂(NbGa)₂Ga₂O₁₂:Nd³⁺, Nd³⁺ ions, two channels of stimulated emission 7-22285
Ca_xNbO_{2+x}, defect structure, Raman spectroscopy 7-63604
Ca_{2-x}Nd_xGa_{2+x}Si_{1-x}O₇, Ga gehlenite, cryst. struct. and optical props. 7-16525
Ca₂Nd₂(SiO₄)₆O₂:Cm, radiation effects, appl. for nuclear waste disposal 7-32522
Ca₂Nd₂(SiO₄)₆O₂:Cm ceramic simulated nuclear waste forms, radiation effects on microstruct. and fracture props. 7-58373
CaO, adsorbed butylamine, thermal desorption and IR study 7-39110
CaO, light sensitive centres with tetragonal symmetry, EPR study 7-53133
CaO, self-consistent electronic structs. 7-32910
CaO, self-trapped hole centres, ODMR and spin coherence studies 7-7612
CaO, solidification point, reinvestig. by digital pyrometry 7-38168
CaO, XANES spectra, band struct. calcs. 7-64738
CaO:OH²⁻, EPR spectrum 7-17217

calcium compounds continued

CaO-Al₂O₃ glass, 3-5 μm transmission, rain erosion resist., surface crystallisation treatment 7-37070
CaO-Al₂O₃-B₂O₃ glass, constitution 7-21120
CaO-Al₂O₃-SiO₂-H₂O hydrated inorganic salts found in concrete, thermal energy storage appls. 7-17922
CaO-Al₂O₃-SiO₂ cement, macro-defect-free processing and low freq. dielec. response 7-13081
CaO-BaO-P₂O₅ glass fibres, stress optical studies 7-7673
CaO-Fe₂O₃ system, solid state reactions, ferrite growth and morphology 7-3236
CaO-Ga₂O₃ system, comp., structural props., X-ray diffr. study 7-37942
CaO-SiO₂ polycryst. silicates, FTIR and Raman spectra, isotopic shifts and force consts. 7-53341
CaO-SiO₂-CaF₂, structural analysis for fluorosilicate glasses by X-ray photoelectron spectroscopy (Japanese) 7-33510
CaO-Sr(Ba)(Mg)(Zn)O-P₂O₅ glasses, internal friction investig. 7-6721
CaO-TiO₂-SiO₂:Eu³⁺ sphere ceramic, impurity laser-excited site-selective fluorescence line-narrowing spectra 7-13200
CaO-ZrO₂, defect struct., EXAFS studies 7-63608
CaO+U₂MoO₆=CaMoO₄+¹/₃U₃O₈+¹/₆O₂, free energy of form., thermodynamic feasibility 7-13753
CaO₂, time resolved picosecond Raman induced phase conjugation 7-13141
CaO₃, induced morphology crystal aggregates, structures, wheatsheaf morphologies 7-51687
(CaO)₂₅(BaO)₂₅(P₂O₅)₅₀ glass fibres, struct., birefringence, density and thermal shrinkage, drawing parameters depend. 7-6536
Ca(OH)₂ and CaCO₃ used in dry additive process for flue gas desulphurisation in power plants, use of Ca(OH)₂ and CaCO₃ (German) 7-46980
Ca(OH)₂·2Zn(OH)₂·2H₂O, chem. comp., solubility in KOH, thermodynamic props., reaction equilib. const. 7-26962
(CaO)₃SiO₂ solid solns., hydration investig. 7-3583
Ca₃OSiO₄, crystallochemistry of phases 7-1965
Ca_{2-x}P_{1-x}Cl_{1+x} and Ca₂PCl₃, prep., crystal struct., thermal behaviour (German) 7-26717
CaPO₃ crystal formation in tissues, SEM studies 7-28445
CaPO₃, EXAFS, multiple scatt. processes 7-64777
Ca(PO₃)₂:Duo₃²⁺ glass, highly doped, fluorescence spectral width of ³D₀-⁷F₀ transition 7-13189
Ca₃(PO₄)₂ polymorph form. from apatite decomp. 7-44796
Ca₃(PO₄)₂:CaF₂, apatite, carbonated crystallites, high resolution TEM study 7-6643
Ca₃(PO₄)₂:CaF₂(OH)_x, hydroxyapatite, morphology of F faces 7-51686
Ca₁₀(PO₄)₆(OH)₂, thermal lattice expansion, 20-600 °C 7-58510
Ca₂(PO₄)₂OH, EXAFS spectrum anal., spherical wave theory 7-33485
CaPuTiO₇, substituted zirconolite, high level waste, self-irrad. effects, mech. props. 7-805
CaRAlO₄ (R=Y, La, Gd, Tb Lu), growth by Czochralski method 7-22460
CaS:Sm³⁺, photolum. of Sm³⁺ ions 7-59246
CaSO₄ crystal size distrib. from double-draw-off FGD liquor crystalliser 7-63533
CaSO₄, exoelectron spectroscopy under photon and low energy electron excitation 7-27873
CaSO₄, gypsum, thermal breakdown and crack form. 7-2178
CaSO₄, hemihydrate crystals, continuous crystallisation in conc. H₃PO₄ 7-53535
CaSO₄, solubilities calcs. 7-9625
CaSO₄:Dy, gamma radiation damage on thermolum. 7-38059
CaSO₄:Dy phosphor, thermoluminesc. props. of a new prep., dosimetry appl. 7-28701
CaSO₄:Mn, thermoluminescent dosimeter, phys. characts. (Korean) 7-34278
CaSO₄·¹/₂H₂O crystal nucleation and growth from simulated FGD liquors 7-63534
CaSO₄·¹/₂ H₂O:Cd, crystallisation from phosphoric acid 7-27882
Ca₃Sc₂Ge_{3-x}Si_xO₁₂:Tb, cathodoluminescence, photoluminescence props. 7-53404
CaSiO₃, perovskite type, cryst. struct., lattice dynamics and eqn. of state 7-58248
CaSiO₃, wollastonite-2M, cryst. struct. 7-6612
Ca(SiO₃)₂, cryst. struct., vibr. spectra, force consts., Si-O bond charact. 7-37932
Ca₂SiO₄, β to α' to β transition, modulated struct. 7-16724
β-Ca₂SiO₄, prep. by firing at 950 °C 7-3238
Ca₂Si₆O₁₈H₂.4H₂O, tobermorite, ion exchange props. 7-59752
Ca₂Sr_{1-x}F₂ layers, epitaxial growth on CaF₂ by vac. evap. 7-22498
Ca₂Sr_{1-x}F₂, mixed crystals, microhardness study 7-51928
Ca₂Sr_{1-x}F₂/GaAs SOI structures, epitaxial GaAs films, antiphase disorder 7-52315
CaTe, vapourisation thermodynamics and formation enthalpies (German) 7-26930
CaTiO₃ (perovskite), high press. phase transformations and isothermal compressibility 7-14269
CaTiO₃, electronic struct., special features (Russian) 7-45146
CaTiO₃, ion implantation, crystallisation of amorphous surface layers 7-58304
CaTiO₃, perovskite, TEM study of dislocations 7-38003
Ca₂Ti₂O₆, pyrolysis product of CaO-TiO₂ system, cryst. struct., X-ray powder diffr. data 7-32394
CaTiSiO₅, sphene crystals, melt growth and character. 7-7840
Ca(UO₂)₂(SiO₃OH)₂.5H₂O, β-uranophane, refined cryst. struct., thermal anal., IR spectra 7-55031
Ca₃Y₂Ge_{3-x}Si_xO₁₂:Tb, cathodoluminescence, photoluminescence props. 7-53404
Ca₈Y₂(PO₄)₆(OH)₂-xO_x, synthesis, struct., dielec. props., AC elec. cond., IR spectra 7-3235
(Ca₂Y)Sn₂Fe₂O₁₂, ion distrib., Mossbauer spectra anal. 7-33306
Ca₂Yb₁₀F₆₄ fluorites, superlattice structs. 7-44485
CaZrO₃, sintering, porosity, mech. props., corrosion resist. 7-39664
CaZrO₃, valence band struct., X-ray-electron spectra studies 7-12604
CaZrTi₂O₇, zirconolite, alpha-recoil damage 7-6692
CaZrTi₂O₇:Cm, radiation effects, appl. for nuclear waste disposal 7-32522
CeF₂:Ho³⁺, fluorescence decay characts. of Green emission 7-7747
CeO₂-CaO, ceria-calcia ceramics, ionic cond., effect of microstruct. 7-38250
Co_{1-x}Ca_xFe₂O₄, single domain-superparamagnet transition 7-17203

calcium compounds continued

- CsCaCl₃, cubic to tetragonal phase transition, space group determ., X-ray studies 7-16736
 CsCaF₃:Gd³⁺, transferred hyperfine interaction of impurity centres, ENDOR, EPR meas. 7-32946
 CsCaF₃:Gd³⁺, transferred hyperfine interactions, ¹⁹F ENDOR studies 7-53177
 CsCaH₃, ternary hydride, crystal struct. 7-26729
 Dy₂O₃-CaO solid solutions, dipole complexes, dielectric relax. 7-53231
 FeO₂-CaO-MgO-BaO-Na₂O, wustite solid solns., interdiffusion coeffs., 1073-1473K (*Japanese*) 7-12357
 Fe₃O₄-CaO-SiO₂ amorphous oxides, magnetic props. and struct., Mossbauer spectra study 7-7538
 Fe₂O₃:CaO, synthetic wustite, elec. cond., doping elements effect (*Korean*) 7-2609
 GaAs-CaF₂, interface struct., dielectric film mol. beam epitaxial growth 7-38360
 Gd₂CaSb₂Zn₃O₁₂, rare-earth activated garnets, cathodolum. 7-7763
 Ge-CaF₂-Si epitaxial structures, growth, structural and electrical props. 7-38356
 Ge-CaF₂-Si heteroepitaxial structures, MBE grown, twinning, topography, channelling, TEM, SEM 7-12566
 K-Ca-NO₃-H₂O glasses, low temp. dielectric study 7-38999
 KCl:CaCl₂, internal friction 7-38114
 K₂O-CaO-SiO₂ system, cryst. growth kinetics, morphology, melt comp. depend. 7-46303
 (La,Ca)(Co,Mn)O₃, sinterability, phase composition and microstructure 7-33622
 La_{1-x}Ca_{0.55x}Ba_{0.45x}FeO_{3-α}, elec. cond. props. rel. to struct. 7-63871
 La_{1-x}Ca_xCr_{1-y}Ni_yO₃, production and elec. parameters 7-33007
 Li₂O-CaO-Al₂O₃-SiO₂, multicomponent glasses, sequence of cryst. phases 7-26648
 Li₂O-CaO-B₂O₃, ion conducting glass, effect of CaO substitution on transport and physical props. 7-58535
 Li₂O-CaO-B₂O₃:VO²⁺, borate glasses, ESR of VO²⁺ ion 7-59110
 MgCl₂-CaCl₂ melts, thermodynamic props. 7-26977
 MgF₂-CaF₂ mixtures, films, prep., physicochemical and optical props. 7-3178
 MgO-CaO, activated sintering, densification, microstruct. (*Chinese*) 7-13410
 Mg₂Si₂O₆-CaMgSi₂O₆ system, solid solutions, dilatometry and elec. conductivity meas. 7-2175
 Na₂CaAl₂Si₂O₁₂·6H₂O, zeolite, adsorption and desorption of ethylene, TPD study 7-32826
 Na₂Ca₂Al₆Si₆O₃₀·8H₂O, mesolite, cryst. struct. X-ray refinement 7-1958
 Na₄Ca₄(Si₆O₁₈), cryst. struct. determ. 7-1957
 Na₂O-CaO-Al₂O₃-SiO₂ glass ceramic system, spherulitic growth, mech. props. 7-46405
 Na₂O-CaO-Al₂O₃-SiO₂ system, synthesis of glasses by sol-gel process 7-64997
 Na₂O-CaO-Al₂O₃-TiO₂-SiO₂:Eu³⁺ glass ceramic, impurity laser-excited site-selective fluorescence line-narrowing spectra 7-13200
 Na₂O-CaO-SiO₂, high-silica glass, sol-gel prep. method 7-46402
 Na₂O-CaO-SiO₂ coating glass for optical fibres, preparation 7-7949
 Na₂O-CaO-SiO₂ glass, indentation strength comparisons 7-3410
 Na₂O-CaO-SiO₂ glass, grinding, crack branching, crushing mechanism 7-3472
 Na₂O-CaO-SiO₂ glass, melting using natural fine-powdered quartz 7-7950
 Na₂O-CaO-SiO₂ glass, hydration, fluid flow effects 7-13758
 Na₂O-CaO-SiO₂ glass, cracktip blunting kinetics, annealing, corrugated surface 7-46611
 Na₂O-CaO-SiO₂ glass, dynamic fatigue, indentation flaws, surface treatment 7-46629
 Na₂O-CaO-SiO₂ glass with subthreshold flaws, dynamic fatigue 7-8111
 Na₂O-CaO-SiO₂ glasses, IR spectra 7-3036
 Na₂O-K₂O-CaO-SiO₂ glass, mixed alkali effect on chemical durability 7-8145
 Na₂O-Y₂O₃-CaO-SiO₂ glass, Na⁺ conductivity 7-52134
 Nd³⁺, Sm²⁺: CaF₂ lasers, Sm²⁺ sensitisation 7-10962
 NiO-CaO eutectic, directionally solidified, struct. imperfections 7-65026
 Pb₆Ca₄(PO₄)₆(OH)₂, apatite struct., Pb substitution, HREM study 7-16530
 Pb₆Ca₄(Si₆O₁₈)Cl₂, apatite struct., Pb substitution, HREM study 7-16530
 Si (111):CaF₂, interface and surface phonons, high resolution EELS study 7-38319
 Si-CaF₂-Si heteroepitaxial structures, MBE grown, twinning, topography, channelling, TEM, SEM 7-12566
 Si-CaF₂-Si MOSFET structures, heteroepitaxial growth, struct., elec. props. 7-12567
 Si-CaF₂-Si structure, reduction of Ca and F surface segregation by solid phase epitaxy of Si 7-38357
 Si-GaF₃-Si epitaxial structures, growth, structural and electrical props. 7-38356
 SiO₂-K₂O-CaO-MgO-CdO glass melts, evaporation 7-2160
 SiO₂-Al₂O₃-CaCO₃-Na₂CO₃ glass system, Ar⁺ ion beam effects 7-32521
 SiO₂-CaO-MgO-Na₂O glasses, frequency dependent equation of state 7-51987
 SiO₂-Na₂O-CaO-Al₂O₃-MgO glasses, heavy ion irradiation, enhanced diffusion, preferential sputtering 7-32523
 SiO₂-Na₂O-CaO-MgO-Al₂O₃-BaO-FeO₃ glass, elec. field stimulated Na depletion 7-6897
 SiO₂-Na₂O-CaO-MgO glass, reaction in isotopically labeled water, D₂O 7-26993
 Y_{1-x}Ca_xCrO₃, electrical and thermal transport props 7-45319
 Y₂CaSb₂Zn₃O₁₂, rare-earth activated garnets, cathodolum. 7-7763
 (YEuLuCa)₃(FeGe)₅O₁₂ films, mag. bubble motion in the presence of a modulated bias field 7-53098
 (YEuTmCa)₃(FeGe)₅O₁₂ films, planar anisotropy and magnetisation, ion irradiation effects study 7-2906
 (YEuTmCa)₃(FeGe)₅O₁₂, epitaxial films, O ion adsorpt. bubble diameter variation effect 7-22125
 (YEuTmCa)₃(FeGe)₅O₁₂/(YLa)₃Fe₅O₁₂ ferrite/garnet layered structs., domain wall and ferromag. reson. props. (*Russian*) 7-45828
 (YEuTmCa)₃(FeGe)₅O₁₂ films, double layer, mag. bubbles, translational velocity 7-45781
 (YLuSmCa)₃(FeGe)₅O₁₂ epitaxial films, transition layer 7-45779
 (YSmLuCa)₃(FeGe)₅O₁₂ epitaxial layer, conversion electron Mossbauer spectra 7-48926
 (YSmLuCa)₃(FeGe)₅O₁₂, epitaxial films, Faraday rot., Sm³⁺ conc. effect. 7-53070

calcium compounds continued

- (YSmLuCa)₃(FeGe)₅O₁₂, film, stripe domain stabilisation for Bloch line modes 7-59087
 ZrO₂-CaO-P₂O₅-SiO₂ glass ceramics, prep. and mech. props. (*Japanese*) 7-7942
calculating *see* calculation
calculating apparatus
 No entries
calculating machines *see* calculating apparatus
calculation
see also graphs; nomograms
 No entries
calculator program listings *see* complete computer programs
calculators *see* calculating apparatus
calculus
see also differentiation; integration; variational techniques
 balloons, pot. energy, elementary calculus appl. 7-29623
 fractional calculus operators, appls. to classes of analytic and multivalent functions 7-61016
 geometry of differential equations, secondary differential calculus and quantum field theory 7-56408
 graded calculus of variations, algebraic model 7-29672
 moment inequalities via optimal design theory 7-24404
 operational calculus, application to initial and boundary value problems 7-55984
calibration
see also measurement standards; standardisation
 12-pole reflectometer calibration analysis 7-325
 Si:O, heavily doped, SIMS meas. of O conc. 7-17388
 absolutely calibrated time-resolving X-ray spectrometer 7-18962
 AC-DC difference meas. system establishment at NPL, Israel, using multijunction thermal converters 7-18837
 accelerometers testing and calibration in frequency range 20 to 600 Hz 7-4820
 accuracy verification of meas. instrument scales, member of check points determ. 7-4804
 acoustic emission piezoelectric receiving transducer, reciprocity calibration 7-62937
 aerial survey cameras, rotationally symmetrical lens distortion and image deformation 7-37086
 aeroacoustic high intensity field meas. using cooling power anemometer 7-16039
 anemometer, accuracy aspects (*Rumanian*) 7-26368
 anemometers, mechanical, in wind tunnels (*Rumanian*) 7-6337
 angle meas., NPL role in standardisation and calibration 7-18747
 angle meas. by multireflected autocollimation 7-35495
 angular encoder automatic calibration system (*Japanese*) 7-56213
 aromatic seeding agents for laser ionization in counting gases 7-42294
 arterial mean pressure, simple device for meas. and for calibration of arterial press. monitors. 7-8731
 attenuated total reflection spectrophotometry, calibration 7-24715
 audit organisation, criteria and procedures 7-14912
 automated DC meas. at NPL, India 7-18842
 black-body radiation densities estimation 7-4890
 broadband pyrometer calibration, bandwidth effective emissivities of nonisothermal blackbody furnace 7-56271
 calibration of neutron probe for soil humidity measurement (*French*) 7-47581
 calorimeter coaxial, and its use as reference standard in automated microwave power calibration system 7-48744
 capacitance strain gauges, CERL planer, calibration errors 7-29993
 certification of an infralow-frequency vibrator for seismic vibrations meas. 7-4207
 CHARM fine-grained calorimeter, calibration 7-49796
 chemometric analysis of multisensor arrays 7-8344
 circular gauge, systematic errors correction, computerised calibration procedure 7-56244
 cloud physics instrumentation, using holographic imaging 7-23897
 combined thermocouple-noise thermometry 7-14944
 computer controlled blackbody calibration facility for steel industry in Australia 7-14950
 correlation counter calibration by calorimetry and γ-ray meas. 7-30905
 cosmic ray EAS, scintillation detector calibration for ANI instrument 7-14466
 CR39 plastic track detector, calibration for 2.45 MeV neutrons 7-49817
 CR-39, automatic α-track acquisition with Frascati PEPR 7-30882
 CR-39, bulk etch meas., standard method 7-19658
 cryogenic radiometric and interferometer system, linearity calibration 7-18858
 crystal integrated reflectivity calibration, using uncollimated, point X-ray source 7-26591
 cylindro-inner cones, freezing point, radiant emission characts. 7-56254
 data acquisition suites, multichannel, with time-scale conversion and storage CRT, design 7-61321
 diagnostic radiology, absolute kVp calibration using characteristic X-ray yields 7-40268
 diamond anvils, sintered, ultrahigh pressure generation, X-ray diffraction calibration 7-18799
 dielectric water-content meter, methodological error in checking by use of water content simulators 7-48757
 differential scanning calorimeters, standard operating procedures development 7-18786
 diffused wide-angle calibration source for remote sensors 7-18862
 digital subtraction angiography systems, acceptance testing and calibration 7-47239
 displacement sensor with two-beam interferometry, US nondestructive evaluation of composite materials 7-13716
 dose calibrator ionisation chamber standards for radionuclide assay 7-40310
 dose calibrators, accuracy testing 7-3879
 drift chamber calibration using lasers, review 7-42284
 droplet surface temperature meas. with IR technique (*Chinese*) 7-48733
 dual energy gamma radiation system for soil water content meas., calibration 7-23917
 dynamic calibration in time domain, expt. data processing method (*Chinese*) 7-48679
 dynamometer machines, three-level standard system 7-302
 eddy current electrical cond. meter graduation without specimens 7-28243

calibration continued

eddy current flaw inversion algorithm, experimental verification 7-54059
 electric field meas., low frequency, antenna calibration 7-56233
 electrical quantities meas. 7-18738
 electron spectrometer calibration and quantitative Auger anal. 7-24729
 endurance of specimens with small cracks, method and calibration 7-22946
 Eppley pyrgeometer calibration for airborne meas. 7-60393
 ERASME airborne side-looking C-band radar, data processing and calibration 7-9205
 errors, upper confidence limit for uniform distrib. parameter 7-56205
 ERS-1 wind and wave calibration workshop, Schliersee, Germany (June 1986) 7-24305
 field strength meters calibration using loop antenna, conductive objects effect determ. 7-18822
 FIRECRACKER 3, computer program for X-ray powder diffractometers calibration 7-14931
 flight simulation, vestibular and visual perception cues, coordination 7-14011
 flight-time-focused time-of-flight atom probe 7-18906
 flow, large-range, calibration by changeable water level system with computer simulation 7-37592
 flowmeter calibration, computer-aided test system 7-37591
 flowmeters, turbine type, calibration curve prediction 7-37598
 force-balance linear standard accelerometer, low-frequency 7-41358
 FTIR spectrometer sample cell, Invar, thermal calibration 7-41507
 galaxies automated surface photometry, calibration and validation of photometric technique 7-60575
 gamma spectrometry, inexpensive and multipurpose calibration phantom for in-vivo measurements of internal contaminants 7-54746
 gas analysis instrumentation (*Spanish*) 7-56208
 gated spectrometer for X-ray lasers, wavelength and efficiency calibration 7-24749
 glasses, entrapped gas bubbles, calibration of dynamic small-sample analysis systems 7-65370
 glasses, turbid, for calibration and checking of nephelometers and turbidimeters 7-20141
 grating calibration facilities for Extreme Ultraviolet Explorer 7-24712
 grazing incidence spectrometer with multielement spectral detector, absolute calibration from 20 to 430 Å 7-25301
 heterogeneous materials, multikilogram capacity calorimeter, design and construction 7-41390
 HHIRF tandem accelerator energy analysing magnet, calibration 7-49765
 high pressure rolling-ball viscometer up to 1 GPa 7-1655
 Hipparcos project, grid pattern calibration by e-beam 7-29403
 hot-film anemometers, const. temp., calibration in water 7-11567
 hot-wire anemometer compensated for ambient temperature variations 7-16275
 hot-wire probes calibration, using self-contained motorised cart 7-31899
 Hubble Space Telescope calibration, IUE spectra of UV standard stars 7-60735
 hydrophones for use in medical US fields 7-60063
 hydrostatic pressure electric resistance cell, for 30 kbars (*Korean*) 7-24656
 indirect manometers, calibration by static expansion of gas 7-30026
 inductance standard calibration method, using ratio transfer unbalanced bridge 7-18833
 ion signal calibration in imaging atom-probe with time-gated intensifier 7-48911
 far-IR blackbody source of variable temperature, for use in IR astronomical radiometry 7-40713
 IR imagers laboratory characterisation 7-24703
 IR K-100 comparator for calibration of IR emitters 7-35564
 IR low-background bolometers, calibration system 7-9899
 IR spectroradiometry, using IBM PC 7-18859
 IR vision systems for biomedical use, calibration from thermal emissivity standards 7-60117
 Josephson voltage standard, computer controlled 7-14970
 KEK TOPAZ barrel TOF counters, laser calibration system 7-62214
 laboratory accreditation in the UK 7-14911
 laser energy absorpt. meas. using differential joulemeter and optoacoustic cell calibration appl. 7-41500
 laser induced two-photon ionisation absorption, seeding agents for particle track simulation 7-5540
 laser interferometer syst. comparison and calibration 7-14997
 laser power standard, automatic calibration system, expt. (*Japanese*) 7-11019
 leak detectors, gross leak calibration 7-18794
 lenses for photogrammetry, 35mm camera lens distortions and calibration 7-40393
 light scattering particle counters, quantitative count calibration 7-56397
 light source, spectrally-broad picosecond for calibrating photonics equipment 7-20378
 Los Alamos X-ray characterization facilities for plasma diagnostics 7-20938
 low temperature measurement methods, thermometers and magnetic effects (*German*) 7-24652
 low-temperature measurement principles, thermodynamics and thermometer functions (*German*) 7-24651
 Magellan SAR, system test and calibration 7-48681
 magnetometers for simultaneous magnetic and resistive meas. at low temp. high magnetic field 7-48788
 mass spectrometers, calibration and applications, conference, Oak Ridge, TN, USA (April 1986) 7-60864
 mass spectrometers, calibration for quantitative gas mixture anal. 7-65369
 meteorological satellite, radiometers, IR detectors and their calibration 7-23898
 methylene, $^1\text{A}_1$ - $^3\text{B}_1$ separation, full CI calcs. 7-36486
 microanemometers for meas. at very low air velocities, calibration 7-44069
 micronozzles for flow rate meas., calibration system 7-51347
 Multichannel Infrared-Red Temperature Micro-Analyzer for multi-wavelength pyrometry 7-41392
 NBS 50 kHz phase angle calibration standard 7-14963
 near-IR reflectance analysis, calibration methods 7-29963
 neutron calibration field from moderated ^{252}Cf source, design and calcs. 7-49852
 neutron calibration field from moderated ^{252}Cf source, expt. characterization 7-49853

calibration continued

neutron dosimeters, evaluation and calibration for class F neutron spectra (*Russian*) 7-15419
 non-metric cameras, calibration using finite element method 7-3969
 ocean imagery, dual-freq. SAR, calibration 7-4244
 ocean remote sensing by microwave radiometry, calibration of multichannel systems 7-60409
 ocean wave period determ. by visual observation, calibration of method 7-55312
 oceanographic current profiling system design and calibration, HF volumetric backscattering 7-9270
 online pressure and temperature calibration based on well-known phase transition 7-4853
 ophthalmic applicators, B-particle, calibration of US National Bureau of Standards 7-47259
 optical convertor for marine quartz gravimeter 7-29262
 optical fibre calibrated Faraday rotation current and mag. field sensor 7-25980
 optical nondestructive evaluation at the National Bureau of Standards 7-39835
 optical particle counters, method for cross calibration 7-56398
 optical system calibration for laser beam divergence measurement (*Russian*) 7-20305
 Penning discharge source for extreme ultraviolet calibration 7-25919
 photodiode arrays for a-Si:H solar cells testing 7-28403
 photometer, stable source of IR radiation 7-56317
 photon counting imaging microchannel plate detectors calibration, for EUV astronomy 7-29404
 photon-radiation absorbed dose rates meas. by water calorimeter 7-5489
 physiological pressure transducers, standard press. source for calibration 7-8732
 piezoelectric actuators for scanning tunnelling microscopy, behaviour and calibration 7-18926
 plasma diagnosis, optical techniques, absolute calibration, geometrical parameters 7-26511
 polycarbonate detectors, Rn/decay product dosimetry by electrochemical etching, calibration (*German*) 7-15418
 positron emission CT, quantitation, technique to reduce noise in accidental coincidence meas. and coincidence efficiency calibration 7-14118
 precision instrument calibration, criteria for neglect of small errors 7-290
 pressure measurement in a blow-down wind tunnel, automatic system 7-16280
 pressure transducer for calibration usage, response character rel. to shock-wave struct. (*Chinese*) 7-48701
 prisms certification for standard angular meas. 7-294
 pyrometers, apparatus with high-aperture black bodies, for -20 to 1000°C range 7-312
 quantitative mass spectrometer analysis of very low impurity concentrations in gases 7-17841
 quartz thermometer calibration method 7-41379
 quartz tuning fork resonator transducers 7-35512
 radial grating meas. systems, accuracy improvement using fibre optic whole circumference sensor 7-31511
 radiation absorbing materials in 1-3 GHz range certification, modulus of reflection coeff. determ. 7-4866
 radiation survey meter calibration tardiness alarm 7-8695
 radioactive check device, exposure rate, calibration methods uncertainty 7-23464
 radioastronomical images, very large array phase data modelling by Box-Jenkins method 7-14504
 radiotelescope calibration, automated system (*French*) 7-60542
 real-time shadow moiré vibr. meas., simple setup, high sensitivity and exact calibration 7-20668
 reduction of calibration points via QR factorization of linear models 7-18737
 resistors, computer-controlled AC bridge for precision resistance meas. 7-18832
 RF field strengths and proton multiplicities, determ. by 2D NMR pulse techniques 7-24677
 RF noise meas. in radioastronomy (*Spanish*) 7-4336
 rotational viscometers, whole-blood appl. 7-40372
 ruby, luminescent R-line emission, pressure calibration to shock wave eqn. of state of Au and Cu 7-18802
 scanning spectrometer design and props. 7-56353
 scintillation detector evaluation and calibration using cyclotron and ECR source 7-42312
 scintillator-photodiode hodoscope, electromagnetic shower position detection 7-42442
 seismograph calibration, transducer inductance effects 7-40613
 seismometers certification, infralow-frequency vibration parameters meas. using microcomputers 7-4208
 SIMS, quantitative anal. of $\text{Ga}_{1-x}\text{Al}_x\text{As}$ (*Chinese*) 7-54239
 small-angle neutron scatt. data, absolute calibration 7-51579
 soft X-ray calibration of diffracting materials 7-26514
 soft X-ray sources and instruments calibration, 1986 status 7-25322
 soft X-ray streak camera, absolute calibration 7-18963
 soft X-ray/EUV calibration facility at the University of Colorado 7-20479
 solar cell calibration and efficiency meas. procedures 7-23160
 solar cell calibration expt. on Chinese scientific satellite 7-13874
 solar cell optical and electrical characts., meas. systems 7-13906
 solar cell short-circuit current meas. as method for efficiency calc. 7-13872
 solar cells, AM 1.5 global and direct solar simulation and secondary reference cell calibration 7-23175
 solar cells, calibration, indoor and outdoor methods 7-59843
 solar EUV instrumentation, calibration in space 7-24009
 solar radiometry instrumentation, calibration techniques, and standards 7-55326
 sound level meters, Japanese testing and calibration methods 7-1334
 spark chambers for SSNTD track counting, cross calibration of independently built devices 7-19654
 SPATE stress measurement system, calibration and qualitative assessment 7-31726
 SPRED VUV spectrograph, synchrotron radiation calibration 7-24711
 sputter depth profile calibration of multilayer structures 7-39382
 strain gauge, bonded resistance type, dynamic characts. exam. method 7-18772
 strain gauge calibration procedure for modal analysis, correction 7-56251
 surface residual stress measurement using blind-hole strain gauge method 7-65249

calibration continued

- sweep-nonlinearity correction procedures in picosecond streak camera measurements 7-15024
- Swiss Institute of Measures, weighing and calibration studies (*German*) 7-297
- synchrotron radiation beam lines as X-ray calibration sources 7-18965
- thermal conductance apparatus, large-scale, commissioning trials 7-14940
- thermal conductivity cell for para-H₂ conc. meas. 7-54229
- thermal detectors of radiation, anal. algorithm 7-48726
- thermal expansion of solids, three-terminal capacitance cell construction and calibration 7-29966
- thermoelectrode materials certification practices 7-304
- thickness-mode piezoelectric transducer constants, automatic meas. and calibration system 7-1369
- thin film filters for Extreme Ultraviolet Explorer Satellite, 68 to 912 Å 7-24015
- time and frequency transfer, NBS calibration service based on GPS common view data 7-14926
- TMX-U, plasma potential diagnostic, hardware and calibration system 7-25224
- Tokamak as an X-ray/XUV light source 7-20926
- TOPAZ time projection chamber, design, construction and calibration 7-30848
- track detectors, thermal neutron calibration curves from ²⁵²Cf irradiation facilities 7-30719
- transverse piezoresistance gauges, stress meas. in shock loaded targets 7-29999
- N-trifluoroacetylated poly(ϵ -caprolactam), gel permeation chromatographic anal., calibration procedure 7-65374
- turbulence measurement with inclined hot wire probe, 3D angle calibration method (*Japanese*) 7-6338
- US physiotherapy transducers, performance of the NPL US beam calibrator 7-60062
- UV telescope with normal incidence concave diffraction grating spectrometer 7-29400
- vacuum, leak calibration using mass spectrometer 7-61348
- vacuum, leak standards, National Bureau of Standards program 7-61347
- vacuum, residual gas analysers, quadrupole and mag. sector mass spectrometers appl. 7-61350
- vacuum, residual gas analyzer calibration, gas dynamics 7-61349
- vacuum, residual gas analyzers, online calibration, pulsed gas injection 7-61351
- vacuum technology survey, applications and prospects (*French*) 7-322
- viscometers, discharge time constant determ. 7-6336
- VUV spectrometer-detector system calibration using synchrotron radiation 7-24710
- VUV-soft X-ray beamline for spectroscopy and calibration 7-18966
- wall shear stress meas., hot film surface gauge improvement 7-37405
- water meter, weighted mean error components analysis and standardisation 7-57949
- waveguide below cutoff attenuation standard calibration, using repeatable attenuation step 7-14972
- wavelength stabilization of tunable diode lasers using an internally-coupled Fabry-Perot interferometer 7-31353
- Wolter X-ray microscope calibration 7-24750
- X-ray calibration of CCD sensors and photodiode array cameras, plasma diagnostics appl. 7-20939
- X-ray calibration techniques, sources and detectors, conf., San Diego, CA, USA (Aug. 1986) 7-24286
- X-ray detector, energy-dispersive, mineral standards for calibration 7-23105
- X-ray diagnostic calibration facilities for 100 eV to 100 keV range 7-18964
- X-ray elliptical analyzer spectrograph appl. to laser produced plasma 7-32088
- X-ray interferometer for surface roughness transducers calibration 7-35649
- X-ray laser research, in situ calibrations of grazing incidence vacuum monochromators 7-41570
- X-ray spectrometer calibration, electron-impact high-intensity line source 7-24745
- XUV radiometric standards at NBS 7-18860
- Au cathode photoelectric detectors, absolute photon sensitivity characterisation 7-24704
- ²⁵²Cf neutron calibration flux distrib., Monte Carlo simulation 7-30805
- ⁵⁷Fe isomer shifts and the problem of calibration 7-61310
- Ge gamma-ray spectrometer, calibration using ¹⁵²Eu decay 7-42275
- He, liquid, flow rate meas., IMGC calibration facilities 7-63234
- InP/InGaAs near-IR detector self-calibration feasibility determ. 7-15002
- N₂ thermometry, CARS 7-62377
- PH₃, accidental IR double reson. transition obs., electric field standards appl. 7-10644
- Pb salt diode laser calibration, wavemeter 7-5930
- Pt thin film resistance thermometer, low temp. high mag. field use 7-14941
- Si PIN diode X-ray detector, pulse calibration technique (*Chinese*) 7-5534
- Si photodiode quantum efficiency as absolute radiometric standard 7-14991
- Si surface barrier telescope for solar particles, characts. and calibration 7-62217
- Si vertex detector, calibration 7-62211
- SiO₂, Fourier transform IR spectroscopy and SIMS calibrations for O conc. meas. 7-16606
- ¹³⁰Te, reference line absolute calibration for positronium spectroscopy 7-25685
- Yb vapour deposited foils, piezoresist. response of stress gauges 7-32986

californium

see also nuclei with

- ²⁵²Cf neutron brachytherapy, complications: review of reported experiences 7-28667
- ²⁵²Cf RBE and PLD-like effect of mag. fields in haemopoietic tissue, CFU-S assay 7-28590
- ²⁵²Cf therapy at the Cancer Inst. Hosp., Tokyo: facility design, environmental protection and planning method 7-28668
- aqueous soln., reaction rate const. of radiation-produced transients 7-60903
- diffusion in Ta-Cf dilute alloy 7-12353
- solid state and thermodynamic props., f-electron bonding and struct., review 7-12321

californium continued

- TURF Californium Facility at ORNL 7-30581
- ²⁵² irradiation rel. to testis wt. loss in mice 7-28592
- ²⁵²Cf, α -particle source, absolute energy meas. 7-42276
- ²⁵²Cf brachytherapy, facilities and remote afterloading 7-28669
- ²⁵²Cf brachytherapy, fast neutron beam therapy and radiobiology, conf., Lexington, KY, USA (April 1985) 7-24273
- ²⁵²Cf brachytherapy of the brain, high LET, B enhancement 7-28670
- ²⁵²Cf γ -neutron radiation biological effects, USSR studies 7-28611
- ²⁵²Cf, historical review of discovery and development, radiotherapy appl. 7-24348
- ²⁵²Cf implant neutron effects on dog brain 7-28593
- ²⁵²Cf irradiation facilities, thermal neutron calibration curve meas. 7-30719
- ²⁵²Cf irradiation of lymphoid organs 7-28591
- ²⁵²Cf irradiation rel. to testis wt. loss in mice 7-28592
- ²⁵²Cf, microdosimetric studies 7-28709
- ²⁵²Cf neutron calibration flux distrib., Monte Carlo simulation 7-30805
- ²⁵²Cf neutron therapy, time and dose considerations for clinical trials 7-28712
- ²⁵²Cf neutrons, review of RBE and OER values, brachytherapy appl. 7-28666
- ²⁵²Cf physics and dosimetry 7-28708
- ²⁵²Cf radiation, phys. and biological dosimetries 7-28711
- ²⁵²Cf radiation dosimetry, studies in the USSR 7-28710
- ²⁵²Cf, tumour and normal tissue effects and therapeutic gain ratio 7-28587
- ²⁵²Cf, props. and prod. 7-28700
- ²⁵²Cf-exposed human cells, pot. lethal damage and radioprotection 7-28612
- ²⁵²Cf RBE expt. on human T-1 cells, inverse γ -ray dose rate effect 7-28616

californium compounds

- Cf oxides, Cf₂O₃, Cf₇O₁₂, CfO₂, BaCfO₃, mag. susceptibility meas. 7-12937
- CfX (X=N,As,Sb), mag. susceptibility meas. 7-12939

calorimeters

see also calorimetry

- A-150 plastic radiometric calorimeter for charged particles and other radiations 7-25264
- ALEPH hadron calorimeter, high voltage network for streamer tubes 7-5549
- Aleph test hadron calorimeter, pion/muon identification using discriminant analysis 7-15464
- BGO calorimeter, performance in electron beam 7-62224
- BGO calorimeter at LEP, characteristics improvement (*French*) 7-49839
- CHARM fine-grained calorimeter, calibration 7-49796
- coaxial, and its use as reference standard in automated microwave power calibration system 7-48744
- commissioning trials on large-scale thermal conductance apparatus 7-14940
- conf., Vienna, Austria, February 1986 7-40989
- continuous-flow calorimeter for local heat transfer coeff. meas. 7-11412
- differential scanning calorimeter automation 7-24654
- differential scanning calorimeters, standard operating procedures development 7-18786
- electromagnetic calorimeter for L3 detector, energy and position resolution (*French*) 7-19664
- electromagnetic calorimeter with wavelength shifting fibre readout 7-49804
- gaseous readout techniques, comparisons with alternatives 7-42440
- heterogeneous materials, multikilogram capacity calorimeter, design and construction 7-41390
- Janus, a bidirectional, multifunctional plasmadiagnostic for Alcator C Tokamak 7-1739
- large plotted circuit board production, delay lines for particle calorimeter 7-25330
- laser power meas. in μ W range, sensitive calorimeter with isothermal temp. control 7-15918
- laser power meas. standards scales intercomparison 7-15917
- liquid TMS calorimeter, performance test, charge yield and stability 7-25307
- macroscale heat flow calorimeter for studying chemical processes 7-41391
- massive fine grained detector for neutrinos in GeV energy region 7-62222
- modeling response variation for radiometric calorimeters 7-30573
- photon-radiation absorbed dose rates meas. by water calorimeter 7-5489
- photothermal spectroscopy using a pyroelectric calorimeter 7-15011
- rectangular waveguide calorimeter for single intensimicrowave pulses 7-9847
- solar test facility for high concentration solar cells, water cooled black-body calorimeter 7-13849
- Soudan 2 nucleon decay experiment, status 7-36428
- thermal neutron flux, device for calorimetric meas. 7-5552
- thermographic laser calorimeter for absorptance meas. in optical coatings 7-41389
- Pb scintillation calorimeter for electron and pion detection, radiation damage props. 7-15451
- Pb-glass calorimeter, low noise amplification chain for vacuum phototriode readout 7-49813
- Si sampling calorimeters, position resolution 7-15465
- Si(Li)-W 4 inch sandwich calorimeter for pp collider expts. 7-5548
- U gas sampling hadron calorimeter, performance 7-5547
- ²³⁸U hadron calorimeters, nuclear fission contrib. to signal, expt. study 7-25306

calorimetry

see also calorimeters; specific heat; thermal analysis

- absorptance characts. of mirrors meas., by photoacoustic calorimetry 7-31432
- adsorption, beginners course (*Japanese*) 7-35182
- 3,3-dimethylbutan-1-ol-n-hexane mixtures, excess molar enthalpy, heat capacity and molar vol. 7-44850
- ethanol-water, excess enthalpies at 323.15, 333.15, 348.15 and 373.15K and from 0.4 to 15 MPa 7-26958
- halocarbons, solubility, interaction with human serum albumin, NMR and microcalorimetric obs. (*French*) 7-65701
- heat of mixing, high temp. calorimetric meas. (*Japanese*) 7-14949
- heat theory principles, historically and critically elucidated, book 7-48265

calorimetry continued

- hexamethylbenzene, phase transition, calorimetric obs. (*Japanese*) 7-16733
high temperature gases in annular channel with cold walls, heat transfer in turbulent flow (*Russian*) 7-1557
instrument realisation of calorimetric check of qualitative parameters in microelectronics (*Russian*) 7-35521
metal mirrors, absorbance meas. at glancing incidence, photoacoustic calorimetry 7-20380
methylammonium iodide, phase transitions, calorimetric and dilatometric studies 7-12261
microwave power meas., microcalorimetric technique with X-band load 7-18817
parabolic cylinder solar unit energy module, luminous flux density meas., calorimetric tests 7-54263
1-phenylcyclohexene, triplet energy state meas., photoisomerisation, time-resolved photoacoustic calorimetry study 7-28319
polyester thermoelestoplastics, softening, thermodynamics (*Russian*) 7-63847
polyethylene oxide-melaminofomaldehyde cocured copolymer, crystallisation and melting (*Russian*) 7-26923
polyethylene oxide-water system, high molecular, calorimetric obs. (*Russian*) 7-12325
polypropylene, isotactic, crazing, energetic characts. (*Russian*) 7-12201
power transmission and shine-through calorimetric meas. during NBI in TFR 7-58056
pyromagnetic detector, pulsed-periodic radiation behavior (*Russian*) 7-35509
solid deformation heat meas., by quick-response calorimetry 7-1522
thermal diffusivity, meas. by light-irradiated AC calorimetry (*Japanese*) 7-14946
thermal diffusivity measurements, AC calorimetric technique (*Japanese*) 7-18787
thermobalance apparatus, metal sulphidation kinetics meas. 7-30013
thermophysical meas. automation, universal microcomputer-controlled system 7-4854
tube banks, staggered, heat transfer characts. in crossflow of air with varying temp. differences (*Russian*) 7-1556
water in benzene and some n-alkanes, heat of soln. at 298.15, 308.07 and 313.14K 7-26959
FeSb₂O₄, thermodynamics studies, 10 to 300K 7-2231
Ge IR absorpt. coeff. meas. with compensating calorimeter 7-56270
GeSe₂, vitreous and crystalline states, energy difference, bond energy, calorimetry study 7-59775
(GeSe₂)₇₀(GeTe)₁₅(Sb₂Te₂)₁₅, glass transition, thermodynamic and thermokinetic characts. 7-26953
H₂ cluster detection at 4.2K 7-36843
In-Bi, liq., heat of mixing, calorimetric study 7-12283
Kr clathrate hydrates, sp. heat, compositions and heat of dissoc. in range 85 to 270K, calorimetric determ. 7-26974
Li/SOCl₂ cell, corrosion, calorimetric study 7-46929
Mn_{0.794}Cr_{0.206} alloy, sigma phase, heat capacities 7-52073
NiSb₂O₄, thermodynamics studies, 10 to 300K 7-2231
O₂, triple point in sealed transportable cells 7-41331
PdTi, enthalpy of form. by high temp. calorimetry 7-21410
RbCN, cryst., phase transition and glass transition 7-12260
ThBe₁₃, high temp. sp. ht. meas. (*French*) 7-16786
UBe₁₃ and UBe₄, high temp. sp. ht. meas. (*French*) 7-16786
Xe clathrate hydrates, sp. heat, compositions and heat of dissoc. in range 85 to 270K, calorimetric determ. 7-26974
YBa₄, enthalpy of form., high temp. calorimetric meas. 7-39909

calorimeters *see calorimeters*

CAMAC

- HERB high-rate CAMAC acquisition system 7-42444
IKAR-16 automated solar spectral-polarisation complex of RATAN-600 radio telescope, configuration and software 7-66460
intelligent multichannel analyzer for themeasurement of gamma spectra 7-5533
KEK e⁺ generator, magnet power supply control system (*Japanese*) 7-19580
minicomputer appl. for radiocarbon anal. control and meas. 7-34682
nuclear micro-beam probe for the investigation of surfaces, microprocessor-controlled 7-8352
pellet injectors, control and data acquisition system, design 7-36254
TFR CAMAC data-acquisition system 7-5426
thermophysical meas., computerised instruments interfaces standardisation 7-4857

camera lenses *see photographic lenses*

camera tubes, television *see television camera tubes*

cameras

- see also coronagraphs; television cameras*
35mm camera lenses used for photogrammetry, lens distortions and calibration 7-40393
aerial photography, comparison of three modern aerial cameras (*French*) 7-47307
aerial photography, retractable camera rig for light aircraft 7-29304
aerial survey camera trials, for Wild RC10A and Zeiss RMK A 15/23 cameras 7-28817
astronomical instruments and techniques, conf., Tucson, AZ, USA (March 1986) 7-48162
automatic amateur camera, program efficiency, probability evaluation 7-41519
automatic focusing systems, IC testing 7-41517
CCD array for Hubble Space Telescope 7-29407
disc format cameras, gradient-index lens system design 7-30105
echelle spectrograph, camera lens system design 7-55475
exposure-measuring systems, photoresistors 7-41518
fast framing camera with independent frame adjustments 7-18894
femtosecond streak camera, struct., operating characteristics (*Japanese*) 7-357
femtosecond streak camera 7-18895
fibre optic streak camera system to monitor X-ray refl. changes in metal multilayers 7-30135
forestry and range applications of high altitude reconnaissance technology 7-23905
gamma camera, electronically collimated, gas scintillation utilisation 7-65845
green light 2w as an X-ray streak camera fiducial 7-11771
Guinier high temp. camera conversion to low temp. device 7-15041

cameras continued

- Halley Multicolour Camera, vibration effects in flat mirror, analysis and reduction 7-18355
high-speed photography, videography and photonics, conf., San Diego, CA, USA (Aug. 1985) 7-18486
holographic display element using polyvinyl carbazole material in 8mm movie camera 7-25745
holographic interferometry, camera using photothermoplastic film 7-43016
human gait data acquisition and processing using digital camera 7-65809
imaging techniques utilizing optical fibres and tomography 7-25977
imploding plasma expts., optical, and UV/X-ray imaging diagnostics 7-11784
IR camera with hybrid 32X32 HgCdTe CCD array for astronomy 7-60560
IR streak camera for use in 1.0 to 1.6 µm region 7-18896
IR zoom lens for thermal cameras (*Japanese*) 7-57515
JEOS, JANUS Earth Observation Satellite camera characts. 7-34824
Kinor film camera, crystal controlled electric drive use (*Russian*) 7-35617
KS-147A LOROP camera integration into RF-5E aircraft 7-18898
KS-147A LOROP camera system, photographic reconnaissance appl. 7-18897
KS-147A LOROP camera system for RF-5E aircraft 7-18899
laser scanner, image capture capabilities and PCB inspection applic. 7-57601
light velocity meas., using streak camera and ring laser 7-18766
MTF analyzer, microcomputer and dynamic RAM chip camera based 7-47
multilens cameras for high velocity/low altitude photoreconnaissance 7-41515
multipinhole camera, phase object obs. 7-41513
neutron penumbral imaging camera, optimisation and simulation 7-1017
non-metric cameras, calibration using finite element method 7-3969
oblique CCD reconnaissance camera operation, atmospheric effects 7-18900
ophthalmological, wide-angle RCS-310 retinal camera, prototype experience 7-8745
ophthalmological, wide-angle RCS-310 retinal camera design 7-8744
optical fiducials for X-ray streak cameras at LLE 7-11772
photoreceiver exposure measuring system for high-quality cameras 7-41516
picosecond electronic framing camera 7-20465
positron camera, multiwire proportional chamber, development of high-efficiency cathode converters 7-40271
Read camera appl. to thin film X-ray anal. 7-58103
reflex, viewfinders, testing and adjustment 7-41520
scanning systems, Sawyer motors use 7-57602
secondary ion imaging, with charge-coupled device camera 7-48912
soft X-ray streak camera, absolute calibration 7-18963
soft X-ray streak cameras, resolution characteristics 7-9931
spaceborne camera using TI TC-104 linear CCD array 7-29406
streak and framing camera designs using SAW-CTD imagers 7-56368
streak camera performance characts., with cooled CCD 7-19425
streak cameras, technological developments 7-61393
streak recording of picosecond pulses 7-15026
sweep-nonlinearly correction procedures in picosecond streak camera measurements 7-15024
synchronously operated streak camera driven by a GaAs photoconductive device 7-18903
thermal camera without liquid N₂ coolant (*Swedish*) 7-35514
time-lapse underwater photography system with event sensor capability 7-60432
X-ray calibration of CCD sensors and photodiode array cameras, plasma diagnostics appl. 7-20939
X-ray camera using a 2D multiwire proportional chamber 7-51570
X-ray framing camera for laser fusion expts. 7-20944
X-ray framing camera for laser plasma diagnostics 7-11779
InSb array IR imaging camera, for astronomical appls. 7-34865
X-ray film calibration, imaging, spectroscopy, dynamic range modification 7-9932
- candoluminescence** *see luminescence*
- canted spin arrangements**
see also weak ferromagnetism
bis(methyl ammonium) iron tetrachloride, mag. susceptibility rel. to thermal and mag. history 7-22095
phase transitions in two-dimensional uniformly frustrated XY spin systems 7-2875
Cd_{1-x}Cu_xFe₂O₄, canted spin arrangements 7-45618
Ce (Fe_{1-x}Al_x)₂, Fe-rich intermetallics, mag. and elec. props. 7-45621
CrTe-CrSe system, mag. phase diagram 7-22105
Dy_xCo_{1-x} thin films, ferrimagnetic reson. in region of spin-reorientation transitions 7-45824
Fe₇Si₈O₂₂(OH)₂, grunerite, mag. order, quasi-one dimensional antiferromag. with spin canting transition 7-58983
FeTiO₃, mag. struct. 7-7484
GdMn₂, magnetic structure, tight binding approx. 7-2819
La₂NiO₄, quasi-2D, canted antiferromag. order studies 7-33153
LaZnFe₁₀O₁₉, cation distribution and random spin canting 7-37945
NiFeAlO₄, cation distrib. and canted spin alignment, Mossbauer obs. 7-22169
Ti_xCo_{1-x}Fe_{2-x}O₄ spinel solid soln., mag. props., Mossbauer effect study 7-12685
- capacitance**
see also photocapacitance
composite, thin-walled structure, growth of through cracks monitoring arrangement, capacitive method 7-22968
double Schottky barrier, grain boundaries, elec. props. in presence of deep bulk traps, appl. to ZnO varistors 7-7334
electrostatic field and capacitance calcs. for spheroidal shells (*Russian*) 7-42836
flat laminae, capacity anal. 7-62565
liquid cryst. display, SBE type, fundamental characteristics (*Japanese*) 7-7670
MOS capacitance in strong inversion at high temp., freq. depend. 7-7403
MOS systems, freq. spectrum of reciprocal capacitance 7-38741
nematic liquid crystal in switched DC electric field, time response 7-32271
paraxial cylinders, resistance and capacitance, undergraduate laboratory expt. 7-44

capacitance continued

- perpendicular conducting planes separated by gap, comments and reply 7-42832
- polystyrene film, electron thermalisation and trapping 7-27343
- potential coefficient equations for non-parallel, non-orthogonal cells 7-15798
- restricted primitive model for electrical double layers; modified HNC theory of density profiles and Monte Carlo study of differential capacitance 7-11868
- SAW transducer, layered struct. tempering (*German*) 7-31615
- semi-insulators, low-freq. dispersion phenomena anal. 7-38991
- SOI struct., implanted buried oxide elec. props., high temp. annealing effects 7-58904
- Ag electrode in NaClO_4 soln., capacitance, pH depend. 7-54135
- Ag electrodes, galvanostatic oxidation, relax. spectrum anal. 7-13788
- AlGaAs-GeAs n-n heterojunction, thermionic current and capacitance, effect of subband quantisation in 2D electron gas 7-17090
- AlInAs-GaInAs superlattices, electronic transport and depletion by tunnelling 7-27395
- $\text{Ba}_{1-x}\text{Gd}_x\text{F}_{2+x}$ defect struct., ionic thermocurrents, dielec. meas., EPR obs. 7-44907
- BaTiO_3 capacitor material, elec. field distrib. around flaws, finite difference modelling 7-64574
- CuInSe_2 -CdS solar cells, capacitance determ. of interfacial states 7-13916
- Fe electrodes, passivated, capacitance under simulated erosion-corrosion conditions 7-3514
- GaAs device structures, γ -ray effects, surface generation-recombination processes 7-64349
- GaAs junction, temp. meas. using capacitance change of space-charge region 7-48742
- n-GaAs metal-dielectric-semiconductor system, field effect, transistor studies 7-52841
- GaAs/ $\text{Al}_x\text{Ga}_{1-x}$ As heterostruct., 2-D density of states in extreme quantum limit 7-2455
- GaAs/ AlAs /GaAs:Se heterojunctions, elec. behaviour, DLTS studies 7-7360
- n-GaAs/Ti-Pt system, Schottky barrier height, doping depend. 7-2708
- GaAs-AlGaAs heterostructures, density of states of Landau levels 7-52822
- $\text{Ga}_{1-x}\text{In}_x\text{P}$ /GaAs heterojunction band discontinuity determ., C-V profiling 7-58880
- InAsSb/GaSb n-n heterojunctions, band discontinuities, C-V and I-V meas. 7-7366
- InP MIS structures, prep. by RF plasma oxidation, interface elec. props. 7-2731
- InP/Al UHV-cleaved and laser annealed interface, acceptor-like electron traps 7-7310
- $\text{Na}_2\text{O-SiO}_2$ glass, longitudinal electrostriction tensor component 7-2982
- $\text{Na}_2\text{O-SiO}_2\text{-Al}_2\text{O}_3$ glass, longitudinal electrostriction tensor component 7-2982
- Pb-acid battery, effect of chemisorbed H_2O on positive plate elec. capacity 7-54284
- Si, impurity and carrier conc. profiles, electrochem. C-V method (*Chinese*) 7-12105
- Si metal tunnel-thin insulator-semiconductor structures, effects of high field corners 7-64348
- a-Si:H, metastable defect states, capacitance studies 7-45225
- a-Si:H/CuInS₂ heterojunctions, photovoltaic behaviour, c-v meas. 7-7340
- a-Si:H/ SiO_2 /metallic gate struct., capacitance-volt. characts. 7-45515
- Si/NiSi₂ heterojunction, interface states, DLTS and hydrogenation studies 7-12777
- Si-SiO₂ interface, MOS capacitance derivative freq. depend., surface state densities and capture cross section 7-45507
- SiO₂/SiC interface. elec. characts., MOS conductance technique meas. 7-12873

capacitance measurement

- bridge for low-temp high-resolution dielectric meas. 7-48778
- deep levels, capacitance method 7-45205
- farad absolute determ. at LCIE, using quadrature bridge 7-14909
- HV capacitance meas. bridge, frequency dependent errors 7-18813
- HV compressed gas capacitors appl. 7-18814
- MIS narrow gap structures, evaluation theory of C-V meas. 7-64355
- MIS structures, minority carrier lifetime meas. (*German*) 7-56306
- plant stem water potential measurement and simulation (*Japanese*) 7-28799
- polyetherimide, RF elec. props., 10 kHz to 1 MHz 7-48779
- polyethylene terephthalate, RF elec. props., 10 kHz to 1 MHz 7-48779
- polyimides, RF elec. props., 10 kHz to 1 MHz 7-48779
- semiconductor junction capacitance meas. for complex systems 7-38681
- squeezable tunnelling junctions 7-7447
- stabilised oct. for equivalent parallel resistance and capacitance and small changes meas. 7-18804
- thickness-mode piezoelectric transducer constants, automatic meas. and calibration system 7-1369
- void fraction meas. by capacitance transducers, parametric effects 7-1652
- Si detectors, large area, properties and radiation stability, capacitance-voltage meas. 7-42333

capacitance meters *see capacitance measurement***capacitor storage**

- fuse and resistor characts. for multi-megajoule capacitor bank appl. 7-30792
- high voltage capacitor low inductance, high energy density, units of different elements, breakdown and life tests (*Japanese*) 7-11796
- plasma erosion opening switch, long conduction time 7-51519
- plasma focus, inductive-capacitive energy storage supply 7-63370
- plasma focus drivers, efficiency parameters for reactor conditions 7-63373
- pulsed power supplies, IEEE conf., Arlington, VA, USA (1985) 7-35110
- pulsed power supply, high power, for proton synchrotron 7-25274
- RFX fusion expt., Italy, power supply protection against plasma disruption and fault conditions 7-30668
- surface discharges as intense photon sources for light-ion fusion acceleration cleaning 7-37800

capacitor stores *see capacitor storage***capacitors**

- see also electrolytic capacitors; power capacitors; thin film capacitors; varactors*
- cylindrical, magnetic field components meas. 7-18847

capacitors continued

- field-effect capacitor, carrier ambipolar drift vel., field control study 7-52840
- HV compressed gas capacitors, precise capacitance meas. appl. 7-18814
- MOS capacitors, interface trap charge effect on C-V and I-V characts. 7-27437
- parallel disc capacitors, fringing fields and total capacitance calc. 7-10814
- photoemf measurement in semiconductor, by two-capacitors method 7-30037
- polymer film capacitors, radiation-induced space charge 7-45516
- quantum Hall resistance value determ., using calculable capacitor at ETL 7-14968
- BaTiO_3 based multilayer ceramic capacitors, chemical processing 7-46399
- n⁻-GaAs/ $\text{Al}_x\text{Ga}_{1-x}$ As/n⁺-GaAs capacitors, accumulation layers magnetotunnelling obs. 7-12880
- Sb_2S_3 amorphous condensers, electroelectret state and local levels studies (*Russian*) 7-45923
- Si/ SiO_2 /TiSi_x(WSi_x) MOS capacitors, radiation-induced interface traps 7-58897

capacity management (computers) *see DP management***capillarity**

- see also bubbles; contact angle; drops; foams; liquid films; surface tension*
- air finger rise in cylindrical tube, rate determ. 7-57910
- binary alloy in 1D lattice, density oscillations model 7-9800
- bubble motion in capillary tubes, wetting film thickness anal. 7-44952
- capillary impregnation kinetics of initial stage 7-63218
- capillary liquids, static problems, soln. methods 7-44950
- condensation in cylindrical pore, stability 7-1623
- crystal violet in ethanol, spreading layer, capillary convection 7-6925
- cylindrical capillary, rise of generalised Newtonian liq. 7-6922
- diameter meas. of capillary holes, in 0.2 to 2 mm range 7-4807
- difluoroethane resonant mols., capillary flow, laser light effects in transitional flow regions 7-57927
- dispersive transport modelling in porous media, solute motion in pipes and capillary tubes 7-23753
- drop generation from capillary streams 7-57913
- drying, filtration process, hydrodynamics 7-57918
- dynamic thermocapillary liquid layers instability mechanism 7-38303
- electrified menisci, cone-like shapes, emitted charge effects 7-31888
- fibre suspensions in Newtonian fluids and polymer solns., capillary flow 7-6318
- floating liquid zones expt. on Spacelab D1 mission 7-22971
- fluid interfaces, phase transitions, local density approx. and smoothed density approx. study 7-63912
- fluid jet models, one-dimensional, numerical comparisons, appl. to drop-on-demand ink-jet printing 7-31851
- fluids, equilib. and stability 7-58567
- gas-liquid flows, capillary waves, spectral behaviour 7-11521
- glow discharge cathode spot, entry into capillary hole 7-32160
- heat pipes, sintered capillary structures, wetting, macroscopic boundary angles 7-12397
- Hele-Shaw cells, imperfect, flow properties 7-6184
- hydrodynamic nature of the fixation of a cathode spot 7-57859
- hydrology, capillary hysteresis model for intermittent flux studies in unsaturated soils 7-29096
- hydroxypropyl guar gels in capillary tubes, slip vels. meas. 7-11550
- isobutane, capillary const. and surface tension 7-12395
- kidney, artificial, press. losses in apparatus with capillary channels made of semipermeable film 7-28772
- liquid crystal capillary cell, orientational and struct. effects in conical elec. field 7-44370
- liquid flow, nonequilibrium thermodynamic appls. 7-6920
- mass transfer in capillaries with absorbent walls, anal. 7-27059
- microcapillaries, partitioning of hard-sphere fluids, Monte Carlo and mol. dynamics simulations 7-63416
- oil-water gravitational separation in beds of limited thickness 7-51299
- porous materials for heat pipes, struct. and hydraulic props. 7-44039
- porous minerals, N₂ adsorption, isotherm calcs. 7-6969
- porous solid-liquid systems, mass exchange in elec. field 7-12398
- profiled crystals, Stepanov growth, conf., Leningrad, USSR (March 1985) 7-29573
- propane capillary const. and surface tension 7-12395
- rubber-glass interfaces, form. and rupture (*French*) 7-54072
- Saffman-Taylor meniscus during flow between plates, gravity effect 7-63915
- simple fluids in cylindrical and slit-like pores, capillary condensation and adsorption 7-32756
- single capillaries, droplet formation in the jet regime of a liquid/liquid system (*German*) 7-16227
- slot, 2D with inclined walls, steady pot. flow, contraction coeff., capillarity effect 7-57891
- Stepanov method crystallisation on a rotating seed 7-33540
- superheated liq., flashing in glass capillaries 7-13797
- surface diffusivity variation on surface morphology and electromigration 7-63920
- thermocapillary and thermogravitational convection in a horizontal liquid layer 7-63909
- thermocapillary convection in a rectangular cavity with a deformable interface 7-43911
- thermocapillary convection in two-layer system, surface active agent effect 7-51121
- thermocapillary movements under microgravity at a minimum of surface tension 7-20721
- thermogravitational and thermocapillary convection in a rectangular cavity 7-63910
- thin films, thermocapillary convection and stability 7-12409
- thin liquid films, thermocapillary flow 7-63908
- time-depend. rise, Newton's motion law for variable mass systems 7-48238
- tip shape evolution, capillarity induced matter transport by surface diffusion 7-58592
- two-layer systems, thermocapillary convection, numerical anal. 7-63911
- viscous incompressible fluid, partial cavity form., cavitation flow calcs. 7-31846
- water flow in capillary, surface and kinetic energy, laboratory exercise 7-18528

capillarity continued

zero gravity conditions, liquid column rise into vertical tubes (*German*) 7-12396
22 NaCl, aq. soln., adsorpt. and diffusion at low concs. 7-27106
H, spin polarised, enhanced capillary flow and vanishing sticking probabilities on liquid He surface 7-27054
4He, superfluid, fractal surface, third sound, capillary condensation 7-27041
LiNbO₃, crystal growth from liquid, physical consts. determ. 7-32322
SF₆ resonant mols., capillary flow, laser light effects in transitional flow regions 7-57927
Si, Stepanov reverse method cryst. growth, thermal and capillary conditions 7-33545
Si, thin sheets, EFG, thermal capillary mechanism for growth limit 7-17407
Si, ultrasonic shaping during pulling cryst. growth 7-33541
SiC, carbide form. in Stepanov cryst. growth 7-33544

capillary phenomena see capillarity

capillary waves

capillary, time-depend. rise, Newton's motion law for variable mass systems 7-48238
capillary-gravity wave at free surface of viscous incompressible liq., dispersion eqn. 7-43943
capillary-gravity waves, symmetry and bifurcation 7-43941
deep-water gravity-capillary waves fourth-order evolution eqn. 7-37482
gravity-capillary waves, wind-generated, period-doubling 7-43952
laser annealing, pulsed, surface structure formation 7-58322
laser-induced instabilities in semiconductor and metal surfaces, nonlinear optical diagnostics 7-2061
liquid drop, instability development in elec. field 7-31850
liquid metals, capillary wave dispersion relation modifications due to electric charge, surface Green fn. matching method 7-21575
nonlinear 2D gravity-capillary waves, 3D instabilities 7-51194
nonlinear gravity waves and capillary waves on surface of infinitely cond. liq., MHD effects 7-44058
nonlinear gravity-capillary waves, free surface accel. 7-43955
nonlinear waves sheets of fluid, highest waves criteria study 7-43953
ocean, capillary-gravity ripples generation by strongly non-linear waves on deep fluid surface (*Russian*) 7-29040
oil surface deformation by laser heating, laser-beam self-focusing and capillary wave generation 7-50656
plate oscils. across liquid interface, contact-angle hysteresis effects 7-52189
single capillaries, droplet formation in the jet regime of a liquid/liquid system (*German*) 7-16227
soliton solutions for capillary waves on deep water 7-43942
stability of nonlinear gravity-capillary waves 7-16161
stationary potential waves of finite amplitude 7-51186
surface waves, thermal fluctuations, photon correlation spectroscopy 7-51197
vapour-liquid interface, scaling laws and universality of critical phenomena 7-14906
viscous liq. drop breakup, capillary wave instabilities, transient effect 7-43954

capture cross-sections, nuclear see nuclear reactions and scattering

Caratheodory's principle see thermodynamics

carbon

see also nuclei with
see also carbon fibres; charcoal; diamond; graphite
14C seasonal variations in atmosphere caused by bomb tests 7-23256
ablation plasmas, laser induced, emission spectra 7-26530
abundance in P/Comet Halley (1982i), rocket-borne UV spectroscopy 7-47784
activated, adsorbed toluene layers, IR spectra 7-10573
activated, heterogeneity, benzene adsorption 7-28342
activated surface, adsorption of Ag, mathematical model 7-44999
adlayers on Fe (100), gasification by O, CO desorption 7-6993
adsorbed on Mo (100), hydrocarbon adsorption and reaction 7-28345
adsorbed on Ni (100), electronic struct. 7-7315
adsorbed on Si surfaces, annealing behaviour, XPS and AES studies 7-27108
adsorption on Mo (100), surface atom oxidation states, ESCA meas. 7-28333
Amazon River, continental shelf organic C accumulation, stable isotope chars. 7-34463
amorphous, origin of extragraphtic low angle peaks in X-ray diffr. patterns 7-37859
amorphous film, modification by inert gas ion irradiation 7-64018
amorphous films, crystallisation influence of residual stresses and density fluctuations 7-21750
amorphous films, laser generated, struct. and bonding, Raman and electron energy loss spectra study 7-27800
amorphous films, plasma fluorination, surface structure determ. 7-27196
amorphous films for InP MIS structs., ion-beam sputtering and plasma deposition 7-7400
amorphous submicron grains, extinction spectra in UV-visible range 7-35023
amorphous submicron grains, far-IR extinction meas. and props., astro-physical appl. 7-47699
amorphous thin films, bonding core-EELS and 13C NMR studies 7-21099
amorphous-metal thin multilayer struct., vacuum condensation, interface development, sheet cond., thickness 7-21681
atom, electron inelastic scatt. cross-sections 7-5775
atom, photoionis. cross section, generalised RPAB calcs. 7-42574
atom, spin and charge densities, HF and UHF calcs. 7-19684
atomic, double excitation and ionisation by strong pulsed laser 7-42571
Auger backscattering factors, prediction from meas. of spectral back-ground 7-28378
AB Aur, Herbig Ae star, wind rot. modulation, C IV and Mg II UV obs. 7-47870
Be stars, C IV reson. lines and IUE obs. 7-55678
black, in styrene-butadiene rubber soln. relax. properties 7-8317
black filled polycarbonate composites, TEM obs. of percolation threshold 7-12771
C_n and C_n⁺ abundance distribts., magic nos. 7-42815
carbonisation of phenol formaldehyde resin, product mech. props. 7-46802
cathode, chem. sputtering in H₂ and O₂ plasmas 7-32171
cathode erosion and power flow in vac.-arc centrifuge 7-26562

carbon continued

cathode performance improvement in Ca(AlCl₄)₂-SOCl₂ cells 7-13851
cathodes for Ca-SOCl₂ cell performance improvement, Ca(AlCl₄)₂-SOCl₂ electrolyte 7-65444
chemisorption on Al, interaction with surface, cluster approx., total energy calcs. 7-52265
cluster ions, trapped FT ICR mass spectrometry 7-1000
clusters, form. in laser vaporisation source, kinetics 7-5808
coadsorption with Si on W (100), Auger spectra studies 7-63954
coating for heat damage prevention of electron microscopy specimens 7-22864
coatings, ion plating, amorphous struct., wear resist. 7-22580
coatings, plasma exposure in mag. fusion devices 7-42193
coke, metallurgical, microstruct. analysis and intercalated species 7-28008
cubic crystals, electron struct., cluster approx., Xalpha calcs. 7-38445
Devonian shales from Appalachian Basin, C and S relations as indicator of deposition environment 7-65988
diamond-like films, intrinsic stress, depend. on deposition parameters 7-58721
diamond-like films, microwave plasma CVD process 7-17435
diamond-like films, stresses, energy depend. 7-45097
diamond-like films for erosion protection of fused silica slides 7-46673
diamond-like layers deposited from C ion beams, struct. (*Russian*) 7-17475
diamondlike coatings, ion beam induced conductivity and structural changes 7-22053
diamondlike films, deposition with C⁺ and hydrocarbon ion beams, mechanical props., comparison 7-59417
diamondlike films, sputtering, appls. 7-39374
dielectric film growth, on GaAs and InP substrates 7-39420
early A-type stars, meridional mixing and C abundances 7-40815
EELS analysis, inner shell excitation profiles visibility 7-22403
electrode, glassy, anodic process in LiF-NaF-KF eutectic, Cl⁻ effect 7-23028
electrodes, adsorpt. of Cl, theory 7-12462
electrodes in Li-SO₂ rechargeable cell 7-65443
electron microscopy, past, present, future 7-16379
electron probe analysis, automatic, in case-hardened steel parts, software (*French*) 7-46889
electron probe microanalysis, quantitative 7-46886
fibre, laser produced plasma, XUV expansion coded recombination lasers 7-62679
fibre plasma, laser produced, population inversion and gain meas. 7-26505
films, CKα spectra and interatomic bonding (*Russian*) 7-58705
films, diamond crystallisation, conf., Warsaw, Poland (June 1985) 7-18469
films, diamond like, prep. and props. 7-22472
films, diamond-like, empirical categorization and naming 7-16919
films, mech. props., relation between different quantities 7-8041
films, plasma deposited from methane, elec. conductivity, optical absorpt. 7-38786
films, transparent, sputter- and plasma-deposition 7-22474
fluorination, thermobalance for investig. 7-41349
foil, H⁺ induced ridge electrons emission 7-46270
foil, secondary electron emission from fast ion bombardment 7-53459
foils, beam-foil convoy electron double differential distribts. for proton irradi. 7-22408
foils, charge equilb. of swift H beams 7-22409
foils, electron absorpt. and scatt. energy spectra, Monte Carlo calcs. 7-22399
fractographic studies 7-17645
fusion machine wall material erosion and impurity prod. 7-62074
fusion reactor first walls, ion debris and X-ray energy deposition and response 7-49639
geochemical C cycle, atmospheric disturbance and impact upon biosphere 7-40546
glass state, stopping cross section of 12C projectiles 7-51899
glass-like, heat treatment, pore growth kinetics 7-58147
glassy, anodic oxidation of surfaces 7-46850
glassy, substrates for IR external refl. spectroscopy characteris. of thin films 7-41509
grain boundary internal adsorption in Fe-base alloys, segregation study (*Russian*) 7-6961
graphitic and non-graphitic, amorphous struct., X-ray diffr. studies 7-58143
hard type, B-doped, prep., phys. and mech. props. 7-39571
HD 109995, field horizontal branch A-type star, CNO comp., UV spectral obs. 7-47862
implantation and diffusion in fusion reactor structural materials, Mo and W 7-49658
insulating films for MIS struct., interfacial characts. 7-2732
interaction, with reduction products of MoO₃, formation of Mo₂C 7-8260
interstellar C abundance, determ. toward ρ Oph and β Sco. 7-9531
interstellar C I, 809 GHz fine-structure line obs. in dense mol. clouds 7-66717
ion implantation into bearing steel, enhanced lubricated sliding wear resistance 7-53916
kerma factor for 18 and 20 MeV neutrons, exact meas. 7-36302
layers, arc plasma deposition, struct., mech. props. (*Russian*) 7-22581
layers, deposition, by RF plasma decomp., physical props. 7-22508
layers, nucleation in HF hydrocarbon plasma 7-17476
mass spectroscopic analysis of stable isotopes, at nanomole level 7-17842
meteorites, carbonaceous chondrite C isotopes and element abundances 7-24086
microanalysis, in steels, statistical method of brief countings (*French*) 7-46888
MIS structures, form. by reactive pulse plasma method, on Si or SiO₂ substrates, phys. props., annealing effects 7-22023
molecule, intercombination transition probabilities between levels X¹Σ_g⁺ and a³Π_g 7-25607
multielectron atoms, multiphoton excitation and ionisation 7-19796
NMR spectral line broadening in lanthanide paramagnetic systems, magnetic suscept. anisotropy effects 7-27624
Paleozoic ocean, O and C isotopic records anal. 7-9029
particulates in marine atmosphere, long-range transport from continents 7-55221
planetary nebulae, abundances of C III and N IV, C II and N III recomb. lines anal. 7-4538
plasma, nonuniform, shock wave propag. investig 7-44174

carbon continued

- plasma deposited thin films, electrophys. props., MIS struct. as tool for anal. 7-17268
 polyimide surface, in situ anal. of H,C,N and O using direct recoil time-of-flight technique 7-54242
 Population II giant stars, C isotopic ratios determ. 7-60654
 protective film on ZnS and ZnSe IR transmitting windows 7-46731
 PS-3.5 spheromak, flow field study by C impurity spectral line shifts 7-26403
 pyrolytic, low temp. growth with highly ordered graphite structure by CVD (*Japanese*) 7-13384
 QSOs, C IV absorpt. systems characts. 7-66780
 redistribution in austenitic steel weldments, general soln. 7-21506
 resistors for cryogenic thermometry 7-56267
 CV Ser, WC8 star, wind modelling, C III UV and visible spectra anal. 7-66625
 Sh2-235, mol. cloud-ionised emission nebula interface modelling, C recomb. lines obs. anal. 7-48012
 single-particle excitations, dynamic correl. corrections, local density theory 7-45115
 solar wind C, N and O ions in magnetosheath of Earth 7-9318
 soot, trapping of inert gases, possible occurrence in meteorites 7-50436
 sputtered films, ion enhancement, struct. prop. relationships studies 7-52332
 strength and structure in carbons and graphite, conf., Liverpool, England (Sept. 1985) 7-24257
 structure, determ. by radial distrib. function 7-16485
 Sun, filaments, oscillations in H α and C IV lines 7-60614
 Sun, quiescent filament, H α and C IV vel., centre-limb anal. 7-14551
 thin films, RF discharge deposition, mech., elec. and optical props. 7-22509
 thin films, sputtering yields for O and Ne ions 7-59341
 thin surface layers on steel substrates, anticorrosion props., ion bombardment effects study 7-27202
 trace anal. in thin films using extremely high vacuum SIMS 7-54243
 ultrathin foils for Coulomb-explosion experiments 7-57184
 vacuum methods of film deposition (*Polish*) 7-64901
 Al₂O₃:C,S CVD layers, C and S distrib., SIMS anal. 7-6668
 C cage molecules of icosahedral symmetry, stability anal. 7-20088
 C I 538 nm line in solar spectrum, appl. as temp. diagnostics for photospheric inhomogeneities 7-66553
 C I isoelectronic sequence, short wavelength laser calcs. 7-20214
 C III, Z-pinch plasma, Stark broadening of spectral lines 7-36537
 C III vacuum arc discharge, reson. photoexcitation, fluoresc., X-ray laser prototype 7-20987
 C IV emission line behaviour in active galactic nuclei, IUE spectra 7-60790
 C IV in galactic halo, implications for interstellar gas props. 7-24171
 C IV in local interstellar medium, evidence from IUE obs. of late B-type stars 7-60771
 C IV in OB-type stars, ionisation fraction determ. from UV line profiles and IR excesses 7-47884
 C IV resonance line investig. using gas-liner pinch 7-9868
 C particle laden O₂ gas, normal shock wave anal. 7-51288
 C V, electron impact excitation of inelastic transitions 7-979
 C VI, soft X-ray laser beam, divergence meas. 7-1210
 C VI, XUV laser numerical modelling 7-20213
 C VI recombination laser, X-ray laser schemes 7-20206
 C⁻ negative-ion-beam deposition system, mass-separated 7-3170
 C⁺, electron impact excitation meas., ion beam apparatus 7-57190
 C⁺, electron scatt., plasma screening effect, distorted wave approach study 7-62532
 C⁺, plasma, Balmer line Stark broadened profiles 7-26513
 C⁺ projectile on C foil, convoy electron yield, target thickness depend. 7-27839
 C:Au(Bi) films, ion implanted, projected ranges and range straggling, RBS anal. 7-63690
 a-C:H, diamondlike, dielectric film, props. rel. to deposition parameters 7-39419
 a-C:H, film, optical and compositional props. 7-39206
 a-C:H, film, optical and electronic props. rel. to deposition parameters 7-38406
 a-C:H, film, optical energy gap, density, hardness 7-39204
 a-C:H, film, plasma emission spectroscopy, chem. anal. 7-38407
 a-C:H, films, plasma deposition characterisation of hydrocarbons used 7-39422
 C:H, homogeneous and heterogeneous chemistry of methane deposition plasma 7-39424
 a-C:H, props., review 7-51630
 C:H amorphous film's, plasma deposition, discharge elec. characteristics 7-46344
 C:H amorphous films, glow discharge deposited from CH₄+H₂, annealing behaviour 7-64922
 a-C:H diamond-like coating on Ge, rain erosion resistance improvement obs. 7-31435
 C:H films, carbonization in acetylene discharge 7-17444
 a-C:H films, glow discharge deposited, valence electron props., electron energy loss spectra study 7-13288
 a-C:H films, plasma deposited, optical props. 7-27799
 a-C:H plasma grown films, struct., physical props. 7-58713
 a-C:H polymeric layers, plasma-activated CVD produced, spectroscopic investigations 7-22572
 a-C:H polymeric plasma-activated CVD films, tribological and mechanical props. studies 7-16920
 C:K, NO adsorpt. and reduction 7-63946
 C:Ne⁺, ion implantation in elemental solids, range profile, gamma-ray spectra 7-2959
 C/methanol, activated, solar-powered solid-adsorption ice maker design 7-65585
 C/N ratio in Lake Karewa sediment, India, palaeoclimate characts. determ. 7-4175
 C-glass resistance thermometer for low temps. and mag. fields up to 7T 7-61331
 C-graphite heat-shielding coating, destruction and heat transfer in N₂ plasma flow 7-63263
 C-Li rechargeable batteries, characts. 7-59835
 C-O₂ suspension, parameters affecting postshock wave relax. zone 7-51289
 C-Se plasma, radiation cooling and gain calc. for C VI 182 Å line 7-6360

carbon continued

- C-Sn composite sputtered films, ion enhancement, struct. prop. relationships studies 7-52332
 C-Ti composite sputtered films, ion enhancement, struct. prop. relationships studies 7-52332
 C-W multilayers, sputtered, ellipsometry monitoring, X-ray refl., XPS 7-39376
 C-W ultrathin layered stacks, sputtering techniques, in situ ellipsometry control system 7-1292
 C-Zn batteries, selection guidelines 7-3633
 C-Zn dry battery with outer metallic jacket (*Japanese*) 7-65427
 C-ZnX (X=S, Se), adherence of diamondlike C films, use of intermediate layers 7-46624
 C+Fe(Ti), thick target bombardment, X-ray production cross sections 7-20025
 C+H(H⁺), methane form. kinetics model 7-5745
 C+HeH⁺(NH⁺), fast mol. ion dissoc., charged fragment wake effects (*French*) 7-50345
 C+U⁶⁸⁺(U⁸³⁺)(Xe⁴⁵⁺), electron stripping, cross section meas. 7-64849
 C⁺+H₂(D₂), rate const. determ. 7-17774
 C³⁺+H, pot. energy curves, spin-coupled VB theory 7-957
 C³⁺+He, transfer excitation, electron emission, forward-backward asymmetries 7-973
 C⁴⁺+He, double charge transfer process, differential cross sections, quantal study 7-62512
 C⁴⁺+He, two-electron capture cross sections, comparison of calc. methods 7-15703
 C⁴⁺+He(H₂)(Ar)(Xe), one-step double electron capture 7-50344
 C⁶⁺+He, (quasi)-two-electron collision systems 7-5764
 C⁶⁺+He, electron capture, Coulomb integral eval. 7-15679
 C⁶⁺+He, intermediate energy collisions, electron capture cross sections, AO expansion method calcs. 7-25381
 C₂, a ³ π_u radical, form. and decay in methane pulse discharge 7-23003
 C₂, chem. bonding, kinetic energy anisotropy investig. 7-10396
 C₂ cluster, Swan band emission obs. 7-62558
 C₂, Coulomb and exchange-correlation energies, local density functional calcs. 7-20087
 C₂ in interstellar space, rotational excitation processes 7-24198
 C₂, interstellar, (3,0) Phillips band detect. towards ζ Oph 7-48043
 C₂ ion, low lying quartet states, radiative transition probabilities, CASSCF and MC-CI electronic wavefunctions 7-49946
 C₂ spectra in comets, synthetic Swan band profiles of ¹²C¹²C and ¹²C¹³C 7-60532
 C₂⁺, excited state, prod., ion-mol. reactions, FT mass spectra investig. 7-54087
 C₂+H₂, vibr.-translation energy transfer determ. 7-57160
 C₂⁺+inert gas, high Rydberg fragments, kinetic energy spectra 7-42745
 C₄, struct., energies, single reference CI calcs. 7-19720
 C₅, C₇, C₉, interstellar, possible carriers of diffuse interstellar bands 7-48020
 C₆, cyclic ground state, struct., ab initio calcs. 7-42819
 C₆₀ and similar substances, inert gas trapping, possible occurrence in meteorites 7-50436
 C₆₀, cage-like struct., HMO calcs. 7-15520
 C₆₀ cluster, electronic structure, LMTO calcs. 7-19682
 C₆₀ cluster, spherical, DV-X α electronic struct. 7-10806
 C₆₀, interstellar, effect of internal cavity on UV extinction peak 7-4546
 C₆₀, localised mol. orbitals and electronic struct., PRDDO calcs. 7-49925
 C₆₀, clusters, rovibrational spectral fine struct. 7-50055
 C_n clusters, spheroidal clusters, rehybridisation and π -orbital alignment 7-25695
 C_n icosahedral clusters, struct. anal. and magic numbers 7-31202
 C_n⁺, (n=1 to 110), laser vaporisation prod., TOF mass spectrometric detect. 7-15760
 C_n⁺, mass resolved cluster ions, photofragmentation 7-15789
 C_n⁺, (a=+or-), clusters, mass resolution, photofragmentation and photodetachment spectroscopy 7-15795
 C_n⁺-D₂(O₂) cluster ions, ion+mol. reactions 7-50432
 C⁶⁺He, electron capture, bound and continuum states, impulse approx. 7-50329
 CNO abundances evol. in galaxies 7-40934
 C(D), excited atom reaction dynamics, charactn. by laser induced fluoresc. 7-46836
¹²C/¹³C ratio in solar photosphere, determ. from CO vibr.-rot. bands 7-55598
¹³C laser isotope separation using reactor for IR multiphoton dissociation 7-991
¹³C NMR imaging, phantom expts. 7-54624
¹³C/¹³C ratio in Lake Karewa sediment, India, palaeoclimate characts. determ. 7-4175
¹⁴C, activity meas. in atmosphere, anal. methods 7-54214
¹⁴C activity of atmosphere, response of hydrological systems 7-23253
¹⁴C, concentration meas. in atm. around nuclear power reactors 7-23257
¹⁴C labeled compounds, gasoline as primary solvents in liquid scintillation counting 7-36417
¹⁴C, radiocarbon dating using low energy cyclotron 7-55310
¹⁴C, T corrected, use for mixed groundwaters dating 7-9044
 C_n⁺(a=+or-), abundance distrib., magic numbers, photoionis. mass spectroscopic investig. 7-15759
 Co-C alloy, α -phase struct., influence of C, polymorphic transformation 7-52033
 Cr³⁺ dielectronic recombination, photon/ion coincidence meas. 7-10756
 Cr:C/O films, growth by laser photolysis of carbonyls, C and O incorporation mechanisms 7-58685
 Cu:C, single crystal, ion implantation, damage profile anal. using Auger electron spectroscopy 7-51802
 Fe-Ti-C multilayered films, ion bombard., microstructure, TEM obs. 7-12165
 Fe_{81.5}B_{13.5}Si_{3.5}C₂, amorphous ferromag. alloy, acoustic waves, mag. field induced changes 7-2917
 Fe₇₆Cr₄P₈C₁₂, amorphous alloy, mag. short range order above T_c, paramag. phase 7-45623
 GaAlAs/GaAs:C quantum wells interface struct. and luminesc. efficiency 7-7735
 GaAs:C, impurity content meas., IR absorpt., room temp. meas. 7-22289
 GaAs:C, impurity levels determ. 7-32949
 GaAs:C, LVM absorpt. temp. depend. (*Chinese*) 7-59225
 GaAs:C, low C conc., crystal growth using pyrolytic BN coated graphite 7-59398
 GaAs:C, O, trace determ. by ³He-activation anal. 7-58308

carbon continued

GaAs:C epilayers, low pressure MOCVD growth, impurity incorporation 7-59442
H-C-C relay investig. of unprotonated C atoms 7-35558
Li-rich supergiant stars HR 7008 and HD 174104, CNO abundances 7-4453
LiF:C⁶⁺, ion implanted, impurity defects outside implantation zone 7-7773
MgO:C, single crystals, solute C and C segregation, SIMS study 7-16759
MgO:C, single crystals, solute C and C segregation, SIMS study 7-16761
MgO:C single crystals, solute C and C segregation, SIMS study 7-16760
MgO:H, C single crystals, ion implanted, C and H diffusion behaviour, SIMS studies 7-32714
Mo-C:O films, growth by laser photolysis of carbonyls, C and O incorporation mechanisms 7-58685
Mo/C multilayered structs., high resolution electron microscopy studies 7-63968
Ni-C multilayer monochromator characterization using 200-900 eV synchrotron radiation 7-41558
Ni-C multilayers, X-ray reflectivity and photoelectron yield 7-13321
Ni-Cr-W-Si-Al-C, heat resistant coatings on Ni alloys 7-3498
Pd/C model catalyst supported on TEM grids, in-situ heating and microanalysis expts. 7-23098
ReW-C multilayer mirrors as X-ray filters for slit scan radiography 7-34243
Si, neutron irradiated, EPR study on C₂ symmetry defect 7-27602
Si surface, 100, in situ anal. of H,C,N and O using direct recoil time-of-flight technique 7-54242
Si:B,C,O, O clustering and thermal donor formation kinetics 7-17566
Si:C, carbide form. in Stepanov cryst. growth 7-33544
Si:C, conf., Boston, MA, USA (Dec. 1985) 7-14711
Si:C, Czochralski grown, incorporation and disposition of C 7-32484
Si:C, electron irradiated, photolum. defect spectra, obs. of interstitial C 7-59253
Si:C, impurity concentration determ. by photoluminesc. method 7-46084
Si:C, impurity content determ. IR absorpt.-charged particle activation anal. conversion factor 7-26788
Si:C, neutron irradiated, EPR study on C₂ symmetry defect 7-27602
Si:C, photolum. detection of impurities introduced by dry etching processes 7-27748
Si:C, polycrystalline, electrical and structural properties 7-12106
Si:C,H, amorphous alloy fabrication and characterisation 7-8389
a-Si:C,H, annealing of metastable defects 7-3343
Si:C,N, ion implanted, C surface contamination, AES and XPS studies 7-38312
Si:C,O, heat-treated, photoconductivity relax., α traps 7-52677
Si:C,O, luminescence props. of shallow donor centre 7-17347
Si:C,O, photoluminescence of C-O related complex defects 7-22346
Si:C,O, solubility, segregation, diffusion and precipitation 7-16777
Si:C,O,P, C precipitation after P junction diffusion 7-16779
Si:C,O grown by gas-assisted solidification, impurities determination 7-16586
Si:C,O wafers, C and O contents, Fourier transform IR spectra studies, book contrib. 7-44596
Si:C,O wafers, defect generation, O precipitation effects (*Chinese*) 7-12058
Si:C crystals, Stepanov method growth, defect structs. 7-32421
Si:C(C,P), C diffusion during annealing and P in-diffusion 7-16812
Si:Gd,C profiled single cryst., electronic parameters and SiC inclusions 7-32944
a-Si:H, C superlattice struct., solar cell performance 7-46945
Si:H,C alloy thin films, optical constants determ., device modelling appl. 7-7666
Si:N,O, impurity interactions in optical defects 7-17348
Si:O, C, low temp. precipitation, IR and SANS meas. 7-32666
Si:O, C, precipitation, microstructures, TEM studies 7-32668
Si:O, C, thermal donor form., T<800K 7-27294
Si:O,C, impurity aggregation, SIMS 7-16778
Si:O,C, intrinsic point defects and impurity interactions 7-16611
Si:O,C, O precipitation, thermal donor generation and annihilation effects 7-16773
Si:O,C, yield stress, impurities and O precipitate morphology effects 7-16674
Si:O,C,N, precipitation phenomena, TEM studies 7-16768
n-Si:P,C, electron-irradiated and injection-annealed, vacancies, dislocations and C interstitials 7-51815
TiN-C, hard composite coatings, deposition and props. 7-46623
W:C,O films, growth by laser photolysis of carbonyls, C and O incorporation mechanisms 7-58685
W/C amorphous multilayer X-ray reflectors, layer imperfections effects 7-25936
W/C multilayer films, thermal stability, X-ray diffr. studies 7-27169
W/C multilayer films for X-ray reflectors, thermal stability 7-32871
W/C multilayered structs., high resolution electron microscopy studies 7-63968
W/C multilayers for X-ray optics, anomalous expansion 7-21782
W/C multilayers subject to high radiation flux, X-ray optics changes 7-30135
W-C multilayer structures, X-ray standing wave enhanced scatt. 7-58095
W-C multilayer X-ray dispersing devices, comparison with natural crystals 7-9929
W-C multilayer X-ray mirrors, optical constants of layers 7-20389

carbon compounds

see also organic compounds
7-36512
¹⁴CO⁺, rot.-vibr. anal., UV spectra 7-19821
chemisorption on TiO₂(110) stoichiometric and defective surfaces 7-6983
CN⁻-H₂O, quantum-chem. MO SCF calcs. 7-5597
CO₂, isotopic species, vib. transition consts., IR emission spectra 7-19849
CO₂, phododesorption from Si(100) 7-52290
CO₂, vibr. levels kinetics, rotational states influence 7-31186
(CO₂)⁺ (n=2 to 4), cluster ion decay kinetics, mol. beam spectroscopy 7-13735
CO₂-N₂ laser containing isotopically substituted molecules, active medium props. 7-43055
CO adsorption on Ni(100), X-ray induced secondary electron emission 7-27866

carbon compounds continued

formation of carbamic acid, urea and carbonic acid from CO₂, H₂O and NH₃ 7-8268
HTGR, adsorpt. removal of CO₂ from He coolant 7-30514
laminar and turbulent mixing, vibr. relax. 7-11459
AlCl₃-CO₂, rate coefficient meas., HT FFR kinetics study 7-46793
Ar:Co₂, electronic energy transfer investig. 7-31149
Ar-CO mixtures adsorbed on graphite, ordering and phase separation 7-21651
Ar-CO₂ interface, wetting, model 7-2303
Ar-N₂(CO) molecular beams, shock heated, vibrational relaxation 7-10717
BI₃-COS, vapour phase flash photolysis, electronic absorpt. spectra 7-23041
BI₃-CS₂, vapour phase flash photolysis, electronic absorpt. spectra 7-23041
CBe₂ struct., stability and bonding 7-10392
C₂Be₂ struct., stability and bonding 7-10392
CF radical, far IR laser mag. reson. spectrum 7-50202
CF⁺, near-equilib. pot. and electric dipole moment calc. by SCEP-CEPA method 7-25368
CF₃ chemisorption on GaAs(001), electronic struct., RHEED, photoelectron spectra, HF SCF calcs. 7-53497
CH⁺, orbital energies, multipole moments and electric field gradients, HF calcs. 7-62270
CHe⁺, mass spectrometric obs. 7-49956
C₂He⁺, mass spectrometric obs. 7-49956
CN, A²Π v=0 rot. levels, laser excited, B-X emission 7-25584
CN adsorbed on PD(111) and (100), hydrogenation 7-6985
CN chemisorbed on Cu(100), field induced vibr. freq. shifts 7-45991
CN, collisional interelectronic and intraelectronic energy transfer involving rot. levels 7-36729
CN, electron affinities evaluation 7-5591
CN, generation by photolysis of NCNO, removal by H₂, HCl and HBr, fluoresc. 7-46812
CN in metal rich globular clusters, characts. 7-14614
CN in solar spectra, facula models 7-24112
CN, in solar spectrum, identifications of weak CN lines in 413.9 to 421.5 nm region 7-4412
CN, in solar spectrum, oscillator strengths and dissociation energies 7-4327
CN jets in Periodic Comet Halley (1982i), imaging obs. 7-47788
CN radical, anal. of perturbation between B²Σ⁺ v=5 and A²Π_i v=17 levels 7-50067
CN⁺, electron affinity calc. with fourth order many body perturbation theory 7-42471
CN⁺, oxidation at Pt electrode, polarisation modulation IRRAS 7-17836
CN-strong stars, origin due to binary coalescence 7-66601
CN+Ar, rot. levels, collisional energy transfer, state-resolved study 7-10713
C₂N₂ adsorbed on Pt(111), reaction with coadsorbed H₂ 7-54186
C₂N₂-Ar gaseous mixture, collision-induced absorpt., quadrupole moments, IR and microwave spectra 7-50098
CN(B²Σ⁺) form. from HCN, in discharged He flow 7-25476
CNH₂⁺, laboratory generation, mass spectra 7-46811
CO + OH, reaction kinetics at atmospheric conditions 7-40529
CO + vinylidene radical, collisional quenching, rate consts., time resolved spectra 7-31104
CO 2.3 μm band synthesis in supergiant stars, appl. to band strengths interpretation in Magellanic Cloud stars 7-66577
CO, 4.7 μm band, vibr. temp. determ., registration region 7-10550
CO, 4.7 μm band absorpt. of sunlight in Venus and Mars atmospheres 7-4358
CO, 5σ photoionis., reson. effects calcs. 7-36705
CO, A¹Π-X¹Σ⁺ system, UV obs. 7-62396
CO adsorbed on Pt₃Ti(111), surface core level shifts 7-22448
CO abundance in P/Comet Halley (1982i), rocket-borne UV spectroscopy 7-47784
CO, adsorbate on a-Si₃C_{1-x}H films, influence on conductance 7-33115
CO, adsorbed, integral absorpt. coeff., IR vibr. spectroscopy 7-53323
CO adsorbed monolayers on Ru(100), surface spectroscopy 7-15931
CO adsorbed on Ag film, surface enhanced Raman scattering study 7-3037
CO adsorbed on Fe(100), UPS characterisation of a and b adsorption states 7-27126
CO adsorbed on Fe(100), tilted dissociation precursor 7-58642
CO adsorbed on graphite, pinwheel and herringbone structs. 7-7015
CO, adsorbed on highly dispersed Pd and Pt, vibr. spectra 7-12475
CO adsorbed on Ni(111), molecular orbital anal. of precursor state, activation barrier for chemisorption 7-21654
CO, adsorbed on Ni, Raman spectra 7-17324
CO, adsorbed on Ni(001), 7-52235
CO adsorbed on Ni(110), bremsstrahlung isochromat spectroscopy 7-27379
CO adsorbed on Ni clusters, surface electronic and mag. struct. 7-21969
CO adsorbed on Pt, vibr. spectrum, electrochemical pot., stark tuning rate 7-10570
CO adsorbed on Pt(111), vibr., site conversion, IR spectra 7-58613
CO adsorbed on Pt(111), LEED structural anal. 7-2376
CO, adsorbed on Pt(111), He thermal beam scattering 7-53475
CO, adsorbed on Pt(111), molecule-substrate vibr. mode, IR emission spectra study 7-57126
CO adsorbed on stepped Pt surfaces, coupled harmonic oscillator models 7-52230
CO adsorbed on W(100), electron-stimulated desorption, metastable particle production 7-21628
CO, adsorpt. on KCl film, IR investig. 7-63945
CO, adsorpt. on Ni(100), diffusion, investig. 7-6960
CO, adsorpt. on stainless steel, kinetics and laser-stimulated surface oxidation 7-63958
CO adsorption and desorption on Pt(111) 7-21643
CO, adsorption and oxidation on clean and oxidised Au(110), surface reactions 7-59782
CO, adsorption on Al(100), EELS and thermal desorpt. 7-17815
CO, adsorption on amorphous Ni₃B, surface electronic struct. 7-7308
CO adsorption on Cu(111)-Fe cryst. 7-21616
CO adsorption on ethylidyne covered Pd/Al₂O₃ surfaces, IR spectra studies 7-2371
CO, adsorption on K covered Co foil, XPS and AES studies 7-8296
CO adsorption on K-doped Cu(110) surface, EELS study 7-7006

carbon compounds continued

- CO, adsorption on Mo (100), surface atom oxidation states, ESCA meas. 7-28333
 CO, adsorption on Ni (100), poisoning in heterogeneous catalysis, role of electronegativity 7-13818
 CO, adsorption on Ni (111), well defined gas-solid interphase, statistical rate theory approach 7-21655
 CO adsorption on Ni covered Cu (111) 7-21658
 CO, adsorption on NiO (100), surface reactions 7-23055
 CO adsorption on Pt-S, effect of S-induced surface reconstruction 7-6987
 CO adsorption on Pt/TiO₂, thermally treated model catalysts 7-54184
 CO adsorption on Pt-Rh, temp. depend. and work function studies 7-33960
 CO adsorption on small PD crystallites, stoichiometry, effect of particle size 7-6984
 CO, adsorption on ZnO-supported Cu particles, vibr. spectra, operation of metal surface selection rule 7-53350
 CO adsorption/desorption on Ni (111), EELS 7-6971
 CO, adsorption-desorption on polycryst. Ni kinetics 7-16873
 CO and K coadsorbed on Ni (111), adsorbates electrostatic interaction, IR reflection-absorption spectra, TPD, LEED obs. 7-32824
 CO, and mixtures, line interaction effects in IR absorpt. spectra 7-31038
 CO, approximate coupled cluster doubles approx. 7-25348
 CO, Ar matrix isolated, librovibr. spectra, indirect dephasing model 7-15582
 CO, atmospheric remote sensing, gas filter radiometer method 7-18317
 CO, B and C $^2\Sigma^+$ states, radiative lifetimes 7-62451
 CO, B $^2\Sigma^+$ state, electronic autoionis., cross section calc. 7-15656
 CO, b $^2\Sigma^+$ -a $^1\Pi$, system, Kaplan bands, UV obs. 7-62395
 CO band heads emission in premain sequence stars 7-66584
 CO, band intensities, IR absorpt. 7-36619
 CO, C and D states, mol. dissoc. mechanisms, photoelectron-ion coincidence spectra 7-15664
 CO catalytic oxidation on Pt (110), kinetic oscillations 7-28346
 CO, chem. shifts meas. in zero-pressure limit 7-62408
 CO, chemisorbed, bonding, comment and reply 7-12472
 CO, chemisorbed, ionisation phenomena, ab initio wave functions 7-36444
 CO chemisorbed on Cr (110), electron stimulated desorption 7-63965
 CO chemisorbed on Cu (100), field induced vibr. freq. shifts 7-45991
 CO chemisorbed on metals, affinity levels, energy and composition 7-59780
 CO, chemisorbed on Ni (111), mol. orientation, effect of adsorbed K, ESDIAD study 7-32825
 CO chemisorbed on Ni (110), mag. props. investigated by spin-polarised electron beams 7-58994
 CO, chemisorbed on Pt (111), adsorbate vibr. modes, inelastic He atom scatt. obs. 7-32782
 CO, chemisorption bond energies on chemically modified Mo (100) surface 7-23056
 CO, chemisorption on Al, interaction with surface, cluster approx., total energy calcs. 7-52265
 CO chemisorption on clean and partly oxidised Pt₃Ti 7-27131
 CO chemisorption on Li, molecule-cluster interaction ab initio SCF-CI calcs. 7-45013
 CO, chemisorption on Ni (001) and Fe (110), bonding, pseudofunctional electron muffin-tin approach 7-2348
 CO, chemisorption on Ni (100), cluster model calcs. 7-23058
 CO chemisorption on Ni (100), precursors and trapping 7-58643
 CO chemisorption on Pd (111) and Ru (001), inverse photoemission spectra 7-21638
 CO, chemisorption on W (100), free carrier surface scatt., IR obs. of adsorbate induced changes 7-22268
 CO coadsorbed with K on Pt (111), inverse photoemission 7-52726
 CO, coadsorpt. with H₂ on Rh (100) surface, adsorbate-adsorbate interactions effects 7-44997
 CO, coadsorpt. with O and NO on Rh (111), EELS 7-16860
 CO coadsorption with H₂ on Ni (100) 7-27117
 CO, coadsorption with K on Ru (001), angle resolved Auger lineshapes 7-2372
 CO, coadsorption with K on Pt (111), structural and vibrational studies 7-52266
 CO coadsorption with NH₃ on Ni (111), multilayer formation studied by metastable quenching spectroscopy 7-21639
 CO coadsorption with O on Pd (111), SIMS and TPD studies 7-27137
 CO, coherent anti-Stokes Raman spectra calcs. 7-50145
 CO components of flue gas, continuous emission monitoring and meas. procedures (German) 7-28436
 CO, desorption from Ni (111) during laser bombardment 7-58628
 CO detection in environment with submm heterodyne spectrometer 7-60562
 CO dil. soln. in liq. Ar, linear biased correlated walk, general soln. 7-61237
 CO, dissociative electron attachment, ang. distrib. of O $^-$ 7-25674
 CO, dissociative single and double photoionisation, photoion spectra anal. 7-19984
 CO electroionisation lasers, injection of laser mixture in liquid phase 7-10921
 CO, electron impact, fragment ion kinetic energy determ. 7-25673
 CO electron impact ionisation efficiency curves, reson. struct. 7-5774
 CO, electron mobility to diffusion coeff. ratio meas. 7-20840
 CO electronically stimulated adsorbate rotation and desorpt. studies 7-45006
 CO, electrostatic autoionis., review 7-951
 CO emission from evolved stars 7-47951
 CO emission from Perseus dark clouds 7-14623
 CO, free and adsorbed mol., valence wavefunctions, deexcitation electron spectroscopy 7-36756
 CO gas, K-shell EXAFS studied by EELS 7-62403
 CO gas, thermalised free positron annihilation rate studies 7-50390
 CO gas dynamic lasers using microwave excitation, design and operation (German) 7-36986
 CO gas phase molecules, O K-edge absorption spectra 7-62405
 CO, ground state, vibr.-rot. matrix elements 7-912
 CO, IR active gas at high press., absorpt. props. 7-10578
 CO IR atmospheric transmittance, band model 7-40563
 CO, IR transitions, vibr.-rot. matrix elements 7-50131
 CO in Arp 220, molecular gas, mm interferometry of galaxy nucleus 7-55815

carbon compounds continued

- CO in atm. over United States E and Gulf coasts, conc. and sources 7-55197
 CO in atmosphere, tracer horizontal spectra in global stratosphere and troposphere 7-29164
 CO, in atmosphere of Kislovodsk, USSR (Russian) 7-54388
 CO in combustion flows, two-photon digital imaging using planar laser-induced fluorescence 7-46896
 CO in interacting and isolated galaxies, star formation efficiency rel. to molecular content 7-55812
 CO in interstellar cold clouds, radio-line profiles anal. 7-4544
 CO in LDN 1551-IRS 5 and B 335, EHF obs. 7-47893
 CO in Seyfert galaxies, spatial distrib. and central source 7-55808
 CO in streets of Thessaloniki, Greece, prediction models based on meas. 7-59897
 CO in troposphere, November 1981, concentration observations 7-29154
 CO in troposphere of Saudi Arabia, India, Arabian Sea, conc. obs. 7-18291
 CO in Virgo Cluster spiral galaxies 7-55800
 CO, insertion reactions, electron correl. effects, MP2 and CAS SCF calcs. 7-65289
 CO, isotopic species, B $^1\Sigma^+$ -X $^1\Sigma^+$ transition, vacuum UV obs. 7-62401
 CO laser amplifier, electroionisation, saturated amplification mode 7-5876
 CO laser discharges, electron-beam-controlled, maximum input energy and field intensity 7-44285
 CO lasers, condensed and compressed, review 7-36952
 CO lasers, electroionisation radiation, spectral brightness increase 7-5875
 CO mapping of M17 molecular cloud, vel. struct. anal. 7-60745
 CO mapping of mol. complex (in M31) 7-66734
 CO mapping of NGC 7023 outflow source 7-60772
 CO, methane and OH concentrations in AD 1980 to 2035 period, model 7-29153
 CO molecules, jet cooled IR laser spectroscopy 7-41495
 CO, monolayer, physisorbed on Cu, laser-induced thermal desorption 7-17817
 CO monolayer on Si (111), electronic props., pseudofunction method calcs. 7-2659
 CO, obs. of optical H II regions 7-40887
 CO obs. of Per A and Vir A 7-60774
 CO observations of galactic centre neutral disk 7-35040
 CO observations of late type giants and supergiants 7-60649
 CO oxidation on Pt(100), kinetic oscillations, computer simulations 7-23061
 CO oxidation over shock-compressed ZnO powder catalysts 7-39919
 CO, personal exposure monitor with automatic data-logging 7-3943
 CO, perturbed triplet states, lifetime meas. of rot.-vibr. levels 7-19951
 CO photodesorption from Si (100) 7-52290
 CO photoelectron spectra, CIs satellites, near threshold meas. 7-10668
 CO photofragment, rot. state distrib., fluoresc. study 7-23039
 CO, photoionisation cross sections, ground state inversion pot./diff. theory 7-946
 CO, potential energy curves, numerical basis function calcs. 7-25438
 CO, RF molecular plasma, electron energy distrib. functions 7-37636
 CO, Raman intensity of adsorbate vibr., cluster-model calc. 7-27089
 CO, reaction with different Cu surfaces with adsorbed O 7-59784
 CO reactions on Ru surfaces, Ru(CO) $_x$ $^{n+1}$ formation, field desorption study 7-54183
 CO removal from flue gases in heat and power generation from coal (German) 7-65653
 CO, rovibr. lines, IR spectral linewidth collisional broadening 7-36621
 CO, selected rovibronic triplet levels, radiative lifetimes, fluoresc. 7-42686
 CO, selection rule in two-photon absorption spectra 7-10693
 CO, short range interactions 7-19999
 CO, soft X-ray induced fragmentation, Auger electron-ion coincidence study 7-36700
 CO solid films, Fourier transform IR spectra 7-59214
 CO submm mapping of M17SW mol. cloud 7-60748
 CO, submm spectroscopy 7-31041
 CO, submm transitions for astronomy 7-47698
 CO temp. programmed desorpt. on powder and exfoliated MoS₂, adsorpt. sites study 7-2385
 CO, terminally bonded on Ru (001), vibr. dephasing 7-17318
 CO towards quasar PHL 61, EHF obs. (Russian) 7-40957
 CO, vibr. energy exchange rates, IR and UV emission 7-966
 CO, vibr. excitation reaction study in CO-He mixture 7-57162
 CO visible multiline laser, lifetime improvement 7-50582
 CO, weakly ionised collision-dominated RF plasmas, electron kinetics 7-20856
 CO, X-ray emission spectra, ab initio MO HF calcs. 7-36642
 CO $^+$ + CO + M, where M = CO, Ne and He, association reactions, third-order kinetics, temp. depend. 7-46817
 CO $^+$, comet tail bands, charge transfer, spectroscopy 7-15702
 CO $^+$, search for MM-wave transitions in Periodic Comet Halley (1982i) 7-24081
 $^{12}\text{C}^{18}\text{O}$, E $^1\Pi$ -A $^1\Pi$ and B $^1\Sigma^+$ -A $^1\Pi$ transitions, emission spectra 7-50095
 CO-air mixture flame front propag. convective vertex form. 7-13777
 CO-Ar system phase diagram, critical point determ., X-ray diff. study (Russian) 7-6776
 CO-induced struct. changes in Al₂O₃ supported Rh, IR study, H₂ effect 7-23063
 CO-N₂O mixtures, adsorption on ZnO-supported Cu particles, vibr. spectra, operation of metal surface selection rule 7-53350
 CO-Xe(NH₃) mixtures, photoionis. discharge, energy characts. 7-21027
 CO+Ar $^+$, charge exchange cross-sections meas. 7-62519
 CO+Cs $^-$, low-energy collisions, absolute total cross section meas., curve-crossing model anal. 7-36749
 CO+H. rot. distrib. from reson. and direct scatt., coupled channel scatt. calcs. 7-46826
 CO+H. scatt., rot. distrib. and collision lifetimes calcs. 7-25638
 CO+H. vibr. excitation, pot. function, classical trajectory study 7-17783
 CO+H₂O, line broadening meas. 7-50330
 CO+He, vibr. relax., coupled states calcs. 7-50317
 CO+He $^+$, metastable state, collisional quenching cross section 7-62315
 CO+N₂, nonequib. vibr. kinetics, IR spectra 7-57158
 CO+N₂, vibr. excitation, operator algebra study 7-20018
 CO+N₂, vibr. transition probabilities, semiclassical algebraic description 7-25636
 CO+N₂, nonequib. vibr. kinetics study 7-57157

carbon compounds continued

- CO+N₂+Ar, submonolayer mixtures physisorbed on graphite, LEED study 7-2364
- CO+N₂(O₂)(air), J=1-0 rot. transition, press. broadening 7-5722
- CO+Na⁺, dissoci., rot. rainbow effect, time-of-flight spectra 7-54117
- CO+O, recomb. chemiluminesc. spectrum calc. 7-46807
- CO+O, surface catalysed reaction, surprisal anal. 7-3601
- CO+O→CO₂ in dense interstellar mol. clouds, role of grain surface reactions 7-24179
- CO⁺+H, ion reaction at interstellar cloud conditions 7-23008
- CO₂, ¹⁴C activity of atmosphere, response of hydrological systems 7-23253
- CO₂, ¹⁴C seasonal variations in atmosphere caused by bomb tests 7-23256
- CO₂, 4.3 μm band, low resolution IR gas transmissivities 7-51386
- CO₂, 4.3 μm band, vibr. temp. determ., registration region 7-10550
- CO₂, 4.3 μm band absorpt. of sunlight in Venus and Mars atmospheres 7-4358
- CO₂, 4.3 μm band microwindows, temp. and freq. depend., line coupling 7-36580
- CO₂ (10⁰)_I-(10⁰)_{II} transition, line strengths and self-broadening parameters 7-10672
- CO₂, adsorbate on a-Si₃C_{1-x}H films, influence on conductance 7-33115
- CO₂ adsorption and dissociation on Fe (111), ARUPS 7-63961
- CO₂ adsorption and reaction, and coadsorption with ²O, on Ni (110) 7-52289
- CO₂, adsorption on Fe (110), (111) and stepped (110) surfaces, UPS, work function meas. 7-12484
- CO₂, air pollution, total production due to wood fuel burning 7-54386
- CO₂ air pollution on global scale, rel. to global fossil fuel consumption scenarios 7-40071
- CO₂, air-sea exchange in coastal areas 7-55083
- CO₂, amorphous solid, mol. vibr., IR spectra anal. 7-53307
- CO₂ amplifier with mirror utilizing degenerate four-wave interaction 7-25837
- CO₂, and mixtures, line interaction effects in IR absorpt. spectra 7-31038
- CO₂, angle-resolved photoelectron spectra excited with focussed polarised reson. radiation 7-50244
- CO₂ annular gain laser, multiple pass unstable resonator 7-36991
- CO₂ atmosphere conc. in Cenozoic, effect on climate 7-34666
- CO₂, atmospheric increase, response of ocean-atmosphere system (*Russian*) 7-23834
- CO₂, autoionisation and isotope effect in threshold UPS 7-19948
- CO₂, CW laser, unsaturated gain coeffs., saturation intensity (*Korean*) 7-25797
- CO₂ CW lasers, DC discharge in pin plate electrode configuration with auxiliary electrode 7-51526
- CO₂ charged walls, condensation of HCl, Stockmayer model calcs. 7-63784
- CO₂, chemisorpt. on η-Al₂O₃, thermal desorpt. spectrosc. obs. 7-16872
- CO₂ climate sensitivity and model dependence of results 7-66298
- CO₂ closed shell configs. SINDO method calcs. 7-19705
- CO₂ coadsorption with ethylene on (001) surface 7-32789
- CO₂ compact wide-aperture single-mode TE laser with low chirp rate 7-50580
- CO₂ conc. profiles of axisymmetric combustion gas flow, IR spectra, temp. profile meas. 7-3591
- CO₂ concentration in lower troposphere, simultaneous meas. at neighbouring mountain stations 7-55199
- CO₂ continuous-flow laser with unstable resonator, acoustic vibrs. 7-25796
- CO₂ degassing problem in soil water extractors 7-23916
- CO₂ desorption from Ni (111) during laser bombardment 7-58628
- CO₂ emission reduction from fossil fuels in future energy planning (*French*) 7-40053
- CO₂, exchange rate between atmos. and ocean, isotopic meas. techniques 7-23884
- CO₂ excited with polarised reson. radiation, angle resolved photoelectron spectrum 7-50245
- CO₂ FTIR spectra, band intensities 7-50264
- CO₂ gas, K-shell EXAFS studied by EELS 7-62403
- CO₂ gas, radiation absorpt., generalised ang., coeffs. 7-11257
- CO₂ gas, supercontinuum generation with femtosecond pulses 7-25908
- CO₂ gas dynamic lasers using microwave excitation, design and operation (*German*) 7-36986
- CO₂, gas exchange between air and sea, effect of breaking ocean waves 7-23704
- CO₂ gas laser, double coupled waveguide, RF excitation expt. exam. 7-31361
- CO₂ gas laser, preionisation using α particles study 7-62508
- CO₂ gas mixtures, ν₃ band, rot. relax., IR spectra 7-42613
- CO₂ gas phase molecules, O K-edge absorption spectra 7-62405
- CO₂ high intensity absorpt., mod. rot. effect, lasing transitions 7-62473
- CO₂ high power laser, pumping by self-sustained volume discharge, electron beam initiated 7-57297
- CO₂ high-pressure discharge laser with plasma cathode 7-57298
- CO₂ high-pressure laser, direct optical pumping with pulsed HF pump laser 7-50533
- CO₂ homogeneously broadened ring laser, optical bistability and instabilities due to mode-mode competition 7-62735
- CO₂ hot bands, UV absorpt. spectrum 7-25535
- CO₂ hybrid laser, longitudinal mode selection for subthreshold operation 7-25795
- CO₂, hyperpolarisability dispersion meas. 7-15940
- CO₂, IR absorption spectrum, 2.7 μm and 4.8 μm band intensities 7-50130
- CO₂ ice, absorpt. coeff. and refr. index, laboratory meas. UV to microwave, review 7-3008
- CO₂ in atm. and land biota destructivity 7-34640
- CO₂ in atmosphere, 19th-century vars. in W Europe and British Isles from anal. of contemporary air masses 7-9144
- CO₂ in atmosphere, concs. during preindustrial times (*Russian*) 7-9081
- CO₂ in atmosphere, effect on climate, general circulation model anal. 7-66285
- CO₂ in atmosphere, emission from tropical forest soils 7-40528
- CO₂ in atmosphere, geochemical C cycle disturbance and impact on biosphere 7-40546
- CO₂ in atmosphere, ice core record of ¹³C/¹²C ratio in past two centuries 7-34637

carbon compounds continued

- CO₂ in atmosphere, study of greenhouse effect with CO₂ enhanced biological methanogenesis 7-29152
- CO₂ in middle and upper atmosphere, 15 microns band IR spectra 7-23923
- CO₂ in primordial atmosphere, climatic consequences 7-66271
- CO₂ in situ modelling using FTIR at high press. 7-54221
- CO₂ interface evolution in shock tube, turbulent mixing zone 7-11460
- CO₂, intramode and Fermi relax. influence on multiple-pass short pulse energy extraction 7-57156
- CO₂ laser, 4.3 μm, longitudinal-discharge output parameters 7-43056
- CO₂ laser, active medium vibr. relax., decay rate, phase absorpt. method 7-43058
- CO₂ laser, chaotic attractors in crisis 7-43178
- CO₂ laser, compact axial flow, multikilowatt operation 7-57295
- CO₂ laser, continuous electroionis., output characts. (*Russian*) 7-20182
- CO₂ laser, form. of self-maintained volume discharge using compact electrode system 7-63394
- CO₂ laser, gain-modulated single mode CW laser instabilities and chaos 7-43057
- CO₂ laser, gas transport, cylindrical geometry, high power, development 7-43149
- CO₂ laser, high-power industrial, operation 7-43054
- CO₂ laser, high-power transverse-flow, props. 7-36935
- CO₂ laser, hot-cell-free, at 4.3 μm 7-15891
- CO₂ laser, intracavity optically controlled cryst. modulators 7-10911
- CO₂ laser, line centre stabilised, frequency shift 7-15839
- CO₂ laser, longitudinal, with multisegment hollow cathode discharge 7-1075
- CO₂ laser, modulated, single-mode, dynamic behaviour and dimens. chaos 7-1074
- CO₂ laser, optical bistability, regular- to sequence-band switching 7-5947
- CO₂ laser, optogalvanic Lamb dip freq. stabilisation 7-31301
- CO₂ laser, piezoelectric Q switching 7-50608
- CO₂ laser, pulse generator supply 7-1195
- CO₂ laser, Raman conversion from far-wave mixing in p-H₂ 7-25877
- CO₂ laser, short pulse cold-cathode glow-discharge electron beam pumped 7-43150
- CO₂ laser, single-mode operation, inertial props. effect 7-62660
- CO₂ laser, synchronisable, injection locked, Q-switched, mode-locked, cavity dumped 10 atmosphere 7-62736
- CO₂ laser, TE CW, influence of electrical discharge homogeneity 7-50537
- CO₂ laser, TEA, tunable multiline and single line operation at 10.6 μm and 9.4 μm 7-31300
- CO₂ laser, TEA, with three cavity mirrors, two-line operation 7-5869
- CO₂ laser, TEA, with unstable resonator, influence of external radiation injection 7-36936
- CO₂ laser, transverse flow, elec. discharge parameters 7-20279
- CO₂ laser, ultrashort pulse generation by square-wave mode locking and cavity dumping 7-43177
- CO₂ laser amplifier, multiatmosphere high gain, characts. and gain at 9.294 μm 7-57366
- CO₂ laser array, 2D effective phase locking studies 7-50607
- CO₂ laser beam, kinetic self-focusing in air 7-20299
- CO₂ laser cathode systems, characts 7-15900
- CO₂ laser detection, using CdHgTe detector 7-5915
- CO₂ laser discharges, electron-beam-controlled, maximum input energy and field intensity 7-44285
- CO₂ laser emission freq. continuous tuning band, widening using combined resonators 7-25847
- CO₂ laser gas transport system, compact axial flow 7-57367
- CO₂ laser P(16) transition, temp. variation of linewidth 7-36934
- CO₂ laser pulse duration control by intracavity IR absorbing gas cell 7-43174
- CO₂ laser pulse shaping and passive mode-locking with nonlinear Michelson interferometer 7-15914
- CO₂ laser pump injection into FIR laser resonator using Al₂O₃ waveguide 7-43356
- CO₂ laser pumping source for CH₂F₂ laser, Stark cell stabilisation 7-43134
- CO₂ laser spectrum monitoring and displaying instrument 7-5935
- CO₂ laser TE, tunable using near grazing incidence grating, performance 7-43052
- CO₂ laser welding, nuclear reactor fuel cladding repair (*Japanese*) 7-15243
- CO₂ laser-induced fluoresc. appl. to HCl detection in atm. 7-46993
- CO₂ lasers, CW, tunable, length reduction using Fabry-Perot resonators 7-11010
- CO₂ lasers, condensed and compressed, review 7-36952
- CO₂ lasers, high energy picosecond 10 μm pulses 7-62665
- CO₂ lasers, SiC ceramic optical waveguide (*Japanese*) 7-6001
- CO₂ lasers with high pressure volume discharges, review 7-36953
- CO₂ lasing characts., effect of waveguide statistical surface roughness 7-50536
- CO₂ lidar systems, high speed tuning mechanism 7-36978
- CO₂, linear triatomic molecules, collisions with Ag (111), energy transfer processes 7-22423
- CO₂, liq., neutron radial and partial distrib. fns., Lennard-Jones pot. 7-58126
- CO₂ liq. finite sink for atmospheric heat engine 7-40022
- CO₂, microwave spectrum laboratory meas. of constituent gas opacities, Venus atmosphere 7-47744
- CO₂ mini-TEA lasers, He-free emissions 7-50535
- CO₂ mixtures, gas density effect on Q branch in IR spectra 7-42612
- CO₂, mol. photodissoc. resons. 7-952
- CO₂ molecules colliding with Pt and Ag surfaces, quantum theory of energy exchange 7-64865
- CO₂, ocean-atmosphere gas transfer in tropical Atlantic 7-29076
- CO₂ output, respiratory gas anal. (*Japanese*) 7-28560
- CO₂, photoionisation cross sections, ground state inversion pot./diff. theory 7-946
- CO₂, positron scattering, cross-section meas. 7-20054
- CO₂, powerful stable laser, optical pumping of methanol FIR laser 7-10993
- CO₂, pulse-periodic laser, gas mixture comp. stabilisation by hopcalite 7-25838
- CO₂, pulsed laser, medium repetition rate, materials processing appls. 7-20184
- CO₂, pulsed laser freq. dynamic tuning, multispike lasing using intracavity cell with IR absorbing gas 7-62663

carbon compounds continued

- CO₂ pump laser cavity for compact high-power NH₃ laser 7-5907
 CO₂, reducing build-up in Earth atmosphere 7-65669
 CO₂ rel. to outburst of P/Comet Halley (1982i) 7-47783
 CO₂ removal by membrane lung at low blood flow, performance model 7-8772
 CO₂ round-trip amplifier with wavefront-reversing mirror, energy characts. 7-43053
 CO₂ saturated liq., sp. ht. meas. 7-16783
 CO₂, self-broadened spectral line shape in low-frequency wing 7-57134
 CO₂ single and multilongit. mode laser emissions, SHG in CdGeAs₂ 7-43211
 CO₂, slow neutron interaction near vaporisation crit. point, cross section temp. depend. 7-52021
 CO₂ sorption in uniaxially drawn atactic polystyrene 7-32812
 CO₂ TEA laser, characteristics of confocal unstable resonator (*Korean*) 7-25848
 CO₂ TEA laser, high-power modulation by injection-locked mode-beating 7-62738
 CO₂ TEA laser, self-sustained volume discharge initiation in lasers by radioisotopes 7-50534
 CO₂ TEA laser, single-mode, using self filtering unstable resonator configuration 7-25850
 CO₂ TEA laser, tunable travelling-wave, single mode operation 7-15840
 CO₂ TEA laser emitting in 11 µm region, gain and output parameters 7-1073
 CO₂ TEA lasers, spectral control by injection-seeding 7-25857
 CO₂ temp. programmed desorpt. on powder and exfoliated MoS₂, adsorpt. sites study 7-2385
 CO₂ thin film-coated waveguide lasers, output power characteristics 7-62664
 CO₂ thin-film-coated waveguide laser, RF excited 7-5908
 CO₂ tunable waveguide laser with expanded tuning range 7-36981
 CO₂, turbulent pipe flows, forced convection correl. in near-critical region 7-51093
 CO₂ ultrashort laser pulse optical free induction decay, freq. spectrum 7-31405
 CO₂, vibr., hyperspherical coordinates, semiclassical SCF calcs. 7-5584
 CO₂, vibr. relax. during injection into ionosphere 7-34087
 CO₂ waveguide laser, anomalous refr. indices of amplifying medium 7-36933
 CO₂ waveguide laser, Cohen model 7-20183
 CO₂ waveguide laser, design and performance 7-15906
 CO₂ waveguide laser, tunable, for optical pumping 7-20263
 CO₂ waveguide laser as tunable IR radiation source 7-31298
 CO₂ waveguide lasers, DC and RF-excited, life problems 7-11000
 CO₂ waveguide lasers with RF excitation, emission freq. tuning 7-43147
 CO₂, X-ray emission spectra, ab initio MO HF calcs. 7-36642
 CO₂⁺ abundance in Periodic Comet Giacobini-Zinner (1984e) 7-47793
 CO₂⁺ v₂ band, diode laser absorpt. 7-10580
¹²C¹⁶O₂, vibr. energy levels and parallel band intensities determ. 7-5657
¹³CO₂/¹²CO₂, abundance meas. by nondispersive IR heterodyne ratio-metry 7-15731
 CO₂-He dilute mixtures, liq.-vapour curve, ³He partial contrib. 7-32625
 CO₂-Ar gaseous mixture, collision-induced absorpt., quadrupole moments, IR and microwave spectra 7-50098
 CO₂-Ar interface, wetting transitions, density functional theory and modified hypernetted chain calcs. 7-63913
 CO₂-CS₂-N₂ mixture, calc. of gains for vibrational transitions 7-1087
 CO₂-ethane gaseous mixture, determ. of virial coeffs., ref. index meas. method 7-51362
 CO₂-H₂O, mass transfer coeff., turbulence in open absorpt. channel 7-6189
 CO₂-He-N₂, vibr. nonequib. flow in axisymmetric channel with glow discharge 7-20741
 CO₂-He-N₂ laser glow discharge, influence of magnetic fields on instability growth 7-5868
 CO₂-methane thermochemical energy transport system, closed-loop mode 7-65640
 CO₂-N₂-H₂ gasdynamic laser with 2D nozzles, gain optimisation 7-50541
 CO₂-N₂-H₂O gasdynamic lasers, collisional relaxation mechanisms 7-20181
 CO₂-N₂-He mixtures, self-sustained and nonself-sustained glow discharges 7-44290
 CO₂-n-hexadecane supercritical system, phase equilib. and vapour density meas., high-pres. multiproperty apparatus appl. 7-12249
 CO₂-Ne soln. thermodynamic props. near CO₂ vaporisation crit. point 7-12316
 CO₂-pentane, excess enthalpies at 348.15, 373.15, 413.15, 470.15 and 573.15K 7-44826
 CO₂-Xe(NH₃) mixtures, photoionis. discharge, energy characts. 7-21027
¹⁴CO₂/¹²CO₂ isotope laser 7-31299
 CO₂+amines, in nonaqueous solvents, reaction kinetics 7-46803
 CO₂+Ar⁺, charge exchange cross-sections meas. 7-62519
 CO₂+Cs⁺, low-energy collisions, absolute total cross section meas., curve-crossing model anal. 7-36749
 CO₂+H, Rydberg atom depopulation, scattering cross section, 7-10732
 CO₂+H₂, rot. resolved hot atom collisional excitation by time-resolved diode laser spectra 7-10731
 CO₂+H⁺, charge transfer reaction cross section and pot. energy curve meas. 7-54086
 CO₂+H⁺, rot. energy transfer, pot. energy surface 7-967
 CO₂+He₂⁺, charge transfer reaction rate consts. 7-22983
 CO₂+Na⁺, rot. rainbow effect, time-of-flight spectra 7-54117
 CO₂+NaO, assoc. reactions with third body N₂ or N₂O, kinetics, atm. appl. 7-59748
 (CO₂)₂⁺, photodissoc. dynamics mechanisms and product energy disposal 7-20083
 (CO₂)₂, complexes free jet spectroscopy by coherent Raman methods 7-15003
 (CO₂)_n⁻ clusters, photodissociation 7-1001
 CO₂ laser emitting in 4.2 µm range, construction and props. 7-1186
 (CO₂)_n⁺ cluster ions, recording by secondary electron multiplier 7-42827
 COF₂, electron impact dissociative ionis., cross section estimation 7-20066
 COF₂ in stratosphere, concentration determined by IR solar absorpt. observations 7-9077
 CO, He⁺, vibr. relax., coupled states calcs. 7-50317
 COSe, photodissoc., CARS 7-11062

carbon compounds continued

- ((CO)₂-W-H-W(CO)₃)⁻, struct., H atom dynamics, spectrosc. investig. 7-15613
 CS, ³²S⁺-a^{II} band system, reson. enhanced multiphoton ionis. detect. 7-5663
 CS observations of galactic centre neutral disk 7-35040
 CS, singlet and triplet excitations, selective control, coherent multicolor laser spectroscopy 7-42629
 CS, vibr. excited, mm-wave rot. spectrosc. obs. 7-36595
 CS⁺, upper limits in diffuse interstellar clouds 7-35020
 CS₂, Ar⁺ ion irradi., S₂ sputtered mol. props. 7-936
 CS₂ binary mixtures, free length theory and collision factor theory comparisons 7-44692
 CS₂, dissociative attachment bands, impact electron and fragment ion energy spectra anal. 7-50386
 CS₂, dynamical model for lattice frequencies and cryst. field splittings 7-16699
 CS₂, dynamically compressed liq., UV-visible spectrum, effects of temperature 7-22284
 CS₂, imbibition in PMMA, light scatt. investig. 7-62628
 CS₂, ionisation spectra calc., Green's function method 7-36684
 CS₂, liq., isotopic thermal diffusion meas. 7-44880
 CS₂, liq., reorientation, vibr. relax., Raman spectra 7-62379
 CS₂ liquid, time-resolved IR spectral photography of shock-induced chemistry 7-27727
 CS₂, phase conjugation of laser beams 7-25903
 CS₂, phase conjugation of laser beam 7-25904
 CS₂, photoabsorpt. and photofragmentation meas. 7-62460
 CS₂, photodissoc. dynamics, VUV laser induced fluoresc. 7-23044
 CS₂, photodissociation, using pulsed supersonic nozzle beam source 7-15665
 CS₂, photofragmentation dynamics using coherent VUV for product detect. 7-19976
 CS₂, shocked liquid, absorpt. spectra 7-27743
 CS₂, spectroscopic studies at high press. 7-27742
 CS₂, sputtering by Ar⁺, S₂ rotational, vibrational and translational energy distrib. 7-993
 CS₂, stimulated Brillouin scattering, phase conjugation efficiency, focal length depend. (*Korean*) 7-31400
 CS₂, stimulated Raman measurements, time-resolved 7-15928
 CS₂, time resolved picosecond Raman induced phase conjugation 7-13141
 CS₂, use in nonlinear light guides of nonresonant type (*German*) 7-57609
 CS₂-benzene mixtures in soln., CARS study of vibr. dephasing 7-42624
 CS₂-CO₂-N₂ mixture, calc. of gains for vibrational transitions 7-1087
 CS₂-nitromethane liq. mixture, on glass, wetting 7-6927
 CS₂+F₂, reaction, mol. electronic emission spectrum 7-3577
 CS₂⁺+atom(molecule), (q=2, 3), electron capture 7-5763
 (CSe)_n, polymerised, metallic and supercond. 7-7433
 (CSe)_n, poly(carbon diselenide), metallic conductor, characterisation 7-2595
⁴⁰CO, A=12, 13, adsorbed on Ni (100), surface charactn. by Raman spectroscopy 7-42625
⁴⁰CO, A=12,13, in atm. and astron. environments, detect. with high-resolution submillimetre heterodyne spectrometer 7-353
 Co in atmosphere of Antarctica, concentration in AD 1977 to 1985 period (*Russian*) 7-18276
 Co, physisorbed multilayer, near-threshold electronic excitation, EELS spectra anal. 7-45001
 Co₂, adsorption and oxidation on clean and oxidised Au (110), surface reactions 7-59782
 Co₂, intensity and press. broadening meas. in ν₃ fund. 7-50265
 CO₂-N₂-He laser mixture, beam-driven discharge, gasdynamic processes 7-50538
 CsCl:CN⁻, F_H(CN⁻)-centre absorption bands, pseudopotential method calcs. 7-22292
 DF-CO₂ pulsed laser performance, gas mixture composition depend. 7-62682
 H-CO₂ binary mixtures, H fugacity coeff. meas., physical equilib. technique 7-16296
 H₂-CO₂ binary mixtures, H component fugacities, press. depend. 7-51367
 K⁺-CO₂ system, pot. energy surfaces calc. 7-57015
 KBr:CN⁻, persistent IR hole burning in vibr. spectrum 7-37057
 KTA_{1-x}Nb_xO₃:CO₂²⁻, impurity detection, IR transmission and Raman scatt. studies 7-13164
 Li-CO₂ complex, pot. energy surface, covalent ionic nature 7-30967
 N₂-CO₂, vibr. relax. in N₂ post discharge 7-20023
 N₂O-CO-Ar, superequilibrium pumping, Ar dilution effects 7-25611
 N₂O-CO-H₂-Ar, superequilibrium pumping, Ar dilution effects 7-25611
 Na⁺-CO₂ system, pot. energy surfaces calc. 7-57015
 NaBr:CN⁻, IR vibrational fluoresc. obs. 7-27775
 NaCl:CO₂²⁻ cryst. surface, localised intramol. vibrations, IR transmission spectra study 7-2132
 NaI:TiOH⁻, NO₃⁻, CO₂²⁻ crystals, scintillation props., vibrational spectra, anion impurity effects (*Russian*) 7-22348
 OCS, jet-cooled, ¹²S⁺-a^{II} transition, spectrosc.-investig. 7-62400
 OCS, line strengths and collisional half-widths, IR spectra 7-36620
 OCS, photodissoc. dynamics, VUV laser induced fluoresc. 7-23044
 OCS, reson. IR radiation interaction, 1 doubling, microwave spectrum 7-42604
 OCS, rot.-vibr. anal., electronic ground state, MW, IR and Raman spectra 7-19820
 OCS, rot.-vibr. anal., dipole moments, Stark spectra. 7-19910
 OCS, triple photoionisation and photodissociation, mass spectrometer and coincidence studies 7-19965
 OCS, vibr. excitation, non-Condon anal. 7-50062
 OCS+Ar semiclassical press. broadening calcs. 7-965
 OD-CO₂ chemical laser, energy capabilities study 7-62683
 Sc-CO, mol. bonding, pseudopot., and singles-and-doubles CI calcs. 7-10440

carbon fibre reinforced composites

- see also carbon fibre reinforced plastics
 automatic ultrasonic materials testing system, US-1000 for C-fibre composite aircraft components 7-22965
 conversion of acrylonitrile based precursor, review 7-59475
 conversion of acrylonitrile precursors 7-59476
 graphite fibre reinforced Al, fatigue crack propag., effect of aq. environments 7-17624

carbon fibre reinforced composites continued

- graphite fibre reinforced Al matrix composites, interface charactn., TEM obs. 7-44554
 graphite fibre reinforced Al or Mg, corrosion protection to NaCl soln. exposure 7-3488
 graphite fibre reinforced Al-Mg-Fe, unidirectional and angle-ply, strength and fracture anal. 7-59605
 graphite fibre reinforced borosilicate glass matrix composites, thermal expansion, laminate theory anal. 7-52087
 graphite fibre reinforced epoxy, fluid-coupled, anomalous US dispersion 7-1296
 graphite fibre reinforced epoxy composite, characterisation by diffuse reflectance Fourier transform IR 7-53332
 graphite fibre reinforced glass sandwich reflectors for far-IR astronomy, thermal stability 7-37093
 graphite fibre reinforced metal matrix composites, liq. metal infiltration prep., wetting 7-46372
 graphite fibre reinforced Mg matrix composites, fabrication, fibre coatings, wetting, adhesion 7-46374
 induced EM fields, 2D model prediction 7-25703
 panels, cylindrical, instability, effect of centrally located midplane delamination 7-63022
 polyetheretherketone, crystalline/amorphous ratio in carbon fibre composite 7-11947
 relaxation property anisotropy 7-46534
 Resiform RTF biocompatible material for implanted prostheses (*German*) 7-60121
 strength and structure in carbons and graphite, conf., Liverpool, England (Sept. 1985) 7-24257
 surface analysis using XPS and electrochemistry 7-28370
 Al matrix, segregation of doping elements, Si, Bi 7-65046
 Al-Cu(Mg) matrix, tensile strength, fracture, interfacial bond strength 7-33744
 Al-Zn-Mg alloy matrix, linear thermal expansion coeff., 25 to 400°C 7-52093
 C matrix, 3D, residual stress 7-52090
 C matrix, multidirectional composites, macroporosity and interface cracks 7-46513
 C matrix, oxidation inhibition by B_2O_3 7-8139
 C matrix, oxidation protection by carbide incorporation 7-46671

carbon fibre reinforced plastics

- binder content in impregnated reinforcement, contactless US inspection use 7-3565
 cemented lap joint, stress-strain state and strength 7-33794
 cylindrical interface crack study 7-26201
 damage states, US and acoustic emission study (*German*) 7-22828
 designing with plastics and advanced plastic composites, book 7-4642
 epoxy laminates, cross-ply cracking 7-39617
 epoxy matrix, average stress-strain curves 7-33733
 epoxy matrix, Ba labelled, XPS anal. 7-28163
 epoxy matrix, electrodeposition of polymer interphase 7-13592
 epoxy matrix, failure in static and fatigue loading 7-17632
 epoxy matrix, laminates, quasi-isotropic, response to biaxial stress 7-33732
 epoxy matrix, matrix splitting, K_I - K_{II} interaction (*German*) 7-22829
 epoxy matrix, polymer-coated C fibres 7-22632
 epoxy matrix with internal stresses under control 7-3383
 epoxy resin matrix, fractography 7-8080
 epoxy resin matrix, laminates 7-39474
 epoxy resin matrix, thin laminated plate bending 7-57708
 epoxy-amine matrices, improvement of phys. and mech. props. 7-39574
 GIOTTO spacecraft high gain antenna mechanical design and development 7-23974
 glass/C hybrid fibre reinforced epoxy, tensile, compressive, flexural and shear props., review 7-39532
 graphite fiber reinforced epoxy, delamination fracture toughness 7-53900
 graphite fibre reinforced epoxy, cross-ply plates, micromech. initial failure anal. 7-62975
 graphite fibre reinforced epoxy, energy absorpt. capability, effect of specimen geometry 7-3315
 graphite fibre reinforced epoxy, interface modified, moisture effects 7-3476
 graphite fibre reinforced epoxy, interlaminar fracture toughness, effects of rad. 7-33773
 graphite fibre reinforced epoxy, NDT by OTDR in embedded optical fibres 7-28255
 graphite fibre reinforced epoxy, reflectance and thermal response during high-power CO_2 laser irradi. 7-32496
 graphite fibre reinforced epoxy, strain energy release rate of edge delamination 7-1508
 graphite fibre reinforced epoxy, subjected to cyclic thermal loading, damage-induced prop. changes 7-46600
 graphite fibre reinforced epoxy, thermal and thermomech. response 7-8150
 graphite fibre reinforced epoxy, thermomech. behaviour, space rad. effects 7-51828
 graphite fibre reinforced epoxy and polyamide matrix composites, thermal expansion, laminate theory anal. 7-52087
 graphite fibre reinforced epoxy column, Euler load determ. by direct computation 7-62976
 graphite fibre reinforced epoxy composites, crack growth under biaxial loading 7-33762
 graphite fibre reinforced epoxy laminate, dynamic moire interferometry of stress wave propag. 7-59717
 graphite fibre reinforced epoxy laminates, dynamic response at high shear strain rates 7-3371
 graphite fibre reinforced epoxy laminates, fatigue damage mechanisms and residual props. 7-44671
 graphite fibre reinforced epoxy laminates, holographic interferometry analysis of bending rigidity loss 7-59733
 graphite fibre reinforced epoxy laminates, holographic investigation of stressing techniques for detecting flaws 7-59732
 graphite fibre reinforced epoxy laminates static or fatigue loading, fracture surface anal. (*German*) 7-22826
 graphite fibre reinforced epoxy resin composites, multidimensionally braided, tensile, compressive and flexural props. 7-33726
 graphite fibre reinforced PEEK, quasi-isotropic laminate, shear strain meas. by moire interferometry 7-65253
 graphite fibre reinforced plastics, energy absorpt., effect of fibre and matrix max. strain 7-3314

carbon fibre reinforced plastics continued

- graphite fibre reinforced polyethersulphone, laminates, temp.-dependent behaviour of matrix 7-17620
 graphite fibre reinforced polyimide, laminates, temp-dependent mech. behaviour of matrix 7-17620
 hardness anisotropy 7-8081
 hybrid composite, sunhemp-C fibre reinforced polyester, tensile strength and fracture 7-13522
 laminate; impeding edge-delamination development effect on tension-tension loading (*German*) 7-22827
 laminates, ply failure under moisture and temp. influences (*German*) 7-22744
 mirrors for IR astronomy 7-57519
 NDT, optothermal method, degree of cure 7-59728
 nonhomogeneous anisotropic elastic body, under axially symm. torsion, cylindrical interface crack 7-26841
 PEEK matrix, potential as bioimplants 7-60126
 PEEK/carbonaceous fibre composite, wide-angle X-ray scatt. 7-21131
 polyester matrix hybrid laminates, impact and perforation props. (*Japanese*) 7-13569
 polyetheretherketone matrix, penetrant durability rel. to processing and struct. 7-65168
 polymer matrix cracks, lightweight construction appl. (*German*) 7-22825
 post-buckling behaviour under compression and shear (*German*) 7-20615
 sandwich panels for far-IR telescope mirrors, thermal stability tests 7-40705
 steel/composite, double-lap joints, stress anal. and failure props. 7-33769
 strength, thermomech. props. thermal spiking and moisture absorpt. effect 7-28085
 stress transfer in single fibre-resin tensile tests 7-28074
 thermal fatigue, flexure strength (*Japanese*) 7-13568
 thermally conductive polymer compositions 7-2284
 thermoplastic laminates, unidirectional, compressive strength 7-39580
 thin plate two-dimensional diffusivity tensor meas. by thermal pattern analysis 7-2285
 unidirectional, fracture strength, role of matrix resin 7-53845
 US wave attenuation for monitoring quality 7-8240
 Young's modulus, effect of heating and environment 7-33720
 C/glass fibre reinforced hybrid composites, aligned short fibres, SCC prop. 7-13615

carbon fibres

- see also carbon fibre reinforced composites; carbon fibre reinforced plastics
 Celion, elec. resist., temp. depend. 7-65073
 Celion, mechanical and fracture behaviour 7-22786
 continuous filament, strength and modulus eval. methods 7-28061
 conversion of acrylonitrile based precursor, review 7-59475
 conversion of acrylonitrile precursors 7-59476
 field emission cathodes, effect of forming on structure 7-39365
 graphite, benzene-derived, exfoliation and characters. 7-46663
 graphite, intercalated fibre elec. conductors, passivating coatings 7-8140
 high electrical conductivity C fibres, intercalation treatment (*French*) 7-59646
 melt spun, non-circular, elastic modulus, tensile strength 7-7908
 microvoid charactn., SAXS obs. 7-26739
 polymer coated, charactn. and pot. for composite appl. 7-22632
 pretorsional deform., annealing, acid treatment, struct., mech. props 7-22768
 production, from polyacrylonitrile fibre, XPS obs. 7-32541
 strength and structure in carbons and graphite, conf., Liverpool, England (Sept. 1985) 7-24257
 tensile strength distrib., statistical model, electrodeposited coating effect 7-39585
 B modified, effect on mech. props. 7-17570
 C_xSO_3F fibre intercalation cpds., enhanced elec. cond. 7-33927

carbon microphones see microphones**carbon steel**

- α -martensite, electrolytically-separated, diff. study of struct. (*Russian*) 7-51702
 abrasive wear mechanism, wear process successive obs. in SEM 7-8229
 arc welds, as-deposited strength, toughness, microstruct. 7-13555
 austenite nuclei growth (*Russian*) 7-59515
 austenite range, hot deform. resist., math. model (*Japanese*) 7-17558
 bar, collision with Pb bar, contact duration study 7-37393
 bimetal of C steel-cast Fe-Cr, interface bonding strength (*Korean*) 7-17618
 bimetallic plate, cold-clad corrosion-resistant, diffusion processes in pre-boundary zone 7-46708
 boriding effect on thermo-EMF 7-8177
 boronised, boride-substrate interface morphology 7-53984
 boronising with heating by laser radiation 7-8173
 boronizing and alloying elements influence 7-59661
 brass plated steel cords, mech. and cohesion props. in sulphurising environment 7-39740
 brittle fracture micromechanism in specimens containing intergranular cementite (*Russian*) 7-59621
 carburised, microstructural constituent in high C layers 7-54006
 carburising process for dense and porous materials, math. model 7-39745
 casting, thin strip continuous, finite element model and thermal feasibility 7-13403
 CEBG single-phase erosion-corrosion research programme for AGR boilers 7-59679
 cold-rolled, texture and lattice deform. states (*German*) 7-53765
 constructional, original charge purity influence on microstruct., hardenability and mech. props. 7-46521
 corrosion, microbiologically induced 7-46683
 corrosion acceleration in boiling annular crevices, 100°C chloride solns. 7-65219
 corrosion fatigue in aq. environments in Kuwait 7-46711
 corrosion in aq. sour gas environments 7-39713
 corrosion inhibition by molybdate in deaerated and low O_2 water 7-39731
 corrosion inhibitor development 7-17684
 corrosive wear in NaCl soln. 7-8191
 creep, glide plane stresses, yield point, dislocation theory (*Russian*) 7-59580
 damage process, thermometric investig. (*German*) 7-3439
 deformation behaviour, influence of mech. twinning (*German*) 7-17603
 diffusion interaction with cast Fe in forging, explosive treatment and thermal cycling 7-28070

carbon steel continued

- directional solidification, δ/γ transform., P and Mn solute distrib. in dendrites 7-65020
 dislocation structure, rolling temp. effects (*Russian*) 7-44552
 dual-phase, Mn-partitioning, austenite form. 7-39552
 electric spark alloying with $\text{TiB}_2\text{-MoB}$ 7-28205
 electrospark alloying of $\text{TiB}_2\text{-Mo}$ coatings, form. kinetics and high-temp. oxidation 7-65210
 electrospark alloying with carbides, electron nature of interaction, phase comp. 7-8182
 environmental fatigue stress rules appl. to reactor piping 7-13600
 eutectoid, 1.3 wt.% Cr, specimen prep. technique influence on analytical TEM obs. of partitioning 7-22950
 eutectoid, continuous cooling austenite-to-pearlite transform. kinetics, prediction using isothermal data 7-17524
 eutectoid, fully pearlitic, cleavage fracture stress, microstruct. effects 7-28123
 eutectoid, phase rot., effect of recrystn. processes during heat deform. (*Russian*) 7-53760
 extra mild, annealed sheets, quantitative surface analysis by glow discharge optical spectrometry 7-28373
 fatigue, low-cycle, expt. and anal. (*Chinese*) 7-13556
 fatigue, statistical anal. of pooled S-N data 7-65136
 fatigue crack growth behaviour at US freq., influence of temp. 7-39622
 fatigue crack resistance, influence of stress conc. 7-33792
 fatigue fracture surface at elevated temps., X-ray fractographic study (*Japanese*) 7-8098
 fatigue lifetime measurements for random loading in very high cycle range 7-22790
 fatigue resistance under combined effect of cyclic bending and cyclic torsion 7-28131
 ferrite-pearlite, H occlusivity and embrittlement, effect of C content 7-3417
 ferritic-pearlitic, heterogeneous microstruct., near-threshold fatigue crack propag. 7-46602
 fracture toughness, J-integral, under modes I, II and III, effect of notch root radius 7-63060
 fretting fatigue, crack propag. behaviour 7-39615
 hardened and tempered, struct. aspects of cyclic crack resist. 7-17613
 hardening process modelling, stresses effect on struct. transform. 7-39555
 heat resistance of composite electrochemical coatings based on Ni-B system 7-3499
 high C, grinding balls, jet slurry corrosive wear 7-39676
 high C, quenched, structural changes, tempering effects (*Russian*) 7-17556
 high strength, fracture toughness, US meas. 7-28238
 high strength line pipe, H induced cracking susceptibility, comp. and treatment effect 7-39619
 high-C, hardened, mech. prop. changes on tempering, martensite decomp. role 7-3375
 high-strength low-C weldable, C content effect on struct. and mech. props. 7-46583
 hypoeutectoid, accelerated spheroidisation by decomp. of supercooled austenite 7-3337
 Inconel welds joining dissimilar metals, radiographic evaluation 7-39828
 interaction with H_2 investig. (*Russian*) 7-13552
 inverse magnetostrictive effect and electromagnetic non-destructive testing methods 7-13714
 isothermal austenite transform. near martensite point, kinetic anomaly 7-46467
 joints of dissimilar metals, adhesively bonded strength evaluation 7-46791
 laminated composite with unique microstruct., development by C diffusion control 7-17501
 line hardening by low-power CO_2 lasers 7-13653
 low C, Al killed sheet, overaging, continuous annealing, carbide precip., hardness (*Korean*) 7-46474
 low C, Al-killed, H diffusion 7-6886
 low C, Al-killed sheet, cold-rolled, batch-annealed, recrystn. model for controlling mech. props. 7-13474
 low C, alloying using high-intensity sources 7-28179
 low C, boronized, conversion electron and X-ray Mossbauer studies under corrosion and oxidation conditions 7-27632
 low C, capped, grain growth during subcritical annealing 7-46519
 low C, cold forgeability, notches, geometry, friction conditions, microstruct. 7-33697
 low C, cold rolled lamination, mag. props., Mn and S contents effect 7-7550
 low C, dynamic recrystn., transition of flow behaviour 7-53756
 low C, fatigue fracture surface, plastic deform., X-ray diff. study (*Japanese*) 7-8097
 low C, H diffusion and trapping by TiC precipitates (*Chinese*) 7-7998
 low C, low alloy, tempering investig., epitaxial ferrite stability studies (*Russian*) 7-13479
 low C, magnetoacoustic emission, magnetisation, Barkhausen effect in decarburised steel 7-33207
 low C, mech. props., effect of cold working and annealing (*Chinese*) 7-13473
 low C, microhardness, temp. depend. on coarse-plastic transition region (*Russian*) 7-46638
 low C, mild, statistical analysis of cleavage fracture ahead of sharp cracks and rounded notches 7-13540
 low C, resulphurised, free-machining, MnS precip. 7-46482
 low C, sheets, yielding rel. to prestrain, uniaxial tension 7-46553
 low C, small fatigue crack growth, effects of microstruct. and limitations of linear elastic fracture mechanics 7-39625
 low C, spheroidised, H degradation 7-8104
 low C, strain ageing, internal stress, Bauschinger effect 7-39612
 low C, struct. rel. to deform. method (*Russian*) 7-46580
 low C, structurally free cementite form. rel. to Cr and Mn addition 7-22675
 low C, vacuum carburising with methane 7-54009
 low C, work hardening, softening and dislocation multiplication 7-3324
 low C, Zn-Al coated sheet, Zn quenching technique 7-33847
 low C lamination, decarburization, grain size, carbide morphology 7-8016
 low C pearlitic, microstruct.-flow stress relationship 7-33739
 low-C, cast, failure micromechanism in fatigue crack propag. after different heat treatments 7-46641
 low-C, mech. prop. change after cold deform. and ageing 7-33696

carbon steel continued

- low-C, Ni influence on struct., fracture resist., and fractographic features 7-3420
 low-C, polymorphic transform. kinetics 7-33653
 low-C, wrought, thermal strengthening methods effectiveness 7-46524
 low-field mag. hysteresis 7-64483
 low-tensile, crack resist. in elastoplastic region under static loading 7-33793
 LWR piping, flaw evaluation 7-46652
 medium, H degradation by disc. press. test 7-53855
 medium and high C 7-46515
 medium C, impact toughness and fracture, prolonged high tempering effects (*Russian*) 7-8083
 medium C, rolling contact fatigue, asperity interacting frequency effect 7-39616
 medium C, wear, influences of materials and operating parameters 7-8133
 microhardness load depend., influence of surface roughness (*Japanese*) 7-46622
 mild, acoustic emission during corrosion in FeCl_3 soln. 7-39814
 mild, brittle fracture, microcracks effect (*Russian*) 7-59618
 mild, cold-form-rolled, rotary bending fatigue behaviour (*Japanese*) 7-53866
 mild, corrosion fatigue in 3.5% NaCl soln., investig. of transient polarisation investig. of transient polarisation currents 7-46680
 mild, corrosion in sea water, calcareous deposits form. 7-3485
 mild, corrosion inhibition by Schiff bases in HCl soln. 7-17680
 mild, crit. stress intensity factor, influences of grain size and precracking load 7-59607
 mild, erosion-corrosion control using $\text{O}_2\text{-NH}_4\text{-hydrazine}$ dosed feedwater in reactor boilers 7-59675
 mild, fast fracture, crack arrest behaviour (*Japanese*) 7-59610
 mild, H diffusivity meas. using electropermeation transients 7-22903
 mild, ion nitriding process with variations 7-53989
 mild, J-crack-opening displacement relationship depend. on work hardening exponent 7-16120
 mild, plastic deform. modelling under nonproportional deform. path 7-13535
 mild, radiation enhanced corrosion of radwaste containers 7-30710
 mild, tensile ductility limit calc. (*Russian*) 7-39597
 mild, tensile tests, nonisothermal, anal. using measured temp. distrib. 7-65245
 mild steel testpiece, SPATE stress measurement system, calibration and qualitative assessment 7-31726
 nickel, surface saturation with B by laser radiation 7-8172
 nitriding temperature in glow discharge effect on nitride zone thickness and comp. 7-8176
 nuclear power station use of neutral/oxygen water treatment 7-30537
 on-site oxidation monitoring in AGRs 7-59677
 oxidation performance of Magnox and AGR boiler materials in high press. CO_2 7-59676
 particles in superconducting samples critical current enhancement 7-2796
 pearlite-austenite transformation during heating, kinetics problems 7-33633
 plain C, lower yield stress, strain rate depend. at high strain rates (*Japanese*) 7-53801
 plain C, peritectic reaction, temp. and comp., influence of alloying elements 7-13435
 plastic deform., plane load wave, elastic precursor decay, eqn. of state 7-33751
 powder metallurgical, heat treatment effect on strength and yield parameters 7-53775
 power plant components, remaining creep life assessment 7-8220
 reactor pipe fracture safety analysis using limit load and J-integral techniques 7-13585
 S45C, fretting fatigue damage accumulation, cycle and stress ratio effect 7-28232
 shearing properties, axial compressive stress effects 7-8063
 sheet, hot-dipping into Al-Zn eutectoid base superplastic alloy (*Japanese*) 7-59664
 shock compressed unloading above phase transition point 7-12266
 solution kinetics in molten Zn 7-16752
 steel, C, laser treatment on fatigue and wear resistance 7-39672
 stress-strain curves, approx. functions 7-59591
 structural, diffusion chromised, elevated temp. effect on comp., struct. and mech. props. 7-8178
 structural, welds, dynamic fracture toughness by instrumented impact testing (*Korean*) 7-28235
 surface fatigue cracks, growth and threshold characts. 7-17607
 surface layer repeated thermomechanical strengthening, mech. props. and failure character 7-53994
 thermodynamics of phase boundaries 7-65007
 thin walled square pipes subjected to compressive load, local buckling strength 7-17578
 US inspection signal rel. to microstruct. and surface condition 7-3556
 Vasco X-2M, precipitation during tempering, rel. to impact toughness 7-46494
 wear, effect of normal stiffness in loading system 7-17649
 wear behaviour with US vibr. effect superimposed on static contact load 7-3452
 wear resistance of chromium and eutectic coatings in corrosive medium 7-17694
 wear resistance under wet-abrasive erosion conditions 7-22848
 weld metal, creep crack growth 7-17623
 welded, corrosion fatigue testing, NaCl conc. and test freq. effects (*German*) 7-8230
 welded joint with austenitic steel, microhardness, effect of C redistrib. 7-13571
 welded joints with austenitic steel, thermally loaded, struct. and mech. props. 7-8102
 XC 80, pearlitic transformation in continuous cooling calc., thermal stresses contrib. (*French*) 7-46410
 Al-killed 1006 steel, H diffusion effect on enamelling 7-33816
 C-Mn, cold-formed, creep crack growth 7-53872
 C-Mn, creep crack growth at 360°C , effect of microstruct. 7-28113
 C-Mn, hot ductility, influence of grain size 7-3374
 Cr-Ni, low-C, butterfly martensite, crystallographic characts. (*Russian*) 7-6580
 Fe-Cr-C steels, martensite and bainite transforms. (*Russian*) 7-13448

carbon steel continued
H diffusivity from electropermeation transients under galvanostatic charging 7-6887
TiN coating, ion-plasma appl., laser alloying, dynamic surface strength 7-17730

carbon tetrachloride, CCl₄ *see organic compounds*

carbonitriding *see surface hardening*

carburising *see surface hardening*

carcinotrons
submm heterodyne spectrometer for UKIRT and UK-NL telescope 7-34883

cardiology
see also blood; electrocardiography; haemodynamics
action potential in beating heart cells, regulation of Na-conducting Ca channel 7-54528
acute myocardial infarction, spectral anal. of heart rate fluctuations in evaluation of autonomous control 7-34313
angiographic images, anal. and interpolation by use of fractals 7-34271
anisotropic cardiac tissue, electronic interactions 7-13989
aortic porcine valves, orifice area flow dependency obs. 7-34185
aortic valve tissues, relative vols. of struct. components rel. to biochem. components 7-34182
arrhythmia haemodynamics, simulation with a real-time computer model 7-3826
arterial blood pressure and heart rate variability signals, normal and pathological subjects evaluation appl. 7-34312
artificial heart, adaptive control technique, rel. to blood press. and flow 7-3933
atrial and venous press. waves spectral anal.: methods and results 7-65795
atrial heart cell aggregates, embryonic chick, repolarisation currents 7-28491
automatic left ventricular cineangiograms analysing system 7-47258
background correction in first-pass radionuclide angiography: comparison of several approaches 7-40264
bioelectrical sources localisation, accuracy, magnetocardiography appl. 7-54542
bioprosthetic heart valves, computer simulations of closing sounds 7-34343
bioprosthetic valves, closed, influence of stent height upon stresses on cusps, finite element model 7-23387
bioprosthetic valves, porcine, leaflet stiffening effect on leaflet stresses 7-65889
biplane multidirectional angiocardiology with a new X-ray system 7-14111
blood flow phase detection on digital subtraction angiography 7-47257
blood pressure and heart rate, closed-loop identification of beat-to-beat interactions 7-8640
blood pressure sensor for fibrillation detect. method, implantable defibrillator output circuit evaluation (*Japanese*) 7-14160
blood rheology in myocardial infarction and hypertension 7-65788
CAI program for teaching cardiac rhythms and arrhythmias 7-48247
cardiac action potentials and twitches, real time acquisition and analysis 7-65737
cardiac defibrillators, safety and reliability (*Spanish*) 7-65892
cardiomagnetism, inverse problem soln. using a current multipole expansion of primary sources 7-54641
cardiopulmonary rate monitor, microprocessor-based, using low-power Doppler microwaves 7-65828
cardiovascular devices—past, present and future direction 7-65674
cardiovascular disease detection, blood flow meas. using NMR imaging technique 7-54694
cardiovascular models for real time applications 7-34094
chest auscultation, reduction of heart sounds from lung sounds by adaptive filtering 7-54685
cine CT, 3D reconstruction of contracting canine heart 7-28759
colour display of quantitative blood flow and cardiac anatomy in a single NMR cine loop 7-60065
computerized autoradiographic technique for the simultaneous high-resolution mapping of myocardial blood flow and metabolism 7-60113
computers in cardiology, conf., Linköping, Sweden (Sept. 1985) 7-24309
conference on bioengineering, New Haven, CT, USA (March 1986) 7-16
conference on biomechanics, Mons, Belgium (Sept. 1986) (*French*) 7-9578
contractile rate of isolated frog hearts, effects of pulsed microwave radiation 7-34192
contracting cardiac muscle, nonlinear viscoelastic behaviour 7-8642
coronary angiograms, digitised, computer anal. for assessment of changes in poststenotic coronary flow 7-28687
coronary angiography, quantitative, accuracy of the catheter as a reference for arterial dimensions 7-28685
coronary angiography, quantitative, improvement by exact calc. of radiological magnification factors 7-40288
coronary arteries densitometry in radiographs, improved phys. model 7-28689
coronary arteries microembolisation, computer simulation of hyperemic flow 7-18007
coronary arteriography, quantitative, state of the art, book 7-54742
coronary artery diameter meas. by angiography, Monte Carlo assessment of precision 7-47240
coronary artery opacification improvement with gated injections and digital subtraction angiography 7-28690
coronary blood flow, absolute, online computer meas. using a H₂ dilution catheter 7-28742
coronary blood vel., phasic, clinical assessment using digital subtraction angiography 7-3873
coronary sinus haemodynamics in transient ischaemia 7-40205
CT, 3D reconstruction from few projections, practical implementation of McKinnon-Bates algorithm 7-47219
CT, heart images in motion 7-14142
defibrillators, technological development (*Spanish*) 7-3939
diagnostic potentials of NMR in heart disease 7-28655
digital radiographic assessment of coronary arterial geometric diameter and videodensitometric cross-sectional area 7-28675
digital sampling of cardiac Purkinje fiber action potentials, maximum frequency components 7-18085
digital subtraction angiography of the heart and coronary arteries 7-18064
Doppler US signals, freq. transformed TAV, cardiac indices meas. 7-28626

cardiology continued
dynamic changes in regional vel. of shortening, anal. 7-40203
echocardiograms, 2D, automatic and intelligent left ventricular contour detect. 7-34212
echocardiographic assessment of ventricular volume microcomputer based method 7-40237
echocardiographic scan images, cine, spatial and temporal processing: automated myocardial border tracking 7-28638
echocardiographic visualisation of acute myocardial ischaemia 7-28631
echocardiography, 2D,, microcomputerised image processor and 3D reconstruction of left ventricle 7-34213
echocardiography, 2D, in infants and children, book 7-60061
echocardiography, attenuation correction 7-23417
echocardiography, computer assisted anal. of left ventricular function 7-34211
echocardiography, versatile digitisation and processing system 7-34216
electrical shock, heart muscles effect (*German*) 7-3776
electrical shock, safety criteria, conf., Toronto, Ontario, Canada (Sept. 1983) 7-18500
electrocardiology, inverse soln. in 1D using a membrane model 7-8554
electrodes, optimal design for electrosurgery, defibrillation, and external cardiac pacing: finite-element computer model 7-3928
electrophysiological stimulation and online processing, automated system 7-34324
endoscopic micromanipulator for multiplanar transesophageal imaging 7-47190
excitable medium models, rotating spiral waves 7-46995
external counterpulsation in the presence of arrhythmias, computer simulation anal. 7-14156
force-interval relationship in heart muscle of mammals, Ca²⁺ compartment model 7-54648
gap junctions, single channel currents, embryonic heart obs. 7-8550
gated radionuclide ventriculography with a slant-hole collimator, fully-automated contour detect. 7-40252
haemodynamically compromised subjects, exercise test protocols, digital filtering and data processing 7-8727
heart's pathological sinus mode modelled by system of interconnected pacemaker cells 7-54518
heart rate and arterial blood press. variability signals, auto-spectral and cross-spectral anal. 7-47270
heart valves, prosthetic, flexible support frame 7-3938
heartbeat rhythms of chick embryos, temp. effects 7-54479
hemodynamic regulation modelling 7-54667
Hofkessel: an artificial afterload for cardiovascular research 7-18096
image processing in cardiovascular radiology 7-65833
impedance cardiography, motion artifact from spot and band electrodes 7-28732
impedance cardiography during treadmill exercise for cardiac output monitoring 7-28733
impedance differential loop and its clinical significance (*Chinese*) 7-18088
impedance measurements in cardiac tissue, tissue struct. model 7-13985
implantable devices for the treatment of cardiac arrhythmias 7-34340
implanted cardiostimulators, polymeric insulation degradation (*Czech*) 7-23487
intracellular long-term measurements on contracting isolated hearts, expt. set-up 7-65902
IR fibre optic device for cardiac cycle timing and photoplethysmography 7-3856
ischaemia, remote, after acute myocardial infarction, detect. by ²⁰¹Tl emission CT 7-34264
isovolumetric contraction, 1st heart sound 7-54424
isovolumic contraction, left ventricular wall stresses determination using FEM 7-23378
Kent bypass pathway electronic simulator for cardiac arrhythmia study (*Spanish*) 7-8733
laser angioplasty, excimer lasers in medicine 7-60073
left ventricle, ²⁰¹Tl perfusion imaging simulated by a dynamic model 7-34267
left ventricle, spatial energy balance within a struct. model 7-54502
left ventricle and aorta of chronically instrumented dogs, beat-to-beat anal. of high-fidelity signals 7-18008
left ventricle over cardiac cycle, simulation model (*Japanese*) 7-47146
left ventricular assist device, computerised 7-40369
left ventricular assist device, pulsed US Doppler rel. obs. 7-8667
left ventricular contraction charactn., comparative study of quantitative methods 7-34261
left ventricular diastolic function, scintigraphic meas., effects of ECG gating 7-34265
left ventricular ejection fraction, continuous monitoring using a miniature NaI detector and microcomputer 7-34305
left ventricular ejection fraction calc. through anal. of model, effect of scintigram background correction 7-54728
left ventricular function after heart transplantation, anal. from myocardial markers 7-34263
left ventricular pressure decay in the myocardial wall 7-34186
left ventricular regional function, objective detect. algorithm, radionuclide blood pool studies 7-40287
left ventricular regional wall motion, quantification using multiple-view radionuclide angiography and the centerline method 7-34268
left ventricular vol. determ. using radionuclide ventriculography (*Russian*) 7-8682
left ventricular wall sequences, 3D, asynergic regions detect. by a clustering technique 7-40357
left ventriculograms, digital subtraction, automated edge detect. method 7-34269
left-to-right shunts, quantitation using digital subtraction angiography 7-40285
left-ventricular regional wall motion assessment, comparison of 2 nuclear cardiology techniques 7-3862
local spatial phase analysis of left ventricular wall motion using Hilbert transform (*Japanese*) 7-47145
magnetic resonance imaging role in cardiovascular disease detection 7-54706
magnetocardiographic data measurement and its movie display (*Japanese*) 7-14073
magnetocardiographic isofield maps, torso geometry effect, computer model study 7-54640
magnetocardiography based method for cardiac activity investig. 7-40351
mathematical model of the cardiac cond. system included external pacemakers 7-40129

cardiology continued

- medical electronics developments, review (*Italian*) 7-18094
 microwave effects on isolated chick embryo hearts 7-28600
 mitochondria from bovine heart, electrophoretic behaviour of H^+ +AT-Pase proteolipid 7-59946
 mitral valve, remote-controlled, development and use 7-14159
 monitoring heart and respiratory activity by impedance change using neck electrodes 7-65869
 myocardial cells, rat, Fe overload 7-59945
 myocardial contractility anal., computational method 7-14140
 myocardial electrical propag., 3D anisotropic model 7-40131
 myocardial infarction, acute, computer-aided decision in haemodynamic-based treatment 7-40360
 myocardial ischaemia studies using epicardial array ECG signals 7-14149
 myocardial ischaemia studies using epicardial array ECG signals 7-14150
 myocardial metabolism, fatty acid kinetics study technique using sequential sampling radioisotope technique 7-65837
 myocardial proton spin-lattice relaxation time in vitro: effect of elapsed time after excision 7-47136
 myocardial scintigrams, symbolic reasoning in PROLOG 7-40253
 myocardial signature: absolute backscatter, cyclical variation, frequency variation, and statistics 7-23418
 myocardium, ^{201}Tl tomography, developments toward quantitative anal. 7-34266
 myocytes, Na^+/Ca^{2+} exchange, effect of ouabain on voltage dependence 7-59958
 myocytes, single isolated, simple technique to meas. rate and magnitude of shortening 7-23494
 NMR imaging, cardiac gating 7-40241
 NMR imaging, optical detection of respiration and heart beats 7-47277
 nuclear medicine images, length-based Fourier anal. in pre-excitation syndrome 7-65879
 nuclear techniques in diagnostic medicine, book 7-24312
 nuclear ventriculography, ejection fraction determ. by combined inverse Fourier anal. and second-derivative technique 7-40254
 opacified myocardium, spatial reconstruction from a small number of projections 7-34270
 output determination, first-pass radionuclide, effect of region of interest selection 7-40256
 papillary muscle, method for generation of rapid step in temp. 7-3753
 pericardium, natural and chem. modified, relative extensibility rel. to gauge length standardisation 7-40194
 pneumatic portable artificial heart drive system, design based on efficiency anal. 7-65893
 positron-emission tomography evaluation of heart membrane pot., use of ^{11}C -triphenylmethylphosphonium 7-14113
 preexcitation syndromes, book 7-41020
 programmed stimulation, real time data collection 7-34329
 propagation through electrically coupled cells, how a small SA node drives a large atrium 7-40128
 prosthetic heart valve, Ionescu-Shiley aortic, in vitro vel. obs. downstream 7-3936
 prosthetic heart valve test apparatus, microcomputer-based data acquisition system 7-40364
 prosthetic heart valves, Ionescu-Shiley, freq. anal. of closing sounds 7-28770
 proton relaxation times in mouse liver, heart and kidney, temporal fluctuations 7-47005
 pulse sequence generated oblique NMR imaging, cardiac imaging appl. 7-40246
 Purkinje fibres, rabbit, voltage-dependent block by tetrodotoxin of Na^+ channel 7-54527
 Purkinje strands, K^+ -activated electrogenic Na^+ pumping 7-28490
 radionuclide, ejection fraction, geometrical depend. 7-65852
 radionuclide left ventricular ejection fraction determ., influence of background correction that considers heart vol. 7-14109
 radionuclide ventriculograms, cardiac activation movies generation using Walsh-Hadamard phase spectrum 7-54743
 radionuclide ventriculography, computer program for data acquisition 7-40289
 regurgitant flow through heart valves: hydraulic model applicable to US Doppler meas. 7-28563
 right ventricular ejection fraction, automated determ. by digital processing of ^{81m}Kr scintigrams 7-65835
 right ventricular regional wall motion, meas. from biplane contrast angiograms using the centerline method 7-34262
 sarcoplasmic reticulum Ca channel, cardiac, single channel $^{45}Ca^{2+}$ obs. 7-28477
 semi automatic computerised system for producing heart and coronary arteries images 7-3875
 sinoatrial node cells, charactn. of single pacemaker channels 7-47024
 some emerging issues in electrocardiology 7-65675
 stroke volume, in vivo meas. using multiple 2D echo views from 1 echo window 7-34215
 superior vena caval blood flow vels. in adults, Doppler echocardiographic study 7-8623
 Swedish perspectives on the use of computers in cardiology 7-28741
 systolic and diastolic cardiac function, rapid radionuclide-derivation using cycle-dependent background correction and Fourier anal. 7-40286
 tachyarrhythmias surgery, programmable stimulator: data acquisition, processing and display system 7-34330
 third heart sound in children, spectral anal., comparative study of max. entropy method and FFT 7-65818
 time dependent anatomically detailed model of cardiac cond. 7-40130
 transient ischaemic attacks and strokes, rel. to interactions between biochem. and haemodynamic factors 7-65786
 US cardiac Doppler diagnosis, book 7-29
 US sector scanning cardiac tissue imaging, spectral anal. method 7-34214
 valves, mech. bileaflet and tilting disc., comparative test 7-3932
 ventricular assist device, elec., power consumption minimisation by design of optimal controller 7-8769
 ventricular fibrillation, 60 Hz, thresholds for large-surface-area electrodes, animal expts. 7-3931
 ventricular mechs., model selection, sensitivity anal. approach 7-40196
 ventricular pressure-volume relationships, automated anal. by digital ventriculography 7-28692
 ventricular wall motion anal., tests of methods 7-40204

cardiology continued

- ventriculograms, normal, curvature anal.: fundamental framework for assessment of shape changes in man 7-34260
 wall motion abnormalities detect., combined amplitude and phase anal. 7-28566
 wall motion abnormality visualised in the 30° RAO and 60° LAO projections, comparison of magnitude 7-28688
 wall motion during exercise, computerised quantitative segmental anal. from 2D echocardiograms 7-34321
 Wolff-Parkinson-White preexcitation syndrome, computer simulation with a modified Miller-Geselowitz heart model 7-3765
 Ca^{2+} current in single heart cells, opposite effects of cyclic GMP and cyclic AMP 7-40135
- carrier avalanches see impact ionisation
 carrier concentration see carrier density
 carrier density
 see also current density; electron density; electron density (metals)
 1/f noise, carrier mobility fluctuation origin 7-38653
 p-AlGaAs/GaAs modulation-doped heterostruct., liq. phase epitaxy and carrier props. 7-33074
 amorphous semiconductors, photoconductivity behaviour during the approach to steady state 7-38637
 anthanthrone-Ag struct., charge carrier photogeneration (*Japanese*) 7-38610
 binary compound polar semiconductors with nonparabolic energy bands, electronic struct. 7-2478
 chalcogenide glasses, field dependent negative U-model and switching 7-7252
 contactless measurement of carrier mobility and concentration in semiconductors 7-30036
 copper phthalocyanine-anthanthrone heterojunction, charge carrier photogeneration (*Japanese*) 7-38610
 degenerate semiconds., anisotropic hot carrier distrib., transport eqn. solns. anal. 7-58815
 disordered media, small polaron charge transport model, density-matrix formalism calcs. 7-52612
 electron-positron systems, two-component density-functional theory, self-consistent density calcs. 7-27277
 epitaxial layers grown directly on Si (100) by low press. MOVPE 7-27924
 field-effect capacitor, carrier ambipolar drift vel., field control study 7-52840
 graphite films, pyrolysed from polyoxadiazole condensation polymer, elec. and thermal props. 7-2736
 graphite-AsF₃ intercalation cpd., galvanomag. props. 7-58822
 III-V semiconductors, carrier concentration and mobility profiling 7-45315
 metal- p^+n structures, Schottky barrier height enhancement, calcs. including free carriers 7-2709
 MIS structure, carriers in insulator and at semiconductor-insulator interface, EEPROM appl. 7-2730
 nondegenerate semiconds., charged dislocation hole capture, hole thermal ionisation and free density calcs. 7-38574
 photoexcited semiconductor, fast carrier dynamics using modified Fresnel formula 7-31238
 photopolymer characteristics, theoretical anal. 7-21931
 polymer dielectrics, injection role in charge accumulation process 7-33026
 Poole-Frenkel effect, field-dependent behaviour 7-12727
 quantum well structures, metal-insulator transition due to surface roughness scatt. 7-27400
 Schottky surface layers, carrier conc., spatial depend. (*German*) 7-2670
 semiconductor, surface recombination vel. calc. 7-38587
 semiconductor 2D struct., time-depend. soln. 7-2755
 semiconductor doping superlattices, n-i-p-i crystals 7-7348
 semiconductor electrical characterisation, non-contacting methods, book contrib. 7-45335
 semiconductor electron-hole plasma, noise spectrum calcs. near slow recomb. wave excitation threshold 7-38649
 semiconductor IR detectors, non-equilibrium modes of operation 7-9898
 semiconductor size-effect modulation laser, three-terminal, gain-switching charact., fast transient response 7-10936
 semiconductors, 1/f noise and number fluctuations 7-38651
 semiconductors, charge carrier distrib., nonlinear eqn. 7-33028
 semiconductors, dispersive transport under conditions of maximum population of localized states 7-52605
 semiconductors, extrinsic, thermal gradient magnetoconc. effect 7-52659
 semiconductors, extrinsic n-type, stochastic self-oscillations under intense illumination 7-2639
 semiconductors, highly doped and excited, electron-phonon mobility variation with carrier density 7-64249
 semiconductors, nonequilibrium carrier recomb. processes, plasmon effects, luminesc. spectra calcs. 7-58818
 semiconductors, photoelectrons subjected to parallel elec. and quantising mag. fields 7-64280
 semiconductors, zero-gap, carrier temp. and density, nonequib. fluctuations 7-38576
 semiconductors with parabolic density of states, activity coeffs. of electrons and holes 7-27324
 temperature dependent data, donor and acceptor behaviour 7-64263
 transient photocond. responses, surface carrier recombination, excitation effects (*French*) 7-7286
 AlAs:Si films and AlAs:Si-GaAs:Si superlattices, MBE growth and electrical props. 7-22052
 AlAs/GaAs:Si super-doped structs., short-period superlattice electrical and defect props. (*Japanese*) 7-7353
 AlGaAs epitaxial layers, large scale MOVPE growth 7-22552
 AlGaAs intraband relaxation dynamics of photo-excited carriers 7-52691
 AlGaAs, MOVPE, laser assisted, selective area irradi., carrier conc. 7-22545
 AlGaAs:Mg LPE layers, Mg doping and injection laser threshold current 7-12092
 AlGaAs/GaAs modulation-doped heterojunctions, 2D electron gas, DX centres 7-38694
 AlGaAs/GaAs/AlGaAs selectively doped double heterostruct., electron conc. and mobility 7-12839
 AlGaAs-GaAs heteroepitaxial wafer for solar cell appls., uniform growth by MOCVD 7-64929
 Al_{1-x}Ga_xAs:Te, low press. OMVPE, Te doping, Hall effect, carrier conc., photolum. 7-21242

carrier density continued

Al_xGa_{1-x}N MOVPE growth, struct. and elec. props. 7-21729
Ba₂NaNb₂O₁₅ cryst., elec. cond. small signal amplification 7-27333
Bi₂Te₃ and Bi₂Fe₃-derived solid solns., carrier density, depend. of anisotropy parameter 7-7226
Bi₂Te₃ doped crystals, energy formation of antisite defects 7-21204
Cd_{1-x}Hg_xTe crystals., impurity band elec. conduction, Fermi glass model anal. 7-27328
CdIn₂O₄ RF sputtered films, transparent heat mirror characts., elec. and optical meas. 7-39199
CdIn₂O₄ thin films, DC reactive sputtered, elec. and optical props. 7-38788
CdIn₂S₂Se₂, semicond., optical and elec. props. 7-33010
n-Cd_{1-x}Mn_xSe, magnetoresist. and Hall effect meas. near metal-insulator transition 7-12741
CdS, nonradiative recomb., elec. transport, combined photoacoustic and photoconductive spectra, theory 7-38583
CdS thin films, preparation and thermoelec. props. 7-64374
CdSe crystals, laser beam defocusing, rel. to Hall mobility and carrier density 7-52652
CdSe, strongly excited, electron-phonon interaction screening, luminesc. meas. 7-38606
CdTe films, electrochemically deposited, resistivity, carrier conc. and carrier mobility 7-7419
CdTe grown on Si by LPMOCVD, physical props., Hall meas. 7-27181
CdTe MOVPE growth on InSb substrate, characts. 7-27920
CdTe:P-CdS solar cells, control of open circuit voltage by carrier density variation 7-17887
CdTe:Sn, impurity compensation effect on elec. resist. and mobility 7-52614
CoSi₂, thin film, electrical transport props. 7-27442
FeS₂-electrolyte photoactive interface, electronic props. 7-33086
GaAs:Be, MOVPE, diethylberyllium dopant source, elec. characts. 7-22521
GaAlAs channelled-substrate-planar laser, measuring modulus and phase of chirp/modulated power ratio 7-57391
n-GaAs, depletion and accumulation layer profiles, self-consistent Hartree approx. calcs. 7-27375
GaAs, electron beam irradi., carrier density, anomalous temp. depend. 7-52610
GaAs epitaxial films, growth by close-spaced vapour transport, unwanted doping, X-ray diffr., SEM obs. 7-27187
GaAs epitaxial films, MOCVD growth using tertiarybutylarsine source 7-59439
GaAs epitaxial layers, OMVPE growth on Si (100) 7-3190
GaAs, epitaxial layers, large scale MOVPE growth 7-22552
a-GaAs films, dynamics of laser annealing by transient grating method 7-12122
GaAs films on oxidised Si, zone melting recrystallisation 7-38396
GaAs, heavily doped, carrier-carrier and carrier-dopant interactions 7-21903
GaAs highly doped quantum wells, mobility enhancement 7-64325
GaAs, hot-electron 1/f noise 7-21927
GaAs injection laser, twin-stripe, lateral behaviour, self-consistent model 7-15861
GaAs intraband relaxation dynamics of photo-excited carriers 7-52691
GaAs, inversion layers, hot free electron gas, intraband absorpt. coeff. calc. 7-33083
GaAs, ion irradi. high-resistivity layer, thickness and resistance, free carrier density and cryst. orientation dependence 7-58354
GaAs LPE layers, heavily doped and compensated, hopping cond., density of states at Fermi level, carrier conc. determ. 7-2753
GaAs, laser MOVPE growth 7-33580
GaAs, laser material, intervalence band absorpt. coeff. calc. 7-3015
GaAs, MBE layers, deep level defects, passivation by H₂ plasma exposure 7-21850
GaAs, MOVPE, laser assisted, selective area irradi., carrier conc. 7-22545
GaAs, neutron transmutation doped, variable range hopping studies 7-33012
GaAs, OMVPE, low pressure growth from trimethylgallium+AsH₃ 7-17439
GaAs, plastically deformed, Hall effect meas. 7-27351
GaAs quantised inversion layers, hot 2D electron gas, spectral acoustic phonon emission intensity 7-52452
GaAs, semiinsulating, electrophysical props., dislocation effects 7-16557
GaAs thin films, on glass substrates, transport props. 7-2742
GaAs:Bi, epitaxial layers, purification by Bi doping 7-58301
GaAs:MG, MOVPE, p-type doping using an organometallic Mg precursor 7-22522
GaAs:S surface elec. props. modification by plasma exposure 7-27346
GaAs:Si, MBE growth, carrier concentration, dislocation effects 7-58682
GaAs:Si₂Se MOCVD epitaxial layer photolum. spectral shift and doping efficiency obs. (Japanese) 7-45076
GaAs:Si heteroepitaxial growth on sapphire, low press. MOCVD three-step method 7-27927
GaAs:Si(S), LEC grown, struct. defects, influence of Si and S doping 7-53550
GaAs:Sn(Te)(Zn) surface layers, luminesc., electrophys. parameters, effect of annealing 7-64680
GaAs:Te, low press. OMVPE, Te doping, Hall effect, carrier conc., photolum. 7-21242
GaAs:Te films, flash evaporation, annealing, elec. props. 7-64373
GaAs:Zn epilayers, metalorganic CVD, Zn incorporation 7-63996
GaAs/Al_xGa_{1-x}As heterostructures., 2D electron gas, polaron screening effects, optical absorpt. calcs. 7-2511
GaAs/AlGaAs 2D electron gas MBE structures, carrier mobility and density meas. 7-64321
GaAs/GaAlAs 2D electron gas, cyclotron resonance study 7-2676
n-GaAs/In_xGa_{1-x}As compositionally graded non-alloyed ohmic contacts 7-38695
GaAs-Al_xGa_{1-x}As heterojunctions, subband Landau-level spectroscopy 7-21996
GaAs-Al_xGa_{1-x}As quantum well structure, recomb. dynamics, photolum. obs. 7-12809
GaAs-AlGaAs heterojunctions, Be⁺, O⁺ ion implantation, impurity profiles, elec. characts. meas., SIMS, annealing 7-12813
GaAs-AlGaAs MQW, intraband relaxation dynamics of photo-excited carriers 7-52691
GaAs-GaAlAs heterostructure, LPE grown, interface photoluminescence spectra 7-53390

carrier density continued

GaAs-GaAs MOVPE epitaxially-grown interfaces, anomalous C-V carrier conc. profiles, model 7-52648
GaAs_{1-x}P_xN, cathodoluminesc. efficiency, N-bound excitons influence 7-7768
n-GaAs_{1-x}Sb_xP, epitaxial film, impurity distrib., cond. and Hall mobility study 7-51808
Ga_{0.47}In_{0.53}As, laser material, intervalence band absorpt. coeff. calc. 7-3015
Ga_{0.47}In_{0.53}As:Be epitaxial films, ion implanted, rapid thermal and furnace annealing 7-22729
Ga_{0.47}In_{0.53}As-InP heterojunction, with three electron subbands, hydrostatic press. effect 7-2695
Ga_{0.47}In_{0.53}As-InP heterojunction, MOCVD grown, 2D hole gas 7-21992
Ga_{1-x}In_xAs/InP heterostructures, MOVPE, electron mobility, exciton peak, magnetotransport 7-58883
Ga_{0.28}In_{0.72}As_{0.6}P_{0.4}, laser material, intervalence band absorpt. coeff. calc. 7-3015
GaN films, epitaxial growth by reactive ion plating, elec. props. 7-3206
GaN:Zn, pure and doped, electrophysical props., nonhomogeneous semicond. model 7-27292
n-GaAs impurity Auger hole recomb. via deep acceptor, electron density depend. calcs. 7-38573
GaSb:Te(Si)(Ge) single crystals., Czochralski growth, carrier conc. rel. to dopant conc. 7-22462
GaSb/InAs/GaSb quantum wells, carrier densities and mobilities, magnetotransport meas. 7-12846
Ge, drag thermoelec. power, anisotropy parameter, carrier density depend. 7-38603
a-Ge films, dynamics of laser annealing by transient grating method 7-12122
Ge, mag. gradient effect (Russian) 7-17040
Ge, muon channelling, evidence for ponium formation 7-51897
Ge surface state characts., surface struct. and low temp. annealing effects 7-45426
Ge:O, γ-irrad., majority carrier mobility meas. 7-27334
Ge_xSi_{1-x}Si strained layer heterojunctions, selectively doped, hole mobilities, temp. depend. 7-7383
GeTe, slight nonstoichiometry and high free carrier density, phase diagram study (Russian) 7-2191
HgCdTe epitaxial layers and structures, characterisation of intentional dopants 7-12552
HgCdTe epitaxial layers, Hall effect and elec. resist. characterisation 7-64375
HgCdTe IR photodetectors, magnetoresist. and cyclotron resonance characterisation 7-64054
p-HgCdTe, minority carrier characterisation using light-modulated Hall effect 7-21934
HgCdTe:B⁺, ion implanted n⁺p junction, lifetime and carrier conc. profile 7-45450
n-Hg_{0.8}Cd_{0.2}Te, magnetic field-induced metal-insulator transition, threshold field electron density depend. 7-52427
Hg_{1-x}Cd_xTe, epitaxial growth by low temp. metalorganic CVD 7-27911
Hg_{1-x}Cd_xTe films, LPE using a semiclosed rotational boat 7-64937
HgCr₂Se₄ spinel magnetic semicond., electronic struct., elec. props., defects and ferromag. anisotropy 7-38857
Hg_{1-x}Mn_xTe, magnetoresist. meas., effect of valence band spectrum quantisation at low temps. 7-52653
In-Ga-As-P films highly excited, ps band filling 7-43261
In_{0.5}G_{0.5}P layers, LPE, elec. and optical props. 7-17119
InGaAs epitaxial films, MO-chloride VPE growth 7-22566
InGaAs/InP single quantum wells, transport and persistent photocond. props. 7-27385
InGaAs-GaAs MOVPE epitaxially-grown interfaces, anomalous C-V carrier conc. profiles, model 7-52648
In_{1-x}Ga_xAs, MOCVD, optical and elec. props. rel. to growth temp. 7-53613
InGaAsP-InP bistable lasers, temp. depend. 7-5887
In₂O₃:Sn films, electron effective mass determ., refractive index carrier density depend. meas. 7-38440
In₂O₃:Sn vapour deposited films, growth, struct., electronic props. 7-12535
InP, electrochemical C-V profiling 7-27325
InP, electron irradi. damage, impurity effects 7-12154
InP epitaxial films, MO-chloride VPE growth 7-22566
InP epitaxial layers, MOVPE, elec. characts., photolum. 7-22519
InP films on oxidised Si substrate, laser recrystallisation 7-38398
InP, MOVPE; morphology, photolum., carrier conc. and mobility 7-22518
InP synthesis by modified horizontal Bridgman method, elec. props. 7-58821
InP:Fe wafer, semi-insulating, elec. characteristics 7-45323
InP:Hg ion implanted at 200°C, rapid thermal annealing, carrier conc. and mobility 7-32469
InP:Mn, LPE growth, carrier conc. control and appl. to buried heterostructure laser diodes 7-21774
InP:Yb LPE layers, luminesc. and elec. props. 7-59464
n-InSb low-temp. growth by plasma process (Japanese) 7-7061
n-InSb, impact ionisation electron-hole pair generation, high power optical wave elec. field effect. luminesc. obs. 7-33025
InSb:Te(Ge)(Cd)(Si), heterogeneity study 7-21476
InSb/CdTe interface, quasi-2D electron gas obs. 7-21987
InSe single crystals., growth by travelling heater method, carrier conc., photoelectrochemical props. 7-59410
Mg₂Si(Ge)(Sn)(Pb), Hall effect in solid and liq. states 7-38647
NiSi₂, thin film, electrical transport props. 7-27442
Pb_{0.7}Sn_{0.3}Te:In, Ge(S)(Se), elec. resist., photocond., Hall effect meas. 7-17050
Pb_{1-x}Sn_xTe films prepared by MOCVD, elec. props. 7-27919
Pb_{1-x}Sn_xTe narrow-gap semicond., electron-electron interaction, effect on permitt., two-band model 7-52420
Pb_{1-x}Sn_xTe:Bi, free carrier density 7-38572
PbTe doping superlattices, transport and magneto-optical props. 7-12852
PbTe:Ti(Tl,Na) films, superconducting transition 7-38797
Pd₂Si formation, dopant redistrib. in Si substrate 7-21255
PdTe:Cd, free charge carrier conc., donor action and Te precipitates effects (Russian) 7-16592
Sb₂Te₃ doped crystals, energy formation of antisite defects 7-21204
Sb₂Te₃ crystals., pure and Cd-doped, point defects, reflectivity and elec. props. room temp. meas. 7-33008

carrier density continued

- SeN compensated semimetal single crystals, electronic struct., reflectivity and elec. props. meas. 7-27253
 p-Si conductivity and Hall mobility calcs., impurity scatt., anisotropic-nonparabolic effects 7-12720
 Si defect annealing and impurity activation during high-intensity As⁺ implantation doping 7-58295
 a-Si, electron and hole concentration modelling 7-64269
 Si, epitaxial growth using photochem. vapour deposition at 200°C 7-39431
 Si epitaxial layers, free carrier conc., optical interference determ. 7-2745
 Si exciton transport, optical time-of-flight investigation 7-64244
 n-Si, heavily doped, carrier conc. and activation energy, Lee-McGill model calcs. 7-58819
 Si, high temp. drift mobility, determ. 7-52621
 Si, hot-electron 1/f noise 7-21927
 Si, impurity and carrier conc. profiles, electrochem. C-V method (*Chinese*) 7-12105
 Si p-amorphous/n-cryst. anisotype heterojunction characts., acceptor doping level depend. 7-7355
 Si polycrystalline CVD film, etch rate free carrier depend., doping level and grain size depend. meas. 7-28219
 Si quantised inversion layers, hot 2D electron gas, spectral acoustic phonon emission intensity 7-52452
 Si quantum well struct., 2D electron gas, transport props. 7-52774
 Si SOI structure, O⁺ implantation and high temp. annealing 7-44579
 Si shallow p-n junctions, reactive ion etching damage, defects and leakage current studies 7-27411
 Si, spin-dependent recombination and low-freq. ESR studies 7-38577
 Si strips, grown by Stepanov's reversed method, strength, struct., electrophysical props., effects of thermal conditions during growth, photocell appl. 7-32325
 Si, transmutation-doped, carrier recomb. props. at gamma-irrad. defects, transport meas. 7-38575
 Si:Ar laminated structure formed by Ar ion doping, electroreflectance 7-7676
 Si:Au n-n⁺ isotype junction, enhanced magnetosensitivity 7-7370
 Si:B, critical supercond. current induced by proximity effect, mag. field depend. 7-22069
 Si:B layers, preamorphised and ion implanted, structural and elec. characterisation 7-52347
 Si:B p-n⁺ junction, injection annealing of radiation defects 7-12161
 Si:B⁺(BF₃⁺), ion implanted, characterisation by IR attenuated total reflection spectroscopy 7-17327
 Si:B(BF₃) wafers, activated carrier density profile and scatt. rate meas., nondestructive IR attenuated total refl. technique 7-22207
 Si:Ga MBE layers, ion implantation doping using liq. metal ion source, carrier conc., spreading resist., SIMS profiles 7-12563
 a-Si:H, photoinduced absorpt., ps decay 7-27684
 Si:H and near-surface damage of Si caused by H ions, review 7-16813
 Si:Na MOSFET struct., hopping cond. in 2D impurity band 7-45512
 Si:O, γ-irrad., majority carrier mobility meas. 7-27334
 Si:O, oxide precipitate nucleation, thermal donor formation kinetics 7-32667
 Si:O,B⁺, ion implanted, reverse annealing 7-16617
 n-Si:P, nonlinear optics near metal-insulator transition 7-20322
 Si:Sb MBE film, doped by electron impact ion source, improved doping characts. 7-12101
 Si/Nb, proximity effect, superconducting transition temp. meas. 7-45566
 Si-Al struct., cond., transverse elec. field depend. 7-27417
 Si-SiGe strained layer superlattices, electric subbands 7-2700
 β-SiC CVD film growth and props., gas phase comp. depend. simulation and meas. 7-22516
 β-SiC crystals, free carrier conc., Raman scattering 7-59197
 SiC, cubic, epitaxial films, compensation 7-7268
 3C-SiC, n- and p-type epitaxial CVD layers, elec. props. temp. depend. studies 7-58917
 SiC:P(N)(B)(Al) thin films, impurity 7-27192
 β-SiC(N) single crystals, CVD grown, elec. props., temp. dependence 7-2740
 SnO₂, nonstoichiometry and defect equilib. rel. to cond. props. 7-52069
 SnO₂, oriented thin films, elec. props. 7-17123
 SnO₂F films, CVD growth using hydrofluoric acid as doping material 7-7871
 SnO₂F thin films, CVD deposition, elec. and optical props. 7-7425
 SnS, photoacoustic response and transmission spectra, thermoacoustic meas. 7-46014
 SnTe:Bi epitaxial layers, vacuum deposition, optical and electrical props. 7-59430
 SrTi_{0.97}Zr_{0.03}O₃, superconductivity at low carrier conc. and indications of charged Bose gas 7-27453
 Te (0001), conductivity of size-quantised holes, hydrostatic pressure effects 7-45428
 TiN_x epitaxial layers, atomic and electronic struct., growth, physical props. 7-32854
 Y_{1-x}M_xCrO₃ (M=Mg, Ca, Sr, Ba), electrical and thermal transport props 7-45319
 Zn_{0.9}Hg_{0.1}Se, electrophysical props. and carrier scatt. mechanisms 7-17024
 ZnO films, elec. props., decomp., chemisorption of O⁻, photocond. meas. 7-27445
 ZnO varistor, grain junction barrier height, majority carrier effects (*French*) 7-17033
 ZnO varistor, single grain junction barrier height, minority carrier effects (*French*) 7-21929
 ZnO with tri-valent donor impurities, elec. props., heat treatment effects 7-2611
 ZnO:In films, microstruct., elec. and optical props., film thickness depend. study 7-16895
 ZnSe layer growth by plasma-assisted epitaxy 7-52365
 ZnSe:Cl layers grown by MBE, blue photoluminesc. 7-52364

carrier diffusion length *see carrier lifetime***carrier lifetime**

- hierarchical lattices, phase transition universality sputtered, photoelec. props. 7-35486
 MIS structures, minority carrier lifetime meas. (*German*) 7-56306
 organic semiconductors, electrical transport props., electron bombardment method 7-52641
 p-n structures, electron-probe analysis using the dependence of the induced current on the acceleration voltage 7-38348

carrier lifetime continued

- p-n-p-n structures, on state spreading, diffusion and drift ratio 7-21937
 photoconductive insulators, diffusion length meas. using photocarrier gratings 7-12750
 photon detector devices, local investig. by scanning laser microprobe 7-30083
 polydiacetylene pTS-FBS single crystal, electric field induced SHG 7-43214
 polyethylene films, charge storage lifetime, structural effects 7-27344
 polypropylene films, charge storage lifetime, structural effects 7-27344
 quantum well structs., electric field effect for luminescence (*Japanese*) 7-13236
 relaxation semiconds., minority carrier injection, boundary conditions effects, numerical computation 7-21935
 semiconductor bicrystal, diffusion length and grain boundary recomb. vel. determ. by laser excitation 7-41402
 semiconductor doping superlattices, n-i-p-i crystals 7-7348
 semiconductor double heterostructures, luminescence radiation photon recycling 7-13208
 semiconductor electrical characterisation, non-contacting methods, book contrib. 7-45335
 semiconductor electron-hole plasma, noise spectrum calcs. near slow recomb. wave excitation threshold 7-38649
 semiconductor epitaxial layers, recombination lifetime profiles meas., injection level depend. 7-52874
 semiconductor fast surface state parameter meas. using SAWs 7-11230
 semiconductor grain boundary photovoltaic effect, scanning laser beam obs. anal. 7-12766
 semiconductors, extrinsic, thermal gradient magnetoconc. effect 7-52659
 semiconductors, space charge stratification, transient processes 7-64313
 SOI struct., implanted buried oxide elec. props., high temp. annealing effects 7-58904
 SOI structures, ion beam synthesised, carrier lifetime increase 7-12865
 solar cells, recombination and transport parameters, advanced measurement techniques 7-54316
 Al_{0.3}Ag_{0.7}As, femtosecond carrier dynamics 7-58829
 Al_{0.1}Ga_{0.9}As homojunctions, minority-carrier diffusion, TOF studies 7-12797
 Bi quasi-1D system, Einstein relation modification 7-33013
 Bi_{1-x}Sb_x narrow-gap semicond., intraband breakdown, current-voltage characts., size effect conditions 7-52624
 n-Cd_{0.8}Hg_{0.2}Te, doped and undoped, minority-carrier lifetime 7-21932
 p-Cd_{0.8}Hg_{0.2}Te, doped and undoped, minority carrier lifetime 7-45353
 CdS films, superlinearity of light-current characts. 7-64282
 CdSe thin film liquid-junction photovoltaic cell, photoelectrochem. charactn. 7-54331
 CdZnS-InP heterojunction solar cell, numerical anal. 7-23155
 CoSi₂, thin film, electrical transport props. 7-27442
 CuInSe₂-based photoelectrochem. solar cells, optical and electronic props. studies 7-46958
 FeS₂-electrolyte photoactive interface, electronic props. 7-33086
 GaAlAs-GaAs solar cells grown by MBE, material props. and device parameters 7-23164
 Ga_{0.60}Al_{0.40}As, electron-hole plasma diffusion and carrier density profiles 7-12747
 Ga_{0.96}Al_{0.04}Sb layers, liq. phase epitaxial growth, elec. and photoelec. characterisation 7-39443
 GaAs, Czochralski grown, defect. conc., spatially resolved photoluminesc. 7-22341
 GaAs doping superlattices, photorefectance 7-53368
 GaAs, electron-hole plasma diffusion and carrier density profiles 7-12747
 GaAs, emission lines, lifetimes and ionisation energies 7-22306
 GaAs epitaxial film shallow homojunction solar cells fabrication by Zn solid state diffusion method 7-17860
 GaAs, femtosecond carrier dynamics 7-58829
 GaAs, length scale near metal-insulator transition 7-52425
 GaAs multiple quantum wells, charge-carrier dynamics, contactless microwave photocond. meas. 7-21998
 GaAs polycrystalline solar cell, electron beam generated carriers, in presence of grain boundaries 7-64262
 GaAs sawtooth doping superlattices, prep., LED and laser appls. 7-7372
 GaAs, surface recombination velocity and bulk minority carrier lifetime 7-17037
 GaAs, transport props., charge collection microscopy 7-52649
 GaAs:Si(Be)(Mg), rapid annealing, temp. depend. of damage removal and carrier activation 7-17032
 GaAs/AlAs single quantum well heterostructures confined by short-period superlattices, photoluminesc. 7-22296
 GaAs/Au(Cr) Schottky barriers, hole diffusion length, photon and electron excitation studies 7-2707
 GaAs-Al_{0.7}Ga_{0.3}As single quantum well, photolum., transient response to electric field, carrier lifetime 7-7757
 GaAs-Al_{0.7}Ga_{0.3}As SQW structure, photolum. switching by pulsed elec. field 7-13197
 GaAs-AlGaAs SCH lasers, lasing gain and threshold current 7-31327
 GaAs-GaAs-Al_xGa_{1-x}As heterostructures, photosensitivity spectra 7-64319
 GaAs-Si thin film solar cells, radiation damage 7-65465
 GaAs_{0.12}P_{0.88}N, Te and GaP:N, Si(Te) epitaxial layers, minority carrier lifetimes, surface and interface recombination effects 7-7424
 GaAs_{1-x}P_x:Be⁺-GaP:Be⁺ strained layer superlattices, ion implantation doping, optical and elec. props., device appls. 7-44583
 GaAs_{1-x}P_xN, cathodoluminesc. efficiency, N-bound excitons influence 7-7768
 GaInAs, Czochralski-grown, dislocation effects investig. 7-7261
 GaSb-AlSb multiple quantum well structs., size-induced direct to indirect gap transition 7-7373
 GaSe amorphous film, high field kinetics of photocurrent 7-2748
 Ge, reverse recovery experiments, diode geometry effect 7-34038
 Ge:Ga(Be)(Zn) extrinsic photoconductor material, cryst. growth and characterisation 7-64893
 Ge-Si, p-n junctions, photoelectric props., effects of electron bombardment 7-7351
 a-GeSi:H:F double Schottky barrier structures, surface photovoltage meas. and calc. 7-17093
 HgCdTe, ambipolar diffusion and free carrier recombination studied by transient grating technique 7-12731
 p-HgCdTe, minority carrier characterisation using light-modulated Hall effect 7-21934
 HgCdTe:B⁺, ion implanted n⁺p junction, lifetime and carrier conc. profile 7-45450

carrier lifetime continued

- InGaAs:Si LED, electrical and luminesc. props., ultrasonically-induced changes 7-22350
- InGaAsP/InP heterostructures, carrier lifetimes and quantum efficiencies, photoluminesc. studies 7-64675
- n-InP, minority carrier diffusion length meas. using a photoelectrochemical technique 7-33030
- InP room temp. band edge photolum. intensity interpretation 7-27762
- InP, surface recombination velocity and bulk minority carrier lifetime 7-17037
- InP thin film solar cells on Si substrate, high efficiency and high radiation resistance 7-59852
- InSb, carrier lifetime, pressure depend. 7-52644
- InSb, Dember EMF contrib. to capacitor photo-EMF 7-38621
- InSb, length scale near metal-insulator transition 7-52425
- InSb MOS structures, heat treatment effects 7-8031
- InSb, intrinsic grating formation under two-photon excitation 7-11037
- LiNbO₃, pure and Mg, Fe doped crystals, photoconductivity props. studies 7-38624
- NiSi₂, thin film, electrical transport props. 7-27442
- Pb_{1-x}Sn_xTe-PbTe graded-gap heterostruct., spectral photoelec. quantum efficiency 7-36961
- PbTe doping superlattices, transport and magneto-optical props. 7-12852
- SOI films, halogen lamp recrystallised, minority carrier lifetime studies 7-33101
- SeO, electrophotographic props., doping depend. (Japanese) 7-12752
- p-Si, alpha-particle irradi., defect form. and thermal stability 7-38073
- Si, amorphous, p-i-n solar cells, light-induced defects influence on performance 7-17910
- Si, Auger recombination at low carrier densities 7-7328
- Si BSF solar cells, Rose-Weaver meas. technique 7-8423
- Si bifacial solar cells, minority carrier diffusion length and surface recomb. vel. determ. 7-8407
- Si, bulk free-carrier lifetime, IR absorpt., contactless spatially resolved meas. 7-52650
- Si, CVD thin film backside gettering effectiveness 7-38217
- Si, defect states on the surface and in the bulk, H passivation 7-13665
- Si dendritic web ribbon, electrical and struct. props. 7-16922
- Si dendritic web solar cells, twin plane effects on minority carrier diffusion length 7-13868
- Si diffused p-n structs., recomb. props. of base region, effect of thermal and radiation defects 7-17089
- Si, diffusion length depend. on cooling rates and bulk resistivity 7-7266
- Si, dislocated, charge carrier recomb. processes 7-7264
- Si for solar cells, characterisation by electrolyte-semiconductor interphase and SERS investigation 7-13887
- Si, high purity, charge carrier lifetime meas. 7-45351
- Si high-low junction emitter solar cell, quantum efficiency improvement 7-3681
- Si interdigitated back contact solar cells development 7-8386
- Si layers, electron irradiation-induced defect levels, annealing behaviour, DLTS studies 7-52493
- Si MIS device diffusion length meas. by spectral response 7-8424
- Si MOS capacitor elec. parameters, effects of process chemical purity 7-33103
- Si, microcrystalline films, carrier lifetime from transient photoconductivity meas. 7-7290
- Si, minority carrier lifetime and resist. mapping, flying-spot scanning method 7-4867
- p-Si n⁺pp⁺ solar cell structs., quasisurface recomb. vel. determ. in contact layers 7-58875
- Si, neutron transmutation doped p-n-p-n structs., fast electron irradiated, minority carrier lifetime variations 7-45352
- Si, neutron-transmutation doped, spatially resolved carrier lifetime meas. 7-7257
- Si, nondegenerate, minority carrier diffusion length and doping density 7-33031
- Si, polycrystalline cast ingots, bulk free-carrier lifetime, contactless meas. 7-7258
- Si, polycrystalline p-type, Al and Cu diffusion effects on electronic properties 7-17038
- Si polycrystalline solar cell p-n junction, carrier lifetime, effective recomb. vel. and diffusion length, EBIC meas. 7-23138
- Si solar cell, improved determ. of lifetime and surface recomb. vel. by transient methods 7-13870
- Si solar cells, high efficiency, identification of key parameters limiting perform. 7-59846
- Si solar cells, metal insulator n on p, radiation damage 7-3703
- Si solar cells, multicrystalline, thermal annealing for fabrication 7-17865
- Si space solar cells, damage coeffs. of 1 MeV electron fluences 7-13880
- a-Si technology, review of developments 7-38551
- Si, thermal and electronic transport, photothermal deflection spectroscopy 7-32731
- Si, transmutation doped, carrier lifetime and hall effect, high temp processing effects 7-33027
- Si, transmutation-doped, carrier recomb. props. at gamma-irrad. defects, transport meas. 7-38575
- p-Si wafer, minority-carrier diffusion length determ., photocurrent generation method 7-38579
- Si wafers, doped by neutron transmutation, minority carrier lifetime, photocond., annealing 7-38785
- Si:B, carrier lifetime meas., capture and recombination 7-38585
- Si:Co, minority carrier lifetimes meas. (Japanese) 7-52647
- a-Si:H, glow discharge deposited, light soaking effects 7-52872
- a-Si:H, light soaked, dangling bond creation 7-12150
- a-Si:H, localised electronic state, light soaking and current injection 7-16994
- a-Si:H,B films, hole transport, time-of-flight meas. 7-45320
- a-Si:H,F/a-Si:Ge:H,F superlattices, elec. transport studies 7-38716
- a-Si:H,F/a-Si:Ge:H,F multiple layered films for enhancement in photoresponse in near IR spectrum 7-52668
- a-Si:H,O films, RF sputtered, photoelec. props. 7-38627
- a-Si:H,P, electron lifetime, excitation energy depend. 7-45349
- a-Si:H films, CVD, optical and electronic props. 7-33597
- a-Si:H films, electronic props., effects of γ -irradiation 7-38584
- a-Si:H films deposited in He atmosphere, charact. 7-45056
- a-Si:H material and p-i-n cell, light-induced charge 7-17055
- a-Si:H p-i-n solar cells, behaviour after light soaks through p-layer and n-layer 7-8398
- a-Si:H solar cells, radiation damage by 12 MeV protons and annealing 7-13895

carrier lifetime continued

- a-Si:H/SiO_x:N,H heterostruct., transport props 7-38768
- a-Si:H/a-Ge:H multilayer films, photoconductivity enhancement 7-27443
- n⁺-Si:H, O precipitation and minority carrier generation lifetimes 7-16774
- Si:O Czochralski wafers, electron traps resulting from O precipitation 7-21866
- Si:P, meas. of heavy doping parameters 7-12855
- Si:Ti(V)(Cr)(Fe)(Zr) polycrystalline solar cells, structural, elec., photovoltaic props., impurity effects 7-39990
- Si-SiO₂, MIS struct., temp. stress influence (Slovak) 7-7389
- a-Si:Ge:H, F glow discharge films, elec. and optical props. 7-46169
- a-Si:Ge:H,F glow discharge films, electronic transport and density of states 7-45114
- a-Si_{1-x}Ge_x:H, electron and hole transport 7-7259
- SiO₂ CVD photox layers, Hg-sensitised, elec. props. 7-64379
- carrier mean free path**
see also *electron mean free path (metals)*
amorphous superlattices, mean free path and size quantisation 7-22003
hexatriacantone, hot electron cond. and relax., internal photoemission for transport anal. method 7-45340
Bi, filamentous single crystals, static skin effect and acoustoelectric instability 7-38644
Bi, liq., elec. resist. meas. 7-38532
GaAs, impact ionisation, soft-threshold lucky drift theory, mean free path calcs. 7-64256
Ge, electron mean free path needed for excitation of volume and surface plasmons 7-21838
Si/CoSi₂/Si structs., parallel and perpendicular transport, supercond. props. 7-45518
- carrier mobility**
see also *carrier mean free path; carrier relaxation time; current density; electron-hole recombination; electron mobility (metals)*
1/f noise, carrier mobility fluctuation origin 7-38653
p-AlGaAs/GaAs modulation-doped heterostruct., liq. phase epitaxy and carrier props. 7-33074
amorphous semiconductor superlattices, stochastic carrier transport props. (Chinese) 7-12791
anthracene: acridine crystals, conduction mechanism and trap levels, TSC meas. 7-27342
aromatic hydrocarbons, semicond., nondispersive transport, model of difficult jumps 7-58812
atomic liquids with mol. impurities, similarity law for kinetic coefficients of hot electrons 7-16999
carrier concentration, temperature dependent data, donor and acceptor behaviour 7-64263
conducting polymer films produced by Ar⁺ irradiation of HPR-204, physical and elec. props. 7-26808
contactless measurement of carrier mobility and concentration in semiconductors 7-30036
copper phthalocyanine evaporated thin films, mobility and trap concentration 7-2746
degenerate semicond., diffusivity-mobility ratio, modified form of Einstein rel. in presence of electric and mag. field 7-45356
disordered media, small polaron charge transport model, density-matrix formalism calcs. 7-52612
disordered solids, dispersive hopping and trapping transport, mean field theory 7-38554
DNA, electric charge transfer phenomena, TSC investig. (Czech) 7-13948
double quantum well structs., parallel electron transport studies 7-45474
drift velocity, direct demonstration using the Hall effect 7-48229
electrical characterisation, non-contacting methods, book contrib. 7-45335
electrophotographic films, small charge drift current characteristics 7-33047
epitaxial layers grown directly on Si (100) by low press. MOVPE 7-27924
field-effect capacitor, carrier ambipolar drift vel., field control study 7-52840
glass, ideal homopolar, delocalised charge carrier mobility, temp. depend. 7-52613
graphite films, pyrolysed from polyoxadiazole condensation polymer, elec. and thermal props. 7-2736
graphite-AsF₅ intercalation cpd., galvanomag. props. 7-58822
hierarchical lattices, phase transition universality sputtered, photoelec. props. 7-35486
high resistivity semiconductors, xerographic time of flight technique for drift mobility determ. 7-58807
hole quasienergy spectrum, anisotropic photocond. and nonlinear optical props. calcs. 7-38619
III-V semicond. alloys, vel.-field charact., band struct. effects, CPA calcs. 7-64243
III-V semiconductors, carrier concentration and mobility profiling 7-45315
III-V semiconductors, negative magnetoresistance and nonequilib. electron cooling 7-17042
In_{0.53}Ga_{0.47}As:Fe metalorganic CVD epitaxial growth and elec. props. 7-63993
liquid methane, mobility of injected electrons, calc. 7-38564
measurement techniques 7-58800
methane nonpolar fluid, electron mobility near crit. point 7-7243
minority carrier transport TOF study 7-45310
modulation doped heterostructures, 2D electron gas, transport coeffs., parallel conduction effects 7-2677
multidimensional semiconductor equations, LBI techniques 7-58803
organic layers, carrier drift mobility, anomalous field depend. 7-58928
organic polycrystalline solids, TOF carrier mobility 7-45332
organic semiconductors, electrical transport props., electron bombardment method 7-52641
p-n-p structures, on state spreading, diffusion and drift ratio 7-21937
parabolic semiconducting quantum wells, electrical and optical props. 7-22002
PET films, low frequency dielectric response 7-13091
phenazine, drift mobilities, photovoltaic appls. 7-21906
polycarbonate, molecularly doped polymer, hole transport 7-52616
polycarbonate doped with pyrazolines, photoconductivity and carrier mobility, press. effects 7-27363
polychlorophenylacetylene, elec. cond., carrier mobility, doping effect 7-52875

carrier mobility continued

- polyethylene, electron beam charged, space charge decay currents 7-27338
- polymer, molecularly doped, charge carriers, pseudo-percolation, Monte Carlo study 7-2613
- polymers, conjugated, elec. cond., chain rigidity effects 7-64230
- polyvinylacetylene, elec. cond., carrier mobility, doping effect 7-52875
- polyvinylcarbazole, photoconduction, transition from dispersive to nondispersive transport 7-64283
- quantum wells, optical high-field transport expts. 7-52638
- quasi-one-dimensional semiconductor, electron mobility investig. 7-2616
- semiconductor, carrier transport in built-in and external fields 7-52634
- semiconductor heterostructures, 2D electron and hole mobilities 7-7350
- semiconductors, disordered, with dispersive transport, elec. transient process 7-17074
- semiconductors, highly doped and excited, electron-phonon mobility variation with carrier density 7-64249
- semiconductors, plasmon linewidth, memory-function approach 7-45193
- semiconductors, unoriented cubic, mobility anisotropy coeff. determ. 7-12715
- semiconductors and quantum wells, electron-electron scatt. and mobilities, determ. 7-33003
- semiconductors with parabolic density of states, activity coeffs. of electrons and holes 7-27324
- SOI films, inhomogeneous carrier transport props., influence of temp. 7-33094
- SOS, ion beam improved, elec. characts. 7-17114
- strongly disordered systems, conductor-insulator transition 7-64087
- superlattices, microstructures and microdevices, conf., Goteborg, Sweden (Aug. 1986) 7-35097
- TCNQ salt, conducting Langmuir-Blodgett film, electronic transport props. 7-38782
- ternary semicond. alloy ultrathin wires, alloy scatt. limited mobility calcs. 7-12724
- tetrazenzofulvalene, polycrystalline thin films, TOF expts. 7-45333
- thin short-circuited dielec. films, dispersive charge transport, space charge dynamics calcs. 7-39038
- (TMTSF)₂BF₄, anion ordering, press. effects 7-2596
- triphenylamine derivatives, guidelines for improving charge transport props. (Japanese) 7-38555
- AlAs/Si films and AlAs/Si-GaAs/Si superlattices, MBE growth and electrical props. 7-22052
- AlGaAs/Sb, MBE growth, Sb doping 7-2038
- AlGaAs/Si-GaAs 2D electron gas structure, scatt. mechanisms 7-38718
- AlGaAs/GaAs/Si heterostruct., MBE growth on polar surfaces 7-7863
- AlGaAs/GaAs/AlGaAs selectively doped double heterostructs., electron conc. and mobility 7-12839
- AlGaAs/GaAs/AlGaAs single quantum well, negative differential mobility and drift vel. overshoot 7-52803
- AlGaAs-GaAs 2D electron gas strucs., scatt. mechanisms 7-52783
- AlGaAs-GaAs-AlGaAs single quantum well heterostruct., negative differential mobility and drift velocity overshoot 7-52787
- Al_{0.2}Ga_{0.8}As/GaAs heterojunction, high mobility 2-D hole gas 7-2679
- Al_{0.1}-_{0.5}-As-GaAs heterostructures, 2D electron space charge layers, plasmon and magnetoplasmon excitation 7-38696
- Al_{0.1}Ga_{0.9}N MOVPE growth, struct. and elec. props. 7-21729
- Al₂O₃:Fe₂Y, high temp. DC elec. cond. rel. to superalloy oxide scale adherence 7-52615
- Ar, liq., effective momentum transfer cross section for excess electrons 7-21956
- Ar nonpolar fluid, electron mobility near crit. point 7-7243
- As₂Se₃:Ni films, electronic struct. and transport props. 7-12595
- Au, discontinuous films, charge carrier mobility, temp. depend. 7-22035
- BaTiO₃, photo-excited holes, photorefractive meas. of mobility anisotropy 7-21918
- Bi band parameter temp. depend. galvanomag. coeffs. and mobility, L-hole effect calcs. 7-2461
- Bi quasi-1D system, Einstein relation modification 7-33013
- Bi₁₂GeO₂₀ piezoelec. semicond., photovoltaic displacement current, Hall component meas. 7-64286
- CdGeAs₂, n-channel inversion layers, oscillatory diffusivity-mobility ratio, quantising mag. field 7-45419
- p-CdGeAs₂ semicond., hole mobility and scatt., temp. depend. study 7-52609
- Cd_{1-x}Hg_xTe crystals, impurity band elec. conduction, Fermi glass model anal. 7-27328
- Cd_{1-x}Hg_x-Te, p-type, minority carrier exclusion 7-64242
- CdIn₂O₄ RF sputtered films, transparent heat mirror characts., elec. and optical meas. 7-39199
- CdIn₂O₄ thin films, DC reactive sputtered, elec. and optical props. 7-38788
- CdIn₂S₂Se₂ semicond., optical and elec. props. 7-33010
- CdS films, spray deposited, laser annealing, struct., carrier mobility 7-58318
- CdS films, superlinearity of light-current characts. 7-64282
- CdSe crystals, laser beam defocusing, rel. to Hall mobility and carrier density 7-52652
- CdSe, optimally annealed in molten Cd, DC galvanomagnetic props. 7-27352
- CdSnO₄:PbO highly conducting films, characterisation 7-22049
- p-CdTe, complex-formation processes at high concentrations of intrinsic defects 7-37963
- CdTe films, electrochemically deposited, resistivity, carrier conc. and carrier mobility 7-7419
- CdTe grown on Si by LPMOCVD, physical props., Hall meas. 7-27181
- n-CdTe:In, high mobility, growth by photoassisted MBE 7-22485
- CdTe:Sn, impurity compensation effect on elec. resist. and mobility 7-52614
- CdZnS-InP heterojunction solar cell, numerical anal. 7-23155
- CuInS₂ films, RF sputtering, struct. and elec. props. 7-3169
- CuInS₂:P, ion implanted, pulsed electron beam annealing 7-16644
- CuInSe₂ thin films, polycrystalline, elec. props., effect of excess Cu 7-52871
- GaAs, chemical beam epitaxial growth investig. 7-7878
- GaAs diode, active layer <1 μm, low temp. current flow 7-52575
- GaAs, electron drift vel.-elec. field characts. 7-38569
- GaAs epilayers, plasma enhanced metalorganic CVD 7-46336
- GaAs epitaxial films, MOCVD growth using tertiarybutylarsine source 7-59439
- GaAs epitaxial layers, OMVPE growth on Si (100) 7-3190

carrier mobility continued

- GaAs epitaxial layers, MOCVD grown, influence of growth parameters on residual impurities 7-7047
- GaAs films on oxidised Si, zone melting recrystallisation 7-38396
- n-GaAs, Hall factor calcs. 7-52657
- GaAs high quality layers grown on Si by MOCVD, high electron mobility 7-27922
- GaAs highly doped quantum wells, mobility enhancement 7-64325
- GaAs, horizontal Bridgman growth, semi-insulating props. characts. 7-64896
- GaAs, hot-electron 1/f noise 7-21927
- GaAs, MBE growth, acceptor impurity background reduction 7-3173
- n-GaAs metal-dielectric-semiconductor system, field effect, transistor studies 7-52841
- GaAs, mixed electron-hole conductivity 7-58808
- GaAs, OMVPE, low pressure growth from trimethylgallium+AsH₃ 7-17439
- GaAs, plastically deformed, Hall effect meas. 7-27351
- GaAs quantum wells, 2D hot-electron mobility 7-45470
- GaAs quantum wells, n-modulation-doped, negative absolute mobility of holes 7-7337
- GaAs, seminsulating, electrophysical props., dislocation effects 7-16557
- GaAs single domain layer growth on Si wafers by MOCVD/MBE, heteroepitaxy 7-52357
- GaAs thin films, on glass substrates, transport props. 7-2742
- n-GaAs:Co, impurity double acceptor state, Hall effect and resistivity meas., temp. and press. depend. 7-12656
- GaAs:Mg⁺, formation of p-type layers using ion implantation and rapid thermal annealing 7-45311
- GaAs:Si surface elec. props. modification by plasma exposure 7-27346
- GaAs:Si, ion implanted, rapid thermal annealing effects 7-21259
- GaAs:Si heteroepitaxial growth on sapphire, low press. MOCVD three-step method 7-27927
- GaAs:Si(Be)(Mg), rapid annealing, temp. depend. of damage removal and carrier activation 7-17032
- GaAs:Te films, flash evaporation, annealing, elec. props. 7-64373
- GaAs/Al_{1-x}Ga_xAs modulation-doped heterostructs., 2D electron gas mobility meas. and calcs. 7-12840
- GaAs/Al_{0.1}Ga_{0.9}As modulation doped heterostruct., high temp. annealing effects (Chinese) 7-12805
- GaAs/AlGaAs 2D electron gas MBE structures, carrier mobility and density meas. 7-64321
- GaAs/AlGaAs heterostructs. on Si substrate, MOCVD and MBE growth 7-7883
- GaAs/AlGaAs modulation doped heterostructs., transport props. studies 7-52752
- GaAs/GaAlAs double quantum well structures, ambipolar carrier transport, optical TOF study 7-12802
- GaAs/GaAlAs graded gap superlattices, high velocity vertical transport 7-52802
- GaAs-Al_{1-x}Ga_xAs, superlattices, carrier behaviour, mag. field. effect 7-45449
- GaAs-Al_{0.1}Ga_{0.9}As modulation-doped structure, parallel cond. in quantum limit 7-12808
- GaAs-Al_{0.1}Ga_{0.9}As semicond. superlattice, exciton transitions study 7-52432
- GaAs-AlGaAs DH injection laser, optical and transport props., emission energy shift, threshold current meas. 7-1101
- GaAs-AlGaAs heterostructures, density of states of Landau levels 7-52822
- GaAs-Ga_{1-x}Al_xAs heterojunction, 2D electron and hole mobilities 7-7350
- GaAs-GaAlAs:Si modulation doped quantum wells, electron mobility, temp. depend. 7-45473
- GaAs_{1-x}P_x:Be⁺-GaP:Be⁺ strained layer superlattices, ion implantation doping, optical and elec. props., device appls. 7-44583
- n-GaAs_{1-x}Sb_xP_y epitaxial film, impurity distrib., cond. and Hall mobility study 7-51808
- GaInAs/GaAs single quantum well pseudomorphic strucs., high electron mobility meas. 7-12841
- GaInAs/InP heterostructures, VPE, homogeneity, mobilities 7-58882
- Ga_{0.47}In_{0.53}As/InP heterojunction, chem. beam epitaxy grown, 2D electron gas 7-12803
- Ga_{0.47}In_{0.53}As-InP heterojunction, with three electron subbands, hydrostatic press. effect 7-2695
- Ga_{0.47}In_{0.53}As-InP heterojunction, MOCVD grown, 2D hole gas 7-21992
- Ga_{1-x}In_xAs/InP heterostructures, MOVPE, electron mobility, exciton peak, magnetotransport 7-58883
- Ga_{0.1}In_{0.9}As, low-pressure MOVPE growth 7-7873
- GaN:Zn, pure and doped, electrophysical props., nonhomogeneous semicond. model 7-27292
- GaP, floating zone melting prep., elec. props. 7-64238
- GaP LPE layers, reuse of Ga melt for LED prep., effect on electrical characts. 7-22592
- GaSb:Te(Si)(Ge) single crystals, Czochralski growth, carrier conc. rel. to dopant conc. 7-22462
- GaSb/InAs/GaSb quantum wells, carrier densities and mobilities, magnetotransport meas. 7-12846
- GaSe amorphous film, high field kinetics of photocurrent 7-2748
- Ga₂Se₃ films on GaAs substrates, insulating coating, stoichiometric vacancies, carrier mobility 7-52846
- Ge crystal, carrier mobility meas. using Haynes-Shockley expt. for student laboratory 7-55933
- p-Ge, Hall effect, mag. field and temp. depend., transport eqn. soln. 7-52651
- p-Ge, hot electron transport, perturbed acoustic phonon distrib. effects, Monte Carlo anal. 7-64254
- Ge, MBE growth on CaF₂/Si (111), structural and electrical characteristics 7-45051
- Ge, n-type and ultrapure samples, electron transport and press. coeffs. 7-2615
- Ge surface state characts., surface struct. and low temp. annealing effects 7-45426
- Ge:Ga(Be)(Zn) extrinsic photoconductor material, cryst. growth and characterisation 7-64893
- Ge:O, γ-irrad., majority carrier mobility meas. 7-27334
- Ge:Sb, mobility anisotropy coeff. determ. 7-12715
- Ge₂Si_{1-x}-Si strained layer heterojunctions, selectively doped, hole mobilities, temp. depend. 7-7383
- n-HgCdTe, acceptor densities, photo-Hall determ. 7-58836

carrier mobility continued
p-HgCdTe, minority carrier characterisation using light-modulated Hall effect 7-21934
p-Hg_{0.78}Cd_{0.22}Te:Sb LPE films, elec. props. 7-7426
Hg_{1-x}Cd_xTe, epitaxial growth by low temp. metalorganic CVD 7-27911
Hg_{1-x}Cd_xTe films, LPE using a semiclosed rotational boat 7-64937
Hg_{1-x}Cd_xTe films, organometallic epitaxial growth on CdTe and characterisation 7-22579
Hg_{1-x}Cd_xTe, zero gap, acceptor levels 7-27287
Hg_{1-x}Cd_xTe/CdTe superlattices, MBE growth and props. 7-53602
Hg₂ detector, electrical characteristics 7-49838
HgTe based superlattice, MBE growth and props., high hole mobility problems 7-7345
HgTe-based solid solns., low temp. electron mobility, resonance scatt. 7-38558
p-HgTe-CdTe superlattices, magnetotransport props. 7-33076
HgTe-Hg_{1-x}Cd_xTe heterojunctions, hole Hall mobility enhancement 7-33077
InAlAs/InGaAs modulation-doped heterostructs., 2D electron gas mobility meas. 7-12842
n-InAs, Kane-type semiconductors, Einstein relation, mag. quantisation effect 7-52603
InGaAs epitaxial films, MO-chloride VPE growth 7-22566
InGaAs/InP single quantum wells, transport and persistent photocond. props. 7-27385
In_{0.53}Ga_{0.47}As-In_{0.52}Al_{0.48}As modulation-doped heterostructs., interface roughness scatt. 7-2678
In₂Ga_{1-x}As, gas source MBE growth 7-52361
In₂O₃/Sn vapour deposited films, growth, struct., electronic props. 7-12535
In₂O₃/Sn(In)(Cd) films, optical and elec. props. 7-22365
InP, chemical beam epitaxial growth investig. 7-7878
InP epitaxial films, MO-chloride VPE growth 7-22566
InP epitaxial films, MOCVD grown, identification of acceptors and donors 7-58688
InP epitaxial layers, MOVPE, elec. characts., photolum. 7-22519
InP films on oxidised Si substrate, laser recrystallisation 7-38398
InP, floating zone melting prep., elec. props. 7-64238
n-InP, Hall factor calcs. 7-52657
InP, MOVPE; morphology, photolum., carrier conc. and mobility 7-22518
InP pure and Er doped liquid phase epitaxial films, elec. props. in strong elec. fields 7-38779
InP room temp. band edge photolum. intensity interpretation 7-27762
InP synthesis by modified horizontal Bridgman method, elec. props. 7-58821
InP, ultrapure, atmospheric pressure OMVPE growth 7-13375
InP, undoped and Zn(Cd) doped thin films, prep. and characts., appl. for solar cells 7-17895
InP, VPE using flow modulation 7-7039
InP:Fe wafer, semi-insulating, elec. characteristics 7-45323
InP:Hg ion implanted at 200°C, rapid thermal annealing, carrier conc. and mobility 7-32469
InP:Yb LPE layers, luminesc. and elec. props. 7-59464
InP/InGaAs:Zn, PIN detectors, OMVPE growth 7-27931
InP-InGaAs single quantum wells, transport and persistent photoconductivity 7-38709
InSb, coherent spontaneous oscills. under transverse breakdown conditions, high frequencies 7-17046
InSb, conduction band, deformation potential constant 7-7112
InSb films, preparation of highly sensitive magnetoresistance elements 7-7859
InSb/CdTe interface, quasi-2D electron gas obs. 7-21987
InSe single crystals, growth by travelling heater method, carrier conc., photoelectrochemical props. 7-59410
Kr, liquid, electron mobility meas. 7-2614
LaS, NaCl type lattice, current carriers and cond. 7-45346
Mg₂Si(Ge)(Sn)(Pb), Hall effect in solid and liq. states 7-38647
Mn_{0.61}Zn_{0.26}Fe_{2.13}O₄, ferrite, conductivity study 7-21909
MoS₂ films, RF magnetron sputtered, elec. and optical props. 7-2747
Pb_{0.75}Sn_{0.25}Te:In, Ge(S)(Se), elec. resist., photocond., Hall effect meas. 7-17050
Pb_{0.9}Sn_{0.1}Te thin films, structural and elec. props., pulsed laser-irrad. effects study 7-21270
PbTe, thermoelectric props., effect of dielectric inclusions 7-12746
PbTe:Ti(Tl,Na) films, superconducting transition 7-38797
Pb_{1-x}Te:Ti, quasilocal level and transport props. 7-38492
ReS₂, single cryst. growth by chem. vapour transport, elec. resist., Hall mobility meas. 7-64251
ReSe₂, single cryst. growth by chem. vapour transport, elec. resist., Hall mobility meas. 7-64251
Se:O, electrophotographic props., doping depend. (Japanese) 7-12752
Si cold cathode for high current densities 7-12816
p-Si conductivity and Hall mobility calcs., impurity scatt., anisotropic-nonparabolic effects 7-12720
Si doping superlattices, anomalous mobility enhancement 7-7381
Si, epitaxial growth using photochem. vapour deposition at 200°C 7-39431
Si exciton transport, optical time-of-flight investigation 7-64244
Si films, solid epitaxial regrowth, structural and electrical characteristics 7-38403
Si films, solid phase epitaxial regrowth on epitaxially grown MgO.Al₂O₃ 7-38399
Si, high temp. drift mobility, determ. 7-52621
Si, hot-electron 1/f noise 7-21927
Si interdigitated back contact solar cells development 7-8386
Si, MBE growth on CaF₂/Si (111), structural and electrical characteristics 7-45051
Si membrane (suspended), base carrier accumulation solar cell, fabrication 7-3664
Si polycrystalline film, mobility temp. depend. (Chinese) 7-2744
Si quantum well struct., 2D electron gas, transport props. 7-52774
Si strips, grown by Stepanov's reversed method, strength, struct., electro-physical props., effects of thermal conditions during growth, photocell appl. 7-32325
Si:As, ion implanted, electronic transport props. 7-7233
Si:As films, heavily doped, grown by partially ionised MBE, phys. and elec. characts. 7-12561
Si:B, F implanted amorphous layers, struct. and elec. props., ESR and Hall effect meas. 7-26634

carrier mobility continued
Si:B(BF₃) wafers, activated carrier density profile and scatt. rate meas., nondestructive IR attenuated total refl. technique 7-22207
Si:Gd, grown from melt, electrical and optical props., residual impurities 7-63636
a-Si:H, electronic transport 7-33004
a-Si:H, extended state mobility and tail-state distrib. 7-2617
a-Si:H, glow discharge deposited, light soaking effects 7-52872
a-Si:H, intrinsic glow-discharge, elec. noise meas. 7-64297
a-Si:H, localised electronic state, light soaking and current injection 7-16994
a-Si:H,B films, hole transport, time-of-flight meas. 7-45320
a-Si:H,F films, H-radical-assisted CVD, hole transport 7-64264
a-Si:H,F/a-Si,Ge:H,F superlattices, elec. transport studies 7-38716
a-Si:H,F/a-SiGe₂H,F multiple layered films for enhancement in photore-sponse in near IR spectrum 7-52668
a-Si:H,F-Si_{0.4}Ge_{0.6}H,F superlattices, carrier scatt., optical absorpt. study 7-38711
a-Si:H,O films, RF sputtered, photoelec. props. 7-38627
a-Si:H biased activated reactive layer evaporation and charactn. 7-59428
a-Si:H CVD coating, high temp. elec. cond. meas. 7-45336
a-Si:H films, carrier transport 7-17023
a-Si:H films, electronic props., effects of γ -irradiation 7-38584
Si:H films, ion implant redistribution 7-16921
a-Si:H material and p-i-n cell, light-induced charge 7-17055
a-Si:H n⁺-i-n⁺ struct., freq.-depend. noise studies 7-45484
a-Si:H p-i-n solar cells, behaviour after light soaks through p-layer and n-layer 7-8398
a-Si:H photo-CVD coatings, characterisation using TFT structure 7-38561
a-Si:H/SiO₂:N,H heterostruct., transport props 7-38768
n⁺-a-Si:H/a-Si:H/a-SiC:H heterostructures, electrophotographic props. 7-45485
a-Si:H/a-SiN_x:H interface, deep states and photoluminescence spectra, transistor characts. 7-39186
Si:O, γ -irrad., majority carrier mobility meas. 7-27334
Si:O,B⁺, ion implanted, reverse annealing 7-16617
Si:P, polycrystal. thin film, carrier transport, temp. depend. study 7-22043
Si:P, self-consistent multi-ion screening formalism 7-38505
Si/Si_{0.55}Ge_{0.45} strained layer superlattices, 2D electron systems 7-7380
Si/SiO₂ interface, digital control of avalanche injection method for studying carrier transport 7-64350
Si-Si_{0.55}Ge_{0.45} modulation doped superlattice, MBE grown, electron mobility enhancement, Hall meas. 7-7382
Si-Si₃N₄ and Si-Si₃N₄-SiO₂ SOI structures, laser recrystallisation, effects of different capping layers, characterisation 7-45511
Si-SiGe strained-layer superlattices, optical and electronic props. 7-53353
Si-SiGe, MBE SOI formation, Auger study 7-32876
Si-SiO₂ interfaces, microstruct. and electronic props. 7-38359
Si-SiO₂ structs., low and high temp. oxidised, inversion electron mobility study 7-22019
3C-SiC, n- and p-type epitaxial CVD layers, elec. props. temp. depend. studies 7-58917
 β -SiC(N) single crystals, CVD grown, elec. props., temp. dependence 7-2740
a-SiGe:H, F glow discharge films, elec. and optical props. 7-46169
a-SiGe:H,F glow discharge films, electronic transport and density of states 7-45114
a-Si_{1-x}Ge_x:H, electron and hole transport 7-7259
a-SiN:H, electrical behaviour 7-2627
SnO₂, oriented thin films, elec. props. 7-17123
SnO₂:F films, CVD growth using hydrofluoric acid as doping material 7-7871
SnO₂:F thin films, CVD deposition, elec. and optical props. 7-7425
SnTe:Bi epitaxial layers, vacuum deposition, optical and electrical props. 7-59430
Ta-Ta₂O₅-electrolyte system, conduction processes 7-38725
(TaSe₂)₂I quasi-1D chain cpd., thermoelec. power temp. depend. meas. 7-17045
Te (0001), conductivity of size-quantised holes, hydrostatic pressure effects 7-54528
TiN_x epitaxial layers, atomic and electronic struct., growth, physical props. 7-32854
Xe, liquid, thermal electron mobility calc. 7-17027
Xe nonpolar fluid, electron mobility near crit. point 7-7243
YIG single crystals, thermodepolarisation studies (Russian) 7-33029
Y₂Ti₂O₇, small-polaron conduction 7-21915
ZnO varistor, grain junction barrier height, majority carrier effects (French) 7-17033
ZnO varistor, single grain junction barrier height, minority carrier effects (French) 7-21929
ZnSe epitaxial layers, MOVPE grown, elec. and photolum. props. 7-7420
n-ZnSe, heavily doped strongly compensated crystals, electron mobility 7-7247
ZnSe layer growth by plasma-assisted epitaxy 7-52365

carrier relaxation time
see also electron relaxation time (metals)
narrow energy band systems, insulator-metal transition 7-38455
polar semicond., carrier-carrier interaction and picosecond phenomena 7-45309
semiconductor heterojunctions, 2D hot electron time-depend. energy relax., nonequilibrium optical phonon effects 7-64102
semiconductor superlattices, amorphous, carrier relax. processes (Chinese) 7-58864
semiconductor thin films, weakly absorbing, thickness, optical consts. and relax. time determ. 7-39194
semiconductors, highly doped and excited, electron-phonon mobility variation with carrier density 7-64249
semiconductors, hot-carrier transport, Monte Carlo and Davydov calcs. 7-45341
semiconductors, plasmon linewidth, memory-function approach 7-45193
SOI struct., implanted buried oxide elec. props., high temp. annealing effects 7-58904
GaAs/AlGaAs multiple quantum well structures, hot-carrier relaxation, femtosecond optical meas. 7-52750
Ge, tubular hole distrib. under streaming conditions, scatt. anisotropy effects calcs. 7-58802
n-Hg_{0.8}Cd_{0.2}Te, condensed electron system, heat capacity, comment 7-58503

carrier relaxation time continued

- Hg_{0.9}Cd_{0.1}Te, low temp. hot electron energy relax. time in extreme quantum limit mag. fields 7-33035
 LaS, NaCl type lattice, current carriers and cond. 7-45346
 NbO₂, semicond., AC cond. meas., 4-196K, 5-92 kHz 7-45327
 Si, tubular hole distrib. under streaming conditions, scatt. anisotropy effects calcs. 7-58802
 YIG single crystals, thermodepolarisation studies (*Russian*) 7-33029

carrier scattering at surfaces *see surface scattering***carrier scattering by dislocations** *see dislocation scattering***carrier scattering by impurities** *see impurity scattering***carrier scattering by point defects** *see point defect scattering***carrier traps** *see electron traps; hole traps***carry circuits** *see adders***CARS** *see coherent antiStokes Raman scattering***cars (vehicles)** *see automobiles***cartography**

- aerial photographs, potential precision of monocular and stereoscopic obs. 7-47317
 airborne reconnaissance, operational cartography appl. 7-23517
 Atlas AMP, Map-Master, and Randmap, mapping packages for IBM PCs 7-28815
 Atmospheric Release Advisory Capability for radioactive materials, contour-to-grid methods 7-40078
 automation conf. London, England (Sept. 1986) 7-35105
 basins tectonic maps, principles of tectonic classification and structural units description 7-34435
 cameras for aerial photography, comparison of three modern aerial cameras (*French*) 7-47307
 Canada's electronic atlas 7-40407
 computer mapping, minimal requirements for CAD 7-40402
 computerised line-matching problem in digital cartography and photogrammetry 7-47315
 coordinate transformation (geodetic to grid coords.), the Lambert conical orthomorphic projection 7-65917
 developing nations, role of computerised cartography 7-40409
 digital cartographic data, electronic delivery for users of data 7-66306
 digital elevation models, comparative test of photogrammetrically sampled models 7-47316
 digital elevation models 7-40403
 digital merging of Landsat TM and digitized NHAP data for 1:24000-scale image mapping 7-40607
 digital terrain model for flat areas by least squares techniques on mini-computer 7-40410
 digital terrain models, accuracy 7-40404
 generalisation, cartographic, data types 7-47323
 generalisation from large to medium and small scale Ordnance Survey maps using expert systems techniques 7-47324
 generalised cartography, computer aided 7-47322
 geographic database, Minute Man National Historical Park, map input software 7-47319
 graphical display and manipulation 3-dimensions of cartographic data 7-40408
 hydrogeological map production using remote sensing, methodological problems 7-55295
 hydrographic data, digital, requirements 7-47422
 hydrographic survey information processing system 7-47421
 land-cover mapping from synthetic aperture radar obs., importance of radiometric correction 7-4200
 Landsat and SPOT high resolution satellite images: a new component for geographic data bases 7-40405
 Landsat data, Fourier filtering for information extraction in surveying and mapping 7-47582
 landscape mapping using space photo imagery 7-60153
 littoral cartography, SPOT remote-sensing image segmentation 7-29307
 meteorological fields mapping, developments in use of empirical orthogonal functions 7-29142
 nautical charting system II for National Ocean Service 7-47423
 planetary satellites, cartographic coordinates and rotational coordinates (1985) 7-34893
 planets, cartographic coordinates and rotational coordinates (1985) 7-34893
 polar coordinate transformation to new pole 7-54846
 projective transformation of space imagery into mosaics and photomaps, minimisation of Earth curvature effect 7-65922
 push-broom linear array scanner, design of all-reflective flat-field objective 7-55320
 quasi-ideal spatial filters for large maps, algorithm for 2D digital signals 7-28808
 radarclinometry, mathematical theory and algorithm 7-34372
 radionavigation methods, differences between nautical charts and the geodetic datum (*Japanese*) 7-66353
 real-time photogrammetric input versus digitised maps: accuracy, timeliness and cost 7-40406
 remote sensing, cartographic projection for reference TV mosaic data bank 7-55048
 remote sensing, multipurpose space experiment for land studies 7-66336
 remote sensing for soil surveys, symposium, Wageningen, Netherlands (March 1985) (*French English*) 7-18476
 remote sensing of power station thermal discharges 7-40503
 SAR data, spaceborne, registration to topographic maps 7-4237
 satellite passive microwave ice map, near real-time data system 7-4242
 smoothing error dynamics in mapping problems 7-8788
 soil mapping, utility of Landsat imagery in data base for small-scale mapping 7-4205
 spatial diversity index mapping, for classes in grid cell maps 7-4221
 terrain data interactive image processing, digital SM-4 Omega system 7-66334
 thematic mapper data geodetic correction to cartographic standards 7-60425
 Thematic Mapper used for map production 7-28816
 thematic mapping from Landsat and collateral data, past experience and future potential 7-3967
 topographic mapping, digital, of Victoria Australia 7-47321
 undersea features name file for personal computer, database description 7-65927
 USA geological survey, digital system development, MARK II 7-47320
 Venus Radar Mapper, implications of Gestalt formation in stereoradargrammetry 7-9379

cartography continued

- Venus surface photographic map, Plate V-4, geological and morphological description of Lakshmi Planum 7-66485
 Venus surface photographic map, Plate V-5, geological and morphological description of Ishtar Terra 7-66486
 watersheds, topographic partitioning via digital elevation models 7-23723
 World projections for environment mapping, application 7-14399
 Zambia, provisional metamorphic maps and explanatory notes 7-18184
 Zeiss/Oberkochen PLANICOMP family for digital mapping 7-40619
 Zeiss/Oberkochen PLANIMAP system extensions 7-40620

cascade control

- hog fuel predrying by flue gas heat recovery 7-8356
 nuclear power plant cascaded state feedback control 7-56776

cascade networks

- electrical networks, 1/f noise, log-normal distrib. and cascade processes 7-48573

cascade showers *see cosmic ray showers and bursts***Cassegrain antennas** *see reflector antennas***cast iron** *see iron alloys***casting**

- brass, two-phase, Al-B Masteralloy addition, B redistrib. during solidification, grain refining effect 7-22664
 epoxy polymers, compact tension specimen casting, fatigue crack growth rate testing 7-13681
 fibre-reinforced Al alloy-matrix composites fabrication process 7-46377
 IN 100, rheocasting and vacuum are double electrode remelting, solidification struct. 7-39497
 inverse problems in solidification and cooling processes, casting 7-58442
 metal-ceramic particle composites, cast, solidification, struct. and props. 7-7932
 metallic mould/casting thermal response characts., transient temp. field anal. 7-65019
 mirror, honeycomb sandwich, borosilicate, blank prep. by spin casting 7-37225
 planar flow casting machine for rapid solidification processing 7-3213
 polyoxy-2,6-dimethyl-1,4-phenylene, sulphonated, ultrafiltration membrane prep. 7-54174
 poly[bis(trifluoroethoxy)phosphazene] membranes, synthesis, casting, diffusion testing 7-13812
 rapidly solidified alloys, developments and engng. design implications, review 7-27967
 steel, C, casting, thin strip continuous, finite element model and thermal feasibility 7-13403
 steel, stainless, martensitic, cooling rate and heat treatment effect on chem. microinhomogeneity 7-3294
 stirred solidification, Taylor vortices influence on morphology 7-22657
 York, England (Jul. 1986) 7-48142
 Zerodur, lightweight large mirror blanks prod. 7-37223
 Al alloy, binary, alloying capacity for solid soln. obtained by casting under press. 7-53716
 Al alloys, wear, comparative investigs. and prep. method role 7-13605
 Al based composite, rheocasting, microstruct., fracture, worn surface (*Chinese*) 7-13407
 Al, grain refinement by horizontal circular vibration 7-22650
 Al-Al₃Cu eutectic alloys, chill cast, directionally solidified, hot rolling microstruct. 7-46447
 Al-Cu (3.76 wt.%), rheocast, partially homogenised, ageing response, microhardness 7-46499
 Al-Cu-Mg, cast composite, mica particle distrib. 7-46375
 Al-Mg-Si, Al-Mg, cast, mica particle dispersed composites, struct., strength, hardness 7-59574
 Al-Mg-mica particle composites, prep. and props. 7-22613
 Al-Si LM 13 alloy with graphite particles, gravity die cast, dispersed graphite effect on freezing rate 7-59506
 Al-Si; graphite particle reinforced composite, solidification, microstruct. 7-28028
 Al₂O₃ ceramic casting by doctor-blade method, effect on props. of green tape (*Japanese*) 7-22620
 Au-Ag-Cu-Pd, cast microstruct. segregation, TEM obs. 7-39495
 Cu-B, cast struct., segregation, conc. undercooling 7-3291
 Cu-Ce, cast struct., segregation, conc. undercooling 7-3291
 Cu-Sn (11 wt.%), stir cast, torsion behaviour 7-46567
 Fe, chromium type, duplex nature of eutectic carbides 7-13440
 Fe, grey cast, skin casting under microgravity conditions 7-22661
 Fe, nodular, ferritising action of increased Mg content on struct. 7-3292
 Fe-Cr-Co permanent magnetic alloys, casting 7-53051
 Fe-Si (3 wt.%), continuously cast slabs, high temp. grain growth during reheating 7-8019
 Fe-TiB, eutectic system, microhardness, modulus of elasticity (*Russian*) 7-39648
 Ni-Al (20 wt.%) alloy, planar flow cast, cooling rates and microstruct. 7-59505
 Ni-Al-Co-Cr-Ta, polycrystalline superalloys, microstruct. rel. to Ta content 7-46446
 Ni-base superalloys, cast, solidification behaviour w.r.t. Hf additions (*Chinese*) 7-7984
 Ni-Ti-Nb, shape memory alloy, cast microstruct. 7-7988
 Si, ingot and foil casting 7-53711
 Si, ramp assisted foil casting and photovoltaic appls. 7-16609
 Si solar cell fabrication by sheet casting 7-17868
 Ti and its alloys, casting technology 7-7914
 U, texture anisotropy, as-cast and heat treated 7-46518
- castings**
 brass, two-phase, Al-B Masteralloy addition, B redistrib. during solidification, grain refining effect 7-22664
 castings, strength and elec. props. 7-27971
 electroradiography inspection method for castings 7-65262
 plate with thin regions, stress conc., theoretical and photoelastic studies 7-57697
 rapidly solidified alloys, developments and engng. design implications, review 7-27967
 steel, high-speed, cast and wrought, impact-fatigue strength 7-39656
 steel, low-C, failure micromechanism in fatigue crack propag. after different heat treatments 7-46641
 steel, nonmetallic inclusions influence on fracture character 7-3421
 steel, stainless, martensitic, cooling rate and heat treatment effect on chem. microinhomogeneity 7-3294
 Al alloy, binary, alloying capacity for solid soln. obtained by casting under press. 7-53716
 Al alloys, wear, comparative investigs. and prep. method role 7-13605

castings continued

Al-Li-Be alloys, arc-melted, microstruct. evaluation 7-22655
Al-Si eutectic alloys, partial modification mechanism 7-59498
Al-Si LM 13 alloy with graphite particles, gravity die cast, dispersed graphite effect on freezing rate 7-59506
Al-Si-Cu castings, fatigue strength improvement by shot peening (*Japanese*) 7-8100
Al-Si-Mg (7, 0.3 wt.%), strength and ductility, effect of macroporosity 7-3386
Al-Si-Zn-Mg-Ti-(Sr) system alloys, mech. props., Sr microalloying effect 7-3377
Cu-Al-Ni-Fe-Mn bronze, cast, laser surfacing, improved corrosion resist., microstruct. characteris. 7-13651
Fe chem. analysis with VRA-30 sequential X-ray fluoresc. spectrometer 7-8333
Fe, Cr-type, duplex nature of eutectic carbides 7-13440
Fe, high-Cr, wear-resistance, laser and heat treatment effect on struct. and props. 7-8174
Nb-Zr (1 wt.%) alloy, hydroextruded, optimum degree of deform., microstruct. 7-3325
NbC_x, ordering behaviour, superstruct, refl. obs. 7-3267
Ni-Al (20 wt.%) alloy, planar flow cast, cooling rates and microstruct. 7-59505
Ni-base superalloy, IN-100, rheocast, processing-struct. charactn. 7-46449
Ni-Cr-Ti-Al-(Mo), dendritic single crysts., microsegregation 7-46477

cataclysmic binary stars

see also dwarf novae; novae; symbiotic stars
accretion disk boundary layer, 2D numerical models 7-60667
accretion disks, model of hydromagnetic turbulence in differentially rotating disks 7-18354
accretion from inhomogeneous medium, general case and observational consequences 7-9460
amplitude-period length relation 7-4472
FO Aqr (H2215-086), intermediate polar, origin of visual and IR pulsations from polarimetric obs. 7-47985
astrometric positions of 20 cataclysmic binary stars 7-18345
V834 Cen (E 1405-451), phase-resolved spectroscopy of AM Her star 7-66675
U Cep, interacting and eclipsing binary star 7-9482
AT Cnc, cataclysmic binary star behaviour in AD 1985/6 season 7-9486
AC Cnc, UBV_R obs. of eclipsing cataclysmic binary 7-29489
T CrB, recurrent nova, UVB photometry rel. to short-term light vars. 7-55660
T CrB, recurrent nova, UV obs. by IUE (1978 to 1986) 7-47941
E 2003+225, AM Her star, mass transfer and mag. field characts., spectrophotometric obs. 7-60722
EXO 023432-5232.3, discovery of probable AM Her binary 7-47980
H 0534-581, DQ Her star, identification, X-ray and visible obs. 7-60837
IH 0542-407, DQ Her star, identification, X-ray and visible obs. 7-60837
HDE 310376, novalike variable, differential photometry 7-66622
AM Her, 1985 light curve and colour indices characts. 7-66670
AM Her, optically variable X-ray binary star 7-4481
AM Her, periodic X-ray minima disappearance 7-66656
AM Her stars, asymmetric light curves model 7-55709
DQ Her stars and other cataclysmic variables, polarisation obs. 7-9491
hot spots flickering in cataclysmic variables, effects of scatt. cloud on flicker freq. spectrum 7-55667
IR photometry, evidence for ellipsoidal vars. in CW Mon, X Leo, IP Peg, and AF Cam 7-4471
IUE-Voyager observations of luminous accretion disk systems 7-66623
Lanning 10 (V363 Aur), eclipsing cataclysmic binary, component masses and spectrophotometric obs. 7-66602
ST LMi, AM Her star, B-photometry and light curve anal. 7-55717
ST LMi, polarimetry of AM Her-type system 7-18438
low-mass close binary stars, evolution with orbital ang. momentum losses 7-24121
LSI +65°010 (=2S 0114+650), visible and UV spectra of X-ray binary indicating mass ejection 7-29516
magnetic braking, ang. momentum transport in accretion disks magnetospheres 7-47918
observational selection in magnitude-limited sample, relation to space distrib. 7-29479
V2051 Oph, possible low-field polar, high-speed photometric obs. 7-60694
RS Oph, recurrent nova, optical spectrum and photometry in quiescence 7-24139
RS Oph, recurrent nova, radio obs. rel. to conditions in nova remnant 7-60695
RS Oph (Nova 1985), coronal lines obs. in post-maximum spectrum 7-9499
GK Per (Nova 1901), IUE spectra and visual magnitude estimates (November to December 1986) 7-47905
PG 0244+104, 0834+488, 1550+131, 1550+191, 1717+413, 2240+193, photoelectric photometry 7-40828
polarisation observations of DQ Her stars and other cataclysmic variables, linear and circular polarisation obs. 7-9491
possible cataclysmic variable in globular cluster NGC 6637, spectroscopic identification as Mira variable 7-47906
precataclysmic binary stars, evol. and orbital characts. 7-34981
T Pyx, UV continuum and spectra 7-34992
recurrent novae, amplitude-period length relation 7-4472
space densities and evol. 7-60672
space density of classical nova in The Galaxy 7-40832
AN UMa, AM Her star, light curve var. due to accretion flow channelling by white dwarf mag. field 7-60720
QQ Vul, long-period AM Her star, period determ. using new minima from old plates 7-66672
white dwarf components, formation and evolution 7-9474
white dwarf components, mass spectrum determ. 7-29476
wind-formed resonance lines, inclination and orbital phase dependent resonance line profile calcs. 7-60692
X-ray sources in ω Cen, soft X-ray obs. with EXOSAT 7-29506

cataloguing

NASA Ocean Data System, computer-based online data information system 7-66307

catalysis

see also catalysts; reaction kinetics
Belousov-Zhabotinski reaction, Mn-catalysed, complex periodic oscills., Farey arithmetic anal. 7-39853
Belousov-Zhabotinsky reaction, catalysed, ion induced oscills. 7-65301
3D chemically nonequilibrium viscous shock layer on catalytic surface 7-20810
dehydrogenase catalysed redox reaction, equilibria, spectroscopic anal. (*German*) 7-54159
1,3- dioxo-2-silacycloalkanes, X-ray diffr., struct., chemical reactions 7-21185
disperse media flow with internal degree of freedom, nonequilib. gasdynamics, kinetics and catalysis 7-44019
enzymatic reaction kinetics, rate const. calc. 7-59741
ethylene, hydroformylation, in situ IR and EXAFS 7-59755
glycol/air fuel cells, electrode catalyst and fuel electrolyte soln. 7-39987
heterogeneous catalysis in low-pressure plasmas 7-28341
heterogeneous reactions, FT IR spectrosc. investig. systems 7-35606
heterogeneous reactions, kinetic studies, computerised conc.-controlled recycle reactor 7-54164
ion exchange resins, effects of metallic impurities on oxidation, catalytic activity 7-30677
isothermal autocatalytic reactions, singularity theory appl., uncatalysed reaction influence 7-65285
oblate ellipsoids, diffusion, shape effect on consumption in fluid-particle processes 7-33930
oxides, elec. props. under conditions of oxidation, reduction and catalysis 7-7250
phase transfer catalysed organic reactions, appls. of US 7-50901
phosphoglucomutase, crystn. at high salt conc., catalytic effect of polyethylene glycol 7-23278
phthalocyanine thin films, gas-surface reactions, elec. cond. meas., ESCA 7-52262
polymers, autocatalytic replication 7-54121
polymers, conjugated, elec. cond., chain rigidity effects 7-64230
Raman spectroscopy, role in study of energy sources, literature review since 1977 7-59827
rhodopsin, catalysis of light-depend. nucleotide exchange at photoreceptor membrane (*German*) 7-8495
silica, sol-gel processing, role of catalysts 7-22630
Silica aerogels, ethyl versus methyl sol-gel comparison, polar nephelometry studies 7-8312
solid surfaces, chemistry and physics, book 7-60891
solid-state gas sensors, role of catalysis, review 7-48718
spacecraft glows, surface-catalysed reactions role 7-14401
surface and interface analysis, appls. conf., Veldhoven, Netherlands, (Oct. 1985) 7-24289
CO oxidation on Pt(100), kinetic oscillations, computer simulations 7-23061
CO₂ pulse-periodic laser, gas mixture comp. stabilisation by hopcalite 7-25838
Co catalyst, O₂ adsorpt. and oxidation of Si at CoSi (100) surfaces 7-46865
Cu, reduction, electrochem., autocatalytic, by formaldehyde 7-54138
H, ortho-para conversion, new channel 7-36502
Hg₂Cl₂, photocatalytic props., O₂ photogeneration from water 7-54151
MoS₂, surface chemistry and props., photoemission, SIMS and SEM anal. 7-44971
Na₂CaAl₂Si₄O₁₂·6H₂O, zeolite, adsorption and desorption of ethylene, TPD study 7-32826
Ni (100), adsorption of CO, poisoning in heterogeneous catalysis, role of electronegativity 7-13818
Ni (111) surface, electronic structure, S effects on heterogeneous catalysis 7-54185
NiO (100), adsorption of CO, ethylene and H₂O, surface reactions 7-23055
O+CO adsorbed on Pt, surface catalysed reaction, surprisal anal. 7-3601
O₂, electroreduction, cobalt porphyrin effect, cyclic voltammetry and UV-absorpt. spectroscopy 7-59778
Os (0001), coexistence of mono- and diatomic steps 7-52204
Pd (111), CO and O co-adsorption, SIMS and TPD studies 7-27137
Pd tubes, diffusion of H₂ 7-20828
Pt catalysed crystallisation of Li₂O-SiO₂ 7-6524
Pt particle/Al₂O₃ surface, ethylene hydrogenation, intrinsic size effects 7-3607
Rh (111) surface, electronic structure, S effects on heterogeneous catalysis 7-54185
Rh-Ru alloys, electroreduction, electrocatalytic activity 7-54137
Si-SiO₂ interface formation by catalytic oxidation using adsorbed alkali metals 7-54017
SiO₂:Na with adsorbed SO₂ and H₂S, FTIR and Raman spectra obs., Na promotion of Claus process 7-46869
TiO₂ on glass substrate, photocatalysis 7-23066
UF₆, fluorination kinetics, catalysts and impurities effect 7-42120
WO₃, carburized, surface composition at catalytic activity 7-21594
Zn-air button type battery for hearing aids (*Japanese*) 7-65890

catalysts

see also catalysis
adsorbed mol. complexes, NH₃ adsorpt., vibr. study, IR spectra anal. 7-36607
n-butyltitanate/triethylaluminium catalyst for polyacetylene film synthesis, ESR study 7-65317
catalyst surfaces, characterisation by neutron inelastic scatt. from adsorbates 7-7000
electrochemical H₂ production, electrocatalytic materials comparison and eval. 7-65645
materials design using a hierarchy of structural models 7-16350
metal oxide catalysts, IR emission spectrosc. 7-39098
molecular clusters, review, materials, architectures and uses (*French*) 7-15765
oxides, elec. props. under conditions of oxidation, reduction and catalysis 7-7250
porous catalysts, temp.-programmed desorpt., modeling and expt. verifications 7-13799
Raman spectroscopy, role in study of energy sources, literature review since 1977 7-59827
resorufin adsorbed on γ -Al₂O₃, fluoresc. line narrowing and site-selection expt. 7-10655

catalysts continued

- small particles, atomic struct. and props., conf., Wickenburg, AZ, USA (Jan. 1986) 7-29592
- solvent-dried coal liquefaction reactivity improvement by disposable catalyst 7-39953
- structure of catalytic particles, TEM studies 7-32241
- surface, fractal clustering of reactants 7-3605
- TEM, conference, Boston, MA, USA (Dec. 1985) 7-35119
- transition metal alloys, glassy and cryst., catalytic activity and selectivity 7-28348
- transition metal oxides, catalysts, laser Raman spectra 7-53295
- Al_2O_3 , catalysts, small angle X-ray scatt. anal. 7-16352
- Al_2O_3 surfaces, catalytic reactions, studies by positron annihilation 7-39309
- Au small particles on amorphous substrates, dynamic atomic-level rearrangements 7-12542
- Co catalyst, O_2 adsorpt. and oxidation of Si at CoSi (100) surfaces 7-46865
- Fe particles on planar Al_2O_3 supports, low rate growth 7-32779
- $\text{Fe}_{83}\text{B}_{17}$, amorphous powder, surface struct. rearrangement by pulverisation, CEMS obs. 7-13065
- $\text{Fe}_{90}\text{Zr}_{10}$, amorphous powder, surface struct. rearrangement by pulverisation, CEMS obs. 7-13065
- $\text{HCo}(\text{CO})_3$, hydroformylation, quantum chem. calcs. 7-54115
- $\text{HCo}(\text{CO})_4$, hydroformylation, quantum chem. calcs. 7-54115
- MoO_3 crystals, surface structure, implications for catalytic oxidation of hydrocarbons 7-6942
- MoS_2 , surface chemistry and props., photoemission, SIMS and SEM anal. 7-44971
- MoS_2 -Co catalyst-promotor interaction, UPS, XPS, LEED studies (Chinese) 7-39913
- Pd/C model catalyst supported on TEM grids, in-situ heating and microanalysis expts. 7-23098
- Pd-Pt, mixed layers, electroplated on stainless steel support, oxidation catalyst appl. 7-22596
- Pt (100) surface, defect struct. rel. to catalytic behaviour, scanning tunnelling microscopy study 7-6930
- Pt (110), catalytic CO oxidation, kinetic oscillations 7-28346
- Pt, catalyst particles, adsorbed S-induced faceting, TEM study 7-27109
- Pt catalysts, SiO_2 supported, muon relax. rate rel. to temp. and loading 7-33315
- Pt clusters in Y-zeolite, atomic and electronic struct. and chemical reactivity 7-32677
- Pt crystallites supported on C black, surface struct., TEM study 7-32778
- Pt microcrystals, charact. using high resolution electron microscopy 7-32676
- Pt/ TiO_2 thermally treated model catalysts, CO adsorption 7-54184
- Pt- Al_2O_3 catalysts, small angle X-ray scatt. anal. 7-16352
- Pt- SiO_2 catalysts, small angle X-ray scatt. anal. 7-16352
- Rh, Al_2O_3 supported, CO-induced struct. changes, H_2 effect, IR study 7-23063
- Rh-Re/ SiO_2 catalysts, metal dispersion 7-39918
- RuO_2 - TiO_2 , thin films, microheterogeneous struct. 7-12541
- SiO_2 , porous catalysts, small angle X-ray scatt. anal. 7-16352
- SiO_2 :Na with adsorbed SO_2 and H_2S , FTIR and Raman spectra obs., Na promotion of Claus process 7-46869
- Sn- Sb_2O_3 catalyst, O adsorpt. and desorpt. kinetics 7-63944
- ZnO shock compressed powders, catalytic activity for CO oxidation and methanol synthesis 7-39919

cataphoresis *see electrophoresis***catastrophe theory**

- bound states of Hamiltonian systems, catastrophes and stable caustics 7-41130
- crystals, form. of phonon-focusing caustics, rel. to catastrophe theory 7-2116
- dielectric closed shell quantum systems, SCF energy surface, catastrophe theory anal. (Rumanian) 7-14832
- forced relaxation oscillations, chaotic blue sky catastrophe 7-4768
- liquid mixture phase transitions and singularities, catastrophe modelling 7-26903
- new kinds of catastrophe substructure macro in system dynamics models 7-61075
- phonon concentrating, catastrophe theory for caustic behaviour 7-2113
- quantum cusp, catastrophe pot. 7-132
- Au crystal, H^+ ion channelling, catastrophe theory 7-21312
- Pd-H system, struct. changes, phase rels. 7-22643

cathode-ray oscilloscopes

- see also oscillographs*
- configuration, functions and operation (Spanish) 7-35510
- sampling oscilloscopes use for economical HF fast-rise-time signal meas. 7-48775
- Tektronix 11000 Series of digitising and analogue CROs 7-61324

cathode-ray tube displays

- see also cathode-ray oscilloscopes*
- choosing colors and luminances for a CRT map display 7-8571
- color-difference prediction of legibility performance for CRT raster imagery 7-8574
- data acquisition suites, multichannel, with time-scale conversion and storage CRT, design 7-61321
- effective colour image encoding 7-8575
- effects of transient adaptation in simulated VDT operations 7-8577
- energy transfer between Ce and Tb ions in $\text{LaOBr}:\text{Ce},\text{Tb}$ 7-5644
- evaluation of colour sets for CRT displays 7-8573
- human colour perception, display technology implications 7-14005
- legibility and symbol-background colour difference relationship 7-14018
- measurement of resolution of shadow-mask CRTs 7-1039
- psychophysical research into resolution and addressability of CRT displays 7-1040
- retinal adaptation to non-uniform fields: average luminance or symbol luminance? 7-54562
- variable focus, single lens, 3 CRT dichroic color graphics projector 7-25933
- VDU image polarity, ergonomic aspects 7-54571
- VDU perceived flicker prediction method 7-54572
- VDU visibility aspects, contrast and luminance 7-54570
- VDUs, practical guide to flicker measurement: using the flicker-matching technique 7-54573

cathode-ray tube displays continued

- visual performance evaluation of liquid-crystal shutter and shadow-mask CRTs 7-8579
- vocal fold vibration and speech signal, simultaneous high speed digital recording 7-47129

cathode-ray tube screens *see cathode-ray tubes; fluorescent screens***cathode-ray tubes**

- see also image converters; image intensifiers; image storage tubes; television camera tubes*
- limited angle reflection mode computerized tomography 7-28635
- nuclear power plants, CRT displays of plant operation 7-49567
- printer, exposures from digital images onto colour photographic paper 7-354

cathode rays

- No entries

cathodes

- see also electron emission; oxide coated cathodes; photocathodes; thermionic cathodes*
- aberration coefficients of complicated electron-optical cathode systems 7-57263
- arc plasma flow in Knudsen layer 7-58088
- Aurora KrF laser system, design and performance of large area monolithic electron guns 7-36987
- bipolar batteries with common electrolyte paths, leakage currents 7-28392
- collective drifting motion of cathode spots in an axial magnetic field 7-32162
- electron beam in combined electromagnetic focusing-deflection system with spherical cathode, relativistic aberration theory 7-62613
- electron beam quality, surface roughness effects 7-57225
- electron beams combined in focusing system with spherical cathode, aberration theory 7-62612
- field-emission cold cathode for oscillator gauge (Chinese) 7-48767
- glow discharge cathode spot, entry into capillary hole 7-32160
- hollow cathode effect, modelling 7-21006
- layer dynamics, effect on externally sustained discharge current 7-21024
- magnetically insulated transmission line in PROTO II accelerator, anode and cathode joints, gap closure 7-30756
- magnetised virtual cathode microwave generator, high-efficiency 7-20964
- magnetron sputtering cathode, CAD using finite-element program 7-46316
- metal cathode, hot, evaporating, in stationary vacuum arc with diffuse cathode emission, thermal conditions 7-58087
- metal surfaces, ion-electron emission mechanism 7-7825
- MIM cathodes, emissivity, temperature and area effects 7-13336
- MIM structures, explosive electron emission 7-13335
- molten carbonate fuel cells, fabrication of bubble press. barriers 7-13856
- multiple-cavity hollow cathode, arc discharge, gas containing alkali metal atom additions 7-32179
- multitip explosive emission cathode plasma generation dynamics, probe meas. 7-51478
- plasma edge cathode for pulsed electron extraction 7-32106
- polyacrylonitrile-based cathodes, performance in Li-I_2 solid state batteries 7-54282
- transition metal dichalcogenides, low-dimens., as secondary cathodic materials, book contrib. 7-28394
- Ar, gas pressure effect on arc cathode erosion and cathodic plasma expansion 7-32164
- Ar, hollow cathode arc, steady-state low-press., diagnostics 7-26561
- Au cathode photoelectric detectors, absolute photon sensitivity characterisation 7-24704
- C, cathode, chem. sputtering in H_2 and O_2 plasmas 7-32171
- C, cathode erosion and power flow in vac.-arc centrifuge 7-26562
- C cathode performance improvement in $\text{Ca}(\text{AlCl}_4)_2\text{-SOCl}_2$ cells 7-13851
- C cathodes for Ca-SOCl_2 cell performance improvements, $\text{Ca}(\text{AlCl}_4)_2\text{-SOCl}_2$ electrolyte 7-65444
- C field emission cathodes, effect of forming on structure 7-39365
- CO_2 laser cathode systems, characts 7-15900
- Cd cathode sinter effects on Ni-Cd secondary cell performance 7-65448
- Cu II laser with spherical and circularly slotted hollow cathodes, output power and operation period 7-50587
- Cu II laser with tulip shaped hollow cathode 7-43145
- CuMo_4S_8 , porous film, prep. on Cu_2S by solid-gas reaction, secondary battery appl. 7-27897
- Fe cathode surface, plasma nitriding, N conc. profile modelling 7-54188
- Fe, cathodic charging, H trapping 7-21256
- H_2 discharge, electron beam energy relax. mechanism in electrode sheath 7-51464
- He, gas pressure effect on arc cathode erosion and cathodic plasma expansion 7-32164
- LaB_6 cathodes in Dudnikov type Penning source 7-56375
- LaB_6 pulsed hot cathode discharge, for uniform plasma production 7-32006
- $\text{La}_{0.7}\text{Sr}_{0.3}\text{CoO}_3$ cathodes for CO_2 waveguide lasers, electrical and emission characts. 7-59383
- Li- LiNO_3 thermal battery cell discharge lifetime with soluble cathode materials 7-3630
- Li_2TiS_2 , intercalation in solid-state battery cathode, TEM study 7-17854
- Mg, cathode erosion and power flow in vac.-arc centrifuge 7-26562
- NbS_3 cathode, prep. under high press., use in Li secondary battery, performance 7-13853
- $\text{Nd}_{0.7}\text{Sr}_{0.3}\text{CoO}_3$ cathodes for CO_2 waveguide lasers, electrical and emission characts. 7-59383
- NiO porous cathode model for molten carbonate fuel cell 7-3640
- Pb-acid battery, effect of chemisorbed H_2O on positive plate elec. capacity 7-54284
- Pb-acid battery, study of positive plates by photoacoustic spectrophotometry 7-54283
- β -PbO as cathode materials for voltage compatible Li cells 7-3632
- β - PbO_2 as cathode materials for voltage compatible Li cells 7-3632
- PbO_2 cathodes of Pb-acid battery, SnO_2 conductor stability 7-65440
- SF_6 , gas pressure effect on arc cathode erosion and cathodic plasma expansion 7-32164
- Si cold cathode for high current densities 7-12816
- V Redox cell, eval. of electrode materials 7-54286
- WC cathodes in acid electrolytes for H_2 production 7-3729

cathodes, electrochemical *see electrochemical electrodes*
cathodic protection *see corrosion protection*
cathodic sputtering *see sputtering*
cathodochromism
polymer films, optically transparent, radiation-induced transient darkening 7-39056
cathodoluminescence
analytical electron microscopy of thin films, review (*Czech*) 7-59261
anthracene, cathodoluminescence, scintillation decay laws, electron track model appl. 7-53416
cathodoluminophors, structuring principles 7-33460
ceramic wear behaviour, cathodolum. mode appl. in SEM 7-8228
conference, Rovno, USSR (Nov. 1984) 7-24263
diamond, radiation damage prod. of 5RL centres, phonons, absorpt. spectra, cathodoluminescence studies 7-33461
double heterostructures, microcathodoluminescence studies 7-39189
film, thin, cathodolum. spectrum in STEM 7-22355
inert gas crystals, surface or bulk location of self-trapped excitons, luminesc. 7-46129
metal oxides, intrinsic shortwave luminescence and electron excitation properties 7-33430
quartz, α -phase, cathodoluminescence of intrinsic defects 7-7766
scanning electron microscope cathodoluminescence technique for anal. of band structure in solids 7-51595
semiconductor materials characterisation techniques, review 7-51598
AlN, undoped and control doped films, luminesc. studies 7-27790
Al₂O₃ surface electrocathodolum., defect state transitions under high voltage stress 7-39187
ArF laser, electron-beam-excited, investig. 7-43074
Ca₃Al₂Ge_{3-x}Si_xO₁₂:Tb, cathodoluminescence, photoluminescence props. 7-53404
Ca₃Ga₂Ge_{3-x}Si_xO₁₂:Tb, cathodoluminescence, photoluminescence props. 7-53404
Ca₃Se₂Ge_{3-x}Si_xO₁₂:Tb, cathodoluminescence, photoluminescence props. 7-53404
Ca₃Y₂Ge_{3-x}Si_xO₁₂:Tb, cathodoluminescence, photoluminescence props. 7-53404
CdS evaporated films, cathodolum., effect of thermal annealing 7-22353
CdS, light emission under voltage pulses 7-7764
CdS single crystals, cathodoluminescence, memory effect 7-22352
CdS, with compensated i-layer, photosimulated deep level transient spectroscopy 7-7765
CuGaS₂, cathodoluminescence from iodine transport method grown crystals (*Japanese*) 7-3096
Cu₂O films, annealing of Cu and O vacancies, cathodoluminescence study 7-59263
GaAlAs-GaAs laser diodes, catastrophic optical damage, electrolum., cathodolum., EBIC and TEM obs. 7-57329
GaAs LEC wafers, cathodolum. mapping, IR absorpt., X-ray topography obs. 7-33462
GaAs, seminsulating LEC substrates, defect etching 7-59694
GaAs, substrates, multi-technique approach to defect microstructure characterisation 7-52215
GaAs:Sn(Te)(Zn) surface layers, luminesc., electrophys. parameters, effect of annealing 7-64680
GaAs-GaAlAs, quantum well wires and boxes, optically detected carrier confinement, cathodolum 7-39188
GaAs_{1-x}P_xN, cathodoluminesc. efficiency, N-bound excitons influence 7-7768
GaInAs, Czochralski-grown, dislocation effects investig. 7-7261
GaN, undoped and control doped films, luminesc. studies 7-27790
GaP, deep level centres at excited states, study by transient optical absorpt. spectroscopy 7-13188
Gd, optical radiation generated by electrons (*Russian*) 7-53415
Gd₂MSb₂Zn₃O₁₂ (M=Sr,Ca), rare-earth activated garnets, cathodolum. 7-7763
Gd₃Te₂Li₃O₁₂:R, cathodoluminescence study (*German*) 7-22354
H₂ electron beam ionisation luminesc. in high-current discharge, vacuum-UV radiation props. 7-57183
In-Ga-P-As, gap width, temp. depend. 7-12602
InP substrates, influence of inhomogeneities on quality of quaternary layers 7-32770
InP:Fe, Czochralski-grown, stoichiometric-related faulted loops, struct. and lum. props. 7-51772
MgO, deformed and annealed, red cathodoluminescence spectrum 7-27792
MgO:Al crystals, cathodolum., effect of heat treatment 7-7767
Ne, solid, electron beam-induced luminescence, time-resolved studies 7-64702
Si MBE layers, defect characterisation, luminesc., TEM studies 7-13227
SiO₂, amorphous layers, cathodoluminescence, kinetic effects 7-13237
SiO₂, glassy and thermal films, cathodoluminescence of intrinsic defects 7-7766
UO₂, thin films form by oxidation, luminesc. studies 7-22351
Y₃MSb₂Zn₃O₁₂ (M=Sr,Ca), rare-earth activated garnets, cathodolum. 7-7763
Y₂O₂S₂:Tb³⁺, phosphor, electronic struct., cathodoluminescence meas. 7-17350
Y₃Te₂Li₃O₁₂:R, cathodoluminescence study (*German*) 7-22354
ZnCdSe, electron beam pumped, cathodolum., gain and stimulated emission 7-64701
ZnSe hydrothermal growth, cathodolum. props. 7-63531
ZnSe:Al(Ca)(In), impurity diffusion coefficients, cathodoluminesc. study 7-27017
ZnSe:Er³⁺, ion implanted, identification of cathodolum. centres 7-53417
ZnTe, cathodoluminescence, Zn-vapour and Te-vapour heat treatment effects 7-46151
ZnTe:O, red cathodolum. kinetics, two-step electron capture model calcs. 7-59262
cathodophosphorescence *see cathodoluminescence*
cathodothermoluminescence *see cathodoluminescence*
catholytes *see electrolytes*
Cauer filters *see passive filters*
causality *see physics fundamentals*
causticity *see pH*
cavitation
see also bubbles; vortices
acoustic turbulence, cavitation effects 7-11206

cavitation continued
axisymmetric headforms, cavitation inception, turbulence simulators effect 7-16223
bubble interactions and radiated pressure waves 7-16018
bubbles, generating impact pressure, nonspherical collapse (*Chinese*) 7-20765
buoyant vapour bubbles modelling growth and collapse, rigid boundary, stagnation flow 7-16220
damage and noise spectra in a polymer soln. 7-62887
defects, stress- and fatigue-induced, small angle neutron scatt. studies 7-58273
ethylene glycol, rapid cavitation induced by shock-wave refl., tensile strength meas. 7-31848
excitation of surface waves by sound in a liquid containing gas bubbles 7-62883
flow in duct, high speed cine photographic obs. 7-51240
fluid separation in rotating tube, cavitation investig. by Runge-Kutta method (*German*) 7-51245
free radical production in aqueous solns. due to diagnostic US 7-50900
HF travelling-bubble cavitation noise generation 7-16221
impact erosion, continuum model 7-11479
jet flow gate valve, cavitation pressure pulse meas. 7-51242
liquid flow, electrical effects 7-37501
metal solidification, effect of high intensity US 7-62888
nonlinear waves of different physicochemical nature in finite continua 7-18604
optical system for cavitation nuclei meas. 7-51243
perturbed flows in a longitudinal gravity field 7-1594
phase transfer catalysed organic reactions, appls. of US 7-50901
physics of acoustic cavitation 7-11207
polymer solutions, bubbles growth and collapse 7-37531
pressure pulse reflection at free surfaces of water 7-11480
pressure-wave and microjet cavitation damage, rotating-disc expts. 7-26225
pump cavitation monitoring by single fluid-borne noise meas. 7-37502
residual creep life, cavitation effects 7-50962
shear layer behind 2D sharp-edged plate, cavitation phenomena 7-51244
sluice valves and chokes, cavitation studies (*Japanese*) 7-6261
stagnant zone, form. at different Bernoulli numbers, nonlin. num. soln. 7-51241
surface protrusion, desinent cavitation, press. gradient influence 7-16222
thermodynamic aspects (*Russian*) 7-51153
tunnel, flow meas. using laser Doppler velocimeter 7-37607
US cavitation, sonochemical reaction and local temp. determ. 7-3594
viscous incompressible fluid, partial cavity form., cavitation flow calcs. 7-31846
viscous Rayleigh-Plesset equation investigation, cavitation press. correl. to fluid viscosity 7-31847
water, rapid cavitation induced by shock-wave refl., tensile strength meas. 7-31848
Ar-H₂O, two-phase mixture, voids fraction meas. 7-44072
cavitation erosion *see wear*
cavities (solid) *see voids (solid)*
cavity resonators
see also acoustic resonators; laser cavity resonators
associative memory using optical resonator 7-20157
atomic metastable states produced during cooperative self-diffraction in a resonator, Maxwell eqn. solns. 7-42558
diffraction radiation generator, electronic efficiency, microwave field distribution, phase nonuniformities effect 7-37124
EM fields in cavities with current normal to walls, monochromatic solns. 7-42849
ENDOR electron spin echo resonator, variable temp., for single-crystal studies 7-30059
Fabry-Perot interferometer, mirror random phase inhomogeneity influence, resonator use 7-24689
Fabry-Perot resonator, transversely coupled fiber device 7-56325
Fabry-Perot resonator with active Sagnac interferometer, multistable 7-50626
Fabry-Perot resonator with volume-distributed phase inhomogeneities 7-25929
Fabry-Perot resonators with phase-conjugate mirrors, dynamics 7-50649
fibre optic hydrophone with dual in-line resonant cavity 7-43600
fibre-optic passive-loop resonator, optical multistability 7-1278
MM-wave cavity spectrometer for gas mixture anal., 26.5-40 GHz, design and operation 7-13836
mode conversion, Bloch oscillations and Zener tunneling with light by means of the Sagnac effect 7-36877
monochromatic EM radiation, wave structure 7-50466
multipass systems with mirrors of different radii, general eqns. 7-11093
open resonators, Huygens-Fresnel principle and integral eqns. 7-31244
optical bistability for single-photon excitation by random field 7-57397
optical frequency conversion efficiency in cavities filled with inhomogeneous nonlinear media 7-50641
optical passive resonators, transverse modes, reference light field choice (*Chinese*) 7-5965
optical passive ring resonator gyro, reson. characts. of backscatt. 7-50753
optical passive ring resonator gyroscope, semiconductor laser and integrated optics use 7-25998
optical resonators, coupled-mode theory 7-54513
optical single-mode fibre resonant cavity calcs. (*French*) 7-50745
permittivity meas. by cavity perturbation method 7-14980
phase conjugate, probe fluctuations 7-20361
phase conjugate mirror, non-degenerate, for resonator system, mode selectivity and misalignment sensitivity 7-20356
phase conjugate optical resonators, eigenmodes, orthogonality props. (*Korean*) 7-1234
plasma density measurement in an imperfect microwave cavity 7-63350
rectangular cavity for EPR in TE₁₀₂ mode 7-48823
reentrant cavity as a low-power plasma source 7-44199
reflecting multibeam interferometer with anisotropic elements, characts. 7-9891
ring resonator fabricated in phosphosilicate glass films deposited by CVD 7-15968
semiconductor in low finesse cavity, optical transistor dynamic gain 7-57418
SHG and parametric amplification in resonator with mirrors with random inhomogeneities 7-25888
soliton amplitude bistability in ring resonator 7-43197
stable, approx. method for solving integral equations 7-20382

cavity resonators continued

- stratified medium, output characts. in case of bilateral incidence of monochromatic waves 7-31241
- telescopes, resonator diff. losses 7-43292
- three mirror axisymmetric quasi-optical resonance system 7-5972
- unstable cavity, aberration sensitivity, second-order theory 7-31256
- unstable-cavity sensitivity to spatially localized intracavity phase aberrations 7-25717
- wheat seeds, germinating, dielec. response meas. using resonant cavity 7-34127
- YIG single-crystal ferrites, relation between biasing magnetic field and linewidth 7-4868
- BaTiO₃ imaging threshold detector using phase-conjugate resonator 7-6019
- Cs alkali gas cell atomic freq. standards 7-41357
- GaAs-GaAlAs passive MQW waveguide resonators, all-optical switching effects, expt. study 7-15967
- Rb alkali gas cell atomic freq. standards 7-41357

CCD *see charge-coupled devices*CCD circuits *see charge-coupled device circuits*

CCD image sensors

- airglow (OH) imaging system, using image intensifier and solid state sensor 7-29288
- astronomical instrumentation and techniques, conf., Tucson, AZ, USA (March 1986) 7-48162
- astronomy, CCD imaging at low-light-levels 7-47703
- aurora CCD-image intensifier camera, for all-sky observation 7-40603
- CCD photodetector, absolute spectral sensitivity 7-18876
- colour endoscope image motion related blur compensation 7-47282
- conference on solid-state arrays, San Diego, CA, USA (Aug. 1985) 7-29582
- fibre optic coupled CID-MCP detectors for scientific appls. 7-30087
- gain meas. in discharges, spontaneous emission amplification obs. 7-14989
- Halogen Occultation experiment, Si photodiode array for solar edge tracking 7-23900
- high-energy particle tracking, NA32 charm production expt. 7-25325
- high-speed photography, videography and photonics, conf., San Diego, CA, USA (Aug. 1985) 7-18486
- IR camera with hybrid 32x32 HgCdTe CCD array 7-60560
- length measuring systems with CCD arrays, resolution improvement (*German*) 7-61312
- light intensity distrib. meas. system, image processing unit (*Japanese*) 7-4881
- matrix CCD photodetector in modulation spectrometer, synchronous integration 7-18885
- neutral-beam performance analysis using a CAD camera 7-1766
- oblique CCD reconnaissance camera operation, atmospheric effects 7-18900
- programmable spatial filtering function using CCD technology (*Japanese*) 7-25715
- Raman spectroscopy, CCD detector for low-light-levels 7-41499
- ROSAT star sensors appl., testing and characterisation 7-29401
- scanning camera with line CCD sensor for use in schools (*Slovak*) 7-29646
- secondary ion imaging, with charge-coupled device camera 7-48912
- spaceborne camera using TI TC-104 linear CCD array 7-29406
- star camera and aspect determ. system for balloon-borne payloads 7-55418
- streak and framing camera designs using SAW-CTD imagers 7-56368
- streak camera performance characts., with cooled CCD 7-19425
- technology and appls., conf., Cannes, France (Nov. 1985) 7-24288
- Tektronix CCD array for Hubble Space Telescope 7-29407
- time-resolved stellar photometry appl. 7-9381
- velocity meas. device using CCD image sensors 7-48705
- X-ray calibration of CCD sensors and photodiode array cameras, plasma diagnostics appl. 7-20939
- X-ray image sensors based on optical time-delay-and-integration CCD imager 7-24753
- X-ray performance enhancement, X-ray astronomy appl. 7-30149
- HgCdTe IR CCD coupling structure for space appls. 7-29309
- InSb charge injection device arrays, IR camera for astronomical imaging 7-34872
- Pb_{1-x}Sn_xTe(Se)IR photodiodes for 3 to 14 μ m, comparison 7-41466
- Si₃-dimensional reconstruction in high energy particle physics 7-25323
- Si:Bi hybrid array for photometric near-IR spectrometer 7-30103

CCD imagers *see CCD image sensors*CCTV *see closed circuit television*CDW *see charge density waves*

celestial mechanics

- 3D inverse problem soln. 7-23983
- N-body hierarchical force calc. algorithm with $N \log N$ growth 7-47673
- adiabatic-invariant change due to separatrix crossing 7-31932
- apocentric librators and the reducing transform. 7-23981
- artificial Earth satellites theory, connection between Tisserand's polynomials and inclination functions 7-47664
- artificial satellites, determ. of geopotential harmonics of order 15 and 30 from orbital resonances anal. 7-65923
- artificial satellites, orbits, perturbation by Earth zonal harmonics 7-23984
- artificial satellites, relativistic eqns. of motion about finite-size rotating Earth 7-34826
- artificial satellites, second order trajectory predictor derivation in terms of geometrical variables 7-23969
- artificial satellites, struct. of higher-order reson. zones in rot. in plane of elliptical orbit 7-34829
- artificial satellites motion, problem of critical inclination and commensurability (*Chinese*) 7-4284
- asteroid belt, secular resonance ν_6 , orbital evolution 7-14515
- asteroid orbits near 3:1 resonance, hyperbolic twist mapping model 7-34909
- asteroids, effects of secular resonances ν_{16} and ν_5 on orbits 7-47748
- asteroids, effects of subtle planetary perturbations by Earth-Moon system 7-4297
- asteroids, orbit integrations 7-34908
- axisymmetric satellite on elliptical orbit, resonant periodic motion 7-34830
- binary stars formation, two-body tidal capture of main sequence stars and white dwarfs 7-4500

celestial mechanics continued

- comet clouds in the solar system, chaotic motion 7-4372
- P/ Comet Halley (1982), coma morphology and dust emission pattern modelling 7-14526
- comet-Sun-Galaxy system, solar system boundary radius: from King-Innanen formula 7-4357
- comet-Sun-solar companion system, outer boundary radius for solar system 7-34890
- cometary dust halo formation, time-dependent numerical modelling 7-55536
- cometary motion, effects of subtle planetary perturbations by Pluto and Earth-Moon system 7-4297
- comets, effect of galactic perturbations on long-period cometary orbits 7-34935
- comets, short-period, nongrav. forces calcs. for high equatorial obliquities 7-47765
- comets, short-period, nongrav. forces calcs. for low equatorial obliquities 7-47764
- comets with short periods, planetary perturbations, Tisserand criterion appl. 7-29383
- Dynamical Astronomy Division, 17th regular meeting, Santa Barbara, California (April 1986) 7-29571
- Earth satellite motion, relativistic effects in generalized Fermi frame 7-23985
- Earth-Moon system, theoretical estimates of tidal decelerations 7-18348
- Eccentricid system of asteroids and meteoroids, orbital evolution 7-24085
- elliptic motion of arbitrary eccentricity and semi-major axis, expansion theory, general periodic function 7-60510
- elliptical motion of arbitrary eccentricity and semi-major axis, elliptic expansions in terms of sectorial variables 7-4300
- elliptical restricted three-body problem, periodic solns., arc solns. and double collision orbits 7-34838
- equatorial satellites, librational motion in gravit. field of rot. nonspherical planet 7-34831
- Extended Semianalytical Kalman Filter and its application to synchronous orbits 7-29386
- external potentials expansions of ellipsoidal bodies, analytical continuation 7-47719
- four-body problem, restricted case, periodic orbits 7-23978
- Galilean satellites, orbital theory compared with occultation obs. 7-47754
- game theoretical estimation problem with unmodelled accel., soln. algorithm 7-55434
- Geminid meteor stream, combined action of cometary ejection process and gravit. perturbations 7-47796
- generalised problem of two fixed centres, coordinates trigonometric expansions 7-4298
- geodynamic twin satellite, relative motion anal. 7-4285
- Germinid meteor swarm, spatial struct. determ. 7-66519
- giant planets satellites, orbital stability 7-34898
- gravitational field, Earth-Moon system, momentum current picture 7-55934
- Henon mapping with Pascal, dynamical systems simulation 7-34836
- Hori method for rotation of celestial body about mass centre 7-66437
- Kepler's equation solution, procedures using FORTRAN 7-24018
- Kepler problem, new integrated general time transformation 7-4301
- Kepler problem spinor regularization and pre-quantization of the negative-energy manifold 7-4304
- Keplerian ellipse under perturbation, perihelion precession (*Chinese*) 7-29381
- Kirkwood gaps origins (*French*) 7-4359
- Kolmogorov-Arnold-Moser theorem, appl. to topological stability of finite-length mag. flux tubes 7-66556
- LAGEOS, sensitivity to changes in Earth's (2,2) gravity coeffs. 7-34825
- lunar natural satellites collision orbits with Moon via method of surface of section 7-9387
- lunar secular acceleration measurements, implications for tidal energy dissipation 7-14301
- lunisolar precession-nutation with time-varying second zonal harmonic, dynamical theory 7-28810
- meteoroid complexes near orbit of Earth, spatial-probability characts. 7-24084
- meteoroids, phase density distrib. function rel. to distrib. of meteoric material in solar system 7-66518
- minimum distance between two Keplerian orbits with common focus 7-23982
- n-dimensional Kepler problem, spinor regularisation, Clifford algebraic construction 7-61089
- Neptune arc rings, satellite corotation resonances theory 7-4363
- Newton's law of gravity modified, celestial mechanical consequences 7-9661
- optimum trajectory problem in gravit. field 7-23980
- orbital inclination function, trigonometric series representations 7-4299
- outer planets, semimajor axes secular var. 7-60587
- particle motion in field of two rotating mag. dipoles, equilb. points stability 7-34839
- periastron precession in general relativity 7-48244
- periodic solutions of Hamiltonian systems, appl. in satellite dynamics 7-66435
- perturbed elliptic motion 7-29631
- perturbed Keplerian motions, linearisation of 3D problems in non-centered force fields 7-34837
- planetary gravitational potential expansion, convergence improvement methods 7-47742
- planetary motion about nearby binary stars, restricted elliptical three-body problem 7-29517
- planetary N-body problem, Hamiltonian eqns. in post-Newtonian approximation 7-47672
- planetary orbits, secular perturbations due to polar flattening of Sun 7-29452
- planetary rings, nonlinear density waves struct. 7-55506
- planetary rings, numerical simulation of binary encounters 7-66499
- planetary rotation, analytical study of rot. axes inclinations 7-9388
- planetary systems with spheroidal star, stability of resonant orbits 7-47670
- radio galaxies, radio trails bending by winds and rot. in slingshot model 7-35045
- relative equilibrium configurations in n-body problem (*French*) 7-66434
- restricted three-body problem, generating soln. in three dimensions 7-4302
- retrograde resonance rotation of natural celestial bodies, instability 7-47671

celestial mechanics continued

- Salyut-6/Kosmos 1267 and Salyut-7/Kosmos-1443 orbital complexes, generalised gravit. orientation regime 7-34832
 satellite in circular orbit, autonomous Hamiltonian systems, explicit formula for stability study 7-34841
 satellite motion, reduction of magnitude of correl. coeffs. between orbital elements 7-29384
 satellite motion about mass centre in circular orbit 7-66438
 satellite orbital period calcs. in relativistic gravit. and general relativity 7-40690
 satellite orbits with periodic flights around Moon, use in very long base-line radio interferometry 7-34833
 satellites of Mercury and Venus, limiting direct and retrograde orbits 7-24035
 Saturn E-rings, dynamical evolution 7-9408
 Saturn ring system, nonlinear study of Mimas 5:3 density wave 7-24057
 Saturn ring systems, large-amplitude stationary periodic wave theory rel. to rings fine struct. 7-23987
 solar system dynamics, implications of relativistic gravitation theory (*Russian*) 7-60533
 symmetric satellite with viscoelastic antenna in circular orbit, evolution of spin about mass centre 7-34828
 Szebehely's problem extended to holonomicsystems with a given integral of motion 7-4303
 three-body problem, averaged elliptical case, internal variant nearly circular orbits family 7-55435
 three-body problem, elliptic restricted case, critical orbits, appl. to planets in binary systems 7-23979
 three-body problem, generalized photogravitational restricted problem 7-29385
 three-body problem, generalized two-fixed centres problem Poisson series expansion 7-29382
 three-body problem, photogravitational restricted circular case, coplanar libration point stability (*Russian*) 7-14475
 three-body problem, restricted case, rotation of rigid body at libration point 7-40675
 three-body problem, restricted elliptical case, planetary motion about nearby binary stars 7-29517
 three-body problem, restricted elliptical case, satellite stability at triangular libration point 7-66436
 two triaxial rigid body problems, existence and stability of equilib. points 7-34840
 two-body problem, motion about rotationally symmetric primary 7-40676
 Uranus and Neptune, long-term orbit evol. and mass 7-34929
 Uranus satellite system, mass determ. and orbital characts. 7-34928
 Uranus satellites, general theory 7-14518
 Venus/Earth orbital resonance, contrib. to recurrent phenomena of Venus 7-66489

cell model (liquids) see liquid theory**cell motility**

- bacteria, swimming, rapid rot. of flagellar bundles 7-59950
 cochlear vibrations, model of effect of outer hair cell motility 7-8586
 dissociated cytoplasm, mechs. of motility, dynamical behaviour simulation 7-40123
 intracellular motility and phagocytosis rate, mag. particle probe behaviour 7-47139
 micro-organisms, swimming, individual and collective fluid dynamics 7-47141

cells (electric)

- see also fuel cells; photoelectric cells; photoelectrochemical cells; primary cells; secondary cells*
 advanced high energy density battery with NaAlCl₄ and β -alumina solid electrolyte 7-39981
 automated DC meas. at NPL, India 7-18842
 battery usage and selection criteria (*Japanese*) 7-65421
 construction and characts., review (*French*) 7-3629
 discharge capacity dependence on electrode fractality 7-3631
 electricity and modern techniques, conf., Bordeaux, France (Oct. 1985) 7-14708
 Raman spectroscopy, role in study of energy sources, literature review since 1977 7-59827
 synthetic metals science and technology, conf., Kyoto, Japan (June 1986) 7-60872
 technology breakout in energy conversion, conf., San Diego, CA, USA (Aug. 1986) 7-60875
 Ca(AlCl₂)₂-SOCl₂ cells, cond., C cathode performance improvement 7-13851
 Cd electrodes, electrotechnological aspects and alkaline battery appls., review 7-3638
 Cl₂-H₂ cells containing PbCl₂ solid electrolyte, cathodic characts; effect of vac. deposited FeCl₃ (*Japanese*) 7-13850
 Li₂TiS₂ intercalation in solid-state battery cathode, TEM study 7-17854
 TiO₂-redox polymer detector junctions, flatband pot. meas. 7-13787

cellular arrays

- gate array appls. in implants for nerve stimulation in paraplegic patients 7-34339
 integrated optical combinatorial logic using electro-optic Bragg gratings 7-26040
 optical cellular array processors 7-25720
 optical parallel array logic system, architecture without memory elements 7-20144
 position sensitive detectors, 2D detector data for crystallography, fast treatment using processor arrays 7-10354
 symbolic substitution logic for digital optical computing 7-10859
 tyred wheels, noise investigation, array processor use (*German*) 7-6041

cellular automata see finite automata**cellular biophysics**

- see also biomembrane transport; biomembranes; cellular effects of radiation; cellular transport and dynamics; lipid bilayers*
 abstract delay-differential equation modelling size dependent cell growth and division 7-61049
 actin system and the rheology of peripheral cytoplasm 7-65787
 activated platelets, human, soft X-ray microscopy studies 7-40124
 alkali metal distribution, intracellular, in ICRP Reference Man 7-65861
 analytical ion microscopy for cell biology and tissue studies 7-40386
 Antibio experiment on E. coli on Spacelab D1 mission, preliminary results 7-8709
 Arrhenius analysis of the heat response of human melanoma xenografts 7-47011
 astral mitotic spindles, phys. theory of orientation 7-65727

cellular biophysics continued

- atrial heart cell aggregates, embryonic chick, repolarisation currents 7-28491
 automated classification techniques, imaging flow cytometer 7-8774
 autoradiographic images, digital cluster anal. system to locate labelled cell regions 7-3958
 autoradiography, paired compartments comparison, probability models and null hypothesis testing 7-40255
 Bacillus subtilis, growth and differentiation under microgravity 7-8710
 bacteria, stereomicroscopy of isolated R-bodies from Pseudomonas taeniospiralis and Caedibacter taeniospiralis 7-65724
 bacteria, tethered, computerised video analysis 7-59957
 bacterial activity during spring bloom off Newfoundland, temp. regulation 7-4057
 bacterial photosynthetic reaction centres, charge recombination, ultrafine interaction, mag. field effect 7-8516
 bacteriochlorophyll, excitation energy transfer to reaction centre in photosynthesis 7-8517
 bacteriorhodopsin in polymer matrices, photochemical activity rel. to hydration 7-8518
 Biorack experiments on Spacelab D-1, results 7-8704
 blood, phase separation of erythrocytes, platelets and plasma at branches 7-54664
 blood filtration rates, review 7-54654
 book, annual review of biophysics and biophysical chemistry 7-30
 cell structure imagery, defocus and partially coherent illumination influence (*German*) 7-10845
 Chinese hamster ovary cells, temp.-dependent induction of thermotolerance 7-59940
 Chlamydomonas reinhardtii, circadian rhythm in a Zeitgeber-free environment, space flight obs. 7-8708
 chloroplast membranes, spectral effects of interaction with H⁺, absorpt. and fluoresc. spectra obs. 7-54503
 CHO cells, thermal adaptation at 40°C, rel. to growth conditions and heat shock proteins 7-17953
 chromatity horizontal cells in retina of freshwater turtle 7-47063
 chromatin content of cervical cancer cells, image processing technique 7-34119
 coherent excitation in polarisation wave band, Frohlich kinetic eqn., appl. to cellular membranes 7-54494
 colour pattern of animals, morphogenesis, cell interaction 7-13977
 commensalistic cultures grown in continuous stirred tank reactor, static and dynamic behaviour 7-13973
 continuous mixed cultures, steady states and bifurcation anal., multiplicity and local stability 7-13949
 cultured endothelium, apparatus to study response to shear stress 7-65907
 cytoarchitectonics, nervous tissue struct. inhomogeneities, software and hardware aspects of evaluation and anal. system 7-34360
 cytoskeleton and mechanoreception thresholds 7-40177
 diaphanography, breast cancer detect. by transillum., IR scatt. and absorpt.-obs. on cell suspensions 7-47211
 digital microscopy for cellular/subcellular features identification 7-54821
 DNA content of cells, distrib. modelling problem 7-47303
 DNA distributions with abnormal stemlines determined by flow cytometry, automatic analysis 7-59949
 dorsal root ganglion cells, chick, activation of a transient inward current by step reductions in extracellular Ca²⁺ 7-23326
 E. coli, effects of microgravity on genetic recombination 7-8711
 electrofusion and other electrophysiological treatments, versatile low-cost apparatus 7-14164
 electron microscopy of cell components, computer environment for 3D shaded perspective display 7-65905
 epithelial morphogenesis, phys. mechanism determining spatial organisation 7-40120
 erythrocyte, live cell, shear elasticity, entropic nature 7-65725
 erythrocyte marginal bands, newt, extensional and flexural rigidity obs. 7-8631
 erythrocyte membranes, viscosity and order, ns fluorimetry obs. 7-40185
 erythrocyte receptors, human, adrenoreceptive function, fluoresc. probe 7-8501
 erythrocytes, human, packing in centrifugal field 7-65721
 erythrocytes agglutinated by antibody, hydrodynamic force of breakup 7-40122
 erythrocytes agglutinated by antibody, interaction forces between 7-40121
 flow system for the study of shear forces upon cultured endothelial cells 7-65908
 Fourier transform IR spectroscopy of live bacterium A. laidlawii cells 7-54507
 ganglion cells, constant dendritic coverage with growth of goldfish's retina 7-40145
 genetic coding logic 7-65723
 Gompertz empirical eqn. for describing cell kinetics 7-17962
 horizontal cells, c-type, in bowfin retina, response props. 7-47053
 horizontal cells in eyecup and isolated retina, differing effects of excitatory amino acids 7-47056
 hyperthermia, chemotherapeutic agents and oncogenic transformation 7-13968
 hyperthermia cell survival data, model-free way of representation 7-17960
 hyperthermic radiosensitisation of thermotolerant Chinese hamster ovary cells 7-17961
 injury currents, elec. and math. props. in wound healing 7-8552
 instrumentation and cell physiology (*Japanese*) 7-14171
 interleukin-2, human recombinant, crystn. 7-65679
 intracellular long-term measurements on contracting isolated hearts, expt. set-up 7-65902
 intracellular microelectrode measurements in small cells evaluated with the patch clamp technique 7-40371
 intracellular water volume, NMR meas. 7-54505
 laser cancer therapy, optimum wavelength, cell components and mucous membrane absorptive spectrograms (*Chinese*) 7-28641
 lateral geniculate nucleus cells, macaque, mesopic spectral responses and Purkinje shift 7-47054
 leaves of higher plants, fluoresc. induction transitions, photosynthesis 7-8519
 light-dependent synaptic delay between photoreceptors and horizontal cells in the tiger salamander retina 7-59983
 lymphocyte, free energy of accumulation of a fluoresc. cation probe within the mitochondria 7-40118

cellular biophysics continued

- lymphocytes, human, sensitivity to gravity obs. (*German*) 7-8705
magnetic characteristics alterations produced by intracellular particles 7-65781
magnetotactic bacteria, mag. props., SQUID obs. 7-8610
mammalian cell polarisation at the ultrastruct. level, effect of microgravity, Spacelab D1 mission obs. 7-8707
mammalian cells, modification of thermal and thermochem. responses by adaptation to low pH 7-47018
membrane physiology and neural connections (*Japanese*) 7-13975
microcalorimetric measurements on tissue cells attached to microcarriers in stirred suspension 7-23311
microvessels, flow control coordination by intercellular cond. 7-65797
mitochondria, math. model of regulation of steady values of vol. and ΔpH 7-40119
mitochondria from bovine heart, electrophoretic behaviour of H^+ + AT-Pase proteolipid 7-59946
mouse liver cells, membrane pot. stability rel. to damaging agents exposure 7-8535
myocardial cells, rat, Fe overload 7-59945
neural cell adhesion mol., differentiation state-dependent surface mobilities 7-47019
Nitellopsis obtusa and Nitella translucens cells, membrane between chloroplast layer and moving cytoplasm, elec. obs. 7-40117
nuclear protein following heat shock: protein removal kinetics and cell cycle rearrangements 7-8522
nuclei, erythrocytes and hepatocytes, small angle scatt. obs. 7-17959
nucleoids, restoration of hyperthermia-associated protein to DNA ratio 7-65720
nucleoli, extraction from images of leucocytes by computerised image analysis 7-23505
online spike form discriminator for extracellular recordings based on an analog correlation technique 7-3952
orcein dye treatment, fluoresc. reactions and appls. 7-60140
pancreatic β -cells, elec. activity rel. to glucose 7-54504
Paramecium experiment on D1 mission of Spacelab 7-8706
particle sizing, high resolution, using time-of-flight and light scatt. meas. 7-48684
phospholipid bilayers, solvent-mediated interaction, nonlocal electrostatic theory of hydration force 7-17958
photoelectron microscopy, applications to biological surfaces 7-8773
photoreceptor cells from retina of domestic pig, comparison of size as determ. by light and scanning electron microscopy 7-13999
Physarum polycephalum, steady compensation of gravity effects 7-8712
phytoplankton, intra- and interspecific single cell optical variability, obs. 7-47015
plant protoplasts, cell fusion by elec. stimulation (*Japanese*) 7-47022
plant vegetative tissue, cell wall elastic constitutive laws and stress-strain behaviour 7-40184
platelet adhesion to fibrinogen-coated glass at an abrupt tubular expansion viewed with fluorescent video-microscopy 7-40183
platelet volume heterogeneity in acute thrombocytopenia, aperture impedance obs. on rats 7-3756
propagation through electrically coupled cells, how a small SA node drives a large atrium 7-40128
radiation dosimetry, picture-processing-based automated system 7-28713
red blood cells suspended in carbohydrate-saline solns., deformability, effect of transmembrane pot. 7-34118
retina, functional architecture 7-59974
retina, whole mount method for sequential anal. of photoreceptor and ganglion cell topography 7-40382
retinal ganglion cells, turtle, photoreceptor input and temporal summation 7-17984
retinal horizontal cells, changes in response waveform during dark and light adaptation 7-47060
retinal pigment epithelial cells, acetazolamide-induced changes of membrane pots. 7-28509
ribosome particles, electron microscopical 3D reconstructions of individual particles 7-41546
scanning laser microscope, real-time, for biological research 7-47292
silicate surface layer of yellowed rice plant leaf, IR refl. spectra 7-3837
Simian Virus 40 assembly 7-34117
spatio-temporal vision of macaques, with severe loss of P_{β} retinal ganglion cells 7-23344
stereology for anisotropic cells, appl. to growth cartilage 7-3947
stria vascularis, DC pots. in different cells, in vitro obs. 7-54586
T lymphocytes, human cloned helper, single-channel and whole-cell recordings of mitogen-regulated inward currents 7-40134
thermotolerance development in L1A2 tumour cells in vitro, evidence for an upper temp. limit 7-13967
thermotolerance in CHO cells, development and modification by procaine 7-65710
three-dimensional morphometric cytology, pictorial pattern recognition 7-28801
tissue culture cells, imaging intracellular elemental distrib. and ion fluxes using ion microscopy, freeze-fracture 7-60139
two-parameter data-acquisition system for slit-scan chromosome analysis 7-35501
ultra-soft X-ray contact microscopy, plant and animal cytology appls. 7-40388
vertebrate retina, physiological and morphological differences between On- and Off-centre bipolar cells 7-47050
visual neurons of macaques, reconstruction of equidistant colour space from responses 7-28514
yeast, elec. impedance change during growth and fermentation (*Japanese*) 7-47021
 Ca^{2+} current in single heart cells, opposite effects of cyclic GMP and cyclic AMP 7-40135

cellular effects of radiation

- see also *biological effects of ... (type of radiation)*
see also *photosynthesis*
adaptive response to ionising radiation induction (*Russian*) 7-14052
aortic endothelial cells, bovine, cell cycle changes and cytotoxicity in irradiated cultures 7-40230
binucleate cell form, in X-irrad. cultured mammalian cells, correl. to loss of colony-form. ability 7-60057
bladder urothelium, mouse, electron irradiation effects, SEM obs. 7-60058
bone marrow cells of BALB/c mice irradiated with ^{252}Cf or ^{60}Co , micronuclei prod. 7-28615

cellular effects of radiation continued

- bone marrow granulocyte-macrophage progenitor cells and stromal colony-forming cells, human, effect of dose rate 7-8662
C3H10T1/2 cells, transformation by UV irradiation to a unique, suppressible phenotype 7-65817
cancer induction and nonstochastic effects 7-54679
chemical modifiers of cancer treatment, conf., Clearwater, FL, USA (Oct. 1985) 7-18475
Chinese hamster cells, modification by mesoporphyrin-IX derivatives of damage by He ions and protons (*Russian*) 7-14064
Chinese hamster cells survival rel. to biological effectiveness of low energy protons 7-40221
chlorophyll a/b-protein complex II, light-harvesting, of higher plants, review 7-59951
chlorophyll chloroplasts, temp. damage and acclimation mechanisms of photosynthetic apparatus 7-59955
chlorophyll chloroplasts, temp. stress and prolonged darkening effect on photosynthetic apparatus 7-59956
chlorophyll in vivo, exciton states and exciton interaction processes, non-linear transmission effects 7-59931
chlorophyll in vivo, large absorpt. unit reflected in fluoresc. enhancement effect 7-59932
chlorophyll-protein complex II, light-harvesting, long-wavelength fluoresc. emission 7-59933
chlorophylls a and b and aggregates, spectra in nematic liq. crystals and polyvinyl alcohol films 7-59930
chloroplast matrix, pea, protein-synthesising apparatus, light quality effect, sedimentary props. 7-59952
chromosome aberrations and reproductive death of mammalian cells: quantitative correl. between these effects (*Russian*) 7-14054
chromosome aberrations induced in human lymphocytes by acute X- and γ -radiation in vitro 7-3843
clonogenic capacity of irradiated cells, factors influencing, computer simulation study (*Russian*) 7-14061
clonogenic cells of Lewis lung carcinoma, survival after γ - and γ -neutron irradiation (*Russian*) 7-14055
contact effects absence in irradiated EMT6-Rw tumours 7-18033
cytogenetic effectiveness of the therapeutic fast neutron beam emitted by cyclotron U-120 (*Russian*) 7-13976
cytogenetic effects of microwave irradiation of male mouse germ cells 7-23404
dissolved gases, influence on biological and chem. effects of US 7-14044
DNA injury in continuous long term low-dose irradiation, fluorometric obs. in rats, mice and men (*Russian*) 7-54506
DNA lesions, role in form. of radiation damage in chromosomes (*Russian*) 7-47170
DNA repair characts. of hybrid cell clone between xeroderma pigmentosum and Potorous tridactylis 7-60045
DNA repair kinetics after exposure to X-irradiation and to internal β -rays in CHO cells 7-28619
DNA repair mechanisms and their potential modification radiotherapy 7-23314
E. coli, L-arabinose isomerase induction by γ -irradiation 7-40229
E. coli cells, thermoinduced radioresistance and heat shock proteins (*Russian*) 7-13969
egg production and fertilisation of copepod Tisbe Holothuriae, laser irradiation effects 7-8650
Ehrlich ascites clonogenic tumour cells exposed to ^{60}Co γ -rays in hypoxic conditions, radiosensitivity (*Russian*) 7-47180
Ehrlich ascites tumour clonogenic cells forming colonies in agar cultures in diffuse chambers, radiosensitivity (*Russian*) 7-47176
embryo, pre-implantation, mouse, radiotoxicity of 3H -thymidine and 3H -arginine 7-60051
erythrocyte membrane, effects of γ -irradiation as shown by ESR, NMR and biochem. studies 7-60041
erythrocytes, effects of He-Ne laser light 7-3840
erythrocytes, human, ferricyanide reduction in the presence of methylene blue, influence of a UHF EM field 7-40217
erythroid units in canine bone marrow cells, survival on neutron or γ -irradiation 7-60056
erythroleukemic cells, murine, differentiation during exposure to microwave radiation 7-40218
fibroblasts, human, mutation induction, evaluation of a specific quality function 7-3842
fish cells, primary cultured with different ploidy, radiosensitivity obs. 7-60044
haematopoiesis and radiation in Harwell steel mice 7-40222
hair cell damage produced by acoustic trauma in the chick cochlea 7-54597
Halobacterium halobium phototaxis, excitation signal processing 7-28602
heat and radiation interaction anal., CHO cells expts. 7-18028
HeLa cells, changes in UV-fluoresc. intensity in irradiated cells (*Russian*) 7-14056
HeLa cells, X-irradiated, action of caffeine, recovery from potential lethal damage 7-8666
hepatoma cells, γ -irradiation, change in initiation of DNA synthesis at a nuclear matrix and its DNA-protein content (*Russian*) 7-47174
hyperglycemia, short-term induced, influence on effectiveness of X- and neutron-radiation on HeLa cells (*Russian*) 7-14065
hyperthermic cell killing, enhancement by nonthermal effect of US 7-60035
hypoxic cells, radiosensitisation at low doses 7-23409
immune response, functional activity of involved cell systems at long times following sublethal irradiation (*Russian*) 7-14057
intestinal cell death induced by HTO in mice, obs. using a new 3H safety clean cabinet 7-60054
jejunal crypt cells, mouse, response to ^{137}Cs γ -rays and ^{252}Cf neutron irradiation 7-28613
Jejunal crypt stem-cell survival after fractionated γ -irradiation performed at different dose rates 7-60042
keratinocytes, cultured, human and mouse, radiosensitivity obs. 7-8656
lethal and mutagenic effects of fast neutrons of different energy of Streptomyces griseus spores (*Russian*) 7-14041
living cell model for electric field and overvoltage effects (*Polish*) 7-60031
lymphocyte subclasses and immunoglobulins, in adults receiving radiation treatment in infancy for thymic enlargement 7-18032
lymphocytes, human, cell survival and radiation induced chromosome aberrations 7-47168
lymphocytes, human, chromosome aberrations yield rel. to dose (*Russian*) 7-18027

cellular effects of radiation continued

- lymphocytes, human, lower limits of dose detect. after X-irrad. 7-34196
 lymphocytes, low-dose-irrad., decreased nucleic acid synthesis, effect of TCGF addition 7-8661
 lymphocytes, peripheral, human, effect of low-level 60 Hz EM fields 7-28582
 lymphoid cells, rat, effect of ionising radiation on lipid metabolism 7-60040
 mammalian cell culture, DNA single- and double-strand breaks by thermal neutrons 7-23392
 mammalian cells, amplification of oncogenes and integrated SV40 sequences by ^{125}I decay 7-40224
 mammalian cells, cultured, induction of cell killing, mutation and oncogenic transformation following exposure to tritiated water 7-60049
 mammalian cells, heat-induced cell killing rel. to heat radiosensitization 7-8521
 mammalian cells, irrad. with ^{252}Cf and ^{60}Co , effects of alternating mag. fields on survival 7-28594
 mammalian tissues, particulate radiation damage, electron microscopy appls. 7-28623
 mammary carcinoma cells, murine, thermal radiosensitisation and thermotolerance 7-59937
 meiotic abnormalities induced in tetraploid and hexaploid wheat by γ -rays and ethyl methanesulphonate 7-65719
 melanoma cells, cultured, RBE of thermal neutron beam and the $^{10}\text{B}(\text{n}, \alpha)^7\text{Li}$ reaction 7-60028
 membrane reception of prostaglandin E_2 in mouse tissues, effect of various doses of ionising radiation (*Russian*) 7-47173
 mesophyll chloroplasts from sugar cane, photosynthetic electron transport 7-59953
 mesophyll plastid, maize, greening under 'extreme low-light intensity 7-59954
 microdosimetric approach in radiation biology, correctness (*Russian*) 7-14063
 micronuclei induced during interphase of 4-cell mouse embryos in vitro after X-irrad. 7-28620
 mitochondria, isolated, rat liver, effects of up to 475 Gy γ -rays 7-60043
 mitogenic response of peripheral blood mononuclear cells, effect of ELF pulsed mag. fields 7-28580
 mononuclear phagocyte system, effects of therapeutic US on activity in vivo 7-14043
 multicellular spheroids initiated from human melanoma xenograft lines 7-14049
 mutation induction in spores of *Bacillus subtilis* by accelerated very heavy ions 7-28618
 mutational extinction induced by sequential X-irrad. and actinomycin D treatments in CHO cells 7-8663
 neoplastic transformation, induction by low-dose-rate exposure to tritiated water 7-8664
 nuclear protein content and cell progression kinetics following X-irrad. 7-40225
 oncogenic transformation of cells in culture: pragmatic comparisons of oncogenicity, cellular and mol. mechanisms 7-60855
 peripheral blood, lymphocytes from ageing donors, sensitivity to X-irrad. 7-8655
 peripheral blood lymphocytes of atomic bomb survivors, anal. using monoclonal antibodies 7-59947
 phototactic microorganism *Haematococcus pluvialis*, transient photoreponses revealed by light scatt. 7-28481
 plasmid damaged at a specific region by UV light, mutational DNA base sequence changes 7-59948
 population kinetic parameters for acute epidermal reactions in man 7-40227
 potentially lethal damage in plateau-phase V790 cells after exposure to neutrons or γ -rays 7-40212
 predictive models of cell death by exposure in vitro to X-rays and 1,3-bis(2-chloroethyl)-1-nitrosourea 7-60046
 protozoan reproduction, promotion by ionising radiation 7-40231
 radiosensitisation of Chinese hamster cells by O_2 and misonidazole at low X-ray doses 7-40219
 radiotherapy, dose distrib. of high-energy electron beam, chromosome aberration freqs. 7-14131
 retinal rod outer segment suspensions, effect of sonication on nucleotide-dependent light scatt. changes 7-23398
 rhabdomyosarcoma tumor cells, rat, pot. lethal damage repair after X-ray or Ne ions 7-18031
 rotating electric fields, cell behaviour rel. to surface charges and cell structs. 7-28584
Saccharomyces cerevisiae cells, effect of mm-wave irrad. on growth 7-28604
 somatic mutations induction in *Tradescantia*, effects of low dose tritiated water and tritium labelled compounds 7-60048
 spermatogonial stem cell population, mouse, variation in sensitivity to fission neutron irrad. 7-60032
 stereocilia, tip links, vulnerability to acoustic trauma in the guinea pig 7-54590
 stromal tissue, mouse, influence of prior heat treatment on effects of heat alone or combined with X-rays 7-59938
 survival and radiation induced chromosome aberrations 7-47167
 synergistic effect of γ -radiation and quinoidradiotoxins on mice and lymphoid cells in culture (*Russian*) 7-14062
 T-1 cells, human, inverse γ -ray dose rate effect in ^{252}Cf RBE expt. 7-28616
 thylakoid membrane, light scatt., photo-induced changes, surface charge effect 7-59934
 thylakoid membrane, light scatt., photo-induced changes, temp. treatment effect 7-59935
 thylakoid membranes and functional subunits, organisation, linear dichroism and fluoresc. polarisation obs. 7-59944
 thymidine synchronised bovine lymphocytes exposed to 7.25 GHz microwaves, cytogenetic obs. 7-14048
 tumour cell heterogeneous population model, radiation therapy optimisation 7-60074
 tumour cell reproductive capability rel. to neutron RBE of cyclotron Y-120 (*Russian*) 7-54673
 X-ray sensitivity in different regions of the sandwich, a diffusion-limited system for cell growth 7-40226
 yeast, wild-type and repair-deficient strain, fast neutron RBE for lethality and genotoxicity 7-23393
 yeast cells, photoreactive damage rel. to O_2 effect in radio- and UV-sensitive mutants (*Russian*) 7-14053

cellular effects of radiation continued

- yeast cells, X-ray induction of DNA double-strand breaks 7-8657
 ^{252}Cf brachytherapy treatment of localised tumours, B neutron capture enhancement, Chinese hamster cell obs. 7-28589
 ^{252}Cf γ -neutron radiation biological effects, USSR studies 7-28611
 ^{252}Cf -exposed human cells, pot. lethal damage and radioprotection 7-28612
 HTO β -rays, RBE measured by effects on cultured mouse embryos at pre-implantation stage 7-60050
 HTO, RBE on cultured mammalian cells at mol. and cellular level 7-60047

cellular method

- ZnS, clusters, electronic struct., variational cellular method 7-45120

cellular transport and dynamics

see also cell motility

- cardiac gap junctions, single channel currents, embryonic heart obs. 7-8550
 cardiac myocytes, $\text{Na}^+/\text{Ca}^{2+}$ exchange, effect of ouabain on voltage dependence 7-59958
 cardiac myocytes, single isolated, simple technique to meas. rate and magnitude of shortening 7-23494
 cardiac Purkinje strands, K^+ -activated electrogenic Na^+ pumping 7-28490
 cardiac sino-atrial node cells, charactn. of single pacemaker channels 7-47024
 CCD line-scan image sensor for meas. of red cell vel. in microvessels 7-8777
 cell membrane permeability and cell inactivation of transformed mouse fibroblasts, heat-induced alterations 7-47023
 chromatin domains and nucleoli in neuronal interphase nuclei, curvilinear 3D motion 7-65726
 deposition of cells on inclined plate, effect of gravity 7-34120
 erythrocyte cells, dynamic studies using laser-projection microscopy 7-14172
 extracellular potentials around active excitable structures with short geometric inhomogeneities 7-8538
 gap junction channel, its aq. nature as indicated by D_2O effects, temp. coeff. obs. on earthworm 7-28492
 gap junctional cond., linear relationship with permeability, frog blastomere obs. 7-40127
Halobacterium halobium phototaxis, excitation signal processing 7-28602
 highly permeable contact membranes, role of microtubules in activity regulation 7-40125
 immunological tumour escape, Monte Carlo simulation 7-13947
 lymphocytes, T, abnormal, from mice with lpr gene mutation, altered K^+ channel expression 7-28487
 mesophyll chloroplasts from sugar cane, photosynthetic electron transport 7-59953
 nerve cell, membrane pot. clamping, cyclic nucleotide injection, intraneurone information processing 7-8527
 neutrophil dynamics, normal, 1/f-like scaling, implications for haematological monitoring 7-3757
 ohmic conductance through the inwardly rectifying K channel and blocking by internal Mg^{2+} 7-47026
 pancreatic β -cell, bursting, effect of intracellular Ca^{2+} -sensitive K^+ channel 7-28483
Paramecium behaviour during video centrifuge-microscopy 7-3758
 photoreceptor membrane currents, inositol trisphosphate regulation, *Hermisenda* obs. 7-28518
 phototactic microorganism *Haematococcus pluvialis*, transient photoreponses revealed by light scatt. 7-28481
 plant cell membranes, water movement, cell wall deform., cooling effect 7-8525
 plant cells water transport props. determ., using automated pressure probe 7-23503
 platelet aggregation, shear-induced, anal. with population balance maths. 7-8614
 platelet diffusivity in flowing blood, fluid shear as a possible mechanism 7-28552
 potential depend. Na channels regulation, spectroscopy of combination scatter 7-8524
 radiolabelled pulse for the simultaneous study of anterograde and retrograde axonal transport 7-3951
 retinal glial cells, higher density of ion channels that mediate K^+ buffering in endfeet 7-47048
 rotating electric fields, cell behaviour rel. to surface charges and cell structs. 7-28584
 skeletal muscle, developing rat, functional differences between 2 classes of Na^+ channels 7-3759
 skeletal muscle sinusoidal oscills., energy stored and dissipated, frog obs. 7-40113
 stereocilia micromechanics, changes following overstimulation in metabolically blocked hair cells 7-40164
 stratum corneum, lipophilic pathway, Fourier transform IR spectroscopy studies 7-54510
 system cells, grapevine shoot, water crystallisation, nystatin treatment, plasma membrane pore size and hardening 7-8497
 tissue culture cells, imaging intracellular elemental distrib. and ion fluxes using ion microscopy, freeze-fracture 7-60139
 transplasmalemma electron transport changes in simian virus 40 transformed liver cells 7-59959
 vascular muscle cells, spontaneously contracting, Ca^{2+} and Na^+ channels 7-3760
 yeast, voltage-dependent ion channel obs. 7-28486
 K^+ channels, voltage-activated, twinning with Ca^{2+} channels in *Drosophila*, rel. to occult Ca^{2+} channels 7-17966
 Na^+ translocation by Na^+/K^+ pump, voltage dependence 7-17957
 Na-conducting Ca channel, regulation in beating heart cells during action pot. 7-54528
 Ra adsorptive uptake by waste inactive microbial biomass 7-40313

cement industry

- metallic corrosion of cement plant facilities, cathodic protection 7-28210
 refractory brick in rotary kiln burning zones, failure mode anal. 7-28140
 waste fuels in the cement industry 7-28386
 Hg emissions from cement factory, influence on environment 7-40060

cementation steel *see alloy steel*

cemented carbides *see cermets*

cements (building materials)

used only for those materials which bind together particulate matter so as to form a coherent mass of considerable strength. For cements that cause two or more separate masses to adhere see adhesion
bending stress determ. from density of localised cracks (German) 7-22935
composite, cement-based, strain rate effects on fracture, conf., Boston, USA (Dec. 191985) 7-14712
gypsum, initial hardening with cement, pulse rheometry investig. 7-37411
paste, low-porosity, subcrit. crack growth in alcohol media 7-59650
pore structure of cement stone in contact with a large filler 7-8244
slag cement-low level radioactive waste forms at Savannah River Plant 7-42197
water leachability of cement forms for medium-level waste immobilization 7-49687

centrifuges

gas centrifuge, separative power, aspect ratio and feed flow rate effect 7-9828
gas-solid reactions, transport and mixing charact., thermocentrifugometric anal. 7-54095
Parametric behaviour during video centrifuge-microscopy 7-3758
photometric analyser with chain-driven continuous feed system 7-24683
PWR power station appls. of centrifugal separators (French) 7-25102
separation of fine particles, using rotating tube with alternate flow 7-35502
ultracentrifuge enrichment plants, flow induced vibrations in gas tube assembly 7-30570
vacuum-arc centrifuge, rotational props. 7-56253

cepstral analysis *see spectral analysis*

ceramics *see cermets*

ceramic industry

US flaw detection of refractory products 7-22960

ceramics

see also ceramic industry; refractories

abrasive wear, fine-scale, by plastic cutting process 7-3458
advanced ceramics, developments and research on cracking tendency 7-27989
alumina, birefringent, millimeter wave dielectric meas. 7-14978
alumina, polycrystalline ceramics, spall strength, plate impact meas., spall zone model calcs. 7-33797
alumina polycrystalline ceramics, shock fracture and recompaction, double impact technique study 7-33880
anisotropic piezoceramics for US probes 7-1362
apatite ceramics, with microstruct. controlled by Y^{3+} substitution, elec. props. 7-21523
bending fatigue, room temp. (Japanese) 7-13597
beryllium, birefringent, millimeter wave dielectric meas. 7-14978
biomedical US transducer array performance with PZT-polymer composite piezoceramic 7-3850
birefringent, millimeter wave dielectric meas. 7-14978
brittle, non-oxide, flaw charactn., computer-aided US testing 7-54064
cation-conductive ceramics examined by 1 MV HRTEM 7-2258
ceramic-metal interfaces, grain boundaries, bonding and interfacial structure 7-26765
ceramic/metal jointed interface, strain distrib. determ., laser speckle photography (Japanese) 7-54037
chemical synthesis from molecular precursors, conf., Palo Alto, USA (Apr. 1986) 7-35113
coal conversion and heat-engine ceramic technology, US instrumentation 7-1344
coatings, plasma sprayed on stainless steel, hot isostatic pressing, hardness, bond strength 7-13624
coaxial ceramic pulse-forming line for XeCl laser 7-43061
colour standards, thermochromism 7-9867
compactum under quadrilateral compaction press. 7-13397
composite ceramics, multiphase interaction, sensor appls. 7-64996
composite electroceramics, book contrib. 7-27645
composite frictional stress evaluation along fibre-matrix interface 7-28143
composite materials, CVD processing 7-64992
composite piezoelectric sensors, elec. charact., hydrophone appl. 7-62943
composites, binary elastic, effective transform. strain 7-44660
composites, laminated, struct.-performance maps 7-17574
composites, liq. phase sintered, hot isostatic pressing 7-64989
composites, non-oxide, CVD fabrication 7-64993
composites, sintering, role of shear deform. 7-64988
cordierite glass and glass-ceramic, comparative single-point diamond scratching behaviour 7-46654
crack propagation by double-torsion method (Japanese) 7-59614
creep modelling for engineering design 7-22776
cutting tool materials, mech. props., wear-resist. relations 7-3443
cylindrical nuclear fuels, computer modelling, review 7-720
data compilation for radiation effects on ceramic insulators 7-58350
defects, stress- and fatigue-induced, small angle neutron scatt. studies 7-58273
density gradients in ceramic pellets measured by computed tomography 7-39840
determination of the thermal conductivity of ceramic materials by the 'hot wire' method (Polish) 7-52894
electrical ceramics, high-alumina, sintered state range widening, temp. depend. of melt apparent viscosity 7-46396
electrical insulators, low thermal expansion 7-2237
electroceramic composites, props. and struct. 7-64558
electroceramic transducers, sensors, and actuators 7-20557
electron irradi. induced transforms. 7-2065
electron microscopy studies, symposium, Nantes France (July 1986) 7-18479
engine appl., conf., London, England (Nov. 1985) 7-5
engine component fabrication techniques 7-3243
engineering, rel. between Rockwell hardness and Vickers hardness (Japanese) 7-65140
engineering ceramics, gas turbine engine appls. 7-3241
engineering ceramics evaluation by gamma-ray computerised tomography 7-28258
engineering performance prediction, fracture mechanics 7-3416
eutectic composites, microstruct. and mech. props. 7-64991
fatigue, static and dynamic (Japanese) 7-46619
ferrite ceramics, AC and DC cond. (Spanish) 7-52560

ceramics continued

ferroelectric, elec. field-excited acoustic waves parametric instability, wave eqn. calcs. 7-6727
ferroelectric, electromagnetic wave scatt. from dielec. permittivity tensor inhomogeneities 7-7629
ferroelectric ceramic bar, normal mode responses, influences of domain switching and dipole dynamics 7-45945
fibre reinforced ceramics, test techniques for mech. props. 7-13698
fission and fusion reactor materials and technology survey 7-10215
fracture toughness evaluation using chevron-notched specimens (Japanese) 7-59613
fusion reactor materials, conf., Chicago, IL, USA (Apr. 1986) 7-48145
fusion solid breeders, T recovery and inventory, surface desorption effect 7-49651
gilsonite, microstructure and mechanical props. 7-44838
glass, failure kinetics using composite glass-crystal system model 7-59631
glass ceramic materials, liq. phase separation, nucleation and crystn., book 7-24327
glass ceramic optical components, prod. using precision machining/metrology facility 7-37222
glass ceramic standards, geometrical dims. stability with time 7-41328
glass ceramics, development in China, review 7-6527
glass ceramics, struct., phase relations 7-7982
glass frit, SIMS 7-9919
glassy phase formation in ceramic-like coatings 7-3257
grain boundary ledges, cavity nucleation 7-21217
green and sintered, elasticity calc. from US velocity meas. 7-2085
grinding, crack branching, crushing mechanism 7-3472
gypsum systems, Young's modulus rel. to porosity 7-46533
hard materials, frictional behavior of diamond and cubic BN abrasives 7-3461
hard materials, fundamentals of wear 7-3456
heat resistance of parts under two-dimens. strain conditions 7-59630
heterogeneous ceramics, processing for dielectric appls. 7-64984
HLLW solidification, review of alternative wasteforms and processes 7-36296
HLW immobilisation in ceramic waste forms. SYNROC props., leaching 7-5459
hollow spherical particles, struct. and strength 7-3234
interfacial bonding and adhesion, conf., Aspen, CO, USA (Aug. 1985) 7-24269
interferometry applied to ceramics 7-39813
intergranular glass phases, equilib. film thickness 7-46433
internal voids, detection by microfocus X-radiography 7-59736
ion implantation and near surface microstructures, analytical electron microscopy 7-37816
ionic conducting ceramics, elec. resist. meas. by impedance spectroscopy 7-9844
laser production of ultra-fine metallic and ceramic particles 7-13406
lifetime prediction of ceramic materials 7-8218
long-spindle insulator damage by shotgun (Japanese) 7-22787
machining of stainless steels, failure mechanisms of ceramics and coated carbides 7-3432
materials science and processing, outline of trends 7-46282
metal-ceramic composite, dynamic fracture toughness (Japanese) 7-13559
metal-ceramic interfacial props., thermodynamics 7-12506
metal-ceramic particle composites, cast, solidification, struct. and props. 7-7932
MgO-monticellite ceramic, high resoln. TEM and STEM study 7-22738
microfracture prediction via microcontact model 7-16678
microstructure characterisation by image anal. 7-3547
model particle packings having multiple generations of agglomerates, fractal dimensions 7-39451
moistened and pyrolyzed materials in strong RF fields, computer-aided permittivity meas. 7-48769
monolithic fuel cell tapes, three-layer ceramic composite, stress and fracture analysis 7-3407
mullite, Al_2O_3 and ZrO_2 particle reinforced, prep. by reaction sintering, fractographic study 7-22800
mullite powders, props. and microstruct. of fired bodies (Japanese) 7-22626
mullite-alumina composites, sintering and charactn. 7-3252
multiphase, quantitative microstruct. charactn. and description 7-65254
multiphase, sintering 7-64963
multiphase and composite, conf., University Park, PA, USA (July 1985) 7-60880
NDT by acoustic microscopy with single zoom lens 7-3570
nondestructive evaluation, converging-surface-acoustic-wave technique investig. 7-54049
nuclear fuels, diffusion processes, review 7-19350
oxide powders, mag., dispersion and particle packing 7-3233
oxides, complex ABO_3 cpds., thermal expansion data 7-12330
oxides, cond., for use as molten carbonate fuel cell electrodes 7-13854
oxynitride ceramics, anal. by electron microscopy 7-16428
parameter meas. by laser interferometry 7-9888
perovskite-like ferroelectrics, optical and electrophysical props. 7-3002
piezoceramic narrow-strip element resonance freq. dispersion diagrams, texture and ionic substitution effects 7-1363
piezoceramic shell, applied theory modification 7-43750
piezoceramic-polymer-composites, damping props. 7-64575
piezoceramics, electrical response to shock waves 7-63178
piezoelectric, equiv. cts. for thickness mode (French) 7-2976
piezoelectric, with low Q coeff., equiv. cts. (French) 7-2977
piezoelectric ceramic shell, high frequency vibrations 7-22191
piezoelectric ceramics, prep. and industrial appls. 7-13096
plasma parameter gradients near ceramic surfaces, origin investig. 7-20900
plasticity, model representations 7-11368
poly(acrylic acid)-ceramic filler composite, filler chem. influence on T_g behaviour, dynamic mech. spectroscopy 7-59559
porcelain, sintering kinetics, struct. evolution 7-28004
porosity and thermal shock behaviour (German) 7-22707
powder compaction response diagrams, generation 7-39450
powder prep., sintering and compaction, internal combustion engine appl. 7-3240
powder size and distrib., surface texture, thermal props., interferometric meas. 7-9818
powders, green state, real-time US NDE during compaction 7-22955
powders, tapping behaviour, numerical analysis 7-46360
properties meas., conf., Soverato, Italy (Sept. 1986) 7-9582

ceramics continued

- PZT piezoceramics, reorientational polarization effects on stability and isotropy (*French*) 7-59153
 quartz, birefringent, millimeter wave dielectric meas. 7-14978
 quartz ceramic reflectors, γ -irrad. effects on Nd:YAG laser energy char-acts. 7-50575
 radiation induced products, STEM microanalysis 7-16639
 reciprocating engine requirements 7-3242
 resistors for noise thermometers 7-4851
 sapphire, birefringent, millimeter wave dielectric meas. 7-14978
 sapphire, ion implantation, mechanical surface property modifications 7-32473
 SCARE postprocessor program to MSC/NASTRAN, ceramic components reliability anal. 7-17750
 semiconductor materials, granular struct. and elec. props. (*German*) 7-58495
 SH wave propag. in piezoelectric ceramic plates 7-21603
 sialon, abrasive polishing problems 7-53939
 sialon, commercial, static fatigue and creep resist. 7-59601
 β -sialon, engineering ceramics, prep., fabrication, appls. 7-53683
 sialon, sliding and abrasive wear mechanisms, comparison 7-3463
 sialon, wear resist., comparative study of hard materials 7-3457
 α - β -sialon ceramic composites, fabrication 7-64990
 sialon ceramics, processing, Al ion redistrib., crystallisation EDX analysis 7-3237
 β -sialon composite ceramics, microstruct., hardness, tool appls. 7-65144
 SIMS 7-9919
 SIMS depth profiling 7-13314
 sintering, intermediate and final-stage, microstruct. development 7-64952
 sphene ceramics containing substituted radionuclides, leaching, CANDU waste disposal 7-811
 sphene glass ceramics, radioactive waste immobilisation, sintering, porosity 7-27984
 static-fatigue limit of materials containing small flaws 7-39620
 strip, cracked, thermal shock, temp. depend. material props. 7-16114
 structural, flaw size distrib. 7-22818
 structural ceramics, flaw detection, holographic interferometry techniques 7-46760
 structure statistical parameter evaluation, image processing automation (*Russian*) 7-10877
 substrates, decohesion of thin films 7-21711
 surface and interface analysis, appls. conf., Veldhoven, Netherlands, (Oct. 1985) 7-24289
 Syalon, bonding investig., active Ti additive role, fracture strength and microstruct. 7-39846
 TEM, conference, Boston, MA, USA (Dec. 1985) 7-35119
 TEM, prep. by ion milling grain boundary glassy phase 7-44327
 thermal diffusivity and cond. 7-12381
 thermal inertia measurement, reflective-cavity method investig. 7-46753
 thermal shock testing of ceramics with pulsed laser irradiation 7-32491
 toughening by strong reinforcements, fracture toughness, microstruct. 7-22783
 transformation toughening, shear, shape and orientation effects 7-39626
 transparent ferroelectrics, appl., theory and props., conference, Latvian State University, Latvian SSR (April 1985) 7-4622
 transparent ferroelectrics, comp., struct. and props. characts. anal. 7-7647
 transparent ferroelectrics, cryst. chem. and struct. props. and modifications 7-6590
 tribochemistry, chemical reaction increase by friction 7-46868
 tubes, acoustic anal., nondestructive examination method 7-13705
 two-phase and porous materials, microstructure-thermomech. prop. correls. 7-12380
 ultrahigh-temperature thermionic conversion in space nuclear power, material considerations 7-65506
 US flaw detection, appl. to model-defect test pieces (*Japanese*) 7-59730
 US flaw detection, effects of coupling layer on sensitivity (*Japanese*) 7-17758
 vitreous ceramic materials, interaction of Si and Ti oxides, carbides, nitrides with phosphate binder 7-3260
 wear behaviour, cathodolum. mode appl. in SEM 7-8228
 wear mechanism in dry rolling friction 7-59643
 Yb ceramic emitter for thermovoltaic energy conversion 7-65481
 Zerodur, lightweight large mirror blanks prod. 7-37223
 Zerodur glass ceramic, long-term dimensional stability as consequence of diffusion (*German*) 7-63488
 ZrN films, supercond. props. (*Russian*) 7-38836
 $\text{Ag}_2\text{O-Al}_2\text{O}_3$ ceramics and single crystals, cond. fluctuations and contact noise meas. 7-58840
 AlN, hot pressed ceramic, porosity effect on elec. cond. 7-7223
 Al_2O_3 , bicrystals, high-purity, grain boundary structures 7-58668
 Al_2O_3 , CVD, morphology rel. to growth conditions 7-17431
 Al_2O_3 ceramic, grain boundaries, microanal. 7-16577
 Al_2O_3 ceramic diaphragm differential-pressure transducer 7-61354
 α - Al_2O_3 , ceramic matrices, precip. morphology 7-65049
 Al_2O_3 ceramics, friction and wear measured by a pin-on-disk method (*Japanese*) 7-22850
 Al_2O_3 ceramics, grindability, effect of microstruct. 7-22862
 Al_2O_3 ceramics, microstruct.-mech. prop. relationship 7-65147
 Al_2O_3 discs, thermal shock reliability, Weibull parameters, bending and fracture testing 7-3408
 Al_2O_3 , engineering ceramics, texture 7-28057
 Al_2O_3 film, transparent, growth from ultrafine alumina sol characteris. 7-13395
 Al_2O_3 film-stainless steel adhesion, improvement using surface precipitates (*Japanese*) 7-22880
 Al_2O_3 , fretting wear in seawater 7-8124
 Al_2O_3 , Na-S cell reliability models using ceramic degradation mechanisms 7-59831
 Al_2O_3 , porous, elec. cond. and fluid flow permeability correls. 7-38566
 Al_2O_3 , reflection scanning acoustic microscopy of partly embedded cracks 7-46769
 Al_2O_3 refractory ceramic, wettability and contact angle with Al melt, nitride additive effects (*Russian*) 7-12402
 Al_2O_3 , sintered, small-angle neutron scatt. from porosity 7-39825
 Al_2O_3 , sliding and abrasive wear mechanisms, comparison 7-3463
 Al_2O_3 , spinel growth, interface struct. investig. 7-16566
 Al_2O_3 , wear resist., comparative study of hard materials 7-3457
 $\text{Al}_2\text{O}_3\text{-Fe}_2\text{Y}$, high temp. DC elec. cond. rel. to superalloy oxide scale adherence 7-52615
 $\text{Al}_2\text{O}_3\text{-Cr}_2\text{O}_3\text{-ZrO}_2$ system, subsolidus, high temp. phase relation 7-17519

ceramics continued

- $\text{Al}_2\text{O}_3\text{-MgO}$, diphasic xerogels, densification, sintering, isostructural seed, epitaxy 7-27987
 $\text{Al}_2\text{O}_3\text{-MgO-TiO}_2\text{-Na}_2\text{O}$ system, sintering and creep, Na_2O influence, Cable and Reijnen-Readley models (*German, English*) 7-7933
 $\beta\text{-Al}_2\text{O}_3\text{-Na}_2\text{O}$ ceramics, electrophoretic deposition 7-13390
 $\beta\text{-Al}_2\text{O}_3\text{-Na}_2\text{O}$ ceramic electrolyte; electrophoretic deposition 7-13411
 $\text{B}^+\text{-Al}_2\text{O}_3\text{-Na}_2\text{O}$ solid electrolytes, degradation in Na-S batteries 7-3466
 $\text{B}^+\text{-Al}_2\text{O}_3\text{-Na}_2\text{O-ZrO}_2$ ceramics, transform toughened, fabrication, mech. props. ionic resist. 7-65143
 $\text{Al}_2\text{O}_3\text{-Nb}$ interface, grain boundary struct., elemental comp. determ., TEM obs. 7-21225
 $\text{Al}_2\text{O}_3\text{-SiC}$ composites, microstruct. and mech. props. (*Japanese*) 7-22821
 $\text{Al}_2\text{O}_3\text{-SiO}_2$, mullite ceramics, sol mixture prep., drying method effect (*Japanese*) 7-7944
 $\text{Al}_2\text{O}_3\text{-SiO}_2\text{:Cr}$ mullite transparent glass ceramics, Cr^{3+} luminesc. 7-46102
 $\text{Al}_2\text{O}_3\text{-SiO}_3$, mullite, prep. by sol-gel method, microstruct. and mech. props. 7-46386
 $\text{Al}_2\text{O}_3\text{-TiC-TiN}$ composite ceramics, microstruct., hardness, tool appls. 7-65144
 $\text{Al}_2\text{O}_3\text{-TiN}$ powder composites, densification kinetics and struct. form. during sintering under high press. 7-53687
 $\text{Al}_2\text{O}_3\text{-TiO}_2$, mech. props. and microstruct., influence of TiO_2 additions. (*Japanese*) 7-22706
 $\text{Al}_2\text{O}_3\text{-TiO}_2$ system detonation coatings, struct. and phase characts., physico-mech. props. 7-65212
 $\text{Al}_2\text{O}_3\text{-TiO}_2\text{-NaO}_{1/2}$ system, elec. cond. meas. to detect suspected liq. phase 7-39467
 $\text{Al}_2\text{O}_3\text{-TiO}_2\text{-SiO}_2$ composite, thermal shock resist. 7-33771
 $\text{Al}_2\text{O}_3\text{-ZrO}_2$ ceramics, densification kinetics 7-27992
 $\text{Al}_2\text{O}_3\text{-ZrO}_2$ ceramics, hot forging characts., grain size 7-3370
 $\text{Al}_2\text{O}_3\text{-ZrO}_2$ composites, high temp. behaviour and microstruct. study with HVEM (*Japanese*) 7-22819
 $\text{Al}_2\text{O}_3\text{-ZrO}_2$ toughened ceramics, dry friction and wear against steel 7-8125
 $\text{Al}_2\text{O}_3\text{-ZrO}_2\text{-Y}_2\text{O}_3$ system, synthesis and props. 7-22614
 $\text{Al}_2\text{O}_3\text{-ZrO}_2$ composite ceramics, microstruct., hardness, tool appls. 7-65144
 Al_2O_3 ceramic casting by doctor-blade method, effect on props. of green tape (*Japanese*) 7-26220
 $\text{Al}_2\text{O}_3\text{-ZrO}_2$ composites, microstruct. charactn. by Raman spectroscopy (*Japanese*) 7-22684
 AlPO_4 , cryst., prep. by reaction using BPO_4 7-46388
 $\text{Al}_2(\text{TiO}_3)_3$ ceramics, sintering, microstruct., bending strength, additives effect (*Japanese*) 7-17601
 Al_2TiO_5 ceramics, form. by solid state reaction of Al_2O_3 and TiO_2 powders 7-46385
 Al_2TiO_5 -mullite composites, thermal and mech. props., effect of comp. (*Japanese*) 7-26987
 B,C ceramics, pressureless sintering with polycarbosilane addition 7-46389
 BN, cubic, aggregate tools, microstruct. and wear 7-3462
 BN, cubic, polycryst., influence of sintering conditions on phys. props. 7-22618
 BN, engineering ceramics, prep., fabrication, appls. 7-53683
 c-BN, high press. sintering 7-22615
 c-BN, phase diagram, p,T,E 7-17517
 BN polycrystals, heat treatment conditions effect on mech. and service props. 7-53894
 BN ultrafine powder synthesis at -75 to 750°C 7-22629
 BN, wurtzite, sintered polycryst., texture form. during hot compacting at high press., sphalerite transition 7-53685
 BN, wurtzite-type and zincblende-type, struct. changes by shock treatments 7-22676
 BN, wurtzitic compacts, sintered, particle size distrib., hardness, phase comp. 7-59603
 $\text{Ba}(\text{Ca}_{1/3}\text{Nb}_{2/3})\text{O}_3\text{-PbZrO}_3\text{-PbTiO}_3$ ceramics, hot-pressed, ferroelectric phase transitions 7-7652
 $\text{BaFe}_{12}\text{O}_{19}$, microcrystalline powders, prep. by glass synthesis method (*French*) 7-46394
 $\text{BaFe}_{12}\text{O}_{19}$, synthesis by hydrolysis of barium acetate and tris (acetylacetonate) iron (*Japanese*) 7-46392
 $(\text{Ba}_{1-x}\text{La}_x)\text{TiO}_3$ semiconducting ceramic props., grain boundary and dopant effects (*Japanese*) 7-6631
 $(\text{Ba}_{1-x}\text{La}_x)(\text{Ti}_{1-y}\text{Zr}_y)_{1-x/4}\text{O}_3$ ceramics, electrostrictive effect 7-53240
 $\text{BaO-Fe}_2\text{O}_3\text{-B}_2\text{O}_3$ -based glasses, crystallisation behaviour, nucleating agent effects 7-51650
 $\text{BaO-TiO}_2\text{-B}_2\text{O}_3(\text{V}_2\text{O}_5)(\text{MoO}_3)$, phase equilib. 7-46430
 $\text{BaO-Nd}_2\text{O}_3\text{-5TiO}_2$ ceramics, matrix phase struct. 7-39488
 $\text{Ba}(\text{Pb, Bi})\text{O}_3$ superconducting ceramics, surface resistance 7-38829
 $\text{BaPb}_{0.73}\text{Bi}_{0.27}\text{O}_3$ ceramic granular superconductor, infinite cluster detection, local heating method 7-2797
 $\text{Ba}(\text{Ti, Zr})\text{O}_3$ powders, hydrothermal prep. 7-64957
 BaTiO_3 based ceramics for multilayer ceramic capacitors, chemical processing 7-46399
 BaTiO_3 capacitor material, elec. field distrib. around flaws, finite difference modelling 7-64574
 BaTiO_3 ceramics, grain struct. and phase anal. (*German*) 7-58496
 BaTiO_3 ceramics, Maxwell-Wagner relax. and degradation 7-2970
 BaTiO_3 ceramics, sintering, liq. phase enhanced discontinuous grain growth control 7-46384
 BaTiO_3 ceramics, zone sintering, dielec. props. rel. to microstruct. 7-13078
 BaTiO_3 composites, dielec. and elec. props., rel. to prep. and microstruct. 7-64559
 BaTiO_3 , electronic struct., special features (*Russian*) 7-45146
 BaTiO_3 , fine-grained superplastic creep in reducing environment 7-28075
 BaTiO_3 , form. from metallo-organic precursors, kinetics 7-39465
 BaTiO_3 , grain boundary inhomogeneity phenomena, microcontact meas. (*German*) 7-58893
 BaTiO_3 , PTCR ceramics, SIMS 7-9919
 BaTiO_3 piezoelectric ceramics, studies for appl. in electromechanical filters 7-20558
 BaTiO_3 , polycryst., glasslike behaviour at very low temp. 7-27647
 $\text{BaTiO}_3\text{:Nb}(\text{Ca})$, ferroelec. domains, SEM and TEM obs. 7-2998
 $\text{BaTiO}_3\text{:Nd}$ ceramics, diffuse phase transform 7-16731
 $\text{BaTiO}_3\text{:Ni}$ ceramic, H defect diffusion 7-58545
 BaTiO_3 -based ceramic, nonlin. electromechanical parameter meas. 7-13094
 $\text{Ba}_2\text{Ti}_{5-x}\text{Zr}_x\text{O}_{12}$, synthesis, stability, cryst. chem. 7-53681

ceramics continued

- BeO, beryllia, polycrystalline ceramics, spall strength, plate impact meas., spall zone model calcs. 7-33797
 BeO, TSEE, pyroelectric properties influence 7-13340
 BeO/Li ceramic, sphere-pac forms, T breeder materials, thermal cond. 7-52163
 Bi₂Ti₃O₁₂ ceramic fabrication, grain-oriented, by normal sintering, sintering mechanisms (*Japanese*) 7-22619
 Bi₂V₂TiO₁₄, layered cpd., crystal-chemical and dielectric props. 7-6595
 Ca-SiAlON ceramic system, A' = β' transition study 7-16738
 CaCO₃, calcite, grain growth, effect of second-phase particles 7-39476
 CaLa₂Si₂O₁₀ optical ceramic, powder synthesis 7-37067
 Ca₂Na₂K₂Si₂O₃₀F₄, chain-silicate canasite glass-ceramic, thermal shock behaviour, effect of crystn. 7-46613
 Ca₂Nd₈(SiO₄)₆O₂:Cm ceramic simulated nuclear waste forms, radiation effects on microstruct. and fracture props. 7-58373
 CaO-TiO₂-SiO₂:Eu³⁺ sphere ceramic, impurity laser-excited site-selective fluorescence line-narrowing spectra 7-13200
 β-Ca₂SiO₄, prep. by firing at 950°C 7-3238
 Ca₈(PO₄)₆(OH)₂-xO_x, synthesis, struct., dielec. props., AC elec. cond., IR spectra 7-3235
 CaZrO₃, sintering, porosity, mech. props., corrosion resist. 7-39664
 Cd₂Nb₂O₇ ceramic, high press. phase transition and dielec. props. 7-2177
 CdS based ceramics, radiative recomb. at high excitation levels (*Russian*) 7-3090
 CeO₂, doped with trivalent cations, grain boundary effect, microstruct. and microanal. 7-38249
 CeO₂:Y³⁺(Gd³⁺)(La³⁺), grain boundary effect, elec. meas. 7-38248
 CeO₂-CaO, ceria-calcia ceramics, ionic cond., effect of microstruct. 7-38250
 CeO₂-ZrO₂ solid solutions, O self-diffusion, effect of grain boundary movement 7-21522
 CeO_{2-x}, thermodynamic model for nonstoichiometric ionic phases 7-32673
 Co-MnO system, thermodynamic props., phase diagram, miscibility gap 7-53706
 CoO-NiO system, immiscibility 7-38202
 Cr₂O₃, in mullite transparent glass-ceramics, X-ray absorpt., emission and EPR spectra 7-7728
 Cr₂O₃, in transparent glass-ceramic, crystn. and spectroscopic props., melting conditions and heat treatment influence 7-7588
 CuO and magnesia ceramic, direct bonding region, thermal resistance 7-37395
 Er-Cr-B system, phase equilibr., isothermal section at 1270°C 7-22647
 Fe-Nb mag. moments and bulk prep. by reduction-sintering method with heat treatment 7-7936
 (FeMg)₂SiO₄, spinel growth, interface struct. investig. 7-16566
 FeTiO₃, ceramic matrices, precip. morphology 7-65049
 Gd₂O₃-ZrO₂-Nb₂O₅ structure investig. 7-46427
 K₂Pb₁₀Nb₁₀O₃₀-K₆Li₄Nb₁₀O₃₀ solid soln., density and struct. studies 7-1973
 (La,Ca)(Co,Mn)O₃, sinterability, phase composition and microstructure 7-33622
 La-Co-O system, nonstoichiometric K₂NiF₄-type phases 7-37936
 La_{1-x}Ca_xCr_{1-y}Ni_yO₃, production and elec. parameters 7-33007
 LaMgAl₁₁O₁₉-LaMgGa₁₁O₁₉-LaMgFe₁₁O₁₉ system, solid solns. 7-39491
 La₂O₃, thermal expansion coeff. below room temp. 7-12332
 Li based ceramics, fusion breeder blanket, irradi., high burnup, large temp. gradients 7-49644
 Li based oxide ceramics, fusion breeders, chemical compatibility with stainless steels 7-49646
 Li ceramics, thermal stability with fusion reactor structural materials 7-38227
 Li containing ceramic, T breeder material, thermal cond. 7-10280
 Li-Na-K-CO₃/MgO salt/ceramic phase change material for high temp. thermal storage, thermoanalytic investigation 7-65631
 γ-LiAlO₂, ceramic, T breeding material, compatibility with austenitic stainless steel 7-53966
 LiAlO₂ ceramic breeder material, fabrication for NET programme 7-798
 LiAlO₂ ceramic breeder material, post irradi. T recovery 7-49647
 LiAlO₂ ceramics, fast neutron irradi., T and He retention, high temp. vacuum extraction 7-49649
 LiAlO₂ ceramics, near surface T depth profiling, low energy nuclear reactions 7-49653
 LiAlO₂, Li₂SiO₃ and Li₂O, breeder ceramics, fabrication, irradi., T release, EXOTIC expts. 7-49648
 γ-LiAlO₂, neutron irradi. effects 7-51841
 LiAlO₂, T ceramic breeder material, Italian fusion technology programme review 7-10279
 Li₂O, elastic and creep props., porosity and temp. depend. 7-53780
 Li₂O, ceramic breeder material, post irradi. T recovery 7-49647
 Li₂O, ceramics, fast neutron irradi., T and He retention, high temp. vacuum extraction 7-49649
 Li₂O ceramics, near surface T depth profiling, low energy nuclear reactions 7-49653
 Li₂O-ZrO₂-P₂O₅ system, phase equilib. and cpd. form. 7-28024
 Li₂SiO₃, Li₄SiO₄, Li₆SiO₅, breeder materials, prep. in alcoholic media 7-49654
 Li₂ZrO₃, ceramics, fast neutron irradi., T and He retention, high temp. vacuum extraction 7-49649
 Mg sialon ceramics, SIMS 7-9919
 MgO single crystals, vibr. polishing in water 7-3479
 MgO, sinterability, microstruct. changes during sintering 7-22624
 MgO, sinterability, prep. and charactn. of sample powder 7-22623
 MgO-Al₂O₃-SiO₂ glass-ceramics, nucleation crystallisation, modulus of rupture, acousto-US obs. 7-59723
 MgO-Al₂O₃-SiO₂-GeO₂ cordierite ceramics, sintering, microstruct., thermal props. 7-52088
 MgO-CaO, activated sintering, densification, microstruct. (*Chinese*) 7-13410
 MgO-Cr₂O₃-ZrO₂ system, subsolidus, high temp. phase relation 7-17519
 MgO-M₂O₃-ZrO₂ 7-17519
 MgO-ZrO₂, dispersed, phase transform., toughening 7-65034
 Mg₂SiO₄, forsterite-based ceramic with BaO addition, synthesis, sintering, struct. and props. 7-46397
 Mg₂SiO₄, laser-heated, temp. distrib. meas. 7-9837
 MnO₂-BaMnO₃ system, pseudo-binary, phase relation and thermal behaviour of synthetic hollandite, Ba₂Mn₈O₁₈ (*Japanese*) 7-28026
 NaGe₂P₃O₁₂ glass-ceramic, synthesis, thermal expansion meas. 7-46406
 (Na_{0.5}K_{0.5})NbO₃, sintering, densification and elec. props., effect of Ba additions 7-46387

ceramics continued

- NaLa(MoO₄)₂ single crystals and ceramic, elec. cond. meas., disordering mechanisms 7-6863
 Na₂O-B₂O₃-SiO₂ glass ceramic, prep., SiO₂ replacement, phase separation, struct. 7-13428
 Na₂O-B₂O₃-SiO₂ ThO₂-rich porous glass ceramic, phase separation (*Afrikaans*) 7-13439
 Na₂O-CaO-Al₂O₃-SiO₂ glass ceramic system, spherulitic growth, mech. props. 7-46405
 Na₂O-CaO-Al₂O₃-TiO₂-SiO₂:Eu³⁺ glass ceramic, impurity laser-excited site-selective fluorescence line-narrowing spectra 7-13200
 Na₂O-WO₃-B₂O₃ glass ceramics, containing W bronze, prep. and elec. props. (*Japanese*) 7-3261
 Na₂O-nAl₂O₃, mullite struct., form. by solid state reaction 7-7937
 Na₃Ti_{0.75}Si₂P₂O₁₂, NASICON-based glass and glass ceramics, synthesis and characterisation 7-44908
 Na₄Zr₂Si₂O₁₂-Y₂Fe₂O₁₂ composite ceramics, prep., thermal expansion 7-63853
 Nb-Ti-O ceramic coatings, synthesis by reactive ion plating and sputter deposition, struct., electrophysical props. 7-64031
 Ni₃Co₂-yO₄ spinels, prep. by thermal decomposition of mixed hydroxide nitrates 7-13424
 NiMn₂O₄, elec. cond. and cation distrib. 7-33009
 NiO, grain boundary struct., TEM obs. 7-21225
 NiO, spinel growth, interface struct. investig. 7-16566
 NiO-based aligned eutectics, microstruct., crystallography and interfaces 7-65025
 PLZT ceramics, grain growth during hot pressing 7-3232
 PLZT ceramics, hot pressed, chemically induced grain boundary migration and recrystallisation 7-27027
 PLZT ceramics, mechanical strength, composition and polarisation depend., microindentation meas. 7-6697
 PLZT ceramics, optical second harmonics, temp. and elec. field depend. meas. 7-5952
 PLZT ceramics (*Japanese*) 7-2981
 PLZT, elastic-plastic contact damage 7-39627
 PLZT, electrically excitable mechanical resonant mode shapes 7-26854
 PLZT electro-optical ceramics, electron pulse irradiation-induced transient optical absorpt. study 7-6682
 PLZT ferroelec. ceramics, IR optical and electrooptical props. studies 7-7675
 PLZT, ferroelec. ceramic, laser-induced surface metallisation 7-53924
 PLZT ferroelec. polycomponent oxides, controllable powder synthesis, HP and PHP methods 7-7935
 PLZT ferroelectric ceramics, gamma, electron and neutron irradi. effects study 7-6677
 PLZT hot pressed ceramic, polarisation reversal studies under hydrostatic press. 7-59160
 PLZT polarised ceramics, electroconductivity asymmetry obs. 7-7225
 PLZT rhombohedral ceramics, electrocaloric effect study, diffuse phase transition intermediate state 7-7645
 PLZT transparent ceramic modulator, visual classroom demonstrations appl. 7-4647
 PLZT transparent ceramics, laser beam self-deflection and self-focusing meas. 7-5960
 PLZT transparent ferroelec. ceramics, low freq. dielec. props. study 7-7630
 PLZT, transparent ferroelectric ceramic, surface composition and structure 7-32765
 PLZT, transparent ferroelectric ceramic, irradiation effects 7-59157
 PLZT-PZN electro-optic ceramics, elec., opt. and switching props. 7-7646
 PZT ceramic, pressure induced ferroelectric-antiferroelectric transition 7-22201
 PZT ceramic SAW interdigital transducers, anal., validity of model of Tancrrell and Holland 7-6068
 PZT ceramics, ordered void struct., dielec. const., flexure strength 7-63607
 PZT ceramics, pulsed TEA CO₂ laser irradi., signal generation 7-16623
 PZT composites, hydrostatic piezoelec. response, finite element modelling 7-64574
 PZT piezoelectric ceramic prop. meas., applied compressive stress parallel to polar axis 7-45939
 PZT, prep. by oxalate method in ethanol soln. (*Japanese*) 7-3245
 PZT:Bi piezoelectric ceramics, vacancies, positron lifetimes 7-37980
 PZT:Mn, dielec. dispersion 7-13076
 PZT:Nb ceramics, sintering, pair doping, elec. characts. 7-39469
 PbLaZrO₃TiO₃, electrostrictive ceramics, SAW transduction, electronic control 7-12450
 Pb(Mg_{1/3}Nb_{2/3})₃ perovskite, prep. using Pb₃Nb₂O₇ and MgO 7-39468
 Pb(Mg_{1/3}Nb_{2/3})₃O₃ ceramics for microdisplacement actuators, electrostrictive characts. (*Japanese*) 7-17270
 Pb(Mg_{1/3}Nb_{2/3})₃O₃ ceramics, dielec. props. 7-46382
 PbMg_{1/3}Nb_{2/3}O₃ ceramic, elastic moduli and diffuse ferroelec. phase transition, press. depend. 7-63717
 PbMg_{1/3}Nb_{2/3}O₃, single cryst. and ceramic samples, isotropic elastic moduli 7-6701
 PbMg_{1/3}Nb_{2/3}O₃, thermal expansion, effect of Mg and Nb substitution by divalent, trivalent, tetravalent and W⁶⁺ ions 7-63851
 PbMg_{1/3}Nb_{2/3}O₃-PbTiO₃, MnO doped, relaxor ferroelec. ceramics, dielec. ageing effects 7-22195
 Pb(Mg_{1/3}Nb_{2/3})₃O₃-Pb(Zn_{1/3}Nb_{2/3})₃O₃, ferroelec. powder, prep., solid solubility, Curie point (*Japanese*) 7-7945
 PbMgO₃NbO₃, electrostrictive ceramics, SAW transduction, electronic control 7-12450
 PbNb₂O₆-BiTiMO₆ (M=Nb, Sb), solid soln. ceramics, piezoelec. const. studies 7-2980
 PbO-Fe₂O₃-B₂O₃ glass ceramics, mag. props. and EPR spectra of precipitated mag. phases 7-45748
 PbO-Nb₂O₅ oxide mixture transparent ferroelec. ceramics, phase form. during solid state reaction 7-6591
 PbO-Nb₂O₅-Sc₂O₃ oxide mixture transparent ferroelec. ceramics, phase form. during solid state reaction 7-6591
 Pb(Sc_{0.5}Nb_{0.5})O₃ ferroelectric ceramics, gamma, electron and neutron irradi. effects study 7-6677
 Pb(Sc_{0.5}Nb_{0.5})O₃ transparent ferroelec. ceramic production by hot pressing and props. 7-7934
 Pb(Sc_{0.5}Nb_{0.5})O₃, transparent ferroelectric ceramic, irradiation effects 7-59157
 Pb(Se_{1-x}Nb_x)O₃ ferroelec. ceramics, IR optical and electrooptical props. studies 7-7675

ceramics continued

- Pb(Si_{1/2}Ta_{1/2})O₃, single crystals, an hot pressed ceramics, ordering, domain struct., TEM obs. 7-26936
 PbTiO₃ based glass ceramics piezoelectricity, pyroelectricity and ferroelectricity 7-7654
 PbTiO₃ ceramic; complex piezoelec. d₃₁ coeff., temp. behaviour 7-13097
 PbTiO₃, distorted cubic, crystn. and phase transform. 7-39548
 PbTiO₃, form. from metallo-organic precursors, kinetics 7-39465
 PbTiO₃ gels and films, hydrolysis conditions effect on characts. 7-46400
 PbTiO₃-Cr₂S₃ ceramic, EPR, ENDOR, ESE investigations. 7-13020
 PbTiO₃-La piezoelectric ceramics, vacancies, positron lifetimes 7-37980
 PbTiO₃-PbZrO₃-Pb(Mg_{1/3}Nb_{2/3})O₃ system, comp. fluctuation in solid soln. (Japanese) 7-28025
 PbTi_{1-x}Zr_xO₃ piezoceramics, annealing in gaseous media with controllable comp., effect on electrophysical props. 7-8012
 Pb(Zn_{1/3}Nb_{2/3})O₃-PbTiO₃, perovskite ceramic powder, prep. dielec. and piezoelec. props. 7-46380
 Pb(Zr_{0.58}Fe_{0.20}Nb_{0.20}Ti_{0.02})_{0.995}U_{0.005}O₃ ferroelec. ceramic, TEM study 7-17272
 PbZrO₃-based piezoelectric ceramics containing Pb(Zn_{1/3}Nb_{2/3})O₃ 7-2984
 Pb(Mg,Zn)_{1/3}Nb_{2/3}O₃, prep. and ferroelec. props. (Japanese) 7-27993
 Ru-Ti-O ceramic coatings, synthesis by reactive ion plating, struct., electrophysical props. 7-64031
 Si ceramics, SIMS 7-9919
 Si, technology and electronic materials (Japanese) 7-22466
 SiAlON composites, interfacial microstruct. 7-16429
 SiAlON-YAG ceramics, Auger electron microscopic quantification of phase comp. 7-22951
 SiC ceramic optical waveguide for CO₂ lasers (Japanese) 7-6001
 SiC ceramics, friction and wear measured by a pin-on-disk method (Japanese) 7-22850
 SiC ceramics, hot pressed, grinding, surface damage, bending strength (Japanese) 7-17602
 SiC ceramics, joining with Si₃N₄-Y₂O₃-La₂O₃-MgO mixture (Japanese) 7-65280
 SiC ceramics, reactivity with various additives, uses as effective sintering aids 7-46383
 SiC corroded, scanning Auger microscopy study 7-13617
 SiC, cubic (3C) polypoly, thermal expansion 7-21493
 SiC, deformed, microstructural changes, creep mechanisms 7-46591
 SiC, engineering ceramics, tensile strength (Japanese) 7-53800
 SiC fibre reinforced Li₂O-Al₂O₃-SiO₂ glass ceramics, tensile and flexural strength 7-13520
 SiC fibre reinforced Li₂O-Al₂O₃-SiO₂ glass ceramic composite, thermomech. mismatch 7-46538
 SiC fibre reinforced SiC, high heat flux, low activation struct. materials 7-49635
 β-SiC fibres, chem. and phys. props. (Russian) 7-46284
 SiC fibres, continuous, synthesis from polycarbosilane 7-22616
 SiC fibres, prep. from polycarbosilane, heat treatment, Raman study 7-65062
 SiC fibres, stability, thermomechanical analysis 7-33627
 SiC, high-press. self-combustion sintering from fine mixed powders of Si and C (Japanese) 7-3249
 SiC, instrumented impact testing, absorbed energy 7-28237
 SiC, polycryst., oxidation 7-28159
 SiC powder, dynamic compaction 7-39452
 β-SiC powder, sintering, phase transform. rel. to additives (Japanese) 7-17527
 SiC powder compacts, formed by cold isostatic pressing, influence of shape and size on homogeneity (Japanese) 7-64981
 SiC powders, prep. by CVD method using RF-plasma (Japanese) 7-3250
 SiC powders, surface charactn. and treatment 7-2306
 SiC refractory materials, passive oxidation 7-13612
 SiC, single crystals, and polycrystals, oxidation kinetics in dry O₂ 7-39683
 SiC, sintered, fracture after Li exposure 7-28103
 α-SiC, sintered, hot corrosion by molten salts, strength degradation mechanism 7-33813
 SiC, sintered, microstruct. and props., influence of fabrication method (Japanese) 7-22622
 α-SiC, sintered, non-equilib. surface conditions and microstruct. changes following pulsed laser irradi. and ion beam mixing of Ni overlayers 7-65170
 α-SiC, sintered, occurrence and distrib. of B-containing phases 7-39466
 SiC, sintering phenomena 7-17504
 SiC, sliding and abrasive wear mechanisms, comparison 7-3463
 α-SiC, static fatigue limit at elevated temps., thermodynamics 7-17629
 SiC, static-fatigue limit of materials containing small flaws 7-39620
 SiC, stress intensity factor meas. using notched and surface flaw specimens 7-65251
 α-SiC, thermal expansion of hexagonal polypoly, 20-1000°C 7-52089
 SiC, wear resist., comparative study of hard materials 7-3457
 SiC:Si, reaction bonded composite, mech. props. and microstruct. anisotropy 7-65146
 SiC:Si reaction bonded composite ceramics, interface struct., grain boundaries 7-64995
 SiC-AlN ceramics, elevated temp. creep, role of grain size 7-39584
 SiC-based ceramics, sintered and hot isostatically pressed, microanalytical investigation 7-27991
 SiC-based materials, high-temp. oxidation 7-65161
 SiC-Si₃N₄ fibres, prep. by polycarbosilane precursors pyrolysis 7-27988
 Si₃N₄ ceramic, bonding to stainless steel, using Cr and Mn pre-diffusion (Japanese) 7-8147
 Si₃N₄ ceramics, friction and wear measured by a pin-on-disk method (Japanese) 7-22850
 Si₃N₄ ceramics, hot pressed, fatigue test with Knoop indentation, residual stress effects (Japanese) 7-17640
 Si₃N₄ ceramics, joining with glass solder in CuO-SiO₂-TiO₂ system 7-22974
 Si₃N₄, deformed, microstructural changes, creep mechanisms 7-46591
 Si₃N₄, engineering ceramics, prep., fabrication, appls. 7-53683
 Si₃N₄, engineering ceramics, tensile strength (Japanese) 7-53800
 Si₃N₄ fine particles, aggregate struct. and compacting process (Japanese) 7-46393
 Si₃N₄, fracture toughness measured with short-bar chevron-notched specimens 7-59599
 Si₃N₄, fracture toughness evaluation using chevron-notched specimens (Japanese) 7-59613
 Si₃N₄, fretting wear in seawater 7-8124
 Si₃N₄, grain boundary phases, EM anal. 7-16569
 Si₃N₄, hot-pressed, friction and wear at 150 to 800°C 7-28142
 Si₃N₄, hot-pressed, friction and wear 7-59642
 Si₃N₄, hot-pressed, tensile strength at room and elevated temp. (Japanese) 7-65139
 Si₃N₄ layers, electrographic effect 7-46675
 Si₃N₄, nanostruct. defects, high-resolution electron microscopy studies 7-12302
 Si₃N₄, nitridation of Si powder compacts in N₂-H₂ gas mixture (Japanese) 7-3247
 α-Si₃N₄, planar defect displacement vector determ. by HREM 7-2444
 Si₃N₄ powder, physico chem. characts. before sintering (Japanese) 7-64980
 Si₃N₄ powders, high press. not pressing, mech. props., thermal cond. temp. depend. 7-3231
 Si₃N₄, reaction bonded, thermal cond. (Japanese) 7-6902
 Si₃N₄, reaction bonded ceramic, combined RHEED and SEM studies 7-16432
 Si₃N₄, sintered, microstruct., mech. props., Pr₆O₁₁ additive effect 7-17506
 Si₃N₄, sintering, under rotary bending, mirrorlike region of fractured surface (Japanese) 7-3436
 Si₃N₄, sliding and abrasive wear mechanisms, comparison 7-3463
 Si₃N₄, static-fatigue limit of materials containing small flaws 7-39620
 Si₃N₄, surface flaws effect on strength 7-59638
 Si₃N₄, wear properties in rolling contact 7-8126
 Si₃N₄, with MgO addition, phys. and tribological props., effect of hot-pressing temp. (Japanese) 7-65150
 Si₃N₄, yield at elevated temps. (Japanese) 7-3388
 Si₃N₄-AlN, grain boundary phases, EM anal. 7-16569
 Si₃N₄-Y₂Al₂O₁₂, grain boundary phases, EM anal. 7-16569
 Si₃N₄/Al/Invar ceramic/metal joints, rel. between tensile and three-point bending strengths 7-39583
 Si₃N₄-Al₂O₃-Y₂O₃(CeO₂)(La₂O₃) ceramics, sintered, IR and Raman spectra 7-46000
 Si₃N₄-AlN-rare earth oxide systems, subsolidus phase relationships 7-39489
 Si₃N₄-SiC film, hybrid material prepared by plasma CVD, microhardness and internal stress 7-13616
 Si₃N₄-SiC film, hybridisation by plasma CVD 7-13379
 Si₃N₄-SiC reaction sintered ceramics, oxidation effect on strength 7-65163
 Si₃N₄-TiC composites, densification, matrix-dispersoid reaction, mech. props. microstruct., impurities effect 7-64994
 Si₃N₄-TiC composites, mech. props., wear resist., dispersoid-matrix interaction 7-65145
 Si₃N₄-Y₂O₃, hot pressed, fracture, flexural strength, temp. degradation 7-13546
 Si₃N₄-Y₂O₃-Al₂O₃, pressureless sintering 7-17503
 Si₃N₄-ZrO₂ composites, thermal instability 7-28158
 SiO₂

ceramics continued

- WC-Co composite, grain boundary films, mean inner pot. determ. by Fresnel technique 7-16431
- Y-Si-Al-O-N ceramics, phase relationships 7-65011
- $Y_4Al_2O_9$, $Y_3Al_5O_{12}$, $YAlO_3$, synthesis by sol-gel process 7-13420
- YIG, multicomponent systems, synthesis, microwave characts., mathematical modelling 7-33626
- Y_2O_3 , DC cond. as function of water vap. press. 7-45317
- Y_2O_3 , elec. cond. as function of O_2 partial press. in wet and dry atm. 7-45405
- Y_2O_3 powders, agglomerate strength distrib., US meas. 7-46379
- Y_2O_3 - TiO_2 system, fluorite type solid soln. crystallisation 7-1882
- ZnO based varistors, sintering, multiparametric anal. 7-64978
- ZnO ceramics ageing under AC voltage (French) 7-39564
- ZnO, glass-doped, prep., elec. props. and degradation phenomena 7-13425
- ZnO, grain boundary inhomogeneity phenomena, microcontact meas. (German) 7-58893
- ZnO, grain growth kinetics during synthesis, optimum elec. props. 7-46398
- ZnO varistor, grain boundary pot. barrier, effects of annealing 7-16568
- ZnO varistor props., grain boundary characts. (Japanese) 7-6631
- ZnO- Bi_2O_3 mixtures, lattice parameters, depend. on Bi_2O_3 conc. 7-1974
- ZnO- Bi_2O_3 system, sintering, role of Bi_2O_3 7-64977
- ZrO₂ advanced ceramics, props. and appl. 7-13416
- ZrO₂ base ceramic thermal barrier coatings, erosion rel. to processing and microstruct. 7-3450
- ZrO₂, CeO₂ containing tetragonal polycrystals, thermal stability, mech. props. 7-28101
- ZrO₂ ceramic, grain boundaries, microanal. 7-16577
- ZrO₂ ceramic, partially stabilised, friction and wear meas. by a pin-on-disk method (Japanese) 7-22850
- ZrO₂, ceramic matrices, precip. morphology 7-65049
- ZrO₂ ceramics, displacive transform. mechanism 7-65031
- ZrO₂ ceramics, hot forging characts., grain size 7-3370
- ZrO₂ ceramics, strength, effect of freeze-drying of $Zr(OH)_2$ 7-13415
- ZrO₂ ceramics, wettability of metals 7-52191
- ZrO₂ ceramics stabilised by rare earth oxides, thermal shock resistance (Japanese) 7-22736
- ZrO₂ crystals, stabilised, vap. phase cryst. growth by hydrolysis of ZrF_4 7-46286
- ZrO₂, MgO partially stabilised, cryogenically induced martensitic transform. of precipitates 7-28037
- ZrO₂, MgO partially stabilised, SrO sintering aid addition, microstruct. and chem. aspects 7-64983
- ZrO₂, MgO partially stabilised ceramics, thermal treatment, mech. props., microstruct. 7-65067
- ZrO₂, nondestructive phase transform. of single cryst. at high press. 7-59511
- ZrO₂, partially destabilised, thermal shock behaviour 7-3392
- ZrO₂, partially stabilised, instrumented impact testing, absorbed energy 7-28237
- ZrO₂, partially stabilised, phase stability, elec. cond., fusion reactor elec. insulator appl. 7-52618
- ZrO₂ partially stabilised, engineering ceramics, tensile strength (Japanese) 7-53800
- ZrO₂, solid electrolytes, effect of admixture cation radius on sintering 7-13398
- ZrO₂, tetragonal, cryst. growth 7-17417
- ZrO₂, tetragonal, ferroelastic domain switching as toughening mechanism 7-33712
- ZrO₂, tetragonal form, stability 7-6567
- ZrO₂ thin films, monoclinic polycryst., sol-gel process, form. and thermal change (Japanese) 7-22470
- ZrO₂ transform. toughened ceramics, fracture toughness rel. to transform. temp. 7-46614
- ZrO₂, Y_2O_3 partially stabilised, thermal shock behaviour (Japanese) 7-8115
- ZrO₂, Y_2O_3 partially stabilised, stress-induced phase transform., obs. by Raman microprobe (Japanese) 7-22683
- ZrO₂, Y_2O_3 partially stabilised, hot isostatic pressing, high temp. mech. props. 7-28082
- ZrO₂, Y_2O_3 partially stabilised, tetragonal phase stability in molten fluoride salts (Japanese) 7-28164
- ZrO₂, Y_2O_3 partially stabilised, phase diagram, microstruct. (Japanese) 7-53707
- ZrO₂, Y_2O_3 partially stabilised, microstruct. after ageing at high temp. 7-65061
- ZrO₂, Y_2O_3 partially stabilised, crack config. (Japanese) 7-65138
- ZrO₂, Y_2O_3 stabilised, fracture toughness and transformability, grain size depend. 7-13566
- ZrO₂, Y_2O_3 stabilised, CeO₂ doped on surface, thermal stability improvement 7-13619
- ZrO₂, Y_2O_3 stabilised powder, spray pyrolysis, sintering, microstruct., fracture toughness 7-27983
- ZrO₂, Y_2O_3 stabilised, amorphous second phase, sintering, grain morphology, fracture roughness, surface degradation 7-46612
- ZrO₂, Y_2O_3 stabilised, phase transform., mech. props., surface struct. rel. to polishing (Japanese) 7-53791
- ZrO₂, Y_2O_3 -doped, powders, sinterable, chemically coprecipitated in non-aq. medium 7-64982
- ZrO₂:Ti, ion implantation, mech. props. 7-28102
- ZrO₂/Al₂O₃ ceramic incoherent interface struct. 7-16430
- ZrO₂/mullite composite ceramic, grain boundary HREM study 7-16427
- ZrO₂-Al₂O₃ composite powder, thermal decomposition prep. for porous ceramics 7-13422
- ZrO₂-Al₂O₃ composite, Y_2O_3 -stabilised, compressive deform. 7-28100
- ZrO₂-CaO-P₂O₅-SiO₂ glass ceramics, prep. and mech. props. (Japanese) 7-7942
- ZrO₂-MgO toughened ceramics, dry friction and wear against steel 7-8125
- ZrO₂-MgO-P₂O₅ system, phase equilib. at 1573K 7-28023
- ZrO₂-SeO₃, cubic to β martensitic transform. 7-22681
- ZrO₂-TiO₂, solubility of TiO₂ in ZrO₂ 7-39490
- ZrO₂-TiO₂ system, low-temp. phase relationships 7-46431
- ZrO₂- Y_2O_3 , arc melted, cubic to tetragonal transform. herringbone struct. 7-28042
- ZrO₂- Y_2O_3 , Y-TZP, toughened, microstruct., TEM and electron diffraction study (Japanese) 7-22634
- ZrO₂- Y_2O_3 , Y-TZP, superplastic, compressive deform. props. and microstruct. (Japanese) 7-22774

ceramics continued

- ZrO₂- Y_2O_3 ceramic system, phase equilib. and transform 7-22682
- ZrO₂- Y_2O_3 ceramics, toughened, prep., microstruct., mech. props. 7-3409
- ZrO₂- Y_2O_3 ceramics, with straight, uniform-sized channels 7-22627
- ZrO₂- Y_2O_3 partially stabilised, Al₂O₃ effect on retaining tetragonal particles, matrix toughening 7-59485
- ZrO₂- Y_2O_3 system, microstruct. resulting from diffusionless cubic to tetragonal phase transform. 7-39501
- ZrO₂- Y_2O_3 toughened ceramics, dry friction and wear against steel 7-8125
- ZrO₂- Y_2O_3 -Co₃O₄ materials, Co₃O₄ effect on struct. and phase comp. 7-27990
- ZrO₂- Y_2O_3 -TiO₂ ceramics, transport, sintering behaviour 7-13421
- ZrSiO₄, burnt zircon with alkali hardeners, humidity sensitivity 7-18793

Cerenkov counters see Cerenkov counters

Cerenkov radiation see Cerenkov radiation

cerium

- see also nuclei with
- core and valence photoemission, calc. 7-33516
- electronic struct. and superconducting transition temp. calcs. (Chinese) 7-27244
- glass:Ce, stable and metastable impurity valence states, spectral props. (Russian) 7-27747
- impurity system, degenerate Anderson model, Bethe-ansatz soln. 7-2559
- ions, Ne-like, precision wavelength meas. in X-ray spectra 7-36525
- isostructural transformations, EMF pulses (Russian) 7-52038
- overlayers on Si (100), oxidation enhancement, CeSiO₃ formation 7-28226
- photoelectron and bremsstrahlung isochromat spectra 7-7817
- plate, isostructural $\gamma \rightleftharpoons \alpha$ transformation, shape changes (Russian) 7-46464
- surface (001), H₂ adsorption, initial stages of hydride form., UPS, LEED and EELS studies 7-21629
- BaTiO₃:Ce, Mg, Ga(Cr)(Cu), double doping study 7-2037
- CaF₂:Ce, Mn crystals, energy transfer, optical absorpt. and luminesc. studies, X-ray irradi. effects 7-27773
- CaF₂:Ce,Mn, optically active sites, optical spectra 7-22305
- CaF₂:Ce³⁺, impurity ion-ligand nuclei interactions, ENDOR meas. and operator method calcs. 7-52538
- CaF₂:Ce³⁺, two-photon absorpt. cross section, anal. of lowest 4f-5d transition 7-46081
- Ce³⁺ doped fluorite elpasolites, 5d-4f spectra, impact of ion-host interactions 7-39143
- Ce³⁺ in dielectric crystal, 5d-4f spectra, phenomenological cryst. field model 7-39148
- Gd:Ce, hyperfine field and relax. rate, intermediate valence model 7-7184
- GdSiO₃:Ce, Czochralski growth 7-53556
- NaGdF₄:Ce, Eu, UV ³H₃ and visible ³Dy luminesc. 7-64676
- Nb-Ce-Nb epitaxial film sandwiches, metastable phases 7-32857
- Nd,Ce:YAG, single crystals, luminesc. and laser props. 7-10967
- SrBaNb₂O₆:Ce as self-pumped phase conjugator 7-5957
- SrBaNb₂O₆:Ce crystal optical oscillator based on frequency-degenerate pumping 7-25887
- Sr_{0.6}Ba_{0.4}Nb₂O₆:Ce, photorefractive props. 7-22205
- Sr_{0.6}Ba_{0.4}Nb₂O₆:Ce(Fe), photorefractive props. 7-45955
- Sr_{0.6}Ba_{0.39}Nb₂O₆:Ce crystals, light emission obs. during freq.-degenerate laser pumping 7-15947
- Sr_{0.75}Ba_{0.25}Nb₂O₆:Ce self-starting passive phase conjugate mirror 7-43243
- YAG:Nd, Ce, energy transfer mechanisms between Ce³⁺ and Nd³⁺ at low temp. 7-64691
- YAlO₃:Ce, single cryst., birefringence spectra, 2-5 eV 7-13124

cerium alloys

- cubic Laves phases, electronic struct., self-consistent APW calcs. 7-12599
- electronic struct., pseudopotential method 7-27245
- electronic structure, spectroscopic and thermodynamic props., impurity Anderson Hamiltonian 7-32900
- kondo effect versus crystal field 7-2602
- Kondo systems, thermopower, elec. resist. and cryst. field effects 7-21900
- photoemission and bremsstrahlung isochromat spectra 7-3155
- Al-Fe-Ce, quasicrystalline decagonal phase, TEM 7-46492
- Al-Fe-Ce-La-Nd-Rr alloys rapidly quenched, positron annihilation studies 7-46184
- Al-Fe-Mischmetal, wear, comparative investigs. and prep. method role 7-13605
- Al-Mg-Ce system, liquidus, intermetallic compound (Chinese) 7-7960
- Ce (Fe_{1-x}Al_x)₂, Fe-rich intermetallics, mag. and elec. props. 7-45621
- Ce metallic systems, valence band photoemission spectra anal. 7-13332
- Ce-(Fe,Co)-(B,Si) system alloys, melt spun ribbons, mag. props. (Japanese) 7-53052
- Ce-Co, amorphous, electronic configuration of Ce 7-7191
- Ce-Cu amorphous alloys, mag. and transport props., Ce-derived anomalies 7-52601
- Ce-Fe-Si system. electron struct. of ternary intermetallic epds. (Russian) 7-38525
- Ce-Ni, amorphous, electronic configuration of Ce 7-7191
- Ce-Sc, shape memory effect (Russian) 7-59583
- Ce-Sc (B at.%), γ to α transition, EMF generation, press. depend. near crit. point (Russian) 7-53723
- Ce-Si, amorphous, electronic configuration of Ce 7-7191
- Ce-Sn alloys, intrinsic magnetic behaviour, influence of stoichiometry 7-45747
- CeAg_{1-x}In_x, magnetisation process, strain effects 7-64488
- CeAl₂, electronic struct. determ. 7-52417
- CeAl₂, Hall effect meas. 7-12702
- CeAl₂, low-temp. high-field magnetoresist. meas. 7-38541
- CeAl₂-Mo point contacts, low temp. I-V characts., thermoelec. effects obs. 7-27382
- CeAl₃, heavy fermion system, fluctuating bands 7-58736
- CeAl₃, Kondo lattice, coherent regime, Hall effect temp. depend. study 7-52581
- CeAl₃ nonmagnetic Kondo lattices, coherent regime, Hall effect temp. depend. meas. 7-52582
- CeAl₃, properties of heavy electron metals 7-45535
- CeAl₃, quasiparticle band struct., local-density approx. anal. 7-27250
- CeB₆, Fermi surface, 2D angular correlation of positron annihilation radiation 7-39241
- CeB₆ heavy fermion system, muon Knight shift study 7-45886

cerium alloys continued

CeB₆-Mo point contacts, low temp. I-V characts., thermoelec. effects obs. 7-27382
CeBe₁₃, band struct. calc. 7-32905
CeBe₁₃, Hall effect meas. 7-12702
Ce(Co,Cu,Fe)₆, magnetically hard, heat treatment effects on struct. and mag. characts. 7-27564
CeCo₅, magnetocrystalline anisotropy, rare earth contribution 7-45659
CeCu₆, heavy fermion substance, magnetoresistance under press. 7-52579
CeCu₆, heavy fermion system, temp. and mag. field depend. of Hall effect 7-2579
CeCu₆, heavy fermion system, photoemission and inverse photoemission studies 7-3148
CeCu₆, heavy-electron compound, de Haas-van Alphen effect 7-12587
CeCu₆, heavy-fermion material, coherent and incoherent behaviour, Hall effect and magnetoresist. 7-32992
CeCu₆-Mo point contacts, low temp. I-V characts., thermoelec. effects obs. 7-27382
CeCu_{2-x}Ni_xSi₂, Kondo-lattice system, resist. anomalies 7-58799
CeCu₂Si₂, Hall effect meas. 7-12702
CeCu₂Si₂, heavy fermion superconductors, Fermi surface and cooperative phenomena 7-2771
CeCu₂Si₂, heavy fermion superconductor, magnetic field penetration, muon spin relax. studies 7-45886
CeCu₂Si₂, heavy-fermion superconductors, induced moment mag. form factors 7-12909
CeCu₂Si₂, kondo effect versus crystal field 7-2602
CeCu₂Si₂, Kondo lattice heavy fermion system, quasi-particle-phonon interactions 7-2521
CeCu₂Si₂, lattice gas heavy fermion-boson model anal. of specific heat, entropy and magnetic susceptibility 7-58505
CeCu₂Si₂, nonmagnetic Kondo lattices, coherent regime, Hall effect temp. depend. meas. 7-52582
CeCu₂Si₂, quasiparticle band struct., local-density approx. anal. 7-27250
CeCu₂Si₂, Raman scatt. study of electronic and vibr. excitations 7-33387
Ce₂Fe₁₄B, anisotropy constants, temp. depend. (Chinese) 7-59003
CeH₇, heavy electron system, muon spin rot., Knight shift and relax. studies 7-45885
CeIn₃, antiferromagnetic alloys, thermoelec. power meas., band gap form. 7-38543
Ce_{0.8}La_{0.2}Al₃ nonmagnetic Kondo lattices, coherent regime, Hall effect temp. depend. meas. 7-52582
Ce₂La_{1-x}Al₃ solid solns., magnetic and thermoelectric props. 7-7212
Ce₂La_{1-x}Cu₆, electronic states, resonant photoemission study 7-53496
(Ce_{1-x}La_x)In₃ antiferromagnetic alloys, thermoelec. power meas., band gap form. 7-38543
CeNi₅ based hydride systems, hydriding characts. and stability 7-40051
CeNi₅, intermediate-valence intermetallic cpd., point contact spectroscopy 7-38139
Ce(Ni_{1-x}Cu_x)₂Si₂, mag. susceptibility, scaling behaviour, cryst. field effects 7-45616
CeNi_{5-x}Fe_x, mag. and cryst. props., effect of H absorpt. 7-33168
CeNi_{5-x}Mn_x, mag. and cryst. props., effect of H absorpt. 7-33168
CeNi₂P₂, 4f-magnetism study by susceptibility and NMR 7-22154
CeOs₂, electronic struct. determ. 7-52417
CePb₃ heavy fermion material, magnetism and superconductivity 7-52880
CePb₃ heavy fermion system, theory of mag. field induced supercond. state 7-45546
CePb₃, possible superconductivity in nearly antiferromagnetic itinerant fermion systems 7-38802
CePb(Al)₃ heavy fermion system, muon Knight shift study 7-45886
CePd₃, electronic structure and intrinsically selective absorption 7-38444
CePd₃, Hall effect meas. 7-12702
CePd₃, mixed valence system, conduction carrier density, energy and temp. depend. 7-21882
Ce(Pd_{0.88}Ag_{0.12})₃, Hall effect meas. 7-12702
Ce_{1-x}Pr_xNi₅ mixed valence cpd., cryst. field at paramag. Pr³⁺ ions 7-45241
CeRh₃, Hall effect meas. 7-12702
CeRh₃(Bi_{1-x}Si_x)₂, 4f shell dehybridisation, Curie temp. and mag. moments 7-45679
CeRh₂Si₂, Neel temp., chem. press. effects, partial substitution depend. meas. 7-59011
CeRu₂Si₂, heavy fermion, magnetism and spin fluctuation effects induced by partial substitution 7-38850
CeRu₂Si₂, heavy-fermion system, magnetoacoustic effects in high mag. fields 7-64506
CeRuSn₃, cage-like void structures (German) 7-32365
CeSc alloys, gamma to alpha transform., press. and alloying effects (Russian) 7-12257
CeSi₃, galvanomag. and thermoelec. props. 7-38537
CeSn₃, comparison of polarised and unpolarised inelastic neutron scatt. data 7-7478
CeSn₃, comparison of polarised and unpolarised neutron inelastic scatt., comment 7-7479
CeSn₃, Hall effect meas. 7-12702
CeZn₂, Kondo anomaly and metamagnetism 7-64234
Co-Ce liquid alloys, variable valency investig. 7-7192
Cu-Ce, cast struct., segregation, conc. undercooling 7-3291
CuCu₂Si₂-Mo point contacts, low temp. I-V characts., thermoelec. effects obs. 7-27382
Eu,Ce_{1-x}Cu_xSi₂ cryst., mixed valence state and Kondo system coexistence (Russian) 7-7185
Fe-B-Ce-based metallic glasses, mag. domain structs. and annealing embrittlement 7-27586
Fe-Ce amorphous alloys, mag. props. and elec. resist. 7-59010
Fe-Ce liquid alloys, variable valency investig. 7-7192
Fe-Cr-Al-Ce, microstruct., high temp. corrosion rel. to Ce additions 7-13648
Fe₁₄Ce₂B fine particles prep. by hydriding, mag. props., recording appls. 7-53660
Fe₇₀(CeNdPr)₂₀B₁₀, rapidly quenched ribbons, hard mag. props. 7-27562
Ir-Ce, cathodes, thermal emission and sublimation 7-13317
La₂Ce_{1-x}B₆, Zeeman splitting, thermodynamics of Coghlin-Schrieffer model 7-58783
(La_{1-x}Ce_x)₂Fe₁₄B rapidly quenched ribbons, hard mag. props. 7-27549
La_{1-x}Ce_xNi, Kondo lattice form., elec. resist. and susceptibility meas. 7-21899
Ni-Ce liquid alloys, variable valency investig. 7-7192
Pd-Ce-H, electrical resistance meas. 7-32984

cerium alloys continued

PdCe, Ce impurity, ground state studies, multiplet effects, near-edge XAS 7-64803
Pd₂CeH₂, H solubility in ordered/disordered Pd alloys 7-21473
ScCe, Ce impurity, ground state studies, multiplet effects, near-edge XAS 7-64803
VCE formed by Ce ion implantation, lattice-location studies of Ce ions 7-2042

cerium compounds
see also cerium alloys
band description with localising orbitals 7-45121
heavy-fermion state in the Anderson lattice 7-7476
intermediate valence and Kondo lattice models 7-2560
kondo effect versus crystal field 7-2602
mixed valence cpds., many body theory for spectroscopies 7-64790
moderately delocalised, mag. behaviour, anisotropy of crit. correlations 7-7474
monopnictides, valence fluctuations and c-f mixing interaction 7-2558
photoemission and bremsstrahlung isochromat spectra 7-3155
valence fluctuations and c-f mixing interaction 7-2558
X-ray absorpt. edges, many body effects, determ. 7-64789
Au/CeO₂ thin films on Ni-Cr Inconel superalloy substrates, diffusional processes 7-45098
BaTiO₃:Ce₂O₃, semiconductor props., influence of dopant oxides 7-6650
CaF₂-CeO₂, dispersed solid electrolyte systems, enhanced ionic conduction 7-16801
CeAs, antiferromag., anisotropic exchange and spin dynamics, neutron study 7-33147
CeB₆, cryst. struct. determ., defect content 7-58245
CeB₆, light, insulating cpds., core hole screening, X-ray absorpt. studies 7-64796
CeB₆, optical props. and band struct., spectroscopic ellipsometry meas. 7-13157
CeB₆, radiative decay of 4d⁹4fⁿ⁺¹ excited states 7-39321
Ce_{1-x}Bi_xF_{3-2x} solid solns., O substitution, influence on struct. and elec. props. (French) 7-12019
Ce₂Co₄P₁₂, synthesis, cryst. struct., X-ray diffr. study 7-32387
CeCo_{1-x}Si_{2+x}, cryst. struct., homogeneity range, X-ray diffr., electron probe anal. 7-37939
CeF₃, epitaxial growth on Si (111), photoluminescence, Raman scattering
Rutherford backscattering/channeling 7-59437
CeH_{2.7}, photoelectron spectra 7-22442
CeLiGe₂ isostructural cpds., crystal structure (Ukrainian) 7-12009
CeMRu₂Si₂ (M=La,Y), high energy EXAFS and XPS studies 7-64801
CeMn(Fe)Si₂, struct. and mag. props. studies (French) 7-37950
Ce₂Mo₆Si₈, crystal growth and struct., susceptibility and transport props. 7-64889
CeN, narrow band material, high resolution photoemission 7-33512
CeNi₂H₈, stoichiometry deviation and structural disorder, H content depend., EXAFS study 7-64815
Ce₂Ni₆P₁₇, bonding relationships and electronic struct. calcs. 7-16941
CeO₂, bond lengths, Ce K-edge EXAFS meas. 7-64753
CeO₂, doped with trivalent cations, grain boundary effect, microstruct. and microanal. 7-38249
CeO₂, films, optical absorption edge and energy gap 7-33471
CeO₂, intermediate valence state, XANES 7-52545
CeO₂, light, insulating cpds., core hole screening, X-ray absorpt. studies 7-64796
CeO₂, reduction by thermal treatment in vacuum or H₂ atmosphere, IR, PMR and ESR spectra 7-59756
CeO₂, with/without colloidal SiO₂, polishing cpd. used on GdGG 7-37212
CeO₂Y³⁺(Gd³⁺)(La³⁺), grain boundary effect, elec. meas. 7-38248
CeO₂-BaO, phase relations, thermodynamic parameters 7-6829
CeO₂-CaO, ceria-calcia ceramics, ionic cond., effect of microstruct. 7-38250
CeO₂-doped glass, solar cell coverglass thermal characts., improvements by thin film coatings 7-13884
CeO₂-Y₂O₃-ZrO₂, phase relations, solubilities, 1100-1600°C 7-46435
CeO₂-ZrO₂ solid solutions, O self-diffusion, effect of grain boundary movement 7-21522
CeO₂-ZrO₂-Y₂O₃ thermal barrier coating, plasma-sprayed, thermal and mech. props. (Japanese) 7-27899
CeO₂, thermodynamic model for nonstoichiometric ionic phases 7-32873
Ce(OH)₄, light, insulating cpds., core hole screening, X-ray absorpt. studies 7-64796
Ce(OH)₃⁺ cluster, 5d-4f excited states, X_α mol. orbital calcs. 7-62284
CePd₃B₆, heavy fermion cpd., thermal and mag. anomalous cryst. field effects 7-45239
CePd₃Si, heavy fermion cpd., thermal and mag. anomalous cryst. field effects 7-45239
CeRh₃B₂, valence fluctuations and c-f mixing interaction 7-2558
Ce(Rh_{1-x}Co_x)₃B₂ ferromag. Kondo system, anomalous elec. resist. temp. depend. 7-2601
CeS, continuous valence transition under high press. 7-32965
Ce(SO₄)₂.4H₂O, intermediate valence state, XANES 7-52545
CeSb, antiferromag., anisotropic exchange and spin dynamics, neutron study 7-33147
CeSb, mag. ordering and critical fluctuations, uniaxial pressure effects 7-33174
CeSc₃(BO₃)₄, preparation, struct. and props. 7-1968
CeSe₂O₆, cryst. struct., X-ray diffr. study (French) 7-26706
Ce₂(SeO₄)₃.5H₂O, vibr., IR and Raman spectra 7-3046
KCeF₄, gagarinite-type superstruct., X-ray diffr. studies (French) 7-58231
La₃₀Ce₆Li₂₄O₆₉, Li₂₄Ce₁₂Li₂₄O₇₂ and La₃₀Th₆Li₂₄O₆₉, cubic and tetragonal phases, structures 7-26725
Na₂(Ce,Co)ZrP₃O₁₂, Nasicon analogues, cryst. data 7-12014
Nd₃₀Ce₆Li₂₄O₆₉ and Nd₂₄Ce₁₂Li₂₄O₇₂, cubic and tetragonal phases, structures 7-26725
Nd₄Ce_{1-x}P₃O₁₄ cryst. growth and characterisation, X-ray diffr., Raman scatt., visible and IR absorpt. meas. 7-44423
Si₃N₄-Al₂O₃-CeO₂ ceramics, sintered, IR absorpt. and Raman spectra 7-46000
SrCeO₃ based proton conductive solid electrolyte in high temp steam electrolysis for H₂ production 7-54364
(U,Ce_{1-x}) O_{2-x}, struct. determ., EXAFS studies 7-63581
UO₂-CeO₂, sintering, solid soln. form. 7-3289

cerium compounds continued

- ZrO₂, CeO₂ containing tetragonal polycrystals, thermal stability, mech. props. 7-28101
ZrO₂, Y₂O₃ stabilised, CeO₂ doped on surface, thermal stability improvement 7-13619

cermets

- carbide electrospray alloying with steel, electron nature of interaction, phase comp. 7-8182
cemented carbide cutting tool materials, mech. props., wear-resist. relations 7-3443
cemented carbides, CVD Al₂O₃/TiC coatings, diffusion of Co and W, TEM/AES study 7-27942
DC cond. and percolation threshold calcs., metal-insulator composite mean-field theories 7-45253
electromagnetic wave propag., multiple scatt. approach 7-1031
frictional behavior of diamond and cubic BN abrasives 7-3461
granular metals with potential disorder, conduction 7-52554
hard alloy, cyclic cracking resist. determ. method 7-13682
hard metal parts, sintered, local alloying 7-27997
metal-carbide composites, implantation modified, friction, surface chemistry 7-46660
powder, surface treatment and surface props. (*Japanese*) 7-46666
steel-VC composites, cold sintered, mech. props., bonding integrity 7-39471
structural materials, cyclic strength 7-59624
Super Invar-Ta₁₆W₁₈O₉₄ composite, thermal expansion coeff. 7-12331
surface modifications and coatings, conf., Toronto, Ont., Canada (Oct. 1985) 7-41004
tandem deposition of small metal particle composites 7-33629
Al-Si-C(Si₃N₄), composites, thermal props. (*Japanese*) 7-52164
Cr-Ti-C system, existence of quasibinary section Cr-TiC 7-3288
Cr₃C₂-Ni-P hard metal, Cr₃C₂ solution in Ni matrix, liq. phase influence 7-53689
Fe-VC composites, cold sintered, mech. props., bonding integrity 7-39471
HfC, HfN, refractories, basic props., survey 7-64883
LaCrO₃-Cr cermets, mech. props., interparticle welding 7-39630
Mn/SiO, thin cermet films, electroformed characts. in dielec. range 7-12892
Ni-Al₂O₃ composites, small metal particles, high resolution electron microscopy and X-ray diff. meas. 7-46376
Pt-Al₂O₃ composites, small metal particles, high resolution electron microscopy and X-ray diff. meas. 7-46376
(Ti,W)-C-Ni₃Al composite prep. by liq. phase sintering, wettability of carbide by molten Ni₃Al, 7-64987
TiB₂-Mo electrospray coatings on steel, form. kinetics and high-temp. oxidation 7-65210
TiC based hard metals, abrasive polishing problems 7-53939
TiC coated cemented carbide cutting tool inserts, performance and material props. 7-46712
TiC-Fe-Cr alloyed with Si, high-Cr, sinterability and mech. props. improvement 7-64986
TiC-Mo₂C-Ni hardmetals, high temp. strength 7-3404
TiC-Ni hard metal, Ni-Ti-C phase diagram analysis 7-28016
TiC-Ni-Mo sintered carbides, struct. and physicochem. props. 7-3256
Ti-steel hard alloys, abrasive and hydroabrasive wear 7-17656
TiC-TaC-WC system, γ - α -solubility line, 1723K, thermochemical estimation 7-39526
TiC-WC-TaC-Co three-phase sintered carbides, Ta content influence on struct. and props. 7-65097
TiCN-Ni-Mo composite powders and coatings, prep. and characteris. 7-3255
TiN-Ni heterophase materials, strength rel. to sintering characts. and components conc. 7-53822
VC_x uses in cemented carbides and coating developments, review 7-39456
W base heavy metal alloys, mech.-props., porosity, impurity effects 7-17495
W-Al₂O₃ emitter for combustion heated thermionic energy converter 7-65509
WC cemented carbides, sintering, impurities, powder quality 7-3253
WC-Co, abrasive wear, 3D shape effect 7-17652
WC-Co, cemented carbides, abrasion, controlling mechanism 7-3460
WC-Co, erosion, effect of hardness 7-17648
WC-Co, erosion rate 7-3464
WC-Co, high press, sintering, microstruct. 7-39470
WC-Co, phenolformaldehyde polymer friction, physicochem. processes 7-28149
WC-Co, plasma sprayed coatings, wear, adherence, heat treatment effect 7-33555
WC-Co, sliding and abrasive wear mechanisms, comparison 7-3463
WC-Co, TiN-coated, residual stress and strength, X-ray diff. study (*Japanese*) 7-8101
WC-Co, tool materials, statistical wear model, appl. to machining 7-33804
WC-Co, wear resist., comparative study of hard materials 7-3457
WC-Co cemented carbides, tensile creep, 800-900°C, grain boundary sliding 7-17585
WC-Co cemented carbides, compression fatigue crack growth 7-28119
WC-Co cermet particle reinforced low alloy steel composite, elastic const., laser US technique 7-65268
WC-Co compact, stereological analysis of struct. form. during consolidation of carbide powder 7-53688
WC-Co composites, fracture toughness rel. to hardness, microstruct. model 7-17637
WC-Co hard metals, thermal conductivity and thermal diffusivity (*German*) 7-27036
WC-Co powder mixtures, electrolytic Co plating effect on densification and strength props. 7-53686
WC-Co sintered carbides, X-ray diff. obs. of microstruct. after hardening, optimum heat treatment cycle 7-65063
WC-FeNi cemented carbides, abrasion, controlling mechanism 7-3460
WC-Ni, wear resist., comparative study of hard materials 7-3457
WC-Ni hard metal parts, sintered, local alloying 7-27997
WC-stainless steel composites, corrosion-resistant optimum prod. conditions 7-65164
WC-TaC-Co, N contained cemented carbides, sinterability, mech. props. rel. to prep. 7-17507
WC-TiC-Co hard alloy Ti5K6, heat treatment effect on failure mechanism 7-13550
WC-TiC-Co TK type hard metal prod. using Ti alloy swarf 7-27996

CESR

- (BEDT-TTF)₂I₃, α and β phases, CESR 7-2930
n-Cd_{1-x}Mn_xSe, electric-dipole-induced spin resonance 7-27592
GaInAs-InP quantum well, CESR of 2D electrons 7-38941

CFRP see carbon fibre reinforced plastics

chalcogenide glasses

- AC conduction, theoretical models and expt. data, review 7-64252
chalcogenide-metal contacts, interdiffusion, struct., comp., electron irradi. effects 7-21686
dangling-bond and void-like structs., microscopic structural model 7-21803
defects and microheterogeneity, positron annihilation studies 7-46220
electrons in mobility gap, spectra and thermodynamic props. 7-2471
field dependent negative U-model and switching 7-7252
films, metal ion doped, impurity effects 7-11943
hollow and glass core chalcogenide fibres, comparison 7-37196
integrated and fibre optics, appls. of chalcogenide glasses, review 7-31412
IR optical fibres, meas. system for dispersion, attenuation, numerical aperture, optical time-domain reflectometry 7-37229
IR optical fibres development and appls. 7-20456
multicomponent alloy, threshold switching phenomena 7-52709
nonequilibrium phonons and photostruct. transforms., energy transfer characts. 7-6742
optical recording on chalcogenide layers, physical basis (*Russian*) 7-50667
photodarkening process and defects 7-13112
photostructural conversions, local phonon modes 7-58427
photostructural transformations, energy accumulation (*Ukrainian*) 7-13110
rapidly condensed highly dispersed films and glasses, phase size effect 7-2149
thin films, glass-crystal transitions, photoacoustic studies 7-45073
Ag/amorphous chalcogenide, Ag photodiffusion, semiconductor heterojunction formation 7-45026
Ag-As-Se glasses, electrical conductivity studies 7-27369
Ag_{0.15}As_{0.425}Se_{0.425-x}Te_x chalcogenide glasses, ionic and electronic cond., comp. depend. study 7-12768
Ag₂S-Ag₂Se-Ag₂Te, quasi-binary systems, elec. conductivity, thermoEMF 7-21908
Ag₂S(Se)-Ag₂Te(Se) liq. and glassy semicond., activation energy of carrier thermal generation, elec. meas. 7-17035
Ag₂S(Se)(Te)-Cu₂S(Se)(Te) liq. and glassy semicond., activation energy of carrier thermal generation, elec. meas. 7-17035
As-Ge-Se-Te chalcogenide glass fibres for thermal IR transmission 7-37193
As-S (Se) chalcogenide glasses, far-IR absorption spectra and spatial charge fluctuation 7-7696
As-S glass IR fibre, Teflon clad, optical loss due to water diffusion 7-57556
As-S:Ag photodoping, energy expenditure determ. (*Russian*) 7-21261
As-S-I semicond. glass system, IR and Raman spectra studies 7-3058
As-Sb-Se glasses, calorimetric meas. 7-26652
As-Se, amorphous, short range structures, EXAFS studies (*Chinese*) 7-37871
As-Se and As-Se-Te IR chalcogenide tube waveguides 7-37195
As-Se glass, IR optical materials, production 7-37075
As-Se glasses, defect levels and photoconductivities 7-12673
As-Se:Ag amorphous films, Ag doping profiles, ellipsometric studies 7-7779
As-Te-based glasses, small polaron hopping and transport props. 7-21911
AsGeSe, IR transmitting fibre optics, spectral props. 7-37179
As₁₀Ge_{22.5}Se_{67.5} glass grating couplers, fabrication using electron beam induced Ag doping (*Japanese*) 7-62817
As₂Ge_{20-x}Se₈₀ amorphous struct. study, positron lifetime spectra meas. 7-37886
As₄₀Ge₁₀Se₂₅S₂₅ glass grating couplers, fabrication using electron beam induced Ag doping (*Japanese*) 7-62817
As₂S₃, viscosity, rel. to intensity and spectral comp. of light 7-12342
As_{1-x}S_x:Ag film, coordination distance determ., EXAFS study 7-64004
As₂S₃, amorphous, bulk glass and thin films, photostructural changes, EXAFS meas. 7-39314
As₂S₃, amorphous, characts. control using acoustic domain 7-20576
As₂S₃ amorphous chalcogenide optical grid, submicron resolution, VLSI appls. 7-48899
As₂S₃ amorphous films, persistent photocurrent 7-45389
As₂S₃ chalcogenide glass, photoinduced gradient waveguide form. (*Russian*) 7-43374
As₂S₃ chalcogenide glass, Zn vacuum deposition rate, photostimulated changes 7-45075
As₂S₃ glass, photostructural effects, EXAFS study 7-64758
As₂S₃, glassy photodeformation 7-44654
As₂S₃ thin films, dissolution investig., surfactant effects 7-6802
As₂S₃ thin films, natural paramagnetic centres obs. (*Russian*) 7-45799
As₂S₃ thin films, photodarkened, reversible recording and erasure of holograms 7-50511
a-As₂S₃ vapour deposited films, thermostructural and photostructural changes, EXAFS study 7-64003
As₂S₃, vitreous, γ -irradiated, EPR of radiation-stimulated paramag. centres (*Russian*) 7-2929
As₂S₃:Ag, amorphous, charge fluctuation, Ag doping effects 7-7700
As₂S₃, glassy, bond strength anal., EXAFS temp. depend. study 7-64763
As₄₀Se₃₀Se₃₀ glasses, surface pot. relax., TSC meas. 7-64261
As₂S₃ amorphous films, persistent photocurrent 7-45389
As₂Se₃ amorphous thin film, bulk trap spectroscopy by temp.-modulated space-charge-limited current meas. 7-45338
As₂Se₃, non-exponential photocurrent decay, anal. 7-38633
As₂Se₃:Ni films, electronic struct. and transport props. 7-12595
As₅₀Se₅₀ amorphous films used for optical recording, structural transformation mechanisms (*Russian*) 7-51823
As₂Se_{100-x} vitreous chalcogenide semicond. layers, deep trapping levels, photostimulated effects (*Russian*) 7-2754
As₂Se_{100-x} chalcogenide glass, Vickers microhardness indentation and fracture mechanics 7-21342
(As₂Se₃)(As₂Te₃)_{1-x/2} glasses, molecular struct., chemical equivalence of ¹²⁵Te absorpt. and ¹²⁵I emission Mossbauer spectroscopy 7-59129
As₂Se_{0.5}Te_{0.3} chalcogenide glass, struct. models, X-ray diff. and Monte Carlo calcs. 7-6548
As_{40.45}Se₁₀Te_{49.55} glassy alloy, struct. model and switching props. 7-1904

chalcogenide glasses continued

- (As₂Se₃)_{1-x}Tl_x, elec. and thermal transport props., effect of Tl addition 7-38200
- α-As₂Te₃ films, hole transport investigation by transient field-effect and time-of-flight methods 7-22040
- As_{2-x}Te_{3-x}In_{2x} and As_{20-x}Te_{80-x}In_{2x} systems, chalcogenides, thin films, optical and electrical props. 7-27446
- a-As₂Te(se)₃, surface phonon generation and picosecond light pulse detection 7-12456
- Bi-Ge-S chalcogenide glasses doping mechanism and structural effects, EXAFS study 7-1909
- CdS-In-glass, spray pyrolysed, photoelectrochemical studies 7-52830
- Cu₁₂As₃Se₅₁, glassy semiconductor, tetrahedral bonding 7-32304
- Ga-Se-Te, phase change optical recording, write erase characteristics 7-57491
- Ga₂₀Te₈₀, double glass transition and double stage crystn., X-ray diffr. studies 7-58157
- Ge-As-S, glasses, elastic properties 7-21323
- Ge-As-Se and As-Se chalcogenide optical glass fibres, prep. and characterisation 7-37194
- Ge-As-Se chalcogenide glasses, structural models, medium range order and interference functions, first sharp diffr. peak calcs. 7-6540
- Ge-As-Se-Te chalcogenide glass fibres for transmission in the 8 to 12 μm range 7-37192
- Ge-based chalcogenide thin films, amorphous, anomalous photoinduced transformations study 7-45070
- Ge-S+bi chalcogenide glasses, struct., DTA and X-ray diffr. studies 7-6543
- Ge-Sb-S glasses, bulk and thin film samples, optical and photo-acoustic props. study 7-22211
- Ge-Sb-Se glasses, crystallisation ability, high energy electron irradi. effects (Russian) 7-32306
- Ge-Sb-Se IR chalcogenide tube waveguides 7-37195
- Ge-Se-Ag amorphous films, Ag doping profiles, ellipsometric studies 7-7779
- Ge-Se-As glasses, elastic constants, rigidity percolation 7-44648
- Ge₃₀As₂₀Se₅₀, glassy semiconductor, structural models 7-44393
- Ge₁₀As₄₀Se₅₀ and Ge₂₂As₁₅Se₆₃ glass films, photodarkening effect, exposure characts. (Japanese) 7-64706
- Ge₂₈Sb₁₅Se₅₆S glasses, surface pot. relax., TSC meas. 7-64261
- GeS and GeSe, chalcogenide glasses for IR fibres, plasma deposition 7-37191
- GeS₂ amorphous films, persistent photocurrent 7-45389
- GeS₂ glass, photostructural effects, EXAFS study 7-64758
- GeS₂ amorphous system, struct. anal. by X-ray spectroscopy 7-26653
- Ge₂₀S₈₀Bi chalcogenide glasses, doping, coordination number and cond. transition, EXAFS study 7-64764
- a-Ge₃₀S₇₀ films, irreversible photobleaching 7-17353
- Ge₃₀S₇₀-Ag chalcogenide films, Ag photodoping, optical transmission spectra 7-59231
- Ge₃₅S₆₅ films, evaporated, structural changes on illumination and heat treatment (Japanese) 7-22489
- Ge₄₀S₆₀, amorphous film, photoinduced bleaching 7-13618
- Ge₂₀S_{80-x}Bi_x, amorphous, electronic cond. props. under high press. 7-45328
- Ge₂₀S_{80-x}Bi_x, n-type amorphous semiconductors, morphological struct. 7-51652
- Ge₂Si_{1-x}(Se_{1-x}), glass, ordered phases, effective microscopic cross charge 7-13077
- GeSe amorphous films, persistent photocurrent 7-45389
- GeSe₂ amorphous films, persistent photocurrent 7-45389
- GeSe₂ glass, photostructural effects, EXAFS study 7-64758
- GeSe₂ glasses, short and medium range order, Mossbauer studies 7-13069
- a-Ge₂₀Se₇₀Bi films, n-type, electron transport props. studies 7-7422
- Ge₂₅Se₇₅ glass films, photodarkening effect, exposure characts. (Japanese) 7-64706
- Ge_{20-x}Se_{80-x}In_{2x} system, chalcogenides, thin films, optical and electrical props. 7-27446
- GeSeSb, IR transmitting fibre optics, spectral props. 7-37179
- Ge₄Se_{6-x}Te_x, amorphous chalcogenide, elec. cond., prep. technique effects 7-7237
- Ge₄Se_{6-x}Te_x, amorphous chalcogenide, elec. cond., bulk and thin film effects 7-7238
- Ge_{1-x}Sn_xSe₂ glasses, elec. cond. rel. to Mossbauer and Raman spectra 7-64250
- (Ge_{1-x}Sn_x)_{1-x}Se_x(S_x) glasses, percolation transition and strain accumulation 7-11939
- GeTe₂ amorphous films, struct. changes by annealing 7-63467
- a-Ge_{1-x}Te_x films, crystallisation behaviour and local order 7-44386
- Ge₂₀Te₈₀ glasses, heat capacity, relax. and thermodynamic kinetics during annealing 7-44843
- Ge₅₀Te₅₀, Auger elemental depth profiling, preferential sputtering 7-54247
- Ge_xX_{1-x} (X=S,Se), chalcogenide glasses, stochastic random network model 7-63493
- La₂S₃-La₂O₃-Ga₂O₃-Ga₂S₃ glassy and crystalline chalcogenides, EXAFS structural study 7-63481
- Pb₉₅Ge₀₅Te, glassy and cryst., defect struct., positron annihilation studies 7-46221
- Sb-Ge-Se-Mn, effect of Mn impurity on comp. and physicochemical props. 7-11922
- Sb-S, thin films, amorphous and thermally annealed, optical props. (Russian) 7-17352
- Sb-Se, thin films, amorphous and thermally annealed, optical props. (Russian) 7-17352
- SbS₃ thin films, vacuum deposited, elec. and photoconductive props. (Korean) 7-52682
- Se, glassy state, phys. props., chem. bonds and defects 7-6530
- a-Se-Te films, space-charge depletion studies of deep states 7-59148
- Se-Te, glass forming melts, nonisothermal crystn., DTA, crit. cooling rate 7-44394
- Se_{100-x}Ge_x, amorphous alloy, photodarkening, structure model anal. 7-3003
- Se₅₀Te₅₀, Auger elemental depth profiling, preferential sputtering 7-54247
- Si-Te-As-Ge chalcogenide glass film, electronic processes in strong elec. field 7-45524
- Si₂Se_{1-x} glass system, diffr. isosbestic points and structural systematics 7-44390
- Si₂Se_{1-x} glasses, intermediate range order 7-11938

chalcogenide glasses continued

- Si₂Se_{1-x} low dimensional inorganic polymer glasses, cross-linked chain cluster model 7-11937
- Si₂Te_{100-x} glasses, crystallisation, DSC studies 7-6542
- Si₂X_{1-x} (X=S,Se), chalcogenide glasses, stochastic random network model 7-63493
- Te-As-S chalcogenide system, annealing, crystalline precipitate phase form., X-ray diffr. anal. 7-16751
- Te-Ge alloy glass, isothermal surface crystallisation 7-58576
- Te_{1-x}Ge_x amorphous films as reversible phase-change optical data storage materials 7-1242
- (Te₉₀Ge₁₀Se₁₀)_{100-x}O_x, Auger elemental depth profiling, preferential sputtering 7-54247
- Tl-Ge-Se, bulk glass formation region, elec. and struct. characts. 7-58159
- Tl₂Se_{100-x} glasses, glass transition, melting, recrystallisation, elec. transport 7-64246
- V₂O₅-As₂O₃-B₂O₃, vitreous, elec. cond., semiconducting props. 7-2620

change of state *see phase transformations***channel flow**

- see also pipe flow*
- air-water upflow in vertical annular channels, true gas content expr. 7-16265
- annular two-phase flow, void fraction 7-44023
- axial flow in square lattice rectangular rod bundle, wall shear stress meas. 7-16282
- axisymmetric flows in swirlers, difference method 7-51166
- baroclinic flow transitions in annulus 7-26351
- Bass Strait, tidal and storm surge model 7-18206
- bounded-volume chambers, convective heat transfer 7-43906
- branched gas circuits, acoustical charact. anal. using signal graphs 7-63219
- bubble growth and collapse, transient boiling heat transfer in narrow channel 7-26346
- cavity flows of multi-cavity channel, self-excited shear layer oscillations 7-51317
- cavity-mounted press. transducer, input press. effects on freq. characts. 7-37595
- circular channels, variable cross section, momentum, energy and mass transfer (Russian) 7-11549
- combined free and forced laminar convection in thermal entrance region of channel, Prandtl no. effect 7-37453
- composite channel flow, periodical large surface eddies generation 7-20803
- corner flow, incompressible fluid with suction, heat transfer eval. 7-26277
- curved channels, flow calcs. 7-44047
- curved rectilinear channels, drag creeping flow, asymptotic soln. 7-37541
- curved square duct, mean vel. and press. distrib. (Chinese) 7-11544
- curved square duct with different Reynolds nos., press. loss and mean velocity field meas. (Chinese) 7-11545
- curvilinear coordinates for 3D laminar, duct flow 7-16269
- cylinder translation between 2 parallel walls, viscous flow in Stokes regimes (French) 7-31885
- dielectric liquids, stressed, transient EHD motion, computer simulation 7-1643
- drag reduction in flow in longitudinally grooved channel 7-51060
- droplet entrainment in vertical annular flow and its contrib. to momentum transfer 7-11492
- droplets, accelerated, in nonisothermal flow, heat transfer (Russian) 7-16179
- duct, rectangular, turbulence promoters, geometric shapes effect 7-37443
- duct with moving walls, longitudinal dispersion 7-51319
- ducts, axisymmetric or plane, flow bifurcation at a wall sink, vorticities for Stokes flow 7-31884
- ducts, finned, triangular, fully developed flow, friction factors 7-63224
- dusty gas, conducting, channel flow, graphical anal. 7-63214
- electric arc in flow with well-developed turbulence, investig. 7-26566
- entrainment and mass transfer at the density interface in a trough 7-11539
- fluid flow in channel, nonsteady heat transfer calc. method 7-63223
- forced-convection heat transfer, 2D transient anal. 7-20724
- free inertia motion of a rotating nonhomogeneous fluid (French) 7-63158
- free inertial movements in a rotating fluid (French) 7-16185
- free surface unsteady flows having shocks or bores, explicit numerical schemes 7-60302
- fully developed combined convection, theory, flow reversal 7-1566
- gas dynamics, quasi-equilibrium, thermodynamic theory for duct flow 7-51204
- gas flow in thin, rectangular channels 7-63221
- gas jet impacting a cavity, temp. and velocity meas., flow anal. 7-43999
- gas mixture nonequib. flow through narrow channels, phonon drag effects 7-16253
- gas-liquid mixture, bubbly flow parameters, bubble breakup effect 7-44021
- haemorrheology, effect of couple stresses on unsteady convective diffusion in fluid flow through a channel 7-3811
- heat transfer around sharp 180-deg turns in smooth rectangular channels 7-63144
- heat transfer from two elliptic cylinders in tandem arrangement 7-63145
- heat transfer in unsteady MHD Couette flow of electrically conducting viscous incompressible rarefied gas, theory 7-66448
- heated parallel channels, flow distrib. calcs., PWR appl. (German) 7-25107
- high temperature gases in annular channel with cold walls, heat transfer in turbulent flow (Russian) 7-1557
- homogeneous rotating fluid flow through rectangular opening 7-18189
- hydromagnetic channel flow in inclined magnetic field, Hall effects 7-51334
- inclined porous channel, viscous MHD flow in the presence of a mag. field 7-6320
- incompressible flow in forward-facing step geometries, Navier-Stokes solns. 7-6180
- incompressible fluid, flow eqn. soln. 7-6179
- incompressible fluid flow from annular slit, flow pot. determ., unsteady axisymmetric problems 7-20796
- incompressible viscous flow, Green's function method for nonlinear problems (Chinese) 7-26342
- incompressible viscous fluid, MHD flow in infinite channel 7-6326
- internal flow, Navier-Stokes eqn. num. soln. (French) 7-57872

channel flow continued

internal turbulent flow, separated flow region, Navier-Stokes solver 7-51069
 inviscid fluids in channel under localised perturbations, steady flows 7-11546
 jets, confined, mixing 7-6263
 Karman vortex flowmeter, fluid flow around bluff body 7-37601
 laminar channel flow with stepwise variations of wall temp., transient forced convection 7-37426
 laminar forced convection inside ducts with temp. periodic variation 7-31736
 laminar heat transfer and flow in curved square channels, elliptic nature, numerical visualisation 7-37432
 laminar jet, in narrow slot at large Reynolds number 7-1599
 laminar mixed convection in a partially blocked, vertical channel 7-43842
 laminar natural convection flow in square enclosure thermal cond. effect 7-51115
 laminar natural convection in square channel, penalty FEM 7-51132
 laminarisation and reversion to turbulence of low Reynolds no. flow 7-51039
 laser Doppler anemometer meas. corrections for curved channel flow 7-37608
 Laval nozzles, acoustic disturbance propag. in transonic zone 7-62882
 linearly stratified, rotating flow over long ridges in a channel 7-6224
 longitudinal vortices in straight open channel, flow visualisation 7-37476
 meandering channels, flow and pollutant dispersion, 3D modelling 7-44052
 meandering rivulet flow transition in vertical parallel plate channels 7-16268
 MHD channel flow through porous medium 7-57932
 MHD flow in liquid metal blanket with nonuniform thickness liner (Japanese) 7-16271
 mixed laminar correction in entrance region of inclined rectangular channels 7-63148
 molecular dynamics simulation 7-37418
 multilayer ideal incompressible heavy fluid flow past body 7-1601
 natural convection, book 7-60909
 natural convection in channel with corrugated confining walls 7-51113
 natural convection in partially divided enclosures 7-63146
 Newtonian fluid, channel flow, press. gradient 7-63213
 Newtonian fluids in curved rectangular ducts, bifurcation phenomena 7-16154
 non-Newtonian flow in helical channels with constant pitch, var. calcs. 7-43988
 nonequilibrium gas-solid system, transport processes, kinetic theory calcs. 7-16254
 nonuniform bottom, linearised soln. 7-1637
 numerical simulation of viscous flows in hydraulic turbomachinery by the finite element method 7-26256
 oblique shock waves and turbulent boundary layer interactions, meas. and model 7-16208
 oceans, depth-dependent channel flow modelling 7-18325
 open-channel network flow model (Japanese) 7-35285
 oscillatory rectangular duct flows with turbulence transition, laminar phase vel. distrib. 7-16257
 oscillatory turbulent flow in a cylindrical channel 7-57820
 passive tapered channel for wave kinetic energy conversion 7-46917
 perturbation propag. in boundary layer on flat channel walls 7-51045
 plane jet at low Reynolds number confined in rectangular channel, numerical analysis 7-37507
 polymer fluids, nonlinear, elastic props, convective transfer processes 7-43824
 potential flow, 2D with separation in unsymmetrical bends 7-11538
 power-law fluid in horizontal ducts, laminar mixed convection heat transfer 7-37427
 pressure losses in channel with injection of jet system (Ukrainian) 7-11542
 Rayleigh's inflexion-point theorem and its extensions 7-11384
 rectangular turbulent promoters, computer generation 7-37549
 relaxed gases, nonsteady-state flow in channels 7-11552
 ribbed wall channel, turbulent flow study using 2-component laser Doppler anemometry 7-37547
 rigid boundary channels carrying sediment-laden flow, resistance to flow and vel. distrib. 7-20802
 rise velocity of large bubbles in stagnant liquid in non-circular ducts, estimation 7-37524
 Rivlin-Ericksen fluid MHD flow in open inclined channel 7-1639
 rotating channels, turbulence, spectral characts. 7-43869
 second-order fluid flow between two porous coaxial circular cylinders, finite element method 7-11530
 second-order fluid flow through channel with porous walls under mag. field 7-20762
 secondary flow in MHD generator channel with mag. field 7-1635
 secondary flow patterns, flow visualization and centrifugal instability in curved tubes 7-37550
 separation of droplets of lower channels, channel profile geometry effect 7-44017
 skin friction and wall shear stress meas. instrument 7-37406
 solar air heater design for cost-effectiveness 7-3626
 sound, nonisentropic propag. in uniform ducts using Euler eqns. 7-6314
 stationary flow in channel, chem. reacting similarity wave propag., viscosity change effects 7-31886
 stationary planar Euler flows in an unbounded strip, nonlinear stability 7-31883
 stirrers and induction pumps, liquid metal velocity distrib. effects on electrodynamic forces (Polish) 7-63231
 Stokes equations, soln. for incompressible fluid in multiconnected domain 7-20797
 subcooled boiling flow in vertical eccentric annular channel, heat transfer study 7-51310
 subcooled liquid, film boiling in channels, heat transfer and hydraulic resistance 7-51145
 supercritical fluid, diffusion and mass transfer 7-63106
 surface-mounted obstacles, wakes, tailing vortices, channel-flow expts. and num. simulation 7-57844
 Sutterby fluid, steady laminar flow in rectangular duct inlet region 7-43990
 thermally stratified fluid, vertical through-flow between flows, Navier-Stokes eqn. 7-31857

channel flow continued

thermogravitational and thermocapillary convection in a rectangular cavity 7-63910
 three-dimensional Cauchy-Poisson problem for variable depth domain 7-44044
 topographic Rossby waves, 1D models, elongated basins, various lake cross sectional distributions 7-18220
 transient dispersed-film flows in channels containing fuel rod bundles 7-10236
 transonic, numerical solution, finite element method, multigrid technique 7-6240
 travelling thermal wave induction of convective heat transfer and fluid flows, nonlin. study 7-1546
 tubes and channels, porous-walled, injection-induced flows 7-31876
 turbulence, curvature effect, num. simulation 7-57926
 turbulence duct flow with nonuniform inlet conditions, 3D calcs. 7-51066
 turbulence models, statistical refinement 7-1537
 turbulence near a wall, limiting behaviour, Navier-Stokes computational models 7-16170
 turbulent, fully developed 2D channel flow, visualisation and image processing 7-37574
 turbulent, mixing in 2D ducts with transverse jets 7-31757
 turbulent boundary layer in channel, injection through porous wall, accel. and turbulence influence, investig. 7-26263
 turbulent channel flow, 3D coherent structures in near-wall region 7-37548
 turbulent channel flow, ejections and bursts, struct. and timescales 7-51088
 turbulent channel flow, heat and mass transfer modelling 7-26257
 turbulent channel flow, rotating system strong effects 7-1580
 turbulent flow and mass transfer of unstabilised stream in channel with obstacle 7-11391
 turbulent flow meas. in ribbed-wall flow channel and comparison with model 7-57947
 turbulent gas flow in cylindrical channel, interactions of electric arc 7-44056
 turbulent open-channel flow, struct., flow visualisation study 7-51071
 twisted circular-sector ducts, fluid flow and heat transfer anal. 7-11374
 two-dimensional, instabilities and bifurcations 7-26352
 two-layer fluid in cylinder and channel nonlinear wave reductive method 7-20776
 two-phase boundary layer, frictional stress meas. 7-44018
 two-phase flow, rod bundle, parameter distrib., expt. study 7-26337
 viscoelastic fluid, unsteady flow through ducts, impulsive pressure gradient 7-57885
 viscous, incompressible fluid in closed cavity, free convection, numerical simulation 7-63134
 viscous flow, Navier-Stokes eqns., 3D elliptic soln. 7-51318
 viscous gas flow, intense heat release in channels 7-31797
 viscous incompressible flow in a narrow channel with one free wall and fluid supply through a porous insert 7-1636
 wall shear stress meas., hot film surface gauge improvement 7-37405
 water, cold, natural convection near its density maximum in rectangular enclosure 7-57836
 water, turbulent flow at supercritical press. in smooth channel, drag coeffs. determ. 7-43866
 CO₂-H₂O, mass transfer coeff., turbulence in open absorpt. channel 7-6189
 CO₂-He-N₂, vibr. nonequib. flow in axisymmetric channel with glow discharge 7-20741
 He, channelled cryogenic liquids, heat transfer and hydrodynamics 7-16261
 He, free convective heat transfer from horizontal cylinder with large temp. head 7-63142
 He II, pressurized, confined to channel, boiling phenomena 7-38280
 He, liq., flow stability at supercrit. press., nonuniform heat flux distrib. in channel 7-51058
 He, liquid, heat transfer with nucleate boiling in channels 7-11524
⁴He, superfluid, flow properties w.r.t. cryogenic appls. 7-52171
³He, superfluid, dissipative flow through thin channels 7-38288
³He, superfluid, dynamics in flow channels with restricted geometries 7-38287
 N₂, channelled cryogenic liquids, heat transfer and hydrodynamics 7-16261

channel substrate planar lasers see semiconductor junction lasers

channeling radiation see channelling radiation

channelling

see also energy loss of particles
 bent crystals, channelling effects, sine-squared pot. anal. (Chinese) 7-12177
 channelling contrast microscopy, He⁺ microbeam, semiconductor impurity profiles 7-51587
 charged particle channelling in solids 7-38081
 computer aided analysis of electron channelling patterns 7-16664
 crystals, fast charged particles channelling rel. to surface layer distortion distrib. (Russian) 7-63687
 curved cryst., vol. capture of particles to channelling, reversibility principle calcs. 7-51900
 diamond, planar channelled protons, breakthrough angles 7-21308
 electron and positron small angle incidence on cryst., radiation processes, incoherent multiple scatt. effects calcs. 7-44625
 electron channelling patterns, many beam effects and phase information 7-32534
 epitaxial growth on CaF₂/Si (111), film quality improvement by Ge predeposition 7-7070
 fast ion dechannelling, electronic diffusion coeff. calc. 7-44635
 grain growth, local texture development, STEM selected area channelling 7-16575
 high-energy charged particles, vol. refl. in quasi-channelling stokes in bent crystals 7-63693
 InP:Si, ion implanted, rapid thermal annealing and solid phase epitaxy 7-21296
 interface and surface struct. characterization, ion scatt. and channelling, scanning tunnelling microscopy and computer simulation (Japanese) 7-7803
 ion backscattering yield under axial channelling with slowing down 7-22415
 ion beam channelling, in semiconductor superlattices, review 7-51902
 ions implanted into single crystals, depth distributions 7-6667

channelling continued

negatively charged high-energy particles, recapture into a channel 7-21305
proton beam deflection by bent Si cryst. 7-44632
radiative energy loss by relativistic electrons and positrons in crystals 7-21306
rare earth silicide epitaxial formation by rapid annealing 7-21768
review of channelling processes 7-51898
semiconductor structures, MeV He⁺ microbeam analysis 7-13315
steel, stainless, laser alloying with Au(Mo), Rutherford backscattering and channelling studies 7-28206
superlattices, diffraction and channelling of photons and neutrons 7-6480
Al, US deform, modelling of reduced bandwidth distortion to wide-area electron channelling mapping 7-16694
AlAs-GaAs superlattices, Si ion implantation, dose-dependent mixing 7-12500
β-Al₂O₃, diffusion of implanted ions (*Chinese*) 7-51798
α-Al₂O₃:Br, ion implanted, RBS and annealing studies 7-32515
As (0001), laser pulsed oxidation modification 7-58320
Au crystal, H⁺ ion channelling, catastrophe theory 7-21312
Bi, electronic structure, effect of ion implantation 7-45143
CaF₂ epitaxial films on Si, structural and electrical props. improvement by rapid thermal annealing 7-38400
CaF₂, epitaxial growth on GaAs (100)(111) 7-59437
CaF₂-BaF₂ epitaxial bilayers on Si (111), characterisation 7-12521
CaF₂-Si interface, strains in MBE grown insulator films, MeV ion channelling meas. 7-7080
CdS:Ri⁺(Kr⁺)(Ar⁺)(Ne⁺), ion implantation damage 7-26812
CeF₃, epitaxial growth on Si (111) 7-59437
CoSi₂-Si epitaxial heterostructures, growth and characterisation 7-27212
Cr single crystals, surface and deeper layers, struct. changes due to laser irradiation 7-6937
Cu, ion irradiat., sputtering and lattice damage, cryst. orientation effect 7-64843
Cu, pion decay site spectroscopy, interstitial sites 7-53191
Cu single cryst. target, atomic and mol. ion surface semichannelling, Lindhard atomic string model calcs. 7-63697
Cu surface, ion irradiat., sputtering and lattice damage, cascade simulation 7-59327
Cu:Ar(Ne)(C), single crystal, ion implantation, damage profile anal. using Auger electron spectroscopy 7-51802
EuS-SrS mag. superlattices grown on Si(111), strain, study by He ion channelling 7-27215
GaAs, impurity atom site location using channelling enhanced microanalysis 7-38023
GaAs, ion implant depth profiles, channelling, Monte Carlo simulation 7-51811
GaAs, Laue zone effects, nonzeroth order, atom location by channelling enhanced microanal., X-ray fluorescence anal. 7-46905
GaAs MBE layers on Si (100), crystalline quality, rapid thermal annealing effects, RBS/channelling studies 7-12519
GaAs, neutron transmutation doped, thermal annealing effects, channelling anal. (*Chinese*) 7-12178
GaAs:Al⁺(P⁺), ion implantation damage 7-38024
GaAs:Si⁺ wafers, implant at. profiles, planar and residual channelling effects 7-12181
GaAs_{1-x}P_x:Be⁺-GaP:Be⁺ strained-layer superlattices, ion implantation doping, structural study 7-38030
GaP single crystals, high energy ion implantation, damage profiles 7-16590
(GaSb)_{1-x}(Ge)_x metastable thin film alloys, struct. phase transitions, ion-channelling studies 7-58462
Ge, channelling effects in radiative emission of electrons 7-2074
Ge ion beam deposition on (100) single cryst. substrate, interface, thin film and damage form. 7-17423
Ge, MBE on Si, role of surface reconstruction, LEED, Rutherford backscattering, channelling meas. 7-7034
Ge, muon channelling, evidence for pionium formation 7-51897
Ge-CaF₂-Si heteroepitaxial structures, MBE grown, twinning, topography, channelling, TEM, SEM 7-12566
Ge₂Si_{1-x}-Si multilayers, MBE grown, thermally annealed, Ge diffusion, strain relax., ion channelling, backscattering anal. 7-6896
In_xGa_{1-x}As, atomic displacements detection using channelled electron induced X-ray emission 7-21311
InP, impurity atom site location using channelling enhanced microanalysis 7-38023
InSb metalorganic magnetron sputtered films, structural and compositional characts. 7-21725
InSe, photoluminescence, defects effects 7-39161
KCl, heat treated, alpha particle dechannelling, range meas. by F-coloration depth determ. 7-32512
LaB₆, lattice dynamics studied by ion channelling, La in Einstein model 7-44710
LaF₃, epitaxial growth on Si (111) 7-59437
LaNi₅, anisotropic H migration, deposition potentials, hardness, brittleness meas. 7-6873
Nb film microstruct., nonnormal incidence ion bombardment effects 7-12174
Nb-D, implanted, lattice distortion, channelling method 7-58382
NdF₃, epitaxial growth on Si (111) 7-59437
Ni, ion implantation and pulsed laser melt quenching, metastable phase and defect struct. form. studies 7-16625
Ni-Al-B-based alloys, site occupations, APFIM and channelling studies 7-32367
Ni₃B, amorphisation by ion implantation, RBS/channelling studies 7-11912
NiSi₂-Si (111) epitaxial interface, strain meas. by MeV ion channelling 7-27157
Sc, single crystal surface characterization, RBS/channelling, SEM and LAMMA anal. 7-12425
Si (111), convergent beam RHEED studies 7-32764
Si, amorphised and rapidly thermally annealed, extended defects 7-16660
Si, amorphous and single cryst., etching rate, ion backscatt. and channelling meas. 7-28231
Si crystals, low energy Ag⁺ implantation-induced deep centre depth distrib., DLTS study 7-26820
Si, dislocation loops, generated by ion implantation and furnace annealing, depth profiles, RBS, X-ray diffr., TEM anal. 7-51882
Si, disorder generation by Ar⁺ implantation, Rutherford backscatt.-channelling meas. 7-63680

channelling continued

Si films, grain size and texture enhancement by seed selection through ion channelling 7-38401
Si ion beam deposition on (100) single cryst. substrate, interface, thin film and damage form. 7-17423
Si, ion beam induced recrystn., channelling effect 7-16650
Si MBE growth on Si (100) and (111), interface formation 7-21773
Si, MBE on Si, role of surface reconstruction, LEED, Rutherford backscattering, channelling meas. 7-7034
Si, planar channelled protons, breakthrough angles 7-21308
Si, proton channelling, energy loss and straggling, inner shell electron collision calcs. 7-63699
Si, reactive ion etching, near-surface disorder, surface residues 7-16846
Si, reactive sputter etching, damage removal methods 7-17742
Si, self-implanted, defects and amorphisation 7-2041
Si single cryst., electron axial and planar channelling, gamma-ray emission studies 7-44636
Si single crystals, insulating cpd. form. by ion beam synthesis, RBS, SIMS and cross-sectional TEM studies 7-26779
Si substrate, anisotropic dry etching effects on surface props., XPS, ion channelling and Raman scatt. studies 7-28229
Si, surface damage induced by low energy ion sputtering (*Chinese*) 7-6693
Si wafers, self and ion beam annealing, epitaxial growth and damage layer, TEM study 7-12172
Si:Al, atom and acceptor depth distributions of channelled Al as a function of ion energy and crystal orientation 7-21247
Si:As, ion implanted, rapid thermal annealing, metastable activation 7-16616
Si:As⁺, heavily doped, ion implant deactivation 7-17567
Si:B, ion implanted, defect and dopant depth profile studies 7-2045
Si:BF₄⁺(PF₆⁺), ion implantation damage, backscattering channelling meas. 7-63675
Si:D, ion implanted, channelling meas. 7-16597
Si:In, substitutional ion implanted dopants, electron and positron channelling studies 7-26778
Si:P(Al), random and channelled implantation profiles and range parameters of dopants 7-21246
Si:Sn, ion implanted, annealing behaviour, channelling and conversion electron Mössbauer spectroscopy 7-13485
Si:Zn, amorphous-crystalline interface, backscattering and channelling study 7-6663
Si/a-SiO₂/ZrO₂-Y₂O₃, SOI system fabrication, charact. 7-22025
Si-CaF₂-Si heteroepitaxial structures, MBE grown, twinning, topography, channelling, TEM, SEM 7-12566
Si-Fe, ion implanted, channelling/RBS studies 7-2039
Si-Ge-Si epitaxial layer structs., particle channelling study, statistical equil. 7-58386
β-SiC monocryst. thin films, ion implantation and annealing, amorphisation and recrystn. processes study 7-16596
SiC single cryst., electron channelling patterns, lack of centrosymm. effects obs. and calcs. 7-51901
SiO₂ native oxide, ion and electron bombardment induced surface modifications studies 7-12175
TaH_{0.07}, lattice location of H by channelling method 7-1975

channelling radiation
atomic displacements detection using channelled electron induced X-ray emission 7-21311
charged particle channelling in solids 7-38081
diamond, channelling radiation spectra of high-energy electrons and positrons 7-27806
diamond, positron planar channelling radiation energy levels. variational calcs. 7-63696
diamond crystal, X-ray radiation generated by transmitting electrons, ang. distrib. and energy depend. 7-26819
diamond single crystals, relativistic positron channelling radiation, spectral density peak splitting studies (*Russian*) 7-21310
diamond struct., axial channelling radiation from positrons, dislocation effects 7-12180
electron radiation during channelling in crystals with a superlattice (*Russian*) 7-2077
emission spectrum of hyperchannelled positrons 7-21309
macroscopic scale systems, electron, positron and radiation quasi-channelling 7-63695
parametric X-ray channelling radiation spectral and ang. distrib. with extreme asym. diff. 7-44637
radiative energy loss of relativistic electrons and positrons in crystals during channelling, temp. depend. 7-21307
relativistic nuclei transmission through condensed matter, monochromatic photon source 7-64724
review of channelling processes 7-51898
strained layer superlattices, struct. effects on positron channelling radiation 7-63979
thin crystals, electron irradiat., Pendellosung radiation and coherent Bremsstrahlung 7-33476
Ge, electron channelling 7-21305
Ge, positron planar channelling radiation energy levels. variational calcs. 7-63696
Si, channelling radiation spectra of high-energy electrons and positrons 7-27806
Si, electron channelling 7-21305
Si, electron planar channelling radiation, temp. depend. 7-46172
Si, positron planar channelling radiation energy levels. variational calcs. 7-63696
Si single cryst., electron axial and planar channelling, gamma-ray emission studies 7-44636
Si single crystals, relativistic positron channelling radiation, spectral density peak splitting studies (*Russian*) 7-21310
W, electron channelling 7-21305

chaos
see also random processes
AC-driven damped 1D sine-Gordon system, phase-pulling and space-time complexity 7-48440
acetylene vibr. excited, chaos and dynamics on 0.5 to 300 ps time scale, Fourier transform spectra 7-42634
active media, quantum chaos 7-1062
anharmonic oscillator with two external periodic forces, chaotic behaviour 7-18624
anharmonic oscillators, dynamical behaviour 7-9707
anisotropic convective fluid, singularities in chaos transition 7-43915

chaos continued

annular chaotic areas, existence and properties 7-29901
 asymmetric map, inverse cascades obs., road to chaos 7-41258
 attractor lifetime in noisy co-dimension-two bifurcation 7-24545
 ball, bouncing, chaotic dynamics 7-35160
 Banach spaces, nonlinear integral operators and chaos 7-24543
 baroclinic chaos numerical anal. 7-57893
 beam, elastic, harmonically excited, chaos 7-43756
 Bianchi-IX cosmological model, chaotic behaviour 7-24509
 Bianchi-type VIII models, chaos in the long-term behaviour 7-60843
 bifurcations in a piecewise linear system 7-9769
 bifurcations in Lorenz's symmetric fourth-order system 7-18699
 binary mixtures near codimension-two point, externally modulated
 Rayleigh-Benard system, phase diagram 7-32602
 biochemical systems, chaos and noise effects 7-65680
 bis(methylammonium) copper tetrachloride, ferromag., parallel-pumped
 magnons, deterministic chaos obs. 7-52962
 bistable system, equistability criterion 7-35418
 Canard chaos in van der Pol's Equation 7-61254
 CDW systems, chaos 7-27321
 chain of coupled generators, chaos development, spatial synchronisation,
 bifurcation 7-48556
 chaotic dynamical processes, coexisting sinks 7-9759
 chaotic spin-glass phase, description in terms of $T=0$ fixed point
 7-45716
 characteristic exponents of chaotic repellers as eigenvalues 7-41250
 charged particle dynamics near parabolic magnetic field reversal, determi-
 nistic chaos 7-26389
 chemical kinetics, time delay effects in rate processes 7-39849
 circle mappings, renormalisation group methods 7-56168
 circle maps with bistable dynamics, basin-struct. invariance 7-9708
 circular cylinder in fluid flow, turbulence transition, wakes 7-6191
 coherent tunnelling, squeezing, chaotic behaviour and fractal dimension in
 a bistable potential 7-35410
 coherent tunnelling propagator and chaotic bistability 7-35315
 comet clouds in the solar system, chaotic motion 7-4372
 complex dynamics, chaotic and Newton's method 7-61241
 connectance effect on Lyapunov charact. exponents of products of sym-
 plectic random matrices 7-9768
 conservative dynamical systems, apparent fractal dimensions 7-24555
 convection, static, wavelike and chaotic, in spherical systems 7-1558
 cosmos, relaxation time for transition from isotropic turbulence to micro-
 scopic chaos (*German*) 7-29848
 Couette-Taylor flow, quasiperiodic to turbulent transition, strange attrac-
 tors 7-63120
 coupled anharmonic oscillators, algebraic reson. quantisation 7-24450
 coupled logistic maps for physico-chem. process modelling 7-59824
 coupled oscillator chain, random attractors, dimensionality and phys.
 props. 7-9774
 coupled oscillators, energy level statistics 7-41267
 coupled ring laser Lorenz systems, periodic-chaotic transition, stability
 anal. 7-62732
 cutting processes, chaotic oscillations 7-4764
 Cvitanovic-Feigenbaum eqn., complete soln. classes 7-14893
 delay-differential systems, statistics and dimensions 7-48572
 delayed circle map, torus oscillations and collision torus-chaos 7-9776
 deterministic representation of chaos in classical dynamics, with appl. to
 turbulence 7-61091
 diamagnetic Kepler problem transition to chaos 7-41247
 dielectric crysts., inelastic light scatt., chaotic behaviour 7-3062
 directly modulated semicond. lasers, gain nonlinearity effects calcs.
 7-20218
 disordered chains, fractal behaviour, 2D stochastic maps 7-41268
 dissipative dynamical systems, review 7-29909
 dissipative quantum maps 7-41266
 dissipative systems, transient chaotic distributions 7-4769
 driven quantum systems, level statistics and stochasticity 7-24561
 dye laser, synchronously pumped periodicity multiplication, optical chaos
 phenomena 7-31311
 dynamical system, chaotic, temporal intermittency as multifractality in
 history space 7-24549
 dynamical system, fractal dimension universality at period-doubling chaos
 onset 7-48570
 dynamical system with delayed feedback (*Chinese*) 7-35263
 dynamical systems describing turbulence, moments calc. 7-20692
 ergodic theory 7-62657
 exciton-biexciton two-oscillator model, chaos 7-31390
 exciton-phonon system, quantum chaos model 7-61231
 fat fractals in quantum chaos 7-4713
 Feigenbaum attractor, fractal dimension, calc., comments 7-35413
 finite Hubbard model with phonon coupling 7-12582
 finite subharmonic bifurcations and horseshoes in centrally symm. systems.
 (*Chinese*) 7-48549
 finite-state machines, chaotic behaviour, simulation 7-29905
 flow, chaotic, fast magnetic dynamos 7-37557
 fluid mixing (stretching) by time periodic sequences for weak flows
 7-31733
 forced plasma-maser effects, stochastic motion 7-51434
 forced relaxation oscillations, chaotic blue sky catastrophe 7-4768
 forced Selkov systems, chaos 7-4771
 fractal measures, scaling indices and routes to chaos 7-48624
 frontiers in fluid mechanics, book 7-4640
 gas lasers, multimode, total electric field strength, temporal evolution
 7-15848
 gas lasers, positive P representation and the laser equations 7-10909
 generalized dimensions and entropies from a measured time series
 7-41256
 generating function and its formal derivatives for dynamical systems
 7-18705
 geomagnetic attractor and 3-disc dynamo system, strange attractor, dimen-
 sions and K_2 entropies 7-3978
 Ginzburg-Landau eqn., spatial struct. of time-periodic solns. 7-48576
 Ginzburg-Landau eqn. soln. integrability and structural stability 7-37480
 global spectral characterization of chaotic dynamics 7-41272
 Hamiltonian systems of n dimens., stability-instability transitions
 7-56159
 Henon's dissipative map, quantized, period doubling, renormalization
 group anal. 7-56067
 HF power spectra for systems subject to noise 7-61247
 high energy particle reactions, approach to chaos 7-49187

chaos continued

high-dimensional chaotic attractor in infinite-dimensional phase space
 7-9765
 homogeneous chem. system, entropy prod. rate 7-13721
 hybrid optically bistable device, characterization of chaos 7-9773
 inflation, effects of nonrenormalisable terms 7-29558
 information processing using chaotic strange attractors 7-48578
 intermittency, symbolic approach 7-61242
 intermittency caused by chaotic modulation, anal. using multiplicative
 noise model 7-35416
 intermittency in chaotic systems and Renyi entropies 7-24550
 intermittency-type chaos, pattern competition as origin 7-61239
 intermittent chaos, global spectral structs. for periodic laminar motions
 with turbulence 7-41271
 intermittent chaos, spectral structure 7-4767
 internally resonant double pendulum, parametric excitation, chaotic behav-
 iour 7-29748
 inverse Poincare halfmaps 7-61251
 islands around islands, class renormalisation 7-222
 iterated mappings, one-dimensional, chaos and fractal dimension of
 strange repellers 7-9775
 Josephson junction with time-independent driving current, chaotic behav-
 iour 7-52904
 Josephson junctions, chaos, quantum effects 7-52905
 kicked pot, classical and quantum chaos 7-41277
 Kolmogorov flow, 2D turbulence, nonlinear chaotic eqn., asymptotic study
 (*French*) 7-37440
 Kolmogorov-Arnol'd-Moser barriers in the quantum dynamics of chaotic
 systems 7-35336
 large-scale neuron-glia network dynamics, chaotic behaviour 7-23327
 laser, Lorenz-type chaos 7-36932
 laser model, Lorenz equation with symmetry breaking, quantum chaos
 7-50525
 laser-driven molecules, bistability and chaos 7-15920
 lasers, chaotic dynamical behaviour 7-10907
 Lorenz attractor, effective noise, stochastic differential eqn. 7-223
 Lorenz laser, time averaged output power in self-pulsing and chaotic
 regime 7-62652
 Lorenz system, phase description method for time averages 7-18704
 Lorenz-type flows, universal scenarios for chaos onset 7-230
 loudspeaker, direct radiation, bifurcation and chaos 7-31608
 low-dimensional chaotic attractor, appl. to characterisation of solar radio
 pulsation event 7-66552
 magnetic systems, Monte Carlo simulations, digital dynamics and chaotic
 behaviour 7-22083
 metric entropy estimation 7-61244
 Mixmaster universe, quantum chaos 7-9742
 multimode lasers, bifurcation successions 7-57294
 near integrable PDE, quasiperiodic route to chaos 7-41269
 nematic liquid crystals, EHD instabilities (*Japanese*) 7-1879
 noisy maps, probability distrib. moments 7-41257
 nonlinear conservative oscillatory system, route to chaos 7-29903
 nonlinear dynamical systems, chaotic transients critical exponent calcs.
 7-232
 nonlinear dynamical systems, fat fractals and scaling exponents 7-24559
 nonlinear oscillator, 1/2 subharmonic resonance and its transition to chaos
 7-29741
 nonlinear oscillators, weakly coupled systems, chaos and order 7-56164
 nonlinear time evolution eqns., bifurcating periodic solns. 7-48562
 nonlinear waves, bifurcation, stability and symmetry 7-41116
 nuclei, chaotic motion, stat. props. 7-30402
 Onchidium pacemaker neuron, harmonic response instability 7-23330
 one-dimensional maps, dynamical fractal props. 7-41255
 one-dimensional modal maps, topological entropy (*Chinese*) 7-35397
 one-dimensional quantum systems, spatial structures and dynamic excita-
 tions, self-consistent theory 7-44755
 one-way coupled subsystems, critical behaviour at the transition to chaos
 7-41314
 open-flow systems, rel.-depend. Lyapunov exponents as measure of chaos
 7-61240
 optical bistability, chaotic motion, dimension meas. 7-62768
 optical cavity with phase conjugate mirror, transverse-mode instability and
 chaos 7-37052
 optically bistable and tristable systems, self pulsing and chaos 7-11049
 order to chaos transition, expt. 7-41
 Pacific Ocean, chaotic behaviour in large and mesoscale motions of Kuro-
 shio current 7-55073
 parallel pumping in ferromagnets, nonlin. dynamics 7-53145
 pendulum period doubling route, critical line, scaling relations 7-79
 pendulums, deterministic chaos, investig. 7-4762
 period-doubling bifurcations, crossover from dissipative to conservative
 behaviour 7-233
 period-doubling systems, chaotic band merging, spectral peak broadening
 7-218
 periodic chaos, characteristic structs. of power spectra, universal recursion
 relations 7-41270
 periodic trajectories for nonintegrable 2D Hamiltonians 7-48448
 periodically, driven particle, in asymmetric pot. well, chaotic motion
 7-29904
 perturbed periodic Toda chain, chaos upon soliton decay 7-41299
 phase space exploration, quantum localisation 7-61245
 photon statistics of damped harmonic oscillator with initial squeezed state
 7-43027
 pictorial nonlinear feedback, chaos, cooperation and quantised feedback
 7-42947
 pictorial nonlinear feedback, chaos, cooperation and stability 7-42946
 pictorial nonlinear feedback, chaos and cooperation 7-42945
 Poincare halfmaps, separating mechanisms 7-48580
 predator-prey eqns., global anal. 7-14757
 primordial inflation with broken symm. gravit. theory 7-14840
 propagation of molecular chaos theorem, hierarchies 7-56047
 pseudosphere, chaos, quantal description, review 7-24556
 quadratic map with swept parameter, postponed bifurcations 7-14865
 quantum chaos with nonergodic Hamiltonians 7-200
 quantum description of chaotic systems, complete integrability 7-9705
 quasi-periodic motion, chaotic transition, expt. observation 7-48566
 quasiperiodic maps, renormalisation procedure 7-220
 randomness, chaos and prediction 7-56165
 renyi dimensions from local expansion rates 7-61243
 repellers, chaotic, smooth stationary distrib. 7-225

chaos continued

RF driven plasma, low-dimensional chaos in a driven damped non-linear Schrödinger equation 7-6408
scaling factors $\alpha(z)$ and $\delta(z)$, for period-doubling route to chaos 7-35411
semiconductor lasers, nonlinear dynamics and chaos 7-62703
semiconductor self-pulsing lasers, quasiperiodic route to chaos under large signal current modulation 7-62706
shear flow, resonant fast dynamo 7-20808
simulating chaos in lasers 7-61253
sine-Gordon chain, driven, bispectral anal. 7-29773
sine-Gordon soliton, pinned to impurity, chaotic motion 7-103
sine-Gordon system, space-independent, horseshoe chaos 7-56451
smooth Smale horseshoes, statistical props. 7-48584
spatial chaos, in 1D patterns, complexity 7-41262
spatio-temporal coherence and chaos, conf. Los Alamos, USA, Jan. 1986 7-48158
spin systems, quantum chaos nature 7-18698
spiral waves in the Belousov-Zhabotinskii reaction 7-8271
SQUID, DC, noise effect on instabilities and chaotic solns. 7-52908
SQUID, DC, noise effect on instabilities and chaotic solns. 7-52909
stable attracting sets, in dynamical systems and in their one-step discretizations 7-35417
statistical physics and field theory conf., Groningen, Netherlands, Aug. 1985 7-55899
stochastic transitions through quasiperiodic oscillations, num. and expt. investg. 7-35419
Stokes flow, chaotic advection 7-31737
Stokes flow, Lagrangian turbulence, chaotic particle motion 7-31754
storage rings, dynamic aperture and transition to chaos 7-36348
strange attractors in self-excited ring systems with inertial links 7-41278
superconducting quantum interferometer, anal. 7-18873
surface waves in cylinder of fluid oscillated vertically, low-dimensional chaos 7-11442
symmetry-breaking bifurcations for the standard mapping 7-29906
Taylor-vortex flow, dynamical system 7-11434
tent map, invariant distrib. of non-fully developed chaos 7-4760
three-body problem, chaotic instability 7-41246
topological entropy and chaos of interval maps 7-56158
trajectories near a separatrix using the matching method 7-56166
transition to chaotic convection 7-11422
transition-strength fluctuations and the onset of chaotic motion 7-35335
turbulent diffusion, chaos-induced, diffusivity 7-43885
two-frequency dynamical systems, rotation interval from a time series 7-61088
two-level atoms, coherently driven superradiant system, symmetry breaking, metastable chaos 7-50524
two-level system coupled to a boson mode, large- n limit, chaos 7-35403
two-level system in semiclassical radiation field, quantum chaos 7-9770
universal strange attractor underlying Hamiltonian stochasticity 7-56163
universal transition between Hamiltonian and dissipative chaos 7-228
weakly turbulent interfaces, order and complexity in Kuramoto-Sivashinsky model 7-43864
whisker mapping, 1/f noise spectrum of chaotic motion 7-4765
Ba₂NaNbO₅ single crystals, spatio-temporal electrical instabilities 7-52632
BaTiO₃ self-pumped phase conjugate mirror, instabilities 7-62790
CO₂ laser, chaotic attractors in crisis 7-43178
CO₂ laser, gain-modulated single mode CW laser instabilities and chaos 7-43057
CO₂ laser, modulated, single-mode, dynamic behaviour and dimens. chaos 7-1074
CsMnF₃ antiferromagnet, parametrically excited magnon redistrib. and chaos 7-17167
n-GaAs, oscillations and chaotic current fluctuations 7-64253
p-Ge, electric avalanche breakdown, chaotic and hyperchaotic states 7-52630
Ge, extrinsic, freq. locking, quasiperiodicity and chaos 7-2618
Ge, extrinsic photoconductors, nonlinear dynamics and chaos 7-52685
p-Ge, nonlinear I-V characts. and spontaneous current oscillations 7-52631
p-Ge, spatial correlations of chaotic oscillations in post-breakdown regime 7-64255
H atom, energy levels in mag. field, quantum chaos and statistical props. 7-19765
H, Hamiltonian system, regularity and irregularity transition 7-56083
H, microwave ionisation below classical chaos border 7-57142
³He, superfluid, driven longitudinal nuclear spin resonance, Smale's horseshoes 7-2292
LiNbO₃ SAW bifurcation and chaotic state obs. 7-2333
NH₃ lasers, FIR, instabilities and chaotic emission 7-15849
NH₃ Raman laser, single-mode homogeneously broadened, self-pulsing instabilities 7-10922
Nb-In point contact, observation of chaotic noise 7-7445
NbSe₃, CDW conductor, broken coherence, chaos, noisy precursors 7-64126
NbSe₃, CDW conductors, mode locking phenomena and routes to chaos 7-52474
Nd doped Z, 7-62713
TaS₃, CDW conductors, mode locking phenomena and routes to chaos 7-52474
YIG, charact. of chaotic states of parallel-pumped magnons 7-52961

characteristic temperature see Debye temperature

characteristics measurement

see also headings for specific characteristics, e.g. gain measurement;
viscosity measurement
cavity-mounted press. transducer, input press. effects on freq. characts. 7-37595
ceramics, props. meas., conf., Soverato, Italy (Sept. 1986) 7-9582
FEU-130 photomultiplier characts. meas. 7-30889
LEED intensity meas. using real-time digital video processor 7-44317
liquids complex adiabatic compressibility and adiabatic pressure-induced temp. variation meas. 7-21316
photomultiplier with bialkali photocathode, wavelength dependence of quantum efficiency determ. 7-18879
photovoltaic array I-V characteristic measurement error 7-3688
piezoelectric actuators for scanning tunnelling microscopy, behaviour and calibration 7-18926
piezoelectric solids elastoelectric response to cyclic stresses obs., using computerised system 7-39810

characteristics measurement continued

scanning camera with line CCD sensor for use in schools (Slovak) 7-29646
solar cell volt-ampere characts. meas., generator of intense millisecond light pulses 7-34042
solar cells volt-ampere characts. meas. (Slovak) 7-39994
spectral response meas. apparatus, microcomputer controlled, for large area solar cells 7-3642
thermodynamic props. of solids determ., by adiabatic pressure variation method 7-2230
thermoelectric rapid inspection, contacts temp. effects 7-2580
transient time constants determ., three point method 7-286
Al_{1-x}Ga_xAs bandgap determ. by Schottky barrier spectral response meas. 7-2667
Si solar cell parameters evaluation method 7-23159
a-Si:H thin film solar cells, accelerated stress testing using photodiode array 7-28403
charcoal
see also carbon
fusion reactors, charcoal sorbents for He cryopumping 7-62077
charge (electric) see electric charge
charge compensation
see also crystallography
alumina, ion-rich β - and β'' -phases, superionic props., local and long-range order determ. 7-21519
CaF₂:Ce³⁺, two-photon absorpt. cross section, anal. of lowest 4f-5d transition 7-46081
CuInSe₂ thin films, polycrystalline, elec. props., effect of excess Cu 7-52871
GaN:Zn, pure and doped, electrophysical props., nonhomogeneous semiconductor, model 7-27292
InP:Ti, Hg, semi-insulating, impurity electron state compensation mechanism, SIMS, SSMS, EPR and Hall effect meas. 7-64164
LiF, electrification mechanism during cleaving 7-44621
Li_x(NH₄)_y(NH₃)_zTiS₂(³⁺)⁺ intercalation cpd., NH₃ oxidation, charge compensation 7-32354
Si:P, quenching thermoelect. prod. Hall effect, EPR meas. 7-27293
ThCl₄:Gd³⁺, impurity-vacancy centre EPR probe for incommensurate phase 7-17220
 β -ThCl₄:Pr³⁺, site selective laser fluorescence spectroscopy 7-64687
Y_{4-x}Zr_{1-4x}O_{2-2x}, ionic cond., defect struct., self-diffusion calcs. 7-12356
ZnS, rare earth impurities, electrolum. of Schottky barriers, photolum., charge compensation, and impurity electron states 7-64700
charge-coupled device arrays. see charge-coupled device circuits
charge-coupled device circuits
see also CCD image sensors
vertex detection in high energy physics expt., use of CCDs 7-42334
charge-coupled device imagers see CCD image sensors
charge-coupled devices
see also charge-coupled device circuits
line-scan image sensor for meas. of red cell vel. in microvessels 7-8777
AlGaAs-GaAs MQW CCD spatial light modulators using electroabsorption effects 7-20407
GaAs CCD, high resistivity gate struct., radiation effects 7-6683
charge density waves
7-33386
1D CDW systems, collective modes and impurity effects 7-21832
1D electron-phonon systems, nearly quarter-filled, CDW struct. 7-45186
3d- and 4f- metals, periodic spin structs., critical props. calcs. (Russian) 7-59031
alkali metals, CDW instabilities and thermoelec. parameters 7-12707
(BMDT-TTF)TCNQ, molecular conductor, dimensionality, struct. and electrical props. 7-52595
breakable CDWs in quasi-1D systems 7-64124
bronzes, structs., sliding motion of CDW 7-64129
chaos in CDW systems 7-27321
d- and f-metals and alloys, anomalous props. due to charge density fluctuations 7-7132
deformable sliding CDW, mode locking and interference phenomena 7-21836
dense Kondo heavy fermion systems, Cooper pairs attractive interactions freq. depend. 7-58951
depinning and quasi-commensurate transition, plastic deformation analysis 7-12628
depinning by quantum tunnelling 7-64121
dissipative incommensurate chain, response to large driving pulses 7-7215
dynamics, model, nonuniversal crit. behaviour 7-12632
dynamics and finite size effects in CDW conduction 7-64221
dynamics and finite-size effects 7-45292
elasticity, phenomenological model 7-52472
electron plasma, pure, strong mag. field states 7-45185
electron-phonon system in 1D (Rumanian) 7-16960
electronic cond. in presence of ϕ solitons 7-27322
electronic struct. of density wave systems effect of mag. fields 7-52467
fractional quantum Hall effect of a multicomponent fermion system, collective excitations 7-21835
frequency depend. response of pinned CDW condensates 7-64135
Ginzburg-Landau theory for hysteresis in CDW systems 7-7136
glassy CDW in 3D, numerical studies 7-64128
high-current electron beams, Buneman instability in neutral gas, ion collective acceleration 7-49749
impurity pinning and depinning, quantum effects 7-52464
impurity pinning of 1D-CDW, role of commensurability energy 7-52456
incommensurate, kink lattice structure and midgap band 7-45187
incommensurate CDW systems, discommensuration domain walls, coherent polaron superlattices and long-range Coulomb forces 7-45184
incommensurate CDW systems, long-range Coulomb effects 7-45189
incommensurate one-dimensional CDW systems, localised electronic state form. due to phase and single particle excitations 7-21834
kink dynamics, breathers, narrow band noise 7-52463
layer crystals dynamics, long wavelength vibr., factor group anal. 7-58424
metal chalcogenides, low-dimensional, synthesis and CDW props. 7-32926
metals, positron annihilation studies, review 7-46180
metastability and nonlinear dynamics of sliding charge density waves 7-52470
microscopic theory in path integral formulation 7-27273
mode locking in an infinite set of coupled circle maps 7-52457

charge density waves continued

- morpholinium TCNQ₂ salts, optical phonon mediated charge transport 7-52596
- nonlinear AC and DC conduction of CDW systems, Fukuyama-Lee-Rice model 7-64214
- nonlinear transport due to driven collective modes 7-52473
- one-dimensional CDW states, self-similar band structure and electron-phonon coupling 7-21833
- one-dimensional conductors, conf., Kyoto, Japan (June 1986) 7-60872
- one-dimensional conductors, electron-phonon backscatt. and phonon dynamics calcs. 7-38468
- one-dimensional electron-phonon Peierls condensate, amplitude solitons 7-52449
- one-dimensional electron-phonon system, CDW structure 7-52444
- one-dimensional incommensurate systems, Stark-Wannier resonances and delocalisation in finite elec. field 7-12671
- one-dimensional interacting electron systems, charge density and superconducting fluctuations 7-22061
- Peierls instabilities, soliton lattice in the relative phase of two coupled charge-density waves 7-21816
- Peierls-CDW state, 1D, impurity distrib., 2k_F distortion 7-44593
- phase slip centre as a dynamic amplitude soliton 7-52465
- pinned CDW, disequilibrium by slight temp. changes 7-64131
- polar semiconductors, negative momentum relaxation rate and transport 7-12712
- polyacetylene, alkaline metal doped, ab initio SCF MO calc. of electronic struct. 7-64048
- polyacetylene, CDW, interaction and disorder 7-64136
- polyacetylene, Raman scatt. from CDW, ab initio calcs. 7-46015
- quasi 1D conductors, anisotropy and Peierls transition 7-45297
- quasi-1D conductors, conf., Yamanashi, Japan (May 1986) 7-60868
- quasi-1D conductors, Peierls state, mechanisms of nonlinear conductivity, electrodynamics (Russian) 7-32997
- quasi-2D strongly-coupled electron-phonon systems, CDW and superconductivity, polaron theory 7-58750
- quasi-one-dimensional density-wave systems, electronic struct., high mag. field effects 7-58754
- quasi-one-dimensional system, CDW and singlet-supercond. phases 7-7219
- quasi-one-dimensional system, simulation of CDW transition 7-32928
- resistivity saturation in metals with structural instabilities 7-45277
- sliding CDW in low-dimensional conductors 7-17018
- sliding CDW systems, dielectric relax. freq. 7-45293
- sliding CDWs, dynamics 7-64122
- spatio-temporal coherence and chaos, conf. Los Alamos, USA, Jan. 1986 7-48158
- statics and dynamics, study based on Fukuyama-Lee-Rice model 7-64127
- strong coupling electron systems, CDW, supercond., effect of randomness 7-27459
- structural and magnetic instabilities in low-dimensional systems 7-59034
- superconducting materials, advances and developments (French) 7-27476
- surface (110), calculated photoemission spectra 7-3151
- switching, phase-slip model 7-52700
- transition metal chalcogenides, low dimensional, charge density waves, formation and characts. 7-2515
- transition metal compounds, layered, structural phase transitions, book 7-41021
- transition metal dichalcogenides, CDW states 7-44810
- transition metal dichalcogenides, CDW transition effects of lattice fluctuations 7-21831
- transition metal dichalcogenides, layered cpds., CDWs 7-2523
- transition metal layered compounds, CDW phase transitions; Landau theory 7-44809
- transitional metal layered compounds, structures phase transitions, lattice fluctuations, microscopic theory 7-44808
- transport properties, effect of inertial term, existence of subharmonic steps, perturbation anal. 7-64119
- TTF-TCNQ, dielec. function in submillimetre range 7-27282
- TTF-TCNQ, nonlinear elec. transport effects driven through CDW commensurability 7-45295
- TTF-TCNQ, nonlinear electrical transport effects, CDW commensurability 7-64217
- two dimensional, electron gas, partially occupied Landau level, dielec. const. RPA calcs. 7-64139
- uncommensurate charge density wave system, phenomenological Lagrangian 7-38474
- Ag-Mg, commensuration and discommensuration characteristics, modulation periods 7-46463
- BaPb_{1-x}Bi_xO₃, semicond. phase, CDW gap, optical meas. 7-53328
- BaPb_{1-x}Bi_xO₃, superconductivity and metal-semicond. transition 7-58940
- Cr alloys, charge and spin density waves (Russian) 7-2514
- Cr, zero field muon spin rotation study 7-45871
- K, CDW phason anisotropy, NMR linewidth 7-27614
- K, charge density waves, satellite patterns 7-38471
- K film, clean and contaminated, CDW search using EELS 7-53462
- K₃CuS₆, mixed valence 2D metal, CDW 7-45294
- K_{0.3}MoO₃, blue bronze, microwave conductivity 7-45370
- K_{0.3}MoO₃, blue bronze, CDW state, nonlinear transport 7-64222
- K_{0.3}MoO₃, blue bronze, broadband noise 7-64223
- K_{0.3}MoO₃, CDW conductor, elastic anomalies 7-44652
- K_{0.3}MoO₃, CDW current density-voltage relation near the depinning threshold 7-58798
- K_{0.3}MoO₃, CDW state, metastable EPR study 7-53125
- K_{0.3}MoO₃, CDW state, metastability and dynamics 7-64130
- K_{0.3}MoO₃, CDW system, stretched exponential dielec. relax. 7-45929
- K_{0.3}MoO₃, CDW transport, crystal quality, inhomogeneous conductivity, contact geometry 7-52587
- K_{0.3}MoO₃, electric field hysteresis and relax. 7-52462
- K_{0.3}MoO₃, electric field induced deformation of sliding CDW 7-64133
- K_{0.3}MoO₃, excess low-temp. sp. ht., CDW state 7-12311
- K_{0.3}MoO₃, nonlinear conduction below 4.2K 7-52588
- K_{0.3}MoO₃, nonlinear effects and inductive response of dissipative incommensurate chain 7-52471
- K_{0.3}MoO₃, quasi-1D cpd., depinning of CDW, analogy with elastic-plastic transitions in metallurgy 7-64132
- K_{0.3}MoO₃, switching, intermittent oscillations 7-52699
- K_{0.3}MoO₃/Fe, CDW state, Mossbauer studies 7-53112
- K_{0.5}MoO₃, electronic struct., room temp. UV photoemission spectra study 7-46272
- K₂Pt(CN)₄Br_{0.3}·3.2H₂O, disordered CDW cpd., Coulomb-induced pseudo-critical behaviour 7-45188

charge density waves continued

- La₂Mo₂O₇, quasi-2D single cryst. struct. and electronic props. studies 7-58238
- (Li_{1-x}M_x)_{0.9}MoO₃ (M=K,Na), superconductivity and CDW 7-45541
- Li_{0.9}(Mo_{1-x}W_x)O₁₇, superconductivity and CDW 7-45541
- Mo₈O₂₃, low-dimensional conductors, inelastic neutron scatt. study 7-52701
- Mo_{0.9}W_{0.1}O_{3n-1}, electrical conductivity, mag. susceptibility and IR spectra 7-38546
- NbSe₃, nonlinear effects and inductive response of dissipative incommensurate chain 7-52471
- Na, induced torque and CDW ground state 7-2838
- NbSe₃, CDW motion and relax., thermally initiated phase-slip 7-38544
- NbSe₂, 2H polytype, CDW phase transition study by means of positron annihilation 7-38476
- NbSe₃, CDW and magnetotransport, mag. field effects to 230 kG 7-64215
- NbSe₃, CDW coherence, breaking under inhomogeneous conditions 7-64125
- NbSe₃, CDW conduction and periodic current noise 7-21896
- NbSe₃, CDW conductor, nonlinear charge transport mechanism 7-2599
- NbSe₃, CDW conductor, interference effects with AC+DC excitations 7-52475
- NbSe₃, CDW conductor, broken coherence, chaos, noisy precursors 7-64126
- NbSe₃ CDW conductor, magnetothermopower studies 7-64226
- NbSe₃, CDW conductors, mode locking phenomena and routes to chaos 7-52474
- NbSe₃, CDW depinning under mag. field 7-64216
- NbSe₃, CDW gap, tunnel junction spectra 7-21897
- NbSe₃, CDW magnetodynamics, complex AC cond. meas. 7-32998
- NbSe₃, conduction noise obs., pulsed electric field, nonohmic regime 7-64219
- NbSe₃, current oscillations in CDW transport 7-32999
- NbSe₃, differential resist., expt. versus classical model of deformable CDWs, interference phenomena and mode locking 7-64212
- NbSe₃, harmonic mixing at large microwave power levels 7-64141
- NbSe₃, inertial dynamics of pinned CDW condensates 7-7217
- NbSe₃, microwave harmonic mixing below threshold 7-64140
- NbSe₃, NMR study of CDW struct. and motion 7-2518
- NbSe₃, scaling behaviour, high field CDW transport, role of free carrier damping 7-64224
- NbSe₃, thermally initiated phase-slip in CDWs 7-64123
- NbSe₃-I-Pb, tunnel junctions under press. 7-52594
- (NbSe₄)_{0.3}/I, AC conductivity, dielectric constant 7-52591
- (NbSe₄)₂, lattice vibrs. at CDW transitions 7-51973
- (NbSe₄)₃, quasi-1D, sp. ht., phason and low-energy excitation contribs. 7-21479
- NbTe₄, quasi-1D conductivity, CDW state effects 7-64213
- Pt complex, (H₃O)_{0.33}Li_{0.8}(Pt(C₄N₂S₂))_{1.67}·H₂O, synthetic conductor, spin-carrying defects 7-44524
- Rb_{0.3}MoO₃, blue bronze, CDW state, nonlinear transport 7-64222
- Rb_{0.3}MoO₃, CDW current rigidity under inhomogeneous conditions 7-45303
- Rb_{0.3}MoO₃, CDW current density-voltage relation near the depinning threshold 7-58798
- Rb_{0.3}MoO₃, CDW transport, crystal quality, inhomogeneous conductivity, contact geometry 7-52587
- Rb_{0.3}MoO₃, IR reflectivity and Raman scatt. from midgap-state exciton-polaritons 7-33386
- Rb_{0.3}MoO₃, NMR evidence of Frohlich mode 7-53156
- Rb_{0.3}MoO₃, sliding motion of CDW, NMR study 7-64134
- TaS₂, 1T polytype, CDW transition obs. by positron annihilation 7-39267
- TaS₃, CDW conduction and periodic current noise 7-21896
- TaS₃, CDW conductors, mode locking phenomena and routes to chaos 7-52474
- TaS₃, current oscillations in CDW transport 7-32999
- TaS₃, disequilibrium of pinned CDW state 7-32927
- TaS₃, monoclinic, CDW conduction under RF field 7-52590
- TaS₃, nonlinear effects and inductive response of dissipative incommensurate chain 7-52471
- TaS₃, orthorhombic, CDW state, point contact study 7-52468
- TaS₃, orthorhombic, inertial dynamics of pinned CDW condensates 7-7218
- TaS₃ quasi-1-D conductor, nonlinear effects in small samples 7-17020
- TaS₃ quasi-1-D conductor, laser-induced EMF and CDW effects 7-17053
- TaS₃, quasi-1-dimens. conductor, dynamic behaviour, possible electronic appls. 7-38548
- TaS₃, quasi-1D conductor, submicron transverse dimensions, jumps between metastable resistance states 7-38547
- TaS₃, scaling behaviour, high field CDW transport, role of free carrier damping 7-64224
- TaS₃ sliding CDW conductor, narrow-band noise freq. modulation and AC-DC mixing 7-52711
- TaS₃, small orthorhombic samples, nonlinear effects 7-64220
- TaS₃, uniaxially deformed, DC induced voltage oscillations 7-52589
- TaSe₂, 1T, submillimetre conductivity, dielectric function 7-12749
- TaSe₂, 2H polytype, CDW transition obs. by positron annihilation 7-39267
- TaSe₂ crystals, 2H polytype, positron meas., CDW phase transition 7-46202
- (TaSe₄)₂I, AC conductivity, dielectric constant 7-52591
- (TaSe₄)₂I, chain-like conductor, Peierls gap, optical study 7-52469
- (TaSe₄)₂I, ID CDW system, positron annihilation 7-39272
- (TaSe₄)₂I, lattice vibrs. at CDW transitions 7-51973
- (TaSe₄)₂I, linear chain conductor, elastic behaviour 7-52466
- (TaSe₄)₂I, low-dimensional conductors, inelastic neutron scatt. study 7-52701
- (TaSe₄)₂I, quasi-1D, sp. ht., phason and low-energy excitation contribs. 7-21479
- (TaSe₄)₂I quasi-1D chain cpd., thermoelec. power temp. depend. meas. 7-17045
- TaTe₄, quasi-1D conductivity, CDW state effects 7-64213
- TiSe₂, 1T polytype, CDW transition effects of lattice fluctuations 7-21831
- URu₂Si₂, heavy electron system, competing electronic correlations, press. effect 7-45539
- VSe₂-1T, distorted struct., convergent beam diffraction study 7-16528

charge exchange

for charge exchange in particle and nuclear physics see elementary particle interactions and nuclear reactions and scattering
 see also charge transfer states; ionisation
 aliphatic amines, proton affinities anal. using Kitaura-Morokuma scheme and MINDO/3 method 7-62286
 alkali halides, interionic potentials based on charge transfer model 7-58197
 atom-ion, reaction dynamics, crossed mol. beam collisions 7-57167
 atom-ion collisions, electron capture, first order Born perturbation theory 7-10746
 atom-ion collisions, electron capture, off-shell Coulomb radial wavefunctions soln. 7-62520
 atom-ion collisions, electron transfer, bibliography of investigs. 7-20007
 atom-ion collisions, K shell charge transfer cross sections, symmetric eikonal theory 7-50328
 BAs, structural and electronic props., pseudopotential method, local density approx. 7-32353
 benzenoid hydrocarbons, charge transfer spectra and struct. reson. theory 7-57165
 benzophenone in diethylaniline, photolysis, excited triplet state with charge transfer struct. 7-42753
 biferrocene, intervalence transfer electronic absorpt. band energy, press.-induced freezing effect 7-25507
 biferrocenium hexafluorophosphate, intervalence transfer electronic absorpt. band energy, press.-induced freezing effect 7-25507
 biferrocenium triiodide, intervalence transfer electronic absorpt. band energy, press.-induced freezing effect 7-25507
 binary crystals, structural stability, chem. trends 7-21153
 bipolar batteries with common electrolyte paths, leakage currents 7-28392
 bis(4-aminophenyl)sulphone, twisted intramol. charge transfer and solvent dynamics, time resolved fluoresc. spectra 7-50232
 9,9-bis(acridizinium-yl), fluorese. quenching, solvent depend. (German) 7-940
 1,3-bis(dicyanomethylene)-2-[4'-(N,N-diethylamino)phenylimino]indane, X-ray diffr. struct. determ. 7-12044
 bound state existence confirmation for atomic and mol. projectiles inside solid targets, expt. investig. (French) 7-22427
 ((bpy)₂ClRu)₂pyz(PF₆)₂, intervalence transfer electronic absorpt. band energy, press.-induced freezing effect 7-25507
 charge exchange cross section meas. (Chinese) 7-5765
 chemical reaction and charge-transfer processes, RIOSA quantum-mechanical study. 7-31159
 chlorophyll photoelectrochemical solar cell, photoresponse, temp. effect 7-54324
 cobaltocene, gaseous, self-exchange electron-transfer kinetics, Franck-Condon barriers 7-36745
 cyclobutenediylic dyes, electron transfer rate consts. and fluorese. lifetime determ. 7-25587
 cytochrome c, electron transfer rate meas. 7-5760
 dicyanoethylene electron affinity, electron transfer equilibria 7-10741
 diffuse interstellar bands, charge transfer model 7-55787
 dimethyldioctadecylammonium bromine, charge-transfer-to-solvent transition, far-UV absorpt. spectra 7-57081
 dimethyldioctadecylammonium chloride, charge-transfer-to-solvent transition, far-UV absorpt. spectra 7-57081
 dimethyldioctadecylammonium iodide, charge-transfer-to-solvent transition, far-UV absorpt. spectra 7-57081
 DNA, electric charge transfer phenomena, TSC investig. (Czech) 7-13948
 electrochemical, electrode pot. effects 7-13784
 electronic nonequilibrium, kinetic eqns. (German) 7-3593
 elements, charge distrib. in ion beam produced from RF-spark ion source 7-46883
 ethane, intramol. interactions, NOLMO calcs. 7-10411
 ferrocene, gaseous, self-exchange electron-transfer kinetics, Franck-Condon barriers 7-36745
 graphite-K intercalation cpd., C₈K, electronic band struct., angle resolved UPS study 7-27232
 haeme proteins, ligand binding and electron transfer rates, spin-boson models 7-13952
 HMTTeF-TCNQF₄ solid complex, partial charge transfer, Raman and XPS studies 7-32967
 ice biological charge transfer processes, IR and microwave spectra 7-3749
 interstellar 220 nm extinction feature, charge transfer model 7-55787
 ion+molecule, reaction dynamics, crossed mol. beam collisions 7-57167
 ion+surface slow collision, neutralisation probability, complex energy Demkov model 7-22432
 ion transfer across interfaces between two media, kinetics 7-32687
 ion-scattering spectroscopy, shadowing and focusing effects 7-53491
 ion-surface collisions, excited state form. dist., reson. charge exchange, multichannel theory 7-46266
 laser assisted charge exchange reactions, theoretical and expt. investig. (French) 7-5759
 lattice geometry changes upon charge transfer 7-6564
 low vel. charged microspheres, interaction with extended surfaces 7-59308
 (M-OH₂)⁺ complexes, charge transfer and electric mobility, ab initio SCF calcs. 7-62253
 mammalian ferritin, binding of Fe²⁺ 7-59917
 manganocene, gaseous, self-exchange electron-transfer kinetics, Franck-Condon barriers 7-36745
 metal surfaces, field adsorption of rare gases 7-21648
 metalloporphyrin polystyrene covalent complex, electron transfer reaction 7-39879
 metalloporphyrins, electron transfer rate meas. 7-5760
 methane anion+methane, internal energy depend. of cross section and mechanism branching, TESICO investig. 7-28298
 1-methyl-2,4,6-triphenylpyridinium iodide, charge transfer complex, UV absorpt. spectra 7-36640
 molecular beam studies of elementary photophysical processes 7-15700
 molecular chain, electron transfer kinetic coeff., supersonic Davydov soliton mechanism 7-10751
 News-Anderson model, time-depend., for moving particles on metal surfaces 7-52263
 nitroaromatic radical anions in aqs. solns., electron transfer kinetics, temp. and steric configuration effect 7-39872
 organic charge transfer solids, review 7-7222

charge exchange continued

oriented atoms and molecules scattered from surfaces, anisotropic charge transfer rates 7-59366
 Peierls-Hubbard model, exact and approximate solns. 7-52383
 perfluorobenzene, electron transfer reaction kinetics, binding energy role 7-22989
 perfluoromethylcyclohexane, electron transfer reaction kinetics, binding energy role 7-22989
 phenothiazine derivative-methylviologen systems, charge separation yield 7-28323
 1-phenyl-3-methyl-5-pyrazolone, conform. and charge transfer, UV spectra 7-57168
 photosynthetic bacteria reaction centre, electron transfer mechanism 7-23315
 positron-gas collisions, charge exchange, ortho-positronium form. 7-62513
 protein globule, charge transfer activation energy and heterogeneous medium reorganisation 7-28440
 proteins, aperiodic, electronic struct., ab initio calcs. 7-23273
 quinones, electron-transfer reactions, kinetic ESR spectra, computer simulation 7-25568
 radiation induced electrostatic instability on surface of ionic crystals 7-46816
 relativistic particle beams, high power, collision effects calcs. 7-30117
 ruthenocene, gaseous, self-exchange electron-transfer kinetics, Franck-Condon barriers 7-36745
 semiconductor-fluid interfaces, illum., adsorption, competition for photogenerated charge carriers 7-27105
 trans-stilbene-fumaronitrile ion pair, back-electron transfer, solvent effects 7-39873
 symmetric heavy ion collisions, K X-ray prod., target thickness fn., X-ray spectra anal. 7-30978
 TCNQ-TTF powdered mixtures, strong solid-state charge transfer reaction 7-46835
 tetracyanoethylene, electron affinity, electron transfer equilibria 7-10741
 tetraethylmethylenediamine-I₂ charge transfer complex, electronic struct. influence, electronic absorpt. spectra 7-10611
 tetramethylmethylenediamine-I₂ charge transfer complex, electronic struct. influence, electronic absorpt. spectra 7-10611
 1,2,4,6-tetraphenylpyridinium perchlorate, charge transfer complex, UV absorpt. spectra 7-36640
 TTF-chloranil, neutral-ionic transition, phenomenological theory 7-26939
 TTF-TCNQ complexes, intramolecular charge transfer 7-7241
 vitamins, electron-transfer reactions, kinetic ESR spectra, computer simulation 7-25568
 Al (110), H₂⁺ scatt., charge exchange 7-3133
 Al (110), scatt. of H₂⁺ ions, resonant transition rates for charge transfer 7-3134
 Al, chemisorption, interaction of atoms and mols. with surfaces, cluster approx., total energy calcs. 7-52265
 Al³⁺H, charge-transfer reaction, mol. representation, CI calcs. 7-36485
 Ar⁺ average equilb. charge state determ., H⁺ secondary ion yield meas. on Au and C target surfaces 7-42757
 Ar+H⁺ two-electron charge exchange mol. states, nonorthogonal CI calcs. 7-50339
 Ar+N₂⁺→Ar⁺+N₂, electron transfer reaction, state-to-state study 7-36746
 Ar⁺+H₂, chemical reaction and charge-transfer processes, RIOSA quantum-mechanical study. 7-31159
 Ar⁺+Kr (CO)(CO₂), charge exchange cross-sections meas. 7-62519
 Ar⁺+N₂, charge exchange reactions, TEPCO method anal. 7-20076
 Ar⁺+N₂, charge transfer collision, Franck-Condon principle at low collision energies study 7-62511
 Ar⁺+N₂ collisions, low energy charge transfer reactions, time-of-flight spectra studies 7-31163
 Ar⁺+O₂ collisions, low energy charge transfer reactions, time-of-flight spectra studies 7-31163
 Ar⁴⁺+D₂(D), collision parameters, energy-gain spectra meas., multichannel Landau-Zener model anal. 7-36752
 Ar₂⁺+N₂, charge-transfer, mol. dynamics study 7-50335
 Ar₂⁺He(Ne), charge exchange into excited states in collisions 7-31155
 ArN₂⁺, charge transfer dynamics, vibronic approach 7-50333
 Be⁴⁺+He, charge exchange cross sections, quasimolecule Feshbach method calcs. 7-36754
 Br₃⁺, electrical cond. mechanism, tight-binding and ab initio pseudopot. calc. 7-52546
 C³⁺+He, transfer excitation, electron emission, forward-backward asymmetries 7-973
 C⁴⁺+He, double charge transfer process, differential cross sections, quantal study 7-62512
 C⁴⁺+He, two-electron capture cross sections, comparison of calc. methods 7-15703
 C⁶⁺+He, (quasi)-two-electron collision systems 7-5764
 C₂⁺, excited state, prod., ion-mol. reactions, FT mass spectra investig. 7-54087
 CO⁺, comet tail bands, charge transfer, spectroscopy 7-15702
 CdS anodic film growth, initial stages, voltammetry and computer simulation studies 7-28216
 Cl⁺, charge transfer reactions with organic mols., cross section anal. 7-15701
 Cl₂²⁺ electronic states, double charge transfer technique 7-841
 Cr²⁺ dielectronic recombination, photon/ion coincidence meas. 7-10756
 Cr₂Br₃⁺, singly and doubly excited states, exchange interaction, theoretical study 7-10749
 Cr₂Cl₃⁺, singly and doubly excited states, exchange interaction, theoretical study 7-10749
 Cs⁺, low-energy collisions with atoms and mols., absolute total cross section meas., curve-crossing model anal. 7-36749
 Fe complexes, (Fe₂O(acetate)₆(pyridine)₃(pyridine), intramol. electron transfer, phase transition mechanism 7-10742
 Fe II, contrib. of charge transfer to UV doubly excited lines 7-66585
 Fe, passive, adsorption and absorpt. of Cl⁻ ions 7-28340
 H, ion recomb. and level pops., role of charge exchange 7-31925
 H plasma, ion collisions, low-energy charge exchange, XUV spectra 7-20032
 H, Rydberg atoms, low-velocity charge transfer, classical scaling failure 7-15707
 H⁻ formation by H⁺ bombardment of cesiated W surface 7-17390
 H⁻ formation in H⁺-surface collisions 7-17389
 H⁺, vibr. excitation by charge exchange with mols., TOF anal. (German) 7-57170
 H+C³⁺, pot. energy curves, spin-coupled VB theory 7-957

charge exchange continued

- H+H, ion-pair form. reaction, mol. treatment 7-50340
H+H⁺, charge transfer processes, H₂⁺ autodetaching states 7-15705
H+H⁺, reson. electron capture from excited 2 s states, cross section calcs. 7-36747
H⁺+He, collisional detachment neutralization at high energy 7-15685
H⁺+Al⁺(Ga⁺)(In⁺)(Tl⁺), charge transfer and ionis. 7-31162
H⁺+Cs charge transfer collisions, laser radiation influence 7-25646
H⁺+H, symmetric resonant charge transfer collisions in ultralow collision energy range 7-31164
H⁺+H₂ double capture; collisions, H⁺ ion excitation energy meas., Franck-Condon calcs. 7-36751
H⁺+H₂(D₂), charge transfer into 2S state, differential cross sections meas. 7-36750
H⁺+H₂(He)(N₂)(Ne)(Ar), 20-100 keV, charge exchange cross section meas. (Chinese) 7-5765
H⁺+HF, charge transfer processes, ab initio calcs. 7-5744
H⁺+H(Ar), capture theory, first-order Born approx. Coulomb boundary conditions 7-10745
H⁺+H(Ar), electron capture, K-shell cross sections 7-10752
H⁺+inert gas, electron transfer and ionis., δ -electron spectrosc. 7-42685
H⁺+K, ionisation and charge transfer collisions, cross section meas. 7-20031
H⁺+K charge transfer collisions, laser radiation influence 7-25646
H⁺+Na charge transfer collisions, laser radiation influence 7-25646
H⁺+O₂ charge transfer collisions, vibr. state resolved meas. 7-5762
H⁺+Ru charge transfer collisions, laser radiation influence 7-25646
H₂⁺+Cs, dissociative charge exchange, H₂ predissociation, fragment spectra anal. 7-36753
H₂⁺+He, elastic and inelastic scatt. mechanisms, energy loss spectra 7-15671
H⁺CO₂, charge transfer reaction cross section and pot. energy curve meas. 7-54086
H₂O biological charge transfer processes, IR and microwave spectra 7-3749
(H₂O)₂O₂⁻ clusters, charge transfer interaction investigated using ab initio MO theory, binding energy calc. 7-5809
He⁺+Ne(Ar), charge exchange into excited states in collisions 7-31155
He, collisions with fast, highly charged ions, electron capture to the continuum meas. 7-20026
He plasma, ion collisions, low-energy charge exchange, XUV spectra 7-20032
He⁺, vibr. excitation by charge exchange with mols., TOF anal. (German) 7-57170
He²⁺, charge exchange collisions, multiply charged closed K shell targets, exponential model study 7-25426
He+B²⁺(O²⁺)(Si²⁺), double- and single-electron capture and loss cross section meas., OBK scaling calcs. 7-42756
He+C⁶⁺(Ne¹⁰⁺) electron capture, bound and continuum states, impulse approx. 7-50329
He+C⁶⁺(O⁸⁺), intermediate energy collisions, electron capture cross sections, AO expansion method calcs. 7-25381
He+H⁺, charge transfer, second-order Born and Faddeev-Watson approx. 7-62516
He+Li³⁺(C⁶⁺)(O⁸⁺), electron capture, Coulomb integral eval. 7-15679
He⁺+Ca(Cr)(Cu), target K-shell ionis., cross-sections and probabilities 7-50343
He⁺+Cd(Zn), exothermic charge exchange with excitation cross sections 7-42755
He⁺+H⁺ ionis., beam-pulsing expt. 7-31160
He⁺+He⁺, electron capture cross sections, SCF-CI calcs. 7-15526
He²⁺+He, symmetric resonant charge transfer collisions in ultralow collision energy range 7-31164
He²⁺+K, ionisation and charge transfer collisions, cross section meas. 7-20031
He²⁺+Ne(N₂)(CO₂), charge transfer reaction rate consts. 7-22983
HeH⁺+Cs, dissociative charge exchange 7-5766
HgBr, excited state, charge transfer absorpt. spectrum 7-5761
I₃, electrical cond. mechanism, tight-binding and ab initio pseudopot. calc. 7-52546
Ir complex, (NEt₄)₄(Ir(CO)₂4,4',5,5'-tetracyano-2,2'-biimidazole) mixed valence cpd., anisotropic conductor precursors identified by intermolecular charge transfer 7-7190
KH₄ graphite intercalation cpd., struct. and electronic props. 7-27234
Kr, ultrasensitive laser isotope anal. 7-19803
Kr⁺, average equil. charge state determ., H⁺ secondary ion yield meas. on Au and C target surfaces 7-42757
Li+He²⁺, electron capture, Coulomb integral eval. 7-15679
Li⁺+He, n=Z levels, alignment and orientation (French) 7-10723
Mg+H₂⁺, direct dissociative charge exchange investig. 7-50332
Mo (100), chemically modified by adsorption of B, C, O, CO, surface atom oxidation states, ESCA meas. 7-28333
N³⁺+H₂, electron transfer rate const. calc. 7-33917
N₂⁺, Meinel bands, charge transfer, spectroscopy 7-15702
N₂+Ar, electron transfer, state-to-state study 7-10714
N₂+N₂⁺(Ar⁺), charge transfer, crossed mol. beam study 7-57166
N₂⁺+N₂, charge transfer reaction, calc. of vibr. levels for neutral mols. 7-42759
N₂⁺+O₂, charge exchange reaction in temp. range 8 to 163 K, rate coeff. meas. 7-46810
NH₃+HX where X=Cl, Br, I, gas phase charge transfer complexes, pot. curves 7-13733
NH₃⁺+NO, cross section as a fn. of ion vibr. level, REMPI time of flight spectra, mass spectra 7-20028
NO⁺+iodomethane (NO₂), charge exchange, ground state radiative lifetimes, ion cyclotron reson. spectra anal. 7-31114
NO⁺+NH₃, cross section as a fn. of ion vibr. level, REMPI time of flight spectra, mass spectra 7-20028
Na, optically excited target, charge exchange with proton beam 7-50342
Na+He²⁺, charge transfer, excitation processes coupled state impact parameter model 7-62518
Na+Li⁺, charge exchange collisions, cross sections calcs., atomic-orbital expansions method 7-36460
Na+Ne⁺(Ar⁺)(Xe⁺), Rydberg electrons removal, cross section meas. 7-36742
Na⁺+Li, charge exchange collisions, cross sections calcs., atomic-orbital expansions method 7-36460
Ne+Ar⁺, time of flight energy spectra, long lived excited Ar⁺ state 7-62486

charge exchange continued

- Ne+R⁸⁺(F⁹⁺), k-k charge transfer, excitation patterns, Auger spectra 7-15682
Ne⁺+He(Ar), charge exchange into excited states in collisions 7-31155
Ne⁴⁺+D₂(D), collision parameters, energy-gain spectra meas., multichannel Landau-Zener model anal. 7-36752
Ni (100), (111) and (110), N₂ chemisorption, molecular cluster calcs. 7-52280
Ni₂H clusters, charge distrib., Hartree-Fock SCF INDO calcs. 7-52411
O⁺+H₂→H⁺+O, ion reaction at interstellar cloud conditions 7-23008
O⁶⁺+He, (quasi)-two-electron collision systems 7-5764
Pb²⁶⁺+Sn(Xe), impact parameter depend. target K X-ray emission, XES spectra anal. 7-62314
Pb⁸⁺+Xe, electron capture, K X-ray emission spectra study 7-36524
Pd (111), chemisorption of NO, photoemission study using synchrotron radiation 7-22446
Ru complex, outer sphere electron transfer, solvent relax. dynamics effect 7-65290
SF₆, charge transfer, time-resolved study 7-10748
SF₆, electron transfer reaction kinetics, binding energy role 7-22989
Si (100) and (111), adsorption of K, AES, work function meas. 7-32818
a-Si:H multilayer films, charge transfer doping, cond., photocond. meas. 7-38735
a-Si:H/a-Ge:H multilayer films, photoconductivity enhancement 7-27443
Sn⁴⁺+Xe collisions, q=34 to 52, resonant electron transfer and L-shell excitation, X-ray spectra study 7-30979
Sr⁺+Ba, laser-induced charge exchange, quasi-mol. model, fluorens. anal. 7-36748
Ta complex, (BEDT-TTF)₃Ta₂F₁₁, optically enhanced phase transition, EPR investig. 7-64454
(Ti,M)O₂ (M=V, Nb, Ta) rutile solid solns., charge transfer and ligand fields, XANES studies 7-64782
TiO₂ electrode, illum., elementary steps in charge transfer mediated by surface states 7-12780
U⁹⁺+Sn, electron capture, K X-ray emission spectra study 7-36524
Xe:Cl₂ (n=1 or 2) 7-28297
Xe:HCl, cooperative photoabsorpt. induced charge transfer reaction dynamics 7-28297
Zn+He⁺(He⁺), Penning and charge transfer reactions, Zn²⁺ levels excitation 7-5746
ZnCdS:Ag/Cd(S,Se):Cu mixed photoconductor system for electrophotography 7-2636
- charge-injection device arrays** *see charge-coupled device circuits*
charge-injection devices *see charge-coupled devices*
charge measurement
see also electrometers
antistatic materials, charge dissipation measurement 7-56304
fractional charge searches, rotor electrometer design 7-14964
fractional electric charge search on niobium samples in liquid He 7-35785
nonequilibrium charge method of measuring MOS-structure parameters 7-2728
rotor electrometer for bulk matter quark search expts. 7-30913
- charge-ordered states**
No entries
- charge storage diodes**
No entries
- charge transfer** *see charge exchange*
charge-transfer device arrays *see charge-coupled device circuits*
charge-transfer devices *see charge-coupled devices*
charge transfer states
alcohol dehydrogenase, liver, Cu substituted, ligand and coenzyme effects, resonance Raman spectra 7-62548
alkali halides, Schottky defect energy, effect of three-body forces 7-21864
anthracene, cryst., charge-transfer transitions, freq. and intensity eval. 7-52543
anthracene-NH₃, jet-cooled clusters, van der Waals complexes, exciplexes, visible fluoresc. spectra 7-19936
bicalicene, cyclic, electronic structure, SCF CI calcs., NMR and PMR 7-50185
chloranil-mesitylene(benzene), charge transfer complexes, thermodynamic and spectrophotometric study 7-33950
crystalline donor-acceptor complexes, vibronic coupling in charge-transfer states 7-52542
crystalline solids, electrostatic Madelung and cohesive energies 7-44442
crystallisation of charge transfer excitons under strong excitation conditions 7-45160
cyclophane-fluoranyl charge transfer complexes, struct. and stability, IR spectra anal. 7-50143
4,4'-diaminophenyl sulphone, intramol. charge transfer state, H-bonded cluster importance, fluoresc. and IR spectra 7-50213
2-dicyanomethylene-1,3-indanedione-methylated[2,2]paracyclophanes charge transfer complexes, IR and mass spectroscopy 7-25523
4-(N,N-dimethylamino)benzonitrile, solvated, charge-transfer state form., structural demand, fluoresc. 7-15637
2-dimethylamino-6-propionyl naphthalene, twisted charge transfer state, fluoresc. quantum chem. study 7-863
DMT(CF salts, electronic and vibr. absorption spectra, electronic correlations 7-46034
DNA electronic structure and cond. props., calcs. 7-23296
donor-acceptor complexes, interstack and intrastack forces 7-63594
excitons, spatial ordering during intensive excitation 7-64097
fluorene-1,2,4,5-tetracyanobenzene, charge transfer cryst., triplet excitons, ODMR and ESR 7-7611
graphite, intercalation cpds., staging walls charge profile, Thomas-Fermi description 7-12687
Heisenberg chains with random exchange, thermodynamic and dynamic props. 7-59048
impurity electron transfer selection rules (Russian) 7-16983
indole:naphthalene(anthracene)(tetracene) crystals, impurity complexes, photolum., thermolum. and absorpt. spectra studies (Russian) 7-46139
magnetic insulators, light absorpt. by intersublattice charge transfer 7-46065
metal phthalocyanine films, electro-absorpt. spectra, charge transfer excitation 7-27695
metal-ligand complexes, nonvibronic d-d intensities, charge-transfer manifold props., simplified group function, MO calcs. 7-19698

charge transfer states continued
 organic charge transfer complex, neutral-ionic transition (*Japanese*) 7-45249
 organic conductors, positron annihilation 7-39277
 organic crystals, neutral-ionic transition, effect of electron-lattice interaction 7-2556
 organic crystals, neutral-ionic transition, effect of intersite Coulomb interaction 7-2555
 organic crystals, neutral-ionic transition, Monte Carlo simulation of modified Hubbard model 7-2554
 perylene, jet-cooled clusters with ammonia, van der Waals complexes, exciplexes, visible fluoresc. spectra 7-19936
 perylene-NH₃, jet-cooled clusters, van der Waals complexes, exciplexes, visible fluoresc. spectra 7-19936
 picolyltricyanoquinodimethane, mol. cryst., charge transfer transitions, electronic spectra 7-22279
 porphyrin, water-soluble dimers, excited-state props. fluoresc. spectra, EPR, ODMR 7-19925
 proteins, electronic structure and cond. props., calcs. 7-23296
 segregated-stack organic charge transfer solids, mag. props. 7-17151
 semiconductor and insulators, charge transfer electron-exciton complexes 7-27258
 TCNQ salts, quarter-filled band, optical absorption studies 7-46033
 tetracyanoethylene-methylated [2.2]paracyclophanes charge transfer complexes, IR and mass spectroscopy 7-25523
 tetraethylammonium chlorofluorooximates, charge transfer transitions, UV-visible spectra 7-22283
 2,6,N,N-tetramethylcyananiline, charge transfer states, solvent effects, fluoresc. 7-31111
 tetrathiofulvalene-p-chloranil, mixed-stack charge-transfer cryst., elec. cond. and phase diagram 7-52586
 3,3',5,5'-TMB-TCNQ charge transfer complexes, electronic props. studies 7-64185
 TMTCT salts, electronic and vibr. absorption spectra, electronic correlations 7-46034
 transition metal alloys, amorphous, short-range order, approx. to coherent locator (*Russian*) 7-58731
 transition metal phosphorus trisulphides, electronic, structural and mag. props., intercalation cpds. and chemical props. 7-44499
 TTF(Ni(dmit)₂)₂ molecular supercond., BCS and small supercond., lattice parameters (*French*) 7-2759
 Al_xGa_{1-x}As/GaAs photoexcited heterojunction, charge transfer calcs. 7-12688
 ArXe⁺, DC discharge in supersonic jet, UV-visible emission spectra anal. 7-19874
 BH+H⁺, charge transfer dynamics 7-50331
 B₂H₆, mol. vibr. coupling, dynamic electron transfers, variational method calcs. 7-36585
 BaFCl:Sm³⁺(Eu³⁺)(Gd³⁺)(Ho³⁺)(Er³⁺)(Yb³⁺), charge transfer excitation and emission spectra 7-64688
 CaF₂:Ce³⁺, impurity ion-ligand nuclei interactions, ENDOR meas. and operator method calcs. 7-52538
 Cs₂UO₂(NO₃)₃, charge transfer bands position, ionisation pot. effects, luminesc. spectra anal. 7-46146
 Cu cluster surface, Na atom adsorpt. SCF ab initio and CI calcs. 7-52259
 Cu(I) complexes, UV absorpt. and reson. Raman spectra 7-10593
 Cu(PH₃)₂(BH₄)₂, mol. vibr. coupling, dynamic electron transfers, variational method calcs. 7-36585
 ErSi₃, electronic struct., X-ray emission spectra studies 7-52419
 EuSi₃, electronic struct., X-ray emission spectra studies 7-52419
 Fe₂Ge_{1-x} amorphous magnetic alloys, d-band occupancy, EELS study 7-64059
 Fe₂Si_{1-x} amorphous magnetic alloys, d-band occupancy, EELS study 7-64059
 GaAs (001), chemisorption of CF₃ radicals, RHEED, photoelectron spectra, HF SCF calcs. 7-53497
 p-GaAs:Cr, excited and metastable states of Cr-related double centres 7-7153
 KUO₂(NO₃)₃, charge transfer bands position, ionisation pot. effects, luminesc. spectra anal. 7-46146
 Li-TaS₂ intercalation cpds., room temp. optical transmission spectra, charge transfer and band struct. modification 7-45962
 Li_x(NH₄)_{1-x}(NH₃)₂TiS₂^{(x+y)-} intercalation cpd., NH₃ oxidation, charge compensation 7-32354
 Mn₂Sn_{1-x}Mo_xS₈, Mn dopant props., supercond. transition temp., EXAFS, XANES, photoemission studies 7-46236
 NH₃⁺+NO, cross section as a fn. of ion vibr. level, REMPI time of flight spectra, mass spectra 7-20028
 (NH₄)_{0.22}TiS₂^{0.22-} ionic intercalation cpd., synthesis, characterisation by thermal anal., mag. 7-45244
 NH₄UO₂(NO₃)₃, charge transfer bands position, ionisation pot. effects, luminesc. spectra anal. 7-46146
 NO⁺+NH₃, cross section as a fn. of ion vibr. level, REMPI time of flight spectra, mass spectra 7-20028
 NaCl:Co, doped and undoped, thermoluminescence and X-ray fluorescence spectra 7-22356
 Ni alloys, core-level shifts anal., LMTO energy band calcs. 7-38487
 PdH_x, electronic density of states, recursion method 7-64043
 RbUO₂(NO₃)₃, charge transfer bands position, ionisation pot. effects, luminesc. spectra anal. 7-46146
 Ru complex, Ru(bpy)₃²⁺, charge transfer states assignments, MCD and CD spectra anal. 7-31056
 Si, amorphous, IR absorpt., local phonon-induced bond angle distortion model 7-26642
 SrTiO₃:Fe³⁺(V⁵⁺), impurity energy levels, tight binding model, Green's function method calcs. 7-21856
 TaC_x, substoichiometric, core-level binding energies and valence-band struct., XPS 7-22450
 (V_{1-x}Cr_x)₂O₃ single crystals, elastic const. temp. depend., ultrasonic strain-induced electron transfer effects 7-2082
 W complex, pentacarbonylpyridine W(O), single cryst., polarised low temp. luminesc. 7-3094
 ZnO:Co(Ni)(Cu), impurity electron states, optical spectroscopy 7-46127
 ZnS:Cr³⁺, Fe³⁺ single crystals, impurity center charge exchange, plastic deform. effects, ESR spectra studies 7-16984

charge transfer transitions see *charge transfer states*

charged currents

fermion+fermion→fermion+fermion+W⁺+W⁻, charged current sector calc., effective W approx. comparison 7-24822

charged currents continued

Monte Carlo simulation of charged-particle analyser line shapes 7-30803
 Skyrme model, expressions for various currents using gauge transformations 7-30162
 $\mu^+\rightarrow e^+1$, search for right-handed currents 7-15151
 $\nu(\bar{\nu}P)$, 400 GeV, neutral to charged current cross section ratios 7-15144
 ν_e, ν_μ coupling to charged weak currents, universality test 7-24872
 $\nu_e d \rightarrow \mu^+ pp$, pion exchange current effects 7-56559
 $\nu_\mu N$ semileptonic interactions, electroweak mixing angle determ. 7-5084
 ^{12}N -strange particles, inclusive production rates 7-528
 $^{12}C(\nu_\mu, \mu^+ X)$, charged current interactions, cross section meas. 7-35852
 $\bar{\nu}N \rightarrow \rho^0$, tensor polarization meas. of ρ^0 , charged current interaction 7-5083

charged dislocations see *dislocation dipoles*

charging, contact see *static electrification*

charm particles

see also *D mesons*

charm hadroproduction in H and Be, nuclear depend. 7-61719
 charmonium and bottomonium spectra, introductory physics course 7-18534
 cosmic ray showers, charmed particle prod. and long-range avalanches 7-14446
 hadron spectrum, stochastic approach, link with quarkonium model 7-49121
 NA32 charm production expt., CCDs for high-energy particle tracking 7-25325
 nonresonant three body decays in chiral perturbation theory 7-10058
 photoproduction processes, quark model with charm and colour 7-41737
 weakly decaying charmed baryon lifetime differences due to preasymptotic bound state effects 7-41801
 $B_c^-\rightarrow\rho^0 D^0(K^0F^-)$, partial decay rate asymmetries and CP violation 7-41792
 $F^+\rightarrow\pi^+\rho^0$, obs. level from D⁺ decay 7-49136
 $\gamma\gamma\rightarrow\eta_c(2980)$, recent results on two-photon processes from DESY 7-61786
 $\Delta_c\rightarrow pK^+\pi^+$, lifetime meas. 7-61669
 Δ_c^+ semi-leptonic branching ratio calcs., statistical model anal. 7-15148
 $\Delta_c^+\rightarrow 1/2^+ +$ mesons, generalised chiral lagrangian method 7-24883
 Δ_c^+ hadronic decay, statistical model anal. 7-15148
 $\Delta_c^+\rightarrow \Delta_{c\nu}$, chiral lagrangian method, partial widths and branching ratio 7-35867
 $\mu N\rightarrow CCX$, nonperturbative, CC component in quark fragmentation function 7-30273
 $\nu N\rightarrow X$, multiplicity of charmed mesons and baryons, quark parton model 7-41783
 $\pi^-p\rightarrow$ charm hadrons, 360 GeV/c, hadron decay props. 7-562
 $F^+\rightarrow K^0\phi K^+$, decay obs. using ARGUS, decay rates 7-24880
 Δ_c^+ , polarisation determination from cascade decays 7-41865

Charpy testing see *dynamic testing*

charring see *combustion*

Chebyshev approximation

free convection at high Reynolds number, spectral Chebyshev solns. 7-37466
 initial-boundary value problems, pseudospectral method of soln. (*Russian*) 7-56006
 multispectral imagery dimension reduction and interpretable, Chebyshev polynomials 7-4236
 Navier-Stokes equations, two-dimensional, soln. using pseudospectral method, primitive variable formulation 7-29762
 piecewise-Chebyshev approximation of exptl. data (*Russian*) 7-56206
 polynomial, generalised, determ. of zeros by Chebyshev system method (*Russian*) 7-61080
 Stokes equations, collocation method, variational problem (*French*) 7-55973

chelates see *coordination complexes*

chemical analysis

see also *chemical analysis by nuclear reactions and scattering; chromatography; electrochemical analysis; electron probe analysis; ion microanalysis; mass spectroscopic chemical analysis; polarimetry; pollution detection and control; radioactive chemical analysis; spectrochemical analysis; thermal analysis; X-ray chemical analysis*
 acoustic gas analyser for binary mixtures 7-39939
 adatom abundance determ. using elastic recoil detect anal. 7-33984
 alkali metal layered Mo bronzes, (A⁺(H₂O)_x)₂MoO₃²⁻, (A=Li, Na, K, Rb, Cs), composition and struct. 7-16518
 applied materials charact., conf., San Francisco, CA, USA (April 1985) 7-18495
 binary mixtures, neutron-gamma transmission based composition meas. 7-54215
 BWR, neutral water-chemistry treatment with H₂O₂ dosing 7-10223
 cadmium dithiocarbamate dichloride, intermediate cpd. in formation of CdS films by spray pyrolysis, characterisation 7-39372
 carboxylated rubber, study of maleic acid residue and vinylic monomer on props. 7-39902
 depth profiling, resolution improvement by superposition of original signals 7-54219
 EELS, chemical analysis in electron microscope, book 7-55903
 fluorophosphate glass, type OK1, interrelationship of refr. index, viscosity and F content 7-57492
 FTIR microanalysis principle and appls. 7-24699
 gas analysers (*Spanish*) 7-59799
 gas analysis instrumentation, calibration (*Spanish*) 7-56208
 gas mixtures, standard, specifications for pure gases as initial components 7-56212
 gasdynamic focusing in supersonic jets, chemical anal. appl. 7-20752
 gilsonite, microstructure and mechanical props. 7-44838
 igneous rocks, chemical analysis, CIPW norm calculations, FORTRAN listing 7-29263
 ion-selective electrodes for ion conc. measurement, operation in nonlinear suboptimal response range 7-56246
 laboratory robot for analytical samples preparation 7-29990
 materials characterisation, conf., Palo Alto, USA (Apr. 1986) 7-48184
 materials microanalysis, techniques, review 7-54244
 multilayered structures, physical and chemical charact. 7-38376
 optical fibre sensors chemical sensing, particularly in biomedical field, areas for use and techniques 7-31472
 oxide scales, chem. mapping using electron energy loss imaging microscope 7-37812
 phosphate rock standard, anal. 7-33982

chemical analysis continued

- piezoelectric sensor and sensor array characterisation 7-54200
 practical applications of surface analysis 7-8329
 quartz crystal microbalance, use for surface anal. in combination with surface sensitive spectroscopies 7-27076
 saline feedwater composition and physical properties determ., experimental methods 7-28364
 secondary ion energy distrib., surface chem. anal. 7-53486
 semiconductor epitaxial layers, sharp doping profiles determ. 7-12111
 soil, water and chloride content meas. using neutron counting 7-56291
 solid-state resistive and electrochemical sensors in gas anal., review (*Spanish*) 7-39936
 stainless steel, ferritic, for selective solar absorbers, conversion coating anal. 7-23224
 surface analysis, AES, XPS, ISS and SIMS, review 7-28372
 surface analysis, sputter depth profile calibration of multilayer structures 7-39382
 surface and interface analysis, appls. conf., Veldhoven, Netherlands, (Oct. 1985) 7-24289
 ternary mixtures, qualitative and quantitative resolution 7-54201
 thin films, structural, mech., and comp. props., charactn. and meas. 7-38378
 thin films composition determ., using TESLA BS 613 TEM with Si:Li detector (*Czech*) 7-65371
 transmission electron microscopes features and capabilities 7-15033
 1,4,10-trioxo-7,13-diazacyclopentadecane-N,N'-diacetic acid metal complexes, NMR investig. 7-57091
 two-parameter data-acquisition system for slit-scan chromosome analysis 7-35501
 ultrasonic techniques 7-50896
 volcanic fumarole gas chemical analysis methods 7-4202
 weld metal, self-shielded FCAW, nitride and N contents estimation method 7-59710
 O₂ composition between 500 and 20000K 7-39944
 As speciation in natural waters and sediments 7-23250
 B, powdered, and cpds., O and H content eval. 7-27964
 C fluorination, thermobalance for investig. 7-41349
 Ca(OH)₂·2Zn(OH)₂·2H₂O, chem. comp., solubility in KOH, thermodynamic props., reaction equilb. const. 7-26962
 CuSO₄ soln., double diffusive convection, conc. meas., optical technique. 7-57825
 H sensors using MOS structures with Pd-Ag gates 7-65364
 H₂ cluster detection at 4.2K 7-36843
 H₂ composition between 500 and 20000K 7-39944
 LiNbO₃:MgO, melt growth and charactn. 7-58170
 MoS₂, high press. synthesis, characterisation 7-26716
 Na particles in N₂ flow, size determ. by optical method, radiation loss 7-17837
 NO₂·nSiO₂+propylene carbonate, gels form., comp. of phases and rheological props. meas. 7-39875
 P content of seawater, determ. method involving nitrate oxidation 7-4227
 Pd-H system, H conc. determ. in absorbing metallic thin films 7-23117
 SAW device, coating responses, rel. to solubility and chem. struct., pattern recognition 7-54162
 Se speciation in natural waters and sediments 7-23250
 Si·O·N, small particles, elemental and chem. anal., EELS method 7-17379
 Si-SiO₂ interface, microchemistry 7-32850
 TeO₂-ZnCl₂ system, glass prep. and composition 7-46403
 W, electrothermal atomiser, temp. distrib. 7-8349
 (WCl₃)_n, (n=1,2,3), electrographic investig. 7-13844

chemical analysis by mass spectrometry *see mass spectroscopic chemical analysis***chemical analysis by nuclear reactions and scattering**

- see also chemical effects of nuclear reactions and scattering; neutron activation analysis; radioactive chemical analysis*
 binary alloys, crystal-amorphous transformation, thermodynamics and kinetics 7-21108
 biological total body O, N, and C, meas. in vivo by photon activation anal. 7-54827
 conference, nuclear and radiochemistry, Beijing, China (Sept. 1986) 7-18494
 external beam proton-induced gamma-ray emission analysis, C and O determ. 7-23088
 instrumental elementary anal., fission research reactor equipment complex 7-39932
 metallic materials, nucl. anal. (*German*) 7-54211
 neutron-induced particle track mapping of elemental distributions 7-54255
 nuclear micro-beam probe for the investigation of surfaces, microprocessor-controlled 7-8352
 photofission effects in γ -activation anal. 7-54207
 photon activation analysis, photonuclear reaction yields 7-23115
 proton bombardment elemental analysis, reliability using air mounted sample 7-59815
 quantitative determination, minimum mass limits 7-59813
 scanning electron microscopy and microanalysis, conf., Leuven, Belgium (May, 1986) 7-40988
 steel, implanted with N ions, physicochem. characters. of surfaces, wear resist. (*French*) 7-28209
 steel, surface analysis by charged particle activation 7-46893
 teeth, laser irradiated, nuclear microprobe anal. (*French*) 7-46890
 trace elements anal., neutron cross-section determ. 7-13840
 Au archaeological artifacts, light element determ. by nuclear reactions 7-59814
 B detection in vegetable samples and solutions using (n, α) technique 7-33980
¹⁰Be analysis, using (p,n) reaction 7-28368
 Fe, passivated, comp., electron backscattering Mossbauer spectra, XPS studies 7-28193
 Ga_{1-x}Al_xAs, Al concentration profiling using nucl. resonances 7-6811
 GaAs:C, O, trace determ. by ³He-activation anal. 7-58308
 H₂ depth profile meas. by reson. nucl. reactions 7-3617
 MoO₃, adsorption of methanol, influence of photoinjected H on adsorptivity 7-63942
¹⁵N(p, γ) resonance reaction for surface depth profiling, energy and width 7-59812
 Ni (110), adsorption of D₂, LEED, TDS, RBS, nucl. reaction anal., work function meas. 7-58638
 Ni (110), adsorption of O, surface phases, absolute coverages 7-12486

chemical analysis by nuclear reactions and scattering continued

- ²¹⁰Po α -source, use in determining Al, F, N content in samples 7-65360
 Pu content of Mururoa Atoll coral samples, nucl. techniques 7-54415
 Si, plasma passivated, subsurface H barrier layer obs. after surface adsorption of Al 7-17745
 Si, self-implanted, defects and amorphisation 7-2041
 Si, thermal nitridation in NH₃, atomic transport mechanisms 7-8201
 Si:B, ion implanted, defect and dopant depth profile studies 7-2045
 Si:C, impurity content determ. IR absorpt.-charged particle activation anal. conversion factor 7-26788
 Si:F, implanted, dry oxidation kinetics, impurity effects 7-13667
 a-Si:H,B(P) films, dopant conc. meas. and depth profiling by means of (p, γ) resonant reactions 7-12555
 Si:H films, H content meas. 7-12553
 Si:O, diffusivity and solubility of O review 7-16809
 SiO₂ films, effects of nitridation press. on props. 7-33818
 Ta₂O₅, amorphous layers, H content determ. by nucl. reactions 7-23097
 TiN-coated gear cutting hobs, wear characteristics, mechanical and structural props. 7-53980
 TiT₄, T depth profiling using the T(d, α)n reaction, neutron source target 7-23084
 U contamination in Al foils, CR-39 track detector study 7-54218
 V₂O₅, adsorption of methanol, influence of photoinjected H on adsorptivity 7-63942
 WO₃, adsorption of methanol, influence of photoinjected H on adsorptivity 7-63942

chemical association *see association***chemical batteries** *see cells (electric)***chemical bonding** *see bonds (chemical)***chemical bonds** *see bonds (chemical)***chemical composition** *see chemical analysis***chemical diffusion** *see diffusion***chemical effects of nuclear reactions and scattering***see also chemical analysis by nuclear reactions and scattering; radiation chemistry*⁵⁷Co EC decay chemical effects in Co(III) complexes 7-23048⁶Li (n, α)³H, chemical effect in Li₂C₂O₄ and Li₂CO₃ mixed with iron compounds 7-21289U minerals, α -decay, chemical effects 7-19544**chemical effects of radiation** *see radiation chemistry***chemical elements** *see elements (chemical)***chemical energy conversion**

- biomass thermochemical liquefaction research sponsored by US Department of Energy, overview 7-65511
 coproduction of methanol in integrated-gasification-combined-cycle electric power generation 7-17920
 direct work output from thermochemical energy transfer systems 7-54334
 electrochemical generators and chemical current sources (*Russian*) 7-59864
 explosive MHD generators, assessment 7-65497
 renewable resources, microbiological conversion into liquid fuels 7-65512
 solar H₂ production, S-I₂ cycle versus water vapour electrolysis 7-65651
 solar methane reforming reactor for chemical energy transport 7-65589
 solar receiver/reactors for thermochemical transport of solar energy 7-65591
 solar thermal dish appls., sensible and thermochemical energy transport systems, economics 7-65414
 solar thermochemical conversion by steam reforming of methane 7-8426
 thermal energy storage by thermochemical energy conversion and heat pumps 7-65568
 thermochemical energy transport for a large heat utility 7-65638
 CO₂-methane thermochemical energy transport system, closed-loop mode 7-65640
 H₂ production from coal and petroleum coke, technical and economical perspectives 7-40050
 H₂SO₄ decomposition and synthesis for chemical energy storage and transportation system 7-65639
 H₂SO₄, kinetics of heterogeneous reactions for chemical storage of energy 7-23229
 K₂S₂O₇ for chemical storage of solar energy 7-23228
 NH₃, kinetics of heterogeneous reactions for chemical storage of energy 7-23229
 Na₂S₂O₇ for chemical storage of solar energy 7-23228

chemical engineering *see chemical technology***chemical engineering computing**

- see also computerised control; computerised instrumentation*
 gas pulsation calculations for pipeline systems 7-44043
 photochemical reactors, industrial, using transparent particles, Monte Carlo modelling 7-59773
 polymerisation kinetics, simulation 7-54122
 polymerisation process computer control, using US sensors 7-8278
 reaction kinetic parameters, estimation by local online experimentation 7-8288
 Cd₂Hg_{1-x}Te heterostructures, MOVPE, computer controlled reactor, charactn. 7-59446

chemical equilibrium

- see also chemical reactions; reaction kinetics*
 acetaldehyde, combustion, oxidation, radical concs. and phase rels. 7-54126
 acid-base equilb. in soln., thermodynamic props., SCF theory 7-54156
 alkali metal hydroxide vapour, ion clustering struct., chem. equilb., mass spectra 7-17814
 alkyl nitriles, conformational kinetics calcs., gas and liquid phases, MR spectra 7-19896
 alkyl nitriles gas and liquid phases, syn-anti conformer equilb., MR chem. shift study 7-19895
 Belousov-Zhabotinsky reaction, induction period, excitability bifurcation 7-65286
 Belousov-Zhabotinskii reaction, Farey triangle 7-65288
 Belousov-Zhabotinskii reaction, Fe³⁺ impurity effect 7-46800
 Belousov-Zhabotinskii reaction, Mn-catalysed, complex periodic oscills., Farey arithmetic anal. 7-39853
 Belousov-Zhabotinskii reaction, O₂ influence, theoretical anal. 7-54080
 Belousov-Zhabotinsky reaction, catalysed, ion induced oscills. 7-65301
 Belousov-Zhabotinsky reaction, oscillating, statistical exptl. study of target patterns (*French*) 7-28279
 benzene+ethylene, isomer group equilb. mole fractions, calcs. 7-13738
 3,3-bis(nitratomethyl)oxetane, solid and soln., IR lineshape 7-3047

chemical equilibrium continued

- charge exchange, electronic nonequilibrium, kinetic eqns. (*German*) 7-3593
- dehydrogenase catalysed redox reaction, equilibria, spectroscopic anal. (*German*) 7-54159
- dicarboxylic acids undergoing conformational transitions, ionisation equilibria, ^1H NMR 7-13757
- donor-acceptor complexes, equilib. const., extinction coeff., spectrophotometric data evaluation 7-33951
- extended Brusselator, multiple attractors 7-17777
- geometric programming technique for computing equilibria 7-39850
- Gibbs free energy calc., symmetric minimum-norm updates 7-39912
- Ginzburg-Landau critical regimes, periodic perturbation entrainment 7-3575
- intermolecular fast exchange equilib., NMR spectroscopy 7-28332
- malonic acid, Belousov-Zhabotinsky reaction, oscillatory states transition 7-17765
- methanol-n-hexane, equilib. assoc. consts., NMR 7-932
- multiphase, calc. using MPEC2 FORTRAN-77 code 7-54155
- open reactive systems, centre manifold onset, far-from-equilib. fluctuations scaling, virtual size parameter calcs. 7-35484
- Oregonator model, excitability thresholds, Hopf and SNIPER bifurcations 7-65287
- oxidation equilibrium diagrams, atlas prep. 7-24324
- partially dissociated and ionised gas mixtures, chem. equilib. flow, effective transport coeffs. calcs. 7-31917
- periodic systems, sensitivity anal., Floquet theoretic approach 7-39854
- polymerisation, equilib., biccritical phenomenon 7-3588
- positive ion clustering with acetonitrile in atm. 7-999
- ring dynamics and percolation in an excitable medium 7-28277
- spiral waves in the Belousov-Zhabotinskii reaction 7-8271
- surface reactions, irreversible, kinetic phase transitions, mean-field theory 7-33962
- thermodynamic properties of reaction involving minerals and aqueous solutions, program 7-28330
- two-step chemical reaction, nonequilib. conc., steady state fluctuations and struct. factor 7-13726
- Al complexes, Al (III)-amino acid complexes, stability const. determ., ionophoretic technique investig. 7-28381
- AlOH, enthalpy of form., mass spectrometric determ., equilib. const., ionisation pot. 7-59777
- BaO-RuO₂-Fe₂O₃ system, equilibria description 7-65340
- Cl⁻+H₂O (methanol)(acetonitrile), clustering reactions, van 't Hoff plots based on ab initio MO calcs. 7-28288
- Cr complex, Cr (II)-amino acid complexes, stability const. determ., ionophoretic technique investig. 7-28381
- FeF₂-FeF₃, ion-molecule equilibria, mass spectra, heat of form., electron affinity 7-46862
- FeS₂, pyrite cryst., chemical vapour transport with halogens 7-53513
- GaAs epitaxial films, growth by close-spaced vapour transport, unwanted doping, X-ray diffr., SEM obs. 7-27187
- H₃AsO₃+IO₃⁻, stirring effects and bistability, coalescence-dispersion model 7-46801
- Hg+Xe, complex form., equilib. const. 7-19752
- Hi-H₂O-I₂ system vapour pressure determ. using static phase equilib. apparatus 7-23049
- N-HO bond complexes, association equilib. const. using dielectric relax. data 7-65291
- N₂, shock-induced molecular dissociation 7-23022
- N₂H, MCSCF equilib., transition struct. and reaction path determ. 7-8251
- N₂H₂, MCSCF equilib., transition struct. and reaction path determ. 7-8251
- Na₂O-SiO₂ binder solns., ester curing, equilibria and kinetics, NMR study 7-8311
- O₂, shock-induced molecular dissociation 7-23022
- Th complex, Th (IV)-amino acid complexes, stability const. determ., ionophoretic technique investig. 7-28381

chemical exchanges

- see also ion exchange; isotope exchanges*
- adsorption dynamics, exchange reactions and defect form. at solid surfaces, computer simulations 7-32823
- alkylamines, interaction with layered compounds 7-46838
- allenes, monosubstitution, stabilisation energies, isodemic methyl exchange reaction study, ab initio LCAO SCF calcs. 7-25389
- ascorbic acid radical anion, Ca²⁺ exchange, ESR line broadening meas. of rate const. 7-28270
- atom-molecule collinear reactive collisions, transition state calcs. 7-59746
- benzene, chemisorbed on Pt {110}, influence of orientation on H-D exchange reactions 7-59781
- benzoic acid:thioindigo(selenoindigo) impurity-induced double proton transfer, fluorescence decays 7-33420
- borane tetrahydrofuran, form. of borane adducts, ^{11}B NMR study. 7-50199
- carbon tetraiodide, crystal synthesis by trifluoroiodomethane+CO₂ IR irradiation 7-46831
- carboxylated rubber, study of maleic acid residue and vinylic monomer on props. 7-39902
- chloromethane+Cl⁻, substitution reaction, mol. dynamics, pot. energy surface, frozen solvent theory calcs. 7-54109
- cyclophane-fluoranyl charge transfer complexes, struct. and stability, IR spectra anal. 7-50143
- dichloroacetic acid complex with substituted pyridines, solvent effects, IR and ^1H NMR spectra anal. 7-62365
- dimethyl sulfone, rotating solid, NMR, chem. exchange effects 7-17227
- donor-acceptor pairs, electron transfer, orientational fluctuations influence 7-20002
- electrophilic aromatic substitution, relative activating ability of ortho and para directors 7-9635
- fluorenicarboxylic acids, and esters, solvent and pH effects, absorpt. and fluoresc. spectra anal. 7-50237
- hexamethylbenzene, proton transfer, high press. mass spectroscopy 7-54083
- 3-hydroxyflavone, ground state tautomer, proton transfer relax., laser fluoresc. spectroscopy 7-15640
- 2-(o-hydroxyphenyl)benzimidazole, excited state proton transfer, pulsed liq. lasers, pop. inversion obs. 7-50549
- ice, cubic, proton transport, FTIR obs. 7-53340
- indolecarboxylic acids, proton transfer reactions in excited singlet state, fluoresc. spectra study 7-22318

chemical exchanges continued

- mesitylene, proton transfer, high press. mass spectroscopy 7-54083
- metalloporphyrin polystyrene covalent complex, electron transfer reaction 7-39879
- 3-methoxybenzanthrone in soln., picosecond spectroscopy of intermolecular proton phototransfer 7-54150
- multisite magnetization transfer experiments 7-48822
- Nile blue, oxazine dye, luminesc. and H⁺ phototransfer in solns. 7-13762
- nitrophenol-trialkylamine ionic complexes, spectral characts. 7-15596
- NMR longitudinal magnetisation recovery curve, chemical exchange effects 7-38957
- organic cpds. excited state H⁺ transfer, state orbital correls. 7-13760
- pentamethylbenzene, proton transfer, high press. mass spectroscopy 7-54083
- PET, ester interchange reactions, small-angle neutron scatt. obs. 7-23004
- pyridine, chemisorbed on Pt {110}, influence of orientation on H-D exchange reactions 7-59781
- quadrupole echo NMR, chem. exchange effects during RF pulses 7-13058
- trans-retinylidene Schiff base, protonation on crystal surfaces, attenuated total refl. IR study 7-50102
- sodium nitrophenolates-crown ethers, proton transfer complexes, spectral characts. 7-15596
- sodium salicylate, excited state proton transfer, pulsed liq. lasers, pop. inversion obs. 7-50549
- Swift-Connick equations for intermediate exchange region 7-13740
- 1,2,3,5-tetramethylbenzene, proton transfer, high press. mass spectroscopy 7-54083
- transition metal phosphorous trisulphides, electronic, structural and mag. props., intercalation cpds. and chemical props. 7-44499
- trifluoroacetic acid-isooquinoline complexes, H bond, H⁺ transfer, medium effects 7-46833
- viomycin polypeptide, H exchange rate, NOESY expt. 7-10790
- zero field NMR, two-site flips 7-22149
- Cl⁻+chloromethane, substitution reaction, solvent effects nonadiabatic solvation, frozen solvent model study 7-54110
- F+H₂(HD)(D₂), quantum reaction probabilities, hyperspherical coordinates 7-13754
- F+I₂, reactive collision, IF laser induced fluoresc. (*French*) 7-13727
- Gd₂Si₂H₇, H-D exchange, H desorption 7-28304
- H+F₂(Cl₂), kinetic isotope effects, dynamics calcs. 7-54098
- H+H₂ collinear exchange reaction, time depend. arrangement channel quantum mechs. eqns. 7-17780
- H₂+D, mol. beam scatt. study, differential cross sections meas. 7-39860
- H₂⁺+H₂, H₃⁺ form., quasiclassical trajectory surface hopping method 7-59750
- HO₂+H, abstraction reaction, saddle point geometries and barrier heights, ab initio SDCI calcs. 7-46806
- H₂POOH, bonding, ab initio calcs., proton exchange reactions 7-5589
- H₂POSH, bonding, ab initio calcs., proton exchange reactions 7-5589
- H₂PSSH, bonding, ab initio calcs., proton exchange reactions 7-5589
- He+H₂⁺ reaction, expt. and quantum mech. results 7-3584
- He+H₂→HeH+H, quasiclassical trajectory calcs. 7-39876
- Ho₂Si₂H₇, H-D exchange, H desorption 7-28304
- K+iodomethane→KI+Methyl radical, orientation depend., classical trajectory calcs. 7-39866
- Li+HCl, laser catalysed reaction, pot. surfaces and transition dipoles 7-39861
- Li+HCl quenching reaction, electronic struct., ab initio SCF CI calcs. 7-56995
- LiCl(H₂O), ion pairs, struct. and stability, H⁺ transfer reaction path, SCF-CNDO/2 calcs. 7-25400
- LiF(H₂O), ion pairs, struct. and stability, H⁺ transfer reaction path, SCF-CNDO/2 calcs. 7-25400
- Mu+F₂(Cl₂), kinetic isotope effects, dynamics calcs. 7-54098
- N₂+O→NO+N, reaction rate const., vibr. excitation effect, information theory approx. 7-46832
- NH₃ dimer, ionis., proton transfer, ab initio pot. energy surface calc. 7-42518
- NaI, radiochemical purity, investigation of method (*Chinese*) 7-8340
- O+CH₃, exothermic reactions, rate consts., classical trajectory study 7-17783
- O+HD reaction rates, variational transition state theory 7-59749
- SO₂ removal by injected limestone sorbents, graphite element drop-tube reactor design 7-22978
- SO₂+Al→AlO+SO, pulsed crossed supersonic beam expt., energy threshold determ. (*French*) 7-33915
- SOF₂, gas-phase hydrolysis, reaction rate consts. 7-13744
- SOF₂, gas-phase hydrolysis, reaction rate consts. 7-13744
- UO₂²⁺+2RH→R₂UO₂+2H⁺, ion exchange equilibria and kinetics 7-25071
- Xe+Cl₂(Br₂)(I₂), atom and excitation transfer, energy disposal, product rot. alignment 7-31158

chemical industry

- fibre optic sensors for chem. industry, industrial meas. of press., temp., and level 7-57579
- hazardous gas monitoring system in chem. manufacturing facility, open path FTIR air monitor 7-54416

chemical kinetics see reaction kinetics**chemical lasers**

- conf., Rochester, NY, USA 7-9595
- conference, laser science advances, Dallas, TX, USA (Nov. 1985) 7-9573
- CW visible chemical laser with reagent jet agitation (*Russian*) 7-15857
- I photodissociation laser using pentafluoroethyl iodide, low-threshold solar-pumped laser operation 7-1091
- strategic defense application of chemical lasers 7-10980
- Cs, atom, lasing action in Kr gas 7-15855
- DF chemical lasers, mixing enhancement using supersonic nozzle design 7-5878
- DF pulsed laser performance, gas mixture composition depend. 7-62682
- DF-CO₂ pulsed laser performance, gas mixture composition depend. 7-62682
- H+N₂O, hot atom reaction, chem. laser, nonequilib. processes 7-1092
- H₂F₂ laser, atmospheric pressure, feasibility of short radiation pulse generation 7-25807
- HF, chem. laser, modeling based on standing detonation wave 7-62681
- HF laser radiation stimulated Brillouin scattering in Xe, high reflectivity 7-15938
- HF-DF chemical laser, electrically initiated (*Chinese*) 7-5879

chemical lasers continued

- Hg halide photodissociation laser pumped by wide-band optical radiation, three-colour emission 7-50548
 Hg₃, superfluorescent laser action around 495 nm 7-15856
 HgCl laser pumped by wide-band optical radiation emitting at 558 and 559 nm; 7-36955
 HgI/HgI₂ laser at 442, 443, 444 nm with wide-band optical pumping 7-25806
 I, active mode locking, acousto-optic modulator (Korean) 7-25852
 I IR laser, IR laser, wide-aperture freq. multipliers based on KH₂PO₄, KD₂PO₄ 7-57469
 I laser, solar-pumped, beam profile meas. 7-37006
 I, laser amplifier, free running operation mode 7-57307
 I photodissociation laser, solar-pumped 7-15854
 I₂ photodissociation laser using I₂+C₃F₄ and I₂+O₃ mixtures 7-50547
 ICl photodissociation laser at 11.35 μ m, gain and energy 7-43082
 IF hybrid chemical-laser, quenching of NF singlet states 7-43081
 O₂-I chemical laser, singlet O₂ generation using porous pipe 7-57363
 O₂-I chemical lasers, singlet O₂ generator 7-20217
 O₂-I₂ chemical laser, influence of water vapour on output energy 7-25808
 O₂-I₂ chemical lasers, review 7-15852
 O₂-I₂ laser active medium, theoretical model 7-1093
 OD-CO₂ chemical laser, energy capabilities study 7-62683
 S atomic laser, VUV, antiStokes Raman 7-15850
 Se atomic laser, VUV, antiStokes Raman 7-15850
 SiF chemical laser, feasibility 7-15853

chemical potential *see thermodynamic properties*

chemical reactions

- see also association; atom-atom collisions; atom-ion collisions; atom-molecule reactions; atomic inelastic collisions; catalysis; charge exchange; chemical exchanges; chemically reactive flow; chemiluminescence; chemisorption; CIDEF; CIDNP; corrosion; dissociation; electrolysis; free radical reactions; heat of reaction; ion-molecule reactions; isomerisation; molecule-molecule reactions; oxidation; photochemistry; polymerisation; pyrolysis; radiolysis; reaction kinetics; reduction (chemical); solvation*
 acetonitrile-water mixtures, stratosphere-related aspects of gas phase ion chemistry 7-13775
 acetylene black, prod. in plasma reactor, design and energy concepts 7-20965
 actinides, physics and chemistry, handbook 7-24317
 addition reactions symmetrisation order transform. to nucl. spin magnetisation 7-42649
 advection-diffusion eqns., shock layer solns., stability 7-28314
 ajoene, antithrombotic cpd. from garlic, struct., mechanistic and synthetic studies 7-54449
 atoms and groups, relationship between charge capacity and hardness 7-49972
 Belousov-Zhabotinsky reaction, induction period, excitability bifurcation 7-65286
 Belousov-Zhabotinskii reaction, Farey triangle 7-65288
 Belousov-Zhabotinskii reaction, Fe³⁺ impurity effect 7-46800
 Belousov-Zhabotinskii reaction, Mn-catalysed, complex periodic oscills., Farey arithmetic anal. 7-39853
 Belousov-Zhabotinskii reaction, O₂ influence, theoretical anal. 7-54080
 Belousov-Zhabotinsky reaction, catalysed, ion induced oscills. 7-65301
 Belousov-Zhabotinsky reaction, oscillating, statistical exptl. study of target patterns (French) 7-28279
 benzene, in liq. isopentane soln., quantum tunnelling of muonium reactions 7-50414
 benzene+NO⁺, struct. and energetics, calc. by ab initio MO computations 7-8267
 bimolecular fast reversible reactions diffusion influenced, kinetics study 7-65282
 bimolecular reactions, diffusion influenced, kinetics study 7-65283
 binary metal alloy clusters, generation and reactivity 7-15784
 trans-bis(diphenylalkylphosphine)(pentaahalophenyl)nickel(II) bromide, nucleophilic substitution reactions and struct. investg. 7-59754
 bond order and valence indices, rel. to Mulliken's population anal. and covalent chemical reactivity 7-56948
 ditert.-butyl malonate in dioxane-water media, acid-catalysed hydrolysis, kinetic and mechanistic studies 7-39884
 t-butyl nitric oxide, singlet and triplet surfaces, unimol. reactions, spectroscopy, rate meas. 7-28300
 calcium monocyclopentadienide, prod. in gas-phase reaction, laser spectroscopic obs. 7-17775
 CARS, applications in chemical reactors, combustion and heat transfer 7-17788
 catalysis, heterogeneous reactions, computerised conc.-controlled recycle reactor 7-54164
 chain molecules, 1D, unimolecular reaction dynamics, RRKM theory 7-8246
 chemical boiling, heat and mass transfer, gas liberation and free convection 7-43907
 chemical reaction and charge-transfer processes, RIOSA quantum-mechanical study. 7-31159
 chemically anisotropic molecules, reaction rates, orientation relax. 7-65303
 coherent pulse sequence induced control of selectivity of reactions, exact quantum mechanical calcs. 7-28274
 complex scaling methods 7-46819
 composite system, design problems with allowance for interphase reactions 7-43661
 concerted reaction process, Woodward-Hoffmann rule, topological mapping explanation 7-59753
 condensed phase, curve crossing, dissipation, tunnelling and adiabaticity criteria 7-65284
 conjugated systems, computer reaction simulation, hybrid model 7-49874
 continuous periodic reactor, adaptive model following control algorithm 7-8254
 cycloadditions, reactivity, perturbation theory 7-49909
 dense gases, viscosity, chem. reaction effects 7-26375
 dense molecular clouds, abundances modelling 7-35029
 di-tert-butyl ketone, laser flash photolysis, time resolved CIDNP, multiplet and net effects 7-10617
 diffusion controlled reactions, Monte Carlo study 7-22994
 diffusion-controlled reactions among static reactive sinks, conc. depend. 7-39868

chemical reactions continued

- diffusion-reaction systems, fluctuations, adiabatic elimination of transport modes 7-39855
 5,6-dihydrobenzo(c)xanthylum salts, synthesis, struct. and spectral props. 7-57050
 dilute gases, chem. reaction rate, viscous flow and thermal flux effect calcs. 7-28268
 1,3-dioxo-2-silacycloalkanes, X-ray diffr., struct., chemical reactions 7-21185
 drug transport kinetics in membranes, simulation in organized assemblies 7-54511
 dual temperature thermal storage with complex compounds 7-65620
 electroactive species, Fourier transform IR reflectron absorpt. spectra 7-23093
 electronic struct. and dynamics, conf., Snowbird, UT, USA (April 1986) 7-55877
 energy hypersurfaces, N-dimensional, gradient extremals 7-13723
 engineering polymers, hydrophilic modification 7-23012
 ethylene, hydroformylation, in situ IR and EXAFS 7-59755
 excitation transfer between donors and acceptors in fluid soln., donor fluorescence decay meas. (French) 7-59236
 excitation transfer between donors and acceptors in fluid soln., theoretical anal. (French) 7-59745
 exothermic, in coupled nonisothermal continuous stirred tank reactors, dynamics 7-13732
 extended Brusselator, multiple attractors 7-17777
 fluid-fluid interface, multicomponent mass transfer 7-8255
 formation of carbamic acid, urea and carbonic acid from CO₂, H₂O and NH₃ 7-8268
 gas phase reaction kinetics, rapid scanning FTIR time-resolved spectrometry technique 7-48886
 gas-liquid kinetics, meas. using press-response method 7-13821
 gas-phase chemistry in dense clouds, complex molecule synthesis 7-18444
 gas-solid reactions, transport and mixing characts., thermocentrifugometric anal. 7-54095
 gaseous swarms, reactive phenomena theory 7-13749
 gels, drying induced shrinkage, liquid flow and chem. reactions 7-23069
 Ginzburg-Landau critical regimes, periodic perturbation entrainment 7-3575
 homogeneous, wall to gas heat transfer coeffs. 7-8258
 homogeneous chem. system. entropy prod. rate 7-13721
 homogeneous gas phase mechanism for regional acid deposition model 7-3737
 hopping-controlled reactions with variable hopping range, models 7-33924
 II-VI-III-V systems, thermodynamics and reactivity 7-16790
 inorganic layered cpds., reactivity, conf., New York, NY, USA (Apr. 1986) 7-41003
 intercalation cpd. struct., enthalpy of reaction 7-46841
 interstellar D chemistry 7-35030
 interstellar medium, role of dust grains in chemical evolution of molecules 7-48014
 interstellar molecular clouds chemistry, grain surface reactions anal. from matrix isolation study 7-24179
 interstellar polyynes and related species, interstellar chem. investg. 7-48031
 interstellar processes and submm astronomy 7-48060
 interstellar S chem. in mol. shocks 7-48048
 kinetics of H₂SO₄ and NH₃ reactions for chemical storage of solar energy 7-40048
 macrotransport processes in the presence of bulk and surface chemical reactions 7-8299
 malonic acid, Belousov-Zhabotinsky reaction, oscillatory states transition 7-17765
 materials synthesis under high-press. shock loading 7-33934
 mechanisms, pot. energy surface, symmetry selection rules, transition state theory 7-3573
 metal clusters, formation, energetics and reactions 7-15776
 methanimine, fluorination effect on double bonds, SCF HF and MP2 ab initio calcs. 7-10384
 methanol synthesis over shock-compressed ZnO powder catalysts 7-39919
 mixing, imperfect, model, CSTR 7-8286
 molecular dynamics of the A+BC reaction in rare gas solution 7-28273
 monomolecular reactions, diffusion-induced, fluctuations and rotation 7-39864
 Monte Carlo simulations of reaction kinetics on clusters and islands 7-22977
 multidimensional systems, electronically nonadiabatic transitions 7-28302
 multiple stationary states, oscillations and macroscopic spatial struct. in far from equilib. systems 7-28280
 muon spin resonance, conference, Uppsala, Sweden (June 1986) 7-48141
 nighttime chemistry for offshore oceanic environment and dry environment 7-34584
 nitromethane, shocked, condensed, ignition, rate determining step 7-54124
 nonisothermal continuous stirred tank reactor, multivariable, global control using moving model 7-13729
 nonlinear characteristics and control of chemical processes (Japanese) 7-65302
 B-nor-D-homo-8-isoanalogs, of steroid oestrogens, synthesis, biological activity (Russian) 7-23293
 Oregonator model, excitability thresholds, Hopf and SNIPER bifurcations 7-65287
 organic crystals, chem. transformations, phase transition effects (Russian) 7-28309
 organic solid state chemistry and X-ray crystallography 7-58098
 organic vapours, thermally induced nucleation 7-23051
 organometallic sonochemical synthetic reactions, new trends 7-50902
 perfluorobenzene, electron transfer reaction kinetics, binding energy role 7-22989
 perfluoromethylcyclohexane, electron transfer reaction kinetics, binding energy role 7-22989
 periodic systems, sensitivity anal., Floquet theoretic approach 7-39854
 phosphamethane, fluorination effect on double bonds, SCF HF and MP2 ab initio calcs. 7-10384
 photosynthetic bacteria reaction centres, recomb. kinetics, electric field depend. 7-47017
 plasma etching reactors, energy distrib. of ions 7-37759
 polyacetylene, p-type doped, reaction with H₂O 7-65316
 polycyclic organic matter in atm., evidence for transformation 7-3735

chemical reactions continued

polyurethane biomaterials, hydrolytic stability in model biological media, surface morphology changes 7-17673
 polyurethane foam, form., exotherm data acquisition using microcomputer 7-54118
 polyurethane-polysiloxane interpenetrating polymer network, morphology, dynamic mech. investig. 7-37901
 positive ion clustering with acetonitrile in atm. 7-999
 o-positronium, quenching reactions, solvent dielec. const. role 7-54077
 potential energy surface homology 7-13725
 potential energy surfaces, LCAO, MO and SCF calcs. 7-17764
 pyroxenes, synthetic, exsolution and phase transforms., X-ray and TEM obs. 7-16725
 radiative heat fluxes in supersonic flow of inviscid gas over 3D bodies 7-43972
 rapid reactions, microdroplet mixing technique investig. using Raman spectrosc. 7-54082
 reaction channel with attractive Coulomb force, threshold continuity theorems 7-10697
 reaction kinetic parameters, estimation by local online experimentation 7-8288
 reaction mechanisms, group theory, global anal. 7-59743
 reaction-diffusion eqns., semidiscrete approx. asymptotic behaviour 7-39880
 reactive ion etching, AES, photoluminescence, SEM obs. 7-65241
 reactive scattering, quantum mechanical, via exchange kernels, exchange interaction calcs. 7-28284
 reactive scattering by large systems, space-time correl. fn. representation 7-28281
 riemann geometrical formulation of the principle of least electronic motion in chemical reactions 7-65281
 ring dynamics and percolation in an excitable medium 7-28277
 rotational and vibrational energy transfer, exponential model 7-10715
 Sb₂O₃, thermodynamic stability, EMF obs. 7-46828
 shocked molecular systems, energy transfer, mol. dynamics simulations 7-39895
 Shuttle glow, chemilum. processes 7-47602
 sodium tetraethylaluminate with NaH, thermodynamic characterisation using phase diagrams and electrochemical meas. for H₂ storage 7-54366
 solid state reactions, heterogeneous, structural features influence (*German*) 7-17766
 solid state reactions, real-time neutron powder diff. 7-16361
 sonochemical hot spot 7-12211
 sonochemically enhanced Ullmann reactions 7-50903
 sonochemistry: historical developments and modern aspects 7-50895
 spiroindolinonaphthoxazine, in glassy polymer matrix, thermal reaction anal. by photochromism 7-54088
 static reaction-diffusion structures in folded slow manifold systems 7-22980
 strontium monocyclopentadienide, prod. in gas-phase reaction, laser spectroscopic obs. 7-17775
 synthesis, micro and semimicro methods, time efficiency study 7-9642
 tetramethyldioxetane in free jet expansion, overtone vibr. initiated unimol. reaction, RRKM theory 7-28299
 thermal stability of chem. reactor, dynamic system stability estimate based on quasistationary principle 7-81
 thermodynamic properties of reaction involving minerals and aqueous solutions, program 7-28330
 thyatron plasmas, self-consistent modeling 7-32122
 toluene, mixed acid nitration, isomer distrib., mass transfer effects on selectivity 7-54094
 transition metal impurities, interstitial, enhanced mobilities and reactivities 7-17769
 transition state identification, statistical method 7-22991
 transition states location using algorithm for ab initio program package Gaussian 82 7-13720
 4-(2,4,6-trimethyl)benzylidene-2-phenyloxazolin-5-one, cryst. struct. determ. and reaction investig. 7-54084
 two-step chemical reaction, nonequilib. conc., steady state fluctuations and struct. factor 7-13726
 unimolecular reactions induced by vibr. overtone excitation, collisional energy transfer 7-39863
 urea-formaldehyde polymer, struct. swelling and titration (*Russian*) 7-6500
 US cavitation, sonochemical reaction and local temp. determ. 7-3594
 VX model compound, reactive props., electrostatic pot. calcs. 7-56954
 AgNO₃, countercurrent diffusion with HCl in cellulose and Nafion films 7-12377
 Al-Ni powder mixtures, shock-induced chemical reactions, optical meas. 7-39463
 Al_nM chem. reaction, M=refractory metal, for Si LPE layer form. 7-7043
 Ar-NO₂ system, muon spin relax. in transverse and longit. mag. fields 7-50413
 Ar+N₂⁺, absolute state to state total cross sections meas. 7-46825
 BN ultrafine powder synthesis at -75 to 750°C 7-22629
 Be, insertion in H₂ and H₂O, C₂ pathway, CI calcs. 7-10445
 C₂MnCl₂·2.4NH₃+4.8NH₃, thermochemical energy storage, kinetic study (*French*) 7-17782
 CO, insertion reactions, electron correl. effects, MP2 and CAS SCF calcs. 7-65289
 CO₂+amines, in nonaqueous solvents, reaction kinetics 7-46803
 CdO-Al₂O₃-P₂O₅ glasses, EPR spectra, synthesis effects 7-64530
 Cl atom conc. meas. in plasma etching reactor 7-37760
 Cl⁻+H₂O (methanol)(acetonitrile), clustering reactions, van 't Hoff plots based on ab initio MO calcs. 7-28288
 Cr-rich oxides, dissolution using H₂SO₄-Ce(IV) soln., radiation decontamination appl. 7-6803
 Cu(II)-alkyl persulphide complex prod., mol. and electronic struct. 7-15590
 Fe clusters+NH₃, reaction kinetics, cluster binding sites and adsorbate binding energies 7-54106
 Fe complex, nucleophilic attack, activation mechanism, EHT and INDO calcs. 7-39847
 Fe(NO₃)₃ reactions with catechol and Na₂S₂O₂, dispersive mode stopped flow X-ray absorption spectroscopy 7-61416
 Fe₃-O₄, diffusion-controlled form. during reactions, defects effects 7-17768
 γ-FeOOH-LiCO₃, mixture, mechanochem. transform. and γ-Fe₂O₃ form. 7-59478
 GaAs, VPE growth, reaction mechanisms 7-58693

chemical reactions continued

GaAs-thermal oxide interfacial chem. reactions, Raman spectra, AES 7-27145
 H transfer in double minimum potential, kinetic props. and quantum dynamics 7-54104
 H₃AsO₃+IO₃⁻, stirring effects and bistability; coalescence-dispersion model 7-46801
 HCl, countercurrent diffusion with AgNO₃ in cellulose and Nafion films 7-12377
 HCo(CO)₃, hydroformylation, quantum chem. calcs. 7-54115
 HCo(CO)₄, hydroformylation, quantum chem. calcs. 7-54115
 (HF)₂, degenerate rearrangement, tunneling splitting, reaction-path anal. 7-22979
 H₂P₂, unimol. rearrangement, ab initio investig. 7-25342
 H₂P₂⁺, unimol. rearrangement, ab initio investig. 7-25342
 H₃(n)(PV_nMo_(12-n)O₄₀).XH₂O, stability to dehydration in air and vacuum, ESR study 7-38929
 H₂SO₄, kinetics of heterogeneous reactions for chemical storage of energy 7-23229
 Hg+Xe, complex form., equilib. const. 7-19752
 I⁻+ClO₂⁻, oscillatory reaction, stirring and premixing effects 7-28278
 I₂, in liquid Xe, vibr. relax. following geminate recombination 7-10712
 InGaAs, reactive ion etching 7-65241
 InP, reactive ion etching, AES, photoluminescence, SEM obs. 7-65241
 (Ir(H₂O)₆)³⁺, substitution inertness, rate const. meas. 7-59742
 K₂S₂O₇ for chemical storage of solar energy 7-23228
 Mg₂Ni dehydrogenating kinetic rates, use as H₂ storage material 7-54363
 Mo electrodes, porous, role of O in alkali metal thermoelec. convertor 7-13925
 N₂ afterglow, U cpd. interaction appl. to laser isotope separation 7-39898
 NH₃, kinetics of heterogeneous reactions for chemical storage of energy 7-23229
 (NH₄)_{0.32}H₂O₁₆WO₃, intercalation cpd. struct., enthalpy of reaction 7-46841
 (NH₄)_{1.84}V₃O₈, intercalation cpd. struct., enthalpy of reaction 7-46841
 NaH, thermodynamic characterisation using phase diagrams and electrochemical meas. for H₂ storage 7-54366
 Na₂O.nAl₂O₃, mullite struct., form. by solid state reaction 7-7937
 Na₂S₂O₇ for chemical storage of solar energy 7-23228
 Ne+He₂⁺, charge transfer reaction rate const. 7-22983
 Ni alloys, thermodynamic anal. of gas phase in thermal diffusion alumino-siliconising 7-1660
 O+unsaturated hydrocarbon, relative rate const. at room temp. 7-28283
 O₂, glow discharge, metastable at. and mol. processes 7-16342
 O₂+K. O₂⁻ ion form., rate const. 7-33926
 O₃ form. in atm. effect of urban areas traffic pollution 7-3736
 O₃, synthesis in charged particle induced inert gas-O₂-(SF₆) discharges 7-3587
 OH+cytosine, ab initio SCF MO calcs. 7-8478
 POBr, gaseous, form., mass spectrometric and matrix IR investig. 7-39908
 S₂, liq., chem. reactions, mol. dynamics simulation 7-39862
 SF₆, corona and glow discharges, electrode-F reaction influence 7-26565
 SF₆, electron transfer reaction kinetics, binding energy role 7-22989
 Si, polycrystalline, chemistry of plasma etching with H₂ and Cl₂ 7-54021
 Si-transition metal interfaces, competing initial chemical reactions 7-21693
 SiO₂ films, hydrogenation during thermal nitridation in NH₃ 7-13763
 SiO₂ xerogels, structural changes during low temp. dehydration 7-28366
 SiO₂:Cl films prod. by Si oxidation in Cl containing ambients, impurity distrib. 7-26787
 Sn IV complex, form. in mixed Na pyrophosphate/SnCl₂ soln., ¹¹⁹Sn NMR 7-10624
 TaS₂, electrochem. intercalation reactions with Li, K, H, In, Ga, In_{0.17}Ga_{0.83}, nucl. quadrupole interactions, TDPAC meas. 7-17245
 Ti-SiO₂-TiSi₂-Si, high temp. reaction between Ti and SiO₂, XPS, sputtering (*Japanese*) 7-7022
 Ti₃Mo₂C₂-TiO₂-C black mixture, complex carbide interactions on heat treatment, homogenisation 7-53684
 TiO₂ gel, formation by hydrolysis of Ti alkoxides, molecular precursor modification by acetic acid 7-59793
 U, reaction rate with water vapour, 30-80 °C 7-42119
 U_{0.86}Gd_{0.14}O_{2+x} pellets, reaction with Cs fission product, annealing, diametral expansion 7-56756
 UO_{2+x} pellets, reaction with Cs fission product, annealing, diametral expansion 7-56756
 V-Ti-Fe-H₂ system, V-rich, dihydride form., lattice parameters, thermodynamics 7-32369
 VO⁺+inert gases, collision-induced dissoc. studied by ion beam tandem mass spectrometer 7-23001
 WF₆, in plasma centrifuges, W recovery 7-46846
 ZnSO₄-Na₂SO₄ reactions in CoCrAlY hot corrosion 7-28188

chemical reactivity see chemical reactions

chemical relaxation

gas phase relaxation process, bulk props. at early times, anal. soln. 7-50319
 H₂-F₂-HF gaseous mixture, light initiated chain reaction, stimulated light scatt. study 7-62778

chemical shift

see also isomer shift

n-alkanes, urea inclusion cpds., chemical shift chain length depend, CPMAS NMR spectra anal. 7-25557
 acetonitrile, dissolved in rapidly spinning nematic matrix, mol. orientation in strong external mag. field (*Russian*) 7-15626
 alkanes, prediction of ¹³C NMR spectra, rigid hydrocarbons geometrical parameters anal. 7-31068
 alkyl nitriles, conformational kinetics calcs., gas and liquid phases, MR spectra 7-19896
 alkyl nitriles gas and liquid phases, syn-anti conformer equilib., MR chem. shift study 7-19895
 4-n-alkyl-4-cyanobiphenyls, nematic ordering, off magic angle spinning ¹³C NMR 7-22153
 4-n-alkylbicyclo (2,2,2)-octan-1-carboxylic acids, spin-spin relax. 7-59121
 alkynyl(trimethyl)mercurials, synthesis, ¹³C, ²⁹Si and ¹⁹⁹Hg NMR 7-31071
 aluminosilicates, at. charges, SCF and semiempirical calcs. 7-2942
 aminosilanes, coupling const., chem shift, ¹⁵N NMR study 7-31072
 aminostannanes, coupling const., chem shift, ¹⁵N NMR study 7-31072

chemical shift continued

- L-asparagine, H_2O , ^{15}N chemical shift tensor, MASS NMR spectra anal. 7-53164
- automated analysis of two-dimensional NMR spectra of mixtures by pattern recognition 7-24635
- 1-azabicyclo[2.2.2]octane, binary solvent system, solute-solvent interactions, ^{13}C and ^{14}N spin-lattice relax. study 7-31069
- 8-azabicyclo[3.2.1]octan-3-ones, derivatives, conform. study, ^1H and ^{13}C NMR spectra anal. 7-36647
- benzene, ^1H chem. shift, D isotope effects, conc. depend. additivity rule 7-50196
- benzenes monosubstituted, H-bonded, complexes with fluoroalkanol and fluoroalkyl ethers, ^1H NMR study 7-42651
- bicalicene, cyclic, electronic structure, SCF CI calcs., NMR and PMR 7-50185
- bis(pentafluorophenyl)telluride and its dihalide, ^{125}Te Mossbauer and NMR chemical shift 7-7615
- bis(trifluoromethyl)telluride and its dihalide, ^{125}Te Mossbauer and NMR chemical shift 7-7615
- bleomycin A_2 , ^{15}N NMR resonance assignments, ^1H - ^{15}N shift correlation spectra anal. 7-25548
- borate esters, in aq. solns. and wine, ^{11}B NMR 7-934
- borate minerals, unoccupied mol. orbitals of B-O bond mol. orbital calcs., XANES, NMR and electron transmission spectra 7-33281
- broadband decoupled zero-quantum coherence for NMR spectroscopy and imaging 7-9858
- chalcocarbonyl(5,10,15,20-tetraphenylporphinato) iron II complexes, IR and NMR spectra 7-33394
- cobaltocenium hexafluorophosphate- d_{10} , ^2H MAS NMR spinning sideband spectra study 7-33282
- cyclohexyl halides, thiourea inclusion compounds, substituted cyclohexane conform., ^{13}C CP/MAS NMR spectra 7-19889
- cytidyl-(3'-%)guanine-methylmercuric cation, aq. soln. interaction, NMR chem. shifts and coupling consts. determ. 7-50179
- deoxycytidyl-(3'-5')guanine-methylmercuric cation, aq. soln. interaction, NMR chem. shifts and coupling consts. determ. 7-50179
- di(2-pyridyl)dichalcogenides, conform. and rot. isomerism ^{13}C NMR spin-lattice relaxation study 7-19888
- dichloroacetic acid complex with substituted pyridines, solvent effects, IR and ^1H NMR spectra anal. 7-62365
- dimethyl tin diacetate, solid-state and soln. struct., ^2H and ^{13}C NMR spectra study 7-25431
- dimethyl tin diacetate hydrolyzate, solid-state and soln. struct., ^2H and ^{13}C NMR spectra study 7-25431
- dimethyldioxirane, electronic struct. and geometry, NMR chem. shifts 7-62406
- dimethylthallium(II) cation, aq. soln., mol. motion, NMR spin relax. time meas. 7-57088
- 2,4-dinitro-6-diazophenol, and analogues, struct. investig. 7-57087
- dipalmityl phosphatidyl chloride, low temp. phase, headgroup mobility, NMR study 7-1856
- 1,3-diphenylthiureas, ^{13}C NMR spectra, chemical shifts and mol. conform. study 7-42650
- 1,3-dipyridyl thiureas, ^{13}C NMR spectra, chemical shifts and mol. conform. study 7-42650
- estrone, long range H^+ coupling, chem. shift, ^1H NMR 7-19903
- ethyl acetate-6-o-acetylmorphine adduct, PMR chem. shift charactn. 7-57084
- fluorocyclohexane, thiourea inclusion compounds, substituted cyclohexane conform., ^{13}C CP/MAS NMR spectra 7-19889
- globoside, oligosaccharide headgroup, soln. conform. study, ^1H NMR spectral methods anal., pot. energy calcs. 7-25361
- group IV organotellurides, ^{125}Te and ^{119}Sn Mossbauer and NMR study 7-7614
- n-hexane, partially oriented in liq. crystal, dipolar coupling consts., NMR methods study 7-25547
- hydrides, first and second row, NMR chem. shift bond length derivatives 7-42644
- L-iduronic acid, sulphated residue in heparins, conformer struct. and population study, ^1H NMR spectra anal., force field calcs. 7-25546
- II-VI semiconductors, shallow donor problem, pseudopot. approach 7-45216
- imaging in high mag. field using chemical shift-specific slice selection 7-48819
- [IN-(2-1) furylidene)- β -(2-furyl)serine methyl ester, diastereomeric forms, tautomeric equil., solvent effects ^1H and ^{13}C NMR spectra 7-19893
- merocyanine dyes, J aggregate form. in mixed monolayers, visible spectra and surface pressure-area isotherms anal. 7-31059
- 2-methoxy-2-oxo-1,3,2-oxazaphosphorinane, conformer struct. and populations, IR, NMR and X-ray spectra anal. 7-25509
- methyl alcohol, ^{13}C NMR chem. shifts, intermol. interactions effects 7-50193
- methylcyclohexane, thiourea inclusion compounds, substituted cyclohexane conform., ^{13}C CP/MAS NMR spectra 7-19889
- methyldichlorophosphine, struct., and orientation in mixed nematic liq. crystals, NMR spectra anal. 7-53165
- monosubstituted ammonium compounds, ^1H NMR chemical shifts of solvent water 7-36648
- multiple chemical shift selective NMR imaging using stimulated echoes 7-14097
- NMR chemical shift imaging, phase-encoded, generalisation 7-47193
- NMR imaging, phase contrast, chemical shift imaging 7-18043
- NMR magic angle spinning technique, chem. shift tensor anal. 7-24665
- nuclear spin relaxation, dipolar and chem. shift anisotropy contribs., interference terms appls. 7-50191
- organic systems, ^1H - and ^{13}C -NMR chemical shifts, elucidation of structures 7-50181
- orthophosphates, ^{31}P NMR chem. shift, anisotropies, struct. and cation effects 7-50187
- paraffins, cyclic, with long chain lengths, ^{13}C NMR chem. shift meas., cryst. structures 7-64537
- peptides, struct. anal., NMR meas. 7-54452
- 1-phenyl-2-pyrrolidinone, substituted, nucl. coupling consts., NMR chem. shifts 7-931
- phosphates, ^{17}O , ^{31}P , ^1H and ^{13}C NMR spectra study 7-25544
- phosphites, ^{17}O , ^{31}P , ^1H and ^{13}C NMR spectra study 7-25544
- platinum-cyanoalkene complexes, mol. vibr. study, Raman and IR spectra anal. 7-42626
- polydimethylsiloxane elastomeric networks, ^{29}Si NMR 7-44402
- polyhalomethanes, X-ray photoelectron spectra, chem. shifts 7-15648
- proteins, struct. anal., NMR meas. 7-54452

chemical shift continued

- proton chemical-shift NMR imaging with nonuniform fields 7-14089
- 1,3-pyridylphenylthiureas, ^{13}C NMR spectra, chemical shifts and mol. conform. study 7-42650
- salt/water/aprotic solvent mixtures, alkali cation influence, IR spectra anal. 7-19856
- short-chain molecules, liquid-phase, motion, ^{13}C and ^1H NMR investig. 7-15624
- single quantum J resolved spectra, zero-quantum coherences 7-9859
- slice selection in the presence of chemically shifted species 7-48821
- spatial localization with surface coils using multiple-pulse chemical-shift scaling 7-24671
- sulphone derivatives, α,β -unsaturated, substituent induced chem. shift, NMR 7-19900
- sulphones, ^{33}S NMR spectrosc 7-5700
- T4 lysozyme, ^1H amide resonance assignment, ^{13}C , ^{15}N DNMR spectra anal. 7-25572
- tetramethylsilane, ^{13}C NMR chemical shifts, solvent effects 7-50198
- 4-thiacyclohexanones, 2,6-disubstituted, stereochemistry, ^1H and ^{13}C NMR 7-57096
- 2-thio-1,3,2-oxazaphosphorinane, conformer struct. and populations, IR, NMR and X-ray spectra anal. 7-25509
- thiophosphates, ^{17}O , ^{31}P , ^1H and ^{13}C NMR spectra study 7-25544
- thiosemicarbazide, bonding and struct., effect of protonation, ^{14}N quadrupole reson. spectra anal. 7-33295
- thiosemicarbazide hydrochloride, bonding and struct., effect of protonation, ^{14}N quadrupole reson. spectra anal. 7-33295
- N-vinylcarbazole, halogeno and nitro derivatives, struct., PMR, MNDO calcs. 7-933
- $\text{Al}_2\text{O}_3\text{-TiO}_2$ amorphous films, thermal expansion and coordination state of cations 7-44860
- 1-aminocyclopropane-1-carboxylic acid, chem. shifts, PMR 7-19902
- AsS_3 , realger, X-ray chemical shift, K absorpt. spectra anal. 7-46239
- As_2S_3 , orpiment, X-ray chemical shift, K absorpt. spectra anal. 7-46239
- Bi chalcogenides, binding energies, chem. shifts XPS and diffuse refl. spectra (German) 7-1943
- CO , chem. shifts meas. in zero-pressure limit 7-62408
- $\text{CdO-B}_2\text{O}_3\text{-Si}(\text{Ge})\text{O}_2$ network struct., coordination and bonding, comp. depend., NMR study 7-6535
- CoAs_3 , smaltite, X-ray chemical shift, K absorpt. spectra anal. 7-46239
- $\text{Cu}_2(\text{OH})_2\text{CO}_3$, malachite, X-ray K-absorpt. study 7-7790
- DI, Ar matrix, conc. effects, binary complexes with impurities, IR spectra anal. 7-31034
- Dy compounds, L_{III} X-ray absorption spectra 7-39312
- FeAsS , arsenopyrite, X-ray chemical shift, K absorpt. spectra anal. 7-46239
- GaAs (100), chemical etching and oxidation, XPS characterisation 7-21591
- n-GaAs films, magneto-optical studies under high hydrostatic press. 7-13247
- HI, Ar matrix, conc. effects, binary complexes with impurities, IR spectra anal. 7-31034
- $\text{H}_2\text{O-DMSO-1,4-dioxan}$, chem. shift, NMR spectroscopy 7-25559
- ^1H 2D chemical shift correlation spectra, image anal., symm. rules 7-35559
- LiClO_4 , solns., chem. shift, NMR 7-57085
- $\text{Na}_2\text{O-Al}_2\text{O}_3\text{-SiO}_2\text{-H}_2\text{O}$, zeolite ASM-5, framework site resolution and assignment by X-ray and NMR meas. correl. 7-25541
- Ni complex, $\text{Ni}(\text{nonamethylimidodiphosphoramide})_3(\text{ClO}_4)_2$, stereochemically nonrigid, proton NMR study 7-25551
- Ni complex, $\text{Ni}(\text{octamethylpyrophosphoramide})_3(\text{ClO}_4)_2$, stereochemically nonrigid, proton NMR study 7-25551
- Ni II complex, (salicylaldehyde)(acetylacetonate)ethylenediimino nickel(II), mixed and non-mixed complexes, PMR 7-31075
- Ni-Mo (6 at %), oxidation, ESCA study 7-22897
- PF_3 , ^{19}F NMR chem. shifts and NQR coupling consts. 7-50188
- $\text{Pd}(\text{II})$ complexes, X-ray absorpt. near-edge struct., ligands influence 7-22380
- Pt complex, $[\text{Pt}(\text{NH}_3)_2(\text{OH})_2(\text{C}_5\text{H}_7\text{N}_3\text{O}_2)](\text{NO}_3)_2 \cdot 2\text{H}_2\text{O}$, metal stabilised cytosine iminoxo tautomer, form. and geometry 7-26710
- PtBr_6^{2-} , NMR chemical shift, nuclear shielding, ro vibr. averaging 7-25550
- PtCl_6^{2-} , NMR chemical shift, nuclear shielding, ro vibr. averaging 7-25550
- Ru (II) complexes, Ru NMR chem. shifts 7-50190
- SF_6 , NMR, ^{77}Se , ^{125}Te and ^{19}F shielding and isotope shifts, temp. depend. 7-25549
- SF_6 , NMR chemical shift, nuclear shielding, ro vibr. averaging 7-25550
- SeF_6 , NMR, ^{77}Se , ^{125}Te and ^{19}F shielding and isotope shifts, temp. depend. 7-25549
- SeF_6 , NMR chemical shift, nuclear shielding, ro vibr. averaging 7-25550
- Si, group III acceptors, neutral and ionised states, deep dopant description 7-64155
- Si surface, Ar^+ ion impact, LMM and LVV Auger electron emission 7-59320
- SiF, core-excited Rydberg state, SCF calcs. 7-851
- SiH_3F_3 ($a+b=4$), NMR shielding consts., ab initio coupled HF calcs. 7-42646
- $\text{Si}_2\text{O}(\text{PO}_4)_6$, chem. shift meas., solid-state ^{29}Si MAS NMR 7-53163
- Sn IV complex, form. in mixed Na pyrophosphate/ SnCl_2 soln., ^{119}Sn NMR 7-10624
- Te cpts., valence electron configs., X-ray chemical shift and Mossbauer isomer shift, SCF anal. 7-32893
- TeF_6 , NMR, ^{77}Se , ^{125}Te and ^{19}F shielding and isotope shifts, temp. depend. 7-25549
- TeF_6 , NMR chemical shift, nuclear shielding, ro vibr. averaging 7-25550
- (Ti,Ta) $_2$ solid solns., chem. shift and cryst. field splitting rel. to valence charge, EXAFS 7-27818
- TiN_x , characterisation by X-ray emission spectroscopy (French) 7-46244
- Tl oxides and halides, covalency and NMR chem. shift correls. 7-2941
- Tl_2MnI_6 , paramag. suscept. w.r.t. NMR chem. shift, hyperfine coupling const. determ. 7-2941
- U cpts., metallic and nonmetallic, X-ray absorpt. at various thresholds 7-64793
- W complexes, W (VI) isopropylimido, cryst. and mol. structs. 7-51722
- WF_6 , NMR, ^{77}Se , ^{125}Te and ^{19}F shielding and isotope shifts, temp. depend. 7-25549
- WF_6 , NMR chemical shift, nuclear shielding, ro vibr. averaging 7-25550

chemical structure

- see also *bonds (chemical)*; *crystal atomic structure*; *crystal chemistry*; *molecular configurations*
- bond index, definition 7-877
- chemical graph-theoretic cluster expansions 7-46794
- chlorophyll *a*, intact and metal-substituted, metal-sensitive bands in Raman and IR spectra 7-25520
- chlorophyll forms, vib. state and struct. anal., Raman spectra 7-19867
- clay constituents, apportionment into structural formula 7-65999
- conference, Marineland, Florida, USA (March 1986) 7-40985
- double bonds, through space interactions, UV photoelectron spectrosc. investig. 7-57130
- graph theory, theoretical concepts and appls. 7-39848
- hydrophobicity parameters from partition coeffs. 7-13954
- identification numbers 7-46795
- information retrieval system, microcomputer based 7-10774
- inorganic layered cpds., reactivity, conf., New York, NY, USA (Apr. 1986) 7-41003
- ion-selective membranes, with chelating agents, stoichiometry of current-carrying complexes 7-33955
- macromolecules, chem. inhomogeneous mixtures, fractionation efficiency anal. (*Russian*) 7-26928
- muonic complexes with atoms and molecules, chem. stability calcs. 7-36827
- organic chemistry, Mobius systems, graph theoretical approach 7-46796
- poly-p-phenylene sulphide, conducting polymer solution, chemical structure, EPR and ¹³F NMR studies 7-2938
- polyacrylonitrile, XPS studies 7-53507
- polyacrylonitrile fibres, stabilised, chem. struct., XPS obs. 7-32541
- polybutadiene acrylates, UV-curable optical fibre coating material, low-temp. modulus 7-51911
- polyethylene oxide-melaminoformaldehyde cured copolymer, crystallisation and melting (*Russian*) 7-26923
- polyethyleneoxide, cryst., eqn. of state, anharmonic theory calcs. 7-32596
- polymer representation, matching polynomial of a polygraph 7-5796
- polymers, molecular weight, distrib. between crosslinks 7-50425
- polyoxymethylene, cryst., eqn. of state, anharmonic theory calcs. 7-32596
- polypyrrene fusenes, subgraph enumeration, transfer-matrix method 7-10377
- polystyrene-divinylbenzene, 2,2'-dipyridylamine binding, transition metal complexes form. 7-23014
- polytetrahydrofuran, cryst., eqn. of state, anharmonic theory calcs. 7-32596
- positronic complexes with atoms and molecules, chem. stability calcs. 7-36827
- violacein, thin layer chromatography and FTIR analysis 7-54469
- Cu complex, CuCl₂-2-phenyl-4,4,5,5-tetramethylimidazoline-1-oxyl-3-oxide, mag. props. 7-51715
- Fe complexes, Fe(II)-neutral N bases, reactivity, basket-handle super-struct. effects 7-54100
- E-glass, coord. of iron, ESR and mag. meas. 7-13021
- Na complex, NaI diglyme, cryst. struct., bond bridging 7-51724
- SAW device, coating responses, rel. to solubility and chem. struct., pattern recognition 7-54162
- Si₃N₄ films prep. by plasma anodisation, XPS depth profiling 7-58667

chemical technology

- see also *chemical industry*; *chemical variables control*; *chemical variables measurement*
- absorption into water in packed tower, mass transfer coeffs. meas 7-266
- boiling curves, calcs. from unsteady-state quenching tests 7-54257
- bulk gas separation by pressure swing adsorption 7-54258
- ceramic synthesis from molecular precursors, conf., Palo Alto, USA (Apr. 1986) 7-35113
- column crystallisation, thermal countercurrent process (*German*) 7-52002
- continuous periodic reactor, adaptive model following control algorithm 7-8254
- fixed-bed reactor, robust multivariable control system design 7-54256
- foam behaviour of liquids in downcomers, expts. (*German*) 7-54192
- leaching processes, 3D diffusion eqn., numerical soln. 7-48638
- macromolecules, chem. inhomogeneous mixtures, fractionation efficiency anal. (*Russian*) 7-26928
- macroscale heat flow calorimeter for studying chemical processes 7-41391
- nonlinear characteristics and control of chemical processes (*Japanese*) 7-65302
- pipe extraction column, operating with two-phase drops, design (*German*) 7-51311
- polymerisation process computer control, using US sensors 7-8278
- reacting flows, combustion and chem. reactors, book 7-4644
- reaction kinetic parameters, estimation by local online experimentation 7-8288
- refrigerant-12 evaporator, swirl flow press. drop calcs. 7-51162
- thermodiffusion apparatus, counterflow, closed stream motion 7-43908
- zeolites use, conf., Burgas, Bulgaria (June 1985) 7-60885
- CaCO₃, formation in cooling water, critical pH depend. 7-54158
- D₂O distillation process, steady and unsteady state models 7-6340

chemical vapour deposited coatings see *CVD coatings***chemical vapour deposition**

- see also *vapour phase epitaxial growth*
- activated reactive evaporation 7-33576
- Al₂O₃, CVD technologies, rate controlling mechanisms, growth morphology 7-33575
- amorphous hydrogenated semiconductors, NMR studies, rel. to growth process 7-38405
- amorphous semiconductor films, photo-assisted CVD and opto-electronic characterisation 7-33595
- C coating effect on ICRH in tokamaks 7-6418
- C thin films, RF discharge deposition, mech., elec. and optical props. 7-22509
- cascade solar cells, efficient two-junction monolithic, grown by MOCVD 7-65483
- ceramic composites, non-oxide, CVD fabrication 7-64993
- ceramic-ceramic composite materials, CVD processing 7-64992
- crystal growth, ion/surface interactions, photo-induced reactions, review 7-53609
- diamond, layers, growth kinetics (*Russian*) 7-22506
- diamond, synthesis by laser induced CVD, low press. 7-13371
- diamond crystallisation, conf., Warsaw, Poland (June 1985) 7-18469
- diamond layers, crystallisation from gas phase, growth kinetics (*Russian*) 7-22505

chemical vapour deposition continued

- diamond layers, growth in laser heated substrate (*Russian*) 7-22507
- dielectric films preparation, activated reactive evaporation using resistively heated sources 7-13383
- electronic materials, CVD methods (*French*) 7-33589
- etching and deposition, basic mechanisms, review 7-53923
- fibre optics, construction technology, materials, technique and future prospects (*Italian*) 7-1274
- films, laser-assisted CVD, surface undulations, Raman microprobe analysis 7-12430
- fine oxide particle VAD for optical fibre preforms (*Croatian*) 7-20481
- gas mixture-laser interaction model, appl. to thermally activated laser-induced CVD 7-46333
- glass:TiO₂, Faraday rotator low loss single mode fibres, MCVD fabrication 7-25993
- glass-making, review 7-3259
- high-power single mode operation of index-guided inner stripe (I²S) laser by MOCVD 7-50592
- II-VI semiconductor films, prep., electronic props., solar cell appl. (*Japanese*) 7-54299
- II-VI semiconductors, low-temperature epitaxial growth, MBE and MOCVD 7-64906
- III-V semiconductors, organometallic CVD using metalorganic halides 7-33587
- In_{0.53}Ga_{0.47}As:Fe metalorganic CVD epitaxial growth and elec. props. 7-63993
- integrated optics use in telecommunications (*German*) 7-43446
- IR Fourier transform spectroscopy for investigating elementary processes in gas-solid interaction 7-33986
- laser direct writing and laser-assisted CVD of III-V cpds. on GaAs 7-13373
- laser materials processing developments at GEC Hirst Research Centre (UK) 7-53581
- laser processing of high-tech materials at high irradiance, review 7-13342
- laser processing of materials, conf., London, England (Dec. 1986) 7-48185
- LPCVD, film thickness distrib., 3D computer simulation 7-17451
- LPCVD on Si-Ge alloy for interconnect appls. 7-17472
- mechanisms, physics and chem. 7-17474
- metal nitride films, prep., props., microelectronics appls. 7-33557
- metallic films, growth by laser photolysis of carbonyls, C and O incorporation mechanisms 7-58685
- metallic thin films, plasma-enhanced CVD for metallisation appls. 7-17459
- MOCVD, control parameters, parametric anal. 7-22543
- MOCVD, horizontal reactors, complex flow phenomena 7-22530
- MOCVD growth processes, in situ charactn. by light scatt. techniques 7-22539
- MOCVD in inverted stagnation point flow 7-22531
- MOCVD laboratory, integrated safety system 7-22528
- MOCVD reactor, vertical vs. horizontal design, optical study of gas phase 7-22534
- MOCVD reactor cell, visualisation of flow and temp. profiles, appl. of holographic interferometry 7-22532
- MOCVD technology 7-3195
- multi-flame VAD process for high-rate fabrication of optical fiber preforms 7-43461
- nanometer structure fabrication (*Japanese*) 7-12545
- noncircular core optical fibres made by pressurized MCVD method 7-57612
- optical coatings, CVD prep., optical characts. 7-43456
- optical fibre fabrication by plasma activated CVD, review 7-11132
- optical fibre manufacture at AT&T by MCVD 7-11129
- optical fibre preform fabrication using MCVD process control technique 7-15981
- optical fibre preform manufacturing, homogeneous heating technique in MCVD 7-31534
- organometallic compounds, laser mass spectroscopy, laser CVD appl. 7-22573
- photoformation of dielectric materials, review 7-53633
- plasma assisted CVD deposited thin films for microelectronic appls. 7-22562
- plasma processing, conf., Palo Alto, CA, USA (April 1986) 7-35109
- plasma-enhanced, plasma-surface interactions, book contrib. 7-27943
- polymerisation, beam-induced, time constants and reaction cross sections meas. 7-7875
- polyphenylacetylene thin films, photochemical polymerisation 7-17441
- radical and ion assisted CVD, step smoothing 7-22565
- RF plasma CVD reactor, flow, temp., conc. fields, num. simulation 7-26501
- semiconductor complementary self-aligned laser arrays, MOCVD growth 7-31339
- semiconductor processing and fabrication techniques, laser diagnostic methods 7-22500
- semiconductors, MOCVD, organometallic precursors monitoring by laser mass spectroscopy 7-22547
- single-mode optical fibre preforms, dimension control in VAD process 7-6025
- solar panels with LPE and metal organic CVD circuits, satellite power 7-65493
- solid-state devices and materials, conf., Tokyo, Japan (Aug. 1986) 7-48173
- surface engineering for corrosion protection 7-3478
- tokamaks, carbonisation, plasmachemical in situ deposition 7-63296
- trimethylgallium CVD reaction, Ga atom detection by multiphoton-ionisation and mass spectrometry 7-25471
- trimethylgallium decomposition during CVD, effect of added hydrazine, multiphoton and electron ionisation mass analysis 7-23010
- tubular reactor, deposition rate and uniformity, diffusion and convection effects, mathematical model 7-22559
- ultra-thin semicond. film growth techniques, review (*Japanese*) 7-7857
- vacuum pump damage solutions for etch and CVD processes 7-35528
- vacuum symposium, Tokyo, Japan (1985) (*Japanese*) 7-14698
- York, England (Jul. 1986) 7-48142
- Al film, laser deposition for metallisation 7-53631
- Al film deposition using magnetron-plasma CVD system 7-64931
- Al MOCVD from trimethylaluminium, pyrolysis and photolysis 7-7881
- Al, selective CVD technology 7-53629
- AlGaAs BH laser with flared waveguides, high power operation, MOCVD growth 7-57352

chemical vapour deposition continued

- AlGaAs, MOCVD growth, refractive indices meas. by in situ reflectometry 7-59270
 AlGaAs:Mg-GaAs:Se concentrator solar cells, 26 percent efficient 7-3699
 AlGaAs-GaAs heteroface space solar cells with 21 percent conversion efficiency 7-3694
 AlGaAs-GaAs heteroface solar cells, role of window layer 7-3695
 AlGaAs-GaAs solar cells, high efficiency DH cells fabrication using MOCVD 7-3693
 AlGaAs-GaAs solar cells, fabrication on Si substrates 7-46937
 Al_{1-x}Ga_xAs films and multilayer structures, MOCVD growth and characterisation, review 7-33586
 Al_{1-x}Ga_xAs, MOCVD, equilib. gas phase species 7-22542
 Al_{1-x}Ga_xAs solar cells, MOCVD growth and characterisation, review 7-34043
 Al_{1-x}Ga_{1-x}As-GaAs heteroface solar concentrator cells, space and terrestrial appls. 7-65486
 Al₂O₃, CVD, morphology rel. to growth conditions 7-17431
 α-Al₂O₃, CVD coating morphology, trace impurity effects 7-3191
 Al₂O₃, film, prep. by pyrolysis of Al isopropylate 7-17448
 Al₂O₃ insulating thin films, normal press. CVD (*German*) 7-59453
 (Al₂O₃)_{1-x}(AlN)_x film, optical and elec. props., comp. depend. 7-38766
 Au by laser induction 7-22564
 Au films, CVD from Au complexes 7-64915
 Au, laser deposition from triphenylphosphine complexes 7-46341
 BeAl₂O₄Cr³⁺ crystals, growth and laser performance 7-15870
 C layers, deposition, by RF plasma decomp., physical props. 7-22508
 C, pyrolytic, low temp. growth with highly ordered graphite structure by CVD (*Japanese*) 7-13384
 CdGa₂S₄ single crystals, chemical vapour transport growth, microhardness, crack patterns 7-7833
 CdS skeletal and hollow crystals grown under time-increasing supersaturation 7-21144
 CdS-InP solar cells, high efficiency, with thermally evaporated window layers 7-3701
 Cd₂SnO₄, struct., elec. and optical props. (*Korean*) 7-27940
 CdTe, closed tube CVD growth using NH₄Cl transport agent 7-27913
 Co, siliconisation using Si₂Cl₆ source by diffusion and CVD processes 7-17700
 CoB layers and crystals, prep. by diffusion and CVD processes 7-17434
 CoGa₂O₄, crystal growth, chemical vapour transport, struct., mag. and electronic props. 7-53517
 Cu films, photochemically deposited, C contamination, surface processes 7-53617
 CuInS₂, chemical transport, thermodynamics 7-7832
 Fe, layer growth on polysiloxane surface in stream of H₂-Cl₂ mixture (*Russian*) 7-65353
 Fe(CO)₅, laser stimulated CVD, kinetics 7-64925
 Fe₂O₃ amorphous film deposition by laser CVD 7-39416
 GaAlAs/GaAs TJS lasers on Si substrates, MOCVD growth 7-62691
 GaAs, AlGaAs, MOCVD, design of safe facility 7-22529
 GaAs epilayers, plasma enhanced metalorganic CVD 7-46336
 GaAs excimer-laser-stimulated CVD, polycryst. thin film growth and props. 7-64912
 GaAs, MOCVD, gas phase depletion and flow dynamics in horizontal reactors 7-17433
 GaAs, MOCVD, uniform growth on multi-wafers 7-22536
 GaAs, MOCVD growth, thermal decomp. rates 7-22540
 GaAs, MOCVD layers on Si substrates with superlattice intermediate layers, DLTS studies 7-38501
 GaAs space qualified solar cell production by organic metal CVD, performance testing 7-65492
 GaAs/AlGaAs heterostruc. on Si substrate, MOCVD and MBE growth 7-7883
 GaAs/GaAlAs ultrathin layer systems, MOCVD growth and struct. props. 7-7063
 GaAs-AlGaAs superlattices and superstructures, growth by metal organic CVD (*Japanese*) 7-13386
 GaAs-Ge crystal growth on Ta₂O₅-coated Si substrates, zone melting and MOCVD 7-53579
 GaAsP, MOCVD growth, IR laser assisted grading 7-27945
 GaAsP-GaAs(P) strained-layer superlattices, MOCVD and device prep. 7-7876
 GaAs_{0.75}P_{0.25} solar cells, high efficiency, grown by one atmosphere MOCVD 7-3697
 GaInAsP-InP CW phase-locked semiconductor laser array, MOCVD growth 7-57351
 Ge polycrystalline films, photoassisted CVD prep. 7-3200
 Ge, vapour phase growth on Ge substrates, influence of p and n doping 7-3198
 GeCl₄ + X⁺ (X=He,Ne,Ar,H), optical emission spectra rel. to PCVD 7-26531
 GeF₄ + X⁺ (X=He,Ne,Ar,H), optical emission spectra rel. to PCVD 7-26531
 GeO₂-core/SiO₂-cladding optical fibres, modified CVD deposition and stimulated Raman appl. 7-43378
 GeS and GeSe, chalcogenide glasses for IR fibres, plasma deposition 7-37191
 H, excited state, translational energy distrib. in DC discharge, spectroscopic meas. 7-20946
 HgGa₂S₄-HgIn₂S₄ system, new multinary layered compound 7-53516
 HgTe films, deposition by photolysis of (t-butyl)HgTe(t-butyl) 7-3197
 InGaAlP transverse mode stabilized visible laser diodes fabricated by MOCVD selective growth 7-50591
 InGaAs, CVD growth by VPE, review 7-39417
 InGaAs films, organometallic CVD growth mechanisms, adduct formation 7-33588
 InGaAs/GaAs GRIN SCH SL quantum well laser, MOCVD grown 7-50557
 InGaAs/InP multiple quantum well waveguides, low loss, MOCVD growth 7-43358
 InP films, MOCVD growth using plasma pre-cracking 7-7880
 InSb-SiO₂ MIS structures, photo-CVD fabrication 7-38739
 MO, micrometer-scale line deposition using near UV laser light 7-59438
 MoO₃, amorphous electrochromic films, plasma enhanced CVD 7-22561
 Ni-NiAl, formation of NiAl coatings by CVD, kinetics 7-59451
 Pt, micrometer-scale line deposition using near UV laser light 7-59438
 Si alloys, amorphous, CVD, electrical and optical props. 7-33596
 Si, CVD, adsorption on Si (111) of Si-H system species, rel. to temp., supersaturation, bond strength and press. 7-33583
 Si, CVD, thermal diffusion effects, math. model 7-2410

chemical vapour deposition continued

- Si, CVD in annular tubes, film thickness profiles in mixed convection-diffusion regime 7-27190
 Si, deposition by photolytic or pyrolytic disoc. of SiH₄ under laser irradi. 7-13388
 Si doped, laser deposition for interconnections 7-53632
 Si, film deposition by radical jet laser-induced CVD 7-59457
 Si film growth for MOS-VLSI, Ti and Pt silicide form. 7-7870
 Si films, plasma-enhanced chemical vapour deposition model anal. 7-27937
 a-Si films, superlattice structure, photo-CVD deposition; solar cell fabrication 7-59450
 Si growth for electronic industry 7-33590
 a-Si high quality films and superlattice solar cells, prep. method 7-46346
 Si LPCVD films properties when formed from SiH₄ in vertical flow reactor 7-22563
 a-Si, large are uniform thin films, production by scanning plasma method (*Japanese*) 7-17449
 Si, laser-induced CVD for direct writing of Si lines 7-64921
 a-Si p-i-n solar cells, CVD deposition from Si₂H₆ 7-59841
 Si, polycrystalline, fabrication and use, overview 7-32879
 Si, polycrystalline films, low press. CVD growth and annealing, morphology obs. 7-3187
 a-Si solar cell modules fabricated with single-chamber load-lock deposition system 7-59860
 a-Si solar cells, fabrication methods using UHV reaction chamber system, high conversion efficiency 7-54293
 Si, technology and electronic materials (*Japanese*) 7-22466
 Si:B, low temp. epitaxial films, nonequilib. doping effects 7-58672
 Si:B(P), microcrystalline, LPCVD production, anal and solar cell appls. 7-17452
 a-Si:H, form. by ion flux control under toroidal mag. field (*Japanese*) 7-17446
 a-Si:H, laser-assisted CVD growth, optical props. 7-22210
 Si:H, microcrystalline, photo-CVD growth 7-13382
 a-Si:H, photo-CVD deposition, initial processes (*Japanese*) 7-7053
 a-Si:H, plasma enhanced CVD, integrated model 7-39423
 Si:H,F by thermal CVD, photosensitivity, spin density, conductivity and p-n type 7-17454
 a-Si:H,F films, H-radical-assisted CVD, hole transport 7-64264
 a-Si:H,F films, prep. using H radical assisted CVD (*Japanese*) 7-17430
 a-Si:H film, photoenhanced deposition and characts. 7-53635
 a-Si:H films, CVD, optical and electronic props. 7-33597
 a-Si:H films, discharge and CVD deposition, surface reactions 7-33601
 a-Si:H films, high rate deposition and impurity doping effects (*Japanese*) 7-13385
 a-Si:H films, laser induced CVD using SiH₄ photodecomposition 7-13376
 a-Si:H films, photo-CVD from SiH₄-H₂ 7-39394
 a-Si:H films, photo-enhanced CVD 7-33594
 a-Si:H films, photochemical vapour deposition from SiH₄-H₂ 7-64916
 a-Si:H films, plasma CVD, deposition kinetics (*Japanese*) 7-17450
 a-Si:H films, reactive deposition 7-33592
 a-Si:H films photo-CVD, photoelectric and structural props. 7-7869
 a-Si:H/a-SiGe:H multilayers, reactive deposition 7-33592
 a-Si:H-based films, photochemical vapour deposition, review 7-46345
 Si:H(F)-SiGe:H(F) amorphous multilayer struct., fabrication and near IR photoconductivity characts. 7-52797
 SiO, deposition from SiH₄-N₂O, role of adsorption stages 7-17447
 Si-based sensors, deposition methods and appls., review 7-48715
 Si-C-W hot shells for thermionic energy converters, CVD deposition 7-27914
 Si-W, buried conductor formation, low press. CVD W deposition on porous Si 7-32877
 a-Si_{1-x}C_xH films prepared by plasma CVD method, props. (*Japanese*) 7-12543
 Si₃N₄ insulating thin film deposition, remote plasma enhanced low temp. CVD process 7-13389
 SiC, CVD, microstruct. around indentation, TEM obs. (*Japanese*) 7-22822
 SiC CVD coatings, production at medium deposition temperatures (*German*) 7-27915
 β-SiC CVD film growth and props., gas phase comp. depend. simulation and meas. 7-22516
 β-SiC dendrites, CVD, propag. mechanism 7-38423
 SiC film, laser deposition for solar cell use 7-53634
 β-SiC films on substrates, CVD, X-ray topography 7-63998
 SiC polypolyte heteroepitaxial growth, and identification by Raman scatt. study 7-63992
 SiC powders, prep. by CVD method using RF-plasma (*Japanese*) 7-3250
 β-SiC, ultrafine powder synthesis in thermal arc plasmas 7-27916
 a-Si_{1-x}C_xH, Si-Kβ spectra, soft X-ray emission spectra (*Japanese*) 7-13268
 SiCl₄ + X⁺ (X=He,Ne,Ar,H), optical emission spectra rel. to PCVD 7-26531
 SiF₄ + X⁺ (X=He,Ne,Ar,H), optical emission spectra rel. to PCVD 7-26531
 SiGe:H, amorphous, solar cell efficiency improvement using graded band-gap layer at i/n interface 7-54327
 a-SiGe:H,F alloys for solar cells, prep. by DC and RF discharge deposition 7-17900
 SiH₄ pyrolysis rates, modelling of CVD 7-64911
 SiH₄/Si₂H₆ RF discharges, radical fluxes, plasma enhanced CVD 7-26580
 Si₂H₆ generation device for amorphous Si deposition system 7-22501
 SiN films, plasma CVD deposition and props. (*Japanese*) 7-13381
 Si₃N₄, CVD on Si surface, RIE 7-59691
 Si₃N₄, deposition in SiCl₄-H₂-O₂-N₂ system, dimensional effects 7-64910
 Si₃N₄ films, excimer laser-induced CVD 7-59441
 Si₃N₄ films, photo-ionisation assisted photo-CVD 7-17442
 Si₃N₄ films, plasma-enhanced CVD deposition from SiH₄/NH₃/N₂ mixtures 7-39414
 Si₃N₄, glow-discharge electron beams appl. (*Czech*) 7-56373
 Si₃N₄ LPCVD optical waveguides on Si substrate 7-20414
 Si₃N₄, laser activated CVD, deposition rate, refractive index 7-33591
 Si₃N₄ localised films on Si substrate, laser deposition 7-39418
 Si₃N₄, low temperature photo-CVD, characterisation 7-13377
 Si₃N₄ MNOS struct., CVD, elec. props., effects of deposition variables 7-52843
 Si₃N₄, plasma CVD on steel substrate (*Japanese*) 7-27939
 Si₃N₄ thin films, growth by microwave-excited plasma 7-59458

chemical vapour deposition continued

a-Si₃N₄:H films, plasma enhanced CVD, chemical and mech. props. 7-38420
a-Si₃N₄:H films deposited by plasma enhanced CVD, optical and elec. props. 7-39205
Si₃N₄-SiC film, hybridisation by plasma CVD 7-13379
Si₃N₄, remote plasma enhanced CVD 7-39425
Si₃N₄H₂ films, synchrotron radiation excited CVD, deposition mechanisms and H content 7-52369
SiO₂, CVD, low temp., low press. 7-46335
SiO₂ deposition by photo-initiation 7-59454
SiO₂, deposition from SiH₄-N₂O, role of adsorption shapes 7-17447
SiO₂ films, LPCVD from diacetoxymethyltrimethoxysilane in temp. range 450 to 600°C 7-53622
SiO₂ films, low-temperature plasma-enhanced CVD deposition 7-33581
SiO₂ films, prod. by low temp. CVD, role of carrier gas in deposition kinetics 7-59452
SiO₂, glow-discharge electron beams appl. (Czech) 7-56373
SiO₂ insulating thin film deposition, remote plasma enhanced low temp. CVD process 7-13389
SiO₂, laser activated CVD, deposition rate, refractive index 7-33591
SiO₂ layers obtained by plasmochemical decomposition, optical props. 7-20390
SiO₂ monomode fibres with F-doped cladding, prep. by MCVD process 7-1289
SiO₂ thin films, production from glow discharge decomp. of NO-SiH₄ mixtures, elec. props. 7-22512
SiO₂:F, P fibres, dopant materials behaviour in MCVD process 7-20462
SiO₂:F layers, modified CVD 7-53608
SiO₂:Ge integrated optical waveguides, plasma CVD 7-27941
SiO₂:Hg films, Hg-sensitized photo-CVD, X-ray fluorescence anal. 7-17440
SiO_x, deposition in SiCl₄-H₂-O₂-N₂ system, dimensional effects 7-64910
SiO₂:P films, pure and doped, low press. CVD growth, structural, optical, elec. props. 7-27186
Si₃O₄, remote plasma enhanced CVD 7-39425
SiO₂:N₂ films, deposited by plasma-enhanced CVD, charact. 7-2413
SiO₂:N₂ films, low press. CVD and composition analysis 7-12554
SiO₂:N₂ films, plasma-enhanced CVD growth 7-22514
SiO₂:N₂, plasma-enhanced deposited oxynitride films, IR and UV transmission 7-33474
Si₃O₄N₂, plasma enhanced CVD, characterisation 7-39426
Si₃O₄N₂, remote plasma enhanced CVD 7-39425
SnO₂ films, CVD deposition, elec. and optical props. 7-7429
SnO₂ films for solar cells, struct., elec., and optical props. 7-40003
SnO₂:F films, CVD growth using hydrofluoric acid as doping material 7-7871
SnO₂:F thin films, CVD deposition, elec. and optical props. 7-7425
SnO₂:F-n-Si(poly) solar cells fabricated by CVD, characterisation 7-59859
Ta films, maskless ion beam assisted deposition 7-46342
TaSi₂, LPCVD process 7-59449
TiAlO₂ coatings, CVD, composition, struct. and wear resistance 7-53929
TiB₂ coated B fibre reinforced Al matrix composite, prep. using liq. phase infiltration 7-3229
TiC, CVD technologies, rate controlling mechanisms, growth morphology 7-33575
TiC coated cemented carbide cutting tool inserts, performance and material props. 7-46712
TiC-coated cemented carbide cutting tools, role of interface development during CVD 7-53930
TiN, CVD technologies, rate controlling mechanisms, growth morphology 7-33575
TiN hard coatings deposition onto tool steel substrates by plasma-assisted CVD 7-53977
TiN, plasma enhanced CVD, rel. to reactive sputtering 7-39427
Ti(O,C,N) hard coatings deposition onto tool steel substrates by plasma-assisted CVD 7-53977
TiO₂ films, low temp. CVD for Si/TiO₂ MIS structures 7-17105
TiO₂ thin dielec. film, deposition on Kodial glass, optical props. 7-7872
TiO₄ films, CVD 7-53620
TiSi₂, filament growth during LPCVD 7-16908
TiSi₂ thin films, production by LPCVD, charact. (French) 7-7888
TiSi₂ ultrafine powder prep. and film charact. 7-64975
W and refractory metals, VLSI appls., conf., Albuquerque, NM, USA (Nov. 1984 and Oct. 1985) 7-14715
W, CVD on porous Si for buried conductor formation 7-3189
W, CVD on Si substrate, effects of dopants and cryst. perfection 7-16912
W, filament growth during LPCVD 7-16908
W film deposition by photolytic dissoc., charactn. 7-17466
W films, CVD on Si by Si reduction of WF₆, effect of substrate dopants and crystal perfection 7-22576
W films, LPCVD deposition kinetics in single wafer vacuum reactor 7-59448
W films, LPCVD growth on Si substrates by H₂ reduction of WF₆ 7-17470
W films, maskless ion beam assisted deposition 7-46342
W films, selective deposition on self-aligned CoSi₂ by low pressure CVD 7-53606
W films by selective LPCVD, struct. charactn., diffusion barrier appls. 7-17468
W growth kinetics on thermal oxide 7-16910
W LPCVD equipment for selective deposition, use of NF₃ as in-situ tube clean 7-17463
W LPCVD film thickness depend. on native oxide thickness 7-17473
W LPCVD films by WF₆/Si reduction method, influence of deposition variables 7-17461
W, LPCVD from W(CO)₆ in hot-wall environment 7-17465
W, LPCVD on Si-Ge alloy for interconnect appls. 7-17472
W, micrometer-scale line deposition using near UV laser light 7-59438
W, selective CVD for VLSI device appls. 7-17455
W, selective CVD for VLSI appls. 7-17457
W, selective deposition by APCVD 7-17460
W, selective LPCVD by WF₆ reduction, reaction kinetics 7-16914
W, selective LPCVD for MOS VLSI appls. 7-17456
W, selective LPCVD for CMOS VLSI, appls. 7-17471
W, selective LPCVD from WF₆ and H₂ 7-17464
W, selective LPCVD kinetics 7-17469
W, selective LPCVD on self-aligned Ti and PtNi silicides 7-17458
W, selective LPCVD on Si substrate, elec. and struct. props. 7-17467

chemical vapour deposition continued

W selective low press. CVD growth on Ti, TiSi₂ and PtNiSi, surface reactions, struct. 7-27183
WF₆, physicochemical props. rel. to CVD for VLSI appls. 7-17462
WO₃, amorphous electrochromic films, plasma enhanced CVD 7-22561
ZnCr₂O₄, crystal growth, chemical vapour transport, struct., mag. and electronic props. 7-53517
ZnS, CVD films on sapphire substrates, epitaxial nature 7-3199
ZnS, ZnSe, crystal growth by chem. transport using NH₄Cl transport agent 7-59385
ZnS_{0.5}Se_{0.5}, gradient IR optical material prepared by CVD 7-31408
ZnSe films; CVD 7-64909
ZnSe-ZnS electroluminescent MIS structures, MOCVD growth and charactn. 7-59443
ZrC and ZrO₂, chemical vapour deposition, thermodynamic conditions (French) 7-27938

chemical variables control
see also pollution detection and control
MOCVD, control parameters, parametric anal. 7-22543
nonisothermal continuous stirred tank reactor, multivariable, global control using moving model 7-13729
plasma spray deposition process parameters control, math. model 7-3477
He gas recovery system, automatic control of gas purity 7-318
U atomic vapour laser isotope separation data acquisition and control system 7-15735

chemical variables measurement
see also chemical analysis; moisture measurement; pollution detection and control
acoustic gas analyser for binary mixtures 7-39939
chemometric analysis of multisensor arrays 7-8344
dew point sensor for gas mixtures and pure gases (German) 7-56248
environment quality monitoring instrumentation 7-17933
fibre optic sensors and their appls., conf., Cannes, France (Nov. 1985) 7-40999
gas analysers (Spanish) 7-59799
gas analysis instrumentation, calibration (Spanish) 7-56208
gas concentration and gradient meas. in photoacoustically perturbed jet 7-37560
ion+ molecule reaction rates at low-temperature, ion drift-tube method 7-23007
ion-selective electrodes for ion conc. measurement, operation in nonlinear suboptimal response range 7-56246
ions activity meas., using digital device 7-3614
katharometer bridge circuit with linearising feedback 7-17840
laser nephelometer, computer controlled for liquid conc. determ. 7-61365
liquids, mixing, conc. meas. by fluoresc. technique 7-65366
MOSFET, Pt-gate, ammonia sensitivity, dependence on gate electrode morphology 7-61330
odour sensing (Japanese) 7-54623
oil traces in turbid water monitoring, using online IR analyser 7-34091
optical fibre sensors chemical sensing, particularly in biomedical field, areas for use and techniques 7-31472
optical particle sizing and concentration meas. system 7-48694
polymers, gaseous uptake at high pressure, meas. technique 7-41348
pump gauges, leakage characteristics 7-48766
salinity distrib. meas. in salt-stratified, double-diffusive systems, by optical deflectometry 7-23092
SAW chemosensor, processes involved at chemical interface 7-65376
SAW gas sensors, design aspects, review 7-48716
seawater effective salinity determ., conductivity comparator 7-4209
sensor technology and appls., conf., Bad Nauheim, FRG (March 1986) (German) 7-24271
sensors, research and development trends (German) 7-24645
solid-state gas sensors, role of catalysis, review 7-48718
taste sensing system (Japanese) 7-54622
Ag/AgCl electrodes fabricated with IC-compatible technologies, chemical sensor reference appl. 7-8343
CO components of flue gas, continuous emission monitoring and meas. procedures (German) 7-28436
CO concentrations, prediction models based on meas. 7-59897
CO, personal exposure monitor with automatic data-logging 7-3943
CaCO₃, formation in cooling water, critical pH depend. 7-54158
CuSO₄ soln., double diffusive convection, conc. meas., optical technique. 7-57825
F₂ detector, excimer laser monitor appl. 7-20216
para-H₂ concentration meas. using thermal conductivity cell 7-54229
NA vapour sensor using Au and Sb intermetallic compounds 7-18774
Na particles in N₂ flow, size determ. by optical method, radiation loss 7-17837
O₂ detection based on fluorescence quenching 7-43426
O₂, singlet, optical monitoring of generation during photodynamic treatment of tumours 7-65897
ZnO-SiO₂-Si SAW chemosensor for NO₂ gas concentration meas. 7-3621

chemically reactive flow
aerial suspension combustion, wave propag. 7-54125
annular premixed propane flame, mass transfer, residence time in recirculation zone 7-17790
atomised liquid fuel, turbulent diffusion flame, fine struct., using pneumatic nozzle 7-17791
behaviour during cylindrical vessel explosions 7-59760
buoyant and combustng flow, turbulence model 7-51083
chemical wave transport expt. on Spacelab D1 mission (German) 7-20814
3D chemically nonequilibrium viscous shock layer on catalytic surface 7-20810
combustion, flow simulation in vortex struct., variational entropy method (French) 7-44064
convective dispersion and interphase mass transfer 7-51269
coupled viscous flow/transport problems, numerical computation 7-44065
critical heat flux prediction via Katto's corrls. and Whalley's model 7-51339
detonation, time dependent 2D, interaction of edge rarefactions with finite length reaction zones 7-26363
diatomic molecules in flows with convective and diffusive particle transport, nonequib. dissoc. 7-20811
dissipative systems, stationary soliton soln. investig. 7-51034
dust-gas mixture, slow burning conditions 7-13778
equilibrium adiabatic flow, thermodynamic existence conditions for phases 7-31891
excitable reacting media, spiral waves, geometrical theory 7-48390

chemically reactive flow continued

- flame, premixed, struct. and extinction limit, Lewis no. effects (*Chinese*) 7-11559
- flame front propag. convective vertex form. 7-13777
- flame propagation, unsteady and 1D, mathematical anal. 7-57944
- flames, curved, nonlinear thermal diffusive theory 7-57941
- flames, diffusion, bluff-body stabilised, near-wake region, CARS meas. 7-8282
- flames, hydrodynamic instability, nonlinear theory, weak thermal-expansion approx. calcs. 7-59764
- flames, Linan's premixed flame regime, stability 7-17797
- flames, one-dimensional premixed, wave characts. 7-8279
- flames, turbulence generation and suppression 7-8281
- fluidised beds, turbulent, mass transfer, burning rate 7-59761
- fluids, acoustic wave propag. 7-6351
- fractal patterns from chemical dissolution 7-44061
- fuel drop, liq., moving, combustion, thin-flame theory, variable density effect 7-26364
- fuel drop-air mixtures, flame propag. 7-23018
- fuel spray ignition by hot surface 7-51337
- gas absorption with instantaneous chemical reaction in a laminar falling film 7-37558
- gaseous mixture wrinkled flames, reactive-diffusive model 7-46849
- gases, premixed turbulent combustion, second-order closure prediction 7-57942
- granular propellants, combustion, two-phase transient flow, modelling 7-37520
- homogeneous turbulence, chem. reactive species spectra 7-6204
- hydrocarbon fuel, combustion products flow in explosive type impulsive setup 7-17792
- internal combustion engine, flow field using Lagrangian-Eulerian method (*Chinese*) 7-20813
- jet diffusion flames, swirl effect on stability 7-23017
- mean mass temp and conc. in turbulent chemically nonequilibrium pipe flow (*Russian*) 7-51342
- methane and propane in diluted air, diffusion flames, extinction limits 7-3590
- methane-air laminar counterflow diffusion flames, struct., CARS meas. 7-57939
- methane-air laminar diffusion flames, struct. 7-65327
- methane-air turbulent diffusion flames laminar-flamelet modelling 7-57938
- MOCVD, control parameters, parametric anal. 7-22543
- MOCVD, horizontal reactors, complex flow phenomena 7-22530
- MOCVD in inverted stagnation point flow 7-22531
- MOCVD laboratory, integrated safety system 7-22528
- MOCVD reactor, vertical vs. horizontal design, optical study of gas phase 7-22534
- MOCVD reactor cell, visualisation of flow and temp. profiles, appl. of holographic interferometry 7-22532
- MOVPE, reaction processes, Raman spectroscopy investig. 7-22538
- MOVPE growth, flow patterns in vertical reactors 7-22535
- multi-component convection/diffusion/reaction systems, FEM 7-44063
- noncatalytic gas-solid reactions in vertical transport reactor anal. 7-44060
- nonequilibrium gas dynamics, chem. kinetics and turbulence 7-1647
- nonlocal conservation law in combustion theory 7-63233
- nonpremixed gases, turbulent diffusion combustion 7-1648
- partially dissociated and ionised gas mixtures, chem. equilib. flow, effective transport coeffs. calcs. 7-31917
- photoelectric aerosol sensor, chemical response to different aerosol systems 7-11514
- physical vapour transport in rectangular horizontal enclosures, surface reactions, convection 7-17398
- plane detonation wave at convex corner, diff. 7-57880
- plane detonation wave in combustible gas mixture, direct initiation 7-31836
- polymer solutions, gelling, rheology, mol. network model 7-51016
- porous medium, chemical dissolution by reactive fluid 7-44062
- porous medium, material transfer and absorpt., boundary regime optimisation 7-26341
- power plant combustion chamber, combustion stability 7-31890
- propane jet flames, near-nozzle region, flow struct. 7-8280
- propane-air flames, explosion venting, 2D Navier-Stokes eqns. 7-51340
- prototype physicochemical processes in shock layer during flow past hypersonic wind tunnels 7-63175
- pulverised coal combustors, NO emissions, swirling flow effect 7-51155
- random choice method for reactive gas with many chemical species 7-20812
- reacting and non-reacting turbulent liquid mixing layer, entrainment and mixing, composition meas. 7-16174
- reacting flows, combustion and chem. reactors, book 7-4644
- reaction zone measurements in high explosive detonation waves by means of shock-induced polarization 7-11558
- reactive plane Poiseuille flow, criticality disappearance in thermal ignition 7-1650
- shock waves, theoretical and num. structure 7-20759
- solar cooling by direct evaporation from sprays 7-37532
- solid-liquid contacting, pulsed packed column, solids holdup 7-11495
- stationary flow in channel, chem. reacting similarity wave propag., viscosity change effects 7-31886
- supersonic combustors, flow, mobile CARS instrument for combustion and plasma diagnostics 7-44238
- supersonic flowfield modelling using spectral methods 7-20747
- suspensions, reactive, flames, radiative transfer as propag. mechanism 7-17796
- thermal explosion critical conditions, turbulent natural convection effects 7-63122
- transverse turbulent jet, flame struct. and vorticity 7-20809
- turbulence, spectral functions 7-1646
- turbulent afterburning jets, temp. and conc. fluctuations, num. investig. 7-26362
- turbulent channel flow, heat and mass transfer modelling 7-26257
- turbulent nonpremixed series parallel reaction, mixing effect 7-31889
- turbulent reacting flow simulation, based on spectral characts. eqns. 7-26361
- turbulent reactive flow, num. computation (*French*) 7-57943
- turbulent shear flows, chemically reacting passive scalars, statistical anal. 7-63127
- two layer fluid, chemically reacting mixing layer, vortical struct., flow visualisation anal. 7-44007

chemically reactive flow continued

- VPE, organometallic, reactor design optimisation, flow visualisation studies 7-22533
- Al particles, ignition, behind detonation and shock waves 7-8287
- C particle laden O₂ gas, normal shock wave anal. 7-51288
- C-O₂ suspension, parameters affecting postshock wave relax. zone 7-51289
- CO₂ conc. profiles of axisymmetric combustion gas flow, IR spectra, temp. profile meas. 7-3591
- CO₂-He-N₂, vibr. nonequil. flow in axisymmetric channel with glow discharge 7-20741
- DF chemical lasers, mixing enhancement using supersonic nozzle design 7-5878
- GaAs, AlGaAs, MOCVD, design of safe facility 7-22529
- GaAs, MOCVD, gas phase depletion and flow dynamics in horizontal reactors 7-17433
- GaAs, MOCVD, uniform growth on multi-wafers 7-22536
- H swirling turbulent diffusion flames, turbulence intensity study 7-26287
- H₂, turbulent jet diffusion flame, conserved scale probability density functions 7-26260
- H₂-O₂-N₂ flames, one-dimensional simulation, mathematical and numerical aspects 7-39893
- HF, chem. laser, modeling based on standing detonation wave 7-62681
- NO+O₃, chemically reacting mixing layer struct., conc. field meas., entrainment and mixing anal. 7-44006
- N₂O₄ condensation in equilibrium maintaining chemical reaction, heat and mass transfer (*Russian*) 7-51341
- O₃ swirling flow combustor, gas densities, laser scatt. meas. 7-6218

chemiluminescence

- benzene, shock decomposition products detection by chemiluminescence 7-23023
- bioluminescence from phytoplankton, diurnal variation and inhibition due to daylight 7-34558
- blood serum and its components, comparative study of chemiluminesc. and resistance on ionising irradi. (*Russian*) 7-14066
- formaldehyde, oxidation, ESR and IR chemiluminescence. obs. 7-36655
- α -phenyl-N-tert-butyl nitron+O₂, solvent effect and temp. depend., luminesc. kinetics meas. 7-54130
- Shuttle glow, chemilum. processes 7-47602
- tetrafluoroethene+O₂, oxidation, laser photosensitised, chemiluminesc. 7-65328
- tetramethyldioxetane, homogeneous and inhomogeneous struct., vibr. overtone spectrum 7-25483
- tetramethyldioxetane in free jet expansion, overtone vibr. initiated unimol. reaction, RRKM theory 7-28299
- trifluoromethyl group, chemiluminesc. 7-33935
- Ba + N₂O, chemiluminescence, vibr. and rot. modes, translational energy and internal state influence 7-13780
- Ba + Cl₂(Br₂)(N₂O)(NO₂) (carbon tetrachloride) 7-13781
- Ba + Cl₂→BaCl₂, mechanism, chemiluminesc. 7-28292
- Ba+N₂O, oriented reactants, product polarised emission, chemiluminesc. 7-22992
- Cs+trichlorotrifluoroethane, vapor phase reactions, chemiluminesc. obs. 7-59767
- Cu+N₂O, collisional quenching, time-resolved emission and chemiluminescence 7-28285
- F₂ detector, excimer laser monitor appl. 7-20216
- F₂+I₂, room-temp. reaction, obs. of I, IF chemiluminesc. 7-28289
- IF, chemiluminesc. 7-31089
- K+tetrachloroethene (tetrafluoroethene), vapor phase reactions, chemiluminesc. obs. 7-59767
- NH(ND), isolated in solid Ne(Ar)(Kr)(Xe), radiative decay and radiationless relax., lifetime meas. 7-10653
- N₂O+Ba reaction, chemiluminesc. study, N₂O electric dipole moment sign meas. 7-54116
- O+CO, recomb. chemiluminesc. spectrum calc. 7-46807
- O+NO₂ (ClO) stratospheric reactions, rate const. meas. 7-8265
- O₂, soln., time-resolved chemiluminesc. 7-8289
- O₂+B(BO), gas-phase oxidation, rate consts., fluoresc. and chemiluminesc. study 7-22985
- Rb+perfluoroheptene, vapor phase reactions, chemiluminesc. obs. 7-59767
- Xe+Cl₂(Br₂)(I₂), atom and excitation transfer, energy disposal, product rot. alignment 7-31158
- XeCl, excitation fns., fluoresc. 7-17773
- XeI, excitation fns., fluoresc. 7-17773

chemioception

- cortical responses to painful CO₂ stimulation of nasal mucosa; a magnetoencephalographic study in man 7-54620
- EEG spatial patterns classification with a tree-structured methodology, rabbit olfaction appl. 7-54420
- neural computation, sigmoid nonlinearity, rat olfactory bulb obs. 7-54619
- odour sensing (*Japanese*) 7-54623
- olfactory bulb of rabbits, oscillating network model of pattern recognition 7-54618
- taste sensing system (*Japanese*) 7-54622

chemisorption

- activated, internal degrees of freedom and measured activation energies, activation mechanism determ. 7-27113
- adatom clusters, formation under coadsorption of reactants 7-6974
- alkaline earth orthovanadates, solid solns., defect struct. and electrochem. changes of O 7-32787
- alkaline earth orthovanadates, surface electrochem. of O, cyclic voltammetric obs. 7-33957
- benzene, chemisorbed on Pt {110}, influence of orientation on H-D exchange reactions 7-59781
- bond making and breaking at surfaces 7-28335
- bond-order conservation, bond making and breaking on transition metal surfaces 7-21653
- catalyst surfaces, characterisation by neutron inelastic scatt. from adsorbates 7-7000
- chlorodimethyl(triethylarsine) gallium, MOCVD adduct, chemisorption and thermal heterogeneous decomp. 7-22558
- coadsorption, promotion and poisoning effects, analytic modelling based on band-order conservation 7-27121
- conference, Oconomowoc, WI, USA (April-May 1985) 7-18468
- critical phenomena in chemisorbed layers 7-27067
- Cu, clean surface with chemisorbed benzotriazole, UPS study 7-21656
- drug absorption, open 2-compartment model for double site 7-59908

chemisorption continued

- ferromagnetic transition metal surface, of H_2 , self-consistent model 7-16862
- generalised Bethe lattices, chemisorpt. theory 7-7318
- graphite, chemisorption of N on basal plane, ab initio calcs., finite cluster models 7-16869
- laser-induced molecular processes on surfaces 7-53452
- metal clusters with chemisorbed H ionisation threshold, photoionisation TOF mass spectra 7-20085
- metal surface, adatom electronic struct. and tunnelling current 7-6962
- metal surfaces, adsorbate binding 7-12491
- metal surfaces, chemisorpt., surface bond length anal. 7-23057
- metal surfaces, oxidation, Ar^+ ion bombardment effects 7-39755
- metals, adsorbed H_2 , kinetics model of chemisorption layer (*Korean*) 7-32813
- metals, chemisorbed CO, affinity levels, energy and composition 7-59780
- molecules, NEXAFS and SEXAFS, studies 7-13261
- noble metal surfaces, chemisorbed state of acetylene, ethylene and ethane 7-52261
- olfactory discrimination, dynamic models 7-54160
- PTCR, high temp., interaction with O models 7-58861
- (10-(3-pyrenyl)decyl)dimethylmonochlorosilane, chemically bonded to silica surfaces, solvent effects on config., excimer decay profiles 7-22329
- pyridine, chemisorbed on Pt (110), influence of orientation on H-D exchange reactions 7-59781
- sapphire, stress corrosion, crack tip, dissociative chemisorpt. 7-33812
- semiconductor-fluid interfaces, illum., adsorption, competition for photogenerated charge carriers 7-27105
- SEXAFS studies of clean surfaces and chemisorption systems 7-13262
- simple cubic lattice, inelastic scatt. and trapping of an atom 7-27122
- solid surfaces, chemisorpt. of atoms binding energy, sum rules 7-16868
- solid surfaces, chemistry and physics, book 7-60891
- substrate impurity effects 7-63964
- tight-binding approach, s-orbital hopping parameters calc. 7-21625
- transition metal clusters, chemisorpt. patterns, charge depend. 7-15763
- transition metal surface, chemisorpt. of H, binding energy, sum rules 7-16868
- transition metal surfaces, dissociative adsorption of H_2 , effect of impurities 7-16876
- transition metal-H system, heats of soln. and vacancy trapping 7-6804
- {100}, of I, surface phases, SEXAFS, multishell simulation anal. 7-59303
- Ag (100), adsorption of Cl, Auger, LEED, XPS, thermal desorption studies 7-58635
- Ag (110), adsorption of NO_2 and surface nitrate formation 7-52286
- Ag (110), O and O_2 adsorption, dispersion, bonding and precursor state 7-6991
- Ag (110), of Br_2 , adsorpt. and reaction states, UV photoemission study 7-45014
- Ag (111), of O_2 , XPS studies 7-2374
- Ag, of H_2O on (100) surface, quantum chem. CNDO calcs. (*German*) 7-859
- Ag surface, O_2 chemisorption, flash desorption spectra (*Chinese*) 7-52294
- Al, thin films, chemisorption of O, electrical resistivity meas. 7-33110
- Al (100), CO adsorption, EELS and thermal desorpt. 7-17815
- Al films, of O, Al-O bond lengths, photoemission EXAFS meas. 7-64871
- Al, interaction of atoms and mols. with surfaces, cluster approx., total energy calcs. 7-52265
- Al surface, O_2 adsorption, electron beam effects, AES and secondary electron emission studies 7-27835
- $\eta-Al_2O_3$, of CO_2 (ethene), thermal desorpt. spectrosc. obs. 7-16872
- C containing compounds, on cold rolled steel sheets, XPS characterisation (*French*) 7-44965
- C fibre-epoxy composite, Ba labelled, XPS anal. 7-28163
- CO, chemisorbed, ionisation phenomena, ab initio wave functions 7-36444
- CO, chemisorbed on Ni (111), mol. orientation, effect of adsorbed K, ESDIAD study 7-32825
- CO, chemisorbed on Pt (111), adsorbate vibr. modes, inelastic He atom scatt. obs. 7-32782
- CO on TiO_2 (110) stoichiometric and defective surfaces 7-6983
- Cl, chemisorption, on Cu (111), site info. from EXAFS and photoelectron diffraction 7-32788
- Co, O_2 chemisorpt., influence of Ar^+ ion bombardment (*Russian*) 7-52253
- Cr (100) surface, evidence for two O chemisorption sites, at room temp. 7-6980
- Cr (110), chemisorption of O_2 7-21662
- Cr (110), O_2 dissociative chemisorpt. studies 7-2377
- Cu (100), field induced vibr. freq. shifts of chemisorbed CO and CN 7-45991
- Cu (100), of linear hydrocarbons, σ -shape and π resonances, XANES 7-53448
- Cu (110) with chemisorbed O, synchrotron X-ray scatt. study 7-7003
- Cu, O_2 chemisorpt., influence of Ar^+ ion bombardment (*Russian*) 7-52253
- Cu, O_2 chemisorption kinetics as function of ion bombardment and temp. (*Russian*) 7-58622
- Cu, of H_2O on (100) surface, quantum chem. CNDO calcs. (*German*) 7-859
- Cu particles, ZnO-supported, of CO, ethylene, and $CO-N_2O$ mixtures, vibr. spectra, operation of metal surface selection rule 7-53350
- Cu surface, interaction with Cl_2 7-21642
- Cu_2O surface with chemisorbed benzotriazole, UPS study 7-21656
- Fe (110), chemisorptive bonding of CO, pseudofunctional electron muffin-tin approach 7-2348
- Fe (111) surface, chemisorption of N_2 , adsorbate geometry, angle resolved XPES anal. 7-45009
- Fe, O_2 chemisorpt., influence of Ar^+ ion bombardment (*Russian*) 7-52253
- Fe surface, I retention modelling, role in source term reduction, reactor accident anal. 7-33961
- Fe surface, oxidised, chemisorption of pyridine and pyrrole, XPS 7-27128
- Fe-H system, electron and neutron irradi., positron lifetime meas. 7-44603
- GaAs (001), of CF_3 radicals, RHEED, photoelectron spectra, HF SCF calcs. 7-53497
- GaAs (110), of O_2 , photoemission evidence for surface growth 7-2356
- Ge (111), adsorbed Pb, atomic geometry, surface X-ray diffr. 7-52277

chemisorption continued

- Ge (111), chemisorption of atomic H, nonempirical cluster-model study 7-38332
- $Ge_{31-x}Si_x$ alloys, (100) surface, shape resonances of chemisorbed OH groups 7-6998
- H-permeation and recycling, molecular chemisorption model 7-8302
- H_2 on Ni and Cu surfaces, dissociative chemisorpt. dynamics, morphology and surface temp. effects 7-13808
- H_2 on TiO_2 (110) stoichiometric and defective surfaces 7-6983
- H_2O , effect on elec. capacity of Pb-acid battery positive plate 7-54284
- InP electrodes, of Ru, time resolved photoelectrochemical meas. 7-27415
- $KMnO_4$, thermal stability changes upon adsorption of water vapour in an electric field 7-8262
- Li surface, of CO, molecule-cluster interaction ab initio SCF-CI calcs. 7-45013
- Li-H systems, localised nature of chemisorption bond, calc. of chemisorption energies 7-2361
- MgF_2 , stress corrosion, crack tip, dissociative chemisorpt. 7-33812
- Mo (100), chemically modified, chemisorption bond energies of Lewis acids and bases 7-23056
- Mo (100), chemically modified by adsorption of B, C, O, CO, surface atom oxidation states, ESCA meas. 7-28333
- Mo (100), clean and with S or C overlayers, adsorption and reactions of hydrocarbons 7-28345
- Mo-H system, neutron irradi., H-void interactions 7-44604
- Nb(100) surface, H_2 chemisorption, LEED, EELS and work function meas. 7-32815
- Ni (001), chemisorptive bonding of CO, pseudofunctional electron muffin-tin approach 7-2348
- Ni (001) and (110) surfaces, adsorbed O, He diffr. results 7-7809
- Ni (100), (111) and (110), N_2 chemisorption, molecular cluster calcs. 7-52280
- Ni (100), CO chemisorption, cluster model calcs. 7-23058
- Ni (100), chemisorbed H and D, vibr. motion, high resolution EELS 7-12458
- Ni (100), chemisorption and decomposition of ethylene 7-59785
- Ni (100), dissociative chemisorption of alkanes studied by supersonic molecular beam techniques 7-52287
- Ni (100), molecular chemisorption of CO, precursors and trapping 7-58643
- Ni (100), O chemisorption, cluster model convergence 7-12461
- Ni (100) stepped surface, of H_2 7-21632
- Ni (100) stepped surface, chemisorbed W, tunneling current calcs. 7-52742
- Ni (110), adsorption of O, electron stimulated ion desorption O^+ yield meas. 7-12487
- Ni (110), chemisorbed H induced (1 \times 2) reconstruction 7-58851
- Ni (111), chemisorption of acetonitrile or benzonitrile, XPS 7-21641
- Ni (111), N_2 adsorption, XPS, UPS, work function and TPD studies 7-52272
- Ni {100}, of I, surface phases, SEXAFS, breakdown of Fourier filtering single shell anal. 7-59304
- Ni, O_2 chemisorpt., influence of Ar^+ ion bombardment (*Russian*) 7-52253
- Ni, of H, tight-binding approach, s-orbital hopping parameters calc. 7-21625
- Ni surface, Ni_2OH model for OH chemisorption, bonding study 7-52240
- Ni-Fe (100) surface, break-up of oxide films by S_2 impingement, LEED and AES meas. 7-46260
- $Ni_{50}Fe_{50}$ (100) alloy, segregation and adsorption of S 7-21617
- O, chemisorbed on oxides, elec. Props., role in gas sensing mechanism 7-7250
- O_2 , chemisorbed on MgO , photostimulated desorption 7-27107
- Pd (100), adsorption of cyanogen, Penning ionisation electron spectroscopy, UPS, TPD studies 7-52268
- Pd (110) with H chemisorption phases, selective population of H subsurface sites, He diffr., thermal desorption spectra study 7-6958
- Pd (111), CO chemisorption, inverse photoemission spectra 7-21638
- Pd (111), chemisorption of NO, photoemission study using synchrotron radiation 7-22446
- Pd (111), of O_2 , EELS and LEED studies 7-2378
- Pd, of H, tight-binding approach, s-orbital hopping parameters calc. 7-21625
- Pt clusters in Y-zeolite, atomic and electronic struct. and chemical reactivity 7-32677
- Pt electrode, in anhydrous methanol solns., added water effects 7-33936
- Pt, of Si, Pt-Si interfacial growth, intermixing, SEXAFS obs. 7-64772
- Pt_3Ti (111), chemisorption induced surface core level shifts 7-22448
- Pt_3Ti (111), chemisorption of CO and O_2 7-27131
- Rh-Re/ SiO_2 catalysts, metal dispersion 7-39918
- Rh(110), adsorpt. of H(D), form. of high density chemisorbed phase, LEED investigations 7-27094
- Ru (001), CO chemisorption, inverse photoemission spectra 7-21638
- Ru (001), clean and O covered, of NO_2 , EELS, thermal desorption mass spectrometry 7-52267
- Ru (001), H_2 chemisorption, effect of coadsorbed O_2 , LEED spectra anal. 7-33959
- Ru (001), of Li, rot. epitaxy, LEED, TDS obs. 7-12479
- Ru (1010) with K overlayers, struct. and energetics, chemisorption and desorption studies 7-21659
- Ru, surfaces, CO reactions, $Ru(CO)_x^{n+1}$ formation, field desorption study 7-54183
- Si (100), chemisorption of water, MNDO calcs. 7-63963
- Si (100), propylene chemisorption, reaction chemistry, active-site manipulation 7-39916
- Si (100), UV-stimulated interaction with Cl_2 , reaction mechanisms for photon-enhanced etching 7-22926
- Si (100) surface, chemisorption of H_2O (*Chinese*) 7-33954
- Si (100)2 \times 1, interaction with O_2 and N_2O 7-63962
- Si (111), Br chemisorption, SCF HF cluster calculation 7-52251
- Si (111), chemisorption of atomic H, nonempirical cluster-model study 7-38332
- Si (111), of benzene, pyridine and thiophene, surface vibr. studies 7-21615
- Si (111), of H, generalised Bethe lattices, chemisorpt. theory 7-7318
- Si (111), of Pt, interface form., EXAFS and X-ray absorpt. resonance spectra studies 7-38336
- Si (111) surface, H_2 dissociative chemisorption dynamics 7-54169
- Si (111) with adsorbed Cs or Na, oxidation 7-54025
- Si (111)2 \times 1, of thiophene, annealing-induced mol. fragmentation, surface vibr. spectra, HREELS study 7-27088

chemisorption continued

- Si, electron stimulated oxidation, surface effects, macroscopic continuum model 7-65236
- Si surface, atomic and mol. F reactions, XPS studies 7-28350
- Si surface, of benzene and pyridine, temp. depend., annealing effects on sorption states 7-2360
- Si surfaces, (111) and (100), chemisorption of halogen atoms 7-6979
- Si₃N₄, surface structure and chemisorption, XPS, AES and direct recoiling studies 7-32790
- Si(111), H₂ chemisorption, dihydride phases; TDS studies (*Chinese*) 7-38321
- W (100), chemisorption of N₂, O₂, CO, H₂, D₂, free carrier surface scatt., IR obs. of adsorbate induced changes 7-22268
- W (110), chemisorption of H, O, surface barrier structure 7-21663
- W (211), activated chemisorption of methane 7-52279
- W, of N₂, dissociative, activated, on (110) surface, dynamics, mol. beam obs. 7-38323
- W surface, field adsorption of He 7-32816
- ZnO films, elec. props., decomp., chemisorption of O⁻, photocond. meas. 7-27445
- ZnO:Ga thin films, temp. depend. of conductivity, effect of H₂O vapour chemisorbed states 7-7427
- Zr surface, chemisorption of Cl, neutral and negative ion thermal desorption spectroscopy 7-6988

chemistry

- see also atmospheric chemistry*
- constituents of matter, acids and bases, first year university students conceptions 7-9616
- photographic process material management/quality control 7-54148
- PWR, water chemistry guidelines 7-25029

chemistry, physical *see physical chemistry***chemistry computing**

- see also computerised instrumentation; spectroscopy computing*
- chromatography, computer simulation of physico-chemical stochastic processes 7-65379
- coding of relational descriptions of molecular structures 7-50399
- combustion research, reaction rate constants computing, using Harris Super minicomputer 7-33912
- conductometer, microprocessor HF contactless, design 7-59808
- conference, Marineland, Florida, USA (March 1986) 7-40985
- conjugated systems, computer reaction simulation, hybrid model 7-49874
- corrosion, knowledge 7-3470
- corrosion knowledge, computer modelling, expert systems, decision tree 7-3469
- distance geometry conformational configuration 7-49919
- DNA-ligand interactions, groove binding, computer simulations 7-54447
- electron microprobe use as digital image analyser (*French*) 7-46746
- EPR, microcomputer-based data acquisition and analysis system 7-48794
- equilibria computation using geometric programming technique 7-39850
- equilibrium, multiphase, calc. using MPEC2 FORTRAN-77 code 7-54155
- graph theory in chemical investigations 7-30916
- igneous rocks, chemical analysis, CIPW norm calculations, FORTRAN listing 7-29263
- molecular conformational studies, topology manipulation and coordinates algorithm using MOLTW program 7-50398
- molecular modeling system for the IBM PC, user-friendly CAMSEQ/M system 7-24633
- molecular structure information retrieval system, microcomputer based 7-10774
- optimizing interpreter for multidimensional products in computational chemistry 7-39947
- polyurethane foam, form., exotherm data acquisition using microcomputer 7-54118
- radioactive disposal, chemical modelling 7-10297
- thermochemical data base 7-18511
- thermodynamic properties of reaction involving minerals and aqueous solutions, program 7-28330
- trace metals in seawater, interaction with humic acid 7-54383
- transition states location using algorithm for ab initio program package Gaussian 82 7-13720
- Fe, inductively coupled plasma, emission, computer simulation 7-8348
- Hg electrode-soln. interface, 2-anion simultaneous adsorpt., elec. double laser parameters algorithm 7-54132

Cherenkov counters

- cosmic ray measurement by atmospheric Cherenkov technique 7-66470
- DELPHI barrel RICH detector, electron attachment of C₅F₁₂ as gas radiator 7-42296
- MuSR measurement in pulsed muon beam, Cherenkov imaging method 7-49842
- photosensitive gas detectors for Ring-Imaging Cherenkov technique, DELPHI barrel RICH prototype 7-42285
- single photon detectors with optically shielded wires, operation in transverse mag. fields 7-30847
- UV radiation detection efficiency increase using transparent wavelength shifters 7-15453
- water Cherenkov counter sensitive to nonwavelength shifted ultraviolet Cherenkov photons 7-25314
- D₂O Cherenkov detector for solar neutrinos 7-40695
- NaCl solution, Cherenkov light meas. for detector appl. 7-62219
- Pb-glass detectors, calibrating light pulser 7-49811

Cherenkov detectors *see Cherenkov counters***Cherenkov radiation**

- see also Cherenkov counters; electron radiation*
- acoustic, excitation in moving relax. media, appls. 7-37237
- atomic spectral lines, Cherenkov radiation effect 7-15549
- beam-generated waves in a large plasma chamber 7-57994
- diamond crystal, ultrarelativistic electron beam, parametric quasi-Cherenkov radiation 7-46174
- electro-optic media, Cherenkov radiation generation by femtosecond optical pulses 7-27808
- electron beam produced, calcs. 7-20118
- gamma-ray telescope, 1TeV, design and evaluation 7-34884
- hodoscopic scintillation gamma spectrometers with light-guide spectrum mixers 7-10351
- ionospheric plasma traversed by geomag. field, Cherenkov class of radiation 7-9286
- magnetoactive plasma waveguides, non periodic waves 7-63287
- microtron Cherenkov free electron laser 7-10970

Cherenkov radiation continued

- molecular clouds, plasma characts. and Cherenkov microwave emission-line mechanism (*Chinese*) 7-66690
- optical transition radiation for charged particle inclined flight through finite thick plate 7-1018
- photomultiplier anode current variation obs., for continuous and pulsed gamma radiation 7-30888
- radiation by uniformly moving sources 7-48456
- relativistic electron beams, time-resolved studies with subnanosecond Cerenkov electro-optic shutter 7-49757
- stimulated collective inelastic stopping effect 7-36781
- stimulated-Cherenkov free electron laser, multiple scatt. effect 7-25832
- synchrotron and Cherenkov radiation interference 7-25705
- ultra-high energy EAS, spectrum irregularity 7-14434
- Vavilov-Cherenkov radiation, bistability in nonlinear media 7-42871
- Vavilov-Cherenkov radiation, elec., mag. and toroidal dipole moments in thin channels 7-56059
- NaCl solution, Cherenkov light meas. for detector appl. 7-62219

chilling *see cooling***chip carriers *see integrated circuit technology; packaging*****chiral symmetries**

- see also SU_n theory*
- σ model, chiral, meson analysis, coupling to GSW bosons 7-48995
- σ -model, vacuum instability 7-48982
- σ -models, two-dimensional, supersymmetric, ultraviolet props. 7-48972
- anomalies in gauge and gravitational interactions, ID SUSY path integral approach 7-41661
- bag model, collision processes 7-30253
- baryon observables in chiral bag model 7-61606
- bound quark-meson system, RPA calcs., solitons, chiral model of nucleon 7-18989
- charged meson nonresonant three body decays in chiral perturbation theory 7-10058
- chiral bag model, cranking procedure, moment of inertia calcs. 7-24847
- chiral bag plus Skyrmin model, axial coupling g_A at large bag radius 7-10035
- chiral gauge theories, anomalies and Weyl modes 7-56447
- complex Langevin simulation of chiral symmetry restoration at finite baryonic density 7-35734
- covariant and consistent anomalies in even-dimensional chiral gauge theories 7-19019
- dilaton, technicolour model, mass and lifetime estimates 7-41712
- dimensional regularization and perturbative solution of the chiral Schwinger model 7-41662
- Dirac fermion, chiral anomalies, dimensional regularisation 7-9990
- Dirac operator coupled to non-Abelian gauge fields, two-dimensional chiral anomaly calc., validity 7-61463
- dynamical chiral symmetry breaking in Nambu-Jona-Lasinio model, pion props. 7-437
- effective Lagrangians for the chiral quark phase and the Skyrmin parameters 7-19069
- electroweak form factors of the Skyrmin 7-415
- electroweak interaction with two quark generations, chiral bosonisation (*Russian*) 7-24825
- electroweak signals in circuits, chiral anomaly induced spin waves as QED probes 7-460
- exact parapositronium like solution to two-body Diracequations 7-5039
- fermion guides, chiral symmetry spontaneous breakdown in QCD, pseudoscalar correl. functions 7-41727
- fermion propagation on 2D fractal structs. 7-48981
- fermion-gauge field interactions, regularized determinants and non-perturbative definition of chiral anomalies 7-30176
- fermionic string models in 4D, construction 7-15136
- finite temperature lattice QCD, deconfinement and chiral symmetry restoration 7-41724
- finite temperature phase transition in chiral limit of lattice QCD 7-61561
- first order chiral transition in QCD 7-41729
- form factors and static props. in relativistic potential model 7-15157
- fractional electric charge induced on GUT monopoles, chiral anomaly effects 7-19044
- gap equation models for chiral symm. breaking in QCD 7-35738
- gauge fields, analytic structure in presence of fermions in arbitrary symmetry 7-30170
- gauge invariant spin-3/2 anomaly in arbitrary dimension 7-178
- gauge theories, gauge-invariant point-splitting procedure 7-56425
- gauge theory, chiral, anomalous, quantization and inclusion of anomaly cancelling fermions during regularization 7-56428
- gauge theory, dimensional reduction, spontaneous symm. breaking and absence of chiral fermions 7-41594
- geometrical aspects of chiral models, superstring theory 7-61496
- hedgehog chiral soliton bags, spin-isospin projection using collective coordinates, nucleons 7-19074
- hypercolour, flavour changing neutral currents, chiral hierarchies 7-465
- instantons and the U(1) anomaly in QCD, review 7-5048
- Kac-Moody algebras, Yang-Baxter-Zamolodchikov-Faddeev algebras and integrable field theories 7-411
- Kaluza-Klein ansatz for chiral N=2 D=10 supergravity on round 5-sphere, truncations 7-183
- Kaluza-Klein theory, torsion and chiral fermions on topologically nontrivial Yang-Mills fields 7-48994
- kink-bag system in (1+1) dims., breathing motion, inertia of confined vacuum 7-19070
- KSFR relation and strength of the nonSkyrme term 7-4968
- lattice fermion derivative formulation, locality and chirality without spectrum doubling 7-41632
- lattice gauge theory, disordered fermion couplings and fermion doubling problem 7-9964
- lattice gauge theory, propagator of Susskind fermions 7-35683
- lattice gauge theory simulations, conf., Wuppertal, Germany, Nov. 1985 7-60883
- lattice Gross-Neveu model, recovery of chiral symm. 7-19010
- lattice Monte Carlo simulations of QCD at finite baryonic density 7-49082
- lattice QCD, chiral symm. breaking in strong coupling limit 7-56514
- lattice QCD, quenched SU(2) simulation with staggered fermions, chiral limit 7-61602
- lattice QCD sum rules and spontaneous chiral symm. breaking, Monte Carlo simulation 7-61603
- lattice QCD with staggered fermions, chiral props. 7-61576

chiral symmetries continued

lattice SU(2) chiral model, complex Langevin simulation on non Abelian group 7-61479
lattice SU(N)×SU(N) chiral models, two-loop coupling constant renormalization 7-424
lattice theory, Hamiltonian formulation for gauged nonanomalous chiral theories 7-19001
lattice theory, weak matrix element calcs., chiral behaviour and multipoint Green's fns. 7-61484
light quarks at low temperatures, QCD partition functions from chiral symmetry 7-61584
low energy meson action from QCD, extended Skyrme model, anomaly terms 7-5052
low energy meson physics in the superconducting quark model 7-35811
low momentum penguin loop contribs. and $\Delta I=1/2$ rule 7-41647
massive Schwinger model with Wilson fermions, chiral condensate calcs. 7-61541
meson-baryon system, Skyrme model results using chiral Lagrangian 7-41576
mirror fermion production near Z^0 peak in e^+e^- collisions 7-49128
multiplicative renormalisation of 2D chiral theories 7-30216
N=1 supergravity, flat potential, Klein's model of Lobachevsky plane 7-41226
N=2 twisted supersymmetric σ models, four loop divergence 7-30158
Nambu-Jona-Lasinio model, phenomenological lagrangian for strong interactions 7-35799
nonAbelian chiral anomaly from lattice regularization 7-15072
nonleptonic K decays in broken SU(3)×SU(3) 7-49134
nonlinear Σ -models, electroweak interactions in gauged hidden symmetry 7-48950
nonrenormalization theorems for chiral anomalies in N=1 supersymmetry 7-4963
nuclear matter, chiral invariant fermionic field theory 7-61831
nuclear matter, thermodynamic properties, anal using saturating chiral field theory 7-24948
nucleon, chiral invariant colour dielectric model 7-463
nucleon size, density dependence of f_π in nuclear medium, QCD sum rule anal. 7-480
open bosonic Polyakov string, saddle-point spectrum anal. and chiral anomaly 7-56528
perturbation theory, possible systematic controls 7-49011
phase transition in a supersymmetric theory 7-5000
pions and H(1190) meson, polarisabilities, sum rules 7-10087
principal chiral field, Bethe-ansatz soln., complete S-matrix and bootstrapping props. 7-48961
QCD₂, chiral symmetry breakup and gluon condensate 7-41731
QCD, chiral perturbation theory and effective lagrangians 7-49055
QCD, chiral symmetry, Wigner-Weyl and Nambu-Goldstone realizations 7-35803
QCD, dynamical symmetry breaking 7-24843
QCD, gauge configuration props. in 3D 7-35783
QCD, order of the finite temp. chiral phase transitions, renormalisation group eqn. 7-15119
QCD, quark condensates in spontaneous chiral SU(2)×SU(2) symm. breaking 7-471
QCD, scalar confinement implications for chiral symmetry breaking 7-61550
QCD, topological anomalies from Dirac equation 7-49051
QCD and CP^N model, collective phenomena, deconfining and chiral transitions 7-15120
QCD based models of hadron structure, book 7-48217
QCD in 2D, chiral symm. breaking and condensate calcs. 7-49073
QCD sum rules for exotic qqG states 7-41733
QCD-like theories, stability of chiral symm. breaking solns. 7-49076
QED, stochastic regularization, gauge and chiral covariant Langevin equations 7-35775
quark currents, complete bosonisation, quantum theory based on anomalies 7-30240
quark-gluon plasma, perturbative and nonperturbative theory, review 7-56510
quark-lepton generation as hypercolor degrees of freedom 7-24850
quenched ACD, chiral props. and hadron spectrum in alternate directions implicit method 7-61577
random lattice, doubling problem and chiral symm. breaking 7-394
Roper resonance and πN phase shift in the Skyrme model with defect 7-18988
scalar-isoscalar two-pion exchange force in the quark model 7-49053
Schwinger model, chiral, space-time formulation 7-24795
Skyrme model, recent developments in context of QCD, review 7-414
Skyrme model of proton-neutron mass difference 7-49145
Skyrme parameter calcs. from QCD sum rules 7-30186
Skyrmion model, vector and scalar mesons 7-35788
SO(5)×SO(5) chiral model, two-dimensional, magnetic props. 7-9968
SO(N)×SO(N) chiral model, two-dimensional, Bethe-ansatz procedure 7-9968
spin structures in string theory 7-5070
SQCD with $N_{\text{colour}} < N_{\text{flavour}}$ symmetry breakings 7-49085
statistical QCD, deconfinement and chiral symm. restoration, Monte Carlo anal. 7-61569
strict QCD inequality and mechanisms for chiral symmetry breaking, instantons role 7-30241
SU(2)_{global}×SU(1)_{local} gauge-Higgs model, phase props., chiral symmetry breaking 7-398
SU(2)×SU(2) 2D chiral Wess-Zumino model, operator algebra and correl. functions 7-19016
SU(2)×SU(2) algebraic description of the skyrmion, SU(4) quark model recovery 7-56440
SU(2)×SU(2) asymmetric linear σ model, symm. restoration at finite temp. 7-41650
SU(2)×SU(2) chiral σ model, phase structure of fermionic system 7-15074
SU(2)×SU(2) lattice theory with spin 3/2 action in 2D, Monte Carlo anal. 7-15067
SU(2) chiral model in external field, complex stochastic process on nonAbelian group 7-393
SU(2) lattice gauge theory, spontaneously broken, chiral symmetry realization 7-9958
SU(2) Skyrme Lagrangian, collective-coordinate quantization and new mass term 7-56439
superstring models with vacuum expectation values for conjugate sneutrinos 7-24863

chiral symmetries continued

supersymmetric chiral model with Wess-Zumino term, integrability 7-4962
supersymmetric Yang-Mills theory, harmonic superspace formalism and consistent chiral anomaly 7-18999
symmetric-space fields reduced from axially symmetric Einstein and Yang-Mills eqns., integrability 7-4971
technicolour theories, chiral hierarchies, perturbation and breaking 7-41728
technicolour theory with pseudo-Goldstone bosons, one-loop corrections 7-56525
three phase model, phenomenology of deconfinement and chiral symmetry restoration 7-35794
topological bags, projections and chiral vac. effects 7-491
triangle anomaly in the light-cone gauge 7-9975
two-dimensional gravit. coupled to chiral fermions, Lorentz anomaly cancellation 7-18674
two-dimensional model for strongly interacting matter at high particle density 7-5045
two-pion exchange three-nucleon potential, modifications, relevance of chiral symmetry 7-49251
U(3)×U(3) symmetric effective chiral Lagrangian for baryons 7-49084
variational approach to chiral-symmetry restoration 7-433
vibrating skyrmions; quantum corrections to masses 7-15054
VPP-interaction, chiral anomalies, low-energy theorems and form factors 7-41813
Ward identities and chiral anomalies in stochastic quantization 7-24774
Ward identities on the lattice for Wilson fermions 7-56419
Weinberg, chiral model, saddle points and skyrmion solns. 7-15100
Weinberg CP violation model, chiral props. of weak amplitudes 7-449
Wess-Zumino term in the chiral bag model 7-49091
Wess-Zumino terms and chiral jacobians, boundary conditions 7-9963
Weyl-Dirac equation for an SU(2) gauge theory with spherical symmetry 7-41622
Yang-Mills theories, supersymmetric, coupled chiral and supersymmetric anomalies 7-41600
 e electric dipole moment bounds in a wide class of models 7-41815
 $e^+e^- \rightarrow X$, sparticle pair prod. with polarized beams 7-61493
 $\gamma\gamma\gamma$, constraints due to topological susceptibility and chiral Ward identities 7-5097
K $\rightarrow\pi\pi$ amplitude, kaon-to-vacuum weak matrix element, soft pion techniques 7-49135
K_L $\rightarrow\gamma\gamma$, chiral perturbation theory corrections to SU(3) terms 7-15160
K_L-K_S mass difference in the chiral quark-loop model 7-61684
N octet magnetic moments, relativistic chiral quark model calcs. 7-19110
($\pi, 2\pi$) reactions, contact term in $\pi\pi\rightarrow\pi^+\pi^-\pi$ reaction 7-49479
 π , quark confinement theory, Nambu-Goldstone scalars and symm. restoration 7-35808
 $\pi^+\rightarrow ae^+\nu$, a=axon, branching ratio calc., chiral Lagrangian anal. 7-511
q-q pair condensation, 3P_0 , QCD anal. using Coulomb plus Breit potential 7-61597
qq condensate, truncation of operator product expansion 7-35791
 2H , magnetic form factor, topological exchange current contrib. 7-35941
 π field around static source, chiral invariant model 7-10034

chlorine

see also nuclei with
adsorbed on Ag, surface enhanced Raman spectrum pot. depend., surface coverage and mutual depolarisation effects 7-7686
adsorbed on Ag (111), weakly ordered and disordered, struct. studies 7-2365
adsorbed on Ag single crystals, adsorbate-substrate bond lengths, coverage depend., SEXAFS 7-63948
adsorption on Ag (100), Auger, LEED, XPS, thermal desorption studies 7-58635
adsorption on C electrodes, theory 7-12462
adsorption on Cu (111), surface struct., SEXAFS, photoelectron diffr. studies 7-64775
arc plasma, Stark broadening of spectral lines study 7-36536
atmosphere pollutant, implications for Antarctic O₃ depletion 7-55173
atom, electron impact ionisation cross sections meas., TOF spectra 7-42770
atom, g_f factors, many-body calcs. 7-62265
atom, K $\alpha_{1,2}$ X-ray emission lines, many electron effects 7-887
atom, photodissoc., third harmonic interference, polarisation effects, MPI spectra 7-50045
atom, Rydberg states transition, 6.7 μ m, obs. 7-42538
atom and mol., photoionisation cross section at 584 Å 7-36702
atom conc. meas. in plasma etching reactor 7-37760
chemisorption, on Cu (111), site info. from EXAFS and photoelectron diffraction 7-32788
chemisorption on (111) and (100) surfaces of Si 7-6979
chemisorption on noble metal surfaces, laser stimulated desorption 7-53453
chemisorption on Zr, neutral and negative ion thermal desorption spectroscopy 7-6988
discharge, 13.56-MHz, optogalvanic effect 7-32148
etching of InP, rare gas ion-enhanced etching 7-22918
excited state, in Ar matrix, internal dynamics and fluoresc. 7-25589
excited state spin-orbit interaction 7-49962
Great Artesian Basin, Australia, very old groundwater ^{36}Cl dating and chem. 7-66194
interaction with Si (100), UV stimulated 7-22926
isoelectronic sequence, allowed 3-3 transitions, Slater parameter optimisation, HF CI calcs. 7-48205
low energy X-ray fluorescence anal. using annular ^{55}Fe source, Monte Carlo approach 7-8335
milk River aquifer, Canada, old groundwater ^{36}Cl dating and chem. 7-66195
molecule, dissoci. state, pot. curve determ. 7-57013
molecule, photoionis. cross section meas. 7-62461
molecule, photoionisation cross section, ground state inversion pot. method/diffr. theory 7-944
molecule, spectral moments, dissoci. band 7-36695
molecule, X state, polynomial and near-dissoc. representations for spectral data 7-5714
photodissociation laser at 11.35 μ m, gain and energy 7-43082
plasma, photo-excitation and ionisation, transition energies, orbital relax. effect 7-37651
plasma etching reactor, atomic Cl conc. and gas temp., laser spectroscopic meas. 7-58069

chlorine continued

- reaction with Cu films, bulk diffusion processes 7-21783
 reaction with Cu surface 7-21642
 tektites, F and Cl contents 7-34501
 third-harmonic generation, nonadiabatic effects, coupled eqns. calcs. 7-1222
 total body, meas. by prompt γ in vivo neutron activation analysis 7-65848
 $\text{Ba} + \text{Cl}_2 \rightarrow \text{BaCl}_2$, mechanism, chemiluminesc. 7-28292
 $\text{CdS}:\text{Cu}:\text{Cl}$ photoconducting films, photolum. spectra studies (*Russian*) 7-46140
 $\text{CdS}:\text{Gd}$, Cl film solar cells, gamma radiation effects on photoelectric properties 7-34032
 Cl^- + methyl iodide, excitation function, microcanonical variational transition state theory 7-22995
 Cl^- VI, forbidden and allowed transition, electron impact excitation 7-62529
 Cl^- , effect on anodic process at C electrodes in $\text{LiF}:\text{NaF}:\text{KF}$ eutectic melt 7-23028
 Cl^- , electron affinity calc. with fourth order many body perturbation theory 7-42471
 Cl^- laser photodetachment spectroscopy 7-19790
 Cl^- , limiting ionic cond. in aq. soln., mol. dynamics simulation 7-44879
 Cl^+ solns., positronium form. and hydrated positron reactions 7-17809
 Cl^+ , charge transfer reactions with organic molcs., cross section anal. 7-15701
 $\text{Cl} + \text{Be}^+$, K-shell X-ray prod. cross section meas. 7-15680
 $\text{Cl} + \text{HCl}$, prod. rot. distrib., centrifugal sudden distorted wave study 7-46808
 Cl^- + chloromethane, substitution reaction, mol. dynamics, pot. energy surface, frozen solvent theory calcs. 7-54109
 Cl^- + chloromethane, substitution reaction, solvent effects nonadiabatic solvation, frozen solvent model study 7-54110
 $\text{Cl}^- + \text{H}_2$, reactive collisions, trajectory surface-hopping study 7-3576
 $\text{Cl}^- + \text{H}_2\text{O}$ (methanol)(acetonitrile), clustering reactions, van 't Hoff plots based on ab initio MO calcs. 7-28288
 Cl_2 , dopant in Ar, ArCl and Cl_2 formation and excited states anal., mol. fluoresc. study 7-19946
 Cl_2^+ , $\text{A}^1\Pi_u$, vibr. levels, radiative lifetime meas. 7-36677
 Cl_2^+ , electronic states, double charge transfer technique 7-841
 $\text{Cl}_2\text{-H}_2$ cells containing PbCl_2 solid electrolyte, cathodic characts; effect of vac. deposited FeCl_3 (*Japanese*) 7-13850
 $\text{Cl}_2 + \text{Ba}$, chemiluminescent reactions; spin orbit state effect 7-13781
 $\text{Cl}_2 + \text{Xe}$, atom and excitation transfer, energy disposal, product rot. alignment 7-31158
 Cl_3 , electronic struct., ab initio SCF and CI study 7-5605
 ^{36}Cl , conc. in meteorite, AMS meas. 7-66524
 ^{36}Cl concentration in groundwater using liquid scintillation counting 7-23892
 $\text{In}_2\text{O}_3:\text{Sn}-\text{ZnS}:\text{Cu}, \text{Cl}, \text{Mn}-\text{Al}$, surface electrical conductivity, in $\text{ZnS}:\text{Cu}, \text{Cl}, \text{Mn}$ thin films 7-38672
 $\text{KI}:\text{Cl}$, electron excitation self-trapping 7-32594
 $\text{a-Si}:\text{H}, \text{Cl}$ glow discharge films, Raman scatt. 7-39116
 $\text{SiO}_2:\text{Cl}$, ion implanted, Cl ion redistrib., SIMS studies 7-21249
 $\text{SiO}_2:\text{Cl}$ films prod. by Si oxidation in Cl containing ambients, impurity distrib. 7-26787
 $\text{a-SiSn}:\text{Cl}, \text{H}$ glow discharge films, elec. and optical props. (*Chinese*) 7-58805
 $\text{SnO}_2:\text{Cl}$ coatings, electrical and optical props. 7-58925
 U_2^+ , superslow mol. motions, EPR spectra 7-62421
 $\text{Xe}:\text{Cl}_2$ ($n=1$ or 2) 7-28297
 $\text{Xe}-\text{CO}_2$, van der Waals, two-photon excitation intermediate states, obs. 7-15638
 $\text{ZnSe}:\text{Cl}$ layers grown by MBE, blue photoluminesc. 7-52364
 $\text{ZnTe}:\text{Cl}$, crystals, vacancy-impurity complexes, ODMR studies 7-2530

chlorine compounds

- in Antarctic stratosphere, impact of OCIO and Cl_2O_2 on O_3 concs. 7-55164
 polyacetylene: AsF_6^- (ClSO_3^-) (FeCl_4^-) metallic, elec. cond. studies 7-64231
 in stratosphere, interaction with meteoric material rel. to O_3 in polar upper stratosphere 7-55166
 CIBS^+ , electron impact prod., $\tilde{\Lambda}^2\Sigma^+$ to $\tilde{X}^2\Pi$ emission spectrum 7-50158
 ClCN^+ , gas phase $\text{B}^2\Pi_u - \tilde{X}^2\Pi$ laser excitation spectrum 7-25529
 ClF , FT IR spectra, rot. struct. 7-922
 ClF_3 intercalated with graphite, electrical conductivity 7-7295
 CH_2^+ ion, ν_2 band, mag. field modulated IR laser spectrosc. 7-36605
 CINC isomerisation to ClCN , MINDO calcs. 7-56979
 ClO , electric dipole moment fn. calcs. 7-10442
 ClO , stratospheric composition 7-60324
 $\text{ClO} + \text{ClO}$ reaction kinetics, implications for Antarctic O_3 7-54090
 $\text{ClO} + \text{HNO}_3$ in stratosphere, implications for HCl content 7-14363
 $\text{ClO} + \text{O}$, stratospheric reactions, rate const. meas. 7-8265
 ClO_2 , struct., pot. functions, electron diff. and spectroscopic data 7-15708
 ClO_4^- , effect on Raman bands of dimethyl sulphoxide (acetonitrile) 7-5686
 ClO_2F , vibr., centrifugal distortion const. 7-19815
 ClONO_2 , stratosphere conc. profile from IR spectral observation 7-9167
 $\text{ClONO}_2 + \text{HCl}$, homogeneous and heterogeneous components, kinetics, implications for stratosphere chem. 7-54091
 $\text{ClONO}_2 + \text{HCl}(\text{H}_2\text{O})$, kinetics, implications for stratospheric O_3 7-54089
 ClOO , low-lying electronic states, SCF- X_{∞} -MS calcs. 7-49922
 HX-XCN complexes ($\text{X}=\text{F}, \text{Cl}, \text{Br}$) H bonding ab initio calcs. 7-56960
 $\text{I}^- + \text{ClO}_2$, oscillatory reaction, stirring and premixing effects 7-28278
 $\text{kBr}:\text{ClO}_4^-$, X irradiation, paramag. defect prod., EPR, Raman and IR spectra 7-22142

chokes see inductors**cholesteric liquid crystals**

- acetoxypropyl cellulose, liq. cryst. props., effect of chain length and degree of acetylation 7-44353
 biaxial, distorted, mol. field theory 7-1851
 bistable cholesteric twist cell, anisotropic domain growth 7-1865
 blue phase, frustrated, Kassel diagrams show elec. field-induced cubic-tetragonal struct. transition 7-32649
 blue phase liq. cryst., phase transition, chiral strain and reentrancy 7-58470
 blue phases, molecular organisation and geometric frustration 7-16399
 blue phases, refractometric meas. 7-7664

cholesteric liquid crystals continued

- blue-phases, orientation in an electric field, BP II transition to tetragonal phase 7-16397
 chiral liq. cryst. systems, blue phases, solitons 7-21097
 chiral smectic C liq. crystals, mol. theory 7-1867
 cholesteric and nematic to isotropic phase transitions, dynamic effects of elec. fields 7-16740
 cholesteric-nematic mixtures, supermolecular structure, spiral pitch 7-44356
 cholesteric-nematic phase transition, appl. in CO_2 laser light modulation, liq. crystal cell. 7-62745
 cholesteric-nematic transition, electrooptic characteristics, control (*Russian*) 7-16741
 cholesterolly acetylferulate, liq. cryst. transitions, glass transition and cold crystn., DSC study 7-63814
 cholesterolly hydrogen phthalate, glass transition study, positron lifetimes meas. 7-38201
 cholesterolly myristate-cholesterly benzoate mixtures, cholesteric/smectic A tricritical point, critical pitch exponents 7-38193
 defects in liquid crystals, structures, energies and interactions, review 7-63441
 DNA, helical polymer, cholesteric liquid crystalline phases 7-6506
 dye lasers, tuning by a cholesteric liquid crystal device 7-15858
 freeze-fracture in cholesteric liquid crystals 7-1906
 helical biological polymers, liq. cryst. phases, columnar textures 7-34106
 helicoidal instability of A $\chi+1$ disclination line in a cholesteric (*French*) 7-16398
 icosahedral ordering, light scatt. and Landau theory calcs. 7-51627
 imperfect, reflection coeffs. and light depolarisation 7-45963
 mechanical shear deformation, time-depend. behaviour 7-26631
 mixtures, pitch, struct., phase transition point and optical props. studies 7-1881
 nematic solvent, induced cholesteric mesophases 7-2195
 nematic-cholesteric liq. cryst. mixtures, optically active additive, optical storage 7-36901
 nematocholesteric mixtures with two-freq. control, electro-optical props. 7-59183
 photoinduced periodic grating obs. 7-37127
 physical props. and mol.-statistical theories 7-37849
 poly γ -benzyl L-glutamate film, solidified, cholesteric struct., colour rel. to stretching and temp. 7-44354
 poly γ -methyl L-glutamate film, solidified, cholesteric struct., colour rel. to stretching and temp. 7-44354
 poly- γ -benzyl-L-glutamate, helical polymer, cholesteric liquid crystalline phases 7-6506
 polymers with chiral phases, prep. 7-63453
 polysiloxane liquid crystals, colour gamut 7-1857
 pretransition phenomena, circular dichroism method study 7-51628
 sheared cholesteric polymer refractive index evolution mechanisms study 7-13120
 sitosteryl chloride-cholesterly laurate binary mixture, polymorphism 7-12267
 solitons, D NMR spectra 7-21096
 structure and mesomorphism of cholesteric liquid crystals 7-16409
 thin films, light propagation, beam polarisation rotation calcs. 7-13245
 ultrasonic absorption, comparison with Fixman theory 7-44693
 xanthan, helical polymer, cholesteric liquid crystalline phases 7-6506

chondrites see meteorites**choppers (circuits)**

- MOSFET chopper amplifier based signal source, brain voltage changes meas. appl. 7-23480

chopping see cutting**CHP generation** see cogeneration**chromatic aberration** see aberrations**chromatography**

- acrylic acid, electron capture gas chromatographic determ. 7-33974
 batch and semicontinuous liq. chromatographic systems comparison 7-13837
 block copolymers, mol. wt. and comp. heterogeneity, determ. 7-6556
 coiling-induced secondary flow in capillary supercritical fluid chromatography 7-33975
 computer simulation of physico-chemical stochastic processes 7-65379
 14,4'-diphenylmethane diisocyanate 1,4'-butanediol, thermal degradation 7-8272
 flexible ring macromolecules, chromatography theory (*Russian*) 7-46906
 Fourier domain processing, mathematics of spectral treatment 7-48870
 gas chromatograms, reconstruction from GC/IR spectrometry data 7-17832
 gas chromatograph/FTIR system, optimal design 7-48891
 generator overheating faults in insulation, detection by gas and capillary chromatography 7-28382
 glasses, entrapped gas bubbles, calibration of dynamic small-sample analysis systems 7-65370
 glucose-fructose, separation using batch and semicontinuous liq. chromatographic systems 7-13837
 glucose-fructose-dextrane mixtures, separation using batch and semicontinuous liq. chromatographic systems 7-13837
 high temperature pulsed nozzle for supersonic jet spectrometry, gas chromatographic appls. 7-15005
 p-hydroxybenzoic acid-based polymers, pyrolysis, thermal stability, thermogravimetric and gas chromatographic mass spectral anal. 7-54208
 hydroxymethanesulfonate, determination in wet deposition by chromatography method 7-54406
 laboratory information management, IBM PC package 7-24631
 liquid, high-performance, detection and identification using SPECORD-M40 UV-VIS spectrophotometer 7-8332
 liquid, pharmaceutical analysis appl. 7-18099
 low-molecular ingredients, migration in elastomer compositions (*Russian*) 7-39942
 DL-lysine, optical resolution by polymers with L-lysine pendant group 7-64601
 macromolecules, linear and cyclic, scaling theory (*Russian*) 7-10801
 multimode ionization cell for gas chromatographic detection 7-54228
 multiwire position sensitive chambers for compound anal. in thin layer chromatography 7-19643
 organic compounds, atmospheric, thermal desorpt./gas chromatographic anal. using hollow tube collectors 7-17928
 organic samples analysis, modular instrument for SIMS and direct chromatography 7-13841

chromatography continued

- photoionisation detector for capillary column gas chromatography 7-48702
- polycyclic aromatic hydrocarbons, characterisation from reference air particulate samples 7-54385
- polycyclic aromatic hydrocarbons, diesel particulate matter identification, chromatography 7-34079
- polyethylene glycol, tetrahydrofuran soln., mol. weight determ., size exclusion chromatography 7-50424
- polyethylene glycols, adsorpt.-exclusion behaviour during chromatography (*Russian*) 7-23095
- polymer films, multicomponent gas permeation, meas. method 7-51304
- polymers, chromatography, adsorption effects (*Russian*) 7-46907
- polyphenylmethylsiloxane, cyclic, preparation and fractionation 7-23013
- portable gas chromatograph evaluation for transformer site polychlorinated biphenyl meas. 7-46994
- rare earth phosphate glasses, structural investigation 7-6522
- reflection-absorbance FT IR spectra of chromatograph effluent, continuous recording 7-15016
- sample transfer accessory for thin-layer chromatography/Fourier transform infrared spectrometry 7-30101
- selenoproteins in bovine kidneys, anal. using gel chromatography and neutron activation 7-34363
- target transformation factor analysis with linear inequality constraints applied to spectroscopic-chromatographic data 7-33973
- Total Diet Program, residue identification by mass spectroscopy 7-54205
- N-trifluoroacetylated poly(ϵ -caprolactam), gel permeation chromatographic anal., calibration procedure 7-65374
- violacein, thin layer chromatography and FTIR analysis 7-54469
- water content of solids, meas. by chromatographic method 7-48759
- Be, determ. in natural water, by electron capture detect. gas chromatography 7-13932
- Fe₂O₃, adsorpt. of pyridine, gas chromatography and IR spectro study 7-39917
- Fe(OH)₃, adsorpt. of pyridine, gas chromatography and IR spectro study 7-39917
- LiH, ¹¹C and ¹³N implantation, chemical effects, radiochromatography study 7-28324
- NaI, radiochemical purity, investigation of method (*Chinese*) 7-8340
- NiO, adsorpt. of pyridine, gas chromatography and IR spectro study 7-39917
- Ni(OH)₂, adsorpt. of pyridine, gas chromatography and IR spectro study 7-39917
- P₂O₄-B₂O₃-SiO₂ CVD glass films, components characterization 7-45085
- PbO-Fe₂O₃-P₂O₅ glasses, liquid chromatography and Raman scattering studies 7-11946
- Pb(PO₃)₂-Fe₂O₃ glass, struct. props., chromatography and Raman spectra studies 7-21112
- SO₂, in humid air, level meas. by chromatography 7-34078
- ZnSe, MOCVD, chemical reactions monitoring 7-53611

chromising see *surface hardening***chromium**see also *nuclei with*

- Al₂O₃:Cr,Ga, Cr-Ga complexes, energy transfer 7-22321
- atom, matrix isolated, magnetisation props., MCD meas. 7-57112
- band structure 7-7105
- borate glass: Cr³⁺, Nd³⁺, energy transfer, emission spectra 7-33440
- carbonaceous films, prod. in situ in Tokamak TEXTOR, depth profiling 7-22893
- catalyst on γ -Al₂O₃ surfaces, reaction, studies by positron annihilation 7-39309
- coatings on gun tubes, cylindrical geometry ion plating technique 7-53638
- corrosion resistant coating on GdTbFe, mag. props. 7-53952
- Cr³⁺-K₂NaScF₆ laser material, tunable, crystal growth and spectroscopy 7-13347
- crystalline and magnetic states, effect of neutron irradiation in reactor (*Russian*) 7-51866
- deformation interaction of incorporation and substitution atoms 7-46556
- dopant in ruby, alternating-sign resonant photocond., impurity ion excitation 7-2643
- EELS studies of Cr-L_{2,3} core levels 7-46258
- electrode, interaction with Li₂S₈, cyclic voltammetry study 7-13786
- electrodeposited, groove adhesion tests 7-46789
- electrodeposits from Cr₂(SO₄)₃-potassium formate baths, hardness (*Japanese*) 7-59471
- electroplated deposits, hardness rel. to C content, heat treatment, bath comp. (*Japanese*) 7-17480
- emerald, Cr³⁺ absorption spectrum, spin-orbit interaction effects 7-13182
- evaporated and ion assisted deposited coatings, microstruct., electron microscope obs. 7-52335
- evaporated films, photoemission spectra, correl. effects 7-39363
- extended appearance potential fine structure anal. 7-27825
- Fermi surface, 2D angular correlation studies 7-39236
- films, acoustic emission during electrodeposition 7-52329
- films, characterisation by SIMS, Auger spectroscopy and TEM 7-12550
- films, thin polycrystalline sputtered, oxidation by CW CO₂ laser irradiation 7-13642
- grain boundaries, interaction with doping atoms (*Russian*) 7-51781
- He production in HFIR neutron irradiated pure elements 7-51852
- high-temperature corrosion film characterization using Raman microscopy 7-46772
- Hubbard model, degeneracy and quantum effects 7-7469
- impurities in Ge-Sb-Te system, diffusion 7-21527
- impurity in ordered perovskites, photolum. thermal quenching, linear and quadratic coupling model calcs. 7-3085
- impurity ions, d-p electronic energy, coord. sphere radius depend. 7-16971
- intergranular corrosion, inhibition mechanism of S-containing additives 7-53946
- Knight shift spin and orbital contribs., real-space formulation, Green's function method 7-2940
- magnetovolume, thermal expansion and Grüneisen parameters 7-33260
- metallic electron charge density to electron momentum density transformations 7-27249
- metallisation of Si₃N₄ ceramic by prediffusion, prior to bonding to stainless steel (*Japanese*) 7-8147
- Neel temp. and thermal expansion press. depend., strain gauge meas. 7-6724

chromium continued

- overlayer, on SiC, Si₃N₄, Al₂O₃, SiO₂, mixing phenomena 7-58330
- oxidation, accelerated, NaCl-induced 7-17715
- oxidised overlayer on Si (111), CrSi₂ formation and reduction of Cr₂O₃ during annealing 7-58660
- paramagnetic, two-photon momentum distrib. 7-45128
- passivation, reversibility limit 7-13626
- position annihilation studies, SDW and CDW instability 7-46180
- positron annihilation radiation, 2D angular correlation distrib. 7-53440
- power metallurgy coatings obtained by impact wave method, struct. form. 7-65211
- residual macrostress distrib. after cyclic heat treatment, US and X-ray study (*Russian*) 7-53772
- ruby, Cr³⁺ absorption spectrum, spin-orbit interaction effects 7-13182
- ruby, Cr³⁺ ground state, superposition-model analyses of EPR data 7-7158
- single crystals, action of α -particles (*Russian*) 7-51880
- single crystals, single modulating mag. state form., neutron obs. (*Russian*) 7-58982
- single crystals, thermoelec. power near the Neel temp., precursor behaviour 7-64209
- spin density waves, inelastic neutron scatt. (*Russian*) 7-58998
- surface, (001), hyperfine fields 7-58847
- surface, (001), near-surface antiferromagnetism and surface ferromagnetism, photoelectron spectroscopy 7-59381
- surface, (100), evidence for two O chemisorption sites, at room temp. 7-6980
- surface, (110), O₂ dissociative chemisorpt. studies 7-2377
- surface, (110), with chemisorbed CO, electron stimulated desorption 7-63965
- surface, low energy positron interactions, elastic and inelastic scatt. calcs. 7-39330
- surface, passivity, coulometric investig. 7-13625
- surface (100), electronic struct. and surface magnetism at finite temps. 7-12776
- surface (110), chemisorption of O₂ 7-21662
- surface EM wave absorpt., 4-350K 7-33354
- surface extended energy loss fine structure above L_{2,3} edge 7-17377
- surface magnetism, effect of adsorbed O 7-58973
- surface oxide films, spectral polarised directional emissivity meas., stratified media theory interpretation 7-17291
- surfaces and overlayers, mag. and electronic props. 7-58985
- target with physisorbed SF₆, coverage effect on sputtering behaviour 7-64845
- TGS:Cr³⁺ single crystals, valence bands and impurity levels, absorpt. edge meas. 7-33350
- thin films, crystallographic props., electron diffraction patterns 7-21751
- thin films, intrinsic stress, elasticity modulus, thermal expansion and struct. 7-16889
- thin films, struct. and compositional characts, electron diffraction patterns 7-21752
- vacancy formation enthalpy, positron annihilation studies 7-44536
- vacuum condensates, microstruct., phase comp., deposition parameters 7-27907
- vacuum deposition, Wheatstone bridge with two thin film arms, dynamic balancing 7-22491
- vacuum-deposited, hardness and struct. studies 7-33761
- vapour deposition on polyimide, interface chemistry 7-46871
- X-ray emission K $\alpha_{1,2}$ spectra 7-64825
- zero field muon spin rotation study 7-45871
- zone-axis critical voltages in HEED, accidental Bloch wave degeneracies obs. 7-63409
- zone-axis critical-voltage effect obs. 7-63408
- AlNbO₄:Cr³⁺ tunable IR laser crystals, fluorescent spectra 7-43110
- Al₂O₃:Cr, lattice relaxation induced by electronic relax. 7-44622
- Al₂O₃:Cr³⁺, radiation colour centres, excitation energy transfer 7-21200
- Al₂O₃:Cr³⁺, ruby, optically excited crystals, critical Cr conc. depend. of electrical instability 7-7280
- Al₂O₃:Cr³⁺, surface temp. meas., fluoresc. appl. 7-19947
- Al₂O₃:Cr³⁺, v³⁺, electron-phonon interaction and impurity energy levels, APR and EPR studies (*Russian*) 7-45814
- Al₂O₃:SiO₂:Cr mullite transparent glass ceramics, Cr³⁺ luminesc. 7-46102
- Al₂O₃:Cr,Ga, ruby, Cr-Ga complexes, luminesc. study 7-22320
- AlTaO₄:Cr³⁺ tunable IR laser crystals, fluorescent spectra 7-43110
- Al₂(WO₄)₃:Cr³⁺, tunable IR laser crystals, fluorescent spectra 7-43110
- Au-Cr superlattices, elastic props., effect of strain 7-52376
- Au-Cr superlattices, electrical resistivity 7-27384
- AuBe-Cr-Au-InP, improved ohmic contact 7-64310
- BaTiO₃:Ce,Cr,Cu, double doping study 7-2037
- BaTiO₃:Cr, impurity electronic struct., molecular-orbital calcs. 7-45213
- BeAl₂O₄:Cr³⁺, alexandrite, excited, absorpt. spectra, 220-900 nm 7-46075
- BeAl₂O₄:Cr³⁺, solid laser material, active ion distributions 7-57342
- BeAl₂O₄:Cr³⁺ tunable laser output pulse kinetics, spectral condensation characts. 7-50570
- Be₃Al₂(SiO₃)₆:Cr³⁺, emerald, spectral energy transfer, fluorescence line narrowing 7-33441
- Bi₁₂GeO₁₂:Cr, three-phonon interactions 7-2127
- Bi₂SiO₅:Mn,Cr single crystals, photoconductivity 7-33044
- Ca₂Ga₂Ge₂O₁₂:Cr³⁺ garnet, ESR and ultrasonically modulated ESR studies 7-22139
- Co/Cr compositionally modulated layered films, saturation magnetisation and FMR, thickness depend. 7-7565
- Cr,Nd:(Gd,Sc)₂Ga₂O₁₂ laser crystals, growth and quality 7-13346
- Cr,Nd:GdScGa₂O₁₂ laser Q switching for optimising use of stored energy 7-25851
- Cr,Nd:GdScGa₂O₁₂ laser rods losses and efficiency meas. 7-43106
- Cr,Nd:LaMgAl₁₁O₁₉ laser material, optical props. 7-10958
- Cr single crystals, surface and deeper layers, struct. changes due to laser irradiation 7-6937
- Cr XIII, electron impact excitation, LS coupling, distorted wave approx. 7-42767
- Cr XVII-XIX, tokamak plasmas, inner-shell X-ray line spectra 7-6371
- Cr²⁺, dielectronic satellite spectra CI HFS calcs. 7-42506
- Cr³⁺ impurity ions in low-symm. fields, energy levels, interconfig. interactions 7-58780
- Cr:C/O films, growth by laser photolysis of carbonyls, C and O incorporation mechanisms 7-58685
- Cr:ScBO₃ laser, tunable over 785 to 892 nm 7-15872

chromium continued

- Cr³⁺:BeAl₂O₄, alexandrite, laser material, nonradiative relaxation, picosecond time resolved studies 7-10956
 Cr³⁺:BeAl₂O₄, alexandrite, emission spectrum conc. of broad-band solid-state lasers 7-43114
 Cr³⁺:BeAl₂O₄, alexandrite, nonradiative transition dynamics 7-1102
 Cr³⁺:BeAl₂O₄, alexandrite, lasers using low-magnification unstable resonators 7-36997
 Cr³⁺:BeAl₂O₄ crystals, growth and laser performance 7-15870
 Cr³⁺:BeAl₂O₄ laser, tunable, characts. (*Chinese*) 7-5902
 Cr³⁺:Gd₂Sc₂Al₃O₁₂ laser, flash-lamp pumped 7-15902
 Cr³⁺:SrAlF₆ laser emission tunable from 825 to 1010 nm 7-10964
 Cr/Cu multilayer struts., scanning Auger microprobe depth profiling, sputtering effects 7-58659
 Cr/GaAs Schottky barriers, hole diffusion length, photon and electron excitation studies 7-2707
 Cr/Ni interface broadening and topography of Auger sputtered profiles 7-53485
 Cr/Ni multilayer films, AES sputter profiling, depth resolution 7-59358
 Cr/Si interfaces, silicide form. kinetics during thermal annealing 7-16897
 Cr/SiO₂/Si struts., Fowler-Nordheim tunnelling oscil., I-V characts. meas. 7-38745
 Cr-Al system, diffusion markers in thin, film CrAl₃ formation 7-58549
 Cr-CrO₂/Zn multilayer electrogalvanised coating on steel, XPS analysis 7-28290
 Cr-Ge thin film interface, interdiffusion, reaction and intermixing, soft X-ray photoemission study 7-27028
 Cr-graphite powder mixture, coatings form. in shock wave treatment 7-8183
 Cr-Ni multilayer thin films structures, AES depth profiling during sample rotation 7-27829
 Cr-polyethylene, adhesion of metal films, effects of Ar⁺ bombardment 7-28267
 Cr-Si, lateral growth of CrSi₂, role of Si transport 7-38272
 Cr+He⁺, target K-shell ionis., cross-sections and probabilities 7-50343
 Cr⁺+H₂(HD)(D₂), kinetic and electronic energy effect, mass spectra 7-65293
 Cr₂, bonding, appl. of local spin density approx., comparison with other studies 7-25371
 Cs₂CdF₄:Cr³⁺, Li⁺, Cr³⁺ centres, EPR study 7-7589
 Cs₂NaAlF₆:Cr³⁺, impurity ion spin Hamiltonian parameters, EPR determ. 7-64523
 Cs₂NaInCl₆:Cr³⁺, elpasolite lattice, broadband near-IR luminesc. 7-17338
 Cs₂NaYBr₆:Cr³⁺, elpasolite lattice, broadband near-IR luminesc. 7-17338
 Cs₂NaYCl₆:Cr, impurity photolum. spectra and lifetimes, thermal quenching and temp. depend. studies 7-3084
 Cs₂NaYCl₆:Cr³⁺, elpasolite lattice, broadband near-IR luminesc. 7-17338
 Cu-Cr matrix, electronic struct. calcs. 7-16976
 Cu/Ni/Cr, multilayer deposits, corrosion protective props. 7-8187
 Cu-Cr multilayers, laser alloying 7-45025
 Cu-Ni-Co-W-Cr system, Cr plating, roughness and wear (*Russian*) 7-33801
 Fe-Cr-Fe double layers, exchange coupling 7-27510
 GaAs:Cr, deep levels characterisation using photo-induced transient spectroscopy 7-16973
 p-GaAs:Cr, excited and metastable states of Cr-related double centres 7-7153
 GaAs:Cr, meas. of residual stress by Cr-related luminesc. lines 7-7726
 GaAs:Cr, microdefects obs. by IR light scatt. tomography 7-32662
 GaAs:Cr, photorefractive behaviour using two-beam coupling 7-31387
 GaAs:Cr,Se, impurity complex, luminescence study 7-53396
 GaAs:Cr free and metallised surfaces, SAW absorpt. meas., hybrid SAW semicond. device appls. 7-52217
 GaAs:Cr impurity level studies 7-33084
 GaAs:Cr semiinsulating LEC wafers, microhardness cartography 7-32886
 GaAs:Cr/ZnSe heterostructure, interface stress 7-38352
 GaAs:Cr³⁺ single crystals, acoustic relax. phenomena, phonon-impurity coupling, ultrasonic attenuation meas. 7-32581
 GaAs:Cr(Te)-GaAs, VPE grown, photoluminescence study, effect of substrate doping 7-27771
 β-Ga₂O₃:Fe³⁺(Cr³⁺), zero-field splittings and site distortions 7-59119
 GaP:Cr, impurity ion-lattice coupling, reson. phonon scatt. spectra 7-58420
 GaP:Cr, optically induced changes in impurity-related absorpt. line struct. 7-17334
 GdScGa₅O₁₂:Cr, Tm crystals., dual freq. lasing study 7-43117
 Gd₂Sc₂Ga₅O₁₂:Cr³⁺ garnet, laser spectral analyser 7-31362
 H and D diffusion in metallic and surface-oxidised 7-6888
 H⁺+Cr, k-shell ionization cross sections and theoretical models 7-5627
 Ho,Cr,Tm:YAG laser spectroscopic pumping scheme for 2 μm band 7-36968
 InGaPAs/GaAs interface stress, Cr-related luminescence study 7-46101
 InP:Cr, impurity ion-lattice coupling, reson. phonon scatt. spectra 7-58420
 InP:Cr, single crystals, LEC growth, precipitate identification 7-16754
 KAl(MoO₄)₂:Cr³⁺ tunable IR laser crystals, fluorescent spectra 7-43110
 KAl(SO₄)₂.12H₂O:Cr³⁺, optical absorpt. spectrum study, cryst. field and site symm. determ. 7-59232
 K₂NaSe(Ga)F₆:Cr, impurity photolum. spectra and lifetimes, thermal quenching and temp. depend. studies 7-3084
 KZnF₃:Cr³⁺ tunable laser with nonselective pumping 7-43113
 LaCrO₃-Cr cermet, mech. props., interparticle welding 7-39630
 LiNbO₃:Cr³⁺, EPR of axial and low-symmetry paramagnetic centres 7-38925
 Li₂O-B₂O₃-WO₃:Cr glasses, optical props. 7-46079
 LiTaO₃:Cr crystal, photoinduced light scatt., noise holographic grating mechanism 7-62775
 Lu₃Al₅O₁₂:Cr³⁺,Fm³⁺,Ho³⁺, 2 μm stimulated emission of Ho³⁺ ions, spectral composition and kinetics 7-46073
 MgO:Cr, Cr³⁺ absorption spectrum, spin-orbit interaction effects 7-13182
 MgO:Cr, positron lifetime spectra, impurity effects 7-39278
 NH₄Al(SO₄)₂.12H₂O:Cr³⁺, X-ray radiation damage, EPR and optical absorption studies 7-26799
 β-Na₂O-Al₂O₃-CdO:Cr³⁺, luminescence spectra 7-33448
 Nd,Cr:(Gd,Sc)₂Ga₅O₁₂, spectroscopic, optical and thermo-mechanical props. and laser performance 7-10963

chromium continued

- Ni/Cr alternating layers, ion beam mixing 7-21303
 Ni-Cr multilayer structures, Auger depth profiles using a dual ion gun system 7-22429
 Ni-Cr multilayers, interface resolution in Auger depth profiles 7-27830
 PbTiO₃:Cr³⁺, ceramic, EPR, ENDOR, ESE investigs. 7-13020
 Pd-Cr-SiO₂-p-Si MIS electrodes for electrochemical solar cells 7-34048
 RbCdF₄:Cr³⁺ tetragonal phase, ENDOR study 7-2952
 Rb₂CdF₄:Cr³⁺, Li⁺, Cr³⁺ centres, EPR study 7-7589
 Rb₂ZnF₄:Cr³⁺, Li⁺, Cr³⁺ centres, EPR study 7-7589
 Si:Cr,B, optically-induced spin orientation, EPR study 7-2927
 Si:Cr MOS capacitor elec. parameters, effects of process chemical purity 7-33103
 Si:Cr polycrystalline solar cells, structural, elec., photovoltaic props., impurity effects 7-39990
 SiO₂-Al₂O₃-Li₂O-ZnO-TiO₂-ZrO₂-As₂O₃-Cr₂O₃:Cr, glass ceramic, time resolved spectra 7-63478
 SiO₂-Al₂O₃-ZnO-Li₂O:Cr³⁺ gahnite type glass ceramics, laser excited emission spectra 7-22288
 SrAlF₆:Cr³⁺, laser material, EPR study 7-45807
 TiO₂:Cr, absorption and photolysis spectra 7-22290
 TiO₂:Cr, sol-gel process, ESR study 7-59108
 TiO₂:Cr thin films, extension of optical absorpt. range by doping 7-39144
 (Y,Sc)₃Ga₅O₁₂:Cr³⁺,Er³⁺, spectral, luminesc. and lasing props., Stark sublevel lifetimes 7-25827
 Y₃Al₅O₁₂:Tm³⁺,Cr³⁺,Ho³⁺, 2 μm stimulated emission of Ho³⁺ ions, spectral composition and kinetics 7-46073
 ZnAl₂O₄:Cr³⁺ laser excited emission spectra 7-22288
 ZnS:Al, Cr, Fe crystals, recomb. luminesc., EPR and photocond. meas. 7-3076
 ZnS:Cr³⁺, Fe³⁺ single crystals, impurity centre charge exchange, plastic deform. effects, ESR spectra studies 7-16984
 ZnS:Cr³⁺, Cr excitation spectrum interpretation 7-58775
 ZnSe-GaAs:Cr, meas. of residual stress by Cr-related luminesc. lines 7-7726
- chromium alloys**
 see also *chromium compounds*
 Alloy 600, intergranular SCC, in aq. soln. containing dissolved H₂, activation energy 7-59683
 Alloy 600, reactor steam generator material, properties and performance 7-30556
 alloy 600 nuclear steam generator tubes, local pitting conditions using Pourbaix diagrams 7-46716
 Alloy 600 PWR steam generator tubing, intergranular attack and SCC remedial methods 7-8199
 alloy 600 tubes, intergranular attack, cause evaluation 7-59685
 alloy 600 tubes in PWR steam generators, localised electrochem. corrosion 7-39760
 alloy 600 tubing in nuclear steam generators, intergranular attack, environmental effects eval. 7-39761
 Alloy 690, thermally treated nuclear steam generator tubes 7-5334
 Alloy 718, Ni-base superalloy, fatigue crack propag. under hold-time cycling, effect of grain size 7-28106
 Alloy 800 H, high temp. fatigue, damage mechanism (*German*) 7-17604
 Astrology, LC, Nirbase superalloy, hot isostatic pressing, powder metallurgy, second phase particle anal. 7-17497
 Astrology, fatigue crack growth, closure anomalies 7-3403
 charge and spin density waves (*Russian*) 7-2514
 Cr-MoVW ferritic steel, ductile-brittle transition temp., irradi. flux depend. 7-56825
 Fecralloy, interaction with Na₂O.2SiO₂ glass 7-3501
 first wall candidate alloys, HFIR irradi. microstruct. development 7-56824
 first wall candidate ferrite alloys, Ni doped, postirrad. tensile behaviour 7-56827
 Hastelloy alloys, C-4, C-22 and C-276, welding metallurgy 7-46448
 Hastelloy G-3, polarization effects in galvanic corrosion 7-39706
 Hastelloy X, thermomech. response, viscoplastic constitutive model 7-8059
 high alloy Cr-base alloys, plasticity, effect of twinning (*Russian*) 7-46582
 HT-9 martensitic steel, radiation induced segregation 7-56830
 HTR alloys, carburisation behaviour 7-10234
 IN738LC, Ni base superalloy, low cycle and thermal fatigue, small crack initiation and growth (*Japanese*) 7-13567
 IN 100, cast superalloy, creep strain and life prediction 7-33741
 IN 100, rheocasting and vacuum are double electrode remelting, solidification struct. 7-39497
 IN 100 superalloy, MC carbide props. rel. to transition element doping 7-13456
 Incoloy 800 H, oxidation, EMPA profiles in depletion zone 7-17727
 Incoloy 800 H, permeability of ³H and H in heat exchanger tubes (*German*) 7-56759
 Incoloy 800H, corrosion protection by plasma assisted vapour deposited and laser fused silica coatings 7-28208
 Incoloy 800H, multilayer oxide scales in gas atmosphere, Ti distribution 7-53972
 Incoloy 904, precipitate size, magnetoacoustic and Barkhausen emission study 7-45749
 Inconel 600, corrosion resist., effects of BF₂⁺ ion implementation 7-39734
 Inconel 600, H permeation studies for fusion reaction 7-5435
 Inconel 600, recovery kinetics, X-ray determ. 7-22722
 Inconel 600, specific heat capacities (*German*) 7-2228
 Inconel 600 and 690, SCC under high temp. NaOH, comp. and annealing effect 7-39710
 Inconel 600 in direct absorption received, optical props. at high temp. 7-40042
 Inconel 601/Mo bimetallic strips, explosively welded, thermal effects (*German*) 7-27144
 Inconel 617, H₂ permeation in high temp. alloys, oxide layer effects (*German*) 7-30568
 Inconel 617, oxidation, EMPA profiles in depletion zone 7-17727
 Inconel 625 matrix-carbide particle composite surface layers, wear resistance improvement 7-53912
 Inconel 718, Ni-base superalloy, creep deform., back stress determ. 7-46564
 Inconel GH39, thermal desorption study (*Chinese*) 7-52295
 Inconel MA 6000, oxide dispersion strengthened superalloy, cyclic creep, HF effect, anelastic model 7-53827

chromium alloys continued

- Inconel MA 6000, oxide-dispersion hardened superalloy, cyclic creep and anelastic relax anal. 7-17596
 Inconel welds joining dissimilar metals, radiographic evaluation 7-39828
 Inconel X-750, air environment/creep interactions, prior exposure times effect 7-13499
 Inconel X-750, elevated temp. fatigue crack growth under displacement control conditions 7-46608
 Inconel X-750, Ni-base superalloy, SCC susceptibility in high-temp. water, effect of chloride 7-39729
 low alloy, strength parameters, effect of dynamic strain ageing (*Russian*) 7-46505
 low alloyed, elastobrittle failure under thermal loading stresses 7-33790
 LWR, corrosion product release, radiation build-up effects 7-10225
 Ni addition effect on void formation following irradiation 7-56822
 Nimonic 105, Ni-base superalloys, precip. and tensile deform. behaviour 7-65078
 Nimonic 80, coupled plastic and creep damage at finite deform. (*Japanese*) 7-33736
 Nimonic 80A, crack growth under sulphidising conditions, metallography 7-59680
 Nimonic 86, carburised, heat treatment, creep behaviour rel. to carbide precip. (*Korean*) 7-46560
 Nimonic PE 16, Ni-base superalloy, duplex γ' particle hardening 7-28053
 oxidation studies using EELS and EDX in the TEM 7-17734
 Rene 80, aluminised coatings, high temp. oxidation, TEM obs. 7-28202
 Rene 80, first stage aluminised coating microstruct., STEM obs. 7-17709
 Rene 80, Ni-base superalloy, creep rupture props., influence of coating treatment and directional solidification 7-28116
 steel, Cr-Mo, elevated temp. strength, H attack resistivity and stress relief cracking suscept. improvements 7-13583
 steel, Ni-Cr-Mo, ΔK_{th} testing method for plastic zone size at fatigue crack tip 7-17748
 steel, X8CrNiTi18.10, corrosion product layers in PWRs at pH 7 (*German*) 7-19356
 surfaces and overlayers, mag. and electronic props. 7-58985
 textured sheets, Young's modulus anisotropy, elastic consts. calc. 7-46535
 Tokamak de Varennes, disruption-induced currents in Inconel vessel liner 7-15352
 Udimet 700, Ni-base alloy, solidified, dendrite arm spacing rel. to cooling rate 7-53713
 Waspaloy, γ - γ' partitioning behaviour, energy dispersive spectrometry 7-17534
 Al-Cr, quasicrystalline and crystalline alloys, temp. dependence of elec. resistivity 7-2574
 Al-Cr, quasicrystals, diffraction pattern simulations 7-6585
 Al-Cr amorphous films, quasicrystalline transformation by ion irradiation 7-2071
 Al-Cr quasicrystalline alloys, isomorphism, neutron diff. meas. 7-51638
 Al-G brazing alloys with active Ti additive, bonding of Syalon 7-39846
 Al-Mg-Bi-Cr, low activation alloy development for reacting plasma experiment 7-15384
 Al-Mn-Cr-Si quasicryst. atomic struct., pulsed neutron scatt. meas. 7-51639
 Al₈₆Cr₁₄, quasicrystals, EXAFS studies 7-64804
 Al₈₅Mn₇Cr₈, quasicrystals, EXAFS studies 7-64804
 AuCr, competing antiferromagnet, mag. phase diagram 7-59023
 AuCr spin glass, remanent magnetization reduction, Heisenberg and Ising comparison 7-53019
 Au₄Cr, atomic ordering, X-ray struct. anal. (*Russian*) 7-1933
 Co-Cr, continuously sputtered films, crystallographic orientation and mag. props. 7-27176
 Co-Cr, high temp. corrosion in sulphidising/oxidising environments, review 7-39737
 Co-Cr film, mag. domain obs. by colloid-SEM method (*Japanese*) 7-7533
 Co-Cr films, continuous fabrication by sputtering, substrate degassing effects 7-27904
 Co-Cr films, deposition by exposed pole magnetron sputtering 7-27903
 Co-Cr films, film growth and magnetisation reversal mechanism 7-27585
 Co-Cr films, mag. parameters, Brillouin light scattering study 7-53357
 Co-Cr films, sputter deposition and characterisation 7-27178
 Co-Cr films, sputter deposition, microstructure and its growth mechanism 7-27179
 Co-Cr films, sputter deposited, effects of additive gases on mag. props. 7-27575
 Co-Cr films for perpendicular mag. recording media, deposition in facing targets sputtering system 7-64899
 Co-Cr magnetic thin films, facing targets sputter deposition, microstruct. model 7-27905
 Co-Cr perpendicular recording media with oxidised surface layer, wear resistance 7-28185
 Co-Cr perpendicular recording media, props., effect of impurity gases 7-59069
 Co-Cr sputtered films, microstructural inhomogeneity, mag. props. 7-45768
 Co-Cr sputtered films, segregated microstructure, TEM studies 7-12538
 Co-Cr surgical implant alloy, mech. props., effects of N additions 7-59573
 Co-Cr thin films, DC magnetron sputtered, mag. props., effect of substrate and deposition rate 7-59067
 Co-Cr thin films, mag. props. and microstructure 7-27514
 Co-Cr thin films, sputter etching and annealing, FMR study 7-59112
 Co-Cr thin films for mag. recording, by facing targets sputtering, C-axis orientation 7-59418
 Co-Cr thin films prepared by fracture, microtome and ion-beam thinning methods, microstructure obs. 7-2427
 Co-Cr-Al-Hf(Y), high temp. oxidation rel. to alloying additions, ion implantation, Rutherford backscatt. 7-53987
 Co-Cr-Fe sputtered films, dilute, Mossbauer effect 7-22167
 Co-Cr-N, surgical implant alloy, mech. props., microstruct. rel. to N addition 7-60125
 Co-Cr-Re system, phase equilib., struct., microstructural, X-ray phase and durometric analyses 7-17513
 Co-Cr-W, Stellite, tool materials, statistical wear model, appl. to machining 7-33804
 Co-Cu, Y ion-implant, growing Cr₂O₃ film, obs. of coherent perovskite particles 7-39738
 Co-Mo-Cr-Si, wear resist. alloy development 7-3440
 CoCr corrosion-resistant alloy films, mag. props. and longitudinal recording performance 7-33226

chromium alloys continued

- CoCr double-layered film, sputter deposition 7-27177
 CoCr evaporated films, mag. props. 7-33225
 CoCr films, corrosion in H₂SO₄ 7-33824
 CoCr films, magnetisation reversal mechanisms 7-59068
 CoCr films, sputter deposition, mag. characteristics of initial deposition layer 7-27574
 CoCr films, texture formation, appl. for perpendicular mag. recording 7-39539
 CoCr films, vacuum evaporation, thickness depend. of mag. props. 7-27576
 CoCr layers, domain obs. with digitally enhanced Kerr-microscope 7-45726
 CoCr magnetic thin films, magnetron co-sputtered, microstructure 7-33558
 CoCr Permalloy films, weather resistance 7-28183
 CoCr RF sputtered magnetic films, Cr segregation, STEM study 7-44827
 CoCr sputtered film recording media, wear resistance, mech. strength and microstruct. 7-32859
 CoCr sputtered films, struct. and mag. props., role of atomic mobility during film growth 7-33224
 CoCr sputtered perpendicular recording media, with columnar microstruct., reversal mech. 7-7552
 CoCr thin films, microstructure and corrosion resistance, effect of SiO₂ protective film 7-28184
 CoCr thin films for recording media, perpendicular anisotropy 7-33202
 CoCr thin films on metallic underlayers, mag. characts. 7-27573
 CoCr-based thin films, growth and mag. props., nucleation layer effects 7-45065
 Co₈₀Cr₂₀, sputtered thin film recording media, micromag. and struct. studies 7-33243
 CoCrAl alloys, microstruct., atom probe FIM and TEM studies 7-33636
 CoCrAlY electron beam physical vapour deposition coating microstruct., TEM characterisation 7-52334
 CoCrAlY, hot corrosion, ZnSO₄-Na₂SO₄ reactions 7-28188
 CoCrAlY, sputter ion plated coatings for gas turbines 7-53971
 Co_{70.5}Cr₂₁B_{2.4}Si_{1.6}W_{4.5}, amorphous material behaviour in friction 7-28151
 CoCrTa corrosion-resistant alloy films, mag. props. and longitudinal recording performance 7-33226
 CoCrTa sputtered films, microstruct. and mag. props. studies 7-12575
 CoFeCr sputtered films, struct. and mag. props. 7-27175
 Co₆₉Fe_{4.2}Cr_{7.5}Si_{2.5}B₂₂ metallic glasses, long-time tunnelling heat relaxation meas. 7-38223
 CoNiCr-Cr sputtered thin films, film struct., mag. props. 7-33227
 Cr-Al dilute alloys, mag. phase diagram, mag. susceptibility studies (*Russian*) 7-2840
 Cr-BN amorphous films, supercond. transition temp. 7-27454
 Cr-C, deposited on Fe, surface amorphous alloys, Ar⁺ and Xe⁺ bombardment (*Chinese*) 7-51885
 Cr-Fe (28.5 at.%) superparamag. particles formed during solid soln. decomp., mag., transitions (*Russian*) 7-33220
 Cr-Ga intermetallic cpds., mag. suscept. meas. 7-12942
 Cr-Ge dilute alloys, elec. resist. temp. and press. depend. studies 7-32980
 Cr-Mo, deposited on Fe, surface amorphous alloys, Ar⁺ and Xe⁺ bombardment (*Chinese*) 7-51885
 Cr-Mo dilute alloys, magnetoelasticity, antiferromagnetism disappearance effects 7-45789
 Cr-Mo ferritic steel, 14 MeV neutron irradiation, mech. prop. changes 7-56821
 Cr-Mo ferritic steel, rust chemical reduction 7-30565
 Cr-Mo-Ni ferritic-martensitic steel, irradiation in RTNS-II, TEM study 7-58345
 Cr-Ni, electrodeposition, role of Cr(II) 7-33614
 Cr-Ni (45 wt.%) amorphous free-standing thin films, struct. transformations, pulse laser irradiation 7-38382
 Cr-Os-Ta-La system, anomalous elastic and thermal props. in region of phase transform. (*Russian*) 7-53783
 Cr-Ru, BCC alloys, supercond. and mag. props. 7-7443
 Cr-Si dilute alloys, magnetic phase diagram near tricritical point, neutron diff. meas. 7-2856
 Cr-Si silicide, quantitative Auger anal., correction factors 7-27831
 Cr-Ta-C, ageing, hardening processes, carbide separation and dissolving (*Russian*) 7-59541
 Cr-Ti-C system, existence of quasibinary section Cr-TiC 7-3288
 Cr-V alloy, magnetovolume, thermal expansion and Grüneisen parameters 7-33260
 (Cr_{1-x}Al_x)₉₅Mo₅, antiferromagnetism disappearance, comp. depend., elec. resist. and sound rel. meas. 7-2843
 Cr₃C₂-Ni-P hard metal, Cr₃C₂ solution in Ni matrix, liq. phase influence 7-53689
 CrCo-porcelain and CrNi-porcelain dental prostheses, strength rel. to surface roughness of metal frames 7-40365
 Cr_{1-x}Mn_xGe, cryst. and amorphous, mag. characts., substitution effects 7-59009
 CrMoV ferritic steels, He containing, fatigue behaviour in fusion reactor 7-56828
 CrMoVNbNi steel, Ni addition effect on void formation following irradiation 7-56822
 CrNi corrosion resistant coating on GdTbFe, mag. props. 7-53952
 Cr_{1-x}Re_x, antiferromag. superconductor, upper crit. mag. field (*Russian*) 7-58963
 Cr₂Si, Al₁₅ cpds., 2D angular correlation of positron annihilation radiation 7-39238
 Cr₂Si, Ar⁺ ion beam induced surface and subsurface modifications, AES study 7-64846
 Cr₇₅Si₂₅ thin films, microstruct. and resist., room temp. to 950°C 7-38410
 Cu-Cr bronze, decomp. kinetics of supersaturated solid solns. 7-3320
 Cu-Cr powders, sintering, densification rel. to Cr content 7-13405
 Cu-Ni-Cr, spinodal decomp., X-ray diff. and TEM study 7-22732
 CuCr dilute alloys, electron struct., X-ray La emission spectra studies 7-12598
 Fe-Cr coatings for gun bores, morphology and erosive wear 7-46697
 Fe-9Cr ferritic steel, 40 keV Cu⁺, Fe⁺ and fission neutron irradiation effects. 7-56823
 Fe-B-Si-Cr-Mo-W, finely cryst. and amorphous structs. on surface by laser treatment 7-8175
 Fe-Co-Cr-Mo alloys, electronic struct. and mag. props., X-ray spectra studies (*Russian*) 7-32902

chromium alloys continued

- Fe-Cr, chromium cast Fe, duplex nature of eutectic carbides 7-13440
 Fe-Cr, high temp. oxidation, effect of various amounts of Ce and CeO₂ 7-53945
 Fe-Cr, high-Cr cast iron, wear-resistance, laser and heat treatment effect on struct. and props. 7-8174
 Fe-Cr, high-temp. air corrosion products, distrib. and charactn. by Raman microscopy 7-65205
 Fe-Cr, intergranular corrosion, inhibition mechanism of S-containing additives 7-53946
 Fe-Cr, liquid alloy, N activity coeff., soln. model for nonmetallic solutes 7-65043
 Fe-Cr, neutron irradiated, defect clusters, positron annihilation lifetime meas. 7-51853
 Fe-Cr, oxide film form., FTIR reflectance spectroscopy characteris. 7-46043
 Fe-Cr, P implanted amorphous alloys, corrosion, passivation, microstruct. 7-65180
 Fe-Cr, passive anodic oxide form., surface anal., XPS, ion scatt. spectra 7-22895
 Fe-Cr, passive current fluctuations, statistical anal. 7-28190
 Fe-Cr, thin oxide film form., XPS study 7-22898
 Fe-Cr (12 at.%), ferritic alloy, He⁺ implantation and Fe⁺ irradiat., bubble nucleation and growth 7-58362
 Fe-Cr (3 wt.%), oxidation behaviour 7-17716
 Fe-Cr alloy films, oxide film form. by aqueous corrosion, EXAFS study 7-64007
 Fe-Cr alloys, H diffusion and trapping 7-27018
 Fe-Cr alloys in acidic electrolytes, effects of P implantation on passivity 7-59658
 Fe-Cr coating, ion plating on steel, deposition conditions effect on coating struct. 7-39748
 Fe-Cr surface oxide scales, XANES 7-65193
 Fe-Cr system, thermodynamic characts., mass spectrometry 7-53736
 Fe-Cr-Al, C solubility, influence of Ti and Nb, high-temp. oxidation resist. 7-22876
 Fe-Cr-Al alloys, Al₂O₃ scale growth 7-65214
 Fe-Cr-Al-Ce, microstruct., high temp. corrosion rel. to Ce additions 7-13648
 Fe-Cr-B, amorphous, Cr redistribution between phases during crystallisation, Mossbauer spectroscopy 7-21100
 Fe-Cr-B metallic glasses, imperfection struct., positron annihilation studies 7-37885
 Fe-Cr-B-Si, amorphous, annealing effects on Curie temp. 7-45675
 Fe-Cr-C, martensite nucleation, dislocations, grain boundaries, plastic accommodation 7-28040
 Fe-Cr-C steels, martensite and bainite transforms. (Russian) 7-13448
 Fe-Cr-C system, phase diagrams, thermodynamic modelling, direct use of chem. pot. function 7-7970
 Fe-Cr-C-B hard surfacing weld deposits, abrasive wear resist. and microstruct. 7-22847
 Fe-Cr-Co permanent magnetic alloys, casting 7-53051
 Fe-Cr-Co solid soln., uniaxial tensile stress in spinodal decomp. effect on coercive force, thermomag. treatment effects 7-7555
 Fe-Cr-Co-Mo alloy struct., 2D scatt. X-ray intensity distrib. patterns, anal. by direct variation method 7-64734
 Fe-Cr-Co-Mo permanent magnet ribbons, mag. props., influence of modulated structure 7-53043
 Fe-Cr-Co-Si-Ti, permanent mag. alloy, ductile, effect of heat treatment on mag. props. (Korean) 7-8137
 Fe-Cr-Co-(Si), permanent magnet alloys, microstruct., mag. props., Si content effect 7-22117
 Fe-Cr-Mn, may susceptibility and elec. resist. (Russian) 7-52952
 Fe-Cr-Mn-C, laser clad, microstruct. and wear props. 7-13652
 Fe-Cr-Mn-Ni-C system, phase relationships at solidification temps. 7-28014
 Fe-Cr-Mo, oxidation, boric acid coatings effect 7-65197
 Fe-Cr-Mo, surface segregation, Auger anal. 7-16844
 Fe-Cr-Mo (9.1 wt.%), initiation of breakaway oxidation in high press. CO₂ atm. 7-33845
 Fe-Cr-Mo system, phase boundaries of intermetallic compounds (Japanese) 7-53697
 Fe-Cr-Mo-Mn-C-P, sintered, ageing and steam oxidation, effect of P 7-7930
 Fe-Cr-Mo-Zr amorphous alloys, corrosion resistance (Japanese) 7-65194
 Fe-Cr-Ni, austenitic, electron irradiat., conversion of stacking fault tetrahedra to voids 7-58342
 Fe-Cr-Ni, Ferralium 255, polarization effects in galvanic corrosion 7-39706
 Fe-Cr-Ni, hardening at low temp. (Russian) 7-39554
 Fe-Cr-Ni, intergranular corrosion, inhibition mechanism of S-containing additives 7-53946
 Fe-Cr-Ni, low temp. mag. susceptibility and mag. transitions (Russian) 7-45628
 Fe-Cr-Ni alloys, FCC, dilation by interstitial C and N 7-44451
 Fe-Cr-Ni alloys, local ordering, neutron irradiat. effects, elec. resist. meas. 7-2070
 Fe-Cr-Ni-Al-Si-Mn, oxidation from 700 to 1000°C 7-65207
 Fe-Cr-Ni-C system, phase relationships at solidification temps. 7-7969
 Fe-Cr-Re system, interaction of intermediate phases, phase equilibria 7-17514
 Fe-Cr-Si-B metallic glass wires, corrosion rel. to crystallinity and comp. 7-46701
 Fe-Cr-(Al), high temp. corrosion in sulphidising/oxidising environments, review 7-39737
 Fe-Mn-Al-Cr system, rel. between $\gamma \rightarrow \epsilon$ transform. temp. and comp. of metastable austenite region (Chinese) 7-7993
 Fe-Ni-Cr, high-purity, irradiat., void swelling and nucl.-induced phase transforms. 7-58340
 Fe-Ni-Cr, oxidation, TEM study, nonprotective oxide growth 7-8180
 Fe-Ni-Cr, oxidation study, protective oxide growth 7-8179
 Fe-Ni-Cr, reactor bolting material A-286, failure analysis 7-30536
 Fe-Ni-Cr, structural materials, welding after neutron and ion irradiat., comparison 7-58357
 Fe-Ni-Cr (25.15 wt.%), MC stabilized, fatigue life, effects of implanted He 7-53852
 Fe-Ni-Cr alloys, internal carburisation, effect of S 7-33839
 Fe-Ni-Cr-Mo-Ti-C, JPCA, He injected and creep ruptured, microstruct. obs. 7-53853
 Fe-Ni-Cr-P, ion irradiat., swelling suppression, effect of P modification 7-58358

chromium alloys continued

- Fe-Ni-Cr-Ti-B, constant elastic alloy, torsion reson. freq. temp. coeff. rel. to B content (Chinese) 7-13488
 Fe-Si-Cr, atomic ordering and mechanical props. 7-11990
 Fe-Si-Cr, high-Si, alloy elements influence on plasticity and mag. props. 7-8067
 Fe-Si-Cr system, ordering process, thermal expansion studies (Russian) 7-1932
 Fe₅₀Ni₃₂Cr₁₀P₁₈ metallic glasses, spin waves, study by polarised neutron scatt. 7-12962
 Fe₇₇B₁₆Si₅Cr₂ metallic glass, crystallisation, DSC and X-ray diffr. studies 7-11932
 Fe₇₄Co_{10-x}Cr_xB₁₆ amorphous alloys, form. and crystn. 7-11930
 Fe₇₄Co_{10-x}Cr_xB₁₆, amorphous, prep. by melt spinning, X-ray diffr., DSC, Mossbauer studies 7-46369
 Fe₃Co_{70-x}Cr_xSi₁₀B₁₅, x=0, 3, 6, 9, amorphous ferromagnet, 180° domain wall (Korean) 7-33198
 Fe_{0.92}Cr_{0.08}, near surface layer conc. profile, XPS (Russian) 7-58582
 FeCrAlY, Al₂O₃ adhesion mechanism 7-33843
 FeCrAlY coatings, ion-implanted, oxidation behaviour 7-53974
 Fe_{80-x}Cr_xB₂₀ metallic glasses, electron transport props., disorder and mag. effects 7-52563
 Fe_{83-x}Cr_xB₁₇, amorphous, mag. contrib. to thermopower 7-45287
 Fe_{85-x}Cr_xB₁₅(Ni₁₅) metallic glasses, mag. and elec. props. 7-13002
 FeCrNi, oxide film thin overlayers, quantitative AES depth profiling studies 7-7796
 Fe_{82-x}Cr₁₈Ni_x, single cryst. alloys, short range atomic ordering (Russian) 7-63558
 Fe₃₀Cr₁₀Ni₄₀B₂₀ metallic glass, fracture toughness rel. to prep. and struct. 7-53870
 Fe₄₃Cr₂₅Ni₂₀B₁₂ glass, devitrification, mag. meas. and X-ray diffr. studies 7-21128
 FeCrNiW amorphous alloys SCC behaviour 7-39727
 FeCrNiWMo alloys, sputtering effects on props 7-36240
 FeCr₁₀P₁₅C₇ amorphous alloy, surface layer chemical bonds, XPS studies 7-12417
 Fe₇₆Cr₄P₈C₁₂, amorphous alloy, mag. short range order above T_g, paramag. phase 7-45623
 Fe₇₀Cr₅Si₁₀B₁₅ metallic glass, field electron emission 7-33530
 Fe_{75-x}Cr_xSi₁₀B₁₅, x=0, 2, 4, 6, amorphous ferromagnet, 180° domain wall (Korean) 7-33198
 Fe_{80-x}Cr_x(SiB)₂₀ amorphous alloy, induced anisotropy, melt spinning effects (Russian) 7-59004
 FeNiCr disordered FCC alloys, paramagnetic-antiferromagnetic-spin glass reentrant transition obs. 7-17175
 FeNiCr, grain boundary solute segregation 7-56833
 FeNiCr spin glass, Edwards-Anderson order parameter temp. depend. meas. (Russian) 7-2866
 FeNiCr spin glasses, nonlinear mag. suscept. study 7-52991
 FeNiCr, strain measurement in convergent beam electron diffraction 7-16562
 FeNiCrSbP, grain boundary segregation, Auger and energy dispersive X-ray mapping 7-16571
 FeNiCr₂₀, spin glass, phase transition, mag. suscept. study 7-53004
 Fe₂Ni_{0.8-x}Cr_{0.2} spin glasses, critical dynamics 7-45683
 Fe₃₀Ni₃₆Cr₁₂Mo₂Si₅B₁₅, amorphous alloy, Curie temp., press. effect 7-52976
 Fe₃₂Ni₃₆Cr₁₄P₁₂B₆ metallic glasses, corrosion in H₂SO₄, alloying effect 7-28201
 Gd-Cr-C system, phase equilib., struct. 7-46423
 La(Cr_xMn_{1-x})₂Ge₂, layer struct. intermetallic cpd., mag. props. comp. depend. studies 7-7489
 Mn_{0.794}Cr_{0.206} alloy, sigma phase, heat capacities 7-52073
 Nb₇₆Al_{24-x}Cr_x, A-15 supercond., transition temp. and mag. susceptibility 7-2768
 NbCr based alloys, grain boundary internal friction investig. (Russian) 7-13490
 Nd₂Fe_{14-x}Cr_xB, crystallographic and mag. props. 7-27522
 Ni base high temp. alloys, corrosion in simulated HTGR He environments 7-17703
 Ni base superalloys, pressure vessel performance, strength, ductility, comp. struct. 7-3365
 Ni-Al-Co-Cr-Ta, polycrystalline superalloys, microstruct. rel. to Ta content 7-46446
 Ni-Al-Cr, melt spun ribbons, microstruct., mech. props., Cr conc. effect 7-28031
 Ni-Al-Cr based alloy plasma-sprayed thermal barrier coatings, sp. ht. and thermal cond. meas. and 2D computer simulation 7-7076
 Ni-base alloy 718, cast, weld heat-affected zone liquation morphology 7-53715
 Ni-base superalloy, cast, high Al-Ti, eutectic form. and σ -phase control (Chinese) 7-7983
 Ni-base superalloy, IN 939, high Cr, effects of heat treatment on mech. props. 7-13526
 Ni-base superalloy, IN-100, rheocast, processing-struct. charactn. 7-46449
 Ni-base superalloy, oxidation in steam at 800°C, role of Al and Ti 7-65203
 Ni-base superalloy, single cyst., SRR99, creep behaviour 7-17587
 Ni-base superalloys, cast, solidification behaviour w.r.t. Hf additions (Chinese) 7-7984
 Ni-base superalloys, creep resist. improvement, role of Re additions, APFIM study 7-22772
 Ni-base superalloys, γ' strengthened, creep and microstruct. rel. to refractory elements 7-3364
 Ni-base superalloys, mag. clusters, calorimetrically determined 7-12977
 Ni-base ternary alloys and superalloys, hot corrosion in SO₂/O₂ atm. 7-65175
 Ni-base ternary alloys and superalloys, hot corrosion mechanism in SO₂/O₂ atm. 7-65176
 Ni-base weld metals, SCC in simulated BWR environments 7-46682
 Ni-Co-Cr-Al-Y, plasma sprayed, high temp. tensile and creep behaviour 7-28083
 Ni-Co-Cr-Al-Y coatings, electron beam deposition, oxidation rel. to pretreatment 7-46702
 Ni-Co-Cr-Mo-Al-Ti prealloyed powder, parts prod. by hot pressing (French) 7-13400
 Ni-Cr, bonding to dental glass 7-39844
 Ni-Cr, carburisation, kinetics, diffusion and precipitation (German) 7-8194
 Ni-Cr, form. by ion beam mixing of alternating layers 7-21303

chromium alloys continued

- Ni-Cr, high temp. alloys, carburisation, finite difference model of C diffusion 7-39712
 Ni-Cr, high temp. corrosion in sulphidising/oxidising environments, review 7-39737
 Ni-Cr, Inconel superalloy, substrates for Au/CeO₂ thin films, diffusional processes 7-45098
 Ni-Cr, oxidation, laser surface treatment and its influence on development of healing Cr₂O₃ scales 7-65204
 Ni-Cr, reaction with Si studied by RBS and TEM 7-21704
 Ni-Cr, struct.-sensitive props., effect of external thermal action 7-46558
 Ni-Cr, wrought, Hf effect on struct. and mech. props. 7-33689
 Ni-Cr (1 wt.%), internal oxidation, two-phase region form. kinetics in diffusion zone (*Russian*) 7-46497
 Ni-Cr alloy, surface segregation, scanning Auger microprobe study 7-22703
 Ni-Cr alloys, phase transformations, C, B, Nb alloying effects (*Russian*) 7-7989
 Ni-Cr based alloys, low impurity content, microanalytical charactn. of microscopic defects 7-58261
 Ni-Cr fibre, porous, physicomech. props. and model prediction 7-3353
 Ni-Cr films, sputter deposition and ion beam mixing, microstruct. 7-44630
 Ni-Cr Inconel alloy, SiO₂ corrosion protective coatings 7-39754
 Ni-Cr superalloy, heat-resistant, heat treatment effect on ductile props. in cold deform. 7-46584
 Ni-Cr superalloy, high-temp. material, microstruct. and mech. props. with high-temp. heating 7-3341
 Ni-Cr vacuum deposition for reproducible thin film resistors, book contrib. 7-46332
 Ni-Cr wire, irreversible magnetisation, effect of plastic deformation 7-53041
 Ni-Cr-Al (20, 12.5 wt.%), coatings containing dispersed oxides, high temp. oxidation 7-33842
 Ni-Cr-Al films, thin film resistor appl., struct., temp. coeff. of resist. props. 7-58912
 Ni-Cr-Co-Mo superalloys, interphase boundary, FIM atom probe study 7-33683
 Ni-Cr-Co-Mo-Ti-Nb-Al, heat-resisting, supersaturated solid soln., isothermal decomp. kinetics 7-33682
 Ni-Cr-Co-Mo-Ti-Nb-Al, heat-resisting, hot strain rate effect on microstruct. and mech. props. 7-39559
 Ni-Cr-Mo-Fe system, pitting corrosion, temp. depend. 7-65186
 Ni-Cr-Si thin films, influence of Si on props. 7-22493
 Ni-Cr-Ti-Al-(Mo), dendritic single crystals, microsegregation 7-46477
 Ni-Cr-W superalloy, experimental, tensile props., effect of carburisation and aging 7-59576
 Ni-Cr-W-Si-Al-C, heat resistant coatings on Ni alloys 7-3498
 Ni-Fe-Cr, age hardenable, SCC in PWR coolant water, heat treatment and Zr additions effect 7-39708
 Ni-Fe-Cr, Inconel 600 and Incoloy 800, fracture toughness 7-59596
 Ni-Mo-Cr-B powders, amorphous and microcrystalline, shock consolidated, wear props. 7-46655
 Ni-Mo-Fe-Cr alloy, transient phase obs during long range ordering to Ni₄Mo, electron diffr. study 7-63806
 Ni-W-Co-Cr superalloy single crystals, fatigue crack propag. under multiaxial cyclic loads 7-28122
 Ni-W-Co-Cr superalloys, creep rupture and tensile props. rel. to hot pressing or aluminising 7-3363
 NiAlCrY, high temp. oxidation, alumina scales, markers and tracer anal. 7-17724
 NiCoCrAlY, plasma sprayed coatings, low cycle fatigue behaviour 7-22793
 NiCr, oxide film thin overlayers, quantitative AES depth profiling studies 7-7796
 NiCr-CuFe thermocouple, mag. field effects (*Chinese*) 7-24646
 NiCr, short range order and atomic interactions, neutron studies 7-51707
 Ni₂Cr, order-disorder transform. kinetics, P content effect 7-13446
 Ni₂Cr, recrystn. kinetics and mech. props., influence of P 7-22718
 Ni₆₀Cr₄₀ alloy, plastic strain rate difference with Cr₂O₃ oxide (*French*) 7-17682
 NiCrAlTi, sputter ion plated coatings for gas turbines 7-53971
 NiCrAlY, Al₂O₃ adhesion mechanism 7-33843
 Ni₇₇Cr₂₃, amorphous, mag. scatt. influence on transport props. 7-33001
 Ni₇₀Cr₇Fe₃Si₈B₁₂ ribbon, rapidly quenched from melt, struct. inhomogeneity and crystallised metastable phase (*Chinese*) 7-63477
 Ni₈₃Cr₇Fe₃Si₈B₃, amorphous alloy, crystallisation (*Chinese*) 7-6518
 NiCrSiB alloy coatings, sputter deposition, microstruct. variations 7-46351
 Ni₆₉Cr₆Si₁₃B₇Fe₂, amorphous alloy, 70 MeV Ni⁶⁺ ion irradi., surface swelling 7-16646
 Ni₃FeCr, atom pair interaction energy and Kurnakov temp. (*Russian*) 7-1938
 (Ni₃Fe)_{1-x}Cr_x alloys, ordering study, comp. depend., electron diffr. and Mossbauer meas. 7-51690
 Ni₃Mn-NiCr tie line, disordering kinetics, neutron diffr. investig. (*Russian*) 7-32347
 Ni₄Mo-Cr, isothermal annealing, structural changes 7-46462
 Ni₅₂Mo₃₈Cr₁₀B_{1.5} metallic glass, shock consolidated, wear props. 7-28154
 NiCr₄Al_{8-x}, mag. props., Mossbauer effect and neutron diffr. 7-59127
 Pt-Al-Cr coatings, structure and 700°C hot corrosion behaviour 7-53973
 TbCr, dilute alloys, hyperfine fields and local moment form. 7-64433
 Ti-Al-Cr-FeSi, AT3 alloy, corrosion resist. and hydrogenation susceptibility in dil. H₂SO₄ soln. 7-17685
 Ti-Al-Cr-Mo, VT3-1 mech. props. depend. on decomp. product morphology for metastable phases 7-39655
 Ti-Al-Mo-Cr, VT3-1, struct. changes during US case hardening (*Russian*) 7-53991
 Ti-Al-Mo-Cr, VT3-1, two-phase, microstruct. and failure nature correl. 7-8110
 Ti-Al-Mo-Cr, VT3-1, vac. annealing of blanks after isothermal deform., hydrogen plasticising effect 7-8027
 Ti-Al-Mo-Cr VT3-1, cooling regimes in heat treatment effect on mech. props. 7-8026
 Ti-Al-Mo-V-Cr, VT22, metallographic study of β -solid soln. decomp. 7-39523
 Ti-Al-V-Mo-Cr, VT23, gas impregnation influence in heat treatment, rapid heating effect 7-17696

chromium alloys continued

- Ti-Cr, β -eutectoid, deform. behaviour of retained β phase 7-39589
 Ti-Cr, nucleation, sympathetic, morphology, crystallography and kinetics 7-65035
 Ti-Cr (6.6 at.%), grain boundary allotriomorphs, nucleation, growth and transform. kinetics 7-28035
 Ti-Cr alloys, cryst. and electronic struct., decomposition of β -solid soln. 7-37931
 Ti-Cr system, oxidation behaviour, role of N 7-28198
 TiC-Fe-Cr alloyed with Si, high-Cr, sinterability and mech. props. improvement 7-64986
 TiCr_{2-x}Fe_x alloys, H absorption and storage investig. 7-32832
 Ti₇₅Sb₂₅Cr_x, A-15 supercond., transition temp. and mag. susceptibility 7-2768
 V-CR-Ti (15, 15 wt.%), mech. props., effect of heat treatment and impurity conc. 7-53857
 V-Cr-C, dispersion hardened, strength changes and recrystn. 7-17545
 V-Cr-Fe(Ti), corrosion in pressurised water, 288°C 7-53967
 V-Cr-Ti, fusion reactor blanket, surface alloying, oxidation resist. to high temp. He coolant 7-53964
 V-Cr-Ti, fusion reactor first wall, oxidation and volatility 7-53965
 V-Cr-Ti, ion-irrad., swelling and microstruct. evolution, effect of He 7-58359
 V-Cr-Ti, thinning treatment, TEM appls. 7-8190
 V-Cr-Ti, V-Cr, oxidation in moist He coolant gas 7-53963
 VCrSi solid solns., elec. resist. (*Russian*) 7-45273
 (VCr)₂Si, neutron irradi., supercond. investig. (*Russian*) 7-12926
 W fibre reinforced Fe-Cr-Al superalloy, surface cladding and matrix deform., thermomech. loading 7-46568
 Zr-Cr-Fe, polypoly structures, TEM, electron diffr. obs. 7-37925

chromium compounds

- see also chromium alloys
 carborundum refractory provisions with aluminium-chromium phosphate binder 7-46395
 K β /K α X-ray intensity ratios, chem. effects 7-17365
 sputtering of Cr atoms, laser-induced fluorescence spectra studies 7-59334
 total angular momentum, atomic mag. moments, calc. 7-62540
 AgCrS₂ two dimens. superionic conductor, DC cond. theory 7-16804
 Al₂O₃-Cr₂O₃ ceramic coatings, thermo-sprayed, microstruct. studies (*Japanese*) 7-22628
 Al₂O₃-Cr₂O₃-ZrO₂ system, subsolidus, high temp. phase relation 7-17519
 CdCr₂Se₄, band structure characteristics and props. of nonequilibrium carriers, cathodoabsorption 7-46064
 CdCr₂Se₄, Cd vapour pressure determ. by atomic absorption method 7-63790
 p-CdCr₂Se₄ ferromag. semicond., photocond. relax. time tempt. depend. meas. 7-45383
 CdCr₂Se₄, ferromag. semiconducting thin films, influence of electric field on magnetisation 7-45738
 CdCr₂Se₄ thin films, ferromagnetic semicond., multielectron energy struct., absorpt. spectrum, temp. and doping depend. 7-38488
 CdCr₂(Se_{1-x}S_x)₄ spinel, mag. prop. anomalies 7-64453
 CdSO₄·8H₂O:CrO₄²⁻, optical absorption spectra, electronic transitions 7-27740
 CeGe_{1-x}Si_x nearly ferromag. props., temp. and comp. depend. study 7-7493
 Co+Cr₂O₃, wear protective dispersion coating for use at high temp. 7-46667
 Co_{0.55}Cu_{0.45}Cr₂S_{4-y}Se_y spinels, X-ray diffr. study 7-44475
 Co_{0.55}Cu_{0.45}Cr₂S_{4-y}Se_y high field susceptibility 7-45630
 Cr (NH₃)₆ ligands, trigonally distorted, ⁴A_{2g}⁻, ²T_{1g} spectra and ligand field calcs. 7-57077
 Cr complex, Cr (III)-amino acid complexes, stability const. determ., ionophoretic technique investig. 7-28381
 Cr complex, luminescence line narrowing, exchange parameter evaluation 7-64677
 Cr Lu₄S₇, synthesis, physicochemical props. 7-44470
 Cr-compounds, Auger and absorpt. spectra involving M_{2,3} levels, atomic effects 7-59311
 Cr-CrO₂/Zn multilayer electrogalvanised coating on steel, XPS analysis 7-22890
 Cr-Fe-C system, EELS fine struct. 7-39333
 Cr-Li-K-C-O system, phase relationships at 650°C, appl. to corrosion processes in molten carbonate fuel cells 7-28020
 Cr-rich oxides, dissolution using H₂SO₄-Ce(IV) soln., radiation decontamination appl. 7-6803
 Cr-Si system, thin film silicide phases, formation and microstructure 7-2435
 Cr-Te, oxidation process, thermodynamic anal., partial sublimation of Te 7-8202
 CrAs, local spin density and paramagnetic susceptibility 7-38844
 Cr₂BeO₄ multi-sublattice antiferromag., elec. polarisation, magnetoelec. effect calcs. (*Russian*) 7-7577
 Cr₂BeO₄ orthorhombic antiferromagnet, double exchange long-period magnetic struct. calcs. 7-2818
 Cr₂Br₃⁻, singly and doubly excited states, exchange interaction, theoretical study 7-10749
 CrC coatings on high speed steel, deposition process and mechanical props. 7-64011
 Cr₂C₃ coatings, tribological props., comp. depend. studies 7-53914
 Cr₂₃C₆, high-resolution Auger spectra, discrete variational X α method 7-16942
 Cr₂C₂-based tribological coating for use to 900°C, appl. to Stirling engine 7-46696
 Cr(CO)₆, electronic struct., X-ray and photoelectron spectra 7-5699
 Cr(CO)₆, photodissoc. in soln., Cr(CO)₅(methanol) form. 7-62399
 Cr(CO)₆, SCF-SW-Xalpha ab initio XANES calcs. 7-64776
 Cr(CO)₅(methanol), form. by photodissoc. of Cr(CO)₆, time-resolved spectrosc. 7-62399
 CrCl₃, ionic crystals, optical and electron energy loss studies 7-3066
 CrCl₃, layer struct., IR vibr. spectra 7-13151
 Cr₂Cl₆⁻, singly and doubly excited states, exchange interaction, theoretical study 7-10749
 Cr_xCy formation in coating of steel with Cr-graphite powder mixtures under shock wave loading 7-8183
 CrDy₄S₇, synthesis, physicochemical props. 7-44470
 CrEr₄S₇, synthesis, physicochemical props. 7-44470
 CrGa_{1.6}S₄ layer cpd. mag. props. and ionic distrib., 2D magnetic system models 7-38880

chromium compounds continued

- CrGd₄S₇, synthesis, physicochemical props. 7-44470
 CrHo₄S₇, synthesis, physicochemical props. 7-44470
 Cr(III) complexes coordinated with macrocyclic tetraamine ligands, low-temp. luminesc. 7-22330
 CrNH₄P₂O₇ and α - and β -CrNH₄HP₃O₁₀, preparation and charact. 7-3161
 CrNbO₄-VO₂-MoO₃ system, rutile phases, prep. and props. 7-6806
 Cr_{1/3}NbS₂, long-period helical spin struct. (*Japanese*) 7-45626
 Cr_{1+x}Nb_{1-x}Se₁₀, resistivity, mag. susceptibility, influence of stoichiometry 7-52426
 CrO, ⁵Π(int)-⁵Π(int) transition, rot. line strengths 7-50050
 CrO₂, half-metallic ferromagnet, band struct. calcs. 7-7091
 CrO₂ particles, LIPS tape prep. and charact. 7-53061
 α -CrO₃, regulator of CdS polycryst. layer photoelec. props. 7-45378
 Cr₂O₃ film, growing on Y ion-implanted Co-Cu alloy, obs. of coherent perovskite particles 7-39738
 Cr₂O₃ film form. on Fe alloys, XPS study 7-22898
 Cr₂O₃, in mullite transparent glass-ceramics, X-ray absorpt., emission and EPR spectra 7-7728
 Cr₂O₃, in transparent glass-ceramic, crystn. and spectroscopic props., melting conditions and heat treatment influence 7-7588
 Cr₂O₃, plastic strain rate difference on Ni₆₀Cr₃₄ (*French*) 7-17682
 Cr₂O₃, pure and MgO doped, sintering kinetics 7-13418
 Cr₂O₃ scale adhesion and growth mechanisms, S effect 7-65206
 Cr₂O₃-GaAs, struct. and electrophysical props. 7-17109
 Cr₂O₃-Nb, high temp. interactions, X-ray diff., DTA studies 7-8259
 CrO₂Cl₂ vibronic anal., CCl₄ and SnCl₄ matrices, emission and excitation spectra, MODOR spectra 7-15542
 CrO₃Cl₂ vibronic anal., phosphorescence and Raman spectra 7-15605
 CrSi₂Ar⁺ ion beam induced surface and subsurface modifications, AES study 7-64846
 CrSi₂ form. by ion implantation in Si, RBS and X-ray diff. studies 7-16656
 CrSi₂/Si Schottky diodes, surface imperfection induced elec. leakage paths 7-2719
 CrSi_x, EELS studies of Cr-L_{2,3} core levels 7-46258
 CrTb₄S₇, 7-44470
 CrTe-CrSe system, mag. phase diagram 7-22105
 Cr₂TiS₂, intercalated dicalchogenide, electronic struct. 7-52387
 CrTm₄S₇, synthesis, physicochemical props. 7-44470
 CrVO₄, magnetic phase transitions, mag. suscept. and sp. ht. meas. 7-2842
 CrVO₄-Li₃VO₄ system, study for solid solns. (*French*) 7-44833
 CrYb₄S₇, synthesis, physicochemical props. 7-44470
 Cs₃Cr₂X₉ (X=Cl,Br,I), synthesis, struct., mag. props. 7-6601
 Cu₂Cr₂Sn_{2-2x}S₄ spinels, Cu-Cu distances, EXAFS studies 7-63585
 Er-Cr-B system, phase equilibr., isothermal section at 1270°C 7-22647
 Fe-Cr oxide film struct., in- and ex-situ fluorescence EXAFS study 7-64007
 FeCoCr₄S₈, crystallographic and mag. props., Mossbauer study (*Korean*) 7-33310
 Fe_{3-x}Cr_xO₄, substituted magnetite, reactivity in O₂, relation with cation distrib. (*French*) 7-46829
 Fe_{1-x}Cr_xBO₃, weak ferrimagnetism, antisymmetric exchange 7-45741
 Gd_{2.815}Tm_{0.17}Ho_{0.017}Sc_{0.005}Ga_{4.95}O₁₂, laser active medium operating in 2 μ m range 7-50568
 HgCr₂Se₄, ferromag. semiconductor, sp. ht. 7-45684
 HgCr₂Se₄, magnetisation, temp. depend. 7-45629
 HgCr₂Se₄, stoichiometry and phys. props. investig. 7-2218
 InVO₂-CrVO₄ system, study for solid solns. (*French*) 7-44833
 KCl:Cr(CN)₆³⁻, phosphorescence spectrum, temp. dependence 7-7742
 K₂SO₄-Cr(SO₄)₃·24H₂O, alum. optical spectra, press. shifts 7-64666
 Mg_{1-x}Cr_xFe₂O₄, Barkhausen noise parameters correl. with strength 7-22963
 MgO-Cr₂O₃-ZrO₂ system, subsolidus, high temp. phase relation 7-17519
 Mn_{0.615}Cr_{0.385}As, press.-induced helimagnetic-ferromagnetic transition 7-52984
 Mn_{0.63}Cr_{0.37}As, thermal, mag. and struct. props. of transitions, thermodynamics, 10 to 350 K 7-64463
 Mn_{1-x}Cr_xAs, phase transitions, effect of external press. and chemical substitutions 7-63798
 Nd₄Cr_{1-x}P₂O₁₄ cryst. growth and characterisation, X-ray diff., Raman scatt., visible and IR absorpt. meas. 7-44423
 Pb₃CrF₉, nonlinear optic, lattice const., ferroelec. Curie temp., phase transition obs. at 555K 7-17275
 Pb_{1-x}Cr_xTe, prep. and electrical props. 7-12721
 Rb₂KCrF₆, structural phase transitions 7-52044
 Rb₂Mn_{0.7}Cr_{0.3}Cl₄, randomly disordered mag. system, mag. cluster excitations and wave-like magnons 7-38881
 Rb₂Mn_{1-x}Cr_xCl₄, reentrant spin glass state, quasi-2D XY system, Cl³⁵ NMR spectra study 7-27613
 Rb₂Mn_{1-x}Cr_xCl₄ mixed crystals, mag. props. 7-2897
 SiO₂-Al₂O₃-Li₂O-ZnO-TiO₂-ZrO₂-As₂O₃-Cr₂O₃:Cr, glass ceramic, time resolved spectra 7-63478
 SiO₂-Al₂O₃-MgO-Cr₂O₃ glass, magnetism of spinel microcrystals, ESR study 7-27594
 SiO₂-Al₂O₃-MgO-TiO₂-Cr₂O₃ based glass ceramics, Cr³⁺ laser emission and excitation spectra 7-22299
 (Ti,Cr)B₂ sintered electrode exposed to liq. Al, degradation, effect of segregated Cr 7-28045
 TiCrNb₂Se₁₀, resistivity, mag. susceptibility, influence of stoichiometry 7-52426
 (V_{1-x}Cr_x)₂O₃ single crystals, elastic const. temp. depend., ultrasonic strain-induced electron transfer effects 7-2082

chromosomes see cellular biophysics**chromosphere**

- 1982 December 2 flare, semi-empirical time-varying models (*Chinese*) 7-66528
 active region loops 7-4418
 coronal material in interspersal region 7-24117
 energetic particle emission regions, temp. conditions determ. 7-66532
 flare eruption, 1985 September 12, prominence spectrograph obs. and interpretation (*French*) 7-60617
 flares, collisional heating by nonthermal electrons in tapered mag. loop 7-66557
 flares, H non-thermal excitation and ionisation 7-34843
 flares, statistical relationship with sunspots 7-66536
 heating, chromosphere and corona, fast magnetosonic surface wave dissipation 7-31969

chromosphere continued

- IR emission lines near 12 microns, non-LTE study 7-66534
 limb flare, 1982 January 22, X-ray imaging 7-66559
 limb spectra, Fe II emission curve of growth 7-24116
 outflows and ejections in the solar transition zone 7-47807
 quiet transition region mag. struct. 7-4417
 spectral lines in 430 to 670 nm wavelength range with large Stokes V-amplitudes outside sunspots, catalogue 7-66554
 spicules, continuous spectral obs. 7-24115
 sunspots, simultaneous meas. of umbral oscills. in photosphere, chromosphere and transition region 7-66542
 temperature density model, results from submillimetre limb brightness profile anal. 7-55590
 transition region, cool loops flow model for fast downflows 7-66537
 transition region, EUV spectroheliograms and time-varying sources 7-24104
 transition region, relative emission-line strengths for Al III and Si IV 7-47799
 transition region spectra, identification of forbidden lines of N I like ions Si VIII, S X and Ar XII 7-66441
 two-ribbon flare, spectra and chromosphere dynamics (*Chinese*) 7-29443
 Ca II K-line shifts in He I 1083 nm dark points, implications for chromospheric vel. field 7-66555
 Ca plages rot. (1967-70) 7-4427
 H β line form. in chromosphere magnetic field (*Chinese*) 7-29441

chronographs see chronometers**chronometers**

- flow visualization and meas., chronographic technique based on split-timer cct. 7-51353

CI calculations (atoms) see atomic electron correlations**CI calculations (molecules) see molecular electron correlations****CIDEP**

- camphorquinone radical anion, photogenerated, time-resolved CIDEP spectra 7-57102

CIDNP

- di-tert-butyl ketone, laser flash photolysis, time resolved CIDNP, multiplet and net effects 7-10617
 hyperfine interactions, semiclassical theory, rel. to mag. field depend. 7-928

cinemafilm see cinematography**cinematography****see also cameras**

- aspect ratio choosing for electronic cinematography (*Russian*) 7-35615
 brightness perception scaling, double-comparison method (*Russian*) 7-4906
 colour display of quantitative blood flow and cardiac anatomy in a single NMR cine loop 7-60065
 colour film development (*German*) 7-15021
 echocardiographic scan images, cine, spatial and temporal processing: automated myocardial border tracking 7-28638
 edit film/conform tape, EFLM/CTAP, film-maker's video system 7-30107
 Electron Beam Recording: the transfer of HDTV signals onto 35 mm film (*German*) 7-9912
 film and video techniques: new directions for the production of programmes for the 1990s (*German*) 7-15020
 film loop noise levels in cameras and projectors (*Russian*) 7-62913
 film theatres, picture and sound improvements (*German*) 7-9913
 heart, contracting, canine, 3D reconstruction using cine CT 7-28759
 holographic cinematography, single and double exposure recording 7-25767
 Marconi B3410 telecine, digital progress 7-15019
 microhardometer for film material testing (*Russian*) 7-61395
 photogrammetric techniques using high-speed cineradiography, biomechanics research appl. 7-23500
 projection equipment, wearout in Geneva mechanisms (*Russian*) 7-11096
 projector, 35-mm, lens design 7-43284
 Soviet Union, history of sound cinema (*Russian*) 7-61397
 special effects, development prospects (*German*) 7-35609
 special effects, mask processes (*German*) 7-24716
 special effects techniques for integral holograms 7-25775
 stereophonic system improvement of 70 mm cinematography (*Russian*) 7-9914
 Video Assisted Film Editing system using 80-bit time code (*German*) 7-9911

circuit analysis see network analysis**circuit analysis computing****see also circuit CAD**

- biomembrane excitation, pulse and const. current stimulation, electrical circuit simulation 7-28479
 metal-insulator-metal (semiconductor) structs., circuit anal., automated 7-27438

circuit breakers

- see also circuit breaking arcs; gas blast circuit breakers**
 earth leakage circuit-breaker protection (*German*) 7-3782
 RFX fusion expt., Italy, design criteria for switching units 7-30667

circuit-breaking arcs**see also circuit breakers; sparks**

- ablation controlled arcs, stagnation press. elec. field strength 7-26332
 asymmetric dual-flow interrupter nozzles, flow field study 7-26331
 gas-blast circuit breaker, nozzle arc dynamic behaviour 7-26556
 mantle studies in dual flow plasmas 7-26559
 post-arc cond., circuit breaker arc, plasma parameters meas. 7-32183
 SF₆ puffer-type circuit breakers, effects of aerodynamic shocks on performance 7-51223

circuit CAD**see also circuit analysis computing**

- finite element modelling of integrated optical waveguides 7-43362

circuit design see network synthesis**circuit oscillations****see also circuit resonance**

- flow/pressure meas. using oscillating fluidic LPA 7-37563

circuit resonance**see also circuit oscillations**

- No entries

circuit simulation *see circuit analysis computing*

circuit synthesis *see network synthesis*

circuit theory

see also filters; network analysis; network synthesis; network topology; time-varying networks

cable theory applied to blowfly receptor cells and large monopolar cells 7-47038

field fluctuations of laser oscillator, electrical circuit theory 7-15886

series circuits, students' approaches 7-24339

circuit topology *see network topology*

circuits *see networks (circuits)*

circular polarisation *see polarisation*

circular waveguides

Doppler-shifted cyclotron resonance maser, theory, TE and TM modes 7-43040

mode converters, optimised overmoded TE₀₁ to TM₁₁, high power appls. at 70, 140 GHz 7-37708

waveguide below cutoff attenuation standard calibration 7-14972

circumstellar shells

A to F-type shell stars, profiles of H α and near-IR spectral lines 7-9497

accretion flows onto massive protostars, temp. struct. 7-29471

δ And (K3 III), primordial dust shell model for IR excess 7-55623

V1343 Aql (SS 433), evidence for optically thick envelope from absence of high-speed light vars. 7-66596

IM Aur, Algol-type eclipsing binary, UV spectrum rel. to gas shells 7-4509

ϵ Aur, eclipsing binary system, high-resolution spectroscopy rel. to massive disk model 7-4519

B 335, compact bipolar outflow source, EHF obs. 7-47893

late B-type stars, nearby, evidence for interstellar or circumstellar C IV and Si IV from IUE obs. 7-60771

Be star, rot. and shell form. (Chinese) 7-66467

Be stars, H α profiles atlas and shell struct. 7-14577

Be stars, shell characters, rot. and spectral obs. (Chinese) 7-4459

Be-type stars of later types, profiles of H α and near-IR spectral lines 7-9497

Becklin-Neugebauer objects, evolution and structure 7-48028

η Car, dust shell internal struct. from six-channel 8 to 13 micron mapping 7-55650

η Car, grain size and geometrical effects in dust shell rel. to 8-13 μ m feature 7-9494

γ Cas, Be star, interferometric meas. of circumstellar envelope in H α line 7-4466

XZ Cep, eclipsing binary, shell electron density characts. 7-4511

CQ Cep, eclipsing Wolf-Rayet star, atmosphere extent from spectrophotometric studies 7-66618

U Cep, photometric asymmetry of disturbed eclipses rel. to distrib. of circumstellar matter 7-47991

μ Cep, red supergiant star, image of circumstellar envelope in Na I 589.0 nm line 7-4442

σ Cet stars, circumstellar shell vel. fields, two-fluid model (Chinese) 7-66591

close binary systems, particles ejection owing to sudden increase in initial vels. (Chinese) 7-4502

conference, Dublin, Ireland (September 1985) 7-24261

R CrB, IRAS detect. and study of fossil circumstellar shell 7-55649

R CrB stars, explosive phenomena rel. to dust form. and brightness decreases 7-24137

R CrB stars, IRAS obs. of cool circumstellar dust 7-9495

R CrB stars and planetary nebulae, IRAS obs. 7-66600

V1057 Cyg, circumstellar dust nature and existence, photometric anal. 7-4463

C Cyg, eclipsing symbiotic star, shell ionisation and radio emission (Russian) 7-40847

CH Cyg, symbiotic star, contrib. of white dwarf and dust shell to spectral energy distrib. 7-47926

V1016 Cyg, symbiotic star, photometric obs. rel. to dust shell form. (summer 1983) 7-47897

dust grains, SiC and amorphous C, laboratory expts. 7-47699

dust in dense regions of interstellar matter, Jena workshop, Georgenthal, DDR (March 1986) Jena workshop, Georgenthal 7-40981

dust shells around late type stars, models for IRAS obs. 7-9461

dust shells around very young and massive stars 7-48026

Egg Nebula (CRL 2688) NH₃ disk characts. 7-4540

evolved stars circumstellar shells, FIRST obs. possibilities 7-47891

G-type stars with IR excesses, IRAS survey 7-66575

Herbig Ae/Be stars, envelopes characts. 7-4473

HH 1-2 exciting star, IR emission from warm circumstellar dust 7-60661

high-mass loss rate stars, projected FIRST obs. 7-47842

HR 5999, Herbig Ae star, circumstellar absorpt. 7-55631

interstellar bubbles, wind driven, soft X-ray spectra 7-4545

IRAS 00193-4033, 22231-4529, O-rich unidentified IRAS sources, optical and IR obs. 7-55853

IRAS 1912+172P09, new binary planetary nebula, spectroscopy and JHKL photometry 7-48046

IRC-10216, ²⁸SiC₂ and ³⁰SiC₂ detect. in millimetre-wave spectrum 7-29474

IRC-10216, brightness distrib. at various wavelengths, radiative transfer in shell 7-60520

IRC-10420, detection of HCN in circumstellar shell of peculiar O-rich evolved supergiant 7-9464

IRC +10420, post AGB star, mass-loss region, circumstellar environment and atm. characts. 7-66583

IRS 16 NW+object A in Sgr A* direction, interpretation 7-40959

late M-type giants and supergiants, dust condensation and stellar UV radiation 7-14565

LDN 1551-IRS 5, circumstellar CO abundance characts. 7-47893

luminous red giant stars, circumstellar dust and gas props. from IRAS and mol. obs. 7-55609

M8 E, IR spectrum obs. rel. to evidence for circumstellar CO 7-48040

M-type giants and supergiants, shell and mass loss characts., CO obs. 7-60649

massive stars in high-lumin. IRAS galaxies, evol. and dust shell form., contrib. to lumin. of galaxy 7-66767

molecular abundances and processes, submm astronomy 7-47892

molecular astrophysics, NATO conf., Bad Windsheim, Germany (1984 July) 7-9589

Nova Cen 1986, IR photometry rel. to dust shell form. (1986 December 30 to 1987 January 5) 7-47913

circumstellar shells continued

Nova Del 1967 (HR Del), spatial shell struct. 7-4462

Nova Her 1934 (DQ Her), spatial shell struct. 7-4462

Nova Vul 1984 No.1, shell ejection, radial vel. anal. (Russian) 7-40848

NS3, NS12, possible bipolar nebulae, optical polarisation study 7-48047

OH-IR stars at Galactic Centre, SiO maser emissions 7-60666

RS Oph (Nova 1985), coronal lines obs. in post-maximum spectrum 7-9499

V346 Ori, antinflame star, circumstellar dust characts., light curve anal. 7-4441

α Ori, circumstellar dust scatt. model for optical polarisation 7-47852

α Ori, dust shell Si fractional condensation, mass loss rate and grain characts., polarisation anal. 7-34972

α Ori, dust shell UV polarisation meas. 7-34971

α Ori, Mg II emission lines flux modulation rel. to atmospheric disturbances 7-47877

α Ori, outer atm. and circumstellar material characts., far-IR spectral obs. 7-60690

Ori IRC 2, SiO maser emission from expanding shell 7-60646

57 Peg, semiregular variable, evidence for expanding chromosphere and envelope 7-55664

pentynylidyne radical (C₅H), detect. of ² $\Pi_{3/2}$ state (in IRC+102.16) 7-23988

β Pic, circumstellar gas cloud, Ca II and Na I obs. anal. 7-24130

β Pic, circumstellar shell characts., UV lines anal. 7-66590

compact planetary nebulae, wind-shell model for radio continuum spectra 7-55751

pre-main sequence, CO band heads emission 7-66584

pre-main-sequence stars, bipolar sources formation in dense mol. clouds 7-24182

pre-main-sequence stars, planets form. in gaseous nebula around 1 solar mass star 7-55497

rapidly rotating gas disks, struct. determ. via versatile two-dimensional method 7-9457

red giants undergoing mass loss, expanding shells IR continuum radiation modelling 7-66582

refractory grain processing in circumstellar shells, diagnostic IR signatures 7-55611

VX Sgr, VLBI obs. of SiO masers rel. to physical conditions in circumstellar envelope 7-55619

solar nebula, pre-planetary disk, radiation press. effects 7-14506

sub-mm astronomy and astrophysics 7-14637

submillimetre astronomy, conf., Segovia, Spain (June 1986) 7-41013

supernovae, type Ib, spectra rel. to supernebulae and nucleosynthesis 7-40854

symbiotic stars, nebular emission location from IUE obs. of HBV 475 (V1329 Cyg) 7-55687

28 Tau (=Pleione), changes in circumstellar shell of Be shell star 7-18412

RY Tau T, Tau star, circumstellar extinction 7-55632

4U 1907+09, spectroscopic obs. rel. to neutron star interaction with Be-star disk 7-18440

Vega-like stars from IRAS point-source catalogue, evidence for circumstellar disks 7-4456

Vel X-1 (4U 0900-403), X-ray probing of circumstellar matter during eclipse phase 7-55726

Vel X-1/HD 77581 system, circumstellar matter characts. from X-ray energy spectra 7-24168

C stars, self-consistent models for dust-driven stellar winds 7-55641

C stars with circumstellar silicate dust, spectral characts. 7-40834

OH circumstellar masers assoc. with IRAS sources, Nancay radiotelescope obs. 7-34978

OH-IR stars, circumstellar shells dimensions from H₂O maser emission obs. 7-24140

OH-IR stars, IRAS obs. rel. to determ. of absolute luminosities and mass loss rates 7-29475

FU Ori, eruptive pre-main sequence star, IUE obs. rel. to wind and extended envelope 7-47875

SO₂ and SO in circumstellar envelopes, millimetre-wave obs. 7-4429

SiO emission from evolved stars 7-47951

SiO maser sources, monitoring obs. at 7 mm wavelength (1977 to 1979) 7-4449

citation analysis *see information analysis*

civil engineering

see also architecture; building; dams

beams, finitely deformed 3-D, tangent-stiffness expression, use in space frame analysis 7-6104

beams/plates under combined loading, finite element dynamic inelastic analysis 7-63002

columns subjected to intermediate concentrated load with axially restrained ends, FEM stability analysis 7-57718

columns with elastic axial restraint, FEM-based stability analysis 7-50964

earthquake-resistant raised floor systems, seismic support of electronic and computer equipment 7-4003

earthquakes, analysis of damage to buildings by OR techniques 7-60169

EM subsurface radar using transient field radiated by wire antenna 7-23866

Histos network for hydrological and meteorological measurement for East-Scheldt storm surge barrier construction 7-47557

plates/shells, two-dimensional FEM model for buckling analysis 7-57717

ship-board echo location system accuracy and system for East-Scheldt storm barrier construction 7-47558

civil engineering computing

see also architectural CAD; town and country planning

beams, cold-bent, flowchart for overbend prediction 7-6103

beams, thin-walled open, elastic nonlinear static analysis 7-62984

curved members, consistent discrete elements technique 7-50948

elasticity versus finite strip analysis of orthotropicfolded plates 7-1427

finite element analysis of steady nonlinear harmonicoscillations of axisymmetric shells 7-6133

frame response to a harmonic excitation, taking intoaccount the effects of shear deformation and rotaryinertia. Timoshenko beam theory 7-6132

I-beams, inelastic distortional buckling analysis using FEM 7-43722

linear elastic fracture mechanics, computerised R-functions method 7-63066

soil testing, BASIC program 7-34735

turbulent flowfield visualisation, computer generated, for flow around cubic model 7-37447

cladding techniques

- steel bimetallic plate, cold-clad, diffusion processes in preboundary zone 7-46708
- Cu-Al-Ni-Fe-Mn bronze, cast, laser surfacing, improved corrosion resist., microstruct. characteris. 7-13651
- Cu-Be, explosive cladding, martensitic transform., electron diffr. 7-46468
- Fe-Cr-Mn-C alloy, laser clad, microstruct. and wear props. 7-13652

claddings

- see also fission reactor fuel claddings*
- optical fibre, mode propagation in case of cladding limited by plane 7-1271
- planar optical waveguide, Si-clad, numerical anal. (Japanese) 7-6000
- semiconductor clad dielectric guided-wave bistable devices, periodic coupling 7-57426
- steel, stainless, chemical compatibility with Li based oxide ceramic fusion breeders 7-49646
- steel bimetallic plate, cold-clad, diffusion processes in preboundary zone 7-46708
- Teflon clad 'As-S glass IR fibre, optical loss due to water diffusion 7-57556
- SiO₂ core optical fibres, triple clad, with zero total dispersion at wavelengths of 1.3 and 1.55 μm (Japanese) 7-50781
- W fibre reinforced Fe-Cr-Al superalloy, surface cladding and matrix deform., thermomech. loading 7-46568

classical algebra *see algebra***classical field theory**

- see also classical mechanics; electromagnetic field theory; gravitation; special relativity*
- field correls. in a fluctuating homogeneous medium, spectral coherence, dynamical struct. factor determ. 7-41119
- fluctuating field systems of finite size, effective classical pot. 7-14866
- gravitational field, Earth-Moon system, momentum current picture 7-55934
- Hamiltonian differential operators, canonical form, Dirac's theory of constraints 7-18607
- potential energy and the field concept in A-level physics 7-14744
- ultraviolet problem and analytical properties of classical field theories 7-61134

classical mechanics

- see also classical mechanics of continuous media; classical mechanics of discrete systems; classical theories of fluid structure*
- book, foundations for classical mechanics 7-14723
- computational continuum dynamics, parallel algorithms 7-4683
- periodic orbits class in classical mech. 7-48349
- photoelasticity and classical mechanics, link, Lorentz group 7-11366
- problem solving by the numerical integration of Hamilton's equations 7-35173
- time-dependent systems, density functional theory 7-41254

classical mechanics of continuous media

- see also elasticity; fluid mechanics; mechanical contact; plasticity*
- arbitrary Lagrangian-Eulerian finite element method for path-dependent materials 7-14766
- asymmetric dynamic problems, higher-order boundary perturbation method 7-41098
- bar, exact soln. of approx. differential eqn. under conditions of nonlinear equilibrium 7-31636
- bar material, dilutely voided, instability in uniaxial tension 7-53787
- beam element, curved isoparametric quadratic thick 7-4684
- beamlike lattice trusses, anisotropic continuum models 7-6085
- beams, naturally twisted, rectilinear, theoretical anal. 7-96
- bifurcation by shear band localisation, incrementally nonlinear constitutive eqns. (French) 7-1441
- biharmonic equation, reduction of boundary value problem to Stokes-type problem 7-18566
- cantilever beam, large deflection anal. with end rotational load 7-29761
- classical space-times, vorticity-preserving motions 7-18595
- composite material failure under compression, complex stressed state case, continuous theory 7-62974
- composite micromechanics, simplified, 3D finite element anal. 7-31637
- composite system, one dimens., with random parameters, dynamic processes 7-107
- composite systems with randomly oriented short fibres, mech. response, microstruct. approach 7-20593
- Cossierat media, inelastic behaviour of plane frictionless block-systems 7-1432
- crack initiation at grain-boundary triple points in high-temp. deform., continuum mech. model 7-28104
- creep rupture mechanics 7-53835
- cylinder, hollow composed, axisymm. problem, approx. soln. (Ukrainian) 7-11277
- cylinder weakened by system of reduced strength layers under dynamic loading, behaviour 7-11345
- cylinders, hard/soft mixture, uniaxial compression effects 7-26135
- damage parameter, effects of interacting cavities 7-43796
- defect and fracture mechanics, conf., Bad Honnef, Germany (Jan. 1985) 7-24260
- direct methods of solution for problems in mechanics from invariance principles 7-77
- discontinuity surfaces in a rigid plastic anal. 7-43697
- discs with fluctuating radii, simulation of elastic response 7-56040
- dislocations, nonlinear continuous medium model for stress, strain and displacement fields 7-6623
- elastic beam on elastic base, optimal design 7-4690
- elastic dielectric, conservation laws and material momentum tensor 7-6086
- elastoplastic systems, linearly strengthened, extremum principles and optimisation problems 7-63015
- elementary beam theory, existence and completeness of conservation laws 7-26134
- energy minimization for nets with slack 7-35279
- equations of motion of granular media 7-1405
- equations of state and constitutive equations 7-21389
- Euler-Bernoulli beam, inverse problem 7-4688
- fluid-and-gas-filled elasto-plastic solids, anal. 7-43657
- fluid-structural vibration studies using boundary element method 7-99
- force-deflection anal., eigenvalue convergence in the finite element method 7-24420
- frame-independent description 7-24417
- frictional materials, theoretical framework for modelling behaviour 7-43706

classical mechanics of continuous media continued

- fundamental equations of continuous structural media 7-56035
- fundamental equations of continuous structural media 7-56036
- incremental harmonic balance method and harmonic balance-Newton Raphson method equivalence 7-4677
- inelastic state-variable theory, large strain 7-4686
- inextensible cloth or cable networks with bending stiffness, continuum theory 7-1400
- kinematics of submanifolds and the mean curvature normal 7-41305
- kinetic theory and material frame-indifference principle 7-24422
- Lagrangian, second-order, duality under dependency inversion and Noether theory 7-24426
- Lagrangian densities, conservation laws 7-91
- Lagrangians for certain classes of inelastic solids 7-43658
- laminare, continuum theories for transient wave propag. and dynamic moire interferometry 7-59717
- lattice element, explicit form of stress constraints (French) 7-14767
- local approach of fracture, continuum damage mechanics 7-50988
- logarithmic strain, material time derivative 7-24421
- mathematical models in mechanics, book 7-55906
- mechanics of deformable media, book 7-35135
- mechanics of solids—equivalent response of structure under cyclic loadings (French) 7-63006
- microelastic continuum theories, relationships and appl. possibilities 7-24423
- mixtures, continuum theory, motivation from discrete considerations 7-57680
- multiphase flow, forces on solid constituent, continuum mechanics 7-37528
- multipolar rod model, virtual power method appl. 7-57684
- nonhomogeneous boundary conditions, reduction method 7-4689
- panel, composite, min. wt., optimum design w.r.t. arbitrary loads 7-1397
- plate, annular, with cyclically symm. curvilinear notches, stress state anal. 7-1420
- plate, cracked, description using Lagrange method (Polish) 7-43793
- plate, three-dimensional, thermoelasticity problem, effect of matching conditions 7-29757
- plate, trapezoidal, on elastic base, vibration and buckling 7-48365
- plate bending elements, nonconforming shape functions (Chinese) 7-50958
- plate theory, matched asymptotic expansions, clamped edge (French) 7-1412
- plates, biharmonic eqn. general soln., generalised Levy's method 7-1396
- plates, elastic with variable flexural rigidity, inverse problems 7-26148
- plates, flexible, rectangular, on nonlinearly elastic base, optimal design 7-62995
- plates, sectorial, laminar, orthotropic, flexure anal. on basis of finite-shear theory 7-63014
- plates, shallow anchor, calc. 7-9673
- plates and envelopes, nonlinear theory and net approx. 7-18597
- plates and shells, finite strain large deformation, nonlinear theory 7-20602
- plates and shells, hybrid strain technique for FEA 7-20603
- porous body, deformability criterion based on continual model 7-64958
- porous media, wave features of nonlinear theory 7-56054
- probabilistic structural modelling in linear dynamic anal. of complex mechanical systems (French) 7-61098
- probabilistic structural modelling in linear dynamic anal. of complex mech. systems (French) 7-61099
- rectangular elastic-plastic cantilever, deflection anal. (Chinese) 7-48358
- refined transverse shear deformation theory for multilayered anisotropic plates 7-1434
- rocks, fracture anal. 7-66106
- rods, elastic, stationarity for non-selfadjoint problems 7-26178
- rods, reinforced, curvilinear, limiting condition under multiparametric external forces 7-1399
- rough disks, shear flow, constitutive relations 7-35267
- shear center of nonsymmetric open thin-walled sections 7-37337
- shear deformation plate continua of large double layered space structs. 7-43660
- shell, spherical, subject to external pressure, stiffening anal. 7-9670
- shell element, curved C¹, based on assumed natural-coordinate strains 7-11313
- shell elements, 3-node triangular, improvements 7-4685
- shell elements, degenerated, implementation with transverse shear and membrane strains 7-50944
- shell of revolution, stiffened, soln. of geometrical nonlinear problem 7-9669
- shell structures, eccentricity of normal forces and initial imperfections 7-26174
- shell with rigid inclusion, finite deformation 7-9667
- shells, cylindrical, calc. by finite-element method 7-95
- shells, cylindrical, thick-walled, nonlinear cross section, stress state anal. 7-62993
- shells, cylindrical, weight optimization for variable stiffness 7-9668
- shells, hollow flexible multilayer orthotropic, nonlinear theory, Bubnov-Galerkin method 7-24430
- shells, mixed variational theoretical formulation 7-35278
- shells, shallow, of variable thickness, differential eqns. 7-11278
- shells coaxial, orthotropic, cylindrical, with flowing fluids, axisymm. normal wave propag. 7-106
- sliding inclusions, anomaly 7-37323
- solid deformable body mechanics, modern directions 7-1398
- strain concentration in inhomogeneous boundless thin plate with circular opening 7-29754
- stress functions for plane problem of couple elasticity theory (Ukrainian) 7-11283
- stress invariants, stationary behaviour 7-14776
- structural reliability anal., nonlinear resistance function (Chinese) 7-1404
- surfaces and interfaces, singular, virtual power method appl. 7-4682
- thin plate, stretching deformation, method of generalized plane stress 7-29760

classical mechanics of discrete systems

- see also N-body problems*
- adiabatic invariant for 1D periodic motion, simple proof 7-4676
- averaged Kolmogorov-Fokker-Planck eqns. in random vibr. theory, integrability condition 7-88
- balancing toy, centre of gravity, oscills. about equilb. 7-48243
- ball rolling on rotating plane, inclusion of viscosity and friction, diff. eqn. soln. 7-41097

classical mechanics of discrete systems continued

- ball rolling without slipping on horizontal table (*French*) 7-29626
 beam-point mass system. stability of 1D unbounded elastic systems 7-26185
 billiard ball problem, instability of boundary 7-61083
 Birkhoff-Gustavson normal form in classical and quantum mechanics 7-18623
 body suspended on string with impact interactions, stability of permanent rotations 7-41090
 bouncing ball, period double boundaries 7-4669
 bowed string vibration, friction-vel. characts. 7-50943
 brachistochrone, unrestrained problem soln. 7-18523
 bubble-tube accelerometer for elementary mechanics teaching 7-14739
 canonical transformations and the equivalence problem 7-18591
 cell mapping method for nonlinear deterministic and stochastic systems 7-35271
 cell mapping method for nonlinear deterministic and stochastic systems, appl. 7-35272
 cellular automata, Langevin equations, and unstable states 7-18703
 chain of anharmonically coupled oscillators, broken ergodicity 7-61087
 Chebyshev polynomials and quadratic path integrals 7-41093
 classical dynamical systems, geometric description 7-24407
 complex mechanical systems, control algorithm synthesis by method of inverse dynamics problem (*Ukrainian*) 7-9660
 constrained systems, equivalence between Lagrangian and Hamiltonian formalism 7-41092
 cylinder, unsteady boundary layer eqns., frictional forces 7-1392
 cylinders, hard/soft mixture, uniaxial compression effects 7-26135
 damped driven Lennard-Jones chain, interacting solitary waves 7-41094
 delay force systems, parametrically excited oscils. 7-11268
 direct methods of solution for problems in mechanics from invariance principles 7-77
 dissipative systems, transient chaotic distributions 7-4769
 dynamic system stability estimate based on quasistationary principle 7-81
 dynamic systems, conservative and non-conservative, conservation laws 7-35269
 dynamic systems, multiple parameter, time-varying, stability 7-37320
 dynamics and the calculus of variations 7-61085
 dynamics formulation without accelerations (*French*) 7-61086
 ellipsoid, heavy rigid, motion along smooth plane, non-existence of additional integral 7-83
 elliptic motion of arbitrary eccentricity and semi-major axis, expansion theory, general periodic function 7-60510
 ergodic properties of linear dynamical systems 7-61044
 essentially nonlinear systems, simplified asymptotic integration algorithm 7-41091
 ferromagnetic rigid body in magnetic field, rotation problem 7-41087
 finite-dimensional integrable systems, master symmetries, Calogero-Moser system 7-4674
 flight vehicle aeroelasticity, 3D motion, nonlinear integrodifferential eqns. 7-43737
 forced van der Pol oscillator, quasi-periodic oscill. destabilisation 7-29744
 free asymmetric top motion in n dimension 7-24416
 free rigid body, eqns. of motion, matrix forms 7-41089
 Frenkel-Kontorova Aubry Model, driven dynamics 7-9662
 generalised problem of two fixed centres, coordinates trigonometric expansions 7-4298
 generalized dynamics, extension to unidimensional phase space 7-61093
 gyrocompass, integration of eqns. of motion 7-43652
 gyroscope, noncontact, in resistive medium, run-up system 7-43653
 gyroscope with small self-excitation, motion, rotation evolution 7-43654
 gyroscopic systems, complete separation of motion 7-11267
 gyroscopic systems, periodically perturbed linear, dynamic behaviour 7-11273
 gyroscopic systems, periodically perturbed nonlinear bifurcation behaviour 7-11274
 Hamilton-Jacobi equation, maximal symmetry group, relativistic particle in flat spacetime 7-18592
 Hamilton-Jacobi theorem in Poincare-Chetaev variables, generalization for linear holonomic systems 7-29747
 Hamiltonian equivalence leading to Newtonian equations 7-78
 Hamiltonian formulation with respect to an observer's light cone 7-48350
 Hamiltonian systems with indefinite kinetic energy 7-18594
 Hamiltonian systems with two degrees of freedom, problem of four point vortices 7-61084
 Hamiltonization as a twofold procedure 7-35266
 Helmholtz conditions and trace theorem 7-14764
 Henon-Heiles and two coupled quartic anharmonic oscillator systems, invariance and integrability 7-24412
 incremental harmonic balance method and harmonic balance-Newton Raphson method equivalence 7-4677
 inertial moment, slip method determ. using functional force and impulse 7-41038
 integrable multiwave interaction systems of ordinary differential equations 7-4671
 interacting self-oscillators, discrete-time population dynamics 7-4675
 inverse problem, Euler-Lagrange form of eqns. of motion 7-29740
 Keplerian ellipse under perturbation, perihelion precession (*Chinese*) 7-29381
 Kovalevskaya top perturbed motion, Lie series 7-84
 Langevin equation, generalised, for oscillator 7-29746
 Lienard 4-resonance forced oscillator, numerical anal. (*French*) 7-14762
 Lorentz-force-induced motion of a solid object with a fixed point 7-41086
 Lorenz equations, second order dynamical system 7-4659
 massive rigid body motion around fixed points, topology, bifurcation sets (*French*) 7-29743
 mathematical models in mechanics, book 7-55906
 mathematical properties of statistical mechanics and dynamics 7-48203
 minimum time problem 7-41042
 modal synthesis method considering rotational effects (*Chinese*) 7-11270
 multidimensional discrete mech. system, freq. spectrum depend. on elasticity parameters 7-1395
 multidimensional Hamiltonian systems, Lyapunov stability 7-80
 multidimensional mechanical systems with freq.-independ. friction, identification problems 7-87
 multiline mechanisms, mathematical model 7-11275
 Neumann-type dynamical systems and their integrability 7-41085
 Newton's laws of rigid body mechanics, proof using stroboscopic photograph 7-55927
 Newton third law, conceptual change, alternative frameworks 7-9614

classical mechanics of discrete systems continued

- Newtonian dynamics; predictability failure 7-4672
 non-autonomous mechanical systems, Fokker-Planck-Kolmogorov eqns., random oscils. 7-85
 nonconservative dynamical systems, stability criteria, appl. to wing flutter 7-18590
 nonlinear mass-spring chains, dynamics near continuum limit 7-24414
 nonrelativistic two-particle Coulomb Green's function at positive energy with explicitly separated singularities (*Ukrainian*) 7-9659
 particle in fixed dispersed layer, fluctuation hydrodynamics of Brownian motion 7-24560
 path integral quantisation of constrained systems, Senjanovic measure 7-61140
 pendulum, gyroscopic, with ideal unilateral constraint, motion with respect to angle of nutation 7-43655
 penetration of compressible liquid by axially symmetric solid 7-11370
 periodic systems, nonlinear. localization of solutions 7-29742
 planetary potential, representation as convergent series 7-4678
 plates and shells, perforated, with system of attached masses, eqns. of motion 7-1393
 primary Hamiltonian constraints for singular N-body Lagrangian 7-24410
 quasienergy integral for canonical maps 7-56029
 rectangular rigid frame, structural anal. by the ϵ -method using a digital computer 7-14761
 rigid body, heavy symmetrical, suspended on string, stationary motions 7-11266
 rigid body dynamics, general integrable cases for problems with no axial symmetry 7-24413
 rigid body in resistive medium, eqns. of free motion, stability control of numerical integration 7-41088
 rigid body undergoing motion, constancy of angular momentum vector 7-41096
 ring motion along straight and cosinusoidal smooth rod (*Ukrainian*) 7-11265
 rope, vertical in circular orbit around Earth, config. strain energy 7-1391
 rough disks, shear flow, constitutive relations 7-35267
 scalar comparison eqns. in stability of motion theory 7-86
 shear deformation plate continua of large double layered space structs. 7-43660
 slow motion extraction from nonlinear equations of motion 7-14763
 solid body hinge-suspended in a fluid flow, vibrations 7-1394
 stability degree, indices of estimation 7-56027
 stability of length of rods in orbit, rigidity and tension conditions 7-61095
 stability of overhanging pile of heavy objects, demonstration 7-48255
 stochastic and variational processes, in classical and quantum mechanics 7-4761
 strictly invariant Lagrangians, determ. from gauge invariant Lagrangians 7-61092
 string objects, vibr. anal. using a diffraction technique, multimode optical fibre appl. 7-11364
 symplectic manifolds with Lagrangian fibration 7-29745
 time-dependent oscillator, constants of motion 7-24408
 truss, three-bar, elastic/perfectly plastic, nonuniqueness, causes and consequences 7-11276
 tubular cantilevered beams conveying compressible fluid, unstable oscillation 7-4670
 two point masses joined by an elastic bar, difference eqns. (*Spanish*) 7-61094
 two-beam problems, sixth-order multidervative method 7-24409
 variable mass nonholonomic systems, higher order Nielsen and Euler operators (*Chinese*) 7-48345
 vibration-impact systems with moving limiters, nonsmooth transforms. 7-11269
- classical theories of fluid structure**
see also kinetic theory; liquid theory
 binary hard sphere mixtures eqns. of state, van der Waals perturbation term calcs. 7-12226
 hard sphere fluid, extended-mode coupling theory, shear viscosity near solidification 7-11875
 hard sphere fluids, bridge fn. calc. 7-63418
 liquid, polar hard dumbbell type, struct. and props., site-site Ornstein-Zernike eqn. soln. 7-63417
 model suspensions, 2D, interactive and non-interactive rigid spherical particles, hydrodynamic interactions, viscosity calculus (*French*) 7-8306
 phase transitions at interfaces, local density approx. and smoothed density approx. study 7-63912
- classification**
see also indexing
 atmospheric turbulence classification, computer program 7-55247
 colour, direction and speed of motion, perceived relations 7-47078
 complexity 7-41051
 dwarf galaxies, luminosity classification anal. 7-60794
 Markarian galaxies, deficiency of normal elliptical galaxies from morphological classification 7-24201
 parts production by hot isostatic pressing, applic. of rheological model for porous materials (*French*) 7-13400
 peculiar stars, UV classification from IUE low-dispersion spectra reference atlas 7-60636
 planetary nebulae, spectroscopic obs. of 21 genuine and misclassified objects 7-66703
 remotely sensed data, classification improvement using additional variables and hierarchical struct. 7-4222
 Ni-Co-Cr-Mo-Al-Ti prealloyed powder, parts prod. by hot pressing (*French*) 7-13400
- classification, pattern** *see pattern recognition*
clathrates *see molecules; organic compounds*
clay
 Amazon River, continental shelf, clay mineral reactions effect on Al distrib. in sediments and waters 7-34551
 argillaceous media, geochemical barrier capacity for radwaste disposal 7-5466
 S Bulgarian Black Sea coast, abraded cliffs heavy minerals characts. (*Russian*) 7-34483
 chemical analyses, clay constituents, apportionment into structural formula 7-65999
 fracture permeability study for radioactive waste repositories 7-10293
 geological radwaste isolation in clay formations, fractures and faults 7-36295

clay continued

- kaolinite particles in aq. suspension, amplification of shock waves 7-43978
- magnetic fabric of clay from compressional zones in Greece and Taiwan 7-23638
- mechanical behaviour of anisotropically consolidated clay, plasticity model 7-14265
- nontronite, effects of shock and thermal alteration on physical props., and implications for Martian surface 7-55024
- pelagic clay from South Pacific, remanent magnetization 7-60161
- porous material prep. from montmorillonite- α -naphthylamine complex, oxidation, struct. 7-27986
- radionuclide migration barrier, use for radwaste disposal 7-56861
- radwaste disposal in shallow tunnels in glacial till or clayey soil, geotechnical considerations 7-42217
- salt marsh creek, clay particles swelling rel. to seasonal changes in surface level 7-8914
- sandstones, porosity and clay content effects on wave vels. 7-47429
- shallow land LLW and ILW repository on a clay site in the UK 7-42219
- slurries, clay-rich, cohesion energy 7-66105
- soil, filtration prop. form., adsorbed H₂O struct. role 7-51297

cleaning *see surface treatment*cleanliness *see hygiene*cleavage fracture *see brittle fracture*cleaved coupled cavity lasers *see semiconductor junction lasers***Clebsch-Gordan coefficients***see also elementary particle theory*

- SO_n, symmetric representations, coupling and recoupling coefficients 7-48425
- SU(2,1) group, Clebsch-Gordan series 7-61499
- Wigner coefficients, nontrivial zeros, nonlinear solns. 7-48421

climatology

- aerosol effects (*Italian*) 7-60372
- aerosol in Late Quaternary atmosphere, Antarctic ice core record 7-55208
- aerosol profile in stratosphere between 1977 and 1984 AD, and relation to climate 7-4136
- E Africa, climate prediction for averting drought-caused famines 7-9158
- S Africa, summer rainfall distrib., effects of circulation and humidity 7-47492
- Africa (southern and equatorial), rainfall spatial variability since 1901 AD 7-23837
- African rainfall anomalies (1901-73), spatial patterns 7-66292
- air quality simulations, nonGaussian climatological model 7-55243
- Alaska, permafrost temp. profile, evidence for climate change 7-66299
- Alberta, Canada, Holocene vegetation and climate changes 7-23840
- alpine snowfields, influence of longwave radiation on energy balance 7-23727
- N Amazon Basin, Holocene fires as climatic indicators, dating 7-47531
- N America, climate change influences on future grain corn yields 7-55047
- anthropogenic factors in climatic change (*Russian*) 7-9163
- Arab Gulf states, climate effect on economic activity 7-9160
- Arctic anthropogenic aerosols, climatic effects 7-55193
- central Arctic Ocean, Pleistocene calcite lysocline and palaeocurrents, climatic implications 7-23696
- areal quality control of min. temp. and sunshine duration, principal component and near neighbour methods 7-4141
- S Asia, local rainfall rel. to southern Oscillation Warm Events 7-34628
- Athens, Greece, air temp. and climatic change 7-66287
- S Atlantic, Oligocene palaeocean and palaeoclimate conditions 7-23698
- North Atlantic deep water production, sporadic shutdown during Glacial-Holocene transition 7-34538
- Atlantic Ocean, mean sea-surface temperature variations (0-20000 BP) 7-18201
- attractor existence in present and Quaternary climates 7-18301
- Australia, major droughts prediction from temp. anal. 7-4170
- S Australia, Precambrian periglacial varvites, palaeomagnetism, palaeoaltitude and palaeoclimate 7-8798
- Austria, precipitation climate regionalization 7-66295
- Baffin Bay, land-ocean correls. during last interglacial-glacial transition 7-34568
- Bangladesh, rainfall probabilities during monsoon period 7-14337
- Birmingham, England, occurrences of very warm and very cold spells 7-55232
- Black Sea region, climatic implications of abyssal waters temps. (*Russian*) 7-66156
- black shale, climatic cycle evidence (*French*) 7-66288
- blocking events, climatology in perpetual January simulation of spectral general circulation model 7-29137
- Bremen, West Germany, summer temp., precipitation and sunshine characts. 7-9162
- Britain, temperature changes since 22000 years BP, beetle remains record 7-60373
- W Canada, temperatures existing 42000 and 34000 years BP 7-23833
- Cenozoic humidity and environments deduced from the variations of kaolinite in East-Atlantic sediments (*French*) 7-66090
- Cenozoic temperature variations, stratospheric aerosol effects 7-34666
- change detection using weighted average of data 7-29235
- China, loess deposits, palaeomagnetism, palaeoclimate and sedimentary history 7-40557
- E China, summer rainfall and temp. rel. to Eurasian snow cover 7-29238
- cirrus cloud, influence on climate and weather processes, global perspective 7-4157
- cloudiness increase in warming atmosphere 7-55249
- coastal wave climate categorization, software packages 7-55254
- convective boundary-layer parameters, climatology over Ontario, Canada 7-40512
- coupled atm.-ocean general circulation climate models 7-55076
- cumulus moisture transport effect on GCM climate simulation 7-66291
- data banks for climatological data, design and use for monthly data records 7-9178
- Dead Sea, high level of lake at 6700 yr BP, salt deposit evidence 7-55087
- Deccan upland region, India, late Quaternary alluvial history and climate 7-60287
- desertification, review and definitions of concept 7-9157
- desertification indicators 7-8452
- climatology continued
 - desertification process, importance of drought in intensification of desert conditions 7-8453
 - desertification processes responsible for land degradation 7-8449
 - drought occurrence in desert border areas, rain-albedo-vegetation feedback process 7-9159
 - drought prediction by use of teleconnection and numerical models 7-9071
 - Earth Radiation Budget Experiment (ERBE), meas. data (1984 November 15) 7-9067
 - East Germany, evaporation height rel. to air temp., global radiation and saturation deficit (*German*) 7-9055
 - El Nino, decay predictability (1982-3) 7-4174
 - El Nino-Southern Oscillation, 1877-8 event rel. to 1982-3 event 7-4051
 - El Nino-Southern oscillation occurrence and New Caledonia rainfall, Pacific Ocean 7-4154
 - El Nino/Southern Oscillation system, role of stratospheric aerosols 7-55196
 - Elatina varve record of solar activity, Hilbert transform anal. 7-47811
 - energy balance model climate, effects of altered exchange coeffs. 7-4176
 - W Europe, climate simulation and CO₂-induced climate change 7-66285
 - Europe and N Hemisphere, nineteenth century climate changes 7-9154
 - Europe climate in winter, influenced by Gulf Stream variability 7-4173
 - extraterrestrial object impacts and triggering of geomagnetic reversals, mechanism involving climate 7-40413
 - fossils and climate, conf., Glasgow, Scotland (Sept. 1982) 7-35121
 - general circulation model of climate, with improved parameterizations 7-40558
 - general circulation models, influence of surface and vegetation 7-9152
 - global temperature changes, annual and seasonal (1960 to 1985) 7-47527
 - Great Britain, windiness (1881-1980) 7-66251
 - Greece, sunshine duration rel. to altitude, latitude and longitude 7-66296
 - greenhouse effect, radiation absorption in Earth's atmosphere causing heating 7-40556
 - greenhouse gases and climate change in twentieth and twenty-first centuries (*Russian*) 7-55250
 - Holocene and late Pleistocene climate of Britain, beetle remains record 7-60373
 - Holstein interglaciation, time-stratigraphic position and correl. to deep-sea sediments stable isotope stratigraphy 7-47529
 - Holsteinian interglaciation, N Germany, stratigraphy and ESR dating 7-34669
 - homogeneity test applied to precipitation data 7-47565
 - NW Iapetus Ocean, Early Palaeozoic climate 7-23694
 - ice age northern hemisphere ice sheet and climate cycles 7-23708
 - India, daily monsoon rainfall persistence anal. 7-47495
 - India, droughts and floods in summer monsoon season, AD 1871 to 1984 period 7-66294
 - India, droughts in Maharashtra State 7-29093
 - India, droughts incidence, seasonal aridity index anal. 7-9049
 - SW India, monsoon fluctuations in 20000 yr BP O isotope/pollen records 7-47532
 - India, monsoonal fields sequential evol. 7-29203
 - Indian Ocean, Quaternary temps. var. due to climatic changes 7-29074
 - interdecadal climate changes, use of ship obs. 7-4217
 - Israel, weather modification by artificial land surface albedo changes 7-9072
 - January climate simulation, general circulation model, removal of zonally-uniform sea surface temp. 7-47526
 - Keweenaw palaeoclimate (1.1 Gyr) of Michigan, implications of CaCO₃ cement (caliche) in sedimentary rocks 7-29024
 - Kuhlungsborn Observatory, East Germany, 27 kHz noise temporal var. rel. to temp. 7-9149
 - Lake Karewa, India, sediments ¹³C/¹²C and C/N ratios, palaeoclimate characts. determ. 7-4175
 - land surface remote sensing and climate, conf., Rome, Italy (Dec. 1985) 7-23921
 - late-glacial climatic oscillation in Atlantic Canada equivalent to the Allerod/younger Dryas event 7-40559
 - Little Ice Age, record in stratigraphy of tropical Quelccaya Ice Cap, Peru 7-34670
 - 'Little Ice Age', ¹⁴C dating and palaeoenvironment of glacier advance of Nigardsbreen, SW Norway 7-9037
 - Manchester, England, major snowfalls (since 1880) and assoc. synoptic conditions 7-9147
 - mean values of atmospheric parameters, satellite retrievals, systematic errors 7-66266
 - Mediterranean Sea, climatic series of sea level oscills. at Trieste and Cagliari 7-40484
 - melanin content of human skin, evidence for past climates? 7-66289
 - microwave communication, equatorial and tropical regions, rain effects 7-66281
 - Miocene climates in Hungary, evidence from tree rings for 7-year cycle 7-9456
 - modelling using Freons, band strengths temp. depend. meas. 7-55252
 - modification of climate by land surface albedo alteration by man 7-18300
 - monthly 700 mbar heights prediction 7-29192
 - Mount Kenya, origin and palaeoclimatic-ecological significance of sand dunes in Mutonga drainage 7-18186
 - neogene paleocirculation and paleoclimate record of ODP Leg (tropical and subtropical east Atlantic) (*French*) 7-66091
 - NE Nevada, precip. reconstruction, 1600 to 1982, using tree ring indices 7-29145
 - New Mexico, USA, Pleistocene climate indicated by groundwater isotopes 7-23838
 - New South Wales, Australia, rainfall characts. 7-29083
 - Northern Hemisphere, climatological consequences of Arctic Ocean halocline degeneration 7-34534
 - Northern Hemisphere, press. var. 7-4171
 - Northern Hemisphere, volcanic activity and climate since 1500 AD (*German*) 7-9161
 - Northern Hemisphere Quaternary glaciations 7-55051
 - Northern Hemisphere surface press. and temp. 7-34665
 - Norway, avalanche winters (1855-1985) 7-4172
 - Norway, models of solar radiation climate for graphical database 7-47514
 - Norwegian and Greenland seas during Pleistocene, ice shelf existence and climate 7-23699
 - Norwegian Sea, volcanism, continental crust rifting, climatic fluctuations (*French*) 7-66089

climatology continued

- nuclear war climate perturbations, indirect effects due to smoke from fires 7-14323
- nuclear winter, protracted climatic effects of massive smoke injection into atmosphere 7-66297
- nuclear winter studies, effects of uncertainties in smoke source term 7-34668
- ocean-atmosphere system, response to increased atmospheric CO₂ cone. (Russian) 7-23834
- Ossau Valley, France, sedimentology and morphology (French) 7-66177
- N Pacific Ocean-atm. system, Pliocene-Pleistocene evol., fossil diatoms anal. 7-23695
- periods of normals appl. (German) 7-9164
- Pleistocene climate and vegetation of S central British Columbia, Canada 7-23833
- Pleistocene climate of American Southwest 7-23838
- Middle Pleistocene cold period, age and duration from ⁴⁰Ar/³⁹Ar ages from Eifel volcanic field 7-47392
- Late Pleistocene-Recent ¹⁸O isotope record, implications of K-Ar dating of volcanics from S Italy 7-47393
- Precambrian palaeoclimates, implications of Precambrian permafrost horizons 7-29023
- Precambrian palaeopedology, conference, Raleigh, North Carolina (June 1985) 7-24275
- prediction models, group method of data handling method 7-29125
- primordial atmosphere, climatic consequences of high CO₂ levels 7-66271
- early Proterozoic palaeoclimate of South Africa, reappraisal of 2200-Myr palaeosol near Waterval Onder 7-29022
- Puerto Rico airport site at San Juan, temp. trends between 1956 and 1983 AD 7-60316
- Qi-Lian mountain area, Nanshan, China, air temperature climate (Chinese) 7-18299
- Qingdao coast, China, climatic and palaeogeographical changes during past 20000 years (Chinese) 7-55011
- Qinghai-Xizang (Tibet) Plateau, Quaternary lakes retreat and climatic significance (Chinese) 7-55104
- Late Quaternary monsoon winds, Arabian Sea sediment records 7-9139
- Late Quaternary palaeoclimates, implications of sediment accumulation in Morocco Basin 7-14259
- N Queensland, Australia, daily rainfall rel. to topography and circulation 7-23810
- Sahara climate by general circulation model dependence on wet or dry initial conditions 7-34644
- Sahel, climatic effects of surface albedo change 7-66290
- Scotland, Eastern Highlands, snow supply during AD 1954 to 1984 period 7-66276
- sea level changes rel. to coastal flooding 7-60271
- S Sierra Nevada, California, Late Holocene upper timberline var. rel. to temp. changes 7-55251
- simulations to BP 18000 years, Earth orbit and surface condition effects 7-29236
- Snake River Plain, United States, contrasting climatic histories resulting from multiple thermal maxima 7-47530
- solar insolation data analysis by means of Allan variance and Fourier transform 7-60371
- South China Sea, palaeoclimate and palaeoceanography during Holocene, sediment O isotopic anal. (Chinese) 7-55264
- Southern Hemisphere, surface air temp. vars. (1851 to 1984) 7-29237
- Southern Oscillation and S Pacific tropical cyclones 7-4155
- standard errors of aeroclimate characts. of related observation series 7-23818
- stratospheric tropical winds, observed quasi-biennial oscill. (1953-84) 7-34594
- stratus cloud parameterization for climate general circulation model 7-9153
- synoptic-scale influences of sea ice and snow cover 7-47498
- temperature global trends in AD 1957 to 1979 period, for 850 to 30 mbar altitudes 7-40532
- temperatures on different time scales, scale invariance 7-9155
- Tianmushan glacial table, paleoclimatological significance 7-55098
- Tibet Plateau, floods, droughts and snowstorms in historical times (Chinese) 7-18255
- Triassic climate, orbital forcing indicated by lake sediment record 7-66300
- tropics, climate prediction 7-9156
- typical climate for Earth (Russian) 7-47528
- United States, summer monthly mean surface temp. field rel. to 700 mb height field 7-34667
- urban warming in North America, average warming rate (1941 to 1980) 7-29146
- USA, cloud increase in warming world atmosphere 7-55249
- SE USA, Palmer drought severity index for AD 1931 to 1982 period 7-66293
- E USA, tree-ring record of past climate 7-23839
- USA and Canada Interior Plains, anomalous moisture conditions persistence 7-23835
- USA and Canada Interior Plains, drought spatial patterns 7-23836
- Venetian Lagoon, freezing since 9th century AD rel. to climate of W Europe and England 7-66286
- West Bengal, India, rainfall correl. with sunspot activity 7-9130
- Western Ghats, India, water supply and hydroclimatology 7-29091
- World Climate Research Programme objectives and plans 7-66303
- Yukon Territory, stratigraphic, isotopic and micrological evidence for early Holocene thaw unconformity 7-9034
- CO₂ climate sensitivity and model dependence of results 7-66298
- CO₂ pollution associated climate change, review 7-55253
- CO₂ problem and increase in global temperatures (French) 7-40515
- CO₂-induced warming and basal melting of E Antarctic ice sheet 7-66181

climb, dislocation *see* dislocation climbclinical equipment *see* biomedical equipmentclinical measurement *see* biomedical measurementclipping circuits *see* limitersclock paradox *see* special relativity

clocks

see also atomic clocks; chronometers; time measurement

digital reverberation time meter 7-20506

inertial clock based on computer controlled servo-driven corotation system with superconducting suspension 7-14927

clocks continued

- passive TV techniques for time transfer via Indian satellite INSAT-1B 7-18764
- viscometer timer using low-cost electronic stopwatch 7-51354

closed circuit television

- radioactive waste vitrification facilities, closed circuit TV and remote crane control 7-42204
- solar unit focal spot analyser based on CCTV 7-54264

closed loop control systems *see* closed loop systems

closed loop systems

see also feedback

- haemodynamic control systems, closed loop identification 7-60027
- muscles, electrically stimulated, effect of muscle nonlinearities on control 7-8644
- myoelectric signal of elec. stimulated muscle during recruitment, rel. to closed-loop control 7-3777
- vertical ground coupled heat pump system design and performance 7-8431

cloud chambers

see also position sensitive particle detectors

No entries

clouds

- acetic acid source determ. 7-55195
- acidification of clouds, numerical model calculation (Chinese) 7-9063
- acidification of clouds over Ontario, Canada, chemical and microphysical observations 7-40530
- aerosol concentration in drops, changes due to particle scavenging and redistrib. by coagulation 7-55201
- aerosols, attachment to cloud droplets 7-4086
- airborne particles scavenging by collision with water drops, combined effects of microdynamic mechanisms 7-55200
- Antarctic polar stratospheric clouds and aerosols, SAM II meas. 7-55160
- Arctic polar stratospheric clouds, airborne lidar meas. 7-60334
- artificially produced clouds, by 1000 MW heat source, microphysics study 7-18286
- E Asia, dynamic and thermodynamic influences of Tibetan Plateau on general circulation model 7-29135
- S Atlantic cloud amounts from Meteosat I images 7-47521
- NW Australia, evening glory wave-cloud lines, formation characts. 7-29124
- automatic cloud classification 7-9214
- Canada, cloud shade to point cloudiness, empirical relationship 7-47513
- chemistry of cloud condensation nuclei, anal. technique 7-3589
- cirriform cloud at -83°C, ice particles characts. implications for polar stratospheric clouds 7-4123
- cirrostratus and complex solar halo over Arnhem, Netherlands (1985 February 26) 7-23841
- cirrus, sunlight absorption by H₂O vapour and O₂ 7-60375
- cirrus cloud, influence on climate and weather processes, global perspective 7-4157
- climate change, increasing cloud accompanying global temperature rise 7-55249
- climatic effects (Italian) 7-60372
- cloudwater at Scandinavian clear air site, chemical composition meas. 7-55223
- comma cloud development in E Pacific 7-34632
- comma cloud in eastern Pacific, development 7-34633
- concentration of cloud condensation nuclei, obs. and prediction discrepancies 7-4088
- convective cloud forecasts from the Meteorological Office fine-mesh model 7-29188
- convective systems of 100 km scale during GATE, heat and moisture transport 7-29189
- Crimean mts., orographic wave clouds (Russian) 7-4114
- Cumbria, England, characts. of airflow, aerosols, precipitation and clouds in boundary layer 7-4096
- cumulonimbus clouds, introductory review 7-4142
- cumulus, intermittent convection in boundary layer 7-66254
- cumulus, spatial inhomogeneities analysis using Landsat data 7-66235
- cumulus cloud amount parameterization scheme 7-4104
- cumulus cloud base heights in S England 7-4144
- cumulus convection, heating of vortices, nonlinear response 7-9101
- cumulus convection Kuo parameterization, general circulation model, sensitivity 7-66221
- cumulus ensemble effects on GATE large-scale vorticity and momentum 7-9105
- cumulus moisture transport effect on GCM climate simulation 7-66291
- Delhi region, India, cumulonimbus clouds occurrence freq., radar obs. 7-9128
- downdraught from convective clouds, vel. and temp. 7-9131
- drop size distribution in tropical warm cumulus clouds 7-29209
- droplet size distribution and mixing in continental convective clouds 7-40526
- drops, capture of sulphate aerosol 7-40059
- drops, exposure by camera technique 7-55277
- Earth Radiation Budget Experiment (ERBE), clouds temp. and reflectivity meas. 7-9067
- electrical fields prod. by convective clouds, airborne meas. using field mill sensors 7-55213
- electrical properties of precipitating clouds 7-29212
- electrification process for thunderclouds of abnormal polarity 7-29227
- electrostatic field measurements and the mechanism of intracloud discharges 7-55121
- NE England and North Sea, May 1986 cool seas and clear skies 7-55231
- W Europe, 1985 noctilucent clouds 7-29187
- explosive mid-latitude synoptic-scale storms dynamics, effects of intense cumulus convection 7-4164
- extinction profile meas. by lidar using Klett's inversion method 7-9184
- formation over snow-covered surface 7-4089
- formic acid, atmospheric chemistry model for clouds 7-18290
- formic acid source determ. 7-55195
- France and S Britain, summer 1983, total and low cloud amounts 7-9079
- funnel-producing indented cloud-base swirl of severe thunderstorm of USA 7-34636
- GATE waterspouts, interacting cumulus processes 7-4120
- global cloud cover, zonal struct. and correl. 7-34612
- Great Dun Fell, England, meteorological conditions 7-34661

clouds continued

- Gulf of Carpentaria, 1984 October 25-6 cloud line and morning glory wind surges 7-4091
 Gulf of Carpentaria cloud line disturbances caused by sea breezes 7-29140
 hail cell radar reflectivity profiles in Switzerland 7-14348
 hail embryo definition, morphology and growth in clouds (*Chinese*) 7-18260
 hail growth in 3D storm cloud model (*Chinese*) 7-4081
 hail suppression by cloud seeding, Grossversuch IV expt. in Switzerland 7-14344
 hailstone embryo types rel. to hailstorm cell form (*Chinese*) 7-18266
 hailstone two-stage growth and accreted ice props. 7-34647
 hailstones, density of accreted ice, laboratory expts. 7-34648
 height estimation of cloud bases, use of condensation levels calc. from ground instruments 7-4144
 ice, microscopic filament form. in elec. field 7-14362
 ice nucleation studies of AgI-AgCl solid solns., X-ray diffr. obs. 7-58179
 ice splinter production, importance of rimmer surface temperature 7-34657
 ice-forming nuclei concentration, dependence on temperature and supersaturation (*Russian*) 7-18278
 image of clouds from satellites, structural-stochastic model for imaging 7-14391
 Lagrangian time scales 7-55190
 laser beam in medium containing droplets, nonlinear refraction phase compensation 7-4183
 lidar equation taking account of polarization, second order scattering and travelling time effects 7-60380
 lidar investigation 7-55135
 marine boundary layer, entrainment instability and cloud break up 7-23798
 maximum droplet size dependence on dilution and cloud age 7-40527
 meteosat IR meas., surface and cloud-top temp. determ. atmospheric correction scheme 7-18310
 mixing processes, critical supersaturation and droplet size 7-66225
 Montana thunderstorm, precipitation particles growth trajectories 7-4124
 morning glory cloud line disturbances caused by sea breezes 7-29140
 multiple scattering approx. 7-4181
 nighttime chemistry, role of NO_3 , reevaporation effects 7-55198
 noctilucent clouds, observational props. rel. to behaviour of upper atmosphere 7-23925
 noctilucent clouds, pictures and characts. 7-4249
 noctilucent clouds and fireballs, search for correlation 7-29437
 North Australian Cloud Line caused by sea breezes 7-29140
 optical radiation intensity for horizontally inhomogeneous clouds (*Russian*) 7-40564
 Pacific Ocean, zones of storm waves and stillness identification from satellite clouds imaging 7-34731
 particles size and concentration determ., cloud physics instrumentation calibration using holographic imaging 7-23897
 peninsula convection over S British Isles, 13 May 1986 case 7-4145
 N Peru, convection, in clouds and rain in coastal areas, AD 1983 obs. 7-60350
 polar mesospheric clouds, altitudes, SME obs. 7-60434
 polar mesospheric clouds, existence regions calc. from zonally averaged model of middle atmosphere 7-47596
 polar mesospheric clouds 7-9276
 polar stratospheric cloud, implications of ice in -83°C cirriform cloud 7-4123
 polar stratospheric clouds, characts. during form. of Antarctic O_3 hole 7-55163
 polar stratospheric clouds, detect. from satellite data 7-55156
 polar stratospheric clouds, role of HNO_3 and HCl condensation in winter stratospheres 7-55162
 radar echo characteristics over Black, Kara and E Siberian seas 7-34615
 radiation interaction in 3D model of mesoscale processes of oceanic energy-active zones (*Russian*) 7-23808
 radiative transfer, effects on column weighting model technique for outgoing longwave irradiance estimation 7-29242
 radiative transfer, relation to atmospheric vertical temp. distrib. (*French*) 7-14338
 radiative transfer theory, small-angle approx. and numerical soln. 7-36878
 radiatively interactive clouds in cumulus convection Kuo parameterization 7-66221
 radioactive cloud, dose reduction factors for large buildings, computer codes 7-54759
 radiowave scattering, effect of meteorological conditions on satellite radar images of Earth's surface 7-66217
 rain drops, kinetic Smolouchowski eqn. for coagulation of spatially nonuniform systems 7-46873
 rain rate by microphysical model 7-29210
 remote sensing, cloud cover estimation using bispectral satellite measurements 7-29148
 remote sensing by satellite, cloud and rainfall monitoring methods used by Bristol University 7-47562
 remote sensing method for height of cloudtop, using Meteor satellite 7-60400
 roll clouds over southern Australia, assoc. with atmospheric bores and cold front 7-55127
 satellite images of cloud systems, synoptic analysis and diagnosis methods (*German*) 7-40542
 scavenging of N and S, assoc. chem. processes 7-55192
 scavenging of N and S in rain 7-55191
 seeding, ice nucleation by AgI-AgBr-CuI system, UV irradiation effect 7-66247
 seeding with NaI, delayed effects 7-66239
 shading, effects on generation and modification of mesoscale circulations 7-34617
 Central Sierra Nevada, United States Winter storms ice-phase water capture regions identification, use of snow O isotopic comp. 7-4084
 solar radiation field modified by dispersive cumulus cloud 7-4105
 solar radiation prediction and cloud cover effects 7-23828
 solar radiation prediction and cloud cover effects 7-23829
 split cold front and associated rainfall pattern seen over UK on FRONTIER radar 7-55207
 stratiform cirrus, radiative props. and ice crystal growth 7-66222
 stratocumulus model with an internal circulation 7-66227
 stratocumulus-topped boundary layer, third-order turbulence closure model stability 7-9102

clouds continued

- stratus, mixing processes, critical supersaturation and droplet size 7-66225
 stratus clouds evolution, numerical modelling 7-9132
 sulphate production in hill cap clouds and subsequent deposition to hill 7-14331
 sunlight spectral absorpt. and total vertical water vapour determ. 7-4087
 supercell thunderstorms, vertical circulation influenced by precipitation development (*Chinese*) 7-18261
 supercooled clouds, supersaturation field around growing graupel 7-34591
 supercooled liquid water in clouds at mountaintop sites, meas. in Colorado Rockies 7-29147
 thundercloud, cloud top dynamics from satellite obs. and cloud top parcel model 7-40525
 isolated thundercloud over mountains, microphysics, kinematics and electrification 7-34602
 thunderclouds, elec. field and precip. growth in finite cloud 7-29206
 thunderstorm anvil clouds, elec. characts. and dynamics (*Chinese*) 7-29121
 thunderstorms, electrochemical charge separation mechanism 7-40511
 E Transvaal, rainfall amounts and possible influence of hail suppression programme 7-18279
 tropical cloud clusters, relation to interaction between meridional and zonal disturbances in tropical easterly flow 7-40509
 tropical squall line, cloud water and water vapour content retrieval 7-4212
 tropical squall line, diagnostic modelling study of stratiform cloud region 7-29136
 unusual clouds over Perth, Western Australia 7-23832
 Urea used for cloud seeding in China (*Chinese*) 7-18264
 USA, cloud increase in warming world atmosphere 7-55249
 variability, contrib. to vars. of Earth-emitted radiation from one year of Nimbus-6 ERB data 7-9092
 warm precipitating stratiform clouds, soluble gas removal 7-55230
 warm shallow convective clouds, large raindrops obs. 7-47479
 HSO_3^- formation in atmospheric clouds, model 7-18290
 OH in tropical clouds, cloud chemistry model 7-18290
 SO_2 , O_3 -induced oxidation to aqueous sulphate in warm cloud conditions 7-54114
Clusius-Dickel columns see isotope separation
cluster analysis see pattern recognition
cluster approximation
 alkali halides, colour centres, Hartree-Fock cluster computations 7-16985
 alkali halides, XANES K-spectra, cryst. pot. and size effects 7-64748
 alkaline earth oxides, colour centres, Hartree-Fock cluster computations 7-16985
 atomic and molecular systems, static electronic props., bivariational coupled-cluster approach 7-15471
 borate glasses, basicity and geometry studies, MNDO calcs. 7-6529
 chemical bonding, validity of formal electron counting rules 7-63544
 covalent cryst., electronic struct., cluster approx. 7-52403
 diamond, KVV Auger electron spectra calcs., band and cluster approx. methods 7-46252
 diamond, muonium-related paramagnetic centres, UHF calcs. 7-38980
 diamond, normal muonium, lattice relax. calcs. 7-51789
 disordered alloy surfaces, density of states calc. 7-21961
 electronic struct. and dynamics, conf., Snowbird, UT, USA (April 1986) 7-55877
 flux growth, metastable zone, mixed cluster model 7-44432
 general coupled-cluster methods, MBPT, analytic energy gradients 7-19674
 growth oscillations, phenomenology and origin, simple stochastic model 7-35414
 Ising systems, semi-infinite, critical and multicritical phenomena 7-59044
 linked cluster expansion in MBPT and coupled-cluster theory 7-49871
 liquid and amorphous metals, multiple scattering effects, cluster calcs. 7-7100
 Migdal-Kadanoff renormalisation, appl. to Potts model 7-24600
 muonium energy profiles, unrestricted Hartree-Fock cluster calcs., comment and reply 7-45907
 quartz, E'_g -centres, conversion rate into E'_2 -centres 7-52517
 quartz, exoemission centre with O vacancies, cluster model 7-12651
 semiconductor-alloy phase diagram, first-principles self-consistent local-density total-energy calcs. 7-44751
 site percolation in a honeycomb lattice, renormalisation group calcs. 7-9798
 stoichiometric solid state-cluster orbital models 7-16928
 transition metal carbides, discrete X_α calcs. and high resolution Auger spectra 7-16942
 transition metal cpds., high press. metal-insulator insulator transition, extended Hubbard model calcs. (*Russian*) 7-32917
 wave functions, coupled cluster calculations 7-24481
 Ag adsorbed layer on Si (111), geometric struct. and density of states, cluster model and charge self-consistent extended Huckel method calcs. 7-21619
 AgCl, electronic struct. of intrinsic interstitial defects 7-21852
 Al atomic cluster, trapping regions around impurity atoms, charge density 7-53195
 Al, chemisorption, interaction of atoms and mols. with surfaces, cluster approx., total energy calcs. 7-52265
 Al, grain boundaries, Na and H impurities, small cluster quantum chemical calcs. 7-38017
 Ar, excitation energies, coupled cluster method calcs. 7-49893
 C cubic crystals, electron struct., cluster approx., α -phase calcs. 7-38445
 Cu, X-ray photoelectron diffr., temp. depend., surface and bulk effects 7-39356
 Cu^{2+} impurity ion in octahedral environment, EPR spectrum, MM field freq. and temp. depend. 7-27596
 Cu-Ni alloys, surface segregation, tight-binding Hartree Hamiltonian, cluster-Bethe-lattice approx. calcs. 7-38665
 Fe sites in minerals, electronic struct., iterative EHT, multiple scatt. X_α calcs. and Mossbauer meas. 7-17244
 Fe-Te cluster, localised props., multiple scatt. X_α SCF method 7-21848
 Fe_{13} clusters, icosahedral and cubo-octahedral coordination, electronic struct., first-principles method calcs. 7-45132
 γ - Fe_4N , Auger spectra, electronic struct. (*Russian*) 7-64832
 Fe_{1-x}O , wustite, electronic struct. and X-ray absorption spectra 7-2479
 GaAs, covalent cryst., electronic struct., cluster approx. 7-52403
 a-GaAs:H:F, electronic struct., dangling bonds, cluster-Bethe lattice method calcs. 7-12592

cluster approximation continued

- GaAs:Mo (W), impurity electronic struct. excitation and ionisation, cluster approach, $\chi\alpha$ multiple scatt. calcs. 7-2535
 GaAs:Si, distorted impurity configuration 7-52501
 GaP finite cluster, local electronic struct., recursion method calcs. 7-2464
 Ge cubic crysts. electron struct., cluster approx., χ alpha calcs. 7-38445
 H₂O dimer, MBPT, coupled cluster study 7-49892
 KSCN, K X-ray $\chi\alpha$ spectra, hidden satellites, chem. effects, DV- $\chi\alpha$ cluster calcs. 7-46245
 K₂SO₄, K X-ray $\chi\alpha$ spectra, hidden satellites, chem. effects, DV- $\chi\alpha$ cluster calcs. 7-46245
 K₂TiF₆, K X-ray $\chi\alpha$ spectra, hidden satellites, chem. effects, DV- $\chi\alpha$ cluster calcs. 7-46245
 Li, crystal and electronic struct., ab initio HF cluster method 7-44443
 Li-Mg disordered, phonons and martensitic phase transitions 7-58423
 LiH, electronic struct., mol. cluster calcs. 7-7110
 Li₁₂Si₇, chemical bonding, validity of formal electron counting rules 7-63544
 Li₂Si₅, electronic struct., INDO calcs. 7-38437
 Mg, excitation energies, coupled cluster method calcs. 7-49893
 Nb_{1-x}(Mo)_xH_x random field system, disorder-disorder phase transition, cluster variation calcs. 7-63803
 Ni diatomic coupled cluster method, MBPT 7-56996
 Ni (100), (111) and (110), N₂ chemisorption, molecular cluster calcs. 7-52280
 Ni:B(s), grain-boundary cohesion, impurity segregation effects, density-functional cluster model calcs. 7-44835
 Ni-He, electronic state or interstitial He atoms, MO calcs. of model clusters 7-16969
 Ni_{1-x}P_x metallic glass, electronic struct. and props., LMTO calcs. 7-52409
 O chemisorbed layer on Ni (001), self-consistent field He scatt. cluster model calcs. 7-53471
 PdH_x, nonstoichiometric, electron density of states, analytic CPA model calcs. 7-52400
 Si (100), chemisorption of water, MNDO calcs. 7-63963
 Si (111), surface reconstruction, benzene-like ring model 7-16851
 Si cubic crysts. electron struct., cluster approx., χ alpha calcs. 7-38445
 Si, normal muonium, location and hyperfine props., Hartree-Fock cluster calcs. 7-52539
 a-Si:H, broken bond local environment relax., g-factor, cluster calcs. 7-37876
 a-Si:H, divacancy electron struct., semiempirical CNDO/2 cluster calcs. 7-38495
 Si:N(O), pseudo Jahn-Teller effect and chemical rebonding 7-16992
 Si:O, cluster computations related to thermal donors 7-16990
 SiC, covalent cryst., electronic struct., cluster approx. 7-52403
 SiO₂, vitreous, electron struct. 7-12591
 SiO₂:F, vitreous, substitutional impurity, semiempirical calcs. 7-32464
 Ti clusters, electronic props., CNDO method 7-27247
 TiH₂, electronic struct., cluster method (*Russian*) 7-64071
 TiO₂ clusters, electronic props., determ. using Ti CNDO parameters 7-27247
 W, He field adsorption and evaporation 7-32802
 W surface, field adsorption of He 7-32816
 ZnS, covalent cryst., electronic struct., cluster approx. 7-52403
 ZnS:Cu, pure and doped, defects in solids, mol. cluster calc. with modification 7-21857

cluster model (nuclear) *see nuclear cluster model*clustering, impurity *see segregation*clustering, solute *see segregation*clusters, atomic *see atomic clusters*clusters, globular (stellar) *see globular star clusters*clusters, metal *see metal clusters*clusters, molecular *see molecular clusters*clusters, stellar *see stellar clusters and associations*

clusters of galaxies

see also galaxies; intergalactic matter

- Abell 2199 and components of NGC 6166 multiple-nucleus galaxy 7-55803
 Abell 2218, 5C20 deep survey at 408 and 1407 MHz 7-18456
 Abell 2218, limits to Sunyaev-Zel'dovich effect 7-60821
 Abell 370, arc structure in cluster of galaxies 7-60815
 Abell clusters, spatial correls. anal. 7-9548
 Abell clusters local radio luminosity function at 102.5 MHz 7-29543
 Abell galaxy clusters, 11.1-cm radio maps and obs. at 6.3 and 2.8 cm 7-18454
 alignments in hierarchically clustered populations, implications for QSOs triple alignments 7-60830
 brightest cluster galaxies, gravit. amplification by foreground clusters 7-24206
 bubble type galaxy distribution, explosion model of formation 7-60820
 burnt-out galaxies and galaxy clusters, relation to quasar pairs 7-35051
 Centaurus cluster, struct. and distrib. of different galaxy types 7-9547
 Cl 0024+1654, members three colour CCD photometry 7-14665
 cluster-cluster correlation function, sampling errors and significance levels 7-48092
 clustering, non-Gaussian fluctuations, large-scale matter distrib. 7-24232
 collision/merger origin of powerful radiogalaxies 7-60788
 collisionless gravitating systems, spherical collapse stability 7-40678
 Coma cluster, distance from Virgo cluster using more precise L- σ distance indicator 7-9541
 Coma cluster, mass determ. from galaxies positions and vels. 7-40945
 Coma/A 1367 Supercluster, radio continuum props. of galaxies in different density environments 7-29547
 compact groups of galaxies as chance alignments of galaxies in loose groups 7-66773
 core 7-66741
 Corona Borealis region, large-scale struct. probes using redshift survey 7-40922
 cosmic strings, fractal geometry and galaxy and cluster correlation functions 7-56115
 cosmological mass density fluctuations, mode coupling 7-55861
 dark matter in the Universe 7-60851
 disk galaxies, populations of subclasses of ordinary and barrel spirals in various environments 7-24215
 distribution and red shifts 7-60818
 double clusters and gravitational lenses 7-9549

clusters of galaxies continued

- elliptical galaxies in groups and clusters, mass determ., X-ray emission anal. 7-4552
 filamentary structure 7-55842
 formation, implications of baryon concentration in string wakes (at $z \geq 200$) 7-14687
 galaxies orbits within galaxy clusters, numerical expts. 7-24231
 galaxy correlation scales, effects of percolation of explosive galaxy form. 7-29533
 galaxy correlations at high redshift, implications for quasars environment 7-24216
 galaxy two-point angular correl. function, determ. from faint galaxy photometry 7-60915
 GC 1556+335, quasar, intervening cluster model for absorpt. line spectrum 7-29552
 general textbook contribution 7-60912
 Hercules Supercluster, ring galaxies detect. 7-14652
 hierarchical structure in the distribution of galaxies 7-55839
 Hubble flow, evidence for non-uniform vel. field 7-24225
 Hydra I cluster, red shifts determ. 7-60816
 intracluster medium, equilib. of gas in gravit. field of cD-type galaxies 7-24204
 large-scale clustering of galaxies with massive dark halos, general struct., two-point correls. and binaries 7-29544
 large-scale structures, peculiar vels. and geometrical elongation 7-55840
 Local Group, dark/luminous matter ratio, Galaxy scale change repercussions 7-14659
 Local Group, motion 7-55835
 local Group, perturbation of nearby extragalactic vel. field 7-40917
 Local Supercluster, orientation of galaxy rot. axes 7-14662
 Local Supercluster, tidal velocity field 7-40946
 M101 group, gr CCD photometry of UGC 8508 assoc. dwarf galaxy 7-9550
 NGC 4005 group, H I 21 cm line obs. rel. to system rotation 7-55841
 objective prism spectra wide-angle samples use for large-scale galaxy distrib. anal. 7-66771
 opposite pairs effect in 'small universe', relation to topological struct. of Universe 7-60844
 PHL 957, quasar, absorpt. line systems nature 7-35061
 Pisces-Perseus supercluster, 21-cm survey in declination zone +21.5° to +27.5° 7-4576
 poor galaxy clusters, photometric props. 7-55843
 protocluster pancakes, IR line emission of H I and H₂ 7-4600
 Q 1548+114A, B, QSO pair, implications of gravit. lens effects of assoc. cluster 7-9554
 QSO clustering and evolution, optically selected sample study, dissertation 7-66785
 QSO fields at $z=1-1.5$, assoc. galaxy clustering 7-14667
 quasar distribution clustering, objective-prism survey rel. to superclusters dimensions (*Chinese*) 7-4581
 quasars association, binaries of intermediate-redshift quasars fields 7-55495
 radial velocities of galaxies near groups of galaxies 7-4550
 red shifts determ. for component galaxies 7-60817
 RI photometry of three distant galaxy cluster, results rel. to BVRI photometry in comparison fields 7-29542
 rich clusters, evolution and clustering theory 7-9546
 rich clusters automatic detect. 7-14502
 rich southern clusters, galaxy redshifts and stellar vel. dispersions 7-60819
 second-order clustering 7-55836
 Seyfert galaxies nearest neighbour analysis (*Chinese*) 7-4549
 Shane-Wirtanen counts, observer and time-depend. effects 7-55838
 Shane-Wirtanen counts, plate correction factors and correl. function 7-55837
 small groups and pairs, H I spectral spectral characts. 7-14669
 small-scale cosmic background radiation anisotropy and galaxy clustering, galaxy origin constraints 7-48082
 South Galactic Pole, galaxy and quasar candidates, correl. studies (*Chinese*) 7-66731
 southern clusters, optical spectra of central galaxies rel. to evidence for star form. 7-55821
 spatal distrib., model 7-40969
 Sunyaev-Zeldovich effect, EHF search 7-48109
 supercluster probing using marginal gravitational lenses 7-55456
 superclusters formation, density perturbations evolution rel. to early star and galaxy form. 7-66794
 Tully-Fisher relation distance determ., effect of cluster population incompleteness bias 7-66772
 two-dimensional covariance function for IRAS sources, implications for galaxy clustering scales 7-14677
 two-point correlations of galaxies and rich clusters, effects of non-Gaussian mass density fluctuations 7-29545
 Ursa Major galaxy clouds, luminosity profiles of galaxies using spheroid-disk composite models 7-55817
 Ursa Major I(S) galaxy group, ¹²CO and far-IR obs. 7-29548
 Virgo Cluster, 2.8 cm radio continuum emission distrib. in four spiral galaxies 7-9540
 Virgo cluster, colour distrib. in eight elliptical galaxies 7-48070
 Virgo cluster, distance from Coma cluster using more precise L- σ distance indicator 7-9541
 Virgo Cluster, dwarf irregular and elliptical galaxies, comparative photometric parameters 7-35053
 Virgo cluster, effect of Virgo-centric flow model on observed rels. of nearby galaxies 7-40723
 Virgo Cluster, elliptical galaxies NGC 4486, 4472 and 4406 colour gradients 7-35054
 Virgo cluster, gravitational waves emission rel. to antenna patterns of interferometric detectors 7-55453
 Virgo cluster, H I content of lenticular and early-type galaxies 7-4559
 Virgo cluster, H I synthesis obs. of two low surface brightness dwarf galaxies 7-4560
 Virgo Cluster, luminosity profiles of galaxies using spheroid-disk composite models 7-55817
 Virgo cluster, orbits of H I deficient spiral galaxies 7-24230
 Virgo cluster, quasars distrib. in cluster core 7-35063
 Virgo cluster, relation of M87 jet to nearby galaxies 7-35047
 Virgo Cluster, struct. and use of lumin. index as distance indicator 7-14668
 Virgo Cluster irregular galaxies, UVB characts. 7-14666
 Virgo Cluster motion 7-55835

clusters of galaxies continued

- Virgo Cluster spiral galaxies, threshold in star formation processes 7-60776
 virial parameters 7-9545
 whole-sky distribution of galaxies, MCG-ESO(B)-UGC comparison 7-9551
 Zwicky galaxy clusters, data on assoc. Markarian galaxies 7-4567

clutches

- see also drives*
 electrorheological fluids, optimisation for electrical control of viscosity and torque 7-44641

CMOS integrated circuits

- charge sensitive amplifier-cable driver, monolithic detector readout electronics 7-42438
 CMOS/SOI devices, laser recrystallisation 7-8014
 integrated detector electronic with CMOS compatible devices 7-42437
 radio astronomy, wideband very fast FFT spectrum analyzer 7-47710
 SOI formation, high dose O^+ ion implantation, lamp annealing 7-32527
 W, selective LPCVD for CMOS VSLI, appls. 7-17471

CNDO calculations

- acetone, CS_2 soln., internal pot. energy surface, CNDO calc. 7-42486
 1-acetylcyclohexene, rot. barrier, conform. stability, MINDO/3 and MNDO calcs., UV spectra anal., CNDO calcs. 7-25405
 acyclic alcohols, hydroxyl stretching freqs., rotamer pop., CNDO calcs., IR spectra anal. 7-36611
 aluminosilicates, at. charges, SCF and semiempirical calcs. 7-2942
 anilinium, long range interactions, near UV spectra, MNDO and CNDO calcs. 7-19879
 aromatic molecules, planar, electronic transition energies and oscill. strengths calcs. 7-19706
 benzene, vibronic activity, CNDO/S and INDO/S calcs. 7-49926
 benzene, vibronic perturbations, pseudoparity propensity rules 7-25397
 benzene, vibronically induced intensities, CNDO/S calcs. 7-19704
 butadiene, lowest electronic states, vibronic coupling, quantum-mechanical calcs. 7-19712
 N-cyanopyrrolidine, pot. surface calcs., geometrics calc. using CNDO/2 method 7-30951
 cyclohexanols, hydroxyl stretching freqs., MM2/CNDO model calcs., IR spectra anal. 7-36610
 cyclopentane, pot. surface calcs., geometrics calc. using CNDO/2 method 7-30951
 decapentane, lowest electronic states, vibronic coupling, quantum-mechanical calcs. 7-19712
 diamond, large unit cell CNDO calculations 7-7106
 2,6-dichloroaniline, solid, vibr., IR spectra, CNDO/2 calcs. 7-3050
 2,4-dihydroxyquinoline, gas phase, prototropic equilib., electron impact fragmentation spectra anal., LCAO-CNDO calcs. 7-36479
 2-dimethylamino-6-propionyl-naphthalene, twisted charge transfer state, fluoresc. quantum chem. study 7-863
 2,4-dinitro-6-diazophenol, and analogues, struct. investig. 7-57087
 diphenylamine, geometry optimisation, semiempirical quantum chem. methods 7-10433
 electronic transition energies and oscillator strengths, CNDO/S-RPA calcs. 7-19706
 ethane, substituted, inductive effect in quantum-chem. calcs., perturbation theory appl. 7-5600
 ethyl 2-bromopropionate, mol. orbital study, Raman and IR spectra anal., CNDO calcs. 7-49931
 ethyl 2-chloropropionate, mol. orbital study, Raman and IR spectra anal., CNDO calcs. 7-49931
 fluorophenols, torsional far IR spectra, tilt influence, use of CNDO/2 method 7-56982
 guanine-metabolite adducts, ab initio and CNDO/2 and MINDO/3 calcs. 7-49928
 hexahalo complexes, vibronic coupling and state Jahn-Teller effect 7-19725
 hexatriene, lowest electronic states, vibronic coupling, quantum-mechanical calcs. 7-19712
 inorganic Cl compounds, NQR freqs., SCF MOLCAO CNDO/2 calcs. 7-30952
 metapyridinophanes, electronic struct. and transitions classification 7-10430
 methanol, associates, H bonding, struct. CNDO/BW calcs. 7-56985
 methanol mol. vibr. spectrum, CNDO/2 FORCE calcs. 7-49924
 methanol-trimethylamine, associates, H bonding, struct. CNDO/BW calcs. 7-56985
 methyl ether, mol. charge similarity index study, appl. to isosteric cpds. 7-56978
 methyl sulphide, mol. charge similarity index study, appl. to isosteric cpds. 7-56978
 5-methylcytosine, incorporation in nucleic acids 7-54441
 nitroimidazoles, UV spectra, CNDO/S calcs. 7-19878
 nucleic acid purine bases, electrooptical props., finite perturbations CNDO/S3 calcs. (Russian) 7-25407
 octatetraene, lowest electronic states, vibronic coupling, quantum-mechanical calcs. 7-19712
 octatetraene, vibronic perturbations, pseudoparity propensity rules 7-25397
 organic Cl compounds, NQR freqs., SCF MOLCAO CNDO/2 calcs. 7-30952
 photographic process, quantum chem. CNDO calcs., latent image growth and structure model 7-28321
 polyenes, mol. polarisability, CNDO/2, CNDO/C, α (VPT) and α (SCPT) calc. comparisons 7-49932
 porphyrins, proton motion, electrostatic pot. distrib., SCF-MO-LCAO calcs. 7-57147
 propane, mol. charge similarity index study, appl. to isosteric cpds. 7-56978
 pyrazine, successive protonation, ab initio quantum chem. calcs. 7-56957
 quinones, polarisability and second hyperpolarisability, intramol. interactions effect 7-19707
 squaraine dye, struct. and electronic props., NDO CI calcs. 7-857
 7,7',8,8'-TCNQ, semicond., fluorescence spectra and electronic energy levels 7-27769
 vinylene carbonate, struct. and vibr. spectra, ab initio CNDO/2 and INDO calcs. 7-49930
 AgCl, electronic struct. of intrinsic interstitial defects 7-21852
 $Al_2Si_2O_7H_{12}$ cluster, electronic struct. and state densities, MINDO/3 and CNDO/2 calcs. 7-57201

CNDO calculations continued

- $Al_2Si_2O_7H_{12}$ cluster, electronic struct. and state densities, MINDO/3 and CNDO/2 calcs. 7-57201
 closo- $B_nH_n^{n-}$ clusters, bond indices, enthalpies, CNDO calcs. 7-10431
 H_2O , associated species, stretching force consts., mol. interaction effects, CNDO calcs. 7-25396
 H_2O chemisorpt. on Cu or Ag (100) surfaces, quantum chem. CNDO calcs. (German) 7-859
 LiCl(H_2O), ion pairs, struct. and stability, H^+ transfer reaction path, SCF-CNDO/2 calcs. 7-25400
 LiF(H_2O), ion pairs, struct. and stability, H^+ transfer reaction path, SCF-CNDO/2 calcs. 7-25400
 Se, CNDO/2 parameterisation 7-49929
 Si, large unit cell CNDO calculations 7-7106
 Si, oxidation, transport processes 7-65232
 Si, oxidation, transport processes 7-65233
 a-Si:H, divacancy electron struct., semiempirical CNDO/2 cluster calcs. 7-38495
 Si:H, Si-H IR stretching bands, models, CNDO calc. 7-53314
 Ti clusters, electronic props., CNDO method 7-27247
 TiO_2 clusters, electronic props., determ. using Ti CNDO parameters 7-27247
 TiCl crystal, electronic struct. 7-38449

coagulation

- aerosols, Brownian diffusion and particle coagulation 7-48564
 bentonite clay suspension, thixotropic-coagulation struct., shock waves 7-6253
 blood, hypercoagulation syndrome in mobility-restricted rats, effect of a weak variable mag. field 7-54669
 equation with separable solutions 7-59792
 heterocoagulation by bubbles in a turbulent multiphase flow. 7-37529
 kinetic Smoluchowski eqn. for coagulation of spatially nonuniform systems 7-46873
 methylated Aerosil R-972, organophilic, alcoholic dispersions, coagulation by additions of water and electrolytes 7-8325
 photocagulation in ophthalmic therapy, argon laser coagulator use 7-8674
 photocagulation in ophthalmic therapy, LAK argon laser coagulator design and use 7-8673
 polydispersed MHD flow in a cylindrical vessel 7-51285
 polystyrene latex, gradient coagulation under microflotation conditions 7-8319
 polystyrene lattices, soln., salt-induced aggregation kinetics, quasielastic light scatt. 7-59796
 Smoluchowski's eqn., const. kernel to coalescence 7-23068
 in-undecane, emulsion in sodium oleate stabilised water, conc. effect on aggregation 7-39926
 SiO_2 in aqs. solns. of cetylpyridinium bromide and inorganic salts, coagulation, thermodynamic stability 7-8326

coal

- see also mining*
 Appalachian low-S coal reserves and supply prospects 7-39951
 ash-agglomerating gasifier, fluidised-bed, high pressure operation 7-65394
 biological coal beneficiation micro-organisms 7-65387
 book, economics and applied geology 7-29609
 China, coal prospecting, use of seismic refl. method (Japanese) 7-23854
 coke, metallurgical, microstruct. analysis and intercalated species 7-28008
 combustion, in fluidised bed furnace, mechanism investig., balance eqn. formulation 7-65322
 conversion and heat-engine ceramic technology, US instrumentation 7-1344
 coproduction of methanol in integrated-gasification-combined-cycle electric power generation 7-17920
 desulphurisation by selective oxidation of pyrites 7-39954
 energy issues of various countries, cogeneration, oil, gas, coal gasification, book 7-48200
 flame acceleration in coal dust, feedback control model for unsteady flow 7-65326
 fluidised-bed combustion, mathematical model 7-6308
 frictional flow properties of coal-oil slurries at low Reynolds number 7-20801
 gasification activities in Europe 7-65393
 gasification characteristics of de-ashed and desulfurized coals 7-65390
 gasification using energy from high temp. solar central receivers 7-65592
 gasification-combined-cycle plant thermoeconomic anal. 7-23206
 gasification-combined-cycle systems for commercial power production 7-17921
 Indian coal-mines, induced seismicity anal. 7-23568
 integrated coal gasification combined cycle power generation (Japanese) 7-65510
 kaolinite quantitative determination by infrared spectroscopy (Rumanian) 7-17847
 liquefaction process, fluid-phase equilibrium prediction 7-40021
 low-grade coal-liquid CO_2 slurry plastic viscosity and yield stress obs. 7-39952
 MHD slagging coal combustors 7-63363
 mild coal gasification yielding gaseous, liquid and solid products 7-28408
 mines, in-seam seismic exploration technique (Hungarian) 7-60416
 Pennsylvania bituminous coal, depolymerization 7-65391
 powdered fuel, combustion characts. in adiabatic diesel engine 7-65596
 pulverised coal/air two-phase flowmeter 7-37580
 Raman spectroscopy, role in study of energy sources, literature review since 1977 7-59827
 Rocky Mountain I underground coal gasification project 7-28407
 seams, tectonic disturbances and quality changes, geoelectric anal. method 7-34712
 seismic exploration of coal mines, in seam reflection technique (Hungarian) 7-66351
 seismic reflection profiling of coal measures, use of discriminant analysis method 7-4211
 seismic reflection prospecting method for lignite seams, shear wave profiling 7-14385
 solid-gas two-phase flowmeter for blast furnace pulverized coal injection 7-37578
 solvent-dried coal liquefaction reactivity improvement by disposable catalyst 7-39953
 structure, determ. by radial distrib. function 7-16485

coal continued

- technology breakout in energy conversion, conf., San Diego, CA, USA (Aug. 1986) 7-60875
- thermal charactn., piezoelectric photoacoustic microscopy 7-44643
- thermal properties, scanning photoacoustic microscopy 7-23089
- underground coal gasification, mechanical considerations of rocks (*Dutch*) 7-59865
- US DOE coal gasification program overview 7-65392
- USA, lignite deposits of Texas to Georgia region 7-18139
- H₂ production from coal and petroleum coke, technical and economical perspectives 7-40050
- Tl, determ. by atomic absorption spectrometry for river sediment, coal, coal fly ash 7-59801

coating processes *see* **coating techniques****coating techniques**

- see also anodisation; cladding techniques; coatings; electrodeposition; electroless deposition; electrophoretic coating techniques; encapsulation; epitaxial growth; metallisation; spray coating techniques; vapour deposition*
- diffusion saturation, coating form, kinetics in metal solns. under isothermal conditions 7-17670
- electrospark deposition coating process 7-53978
- fibre-optic mirror fabrication 7-37214
- graphite fibre reinforced Mg matrix composites, fabrication, fibre coatings, wetting, adhesion 7-46374
- ion beam enhanced deposition and dynamic ion mixing for surface modification 7-64027
- langmuir trough with four movable barriers 7-59416
- Langmuir-Blodgett film deposition system, hydraulic with adjustable speed 7-59415
- metal pretreatment, surface coating and post-treatment methods 7-22905
- multilayer X-ray mirrors, fabrication, in situ monitoring system 7-37217
- nonlinear mechano diffusion in solids with coatings 7-17669
- optical coating with open-cup applicators, slip mechanism 7-15985
- optical fibre drawing, high speed and coating, review 7-11134
- optical monitor for control of thin-film deposition 7-11182
- protective coatings, physics and chemistry, conf., Universal City, CA, USA (Apr. 1985) 7-29568
- steel, low C, Zn-Al coated sheet, Zn quenching technique 7-33847
- Al film growth by UV laser photolysis of trimethylaluminium 7-54153
- Al₂O₃ coatings made by sol-gel process, mechanical props. 7-22867
- As₂S₃ films, prep. by spin coating or melt quenching, optical props. 7-39208
- CdS thin films, deposition by dip technique 7-3210
- CuMoS_{8-y} porous film, prep. on Cu₂S by solid-gas⁺ reaction, secondary battery appl. 7-27897
- Cu₂S-CdS solar cells, comp. of differing junction types, AES, SIMS determ. 7-23167
- In₂O₃/Sn films, prep. by thermal decomposition of organometallic cpds., optical and electrical props. 7-17483
- LiNbO₃ polycrystalline films, prep. by hydrolytic decomp. of metal alkoxide alcoholic solns., SEM obs. 7-7044
- NaNbO₃ polycrystalline films, prep. by hydrolytic decomp. of metal alkoxide alcoholic solns., SEM obs. 7-7044
- NiS thin films, deposition by soln. growth techniques, X-ray diffr., optical, elec. meas. 7-32870
- NiSe thin films, deposition by soln. growth techniques, X-ray diffr., optical, elec. meas. 7-32870
- Zn alloy films on Al, growth and adhesion rel. to application technique 7-13396

coatings

- see also anodised layers; antireflection coatings; claddings; decorative coatings; electrodeposits; electroless deposited coatings; electrophoretic coatings; epitaxial layers; insulating coatings; protective coatings; spray coatings; sputtered coatings; vapour deposited coatings; varnish*
- activated reactive evaporation 7-33576
- balloon, hot air, flight duration, surface characts. effects 7-50906
- composition of coatings of dissimilar metals interacting through melt 7-3490
- dielectric, mol. struct. and phys. props. Raman studies 7-45063
- effect of ion irradi., 7-28160
- friction and adhesion meas. using microtribometer 7-46742
- metallurgical coatings, conference (San Diego, CA, USA, April 1986) 7-48149
- microindentation hardness testing, techniques and data interpretation 7-33868
- multilayer coating X-ray mirrors, design, fabrication and performance 7-25935
- multilayered structures, physical and chemical charact. 7-38376
- nonlinear mechano diffusion in solids with coatings 7-17669
- plasma exposure in mag. fusion devices 7-42193
- polybutadiene acrylates, UV-curable optical fibre coating material, low-temp. modulus 7-51911
- radar cross-sections calc., equivalent currents, flat plates with surface impedance coatings anal. 7-42867
- selective absorbers conversion coating surface characterisation 7-23224
- solar cell coverglass thermal characts., improvements by thin film coatings 7-13884
- split point drills, TiN and ZrN coatings performance charact. meas. 7-65244
- thermally affected layer caused by friction, temp. field, calc., experimental study 7-45095
- thickness meas., thermo-EMF obs., method of division 7-48687
- thin films, conference, India (Jan. 1985) 7-4619
- thin hard coatings, adhesion test methods, review 7-46741
- ultralow load hardness testing in a scanning electron microscope 7-46740
- viscoelastic coating for reducing sound wave reflection, gradient techniques 7-62874
- Ag films, SERS-active, chem. prep. method 7-53293
- B₂O₃-SiO₂ glass coating films, prep. by sol-gel method 7-46310
- CoSi, CoSi₂, thin films, study by ultrasoft X-ray spectroscopy (*Russian*) 7-52345
- Fe oxide coatings on Invar, IR emission, absorpt. modes effect 7-27708
- Fe oxides, coatings on Fe, IR emission, absorpt. modes effect 7-27708
- Fe-Si (3 wt.%), mag. props., influence of elastic-stress state produced by coatings 7-12990
- HfC, HfN, refractories, basic props., survey 7-64883
- MoS₂ coatings, thickness meas., nondestructive methods performance 7-18751
- Nb alloys, borosilicide coatings, X-ray obs. (*Russian*) 7-45066

coatings continued

- Ni overlayers on α -SiC, non-equilib. surface conditions and microstruct. changes following pulsed laser irradi. and ion beam mixing 7-65170
- SiO₂, silica sol-gel derived coatings, thickness, prep. by dipping 7-27193
- Ti-Ru oxide anodes, durability in Cl cells with Hg anodes 7-32562
- VC_x uses in cemented carbides and coating developments, review 7-39456
- WO₃ thin films, transparent, amorphous, prep. by dip-coating method 7-53644
- ZrO₂ base ceramic thermal barrier coatings, erosion rel. to processing and microstruct. 7-3450
- ZrO₂ thin films, monoclinic polycryst., sol-gel process, form. and thermal change (*Japanese*) 7-22470

coatings, protective *see* **protective coatings****coaxial cables**

- asymmetrically driven coaxial line, field asymmetry calc. 7-32076
- broadband analysis of a coaxial discontinuity used for dielectric measurements: solutions of direct and inverse problems 7-35540
- ceramic pulse-forming line for XeCl laser 7-43061
- magnetic pressure variation in coaxial plasma experiments with low inductance drivers 7-32077
- primary broadbanded coaxial thermal noise standard, watt unit realisation 7-18819
- pulsed power system, high voltage coaxial cable, polyethylene-insulated, breakdown properties, cable terminals (*Japanese*) 7-11797
- spherical tissue-equivalent proportional counter with coaxial electric field 7-3868
- time domain spectroscopy for dielectric props. meas., human skin in vivo meas. appl. 7-14961

coaxial lines *see* **coaxial cables****cobalt**

- see also nuclei with*
- adsorbed on Cu (111), surface EXAFS investig. (*French*) 7-6957
- γ -Al₂O₃/Co, spinel phase composite, study of γ -ray irradi. effects on optical absorpt. spectra 7-46071
- Apollo 16 highland breccia, komatiite component, abundance characts. 7-60583
- atom, L_{2,3}M_{4,5}M_{4,5} Auger process, meas. 7-57038
- Auger spectra, extended fine structures 7-64831
- BCC and FCC forms, ferromag. phases investig. 7-2851
- boronising, CoB layers prep. by diffusion and CVD processes 7-17434
- BWRs, methods for dose rate reduction, ^{58,60}Co concs. in coolant 7-42187
- catalyst on γ -Al₂O₃ surfaces, reaction, studies by positron annihilation 7-39309
- clusters, small, reactivity 7-15781
- determination in steel, by X-ray fluoresc. anal. 7-23075
- diffusion of ⁴⁸V, mag. anomalies, quasi-chemical model 7-6862
- diffusion of ⁶⁰Co in Fe, mag. anomalies, quasi-chemical model 7-6862
- electroplated on WC, plating effect on WC-Co powder mixture props. 7-53686
- evaporated films, photoemission spectra, correl. effects 7-39363
- ferromagnetic thin layer on Au(111), cryst. struct., TEM study 7-64015
- foil surface, preadsorbed K, CO adsorption, XPS and AES studies 7-8296
- HD 101065 (Przybylski's star), element identifications 7-55684
- internal friction and linear expansion coeff. in phase transition region 7-44857
- ion implantation, of Si, struct. and phase modifications 7-12095
- JMTR OWL-1 loop water, crud behaviour, ⁶⁰Co chemical form 7-19390
- liquid, O solubility 7-12284
- low-field mag. hysteresis 7-64483
- magnetic phase location, total energy spin polarised band calcs. 7-17176
- metal films, mech. props., relation between different quantities 7-8041
- metallic mag. film, mag. anisotropy field freq. dispersion 7-33240
- monolayer on Cu (111), Debye-Waller factor anisotropy, SEXAFS study 7-63936
- monolayer on Cu Debye-Waller factor in surface EXAFS 7-39316
- optical props., electronic struct. depend. (*Russian*) 7-33356
- optical props., refl. and spectroscopic ellipsometry meas., hybridisation effects 7-39073
- oxidation kinetics, laser control 7-28174
- particles, magnetic structure and thickness distrib., holographic interference electron microscopy appl. 7-5860
- particles, ultra fine, ferromag., growth rel. to mag. field 7-53515
- polycrystalline, flow stress, work hardening coeff., temp. depend., 15 to 300K 7-59575
- powder, very fine, electrodeposition from electrolytes of various anion comps. 7-3224
- powder and thin film samples, nuclear spin-lattice relax. studies 7-38955
- siliconisation using Si₂Cl₆ source by diffusion and CVD processes 7-17700
- single cryst., NMR freq. temp. depend. anomaly, spin-wave stiffness const. determ. 7-53154
- single crystal and polycrystalline, mag. relax. following electron irradiation 7-53067
- single crystal foils, α - and β -phase, ion transmission and sputtering 7-59322
- slip, fractal nature 7-16561
- spin wave excitations and magnetisation temp. depend. 7-45642
- surface, metal atom catalysed oxidation, UPS and AES studies 7-46865
- surface (001), metastable BCC phase, electronic struct. and magnetism 7-45418
- surfaces and overlayers, mag. and electronic props. 7-58985
- thermal equilibrium vacancies, muon spin resonance studies 7-51757
- thick and thin films, K α satellites of X-ray spectra during electron bombardment (*Russian*) 7-53449
- thin films, nucl. spin echo, effect of nonresonance pulsed mag. field 7-45839
- thin films on Au, ferromag. resonance studies 7-2932
- total angular momentum, atomic mag. moments, calc. 7-62540
- X-ray emission K $\alpha_{1,2}$ spectra 7-64825
- Al₂O₃-Co solar absorber coating, spectrally selective surfaces 7-23223
- CdTe:Co, Jahn-Teller interaction, influence of mag. field 7-16995
- CdTe:Co, segregation coeff., recoil implanted tracer technique 7-21461
- Co complex, cobalt(3-amino-5-methyl isoxazole)₂dichlorine, mol. motion detect., PMR 7-31066
- Co:Ne⁺, ion implantation in elemental solids, range profile, gamma-ray spectra 7-2959

cobalt continued

- Co/Ag, compositionally modulated layered films, saturation magnetisation and FMR, thickness depend. 7-7565
 Co/Cr compositionally modulated layered films, saturation magnetisation and FMR, thickness depend. 7-7565
 Co-Al system, diffusion markers in thin films Co_2Al_3 formation 7-58549
 Co-Au compositionally modulated multilayered films, magneto-optical Kerr rot., wavelength depend. 7-3100
 Co-CoO multilayered films, exchange anisotropy 7-27579
 Co-Cu compositionally modulated multilayered films, magneto-optical Kerr rot., wavelength depend. 7-3100
 Co-Fe bilayer thin films, annealing behaviour, mag. props. 7-59079
 Co-MoS₂ promoter-catalyst interaction, UPS, XPS, LEED studies (Chinese) 7-39913
 Co-Pt bilayer thin films, annealing behaviour, mag. props. 7-59079
 Co-Sb superlattices, NMR study (Japanese) 7-13046
 Co-Si, high energy density pulsed ion beam irradiation, study of reacted layers 7-52151
 Co-Si bilayered films, chem., elec., and struct. charges upon annealing 7-22037
 Co-Sn multilayers, amorphisation and interdiffusion, EXAFS and XANES studies 7-64812
 Co-WC composites, plastic deform. mechanisms, dislocation struct., TEM obs. (French) 7-22765
⁵⁷Co, Mossbauer spectra area meas., use of internal standard 7-36426
⁶⁰Co and ¹²⁵I in eye plaque therapy, Monte Carlo dosimetry 7-40300
⁶⁰Co ion adsorption on hematite particles, BWR radiation field build-up 7-49588
⁶⁰Co irradiation of lymphoid organs 7-28591
⁶⁰Co irradiation rel. to testis wt. loss in mice 7-28592
⁶⁰Co irradiator at Hiroshima Univ., dose rate distrib. (Japanese) 7-40295
⁶⁰Co, migration in pH 12 solution through sandy soil layer 7-19540
⁶⁰Co radiation control in BWR using thin film coatings 7-49590
 γ -Fe₂O₃/Co, microstructural defects 7-58497
 Fe₂O₃/Co sputtered films, X-ray diffraction anal. 7-58675
 n-GaAs/Co, impurity double acceptor state, Hall effect and resistivity meas., temp. and press. depend. 7-12656
 Gd-Co compositionally modulated mag. film props. study 7-7566
 H⁺ + Co, k-shell ionization cross sections and theoretical models 7-5627
 p-InP/Co(Pt) photocathodes for photoelectrochemical solar cells, H₂ evolution from alkaline solns. 7-13922
 In₂S₃/Co, photoconductivity, Co impurity energy levels (Korean) 7-33049
 LiF:Mg(Ni)(Co) R' colour centres, spectral holeburning props., depend. on doping and irradiation 7-26743
 LiGa₂O₄/Co²⁺, photon-gated spectral hole burning 7-1240
 α -LiIO₃/Co²⁺, ESR and optical absorpt. studies of impurity ions 7-45803
 LiNbO₃/Co²⁺, ESR and optical absorpt. studies of impurity ions 7-45803
 Li₂O-B₂O₃-WO₃/Co glasses, optical props. 7-46079
 MgF₂/Co laser, mode locking and Q-switching by loss-modulation freq detuning 7-62711
 MgO/Co, positron lifetime spectra, impurity effects 7-39278
 MoS₂ single crystals grown in presence of Co, photoelectrochemical props. 7-8294
 NH₄H₂PO₄/Co²⁺, optical absorption spectrum 7-46077
 NaCl/Co, doped and undoped, thermoluminescence and X-ray fluorescence spectra 7-22356
 NiFe-Co-Au trilayer film, structural depth profiling by glancing angle X-ray diffraction 7-26593
 O₂ chemisorpt., influence of Ar⁺ ion bombardment (Russian) 7-52253
 Rb₂Mg(SO₄)₂·6H₂O/Co²⁺ optical absorption spectrum 7-13180
 Si(BiAs)₃/Co, silicide formation using rapid thermal processing, defect behaviour 7-32726
 Si/Co, impurity energy levels, Hall and DLTS meas. 7-52509
 Si/Co, minority carrier lifetimes meas. (Japanese) 7-52647
 Si/Co, supersaturated solid solution, annealing 7-63642
 Si-Co interfacial atomic struct. and cpd. form., FIM studies 7-32846
 WC-Co composite, grain boundary films, mean inner pot. determ. by Fresnel technique 7-16431
 ZnO/Co, impurity electron states, optical spectroscopy 7-46127
 ZnO/Co, pulsed-laser induced phototops., time evolution, electron-hole recombination 7-45379
 ZnS-CdS:Ag,Ni,Co phosphors, photolum., energy level model 7-59245

cobalt alloys

see also cobalt compounds

- Alnico 5, Fe-Co-Ni-Al-Cu, microstruct. and mag. props., effects of heat treatment (Korean) 7-8138
 amorphous alloys, cold shortness (Russian) 7-39649
 Astrology, LC, Nirbase superalloy, hot isostatic pressing, powder metallurgy, second phase particle anal. 7-17497
 Astrology, fatigue crack growth, closure anomalies 7-3403
 electrical transport props. 7-58908
 IN738LC, Ni base superalloy, low cycle and thermal fatigue, small crack initiation and growth (Japanese) 7-13567
 IN 100, cast superalloy, creep strain and life prediction 7-33741
 IN 100, rheocasting and vacuum are double electrode remelting, solidification struct. 7-39497
 IN 100 superalloy, MC carbide props. rel. to transition element doping 7-13456
 Inconel 617, H₂ permeation in high temp. alloys, oxide layer effects (German) 7-30568
 Inconel 617, oxidation, EMPA profiles in depletion zone 7-17727
 mag. suscept. and cryst. struct. determ. (Russian) 7-1952
 metallic glasses, flash annealing under stress 7-52971
 Millstone-2 PWR, wear and neutron activation of positioning pins, ⁶⁰Co buildup 7-15247
 Nimonic 105, Ni-base superalloys, precip. and tensile deform. behaviour 7-65078
 Pd(Fe,Co,Ni)_{0.05-0.15}Si_{0.17} metallic glasses, crystallization kinetics, elec. resist. obs. (Chinese) 7-11919
 polymorphic transformations, 1D disordered struct. form. (Russian) 7-16478
 rare earth alloys, R₂(Fe,Al,Co)₁₄B, mag. props., composition depend. 7-53030
 rare earth alloys, R-Co-Fe system between 2:1 and 2:7 phase regions, phase equilibria, metallography, X-ray diff., thermomagnetic anal. 7-17511
 rare earth-Co alloys, magnetic moment irreversibility from temperature cycling 7-33194
 Rene 80, aluminised coatings, high temp. oxidation, TEM obs. 7-28202

cobalt alloys continued

- Rene 80, first stage aluminised coating microstruct., STEM obs. 7-17709
 Rene 80, Ni-base superalloy, creep rupture props., influence of coating treatment and directional solidification 7-28116
 spin wave excitations and magnetisation temp. depend. 7-45642
 surfaces and overlayers, mag. and electronic props. 7-58985
 thin film disks, DC magnetron sputtered, anisotropy induced signal waveform modulation 7-33229
 Waspaloy, γ - γ' partitioning behaviour, energy dispersive spectrometry 7-17534
 Al-Co, melt spinning, microstruct., precip., microhardness (Korean) 7-64644
 Al-Co icosahedral alloys, struct., elec. and mag. props. 7-6583
 Al-Co quasicrystalline alloys, isomorphism, neutron diff. meas. 7-51638
 Al-Ge-Co and Al-Si-Co, amorphous ductile, with two separate phases 7-59493
 Al-Ni-Fe-Co powders, cold sintering 7-64972
 AlCo powders, dynamic consolidation 7-39457
 Co-GE, disordered ϵ' martensite struct. (Russian) 7-58207
 CO-H system, magnetisation study 7-38901
 Ce-(Fe,Co)-(B,Si) system alloys, melt spun ribbons, mag. props. (Japanese) 7-53052
 Ce-Co, amorphous, electronic configuration of Ce 7-7191
 Ce(Co,Cu,Fe)₆, magnetically hard, heat treatment effects on struct. and mag. charact. 7-27564
 CeCo₂, electronic structure, spectroscopic and thermodynamic props., impurity Anderson Hamiltonian 7-32900
 Co-Al, 1D disordered structural states, form., quenching, X-ray diff. study 7-44784
 Co-Al, ageing kinetics, precipitation studies (Russian) 7-3332
 Co-Al, precipitation product dissolution (Russian) 7-58479
 Co-Al (10.9 at.%), cellular prep. from supersaturated solid soln. (Russian) 7-65045
 Co-Al alloys, magnetic hardening 7-33209
 Co-Al solid solutions, porous decay, temp. conc. existence limits (Russian) 7-33680
 Co-Al-Fe(Ni), B2, slow plastic flow props. between 1100 and 1400 K 7-46565
 Co-B, amorphous, thermodynamic, thermomag. and struct. studies (French) 7-16438
 Co-B amorphous alloys, ⁵⁹Co hyperfine field distrib., NMR spin echo studies 7-53174
 Co-base alloys, N and H solubility, equivalent influence of alloying elements 7-59495
 Co-base amorphous metallic films, SAX investig. (Russian) 7-51576
 Co-based amorphous alloys, anisotropic electrical magnetoresistivity at 295 K 7-58796
 Co-based metallic glasses, magnetic relaxation and struct. transformations 7-27557
 Co-based metallic glasses, magnetic aftereffect and magnetostriction studies 7-27571
 Co-C, long period struct. development (Russian) 7-63559
 Co-C alloy, α -phase struct., influence of C, polymorphic transformation 7-52033
 Co-Ce(Pr) liquid alloys, variable valency investig. 7-7192
 Co-Cr, continuously sputtered films, crystallographic orientation and mag. props. 7-27176
 Co-Cr, high temp. corrosion in sulphidising/oxidising environments, review 7-39737
 Co-Cr film, mag. domain obs. by colloid-SEM method (Japanese) 7-7533
 Co-Cr films, continuous fabrication by sputtering, substrate degassing effects 7-27904
 Co-Cr films, deposition by exposed pole magnetron sputtering 7-27903
 Co-Cr films, film growth and magnetisation reversal mechanism 7-27585
 Co-Cr films, mag. parameters, Brillouin light scattering study 7-53357
 Co-Cr films, sputter deposition and characterisation 7-27178
 Co-Cr films, sputter deposition, microstructure and its growth mechanism 7-27179
 Co-Cr films, sputter deposited, effects of additive gases on mag. props. 7-27575
 Co-Cr films for perpendicular mag. recording media, deposition in facing targets sputtering system 7-64899
 Co-Cr magnetic thin films, facing targets sputter deposition, microstruct. model 7-27905
 Co-Cr perpendicular recording media with oxidised surface layer, wear resistance 7-28185
 Co-Cr perpendicular recording media, props., effect of impurity gases 7-59069
 Co-Cr sputtered films, microstructural inhomogeneity, mag. props. 7-45768
 Co-Cr sputtered films, segregated microstructure, TEM studies 7-12538
 Co-Cr surgical implant alloy, mech. props., effects of N additions 7-59573
 Co-Cr thin films, DC magnetron sputtered, mag. props., effect of substrate and deposition rate 7-59067
 Co-Cr thin films, mag. props. and microstructure 7-27514
 Co-Cr thin films, sputter etching and annealing, FMR study 7-59112
 Co-Cr thin films for mag. recording, by facing targets sputtering, C-axis orientation 7-59418
 Co-Cr thin films prepared by fracture, microtome and ion-beam thinning methods, microstructure obs. 7-2427
 Co-Cr-Al-Hf(Y), high temp. oxidation rel. to alloying additions, ion implantation, Rutherford backscatt. 7-53987
 Co-Cr-Fe sputtered films, dilute, Mossbauer effect 7-22167
 Co-Cr-N, surgical implant alloy, mech. props., microstruct. rel. to N addition 7-60125
 Co-Cr-Fe system, phase equilib., struct., microstructural, X-ray phase and durometric analyses 7-17513
 Co-Cr-W, Stellite, tool materials, statistical wear model, appl. to machining 7-33804
 Co-Cu, 1D disordered structural states, form., quenching, X-ray diff. study 7-44784
 Co-Cu, Y ion-implant, growing Cr₂O₃ film, obs. of coherent perovskite particles 7-39738
 Co-Fe-B amorphous powders, flame-spray quenching process for continuous prod. 7-53679
 Co-Fe-Ni-V alloys, Invar props. and mag. field distrib. (Russian) 7-45733
 Co-Fe-Si-B amorphous alloys, struct. evolution during heating (Russian) 7-16418

cobalt alloys continued

- Co-Fe-V-Si-B metallic glass, Co-rich, temp. and annealing dependences of magnetostriction const. 7-33255
- Co-Gd-Tb-based thin films, properties and stability for magneto-optic recording 7-53075
- Co-Ge, 1D disordered structural states, form., quenching, X-ray diff. study 7-44784
- Co-Mg coevaporated films, prep. and mag. props. 7-53082
- Co-Mo-Cr-Si, wear resist. alloy development 7-3440
- Co-Ni, aq. and atmospheric corrosion 7-39696
- Co-Ni 1D disordered structural states, form., quenching, X-ray diff. study 7-44784
- Co-Ni evaporated recording media, improvement of mag. props. and corrosion resistance by Pr additions 7-33825
- Co-Ni-As mixtures, phase diagram isothermal sections, binding 7-46418
- Co-Ni-Fe underlayer for double-layer perpendicular media, vacuum deposition and mag. props. 7-27577
- Co-Ni-Mn system, thermodynamics and phase equilib. 7-65008
- Co-Ni-P electroless plated thin films, microstructure, mag. props., mag. recording appl. 7-27581
- Co-Ni-Re-P films for perpendicular mag. recording media, electroless deposition and mag. props. 7-27580
- Co-Ni-Ti-based alloys, critical shear stress asymmetry during stretching and compression (Russian) 7-8054
- Co-P, amorphous, Curie temp. meas. 7-45669
- Co-P, amorphous, pulse plated, electrochemical props., corrosion resist. (Japanese) 7-53954
- Co-P electroless plated thin films, microstructure, mag. props., mag. recording appl. 7-27581
- Co-Pt sputtered films, mag. props., O impurity effects 7-33238
- Co-Pt thin films, sputtered, TEM study 7-21757
- Co-Pt-M (M=Cs,Mo,W,V,Nb,Ta,Ti,Zr,Ge), thin film media for high density recording (Japanese) 7-7567
- Co-rich amorphous ferromag. alloys, aftereffect of mag. permeability 7-33223
- Co-rich metallic glasses, magnetostriction, anomalous temp. depend., single ion model 7-33261
- Co-Sb system, α -solid soln., interdiffusion (Japanese) 7-6861
- Co-Si-B, change of elongation, rel. to conditions for hot working 7-3384
- Co-Si-B amorphous alloys, mag. props., annealing effects 7-27513
- Co-Ta, 1D disordered structural states, form., quenching, X-ray diff. study 7-44784
- Co-Ta, cryst. struct. of α -martensite, effect of Ta conc. (Russian) 7-44452
- Co-Ta alloy, 1D disordered α -martensite states (Russian) 7-51703
- Co-Ta amorphous magnetic thin films, sputter deposition methods 7-22483
- Co-TaC, rapid quenching, microstruct. 7-65023
- Co-Te system, phase diagram, DTA 7-46425
- Co-Ti sputtered films, mag. props., O impurity effects 7-33238
- Co-transition metal amorphous films, mag. and galvanomag. props. 7-53079
- Co-W, ageing, polymorphism, cellular mechanism (Russian) 7-59514
- Co-W-P electroplated alloys, struct. and mag. props. (Russian) 7-2428
- Co-Y alloys, low temp. sp. ht. study, crystalline and amorphous phases 7-52995
- Co-Y amorphous alloys, high-field susceptibility, spin wave stiffness const. 7-33150
- Co-Y amorphous alloys, mag. props. 7-58990
- Co-Zr amorphous films, low energy ion beam sputtering, mag. props. 7-53081
- Co-Zr amorphous magnetic thin films, sputter deposition methods 7-22483
- Co-Zr(Ti) amorphous films, induced anisotropy, relax. process 7-53080
- CoAl, combustive synthesis, physicochemical props. 7-7918
- CoAl, electronic struct. of antistructure Co atoms and Co-vacancies 7-7165
- CoAl, electronic struct. of vacancies 7-16975
- CoAl, ordered B2 polycryst., Young's modulus, temp. and comp. depend. 7-33716
- CoAl_M phases, binding anal. 7-44445
- Co_{100-x}B_x amorphous sputtered thin films, magnetic anisotropy origins 7-27583
- Co₇₀B₃₀ amorphous films, ferromag., induced mag. anisotropy (Russian) 7-52974
- Co₉₂B₈ amorphous alloy, reminiscent devitrification, X-ray diff. studies 7-6547
- CoCr corrosion-resistant alloy films, mag. props. and longitudinal recording performance 7-33226
- CoCr double-layered film, sputter deposition 7-27177
- CoCr evaporated films, mag. props. 7-33225
- CoCr films, corrosion in H₂SO₄ 7-33824
- CoCr films, magnetisation reversal mechanisms 7-59068
- CoCr films, sputter deposition, mag. characteristics of initial deposition layer 7-27574
- CoCr films, texture formation, appl. for perpendicular mag. recording 7-39539
- CoCr films, vacuum evaporation, thickness depend. of mag. props. 7-27576
- CoCr layers, domain obs. with digitally enhanced Kerr-microscope 7-45726
- CoCr magnetic thin films, magnetron co-sputtered, microstructure 7-33558
- CoCr Permalloy films, weather resistance 7-28183
- CoCr RF sputtered magnetic films, Cr segregation, STEM study 7-44827
- CoCr sputtered film recording media, wear resistance, mech. strength and microstruct. 7-32859
- CoCr sputtered films, struct. and mag. props., role of atomic mobility during film growth 7-33224
- CoCr sputtered perpendicular recording media, with columnar microstruct., reversal mech. 7-7552
- CoCr thin films, microstructure and corrosion resistance, effect of SiO₂ protective film 7-28184
- CoCr thin films for recording media, perpendicular anisotropy 7-33202
- CoCr thin films on metallic underlayers, mag. charact. 7-27573
- CoCr-based thin films, growth and mag. props., nucleation layer effects 7-45065
- CoCrAl alloys, microstruct., atom probe FIM and TEM studies 7-33636
- CoCrAlY electron beam physical vapour deposition coating microstruct., TEM characterisation 7-52334

cobalt alloys continued

- CoCrAlY, hot corrosion, ZnSO₄-Na₂SO₄ reactions 7-28188
- CoCrAlY, sputter ion plated coatings for gas turbines 7-53971
- Co₇₀Cr₂₀B₂₄Si_{1.6}W_{4.5} amorphous material behaviour in friction 7-28151
- CoCrTa corrosion-resistant alloy films, mag. props. and longitudinal recording performance 7-33226
- CoCrTa sputtered films, microstruct. and mag. props. studies 7-12575
- Co₃Er noncrystalline alloy, local atomic order, magnetism 7-32286
- Co₉₂Fe_{0.08}, FCC, Fermi surface, de Haas-van Alphen studies 7-52406
- Co₇₄Fe₂₀B₂₀ amorphous sputtered thin films, magnetic anisotropy origins 7-27583
- CoFeCr sputtered films, struct. and mag. props. 7-27175
- Co₆₉Fe_{4.5}Cr₂Si_{2.5}B₂₂ metallic glasses, long-time tunnelling heat relaxation meas. 7-38223
- CoFeMoB amorphous thin films, prep. and high-freq. impedance studies 7-53585
- (Co₈₅Fe_{0.06}Ni_{0.08}Nb_{0.01})₇₅Si₁₀B₁₅ amorphous alloys, structural relax. and crystn., positron annihilation studies 7-37869
- Co₅₇Fe₂Ni₁₀Si₁₁B₁₇, metallic glasses, superplastic deform. (Russian) 7-39599
- Co₅₈Fe₂Ni₁₀Si₁₁B₁₆, metallic glasses, multiplet splitting, XPS study 7-27588
- Co₆₈Fe₂Ni₁₂Si₇B₅, amorphous alloy, superplasticity 7-3368
- CoFeSiB inhomogeneous magnetic alloys, anomalous Hall effect-magnetic polarisation correl. 7-7208
- (Co₉₅Fe_{0.05})₇₅Si₁₅B₁₀ amorphous alloy, mag. saturation 7-45632
- Co_{70.4}Fe_{4.6}Si₁₅B₁₀, amorphous alloy, mag. props. rel. to mag. coating 7-22123
- Co₇₁Fe₂Si₁₅B₁₀ and Co₇₅Si₁₅B₁₀ amorphous alloys, mag. props., stress and annealing depend. 7-33250
- Co₈₅Fe₂Si₈B₂ amorphous alloys, annealing, positron annihilation parameters anal. 7-39303
- Co_{83.5}Fe₂Si_{7.5}Ge_{1.5}B_{2.5}, amorphous alloy, struct. changes after γ -irrad. (Russian) 7-58336
- CoGa, electronic struct. of vacancies 7-16975
- Co₅₀Ga₅₀ film samples, interband optical conductivity (Ukrainian) 7-13244
- Co₈₀M₂₀ (M=Cr,Sm) sputtered thin film recording media, micromag. and struct. studies 7-33243
- Co₈₀M₁₀ (M=Pt,Re) sputtered thin film recording media, micromag. and struct. studies 7-33243
- (Co_{1-x}Mn_x)₂B, crystalline and amorphous, mag. and elec. props. 7-2827
- Co₈₄Nb₁₀B₆ fully crystallised metallic glass, fracture processes 7-22841
- CoNbTi/SiO₂ amorphous layered films, high freq. permeability 7-53078
- Co₈₀Nb₁₀Ti₁₀ two-layered films, mag. domain structures, transmission Lorentz microscopy 7-53096
- Co₈₀Nb₁₀Ti₁₀SiO₂, amorphous multi-layered films, mag. props. rel. to film thickness 7-2912
- CoNbZr films, deposition by DC opposing-target sputtering method 7-13352
- CoNi equiatomic ferromag. alloy, local mag. form factor determ., neutron scatt. study 7-38849
- CoNi sputtered films on Cr and polyimide, mag. props., relation to struct. 7-33228
- CoNi thin films, oblique-deposited, mag. props., O impurity effects 7-33244
- Co₈₀Ni₂₀ magnetic thin films, obliquely deposited, oxidation behaviour 7-65217
- CoNiCr-Cr sputtered thin films, film struct., mag. props. 7-33227
- Co₈₅Ni₁₀Fe₅B₁₆Si₁₁, metallic glass, reversible struct. transformation 7-1907
- Co₈₅Ni₁₀Fe₅B₁₆Si₁₁ amorphous ferromag. alloy struct., shock loading effects, mag. struct. anal. 7-2100
- Co₈₅Ni₁₀Fe₅B₁₆Si₁₁ amorphous ferromagnet, prep. and struct. 7-22605
- γ -CoNiMn alloys, mag. phase diagram, neutron diff. methods (Russian) 7-45667
- CoNiReP alloy films for perpendicular mag. recording, thickness depend. of perpendicular coercivity 7-59066
- (Co_{0.4}Ni_{0.4})₇₈Si₈B₁₄, amorphous, itinerant electron charact., current induced reson. mag. field shift obs. 7-27590
- (Co_{1-x}Ni_x)₇₅Si₁₅B₁₀ amorphous alloys, magnetostriction and other mag. props. 7-45787
- CoO-NiO system, immiscibility 7-38202
- CoP amorphous films, FMR spectra during crystallisation 7-53142
- Co₈₀P₂₀, amorphous films, electrodeposited, optical and NMR spectra, annealing effect (Russian) 7-45831
- CoPtTi thin films, magnetic and microstructural props. 7-33230
- CoR alloys, R=rare earth, permanent quadrupole magnets, construction and calcs. 7-19578
- CoSi, CoSi₂, thin films, study by ultrasoft X-ray spectroscopy (Russian) 7-52345
- CoSi₂ epitaxial layer on Si, X-ray diff. analysis 7-21047
- CoSi₂ films, electrical transport props. 7-58908
- CoSi₂ films, structural analysis by X-ray diff. in the grazing Bragg-Laue geometry 7-7042
- CoSi₂, MBE growth of epitaxial insulator-metal-semicond. struct., CaF₂-CoSi₂-Si 7-22496
- Co₇₀Si₃₀, amorphous films, ferromag., induced mag. anisotropy (Russian) 7-52974
- Co₇₀Si₃₀ amorphous films, coercive force rel. to crystallisation (Russian) 7-59078
- CoSi_{1-x} polycrystalline alloys, positron lifetime, Doppler studies 7-33480
- Co₇₅Si₁₄B₁₅, amorphous powder, static consolidation, mechanical and mag. props. 7-3217
- Co₇₁Si₁₀B₁₃, amorphous, structural anal. (Korean) 7-26637
- CoTa sputtered magnetic thin film, ion beam irrad., struct. studies 7-22588
- CoTi soft ferromagnetic thin films, structure-related induced anisotropy 7-45663
- CoTi-CoNb amorphous alternating layers, magnetic and diffusional props. study 7-7563
- Co₂Ti₇₅, amorphous struct., neutron and X-ray diff. 7-58149
- Co₃Ti, alloying behaviour, phase equilib. 7-7968
- Co₃Ti, effect of plastic deformation on mag. props. 7-33259
- Co₃Ti, L1₂ ordered alloys, grain boundary strength and fracture, electronic and struct. studies 7-33756
- CoZr sputtered magnetic thin film, ion beam irrad., struct. studies 7-22588

cobalt alloys continued

- Cr-Co-porcelain dental prostheses, strength rel. to surface roughness of metal frames 7-40365
- Cu-⁵⁷Co Mossbauer source in low temp. He, oscillations after heating by an RF pulse 7-59128
- Cu-Al-Co, stacking fault energy determ. (Russian) 7-12082
- Cu-Be-Co, elec. resist., decomposition and coarsening effects 7-2573
- Cu-Co, age hardened, tensile deform., acoustic emission characts. 7-13536
- Cu-Co, dynamic fracture characts., void nucleation at incoherent precipitates 7-17628
- Cu-Co (2 at.%), age-hardened, fatigue behaviour 7-33786
- Cu-Co (2 at.%), underaged, fatigue props., comparison of single crystals and polycrystals. (German) 7-46648
- Cu-Co (2.7 at.%), decomp., atom probe FIM 7-3268
- Cu-Co alloy, coherent precipitate strain contrast under high order refl. excitation 7-3306
- Cu-Co alloy decomposition, TEM, FIM and SANS studies 7-53749
- Cu-Ni-Co-W-Cr system, Cr plating, roughness and wear (Russian) 7-33801
- (CuAu)-Co single crystals, under- and over-aged, additivity of precip. and solid soln. hardening 7-65051
- CuCo, Cu-rich alloy, precipitation, critical nuclei size, neutron scatt. studies 7-12294
- CuCo dilute alloys, electron struct., X-ray L α emission spectra studies 7-12598
- Dy-Co-Re, intermetallic-based solid solns., phase equilib. and mag. props. 7-22639
- Dy, Co_{1-x} thin films, ferrimagnetic reson. in region of spin-reorientation transitions 7-45824
- Dy₂Co₂Sn₂₃ cryst. struct. and mag. suscept. studies (Russian) 7-21161
- Er₂Co glasses, electronic struct., photoemission and magnetism 7-64060
- ErCo₂Ni₂, ferrimag. cpds., mag. anisotropy, temp. depend. 7-64450
- Er₂CoSn₂₃ cryst. struct. and mag. suscept. studies (Russian) 7-21161
- Er₂(FeCo)₁₄B, struct., composition depend. 7-51701
- (FeCo,Ni)-P layers, electrochemical deposition, struct. (Chinese) 7-7037
- Fe-Al-Co ordering alloys, phase separations 7-33634
- Fe-C-Co, ferrite nucleation at austenite grain edges, kinetics 7-7991
- Fe-C-Co, nucleation of proeutectoid ferrite at austenite grain boundaries 7-8003
- Fe-Co, atomic short-range order, temp. depend., neutron diffuse scatt. studies 7-51708
- Fe-Co, liq., thermodynamic mixing functions, Knudsen cell mass spectrometry (German) 7-21470
- Fe-Co, liq. alloys, density of electron states, calc. (Russian) 7-45110
- Fe-Co, thermal equilibrium vacancies, muon spin resonance studies 7-51757
- Fe-Co alloys, powder and thin film samples, nuclear spin-lattice relax. studies 7-38955
- Fe-Co alloys, powder metallurgy produced, mag. props. 7-33211
- Fe-Co dil. alloy, ^{56,57,60}Co isotopes, hyperfine anomalies, α -factors NMR/ON obs. 7-33278
- Fe-Co-As mixtures, phase diagram isothermal sections, binding 7-46418
- Fe-Co-B films, phase transition, microstruct. 7-33568
- Fe-Co-B powders, amorphous mag. state, Mossbauer spectra study 7-45846
- Fe-Co-Cr-Mo alloys, electronic struct. and mag. props., X-ray spectra studies (Russian) 7-32902
- Fe-Co-Mn(V) films, ion beam sputtered, soft mag. props. 7-33237
- Fe-Co-Mo alloys, liq., H solubility meas. and estimates (German) 7-58487
- Fe-Co-Ni amorphous alloys, anisotropic magnetoresist. studies 7-58793
- Fe-Co-Ni based alloys, crystalline and amorphous, magnetoresistance 7-38538
- Fe-Co-Ni cryst. alloys, anisotropic magnetoresist. studies 7-58794
- Fe-Co-Ni powder, fine, corrosion resist. and mag. prop. changes, surface-active agent use in prep. 7-54001
- Fe-Co-Ni-Al-Cu metallic alloy ordering and spinodal decomposition, atom probe FIM study 7-33676
- Fe-Co-Ni-Ti (34.9, 20.0, 10.2 wt.%), thermoelastic martensite transformation 7-52032
- Fe-Co-Si-B glass, liq.-quenched, cooling condition depend. of saturated mag. flux density 7-58991
- Fe-Co-V, atomic ordering mechanism, neutron diffr. study (Russian) 7-46459
- Fe-Co-V, ordered alloy, plastic deform., antiphase boundaries (Russian) 7-39596
- Fe-Co-based ternary alloys, atomic and mag. moment mutual ordering (Russian) 7-33169
- Fe-Cr-Co permanent magnetic alloys, casting 7-53051
- Fe-Cr-Co solid soln., uniaxial tensile stress in spinodal decomp. effect on coercive force, thermomag. treatment effects 7-7555
- Fe-Cr-Co-Mo alloy struct., 2D scatt. X-ray intensity distrib. patterns, anal. by direct variation method 7-64734
- Fe-Cr-Co-Mo permanent magnet ribbons, mag. props., influence of modulated structure 7-53043
- Fe-Cr-Co-Si-Ti, permanent mag. alloy, ductile, effect of heat treatment on mag. props. (Korean) 7-8137
- Fe-Cr-Co-(Si), permanent magnet alloys, microstruct., mag. props., Si content effect 7-22117
- Fe-Ni-Al-Co system, miscibility gap, phase decomp. in Alnico mag. alloys 7-17537
- Fe-Ni-Co alloy, H damage, lattice distortion, defect and crack generation, positron lifetime study 7-39675
- Fe-Si-Co, atomic ordering and mechanical props. 7-11990
- FeAlNiCoCu permanent magnetic material, phase decomposition kinetics, atom probe FIM study 7-33669
- FeCo alloy, electronic struct., effect of ordering, positron annihilation and Mossbauer effect study 7-45142
- FeCo alloys, critical mag. phenomena, results from μ SR studies 7-45872
- Fe_{1-x}Co_x, spin-polarised positron annihilation and mag. moments 7-53439
- Fe₇₀Co₃₀-SiO₂ compositionally modulated mag. film props. study 7-7566
- (FeCo)₈₀B₂₀ amorphous ultrafine particles, mag. props. 7-53063
- (Fe_{1-x}Co_x)₈₀B₂₀, amorphous alloy, crystallisation kinetics (Korean) 7-26638
- (Fe_{1-x}Co_x)₈₄B₁₆ amorphous alloy, temp. depend. of the resistivity (Chinese) 7-27314
- (Fe_{1-x}Co_x)₈₄B₁₆ thermoelectric power, influence of Ci(Ni) additives 7-32995

cobalt alloys continued

- Fe₆₇Co₁₈B₁₅S metallic glass, magnetic aftereffect, thermal treatment, positron lifetime study 7-38907
- (Fe_{1-x}Co_x)₇₇B₁₃Si₁₀ amorphous alloys, Mossbauer study 7-7623
- Fe₆₇Co₁₈B₁₅Si, amorphous mag. alloy, crystallisation, elec. resist., TEM obs. 7-11927
- Fe₆₇Co₁₈B₁₅Si, metallic glasses, corrosion in H₂SO₄, alloying effect 7-28201
- Fe₇₄Co_{10-x}Cr_xB₁₆ amorphous alloys, form. and crystn. 7-11930
- Fe₇₄Co_{10-x}Cr_xB₁₆, amorphous, prep. by melt spinning, X-ray diffr., DSC, Mossbauer studies 7-46369
- Fe₂Co_{70-x}Cr_xSi₁₀B₁₅, x=0, 3, 6, 9, amorphous ferromagnet, 180° domain wall (Korean) 7-33198
- Fe_{5.85}Co_{72.15}Mo₂B₁₅Si₅ amorphous ribbons traversed by DC electric currents excess resistance, collective motion of ferromag. domain walls 7-32989
- (Fe_{1-x}Co_x)₇₀Si₃B_{12.5} amorphous alloys, density of states, XPS studie (Chinese) 7-13320
- Fe₆₇Co₁₈SiB₁₄S, mean positron lifetimes after annealing (Chinese) 7-27814
- FeNiAlCoTiCuS permanent magnetic material, phase comp. and ordering, atom probe FIM and TEM studies 7-33635
- Gd-Co, amorphous, influence of hydrogenation or mag. props. 7-2899
- Gd-Co, amorphous and crystalline, hydrogenation, pressure-composition isotherm 7-3606
- Gd-Co, anisotropic ferrimagnets in high mag. fields 7-17200
- Gd-Co films, amorphous, spontaneous spin-reorientation transition (Russian) 7-45763
- Gd-Co-Mo amorphous magnetic thin films, spin wave mode linewidth meas. 7-45826
- Gd-Fe-Co, amorphous Faraday rotation 7-64612
- Gd-Tb-Co-Fe sputtered amorphous films, Kerr magneto-optical effect, anisotropy dispersion effects 7-38913
- Gd₂(Co_{1-x}Mn_x)₁₇, Co contribution to magnetocrystalline anisotropy, point charge model 7-45665
- GdCo amorphous, Faraday rotation 7-64612
- GdCo amorphous films with perpendicular anisotropy, Hall loop meas., mag. struct. studies 7-7205
- GdCo amorphous thin films, electrical conductivity, influence of mag. order 7-7409
- GdCo and GdTbFeCo alloys, amorphous thin films, thermomag. recording, magnetisation reversal, coercivity 7-64459
- GdCo-based glasses, double transition behaviour induced by anisotropy 7-22109
- GdCo₂, ¹⁵⁵Gd 105.3 KeV transition, Mossbauer effect study 7-38971
- Gd₂Co glasses, electronic struct., photoemission and magnetism 7-64060
- GdCoSi, amorphous film, mag. and magnetoopt. props., thickness depend. 7-33239
- Gd(Cu_{1-x}Co_x)₂, mag. and crystallographic props. 7-38903
- Gd₂La_{65-x}Co₂B₁₀ mixed glasses, mag. props., phase transitions, microstruct. effects 7-64465
- Hf₂Co, surface oxidation, XPS 7-8184
- HoCo₁₇, intersublattice mol. field calc. 7-27511
- HoCo₂Co₂, ferrimag. cpds., mag. anisotropy, temp. depend. 7-64450
- Ho₂(CoFe)₁₇ intermetallics, high field magnetisation studies 7-53038
- Ho₂Co₂Sn₂₃ cryst. struct. and mag. suscept. studies (Russian) 7-21161
- Ho₂Fe₄, amorphous ribbons, mag. props. 7-33177
- Ho_{1-x}Y_xCo₃, orientational phase transitions and elec. resist. (Russian) 7-7506
- La_{0.8}Nd_{0.2}Ni_{2.5}Co₂Si_{0.1} electrode, storage capacity investig. 7-33946
- Lu₃Co₂Si₁₄, monoclinic struct. type, rel. to Sc₃Co₂Si₁₀ and La₃Co₂Sn₇ 7-1944
- Mo-Ni-Co-Sn, liq. phase sintering, grain boundary migration, coherency strain effect 7-22604
- Nd-Fe-B-Co-Al based permanent magnets, mag. props. and temp. characts. 7-53045
- Nd-Fe-Co, amorphous films, perpendicular magnetic, mag. and magneto-optical props. 7-64496
- Nd₂Co₁₄B, NMR study 7-64544
- Nd₂Co₁₄B, spin arrangements, 4.2-1100K 7-22094
- Nd_x(Co_{0.9}Fe_{0.1-x})₁₄B alloys, mag. struct., preferential site occupation 7-45619
- Nd₆Co₂Ge₂₂, cryst. struct., X-ray diffr. studies 7-44450
- NdFeBCoAl magnets, Curie temp., coercive force and magnetisation 7-52982
- Nd₂Fe_{14-x-y}Co_xAl_yB alloys, permanent mag. props. 7-45755
- Nd₂Fe_{14-x}Co_xB, crystallographic and mag. props. 7-27522
- Nd₂Fe_{14-x}Co_xB system, mag. phase transitions and anisotropy 7-27524
- Nd₂Fe_{12-x}R_xMn₂Co₂B, mag. props. 7-52946
- Nd_{2-x}R_xFe₁₂Co₂B, mag. characts. 7-45670
- Ni base superalloys, pressure vessel performance, strength, ductility, comp. struct. 7-3365
- Ni-Al-Co-Cr-Ta, polycrystalline superalloys, microstruct. rel. to Ta content 7-46446
- Ni-Al-Co-Nb superalloy, interphase boundary, FIM atom probe study 7-33683
- Ni-base superalloy, cast, high Al-Ti, eutectic form. and σ -phase control (Chinese) 7-7983
- Ni-base superalloy, IN 939, high Cr, effects of heat treatment on mech. props. 7-13526
- Ni-base superalloy, IN-100, rheocast, processing-struct. charactn. 7-46449
- Ni-base superalloy, single cryst., MAR-M200, with bimodal γ' distrib., low cycle fatigue at 750 and 870°C 7-17627
- Ni-base superalloy powder, IN-100, shock consolidation 7-39459
- Ni-base superalloys, cast, solidification behaviour w.r.t. Hf additions (Chinese) 7-7984
- Ni-base superalloys, γ' strengthened, creep and microstruct. rel. to refractory elements 7-3364
- Ni-base superalloys, mag. clusters, calorimetrically determined 7-12977
- Ni-CO, limitations of dynamic recovery as revealed by temp. change tests at large strains 7-22723
- Ni-Co based refractory alloys, γ' -phase strengthening rel. to comp 7-46496
- Ni-Co-Cr-Al-Y, plasma sprayed, high temp. tensile and creep behaviour 7-28083
- Ni-Co-Cr-Al-Y coatings, electron beam deposition, oxidation rel. to pretreatment 7-46702
- Ni-Co-Cr-Mo-Al-Ti prealloyed powder, parts prod. by hot pressing (French) 7-13400
- Ni-Cr-Co-Mo superalloys, interphase boundary, FIM atom probe study 7-33683

cobalt alloys continued

- Ni-Cr-Co-Mo-Nb-Ti-Al superalloy, microstruct. and mech. props. with high-temp. heating 7-3341
 Ni-Cr-Co-Mo-Ti-Nb-Al, heat-resisting, supersaturated solid soln., isothermal decomp. kinetics 7-33682
 Ni-Cr-Co-Mo-Ti-Nb-Al, heat-resisting, hot strain rate effect on microstruct. and mech. props. 7-39559
 Ni-Pt, order-disorder transformation kinetics 7-52047
 Ni-W-Co-Cr superalloy single crystals, fatigue crack propag. under multiaxial cyclic loads 7-28122
 Ni-W-Co-Cr superalloys, creep rupture and tensile props. rel. to hot pressing or aluminising 7-3363
 Ni₇₇Co₂₃B₂₀, amorphous, mag. scatt. influence on transport props. 7-33001
 NiCoCrAlY, plasma sprayed coatings, low cycle fatigue behaviour 7-22793
 NiCoGa, thermal vacancies 7-51764
 NiCoP onefold layer, domain propag. along hard axis 7-45727
 NiFe/SiO₂/CoPt multilayer magnetoresistors sensitivity anal. 7-48786
 PdSiCo inhomogeneous magnetic alloys, anomalous Hall effect—magnetic polarisation corrls. 7-7208
 Pr-Co rapidly quenched ribbons, mag. props. 7-27551
 Pr-Co-B system, phase diagram over complete conc. range 7-3281
 Pr₂Fe_{14-x}Co_x B system, struct. and magnetism 7-45631
 PrCo₅, microstructure and coercivity, effect of annealing, 650-850°C 7-38905
 Pr₇Co₆Al₇, crystal struct. determ. 7-16494
 Pr₂Co₁₄B, spin arrangements, 4.2-1100K 7-22094
 PrCo_{4-x}Fe_xB, crystallographic and mag. props. 7-45671
 Pr₂(Fe_{1-x}Co_x)₁₄B, mag. props. 7-64549
 Pr_{2-x}R_xFe₁₂Co₂B, (R=Dy, Tb), mag. characts. 7-45670
 PtCo, order-disorder transform. kinetics, temp. depend., magnetisation meas. 7-63797
 R-Co, 4f Co rich intermetallics, basal plane magnetocrystalline anisotropy 7-52972
 RCo₅, (R=Tb,Dy,Ho, Pr,Nd,Ce,Sm,Gd,Er,Tm,Yb), magnetocrystalline anisotropy, rare earth contribution 7-45659
 R₂Co₁₄B, permanent magnet, props. and struct. 7-53053
 R₂Fe_{14-x}Co_xB, spin reorientations 7-64484
 R₂Fe_{12-x}Mn_xCo₂B (R≡Pr, Gd), mag. props. 7-27500
 RGa₂Co₂ (R=Ce, Pr, Eu), cryst. struct., mag. props. 7-45614
 Sc(Co_{1-x}Al_x)₂, pseudobinary system, weak itinerant ferromagnetism 7-2825
 Sc(Co_{1-x}Al_x)₂, anomalous high field magnetisation 7-64438
 Si-Co₅₀Mo₅₀-Au, amorphous Co₅₀Ta₅₀ alloys as diffusion barriers 7-44923
 Si-Co₅₀Ta₅₀-Al, amorphous Co₅₀Ta₅₀ alloys as diffusion barriers 7-44923
 Sm-Co amorphous thin films, low temp. mag. props. (Chinese) 7-38910
 Sm-Co-B rapidly quenched ribbons, hard mag. props. and struct. 7-53048
 Sm-Co-Fe-transition metal permanent magnets, magnetisation 7-53033
 Sm-Fe-Co-B-Si melt-spun alloys, mag. props. 7-27553
 Sm₂(Co, Fe, Cu, Zr)₁₇ sintered compact permanent magnet, mag. props., comp. and heat treatment effects (Korean) 7-2894
 SmCo permanent magnet linear undulator for ENEA free electron laser expt., dipole moment meas 7-43151
 SmCo₅ aligned deposits, plasma spraying 7-39371
 SmCo₅ and Sm₂Co₁₇ plastic magnets, magnetisation process, depend. of surface flux density 7-27548
 SmCo₅, anisotropic permanent magnet, prep. and investig. 7-52969
 SmCo₅ fine particles, produced by ball milling, strain and domain wall energy (Japanese) 7-7556
 SmCo₅ powder in nylon-12 and polybutylene tetrathalate, thermoplastic magnet, heat resistance 7-27567
 SmCo₅ powder magnet, texture form. in alternating and steady mag. fields 7-27977
 Sm₂Co₁₇ single domain particles, SEM domain obs. 7-27566
 Sm₂(CoCu)₁₇ magnets, cast, coercivity and microhardness 7-53880
 Sm₂(Co_{1-x}M_x)₁₇ (M=Fe,Mn), rapidly quenched ribbons, mag. props. 7-27552
 Tb-Co amorphous films, magneto-optic props. 7-64611
 Tb-Co thin films preparation for erasable optical memory disk (Japanese) 7-7049
 TbCo, amorphous sputtered films, mag. props., film struct., comp., internal stress meas. (Japanese) 7-7570
 TbCo, dilute alloys, hyperfine fields and local moment form. 7-64433
 TbCo film, optical disc memory struct., mag. props., underlayer film treatment effect 7-45767
 TbCo sputtered films, compositionally modulated, mag. props. 7-64495
 TbCo sputtered films, mag. and magneto-optic props., stability 7-53076
 TbCo sputtered films, stability of mag. and magneto-optical props. (Japanese) 7-33241
 TbCo₂, NMR of ¹⁵⁹Tb (Russian) 7-45832
 Tb₂Co₁₄B, spin arrangements, 4.2-1100K 7-22094
 Tb₃Co₂Ge₄, crystal struct. determ. 7-16495
 Tb₂Co₅Sn₂₃ cryst. struct. and mag. suscept. studies (Russian) 7-21161
 TbFeCo amorphous film sputtered onto polycarbonate substrate, depth profile, XPS 7-65362
 TbFeCo/dielectric interface, chemical stability, interdiffusion and oxidation, AES, XPS and RBS depth profile studies 7-12513
 TbFeCo-based amorphous films, magneto-optical recording appls. 7-53074
 Tb(Fe_{1-x}Co_x)₃, struct. and mag. props. 7-1950
 (Tb_{1-x}Y_x)Co₂ ferrimagnetic alloy, sp. ht., Curie temp. and density of states comp. depend. meas. 7-7514
 (Tb_{1-x}Y_x)₃Co, magnetoelastic interactions and thermal expansion (Russian) 7-17211
 Ti-Co, amorphous phases, mechanical alloying 7-27972
 Ti-Co, liq-alloys; thermodynamic props., mass spectrometry (Japanese) 7-52084
 Ti-Co (3.2 at.%), grain boundary allotriomorphs, nucleation, growth and transform. kinetics 7-28035
 TiC-WC-TaC-Co hard metals, Ta conc. effect on comp. and physicochem. of carbide and Co phases 7-53708
 TiC-WC-TaC-Co three-phase sintered carbides, Ta content influence on struct. and props. 7-65097
 U-Co system, mag. props., influence of hydriding 7-45750
 UAl(Ga)(Sn)Co ternary alloys, magnetic behaviour, elec. resist. and sp. ht. meas., 5f electron effects 7-12999
 U₆Co, heavy fermion superconductor; penetration depth rel. to saturation spin moment 7-52893

cobalt alloys continued

- VCoSi, VCoGe, solid solns., elec. resist. (Russian) 7-45273
 W-Co alloy, gamma-irradiated, anomalous effect of small doses 7-12151
 W-Fe-Co-Ni system, isotherms of solidus and phase comp. above 1200°C 7-65006
 W-Fe-Co-Ni system, phase equil., peritectic transform. 7-53701
 WC-Co, abrasive wear, 3D shape effect 7-17652
 WC-Co, cermet, structural materials, cyclic strength 7-59624
 WC-Co, erosion, effect of hardness 7-17648
 WC-Co, erosion rate 7-3464
 WC-Co, high press, sintering, microstruct. 7-39470
 WC-Co, phenolformaldehyde polymer friction, physicochem. processes 7-28149
 WC-Co, plasma sprayed coatings, wear, adherence, heat treatment effect 7-33555
 WC-Co, sliding and abrasive wear mechanisms, comparison 7-3463
 WC-Co, TiN-coated, residual stress and strength, X-ray diff. study (Japanese) 7-8101
 WC-Co, tool materials, statistical wear model, appl. to machining 7-33804
 WC-Co, wear resist., comparative study of hard materials 7-3457
 WC-Co cemented carbides, abrasion, controlling mechanism 7-3460
 WC-Co cemented carbides, tensile creep, 800-900°C, grain boundary sliding 7-17585
 WC-Co cemented carbides, compression fatigue crack growth 7-28119
 WC-Co cermet particle reinforced low alloy steel composite, elastic const., laser US technique 7-65268
 WC-Co compact, stereological analysis of struct. form. during consolidation of carbide powder 7-53688
 WC-Co composites, fracture toughness rel. to hardness, microstruct. model 7-17637
 WC-Co hard metals, thermal conductivity and thermal diffusivity (German) 7-27036
 WC-Co powder mixtures, electrolytic Co plating effect on densification and strength props. 7-53686
 WC-Co sintered carbides, X-ray diff. obs. of microstruct. after hardening, optimum heat treatment cycle 7-65063
 WC-Co-B system, formation mechanism of composite coating, electrophoresis 7-3208
 WC-TaC-Co, N contained cemented carbides, sinterability, mech. props. rel. to prep. 7-17507
 WC-TiC-Co hard alloy Ti5K6, heat treatment effect on failure mechanism 7-13550
 WC-TiC-Co TK type hard metal prod. using Ti alloy swarf 7-27996
 Y-Pd-Co, intermetallics, interaction characts. and props. 7-46414
 Y₂(Co_{1-x}Mn_x)₁₇, Co contribution to magnetocrystalline anisotropy, point charge model 7-45665
 YCo₅, ferromag. resonance, local Co anisotropy effects 7-53143
 Y₂Co₁₇, local orbital moment, recursion method calcs. 7-45640
 Y₂Co₁₇, electronic struct. and mag. props. 7-7104
 Y₂Co₁₇ mag. supercond., ⁵⁹Co NMR and nuclear relax. studies 7-64401
 Y₂Co₁₇, resistivity and Hall effect temp. depend. meas. 7-52568
 Y₂Co₁₄B alloys, magnetic anisotropy and spin reorientations 7-38855
 Y₂Co₁₄B intermetallic cpd., electronic struct. and mag. props., tight-binding calcs. 7-2450
 YCo₅H₂, mag. props. meas. 7-33217
 YCo₅H₂, mag. props. meas. 7-33217
 Y₂Co₁₇H₂, mag. props. meas. 7-33217
 Y(Co_{0.9}Ni_{0.1})₅, magnetocrystalline anisotropy studies (Russian) 7-45656
 Y₂Co₁₄B, NMR study 7-64544
 Y₂Co₅Sn₂₃ cryst. struct. and mag. suscept. studies (Russian) 7-21161
 Y₂(Fe,Al,Co)₁₄B, mag. props., composition depend. 7-53030
 (Y,Zr_{1-x})Co₂, cryst. struct., mag. props. 7-51719
 YbCoB₄, YCrB₄-type structure, formation in Yb-Co-B ternary systems 7-6581
 Zr-Co, amorphous alloys, microhardness and struct. relax. (Chinese) 7-65069
 Zr-Co, electronic struct., supercond. and magnetism 7-64398
 Zr-Co (2 at.%), Co fast diffusion, quasielastic neutron scatt. study 7-63883
 Zr-Co amorphous alloys, superconductivity, normal-state resistivity and mag. susceptibility 7-12900
 β-Zr-Co system, fast Co diffusion, quasielastic neutron scatt. studies 7-52120

cobalt compounds

- see also cobalt alloys
 acetate soln., ion exchange with 2,9-dimethyl-1,10-phenanthroline intercalated in α-Zr(HPO₄)₂ 7-65305
 diffusivity, conc. and temp. depend. 7-21518
 Al-CoSi₂-Si contacts, four-terminal resistor structs. for contact resist. determ. from end resist. meas. 7-38730
 BaCo₂Fe₁₆O₂₇, Curie temp., magnetization, susceptibility, mag. anisotropy meas. (French) 7-27507
 BaCo₂Fe₁₆O₂₇, hexagonal ferrites, neutron diff. studies 7-45622
 BaCo₂Fe₁₆O₂₇, W-type hexagonal ferrite, cryst. struct. and Co location 7-6605
 BaZn₁₁Co₉Fe₁₆O₂₇ hexaferrite, competing anisotropies, first order magnetisation processes and spin transitions obs. 7-38856
 CO complexes, struct. ang. distortions, stretching modes. IR spectra 7-3052
 Ca₂Co_{1-x}Fe_xO₄ substituted ferrite system, mag. props., comp. depend., Mossbauer study 7-7618
 Ce₂Co₂P₁₂, synthesis, cryst. struct., X-ray diff. study 7-32387
 CeCo_{1-x}Si_{2+x}, cryst. struct., homogeneity range, X-ray diff., electron probe anal. 7-37939
 Ce(Rh_{1-x}Co_x)₃B₂ ferromag. Kondo system, anomalous elec. resist. temp. depend. 7-2601
 Co (II) azelaic acid bis(phenylhydrazide), X-ray absorpt. near-edge struct. obs. 7-19881
 Co (II) complexes, spin-exchange processes 7-12677
 Co (II) diethiocarbamates, X-ray photoelectron spectra 7-50256
 Co (II) sebacic acid bis(2,4-dinitrophenylhydrazide), X-ray absorpt. near-edge struct. obs. 7-19881
 Co catalyst, O₂ adsorpt. and oxidation of Si at CoSi (100) surfaces 7-46865
 Co complex, CO(II)-5' IMP, struct., hydration, mag. suscept. and Mossbauer emission obs. 7-36660
 Co complex, Co (II) nonamethylimidodiphosphoramide, struct., mag. props., NMR 7-50197

cobalt compounds continued

- Co complex, Co (II) octamethylpyrophosphoramide, struct., mag. props., NMR 7-50197
- Co complex, cobalamine, ESR, unpaired electrons interspin distance, Eatons' formula calc. 7-25569
- Co complexes, bis(dimethylglyoximate)cobalt(II), frozen soln., EPR and ENDOR investig. 7-57097
- Co complexes, Co (II) hydroxo, in KOH solns., diffusion coeffs. determ. 7-52096
- Co complexes, dimeric, bonding and struct. 7-56939
- Co complexes, tris(aminoacido) cobalt (III), crystal field theory failure 7-12674
- Co complexes and related cpds., aq. soln., densities, viscosities and electrolytic cond. (Japanese) 7-12347
- Co²⁺, complexes, IR spectra, coordination bond length correlation 7-13160
- Co-Ba-Ni-O₂ thermal resistance thermometer study (Chinese) 7-24650
- Co-Co multilayered films, exchange anisotropy 7-27579
- Co-O cluster ions, collision-induced dissociation, struct. calcs., mass spectral anal. 7-54107
- Co-Si, direct silicidation, on Si:B(As)(P), rapid thermal annealing 7-21546
- Co+Cr₂O₃, wear protective dispersion coating for use at high temp. 7-46667
- CoAlFeO₄, cubic spinel, Mossbauer anal. 7-33304
- CoB layers and crystals, prep. by diffusion and CVD processes 7-17434
- Co(C₂H₃O₂)₂·4H₂O, liquid optical filter anal. for hybrid solar energy conversion 7-50724
- Co(CO)₃NO, photofragmentation dynamics using coherent VUV for product detect. 7-19976
- Co_{1-x}Ca_xFe₂O₄, single domain-superparamagnet transition 7-17203
- CoCl₂ 3p-3d hybridisation eval., valence band photoelectron spectra meas. 7-53495
- CoCl₂, electronic transitions, IETS 7-50099
- CoCl₂-graphite intercalation cpds., mag. susceptibility meas. 7-45638
- CoCl₂-graphite intercalation compound, obs. of magnetic state, high magnetic field 7-59008
- CoCl₂·6H₂O, liquid optical filter anal. for hybrid solar energy conversion 7-50724
- CoCo₂O₄, fine-particles, low temp. prep. by solid solution precursor method 7-59486
- Co_{0.55}Cu_{0.45}Cr₂S_{4-y}Se_y spinels, X-ray diff. study 7-44475
- Co_{0.55}Cu_{0.45}Cr₂S_{4-y}Se_y, high field susceptibility 7-45630
- CoF₂, antiferromag. insulator, H-odd linear dichroism of exciton-magnon transitions 7-53282
- (CoF₂)_{0.5}(BaF₂)_{0.2}(NaPO₃)_{0.3}, AC magnetic susceptibility and acoustic wave attenuation meas. 7-59020
- Co_{1-x}Fe_xCr₂S₄, paramag. susceptibility study 7-52934
- Co₂Fe_{1-x}Cr_{2-x}S₄ mixed spinel system, temp. depend. Mossbauer studies 7-38976
- CoFe₂O₄ (100)-textured thin films, anisotropy study 7-7568
- CoFe₂O₄ ferrite epitaxial layers, high coercivity (Chinese) 7-38908
- CoFe_{3-x}O₄ ferrites, polycrystalline, Verwey transition 7-7120
- CoGaInS₄, cpd. with FeGa₂S₄ struct., prep. and characts (German) 7-1984
- CoGaInS₄ layer cpds., struct. and mag. props., XPS studies 7-44498
- CoGaInS₄ pseudoternary layers cpds., optical props., comp. depend. studies 7-39072
- CoGa₂O₄, crystal growth, chemical vapour transport, struct., mag. and electronic props. 7-53517
- CoGa₂O₄ substrates for hexaferrite film growth 7-52320
- Co_{0.2}Ga_{0.8}S₂ single crystals, optical props. and impurity energy levels meas. 7-13122
- Co₂Ge, chemical bond, struct., short range order 7-32350
- CoH system, ferromag., heat of formation, total energy calcs. 7-45198
- CoI₂, Raman scatt. from phonons and electronic excitations 7-53312
- Co₂In₂S_{3+x} thin films, spray pyrolysis deposited, structural and optical props. 7-22468
- Co₂Mg_{1-x}O, Neel temp., var. with mag. dilution 7-27516
- CoN₂ thin films, magnetic props. 7-13008
- CoN₂ thin films, sputter-synthesized, crystal structure 7-52313
- Co(NO₃)₂·6H₂O, electrical resistance effects accompanying high pressure and temperature melting and decomposition 7-16719
- Co(NO₃)₂·6H₂O, liquid optical filter anal. for hybrid solar energy conversion 7-50724
- CoO (100), LEED intensities, quasidynamical approx. calc. 7-12428
- CoO, band structure and optical absorption edge 7-45147
- CoO, defect processes, calc. using SHEOL code 7-58267
- CoO, deformed, dislocation struct., TEM study 7-21209
- CoO, diffusion, isotope effect, quasi-harmonic calcs. 7-26996
- CoO, heat capacity in vicinity of strong fluctuations, nonpower-law behaviour 7-2865
- CoO single crystals, ¹⁸O diffusion coeff. meas. 7-32707
- CoO, subgrain size after creep 7-39603
- CoO-Al₂O₃ dispersed oxides, positron annihilation 7-39275
- CoO-H₂O and Co₃O₄-H₂O systems, hydrothermal equilib. thermodynamic props. of Co(OH)₂ 7-39492
- CoO-MnO system, thermodynamic props., phase diagram, miscibility gap 7-53706
- CoO₂, sputtered thin, annealing effects on mag. props. and structure, Co-CoO layer separation 7-27180
- CoO₂-FeO_x selective coatings, spray pyrolysis for high temp. appls. 7-5974
- Co_{1-x}O, defect cluster energies, MO calc. 7-2010
- Co_{1-x}O, dopant cations interaction with 4:1 defect clusters, theoretical study 7-63644
- Co₃O₄ sputtered films, optical props. 7-46167
- Co₃O₄-Al₂Si₂O₅(OH)₄, X-ray anomalous scatt. difference patterns in powder diff. anal. 7-16356
- Co₃O₄-P₂O₅ glass system, thermal analysis from room temp. to softening pt., vibr. anharmonicity, US vel. 7-12221
- Co_{1-x}Rh_x(Ru_x)S₂, prep., mag. and crystallographic props. 7-33154
- CoS_{1.035} film, soln. growth, optical absorpt. coeff. 7-39446
- CoSO₄·7H₂O, liquid optical filter anal. for hybrid solar energy conversion 7-50724
- CoSi form. by ion implantation in Si, RBS and X-ray diff. studies 7-16656
- CoSi, heat of form. evaluation from X-ray emission spectra (Russian) 7-59776
- CoSi layers, prep. by Co silicidation using Si₂Cl₆ source by diffusion and CVD processes, microhardness meas. 7-17700

cobalt compounds continued

- CoSi₂, epitaxial growth, conf., Toronto, Ont., Canada (May 1985) 7-9588
- CoSi₂, MBE growth, struct. props. and device appls. 7-21738
- CoSi₂ optical props., refl. and spectroscopic ellipsometry meas., hybridisation effects 7-39073
- CoSi₂, self-aligned silicide technology using rapid thermal processing 7-52154
- CoSi₂, thin film, electrical transport props. 7-27442
- CoSi₂, thin films, self-diffusion of Si, study using radioactive ³¹Si tracers 7-2263
- CoSi₂-Si, mesotaxy, single crystal growth of buried CoSi₂ layers 7-58671
- CoSi₂-Si, solid phase epitaxial growth of CoSi₂, nonultrahigh vacuum method 7-45043
- CoSi₂-Si epitaxial heterostructures, growth and characterisation 7-27212
- CoSi₂-Si heterostructures, MBE or solid phase epitaxially grown, Schottky barrier heights, DLTS spectra 7-12859
- CoSi₂-Si heterostructures, epitaxial growth 7-39387
- CoSi₂-Si Schottky barriers, epitaxially grown, supercond. below 1.05K, tunnelling spectra 7-12860
- CoSi₂, Mossbauer spectroscopy 7-59126
- CoSi₂ layers, prep. by Co silicidation using Si₂Cl₆ source by diffusion and CVD processes, microhardness meas. 7-17700
- CoSiF₆·6H₂O, phase transitions detected by positron lifetime meas. 7-38191
- Co₂SiO₄, decomp., O₂ pot. gradient, stability investig. (German) 7-17767
- Co₂Ta₂S₆, channel structs., 3d metal pairing 7-26719
- Co₂TiS₂, intercalation cpd., elec. resist. and thermopower studies 7-45331
- Co_{0.46}Zn_{0.54}In₂S₄ layer cpd. mag. props. and ionic distrib., 2D magnetic system models 7-38880
- Co₂Zn_{1-x}In₂S₄ pseudoternary layers cpds., optical props., comp. depend. studies 7-39072
- Co₂Zn_{1-x}In₂S₄ solid soln. layer cpd., site coordination and short range magnetic order, XPS anal. 7-26724
- ⁵⁷Co EC decay chemical effects in Co(III) complexes 7-23048
- CoCoCl₂·2H₂O, 1D antiferromagnet, exciton transfer, absorpt. spectra 7-27254
- Co₃Co₄NO₃, synthesis and cryst. struct. (French) 7-32401
- Cu₂Co₃O₄, cationic distribution and mag. props. 7-26726
- FeCo oxides, oxidation state and site symmetry, EXAFS and XANES studies 7-63584
- Fe_{1-x}Co_xCl₂, Fe²⁺ localised excitation and spin orientation, ESR studies 7-64524
- Fe_{1-x}Co_xCl₂, random-field and competing-anisotropy effects, sp. ht. study 7-2872
- FeCoCr₂S₈, crystallographic and mag. props., Mossbauer study (Korean) 7-33310
- Fe₃Co₃Si₁₀B₁₂, magnetic induced anisotropy, crossover effect 7-17169
- KCoF₃ antiferromagnetic cryst., electronic Raman scatt. by high-energy magnetic excitons 7-46016
- K₂Co₂Fe_{1-x}F_x, oblique antiferromag. phase, spin waves, inelastic neutron scatt. study 7-64443
- La-Co-O system, nonstoichiometric K₂NiF₄-type phases 7-37936
- La₂Co₄P₁₂, synthesis, cryst. struct., X-ray diff. study 7-32387
- La₂Li_{0.5}Co_{0.5}O₄·⁵⁷Co, Ti, ⁵⁷Fe⁴⁺, anomalous charge state obs., ⁵⁷Co³⁺ nuclear decay studies 7-21881
- LuCo_{1-x}Si₂, cryst. struct., homogeneity range, X-ray diff., electron probe anal. 7-37939
- Mn_{1-x}Co_xAs, phase transitions, effect of external press. and chemical substitutions 7-63798
- Na₂(Co,Co)ZrP₃O₁₂ and Na₂(La,Co)TiP₃O₁₂, Nasicon analogues, cryst. data 7-12014
- Nd₂Co₄P₁₂, synthesis, cryst. struct., X-ray diff. study 7-32387
- NiCoFe ferrite, perminvar, wall displacements, induced anisotropy effect. 7-52968
- Ni_{1-x}Co_xFe₂O₄ polycryst. magnetostrictive ferrite, long-term bulk acoustic wave memory 7-59099
- Ni_{1-x}Co_xO₄ spinels, prep. by thermal decomposition of mixed hydroxide nitrates 7-13424
- Pr_xCo₄P₁₂, synthesis, cryst. struct., X-ray diff. study 7-32387
- Se₃Co₄, cryst. struct. determ. 7-58241
- Si-CoSi₂-Si, heterostructure transistor, electrical transport props. 7-27442
- Si-CoSi₂-Si, transistor current modulation (French) 7-58894
- SrFe_{1-x}Co_xO₃, Mossbauer spectroscopic studies 7-59130
- Ti₂Co_{1+x}Fe_{2-2x}O₄ spinel solid soln., mag. props., Mossbauer effect study 7-12685
- Ti₂Co(SeO₄)₂·6H₂O·Mn²⁺, electron spin resonance studies 7-45809
- UCoGa₅, structural chemistry, mag. behaviour 7-16513
- Y₂Co₇H₈ hydrides, cryst. struct. and mag. props., H effects (Russian) 7-44468
- Yb₂Co₄P₁₂, synthesis, cryst. struct., X-ray diff. study 7-32387
- Zn_{0.5}Co_{0.5}FeCrO₄, cluster spin glass, spin freezing 7-27531
- ZrO₂-Y₂O₃-Co₃O₄ materials, Co₃O₄ effect on struct. and phase comp. 7-27990

cochlea see ear**codes**

see also encoding

- functional neuromuscular stimulated hand orthoses, sensory feedback using electrodes fitted to shoulder 7-34354
- impulse response measurement using Golay codes 7-37304
- pitch perception model 7-40174

coding see encoding**coefficient of thermal expansion** see thermal expansion**coercive force**

see also magnetic hysteresis

- alumite disc prep. using anodic oxidation (Japanese) 7-46672
- bubble films, coercive force control mechanism (Russian) 7-45776
- bubble garnet films, coercive force determ., microwave absorpt. meas. 7-59096
- ferromagnetic hysteresis, domain wall pinning, mathematical model anal. 7-7544
- films, coercive force establishment, magnetoelastic interaction effects (Russian) 7-7558
- magnetic stripe domain structs., stability and temp. hysteresis model calcs. 7-7535
- magnetics, conf., Japan (Nov.1985) 7-24259
- magnetisation coercive force for industrial alloys YuN14DK34T5, YuNDK15, YuN14DK24 and YuN14DK25BA 7-17202
- meter with U-shaped electromagnet, operation rel. to test piece cross-section area 7-329

coercive force continued

- misc metal-Fe-B melt-spun magnets, mag. and structural props.
 7-53032
 particulate magnetic recording tapes, hysteretic props. ang. depend. studies
 7-53058
 particulate recording media, magneto-optic Kerr effect hysteresis loop
 meas. 7-48782
 Permalloy thin films heads, RF sputtered, mag. props. 7-33235
 phase analysis, porosity, mag. meas. methods 7-28240
 polycrystalline permanent magnet, texture influence on coercive field
 strength computation (German) 7-2902
 rare earth alloys, $R_2(Fe,Al,Co)_{12}B$, mag. props., composition depend.
 7-53030
 rare earth-Fe-B alloys, sintered permanent magnets, depend. of coercivity
 on anisotropy field 7-45744
 sputtered magnetic thin film, ion beam irradi., struct. studies 7-22588
 steel, austenitic, cold deformed, mag. props. (Russian) 7-45734
 steel, Cr-Si type parts, mag. characts. after isothermal hardening, heat
 treatment quality inspection method 7-65261
 steel, dual-phase, Bauschinger effect and coercivity, effect of ageing
 (Chinese) 7-8045
 steel, low C, magnetoacoustic emission, magnetisation, Barkhausen effect
 in decarburised steel 7-33207
 steel, structural, heat treated, coercivity in various remanent magnetization
 states, NDT method development 7-65259
 structural steels, coercivity and Barkhausen noise power spectrum, stress
 depend. meas. 7-7548
 surface magnetism, study by spin polarised electrons 7-2901
 Ba ferrite filled styrene-isoprene-styrene composite, dynamic mech., elec.
 and mag. props. 7-13001
 $BaFe_{12-2x}Co_xTi_xO_{19}$ superfine particles, coercivity conc. and aspect ratio
 depend. meas. 7-53054
 $BaFe_{12}O_{19}$ films, RF diode sputtering prep. and mag. props. (Japanese)
 7-7852
 $BaFe_{12}O_{19}$ fine powder for particulate perp. mag. recording media, coer-
 civity meas. method 7-59062
 $BaFe_{12}O_{19}$ particulate coatings, pigment-to-binder loading effects
 7-53056
 Ce-(Fe,Co)-(B,Si) system alloys, melt spun ribbons, mag. props.
 (Japanese) 7-53052
 Ce(Co,Cu,Fe)₆, magnetically hard, heat treatment effects on struct. and
 mag. characts. 7-27564
 Co-Al alloys, magnetic hardening 7-33209
 Co-CoO multilayered films, exchange anisotropy 7-27579
 Co-Cr, continuously sputtered films, crystallographic orientation and mag.
 props. 7-27176
 Co-Cr films, sputter deposited, effects of additive gases on mag. props.
 7-27575
 Co-Cr perpendicular recording media, props., effect of impurity gases
 7-59069
 Co-Cr sputtered films, microstructural inhomogeneity, mag. props.
 7-45768
 Co-Cr thin films, DC magnetron sputtered, mag. props., effect of sub-
 strate and deposition rate 7-59067
 Co-Fe bilayer thin films, annealing behaviour, mag. props. 7-59079
 Co-Gd-Tb-based thin films, properties and stability for magneto-optic
 recording 7-53075
 Co-Mg coevaporated films, prep. and mag. props. 7-53082
 Co-Ni-Fe underlayer for double-layer perpendicular media, vacuum
 deposition and mag. props. 7-27577
 Co-Ni-P electroless plated thin films, microstructure, mag. props., mag.
 recording appl. 7-27581
 Co-P electroless plated thin films, microstructure, mag. props., mag.
 recording appl. 7-27581
 Co-Pt bilayer thin films, annealing behaviour, mag. props. 7-59079
 Co-Si-B amorphous alloys, mag. props., annealing effects 7-27513
 Co-Ti(Pt) sputtered films, mag. props., O impurity effects 7-33238
 Co-W-P electroplated alloys, struct. and mag. props. (Russian) 7-2428
 Co-Zr amorphous films, low energy ion beam sputtering, mag. props.
 7-53081
 $Co_{100-x}B_x$ amorphous sputtered thin films, magnetic anisotropy origins
 7-27583
 CoCr corrosion-resistant alloy films, mag. props. and longitudinal record-
 ing performance 7-33226
 CoCr evaporated films, mag. props. 7-33225
 CoCr films, magnetisation reversal mechanisms 7-59068
 CoCr films, sputter deposition, mag. characteristics of initial deposition
 layer 7-27574
 CoCr films, vacuum evaporation, thickness depend. of mag. props.
 7-27576
 CoCr Permalloy films, weather resistance 7-28183
 CoCr sputtered films, struct. and mag. props., role of atomic mobility
 during film growth 7-33224
 CoCr sputtered perpendicular recording media, with columnar micros-
 struct., reversal mech. 7-7552
 CoCr thin films on metallic underlayers, mag. characts. 7-27573
 CoCrTa corrosion-resistant alloy films, mag. props. and longitudinal
 recording performance 7-33226
 $Co_{74}Fe_{26}B_{20}$ amorphous sputtered thin films, magnetic anisotropy origins
 7-27583
 CoFeCr sputtered films, struct. and mag. props. 7-27175
 $CoFe_2O_4$ ferrite epitaxial layers, high coercivity (Chinese) 7-38908
 $Co_{70}Fe_{46}Si_{13}B_{10}$ amorphous alloy, mag. props. rel. to mag. coating
 7-22123
 $Co_{71}Fe_{25}Si_{13}B_{10}$ and $Co_{75}Si_{13}B_{10}$ amorphous alloys, mag. props., stress and
 annealing depend. 7-33250
 $CoNbTi/SiO_2$ amorphous layered films, high freq. permeability 7-53078
 $Co_{80}Nb_{10}Ti_{10}SiO_2$ amorphous multi-layered films, mag. props. rel.
 to film thickness 7-2912
 CoNi sputtered films on Cr and polyimide, mag. props., relation to struct.
 7-33228
 CoNi thin films, oblique-deposited, mag. props., O impurity effects
 7-33244
 CoNiCr-Cr sputtered thin films, film struct., mag. props. 7-33227
 CoNiFeCr alloy films for perpendicular mag. recording, thickness depend.
 of perpendicular coercivity 7-59066
 CoO_x sputtered thin, annealing effects on mag. props. and structure,
 Co-CoO layer separation 7-27180
 CoPtTi thin films, magnetic and microstructural props. 7-33230
 $Co_{70}Si_{30}$ amorphous films, coercive force rel. to crystallisation (Russian)
 7-59078

coercive force continued

- CoTi-CoNb amorphous alternating layers, magnetic and diffusional props.
 study 7-7563
 Cu-Fe-Al, cold rolled, γ to α transform. of fine α -Fe precipitates, mag.
 props. 7-3300
 Cu-Mn-Al alloys, mag. and structural props. study 7-2895
 $CuFe_{2-x}Al_xO_4$ system, mag. props. 7-45740
 $Dy_{1-x}Al_x$, intrinsic coercive field 7-45728
 DyFe alloys, amorphous thin films, thermomag. recording, magnetisation
 reversal, coercivity 7-64459
 DyIG:Ga,Bi, RF sputtered films for magneto-optical memory, mag. props.
 7-64613
 DySe-USe system, mag. props. of solid solns. 7-22121
 $Dy_xY_{1-x}Al_2$, intrinsic low field susceptibility studies 7-45633
 $Dy_xY_{1-x}Al_2$, intrinsic coercive field 7-45728
 $ErAl_2$, intrinsic coercive field 7-45729
 $Er_{0.135}Fe_{0.813}B_{0.052}$ melt spun ribbons, mag. and struct. props. 7-59059
 Fe thin films, sputter deposited at oblique incidence, microstruct. and
 mag. props. (Japanese) 7-33560
 Fe-based thin films, saturation magnetisation and coercive force 7-59074
 Fe-Co alloys, powder metallurgy produced, mag. props. 7-33211
 Fe-Co-Mn(V) films, ion beam sputtered, soft mag. props. 7-33237
 Fe-Cr-Co solid soln., uniaxial tensile stress in spinodal decomp. effect on
 coercive force, thermomag. treatment effects 7-7555
 Fe-Cr-Co-Mo permanent magnet ribbons, mag. props., influence of modu-
 lated structure 7-53043
 Fe-Cr-Co-Si-Ti, permanent mag. alloy, ductile, effect of heat treatment on
 mag. props. (Korean) 7-8137
 Fe-Dy-C high coercivity permanent magnet materials 7-2903
 Fe-Mo (14.5 wt.%), ageing, discontinuous dislocational transform., coer-
 civity obs. 7-3305
 Fe-Nd-B magnets, microstructure and mag. props. 7-53049
 Fe-Nd-B permanent magnets, prep. by liquid dynamic compaction
 7-53661
 Fe-Ni evaporated films for a back layer of perpendicular mag. recording
 media, origin of high coercivity 7-27578
 Fe-Ni evaporated films for a back layer of perpendicular mag. recording
 media, prep. 7-27908
 Fe-Pt (36 at.%), cryst. struct., permanent mag. props. (Japanese)
 7-53036
 Fe-R-B (R=rare earth) metallic glass permanent magnets, struct. and
 mag. props. 7-27565
 Fe-Si, rapidly quenched ribbons, grain growth, mag. props. 7-8017
 Fe-Si, structure, texture and mag. props. 7-12995
 Fe-Si (3.2 wt.%), mag. props., influence of substructural features
 7-12996
 Fe-Si-Al, Sendust films, DC opposite sputtered, mag. and crystallographic
 characteristics 7-7847
 Fe-Si-B amorphous alloys, hypoeutectic, thermal stability and soft mag.
 props. 7-11928
 Fe-SiO₂ compositionally modulated mag. film props. study 7-7566
 Fe-Tb amorphous alloys, film and bulk mag. props. and thermal expansion
 meas. 7-7540
 Fe-X, X=Al, Si, Nb, Ti, Zr, coercive field measurements 7-64491
 (Fe-B)₈₅Nd₁₅ amorphous films, soft mag. props. 7-53077
 $Fe_{78}B_{13}Si_9$ amorphous ribbons, ferromag. resonance 7-27606
 $Fe_{78}B_{13}Si_9$, magnetron sputtered amorphous alloys, thermal, mag. and
 magnetomechanical props. 7-33249
 $Fe_{80}Si_{18}B_2$ amorphous alloy ribbons, processing conditions rel. to mag.
 prop. changes (Korean) 7-7919
 $Fe_{80}C_{20}Si$ compositionally modulated amorphous struct., mag. and diffu-
 sional props. study 7-7564
 $Fe_{70}(CeNdPr)_{20}B_{10}$, rapidly quenched ribbons, hard mag. props. 7-27562
 $Fe_{70}Co_{30}SiO_2$ compositionally modulated mag. film props. study 7-7566
 (FeCo)₉₀B₁₀ amorphous ultrafine particles, mag. props. 7-53063
 $Fe_{14}Nd_{16}B$ permanent magnet, Dy substituted positron annihilation studies
 7-3108
 $Fe_{16}Nd_{16}B_8$ plasma sprayed permanent magnets, characts. 7-45754
 FeNiAlCoTiCuS permanent magnetic material, phase comp. and ordering,
 atom probe FIM and TEM studies 7-33635
 $Fe_{40}Ni_{40}B_{20}$ amorphous thin films, coercive field, annealing effects
 7-7553
 $Fe_{40}Ni_{40}B_{20}$ amorphous alloy, effect of plastic deform. on mech. and mag.
 props. (Russian) 7-53810
 γ -Fe₂O₃ acicular particles, magnetisation reversal by flipping mechanism
 7-7545
 γ -Fe₂O₃ films, CVD deposited, uniaxial mag. anisotropy 7-33234
 γ -Fe₂O₃ particles, microstructure, X-ray diff., magnetisation props.
 7-45757
 γ -Fe₂O₃ reactive RF sputter deposition, struct., elec. and mag. props.
 studies 7-17421
 γ -Fe₂O₃ thin films, mag. props. 7-33233
 Fe₂O₃ Co particles, coercivity time-scale depend., magnetic switching units
 vol. determ. 7-53059
 $Fe_{67}Si_{33}$ amorphous films, coercive force rel. to crystallisation (Russian)
 7-59078
 $Fe_{77}Si_{16}B_{13}$, as-quenched and cold-rolled amorphous alloy, mag. props.
 7-33219
 $Fe_{78}Si_{12}B_{10}$ amorphous alloys, surface crystallisation and mag. props.
 7-51649
 $Fe_{80}Si_{20-x}$ amorphous alloys, struct., mag. and elec. props. (Korean)
 7-2893
 $Fe_{0.458}Sn_{0.088}O_{0.454}$ film, mag. props., appl. in perpendicular mag. record-
 ing 7-59005
 $Fe_{84-x}V_xB_{16}$ amorphous alloys, crystn., products and kinetics 7-51677
 Gd-Co compositionally modulated mag. film props. study 7-7566
 GdCo and GdTbFeCo alloys, amorphous thin films, thermomag. record-
 ing, magnetisation reversal, coercivity 7-64459
 $Gd_{1-x}Si_x$, x=0.18, 0.59, 0.87, amorphous, thermal, elec. and mag. props.
 7-53039
 GdTbFe, corrosion resistance improvement by metal coatings 7-53952
 Ho₂Fe₄ amorphous ribbons, mag. props. 7-33177
 Li ferrites, microstruct. effects on mag. props. (German) 7-59052
 $(Mn_{0.9}Fe_{1-m})_{100-x}B_{1-x}$ films, evaporated, structure and mag. props.
 (Japanese) 7-59077
 (Nd,Tb)_{16.7}Fe_{75.5}B_{7.8}, magnetisation meas., spin reorientation temp.
 7-17161
 Nd-Dy-Fe-B-based sintered magnet, microstruct., heat treatment effects
 7-53767
 Nd-Fe-B amorphous ribbons, effect of crystallisation conditions on hard
 mag. props. 7-27561

coercive force continued

- Nd-Fe-B based permanent magnets, hysteresis loop and mag. anisotropy 7-53031
 Nd-Fe-B liquid-quenched alloys, mag. props. 7-27550
 Nd-Fe-B permanent magnet, microstructure and coercivity 7-27559
 Nd-Fe-B rapidly solidified permanent magnet materials, magnetisation processes and domain wall motion 7-38902
 Nd-Fe-B rapidly solidified ribbons, magnetisation, quench rate depend. 7-53034
 Nd-Fe-B sintered magnets, hysteresis loops, anal. 7-33215
 Nd-Fe-B system, permanent magnet, mag. props. (Korean) 7-7554
 Nd-Fe-B system, temp. depend. of coercive force, effect of annealing, aging and sintering 7-27560
 Nd-Fe-B-Co-Al based permanent magnets, mag. props. and temp. characts. 7-53045
 NdFeB, anisotropic permanent magnet, prep. and investig. 7-52969
 Nd₂Fe₁₄B sputtered films, perpendicular anisotropy 7-53073
 NdFeB/CoAl magnets, Curie temp., coercive force and magnetisation 7-52982
 Nd₂Fe_{14-x-y}Co_xAl_yB alloys, permanent mag. props. 7-45755
 Nd₂(Y₂)(Fe_{1-x}Al_x)₁₄B, intrinsic and permanent mag. props. (Chinese) 7-13003
 Ni, dislocation structure after US deformation, physical props. (Russian) 7-44699
 Ni-Fe-In ternary Permalloy electroplated films, mag. props. and thermal stability 7-33236
 Ni-Zn ferrite and Ni ferrite films, prep., mag. props. 7-13378
 NiCoP onefold layer, domain propag. along hard axis 7-45727
 PbO-Fe₂O₃-B₂O₃ glass ceramics, mag. props. and EPR spectra of precipitated mag. phases 7-45748
 Pr-Co rapidly quenched ribbons, mag. props. 7-27551
 PrCo₅, microstructure and coercivity, effect of annealing, 650-850°C 7-38905
 Sm-Co amorphous thin films, low temp. mag. props. (Chinese) 7-38910
 Sm-Co-B rapidly quenched ribbons, hard mag. props. and struct. 7-53048
 Sm-Fe amorphous thin films, low temp. mag. props. (Chinese) 7-38910
 Sm-Fe-Co-B-Si melt-spun alloys, mag. props. 7-27553
 Sm₂(Co, Fe, Cu, Zr)₁₇ sintered compact permanent magnet, mag. props., comp. and heat treatment effects (Korean) 7-2894
 SmCo₅, anisotropic permanent magnet, prep. and investig. 7-52969
 Sm₂(CoCu)₁₇ magnets, cast, coercivity and microhardness 7-53880
 Sm₂(Co_{1-x}M_x)₁₇ (M=Fe,Mn), rapidly quenched ribbons, mag. props. 7-27552
 Sr ferrite fine particles, prep., mag. props. (Japanese) 7-53065
 SrO.56Fe₂O₃, doped with kaolin and BaB₂O₄, sintering temp., effect on structural and mag. parameters 7-7543
 TbCo film, optical disc memory struct., mag. props., underlayer film treatment effect 7-45767
 TbCo sputtered films, compositionally modulated, mag. props., magneto-optical storage appl. 7-64495
 TbFe and GdTbFeCo alloys, amorphous thin films, thermomag. recording, magnetisation reversal, coercivity 7-64459
 TbFeCo/dielectric interface, chemical stability, interdiffusion and oxidation, AES, XPS and RBS depth profile studies 7-12513
 TbFeCo-based amorphous films, magneto-optical recording appls. 7-53074
 Tb₂Gd_{1-x}Al_x, intrinsic low field susceptibility studies 7-45633
 Tb₂Gd_{1-x}Al_x, intrinsic coercive field 7-45729
 Tb₂Si_{1-x}, x=0.18, 0.59, 0.87, amorphous, thermal, elec. and mag. props. 7-53039
 Ti-N-Permalloy ferromag. multilayers, prep. and props. 7-64497
 Y-Fe-B system alloys, mag. props. 7-27563
 Y₂(Fe,Al,Co)₁₄B, mag. props., composition depend. 7-53030
 YIG:Ga, Bi, RF sputtered films for magneto-optical memory, mag. props. 7-64613
 Zn_{1-x}Ge_xFe₂O₄, ferrites, atomic, mag. and electronic disorder (French) 7-44477

coercivity *see* **coercive force****coexistent superconductors** *see* **magnetic superconductors****cogeneration**

- energy issues of various countries, cogeneration, oil, gas, coal gasification, book 7-48200
 flue gas purification develop. in coal-fired heat power plants (German) 7-46981
 heat storage from cogeneration processes, basin construction and measuring concept, west Berlin 7-65614
 technology breakout in energy conversion, conf., San Diego, CA, USA (Aug. 1986) 7-60875

cognitive systems

- see also* **adaptive systems**; **artificial intelligence**; **automata theory**
 brain organisation in cognition, matrix and convolution models 7-47058

coherence*see also* **light coherence**

- electron, coherency matrix description 7-15811
 field correls. in a fluctuating homogeneous medium, spectral coherence, dynamical struct. factor determ. 7-41119
 free electron lasers, self-amplified spontaneous emission and coherent amplification 7-15881
 inverse optics, conf., San Diego, CA, USA (Aug. 1985) 7-60869
 inverse source problem comparison for quasihomogeneous, partially coherent sources in two and three dimensions 7-62597
 laser radiation, diffusely scattered, spatial coherence and its meas. 7-20134
 phase problem, complex coherence function 7-9710
 quantum dissipative system, dynamics and phase coherence 7-9709
 radiation coherence influence on nonlinear optical phenomena (Rumanian) 7-15924
 radiometry and radiative transfer theory, general mapping of cross-spectral densities in second-order coherence theories 7-4879
 relativistic charged particles, coherent curvature radiation pulse duration 7-1015
 soft X-rays from lasers, undulators and plasmas, coherence props. 7-18956
 X-ray partially coherent radiation, props. and appls. 7-24738

coherence distance *see* **coherence length****coherence length**

- Ginzburg-Landau equations for triplet local-electron-pair systems 7-45547

coherence length continued

- heavy electron superconductors, normal impurity effects, excitation spectrum 7-27462
 thin films, critical temp. enhancement, coherence length mag. field depend. effects 7-58944
 thin supercond. films, parallel nucleation field determ., quasiclassical BCS theory calcs. 7-7458
 Nb/n-InAs/GaAs/Nb SNS heterostructure weak link 7-52898
 Si/Nb, proximity effect, superconducting transition temp. meas. 7-45566
- coherent accelerators** *see* **collective accelerators**
- coherent antiStokes Raman scattering**
 acetone, stretching vibrs., CARS study 7-42623
 applications in chemical reactors, combustion and heat transfer 7-17788
 benzene, CARS, shock-compression induced frequency shifts 7-22272
 benzene, stretching vibrs., CARS study 7-42623
 benzene-CS₂ mixtures in soln., vibr. dephasing 7-42624
 chloroethane, IR multiphoton excitation probed by CARS, vibr. population distrib. 7-10591
 coherent UV- and VUV- radiation generation, antiStokes Raman process 7-11062
 combustion and plasma diagnostics appl. 7-16332
 cycloheptatriene, isomerisations, kinetic CARS appls. 7-36630
 drops, micron-size, nonlin. optical processes 7-11063
 dye solution, reson. CARS line shape anal. for conc. series 7-15611
 flames, diffusion, bluff-body stabilised, near-wake region, CARS meas. 7-8282
 free jet spectroscopy by coherent Raman methods 7-15003
 liquids, molecular, CARS, femtosecond pulses appls. 7-62375
 methane in supersonic molecular beams CARS of ν_3 band 7-25876
 methane-air laminar counterflow diffusion flames, struct., CARS meas. 7-57939
 mobile CARS instrument for combustion and plasma diagnostics 7-44238
 nitromethane, CARS, shock-compression induced frequency shifts 7-22272
 non-thermal pump effects in broadband CARS 7-43228
 phenol adsorbed on ZnO surface, surface CARS spectroscopy 7-46036
 plasma, gaseous, cubic optical nonlinearities 7-1703
 pyridine adsorbed on ZnO surface, surface CARS spectroscopy 7-46036
 rhodamine 6G in ethanol reson. CARS line shape anal. for conc. series 7-15611
 rotational CARS generation through multiple four-colour interaction 7-50632
 single-pulse, noise props. with multimode pump sources 7-48866
 spontaneous Raman temp. sensor, based on signal backscattering from multimode fibre 7-41387
 surfaces with adsorbed molecules, surface coherent antiStokes Raman spectroscopy as analytical tool 7-1233
 third-order nonlinear susceptibility, dispersion formula validity 7-15929
 three-laser CARS meas. of two species 7-46897
 VUV radiation generation by antiStokes Raman laser process 7-11050
 CS₂-benzene mixtures in soln., vibr. dephasing 7-42624
 D₂, hyperpolarisabilities, vibr. contribs., CARS 7-57074
 GaP, phonons, ps laser induced transient dynamics 7-39113
 H₂, hyperpolarisabilities, vibr. contribs., CARS 7-57074
 H₂, photodissociation processes, CARS (French) 7-5726
 H₂ rovibrational population in H⁺ source, CARS time-resolved meas. 7-10605
 H₂ VUV anti-Stokes Raman line generation using excimer lasers 7-57450
 H₂-He, photodissociation processes, CARS (French) 7-5726
 H₂O, third-order nonreson. susceptibility relative value, CARS meas. 7-50633
 N₂ 7-26268
 N₂, coherent anti-Stokes Raman spectra, two-colour, theoretical modelling 7-25879
 N₂, flowing and post discharge, vibr. level, CARS spectroscopy (French) 7-11810
 N₂ fluid, high temp. and press. vibrational spectra, CARS study 7-53326
 N₂ gas in thermal equilib. at 3467 K, CARS spectrum 7-62377
 N₂, hyperpolarisabilities, vibr. contribs., CARS 7-57074
 N₂ in gas discharge, vibr. levels excitation, CARS obs. 7-20021
 N₂ multiplex CARS temperature meas. precision using single-mode and multimode pump lasers 7-41376
 N₂, nonequilib. vibrational states distrib. kinetics, wide-band CARS study 7-31154
 N₂ plasma diagnostics using coherent anti-Stokes Raman spectroscopy 7-16333
 N₂ self-broadening at high temp. with inverse Raman spectroscopy 7-5723
 Na+H₂, energy transfer expts., CARS 7-10719
 O₂, hyperpolarisabilities, vibr. contribs., CARS 7-57074
 O₂, IR multiphoton excitation probed by CARS, vibr. population distrib. 7-10591
 SF₆, IR multiphoton excitation probed by CARS, vibr. population distrib. 7-10591
 Si optical phonon spectrum transform. obs. under laser pulse bombardment, CARS study 7-51967
 TiO₂ film on Nb₂O₅ waveguide, surface CARS spectroscopy 7-46036
 W lamp, temperature and pressure profiles, high-resolution CARS measurements 7-41377
 ZnSe, phonons, ps laser induced transient dynamics 7-39113

coherent optical transients *see* **optical coherent transients****coherent potential approximation** *see* **CPA calculations****cohesive energy** *see* **binding energy****coils***see also* **inductors**; **solenoids**

- 3D, conducting structures with pulsed excitation, time domain anal. of eddy current effects 7-62573
 CANDU nuclear reactor, EM pulse power coils for coolant tube spacer repositioning 7-49566
 complete localization of in vivo NMR spectra using two concentric surface coils and RF methods only 7-28751
 constant determ. in γ - π expt. at PTB 7-18739
 Helmholtz coils for generating mag. fields, optimisation using computational method 7-48791
 Lisitano coils, Al and Cu, plasma production, comparisons (Japanese) 7-11655
 lumbar spine NMR imaging, comparison of circular and elliptical coils 7-3858

coils continued

- medical NMR, breast coil, design modification 7-14085
 NMR imaging of breasts, receiver coil 7-65831
 quadrature coil for NMR imaging 7-14087
 receiver coils in NMR imaging, phase and sensitivity 7-54700
 RF coils, importance for NMR tomography 7-3854
 spheromak shift instability, critical field index for passive coil stabilisation 7-44230
 surface coil design for a vertical field MRI system, breast imaging appl. 7-18048
 surface coil for in vivo ^1H NMR, pulse sequences 7-14166
 surface coil proton NMR imaging at 2T, coil design and appl. 7-28653

coincidence circuits

- see also counters
 electron microscopy, analytical, coincidence counting techniques 7-23104
 priority switching in measurement of time spectra of gamma-gamma coincidences 7-10369

coincidence techniques

- 16 discriminator and 16 strobed coincidence ECL (*Italian*) 7-25334
 accidental-coincidence corrections, discrepancies determ. 7-49858
 accidental-coincidence corrections 7-30908
 anticoincidence counting system, absolute activity meas. (*Korean*) 7-25329
 atomic beams, resonance ionisation spectroscopy, coincidence detection 7-57188
 1,3-butadiene ions, photodissoc., photoelectron photoion coincidence study, isomerisation barrier meas. 7-36711
 hybrid Monte Carlo-analytical model of neutron coincidence counting 7-30906
 in-plant neutron coincidence counting in nucl. materials processing plants, status 7-30904
 modular acquisition system for coincidence data 7-49850
 priority switching in measurement of time spectra of gamma-gamma coincidences 7-10369
 selective sampling method, activity standardisation 7-56917
 small molecules, multiple photoionisation and photodissociation, mass spectrometer and coincidence studies 7-19965
 spectrometer with scintillation and planar detectors, time characts. 7-36438
 thermal in coincidence counting, rejection of outliers 7-30909
 BeO, neutron multiplication study by shift register coincidence technique 7-30467
 Ge detectors, high pressure large volume, pulse shaping system for fast coincidence 7-49814
 H_2O , positron age-momentum correlation meas. 7-36440
 N_2 soft X-ray-induced fragmentation, Auger electron-ion coincidence studies 7-42697
 NH_3 , double photoionisation and fragmentation, PIPICO method anal. 7-19985
 NaI:TL, triple-coincidence spectrometer for ^{26}Al , ^{22}Na 7-25317
 $^{16}\text{O}(\pi^+, \pi^+ p)$ cross section, coincidence meas. 7-42078
 ^{103}Pd decay, absolute photon intensities determ. by coincidence method 7-5569
 a-Si:H films, depth profiling of constituents and impurities, elastic proton scatt. 7-45044

cold-cathode tubes

- see also counting tubes; photomultipliers; phototubes
 No entries

cold rolling

- cold heading workshop noise 7-20505
 polyethylene, cold-rolled low-density, morphology and transport props. 7-13519
 steel, austenitic stainless, microstructure rel. to cathodic H charging 7-28039
 steel, cold rolled, Ni activated phosphating, corrosion resist., durability, strength 7-28187
 steel, cold-rolled, corrosion investig. by thermal-wave microscopy 7-28169
 steel, Cr type, dislocation struct. after hydraulic pressing followed by austempering 7-3334
 steel, deep drawing, recrystn. texture development, investig. by ODF anal. 7-13466
 steel, low C, cold rolled lamination, mag. props., Mn and S contents effect 7-7550
 steel, low C lamination, decarburization, grain size, carbide morphology 7-8016
 steel, mild, cold-form-rolled, rotary bending fatigue behaviour (*Japanese*) 7-53866
 steel, plain C, cold-rolled, texture and lattice deform. states (*German*) 7-53765
 steel sheet, low C, Al-killed, cold-rolled, batch-annealed, recrystn. model for controlling mech. props. 7-13474
 Al, repeated cold rolling effect on recrystn. Vickers hardness obs. 7-59543
 Cd, polycrystalline rolled sheets, flow stress, hydrostatic press. effect, 600 MPa (*Japanese*) 7-33735
 Cu-Fe-Al, cold rolled, γ to α transform. of fine α -Fe precipitates, mag. props. 7-3300
 Cu-Ni-Al (7.5, 2.5 at.%), thermomech. treatment (*Japanese*) 7-8013
 Er-Cu (Ni) metallic glass form. by near-isothermal cold rolling 7-22610
 Fe, rolling texture, effect of parity 7-59548
 Fe-Al(Si) cold-rolled nonbrittle powder strip prep., texture and mag. props. 7-46370
 Fe-B, amorphous, structural characterisation by laboratory EXAFS spectrometer 7-1911
 Fe-Mn-Al, processing and props., effect of Si and C additions 7-17707
 Fe-Si, plasticity, influence of thermomechanical parameters 7-13512
 Fe-Si (3 wt.%), secondary recrystallisation, sharp ribbed texture formation 7-13469
 Fe-Si (3 wt.%), secondary recrystallisation, seed grain formation, influence of elastic anisotropy energy 7-13470
 $\text{Fe}_{40}\text{Ni}_{40}\text{B}_{20}$ amorphous alloy, effect of plastic deform. on mech. and mag. props. (*Russian*) 7-53810
 Nb-N, internal friction rel. to quenching temp. (*Russian*) 7-46543
 Ni-Cr superalloy, heat-resistant, heat treatment effect on ductile props. in cold deform. 7-46584
 Ni-Si-B, nonferromagnetic amorphous wide ribbons, Young's modulus anisotropy 7-3354
 Ni_2Cr , recrystn. kinetics and mech. props., influence of P 7-22718
 Pd membrane, diffusion of H_2 , transport coeffs. and energetics 7-21533

cold rolling continued

- Pd-Si, nonferromagnetic amorphous wide ribbons, Young's modulus anisotropy 7-3354
 δ -Pu-Ga (1.5 wt.%) foils, cold rolling, annealing, microstruct., TEM obs. 7-59544
 Ti alloy metastable phases, plasticity (*Russian*) 7-33729
- cold shortness** see brittleness
- cold working**
 see also bending; cold rolling; plastic deformation; slip; work hardening
 metal, cold-deformed, microcrack development (*Russian*) 7-39652
 steel, austenitic stainless, amplitude depend. damping (*German*) 7-13498
 steel, austenitic stainless, cold-worked, irradi. and unirradi., liq. Cs, Te-induced fatigue embrittlement 7-46637
 steel, austenitic stainless, cold-worked, SCC and hydrogen embrittlement 7-13637
 steel, austenitic stainless, electron irradi., cold working, vacancy swelling, void form., carbide precip., electron microscopy 7-21282
 steel, austenitic stainless, strain martensite determ., eddy current method 7-3559
 steel, austenitic stainless, surface phase transform. rel. to H charging and ageing 7-17530
 steel, austenitic stainless, Ti addition effect on swelling under HVEM conditions 7-58343
 steel, Cr-Mo type, ageing effect on heat resist. props. after cold deform. and tempering 7-22813
 steel, Cr-Ni-Ti-Al, cold-prestrained, length changes during annealing 7-65058
 steel, high-speed W-Mo, nitrogen effect of stabilisation of austenite 7-8021
 steel, low C, cold forgeability, notches, geometry, friction conditions, microstruct. 7-33697
 steel, low C, mech. props., effect of cold working and annealing (*Chinese*) 7-13473
 steel, low-C, mech. prop. change after cold deform. and ageing 7-33696
 steel, stainless, ductility rel. to cold working 7-22759
 steel, stainless, transition class, deform. method effect on microstruct. 7-3299
 superalloy single crystals, directional solidification, mech. anisotropy, fatigue, creep 7-3293
 superalloys, columnar grained and single-crystal, high-temp. strength with surface recrystallised layer (*Japanese*) 7-53788
 Zircaloy-2, cold worked, irradi. growth, point defect trapping, computer simulation 7-16613
 Zircaloy-4, cold worked, anelastic contrib. to high temp. stress relax., model 7-65072
 Al-Mg (0.2 wt.%), subgrain growth rel. to prior cold work and annealing temp. 7-17551
 Al-Mn-Fe alloy, aging characteristics, pre-cold working effects 7-53758
 Al-Si, cold worked, damping characts. 7-28064
 Fe, Armco, annealed and cold worked, neutron irradi. damage 7-2067
 Fe, pure, diffusion of H, dislocation trapping, interstitial impurities effect (*Japanese*) 7-52140
 Fe-Ti-N, mech. props. rel. to cold working 7-28089
 Mo single crystal, cold worked, He pipe diffusion along dislocation, thermal desorption spectra 7-52142
 Nb-Zr (1 wt.%) alloy, hydroextruded, optimum degree of deform., microstruct. 7-3325
 $\text{Ni}_{40}\text{Nb}_{60}$ glass ribbons, H embrittlement susceptibility, effects of cold working 7-46503
 Pb-Sn α -phase alloys, cold-worked and splat-cooled, X-ray diffraction line anal. 7-46502
 $\text{ZrC}_{0.98}$, sintered polycryst., primary recrystn. process 7-28056
- collagen** see proteins
- collections of physical data**
 A=122, nuclear data sheets, levels J^π , transitions, decays 7-41024
 A=133, nuclear data sheets, levels, J^π , transitions, decays 7-60906
 A=143, nuclear data sheets, levels, J^π , transitions, decays 7-14720
 A=145, nuclear data sheets, levels, J^π , transitions, decays 7-29604
 A=156, nuclear data sheets, levels J^π , transitions, decays 7-41025
 A=16, 17, energy levels, EM transitions, J^π , and resonances 7-35132
 A=201, nuclear data sheets, levels, J^π , transitions, decays 7-60907
 A=216, nuclear data sheets, levels, J^π , transitions, decays 7-29605
 A=220, nuclear data sheets, levels, J^π , transitions, decays 7-29605
 A=224, nuclear data sheets, levels, J^π , transitions, decays 7-29605
 A=228, nuclear data sheets, levels, J^π , transitions, decays 7-29605
 A=237, nuclear data sheets, levels, J^π , transitions, decays 7-29606
 A=244, nuclear data sheets, levels, J^π , transitions, decays 7-60908
 A=46, nuclear data sheets, levels, J^π , transitions, decays 7-41023
 A=49, nuclear data sheets, levels, J^π , transitions, decays 7-14718
 A=83, nuclear data sheets, levels, J^π , transitions, decays 7-60905
 A=99, nuclear data sheets, levels, J^π , transitions, decays 7-14719
 actinides, aq. soln., reaction rate consts. of radiation-produced transients 7-60903
 alkyne isomer groups, chemical thermodynamic props. data 7-60901
 atomic positive ions, $Z=2$ to 50, quantum defect values 7-24323
 atoms, electron bremsstrahlung energy spectra 7-24319
 atoms and ions, electron impact total and partial ionisation cross sections 7-60897
 chemical and electrochemical equilibrium diagrams, atlas prep. 7-24324
 D₂, triple-point measurements 7-60902
 even-even nuclei, ground-first excited 2^+ state transition probability B(E2) 7-48204
 geomagnetic fields variations at Hurbanovo, Czechoslovakia, during 1984 AD 7-32
 n-heptane, thermal cond., standard reference data 7-18515
 Integrated Lake-Watershed Acidification Study database documentation 7-46976
 ion-molecule association and clustering form., thermochemical data 7-18514
 Jupiter, Galilean satellite eclipse timings, for AD 1983 to 1985 period 7-55524
 material properties databases, nonbibliographic, cluster anal. 7-41026
 metallography, interference layer technique, phase optical consts., data collection construction (*German, English*) 7-4645
 methane and related cpds., combustion and pyrolysis 7-18516
 nuclear data sheets, recent references May-August 1986 7-35131
 nuclear data sheets, recent refs. Jan. to April 1986 7-31
 OEKFAK factual database on nuclear technology (*Russian*) 7-35133
 office information retrieval system using concepts of the AIR/PHYS physics data bank (*German*) 7-14721

collections of physical data continued

- optical spectroscopy, names, symbols, definitions and units 7-48208
- organic O O contrary comps. in C₁ to C₄ range, ideal gas thermodynamic props. 7-60904
- physical sciences databases, new developments 7-24325
- semiconductor interatomic potentials, handbook 7-35130
- toluene, thermal cond., standard reference data 7-18515
- USA Water Supply Computerised Information Directory 7-66204
- water, thermal cond., standard reference data 7-18515
- $\gamma\gamma$ hadrons, data compilation, struct. functions, resonance widths, cross sections 7-14722
- (p,p) reaction and total cross sections below 1 GeV 7-24321
- Ar, fluid, viscosity and thermal cond. 7-60900
- Be I isoelectronic series, atomic and spectral data for typical tokamak plasma conditions 7-24322
- Cl isoelectronic sequence, allowed 3-3 transitions, Slater parameter optimisation, HF CI calcs. 7-48205
- Fe thermodynamic props., data tables and reviews 7-18512
- H₂, viscosity, thermal cond., zero density limit data 7-60899
- H₂O ordinary fluid, thermal cond., viscosity and density data 7-60898
- H₂, transition probabilities and oscillator strengths, for singly excited states 7-48207
- Mg-like ions, energy levels, model-pot. relativistic perturbation calcs. 7-24320
- N₂, electron and photon collision cross section 7-18513
- Si isoelectronic sequence, allowed 3-3 transitions, Slater parameter optimisation, HF CI calcs. 7-48206
- Si, thermodynamic props., data tables and reviews 7-18512
- TiCl₂, crystn. heat of form. and entropies data base 7-18511
- TiCl₃, crystn. heat of form. and entropies data base 7-18511
- TiCl₄, heat of form. and entropies data base 7-18511

collective accelerators

- atomic physics expts. appls. 7-19561
- beat-wave plasma accelerator, particle acceleration using microwaves 7-56885
- cluster ion accelerator using triangle-shaped accelerated waves 7-42246
- current sheet dynamics, coaxial plasma accelerator, atm. initial press., num. anal. 7-31945
- cyclotron resonance laser acceleration of electron beam by a large amplitude EM wave in a uniform magnetic field 7-10308
- electron acceleration by laser plasma beatwave accelerator 7-62141
- electron acceleration in vacuum by two laser beams 7-50480
- electron accelerator, wake field acceleration by proton bunches 7-62140
- EM projectile accelerators, arc-driven, 3D plasma model 7-32117
- EM wakefields for axisymmetric charge distrib. moving through cold uniform plasma, 2D dynamics 7-44263
- HELIA-high energy linear inductor accelerator, design and performance of pulsed power driver 7-30744
- high-current electron beams, Buneman instability in neutral gas, ion collective acceleration 7-49749
- induction linac accelerators, current pulse shortening 7-49750
- inductive acceleration of plane bodies 7-30739
- inverse noncollinear Compton laser for electron acceleration 7-49744
- ion focused linear induction accelerator, design and operation 7-36344
- IR laser particle accelerators with oversized DBR and HFB waveguides 7-10309
- laser acceleration of particles, strong internal elec. fields in nonlinear force produced cavitons 7-11662
- laser-controlled collective ion accelerator 7-49745
- laser-irradiated plasma, electron acceleration 7-11651
- linear induction accelerators for gamma ray simulation, megamp accelerator and beam expt. 7-30745
- magnetically insulated transmission line in PROTO II accelerator, anode and cathode joints, gap closure 7-30756
- modulated intense relativistic electron beam powered 7-5494
- parallel plate accelerator, time evolution of plasma column 7-19562
- particle acceleration using lasers (*German*) 7-5495
- plasma beat-wave accelerator, collinear optical mixing of relativistic electron plasma waves 7-11614
- plasma impulse accelerators with cylindrical electrodes 7-36340
- power flow eval. for HERMES III linear induction accelerator 7-30761
- PROTO II accelerator power flow modification in insulator stack 7-30669
- pulsed induction acceleration, expt. study 7-36341
- rail gun, electrical characteristics of an EDMA device 7-32116
- rail gun, operation of an EDMA device 7-32115
- rail plasma accelerator, accelerating process, variational formulation 7-30741
- relativistic electron beam diodes, electrode design and appls. 7-20967
- relativistic electrons, determ. in electron-ion ring using bremsstrahlung 7-19559
- vortex structures, pulsed plasma stream, snow-plow model calcs. 7-31953
- wake field accelerator, central beam transverse stability (*Chinese*) 7-49774
- wakeless triple-soliton accelerator 7-10312

collective states, nuclear *see nuclear collective states and giant resonances***collimators (optical)** *see optical collimators***collision processes**

- see also atom-surface impact; atomic inelastic collisions; charge exchange; chemical reactions; elastic scattering of atoms and molecules; elastic scattering of electrons by atoms and molecules; electron attachment; electron impact; elementary particle interactions; intermolecular mechanics; ion-surface impact; molecular inelastic collisions; molecule-surface impact; negative ions; nuclear reactions and scattering; Penning ionisation; plasma collision processes; potential energy surfaces for collision processes; quantum field theory; quasimolecules; radiation quenching*
- aerosol particles scavenging by water drops, nonlinear stochastic collisions model 7-55200
- binary star collisions in globular clusters, head-on collision probabilities 7-60739
- charged microspheres, interaction with extended surfaces 7-59308
- charged particles motion, bounded systems with collisions 7-48521
- collision cross sections, centrifugal sudden approx. integral eqn. approach 7-10696
- collision-induced absorption, bibliography 7-13271
- cometary nuclei, collisions rel. to nature of P/Comet Halley (1982i) 7-34936
- cross sections, centrifugal sudden approx. integral eqn. approach 7-10696

collision processes continued

- elliptical restricted three-body problem, consecutive collisions solns. and double collision orbits 7-34838
- galactic disks collisions with high-velocity clouds, 2D hydrodynamic simulations 7-48065
- galaxies, binary collisions rel. to populations of subclasses of ordinary and barred spirals 7-24215
- galaxy mergers, implications of globular cluster frequencies in ellipticals and spirals 7-4572
- galaxy mergers, two-body simulations rel. to shells form. around elliptical galaxies 7-9536
- gas mixtures, electron transport, collision cross section and dielectric strength 7-63244
- interstellar cloud-cloud collisions, contrib. to high-mass stars formation 7-55610
- interstellar clouds collisions, contrib. to damping of spiral density waves in galaxies 7-66755
- Lippmann-Schwinger-type eqns. iterative soln. 7-15669
- lunar natural satellites collision orbits with Moon via method of surface of section 7-9387
- Markarian 231, Seyfert galaxy/QSO, CO and optical obs. rel. to galaxy merger model 7-66757
- Mars, impact-induced mantle convection rel. to origin of Tharsis region 7-14514
- momentum, relativistic, alternate derivation 7-42
- neutron stars-giant stars collisions in globular clusters, contrib. to ultra-short period binaries form. 7-66667
- NGC 4214, 4449, blue irregular galaxies, collision model rel. to kinematics of H II regions 7-40925
- particle bombard. induced erosional and depositional phenomena 7-63652
- plane jets, of ideal incompressible fluid, nonsymm. collision 7-31853
- planetary rings, numerical simulation of binary encounters 7-66499
- planetesimals collisions, contrib. to evolution of planetary rot. axes inclinations 7-9388
- predispersive electron gun for an electron monochromator appl. 7-15034
- quantum close-coupled eqns., linear reference pot. algorithm 7-62477
- reaction channel with attractive Coulomb force, threshold continuity theorems 7-10697
- relativistic particle beams, high power, collision effects calcs. 7-30117
- statistical mechanics of point particles, hyperbolicity and Moller-morphism 7-48531
- stellar collisions in globular cluster cores, effects on dynamical evolution 7-4500
- stellar encounters, cross sections for tidal capture binary form. and stellar merger 7-29519
- stellar encounters in open clusters, effects on dynamical evolution of N-body clusters 7-55748
- structureless particle surface scattering, classical differential cross-sections 7-39323
- supernova remnants, colliding, oblique shock refls. rel. to anomalous H I vel. features 7-24175
- surface scatt., effects of detector geometry on measured lineshapes and intensities 7-64827
- water drops in atmosphere, aerosols redistrib. by drops coagulation 7-55201

collision sequences, focused *see sputtering***colloid chemistry** *see colloids***colloids**

- see also Brownian motion; coagulation; electrophoresis; electroviscous effect; emulsions; gels; magnetic fluids; thixotropy*
- 1-acetonaphthone-*d*-diphenylamine, micellar soln. photoinduced electron transfer, mag. field effects 7-3579
- acridine cation, in micellar soln. fluoresc. quenching 7-62447
- agar phantom electrically adaptable for tissue simulation in 5-40 MHz range, hyperthermia cancer treatment 7-65713
- alkylamines, interaction with layered compounds 7-46838
- alkylbenzenesulfonates microdisperse organosols, struct., small-angle X-ray diff. investig. 7-39925
- alkylsalicylates microdisperse organosols, struct., small-angle X-ray diff. investig. 7-39925
- ammonium perfluorononanoate-H₂O system, micellar nematic phase, conductivity, relax. times 7-38230
- anil brown, anisotropy in elec. cond. induced by external field 7-39924
- ballistic aggregate growth theory 7-39928
- ballistic deposition on surfaces, num. simulation 7-39929
- Brownian particles, interacting, stochastic descriptions 7-29900
- caesium pentadecafluorooctanoate-water discoid micelle solns., order-disorder transitions, X-ray scatt., elec. cond., NMR meas. 7-26949
- charge-stabilised, Yukawa systems, phase diagram 7-32606
- charged colloidal dispersions, elastic scatt., static struct. factor, RPA calcs. 7-65357
- charged colloidal particles, mean-squared displacement and self-diffusion coeff. 7-28360
- colloidal crysts., lattice dynamics, pot. and long range hydrodynamic interactions 7-13831
- colloidal suspensions, solitary wave model anal. of sedimentation 7-57911
- cross-correlation intensity fluctuation spectroscopy and laser trapping studies 7-28359
- crystals, shear melting and Taylor instabilities 7-43858
- dodecyl hexaoxyethylene ether, phase diagram vanishing miscibility loop obs. 7-28352
- n-dodecyl-octaoxyethylene glycol monoether micellar solns., long-range crossover 7-21068
- double-layer interaction between curved surfaces bearing pot., Derjaguin approx. 7-17819
- dynamics under shear 7-6258
- enzyme recovery by liquid-liquid extraction using reversed micelles 7-40086
- flowing colloidal crystals rheological props. 7-8305
- fractal cluster form. by aq. nanodroplets in apolar media, dielec. 7-39921
- gel-like sediment form., Brownian dynamics simulation, colloidal and hydrodynamic interaction effect 7-13825
- groundwater radiocolloids in the vicinity of some Australian uranium ore bodies 7-28430
- hexadecyldimethylammoniumbromide micelles, aq. solns., shape, neutron and X-ray scatt. 7-46872
- interfacial particles, electrostatic trapping mechanism 7-13828
- ionic micelles, static and dynamic properties 7-28353
- latexes, colloidal and film-forming props., phase inversion obs. 7-8277

colloids continued

- lithium dodecyl sulphate, micellar dynamics, ^{13}C - ^2H scalar relax., NMR 7-27622
- macromolecular charged fluids, struct. and dynamics 7-11892
- micellar aggregates, packing of semi-flexible chains, statistical thermodynamics approach 7-28357
- micellar and hard sphere solutions, concentrated, diffusion 7-8316
- micellar and microemulsion globules solvent induced attractions 7-54195
- micellar liq. cryst., isotropic phase, temp.-depend. supercooling limit, mag. birefringence meas. 7-63815
- micellar solns., intermicellar struct. factors, hypernetted chain Percus-Yevick approx. 7-3611
- micellar solutions, equilib. thermodynamic props. and phase separation theory 7-46876
- micellar solutions, marginalism, quasi-marginalism and critical phenomena 7-58437
- micellar solutions, origin of nonuniversality 7-46879
- micellar systems, isotropic-nematic transition temps., conc. depend. 7-2199
- micelle solutions, isotropic-nematic phase transition, micellar flexibility effects 7-58467
- micelles, cylindrical, intramicellar fluoresc. quenching rate const. 7-54189
- micelles, monodisperse confinements, fluorescence decay kinetics anal. 7-19937
- micelles, spherical and nonspherical, asymmetrisation, free energy, conc. depend. 7-8321
- micelles and bilayers, chain statistics, surface roughness and internal energy effect 7-23052
- micelles synchronous wavelength scanning room temp. phosphoresc. 7-33452
- modulation transfer function meas. using moire deflectometry 7-31265
- nucleation and growth of colloidal crystals 7-12243
- particle motion study in concentrated dispersions, tracer diffusion method 7-51351
- polydisperse colloidal crystals, stability anal. 7-8315
- polyhexazocyclane, solns., viscosity props. (Russian) 7-63864
- polymeric colloidal suspensions in polymeric suspending fluids, dichroism and birefringence meas. 7-11478
- polystyrene, colloidal cryst. in semidilute aq. suspension, ordering process 7-13829
- polystyrene, cryst. colloidal array filter 7-37117
- polystyrene latex spheres, colloidal dispersion, high freq. elastic moduli calc. 7-38083
- polystyrene latex suspensions, aq., semidilute, ordering process of colloidal crystals. 7-17829
- polystyrene-b-(ethylene-co-propylene) diblock copolymers, micelle form., small angle neutron scatt. 7-11887
- programmed symmetry lowering in 2D colloids 7-65354
- propanol-2 radical+ CdS, photochemistry and radiation chemistry, non-linear optical effects 7-46858
- radioactive waste, colloid migration 7-5477
- reaction-limited cluster aggregation kinetics, Smoluchowski eqns. modeling 7-41261
- rhodamines, aq. micellar solns., flash lamp excitation, photostability, lasing props. 7-57308
- shear viscosity, interaction corrections 7-63197
- silica, colloidal, gelation 7-46877
- sodium p-n octylbenzenesulphonate, aq. solns., micelle form., acoustic and rheological props. 7-13823
- sodium salicylate, in viscoelastic micelles, PMR, spin-spin splitting and relax. effects 7-53150
- spherical mols. model mixtures, phase equilib. 7-38203
- statistical methods, conf., Oaxtepec, Mexico, Jan. 1986 7-24268
- statistical physics, conference, Oaxtepec, Morelos, Mexico (Aug. 1985) 7-9584
- strongly interacting colloids in suspension, viscosity and shear modulus calcs. 7-1617
- surfactant systems, drag reduction, physico-chem. props., rheology 7-43992
- surfactant-water-nonaqueous liq. systems, elec. cond. study 7-13789
- suspension, dilute macro-ions, effective charge and diameter, Gibbs-Bogoliubov inequality calcs. 7-65356
- tracer diffusion in concentrated colloidal dispersions 7-8303
- transition metal oxides, sol-gel process synthesis, electronic and ionic props. 7-33618
- water, molecular motion in small reversed micelles 7-59791
- Ag, adsorbed flavins, SERS 7-64626
- Ag colloid particles, SERS of adsorbed quinoxaline, adsorbate orientations 7-22265
- Am behaviour in aqueous solns. containing Fe, radwaste treatment appl., colloids 7-19529
- Am pseudocolloids, formation and transport in aqueous systems 7-5476
- Au, aqueous, diffusion- and reaction-limited kinetic aggregation, cluster-mass distrib. meas., dynamic scaling 7-21467
- Au colloidal particles, optical nonlinearities, surface resonances and quantum size effects 7-50648
- CdS on synthetic clay, luminesc. lifetimes, UV spectra 7-22297
- CuCl₂Br_{1-x} colloids in glasses, x=0-1, exciton spectrum (Chinese) 7-38459
- FeCO colloids, anisotropy in elec. cond. induced by external field 7-39924
- $\gamma\text{-Fe}_2\text{O}_3$ particles, colloidal suspension, mag. props. of ionic ferrofluids 7-45758
- Na-colloid in NaCl, low freq. surface enhanced Raman scatt. from NaCl-Na interface localized fractal vibrational modes 7-59195
- Na₂O-SiO₂ binder solns., ester curing, equilibria and kinetics, NMR study 7-8311
- PbI₂ aggregated microcrystallites, Raman scatt. 7-22233
- Si, colloidal, prep., photochem. expts. 7-65332
- SiO₂ aggregates, fractal props., light scatt. studies 7-28358
- SiO₂ colloidal fractal aggregates, hydrodynamic behaviour 7-59797
- SiO₂ in aqs. solns. of cetylpyridinium bromide and inorganic salts, coagulation, thermodynamic stability 7-8326

colorimeters

- see also colorimetry
- skin colour measurement device based on photoelec. colorimeter 7-60136

colorimetry

- see also colorimeters; spectrochemical analysis; spectrophotometry
- ceramic colour standards, thermochromism 7-9867

colorimetry continued

- chromance and photochromic coefficient, new terms proposed for use in colorimetry 7-18854
- dyestuff, optical density determ. with multi-reflection, correction eqn. (Japanese) 7-35563
- influence of changes in the reflectance spectra of the test samples on the colour rendering index (Hungarian) 7-18856
- natural scene colour and spatial structure, photographic colorimetry 7-41420
- polyethylene, oriented in heptane, uniaxial stretching, thermodynamics (Russian) 7-63731
- polymer solutions cloud points meas., using pressurised apparatus 7-9871
- powder sample colour measurement in the medical industry (Hungarian) 7-18857
- TV, scene-by-scene colour correction using phase domain signal processing 7-24685
- Xe lamp spectral distribution as standard white light source (Japanese) 7-1244
- P₂O₅-B₂O₃-SiO₂ CVD glass films, components characterization 7-45085
- U concentration determ. in natural water, comparison with fission track method 7-54217

colour

- see also colour vision
- 3D CT image reconstruction and display (Chinese) 7-60118
- apochromatic optical system design 7-43312
- ceramic colour standards, thermochromism 7-9867
- colour endoscope image motion related blur compensation 7-47282
- Danaines golden pupae, natural broad-band interference reflector microspectrophotometry 7-54676
- dichromated gelatin achromatic reflection display holograms 7-25750
- Dirac equation, generalisation admitting isospin and colour symmetries 7-9941
- garnets, ornamental, general method of formulation and crystal growth 7-53252
- glass, colour, origins 7-13114
- image processing for bronchus endoscopic image restoration 7-47281
- image recording, computer generated linear tricolour sampling pattern 7-42952
- metallic oxide thermostable reversible thermochromic materials (Japanese) 7-13140
- natural scene colour and spatial structure, photographic colorimetry 7-41420
- ocean colour spectral variability measurement using solar-induced chlorophyll fluoresc., intraspectral correlation technique 7-47547
- perceived relations between colour, direction and speed of motion 7-47078
- poly γ -methyl L-glutamate film, solidified, cholesteric struct., colour rel. to stretching and temp. 7-44354
- poly γ -benzyl L-glutamate film, solidified, cholesteric struct., colour rel. to stretching and temp. 7-44354
- polysiloxane liquid crystals, colour gamut 7-1857
- quartz: Cu⁺ (Fe³⁺)(Nb⁵⁺), ion implanted, coloration and transparency (Japanese) 7-15656
- refractory metal nitride, sputtered coatings, wear and friction 7-33800
- Triassic sediments of Betic Cordillera, Spain, colour meas. rel. to Fe oxides mineralogy determ. 7-66098
- Bi₄Ge₃O₁₂, high quality large cryst. growth, colour and precip. form., pulse height resolution 7-53554
- GeO₂-Bi₂O₃-ZnO glass, coloration mechanism due to Bi₂O₃ and effects of ZnO addition 7-22291
- HfN films, colour, aging and tempering effects 7-46159
- TiN coatings, N partial pressure effects on composition, spectral reflectance and colour 7-53420
- TiN film deposition by reactive sputtering, hardness and optical props. 7-22481
- TiN films, colour, aging and tempering effects 7-46159
- TiN films, reflectance and colour 7-46160
- TiN ion plated films, tempering effects 7-59461
- ZnWO₄, Czochralski grown, quality, colour rel. to scintillation output 7-59407

colour blindness see colour vision; vision defects

colour cameras, television see colour television cameras

colour centre lasers

- alkali halide crystals, active media for tunable crystal lasers 7-25823
- development, characts., use in selective spectroscopy of disordered media 7-25822
- (F₂)_A centre in KI:Li selective two-step photoionisation using 1.06 μm radiation 7-38053
- F_A(II) colour centre laser at 2.653 μm , synchronously pumped, mode-locked, cavity length meas. 7-5920
- IR laser developments with tunable crystals and diodes 7-15887
- kinetic spectroscopy using a color center laser 7-15013
- luminescence, conference, Rovno, USSR (Nov. 1984) 7-24263
- molecular velocity modulation laser spectroscopy using colour centre lasers 7-48867
- N₁⁺ centre in KBr, selective two-step photoionisation using 1.06 μm radiation 7-38053
- sapphire colour-centre crystal, laser appls. 7-43120
- sapphire laser crystal, with colour centres, radiation generation 7-10968
- soliton laser stabilisation, feedback from pulse-shaping fibre 7-50602
- KCl:Li₂F₄(II) colour centre laser, synchronously pumped, mode locking 7-62710
- KCl:Li F_A(II) colour centre lasers appl. to intracavity laser spectroscopy 7-43189
- KCl:Ti crystals, optical and lasing characts. of Ti³⁺(I) colour centres 7-50569
- LiF crystals with F₂⁻ centres, inactive losses, investig. of mechanism 7-3072
- LiF, F₂ laser active element, optically stable component 7-43116
- LiF F₂ color center lasers, review 7-36971
- LiF F₂ laser, coatings for multiwavelength solid state lasers, laser beam testing expts. 7-57522
- LiF:F₂ laser, room temperature, active element, thermal effects 7-62714
- NH₂ + NO reaction, kinetic spectroscopy using a color center laser 7-9901
- NaCl:Ti colour centre laser, structural, optical and prod. props. 7-57340
- NaF:F₂⁺, F₃⁻, intracavity spectrum analyser, long-wavelength IR region 7-48897
- Pb²⁺:KMgF₃ colour centre laser, tunable for 855 to 965 nm 7-15874

colour centres

- see also *F-centres*; *OH⁻-centres*; *paramagnetic resonance of colour centres*; *U-centres*; *V-centres*
alkali halides, colour centres, Hartree-Fock cluster computations 7-16985
alkaline earth oxides, colour centres, Hartree-Fock cluster computations 7-16985
borates and halogenoborates, cryst. and vitreous, X-ray irradi., ESR centres, review 7-7586
fluorapatite, relative defect-production efficiency for fission fragments, alpha decay and electron irradiation 7-12167
glass, laser exposure, repeated, absence of below-threshold ionisation and cumulation effect 7-63653
optical glass fibre waveguides, colour centres 7-11081
optical glass fibres, UV-radiation induced colour centres 7-11082
photochromic glasses, degree of darkening depend. on radiation absorpt. cross section 7-37078
 α -quartz, neutron damaged, static paramag. susceptibility studies 7-33140
quartz, radiation damage, rel. to trace water 7-32489
topaz, radiation damage, rel. to trace water 7-32489
zircon, radiation damage, rel. to trace water 7-32489
 Al_2O_3 , leucosapphire single crystals, transformation of colour centres 7-37986
 $\text{Al}_2\text{O}_3:\text{Cr}^{3+}$, radiation colour centres, excitation energy transfer 7-21200
 $\text{Ba}(\text{PO}_3)_2$ -LiF gamma irradiated activated glasses, optical absorpt. and ESR spectra correls. 7-13030
 BaSO_4 , barite, X-irrad., thermally stimulated luminesc., trap distrib. 7-59266
 CaO , light sensitive centres with tetragonal symmetry, EPR study 7-53133
 $\text{GeO}_2\text{-Bi}_2\text{O}_3\text{-ZnO}$ glass, coloration mechanism due to Bi_2O_3 and effects of ZnO addition 7-22291
 KBr N_2^+ centre, selective two-step photoionisation using 1.06 μm radiation 7-38053
 KBr:Cu , visible absorpt. spectra 7-3073
 KBr:Ti(In) , defect creation by excitons, room temp. (*Russian*) 7-16946
 KCl , γ -irradiated, influence of plastic deformation on colour centre conc. 7-44538
 KCl:Cu visible absorpt. spectra 7-3073
 KCl:I , electron excitation self-trapping 7-32594
 KCl:Ti crystals, optical and lasing characts. of $\text{Ti}^0(1)$ colour centres 7-50569
 KCl-En solid soln. crystals, thermal and radiation induced decay, impurity aggregation study (*Russian*) 7-2216
 KI:Cl , electron excitation self-trapping 7-32594
 Li-W-O films, electrochromic props., UV radiation effects study 7-22222
 LiF , γ -irradiated, influence of plastic deformation on colour centre conc. 7-44538
 LiF , N ion implanted and X-irrad., microhardness response 7-21344
 LiF:Mg(Ni)(Co) R' colour centres, spectral holeburning props., depend. on doping and irradiation 7-26743
 $\text{Li}_2\text{O-B}_2\text{O}_3\text{-WO}_3\text{:Co(Cr)}$ glasses, optical props. 7-46079
 MoO_3 , amorphous films, X- and γ -irradiated, color center form. 7-44541
 NaCl , thermolum. of colloids centres 7-7772
 NaCl:Cu , visible absorpt. spectra 7-3073
 NaCl:Eu^{2+} crystals, γ -irradiated, colourability 7-12062
 NaCl:Mg , X-ray irradi., exciton interactions with impurity-vacancy dipoles, absorpt. and luminesc. spectra 7-45162
 NaF:Mg , doped and undoped, electron beam irradiated, thermoluminescence and thermally stimulated conductivity 7-7771
 $\text{Na}_2\text{O-SiO}_2$ glass, relative defect-production efficiency for fission fragments, alpha decay and electron irradiation 7-12167
 $\text{Na}_2\text{O-SiO}_2\text{-Tb}^{3+}$ glasses, colour centre formation during UV irradiation 7-2049
 Nd^{3+} :YAG laser radiation generation, influence of unstable defects 7-1103
 Si:H , impurity effects on IR absorpt. bands of Si-H centres, irradi. and unirrad. crystals. 7-53379
 SiO_2 , amorphous, intrinsic defects, theory 7-11936
 $\alpha\text{-SiO}_2$, quartz, E'_1 centre, nonradiative charge transfer rate 7-12659
 $\text{YAlO}_3\text{:Pr}^{3+}$ single crystals, colour centres, optical absorption spectra studies 7-63610
 $\text{Y}_3\text{Al}_5\text{O}_{12}$, room temp. γ -irrad., colour centre investig 7-6621

colour filters see optical filters

colour model

- Abelian quark-gluon plasma, gauge invariant eqns. of motion, QED derivation 7-61823
axion-EM coupling, implications for cosmic background radiation 7-439
backwards evolved initial state parton showers, Monte Carlo model 7-15128
bare pomeron trajectory calcs., vacuum Regge singularity Green's function in QCD 7-41773
baryon mass spectrum, convexity props. in pot. models with flavour independence 7-503
baryon rich quark-gluon plasma produced in rel. heavy ion collisions, decay 7-5175
baryon-baryon multiple scattering matrix elements, color parts, $\text{SU}(3)$ group 7-41827
baryonic matter, mean field anal. of critical behaviour, QCD system anal. 7-61830
baryons, electroweak properties in QCD 7-56522
baryons in relativistic quark model with chromodynamics 7-19075
baryons structure, hyperfine interactions 7-56518
bound states and asymptotically free quarks, duality relations 7-5050
BRS transformations and colour confinement number of generations 7-35800
chiral QCD, topological anomalies from Dirac equation 7-49051
chiral symm. breaking and condensate calcs. 7-49073
chiral symmetry breakup and gluon condensate in QCD_2 7-41731
chromomagnetism and quasiparticles at finite temperature 7-56506
cold nuclear matter at high densities 7-56502
colour dielectric model for nuclear binding and quark confinement 7-35936
conference, strong interactions and gauge theories, Les Arcs, Savoie, France (March 1986) 7-60876
consistent quark model with chromodynamics, baryon spectrum calcs. 7-30249
cosmic ray, multijet family event at super-high energy (*Chinese*) 7-14443
cosmological quark-hadron transition, effects on primaeval nucleosynthesis 7-47677

colour model continued

- Coulomb-like gauge for massive gauge fields, $\text{SU}(2)$ model appl. 7-4957
currents acting at finite length, electromagnetic and hadron radiation 7-10031
Cyg X-3, cosmic glueballinos source, discussion 7-48105
dibaryons, positive parity, strangeness -1 potential model anal. 7-24846
dielectric model, numerical solns. 7-469
dilaton, technicolour model, mass and lifetime estimates 7-41712
dilepton emission and the QCD phase transition in ultrarelativistic nuclear collisions 7-5219
Dirac eqn., supersymmetry in nonabelian, chromomagnetic field 7-35726
Dirac equations, exact solutions in constant chromomagnetic fields 7-61434
Dirac neutrinos and techniphotons, minimal model in technicolour framework 7-10020
direct photon production, nuclear depend. for large P_T , parton distrib. gluon distrib. 7-5063
dual description of a confined colour field 7-61565
dynamical symmetry breaking in QCD 7-24843
early Universe, bubble growth and droplet decay in quark-hadron phase transition 7-9562
effective action for π and vector mesons 7-15117
effective chiral Lagrangian with $\text{U}(3)\times\text{U}(3)$ symmetry for baryons 7-49084
effective gauge theory for low energy mesons, stable and unstable classical solns. 7-427
effective Lagrangians for the chiral quark phase and the Skyrmin parameters 7-19069
electric source problem in Hermite-symmetric Einstein field theory 7-29838
electromagnetic struct. of nuclei and nucleons, review 7-30315
electroweak symmetry breaking, phenomenology of colour exotic fermions 7-10009
EMC effect, QCD and Fermi gas model interpretations 7-15188
EMC effect, QCD and Fermi gas model interpretations 7-49086
EMC effect, SLAC data reanalysis and x rescaling, perturbative QCD comparisons 7-49233
European Hadron Facility, conference, Mainz, Germany (March 1986) 7-48154
exact QCD matrix element incorporation into QCD parton cascade models 7-61566
extended technicolour model, exptl. constraints on detection of light scalar particles 7-484
extended technicolour model based on $\text{SO}(10)^2$, fermion mass spectrum 7-61520
Fermilab Antiproton Source, physics workshop report 7-49174
fermion guides, chiral symmetry spontaneous breakdown in QCD, pseudoscalar correl. functions 7-41727
finite temperature lattice QCD, deconfinement and chiral symmetry restoration 7-41724
finite temperature Monte Carlo simulations 7-61567
finite temperature phase transition in chiral limit of lattice QCD 7-61561
finite temperature QCD, flavour dependence of phase transition 7-61554
finite temperature $\text{SU}(2)$ gauge theory, correlation length temp. depend., screening, deconfinement 7-41606
finite-order QCD calcs., optimized perturbation theory for factorization scheme depend. 7-15118
first order chiral transition in QCD 7-41729
flux-tube model, spin interactions and hybrid meson masses 7-61593
four-quark two-gluon amplitude, extension to equal flavour quarks 7-482
gamma-families formed at ultrahigh energies, spatial characts., Monte Carlo calcs. 7-14431
gap equation models for chiral symm. breaking in QCD 7-35738
gauge-invariant variables and infrared confinement in finite space-time 7-61564
GF11 supercomputer for QCD calcs. 7-61556
globally supersymmetric preon models with gauged colour-flavour symm. 7-19079
glueball, 0^{++} , quarks, decay width calcs. 7-516
glueball (0^{++}), mass scaling, $\text{SU}(N)$ Hamiltonian lattice calcs., Monte Carlo anal. 7-35807
glueball mass inequalities, QCD anal. 7-10029
glueball mass spectrum calculation by light-cone quantization (*Russian*) 7-61594
glueball search, QCD spectroscopy beyond the quark model 7-56521
glueball wave functional calcs. using lattice technique 7-61580
glueballs, tensor and scalar, mass calcs., in lattice gauge theory 7-61587
gluon, magnetic mass in QCD_4 , two loop approx. 7-61563
gluon bremsstrahlung in supersymmetric QCD 7-461
gluon condensate, effective QCD Lagrangian 7-485
gluon condensate and the effective gluon mass, QCD anal. 7-61598
gluon condensate modification in nuclei 7-49279
gluon condensation, detection from heavy quarkonia spectra 7-488
gluon mass, gluon propagator calcs. in Landau gauge, $\text{SU}(3)$ lattice anal. 7-61588
gluon mass in quenched Eguchi-Kawai model, momentum-space Monte Carlo method 7-19065
gluon thermodynamics with an extended plaquette action, deconfinement in lattice QCD 7-41723
gluon-quark confinement, gluodynamics IR behaviour 7-5056
gluons, properties in hadrons, gluonic structure functions, review (*Polish*) 7-30243
gluons in nuclei and pions 7-30250
hadron masses in quenched QCD 7-61581
hadron spectroscopy, European Hadron Facility 7-49185
hadron spectroscopy, gluonic containing hadrons 7-49078
hadron spectroscopy, QCD aspects 7-30245
hadron spectroscopy in lattice QCD with dynamical quark loops 7-464
hadronic low transverse momentum transfer reactions, colour superconducting treatment 7-41738
hadronic photoabsorption, energy depend. of total cross section, gluonic character 7-19113
hadronization of quarks and gluons into hadron jets at high energies 7-41749
hadrons as collective excitations of a superfluid-coloured-quark liquid 7-5044
Hamiltonian lattice $\text{SU}(N_c)\text{QCD}$, mechanism to lift the Goldstone degeneracy 7-49081
hard processes involving two quarks and four gluons, cross section, QCD tree approx. calcs. 7-49083

colour model continued

heat-kernel regularization of gauge theory, vanishing gluon mass 7-41624
heavy ion collisions, relativistic hydrodynamics, entropy, π prod., quark-gluon plasma, review 7-615
heavy narrow QQ resonances, gluonic prod., parton cross sections 7-61585
heavy quark condensation in QCD sum rule approach, quark expansions 7-5054
heavy quark dynamical mass, electroweak symmetric breaking, extended technicolour sector simplification 7-24837
heavy quarkonia, QCD scale parameter 7-35809
hidden colour dynamics in the flip-flop model of confinement for 2N systems 7-24836
high energy spin physics and QCD tests 7-30236
high mass dilepton production in hadron collisions, review 7-56574
hot QCD, nonAbelian Debye screening, singlet pot. and gauge symm. breaking 7-49075
hypercolour, flavour changing neutral currents, chiral hierarchies 7-465
inclusive jet cross sections and production in the UA2 detector 7-61775
infrared behaviour, Wilson loop renormalisation beyond leading order 7-61451
initial state radiation effects on W and jetproduction 7-5064
instantons and the U(1) anomaly in QCD, review 7-5048
jet physics in the UA1 experiment 7-61773
kink-bag system in (1+1) dimens., breathing motion, inertia of confined vacuum 7-19070
Klein-Gordon equation, gluonium and Regge trajectories 7-9974
Langevin QCD with dynamical quarks, numerical study 7-49062
large-N QCD, Eguchi-Kawai approach and Monte Carlo simulations 7-61574
lattice gauge theories with matter fields, order parameter 7-61486
lattice gauge theory, high-temperature QCD and quark matter 7-56416
lattice gauge theory, static screening lengths in finite-temperature pure gluon plasma 7-19003
lattice gauge theory simulations, conf., Wuppertal, Germany, Nov. 1985 7-60883
lattice Gross-Neveu model, recovery of chiral symm. 7-19010
lattice Monte Carlo simulations of QCD at finite baryonic density 7-49082
lattice QCD, $\beta=5.7$, evidence for scaling, SU(3) deconfinement temp. anal. 7-19072
lattice QCD, chiral symm. breaking in strong coupling limit 7-56514
lattice QCD, connection with nuclear many-body problem 7-35802
lattice QCD, deconfining phase transition and continuum limit 7-61568
lattice QCD, deconfining transition 7-56508
lattice QCD, finite temperature, phase transitions 7-35804
lattice QCD, improved actions, redundant operators and scaling 7-56513
lattice QCD, large N with Susskind fermions, continuous flavour symmetries 7-15123
lattice QCD, large scale computing aspects 7-49068
lattice QCD, light hadron and quark masses, large lattice results 7-15139
lattice QCD, numerical simulation of interacting fields and static inter-quark pot. 7-61575
lattice QCD, problems with finite density simulations 7-5058
lattice QCD, quenched SU(2) simulation with staggered fermions, chiral limit 7-61602
lattice QCD, strongly coupled, fermions in Euclidean formulation 7-30247
lattice QCD, t-expansion method 7-61573
lattice QCD, weak Hamiltonian, eye diagrams, calculational technique 7-477
lattice QCD, with Wilson fermion action, finite temp. behaviour, implication on spectroscopic studies 7-19066
lattice QCD at finite density 7-56509
lattice QCD in 2D, Monte Carlo simulation 7-35782
lattice QCD sum rules and spontaneous chiral symm. breaking, Monte Carlo simulation 7-61603
lattice QCD with quark loops, Lanczos algorithm simulation 7-61571
lattice QCD with staggered fermions, chiral props. 7-61576
lattice QCD with Susskind fermions, current algebra relation 7-41730
lattice QCD with Wilson fermions, fast fermionic algorithms 7-61572
lattice SU(3) gauge theory, deconfined phase, gluon plasma thermodynamic props. 7-41741
lattice SU(N) QCD study at finite chem. pot. and baryon density 7-474
lepton pair angular distn. in Drell-Yan-like processes 7-24920
lepton-hadron deep inelastic scattering, higher-order QCD perturbative corrections, exponentiation 7-49158
light cone gauge, integral equation for multiplicity distribution 7-15115
light quarks at low temperatures, QCD partition functions from chiral symmetry 7-61584
lightest glueball mass in SU(2) and SU(3) gauge theories, lattice size depend. 7-41722
low energy meson action from QCD, extended Skyrme model, anomaly terms 7-5052
low mass dilepton production in heavy ion collisions, background from quark-gluon plasma 7-35795
low-energy theorems for scalar gluonic currents between quarkonium states 7-10024
magnetic monopole interactions with quark's dipole moment 7-61578
massive confined quark, QCD and QED energy shifts, cavity perturbation theory 7-15116
massless SUSY QCD, vacuum stability, instanton-anti-instanton contrib. to vacuum energy 7-41725
meson decays, chromoelectric flux-tube breaking 7-41742
meson dynamics beyond the quark model, final state interactions, glueballs, CC anal. 7-24844
meson-baryon system, Skyrme model results using chiral Lagrangian 7-41576
mesons structure, hyperfine interactions 7-56518
Monte Carlo simulation of hard hadronic processes, review 7-56563
multiflavour QCD, nonAbelian bosonization and baryon mass formulae 7-61579
multijet events at CERN pp collider 7-61774
multijet production in e^+e^- annihilation at PETRA energies 7-61715
multiquark states in QCD-like pot. model 7-41718
Nambu-Jona-Lasinio model, phenomenological lagrangian for strong interactions 7-35799
non-interacting quarks and gluons in a slab, thermodynamics, plasma in HI collisions 7-49444

colour model continued

non-perturbative QCD, algorithm for transport coeffs. using lattice Monte Carlo methods 7-49071
nonAbelian chiral anomaly from lattice regularization 7-15072
nonperturbative hadron phase, chromoelectric flux and action quantisation 7-41736
nuclear matter binding energy, dependence on number of colours 7-61828
nuclear structure studies with high energy projectiles and probes 7-56611
nuclear-like states of quark matter in QCD 7-41924
nucleon, chiral invariant colour dielectric model 7-463
nucleon axial vector form factor in perturbative QCD 7-522
nucleon size, density dependence of f_π in nuclear medium, QCD sum rule anal. 7-480
nucleon wavefunctions and QCD sum rules 7-30248
numerical simulation using Cray supercomputers 7-61557
one-plaquette U(N) gauge model with fermions, leading order topological expansion 7-35721
Pamir expt. data, comparison with strong interaction model with QCD jets 7-10038
perturbative QCD, anomalous dimens. of multi-quark bound states 7-41719
perturbative QCD and jets 7-61600
photon structure function, meas. and QCD anal. 7-49148
photoproduction processes, quark model with charm and colour 7-41737
pions, quark-gluon substructure in nuclei 7-49064
preon model with three SU₃ hypercolours and three SU₃ hyperflavours 7-49026
prompt meson production at large p_T 7-41707
pseudoscalar lattice mesons, relative charge distribts. for qq pair 7-49072
pseudoscalar meson charge radii from QCD sum rules, SU(3) breaking 7-10033
pseudoscalar meson electric form factor calcs. lattice QCD anal. 7-35801
QCD₂ ($N_c \rightarrow \infty$), spectrum of states, low-energy theorems and sum rules 7-61595
QCD₃, homotopy theory applications, review 7-24793
QCD, anal. of anomalous Ward identities, $\alpha(1440)$ contributions and topological susceptibility 7-19071
QCD, chiral perturbation theory and effective lagrangians 7-49055
QCD, chiral symmetry, Wigner-Weyl and Nambu-Goldstone realizations 7-35803
QCD, damping of plasma oscillations in hot gluon matter 7-49063
QCD, dynamics of confinement, asymptotic freedom 7-49057
QCD, explicit formulae for heavy flavour production 7-41739
QCD, finite energy sum rules for light quark systems 7-24841
QCD, gauge configuration props. in 3D 7-35783
QCD, gauge theories with imaginary chemical potential 7-35781
QCD, implications of nucleon struct. determ. by deep inelastic lepton scatt. 7-10028
QCD, lattice quantum field theory (Czech) 7-5042
QCD, longitudinal structure function, fermionic next-to-leading-order contributions 7-41708
QCD, nonperturbative aspects 7-49069
QCD, nucleon spin conservation at short distances 7-490
QCD, order of the finite temp. chiral phase transitions, renormalisation group eqn. 7-15119
QCD, perturbative, IR asymptotic, behaviour, contour gauges, renormalization group anal. 7-61596
QCD, quark condensates in spontaneous chiral SU(2) \times SU(2) symm. breaking 7-471
QCD, scalar confinement implications for chiral symmetry breaking 7-61550
QCD, spectral function sum rules and SU(3) violation of quark condensates 7-466
QCD and CP^N model, collective phenomena, deconfining and chiral transitions 7-15120
QCD and higher twist, anal. of xF_3 7-35793
QCD and the lattice, introductory remarks 7-56507
QCD based models of hadron structure, book 7-48217
QCD condensates, corrections to Goldberger-Treiman relation 7-10025
QCD corrections for semiphenomenological treatment of heavy-quark decay 7-483
QCD effects in semi-inclusive deep inelastic scattering from a polarised target 7-10032
QCD evolution of structure functions, EMC effect study 7-61601
QCD flux tubes and glueballs, soliton interactions in gauge theories 7-5051
QCD gluon Wigner operator, quantum transport eqns. derivation 7-5046
QCD inspired models of multiparticle production 7-24840
QCD lattice gauge theory, updating fermions with Lanczos method 7-49052
QCD nonperturbative effects modelling, 2D sigma models and 4D gauge theories 7-35664
QCD plasma, effect of dynamical quarks 7-61555
QCD spin-depend. static pots., SPINSUB vectorised code for Monte Carlo computation 7-41721
QCD string, origin in Yang-Mills theory 7-61552
QCD SU(N) quark Wigner operator, transport equations 7-475
QCD sum rules, analytic continuation by duality 7-15114
QCD sum rules, quark operator classification, gluon condensate contrib. to quark vacuum polarization 7-61599
QCD sum rules and the Skyrme model at large N_c 7-61583
QCD SVZ sum rules, compatibility with expt. sum rules 7-5055
QCD vacuum, colour ferromagnet model, light quark mass effect 7-24842
QCD with fermions, Langevin simulations 7-61570
QCD with Wilson fermions at finite chemical potential and temp., comparisons with SU(3) spin model 7-61589
QCD-based relativistic Hartree-Fock calculations for identical quarks 7-15112
quantum field theory, progress, book 7-9602
quantum-chromodynamic evolution of six-quark states 7-472
quark currents, complete bosonisation, quantum theory based on anomalies 7-30240
quark distribution amplitudes for the nucleon from perturbative QCD and QCD sum rules 7-41745
quark mass and spin effects in meson wave functions 7-41744
quark mass matrix under S_N symmetry 7-61510
quark matter, conference, Pacific Grove, CA, USA (April 1986) 7-55881
quark matter as ground state in Universe 7-56503
quark plasma theory 7-24947

colour model continued

quark propagators on large lattices, extension in time by distant source method, quenched QCD 7-61559
 quark structure functions measured with Drell-Yan process 7-49079
 quark-gluon plasma, dynamical evolution and phenomenology 7-56500
 quark-gluon plasma, perturbative and nonperturbative theory, review 7-56510
 quark-gluon plasma, rehadrization, thermodynamical considerations 7-49278
 quark-gluon plasma, strange particles as signature 7-56504
 quark-gluon plasma droplets, finite size effects, partition function 7-24839
 quark-gluon plasma formation, pre-equilibrium plasma dynamics 7-56578
 quark-gluon plasma in SU(2) T=200-300 MeV, reduction of degrees of freedom from T, Q, Y effects 7-5062
 quark-gluon plasma undergoing a phase transition, rel. hydrodynamic eqns. 7-19184
 quarkless QCD, transport coeffs., lattice estimates 7-35798
 quarkonia, covariant soliton dynamics, role of gluon condensate 7-35790
 quarkonium \rightarrow ggg, gggg, colour factor weight calcs., QCD anal. 7-56519
 quarkonium energy splittings in perturbative QCD 7-15126
 quarks, four generation mass fixing 7-61511
 quenched ACD, chiral props. and hadron spectrum in alternate directions implicit method 7-61577
 quenched QCD hadron mass calcs. on 16^4 spacetime lattice 7-61604
 Rubakov-Callan effect, nonabelian interactions 7-10013
 S-wave nonleptonic hyperon decays in quantum chromodynamics 7-15149
 Savvidy model, absence of deconfining phase transition at one-loop order 7-41735
 scalar glueball mass estimate, pure gauge lattice QCD calcs., four-parameter improved action 7-487
 scalar gluonium, local duality constraints, Gauss-Weierstrass QCD sum rule anal. 7-489
 scalar lattice QCD, hadron static props., form factors, charge radii, lepton widths 7-49080
 scalar meson is a dilaton in QCD 7-41748
 scalar sector of gauge theories and the quest for unified theory 7-10007
 scale fixing, lattice Monte Carlo calcs. 7-30239
 Schrödinger equation, local equivalent, with relativistic kinematics, WKB approximation 7-56406
 sextet quarks and light pseudoscalars 7-5047
 short-distance hadronic cross sections, soft-gluon corrections 7-24907
 short-distance hadronic cross-sections, soft gluon corrections 7-41840
 short-range rapidity fluctuations in high energy collisions 7-61781
 six-quark subprocesses in QCD 7-470
 Skyrme model, recent developments in context of QCD, review 7-414
 Skyrme parameter calcs. from QCD sum rules 7-30186
 skyrmion scattering in an axially symmetric system 7-61445
 skyrmion-skyrmion interaction struct., zero-range boson-exchange interpretation 7-581
 soliton bag model, characteristics using BAG program 7-49087
 soliton solutions in confining colour dielectric model 7-41713
 spin-dependent structure fns. for polarized nucleons, perturbative QCD calcs. 7-56553
 spinor propagators in anti-de Sitter space-time 7-35797
 SQCD with $N_{\text{colour}} < N_{\text{flavour}}$ symmetry breakings 7-49085
 squark mixing angles in supergravity theories, gluino flavour changing in SU(5) 7-56136
 stability of chiral symm. breaking solns. 7-49076
 state dependent bag constant at large-N limit of QCD 7-10022
 static potential for smooth strings 7-41769
 static potentials from an extended gauge symmetry, confinement mech. 7-24838
 static quark pot. in dual superconductor calcs. 7-49074
 statistical QCD, deconfinement and chiral symm. restoration, Monte Carlo anal. 7-61569
 strict QCD inequality and mechanisms for chiral symmetry breaking, instantons role 7-30241
 string model with extrinsic curvature effects, static quark pot. 7-61610
 string tension and plaquette-plaquette correlation from QCD sum rules 7-478
 structure function, sensitivity to QCD scale parameter 7-35877
 SU(2) \times SU(2) algebraic description of the skyrmion, SU(4) quark model recovery 7-56440
 SU(2) deconfining phase transition, correlation length and susceptibility, Monte Carlo methods 7-56515
 SU(2) flux-tube model of quark deconfinement at high temperature, effective string tension calcs. 7-473
 SU(2) gauge theory, Monte Carlo renormalisation study of deconfining transition 7-15073
 SU(2) lattice gauge theory, renormalisation and continuum limit of composite operators 7-19017
 SU(2) nonAbelian gauge theory, quantum fluctuations of Copenhagen vacuum 7-61436
 SU(3) gauge theory for quark-gluon plasma 7-41623
 SU(3) lattice gauge theory, scaling behaviour of heavy-quark potential 7-486
 SU(3) lattice QCD, β -function at large β , Monte Carlo renormalisation group anal. scaling deviations 7-24781
 SU(4) \times SU(4) composite model of weak interactions (Chinese) 7-10037
 SU(N) gauge theories, effects of self-dual fourth-rank tensor scalar fields on asymptotic freedom, broken QCD appl. 7-390
 SU(N) SUSY QCD, instanton superfield calcs. in Higgs phase 7-56512
 sum rules for exotic qqg states 7-41733
 supersymmetric QCD, consistency of instanton calculus 7-61551
 supersymmetric QCD, effective Lagrangian in 1/N approx. 7-30244
 SUSY QCD, nucleon spin conservation at short distances 7-490
 SUSY Yang-Mills theories and QCD, structure fn. comparisons in leading log approximation, second moments 7-5095
 SVZ method applied to Schrödinger equation with $V=\lambda \text{ctg}^2\pi x$ pot. 7-61135
 swelling nucleons in QCD, superconducting state, string tension 7-15124
 technicolour theories, chiral hierarchies, perturbation and breaking 7-41728
 technicolour theory with pseudo-Goldstone bosons, one-loop corrections 7-56525
 technidilation from technicolour model, $\xi(2,23)$ resonance 7-15098
 technipion production and decay, order- α_s QCD effects 7-35806
 tensor gluonium spectrum, QCD sum rules framework 7-19073
 three gluon vertex in light cone gauge, nonlocal BRS counterterms 7-5060

colour model continued

three gluon vertex in light cone gauge, renormalisation anal., nonlocal terms 7-5059
 topologically massive chromodynamics at finite temperature 7-41726
 toponium and QCD scale parameter Λ_{ms} 7-61787
 transformation of elementary particle physics into many-body physics 7-49042
 transition to quark matter by light ion expts. 7-56501
 transverse plasmon effect, proof of nonexistence 7-479
 U(1) problem on a lattice, massless π^0 and massive η 7-48996
 ultra-heavy quarks, prod. and decay props., quarkonia prod. in hh and e^+e^- 7-30242
 ultra-relativistic heavy ion collisions, strangeness in the central region 7-56691
 ultrarelativistic heavy-ion collisions, flavour composition in scaling hydrodynamics 7-15178
 vector glueball, algebraic approach consistent with QCD 7-41743
 vector meson radiative decay in lattice QCD 7-35879
 wave function, nonlocal condensates and QCD sum rules 7-41747
 x-space sum rules and π wave function 7-41734
 B $\rightarrow\gamma$ X, helicity suppression and colour thaw problem 7-61590
 B mesons, QCD probes of charge radii and possible sum rules 7-35805
 B-meson decays without charmed particles in the finalstate 7-517
 B \rightarrow D $\bar{D}^0\pi^\pm$, CP violation anal. 7-61657
 $\bar{c}c$, QCD sum rules for S-wave charmonium 7-41732
 D-mesons, vacuum insertion and nonperturbative effects 7-10057
 $e(\bar{e})p$, nucleon structure fns., SUSYQCD anal. 7-61689
 ed interactions, nonperturbative QCD corrections to $R=\sigma_L/\sigma_T$, use of MIT bag model 7-481
 $e^+e^- \rightarrow 2$ mesons $+\gamma$, high energies, QCD perturbation theory anal., cross sections, wave functions 7-19123
 e^+e^- annihilation, charged particle multiplicities at 29 GeV in central rapidity regions 7-61713
 $e^+e^- \rightarrow e^+e^- +$ hadrons, 7-70 (GeV/c) 2 , photon structure fn. meas. QCD, parton model comparisons 7-540
 $e^+e^- \rightarrow \gamma + 2$ jets, quark charge test 7-61706
 $e^+e^- \rightarrow \gamma\gamma\gamma$, heavy flavor production with gluon bremsstrahlung 7-15125
 $e^+e^- \rightarrow$ hadrons, 35 GeV, α_s determ., corrections to corrected data, second-order QCD anal. 7-30275
 $e^+e^- \rightarrow$ heavy baryons, perturbative QCD anal. 7-35887
 e^+e^- high energy annihilation, quark and gluon fragmentation, Feynman diagrams 7-24901
 $e^+e^- \rightarrow$ jets, geometric struct. anal. review, QED tests, review 7-541
 $e^+e^- \rightarrow$ jets, hadronic final states, QCD and string model comparisons, review 7-30274
 $e^+e^- \rightarrow$ leptons, strong interaction contributions to four-lepton processes in electroweak SU(2) \times U(1) 7-61644
 $e^+e^- \rightarrow q\bar{q}$, invariant amplitudes in QCD 7-537
 $e^+e^- \rightarrow q\bar{q}$, three-jet event cross-section, transverse momentum distribution, first order QCD calcs. 7-24895
 $e^+e^- \rightarrow q\bar{q}\gamma\gamma$, scalar quark production, Monte Carlo QCD simulation 7-35888
 $e^+e^- \rightarrow X$, multijet production studies 7-35891
 $e^+e^- \rightarrow e\Delta$, high Q^2 , N- Δ form factors, perturbative QCD anal. 7-19119
 ep \rightarrow hadrons + jets, cross sections, perturbative QCD calcs. 7-24869
 ep interactions, nonperturbative QCD corrections to $R=\sigma_L/\sigma_T$, use of MIT bag model 7-481
 η' effects and instanton physics in low energy axion dynamics 7-30191
 $g(2050-2350)$, glueball candidate, coupling const. estimate 7-41710
 $gg \rightarrow Z^0 + L_j$, helicity amplitude formalism, cross-section formulae 7-61586
 $gg \rightarrow Q\bar{Q}g(\bar{g}g)$, heavy flavor production with gluon bremsstrahlung 7-15125
 $\gamma e \rightarrow$ hadrons + jets, cross sections, perturbative QCD calcs. 7-24869
 $\gamma\gamma$ annihilation, nondiffractive meson pair prod., perturbative QCD and resonance contribs. 7-41826
 $\gamma\gamma \rightarrow B\bar{B}$, baryon production, Q^2 dependence, QCD anal. 7-19148
 $\gamma\gamma \rightarrow \gamma\gamma$, elastic scatt., worden sum rule and perturbative QCD 7-24924
 $\gamma\gamma \rightarrow M^+M^-$ ($M=\pi, K$), next-to-leading-order perturbative QCD calcs. 7-61591
 $\gamma p \rightarrow$ hadrons + jets, cross sections, perturbative QCD calcs. 7-24869
 γq Compton scatt., NA14 expt. results 7-61785
 H $^-$ meson investigation by QCD sum rule method 7-41751
 hh \rightarrow hh, inelastic scatt., flux tube or bremsstrahlung 7-35893
 hh large angle scatt., spin effects 7-24912
 hh \rightarrow W(Z)+jet, QCD parton shower Monte Carlo model 7-41852
 hN $\rightarrow\gamma\gamma\text{pp}+X$, qq $\rightarrow\gamma\gamma$, gg $\rightarrow\gamma\gamma$, qg $\rightarrow\gamma\gamma$ mechanisms, perturbative QCD anal. 7-61592
 $i(146\phi) \rightarrow \gamma\gamma(0\gamma)$, radiative decays and SU(3) flavour structure 7-15161
 K $\rightarrow 2\pi$, vacuum insertion and nonperturbative effects 7-10057
 K $\rightarrow \pi\pi$ amplitudes in QCD duality approach, $|\Delta I|=1/2$ rule problems in standard model 7-10056
 K 0 -K 0 mixing, short-distance contrib. from QCD sum rules 7-15122
 K $^+$ $\rightarrow \pi^+\pi^0$, amplitude in quenched approx., lattice calculation 7-35857
 K 0 $\rightarrow \pi^0\pi^0$, quark contribution to nuclear force 7-551
 (L) † , deep inelastic process, colour conductivity model anal., nuclear shadowing phenomenon and binding energy comparisons 7-49385
 (L) ϕ (X), nuclear enhancement effect, colour oscillation mechanism 7-41987
 IN \rightarrow X, deep inelastic scatt., impulse approx. and scaling variable modification 7-527
 IN \rightarrow X, structure functions and parity violation in supersymmetric QCD 7-61700
 $\mu N \rightarrow X$, inclusive deep inelastic scatt., structure function meas., QCD comparison 7-529
 μp deep inelastic scatt., jet profiles, QCD effects 7-61699
 N form factor, QCD anal. 7-61686
 N form factor, QCD and perturbation theory calcs. 7-61685
 NN elastic scattering, new mechanism for spin effects 7-61744
 NN \rightarrow NN, six-quark resonance structures in QCD 7-545
 NN \rightarrow NN π , quark interchange in pion prod. 7-30286
 NN \rightarrow X, quark-gluon plasma formation 7-56579
 np scattering, spin and isospin nonconservation by a colour force 7-30285
 Ωp elastic scatt., Chou-Yang model for differential cross section 7-41833
 $p \rightarrow \pi^0 e^+$, lattice QCD Monte Carlo simulations 7-35763
 pp, $\sqrt{s} = 630$ GeV, jet, W $^\pm$ and Z 0 prod. at UA2 7-10075
 pp, one-jet events, colour scalar bosons as source of jets 7-5134
 pp, SPS energies, fragmentation props. of quark and gluon jets 7-5129
 pp \rightarrow heavy leptons, missing- p_T -plus-jets signal anal. 7-61761
 pp \rightarrow jets, W $^\pm$, Z comparison with QCD and standard model 7-10086

colour model continued

- $pp \rightarrow$ quark+gluon jets, fragmentation props., gluon radiation effects, model comparisons 7-61772
 pp scattering, cross section increase due to parton-parton scatt., diffraction formalism 7-41843
 $pp \rightarrow W^+X$, transverse hadronic energy distrib. anal. 7-19144
 $pp \rightarrow X$, cross-sections for supersymmetry production 7-560
 $pp \rightarrow X$, inclusive minijet cross section and the bare pomeron in QCD 7-41740
 $pp \rightarrow X$, KNO scaling, multiplicity fluctuations, strange particle production 7-56580
 $pp \rightarrow X$, search for quark-gluon plasma at TeV I 7-56577
 $pp \rightarrow X$, three-jet prod. due to QCD fragmentation process 7-19141
 $pp \rightarrow Z^0X$, transverse hadronic energy distrib. anal. 7-19144
 π , QCD probes of charge radii and possible sum rules 7-35805
 π distribution amplitude moments and QCD sum rules 7-30246
 π form factor, QCD anal. 7-61686
 $\pi \rightarrow \gamma\gamma$, partial decay widths in QCD with coloured light scalars 7-19105
 π -hadrons, partial decay widths in QCD with coloured light scalars 7-19105
 π structure function, Fock state expansion of hadronic wave function in QCD (Chinese) 7-24887
 π structure functions, second moments, QCD sum-rule calcs. 7-5094
 π - η mass difference in lattice QCD, U(1) problem, strong coupling expansion 7-41810
 π^0/γ ratio meas. using dileptons, quark-gluon plasma diagnostics 7-41746
 $\pi^+-\pi^0$ mass difference and Weinberg sum rules, phenomenological anal. 7-41809
 $\pi\pi$ - $\pi\pi$, dibaryon state search in kinematically complete meas. 7-5120
 π -N, parity-violating coupling constant, determination from nonleptonic Hamiltonians 7-4993
 π - π N, isospin-even forward scatt. amplitude as low-energy QCD test 7-56572
 $\pi^-N \rightarrow p^0X$, 300 GeV/c, $p_T > 2$ GeV/c, evidence for QCD higher twist mechanisms 7-61740
 $\Psi = e^+e^-$, $R_2 = \Gamma(T \rightarrow e^+e^-)/\Gamma(\Psi \rightarrow e^+e^-)$ calcs. bound state quark model anal. 7-61582
 $\psi = \eta(\eta')$, gluonium content in phenomenological model with SU(3) breaking 7-19108
 q - q pair condensation, 3P_0 , QCD anal. using Coulomb plus Breit potential 7-61597
 qq pair exchange transition pot. in constituent quark model (Chinese) 7-5057
 qq plasma near equilibrium, kinetic coeffs., colour density matrix 7-10023
 qq realistic pot. with running coupling constant, fine and hyperfine splitting 7-19068
 $\rho \rightarrow \pi\gamma$, partial decay widths in QCD with coloured light scalars 7-19105
 Σp elastic scatt., Chou-Yang model for differential cross section 7-41833
 \bar{t} resonance, one-loop electroweak radiative corrections 7-41819
 $\tau \rightarrow \rho\nu$, $K^*\nu$, branching ratios, effects of asymptotic flavour symmetry, QCD anal. 7-49143
 $T \rightarrow e^+e^-$, $R_2 = \Gamma(T \rightarrow e^+e^-)/\Gamma(\Psi \rightarrow e^+e^-)$ calcs., bound state quark model anal. 7-61582
 $T \rightarrow T\pi\pi$, $3S$ to 1^1P_1 transition, QCD multipole expansion 7-41797
 $V \rightarrow \rho\gamma$, decay amplitude calcs., lattice QCD anal. 7-35801
 W and Z production properties 7-61777
 $\bar{E}p$ elastic scatt., Chou-Yang model for differential cross section 7-41833
 $D^+ \rightarrow \mu^+\nu_\mu$, $R_1 = \Gamma(\eta_c \rightarrow \gamma\gamma)/\Gamma(D^+ \rightarrow \mu^+\nu_\mu)$ calcs. bound state quark model anal. 7-61582
 $^2H(e^+e^-)$, tensor polarisation and spin observables as perturbative QCD test 7-35998
 3He , quark induced three body forces in 3N systems, nonrelativistic potential model anal. 7-56615
 4He , quark induced three body forces in 3N systems, nonrelativistic potential model anal. 7-56615
 $^AHe(e,e')^AHe$, $A=3,4$ effect of hidden colour 7-49382
 J/ψ suppression by quark-gluon plasma formation 7-10030
 $K^-p \rightarrow AX$, Δ polarization, energy dependence and p_T variance, QCD comparisons 7-61754
 $pp \rightarrow W+2$ jet events, standard model expectations for large transverse momentum 7-24917
 π N low energy scatt., isospin-even forward scatt. amplitude as QCD test 7-41835
 $W \rightarrow qq$, reconstructing jet-jet invariant masses 7-10060

colour perception see colour vision

colour photography

- Cibachrome materials, permanence improvements under adverse display conditions 7-355
 CRT printer, exposures from digital images onto colour photographic paper 7-354
 negative film technology, recent progress (Japanese) 7-56364
 printing, digital image layout system 7-15027
 reflection holography, recording and reconstruction 7-25781
 special effects, mask processes (German) 7-24716
 step-focus photographic technique for recording stellar colour 7-14505
 violet light photographic technique for studying Mars atmosphere 7-18364
 Ag halide colour photographic materials (Japanese) 7-56358
 Ag-based sensitive materials in colour photography (Japanese) 7-56365

colour receivers, television see colour television receivers

colour television cameras

- proximity image intensifier persistence improvements with $Y_2O_3:Sb$ phosphor 7-57598

colour television receivers

- HDTV and 525-line viewing, sight-line displacements, eye movements eval. 7-59992
 projection lens, wide-angle, design 7-50699
 projection lens, wide-angle having aspherical surfaces 7-50698

colour tv receivers see colour television receivers

colour vision

- see also eye
 adaptation and colour matching 7-54566
 ambient illumination and the determ. of material changes 7-28532
 chromatic adaptation and colour constancy, possible dichotomy 7-28520
 chromatic adaptation rel. to central binocular mechanism 7-59993
 chromaticity differential thresholds and general metamerism indexes 7-40150

colour vision continued

- chromaticity horizontal cells in retina of freshwater turtle 7-47063
 chromostereopsis and chromatic dispersion 7-34145
 cone photoreceptors, human, spectral sensitivity obs. 7-59991
 cones and opponency 7-17991
 contrast threshold measurement system 7-54563
 CRT display, legibility and symbol-background colour difference relationship 7-14018
 defects rel. to eye disease 7-17994
 dichromatic confusion lines and colour vision models 7-54565
 display colour parameters modelling and algorithmic colour selection 7-28538
 display technology implications of colour perception 7-14005
 displays, colours description w.r.t. natural colour system 7-23356
 equidistant colour space, reconstruction from responses of visual neurons of macaques 7-28514
 ethyl alcohol, effects on electrooculogram and colour vision 7-28501
 event-related pots. to coloured patterns and colour names 7-23349
 evoked potentials, comparison of fibre optical and video monitor stimulators in normals and multiple sclerosis patients 7-65865
 flicker photometry, residual minimum flicker 7-34150
 HDTV and 525-line viewing, sight-line displacements, eye movements eval. 7-59992
 heterochromatic boundary in stabilised retinal image, effect of imposed retinal image movements on colour vision 7-23351
 horizontal cells, c-type, in bowfin retina, response props. 7-47053
 human colour-discrimination, Stiles's anal. on Apple II 7-8562
 increment spectral sensitivities for spatial periodic grating patterns: evidence for variable tuning of the chromatic system 7-23353
 lateral geniculate nucleus cells, macaque, mesopic spectral responses and Purkinje shift 7-47054
 lateral geniculate nucleus chromatic data, macaque, principal component anal. 7-28515
 lightness algorithms, formal connections 7-28523
 long-wavelength flashes detect., spatial and chromatic antagonism between long- and middle-wavelength cones 7-54567
 luminance contrast and colour systems in human vision 7-47068
 mechanisms of colour constancy 7-28530
 natural scene colour and spatial structure, photographic colorimetry 7-41420
 neural coding and colour discrimination in colour deficient 7-59995
 pattern vision, neural mechanisms (Japanese) 7-28527
 perception, functions and characts. between brightness channel and chromaticity channel (Japanese) 7-28521
 personal-computer based color monitor system for color anomaly inspection (Japanese) 7-47066
 photopigment spectra, unifying presentation 7-17992
 polymorphism of the long-wavelength cone in normal human colour vision 7-17990
 primary colours spatial array, visual colour shifts (Japanese) 7-3785
 reaction time, spatial and chromatic dependences 7-8569
 retina, central part, distrib. of sensitivity to coloured light (Japanese) 7-65755
 retinal ganglion cells, turtle, photoreceptor input and temporal summation 7-17984
 retinex theory of colour vision, anal. rel. to human colour constancy 7-28529
 retinol in insect photoreceptors, sensitising function 7-23352
 retrobulbar neuritis afflicted patients, chromatic visual field (Italian) 7-28519
 scene-illuminant chromaticity, method for computation for specular high-lights 7-28531
 short-wavelength-sensitive cone photoreceptors, isolation in 4-6-week-old human infants 7-59994
 simultaneous colour constancy obs. 7-28534
 simultaneous colour induction, mechanisms 7-28525
 sinusoidal spectral power distrib., human colour mechanisms anal. appl. 7-28524
 spectral information coding by IR photoreceptors, colour vision and neural network analogues 7-35593
 spectral luminous efficiency functions by heterochromatic brightness matching 7-47064
 spectral sensitivity, intense spectral light studies and the colour receptor mosaic of primates 7-17993
 spectrally selective flash early receptor pot. in dichromats 7-28510
 standards within the transport industry, origins 7-23350
 stereopsis, chromatic and luminance difference control 7-54568
 surface spectral reflectance, evaluation of linear models 7-28522
 temporal integration of chromatic double pulses for detection of equal-luminance wavelength changes 7-47065
 von Kries colour constancy, heuristic anal. 7-28533

columbium see niobium

coma see aberrations

combination locks (electronic) see safety systems

combination scattering spectra see Raman spectra

combinational circuits see combinatorial circuits

combinational mathematics see combinatorial mathematics

combinatorial circuits

- integrated optical combinatorial logic using electro-optic Bragg gratings 7-26040

combinatorial mathematics

- see also graph theory; trees (mathematics)
 evolution, test of phylogenical predictions using combinatorial optimisation 7-40084
 NP-complete problem without local minima 7-29673
 radioactive waste containers store, radiation minimisation 7-10290

combined cycle power stations

- coal gasification-combined-cycle plant thermoeconomic anal. 7-23206
 heat and power generation from coal, SO_2 , SO_3 , NO , NO_2 and CO removal from flue gases (German) 7-65653
 integrated coal gasification combined cycle power generation (Japanese) 7-65510

combined heat and power generation see cogeneration

combustion

- see also explosions; flames; heat of combustion; reaction kinetics
 acetaldehyde, combustion, oxidation, radical concs. and phase rels. 7-54126
 aerial suspension combustion, wave propag. 7-54125
 aerosols, monofuel, combustion, num. investig. 7-8283

combustion continued

- analysis of the stability of heating processes from the point of view of measurement (*Hungarian*) 7-59765
 annular premixed propane flame, mass transfer, residence time in recirculation zone 7-17790
 atomised liquid fuel, turbulent diffusion flame, fine struct., using pneumatic nozzle 7-17791
 benzene, combustion processes under intense mag. fields, living organisms appl. 7-8285
 buoyant and combusting flow, turbulence model 7-51083
 burner, flashback-resistant, for combustion diagnostics and anal. spectrometry 7-35598
 burner nozzle combustion noise expts. 7-50843
 CARS, applications in chemical reactors, combustion and heat transfer 7-17788
 coal, fluidised-bed combustion, mathematical model 7-6308
 coal, in fluidised bed furnace, mechanism investig., balance eqn. formulation 7-65322
 coal char combustion in fluidised bed 7-37537
 coal dust flame acceleration, feedback control model for unsteady flow 7-65326
 coal particles, holographic interferometry 7-25734
 cobaltites, fine-particles, low temp. prep. by solid solution precursor method 7-59486
 coke dust, polydisperse, combustion kinetics 7-13776
 cross-beam polarisation spectroscopy with pulsed dye laser 7-13771
 developing simplified models of combustion chemistry by simulation with detailed chemical kinetics models 7-13779
 diagnostics by pulsed photothermal and photoacoustic deflection spectroscopy 7-23016
 dust-gas mixture, slow burning conditions 7-13778
 flame front propag. convective vertex form. 7-13777
 flame propagation, unsteady and ID, mathematical anal. 7-57944
 flames, diffusion, bluff-body stabilised, near-wake region, CARS meas. 7-8282
 flames, one-dimensional premixed, wave characts. 7-8279
 flames, turbulence generation and suppression 7-8281
 FLARE code for two-dimens. turbulent combustion 7-20815
 flow simulation in vortex struct., variational entropy method (*French*) 7-44064
 fluidised beds, turbulent, mass transfer, burning rate 7-59761
 free-resistant material, Sb_2O_3 influence on effectiveness, chem. anal. (*Russian*) 7-65378
 fuel drop, liq., moving, combustion, thin-flame theory, variable density effect 7-26364
 fuel drops combustion, stability loss mechanism in stream of oxidising gas 7-31892
 gasdynamic model, heat exchange, press. distrib. in high enthalpy air stream 7-1587
 gaseous and solid fuel combustion, energy efficiency calc. (*German*) 7-8354
 gases, premixed turbulent combustion, second-order closure prediction 7-57942
 granular propellants, combustion, two-phase transient flow, modelling 7-37520
 hydrocarbon fuel, combustion products flow in explosive type impulsive setup 7-17792
 hydrocarbon fuels, combustion, chem. kinetic modelling 7-54123
 ignition criterion in combustion problem with heat source 7-33933
 internal combustion engine, flow field using Lagrangian-Eulerian method (*Chinese*) 7-20813
 magnetic field effects on biological and chem. processes 7-47135
 metal bulk sample, laser heating and combustion by obliquely incident radiation 7-26795
 methane, combustion kinetics with Pd, Pt catalysts 7-39894
 methane and propane in diluted air, diffusion flames, extinction limits 7-3590
 methane and related cpds., combustion and pyrolysis 7-18516
 methane-air mixture, minimum ignition energy, spark discharge characteristics 7-39896
 methane-air turbulent diffusion flames laminar-flamelet modelling 7-57938
 MHD slagging coal combustors 7-63363
 mobile CARS instrument for combustion and plasma diagnostics 7-44238
 multiphoton excitation techniques for combustion diagnostics 7-17789
 nonlinear Raman spectroscopy combustion and plasma diagnostics appl. 7-16332
 nonlocal conservation law in combustion theory 7-63233
 oblate ellipsoids, diffusion, shape effect on consumption in fluid-particle processes 7-33930
 peat bog fires, simulation and control 7-13773
 plane detonation wave in combustible gas mixture, direct initiation 7-31836
 plane premixed flame, nonlinear differential system modelling (*French*) 7-28313
 porous granular systems, convective combustion 7-13772
 power plant combustion chamber, combustion stability 7-31890
 premixed laminar flames in stagnation point flow, calculation of extinction limits 7-59762
 propane jet flames, near-nozzle region, flow struct. 7-8280
 pulse combustion, characts., appls., and research needs 7-65594
 reacting flows, combustion and chem. reactors, book 7-4644
 reaction rate constants computing using Harris Super minicomputer 7-33912
 Stirling engines, shaft power producing combustor for thermal efficiency improvement 7-65560
 thermionic energy convertor, combustion heated, materials and preliminary design 7-65509
 transient ignition on a flat plate 7-17794
 turbulent flames, struct. calc. 7-65321
 unitary fuel aerosol, burning in closed region, planar problem 7-13833
 wall jet diffusion combustion, heat exchange process, num. investig. 7-26266
 waste fuels in the cement industry 7-28386
 weak disturbance velocity measurement, bulk density in porous media 7-31826
 C particle laden O_2 gas, normal shock wave anal. 7-51288
 CO in combustion flows, two-photon digital imaging using planar laser-induced fluorescence 7-46896

combustion continued

- CO_2 conc. profiles of axisymmetric combustion gas flow, IR spectra, temp. profile meas. 7-3591
 CoAl, combustive synthesis, physicochemical props. 7-7918
 FeAl_3 , Fe_2Al_3 , combustive synthesis, physicochemical props. 7-7918
 H flame-out in air flow, gas dynamic struct., interaction effect 7-26315
 H_2 -air mixtures, 1-D tube combustion processes, numerical calc. 7-65647
 Li- SO_2 batteries, effect of water during incineration 7-39983
 NO_x in-furnace reduction, reburning, bench scale process evaluation 7-17798
 NiAl , Ni_2Al_3 , combustive synthesis, physicochemical props. 7-7918
 O atom, flame diagnostics by two-photon fluoresc., UV laser appl. 7-23015
 O_3 swirling flow combustor, gas densities, laser scatt. meas. 7-6218
 Ti nonisothermal carbiding mechanism, combustion with carbonaceous material, thermal wave propag. vel. determ. 7-46381
 Ti plate, ignition in air under CW laser radiation action 7-32492

comets

- 1984 comets, observations and designations 7-47790
 P/ (1982i), inner coma critical ionization velocity effects 7-9424
 P/Halley (1982i), dust emission ground-based obs. 7-18384
 abundance correlations 7-47766
 abundant small comets impacting Earth and Moon 7-40727
 advanced image processing and planetological appl., conference, Vulcano, Italy (September 1985) 7-24270
 American Astronomical Society, 18th annual meeting of Division for Planetary Sciences, conf., Paris, France (November 1986) 7-24255
 AMPTE artificial comet, study of plasma waves and elec. field 7-9355
 ancient comets and meteor showers, temporal correlations and genetic associations 7-55543
 inner atmosphere, modelling of dust and neutral gas 7-24083
 Bennett (1970II), Na atom coma conditions (*Chinese*) 7-4366
 breakup as possible cause of formation of group of impact structures Earth's surface 7-55544
 breakup hypothesis re-examination 7-60605
 brightness outbursts, model of icy bodies fragmentation in solar wind high-speed streams 7-47768
 P/Bus (1987f), recovery, astrometry, orbital elements and ephemeris (1987 January to May) 7-55558
 chaotic motion and existence of comet clouds 7-4372
 chemistry of atmospheres of planets and comets, book 7-48210
 comae, electron impact ionization effect 7-40766
 comae, molecular physics and chemistry 7-14541
 comet nucleus sample return mission, conf., Canterbury, England (July 1986) 7-48180
 P/Crommelin (1984 IV), scanner spectral obs. 7-34934
 P/d'Arrest (1976 XI), search for periodic photometric vars. 7-55564
 dirty ice grain characts. 7-18387
 dirty ice grains, albedos evol. 7-24067
 P/Du Toit-Hartley (1986q), recovery, astrometry and total visual magnitude estimate 7-47775
 dust halo formation, time-dependent numerical modelling 7-55536
 dust particle impact on metal targets, ion form. studies 7-46259
 dust studies using ground-based near-IR obs. (*Chinese*) 7-18357
 dust tail interaction with solar wind sector boundaries 7-66416
 dust tails, density and brightness distrib. 7-60597
 dust tails interpretation, use of Finson-Probststein method 7-60563
 P/Encke, spectroscopic observations during 1984 apparition 7-66508
 P/Encke from progenitor breakup, hypothesis re-examination 7-60605
 exosphere model, analogue in planetary fast neutral atoms emission and effects on solar wind 7-55521
 experimental modelling of cometary phenomena, conformity to similarity criteria 7-66506
 flare activity, relation to velocity waves in solar wind 7-4371
 Geminids parent comet, combined action of cometary ejection process and gravit. perturbations on meteor stream struct. 7-47796
 Germinid meteors parent body, orbital elements, mass and size from spatial struct. of meteor swarm 7-66519
 P/Giacobini-Zinner, solar wind flow past comet 7-9426
 P/Giacobini-Zinner, ground based and in-situ observations 7-9433
 P/Giacobini-Zinner, heating of tail electrons 7-66510
 P/Giacobini-Zinner, ion tail struct. and interaction with solar wind 7-40778
 P/Giacobini-Zinner, linearly polarized magnetic fluctuations 7-55565
 P/Giacobini-Zinner, plasma wave turbulence in strong coupling region 7-9430
 P/Giacobini-Zinner, plasma waves in shock interaction region 7-23965
 P/Giacobini-Zinner (1984e), column densities, prod. rates and spectral obs. 7-47767
 P/Giacobini-Zinner (1984e), COSPAR symposium 12, Toulouse, France (1986 June-July) 7-35080
 P/Giacobini-Zinner (1984e), electron impact ionization effect in coma 7-40766
 P/Giacobini-Zinner (1984e), H_2O prod., CO_2^+ and plasma concentrations, spectrophotometric obs. 7-47793
 P/Giacobini-Zinner (1984e), high dispersion spectral obs. 7-47792
 P/Giacobini-Zinner (1984e), ICE energetic ion obs. 7-40763
 P/Giacobini-Zinner (1984e), ICE radio receiver meas. 7-40765
 P/Giacobini-Zinner (1984e), International Cometary Explorer project 7-40665
 P/Giacobini-Zinner (1984e), ion comp. and upstream solar wind obs. 7-60604
 P/Giacobini-Zinner (1984e), ion tail structures and vel. fields near ICE encounter time 7-18376
 P/Giacobini-Zinner (1984e), origin of metal ions in cometary coma 7-9415
 P/Giacobini-Zinner (1984e), plasma characts. 7-14510
 P/Giacobini-Zinner (1984e), plasma regime, ICE sampling 7-40764
 P/Giacobini-Zinner (1984e), possibility of strong Draconid meteor shower (1986 October 8 to 9) 7-4385
 P/Giacobini-Zinner (1984e), spectral obs. during ICE encounter 7-18380
 P/Giacobini-Zinner (1984e), thermal IR and visual imaging 7-24073
 PI Giacobini-Zinner (1985 XIII), astrometric positions (June to October 1985) 7-66504
 P/Giacobini-Zinner (1985 XIII), periodic photometric variations in near-nucleus zone 7-55564
 P/Giacobini-Zinner (1985 XIII), stability of sunlit ionopause 7-60599
 P/Grigg-Skjellerup, 1987 predictions, orbit improvement and ephemeris 7-40761

comets continued

- P/Grigg-Skjellerup (1986m), January and February 1987, spectra and magnitude 7-55560
 P/Grigg-Skjellerup (1986m), recovery observations 7-4368
 P/Halley, 1910 and 1986 apparitions, electrostatic charging effect on dust distrib. 7-66507
 P/Halley, (1982i), bacterial grain model for 2 to 4 μm spectrum 7-34937
 P/Halley, (1982i), energetic particles obs. by Giotto spacecraft 7-14529
 P/Halley, (1982i), in situ photopolarimetric meas. of dust and gas in coma 7-14527
 P/Halley, (1982i), IR heating of cometary atmosphere 7-34933
 P/Halley, (1982i), optimum orbit determ. via ground-based astrometry and Vega spacecraft obs. 7-14525
 P/Halley, (1982i) results of Giotto radio science expt. 7-14528
 P/Halley, shape, rotation state and puzzling observational findings 7-29434
 P/Halley, spacecraft exploration missions and results 7-55573
 P/Halley, USNO astrometric catalogue 7-34888
 Halley's Comet, images 7-9439
 P/Halley 7-47788
 P/Halley (1910 II), astrometric obs. by J. Tebbutt 7-55943
 P/Halley (1910 II), spin vector refinement and discrete dust sources map (May-June 1910) 7-4365
 P/Halley (1982i), 1986 March spectral characts. (*Chinese*) 7-29426
 P/Halley (1982i), 3 μm spectroscopy and photometry 7-24070
 P/Halley (1982i), a priori position prediction error from terrestrial and space-probe meas. 7-4370
 P/Halley (1982i), accurate positions (*Chinese*) 7-29425
 P/Halley (1982i), Astron UV obs., gaseous coma model (*Russian*) 7-14540
 P/Halley (1982i), attitude and orbit control systems of Japanese spacecraft Sakigake and Suisei 7-55568
 P/Halley (1982i), bow shock position and struct. during Vega encounters 7-9423
 P/Halley (1982i), coma mag. field characts., Vega obs. (*Russian*) 7-4381
 P/Halley (1982i), coma morphology and dust emission pattern modelling 7-14526
 P/Halley (1982i), cometary ion obs. at and within cometopause region 7-14530
 P/Halley (1982i), cometary tail discontinuity rel. to tangential discontinuity in solar wind rel. field (*Russian*) 7-55570
 P/Halley (1982i), COSPAR symposium 12, Toulouse, France (1986 June-July) 7-35080
 P/Halley (1982i), dust and gas impact on spacecraft causing electron emission 7-9432
 P/Halley (1982i), dust coma meas. by Vega (*Russian*) 7-4380
 P/Halley (1982i), dust environment, Vega SP-2 expt. obs. (*Russian*) 7-4378
 P/Halley (1982i), dust high-velocity impacts on space probes 7-34946
 P/Halley (1982i), dust IR characts. 7-18385
 P/Halley (1982i), dust particles, Vega spacecraft Puma obs. (*Russian*) 7-4375
 P/Halley (1982i), dust tail interaction with solar wind sector boundaries 7-66416
 P/Halley (1982i), electron impact ionization effect in coma 7-40766
 P/Halley (1982i), ELF plasma waves, Vega APV-N detections (*Russian*) 7-14539
 P/Halley (1982i), Fabry-Perot ground-based obs. 7-18377
 P/Halley (1982i), far UV spectral images from sounding rockets 7-47785
 P/Halley (1982i), far-IR photometry obs. 7-18386
 P/Halley (1982i), gas phenomena 7-14531
 P/Halley (1982i), Giotto encounter 7-24082
 P/Halley (1982i), Giotto Radio Science Experiment at Parkes 7-55571
 P/Halley (1982i), ground-based obs. of 3.2-3.6 μm emission features 7-24071
 P/Halley (1982i), H α and 630 nm meas. 7-18378
 P/Halley (1982i), H alpha and O'D spectra observations 7-66509
 P/Halley (1982i), H coma, Dynamics Explorer 1 observations 7-9431
 P/Halley (1982i), H coma obs. by Suisei 7-40768
 P/Halley (1982i), HCN production 7-24072
 P/Halley (1982i), high dispersion spectral obs. 7-47792
 P/Halley (1982i), highlights of Japanese spacecraft observations 7-9417
 P/Halley (1982i), hydromagnetic waves near O $^+$ or H $_2$ O $^+$ ion cyclotron freq. 7-9419
 P/Halley (1982i), ICE plasma wave measurements in ion pick-up region 7-9427
 P/Halley (1982i), International Cometary Explorer project 7-40665
 P/Halley (1982i), ion dynamics and distrib., Suisei spacecraft observations 7-9420
 P/Halley (1982i), ion tail bending and solar wind plasma flow 7-40767
 P/Halley (1982i), ion tail disturbance, 31 Dec. 1985 event 7-9418
 P/Halley (1982i), ion tail structures and vel. flows, optical obs. 7-18374
 P/Halley (1982i), JHK IR magnitudes (1986 November 16) 7-24080
 P/Halley (1982i), JHK photometry and visual magnitude estimates (1987 January 28 to February 12) 7-66512
 P/Halley (1982i), kilometric radio waves and plasma waves; Sakigake obs. 7-40769
 P/Halley (1982i), line profiles and images 7-18356
 P/Halley (1982i), linear features rel. to thermomechanical stresses and surface cracks on nucleus 7-40772
 P/Halley (1982i), linear polarisation obs. 7-47782
 P/Halley (1982i), magnetic field free cavity form. 7-60606
 P/Halley (1982i), MMT spectroscopic obs. (1986 Nov.) 7-47771
 P/Halley (1982i), molecules, gas and dust in inner coma 7-40773
 P/Halley (1982i), multiple light scattering near nucleus 7-40770
 P/Halley (1982i), nature of cometary nucleus 7-34936
 P/Halley (1982i), near IR obs. from Vega-2 spacecraft 7-14520
 P/Halley (1982i), nucleus albedo rel. to total cometary mass in solar system 7-24077
 P/Halley (1982i), nucleus and jets, Vega 1 and 2 results 7-40771
 P/Halley (1982i), nucleus characts. review 7-18383
 P/Halley (1982i), O, C and CO prod. rates determ., UV spectra anal. 7-18379
 P/Halley (1982i), obs. of nucleus and jets by Vega missions 7-9438
 P/Halley (1982i), occultation of PKS 2314+03, scintillation meas. 7-18381
 P/Halley (1982i), OH emission and absorption meas. at 18 cm 7-55572
 P/Halley (1982i), period from pre-perihelion light curve 7-29427

comets continued

- P/Halley (1982i), photoelectric discovery of 52-hour periodicity in nuclear activity 7-55563
 P/Halley (1982i), photometry and activity of nucleus at pre-perihelion heliocentric distances > 4.6 AU 7-47763
 P/Halley (1982i), photometry of solar analogues along path 7-9416
 P/Halley (1982i), Pioneer Venus obs. during inferior conjunction 7-18382
 P/Halley (1982i), plasma and neutral gas meas. from Vega 1 and 2 spacecraft 7-14523
 P/Halley (1982i), polarimetry of visible and UV molecular bands 7-66503
 P/Halley (1982i), post-perihelion obs. of H $_2$ O from KAO 7-47786
 P/Halley (1982i), pre-perihelion photometry at Catania (Italy) Observatory 7-34930
 P/Halley (1982i), pre-perihelion tail characts. and solar wind effects 7-24068
 P/Halley (1982i), preperihelion IRTF monitoring program obs. 7-34931
 P/Halley (1982i), radio source scintillation obs. through cometary tail 7-66516
 P/Halley (1982i), rocket-borne UV spectroscopy, CO and C abundances 7-47784
 P/Halley (1982i), role of CO $_2$ in outbursts 7-47783
 P/Halley (1982i), rot. period determ. from photometric obs. 7-47787
 P/Halley (1982i), rotation model involving 2.2 day precession 7-55567
 P/Halley (1982i), search for CO $^+$ MM-wave transitions 7-24081
 P/Halley (1982i), search for H $_2$ O $^+$ emission 7-9524
 P/Halley (1982i), solar wind interaction meas. by Vega spacecraft 7-14522
 P/Halley (1982i), sources of visual photometry 7-34941
 P/Halley (1982i), spacecraft charging effects in cometary environment 7-14473
 P/Halley (1982i), spacecraft encounters and international cooperation 7-55427
 P/Halley (1982i), spatial structures imaging from Catania Observatory 7-18375
 P/Halley (1982i), spectral and visible magnitude obs. 7-55554
 P/Halley (1982i), spectroscopy of 3.4 μm emission feature 7-55537
 P/Halley (1982i), stability of sunlit ionopause 7-60599
 P/Halley (1982i), Suisei and Sakagake project overview 7-40666
 P/Halley (1982i), Suisei spacecraft observations of pickup ions 7-9422
 P/Halley (1982i), TA reports (1986 May-June) 7-24069
 P/Halley (1982i), tail phenomena and solar wind interactions 7-18373
 P/Halley (1982i), three-channel spectrophotometric study by Vega project 7-14472
 P/Halley (1982i), total visual magnitude estimates (1986 August to October) 7-29429
 P/Halley (1982i), total visual magnitude estimates (1986 November 3 to December 4) 7-40781
 P/Halley (1982i), upstream cometary pick-up observations 7-9428
 P/Halley (1982i), UV spectrum evol. (1985 September to 1986 June) 7-47794
 P/Halley (1982i), UV variability and H $_2$ O production rates 7-9421
 P/Halley (1982i), Vega 1 and 2 dual freq. radio sounding (*Russian*) 7-14537
 P/Halley (1982i), Vega 1 and 2 plasma and neutral gas meas. (*Russian*) 7-14536
 P/Halley (1982i), Vega 1 IKS IR obs. of nucleus 7-40774
 P/Halley (1982i), Vega APV-V electric field and plasma meas. (*Russian*) 7-14538
 P/Halley (1982i), Vega IKS IR spectrum 7-40775
 P/Halley (1982i), Vega IR spectral obs. (*Russian*) 7-4376
 P/Halley (1982i), Vega SP-1 obs. of dust coma (*Russian*) 7-4379
 P/Halley (1982i), Vega three-channel spectroscopy in visible and near-UV ranges 7-14519
 P/Halley (1982i), Vega TV obs. (*Russian*) 7-4374
 P/Halley (1982i), Vega-1 and 2 encounters (*Russian*) 7-4373
 P/Halley (1982i), Vega-1 meas. of secondary electron currents induced by impacts 7-14521
 P/Halley (1982i), Vega-1 neutral gas obs. (*Russian*) 7-4382
 P/Halley (1982i), Vega-1 obs. of energetic particles (*Russian*) 7-14535
 P/Halley (1982i), Vega-2 TKS expt. obs. (*Russian*) 7-4377
 P/Halley (1982i), visual magnitudes, Dec. 1986 and Jan. 1987 observations 7-55546
 P/Halley (1982i), wave and plasma meas. on Vega-1 and Vega-2 spacecraft 7-14524
 P/Halley (1982i) 7-40777
 P/Halley (1982i) 7-55479
 P/Halley (1982i) HCN detect. 7-60598
 Hartley-Good (1985 XVII), polarimetry of visible and UV molecular bands 7-66503
 ice particle condensation and sublimation, hydrodynamic study 7-40782
 icy nuclei, optical constns. of H $_2$ O-NH $_3$ ice mixtures 7-23993
 icy-glue model of cometary nuclei 7-34943
 impacts, fulgurites form. 7-47439
 interaction with solar wind, model 7-29373
 interstellar particle impacts upon Oort Cloud comets 7-40783
 ion acceleration processes, due to solar wind interaction 7-34945
 ionised tail rays creation 7-47789
 ionopause instability, consequences of collisions and compressibility 7-9437
 ionospheres, electron cooling by vibr. and rot. excitation of water vapour 7-29435
 ions interacting with solar wind, evol. 7-60600
 IRAS-Araki-Alcock (1983 VII), $^{32}\text{S}_2$ photodissoc. lifetime determ. 7-24075
 IUE observations and UV characts. 7-47791
 Levy (1987a), discovery, orbital elements, magnitude eqn. and ephemeris (1987 January 25 to March 6) 7-55539
 Levy (1987a), discovery, rough positions and total visual magnitude estimates 7-47777
 Levy (1987a), obs., orbital elements and ephemeris (1987 January 5 to February 4) 7-47779
 Levy (1987a), position in January 1987 and ephemerides 7-60602
 Levy (1987a), positions and magnitudes (1987 January) 7-47780
 light scattering by cometary grains, wavelength depend. 7-55535
 long-period cometary orbits, effect of galactic perturbations 7-34935
 P/Lovas 2 (1986p), astrometric positions, orbital elements and ephemeris 7-47778
 P/Lovas 2 (1986p), positions, orbital elements and ephemeris 7-47774
 Lovas (1986p), Nov. 1986 comet discovery 7-34940

comets continued

- Lovas (1986p), positions, elements, and ephemeris (1986 Nov.-Dec.) 7-40780
- Machholz (1986e), TA reports (1986 May-June) 7-24069
- magnitude distribution, implications for fading of comets 7-55566
- magnitudes, coma and tail details for 24 objects (1982 Sep.-1986 Jul.) 7-34942
- magnitudes, coma and tail details for eleven objects (1985 08 to 1986 06) 7-14534
- magnitudes distribution 7-24066
- Minor Planet Circulars, precise positions for ten objects, elements and ephemerides 7-24046
- Minor Planet Circulars, precise positions for ten objects, elements, and ephemerides 7-40743
- Minor Planet Circulars 11275-11374, precise positions for 18 objects, elements, and ephemerides 7-40742
- Minor Planet Circulars 11465-11560, precise positions for Minor Planet Circulars 11465-11560 objects, elements, and ephemerides 7-55520
- Minor Planet Circulars 11561-11680, precise positions for 22 objects, elements, and ephemerides 7-66495
- molecular astrophysics, NATO conf., Bad Windsheim, Germany (1984 July) 7-9589
- Moon, abundant small comet impacts NOT causing seismic waves 7-40727
- mystery of comets, book 7-24330
- Nishikawa-Takamihawa-Tago (1987c), total visual magnitudes (1987 Jan.-Feb.) 7-66515
- Nishikawa-Takamizawa-Tago (1987c), discovery positions 7-55547
- Nishikawa-Takamizawa-Tago (1987c), positional observations, orbit and ephemeris 7-55549
- Nishikawa-Takamizawa-Tago (1987c), positional observations and improved orbit and ephemeris 7-55552
- Nishikawa-Takamizawa-Tago (1987c), total visual magnitude estimates (1987 January) 7-55555
- Nishikawa-Takamizawa-Tago (1987c), discovery, elements and ephemeris (1987 January 25 to March 1) 7-55538
- nongravitational forces on short-period comets, model calcs. for low equatorial obliquities 7-47764
- nongravitational forces on short-period comets, model calcs. for high equatorial obliquities 7-47765
- Oort cloud, outer boundary radius set by hypothetical companion star 7-34890
- Oort cloud, struct. characters. 7-34944
- Oort cloud comets injection to inner Solar System by galactic tidal fields 7-47738
- Oort cloud outer radius, boundary set by Galaxy according to King Innanen formula 7-4357
- orbital elements, calcs. from 1982-3 obs. 7-66505
- orbital motion, effects of subtle planetary perturbations by Pluto and Earth-Moon system 7-4297
- origin and evolution 7-55569
- planetary perturbations, Tisserand criterion appl. 7-29383
- plasma conf., Sukhumi, USSR (May 1986) 7-48174
- plasma tail acceleration mechanism, theory 7-9425
- plasma tail and tail rays stability, effect of plasma-neutrals coupling 7-24076
- precise posns. on Minor Planet Circulars 10781-10884 for eight objects 7-9399
- precise posns. on Minor Planet Circulars 10885-10988 for 17 objects 7-9400
- precise posns. on Minor Planet Circulars 10989-11094 for nine objects 7-9401
- precise posns. on Minor Planet Circulars 11095-11198 for 16 objects 7-9402
- P/Schwassmann-Wachmann 2 (1986h), visual magnitude estimates (1986 Dec.-1987 Jan.) 7-55562
- short period comets, origin and near-parabolic flux 7-34944
- P/Skiff-Kosai (1976 XVI)=1977 DV3, precise positions and orbital elements 7-9435
- small comet influx to Earth rel. to airglow holes and H₂O conc. in mesosphere 7-40622
- small comets, influx into Earth's upper atmosphere, comments and reply 7-60601
- solar wind - comet surface interactions 7-40691
- solar wind interaction, rapid pickup of ions from comet due to turbulence 7-9429
- solar wind interactions, review (Russian) 7-40663
- solar wind-comet interaction, MHD simulation model 7-24078
- solar wind-comet plasma interaction, laboratory simulation expt. 7-9434
- Sorrells (1986n), discovery, total visual magnitude estimates and positions 7-29428
- Sorrells (1986n), ephemeris (1986 November 26 to 1987 January 10) in 5-day steps 7-47769
- Sorrells (1986n), MMT spectroscopic obs. (1986 Nov.) 7-47771
- Sorrells (1986n), Nov. 1986 discovery and ephemeris 7-40776
- Sorrells (1986n), Nov. and Dec. 1986 magnitude observations 7-47773
- Sorrells (1986n), orbital elements, magnitude eqn. and ephemeris (1987 January 25 to March 1) 7-55541
- Sorrells (1986n), orbital elements and ephemeris 7-29432
- Sorrells (1986n), precise positions, parabolic orbital elements, and ephemeris 7-29430
- Sorrells (1986n), total visual magnitude estimates 7-55556
- Sorrells (1986n), total visual magnitude estimates (1986 November) 7-34938
- Sorrells (1986n), total visual magnitude estimates (January-February 1987) 7-66514
- stability of sunlit ionopause 7-60599
- submm spectroscopy 7-47795
- surface materials characts. 7-40729
- TA reports (1985 November-1986 August) 7-14533
- TA reports (1986 Aug.-Nov.) 7-55533
- TA reports (1986 January-June) 7-14532
- TA reports (1986 November-1987 January) 7-55534
- tail formation, laboratory simulation expt. of solar wind-comet interaction 7-9434
- P/Tempel 2 (1987g), recovery positions and ephemeris 7-55561
- Terasako (1987d), discovery and approximate positions 7-55550
- Terasako (1987d), ephemeris (1987 January-March) 7-55542
- Terasako (1987d), orbital elements, ephemeris and visual observations 7-60603

comets continued

- Terasako (1987d), positions, elements, ephemeris, and magnitude (1987 Jan.-Feb.) 7-55553
- thermomechanical stresses and surface cracks on nucleus 7-40772
- total cometary mass in solar system, implications of albedo of Halley's Comet 7-24077
- P/Tsuchinshan 1 and 2, improved orbits and ephemerides 7-40762
- Tunguska body, cometary breakup hypothesis re-examination 7-60605
- Tunguska event, cometary model rel. to meteors with terminal flares 7-9449
- P/Urata-Nijijima (1986o), ephemeris (1986 December 1 to 16) in 5-day steps 7-47770
- P/Urata-Nijijima (1986o), independent discovery and ephemeris (1986 November 16 to 1987 January 15) 7-40779
- P/Urata-Nijijima (1986o), MMT spectroscopic obs. (1986 Nov.) 7-47771
- Urata-Nijijima (1986o) (=1986 UD), precise positions, parabolic orbital elements, and ephemeris 7-29431
- UV spectra, S compounds identification 7-55574
- Vesta mission to Venus, comet and asteroids for 1990s 7-40667
- P/Wild 3 (1987e), orbital elements and ephemeris 7-55559
- P/Wild 3 (1987e), recovery positions (1987 January-February) 7-55557
- Wilson (1986i), predicted occultation of SAO 125375 (1986 October 28) 7-18389
- Wilson (1986i), ephemeris (1986 October 17-December 26) 7-24074
- Wilson (1986i), ephemeris for 17 Sept. to 16 Dec. 1986 period 7-4369
- P/Wilson (1986i), Feb. 1987 visual magnitudes 7-66513
- Wilson (1986i), IR and visual magnitudes (1986 September) 7-9436
- Wilson (1986i), MMT spectroscopic obs. (1986 Nov.) 7-47771
- Wilson (1986i), OH emission obs. and visual magnitude estimate 7-66511
- Wilson (1986i), OH production rate from 1667 MHz obs. and visual magnitudes 7-29433
- Wilson (1986i), orbital elements, magnitude eqn. and ephemeris (1987 January 25 to March 31) 7-55540
- Wilson (1986i), Sept. and Oct. 1986 visual magnitudes 7-18388
- Wilson (1986i), total visual magnitude estimates, spectra and CCD imaging 7-4367
- Wilson (1986i), total visual magnitude estimates (1986 December 20 to 27) 7-47781
- Wilson (1986i), total visual magnitude estimates (1986 November) 7-34939
- Wilson (1986i), total visual magnitude estimates (1986 November 25 to December 7) 7-47772
- Wilson (1986i), total visual magnitude estimates (1986 October 17 to 23) 7-24079
- Wilson (1986i), visual obs. and positions (1986 Aug.-Sep.) 7-34932
- Wiseman-Skiff (1987b), discovery observations 7-55545
- P/Wiseman-Skiff (1987b), total visual magnitude estimates (1987 January 22 and 26) 7-55551
- P/Wiseman-Skiff (1987b), astrometry, elements and ephemeris 7-55548
- P/Wilson (1986i), orbital elements and ephemeris 7-47776
- zodiacal dust cloud source, implications of solar flare track densities in interplanetary dust particles 7-55531
- C₂ spectra, synthetic Swan band profiles of ¹²C¹²C and ¹²C¹³C 7-60532
- H₂O⁺ origin 7-66517
- ³²S₂ photodissociation lifetime, implications for ³²S₂ prod. rate 7-24075

commensurate-incommensurate transformations

- 3d- and 4f- metals, periodic spin structs., critical props. calcs. (Russian) 7-59031
- Ag-Mg, modulation periods 7-46463
- anisotropic honeycomb domain wall networks in uniaxial systems 7-26900
- bi-tetramethylammonium copper tetrachloride, phase transitions, microwave permitt. meas. 7-2184
- bis-methylammonium zinc tetrachloride, lock-in transition, X-ray topography studies 7-32630
- CDW, depinning and quasi-commensurate transition, plastic deformation analogy 7-12628
- continuous phase transitions to incommensurate structures 7-21402
- dimer pair correlations on the brick lattice, commensurate-incommensurate transitions 7-9789
- discommensuration patterns, dynamics 7-44749
- displacive surface reconstructions, incommensurate sandwiches 7-52223
- domain wall kinetics, space-time complexity and nonlinear field eqns. 7-51996
- electric field induced, Landau-type thermodynamic pot. 7-63766
- epitaxial overlayers, structural transitions 7-27194
- graphite intercalated with Br, struct. and phase transitions, review 7-52041
- graphite surface, adsorbed Kr incommensurate phase, computer simulation studies 7-7009
- icosahedral phases, discommensurations 7-44437
- incommensurate antiferromagnetic struct., equilb. states and precession excitation spectra, phase diagram study (Russian) 7-27521
- incommensurate CDW systems, long-range Coulomb effects 7-45189
- incommensurate phases, phasons, dynamic pinning mechanisms 7-45941
- incommensurately modulated phases, scatt. theory 7-26938
- methane monolayer on graphite, thermodynamic study 7-16863
- noise suppression 7-44752
- one-dimensional quantum systems, spatial structures and dynamic excitations, self-consistent theory 7-44755
- p=2 lock-in phase transition in surface reconstruction, theory 7-32628
- phase and amplitude modulation 7-32600
- propylammonium tetrachloromanganate, incommensurate γ phase, elastic neutron and X-ray scatt. 7-16538
- quartz, incommensurate phase, temperature dependent low-frequency modes 7-6737
- quartz, phonon dispersion and mode coupling near incommensurate phase transition 7-58421
- quartz, stress induced, incommensurate 3q-1q transition 7-63794
- soliton line formation, kinetics 7-38157
- steric interaction between wandering walls, mean field theory 7-27058
- sublattice model, incommensurate phase sandwiched by reentrant commensurate phases 7-51991
- submonolayer adsorbed film, phase diagram, intrinsic and extrinsic ordering forces, density functional theory calcs. 7-63952
- submonolayer film, phase diagram, relax. mechanisms, density functional theory calcs. 7-63953
- surface reconstruction phase transformations 7-2326

commensurate-incommensurate transformations continued
 tetrafluoromethane on graphite, phase diagram, phase transitions 7-38338
 bis(tetramethylammonium) bromochlorocuprate single cryst. solid solns., phase diagram study 7-26944
 tetramethylammonium tetrachlorozincate, ferroelec., optical activity, high accuracy universal polarimeter meas. 7-17300
 tetramethylammonium tetrachlorozincate, ferroelec., optical activity in incommensurate phase 7-64602
 tetramethylammonium tetrachlorozincate, X-ray radiation damage, satellite reflections 7-51827
 thiourea, paraelectric phase, mol. dynamics simulation 7-37920
 transition metal dichalcogenides, CDW states 7-44810
 transition metal dichalcogenides, layered cpds., CDWs 7-2523
 transition metal layered compounds, CDW phase transitions, Landau theory 7-44809
 TTF-TCNQ, incommensurate phase transition, symmetry theory (*Chinese*) 7-63793
 wall orientation near the commensurate-incommensurate transition 7-58438
 Xe monolayers on graphite, low temp. struct. and incommensurate-commensurate transition, electron diff. study 7-38335
 Ag₃AsS₃, incommensurate phase, electroacoustic echo obs. 7-45400
 Ag₃SbS₃, pyrrargyrite, incommensurate phase, NQR study 7-45837
 AlPO₄, berlinite, growth defects and incommensurate phase obs. by high temp. X-ray topography 7-32423
 AlPO₄, modulated phase, electron microscopy study 7-26937
 BaZnGeO₄, phase transitions, X-ray study 7-52036
 Cd₂Nb₂O₇, soft mode damping in incommensurate phases, anomalous behaviour 7-38149
 Cr-Ge dilute alloys, elec. resist. temp. and press. depend. studies 7-32980
 Cs₂HgBr₄, phase transitions, microwave permitt. meas. 7-2184
 Cu_{1+x}Pd, long-period superstructures 7-21430
 o-D₂ monolayers, physisorbed on graphite specific heat studies 7-52271
 KC₂₄ intercalation cpd., low temp. structural transition 7-21431
 K₃Cu₈S₆, mixed valence 2D metal, CDW 7-45294
 K₂SeO₄, soft mode damping in incommensurate phases, anomalous behaviour 7-38149
 K₂ZnCl₄, phase transitions, Raman-scattering study 7-52035
 Kr adsorbed on graphite, adsorption isotherm meas. near commensurate-incommensurate transition 7-38337
 Mo surface, struct. phase transitions 7-2327
 Mo₈O₂₃ low-dimensional conductor, cryst. struct. and commensurate-incommensurate transition, X-ray diff. study 7-58230
 N₂ surface layer on graphite, motion investig. 7-32792
 NH₄HSeO₄, X-ray irradiat., existence of incommensurate phase, permitt. meas. 7-33338
 Na₂CO₃, incommensurate crystal, Raman and IR spectra 7-17315
 NaNbO₃, incommensurate ferroelec., in transverse elec. field, virtual Lifshitz point 7-45947
 NpAs single crystal, neutron diff. study 7-17158
 Pd monolayers on Ta(110), morphology and struct. phase transitions 7-38374
 Rb_{1-x}Cs_xFeCl₃, random singlet-magnetic ground state system, mag. ordering effects 7-33167
 Rb₂ZnBr₄, soft mode damping in incommensurate phases, anomalous behaviour 7-38149
 Rb₂ZnCl₄, commensurate-incommensurate phase transition, X-ray and dielec. studies 7-63800
 Rb₂ZnCl₄, cryst., incommensurate modulation, light propag. 7-22196
 Rb₂ZnCl₄, incommensurate transition, pot. energy and mol. dynamics ab initio calcs. 7-21435
 SiO₂, modulated phase, electron microscopy study 7-26937
 Sr_{0.95}Ba_{0.05}Nb₂O₆, incommensurate superstructures, phase transition, electron diff. study 7-63792
 TaS₂: 1T, submillimetre conductivity, dielectric function 7-12749
 2H-TaSe₂, triply incommensurate phase, phase slip region 7-44811
 Ti-Cr, β -eutectoid, deform. behaviour of retained β phase 7-39589
 TiNi-X, X=Fe, Ge, Re or Ni, struct. transitions in premartensitic range (*Russian*) 7-39504
 TiGaSe₂ crystals, exciton spectrum, phase transitions 7-7124
 U, modulated phases, superspace symm. anal. 7-38186
 UAs_{0.95}Se_{0.05}, disappearance of type-I antiferromag. struct., neutron diff. study 7-45620
 UAs_{1-x}Se_x system, mag. phase diagram, neutron diff. study 7-12971
 W (001), adsorbed H, displace surface reconstructions, incommensurate sandwiches 7-52223
 W (001), H adsorption, commensurate-incommensurate phase transitions 7-7010
 W surface, struct. phase transitions 7-2327
 Xe, adsorbed on graphite, incommensurate-commensurate phase transition, X-ray diff. obs. 7-32793
 Xe-Kr mixtures adsorbed on graphite, X-ray diffraction studies 7-6966
 α -ZnP₂, incommensurate phase, phase transformations and lattice modulation 7-6777

commerce

see also investment; marketing
 Space Remote Sensing Center projects and commercial prospects 7-60258

commissioning

see also installation
 thermal conductance apparatus, large-scale, commissioning trials 7-14940

communication aids for handicapped *see handicapped aids*

communication cables *see telecommunication cables*

communication channels *see telecommunication channels*

communication theory *see information theory*

communications applications of computers *see telecommunications computing*

communications computer control *see telecommunications computer control*

communications computing *see telecommunications computing*

community planning *see town and country planning*

commutators

planar acoustooptic 2x2 commutator switch 7-50741

compact discs *see video and audio discs*

compacting *see densification*

comparators (circuits)

amplitude comparator for RF signals analogous to cricket's auditory system 7-14024

compasses

see also navigation

gyrocompass, integration of eqns. of motion 7-43652

gyromagnetic compass bearings anal., appl. of current flow junction (*Polish*) 7-30051

magnetic flux-gate compass for automobile navigation 7-330

North azimuth determination using suspended gyrocompasses 7-66309

compensation

see also error compensation

compensator for the time dispersion in monochromator 7-1253

crosstalk optical sensors accuracies improvement 7-43434

fan shaped SAW transducers, characts. distortions, anal. and compensation 7-20554

ions activity meas., using digital device 7-3614

MA 5964 laboratory microprocessor-controlled conductivity meter (*Slovenian*) 7-18803

magnetic suspension systems with digital controllers 7-332

magnetometer for geophysical exploration, compensation display device (*Russian*) 7-30045

speckle-shearing interferometry, compensation for rigid and deformational displacements 7-48841

thermometric characts. of planar semiconductor diodes correction (*Czech*) 7-61334

zoom convertor with focusing and thermal compensation functions 7-31516

- 7-38565

compensation, charge *see charge compensation*

compilers (program) *see program compilers*

compiling programs *see program compilers*

complementarity

No entries

complementary metal-oxide-semiconductor integrated circuits *see CMOS integrated circuits*

complete computer programs

see also APL listings; BASIC listings; C listings; FORTRAN listings; macros; Pascal listings; subroutines

dbASE II program for using archival files of geological subsurface files 7-40584

flow, determinacy of degenerate equilibria 7-57782

HP program to determ. centre thickness of convex spectacle lenses 7-14158

plates structures, 3D, elastostatic anal., CAD, stress anal. 7-37334

sea bed contour map construction from random data, spline method 7-34726

NS, spin-orbit coupling const. calc. using restricted HF wavefunctions 7-56949

SiF, spin-orbit coupling const. calc. using restricted HF wavefunctions 7-56949

complex angular momentum plane

see also angular momentum theory; Pomeranchuk poles and trajectories; Regge poles and trajectories

No entries

complex systems *see large-scale systems*

compliance constants *see elastic constants*

composite insulating materials

electroceramics, book contrib. 7-27645

glass fibre reinforced epoxy resin insulator, interface treeing phenomena study 7-39012

mica-epoxy composite dielectric strength obs. 7-64570

polyester fibre-epoxy resin insulator, prebreakdown space charge injection meas. 7-39017

quartz-filled epoxy resin, charged, photoemission meas. in insulating gases 7-27871

PbZr_{1-x}Ti_xO₃-polyethylene 3-0 connected composite, dielec. and piezoelec. props. 7-45937

composite material interfaces

see also delamination

7-28112

aramid fibre reinforced epoxy, delamination fracture toughness 7-53900

barrier coatings on unidirectional fibres, diffusional interaction of compounds effect on cond. 7-52167

C fibre reinforced Al, segregation of doping elements, Si, Bi 7-65046

carbide/ α -Fe matrix interface, void nucleation mechanism 7-38354

ceramic eutectic composites, microstruct. and mech. props. 7-64991

ceramic matrix composite frictional stress evaluation along fibre-matrix interface 7-28143

composite laminates, first ply failure anal. 7-44670

conductivity, effective, of composites with imperfect thermal contact at constituent interfaces 7-6901

continuous composite materials, interface response theory 7-64039

design problems with allowance for interphase reactions 7-43661

duplex fibre reinforced materials, fracture toughness development 7-22804

electroceramics, book contrib. 7-27645

electromagnetism, interface response theory in composite dielectric materials 7-62564

epoxy composites, Fe powder reinforced, flexural props., water condition temp. depend. 7-59587

fibre reinforced composites, compressive-fluxural/shear failure mode transition, interface strength 7-39586

fibre reinforced composites, damage constitutive relations 7-43765

fibre reinforced composites, fracture, micromechanical and macromech. criterion 7-17609

fibre reinforced metal, subjected to uniform temp. change, dislocations punched out around short fibre 7-21491

fibre reinforced Ti-base alloy, development of creep-resisting composites 7-3228

E-glass fibre composite interfaces, surface studies using diffuse reflectance and photoacoustic FTIR spectra 7-46044

glass fibre reinforced epoxide resin, tensile props. under superposed hydrostatic press., failure mechanisms 7-28078

glass fibre reinforced epoxy and polyester composites, flexural failure mechanisms, global stress plane 7-8082

glass fibre reinforced epoxy resin insulator, interface treeing phenomena study 7-39012

glass fibre reinforced PVC matrix, acoustic emission during irreversible deform. 7-3380

graphite fiber reinforced epoxy, delamination fracture toughness 7-53900

composite material interfaces continued

- graphite fibre reinforced Al matrix composites, interface charactn., TEM obs. 7-44554
 graphite fibre reinforced epoxy, interface modified, moisture effects 7-3476
 graphite fibre reinforced epoxy laminate, dynamic moire interferometry of stress wave propag. 7-59717
 graphite fibre reinforced epoxy laminates, dynamic response at high shear strain rates 7-3371
 graphite fibre reinforced Mg matrix composites, fabrication, fibre coatings, wetting, adhesion 7-46374
 graphite fibre reinforced PEEK, quasi-isotropic laminate, shear strain meas. by moire interferometry 7-65253
 jute fibre reinforced polyester resin with fillers, fibre matrix interactions, absorbed water influence 7-3263
 Kevlar 29 fibre reinforced bone and dental cements, mech. props. 7-28080
 laminate, dynamic moire interferometry of stress wave propag. 7-59717
 metal matrix composites, fatigue crack propag., effect of aq. environments 7-17624
 metal matrix composites, liq. metal infiltration prep., wetting 7-46372
 metal matrix composites, thermal residual stress 7-63848
 metallic glass reinforced Al composite fabrication by multi-lamina explosive compaction 7-59482
 mother-of-pearl, fracture surfaces, analytical techniques appl. 7-8781
 photoelastic analysis of composites and other bonded-material structures, limitations 7-63094
 pineapple leaf fibre reinforced rubber, phys. and mech. props. 7-3378
 plastic composites, layered, periodic necking instability 7-43709
 polyethylene, chlorinated, rutile-filled, 7-39573
 polymer composites, particle filled, mechanical strength/filler content relationship 7-13594
 polymers, ferrite-filled, highly loaded, melt rheology 7-12345
 polypropylene, mica-reinforced, fracture behaviour, effect of coupling agent, flake orientation and degradation 7-13593
 polyurethane-CaCO₃ composites, segmented, dielec. relax., glass transition 7-45926
 single fibre composites, stress transfer, critical fibre length, Young's modulus ratio 7-59558
 single fibre-resin tensile tests, stress transfer 7-28074
 steel fibre reinforced Cu composites, extruded, struct. and fractography 7-13595
 styrene-isoprene-styrene block copolymer system, ferrite-filled, matrix-filler interactions 7-3352
 sunhemp fibre reinforced polyester composites, tensile and impact props. 7-39592
 wood pulp fibre-cement paste composites, fibre-matrix interface, SEM obs. 7-64985
 Ag₃S-Al₂O₃ composites, stoichiometry and homogeneity, interfacial effects 7-6815
 Al based composite, rheocasting, microstruct., fracture, worn surface (Chinese) 7-13407
 Al-Mg-Si, Al-Mg, cast, mica particle dispersed composites, struct., strength, hardness 7-59574
 Al-Si-SiO₂ sand composites, prep. and mech. props. 7-17500
 B fibre reinforced Al, bond form. between alitized B fibres and matrix in rolling 7-3331
 B fibre reinforced Al, strength characts. 7-33768
 B fibre reinforced Al matrix composites, transverse mech. props., isothermal exposure effect 7-39688
 C fibre reinforced Al-Cu(Mg) composites, tensile strength, fracture, interfacial bond strength 7-33744
 C fibre reinforced C, 3D, residual stress 7-52090
 C fibre reinforced C, multidirectional composites, macroporosity and interface cracks 7-46513
 C fibre reinforced epoxy, electrodeposition of polymer interphase 7-13592
 C fibre reinforced epoxy resin laminates, curing characts., fibre kinking 7-39474
 C fibre reinforced plastics, cylindrical interface crack study 7-26201
 C fibre reinforced plastic, cemented lap joint, stress-strain state and strength 7-33794
 C fibre-epoxy composite, Ba labelled, XPS anal. 7-28163
 Cr₃C₂-Ni-P hard metal, Cr₃C₂ solution in Ni matrix, liq. phase influence 7-53689
 Mo fibre reinforced Cu or Fe composites, extruded, struct. and fractography 7-13595
 Ni reinforced Al, matrix crystn. and sintering, role of reinforcing phase 7-33625
 Ni reinforced LiF-NaF, matrix crystn. and sintering, role of reinforcing phase 7-33625
 NiO-based aligned eutectics, microstruct., crystallography and interfaces 7-65025
 NiO-CaO eutectic, directionally solidified, struct. imperfections 7-65026
 SiC fibre reinforced Al alloys, whisker or particulate hybrids, mech. props. 7-13537
 SiC fibre reinforced Li₂O-Al₂O₃-SiO₂ glass ceramic composite, thermomech. mismatch 7-46538
 SiC whisker or particle reinforced Al composites, deform. thermal expansion, strengthening mechanisms 7-3373
 SiC whisker reinforced Si₃N₄, microstruct. and props. 7-22824
 SiC whisker reinforced Si₃N₄ ceramics, fracture toughness (Japanese) 7-28138
 SiC whisker reinforced Al, flame spraying fabrication and forging, whisker distrib. and strengths 7-59483
 W fibre reinforced Fe-Cr-Al superalloy, surface cladding and matrix deform., thermomech. loading 7-46568

composite materials

- see also *cermets; composite insulating materials; composite material interfaces; composite superconductors; concrete; eutectic alloys; fibre reinforced composites; fibres; laminates; particle reinforced composites*
 advanced composite developments 7-27956
 aerospace material advances 7-27875
 anisotropic, interface crack, singularities 7-26218
 anisotropic, kinetic Hall and seebeck coeffs., critical behaviour calcs. 7-45411
 anisotropic materials of different moduli, cylindrical shell theory 7-43684
 anomalous transport in random resistor-capacitor network, appl. to composite materials 7-27312
 asbestos-brucite-polyphenylene sulphide composites 7-53925

composite materials continued

- beam, two-layer cpd., damping characts., influence of quality of adhesion 7-50972
 binary elastic effective transform. strain 7-44660
 breakdown in high-temperature gas flow 7-26383
 bronze/Pb composite matrix for small closed cycle refrigerators 7-61340
 cement-based, strain rate effects on fracture, conf., Boston, USA (Dec. 1985) 7-14712
 ceramic composites, multiphase interaction, sensor appls. 7-64996
 ceramic-ceramic, CVD processing 7-64992
 ceramic-polymer composites, piezoelec. sensors, elec. characts., hydrophone appl. 7-62943
 ceramics, conf., University Park, PA, USA (July 1985) 7-60880
 ceramics, liq. phase sintered, hot isostatic pressing 7-64989
 ceramics, non-oxide, CVD fabrication 7-64993
 ceramics, sintering, role of shear deform. 7-64988
 columnar, subjected to impulsive loading, dynamic response testing 7-59708
 conductivity, effective, of composites with imperfect thermal contact at constituent interfaces 7-6901
 cracked matrix, strength 7-46609
 cylinder, non-homogeneous, elastic-plastic and limit soln. under internal pressure (Chinese) 7-43693
 DC cond. and percolation threshold calcs., metal-insulator composite mean-field theories 7-45253
 design problems with allowance for interphase reactions 7-43661
 dielectric function, momentum depend. effective medium approach 7-27281
 diffusion and heat transfer, practical eqns. 7-6855
 digital image correlation methodology use for deform. quantification 7-59718
 effective elastic moduli of isotropic multicomponent composites, Walpole bounds 7-6704
 effective thermal conductivity determ. method 7-52160
 elastic, linear elasticity rel. to homogenisation and optimal bounds 7-31645
 elastic wave scattering by spherical inclusions, with appl. to low frequency wave propag. in composites 7-6719
 electrical conductivity, quantitative microstruct. effects (German) 7-17666
 electricity and modern techniques, conf., Bordeaux, France (Oct. 1985) 7-14708
 electroceramics, book contrib. 7-27645
 electron microscopy studies, symposium, Nantes France (July 1986) 7-18479
 fabric dependence of anisotropic strength criterion 7-38084
 failure criteria, tensor-polynomial type, exptl. verification of efficiency 7-22812
 failure under compression, complex stressed state case, continuous theory 7-62974
 fatigue life and residual strength, lognormal distribution model 7-17616
 ferrofluid-Al particle composite, microwave absorption studies 7-59306
 fibre optic sensor development for high speed material diagnostics 7-65250
 fibrous composites, influence of thermal effects of struct. and props. during explosive welding 7-17793
 fibrous composites with weak bonding, elastic response 7-31646
 fibrous materials, definition, class and elaboration (French) 7-17539
 fibrous reinforced composites for electronics and electric technology appls. (French) 7-17540
 flexure specimen, end-notched, for mode II testing, design and anal. 7-51005
 formulation of new materials 7-13341
 fracture, critical element model, modelling philosophy 7-43767
 granular, failure anal. in conditions of adverse medium 7-33686
 granular metals, conc. depend. of hopping conductivity 7-32969
 halide eutectic composites, growth, struct., mech., elec. and optical props. 7-33648
 high-speed mechanisms fabricated with composite laminates, mechanical tests 7-37404
 hygrothermal behaviour, new prediction methods 7-21492
 IR imaging of subsurface structures, using pulse video thermography 7-33899
 lamellar composite materials, elastic properties (Japanese) 7-13489
 laminated, method for predicting nonlinear viscoelastic props. 7-63020
 laminated composite plate theory, with improved inplane response 7-37354
 laminated composite wedges, stress singularities 7-43659
 lateral pressure coefficient of linear-elastic anisotropic media and composites 7-1416
 layered, thermal diffusivity, laser flash meas. method (Japanese) 7-16831
 macroscopic relaxation kernels determ. 7-16073
 materials science and processing, outline of trends 7-46282
 materials with heterogeneous and anisotropic microstructures, wear description models 7-16682
 metal matrix composites, crack detection, structural inhomogeneities, multi-freq. eddy current testing 7-22954
 metal matrix composites, liq. metal infiltration prep., wetting 7-46372
 metal-ceramic composite, dynamic fracture toughness (Japanese) 7-13559
 metal-insulator, composite microemitters, hot electron emission 7-33532
 metal/ceramic, diffusion welded layered composites, transition zone metallography, struct., hardness (German, English) 7-8226
 microstructure characterization and bulk properties of disordered two-phase media 7-52068
 mode I edge delamination, stress distrib. ahead of crack, thermal residual stress 7-6151
 monolithic fuel cell tapes, three-layer ceramic composite, stress and fracture analysis 7-3407
 mother-of-pearl, fracture surfaces, analytical techniques appl. 7-8781
 mullite-alumina composites, sintering and charactn. 7-3252
 multilayer composite material for X-, γ - and β -ray detector windows 7-5570
 multiphase composites, effective thermal conductivity, three phase results 7-31634
 nondestructive measurement of dielec. permeability by nonsteady frequency-phase method 7-33888
 one-dimensional periodic composite piezoelectric materials, Floquet matrix and US propagation 7-2109
 optical methods in composites, conf., Keystone, USA (Nov. 86) 7-55894
 optical nonlinearities in small particles and composite materials 7-50631

composite materials continued

- panel, in situ testing of mech. props., flexural wave phase changes obs. 7-63095
- panel, min. wt., optimum design w.r.t. arbitrary loads 7-1397
- panel, whole-field strain determ. using coherent opt. processing 7-57779
- paperboard, constitutive behaviour under uniaxial and biaxial loading 7-63019
- periodic, elastic and instantaneous elastoplastic and moduli, overall, bounds 7-37349
- periodic composite materials, effective transport props., multipole coeffs. 7-32974
- periodic structure, coupled problems of thermoviscoelasticity 7-16074
- photoelastic analysis of composites and other bonded-material structures, limitations 7-63094
- plane wave propagation, T-matrix calcs. 7-14795
- plastic, advanced, design methods and appls., book 7-4642
- plastic film covered steel plates, thermoelastic props. meas. 7-33713
- plate, spectral analysis of natural grid features for surface analysis 7-63096
- plates, composite, impact tensile loading, crack bifurcation modes 7-50993
- plates, corner-supported, vibration analysis 7-37375
- plates, orthotropic folded, elasticity versus finite strip analysis 7-1427
- plates, thick composite, loading, nonlinear finite element anal. using cubic spline functions 7-31643
- poly-p-phenylene benzobisthiazole-epoxy composite, adhesive behaviour 7-65278
- polychlorotrifluoroethylene-Au composite films, optical response in visible region, effective medium approach 7-53433
- polycomponent composite materials, fracture toughness estimation (Chinese) 7-8075
- polymer, thermoviscoelastic properties prediction in complex stressed state 7-17573
- polymer based composites, stress relax., bond breaking, free vol. effects 7-22742
- polymer composite structure, thermal and thermomech. response 7-8150
- polymer-metal composite thin films, plasma deposition, optical props. 7-27947
- polyvinylidene fluoride/PZT, composites, dielec. behaviour 7-38992
- porous, transport props., pore-size parameter studies 7-38657
- porous and dense, prep. from sol-gel 7-65002
- protective coatings based on composite materials 7-3471
- PVC based powder mixtures, shock consolidation, densification, industrial appls. 7-39473
- recrystallised dielectromagnetics for AC machine magnetic circuits 7-22725
- response in adverse environment, reliable modelling, implication of 7-65169
- rubber-modified epoxy resins, toughening mechanism 7-28112
- shear testing methods for composites 7-46745
- shell, conical, stability calc. with allowance for cracking of binder in layers 7-16084
- shell of revolution, flexible, weakened by notches, stress-strain state, num. method 7-16075
- shells, layered composite, thermoelasticity 7-31649
- shells, shallow sandwich, finite deflection eqns. and linear stability problem (Chinese) 7-43721
- O'- β -sialon ceramic composites, fabrication 7-64990
- slab, transient heat conduction, convective and radiative cooling 7-11246
- spark discharge anodic oxidation layers and composites, appl. fields 7-65189
- spherical inclusions in periodic array, elastic coeffs. 7-50952
- steel reinforcement, hot-rolled, strength characts. eval. using mag. method 7-39824
- stress analysis, methodologies, new expt. approaches 7-37326
- stress analysis, methodologies 7-37325
- subsurface defect acoustic imaging in composites and roughened samples 7-3568
- synchrotron beam line critical elements, heat transfer studies 7-42255
- thermoelastic waves, photothermal generation 7-44685
- transient wave propagation in a viscoelastic layered composite—an approximate theory 7-62872
- two-component, elec. and thermal cond., Bergman-Milton theory of bounds appl. 7-23635
- two-phase and porous materials, microstructure-thermomech. prop. correls. 7-12380
- n-undecane, emulsion in sodium oleate stabilised water, conc. effect on aggregation 7-39926
- unidirectional reinforcing elements, scale effect of strength in tensile loading 7-31640
- US NDT for transverse cracking 7-59734
- US nondestructive evaluation, displacement sensor with two-beam interferometry 7-13716
- winding, stress form. in frontal hardening 7-17491
- Ag coated glass-Teflon composite, 3D continuum percolation system, nonuniversal behaviour of conductivity exponent, exptl. obs. 7-38656
- Ag-Teflon composites, temp. depend. far-IR absorpt. of Ag smoke 7-3041
- AgI/ α -Fe₂O₃ composite electrolytes, phase transition temperatures (Chinese) 7-38244
- Al powder-steel composite coatings, prod. by compacting electrophoretic and electrostatic deposits protective props. 7-3491
- Al-Al₂O₃-MgO, cast particulate composites, microstruct. and mech. props. 7-65086
- Al-epoxy laminated composites, US dispersion studies 7-26871
- Al₂O₃-stainless steel composite 7-3464
- Al₂O₃, strengthening, mech. props. and microstruct. (Japanese) 7-22820
- Al₂O₃-CaO cement-glass microsphere composites, relative dielectric permittivity 7-33319
- Al₂O₃-SiC composites, microstruct. and mech. props. (Japanese) 7-22821
- Al₂O₃-TiN powder composites, densification kinetics and struct. form. during sintering under high press. 7-53687
- Al₂O₃-TiO₂-SiO₂ composite, thermal shock resist. 7-33771
- Al₂O₃-ZrO₂ composites, high temp. behaviour and microstruct. study with HVEM (Japanese) 7-22819
- Al₂O₃-ZrO₂ composites, microstruct. charactn. by Raman spectroscopy (Japanese) 7-22684
- Al₂TiO₅-mullite composites, thermal and mech. props., effect of comp. (Japanese) 7-26987
- BaTiO₃ composites, dielec. and elec. props., rel. to prep. and microstruct. 7-64559

composite materials continued

- BaTiO₃-graphite-rubber composites, varistors fabrication 7-58841
- Bi alloy impregnated Ti, composite pseudoalloy, mech. props., Bi alloy content depend. 7-28095
- C-Sn composite sputtered films, ion enhancement, struct. prop. relationships studies 7-52332
- C-Ti composite sputtered films, ion enhancement, struct. prop. relationships studies 7-52332
- CaF₂-Al₂O₃ (ZrO₂) dispersions, single and polycrystalline, elec. conductivity 7-27005
- CdS/polymer composites, degenerate four-wave mixing 7-62795
- Co+Cr₂O₃, wear protective dispersion coating for use at high temp. 7-46667
- Cu/Ag composite discontinuous thin films, aging and field effect studies 7-7413
- Cu-composite material contact, sliding characts. and contact resistance (Japanese) 7-8120
- In-glass composite 7-38656
- MgF₂-MF₂ mixtures, (M=Ca,Sr,Ba), films, prep., physicochemical and optical props. 7-3178
- MgO-SiO₂ high-temperature composites, calcination temp. and mech. strength 7-33651
- NaGe₂P₃O₁₂ glass-ceramic, synthesis, thermal expansion meas. 7-46406
- Na₄Zr₂Si₃O₁₂-Y₃Fe₃O₁₂ composite ceramics, prep., thermal expansion 7-63853
- Ni reinforced Al, matrix crystn. and sintering, role of reinforcing phase 7-33625
- Ni reinforced LiF-NaF, matrix crystn. and sintering, role of reinforcing phase 7-33625
- PZT composites, hydrostatic piezoelec. response, finite element modelling 7-64574
- PZT-epoxy composites, thinning, ceramic width, acoustic impedance study 7-51954
- Pd/Al composite film MOS structure, H₂ sensitivity 7-52842
- SiC:Si, reaction bonded composite, mech. props. and microstruct. anisotropy 7-65146
- SiC:Si reaction bonded composite ceramics, interface struct., grain boundaries 7-64995
- Si₃N₄ based composites, design and wear resist. 7-3459
- Si₃N₄-TiC composites, densification, matrix-dispersoid reaction, mech. props. microstruct., impurities effect 7-64994
- Si₃N₄-TiC composites, mech. props., wear resist., dispersoid-matrix interaction 7-65145
- Si₃N₄-ZrO₂ composites, thermal instability 7-28158
- TiB₂-TiC composite, hot pressed, degradation in liq Al 7-28156
- TiN-C(BN), hard composite coatings, deposition and props. 7-46623
- W-Cu compacted pseudoalloys, elastic props., deform. diagram and pores effect 7-33722
- WC-Co composites, plastic deform. mechanisms, dislocation struct., TEM obs. (French) 7-22765
- WC-Co-B system, formation mechanism of composite coating, electrophoresis 7-3208
- ZnO, glass-doped, prep., elec. props. and degradation phenomena 7-13425
- ZrO₂-Al₂O₃ composite powder, thermal decomposition prep. for porous ceramics 7-13422
- ZrO₂-Al₂O₃ composite, Y₂O₃-stabilised, compressive deform. 7-28100

composite models of elementary particles

see also composite models of hadrons

- Abelian composite vector boson model, spontaneous symmetry breaking 7-41754
- composite vector bosons, unstable particle case 7-41711
- diquark model, proton mass, diquark radius calcs. 7-49101
- electroweak bosons, leptons and Han-Nambu quarks in a unified spinor-isospinor preon field model 7-49102
- family replication constraints on preonic model from lepton anomalies mag. moment 7-49098
- fermion-scalar preon models, unification of interactions and charge constraints 7-49100
- field theoretic model of composite particles, variational approach 7-19080
- fractional statistics, exceptional preons, scalar dark matter, lepton number violation, neutrino masses, and hidden gauge structure 7-10021
- geometrical rishon model, quark and lepton generations 7-497
- globally supersymmetric preon models with gauged colour-flavour symm. 7-19079
- Higgs boson-quarks composite model 7-10008
- left-right symmetric model, spectroscopy of Higgs scalars and exotic mesons 7-35767
- leptogluons and exotic coloured vector bosons 7-41756
- leptoquark bosons, decay in lepton+quark 7-10019
- low-energy phenomenology of a realistic composite model 7-15131
- masses of first and second generations of quarks in minimal composite model 7-49096
- masses of quarks and leptons in minimal composite model, square-root sum rule 7-49097
- neutron, mean decay rate, composite model 7-19078
- preon dynamics, relevance of Higgs field mass parameter variation to fermion mass generation 7-408
- preon model with three SU₃ hypercolours and three SU₂ hyperflavours 7-49026
- preons, vertical and horizontal, in SU(5) model 7-56524
- quark-lepton generation as hypercolor degrees of freedom 7-24850
- SO(10)×SO(10) theory, composite and elementary quarks and leptons 7-9997
- SU(4)×SU(4) composite model of weak interactions (Chinese) 7-10037
- SU(7) preon model with complementarity, constraint on 't Hooft indices 7-49099
- superstrings and preons, uniqueness, parameterlessness and good quantum gravity 7-9738
- supersymmetric composite quark-lepton model, effective Lagrangian 7-41755
- pp→X, KNO scaling in fire ball model (Chinese) 7-10077
- W, composite particle, magnetic moment calcs. 7-49149
- Y bosons, signatures in pp and pp colliders 7-24851
- Z boson, internal structure, composite nature 7-496
- Z→ggg, gq \bar{q} , l \bar{l} γ , preon-composed bosons 7-24885
- Z→H γ (HH γ), composite model study 7-24886
- Z→ $\bar{\nu}\nu\gamma$, composite model study 7-24886

composite models of elementary particles continued

- $W^{\pm}Z^0$ self interactions, Lagrangian containing quadrupole terms, $e^+e^- \rightarrow W^+W^-$ anal. 7-61515
 $Z \rightarrow \nu\bar{\nu}H$, composite model study 7-24886

composite models of hadrons

- see also parton model; quark models*
 fermion-scalar system, potential model anal. of magnetic moment and form factors 7-61691

composite particles

- see also alpha-particles; deuterons; nuclei with mass number 1 to 5; tritons*
 No entries

composite superconductors

- AC losses, modified boil off method 7-17130
 bilayer composite excitation spectrum, density of states, Bogoliubov eqns. 7-52892
 filamentary superconductors, hard, transport props. in vicinity of H_{c2} (Russian) 7-38827
 granular superconductors, 3D, short-range order and phase diagrams 7-22062
 granular superconductors, phase-locking transition, phase-number representation 7-38803
 internal fields in magnetic materials and superconductors 7-17131
 multifilament superconductor fabrication, superconductivity of ternary materials (French) 7-2777
 multifilamentary superconducting conductors, AC eddy current losses caused by tangential magnetic field (Slovak) 7-58952
 multifilamentary superconducting wires, hysteresis losses 7-22064
 scale effect on transition temp. 7-7432
 stability, forced cooling by coolant stream 7-33126
 stabilized superconductor carrying current in varying mag. fields 7-22063
 thermal processes and charact. thermal length of composite, math. model 7-64389
 Al-Pb disordered 3D normal metal-superconductor composite, elec. transport, magnetisation meas. 7-64383
 BaPb_{0.75}Bi_{0.25}O₃ ceramic granular superconductor, infinite cluster detection, local heating method 7-2797
 Cu-Nb, composite struct., filamentary medium, cond. anisotropy and crit. current 7-22081
 Cu-Nb, supercond. composites, low temp. plasticity, annealing hardening, strength (Russian) 7-59579
 Cu-Nb composite superconductors, critical parameters and surface flux pinning studies 7-38830
 Cu-Nb microcomposite superconductors, in situ, nature of connection (Russian) 7-45585
 Nb/Si multilayered thin films, supercond. props. (Japanese) 7-64405
 Nb-Sn composite wires, effectiveness of V as diffusion barrier material 7-15353
 Nb-Sn liq.-infiltrated superconducting composite wire, T_c and sp. ht. meas. studies 7-45560
 Nb-Ti, superconducting composites, critical current distributions 7-38833
 Nb-Ti composite superconductors, influence of heat transfer on current carrying capability 7-64422
 Nb-Ti multifilamentary superconductors develop. 7-7456
 Nb₃Sn bronze process multifilamentary wire, cooling stress and supercond. (Chinese) 7-12894
 Nb₃Sn filamentary superconductor with high bending strength, fabrication (Slovak) 7-58965
 Nb₃Sn fine filament internal-tin superconductors, hysteresis losses 7-2778
 Nb₃Sn, heat treatment for in-situ processing, Cu, Nb, Sn, distrib. (Chinese) 7-12924
 Nb₃Sn multifilamentary composite superconductor, bronze processed, global pinning force, critical mag. field, grain size 7-22078
 Nb₃Sn multifilamentary superconductor, AC props. 7-38834
 Nb₃Sn multifilamentary wire superconductors, development at SLE 7-64421
 Nb₃Sn, superconducting composites, critical current distributions 7-38833
 Nb₃Sn-Ti(In) multifilamentary superconducting composites, growth dynamics, struct. and props., additive and heat treatment effects 7-22056
 NbTi/Cu stabilised wires, wiggler design for ESRF 7-42253
 (NbTi)₃Sn multifilamentary superconductors develop. 7-7456
 Sn-GeO granular films, struct., resistivity and superconducting props. study 7-45082

composite systems *see large-scale systems***composition measurement** *see chemical analysis***compressibility**

- see also compressibility of gases; compressibility of liquids; compressive strength*
 alkali cyanides, multipole interaction effects on cohesive and anharmonic props. 7-1942
 alkali halide mixed crystals, phys. props., review 7-37943
 beryl, high press. cryst. struct. and compressibilities 7-16505
 dl-borneole, mol. reorientation dynamics, proton NMR study under hydrostatic press. 7-50175
 composite material failure under compression, complex stressed state case, continuous theory 7-62974
 compression approximations in computer tomography (Russian) 7-54717
 cylinders and spheres, hollow, internally pressurised, finite deform. for class of compressible elastic material 7-43676
 elastic-plastic problem soln. with increasing strain hardening of material 7-11304
 finite compression of solids, second order thermoelastic anal. 7-43708
 freons, liquid-vapour system, shock wave compression 7-31874
 gas-vapour-liquid mixtures, shock compression 7-43713
 granular materials, shear band analysis by Cosserat theory (German) 7-20598
 homogeneous spinodal phase, stability boundaries, thermodynamic functions homogeneity (Russian) 7-41325
 ice I, pre-melting second-order transform., isothermal compressibility and expansivity meas. 7-32631
 linear elastic beam elements of MODULEF library (French) 7-31655
 materials with defects, brittle compressive failure criterion 7-43762
 metals, BCC refractory, mag. susceptibility, elastic const. and compressibility 7-33142
 metals, compression pulses, nanosecond, attenuation 7-58413
 metals, liquid and solid, thermal properties and compressibility 7-58509
 Mg-Al alloys, precipitation and recrystallisation rates under small external stress 7-17532

compressibility continued

- network polymers, deform. under compression, resistance, struct. factors (Russian) 7-13538
 organic mol. cpds., pre-melting second-order transform., isothermal compressibility and expansivity meas. 7-32631
 plastic subsurface failure in compression along macrocracks, spatial problem 7-26159
 plates, bimodulus thick circular, axisymmetric buckling analysis using FEM 7-57716
 polymers, partially crystalline, viscoelastic and acoustic props. on hydrostatic compression 7-33719
 rectangle, elastic, compressible object, contact interaction of two stressed half-planes 7-1518
 rock compressibility and pore volumes, micromechanical model 7-40467
 rubber, natural, low temp. crystallisation, shear and compressive strain 7-6559
 sintering, viscous under uniaxial load 7-27959
 sphere, elastic isotropic, of compressible material, dynamics under cubic initial loading 7-1480
 steel, HSLA, high strain-rate behaviour, Bodner-Partom viscoplastic constitutive model description 7-33754
 thin flat-walled structures, buckling, spline finite strip method 7-1459
 (TMTSF)₂PF₆, cryst. struct., neutron low temp. and X-ray high press. diff. studies 7-44502
 type II superconductors, flux-line lattice, elastic and plastic props. 7-27481
 vortices, interaction, MHD, current layer form. 7-51178
 Al, shock adiabats, shell effects 7-2104
 B₂O₃ glass, thermal expansion, sp. ht. meas. 7-44862
 BeAlSiO₄OH, euclase, high press. cryst. struct. and compressibilities 7-16505
 CaSiO₃, perovskite type, cryst. struct., lattice dynamics and eqn. of state 7-58248
 CaTiO₃ (perovskite), high press. phase transformations and isothermal compressibility 7-14269
 D₂, solid, compressibility and pressure, LOCV calc. 7-52182
 Fe powder, quality assessment method 7-53671
 Fe powder, ultrafine, and hot forged specimens, reduction temp. effect on struct. form. and props. 7-53670
 Fe₂O₄, magnetite, cryst. struct. under press. 7-16524
 Fe₂O₄, magnetite, high press. cryst. chemistry 7-16521
 n-GaAs, intervalley processes, nonequib. phonon spectroscopy and hydrostatic compression, Monte Carlo study 7-58425
 H atom, compressed, energy shift calcs. 7-35175
 H, liq. and solid, cryogenic, high press. eqn. of state, laser interferometric meas. method 7-30027
 H₂, solid, compressibility and pressure, LOCV calc. 7-52182
 H₂, solid, dynamic isentropic loading, high press. eqn. of state, computational simulations 7-32747
 K, compression and polymorphism, up to 400 kbar 7-32632
 MgAl₂O₄ spinel, high press. cryst. chemistry 7-16521
 MgSiO₃, perovskite type, cryst. struct., lattice dynamics and eqn. of state 7-58248
 NH₃, pre-melting second-order transform., isothermal compressibility and expansivity meas. 7-32631
 Na₂O-B₂O₃ glasses, effect of Na₂O addition, thermal expansion, sp. ht. meas. 7-44862
 Pb, shock adiabats, shell effects 7-2104
 PbTiO₃, spontaneous strain, anomalous press. depend. 7-26833
 Sn, high press. phase transitions and compressions, in situ X-ray diff. study 7-6722
 Xe adsorbed on graphite, thermodynamics of first-order and continuous melting 7-2358

compressibility of gases

- see also high pressure phenomena and effects*
 bromotrifluoromethane, liq. and gaseous phases, compression factor, vapour press. meas. 7-51905
 compressible gas dynamical eqns., rapidly oscill. solns. (Russian) 7-55181
 methanol, compressed gas and liq. PVT props. meas., pseudoisochores determ. 7-16713
 molecular fluids, mixing, statistical mech., Kirkwood-Buff soln. theory 7-58480
 n-pentane, vol. ratios, compressibilities, 278-338K, pressures up to 280 MPa 7-51906
 Ar-Ne mixture, density meas. up to 8000 bar, Lennard-Jones comparison 7-1669
 CO₂-ethane gaseous mixture, determ. of virial coeffs., ref. index meas. method 7-51362
 He-Ar mixture, density meas. up to 8000 bar, Lennard-Jones comparison 7-1669

compressibility of liquids

- alcohol-water mixture, volumetric behaviour, high press. study 7-51904
 alcohols, compressibility, US sound vet., topological indices 7-21359
 alkanes, compressibility, US sound vet., topological indices 7-21359
 alloys, isothermal compressibility, theoretical analysis (Russian) 7-58391
 benzene, acoustic and thermodynamic props., press. and temp. depend. 7-63745
 bromotrifluoromethane, liq. and gaseous phases, compression factor, vapour press. meas. 7-51905
 butoxybenzylidene phenylazoaniline, liq. cryst. transitions, density and US vel. studies 7-32266
 t-butyl alcohol-H₂O mixtures, X-ray scatt., Kirkwood-Buff parameters 7-44337
 carbohydrate solns., aqs., molar vols., isobaric expansion coeffs. and compressibilities 7-12183
 carbohydrate solns., non-aqs., molar volumes, isobaric expansion coeffs., compressibility 7-12184
 complex adiabatic compressibility and adiabatic pressure-induced temp. variation meas. 7-21316
 complex adiabatic compressibility meas. at low freq. 7-21313
 cumene/1-butanol mixtures, US studies 7-58414
 cyclohexane, acoustic and thermodynamic props., press. and temp. depend. 7-63745
 dense liq. departures from Joule's law near freezing w.r.t. vacancy props. of hot crys. 7-63840
 N,N-dimethylformamide-n-alcohols, binary mixtures, excess isentropic compressibilities at 303.15K 7-21315
 n-dodecane-hexane isomer mixtures, ultrasonic speeds and isentropic compressibilities 7-51943

compressibility of liquids continued

- ethyl-alcohol in water, dil. solns., isentropic compressibility behaviour 7-58392
- N(p-n-heptyloxybenzylidene) p-n-pentylaniline, liq. cryst. phase transitions, density, US vel. meas. 7-1874
- interfacial turbulence and mass transfer, importance of surface compression elasticity modulus and Reynolds number 7-63128
- liquid metals, compressibility, coexistence line and critical characts. 7-44350
- liquids, entropy changes and fluctuations near tensile instability 7-6830
- metals, liquid and solid, thermal properties and compressibility 7-58509
- methane nonpolar fluid, electron mobility near crit. point 7-7243
- methanol, compressed gas and liq. PVT props. meas., pseudoisochores determ. 7-16713
- molecular fluids, mixing, statistical mech., Kirkwood-Buff soln. theory 7-58480
- nematic liquid crystals, Frank constants, effects of compression 7-63702
- penetration of compressible liquid by axially symmetric solid 7-11370
- n-pentane, vol. ratios, compressibilities, 278-338K, pressures up to 280 MPa 7-51906
- polyelectrolytes, highly asymmetrical, spinodal curve 7-21466
- polymer melt struct., nonperturbative integral eqn. theory calcs. 7-44345
- polymer nets, high elasticity, mol. theory with allowance for topological constraints 7-37839
- polystyrene-cis-decalin gels, isotactic, compression modulus, conc. depend. 7-32536
- smectic-A-smectic-C phase transition, Frank const. corrections, renormalisation-group method calcs. 7-16742
- sodium p-n octylbenzenesulphonate, aq. solns., micelle form., acoustic and rheological props. 7-13823
- sulpholane-benzene (toluene)(p-xylene)(mesitylene), ultrasonic speeds, compressibility and excess molar quantity at 303.15K 7-26870
- 1,1,2,2-tetrachloroethane-alkane binary mixture, US behaviour and isentropic compressibility 7-21358
- toluene-n-decane (n-dodecane), isothermal compressibility at various temp., excess functions calc. 7-26822
- 1,3,5-trimethylbenzene, melting point meas., liq. self-diffusion study, hard-spheres method 7-52003
- water-organic mixtures, positron annihilation and compressibility 7-39227
- Ag chalcogenides, molten, US vel. investig. 7-38124
- Ar nonpolar fluid, electron mobility near crit. point 7-7243
- Xe nonpolar fluid, electron mobility near crit. point 7-7243

compressible flow

- see also compressibility*
- 3D flow obs. by interferometry and image processing 7-37576
- 4-cylinder internal combustion engine, 2D intake manifold flow digital simulation 7-63170
- ablation front instability in presence of layer acceleration 7-1536
- axisymmetric dual-flow interrupter nozzles, flow field study 7-26331
- atmosphere, manifestations of Charney baroclinic-instability with Rossby wavetrains 7-18287
- axisymmetric vortex sound, acoustic wave field determ. 7-51182
- boundary layer excitation by surface heating or cooling, numerical simulation 7-6181
- boundary-layer transition, first and second role modes 7-11452
- Cauchy problem for linearised Navier-Stokes eqns. with allowance for compressibility 7-43964
- compressible gas dynamical eqns., rapidly oscill. solns. (Russian) 7-55181
- cylindrical compressible flow, circumferential distortion, surge interaction and rotating stall (French) 7-1638
- detached flow problems, soln. using finite element method 7-18599
- discontinuous flows, teaching using interactive techniques and windowing 7-60923
- electrodynamic effect on small perturbation development in the boundary layer on thin airfoil 7-1641
- Euler and Navier-Stokes eqns., finite element flux, corrected transport algorithm 7-43959
- Euler equations, compressible, soln. by time-marching scheme 7-26311
- finite element methods in flow problems, conference, Antibes, France (June 1986) 7-41009
- finite element solution of flows through cascades of profiles in a layer of variable thickness 7-26307
- flow rates for compressible and immiscible viscous filtration fluids 7-98
- fluidic resistance ccts with compressible flow throughput (German) 7-51205
- forced oscillatory compressible flow past yawed cylinder, heat transfer 7-1585
- gas jet impacting a cavity, temp. and velocity meas., flow anal. 7-43999
- gas-dynamics equations, invariant difference schemes (Russian) 7-63173
- gas-dynamic model, heat exchange, press. distrib. in high enthalpy air stream 7-1587
- heated gas flow in circular tube, friction factor studies (Japanese) 7-57924
- ideal fluid, press. waves, nonstationary interaction 7-31823
- ideal isothermal gas, 2D unsteady viscous compressible flows, global solns. 7-26304
- incompressible fluid eqns., oscillations and concentrations in weak solns. 7-57802
- inverse integral equation method, appl. to compressors and turbines in compressible flow 7-6244
- inviscid compressible flow, mech refinement for adaptive FEM 7-37485
- inviscid compressible fluid, flow past cylinder (Chinese) 7-26306
- isentropic Navier-Stokes eqns. in one space dimension with nonsmooth initial data, solns. 7-26244
- isentropic spiral flow between two coaxial circular cylinders, instability 7-6216
- Kelvin waves, cylindrical, in compressible stratified fluid (Russian) 7-43957
- Kelvin waves in compressible stratified fluids (Russian) 7-63168
- laminar boundary layer eqns. stream function numerical soln. 7-6183
- laminar boundary layer flow with heat transfer, quasilinearization technique 7-26247
- laminar boundary-layer flow past a cylinder with massive blowing 7-31742
- laminar compressible MHD boundary layer at wedge 7-6325
- lifting bodies, 2D and 3D Euler computations, finite element method 7-43961
- Liouville eqn., real periodic solns. in the μ -representation 7-48318
- moving finite element modelling of compressible flow 7-51222

compressible flow continued

- Navier-Stokes eqns., pseudo-time algorithm for integration to steady state 7-26302
- Newtonian fluid in a pipe, Navier-Stokes eqn. soln. 7-11551
- nonisothermal plane point jet, single-parameter self-similar problem 7-44002
- nonlocal conservation law in combustion theory 7-63233
- nonuniform-mesh schemes, accuracy 7-51202
- one-dimensional unsteady gas motions, stability 7-20687
- percolation of a compressible fluid in a nondeformable porous medium 7-44035
- perfect gas flow rate through slit in plane wall 7-20746
- quasi-steady state isochoric plane flow meas., noisy data anal. 7-63727
- reacting shock waves, theoretical and num. structure 7-20759
- rectangular tube, oscillatory flow of incompressible viscous fluid, exact solns. (Chinese) 7-51308
- rotating compressible flow, nonself adjoint operator, eigenvalue problem 7-57861
- rotational inviscid flows, 3D, finite element method 7-43940
- separated turbulent shear flow, mixing, flow meas. 7-51080
- shear layer entrainment, 2D 7-31770
- smoothed particle hydrodynamics, hypersonic flow appl. 7-16206
- spherical segment entering compressible fluid, surface press: distrib. 7-51203
- star-shaped 3D body penetration in liq. with free surface 7-11446
- Stirling engine, pressure drops anal. under reversing flow conditions 7-65548
- Stokes equations, soln. for incompressible fluid in multiconnected domain 7-20797
- subsonic flow, incremental multigrid strategy for fluid dynamic eqn. soln. 7-51019
- supersonic turbulent flow through square duct, cross-flow vel. profiles 7-20748
- thermal boundary layer on a plate 7-37451
- transition to time-dependent free convection in an inclined air layer 7-20708
- tubular cantilevered beams conveying compressible fluid, unstable oscillation 7-4670
- turbulent boundary layer, supersonic flow, investig. 7-57877
- turbulent flows, 2D, Navier Stokes eqns. solved using finite element method 7-43960
- turbulent free shear layer interaction 7-51078
- two-dimensional, unsteady flows, technique for integrating Euler eqns. 7-51225
- unsaturated flow of liquids in porous media, free boundary problem 7-37538
- unsteady compressible cascade flows anal. using boundary element and free vortex method 7-43962
- unsteady compressible viscous flow over airfoils, integro-differential and finite-difference methods 7-31821
- vectorised finite element codes 7-37488
- viscous compressible heat conducting fluid, 1D motion, Navier-Stokes weak soln. (French) 7-37486
- viscous flow in transonic nozzles, Navier-Stokes eqn. 7-31827
- vortex dynamics and singularities, simulation, appl. to incompressible Euler eqns. 7-51183
- CO₂-He-N₂, vibr. nonequilib. flow in axisymmetric channel with glow discharge 7-20741
- compression, bandwidth** *see bandwidth compression*
- compressive strength**
- see also compressibility*
- adhesive lap joints, yield strength in tension, compression and torsion, Poisson ratio 7-39591
- Aramid fibre reinforced composite beams, viscoelastic-plastic anal. in flexure 7-33717
- bone, mech. props. and morphology, effects of Ca deficient diet, goose obs. 7-3822
- carburendum refractory provisions with aluminium-chromium phosphate binder 7-46395
- ceramics, made of hollow spherical particles, struct. and strength 7-3234
- composite materials, energy absorpt. capability, effect of specimen geometry 7-3315
- composites, compressive failure modes 7-6717
- concrete, insulating cellular, compressive strength, in situ evaluation using impact device 7-39800
- corundum-graphite refractories, thermomech. props. 7-22806
- diamond semiconductors, synthesis and props. (Russian) 7-16588
- dynamically overloaded cold profiled cylindrical compression springs calc. using Spectrum 48 k (Croatian) 7-22705
- epoxy-amine matrices, improvement of phys. and mech. props. 7-39574
- fabric dependence of anisotropic strength criterion 7-38084
- fibre reinforced composites, compressive-flexural/shear failure mode transition, interface strength 7-39586
- fibre reinforced composites, energy absorpt. capability, effect of specimen geometry 7-3315
- fibre reinforced plastics, hybrid, tensile, compressive, flexural and shear props., review 7-39532
- glass fibre reinforced epoxy and polyester composites, flexural failure mechanisms, global stress plane 7-8082
- glass fibre reinforced plastic, cross-layered reinforcement strength criteria 7-17631
- graphite fibre reinforced epoxy resin composites, multidimensionally braided, tensile, compressive and flexural props. 7-33726
- graphite fibre reinforced plastics, energy absorpt., effect of fibre and matrix max. strain 7-3314
- low density materials, mechanics 7-38089
- metals, sheet, press formability and anisotropic yield, Bassani-type criteria 7-28068
- polycarbonate, shock-loaded, tension-recompression response method study 7-33879
- polydiacetylene single crystal fibres in composites, stress-induced twinning 7-16567
- porous brittle solid, strength and elastic modulus, acousto-US study 7-21321
- pulp fibres longitudinal compression device 7-13697
- refractories, compactum under quadrilateral compacting press. 7-13397
- reinforcing bar behaviour under compression, stress-strain relationship 7-1440
- steel, P/M, produced by hot forming, strength characts., influence of porosity, C content and compacting method 7-53823

compressive strength continued

- Al-Si-SiO₂ sand composites, prep. and mech. props. 7-17500
 Al₂O₃ fibre reinforced Al composites, compressive failure modes, dead weight or machine loading 7-39663
 B⁺-Al₂O₃-Na₂O-ZrO₂ ceramics, transform toughened, fabrication, mech. props. ionic resist. 7-65143
 Bi alloy impregnated Ti composite pseudoalloy, mech. props., Bi alloy content depend. 7-28095
 C fibre reinforced epoxy, unidirectional, fracture strength, role of matrix resin 7-53845
 C fibre reinforced plastics, strength, thermomech. props. thermal spiking and moisture absorpt. effect 7-28085
 C fibre reinforced thermoplastic laminates, compressive strength 7-39580
 Co₇Si₁₀B₁₅, amorphous powder, static consolidation, mechanical and mag. props. 7-3217
 LaCrO₃-Cr cermets, mech. props., interparticle welding 7-39630
 Mo alloys, forging, crystallographic texture, X-ray diff. (*Russian*) 7-39538
 Mo, arc melting, impurity content, mech. props. 7-27980
 TiC-Ni-Mo sintered carbides, struct. and physicomech. props. 7-3256
 TiC-WC-Ta-Co three-phase sintered carbides, Ta content influence on struct. and props. 7-65097
 WC-Co powder mixtures, electrolytic Co plating effect on densification and strength props. 7-53686
 ZrO₂-Al₂O₃ composite, Y₂O₃-stabilised, compressive deform. 7-28100
 ZrO₂-Y₂O₃, Y-TZP, superplastic, compressive deform. props. and microstruct. (*Japanese*) 7-22774
 (ZrO₂)_{0.9}(Y₂O₃)_{0.1} fianite crystals, bending and compressive strength temp. depend. meas. 7-44653

compressors

- expansion turbine, miniature cryogenic, gas bearing with tangential feed holes, instability onset speed 7-56289
 expansion turbines, gas-bearing miniature, high-performance dynamic balancing system 7-56288
 heat pump compressor life anal. 7-23211
 heat pump service life and compressor survival in northern climate 7-23212
 high specific centrifugal compressors, flow measurement 7-26371
 piston expander, balanced pressure, ideal cycle analysis 7-56275
 He Joule-Thomson satellite refrigerator, advantages 7-48755
 He liquefier, condensing and freezing purification system 7-56280
 He liquefier with turbo-expanders, prediction method for cool-down characts. 7-56276
 He, regenerative oilfree, for cryopumps 7-56298

Compton effect

- astrophysical supercritical winds, Comptonisation, dynamics and obs. diagnostics 7-55438
 astrophysical supercritical winds, spectral evol. 7-55437
 backward Compton scatt. for electric field probes in high-density relativistic plasma 7-1759
 band occupancy determ. using Fourier-transformed Compton profile 7-21801
 Cen A, thermal Comptonization and synchrotron self-Compton models for MeV gamma-ray emission 7-66754
 Compton profile meas. for TiH₂, Ti using energy dispersive Compton spectrometer 7-15449
 cyclotron line formation in a hot plasma including Compton cooling, appl. to X-ray binary stars 7-60514
 deep inelastic QED Compton scatt., topological isolation, inclusive cross sections 7-49157
 diffraction pattern distortion for plane specimens of weakly absorbent materials 7-21042
 electron and two-photon momentum distrib., ab initio calc. using LMTO formation 7-46182
 electron beam interaction with two counterpropagating laser beams, obs. of enhanced energy transfer 7-42875
 first Born approx. 7-10503
 free electron laser, Compton and Raman regimes, Hamiltonian model 7-57348
 free electron laser, Raman and Compton regimes (*Japanese*) 7-1177
 graphite, electron momenta, Hartree-Fock-Roothaan calc. 7-42466
 highly asymmetric Bragg diff., coherent Compton effect 7-46233
 hydrides, amorphous and crystalline, comparative studies via incoherent scatt. 7-21798
 inverse noncollinear Compton laser for electron acceleration 7-49744
 laser electron acceleration in stimulated Compton scatt. 7-50645
 M87, Compton model for X-ray emission from galactic halo 7-66752
 materials examination, elastic to Compton scattering ratio determ. 7-46892
 metals, metallic electron charge density to electron momentum density transformations 7-27249
 methane, electron momenta, Hartree-Fock-Roothaan calc. 7-42466
 nuclear forward Compton amplitude in GDR and Δ regions, dispersion relation anal. 7-49377
 photon-hadron interactions involving tracer photon beams, multi-particle finite states 7-5101
 PIXE, accurate anal. using INK computer program 7-54216
 plasma, strongly magnetized, Thomson scattering of o-mode and z-mode below cyclotron frequency 7-37650
 polyacetylene, electron momenta, Hartree-Fock-Roothaan calc. 7-42466
 quasars, Compton heating rel. to broad line region energetics 7-9553
 radiative transfer relativistic Compton scatt. kernel 7-35471
 Schrodinger's treatment 7-29620
 spectral flux, resolution, of X-ray spectrometer for inelastic scatt. expts. 7-16355
 Sun, microwave and X-ray bursts, fast time structures, inverse Compton interpretation 7-4401
 time projection Compton spectrometer for medium-voltage flash X-ray sources 7-56391
 Wolf-Rayet stars, new evidence at X-ray and gamma-ray freqs. for non-thermal phenomena 7-55640
 X- and γ -ray scatt. cross section anal. for Z=11-95 7-17359
 X-ray burst sources, influence of Comptonisation on radiation spectra (*Russian*) 7-55724
 X-ray sources, effects of one-generation pair production in synchrotron self-Compton sources 7-55452
 X-ray spectrometer design, performance, inelastic scatt. expts. appl. 7-15040
 γ N $\rightarrow\gamma$ N, cloudy bag model anal. 7-61698
 $\gamma\pi^+\rightarrow\gamma\pi^+$, Compton scatt. cross section meas. 7-5103

Compton effect continued

- CaF₂, directional gamma-ray Compton profile meas. and LCAO calcs. 7-2063
 Cu, X-ray Compton-Raman scatt. from atomic inner shell electrons 7-13257
 Fe, ferromagnetic, spin depend. Compton profile, circularly polarised synchrotron radiation study 7-33477
 Fe, X-ray Compton-Raman scatt. from atomic inner shell electrons 7-13257
 LiH, single cryst., electron momentum density and Compton profiles 7-3113
 MgO, directional Compton profiles and autocorrelation function 7-3103
 Nb, momentum-space props. Compton profiles 7-42505
 Nb and its dihydride, Compton profiles 7-59281
 Nb, polycrystalline, electron momentum distrib. for ang. correlation of positron annihilation radiation 7-46188
 Ni multiple scattering profile, gamma-ray Compton study 7-17356
 Ni₃Ga, momentum density distrib., Compton scatt., positron annihilation, symmetrised APW method 7-64069
 Ta, Compton profiles, APW calcs. 7-27809
 Ti, Compton profiles due to valence electrons, self-consistent calcs. 7-13250
 TiH_{1.98} and Ti, Compton profiles meas. 7-7785
 TiH₂, Compton profiles due to valence electrons, self-consistent calcs. 7-13250
 V and its dihydride, Compton profiles 7-59281
 W, Compton profiles, APW calcs. 7-27809
 W, J-shell electrons, gamma ray Compton scatt., intensity distrib. 7-13252

Compton profile *see Compton effect***Compton scattering** *see Compton effect***computability**

- see also computational complexity*
 physical theories and computability 7-18589

computability and decidability *see computability***computation** *see calculation***computation theory**

- see also automata theory; formal logic; switching theory*
 physical limitations due to quantum mechanics 7-18615
 physical limitations on computational processes 7-18616
 physical limits of computation, reversible computation 7-55919

computational complexity

- see also computability*
 N-body hierarchical force calc. algorithm with N log N growth 7-47673
 PDEs, complexity 7-48385
 remote sensing of land surface, context classifier for pixel analysis of images 7-23873
 tomography, optical microscopic type, constrained resolution enhancement 7-47304

computational geometry

- ocean wave models 7-34503
 ocean wave modeling 7-34502

computer aided analysis

- see also analogue simulation; CAD; circuit analysis computing; digital simulation; electric machine analysis computing; hybrid simulation; power system analysis computing*
 concert halls transient distortion, sound differences anal. (*German*) 7-62929
 echocardiography, computer assisted anal. of left ventricular function 7-34211
 lung air content, regional, analysis by 3D computerised tomography and multinomial models 7-54801
 oligosaccharides, conformational statistics 7-13958
 orchestral instruments, performed transitions anal. 7-43579
 shadow moire topography equipment for skin diagnostics, using Sinclair Spectrum computer (*Czech*) 7-14145
 solar cells, low bulk resist., sensitivity anal. using SPCOLAY computer code 7-8406
 SSYST-3 fuel rod behaviour analysis program (*Hungarian*) 7-56724
 Topographic Air Pollution Analysis System 7-54395
 torsional axially symmetric finite element model for problems in elasticity 7-57701
 InGaAsP epitaxial films, strain mapping by an X-ray diffraction technique 7-21786

computer-aided circuit analysis *see circuit analysis computing***computer-aided circuit design** *see circuit CAD***computer-aided design** *see CAD***computer aided engineering** *see CAD/CAM***computer-aided geometric design theory** *see computational geometry***computer aided instruction**

- see also education*
 atmosphere sulphur deposition, spreadsheet-based model 7-54397
 cardiac rhythms and arrhythmias: a teaching program 7-48247
 computational physics teaching 7-48226
 computer illustrated texts 7-14740
 discontinuous flows, teaching using interactive techniques and windowing 7-60923
 Formula Vision, spreadsheet program for aiding in maths and science formula comprehension 7-35181
 kinematics instruction using microcomputers 7-14732
 meteorology teaching with microcomputers, software packages review 7-60
 physics education, computer use 7-38
 pipe flow studies, microcomputer appl. 7-14733
 remote site instruction in physics: a test of the effectiveness of a new teaching technology 7-18518
 speech anal. devices for speech and hearing people diagnosis and education 7-37280
 speech training devices for profoundly deaf children 7-37278
 speech training systems for handicapped children using vocal tract lateral shapes 7-37279
 TIPS, interactive microcomputer program for teaching digital imaging processing theory 7-18542

computer-aided tomography *see computerised tomography***computer architecture**

- see also logic design; parallel architectures*
 optical parallel array logic system, architecture without memory elements 7-20144

computer architecture continued

- optical relational-graph rule-based processor for structural-attribute knowledge bases 7-10861
- optical single-instruction multiple-data array architectures for digital optical computing 7-42941
- SIMPLE hydrodynamics benchmark, restructuring for CHiP architecture 7-16145

computer bureaux *see computer facilities***computer facilities**

- seismic support of electronic and computer equipment, design of raised floor systems 7-4003

computer-generated holography

- 3D image display using 1D transforms 7-31274
- achromatic single-component kinoform objective, with circular aberration coeff. 7-25737
- cylindrical kinoform lenses for monochromatic light, effect of fabrication errors 7-25923
- defect resistance by object phase manipulation 7-31273
- deflecting focusing kinoform for lasers 7-25736
- distortion-free computer generated holograms for optical element testing (Japanese) 7-10892
- head-up displays, holographic diffractive optics progress 7-25749
- high-dimensionality pattern recognition feature space production 7-25725
- Hough transform optical implementation by matrix of holograms 7-42940
- image lens, optimal design 7-43007
- kinoform lens fabrication errors, effect on pupil function 7-25739
- kinoforms phase structure synthesis 7-25738
- laser image plotter for high-information-density images recording 7-26043
- laser printer for CGH recording 7-43002
- laser pulse spatial modes, direct measurement 7-5931
- real-time computer-generated hologram by means of liquid-crystal television spatial light modulator 7-36918
- reconstruction of curves in 3D 7-36916
- seismic holography, computer simulation 7-18124
- synthetic discriminant function filters, computer-generated and phase-only 7-20392
- wavelengths demultiplexer for optical fibre communications 7-25774

computer graphic equipment*see also plotters*

- colour graphic display systems for power station control rooms 7-56811
- human colour perception, display technology implications 7-14005
- Mossbauer spectrometer and data anal. system, IBM PC-based 7-18959
- photogrammetric acquisition, graphical verification subsystem 7-40618
- reactor colour graphics display system 7-25122
- variable raster and vector display processor, interface with PDP-11/23 7-60003

computer graphics

- see also business graphics; computational geometry; curve fitting; engineering graphics; interactive systems*
- animation of human walking, real-time, for pathological gait evaluation 7-28569
- biopolymer conformation determination using NMR, CONFOR graphics program 7-54455
- cartographic data graphical display and manipulation 3-dimensions 7-40408
- computer illustrated texts 7-14740
- crystallography, 3D intensity data from single crystal reflections, graphical display 7-11829
- discontinuous flows, teaching using interactive techniques and windowing 7-60923
- display of 3-D analysis data 7-4826
- Fishnet graphs generation and character-mapped contour plots on IBM PC 7-24629
- fringe pattern plotting, computer algorithms, speckle analysis 7-50496
- Halley's comet and planets, graphical orbit display in UCSD Pascal 7-55479
- heart images in motion, computerised tomography 7-14142
- human body biomechanics study, technique for superimposition of computer graphics and video images 7-34361
- Jupiter, physical and visual simulation 7-34910
- lens design software, human dimension 7-50675
- meteorological computer graphics, stereo display terminals for McIDAS system 7-60389
- molecular modeling system for the IBM PC, user-friendly CAMSEQ/M system 7-24633
- molecular structures and properties, display system, Winchester Graphical System 7-49875
- motion perception research, use of computer graphics animation 7-59996
- ocean wave models 7-34503
- ocean wave modeling 7-34502
- radiotherapy treatment planning, graphical displays 7-40283
- reactor simulation for operator training, use of computer graphics 7-55940
- streamlines and pathlines, plotting on microcomputer 7-16272
- intelligent FASTBUS, 168/E data acquisition interface system for NA31 experiment 7-18769
- NMR spectrometer, computer control of magnetic field homogeneity 7-48795
- ocean meas. under sea ice, medium-resolution turbulence cluster 7-9271
- photoelectron spectrometer interfacing to microcomputer for data acquisition and processing 7-48919
- World projections for environment mapping, application 7-14399

computer installation management *see DP management***computer interfaces**

- not used for human interfaces for which see "user interfaces"*
- see also CAMAC; data communication equipment*
- Air-track kinematics and ultrasonic ranging module interface for Apple IIe 7-35148
- IEEE-48 instrument bus appl. to tunnelling spectrometer 7-56383
- field emitter FASTBUS, 168/E data acquisition interface system for NA31 experiment 7-18769
- NMR spectrometer, computer control of magnetic field homogeneity 7-48795
- ocean meas. under sea ice, medium-resolution turbulence cluster 7-9271
- photoelectron spectrometer interfacing to microcomputer for data acquisition and processing 7-48919

computer interfaces continued

- Raman spectra obtained with optical multichannel spectrometer, digitisation and processing 7-15010
- rectilinear scanner, interfacing with a microcomputer 7-65858
- strain gauge rosette data acquisition and analysis, microcomputer-data logger interfacing 7-29995
- thermophysical meas., computerised instruments interfaces standardisation 7-4857
- UPS, XPS and Auger spectrometers, digital power supply and counting interface 7-9825
- video/computer technology role in exptl. mech. 7-63093
- VME/VMX parallel multiprocessor system for the data acquisition of the UA1 streamer tubes 7-19665

computer internal arrangement *see computer architecture***computer metatheory** *see computation theory***computer networks**

- see also distributed processing*
- astronomical data networks, CDS meeting Strasbourg, France (1985 November) 7-4617
- IKONET, distributed accelerator and experiment control applications 7-19560
- water level measurement stations prototype network, test and evaluation software 7-66364

computer operator training *see training***computer performance evaluation** *see performance evaluation***computer power supplies** *see power supplies to apparatus***computer printers** *see printers***computer programming** *see programming***computer programs, complete** *see complete computer programs***computer programs (listings)** *see complete computer programs***computer science education**

- computational physics teaching 7-48226

computer simulation by computers *see virtual machines***computer software**

- not used for specific application software for which see relevant applications*
- see also macros; programming; software engineering; software packages*
- No entries

computer storage devices *see digital storage***computer subroutines** *see subroutines***computer vision**

- 4-camera video system, development and use 7-4235
- apparent motion correspondence 7-14015
- automatic seismic wave-field movement anal. 7-23902
- boundary image segmentation, image features 7-14012
- cortical representation of texture primitives 7-14013
- digital image-processing techniques for the display of images and modeling of visual perception 7-59997
- heart images in motion, computerised tomography 7-14142
- life sciences experimentation, autonomous, in space stations, visual monitoring 7-23467
- natural scene colour and spatial structure, photographic colorimetry 7-41420
- neuron tracing system, CARTOS-ACE, 3D reconstruction of electron micrographs 7-23502
- object interpretation using boundary based perceptually valid features 7-23362
- phase discrimination 7-14014
- prosthetics and orthotics, shape sensing by CAD/CAM techniques for fitting 7-34348
- prosthetics fitting, optical noncontact 3D body measurement 7-34350
- retinal functions, simulation with Gaussian derivative model 7-3786
- shape knowledge, use in improving performance of neuron tracing through serial sections 7-3954
- stereo real-time metrology with CCD cameras 7-47314
- stereo vision model based on human binocular vision 7-23361
- texture discrimination characteristics 7-14016
- transparency perception in man and machine 7-14008
- unsteady jets, 3D surface shape estimation by image processing 7-37573
- vision research and image technology, human functions of information processing (Japanese) 7-28499

computerised communications control *see telecommunications computer control***computerised control**

- see also chemical engineering computing; computerised materials handling; control engineering computing; electrical engineering computing; mechanical engineering computing; nuclear engineering computing; power system computer control; telecommunications computer control*
- 16-channel controller for implantable gait stimulation system, design 7-28781
- analytical software in laboratory research 7-24632
- arterial pressure, mean, computer control with Na-nitroprusside: adaptive model-based system 7-40359
- ASTRO-C X-ray astronomy satellite, microprocessor-based attitude control system, development 7-55465
- audiological investigations using microcomputer system 7-65882
- batch cooling crystalliser, microcomputer programming of temp. 7-53522
- bidirectional scattering distrib. function meas. using computer controlled facility 7-41414
- blood pressure regulation during surgery using self tuning controller 7-54805
- common-user submm receiver for UKIRT and UK-NL telescopes 7-34883
- compact quasi-optical dual LO receiver for 300-500 GHz 7-34882
- digital controller for a magnetic suspension system 7-333
- DIH-D tokamak, vacuum control system, design 7-36253
- Doublet H-D tokamak, computerised operation of neutral beams 7-19466
- electrical stimulation open-loop control of human knee during swing 7-28763
- electron linac, control system for Photon Factory 7-5498
- field emitter remodeling, microprocessor controlled 7-29987
- flexible US scanner using industrial robot for NDT 7-22970
- Forth controlled oceanographic instrument 7-55306
- Fourier transform, spectrometer, microcomputer-controlled, path difference control 7-48861
- Fourier transform spectrometer, Los Alamos design with microprocessor control 7-48860

computerised control continued

- hazardous gas monitoring system in chem. manufacturing facility, open path FTIR air monitor 7-54416
 hybrid solar house design and control using microcomputers 7-3627
 implantable gait simulation using microprocessor-controlled trigger switches 7-34353
 implantable gait stimulation system, 16-channel microprocessor-based controller, features 7-28780
 insertion device Beam Line Wunder design at SSRL 7-42256
 IR 2D detector array, microcomputer-based data acquisition 7-9382
 JEM-2000FX TEM control, using LSI-11/23 computer 7-30130
 JT-60, plasma feedback control system 7-36250
 KEK e^+ generator, magnet power supply control system (Japanese) 7-19580
 Langmuir probe plasma diagnostic 7-58063
 laser nephelometer, computer controlled for liquid conc. determ. 7-61365
 life sciences experimentation, autonomous, in space stations, visual monitoring 7-23467
 magnetic confinement expt. control system, design 7-5427
 magnetic hysteresis, low freq. meas., well-defined time depend. of flux density, meas. system 7-29985
 mass spectrometer control system design 7-18905
 medical electronic precision engineering, design considerations (Japanese) 7-60124
 MFTF ICRH system, control and data acquisition 7-15396
 MFTF-B, diagnostic control, data acquisition and data processing 7-5422
 MFTF-B, Q-bus local control computers, upgraded redesign 7-36256
 minicomputer appl. for radiocarbon anal. control and meas. 7-34682
 Mirror Fusion Facility, local control station development 7-19463
 monochromator wavelength automatic setting 7-37120
 MOS device, microcomputer-based instrumentation system for carrier transport study 7-64350
 multilayer soft X-ray reflection coatings, automatic electron beam deposition 7-33571
 optical figure generation using feedback from IR phase-shifting interferometer 7-37219
 optical surfacing unit for rapid fabrication of large aspheric optics 7-37224
 particle beam fusion accelerator I (PBFA I), automated features of control/monitor system 7-30754
 particle beam fusion accelerator II (PBFA II) control/monitor system 7-30751
 pellet injectors, control and data acquisition system, design 7-36254
 phase-shifting speckle interferometry 7-48839
 pipetting device, microvolume, for atomic absorpt. spectrometry 7-4900
 plasma control on the Tokamak de Varennes 7-15336
 potentiostat, modular microcomputer controlled for electrochemical meas. 7-59819
 precision machining/metrology facility for X-ray mirror substrates fabrication 7-37222
 Prognoz-10, instrumentation control 7-55417
 pulse radiolysis equipment, setup for simultaneous multiwavelength kinetic spectroscopy 7-56349
 qualification concepts for instrumentation and control systems of nuclear power plants 7-19419
 quasi-elastic light scattering, data acquisition and evaluation 7-56239
 radio-frequency heating apparatus for JT-60, controlling system 7-19503
 recoil separator, adaptable computer control system 7-5520
 research reactors, computer codes for operational control 7-15232
 robotic US scanning system for NDT of composites 7-22969
 scanning spectrometer design and props. 7-56353
 secondary storage batteries, computerised management system for space vehicle appls. 7-34021
 SEM, automatic method for astigmatism meas. and correction 7-41541
 semi-automatic schistosome eggs detection system, image processing technique 7-47283
 semiconductor lasers, beam location and focusing using computer-controlled spot-centring technique 7-5934
 Siemens texture goniometer, modified with microcomputer controlled stepping motors 7-44306
 sound negative processing 7-4904
 spectrometer, IR, for surface EM waves, computerised control system 7-41511
 Stepanov method cryst. growth, computerised TV system examination 7-33542
 Stereoscan 360, total computer control SEM 7-4924
 TFTR neutral beam computer control system 7-19465
 thermal decomposition study instrument 7-59818
 TMX-U, ECRH control system 7-15397
 TMX-U, Ti-Ta sublimation getter pumping system and performance, computer control 7-25184
 TMX-U diagnostic data base, evolution 7-5423
 tunnelling spectrometer using IEEE-48 instrument bus and IBM PC-XT controller 7-56383
 turbulence measurement with inclined hot wire probe, 3D angle calibration method (Japanese) 7-6338
 ultra-short laser pulse characts., microprocessor-based meas. system 7-41360
 upper arm prosthesis, intelligent control system (Chinese) 7-60127
 velocity meas. device using CCD image sensors 7-48705
 X-ray spectrometer, Cauchois-type, computer-controlled 7-56395
 ZENKEI, JT-60 central control system, design and testing 7-36249
 Cd_{0.8}Hg_{0.2}-Te heterostructures, MOVPE, computer controlled reactor, charactn. 7-59446
 LiNbO₃, Czochralski cryst. growth, computer control 7-27886
 U atomic vapour laser isotope separation data acquisition and control system 7-15735

computerised instrumentation

- see also astronomy computing; astrophysics computing; automatic test equipment; biology computing; chemical engineering computing; chemistry computing; computerised monitoring; computerised spectroscopy; computerised tomography; data acquisition; electrical engineering computing; electronic engineering computing; geophysics computing; nuclear engineering computing; physics computing
 3D surface metrology, interference microscopy, computer controlled instrumentation 7-29975
 AC bridge for precision resistance meas., computer-controlled 7-18832
 AC/DC transfer standard, digital, using differential multijunction thermal convertors 7-18838

computerised instrumentation continued

- AFMS-2, microcomputer-based automatic remote transmitting meteorological station (German) 7-4228
 alpha particle spectroscopy using a magnetic spectrograph and a large SSNTD spark counter 7-19625
 analytical software in laboratory research 7-24632
 angular encoder automatic calibration system (Japanese) 7-56213
 arbitrary waveform generator for turbulence experiments, computer-controlled 7-9846
 automatic holographic particulate meas., fundamental study (Japanese) 7-18745
 automatic sample loader 7-48909
 biomedical microprocessor-based time-of-flight respirometer 7-65866
 blackbody calibration facility for steel industry in Australia 7-14950
 blood-rate detector, one-chip VLSI implementation using PPL 7-28756
 calibration of neutron probe for soil humidity measurement (French) 7-47581
 calorimeter coaxial, and its use as reference standard in automated microwave power calibration system 7-48744
 capacitance dilatometer/oven system, computerized analysis of thermal correlations using Peltier AC-heating 7-18775
 centrifugal photometric analyser with chain-driven continuous feed system 7-24683
 coating thickness meas., XFT-84 microcomputer based X-ray fluorescent instrument (Chinese) 7-4814
 common-user submm receiver for UKIRT and UK-NL telescopes 7-34883
 compact quasi-optical dual LO receiver for 300-500 GHz 7-34882
 composite materials, displacement sensor with two-beam interferometry 7-13716
 computer aided PWR power plant operation, control and meas. (German) 7-19394
 conductometer, microprocessor HF contactless, design 7-59808
 continuous Rn monitor for groundwater research, automated operation and characts. 7-40424
 CR-39 detectors, automatic track counting with an optic RAM-based instrument 7-19652
 cryocrystal thermal expansion meas. automation 7-4845
 cutaneous galvanic reaction parameters, automated recording system 7-40353
 data acquisition suites, multichannel, with time-scale conversion and storage CRT, design 7-61321
 DC meas. at NPL, India 7-18842
 DENSEPACK array of Langmuir probes, Alcator C Tokamak fusion expt. appl. 7-20940
 densitometer, precision with microprocessor-based display unit 7-48697
 DICOM-8 digital imaging computer for pseudo-3D imaging 7-47275
 differential scanning calorimeter automation 7-24654
 digital image counting system for nuclear track detectors 7-19644
 digital upgrades for nuclear plant control and instrumentation 7-30597
 diverse experimental data preliminary processing, interactive system 7-4825
 electrochemical analysis methods improvement 7-8353
 electron microscopes astigmatism detection using radon transform (Japanese) 7-18931
 ellipsometry, computer-based high resolution transmission 7-41428
 EM precision meas., conf., Gaithersburg, MD, USA (June 1986) 7-14710
 emulsion analysis system for nanobarn cross section events 7-19647
 eye, visual adaptation measurement using computer controlled device 7-34144
 eye examination setup, OAP-311, rational refraction system 7-8747
 flow meas., multichannel time counter and data acquisition system 7-37571
 flow measurement by transit time method using radioactive tracers (Finnish) 7-57970
 flowmeter, microcomputerised system, accuracy estimation 7-57956
 frequency and time reproduction standards, automatic 7-41352
 gait, temporal and spatial parameters meas. using a microcomputer system 7-40321
 gait analysis system, portable computerised, force distrib. meas. under foot in walking modes (Japanese) 7-14146
 geological data logger with 8085 microprocessor 7-9179
 hearing aids, prescription technique comparison using computerised filter adjustment for aid simulation 7-34163
 high freq. core loss automatic measuring system 7-48784
 Histos network for hydrological and meteorological measurement for East-Scheldt storm surge barrier construction 7-47557
 HSI digital ocean bottom seismograph (Chinese) 7-29260
 hygrometer, Volna-5 low-inertia type (Russian) 7-41396
 IKAR-16 automated solar spectral-polarisation complex of RATAN-600 radio telescope, configuration and software 7-66460
 impact testing, computer-assisted 7-59707
 inertial clock based on computer controlled servo-driven corotation system with superconducting suspension 7-14927
 inertial surveying missions over short distances, methods for high accuracy 7-4198
 injection laser application for measuring surfacegeometric parameters 7-4816
 integrating sphere spectrometer for high-temperature materials characterization 7-35604
 intelligent multichannel analyzer for the measurement of gamma spectra 7-5533
 ion-selective electrodes for ion conc. measurement, operation in nonlinear suboptimal response range 7-56246
 IR lens elements and assemblies, spectral transmission meas. 7-31429
 IR spectroradiometry, using IBM PC 7-18859
 JEM-2000FX TEM control, using LSI-11/23 computer 7-30130
 Josephson voltage standard, computer controlled 7-14970
 JT-60, plasma feedback control system 7-36250
 KS-147A LOROP camera system, photographic reconnaissance appl. 7-18897
 laboratory robot, decision criteria for purchasing 7-24637
 Langmuir probe plasma diagnostic 7-58063
 Langmuir probe technique for plasma parameter measurement in a medium density discharge 7-11782
 laser Doppler velocimetry, multi-pt. system using phase diffraction grating 7-37605
 laser level for adjustment of RATAN-600 radio telescope, design and performance 7-66468
 LEED intensity meas. using real-time digital video processor 7-44317

computerised instrumentation continued

- left ventricular assist device 7-40369
 light microscope system for morphometric anal. of organ of Corti 7-40373
 lightning surge and transient protection and warning systems 7-34663
 low-cost satellite image reception and analysis facility 7-66305
 low-Q piezoelec. material constants, automated meas. system 7-328
 low-temperature thermophysics systems metrology, applied aspects 7-48745
 MA 5964 laboratory microprocessor-controlled conductivity meter (*Slovenian*) 7-18803
 magnetic hysteresis measurement system, automatic, with high accuracy 7-4871
 microcomputer data-acquisition system for flow rate sensor 7-51349
 microcomputer-controlled two-pulse generator, for use in NQR spectroscopy 7-9863
 micropolariscope for automatic stress analysis 7-43815
 microprocessor controlled microscope for nuclear emulsion meas. 7-19648
 microprocessor meter of radiation attenuation coefficient in solutions 7-4876
 moistened and pyrolyzed materials in strong RF fields, computer-aided permittivity meas. 7-48769
 monochromator, computer-controlled, for qualitative and semiquantitative ICAP-AES anal. 7-30096
 MTF meas. equipment for IR and visible wavelengths, microcomputer-controlled 7-31543
 multi-job, multi-user electron probe X-ray microanalyser, JXA-8600 series 7-33978
 multichannel optoelectronic processor with correlation-function processing 7-25740
 multichannel portable functional electrical stimulation system for spinal cord injured persons 7-28765
 multichannel scaling with a VIC-20 or Commodore 64 7-49841
 MWPC imaging, derandomising buffer and microcomputer memory 7-42309
 NRLM work relating to precision meas. and fundamental constants 7-14915
 nuclear micro-beam probe for the investigation of surfaces, microprocessor-controlled 7-8352
 ocean current meter, inclinometer-type, microprocessor control 7-66365
 ocean meas. under sea ice, medium-resolution turbulence cluster 7-9271
 optical gain meas. in discharges, spontaneous emission amplification obs. 7-14989
 phase-shifting speckle interferometry 7-48839
 photographs processing from bubble chambers 7-35498
 photomultiplier-based track counting system for SSNTDs 7-19655
 picture analysis systems for nuclear emulsion track meas. 7-19649
 plant cells water transport props. determ., using automated pressure probe 7-23503
 plotting probability density function of resultant error with two or more components 7-48673
 polarisation spectrophotometer for meas. of polarised emission and excitation spectra 7-56318
 portable continuous blood pressure monitor utilizing an M68705 microcomputer 7-28755
 potentiostat, modular microcomputer controlled for electrochemical meas. 7-59819
 pressure measurement in a blow-down wind tunnel, automatic system 7-16280
 Prognoz-10, instrumentation control 7-55417
 programmable, multifunction dual-channel waveform generator for visual psychophysics 7-60006
 programmable DC-100 MHz voltage standard 7-18839
 prosthetics and orthotics, shape sensing by CAD/CAM techniques for fitting 7-34348
 prosthetics fitting, optical noncontact 3D body measurement 7-34350
 psychrometer with autocalibration 7-4860
 pulse radiolysis equipment, setup for simultaneous multiwavelength kinetic spectroscopy 7-56349
 qualification concepts for instrumentation and control systems of nuclear power plants 7-19419
 quantized Hall resistance measurement at the National Measurement Laboratory, Australia, using GaAs/GaAlAs heterostructure 7-14965
 quartz sensor for automatic dew-point hygrometry 7-61344
 quasi-elastic light scattering, data acquisition and evaluation 7-56239
 radiation protection measuring equipment, use of microprocessors (*German*) 7-25257
 radio-meteor systems for time-scale synchronisation, accuracy criteria 7-41350
 radiography system TCR 201 7-18067
 radiography system using an imaging plate as an X-ray sensor, TCR-201 7-40282
 radiotelescope calibration, automated system (*French*) 7-60542
 radiotherapy, external beam, on-line electronic portal imaging system 7-14110
 RAS III, modular noise diagnostics system for reactor primary circuit monitoring (*German*) 7-56787
 refractometric water-content meas., systematic error reduction by structural method and microcomputer 7-48832
 refractory materials specific heat, resistivity and integral emissivity meas., high-speed pulse meas. 7-4842
 resistance standard, automated cryogenic current comparator resistance bridge 7-18829
 respiratory gas exchange calc. using mass spectrometer, correction for instrument time constant and transport delay 7-60143
 rock thermophysical characts. determ. 7-9219
 Rossendorf Research Reactor, computer-based γ -ray area monitoring system (*German*) 7-19552
 scanning acoustic microscope, 50-2000 MHz range 7-20544
 scanning laser acoustic microscope with digital data acquisition 7-50882
 scanning tunneling microscope automation 7-18924
 scanning tunnelling microscopy 7-18925
 seismic shallow layer reflecting survey system for Japan Geographical Survey Office (*Japanese*) 7-23855
 SEM, automatic method for astigmatism meas. and correction 7-41541
 SEM stereophotogrammetric method and system for three-dimens. eval. of features on flat substrates 7-40377
 ship-board echo location system accuracy and system for East-Scheldt storm barrier construction 7-47558
 shipboard-three component magnetometer control 7-29276

computerised instrumentation continued

- Siegen automatic measuring system for nuclear track detectors: status and new developments 7-19650
 SIMS, quadrupole, data acquisition and control system 7-24722
 sleep investig., reaction time meter (*Dutch*) 7-23322
 small-angle neutron scatt. spectrometer 7-32227
 smart acoustic current meters, experiences in Lake St. Clair, Canada/USA 7-9255
 soft X-ray/EUV calibration facility at the University of Colorado 7-20479
 spectral response meas. apparatus, microcomputer controlled, for large area solar cells 7-3642
 Stereoscan 360, total computer control SEM 7-4924
 strain gauge rosette data acquisition and analysis, microcomputer-data logger interfacing 7-29995
 streak photography, two-dimensional transients acquisition and processing, using IBM personal computer 7-15025
 stress meas., photoelasticity determ. with aid of computer, in polycrystalline Si ribbon 7-31725
 surface testing by microscope-TV-computer system 7-14922
 sweep-nonlinearity correction procedures in picosecond streak camera measurements 7-15024
 synergistic relationship between computers and robotics 7-24638
 temperature measurement system, multichannel, with built-in microcomputer 7-41381
 thermal decomposition study instrument 7-59818
 thermal radiation flux densities meas., automated metrological support 7-4846
 thermal variables meas., microcomputer data-acquisition and control system 7-4841
 thermophysical laboratory database formation, using pulse heat method 7-4828
 thermophysical meas., computerised instruments interfaces standardisation 7-4857
 thermophysical meas. automation, universal microcomputer-controlled system 7-4854
 thermophysical props. of metals meas., 600 to 4000K range 7-4843
 thermophysical research automation at BSSR Institute of Heat and Mass Transfer 7-4823
 thermophysical variables meas., UNTO systems 7-4847
 thromboelastograph, 2-channel, microprocessor-based 7-3903
 time and frequency standard units automatic comparison, software 7-41353
 time domain spectroscopy for dielectric props. meas., human skin in vivo meas. appl. 7-14961
 tissue blood perfusion, computer-based system for continuous on-line meas. using a thermal method 7-40319
 Tohoku 300 MeV e^- linac cooling system, trouble and warning system 7-19579
 transparent materials, spectral emissivity exam., using fast automatic system 7-4855
 tunnelling spectrometer using IEEE-48 instrument bus and IBM PC-XT controller 7-56383
 two-parameter data-acquisition system for slit-scan chromosome analysis 7-35501
 tired wheels, noise investigation, array processor use (*German*) 7-6041
 UHF water-content meters for cotton materials 7-48758
 ultra-short laser pulse characts., microprocessor-based meas. system 7-41360
 ultrasonic imaging systems for robot object recognition 7-26097
 US displacement meas. system, microcomputer controlled (*German*) 7-56222
 US nondestructive testing, microcomputer appls. in thickness meters and hardness testing (*French*) 7-54068
 US velocity and attenuation meas., microcomputer-controlled phase-sensitive detection 7-50881
 vapour-pressure isotherms, high-precision, apparatus errors and results 7-56252
 velocity meas. device using CCD image sensors 7-48705
 video-electronic device for particle track meas. 7-19651
 viscometer for shear rate meas. at low frequencies 7-1658
 visual display, programmable, for diagnosing, assessing and rehabilitating unilateral neglect 7-65880
 voltage standard using solid-state references 7-18841
 vortex flow meters for computerised vapour-heat flow measurement (*German*) 7-11564
 waveform analyser, programmable, metallurgical test appl. 7-35505
 windmills driving piston pumps, computer aided wind speed meas. field tests 7-39961
 X-band time-domain EPR spectrometer, computer-controlled 7-30054
 X-ray diffractometer for tensometry using SAPI 1 microcomputer and FORTH language (*Czech*) 7-56390
 X-ray equipment automation (*Russian*) 7-4939
 X-ray image acquisition using an IBM-PC, SEM based energy dispersive spectroscopy 7-4942
 X-ray spectrometer, Cauchy-type, computer-controlled 7-56395
 ZENKEI, JT-60 central control system, design and testing 7-36249
 GaAs:In, doped and undoped, EL2 maps from computer based IR image analysis 7-32237
³He melting curve thermometer, automated, pressure meas. appl. 7-14955

computerised manufacturing control *see manufacturing computer control*

computerised materials handling

- canister grapple for the Defense Waste Processing Facility 7-49696
 dielectrophoretic levitation, active feedback-controlled 7-3596
 FBR reprocessing plant using remote maintenance, Japanese design 7-61977
 FFTF interim examination and maintenance cell, remote tool development 7-49547
 FRG nuclear fuel reprocessing plant, remote maintenance aspects, manufacturer's viewpoint 7-49559
 HLW vitrification in a liquid-fed ceramic melter, remote equipment performance 7-42201
 Manipulator Comparative Testing Program for nuclear fuel reprocessing appls. 7-49556
 nuclear fuel pin weighing system, remote maintenance design considerations 7-49548
 nuclear waste glass canisters, remote handling at the Savannah River Plant 7-42200
 PWR steam generator tubing sampling, feasibility study 7-5364

computerised materials handling continued

- radioactive waste vitrification facilities, closed circuit TV and remote crane control 7-42204
- reactor pressure vessel manipulators, functions and basic concepts (*German*) 7-56807
- remote equipment operators in nuclear facilities, training programme requirements 7-49607
- remote handling in hot cells, state of the art and future view 7-49555
- remote handling systems for reprocessing plant maintenance and reactor dismantling, testing and design 7-49614
- remote radwaste canister level and turntable positioning system 7-42202
- remote vacuum cleaner for PUREX cells 7-49557
- remote weighing of irradiated fuel pins at FFTF 7-49546
- remote work vehicle, design rationale, radiological decontamination work 7-49741
- remotely operated TRU waste size reduction and material handling process at SRP 7-49698
- TMI-2, integrated defuelling system, remote tools and support equipment 7-49610
- TOR fast reactor fuel reprocessing facility, integrated remote handling system 7-49558

computerised monitoring

- air pollution monitoring using Commodore 64 home computers 7-54418
- Automated Remote Monitoring System for machinery health assessment 7-20674
- automatic monitoring of nuclear wastes (*French*) 7-36299
- cardiopulmonary rate monitor, microprocessor-based, using low-power Doppler microwaves 7-65828
- cerebral blood flow measurement, indicator elution curves analysis by microcomputer 7-40389
- ECG, arrhythmia typification in a real-time anal. system for monitoring geriatric patients during exercises 7-40337
- ECG, automated arrhythmia anal. combined with ST anal. for exercise monitoring 7-34326
- ECG, continuous vectorcardiography, in acute myocardial infarction 7-34302
- eye, excised crystalline lens, computer assisted scanning laser monitor for optical quality meas. 7-23507
- hazardous gas monitoring system in chem. manufacturing facility, open path FTIR air monitor 7-54416
- Holter monitoring, computer-aided, use for S-T changes detect. 7-40348
- inertial surveying missions over short distances, methods for high accuracy 7-4198
- intracranial pressure monitoring (*Spanish*) 7-34299
- left ventricular ejection fraction, continuous monitoring using a miniature NaI detector and microcomputer 7-34305
- life sciences experimentation, autonomous, in space stations, visual monitoring 7-23467
- microcomputer-based solar and meteorological data acquisition and control system 7-4186
- neonates with low birth weight, data acquisition system for monitoring 7-3920
- nuclear power plant status monitor design and operation 7-15267
- nuclear reactor monitoring system, reliability improvements (*Russian*) 7-25101
- nuclear systems, automatic fault monitoring system 7-833
- oil traces in turbid water monitoring, using online IR analyser 7-34091
- optical fibre transmission loss characteristics during drawing, continuous measurement 7-6004
- patient monitoring 7-40329
- photovoltaic, solar plant, automatic data acquisition system 7-54273
- portable continuous blood pressure monitor utilizing an M68705 microcomputer 7-28755
- respiratory pressure data analysis for detecting breathing circuit faults in ventilated patients 7-40330
- secondary storage batteries, computerised management system for space vehicle appls. 7-34021
- spinal somatosensory evoked pots. monitoring during surgery, microprocessor-based system 7-23482
- sudden infant death syndrome, microprocessor-based home monitor 7-3921
- walking and ECG, computerised system for 24 hr simultaneous recording and anal. 7-40347

computerised navigation

- magnetic flux-gate compass for automobile navigation 7-330

computerised pattern recognition

- 3D reconstruction of median eminence sections 7-34356
- autoradiographic images, digital cluster anal. system to locate labelled cell regions 7-3958
- autoradiographs, grain counting using pattern recognition 7-23490
- boundary image segmentation, image features 7-14012
- carotid angiograms abnormality detection using computerised syntactic pattern recognition 7-40354
- cells, chromatin content of cervical cancer cells, image processing technique 7-34119
- cortical representation of texture primitives 7-14013
- cosmic ray track analysis by expert system using distributed problem solving 7-55388
- digital microscopy for cellular/subcellular features identification 7-54821
- ECG, ST segment shape recognition, automatic method 7-23476
- ECG automatic detect. of ventricular fibrillation 7-18082
- ECG data, Hilbert transforms and Wigner-Ville distributions 7-47265
- EEG automatic classification based on syntactical pattern recognition, ARMA model 7-40328
- expert diagnostic US system, statistical approach 7-23415
- filter with limited rotation invariance for target recognition 7-10872
- high-dimensionality pattern recognition feature space production 7-25725
- hybrid pattern recognition by features extracted from object and Fraunhofer diff. patterns 7-42942
- littoral cartography, SPOT remote-sensing image segmentation 7-29307
- multichannel optoelectronic processor with correlation-function processing 7-25740
- nerves and molecules 3D reconstruction and display using pattern recognition 7-65734
- nucleoli, extraction from images of leucocytes by computerised image analysis 7-23505
- oceanographic image anal. expert system, knowledge-based, features 7-23901
- optical/digital hybrid system for calculating geometric moments 7-25724

computerised pattern recognition continued

- portable continuous blood pressure monitor utilizing an M68705 microcomputer 7-28755
- radiation dosimetry, picture-processing-based automated system 7-28713
- remote sensing of land surface, context classifier for pixel analysis of images 7-23873
- remote sensing of linear features on land surface, using visual model 7-60404
- rock microstructure, image analysis of particles, FORTRAN V program 7-66311
- side scan sonar records, use of image processing 7-66368
- signal image interpretation system, rule-based, seismic data anal. appl. 7-23903
- stereo real-time metrology with CCD cameras 7-47314
- subsurface geology from well logs, color images, Kansas 7-40581
- textural feature extraction procedure for remote sensing 7-9207
- three-dimensional morphometric cytology, pictorial pattern recognition 7-28801
- ultrasonic imaging systems for robot object recognition 7-26097

computerised picture processing

- see also computer-generated holography
- 2D hybrid stress analysis, laser speckle photography, image processing techniques 7-31712
- 3D CT image reconstruction and display (*Chinese*) 7-60118
- 3D flow obs. by interferometry and image processing 7-37576
- 3D reconstruction of median eminence sections 7-34356
- aerial digital images enhancement, high altitude, histogram specification techniques 7-40608
- astronomical instrumentation and techniques, conf., Tucson, AZ, USA (March 1986) 7-48162
- astronomical telescope, image processing technique for Halley Multicolor Camera system 7-9380
- automated analysis of two-dimensional NMR spectra of mixtures by pattern recognition 7-24635
- automatic left ventricular cineangiograms analysing system 7-47258
- automation range of motion meas. in cervical spine using video images 7-28747
- autoradiographic images, digital cluster anal. system to locate labelled cell regions 7-3958
- bandwidth extrapolation through iterative deconvolution 7-62637
- biological thick specimens, computer-assisted video technique for preparing high resolution pictures and stereograms 7-28789
- biomedical image, 3D and 4D, workstation for their display and analysis 7-65885
- blood flow phase detection on digital subtraction angiography 7-47257
- boundary image segmentation, image features 7-14012
- Canadian petroleum exploration, appl. of remote sensing 7-40585
- cancer detection, coding theoretic approach 7-47252
- cardiac activation movies generation using Walsh-Hadamard phase spectrum 7-54743
- cardiac wall motion during exercise, computerised quantitative segmental anal. from 2D echocardiograms 7-34321
- cardiovascular radiology image processing 7-65833
- cartography and photogrammetry, digital computerised line-matching problem 7-47315
- CCD colour endoscope image motion related blur compensation 7-47282
- cell automated classification techniques, imaging flow cytometer 7-8774
- cells, chromatin content of cervical cancer cells, image processing technique 7-34119
- chest radiography, digital image processing 7-23455
- colour image processing for bronchus endoscopic image restoration 7-47281
- colour printing, digital image layout system 7-15027
- composite, digital image correlation methodology use for deform. quantification 7-59718
- composite plate, spectral analysis of natural grid features for surface analysis 7-63096
- computer-aided holography, new developments 7-31285
- coronary angiograms, digitised, computer anal. for assessment of changes in poststenotic coronary flow 7-28687
- coronary angiography, quantitative, accuracy of the catheter as a reference for arterial dimensions 7-28685
- coronary arteries skeleton from cineangiograms 7-18062
- coronary artery quantification by digital radiography 7-28691
- cosmic ray track analysis by expert system using distributed problem solving 7-55388
- CRT printer, exposures from digital images onto colour photographic paper 7-354
- CT, high speed, using Imatron C-100 cine scanner, efficient data archiving and rapid image anal. 7-28683
- CT methods use for nondestructive inspection under conditions of insufficient data 7-39818
- cytoarchitectonics, nervous tissue struct. inhomogeneities, software and hardware aspects of evaluation and anal. system 7-34360
- dam site planning with enhanced satellite imagery 7-17848
- development of a new image processing system for nuclear medicine 'SCINTIPAC-700' (*Japanese*) 7-18074
- diffraction tomography reconstruction, max. entropy method 7-47256
- digital correlation method, optimised appl. to deformation analysis 7-26136
- digital diagnostic imaging, versatile image processor and its appl. in computed radiography 7-28673
- digital image processing techniques used in astronomy, appl. to diff. data 7-11828
- digital representation and evaluation of metallographical microstructural images (*German, English*) 7-39809
- digital subtraction angiography, automated tracking of the vascular tree using a double-square-box region-of-search algorithm 7-28674
- digital subtraction angiography, technique for automatic motion correction 7-23456
- digital subtraction radiography technology, equipment and techniques 7-40267
- discrete Radon transform in a continuous space 7-56235
- display colour parameters modelling and algorithmic colour selection 7-28538
- droplet field visualization and characterization via digital image analysis 7-37577
- echocardiograms, 2D, automatic and intelligent left ventricular contour detect. 7-34212

computerised picture processing continued
 echocardiographic scan images, cine, spatial and temporal processing: automated myocardial border tracking 7-28638
 echocardiography, 2D., microcomputerised image processor and 3D reconstruction of left ventricle 7-34213
 echocardiography, computer assisted anal. of left ventricular function 7-34211
 echocardiography, versatile digitisation and processing system 7-34216
 electron microprobe use as digital image analyser (*French*) 7-46746
 electron microscope molecule images reconstitution, correspondence analysis, struct. interpret. tool 7-60138
 electron microscopy, high resolution, digital image processing 7-4931
 electron microscopy of cell components, computer environment for 3D shaded perspective display 7-65905
 eye rotational movement anal. using template matching, IR image processing (*Japanese*) 7-60111
 facial skin features, image processing algorithms and photographic techniques 7-23501
 fan beam-CT system, high-resolution algorithm 7-8686
 fan-beam CT system, fast reconstruction algorithm 7-8685
 field emission gun scanning electron microscope columns, computer modelling 7-41548
 film digitisation, low cost solutions implementation 7-18893
 flow, multi-point vector measurement by pulsed laser velocimetry with image compression 7-37610
 flow vel. vector, automatic determ. from pathline photograph 7-37575
 Fourier phase retrieval when image is complex 7-62634
 Fourier-based textural feature extraction procedure for remote sensing 7-9207
 fringe pattern analysis using holographic interferometry 7-15817
 gated radionuclide ventriculography with a slant-hole collimator, fully-automated contour detect. 7-40252
 heart images in motion, computerised tomography 7-14142
 holographic interferometry, computer-based fringe interpretation 7-31264
 holographic interferometry fringe anal., automatic 7-31286
 human chest measurement during respiration, using structured light 7-40326
 human gait data acquisition and processing using digital camera 7-65809
 human visual system models appl. to digital colour image compression 7-65744
 hybrid pattern recognition by features extracted from object and Fraunhofer diff. patterns 7-42942
 IBM PC/AT-based image acquisition and processing system for quantitative image anal. 7-28796
 III-V semiconductors, elec. parameter mapping by numerical image processing of light beam induced current topography 7-33051
 image analysis system for quantitative metallography, microprocessor and minicomputer-based 7-1033
 image detection system for Kiso Schmidt plates, appl. to Orion Association 7-55477
 image processing in the reconnaissance revolution 7-50507
 image processing system for electron linac beam diagnosis (*Japanese*) 7-19621
 imagery from satellite, video technology appls. (*Japanese*) 7-66349
 infection diagnosis, computer subtraction of simultaneously acquired dual radionuclide images 7-40274
 interactive proton MR image synthesis 7-65829
 interference automatic fringe pattern analysis, review 7-18869
 interferogram fringe analysis by photodiode array digitizer 7-30073
 interferograms, computer complex for measurement and processing 7-41454
 IR satellite image processing, kinetic temp. image modelling 7-23899
 IUE spectra, VIRIS-VAX interactive reduction 7-40720
 jet flow visualisation, image processing using streamline coordinates 7-37572
 Landsat data, Fourier filtering for information extraction in surveying and mapping 7-47582
 LEED intensity meas. using real-time digital video processor 7-44317
 left ventricular regional wall motion, quantification using multiple-view radionuclide angiography and the centerline method 7-34268
 left ventriculograms. digital subtraction, automated edge detect. method 7-34269
 light intensity distrib. meas. system, image processing unit (*Japanese*) 7-4881
 littoral cartography, SPOT remote-sensing image segmentation 7-29307
 longitudinal ECT imaging using γ -ray camera 7-40281
 lung air content, regional, analysis by 3D computerised tomography and multinomial models 7-54801
 macromolecular diffusion coeffs. meas. using holographic interferometry, digital image processing 7-31272
 macular laser lesions, image anal. 7-34229
 Magellan SAR system, data rate charact. 7-55469
 magnetic microfield 3D reconstruction, computerised microtomography methods 7-4874
 mammography, subtle microcalcifications detect., evaluation of digital unsharp-mask filtering 7-28677
 material surface deformation slope meas., reflection grating method, digital image processing 7-29974
 maximum entropy method deconvolution in astronomy 7-14500
 medical B-mode imaging data sampling, US beamwidth effect on attenuation 7-47191
 medical fluorescence imaging, digital background subtraction 7-40247
 medical images, comparison of discrete cosine transform and vector quantisation 7-28624
 medical images, edge enhancement by 3D processing 7-54803
 medical images, vessels tracking, development of 3D discontinuity detector and linking algorithm 7-8751
 medical IR thermogram processing system using a microcomputer (*Chinese*) 7-28643
 medical microscopy automation blood smear analysis automation 7-65832
 medical NMR, high-speed techniques for estimating T1 and T2 images 7-23429
 medical radiography, image processing technology 7-65856
 MRI and CT images of human body, three dimensional reconstruction of surfaces 7-54804
 multichannel optoelectronic processor with correlation-function processing 7-25740
 multispectral imagery dimension reduction and interpretable, Chebyshev polynomials 7-4236
 myoelectric signals of neck and head, speech information 7-34164

computerised picture processing continued
 NDT, video images, digital enhancement techniques 7-65272
 neuron tracing system, CARTOS-ACE, 3D reconstruction of electron micrographs 7-23502
 NMR imaging, struct. enhancement by subtraction 7-54692
 NOAA data processing system (*Japanese*) 7-4287
 nuclear medicine images, digital restoration by two-step procedure 7-14121
 nuclear ventriculography, ejection fraction determ. by combined inverse Fourier anal. and second-derivative technique 7-40254
 nucleoli, extraction from images of leucocytes by computerised image analysis 7-23505
 object reconstruction over integer field from noisy Fourier intensity data 7-5850
 ocean imagery, dual-freq. SAR, calibration 7-4244
 oceanographic image anal. expert system, knowledge-based, features 7-23901
 optical analysis and simulation, microcomputer-based image processing aids 7-36891
 optical microscopy, tomographic imaging, support constraint 7-41460
 optical-electronic hybrid system with feedback, iterative image reconstruction 7-57252
 optoelectronic system with feedback, software shaping of instrumental function 7-57253
 particle velocity and displacement distribts. from double-exposure holograms using opt. and digital processing 7-31277
 phase retrieval, practical appl. for the space telescope 7-62638
 phase retrieval based on theoretical models for multi-dimens. band-limited signals 7-62636
 phase retrieval method apparent limitations 7-62635
 phase-only image reconstruction from offset Fourier data 7-50509
 photodetection process in optical range finding simulation 7-41467
 photographs processing from bubble chambers 7-35498
 photographs processing from large bubble chambers 7-36411
 plasmas, laser sustained, imaging of continuum emission for diagnostics 7-20930
 programmable spatial filtering function using CCD technology (*Japanese*) 7-25715
 prosthetics fitting, optical noncontact 3D body measurement 7-34350
 quantized images with smooth appearances, vision research tricks 7-59998
 radiation dosimetry, picture-processing-based automated system 7-28713
 radiographs, effect of digital unsharp masking on detectability of interstitial infiltrates and pneumothoraces 7-47248
 radiological images, compression with 512, 1024 and 2048 matrices 7-54738
 radiotherapy, port film enhancement of digital processing 7-47234
 Raman spectra obtained with optical multichannel spectrometer, digitisation and processing 7-15010
 raster-formatted geodata, image processing techniques 7-66367
 Rayleigh-Benard convection, laser speckle velocimetry 7-31902
 real-time programmable image subtractor using a magneto optic device 7-20145
 reconstruction of tomographic images from projections of a small number of views via mathematical programming 7-34245
 rectilinear scanner, interfacing with a microcomputer 7-65858
 remote sensing of land surface, context classifier for pixel analysis of images 7-23873
 renal volume calculation using [125 I]hippuran gamma camera renography and computerised image processing 7-8680
 retina display and reconstruction 7-14000
 right ventricular ejection fraction, automated determ. by digital processing of 81m Kr scintigrams 7-65835
 rock microstructure, image analysis of particles, FORTRAN V program 7-66311
 rock type recognition, computer-aided drainage network anal. form Landsat imagery 7-4238
 SAR data, spaceborne, registration to topographic maps 7-4237
 SAR data processing, high speed, on NEDIPS data flow computer 7-47579
 SAR imagery, geometric filter for reducing speckle 7-50719
 SAR images 3D formulation 7-9208
 SAR sea ice imagery, geophys. anal., computer-assisted techniques 7-4243
 scanning electron microscopy, online digital recording system 7-4933
 scanning laser acoustic microscope high-resolution imaging with digital processing 7-1318
 scanning X-ray imaging system for quantitative arteriography and blood flow meas. 7-40266
 scintigram-standard radiograph superimposition, image processing system, ventilation index determ. 7-40259
 scintigraphic images, automated comparison 7-40258
 secondary ion imaging, with charge-coupled device camera 7-48912
 self-consistent solutions to algebraic reconstruction of image from its projections 7-56237
 SEM, transmitted electron image observation 7-4932
 SEM image, contamination effects removal by homomorphic filtering 7-367
 SEM image analysis, fully automated system 7-56385
 SEM images acquisition and enhancement, using microcomputer 7-377
 semi automatic computerised system for producing heart and coronary arteries images 7-3875
 semi-automatic schistosome eggs detection system, image processing technique 7-47283
 Shuttle Orbiter leeside surface IR imagery, during atmospheric entry, comprehensive analysis 7-29378
 side scan sonar records, use of image processing 7-66368
 signal image interpretation system, rule-based, seismic data anal. appl. 7-23903
 single photon emission CT, automated body contour detect. 7-65841
 single photon emission CT using ^{111}In and ^{123}I , digital image restoration using optimised Metz filters 7-40257
 soft X-ray streak camera, absolute calibration 7-18963
 speckle interferogram inverse filtering for HST roll deconvolution 7-55487
 speckle photography fringes, 2D digital processing, angular determ. accuracy 7-41441
 spinal bone mineral determ. using automated contour detect.: appl. to single and dual energy CT 7-47243
 steel metallurgy, computer-assisted image anal. systems 7-3546
 stereocomputer, three axis, for SEM photogrammetry 7-4934

computerised picture processing continued

- stomach and duodenum, radiographic mag. using computed radiography 7-14126
- strain measurement using moiré by shifting model grating, image processing (*Japanese*) 7-31715
- stress analysis using image processing, (*Italian*) 7-46777
- surface testing by microscope-TV-computer system 7-14922
- Swedish perspectives on the use of computers in cardiology 7-28741
- systolic and diastolic cardiac function, rapid radionuclide-derivation using cycle-dependent background correction and Fourier anal. 7-40286
- TEM, systems design, computer aided image processing, appls. 7-41539
- TEM images mapping, using photogrammetric plotting system 7-41361
- TEM images processing 7-35497
- terrain data interactive image processing, digital SM-4 Omega system 7-66334
- three-dimensional morphometric cytology, pictorial pattern recognition 7-28801
- tissue characterisation from US B-scan data, liver and spleen appl. 7-14072
- tomographic reconstruction consistency by iterative methods 7-47253
- tomography, computer assisted, detector width artifact correction 7-47255
- tomography synthesis, 3D reconstructing algorithm 7-47254
- tomosynthesis using a digital radiographic system 7-23446
- transmitter binding sites, quantitative autoradiography with an image analyser 7-34359
- turbulent, fully developed 2D channel flow, visualisation and image processing 7-37574
- TV, scene-by-scene colour correction using phase domain signal processing 7-24685
- underground object imaging system with computerized reconstruction 7-47580
- unsteady jets, 3D surface shape estimation by image processing 7-37573
- US holography with liquid crystal convertor and image processing system 7-43547
- US tomography, resolution improvement using adaptive filtering (*Japanese*) 7-34202
- VEGA mission, cosmic visual data processing and recording (*German*) 7-66477
- velocity-field measurement by pixel-based temporal mutual-correlation analysis of dynamic image 7-20823
- ventricular pressure-volume relationships, automated anal. by digital ventriculography 7-28692
- vibration measurement using phase-shifting time-average holographic interferometry and image processing techniques 7-35575
- video/computer technology role in exptl. mech. 7-63093
- videograms, field recorded, computerized analysis 7-42943
- vision research and image technology, human functions of information processing (*Japanese*) 7-28499
- visual perception modeling and image display of digital image processing techniques 7-59997
- vocal fold vibration and speech signal, simultaneous high speed digital recording 7-47129
- water pollution, Seto Inland Sea hydraulic model, dye conc. pattern anal. 7-40058
- white light speckle, digital image correlation, image distortion effects 7-42997
- X-ray CT image, 3D display of cerebral ventricle 7-47280
- X-ray image acquisition using an IBM-PC, SEM based energy dispersive spectroscopy 7-4942
- X-ray images, computer processing 7-23435
- zooplankton population analysis, multiple microprocessor system using image processing 7-18103
- Al-Mn, lattice model of quasicrystalline phase, high resolution electron microscope images 7-37866
- Si polycrystalline ribbons, stress meas., photoelasticity determ. with aid of computer 7-31725

computerised power station control *see power station computer control*

computerised power system control *see power system computer control*

computerised process control *see process computer control*

computerised signal processing

- see also biology computing; computerised pattern recognition; computerised picture processing; medical diagnostic computing*
- acoustical communication in animals 7-50854
- bioacoustic, digital signal acquisition, analysis and synthesis, microcomputer based system, PAL 7-54817
- body surface pot. mapping, recursive computation of LF baseline drifts 7-40338
- cardiac electrophysiological stimulation and online processing, automated system 7-34324
- cognitive dysfunction diagnosis, multimicroprocessor-based real-time EEG analyser 7-23475
- digital filter for electron instrumentation 7-47034
- digital sampling of cardiac Purkinje fiber action potentials, maximum frequency components 7-18085
- digital signal processing for noise removal from plasma diagnostics 7-15400
- Doppler US signals, CW, statistical props. and speckle, simulation model 7-43538
- ECG, ambulatory recordings, performance evaluation of algorithms for QT interval meas. 7-40343
- ECG, arrhythmia detect. in Holter records: reliability of multi-lead vs. single-lead anal. 7-40355
- ECG, arrhythmia detector performance, confidence limits estimation 7-40335
- ECG, continuous vectorcardiography, in acute myocardial infarction 7-34302
- ECG, data compression VCG anal., comparison of two algorithms 7-40356
- ECG, dedicated cardiac signal processor 7-34303
- ECG, freq.-domain QRS classification algorithm using an annotated ECG database 7-34307
- ECG, HF, microcomputer-based analyser 7-54787
- ECG, Holter anal., fourth generation computer aided system: Mk4 7-40331
- ECG, multivariate characterisation of normal ST response derived from a computerised exercise ECG system 7-34325
- ECG, P wave recognition, CSE database in the development of a new algorithm 7-40340
- ECG, power line interference estimation and removal 7-65863

computerised signal processing continued

- ECG, quantitative investigation of QRS detect. rules using MIT/BIH arrhythmia database 7-54789
- ECG, RR-intervals during atrial fibrillation, heart rate stratified anal. from ambulatory tape recordings 7-34314
- ECG ambulatory arrhythmia analysis: a dual-channel, Bayesian approach 7-40332
- ECG analysis, long term automated system, low cost microprocessor based implementation 7-40350
- ECG baseline wander reduction using linear phase filters 7-18086
- ECG databases, software interface for arrhythmia detector evaluation 7-40336
- ECG P-wave, algorithm for automatic detect. in single or multiple lead signals 7-28746
- ECG program for anal. of 12 simultaneous leads during an exercise test, precision and accuracy 7-40342
- ECG signal processing methods for microcomputer-based automatic diagnostic system 7-47284
- ECG ST-T segment anal., template matching algorithm 7-34327
- ECG traces, construction of respiratory waveforms 7-18084
- echocardiographic assessment of ventricular volume microcomputer based method 7-40237
- EEG, epileptogenic sharp transients detect., multichannel signal processor 7-54786
- EEG, human, adaptive techniques for signal enhancement 7-34319
- EEG power spectrum anal. of head-injured patients, computer assessment of neurological status 7-34128
- EKG tracings, chronic disease detect., computer-aided technique 7-14151
- electron microscopes astigmatism detection using radon transform (*Japanese*) 7-18931
- EMG, clinical, basic problems of automatic analysis 7-8737
- EMG, computerised, conf., New York, USA (April 1981) 7-4621
- EMG, quantitative, diagnostic yield of automated method 7-8742
- EMG automatic analysis with ANOPS computer, monopolar electrode use 7-8738
- EMG signal on-line analysis, microcomputer based neurophysiological measurements system 7-8739
- exercise ECG anal., versatile computer system 7-28743
- FTIR photoacoustic spectra, phase analysis 7-48878
- FTIR spectroscopy, quantitative, ADC errors 7-48877
- geophysics, EM modelling program for 2D structures 7-34714
- gradient time-shape measurement by NMR 7-14985
- haemodynamically compromised subjects, exercise test protocols, digital filtering and data processing 7-8727
- high temp. crystallisation, flaw form., AE detection, automatic system 7-3557
- Holter ECG processing, distrib. 2-channel system 7-40349
- Holter ECG processing, improvement of morphology clustering through directed search techniques 7-40334
- human vocal tract, real time modelling using multiple DSPs 7-54617
- image processing in the reconnaissance revolution 7-50507
- integral equations in diagnosis problems (*Russian*) 7-34234
- intracranial pressure monitoring unit with computerised signal processing, improved design (*Spanish*) 7-34299
- inverse scattering problem soln. using null field method 7-62595
- laser Doppler velocimetry, multi-pt. system using phase diffraction grating 7-37605
- laser ranging, extended Kalman filter for automatic target following of lunar reflectors (*German*) 7-23521
- microcomputer based system for acoustic analysis of voice characteristics 7-37286
- motor unit potentials with varying loads, automatic analysis 7-8741
- multichannel data acquisition suites with time-scale conversion and storage CRT, design 7-61321
- multi-point signal averager for repetitive bioelectric signals, microprocessor-based 7-18091
- neuromuscular diseases, computerised electromyographic signal processing 7-54541
- neurosurgical intensive care unit, computerised monitoring system 7-34320
- QRS complex detection under strong noise, real-time, medical appl. 7-47266
- SAMICOS, sleep analysing microcomputer system using multichannel EEG 7-23470
- seismic data processing, appl. of homomorphic system concept (*Rumanian*) 7-9244
- seismic tomography for 3D struct. and vel. determ. 7-29268
- selection system for particles with lifetimes of 1-0.1 psec, in vertex detector 7-10364
- SETI, ultranarrowband searches with dedicated signal processing hardware 7-24013
- signal averaging computer system for Perkin-Elmer 577 infrared spectrophotometer 7-48865
- sleep EEG and EMG, computer program for automatic anal. 7-54783
- spinal somatosensory evoked pots. monitoring during surgery, microprocessor-based system 7-23482
- streak photography, two-dimensional transients acquisition and processing, using IBM personal computer 7-15025
- system theory, conf., Knoxville, TN, USA (Apr. 1986) 7-14714
- time-variable signals, computer averaging by autocorrelation 7-18768
- TMS2010 signal processing microprocessor, use in acoustic noise cancellation system 7-37259
- tyred wheels, noise investigation, array processor use (*German*) 7-6041
- US materials charactn. 7-33892
- vascular and urethral parameters meas., microprocessor-based signal processing system 7-54686
- X-ray equipment automation (*Russian*) 7-4939

computerised spectroscopy

- see also spectroscopy computing*
- analysis, computerised, using orthonormalised reference spectra 7-35605
- digital power supply and counting interface for UPS, XPS and Auger spectrometers 7-9825
- DLTS, capacitance transient characterisation 7-18805
- dye laser system, high resolution computer controlled 7-20249
- electron microprobe use as digital image analyser (*French*) 7-46746
- EPR, microcomputer-based data acquisition and analysis system 7-48794
- EPR spectrometer, automated, for structural anal. of disordered solids 7-58109
- Fourier transform, spectrometer, microcomputer-controlled, path difference control 7-48861

computerised spectroscopy continued

- Fourier transform IR spectrometer, research grade, Digilab FTS 60, design and performance 7-48892
- Fourier transform IR spectroscopy, today and tomorrow 7-48876
- Fourier transform spectrometer, Los Alamos design with microprocessor control 7-48860
- GBS hybrid spectrometer, computerised control system design 7-4832
- IBM AT-based FTIR spectrometer 7-24713
- indirect detection experiments, computer-controlled attenuator 7-24679
- IR spectral emittance meas., 2 to 20 μm 7-30104
- IR spectroradiometer, capabilities and appls. 7-30063
- mass spectrometer control system design 7-18905
- matrix CCD photodetector in modulation spectrometer, synchronous integration 7-18885
- 3-methyl-2-phenyl-5-(3-methyl-2-phenyl-1-acetyl-3,4-dehydro-6-piperidyl)piperidine, restrained rot., NMR line form anal. 7-10630
- microcomputer-based optical-displacement spectrometer, for kinetics of transparent fluids obs. 7-4894
- Mossbauer spectrometer and data anal. system, IBM PC-based 7-18959
- NMR flowmeter, front sampling parameters effect on systematic error 7-57952
- NMR spectra phase distortion spectral generation algorithm 7-24664
- NMR spectrometer, computer control of magnetic field homogeneity 7-48795
- peak-separation algorithm for personal computer, appl. to visible emission and IR absorpt. spectra (*Japanese*) 7-31015
- photometric near-IR spectrometer using Si:Bi hybrid array 7-30103
- photon correlator, microprocessor based 7-18887
- picosecond absorption spectrometer time resolution enhancement by laser radiation pulse duration selection 7-61387
- picosecond transient absorption spectrometer, using photodiode arrays as detectors 7-30095
- pipetting device, microvolume, for atomic absorpt. spectrometry. 7-4900
- pulse generator, microcomputer controlled, for electron spin-echo spectrometer 7-35551
- Raman spectrometer for time resolved meas. in gaseous samples 7-18886
- reflection and transmission meas. of semiconductor thin films, using IR spectrophotometer 7-4902
- SETI, ultranarrowband searches with dedicated signal processing hardware 7-24013
- signal averaging computer system for Perkin-Elmer 577 infrared spectrophotometer 7-48865
- SIMS, image depth profiling with high dynamic range, automated method 7-23086
- SIMS, quadrupole, data acquisition and control system 7-24722
- solid surface exam. by ion and electron spectroscopy, with angular resolution 2-6° 7-32773
- spectrofluorimeter, laser pulse, LIS-201, automated ultrashort-time, for UV and visible regions 7-4896
- spectrometer, IR, for surface EM waves, computerised control system 7-41511
- spectrophotometer, SPECORD M40 UV-VIS, computer-aided data acquisition and processing by software cassettes 7-4898
- spectrophotometer for small optical density meas., single-beam, automatic design 7-30062
- thermal desorption expt., microcomputer-controlled mass spectroscopy 7-3619
- time-of-flight molecular-beam spectrometer, with five-stage vacuum system 7-30110
- time-resolved IR spectroscopy system, data acquisition and processing 7-48884
- TOF mass spectrometer, automatically controlled (*Japanese*) 7-56370
- tunable diode laser spectroscopy using the IBM PC 7-18892
- UNIX based computer workstation for spectroscopic data manipulation 7-48859
- water content in liquids, IR spectrochemical anal., standard-signal method and microprocessor technique 7-59809
- CO₂, angle-resolved photoelectron spectra excited with focussed polarised reson. radiation 7-50244
- H₂⁺ isotopes, relative abundance, mass spectrometric meas., computer-assisted null point method 7-25489

computerised test equipment see automatic test equipment

computerised tomography

- 3D CT image reconstruction and display (*Chinese*) 7-60118
- 3D flow obs. by interferometry and image processing 7-37576
- acute localized irradi., use for X-ray and NMR tomography for diagnosis, pig expts. (*French*) 7-3869
- attenuation correction for SPECT (*Japanese*) 7-18071
- blood flow meas. using NMR imaging technique, cardiovascular disease detection appl. 7-54694
- bone mineral assessment with dual energy CT scanning 7-47242
- brain, CT image, 3-D shaded display, high-precision surface form. (*Japanese*) 7-47300
- central venous abnormalities, scintigraphic and CT features 7-18063
- compression approximations in computer tomography (*Russian*) 7-54717
- compression of radiological images with 512, 1024, and 2048 matrices 7-54738
- conference on medical imaging and PACS, Newport Beach, CA, USA (Feb. 1986) 7-18490
- correction for scattered radiation in a PET (*Japanese*) 7-18068
- density gradients in ceramic pellets measured by computed tomography 7-39840
- detector width artifact correction 7-47255
- device providing information on chem. props. of body struct. 7-47217
- diffraction tomography and maximum entropy Fourier synthesis 7-65884
- diffraction tomography in reconstructing marginal spatialfrequency spectra for wave fields 7-3867
- diffraction tomography reconstruction, max. entropy method 7-47256
- discrete Radon transform in a continuous space 7-56235
- display preferences for viewing CT scans, rel. to workstation design 7-28682
- dynamic scan using the Shimadzu single photon emission computed tomograph for heat SET-031 (*Japanese*) 7-18070
- effective dose equivalent, H_e, use as risk parameter in CT 7-40294
- electrooptical computer for reconstruction of CT images 7-3874
- emission CT, quantitative, comparison of recovery coeff. and linearity of detector response 7-47214
- emission CT, statistical noise and spatial resolution in image reconstruction, simulation study (*Japanese*) 7-60085
- energy resolved X-ray diff. CT 7-23447

computerised tomography continued

- engineering ceramics evaluation by gamma-ray computerised tomography 7-28258
- epoxy insulation study using X-ray computing tomograph 7-13679
- fan beam-CT system, high-resolution algorithm 7-8686
- fan-beam CT system, fast reconstruction algorithm 7-8685
- femoral stress anal., 3D, using CT scans and P-version FEM 7-8613
- film based industrial computerized tomography 7-54067
- flow measurement (two-phase flow) by digital tomography 7-16281
- head trauma evaluation, mag. resonance rel. to CT 7-18061
- heart, 3D reconstruction from few projections, practical implementation of McKinnon-Bates algorithm 7-47219
- heart, contracting, canine, 3D reconstruction using cine CT 7-28759
- heart images in motion 7-14142
- high resolution ultrasound computerised tomography 7-34207
- high speed CT using Imatron C-100 cine scanner, efficient data archiving and rapid image anal. 7-28683
- hip joint meas. in children, radiation exposure and image quality in CT 7-23460
- image reconstruction using parallel computation 7-3876
- image resampling on a cylindrical sector grid 7-14114
- integral equations in diagnosis problems (*Russian*) 7-34234
- interactive proton MR image synthesis 7-65829
- inverse digital filtering of radiographic pictures, tomographic props. 7-9930
- IR computerised axial tomography, appl. of IR scanners and inverse heat conduction methods 7-48731
- ischaemia, remote, after acute myocardial infarction, detect. by ²⁰¹Tl emission CT 7-34264
- linear attenuation coeffs., linear dependence of CT numbers 7-47244
- longitudinal ECT imaging using γ -ray camera 7-40281
- lumbar vertebrae, progressive positions visualisation using CAT-scan data 7-3834
- lung, CT assessment of X-ray-induced damage in mice 7-65815
- lung air content, regional, analysis by 3D computerised tomography and multinomial models 7-54801
- magnetic microfield 3D reconstruction, computerised microtomography methods 7-4874
- magnetic resonance tomography using specially designed RF antennas 7-14076
- magnetic-resonance imaging system using superconducting magnet (*Japanese*) 7-23478
- metallic hip implants: CT with multiplanar reconstructions 7-14161
- micro-CT scanner for biomedical appls. 7-47246
- microtomography in scanning electron microscope 7-41543
- microwave diffraction tomography for dielectric constant distribution meas. 7-41401
- MRI and CT images of human body, three dimensional reconstruction of surfaces 7-54804
- myocardium, ²⁰¹Tl tomography, developments toward quantitative anal. 7-34266
- NDT appls. of computed tomography, basic principles 7-28253
- neonates, dedicated CT technique for scanning 7-54736
- neuroimages interpretation, radiologic automated diagnosis (RAD) 7-65857
- neuroradiology, conf., Amsterdam, Netherlands, (Sept. 1985) 7-14706
- NMR, clinical appls. (*Italian*) 7-47272
- NMR computerised tomography, theoretical anal. (*Chinese*) 7-14144
- NMR spectrometer, solid-state, tomographic expts. 7-30052
- nondestructive inspection under conditions of insufficient data, CT methods use 7-39818
- nonlinear parameter imaging CT system using parametric acoustic array 7-34204
- opacified myocardium, spatial reconstruction from a small number of projections 7-34270
- optical microscopic type, constrained resolution enhancement 7-47304
- organ volume determ. using single photon emission CT, thresholding method 7-65838
- physical aspects of X-ray transmission CT, review 7-60080
- plasma multidimensional ion velocity distrib. meas., by optical tomography 7-20942
- polymeric materials, NDT appl. 7-28254
- Positome IIIp, a dynamic positron emission tomograph, imaging performance obs. 7-47215
- positron CT (*Japanese*) 7-65844
- positron emission CT, quantitation, technique to reduce noise in accidental coincidence meas. and coincidence efficiency calibration 7-14118
- positron emission tomography, human visual cortex mapping appl. 7-28516
- positron emission tomography, physico-technical aspects (*Russian*) 7-34241
- positron emission tomography, stationary high resolution, BGO detector unit 7-14119
- positron emission tomography, using in pion radiotherapy 7-28661
- positron emission tomography in neuroradiology—integration of a research tool in clinical routine 7-18079
- positron emission tomography meas. of regional lung density 7-14116
- positron emission tomography measurements of cerebral glucose metabolism, methodological factors affecting 7-40261
- positron-emission tomography evaluation of heart membrane pot., use of ¹¹C-triphenylmethylphosphonium 7-14113
- principles and appls. (*German*) 7-3866
- projections calcs. 7-14115
- pulmonary changes, radiation-induced, acute, assessment by CRT 7-14117
- radiotherapy planning tomographic system 7-34244
- real-time analysis of Doppler waveforms 7-62918
- reconstruction consistency by iterative methods 7-47253
- reconstruction from limited projection data using fuzzy sets 7-28672
- reconstruction of images according to projections (*Russian*) 7-34235
- reconstruction of tomographic images from projections of a small number of views via mathematical programming 7-34245
- reconstruction time, effect on patient throughput in a university setting 7-47245
- RF coils, importance for NMR tomography 7-3854
- self-consistent solutions to algebraic reconstruction of image from its projections 7-56237
- Shimadzu single photon emission computed tomography for whole body, SET-030W (*Japanese*) 7-18069
- single photon emission CT, allowing for variable resolution and constant attenuation 7-60081

computerised tomography continued

- single photon emission CT, automated body contour detect. 7-65841
- single photon emission CT, recommendation on image display standardisation (Japanese) 7-54735
- single photon emission CT imaging with ^{123}I -labelled antibodies, comparison of low- and medium-energy collimators 7-40263
- single photon emission CT using ^{111}In and ^{123}I , digital image restoration using optimised Metz filters 7-40257
- single-photon-emission CT, high resolution, using 511 keV collimation 7-3871
- size discrimination of features on CT images 7-23359
- skull, computer-aided tomogram, multiplex hologram 7-65883
- spatial resolution of X-ray computer-aided tomography 7-48925
- SPECT images by using a multislice fan beam collimator 7-23458
- spinal bone mineral determ. using automated contour detect.: appl. to single and dual energy CT 7-47243
- stationary positron emission tomography and its image reconstruction 7-47216
- supersonic expansion, density meas. using beam-deflection optical tomography 7-44080
- three-phase flow meas., tomographic imaging 7-51355
- thyroid, vol. estimation using single photon emission CT and fan-beam geometry 7-3864
- time-coded aperture tomography: expt. results 7-47218
- tomographic analysis of the evolution of plasma crosssections 7-1741
- tomography synthesis, 3D reconstructing algorithm 7-47254
- trabecular bone density in proximal femur, quantitative CT assessment 7-14129
- tumour metabolism determ., pot. of NMR and PET 7-23424
- two dimensional polar display using SPECT (Japanese) 7-18073
- US nonlinear parameters CT by nonlinear interaction of sound waves (Japanese) 7-14069
- US tomography, resolution improvement using adaptive filtering (Japanese) 7-34202
- X-ray computed tomography for nondestructive industrial testing 7-59719
- X-ray CT image, 3D display of cerebral ventricle 7-47280
- X-ray flux meas., minimising photomemory effects 7-56392
- X-ray micro-tomography, using synchrotron radiation, chem. state mapping 7-54248
- X-ray microtomography with synchrotron radiation 7-47224
- BaF₂ crystals for time resolution improvement in TOF positron emission tomography system 7-47222
- ^{192}Ir dosimetry, use of simulator-based CT 7-14132
- NbH₃, spinodal decomposition, neutron radiography studies 7-58489
- a-Si based integrated type X-ray sensor (Japanese) 7-15456
- Xe enhanced CT 7-18076

concentration measurement *see chemical analysis; chemical variables measurement*

concrete

see also cement industry

- DIORIT research reactor, activation product distrib. in shielding materials (German) 7-49536
- endochronic plasticity theory 7-37351
- failure process, dynamic description 7-57738
- fibre reinforced and plain, shear test specimen geometry 7-46738
- HLLW solidification, review of alternative wasteforms and processes 7-36296
- hydrated inorganic salts found in concrete, thermal energy storage appls. 7-17922
- hydrostatic pressure effects on integrity, monolithic slag/cement under radwaste sea disposal conditions 7-36297
- inelastic behaviour, damage mechanics constitutive theory, FEM model 7-53833
- insulating cellular, compressive strength, in situ evaluation using impact device 7-39800
- micromechanical damage model 7-53837
- microplane model for progressive fracture, microcracking 7-15248
- molted reactor core/concrete interactions in HCDA, mass and heat transfer simulation 7-25138
- NDT, computed tomography appl. 7-28254
- NDT appls. of computed tomography, basic principles 7-28253
- reinforced concrete members, reliability of crack control, fuzz set anal. (Chinese) 7-20655
- reinforced concrete pads for spent nuclear fuel casks, hardness effects on design 7-49700
- reinforced concrete shear walls in nuclear power plants, probab.-based design criteria 7-36078
- shield, fast neutron albedo calcs. 7-30622
- shield, heat-resistant, in nuclear reactor, capture X-ray refl. and transmission 7-49532
- sorption of fission products 7-5471
- strain rate effects on fracture, conf., Boston, USA (Dec. 1985) 7-14712
- strain-space plasticity formulation for hardening-softening materials with elastoplastic coupling 7-26164
- structures, micro- and macroscale damage 7-43766
- vitrified colemanite and impregnated polymer, nuclear shielding materials 7-726
- D-T neutrons transmitted through rare earth mixed concretes, neutron spectrum 7-25158

concurrency (computers) *see multiprocessing systems*

condensation

- alkali halides, neutral molecule incorporation, composite form. at room temp. 7-54101
- binary metal alloy clusters, generation and reactivity 7-15784
- capillary condensation in cylindrical pore, stability 7-1623
- conjugate film condensation on one side of vertical wall and natural convection on other side 7-63147
- converging condensing flows of steam, pulsation characts. 7-6239
- direct contact condensation of R 114 on the vertical falling water column (Japanese) 7-34063
- disperse media flow with internal degree of freedom, nonequilib. gasdynamics, kinetics and catalysis 7-44019
- droplet in high Reynolds no. flow, transport mechanism, stagnant surfactant cap effect 7-51271
- droplet shape and size variations from morphology-depend. reson. in fluorescence spectra 7-29970
- dropwise condensation heat transfer on a horizontal tube 7-20704
- evaporation and condensation heat transfer performance for R 22 and ammonia (Japanese) 7-34062

condensation continued

- film condensation and natural convection along interface between porous and open space 7-43903
- film condensation instability at surface of a cylinder 7-37526
- flowing vapour on horizontal elliptic cylinder 7-58452
- fluid interfaces, phase transitions, local density approx. and smoothed density approx. study 7-63912
- fractionating condensation and evaporation in plate-fin devices 7-43644
- Freon-11 vapour direct condensation on horizontal water surface (Japanese) 7-32623
- freons, liquid-vapour system, shock wave compression 7-31874
- graphite, pyrolytic, surface, sticking probabilities of evaporated C₁, C₂ and C₃ species 7-52273
- HCL, condensation on charged CO₂ walls, Stockmayer model calcs. 7-63784
- heat transfer to surface of vertical tube with crossflow 7-51144
- heterogeneous vapour condensation on ions, dynamical conditions (Russian) 7-63786
- hydrocarbon mixed working fluids for geothermal power plants, vaporisation and condensation 7-65408
- inert gases, condensation in free jets, scaling laws, similarity relations 7-42825
- interphase boundary instability during condensation of moving vapour 7-12250
- kinetic equations, soln. (Russian) 7-26907
- kinetic theory, temp. paradox 7-48660
- kinetics under ideal supersaturation conditions (Russian) 7-63787
- LWR ECCS injection, fluid and pressure oscills. during direct contact condensation 7-5376
- LWR safety anal., steam direct contact condensation on slowly moving water 7-5358
- metal clusters, phase investig. 7-15772
- metal vapours, homogeneous condensation, mechanism of early stages 7-26925
- metals, condensation in free jets, scaling laws, similarity relations 7-42825
- nonecondensable gas behaviour in vapour, macroscopic eqns., boundary conditions and Knudsen layer corrections calcs. 7-31840
- nonequilibrium homogeneous condensation in rarefaction waves 7-51280
- nonequilibrium transitions, mass and energy flux 7-12252
- OTEC, plate type condenser, performance tests (Japanese) 7-54337
- particle metallising, kinetics of vapour condensation 7-2162
- phase flow regimes, heat exchange with vapour condensation in horizontal tubes 7-31858
- pipe, vertical, internally cooled, embedded in porous medium, condensation 7-32624
- polyelectrolytes, counterion condensation, Poisson-Boltzmann eqn. sol. 7-52029
- porous slab, phase change, heat and mass transfer 7-31863
- power plant condensers, 2D flow and heat transfer computation 7-51148
- reactor accident confinement systems, vapour condensation in underheated nonflowing liquid 7-30621
- simple fluids in cylindrical and slit-like pores, capillary condensation and adsorption 7-32756
- spherical droplet condensation in free molecular limit 7-11469
- spiral double-fin tubes with drainage gutters, characts. (Japanese) 7-34060
- spontaneous condensation of vapor in a nonequilibrium supersonic monodisperse flow 7-6286
- stationary vapour on corrugated surface of horizontal tube, heat transfer, condensation 7-50919
- steam, dropwise condensation, heat transfer study, falling drops effect 7-43890
- steam condensation in pool water, press. oscill. threshold 7-26334
- steam-water violent condensation shock mechanism 7-57901
- submonolayer ordering and multilayer adsorption, simple lattice gas models 7-12490
- supercooled vapour condensation, phase boundary velocity 7-21399
- surface exposed to vapour with noncondensable gas, simultaneous melting and condensation 7-51274
- turbulent gas jets, elec. field control 7-11485
- turbulent liq. vapour condensation burst instability 7-1539
- turbulent liq. vapour condensation rate 7-1538
- vapor condensation on an inclined plate within aporous medium 7-1572
- vapour bubble growth rate in turbulent flow, calc. 7-16239
- vapour bubbling of moving underheated liquid, condensation and heat exchange 7-37525
- vapour condensation in cylindrical borehole, heat transfer 7-11408
- vapour flow in low temp. heat pipes, effect of evaporation and condensation zones 7-63136
- vapour-gas mixture, condensation and evaporation of a drop 7-52014
- HCl condensation in winter polar stratospheres, contrib. to Antarctic O₃ hole 7-55162
- HNO₃ condensation in winter polar stratospheres, contrib. to Antarctic O₃ hole 7-55162
- H₂O condensation on glass, growth of breath figures 7-12405
- He liquefaction, condensation heat transfer enhancement for mag. refrigerator performance improvement 7-56283
- He liquefier, condensing and freezing purification system 7-56280
- ⁴He, superfluid, fractal surface, third sound, capillary condensation 7-27041
- K adatoms on Cu (001), two-dimensional condensation, LEED obs. 7-12478
- KCl (100), interaction of NaCl mol. beams with surface, desorption flux meas., SIMS obs. 7-33508

condensers (electric) *see capacitors*

condensers (steam plant)

- hydraulic pump driven by low-level temp. difference 7-54335
- power plant condensers, 2D flow and heat transfer computation 7-51148
- steam turbine condenser leakage detectors (Czech) 7-61988
- Ti in power generation industry 7-46283

condensing *see condensation*

conductance, electric *see electric admittance*

conductance, electric, measurement *see electric admittance measurement*

conductance measurement, electric *see electrical conductivity measurement*

conducting materials

see also bimaterials; electrolytes; metals; semiconductor materials; superconducting materials
 plastics, conductive, continuous milling (Japanese) 7-46408

conduction, heat *see* heat conduction

conduction bands

see also Fermi level; semiconductor materials

band offsets at pseudo-ternary semiconductor-alloy heterojunctions 7-12835

elemental semicond., conduction-band-edge charge density, empirical pseudopot. calcs. 7-64046

f-electron and conduction electron superconductivity, periodic Anderson model, self-consistent calcs. 7-12908

graphite, single cryst., synchrotron radiation-excited angle-resolved photoemission 7-17391

graphite intercalation compounds, first stage, with heavy alkali metals, electronic props. 7-2463

heavy fermion superconductivity, conduction band and virtual bound states, Kondo-like interaction, periodic Anderson Hamiltonian calcs. 7-27460

heterojunction band offsets, two-level model anal. 7-7363

HfTe₂, electronic props. 7-2610

III-V cpd. semicond., conduction-band-edge charge density, empirical pseudopot. calcs. 7-64046

III-V semiconductors, hot-electron photoluminescence, polarisation 7-46118

intermediate valence systems, Ferromagnetic order coexistence, mag. props 7-64187

Kondo lattices, magnetoresistance at low temp. 7-2600

narrow-gap cpd. semicond., weak-coupling polarons, band nonparabolicity effects, comment 7-21830

optical radiation continuous spectrum emitted by at. particle secondary emission products, two-photon form. mechanism 7-42713

parabolic semiconducting quantum wells, electrical and optical props. 7-22002

polyacetylene, N-containing analogues, electronic structs., conduction props., ab initio study 7-32911

s-f model with antiferromag. s-f exchange 7-45653

scheelite structure crystals, optical and elec. props. 7-33431

semiconductor strained layer superlattices, electronic and optical props. 7-7359

superlattices with complex unit cells, conduction band energy levels 7-27402

tetrahedral solids, semicond., dispersion of linear optical props., empirical tight-binding calc. 7-45966

transition metal alloys, disordered, localised and extended state coexistence 7-7175

AlGaAs/AlAs multiquantum-well structs., staggered band alignments 7-7361

AlGaAs/GaAs modulation-doped heterojunctions, 2D electron gas; DX centres 7-38694

Al_{0.5}Ga_{0.5}As/GaAs, multilayer and superlattice structs., electronic sub-bands 7-58877

Al_{0.5}Ga_{0.5}As/GaAs photoexcited heterojunction, charge transfer calcs. 7-12688

Al_{0.5}Ga_{0.5}As-AlAs heterojunctions, band discontinuities meas. 7-27407

AlN formed by N ion implantation of Al, electronic struct. 7-58926

AlN thin crystalline stoichiometric film, electronic struct., electron spectra studies 7-58916

AlSb, hot electron luminesc. 7-46119

C films, plasma deposited from methane, elec. conductivity, optical absorpt. 7-38786

CaF₂/Si interface, with MBE grown insulator, trap states, I-V, C-V meas. 7-7407

CdCr₂Se₄, band structure characteristics and props. of nonequilibrium carriers, cathodoabsorption 7-46064

Cd_{1-x}Mn_xTe, interband Faraday rot. meas. 7-39093

CdSe, optimally annealed in molten Cd, DC galvanomagnetic props. 7-27352

CdTe, d-core transitions, reflectivity spectra 7-53364

n-CdZnS/p-CuInSe₂ polycrystalline solar cells, open circuit voltage 7-17889

CePd₃B_{0.6} heavy fermion cpd., thermal and mag. anomalous cryst. field effects 7-45239

CePd₃Si, heavy fermion cpd., thermal and mag. anomalous cryst. field effects 7-45239

CsI, two-photon induced luminesc. 7-64696

Cu-CdTe interface form., effect of different cation-anion bond strengths 7-27149

Cu-Hg_{0.75}Cd_{0.25}Te interface form., effect of different cation-anion bond strengths 7-27149

FePS₃, layered cpd., valence and conduction bands studied by synchrotron radiation 7-38450

Ga_{1-x}Al_xAs/Ga_{1-y}Al_yAs/GaAs double barrier tunnelling struct., negative resist. calcs. 7-45451

GaAs, conduction band, deformation splitting and intervalley scattering 7-2548

GaAs crystalline and amorphous, L near-edge structure, X-ray photoabsorpt. spectra 7-64766

n-GaAs impurity bands and band tailing 7-21809

GaAs quantum wells, band offsets, inelastic light scatt. studies 7-7362

n-GaAs:O, semi-insulating, impurity centres, electron capture 7-52643

GaAs/Si/AlAs multiquantum well structs., band struct. and photolum. studies 7-12843

GaAs/AlGaAs single and coupled double wells, energy depend. light hole mass, photolum. spectra anal. 7-38691

GaAs/GaAlAs single quantum wells, steady-state photoluminescence studies 7-7750

GaAs-Al_{0.5}Ga_{0.5}As-AlAs, p-type quantum wells, resonant Raman scatt. 7-22259

GaAs-Al_{0.5}Ga_{0.5}As quantum wells, parabolic, light scatt. studies 7-64651

GaAs-AlAs ultra-thin layer semicond. superlattices, energy band and stable structs. study 7-52789

GaAs-AlGaAs multiple quantum well structs., photolum. under high laser excitation 7-13213

GaAs-AlGaAs quantum wells, high electric field, interband transitions, photocurrent spectra obs. 7-7289

GaAs-Ga_{1-x}Al_xAs quantum wells, with indirect gap semicond. barriers, electron tunnelling 7-64340

GaAs-Ga_{1-x}Al_xAs superlattices, in appl. elec. field, interband optical transitions 7-53274

GaInAs/InP quantum wells, atmospheric organometallic vapour phase epitaxial growth 7-27912

conduction bands continued

Ga_{1-x}In_xP/GaAs heterojunction band discontinuity determ., C-V profiling 7-58880

GaSb-AlSb quantum wells, optical transitions, obs. 7-46086

Ge, gamma irradi., photoluminescence spectra, temp. depend. 7-17336

Ge, electron irradi., annealing kinetics, impurity effects 7-16630

Ge_{0.5}Si_{0.5-x}Si strained layer heterojunctions, selectively doped, hole mobilities, temp. depend. 7-7383

HgCr₂Se₄ spinel magnetic semicond., electronic struct., elec. props., defects and ferromag. anisotropy 7-38857

Hg_{1-x}Mn_xTe LPE crystals, magnetophonon reson. recomb. with phonon emission 7-63755

HgTe, d-core transitions, reflectivity spectra 7-53364

InAs-GaSb superlattice, band offset press. depend., magneto-optical studies 7-38698

InAs-GaSb superlattices, band line-up under hydrostatic press. 7-52782

n⁺-InGaAs/InAlAs/n⁻InGaAs, conduction band discontinuity determ. by current-voltage meas. 7-7352

In_{0.5}Ga_{0.5}As quantum wells, quantized energy levels, conduction-band nonparabolicity effects 7-2675

In_{0.52}Ga_{0.48}As/In_{0.52}(Ga_{1-x}Al_x)_{0.48}As heterostructures, conduction band edge discontinuity 7-12815

In_{0.69}Ga_{0.31}As-InP strained-layer effective-mass superlattices 7-7378

InSb, conduction band, deformation potential constant 7-7112

InSb conduction band spin splitting, spin reson. interaction obs., LMTO and k.p. perturbation calcs. 7-12676

InSb, conduction electrons g-factor anisotropy, spin-orbit splitting calcs., comment 7-38441

InSb, cyclotron resonance harmonics in conduction band, obs. 7-53136

K₂CuX₃ (X=Cl, Br), energy band struct., fundamental optical absorption 7-7093

K_{0.3}MoO₃, electronic struct., UPS study 7-53499

Li_{1-x}(NH₄)_x(NH₃)_{1-x}TiS₂(x+y)⁻ intercalation cpd., NH₃ oxidation, charge compensation 7-32354

MnPS₃, layered cpd., valence and conduction bands studied by synchrotron radiation 7-38450

N₂ film, solid, quasielastic hot-electron transport 7-39327

(NH₄)_{0.22}TiS₂^{0.22+} ionic intercalation cpd., synthesis, characterisation by thermal anal., mag. 7-45244

Na (110), calculated photoemission spectra 7-3151

NiPS₃, layered cpd., valence and conduction bands studied by synchrotron radiation 7-38450

PbEuSeTe/PbTe single quantum well diode laser with side optical cavity 7-43105

PbS/PbSe heterostructure, band offsets, photovoltaic study 7-58872

Rb₂AgI₃, energy band struct., fundamental optical absorption 7-7093

Rb₂CuX₃ (X=Cl, Br, I), energy band struct., fundamental optical absorption 7-7093

n-Si, piezoresistance associated with bending of the energy relief at the bottom of the conduction band 7-13095

a-Si:H solar cells, density of states asymmetry effects 7-46946

a-Si:H/a-SiO(N)_xH multilayer films, interface electroabsorpt. meas. 7-2689

a-Si:H/c-Si heterojunctions, energy-band discontinuities, internal photoemission studies 7-58869

Si/Ge_{1-x}Si_x superlattices, conduction band interactions and splitting, envelope-function approx. calcs. 7-64332

Si_{1-x}Ge_xH amorphous alloys, electronic struct., soft X-ray and photoelectron spectra studies 7-27857

Si_{0.5}Ge_{0.5-x} coherently strained bulk alloys on Ge (001) substrate, indirect band gap and band alignment calcs. 7-2481

URu₂Si₂ heavy fermion system, core levels and band struct., electron spectra studies 7-52418

Y, pressure-induced superconductivity, band struct. and sp. ht. press. depend. calcs. 7-7431

Zn_{1-x}Mn_xTe, interband Faraday rot. meas. 7-39093

ZnO-electrolyte interface, electrochrom. under cathodic and anodic pulsed polarisation 7-13235

ZnS:Mn, impact excitation and Auger quenching 7-27827

ZnTe, d-core transitions, reflectivity spectra 7-53364

conduction electron spin resonance *see* CESR

conduction in solids, ionic *see* ionic conduction in solids

conductivity, electrical *see* electrical conductivity

conductivity, thermal *see* thermal conductivity

conductors (electric)

see also bimetal; wires (electric)

elliptic conductors, boundary-matching method 7-36849

EM edge wave, current point source, conducting wedge presence 7-15801

EM scattering, dielectric cylinder partially covered by conductor, anal. 7-50473

flat plate steel conductor impedance to earth fault currents 7-62582

multiconductor transmission line, effect of pulse corona discharge on coupling coeffs. and wave impedances 7-63383

physical optics, fields, perfectly conducting screen aperture, line integrals 7-15802

scattering by large conducting cylinders, moment method 7-50475

configuration interactions (atoms) *see* atomic electron correlations

configuration interactions (molecules) *see* molecular electron correlations

confinement, plasma *see* plasma confinement

connecting *see* joining processes

connectors (electric) *see* electric connectors

conservation laws

see also C invariance; CP invariance; CPT invariance; elementary particle symmetry; P invariance; T invariance

abelian (V-A) theories in 4D, fermion number nonconservation and cold neutral matter 7-41595

angular momentum versus mass 7-14483

approximate random choice method for scalar conservation laws 7-20679

baryon and lepton number-violation in astrophysics 7-55866

baryon-number nonconservation in superstring models 7-453

bosonic closed string theory, hidden superstrings in Poincare supersymmetric sectors 7-35840

computational continuum dynamics, introduction 7-4800

computational continuum dynamics, parallel algorithms 7-4683

cosmological baryon number in homogeneities, effects of quark-hadron transition 7-47677

curvature and torsion from matter, Lorentz gauge symm. 7-41208

Dirac operators, eta invariants and holonomy theorem for elliptic families 7-15049

conservation laws continued

- dynamic systems, conservative and non-conservative, conservation laws 7-35269
- Einstein-Cartan theory, matter field torsion and conservation laws 7-41195
- electric source problem in Hermite-symmetric Einstein field theory 7-29838
- energy-momentum vector of the classical electron 7-24498
- entropy functions for symmetric systems of conservation laws 7-61300
- finite-dimensional integrable systems, master symmetries, Calogero-Moser system 7-4674
- G-parity conservation, limitations of validity, alignment-correlation meas. in ^{12}N and ^{12}B 7-5156
- general relativity, conservation laws in spacetimes with boundary 7-29829
- GUTs and SUSY GUTs, proton decay status, SU(5) model, lifetimes 7-30220
- Hamiltonian systems with even and odd Poisson brackets, conservation laws duality 7-49015
- hyperbolic conservation laws, soln. of Riemann and Cauchy problems 7-18602
- hyperbolic conservation laws with relaxation 7-48373
- hyperbolic conservation law approx., nonoscillatory shock capturing methods 7-26318
- Kaluza-Klein model, conservation laws and integrability conditions for gravitational and Yang-Mills field equations 7-56108
- Klein-Gordon equation, generalized, symmetries in $N \geq 3$ dimensions 7-48957
- lepton number/flavour nonconservation and gauge theories 7-56468
- lepton number/flavour violation, phenomenological implications of gauge theories 7-35728
- local Lorentz symm. breaking and space-time dimens. in gravit. theory 7-24803
- Lorentz, conformal and gauge anomalies in external fields 7-41219
- Lorentz covariant string theories in $D=10$ and $D=18$ 7-19038
- multi-point total variation diminishing difference schemes, construction conditions 7-26317
- $N=1$ supergravity, lepton number nonconservation 7-191
- neutrino mass, lepton flavour and lepton number nonconservation 7-9989
- nondegenerate many-body theory and conservation laws 7-24448
- nonlocal equations of motion and their balance laws 7-35214
- operator ordering in nonlinear Lagrangian formalism of relativistic quantum field theory 7-30180
- partial differential eqns., integration of self-similar eqns., Cole-Hopf transformation 7-18579
- partial differential equations, scale-invariant, conservation laws, resonances and the Painleve test 7-56002
- plane-fronted gravit. waves, isometry groups 7-24501
- Poincare gauge theory of gravit. 7-9741
- Poincare group, group scaling, classical gauge theory and gravit. corrections 7-24762
- proton decay, baryon number nonconservation in GUTs 7-56547
- relativistic rotating spherical mass shells, singularities and gravimetric effects 7-41182
- steady Euler eqns., multiple-grid and Osher's scheme 7-51021
- stochastic particle systems, equilibrium fluctuations 7-48586
- string theory, energy-momentum tensor and conserved currents 7-35833
- supercharge nonconservation, finite-box quantization, SUSY soliton anal. 7-15076
- superstring models, baryon and lepton number violation 7-35817
- superstring models, baryon and lepton number violation 7-48498
- superstring models, neutrino mass and baryon number violation 7-48499
- supersymmetric chiral model with Wess-Zumino term, integrability 7-4962
- symmetry tests in particle and nuclear physics, review 7-30205
- two-body relativistic systems, bound-state solns., invariant scalar products and conserved currents 7-48984
- unified left-right symmetric model of massive neutrinos with conserved lepton number 7-30224
- $\bar{\nu}_e$ decay above $\bar{D}D$ threshold, OZI rule 7-24877
- e^+e^- annihilation, 29 GeV, p-A correls., local baryon number conservation 7-49163
- $\mu \rightarrow 3e(\gamma\gamma)$, rare muon decays, branching ratios 7-56550
- n -n oscillations, baryon number violation 7-56495
- np scattering, spin and isospin nonconservation by a colour force 7-30285
- ν physics, lepton number conservation, review 7-30218
- τ neutrinoless decay, lepton-number and lepton-flavour violation search 7-61675
- ^{76}Ge neutrinoless double β -decay, lepton number nonconservation, Milano expt. 7-56644
- $^{76}\text{Ge} \rightarrow ^{76}\text{Se}$, neutrinoless double beta-decay, limits on lepton number nonconservation 7-49339
- ^{100}Mo , neutrinoless double beta-decay, limits on lepton number nonconservation 7-49339
- $\mu \rightarrow e\gamma$, internal asymmetry parameter and nonstandard weak interaction 7-35870
- Ti(μ, x), muon-electron conversion search at TRIUMF 7-56671

constant current modulation *see amplitude modulation*

constant voltage diodes *see avalanche diodes; Zener diodes*

constants

- see also elastic constants; gravitational constant; lattice constants; optical constants*
- $2e/h$ and h/e^2 determ. from volt and quantised Hall resist. meas. in Si units 7-41332
- acceleration due to gravity, meas. using bouncing rubber ball 7-48237
- Avogadro, Si molar volume results 7-14913
- Boltzmann constant meas. 7-14742
- coil constant determ. in in γ - γ expt. at PTB 7-18739
- e/m experiment, magnetic field and electron trajectory calcs. 7-48228
- EM precision meas., conf., Gaithersburg, MD, USA (June 1986) 7-14710
- fine structure constant, electron self-field interaction and internal resonance 7-41701
- fundamental constants, probability law 7-18544
- fundamental constants derived from two-dimensional harmonic oscillations in an electrically structured vacuum 7-55942
- h/m_e determ., using rotating, superconducting ring 7-14914
- magnetic flux quantum determ., superconducting magnetic levitation system design 7-18846
- measurement uncertainty assessment 7-39

constants continued

- NRLM work relating to precision meas. and fundamental constants 7-14915
- proton gyromagnetic ratio expt. at ETL 7-14917
- proton gyromagnetic ratio in H_2O determ., by low field method 7-14916
- Rydberg constant determ. by two-photon spectroscopy of H Rydberg states 7-25433
- theory 7-55941
- transient time constants determ., three point method 7-286
- constituent interchange model** *see quark models*
- constitution diagrams** *see phase diagrams*
- construction** *see building*
- constructional engineering** *see civil engineering*
- contact (mechanical)** *see mechanical contact*
- contact angle**
 - see also capillarity; surface tension; wetting*
 - capillary fluids, equilib. and stability 7-58567
 - drops, liquid spreading on substrate, nonequilibrium thermodynamic appls. 7-6920
 - drops, surface tension dynamics, laser-induced modification 7-58570
 - drops on planar surface, dislodgment due to surrounding fluid motion 7-52190
 - Fecralloy, interaction with $\text{Na}_2\text{O}_2\text{SiO}_2$ glass 7-3501
 - fluid interfaces, phase transitions, local density approx. and smoothed density approx. study 7-63912
 - Langmuir-Blodgett hydrophobic water-stable monolayers on mica, interaction meas. 7-32759
 - non-wetting melt in free fall, bubble-bridge config., contact angle 7-21572
 - plastic surfaces, wettability control by plasma treatment, etching effects 7-53927
 - plate oscills. across liquid interface, contact-angle hysteresis effects 7-52189
 - poly(n-alkyl methacrylates), surface mobility and struct. transitions, dynamic contact angle meas. 7-32758
 - poly(vinyl alcohol)-poly(dimethylsiloxane) graft copolymers, surface studies 7-32307
 - polydimethylsiloxane, liq., spreading, existence and role of thin precursor film 7-44954
 - polyimide film, etching and surface modification in plasmas, XPS, SEM and contact angle meas. 7-28166
 - polymer surface and interface dynamics study 7-63917
 - porous powdered material, contact wetting angle determ. method 7-52193
 - Teflon, wetting, effect of diphilic polyelectrolytes conc. 7-38302
 - vapour bubble, quasistatic growth on boiling liq. surface, contact angle var. 7-44951
 - zeolite 13X, hydrophobic, generation by exchange with octadecylammonium ion 7-13809
 - Al_2O_3 refractory ceramic, wettability and contact angle with Al melt, nitride additive effects (Russian) 7-12402
 - $\text{Al}_2\text{O}_3/\text{Au}$, wettability of single crystals between metal melting point and 1673 K (French) 7-63902
 - $\text{Al}_2\text{O}_3/\text{Sn}$, wettability of single crystals between metal melting point and 1673 K (French) 7-63902
 - C films, plasma fluorination, surface structure determ. 7-27196
 - SiC, wettability by Al and Al-Si 7-58569
- contact EMF** *see contact potential*
- contact fatigue** *see fatigue; wear*
- contact lenses**
 - intraocular pressure meas., noncontact tonometry through soft contact lenses 7-54780
 - motion during blinking 7-40138
 - optical pachometry with contact lenses in situ, measurement artifact 7-40238
 - soft lenses, changes in contrast sensitivity during first hour of wear 7-14006
 - tinted hydrogel contact lenses, spectral transmittance obs. 7-54807
- contact potential**
 - see also contact resistance*
 - nematic liq. crystals, thermoelectrical effects, temp. depend., contact pot. effects (Russian) 7-21945
 - plasma, surface ion sputtering, rel. to angle to mag. field lines 7-63303
 - Al-SiO₂-Si system, contact pot. difference, effect of processing conditions 7-38746
 - Bi, chemical pot. of electrons, effect of mag. field 7-38682
 - p-crystalline Si/n-amorphous Si heterojunction, electrostatic pot. barrier distrib. calcs. 7-58881
 - Fe-Ni alloy surfaces, sputter-cleaned, work function and dipole barrier 7-38673
 - GaAs (110), O₂ adsorption, electronic props., contact pot. meas. 7-2353
 - GaAs-Al_{0.1}Ga_{0.9}As heterojunction, chemical pot. of electrons, effect of mag. field 7-38682
 - a-Si:H films, metal-semiconductor contacts, characterisation 7-38724
- contact resistance**
 - see also contact potential*
 - four-terminal meas. techniques 7-35537
 - graphite, powder, elec. resistivity, rel. to degree of comminution 7-45257
 - measurement, photothermal radiometry appl. using IR scanners 7-33898
 - metal wire connections, contact resist., effect of fretting 7-21980
 - metal-semiconductor contact resistance, determ. using ring structs. 7-58862
 - metal-semiconductor contacts, current flow, dual-level transmission line model 7-45493
 - PTCR, high temp., interaction with O models 7-58861
 - stearic acid-Langmuir-Blodgett films, boundary lubricant efficiency (Japanese) 7-8118
 - Ag specimen, contact resist. meas., deform., fretting effects 7-9848
 - Al-Ge-Si, heterojunction ohmic contacts 7-27432
 - Al-Si/MoSi₃ stable contacts to shallow junctions 7-52847
 - Al-Sn, bearing alloys, run-in kinetics, friction, contact resist., AE signals 7-17655
 - Al-Ti (CoSi₂)-Si contacts, four-terminal resistor structs. for contact resist. determ. from end resist. meas. 7-38730
 - AlGaAs-GaAs selectively doped heterostructures, orientation effect on contact resistance 7-38680
 - Au-Ge-Ni-GaAs, non-alloyed ohmic contact, solid phase epitaxy 7-27423
 - Au-Ni-Au-Ge-Ni-GaAs, ohmic contacts, alloying, specific contact resistivity 7-27425

contact resistance continued

- Au-TiB₂-Au-Ge-Ni-GaAs, ohmic contacts, alloying, specific contact resistivity 7-27425
 AuBe-Cr-Au-InP, improved ohmic contact 7-64310
 AuNiGe-GaAs ohmic contacts, microstruct. anal. and contact resist. meas. 7-2393
 Bi-Sb, adhesion, elec. phenomena, effect of additions of Bi and Sn in solder 7-12399
 CdTe-AuCu, AC contact impedance, influence on high freq., low temp. on fast transient junction meas. 7-64311
 CoSi₂ self-aligned silicide technology using rapid thermal processing 7-52154
 Cu-composite material contact, sliding characts. and contact resistance (*Japanese*) 7-8120
 Cu-Cu contact, sliding characts. and contact resistance (*Japanese*) 7-8120
 Fe/Ni Reed blades, Au coated, AES/SEM study 7-44972
 GaAs n-i-p-i doping superlattices, selective contacts, MBE growth through shadow mask 7-13356
 GaAs, ohmic contact resist. limitations 7-52838
 GaAs/Au-Ge/Ni ohmic contacts, ion implantation and metallisation prep. 7-22014
 p-GaAs/AuZnNi/Ti/Au ohmic contacts, low-resistance 7-7385
 GaAs-GaAlAs heterojunction bipolar transistors, ²⁴Mg and ⁶⁴Zn implanted profiles 7-44591
 GaAs-InAs, in situ contacts, MBE grown 7-45444
 GaAs-Pt reacted ohmic contact charact., effect of Mg layer 7-7387
 InGaAsP-InP laser diodes, low resist. contacts on p-side 7-20276
 Mo/Al-Si interdiffusion kinetics and contact resistance study for VLSI appls. 7-21714
 Pd-Ag alloy electroplated coating contact and corrosion resistance and wear 7-3509
 Pd-Ge ohmic contacts to InGaAsP-InP, solid-phase epitaxial growth 7-2706
 Pt-R contact, R=Gd, Tb, Dy, Ho, Tm, mag. order destruction by cold current 7-52980
 Si interdigitated back contact solar cells development 7-8386
 a-Si:H, contact resist. meas. technique 7-24658
 Ti, reactively sputtered coatings, oxidation, XPS and contact resistance meas. 7-53934
 TiN_x, reactively sputtered coatings, oxidation, XPS and contact resistance meas. 7-53934
 W, LPCVD on Si-Ge alloy for interconnect appls. 7-17472
 W, selective LPCVD for CMOS VSLI, appls. 7-17471
 W, selective LPCVD on Si substrate, elec. and struct. props. 7-17467
 W-Cu-Ni contact materials, elec. props., particle size effect 7-2672

contacts, electrical *see electrical contacts***content-addressable storage**

- autoassociative neural network, influence of noise on behaviour 7-54525
 neural networks and optical resonators, coupled-mode theory 7-54513
 nonlinear optical associative memories using thresholding devices and volume hologram 7-57408
 optical computing, compound literal implementation via shadow-casting 7-25732
 optical holographic associative memory using a phase conjugate resonator 7-25733
 optical resonators and neural networks 7-54512
 pattern recognition in rabbits, oscillating network model 7-54618

continuum hypothesis *see set theory***continuum mechanics** *see classical mechanics of continuous media***contours, surface** *see surface topography***contracts**

- natural gas industry, open access transportation implications 7-65389

contrast transfer function *see optical transfer function***control engineering applications of computers** *see control engineering computing***control engineering computing**

- see also computerised control; control system CAD*
 nuclear multivariable control system design using CAD package 7-10211

control equipment

- see also actuators; controllers; cryostats; telecontrol equipment; thermostats; valves; variable speed gear*
 solar distillation plants, instrumentation and control devices 7-28410

control facilities

- sound recording control room design incorporating RFZ, LFD and RPG diffusors 7-37249

control rooms, radio *see radio studios***control system CAD**

- nuclear multivariable control system design using CAD package 7-10211

control system computer aided design *see control system CAD***control system synthesis**

- see also Bode diagrams; correlation methods; describing functions; frequency-domain synthesis; frequency response; linearisation techniques; perturbation techniques; phase space methods; piecewise-linear techniques; poles and zeros; root loci; sensitivity analysis; stability; state-space methods; step response; transfer functions*
 fixed-bed reactor, robust multivariable control system design 7-54256
 solar energy system, cycling rate effect on energy collection for bang-bang controllers 7-8438
 very high temperature gas cooled reactor, control system design and dynamics 7-768

control systems

- see also adaptive systems; closed loop systems; delay-differential systems; distributed parameter systems; model reference adaptive control systems; multivariable control systems; nonlinear control systems; optimal control; physical instrumentation control; time-varying systems*
 Doublet III-D tokamak, computerised operation of neutral beams 7-19466
 electron linac, control system for Photon Factory 7-5498
 JFT-2M poloidal field coils, power supply and control system 7-15323
 Mirror Fusion Facility, local control system development 7-19463
 particle beam fusion accelerator I (PBFA I), automated features of control/monitor system 7-30754
 plasma control on the Tokamak de Varennes 7-15336
 qualification concepts for instrumentation and control systems of nuclear power plants 7-19419
 radio-frequency heating apparatus for JT-60, controlling system 7-19503
 recoil separator, adaptable computer control system 7-5520

control systems continued

- solar electric station heliostat field, crossover effect on automatic control system 7-54267
 TFTR neutral beam computer control system 7-19465
 unsteady heat and mass transfer in a heat exchanger with twisted tubes 7-31794
 very high temperature gas cooled reactor, control system design and dynamics 7-768

controllers

- see also cryostats; instruments; programmable controllers; servomechanisms; thermostats*
 16-channel controller for implantable gait stimulation system, design 7-28781
 cryogenic temp. controller, for diffusion coeff. of Kr in liquid Ar determ. 7-30020
 digital controller for a magnetic suspension system 7-333
 electrodynamic drive of Mossbauer spectrometer, controller design 7-35508
 glass melter for nuclear waste, power supply and controls 7-19528
 humidity measuring devices and controllers (*Japanese*) 7-56296
 IBM PC-XT controller use for tunnelling spectrometer 7-56383
 implantable gait stimulation system, 16-channel microprocessor-based controller, features 7-28780
 magnetic suspension systems with digital controllers 7-332
 solar energy system, cycling rate effect on energy collection for bang-bang controllers 7-8438
 thermocouples, bath for reference junctions, using solid-state heat pump 7-14936
 ventricular assist device, elec., power consumption minimisation by design of optimal controller 7-8769

controllers (computer peripherals) *see computer interfaces***convection**

- see also convection in liquids*
 3D convective motion in spherical shells 7-57823
 absorbed polyelectrolytes, effect on convective flow and diffusion in porous membranes 7-11536
 aerial suspension combustion, wave propag. 7-54125
 air-water (hexadecane), natural convection in complex enclosed space, heat transfer 7-11421
 airflow, convective turbulent, light reflection, partial phase conjugation 7-43248
 alloys, binary, freezing, convective and morphological instabilities 7-32615
 anisotropic convective fluid, singularities in chaos transition 7-43915
 annular duct, convective heat transfer, turbulent to laminar reverse transition (*Japanese*) 7-11543
 annular packed-sphere bed with wall effects, fully-developed forced convective flow 7-51110
 approximate random choice method for scalar conservation laws 7-20679
 asymptotic laminar boundary layer, mass transfer effects on transient behaviour 7-4323
 atmosphere, climatology of convective boundary-layer parameters over Ontario, Canada 7-40512
 atmosphere, flow dynamics and stability in severe rainband 7-9096
 atmosphere, periodic solns. of non-stationary eqn. for vertical rel. 7-18296
 atmosphere boundary layer, effects of convection on horizontal plume dispersion 7-40062
 atmospheric convection, comparison of GR FEM models 7-18298
 axisymmetric free convection boundary layer flow of water at 4°C past slender bodies 7-20709
 axisymmetric laminar plume, asymptotic soln. for large Prandtl no. 7-26275
 Benard convection, numbers of degrees of freedom estimation 7-37460
 Benard convection, two-dimens., finite element numerical calcs. 7-37454
 Benard convection in finite cavity, two-dimensional, use of symmetry in bifurcation calcs. 7-31798
 Benard fluid two-component, with surface adsorption accumulation, stability anal. 7-62954
 Benard-Marangoni's instability, nonuniform temp. gradient and Coriolis force effect 7-43886
 biharmonic equation in rectangular prism, vector processing routine, TDPOIS 7-48636
 binary fluid convection, eight-mode Lorenz model of travelling waves 7-37462
 binary fluids, convection, eight-mode Lorenz model 7-41307
 binary-fluid convection in finite geometries, travelling and standing waves 7-37463
 boiling crisis in rod bundles, governing relationships investig. 7-26125
 boundary layer simulation, efficiency of different higher order turbulence models, atm. appl. 7-57819
 bounded-volume chambers, convective heat transfer 7-43906
 buoyancy effects in vertical open tubes, thermal and mass 7-31787
 buoyancy-driven convection in horizontal fluid layer extending over porous substrate 7-51136
 buoyancy-driven flows of gases above liquids with nonuniform heating 7-31790
 cassette radioelectronic apparatus, forced ventilation cooling, optimisation algorithm 7-63138
 channel, smooth rectangular, heat transfer around sharp 180 deg. turns 7-63144
 channel, vertical, partially blocked, laminar mixed convection 7-43842
 chaotically convecting fluid thin layer, temp. field, light scatt. meas. 7-51126
 chemical boiling, heat and mass transfer, gas liberation and free convection 7-43907
 combined free and forced laminar convection in thermal entrance region of channel, Prandtl no. effect 7-37453
 completely confined porous medium, onset of hydromagnetic thermal convection, stability 7-6205
 composite slab, transient heat conduction, convective and radiative cooling 7-11246
 conducting liq., MHD convection, Hall and wall temp. oscils. effect 7-6206
 conference, Cambridge, England (March 1986) 7-40987
 conjugate film condensation on one side of vertical wall and natural convection on other side 7-63147
 conjugate natural convection in air-filled rectangular cavity, numerical soln. 7-57826

convection continued

- conjugated convection-conduction anal. for vertical plate fin, microstruct. effects 7-63149
- convection-diffusion eqn., smoothing of numerical soln. by central difference method (*Japanese*) 7-41312
- convection-diffusion system, global existence 7-11420
- convective flow due to instantaneous heating by horizontal source 7-1571
- coupled viscous flow/transport problems, numerical computation 7-44065
- cryogenics, geometry and rot. effects on convection onset 7-57833
- cryoturbogenerator rotors, heating and convection of boiling fluid 7-31796
- crystal growth, thermocapillary free boundaries 7-46309
- crystals, impurity distrib. due to growth-rate fluctuations 7-44589
- cubic cavity, convection at high Rayleigh number, inclination influence 7-16178
- CVD of Si in annular tubes, film thickness profiles in mixed convection-diffusion regime 7-27190
- Czochralski cryst. growth, simulation of jet cooling effects 7-17408
- diatomic molecules in flows with convective and diffusive particle transport, nonequilib. dissociation 7-20811
- diffusion-convection equations, bracket formulation 7-6214
- diffusive transport in spatially periodic hydrodynamic flows 7-31801
- dispersion, convective, interphase mass transfer 7-51269
- dispersion and convection in periodic porous media 7-51140
- dissipative systems, stationary soliton soln. investig. 7-51034
- double-diffusion convection in completely confined fluids 7-57835
- driven flow in square cavity, Navier-Stokes eqns., finite difference scheme 7-20795
- droplet vaporisation, internal circulation integral eqn. formulation 7-37530
- drops, diffusion-convective vaporisation by intensive optical radiation, quasistationary soln. 7-50914
- Earth lower mantle convection, interaction with mantle dregs rel. to laterally heterogeneous core-mantle boundary 7-66022
- Earth mantle, convection in spherical shell, onset of time-dependence 7-60212
- Earth mantle, heat transfer, 2D model 7-54940
- electrohydrodynamics and electrically induced convective heat transfer 7-63133
- ethanol-water mixture, finite-amplitude travelling wave convection 7-43913
- FEM for study of solidification processes with natural convection 7-14758
- film condensation and natural convection along interface between porous and open space 7-43903
- finite amplitude axisymmetric convection between rigid rotating planes 7-26272
- finite amplitude convection in a rotating porous medium 7-57842
- finite element methods in flow problems, conference, Antibes, France (June 1986) 7-41009
- finite element solution of coupled natural convection and radiation in an axisymmetric cavity 7-37311
- flame front propag. convective vertex form. 7-13777
- flow patterns in cylindrical layer, wave-vector field 7-51352
- flow structure in porous media (*French*) 7-16246
- fluid frame, radiation transfer 7-20587
- fluids, enhanced heat diffusion by oscillation 7-51116
- forced convection boiling of R-12 under swirl flow, heat transfer 7-63162
- forced convection heat transfer loop supported by natural convection loop 7-11406
- forced convection of drag reducing fluids in vertical pipes, buoyancy effect on heat transfer 7-26278
- forced-convection heat transfer, 2D transient anal. 7-20724
- free and forced convective heat transfer, FEM 7-51117
- free convection near continuously moving vertical plate, boundary layer eqns. solns 7-1569
- free convective heat transfer, temp. factor effect 7-63143
- free turbulent flow diffusion theory 7-11401
- free-convection boundary layer at heated vertical plate, heat transfer and temp. profiles 7-31795
- fully developed combined convection, theory, flow reversal 7-1566
- Ganymede, equatorially-symmetric convection cells rel. to tectonic framework of grooved terrain 7-24050
- gas flow struct. and impurity distrib., num. calcs. 7-51124
- gas velocity imaging using photothermal deflection effect 7-20817
- gravitating rotating gaseous disk, nonlinear convective instability development calcs. 7-66766
- heat generating fluid in horizontal cylinder, natural convection 7-20702
- heat transfer in unsteady MHD Couette flow of electrically conducting viscous incompressible rarefied gas, theory 7-66448
- hexadecane-water, natural convection in complex enclosed space, heat transfer 7-11421
- horizontal eccentric annular cavity, natural convective heat transfer reduction by baffles 7-20701
- hot-film anemometers, const. temp., calibration in water 7-11567
- hydromagnetic convection at a heated semi-infinite vertical plate 7-57933
- hydromagnetic free convection flow along porous plate with mass transfer, Hall effects 7-63141
- ice, melting around horizontal cylinder, numerical simulation 7-1604
- ice, melting in porous media, solid-liq. interface motion, temp. distrib. 7-50926
- impulsively started circular cylinder, buoyancy effects on transient flow and heat transfer 7-26279
- inclined square enclosure, natural convection, wall conduction influence 7-26122
- incompressible fluid flow, temp.-vel. coupling 7-20723
- instability in packed or porous beds with throughflow 7-11383
- kink instability in solar convective zone mag. flux tubes 7-14476
- laminar buoyancy-driven convection flow in settling vessels having inclined walls 7-51135
- laminar channel flow with stepwise variations of wall temp., transient forced convection 7-37426
- laminar convective gas flow in vertical slots, steady Navier-Stokes eqns. 7-37461
- laminar duct flow subjected to axial variation of heat transfer coeff. 7-51111
- laminar flow past short, heated cylinder, finite element soln. 7-57789
- laminar forced convection inside ducts with temp. periodic variation 7-31736
- laminar free convective heat transfer in vertical uniform heat flux ducts 7-43891

convection continued

- laminar horizontal fluid flow near vertical heated surface, mixed convection study 7-51133
- laminar mixed convection flow about horizontal cylinder (*French*) 7-1552
- laminar natural convection above horizontal isothermal square cylinder, separation 7-31783
- laminar natural convection flow in square enclosure thermal cond. effect 7-51115
- laminar natural convection in an enclosure 7-20710
- laminar natural convection in annuli between concentric and eccentric cylinders 7-37546
- laminar natural convection in square channel, penalty FEM 7-51132
- laminar natural convective flow along isothermal vertical surface, stability 7-31744
- laminar to turbulent convection transition, 3D spectra evolution 7-57831
- laser-induced convection, instability, laminar to turbulent transition 7-37464
- linear 1D eqn., numerical dispersion by upwind differencing 7-26267
- liquid film downflow, Orr-Sommerfeld eqn. soln., optimal approach 7-51119
- liquid metals, horizontal Bridgman growth in 2D flow 7-64885
- liquid metals, horizontal Bridgman growth in 3D flow 7-64886
- low resolution IR gas transmissivities, line-by-line approach 7-51386
- lung, convective momentum near airway bifurcation, rel. to ventilation distrib. during HF oscill. 7-14037
- magnetoconvection, condition for the validity of Chandrasekhar's conjecture 7-51323
- magnetoconvection, interaction between standing and travelling waves and steady states 7-6328
- mantle diapirs evol., laboratory 7-8890
- Marangoni convection, surface deformation, nonlinear diffusion eqn. 7-51130
- MHD convection, overstability study 7-51333
- micro-organisms, swimming, individual and collective fluid dynamics 7-47141
- micropolar fluid in magnetic field, laminar free convective heat transfer, suction/injection effects 7-57824
- micropolar fluid over isothermal cone, natural convection boundary layer flow 7-43887
- mixed convection flow over horizontal cylinder or sphere in saturated porous medium 7-1562
- mixed laminar correction in entrance region of inclined rectangular channels 7-63148
- MOCVD, horizontal reactors, complex flow phenomena 7-22530
- multi-component convection/diffusion/reaction systems, FEM 7-44063
- natural convection, book 7-60909
- natural convection, heated horizontal surface, numerical anal. 7-31777
- natural convection, partially filled rectangular enclosure, heat transfer study 7-31625
- natural convection, partitioned enclosures, heat transfer study 7-31626
- natural convection enclosure flow, temp. and heat flux distrib. 7-1563
- natural convection experiments in a stratified liquid-saturated Porous Medium 7-63150
- natural convection flow on inclined flat plates with uniform surface heat flux, wave instability 7-20725
- natural convection from cylinder array in water, orientation effect 7-31781
- natural convection from cylindrical heat source in water saturated porous medium, radwaste appl. 7-806
- natural convection heat transfer in horizontal annulus 7-31784
- natural convection in channel with corrugated confining walls 7-51113
- natural convection in narrow-gap spherical annuli, stability to axisymmetric disturbances 7-31789
- natural convection in partially divided enclosures 7-63146
- natural convection in porous media, non-Darcian effects 7-31785
- natural convection in rapidly spinning systems, heat transfer and flow visualisation 7-63161
- natural convection of stably stratified fluid layer with uniform heating from below 7-51141
- natural convection on downward-facing heated plate, average Nusselt number 7-31791
- natural convection on plates with variable surface temp. or heat flux 7-31743
- natural convective heat transfer on vertical plate, heat conduction effect 7-26124
- nematic liquid layers, convective flow, multiple spatial periodicities, EHD instability 7-43909
- network models of porous media, hydrodynamic dispersion 7-1625
- non-Newtonian fluid, buoyancy effects, magnetic field parameter, magnetisation 7-6257
- nonDarcy free convection boundary layer on axisymmetric and 2D bodies of arbitrary shape 7-43904
- nonlinear convection of compressible fluid in rot. spherical shell, theory 7-9459
- nonlinear convection with variable coefficient of thermal expansion 7-6207
- nonlinear heat and wave eqns., symmetries 7-14787
- numerical simulation of two- and three-dimensional Benard convection 7-37465
- olivine-basalt partial melts, rheology and struct. 7-8931
- open-flow systems, rel.-depend. Lyapunov exponents as measure of chaos 7-61240
- optical glasses, radiation heating, radiation source selective props. and temp. effects 7-11255
- oscillating flow past infinite vertical plate, suction and free convection effects 7-1555
- oscillating free-convection flow past infinite porous vertical limiting surface, effects of mass transfer 7-14479
- penalty finite-element analysis of coupled fluid flow and heat transfer for in-line bundle of cylinders in cross flow 7-31792
- penetrative double-diffusive convection, stability anal. 7-57838
- Petrov-Galerkin method for convection-dominated linear and nonlinear parabolic problems 7-18726
- phase change, enthalpy formulation anal. 7-51118
- phase-change material during melting, heat cond. and natural convection, moving boundary problem 7-43900
- physical vapour transport in rectangular horizontal enclosures, surface reactions, convection 7-17398
- pipe laminar thermal energy region, transient unsteady convective heat transfer 7-31775
- plane pipe, nonsteady heat convection study 7-63135

convection continued

planetary and stellar convection at global-scale, zero-gravity expts. 7-29393
 plasma convection in horizontal magnetic field with periodic boundary conditions 7-4328
 plate, inclined, isothermal, natural convection from upper and lower surfaces 7-31782
 plate, nonisothermal flat, free convection flow influenced by blowing or suction 7-11529
 plate, short vertical, free convection heat transfer, Nusselt and Grashof numbers 7-6077
 polymer fluids, nonlinear, elastic props, convective transfer processes 7-43824
 polymer thermal destruction in nonsteady heating in hot gas stream 7-26126
 porous granular systems, convective combustion 7-13772
 power-law fluid in horizontal ducts, laminar mixed convection heat transfer 7-37427
 Prandtl number, turbulent passive scalar field 7-31765
 propane-air flames, explosion venting, 2D Navier-Stokes eqns. 7-51340
 quasisteady free convection regime in a vertical cylindrical vessel 7-20716
 radial transport in tubular polymerization reactors 7-6315
 radiative and convective heat transfer during blowing into layer of two-phase prods. from ablation 7-20755
 radiative convection in stratified atmosphere, anelastic eqns. soln. 7-29389
 ramped Rayleigh-Bernard convection, wavenumber selection 7-26273
 random method with creation of vorticity for free convection near wall, random method with creation of vorticity 7-20728
 Rayleigh-Bernard cell, transition to convective roll pattern 7-57839
 Rayleigh-Bernard convection, laser speckle velocimetry 7-31902
 Rayleigh-Bernard convection patterns, wavenumber distrib. and time dependence 7-43914
 Rayleigh-Bernard expt. metric entropy estimation 7-61244
 rectangular box, oscillatory instability, 3D Boussinesq eqns. 7-51129
 rotating Benard convection, transition to turbulent flow, instability heat transfer meas. 7-26253
 rotating cylindrical annulus, convection, asymptotic theory 7-51169
 rotating cylindrical annulus, imposed temp. gradient, flow regimes study 7-43933
 rotating cylindrical annulus, instabilities of columns 7-51128
 rotating differentially heated annulus with unstable stratification (*Russian*) 7-29129
 rotating hemispherical shell with radial gravity, Spacelab simulation expts. of astronomical bodies 7-55450
 rotating porous medium, unsteady free convective flow 7-51139
 shock waves, weak, Taylor internal struct. 7-51228
 sloped porous layers, 3 D convective cells (*French*) 7-16247
 solar convective zone outer layer, spectral lines pressure shift diagnostic study 7-40793
 solar dryer based on convective heat and mass transfer 7-54354
 solar greenhouse, temperature-humidity regime in inclined thermal-storage channels 7-54269
 solar shed greenhouses, storage of heat by forced air circulation 7-54270
 sparsely packed porous layer, double diffusive convection 7-11531
 sparsely packed porous medium, double diffusive convection, rot. effect 7-1553
 spatial oscillations in confined rotating fluid, temporal development 7-16186
 spatially-forced thermal convection, resonance and phase solitons 7-51138
 spatio-temporal coherence and chaos, conf. Los Alamos, USA, Jan. 1986 7-48158
 spectral Chebyshev solutions for free convection at high Reynolds number 7-37466
 sphere in free convective flow, heat transfer, Navier-Stokes eqns. soln. 7-20705
 spheres in beds in lengthwise flow, fluid friction and convective exchange 7-57917
 spherical fluid inclusion, convective instability 7-43856
 spherical systems, static, wavelike and chaotic thermal convection 7-1558
 steady bimodal convection in a cylinder at large Prandtl numbers 7-57837
 steady heat source moving through stratified flow, resulting flow patterns, atm. appl. 7-4127
 steady-state, 3D problem, numerical soln. (*Russian*) 7-61296
 steam-water dispersed flow heat transfer in vertical round tube, post-dryout regime (*Chinese*) 7-11419
 stellar atmospheres, effect of Hall currents on thermal-convective instability of composite plasma 7-4437
 stellar atmospheres, effect of rot. and mag. field on thermosolutal-convective instability 7-14557
 stellar interiors, convective turbulence with rot. and mag. fields 7-29388
 stellar interiors, non-local convection theory rel. to evolution of massive stars 7-29460
 stratified fluid, thermally, slow flow between rot. eccentric spheres with radial gravit. field 7-26333
 subharmonic and asymmetric convection rolls 7-1570
 subsonic convection, consistent approximation of viscous terms 7-34845
 superconducting magnet system superfluid He II for cooling 7-61343
 supercritical fluid, diffusion and mass transfer 7-63106
 superheater, convection-type, thermal damage minimisation 7-11407
 superersonic wake past blunt body, heat transfer, and drag 7-51214
 surface tension driven convection subjected to rotation and non-uniform temperature gradient 7-6213
 temperature distribution and mass transfer of flow by free convection in enclosures rel. to crystal growth (*Chinese*) 7-11977
 temperature fields, finite elements nonlinear anal. 7-50924
 thermal convection, steady in annular region between two horizontal concentric cylinders 7-51131
 thermal convection, vibr. induced, in weightlessness 7-63132
 thermal diffusion cell, 3D num. study 7-31799
 thermal diffusion column for isotope separation, cut and feed rate effects on circulating flow 7-50393
 thermal energy storage in interior partition walls of buildings, convection coefficient effects 7-28416
 thermal explosion critical conditions, turbulent natural convection effects 7-63122
 thermal problems, time integration, least-squares schemes 7-50908
 thermal storage, phase change material melting process 7-65623

convection continued

thermocapillary and thermogravitational convection in a horizontal liquid layer 7-63909
 thermocapillary convection in a rectangular cavity with a deformable interface 7-43911
 thermocapillary convection in two-layer system, surface active agent effect 7-51121
 thermogravitational and thermocapillary convection in a rectangular cavity 7-63910
 thermohaline convection, finger development, similarity anal. 7-11413
 time-dependent convective flow pattern rotation, comment and reply 7-1560
 toroidal loop, two-phase natural circulation 7-26280
 transient conduction in a plate cooled by free convection 7-51108
 transient heat transfer in porous media—a two-temperature model 7-16181
 transition to chaotic convection 7-11422
 transition to time-dependent free convection in an inclined air layer 7-20708
 transport equation, convective, finite element soln., determ. of optimal upstream weighting parameter 7-29764
 transport processes approximate soln., nonintegral technique 7-9804
 transverse thermal dispersion in forced convective flow through packed bed 7-51105
 travelling thermal wave induction of convective heat transfer and fluid flows, nonlin. study 7-1546
 trichlorofluoromethane, down-flow shell-side forced convective boiling 7-63194
 tubular CVD reactor, deposition rate and uniformity, diffusion and convection effects, mathematical model 7-22559
 tubular thermal solar absorbers, numerical study and THEK appl. (*French*) 7-54353
 turbulence, fully developed, intermittent passive scalar field scaling exponents calcs. 7-26261
 turbulence, two-point-moment closure models 7-6192
 turbulent compressible convection in deep atmosphere, validity of numerical approach 7-47690
 turbulent convection, anal. developed from 2D Boussinesq eqns. 7-16177
 turbulent convection near vertical heated plate, calc. 7-31793
 turbulent incompressible convection, scalar model 7-43912
 turbulent wall pressure spectrum at subconvective wavenumbers 7-51073
 two stratified layers, rectangular enclosure, numerical anal. 7-31778
 two-layer immiscible fluids with thermally insulated boundaries, convective instability 7-51122
 two-layer systems, thermocapillary convection, numerical anal. 7-63911
 unitary fuel aerosol, burning in closed region, planar problem 7-13833
 unstationary flow, particle behaviour in Basset-Boussinesq-Oseen eqn. 7-11404
 unsteady boundary-layer flow, semisimilar solns. 7-57834
 unsteady free-convection flow past accelerated plate, skin friction 7-4321
 unsteady laminar forced convection from impulsively started sphere, temp. field 7-43852
 vaporisation, of irradiated droplets, hydrodynamic description 7-31800
 vapour axial deposited preform stretching, numerical model for internal distortion 7-11133
 vertical cylinder embedded in saturated porous medium, free convection 7-63129
 vibrations effect on convection in horizontal cylindrical layer 7-20714
 viscoelastic rarefied gas, MHD natural convection flows, buoyancy effects 7-6321
 viscous, incompressible fluid in closed cavity, free convection, numerical simulation 7-63134
 viscous fluid, finite difference methods 7-14784
 viscous fluid convective thermal motion instability in tube 7-31804
 viscous fluid in porous medium, stability criteria for convection, eigenvalue problems 7-44033
 vortex instability in natural convection flow on an inclined uniform-heat-flux surface (*Chinese*) 7-11430
 VPE, organometallic, reactor design optimisation, flow visualisation studies 7-22533
 wake, axisymmetric body, velocity and temperature profiles study 7-63155
 wall temperature nonuniformity effect on natural convection in heated enclosure 7-51109
 water, cold, horizontal buoyant flows, multiple steady-state solns. 7-43899
 water, cold, natural convection near its density maximum in rectangular enclosure 7-57836
 water, cold, transient and steady-state vertical natural convection flow, meas. and visualisations 7-43902
 water free and forced convective flow through porous medium 7-11533
 wavenumber selection and dynamics in periodic states of driven systems 7-51137
 weak nonlinear instability of Euler explicit scheme 7-57832
 wet porous beds, natural convection determ. 7-31786
 He, free convective heat transfer from horizontal cylinder with large temp. head 7-63142
 He, turbulent convection at supercritical press. under nonisothermal conditions 7-31805
 He-H₂O, gas/vapour mixtures in porous medium, natural convection 7-1554
 MnBi/Bi eutectic, freezing rates, convection effect on microstruct. 7-22652
 N₂ 7-26268
 N₂-H₂O, gas/vapour mixtures in porous medium, natural convection 7-1554
 Pb-Sn eutectic, spiral structures, convection influence 7-22653

convection in liquids

alcohol-water mixture, Benjamin-Feir turbulence in convective binary fluid mixtures 7-43916
 binary semiconductor alloys, directional solidification, convection, segregation, ampoule and furnace design 7-59501
 centrifuges, cylindrical, with compartments, sedimentation, Coriolis force reduction 7-20736
 coupled oscillators in convective flow, neutron scatt. obs. 7-44366
 crystal growth, Czochralski furnace, numerical calc. of heat transfer 7-53543
 crystal growth, heat and mass transfer in microgravity and on Earth 7-53510

convection in liquids continued

- crystal growth and directional solidification, transport processes, analytical modelling and expt. obs. 7-53541
 crystal growth from soln., holographic interferometry appl. to conc. distrib. and hydrodynamics 7-53526
 crystal violet in ethanol, spreading layer, capillary convection 7-6925
 Czochralski method simulation using tetradecane, Flow transitions visualisation 7-22463
 dielectric liquid, stationary instabilities, unipolar injection and thermal gradient effects 7-26357
 double diffusive natural convection in solar ponds, nonlinear temp. and salinity profiles 7-8445
 ethanol-water convective binary mixture, competing patterns 7-20727
 eutectics, solidification, lamellar spacing, influence of convection 7-17522
 explosive flashing, effective heat of vaporisation 7-1547
 fluid phases, separation, and bubble dynamics in temp. gradient and microgravity conditions 7-20722
 haemorrheology, effect of couple stresses on unsteady convective diffusion in fluid flow through a channel 7-3811
 laser radiation absorpt. producing natural convection 7-26274
 light propag., convection effect, numerical investigation method 7-25711
 Marangoni convection, bubble motions induced by a temperature gradient 7-20717
 Marangoni convection and mass transfer from the the liquid to the gas phase under microgravity conditions 7-20720
 Marangoni convection in an open vessel (*German*) 7-20718
 Marangoni convection in one- and two-liquids floating zones 7-20719
 mixed-convective heat transfer to liquids at supercrit. press. in vertical pipes 7-57830
 molten glass layer, temp. convection, anal. 7-57822
 nematic liquid crystals, EHD instabilities (*Japanese*) 7-1879
 Newtonian fluid in cylindrical pipe, convective heat transfer 7-6210
 protein crystal growth, convective diffusion in parent soln. 7-23287
 salt gradient solar pond performance model 7-54359
 salt-stratified layer, double-diffusive convection induced by discrete heat source 7-43901
 thermal lens oscills. on liq. surface produced by laser beam 7-11403
 thermocapillary movements under microgravity at a minimum of surface tension 7-20721
 thin films, thermocapillary convection and stability 7-12409
 tube bundle with spacers, flow of water, convective heat transfer 7-51146
 two-component fluid-fluid system, convective instability 7-31776
 unsteady MHD flow past vertical porous plate, mass transfer and free convection effects with constant suction 7-54332
 unsteady MHD flow past vertical porous plate, mass transfer and free convection effects with variable suction 7-54333
 viscoelastic liquids, tricritical codimension-2 point near convection onset 7-51055
 water, supercritical, heat transfer and turbulent flow in vertical tube 7-51142
 water, turbulent pipe flows, forced convection correl. in near-critical region 7-51093
 Al-Zn eutectic, oriented crystallisation, buoyancy-driven convection effects 7-27887
 CO₂, turbulent pipe flows, forced convection correl. in near-critical region 7-51093
 CuSO₄ soln., double diffusive convection, conc. meas., optical technique. 7-57825
 He, channelled cryogenic liquids, heat transfer and hydrodynamics 7-16261
³He in superfluid ⁴He, correcting dil. solns.; superfluid turbulence 7-44946
³He-⁴He mixture, Benjamin-Feir turbulence in convective binary fluid mixtures 7-43916
⁴He, convection in variable cylindrical geometry, heat-flow meas. 7-51127
 N₂, channelled cryogenic liquids, heat transfer and hydrodynamics 7-16261
 PbTe crystals, Bridgman growth in centrifuge, convection effects (*French*) 7-53542
 Si, Stepanov reverse method cryst. growth, thermal and capillary conditions 7-33545
 SiO₂, Czochralski cryst. growth, impurity segregation, high axial mag. field effect 7-26960

convergence

- see also *convergence of numerical methods*
 complex domain, behaviour of eigenfunction expansion, pointwise convergence 7-61040
 conservative uniformly accurate difference method for a singular perturbation problem in conservation form 7-48325
 coupled-cluster approach, convergence accel., DIIS method 7-15468
 elastic beam on elastic base, optimal design 7-4690
 Gross-Jackson kinetic model eqn., convergence 7-48642
 interpolatory product integration rules, extension of results to noninterpolatory rules 7-48328
 linear transport equation, inner iteration convergence for finite difference approxs. 7-35482
 Madelung constant, lattice sum definition, conditional convergence and anal. of ambiguity in summation 7-58196
 multivariate aberration series, acceleration of convergence 7-5846
 multivariate Lagrangian aberration functions, singularities 7-5844
 multivariate Lagrangian aberration series, extension of convergence 7-5845
 overdetermined systems of linear inequalities, projection method for least squares solns. 7-61079
 parabolic type integro-differential eqn., time discretisation 7-35251
 passive underwater tracking with nonlinear feedback, convergence anal. 7-31557
 predictor-solver continuation methods, convergence cones near bifurcation 7-35203
 sea bed contour map construction from random data, iterative method 7-34725
 second order nonlinear delay equation, asymptotic decay of oscillatory solns., convergence 7-29684
 semilinear wave equation in 1 space variable with weak damping, convergence to equilib. 7-48386
 symmetric tridiagonal band matrix, explicit inverse, Sturm-Liouville system eigenvalues appl. 7-60959

convergence of numerical methods

- 1/D expansion, convergence props. 7-14830

convergence of numerical methods continued

- acceleration, computation 7-55938
 annular thermal entry problem, num. solns. 7-16180
 axisymmetric elastoplastic torsion problem, num. soln. (*Chinese*) 7-14775
 Babuska-Brezzi conditions for two kinds of rectangular elements (*Chinese*) 7-51029
 boundary integral equation on polygonal domains, superconvergent approxs. to soln. 7-48323
 Burger's eqn., convergence to steady-state of solns. 7-26234
 collocation for singular boundary value problems of second order 7-35252
 compressible flow, accuracy of nonuniform-mesh schemes 7-51202
 computational fluid dynamics, implicit soln. methods 7-51020
 COMTA code for fuel performance, convergence behaviour of nonlinear eqn. solvers 7-15241
 contact problem, dual FEM for elastic bodies with enlarging contact zone 7-57763
 coupled dynamic thermoelasticity, approx. solns. 7-16062
 curved members, consistent discrete elements technique 7-50948
 deconvolution, iterative algorithm with quadratic convergence 7-42969
 dielectric sphere buried in lossy medium, scatt. Sommerfeld integral computation 7-57218
 differential operators, G-asymptotic representation 7-18570
 diffusion eqn., 1D lin., 5-pt. explicit finite difference method 7-14898
 diffusion eqn., iteration scheme convergence in nodal expansion method 7-30465
 discontinuous flows, teaching using interactive techniques and windowing 7-60923
 eddy current flow inversion algorithm, experimental verification 7-54059
 elastic-plastic problem soln. with increasing strain hardening of material 7-11304
 elasticity axisymmetric problems solution using triangular three-node non-conforming elements 7-56042
 elastoplastic strain hardening solids, convergent bounding principle 7-43704
 FEM, inelastic distortional buckling analysis of I-beams 7-43722
 Fokker-Planck equation solns., polynomial expansion and integral eqn. methods 7-61291
 force-deflection anal., eigenvalue convergence in the finite element method 7-24420
 Fornberg's numerical method for conformal mapping 7-48342
 free convection near wall, random method with creation of vorticity 7-20728
 Galerkin finite element analysis of complex viscoelastic flows 7-16143
 geometrical optics, Taylor series for point charact. of refracting plane 7-57113
 heavy gas atoms, particle behaviour simulation 7-9749
 hyperelastic materials, elastostatic equilb., weak convergence of sets of constraints (*French*) 7-61100
 image restoration, linear degradation effects, iterative algorithm 7-42970
 isotropic multigroup problems in half-space geometry, convergence of F_N method 7-61288
 iteration method, convergence (*Russian*) 7-61082
 Navier-Stokes eqns., reduced form, single- and multi-sweep techniques 7-16153
 Navier-Stokes equations, penalty FEM, iterative methods convergence 7-51024
 nonlinear problems, error estimates for mixed finite element approximations 7-4691
 nonpositive definite weights, Monte Carlo and Langevin algorithms convergence comparison 7-75
 oceans, depth-dependent channel flow modelling 7-18325
 parabolic type integro-differential eqn., time discretisation 7-35251
 periodic nonlinear differential eqns., Massera's convergence theorem 7-24390
 plane elasticity, two-grid FEM method 7-6089
 plate, rectangular, on line supports, vibr. analysis, Lagrange multiplier-Fourier expansion 7-6145
 plate/shell element, field-consistent four-noded laminated anisotropic 7-62983
 plates, laminated composite, 3D hybrid stress isoparametric element 7-56020
 plates, prismatic, folding, instability by finite strip method (*Spanish*) 7-20611
 Poisson equation, numer. soln. 7-29774
 reconstruction of tomographic images from projections of a small number of views via mathematical programming 7-34245
 shell elements, 3-node triangular, improvements 7-4685
 small-strain problems, geometrically nonlinear discretization, convergence at infinitesimal element division 7-48362
 soil, infiltration from cavities, num. soln. 7-18254
 steady Euler eqns., multiple-grid and Osher's scheme 7-51021
 thin flat-walled structures, buckling, spline finite strip method 7-1459
 transonic full potential eqn., intermediate boundary condition in Holst AF2 scheme 7-26308
 turbulence measurement with inclined hot wire probe, 3D angle calibration method (*Japanese*) 7-6338
 viscous incompressible fluid in half-plane, Chorin-Marsden product formula convergence 7-11372
 vortex filament method, convergence 7-51179
 weakly singular discrete Gronwall inequalities 7-41081

conversion electron spectra

- backscattered conversion electron Mossbauer spectra, electron intensities calc. 7-53181
 gamma-ray lasers, Mossbauer effect in long-lived nucl. states, observational techniques 7-10124
 proportional detector for high temp. conversion electron Mossbauer spectroscopy 7-48926
 Al₂O₃/Fe interface, ion beam mixing, conversion electron Mossbauer spectra studies 7-63679
²⁰²Pb, conversion electron spectra meas. for anal. of ²⁰²Pb transition multipolarities 7-30375
 Cu-Fe host-impurity system, O ion bombarded, internal oxidation, Mossbauer spectra studies 7-59131
 Fe/H₂O interface, pulsed-laser-induced reactive quenching, FeO metastable phase form. studies 7-45005
 Fe₈₄B₁₆ amorphous alloy, heterogeneous surface struct., Mossbauer differential conversion electron spectra anal. 7-2319
 Fe₅₀Ni₅₀ alloy foils, N₂⁺ implantation, oxidation behaviour, conversion electron Mossbauer spectra study 7-22877

conversion electron spectra continued

- GaAs:Zn, ion damage and recrystn. annealing, conversion electron EXAFS meas. 7-64821
¹⁸⁰Hf, longitudinal conversion-electron polarization 7-30377
¹Hg (d,py), A=202, 204, γ -ray and conversion electron meas., neutron hole states 7-49432
¹⁷³Lu, longitudinal conversion-electron polarization 7-30377
²⁰¹Po, m and g isomers, decay scheme construction from time-sequenced spectra 7-30365
^ARn, A=223, 226, 227, half-life meas. 7-49291
^ASm, A=150,152, electromagnetic decay of O_2^+ and O_3^+ states 7-15199
¹²⁵Tc, Mossbauer isomer shifts and contact densities 7-38966
 (YSmLuCa)₃(FeGe)₅O₁₂ epitaxial layer, conversion electron Mossbauer spectra 7-48926

convertors

- see also Joule-Thomson effect; low-temperature production; magnetic cooling; quenching (thermal); refrigeration; supercooling
 absorption heat pump systems, H₂O-LiBr based, operating temps. and concs. 7-59866
 air flow with fine droplets, evaporative cooling heat transfer 7-11508
 apparatus cooldown using He or N cooling systems, mass flow requirements calc. 7-56281
 atomic gases, ultracold, collective quantum effects by laser-cooling techniques 7-30989
 betatron magnetic circuit temp. distrib. calc. (Russian) 7-42247
 bimetal cylinder, temp. fields and residual stresses in cooling 7-33705
 biological cryo-electron microscopy, cryst. size and cooling rate 7-3949
 cassette radioelectronic apparatus, forced ventilation cooling, optimisation algorithm 7-63138
 closed cycle cooler, simplified cold head design 7-56277
 closed type adsorption cooling system utilising solar heat, simultaneous transport of heat and adsorbate 7-8440
 composite slab, cooling 7-43645
 composite slab, transient heat conduction, convective and radiative cooling 7-11246
 cryogenic current leads cooling, energy losses 7-61342
 cryogenic current leads with current overloads and coolant flow interruption, temp. state 7-61341
 cryogenic systems with long dead-end pipelines, pressure increase 7-31880
 cryopreservation of biological specimens, possibility of using exponential cooling regimes 7-54815
 Czochralski cryst. growth, simulation of jet cooling effects 7-17408
 ethanol, jet-cooled, electron impact induced fluoresc. of dissociation fragments 7-36676
 evaporative cooling thresholds of lizards, effect of hypoxia 7-54486
 far-IR detectors cooling technology (Japanese) 7-56340
 fibre formation, nonsteady regimes, heat removal effect 7-44025
 heat transfer, deflector type effect, blades with cooling gas crossflow 7-43635
 heat transfer with viscous dissipation between infinite parallel plates, functional analysis 7-37459
 heat transfer with viscous dissipation in semi-infinite tube, functional analysis 7-37458
 inverse problems in solidification and cooling processes, casting 7-58442
 jet cooling and finned walls for improved heat transfer in power installations 7-63140
 Lake Norman, NC (USA) application of ecosystem assessment model 7-65654
 laser guided discharges and appls., pulsed power considerations 7-37801
 lighting generators for commercial vehicles, oil cooled, heat transfer coefficients comparison (German) 7-37312
 methane, jet-cooled, electron impact induced fluoresc. of dissociation fragments 7-36676
 methanol, jet-cooled, electron impact induced fluoresc. of dissociation fragments 7-36676
 natural convection, book 7-60909
 nonisothermal continuous stirred tank reactor, multivariable, global control using moving model 7-13729
 nuclear power plant neutral oxygenated water conditions appl. efficiency for corrosion protection (Russian) 7-765
 nuclear power station two-stage coolant system, hydraulic and mechanical transients (Russian) 7-5351
 open-type vortex cooler for power semicond. instruments, thermal resist. study 7-11405
 W equatorial Pacific, evaporative cooling by anomalous winds 7-9023
 passive radiator for cooling IR detectors in geostationary orbit 7-18878
 photovoltaic-thermal solar concentrator receiver system using fin-type absorber, actively cooled, anal. 7-54274
 polyolefines, struct., dielec. props., crystallisation conditions effects (Russian) 7-64564
 polypropylene-polyethylene blends, γ -irrad., mech. and thermal props. 7-21137
 power-generating turbine, cooling systems, flow behavior 7-6221
 pressure losses in finned air coolers during frost formation 7-57829
 pyrimidine, jet-cooled, rot. resolved fluoresc. excitation spectra 7-25597
 radiative cooling in valleys and hollows 7-55134
 radiative heat pumps using narrow-bandgap semiconductors 7-40019
 rolled metal section, light, accelerated cooling rate during TMT, effects of design, hydromech. and temp. factors 7-8011
 semiconductor and electrical engineering devices, cooling device design 7-37314
 solar active cooling systems, comparison using fuzzy decision analysis package 7-59876
 solar cooling by direct evaporation from sprays 7-37532
 solar energy cooling units thermodynamic parameters optimisation using gas turbine transducers 7-34066
 solar panels power improvement by using cooling and light concentration 7-54302

cooling

- see also Joule-Thomson effect; low-temperature production; magnetic cooling; quenching (thermal); refrigeration; supercooling
 absorption heat pump systems, H₂O-LiBr based, operating temps. and concs. 7-59866
 air flow with fine droplets, evaporative cooling heat transfer 7-11508
 apparatus cooldown using He or N cooling systems, mass flow requirements calc. 7-56281
 atomic gases, ultracold, collective quantum effects by laser-cooling techniques 7-30989
 betatron magnetic circuit temp. distrib. calc. (Russian) 7-42247
 bimetal cylinder, temp. fields and residual stresses in cooling 7-33705
 biological cryo-electron microscopy, cryst. size and cooling rate 7-3949
 cassette radioelectronic apparatus, forced ventilation cooling, optimisation algorithm 7-63138
 closed cycle cooler, simplified cold head design 7-56277
 closed type adsorption cooling system utilising solar heat, simultaneous transport of heat and adsorbate 7-8440
 composite slab, cooling 7-43645
 composite slab, transient heat conduction, convective and radiative cooling 7-11246
 cryogenic current leads cooling, energy losses 7-61342
 cryogenic current leads with current overloads and coolant flow interruption, temp. state 7-61341
 cryogenic systems with long dead-end pipelines, pressure increase 7-31880
 cryopreservation of biological specimens, possibility of using exponential cooling regimes 7-54815
 Czochralski cryst. growth, simulation of jet cooling effects 7-17408
 ethanol, jet-cooled, electron impact induced fluoresc. of dissociation fragments 7-36676
 evaporative cooling thresholds of lizards, effect of hypoxia 7-54486
 far-IR detectors cooling technology (Japanese) 7-56340
 fibre formation, nonsteady regimes, heat removal effect 7-44025
 heat transfer, deflector type effect, blades with cooling gas crossflow 7-43635
 heat transfer with viscous dissipation between infinite parallel plates, functional analysis 7-37459
 heat transfer with viscous dissipation in semi-infinite tube, functional analysis 7-37458
 inverse problems in solidification and cooling processes, casting 7-58442
 jet cooling and finned walls for improved heat transfer in power installations 7-63140
 Lake Norman, NC (USA) application of ecosystem assessment model 7-65654
 laser guided discharges and appls., pulsed power considerations 7-37801
 lighting generators for commercial vehicles, oil cooled, heat transfer coefficients comparison (German) 7-37312
 methane, jet-cooled, electron impact induced fluoresc. of dissociation fragments 7-36676
 methanol, jet-cooled, electron impact induced fluoresc. of dissociation fragments 7-36676
 natural convection, book 7-60909
 nonisothermal continuous stirred tank reactor, multivariable, global control using moving model 7-13729
 nuclear power plant neutral oxygenated water conditions appl. efficiency for corrosion protection (Russian) 7-765
 nuclear power station two-stage coolant system, hydraulic and mechanical transients (Russian) 7-5351
 open-type vortex cooler for power semicond. instruments, thermal resist. study 7-11405
 W equatorial Pacific, evaporative cooling by anomalous winds 7-9023
 passive radiator for cooling IR detectors in geostationary orbit 7-18878
 photovoltaic-thermal solar concentrator receiver system using fin-type absorber, actively cooled, anal. 7-54274
 polyolefines, struct., dielec. props., crystallisation conditions effects (Russian) 7-64564
 polypropylene-polyethylene blends, γ -irrad., mech. and thermal props. 7-21137
 power-generating turbine, cooling systems, flow behavior 7-6221
 pressure losses in finned air coolers during frost formation 7-57829
 pyrimidine, jet-cooled, rot. resolved fluoresc. excitation spectra 7-25597
 radiative cooling in valleys and hollows 7-55134
 radiative heat pumps using narrow-bandgap semiconductors 7-40019
 rolled metal section, light, accelerated cooling rate during TMT, effects of design, hydromech. and temp. factors 7-8011
 semiconductor and electrical engineering devices, cooling device design 7-37314
 solar active cooling systems, comparison using fuzzy decision analysis package 7-59876
 solar cooling by direct evaporation from sprays 7-37532
 solar energy cooling units thermodynamic parameters optimisation using gas turbine transducers 7-34066
 solar panels power improvement by using cooling and light concentration 7-54302

cooling continued

- solar pumps, water cooled, expt. laboratory study of dimensioning principles (Rumanian) 7-13930
 solid gas adsorption cooling system, refrigerator and heat pump using natural zeolite 7-65567
 sputtering temperature of cooling cylindrical rod with insulated core, num. results 7-31631
 SQUID, DC, cooled to 4.2 K with hybrid closed-cycle cryocooler, operation 7-56278
 steel, dual phase, continuous cooling, transform. processes and products 7-28034
 superconducting magnet system superfluid He II for cooling 7-61343
 synchrotron beam line critical elements, heat transfer studies 7-42255
 thermal storage sizing methodology for solar cooling/power generation systems 7-65617
 thermoelectric cooling using Peltier elements (Dutch) 7-309
 transformer magnetic circuit temp. distrib. calc. (Russian) 7-42247
 tryptophan, jet-cooled, excited state conformers and intramol. exciplex form., dispersed fluoresc. 7-36671
 two-phase thermosiphons, tests on cooling of semiconductor power devices 7-11504
 water-LiBr absorption cooling system thermodynamic design data 7-23208
 Ar milliwatt laser with modern capillary design (German) 7-20274
 H₂ cluster detection at 4.2 K 7-36843
 H₂O, absorpt. of 2.3 μ m radiation 7-57060
 H₂O vapour, kinetic cooling by CO laser radiation 7-16297
 He cooled high flux heat removal, fusion reactor appl. 7-25194
³He, superfluid, hydrodynamic boundary conditions and cooling 7-63897
 Kr, electron impact, low energy, in afterglow 7-20060
 Li₂O-SiO₂ glass, critical cooling rates for nucleating agents 7-6795
 N₂, liquid, molecular dissociation and shock-induced cooling at high densities and temperatures 7-28307
 OCS, jet-cooled, ¹³C⁺ \rightarrow ¹²C⁺ transition, spectrosc. investig. 7-62400
- cooling, splat see splat cooling
- cooling towers
 see also water supply
 nuclear power station two-stage coolant system, hydraulic and mechanical transients (Russian) 7-5351
- Cooper Hewitt lamps see mercury vapour lamps
- Cooper pairing see Cooper pairs
- Cooper pairs
 see also BCS theory; Josephson effect
³He-A superfluid, chiral anomaly, finite fermion vacuum current calcs. 7-44945
 Anderson Kondo lattices, heavy-fermion superconductivity 7-2775
 cubic systems, superconducting p-wave pair states, collective excitations, spin-orbit interaction and cryst. field effect 7-7440
 dense Kondo heavy fermion systems, Cooper pairs attractive interactions freq. depend. 7-58951
 f-electron and conduction electron superconductivity, periodic Anderson model, self-consistent calcs. 7-12908
 heavy fermion superconductivity, tight binding picture and Cooper pairs 7-2776
 heavy fermion superconductors, spin-fluctuation-mediated even-parity pairing 7-38812
 heavy fermion superconductors 7-33123
 heavy-fermion superconductors, anomalous pairing and superconducting state, review 7-2774
 Josephson tunnel junction, ordered magnetic impurities in barrier region near critical temp. 7-58961
 many-valley superconductors, phase oscils., Fermi liq. effects 7-33124
 superconducting electron pairing, exchange and correl. contributions 7-45574
 superconducting networks, finite width effect on upper critical field 7-45586
 superconducting tunnel junctions, microwave detection, quantum statistical theory 7-2786
 superconducting tunnel junctions, quasiparticle trapping and the quasiparticle multiplier 7-58954
 superconductivity with triplet pairing, diamagnetic limit, critical mag. field determ. 7-64395
 superconductor, sinusoidal magnetic order and superconductivity coexistence 7-7442
 thin films, inelastic electron collision lifetime, surface fluctuating superconducting electron pairing effects (Russian) 7-52890
 tunnelling of triplet pair states 7-38825
 CeCu₂Si₂, heavy fermion superconductors, Fermi surface and cooperative phenomena 7-2771
 Cu, thick proximity induced superconductor, mag. field effects, thickness and temp. depend. 7-52903
 Hg₃-AsF₆, 1D BCS Hamiltonian 7-45558
 Ti_{1-x}V_x quench condensed thin films, supercond. crit. field and fluctuation cond. meas. 7-64415
 UBe₁₃, electron-phonon coupling calcs., unconventional superconductivity mechanism 7-38811
 UBe₁₃, heavy fermion superconductors, Fermi surface and cooperative phenomena 7-2771
 UBe₁₃, heavy-fermion superconductor, muon Knight shift study 7-7628
 UPt₃, anisotropic superconductivity 7-7461
 UPt₃, heavy fermion superconductors, Fermi surface and cooperative phenomena 7-2771
 UPt₃, heavy fermion supercond., Cooper pair states, atomic representation 7-45550
 UPt₃, upper critical field, ang. and temp. depend. 7-7459
 U_{0.967}Th_{0.033}Be₁₃, heavy-fermion superconductor, muon Knight shift study 7-7628
- coordination complexes
 inorganic complexes are indexed under the appropriate metal compound headings
 hexahalo complexes, vibronic coupling and state Jahn-Teller effect 7-19725
 metal-bipyridine complexes, second harmonic generation obs., struct. determ. 7-57454
 metal-pyridine complexes, second harmonic generation obs., struct. determ. 7-57454
 1,4,10-trioxo-7,13-diazacyclopentadecane-N,N'-diacetic acid metal complexes, NMR investig. 7-57091

copolymerisation *see* polymerisation

copolymers *see* polymer blends

copper

- see also* nuclei with
- acoustic emission during corrosion in FeCl_3 soln. 7-39814
- acoustic-jet plating of 7.5 MHz 7-59462
- adsorbed on W (110), thermal desorption spectroscopy 7-27119
- adsorption on W (110), calcs. based on nonadditive effective binding pot. 7-12483
- amorphous, density of states calc., cluster embedding in effective shell 7-2457
- anodic oxidation in Br^- and SCN^- solns., mechanism 7-52052
- anodic oxidation in KOH soln., in situ spectroelectrochemical anal. 7-28192
- atom, photon cross section meas. 7-57016
- atom, resonant photoemission, atomic correl. effect 7-907
- Auger electron spectra, deconvolution calcs. 7-24728
- Auger spectra, extended fine structures 7-64831
- Bauschinger effect, influence of alloying elements and grain size (German) 7-17605
- β -(BEDT-TTF) I_3 /Cu point contact spectra 7-27383
- bicrystals, fatigued at high temp., microstruct. obs. in vicinity of cavitated grain boundaries 7-38019
- bicrystals, isoaxial, with (001) tilt boundaries, dynamic recrystn., effect of grain boundaries 7-17549
- binding energies and elastic constants, one-parameter model pseudopotential calc. 7-44650
- bright plating electrodeposition kinetics, adsorption on cathode surface (Russian) 7-33942
- cable, electrical conduction, comparison with light transmission 7-57594
- candidate materials for high heat load appl. in neutron environments 7-49636
- cascade overlap effect on defect struct. after repeated neutron irradiation 7-51859
- chemisorption, of H_2O , on (100) surface, quantum chem. CNDO calcs. (German) 7-859
- chlorinated surface, laser-induced desorption and etching processes 7-27092
- cluster surface, Na atom adsorpt., SCF ab initio and CI calcs. 7-52259
- clusters on graphite, Auger spectra, size effect on linewidths 7-53455
- coated Nb_3Sn tape, effect on crit. bending diameter (Russian) 7-33747
- coating, ion plating on steel, deposition conditions effect on coating struct. 7-39748
- coating on ultrahigh strength maraging steels, H embrittlement 7-28137
- coating on wire by magnetron sputtering, Auger electron spectroscopy anal. 7-65361
- compression test, high speed, microcomputer system, split Hopkinson bar technique 7-13686
- contact with MoN_x sputtered coatings, tribological props. 7-53911
- colddown mass flow requirements for He or N cooling systems 7-56281
- corrosion, microbiologically induced 7-46683
- corrosion by tartaric acid 7-22902
- corrosion in solar heating systems, water-glycol solns. 7-22900
- corrosion inhibition by Schiff bases in acid media 7-22892
- corrosion inhibition complex study using Raman microscopy 7-46772
- corrosion inhibition in humid environments by azole compounds 7-3484
- corrosion resistant coating on GdTiFe , mag. props. 7-53952
- corrosion-fatigue of single crystals in aq., oxide-forming environment, electrochem. response 7-65115
- creep crack growth, 450-650°C 7-33758
- creep of pure metals, new approach 7-53805
- creep rupture under tri-axial tension 7-53839
- crystal surface and interface, heterophase fluctuations (Russian) 7-58650
- crystals, H_2 diffusion, continuous-time correlated walk with unrestricted jumps model appl. 7-27015
- crystals with edge dislocations, 2D angular correlation of positron annihilation radiation 7-39242
- cubic polycrystals, elastic const., Young's modulus rel. to axial texture (Russian) 7-59562
- current collecting grid on Si solar cells, oxidation and spalling 7-22910
- cyclic stress-strain behavior of single- and (111) multiple-slip-oriented single crystals. 7-26845
- cyclically deformed, positron trapping 7-39260
- cylindro-inner cones, freezing point, radiant emission characts. 7-56254
- damage correlation of high energy neutron and ion irradiation, sub-cascades 7-51860
- DC transport 7-17010
- defect development from displacement cascade damage in low temp. neutron irradiation 7-51851
- deformation, steady state 7-21334
- deformed single crystal, lattice parameter changes through long-range internal stresses (German) 7-16673
- deposition, initial stages, on MgO (001) and ZnO (1010) 7-63959
- deposition on Si (111) surface, Auger electron spectrosc. obs. (Russian) 7-27833
- deuteron irradi., multiple fracture planes, bubble growth 7-58372
- diamagnetic, muon level crossing resonance, general considerations 7-53185
- diffusion bonding, strain-free mounting appl. 7-3572
- diffusion of Zn, electrochemical method 7-44897
- directional solidification, behavior of dispersed Mo and Al_2O_3 , reduced gravity (German) 7-22658
- disc bend test, parameterize anal. 7-54039
- discontinuous films, aging, elec. field and temp. effects 7-64364
- discontinuous films, large scale coalescence, post-deposition DC resistance increase 7-45069
- discontinuous thin films, aging and field effect studies 7-7413
- dislocated single cryst., sub-grain misorientation, de Haas-van Alphen meas. 7-12300
- dislocation assemblies, parameter linking change in internal energy and vol. in creation (Russian) 7-58279
- dislocation mechanism based model for stage II fatigue crack propagation rate 7-21338
- dislocation-diffusion mechanism of wear reduction in selective transfer 7-17658
- dislocation-mechanics-based constitutive relations for material dynamics calcs. 7-63706
- displacement cascade damage computer simulation using binary collision approx. code (Japanese) 7-32535
- copper continued
- dynamic elongation determ. expanding ring test, 2D hydro-plasto-dynamic code anal. 7-33755
- dynamic fracture of ductile solids, internal state variable description 7-26844
- dynamic softening during deform. at high temps. and strain rates 7-33690
- elastic modulus, third-order, effect of plastic deform. (Russian) 7-46544
- elec. resist., strain-induced changes in temp. depend. component, magnetic impurity effects 7-52567
- electrocrystallisation kinetics, surface ion conc. depend. on overvoltage in case of slow adatom surface diffusion (Russian) 7-2429
- electrocrystallisation on indifferent substrates, twinning 7-53639
- electrocrystallisation processes, excluded nucleation zones 7-32318
- electrode, adsorpt. of halide ions, electroreflectance obs. 7-13132
- electrode-electrolyte interface, surface anal., XPS, ion scatt. spectra 7-22895
- electrodeposits, decorated grain boundary dislocations, electron microscopy obs. 7-27185
- electroless deposits, ductility, effect of inclusions 7-58719
- electroless plating, microdistrib., soln agitation, temp. and pH depend. 7-7907
- electroless plating rate rel. to $\text{K}_3\text{Fe}(\text{CN})_6$ in bath 7-22594
- electron beam heating, vapourisation and melting meas. 7-26929
- electron mean-free-path calculations using a model dielectric function 7-52583
- electronic props., spectrosc. investig. 7-59216
- electroplated on ultrahigh strength maraging steel, H embrittlement 7-28136
- electrotechnical grade, acoustic emission characts. in elastoplastic deform. 7-39816
- epitaxial film struct. and surface purity on MgO single cryst. substrates 7-16896
- epitaxial growth on Ni (100) angle-resolved XPS study 7-7823
- erosion by spherical non-friable steel shot, impact angle effect 7-8136
- evaporated films, elec. resist., influence of surface roughness (German) 7-64368
- extrusion, dislocation density determ. (Russian) 7-58285
- fatigue crack propagation rate model based on a dislocation mechanism 7-8093
- fatigue crack size distrib. in single crystals. 7-38101
- fatigue near surface indentations and pits, deform. 7-46628
- FCC structure, multiple grain-boundary contacts (Russian) 7-12079
- fibre, porous, physicochem. props. and model prediction 7-3353
- filament growth on Cu_2Se , superionic transport mechanism 7-45104
- filled polypropylene films, struct. and elec. cond. 7-64301
- film, MT-Z potential, calc. electronic states 7-17064
- film deposition, sputtering method using Ar gas flow (Japanese) 7-22479
- films, characterisation by SIMS, Auger spectroscopy and TEM 7-12550
- films, interaction with Cl_2 , bulk diffusion processes 7-21783
- films, laser-assisted oxidation 7-65208
- films, photochemically deposited, C contamination, surface processes 7-53617
- films, rapid crystn. kinetics under laser irradi., picosec. transient reflectance meas. 7-11915
- films, sputter deposition, effect of ion bombardment of growing film 7-64009
- films, sputter deposition using hollow cathode discharge ion source 7-41536
- films, vapour-quenched, elec. resistivity (Japanese) 7-33107
- films, with surface adsorbed ethylene, adsorbate-substrate bonding 7-52292
- films influence on optical scatter and microroughness of coated surfaces 7-13242
- films on MgO , epitaxial and electronic structures, LEED, AES, and EELS studies 7-52352
- fine powder, synthesis from metallic aerogels 7-3216
- Foametal, high thermal conductivity material, thermal, mechanical and vacuum props. 7-25191
- foil, excimer laser assisted gas phase etching 7-54015
- foils, electron absorpt. and scatt. energy spectra, Monte Carlo calcs. 7-22399
- fourth-order thermal expansion coeff. fn. 7-44868
- Frenkel pair production cross sections, calc. fission-fusion neutron spectrum sensitivity 7-51849
- gamma-irradiated, anomalous effect of small doses 7-12151
- gamma-ray attenuation coeff. obs. incorporating detector resolution 7-63656
- $\text{Ge}_{1-x}\text{Si}_x\text{Cu}$, supersaturated solid solution, decomposition 7-32654
- geological Cu-Ni sulphide deposits, formation conditions 7-23599
- grain boundary cavity-growth kinetics determ. from cavity-size distrib. during creep and continuous nucleation 7-26767
- grain growth, local texture development, STEM selected area channelling 7-16575
- He production in HFIR neutron irradiated pure elements 7-51852
- heat spreader for Si solar cells in high concentration photovoltaic module 7-17874
- hot rolled, recrystallized microstruct., deform. processes 7-13500
- impurity effects on radiation embrittlement of pearlitic steel 7-49535
- indirect-exchange interaction, realistic calc. 7-38854
- initial stages of epitaxy on $\text{Si}(111)$, UHV electron microscopy study 7-27210
- InP:Cu, band-edge photolum. quenching, impurity recomb. centre effects study 7-39177
- interfacial surface energy atomistic estimation and adhesion meas. (Japanese) 7-58657
- ion irradi., sputtering and lattice damage, cryst. orientation effect 7-64843
- ion irradiated, mech. prop. meas. 7-51873
- ion mixing and thermochemical props. of markers 7-26805
- irradiated in FFTF to 16 dpa at 450°C, microstruct. eval. 7-51837
- Johnson Camp, Arizona, Cu-Zn ore bodies determ. from soil and soil gas comp. anal. 7-40591
- joints of dissimilar metals, adhesively bonded strength evaluation 7-46791
- Lamb wave velocity meas. in thin plates by acoustic microscopy 7-2332
- lasing mechanism and energy characts., relax. processes of metastable states 7-62673
- liquid, thermoelectric power calc. 7-12704
- liquid targets, sputtering, mol. dynamics studies 7-3130
- low dose neutron irradiation, spectral effects on yield stress 7-51850

copper continued

low neutron dose effects on tensile props., yield stress 7-51863
materials erosion and redeposition studies at PISCES facility, net erosion under redeposition 7-49637
mechanical instability of single crystals undergoing tension at high temps. 7-13505
metal leaves, 7-12523
metal-metal and metal-dielectric systems, adhesion calc. 7-7023
metallic electron charge density to electron momentum density transformations 7-27249
microlithographically prepared surface, adsorbed 1,2,4-triazole and imidazole, SERS obs. 7-27712
mirror, absorbance meas. at glancing incidence, photoacoustic calorimetry 7-20380
mirrors, Ag⁺ implanted, laser oxidation and optical props. 7-5971
molecule, glow discharge sputtering, laser-excited fluoresc. 7-10647
molecule, STF HF wave function 7-25365
monolayer on Au (111), fluoresc. detected surface EXAFS 7-46235
muon arrhenius jump rates, neutrino emission 7-27643
muon hopping rates, low longitudinal mag. field muon spin relax. studies 7-53198
muon level crossing resonance, muon polarisation function for longitudinal fields 7-53187
muon polarisation function and spin dynamics 7-53188
near-threshold fatigue crack propag. and high cycle fatigue 7-13545
nearest-neighbour host site elec. field gradient, monovacancy effects, muffin tin pot. calcs. 7-2549
neutron irradi. effects, elec. cond., fusion reactor appl. 7-51835
neutron irradiated, 13 dpa, mech. prop. and elec. cond. changes 7-51839
neutron irradiated, thermal stability of cascade defects, annealing expt. 7-51856
neutron-irradiated single crystals, plastic deform. and stress inhomogeneity 7-22746
Newark Bay, New Jersey, USA, heavy metals in water column of estuary 7-55084
nonmagnetic samples, ferromag. behaviour 7-53040
nuclear quadrupole interactions in the presence of muons 7-53192
ordered overlayer on Si (111), surface states, inverse photoemission studies 7-2660
overlayer, on SiC, Si₃N₄, Al₂O₃, SiO₂, mixing phenomena 7-58330
overlayer growth on Ni (100), X-ray induced secondary electron emission meas. 7-27865
overlayer on Si (111), inverse photoemission spectroscopy 7-59280
oxidation, brittle oxide, AE technique, alternative to thermogravimetry 7-65274
oxidation kinetics, laser control 7-28174
particles, ZnO-supported, vibr. spectra of adsorbed species, operation of metal surface selection rule 7-53350
phonon spectra, dynamical pseudopot. shell model calcs. 7-51965
phon decay site spectroscopy, interstitial sites 7-53191
plasma, at. quantities, diagnostic determ., capillary discharge technique 7-11787
plasma, laser-vaporised, X-ray laser expt. 7-63323
plasma, Ne-like, gain expt. 7-20876
plasma, X-ray spectroscopic diagnostics 7-6465
plasma nitriding, sputtering and redeposition of cathode material 7-39752
plastic deform. and supercond. props., 0.5 to 4.2K (Russian) 7-8055
plates, monomer films form. and polymerisation 7-65347
plating, grain density and cyclic stresses (Japanese) 7-7904
point defects in thermal equilibrium, laser interferometry-neutron diffraction studies 7-58274
polished surface, ellipsometric study of reflection 7-13121
poly-vinylacetate-Cu, thin polymer films, Fourier transform IR ellipsometry 7-53334
polycrystalline, annealed, large deform., combined tension-torsion, incremental plasticity theory 7-46554
polycrystalline, cyclic stress-strain curve, grain size effect 7-53803
polycrystalline, flow stress, work hardening coeff., temp. depend., 15 to 300K 7-59575
polycrystalline, high cycle fatigue behaviour, effect of grain size 7-46626
polycrystalline, multiaxial low cycle fatigue, crack initiation, slip bands, damage mechanics 7-53840
polycrystalline, US and neutron irradi., struct. and mech. props. (Russian) 7-3402
polycrystalline target, sputtering by 40 keV Ar⁺ ions, computer simulation 7-64848
porous sintered, rolling technology optimisation 7-53673
positive muon diffusion and hopping rate 7-52111
positron lifetime temp. depend., two-state trapping model, vacancy form. enthalpy calcs. 7-3107
positron trapping by vacancies, high resolution lifetime studies 7-46211
positron-annihilation apparatus for layerwise analysis of defects in solids 7-39219
positronium work function, temp. depend. 7-58859
powder, force characts. of powder compaction process 7-7912
powder, porosity influence on mech. and tribotech. characts. in high-speed friction 7-8119
powders, sintering, densification, grain growth (Japanese) 7-53662
preparation using γ -Cu₂(OH)Cl precursor, X-ray diffraction 7-27970
proximity induced superconductor, mag. field effects, thickness and temp. depend. 7-52903
pulsed ion implantation in Mo 7-51867
quartz:Cu⁺, ion implanted, coloration and transparency (Japanese) 7-7656
quartz:Cu, electrodiffused, radiation-induced conductivity 7-6691
rapidly solidified powder metallurgy, irradi. to 13.5 dpa with neutrons, microstruct. evolution and swelling 7-51840
recrystallisation, deform. threshold, annealing temp. depend. (Russian) 7-59546
recrystallisation texture, deformation temp. effects (Russian) 7-8007
reduction, electrochem., autocatalytic, by formaldehyde 7-54138
resistivity and superconducting transition temp. 7-17013
resonant-like reabsorption in AC arc plasma 7-13842
rod, skin depth and complex mag. susceptibility, expt. 7-51
SCC propagation after exposure to NaNO₂ soln. 7-65174
screen, transmission coeff. depend. on optical radiation incidence angle 7-57528
secondary ion emission mass spectra, cluster ion monomolecular decays 7-13300

copper continued

Severn Estuary, UK, sediment trace metal record for last 2000 years 7-18211
sheets, rolled, US SH wave vel., ang. depend. 7-38126
shock Hugoniot, ab initio interatomic pot. calcs. 7-21395
simple surface states, effective-mass theory 7-38661
single crystal, high intensity positron beam and ang. correl. expts. 7-42274
single crystal, target, atomic and mol. ion-surface semichannelling, Lindhard atomic string model calcs. 7-63697
single crystal, glancing angle ion sputtering, angular depend. 7-13296
single crystals, corrosion fatigue in aq. oxide forming environment 7-33823
single crystals, fatigue crack initiation mechanism, persistent slip band model 7-53869
single crystals with different orientations, strain localisation during high temp. deform. 7-13506
single crystals, low temp. recrystallisation characts. (Russian) 7-17546
sintered powder, ultrasonic attenuation meas., phonon-fracton crossover 7-2105
slip, fractal nature 7-16561
specific heat meas. below 1K 7-16789
spheres, 2D arrays, rearrangement during sintering 7-46361
sputtering yield, weight loss method studies 7-59340
sputtering yield meas. with 3D stylus surface mapping system 7-27850
stabiliser, supercond. mag. material, fusion reactor conditions simulation 7-52922
static compression, basis for ruby pressure scale calibration 7-18802
steel fibre reinforced Cu composites, extruded, struct. and fractography 7-13595
steel/Cu/Si₃N₄ (Japanese) 7-54037
structural elements, corrosion in contact with building materials (German) 7-3522
structural materials, welling after neutron and ion irradi., comparison 7-58357
structure evolution during strong plastic deformation (Russian) 7-3358
substrate, Ag monolayer electronic struct. and binding energy, photoemission studies 7-39359
substrate, depth profile shape of Ag film, influence of crystallographic orientation 7-27205
substrate, gettering effect on hydrogenation of Ni 7-13804
substrate, periodic microrelief, laser irradiation, of nitrocellulose film 7-63927
surface, (001), K adatoms two-dimensional condensation, LEED obs. 7-12478
surface, (001) adsorbed K, valence-electronic struct., work function changes and EELS 7-45002
surface, (100), adsorption of S, (2x2) struct., LEED anal. 7-32827
surface, (100), chemisorption of linear hydrocarbons, σ -shape and π resonances, XANES 7-53448
surface, (100), cross-section anal. of surface and bulk phonons by electron scatt. 7-2336
surface, (100), effective mass of image-potential states 7-64304
surface, (100), electronic props. calc. using layer method 7-45105
surface, (100), field induced vibr. freq. shifts of chemisorbed CO and CN 7-45991
surface, (100), for Fe epitaxial growth 7-52353
surface, (100), H₂(D₂) molecular beam impact, resonant sticking coeff. 7-13308
surface, (100), Pb epitaxial growth, thermal He atom scattering 7-52351
surface, (100), physisorbed H₂ quadrupolar mol. rot. damping due to electron-hole pair excitation 7-23064
surface, (100), with chemisorbed ethylene, C K-edge structure of chemisorbed molecules 7-27824
surface, (100), XANES fluoresc. yield meas. of submonolayer linear hydrocarbon mols. 7-64751
surface, (110), adsorbed O induced reconstruction, XANES 7-53447
surface, (110), O₂ adsorption 7-27132
surface, (111), adsorption of TCNQ, vibr. spectra, EELS, work function meas. 7-52228
surface, (111), Co adsorbed layer, surface EXAFS investig. (French) 7-6957
surface, (111), epitaxial FCC γ -Fe (111)p(1x1) films, surface ferromagnetic order 7-45773
surface, (111), K doped, anomalous surface-state penetration near band edge, photoemission studies 7-39361
surface, Ba covered, adsorbed O, XPS and UPS studies 7-2373
surface, binding energy of image-potential states 7-64303
surface, characterisation with intense positron beams 7-13256
surface, chemisorbed state of acetylene, ethylene and ethane 7-52261
surface, Cu atom sticking and penetration, computer simulation studies 7-59326
surface, desorpt. of Xe, surface temp. determ. using pyroelectric calorimeter 7-52233
surface, glazing-angle scattering and neutralization of positron beam 7-46178
surface, graphite thin absorber layer influence on thermal-wave appls. 7-48723
surface, H₂, dissoci. chemisorpt. dynamics, morphology and surface temp. effects 7-13808
surface, He(H₂)(Ne) scatt., thermal attenuation, multiphonon contrib. 7-39338
surface, interaction with Cl₂ 7-21642
surface, ion bombardment-induced microtopography 7-58588
surface, ion irradi., sputtering and lattice damage, cascade simulation 7-59327
surface, large angle scattering of H, D and He atoms 7-64854
surface, laser stimulated desorption during Cl₂ reactions 7-53453
surface, low energy O⁺ ion bombardment, atom and mol. ejection 7-59325
surface, photon emission from sputtered atoms, temp. effects 7-13312
surface, physisorbed Xe, Ar, O₂ and CO, laser-induced thermal desorption 7-17817
surface, pyridine adsorbed layer; resonance Raman contrib. to SERS in aq. media 7-3055
surface, Raman intensity of adsorbate vibr., cluster-model calc. 7-27089
surface, sputtered neutral atoms, energy distrib. 7-59336
surface, sputtering and surface topography evolution 7-58586
surface (001), N₂⁺ and N⁺ scatt., 2D pattern obs. 7-46269
surface (001), single cryst., inverse photoemission polarisation effects study 7-27812

copper continued

- surface (001), variable temperature angle-resolved photoemission, non-direct transitions 7-64874
 surface (100), adsorbed S, surface struct. determ. using angle-resolved photoemission extended fine struct. 7-7822
 surface (100), c(2x2)N overlayer, surface phonon dispersion, LEED, AES and EELS studies 7-12459
 surface (100), dense Pb monolayer, LEED anal. 7-6989
 surface (100), electron states calc., tight-binding muffin-tin orbital Green's function method 7-52721
 surface (100), Pb overlayer growth, phase transitions and struct., thermal energy He atom scatt. study 7-63943
 surface (100), Rayleigh phonon dispersion, stress-induced freq. shift, EELS studies 7-27090
 surface (100), unoccupied surface states, surface barrier, spectroscopy 7-2651
 surface (110), adsorbed Pb, struct. and melting, X-ray scatt. studies 7-7016
 surface (110), H adsorpt., adsorbate movement-induced subsurface reconstruction, LEED and atom diff. meas. 7-27114
 surface (110), K-doped, CO adsorption, EELS study 7-7006
 surface (110), O (2x1) overlayer, surface reconstruction, mean free path and Debye-Waller factor, SEXAFS study 7-46238
 surface (110), surface characterisation by In probe atoms, electric field gradient 7-2553
 surface (110), surface energy anisotropy, surface reconstruction 7-2346
 surface (110), surface relax., electron states 7-21965
 surface (110) with chemisorbed O, synchrotron X-ray scatt. study 7-7003
 surface (111), adsorbed benzene and azabenzene, electron affinity levels studied by inverse photoemission 7-44991
 surface (111), angle-resolved photoemission spectra, low-energy modelling 7-46275
 surface (111), Cl chemisorb., site info. from EXAFS and photoelectron diffraction 7-32788
 surface (111), Co monolayer, Debye-Waller factor anisotropy, SEXAFS study 7-63936
 surface (111), neutral cluster anisotropic emission 7-59352
 surface (111), Ni covered, CO adsorption studies 7-21658
 surface (111), surface electronic struct., perturbations induced by adsorption of K 7-52720
 surface (111), Tamm surface state 7-58849
 surface (111) with Pb overlayers, spot profile anal. of LEED 7-51586
 surface (115), low temp. behaviour of surface roughness 7-6941
 surface (115), thermal behaviour, molecular dynamics study 7-52222
 surface Co monolayer, Debye-Waller factor in surface EXAFS 7-39316
 surface electronic struct., relativistic effects, high resolution angle-resolved photoemission study 7-52723
 surface friction layers, study by AES method (Russian) 7-59674
 surface modified by Al, electronic struct. and oxidation of surface 7-22443
 surface oxidation, ion-induced secondary emission target current meas. 7-59684
 surface roughening transition, He beam diff. study 7-52202
 surface self-diffusion of H isotopes, substrate motion effects 7-38237
 surface state positron annihilation 2D ang. correl., jellium model calcs. 7-3106
 surface states, phase shifts, image planes 7-21962
 surface struct. anal., use of atomic beam diff. 7-6944
 surface structure minimal disturbance under ion bombardment 7-12419
 surface with chemisorbed benzotriazole, UPS study 7-21656
 surface with Ni/Au bilayer film, Ni out-diffusion 7-12511
 surface with vapour deposited Ni film, SIMS meas. of interdiffusion coeffs., SIMS analysing depth 7-27853
 surfaces, (10,10) and (510), adsorption of Pb, faceting, LEED, AES studies 7-32828
 surfaces, (110) and (111), XANES studies of adsorbed ring mols., orientation determ. 7-64769
 surfaces, (110) and polycrystalline, adsorbed O₂, UPS, XPS, AES, EELS, LEED studies 7-32820
 surfaces, formate adsorpt. site symm. and bond lengths, SEXAFS data, multishell simulation anal. 7-63947
 surfaces, low energy positron diff. pattern calcs., scatt. processes anal. 7-39331
 surfaces, with adsorbed O, Z 7-59784
 surfaces (100) and (110), formate adsorption, bonding, EXAFS studies 7-38341
 surfaces (111) and (110), atomic adsorption of O, inverse photoemission study 7-7783
 target, plasma surface coupling of laser radiation, NaCl effects 7-63318
 tensile test, numerical investig. using finite difference 1D elastoviscoplastic code 7-46747
 tetramethylammonium manganese tribromide:Cu²⁺, emission dynamics, exciton trapping 7-39164
 thermal equilibrium vacancies, positron lifetime studies 7-44535
 thin film, surface electromag. waves damping, deposition technique study 7-59274
 thin film growth, in situ study by internal stress meas. 7-16890
 thin films, crystallographic props., electron diff. patterns 7-21751
 thin films, discontinuous, post-deposition resist., ageing studies 7-58909
 thin films, elec. cond. quantum size effect, Kubo formalism study 7-22034
 thin polycryst. wires, elec. resist. meas., surface induced deviations from Matthiessen's rule 7-27319
 threshold stress meas. in shock-deformed Cu 7-26868
 tubes, creep-fracture tests 7-46739
 tubes, pitting pot. in hot water, oxidising agents effect 7-28207
 two-dimensional systems, lattice and continuum percolation transport exponents 7-45275
 ultra-pure samples, diffusion of positive muons, detection by zero-field muon spin resonance 7-45862
 ultrapure, electrorefining, vacuum switch electrode appl. 7-27966
 vacancy diffusion along (100) twist boundaries (Russian) 7-2265
 vacancy formation enthalpy, positron annihilation studies 7-7787
 vacuum deposition, Wheatstone bridge with two thin film arms, dynamic balancing 7-22491
 vapour laser, four-wave mixing obs. 7-20359
 vapour laser, molecular gas impurities effects 7-36948
 vapour laser, pumping of dye laser, U isotope separation appl. 7-50553
 vapour laser, self-heated, thermal conditions and stimulated emission characts. 7-25802

copper continued

- vapour laser, structure and characts. (Chinese) 7-10994
 vapour laser for U isotope separation 7-50546
 vapour laser using metallic walls for discharge confinement 7-43146
 vapour laser with self-pumped wavefront reversing mirror 7-1185
 vapour laser with unstable resonator, background radiation influence on dye lasing 7-25856
 vapour laser with wavefront-reversing mirror induced in active medium 7-1199
 vapour lasers, resonance radiation trapping effects 7-62669
 vapour press. and heat of sublimation 7-58454
 wettability against ZrO₂ ceramics 7-52191
 whiskers, derivation from Matthiessen's rule, effect of surface condition 7-45276
 wire, size effect of DC resistance (Chinese) 7-12694
 wire connections, contact resist., effect of fretting 7-21980
 wires, thin, sputter-induced cones 7-51881
 wires, very thin, fatigue 7-39671
 wires and strips fabrication, glow-discharge electron beams appl. (Czech) 7-56373
 work fn., temp. depend., anal. 7-52737
 X-ray Compton-Raman scatt. from atomic inner shell electrons 7-13257
 X-ray emission, proton induced Kossel diffraction 7-53451
 X-ray emission K $\alpha_{1,2}$ spectra 7-64825
 X-ray K α emission spectrum 7-22383
 X-ray photoelectron diff., temp. depend., surface and bulk effects 7-39356
 XANES high-energy approximation 7-17364
 XPS, background removal 7-39355
 Ag/Cu interface, metastable solid soln. form. by ion mixing 7-12163
 Al/Cu friction welds, microstruct. and mech. props. (German) 7-46792
 Al-Cu, thin interface regions, EXAFS studies 7-59285
 Al-Cu interface, grazing incidence X-ray study of interfacial reactions 7-21543
 Al-Ti-Cu multilayer films, thickness and composition anal. using X-ray fluorescence 7-46898
 Al₂O₃-Cu, effective thermal cond. determ. 7-27037
 Au-Ni-Cu, diffusion of Au and Cu through Ni layer, depend. on ambient 7-38266
 BaFCl:Cu, thermolum., X-irradiated at room temp. 7-53419
 BaTiO₃:Ce,Cr,Cu, double doping study 7-2037
 CdS:Cu,Cl photoconducting films, photolum. spectra studies (Russian) 7-46140
 CdSe:Cu, deep levels investigated by photoconductivity and space-charge region capacitance techniques 7-7148
 CdSe:Cu, transient photocond. anal. 7-64288
 CdSe,Te_{1-x}:Cu films, deep local levels, photosensitivity, spectral study 7-2371
 CdTe : Cu⁺ ion implantation damage, rapid thermal annealing, photolum. anal. 7-39162
 Cu + He⁺, L shell X-ray prod. cross sections meas., first Born approx. and ECPSSR theory anal. 7-36526
 Cu complex, copper(3-amino-5-methyl isoxazole)₂dibromine, mol. motion detect., PMR 7-31066
 Cu I vapour laser, room temperature operation 7-10919
 Cu II laser with spherical and circularly slotted hollow cathodes, output power and operation period 7-50587
 Cu II laser with tulip shaped hollow cathode 7-43145
 Cu II lines, laser generation in water cooled helical hollow cathode discharge 7-57299
 Cu layer on steel substrate, thickness meas. by transverse surface waves (French) 7-4815
 Cu thin films, CW Ar⁺ laser-induced oxidation 7-39694
 Cu XIII and XVII, excitation rate coeff. meas. in TEXT 7-44223
 Cu²⁺ containing plastocyanin, paramag., spectroscopic and computer simulation study 7-8494
 Cu²⁺, detection in Nafion membranes, H₂O solvent and Zn²⁺ ratio effects, ESR spectra anal. 7-33268
 Cu²⁺ impurity ion in octahedral environment, EPR spectrum, MM field freq. and temp. depend. 7-27596
 Cu³⁺, effective charge, around 4 MeV per nucleon 7-50297
 Cu:Ar(Ne)(C), single crystal, ion implantation, damage profile anal. using Auger electron spectroscopy 7-51802
 Cu:Mn(Cr) matrix, electronic struct. calcs. 7-16976
 Cu:O(He) vacancy cluster stability calcs., void form., O and the impurity effects 7-51763
 Cu/Ag composite discontinuous thin films, aging and field effect studies 7-7413
 Cu/Au thin film systems, interdiffusive kinetics, EXAFS studies 7-16819
 Cu/Cr multilayer structs., scanning Auger microprobe depth profiling, sputtering effects 7-58659
 Cu/Fe/Cu (001), electronic and mag. props. 7-64499
 Cu/Hg_{1-x}Cd_xTe interfaces, morphology, Hg bonding effects 7-7021
 Cu/In thin film couples, interface CuIn₂ cpd. form. and props., gamma ray spectra 7-21688
 Cu/Mo multilayered film growth, RHEED intensity oscils. (Japanese) 7-63987
 Cu/Ni/Cr, multilayer deposits, corrosion protective props. 7-8187
 Cu/NiPd multilayered film, atomic level structural characterisation 7-16900
 Cu/Pb-Sn solder interfacial reactions, Cu₃Sn intermetallic formation 7-44924
 Cu/Pd metallic superlattices, UPS, LEED, AES and ISS studies 7-3153
 Cu/PdNi, single cryst. multilayers, sputter deposition 7-53582
 Cu-Ag sandwich, sputter etching, microprojections growth 7-22885
 Cu-air plasma, composition and conductivity (French) 7-11595
 Cu-Al bilayers, EXAFS and X-ray reflectivity meas. 7-27821
 Cu-Al interfacial interaction, struct., synchrotron radiation photoemission study 7-22444
 Cu-Al₂O₃, interaction, X-ray photoelectron spectroscopy, Auger electron spectroscopy 7-58669
 Cu-CdTe interface form., effect of different cation-anion bond strengths 7-27149
 Cu-chalcogenide contacts, interdiffusion, struct., comp., electron irradi. effects 7-21686
 Cu-Co compositionally modulated multilayered films, magneto-optical Kerr rot., wavelength depend. 7-3100
 Cu-composite material contact, sliding characts. and contact resistance (Japanese) 7-8120
 Cu-Cr multilayers, laser alloying 7-45025

- copper continued**
- Cu-Cu contact, sliding characts. and contact resistance (*Japanese*) 7-8120
- Cu-Cu₂O Schottky barrier solar cells, interfacial layer effects investig. using n -V_{oc} diagram 7-54304
- Cu-Fe compositionally modulated multilayered films, magneto-optical Kerr rot., wavelength depend. 7-3100
- Cu-GaAs (110), electron struct., synchrotron radiation photoelectron spectroscopy 7-27420
- Cu-graphite contacts prep. using atomised Cu powder 7-27976
- Cu-He system, closed swelling layer, internal stress distrib. (*Russian*) 7-59571
- Cu-Hf multilayers, interface EXAFS study 7-64811
- Cu-Hg_{0.75}Cd_{0.25}Te interface form., effect of different cation-anion bond strengths 7-27149
- Cu-K, amorphous multilayer X-ray reflectors, layer imperfections effects 7-25936
- Cu-Mo multilayer film growth, RHEED intensity obs. 7-7051
- Cu-Nb microcomposite superconductors, in situ, nature of connection (*Russian*) 7-45585
- Cu-NbTi superconducting magnet for NMR field cycling 7-41412
- Cu-Ni, compositionally modulated thin films, double positioning twinning 7-38351
- Cu-Ni interface, emission spectrochemical anal. using glow discharge, appl. to in-depth anal. (*Japanese*) 7-63886
- Cu-Ni interface, mag. size effects 7-59081
- Cu-Ni multilayer thin film system, low temp. mutual diffusion (*Russian*) 7-58551
- Cu-Ni superlattices, mech. props. and diffusion 7-52377
- Cu-Ni-CoW-Cr system, Cr plating, roughness and wear (*Russian*) 7-33801
- Cu-polyethylene, adhesion of metal films, effects of Ar⁺ bombardment 7-28267
- Cu-ruby glasses, optical props., transmission and attenuation spectra 7-13177
- Cu-Si interface, surface struct., angle resolved Auger electron emission determ. 7-21672
- Cu-Si₃N₄, effect of Si₃N₄ on deposition of Cu chemical coatings 7-3207
- Cu-SiO₂-Cu sandwich struct., thermal voltage memory effect, time depend. 7-45527
- Cu-Sn thin film diffusion couple, reaction kinetics at room temp. 7-21536
- Cu-W, layered, ion beam mixing, energy and dose depend., RBS 7-38075
- Cu+Cu, projectile and target K X-ray prod., target thickness fn. anal. 7-30978
- Cu+He⁺, target K-shell ionis., cross-sections and probabilities 7-50343
- Cu₁₃, fragmental cluster model and electronic struct. (*Ukrainian*) 7-12597
- Cu₃, assignment of the 5397 Å system, mol. fluoresc. data anal. 7-50217
- Cu₃, cluster formation ion irradiation of Ta-Cu (*Chinese*) 7-53468
- Cu₃, ground state surface, ab initio calcs. 7-42467
- Cu_n (n=1-10), cluster, photoelectron spectra 7-62561
- (Cu)_n clusters, mass distrib., mass spectra 7-50431
- Cu₂(Cu₃), ground state pot. energy surfaces 7-25441
- ⁶⁴Cu, radioisotope enrichment, nuclear recoil appl. 7-62539
- Fe/Cu (001), electronic and mag. props. 7-64499
- Fe/Cu microlaminate condensates, creep and struct. investig. (*Russian*) 7-33749
- Fe/Cu multilayered samples, ion beam mixing-induced metastable phases 7-53777
- Fe-Cu, epitaxially grown Fe films, electronic and crystallographic struct. 7-27214
- Fe-Cu multilayer films, layered mag. domains, Schlieren-Lorentz TEM studies 7-38916
- GaAs-Cu, neutral state of deep acceptors, photoluminescence spectra, Jahn-Teller effect 7-64149
- GaAs-Cu crystals, impurity and defect props., heat treatment, photolum. studies 7-39163
- GaP-Cu, 1.65 eV luminescence, optically detected mag. resonance studies 7-64547
- Ge:Sb, Cu, impurity photoconductivity, field and spectrum dependences, exclusion effect 7-38635
- GeO₂-Cu thin films, optical absorpt. edge 7-53431
- H trapping, positron annihilation spectra 7-33482
- H₂O-Cu(Ni) complexes, binding, SCF CI calcs. 7-56958
- Hg_{0.9}Cd_{0.1}Te-Cu, activation energy of Cu shallow acceptors 7-64153
- In/GaAs-Cu/In struct., I-V characts., carrier recomb. and generation, impurity thermionic field ionisation effects (*Russian*) 7-22030
- In₂O₃-Sn-ZnS-Cu,Cl,Mn-Al, surface electrical conductivity in ZnS-Cu,Cl,Mn thin films 7-38672
- InP-Cu(Au)(Ag), interphase contact interaction 7-33087
- KBr-Cu, visible absorpt. spectra 7-3073
- KCl-Cu visible absorpt. spectra 7-3073
- KCl(Br):Cu²⁺, diffusion, nuclear spin-lattice relax. rate meas. (*German*) 7-6885
- K₂ZnF₄:Cu²⁺ crystal, possible ligand spin-orbit coupling in CuF₄ clusters 7-38520
- Li₂B₄O₇:Cu, TLD, thermal neutron response 7-5491
- LiF:U-Cu, X-irradiated crystals, absorpt. bands of U⁴⁺ and U³⁺ ions 7-13183
- LiNbO₃:Cu, γ -irradiated, ESR spectra of impurity centres 7-17218
- LiNbO₃:Er, laser-induced grating characteristics 7-62746
- Mo fibre reinforced Cu composites, extruded, struct. and fractography 7-13595
- NH(D)₂Cl:Cu²⁺ crystals, impurity optical absorpt. spectrum temp. depend. study 7-53374
- NaCl:Cu, nuclear quadrupole spin-phonon interaction 7-22155
- NaCl:Cu, visible absorpt. spectra 7-3073
- NaCl:Cu²⁺, lattice relax. around cuprous ion, EXAFS studies 7-64788
- NaF:Cu, nuclear quadrupole spin-phonon interaction 7-22155
- Nb/Cu artificial superconductive metallic superlattices, electron density, pair tunnelling studies 7-58959
- Nb/Cu Fibonacci 1D quasiperiodic superlattice struct., X-ray diffr. meas. 7-52307
- Nb-Cu, superlattices, elastic props., effect of strain 7-52376
- NbTi/Cu stabilised wires, wiggler design for ESRF 7-42253
- NbTi-Cu Al stabilised superconducting detector magnet technology for high energy accelerators, review 7-49779
- Ni-Cu diffusion contact, mass transfer at grain boundaries in fields of diffusion-concentration stresses 7-2272
- copper continued**
- O₂ chemisorpt., influence of Ar⁺ ion bombardment (*Russian*) 7-52253
- O₂ chemisorption kinetics as function of ion bombardment and temp. (*Russian*) 7-58622
- Pb/Nb₂O₅/Nb/Nb/Cu junction, 2D superconductor, pair tunnelling study 7-12916
- Rb₂Mg(SO₄)₂·6H₂O:Cu²⁺, electronic and EPR spectra 7-13019
- Si:Cu, amorphous, explosive crystn., RBS and time-resolved reflectivity studies 7-21265
- Si:Cu, Czochralski grown, interdependence of contamination and defect formation 7-32467
- Si:Cu, deep level position in forbidden gap, charactn. using ionisation Gibbs free energy (*Chinese*) 7-58760
- Si:Cu, ion implantation-amorphised, direct imaging of pulsed laser-induced buried molten layers 7-12130
- Si:Cu thin single crystals, decorated dislocations, X-ray Laue diffr. and scatt. studies (*Russian*) 7-58282
- Si-Cu, interface, Auger electron emission (*Russian*) 7-17100
- Si-Cu interface, atomic bonding 7-58663
- Si-Cu-Au layered struct. reflectivity and EXAFS study 7-59292
- Si-SiO₂-Ag(Cu)(Au)(Pd)(Ti) MOS structures, diffusion coeff. meas. in elec. fields, solid solubilities 7-2279
- Si-SiO₂-Cu, light induced deposition of Cu 7-46354
- Ti-Cu thin films, reaction kinetics, stress, and microstruct. 7-21764
- W-Cu duplex struct., brazed test pieces, durability against thermal fatigue (*Japanese*) 7-56818
- W-Cu bond, mechanical properties, fusion reactor divertor plate appl. 7-26848
- XVIII, Mg-like spectrum 7-25443
- Zn complexes, zinc(II)-bis-histidine:Cu, Jahn-Teller effect induced phase transition, ESR detect. 7-53122
- Zn grain boundary migration, diffusion-induced, effect of thermomech. treatment 7-26764
- ZnCdS:Ag/Cd(S,Se):Cu mixed photoconductor system for electrophotography 7-2636
- ZnO:Cu, impurity electron states, optical spectroscopy 7-46127
- ZnO:Cu(Bi), phosphor electroluminescence mechanism, spectral energy distrib. 7-7760
- ZnO-Cu-SiO₂-Si composite membrane, interdigital transducer generated US Lamb waves 7-11241
- ZnS:Cu, electrophosphors, aging phenomena 7-27791
- ZnS:Cu, Mn (H), electroluminesc., simultaneous action of AC and DC fields 7-64699
- ZnS:Cu, pure and doped, defects in solids, mol. cluster calc. with modification 7-21857
- ZnS:Cu, solid solution, electroluminescent phosphor, compositional inhomogeneities 7-6800
- ZnS:Cu,Mn films, vacuum deposition and DC electroluminescence 7-7868
- ZnS:Cu,Yb phosphor, AC electrolum. study 7-13233
- ZnS:Cu²⁺, multimode Jahn-Teller effect in the luminescence spectrum 7-12675
- ZnS:Fe,Cu, three-centre Auger recombination, EPR study 7-45806
- ZnSe:Cu, cationic substitutional impurities and metal vacancy, microscopic models 7-27296
- ZnSe:Cu,Al,Fe crystals, melt-grown, absorpt. coeff., impurity effects 7-3070
- ZnTe:Cu, impurity related neutral complex with bound exciton, photoluminescence, absorpt., Zeeman meas. 7-45165
- ZnTiF₆:Cu²⁺·6H₂O, Jahn-Teller effect and phase transitions, powder EPR study 7-13023
- copper alloys**
- see also brass; copper compounds*
- Al-Zn-Mg-Cu, impact toughness improvement by intermediate thermomech. treatment 7-53907
- Alnico 5, Fe-Co-Ni-Al-Cu, microstruct. and mag. props., effects of heat treatment (*Korean*) 7-8138
- bronze, powder particle shape effect on stability props. 7-7927
- bronze BrAZh, elec. discharge sintering of powder from swarf, electrophys. and mech. props., microstruct. 7-27974
- bronze powder, regularity of struct. of porous materials 7-53676
- bronze powder production from melts by centrifugal atomisation 7-7924
- bronze-steel pair, friction surface, local X-ray spectra study 7-3449
- bronze/Pb composite matrix for small closed cycle refrigerators 7-61340
- candidate materials for high heat load appl. in neutron environments 7-49636
- commercial alloys, low neutron dose effects on tensile props., yield stress 7-51863
- dilute, with 3d impurities, X-ray absorpt. edges (*German*) 7-46241
- dilute alloys with 3d elements, electronic struct., K-edge XAS study 7-64066
- dispersion hardened, melting and solidification in microgravity environment 7-22659
- divertor materials, heat load expts. with electron beam facility 7-49638
- high-strength, rad.-enhanced recrystn. 7-51871
- irradiated in FFTF to 16 dpa at 450°C, microstruct. eval. 7-51837
- manganin foil stress gauges, piezoresist. response meas. 7-29998
- monel, plasma simulator, first wall damage, H recycling models 7-801
- Monel 400, embrittlement by Hg, effect of prestress 7-3431
- Monel K-500, precip. of intermetallic γ phase and carbide phases 7-33678
- neutron damage microstructs. 7-58347
- neutron irradi. effects, elec. cond., fusion reactor appl. 7-51835
- neutron irradiated, 13 dpa, mech. prop. and elec. cond. changes 7-51839
- neutron irradiated, cond. changes, porosity swelling and transmutation contrib. 7-51838
- powder materials with MoS₂/(Se₂), self-lubricating, tribotech. characts. 7-28146
- rapid solidification, fusion reactor appl. 7-49657
- rapidly solidified powder metallurgy, irradi. to 13.5 dpa with neutrons, microstruct. evolution and swelling 7-51840
- Ag-Cu (12 at.%), supersaturated solid soln., decomp. kinetics, effect of creep (*Russian*) 7-33748
- Ag-Cu (14 at.%), stepped X-ray K absorpt. spectra (*Russian*) 7-39313
- Ag-Cu (15 wt.%), rapidly solidified, microsegregation 7-59524
- Ag-Cu systems, amorphisation induced by ion mixing 7-21300
- AgCu powder, ultrafine, surface segregation of atoms during oxidation 7-54004
- AgCu thin epitaxial films, struct. investig. (*Russian*) 7-12528

copper alloys continued

- Al-Al₂Cu eutectic alloys, chill cast, directionally solidified, hot rolling microstruct. 7-46447
 Al-Cu, corrosion protection by Ce corrosion coatings 7-53988
 Al-Cu, Al-Cu-Si, superplastic strain rate sensitivity index 7-3387
 Al-Cu, creep rupture under tri-axial tension 7-53839
 Al-Cu, dendritic growth models, comparison of theory with expt. 7-22649
 Al-Cu, directionally crystallised, crystallographic texture transform. during wear 7-17660
 Al-Cu, microsegregation, effect of solidification rate 7-46480
 Al-Cu, solidification, microsegregation in coarsened dendritic microstruct. 7-28048
 Al-Cu, superplasticity rel. to grain refining addition elements 7-46561
 Al-Cu (1.87 wt.%), stability of metastable defects at elevated temps. 7-38207
 Al-Cu (2 wt.%) single crystals, rolled, shear band form. rel. to θ' precipitates 7-3385
 Al-Cu (2 wt.%) single crystals, rolled, shear band form., θ precip. 7-28099
 Al-Cu (2.5 wt.%), creep deform., effect of θ precipitates 7-65088
 Al-Cu (2.5 wt.%), electrical resistivity, effect of precipitation 7-12697
 Al-Cu (3 at.%) precip. growth kinetics of θ' - and θ -phases 7-39519
 Al-Cu (3.76 wt.%), rheocast, partially homogenised, ageing response, microhardness 7-46499
 Al-Cu (4.5 wt.%), laser treated, surface solidification with moving heat source 7-22648
 Al-Cu compact, struct. form. during sintering 7-53675
 Al-Cu films, characterisation by SIMS, Auger spectroscopy and TEM 7-12550
 Al-Cu system, trapping and diffusion mechanism, μ SR study 7-45863
 Al-Cu-Be (3, 0.1 wt.%), precip. reactions 7-53738
 Al-Cu-In alloy, deformed, θ' -phase precipitation 7-22691
 Al-Cu-Li, 2020, low-cycle fatigue, effect of environment and temp. 7-28117
 Al-Cu-Li, cryogenic toughness, orientation effects 7-39669
 Al-Cu-Li, liquid dynamic compaction, microstruct. and precipitation, TEM study 7-59529
 Al-Cu-Li, plastic deform. in conditions of quasihydrostatics (Russian) 7-59586
 Al-Cu-Li alloys, cyclic fracture, mechanisms 7-46634
 Al-Cu-Li-Mn-Cd, 2020, micromechanisms governing elevated temp. fracture resist. 7-22803
 Al-Cu-Mg, annealed, creep, 623-723 K 7-53802
 Al-Cu-Mg, 2024, averaged, yield loci, expt. investig. 7-51923
 Al-Cu-Mg, 2024, TEM specimen prep. parallel and perpendicular to machined surfaces 7-39808
 Al-Cu-Mg, 7090, powder metallurgy, fatigue crack growth, influence of load ratio 7-28124
 Al-Cu-Mg, cast composite, mica particle distrib. 7-46375
 Al-Cu-Mg, crack propagation resist., in connection with limiting crack resist. 7-59629
 Al-Cu-Mg, D16T, endurance over wide range of stress variation 7-22811
 Al-Cu-Mg, deformed, dislocation struct., AE obs., electron microscopy (Russian) 7-39832
 Al-Cu-Mg, fatigue crack propagation rate, effect of overloads 7-59623
 Al-Cu-Mg, fracture behaviour, influence of fine transition-metal particles and grain struct. 7-3406
 Al-Cu-Mg, hot workability, recrystallisation during torsional deform. (Korean) 7-46559
 Al-Cu-Mg, IN 9021, corrosion behavior 7-39733
 Al-Cu-Mg, IN 9021, creep crack growth fracture morphology 7-53881
 Al-Cu-Mg, plastic deform., AE, X-ray obs. (Russian) 7-46579
 Al-Cu-Mg, stability of struts in compression in elastoplastic range 7-22771
 Al-Cu-Mg, strip with hole, fatigue resist., effect of multiple local plastic deform. 7-59625
 Al-Cu-Mg r-curve behaviour of double edge notched tensionspecimens in plane stress 7-13701
 Al-Cu-Mg system, D16 alloy, struct. changes during electron bombardment 7-8005
 Al-Cu-Mg-Al₂O₃-Al₄C₃, IN 9021, mechanically alloyed precip. hardened, tensile behaviour 7-13525
 Al-Cu-Mn, fracture toughness, all modes 7-65121
 Al-Li-Cu, precip.-hardened, cyclic stress response and deform. behaviour 7-22791
 Al-Li-Cu, T₂ phase, icosahedral struct. 7-16425
 Al-Li-Cu icosahedral quasicrystals, solid state reaction and rapid solidification prep. comparison 7-37864
 Al-Li-Cu-Mg quaternary alloy, initiation of voiding at second-phase particles 7-39645
 Al-Li-Cu-Mg-Zr, wear, comparative investigs. and prep. method role 7-13605
 Al-Li-Cu-Mg-Zr, yield stress, temp. and strain rate depend. (Japanese) 7-33734
 Al-Li-Cu-Mg-Zr die forgings, mech. props., microstruct. 7-46636
 Al-Li-Cu-Mg-Zr powder alloy, superplastic, high modulus and hardness 7-53816
 Al-Li-Cu-Zr, 2090, small fatigue crack growth 7-22817
 Al-Li-Cu-Zr, fracture, ageing and comp. depend. 7-22784
 Al-Li-Cu-Zr, nucleation of precipitates 7-46476
 Al-Li-Cu-Zr, nucleation of δ' and β' precipitates 7-59527
 Al-Li-Cu-(Mg), fracture, effect of subgrain struct. and ageing practice 7-13563
 Al-Li-Cu-(Mg), stress corrosion-resist. and mech. props. 7-33833
 Al-Li-Zn-Mg-Cu alloys, microstruct. evolution 7-53739
 Al-Mg-Cu, icosahedral quasicrystals, solid state reaction and rapid solidification prep. comparison 7-37864
 Al-Mg-Cu-Zr, low activation alloy development for reacting plasma experiment 7-15384
 Al-Si-Cu castings, fatigue strength improvement by shot peening (Japanese) 7-8100
 Al-Si-Cu sputtered electrode for VLSI, Cu distributions meas. by RBS 7-2415
 Al-Zn-Mg-Cu, 7475, environment sensitive fracture using shadow optical method of caustics 7-39647
 Al-Zn-Mg-Cu, 7475, superplasticity, constitutive eqn., evaluation of parameters 7-65085
 Al-Zn-Mg-Cu, fatigue crack propag., influence of microstruct. (German) 7-22833

copper alloys continued

- Al-Zn-Mg-Cu, high-energy rate powder metallurgy processed, microstruct. evaluation 7-22607
 Al-Zn-Mg-Cu, high-strength alloys, long-term marine atm. stress corrosion tests 7-46679
 Al-Zn-Mg-Cu, microalloying effect on struct. and mech. props. 7-53755
 Al-Zn-Mg-Cu, notched and unnotched bars, macroscopic shear localisation and fracture 7-46633
 Al-Zn-Mg-Cu, strain distrib. within crack tip plastic zones 7-3396
 Al-Zn-Mg-Cu-Ni-Zr, modified 7075, prod. by liq. dynamic compaction, struct. and props. 7-46437
 Al-Zr-Cu, grain boundary struct. and superplasticity, electron microscopy studies (Russian) 7-6630
 AlCuLi alloys, large quasicrystalline dendrites, triacontahedral solidification morphology 7-32345
 AlCuLi quasicrystalline struct., construction 7-37929
 AlCuSiC composite, shock response 7-26867
 AlZnCuMgZr, directional solidification, microstruct. (German) 7-46452
 Au-Ag-Cu-Pd, cast microstruct, segregation, TEM obs. 7-39495
 Au-Cu alloys, polycryst., room temp. interdiffusion 7-2274
 Au-Cu alloys, surface composition, sequential ion scatt. spectroscopy-Auger electron spectroscopy meas. 7-22394
 Au-Cu alloys, vapour deposition on NaCl single crystals, nucleation and growth 7-39391
 Au-Cu sputtered alloys, segregation, surface compositional changes 7-58585
 Au-Cu-Pd, corrosion resist. 7-39739
 AuCu₃, ordered alloy, antiphase boundary form. energy, atomic config., Morse pot. approx. (Russian) 7-46419
 Au₃Cu short range order, EXAFS study 7-63555
 Au₇₅Cu₂₅ and Au₇₀Cu₃₀, local order, X-ray diffuse scatt. meas. 7-26972
 Ba₂CaCuFe₂F₁₄, heteronuclear trimers with ferrimagnetic behavior (French) 7-64448
 C fibre reinforced Al-Cu composites, tensile strength, fracture, interfacial bond strength 7-33744
 Cd(Cu_{1-x}Al_x)₂, mag. and cryst. props. 7-27506
 Cd(Cu_{1-x}Ni_x)₂, mag. and cryst. props. 7-27506
 CdTe-AuCu, AC contact impedance, influence on high freq., low temp. on fast transient junction meas. 7-64311
 Ce-Cu amorphous alloys, mag. and transport props., Ce-derived anomalies 7-52601
 Ce(Co,Cu,Fe)₆, magnetically hard, heat treatment effects on struct. and mag. characts. 7-27564
 CeCu₆, heavy fermion substance, magnetoresistance under press. 7-52579
 CeCu₆, heavy fermion system, temp. and mag. field depend. of Hall effect 7-2579
 CeCu₆ heavy fermion system, photoemission and inverse photoemission studies 7-3148
 CeCu₆, heavy-electron compound, de Haas-van Alphen effect 7-12587
 CeCu₆, heavy-fermion material, coherent and incoherent behaviour, Hall effect and magnetoresist. 7-32992
 CeCu₆-Mo point contacts, low temp. I-V characts., thermoelec. effects obs. 7-27382
 CeCu_{2-x}Ni_xSi₂, Kondo-lattice system, resist. anomalies 7-58799
 CeCu₂Si₂, heavy fermion superconductors, Fermi surface and cooperative phenomena 7-2771
 CeCu₂Si₂, heavy fermion superconductor, magnetic field penetration, muon spin relax. studies 7-45886
 CeCu₂Si₂, heavy-fermion superconductors, induced moment mag. form factors 7-12909
 CeCu₂Si₂, kondo effect versus crystal field 7-2602
 CeCu₂Si₂, Kondo lattice heavy fermion system, quasi-particle-phonon interactions 7-2521
 CeCu₂Si₂, lattice gas heavy fermion-boson model anal. of specific heat, entropy and magnetic susceptibility 7-58505
 CeCu₂Si₂, nonmagnetic Kondo lattices, coherent regime, Hall effect temp. depend. meas. 7-52582
 CeCu₂Si₂, quasiparticle band struct., local-density approx. anal. 7-27250
 CeCu₂Si₂, Raman scatt. study of electronic and vibr. excitations 7-33387
 Ce_{1-x}La_xCu₆, electronic states, resonant photoemission study 7-53496
 Ce(Ni_{1-x}Cu_x)₂Si₂, mag. susceptibility, scaling behaviour, cryst. field effects 7-45616
 Co-Au-Fe, dil., local structural and mag. environments of Fe 7-26965
 Co-Cu, 1D disordered structural states, form., quenching, X-ray diffraction study 7-44784
 Co-Ga binary system, β -phase solid soln., positron annihilation studies 7-46185
 Cu (111)-Fe crystal, CO adsorption 7-21616
 Cu (111)-Fe surface alloys, prep. and oxidation 7-22870
 Cu base, ageing and thermal cycling effects in shape memory alloys 7-3336
 Cu base alloys, rapid solidification technology 7-39493
 Cu based alloy, EELS at 1000 kV 7-1825
 Cu based alloys, internal friction, Young's modulus, amplitude relationship (Russian) 7-65075
 Cu-⁵⁷Co Mossbauer source in low temp. He, oscillations after heating by an RF pulse 7-59128
 Cu-Ag, surface segregation 7-44829
 Cu-Ag alloy thin films, co-deposited, phase form. 7-59492
 Cu-Ag alloys, two-phase, models of tensile behaviour from components 7-46570
 Cu-Ag-Pb system, thermodynamic optimisation 7-46421
 Cu-Ag-Ti brazing alloys with active Ti additive, bonding of Syalon 7-39846
 Cu-Ag-Zr, serrated flow, disappearance 7-17588
 Cu-Al, diffusion coefficients, composition depend. (Russian) 7-32701
 Cu-Al, dynamic recrystallisation, grain boundary bulging 7-39540
 Cu-Al, H trapping, positron annihilation spectra 7-33482
 α -Cu-Al, ordered domain charactn. from dissoln. kinetics study 7-22693
 Cu-Al, rel. between phase comp. and electron conc. (Russian) 7-53700
 Cu-Al (111), S segregation, LEED and AES studies 7-2321
 Cu-Al (25 wt.%), diffusion coeff., segregation, high temp. creep of β -phases (French) 7-32658
 Cu-Al (6 wt.%), erosion by spherical non-friable steel shot, impact angle effect 7-8136
 Cu-Al bronze, hot deform. and annealing, mechanical props. and softening kinetics 7-17552
 Cu-Al bronzes, microstruct., corrosion 7-39697
 Cu-Al film couples, interfacial phase form., in situ annealing X-ray diffraction obs. 7-21705
 Cu-Al film resistivity depend. on thickness and annealing time 7-11242

copper alloys continued

- Cu-Al long-period superlattice, interface struct., TEM and HREM study 7-16499
- Cu-Al₂O₃, dispersion strengthened powder alloys struct. and mech. props. 7-53667
- Cu-Al₂O₃ films, dispersion strengthened, flow stress, temp. depend. (*Russian*) 7-53815
- Cu-Al-Ag (5.4, 5.2 wt.%), ageing, hardness, precip. energy 7-65127
- Cu-Al-Co(Mn)(Fe)(Ni), stacking fault energy determ. (*Russian*) 7-12082
- Cu-Al-Fe, Al bronze, superplasticity, effect of Fe content 7-65109
- Cu-Al-Mg alloys, complex oxide form. and precipitate morphology (*Russian*) 7-33664
- Cu-Al-Mn, surface layers, change in chem. state during annealing investig. using Auger spectroscopy (*Russian*) 7-33834
- Cu-Al-Mn, thermoelastic martensite form., effect of thermal and stress cycling 7-22680
- Cu-Al-Ni, β -phase alloys, fracture rel. to grain boundary precip. and Ni content 7-59604
- Cu-Al-Ni, cryst. struct. of α' , martensite formed during deform. (*Russian*) 7-53814
- Cu-Al-Ni, shape memory alloys, polycrystalline, cyclic deform., fatigue above transform temp. 7-3434
- Cu-Al-Ni shape memory alloys, polycrystalline, cyclic deform. and fatigue above transform. temp. 7-3433
- Cu-Al-Ni-Fe bronze, laser glazing, microstruct. 7-52197
- Cu-Al-Ni-Fe-Mn bronze, cast, laser surfacing, improved corrosion resist., microstruct. characteris. 7-13651
- Cu-Al-Ni-Ti-Zr, shape memory alloy, grain refinement, fracture mode, Ti and Zr additions effect 7-3301
- Cu-Al-Si, rel. between phase comp. and electron conc. (*Russian*) 7-53700
- Cu-Al-Zn, β -phase stability, mech. props. rel. to quenching rate 7-33659
- Cu-Al-Zn, rel. between phase comp. and electron conc. (*Russian*) 7-53700
- Cu-Al-Zn-Mn-Ni shape memory alloy, positron annihilation study 7-46206
- Cu-Au, disordered, short-range ordering, X-ray split diffuse intensity maxima separation 7-2222
- Cu-Au, phase diagrams and short range order, Monte Carlo simulations 7-53704
- Cu-Au quenched alloys, diffuse X-ray scatt., microdomain model anal. 7-6814
- Cu-B, cast struct., segregation, conc. undercooling 7-3291
- Cu-B, rapid solidified and ion implanted, struct. studies 7-21130
- Cu-based binary alloys, Young's modulus, microalloying effects (*Russian*) 7-33711
- Cu-based binary dilute alloys, electron struct., X-ray $L\alpha$ emission spectra studies 7-12598
- Cu-based dilute alloys, low temp. elec. resist. 7-52565
- Cu-Be, explosive cladding, martensitic transform., electron diff. 7-46468
- Cu-Be, serrated flow, disappearance 7-17588
- Cu-Be (2 wt.%), ageing, lattice rearrangement (*Russian*) 7-39553
- Cu-Be (30 at.%), eutectoid decomp., spatial distrib. of α -phase (*Russian*) 7-53694
- Cu-Be-Co, elec. resist., decomposition and coarsening effects 7-2573
- Cu-Ce, cast struct., segregation, conc. undercooling 7-3291
- Cu-Co, age hardened, tensile deform., acoustic emission characts. 7-13356
- Cu-Co, dynamic fracture characts., void nucleation at incoherent precipitates 7-17628
- Cu-Co (2 at.%), age-hardened, fatigue behaviour 7-33786
- Cu-Co (2 at.%), underaged, fatigue props., comparison of single crystals and polycrystals. (*German*) 7-46648
- Cu-Co (2.7 at.%), decomp., atom probe FIM 7-3268
- Cu-Co alloy, coherent precipitate strain contrast under high order refl. excitation 7-3306
- Cu-Co alloy decomposition, TEM, FIM and SANS studies 7-53749
- Cu-Cr bronze, decomp. kinetics of supersaturated solid solns. 7-3320
- Cu-Cr powders, sintering, densification rel. to Cr content 7-13405
- Cu-Dy, thermodynamic props. rel. to glass forming ability 7-38204
- Cu-Er, thermodynamic props. rel. to glass forming ability 7-38204
- Cu-Er metallic glass, ion beam mixing, diffusion and phase separation meas. 7-16659
- Cu-Er metallic glass form. by near-isothermal cold rolling 7-22610
- Cu-Fe, diffusion of Fe studied by Mossbauer spectroscopy 7-2252
- Cu-Fe, dil., local structural and mag. environments of Fe 7-26965
- Cu-Fe, implanted solid solns., Mossbauer study on thermal dynamics of Fe atoms 7-45855
- Cu-Fe, thermomech. treatment, softening rel. to disperse α -Fe particle, size and orientation 7-28054
- Cu-Fe (0.6 to 2.2 at.%), solid solns., decomp. processes, effect of O₂ (*Russian*) 7-33681
- Cu-Fe alloy, BCC and FCC Fe particles, field ion microscopy studies 7-33667
- Cu-Fe alloys, electronic structure and impurity states, optical investigations (*Russian*) 7-32943
- Cu-Fe host-impurity system, O ion bombarded, internal oxidation, Mossbauer spectra studies 7-59131
- Cu-Fe system, diffusion of positive muons, detection by zero-field muon spin resonance 7-45862
- Cu-Fe-Al, cold rolled, γ to α transform. of fine α -Fe precipitates, mag. props. 7-3300
- Cu-Fe-Al alloys, thermoelec. power temp. depend. (*Russian*) 7-12706
- Cu-Fe-Mg-Ni-Al alloy, stress relaxation in tension and creep in torsion 7-44667
- Cu-Ga, random alloys, residual electrical resistivity, first-principles calc. 7-2569
- Cu-Gd, thermodynamic props. rel. to glass forming ability 7-38204
- Cu-Ge, random alloys, residual electrical resistivity, first-principles calc. 7-2569
- Cu-Ge (15.0 wt.%), Fermi surface, 2D angular correlation of positron annihilation radiation 7-39243
- α -Cu-Ge alloys, determ. of quantum mechanical density matrix from angular correlation of positron annihilation data 7-39245
- Cu-Ge-Ga-Al FCC alloys, faulted structure, X-ray diff. studies 7-58292
- Cu-GeO₂, dispersion hardened polycrystals, intermediate temp. embrittlement 7-53903
- Cu-In (15 wt.%), lamellar precipitates, cellular dissolution kinetics, grain boundary diffusion 7-28047
- Cu-In alloys, vacancy-induced elec. field gradient temp. depend., PAC meas. 7-52541

copper alloys continued

- Cu-Kr system, Kr bubble growth, positron annihilation studies 7-39247
- Cu-La, thermodynamic props. rel. to glass forming ability 7-38204
- Cu-Li, prep. and props. 7-53663
- Cu-Mg amorphous alloys, 2D weak localisation effects 7-21871
- Cu-Mn, dilute metallic spin glasses, response time, temp. depend. study 7-2896
- Cu-Mn, metallic spin glasses, local-field rotational correlation length, AC susceptibility 7-17179
- Cu-Mn dil. alloys, electronic struct. of mag. impurities 7-58771
- Cu-Mn dilute alloys, oxidized formation, Auger lines relative intensities 7-17726
- Cu-Mn spin glass, intrinsic remanent magnetisation and anisotropy energy, temp. depend. 7-45690
- Cu-Mn spin glass, remanent magnetization, field dependence 7-59018
- Cu-Mn-Al alloys, mag. and structural props. study 7-2895
- Cu-Mn-Ge system, phase equilib. in Cu-rich alloys 7-3277
- Cu-Mn-Sn, phase conc. nonuniformities rel. to annealing (*Russian*) 7-59494
- Cu-Nb, composite struct., filamentary medium, cond. anisotropy and crit. current 7-22081
- Cu-Nb, supercond. composites, low temp. plasticity, annealing hardening, strength (*Russian*) 7-59579
- Cu-Nb composite superconductors, critical parameters and surface flux pinning studies 7-38830
- Cu-Ni, corrosion inhibition by Schiff bases in acid media 7-22892
- Cu-Ni, dynamic recrystallisation, grain boundary bulging 7-39540
- Cu-Ni, external surface adsorption isotherm 7-6978
- Cu-Ni alloy surface segregation, H chemisorbed monolayer effects calcs. 7-21465
- Cu-Ni alloy surfaces, composition, low energy ion scatt. study 7-32771
- Cu-Ni alloys, chemisorpt.-induced surface segregation, time-of-flight atom probe and AES studies 7-32657
- Cu-Ni alloys, dislocation vel. determ., stress pulse etch pit and slip line cinematography techniques 7-63627
- Cu-Ni alloys, surface segregation, tight-binding Hartree Hamiltonian, cluster-Bethe-lattice approx. calcs. 7-38665
- Cu-Ni electrodeposition, comp. modulated alloy form. 7-59468
- Cu-Ni-Al, two-step ageing, microstruct., mech. props. 7-39565
- Cu-Ni-Al (7.5, 2.5 at.%), thermomech. treatment (*Japanese*) 7-8013
- Cu-Ni-Cr, spinodal decomp., X-ray diff. and TEM study 7-22732
- Cu-Ni-Fe, alloy decomposition and periodic struct. coarsening 7-53735
- Cu-Ni-Fe, irradi., stability of periodic decomp. struct. 7-58366
- Cu-Ni-Fe, specific heat capacities (*German*) 7-2228
- Cu-Ni-Fe-Mn, physical props. rel. to precip. and thermal treatment (*German*) 7-12698
- Cu-Ni-P, P addition effect on struct. and strength 7-53669
- 2-Cu-Ni-Sn solid solutions, ternary diffusion and thermodynamic interactions 7-52159
- Cu-P alloy liquid metal ion sources, ion formation 7-64878
- Cu-P powder, contact form. during liq. phase sintering 7-7925
- Cu-P-Pt-B liquid metal ion source, B⁺ and P²⁺ ion emissions 7-41531
- Cu-Pb, resistance to wear and cavitation erosion of bearingalloys 7-8129
- Cu-Pb-Sn leaded bronze, resistance to wear and cavitation erosion of bearingalloys 7-8129
- Cu-Pd alloy, surface segregation, scanning Auger electron microscopy study 7-21578
- Cu-Pd bimetallic system, electron microscopy 7-16504
- Cu-Pt (25.7 at.%), transform. from short-range order to L₁₂ and L₁₂-s ordered states 7-53726
- Cu-Pt (48.1 at.%), elec. resist. var. during ordering under press. (*Russian*) 7-33810
- Cu-Pt-Pd ternary alloys, L₁-type ordered phases 7-16493
- Cu-Rh, diamag. susceptibility calc. 7-45615
- Cu-Rh, dilute alloy, surface composition, Auger electron spectroscopy 7-16845
- Cu-Ru bimetallic system, electron microscopy 7-16504
- Cu-Sb (1 wt.%), creep crack growth, 450-650°C 7-33758
- Cu-Si, elemental Si inclusion form. in sulphide scale 7-17720
- Cu-Si, microhardness correction procedures evaluation 7-3550
- Cu-Si (6 at.%), secondary grain boundary dislocation nodes at junction of three grains 7-63648
- Cu-Si alloys, thermodynamic props. determ. by Knudsen cell mass spectrometry 7-26976
- Cu-Sn, Bauschinger effect, influence of alloying elements and grain size (*German*) 7-17605
- Cu-Sn, diffusion coefficients, composition depend. (*Russian*) 7-32701
- Cu-Sn, dual phase, struct.-prop. correl., hardness obs. 7-8094
- Cu-Sn, ductility at elevated temps., effect of small amounts of B, P or Mg 7-53904
- Cu-Sn, low cycle fatigue damage, crack initiation (*Japanese*) 7-33780
- Cu-Sn, rapid solidified and ion implanted, struct. studies 7-21130
- Cu-Sn (11 wt.%), stir cast, torsion behaviour 7-46567
- Cu-Sn (14.37 at.%), hypoeutectoid, diffusion coeff. governing high-temp. creep (*French*) 7-46572
- Cu-Sn (14.4 wt.%), diffusion coeff., segregation, high temp. creep of β -phases (*French*) 7-32658
- Cu-Sn alloy coatings, magnetron sputtered, crystal orientation 7-39381
- Cu-Sn alloy thin films, co-deposited, phase form. 7-59492
- Cu-Sn system, atomised metal powders, factors affecting particle size 7-53659
- Cu-Sn-B(Mg)(P), ductility at high temp., alloying additions effect (*Japanese*) 7-13515
- Cu-Sn-Pb system, struct. form. during sintering 7-64967
- Cu-Su, amorphous system, high press. melt quenching, microhardness, X-ray obs. (*Russian*) 7-44396
- Cu-Ti, amorphisation, high resolution electron microscopy 7-44377
- Cu-Ti, early stage precipitation kinetics, SANS studies 7-53746
- Cu-Ti, powdered, dynamic strain ageing, 375-860K 7-28058
- Cu-Ti (5.7 at.%), cellular decomp. (*Russian*) 7-53693
- Cu-Ti (5.7 at.%), diffusion of products of cellular dissoln. (*Russian*) 7-58485
- Cu-Ti alloy system, electron irradi.-induced amorphisation, chemical disordering effects study 7-16640
- Cu-Ti alloys, amorphous and crystalline, H absorption 7-2369
- Cu-Ti brazing alloys with active Ti additive, bonding of Syalon 7-39846
- Cu-Ti-Al single crystals, strain hardening due to multiple twinning (*Russian*) 7-46501
- Cu-V (Nb) (Ta), castings, strength and elec. props. 7-27971
- Cu-Za-Al ribbons, rapidly, quenched, martensitic transform., stabilisation 7-22678

copper alloys continued

- Cu-Zn, Bauschinger effect, influence of alloying elements and grain size (*German*) 7-17605
 Cu-Zn, electrodeposits, comp. rel. to deposition pot. (*Japanese*) 7-27951
 Cu-Zn, embrittlement in solidification process 7-3435
 Cu-Zn, preferential sputtering, AES and SIMS studies 7-53467
 Cu-Zn, random alloys, residual electrical resistivity, first-principles calc. 7-2569
 Cu-Zn (52 wt.%), diffusion coeff., segregation, high temp. creep of β -phases (*French*) 7-32658
 Cu-Zn alloy, cyclic BCC-9R martensitic transform-induced dislocations Burgess vector, electron microscopy studies 7-51775
 Cu-Zn alloys, electron irradiation, interstitial cluster form., diffusion rates, resistivity 7-2013
 Cu-Zn system, diffusion induced grain boundary migration 7-21227
 Cu-Zn system, diffusion induced grain boundary migration, misorientation depend. 7-21229
 Cu-Zn system, phase equilib., thermodynamic evaluation 7-3271
 Cu-Zn-Al, dislocation density and mobility during reversible martensitic transforms. 7-26759
 Cu-Zn-Al, liq. alloys, activity of Zn (*Japanese*) 7-53698
 Cu-Zn-Al, quenched sheets, shape change rel. to thermal cycle (*Japanese*) 7-53790
 Cu-Zn-Al, shape memory alloy, type II twins in self-accommodating martensite plate variants 7-22752
 Cu-Zn-Al, thermoelastic, two way memory effect, dislocation form. model 7-22741
 Cu-Zn-Al, thermoelastic, two-way memory effect, dislocations origin 7-22754
 Cu-Zn-Al (26.4 wt.%), shape memory alloy, martensitic transform. crystallography (*Chinese*) 7-7994
 Cu-Zn-Al (26.4 wt.%), shape memory alloy, crystallography of martensitic transform. (*Chinese*) 7-7995
 β -Cu-Zn-Al alloys, elastic constants and lattice stability 7-13492
 Cu-Zn-Al shape memory alloys, rapidly solidified, microstruct. and props. (*Chinese*) 7-8043
 Cu-Zn-Al shape memory alloys, grain refinement 7-53774
 Cu-Zn-Al-Zr, shape memory alloys, grain-refined, effect of grain size on transform. temp. 7-39512
 Cu-Zn-Ni, liq. alloys, activity of Zn (*Japanese*) 7-53698
 Cu-Zr, amorphisation under action of high press. and shear deform. (*Russian*) 7-58163
 Cu-Zr, compositionally modulated amorphous films, sputter deposition prep. 7-22482
 Cu-Zr, ion irradiated, mech. prop. meas. 7-51873
 Cu-Zr (0.5 wt.%), high strength, high cond., prod. by rapid solidification technology 7-28029
 Cu-Zr amorphous alloy, induced recrystallisation by electron and laser beam irradiation 7-12152
 Cu-Zr brazing alloys with active Ti additive, bonding of Syalon 7-39846
 Cu-Zr metallic glass, elec. cond., annealing effects 7-7198
 CuAl, short-range order-induced equilib. resist. conc. depend. meas. 7-26700
 CuAl-quartz, SAW resonators, annealing behaviour and phase noise performance 7-11242
 Cu_{1-x}Al_x, α -phase, specific heat 7-12312
 CuAlNi deformed single cryst., internal friction amplitude depend. (*Russian*) 7-13491
 CuAlNi, shape memory alloys, mech. props., polycrystal model (*Japanese*) 7-53789
 CuAu I and II, initial ordering stages, twinning, periodic antiphase boundaries, electron microscopy 7-28032
 CuAu, ordering and recrystallisation, TEM studies (*Russian*) 7-16479
 (CuAu)-Co single crystals, under- and over-aged, additivity of precip. and solid soln. hardening 7-65051
 Cu₃Au alloy, displacement cascade collapse at low temp. 7-51892
 Cu₃Au, electron irradiation, long range ordering, recovery, vacancy migration and clustering, positron lifetime study 7-39543
 Cu₃Au, irradiation disordering and reordering by fusion neutrons, electrical resistivity meas. 7-51864
 Cu₃Au, L1₂ ordered intermetallic cpds., symm. tilt boundaries, geometrical models 7-32454
 Cu₃Au ordered alloys, twin boundary structure, TEM anal. 7-2027
 Cu₃Au, quenched, vacancies, ordering and annealing, positron lifetime and elec. resist. meas. 7-39544
 Cu_{70-x}Au₃₀Fe_x, ferromagnetic interactions, EXAFS and XANES anal. of Fe atom environment and clustering 7-64808
 CuB:He, neutron irradiated, annealing behaviour of defects, positron annihilation study 7-39291
 CuBe, oxidised, secondary electron emitters, AES and ESCA studies (*Chinese*) 7-54238
 CuBe, scatt. anisotropy of conduction electrons 7-38536
 CuCo, Cu-rich alloy, precipitation, critical nuclei size, neutron scatt. studies 7-12294
 CuCu₂Si₂Mo point contacts, low temp. I-V characts., thermoelec. effects obs. 7-27382
 CuFe alloys, anomalous Hall effect 7-52577
 CuFe-NiCr thermocouple, mag. field effects (*Chinese*) 7-24646
 Cu_{100-x}Fe_x alloys rapidly quenched, spin glass state 7-12979
 Cu₉₈Fe₂, antiferromagnetic interactions, EXAFS and XANES anal. of Fe atom environment and clustering 7-64808
 Cu₂Hf₄₃ amorphous alloy, local Hf environment, TDPAC spectra study 7-32303
 CuMn and CuMnAu alloys, homogeneous and inhomogeneous spin freezing, μ SR studies 7-45687
 CuMn, short-range order-induced equilib. resist. conc. depend. meas. 7-26700
 CuMn spin glass, remanent magnetization reduction, Heisenberg and Ising comparison 7-53019
 Cu₂MnAl, Heusler alloy, heat and press. processed, changes in phys. props. during heating (*Russian*) 7-59645
 Cu₂MnAl, high press. phase transition, elec. resist., saturation magnetisation, lattice parameters (*Russian*) 7-46457
 CuMnAu spin glasses, crit. behaviour, Dzyaloshinsky-Moriya interactions 7-7525
 CuMn_{0.05}Ni_{0.03}, spin glass, long-time low temp. relaxation 7-38870
 CuNi, substitutionally disordered, electronic struct., LCAO-CPA calcs. 7-64067
 CuNiFe, electron irradi., decomposition kinetics and morphology 7-58491
 CuNiSn, high-strength heterophase cryst., deform. mechanism investig. (*Russian*) 7-13509

copper alloys continued

- CuO-P₂O₅ glass, containing Pr₂O₃, optical props. 7-17292
 CuPd, disordering by 14 MeV Cu ions between 296 and 823 K 7-51877
 Cu₃Pd, alloys with periodic antiphase boundary struct., dislocation motion 7-63620
 Cu_{3±x}Pd, long-period superstructures 7-21430
 Cu₇₅Pd₂₅, partial densities of states determ., valence band photoelectron spectra meas. 7-52390
 Cu_{1-x}Pt, disordered system, X-ray absorpt. edges (*German*) 7-46241
 Cu₂Pt ordering kinetics, comp. depend., X-ray and DTA studies 7-26940
 CuSb(In), vacancy formation enthalpy, positron annihilation studies 7-7787
 Cu₂Se, Cu filament growth, superionic transport mechanism 7-45104
 Cu₃Si, oxidation, XPS and Auger spectra 7-22899
 Cu_{0.85}Sn_{0.15}, amorphous melt-quenched alloys, crystn. (*Russian*) 7-37881
 Cu₄₁Sn₁₁, giant cells, polyhedral packing 7-11992
 CuSnBe bronze sheets, lamination investig., Auger and photoelectron studies (*Russian*) 7-13628
 Cu_{94.6}Tb_{5.4} sputtered alloy, spin glass like behaviour 7-53001
 CuTi molten alloys, evidence of chemical short range order 7-21077
 CuTiH, medium-range structure, ASAXS study 7-58203
 Cu_{1-x}Ti_x metallic glasses, magnetoresist., quantum interference and electron interaction effects 7-2576
 Cu₄Ti₃, electron irradiation induced amorphisation, high resolution electron microscopy 7-44373
 Cu₄₄Ti₅₆ 3D metallic glasses, magnetoconductivity meas., quantum interference effects calcs. 7-17016
 Cu₄₈Ti₅₂, amorphous, crystallisation, intermediate long period superlattice phase form. 7-21098
 Cu₅₀Ti₅₀ amorphous alloys, positron annihilation peakrate temp. depend. meas. 7-39302
 Cu₇₀Ti₃₀ metallic glass, atomic neighbouring struct., EXAFS study (*Chinese*) 7-6519
 Cu_xTi_{1-x} amorphous alloys, neutron diffr., computer simulation studies 7-21109
 Cu_xTi_{100-x}, x=50,66, metallic glasses, crystn., DTA, X-ray diffr., hardness meas. 7-63489
 Cu₃₃Y₆₇ metallic glasses, partial struct. factors, chem. short range order 7-63486
 Cu_xY_{1-x} amorphous alloys, empty and occupied electronic states, inverse and direct photoemission spectroscopies study 7-32899
 CuZn (Ni) Al (Ge) random alloys, positron state, rel. to 2D ang. correlation 7-45230
 CuZn brass alloys, local disorder and premartensitic phenomena, EXAFS study 7-64817
 CuZn, short-range order-induced equilib. resist. conc. depend. meas. 7-26700
 CuZnAl alloys, β -phase, defects study by positron annihilation 7-39297
 CuZnAl, isothermal growth of thermoelastic martensite, quenching and ageing effects 7-53730
 CuZnAl, shape memory alloys, mech. props., polycrystal model (*Japanese*) 7-53789
 CuZr, amorphous and cryst., bond length determ. from EXAFS data 7-63553
 CuZr metallic glass, blistering under He implantation, EELS anal. 7-16593
 Cu₁₀Zr₇, cryst. and amorphous, muon spin resonance studies 7-53196
 Cu₃₃Zr₆₇, glassy metals, peak effect, flux pinning (*Chinese*) 7-12929
 Cu₃₃Zr₆₇ metallic glasses, flux pinning and critical current peak effect studies 7-22079
 Cu₃₉Zr₆₁ 3D metallic glasses, magnetoconductivity meas., quantum interference effects calcs. 7-17016
 Cu₅₀Zr₅₀ amorphous alloys, positron annihilation peakrate temp. depend. meas. 7-39302
 Cu₅₇Zr₄₃ glass metals, temp. depend. of positron trapping effect 7-39292
 Cu₆₀Zr₄₀, amorphous, isothermal crystallisation, nucleation activation energy, DSC obs. 7-11926
 Eu, Ce_{1-x}Cu₂Si₂ cryst., mixed valence state and Kondo system coexistence (*Russian*) 7-7185
 EuCu₂Si₂, Eu valency, effect of Cu or Si replacement by other ions 7-58787
 EuCu₂Si₂, mixed valence system, interconfiguration fluctuation model 7-64188
 Fe-Co-Ni-Al-Cu metallic alloy ordering and spinodal decomposition, atom probe FIM study 7-33676
 Fe-Cu, dilute alloys, electron irradiated, vacancy-solute interaction, positron lifetime, muon spin rotation studies 7-39288
 Fe-Cu, neutron irradi., defect microstruct., SANS and TEM studies 7-58351
 Fe-Cu, pore form. during sintering, effect on mech. props. 7-64970
 Fe-Cu, sintering, form. of Cu pockets in Fe grains 7-7922
 Fe-Cu alloy, neutron irradiation, magnetoacoustic and Barkhausen emission study 7-45749
 Fe-Cu alloys, phase transformations, SANS studies 7-53747
 Fe-Cu evaporated film, composition distrib. and mag. props., Mossbauer meas. 7-7561
 Fe-Cu films, obliquely evaporated, inhomogeneous conc. distrib. 7-38367
 Fe-Cu metastable alloy sputtered films, mag. props., X-ray diffr. and Mossbauer meas. 7-7560
 Fe-Cu powder, contact form. during liq. phase sintering 7-7925
 Fe-Cu sputtered films, thermal stability, X-ray diffr. and Mossbauer studies 7-58679
 Fe-Cu-Ag amorphous alloys produced by vapor quenching 7-7849
 γ -Fe-Cu-C, C activity, effect of Cu 7-13432
 Fe-Cu-Ni, FCC ternary alloys, mag. props. 7-22852
 Fe-Cu-P, sintered, ageing and steam oxidation, effect of P 7-7930
 Fe-Cu-P, sintered atomised powder premixes, mech. props. 7-7931
 GdCu, optical props. and electronic struct. investigations. (*Russian*) 7-13174
 Gd(Cu_{1-x}Co_x)₂, mag. and crystallographic props. 7-38903
 Hf_{1-x}Cu_x metallic glass, thermal stability and phase transformations 7-21125
 HoCo₃Y₂ ferrimag. cpds., mag. anisotropy, temp. depend. 7-64450
 Lu₂Cu₃₇Y_{0.63-x} metallic glasses, low temp. sp. ht. 7-64462
 Mg-Cu alloys, vap. press. meas. by boiling temp. method, thermodynamic props. 7-44778
 Mg-Cu solvated in organic matrices, H absorption studies 7-34073
 Mn-Cu, sintered damping alloy, tempering, & solid soln. breakdown mechanism 7-22692
 Mn-Cu alloy, nonlinear anelasticity and temp. depend. lattice const., nonlinear resonance curve meas. 7-63741

copper alloys continued

- Mn-Cu single crystals, Debye-Waller coeff. behaviour, energy dispersive X-ray diff. study (*Russian*) 7-51983
- Mo-Ag pseudoalloys, Ni and Co effect on interphase interaction 7-27975
- Mo-Cu pseudoalloy obtained by sintering of powdered mixtures, chromising investig. 7-54003
- NbTi-Cu dipole superconducting magnet for accelerators, develop. 7-5510
- NdCu₆, powder and single cryst., magnetic struct. and ordering, neutron diff. studies 7-33146
- Nd₂Fe_{14-x}Cu_xB, crystallographic and mag. props. 7-27522
- Ni-base superalloy powder, IN-100, shock consolidation 7-39459
- Ni-Cu, gamma-irradiated, point defect migration 7-6893
- Ni-Cu, heterodiffusion, effect of γ -rad. (*Russian*) 7-44617
- Ni-Cu, liq. alloys, density of electron states, calc. (*Russian*) 7-45110
- Ni-Cu (10 at.%), stepped X-ray K absorpt. spectra (*Russian*) 7-39313
- Ni-Cu alloy, equilib. segregation, embedded atom simulation 7-17538
- Ni-Cu binary alloys, surface segregation (*Japanese*) 7-12422
- Ni-Cu binary alloys, surface segregation studied by atom-probe 7-44966
- Ni-Cu-Pd ternary system, state-state composition determ. from binary system under sputtering 7-22421
- Ni-Cu-Si, γ' precip. coarsening, bifurcation theory appl. (*Japanese*) 7-53734
- Ni-Fe-Cu, mag. props., hardness, elec. resist., V, Nb and Ta additions effect (*Japanese*) 7-12998
- Ni-Mo-Cu-Fe-Mg, coarse-grained PC permalloys, annealing-twin density (*Japanese*) 7-3330
- (Ni_{1-x}Cu_x)₅ Zr alloys, cryst. struct. study (*French*) 7-26698
- (Ni_{1-x}Cu_x)₇₇B₁₃Si₁₀ pseudobinary metallic glass, low-temp. sp. ht. studies 7-12309
- (Ni_{1-x}Cu_x)₈₀P₂₀ pseudobinary metallic glass, low-temp. sp. ht. studies 7-12309
- Ni₂V-Cu alloys, discontinuous precipitation and ordering (*Russian*) 7-59523
- NpCu₂Al_{8-x}, mag. props., Mossbauer effect and neutron diff. 7-59127
- Pd-Cu-Ag, ordering and precipitation, field emission microscopy studies (*Russian*) 7-46472
- PdCuSi, amorphous, reversible and irreversible changes in the thermal conductivity 7-45267
- Pd_{77.5}Cu_{21.5} glass, cryst. nucleation and growth kinetics 7-11917
- Pd_{78.5}Cu_{21.5} metallic glass, structural relax., vitrification, sp. ht., DSC obs. (*Russian*) 7-37880
- PdSiCu, amorphous, ultrasonic vel., mechanical props. (*Korean*) 7-26874
- Pt-Pd-Cu₂S-Ni₂S system, annealing, phase comp., DTA 7-46412
- RAuCu₄ (R=Gd, Tb, Dy, Ho, Er), cubic alloys, mag. props. 7-52936
- Ru-Cu₂S system, annealing, phase comp., DTA 7-46412
- SiC particle reinforced Al-Cu-Mg composite, failure mechanism, SEM obs. 7-65132
- Sm₂(Co, Fe, Cu, Zr)₁₇ sintered compact permanent magnet, mag. props., comp. and heat treatment effects (*Korean*) 7-2894
- Sm₂(CoCu)₁₇ magnets, cast, coercivity and microhardness 7-53880
- SmCu₂ single cryst., high field transverse magnetoresist. meas., Fermi surface determ. 7-52576
- Ta-Cu, ion irradiated, Cu₃ cluster formation, atomic mixing and demixing (*Chinese*) 7-53468
- Ta-Cu, multilayer systems, temp. depend. of ion beam mixing, 77-book (*Chinese*) 7-51884
- Ta₂Cu_{1-x} amorphous thin-film diffusion barriers on GaAs, thermal and structural stabilities 7-52321
- TbCu_{2.54}, seedy mag. order, neutron scatt. study, mag. meas. 7-33145
- Ti-Cu, H storage, theory 7-34074
- Ti-Cu alloys, Guinier-Preston zones, multi-layer struct., atom probe FIM study 7-33674
- Ti-Cu-Ni-Si amorphous alloys, structural relax. annealing, X-ray diff. studies 7-6537
- Ti-Ni-Cu, martensite cryst. lattice distortions, comp. depend. 7-22679
- Ti-Ni-Cu system metallic glasses, superplastic props. in vitrification temp. range 7-3356
- TiCu-H₂, thermal stability of hydrides 7-26664
- TiNi-TiCu amorphous alloy, thermal devitrification kinetics, DSC obs. 7-21116
- TiNiCu alloys, martensitic transformations, kinetic and morphological laws 7-52031
- TmCu₂, ³H₆ multiplet splitting, cryst. field effect 7-52533
- TmCu₂, magnetic phase transitions, suscept., sp. ht., elec. resist. and magnetisation meas. 7-2857
- UAuCu₄ magnetic props., X-ray diff., NMR and mag. suscept. meas. 7-52948
- UBe_{12.94}Cu_{0.06}, low temp. high mag. field study 7-12911
- UCu₅, heavy-electron state 7-45535
- UCu₅, magnetic heavy electron materials, muon spin rotation studies 7-45884
- UCu_{4.5}Al_{7.5}, antiferromagnetic suscept. meas. 7-12954
- UCu₂Si₂, ThCu₂Si₂, magnetochemistry and crystal chemistry 7-58976
- UPdCu₄ magnetic props., X-ray diff., NMR and mag. suscept. meas. 7-52948
- U₂Sb₃Cu₂, cryst. struct., mag. props. 7-38864
- W-Ag pseudoalloys, Ni and Co effect on interphase interaction 7-27975
- W-Cu, multilayer systems, temp. depend. of ion beam mixing, 77-book (*Chinese*) 7-51884
- W-Cu compacted pseudoalloys, elastic props., deform. diagram and pores effect 7-33722
- W-Cu pseudoalloy, Si alloying effect on solute redistrib. and ductility characts. 7-53741
- W-Cu-Ni contact materials, elec. props., particle size effect 7-2672
- W-Cu-Ti(Zr), saturation rate of porous W with Cu, effect of Ti and Zr 7-3220
- Y₂Fe_{14-x}Si(Cu)B alloys, mag. props. 7-45681
- YBaCu₄, strong electronic correlations 7-45194
- YBaCu₄, strong electronic correlations 7-45194
- Yb₂In_{1-x}Cu_x, Yb valence transition 7-45245
- YbPdCu₄, strong electronic correlations 7-45194
- Zn-Al-Cu, superplastic, cavitation damage 7-65080
- Zn-Al-Cu (ZZ.0.5%), superplastic behaviour 7-28093
- Zr_{1-x}Cu_x amorphous sputtered alloys, low energy excitations, sp. ht. meas., structural relax. effects 7-11913
- Zr₇₀Cu₃₀ melt spun ribbons, collective flux pinning dimensional crossover obs. 7-17143
- Zr₆₈Hf₂Cu₃₀ amorphous and cryst. alloy, elec. field gradient, TDPAC meas. 7-2958

copper compounds

see also copper alloys

- acetate soln., ion exchange with 2,9-dimethyl-1,10-phenanthroline intercalated in α -Zr(HPO₄)₂ 7-65305
- bis(2,4,6-trinitrophenolato)di(pyridine)copper(II), struct., X-ray investig. 7-12033
- calcium copper acetate hexahydrate single crystals, thermal expansion meas. 7-26985
- CdS-CuInSe₂ solar cells fabricated by DC magnetron sputtering of Cu₂Se and In₂Se₃ 7-23170
- Cu₆PS₃Br(Cl), superionic cryst., refractive indices, optical-refractometric correlation (*Russian*) 7-3016
- Cu₂MoS₈, shape memory effect and rhombohedral-triclinic transition (*Russian*) 7-8058
- Cu(H₂PO₄)₂ thermographic materials for laser thermal information recording 7-57496
- halides, excitonic mol., book chapter 7-29610
- halides, photochromic glasses, elastic props., 20-500 °C (*Russian*) 7-21365
- oxide, brittle, formed on Cu, AE technique, alternative to thermogravimetry 7-65274
- oxide films, form. mechanism and struct. 7-33956
- phthalocyanine evaporated thin films, mobility and trap concentration 7-2746
- phthalocyanine thin films, thermoelectroluminescence studies 7-7770
- phthalocyanine-anthanthrone heterojunction, charge carrier photogeneration (*Japanese*) 7-38610
- sputtered atom excitation, optical spectra studies 7-59347
- surface friction layers, study by AES method (*Russian*) 7-59674
- synthetic Cu salts, corrosion on bronze, TEM and SEM study 7-17737
- AgI-AgBr-CuI system, ice nucleating ability, UV irradiation effect 7-66247
- Al₂O₃-B₂O₃-SiO₂-Cu₂O glass, Cu activated, photoconductivity, lumin., influence of radiation defects 7-45381
- Ba-La-Cu-O system, possible high T_c superconductivity 7-2770
- Ba₂CaCu₂Fe₂F₁₄, exchange interactions, mag. susceptibility meas. 7-45654
- α -Ba₂Cu₅F₁₄, crystalline structure (*French*) 7-26730
- BaCuFe₇O₂₇, W-type hexagonal ferrite, intermediate valency, oxidation annealing, magnetisation and neutron diff. studies 7-7187
- BaLaCuO, magnetic susceptibility meas., indication of high-T_c superconductivity 7-58953
- C₁₀CuCl₂ intercalation cpd., Shubnikov-de Hass effect, amplitude behaviour (*Russian*) 7-52571
- Cu₂MoSe_{7.6}, Chevrel phase cpds., positron annihilation studies 7-46201
- Cu₂S, superionic conductor, ionic conductivity and diffusion 7-44899
- Cd₂Cu_{1-x}Fe_xO₄, canted spin arrangements 7-45618
- CdS-CuGaSe₂ solar cell fabrication 7-22047
- CdS-CuInSe₂ Boeing solar cells, I-V characteristics meas. 7-8408
- CdS-CuInSe₂ heterojunctions, struct., elec. and photoelectric props. 7-22001
- CdS-CuInSe₂ thin film solar cell, solid state photovoltaic research status at SERI 7-8389
- CdS-CuInSe₂ thin-film solar cells, junction formation and O role, EBIC studies 7-17915
- CdS-CuInSe₃ backwall solar cells, intrinsic loss mechanisms calc. 7-23187
- CdSe-Cu₂Se heterojunction solar cell, dry formation, electron microscope study 7-17916
- CdZnS/CuInSe₂ solar cells, transient current studies of junction activity 7-8409
- Co_{0.55}Cu_{0.45}Cr₂S_{4-y}Se_y spinels, X-ray diff. study 7-44475
- Co_{0.55}Cu_{0.45}Cr₂S_{4-y}Se_y, high field susceptibility 7-45630
- CsCu₂S₃, Jahn-Teller induced helical deformations 7-7178
- Cu (II) complexes, bis (β -diketonato) and β -diketone ligands, double melting, mesomorphism, long chain substituent effect 7-1862
- Cu (I) iodide complexes, tetrameric, photoluminesc. 7-33437
- Cu complex, 2-acetylpyridine thiosemicarbazone copper(II) complex, mag. moment meas., ESR and spectra investig. 7-57105
- Cu complex, (C₆H₁₁NH₃)CuBr₃, easy-plane ferromag. chain, quantum sp. ht. 7-7522
- Cu complex, aliphatic polyamine Cu (II), ESR hyperfine line width 7-19891
- Cu complex, bi(dithiocarbamate) copper II, struct., NDDO calcs. 7-15515
- Cu complex, bis(1,3-di(p-n-alkoxyphenyl) propane-1,3-dionato) copper (II), discotic liq. cryst. props. 7-37846
- Cu complex, bis(disopropylsilyl)acetylacetonate copper(II) pyridyl nitronyl nitroxide, mol. conform., ESR study 7-57103
- Cu complex, bis(formato)bis(isonicotinamide)diaqua copper(II), X-ray structural anal. 7-51727
- Cu complex, Cu (II) α,ω -dicarboxylato polybutadiene, microstruct. obs. 7-13259
- Cu complex, Cu (II) α,ω -dicarboxylato polybutadiene, microstruct. investig. 7-16450
- Cu complex, Cu II-acetylacetone-substituted 8-hydroxyquinolines, ESR obs. 7-19890
- Cu complex, Cu₄OCl₆(triphenylphosphine)₄, EPR spectrum, Zeeman, hyperfine and mag. dipole effects 7-10642
- Cu complex, CuBr₂·2DMSO, linear chain antiferromag., optical birefringence 7-7679
- Cu complex, CuCl₂·2-phenyl-4,4,5,5-tetramethylimidazoline-1-oxyl-3-oxide, mag. props. 7-51715
- Cu complex, Cu(II) saccharinate, electronic struct. and cryst. struct. 7-27251
- Cu complex, Cu(imidazole)₂²⁺, vibr. spectrum, solvent, protonation and metal ion coord. effects, UV Raman spectra 7-25526
- Cu complex, hexakis (1-methyltetrazole) copper II bis(tetrafluoroborate), Cu(II) sites, Jahn-Teller behaviour, ESR spectra anal. 7-21163
- Cu complex, pyridine 2-aldehyde thiosemicarbazone copper(II) complex, mag. moment meas., ESR and spectra investig. 7-57105
- Cu complex, sulphato aquotris(benzotriazole) Cu (II) benzotriazole, cryst. and mol. struct. 7-21181
- Cu complex, transition of local moments in quasi 1D conductor 7-2815
- Cu complexes, copper(II) cyclodextrin complex, EPR investig. 7-57101
- Cu complexes, dibromotetrapyrrole copper, polycryst. and soln., ESR study 7-38928
- Cu complexes, dichlorobispyrrole copper, polycryst. and soln., ESR study 7-38928
- Cu complexes, dipchlorotetrapyrrole copper, polycryst. and soln., ESR study 7-38928

copper compounds continued

- Cu complexes, ESR, unpaired electrons interspin distance, Eatons' formula calc. 7-25569
 Cu complexes, glutamic acid, struct., EXAFS study 7-19882
 Cu complexes, halogen-substituted 8-hydroxyquinoline Cu II, ESR obs. 7-5709
 Cu complexes, L-phenylalanine salt, EPR study 7-59106
 Cu complexes, single and mixed ligand, bonding parameter, ESR obs. 7-50203
 Cu complexes, with ethanolate, mol. and electronic struct., EPR study 7-19901
 Cu complexes, with polymeric sorbents, ESR investig. (Russian) 7-42812
 Cu complexes, with porphyrin, effect of vinyl groups on meson. Raman spectra 7-15610
 Cu halides, vapour lasers, resonance radiation trapping effects 7-62669
 Cu II complexes, charactn., electronic and ESR parameters 7-2925
 Cu II complexes, dibenzylthiocarbamate copper, bonding, XPS 7-19950
 Cu II complexes, interligand interaction, spectrosc. props. (Japanese) 7-57093
 Cu²⁺ complexes, IR spectra, coordination bond length correlation 7-13160
 Cu²⁺ complexes with phenanthroline, struct., ESR 7-31080
 Cu/n-Si films, LPE growth 7-46359
 Cu-Co complex valence virtual MOs for CI calcs. 7-860
 Cu-Cu₂O Schottky barrier solar cells, interfacial layer effects investig. using n-V_{oc} diagram 7-54304
 Cu-H₂O complexes, bonding, intermolecular electron correl. 7-10449
 Cu-O, laser reduction to metal, effect of heat conduction 7-17674
 Cu-Sb-S cpds., valence bands and semiconducting gaps, nonstoichiometry and phase separation 7-16941
 Cu-Te system, p-T diagram 7-21404
 Cu_xAg_{1-x}InSe₂, liquid-encapsulated Bridgman-Stockbarger melt growth and props. 7-59403
 CuAl_{1-x}Ga_xSe₂, mixed crystals, Raman scatt. spectra 7-13168
 CuAl_{1-x}Ga_xSe₂, chem. transport reactions, growth and morphology 7-7830
 Cu_{1-x}As_xSe₁, glassy semiconductor, tetrahedral bonding 7-32304
 CuBiS₂, thin films, spray pyrolytic deposition, elec. and optical props. 7-7894
 CuBr, X-ray absorption study at higher press. 7-17362
 CuBr-Cu₂S solid solns., fast Cu ion transport 7-52121
 p-CuCNS photocathode for dye-sensitized photoelectrochemical cell 7-3709
 p-CuCNS photocathode, dye-sensitized, stabilisation by Pt deposition 7-27416
 p-CuCNS photocathode sensitized with Acridine Orange, photocurrent quantum efficiency 7-33944
 Cu(CO)_n, (n=1,3) electronic struct. 7-36445
 Cu_{1-x}Cd_xFe₂O₄, irreversible magnetisation. depend. on magnetising field 7-64487
 Cu_{2-x}Cd_xFe₂O₄ system, elec. resist. and cation distrib. 7-7256
 Cu_{2-x}Cd_xTe-Zn_{39.5}Cd_{60.5}TeI, heterojunction solar cells, fabrication and characterisation (Korean) 7-28402
 CuCl, aq., reaction with CdS surface, TEM 7-39920
 CuCl, excitonic particle study by laser spectroscopy 7-16953
 CuCl, giant two-photon excitation of excitonic molecules, nonlinear depolarisation effects 7-64594
 CuCl intercalation cpd. with graphite, ideal resistivity studies 7-32976
 CuCl laser radiation at 510 nm, internal attenuation 7-36949
 CuCl, low-lying electronic states, radiative lifetimes 7-50258
 CuCl, low-lying excited states, HF approx. 7-62254
 CuCl microcrystals, excitons, size quantisation effects, luminesc. spectra anal. 7-53409
 CuCl nanosec. laser etching, time-of-flight study 7-39687
 CuCl, off-centre model, vibr. and struct. props. 7-17316
 CuCl, optical bistability and pulse shaping 7-57433
 CuCl, photo-induced optical activity, nonlinear ellipsometric studies 7-14993
 CuCl polycrystalline layers, nonlinear propagation of nanosecond laser pulses 7-53263
 CuCl π-complexes with hexadiene-1,5 and diallyl ether, cryst. struct. determ. 7-21179
 CuCl single cryst. thin films, resonant two-photon absorption and emission 7-22310
 CuCl solid surface, laser-induced desorption and etching processes 7-27092
 CuCl, time-resolved degenerate four-wave mixing under nanosecond pulsed excitation 7-43206
 (Cu₂Cl₆)²⁻ dimers, electronic struct., mag. props., Xα-SW calcs. 7-10419
 CuCl, Br_{1-x} colloids in glasses; x=0-1, exciton spectrum (Chinese) 7-38459
 Cu₂Cl(OH)₃, atacamite, struct. refinement, X-ray diffr. study 7-32371
 CuCl₂·2H₂O, liquid optical filter anal. for hybrid solar energy conversion 7-50724
 CuCl₂·2DMSO, paramagnetic susceptibility of antiferromagnetic quantum chain 7-52997
 Cu₂Co₃O₄, cationic distribution and mag. props. 7-26726
 CuCo₃Ti₁₀O₂, delafossite type struct. cpd. lattice constant (French) 7-63572
 CuCrO₂:Ca, semiconductor, prep., opto-electronic props. 7-2705
 CuCrO₄, cryst. struct. refinement from single-cryst. data 7-58211
 Cu₂Cr₂Sn_{2-2x}S₄ spinels, Cu-Cu distances, EXAFS studies 7-63585
 CuF, low-lying electronic states, radiative lifetimes 7-50258
 CuFe_{2-x}Al_xO₄ system, mag. props. 7-45740
 CuFe₂ electronic struct., K-edge EXAFS study 7-64079
 CuFe₂S₃, EXAFS meas. under high press. by diamond anvil cell 7-64754
 Cu_{1.80}Fe_{0.05}S, structural phase transitions, X-ray diffr. study 7-1935
 Cu_{0.96}SiF₆·6H₂O Jahn-Teller cryst., glass transition, calorimetry and Mossbauer studies (Russian) 7-26952
 Cu₂FeS₄, stannite, melting, polymorphic transition temp. 7-44764
 CuGa_{1-x}In_xS₂, solid solns., conc. depend. of band gap 7-52423
 CuGa_{1-x}In_xSe₂ mixed chalcopyrite local struct., K-edge EXAFS meas. 7-63574
 CuGaS₂, cathodoluminescence from iodine transport method grown crystals (Japanese) 7-3096
 CuGaSe₂ thin films, flash evaporated, optical and elec. props. 7-7417
 CuGaSe₂ thin films, physical props, and photovoltaic potential 7-22047
 CuGaSe₂-CdS solar cells, physical properties and photovoltaic potential of CuGaSe₂ thin films 7-12889

copper compounds continued

- CuGaSe₂-ZnCdS wide bandgap solar cells for thin film tandem structs. 7-23172
 CuGaSe(S)₂, valence band struct., spin-orbit and cryst. field splittings, p-d hybridisation effects calcs. 7-27252
 CuGaSe₂(1-x)Te_x solid solns., prep. and characteris. 7-21169
 CuGaSe₂, valence band struct., spin-orbit and cryst. field splittings, p-d hybridisation effects calcs. 7-27252
 CuGaTe₂, lattice thermal expansion, 80 to 650K 7-12326
 CuGaTe₂ thin films, elec. cond., 100-300K 7-22042
 CuGe₂P₃, semicond., elastic const., anharmonic props. 7-26830
 CuH, singlet and triplet ²Σ⁺ pot. energy curves investigated by valence-only CI calcs. 7-42495
 CuH, vibr.-rot. spectra obs. using FTIR 7-50139
 CuH(CuF)(CuCl) and their cations, ab initio calcs. chemical reactivity 7-10400
 Cu₂HgI₄, order-disorder transition, differential scanning calorimetry high-press. phase diagrams 7-58463
 Cu(I) complexes, UV absorpt. and reson. Raman spectra 7-10593
 CuI, Debye-Waller factors of ¹²⁹I, Mossbauer study 7-2135
 CuI, Debye-Waller factors, Mossbauer scatt. meas. 7-6746
 Cu(II)-alkyl persulphide complex prod., mol. and electronic struct. 7-15590
 Cu(IO₃)₂·2H₂O, electronic absorption spectra, energy splittings 7-64625
 CuIn(Ga)Se₂ thin film solar cells, ESCA anal. 7-23197
 CuIn_{1-x}Ga_xSe₂ absorber materials, electroplating prep. 7-17894
 CuIn_{1-x}Ga_xSe₂, liquid-encapsulated Bridgman-Stockbarger melt growth and props. 7-59403
 CuInS₂, chem. diffusion, 20-100°C 7-16799
 CuInS₂, chemical transport, thermodynamics 7-7832
 CuInS₂ films, RF sputtering, struct. and elec. props. 7-3169
 CuInS₂, heterogeneous, VLS growth, electronic defects, photocurrent spectra, photolum., EBIC analysis 7-27288
 p-CuInS₂, strongly sublinear photocond. 7-52667
 CuInS₂:P, ion implanted, pulsed electron beam annealing 7-16644
 CuInS₂:a-Si:H heterojunctions, photovoltaic behaviour, c-v meas. 7-7340
 CuInS₂-SnO₂:F sprayed solar cells, photovoltaic props. 7-54322
 CuInS₂ photoelectrodes, thermodynamic stability in electrolytes 7-54330
 Cu_{2-x}In_xS crystals, structural transformations 7-38185
 CuInSe thin films, flash evaporation prep. and characterisation 7-7893
 CuInSe₂ coatings, sputter deposition 7-39377
 CuInSe₂ electrodeposited films, photoelectrochem. solar cells fabrication 7-3710
 CuInSe₂ epitaxial films deposited on GaAs and CdS, RHEED studies 7-12549
 CuInSe₂, flash evaporation, elec. and optical props. 7-7892
 CuInSe₂ large grain (112) oriented thin films grown by RF sputtering, solar cell applications 7-17422
 CuInSe₂, p-type, CdS induced homojunction formation 7-58867
 CuInSe₂, pH effects on surface properties 7-23201
 n-CuInSe₂ photoelectrochemical cells 7-23199
 CuInSe₂ photovoltaic devices, analysis using admittance spectroscopy 7-7171
 CuInSe₂ polycryst. semicond. growth from melt, surface props., ion bombardment and annealing effects 7-46304
 CuInSe₂ polycrystalline thin film solar cells 7-17888
 CuInSe₂ polycrystalline thin film solar cells, donor-acceptor pair luminescence 7-17890
 CuInSe₂, thin film, electron beam evaporation optical props. (Korean) 7-27801
 CuInSe₂ thin film growth 7-13368
 CuInSe₂ thin film photoelectrochemical cells 7-23200
 CuInSe₂ thin films, flash evaporated, electrical cond. and optical absorpt. spectrum 7-33112
 CuInSe₂ thin films, polycrystalline, elec. props., effect of excess Cu 7-52871
 CuInSe₂/CdS, thin film chalcopyrite solar cells, electroplating prep. 7-17894
 CuInSe₂/CdS solar cells, modelling and anal. 7-17893
 CuInSe₂/CdS-CdTe/CdS tandem solar cells 7-17891
 CuInSe₂/CdZnS solar cells, spray pyrolysis prep. and characts. 7-8374
 n-CuInSe₂/I⁻-I₂ acidic electrolyte contact, interphase characterisation 7-2703
 p-CuInSe₂/n-(Cd,Zn)S polycrystalline solar cells, open circuit voltage 7-17889
 CuInSe₂-based photoelectrochem. solar cells, optical and electronic props. studies 7-46958
 CuInSe₂-Cd_{1-x}Zn_xS thin-film solar cells, voltage and light bias-dependent spectral response 7-8375
 CuInSe₂-CdS heterojunctions deposition, in-line sputtering system 7-64900
 CuInSe₂-CdS solar cells and CuInSe₂ thin films, charge transport studies 7-12890
 CuInSe₂-CdS solar cells, capacitance determ. of interfacial states 7-13916
 CuInSe₂-CdZnS solar cell development for space appls. 7-13917
 p-CuInSe₂-CdZnS-ZnO solar cells, device anal. 7-23171
 CuInSe₂-Si:H, tandem modules, thin film design and fabrication 7-13913
 CuInSe₂-Si:H thin film tandem solar cells, energy based perform. and eval. 7-13890
 CuInSe₂-ZnCdS thin film polycryst. solar cell efficiency improvement using antireflection coatings 7-23186
 CuInTe film, amorphous, flash evap., DC cond. mechanisms, density of states 7-22041
 CuInTe₂, lattice thermal expansion, 80 to 650K 7-12326
 CuInTe₂ thin films, flash evaporated, elec. conductivity, optical absorption 7-7428
 CuK₂(SO₄)₂·6H₂O·³He, thermal resist., surface mag. coupling, effect of ³He addition 7-52173
 CuMO₂, (M=Cr, Fe, Al, Co), delafossite-type cpds., mag. props. 7-2879
 Cu_{0.25}Mn_{0.75}PS₃, crystalline lamellar cpds. EXAFS studies of disorder 7-59295
 Cu₂Mo₂O₇, synthesis and cryst. struct. 7-32398
 CuMo₂S₄ porous film, prep. on Cu₂S by solid-gas reaction, secondary battery appl. 7-27897
 Cu₂Mo₂S₈, Chevrel cpd., oxidation study 7-3473
 Cu(NH₃)₄(MnO₄)₂, cryst. struct. determ. 7-1959
 Cu(NO₃)₂·2.5 H₂O, EPR and magneto-microwave birefringence powder spectra 7-45810
 Cu(NO₃)₂·3H₂O, liquid optical filter anal. for hybrid solar energy conversion 7-50724

copper compounds continued

- Cu_2NbSe_2 intercalation cpds., crystal structures and staging 7-12023
 $\text{Cu}_{1-x}\text{Ni}_x\text{Cr}_2\text{O}_4$, heat capacity anomalies, cooperative Jahn-Teller effect 7-6823
 $\text{CuNi}_2\text{S}_2\text{O}_5$, delafossite type struct. cpd. lattice constant (French) 7-63572
 $\text{CuNi}_2\text{S}_2\text{O}_5$, crystal structure determ. 7-26728
 $\text{CuNi}_2\text{S}_2\text{O}_5$, delafossite type struct. cpd. lattice constant (French) 7-63572
 CuO and magnesia ceramic, direct bonding region, thermal resistance 7-37395
 CuO , preparation using $\gamma\text{-Cu}_2(\text{OH})_2\text{Cl}$ precursor, X-ray diffr. 7-27970
 $\text{CuO-Al}_2\text{O}_3$ dispersed oxides, positron annihilation 7-39275
 $\text{CuO-La}_2\text{O}_3\text{-Al}_2\text{O}_3$, phase transformations and solid soln. form. 7-2176
 $\text{CuO-P}_2\text{O}_5$ glasses containing NiO or CoO , elec. cond. 7-17025
 $\text{CuO-V}_2\text{O}_5\text{-Na}_2\text{O-P}_2\text{O}_5$ phosphate glasses EPR of Cu^{2+} and Vo^{2+} ions. 7-59107
 CuO-ZnO p-n contact, sensor appls. 7-64996
 $(\text{CuOCl}_6)_x$ complexes, ($x=1,2$), bonding and configuration, matrix isolation ESR spectra anal. 7-19905
 CuO crystals, diamagnetic excitons, valence band corrugation 7-64546
 Cu_2O electrodeposited film electrodes in photoelectrochemical cells, n-type photocond. obs. 7-17917
 Cu_2O , electronic struct. and binding mech. 7-2482
 Cu_2O film-electrolyte interface, photoelectric effect 7-38723
 Cu_2O films, annealing of Cu and O vacancies, cathodoluminescence study 7-59263
 Cu_2O , long-lived strain-confined paraexciton thermodynamics, recomb. luminesc. and thermalisation 7-2492
 Cu_2O , Raman-like luminescence emission (Japanese) 7-59219
 Cu_2O surface with chemisorbed benzotriazole, UPS study 7-21656
 Cu_2O , use of dynamic electron scatt. for studying O atom position 7-44501
 $\text{Cu}_2\text{O-Al}_2\text{O}_3\text{-Al}$ moisture transducer, design and development 7-41395
 $\text{Cu}_2\text{OCl}_6((\text{C}_6\text{H}_5)_3\text{PO})_4\cdot 0.70\text{CH}_3\text{NO}_2$ crystals, anharmonic atomic thermal vibrs. and pots. X-ray diffr. struct. study 7-63762
 CuOH , metal-OH bonding study 7-52240
 $\text{Cu}_2(\text{OH})_2\text{CO}_3$, malachite, X-ray K-absorpt. study 7-7790
 $\text{Cu}(\text{PH}_3)_2(\text{BH}_4)_2$, mol. vibr. coupling, dynamic electron transfers, variational method calcs. 7-36585
 $\text{Cu}_2\text{P}_2\text{I}_2$, solid electrolyte, prep., props. and cryst. struct. 7-32396
 $\text{Cu}_{1.8}\text{S-CdTe}$ thin film polycrystalline solar transducers, photosensitivity spectra 7-34036
 $\text{Cu}_{1.8}\text{S-SeCdTe}$ thin film polycrystalline solar transducers, photosensitivity spectra 7-34036
 $\text{Cu}_{1.8}\text{S}_2$, digenite, single crystal, structural transitions 7-12259
 Cu_2S films, chemically sprayed, optical and solar selective props. 7-54350
 Cu_2S films, flash-evaporated, optical props. and solar selectivity 7-64719
 Cu_2S , interpretation of AES of sulphide minerals 7-22391
 Cu_2S thin films, form. by electrochem. procedure 7-39445
 $\text{Cu}_2\text{S/CdS}$ large-area solar cells, reactive sputtering 7-46943
 $\text{Cu}_2\text{S-CdS}$ heterojunction, form. by photoelectrochemical process, phys. props. under light irradi. 7-45456
 $\text{Cu}_2\text{S-CdS}$ polycrystalline solar cell, freq. dispersion in admittance 7-65464
 $\text{Cu}_2\text{S-CdS}$ solar cells, all-evaporation processed, characts. 7-8383
 $\text{Cu}_2\text{S-CdS}$ solar cells, SEM and Auger microanalysis 7-23189
 Cu_2S crystals, structural transformations 7-38185
 Cu_2S films, field assisted chemiplating for $\text{CdS/Cu}_2\text{S}$ heterostruct., growth mechanism 7-59470
 Cu_2S , stoichiometry and phase transitions, Cu^{2+} EPR studies 7-17219
 $\text{Cu}_2\text{S-Cd}_{1-x}\text{Zn}_x\text{S}$ thin film solar cells perform., depend. on annealing temp. 7-17861
 $\text{Cu}_2\text{S-CdS}$ solar cells, comp. of differing junction types, AES, SIMS determ. 7-23167
 CuSO_4 soln., double diffusive convection, conc. meas., optical technique. 7-57825
 $\text{CuSO}_4\cdot 5\text{H}_2\text{O}$, liquid optical filter anal. for hybrid solar energy conversion 7-50724
 $\text{CuSO}_4\cdot 5\text{D}_2\text{O}$, indirect nucl. spin-spin interaction above chain crit. field 7-2948
 $\text{CuSO}_4\cdot 5\text{H}_2\text{O}$, indirect nucl. spin-spin interaction above chain crit. field 7-2948
 $\text{Cu}_2\text{S}(\text{Se})(\text{Te})\text{-Ag}_2\text{S}(\text{Se})(\text{Te})$ liq. and glassy semicond., activation energy of carrier thermal generation, elec. meas. 7-17035
 CuSeO_2 , delafossite type struct. cpd. lattice constant (French) 7-63572
 Cu_{2-x}Se , electrical resistivity, temp. and carrier density dependences 7-38556
 Cu_{2-x}Se , struct. phase transition, X-ray diffr. studies 7-2179
 CuSeO_3 , cryst. struct. of three modifications, X-ray diffr. study (German) 7-32410
 CuSeO_3 struct. determ. and refinement, X-ray diffr. study 7-32373
 $\text{Cu}(\text{SeO}_2\text{OH})_2$, synthesis and cryst. struct. 7-2004
 $\text{CuSiF}_6\cdot \text{H}_2\text{O}$ four-sublattice Jahn-Teller crystals., phase transitions, free energy and symm. props. calcs. 7-2544
 $\text{Cu}_6\text{Si}_6\text{O}_{18}\cdot 6\text{H}_2\text{O}$, Diopside crystals., Cu^{2+} EPR and optical absorpt. spectra studies 7-53120
 $\text{Cu}_2\text{SnP}_{10}$, bonding and electronic struct. studies 7-26694
 CuTaS_3 , isomer shift of elec. split 6.2 keV nucl. transition of ^{181}Ta 7-7624
 CuTiH_x , amorphous hydrides, quasi elastic and inelastic neutron scatt. 7-21382
 $\text{CuTiH}(\text{D})$ amorphous hydrides, neutron diffr., computer simulation studies 7-21109
 $\text{Cu}_3\text{Ti}_2(\text{PO}_4)_3$, Nasicon-type phase, struct. and physical props. 7-45804
 $\text{CuTiS}(\text{Se})\text{-AgTiS}(\text{Se})$, solid solutions, phase formation 7-7976
 $\beta\text{-Cu}_2\text{V}_2\text{O}_5$, ESR spectra 7-64517
 $\text{Eu}(\text{Cu}_{1-x}\text{M}_x)_2\text{Si}_2$ ($\text{M}=\text{Au}, \text{Ag}, \text{Ru}, \text{Ni}$), substitution effects on mixed valence behaviour, Mossbauer and XANES studies 7-64183
 $\text{EuCu}_2(\text{Si}_{1-x}\text{Sn}_x)_2$, substitution effects on mixed valence behaviour, Mossbauer and XANES studies 7-64183
 $\text{GeCuH}(\text{D})_2$, acceptor electronic state symm., isotope effects study 7-21863
 $\text{KCu}_4\text{Cl}_3(\text{I}_3)$ and KCu_4I_3 solid electrolytes, elec. conductivity and mag. susceptibility 7-12360
 K_2CuF_4 , 2D ferromagnet, polarised neutron studies of forbidden magnons 7-45693
 $\text{K}_2\text{CuMn}_{1-x}\text{F}_4$, quasi-two-dimensional mixed ferromagnetic-antiferromag. system, mag. phase transitions, intermediate spin glass phase 7-27525
 $\text{K}_3\text{Cu}_8\text{S}_6$, mixed valence 2D metal, CDW 7-45294

copper compounds continued

- K_2CuX_3 , ($\text{X}=\text{Cl}, \text{Br}$), energy band struct., fundamental optical absorption 7-7093
 La-Ba-Cu-O system, superconducting transition above 40 K, high press. 7-58946
 $\text{LaNi}_4\text{CuH}_x$, dynamical disorder of H, quasi-elastic neutron scatt. study 7-21535
 $\text{La}_{1.8}\text{Sr}_{0.2}\text{CuO}_4$, superconducting transition at 36.2 K 7-58947
 Li/CuO -chalcopyrite battery structure and characteristics (Japanese) 7-65424
 $\text{Li}_2\text{B}_2\text{O}_7\text{-CuCl}_2$ crystallised glasses, pure and doped, thermally stimulated exoelectron emission, thermolum. 7-27874
 $\text{Li}_{1-x}\text{Cu}_x\text{MnRuO}_4$ system, prep. and characterisation (German) 7-26721
 $\text{Na}_2\text{B}_2\text{O}_7\text{-Pb}_2\text{O}_4\text{-CuO}$ glasses, elec. props., effect of added CuO 7-2605
 $\text{Na}_2\text{O-B}_2\text{O}_3\text{-CuO}$ glasses, B ions coordination state studied by X-ray and Raman spectroscopy 7-1892
 $\text{Na}_5[\text{Cu}(\text{HIO}_6)_2]\cdot 16\text{H}_2\text{O}$, room temp. reson. Raman spectrum 7-64638
 $\text{Nd}_{2-x}\text{Cu}_x\text{Ru}_2\text{O}_{7-y}$ pyrochlore type phases, elec. and cryst. characts., X-ray fluoresc. anal. (French) 7-45325
 $\text{NdCu}_3\text{Ru}_2\text{Ti}_{4-x}\text{O}_{12}$ and $\text{Nd}_{2+x}\text{Cu}_3\text{Ru}_2\text{Ti}_{4-x}\text{O}_{12}$, electrical conductivity and crystallographic characterisation (French) 7-17057
 $\text{Ni}_{0.97}\text{Cu}_{0.03}\text{Fe}_2\text{O}_3$, ferrite, domain-acoustic echo 7-13014
 NiCuNbO_4 , cryst. data and conductance investig. 7-38550
 NiO-CuO solid solutions, tweed microstruct., investig. using TEM 7-44756
 NiO-CuO solid solutions, evidence for long-range cation order, TEM investig. 7-44757
 RbCuCl_3 single crystals., mag. suscept. meas., exchange interactions, magnetic and crystallographic transitions studies 7-52950
 $\text{Rb}_4\text{Cu}_9\text{Cl}_{13}$, solid electrolyte, elec. cond. and cryst. struct. 7-2257
 $\text{Rb}_4\text{Cu}_9\text{Cl}_{13}$ solid electrolyte single crystals., anisotropic elec. cond. meas., structural model 7-52126
 $\text{RbCu}_4\text{Cl}_{13}$, luminesc. band profile, localised carrier tunnel recomb. effects calcs. 7-3075
 Rb_5CuX_3 , ($\text{X}=\text{Cl}, \text{Br}, \text{I}$), energy band struct., fundamental optical absorption 7-7093
 $\text{Ti}_2\text{Cu}(\text{SO}_4)_2$, glassy γ -modification, structural and electronic props. studies 7-58161
 $\text{Ti}_2\text{S-Cu}_2\text{S}$ melts, ionic-electronic conductivity 7-33057
 $\text{U-Cu-P}(\text{As})$, ternary particles, cryst. struct. and mag. props. 7-12955
 ZnS -based electroluminescent phosphor, influence of surface Cu_2S 7-7759

copper zinc brass alloys see brass

Corbino effect

see also Hall effect

Al, Corbino effect, thickness variations effects 7-38539

core levels see localised electron states; surface electron states

Coriolis force

see also rotation

acetylene, isotopic species, mol. vibr., rot. energy level struct. calcs. 7-50061

atmosphere, effect of Coriolis parameter on vortices formation over ocean surface heat anomalies 7-9134

atom-atom collisions, angular momentum coupling 7-10706

beams, rot., pretwisted, preconed, nonlinear flap-lag extensional vibrs. 7-63036

Benard-Marangoni's instability, nonuniform temp. gradient and Coriolis force effect 7-43886

coriolis coupling constants calculated using the high and low frequency separation method (HLFS) 7-56028

9-cyanoanthracene, intramol. radiationless transitions, rot. effects 7-57116

cyclopropane, IR spectra, combination bands, vibr.-rot. coupling parameters 7-25515

difluorodichloromethane, mol. const., force field study, thermodynamics props. 7-19814

dihalogenanes, mol. dynamics, vibr. anal. 7-50049

falling body, sideways deflection 7-29630

fluoroform-d, Coriolis splitting parameter, vibr. depend., IR double-reson. spectra anal. 7-42616

formic acid, ν_3 band, sub-Doppler laser-stack and Fourier transform spectroscopy 7-62430

fully developed turbulent flow in rot. channel, large-eddy simulation 7-37450

germylacetylene- $\text{d}_0(\text{d}_3)$, vibr. anal., mol. const. study, F-G matrix technique calcs. 7-36578

glyoxal, vibr. and rot. const. meas., stimulated emission polarisation spectroscopy 7-57136

gravity current on sloping bottom, rot. flow interaction, shelf wave generation, flow visualisation expts. 7-43947

hexafluoride mols., vibr. isotope shifts 7-943

hydrostatic atmospheric gravity waves, influence of Coriolis force due to Earth's rot. (French) 7-18271

iodomethane, ν_4 band, high resolution IR spectra 7-5681

iodomethane, IR spectrum, rot. anal. and interaction mechanism 7-57063

methane- $\text{d}_1(\text{d}_3)$, bending mode triad, anal. model, IR spectra 7-19822

methylene chloride, isotope effect, empirical general harmonic force field 7-62346

microwave spectra, quadratic vibr.-rot. coupling terms 7-50089

nitril halides and their isotopes, vibr. anal. 7-50051

ocean dynamics, latit. var. of Coriolis parameter rel. to barotropic continental shelf waves on β -plane 7-8983

propyne, $2\nu_9$ band study, Fourier transform IR spectra anal. 7-50119

pyrazine $\text{S}_1(\text{B}_{3u})$ state, rot. induced vibr. energy redistrib. and K selectivity model 7-10710

rigid particle suspensions, mass and entropy transport 7-32691

rotating plasma, thermosolutal instability, Coriolis force and ion Larmor radius effects 7-44135

turbulent boundary layer with pressure gradient, Coriolis force effects 7-20695

turbulent flow struct. in rot. channel, large-eddy simulation 7-37442

ClO_2 struct., pot. functions, electron diffr. and spectroscopic data 7-15708

D_2CO + inert gas, Coriolis enhanced vibr. energy transfer theory and its appls. 7-31153

$\text{GeH}_3\text{D}(\text{GeD}_3\text{H})$, bending mode triad, anal. model, IR spectra 7-19822

HCN-HF , Coriolis coupling const., eval. for ν_9 estimation 7-5583

HCN-HF , excited vibr. states, gas-phase IR spectrum 7-50108

Coriolis force continued

- HDNNC, rot.-inversion spectrum in region from 100 to 400 GHz 7-25494
 HDO, $\nu_1 + \nu_2$ and $3\nu_2$ bands, energy level and intensity calcs. 7-5654
 H₂GeD, Fourier transform IR spectra, rovibr. anal. 7-25516
 HN₃, rot. anal. for ground, ν_2 and ν_6 states, IR spectra 7-19850
 H₂SiD, Fourier transform IR spectra, rovibr. anal. 7-25516
 H₂SiF, Coriolis coupling, FT IR spectrum, rovibr. anal. 7-5679
 H₂SnBr, rovibr. anal., harmonic force field calc., Fourier transform IR spectra study 7-50122
 H₂SnCl, rovibr. anal., harmonic force field calc., Fourier transform IR spectra study 7-50122
 H₂SnI, rovibr. anal., harmonic force field calc., Fourier transform IR spectra study 7-50122
 IOF₃, excited vibr. state, microwave spectrum, vibr. and rot. parameters 7-25498
 Na₂P₂Se₆, isomeric forms, P₂Se₆⁴⁻ vibr. spectra, normal coordinate anal. (German) 7-22270
 NpF₆, IR-active fundamentals and combination bands, vibr. force consts. 7-25511
 PuF₆, IR-active fundamentals and combination bands, vibr. force consts. 7-25511
 SF₆, mol. vibr.-rot. consts., IR saturated absorpt. spectra anal. 7-50118
 SeO₂, struct., pot. functions, electron diffr. and spectroscopic data 7-15708
 SiH₄, mol. vibr., rot. energy level struct. calcs. 7-50061
 SiH₃D(SiD₃H), bending mode triad, anal. model, IR spectra 7-19822
 SnH₃D(SnD₃H), bending mode triad, anal. model, IR spectra 7-19822
 Ti₄P₂Se₆, isomeric forms, P₂Se₆⁴⁻ vibr. spectra, normal coordinate anal. (German) 7-22270

cornea *see eye***corona**

- see also electric breakdown; flashover*
 3D tuft corona and EHD, num. simulation 7-20983
 1150 kV power lines, acoustic noise due to corona (Russian) 7-1314
 air, negative corona, neutral densities and temps., optical interferometric and thermocouple studies 7-26569
 air, positive corona discharge, influence of water mols., mass spectra anal. 7-32180
 air negative corona discharge current, halobenzene admixture influence 7-32176
 alpha-particle corona streamer counter 7-55333
 back corona, effect in laboratory scale electrostatic precipitator 7-20981
 back-corona discharge, laboratory analysis 7-58083
 bridged-over, control using high-intensity sound 7-20581
 bunched model in gas-dynamical flow 7-20986
 charged aerosol particle motion 7-32156
 coaxial electrode system, steep wavefront discharges 7-51545
 DC ionised field quantities as influenced by coronating conductor surface gradient 7-58074
 discharge inception voltage from free cond. particles in air 7-51544
 double impulse tests of long airgaps, leader decay and reactivation 7-20975
 electrified menisci, cone-like shapes, emitted charge effects 7-31888
 electrostatic precipitators, corona discharges, laboratory analyses 7-58082
 electrostatic precipitators back-corona initiation, anal. 7-51555
 fast electron form. in caviton field, depend. on laser radiation parameters, steady-state corona model 7-44204
 high voltage transmission lines, corona discharges and ion prod. 7-29232
 iced insulator string flashover mechanism; role of water film 7-51556
 insulators, electrical damage, fluorescence probes 7-51525
 inverse bremsstrahlung absorption in the planar corona of a laser target 7-16335
 ion beam incident on pellet, ablative corona generation 7-1803
 laser corona, anomalous filamentation, current instability and excitation 7-26549
 laser-generated pellet coronas, steady ID outflow form. 7-37785
 metallic ground points beneath thunderstorm, calc. of space charge due to corona discharge (Chinese) 7-29222
 microwave discharge, plasma corona, large amplitude plasma waves and particle acceleration 7-63380
 multiconductor transmission line, effect of pulse corona discharge on coupling coeffs. and wave impedances 7-63383
 ozone generation using travelling wave pulse voltage and transmission-line ozonizer, corona prod. 7-20984
 parallel-horizontal cylinder rows under corona discharge, heat transfer 7-43634
 parallel-plate electrodes, corona wire, repulsive forces 7-58081
 photothermoplastic material, electrostatic sensitisation pot. and parameters of scorotron 7-38683
 plasma, emission characteristics, soft X-ray region, plasma diagnostics, radiative-collisional model study 7-62312
 point-to-plane corona discharge, back ionisation 7-26568
 polyethylene films, surface modification by corona discharge 7-39691
 polypropylene film electrets, corona-charge mechanism 7-53227
 positive corona, math. anal. of glow and dark space regions 7-20982
 rod-plane gap, corona, breakdown and humidity effects 7-20979
 rod-plane gap, space-charge behaviour evaluation using Pockels' cells 7-20980
 supersonic expansion, corona excited for cold radicals or ions production 7-9926
 underdense coronal plasma, laser interaction physics 7-26432
 unipolar space charge flow 7-26567
 XLPE, dielectric properties modification due to corona discharges, humidity effects 7-39022
 Z-pinch, corona form. radiative loss, dynamics, ID approx. 7-51483
 Ar-CF₄ mixtures in corona discharges in diffuse discharge switch appls., decomposition 7-37799
 H₂O, deionized, for capacitor insulation, partial discharge and electric breakdown 7-32186
 NO₃⁻ production in negative corona discharge, mass spectra 7-32175
 SF₆ and SF₆ mixtures, streamer, leader and corona formation under positive impulse 7-37773
 SF₆, breakdown and corona, electrode surface processing effect 7-51557
 SF₆, corona and glow discharges, electrode-F reaction influence 7-26565
 SF₆+Freon 113 mixtures in nonuniform field gaps, breakdown 7-51551
 SF₆+O₂, decomp. rate of SF₆, influence of O₂ in corona 7-51548
 ZnO powder-polyvinyl butyral films, dark discharge props. 7-58919

coronagraphs

- see also solar corona*
 No entries

correlation methods

- see also correlators; optical correlation*
 2D target reconstruction using normalisation and recorrelation, noise elimination 7-36908
 central nervous system connections determ. by physiological methods 7-47037
 crosscorrelation for evoked potential analysis 7-8551
 Dhahran, Saudi Arabia, insolation meas., diffuse fraction estimation 7-3625
 digital correlation method, optimised appl. to deformation analysis 7-26136
 digital image correlation methodology use for deform. quantification in composites 7-59718
 disjunctive kriging, appl. to elec. cond. distrib. 7-23755
 disjunctive kriging, estimation and conditional probability 7-23754
 Earth crust investigations, simultaneous correl. anal. of gravity, mag. and seismic data 7-47552
 flowmeter, EM, for liq. metal flow rate meas., error in correl. method 7-57954
 galaxies, effects of non-Gaussian mass density fluctuations on two-point correls. 7-29545
 galaxy cluster-cluster correlation function, sampling errors and significance levels 7-48092
 rich galaxy clusters, effects of non-Gaussian mass density fluctuations on two-point correls. 7-29545
 galaxy correlation functions, closure of BBGKY hierarchy in phase space 7-29546
 galaxy correlation scales, effects of percolation of explosive galaxy form. 7-29533
 general purpose correlator for introductory student demonstration expts. 7-18537
 heat transfer between immersed surfaces and large-particle gas-fluidised beds 7-26127
 komatiites alteration analysis, role of spurious correl. in development of alteration model 7-55039
 limited time-series data, correl. algorithms appl. 7-224
 magnetospheric VLF radio waves spectral estimation, one-bit correlation method 7-9337
 marine paths, correlation props. of signals in 10 cm band with angular diversity reception 7-23823
 Mekometer distance meas., statistical correction methods (German) 7-23519
 moving sound source analysis, orbit determ. using linear sensor array 7-43492
 muscle fibre conduction velocity meas. with surface EMG, cross-correlation method 7-3763
 pump cavitation monitoring by single fluid-borne noise meas. 7-37502
 remote sensing, correl. of spectral radiance parameters measured from multiband space images 7-66339
 sea surface temperature anomaly field in N Atlantic Ocean, autoregression model 7-14309
 stellar speckle interferometry, potential accuracy of ang. dias. and limb darkening meas. 7-47720
 time-variable signals, computer averaging by autocorrelation 7-18768
 velocity-field measurement by pixel-based temporal mutual-correlation analysis of dynamic image 7-20823
 well-logs zoning and correl., computer techniques 7-9195
 Z 7-40583
 H₂O, positron age-momentum correlation meas. 7-36440

correlation theory

- see also correlators; information theory*
 wave field, rough surface with high Rayleigh parameter scattered, intensity correlation 7-57209

correlators

- see also correlation methods; correlation theory; information theory*
 acousto-optical correlators possible appls. in radiointerferometry 7-60569
 nuclear fuel reprocessing, fluid flow meas., microcomputer-based multi-channel polarity cross-correlator 7-42121
 optical fibre characteristics and industrial production techniques (French) 7-1282
 VLBI correlators, signal loss due to imperfect fringe rqt. 7-47722

correspondence principle

- No entries

corrosion

- see also corrosion fatigue; corrosion protection; corrosion testing; electrochemistry; stress corrosion cracking; surface chemistry*
 alloy 600 nuclear steam generator tubes, local pitting conditions using Pourbaix diagrams 7-46716
 alloy 600 tubes, intergranular attack, cause evaluation 7-59685
 alloy 600 tubes in PWR steam generators, localised electrochem. corrosion 7-39760
 alloy 600 tubing in nuclear steam generators, intergranular attack, environmental effects eval. 7-39761
 Alloy 800, pitting corrosion in chloride-sulphate media, potentiodynamic polarisation 7-65184
 alloys, high temp. corrosion in sulphidising/oxidising environments, review 7-39737
 borosilicate glass, dissolution method study using fission track method 7-53937
 borosilicate glasses, fission track etching using deionized water 7-53938
 BR-10 reactor first circuit pipelines, radioisotope distrib. 7-30590
 brass, 63/37, electrochem. behaviour in binary mixtures of N,N-dimethylformamide and water 7-46677
 brass, stress assisted dezincification in NH₃ soln. 7-17675
 breached LMR fuel element, thermal effects of Na₂(U_{1-y}Pu_y)O₄ formation 7-30558
 BWR, mass transfer anal. of corrosion products in water circuit 7-61980
 BWR at Gundremmingen nuclear power station with twin 1300 MW units, corrosion products (German) 7-10241
 BWRs, methods for dose rate reduction, ^{58,60}Co concs. in coolant 7-42187
 Calvert Cliffs Unit 1 tube examination 7-61970
 CEBG single-phase erosion-corrosion research programme for AGR boilers 7-59679
 cement-based nuclear waste forms, leach-test characterisation 7-49691
 computer modelling, expert system, information use 7-3470
 computer modelling, expert systems, decision tree 7-3469

corrosion continued

conference, tribology and lubrication, Tokyo, Japan (July 1985) 7-4631
 cylindrical object, simulated corrosion wastages detection, US waveguide technique 7-59729
 defect mapping by in-water photocorrosion 7-59692
 devitrified simulated HLW glass, leaching, crystalline phases effects 7-49690
 double layer capacity and corrosion rate, relax. technique meas. 7-39680
 electron spectroscopy, role in corrosion science, review 7-22860
 electronic materials and devices corrosion 7-33815
 flue gas scrubber corrosion rel. to pH and trace element concentrations 7-40077
 fusion reactor materials, conf., Chicago, IL, USA (Apr. 1986) 7-48145
 fusion reactor materials, corrosion by liq. Li or Li-Pb blankets, mass transfer obs. 7-49659
 fusion reactor materials, crack growth behavior, appl. of H embrittlement models 7-53850
 graphite, nuclear material, corrosion and irradiation induced porosity 7-51836
 high-temperature corrosion film characterization using Raman microscopy 7-46772
 HLW disposal in salt formations, field expts., groundwater, corrosion 7-5465
 HLW immobilisation in ceramic waste forms. SYNROC props., leaching 7-5459
 immobilised nuclear wastes, diffusing species release by leaching in closed solid/liquid system 7-810
 Inconel 600, corrosion resist., effects of BF_2^+ ion implementation 7-39734
 intermetallic phases, appl. as high temp. materials, review 7-22775
 JMTR OWL-1 loop water, crud behaviour, ^{60}Co chemical form 7-19390
 LaSalle-1 BWR, water chemistry, corrosion products and radiation-field buildup 7-36206
 LWR accident source term expts. deposition samples 7-62047
 marine alloys, polarisation under flowing and quiescent conditions 7-39720
 mass transport effect on corrosion rates determ., polarisation curves 7-28191
 metal depassivation in neutral aq. solns., anion type effects 7-13627
 metallic corrosion of cement plant facilities, cathodic protection 7-28210
 metals, corrosion in contact with thermal insulation (*German*) 7-3524
 metals, corrosion in contact with wood (*German*) 7-3523
 metals, high temp. corrosion in sulphidising/oxidising environments 7-3494
 metals, microbiologically induced 7-46683
 metals, pointed, corrosion, impedance plot methods 7-3486
 metals, positive and negative ion exoemission, physicochemical conception 7-13301
 molten carbonate fuel cells, corrosion, anal. using Cr-Li-K-C-O system phase relationships 7-28020
 New Zealand, sea salt wind-borne transport and deposition, implications for corrosion 7-14361
 Nimonic 80A, crack growth under sulphidising conditions, metallography 7-59680
 nuclear waste glass, comparison of leaching in natural and synthesized groundwaters 7-19530
 nuclear waste/natural glasses, aqueous corrosion, comparative hydration rates in liquid/vapour environments 7-8141
 phosphate glasses, corrosion studies, conventional and glancing angle EXAFS 7-59284
 PNP-500 pebble bed reactor, massive water ingress accidents, computer anal., graphite corrosion (*German*) 7-5371
 polarization effects in galvanic corrosion 7-39706
 polymers, corrosive medium and mech. stress effect (*Russian*) 7-65166
 pressure vessels, high temperature life prediction, computer modelling anal. 7-3391
 PWR, improved water chemistry controls for minimizing degradation of materials 7-30615
 PWR, solubility of simulated primary circuit corrosion products 7-19401
 PWR boiler pipework, effect of feedwater conditioning on corrosion (*German*) 7-25115
 PWR feedwater, Cu oxides, acid chlorides, steam generator denting 7-5333
 PWR secondary water chemistry, corrosion reduction (*German*) 7-62010
 PWR secondary water chemistry, corrosion reduction (*German*) 7-62011
 PWR steam generators, correlation of tube support struct. studies, corrosion 7-10246
 PWR steam generators, review of secondary side tube degradation processes 7-30616
 PWRs, seawater cooled steam generators, tube support corrosion, chlorides effects 7-46715
 reactor steam generator pitting, electrochemical effects on Ni-base alloys 7-10228
 reactor steam generators, crevice hideout return testing, H_3BO_3 and $\text{Ca}(\text{OH})_2$ effects 7-10247
 Savannah River Plant waste glass, interaction with canister and overpack metals 7-8142
 semiconductor interfaces, bonding and adhesion, characterisation techniques, electronic struct. 7-27418
 sphene ceramics containing substituted radionuclides, leaching, CANDU waste disposal 7-811
 stainless steel, exposure to high temp. OWL-1 loop water, corrosion layer characterization 7-8167
 steel, alloy, corrosion resist., influence of thermomech. treatment 7-22873
 steel, austenitic, Al-Mn, mech. props., oxidation and corrosion behaviour 7-65218
 steel, austenitic, fusion reactor first wall material, development and testing 7-53860
 steel, austenitic Cr-Mn, corrosion in thermally convective Li 7-53960
 steel, austenitic stainless, compatibility with liq. and solid T breeding materials 7-53966
 steel, austenitic stainless, corrosion, γ -radiation effect 7-28173
 steel, austenitic stainless, corrosion and grain boundary Cr depletion, comparison in modified strauss test 7-39728
 steel, austenitic stainless, corrosion in flowing PbLi eutectic 7-53958
 steel, austenitic stainless, corrosion in high temp. water containing both dissolved H and O 7-65177
 steel, austenitic stainless, corrosion in Na loop system, downstream effects 7-3504
 steel, austenitic stainless, corrosion product release in lithiated high temp. water, mechanism and kinetics 7-65172

corrosion continued

steel, austenitic stainless, corrosion resist. in Cl^- containing water at high temp. (*German*) 7-3525
 steel, austenitic stainless, crevice corrosion NaCl soln., electrochemical kinetics 7-39701
 steel, austenitic stainless, intercrystalline corrosion causes and counter-measures (*German*) 7-17729
 steel, austenitic stainless, intercrystalline corrosion rel. to chromium carbide precip. 7-53986
 steel, austenitic stainless, microbial pitting mechanism 7-39724
 steel, austenitic stainless, Mo-ion plated, corrosion resist. in flowing Na environment 7-59667
 steel, austenitic stainless, passivation and pitting corrosion rel. to Ti stabilisation and Mn content (*German*) 7-39756
 steel, austenitic stainless, pitting corrosion in NaCl soln., electrochemical obs. 7-39700
 steel, austenitic stainless, sensitised, corrosion in sulphidising atmosphere 7-17710
 steel, austenitic stainless, sensitized, intergranular corrosion, inhibition mechanism of S-containing additives 7-53946
 steel, austenitic stainless and Cr-Mo, corrosion in flowing Li environment, temp. and purity depend. 7-53961
 steel, austenitic stainless and Cr-Mo, corrosion in molten thermally convective Pb-Li 7-53962
 steel, austenitic stainless and CrMo, corrosion in flowing Pb-Li environment 7-53959
 steel, bearing, fretting wear in seawater 7-8124
 steel, boronized low C, conversion electron and X-ray Mossbauer studies under corrosion and oxidation conditions 7-27632
 steel, C, corrosion in aq. sour gas environments 7-39713
 steel, C and austenitic stainless, corrosive wear in NaCl soln. 7-8191
 steel, C type, corrosion acceleration in boiling annular crevices, 100°C chloride solns. 7-65219
 steel, cold-rolled, corrosion investig. by thermal-wave microscopy 7-28169
 steel, corrosion monitoring by AE 7-22956
 steel, Cr containing, elevated temp. combined erosion-corrosion, particle impacts 7-3517
 steel, Cr-Mn and Cr-Mn-Ni types, corrosion and SCC behaviour 7-17683
 steel, Cr-Mo, elevated temp. erosion-corrosion 7-3518
 steel, Cr-Mo, erosion-corrosion, effect of temp. 7-3519
 steel, Cr-Mo, friction pair, surface layer structural modifications (*Russian*) 7-39678
 steel, duplex stainless, electrochem. test for intergranular corrosion susceptibility 7-39794
 steel, ferritic, fusion reactor first wall material, development and testing 7-53860
 steel, ferritic stainless, corrosion resist. in H_2SO_4 soln., alloying effects 7-28172
 steel, galvanised sheet, surface treatment prior to painting, effects on surface comp. and corrosion resist. (*French*) 7-46703
 steel, high C, grinding balls, jet slurry corrosive wear 7-39676
 steel, HSLA, corrosion in sea water, long term exposure tests, alloying elements effect 7-3482
 steel, HSLA, rolled sheets, residual surface stresses, corrosion pot., X-ray obs. 7-39704
 steel, maraging, struct., mech. props. and cavitation-corrosion stability (*Russian*) 7-46684
 steel, mild, acoustic emission during corrosion in FeCl_3 soln. 7-39814
 steel, mild, corrosion in sea water, calcareous deposits form. 7-3485
 steel, mild, corrosion inhibition by Schiff bases in HCl soln. 7-17680
 steel, mild, erosion-corrosion control using O_2 - NH_4 -hydrazine dosed feed-water in reactor boilers 7-59675
 steel, mild, H diffusivity meas. using electropemutation transients 7-22903
 steel, mild, radiation enhanced corrosion of radwaste containers 7-30710
 steel, N^+ implanted layers, in 9Cr18, GCr15 steels (*Chinese*) 7-53996
 steel, stainless, $(\text{Cr}_x\text{Fe}_{1-x})_{23}\text{C}_6$ compact specimens, corrosion-electrochem. and phys. props. w.r.t. comp. 7-54000
 steel, stainless, corrosion behaviour in formic acid (*German*) 7-3526
 steel, stainless, corrosion by Pu in PUREX reprocessing environment 7-25096
 steel, stainless, corrosion films, effect of Zn incorporation 7-39732
 steel, stainless, corrosion resistance, Al and Si alloying effects (*French*) 7-17711
 steel, stainless, duplex, corrosion imaged and welded conditions, microstruct. effect 7-39698
 steel, stainless, high temp. corrosion by oxidising gases (*Korean*) 7-8161
 steel, stainless, microelectrodes, pitting dissolution in NaCl solns., nitrate passivation 7-39703
 steel, stainless, oxide growth mechanisms and corrosion rate for types 405 and 409 7-13649
 steel, stainless, polarisation behaviour and admittance response in NaCl soln. (*Japanese*) 7-22871
 steel, stainless, powder compacts, props., influence of sintering conditions (*Korean*) 7-17496
 steel, stainless, surface corrosion products after exposure to liq. alkali metals, glow discharge optical spectroscopy, SIMS anal. 7-22896
 steel, structural, diffusion chromised, elevated temp. effect on comp., struct. and mech. props. 7-8178
 steel, tool, corrosion resistance in molten Al alloy 7-33835
 steel, wear resist. under wet-abrasive erosion conditions 7-22848
 steel, X8CrNiTi18.10, corrosion product layers in PWRs at pH 7 (*German*) 7-19356
 steel radioactive waste canisters, localised corrosion, mathematical model 7-46709
 steel with chromium and eutectic coatings, wear resist. in corrosive medium 7-17694
 steels, stainless, pitting corrosion behaviour in NaCl solns. under heat transfer conditions (*Japanese*) 7-33832
 steels, surface degradation in elevated temp. gas-particle streams 7-3520
 surface and interface analysis, appls. conf., Veldhoven, Netherlands, (Oct. 1985) 7-24289
 SYNROC-C waste glass, leaching experiments 7-39689
 synthetic Cu salts, corrosion on bronze, TEM and SEM study 7-17737
 TRISTAN e $^+$ e $^-$ colliding beam ring, Al alloys, corrosion resistance to cooling water (*Japanese*) 7-42248
 water leachability of cement forms for medium-level waste immobilization 7-49687
 Zircaloy, corrosion resistance, precipitation of second phase particles effect 7-30564

corrosion continued

- Zircaloy-2, exposure to high temp. OWL-1 loop water, corrosion layer characterization 7-8167
 Zircaloy-2, nodular corrosion behaviour 7-8168
 Zircaloy-4, high temperature corrosion in flowing steam 7-28204
 Ag-Ag₂S, reference electrode, high temp. behaviour in aq. alkaline sulphide solns. 7-39714
 Ag-Zn, corrosion in H₂S, surface analysis, AES, XPS (*Japanese*) 7-53955
 Al, acoustic emission during corrosion in FeCl₃ soln. 7-39814
 Al alloys, corrosion of alloys buried in mortar and concrete, effect of NaCl (*Japanese*) 7-46692
 Al alloys, corrosion of alloys in mortar, effect of Na⁺ and Ca²⁺ ions (*Japanese*) 7-46693
 Al alloys, rapidly solidified, pitting corrosion 7-17678
 Al alloys in mortar, cathodic polarisation (*Japanese*) 7-53969
 Al, anodic oxide films, dissolution kinetics in KF solns. 7-39705
 Al coatings, atmospheric corrosion products in industrial and marine environments 7-39716
 Al, corrosion in carbon tetrachloride, inhibition 7-54010
 Al, corrosion in NaCl solns., influence of hydrostatic press. and salt conc. 7-39721
 Al, pure, 7-65182
 Al, structural elements, corrosion in contact with building materials (*German*) 7-3522
 Al structures, corrosion damage depth meas., eddy current method (*German*) 7-13711
 Al-Cu-Mg, IN 9021, corrosion behavior 7-39733
 Al-Fe-Si, 1060 alloy, corrosion in p-quinone and acetic acid 7-28170
 Al-Fe-V rapidly solidified sheets, mech. props., hot rolling effects 7-22838
 Al-Li-Ge, corrosion rel. to Ge content 7-39715
 AlNiFe_{0.5}, reactor fuel cladding, corrosion resistance, rupture strength, neutron irradiation effects testing 7-59670
 Al₂O₃, fretting wear in seawater 7-8124
 AlSi₉Ni, reactor fuel cladding, corrosion resistance, rupture strength, neutron irradiation effects testing 7-59670
 AlZn coatings, atmospheric corrosion products in industrial and marine environments 7-39716
 Au-Cu-Pd, corrosion resist. 7-39739
 Ba(PO₃)₂-AlF₃-NaF system, glass form. and props. 7-11929
 CaZrO₃, sintering, porosity, mech. props., corrosion resist. 7-39664
 CdSe-polysulphide photoelectrochem. system. corrosion reactions, thermodynamic stability calcs. 7-28320
 CdSe_{0.65}Te_{0.35}/aqueous polysulphide interface, photoelectrochemical props. 7-52829
 CdTe-In, photocorrosion, vacancies, photoluminescence spectra 7-27948
 Co, silicidation using Si₂Cl₆ source by diffusion and CVD processes 7-17700
 Co-Ni, aq. and atmospheric corrosion 7-39696
 Co-P, amorphous, pulse plated, electrochemical props., corrosion resist. (*Japanese*) 7-53954
 CoCr films, corrosion in H₂SO₄ 7-33824
 CoCrAlY, hot corrosion, H₂SO₄-Na₂SO₄ reactions 7-28188
 Cr, NaCl-induced accelerated oxidation 7-17715
 Cr-Mo ferritic steel, rust chemical reduction 7-30565
 Cu, acoustic emission during corrosion in FeCl₃ soln. 7-39814
 Cu, corrosion by tartaric acid 7-22902
 Cu, corrosion in solar heating systems, water-glycol solns. 7-22900
 Cu, corrosion inhibition complex study using Raman microscopy 7-46772
 Cu, structural elements, corrosion in contact with building materials (*German*) 7-3522
 Cu tubes, pitting pot. in hot water, oxidising agents effect 7-28207
 Cu-Al bronzes, microstruct., corrosion 7-39697
 Cu-Si, elemental Si inclusion form. in sulphide scale 7-17720
 Fe and Fe-Co-Ni fine powders, corrosion resist. and mag. prop. changes, surface-active agent use in prep. 7-54001
 Fe, cast, high Cr, grinding balls, jet slurry corrosive wear 7-39676
 Fe, cast, Sn plating, heat diffusion method, corrosion resist. in H₂SO₄ (*Japanese*) 7-53956
 Fe, cast/stainless steel couple, galvanic corrosion NaCl soln., boundary element prediction (*Japanese*) 7-13635
 Fe electrodes, electrodisolution and passivation K₂CO₃-KHCO₃ solns., ionic comp. effect 7-17677
 Fe film, electrodeposition and corrosion, piezoelec. cryst. substrate obs. 7-39707
 Fe, oxygen corrosion in neutral aerated sulphate solns., dynamic systems analysis (*German*) 7-8192
 Fe, pitting corrosion, role of Cl⁻ ions (*Japanese*) 7-33829
 Fe, thin corrosion films, laser Raman spectroscopy at 100 to 150°C in air 7-39722
 Fe-B based metallic glasses, corrosion in H₂SO₄, alloying effect 7-28201
 Fe-Cr, high-temp. air corrosion products, distrib. and charactn. by Raman microscopy 7-65205
 Fe-Cr alloy films, oxide film form. by aqueous corrosion, EXAFS study 7-64007
 Fe-Cr-Al-Ce, microstruct., high temp. corrosion rel. to Ce additions 7-13648
 Fe-Cr-Mo-Zr amorphous alloys, corrosion resistance (*Japanese*) 7-65194
 Fe-Cr-Si-B metallic glass wires, corrosion rel. to crystallinity and comp. 7-46701
 Fe-Mn-Al, processing and props., effect of Si and C additions 7-17707
 Fe_xN thin films, ion beam deposited, mag. props. and corrosion resistance 7-33231
 GdTbFe, corrosion resistance improvement by metal coatings 7-53952
 GeO₂-ZnO-Bi₂O₃ IR transmitting glasses 7-43276
 He corrosion effect on high temp alloy (*German*) 7-30567
 Hf, valve metal, corrosion under influence of Pu, oxide layer formation 7-17699
 Li/SOCl₂ cell, corrosion, calorimetric study 7-46929
 Mo porous electrodes for alkali metal thermoelec. convertor, voltammetric studies 7-28405
 Mo surface, high-field corrosion, field-ion microscopy studies 7-33830
 Mo, tubes, corrosion in flowing water, O₂ conc. effect 7-22906
 Na-circuit materials corrosion, electrochemical potentiokinetic reactivation method (*Czech*) 7-61966
 Na/steel system, NaCrO₂, form. threshold. O level, LMFBF operation 7-42113
 Nb, corrosion behaviour in HBr solns. 7-39725
 Nb corrosion resist. in molten Lr, alloying influence 7-17689

corrosion continued

- Nb-Ti-W (30, 20 wt.%), nitriding, hardness, wear and corrosion resist. 7-46713
 Ni alloys, corrosion behaviour in formic acid (*German*) 7-3526
 Ni, anode, electrochemical behaviour in H₂SO₄ solns., halide ions effect 7-39758
 Ni base amorphous alloys, containing Ti, Zr, Nb, Ta and/or P, corrosion behaviour in boiling conc. HNO₃ and HCl 7-3511
 Ni base high temp. alloys, corrosion in simulated HTGR He environments 7-17703
 Ni base superalloys, techniques for required props. prod. (*Turkish*) 7-59657
 Ni braced joint, corrosion process, involvement of thermophilic bacterium 7-39730
 Ni, electroless plating, outdoor exposure, accelerated atmospheric corrosion (*Japanese*) 7-13633
 Ni, hydrodynamic effects during electrochem. and exposure pitting test with passive films 7-46678
 Ni-base ternary alloys and superalloys, hot corrosion in SO₂/O₂ atm. 7-65175
 Ni-base ternary alloys and superalloys, hot corrosion mechanism in SO₂/O₂ atm. 7-65176
 Ni-Cr-Mo-Fe system, pitting corrosion, temp. depend. 7-65186
 Ni-Mo-B(P), metallic glasses, depth-composition profile, X-ray photoelectron study 7-63928
 Ni-P, electrodeposition, pulse plating, corrosion resist. (*Japanese*) 7-53643
 Ni-P, glassy, dissolution in H₂SO₄ and HCl electrolytes 7-28189
 Ni-P amorphous alloy electrodeposition and corrosion obs. 7-27953
 Ni-P-B electroless coatings, prep. and deposit characts. 7-59671
 (Ni-Pd)₈₃Si₁₈ amorphous alloys, corrosion behaviour, struct. relax. effects. 7-8166
 NiCrSiB alloy coatings, sputter deposition, microstruct. variations 7-46351
 Pb cladding on radwaste containers, corrosion study (*Spanish*) 7-54013
 Pb, dissolution in HNO₃, thermometric obs. 7-8189
 Pb, structural elements, corrosion in contact with building materials (*German*) 7-3522
 Re surface, high-field corrosion, field-ion microscopy studies 7-33830
 SiC corroded, scanning Auger microscopy study 7-13617
 SiC, corrosion pitting by molten salts 7-59695
 α-SiC, sintered, hot corrosion by molten salts, strength degradation mechanism 7-33813
 Si₃N₄, fretting wear in seawater 7-8124
 SiO₂ refractories, corrosion by molten Mn steel (*Japanese*) 7-65167
 SiO₂-B₂O₃-Na₂O-Al₂O₃ glasses, corroded, grazing incidence fluorescence EXAFS, near edge spectroscopy 7-59296
 SiO₂-GeO₂ optical fibre surfaces, formation mechanism of H-associated defect centre 7-65158
 Ti, thermochemical surface treatment using lasers, wear and corrosion resist. 7-22908
 Ta, corrosion behaviour in HBr solns. 7-39725
 Ta, valve metal, corrosion under influence of Pu, oxide layer formation 7-17699
 β-Ti alloy, springs, design and mech. props. 7-46630
 Ti alloy sheet, vac. annealing temp. influence on surface relief 7-17688
 Ti, anodic and cathodic polarisation, surface oxide films, ellipsometric anal. (*Japanese*) 7-33828
 Ti, corrosion behaviour in formic acid (*German*) 7-3526
 Ti, crevice corrosion in NaCl-HCl solns. (*Japanese*) 7-13630
 Ti in power generation industry 7-46283
 Ti, valve metal, corrosion under influence of Pu, oxide layer formation 7-17699
 Ti-Al-Cr-Fe-Si, AT3 alloy, corrosion resist. and hydrogenation susceptibility in dil. H₂SO₄ soln. 7-17685
 Ti-Mo, electrochemical behaviour in brine, gamma radiolysis effect 7-65185
 Ti-Zr, dry corrosion, bistability, thermal oscillations (*French*) 7-65188
 Ti₇₅Ni₂₀Ge₅ metallic glasses, corrosion rates in the H₂SO₄ and HCl solns. 7-28199
 Ti₇₅Ni₂₀Si₅ metallic glasses, corrosion rates in the H₂SO₄ and HCl solns. 7-28199
 TiO₂-RuO₂ in chloride solns., corrosion and electrochem. props. 7-53951
 V-based alloys, alloying and impurity effects 7-53666
 V-Cr-Fe, corrosion in pressurised water, 288°C 7-53967
 V-Cr-Ti, corrosion in pressurised water, 288°C 7-53967
 V-Ti, corrosion in pressurised water, 288°C 7-53967
 W surface, high-field corrosion, field-ion microscopy studies 7-33830
 WC-stainless steel composites, corrosion-resistant optimum prod. conditions 7-65164
 Zn coatings, atmospheric corrosion products in industrial and marine environments 7-39716
 Zn, corrosion promotion and inhibition by organic anions 7-8188
 Zn, electrochem. corrosion in NaClO₃ aq. soln. 7-17702
 Zn electrodes, electrochem. and corrosion props. in mixed aq.-ethanolic media 7-54140
 Zn, structural elements, corrosion in contact with building materials (*German*) 7-3522
 Zn-Al alloys, corrosion behaviour, effect of Al content and cooling conditions 7-54008
 Zn-Al coated steel, corrosion behaviour, effect of matrix struct. (*Japanese*) 7-33826
 Zr, valve metal, corrosion under influence of Pu, oxide layer formation 7-17699
 ZrO₂, Y₂O₃ partially stabilised, tetragonal phase stability in molten fluoride salts (*Japanese*) 7-28164
 ZrO₂-containing glass fibres, alkali corrosion process, XPS study (*Japanese*) 7-3480

corrosion control see corrosion protection

corrosion fatigue

- coatings in high performance gas turbines, high temp. behaviour, laboratory tests 7-46694
 high-strength steels, corrosion-fatigue strength, notch effect 7-26842
 materials fatigue behaviour, influencing factors (*Japanese*) 7-39642
 optical fibres, silicone-coated, influence of pH solns. on strength and dynamic fatigue 7-6006
 PMMA, environmental fatigue, initiation of wavy striation (*Japanese*) 7-33814

corrosion fatigue continued

- power plant components stress corrosion crack model in laboratory tests 7-17732
- steel, 18 Ni maraging, corrosion fatigue crack initiation and growth 7-3413
- steel, austenitic, Mn-Cr, fatigue crack growth behaviour 7-59593
- steel, corrosion fatigue, crack initiation determ. (German) 7-3527
- steel, corrosion fatigue in aq. environments in Kuwait 7-46711
- steel, corrosion inhibitor development 7-17684
- steel, dual-phase, as-rolled, corrosion fatigue behaviour 7-46710
- steel, high strength, modified HY 130, corrosion fatigue and electrochem. reactions 7-65201
- steel, low alloy, fatigue fracture in air and 3.5% NaCl soln., X-ray fractography (Japanese) 7-8099
- steel, low alloy, SCC and corrosion fatigue in artificial seawater, effect of yield strength (Chinese) 7-8152
- steel, mild, corrosion fatigue in 3.5% NaCl soln., investig. of transient polarisation investig. of transient polarisation currents 7-46680
- steel, Ni-Cr-Mo, pressure vessel, environmentally assisted fatigue crack growth 7-17638
- steel, pressure vessel, fatigue crack growth rates under various conditions of loading and environment 7-28203
- steel, stainless, type 316L, fatigue in simulated fast reactor environments 7-39759
- steel, welded, corrosion fatigue testing, NaCl conc. and test freq. effects (German) 7-8230
- steel 65G, microstruct. and mech. props. after low-temp. TMT, tempering temp. influence 7-17554
- steel weld joint, austenitic surfacing-pearlitic transition zone, cyclic crack resist. 7-17691
- Zircaloy-2, low cycle corrosion fatigue in I₂ atmosphere 7-17705
- Al alloy, corrosion effects on fatigue crack propagation 7-39628
- Al alloy, life prediction for corrosion fatigue 7-39629
- Cu, single crystals, corrosion fatigue in aq. oxide forming environment 7-33823
- Cu single crystals, corrosion fatigue in aq., oxide-forming environment, electrochem. response 7-65115

corrosion fatigue testing see corrosion testing

corrosion prevention see corrosion protection

corrosion protection

- see also anodisation; corrosion; corrosion protective coatings; packaging; pH control
- Beaver Valley PWR, water chemistry control with morpholine 7-5362
- brass, corrosion inhibitors evaluation (German) 7-8197
- buried metallic structures, cathodic protection methods (Italian) 7-28175
- Calder Hall, water chemistry control, corrosion prevention 7-56796
- evaluation of corrosion inhibitors in conc. HCl at 93°C, use of linear polarisation meas. 7-65243
- graphite fibre reinforced Al or Mg composite, corrosion protection to NaCl soln. exposure 7-3488
- Incoloy 800H, corrosion protection by plasma assisted vapour deposited and laser fused silica coatings 7-28208
- metal surfaces, ion beam and laser processing for improvement corrosion resist., surface modification program 7-65200
- metal surfaces, ion implanted, durability 7-53918
- metallic corrosion of cement plant facilities, cathodic protection 7-28210
- metallic materials, surface refinement by ion implantation, friction, abrasive and corrosion resist. (German) 7-53949
- nonferrous materials, specific heat capacities (German) 7-2228
- nuclear power plant neutral oxygenated water conditions appl. efficiency for corrosion protection (Russian) 7-765
- nuclear power station use of neutral/oxygen water treatment 7-30537
- power plant life extension using corrosion control 7-54005
- PWR condenser improvements for corrosion impurity protection 7-15250
- PWR secondary coolant system, deaeration of makeup water 7-10242
- PWR secondary water systems, eval. of pH control agents 7-5363
- PWR steam generators, depressurisation procedures for tubesheet crevice flushing 7-10248
- PWR steam generators, tubesheet crevice-flushing effectiveness 7-56797
- PWR steam recirculation systems using brackish water, condensate polishers 7-19400
- PWR water chemistry control with morpholine, USA and foreign experience 7-10245
- PWR water systems, organics identity and concentration survey, corrosion reduction 7-19399
- steel, austenitic stainless, intercrystalline corrosion causes and counter-measures (German) 7-17729
- steel, austenitic stainless, intergranular SCC resist., influence of Si 7-46681
- steel, austenitic stainless, slow strain rate SCC in NaCl soln., cathodic protection 7-39709
- steel, austenitic stainless, surface, S containing corrosion inhibitor removal 7-39717
- steel, cathodic protection mechanism 7-39718
- steel, corrosion in systems containing elementary S, H₂S and Cl⁻, sulphurated fatty-acid derivatives as inhibitors (German) 7-22901
- steel, corrosion inhibition by molybdate in deaerated and low O₂ water 7-39731
- steel, corrosion inhibitor development 7-17684
- steel, duplex stainless, sintered, mech. props., corrosion resist. and high temp. oxidation resist. 7-7928
- steel, ferritic stainless, corrosion resist. in H₂SO₄ soln., alloying effects 7-28172
- steel, galvanised sheet, surface treatment prior to painting, effects on surface comp. and corrosion resist. (French) 7-46703
- steel, high strength, H induced SCC rel. to galvanisation (German) 7-3521
- steel, linepipe weldments, ductility rel. to cathodic protection 7-39578
- steel, Ni-Cr-Mo, turbine disc, Ni electrodeposit, corrosion protection, pot.-pH diagrams 7-39699
- steel, stainless, (Cr₂Fe)₁₂₅C₆ compact specimens, corrosion-electrochem. and phys. props. w.r.t. comp. 7-54000
- steel, structural, diffusion chromised, elevated temp. effect on comp., struct. and mech. props. 7-8178
- steel sheet, hot-dipping into Al-Zn eutectoid base superplastic alloy (Japanese) 7-59664
- steel sheet, PET and PVC coated, corrosion resist. and adhesion strength (Japanese) 7-8165
- Al brass, corrosion inhibition by Schiff bases in acid media 7-22892
- Al, corrosion in carbon tetrachloride, inhibition 7-54010

corrosion protection continued

- Al, corrosion inhibition in HCl by thiosemicarbazide derivatives 7-3487
- Al foil, anodic etching, influence of activators and passivators in electrolyte on surface area increase (Polish) 7-22889
- Al-semiconductor interfaces, form. of active electronic barrier, novel approach in corrosion prevention 7-65178
- Co-Ni evaporated recording media, improvement of mag. props. and corrosion resistance by Pr additions 7-33825
- Cr, metallic and surface-oxidised, H and D diffusion 7-6888
- Cu, corrosion inhibition by Schiff bases in acid media 7-22892
- Cu, polished surface, ellipsometric study of reflection 7-13121
- Cu-Al-Ni-Fe-Mn bronze, cast, laser surfacing, improved corrosion resist., microstruct. characteris. 7-13651
- Cu-Ni, corrosion inhibition by Schiff bases in acid media 7-22892
- Cu; corrosion inhibition in humid environments by azole compounds 7-3484
- Fe and Fe-Co-Ni fine powders, corrosion resist. and mag. prop. changes, surface-active agent use in prep. 7-54001
- Fe, corrosion inhibition by H₂O₂ 7-39695
- Fe-Al, al alloying for oxidation resist. improvement, comparison between ion implantation and laser irradi. 7-22883
- Fe-Cr, P implanted amorphous alloys, corrosion, passivation, microstruct. 7-65180
- Ni, anode, electrochemical behaviour in H₂SO₄ solns., halide ions effect 7-39758
- Ni, siliconised layer form. by diffusion and CVD, oxidation and corrosion resist. 7-59659
- SiC fibre reinforced Al, corrosion protection to NaCl soln. exposure 7-3488
- V-Cr-Ti, fusion reactor blanket, surface alloying, oxidation resist. to high temp. He coolant 7-53964
- Zn, corrosion inhibitors evaluation (German) 7-8197
- Zn, corrosion promotion and inhibition by organic anions 7-8188
- Zn, corrosion resistance improvement by surface modification with organic cpds. (Japanese) 7-8164
- Zr-Nb (1 wt.%), laser irradi., hardness, struct., corrosion resist. 7-3400

corrosion protective coatings

- aluminizing, hot dip, alloy layer growth, influence of Si additions 7-3502
- electrodeposits for high temp. oxidation and corrosion resistance, appl. for gas turbines 7-46358
- graphite, intercalated fibre elec. conductors, passivating coatings 7-8140
- high temp. behaviour, coatings in high performance gas turbines 7-46694
- high temperature gaseous corrosion, development requirements 7-46670
- Incoloy 800H, multilayer oxide scales in gas atmosphere, Ti distribution 7-53972
- metals, pointed, corrosion, impedance plot methods 7-3486
- nuclear power station, steel component surface treatment, detonation-deposition method (Russian) 7-39736
- polyester powder films on Zn coated steel substrates, cratering and pin holes 7-13647
- polymer films, radiation-induced implantation in metallic substrates 7-8163
- polyphenylene sulphide coatings, internal struct., curing effect 7-22861
- Rene 80, first stage aluminised coating microstruct., STEM obs. 7-17709
- rolling bearings, friction, wear and corrosion control 7-46658
- steel, cathodic protection by galvanic coating alloys, electrochemical criterion 7-65187
- steel, cold rolled, Ni activated phosphating, corrosion resist., durability, strength 7-28187
- steel, high strength, H induced SCC rel. to galvanisation (German) 7-3521
- steel, polymer coated, NaCl soln. exposure, interface reactions, impedance spectra 7-3489
- steel, surface conversion, phosphate coatings, corrosion protection during welding 7-8198
- steel, Zn phosphated, corrosion resist., cyclic voltammetry, SEM obs. 7-65181
- steel weld joint, austenitic surfacing-pearlitic transition zone, cyclic crack resist. 7-17691
- superalloys, hot corrosion processes, diffusion and overlayer coating struct. effects 7-53985
- surface engineering for corrosion protection 7-3478
- surface modifications and coatings, conf., Toronto, Ont., Canada (Oct. 1985) 7-41004
- Ag, coating on brass, corrosion protective props. 7-53950
- Al corrosion resistant coating on Gd₂TbFe, mag. props. 7-53952
- Al plasma and powdered, on Cr steel, SCC behaviour 7-17686
- Al powder-steel composite coatings, prod. by compacting electrophoretic and electrostatic deposits protective props. 7-3491
- Al-Zn eutectoid-base superplastic alloy for hot-dipping of steel sheet (Japanese) 7-59664
- AlN corrosion protective coating for TbFe magneto-optical media 7-53953
- C thin surface layers on steel substrates, anticorrosion props., ion bombardment effects study 7-27202
- Ce conversion coatings on Al alloys, corrosion protection 7-53988
- CeO₂-ZrO₂-Y₂O₃ thermal barrier coating, plasma-sprayed, thermal and mech. props. (Japanese) 7-27899
- CoB layers and crystals, prep. by diffusion and CVD processes 7-17434
- CoCr corrosion-resistant alloy films, mag. props. and longitudinal recording performance 7-33226
- CoCrAlY, sputter ion plated coatings for gas turbines 7-53971
- CoCrTa corrosion-resistant alloy films, mag. props. and longitudinal recording performance 7-33226
- Cr and eutectic coatings on steel, wear resist. in corrosive medium 7-17694
- Cr corrosion resistant coating on Gd₂TbFe, mag. props. 7-53952
- Cr-CrO₂/Zn multilayer electrogalvanised coating on steel, XPS analysis 7-22890
- CrNi corrosion resistant coating on Gd₂TbFe, mag. props. 7-53952
- Cu corrosion resistant coating on Gd₂TbFe, mag. props. 7-53952
- Cu/Ni/Cr, multilayer deposits, corrosion protective props. 7-8187
- Cu-Al-Ni-Fe-Mn bronze, cast, laser surfacing, improved corrosion resist., microstruct. characteris. 7-13651
- Fe electrodes, passivated, capacitance under simulated erosion-corrosion conditions 7-3514
- Fe-Cr-Mo, oxidation, boric acid coatings effect 7-65197
- FeCrAlY coatings, ion-implanted, oxidation behaviour 7-53974
- Mo, oxidation-preventing coating, high temperature, low-pressure plasma spraying 7-28182

corrosion protective coatings continued

- Mo-Bi-Si thermodiffusion coating on Nb-Mo-Zr alloy, oxidation protection, heat resist. 7-8156
- Ni base superalloys, techniques for required props. prod. (*Turkish*) 7-59657
- Ni plating basics, electroforming, surface prep. and quality control procedures 7-13638
- Ni-P coating, electrolytic, electron microscope obs. of struct., P content depend., amorphous layer form. 7-8157
- Ni-P electroless coatings, corrosion resistance 7-17484
- Ni-P-B electroless coatings, prep. and deposit characs. 7-59671
- NiCoCrAlY, plasma sprayed coatings, low cycle fatigue behaviour 7-22793
- NiCrAlTi, sputter ion plated coatings for gas turbines 7-53971
- Pd and alloy contact finish performance and cost 7-3508
- Pd-Ag alloy electroplated coating contact and corrosion resistance and wear 7-3509
- Pt-Al-Cr coatings, structure and 700°C hot corrosion behaviour 7-53973
- SiO₂, plasma assisted vapour deposited and laser fused coatings, corrosion protective props. 7-28208
- SiO₂ protective coating on CoCr films 7-28184
- SiO₂, corrosion protective coatings on Ni-Cr Inconel alloy 7-39754
- Sn on Fe, electrolyte tinplate, determ. of reaction time during first stage of FeSn₂ growth 7-53990
- Sn plated on cast Fe, heat diffusion method, corrosion resist in H₂SO₄ (*Japanese*) 7-53956
- Y₂O₃, Al₂O₃ coatings on Ni-based superalloy, appl. as high temp. protective coatings for gas turbines 7-46695
- Zn coatings on steel, effect of Si on stability and growth of Fe-Zn phases 7-54011
- Zn, electroplating in acidic bath, corrosion resist. improvement with Co and Cr additions 7-13640
- Zn-Al (5 wt.%) coating on low C sheet steel, Zn quenching technique 7-33847
- Zn-Al alloys, corrosion behaviour, effect of Al content and cooling conditions 7-54008
- Zn-Al coated steel, corrosion behaviour, effect of matrix struct. (*Japanese*) 7-33826
- Zn₃(PO₄)₂ coating, deposited on cold rolled steel surface, Fe dissolution, X-ray fluoresc. anal. 7-28168

corrosion testing

- acoustic emission applications in struct. testing 7-33883
- BWR, neutral water-chemistry treatment with H₂O₂ dosing 7-10223
- evaluation of corrosion inhibitors in conc. HCl at 93°C, use of linear polarisation meas. 7-65243
- heat transfer effect, dimensionless groups appl. 7-39792
- LMFBR, 316SS fuel cladding tube, stress-loaded corrosion tests in I₂ or Te (*Japanese*) 7-61958
- metals, bend tests for stress corrosion testing 7-54040
- pit depth and positions, meas by semi-automatic device 7-54035
- power plant components stress corrosion crack model in laboratory tests 7-17732
- SCC and corrosion fatigue test procedure problems 7-8215
- steel, austenitic stainless, pitting corrosion rate, meas. by means of 60 Hz Lissajous figure (*Japanese*) 7-8212
- steel, cold-rolled, corrosion investig. by thermal-wave microscopy 7-28169
- steel, duplex stainless, electrochem. test for intergranular corrosion susceptibility 7-39794
- steel, HSLA, partially coated, SCC, non-uniform H charging effect 7-3483
- steel, welded, corrosion fatigue testing, NaCl conc. and test freq. effects (*German*) 7-8230
- Al alloys as heat exchanger materials for OTEC 7-65571
- Fe film, electrodeposition and corrosion, piezoelec. cryst. substrate obs. 7-39707

corundum

- see also *ruby; sapphire*
- carborundum refractory provisions with aluminium-chromium phosphate binder 7-46395
- ceramic matrices, precip. morphology 7-65049
- corundum:V⁴⁺, cryst., luminesc. 7-33454
- corundum-graphite refractories, thermomech. props. 7-22806
- crystal growth from melt, phase boundary displacement mechanism, defect distrib. 7-32328
- elasticity and high pressure instabilities 7-66103
- electrical ceramics, high-alumina, sintered state range widening, temp. depend. of melt apparent viscosity 7-46396
- emerald, Cr³⁺ absorption spectrum, spin-orbit interaction effects 7-13182
- formocorundums abrasive, simulation of polymer binders using organic liqs., bond strength investig. 7-38301
- hexagonal, plate-like, synthesis using hydrated Al₂(SO₄)₃ as starting material (*Japanese*) 7-22454
- ion implantation, crystallisation of amorphous surface layers 7-58304
- monite-corundum refractories, creep behaviour rel. to struct. features 7-22770
- muon spin relaxation, muon bonding versus muonium formation 7-45902
- porcelain, sintering kinetics, struct. evolution 7-28004
- profiled, plastic flow in surface layers during diffusion welding 7-33730
- single crystals, IR absorpt. and transmission spectra study 7-53305
- single crystals, wear rate, influence of annealing 7-53920
- surface segregation of Y and Mg, atomistic lattice simulation 7-58492
- surface structure, identification by electron diffraction 7-27069
- α -Al₂O₃:Br⁻ ion implanted, RBS and annealing studies 7-32515
- Al₂O₃:Cr³⁺, V³⁺, electron-phonon interaction and impurity energy levels, APR and EPR studies (*Russian*) 7-45814
- Al₂O₃:V⁴⁺, UV-visible absorpt. and luminesc. study 7-33447
- Al₂O₃-TiN powder composites, densification kinetics and struct. form. during sintering under high press. 7-53687
- SiO₂-Al₂O₃ powders, prep. by spray pyrolysis, sinterability, effect of chem. comp. (*Japanese*) 7-3246
- Ti³⁺:Al₂O₃ laser, excitation methods, use in intracavity spectroscopy 7-43190

cosmic background radiation

- see also *radiofrequency cosmic radiation*
- anisotropy calculating from anal. of cosmological density perturbations during decoupling era 7-60849
- axion-EM coupling, implications for cosmic background radiation 7-439
- conf., Erice, Italy (April 1986) 7-41001
- diffuse IR galactic background due to dust 7-47699
- far-UV diffuse background, Voyager 2 obs. of NGP 7-60839

cosmic background radiation continued

- fluctuations in ino-dominated Universe, role of baryonic density 7-55858
- Friedmann universes, large-scale anisotropy of cosmic background radiation 7-9561
- galactic gamma-ray line emission, constraint on origin of mass 22 nuclei in astrophysical environments 7-35069
- galactic ridge excess X-ray emission, contrib. from supernova remnants 7-24221
- galactic ridge X-ray emission, galactic nucleus explosion and hot interstellar matter effects 7-40962
- IR galactic and extragalactic diffuse emission study using IR photometer 7-14493
- perturbation by moving gravit. lens 7-35070
- Population III stars, evidence in isotropic background radiation 7-47998
- primordial gas heating by background radiation, effects of presence of H₂ 7-24205
- small-scale anisotropy and galaxy clustering, galaxy origin constraints 7-48082
- soft X-ray background and galactic small-scale H I structure 7-55769
- spectrum, early universe probe 7-48107
- superconducting cosmic strings, hard X-ray and γ -ray background contribs. 7-24518
- UV background, effects on gas props. in galactic halo 7-24171
- X-ray background, relation to nonspherical model for Lyman-alpha clouds 7-60805
- X-ray background, spectral characteristics and spatial fluctuations 7-66792

cosmic dust

see also *meteoroids*

- accretion flows onto massive protostars, radiative transfer rel. to temp. struct. 7-29471
- amorphous C submicron grains, extinction spectra in UV-visible range 7-35023
- amorphous silicate grains, H₂ form. mechanism 7-24184
- δ And (K3 III), primordial dust shell model for IR excess 7-55623
- anomalous interstellar dust in open cluster Trumpler 37, evidence from UV extinction curves 7-48010
- B5, interstellar dark cloud, evidence for large dust grains 7-9529
- in blue ice lakes of Greenland, cosmic dust placers discovery 7-14548
- η Car, dust shell internal struct. from six-channel 8 to 13 micron mapping 7-55650
- η Car, visual features and IR emission characs. 7-60769
- η Car dust shell, grain size and geometrical effects rel. to 8-13 μ m feature 7-9494
- Car II dust scattering and η Car Balmer profiles 7-24153
- Cas A, fast moving knot, IR spectral and photometric meas. 7-66708
- Cas A supernova remnant, contrib. of dust and synchrotron emission to IR spectrum 7-24176
- \circ Cet stars, circumstellar shell vel. fields, role of dust and mass loss (*Chinese*) 7-66591
- charge transfer reactions on grain surfaces, contrib. to interstellar 220 nm feature 7-55787
- China, cosmic dust in Wendermiaio and Bainaimiao groups, heavy minerals characs. 7-14546
- circumstellar dust shells around late type stars, models for IRAS obs. 7-9461
- circumstellar grains around luminous red giant stars, emissivity indices from IRAS obs. 7-55609
- Cn1-1, planetary nebula, dust characs. 7-35019
- comet dirty ice grains, albedos evol. 7-24067
- P/Comet Halley, 1910 and 1986 apparitions, electrostatic charging effect on dust distrib. 7-66507
- P/Comet Halley, (1982i), bacterial grain model for 2 to 4 μ m spectrum 7-34937
- P/Comet Halley, (1982i), in situ photopolarimetric meas. of dust and gas in coma 7-14527
- P/Comet Halley, dust impacts and detectors on space probes 7-34946
- P/Comet Halley (1910 II), spin vector refinement and discrete dust sources map (May-June 1910) 7-4365
- P/Comet Halley (1982i), coma morphology and dust emission pattern modelling 7-14526
- P/Comet Halley (1982i), dust and gas impact on spacecraft causing electron emission 7-9432
- P/Comet Halley (1982i), dust and gas prod. rates from Vega-2 near IR obs. 7-14520
- P/Comet Halley (1982i), dust characs., linear polarisation obs. 7-47782
- P/Comet Halley (1982i), dust coma meas. by Vega (*Russian*) 7-4380
- P/Comet Halley (1982i), dust emission ground-based obs. 7-18384
- P/Comet Halley (1982i), dust environment, Vega SP-2 expt. obs. (*Russian*) 7-4378
- P/Comet Halley (1982i), dust IR characs. 7-18385
- P/Comet Halley (1982i), dust particles, Vega spacecraft Puma obs. (*Russian*) 7-4375
- P/Comet Halley (1982i), dust prod. and impact rates from Giotto radio science expt. 7-14528
- P/Comet Halley (1982i), IR heating of cometary atmosphere 7-34933
- P/Comet Halley (1982i), molecules, gas and dust in inner coma 7-40773
- P/Comet Halley (1982i), organic CHON particles as source of CN jets 7-47788
- P/Comet Halley (1982i), photometry and activity of nucleus at pre-perihelion heliocentric distances > 4.6 AU 7-47763
- P/Comet Halley (1982i), pre-perihelion photometry rel. to gas and dust prod. rates 7-34930
- P/Comet Halley (1982i), Vega SP-1 obs. of dust coma (*Russian*) 7-4379
- P/Comet Halley (1982i), Vega-1 meas. of secondary electron currents induced by impacts 7-14521
- comet nucleus sample return mission, conf., Canterbury, England (July 1986) 7-48180
- cometary comae, micron-size ice grains cloud rel. to exptl. modelling of cometary phenomena 7-66506
- cometary dust grains, wavelength depend. of light scatt. 7-55535
- cometary dust halo formation, time-dependent numerical modelling 7-55536
- cometary dust induced vibrations effects on Halley Multicolour Camera 7-18355
- cometary dust particle impact on metal targets, ion form. studies 7-46259
- cometary dust studies using ground-based near-IR obs. (*Chinese*) 7-18357
- cometary nuclei, dust particles refr. index and packing 7-34936

cosmic dust continued

- comets, dirty ice grain characts. 7-18387
 comets, dust tails, density and brightness distrib. 7-60597
 comets, dust tails interpretation, use of Finson-Probstein Method 7-60563
 compact blue dwarf galaxies, dust content 7-48078
 compact galactic H II regions, extinction and reddening anal. 7-60747
 Crab Nebula, contrib. of dust and synchrotron emission to IR spectrum 7-24176
 R CrB, IRAS detect. and study of fossil circumstellar shell 7-55649
 R CrB stars, explosive phenomena rel. to dust form. and brightness decreases 7-24137
 R CrB stars, IRAS obs. of cool circumstellar dust 7-9495
 CRL 618, proto-planetary nebula, H₂ S(1) line profile, wind and dust effects 7-35031
 V1057 Cyg, circumstellar dust nature and existence, photometric anal. 7-4463
 V1016 Cyg, symbiotic star, circumstellar dust grains comp. from photometric obs. 7-47897
 CH Cyg, symbiotic star, contrib. of white dwarf and dust shell to spectral energy distrib. 7-47926
 in dense interstellar clouds, Jena workshop, Georgenthal, DDR (March 1986) 7-40981
 diffuse galactic 380 μ m emission 7-48090
 diffuse interstellar bands, charge transfer model 7-55787
 emission from star-forming regions, spectral study 7-48029
 ESO 428-G14, new Seyfert 2 galaxy, contrib. of dust to far-IR continuum 7-9538
 evolved stars, circumstellar shells, FIRST obs. possibilities 7-47891
 evolved stars, grain characts. 7-47951
 galactic halo and disk, mass constraints on objects constituting missing mass 7-14650
 galactic IR absorption var. with latitude 7-48089
 in galactic nuclei, relation between 3.28 μ m feature and continuum emission 7-9533
 in galaxies of IRAS minisurvey, effects of dust on near-IR colours 7-40923
 grain formation and growth in C stars, appl. to self-consistent models for dust-driven stellar winds 7-55641
 grain formation in space, simulation using plasma jet 7-66458
 grain growth model, geometrical cross-section of N-mer 7-48016
 grains and photoelectric heating of H II regions 7-18442
 graphite spheres (C₆₀ structure), effect of cavities and mantles on UV extinction peak 7-4546
 Gum Nebula, globules, dark clouds and T Tau stars 7-55750
 Herbig Ae/Be stars, envelopes dust IR excess and H₂O absorpt. 7-4473
 HH 1-2 exciting star, IR emission from warm circumstellar dust 7-60661
 high-mass loss rate stars, projected FIRST obs. 7-47842
 high-velocity clouds, search for dust, IR emission search 7-40893
 IC 443, supernova remnant, thermal dust emission contribs. to IR fluxes 7-40896
 impact on insulators, ion emission, energy deposition and desorption studies 7-29374
 interplanetary dust, interferometric obs. of F-corona radial vel. field between 3 and 7 solar radii 7-66535
 interplanetary dust, IR and visible obs. anal. 7-47762
 interplanetary dust, refractory minerals comp. 7-34823
 interplanetary dust, scatt. phase function determ. from blue light survey of gegenschein 7-24065
 interplanetary dust particles, solar flare track densities rel. to asteroidal or cometary source for zodiacal dust cloud 7-55531
 interplanetary grains, optical constns. of H₂O-NH₃ ice mixtures 7-23993
 interplanetary micro-organisms, heat exposure expt. rel. to entry into planetary atmosphere 7-9275
 interstellar 220 nm feature, interpretation 7-48018
 interstellar ²⁶Mg fossil anomaly rel. to excess in meteorites 7-48036
 interstellar dust, appl. of EXAFS studies 7-24185
 interstellar dust, constraints on grain hypothesis for diffuse absorpt. bands 7-55762
 interstellar dust, light extinction and polarisation 7-40888
 interstellar dust, review (*Russian*) 7-40899
 interstellar dust, small scale distrib. towards NGC 2516 open cluster 7-35043
 interstellar dust, submm characts. 7-48059
 interstellar dust clouds, sub-millimetre/far-IR emission from warm and cold clouds 7-48022
 interstellar dust parameters, relation to gas-phase element depletions 7-48015
 interstellar dust-temps. in IRAS sources assoc. with mol. outflows, implications of far-IR fluxes 7-55766
 interstellar dust-mol. excitation interaction in submm astronomy 7-47698
 interstellar grain compositional model 7-60596
 interstellar grain impact on comets of Oort Cloud 7-40783
 interstellar grain models, comparison with obs. 7-48013
 interstellar grains, IR emission due to grains heating by supernovae 7-48007
 interstellar grains, props. of small C particles and large molecules 7-24189
 interstellar grains, role in chemical evolution of molecules 7-48014
 interstellar grains, sub-millimetre emission from galactic disk ($l = -150^\circ$ to $l = 82^\circ$) 7-4558
 interstellar grains, time-dependent surface reactions in dense mol. clouds 7-24179
 interstellar grains in Cyg X-3 halo, observational props. X-ray scattering effects 7-47977
 interstellar grains opacity in galaxies with different Z, effects on mol. clouds form. 7-40908
 interstellar grains relation to obs. of diffuse absorpt. band at 443 nm 7-24187
 interstellar medium, submm obs. 7-48058
 interstellar paramagnetic grain alignment associated with internal friction and the polarization efficiency 7-48053
 interstellar silicate grains, expl. investigations of astronomically important silicates 7-48017
 interstellar spherical grains, polarization, props., light scattering 7-14631
 interstellar UV extinction curve, IUE anal. of 2175 Å bump 7-48039
 interstellar very broad-band extinction structure, obs. by combined uvby and UVB photometry 7-48019
 IR reflection nebulae in Orion Molecular Cloud 2, dust grains near-IR albedo 7-55765

cosmic dust continued

- IRAS galaxies, dust temps. and luminosities from sub-millimetre obs. 7-9532
 IRC+10216, brightness distrib. at various wavelengths, radiative transfer in shell 7-60520
 L1551 IRS 5, dust scatt. model for IR polarisation of nearby refl. nebula 7-24186
 late M-type giants and supergiants, dust condensation and stellar UV radiation 7-14565
 LDN 1551, bipolar nebula IR emission characts. 7-48061
 LDN 1642, high-latitude cloud, grain characts. 7-48062
 in M31 nucleus, near-UV obs. with ESA Photon Counting Detector 7-4562
 Markarian 3, Seyfert 2 galaxy, dust in emission-line gas 7-66746
 Mars, atm. dust injection mechanism 7-34904
 Mars, conference on atm. and climate, Washington, DC, USA (July 1986) 7-9598
 Mars, global dust storms interannual variability 7-40737
 Martian dust, MECA workshop, Tempe, Arizona (February 1986) 7-29603
 massive stars in high-lumin. IRAS galaxies, evol. and dust shell form., contrib. to lumin. of galaxy 7-66767
 Mercury, surface dust transport due to electrostatic charging 7-40730
 meteoric dust in atmosphere, possible causal relation between fireballs and noctilucent clouds 7-29437
 meteoroid grain ablation, residual mass 7-55577
 Nova Cen 1986, IR photometry rel. to dust shell form. (1986 December 30 to 1987 January 5) 7-47913
 NS3, NS12, possible bipolar nebulae, optical polarisation study 7-48047
 optically thick dust, effect of intervening galaxies on quasar counts and colors 7-55847
 V346 Ori, antilflare star, circumstellar dust characts., light curve anal. 7-4441
 α Ori, circumstellar dust scatt. model for optical polarisation 7-47852
 α Ori, dust shell Si fractional condensation, mass loss rate and grain characts., polarisation anal. 7-34972
 α Ori, dust shell UVB polarisation meas. 7-34971
 α Ori, outer atm. and circumstellar material characts., far-IR spectral obs. 7-60690
 Orion region, extinction and dust characts. 7-66728
 Pleiades, interstellar dust grains IRAS obs. 7-48003
 Population III, heating of dust and radiative spectrum (*Chinese*) 7-66680
 radiative transfer in spherical dust cloud, isotropic scattering 7-66440
 red giant, mass loss, role of dust 7-60651
 reflection nebulae, CCD surface photometry rel. to dust scatt. props. 7-55773
 reflection nebulae, IUE obs. review 7-66726
 refractory grain processing in circumstellar shells, diagnostic IR signatures 7-55611
 Saturn, small particle phenomena in ring system 7-34924
 Saturn E-ring, dynamical evolution of dust grains 7-9408
 Sh2-155, emission region, blue refl. nebula detect., assoc. dust emission, IRAS data anal. 7-66723
 in Shapley-Ames elliptical galaxies, interstellar dust content from IRAS obs. 7-66758
 Sharpless 252, assoc. dust and gas, UVRI polarimetry and molecular line obs. 7-48023
 solar nebula of low mass in laminar phase, particles settling and growth 7-24025
 South Galactic Pole and Magellanic Stream, dust content 7-66721
 in spiral galaxies, IR characts. and implications for existence of very small dust particles 7-24209
 star formation regions, far IR, submm and mm dust emission spectra 7-24180
 T Tau stars, circular polarisation due to grains 7-40810
 Trifid reflection nebulae, dust grain characts. 7-35024
 Tunguska body, cometary breakup hypothesis re-examination 7-60605
 Ursa Major I(S) group galaxies, far-IR obs. rel. to dust and H II regions heating 7-29548
 UV extinction curves towards OB associations, statistical anal. of IUE obs. 7-55785
 UV extinctions towards OB associations and star-forming regions, IUE obs. 7-55786
 Vega-like stars from IRAS point-source catalogue, evidence for circumstellar disks 7-4456
 W3 core region, dust grains size distrib. from millimetre-wave continuum obs. at 6.5 and 4 mm 7-55781
 W3 molecular cloud complex, dust clouds distrib. from stellar colour excesses 7-48004
 in young supernova remnants, shock-heated dust obs. rel. to remnant struct. and dynamics 7-55754
 zodiacal dust cloud structure, comparative study of 3D models 7-55532
 C stars with circumstellar silicate dust, spectral characts. 7-40834
 H II regions, dust characts. 7-40901
 H II regions, galactic electron temp. gradient, dust effects 7-48073
 Li differential depletion in diffuse interstellar clouds, role of dust 7-66706
- cosmic radiation** *see cosmic background radiation*
cosmic radiations, radiofrequency *see radiofrequency cosmic radiation*
cosmic radio waves *see radiofrequency cosmic radiation*
cosmic ray absorption *see cosmic ray propagation*
cosmic ray alpha-particles and helium nuclei *see cosmic ray nuclei*
cosmic ray apparatus
 ANI scintillation detector calibration 7-14466
 Buckland Park cosmic ray air shower array for UHE γ -ray astronomy 7-60565
 Cerenkov pulse width of extensive air showers with energies above 10^{15} eV 7-14459
 cosmic radiation characteristics, Salyut-7 meas. 7-42401
 CR-39 detection of cosmic rays in Spacelab-3 7-42386
 CR-39 detector calibration for Spacelab-3 cosmic ray expt. 7-42387
 CR-39 detector foil meas., cosmic ray LET spectra, automatic scanning technique 7-34809
 CR-39 resolution power for heavy cosmic ions 7-42394
 CR-39 used for cosmic ray measurements aboard Spacelab-1 7-42388
 Cygnus experiment, preliminary results, air shower array performance 7-40714
 DUMAND, neutrino and γ -quanta detector (*Russian*) 7-14497
 EAS, spatial distribns. function of Cerenkov radiation 7-14496
 EAS, transition effect in thick scintillators 7-14463

cosmic ray apparatus continued

- emulsion chambers for high energy cosmic ray proton/He energy spectra meas. 7-15455
- event sampling by particle-number difference, using high-speed A/D processor 7-10365
- gamma ray detection with atmospheric Cherenkov technique 7-66470
- gamma-ray telescope, 1TeV, design and evaluation 7-34884
- hodoscopic scintillation gamma spectrometers with light-guide spectrum mixers 7-10351
- Kamioka solar neutrino search 7-40694
- large-acceptance space spectrometer, toroidal coil configurations 7-40699
- low energy neutrino detection with the Mont Blanc LSD experiment 7-56915
- magnetic scintillation electron spectrometer 7-40715
- magnetic spectrometer experiment, appl. to meas. of primary cosmic anti-matter 7-47647
- phosphate glasses for identification of heavy ions 7-42280
- plastic SSNTD for Spacelab-1 low energy cosmic ray meas. 7-42385
- research, the early history, 1900 to 1927 7-48263
- scintillation counter for EAS meas. 7-66414
- scintillation detector, active charged-particle protection of neutral-radiation detectors with polymethylmethacrylate scintillator 7-10358
- scintillation hodoscopes based on multipliers, load characts. 7-10357
- Sokol detector primary cosmic rays composition and energy spectra study 7-14424
- solar neutrino detection, workshop, Tsukuba-gun, Japan (August 1986) 7-48193
- space-borne detector materials, formation of disintegration products 7-66425
- Sudbury D₂O neutrino detector 7-56914
- time resolution equipment of cosmic ray registration 7-42392
- time resolution of plastic detection in cosmic ray studies 7-42391
- Trapped Ions in Space Experiment 7-42390
- ultralarge detectors in the ocean, atmosphere, and ice masses 7-14465
- AgCl-detectors in space biophysics, biological effects of cosmic ray HZE particles, evaluation methods 7-34295
- D₂O Cherenkov detector for solar neutrinos 7-40695
- Si surface barrier telescope for solar particles, characts. and calibration 7-62217

cosmic ray composition

- see also cosmic ray electrons; cosmic ray mesons; cosmic ray muons; cosmic ray neutrinos; cosmic ray nuclei; cosmic ray photons*
- anomalous correl. between hadrons and electromagnetic particles, Chacaltaya emulsion chamber obs. 7-34816
- cosmions in solar neutrino problem, particle physics models 7-55457
- cosmogenic nuclide production in lunar samples, Monte Carlo simulation 7-23961
- Cyg X-3, cosmic glueballinos source, discussion 7-48105
- Cyg X-3, H dihyperon from high energy muon obs. 7-47992
- cygnat particles associated with Cygnus X-3, flux predictions 7-30303
- EAS, composition anal., distrib. functions for Crab Nebula and Cyg X-3 7-14461
- EAS, energy spectrum of primary cosmic rays 7-14460
- EAS, hadron charge composition and energy spectrum 7-14433
- EAS, spatial distrib. functions at sea level, primary composition 7-14456
- galactic cosmic rays, Mg isotopic characts. 7-60645
- hadron characteristics at Mt. Kambala 7-34813
- hadron families, energy spectra and spatial distrib. at ultrahigh energy 7-14432
- hadron interactions, ang. distrib. and scaling violation 7-14467
- JACEE data on particle primary nucleon spectra 7-9347
- magnetic scintillation electron spectrometer 7-40715
- Marjalahti meteorite minerals, etched track length distributions for $Z \geq 90$ cosmic rays 7-47653
- matter-antimatter symmetry, COSMIC radiation study 7-23958
- penetrative high energy showers, Chacaltaya emulsion chamber obs. 7-34815
- positron/electron ratio from 10 to 20 GeV, balloon-borne meas. using geomag. east-west asymmetry 7-66411
- primary composition around 10^{14} eV (Chinese) 7-55395
- primary cosmic rays, chemical composition and high energy muon groups 7-14423
- primary cosmic rays, comp. determ. from EAS meas. 7-14454
- primary cosmic rays, composition and energy spectra study using Sokol detector 7-14424
- secondary particles with large transverse momentum, X-ray emulsion chamber study 7-14429
- solar cosmic ray particles, heavy ion spectra from mag. flux tube accel. 7-34962
- solar flare particles, element abundances rel. to temp. of energetic particle emission regions 7-66532
- supermassive relic particle search, flux upper limits 7-61516
- tachyons, search in EAS data 7-66414
- ultra-high-energy cosmic rays, proton and Fe energy spectra from accel. in Galactic wind 7-66403
- p/p ratios, antiprotons production models at ultrahigh energies with leaky box propag. model 7-40654
- ⁵⁶Fe initiated EAS, longitudinal characteristics, fireball production and quark-gluon plasma model anal. 7-9348
- H and He isotopes in galactic cosmic radiation, meas. rel. to source abundances and interstellar propag. 7-55394
- ³He/⁴He ratio at high energies, implications of rigidity spectrum of He nuclei 7-66410
- ³He/⁴He ratio rel-to origin of cosmic-ray He nuclei 7-60497

cosmic ray deuterons *see cosmic ray nuclei***cosmic ray effects and interactions**

- see also high-energy cosmic ray interactions*
- acceleration effect on plasma shock waves stability 7-34861
- biological effects of cosmic ray HZE particles, evaluation methods 7-34295
- bombardment of icy grains, high mass ion production, ion desorption study from ice film, TOF mass spectra 7-26815
- cosmogenic nuclide production in lunar samples, Monte Carlo simulation 7-23961
- cosmogenic nuclides in meteorites and terrestrial matter, workshop, Los Alamos, New Mexico (July 1984) 7-29601
- Dhajala chondrite, depth profiles of radionuclide prod. rates 7-29439
- Dhurmsala, LL-chondrite, cosmic ray records 7-9442
- galactic cosmic ray nuclei, time averaged charge and energy spectra, from Marjalahti meteorite 7-60498

cosmic ray effects and interactions continued

- hadron interaction range for $E > 20$ TeV in Pb chambers 7-14470
- hadron interactions, ang. distrib. and scaling violation 7-14467
- interplanetary dust particles, solar flare track densities rel. to asteroidal or cometary source for zodiacal dust cloud 7-55531
- ionisation induced by cosmic rays, intensity meas. 7-40308
- Jilin, H5 chondrite, cosmic ray track density depth profile study 7-55400
- LET spectra, anal. by automatic scanning, meas. of CR-39 detector foils 7-34809
- lunar highland breccias 60018, 67435 and 67455, single-stage exposure histories 7-55501
- Marjalahti meteorite minerals, etched track length distributions for $Z \geq 90$ cosmic rays 7-47653
- meteorite, Cape York iron, cosmic ray produced inert gas isotopes 7-66523
- meteorites, cosmogenic isotope and track records rel. to cosmic ray fluxes 7-29440
- positron annihilation in interstellar H₂ environment, laboratory simulation 7-14426
- shock waves propagation in gas with cosmic rays, instability (Russian) 7-40652
- space-borne detector materials, formation of disintegration products 7-66425
- Trapped Ions in Space expt., linear energy transfer spectra in low Earth orbit 7-60479
- Wethersfield (1982) chondrite, abundances of cosmogenic radionuclides and noble gases 7-34952
- (p,p'), in air, interaction cross section at mountaintop heights 7-14428
- π isolation in group arrival of hadrons at mountaintop heights 7-14430
- ²⁶Al, production rate by cosmic ray protons, Monte Carlo calcs. 7-34842
- ³He in volcanic rocks, of cosmogenic origin, in situ production 7-60500
- ⁵⁵Mn, production rate by cosmic ray protons, Monte Carlo calcs. 7-34842
- ²²Na, production rate by cosmic ray protons, Monte Carlo calcs. 7-34842

cosmic ray electrons

- anomalous e⁻-photon cascade anal. 7-14448
- 3C 273, quasar, particle accel. in jet hotspot rel. to radio to IR spectrum 7-14676
- EAS, μ and e distrib. and shower front struct. 7-18341
- EAS of low energy, characts. 7-34812
- galactic cosmic rays, protons and electrons accel. in EM field of rot. orthogonal mag. dipole 7-9339
- galactic electrons of superhigh energy, spectrum formation 7-4278
- galactic positrons in diffusion model (Russian) 7-40655
- magnetic scintillation electron spectrometer 7-40715
- multidimensional characts. of e⁻-photon showers, analytic solns. 7-14450
- positron annihilation in interstellar H₂ environment, laboratory simulation 7-14426
- positron observations from 10 to 20 GeV, balloon-borne meas. using geomag. east-west asymmetry 7-66411
- primary cosmic antimatter detection, proposed satellite expt. for energy spectra determ. 7-47647
- solar flare electrons exciting type III radio bursts, electron speeds determ. 7-66533

cosmic ray energy spectra

- atmospheric muons of prompt generation, spectra 7-14440
- atmospheric neutrinos, of prompt generation, spectra 7-14440
- cascades, features of hadron component of EAS core 7-14445
- cosmogenic nuclide production in lunar samples, Monte Carlo simulation 7-23961
- EAS, μ energy spectrum and spatial distrib. 7-14452
- EAS, ANI-83 integrated installation for hadron component investigation 7-14453
- EAS, energy spectrum of primary cosmic rays 7-14460
- EAS, hadron charge composition and energy spectrum 7-14433
- EAS, spectra of central densities 7-14462
- EAS maximum, position as function of primary particle energy 7-14451
- electrons of superhigh energy, spectrum formation in Galaxy 7-4278
- flux intensity and integral energy spectrum at mountaintop heights 7-14428
- galactic cosmic ray nuclei, time averaged charge and energy spectra, from Marjalahti meteorite 7-60498
- galactic positrons and gamma rays prod. (Russian) 7-40655
- hadron characteristics at Mt. Kambala 7-34813
- hadron families, energy spectra and spatial distrib. at ultrahigh energy 7-14432
- hadron interaction range for $E > 20$ TeV in Pb chambers 7-14470
- highest energy cosmic rays, energy spectrum, directional anisotropy and origin 7-55389
- LET spectra, anal. by automatic scanning, meas. of CR-39 detector foils 7-34809
- magnetic scintillation electron spectrometer 7-40715
- multijet family event at super-high energy (Chinese) 7-14443
- muon flux, momentum spectra and charge composition 7-14437
- muons, depth-intensity relation in sea water 7-4281
- muons, energy spectra anal., tachyon hypothesis 7-14442
- muons, energy spectra and intensities at great depths 7-14441
- neutrinos in atmosphere, energy spectrum calc. 7-40660
- neutrons of cosmic ray origin, altitude and latitude effects on intensity and energy spectra 7-9346
- nuclear particle flux propagation in atmosphere, model (Russian) 7-66413
- nuclei energy spectra and charge composition at energies greater than 2 TeV 7-66412
- positron observations from 10 to 20 GeV, balloon-borne meas. using geomag. east-west asymmetry 7-66411
- primary composition around 10^{14} eV (Chinese) 7-55395
- primary cosmic antimatter, energy spectra determ. via satellite expt. 7-47647
- primary cosmic ray nuclei, composition and spectra above 10^{14} eV (Chinese) 7-29371
- primary cosmic rays, composition and energy spectra study using Sokol detector 7-14424
- secondary particles with large transverse momentum, X-ray emulsion chamber study 7-14429
- solar cosmic ray particles, heavy ion spectra from mag. flux tube accel. 7-34962
- solar neutrino energy spectra calcs. from supersymmetric relics 7-34814

cosmic ray energy spectra continued

- solar neutrino oscillations, coherent forward scatt. effects on solar V_e flux 7-29372
- solar neutrinos, high energy and cold dark matter 7-34817
- Tien-Shan EAS installation, energy spectrum meas. 7-14444
- ultra-high energy cosmic rays, energy spectrum and anisotropy of intensity 7-14435
- ultra-high energy cosmic-ray spectrum, implications of Fly's Eye detector results 7-4280
- ultra-high energy EAS, spectrum irregularity 7-14434
- ultra-high-energy cosmic rays, proton and Fe energy spectra from accel. in Galactic wind 7-66403
- vertical cut-off rigidities for energy spectrum computations 7-40659
- π isolation in group arrival of hadrons at mountaintop heights 7-14430
- He nuclei, rigidity spectrum rel. to $^3\text{He}/^4\text{He}$ ratio at high energies 7-66410
- ^4He , anomalous component, solar modulation 7-47648

cosmic ray geophysical effects *see geophysical aspects of cosmic rays***cosmic ray mesons**

- π isolation in group arrival of hadrons at mountaintop heights 7-14430

cosmic ray muons

- air showers, equi-intensity cuts in muon fluxes 7-55397
- atmospheric muons of prompt generation, spectra 7-14440
- Cyg X-3, μ flux, possible prod. by sneutrino interactions 7-23962
- Cyg X-3, H dihypon from high energy muon obs. 7-47992
- Cyg X-3, high energy muon detection 7-14612
- Cygnus X-3, underground muons, new evidence from Soudan 1 7-40863
- depth-intensity relation in sea water 7-4281
- diurnal anisotropy, long-term vars. rel. to heliospheric transport parameters 7-66408
- EAS, μ and e distrib. and shower front struct. 7-18341
- EAS, μ energy spectrum and spatial distrib. 7-14452
- EAS, fluctuations in muon density with fixed electron density 7-14455
- electron decay in space-borne detector materials 7-66425
- energy spectra anal., tachyon hypothesis 7-14442
- energy spectra and intensities at great depths 7-14441
- flux, momentum spectra and charge composition 7-14437
- fluxes of transiting and stopped muons, μ - e decay 7-14436
- indoor exposure rate, effect of partition walls and neighboring buildings 7-34277
- inelastic interaction cross section of muons in cosmic rays 7-14438
- intensities at deep underground facilities, atm. effects 7-34811
- multiplicity of muon groups at various zenith angles 7-14439
- primary cosmic rays, chemical composition and high energy muon groups 7-14423
- solar diurnal anisotropy of cosmic rays, secular changes in upper cut-off rigidity 7-66407
- ultra-high energy cosmic ray point sources 7-40653
- underground muons associated with Cygnus X-3 cygnet particle flux predictions 7-30303

cosmic ray neutrinos

- acoustic phonon scattering technique for cosmic-background neutrino detection 7-55476
- atmospheric neutrinos, of prompt generation, spectra 7-14440
- cosmions in solar neutrino. problem, particle physics models 7-55457
- Cygnus X-3, radiation source, role of antineutrinos and photinos 7-24242
- DUMAND, neutrino and γ -quanta detector (*Russian*) 7-14497
- energy spectrum of neutrinos in atmosphere, calc. from 0.2 to 10^8 GeV 7-40660
- Kamioka solar neutrino search 7-40694
- liquid Ar solar neutrino detector, spectrum from direction of Sun, oscillation effects 7-18340
- Mikheyev-Smirnov-Wolfenstein solar ν_e regeneration in the Earth 7-40661
- neutron star formation, neutrino signature of collapse 7-55699
- neutron stars, neutrino lumin., implications of collective effects of nucleon medium 7-47967
- nucleon decay, KAMIOKA experiment, atmospheric neutrino background and pion nuclear effect 7-49140
- pulsars, pulsed $\bar{\nu}_3$ flux anal. 7-36019
- resonant-solar-neutrino-oscillation experiments, electron-neutrino survival probability 7-29459
- SN 1987A in LMC, neutrino signal obs. (1987 February 23) 7-66637
- solar ^8B neutrinos, oscillations, possible expt. using D_2O detector 7-40656
- solar neutrino correlation with reactor expts. 7-41689
- solar neutrino detection, workshop, Tsukuba-gun, Japan (August 1986) 7-48193
- solar neutrino problem, ν_e - ν_τ oscillations, predictions in $\text{SO}(10)$ model 7-61525
- solar neutrino problem, implications of $^7\text{Be}(\text{p}, \gamma)^8\text{B}$ cross section 7-66452
- solar neutrino problem, MSW mechanism of neutrino oscillations 7-41675
- solar neutrino short-time variations rel. to solar activity and core oscillations 7-47826
- solar neutrinos, high energy and cold dark matter 7-34817
- superstring-induced time modulation of solar ν flux 7-35824
- ultra-high energy cosmic-ray spectrum, implications of Fly's Eye detector results 7-4280
- ν_e - ν_μ +majoron, Sun-Earth decay problem, triplet majoron model anal. 7-61673
- D_2O Cherenkov detector for solar neutrinos 7-40695

cosmic ray neutrons

- 11-year modulation seen in neutron monitoring data 7-66406
- diurnal anisotropy, long-term vars. rel. to heliospheric transport parameters 7-66408
- neutrons of cosmic ray origin, altitude and latitude effects on intensity and energy spectra 7-9346

cosmic ray nuclei

- antihelium nuclei of cosmological origin, measurement via proposal satellite expt. 7-47647
- energy spectra and charge composition at energies greater than 2 TeV 7-66412
- galactic cosmic ray nuclei, time averaged charge and energy spectra, from Marjalahti meteorite 7-60498
- high energy collisions, average transverse momentum and energy density meas. in emulsion chamber 7-42063
- JACEE data on particle primary nucleon spectra 7-9347
- outer heliosphere, recovery phase of galactic cosmic ray solar modulation 7-9342

cosmic ray nuclei continued

- primary cosmic ray nuclei, composition and spectra above 10^{14} eV (*Chinese*) 7-29371
- H and He isotopes in galactic cosmic radiation, meas. rel. to source abundances and interstellar propag. 7-55394
- He nuclei, rigidity spectrum rel. to $^3\text{He}/^4\text{He}$ ratio at high energies 7-66410
- $^3\text{He}/^4\text{He}$ ratio rel-to origin of cosmic-ray He nuclei 7-60497
- ^4He , anomalous component, solar modulation 7-47648

cosmic ray-nucleus reactions *see cosmic ray effects and interactions***cosmic ray-nucleus scattering** *see cosmic ray effects and interactions***cosmic ray origin**

- acceleration in supernova remnants, γ -ray evidence for intensity variations 7-18338
- acceleration in supernova remnants, large-scale intensity variations 7-18339
- antiprotons origin, models 7-55390
- antiprotons production at ultrahigh energies rel. to \bar{p}/p ratios, appl. of leaky box propag. model 7-40654
- 3C 273, quasar, particle accel. in jet hotspot rel. to radio to IR spectrum 7-14676
- Cyg X-3, μ flux, possible prod. by sneutrino interactions 7-23962
- Cygnus experiment, preliminary results, air shower array performance 7-40714
- Cygnus X-3, cygnet particle flux predictions 7-30303
- galactic cosmic radiation, H and He isotopes rel. to source abundances and interstellar propag. 7-55394
- galactic cosmic rays, protons and electrons accel. in EM field of rot. orthogonal mag. dipole 7-9339
- generation of very high energy cosmic rays by shock waves (*Russian*) 7-40652
- highest energy cosmic rays, energy spectrum, directional anisotropy and origin 7-55389
- point sources, ultrahigh energy γ -rays 7-14422
- positrons origin in 10 to 20 GeV range, implications of balloon-borne meas. 7-66411
- SN 1987A in LMC, neutrino signal obs. (1987 February 23) 7-66637
- superconducting cosmic strings, contribs. to 10^{20} eV cosmic rays 7-24518
- ultra-high energy cosmic ray point sources 7-40653
- ultra-high-energy cosmic rays, accel. and transport in Galactic wind and termination shock 7-66403
- $^3\text{He}/^4\text{He}$ ratio rel-to origin of cosmic-ray He nuclei 7-60497

cosmic ray photons*see also cosmic ray X-rays; solar cosmic ray photons*

- acceleration in supernova remnants, γ -ray evidence for intensity variations 7-18338
- anomalous e^- -photon cascade anal. 7-14448
- Cygnus experiment, preliminary results, air shower array performance 7-40714
- Cygnus X-3, radiation source, role of antineutrinos and photinos 7-24242
- DUMAND, neutrino and γ -quanta detector (*Russian*) 7-14497
- gamma ray detection with atmospheric Cherenkov technique 7-66470
- gamma-families formed at ultrahigh energies, spatial characts., Monte Carlo calcs. 7-14431
- gamma-ray emission lines at 0.51 and 1.81 MeV from galactic centre, model for common origin 7-24238
- gamma-ray line emission, constraint on origin of mass 22 nuclei in astrophysical environments 7-35069
- gamma-ray telescope, 1TeV, design and evaluation 7-34884
- halo structure of large gamma-families 7-14469
- jet phenomena in a giant superfamily 7-14468
- multidimensional characts. of e^- -photon showers, analytic solns. 7-14450
- Pamir experiment, scaling violation in γ -ray families 7-14447
- Pamir expt. data, comparison with strong interaction model 7-10038
- penetrative high energy showers, Chacaltaya emulsion chamber obs. 7-34815
- point sources, ultrahigh energy γ -rays 7-14422
- ultra-high energy cosmic ray point sources 7-40653
- very-high-energy gamma rays from astronomical objects, obs. of Cyg X-3 and Crab pulsar 7-60916
- H interaction, positrons prod. (*Russian*) 7-40655

cosmic ray propagation

- acceleration by collisionless interplanetary shocks 7-34822
- acceleration by supernova remnant shock-waves, orbit averaged Darwin quasi-neutral hybrid code 7-14425
- acceleration effect on plasma shock waves stability 7-34861
- acceleration in collapsing gas clouds 7-55390
- acceleration in supernova remnants, γ -ray evidence for intensity variations 7-18338
- acceleration in supernova remnants, large-scale intensity variations 7-18339
- daily intensity variations due to anisotropies of solar origin (*Japanese*) 7-40658
- Forbush effects in recurrent high-velocity solar wind streams 7-9345
- galactic cosmic rays. leaky box model rel. to antiprotons prod. and \bar{p}/p ratios 7-40654
- galactic diffusion model and positrons and gamma rays (*Russian*) 7-40655
- geomagnetic activity and local modulations of cosmic rays 7-66404
- heliosphere transport parameters, implications of cosmic rays diurnal anisotropy vars. 7-66408
- interplanetary propagation, effect heliospheric current sheet tilt changes 7-9340
- interplanetary propagation, generalised Compton-Getting transformation for nonrelativistic particles 7-34810
- interplanetary propagation, particle flux vars. rel. to radionuclides in Dhajala chondrite 7-29439
- interplanetary propagation, power spectral density of temporal fluctuations at rigidities 4 to 180 GV 7-14427
- interplanetary propagation including 11-year modulation 7-66406
- interstellar propagation and source abundances, implications of H and He isotopes meas. 7-55394
- magnetosphere, allowed regions for particle motion in superposed dipole and uniform mag. fields 7-14482
- outer heliosphere, intensity variation with heliolatitude 7-9341
- outer heliosphere, recovery phase of galactic cosmic ray solar modulation 7-9342
- relativistic protons, interplanetary propag. anal. 7-66405
- solar electrons in interplanetary space due to type III radiobursts trajectory determ. by radio method 7-47649

cosmic ray propagation continued

- solar energetic particles propag., local scatt. props. of interplanetary medium from particle pitch angle distrib. 7-55392
- solar modulation (*Japanese*) 7-40657
- solar particles, focusing anisotropy 7-9343
- solar wind, cosmic ray aspects 7-35124
- solar wind, mag. field annihilation region and assoc. galactic cosmic rays intensity enhancement 7-23960
- transport equation, approx. solns., use of max. entropy method 7-60564
- ultra-high-energy cosmic rays, accel. and transport in Galactic wind and termination shock 7-66403
- He nuclei interstellar pathlength, implications of He rigidity spectrum and $^3\text{He}/^4\text{He}$ ratio at high energies 7-66410

cosmic ray protons

- antiprotons origin, models 7-55390
- antiprotons production at ultrahigh energies rel. to p/p ratios, appl. of leaky box propag. model 7-40654
- flux intensity and integral energy spectrum at mountaintop heights 7-14428
- galactic cosmic ray-supported corona, model 7-60787
- galactic cosmic rays, protons and electrons accel. in EM field of rot. orthogonal mag. dipole 7-9339
- nonrelativistic particles propagation, generalised Compton-Getting transformation 7-34810
- outer heliosphere, recovery phase of galactic cosmic ray solar modulation 7-9342
- primary cosmic antimatter detection, proposed satellite expt. for energy spectra determ. 7-47647
- relativistic protons, interplanetary propag. anal. 7-66405
- solar flare protons, bremsstrahlung production of hard X-ray and gamma-ray emission 7-55594
- Sun, flare radio bursts, γ -ray lines and proton fluxes correl. 7-4402
- ^{26}Al , production rate by cosmic ray protons, Monte Carlo calcs. 7-34842
- ^{51}Mn , production rate by cosmic ray protons, Monte Carlo calcs. 7-34842
- ^{22}Na , production rate by cosmic ray protons, Monte Carlo calcs. 7-34842

cosmic ray showers and bursts

- air showers, equi-intensity cuts in muon fluxes 7-55397
- anomalous correl. between hadrons and electromagnetic particles, Chacaltaya emulsion chamber obs. 7-34816
- anomalous e^- -photon cascade anal. 7-14448
- atmospheric showers initiated by cosmic accelerators 7-18342
- Buckland Park cosmic ray air shower array for UHE γ -ray astronomy 7-60565
- casades, features of hadron component of EAS core 7-14445
- Cerenkov pulse width of extensive air showers with energies above 10^{15} eV 7-14459
- charmed particle prod. and long-range avalanches in cosmic ray showers 7-14446
- Cyg X-3, Oct. 1985 RF burst and gamma-ray event, cosmic ray shower observations 7-66790
- Cygnus experiment, preliminary results, air shower array performance 7-40714
- Cygnus X-3, radiation source, role of antineutrinos and photinos 7-24242
- EAS, μ and e distrib. and shower front struct. 7-18341
- EAS, μ energy spectrum and spatial distrib. 7-14452
- EAS, ANI-83 integrated installation for hadron component investigation 7-14453
- EAS, cascade curve, uncertainties in reconstruction from optical emission pulse shape 7-55396
- EAS, composition anal., distrib. functions for Crab Nebula and Cyg X-3 7-14461
- EAS, composition of primary radiation and fluctuations in longitudinal development 7-14454
- EAS, energy spectrum of primary cosmic rays 7-14460
- EAS, fluctuations in muon density with fixed electron density 7-14455
- EAS, hadron charge composition and energy spectrum 7-14433
- EAS, initiation by ^{56}Fe primary, longitudinal characteristics, fireball production and quark-gluon plasma model anal. 7-9348
- EAS, investigation of shower 'disk' at great distances from the axis 7-14457
- EAS, radiology 7-14464
- EAS, scintillation detector calibration for ANI instrument 7-14466
- EAS, search for assoc. tachyons 7-66414
- EAS, spatial distrib. function of Cerenkov radiation 7-14496
- EAS, spatial distrib. functions at sea level, primary composition 7-14456
- EAS, spectra of central densities 7-14462
- EAS, transition effect in thick scintillators 7-14463
- EAS, ultra-high-energy, ang. distrib. of Cerenkov light 7-55398
- EAS characts. calcs. using above-critical pomeron theory with additive quark model 7-14449
- EAS maximum, position as function of primary particle energy 7-14451
- EAS of low energy, characts. 7-34812
- halo structure of large gamma-families 7-14469
- jet phenomena in a giant superfamily 7-14468
- multidimensional characts. of e^- -photon showers, analytic solns. 7-14450
- neutrino-induced EAS, detection possibilities 7-9349
- nuclear particle flux propagation in atmosphere, model (*Russian*) 7-66413
- Pamir experiment, scaling violation in γ -ray families 7-14447
- penetrative high energy showers, Chacaltaya emulsion chamber obs. 7-34815
- possibility of reconstructing a hadron cascade of arbitrary form in the atmosphere 7-14458
- Tien-Shan EAS installation, energy spectrum meas. 7-14444
- ultra-high energy cosmic ray point sources 7-40653
- ultra-high energy EAS, spectrum irregularity 7-14434
- ultralarge detectors in the ocean, atmosphere, and ice masses 7-14465

cosmic ray solar modulation

- 3D anisotropies (*Japanese*) 7-40657
- 11-year modulation seen in neutron monitoring data 7-66406
- anomalous component of ^4He 7-47648
- daily intensity variations due to anisotropies of solar origin (*Japanese*) 7-40658
- density gradient perpendicular to ecliptic plane pointing southward, correl. with Sun northern activity excess 7-24111
- diurnal anisotropy of cosmic rays, implications for heliospheric transport parameters 7-66408
- enhanced diurnal variations associated with two-sector struct. 7-55391

cosmic ray solar modulation continued

- Forbush effects in recurrent high-velocity solar wind streams 7-9345
- galactic cosmic ray fluxes, space-time vars. rel. to radionuclides in Dhajala chondrite 7-29439
- galactic cosmic rays, intensity profiles, effects of solar wind compound stream 7-47656
- galactic cosmic rays in atmosphere, north-south asymmetry, solar mag. field effects 7-66409
- galactic cosmic rays in solar wind 7-35124
- galactic cosmic rays intensity enhancement near interplanetary mag. field annihilation region 7-23960
- interplanetary mag. clouds influence on cosmic ray intensity var. 7-23959
- outer heliosphere, recovery phase of galactic cosmic ray solar modulation 7-9342
- solar diurnal anisotropy of cosmic rays, secular changes in upper cut-off rigidity 7-66407
- temporal fluctuations at rigidities 4 to 180 GV, power spectral density (1976 to 1980) 7-14427
- Wethersfield (1982) chondrite, modulation effects on cosmogenic radionuclides abundances 7-34952
- He nuclei, rigidity spectrum rel. to $^3\text{He}/^4\text{He}$ ratio at high energies 7-66410

cosmic ray variations

- see also cosmic ray solar modulation
- acceleration in supernova remnants, γ -ray evidence for intensity variations 7-18338
- acceleration in supernova remnants, large-scale intensity variations 7-18339
- Compton-Getting effect, frame transformation of spherical-harmonic coefficients of differential particle intensity 7-18337
- D_{H} correlated cosmic ray variations 7-4279
- galactic cosmic ray fluxes, implications of cosmogenic isotope and track records in meteorites 7-29440
- galactic cosmic ray fluxes, space-time vars. rel. to radionuclides in Dhajala chondrite 7-29439
- geomagnetic activity and local modulations of cosmic rays 7-66404
- interplanetary propagation, effect heliospheric current sheet tilt changes 7-9340
- long term variations of galactic cosmic rays, Monte Carlo calcs. 7-34842
- outer heliosphere, intensity variation with heliolatitude 7-9341
- outer heliosphere, recovery phase of galactic cosmic ray solar modulation 7-9342
- solar neutrino short-time variations rel. to solar activity and core oscillations 7-47826
- stratospheric level, galactic cosmic ray modulation at mid-latitudes 7-9344
- supernova remnants, long term variations of terrestrial and near-Earth cosmic-ray intensity 7-66402
- temporal fluctuations at rigidities 4 to 180 GV, power spectral density (1976 to 1980) 7-14427

cosmic ray X-rays

- solar X-ray burst stereo observations, thick-target interpretation 7-47651
- solar X-ray bursts from the flare electrons, intensity rel. to mag. field strength 7-47650

cosmic rays

- see also cosmic ray composition; cosmic ray effects and interactions; cosmic ray energy spectra; cosmic ray origin; cosmic ray propagation; cosmic ray showers and bursts; cosmic ray variations; primary cosmic rays
- Cyg X-3, Oct. 1985 RF burst and gamma-ray event, cosmic ray shower observations 7-66790
- interplanetary propagation, effect heliospheric current sheet tilt changes 7-9340
- low-level counting, conference, Bratislava, Czechoslovakia (Oct. 1985) 7-24272
- Pamir Experiment (*Russian*) 7-9338
- particle and nucl. physics intersections conf., Lake Louise, Canada, May 1986 7-29569
- plasma interactions, conf., Sukhumi, USSR (May 1986) 7-48174
- research, the early history, 1900 to 1927 7-48263
- spacelab-2 experiments 7-23973
- track analysis by expert system using distributed problem solving 7-55388

cosmic X-rays see cosmic ray X-rays**cosmogony. see solar nebula; solar system****cosmology**

- 5D space-time-mass gravity in a vacuum, cosmological soln. 7-60842
- 10D superstring theories, cosmology with Ricci-flat compactification 7-40977
- adiabatic perturbations evolution in baryonic Universe, general soln. 7-4597
- alignments in hierarchically clustered populations, implications for QSOs triple alignments 7-60830
- anisotropic cosmological model, Boltzmann and Vlasov kinetic eqns. 7-61189
- anisotropic homogeneous cosmological models, gauge-invariant perturbations 7-48494
- attractor in a higher-dimensional cosmology 7-14696
- attractor in superstring model, Einstein theory, Friedmann universe, inflation 7-41201
- axion decay to photons in microwave and IR regions 7-14695
- Barker's theory of gravit., homogeneous and isotropic cosmological models 7-48495
- barotropic perfect fluid, cosmological shock waves in general relativity 7-66797
- baryon and lepton number violation in astrophysics 7-55866
- baryon asymmetry of Universe, depend. on eqn. of state 7-24243
- baryon concentration in string wakes at $z \geq 200$, implications for galaxy form. and large-scale struct. 7-14687
- baryon diffusion and inhomogeneities in big-bang plasma 7-60848
- Bianchi cosmologies, He production, time scale arguments 7-40972
- Bianchi II vacuum model, relation to vacuum Einstein equation solns., gravitational waves 7-61181
- Bianchi models, does anisotropy suppress inflation 7-29559
- Bianchi type-I Einstein-Cartan cosmological model, inflationary aspects 7-56118
- Bianchi type-II perfect fluid solutions 7-40967
- Bianchi type-V solution in scale-covariant theory 7-48114
- Bianchi type-VI₀ solutions, homogeneous and inhomogeneous 7-48115
- Bianchi types -I-II-III-V-VI₀-VI_h and KS universes in JBD theory. 7-14680

cosmology continued

Bianchi-IX cosmological model, chaotic behaviour 7-24509
 Bianchi-type I space times, appl. of Einstein equations with fourth-order derivative terms 7-48111
 Bianchi-type VIII models, chaos in the long-term behaviour 7-60843
 biased galaxy formation 7-14658
 big bang as the collapse of an ordered spin system 7-66798
 Big Crunch, strong black hole thermodynamics, unified geometrical approach 7-4749
 big-bang nucleosynthesis, standard model with interacting particle species 7-23997
 black minihole evaporation dynamics, estimates and interpretation for high-energy physics 7-66653
 Boltzmann gas, semi-normalistic, fitting formulae for eqn. of state 7-40685
 boson stars, gravitational equilibria of self-interacting scalar fields, maximum mass calcs. 7-24519
 bubble dynamics in the expanding Universe 7-24244
 canonical quantization of gravit., Universe wave function boundary conditions 7-18672
 causality in general relativity, recovery 7-160
 centrally symmetric space-time, Schwarzschild's formula 7-47687
 chaotic inflation, effects of nonnormalisable terms 7-29558
 chaotic inflationary universe, anisotropy effects in Bianchi cosmologies, scalar fields 7-18463
 chaotic inflationary universe model 7-60845
 characteristic actions $\hbar^{(4)}$ in struct. of Universe, implications for time depend. of gravit. const. 7-4602
 chronometric cosmology, flux-redshift relations rel. to quasar luminosity evolution 7-24237
 classical cosmologies from ten-dimensional supergravity 7-9563
 classical model with inflationary expansion 7-48113
 closed universes, dynamical torsion and the indefinite metric, general relativistic anal. 7-9571
 closed-time-path functional formalism in curved spacetime, cosmological back-reaction problems 7-4215
 closed-universe recollapse conjecture 7-48119
 collisionless gravitating systems, spherical collapse stability 7-40678
 conf., Erice, Italy (April 1986) 7-41001
 conf., Neuchatel, Switzerland, April 1986 7-40984
 constant, non-compact symmetries and Weyl invariance 7-4611
 contraction/expansion cycles, anal. using Bekenstein-Hawking thermodynamics 7-48128
 cosmic censorship hypothesis in cosmological space-times 7-48470
 cosmic microwave background, temp. fluctuations induced by gravitational lensing 7-4595
 cosmic strings, evolution and scaling soln. 7-48496
 cosmic strings, superheavy, superconducting, from superstring models 7-60847
 cosmological consequences of strong and gravitational unification 7-14844
 cosmological constant, uncertainty principle limits 7-14685
 cosmological density perturbations, gauge-invariant, evolution during decoupling era 7-60849
 cosmology and particle physics 7-48117
 cosmos, space education, conf., Copenhagen, Denmark (Aug. 1986) 7-48182
 creation of Universe, from before Big Bang to end of Planck era 7-66795
 curved space-time cosmologies, S-matrix approach to interacting quantum field theory 7-47675
 D=11 supergravity theory, cosmological constant contribs. from quantized gravitino sector 7-18678
 dark matter, weak interaction and the large scale structure of the Universe 7-55871
 dark matter and axion rest mass 7-60524
 dark matter in superclusters 7-60818
 dark matter in the Universe 7-60851
 dark matter in Universe 7-9560
 dark matter nature 7-60658
 dark matter particles mass, implications of obs. of wise binary stars 7-66664
 dark matter problem, alternatives in modified gravitation models 7-47692
 de Sitter universe with quadratic lagrangian, stability and cosmic no-hair theorems 7-60846
 deceleration parameter, implications of faint galaxy photometry 7-60915
 deflationary universe as de Sitter universe instability 7-35078
 diffuse microwave background radiation, temp. at 12 cm wavelength 7-55859
 disk galaxies form. at high red-shift 7-55794
 double galaxies in cosmic quantum mechanics, possible mass limits 7-18455
 double inflation, density perturbations in the Universe, bubbles 7-48123
 E_6 supergravity GUT, cosmological constant problem 7-61524
 early Universe, bubble growth and droplet decay in quark-hadron phase transition 7-9562
 early universe, cosmology, phase transitions and inflation 7-48126
 early Universe, evaporation of strange quark matter, dark matter candidate 7-40974
 early Universe, N-vector model for inflationary expansion 7-24247
 early universe, possible violation of thermodynamic equilibrium 7-48118
 early Universe, time variation of fundamental constants, primordial nucleosynthesis and extra dims. size 7-9567
 early Universe, vacuum polarisation a scalar field effects 7-48110
 early Universe structures and microwave background 7-48108
 Einstein's eqns., similarity solns. relevant to the early Universe 7-48481
 Einstein's field equations, dimensional reduction in a multi-dimensional cosmology 7-29830
 Einstein gravity, extended with Gauss-Bonnet term, cosmological solns. 7-24500
 Einstein solutions, spatially inhomogeneous cosmologies with heat flow 7-35075
 Einstein-Born-Infeld theory, duality rotations and type-D solns. 7-47683
 Einstein-Hilbert lagrangian, higher dimensional cosmological solns. 7-14835
 Einstein-Kalb-Ramond cosmology 7-48122
 Einstein-Rosen metrics, generalised soliton solns. 7-41166
 elliptical galaxies formation 7-55795
 entropy production during an isothermal phasetransition in the early Universe 7-4598

cosmology continued

evaporating black holes, back reaction of quantum fields in presence of inflation 7-9506
 expanding universe, redshift, ang. size 7-18527
 extended thermodynamics in the early Universe 7-9557
 extragalactic distance scale, Galaxy scale change repercussions 7-14659
 extragalactic radio sources evolution, implications of spectral index-flux density relation at 408 MHz 7-4578
 faint galaxies as probes for distant Universe 7-4610
 field theories in Robertson-Walker background, consistency of Hamiltonian diagonalisation 7-4969
 finite temperature quantum field theory in curved spacetime, quasilocal effective Lagrangians 7-4216
 finite-temperature instability for compactification 7-9564
 fourth-order theories of gravity and general relativity, equivalence, cosmological singularity 7-41178
 Friedmann cosmology with a cosmological constant in scale covariant theory 7-4608
 Friedmann universe, general conditions for inflation 7-40971
 Friedmann universe and compact internal spaces in 4+N gravity theories 7-9733
 Friedmann universe development, implications of relativistic gravitation theory (Russian) 7-60533
 Friedmann universes, large-scale anisotropy of cosmic background radiation 7-9561
 Friedmann universes, scale factors and critical values of cosmological const. 7-9569
 Friedmann-Lemaitre-Robertson-Walker models in Lyra's manifold 7-40966
 galactic halos, rotation, density and string-seeded spirals 7-29562
 galaxies, dwarf irregular and elliptical, possible evolutionary relationships 7-35053
 galaxies, large-scale distrib. determ. from wide-angle samples of objective-prism spectra 7-66771
 galaxies, origin, evolution and star form. 7-48087
 galaxies, redshift-magnitude formula for Universe with cosmological const. and radiation press. 7-40924
 galaxies clustering, evolution and clustering of rich clusters 7-9546
 galaxies clustering, two-dimensional covariance function for IRAS sources 7-14677
 galaxies explosive formation, percolation rel. to galaxy-galaxy correl. scale 7-29533
 galaxies formation equilibria and instabilities of polytropic configurations within homogeneous background matter 7-4316
 galaxies red shift quantisation 7-60812
 Galaxy age and chemical evolution, general constraints 7-55809
 galaxy cluster-cluster correlation function, sampling errors and significance levels 7-48092
 galaxy clustering, non-Gaussian fluctuations, large-scale matter distrib. 7-24232
 galaxy clusters distribution, spatial correls. of Abell clusters 7-9548
 galaxy clusters evolution, vel.-distance relation in Virgo rel. to mass-age infall models 7-24230
 galaxy correlation functions, closure of BBGKY hierarchy in phase space 7-29546
 galaxy correlations at high redshift, implications for quasars environment 7-24216
 galaxy distrib. of bubble type, explosion model of formation 7-60820
 galaxy formation, cosmic string basis 7-14693
 galaxy formation, recent developments in cosmic string theory 7-14694
 galaxy formation, string-induced, compatibility with inflation 7-66765
 galaxy formation by cosmic strings 7-9543
 galaxy origin, constraints from small-scale cosmic background radiation anisotropy and galaxy clustering 7-48082
 general relativistic models with variable G, Λ , energy nonconservation reanalysis 7-48121
 general relativity, generalised harmonic gauge conditions as field eqns. for lapse and shift 7-47678
 general textbook contribution 7-60912
 generalised field theory and the Kasner universe 7-41186
 generalised inflationary cosmology, gauge-invariant perturbations 7-48112
 geometric effects in cosmological phase transitions 7-14692
 geometrical structures appl. 7-35073
 gravitation and vacuum field 7-172
 gravitational lensing, flux conservation and random lensing in Friedmann universes 7-23994
 gravity, gauge theories and quantum cosmology, book 7-48512
 Green's function in curved space-time, Hadamard construction (German) 7-66444
 heterotic string, vanishing vacuum amplitude, modular forms and cosmological constant 7-15091
 hierarchical structure in the distribution of galaxies 7-55839
 Higgs field coupled gravitation theory, high-freq. perturbations and gravitational collapse 7-40681
 higher dimensional cosmology, initial conditions and attractors 7-29561
 homogeneous anisotropic cosmological models with viscous fluid and magnetic field 7-24503
 homogeneous Kaluza Klein cosmologies, group theoretical classification 7-48491
 hot big bang model, compatibility of zero cosmological const. with obs. 7-24250
 hot Universe with massive unstable leptons, evolution 7-4596
 Hubble constant determ. method involving observation of gravitational waves 7-9559
 Hubble diagram for brightest cluster galaxies, effects of gravit. amplification by foreground clusters 7-24206
 Hubble flow, evidence for non-uniform vel. field 7-24225
 Hubble law derivation from cosmological redshift 7-66796
 Hubble parameter, noncompact symmetries and Weyl invariance 7-29560
 induced causality in astrophysics, alternatives to general relativity 7-47676
 inflation, examination of phase transitions 7-29564
 inflation and bubbles in general relativity 7-35351
 inflation from inhomogeneous initial data in a one-dimensional back-reacting cosmology 7-48125
 inflation in the heterotic $E_6 \times E_6$ superstring model, reheating 7-4604
 inflation with generalized initial conditions of scalar field configs. 7-48124
 inflationary cosmological model, homogenization and isotropization 7-35375

cosmology continued

- inflationary cosmology, age of Universe 7-55868
- inflationary cosmology, dynamical anal. 7-14691
- inflationary cosmology, generation of density perturbations 7-48120
- inflationary Universe, effective grav. Lagrangian and energy-momentum tensor 7-4606
- inflationary Universe, homogeneous cosmological models 7-24249
- inflationary universe, large-scale quantum fluctuations 7-60850
- inflationary universe, phenomenological cosmological model w.r.t. general relativity 7-48130
- inflationary universe, primordial black holes as missing mass candidates 7-4599
- inflationary Universe, progress and problems 7-55867
- inflationary universe models, generation and evolution 7-29565
- inhomogeneous anisotropic cosmologies, general upper limits to age of Universe 7-4603
- inhomogeneous cosmological model, generalized vacuum soliton soln. of Einstein's eqns. 7-9715
- inhomogeneous cosmological models, de Sitter soln. and inflationary scenarios 7-56116
- inhomogeneous universes, gravitational lens effect probabilities 7-40965
- initial conditions in quantum cosmology 7-14690
- ino-dominated Universe, radiation fluctuations, role of baryonic density 7-55858
- intergalactic voids at high redshifts, constraints from QSO Ly α absorbers 7-55823
- IR line emission from protogalaxies and protocluster pancakes 7-4600
- isotropic flat space cosmology, in Jordan-Brans-Dicke theory 7-4601
- isotropization in spatially homogeneous, two-component cosmological models 7-55860
- Kaluza-Klein cosmological model, 5D, density matrix and entropy 7-55865
- Kaluza-Klein cosmologies, surfaces of discontinuity in 5-D 7-41197
- Kaluza-Klein gravitational theory, astrophysical data and cosmological solns. 7-9363
- Kaluza-Klein model, cosmological solns. for homogeneous, spatially isotropic metric 7-9723
- Kaluza-Klein theories, cosmological evolution of degenerate vacua 7-41198
- Kaluza-Klein theory, extra time-like dimens. leading to nonvanishing cosmological constant 7-4753
- Kaluza-Klein theory, quantum cosmological approach and 'no boundary' condition 7-41191
- Klein-Gordon and Weyl equations in the Godeluniverse 7-167
- large number hypothesis, Bekenstein-Hawking entropy and Weizsackers ur theory 7-14686
- large scale structure, consistency problems 7-48127
- large scale Universe structure, origin, evolution 7-55872
- large-scale clustering of galaxies with massive dark halos, general struct., two-point corrs. and binaries 7-29544
- large-scale structure in Corona Borealis region, redshift survey 7-40922
- lightest elements formation in cosmological nucleosynthesis 7-24252
- local Euclidean gravity coupled to σ -model, harmonic maps and submer-sion 7-14843
- magnetic monopole detection, from Stanford to MACRO 7-10014
- magnetized cosmological model for perfect fluid distribution 7-24505
- mass density fluctuations, mode coupling 7-55861
- massive scalar field in the static space-time of a cosmic string 7-41217
- material content of Universe, conference, London, England (October 1985) 7-55884
- matter creation, dynamic meas. system 7-55862
- matter models which violate the strong energy condition, initial singular-ity, construction 7-179
- microwave background, entropy of perturbed background radiation 7-66791
- microwave background radiation, temp. meas. at 3.3 mm wavelength 7-29556
- microwave background radiation anisotropy, review 7-48106
- missing matter problem and weakly interacting massive particles 7-24246
- Mixmaster universe, quantum chaos 7-9742
- models testing, use of large-scale vel. fields 7-4609
- monopole abundance from first order GUT phase transition of early Universe, theory 7-9572
- monopole dilution by inflation and entropy enhancement 7-9734
- N=1 supergravity in 11D, fermionic mass and cosmological constant generation 7-61206
- natural measure on the set of all universes, inflation period 7-55864
- Newtonian cosmology based on Yukawa-type pot. 7-41189
- non-Euclideanism in general relativity and cosmology, mathematical formalism 7-34851
- non-Gaussian mass density fluctuations, effects on two-point correlations of galaxies and rich clusters 7-29545
- non-Hubble velocities of cosmological objects 7-35070
- nonvanishing energy density of vacuum or cosmological constant 7-55870
- nuclei, weak and EM interactions, conference, Heidelberg, Germany (July 1986) 7-48172
- nucleosynthesis, relation between ^4He , ^2H and ^3He prod. 7-40979
- Olber's paradox resolution 7-18346
- open Kaluza-Klein universe, effective pot. of scalar fields 7-40975
- orthogonal perfect fluid and vacuum solutions, self-similar spatially homogeneous cosmologies 7-29824
- paradox resolution using concepts from general relativity 7-35172
- particle creation, intrinsic measures of field entropy 7-35077
- particles in the early universe, conference, Thessaloniki, Greece (June 1985) 7-9596
- phase transitions at late epochs, contrib. to density perturbations genera-tion 7-24248
- phase transitions in the early universe, nonabelian gauge theories 7-9570
- Planck length as cosmological constraint, derivation 7-34852
- population II star (G 64-12), ^7Li abundance indicative of primordial composition 7-60642
- Population III, heating of dust and radiative spectrum (*Chinese*) 7-66680
- Population III stars, evidence in isotropic background radiation 7-47998
- Population III stars, identification with current Population II stars 7-29470
- primary cosmic antimatter detection, proposed satellite expt. for energy spectra determ. 7-47647
- primordial gas heating by background radiation, effects of presence of H $_2$ 7-24205
- primordial He abundance determ. from metal-poor galaxies 7-40978

cosmology continued

- primordial He abundance rel. to He in metal-poor H II regions of dwarf irregular galaxies 7-55804
- primordial nucleosynthesis and photinos 7-66793
- primordial star formation and galaxy form., triggering by evolution of large-scale density perturbations 7-66794
- primordial stars formation, clouds fragmentation and pre-main-sequence evolution 7-47999
- protogalaxies and galaxy clusters burnout, relation to close quasar pairs 7-35051
- quantum cosmological perturbations in pure gravity 7-180
- quantum cosmology, fermionic perturbations and wavefunction of the Universe 7-56128
- quantum cosmology, local laws and boundary conditions 7-29563
- quantum field theory, progress, book 7-9602
- quantum gravity and cosmology, Kyoto, Japan (May 1985), conference 7-24295
- quark matter as ground state in Universe 7-56503
- quark-hadron transition in cosmology, effects on primaeval nucleosynthesis 7-47677
- quasar distrib. on large and super large scales 7-60826
- quasar redshift cutoff 7-55846
- quasars, characts. review 7-48098
- quasars, cosmic evolution at high red shift 7-40954
- quasars, evolution rel. to selection effects 7-18460
- quasars, UV continuum evolution with redshift 7-55849
- quasars space distribution, luminosity-volume test rel. to local hypothesis 7-35064
- R 2 cosmology, inflation without a phase transition 7-40973
- R+R 2 gravity, first order formalism treatment conformally metric theory, early Universe appl. 7-41200
- radiating system of two coupled strings, normal modes, stars 7-18656
- radio sources evolution, evolution function of flat-spectrum sources at 5 GHz 7-14673
- red shift-number test implications 7-35079
- redshift-distance relation for galaxies, perturbation due to Local Group mass 7-40928
- reheating after inflation for classical scalar field with exponentially flat pot. 7-4605
- relativistic astrophysics and gravitation, conference, Potsdam, Germany (October 1985) 7-40980
- relativistic cosmology, conformal potential of stationary axisymmetric vacuum 7-47682
- relativistic cosmology, eqns. of motion for test particles with internal struct. 7-41165
- relativistic cosmology, linear problem for five-dimensional projective field theory 7-47681
- relaxation time for transition from isotropic turbulence to microscopic chaos (*German*) 7-29848
- rotating axisymmetric expanding universe with an electromagnetic field 7-24245
- rotating cosmic string surrounded by grav. radiation, Einstein eqns. solns. 7-18464
- rotation in cosmological solutions to metric gravity theories, comments 7-40970
- scalar-tensor theory and baryonic interaction 7-18350
- scalar-tensor theory of fourth-order gravity, Universe scale factor 7-61190
- scale factor evolution of 5D cosmology 7-14689
- secular redshift variations, effects of cosmological deceleration and peculiar motion 7-60796
- self-creations cosmologies, Raychaudhuri-type equations 7-24251
- self-focusing as a mechanism for the formation of dense structures in Newtonian cosmology 7-40964
- self-similar, galactic scale phenomena and dark matter 7-35076
- self-similar scaling in stellar and atomic systems 7-14683
- self-similarity, scaling eqns. 7-14684
- self-similarity and scale covariance principle 7-48116
- Shane-Wirtanen counts, observer and time-depend. effects 7-55838
- Shane-Wirtanen counts, plate correction factors and correl. function 7-55837
- shear-free homogeneous cosmological model with heat flux 7-55863
- space-time structure, relation to quantum mechanics 7-47679
- spatially homogeneous and anisotropic expanding Universe of Bianchi type-V 7-9558
- spontaneous CP-violating models without strong CP problem, cosmological baryon prod. 7-49037
- static Friedmann-Robertson-Walker vacuum models, solutions 7-14682
- Stephani-Krasinski solution, anal. of viability as model of universe 7-66800
- strings and other topological defects 7-29566
- superconducting cosmic strings, cosmological effects 7-24518
- superconducting cosmic strings, induced ang. momentum 7-9566
- Superconducting Supercollider, elementary particles and cosmology 7-48260
- supergravity GUTs, N=1, Higgs potential minima with vanishing cosmological constant 7-9731
- supernovae as distance indicators, proceedings, Cambridge, MA, USA (September 1984) 7-24296
- superstring in 4D, evolution with temp. and possibility of inflation 7-9728
- superstring model, baryogenesis and entropy generation 7-66801
- superstring models, candidates for inflaton field in cosmology 7-40976
- superstring models with intermediate scale breaking, inflation as cure for cosmological problems 7-56113
- supersymmetric inflationary cosmology in supergravity framework 7-48514
- SUSY electroweak model, N=1 supergravity extension, cosmology of phase transition 7-445
- technibaryon missing mass bounds 7-19042
- theories of Universe, review (*French*) 7-60841
- time varying gravitational constant, no creation and constant rest mass 7-66799
- time-varying coupling constants and primordial nucleosynthesis 7-4607
- Tolman-Bondi model, Hawking mass test in expanding dustlike universe 7-18650
- topological structure of Universe, observational consequences of 'small universe' 7-60844
- Tully-Fisher relation, type effect and Malmquist bias 7-14646
- tunnelling without barriers in curved space-time 7-41196
- universal structure, response to DerSarkissian's 1984, 5 papers 7-14681

cosmology continued

- Universe, average density and Regge law 7-35072
- Universe, large-scale structure, cosmic strings 7-14688
- Universe, mag. field and rot. 7-40963
- Universe, open or closed, evidence from Galaxy chem. modelling 7-35030
- Universe, quantum creation theory 7-14487
- Universe age, constraints from globular clusters and cosmic expansion rate 7-55869
- Universe dominated by relativistic particles 7-29557
- Universe large scale structure, model 7-40969
- Universe mass density 7-40968
- unstable heavy neutrinos, constraints from cosmology 7-34860
- vacuum Einstein eqn. solns., cylindrical waves and cosmic strings of Petrov type D 7-48477
- vacuum fluctuations outside cosmic strings 7-9565
- vacuum Friedman-Robertson-Walker universe, generation of gravitational waves 7-29832
- vacuum Friedmann cosmology based on Lyr's manifold, solns. 7-35074
- vacuum inhomogeneous mixmaster universe, symm. behaviour and cold-started inflation 7-18675
- wave equations in cosmic string spacetime 7-35071
- wave fns. of universe, quantum-classical correspondence 7-9568
- ν mass and nuclear beta-strength, cosmological and astrophysical consequences 7-48129
- H II regions dynamics, implications for photoionisation of intergalactic medium 7-40938
- He primordial abundance, determ. from meas. in H II galaxies 7-40937
- He primordial abundance, implications of collisional effects in He I triplets 7-55446
- ³He primordial abundance and stellar ³He contrib. to interstellar matter 7-60840
- ¹⁸⁷Re, half-life determ., relevance to fine-structure const. 7-49345

cosmotrons

No entries

Costa Ribeiro effect *see dielectric phenomena; phase transformations*

Cotton-Mouton effect *see magneto-optical effects*

Cottrell atmospheres

- Cu based alloys, internal friction, Young's modulus, amplitude relationship (Russian) 7-65075
- GaAs, semi-insulating, photoluminescence imaging using laser scanning microscope 7-53384

Cottrell locking *see Cottrell atmospheres*

Couette flow

see also jets

- axial laminar, characteristics in concentric and eccentric double tube models (Japanese) 7-11379
- axial laminar, characteristics in concentric circular double tube model (Japanese) 7-11378
- axial laminar, characteristics in eccentric circular double tube model (Japanese) 7-11377
- bifurcations near tricritical point in Couette-Taylor flow, Landau model 7-1528
- buoyant and combusting flow, turbulence model 7-51083
- circular, mass transfer at smooth and rough surfaces 7-51163
- circular couette system, formation of dynamical domains 7-37430
- colloidal crystals, shear melting and Taylor instabilities 7-43858
- Couette flow with porous walls of a dilute suspension 7-51037
- Couette-Taylor flow, quasiperiodic to turbulent transition, strange attractors 7-63120
- Couette-Taylor flow, rotating, Eckhaus boundary and wavenumber selection 7-43938
- Couette-Taylor instability, hydrodynamic and phase-transition descriptions, expt. study of connection 7-20691
- crystal growth from melt, Accelerated Crucible Rotation Technique, fluid flows 7-46306
- dense liquids, planar Couette flow, rheological props., mol. dynamics simulation 7-57791
- dense systems of spherical particles under shear dynamics 7-6258
- heat transfer in unsteady MHD Couette flow of electrically conducting viscous incompressible rarefied gas, theory 7-66448
- hydraulic drag coefficient determination in Couette flow at high Re 7-43841
- hydromagnetic channel flow in inclined magnetic field, Hall effects 7-51334
- instability onset, parametric modulation effects 7-43857
- Lennard-Jones fluid, shear thinning, mol. dynamics method calcs. 7-21059
- Lennard-Jones fluids, thermoviscous coupling and nonlinear transport effects on plane Couette flow 7-57793
- liquid, nonsteady properties, phase transition conditions 7-31739
- magnetic fluids, Taylor instability, mag. field effects 7-31738
- MHD Couette flow with heat transfer, Hall effects 7-37554
- microbial suspensions, rheological meas. (German) 7-14035
- modulated Taylor-Couette flow as a dynamical system, linear stability 7-11431
- shear flow, nonequilibrium steady states, transient correl. functions 7-57792
- slightly rarefied gas mixture, behaviour over plane boundaries 7-1592
- slurries, flow curve, rheological props. 7-43833
- smectic A liquid crystals, screw dislocation dynamics 7-21090
- spatial modes characteristics, vertex flow (Korean) 7-26295
- surfactant systems, drag reduction, physico-chem. props., rheology 7-43992
- Taylor-Couette flow, stability limits, flow visualisation and numerical study 7-43844
- Taylor-Couette flows, computation of anomalous modes 7-63108
- Taylor-Couette systems, phase instabilities and end effects 7-11432
- unstationary flow, particle behaviour in Basset-Boussinesq-Oseen eqn. 7-11404
- upper convected Maxwell fluid, plane Couette flow, linear stability 7-16160
- wavenumber selection and Eckhaus instability in Couette-Taylor flow 7-43843
- Cd,Hg_{1-x}Te, Bridgman growth using Accelerated Crucible Rotation Technique 7-46307

counter accessories

see also counting circuits

No entries

counters

see also Cherenkov counters; counting tubes; fission counters; Geiger counters; proportional counters; scintillation counters; semiconductor counters; spark counters

- commercial particle counters, counting efficiencies 7-56396
- models of particle counters with prolonged dead time 7-56905
- Mossbauer spectra meas. with high count rate 7-36425
- multichannel scaling with a VIC-20 or Commodore 64 7-49841

counters (circuits) *see counting circuits*

counting circuits

- see also coincidence circuits; pulse height analysers; scaling circuits*
- anticoincidence counting system, absolute activity meas. (Korean) 7-25329
- conf., Munich, Germany, March 1986 7-40990
- EELS parallel detection setups 7-18943
- flow meas., multichannel time counter and data acquisition system 7-37571
- neutron multiplicity measurements with shift registers, dead-time error reduction method 7-25331
- radiation meter with counter tube or p-i-n-diode detector, design (German) 7-30900
- radioactive radiation meas., detectors construction (German) 7-30834

counting tubes

see also dekatrons

No entries

country planning *see town and country planning*

county planning *see town and country planning*

coupled circuits

- neural networks and optical resonators, coupled-mode theory 7-54513

coupled networks *see coupled circuits*

coupled superconductor devices *see superconducting junction devices*

couplers (electric connectors) *see electric connectors*

couplers (waveguide) *see waveguide couplers*

coupling (process) *see joining processes*

coupling circuits *see coupled circuits*

CP invariance

- axion-EM coupling, implications for cosmic background radiation 7-439
- beta-decay, mixing matrix and CP-violating phenomena 7-476
- CP violation models 7-436
- Fermilab Antiproton Source, physics workshop report 7-49174
- Fermilab E731 experiment, α/α parameter measurement, status 7-41653
- gauge field coupled to axial U(1) charge in gravitational field, CP-effective action anal., spectral asymmetry 7-41601
- hyperon decay, CP-odd observables 7-49138
- Kobayashi-Maskawa hard-CP-violation model with three-generation Majorana neutrinos 7-19027
- Kobayashi-Maskawa matrix, renormalisation group eqns., quark mixing, CP nonconservation 7-5034
- Kobayashi-Maskawa matrix and maximal CP violation 7-19028
- Kobayashi-Maskawa matrix with four-generation quarks and CP violation 7-61497
- left-right squark flavour mixing, effect on CP violation, minimal low energy supergravity anal. 7-35737
- left-right symmetric models and CP invariance 7-56498
- magnetic monopole, CP violating electric charge 7-10004
- models of CP violation, experimental constraints 7-41652
- neutron electric dipole moment, CP invariance 7-56558
- neutron electric dipole moment from cloudy bag model, CP-violating effects 7-24889
- quark mass matrices, model of flavor mixing 7-447
- quark mass matrices in standard electroweak model, maximal CP violation, anal. for many quark generations 7-30215
- quasi standard model physics, strong CP problem 7-56496
- reviews of particle and nuclear physics, book 7-55907
- spontaneous CP-violating models without strong CP problem, cosmological baryon prod. 7-49037
- squark mass matrix constraints from CP-violation 7-24805
- squark mixing angles in supergravity theories, gluino flavour changing in SU(5) 7-56136
- standard model, CP invariance and $\Delta I=1/2$ rule 7-49025
- standard model, CP violation size (Chinese) 7-49027
- strong CP problem, elimination via invisible axion mechanism in E₆ supergravity GUT 7-61524
- SU(2)×U(1) gauge theory, Majorana D and CP violation in leptonic sector 7-24790
- SU(3) × SU(2) × U(1) model, addition of vector-like quarks, CP-violating phases 7-35753
- supergravity, CP-violation in 11D 7-41225
- supersymmetric inflationary cosmology in supergravity framework 7-48514
- supersymmetric standard model, light gluinos and CP violation 7-443
- symmetry tests, T, CP and CPT invariance, review 7-30205
- T, CP, and CPT transformations in the presence of vacuum degeneracy 7-35741
- three-generation phase-invariant measure of CP nonconservation at the unification scale 7-19029
- violating parameter, double penguin-like diagrams for ϵ parameter 7-5028
- violation, present status, review 7-56466
- Weinberg CP violation model, chiral props. of weak amplitudes 7-449
- B→K⁰1⁺, rate and CP-nonconservation asymmetry, standard model calcs. 7-514
- B→K⁰1⁺, rates and CP violation, fourth-generation standard model anal. 7-19099
- B meson decay, mixing matrix and CP-violating phenomena 7-476
- B meson exclusive decays, CP violation, phenomenology 7-41656
- B⁰ - B⁰ system, CP violation, left-right mixing, SUSY standard model comparisons 7-24805
- B⁰ decay, large CP violations 7-35863
- B⁰-B⁰, time-dependent CP violation effects 7-435
- B[±]→D⁰D⁰ π^{\pm} , CP violation anal. 7-61657
- B_s→D⁰ (K⁰F⁻), partial decay rate asymmetries and CP violation 7-41792
- B_s⁰ meson rare decays, CP-odd effects 7-438
- B_s⁰→F⁻D^{0*} (F⁻*D⁰), partial decay rate asymmetries and CP violation 7-41792
- D meson exclusive decays, CP violation, phenomenology 7-41656
- D⁰-D⁰ system, partial decay rate asymmetries, CP violation 7-35864
- ϵ electric dipole moment bounds in a wide class of models 7-41815

CP invariance continued

- e^+e^- →heavy Majorana fermions→ l^+l^- , cross sections, tests for Majorana nature, CP-, CPT-invariance 7-61702
 e^+e^- →neutralinos, CP violation effect, SUSY electroweak model anal. 7-10065
 e^+e^- → W^+W^- , probing the weak boson sector, anomalous couplings search, helicity amps. 7-56533
 e^+e^- →X, CP nonconservation search using jet variables 7-41665
 $K=2\pi$, CP violation in six-quark standard model 7-35740
K decays, CP nonconservation, time depend. perturbation theory for quaternionic quantum mech. 7-5087
 $K\rightarrow\pi\pi$ amplitudes in QCD duality approach, $|\Delta I|=1/2$ rule problems in standard model 7-10056
 $K^0(K^0)$ decay, meas. possibilities for T-, CP-, CPT-violation parameters 7-10053
 $K^0\bar{K}^0$ system, CP and CPT violation 7-30206
 $K_L\rightarrow\mu^+\mu^-$, CP-nonconservation with four generations 7-24875
 K^0 decay, CP violation, experimental anal. 7-41786
 $\nu\rightarrow\nu\gamma$, lifetime in left-right models 7-35764
 $p\bar{p}\rightarrow e^+\mu^-X$, CP violation at the TeV scale 7-19145
 $p\bar{p}\rightarrow e^+\nu X$, CP violation at the TeV scale 7-19145
 $p\bar{p}\rightarrow\Lambda\bar{\Lambda}$, LEAR data anal., CP invariance in $\Lambda\bar{\Lambda}$ system 7-49167
 $p\bar{p}\rightarrow\Lambda\bar{\Lambda}(\Xi\bar{\Xi})$, low energy, CP violation, asymmetry meas. 7-15082
 $p\bar{p}\rightarrow X$, CP nonconservation search using jet variables 7-41665
q-decay ($q=c,b$) and CP violation, electroweak theory status 7-56486
 $SU(2)_L\times SU(2)_R\times U(1)$ electroweak models, constraints from nuclear beta-decay 7-56489
 $W^{(\pm)}\rightarrow tb(\bar{t}b)$, branching ratio comparisons, CP nonconservation 7-10061
 $Z\rightarrow b\bar{s}(bs)$, branching ratio comparisons, CP nonconservation 7-10061
 Z^0 decays, CP nonconservation effects in the standard model 7-5090

CPA calculations

- alloys, binary, short range order, coherent pot. approx. 7-7142
alloys, substitutionally random, electron localisation and metal-insulator transition, CPA calcs. 7-27302
alloys, ternary substitutional, electronic structure, KKR-CPA method 7-64074
band offsets at pseudo-ternary semiconductor-alloy heterojunctions 7-12835
composite materials, dielec. function, momentum depend. effective medium approach 7-27281
concentrated disordered alloys, positron annihilation in vacancies 7-39290
disordered alloy surfaces, density of states calc. 7-21961
disordered materials, optical phonon spectra, CPA calcs. 7-38147
electronic and transport props., coherent potential approx. 7-27241
ferromagnetic, electronic quasiparticle struct., temp. depend. 7-32908
III-V semicond. alloys, val.-field characts., band struct. effects, CPA calcs. 7-64243
metal alloy hydrides, disordered, theory of electronic states 7-27243
MIM junction with disordered insulator, tunnelling current, CPA calc. 7-52850
noble metal alloys, Al- K_{α} XPS intensities 7-27870
one-dimensional periodic Anderson Hamiltonian, effect of disordered conc. nonmagnetic impurities 7-27517
optical absorption lines, influence of exciton motion, appl. to surface vibrations 7-7317
orientationally disordered systems, optical props., CPA approx. calcs. 7-53256
paramagnetic medium, completely disordered, magnetisation fluctuations, CPA approx. 7-2808
quantum paraelectric material with two types of impurity, structural phase transition, CPA calc. 7-44786
quantum wells, electronic struct., interface disorder effects 7-45476
random binary alloys, electronic props., max. entropy method 7-16929
randomly dil. Cayley tree, electronic density of states determ. 7-32890
semiconductor strained layer superlattices, electronic and optical props. 7-7359
transition metal alloys, disordered, electron struct. and positron annihilation (Russian) 7-45133
Ag-Pd, random alloys, residual electrical resistivity, first-principles calc. 7-2569
Au-Pt $_{1-x}$, mag. susceptibility, 77 to 450K 7-17164
Cu-Zn (Ga)(Ge), random alloys, residual electrical resistivity, first-principles calc. 7-2569
CuNi, substitutionally disordered, electronic struct., LCAO-CPA calcs. 7-64067
Fe $_3$ Si, electronic struct. and X-ray spectra, disorder effects (Russian) 7-32903
Ga-In-As-P system, ternary alloys, E_1 energy gap, CPA calc. 7-58740
Mo-Re alloys, electron struct., X-ray spectra studies (Russian) 7-45135
Ni, magnetic props., Hubbard model 7-2806
Ni-Mo, random alloys, residual electrical resistivity, first-principles calc. 7-2569
Pd $_3$ Fe, disordered phase, electronic struct. anal. 7-58735
PdH $_x$, nonstoichiometric, electron density of states, analytic CPA model calcs. 7-52400
 α -Si:H, amorphous, coherent potential approx., potential well analogy 7-27240
a-Si:H, bulk, surface state densities, Bethe lattice method, CPA calcs. 7-32898
 α -SiGeH, electronic and transport props., coherent potential approx. 7-27241
 α -SiH, electronic and transport props., coherent potential approx. 7-27241
ZrN, electronic struct., metal vacancy effects, KKR-CPA method anal. 7-12606

CPT invariance

- Fermilab Antiproton Source, physics workshop report 7-49174
symmetry tests, T, CP and CPT invariance, review 7-30205
T, CP, and CPT transformations in the presence of vacuum degeneracy 7-35741
 e^+e^- →heavy Majorana fermions→ l^+l^- , cross sections, tests for Majorana nature, CP-, CPT-invariance 7-61702
 $K^0(K^0)$ decay, meas. possibilities for T-, CP-, CPT-violation parameters 7-10053
 $K^0\bar{K}^0$ system, CP and CPT violation 7-30206
 $K^0\rightarrow e^+\pi^+\nu$, search for T and CPT violation 7-41787
 $K^0\rightarrow e^+\pi^-\nu$, search for T and CPT violation 7-41787

crack detection*see also cracks*

- AC field meas. for crack detection and sizing 7-46770
acoustic emission applications in struct. testing 7-33883
acoustic emission signal amplitude correlation with material deform. rate 7-33895
acoustic microscopy, subsurface crack analysis 7-20537
AE testing for 7-3563
aircraft structures, using acoustic emission testing 7-33906
alumina surface crack characterisation by scanning acoustic microscopy 7-3567
ceramic wear behaviour, cathodolum. mode appl. in SEM 7-8228
composite, thin-walled structure, growth of through cracks monitoring arrangement, capacitive method 7-22968
composite, US NDT for transverse cracking 7-59734
computerized test system for thermal-mechanical fatigue crack growth 7-39801
electronic materials and their microstructure, thermal wave imaging studies 7-8237
initiation sites, determ. using digital NDE workstation 7-65277
magnetic crack detection using combined AC field magnetisation 7-33886
metallic materials, crack detection, structural inhomogeneities, multi-freq. eddy current testing 7-22954
metallic tubes, longit. crack detect. using EM acoustic transducers 7-22953
NDT applications of laser-generated focused acoustic waves 7-17754
noise emission analysis for determining crackinitiation during instrumental notched bar impact testing (German) 7-8216
photodisplacement techniques for defect detection 7-44865
photothermal methods of optical charactn. 7-28249
planar defect sizing by use of double-angle US beams and tip-echo times 7-17755
PMMA, rubber toughened, dynamic crack propag., high speed photographic, transmitted caustics 7-39638
pulsed holographic microscopy for crack tip propagation measurement (Japanese) 7-46780
radiowave diffraction method of complex quality control of cond. surfaces and dielec. coatings 7-39820
refractory products, US flaw detection 7-22960
residual stress analysis, US techniques 7-65273
SAE interactions with cracks and slots, noncontacting study using lasers 7-46756
scanning acoustic microscopy, NDT appl. 7-3564
scanning acoustic microscopy appl., NPL developments 7-22959
steel, Ni-Mo-Mn, stable crack growth monitoring AC/DC pot. drop technique 7-33887
steel, rotor type, deformed, microcrack dimens. rel. to acoustic emission parameters and struct. 7-65258
steel, stainless, pipe, detection of configuration of surface fatigue crack by DC pot. drop method (Japanese) 7-59726
steel plates, 2D crack meas. using elec. pot. CT method (Japanese) 7-59727
steel weldment defects, quantification techniques by US normal beam testing 7-16044
surface cracks, acoustic microscopy 7-46768
surface-breaking cracks, noncontact detection using laser acoustic source and EM acoustic receiver 7-3551
ultrasonic underwater imaging of cracks in concrete 7-33908
US pitch-catch technique, beam entry point correction 7-33884
welded joint, cracks reflecting characts. and stat. parameters of irregularities 7-8232
Al $_2$ O $_3$, crack imaging using scanning acoustic microscopy 7-28257
Al $_2$ O $_3$, reflection scanning acoustic microscopy of partly embedded cracks 7-46769
Cu, brittle oxide formed during oxidation, AE technique, alternative to thermogravimetry 7-65274
Cu, electrotech. grade, acoustic emission characts. in elastoplastic deform. 7-39816
SiC, stress intensity factor meas. using notched and surface flaw specimens 7-65251
- crack-edge stress field analysis**
see also penny-shaped cracks
7-22742
3D body, subjected to nonproportional loadings, non-uniform growth of plane crack 7-26209
3D crack, surface and through, integral eqns. method 7-1504
3D crack terminating at interface, stress intensity factors 7-11351
3D cracked anisotropic bodies, stress intensity factors, singular isoparametric elements 7-1501
3D structures, largely yielded, J-dominance of crack-tip fields 7-26210
-0 7-17622
analysis of crack emanating from circular hole in loaded plane 7-43775
angled crack problem, second-order terms and strain energy density 7-63062
anisotropic elastic strip, elastodynamic crack, complex variable approach 7-37389
anisotropic materials, crack tip field evaluation, iterative soln. of eigenvalue problem 7-43776
Astroloy, fatigue crack growth, closure anomalies 7-3403
asymptotic small scale yielding and double limits of crack tip fields 7-26215
asymptotic solution of three-dimensional elasticity problems of elongated plane tensile cracks 7-1502
bar, elliptical, with asymm. internal crack under anti-plane shear deform. 7-26208
bars, cylindrical, fatigue crack propag. 7-21346
BCC crystals, tensile crack stress intensity coeff. 7-13591
beam, cracked, of non-circular cross-section, torsional vibr. 7-6136
blunting lines in terms of crack opening displacement, eqns. 7-43778
body with plane crack, elasticity theory three-dimens. problem, variational soln. method 7-63072
bonded half planes in plane and antipane elasticity, multiple crack problems 7-1490
boundary element method for determ. effect of holes on crack stress distribution 7-6154
boundary integral method for crack tip stress intensity factors 7-16129
boundary separating two media, elasticity theory for cracks, singular problems 7-1515
caustic method for stress intensity factor determ. (German) 7-20672

crack-edge stress field analysis continued
 cellulose/asbestos fibre reinforced mortar, strain softening, crack growth resist. curves 7-39640
 ceramic materials, lifetime prediction 7-8218
 ceramics, crack propagation by double-torsion method (*Japanese*) 7-59614
 ceramics, grinding, crack branching, crushing mechanism 7-3472
 ceramics, transformation toughening, shear, shape and orientation effects 7-39626
 cleavage fracture, ductile-brittle transition 7-21339
 coherent-light-shadow spot of crack under mode I loading, theory and expt. 7-63089
 compact tension specimen, crack tip interaction with void, numerical analysis using J_2 corner theory (*Japanese*) 7-31703
 compact tension specimen, J-integral functions for fracture and fatigue anal. 7-63055
 compact tension specimens, crack length measurement by pot. drop method, improved anal. 7-31695
 compliance matrices for cracked bodies 7-31700
 composite, failure in compression, surface delamination along macrocrack 7-6155
 composite crack profile model for CTOD determ., theoretical anal. 7-63058
 composite materials, mode I edge delamination, stress distrib. ahead of crack, thermal residual stress 7-6151
 composite panel, whole-field strain determ. using coherent opt. processing 7-57779
 composites, anisotropic, interface crack, singularities 7-26218
 computerized test system for thermal-mechanical fatigue crack growth 7-39801
 concrete micromechanical damage model 7-53837
 conical crack problem in semi-infinite media with stress-free boundary conditions 7-31697
 contour integration around crack tips in elastic plastic material, mixed mode loading 7-50994
 crack closure integral method with quarter point elements 7-16121
 crack layer stability, anal. 7-43773
 crack-tip field parameters for large and small fatigue cracks 7-11356
 creep crack growth, theoretical-numerical investig. of expts. (*German*) 7-43803
 creep crack growth by grain boundary cavitation 7-21340
 crystalline solid bodies, conditions of elastic equil. of submicrocracks (*Russian*) 7-58407
 crystallites, 2D, crack growth, computer modelling 7-43787
 cyclic loading, crack growth rate, effect of different singularity fields 7-37381
 cylinder, circular, infinite, with penny-shaped crack under transient loading 7-43774
 cylinder, composite with penny-shaped crack, impact response 7-37384
 cylinder, elastic circular containing cavity or penny-shaped crack, thermal stresses 7-26202
 cylinder, hollow, surface compression strengthened, stable crack growth 7-37385
 cylinders, hollow, axial through cracks, stress intensity factors, opening areas, internal press. loading 7-1496
 defect and fracture mechanics, conf., Bad Honnef, Germany (Jan. 1985) 7-24260
 deformation modes of crack flanks due to shear, paradoxes 7-57754
 delayed damage in brittle solids 7-38111
 dielectric medium, crack extension force 7-6152
 discontinuous crack model, constitutive eqn. 7-26223
 discs and rings, subjected to rolling contact, stress intensity factors for small cracks in rim 7-57761
 dislocation around crack tip, image forces and pot. energy 7-26758
 dislocation emission from crack tip, computer simulations 7-37994
 dislocation emission from cracks, electron microscope obs. 7-38005
 dislocation emission from cracks in crysts. or along cryst interfaces 7-37992
 dislocation emission into mode III crack tip plastic zone 7-37995
 dislocation-crack interactions, mathematical modelling 7-37993
 displacement fields for mixed mode elastic-plastic cracks 7-16111
 domain with cut, stress intensity coeffs. in quasistatic temp. problems, asymptotic form 7-26152
 double edge cracks, interference effect on limit moment 7-26203
 ductile crack initiation and void vol. fraction, investig. based on Gurson's yield criterion (*Japanese*) 7-58402
 ductile fracture, plane stress, essential work of fracture vs. energy dissipation rate 7-20649
 ductile instability prediction in compact tension specimens 7-37383
 ductile instability prediction in cracked press. vessels 7-43769
 ductile-brittle fracture mode transition behaviour, kinetic model 7-21337
 dynamic fracture studies by stress intensity factor tracer method 7-63081
 dynamic stress intensity factors, meas. using FFT analyser, appl. to drop weight impact three-point bend testing (*Japanese*) 7-59712
 edge crack propag. and arrest in anti-plane shear 7-43790
 elastic body containing moving crack, dynamics 7-43788
 elastic dielectric, conservation laws and material momentum tensor 7-6086
 elastic media, finite plane, straight-crack tip location 7-43779
 elastic moduli, effective, of crack bodies in plane deform. 7-58395
 elastic unbounded body, cracks, 3D loading, stress intensity factor history 7-50998
 elastic wave scattering from interface crack in layered half space submerged in water, applied tractions at interface 7-11340
 elastic wave scattering from interface crack in layered half space submerged in water 7-11341
 elastic-perfect plastic soln. of antiplane parallel periodical crack field 7-57744
 elastomers, adherence, study by cyclic unloading expt. 7-33909
 elastomers, sliding friction mechanics, asperities adhesion fracture 7-53922
 elastoplastic problem of antiplanar deform. of crack-containing body, discontinuous solns. 7-11343
 elastoplastic stresses at crack tip, experimental-analytical hybrid model 7-63065
 energy release rate in quasi-static crack propag. and J-integral 7-26214
 epoxy polymers, compact tension specimen casting, fatigue crack growth rate testing 7-13681
 exterior Griffith cracks opened by a wedge in a rectangle 7-6149
 fatigue crack, closure behaviour, S-shaped unloading curve method (*Japanese*) 7-13684

crack-edge stress field analysis continued
 fatigue crack closure behaviour, simulation by extended body force, method (*Japanese*) 7-12199
 fatigue crack growth, dynamics factors (*Japanese*) 7-20657
 fatigue crack growth, stochastic modelling based on damage accumulation 7-6715
 fatigue crack growth, two element structural rheological model 7-16128
 fatigue crack growth at notch root in elastic-plastic region (*Japanese*) 7-58404
 fatigue crack growth rate, scatter, new model 7-43777
 fatigue crack growth under general-yielding cyclic loading 7-11355
 fatigue crack length and closure/opening stress, automated estimation 7-43811
 fatigue crack propagation, local crack-tip strain approach 7-63057
 fatigue crack propagation for defects near free surface 7-57743
 fatigue crack propagation rate, plastic deform. effect 7-13561
 fatigue crack propagation under biaxial loading, anal. using inclined strip yield zone model of crack tip plasticity 7-43771
 fatigue cracks, statistical analysis of growth data 7-16115
 fatigue cracks propagation model for random loading, stress ratio effect (*Japanese*) 7-12198
 fatigue failure criterion of mixed model 7-57750
 fatigue failure model, crack initiation and propag. 7-1499
 fatigue non-damaging notches 7-38103
 fibre composites, orthogonally reinforced, fracture criteria 7-1494
 fibre reinforced composite, planar, in tension, optimum crack-resistant design 7-16126
 fibre reinforced composites, delamination growth in angle-ply laminated composites 7-31701
 fibre reinforced composites, fracture, micromechanical and macromech. criterion 7-17609
 fibre reinforced laminates, transverse ply cracking strains 7-39637
 fibre reinforced polymeric composite, cracked orthotropic, long-time strength under constant tensile load 7-6156
 finite element modelling of grinding residual stress effects 7-16113
 finite plane isotropic elastic medium, straight crack, complex path independent integrals 7-43792
 flexure specimen, end-notched, for mode II testing, design and anal. 7-51005
 fracture, in-situ, TEM obs., influence of several parameters 7-6713
 fracture, post-yield, 3D finite element simulation 7-26216
 fracture analysis, brittle and ductile, of surface flaws using crack tip opening displacement 7-63078
 fracture criterion, crack propag. angle, fracture load 7-1506
 fracture dynamics, path-independent integrals using auxiliary fields 7-1495
 fracture mechanics, linear elastic, singular nine-noded distorted isoparametric elements 7-63054
 fracture mechanics and strength size effects, phys. evidence 7-57756
 fracture stress for inclined crack under biaxial load 7-57747
 fracture toughness assessment using elec. pot. method in comparison with standardized multiple specimen method 7-22932
 glass, AE source characteristics from thermal crack 7-21341
 glass fibre reinforced polyester resin composite, fracture toughness and microfractures, AE obs. (*Japanese*) 7-33779
 glass tubing, thermally induced crack propagation (*German*) 7-22805
 graphite fibre reinforced epoxy composites, crack growth under biaxial loading 7-33762
 Griffith's crack, interaction with rigid inclusions in elastic space 7-57741
 half-plane with system of rectilinear thin elastic inclusions, stress-strain state 7-11285
 heating preceded by coding ahead of crack, macrodamage-free zone 7-6716
 Homalite 100, stress intensity factor, crack vel., photoelastic obs. 7-1498
 Hookean materials, nonlinear mode II crack tip fields 7-37392
 hydraulic fracturing mechanics, explicit approx. solns. 7-6158
 IN738LC, Ni base superalloy, low cycle and thermal fatigue, small crack initiation and growth (*Japanese*) 7-13567
 incompatible singular elastic element for two- and three-dimensional problems 7-1503
 incompressible material, semi-infinite initially stressed body, penny-shaped crack, stress distrib. 7-1486
 infinite elastic medium containing penny-shaped crack, stress intensity factors for transient thermal loading 7-20647
 infinite solid weakened by circular crack, asymmetric thermal stress distrib. 7-6150
 inhomogeneous elastic body with circular crack, equil. problem 7-16127
 initiation determ. by standard test methods 7-37999
 initiation parameters, effect of crack closure 7-1493
 interaction with microcrack arrays, damage modelling 7-50991
 interface crack, stress field 7-37378
 interface crack, transient stresses 7-37382
 interface cracks, finite element approach 7-43801
 interface in uniform stress field, crack problem soln. 7-16125
 interfacial bonding and adhesion, conf., Aspen, CO, USA (Aug. 1985) 7-24269
 interfacial crack problems, appl. of conservation integrals 7-37387
 isotropic elastic solid, elliptical cracks under shear loading, polynomial solns. 7-57758
 J_k integral, contradiction 7-20653
 J-crack resistance curves, determ. by use of AC pot. drop technique 7-57773
 J-crack-opening displacement relationship depend. on work hardening exponent 7-16120
 J-integral, estimation using FEM, simplified eqns. (*Japanese*) 7-50999
 J-integral estimates for cracks in infinite bodies 7-63056
 kinked crack solved by Mellin transform 7-43789
 kinked partially closed cracks in compression, stress intensity factors 7-43782
 kinking of crack emanating from free surface of beam under pure bending 7-43783
 ligament, plastic, ahead of edge-crack, combined loading 7-11349
 line spring model, equivalent relation 7-57746
 linear elasticity, post-processing procedures for FEMs 7-14777
 linear elastodynamics for plane crack bodies, theorems 7-37390
 loadings and screenings of cracks with aid of universal wt. functions 7-20650
 local approach of fracture, continuum damage mechanics 7-50988
 macrocrack growth kinetics in aging viscoelastic bodies under variable loads 7-63071
 macrocrack-microdefect interaction, stress field anal. 7-43797

crack-edge stress field analysis continued

material, homogeneous, isotropic, stiffness and strength reduction due to crack development 7-51927
 materials, anisotropic perfectly plastic; plane strain crack tip stress field 7-38106
 materials, transform. toughened, transformed zone size during steady state cracking 7-39641
 mechanics of damage and fatigue, conf., Haifa, Israel (Jul. 1985) 7-48139
 metals, BCC, ductile-brittle transition rel. to dislocation density 7-39668
 metals, creep crack growth prediction by a local approach 7-53841
 microcrack behaviour near low angle grain boundary 7-2096
 microcrack damage theory 7-16124
 microcrack interaction with main crack 7-20651
 microcrack propagation, development of physically based model 7-38109
 microcracked elastic solid, 1D constitutive model 7-1488
 micropolar media, path-independent integrals 7-26213
 mixed mode energy release rate 7-57757
 mode II fatigue crack test specimen, elastic analysis 7-1505
 mode III crack kinking with delay time, analytical approx. 7-26217
 moduli of cracked bodies, calc. using Mori-Tanaka's method 7-16122
 moiré interferometry, crack tip displacement anal. 7-11367
 multiple displacement discontinuities in 2D finite/infinite regions, indirect boundary element method 7-57748
 multiple interacting cracks in elastic material, boundary integral soln. 7-31696
 Nimonic 80A, crack growth under sulphidising conditions, metallography 7-59680
 noise emission analysis for determining crackinitiation during instrumental notched bar impact testing (*German*) 7-8216
 nonhomogeneous anisotropic elastic body, under axially symm. torsion, cylindrical interface crack 7-26841
 nonlinear 3D fracture dynamics, path-independent integrals 7-63069
 nonlinear effect in crack problem, scale 7-43798
 nonlinear fracture problems, path-independent integral, finite element approach 7-63068
 nonlinear materials, energy release rate for crack growth, multiaxial loadings formula (*Japanese*) 7-11346
 notch tips, plane, stress singularity 7-26220
 notch-emanated cracks, small, stress intensity factors 7-63063
 notched specimens, fatigue threshold 7-20652
 orthotropic materials, mode I crack kinking, strain energy release rate calc. 7-50996
 orthotropically damaged elastic solid, effective material consts., constitutive eqn. 7-1489
 panel with uniformly spaced holes, crack stress intensity factors 7-57755
 panels, tensile, elastic-plastic models of surface cracks 7-63077
 path-independent integrals, comparison including plasticity effects 7-31698
 path-independent integrals for the direct determination of stress intensity factors in certain classical crack problems 7-43791
 plane elasticity, singular behaviour at fixed rigid line tip 7-1491
 plane-crack problem, nonunique solution 7-50997
 plastic asymmetric crack growth near single shear band 7-20654
 plasticity-induced crack closure, under plane strain conditions, finite element anal. 7-37379
 plate, center cracked with singularity, finite element mesh 7-20645
 plate, crack growth rel. to geometry and material props. 7-16112
 plate, cracked, bending, stress intensity factor computation via path-independent integral 7-37380
 plate, edge-cracked, subjected to uniform surface heating, thermal shock 7-57752
 plate, elliptically notched semi-infinite, fatigue limits of crack initiation and propag. 7-1500
 plate, heating of cracked edge, variation of stress intensity factors with crack inclination 7-1512
 plate, infinite, of crack-weakened hereditary material, limiting equil. 7-31705
 plate, multilayer reinforced, with through crack, stress state and limiting equil. 7-11344
 plate, orthotropic containing pair of coplanar central cracks, thermal stress 7-1513
 plate, stiffened tension, with eccentric crack, elastic-plastic finite element analysis (*Chinese*) 7-16119
 plate, two-layered, transient response of interface crack 7-43802
 plates, centre-cracked biaxially loaded, plastic plane stress solns. 7-43800
 plates, composite, impact tensile loading; crack bifurcation modes 7-50993
 plates, weakened by cracks, tensile and compressive buckling 7-6124
 plates and cylinders, surface-cracked, J-integral and HRR dominance under large-scale yielding 7-63080
 PMMA, craze zone micromechanics at stationary crack tip 7-33775
 PMMA, environmental stress cracking in methanol, mol. props. effects 7-65153
 PMMA, rubber toughened, dynamic crack propag., high speed photographic, transmitted caustics 7-39638
 polycarbonate, J-integral as fracture criterion 7-39631
 polyethylene, failure prediction from initiation stage of slow crack growth 7-22801
 polyethylene, low density, environmental stress cracking in methanol, heat treatment effect 7-8146
 polymers, glassy, bimaterial interface, cracks, incipient plastic zone shape, elastic consts. effect 7-53874
 polypropylene, glass-flake reinforced, impact fracture 7-39659
 power plant components stress corrosion crack model in laboratory tests 7-17732
 prediction of crack growth increments, NT-criterion 7-63059
 pressure vessel, elastic-plastic J-anal. for inner surface flaw 7-63076
 PWR coolant pump flywheel radial crack testing, caustic curve method 7-15266
 residual stress analysis, US techniques 7-65273
 rubber toughened plastic, surface embrittlement, fracture mechanics 7-28161
 sapphire, stress corrosion, crack tip, dissociative chemisorpt. 7-33812
 scattering of shear and Rayleigh waves by cracks 7-26194
 SCC electrochemical potential profile models 7-46717
 semi-elliptical crack at notch root, stress intensity factor (*Japanese*) 7-31702
 semi-infinite array of cracks in uniform stress field 7-57742
 semi-infinite crack, SCC growth rate rel. to plasticity 7-31704
 semiplane weakened by holes and cracks, elasticity theory 7-11347

crack-edge stress field analysis continued

sharp edge notches, estimations of elastic stress distrib. and stress conc. factors 7-20648
 sheet, orthotropic, adhesively bonded to a stringer, crack tip stress intensity factors 7-1497
 single crystals, anisotropic, crystallographic cracking, effect of cross-slip 7-63735
 small cracks, ΔK_{th} , effect of hardness and crack geometry (*Japanese*) 7-58405
 solid deformable body mechanics, configurational forces 7-26167
 solids with microcracks, fatigue failure self-similarity, static thermodynamics 7-31706
 sphere, twisting, induced stress field 7-11314
 square specimen, compressed, with longit. or diagonal crack, stress intensity factors calc. 7-16118
 stage II fatigue crack growth behaviour of granular bainitic microstructures 7-28134
 statistical analysis of cleavage fracture ahead of sharp cracks and rounded notches 7-13540
 steel, 0.45% C, surface fatigue cracks, growth and threshold characts. 7-17607
 steel, alloy, rel. between crack tip opening displacement, J-integral and stress intensity factor 7-63073
 steel, austenitic stainless, crack tip cyclic plastic work, load ratio, frictional work 7-53897
 steel, austenitic stainless, creep rupture, fatigue cracking in flowing liq. Na 7-53843
 steel, austenitic stainless, low cycle fatigue damage, crack initiation (*Japanese*) 7-33780
 steel, austenitic stainless, SCC, delayed fractures under mode III loading, H induced cracking 7-53898
 steel, austenitic stainless, SCC susceptibility in polythionic acids 7-65183
 steel, austenitic stainless, small fatigue cracks, threshold behaviour at notch root 7-3395
 steel, austenitic stainless, strain distrib. within crack tip plastic zones 7-3396
 steel, C, fretting fatigue, crack propag. behaviour 7-39615
 steel, Cr, high C, notched rods, breaking by heating process, elastic-plastic stress analysis (*Japanese*) 7-33777
 steel, Cr-Mo, tube, fatigue crack growth at high temp. 7-59632
 steel, Cr-Mo, tube, high temp. press. fatigue testing 7-65246
 steel, Cr-Mo-V, creep crack growth at 838 K, displacement-controlled loading behaviour 7-17626
 steel, Cr-Mo-V, creep crack growth at 838K, const. load behaviour 7-17625
 steel, Cr-Ni-W, fatigue striation, macrocrack propag. (*Chinese*) 7-8074
 steel, crack stability in shock loading 7-53871
 steel, cyclic corrosion crack resistance, basic diagrams, electrochemical conditions at crack tip 7-51926
 steel, dual phase, effective grain size, cleavage crack propag. 7-28118
 steel, fatigue crack growth, influence of ambient environment 7-28107
 steel, ferritic, fracture behaviour after warm prestressing, effects of subcrit. crack growth 7-46601
 steel, growth under impact tension 7-28105
 steel, high strength, fatigue crack growth, slip localisation, intergranular fracture 7-28120
 steel, high strength, fracture toughness, US meas. 7-28238
 steel, high strength, H assisted cracking in aq. environment 7-3393
 steel, high tensile, HT55, ΔK_{th} testing method for plastic zone size at fatigue crack tip 7-17748
 steel, low C, cold forgeability, notches, geometry, friction conditions, microstruct. 7-33697
 steel, mild, cold-form-rolled, rotary bending fatigue behaviour (*Japanese*) 7-53866
 steel, mild, crit. stress intensity factor, influences of grain size and precracking load 7-59607
 steel, mild, fast fracture, crack arrest behaviour (*Japanese*) 7-59610
 steel, Ni-Co-Mo, maraging, lath martensite boundary cracking near threshold stress intensity factor (*Japanese*) 7-53846
 steel, Ni-Cr-Mo, ΔK_{th} testing method for plastic zone size at fatigue crack tip 7-17748
 steel, Ni-Cr-Mo, crack branching in H embrittlement (*Japanese*) 7-53847
 steel, Ni-Cr-Mo, pressure vessel, crack tip opening displacement, stretch zone width correl. 7-39670
 steel, Ni-Cr-Mo, pressure vessel, environmentally assisted fatigue crack growth 7-17638
 steel, Ni-Cr-Mo, weldments, dynamic fracture toughness, split Hopkinson bar technique 7-13685
 steel, Ni-Mo-Mn, stable crack growth monitoring AC/DC pot. drop technique 7-33887
 steel, notched specimens, cyclic deform., thermoelastic effect (*German*) 7-33746
 steel, nuclear pressure vessel, dynamic fracture toughness, crack tip strain behaviour, EM force appl. 7-28126
 steel, nuclear reactor pressure vessel, thermal transient, crack arrest in K-gradient 7-46617
 steel, Si-Mn-Mo, austenitising, bainite transform., lump-like composite struct., mech. props. (*Chinese*) 7-13477
 steel, small surface crack propag. 7-65142
 steel, structural, δ_1 and J_1 values, effect of a/W ratio 7-57753
 steel, tool, Cr-Mo-V, hot working, ductility, C content, toughness, eutectic carbide segregation 7-59592
 steel, weld metal, creep crack growth 7-17623
 steel cylinders, thick-walled, stress intensity factors for large arrays of radial cracks 7-26207
 stress distribution around surface crack using scattered-light photoelasticity 7-37403
 stress intensity factor and energy release rate for three-point bend specimen 7-26205
 stress intensity factor determ. by optical methods 7-43816
 stress intensity factor field extent during crack growth under dynamic loading conditions 7-11350
 stress intensity factor of macrocrack, influence of elliptical hole 7-1492
 stress intensity factors, extraction from near-tip photoelastic data 7-63064
 stress intensity factors at the tip of a kinked crack (*French*) 7-20646
 stress intensity factors calc. by quarter-point quadrilateral method 7-50995
 stress intensity factors determ. for wave loadings, integral eqn. method (*German*) 7-1514

crack-edge stress field analysis continued

stress intensity factors of internal radial cracks in rotating discs by method of caustics 7-57745
stress singularity and generalised fracture toughness at vertex of re-entrant corners 7-57749
strip, cracked, thermal shock, temp. depend. material props. 7-16114
strip, displacement loaded, semi-infinite crack, dislocation interaction, nonlinear stress-strain law 7-44676
strip, infinite, with cracks and holes, singular integral eqn. soln. 7-26219
strip with circular hole, stress concentration calc. by singular integral equations 7-16123
structural elements, crit. stresses, theoretical-expt. determ. 7-31707
surface crack, stress intensity factor variation and back surface displacement 7-57762
surface crack configurations, crack tip opening displacement, expt. invest. 7-63079
surface crack growth in lubricated rolling/sliding spherical contact 7-11354
surface crack initiation and growth, determ. using pot. drop method (*German*) 7-8241
surface flaw, stress intensity distrib. and fatigue crack growth predictions 7-63075
surface part-through crack, equivalent through-crack model 7-1487
tensile loaded crack, plastic zone size ahead of crack tip 7-16116
tensile plane-strain nonlinear crack problems, high-order asymptotic field 7-6157
thermally stressed specimen, crack closure integral and J-integral calcs., numerical investig. 7-26211
thermoelasticity, thermodynamic and energetic forces 7-26212
three-point bend ductile fracture specimen, dynamically loaded, anal. 7-26206
transient coupled thermoelastic crack problems 7-37391
unidirectional fibre composites, two in-plane fracture toughnesses relationship 7-53844
universal optimum quarter point element 7-16117
viscoplastic finite element analysis of rapid fracture 7-63061
work-hardening crack tip field, nonlinear dislocation model 7-43772
Zircaloy-2, low cycle corrosion fatigue in I_2 atmosphere 7-17705
Al alloy, small surface crack propag. 7-65142
Al alloy A5083-0, ΔK_{th} testing method for plastic zone size at fatigue crack tip 7-17748
Al alloys, fracture toughness, all modes 7-65121
Al alloys, fretting, fatigue crack growth, spherical particle form. 7-3445
Al, cracking behaviour during liquid Hg embrittlement 7-22816
Al, fracture, size effect tests 7-59595
Al-Cu-Mg, fatigue crack growth, closure anomalies 7-3403
Al-Cu-Mg r-curve behaviour of double edge notched tensile specimens in plane strain 7-13701
Al-Li-Cu-Zr, 2090, small fatigue crack growth 7-22817
Al-Li-Cu-Zr, fracture, ageing and comp. depend. 7-22784
Al-Zn-Mg, 7090, fracture, stress intensity rel. to notch root radius 7-17635
Al-Zn-Mg, small fatigue crack growth from a keyhole notch 7-65133
Al-Zn-Mg-Cu, 7475, environment sensitive fracture using shadow optical method of caustics 7-39647
Al-Zn-Mg-Cu, strain distrib. within crack tip plastic zones 7-3396
 Al_2O_3 , polycrystalline, fracture toughness, R-curve behaviour rel. to grain size 7-46615
 Al_2O_3 , vitreous bonded, crack nucleation and growth at elevated temps. 7-33770
C fibre reinforced epoxy laminates, matrix splitting, K_I - K_{II} interaction (*German*) 7-22829
C fibre reinforced plastics, cylindrical interface crack study 7-26201
C/glass fibre reinforced hybrid composites, aligned short fibres, SCC propag. 7-13615
Cu, creep crack growth, 450-650°C 7-33758
Cu, dislocation mechanism based model for stage II fatigue crack propagation rate 7-21338
Cu, fatigue crack propagation rate model based on a dislocation mechanism 7-8093
Cu, near-threshold fatigue crack propag. and high cycle fatigue 7-13545
Cu, polycrystalline, multiaxial low cycle fatigue, crack initiation, slip bands, damage mechanics 7-53840
Cu single crystals, fatigue crack size distrib. 7-38101
Cu single crystals, fatigue crack initiation mechanism, persistent slip band model 7-53869
Cu-Sb (1 wt.%), creep crack growth, 450-650°C 7-33758
Cu-Sn, low cycle fatigue damage, crack initiation (*Japanese*) 7-33780
Fe, cast, nodular graphite, fatigue crack propag. rel. to microstruct., SEM obs. (*Chinese*) 7-13542
Fe-Si (3 at.%), grain-oriented, fatigue crack growth, direct, real-time obs. (*Japanese*) 7-59615
 MgF_2 , stress corrosion, crack tip, dissociative chemisorpt. 7-33812
 Na_2O - CaO - SiO_2 glass, cracktip blunting kinetics, annealing, corrugated surface 7-46611
Nb, H embrittlement, crack propag., 120-300K, hydride form. 7-33757
Nb, pure, tensile deform., brittle fracture, H effect, SEM obs. (*Chinese*) 7-8078
Ni-W-Co-Cr superalloy single crystals, fatigue crack propag. under multiaxial cyclic loads 7-28122
 Ni_3Al , polycrystalline, grain boundary fracture model 7-53896
Si, dislocation emission from cracks, X-ray topography obs. 7-38004
 α - SiC , static fatigue limit at elevated temps., thermodynamics 7-17629
 Si_3N_4 ceramics, hot pressed, fatigue test with Knoop indentation, residual stress effects (*Japanese*) 7-17640
 Si_3N_4 -TiC composites, mech. props., wear resist., dispersoid-matrix interaction 7-65145
Ti-Al-V (6.4 wt.%), annealed fatigue crack growth in water, SEM fractography (*Chinese*) 7-8076
Ti-Al-V (6.4 wt.%), strain distrib. within crack tip plastic zones 7-3396
TiB₂-TiC composite, hot pressed, degradation in liq Al 7-28156
U-Nb-Zr (7.5, 2-5 wt.%), SCC in gaseous O_2 and H_2 (*French*) 7-17619
W fibre reinforced Fe-Cr-Al superalloy, surface cladding and matrix deform., thermomech. loading 7-46568
WC-Co cemented carbides, compression fatigue crack growth 7-28119
 ZrO_2 , Y_2O_3 partially stabilised, thermal shock behaviour (*Japanese*) 7-8115
 ZrO_2 , Y_2O_3 partially stabilised, crack config. (*Japanese*) 7-65138

crack inspection see crack detection

crack-tip stress field analysis see crack-edge stress field analysis

cracking see cracks; fracture

cracking, stress corrosion see stress corrosion cracking

cracking, thermal stress see thermal stress cracking

cracks

see also crack detection; crack-edge stress field analysis; crazing; fatigue cracks; penny-shaped cracks; stress corrosion cracking; thermal stress cracking
7-28112
arrest with externally bonded ligaments 7-26221
barium oxalate dihydrate single crystals, Vickers microhardness meas. 7-63736
BCC crystals, tensile crack stress intensity coeff. 7-13591
beams, cracked, stress intensity factors, elementary theory 7-62978
brine-saturated fractured rock, elec. cond. for various confirming press. 7-29002
brittle failure in compression, micromechanics, splitting, faulting and brittle-ductile transition 7-13590
brittle material, crack stability and toughness characts., book contrib. 7-26224
brittle materials, contact flaws; strength, lateral crack growth effects 7-8091
brittle materials, fracture toughness, crack front irregularity effect 7-57740
brittle-matrix, fibre-reinforced composites, matrix cracking mechanics 7-65129
BWR piping research in Italy, IGSCC tests, fracture and cracks 7-53890
cast Fe, flake and nodular graphite, breaking behaviour of perforated notched specimens 7-17606
ceramics, structural, flaw size distrib. 7-22818
coherent multilayer structures, damage by dislocation or crack injection 7-21674
components under complex loading, stress anal. incorporating fracture mech. and materials aspects 7-13584
composite laminates, first ply failure anal. 7-44670
composite laminates, with matrix cracking and interior delamination, stiffness props. 7-44669
composite materials, damage constitutive relations 7-43765
composites, response in adverse environment, reliable modelling, implication of 7-65169
concrete, hydrostatic pressure effects on integrity, monolithic slag/cement under radwaste sea disposal conditions 7-36297
concrete, microplane model for progressive fracture, microcracking 7-15248
concrete, structures, micro- and macroscale damage 7-43766
conference on the safety and reliability of reactor pressure components, Stuttgart, Germany, (Oct. 1985) 7-9583
conference on water reactor safety, Gaithersburg, MD, USA, (Oct. 1985) 7-48152
cordierite glass and glass-ceramic, comparative single-point diamond scratching behaviour 7-46654
CR-39 crack detector, treeing during electrochemical etching, fracture mech. study 7-30877
crack arrest specimen, dynamic anal. under reactor pressurised thermal shock conditions 7-13693
defects, stress- and fatigue-induced, small angle neutron scatt. studies 7-58273
dynamic crack extension, dislocation distribution growth by climb and glide over nonplanar surfaces 7-16556
dynamically loaded pipes with circumferential flaws, behaviour under internal pressure and external loads 7-13577
elastic unbounded body, cracks, 3D loading, stress intensity factor history 7-50998
exterior Griffith cracks opened by a wedge in a rectangle 7-6149
fatigue precracked Charpy-type specimens, crack initiation testing, reactor piping appl. 7-13579
fibre reinforced composite laminates, yield and ultimate strengths 7-22785
garnet LPE films, lattice relax. around cracks 7-7054
glass, crack propagation, effect of inhomogeneities (*Japanese*) 7-22823
glass, laser irradiated with picosecond high-power pulses, long-range structural changes 7-12123
glass, microdefect accumulation kinetics during optical irradiation 7-38050
graphite, fracture criterion, acoustic emission studies (*Japanese*) 7-8088
graphite fibre reinforced epoxy, subjected to cyclic thermal loading, damage-induced prop. changes 7-46600
graphite fibre reinforced epoxy laminates, fatigue damage mechanisms and residual props. 7-44671
graphite isotropic, fine grained, oxidation effect on crack extension rate (*Japanese*) 7-56754
Griffith's crack, interaction with rigid inclusions in elastic space 7-57741
Hastelloy alloys, C-4, C-22 and C-276, welding metallurgy 7-46448
heterogeneous materials, cracking mechanisms under compression 7-33777
ice, freshwater, crack resist. determ. 7-12195
infinite plate, plane rectilinear crack, pot. method soln. 7-63070
isotropic elastic solid, elliptical cracks under shear loading, polynomial solns. 7-57758
jointed rock mass, crack tensor rel. to wave vel. anisotropy 7-55016
laminates, cross-ply, cracked, stiffness reduction anal. 7-44644
Love wave scattering by surface-breaking crack 7-43753
LWR heavy section steel technology, crack arrest studies overview, reactor pressure vessels 7-53885
macrocrack growth kinetics in aging viscoelastic bodies under variable loads 7-63071
marble, development of conjugate-shear fracture (*Chinese*) 7-34474
metal, cold-deformed, microcrack development (*Russian*) 7-39652
metal tubes, ductile, no. of cracks in axial splitting 7-59597
metal-H system, internal grain-boundary crack opening by H (*Russian*) 7-33764
metallic and compound films, mech. props., relation between different quantities 7-8041
MPA thermoshock expt. anal. using TRAC PF 1 code, PTS in reactor ECC conditions 7-13588
mullite, Al_2O_3 and ZrO_2 particle reinforced, prep. by reaction sintering, fractographic study 7-22800
notched and precracked ISO-V specimens, loading rate effects on fracture resistance 7-13580
NRC Degraded Piping Programme, LWR piping fracture research, Phase II progress 7-53889

cracks continued

- online acoustic emission monitoring of cracks in nuclear systems, review 7-54066
- optical coatings, thermal conductivity 7-45094
- planar boundary contact problem with cracks (*German*) 7-6166
- plane-crack problem, nonunique solution 7-50997
- plastic subsurface failure in compression along macrocracks, spatial problem 7-26159
- plate, cracked, description using Lagrange method (*Polish*) 7-43793
- plate, elastic, containing two collinear transverse edge cracks, stress distrib. 7-43761
- plate with line crack subject to varying shear load, nonlinear elasticity anal. 7-48367
- PMMA, failure at high loading rates, correlation of relaxation and energy characteristics 7-46598
- PMMA, microdefect accumulation kinetics during optical irradiation 7-38050
- PMMA, surface crack profile measurement method and results 7-22939
- poly(1,4-dimethylene-trans-cyclohexyl suberate) mol. wt. blends, fracture energy and morphology 7-37899
- polycarbonate, failure at high loading rates, correlation of relaxation and energy characteristics 7-46598
- polymer films, stress development during thermal cycling, bending beam technique 7-28063
- polymers, deform. under impact, transient high temp. meas. 7-22802
- polypropylene, mica-reinforced, fracture behaviour, effect of coupling agent, flake orientation and degradation 7-13593
- polystyrene, slow crack propag., crazing and fracture, acoustic emission study 7-32555
- poroelastic medium deform. containing thin internal crack, approx. solns. 7-62990
- porous medium with crack, elastic-hydrodynamic problem of fluid inflow 7-11534
- pressure vessels, high temperature life prediction, computer modelling anal. 7-3391
- propagation in 3D, formulation 7-57739
- propagation resistance, in connection with limiting crack resist. 7-59629
- quartz glass, microdefect accumulation kinetics during optical irradiation 7-38050
- random crack distribution effect on elastic wave propag. consts. 7-16091
- reactor piping systems, cycle-dependent material props. 7-10222
- reactor pressure vessel, crack propag. under cyclic thermal loading, NDT results 7-10219
- regularized integral equations for a two-dimensional body containing a crack of an arbitrary form (*French*) 7-62988
- reinforced concrete members, reliability of crack control, fuzz set anal. (*Chinese*) 7-20655
- ribbon-type crack, scattered ultrasonic fields 7-59731
- rock-like materials, viscoplastic, damage and failure 7-1507
- rocks, crack-seal mechanism as deform. factor in strike-slip faulting 7-29010
- rocks, fracture anal. 7-66106
- rocks subjected to uniaxial compression, crack shape distrib. 7-66112
- rubber, particle reinforced, with distributed damage, micromech. model for nonlinear viscoelastic behaviour 7-43698
- sapphire, crack propagation threshold, surface energy determ. 7-58401
- scattering by a horizontal subsurface penny-shaped crack 7-51000
- slate schist, crack propagation under mode I and II loading 7-8921
- stainless steel electrode surface damage anal. in high energy spark gaps 7-33991
- steel, alloy, crack arrest toughness, moment modified compact tension specimen, PTS conditions 7-13695
- steel, austenitic stainless, biaxial loading, high temp. intergranular crack growth 7-53902
- steel, austenitic stainless, LWR piping, ASME code for flaw eval. 7-13601
- steel, C, LWR piping, flaw evaluation 7-46652
- steel, C-Mn, cold-formed, creep crack growth 7-53872
- steel, C-Mn, creep crack growth at 360°C, effect of microstruct. 7-28113
- steel, C-Mn, Nb-modified, creep crack characts. at 360°C 7-46631
- steel, Cr-Mo, crack initiation under sustained load, effect of impurity segregation 7-65111
- steel, Cr-Mo, creep fracture 7-33784
- steel, Cr-Mo, elevated temp. strength, H attack resistivity and stress relief cracking suscept. improvements 7-13583
- steel, Cr-Mo-Fe-C, crack resist., temp. and comp. depend. study (*Russian*) 7-13553
- steel, Cr-Mo-Ni-Mn, stress relief cracking, impurity effects 7-46635
- steel, ferritic, yielding and fracture in transition region of quasistatic to dynamic loading 7-13581
- steel, heavy section, Ni-Mo, elastodynamic fracture analysis of large crack-arrest experiments 7-53887
- steel, high strength, defect enhanced diffusion process and hydrogen delayed fracture 7-39673
- steel, HSLA, H-induced crack propag., method to evaluate crit. H conc. 7-65116
- steel, low alloy, retarded brittle fracture, crack nucleation stress and internal microstresses (*Russian*) 7-8084
- steel, low C, spheroidised, H degradation 7-8104
- steel, low-tensile, crack resist. in elastoplastic region under static loading 7-33793
- steel, martensitic, intergranular crack nucleation, fractographic and acoustic emission meas. (*Russian*) 7-33766
- steel, mild, brittle fracture, microcracks effect (*Russian*) 7-59618
- steel, Ni-Mo, LWR pressure vessel cladding, irradiation effects and flaw structs. 7-53888
- steel, Ni-Mo, wide plate crack arrest testing using acoustic emission, reactor pressure vessel appl. 7-53886
- steel, nuclear pressure vessel, dynamic fracture toughness, crack tip strain behaviour, EM force appl. 7-28126
- steel, stainless, crack growth in BWR piping, meas. techniques 7-39839
- steel, stainless, heavy section, fracture studies, welds, neutron irradiation, crack arrest 7-13587
- steel, stainless, pipe, subjected to bending deform., fracture instability, effect of multiple circumferential through-wall cracks 7-65122
- steel, stainless, pressure vessel, stress relief cracking, reactor safety 7-8117
- steel, stainless, screw cracks in reformer tube of HK40 alloy (*Chinese*) 7-3412
- steel, stainless, type 316, neutron damage USA-Japan studies 7-56834
- steel, structural, cleavage fracture toughness predictions 7-13544

cracks continued

- steel, V, W2, laser surface melting, effects of prior heat treatment 7-65195
- steels, alloy, crack arrest toughness, proposed ASTM test method, European experience 7-13694
- strip, infinite orthotropic, finite crack, impact response 7-63082
- structural member, endurance in creep conditions, accuracy of prediction 7-32561
- structurally stress concentrated regions, brittle fracture strength eval. method 7-3424
- surface crack, stress intensity factor variation and back surface displacement 7-57762
- surface crack growth with regular and random loading processes 7-43785
- surface crack profile measurement method and results 7-22939
- surface features, thermal wave imaging studies in a SEM 7-44874
- surface fracture during He⁺ ion bombardment 7-21294
- surface layer modification at solid walls in high temp. plasma exp. 7-63343
- surface of transparent materials, submicrocrack role in optical props. form. 7-53255
- surface-breaking discontinuities, Rayleigh wave diffr. 7-27084
- symmetric and asymmetric fully plastic crack growth, macromech. anal. 7-51931
- tensile plane-strain nonlinear crack problems, high-order asymptotic field 7-6157
- thermal shock loadings in PTS accidents, J-integral concept appl. 7-13696
- transient dynamic Green's functions for a cracked plane 7-37388
- transversely isotropic solid, distribution of stress in the neighbourhood of crack 7-11348
- tribochemistry, chemical reaction increase by friction 7-46868
- unstable growth, conditions of normal separation under static loading beyond ultimate strength 7-32559
- vertical interfaces, solid, photothermal beam-deflection imaging 7-48721
- viscoelastic medium, effect of microfractures on behaviour under extension and shear 7-29003
- Zener-Stroh cracks and Zener-Hollomon parameter 7-8086
- Al alloy plates, crack opening after discontinuous growth, laser interferometry studies (*Russian*) 7-46604
- Al alloy sheets, LY12CZ, fracture resist. characts., crack initiation, stable and unstable propag. (*Chinese*) 7-46592
- Al-Li-Cu-Mg quaternary alloy, initiation of voiding at second-phase particles 7-39645
- Al-Zn-Mg, 7020, thin welded joints, ductile crack growth of surface cracks 7-59594
- Al₂O₃, sintered, erosion and strength degradation 7-17663
- B⁺-Al₂O₃-Na₂O solid electrolytes, degradation in Na-S batteries 7-3466
- C fibre reinforced plastic, damage states, US and acoustic emission study (*German*) 7-22828
- C fibres, pretorsional deform., annealing, acid treatment, struct., mech. props 7-22768
- C, fractographic studies 7-17645
- CaF₂-Si interface, with epitaxially grown insulator, post-growth annealing treatments 7-7074
- CaSO₄, gypsum, thermal breakdown and crack form. 7-2178
- CdGa₂S₄ single crystals, chemical vapour transport growth, microhardness, crack patterns 7-7833
- Cr films, acoustic emission during electrodeposition 7-52329
- FE-Cr coatings for gun bores, morphology and erosive wear 7-46697
- Fe, (001) oriented single crystals, hydrogen induced cracking and hydrogen embrittlement (*Japanese*) 7-33782
- Fe, BCC, effective fracture energy assoc. with cleavage crack growth 7-44678
- Fe, cathodic charging, H trapping 7-21256
- Fe-Ni-Co alloy, H damage, lattice distortion, defect and crack generation, positron lifetime study 7-39675
- α-Fe-Si, Zn vapour induced cracking phenomena (*French*) 7-3394
- Fe₉₀B₁₀Si₁₅C₂ metallic glass, laser beam irr., high energy, shear band form. and cracking 7-59606
- Fe₄₀Ni₄₀B₂₀ metallic glass ribbon, failure mechanics and atom probe study correlations 7-28139
- GaAs solar cells, fracture strength as function of manufacturing process steps 7-3696
- GeTe, α-γ phase transformation kinetics, effect of heat treatment 7-63795
- In As_{1-x}Sb_x epitaxial layers, MOCVD, strained-layer superlattices 7-39407
- LiF, fracture, mag. field effects 7-16675
- LiF plastic crystals, formation of cracks at cleavage fracture front 7-44674
- MgAl₂O₄ spinel, electron irradiation, Mg depletion, cubic γ-alumina form. and microcracking 7-26802
- MgAl₂O₄ stoichiometric spinel, electron beam-induced diffusion, cracking and phase separation 7-16641
- Mo-Ti-C system, embrittlement of ingots, role of phase stresses 7-3398
- Ni-base superalloy, single cyst., SRR99, creep behaviour 7-17587
- Ni-based consolidated rapidly solidified alloys, strengthening mechanisms 7-22712
- Ni-Sn-Pb-Bi system, crack form. in diffusion zone 7-3397
- Ni₇₅Si₁₀B₁₂, metallic glass, shear crack propag. 7-65113
- PLZT, elastic-plastic contact damage 7-39627
- Rb_{0.023}WO₃, crystal growth and struct., SEM and TEM anal. 7-46288
- Si, low-angle silicon sheet (LASS) material, microstructure exam. 7-21231
- SiC, CVD, microstruct. around indentation, TEM obs. (*Japanese*) 7-22822
- SiC ceramics, hot pressed, grinding, surface damage, bending strength (*Japanese*) 7-17602
- SiC, deformed, microstructural changes, creep mechanisms 7-46591
- SiC whisker reinforced Si₃N₄ ceramics, fracture toughness (*Japanese*) 7-28138
- SiC-C alloy coated graphite as armour tiles, post-exposure anal. after high heat loadings 7-49632
- Si₃N₄, hot-pressed, tensile strength at room and elevated temp. (*Japanese*) 7-65139
- Si₃N₄-Mg₂O₃, deformed, microstructural changes, creep mechanisms 7-46591
- Si₃N₄-Y₂O₃, deformed, microstructural changes, creep mechanisms 7-46591
- SiO₂-P₂O₅ glass films, deposited by different CVD methods, phys. props. 7-27220

cracks continued

- Ta₂O₅ crystalline films, sputter deposited, phys. and elec. props. 7-2412
 (Ti,Cr)B₂ sintered electrode exposed to liq. Al, degradation, effect of segregated Cr 7-28045
 Ti-Al-Nb (6.2 wt.%), fusion weld, defect regions, cracking, porosity, interstitials analysis 7-28109
 Ti-Mn, alpha and beta phases, yield and tensile strength, ductility, Bauschinger behaviour, fatigue life, crack propag. 7-8052
 Zr alloys, hydride cracking, acoustic emission studies 7-59637
 z-ZrH_x, shape memory effect (*Russian*) 7-59577

cranes

- radioactive waste vitrification facilities, closed circuit TV and remote crane control 7-42204

cranking model *see* nuclear cranking model

crazing

- see also stress corrosion cracking*
 amorphous polymers, craze accumulation during deformation in creep conditions (*Russian*) 7-63740
 glassy polymers, fracture mechanisms, scaling analysis 7-46618
 PMMA, craze zone micromechanics at stationary crack tip 7-33775
 PMMA based materials, craze resist., struct., water absorpt. 7-59602
 polycarbonate-polystyrene-acrylonitrile, coextruded multilayer composites, tensile props. 7-59572
 polycarbonate-polycarbonate blend, crystallising crazes, probable source of solvent stress cracking resist. 7-13621
 polyethylene, failure prediction from initiation stage of slow crack growth 7-22801
 polypropylene, isotactic, crazing, energetic characts. (*Russian*) 7-12201
 polystyrene, monodisperse, fracture, chain scission, mol. wt., temp. depend. 7-33776
 polystyrene, slow crack propag., crazing and fracture, acoustic emission study 7-32555
 polystyrene, tensile impact, craze vol. and microstruct., synchrotron SAXS 7-53893
 polystyrene films, craze microstruct., low angle electron diffr., Fourier transforms of TEM images 7-13560
 rubber toughened plastic, surface embrittlement, fracture mechanics 7-28161
 styrene-butadiene-styrene block copolymer films, crazing, voiding, fibrillation, TEM obs. 7-17672

creation of electron pairs *see* electron pair production

creep

- see also creep fracture; creep testing; diffusion creep; elastic aftereffect; irradiation induced creep; recovery-creep; stress relaxation*
 alloy, structural, creep and stress relax. mechanism 7-46571
 alloys, creep activation energy 7-63732
 alloys, heat resistant gas turbine, creep behaviour (*German*) 7-3389
 amorphous polymers, craze accumulation during deformation in creep conditions (*Russian*) 7-63740
 Aramid fibre reinforced composite beams, viscoelastic-plastic anal. in flexure 7-33717
 austenitic stainless steels, fatigue props., time-depend modes, dislocation concepts appl. 7-28128
 bar material, dilutely voided, instability in uniaxial tension 7-53787
 bisphenol-A-based epoxy resins, physical props. rel. to curing 7-46539
 Bridgman notched bar, creep stresses 7-37350
 cavitation and residual creep life 7-50962
 charge-induced effect on creep and hardness 7-21598
 columns, nonlinear viscoelastic, creep buckling 7-6102
 composite, macroscopic relaxation kernels determ. 7-16073
 composite with periodic structure, coupled problems of thermoviscoelasticity 7-16074
 corundum-graphite refractories, thermomech. props. 7-22806
 crack growth, theoretical-numerical investig. of expts. (*German*) 7-43803
 crack initiation at grain-boundary triple points in high-temp. deform., continuum mech. model 7-28104
 cyclic loading, creep plasticity problem 7-63003
 cyclic plasticity and creep, constitutive modelling using internal time concept 7-1437
 damage localisation theory 7-50990
 discontinuous crack model, constitutive eqn. 7-26223
 elastic-viscoplastic constitutive eqns., modelling of continuum damage 7-43764
 ethyl cellulose films, creep, liq. cryst. soln. casting 7-8069
 ethylene-hexene copolymer, creep and recovery in small uniaxial deform. region 7-13527
 fibre in viscoelastic matrix, stress state of isolated fibre 7-16079
 fibre reinforced Ti-base alloy, development of creep-resisting composites 7-3228
 glassy polymers, time depend. nonlinear deform. 7-63733
 grain boundary cavitation, anal. of creep crack growth 7-21340
 grain boundary cavity-growth kinetics determ. from cavity-size distrib. during creep and continuous nucleation 7-26767
 grain boundary-slip interaction, role in cavity nucleation 7-21219
 graphite, nucl. grade, polycryst., deform. under press., elastic moduli rel. to struct., neutron irradi. effect 7-28069
 Hastelloy X, thermomech. response, viscoplastic constitutive model 7-8059
 heat exchanger tubes, cyclic temperature transient influence on creep behaviour 7-10186
 high temperature structures in reactors, creep curve variation effects on creep behaviour 7-39602
 ice, dynamic recrystallization and fabric development during shear deformation 7-55096
 IN 100, cast superalloy, creep strain and life prediction 7-33741
 Inconel 718, Ni-base superalloy, creep deform., back stress determ. 7-46564
 Inconel MA 6000, oxide dispersion strengthened superalloy, cyclic creep, HF effect, anelastic model 7-53827
 Inconel MA 6000, oxide-dispersion hardened superalloy, cyclic creep and anelastic relax anal. 7-17596
 Inconel X-750, air environment/creep interactions, prior exposure times effect 7-13499
 intermetallic phases, appl. as high temp. materials, review 7-22775
 laser Doppler anemometer for measuring supersonic velocities 7-43812
 LMFBR, French reactor-fatigue design rules 7-49522
 LMFBR class 1 components, design rules and elastic creep-fatigue damage evaluation 7-49540
 membrane deformation under creep conditions 7-1449
 metal, structural, creep and stress relax. mechanism 7-46571

creep continued

- metal powders, hot isostatic pressing, empirical model 7-46365
 metallic materials, high strength, life time prediction in creep-fatigue interaction regime (*German*) 7-53905
 metals, FCC, creep power law breakdown, stacking fault energy effect 7-39609
 metals, irradiated, creep mechanisms, dislocation climb and slip 7-12194
 metals, irradiated, deformation, impurity atmosphere effects (*Russian*) 7-59569
 metals, irradiated, deformation rate, impurity atmosphere effects (*Russian*) 7-33727
 metals, irradiated, deformation rate, radiation swelling and creep (*Russian*) 7-44597
 metals, local and macroscopic viscosities in solid state 7-46555
 metals, steady state creep, strain response to complete unloading 7-59568
 metals pure, new approach to creep 7-53805
 modelling for engineering design 7-22776
 mullite-corundum refractories, creep behaviour rel. to struct. features 7-22770
 Nimonic 80, coupled plastic and creep damage at finite deform. (*Japanese*) 7-33736
 Nimonic 80A, coupled effect of plastic damage and creep damage at finite deform. 7-46599
 Nimonic 86, carburised, heat treatment, creep behaviour rel. to carbide precip. (*Korean*) 7-46560
 olivine-basalt partial melts, rheology and struct. 7-8931
 optical component reliability, effects of solder creep 7-15997
 perforated plates, simplified creep anal. for steady creep conditions 7-28094
 PET, biaxially oriented, effects of thermal treatment 7-12193
 PET films, viscoelastic props. 7-28066
 plasticity constitutive models suitable for thermal loading 7-51925
 plate flexure with creep, inverse problems 7-11303
 plates, inelastic, bending problems, influence functions use (*German*) 7-20606
 polyaminobismaleimide resin, dynamic recovery and embrittlement 7-38108
 polyarylates, amorphous, glassy, plastic deform. in stress relax. and creep regimes (*Russian*) 7-63730
 polyetheretherketone, phys. ageing characts. 7-65110
 polyethylene, creep behaviour, stress relax. expts. 7-46546
 polyethylene, linear high density, creep and recovery in small uniaxial deform. region 7-13527
 polymer, thermoviscoelastic properties prediction in complex stressed state 7-17573
 polymers, amorphous, structured, strain-dependent birefringence under creep conditions (*Russian*) 7-27690
 polymers, creep behaviour, nonlinear isochronous stress-strain rels. (*German*) 7-13529
 precipitation hardening, creep and reverse mechanical aftereffect processes (*Russian*) 7-3317
 pressure vessels, high temperature life prediction, computer modelling anal. 7-3391
 reactor components, asymptotic and reference stresses for design by anal. 7-49518
 reactor construction codes and engineering mechanics conf., Paris, France, Aug. 1985 7-48153
 sea ice, creep behaviour under uniaxial compression (*Chinese*) 7-23673
 shells, cylindrical viscoelastic creep-stability anal. 7-26166
 sialon, commercial, static fatigue and creep resist. 7-59601
 sphalerite single crystals, plastic behaviour between 473 and 873K, differential creep stress, relaxation tests 7-2093
 steel, austenitic Cr-Ni, cylindrical bars, with deviations from ideal form, creep behaviour (*German*) 7-3390
 steel, austenitic stainless, creep, effect of hydrogen charging (*Chinese*) 7-8042
 steel, austenitic stainless, creep and anelasticity at const. homogeneous dislocation struct. 7-17586
 steel, austenitic stainless, creep cavitation rel. to S and P impurity segregation 7-39587
 steel, austenitic stainless, creep strain, resulting changes in subboundary mesh size 7-46575
 steel, austenitic stainless, EP 838, creep study, 773 to 1073 K 7-59567
 steel, austenitic stainless, long term creep, transient strain induced strengthening 7-28090
 steel, austenitic stainless, near-threshold fatigue crack growth and crack closure under creep conditions (*Japanese*) 7-59616
 steel, austenitic stainless, plastic creep, laws of high temp. behaviour (*French*) 7-13523
 steel, austenitic stainless, SCC at const. load in molten NaCl-CaCl₂ at 570°C 7-53944
 steel, austenitic stainless, TiN dispersion hardened, creep below transition stress 7-65079
 steel, austenitic stainless heterogeneities, small angle neutron scatt. studies 7-51580
 steel, C, creep, glide plane stresses, yield point, dislocation theory (*Russian*) 7-59580
 steel, C-Mn, creep crack growth at 360°C, effect of microstruct. 7-28113
 steel, Cr-Mo, cyclic softening, creep and fatigue, fusion reactor appls. 7-53757
 steel, Cr-Mo-V, creep crack growth at 838 K, displacement-controlled loading behaviour 7-17626
 steel, Cr-Mo-V, creep crack growth at 838K, const. load behaviour 7-17625
 steel, Cr-Mo-V, creep curves, exponential descriptions 7-65106
 steel, Cr-Mo-V, creep ductility, impurity and microstruct. effects 7-46587
 steel, Cr-Mo-V, cyclic creep accel. and retardation at room and elevated temp. 7-39581
 steel, Cr-Mo-V, rotor, high temp. creep, prior austenite grain size effect 7-53828
 steel, Cr-Mo-V creep eqns., parameter estimation methods 7-65107
 steel, high Ni, reactor irradi., dislocation struct. and steady-state creep (*Russian*) 7-2068
 steel, Ni-Co-W, maraging, martensite-austenite reversible transforms. during tensile deform. and thermal cycling 7-17528
 steel, stainless, pressure vessel, stress relief cracking, reactor safety 7-8117
 steel, took, Cr-Mo-V, hot working, ductility, C content, toughness, eutectic carbide segregation 7-59592

creep continued

- structural member, endurance in creep conditions, accuracy of prediction 7-32561
- superalloy single crystals, directional solidification, mech. anisotropy, fatigue, creep 7-3293
- superalloys and ceramics, electron microscopy studies, symposium, Nantes France (July 1986) 7-18479
- superplastic to non-superplastic deform., transition at high strain rates 7-46586
- thermal creep and thermophoretic forces acting on a spheroid 7-1666
- time depend. plasticity theory, stress relax., creep, plastic flow 7-43703
- tubes, homogeneous and inhomogeneous conical, torsion under steady-state creep conditions 7-11302
- two dimensional line element for glacier flow problems 7-4063
- uniaxial material laws, generalisation of tensorial constitutive eqns. (*German*) 7-57715
- viscoelastic pulse propag. and stable probability distrib. 7-37353
- yield stress, time depend. prop., meas. tech. 7-43834
- Zircaloy, claddings, creep deform., bulge growth, time to failure 7-59589
- Zircaloy-4, oxide layer thickness anal. post-oxidation creep strain, effect of stress (*Korean*) 7-8160
- Zircaloy-4 fuel sheaths, failure model, circumferential temp. effect 7-728
- Ag-Cu (12 at.%), supersaturated solid soln., decomp. kinetics, effect of creep (*Russian*) 7-33748
- Al alloy, uniaxial transient creep behaviour under varying stress states (*Chinese*) 7-13513
- Al, charge-induced effect on creep and hardness 7-21598
- Al, creep rate, role of grain boundary movements 7-44666
- Al, monocrystalline, Harper-Dorn creep, dislocation network theory 7-22749
- Al, polycrystalline, high temp. creep, strain hardening rates during primary stage 7-65104
- Al sheet, dislocation relax. contrib. to deform., internal friction and dynamic modulus meas. during creep 7-63626
- Al tricroystals, grain boundary sliding, triple point fold form. mechanism 7-65101
- Al-Ag, steady-state creep, effect of isochronal ageing 7-17598
- Al-Cu (2.5 wt.%), creep deform., effect of θ' precipitates 7-65088
- Al-Cu-In alloy, deformed, θ' -phase precipitation 7-22691
- Al-Cu-MG, annealed, creep, 623-723 K 7-53802
- Al-Mg, creep, stress exponent, dynamic strain ageing, dislocation struct. 7-17591
- Al-Mg (5 at.%), creep, interpretation of internal stress determ. from dip tests 7-65091
- Al-Mg alloys, steady-state creep, microstruct. development 7-53817
- Al-Si-Fe, RR 58, electroslag refined, creep 7-39582
- Al-Zn (11 wt.%), dislocation density in high temp. creep 7-39611
- BaTiO₃, fine-grained superplastic creep in reducing environment 7-28075
- BaTiO₃, perovskite, TEM study of dislocations 7-38003
- Be, superplastic flow, electron microscopy studies (*Russian*) 7-3360
- Cd, polycrystalline, steady-state creep, internal and effective stresses 7-38100
- Cu, creep, new approach 7-53805
- Cu-Fe-Mg-Ni-Al alloy, stress relaxation in tension and creep in torsion 7-44667
- Cu-Zn (30 wt.%), anomalous instantaneous creep strain, obs. after stress change 7-46585
- Fe alloys, high-temp. creep, rel. between dislocation density and internal stress 7-13524
- Fe, creep, glide plane stresses, yield point, dislocation theory (*Russian*) 7-59580
- Fe/Cu microlaminate condensates, creep and struct. investig. (*Russian*) 7-33749
- Fe-Ni, creep in vacuum and air, relationships governing deform. and failure 7-28097
- Ge single crystals, plasticity meas. near yield peak (*Russian*) 7-44664
- Ge₂Si_{1-x}-Si multilayers, MBE grown, thermally annealed, Ge diffusion, strain relax., ion channelling, backscattering anal. 7-6896
- LaCrO₃-Cr cermets, mech. props., interparticle welding 7-39630
- LiO₂, elastic and creep props., porosity and temp. depend. 7-53780
- Li₂O single crystals, compressive creep and plastic deform. at high temp. 7-51920
- Mg, high purity polycrystals, creep behaviour, recovery, and stress exponent determ. 7-26840
- MgO single crystals, high temp. creep and dislocation struct. at low stresses 7-21336
- Mg₂SiO₄:V, forsterite, high temp. deform., creep study 7-21332
- Mg₂SiO₄:V forsterite single crystals, creep, 1571-1923K 7-33731
- Mo, creep, stress factors (*Russian*) 7-33750
- Mo, creep behaviour, stress relax. expts. 7-46546
- Mo, recrystallised, microstruct. and creep charact. (*Russian*) 7-39600
- Mo single crystals, high temp. deep following ion thermal treatment (*Russian*) 7-53813
- Mo-Ti-Zr alloy, creep resistance, particle strengthening contribution 7-28073
- Mo-W alloys, creep failure, thermomechanical treatment effects 7-28072
- Ni base superalloys, hot deformed, matrix dislocations, weak beam electron microscopy obs. (*French*) 7-21210
- Ni base superalloys, pressure vessel performance, strength, ductility, comp. struct. 7-3365
- Ni base superalloys, techniques for required props. prod. (*Turkish*) 7-59657
- Ni, creep, T charging, He bubble migration and coalescence 7-65102
- Ni dislocation structure evolution during creep, alternating mag. field effects study (*Russian*) 7-58286
- Ni, intergranular cavitation in high temp. creep, fractographic techniques appl. 7-53804
- Ni, substructure at accelerated high temp. creep (*Russian*) 7-65096
- Ni superalloy IN738LC, creep modelling for engng. design 7-22776
- Ni, T-induced He bubbles on grain boundaries migration and coalescence 7-58289
- Ni-base superalloy, CMSX-2 creep anisotropy, TEM anal. (*French*) 7-22764
- Ni-base superalloy, IN 939, high Cr, effects of heat treatment on mech. props. 7-13526
- Ni-base superalloy, single cystal, SRR99, creep behaviour 7-17587
- Ni-base superalloys, creep resist. improvement, role of Re additions, APFIM study 7-22772
- Ni-base superalloys, γ' strengthened, creep and microstruct. rel. to refractory elements 7-3364
- Ni-base superalloys, stability of lamellar $\gamma-\gamma'$ struct. 7-46566

creep continued

- Ni-Co-Cr-Al-Y, plasma sprayed, high temp. tensile and creep behaviour 7-28083
- NiAl, slow plastic creep props. between 1200 and 1400 K, effect of comp. and grain size 7-65084
- Ni₇₅B₁₇Si₈, ultrafine grained, creep deformation mechanisms 7-22781
- SiC, deformed, microstructural changes, creep mechanisms 7-46591
- SiC:AlN ceramics, elevated temp. creep, role of grain size 7-39584
- Si₃N₄:Mg₂O₃, deformed, microstructural changes, creep mechanisms 7-46591
- Si₃N₄:Y₂O₃, deformed, microstructural changes, creep mechanisms 7-46591
- Si₃N₄:Y₂O₃, hot pressed, fracture, flexural strength, temp. degradation 7-13546
- Ti-Al-Zr-Mo-Si, creep resistance, silicides obs., effect on mechanical props. and fracture 7-8051
- Ti-R (R=rare earth) alloys, rapidly solidified, tensile and creep props. 7-22778
- W, n (*Russian*) 7-51699
- WC-Co cemented carbides, tensile creep, 800-900°C, grain boundary sliding 7-17585
- Zn single crystals, creep, dislocation struct., high press. effect (*Russian*) 7-59578
- Zn-Ag dilute alloy single crystals, thermally activated and quantum creep, impurity effects (*Russian*) 7-26755
- Zn-Al, bicrystals and polycrystals, creep grain boundary strengthening 7-22747
- Zn-Al alloys, transient creep, structural transformation effect 7-22758
- Zn-Au dilute alloy single crystals, thermally activated and quantum creep, impurity effects (*Russian*) 7-26755
- α -Zr, low stress creep at intermediate temps. 7-33745
- Zr, polycrystalline, low temp. creep, dislocation interactions (*Russian*) 7-3359
- creep fracture**
- crack growth, theoretical-numerical investig. of expts. (*German*) 7-43803
- crack growth parameters, finite element and exptl. investigs. comparison 7-39674
- creep-fatigue life, long-term, prediction and evaluation 7-39796
- damage cumulation, self-similarity for different loading conditions 7-20658
- damage localisation theory 7-50990
- damage parameter, effects of interacting cavities 7-43796
- disk, rotating, variable thickness, dynamic creep rupture 7-43781
- elastic-viscoplastic constitutive eqns., modelling of continuum damage 7-43764
- fusion reactor structural alloys, irradi., creep fracture by grain boundary cavitation, modelling 7-53859
- high temperature structures in reactors, creep curve variation effects on creep behaviour 7-39602
- IN 100, cast superalloy, creep strain and life prediction 7-33741
- Inconel X-750, air environment/creep interactions, prior exposure times effect 7-13499
- inhomogeneous materials, 1D strain-dependent creep damage 7-6153
- local approach of fracture, continuum damage mechanics 7-50988
- material, creep rupture mechanics 7-53835
- material anisotropy and creep damage, constitutive eqn. formulation, tensor functions 7-50989
- mechanics of damage and fatigue, conf., Haifa, Israel (Jul. 1985) 7-48139
- metals, creep crack growth prediction by a local approach 7-53841
- modelling for engineering design 7-22776
- Nimonic 80A, coupled effect of plastic damage and creep damage at finite deform. 7-46599
- polyester fibres, fatigue and creep failure under cyclic loading 7-28110
- Rene 80, Ni-base superalloy, creep rupture props., influence of coating treatment and directional solidification 7-28116
- steel, austenitic, fusion reactor first wall material, development and testing 7-53860
- steel, austenitic stainless, creep rupture, fatigue cracking in flowing liq. Na 7-53843
- steel, austenitic stainless, creep rupture properties of heavy section Type 304 forgings for LMFBRs 7-13582
- steel, austenitic stainless, ductile failure under biaxial loading, thermal transients, analytical model 7-59609
- steel, austenitic stainless, FBR material, crack propag. under creep-fatigue interaction condition 7-22837
- steel, austenitic stainless, He-induced creep ductility loss, prediction and anal. 7-53854
- steel, austenitic stainless, in-beam creep rupture props. at 873K 7-53851
- steel, austenitic stainless, low activation, development, mechanical props., fusion reactor structural material 7-53799
- steel, austenitic stainless, precipitation strengthened, creep fracture, 875-975K 7-8046
- steel, austenitic stainless, tensile, creep and low-cycle fatigue props., effect of prestrain (*Japanese*) 7-46621
- steel, Cr-Mn, cold-formed, creep crack growth 7-53872
- steel, Cr-Mn, Nb-modified, creep crack characts. at 360°C 7-46631
- steel, Cr, heat-resisting, mech. props., effect of W (*Japanese*) 7-17617
- steel, Cr-Mo, creep fracture 7-33784
- steel, Cr-Mo, cyclic softening, creep and fatigue, fusion reactor appls. 7-53757
- steel, Cr-Mo, elevated temp. strength, H attack resistivity and stress relief cracking suscep. improvements 7-13583
- steel, Cr-Mo, tube, high temp. press. fatigue testing 7-65246
- steel, Cr-Mo-Ni-Mn, stress relief cracking, impurity effects 7-46635
- steel, Cr-Mo-V, creep crack growth at 838 K, displacement-controlled loading behaviour 7-17626
- steel, Cr-Mo-V, creep crack growth at 838K, const. load behaviour 7-17625
- steel, ferritic, fusion reactor first wall material, development and testing 7-53860
- steel, Mo-Ni-Mn, creep fracture mechanisms and rupture life 7-65137
- steel, stainless, austenitic, low-activation, constitution, struct. and mech. props. 7-42195
- steel, weld metal, creep crack growth 7-17623
- steels, creep-fatigue cracks, high temp., strain range partitioning anal. (*Japanese*) 7-33781
- structural member, endurance in creep conditions, accuracy of prediction 7-32561

creep fracture continued

- super alloys, columnar grained and single-crystal, high-temp. strength with surface recrystallised layer (*Japanese*) 7-53788
 tensile test, creep failure by microstruct. degradation and grain boundary cavitation 7-65117
 tension-torsion creep-fracture testing device 7-46739
 Al-Cu, creep rupture under tri-axial tension 7-53839
 Al-Cu-Mg, IN 9021, creep crack growth fracture morphology 7-53881
 Al₂O₃, vitreous bonded, crack nucleation and growth at elevated temps. 7-33770
 Cu, creep crack growth, 450-650°C 7-33758
 Cu, creep rupture under tri-axial tension 7-53839
 Cu tubes, creep-fracture tests 7-46739
 Cu-Sb (1 wt.%), creep crack growth, 450-650°C 7-33758
 Fe-Ni-Cr-Mo-Ti-C, JPCA, He injected and creep ruptured, microstruct. obs. 7-53853
 Ni, intergranular cavitation in high temp. creep, fractographic techniques appl. 7-53804
 Ni superalloy IN738LC, creep modelling for engng. design 7-22776
 Ni-base alloy, (Nimonic 75), creep-fatigue interaction, SEM and TEM studies (*Chinese*) 7-13543
 Ni-base superalloys, γ' strengthened, creep and microstruct. rel. to refractory elements 7-3364
 Ni-Cr superalloy IN738LC creep induced damage identification using electron backscatt. patterns 7-46748
 Ni-W-Co-Cr superalloys, creep rupture and tensile props. rel. to hot pressing or aluminising 7-3363
 Pb alloy, creep crack growth parameters of model materials 7-39674

creep-recovery see recovery-creep**creep testing**

- constant stress compressive creep machine, modified lever system 7-13687
 creep-fatigue life, long-term, prediction and evaluation 7-39796
 high press. testing in 20 MPa H₂ atmosphere at high temp. 7-3548
 high temperature compression creep equipment for low stresses 7-17751
 machine for tensile and compressive testing of materials with application of pressure 7-33876
 photoviscoelastic experiments (*German*) 7-22936
 rapid prediction, thermoactivation analysis basis, residual life eval. after TMT 7-22941
 refractory, long-term strength characts., parametric methods suitability 7-22942
 steel power plant components, remaining creep life assessment 7-8220
 transformation processes at const. tensile stress, equipment 7-13688
 Ni-Cr superalloy IN738LC creep induced damage identification using electron backscatt. patterns 7-46748
 Pb-Sn eutectic, superplasticity, investig. by impression creep testing 7-3372

crestatrons see travelling-wave-tubes**rimping**

No entries

critical constants, thermal see critical points**critical current density (superconductivity)**

- microcomposite superconductors, in situ, nature of connection (*Russian*) 7-45585
 stabilized superconductor carrying current in varying mag. fields 7-22063
 tetrahydrofulvalene bis(bis-(4,5 dimercapto-1,3-dithiole-2-thione) Ni(II)), 3D mol. supercond. 7-45594
 Al-Si-Pb-Bi, duplex alloys, melt quenching, microstruct. supercond. props. 7-45593
 BaPb_{0.75}Bi_{0.25}O₃ ceramic granular superconductor, infinite cluster detection, local heating method 7-2797
 Cu-Nb composite superconductors, critical parameters and surface flux pinning studies 7-38830
 Cu₃₃Zr₆₇, glassy metals, peak effect, flux pinning (*Chinese*) 7-12929
 Mo₃(SiRe), neutron irradi., supercond. investig. (*Russian*) 7-12926
 (Nb,Ti)₃ Sn, supercond. mag. material, fusion reactor conditions simulation 7-52922
 Nb film, elec. props., temp. cycling effects 7-38804
 Nb-Ti, supercond. mag. material, fusion reactor conditions simulation 7-52922
 Nb₃Al superconducting tape prepared by CO₂ laser beam irradiation 7-17145
 Nb₃Al₁Si_{14.5}Pb_{0.5}, A-15 superconducting tapes for high mag. fields, fabrication 7-33133
 Nb₃Sn multifilamentary wire superconductors, development at SLE 7-64421
 Nb₃Sn-Ti(In) multifilamentary superconducting composites, growth dynamics, struct. and props., additive and heat treatment effects 7-22056
 Ni₃₃Zr₆₇, glassy metals, peak effect, flux pinning (*Chinese*) 7-12929
 Pb-Bi superconducting alloys with Bi precipitates, critical current density 7-17146
 Pt-Bi (22 wt.%), supercond. films, pinning in appl. mag. field (*Russian*) 7-64418
 (VCr)₃Si, neutron irradi., supercond. investig. (*Russian*) 7-12926
 (VMo)₃Si, neutron irradi., supercond. investig. (*Russian*) 7-12926

critical currents

- see also critical current density (superconductivity); flux creep; flux flow; flux pinning
 Chevrel phase cpd. films, upper critical field determination from critical current data 7-38828
 cylindrical samples with ferromag. particles, critical current enhancement 7-2796
 Josephson contacts, critical current quantum renormalisation 7-12921
 Josephson junctions, I-V characts., fluctuation effects 7-52902
 Josephson junctions with microinhomogeneities attracting solitons, crit. currents 7-64406
 upper critical field determination from critical current data 7-38828
 ZrN films, supercond. props. (*Russian*) 7-38836
 Al-Pb disordered 3D normal metal-superconductor composite, elec. transport, magnetisation meas. 7-64383
 Cu-Nb, composite struct., filamentary medium, cond. anisotropy and crit. current 7-22081
 Cu₃₃Zr₆₇ metallic glasses, flux pinning and critical current peak effect studies 7-22079
 HoMo₃S₈ ferromagnetic films, supercond. props., temp. and mag. field depend. 7-45538
 In superconducting film, temp. dependent order parameter relax. time determ., critical DC current meas. 7-17147

critical currents continued

- In-Pb whiskers, critical currents and Ginzburg-Landau parameters 7-17144
 In-Pb whiskers, quasi 1D supercond., weak to strong coupling transition, I-V characts. study 7-38835
 Nb film supercond. props., α particle bombardment and thermal cycling effects 7-33704
 Nb, polycrystalline, US excitation, critical current, dislocation struct., flow limit (*Russian*) 7-58966
 Nb-NbO_x-PbInAu, Josephson tunnelling current depend. on normal state tunnelling resist. 7-22073
 Nb-Ti, superconducting composites, critical current distributions 7-38833
 Nb-Ti composite superconductors, influence of heat transfer on current carrying capability 7-64422
 Nb₃Al superconducting tape prepared by CO₂ laser beam irradiation 7-17145
 NbN microbridges, current-voltage characts., magnetic field effects (*Russian*) 7-7460
 Nb₃Sn filamentary superconductor with high bending strength, fabrication (*Slovak*) 7-58965
 Nb₃Sn film, grain size, grain boundaries and diffusion, TEM study 7-21222
 Nb₃Sn multifilamentary superconductor, AC props. 7-38834
 Nb₃Sn, superconducting composites, critical current distributions 7-38833
 Ni₃₃Zr₆₇ metallic glasses, flux pinning and critical current peak effect studies 7-22079
 Si-B, critical supercond. current induced by proximity effect, mag. field depend. 7-22069
 Sn wide superconducting films, voltage-depend. excessive current, resistive state obs. (*Russian*) 7-12930

critical field, superconducting see superconducting critical field**critical fluctuations**

- see also fluctuations in superconductors
 antiferromagnetic Potts model, simple cubic lattice, critical fluctuations and phase transitions, Monte Carlo simulations 7-35457
 biological membranes, microwave effects, rel. to crit. phase transition 7-40114
 CDW dynamics, model, nonuniversal crit. behaviour 7-12632
 glass transition singularity, dynamical theory 7-58476
 magnetic materials with two sublattices, phase transitions, fluctuation effects 7-38872
 metals, vacancy pore spatial distrib. during continuous irradi. (*Russian*) 7-58268
 polymer melts, viscoelasticity near a critical point 7-57781
 polystyrene-poly(vinyl methyl ether), binary mixtures, spinodal decomposition 7-44822
 1-propanol-water, conc. fluctuations, US absorpt. 7-58416
 spherical model, fluctuation effects and phase transitions 7-33192
 system with coupled order parameters, ring approx. 7-41315
 weakly first-order transition, delayed nucleation 7-26904
 CeSb, mag. ordering and critical fluctuations, uniaxial pressure effects 7-33174
 α -Fe, paramag. and ferromag., critical mag. phenomena, results from μ SR studies 7-45872
 FeCo alloys, critical mag. phenomena, results from μ SR studies 7-45872
 Fe_{0.91}Zr_{0.09} amorphous alloys, critical mag. phenomena, results from μ SR studies 7-45872
 KMnF₃, 2D order parameter fluctuations at antiferrodistortion phase transition, dielec. const. meas. 7-16735

critical mixtures

- acetonitrile-cyclohexane-benzene, crit. solns., nonlinear dielec. effect obs. 7-53213
 binary critical mixtures, universality 7-44758
 binary liquid mixture, wetting transition, order-parameter exponent 7-21574
 binary liquid mixtures, Kerr effect 7-53271
 cyclohexane-methanol, critical soln. temp., dissolved gas effect 7-44759
 dynamic gratings induced by electrostrictive compression of critical microemulsions 7-11032
 gas mixtures, cross-over behaviour for exponent doubling near critical point, light scatt. expt. 7-32611
 guaicol-glycerine critical solutions, viscosity meas. 7-6850
 isobutyric acid-H₂O, near-critical binary fluid mixture, refractive index, Lorentz-Lorenz rel. 7-7659
 liquid state, isotope-induced quantum-phase transitions 7-12295
 methane - 2,2-dimethylbutane - 2,3-dimethylbutane, tricritical behaviour 7-12234
 methane-alkane mixtures, vapour-liq. equilib. Wilson-Wegner expansion, vapour press. calcs. 7-12248
 methanol-isooctane mixture, coexistence curve determ. by meas. refractive index 7-38162
 polystyrene-poly(vinyl methyl ether), binary mixtures, spinodal decomposition 7-44822
 polystyrene-polyvinyl methyl ether, crit. mixture, late stage spinodal decomposition 7-26955
 1-propanol-water, conc. fluctuations, US absorpt. 7-58416
 viscoelasticity near a critical point 7-57781
 CO₂-n-hexadecane supercritical system, phase equilib. and vapour density meas., high-press. multiproperty apparatus appl. 7-12249

critical opalescence

- fluid layer, critical opalescence in multiple scatt., density fluctuation higher correlation contrib. 7-33351

critical phenomena

- see also critical fluctuations; critical mixtures; magnetic transitions; phase equilibrium; phase transformations; renormalisation
 2D criticality, correlation functions and projective transformations 7-41322
 ϕ^4 theory, nonuniversal power laws and critical-to-classical crossover 7-41297
 adhesive-hard-sphere model, crit. behaviour, mean spherical approx. 7-58113
 adsorption of fluid 7-21626
 alternative binary system, two-dimensional, critical state 7-63783
 Anderson localisation, upper critical dimens., wave function anomalous scaling behaviour 7-38428
 anisotropic cubic spin-1 Ising model, linear chain approx. 7-2876
 Ashkin-Teller model, 2D conformal symmetry and critical 4-spin correl. fns. 7-48999
 Ashkin-Teller quantum chain, criticality, finite-size effects and conformal invariance 7-52993

critical phenomena continued

background fluctuations and Wegner corrections 7-281
 baroclinic chaos numerical anal. 7-57893
 Base-Einstein condensation, free boson gas in thermodynamic limit 7-29873
 Bethe lattice, localisation transition 7-29940
 binary fluid mixtures, eqn. of state, high temp. and high press. 7-21385
 binary mixtures near codimension-two point, externally modulated Rayleigh-Benard system, phase diagram 7-32602
 binary random harmonic chains, special freqs. and Lifshitz singularities 7-35404
 Blume-Emery-Griffiths model, 3D semi-infinite, real-space renormalisation group study 7-38156
 Bose fluid, interacting, nonlinear quantum and classical renormalization-group trajectories 7-35396
 Bose-Einstein condensation, critical density and thermodynamic functions 7-29872
 brochard-Leger wall in liquid crystals 7-37855
 Cayley trees, randomly closed, and fractal dimensionality 7-4784
 classical limits and critical properties 7-48457
 complex eigenvalues of differential eqns., critical layer singularities, review 7-4714
 complex Sierpinski carpets, phase transform. 7-61303
 conference, critical phenomena and phase transitions, Brasov, Rumania, (1983) 7-48187
 n-dodecyl-octaoxyethylene glycol monoether micellar solns., long-range crossover 7-21068
 driven diffusive system, critical behaviour, field theoretic renormalisation group study 7-9811
 driven diffusive system, field theory of critical behaviour 7-29949
 dynamic scaling of Eden-cluster surfaces 7-14888
 dynamical systems and statistical physics conf., Koszeg, Hungary, Aug.-Sept. 1984 7-48194
 field theory applications 7-41578
 finite cutoff and higher transient effects on critical behavior 7-282
 finite temperature deconfinement transition, Monte Carlo renormalisation group calcs. of critical exponent 7-49054
 finite volume effects on critical behaviour, exactly solvable model 7-35487
 finite-size scaling in strips, log. corrections, Potts model appl. 7-35429
 fluid hierarchical reference theory, smooth cut-off formulation 7-6491
 free-standing liquid crystal films, smectic A-hexatic B transition, critical exponent study 7-6819
 gelation, 3D kinetic model, critical behaviour 7-14904
 growth probability distribution in kinetic aggregation processes 7-2145
 hard hexagon model, lattice gas generalisation, local densities as elliptic functions 7-9788
 n-heptane-perfluorohexane soln., phase separation, spinodal curves 7-13170
 hierarchical lattices, geometrical phase transitions and universality 7-41321
 hierarchical structures, complexity and relax. 7-18702
 hierarchical vector-valued ϕ^4 model, Maxwell rule and phase separation 7-48634
 higher-order phase field models and detailed anisotropy 7-18732
 infinite strips with periodic boundaries, critical point structure fns., correlation lengths and susceptibility 7-24580
 interfacial profile in external field, ϵ -expansion calcs. 7-197
 interfacial transitions, bifurcation of renormalisation-group fixed pts. 7-27062
 Ising model, critical exponents in non-integer dimensions 7-56172
 Ising model, d-dimens., thermodynamic behaviour in generalized spherical model 7-27536
 Ising model, kinetic two-spin facilitated model on square lattice, Monte Carlo simulation 7-24598
 Ising model, three dimensional, partition fn. calcs. 7-61264
 Ising model, wetting transitions near bulk critical temps., long-range forces effects calcs. 7-58573
 Ising model on hypercubic lattice, critical conditions 7-29941
 Ising model on square superlattice, critical props., real space renormalisation group calcs. (Chinese) 7-27532
 Ising random-field systems, integer optimization and zero-temperature fixed point 7-7530
 Ising strips, correl. lengths universal scaling form calcs., boundary conditions depend. 7-56177
 lattice gas of diffusing interacting particles in concentration gradient, Monte Carlo simulation 7-48596
 letting, 2D, exact decimation-type functional renormalisation 7-44955
 linear polymers, collapse transition, lattice self-avoiding walk model 7-35452
 loop gas model, square lattice, critical behaviour 7-216
 magnetic hard-square lattice gas, multicritical scaling 7-48607
 mean field renormalisation group, length scaling, critical indices 7-61260
 mean-field renormalisation group, unified approach to bulk and surface critical behaviour 7-48665
 micellar solutions, marginalism, quasi-marginalism and critical phenomena 7-58437
 micellar solutions, origin of nonuniversality 7-46879
 Monte Carlo simulations nonuniversal critical dynamics 7-41323
 n-vector model, critical behaviour for $1 < n < 2$ 7-48666
 nonequilib. phase transforms., critical behaviour in fast-ionic-conductor and reaction-diffusion Ising models, Monte Carlo scaling 7-61304
 nonideal Bose gas, chemical pot. and press., perturbation theory anal. 7-61222
 nonlinear dynamical systems, chaotic transients critical exponent calcs. 7-232
 O(n) models, finite-size scaling in higher dimensions 7-14903
 one-way coupled subsystems, critical behaviour at the transition to chaos 7-41314
 percolation, thresholds and critical indices 7-29913
 percolation, two dimensional, Ising-like critical phenomena 7-24581
 percolation at surface, fractal dimension 7-14867
 percolation models, critical exponent inequalities 7-35451
 phase diagram, substance properties for wide range around critical point 7-6757
 planar random surfaces with extrinsic action, critical exponents 7-29938
 Potts model, 2D, critical dynamics 7-18714
 Potts model, 2D, renormalisation by substitution 7-24568
 Potts model, one dimensional, critical dynamics 7-240
 Potts model, triangular, with 2- and 3- site interactions, crit. line 7-24596

critical phenomena continued

Potts models, crit. dynamics at percolation threshold 7-29917
 propane, gas, thermal cond. meas., coaxial cylinder method 7-51369
 quasiperiodic Schrodinger equation, global scaling props. of spectrum 7-283
 random field problem, critical behaviour, Fisher renormalisation 7-41289
 random surfaces, triangulated, intrinsic geometry, mean size fluctuations, Monte Carlo simulation of critical props. 7-61227
 random surfaces on cubic lattice, critical behaviour, phase diagram 7-24582
 resistor-diode percolation on the hierarchical diamond lattice, real space renormalization group anal. 7-243
 scale-invariant description of critical region, Percus-Lebowitz method 7-29962
 scaling laws and universality of critical phenomena in an external field 7-14906
 self dual quantum Z(5) model, finite-size scaling and conformal invariance 7-35428
 self-avoiding random walks on the hexagonal lattice, critical exponent calcs. 7-35405
 self-avoiding walk, Monte Carlo algorithms, dynamic critical exponents 7-213
 semi-infinite ferromagnetic q-state Potts bulks separated by bond diluted interface, criticality 7-33179
 Sierpinski carpets, classification and universal props., Potts model critical points 7-61259
 solid-on-solid models, integrable, automorphic props. of local height probabilities 7-56184
 specific heat, universal critical amplitude ratio estimation from ϵ expansion 7-41320
 specific heat critical exponents, LEED meas., Monte Carlo data anal. 7-6824
 spin models, accelerated hybrid stochastic algorithm for critical slowing down problem 7-2859
 spin-1 Ising model, two and three dimensional, biquadratic exchange interactions, reentrant behaviour, Monte Carlo study 7-12986
 spin-1/2 Heisenberg chains, critical region, finite-size corrections and numerical calcs. 7-59045
 statistical mechanical systems, critical behaviour and random walk representations 7-48532
 statistical mechanical theory, fluctuations, coherent anomalies and scaling exponents 7-48658
 structural phase transitions, correlated random field effects in the quantum displacive limit, critical props. 7-63767
 sulphobetaine polymers, phase behaviour and soln. props. 7-38164
 three dimensional phenomena 7-48526
 three-spin Ising model, conformal invariance and critical behaviour 7-53009
 turbulence transition via spatiotemporal intermittency 7-43861
 two coupled semi-infinite systems near criticality 7-44747
 two-dimensional lattice gas on triangular net, order-disorder transitions, struct. factors, Monte Carlo simulation 7-56176
 two-dimensional melting, defect core-energy depend., Laplacian-roughening model calcs. 7-6765
 XXZ chain, conformal invariance and spectrum 7-63768
 XY model, 3D, critical surface free energy, universal finite scaling amplitude, direct Monte Carlo sampling 7-61305
 Z₂ gauge theory, finite lattice effects 7-389
 Al thin supercond. film, nonlinear RF props., vortex pair creation, critical effects 7-17137
 Ar gas crit. behaviour, modified hypernetted chain eqns., nonuniversal quantities 7-44090
 p-Ge:As, Hall effect and electrical conductivity, temp. corrections 7-38592
 He, Gruneisen parameter at critical points (Chinese) 7-24609
 He, superfluid, flow through tiny orifice, order parameter phase difference 7-63894
 S, equilibrium polymerization and polymer solns. as multicritical phenomena 7-28310

critical phenomena, magnetic *see magnetic transitions*

critical points
see also boiling point; melting point
 ϕ^6 model in 3+1 dimensions, exact solns. 7-41598
 amphiphilic molecules, adsorpt. and orientation, liq.-liq. interface 7-12403
 bifurcations near tricritical point in Couette-Taylor flow, Landau model 7-1528
 binary polymer mixtures, homogeneous, near-critical quenching kinetics 7-13482
 calculations using nonzero interaction parameters 7-32597
 chaotic spin-glass phase, description in terms of T=0 fixed point 7-45716
 Coulomb gases, 2D, hierarchical model with Kosterlitz-Thouless fixed point 7-9797
 crystal order parameter, relax. time near phase transition points, Raman scatt. studies 7-44738
 cyclohexane-methanol, liq.-liq. critical point, eqn. of state 7-12230
 D₂, triple-point measurements 7-60902
 density distribution near gas/liquid critical points under reduced gravity 7-21426
 deuterio-isobutyric acid (coax)-D₂O, critical mixtures, isotope effects 7-12253
 deuterio-isobutyric acid (COOH)-H₂O, critical mixtures, isotope effects 7-12253
 disorder fields in two-dimensional conformal quantum-field theory and N=2 extended supersymmetry 7-41161
 effective renormalised coupling constants and the critical point 7-44745
 electrolyte near critical point elec. struct. of interface, elec. double layer 7-33063
 electron gas, low freq. fluctuation phenomena near metal-dielectric transition point 7-38654
 ethane, thermal diffusivity around crit. point along liquid-gas coexistence curve, light scatt. meas. 7-52098
 ethoxylated alcohol-n-alkane-water mixtures, phase behaviour patterns 7-21406
 ethylene adsorbed on graphite, layering and layer-critical-point transitions 7-12471
 exponents far from T_c, specific heat appl. to hierarchical structures 7-33175

critical points continued

- fermi system, correlation functions of order-parameter fluctuations 7-56145
- ferroelectrics, thermodynamic equilib. critical exponents and stability 7-12237
- ferromagnetic systems, critical point phenomenology and neglect of irrelevant variables, renormalisation group results anal. 7-64468
- finite systems, hyperuniversality and renormalisation group, finite-size scaling 7-56203
- fluids, thermodynamic stability and viscosity behaviour or melting curve 7-12247
- fluids at liq-vapour critical point, many-body interaction effects calcs. and meas. 7-44750
- gas mixtures, cross-over behaviour for exponent doubling near critical point, light scatt. expt. 7-32611
- hard disks and spheres, power series expansions, critical point singularities 7-44333
- hard spheres with Yukawa tail, critical behaviour, mean spherical approx., finite element solns. 7-12251
- Heisenberg antiferromagnets, multicritical points 7-27541
- N(p-n-heptyloxybenzylidene) p-n-pentylaniline, liq. cryst. phase transitions, density, US vel. meas. 7-1874
- hexatic liquid crystals, multicriticality 7-2201
- homogeneous spinodal phase, stability boundaries, thermodynamic functions homogeneity (Russian) 7-41325
- immiscible fluid mixture in shear flow, phase separation, spinodal decomposition under shear 7-21464
- inert gas films, physisorbed on lamellar halides, incipient triple points 7-16722
- Ising generalised mixed spin model, renormalisation group approach (Chinese) 7-9779
- Ising model, random-field, with trimodal distrib., phase diagram 7-56182
- Ising model, trimodal random-field, on Bethe lattice and tricritical point 7-56181
- Ising models with random bonds and crystal field interactions, tricritical point 7-2868
- Ising spin 1/2 lattice model, magnetic susceptibility, critical parameters, shifted ratio method 7-14890
- IV-VI compounds, vibronic theory of struct. phase transition and tricritical point 7-38187
- lead (II) carboxylates, thermotropic phase transitions, DSC meas. 7-21441
- linear scaling theory model and eqn. of state comparison 7-41316
- liquid metals, compressibility, coexistence line and critical characts. 7-44350
- liquid wetting layers equilib. struct. 7-58568
- liquids, surface tension correl. 7-2299
- methane, press., density and temp. meas. in crit. region 7-52000
- methane, vibr. dephasing, critical density broadening, Raman spectra anal. 7-62387
- methane monolayer on graphite, thermodynamic study 7-16863
- methane-alkane mixtures, vapour-liq. equilib. Wilson-Wegner expansion, vapour press. calcs. 7-12248
- methanol-n-hexane near liquid-liquid critical point, mutual diffusion coeff. 7-44876
- methanol-d₀(d₁)(d₄)-cyclohexane-d₀(d₁₂), critical mixtures, isotope effects 7-12253
- methanol-heptane (octane), liq.-liq. phase equilibrium at press. from 0.1 to 150 MPa 7-26931
- methanol-isooctane mixture, coexistence curve determ. by meas. refractive index 7-38162
- Migdal-Kadanoff renormalisation, appl. to Potts model 7-24600
- mixtures, dilute behaviour near crit. pt. of solvent 7-26979
- model microemulsion, phase equilibria and critical endpoints 7-17828
- multicomponent mixtures, vapour-liq. critical points calc. using empirical method 7-38175
- multicritical phenomena and critical dynamics, differential renormalisation group generators 7-38159
- naphthalene solubilities in supercritical CO₂ near upper critical end point, NMR 7-12293
- nematic-smectic A liq. cryst. phase transition, tricrit. point, num. anal. 7-12268
- nematic-smectic A phase transition, calc. of tricritical temp. 7-12276
- nematic-smectic A-smectic C multicritical points, universality 7-2200
- perfluoromethylcyclohexane-carbon tetrachloride, liq.-liq. critical point, dielectric const. 7-13079
- phenol-d₆-D₂O, critical mixtures, isotope effects 7-12253
- polyelectrolytes, highly asymmetrical, spinodal curve 7-21466
- polymer melts, viscoelasticity near a critical point 7-57781
- polymerisation, equilib., bicritical phenomenon 7-3588
- propyne, thermodynamic props. (German) 7-52081
- quartz particles, α - β inversion, structural damage effects, micro DTA study 7-2185
- random field models with long range exchange, scaling theory, 1/n expansion 7-24553
- real fluid in critical region, eqn. of state, thermodynamic props. 7-58430
- reentrant wetting phenomena and crit. behaviour near bulk critical points 7-44956
- reentrant-nematic-smectic C-smectic A multicritical points, universality 7-2200
- spin van der Waals model, specific heat (Korean) 7-27537
- square-lattice-gas model with anisotropic repulsive interactions, multicritical behaviour, transfer-matrix scaling 7-41291
- stability of the isotropic fixed point near one dimension 7-9787
- statistical physics, conference, Oaxtepec, Morelos, Mexico (Aug. 1985) 7-9584
- succinonitrile triple-point cells for temp. ref. standard near 58.08°C 7-35492
- symmetry-breaking transitions, state selection 7-48661
- tetramethyl urea+water system, solid-liq. phase equil., freezing pts. 7-32616
- bis(tetramethylammonium) bromochloroacetate single cryst. solid solns., phase diagram study 7-26944
- two dimensional Heisenberg model, easy-plane exchange anisotropy, Monte Carlo study 7-17196
- two-dimensional, scatt. function lineshape, finite geometry and boundary conditions effects. 7-280
- two-dimensional lattice gas phase diagrams, multi-critical point positions 7-2142
- water, distilled, triple point, prep. of water cells (Korean) 7-24620

critical points continued

- CO-Ar system phase diagram, critical point determ., X-ray diffr. study (Russian) 7-6776
- CO₂, slow neutron interaction near vaporisation crit. point, cross section temp. depend. 7-52021
- CO₂-n-hexadecane supercritical system, phase equilib. and vapour density meas., high-pressure, multiproperty apparatus appl. 7-12249
- CO₂-pentane, excess enthalpies at 348.15, 373.15, 413.15, 470.15 and 573.15K 7-44826
- Fe, phase diagram and Earth interior conditions 7-38179
- LiKSO₄ phase diagram, critical points determ., press. depend., differential thermal anal. 7-6780
- ND₃, elastic consts. and elasto-optic coeffs., Brillouin spectra anal. 7-53359
- N₂O, thermal diffusivity around crit. point along liquid-gas coexistence curve, light scatt. meas. 7-52098
- NaNO₂, incommensurate ferroelec., in transverse elec. field, virtual Lifshitz point 7-45947
- Ne film on Ag, triple-point wetting 7-32760
- Ne triple point, thermodynamic temp. determ. 7-18791
- O₂, triple point in sealed transportable cells 7-41331
- O₃ solid and liq., vapour press. meas. 7-16716
- Pb₃P₂V₂-₂O₈ mixed system, substitution defects, first order transition spreading 7-58458
- SF₆, thermal diffusivity around crit. point along liquid-gas coexistence curve, light scatt. meas. 7-52098
- SiO₂-MgO(SrO)(La₂O₃)(Y₂O₃) systems, liq. immiscibility 7-6807
- Ti-Zr, α - β transform. temp. study 7-38180
- critical temperature, superconducting** see *superconducting transition temperature*
- CRO** see *cathode-ray oscilloscopes*
- crocidolite** see *asbestos*
- crops** see *farming*
- cross-sections (nuclear)** see *nuclear reactions and scattering*
- crossed-field tubes** see *microwave tubes*
- crosstalk**
- biomedical US transducer array performance with PZT-polymer composite piezoceramic 7-3850
- biomedical US transducer design for uniform insonation 7-3847
- electro-optic directional coupler switches, crosstalk due to reversed- $\Delta\beta$ electrode misalignment 7-20471
- fibre couplers composed of unequal cores 7-20420
- fibres, polarisation-maintaining birefringent, polarisation cross talk ultimate limit 7-25970
- high birefringence fibres, crosstalk meas. 7-57566
- MQW optical logic arrays, thermal crosstalk 7-38720
- optical $\Delta\beta$ phase reversal directional coupler switches, crosstalk characts. 7-26037
- optical fibres, high-birefringence type, dichroism eval. using crosstalk meas. 7-20421
- optical multiplexing techniques and equipment (German) 7-1286
- optical sensors accuracies improvement, compensation method 7-43434
- polarisation-maintaining fibre, 26-km length 7-57570
- polarisation-maintaining fibre couplers with low excess loss 7-1269
- semiconductor laser amps. with reduced facet reflectivity, gain props. (German) 7-62687
- SQUID magnetometers, multichannel, flux-transformer crosstalk elimination 7-35541
- LiNbO₃:Ti 4X4 directional coupler switch with permanently attached polarisation maintaining fibre array, low crosstalk 7-31520
- LiNbO₃:Ti integrated electro-optic devices, modelling and beam propag. anal. 7-11177
- crowdions**
- irradiated metals, isochronal annealing PAC monitored defect reactions anal. 7-44623
- void growth, displace stability and size uniformity in void lattice, crowdion migration 7-44521
- CRT** see *cathode-ray tubes*
- crushing**
- mirror, large, prod. using single point diamond crushing combined with polishing 7-37220
- refractory carbide powder, mech. treatment model, energy characts. 7-35653
- γ -FeOOH-LiCO₃, mixture, mechanochem. transform. and γ -Fe₂O₃ form. 7-59478
- crushing strength** see *compressive strength*
- cryobiology** see *biothermics*
- cryogenic cables** see *superconducting cables*
- cryogenic pumps** see *cryopumping*
- cryogenics**
- see also *cryopumping; cryoscopy; cryostats; cryotrons; Joule-Thomson effect; low-temperature production; low-temperature techniques; magnetic cooling; refrigeration*
- accelerating-storage unit superconducting magnet testing using cryogenic equipment 7-48754
- adiabatic boiling, cryogenic flow instability 7-11385
- biological specimen visualisation by cryoHVM 7-40380
- cryogenic engineering conf., Berlin, Germany (April 1986) 7-48183
- current leads cooling, energy losses 7-61342
- dead-end pipelines of cryogenic systems, pressure increase 7-31880
- diffusion coeff. of Kr in liquid Ar determ., temp. controller design 7-30020
- expansion turbine, miniature cryogenic, gas bearing with tangential feed holes, instability onset speed 7-56289
- falling liquid film He separator for T production, design concept 7-800
- Freons, band strengths temp. depend. rel. to stratosphere climate modelling 7-55252
- galvanomagnetic instruments for operation in cryogenic electrical-engineering installations 7-56308
- glass, stabilised, low temp. relax., pot. barrier model. 7-43714
- HERA magnet measurement facility, cryogenic system 7-49781
- history of cryogenics, speculations and reminiscences 7-48266
- K-band receiver, cryogenically cooled HEMT for radio astronomical obs. 7-60548
- liquids, evaporative loss during vibration and transport 7-44776
- microminiature cryogenic refrigerator for compact CdSe laser 7-43153
- multilayer insulation, heat flux, 77 to 277K 7-35523

cryogenics continued

- picosecond electronics and optoelectronics, topical meeting, Lake Tahoe, NV, USA (Mar. 85) 7-41007
 proton source, high purity, pulsed with cryogenic plasma diode 7-30815
 radioastronomy, mm-wave, 230 GHz, low-noise cryogenic receiver, spectroscopic appls. 7-29396
 radiometric and interferometer system, linearity calibration 7-18858
 SCRIBE interferometer atmospheric emission spectra 7-55319
 SIRTf, a cryogenically cooled IR telescope 7-34873
 space systems, impact on cryogenic technology 7-48752
 steel, stainless, cryogenic structural material, low-temp. strength under action of elec. current pulses 7-22814
 Stirling cryocoolers, trends and development 7-65535
 superconducting magnets in fusion reactor design, review 7-49680
 supply and importance to cryoengineering 7-48748
 thermoacoustic oscillations elimination in cryogenic tubes 7-30021
 TORE SUPRA tokamak, cryogenic system design 7-1716
 H maser, operation below 1K 7-1069
 H microwave-pumped cryogenic maser 7-43044
⁴He, superfluid, flow properties w.r.t. cryogenic appls. 7-52171
⁴He, superfluid, props. and appls. 7-48751
 KSnCl₃·H₂O, near IR spectra, polarised overtone-combination bands 7-7684
 K₂SnCl₄·H₂O, near IR spectra, polarised overtone-combination bands 7-7684
 NbTi-Cu Al stabilised superconducting detector magnet technology for high energy accelerators, review 7-49779

cryopumping

- cryogenic engineering conf., Berlin, Germany (April 1986) 7-48183
 CTR, development and evaluation of cryosorption and cryotrapping pumps 7-25185
 fusion reactor cryopumping applications 7-25205
 fusion reactors, charcoal sorbents for He cryopumping 7-62077
 fusion reactors, cryopumping 7-56838
 JT-60 neutral beam injectors, cryopumps and cryogenic systems 7-19519
 optical coating deposition, cryopump conversion advantages 7-3185
 optical coating deposition, pump requirements 7-33570
 He compressor, regenerative oilfree, for cryopumps 7-56298
 He, superfluid, mechanical and fountain-effect pumps for in-orbit transfer 7-61339

cryoscopes see cryoscopy**cryoscopy**

- polydimethylsiloxane, swollen in benzene, network struct., cryoscopic obs. 7-21135

cryosorption see sorption**cryostats**

- 2I-He hybrid cryostat for 690 GHz InSb bolometer 7-30024
 accelerating-storage unit superconducting magnet testing using cryogenic equipment 7-48754
 CEBAF cavity cryostat 7-62183
 coldplates, continuously cooled, for reference temperatures realisation 7-317
 cryorefrigerator for neutron diffractometer, unit for holding and centering on a Eulerian cradle 7-30019
 galvanomagnetic studies of organic metals, at high pressures and low temp. 7-30035
 low-loss, numerical modelling 7-35524
 magnetic circular dichroism meas. of matrix-isolated species, cryostat for 1.5 to 60K range 7-14982
 Mossbauer spectrometers, cryostat design (Chinese) 7-61338
 Mossbauer spectroscopy, hydrostatic pressure effect on the minimum temperature of a helium-3 cryostat 7-18970
 NMR magnetic field meter, high-field meas. at liquid He temp. 7-18849
 Peltier effect based, for X-ray diffractometry at low temp. 7-14956
 sample-rotation mechanism for an ultralow-temperature cryostat 7-48747
 thermal mode optimisation (Russian) 7-48746
 three-terminal capacitance cell construction and calibration for thermal expansion meas. 7-29966
 vacuum cryostat, liq. N₂ cooled, differentially pumped rotary feedthrough 7-18795
 variable temp., steady-state vapour bubble type (Chinese) 7-61337
 He gas recovery system, automatic control of gas purity 7-318
 He subcooled superfluid, for hybrid supercond. mag. system 7-14952
⁴He, for storage Dewars 7-35526

cryotrons

- electrical nonlinearity of a laser-controlled film cryotron 7-18792

crystal atomic structure

- see also crystal atomic structure of alloys; crystal atomic structure of elements; crystal atomic structure of inorganic compounds; crystal atomic structure of organic compounds; electron diffraction crystallography; lattice constants; neutron diffraction crystallography; space groups; superlattices; X-ray crystallography
 atomic struct. refinement, algorithm and program for Borrmann effect 7-21045
 atomic structure models, electron microscope images, computer simulation 7-16380
 chain configs. in MX₅ cpds. with vertex sharing octahedra (German) 7-44460
 coincidence site lattice theory, appl. to cryst. struct. description 7-63535
 computer modelling of materials 7-51676
 coordination numbers and composition 7-58166
 crystalline materials, press-induced first-order phase transition, nearest-neighbour distance changes calcs. 7-6723
 crystallography, conference, Kharagpur, India (Dec. 1982) 7-55876
 cut model reconstructed from a three-dimensional data represented by Miller-Bravais indices and a simulation of Hirano bodies 7-6572
 direct methods of crystal struct. determ., anomalous dispersion 7-11836
 group-theoretical definition of crystal-structure types 7-11970
 magnetic materials, conference, Freudenstadt, Germany (April 1986) 7-48144
 mechanoluminescence studies of crystal structure 7-59268
 neutron scattering from tunneling centres in metals, structure factors 7-21155
 nonconvex, polygonal mesh and quad-tree display algorithms 7-51672
 perfect crystal tensile strength, anisotropy and interatomic pot. effect 7-12187
 phase information from intensity data 7-11971
 polychromatic crystals, mag. props. 7-51683

crystal atomic structure continued

- profiled crystals, Stepanov growth, conf., Leningrad, USSR (March 1985) 7-29573
 reciprocal lattice concept and props. 7-18525
 solid state reactions, heterogeneous, structural features influence (German) 7-17766
 space group band representations, appl. to theory of phase transitions and point defects 7-1927
 square matrices, symmetry, Bravais nets, point groups and plane groups 7-58183
 tetrahedral anion complexes in structures, relation between tetrahedron connections and comp. 7-44457
 three-dimensional polyatomids, classification (Russian) 7-16474
 two-dimensional Penrose lattice, distrib. of vertices and near neighborhoods, decorations 7-37915
 valence cryst., struct., coordination number 7-58167
 X-ray intensity statistics, non-ideal distributions 7-58185
 X-ray intensity statistics, significance of residuals 7-58186
 zone axes in the Miller index space 7-32317

crystal atomic structure of alloys

- Al₅ compounds, cryst. struct. 7-6587
 actinide metal, compound and alloy props., conference, Aix'en Provence, France (Sept. 1985) 7-9579
 alkali metals, structural properties, ab initio calc. 7-21156
 alloys, binary, phase diagrams and short range order, Monte Carlo simulations 7-53704
 amorphous and crystalline, local atomic struct., computer simulation 7-58160
 BCC and FCC crystal structures, H trapping, thermal anal. obs. 7-22830
 brass, Sn alloyed, disordered areas in three component solid solns. 7-21157
 germanides, M-M'-Ge, (M=Ca,Sr,Sc,Y,La-Lu; M'=Co,Rh,Ir), structural and superconducting props. (French) 7-44491
 icosahedral and amorphous structures, fractal coefficients 7-26646
 intermetallic compounds, ternary, equiatomic, cryst. struct. prediction 7-21158
 intermetallic phases, appl. as high temp. materials, review 7-22775
 Laves phases, and struct. rel. cpds., interstitial site occupancy of H atoms 7-16549
 Mg-Al alloys, precipitation and recrystallisation rates under small external stress 7-17532
 Ni₃Al_{0.8}-based alloys, magnetic and structural props. studies 7-45635
 plumbides, M-M'-Pt, (M=Ca,Sr,Sc,Y,La-Lu; M'=Co,Rh,Ir), structural and superconducting props. (French) 7-44491
 quasi-periodic lattice structures, dynamical calcs. 7-16370
 sputtered magnetic thin film, ion beam irradi., struct. studies 7-22588
 steel, Cr-Ni, low-C, butterfly martensite, crystallographic characts. (Russian) 7-6580
 steel, packet martensite deformation, struct. and crystal geometry (Russian) 7-3357
 steel, stainless, austenite ordering struct., X-ray diffr. studies (Russian) 7-6579
 superalloys, crystalline struct. and growth twin of Cr₇C₃, electron diffr. (Chinese) 7-12077
 superalloys, topologically close packed phases, domain struct. (Chinese) 7-11989
 Ag-In, atomic radial distrib. function, close order sorting parameter (Russian) 7-58206
 Ag-Mg (15.0 wt.%), disordered alloy, SRO, X-ray diffr. study 7-16490
 Al alloys, crystal structure and microstructure, metallography studies 7-58204
 Al alloys, quasicrystals, electron diffraction structure anal. (German) 7-37930
 Al two phase alloys, high temp. deformation, microtexture 7-16563
 Al-Co icosahedral alloys, struct., elec. and mag. props. 7-6583
 Al-Cu-Mg system, D16 alloy, struct. changes during electron bombardment 7-8005
 Al-Fe-Ce, quasicrystalline decagonal phase, TEM 7-46492
 Al-Fe-Mg, solidified from liq. phase, struct. (Russian) 7-39498
 Al-Fe-Si, TEM geometric projection of crystal struct. 7-16501
 Al-Mn, lattice model of quasicrystalline phase, high resolution electron microscope images 7-37866
 Al-Mn, periodic and quasiperiodic crystals 7-1928
 Al-Mn, rapidly solidified, decagonal phase morphology 7-39499
 Al-Mn (14 at.%), solidification, icosahedral and T-phase form, temp. rel. to cooling rates 7-53718
 Al-Mn alloy, decagonal phase, struct. model 7-63552
 Al-Mn alloys, local struct., EXAFS study 7-63466
 Al-Mn quasicrystals, 1D translational periodicity and ten-fold rotation axis 7-26643
 Al-Mn quasicrystals, field ion images, computer simulation studies 7-32368
 Al-Mn quasicrystals, local struct., EXAFS and XANES studies 7-6582
 Al-Mn system, quasicrystal form., metallurgy 7-3295
 Al-Pd, rapidly solidified, decagonal phase morphology 7-39499
 Al-Ti alloys, 1D antiphase domain structures 7-63557
 Al-Ti-Gd, rapidly solidified ribbons, aged, ternary phase precipitate identification 7-3311
 Al-transition metal alloys, vacancy-ordered phase and 1D quasiperiodicity 7-63551
 Al-V alloy, amorphous and quasicrystalline state, electron diffr. study 7-63562
 AlCuLi quasicrystalline struct., construction 7-37929
 AlMn icosahedral phase, atomic struct., electron diffr., studies 7-32366
 AlMn quasiperiodic material, disorder systematics, X-ray scatt., studies 7-11995
 Al_{1-x}Mn_x cryst. and quasicryst. alloys, struct. and mag. props. 7-1949
 Al₄Mn alloy, decagonal and icosahedral phase coexistence, electron diffr. studies 7-11991
 Al₄Mn, diffraction approach to the structure of decagonalquasi-crystals 7-6586
 AlMnSi, icosahedral and α-phase structs., EXAFS anal. 7-63554
 Al₁₂Mo precipitate microstruct. and orientation, implantation and annealing effects, electron microscopy study 7-16782
 Au-Sd transition metal alloys, heat of form. and cryst. struct., linear augmented STO calcs. 7-51705
 Au₇₇Ag₂₃, atom sublattices, selective high resolution electron microscopy 7-6486

crystal atomic structure of alloys continued

- Au₂Mn, atom sublattices, selective high resolution electron microscopy 7-6486
- Au₂Zn, non-periodic antiphase boundaries, obs. by HREM 7-63550
- BiAl₃, structural relationship to CaRh₂B₂ 7-16496
- Bi-Te metastable solid soln., fine struct., X-ray diffr. studies 7-44449
- Co-Ge, disordered α' martensite struct. (Russian) 7-58207
- Ca₃Ag₈, giant cells, polyhedral packing 7-11992
- CaIr₂B₂, structural relationship to BaAl₄ 7-16496
- CaRh₂B₂, structural relationship to BaAl₄ 7-16496
- Ce(Co,Cu,Fe)₆, magnetically hard, heat treatment effects on struct. and mag. characts. 7-27564
- CeRuSn₃, cage-like void structures (German) 7-32365
- Co-C, long period struct. development (Russian) 7-63559
- Co-Ta, cryst. struct. of α -martensite, effect of Ta conc. (Russian) 7-44452
- Co-Ta alloy, 1D disordered α -martensite states (Russian) 7-51703
- Co-W, ageing, polymorphism, cellular mechanism (Russian) 7-59514
- CoSi₂ films, structural analysis by X-ray diffr. in the grazing Bragg-Laue geometry 7-7042
- Cs-Se system, phase diagram 7-6759
- Cu-Al long-period superlattice, interface struct., TEM and HREM study 7-16499
- Cu-Be (2 wt.%), ageing, lattice rearrangement (Russian) 7-39553
- Cu-Mn-Al alloys, mag. and structural props. study 7-2895
- Cu-Pd bimetallic system, electron microscopy 7-16504
- Cu-Pt-Pd ternary alloys, L1-type ordered phases 7-16493
- Cu-Ru bimetallic system, electron microscopy 7-16504
- Cu-Zn-Al (26.4 wt.%), shape memory alloy, martensitic transform. crystallography (Chinese) 7-7994
- Cu-Zn-Al (26.4 wt.%), shape memory alloy, crystallography of martensitic transform. (Chinese) 7-7995
- Cu₄Sn₁₁, giant cells, polyhedral packing 7-11992
- CuZr, amorphous and cryst., bond length determ. from EXAFS data 7-63553
- Cu₁₀Zr₇, cryst. and amorphous, muon spin resonance studies 7-53196
- Dy₇Co₆Sn₂₃ cryst. struct. and mag. suscept. studies (Russian) 7-21161
- Er₇Co₆Sn₂₃ cryst. struct. and mag. suscept. studies (Russian) 7-21161
- Er₂(Fe,Co)₁₄B, struct., composition depend. 7-51701
- Er₂(Fe,Mn)₁₄B, struct., composition depend. 7-51701
- Fe-Al, atomic radial distrib. function, close order sorting parameter (Russian) 7-58206
- Fe-B, atomic radial distrib. function, close order sorting parameter (Russian) 7-58206
- Fe-B-based amorphous alloys, struct. evolution during heating (Russian) 7-16418
- Fe-Co-Ni-Al-Cu metallic alloy ordering and spinodal decomposition, atom probe FIM study 7-33676
- Fe-Co(V) alloys 7-51708
- Fe-Mn-C, local instability in FCC struct. (Russian) 7-58208
- Fe-Sc alloys, struct. and mag. props., NMR and X-ray diffr. studies (Russian) 7-6578
- Fe-Si, electrical steels and alloys, conf., Vladimir, USSR (Dec. 1984) 7-9576
- Fe-Si (4.5 to 7.5 wt.%), melt-spun, ordered struct. 7-1951
- Fe-Si-Al(Ga)(Al)(Ni)(Co)(Cr)(Mn)(Nb), atomic ordering and mechanical props. 7-11990
- Fe₇₈B₁₃Si₉ amorphous and partially crystalline alloy, high resolution TEM studies 7-21127
- FeNiAlCoTiCuS permanent magnetic material, phase comp. and ordering, atom probe FIM and TEM studies 7-33635
- Gd-Cr-C system, phase equilib., struct. 7-46423
- Gd(Al_{1-x}Ga_x)₂, cryst. struct., paramag. susceptibility, elec. resist. meas. 7-16492
- HfCo(Ni)Sn, Pauli paramagnet, mag. suscept. and cryst. struct. determ. (Russian) 7-1952
- Ho₇Co₆Sn₂₃ cryst. struct. and mag. suscept. studies (Russian) 7-21161
- K₂Na₃Ga₄₉S₇, synthesis and cryst. struct. 7-6584
- La₁₁Ni₄Ge₆, cryst. struct., trigonal-prismatic coordination of atoms 7-21159
- LaRuSn₃, cage-like void structures (German) 7-32365
- Lu₃Co₂Si₁₄, monoclinic struct. type, rel. to Sc₃Co₂Si₁₀ and La₃Co₂Sn₇ 7-1944
- Mg-Gd supersaturated solid soln., precipitate cryst. struct. (Russian) 7-33665
- Mg₇₆Zn₂₄, amorphous, crystn., X-ray small angle scatt. 7-11935
- Mn-P-B system, isothermal cross section at 1070K, lattice parameters of phases 7-53702
- {Mn₂Ge₂, high temp. phase structs., electron microscopy obs. 7-26697
- {Mn₂Si₁₁Ge₂, cryst. struct. 7-58202
- MnHg_{1-x}Au_x, cubic to orthorhombic transition and mag. suscept. meas. 7-52037
- Mn₃Ni₂Si₇, rapidly solidified, Friauf-Laves phase related quasicrystal, TEM obs. 7-51706
- Mo₃Ir, cryst. struct., X-ray diffr. meas. at 293K and 12.5K 7-16491
- NaCd₃, cryst. struct., matrix algebra calcs. 7-63548
- Nb single crystals, reverse lattice nodes form rel. to N diffusion (Russian) 7-58201
- Nb-Al alloys, struct. and supercond. props. (Russian) 7-1945
- NbNi(Co)Sn, Pauli paramagnet, mag. suscept. and cryst. struct. determ. (Russian) 7-1952
- Nb₃Sn thin films, X-ray diffr. spectra, processing methods 7-44308
- Nb₃Sn₂Ga, crystal growth and superconductivity 7-27451
- Nd-Fe-B liquid-quenched alloys, mag. props. 7-27550
- Nd-Fe-B permanent magnets, BCC phase mag. props. at grain boundaries 7-53044
- Nd_x(Co₉Fe_{1-x})₁₄B alloys, mag. struct., preferential site occupation 7-45619
- Nd₆Co₅Ge_{2.2}, cryst. struct., X-ray diffr. studies 7-44450
- Nd₂Fe₂₃B₃, struct., Curie temp., X-ray diffraction phase 7-11994
- Nd₂Fe_{14-x}M_xB₃ (M=Co,Ni,Cu,V,Al,Cr,Mn), crystallographic and mag. props. 7-27522
- NdRuSn₃, cage-like void structures (German) 7-32365
- Ni powder metallurgical superalloy, intermetallic phase 7-16503
- Ni-Al alloy phase transforms. during ion beam mixing, electron diffr. and microscopy studies 7-16655
- Ni-Al-B-based alloys, site occupations, APFIM and channelling studies 7-32367
- Ni-Be (2 wt.%), ageing, lattice rearrangement (Russian) 7-39553
- Ni-Fe-Mn system, coexistence of Ni₃(FeMn) and Ni(MnFe) superstructures (Russian) 7-1946

crystal atomic structure of alloys continued

- Ni-Ti metallic alloy ordering and spinodal decomposition, atom probe FIM study 7-33676
- β' NiAl, electron charge distrib., HEED meas. 7-16502
- Ni₃B/Ni eutectic, SEM and HREM struct. and chem. anal. 7-17515
- NiCr₂, short range order and atomic interactions, neutron studies 7-51707
- (Ni_{1-x}Cu_x)₂ Zr alloys, cryst. struct. study (French) 7-26698
- Ni₃(FEM) alloys, (M=Nb, V, Ta), atomic short range order, pseudopot. calcs. (Russian) 7-44448
- Ni_{1-x}Fe_xMnSb, half-metallic ferrimag., mag. and crystallographic props. 7-45672
- Ni_{93.35}Sb_{6.65} and Ni_{78.5}Sb_{21.5} alloys, characterisation studies (French) 7-28010
- NpM₄Al_{8-x} (M=Cr,Fe,Cu), mag. props., Mossbauer effect and neutron diffr. 7-59127
- Pd-U-Si glassy state, quasicrystalline phase form., X-ray and electron diffr. studies 7-26645
- Pr₇Co₆Al₇, crystal struct. determ. 7-16494
- PrRuSn₃, cage-like void structures (German) 7-32365
- Pu-Os-B system, phase equilibria and cryst. struct. 7-16781
- Pu-Rh-B system, phase equilibria and cryst. struct. 7-16781
- Pu-Ru-B system, phase equilibria and cryst. struct. 7-16781
- R₂Fe_{12-x}Mn_xCo₂B (R=Pr, Gd), mag. props. 7-27500
- RGa₃Co₂ (R=Ca, Ce, Pr, Nd), cryst. struct., mag. props. 7-45614
- RGa₃Fe₂ (R=La, Ce, Pr, Nd, Sm), cryst. struct., mag. props. 7-45614
- Sc₆Ni₁₈Si₁₁, cryst. struct. determ. 7-58205
- Sm₁₁Cd₄₅, giant cells, polyhedral packing 7-11992
- Sn_{1-x}Dy_{4+x}Os₆Sn₁₈, disordered II' phase, structural study, electron and X-ray diffr. meas. 7-63549
- Sn_{1-x}Tb_{4+x}Rh₆Sn₁₈, disordered II' phase, structural study, electron and X-ray diffr. meas. 7-63549
- SnYb(La-Gd)(Ca)(Sr)(Th)₃Rh₄Sn₁₂ crystals, structural distortion and chem. bonding, X-ray diffr. studies 7-1947
- Tb₃Co₂Ge₄, crystal struct. determ. 7-16495
- Tb₇Co₆Sn₂₃ cryst. struct. and mag. suscept. studies (Russian) 7-21161
- Tb(Fe,Co_{1-x})₃, struct. and mag. props. 7-1950
- Th₂Hg, intermediate phase in Th-Hg system, synthesis, struct., X-ray diffr. study 7-37911
- ThM₂Si₂ (M=Cu, Ru, Os, Ir, Pt), magnetochemistry and crystal chemistry 7-58976
- Th₆Mn₂₃, giant cells, polyhedral packing 7-11992
- Ti alloys, microstruct. and slip characts. 7-8050
- Ti-Al-Sn, silicide precipitates struct. 7-63561
- Ti-Al-V, VT23, α and β phases, temp. relationship of chem. comp. (Russian) 7-39520
- Ti-Cr alloys, cryst. and electronic struct., decomposition of β -solid soln. 7-37931
- Ti-Mo alloy, ordering, effect of interstitial trace elements (Russian) 7-37928
- Ti-Nb alloys, struct. and precipitation under high energy electron irradi. (Russian) 7-44620
- Ti-Ni, shape memory alloys, metastable X-phase, cryst. struct., morphology, TEM, X-ray diffr. 7-37926
- Ti-Ni (51 at.%), aged shape memory alloy, precip. morphology, comp., cryst. struct. 7-28049
- Ti-V-H alloys, struct., X-ray diffr. and ¹H and ⁵¹V NMR studies 7-32364
- Ti_{1-x}Al_x, long period struct. 7-16500
- TiCoSn ferromagnet, magnetisation, mag. suscept. and cryst. struct. determ. (Russian) 7-1952
- Ti₂Ni, giant cells, polyhedral packing 7-11992
- TiNiSn, Pauli paramagnet, mag. suscept. and cryst. struct. determ. (Russian) 7-1952
- Tl₂Sb₂, giant cells, polyhedral packing 7-11992
- Uir, cryst. struct., X-ray diffr. study 7-37927
- UM₂Si₂ (M=Cu, Ru, Os, Ir, Pt), magnetochemistry and crystal chemistry 7-58976
- U₃Sb₃Cu₂, cryst. struct., mag. props. 7-38864
- V-N system, metastable ordered phases, cryst. struct. (Russian) 7-44447
- V-Ti-Fe-H₂ system, V-rich, dihydride form., lattice parameters, thermodynamics 7-32369
- V₃Si, structure factor phase determ. by multiple Bragg diffr. 7-32211
- Y₇Co₆Sn₂₃ cryst. struct. and mag. suscept. studies (Russian) 7-21161
- (Y₂Zr_{1-x})Co₂₉, cryst. struct., mag. props. 7-51719
- YbCoB₄, YCrB₄-type structure, formation in Yb-Co-B ternary systems 7-6581
- YbFeB₄, YCrB₄-type structure, formation in Yb-Fe-B ternary systems 7-6581
- YbNiB₄, YCrB₄-type structure, formation in Yb-Ni-B ternary systems 7-6581
- Zr-Mn-H system, equilibrium props. 7-16756
- ZrCo(Ni)Sn, Pauli paramagnet, mag. suscept. and cryst. struct. determ. (Russian) 7-1952

crystal atomic structure of elements

- actinide metal, compound and alloy props., conference, Aix en Provence, France (Sept. 1985) 7-9579
- bicrystal, grain boundary dislocations, struct., steps, HREM study 7-16488
- crystallographic equivalence between BCT and FCT structs. 7-37924
- diamond, ion implanted, struct. props., EPR and electron diffr. studies 7-32363
- diamond, type Ia, voidites, evidence for crystalline phase containing nitrogen, cell constant determ. 7-2011
- diamond-like layers deposited from C ion beams, struct. (Russian) 7-17475
- grain growth, local texture development, STEM selected area channelling 7-16575
- graphite, mol. dynamics simulation and Raman spectrum, atom configs. and interactions, honeycomb struct. 7-58200
- graphite, neutron irradiation, macrostruct. and porosity studies 7-2069
- metals, BCC and FCC cryst. struct., H trapping, thermal anal. obs. 7-22830
- Pb, tetrahedral bonding and crystal struct., first-principles theory 7-32355
- rare earth metals, high-performance phases, crystal structure models 7-16489
- transition metal crystal, BCC, metal-H bond investig. 7-32360
- Ag, electrodeposit structure rel. to plating from complex electrolytes 7-2406

crystal atomic structure of elements continued

- Al atomic cluster, trapping regions around impurity atoms, charge density 7-53195
 Ar, Lennard-Jones cryst. struct., mol. dynamics method 7-16487
 Be, charge density distrib., local density approx. calcs. 7-6577
 C structure, determ. by radial distrib. function 7-16485
 Cr, cryst. and mag. states; effect of neutron irradi. in reactor (Russian) 7-51866
 Cr single crystals, surface and deeper layers, struct. changes due to laser irradiation 7-6937
 Cs high press. phase, β -Sn-type struct., pseudopot. perturbation calcs. 7-51938
 F₂ solid, high-press. behaviour at low temps. 7-37923
 K, (French) 7-26696
 Kr, defect props. in condensed two-dimensional lattice 7-2018
 Li, crystal and electronic struct., ab initio HF cluster method 7-44443
 Li, large clusters, struct., charge distribution and spin densities, semiempirical study (French) 7-26696
 Mo single crystals, struct. changes during annealing after bending deform. (Russian) 7-44446
 Na, crystals, BCC and FCC, thermophys. props., mol. dynamics calcs. 7-2229
 Na, large clusters, struct., charge distribution and spin densities, semiempirical study (French) 7-26696
 Ni close packed polycryst. struct., stacking order, mol. dynamics computer simulation studies 7-51691
 Rb high press. phase, β -Sn-type struct., pseudopot. perturbation calcs. 7-51938
 Ru, electronic, structural and cohesive props., theoretical study 7-37922
 Si 7-51938
 Si dendritic web ribbon, electrical and struct. props. 7-16922
 Si, Pendellosung intensity beat meas. with γ -radiation 7-46170
 Si powders, prod. from laser-heated silane, cryst. struct. 7-46362
 Si structural EXAFS study 7-64762
 Si, structural props., EXAFS study 7-64760
 Si, X-ray electron charge density distrib. 7-26695
 Si, X-ray structure factor, Pendellosung method meas. 7-32362
 Xe, defect props. in condensed two-dimensional lattice 7-2018

crystal atomic structure of inorganic compounds

- = 7-1986
 actinide metal, compound and alloy props., conference, Aix en Provence, France (Sept. 1985) 7-9579
 alkali metal cyanide halide mixed crystals, orientational glass state 7-21140
 alkali metal cyanide-halide mixed crystals, orientational glass state static props., microscopic model calcs. 7-63591
 alkali metal layered Mo bronzes, $(A^+(H_2O)_n)_x MoO_4^{x-}$, (A=Li, Na, K, Rb, Cs), composition and struct. 7-16518
 alumina, ion-rich β - and β' -phases, superionic props., homogeneity ranges and conductivities 7-21520
 alumina, ion-rich β - and β' -phases, superionic props., local and long-range order determ. 7-21519
 atomic coordination numbers and defects, geometric estimate 7-63571
 beryl, high press. cryst. struct. and compressibilities 7-16505
 bis(2,4,6-trinitrophenolato)di(pyridine)copper(II), struct., X-ray investig. 7-12033
 bromide salt hydrates, H-bonded $(H_2O \cdot Br^-)_\infty$ 7-51738
 ceramic eutectic composites, microstruct. and mech. props. 7-64991
 chain configs. in MX_5 cpds. with vertex sharing octahedra (German) 7-44460
 cordierite, cryst. struct. refinement and thermal expansion, 100-550K 7-6609
 ferrichromites, coordination and oxidation states, XPS and XANES studies 7-63583
 fluorites, superlattice structs. 7-44485
 graphite, pyrolytic, highly oriented, intercalation reaction with K vapour, neutron diff. study 7-1999
 graphite intercalated with Br, struct. and phase transitions, review 7-52041
 graphite intercalation cpd., stage transformation, stochastic model 7-21433
 graphite intercalation cpds., staging, struct., dynamical and magnetic props., review 7-1966
 graphite- $AlCl_3$ intercalation cpd., phases and phase transform., X-ray crystallography (French) 7-44783
 graphite-Fe intercalation cpd., atomic structure, EXAFS studies 7-12011
 graphite- HNO_3 intercalation cpd., $C_{20}HNO_3$, low-temp. struct. 7-51721
 Group VII hydrides, high-press. cryst. struct. 7-21183
 heavy metal phosphates, IR spectrosc. investig. (German) 7-53299
 HfRuSi, equiatomic ternary silicides, superconductivity, rel. to cryst. struct. 7-6607
 hollandites, modelling tunnel-cation displacements using struct.-energy calcs. 7-32374
 ice Ih, X-ray powder spectrum, temp. depend. simulation, Metropolis Monte Carlo sampling 7-16510
 icosahedral boron-rich solids 7-63537
 II-V semiconds., cryst. growth, characterisation and appls., review 7-26685
 II-VI solid solutions with wurtzite structure 7-32348
 inorganic layered cpds., reactivity, conf., New York, NY, USA (Apr. 1986) 7-41003
 ion implanted layers, anal. by X-ray diffraction (Chinese) 7-51801
 kaersutite, cation distrib. and proton location, neutron diff. studies 7-63569
 kaolin-mullite, charactn. of spinel phase formed in thermal sequence 7-37937
 layer crystals dynamics, long wavelength vibrs., factor group anal. 7-58424
 lunar sample 76535, coarse-grained granulitic troctolite, crystal struct. refinement 7-55505
 monazite-type cpds., pentagonal interpenetrating tetrahedral polyhedron nine-coordination geometry 7-1982
 noncentrosymmetric laser crystals, struct. and props. study review 7-62709
 nontronite, effects of shock and thermal alteration on physical props., and implications for Martian surfaces 7-55024
 octahaloaluminates(III) anions, struct. and bonding 7-16508
 oxides, $AM_2O_9(M_2O_4)_n$, derived from the rutile structure by chemical twinning, structural evolution and stability 7-16757
 oxides, near edge struct., local geometry and cation type effects 7-63576

crystal atomic structure of inorganic compounds continued

- oxides, tunnel structure, mixed framework of octahedra and tetrahedra 7-1997
 oxidic actinide cpds., systematic props., oxidation states, fluorite lattice and thermodynamic props., review 7-12013
 paragonite mica, characteristic beam damage in TEM images 7-12159
 perovskite-like ferroelectrics, optical and electrophysical props. 7-3002
 pyrope ($Mg_3Al_2Si_2O_{12}$), melting up to 10 GPa rel. to press.-induced struct. change in pyrope melt 7-8936
 quartz, structural EXAFS study 7-64762
 rare earth cpds., $RSO_4(BO_3)_4$, (R=Ce,Pr,Nd,Sm), preparation, struct. and props. 7-1968
 rare earth hydrides, cryst. and mag. structs., superstruct. form. 7-33148
 rare earth ternary carbides, struct. 7-46423
 rare earth-transition metal-nonmetal ternary phase struct., crystallochem. anal. (French) 7-58234
 silicate phases, $Cs_2MSi_2O_{12}$, M=Be, Mg, Fe-Ni, Zn, Cd, with pollucite struct., cryst. struct., X-ray powder diff. 7-32409
 silicate phases, $Rb_2MSi_2O_{12}$, M=Mg, Fe, (Co, Zn), with pollucite struct., cryst. struct., X-ray powder diff. 7-32409
 stellerite, cryst. struct., X-ray diff. refinement 7-12007
 symmetry of zone-axis patterns in reflection high-energy electron diffraction 7-16373
 ternary material superconductivity, struct. characts. (French) 7-2777
 tetrahedral anion complexes in structures, relation between tetrahedron connections and comp. 7-44457
 transition metal borides, AlB_2 type, electronic struct. study, heats of formation anal., HMO calcs. 7-25409
 transition metal chalcogenides, ternary and quaternary, struct. and substitutional chem. 7-32384
 transition metal phosphorous trisulphides, electronic, structural and mag. props., intercalation cpds. and chemical props. 7-44499
 transition metal silicide form. by ion implantation in Si, RBS and X-ray diff. studies 7-16656
 transition metal sulphides and selenides, metal-rich, high temp. prep. and struct. props. 7-33617
 transparent ferroelectric ceramics, comp. struct. and props. characts. anal. 7-7647
 transparent ferroelectric ceramics, cryst. chem. and struct. props. and modifications 7-6590
 tris(tetrahydroborato)titanium(II)-dimethoxyethane, cryst., X-ray structural investig. 7-51730
 zeolite theta-1, structural TEM studies 7-16534
 $[Ag_6Ge_2P_{12}]Ge(Si)_6$, bonding relationships and electronic struct. calcs. 7-16941
 $[Ag_6Sn_2P_{12}]Ge(Si)_6$, bonding relationships and electronic struct. calcs. 7-16941
 $[Ba_2Cs_2]([Ti_2Al]_{2x+y}^{3+} Ti_{3-2x-y}^{4+}) O_{16}$ hollandites; structural chemistry 7-51726
 AgBr_{1-x}I_x rock-salt solid solns., local struct., X-ray studies 7-63586
 Ag_{1/2}In_{1/2}PS₃ lamellar cpd., cryst. struct. refinement studies 7-58235
 Ag₃NbSe₂ intercalation cpds., crystal structures and staging 7-12023
 AgO, tetragonal, struct. and mag. props. 7-32399
 Ag₂P₂I₂ solid electrolyte, prep., props. and cryst. struct. 7-32396
 Ag₂P₂O₇, high-press. polymorph, characterisation 7-1991
 Ag₂Pb₄Nb₁₀O₃₀, ferroelectric with tetragonal W-bronze struct., first-order transition 7-39048
 Ag_{0.5}V_{0.5}PS₃, struct., metal ordering and mag. props. 7-16517
 Al₁(Al_{1-x}Si_{2-2x})O_{10-x}, mullite, cryst. struct., X-ray diff. data refinement 7-55030
 AlCl₃, layer struct., IR vibr. spectra 7-13151
 AlN corrosion protective coating for TbFe magneto-optical media 7-53953
 γ -Al₂O₃ small particles, HREM, single cryst. struct. anal. 7-1824
 Al(OH)₃ aggregate fractal structs., X-ray scatt. functions 7-32381
 AlPO₄, berlinite, high-temp. X-ray diff. studies 7-12015
 Al₂P₂O₈, synthesis and struct. 7-1969
 AlPO₄·1.5 H₂O, crystal struct., X-ray⁴ studies 7-12003
 As₂Se₃, cryst. struct., X-ray meas., MULTAN anal. 7-2000
 As₂Se₃, crystalline, electronic and geometric struct., ab initio total-energy calcs. 7-12607
 As₂Te₃, metastable state, rhombohedral struct. study (French) 7-44496
 As₂V₄O₁₃, cryst. struct., X-ray diff. study 7-26702
 BN, wurtzite-type and zincblende-type, struct. changes by shock treatments 7-22676
 B(OH)₃, electron density, X-ray diff. determ. at 105 K, ab initio calcs. 7-44458
 Ba₂Al₂Ti_{8-2x}O₁₆, with K, Rb and Cs substitution, cryst. struct., neutron diff. study 7-63563
 BaBr₂H₂O, cryst. struct., comparative study with isotypic halides, bifurcated H bonds 7-63543
 BaCl₂H₂O, cryst. struct., comparative study with isotypic halides, bifurcated H bonds 7-63543
 BaCo₂Fe₁₆O₂₇, W-type hexagonal ferrite, cryst. struct. and Co location 7-6605
 Ba(Cr,Si)O₄, barite struct. type hashemite, cryst. struct. determ. 7-32375
 BaCs₄(PO₃)₆, cryst. struct. determ. 7-1954
 α -Ba₂Cu₂F₁₄, crystalline structure (French) 7-26730
 Ba₂Fe₂²⁺Fe₁₂²⁺O₂₂ hexagonal ferrite, hydrothermal synthesis, elec., magnetic and structural characterisation 7-45637
 Ba_{1.06}Fe_{10.92}Mn_{1.02}O₁₉ and Ba_{1.03}Fe_{11.97}O₁₉, single crystals, white synchrotron radiation topography 7-6606
 BaFe₂O₉ hexaferrite, cryst. struct. formation and transformations 7-44489
 BaFe₂S₄ and Ba₁₃(Fe₂S₄)₁₂, vernier struct. series, high resolution electron microscope study 7-6603
 Ba_{0.65}Ga_{10.8}O_{16.84}, cryst. struct., single cryst. X-ray reflection studies 7-6608
 Ba₉Ge₂₃O₅₃(OH)₄, high press. phase, cryst. struct., X-ray diff. study 7-32412
 BaI₂H₂O, cryst. struct., comparative study with isotypic halides, bifurcated H bonds 7-63543
 BaLaFeO₄, prep. and characterisation 7-1987
 Ba(Li_{0.25}Sb_{0.75})O₃, cubic perovskite, prep. and struct. 7-63589
 BaMnF₄, incommensurate modulated phase, struct. study 7-1993
 BaMn_{1-x}Ta(Zn)_xO₃ phase struct. and transforms., high resolution electron microscopy obs. 7-58237
 Ba(NO₂)₂, cryst. struct., X-ray diff. study 7-32411
 Ba₂NaNb₂O₁₂, atom sublattices, selective high resolution electron microscopy 7-6486
 Ba(Na_{0.25}Sb_{0.75})O₃, cubic perovskite, prep. and struct. 7-63589

crystal atomic structure of inorganic compounds continued

- Ba₂Ni₂Se₃O₁₅, metastable, cryst. struct., X-ray diffr. study (*German*) 7-16514
- BaO-La₂O₃-Nd₂O₃-Al₂O₃ systems, synthesis, characterisation and spectroscopic investigations of mixed hexa-aluminates 7-63827
- BaO-RuO₂-Fe₂O₃ system, equilibria description 7-65340
- Ba₃(PO₃)₃OH, synthetic, cryst. struct. determ. 7-21173
- Ba₃(P₃O₆)₂·4H₂O, cryst. struct. 7-6610
- BaPb β(II)-alumina, superstructure, high resolution electron microscopy study 7-12021
- BaPb_{1-x}Bi_xO₃ soln.-grown single crystals, crystallographic symmetries, effect on supercond. props. 7-37916
- BaPb_{1-x}Bi_xO₃, supercond., struct. and elec. props. 7-58247
- Ba_{0.73}Fe_{0.27}F_{2.27} nonstoichiometric phase struct., neutron diffr. study 7-63587
- Ba₂Sn₂Mn(Ni)(Co)Fe_{10-x}Ga_xO₂₂ hexagonal ferrites, cryst. and magnetic struct. studies 7-44474
- Ba_{0.1}Sr_{1.1}Ca_{0.8}Fe₁₂O₁₉-La₂O₃, hexagonal ferrites, influence of electric field on struct. and props., Mossbauer study 7-7616
- Ba_{0.4}Sr_{0.4}Ca_{0.2}Fe₁₂O₁₉, hexagonal ferrites, influence of electric field on struct. and props., Mossbauer study 7-7616
- BaTiO₃, electronic struct., special features (*Russian*) 7-45146
- BaTi_{2-x}Sn_xFe₄O₁₁, crystal structures and mag. props. 7-12024
- BaTi_{1-x}Zr_xO₁₂, synthesis, stability, cryst. chem. 7-53681
- BaVS₃, low temp. phase transitions, powder neutron diffr. 7-38181
- Be₁₃ and Be₃₅, stability and struct., binding energy, ionisation pot. 7-11988
- BeAlSiO₄OH, euclase, high press. cryst. struct. and compressibilities 7-16505
- Bi oxides, small distortions, EXAFS transmission studies 7-63580
- Bi-O, structural types, influence of Bi³⁺ lone pair electrons 7-1998
- Bi₂Ge₂O₁₂ single cryst. growth, characterisation and appls. 7-33550
- Bi₂(MoO₄)₃, Czochralski growth, monoclinic unit cell (*Korean*) 7-27890
- Bi₃₈Mo₇O₇₈, cryst. struct. characterisation 7-1988
- BiOBr, cryst. struct. refinement 7-1964
- Bi₁₂Si(Ge)O₂₀ crystals, sillenite struct., dielec., elastic and piezoelec. props. calcs. 7-51714
- Bi₁₃V₅TiO₃₄, layered cpd., crystal-chemical and dielectric props. 7-6595
- BiX₂-GaX₄ complex; X=Cl, Br; struct. Raman spectra study 7-46020
- C₂S₂O₂F fibre intercalation cpds., enhanced elec. cond. 7-33927
- Ca₂ErF₇ fluorites, superlattice struct. 7-44485
- CaF₂Er³⁺, H⁻(D⁻), IR excitation and absorpt. spectra anal. of sites 7-53306
- Ca₅(PO₄)₅, struct., spin dynamics, NMR study 7-59124
- CaFeO₇, crystal struct. (*French*) 7-16519
- Ca(HSeO₃)₂·H₂O, cryst. struct., IR spectra, thermal behaviour 7-44479
- Ca₂(HSeO₃)₂(Se₂O₅), cryst. struct., IR spectra, thermal behaviour 7-44479
- Ca_{2-x}Nd_xGa_{2-x}Si_{1-x}O₇, Ga gehlenite, cryst. struct. and optical props. 7-16525
- CaO-ZrO₂, defect struct., EXAFS studies 7-63608
- Ca_{2-x}P_{1-x}Cl_{1+x} and Ca₃PCl₃, prep., crystal struct., thermal behaviour (*German*) 7-26717
- CaSiO₃, perovskite type, cryst. struct., lattice dynamics and eqn. of state 7-58248
- CaSiO₃, wollastonite-2M, cryst. struct. 7-6612
- Ca(SiO₂)_x, cryst. struct., vibr. spectra, force consts., Si-O bond charact. 7-37932
- Ca₂SiO₄, β to α' to β transition, modulated struct. 7-16724
- Ca₂Ti₂O₆, pyrolysis product of CaO-TiO₂ system, cryst. struct., X-ray powder diffr. data 7-32394
- Ca(UO₂)₂(SiO₃OH)₂·5H₂O, β-uranophane, refined cryst. struct., thermal anal., IR spectra 7-55031
- Ca₁₇Yb₁₀F₆₄ fluorites, superlattice struct. 7-44485
- Cd complex, trans-bis(isothiocyanato)-tetrakis-4-methylpyridinecadmium (II), inclusion cpd., cryst. struct. 7-12031
- (CdBi)(M_{1/2}Sb_{3/2})O₇, (M=Cr, Ga, V, Mn, Fe, Rh, Sc, In), pyrochlores, struct. and characterisation 7-1986
- Cd(BrO₃)₂ · 2H₂O(D₂O), H bonding, crystal struct., ¹H and ²D NMR anal. 7-22156
- CdCl₂, cryst. struct., temp. var., determ. from CdCl₂:Mn²⁺ EPR data 7-32382
- Cd(Cu_{1-x}Al_x)₂, mag. and cryst. props. 7-27506
- Cd(Cu_{1-x}Ni_x)₂, mag. and cryst. props. 7-27506
- Cd(NO₂)₂·2H₂O, cryst. struct. 7-58220
- Cd(NO₂)₂·2KNO₃, cryst. struct. 7-58220
- CdO-Bi₂O₃, crystallographic state of CdO lattice during sintering with Bi₂O₃ addition 7-37944
- CdP₂, crystal structures and microphases, devil's staircase 7-11982
- CeB₆, cryst. struct. determ., defect content 7-58245
- Ce_{1-x}Bi_xO₄F_{3-2x} solid solns., O substitution, influence on struct. and elec. props. (*French*) 7-12019
- Ce₂Co₄P₁₂, synthesis, cryst. struct., X-ray diffr. study 7-32387
- CeCo_{1-x}Si_x, cryst. struct., homogeneity range, X-ray diffr., electron probe anal. 7-37939
- CeLiGe₂, isostructural cpds., crystal structure (*Ukrainian*) 7-12009
- CeMn(Fe)Si₂, struct. and mag. props. studies (*French*) 7-37950
- Ce₂Mo₆S₈, crystal growth and struct., susceptibility and transport props. 7-64889
- CeNi_{5-x}Fe_x, mag. and cryst. props., effect of H absorpt. 7-33168
- CeNi_{5-x}Mn_x, mag. and cryst. props., effect of H absorpt. 7-33168
- CeSe₂O₆, cryst. struct., X-ray diffr. study (*French*) 7-26706
- Co alloys, 1D disordered structural states, form., quenching, X-ray diffr. study 7-44784
- CoGaInS₄ cpd. with FeGa₂S₄ struct., prep. and characts (*German*) 7-1984
- CoGaInS₄ layer cpds., struct. and mag. props., XPS studies 7-44498
- Co₂Ge, chemical bond, struct., short range order 7-32350
- Co_{1-x}Rh_x(Ru_x)₂, prep., mag. and crystallographic props. 7-33154
- CoSi₁₀, Mossbauer spectroscopy 7-59126
- Co₂Ta₂S₆, channel structures, 3d metal pairing 7-26719
- Co_{0.46}Ni_{0.54}In₂S₄ layer cpd. mag. props. and ionic distrib., 2D magnetic system models 7-38880
- Co₂Zn_{1-x}In₂S₄ solid soln. layer cpd., site coordination and short range magnetic order, XPS anal. 7-26724
- Cr Lu₄S₇, synthesis, physicochemical props. 7-44470
- CrCl₃, layer struct., IR vibr. spectra 7-13151
- CrDy₄S₇, synthesis, physicochemical props. 7-44470
- CrEr₄S₇, synthesis, physicochemical props. 7-44470
- CrGa_{1.67}S₄ layer cpd. mag. props. and ionic distrib., 2D magnetic system models 7-38880

crystal atomic structure of inorganic compounds continued

- CrGd₄S₇, synthesis, physicochemical props. 7-44470
- CrHo₄S₇, synthesis, physicochemical props. 7-44470
- CrNH₄P₃O₇ and α- and β-CrNH₄HP₃O₁₀, preparation and characts. 7-3161
- CrTb₄S₇, 7-44470
- CrTm₄S₇, synthesis, physicochemical props. 7-44470
- CrYb₄S₇, synthesis, physicochemical props. 7-44470
- Cs₃BiCl₆, cryst. struct., X-ray diffr. study 7-32389
- Cs₃BrN₃, layered struct., X-ray diffr. and Raman spectra study (*German*) 7-26715
- CsCaH₃, ternary hydride, crystal struct. 7-26729
- Cs₃Cr₂X₉ (X=Cl, Br, I), synthesis, struct., mag. props. 7-6601
- CsDSO₄, cryst. struct. and III-III phase transition 7-44484
- Cs₃Fe₂F₉, precise struct. determ. and ferromag. props. anal. 7-1981
- CsH(D)SO₄ struct. and phase transitions, X-ray diffr. studies 7-2170
- CsHSO₄ cryst. struct. IR spectra study 7-63588
- Cs₂H₂V₁₀O₂₈·4H₂O, pseudo-orthorhombic cryst. struct. 7-58222
- Cs₃IN₃, layered struct., X-ray diffr. and Raman spectra study (*German*) 7-26715
- Cs₃K₂ (TeO₅), coordination, cryst. struct., lattice energy (*German*) 7-26714
- CsK₂BiCl₆, cryst. struct., X-ray diffr. study 7-32389
- CsLiCrO₄, ferroelectric phase transition 7-39047
- Cs_{1-x}Lu_xF_{10-x}, cryst. struct., space group, least-squares refinement 7-6604
- CsMCl₃ (M=Cu, Cr), hexagonal Jahn-Teller crystals, struct. phase transitions, face-sharing coupling, ground-state configuration 7-2180
- Cs₃Mn₂NO₃, (M=Zn, Co, Cd), synthesis and cryst. struct. (*French*) 7-32401
- CsMnCl₃ antiferromag. crystals, struct. deform. by exciton self-localisation, luminesc. spectra fine struct. study (*Russian*) 7-27752
- Cs₂Na₁₀(FeO₃)₄ single cryst. prep. and structural characterisation (*German*) 7-37951
- Cs₂Ti_{2-x}O₄ phase struct. and stability, composition depend., X-ray studies 7-58229
- Cs₂V₂O₇, crystals, struct., cathodic reduction from melt, and elec. props. studies 7-58236
- Cs₆Zn₃(MoO₄)₈, cryst. struct. 7-58217
- CsZnPO₄, crystal struct. of three phases 7-1967
- CsZr₂P₃O₁₂, thermal expansion, structural model 7-44858
- Cu complex, bis(formato)bis(isonicotinamide)diaqua copper(II), X-ray structural anal. 7-51727
- Cu complex, CuCl₂-2-phenyl-4,4,5,5-tetramethylimidazoline-1-oxyl-3-oxide, mag. props. 7-51715
- Cu complex, hexakis (1-methyltetrazole) copper II bis(tetrafluoroborate), Cu(II) sites, Jahn-Teller behaviour, ESR spectra anal. 7-21163
- Cu complex, sulphato aquotris(benzotriazole) Cu(II) benzotriazole, cryst. and mol. struct. 7-21181
- Cu-Sb-S cpds., valence bands and semiconducting gaps, nonstoichiometry and phase separation 7-16941
- CuAl₂Ga_{1-x}Se₂, chem. transport reactions, growth and morphology 7-7830
- CuCl π-complexes with hexadiene-1,5 and diallyl ether, cryst. struct. determ. 7-21179
- Cu₂Cl(OH)₃, atacamite, struct. refinement, X-ray diffr. study 7-32371
- Cu₃CO_{3-x}O₄, cationic distribution and mag. props. 7-26726
- CuCrO₄, cryst. struct. refinement from single-cryst. data 7-58211
- Cu₂Cr₂Sn_{2-2x}S₄ spinels, Cu-Cu distances, EXAFS studies 7-63585
- CuGa_{1-x}In_xSe₂ mixed chalcopyrite local struct., K-edge EXAFS meas. 7-63574
- CuGaSe₂(1-x)Te_{2x} solid solns., prep. and characteris. 7-21169
- CuInS₂ films, RF sputtering, struct. and elec. props. 7-3169
- Cu_{0.26}Mn_{0.87}PS₃, crystalline lamellar cpds. EXAFS studies of disorder 7-59295
- Cu₄Mo₅O₁₇, synthesis and cryst. struct. 7-32398
- Cu(NH₃)₄(MnO₄)₂, cryst. struct. determ. 7-1959
- Cu₂NbSe₂ intercalation cpds., crystal structures and staging 7-12023
- CuNi_{0.5}Ti_{0.5}O₂, crystal structure determ. 7-26728
- Cu₂O, use of dynamic electron scatt. for studying O atom position 7-44501
- Cu₄OCl₆(C₆H₅)₃PO₄·0.70CH₃NO₂ crystals, anharmonic atomic thermal vibrs. and pots. X-ray diffr. struct. study 7-63762
- Cu₂P₃I₂, solid electrolyte, prep., props. and cryst. struct. 7-32396
- Cu_{1.85}S, digenite, single crystal, structural transitions 7-12259
- CuSeO₃, cryst. struct. of three modifications, X-ray diffr. study (*German*) 7-32410
- CuSeO₃ struct. determ. and refinement, X-ray diffr. study 7-32373
- Cu(SeO₂OH)₂, synthesis and cryst. struct. 7-2004
- Cu_{0.5}Ti_{0.5}(PO₄)₃, Nasicon-type phase, struct. and physical props. 7-45804
- Er-Cu₂V₂O₅, ESR spectra 7-64517
- Er complexes, (tricarbamidotriscetato)erbium(III) monocarbamide, cryst. struct. 7-12029
- Er₃Ir₄Si₁₃, existence and electrical props. (*French*) 7-17008
- Er₃Os₄Si₁₃, existence and electrical props. (*French*) 7-17008
- ErRh₂B₄, body-centred tetragonal, cryst. struct., X-ray diffr. study 7-26704
- Eu complexes, Eu(NO₃)₃(triphenylphosphine oxide)₃ systems, cryst. and mol. struct. 7-51723
- Eu-Bi-S, synthesis and props. 7-44471
- Eu-Bi-Se(Te), synthesis and props. 7-44471
- Eu-Sb-S, synthesis and props. 7-44471
- Eu-Sb-Se(Te), synthesis and props. 7-44471
- Eu(II)-β"-alumina, luminescence, order-disorder effects, optical, structural and ion transport props. 7-46114
- Eu₂PCl(Br)(I), prep., mag. props. and cryst. struct. (*German*) 7-32379
- Eu₂RuO₇, crystal struct. determ. 7-16520
- Eu₂TiS₂, mixed valence intercalation cpd., low-temp. synthesis and mag. props. 7-17779
- Fe complex Fe(II) trans-bis(dimethyl-glyoximate)bis(dibutyl phenylarsine) cryst. and mol. struct. 7-51711
- Fe-Ge-Te, compound formation, microstructure, X-ray diffraction, dilatometry studies 7-7980
- Fe-O system, struct. transitions, cryst. struct. formation 7-58459
- FeCl₃ layer struct., IR vibr. spectra 7-13151
- FeCl₃MoO₄ layered compound, struct. and mag. props., Mossbauer effect, mag. suscept., and neutron diffr. studies 7-58981
- FeCo oxides, oxidation state and site symmetry, EXAFS and XANES studies 7-63584
- FeCoCr₂S₈, crystallographic and mag. props., Mossbauer study (*Korean*) 7-33310

crystal atomic structure of inorganic compounds continued

- FeF₃, pyrochlore struct., soft chemistry synthesis and thermal transitions 7-17396
 (Fe³⁺_{2-2x}Fe²⁺_{1+x}Ti⁴⁺_x)O₄²⁻, submicron synthetic titanomagnetites, oxidation products, IR spectra 7-27716
 x-FeGa₂S₄ layer cpd. mag. props. and ionic distrib., 2D magnetic system models 7-38880
 Fe₂Ge, chemical bond, struct., short range order 7-32350
 Fe(II) tetraphenylporphyrin bis(tetrahydrofuran), electronic ground state, electron density meas. 7-51716
 Fe_{3-x}M_{3-x}O₄ (M=Ti, Cr, Mn, Al), substituted magnetite, reactivity in O₂, relation with cation distrib. (French) 7-46829
 Fe₂Mn_{1-x}S, high temp. metal-nonmetal transition 7-7117
 FeNb₂O₆, cryst. struct., determ. by neutron diff. 7-6599
 (Fe_{1-x}Ni_x)TiH₃, critical study of β-region 7-27634
 Fe_{1-x}O, double electron exchange, Mossbauer spectroscopy 7-17168
 Fe₃O₄, magnetite, cryst. struct. under press. 7-16524
 FeOOH, poorly-ordered precursors, local struct., EXAFS studies 7-63577
 Fe₂SiO₄, spinels, cryst. struct. as function of temp. and heating duration 7-16522
 Fe₂SiO₄-Zn₂SiO₄, limited solid soln., cation ordering 7-51709
 Fe₂Ta₂O₇, channel structs., 3d metal pairing 7-26719
 Fe₃(1-δ)O₄, magnetite, synthesis, crystal growth and characterisation 7-2647
 GaAs, electron density distrib., X-ray refl. anal. 7-44497
 GaAs, sublattices direct resolution and identification by high-resolution TEM 7-37813
 GaAs, X-ray diff., anomalous dispersion effects, thermal vibr. and bonding charges 7-44733
 GaAs:Te, struct. environment of dopant, study by EXAFS in fluorescence mode. 7-59300
 GaAsSb_{1-y}, relaxed zinc-blende lattice, EXAFS study 7-64759
 GaF₂Mn cubic cryst., local lattice instability near impurity, ESR study 7-53123
 α-Ga₄GeO₈, tunnel structures 7-44480
 Ga₄Ge₃O₁₂, tunnel structures 7-44480
 Ga_{1-x}In_xAs, heterostruct., local composition, CBED anal. 7-16529
 Ga₂O₃-CaO system, comp., structural props., X-ray diff. study 7-37942
 GaP, sublattices direct resolution and identification by high-resolution TEM 7-37813
 Ga₂S₃-MnS phase diagrams, metastable phases, thermal and structural features 7-38165
 GaSb high press. phase, β-Sn-type struct., pseudopot. perturbation calcs. 7-51938
 GaSb_{1-x}As_x 7-16529
 Ga₂Te₂Se₃ solid solns., cryst. struct., X-ray powder diff. studies 7-16526
 Ga₉Tl₃O₁₃, crystal struct. investig. (French) 7-12000
 Gd oxychlorides, phase equilib., X-ray diff. and spectro-luminesc. anal. 7-46143
 Gd-Cr-C system, phase equilib., struct. 7-46423
 GdFe₄B₄, cryst. struct. and interatomic distances 7-32380
 Gd₃Sc₂Ga₃O₁₂, garnets 7-21045
 Gd_{1-x}Sr_xCrO₃, coordination number and elec. cond., EXAFS and XANES studies 7-64785
 GeTe-GeSe₂, polythermal section of Ge-Te-Se, effects of deviations from stoichiometry 7-7977
 GeTe-PbSe, phase transformations, cation-anion substitution, electrophysical props. 7-7978
 H₃PO₄, n=1-3, tetrahedra distortion depend. on H bond length. 7-63542
 HfGeO₄, cryst. struct. determ. 7-26718
 HfOsSi, equiatomic ternary silicides, superconductivity, rel. to cryst. struct. 7-6607
 HfRhSi, equiatomic ternary silicides, superconductivity, rel. to cryst. struct. 7-6607
 Hg chalcogenides of form Hg₃X₂Y₂, phys. characts. review (Russian) 7-53254
 Hg complex, with cis, syn, cis-dicyclohexyl-18-crown-6, cryst. struct. study 7-51713
 Hg_{1-x}Cd_xTe_{1-x}Se_x, existence region of wurtzite struct. 7-53709
 HgK₂P₂O₇, cryst. struct. determ. 7-1955
 Hg(NH₄)₂Na₂(P₃O₉)₂, cryst. struct. determ. 7-1956
 Ho₃Ir₂Si₁₃, existence and electrical props. (French) 7-17008
 Ho₃Os₂Si₁₃, existence and electrical props. (French) 7-17008
 InGaAsP local struct., EXAFS and near-edge struct. studies 7-64006
 In₂Mo₂Se₃, insertion cpd., synthesis and props. 7-32407
 InP, sublattices direct resolution and identification by high-resolution TEM 7-37813
 In₁₈Sn₃S₄, cryst. struct. determ. (French) 7-58214
 Ir₈ complex, (Ir(CO)₂4,4',5,5'-tetracyano-2,2'-bimidazole)⁻, anisotropic conductor, phys. props. 7-7242
 Ir₂Se₉, synthesis, powder diff. characterisation 7-64956
 K(AlSi₂O₆), synthetic pollucite, high temp. X-ray diff. study 7-21176
 K_{1.50}Al_{1.50}I_{6.50}O₁₆ hollandite-type struct. refinement, cation substitution effects study 7-58232
 K(AuBr₄)₂H₂O, cryst. struct. determ. 7-1963
 K₂Bi(MoO₄)₄, palmierite-type cpd., cryst. struct. determ. 7-21174
 (KBr)_{1-x}(KCN)_x, mixed crystals, random strains and struct. 7-32405
 K₂C₈D₂O intercalation cpd., X-ray diff., NMR, EPR and gas phase mass spectra anal. 7-46843
 K₂C₂O₄H₂O, deform. electron density study at 100 K 7-63565
 KCeF₄, gagarinite-type superstruct., X-ray diff. studies (French) 7-58231
 K₂Ce(SO₄)₃H₂O, cryst. struct. calcs. 7-51731
 K₂(WO₄)₂, vibr. characts. of O bonds, IR and Raman spectra 7-32587
 K₂(Fe(CN)₅NO).1.25 H₂O, DTA-TGA, cryst. and mol. struct. and vibr. props. 7-6597
 K₂HfF₆ (x=2.5, 3), homologous anions, crystal struct. anal. 7-26711
 K₄(Ga₂Ga_{2-x}Ti_{16-x}O₅₆), synthesis of new cpd. by flux method 7-27883
 K₄ graphite intercalation cpd., struct. and electronic props. 7-27234
 KH₂(IO₃)₃, proton cond. and cryst. struct., X-ray and neutron diff. studies 7-12026
 K₂H(IO₃)₂Cl, cryst. struct., neutron diff. studies (Chinese) 7-12005
 KHSeO₄ single crystal, polarised IR spectra anal., rel. to cryst. struct. 7-46047
 K₂Hg(CN)₄, cryst. struct. and phase transition 7-26933
 K₂LiFe₂S₂Cl₂, djerfisherite, electrochemically synthesised, cryst. struct., neutron diff. study 7-58224
 K₃Li₃TeO₆, prep., cryst. struct., Madelung lattice energy calc. (German) 7-16515
 K₂Mn₂(MoO₄)₃, synthesis and cryst. struct. determ. 7-44482

crystal atomic structure of inorganic compounds continued

- KMn₂(PO₄)₃ synthetic orthophosphate, cryst. struct., homeotypy with KFe₂(PO₄)₃ 7-21177
 K₂NaHf₅Fe₅³⁺F₆, synthetic Fe³⁺ elpasolite, cryst. struct. 7-51712
 K₂Na₂TeO₆, cryst. struct., X-ray diff., Madelung part of lattice energy (German) 7-37941
 K₂Nd(MoO₄)₄, palmierite-type cpd., cryst. struct. determ. 7-21174
 KPbBr₃H₂O, synthesis, cryst. struct., X-ray diff. study (German) 7-37940
 KPbLaF₆ solid soln. twinned cryst. struct., lattice parameters and point group, X-ray diff. studies (French) 7-58231
 K₂Pb₂Nb₁₀O₃₀, ferroelectric with tetragonal W-bronze struct., first-order transition 7-39048
 K₂Pb₂Nb₁₀O₃₀-K₆Li₂Nb₁₀O₃₀ solid soln., density and struct. studies 7-1973
 K₂SbPO₆, solid-state reaction prep. and cryst. struct. determ., X-ray diff. study 7-1980
 K₂Sb₂P₂O₂₀, 3D framework 7-44492
 K₂SeO₄, β to α' to β transition, modulated struct. 7-16724
 KT₂Nb₂O₇, mixed-valence rutile structures 7-27329
 KTaWO₆H₂O, pyrochlore-type cpd., characterisation 7-1989
 K₂Ti₂O₆, layered, synthesis and struct. 7-32406
 KTiOAsO₄, struct. and nonlinear optical props. studies (French) 7-37948
 KTiOPO₄, IR spectra 7-46025
 KZr₂P₂O₁₂, thermal expansion, structural model 7-44858
 K[(OH)₂PO₂], irradiated single crystal struct. study, ESR and ENDOR anal. 7-38962
 La complexes, (hexaquadecapropionato)tetralanthanum(III) dithiocarbamate dihydrate, cryst. struct. 7-12030
 LaB₆, cryst. struct. determ., defect content 7-58245
 LaCO₃OH polymorphs, prep., cryst. data, X-ray powder diff., IR spectra, TGA curves 7-32392
 La₃₀Ce₆Li₂₄O₆₉, Li₂₄Ce₁₂Li₂₄O₇₂ and La₃₀Th₆Li₂₄O₆₉, cubic and tetragonal phases, structures 7-26725
 La₂Co₂P₁₂, synthesis, cryst. struct., X-ray diff. study 7-32387
 LaMn(Fe)Si₂, struct. and mag. props. studies (French) 7-37950
 La₂Mo₂O₇, quasi-2D single cryst. struct. and electronic props. studies 7-58238
 LaNi₅-H₂ system, γ-phase hydride, in situ X-ray diffractometry study 7-26712
 LaNiAl₁₁O₁₉, magnetoplumbite type cpd., synthesis, cryst. growth and struct., electronic spectra 7-44476
 La₂NiO₄, struct. characterisation of orthorhombic form 7-1990
 LaOB, single cryst. growth, struct., X-ray diff. study 7-44431
 La(OH)₂Br.nH₂O, prep. and characterisation 7-12018
 La₂S₃-La₂O₃-Ga₂O₃-Ga₂S₃ glassy and crystalline chalcogenides, EXAFS structural study 7-63481
 La_{1-x}Sr_xCoO₃, local struct., EXAFS and XANES studies 7-63582
 La₂TiMo₆ (M=Fe, Ni, Cu, Zn), synthesis, struct. and elec. props. 7-2619
 LaZnFe₁₁O₁₉, cation distribution and random spin canting 7-37945
 Li halides, thermal parameters, cryst. struct. determ. 7-12020
 Li₂BN₂, synthesis, polymorph struct., ionic cond. meas. 7-32388
 LiBeH₃ and Li₂BeH₄, cryst. struct. and IR absorption 7-51720
 Li_{1-x-y}Cu_xMnRuO₄ system, prep. and characterisation (German) 7-26721
 LiFeClMoO₄, synthesis, struct. and low temp. magnetism 7-21172
 Li₂Fe₂(MoO₄)₃, insertion cpd., struct., from neutron powder diff. data 7-1985
 LiFeP₂O₇, cryst. synthesis, at. struct., DTA, X-ray diff. study 7-26708
 Li₂Fe₂(PO₄)₃, microtwinning, X-ray struct. investig. 7-44567
 Li_{1-x}H₂NbO₃, struct. and props. 7-12017
 LiIO₃ crystals, iron-group doped, impurity centres, circular dichroism studies 7-45976
 LiInP₂O₇, synthesis and cryst. struct. (French) 7-58223
 LiKSO₄ crystals, low temp. phase transitions, Raman spectra and dielec. const. meas. 7-26943
 Li_{2+x}(Li_{1-x}Mg_{1-x}Sn₃)O₈, ramsdellite type cpds., ionic conductivity and cryst. chemistry 7-32708
 Li₂Mg_{1-x}Fe_{2-x}Sn_{3-x}O₈, ramsdellite type cpds., ionic conductivity and cryst. chemistry 7-32708
 Li_{0.6}Mg_{0.25}Ti₂O₇, crystal struct. refinement 7-44467
 Li₂Mg_{1.5-x}VO₄ solid soln. phase, synthesis, stoichiometry and struct. 7-21168
 Li_{1-x}MnRu_{1-x}Ti_xO₄ system, characterisation of different phases (German) 7-26971
 Li_{1+y}Mn_{1+y}SGeRu_{1-x}O₄, Li insertion cpd., prep. and characterisation (German) 7-26720
 LiMoO₄, synthesis and struct., orthogonal nonintersecting octahedral cluster chains 7-32386
 Li_{0.33}MoO₃, stoichiometric triclinic bronze, cryst. struct. 7-6600
 Li_{0.5}Mo_{0.17} purple bronze, cryst. struct. determ. 7-58239
 Li_{0.9}Mo_{0.17}, superconductivity and CDW 7-45541
 LiMoS₃, synthesis, electrochemistry and struct. 7-33619
 Li₂Mo₆Se_{6-y}I_y, Li electrochemical insertion, struct. studies 7-37947
 Li_{0.5}Mo_{0.5}-W_{0.5}O₁₇, W substitutional effects on elec. resistivity and transport props. 7-45260
 Li₂(NH₄)₂(NH₄)₂Ti₂(x+y)- intercalation cpd., NH₃ oxidation, charge compensation 7-32354
 (Li_{1-x}Na_x(K)_{0.5}Mo_{0.17}), anomalous transport props., resist., mag. suscept., sp. ht., struct. and supercond. transition temp. meas. 7-21913
 Li₂NaK(SO₄)₂, cryst. struct. determ. 7-58212
 Li₂Na₂TiS₂ intercalated dichalcogenides, struct., electrochem. and thermodynamic props. studies 7-21167
 LiNbGeO₅, luminesc. and cryst. struct. 7-32403
 LiNb₂O₆-TiO₂ system, rutile structure solid-solution phase, Ti diffusion into LiNbO₃ 7-44473
 Li₂SO₄H₂O, supercooled melts, cryst. and mol. struct., thermal stability 7-21170
 Li₂Se₂(PO₄)₃, cryst. struct. at 573K, X-ray diff. studies 7-44487
 Li₂Se₂(PO₄)₃, microtwinning, X-ray struct. investig. 7-44567
 Li₂Se₂(PO₄)₃, monoclinic modification, cryst. struct. studies 7-44488
 Li₂SeO₄ single crystal, optic modes, room temp. Raman spectra study 7-53345
 LiV₂O₅, Li inserted, struct., neutron and X-ray powder diff. anal. 7-32391
 LiW₃O₉F, ordered O-F distrib., NMR, Raman spectra, electrostatic energy, site pot. calcs. (French) 7-32390
 LiZnF₃ prep. and X-ray and NMR structural study 7-37953
 LiZr₃P₃O₁₂, thermal expansion, structural model 7-44858

crystal atomic structure of inorganic compounds continued

- LuCo_{1-x}Si₂, cryst. struct., homogeneity range, X-ray diffr., electron probe anal. 7-37939
- Lu₃Ir₄Si₃, existence and electrical props. (French) 7-17008
- Lu₃Os₄Si₃, existence and electrical props. (French) 7-17008
- MF₂ type fluorides, stability under high pressure (French) 7-63568
- MMF₄ type fluorides, stability under high pressure (French) 7-63568
- MgAl₂O₄ spinel, high press. cryst. chemistry 7-16521
- MgCr₂O₄, cation distribution, temp. depend. normality (Korean) 7-32404
- Mg₇Ga₂GeO₁₂, spinelloid related cpd., cryst. struct., powder X-ray diffr. determ. 7-63564
- MgGa₂O₄-Mg₂GeO₄ system, spinelloid phases charact. 7-37946
- Mg_{0.98}Na_{0.02}Fe₂O₄, spinel struct., EXAFS and XANES studies, humidity sensor appls. 7-64784
- Mg₂NiH₄, struct., thermal and elec. props., rel. to covalent bonding 7-21184
- Mg₂NiH₄, twinning at unit cell level, low temp. phase, electron microscopy study 7-26762
- Mg₃(PO₄)₂·8H₂O, synthetic, and bobierite, cryst. structures 7-32376
- MgSO₄·6H₂O, deform. electron density, X-ray and neutron diffr. studies 7-44459
- MgSiO₃, perovskite type, cryst. struct., lattice dynamics and eqn. of state 7-58248
- MgWO₄·2H₂O, cryst. struct., topotactic dehydration, X-ray powder diffr. study 7-32393
- Mn oxides, oxides, Ni- and Co-containing, structural chemistry, EXAFS studies 7-63578
- Mn-Ni-P, equilib. phase diagram at 1070K, X-ray anal. 7-46429
- MnAl₂(SeO₄)₂ layer cpd. mag. props. and ionic distrib., 2D magnetic system models 7-38880
- MnAs, crystal struct. and mag. props. 7-6592
- MnAs, phase transitions, effect of external press. and chemical substitutions 7-63798
- MnAs_{0.9}P_{0.1}, struct. and mag. props. 7-12948
- Mn₂GeS₄, cryst. struct. refinement (French) 7-32402
- Mn(H₂PO₄)₂·2H₂O, cryst. struct., Patterson synthesis 7-2001
- MnNa(H₂PO₃)₃·H₂O orthorhombic struct., bond lengths and angles, X-ray diffr. study 7-32372
- MnNa₃P₃O₁₀·12H₂O, cryst. struct. determ. 7-58210
- Mn_{1-x}Ni_xAs, structural and magnetic phase diagrams 7-6784
- Mn₂Sb₂O₈, synthesis and cryst. struct., X-ray powder diffr. meas. 7-58240
- Mn₃Si₂Te₆ ferrimag. semicond., cryst. struct., X-ray diffr. study 7-1977
- MnZnFe₂O₄, struct., Mossbauer, X-ray, and mag. meas. 7-1971
- Mo ternary chlorides, MMo₆Cl₁₄, M₂Mo₆Cl₁₄ and M³⁺Mo₆Cl₁₃, structural characterisation 7-44493
- Mo₂As₃, cryst. struct. determ. 7-1979
- MoB₂, crystal struct. determ. 7-26713
- Mo₂C, interaction of C with reduction products of MoO₃ 7-8260
- MoO₄-WO₃, H insertion, struct. and thermodynamics 7-16506
- MoO₂, low-dimensional conductor, cryst. struct. and commensurate-incommensurate transition, X-ray diffr. study 7-58230
- NH₄H₂(IO₃)₃, proton cond. and cryst. struct., X-ray and neutron diffr. studies 7-12026
- (NH₄)_{0.23}H_{0.31}MoO₃, intercalation cpd. struct., enthalpy of reaction 7-46841
- (NH₄)_{0.32}H_{0.16}WO₃, intercalation cpd. struct., enthalpy of reaction 7-46841
- (NH₄)₂·Hf₂(O₄OH)(SO₄)₁₀(H₂O)₇, struct. X-ray diffr. 7-6613
- NH₄Np(OH)₃, cryst. struct. determ. (French) 7-16511
- (NH₄)₂SeCl₄, crystal struct. investig. 7-12001
- (NH₄)₃Sn₃F₁₁, high temperature form, crystal structure (French) 7-26727
- (NH₄)₂FeF₃(HCl)_{0.25}(H₂O)_{0.25}, tunnel-type cryst. struct., single cryst. X-ray diffr. meas. 7-44495
- (NH₄)_{1.84}V₂O₈, intercalation cpd. struct., enthalpy of reaction 7-46841
- (NH₄)₃VO₂F₄, cryst. struct., struct. of VO₂F₃²⁻ ion 7-32400
- (NH₄)₃(ZnCl₂)Cl crystals, electron-density distrib. at 120 K 7-58219
- Na complex, Na₂diglyme, cryst. struct., bond bridging 7-51724
- Na₂Al₂Si₂O₁₀, tetranatrolite, cryst. struct., X-ray diffr. studies 7-44481
- Na₂(AlSiO₄)₆(OH)₂, cryst. struct., powder neutron diffr. study 7-58209
- Na₂(AlSiO₄)₆·nH₂O, dehydration, struct. collapse or expansion 7-17770
- Na₂(AlSiO₄)₆·nH₂O, dehydration, struct. collapse or expansion 7-17770
- Na₂B₄O₇, pyroborax, model for short range order of Na₂O-B₂O₃ glass 7-44391
- NaBrO₃, X-ray birefringence and forbidden reflections 7-33475
- Na₂Ca₂Al₆Si₉O₃₀·8H₂O, mesolite, cryst. struct. X-ray refinement 7-1958
- Na₂Ca₄(Si₆O₁₈), cryst. struct. determ. 7-1957
- NaCl:Cu²⁺, lattice relax. around cuprous ion, EXAFS studies 7-64788
- NaFeClMoO₄, synthesis, struct. and low temp. magnetism 7-21172
- NaH(D)SeO₃, neutron diffr., DMR investigation 7-21178
- Na₁₀(H₂W₁₂O₄₂), cryst. and mol. struct. studies 7-6596
- Na₂Hf₂Ge₂O₁₂, ionic conductor, hydrothermal crystallisation and cryst. struct. 7-37935
- Na₂ZrP₃O₁₂ crystals, X-ray powder diffr. data 7-26722
- (Na_{1-x}Li_x)_{0.9}MoO₃, Na substitutional effects on elec. resistivity and transport props. 7-45260
- NaLi₂Si(Ge)(Ti)O₄ isotopic oxides, cryst. struct. determ. lattice energy calcs. (German) 7-37952
- NaLiYb₂F₈, isotopic cpds., cryst. struct. (French) 7-32397
- NaMn₂ZrP₃O₁₂, Na₂(Ce,Co)ZrP₃O₁₂ and Na₂(La,Co)TiP₃O₁₂, Nasicon analogues, cryst. data 7-12014
- Na_{0.9}MoO₃, superconductivity and CDW 7-45541
- Na₂Mo₂O₄ intercalation cpd., struct., mag. suscept., X-ray diffr. and electrochemical anal. 7-46842
- NaMoO₃F, ordered O-F distrib., NMR, Raman spectra, electrostatic energy, site pot. calcs. (French) 7-32390
- Na₃MoO₃F₃, ferroelastic and ferroelectric behaviour 7-44792
- NaNbO₃-Nb₂O₅-WO₃ system, crystal struct., twinning, furling and anti-phase boundary operations 7-63567
- Na₂Nb(PO₄)₃, struct. evolution by vitreous state formation (French) 7-21164
- NaNi₂OH·H₂O·(MoO₄)₂, H atom location, Rietveld refinement, neutron powder time of flight meas. 7-26707
- Na₂O-Al₂O₃, ¹H, ²⁷Al and ²³Na NMR studies 7-22148
- β-Na₂O-Al₂O₃, struct. at 5K, ²³Na NMR 7-7595
- β'-Na₂O-Al₂O₃, structure at 5K, ²³Na NMR 7-7594
- Na₂O-Nd₂O₃-Al₂O₃ system, struct. of single cryst. with magnetoplumbite struct. 7-6602
- Na_{1.7}P₄W₁₄O₅₀ struct. refinement, single cryst. X-ray anal. study 7-58233

crystal atomic structure of inorganic compounds continued

- Na₂Sc₂(PO₄)₃ cryst. struct., tetrahedra disorder and ion-ion correls. studies 7-26723
- Na₆(TeW₆O₂₄)·22H₂O, crystal struct. investig. 7-12002
- Na₂Ti₃S₂O₇(OH)₂(SiO₄)₄, polymorphous modification of natisite, cryst. struct., X-ray diffr. 7-26709
- Na₂V₂O₅ bronze, struct. and valence, XANES studies 7-63579
- Na₂WO₂F₄, ordered O-F distrib., NMR, Raman spectra, electrostatic energy, site pot. calcs. (French) 7-32390
- Na₅Y₂Si₄O₁₂, twinning, crystal struct. 7-21226
- Na₂Zn(SO₄)₂(H₂O)₂, cryst. struct. determ. 7-1960
- Na₂Zr_{1-x}In_xSi_{2-x}P_{1+x}O₁₂ system, chem. composition, cryst. struct. and ionic cond. (Chinese) 7-12006
- NaZr₂P₃O₁₂, thermal expansion, structural model 7-44858
- Na₃Zr₂Si₂PO₁₂ and Na₃M₂(PO₄)₃, rhombohedral structures, crystallographic 7-32377
- Na₆(H₂L₂V₂O₁₆)·10H₂O, cryst. struct. determ. 7-58213
- NbC₃, ordering behaviour, superstruct. refl. obs. 7-3267
- Nb₂C lower carbide, rhombic modification, X-ray diffr. obs. of cell type and dimens. 7-51725
- Nb₂O₅ and Nb oxide cpds., synthesis of fine particles, struct. studies 7-59212
- NbPO₃, β-form, bronzoite, struct. and stability 7-44478
- Nb₂Pd_{0.74}Cu_{0.22}S₅, reactivity, intercalation structural changes, X-ray diffr. exam. 7-46839
- NbS₂(Se₂)-transition metal intercalation cpds., EXAFS 7-53446
- NbTe₄, incommensurate distortion waves, struct. changes on cooling 7-1996
- NbTe₄, incommensurate state microstruct., electron diffr. pattern obs. 7-6598
- Nd₂Ba₂(Si₄O₁₃), cryst. struct. 7-37934
- Nd₃₀Ce₆Li₂₄O₆₉ and Nd₂₄Ce₁₂Li₂₄O₇₂, cubic and tetragonal phases, structures 7-26725
- Nd₂Co₂P₁₂, synthesis, cryst. struct., X-ray diffr. study 7-32387
- Nd_{2-x}Cu_xRu₂O_{7-y} pyrochlore type phases, elec. and cryst. characts., X-ray fluoresc. anal. (French) 7-45325
- NdCu₃Ru₄Ti_{4-x}O₁₂ and Nd_{2(x+3/3)}Cu₃Ru₄Ti_{4-x}O₁₂, electrical conductivity and crystallographic characterisation (French) 7-17057
- NdFe₂B₄, cryst. struct. and interatomic distances 7-32380
- NdFe(Mn)Si₂, struct. and mag. props. studies (French) 7-37950
- Nd₂MgTiO₆, cryst. struct., Rietveld refinement of neutron powder diffr. data 7-26705
- NdPO₄, cryst. struct. determ. 7-58244
- Nd₂RuO₇, crystal struct. determ. 7-16520
- Ni cobaltite, coordination and oxidation states, XPS and XANES studies 7-63583
- Ni complex, bis (S-ethylthiosemicarbazide) nickel (II) iodide, cryst. and mol. struct., X-ray diffr. study 7-2005
- Ni complex, bis(triphenylphosphine) adduct of Ni(NCS)₂, cryst. struct., X-ray study 7-12025
- Ni complex, nickel(II) acyl hydrazones, X-ray structural anal. 7-51729
- Ni complex, tris(ethylenediamine)ethylenediaminetetraacetic acid nickel(II), X-ray structural anal. 7-51728
- NiAl₂O₄, cation distribution, temp. depend. normality (Korean) 7-32404
- Ni₂Cd_{1-x}Mn_xO₄ spinels, cation distrib., structural transitions and Jahn-Teller distortion 7-58227
- Ni₂Cd_{1-x}PS₃, crystalline lamellar cpds. EXAFS studies of disorder 7-59295
- NiCuNbO₄, cryst. data and conductance investig. 7-38550
- NiFeAlO₄, cation distrib. and canted spin alignment, Mossbauer obs. 7-22169
- Ni₂Ge, chemical bond, struct., short range order 7-32350
- NiO-CuO solid solutions, evidence for long-range cation order, TEM investig. 7-44757
- Ni(OH)₂, EXAFS spectra, vacant cationic site model (French) 7-64783
- Ni₈Pb(P₂O₇)₂, cryst. struct. determ. 7-1970
- Ni₂SiO₄ spinels, cryst. struct. as function of temp. and heating duration 7-16522
- Ni₂Ta₂Se₆, channel structs., 3d metal pairing 7-26719
- Np borides and oxycarbides, synthesis and crystallographic studies (French) 7-17487
- NpO₂CO₃, crystal chemistry, Mossbauer studies 7-17249
- Np(OH)₄, cryst. struct., Mossbauer study (French) 7-16511
- P₂As₂S₃, occupationally disordered cryst. struct. 7-58218
- (PBr₄)₂(MBr₄)⁻¹ complex, M=B, Al, Ga, In, mol. vibr., Raman and IR spectra anal. 7-46021
- PLZT ceramics (Japanese) 7-2981
- (PMo₁₀V₂O₄₀)₅, Keggin struct. 7-51732
- (PMo₉V₃O₄₀)₅, Keggin struct. 7-51732
- Pb₆Ca₄(PO₄)₆(OH)₂, apatite struct., Pb substitution, HREM study 7-16530
- Pb₆Ca₄(Si₂O₇)Cl₂, apatite struct., Pb substitution, HREM study 7-16530
- Pb₂Cr₃F₁₉, nonlinear optic, lattice consts., ferroelec. Curie temp., phase transition obs. at 555K 7-17275
- Pb₄In₂Bi₂Si₃, cryst. struct. determ. 7-1962
- Pb(M_{1/2}Sm_{1/2})O₃, perovskite type antiferroelectrics, (M=Sc, Ho-Lu), X-ray and dielec. characts. 7-7649
- Pb₂(MSb)O_{6.5}, M=Ti, Zr, Sn, Hf, pyrochlores, cryst. data 7-21171
- PbMg_{1/3}Nb_{2/3}O₃, cryst. struct., electrocaloric effect, diffuse phase transition 7-22194
- PbMn₂/3MO₃, perovskite-type cpds., (M=Mo, Te, Re), dielec. and mag. props. 7-7650
- PbO-Nb₂O₅ oxide mixture transparent ferroelec. ceramics, phase form. during solid state reaction 7-6591
- PbO-Nb₂O₅-Sc₂O₃ oxide mixture transparent ferroelec. ceramics, phase form. during solid state reaction 7-6591
- Pb₂P₄O₁₃, chemical prep., crystallographic study (French) 7-6589
- Pb_{1-x}(S,Te_{1-x})₂, solid solution, growth from vapour, region of homogeneity 7-46285
- PbTeO₃, tetragonal phase, cryst. struct., X-ray diffr. study (French) 7-44466
- PbTiO₃, distorted cubic, crystn. and phase transform. 7-39548
- PbUO₄, cryst. struct. X-ray diffr. study 7-44464
- Pb₃UO₆ struct. refinement, neutron powder diffr. study 7-32370
- Pb₃(VO₄)₂, β-γ transition, intermediate modulated struct. 7-2183
- PbWO₄, struct., X-ray, IR absorpt. and Raman spectra 7-37954
- Pb₈F₂Y₂O₁₀, cryst. struct. determ. (French) 7-12016
- Pd₁₃Pd_{0.46}, cryst. struct., neutron powder diffraction investig. 7-32416
- Pr₂Co₂P₁₂, synthesis, cryst. struct., X-ray diffr. study 7-32387
- PrMn(Fe)Si₂, struct. and mag. props. studies (French) 7-37950

crystal atomic structure of inorganic compounds continued

- PrO₂, fluorite prototype struct., interfaces and domain form. study 7-58498
 Pr₂O₁₂, related struct., in HREM study 7-16531
 Pt complex, [Pt(NH₃)₂(OH)₂(C₅H₇N₃O)₂](NO₃)₂·2H₂O, metal stabilised cytosine iminoxo tautomer, form. and geometry 7-26710
 Pt complex, platinum(II) diiodo-L-histidine, cryst. and mol. struct. determ. 7-12032
 Pu borides and oxyhalogenides, synthesis and crystallographic studies (*French*) 7-17487
 RNi₂P₂ type cpds. with ZrFe₂Si₂ type struct. (*Ukrainian*) 7-12010
 Rb(AlSi₂O₆), synthetic leucite, high temp. X-ray diff. study 7-21176
 Rb_{1.47}Al_{1.47}Ti_{0.53}O₁₆, hollandite-type struct. refinement, cation substitution effects study 7-58232
 Rb₄Cu₉Cl₁₃, solid electrolyte, elec. cond. and cryst. struct. 7-2257
 Rb₄Cu₉Cl₁₃, solid electrolyte single crystals, anisotropic elec. cond. meas., structural model 7-52126
 Rb₃Gd(MoO₄)₄, palmierite-type cpd., cryst. struct. determ. 7-21174
 RbI₃, cryst. struct., X-ray diff. study 7-44461
 Rb₂IN₃, layered struct., X-ray diff. and Raman spectra study (*German*) 7-26715
 RbMCl₃, (M=Cu, Cr), hexagonal Jahn-Teller crystals, struct. phase transitions, face-sharing coupling, ground-state configuration 7-2180
 Rb₂Pb₄Nb₁₀O₃₀, ferroelectric with tetragonal W-bronze struct., first-order transition 7-39048
 Rb₂SeO₄, cryst. struct. at room temp. 7-58215
 RbSn₂Br₃, cryst. struct., X-ray determ. 7-21182
 RbV₂O₇ crystals, struct., cathodic reduction from melt, and elec. props. studies 7-58236
 Rb_{0.023}WO₃, crystal growth and struct., SEM and TEM anal. 7-46288
 RbZr₂P₃O₁₂, thermal expansion, structural model 7-44858
 Re₂Nb_{1-x}Se₂ layered system, cryst. struct., X-ray diff. studies 7-44486
 ReO₃, bridging angle, high press. EXAFS studies 7-64781
 Re₂Te₁₅, cluster type struct., X-ray diff. study, thermodynamical form. const. determ. 7-44494
 Rh complex, dirhodium tetradecanoate, discotic mesophase struct., optical microscopy, DSC and X-ray diff. study 7-26627
 Rh_{1-x}Ru_xS₂, prep., mag. and crystallographic props. 7-33154
 Ru complex, Creutz-Taube complex with HUO₂PO₄, synthesis, struct. and oxidation, IR and X-ray spectra anal. 7-46840
 Ru complex, K₃[Ru(C₂O₄)₃]·4.5H₂O, cryst. struct. determ. (*French*) 7-1961
 α-RuCl₃, intercalation reactions, electron/ion transfer and exchange reactions 7-46837
 (S₂N₃)(AuCl₄), crystal struct. studies (*German*) 7-12004
 SbBr₂-AlBr₄ complex, struct. Raman spectra study 7-46020
 β-Sb₂O₄·V(Mo), struct. characterisation, X-ray, neutron, and electron microscopy studies 7-32383
 SbX₂-GaX₄ complex, X=Cl, Br; struct. Raman spectra study 7-46020
 ScAl₂C₃, cryst. struct. determ. 7-58242
 Sc₂Cl₆B(N) infinite chain phases, single cryst. struct. studies 7-32385
 Sc₂Cl₂B(N) metal-metal bonded cluster phases, single cryst. struct. studies 7-32385
 Sc₃CoC₄, cryst. struct. determ. 7-58241
 Sc₂V₃Si₄, cryst. struct. determ. 7-58243
 Si, crystal data for high-press. phases 7-16486
 Si, high dose implantation, with Co, Ni, Fe ions struct. and phase modifications 7-12095
 β-SiC epitaxial layers, cubic cryst. struct., electron diff. and microscopy studies 7-27199
 SiC polytypes, lattice imaging studies on struct. and disorder 7-37933
 SiC, structural EXAFS study 7-64762
 Si_{1-x}Ge_x, MBE crystals, ordering study 7-58709
 SiO₂-rich ceramics, intergrowth relationships between SiO₂ polymorphs, quartz, cristobalite and tridymite 7-13445
 SmB₆, cryst. struct. determ., defect content 7-58245
 SmMnSi₂, struct. and mag. props. studies (*French*) 7-37950
 SmOBr, single cryst. growth, struct., X-ray diff. study 7-44431
 Sm₃RuO₇, crystal struct. determ. 7-16520
 Sn-Sb-Te, complex formation, conc. depend. of lattice parameter 7-44472
 α-SnBi₂S₄, congruently melting compound in Sn-Bi-S system, unit cell parameters 7-13437
 SnFe_{0.95}Mo_{0.05}S₈, Chevrel-phase superconductor, collinear ordering, EXAFS studies 7-13258
 SnS₂-Ti₂S₃ phases, ¹¹⁹Su Mossbauer study (*French*) 7-27639
 SnTe, conc. depend. props. in region of homogeneity 7-45366
 SnTe, low temp. iodide method synthesis, X-ray reaction product studies 7-64945
 SrBr₂H₂O, cryst. struct., comparative study with isotypic halides, bifurcated H bonds 7-63543
 SrCl₂H₂O, cryst. struct., comparative study with isotypic halides, bifurcated H bonds 7-63543
 Sr₂FeTiO_{6-x}, defect struct. 7-1992
 Sr_{1.2}H₂O, cryst. struct., comparative study with isotypic halides, bifurcated H bonds 7-63543
 Sr_{0.69}La_{0.31}F_{2.31}, nonstoichiometric phase, atomic struct. 7-21175
 Sr₂Mn_{2-x}Ti_xO_{5+x/2}, struct. and defects 7-44490
 Sr₂Nb_{2-x}O₉, single cryst., bronze-type struct., X-ray diff. study (*German*) 7-37949
 Sr₂P₂O₁₂·6H₂O, cryst. struct. determ. 7-1953
 SrSe₂O₅, cryst. struct. 7-58216
 Sr₂SiO₄, β to α' to β transformation, electron microscope study 7-16723
 Sr₂SiO₄, β to α' to β transition, modulated struct. 7-16724
 Sr₂UO₂(CO₃)₃·8H₂O, cryst. struct., X-ray diff. study 7-44462
 SrZn₂Fe₁₆O₂₇, cryst. struct. refinement, X-ray diff. study 7-32413
 Ta-Cu, multilayer systems, temp. depend. of ion beam mixing, 77-book (*Chinese*) 7-51884
 TaH_{0.07}, lattice location of H by channeling method 7-1975
 TaPO₅, β-form, bronzoit, struct. and stability 7-44478
 TbO₂, fluorite prototype struct., interfaces and domain form. study 7-58498
 Te₂P₃ twinned cryst., space group and lattice constant, X-ray diff. determ. 7-1979
 ThC powders, structural stability, eqn. of state, press. up to 36 GPa 7-16688
 ThGeO₄, cryst. struct. determ. 7-26718
 α-ThSi₂, struct. type, geometrical characteristics 7-2003
 Th₂Zr₂D₂, D distrib., neutron diff. study 7-16512
 (Ti_{1-x}M_x)O₂ (M=V, Nb, Ta) rutile solid solns., charge transfer and ligand fields, XANES studies 7-64782

crystal atomic structure of inorganic compounds continued

- Ti-N system, short-range order 7-63570
 TiAlN coatings, sputter ion plating, struct. and protective props. 7-53976
 TiH₂, struct. and phase transitions, X-ray diff. anal. 7-52034
 TiN_x epitaxial layers, atomic and electronic struct., growth, physical props. 7-32854
 Ti₃N_{2-x}, cryst. struct., X-ray diff. study 7-37938
 Ti_{1-x}Nb_xCo_{0.5}Nb_{0.5} solid solns., prod. factors influence on struct. parameters of variable comp. phases 7-7940
 TiO₂, rutile, dynamical thermal diffuse scatt. of fast electrons, crystal struct. 7-32229
 TiO₂(B) open metastable structure, layered, synthesis and struct. 7-32406
 TiOSi, equiatomic ternary silicides, superconductivity, rel. to cryst. struct. 7-6607
 TiS₂, highly stoichiometric, compositional and struct. studies 7-2224
 TiS₂, prep. in presence of Sb, struct. studies 7-33616
 Ti₂Si₃H(D)_{1-x}, site occupation and local vibration of H isotopes (*Japanese*) 7-12012
 Ti₂Si₃H(D)_{1-x}, site occupation and local vibration of H isotopes 7-12028
 TiD₂PO₄, cryst. struct., X-ray diff. study 7-32414
 TiH₂P(As)O₄, cryst. struct. and polymorphic transformations, X-ray and thermal anal. 7-1972
 TiI₃, cryst. struct., X-ray diff. study 7-44461
 Ti₂PO₄, optical SHG material, cryst. struct., X-ray diff. study 7-44465
 Ti₄UO₂(CO₃)₃, cryst. struct., X-ray diff. study 7-44463
 To₂NiSe₅, reactivity, intercalation structural changes, X-ray diff. exam. 7-46839
 To₂PdSe₅, reactivity, intercalation structural changes, X-ray diff. exam. 7-46839
 U borides and oxyhalogenides, synthesis and crystallographic studies (*French*) 7-17487
 U-Cu-P(As), ternary particles, cryst. struct. and mag. props. 7-12955
 U-Ni-As(P), ternary particles, cryst. struct. and mag. props. 7-12955
 UAsO₅, crystal struct. determ. 7-32378
 UC, high press. struct. study, X-ray diff., synchrotron radiation 7-16729
 (U₂Ce_{1-y}) O_{2-x}, struct. determ., EXAFS studies 7-63581
 UCl₄, spin-density study, covalency effects 7-12947
 UMGa₃ (M=Fe, Co, Ni, Ru, Rh, Pd, Os, Ir, Pt), structural chemistry, mag. behaviour 7-16513
 UO₂, nonstoichiometric, n diffraction meas. of struct. factors (*Rumanian*) 7-12027
 UO₂, struct. determ., EXAFS studies 7-63581
 U₄O₉, struct. determ., EXAFS studies 7-63581
 U₄O₉, superstructure and surface images 7-16532
 (UO)₂ErS₃, crystal struct. and oxidation state (*French*) 7-11999
 UPO₅, crystal struct. determ. 7-32378
 Up(Sb), bulk moduli and phase transforms., high press. X-ray diff. study 7-12206
 V₂H, cryst. struct. of tetragonal and monoclinic forms, X-ray diff. study 7-44456
 V_{3-x}Mo_xS₄, struct. and phase relations, comp. depend., X-ray powder diff. study 7-1978
 VO²⁺ complexes, rhombic symmetry cryst. field and ground state wavefnc. 7-38927
 V₂O₅, cryst. struct. refinement 7-26703
 VO(II) complexes, ENDOR spectra, struct., hyperfine tensors 7-33299
 V₂P₂SiO₁₉, cryst. struct. determ. 7-32395
 VSe₂-IT, distorted struct., convergent beam diffraction study 7-16528
 V₂TiO₅, valency distrib. determ., XANES 7-16509
 W complexes, W(VI) isopropylimido, cryst. and mol. struct. 7-51722
 W-Cu, multilayer systems, temp. depend. of ion beam mixing, 77-book (*Chinese*) 7-51884
 W_{1-x}Mo_xO₃, structure parameters (*French*) 7-16507
 WO₃ containing compounds, nonstoichiometry and struct. disorder 7-63566
 n-WSe₂, single crystal, growth, struct. and photoelectrochem. props. 7-27879
 WS₂, formation by As ion implantation, ion beam mixing (*Chinese*) 7-51797
 Y oxychlorides, phase equilb., X-ray diff. and spectro-luminesc. anal. 7-46143
 Y-Si-Al-O-N ceramics, phase relationships 7-65011
 Y₂Co₂H₂ hydrides, cryst. struct. and mag. props., H effects (*Russian*) 7-44468
 Y₂O₃-Bi₂O₃, local interactions and environments, EXAFS studies 7-63575
 Y₂O₃-ZrO₂, local interactions and environments, EXAFS studies 7-63575
 Y₂O₂Se₂Tb³⁺, phosphor, electronic struct., cathodoluminescence meas. 7-17350
 Yb-Sb-S(Se), synthesis and props. 7-44471
 Yb_{0.06}(NH₃)_{0.33}Ti₂ intercalation compounds, structural and magnetic studies 7-63593
 YbBiS(Te), synthesis and props. 7-44471
 Yb₂Co₄P₁₂, synthesis, cryst. struct., X-ray diff. study 7-32387
 YbD₂, cryst. struct., X-ray diff. study 7-16516
 YbD₃, 2.0 < x < 2.5, cryst. struct., X-ray diff. study 7-16516
 Yb₂Se₄, crystal struct. and mag. props. (*French*) 7-63590
 Yb₂Ti₂, mixed valence intercalation cpd., low-temp. synthesis and mag. props. 7-17779
 Zn_{0.25}Co_{0.75}Se mixed crystals, electron and hole deep level traps 7-16980
 ZnFe₂(H₂O)₂, cryst. struct., mag. and Mossbauer study 7-45845
 Zn_{1-x}Fe_xFe₂O₄, shock synthesised, X-ray diff. 7-39899
 Zn_{1-x}Fe_{2+x}O₄, shock synthesised, electron microscopy 7-37955
 Zn_{1-x}Gd_xFe₂O₄, ferrites, atomic, mag. and electronic disorder (*French*) 7-44477
 ZnIn₂Se₄, crystal struct. 7-2002
 ZnMoO₁₀, synthesis and struct., orthogonal nonintersecting octahedral cluster chains 7-32386
 Zn_{0.98}Na_{0.02}Fe₂O₄, spinel struct., EXAFS and XANES studies, humidity sensor appls. 7-64784
 ZnO piezoelectric thin films, layer struct., RHEED and X-ray diff. studies 7-16888
 ZnO:Al films, RF reactive sputter deposition, struct., elec. and optical props. (*Japanese*) 7-27900
 ZnP₂, crystal structures and microphases, devil's staircase 7-11982
 Zn₃(PO₃(OH))₃·3H₂O, cryst. struct. (*French*) 7-58221
 ZnS:Cu, solid solution, electroluminescent phosphor, compositional inhomogeneities 7-6800
 ZnS:Mn films, struct. and electroluminescence props. (*Japanese*) 7-27783
 β-Zn₇Sb₂O₁₂, structural data 7-12022

crystal atomic structure of inorganic compounds continued

- ZnSe:Si, single crystal growth, chem. transport method (Korean) 7-27880
 β -ZnSeO₃, cryst. struct. determ. 7-6611
 ZnSeO₃ struct. determ. and refinement, X-ray diffr. study 7-32373
 Zr(HPO₄)₂·xH₂O mixed α -layered cpds., crystalline phases, comp. depend., X-ray powder diffr. study 7-1983
 γ -ZrI₄, cryst. struct., X-ray diffr. studies 7-44483
 Zr₃Ir₃, crystal struct., Mn₂Si₃ deform. superstruct. type 7-11998
 ZrO₂, high press. phase, cryst. struct. 7-16523
 ZrO₂ single crystals, stabilised, growth by skull melting technique, char. act. 7-53560
 ZrRhSi, equiatomic ternary silicides, superconductivity, rel. to cryst. struct. 7-6607
 ZrTe₅, struct. polytypes 7-51718
 ZrTiO₄ and Zr₅Ti₇O₂₄, cryst. struct., determ. by neutron diffr. 7-6599

crystal atomic structure of organic compounds

- 2,4-diphenyl-3-azabicyclo[3,3,1] non-2-en-9-ol, cryst. and mol. struct. X-ray exam. 7-12052
 4-trifluoromethyl-6-phenyl-3-cyano-2-pyridone X-ray struct. study 7-21192
 8-quinolinaldehyde thiosemicarbazone, struct. X-ray diffr. and quantum mechanical investig. 7-12050
 α -acetoxybenzoic acid, tetramer, topotactic transitions 7-12264
 N-acetyl-1-aminocyclohexanecarboxylic acid N'-methylamide, conformations, PMR and NOE studies 7-62424
 acetylene, solid, high-press. props., polymerisation paths 7-58412
 N-(P'-1-adamantyl-P'-bis(trimethylsilyl)amino)phosphino-P-iodo-P-P-di(tert-butyl)imidophosphinate, X-ray diffr. structural anal. 7-51744
 alkylamines intercalation into HCa₂Nb₂O₁₂, structural studies 7-65306
 N-meta-allyloxybenzoyl-N',N',N''-N'-diethylene phosphoric acid triamide, crystal and molecule struct. 7-44506
 4-amino-4'-nitrodiphenyl sulphide, nonlinear optical props. 7-25880
 ammonium trisoxalato-chromate (III) trihydrate, crystallochemical study (French) 7-26738
 arachidic acid Langmuir-Blodgett multilayers, profile structs., X-ray diffr. studies 7-21630
 2-azido-1,3-butadiene, vibr. spectra, mol. struct., conform., GPED anal., Raman and IR spectra anal. 7-36608
 barbiturates, cryst. struct. anal., H bond geometry and types 7-23300
 (BEDT-TTF)₂Br₂, synthesis, structure and electrical props. 7-46296
 β -(BEDT-TTF)₂AuBr₂, conducting charge transfer salt, struct. and props. 7-58259
 β -(BEDT-TTF)₂I₂Br, low temp. struct., superconductivity suppression 7-44518
 β^* -(BEDT-TTF)₂I₃, cryst. struct. in high-T_c phase 7-44519
 β -(BEDT-TTF)₂I₃, electronic and struct. props., ¹H NMR meas. 7-53170
 β -(BEDT-TTF)₂I₃, shear-induced superconductivity 7-45583
 α -(BEDT-TTF)₂I₃, struct. charact. and band electronic struct. below metal-insulator transition 7-2007
 β^* -(BEDT-TTF)₂I₃, struct. order and disorder, neutron diffr. obs. 7-58253
 $\alpha(\beta)$ -(BEDT-TTF)₂X (X=I₃, IBr₂), organic conductors, structural and electrical props. 7-63601
 (BEDT-TTF)₂X salts struct., anion length depend., shear transform. anal. 7-37961
 (BEDT-TTF)₂CuCl₂, cryst. struct. 7-58251
 (BEDT-TTF)₂I₃, cryst. struct., X-ray diffr. studies 7-44507
 BEDT-TTF charge transfer salts with tetrahedral anions, elec. props., crystal packing and stoichiometry effects 7-63599
 BEDT-TTF-containing molecular solids, struct. and physical props. 7-44511
 beef liver catalase, refined struct. 7-17938
 benzil, structure factor phase determ. by multiple Bragg diffr. 7-32211
 benzoic acid, crystn. state compression effect on struct. and proton transfer barrier height 7-12042
 6-benzyl-2-thiouacile, conformational study (French) 7-58252
 biopoxycyclopentyl selenium derivatives, partial disorder, X-ray structural anal. 7-51742
 biphenylene-1,2,4,5-tetracyanobenzene charge transfer complex, cryst. struct. and photoexcited triplet excitons EPR study 7-63600
 1,2-bis(4'-pentylcyclohexyl)ethane, cryst. and mol. struct. 7-58257
 bis(5,6-dihydro-1,4-dithiin-2,3-dithiolate) metalates, molecular solids, struct. and physical props. 7-44511
 1,3-bis(dicyanomethylene)-2-[4'-(N,N-diethylamino)phenylimino]indane, X-ray diffr. struct. determ. 7-12044
 bis(ethylenedithio)tetrathiafulvalene, low-temp. phases, X-ray diffr., resistivity and thermopower meas. 7-37962
 bis(tetramethylammonium)Ag₃I₅, O probe, electrical conductivity and struct. 7-52147
 1,3-bis(trimethylsilyl)-2-bis(trimethylsilyl)amino-2,4,4-triphenyl-1,3,2,4-diazaphosphalumetidine, X-ray diffr. struct. determ. 7-12045
 bis (4-(n-heptyloxy)-N-(p-methoxyphenyl) benzaldimino-olate) copper (2+), cryst. struct. 7-44509
 bis-5,6-diseleno-11,12-ditellurotetracene bromide (chloride), struct. and elec. cond. 7-44512
 (BMDT-TTF)₂Au(CN)₂, organic metal, synthesis, struct. and props. 7-32420
 (BPDT-TTF)₂IBr₂, synthesis by electrochemical oxidation, struct. and ESR spectra 7-46856
 α -(BPDT-TTF)(Ni(dmit)₂)₂, struct. phase transition accompanied by change of electronic struct. 7-52704
 brexan-6,7-diol, struct., X-ray study 7-12051
 bromide salt hydrates, H-bonded (H₂O.Br)[∞], 7-51738
 p-bromochlorobenzene/p-chloriodobenzene mixed crystals, crystal data at 293 K 7-51737
 o-bromophenyldibromarsine, X-ray structural anal. 7-51748
 p-butyl-p'-cyanocyclohexyl-cyclohexane, smectic liq. cryst., phase struct., X-ray diffr. 7-21087
 carbazole-TCNQ, molecular complex with charge transfer, cryst. struct. determ. 7-58256
 catenand, monoprotonated, mol. struct., X-ray and PMR study 7-63595
 charge transfer complexes, synthesis, struct. and physical props. 7-44510
 chloro-methyl exchange rule, notation in packing of organic molecular solids 7-2008
 o-(β -chloroethyl)phenyl- α -hydroxycyclopentyl phosphinate, mol. and cryst. struct., X-ray study 7-12054
 p-chloriodobenzene, crystal data at 293 K 7-51737
 1-chloromercurio-1,3-diphenyl-2-carbomethoxy-3-methoxycyclopropane, X-ray diffr. structural anal. 7-51743

crystal atomic structure of organic compounds continued

- 2-(chloromethyl)-2-methyl-1,3-dichloropropane, conformational equilib., Raman and IR spectra study 7-46018
 chloronitroacetic acid, amide, ammonium salt, molecular and defect cryst. struct. 7-21188
 chlorophenoxyacetylpropylbenzenes, X-ray struct. investig. 7-12049
 cholesterol p-n-hexyloxybenzoate mesophase precursor cryst. struct., X-ray study 7-63597
 conducting single crystals, electron irradi., Bragg spot fading 7-12158
 α -cyanoacetohydrazide, crystal struct., neutron diffr. anal., ab initio MO calcs. 7-36458
 cyanocobalt (III) phthalocyanine, conductive crystals prepared by electrolysis 7-2590
 4-cyanophenyl-trans-4-((trans-4-n-butylcyclohexyl)methyl)-cyclohexanoate, nematogenic, cryst. struct., X-ray diffr., conformational anal. 7-2006
 cyclohexanediene:benzene cyclamer, 6:1, solid-state struct. characterisation 7-12040
 1,3-cyclohexanedione, solid-state struct. characterisation 7-12040
 deltic acid, crystal struct., vibr. anal., monoanion props., ab initio SCF calcs. 7-25387
 di(3,4-ethylenedithio-3',4'-dimethyl-2',5',5'-tetrathiafulvalenium) perchlorate, cryst. struct. study 7-58250
 di(propylammonium) mercury tetrachloride, cryst. struct. and Raman study (French) 7-32418
 diacyl peroxides, low temp. photolysis, vib. anal. for CO₂ dimer, IR spectra 7-15597
 1,3-diaza-6,9-dioxo-2-cycloundecanthione, cryst. and molecular struct. 7-21189
 2,3-diazido-1,3-butadiene, vibr. spectra, mol. struct., conform., GPED anal., Raman and IR spectra anal. 7-36609
 2,6-dichloroacetanilide, X-ray diffr. and NQR study, struct. and bond props. 7-12041
 1-difluoronitroacetyl-2,2-dimethylhydrazine, cryst. and mol. struct., X-ray diffr. anal. 7-26735
 dihydrogen triacetate, cryst. struct. study 7-44503
 N,N'-dihydroxyethylidithiooxamide-d₄(d₄), vibr. anal., X-ray diffr., NMR, Raman, IR, visible and UV spectra 7-51741
 1-(3,4-dimethoxyphenyl)-4-methyl-5-ethyl-7,8-dimethoxy-5H-2,3-benzodiazepine, config., X-ray anal. 7-21186
 dimethyl tin diacetate, solid-state and soln. struct., ²H and ¹³C NMR spectra study 7-25431
 dimethyl tin diacetate hydrolyzate, solid-state and soln. struct., ²H and ¹³C NMR spectra study 7-25431
 2,9-dimethyl-1,10-phenanthroline intercalated into α -Zr(HPO₄)₂, ion exchange with Co²⁺, Ni²⁺ and Cu²⁺, dimer formation 7-65305
 1,5-dimethyl-1,5-divinyl-3,3,7,7-tetraphenylcyclotetrasiloxane, disordered cryst. struct. investig. 7-51745
 4,4'-dimethyl-8,9,10-trimor-spiro-2'-2'-borane (1,3-oxazolidine)-3'-oxyl racemic mol. solid soln., phase separation statics and dynamics 7-26737
 1,3-dioxo-2-silacycloalkanes, X-ray diffr., struct., chemical reactions 7-21185
 4,4-dioxo-4-thia-1-acetyl-1,4-dihydropyridine, heteroaromaticity, p-d bonding, NMR, crystallography and calcs. 7-15623
 1,1-diphenylethanol, cryst. struct. 7-12057
 DNA-Eco RI endonuclease recognition complex, struct. at 3 Å resolution 7-65698
 donor-acceptor complexes, interstack and intrastack forces 7-63594
 dotriacontamethylcyclohexadecasilane, cryst. and mol. struct., X-ray determ. 7-12039
 β -(ET)₂X organic superconductors, ambient press., point contact tunnelling studies 7-44517
 α -ethoxyacrolein semicarbazone, cryst. and mol. struct., X-ray diffr. 7-26734
 3-ethyl-5-[2-(3-ethyl-2-benzothiazolylidene)-ethylidene]-rhodanine, polymorphism and electronic props. 7-37959
 p-ethyl-p'-cyanocyclohexyl-cyclohexane, smectic liq. cryst., phase struct., X-ray diffr. 7-21087
 ethylaminodimethylenephosphonic acid, X-ray diffr. cryst. and mol. struct. anal. 7-12046
 ethylenediammonium hexachlorometallates, struct., H bonds and phase transitions 7-16535
 guanidinium aluminium pentafluoride dihydrate single crystals, struct. and symm. determ., X-ray diffr. study (French) 7-37960
 1-(4-n-heptylbenzoyl)-2-(cyanoacetyl)-hydrazine, cryst. and mol. struct. 7-26733
 2,2', 4,4', 5,5'-hexachlorobiphenyl, crystal and energy-refined structs. 7-12035
 2,2', 4,4', 5,5'-hexachlorobiphenyl, crystal struct., X-ray and NMR studies 7-12036
 1,2,3,7,8,9-hexachlorodibenzo-p-dioxan, dipole-dipole interactions and inversion motif 7-26732
 hexacosamethylcyclotrideasilane, cryst. and mol. struct., X-ray determ. 7-12039
 hexakis(trimethylelementyl)benzenes, synthesis and crystal mol. struct., X-ray spectra anal., EFF calcs. 7-25360
 hexanitroethane, crystallographic and vibrational study 7-38131
 4,7,13,16,23,26-hexaoxa-1,10,20,29-tetraazabicyclo [8.8.12]-triacontane-19,30-dithione, cryst. struct. 7-44508
 1-(hydroxy)germatrane, cryst. and mol. struct., X-ray investig. 7-12055
 6-hydroxy-1,2-dihydroquinoline, 2,2,4-trimethyl substituted, cryst. and mol. struct., X-ray diffr. 7-16539
 8-hydroxy-2-piperidinoquinoline, cryst. and molecular struct. 7-21191
 4-hydroxybiphenyl, cryst. packing rel. to mol. geometry and thermal motion 7-26736
 hydroxyiminophenylacetonitrile, cryst. and mol. struct. 7-51746
 ion radical salt, (AsPh₄)_{0.25}(Ni(dmit)₂), synthesis, elec. cond. and cryst. struct. 7-37958
 isoprenaline, cryst. and mol. struct. anal. 7-57008
 isotactic poly-1-butene, crystalline forms, thermodynamic stabilities 7-12038
 β -lactoglobulin, struct. and similarity to plasma retinal-binding protein 7-34108
 lutetium diphthalocyanine, γ -phase, cryst. and molecular struct. 7-21190
 metal dithiolenes, struct., elec. and optical props. 7-44516
 methyl cyanide-d₀(d₃), lattice vibr., Raman and IR spectra study 7-46019
 β -methyl-cellobioside heptanitate, mol. and cryst. struct., X-ray anal. 7-63598
 bis-methylammonium tetrachloro manganese antiferromag. crystals, struct. deform. by exciton self-localisation, luminesc. spectra fine struct. study (Russian) 7-27752

crystal atomic structure of organic compounds continued

- (2-methylsulphanyl ethyl)trifluorosilane, Si-O bond length and cryst. struct. study 7-51734
 mono-AZO pigment, electron microscope studies 7-16543
 2-morpholine-8-hydroxyquinoline, cryst. and molecular struct. 7-21191
 multi-S π donor and π -acceptor charge transfer complexes, struct., elec. and optical props. 7-44513
 p-nitrostyrene oxide, cryst. and molecular struct. 7-58255
 oleic acid, polymorphism, order-disorder phase transition, IR and Raman spectra anal. 7-33379
 organic metals, interstack and intrastack forces 7-63594
 organic superconductors, charge transfer salts, structural aspects 7-6614
 6-oxo-2, 6-dihydroquinoline, 2,2,4-trimethyl substituted, cryst. and mol. struct., X-ray diffr. 7-16539
 paraffins, cyclic, with long chain lengths, ^{13}C NMR chem. shift meas., cryst. structures 7-64537
 paraffins, direct lattice imaging 7-16542
 n-paraffins, electron crystallography 7-16541
 N-paramethoxybenzoyl-N',N'',N'''-diethylene phosphoric acid triamide, cryst. and mol. struct. 7-51733
 (O-phenyl-N-N-di(2-chloroethyl)amidophosphonyl) hydrazone of parachloracetophenone, crystal and molecular struct. 7-44505
 N-phenylsulfonylbenzimidoyl chloride, cryst. and mol. struct., X-ray and calc. investig. 7-51747
 phthalocyanines, halogenated, radiation damage and structural studies 7-6688
 phthalocyanines, polymeric structural arrangements 7-16544
 N-phthalyl-4-bromo-L-glutamic acid, dimethylester, struct. and absolute configuration 7-40092
 polymorphism and nonlinear optical activity in organic crystals 7-57400
 polyoxyethylene-p-dihalogenobenzene intercalates, struct. 7-13154
 potassium hydrogen malonate, crystn., inelastic neutron scatt. 7-32419
 potassium isopropylxanthate, cryst. struct. determ. 7-58254
 DL-(4,4'-H₂) proline, solid state, ring dynamics, crystal struct. and temp. dependence, ^2H NMR study 7-26602
 DL-(4,4'-H₂)proline hydrochloride, solid state, ring dynamics, crystal struct. and temp. dependence, ^2H NMR study 7-26602
 2-(N-prolinol)-5-nitropyridine, nonlinear optical props., mol. and cryst. struct. 7-11056
 purines, cryst. struct. anal., H bond geometry and types 7-23300
 pyrimidines, cryst. struct. anal., H bond geometry and types 7-23300
 quasi-1D conductors, conf., Yamanashi, Japan (May 1986) 7-60868
 radical anions, single cryst., dissoc., struct. investig. 7-33275
 ribonuclease, guanyl-specific, spatial structure studies 7-46999
 sodium succinate hexahydrate, cryst. struct. investig. 7-12034
 solid state chemistry and X-ray crystallography 7-58098
 squaric acid, crystal struct., vibr. anal., monoanion props., ab initio SCF calcs. 7-25387
 squaric acid, press. depend. of cryst. struct. 7-32417
 strontium formate dihydrate single crystals, polarised Raman scatt., water internal modes 7-53311
 sulphonylamide-6-(4,5-dimethoxy)-pyrimidinyl, cryst. and mol. struct. 7-37957
 TCNQ salt, N-n-propyl phthalazinium 7,7,8,8 TCNQ₂, struct., elec., mag. props., EPR meas. 7-33005
 terephthalic acid, linear chain struct., order-disorder phenomena, Raman scatt. study 7-21150
 3,3',5,5'-tetrabromo-4,4'-dioxiphenyldimethylmethane, crystal and molecular struct. 7-16537
 4,4,8,8-tetrafluorotricyclo(5.1.0.0^{3,5}) octane, syn isomer struct., X-ray anal. 7-21187
 3,3,9,9-tetramethyl-6-phenyl-1,3,4,7,9,10-hexahydrodipyrano[4,3-b:3'-d]pyridine, cryst. and mol. struct., X-ray anal. 7-12053
 tetramethylammonium hexachloroplatinate, crystal struct. and theoretical symmetry analysis of phase transition sequence 7-51739
 tetramethylammonium tetrachlorozincate, cryst. form, surface morphology, optical microscopy study 7-63919
 3,3,7,7-tetraoxo-9-oxa-3,7-dithiabicyclo [3.3.1] nonane, mol. and cryst. struct. 7-37956
 tetraphenylphosphonium chloride, cryst. struct. investig. 7-12037
 tetrahydrofulvenes, N-containing, charge transfer complexes, struct. and elec. props. 7-44514
 thiamin thiazolone, cryst. struct., transition state analogue 7-51736
 thiosemicarbazide, bonding and struct., effect of protonation, ^{14}N quadrupole reson. spectra anal. 7-33295
 thiosemicarbazide hydrochloride, bonding and struct., effect of protonation, ^{14}N quadrupole reson. spectra anal. 7-33295
 (TMTCF)_x salts (C=S,Se), crystal struct., press. and temp. depend. 7-44520
 (TMTSF)₂(ClO₄)_{1-x}(ReO₄)_x, organic conductors, competition between structural instabilities 7-51740
 (TMTSF)₂ClO₄, superconducting and spin-density-wave transition temperatures, effect of anion ordering 7-2761
 (TMTSF)₂PF₆O₂, organic conductors, competition between structural instabilities 7-51740
 (TMTSF)₂PF₆, cryst. struct., neutron low temp. and X-ray high press. diff. studies 7-44502
 (TMTSF)₂ReO₄, organic conductors, competition between structural instabilities 7-51740
 (TMTTF)₂Mo₆Cl₁₄, prep. by electrocrystallisation, struct. and spectroscopic characterisation 7-46295
 para-tolylmercury chloride, cryst. struct., X-ray diffr. study 7-63596
 transition metal complexes, M(dmit)₂, conductive and superconductive materials 7-44515
 1,2,3-trichlorobenzene, dipole-dipole interactions and inversion motif 7-26732
 1'-trichlorogermeryl-1,1'-bicyclopentane-2-one, cryst. and mol. struct. 7-12047
 1-(triethylene amide)-phosphazo-1,1-(diethylene amide)-2,2,2-trichloroethane, cryst. and mol. struct. 7-51735
 1,3,5-trigermatris(spiro-1-germa-3,5-disila-3,3,5,5-tetramethyl-4-oxacyclohex)-2,4,6-cyclotrioxane, cryst. and mol. struct. determ. 7-12056
 4-(2,4,6-trimethyl)benzylidene-2-phenyloxazolin-5-one, cryst. struct. determ. and reaction investig. 7-54084
 2,2,4-trimethyl-6-acetoxy-1,2,3,4-tetra-hydroquinoline, cryst. and mol. struct. X-ray diffr. 7-16540
 1,6,12-trioxa-9-aza-9-butyl-5-germa-spiro[4,7]dodecane-2-one, cryst. and mol. struct. 7-12048
 tris-(ethylenedithio) benzene salt, (TEDTB)₂BF₄, C₃ symmetry, synthesis and crystal struct. 7-63602

crystal atomic structure of organic compounds continued

- TSF(Ni(dmit)₂)₃, organic conductor, structure-related magnetism 7-2807
 β -(BEDT-TTF)₂I₃, organic supercond., cryst. and mol. struct., X-ray diffr. study at 9.5 kbar 7-44504
 caesium 4-trifluoromethyl-6-phenyl-3-cyano-2-pyridone, X-ray struct. study 7-21192
 Cu complex, Cu(II) saccharinate, electronic struct. and cryst. struct. 7-27251
 Zn complex, Zn (acetylacetonate)₂·H₂O, Mn²⁺ dopant, crystal struct., EPR spectra study 7-64521
- crystal binding**
 see also binding energy; lattice energy
 anharmonic cryst. stability, Lennard-Jones pairwise pot. anal. 7-32356
 compound semiconds., systematic variation of Szegedi charge with anion radius/nearest-neighbour distance ratio 7-11987
 computer modelling of materials 7-51676
 crystal growth, hkl formation by 2D nucleation 7-44427
 crystallites, 2D, crack growth, computer modelling 7-43787
 graphite crystal interplanar binding, Englert-Schwinger eqn. calcs. 7-21846
 graphite-K intercalation cpd., C₈K, anisotropic binding of K, nuclear resonance photon scatt. of bremsstrahlung 7-51695
 insulators, indirect short-range interactions and lattice vibrs. 7-21154
 ionic crystals, radius ratios, general approach 7-9634
 ionicity in solids, review 7-48201
 ions, in cryst., dipole-quadrupole dispersion coefficients, ab initio coupled HF calcs. 7-11986
 lattice stability and defect form., noncentral forces effects, tight binding parameter calcs., recursion method 7-51694
 layer crystals dynamics, long wavelength vibrs., factor group anal. 7-58424
 metal chalcogenides, low-dimensional, synthesis and CDW props. 7-32926
 metal-H systems, bond weakening 7-63546
 metal-H systems, interatomic forces near H impurity 7-58293
 metal-H systems, statistical thermodynamic aspects of bonding 7-6576
 metals, (s,p)-bonded, atomic interaction theory 7-11985
 mixed stack charge transfer crystals, regular dimerized stack, neutral ionic instability 7-51698
 molecular crystals, electron density distrib. calcs., X-ray diffr. 7-26587
 Phillips and Van Vechten theory, Levin's modifications, d-electron effect on ionicity 7-16482
 quasi-crystallinity, non-uniformity and nanocomposites 7-1926
 rare earth vanadates, XES charact. 7-51693
 semiconductor interatomic potentials, handbook 7-35130
 soft-core Thomas-Fermi pseudopot. for total energy calcs. 7-21845
 surfaces, force sum rules, Hellmann-Feynman theory 7-44989
 thiosemicarbazide, bonding and struct., effect of protonation, ^{14}N quadrupole reson. spectra anal. 7-33295
 thiosemicarbazide hydrochloride, bonding and struct., effect of protonation, ^{14}N quadrupole reson. spectra anal. 7-33295
 transition metal alloys, heat of formation, X-ray emission centres (Russian) 7-37919
 transition metal crystal, BCC, metal-H bond investig. 7-32360
 transition metal phosphorous trisulphides, electronic, structural and mag. props., intercalation cpds. and chemical props. 7-44499
 Al₂O₃-H₂O-based heterogeneous monotype systems, hardening and binding props. 7-65052
 Ar, Lennard-Jones cryst. struct., mol. dynamics method 7-16487
 Ar, solid, pair potential, effective medium approach 7-45201
 C films, CK α spectra and interatomic bonding (Russian) 7-58705
 Ca, cryst., FCC, generalised Morse pot. and mech. stability 7-6575
 CdI₂, layered cryst., Raman scatt. intensities and atomic bonding 7-22257
 Co-Ni-As mixtures, phase diagram isothermal sections, binding 7-46418
 CoAl₃ phases, binding anal. 7-44445
 CsI, press. induced structural instability, ab initio pseudopotential techniques 7-52042
 Fe solid and molten, X-ray K α_1 and K β lines (Russian) 7-39211
 Fe-Co-As mixtures, phase diagram isothermal sections, binding 7-46418
 FeAl₃ phases, binding anal. 7-44445
 GaAs, X-ray diffr., anomalous dispersion effects, thermal vibrs. and bonding charges 7-44733
 GaSe, layered cryst., Raman scatt. intensities and atomic bonding 7-22257
 Ge, structural props., ab initio pseudopotential calcs. 7-44797
 He, solid, pair potential, effective medium approach 7-45201
 HgI₂, red, layered cryst., Raman scatt. intensities and atomic bonding 7-22257
 LaNbO₄, single crystal, elastic props. 7-51915
 Mg₂FeH₆ cryst. complexes, Madelung field effects, quantum chem. calcs. 7-11984
 Mg₂NiH₄ cryst. complexes, Madelung field effects, quantum chem. calcs. 7-11984
 Mo halides, chalcogenides and chalcogenides, Mo₆ octahedral clusters (French) 7-32351
 N substituted crystal structures, Pauling's second cryst. rule 7-37918
 Na₄(AlSiO₄)₆·nH₂O, dehydration, struct. collapse or expansion 7-17770
 Na₈(AlSiO₄)₆·nH₂O, dehydration, struct. collapse or expansion 7-17770
 Nb₂Pd_{0.74}Cu_{0.26}S₂, reactivity, intercalation structural changes, X-ray diffr. exam. 7-46839
 Ne, solid, pair potential, effective medium approach 7-45201
 Ni, spin polarised electronic struct., mag. and bonding props. 7-32904
 Ni-C, C-vacancy binding 7-44601
 NiAl₃ phases, binding anal. 7-44445
 Ni₃(Fe,M) (M=C, Mn, W, Mo), atom pair interaction energy and Kurnakov temp. (Russian) 7-1938
 NiH, spin polarised electronic struct., mag. and bonding props. 7-32904
 P, black, interplanar forces caused by electron-lattice interaction 7-63547
 PbO₂-H₂O-based heterogeneous monotype systems, hardening and binding props. 7-65052
 Ti halides, ionicity-effective radius diagram calcs. interatomic distances determ. 7-1939
 To₂NiSe₃, reactivity, intercalation structural changes, X-ray diffr. exam. 7-46839
 To₂PdSe₃, reactivity, intercalation structural changes, X-ray diffr. exam. 7-46839
 U chalcogenides, ionicity and bond formation 7-32357

ystal binding continued

Yb, cryst., FCC, generalised Morse pot. and mech. stability 7-6575
 $Zr_{68}Hf_{32}Cu_{30}$ amorphous and cryst. alloy, elec. field gradient, TDPAC meas. 7-2958

ystal chemistry

see also *crystallography*
 actinides, physics and chemistry, handbook 7-24317
 ammonium trisoxalato-chromate (III) trihydrate, crystallochemical study (French) 7-26738
 dichalcogenides, low-dimens., as secondary cathodic materials, book contrib. 7-28394
 II-VI solid solutions with wurtzite structure 7-32348
 micas, synthetic, growth spirals and complex polytypism, occurrence frequencies 7-37997
 rare earth-transition metal-nonmetal ternary phase struct., crystallochem. anal. (French) 7-58234
 tetrahedral anion complexes in structures, relation between tetrahedron connections and comp. 7-44457
 transparent ferroelectric ceramics, cryst. chem. and struct. props. and modifications 7-6590
 $[Ba_xCa_{1-x}](Ti,Al)_{2x+y}^{3+}Ti_{8-2x-y}^{4+}O_{16}$ hollandites, structural chemistry 7-51726
 $Ba_2Ti_{1-x}Zr_xO_{12}$, synthesis, stability, cryst. chem. 7-53681
 Ca_3OSiO_4 , crystallochemistry of phases 7-1965
 $K_{1.50}Al_{1.50}Ti_{0.50}O_{16}$ hollandite-type struct. refinement, cation substitution effects study 7-58232
 $Li_{2+2x}(Li,Mg_{1-x}Sn_x)O_8$, ramsdellite type cpds., ionic conductivity and cryst. chemistry 7-32708
 $Li_2Mg_{1-x}Fe_xSn_{1-x}O_8$, ramsdellite type cpds., ionic conductivity and cryst. chemistry 7-32708
 $Li_{2x}Mg_{1.5-x}VO_4$ solid soln. phase, synthesis, stoichiometry and struct. 7-21168
 $Na_{1+x}Zr_{2-(x/2)}Mg_{(x/2)}(PO_4)_3$ solid soln., cryst. chemistry and ionic cond. studies 7-32408
 $Na_3Zr_2Si_2PO_{12}$ and $Na_3M_2(PO_4)_3$, rhombohedral structures, crystallochemistry 7-32377
 $Pb_2(MSb)O_{6.5}$, $M=Ti, Zr, Sn, Hf$, pyrochlores, cryst. data 7-21171
 $Rb_{1.47}Al_{1.47}Ti_{0.53}O_{16}$ hollandite-type struct. refinement, cation substitution effects study 7-58232
 ThM_2Si_2 ($M=Cu, Ru, Os, Ir, Pt$), magnetochemistry and crystal chemistry 7-58976
 UM_2Si_2 ($M=Cu, Ru, Os, Ir, Pt$), magnetochemistry and crystal chemistry 7-58976
 $UO_2-Gd_2O_3$, solid solution, lattice parameters, O/U thermal conductivity meas. 7-21180

ystal classes see *crystal symmetry*
 ystal cleavage see *crystal faces; specimen preparation*
 ystal defects

see also *Cottrell atmospheres; crowdions; crystal inclusions; crystal microstructure; defect electron energy states; disclinations; dislocations; grain boundaries; impurity-defect interactions; phonon-defect interactions; point defects; stacking faults; twinning*
 acoustic properties of solids, defect effects (Russian) 7-26069
 alkali halide crystals, optical breakdown threshold, size depend. 7-44615
 alloys, electron irradi. induced transforms. 7-2065
 amorphous semiconductors, conference, Palo Alto, CA, USA (April 1986) 7-29602
 anharmonic effects in imperfect crystals, self consistent statistical theory 7-51984
 annealing and creation kinetics of defects, ESR transient spectroscopy 7-2928
 austenitic stainless steel, defects study by positron annihilation 7-39296
 binary alloys, TEM study of precipitate growth mechanisms 7-52064
 bis-methylammonium zinc tetrachloride, lock-in transition, X-ray topography studies 7-32630
 CdTe films, MBE growth, photoluminescence and TEM characterisation 7-22376
 CDW, depinning and quasi-commensurate transition, plastic deformation analogy 7-12628
 ceramics, electron irradi. induced transforms. 7-2065
 compound semiconductor multilayered structure, cross-sectional obs. with TEM 7-2416
 computer modelling of materials 7-51676
 continuous two-level media, defects, motion and plastic fields (Russian) 7-58260
 crystal instability, defect-phonon interactions 7-44722
 crystalline rods, thermoelastic stresses and temps., asymptotic calc. 7-32542
 crystallography, conference, Kharagpur, India (Dec. 1982) 7-55876
 crystals with microdefects, dynamic theory of diffuse X-ray scatt. (Russian) 7-51567
 cultured quartz Al defects, IR and laser spectroscopic charactn. 7-59234
 electronic materials and their microstructure, thermal wave imaging studies 7-8237
 ferromagnetic metals, structural defects studies muon depolarisation method calcs. 7-45898
 friction, material compatibility, surface processes 7-26850
 gate oxide defect localisation by tunnelling current microscopy and dielec. breakdown meas. 7-26601
 high resolution electron microscopy in materials science (German, English) 7-39806
 highly excited crystals, mixed state and defect struct. 7-45584
 II-V semiconds., cryst. growth, characterisation and appls., review 7-26685
 III-V semiconductors, defect recognition and image processing, conf., Montpellier, France (July 1985) 7-29596
 III-V semiconductors, lattice defects detection using IR tomography 7-32234
 III-V semiconductors, line defects, TEM obs. 7-51751
 III-V semiconductors, selective photoetching studies of defects 7-32426
 III-V semiconductors, single crystal growth, formation of microinclusions 7-21141
 III-V semiconductors, X-ray topography and diffraction imaging 7-32224
 imperfect crystals, generation of second harmonic near struct. phase transitions 7-2168
 imperfect crystals, strongly absorbent, surface layer defects and flaws, X-ray diffraction (Russian) 7-63923
 incommensurate crystals and mag. crystals, 2D topological vortex-type defects 7-7462
 incommensurate phases, phasons, dynamic pinning mechanisms 7-45941

ystal defects continued

inert gas bubble precipitate solid in Al, defects, high resolution electron microscopy studies 7-32424
 inert gases implanted in solids, model of diffusion and release behaviour (Chinese) 7-38257
 inorganic crystals, atomic coordination numbers and defects, geometric estimate 7-63571
 insulating halide crystals, exciton-defect conversion 7-7122
 interface response theory of discrete composite systems 7-38424
 ionic solids, radiation effects, review 7-26792
 laser tomography, appl. in obs. of crystal defects (Japanese) 7-51750
 lattice damage due to dynamic loading, simulation 7-26835
 lattice stability and defect form, noncentral forces effects, tight binding parameter calcs., recursion method 7-51694
 macrocrack-microdefect interaction, stress field anal. 7-43797
 material analysis, computer-based, conf., Boston, MA, USA (Dec. 1985) 7-14709
 metals, defect profiles, low energy positron meas. 7-64731
 metals, neutron scattering studies, conf., Jülich, Germany (Oct. 1985) 7-48178
 necking development under uniaxial tensile deform., strain hardening, geometric defects, elongation to failure 7-33742
 neutron and synchrotron radiation studies, comparisons 7-51754
 nucleation and growth, crystal defects 7-58169
 organic conducting single crystals, electron irradi., Bragg spot fading 7-12158
 oxides, defect behaviour, computer-based atomistic simulation studies 7-16548
 oxides, nonstoichiometry, metal surface heating by CW laser 7-17721
 plane, elastic, hole-defect interaction, stress distrib., integral eqn. method 7-37964
 positron lifetime meas. methods and apparatus 7-39218
 positron-annihilation apparatus for layerwise analysis of defects in solids 7-39219
 premelting, ionic disorder and defects 7-44763
 profiled crystals, Stepanov growth, conf., Leningrad, USSR (March 1985) 7-29573
 pyroxene, mineral lattice defects and crystalline plasticity, review (French) 7-34476
 α -quartz, synthetic, defects 7-63603
 α -quartz, XX 7-7766
 quartz crystal defect imaging, sound-beam topography method 7-11237
 quartz irradiation effects study using low-temp. dielec. relax. 7-58334
 radiation damage and defects, computer simulation studies 7-2048
 rapid thermal processing, conf., Boston, MA, USA (Dec. 1985) 7-14713
 Rutherford backscattering-particle induced X-ray emission analysis, large residual defects 7-54251
 S^3 blue phase, double twist connection calcs. 7-58134
 scanning electron microscopy, ultra-high vacuum techniques with field emission gun, surface studies 7-24725
 semiconductor interatomic potentials, handbook 7-35130
 semiconductor interfaces, SEM three-dimensional characterisation 7-52312
 semiconductor materials, high resolution microstruct. studies using TEM 7-21055
 semiconductors, ion beam induced epitaxial crystn., kinetics, mechanisms and microstruct. 7-12171
 semiconductors, lattice defect struct. anal. by X-ray diffraction using synchrotron radiation (Japanese) 7-63399
 semiconductors, photothermal spectroscopy, review 7-48732
 semiconductors, processing and charactn. techniques, conf., Los Angeles, CA, USA (Jan. 1986) 7-18489
 Si, intrinsic faults, weak beam contrast study 7-16377
 single crystals, defective structs., appl. of thickness dependencies for integrated intensities of X-ray scatt. (Russian) 7-51561
 β -Sn thin films, high resolution TEM obs. 7-16891
 SOI films, laser recrystallisation, agglomeration, surface roughness and crystal imperfection 7-38389
 solar cell substrate charactn. techniques 7-40004
 steel, Ni alloy, laser-induced C atom directional motion 7-44894
 steel, pressure vessel, small angle neutron scatt. technique studies 7-59735
 superconductivity, anisotropic, group theoretical anal. of lattice distortion 7-58264
 surface electronic function props. charact. from defect heterogeneity dominated small-angle scatt. diffraction pattern, static synergetics algorithm 7-21041
 $TGS:Fe^{3+}$ crystals, spatially distributed defects, luminescence studies 7-26770
 TGS crystals, polarisation relax., defect effects 7-17265
 thin crystal with anisotropic distortion of cryst. lattice, X-ray beam Laue diffraction (Russian) 7-58101
 thin film pulsed heating, thermal and plasma models 7-26946
 two-dimensional melting, defect core-energy depend., Laplacian-roughening model calcs. 7-6765
 X-ray diffuse, scatt. dynamic effects in defect detection (Russian) 7-37803
 X-ray scattering [crystals with lamellar inhomogeneities, X-ray diffusion scatt.] crystal defects [X-ray diffusion scattering in cryst. with lamellar inhomogeneities] (Russian) 7-51568
 Al, heterogeneous shock wave response, holographic interferometry studies 7-32571
 AlGaAs, low press. MOCVD grown, surface morphology and defects 7-64023
 AlGaAs/GaAs/Ge multijunction solar cell, model for calc. of displacement damage by radiation 7-13878
 AlGaAs/GaAs/InGaAs multijunction solar cell, model for calc. of displacement damage by radiation 7-13878
 $Al_{1-x}Ga_xAs$ -GaAs superlattices, ion implanted, defect struct. 7-26783
 $(Al_{0.9}In_{0.9})_2Se_3$, metastable complex defects, ESR studies 7-33270
 $AlPO_4$, berlinite, growth defects and incommensurate phase obs. by high temp. X-ray topography 7-32423
 Au, defects in multiply-twinned particles 7-16558
 Au, neutron irradiated, recoil energy effects on cascade defect structures 7-51855
 B_4C , fast neutron irradiated, thermal cond. meas. 7-6900
 BN, pyrolytic, macrodefects study 7-44523
 $BaFe_{12}O_{19}$, defects created by Kr ion bombardment, HREM study 7-12168
 $Ba_{1-x}La_xF_{2+x}$ solid solutions, thermally stimulated depolarisation currents 7-53226

crystal defects continued

- BaTiO₃, Nd₂O₃-modified, defect struct. and dielec. props 7-37968
 Ba_{1-x}U_xF_{2+x} solid solutions, thermally stimulated depolarisation currents 7-53226
 Bi, positron trapping in deformation induced defects 7-39257
 Bi thin films (111), melt growth, in-situ obs. by TEM 7-53573
 Bi₂Ge₂O₁₂ single cryst. growth, characterisation and appls. 7-33550
 C fibre reinforced C₃ multidirectional composites, macroporosity and interface cracks 7-46513
 Ca₂NbO_{2+x}, defect structure, Raman spectroscopy 7-63604
 Ca₃(PO₄)₂CaF₂, apatite, carbonated crystallites, high resolution TEM study 7-6643
 CdS plastically deformed cryst., reorientable defects, polarised luminesc. study 7-51749
 CdS single crystals, nonequilibrium high-temp. vacuum annealing effects, intrinsic defect transform. 7-58764
 CdSe lattice defects, digital struct. anal. by ion beam thinning for high resolution electron microscopy 7-6616
 CdTe, annealing in Cd or Hg vapour, defect concentrations 7-65064
 p-CdTe, complex-formation processes at high concentrations of intrinsic defects 7-37963
 CdTe crystals, resistive element defect electromigration, flicker noise enhancement. 7-63889
 CdTe, positron annihilation in defects at crystal surface, defect anal. 7-39306
 CdTe single crystals, anisotropy of positron annihilation 7-39214
 CeB₆, cryst. struct. determ., defect content 7-58245
 Co, oxidation kinetics, laser control 7-28174
 CoO, defect processes, calc. using SHEOL code 7-58267
 Co_{1-x}O, defect cluster energies, MO calc. 7-2010
 Cr single crystals, surface and deeper layers, struct. changes due to laser irradiation 7-6937
 CsCuCl₃, Jahn-Teller induced helical deformations 7-7178
 Cu, crystal surface and interface, heterophase fluctuations (*Russian*) 7-58650
 Cu, gamma-irradiated, anomalous effect of small doses 7-12151
 Cu, oxidation kinetics, laser control 7-28174
 Fe, alpha phase, high energy proton and alpha-particle irradi., radiation defects (*Russian*) 7-16645
 Fe-Cr-Ni alloys, local ordering, neutron irradi. effects, elec. resist. meas. 7-2070
 Fe-Mn-C, FCC, energy of complex packing defects, calc. (*Russian*) 7-58263
 Fe-Ni-Co alloy, H damage, lattice distortion, defect and crack generation, positron lifetime study 7-39675
 Fe_{1-x}O, defect cluster energies, MO calc. 7-2010
 Fe_{1-x}O, wustite, defect clustering 7-51787
 Fe_{3-x}O₄, diffusion-controlled form. during reactions, defects effects 7-17768
 Fe₂(SiO₄), defects, Fe³⁺ conc., microscope-spectrometric method 7-17330
 GaAs cleaved semiconductor surfaces scanning tunnelling microscopy 7-21051
 GaAs crystals, selective etching and photoetching of CrO₃-HF aq. solns. 7-32442
 GaAs, defect structure charactn., US meas. 7-21363
 GaAs films, MBE growth and structural characterisation 7-21775
 GaAs, IR tomography and transmission images, numerical processing 7-32236
 GaAs layers, MBE, oval defects 7-59433
 GaAs MBE layers, oval defects, particulate effects during growth 7-21194
 GaAs p-n homojunction diode, photocurrent meas. of defect distribution 7-32851
 GaAs semi-insulating thin wafers, EL2 defect and dislocation mapping, near-IR transmittance meas. 7-63605
 GaAs, strain-induced defects, ERP anal. 7-45821
 GaAs, substrates, multi-technique approach to defect microstructure characterisation 7-52215
 GaAs, surface morphology of crystals grown by gas-source MBE using trimethylgallium and As₄ 7-17424
 GaAs wafers, subsurface structural defects, photon backscattering studies 7-12059
 GaAs, X-ray topographic examination 7-32225
 GaAs:Al, surface layer, degree of disordering, effect of dopant 7-63929
 GaAs:In (B)(Si), dislocation free crystals, LEC grown, microscopic defects, eutectic etching 7-16545
 n-Ga_{1-x}In_xP, light scatt. by free carriers 7-17328
 GaP, defects, optical detection of magnetic resonance studies 7-22165
 GaP on Si substrate, MOCVD growth and characterisation 7-27926
 Ge, Kikuchi lines, contrast reversal near reflex points with same indices in crystals with defects (*Russian*) 7-51582
 Ge, scattering inhomogeneities, two-wavelength probe meas. 7-46063
 Ge, swirl defects formation 7-51753
 Ge:Sb single crystal, extended defects, X-ray topography meas. 7-38020
 HfO₂-R₂O₃, R=Sc, Y, Nd, Gd, Tb, Er, Yb, solid solution single crystal growth 7-7838
 HgCdTe: In, ion implanted, damage and rapid thermal annealing 7-63637
 α-HgI₂ crystals, recent progress in material characterization for X- and γ-ray detectors 7-44577
 InGaAsP/InP laser wafers, pinhole defects, identification of source 7-46356
 n-InGaAsP/p-GaAs diodes, photocurrent meas. of defect distribution 7-32851
 p-InP, electron irradi., atomic displacement threshold energy 7-2066
 InP, grown-in defects, slow positron beam and positron labelling studies 7-44527
 n-InP, light scatt. by free carriers 7-17328
 InP:S, LEC grown, influence of growth conditions on defects 7-32427
 InSe, photoluminescence, defects effects 7-39161
 In₂Te₃/Fe, Fe²⁺ elec. inactivity study, mag. suscept., Mossbauer spectra and XPS anal. 7-52494
 KBr, stable hole defect formation by ionizing radiation 7-63669
 LaB₆, cryst. struct. determ., defect content 7-58245
 LiF, quenched, dielectric props., effect of high AC field and X-ray irradiation 7-38985
 α-LiIO₃ crystals, anomaly of optical props., 100 to 140°C, influence of growth defects 7-59172
 LiNbO₃, anomaly study by X-ray diffraction 7-6588
 LiNbO₃ crystals, struct. defects and etch figures 7-44555
 LiNbO₃, defect structure, Raman spectroscopy 7-63604

crystal defects continued

- LiNbO₃, heterogeneous shock wave response, holographic interferometry studies 7-32571
 LiNbO₃:Ni(Cu), γ-irradiated, ESR spectra of impurity centres 7-17218
 MgFe₂O₄, photoelectrochemical props., effect of defects and doping 7-45385
 MgO, electron irradi., stored energy, differential thermal anal. studies 7-32503
 Mn-Al-C ferromag. alloys, phase, transformations, and struct. defects, positron annihilation study 7-46461
 Mn_{1-x}O, defect cluster energies, MO calc. 7-2010
 Mo (100), ion irradiated, sub-surface defects, study by variable energy positrons 7-39286
 Mo, polygonisation under high press. (*Russian*) 7-51939
 MoN B1 phase sputtered films, mag. susceptibility and defect struct. 7-53087
 Mo_{n-x}W_xO_{3n-1}, electrical conductivity, mag. susceptibility and IR spectra 7-38546
 NaCl, intense nanosecond electron beam irradi., periodic damage struct. form. 7-12157
 NaLa(MoO₄)₂ single crystals and ceramic, elec. cond. meas., disordering mechanisms 7-6863
 Nb, shock-synthesised superconductor, characterisation 7-38116
 Nb-Al alloys, struct. and supercond. props. (*Russian*) 7-1945
 Nb₂O₅, defect structure, Raman spectroscopy 7-63604
 Ni, ion implantation and pulsed laser melt quenching, metastable phase and defect struct. form. studies 7-16625
 Ni, irradi. with energetic ions, defect prod. and recovery 7-58370
 Ni-Al-La, defect form., disordering, strengthening effect of La addition 7-22708
 NiO-CaO eutectic, directionally solidified, struct. imperfections 7-65026
 Ni_{1-x}O, defect cluster energies, MO calc. 7-2010
 PLZT electro-optical ceramics, electron pulse irradiation-induced transient optical absorpt. study 7-6682
 Pb, deforming stress and defect struct. in low temp. anomaly region (*Russian*) 7-38093
 Pb_{0.93}Ge_{0.07}Te, glassy and cryst., defect struct., positron annihilation studies 7-46221
 Pb₂P₂V₂-₂O₈ mixed system, substitution defects, first order transition spreading 7-58458
 PbSe, Te_{1-x}, thin films, localised defect states and Hall effect 7-2752
 PbTe, mag. susceptibility, optical absorpt. spectra, effect of intrinsic defects 7-64670
 Pt complex, (H₂O)_{0.33}Li_{0.8}(Pt(C₄N₂S₂)₂)_{1.67}·H₂O, synthetic conductor, spin-carrying defects 7-44524
 Pt silicide formation, defects study by scanning Auger microscopy 7-21195
 PtSi/Si heterogeneous interface struct., defects, and coherency, HRTEM meas. (*Japanese*) 7-7019
 (Pu, R)O₂, (R=Nd, Y), reactor fuels, thermal conductivity 7-19352
 Re₇B₃, inverse boundaries, rel. to defects in M₇C₃ carbides 7-12083
 Ru₇B₃, inverse boundaries, rel. to defects in M₇C₃ carbides 7-12083
 p-Si, alpha-particle irradi., defect form. and thermal stability 7-38073
 Si, amorphisation and crystallisation 7-11914
 Si, amorphised and rapid thermally annealed, extended defects 7-16660
 Si cleaved semiconductor surfaces scanning tunnelling microscopy 7-21051
 Si, crystal growth, impurity effect on formation of microdefects 7-32340
 Si crystals, radiation defect stabilisation and annealing kinetics study (*Russian*) 7-44608
 Si, Czochralski grown, interdependence of contamination and defect formation 7-32467
 Si, defect free zone, non-destructive microwave reflection decay meas. 7-51755
 Si, defects and device processing, achievements and limitations 7-32428
 Si detector material analysis using back electron beam induced current 7-44319
 Si, external photoelectric effect, Laue diff., anomalous X-ray transmission 7-7811
 n-Si, gamma-irradi., intrinsic defects, Hall effect and elec. cond. meas. 7-6615
 Si, impurity and defect props., processes and characterisation (*Japanese*) 7-7151
 Si, isoelectronic structurally bistable defect configs. study 7-16546
 Si, layers damaged by cutting, struct., X-ray diff. obs. 7-2401
 Si MBE, review 7-33573
 Si materials science and technology, conf., Boston, MA, USA (May 1986) 7-29598
 Si, microdefects, X-ray absorpt. during Laue diff. study 7-2009
 Si, oxidative packing defect form. during high temp. annealing 7-44522
 Si p⁺-i-n⁺ diodes, gamma irradi., capacitance detected mag. resonance 7-17243
 Si, recoil implantation of O₂, characterisation by double-crystal X-ray diffraction, TEM, Monte Carlo simulation 7-51807
 Si, scanning optical fibre microscope, laser beam induced current images 7-48846
 Si, scattering inhomogeneities, two-wavelength probe meas. 7-46063
 Si, self-implanted, defects and amorphisation 7-2041
 Si, solid-phase amorphous to crystalline transformation for shallow junction processing 7-32642
 Si, spin-dependent recombination and low-freq. ESR studies 7-38577
 Si, swirl defects formation 7-51753
 Si, visualisation of microdefects by X-ray topography 7-1811
 Si:As, Rutherford backscattering-particle induced X-ray emission analysis 7-54251
 Si:B, ion implanted, defect and dopant depth profile studies 7-2045
 Si:B(Al)(Ga)(P)(Sb) thermal donor props., impurity effects, DLTS, Hall effect, and admittance spectra meas. 7-21851
 Si:C wafers, defect generation, O precipitation effects (*Chinese*) 7-12058
 Si:C crystals, Stepanov method growth, defect structs. 7-32421
 Si:Ga epitaxial layers, growth induced planar defects 7-38414
 a-Si:H, charge transport and relax., luminesc. long-time tail distrib. anal. 7-39185
 n⁺-Si_{0.5}O_{0.5}, O precipitation and minority carrier generation lifetimes 7-16774
 Si₃N₄, small particles, elemental and chem. anal., EELS method 7-17379
 Si:P, ion implanted defect structs. rel. to implant energy 7-38079
 Si:Ti ion implanted layers, defect form. and precipitation, electron microscopy studies 7-12097

crystal defects continued

- Si-B⁺, Ge⁺, preamorphised shallow junctions, end-of-range and mask edge lateral damage 7-38071
 Si-SiO₂, SOI struct., deep O⁺ implantation, strain and damage in Si 7-32531
 6H-SiC neutron-radiated crystals, green luminesc., electron-vibrational interaction study (*Russian*) 7-59255
 β -SiC thin films, TEM obs. of process induced defects 7-58696
 SiC whiskers, tensile fracture rel. to defects 7-58722
 Si₃N₄ amorphous insulator thin films, defect-enhanced UV etching damage studies 7-26797
 Si₃N₄, nanostruct. defects, high-resolution electron microscopy studies 7-12302
 α -Si₃N₄, planar defect displacement vector determ. by HREM 7-2444
 α -Si₃N₄ whiskers, microstruct. investig. by TEM (*Japanese*) 7-21789
 SiO₂ films, breakdown lifetime meas., defect density determ. 7-22189
 SiO₂ RF sputtered thin films, atomic defects and stresses, optical and elec. props. 7-16898
 SiO₂ thermal films, cathodoluminescence of intrinsic defects 7-7766
 SiO₂ thermally grown on Si substrates, breakdown and defects studies 7-33104
 SiO₂ amorphous insulator thin films, defect-enhanced UV etching damage studies 7-26797
 SiB₆, cryst. struct. determ., defect content 7-58245
 SnO₂, mechanical activation, defect form. and struct. 7-16972
 SnTe, conc. depend. props. in region of homogeneity 7-45366
 SrCl₂:Eu, defect equilibria, site selective laser spectrosc. 7-46078
 Sr₂Mn_{2-x}Ti_xO_{5+x/2}, struct. and defects 7-44490
 SrTiO₃ cryst., electron pulse irradiation-induced transient optical absorpt. study 7-6682
 SrTiO₃ single cryst., H defect diffusion 7-58545
 Ta, Ne implanted, annealing behaviour of H traps 7-46506
 Ti, hardened from β -region, fine struct. study (*Russian*) 7-32450
 TiN reactively RF sputtered coatings, structural defects and porosity, electrochem. polarisation meas. 7-52333
 (U, R₂O₂), (R=Nd, Sm, Eu, Gd, Y), reactor fuels, thermal conductivity 7-19352
 (UPuR₂)O₂, (R=Nd, Eu), reactor fuels, thermal conductivity 7-19352
 V, radiation hardening by 14 MeV neutrons, athermal effects 7-51858
 W, electron and proton irradi., thermal annealing, positron annihilation studies 7-46214
 W, gamma-irradiated, anomalous effect of small doses 7-12151
 W-Co alloy, gamma-irradiated, anomalous effect of small doses 7-12151
 YAG:Ni (Ni, Zr) (Fe), defect and optical props. 7-59258
 YNbO₄, defect structure, Raman spectroscopy 7-63604
 Zn-Al-Mg alloy, defect and grain boundary diffusion-controlled positron trapping study 7-39301
 ZnS, fused polycryst. layers, photocond. and photolum. spectra, defect form. influence 7-46142
 ZnS, single crystal, annealed in O, intrinsic defects rel. to elec. and luminesc. props. 7-12649

crystal dislocations *see dislocations*crystal electron states *see electron energy states (condensed matter)*crystal energy *see lattice energy*crystal etching *see etching*

crystal faces

- apatite, Ising crit. temp. of connected nets and morphological importance of F faces 7-16476
 faceting effects on cryst. shape at crystn. front 7-32335
 organic materials, crystal growth kinetics, tailor-made additives influence 7-58171
 Au particle faces, restructuring TEM study 7-12418
 Ca₃(PO₄)₂CaF₂(OH)_x, hydroxyapatite, morphology of F faces 7-51686
 Ga growth into supercooled melt, faceted solid-liq. interface kinetics, kinetic roughening 7-58172
 n-GaAs, cleaved clean (110) surface initial band bending cause, noble metal deposition 7-22017
 In, equilibrium shapes, critical behaviour of curved regions 7-63529
 KH₂PO₄ crystals, contact nucleation on (100) face 7-51680
 KH₂PO₄ crystals grown at boiling point, surface microtopography 7-21581
 NaCl, equilibrium crystal form 7-16457
 NiSO₄·6H₂O crystals, soln., grown, steps on {001} faces, screw dislocations glide 7-58181

crystal field interactions

see also crystal hyperfine field interactions

- actinide systems, moderately delocalised, mag. behaviour, anisotropy of crit. correlations 7-7474
 ammonium hydrogen-DL-malate monohydrate, dielec. and pyroelec. props. 7-59138
 Anderson model, Bethe ansatz soln., cryst. field and spin-orbit coupling effects 7-2449
 Anderson model, dynamic susceptibility, freq. depend., 1/N_f expansion studies 7-2816
 CoCl₂-graphite, obs. of magnetic state, high magnetic field 7-59008
 cubic crystalline field eigenstates and energies, group-theoretical computational approach 7-21877
 cubic systems, superconducting p-wave pair states, collective excitations, spin-orbit interaction and cryst. field effect 7-7440
 degenerate Kondo lattice, magnetic instability and sp. ht. calcs. 7-58977
 dilute mag. alloy system, external mag. field, thermodynamic props. anomalies 7-45666
 emerald, Cr³⁺ absorption spectrum, spin-orbit interaction effects 7-13182
 ethylsulphate:Nd³⁺, high press. spin-lattice relax. and ground state 7-38934
 heavy fermion superconductivity, tight binding picture and Cooper pairs 7-2776
 bis(2-hydroxyethyl)terephthalate single cryst., benzene ring modes, Raman tensors determ. 7-64642
 ionic crystals, electronic polarisabilities and photoelastic behaviour 7-44444
 Ising chains, spin-S, cryst. field effect on transverse susceptibility 7-45601
 Knight shift, density matrix perturbational approach 7-33283
 lanthanum ethylsulphate: Gd³⁺, spin correlated cryst. fields and zero-field splittings, intersite contrib. calcs. 7-16996
 magnetic ion ground-state tunnelling splitting in cryst. field, mag. field depend. calcs. 7-21876
 metals, Kondo effect amplification by mag. field 7-52602

crystal field interactions continued

- paramagnets, thermodynamics, influence of crystal field anisotropy 7-12988
 permanent magnet materials, props., struct., exchange interactions 7-53053
 polyatomic mols. Rydberg states, cryst. field theory 7-10804
 rare earth adsorbates on metal surfaces, EPR line shapes 7-53129
 rare earth compounds, crystal field parameters in binary systems (*Chinese*) 7-38518
 rare earth compounds, crystal field strength, ligand field effects, angular overlap anal. 7-2543
 rare earth cpd. crystals, magnetooptic anisotropy, ionic polarisability in cryst. field 7-53285
 rare earth metals and intermetallics, Cryst. pot. model for description of cryst. elec. field effects 7-45599
 ruby, Cr³⁺ absorption spectrum, spin-orbit interaction effects 7-13182
 ruby, Cr³⁺ ground state, superposition-model analyses of EPR data 7-7158
 spin-orbit interaction and crystal field effects 7-38806
 tetrakis(1,1,1-trifluoro-4-phenylbutane-2,4-dionato) uranium (IV) magnetochemical study (*French*) 7-12956
 tetraphenylarsonium pentakis(nitrato)ytterbate(III), crystal field levels determ. by neutron spectroscopy 7-45238
 thin noncentrosymmetric crystals, Rayleigh scatt. of light 7-7710
 transition metal compounds, photoelectron spectra, ligand-field theory 7-22440
 transition metal phosphorus trisulphides, electronic, structural and mag. props., intercalation cpds. and chemical props. 7-44499
 tricritical point, Ising models with random bonds and crystal field interactions 7-2868
 Van Vleck paramagnetic susceptibility, cryst. field effect, temp. depend., approximate formulae, review 7-12935
 Ag-Au, valence level splitting 7-45139
 AgGaSe₂, cryst. field and spin-orbit interactions at fundamental gap, reflectivity meas. 7-16997
 AgGaSe(Te)₂, valence band struct., spin-orbit and cryst. field splittings, p-d hybridisation effects calcs. 7-27252
 Au-Er dilute alloys, Er³⁺ crystalline electric fields, screening effects 7-27307
 BaTiO₃:Fe³⁺, ferroelectric transition, EPR 7-33343
 BaYb₂F₈:Er(Tm), energy levels Stark struct., crystn. field interactions 7-58782
 BeAl₂O₄:Ni²⁺, chrysoberyl, laser induced fluoresc. and decay lifetime 7-46135
 CS₂, dynamical model for lattice frequencies and cryst. field splittings 7-16699
 CaF₂:Ce³⁺, two-photon absorpt. cross section, anal. of lowest 4f-5d transition 7-46081
 Ca₃Ga₂Ge₂O₁₂:Cr³⁺ garnet, ESR and ultrasonically modulated ESR studies 7-22139
 CaO-TiO₂-SiO₂:Eu³⁺ sphere ceramic, impurity laser-excited site-selective fluorescence line-narrowing spectra 7-13200
 CdCl₂, cryst. struct., temp. var., determ. from CdCl₂:Mn²⁺ EPR data 7-32382
 Ce compounds, moderately delocalised, mag. behaviour, anisotropy of crit. correlations 7-7474
 Ce cpds. and alloys, kondo effect versus crystal field 7-2602
 Ce doped fluoride elpasolites, 5d-4f spectra, impact of ion-host interactions 7-39143
 Ce impurity system, degenerate Anderson model, Bethe-ansatz soln. 7-2559
 Ce Kondo systems, thermopower, elec. resist. and cryst. field effects 7-21900
 Ce³⁺ in dielectric crystal, 5d-4f spectra, phenomenological cryst. field model 7-39148
 CeCu₂Si₂, Raman scatt. study of electronic and vibr. excitations 7-33387
 CeMRu₂Si₂ (M=La,Y), high energy EXAFS and XPS studies 7-64801
 Ce(Ni_{1-x}Cu_x)₂Si₂, mag. susceptibility, scaling behaviour, cryst. field effects 7-45616
 CePd₃B₆, heavy fermion cpd., thermal and mag. anomalous cryst. field effects 7-45239
 CePd₃Si, heavy fermion cpd., thermal and mag. anomalous cryst. field effects 7-45239
 Ce_{1-x}Pr_xNi₅ mixed valence cpd., cryst. field at paramag. Pr³⁺ ions 7-45241
 Cf oxides, Cf₂O₃, Cf₂O₁₂, CfO₂, BaCfO₃, mag. susceptibility meas. 7-12937
 CfX (X=N,As,Sb), mag. susceptibility meas. 7-12939
 Co complexes, tris(aminoacidato) cobalt (III), crystal field theory failure 7-12674
 Cr³⁺ impurity ions in low-symm. fields, energy levels, interconfig. interactions 7-58780
 CsFeCl₃, quasi-one-dimensional ferromag., mag. field effects on optical spectrum 7-3026
 Cs₂NaHoBr₆, excitation, electronic absorpt. and luminesc. spectra, crystal field splittings 7-46088
 CuGaSe(S)₂, valence band struct., spin-orbit and cryst. field splittings, p-d hybridisation effects calcs. 7-27252
 CuGaSnSe₄, valence band struct., spin-orbit and cryst. field splittings, p-d hybridisation effects calcs. 7-27252
 Cu(IO₃)₂·2H₂O, electronic absorption spectra, energy splittings 7-64625
 CuInSe thin films, flash evaporation prep. and characterisation 7-7893
 Cu₂Si₂O₆·6H₂O, Diopside crystals, Cu²⁺ EPR and optical absorpt. spectra studies 7-53120
 DyAl₂ single crystals, low temp. heat capacity meas. in mag. field, mean field approx. calcs. 7-27530
 Dy₂(SO₄)₃·8H₂O, magnetic and hyperfine props., cryst. field effects calcs. 7-27305
 ErAg, sp. ht. meas. 0.5 to 21 K 7-52994
 ErAl₂ single crystals, low temp. heat capacity meas. in mag. field, mean field approx. calcs. 7-27530
 ErIG, mag. prop. calc. 7-52977
 Er₂(SO₄)₃·8H₂O, magnetic and hyperfine props., cryst. field effects calcs. 7-27305
 Eu²⁺ impurity in garnets, compositional shift of spectral lines 7-53252
 Fe complex, ferric acetyl acetate, EPR studies 7-13024
 Fe-R intermetallics, (R=rare earth), intersublattice mol. field studies 7-27306
 FeTiO₃, oblique easy-axis antiferromag. neutron scatt. study of mag. excitations 7-45643

crystal field interactions continued

- Gd₂(Co_{1-x}Mn_x)₁₇, Co contribution to magnetocrystalline anisotropy, point charge model 7-45665
 GeFe₂O₄, ⁵⁷Fe²⁺ Mossbauer quadrupole splitting and orbit-lattice interaction 7-12684
 HoCl₃, ¹⁵Sm³⁺ cryst. field levels, assignment 7-27766
 Ho₂Co₁₇, intersublattice mol. field calc. 7-27511
 KAl(SO₄)₂·12H₂O:Cr³⁺, optical absorpt. spectrum study, cryst. field and site symm. determ. 7-59232
 KAlSi₃O₈:Fe³⁺, orthoclase, absorpt. and luminesc. spectra 7-53383
 KCl crystals with F_A(Li)-centres, double beam clarification kinetics (*Russian*) 7-53253
 KHo(MoO₄)₂, Ho³⁺ ground state, low temp. sp. ht., Stark components 7-44840
 K₂SO₄·Cr(SO₄)₂·24H₂O, alum, optical spectra, press. shifts 7-64666
 KZnF₃:Mn²⁺, thermal expansion of the Mn²⁺-F⁻ bond 7-6836
 LaF₃:Nd³⁺, energy value calc. of Stark sublevels (*Chinese*) 7-38519
 LiNbO₃:Fe³⁺, Mossbauer spectroscopic evidence of angle-depend. intersystem crossing 7-33312
 LiRbSO₄·VO²⁺, optical absorpt. and EPR spectrum, crystal field parameters 7-59109
 LiYbF₄:Er(Tm), energy levels Stark struct., crystn. field interactions 7-58782
 MgO:Cr, Cr³⁺, absorption spectrum, spin-orbit interaction effects 7-13182
 Mn²⁺-F⁻, ligand field correl. effects ab initio MBPT calcs. 7-21874
 Mn(IO₃)₂, electronic absorption spectra, energy splittings 7-64625
 NH₄H₂PO₄:Co²⁺, optical absorption spectrum 7-64077
 NH₄MnX₃ (X=Cl, F), absorpt. spectra 7-33410
 (NH₄)₂PdCl₄, NH₄⁺ rot. pot., inelastic neutron scatt. study 7-26676
 (NH₄)₂PtCl₄, NH₄⁺ rot. pot., inelastic neutron scatt. study 7-26676
 (NH₄)₂SO₄ crystal, cryst. fields calc., Madelung energies and cryst. pots. 7-64180
 (NH₄)₂SO₄:Ti, mol. orbitals, EHT calc., rel. to absorption spectra 7-64181
 (NH₄)₂SO₄:Ti crystal, temp. depend. of optical absorption bands 7-64671
 Na₂O·Al₂O₃·SiO₂:Eu³⁺ glass, impurity laser-excited site-selective fluorescence line-narrowing spectra 7-13200
 Na₂O·CaO·Al₂O₃·TiO₂:SiO₂:Eu³⁺ glass ceramic, impurity laser-excited site-selective fluorescence line-narrowing spectra 7-13200
 Nd₂Fe₁₄B, cryst. field effects 7-45598
 Nd₂Ga₅O₁₂ garnet, cryst. field studies of excited states 7-33407
 NdZn, antiferromag. skew scatt. Hall effect 7-52578
 Ni (IO₃)₂·2H₂O, electronic absorption spectra, energy splittings 7-64625
 Ni cpds., ionic, ground state studies, multiplet effects, near-edge XAS 7-64803
 NpAs₂, J=9/2 multiplet, tetragonal symmetry, crystal field wavefunction, Hamiltonian 7-12931
 PbV₂O₆, vitreous and crystalline, mag. props. 7-7473
 PbWO₄:Nd³⁺ (Pr³⁺), optical spectra 7-39146
 PrCl₃ cryst. field correlation effects in Pr³⁺-Cl⁻, ab initio calcs. 7-7177
 PrH_{2-x}, (x=0-0.5), low temp. specific heat meas. 7-32681
 Pr₂(SO₄)₃·8H₂O, magnetic and hyperfine props., cryst. field effects calcs. 7-27305
 Pt complexes, CO ligand σ and π interactions 7-64663
 R-Co, 4f Co rich intermetallics, basal plane magnetocrystalline anisotropy 7-52972
 R₂Fe₁₄B, cryst. field effects at rare-earth sites 7-45598
 Rb₂Mg(SO₄)₆H₂O:CO²⁺ optical absorption spectrum 7-13180
 TbAl₂ single crystals, low temp. heat capacity meas. in mag. field, mean field approx. calcs. 7-27530
 Tb₂Ti₂O₇, elastic modulus, low temp. anomalies 7-44651
 β -ThCl₄:Pr³⁺, site selective laser fluorescence spectroscopy 7-64687
 ThNX (X=Se, Te), heat capacity, neutron diff. and crystal field models 7-12976
 ThO₂:Np⁴⁺, absorption and emission spectra of Np⁴⁺ 7-27763
 ThSiO₄:Np⁴⁺, absorption and emission spectra of Np⁴⁺ 7-27763
 (Ti,M)O₂ (M=V, Nb, Ta) rutile solid solns., charge transfer and ligand fields, XANES studies 7-64782
 (Ti,Ta)₂O₃ solid solns., chem. shift and cryst. field splitting rel. to valence charge, EXAFS 7-27818
 TmAl₂ polycryst., low temp. heat capacity meas. in mag. field, mean field approx. calcs. 7-27530
 TmCu₂, ³H₄ multiplet splitting, cryst. field effect 7-52533
 TmH₂, spin-disorder resistivity and cryst. field effects 7-17021
 TmNi₂, singlet ground-state cpd., induced-moment ferromagnetic ordering meas. 7-38866
 UBr(Cl)(I)₃, magnetic transitions, antiferromag. order and cryst. field splitting, neutron scatt. study 7-12974
 UCl₄, cryst. field spectroscopy by neutron inelastic scatt. 7-27304
 UNX (X=Se, Te), heat capacity, neutron diff. and crystal field models 7-12976
 URu₂Si₂, monocrystalline, thermal expansion and sp.ht. 7-44866
 UO²⁺ complexes, rhombic symmetry cryst. field and ground state wavefns. 7-38927
 Y₂(Co_{1-x}Mn_x)₁₇, Co contribution to magnetocrystalline anisotropy, point charge model 7-45665
 YAG:Tb, electron-phonon relax. in ⁵D₄ of Tb³⁺ 7-2130
 YAG:Tb cryst. field anal. of Tb³⁺, site selective polarisation spectroscopy 7-2546
 Y_{1-x}Dy_x dilute alloys, spin density wave antiferromagnetism 7-52947
 Yb impurity system, degenerate Anderson model, Bethe-ansatz soln. 7-2559
 Yb²⁺ impurity in garnets, compositional shift of spectral lines 7-53252
 Yb₂Fe₁₄B, exchange and cryst. field interactions 7-27512
 Yb₂Se₄, crystal struct. and mag. props. (*French*) 7-63590
 Zn(BF₄)₂·6H₂O:Mn²⁺, EPR study 7-64520
 ZnS:Cr²⁺, Cr excitation spectrum interpretation 7-58775
 ZnSiP₂ cryst., exciton absorpt. spectrum, energy gap and exciton binding energy determ. 7-2500
 ZnTiF₆·6H₂O:Mn²⁺, ESR spectrum, axial press. effects 7-22136
 Zr³⁺ impurity in garnets, compositional shift of spectral lines 7-53252

crystal field splitting see crystal field interactions

crystal field theory see crystal field interactions

crystal fields see crystal field interactions

crystal filters

- SAW filters, method for false signal level reduction 7-57640

crystal growth

- see also crystal growth from melt; crystal growth from solution; crystal growth from vapour; crystal purification; crystallisation; dendrites; epitaxial growth; nucleation
 2D nucleation in elec. field, form. free energy 7-58434
 actinides, metals and cpds., crystal prep. for solid state research 7-17395
 alloys, electrochemical deposition, cryst. growth modelling 7-59386
 asymptotic growth shapes developed from 2D nuclei 7-58180
 colloidal crystals, nucleation and growth 7-12243
 conference, York, England (Jul. 1986) 7-48142
 crystalline rods, thermoelastic stresses and temps., asymptotic calc. 7-32542
 crystallography, conference, Kharagpur, India (Dec. 1982) 7-55876
 dendrites, symmetric model of growth, boundary integral formulation 7-45103
 dendritic growth, geometrical model, small velocity limit 7-7081
 dendritic growth, sidebranch generation mechanisms, nonlinear effects 7-64035
 diffusion-controlled interfacial growth, dense branching morphology form. 7-21147
 diffusion-limited aggregation without branching 7-21146
 doped semiconductors, prep. and thermal cond., review 7-38279
 equilibrium crystal shape, numerical evaluation 7-63530
 faceting effects on cryst. shape at crystn. front 7-32335
 fluid structure and surface roughening 7-58606
 glass core fibre with crystal cladding, fibre system fabrication for nonlinear optics 7-37188
 growth shape of crystallite on substrate, Monte Carlo simulation 7-44426
 heat and mass transfer in microgravity and on Earth 7-53510
 high electric fields, review 7-32338
 high purity autoclaves for high temp. cryst. growth and phase diagram studies 7-53511
 high temp. crystallisation, flaw form., AE detection, automatic system 7-3557
 hill formation by 2D nucleation 7-44427
 II-V semiconds., cryst. growth, characterisation and appls., review 7-26685
 III-V semiconductors, X-ray topography and diff. imaging 7-32224
 inorganic layered cpds., reactivity, conf., New York, NY, USA (Apr. 1986) 7-41003
 liquid-solid interface stability, review 7-37912
 magnetic domain studies, review 7-17209
 materials modification with ion beams, review 7-16647
 metal oxides, new routes in their synthesis 7-32339
 microgravity expts. in materials processing (*Japanese*) 7-59737
 monolayer post-deposition cluster growth, nearest-neighbour model, computer simulation 7-58621
 Monte Carlo simulation of continuous-space crystal growth, Monte Carlo simulation 7-6568
 needle crystal formation in two dimensions 7-38421
 nonlinear optical and electro-optical material advances, book contrib. 7-25914
 nucleation and growth, crystal defects 7-58169
 polymer crystals, 1D growth, computer simulation 7-16466
 profiled crystal growth, surface tension as an automatic control parameter 7-32324
 rare earth phosphates, preparative methods and growth, review 7-37913
 refractory metals, crystal growth and surface self-diffusion in high elec. fields, FEM studies 7-37914
 research in China 7-53509
 sapphire, growing crystals, hot zone heat transfer simulation 7-32321
 semiconductor infrared detectors, conf., Innsbruck, Austria (April 1986) 7-60871
 structures, nonconvex, polygonal mesh and quad-tree display algorithms 7-51672
 temperature distribution and mass transfer of flow by free convection in enclosures rel. to crystal growth (*Chinese*) 7-11977
 two-dimensional growth models, interface dynamics, time-reversal invariance and universality 7-63532
 Al₂P₆O₁₈, synthesis and struct. 7-1969
 Ba(Li_{0.25}Sb_{0.75})O₃, cubic perovskite, prep. and struct. 7-63589
 Ba(Na_{0.25}Sb_{0.75})O₃, cubic perovskite, prep. and struct. 7-63589
 Ce₂Co₂P₁₂, synthesis, cryst. struct., X-ray diff. study 7-32387
 CeSe₂O₆, cryst. struct., X-ray diff. study (*French*) 7-26706
 CoCr-based thin films, growth and mag. props., nucleation layer effects 7-45065
 CoGaInS₄, cpd. with FeGa₂S₄ struct., prep. and characs (*German*) 7-1984
 Cr Lu₄S₇, synthesis, physiochemical props. 7-44470
 CrDy₄S₇, synthesis, physiochemical props. 7-44470
 CrEr₄S₇, synthesis, physiochemical props. 7-44470
 CrGd₄S₇, synthesis, physiochemical props. 7-44470
 CrHo₄S₇, synthesis, physiochemical props. 7-44470
 CrTb₄S₇, 7-44470
 CrTm₄S₇, synthesis, physiochemical props. 7-44470
 CrYb₄S₇, synthesis, physiochemical props. 7-44470
 Cu, filament growth on Cu₂Se, superionic transport mechanism 7-45104
 Cu_{1.80}Fe_{0.05}S₃, structural phase transitions, X-ray diff. study 7-1935
 CuGaSe₂(1-x)Te_{2x} solid solns., prep. and character. 7-21169
⁴He crystals, dendritic growth obs. 7-44948
⁴He dendritic growth, spatio-temporal coherence and chaos, conf. Los Alamos, USA, Jan. 1986 7-48158
 HgCdTe materials for infrared detectors, prep. techniques 7-64019
 K₃Cu₂S₆, mixed valence 2D metal, CDW 7-45294
 KH₂PO₄ crystals, contact nucleation on (100) face 7-51680
 K₆LiFe₂₃S₂₆Cl₂, djferisherite, electrochemically synthesised, cryst. struct., neutron diff. study 7-58224
 K₃Li₂TeO₆, prep., cryst. struct., Madelung lattice energy calc. (*German*) 7-16515
 K_{0.3}MoO₃, CDW transport, crystal quality, inhomogeneous conductivity, contact geometry 7-52587
 KPbBr₃·H₂O, synthesis, cryst. struct., X-ray diff. study (*German*) 7-37940
 La₂Co₄P₁₂, synthesis, cryst. struct., X-ray diff. study 7-32387
 Li₂Mg_{1.5-x}VO₄ solid soln. phase, synthesis, stoichiometry and struct. 7-21168
 LiTa_{1-x}Mg_xO_{3-3x}F_{3x}, prep., ferroelec. Curie temp., effect of cationic substitution 7-45946
 LiTa_{1-x}Zn_xO_{3-3x}F_{3x}, prep., ferroelec. Curie temp., effect of cationic substitution 7-45946

crystal growth continued

- Mn allotropic phases nucleation during laser annealing, melting, solidification and regrowth 7-12143
 NH_4Cl , irregular fractal-like crystal growth, diffusion-limited aggregation model 7-2445
 $(\text{NH}_4^+)_{0.22}\text{TiS}_2^{0.22-}$ ionic intercalation cpd., synthesis, characterisation by thermal anal., mag. 7-45244
 $\text{Nd}_2\text{Co}_4\text{P}_{12}$, synthesis, cryst. struct., X-ray diffr. study 7-32387
 $\text{Nd}_2\text{Cr}(\text{Ce})_{1-x}\text{P}_5\text{O}_{14}$ cryst. growth and characterisation, X-ray diffr., Raman scatt., visible and IR absorpt. meas. 7-44423
 $\text{Nd}_2\text{Y}_3\text{-Fe}_5\text{O}_{12}$, garnets, growth anisotropy, Mossbauer study 7-38973
Ni thin strips, cryst. growth 7-53580
 NiAl_2O_4 , spinel growth, thin film Al_2O_3 substrate, topotactic relationships 7-5817
Pd-U-Si glassy alloys, glassy-to-icosahedral polymorphous crystn. transform., X-ray and electron diffr. studies 7-6515
 $\text{Pr}_2\text{Co}_4\text{P}_{12}$, synthesis, cryst. struct., X-ray diffr. study 7-32387
 $\text{Pr}_2\text{P}_5\text{O}_{14}$ cryst. growth and characterisation, X-ray diffr., Raman scatt., visible and IR absorpt. meas. 7-44423
 $\text{Pr}_2\text{Y}_3\text{-Fe}_5\text{O}_{12}$, garnets, growth anisotropy, Mossbauer study 7-38973
Pt small crystals, atomic-resolution study of struct. rearrangements 7-32243
 $\text{Rb}_{0.3}\text{MoO}_3$, CDW transport, crystal quality, inhomogeneous conductivity, contact geometry 7-52587
Si-O system, solubilities of O in liq. and solid Si 7-26961
Sn, crystal growth and Stefan problem, stochastic theory comparison 7-21415
Th₂Hg, intermediate phase in Th-Hg system, synthesis, struct., X-ray diffr. study 7-37911
V₂H, cryst. struct. of tetragonal and monoclinic forms, X-ray diffr. study 7-44456
 $\text{Yb}_2\text{Co}_4\text{P}_{12}$, synthesis, cryst. struct., X-ray diffr. study 7-32387
 $\text{YbD}_{2.6}$, cryst. struct., X-ray diffr. study 7-16516
 YbD_x , $2.0 < x < 2.5$, cryst. struct., X-ray diffr. study 7-16516
 ZrO_2 , tetragonal, cryst. growth 7-17417

crystal growth from gel

- ammonium hydrogen tartrate, dislocation etch pits 7-37999
ammonium hydrogen tartrate, ferroelectric, crystal growth and dislocation etching kinetics 7-51770
didymium tartrate crystals, gel grown, charactn., thermal behaviour 7-39367
 $\text{Cd}(\text{OH})_2$, dendritic structures in agar gel 7-58723
Sb trihalide single crystal growth in gel 7-22458
 SiO_2 , tridymite, form. from colloidal silica, kinetics 7-23053

crystal growth from melt

- see also liquid phase epitaxial growth; zone melting
Accelerated Crucible Rotation Technique, fluid flows 7-46306
accelerated crucible rotation technique for cryst., growth, review of the theoretical models 7-39368
alkali halide, crystal growth in stationary crucible 7-59413
axisymmetric needle crystals, 3-D, solvability condition at large undercooling 7-32337
binary alloy, freezing, morphological instability evolution, model cryst. growth system 7-1925
binary semiconductor alloys, directional solidification, convection, segregation, ampoule and furnace design 7-59501
binary systems, stochastic theory of solidification 7-12238
Bridgman growth, interface temp. distrib., furnace stability, computer calc. 7-53546
chondrule melts of porphyritic and radial pyroxene comp., dynamic crystallisation 7-9368
crystallisation front morphology rel. to inclusions in melt (Russian) 7-64890
Czochralski cryst. growth, simulation of jet cooling effects 7-17408
Czochralski crystal puller, modelling of melt motion in axial mag. field 7-53545
Czochralski furnace, numerical calc. of heat transfer 7-53543
Czochralski growth, cryst. wt. rel to melt temp. variation 7-7841
Czochralski growth, global finite element calc. 7-39370
Czochralski growth, mag., expt. model 7-44428
Czochralski method, controlled crystn. dynamics model anal. 7-27885
Czochralski method, melt level variations effect on crystn. rate 7-3160
Czochralski method, simulations with tetradecane and water, growth instability 7-44424
Czochralski method simulation using tetradecane, Flow transitions visualisation 7-22463
diamond nucleation and growth at high press., colloidal theory 7-46301
directional solidification, asymptotic eqns. and solid-liquid interface struct. 7-52010
domain growth from melt, temp. gradient, form. kinetics study 7-51681
flame fusion, growth of single crystal with dissolution phase (Japanese) 7-53571
Gault process for III-V compound semiconductors 7-46300
ice, pure and doped, US absorpt., dislocation damping 7-26756
ice, single crystal crucible-free growth, weightlessness simulation 7-64888
ice formation on substrates, crystallographic config., cooling rate and direction (Japanese) 7-6569
III-V semiconductors, single crystal growth, formation of microinclusions 7-21141
image processing of Czochralski bulk flow 7-53544
interfacial, surface angles at three phase line, melt solidification conditions, thermodynamic analysis 7-27889
liquid metals, horizontal Bridgman growth in 2D flow 7-64885
liquid metals, horizontal Bridgman growth in 3D flow 7-64886
 $(\text{LuYbPb})_2(\text{FeGa})_5\text{O}_{12}$, crystn. from soln. melt, component distrib. 7-21149
methyl 2-(2,4-dinitrophenyl)aminopropanoate single crystals, travelling-heater Bridgman growth 7-59409
2-methyl-4-nitroaniline single crystalline films, growth for phase-matched frequency-doubling 7-3212
non-wetting melt in free fall, bubble-bridge config., contact angle 7-21572
optical crystals, growth, Bridgman-Stockbarger method, thermal modelling 7-22461
organic molecular crystals, growth, quadratic nonlinearities 7-53569
oxide crystal growth, Czochralski apparatus automation 7-27884
physical constants of melt determ. 7-13348
poly(vinylidene fluoride), α -polymorph, melting behaviour and isothermal lamellar thickening 7-12240
- crystal growth from melt continued
poly- ϵ -caprolactone, crystallisation from melt, real-time pulse NMR meas. 7-27621
profiled crystals, Stepanov growth, conf., Leningrad, USSR (March 1985) 7-29573
quartz, crystal growth, pragmatic model for simulation of self-induced striations 7-11973
rapid solidification, steady and oscillatory cellular morphologies 7-2157
salol melt-grown crystals., decanted surface markings, in situ microscope obs. 7-27068
sapphire:Ti³⁺ laser material, scattering centre formation mechanism 7-10960
sapphire, Stepanov growth, radiative-conductive heat transfer simulation 7-31630
sapphire tube prod. by Stepanov method at high growth rates 7-7837
semi-insulating, nonstoichiometry study, lattice parameter meas. 7-38220
semiconductor crystal growth, industry needs 7-53540
semiconductors, confined vertical growth method 7-17411
semiconductors, Czochralski, growth, slip dislocation generation 7-22467
solid/melt interfaces, cryst. growth, computer simulation studies 7-16469
sphere crystallisation, thermoelastic stresses in weightless conditions 7-1424
Stepanov crystallisation method, stationary state existence conditions 7-32323
Stepanov method cryst. growth, computerised TV system examination 7-33542
Stepanov method crystallisation on a rotating seed 7-33540
Stepanov method growth, dopant evaporation effects 7-32319
supercooled melt, kinetics of crystal growth 7-1924
ternary intermetallic compounds, single crystal, Czochralski growth, charactn. 7-53557
thermal image floating zone method (Japanese) 7-53570
thermocapillary free boundaries 7-46309
transport processes, analytical modelling and expt. obs. 7-53541
YAG: rare earth crystals, impurity content, absorpt., spectrophotometric obs. 7-13843
AgGaS₂(Se₂), chalcopyrite, crystal growth, nonlinear IR props. 7-37040
Al-Cu-Mg, growth by Stepanov's method, macro- and microstructure, strength, plasticity meas. 7-33546
Al-Mn surface icosahedral phase form., ion beam mixing and interdiffusion 7-16653
Al-Zn eutectic, oriented crystallisation, buoyancy-driven convection effects 7-27887
 Al_2O_3 , bicrystals, high-purity, grain boundary structures 7-58668
 Al_2O_3 , cryst. growth from melt, phase boundary displacement mechanism, defect distrib. 7-32328
 Al_2O_3 , profiled cryst. growth, static thermal stability, growth angle determ. 7-32334
 Al_2O_3 , profiled crystals, bubble distrib., cellular struct., residual stresses 7-32422
 Al_2O_3 profiled crystals, prod., quality characts. 7-33615
 Al_2O_3 :Mo, W, Cr, leucosapphire, growth by horizontal directional crystallisation, mass transport of Mo, W 7-22459
B, crystal growth in solar furnace 7-33538
BaF₂, Bridgman-Stockbarger growth and scintillation props. 7-59408
Ba_{2-x}Sr_xK_{1-x}Na₂Nb₂O₁₅, ferroelectric tungsten bronzes, crystal growth and optical appl. 7-39085
BaTi₄O₉ single crystals, growth by floating zone method 7-17415
Bi thin films (111), melt growth, in-situ obs. by TEM 7-53573
Bi-Sb-(Te), single cryst. alloys, component distrib., stratified heterogeneity 7-46302
 $\text{Bi}_4\text{Ge}_3\text{O}_{12}$ crystals, imperfection nature, precipitates and bubbles 7-21463
 $\text{Bi}_4\text{Ge}_3\text{O}_{12}$, Czochralski growth, melt temp. fluctuations 7-53555
 $\text{Bi}_4\text{Ge}_3\text{O}_{12}$, high quality large cryst. growth, colour and precip. form., pulse height resolution 7-53554
 $\text{Bi}_4\text{Ge}_3\text{O}_{12}$ single crystals, shape, melt flow patterns, Czochralski growth conditions 7-16464
 $\text{Bi}_4\text{Ge}_3\text{O}_{12}$ single cryst. growth, characterisation and appls. 7-33550
 $\text{Bi}_2(\text{MoO}_4)_3$, Czochralski growth, monoclinic unit cell (Korean) 7-27890
 $\text{Bi}_{5.8}\text{PO}_{11.2}\text{Nd}^{3+}$, cryst. growth, spectroscopic props. of Nd³⁺ ions 7-46131
 $\text{Bi}_{0.52}\text{Sb}_{1.48}\text{Te}_3$, semiconducting solid soln., thermoelectric props 7-45365
 $\text{Bi}_2\text{Te}_2\text{SeO}_{0.6}$, 7-45365
CaF₂, fluorite residual stress fields in cylindrical Bridgman-Stockbarger crystals 7-11976
CaF₂ profiled crystals, growth by Stepanov's method, appl. for optical components 7-31409
 CaRaIO_4 (R=Y, La, Gd, Tb Lu), growth by Czochralski method 7-22460
 $\text{Cd}_2\text{Hg}_{1-x}\text{Te}$, Bridgman growth using Accelerated Crucible Rotation Technique 7-46307
CdSe cryst., low press. melt growth technique 7-33548
 CdSnAs_2 crystal growth from melt sealed by LiCl-KCl mixture 7-7839
CdTe cryst., low press. melt growth technique 7-33548
 $\text{Ce}_2\text{Mo}_6\text{S}_8$, crystal growth and struct., susceptibility and transport props. 7-64889
 $\text{CrNH}_4\text{P}_2\text{O}_7$ and α - and β - $\text{CrNH}_4\text{HP}_3\text{O}_{10}$, preparation and characts. 7-3161
CsBr-AgBr fibres, growth by Stepanov's method 7-31533
 $\text{Cs}_3\text{Cr}_2\text{X}_6$ (X=Cl, Br, I), synthesis, struct., mag. props. 7-6601
 CsV_2O_7 , crystals, struct., cathodic reduction from melt, and elec. props. studies 7-58236
 $\text{Cu}_2\text{Ag}_{1-x}\text{InSe}_2$, liquid-encapsulated Bridgman-Stockbarger melt growth and props. 7-59403
 $\text{CuInGa}_{1-x}\text{Se}_2$, liquid-encapsulated Bridgman-Stockbarger melt growth and props. 7-59403
 CuInSe_2 polycryst. semicond. growth from melt, surface props., ion bombardment and annealing effects 7-46304
 $\text{Cu}_2\text{Mo}_2\text{O}_{17}$, synthesis and cryst. struct. 7-32398
Eu-Bi-S, synthesis and props. 7-44471
Eu-Bi-Se(Te), synthesis and props. 7-44471
Eu-Sb-S, synthesis and props. 7-44471
Eu-Sb-Se(Te), synthesis and props. 7-44471
Fe crystals, growth shape, effect of melt undercooling (Russian) 7-46308
 $\text{Fe}_3(1-\delta)\text{O}_4$, magnetite, synthesis, crystal growth and characterisation 7-2647
Ga growth into supercooled melt, faceted solid-liq. interface kinetics, kinetic roughening 7-58172
GaAs, Czochralski growth of high quality crystals. 7-53548
GaAs, dislocation density reduction in crystal growth 7-2020

crystal growth from melt continued

- GaAs, horizontal Bridgman growth, semi-insulating props. characts. 7-64896
- GaAs, LEC, semi-insulating, undoped, C origin and melt comp. depend. 7-17410
- GaAs, LEC, undoped, stoichiometry 7-53563
- GaAs, LEC grown, obs. of Ga precipitates 7-32663
- GaAs, LEC grown, threshold for dislocation form., role of cryst. dia. and impurity hardening 7-53551
- GaAs, LEC growth configuration, thermal stresses, effect of liq. encapsulation, thermoelastic anal. 7-59414
- GaAs, LEC growth for IC technology appls. 7-64894
- GaAs, LEC single cryst. homogeneity, effect of strong mag. field 7-53549
- GaAs LEC substrates, EL2 deep donor kinetics under annealing, IR absorpt., DLTS, Hall effect meas. 7-32955
- GaAs, large dislocation-free cryst. growth for LSI appls. 7-64895
- GaAs, melt grown, theoretical and expt. fundamentals of decreasing dislocations 7-53547
- GaAs, semi-insulating, LEC grown, midgap native donor concentration 7-33547
- GaAs:B, as-grown Czochralski crystals, EPR signal 7-38935
- GaAs:C, low C conc., crystal growth using pyrolytic BN coated graphite 7-59398
- GaAs:Cr semiinsulating LEC wafers, microhardness cartography 7-32886
- GaAs:In, B, electrical props., role of residual B impurity, liquid encapsulated Czochralski growth 7-45312
- GaAs:In, LEC growth, annealing, solid soln. hardening, dislocation density, elec. props. 7-17404
- GaAs:In, low In conc., LEC cryst. growth employing thermal stress anal. 7-46305
- GaAs:In (B)(Si), dislocation free crystals, LEC grown, microscopic defects, eutectic etching 7-16545
- GaAs:In crystals, LEC growth, growth-in dislocation elimination 7-22465
- GaAs:Si, semi-insulating, ion implanted, LEC growth, elec. activation efficiency, stoichiometry dependence 7-46298
- GaAs:Si(S), LEC grown, struct. defects, influence of Si and S doping 7-53550
- GaSb, crystal growth and synthesis, thermodynamics, optimisation algorithm appl. 7-16461
- GaSb:Te(Se)(Si)(Ge) single crystals, Czochralski growth, carrier conc. rel. to dopant conc. 7-22462
- (Gd,Sc)₂Ga₂O₁₂: Cr, Nd laser crystals, growth and quality 7-13346
- Gd_{3-x}Bi_xFe₂O₁₂ crystal growth for 0.8 μ m optical isolator 7-57605
- Gd_{2.95}Sc_{0.05}Ga_{3.138}O₁₂ garnet, congruently melting, cryst. growth 7-59412
- Gd₂SiO₃:Ce(Tb), Czochralski growth 7-53556
- Ge, Czochralski growth, cryst. wt. rel to melt temp. variation 7-7841
- Ge large crystal growth by Stepanov method 7-33543
- Ge profiled crystals, growth by Stepanov's method, appl. for optical components 7-31409
- Ge:Ga(Be)(Zn) extrinsic photoconductor material, cryst. growth and characterisation 7-64893
- Ge-transition metal eutectic alloys, cryst. growth by directional crystallisation 7-64887
- HfO₂-R₂O₃, R=Sc, Y, Nd, Gd, Tb, Er, Yb, solid solution single crystal growth 7-7838
- HgCdTe, bulk melt growth and LPE, defect control 7-64940
- HgCdTe, cryst. growth by travelling heater method 7-64892
- HgCdTe, single cryst. growth by travelling heater method 7-64891
- HgI₂ single cryst. growth new technique 7-53562
- InAs₂P_{1-x}, LEC-grown single crystals, growth defects and lattice strains 7-38001
- InP, direct synthesis, growth, liquid encapsulated Czochralski method 7-59397
- InP, dislocation density reduction in crystal growth 7-2020
- InP synthesis by modified horizontal Bridgman method, elec. props. 7-58821
- InP:Fe, Czochralski-grown, stoichiometric-related faulted loops, struct. and lumin. props. 7-51772
- InP:Fe, programmed magnetic field applied LEC crystal growth 7-59399
- InP:Fe:Ga:Sb, LEC growth, dislocation density, resistivity, SIMS obs. 7-53552
- InP:Ga,As,Sb single crystals, LEC growth, isoelectronic doping, dislocation density, X-ray topography 7-33549
- InP:Ge:S, LEC-growth, dislocation-free 7-17409
- InP:S, LEC grown, influence of growth conditions on defects 7-32427
- InP:S,Ga,Sb, LEC growth, appl. mag. field method, dislocation etching 7-53553
- InP:Ti(Cr)(Ni), LEC growth, precipitate phase identification 7-16754
- InSb, Czochralski growth rate and spreading resist. relations (*Japanese*) 7-26679
- InSb:Te, Cd, Zn single crystals, Czochralski growth, solute distrib., mag. field effect on melt 7-3158
- InSb:Te crystals, Czochralski growth, layered heterogeneity, melt temp. fluctuations, mag. field effect 7-27888
- InSe crystals, melt-grown, electron diff. study 7-1994
- InSe single crystals, growth by travelling heater method, carrier conc., photoelectrochemical props. 7-59410
- K_{1.5}Bi_{1-x}Nd_xNb_{0.5}O₁₅, cryst. growth, spectral props. of Nd³⁺ ions 7-53405
- KCl:Ca, γ -irrad., Z₁-centre growth, effect of dislocations, thermolum. study 7-32487
- K₂NaScF₆:Cr³⁺ laser material, tunable, crystal growth and spectroscopy 7-13347
- KNbO₃, single domain cryst. prep., orientation and dielec. polarisation 7-45950
- K₂O-CaO-SiO₂ system, cryst. growth kinetics, morphology, melt comp. depend. 7-46303
- KTiOPO₄, crystal and optical props. 7-17403
- KTiPO₄ crystal growth for high efficiency SHG devices (*Chinese*) 7-7835
- LaB₆ crystals, grown with Xe arc image furnace, subgrains 7-59411
- LaNiAl₁₀O₁₉, magnetoplumbite type cpd., synthesis, cryst. growth and struct., electronic spectra 7-44476
- Li₂BN₂, synthesis, polymorph struct., ionic cond. meas. 7-32388
- LiNbO₃, charactn. by γ -ray diff. 7-54061
- LiBr-LiCl binary mixed crystal system, critical nucleus, melt comp. 7-58445
- LiF profiled crystals, growth by Stepanov's method, appl. for optical components 7-31409

crystal growth from melt continued

- LiF profiled crystals, growth by Stepanov method, shaper material effects 7-32333
- LiF, Stepanov method growth and crystal shaping 7-32320
- LiNbO₃, Czochralski cryst. growth, computer control 7-27886
- LiNbO₃, Czochralski growth, physical constants of melt determ. 7-13348
- LiNbO₃, prod. by Czochralski and Stepanov methods, elec. phenomena accompanying growth 7-32332
- LiNbO₃, profiled cryst. growth by Stepanov's method, regular domain struct. prod. 7-32330
- LiNbO₃ single crystal fibres, ferroelec. domain structs. 7-22202
- LiNbO₃ substrates, growth and composition effects 7-26025
- LiNbO₃:Fe, Czochralski growth and holography appl. 7-59404
- LiNbO₃:MgO, melt growth and charactn. 7-58170
- LiNbO₃:Y single crystal, Czochralski growth, crystal-melt interface stability (*Chinese*) 7-58168
- LiNbO₃Ta₂O₅ single cryst., piezoelec., pyroelec., dielec. and elastic consts. 7-53565
- LiTaO₃, cryst. strip growth and quality, prod. by Stepanov's method 7-32331
- LiTaO₃, Czochralski grown with modulated struct., periodic laminar ferroelec. domains, SHG 7-59405
- LiTaO₃ substrates, growth and composition effects 7-26025
- LiY_{1-x}Yb_xF₄ single cryst. growth, lattice const. and thermal expansion coeff. temp. depend. studies 7-27891
- MgAl₂O₄:Ni²⁺, Czochralski growth and optical props. 7-59406
- MgO-Al₂O₃-SiO₂, leucosapphire, crystal growth by directional crystn., gas inclusions formation 7-33539
- MoSe₂, melt grown layered crystals, optoelectronic props. 7-21946
- NaNbO₃, single cryst. growth by Stepanov's method 7-32329
- Nb₂S₂Se₂, crystal growth and superconductivity 7-27451
- NdGe₂, Czochralski single cryst. growth using tri-arc furnace 7-7836
- oxide bronze single cryst., Bridgman growth in air 7-3162
- Pb-Tl, Bridgman growth, pattern generation at solidification front, forbidden cells 7-22651
- PbBi₄Te₇, synthesis and physicochemical props. 7-13349
- Pb_{1-x}Zn_x single crystals, growth and semicond. behaviour 7-53577
- PbMoO₄, Czochralski grown, crystallisation front rel. to cryst. quality 7-59402
- PbSe:Cd, crystal growth and impurity distrib., electron probe X-ray microanal. studies 7-63639
- PbTe crystals, Bridgman growth in centrifuge, convection effects (*French*) 7-53542
- Rb₂NaScF₆, Ce doped, 5d-4f spectra, impact of ion-host interactions 7-39143
- Rb₂NaYF₆, Ce doped, 5d-4f spectra, impact of ion-host interactions 7-39143
- RbV₃O₇ crystals, struct., cathodic reduction from melt, and elec. props. studies 7-58236
- SbSI, crystals, growth from melt, microhardness study 7-12196
- SbSI, elec. charactn. of crystals, grown from melt by temp. fluctuation technique 7-13104
- SbSI, SbSOI, cryst. growth and elec. charactn. 7-53564
- SbSeI, crystals, grown from melt, microhardness study 7-12196
- Si, axial magnetic Czochralski growth 7-32343
- Si bicrystals, Czochralski growth, tilt boundaries 7-53558
- Si crystal growth, mould shaping, spinning, method 7-53568
- Si crystal growth and epitaxial layer deposition for VLSI devices 7-46299
- Si, crystal growth and solidification, high speed laser heating technique 7-53566
- Si, Czochralski grown, tensile props., 900-1200°C 7-51922
- Si, Czochralski grown crystals, octahedral crystalline inclusions, TEM obs. 7-16581
- Si, Czochralski growth, large diameter crystals, under horizontal or vertical mag. field 7-32342
- Si, Czochralski growth, relax. in point defects system 7-16468
- Si, Czochralski growth of high quality crystals. 7-53548
- Si, diffusion length depend. on cooling rates and bulk resistivity 7-7266
- Si, directional crystallisation, carbon-fabric support 7-13350
- Si for solar cells, growth by horizontal supported web technique 7-17412
- Si growth by SOG method and Stepanov method, stability anal. 7-33602
- Si, mag.-field Czochralski-grown neutron transmutation doped, thermal behaviour 7-53574
- Si, magnetic Czochralski growth, at high pulling rates 7-33551
- Si, magnetic-field-applied Czochralski growth (*Chinese*) 7-59401
- Si ribbon casting for solar cell fabrication 7-13907
- Si self-doping using Stepanov method, elec. resist. meas. 7-32470
- Si sheet, growth by horizontal supported web technique, solar cell efficiency 7-53567
- Si, SiC microdefect generation, melt-interface mechanism 7-53710
- Si, single cryst. temp. distrib. during czochralski growth, computer modelling 7-17414
- Si, single crystal, effects of shape of crystn. front, melting boundary 7-6566
- Si solar cell photovoltaics, edge-defined film fed growth 7-17413
- Si, Stepanov reverse method cryst. growth, thermal and capillary conditions 7-33545
- Si strips, grown by Stepanov's reversed method, strength, struct., electro-physical props., effects of thermal conditions during growth, photocell appl. 7-32325
- Si, technology and electronic materials (*Japanese*) 7-22466
- Si, thin sheets, EFG, thermal capillary mechanism for growth limit 7-17407
- Si tube, growth from shaped seed, struct. development 7-32326
- Si, ultrasonic shaping during pulling cryst. growth 7-33541
- Si:B, impurity transport in mag. Czochralski growth, computer simulation 7-58182
- Si:B, magnetic Czochralski growth, computer simulation of B transport 7-32344
- Si:B(O)(Sb,O), heavily doped Czochralski wafers, O precipitation, 450°C thermal annealing 7-58477
- Si:Bi, solute trapping by lateral motion of {111} ledges 7-44592
- Si:C, carbide form. in Stepanov cryst. growth 7-33544
- Si:C, Czochralski grown, incorporation and disposition of C 7-32484
- Si:C, polycrystalline, electrical and structural properties 7-12106
- Si:C crystals, Stepanov method growth, defect structs. 7-32421
- Si:Gd, grown from melt, electrical and optical props., residual impurities 7-63636
- Si:O, C, thermal donor form., T<800K 7-27294

crystal growth from melt continued
 Si:O, Czochralski cryst. growth, impurity segregation, high axial mag. field effect 7-26960
 Si:O, Czochralski-grown wafers, growth striations, X-ray topography study 7-59400
 Si:O, dendritic web growth, plastic flow, O effects 7-16471
 Si:O Czochralski crystals and melts, internal gettering, review 7-32341
 Si:P, pulsed laser annealing, molten phase local nucleation study 7-63655
 Si-O system, solubilities of O in liq. and solid Si 7-26961
 Sn crystals, Czochralski; growth, dia. control by IR heating method 7-17405
 $\text{Sr}_{1-x}\text{Ba}_x\text{Nb}_2\text{O}_6$ bronze piezoelectric for SAW device applications 7-17271
 $\text{Sr}_{1-x}\text{Ba}_x\text{Nb}_2\text{O}_6$ ferroelectric tungsten bronzes, crystal growth and optical appl. 7-39085
 Ti_3AsSe_3 crystals, Bridgman growth, dislocation etching, thermal stress distrib. 7-21208
 TiBr-TiCl fibres, growth by Stepanov's method 7-31533
 V-W single crystal alloys, directionally solidified, growth structs. 7-3159
 WSe_2 , melt grown layered crystals, optoelectronic props. 7-21946
 YAG, laser crystals, cryst. growth by Czochralski technique (Japanese) 7-53572
 YAG:Nd crystals, high quality, growth by temp. gradient technique 7-22464
 Y_2SiO_5 :R (R=Ce, Pr, Nd, Sm, Gd, Tb, Er, Tm, Yb), Czochralski growth 7-53556
 Yb-Sb-S(Se), synthesis and props. 7-44471
 YbBiS(Te), synthesis and props. 7-44471
 $\text{Zn}_x\text{Cd}_{1-x}\text{Te}$, crystals, grown from non-stoichiometric melts, Zn distrib. calc. 7-51678
 ZnGeP_2 , single crystals, prep. and characterisation 7-2612
 $\text{ZnS}:\text{Cu}$, solid solution, electroluminescent phosphor, compositional inhomogeneities 7-6800
 $\text{ZnS}:\text{Se}_{1-x}$ cryst., low press. melt growth technique 7-33548
 ZnSe cryst., low press. melt growth technique, photolum., laser appl. 7-33548
 p-ZnSnP, single cryst., recombination radiation, cryst. growth effects 7-53394
 ZnWO_4 , Czochralski grown, quality, colour rel. to scintillation output 7-59407
 ZrO_2 , cubic, crystal growth, stabiliser distrib. coeff. 7-53561
 ZrO_2 single crystals, stabilised, growth by skull melting technique, charactn. 7-53560

crystal growth from solution

see also crystal growth from gel; liquid phase epitaxial growth
 α -factor of Jackson 7-44425
 accelerated crucible rotation technique for cryst., growth, review of theoretical models 7-39368
 analcime, hydrothermal cryst. growth, morphology 7-11975
 batch cooling crystalliser, microcomputer programming of temp. 7-53522 (BEDT-TTD), BrI_2 , synthesis, structure and electrical props. 7-46296
 BEDT-TTF complexes with linear chain anions, crystal growth 7-46297
 calcium oxalate, crystal growth and aggregation, computer model, partial size distribution 7-16463
 calcium oxalate, crystallization processes using reverse osmosis 7-53538
 calcium oxalate crystals, precip. by reverse osmosis system, habit modifiers 7-16460
 calcium oxalates, precip. from high ionic strength solns., nucleating phase, additives effect 7-59774
 cro protein-pseudo O_2 complex, studies on crystn. 7-23290
 cyanocobalt (III) phthalocyanine, conductive crystals prepared by electrolysis 7-2590
 dendritic growth is channel from supersaturated soln. 7-44433
 diffusion controlled travelling heater method growth, thermal diffusion effect 7-53527
 electrocrystallisation, kinetics, computer simulation studies 7-58173
 flux growth, metastable zone, mixed cluster model 7-44432
 hevein, protein from latex of rubber tree, crystn. studies 7-23289
 holographic interferometry appl. to conc. distrib. and hydrodynamics 7-53526
 inorganic and protein crystal growth—similarities and differences 7-23283
 lithium rare earth tetraphosphates, $\text{LiR}_2\text{P}_4\text{O}_{12}$, flux cryst. growth 7-13345
 $(\text{LuYBiPb})_3(\text{FeGa})_2\text{O}_{12}$, crystn. from soln. melt, component distrib. 7-21149
 lysozyme, growth kinetics of tetragonal crystals. 7-23281
 lysozyme as a model for protein crystn., cryst. growth studies 7-23280
 membrane protein crystals, growth and charactn. 7-23288
 minimum crystal size producing secondary nuclei 7-21143
 naphthalene, linear growth rate, temp. depend., kinetics of rough crystal face 7-6565
 nucleation in small liq. volumes, high saturation change rate 7-53536
 nucleic acids, role of purification 7-23277
 organic crystals, polymorphism and nonlinear optical activity 7-57400
 organic crystals growth in a microgravity environment 7-22456
 organic materials, crystal growth kinetics, tailor-made additives influence 7-58171
 palmitic acid, crystallisation, K-like twins 7-58288
 phosphoglucomutase, crystn. at high salt conc., catalytic effect of polyethylene glycol 7-23278
 poly-p-phenylene sulphide, solution-grown crystals and crystalline thin films, morphology 7-16441
 polyacetylene, growth, struct., optical props. and photo-induced spin states 7-16455
 polyethylene, single cryst., regime II growth from dil. soln. in n-octane 7-21133
 polyethylene, soln. crystallisation kinetics and morphology 7-21148
 polyethylene single crystals, high temp. soln. growth rates, morphology 7-17402
 potassium hydrogen phthalate, cryst. growth, influence of impurities, in situ obs. of {010} face 7-46289
 protein crystal growth, conf., Stanford, CA, USA (Aug. 1985) 7-18478
 protein crystal growth, convective diffusion in parent soln. 7-23287
 protein crystal growth, feasibility of mapping soln. props. 7-23284
 protein crystal growth, preliminary investigations using the Space Shuttle 7-23286
 protein crystal growth, the future 7-23274
 protein crystals, mechanisms of nucleation and growth 7-23275
 proteins, effects of neutral detergents on crystn. 7-23276
 proteins, role of purification 7-23277

crystal growth from solution continued

α -quartz, cryst. growth from silica gel using alkali halide flux (Japanese) 7-64884
 quartz, cultured, grown from +X seeds, Al and OH^- distrib. 7-58307
 quartz, hydrothermal growth and elec. sweeping for resonators 7-39369
 quartz, hydrothermal growth at low fillings in NaCl KCl solns. 7-46291
 quartz, rose, cryst. synthesis 7-46292
 quartz analogues, family of binary III-V compounds 7-59395
 rare earth mixed ligand crystals, temperature reduction and spontaneous crystallisation prep. 7-46294
 Rochelle salt crystals grown from carbamide-containing soln., dielec. props. study 7-64557
 saturation temperature determination, crystallisation 7-44429
 single crystal growth under microgravity 7-23285
 small molecule organic crystals, growth and charactn. 7-22455
 solar cells with internal reflection, fabrication by solution growth on steel substrates 7-3683
 solvent role in cryst. growth from soln., protein appl. 7-21142
 sphere, diffusion controlled growth from finite size, numerical solns. 7-44889
 stearic acid, B modification, growth kinetics of (001) and (110) faces from n-alkanes 7-58174
 stearic acid soln., cryst. growth modelling 7-59386
 surface coarsening by macrostep formation 7-26683
 synthetic quartz growth, Brazilian lascas charact. for synthetic quartz growth, props. correlation 7-59394
 TGS single crystal solution growth with modulated struct. 7-59388
 thermo-kinetic considerations for cryst. growth of complex mols. from soln. 7-23282
 (TMTSF) $_x$ salt, isolated single cryst. growth, electrochemical technique 7-59393
 (TMTTF) $_x\text{Mo}_6\text{Cl}_{14}$, prep. by electrocrystallisation, struct. and spectroscopic characterisation 7-46295
 triglycine selenate crystals, dielectric props. at high hydrostatic press. 7-7631
 triglycine sulphate nucleation in supersaturated solns., induction period meas. 7-26680
 triorthophosphates, superionic, synthesis and charactn. 7-53530
 trypsin-modified elongation factor from E. coli, effect of chem. impurities in polyethylene glycol on macromol. crystn. 7-23279
 turntable seed holder for low temp. growth 7-53525
 urea crystals, growth kinetics in aq. soln., biuret effect 7-51679
 zeolite, ZSM-5, crystallisation kinetics from organic solvent-water mixture 7-22457
 zeolite ZSM-5, hydrothermal synthesis, nucleation and growth 7-33537
 zinc oxalate, crystallisation, precip. kinetics 7-53537
 AlGaAs layer, separating on GaAs surface, growth mechanism, Auger depth profiling 7-44434
 Al_2O_3 profiled crystals, prod. from gas-saturated liq., struct., effects of growth conditions 7-32327
 AlPO_4 , berlinite, hydrothermal cryst., growth, X-ray topography, bulk acoustic wave device characts. 7-59391
 AlPO_4 , berlinite, synthesis and charactn. of new polymorphic modification 7-53534
 AlPO_4 berlinite: characterization of crystals with a low water concentrations and design of bulk wave resonators 7-59396
 $\beta\text{-BaB}_2\text{O}_4$ single crystals, flux growth, SHG appl. 7-59390
 $\text{BaPb}_{1-x}\text{Bi}_x\text{O}_3$, $0 \leq x \leq 0.30$, hydrothermal cryst. growth 7-46290
 $\text{BaPb}_{1-x}\text{Bi}_x\text{O}_3$ soln.-grown single crystals, crystallographic symmetries, effect on supercond. props. 7-37916
 $\text{BaPb}_{1-x}\text{Bi}_x\text{O}_3$, supercond. crystals, hydrothermal synthesis and props. 7-53532
 CaCO_3 , calcite, hydrothermal cryst. of growth and solubility in nitrate solns. 7-53533
 $\text{Ca}_{18}\text{Mg}_2\text{H}_2(\text{PO}_4)_{14}$, whitlockite, cryst. growth 7-53528
 CaSO_4 crystal size distrib. from double-draw-off FGD liquor crystalliser 7-63533
 CaSO_4 , hemihydrate crystals, continuous crystallisation in conc. H_3PO_4 7-53535
 $\text{CaSO}_3 \cdot 1/2\text{H}_2\text{O}$ crystal nucleation and growth from simulated FGD liquors 7-63534
 $\text{CaSO}_4 \cdot 1/2\text{H}_2\text{O}:\text{Cd}$, crystallisation from phosphoric acid 7-27882
 $\text{Cu}_4\text{Mo}_5\text{O}_{17}$, synthesis and cryst. struct. 7-32398
 CuSeO_3 , cryst. struct. of three modifications, X-ray diffr. study (German) 7-32410
 GaPO_4 orthophosphate crystals, hydrothermal synthesis 7-53531
 HgZnTe bulk crystals, travelling heater method growth and charactn. 7-59387
 HoFeO_3 crystals, flux growth, secondary phase and microdiscs form. 7-13344
 $\text{KAl}(\text{SO}_4)_2 \cdot 12\text{H}_2\text{O}$, alum crystals, habit changes by novel additives to nutrient 7-44439
 $\text{K}_2\text{Cr}_2\text{O}_7$ crystals grown from soln., enantiomorphism 7-51682
 $\text{K}_2\text{Cr}_2\text{O}_7$, surface micromorphology rel. to growth conditions 7-58175
 $\text{K}_2(\text{Ga}_2\text{Ga}_{8-x}\text{Ti}_{16-x}\text{O}_{56})$, synthesis of new cpd. by flux method 7-27883
 KH_2PO_4 , crystal growth spiral morphology on {100} surfaces, impurity effects, step kinetics 7-16459
 KH_2PO_4 crystals grown at boiling point, surface microtopography 7-21581
 K_2HPO_4 , cryst. growth from boiling solns. in presence of impurities 7-53529
 KNO_3 , cryst. growth, top seeded pulling method 7-53524
 $\text{K}_2\text{O} \cdot \text{Fe}_2\text{O}_3 \cdot \text{TiO}_2$ system, cryst. growth of titanates, morphology, ionic cond. 7-53523
 K_2SO_4 , cryst. growth, nucleation kinetics, habit, Cr(III) effect, soln. pH 7-53539
 K_2SO_4 solution, crystallisation in a microcomputer batch coating crystalliser 7-53522
 KTiOPO_4 , crystal and optical props. 7-17403
 KTiOPO_4 crystals, high temp. flux growth, morphology 7-58178
 KTiOPO_4 , solubility in KF aq. soln., high temp. and press., hygrothermal growth 7-58482
 LaCO_3OH polymorphs, prep., cryst. data, X-ray powder diffr., IR spectra, TGA curves 7-32392
 LaOBr , single cryst. growth, struct., X-ray diffr. study 7-44431
 LiFePO_7 , cryst. synthesis, at. struct., DTA, X-ray diffr. study 7-26708
 LiTaO_3 single crystals, synthesis and recrystallisation under hydrothermal conditions 7-3157
 $\text{NH}_4\text{Al}(\text{SO}_4)_2 \cdot 12\text{H}_2\text{O}$ secondary nucleation from soln., effect of insoluble additives 7-26681

crystal growth from solution continued

- (NH₄)₂SO₄, crystal growth, contact nucleation rel. to Cr ion conc. 7-16462
 (NH₄)₂SO₄.Al₂(SO₄)₃.24H₂O crystals, growth rate dispersion from aq. soln. 7-59392
 NaBF₄, orthorhombic, cryst. growth and phys. props. 7-7834
 NaBO₃.4H₂O, primary nucleation in aq. solns. 7-32336
 NaCl, secondary nucleation rate under different stirring conditions 7-44742
 Na₂Hf₂Ge₂O₁₂, ionic conductor, hydrothermal crystallisation and cryst. struct. 7-37935
 NaNi₂OH.H₂O.(MoO₄)₂, H atom location, Rietveld refinement, neutron powder time of flight meas. 7-26707
 Nb₃Sn, Ti-alloyed, cryst. growth from soln. by top seeded soln. growth 7-46293
 NdP₂O₁₄ single crystals, growth from pyrophosphoric acid soln., cold finger technique, defect struct. 7-59389
 NiSO₄.6H₂O crystals, soln., grown, steps on {001} faces, screw dislocations glide 7-58181
 PbO-Fe₂O₃, binary phase diagram, DTA, X-ray diff. meas. 7-46434
 SnO₂, single cryst. growth, struct., X-ray diff. study 7-44431
 ThO₂, prep. and EPR study of actinide and rare earth ions 7-27598
 YAG powders, hydrothermal growth, controlled nucleation, CRT phosphor prep. 7-13412
 ZnO crystals, real struct. during growth process, effect of plastic deformation 7-11974
 ZnSe hydrothermal growth, cathodolum. props. 7-63531
 ZrO₂, tetragonal form, stability 7-6567
 ZrSiO₄, rare earths, luminescence-spectra props., hydrothermal synthesis methods 7-64683

crystal growth from vapour

- see also vapour phase epitaxial growth
 closed-tube chem. vapour transport, interface kinetical limitations, semiempirical calcs. 7-27878
 diphenyl crystal, interaction of anthracene impurities with surface layers, struct. model of quasiliquid layer 7-58191
 ion/surface interactions, photo-induced reactions, review 7-53609
 ionized-cluster-beam deposition apparatus (Japanese) 7-22583
 metal particles, ultra fine, ferromag., growth rel. to mag. field 7-53515
 physical vapour transport in rectangular horizontal enclosures, surface reactions, convection 7-17398
 surface coarsening by macrostep formation 7-26683
 α-Al₂O₃, hexagonal, plate-like, synthesis using hydrated Al₂(SO₄)₃ as starting material (Japanese) 7-22454
 As₂Se₃ single cryst. growth from vapour phase, crucible diameter and sealing press. depend. 7-27877
 BiSeI, dendritic, growth from vapour, characteris. 7-21788
 CdGa₂S₄ single crystals, chemical vapour transport growth, microhardness, crack patterns 7-7833
 CdIn₂S₄ single cryst., chem. vapour transport growth and Vickers microhardness 7-21345
 Cd_{1-x}Mn_xS, crystal growth and charact. (Japanese) 7-7829
 CdS crystal growth and charact. (Japanese) 7-7829
 CdS skeletal and hollow crystals grown under time-increasing supersaturation 7-21144
 CoGa₂O₄, crystal growth, chemical vapour transport, struct., mag. and electronic props. 7-53517
 CuAlGa_{1-x}Se₂, chem. transport reactions, growth and morphology 7-7830
 CuInS₂, chemical transport, thermodynamics 7-7832
 CuInS₂, heterogeneous, VLS growth, electronic defects, photocurrent spectra, photolum., EBIC analysis 7-27288
 FeS₂, pyrite cryst., chemical vapour transport with halogens 7-53513
 Ga₂O₃, chem. transport in Ga₂O₃/H-Cl system 7-17401
 Ga₂O₃, chem. transport in Ga₂O₃/N-H-Cl system 7-53519
 β-Ga₂O₃, chem. transport using Cl₂ as transporting agent 7-17400
 GaSe, single cryst. growth by I₂ vap. transport 7-17399
 GeSe, cryst. growth in Xe atmosphere, expts. performed on Spacelab D1 mission 7-21145
 HgGa₂S₄-HgIn₂S₄ system, new multinary layered compound 7-53516
 HgI₂, evaporation studies and phase stability 7-52025
 HgI₂ single cryst. growth new technique 7-53562
 I, cryst. growth by phys. vap. transport, faceting and rounding during sublimation 7-58177
 α-LiIO₃ single crystals, morphology in relation to growth conditions 7-58192
 Mg, crystal habit of ultrafine particles, gas phase evaporation growth 7-53514
 Mn₃Cr₂Ge₃O₁₂ garnets, cryst. growth, chemical vapour transport, struct. 7-53518
 Mn₃Fe₂Ge₃O₁₂ garnets, cryst. growth, chemical vapour transport, struct. 7-53518
 Mn₃Ga₂Ge₃O₁₂ garnets, cryst. growth, chemical vapour transport, struct. 7-53518
 NaCl, cryst. growth from vap., 2D nucleation 7-16467
 NbSe₄I₃₃, vapour grown, cryst. growth by microsteps 7-58176
 Pb_{1-x}(S₂Te_{1-x}), solid solution, growth from vapour; region of homogeneity 7-46285
 PbTe:Ga, doping during vapour phase growth, elec. props. 7-26774
 Rb_{0.023}WO₃, crystal growth and struct., SEM and TEM anal. 7-46288
 ReS₂, single cryst. growth by chem. vapour transport, elec. resist., Hall mobility meas. 7-64251
 ReSe₂, single cryst. growth by chem. vapour transport, elec. resist., Hall mobility meas. 7-64251
 Sb₂S₃-Sb₂Se₃, hollow mixed crystals vapour growth, morphology and whisker growth 7-7831
 SbSI, hollow cryst. growth from vap. 7-53520
 SbSI single crystals, vapour growth, morphology rel. to temp. gradients 7-46287
 α-SiC, single cryst. growth using furnace with NbC heaters 7-27881
 Sn-In-S ternary system, cryst. growth and charact. (French) 7-33645
 Te-Se, whisker crystals, growth and elec. props. 7-12578
 W, emitter tip radius, condensation-related shape changes 7-13343
 n-WSe₂ single crystal, growth, struct. and photoelectrochem. props. 7-27879
 ZnCr₂O₄, crystal growth, chemical vapour transport, struct., mag. and electronic props. 7-53517
 ZnS, ZnSe, crystal growth by chem. transport using NH₄Cl transport agent 7-59385
 ZnS₂Se_{1-x}, single crystals, growth, exciton luminesc. 7-22453

crystal growth from vapour continued

- ZnSe, single crystals, growth, exciton luminesc. 7-22453
 ZnSe:Si, single crystal growth, chem. transport method (Korean) 7-27880
 ZnSiP₂ and ZnGeP₂, single crystals, prep. and characterisation 7-2612
 ZrO₂ crystals, stabilised, vap. phase cryst. growth by hydrolysis of ZrF₄ 7-46286
- crystal habit see crystal morphology
- crystal hyperfine field interactions
 alkali halides, muonium centres 7-45901
 alkali halides, trapped atomic H and muonium 7-45900
 antiferromagnets, X-ray emission spectra, hyperfine effects 7-13264
 bis arene sandwiches, C₂R₂FeC₆R₆ where k=H or CH₃, and (C₆(CH₃)₆)₂Fe²⁺, hyperfine and mag. props. 7-12680
 closed shell ions, electric field gradient Sternheimer function 7-12681
 cubic lattices, diffusing atoms, Mossbauer spectrum studies 7-64552
 diamond, Mu⁺ hyperfine parameters, absolute sign, muon polarisation studies 7-53204
 diamond, muonium-related paramagnetic centres, UHF calcs. 7-38980
 diamond anomalous muonium, vacancy-associated model 7-51758
 diethyleneterephthalate, high resol. time domain zero field NQR 7-13056
 dimers, antiferromagnetic coupling, ligand spin polarisation, broken symmetry UHF calcs. 7-22084
 electric quadrupole perturbation coefficients for I=4 spin-level in angular correlations (Japanese) 7-21873
 electric quadrupole perturbation coefficients for I=9/2 in Angular correlations (Japanese) 7-12678
 Fe (110) surface, clean and Ag coated, magnetic hyperfine field, local structure 7-21878
 high resol. time domain zero field NQR 7-13056
 l-histidine hydrochloride monohydrate, single cryst., ¹⁴quadrupole coupling, NMR spectra 7-13042
 iron porphyrin complexes, mag. moment susceptibility, Mossbauer study 7-22168
 irradiated metals, isochronal annealing PAC monitored defect reactions anal. 7-44623
 magnetically concentrated crystals, NMR lineshape theory 7-33288
 methyl ammonium boron trifluoride, nucl. quadrupole coupling, electronic struct. NMR 7-13043
 molecular cubic crystals, quadrupolar polarisability and Bether's splitting calcs., local field method (Russian) 7-21879
 muon level crossing resonance, muon polarisation function for longitudinal fields 7-53187
 nuclear hyperfine interactions, appl. of digital filtering techniques 7-38523
 1,2,3,4,5,6,7,8-octahydroanthracene and rel. hydroaromatics, ¹³C NMR, line splittings 7-13044
 orthorhombic paramagnet, J=1, external field induced Jahn-Teller effect (Polish) 7-7179
 paramagnetic systems involving a muon, level crossing resonance 7-45905
 α-quartz: AlO₄, hyperfine and quadrupole interactions, ENDOR study 7-2951
 α-quartz, muonium atoms, diffusion and quadrupole interactions, temp. depend. 7-52138
 rare earth alloys, R₂Fe₁₃B, R=La-Nd, Sm, Gd-Tm, Lu and Y, ⁵⁷Fe Mossbauer spectra 7-64551
 rare earth alloys, RMn₂, R=heavy rare earth, mag. state, spin echo NMR spectra 7-27629
 rare earth-Al alloys, RAl₂, paramagnetic fluctuations, muon spin rotation studies 7-12941
 semiconductors, n-doped insulating phase, ESR line shape studies 7-22134
 silicates, sheet, EFG tensor at Fe sites, room temp. Mossbauer study 7-45851
 surface (110), surface characterisation by In probe atoms, electric field gradient 7-2553
 (TMTSF)₂PF₆(ClO₄), nesting vector, SDW amplitude and anisotropy 7-45125
 transition metal surfaces and interfaces, hyperfine fields 7-58847
 zincblende-structure semiconductors; muonium states, muon spin resonance studies 7-53206
 Ag alloys, dil., EFG, asymmetry parameter calcs. 7-2545
 Ag/In thin film couples, interface AgIn₂ cpd. form. and props., gamma ray spectra 7-21688
 Ag₂Se:Sn, solid electrolyte, microscopic disorder, Mossbauer spectroscopy 7-58533
 Al, nuclear quadrupole interactions in the presence of muons 7-53192
 Al_{1-x}Ga_xAs, Ga interstitial identification by ODMR 7-33302
 Au alloys, dil., EFG, asymmetry parameter calcs. 7-2545
 Au/In thin film couples, interface AuIn₂ cpd. form. and props., gamma-ray spectra 7-21688
 Au-Fe, mag. hyperfine field, temp. and composition depend. 7-45243
 Ba₂Sn₂Mn(Ni)(Co)Fe_{10-x}Ga₂O₂₂ hexagonal ferrites, cryst. and magnetic struct. studies 7-44474
 Bi, rhombohedral, lattice relax. and muon⁺ sites 7-53190
 Ca₂Co_{1-x}Fe₂O₄ substituted ferrite system, mag. props., comp. depend., Mossbauer study 7-7618
 CaF₂:Ce³⁺, impurity ion-ligand nuclei interactions, ENDOR meas. and operator method calcs. 7-52538
 CaF₂:Eu³⁺, ¹⁵³Eu-¹⁵¹Eu quadrupole moment ratio, optically detected NMR studies 7-22164
 CaF₂:Eu³⁺, hyperfine coupling in ⁷F₀ and ⁵D₀ states, ODMR meas., optical hole burning 7-45842
 CaF₂:Eu³⁺, O₂⁻, quadrupole coupling and crystal-field shielding under hydrostatic press. 7-2551
 CaF₂:Li⁺(Na⁺), EPR of colour centres 7-17222
 (Ca_{1-x}Mg_xFe_{0.3}Mn_{0.1})(CO₃)₂, ankerite, ⁵⁷Mossbauer spectra relax. rates 7-27640
 Cd:OH⁻, EPR spectrum 7-17217
 Cd-In alloys, vacancy-induced elec. field gradient temp. depend., PAC meas. 7-52541
 Cd(BrO₃)₂·2H₂O(D₂O), H bonding, crystal struct., ¹H and ²D NMR anal. 7-22156
 CdF₂:Eu³⁺, hyperfine coupling in ⁷F₀ and ⁵D₀ states, ODMR meas., optical hole burning 7-45842
 CdS, powder, metal-loaded, photoinduced electron-hole pair separation 7-59770
 CdS(Se)(Te):Mn, impurity EPR spin Hamiltonian parameter correl. calcs. 7-27597
 Cd_{1-x}Zn_xTe:Mn, hyperfine coupling constant, EPR study 7-22138

crystal hyperfine field interactions continued

- Co thin films, nucl. spin echo, effect of nonresonance pulsed mag. field 7-45839
- Co-Au-Fe, dil., local structural and mag. environments of Fe 7-26965
- Co-Cr-Fe sputtered films, dilute, Mossbauer effect 7-22167
- Co₂Fe_{1-x}Cr_{2x}S₄ mixed spin system, temp. depend. Mossbauer studies 7-38976
- CoSi₂, Mossbauer spectroscopy 7-59126
- CsCaF₃Gd³⁺, transferred hyperfine interaction of impurity centres, ENDOR, EPR meas. 7-32946
- CsCl:CN⁻, F₂(CN⁻)-centre absorption bands, pseudopotential method calcs. 7-22292
- CsDSO₄, superionic transition, NMR 7-38951
- Cs₂FeCl₅H₂O, antiferromagnet, mag. phase diagram, spin wave excitations, Mossbauer spectra 7-45676
- Cs₂NaInCl₆:Cr³⁺, elpasolite lattice, broadband near-IR luminesc. 7-17338
- Cs₂NaYBr₆:Cr³⁺, elpasolite lattice, broadband near-IR luminesc. 7-17338
- Cs₂NaYCl₆:Cr³⁺, elpasolite lattice, broadband near-IR luminesc. 7-17338
- CsSD, mol. reorientation, elec. field gradient ²H NMR 7-13052
- Cu complexes, L-phenylalanine salt, EPR study 7-59106
- Cu, nearest-neighbour host site elec. field gradient, monovacancy effects, muffin tin pot. calcs. 7-2549
- Cu, nuclear quadrupole interactions in the presence of muons 7-53192
- Cu/In thin film couples, interface CuIn₂ cpd. form. and props., gamma ray spectra 7-21688
- Cu-Fe, dil., local structural and mag. environments of Fe 7-26965
- Cu-Fe, implanted solid solns., Mossbauer study on thermal dynamics of Fe atoms 7-45855
- Cu-In alloys, vacancy-induced elec. field gradient temp. depend., PAC meas. 7-52541
- CuTaS₃, isomer shift of elec. split 6.2 keV nucl. transition of ¹⁸¹Ta 7-7624
- Dy₂(SO₄)₃·8H₂O, magnetic and hyperfine props., cryst. field effects calcs. 7-27305
- Er₂(SO₄)₃·8H₂O, magnetic and hyperfine props., cryst. field effects calcs. 7-27305
- Eu²⁺ in crystals, covalency and EPR hyperfine struct. const. 7-45815
- EuS ferromagnetic single cryst., elec. field gradient and magnetic hyperfine interaction, NMR meas. 7-52540
- Fe films on Ni substrates, magnetism and interface processes, in-situ conversion electron Mossbauer study 7-7571
- Fe II complexes, spin transition induced by heat, pressure, light and nuclear decay 7-58785
- Fe, negative muon spin precession and hyperfine field anomaly study 7-45894
- Fe, negative muon spin precession and the hyperfine anomaly 7-45906
- Fe overlayers or sandwiches with Cu (001), electronic and mag. props. 7-64499
- Fe-Ag sputtered films, thermal stability, X-ray diffr. and Mossbauer studies 7-58679
- Fe-Al disordered alloys, electronic struct., mag. props. and Mossbauer spectra 7-64073
- Fe-Au system, low Au conc., low temp. nucl. orientation and NMR-ON studies 7-2936
- Fe-B alloys, metastable crystalline, Mossbauer study of local atomic environments 7-17252
- Fe-B rapidly quenched cryst. alloys, local atomic environments, spin echo NMR studies 7-7606
- Fe-Co dil. alloy, ^{57,60}Co isotopes, hyperfine anomalies, α -factors NMR/ON obs. 7-33278
- Fe-Cu metastable alloy sputtered films, mag. props., X-ray diffr. and Mossbauer meas. 7-7560
- Fe-Cu sputtered films, thermal stability, X-ray diffr. and Mossbauer studies 7-58679
- Fe-Ni, hyperfine mag. fields, temp. dependence 7-12683
- Fe-Sc alloys, struct. and mag. props., NMR and X-ray diffr. studies (*Russian*) 7-6578
- Fe-Zn alloys, sputtered, X-ray diffr., magnetisation and Mossbauer studies 7-59075
- Fe₃BO₄ crystals, Laue diffracted Mossbauer spectra near spin-reversal phase transition 7-38975
- Fe₇₄Co_{10-x}Cr_xB₁₆, amorphous, prep. by melt spinning, X-ray diffr., DSC, Mossbauer studies 7-46369
- FeCoCr₂S₈, crystallographic and mag. props., Mossbauer study (*Korean*) 7-33310
- FeH₃, prep. under high press., Mossbauer obs. 7-33313
- FeNi₅₀ alloy foils, N₂⁺ implantation, oxidation behaviour, conversion electron Mossbauer spectra study 7-22877
- (Fe₆₄Ni₃₃)_{1-x}(Fe₈₄Mn₁₆)_x alloys, low field magnetisation and Mossbauer effect studies 7-33311
- FeOCl, anisotropic layer cpd., hyperfine interactions, Mossbauer spectra 7-58786
- β -Ga₂O₃:Fe³⁺(Cr³⁺), zero-field splittings and site distortions 7-59119
- g-PaP, powder, metal-loaded, photoinduced electron-hole pair separation 7-59770
- Gd:Ce, hyperfine field and relax. rate, intermediate valence model 7-7184
- Ge, anomalous muonium, vacancy-associated model 7-51758
- GeFe₂O₄, ⁵⁷Fe²⁺ Mossbauer quadrupole splitting and orbit-lattice interaction 7-12684
- In_{0.95}Ag_{0.05}Ga_{0.05}, ¹¹¹Cd quadrupole interaction, temp. dependence, lattice electric field gradients (*Chinese*) 7-7183
- In_{0.95}Ag_{0.05}Ga_{0.05} alloy, quadrupole interactions, TDPAC study 7-38521
- InCl₃ mixed valence cpds., nuclear electron capture aftereffects, quadrupole interactions, γ ray ang. correl. anal. 7-53182
- K₂HfF₆, polymorphism, TDPAC investig. 7-2188
- KMgF₃:Dy³⁺, ligand hyperfine interaction of Dy³⁺, ENDOR 7-22163
- La(Fe₄Al_{1-x})₁₃, mag. props. determined via neutron scatt. and Mossbauer spectroscopy 7-2820
- LaZnFe₁₀O₁₉, cation distribution and random spin canting 7-37945
- LiAl₂O₃:Fe³⁺, Mossbauer relaxation spectrum, electric quadrupole shifts dependency on mag. field 7-7182
- LiCl:Fe³⁺, X-ray irradi., EPR spin Hamiltonian parameters 7-45808
- LiFeClMoO₄, synthesis, struct. and low temp. magnetism 7-21172
- Li₂HfF₆, hyperfine interactions, temp. depend. 7-12679
- Li₂ZrF₆, hyperfine interactions, temp. depend. 7-12679
- LuPO₄:Gd³⁺, mag. hyperfine interactions, ³¹P and ⁵¹V ENDOR spectra 7-27630

crystal hyperfine field interactions continued

- LuVO₄:Gd³⁺, mag. hyperfine interactions, ³¹P and ⁵¹V ENDOR spectra 7-27630
- MnF₂, antiferromag., muon level crossing resonance 7-53186
- Mn_{1-x}Fe_x sputtered films, mag. props. 7-38915
- (NH₄)₂HfF₆, thermally activated α - β transition 7-12258
- β -Na₂O-Al₂O₃, struct. at 5K, ²³Na NMR 7-7595
- β'' -Na₂O-Al₂O₃, structure at 5K, ²³Na NMR 7-7594
- Nb-Hf-Ta-O dilute alloy system, O-induced nonaxially symmetric elec. field gradient, TDPAC meas. 7-12686
- Nd complex, tetra dimethyl sulphoxide neodymium nitrate, vibr., Raman. IR and luminesc. study 7-33392
- Nd₂(Fe_{0.67}Al_{0.33})₁₄B, reduction of mag. hyperfine fields and Curie temp. on Al substitution, Mossbauer spectra 7-38859
- Nd₂Fe₁₄B, EFG tensor for interpretation of Mossbauer effect meas. near spin reorientation temp. 7-38968
- Nd₂Fe₁₄B untextured polycryst., magnetic hyperfine fields, Mossbauer spectra anal. 7-12682
- Nd₂(Fe_{0.67}Si_{0.33})₁₄B, reduction of mag. hyperfine fields and Curie temp. on Si substitution, Mossbauer spectra 7-38859
- Ni complex, tetraphenylarsonium-bis(maleonitriledithiolato)nickel(II), Rh complex dopant, hyperfine interactions, EPR-ENDOR study 7-53124
- NiFe_{2-x}Al_xO₄ mixed spinels, electric quadrupole interactions, Mossbauer spectra study 7-2552
- NpM₄Al_{8-x}, (M=Cr,Fe,Cu), mag. props., Mossbauer effect and neutron diffr. 7-59127
- NpO₂CO₃, crystal chemistry, Mossbauer studies 7-17249
- PbTe:Mn²⁺, superhyperfine struct., EPR spectra 7-27595
- Pd₂Fe hydrated ordered alloy, mag. behaviour, Mossbauer studies (*Russian*) 7-2890
- Pr₂(SO₄)₃·8H₂O, magnetic and hyperfine props., cryst. field effects calcs. 7-27305
- RbAg₄I₅, solid electrolyte, microscopic disorder, Mossbauer spectroscopy 7-58533
- RbCdF₃, struct. phase transition, ENDOR study 7-33298
- RbSD, mol. reorientation, elec. field gradient ²H NMR 7-13052
- Ru, quadrupole orientation of ¹⁰³Ru at low temps. 7-38522
- Si, anomalous muonium, vacancy-associated model 7-51758
- Si, normal muonium, location and hyperfine props., Hartree-Fock cluster calcs. 7-52539
- Si, off-centre impurities and defects, local electronic struct. valence-bond theory calcs. 7-2532
- Si:¹¹¹Cd, hyperfine interactions, temp. depend., gamma-ray spectra studies 7-64553
- Si:As,In, formation of In-As complexes, perturbed angular correlation technique obs. 7-17254
- Si:B, B-vacancy complex, electronic and atomic struct., ENDOR studies 7-63649
- Si:Fe, interstitial Fe, spin delocalisation 7-13059
- Si:Fe, interstitial impurity, superhyperfine interaction and spin-lattice relax. 7-53178
- Si:O, magnetic resonance of O-related defects 7-17223
- SiC, paramag. muonium centres, hyperfine freqs. 7-52503
- Sr(BrO₃)₂·H₂O(D₂O), EFG parameters, H bonding, PMR, deuteron mag. reson. 7-27612
- SrF₂:Na⁺, EPR of colour centres 7-17222
- SrF₂:Tm²⁺, g-factor signs, optically detected ESR 7-32948
- TaS₂, electrochem. intercalation reactions with Li, K, H, In, Ga, In_{0.17}Ga_{0.83}, nucl. quadrupole interactions, TDPAC meas. 7-17245
- TbSc(V)(Cr)(Mn)(Co), dilute alloys, hyperfine fields and local moment form. 7-64433
- α -TeO₂:Al single crystals, electron irradi., colour centre ESR obs. 7-33271
- ThO₂, prep. and EPR study of actinide and rare earth ions 7-27598
- Ti, HCP, ⁴⁷Ti and ⁴⁹Ti NMR studies, spin-echo profiles 7-7599
- Ti₂Co_{1-x}Fe_{2-2x}O₄ spinel solid soln., mag. props., Mossbauer effect study 7-12685
- TiH₂, Ti Knight shift meas. 7-38954
- Tl₄MnI₆, paramag. suscep. w.r.t. NMR chem. shift, hyperfine coupling const. determ. 7-2941
- Tm cubic intermetallic cpds., magnetic dynamics, low-frequency, in vicinity of the quadrupolar phase transition pt. 7-17155
- VO(II) complexes, ENDOR spectra, struct., hyperfine tensors 7-33299
- YAlO₃:Eu³⁺ lattice and electronic contributions to the quadrupole interaction of trivalent Eu 7-2550
- Y₃Fe₄Ga_{0.5}O₁₂, single cryst., NMR, ang. depend. 7-53148
- YFeO₃, orthoferrite, Dzyaloshinskii-Morié electron-nuclear interaction, NMR data anal. 7-53162
- YFeO₃-Fe₂O₃ mixed phase system microcryst., anomalous behaviour of mag. hyperfine field 7-45760
- YIG:H, sp. ht. and annealing behaviour, conversion-electron Mossbauer spectroscopy study 7-17253
- (YLuBi)₃(FeGa)₁₂, Ne⁺ implanted, CEMS study, hyperfine field anal. (*Chinese*) 7-7620
- YVO₄:Gd³⁺, mag. hyperfine interactions, ³¹P and ⁵¹V ENDOR spectra 7-27630
- Zn complex, Zn(antipyrine)₂(NO₃)₂:VO²⁺, VO²⁺ orientation, EPR spectra anal. 7-53121
- Zn, electric quadrupole interaction of ⁶⁷Zn, mag. reson. meas. 7-53167
- Zn ferrite, shock-synthesised, Mossbauer spectroscopy 7-38979
- Zn-In alloys, vacancy-induced elec. field gradient temp. depend., PAC meas. 7-52541
- ZnS(Se)(Te):Mn, impurity EPR spin Hamiltonian parameter correl. calcs. 7-27597
- ZnTe:Cl(Al), crystals, vacancy-impurity complexes, ODMR studies 7-2530
- Zr₆₃Hf₇Cu₃₀ amorphous and cryst. alloy, elec. field gradient, TDPAC meas. 7-2958

crystal imperfections see crystal defects

crystal inclusions

- 3D size distributions 7-39802
- acetone-d₆-apocholic acid inclusion cpd., guest dynamics rel. to host lattice symm. 7-26677
- acetone-d₆-deoxycholic acid inclusion cpd., guest dynamics rel. to host lattice symm. 7-26677
- edge dislocation interaction with circular inclusions in infinite medium, elastic const. 7-37989
- edge dislocation-rigid elliptical inclusion, elastic field created 7-12116
- elastic inclusions, stress distrib., 2D soln. 7-62989
- elastic wave scattering by spherical inclusions, with appl. to low frequency wave propag. in composites 7-6719

crystal inclusions continued

- electron diffraction contrast due to large cryst. inclusions, modified Bloch wave theory calcs. 7-51583
 epoxy insulation study using X-ray computing tomograph 7-13679
 III-V semiconductors, lattice defects detection using IR tomography 7-32234
 metallic materials, with elliptic inclusions, plastic deform. 7-28067
 metals, BCC and FCC cryst. struct., H trapping, thermal anal. obs. 7-22830
 optical components microscopic inclusions location, automatic inspection device using Q-switched YAG laser 7-31544
 optical surface defect characts. using pulsed laser damage methods 7-37010
 position diffusion towards spheroidal inclusions (*Russian*) 7-39216
 steel, 18 Ni maraging, corrosion fatigue crack initiation and growth 7-3413
 steel, austenitic stainless, passivation and pitting corrosion rel. to Ti stabilisation and Mn content (*German*) 7-39756
 steel, austenitic stainless, strength and toughness at 4K, fusion energy magnets appl. 7-53793
 steel, austenitic-ferritic stainless, weld metal deposits, final microstruct. form., role of thermal contraction stresses assoc. with inclusions 7-59738
 steel, C-Mn, arc welds, as-deposited strength, toughness, microstruct. 7-13555
 steel, Ca, inclusion globularising, Ba additions effect 7-21193
 steel, constructional carbon type, original charge purity influence on microstruct. hardenability and mech. props. 7-46521
 steel, cost, nonmetallic inclusions influence on fracture character 7-3421
 steel, eutectoid, fully pearlitic, cleavage fracture stress, microstruct. effects 7-28123
 steel, HSLA, submerged arc welds, acicular ferrite nucleation by inclusion phases 7-17525
 steel, linepipe, H-induced cracking 7-22881
 steel, low-alloy, Te-containing, nonmetallic inclusions and austenite grains 7-39522
 steel, low-alloy construction, nonmetallic inclusions influence on impact strength and fracture type 7-8085
 steel, Mn-Cr, case carburising, mech. props., influence of inclusion characts. 7-65135
 steel, pressure vessel, fatigue crack growth rates under various conditions of loading and environment 7-28203
 steel, pressure vessel weld metal, cleavage fracturing stages at inclusion sites 7-8092
 steel, solubility of S in presence of Mn and Si 7-39524
 steel, tool, fracture toughness, effect of nonmetallic inclusions 7-59635
 weld metal, self-shielded FCAW, nitride and N contents estimation method 7-59710
 yttrium formate crystals and solutions, Raman spectra studies 7-46024
 Al-Mg and Al-Zn-Mg alloys, plasma-coated, heat treatment effect on fine struct. and failure mechanism 7-3496
 Al-Mg-Zn system, fracture viscosity rel. to surplus phase morphology 7-46610
 Al₂O₃ profiled crystals, prod. from gas-saturated liq., struct., effects of growth conditions 7-32327
 CdIn₂(Ga₂)S₄ single crystals, phase transforms., photoluminesc. studies 7-2171
 Cu electrodeposits, decorated grain boundary dislocations, electron microscopy obs. 7-27185
 Cu-Si, elemental Si inclusion form. in sulphide scale 7-17720
 Cu-Zn, electrodeposits, comp. rel. to deposition pot. (*Japanese*) 7-27951
 Fe-Ni-B, amorphous, shock loading, inclusions dissolving, domain struct. (*Russian*) 7-63487
 InSe, excitonic luminescence, influence of macroscopic inclusions 7-13204
 KH₂PO₄ crystals grown at boiling point, surface microtopography 7-21581
 MgO-Al₂O₃-SiO₂, leucosapphire, crystal growth by directional crystn., gas inclusions formation 7-33539
 Mo permalloy films, mag. domain walls stability, external mag. field, Lorentz microscopy 7-45780
 NdP₂O₄ single crystals, growth from pyrophosphoric acid soln., cold finger technique, defect struct. 7-59389
 Ni-Cr based alloys, low impurity content, microanalytical charactn. of microscopic defects 7-58261
 Pb_{0.8}Sn_{0.2} Te epitaxial films, vacuum deposition growth in a quasiclosed vol. 7-46329
 PbTe, thermoelectric props., effect of dielectric inclusions 7-12746
 Si, Czochralski grown crystals, octahedral crystalline inclusions, TEM obs. 7-16581
 Si:Gd,C profiled single cryst., electronic parameters and SiC inclusions 7-32944
 SiC:Si reaction bonded composite ceramics, interface struct., grain boundaries 7-64995
 a-SiGe:H,F glow discharge films, microcrystallinity studies 7-45088
 Si₃N₄, surface flaws effect on strength 7-59638
 W monocrystals, with P impurities, removal during chem. and metallurgical treatments 7-6645
 ZrO₂, cubic, crystal growth, stabiliser distrib. coeff. 7-53561
 ZrO₂-Y₂O₃-Co₃O₄ materials, Co₃O₄ effect on struct. and phase comp. 7-27990

crystal internal fields *see crystal field interactions*

crystal interstitials *see interstitials*

crystal lattice structures *see crystal atomic structure*

crystal microphones *see microphones*

crystal microstructure

- for microstructural changes, see also phase transformations, hardening, heat treatment, metalworking*
see also crystal defects; crystal inclusions; crystallites; dendritic structure; domain boundaries; domains; electron microscope examination of materials; eutectic structure; grain boundaries; grain size; Guinier-Preston zones; martensitic structure; mosaic structure (microstructure); noncrystalline state structure; precipitation; segregation; subboundary structure; superlattices; texture; Widmanstätten structure
 7-46439
 2D grain structures, topology, geometry, nucleation conditions 7-32853
 Alloy 718, Ni-base superalloy, fatigue crack propag. under hold-time cycling, effect of grain size 7-28106
 alloys, dislocation glide during ageing, hardening phase particle interaction modelling (*Russian*) 7-38010

crystal microstructure continued

- apatite ceramics, with microstruct. controlled by Y³⁺ substitution, elec. props. 7-21523
 applied materials charact., conf., San Francisco, CA, USA (April 1985) 7-18495
 automatic quantitative microstructure analysis, contrast determ. 7-8227
 bainite reaction 7-3297
 bronze BrAZh, elec. discharge sintering of powder from swarf, electro-phys. and mech. props., microstruct. 7-27974
 cellular precipitation and dissolution, model analysis 7-53743
 ceramic coatings, thermo-sprayed, microstruct. studies (*Japanese*) 7-22628
 ceramic semiconductors, granular struct. and elec. props. (*German*) 7-58495
 ceramics, microstruct. charactn. by image anal. 7-3547
 ceramics, multiphase, quantitative microstruct. charactn. and description 7-65254
 ceramics, toughening by strong reinforcements, fracture toughness, microstruct. 7-22783
 composite materials, dielec. function, momentum depend. effective medium approach 7-27281
 composite materials, plane wave propagation, T-matrix calcs. 7-14795
 composites, periodic, elastic and instantaneous elastoplastic and moduli, overall, bounds 7-37349
 composites, quantitative microstruct. effects (*German*) 7-17666
 concrete, structures, micro- and macroscale damage 7-43766
 continuous intergranular phases, morphological stability, thermodynamic considerations 7-21475
 cracks, small, ΔK_{th}, effect of hardness and crack geometry (*Japanese*) 7-58405
 CVD and PVD coatings, structural, mechanical and tribological props. and applications 7-53935
 diamond, powders, dynamically synthesised, polycrystal microstructure formation during sintering 7-22603
 dielectric coatings, mol. struct. and phys. props. Raman studies 7-45063
 domain growth from melt, temp. gradient, form. kinetics study 7-51681
 electrical treeing, breakdown lifetime and microstruct. sequence 7-13092
 electroceramic composites, props. and struct. 7-64558
 electronic materials and their microstructure, thermal wave imaging studies 7-8237
 epitaxial overlayers, structural transitions 7-27194
 epoxy matrices, microstruct. 7-33632
 ferromagnetic materials, defect and microstructural analyses using TEM 7-37817
 films, grain growth phenomena and microstructural evolution during deposition, Monte Carlo simulation 7-52336
 finely dispersed systems, microstruct. parameters, atom-probe anal. 7-33677
 fractographic features caused by impact load and microstruct. effect of impact vel. (*Japanese*) 7-51929
 gilsonite, microstructure and mechanical props. 7-44838
 glass ceramics, struct., phase relations 7-7982
 halide eutectic composites, growth, struct., mech., elec. and optical props. 7-33648
 heterogeneous ceramics, processing for dielectric appls. 7-64984
 high resolution electron microscopy in materials science (*German, English*) 7-39806
 IN 100, rheocasting and vacuum are double electrode remelting, solidification struct. 7-39497
 IN 100 superalloy, MC carbide props. rel. to transition element doping 7-13456
 Inconel 600 and 690, SCC under high temp. NaOH, comp. and annealing effect 7-39710
 intermetallic phases, appl. as high temp. materials, review 7-22775
 metal tubes, ductile, no. of cracks in axial splitting 7-59597
 metals, dual-phase, simulation of growth process of minor phase grains 7-65050
 metals, struct. changes under action of thermal cycling (*Russian*) 7-53752
 MgO-monticellite ceramic, high resolu. TEM and STEM study 7-22738
 misch metal-Fe-B melt-spun magnets, mag. and structural props. 7-53032
 mullite, Al₂O₃ and ZrO₂ particle reinforced, prep. by reaction sintering, fractographic study 7-22800
 Nimonic 86, carburised, heat treatment, creep behaviour rel. to carbide precip. (*Korean*) 7-46560
 Nimonic PE 16, Ni-base superalloy, duplex γ' particle hardening 7-28053
 pearlite spacings, meas. of spread 7-39804
 pearlite-austenite interface, SEM obs. 7-39505
 porcelain, sintering kinetics, struct. evolution 7-28004
 powder, internal structure of solidified aerosol droplets, etching method 7-7920
 powder metallurgy, modern science and technology 7-7921
 powder plastically worked articles, annealing effect on behaviour in temp. jump and substruct. 7-27961
 power metallurgy coatings obtained by impact wave method, struct. form. 7-65211
 pyroxenes, synthetic, exsolution and phase transforms., X-ray and TEM obs. 7-16725
 rapid thermal processing, conf., Boston, MA, USA (Dec. 1985) 7-14713
 rapidly solidified alloys, developments and engng. design implications 7-27967
 rhombohedral system, coincidence-site lattices 7-51685
 scanning tunneling microscopy of surface microstructure on rough surfaces 7-21580
 semiconductor materials, high resolution microstruct. studies using TEM 7-21055
 semiconductors, ion beam induced epitaxial crystn., kinetics, mechanisms and microstruct. 7-12171
 shape memory alloys, mech. props., polycrystal model (*Japanese*) 7-53789
 shock compression induced modification and synthesis, book contrib. 7-27957
 β-sialon composite ceramics, microstruct., hardness, tool appls. 7-65144
 SOI formation by O ion implantation of Si, ordered precipitate structure and coesite formation 7-52065
 solidification, stirred, Taylor vortices influence on morphology 7-22657
 stage II fatigue crack growth behaviour of granular bainitic microstructures 7-28134

crystal microstructure continued

- steel, alloy, structure evolution during strong plastic deformation (*Russian*) 7-3558
- steel, alloyed structural, struct. rel. to cold deformability, softening heat treatment methods development 7-39556
- steel, austenitic, Mn-Cr, hardening characts. and hydroextrusion parameters (*Russian*) 7-59540
- steel, austenitic stainless, creep cavitation rel. to S and P impurity segregation 7-39587
- steel, austenitic stainless, electron irradi., cold working, vacancy swelling, void form., carbide precip., electron microscopy 7-21282
- steel, austenitic stainless, in-beam creep rupture props. at 873K 7-53851
- steel, austenitic stainless, intercrystalline corrosion rel. to chromium carbide precip. 7-53986
- steel, austenitic stainless, liq. phase sintering, effect of Si additions 7-53678
- steel, austenitic stainless, long term creep, transient strain induced strengthening 7-28090
- steel, austenitic stainless, microstructure rel. to cathodic H charging 7-28039
- steel, austenitic stainless, rapidly solidified, microstruct. characterisation 7-22672
- steel, austenitic-ferritic stainless, weld metal deposits, final microstruct. form., role of thermal contraction stresses assoc. with inclusions 7-59738
- steel, bearing type, quenching temp. rel. to microstruct. and fracture surface morphology 7-8015
- steel, C-Mn, arc welds, as-deposited strength, toughness, microstruct. 7-13555
- steel, C-Mn, creep crack growth at 360°C, effect of microstruct. 7-28113
- steel, carburised, microstructural constituent in high C layers 7-54006
- steel, combined heat treatment, surface layer props. (*Russian*) 7-39742
- steel, composition-treatment-structure property correlation, computer software development 7-3329
- steel, constructional, struct. and props. after high-temp thermomech. isothermal working 7-46522
- steel, Cr type, dislocation struct. after hydraulic pressing followed by austempering 7-3334
- steel, Cr-Mo, high C, bonded carbide, secondary temper hardening, microstruct. 7-17542
- steel, Cr-Mo, mech. stability of retained austenite, absence of H influence 7-28125
- steel, Cr-Mo, normalised, tempered, neutron irradi., 390-550°C, tensile props. 7-17621
- steel, Cr-Mo, normalised heavy section plate, weld cold cracking susceptibility (*Japanese*) 7-3425
- steel, Cr-Mo, plate, directional solidification, rolling, strength, toughness, microstruct., weldability 7-59622
- steel, Cr-Mo, thermodynamic props. of carbides, 985K 7-17536
- steel, Cr-Mo type, deformed, struct. and mech. props. after long ageing 7-8106
- steel, Cr-Mo-V, creep crack growth at 838 K, displacement-controlled loading behaviour 7-17626
- steel, Cr-Mo-V, creep crack growth at 838K, const. load behaviour 7-17625
- steel, Cr-Mo-V, creep ductility, impurity and microstruct. effects 7-46587
- steel, Cr-Mo-V, rail, fatigue crack growth 7-8114
- steel, CR-Mo-V, thermal fatigue resist., effect of initial struct. 7-28132
- steel, Cr-Mo-V type, service props. in different struct. conditions 7-8107
- steel, Cr-Ni high-temp. type, N and heat treatment effect on struct. and mech. props. 7-33688
- steel, Cr-Ni-Co VK56, struct. and mech. characts., effects of Ni, Co and heat treatment 7-8108
- steel, Cr-Ni-Mo, maraging, mech. props. rel. to heat treatment (*Japanese*) 7-53792
- steel, Cr-Ni-W, fatigue striation, macrocrack propag. (*Chinese*) 7-8074
- steel, CrMoV, cold rolled, effects of ageing on mechanical properties (*Russian*) 7-13478
- steel, die, preliminary heat treatment schedule 7-8023
- steel, dual phase, continuous cooling, transform. processes and products 7-28034
- steel, dual-phase, micro alloyed, mech. props. and struct., effect of process variables 7-65108
- steel, duplex stainless, manual metal arc weld metals, microstruct. and phase transform. 7-59526
- steel, eutectoid, microstruct. obs. of bainite stars 7-53695
- steel, eutectoid, phase rot., effect of recrystn. processes during heat deform. (*Russian*) 7-53760
- steel, fatigue, microstruct. changes, thermometric assessment (*German*) 7-17641
- steel, fatigue threshold, effective, influencing factors 7-46607
- steel, ferritic and austenitic welded joints, thermally loaded, struct. and mech. props. 7-8102
- steel, ferritic stainless, He-doped, microstruct. evolution following 14 MeV Ni ion irradi. 7-58363
- steel, ferritic stainless, Mo, welding, heat affected zones, microstruct., thermal history 7-53769
- steel, fine-grained, Zr effect on struct. and phase comp. 7-39525
- steel, fracture toughness of specimens with mixed microstruct., prediction using conc. model 7-13570
- steel, Hadfield, cold-deformed, fine struct. anal., brittle fracture (*Russian*) 7-59570
- steel, hardened and tempered, struct. aspects of cyclic crack resist. 7-17613
- steel, heat treatment method effect on struct. and mech. props. 7-39561
- steel, heterogeneous microstruct., near-threshold fatigue crack propag. 7-46602
- steel, high Si, rapid solidification in double roller method 7-22665
- steel, high speed, powders, transform., struct. and props., prior annealing effect 7-13452
- steel, high speed, service performance rel. to Ca and Zr microalloying 7-3366
- steel, high speed, wear mechanisms and tool life rel. to microstruct. 7-8128
- steel, high-speed, atomised powder, particle size effect on amount of residual austenite 7-3308
- steel, high-speed, powdered, struct. after sintering in presence of liq. phase 7-53677
- steel, high-speed p/m tungstenless, Mo and V effect on microstruct. and operating props. 7-33788

crystal microstructure continued

- steel, high-speed W-Mo, nitrogen effect of stabilisation of austenite 7-8021
- steel, high-strength low-C weldable, C content effect on struct. and mech. props. 7-46583
- steel, linepipe, H-induced cracking 7-22881
- steel, low alloy, arc weld deposits, austenite grain struct. 7-39494
- steel, low alloy, hot forming, transform. behaviour, struct. (*German*) 7-59518
- steel, low alloy, microstruct., mech. props. rel. to cooling rate 7-46514
- steel, low C, cold forgeability, notches, geometry, friction conditions, microstruct. 7-33697
- steel, low C, H diffusion and trapping by TiC precipitates (*Chinese*) 7-7998
- steel, low C, sheets, yielding rel. to prestrain, uniaxial tension 7-46553
- steel, low C, small fatigue crack growth, effects of microstruct. and limitations of linear elastic fracture mechanics 7-39625
- steel, low C, strain ageing, internal stress, Bauschinger effect 7-39612
- steel, low C, struct. rel. to deform. method (*Russian*) 7-46580
- steel, low-C, cost, failure micromechanism in fatigue crack propag. after different heat treatments 7-46641
- steel, low-C, Ni influence on struct., fracture resist. and fractographic features 7-3420
- steel, low-pearlite, rules of austenite decomp. in continuous cooling 7-3339
- steel, managing, 18 Ni, erosion, effect of microstruct. and mech. props. 7-22849
- steel, managing, hydraulically pressed, struct., texture and hardening (*Russian*) 7-3323
- steel, managing, struct., mech. props. and cavitation-corrosion stability (*Russian*) 7-46684
- steel, medium and high C, coalescence recrystallisation, cementite particles effect 7-46515
- steel, microalloyed, abnormal grain growth in austenite range (*German*) 7-7958
- steel, microalloyed, carbonitride charactn. (*German*) 7-13461
- steel, microstrain distribution under simple and complex loading 7-28096
- steel, mild and Cr, surface saturation with B by laser radiation 7-8172
- steel, Mn-V-Mo austenitic, struct. and precipitation hardening (*Russian*) 7-17541
- steel, Mo-base high speed, carbide chem. composition, electron microscopy studies 7-22671
- steel, Ni-Co-Mo, maraging, fracture toughness rel. to heat treatment, precip., Auger spectra 7-65124
- steel, Ni-Cr, deform. dislocation struct., fracture 7-33740
- steel, Ni-Cr, tensile flake form., H damage, dislocation transportation (*Chinese*) 7-8077
- steel, pressure vessel, neutron irradi., defect microstruct., SANS and TEM studies 7-58351
- steel, rail, US inspection signal rel. to microstruct. and surface condition 7-3556
- steel, rotor type, deformed, microcrack dimens. rel. to acoustic emission parameters and struct. 7-65258
- steel, stainless, austenitic, low-activation, constitution, struct. and mech. props. 7-42195
- steel, stainless, austenitic, valve type, heat treatment schedule effect on failure nature 7-3423
- steel, stainless, cold rolled sheet, struct. form. during recrystn., optimum heat treatment schedule 7-3340
- steel, stainless, Cr type, chem. microinhomogeneity of solid solns. effect on brittleness 7-3422
- steel, stainless, duplex, corrosion imaged and welded conditions, microstruct. effect 7-39698
- steel, stainless, films, sputter deposited, vacuum annealing-induced solute depletion 7-64012
- steel, stainless, microstruct., aging effects, atom probe FIM, optical and analytic electron microscopy studies 7-33700
- steel, stainless, neutron irradiated, microstruct. and swelling, Si and N impurity effects (*Russian*) 7-2217
- steel, stainless, Ni-Cr precision alloy, spread of local overloads in microstruct. of aged and nonaged specimens 7-8061
- steel, stainless, passivity rel. to comp. and microstruct. 7-39711
- steel, stainless, pulsed and continuous laser welded, solidification behaviour and microstruct. characts. 7-13444
- steel, stainless, transition class, deform. method effect on microstruct. 7-3299
- steel, stainless, Type 316, microstruct. exam. around weldments 7-22697
- steel, structural, diffusion chromised, elevated temp. effect on comp., struct. and mech. props. 7-8178
- steel, structural, micromechanisms of near-threshold fatigue crack propag. 7-13551
- steel, structural heredity in heat cycling 7-33703
- steel, tool, heat treatment cycles, original struct. and deform. influence on mech. props. 7-39560
- steel, V, thermal softening, carbide structural parameters rel. to alloying 7-22728
- steel, V, W₂, laser surface melting, effects of prior heat treatment 7-65195
- steel 45, hardening coatings, electroerosion alloying 7-17722
- steel 65G, microstruct. and mech. props. after low-temp. TMT, tempering temp. influence 7-17554
- steel filaments, fatigue failure signs 7-46642
- steel foils, H charged, internal friction, quasi-molecular state (*Russian*) 7-59561
- steel-VC composites, cold sintered, mech. props., bonding integrity 7-39471
- steels, tool, M2 and H13, fracture toughness, influence of microstruct. 7-46632
- steels, transformation, improved calc. 7-28009
- stereological counting meas., estimation of dihedral angles 7-39803
- structure statistical parameter evaluation, image processing automation (*Russian*) 7-10877
- structure-dependent optical phenomena 7-45953
- superalloys, crystalline struct. and growth twin of Cr₇C₃, electron diffraction (*Chinese*) 7-12077
- superalloys, topologically close packed phases, domain struct. (*Chinese*) 7-11989
- superplastic deformation, grain-boundary slip velocity and microstruct. (*Russian*) 7-3362
- systematic description 7-22633

crystal microstructure continued

- Udimet 700, Ni-base alloy, solidified, dendrite arm spacing rel. to cooling rate 7-53713
- ultrasonic techniques for microcrystalline struct. examination 7-46765
- visible-near UV spectroellipsometry and spectrophotometry studies 7-46758
- Waspaloy, γ - γ' partitioning behaviour, energy dispersive spectrometry 7-17534
- with lamellar graphite, mech. props. and morphology (*German*) 7-21160
- Al alloy surface, UV laser pulse irradi., microscopic crater form. 7-12124
- Al alloys, crystal structure and microstructure, metallography studies 7-58204
- Al alloys, liquid dynamic compaction, microstruct. and precipitation, TEM study 7-59529
- Al alloys, medium strength, formability rel. to microstruct. 7-17592
- Al alloys, solidification, continuous and interrupted, development of microstruct. and homogenisation (*German*) 7-53719
- Al and alloys, dynamic restoration during hot rolling 7-22724
- Al sputtered thin films, struct. props. 7-21758
- Al, US deform, modelling of reduced bandwidth distortion to wide-area electron channelling mapping 7-16694
- Al/Cu friction welds, microstruct. and mech. props. (*German*) 7-46792
- Al-Ag (5 wt.%), anelastic effects, quench sensitivity, precip. and dissolution 7-53784
- Al-Cu (2 wt.%) single crystals, rolled, shear band form. rel. to δ' precipitates 7-3385
- Al-Cu (3.76 wt.%), rheocast, partially homogenised, ageing response, microhardness 7-46499
- Al-Cu compact, struct. form. during sintering 7-53675
- Al-Cu-Li, 2020, low-cycle fatigue, effect of environment and temp. 7-28117
- Al-Cu-Li-Mn-Cd alloy, 2020, micromechanisms governing elevated temp. fracture resist. 7-22803
- Al-Cu-Mg, 2024, TEM specimen prep. parallel and perpendicular to machined surfaces 7-39808
- Al-Cu-Mg, cast composite, mica particle distrib. 7-46375
- Al-Cu-Mg, hot workability, recrystallisation during torsional deform. (*Korean*) 7-46559
- Al-Fe-Mn powder, rapidly solidified, microstruct. 7-46445
- Al-Fe-Ni, R=Ce, Er, Nd or Gd, rapidly solidified microstruct. 7-59502
- Al-Li, coarsening of δ' precipitates 7-33663
- Al-Li, quenched, ageing, light ion irradi., δ' phase form. and particle growth 7-26807
- Al-Li base system, solid-state phase transform. 7-46456
- Al-Li-Cu-Mg-Zr die forgings, mech. props., microstruct. 7-46636
- Al-Li-Cu-Zr, fracture, ageing and comp. depend. 7-22784
- Al-Li-Cu-Zr, nucleation of precipitates 7-46476
- Al-Li-Zn-Mg-Cu alloys, microstruct. evolution 7-53739
- Al-Mg and Al-Zn-Mg alloys, plasma-coated, heat treatment effect on fine struct. and failure mechanism 7-3496
- Al-Mn (15 wt.%), melt spun ribbons, icosahedral struct., decomp. rel. to annealing 7-28030
- Al-Mn-Si, quasicryst., X-ray diffr., TEM and SEM study 7-12299
- Al-Mn-Zr (7.1 wt.%), rapidly solidified, quasicrystalline phase precip. 7-3310
- Al-Mo (11 at.%), rapidly solidified, equil. phase development 7-46436
- Al-Si eutectic, unmodified, Al grain struct. 7-65012
- Al-Si LM 13 alloy with graphite particles, gravity die cast, dispersed graphite effect on freezing rate 7-59506
- Al-Si/Ti/Al-Si VLSI metallisation, electromigration and microstruct. props. 7-21550
- Al-Si-Pb-Bi, duplex alloys, melt quenching, microstruct. supercond. props. 7-45593
- Al-Si; graphite particle reinforced composite, solidification, microstruct. 7-28028
- Al-Ti-based homogeneous alloy films, elec. resist., microstruct., electromigration, comp. effects 7-21765
- Al-Zn-Mg, TEM specimen prep. parallel and perpendicular to machined surfaces 7-39808
- Al-Zn-Mg-Cu, fatigue crack propag., influence of microstruct. (*German*) 7-22833
- Al-Zn-Mg-Cu, high-energy rate powder metallurgy processed, microstruct. evaluation 7-22607
- Al-Zn-Mg-Cu alloy, microalloying effect on struct. and mech. props. 7-53755
- Al-Zr-V, rapid solidification, age hardening, solid soln. form. (*Korean*) 7-46475
- Al_{1-x}Mn_x cryst. and quasicryst. alloys, struct. and mag. props. 7-1949
- Al₈₈Mn₇Fe₅, Al₈₈Mn₁₄, icosahedral alloys, obs. of mirror-related grains 7-37867
- Al₁₂Mo precipitate microstruct. and orientation, implantation and annealing effects, electron microscopy study 7-16782
- Al₂O₃-SiC composites, microstruct. and mech. props. (*Japanese*) 7-22821
- Al₂O₃-SiO₂, mullite ceramics, sol mixture prep., drying method effect (*Japanese*) 7-1944
- Al₂O₃-SiO₂, mullite, prep. by sol-gel method, microstruct. and mech. props. 7-46386
- Al₂O₃-TiC-TiN composite ceramics, microstruct., hardness, tool appls. 7-65144
- Al₂O₃-TiN powder composites, densification kinetics and struct. form. during sintering under high press. 7-53687
- Al₂O₃-TiO₂ composite powders, prep., transform. temp. 7-27985
- Al₂O₃-TiO₂ system detonation coatings, struct. and phase characts., physico-mech. props. 7-65212
- Al₂O₃-ZrO₂ composite ceramics, microstruct., hardness, tool appls. 7-65144
- Al₂O₃-ZrO₂ composites, microstruct. charactn. by Raman spectroscopy (*Japanese*) 7-22684
- Al₈₉Si₁₀ melt spun ribbons, microstructures and superconducting transition temperatures 7-38222
- Au films, early stages of reaction with amorphous Ni-Nb films 7-21703
- Au polycrystalline tips, grain rotation and grain boundary annihilation, in situ SEM study 7-32460
- B₂C, fast neutron irradiated, thermal cond. meas. 7-6900
- BN, cubic, aggregate tools, microstruct. and wear 7-3462
- BN, cubic, polycryst., influence of sintering conditions on phys. props. 7-22618
- Ba_{0.9}Sr_{0.1}TiO₃Sb, positive temp. coeff. of resist., synthesis method depend. 7-45324
- BaTiO₃ ceramics, grain struct. and phase anal. (*German*) 7-58496

crystal microstructure continued

- Bi-Ga two-layer film compositions, refl. and microstruct., temp. depend. 7-53428
- C and graphite, strength and struct., conf., Liverpool, England (Sept. 1985) 7-24257
- C fibre reinforced C, multidirectional composites, macroporosity and interface cracks 7-46513
- Ca_{1-x}Ba_xF₂ epitaxial layer growth and struct., electron microscopy studies 7-21714
- CaCO₃, calcite, grain growth, effect of second-phase particles 7-39476
- CaFe₂Mn_{1-x}O_{3-y} ferrites, microdomains, role in oxidation, reduction and annealing 7-46830
- Ca₂Fe₂TiO_{8+x} perovskites, microdomains, electron microscopy 7-16533
- Ca₃Mn_{1.8}Fe_{1.2}O_{3+y} perovskites, microdomains, electron microscopy 7-16533
- Ca₂Nd₈(SiO₄)₆O₂·Cm ceramic simulated nuclear waste forms, radiation effects on microstruct. and fracture props. 7-58373
- CaO-Fe₂O₃ system, solid state reactions, ferrite growth and morphology 7-3236
- CaZrO₃, sintering, porosity, mech. props., corrosion resist. 7-39664
- CeO₂, doped with trivalent cations, grain boundary effect, microstruct. and microanal. 7-38249
- CeO₂-CaO, ceria-calcia ceramics, ionic cond., effect of microstruct. 7-38250
- Co-Al, precipitation product dissolution (*Russian*) 7-58479
- Co-Al (10.9 at.%), cellular prep. from supersaturated solid soln. (*Russian*) 7-65045
- Co-Cr magnetic thin films, facing targets sputter deposition, microstruct. model 7-27905
- Co-Cr thin films, DC magnetron sputtered, mag. props., effect of substrate and deposition rate 7-59067
- Co-Cr-N, surgical implant alloy, mech. props., microstruct. rel. to N addition 7-60125
- Co-Cr-Re system, phase equilib., struct., microstructural, X-ray phase and durometric analyses 7-17513
- Co-Pt thin films, sputtered, TEM study 7-21757
- Co-TaC, rapid quenching, microstruct. 7-65023
- CoCr films, vacuum evaporation, thickness depend. of mag. props. 7-27576
- CoCr RF sputtered magnetic films, Cr segregation, STEM study 7-44827
- CoCr sputtered film recording media, wear resistance, mech. strength and microstruct. 7-32859
- CoCr sputtered perpendicular recording media, with columnar microstruct., reversal mech. 7-7552
- CoCr-based thin films, growth and mag. props., nucleation layer effects 7-45065
- CoCrAl alloys, microstruct., atom probe FIM and TEM studies 7-33636
- CoCrAlY electron beam physical vapour deposition coating microstruct., TEM characterisation 7-52334
- CoCrTa sputtered films, microstruct. and mag. props. studies 7-12575
- CoNi sputtered films on Cr and polyimide, mag. props., relation to struct. 7-33228
- Cr evaporated and ion assisted deposited coatings, microstruct., electron microscope obs. 7-52335
- Cr-Ta-C, ageing, hardening processes, carbide separation and dissolving (*Russian*) 7-59541
- Cr₇₅Si₂₅ thin films, microstruct. and resist., room temp. to 950°C 7-38410
- Cu alloys, irradi. in FFTF to 16 dpa at 450°C, microstruct. eval. 7-51837
- Cu alloys, neutron damage microstructs. 7-58347
- Cu alloys, rapidly solidified powder metallurgy, irradi. to 13.5 dpa with neutrons, microstruct. evolution and swelling 7-51840
- Cu bicrystals, fatigued at high temp., microstruct. obs. in vicinity of cavitated grain boundaries 7-38019
- Cu dislocated single cryst., sub-grain misorientation, de Haas-van Alphen meas. 7-12300
- Cu, dislocation mechanism based model for stage II fatigue crack propagation rate 7-21338
- Cu, polycrystalline, US and neutron irradi., struct. and mech. props. (*Russian*) 7-3402
- Cu, structure evolution during strong plastic deformation (*Russian*) 7-3358
- Cu-Al bronzes, microstruct., corrosion 7-39697
- Cu-Al-Ni-Fe-Mn bronze, cast, laser surfacing, improved corrosion resist., microstruct. characteris. 7-13651
- Cu-Al-Ni-Ti-Zr, shape memory alloy, grain refinement, fracture mode, Ti and Zr additions effect 7-3301
- Cu-Al-Zn-Mn-Ni shape memory alloy, positron annihilation study 7-46206
- Cu-B, cast struct., segregation, conc. undercooling 7-3291
- Cu-Be, explosive cladding, martensitic transform., electron diffr. 7-46468
- Cu-Be (30 at.%), eutectoid decomp., spatial distrib. of α -phase (*Russian*) 7-53694
- Cu-Ce, cast struct., segregation, conc. undercooling 7-3291
- Cu-Co, age hardened, tensile deform., acoustic emission characts. 7-13536
- Cu-Co, dynamic fracture characts., void nucleation at incoherent precipitates 7-17628
- Cu-Cr multilayers, laser alloying 7-45025
- Cu-Fe, thermomech. treatment, softening rel. to disperse α -Fe particle, size and orientation 7-28054
- Cu-Ni-Fe-Mn, physical props. rel. to precip. and thermal treatment (*German*) 7-12698
- Cu-Ni-P alloy, P addition effect on struct. and strength 7-53669
- Cu-Sn-Pb system, struct. form. during sintering 7-64967
- Fe, cast, alloyed, pearlite, flake graphite, thermal fatigue resist. 7-46606
- Fe, cast, alloyed pearlitic flake graphite, thermal cond., comp. and microstruct. depend. 7-27317
- Fe, cast, bainitic ductile, microstruct. rel. to comp. and heat treatment 7-39579
- Fe, cast, cavitation resist., microstructure, SEM obs. (*German, English*) 7-59641
- Fe, cast, high-Cr, wear-resistance, laser and heat treatment effect on struct. and props. 7-8174
- Fe, cast, metastable austenite form. rel. to initial treatment and struct. 7-46455
- Fe, cast, nodular, ferritising action of increased Mg content on struct. 7-3292

crystal microstructure continued

- Fe, cast, nodular graphite, fatigue crack propag. rel. to microstruct., SEM obs. (*Chinese*) 7-13542
- Fe foils, H charged, internal friction, quasi-molecular state (*Russian*) 7-59561
- Fe oxide layer on Fe acicular particles morphology and mag. props. 7-52067
- Fe sputtered films, mag. perpendicular anisotropy, Mossbauer studies 7-59076
- Fe thin films, sputter deposited at oblique incidence, microstruct. and mag. props. (*Japanese*) 7-33560
- Fe-Cr-C-B hard surfacing weld deposits, abrasive wear resist. and microstruct. 7-22847
- Fe-Cr-Co(Si), permanent magnet alloys, microstruct., mag. props., Si content effect 7-22117
- Fe-Cr-Mn-C alloy, laser clad, microstruct. and wear props. 7-13652
- Fe-Cr-Re system, interaction of intermediate phases, phase equilibria 7-17514
- Fe-Cu, neutron irradi., defect microstruct., SANS and TEM studies 7-58351
- Fe-Mn alloy, p/m type, martensitic transform. and struct. form. mechanisms 7-33658
- Fe-Mo (14.5 wt.%), ageing, discontinuous dislocational transform., coercivity obs. 7-3305
- Fe-N, implantation at 77 K, surface comp., microstructure, AES, HVEM, transmission HEED studies 7-38033
- Fe-N alloys, phase state and precipitation, plastic deformation effects (*Russian*) 7-46551
- Fe-Nd-B magnets, microstructure and mag. props. 7-53049
- Fe-Ni, martensitic transform., defect form., positron annihilation study (*Chinese*) 7-39213
- Fe-Ni martensite crystals, positions, external stress effects (*Russian*) 7-46409
- Fe-Ni-Al-Co system, miscibility gap, phase decomp. in Alnico mag. alloys 7-17537
- Fe-Ni-Cr-Ti-B, constant elastic alloy, torsion reson. freq. temp. coeff. rel. to B content (*Chinese*) 7-13488
- Fe-Si, electrical steels and alloys, conf., Vladimir, USSR (Dec. 1984) 7-9576
- Fe-Si, grain oriented, hot rolling texture, thickness variations 7-8009
- Fe-Si, structure, texture and mag. props. 7-12995
- Fe-Si (2 wt.%), microstruct., mag. props., thermomech. history effect 7-7551
- Fe-Si (3 wt.%), hot rolling, austenite formation 7-13481
- Fe-Si (3.3 wt.%), grain-oriented, domain refined, core losses 7-33692
- Fe-Si-Al, carbide precip. kinetics, core loss 7-8001
- Fe-Si-B, normalising, decarburisation, secondary recrystallisation, mag. induction obs. 7-8020
- Fe-Si-Ni (6.5, 2 wt.%), development of Goss texture, lowering of core loss 7-33693
- Fe-Ti multilayered films, ion bombard., microstructure, TEM obs. 7-12165
- Fe-Ti-C multilayered films, ion bombard., microstructure, TEM obs. 7-12165
- Fe-Ti-N, mech. props. rel. to cold working 7-28089
- Fe-TiB₂ eutectic system, microhardness, modulus of elasticity (*Russian*) 7-39648
- Fe-VC composites, cold sintered, mech. props., bonding integrity 7-39471
- Fe-Zr, amorphous and microcrystalline, exchange interaction and saturation magnetisation 7-45651
- Fe₁₄Nd₂B permanent magnet, Dy substituted positron annihilation studies 7-3108
- Fe₁₄Nd(Y)(Ce)₂B fine particles prep. by hydriding, mag. props., recording appls. 7-53660
- FeO₂ fine particles, magnetic and morphological props., annealing effects study 7-53766
- γ -Fe₂O₃ particles, microstructure, X-ray diffr., magnetisation props. 7-45757
- γ -Fe₂O₃ particles, pure and Co-modified, microstructural defects 7-58497
- GaAs crystals, selective etching and photoetching of CrO₃-HF aq. solns. 7-32442
- GaAs:Be⁺, ion implanted, residual microstruct., TEM studies 7-32675
- GaAs/metal interface microstruct. and reactions, stability and elec. props., TEM and STEM studies 7-12515
- Gd-Sb, phase diagram, peritectic reactions, congruent melting, DTA, microstructural and X-ray anal. 7-39481
- Ge single crystal, microstruct. of fragments (*Russian*) 7-38107
- HoFeO₃ crystals, flux growth, secondary phase and microdiscs form. 7-13344
- InP:Ti(Cr)(Ni), LEC growth, precipitate phase identification 7-16754
- Ir-Fe₂, vaporisation, torsion-effusion obs., morphology 7-58455
- (La,Ca)(Co,Mn)O₃, sinterability, phase composition and microstructure 7-33622
- LaCrO₃-Cr cermets, mech. props., interparticle welding 7-39630
- Li ferrites, microstruct. effects on mag. props. (*German*) 7-59052
- Mg-Gd supersaturated solid soln., precipitate cryst. struct. (*Russian*) 7-33665
- MgO, sinterability, microstruct. changes during sintering 7-22624
- MgO-Al₂O₃-SiO₂-GeO₂ cordierite ceramics, sintering, microstruct., thermal props. 7-52088
- MgO-CaO, activated sintering, densification, microstruct. (*Chinese*) 7-13410
- Mg₂SiO₄, fosterite-based ceramic with BaO addition, synthesis, sintering, struct. and props. 7-46397
- Mn-Al-C ferromag. alloys, phase, transformations. and struct. defects, positron annihilation study 7-46461
- Mn₃Ni₂Si, rapidly solidified, Frauf-Laves phase related quasicrystal, TEM obs. 7-51706
- Mo, hydroextruded single crystals, nonuniformity of texture deform. (*Russian*) 7-33695
- Mo, recrystallised, microstruct. and creep charact. (*Russian*) 7-39600
- Mo-Nb, a nitride form., particle coalescence (*Russian*) 7-59530
- Mo-ZrO₂, sintered composites, mech. props, microstruct. (*Japanese*) 7-13558
- Na₂O-CaO-Al₂O₃-SiO₂ glass ceramic system, spherulitic growth, mech. props. 7-46405
- Nb film microstruct., nonnormal incidence ion bombardment effects 7-12174
- Nb, H embrittlement, crack propag., 120-300K, hydride form. 7-33757
- Nb-Ge alloys, processed in inert gas in 100 m drop tube 7-7986

crystal microstructure continued

- Nb-Zr (1 wt.%) alloy, hydroextruded, optimum degree of deform., microstruct. 7-3325
- Nd-Dy-Fe-B-based sintered magnet, microstruct., heat treatment effects 7-53767
- Ni alloy, heat-resisting, hot strain rate effect on microstruct. and mech. props. 7-39559
- Ni base superalloys, interphase boundaries, FIM atom probe study 7-33683
- Ni base superalloys, techniques for required props. prod. (*Turkish*) 7-59657
- Ni, dislocation arrangements in single crystals fatigued at low temps. 7-12068
- Ni, foils, H charged, internal friction, quasi-molecular state (*Russian*) 7-59561
- Ni powder plastically worked articles, annealing effect on behaviour in temp. jump and substruct. 7-27961
- Ni, structure evolution during strong plastic deformation (*Russian*) 7-3358
- Ni, substructure at accelerated high temp. creep (*Russian*) 7-65096
- Ni-Al synthesis by shock compression of composite particles 7-39462
- Ni-Al-Co-Cr-Ta, polycrystalline superalloys, microstruct. rel. to Ta content 7-46446
- Ni-base superalloy, IN 939, high Cr, effects of heat treatment on mech. props. 7-13526
- Ni-base superalloys, fatigue endurance at high temps., influence of struct. and surface oxidation 7-59626
- Ni-base superalloys, γ strengthened, creep and microstruct. rel. to refractory elements 7-3364
- Ni-base wrought superalloy, thermal fatigue resist. improvement by laser-glaze 7-22840
- Ni-Co based refractory alloys, γ -phase strengthening rel. to comp 7-46496
- Ni-Cr, carburisation, kinetics, diffusion and precipitation (*German*) 7-8194
- Ni-Cr (1 wt.%), internal oxidation, two-phase region form. kinetics in diffusion zone (*Russian*) 7-46497
- Ni-Cr alloy, wrought, HF effect on struct. and mech. props. 7-33689
- Ni-Cr superalloy, high-temp. material, microstruct. and mech. props. with high-temp. heating 7-3341
- Ni-Cu-Si, γ precip. coarsening, bifurcation theory appl. (*Japanese*) 7-53734
- Ni-P coating, electrolytic, electron microscope obs. of struct., P content depend., amorphous layer form. 7-8157
- Ni-P films, electrodeless deposited, struct., electron microscopy studies 7-7041
- Ni-Sn, ageing, discontinuous coarsening of cellular precipitate at grain boundary 7-39528
- NiAl thin films, ion irradi. induced amorphisation studies rel. to cascade parameters 7-63671
- NiCrSiB alloy coatings, sputter deposition, microstruct. variations 7-46351
- NiO-CuO solid solutions, tweed microstruct., investig. using TEM 7-44756
- PZT, shock-recovery expts. 7-38119
- Pb-Tl, Bridgman growth, pattern generation at solidification front, forbidden cells 7-22651
- Pb(Mg_{1/3}Nb_{2/3})O₃ ceramics, dielec. props. 7-46382
- Pb(Zn_{1/3}Nb_{2/3})O₃-PbTiO₃, perovskite ceramic powder, prep. dielec. and piezoelec. props. 7-46380
- Pt, sputtered film, microstruct., thickness effect studied by X-ray diffr. method 7-21756
- Pt-group metal silicides epitaxial growth on Si (111) 7-21760
- Pt-Zr internally oxidised alloys, morphology, struct. and stability (*Russian*) 7-33687
- δ -Pu-Ga (1.5 wt.%) foils, cold rolling, annealing, microstruct., TEM obs. 7-59544
- Sb₂S₃-PbS systems, non-stoichiometric phases close to Sb₂S₃, structure 7-32674
- Si, charge carrier-lattice interaction, X-ray diffr. study 7-51975
- Si powders, prod. from laser-heated silane, cryst. struct. 7-46362
- Si:As substrate, dopant effects on formation kinetics of Pt silicides 7-21697
- SiO₂, C, precipitation, microstructures, TEM studies 7-32668
- a-Si/c-Si interface, microcrystallites and orientational proximity effect, HREM image interpretation, comment and reply 7-45028
- Si-Al-O-N Syalon, bonding investig., active Ti additive role, fracture strength and microstruct. 7-39846
- Si-Si interfaces, MBE grown, sputter cleaned, microstructure, electron microscopy obs. 7-12512
- SiC fibre composites, structural EXAFS study 7-64762
- SiC fibre reinforced Al composite wires, neutron irradi., mech. props., fusion reactor appl. 7-49628
- α -SiC polycryst., pulsed laser annealing and ion beam mixing surface modification studies 7-16657
- β -SiC powder, sintering, phase transform. rel. to additives (*Japanese*) 7-17527
- SiC, sintered, microstruct. and props., influence of fabrication method (*Japanese*) 7-22622
- α -SiC, sintered, occurrence and distrib. of B-containing phases 7-39466
- SiC whisker reinforced Si₃N₄, microstruct. and props. 7-22824
- SiC whisker reinforced Al₂O₃, ZrO₂ or glass composites, microwave sintering, microstruct. 7-27993
- SiFe, grain oriented, Barkhausen noise behaviour, effect of local strain 7-33205
- Si₃N₄, gas press. sintering, fracture toughness, fibre like struct., additions effect 7-13414
- Si₃N₄, hot isostatic pressing with BeAl₂O₄ addition (*Japanese*) 7-27994
- Si₃N₄, hot pressed, elec. cond., microstruct., fusion reactor insulator appl. 7-52619
- Si₃N₄, nanostruct. defects, high-resolution electron microscopy studies 7-12302
- Si₃N₄, reaction bonded, thermal cond. (*Japanese*) 7-6902
- Si₃N₄ whisker reinforced Al₂O₃ or ZrO₂ composites, microwave sintering, microstruct. 7-27995
- Si₃N₄, with MgO addition, phys. and tribological props., effect of hot-pressing time (*Japanese*) 7-65150
- Si₃N₄-TiC composites, densification, matrix-dispersoid reaction, mech. props. microstruct., impurities effect 7-64994
- Si₃N₄-TiC composites, mech. props., wear resist., dispersoid-matrix interaction 7-65145

crystal microstructure continued

- SiO₂ evaporated and ion assisted deposited coatings, microstruct., electron microscope obs. 7-52335
 SiO₂ powder compacts, densification rel. to sintering atmosphere 7-13417
 SiO₂-rich ceramics, intergrowth relationships between SiO₂ polymorphs, quartz, cristobalite and tridymite 7-13445
 Sm-Co-B rapidly quenched ribbons, hard mag. props. and struct. 7-53048
 Sn-Sb (2 at.%), morphological development of planar solid-liq. interface (Korean) 7-17523
 SnO₂:Sb spray deposited coatings, comp., elec. props. thermal treatments, AES study 7-22393
 SrO.5.6Fe₂O₃, doped with kaolin and BaB₂O₄, sintering temp., effect on structural and mag. parameters 7-7543
 SrTiO₃, spherical fine particles prep. by US spray pyrolysis, microstruct. (Japanese) 7-22625
 Ta₂O₅ crystalline films, sputter deposited, phys. and elec. props. 7-2412
 Ta₂O₅ evaporated and ion assisted deposited coatings, microstruct., electron microscope obs. 7-52335
 Te₆₀Si₃₀As overcoated trilayer struct., laser writing mechanism, microscopy studies 7-20149
 (Ti,Cr)₂B₂ sintered electrode exposed to liq. Al, degradation, effect of segregated Cr 7-28045
 Ti alloy, heat cycling regimes and effects 7-8028
 Ti alloy, two-phase, microstruct. and failure nature correl. 7-8110
 Ti alloys, microstruct. and slip characts. 7-8050
 Ti binary alloys, reduced technological plasticity and struct. (Russian) 7-17583
 Ti, implantation-induced textures, electron diffr. and microscopy studies 7-46507
 Ti, pure, plate, yield strength, H content depend. (Chinese) 7-8044
 Ti Si₂ epitaxial growth kinetics on (111)Si, TEM study 7-58683
 Ti-Al-Cr-Mo alloy VT3-1 mech. props. depend. on decomp. product morphology for metastable phases 7-39655
 Ti-Al-Mo-V-Cr alloy VT22, metallographic study of β -solid soln. decomp. 7-39523
 Ti-Al-Mo-Zr(Si) alloys, superplastic characts., H alloying effect 7-8049
 Ti-Al-Sn-Zr-Mo (6,2,4,2 wt.%) superplastic deform., temp. depend. 7-39588
 Ti-Al-V, pseudo-alpha alloys, BCC lattice hydrides (Russian) 7-53751
 Ti-Al-V, struct., martensitic transform., cooling rate depend. (Russian) 7-46469
 Ti-Al-V (6, 4 wt.%), hardness and alpha/beta ratio, effect of O 7-3430
 Ti-Al-V (6, 4 wt.%), powder metallurgy, fatigue props. rel. to microstruct. 7-8096
 Ti-Al-V (6, 4 wt.%) platés, rolling, heat treatment, microstruct., mech. props., turbine blade appl. 7-17644
 Ti-Al-V (6.4 wt.%), α morphology rel. to thermomech. treatment 7-46520
 Ti-Al-V (6.4 wt.%), powder metallurgy, thermomechanically treated, deform. behaviour 7-53908
 Ti-Al-V (6.4 wt.%) r-values after superplastic strain 7-53806
 Ti-Al-V (6.4 wt.%) superplastic deform., temp. depend. 7-39588
 Ti-Al-Zr, IMI 829, low cycle fatigue 7-22792
 Ti-Al-Zr-Mo-Si, creep resistance, silicides obs., effect on mechanical props. and fracture 7-8051
 Ti-Cu-Ti thin films, reaction kinetics, stress, and microstruct. 7-21764
 Ti-Mn, alpha and beta phases, yield and tensile strength, ductility, Bauschinger behaviour, fatigue life, crack propag. 7-8052
 Ti-R (R=rare earth) alloys, rapidly solidified, tensile and creep props. 7-22778
 Ti₃Al, struct., phase comp. rel. to crystallisation rate and heat treatment 7-46442
 Ti₃Al-Nb-Er rapidly solidified alloy, microstruct. effects and dispersoid stability 7-22669
 TiAlOC coatings, CVD, composition, struct. and wear resistance 7-53929
 TiC-Ni-Mo sintered carbides, struct. and physicomech. props. 7-3256
 TiC-WC-Ta-Co three-phase sintered carbides, Ta content influence on struct. and props. 7-65097
 TiFe, oxidised, bulk and surface phase composition 7-46700
 TiN reactively RF sputtered coatings, structural defects and porosity, electrochem. polarisation meas. 7-52333
 TiN-coated gear cutting hobs, wear characteristics, mechanical and structural props. 7-53980
 TiN(C) hard reactively sputtered and evaporated coatings, composition and microstruct. studies 7-52331
 Ti_{1-x}Nb_xCo_{0.5}Ni_{0.5} solid solns., prod. factors influence on struct. parameters of variable comp. phases 7-7940
 TiO₂ evaporated and ion assisted deposited coatings, microstruct., electron microscope obs. 7-52335
 TiO₂ powders, dispersant use, sintering, microstruct. 7-46378
 V/Ni multilayered superlattice, microstruct., X-ray and neutron diffr. 7-32849
 V₄₁Ni₃₆Si₂₃, rapidly solidified, quasicrystalline and Frank-Kasper phases, tenfold electron diffr. pattern obs. 7-65022
 W base heavy metal alloys, mech.-props., porosity, impurity effects 7-17495
 W doped wire, effect of dopants on microstruct. (Korean) 7-17547
 W, n (Russian) 7-51699
 W-Ni dilute alloy, Ni enrichment at screw dislocations, atomistic calcs. and atom probe FIM meas. 7-33638
 W-Ni-Cu(Fe)(Cr), sintered heavy alloys, contiguity var. in W spheruloids 7-53668
 W-Ni-Fe system, matrix and interfacial precip. 7-46478
 WC, high press. sintering, microstruct. 7-39470
 WC-Co, high press. sintering, microstruct. 7-39470
 WC-Co composites, fracture toughness rel. to hardness, microstruct. model 7-17637
 WC-Co sintered carbides, X-ray diffr. obs. of microstruct. after hardening, optimum heat treatment cycle 7-65063
 WC-TaC-Co, N contained cemented carbides, sinterability, mech. props. rel. to prep. 7-17507
 Y₂O₃ film, electron beam evap., struct. characteris. using TEM, opt. props. 7-21732
 Zn-based alloys, mechanical props., alloying addition effects (Japanese) 7-8090
 ZnO-Bi₂O₃ system, sintering, role of Bi₂O₃ 7-64977
 ZnS_{Se_{1-x}} gradient IR optical material prepared by CVD 7-31408
 Zr cathode, material and structural changes during arc operation in N₂ 7-46866

crystal microstructure continued

- Zr-Ir, hardening by dispersed ω -phase particles, annealing effect (Russian) 7-65053
 Zr-Nb (20 wt.%), ageing behaviour, effect of H 7-46527
 Zr-Os, hardening by dispersed ω -phase particles, annealing effect (Russian) 7-65053
 ZrF₄-BaF₂-LaF₃-AlF₃-NaF glass, crystal growth and microstruct. 7-1896
 ZrN(C) hard reactively sputtered and evaporated coatings, composition and microstruct. studies 7-52331
 ZrO₂ base ceramic thermal barrier coatings, erosion rel. to processing and microstruct. 7-3450
 ZrO₂, MgO partially stabilised ceramics, thermal treatment, mech. props., microstruct. 7-65067
 ZrO₂, Y₂O₃ partially stabilised, hot isostatic pressing, high temp. mech. props. 7-28082
 ZrO₂, Y₂O₃ partially stabilised, phase diagram, microstruct. (Japanese) 7-53707
 ZrO₂, Y₂O₃ partially stabilised, microstruct. after ageing at high temp. 7-65061
 ZrO₂, Y₂O₃ stabilised powder, spray pyrolysis, sintering, microstruct., fracture toughness 7-27983
 ZrO₂, Y₂O₃ stabilised, amorphous second phase, sintering, grain morphology, fracture roughness, surface degradation 7-46612
 ZrO₂-Se₂O₃, cubic to β martensitic transform. 7-22681
 ZrO₂-SiO₂, optical films, struct. modification by coevaporation 7-45064
 ZrO₂-Y₂O₃, rapidly quenched, microstruct. evolution by annealing 7-22737
 ZrO₂-Y₂O₃, Y-TZP, toughened, microstruct., TEM and electron diffr. study (Japanese) 7-22634
 ZrO₂-Y₂O₃ ceramics, toughened, prep., microstruct., mech. props. 7-3409
 ZrO₂-Y₂O₃-Co₃O₄ materials, Co₃O₄ effect on struct. and phase comp. 7-27990
- crystal morphology**
 analcime, hydrothermal cryst. growth, morphology 7-11975
 apatite, Ising crit. temp. of connected nets and morphological importance of F faces 7-16476
 austenitic steels, small precip., moire imaging in TEM 7-46490
 barbiturates, cryst. struct. anal., H bond geometry and types 7-23300
 binary alloys, TEM study of precipitate growth mechanisms 7-52064
 calcium oxalate crystals, precip. by reverse osmosis system, habit modifiers 7-16460
 Czochralski cryst. growth, simulation of jet cooling effects 7-17408
 diffusion-controlled interfacial growth, dense branching morphology form. 7-21147
 diphenyl crystal, interaction of anthracene impurities with surface layers, struct. model of quasiliquid layer 7-58191
 field ion microscope specimen preparation technique, combined TEM/FIM examination 7-29988
 high polymers, spherulite crystallization and spherulitic morphology 7-11967
 metallic and ceramic ultrafine, particles, laser prod. 7-13406
 metallic fine particles, surface free energy anisotropy determ. 7-32783
 modulated structures, cryst. form and surface morphology 7-58190
 poly(vinylidene fluoride)-poly(ethyl acrylate) blends, phase diagram and morphology 7-63538
 poly-p-phenylene sulphide, solution-grown crystals and crystalline thin films, morphology 7-16441
 polyethylene, soln. crystallisation kinetics and morphology 7-21148
 polypropylene-ethylene-propylene copolymer blends, isotactic, mechanical props. and morphology 7-63539
 purines, cryst. struct. anal., H bond geometry and types 7-23300
 pyrimidines, cryst. struct. anal., H bond geometry and types 7-23300
 SOI laterally seeded epitaxial films recrystallised by electron beam, sub-grain boundaries charactn. 7-53779
 solid state reactions, heterogeneous, structural features influence (German) 7-17766
 steel, Cr-Ni, low-C, butterfly martensite, crystallographic characts. (Russian) 7-6580
 tetramethylammonium tetrachlorozincate, cryst. form, surface morphology, optical microscopy study 7-63919
 urea crystals, growth kinetics in aq. soln., biuret effect 7-51679
 with lamellar graphite, mech. props. and morphology (German) 7-21160
 Al-Si eutectic, Sr-modified, fibrous Si cryst. morphology, TEM study 7-28015
 AlCuLi alloys, large quasicrystalline dendrites, triacontahedral solidification morphology 7-32345
 Al₆Mn, icosahedral, fine line struct. in convergent beam electron diffr. 7-63560
 AlPO₄, berlinite, synthesis and charactn. of new polymorphic modification 7-53534
 Au polycrystalline tips, grain rotation and grain boundary annihilation, in situ SEM study 7-32460
 Au tip crystals, morphological evolution and surface self-diffusion, in situ scanning electron microscopy study 7-32239
 Bi₄Ge₃O₁₂ single crystals, shape, melt flow patterns, Czochralski growth conditions 7-16464
 BiSeI, dendritic, growth from vapour, characteris. 7-21788
 CaCO₃-MnCO₃ mixed cryst., metastable formation range and morphology 7-26910
 CaO₃, induced morphology crystal aggregates, structures, sheaf morphologies 7-51687
 Ca₃(PO₄)₂CaF₂(OH)₂, hydroxyapatite, morphology of F faces 7-51686
 CaSO₄ crystal size distrib. from double-draw-off FGD liquor crystalliser 7-63533
 Cd(BrO₃)₂ · 2H₂O(D₂O), H bonding, crystal struct., ¹H and ²D NMR anal. 7-22156
 Cd(OH)₂ dendritic structures in agar gel 7-58723
 CdS skeletal and hollow crystals grown under time-increasing supersaturation 7-21144
 CuAlGa_{1-x}Se₂, chem. transport reactions, growth and morphology 7-7830
 CuNiFe, electron irradi., decomposition kinetics and morphology 7-58491
 FeNiAlCoTiCuS permanent magnetic material, phase comp. and ordering, atom probe FIM and TEM studies 7-33635
 GaAlAs, MOVPE growth rate, orientation depend. 7-22556
 GaAs, MOVPE growth rate, orientation depend. 7-22556
 KAl(SO₄)₂ · 12H₂O, alum crystals, habit changes by novel additives to nutrient 7-44439
 KH₂PO₄, crystal growth spiral morphology on {100} surfaces, impurity effects, step kinetics 7-16459

crystal morphology continued

- KH₂PO₄ crystals, contact nucleation on (100) face 7-51680
 K₂SO₄, cryst. growth, nucleation kinetics, habit, Cr(III) effect, soln. pH 7-53539
 KTiOPO₄ crystals, high temp. flux growth, morphology 7-58178
 LaB₆ dispersed powders and compact specimens, struct. and morphology 7-64976
 α -LiIO₃ single crystals, morphology in relation to growth conditions 7-58192
 Mg, crystal habit of ultrafine particles, gas phase evaporation growth 7-53514
 NaCl, equilibrium crystal form 7-16457
 Ni-Fe film, ion beam sputter deposition, ion bombardment effect on preferred orientation 7-64010
 Ni-Ta amorphous alloy, struct. changes and crystallization during heating (*Russian*) 7-16419
 NiAl₂O₃, spinel growth, thin film Al₂O₃ substrate, topotactic relationships 7-58717
 Sb trihalide single crystal growth in gel 7-22458
 Sb₂S₃-Sb₂Se₃, hollow mixed crystals vapour growth, morphology and whisker growth 7-7831
 SbSI single crystals, vapour growth, morphology rel. to temp. gradients 7-46287
 SiC short fibred filamentary crystals, phase comp. and morphology 7-65010
 Sn-In-S ternary system, cryst. growth and charact. (*French*) 7-33645
 Ti-Ni, shape memory alloys, metastable X-phase, cryst. struct., morphology, TEM, X-ray diffr. 7-37926

crystal orientation

- alkali metal cyanide-halide mixed crystals, orientational glass state static props., microscopic model calcs. 7-63591
 BCC lattice crystal, rolling, interrelationship between struct. and orientation changes (*Russian*) 7-53773
 ceramic eutectic composites, microstruct. and mech. props. 7-64991
 grain rotation, FCC {111} traces and Euler angles (*Korean*) 7-6573
 graphite layers on diamond surfaces, optical anisotropy, effect of crystallographic orientation 7-53267
 intragranular heterogeneity of deformation and crystal rotation 7-53786
 ion sputtering, high depth resolution problem 7-27849
 Laue indexing, orientation matrix approach 7-16346
 metallic materials, electron diffr. anal., appl. of theoretical diffr. patterns 7-11853
 MgO films, prep. by RF sputtering, orientation and microstruct. (*Japanese*) 7-22480
 misorientation angle determination, near surface layers of crystal cuts 7-16842
 nucleation, sympathetic, morphology, crystallography and kinetics 7-65035
 quartz, topography of etched rhombohedral faces, evidence for orientation effects 7-16840
 rhombohedral system, coincidence-site lattices 7-51685
 semiconductor thin layers, orientation determ. using Raman scatt. light 7-61320
 SOI laser recrystallisation, orientation control 7-53777
 steel, Cr-Ni, low-C, butterfly martensite, crystallographic characts. (*Russian*) 7-6580
 tetramethylammonium tetrachlorozincate, cryst. form, surface morphology, optical microscopy study 7-63919
 Widmanstätten crystallography in Fe meteorites, habit planes and lattice orientations 7-9448
 X-ray and Auger electron microanalysis, cryst. orientation effects 7-23109
 Ag surface, binding energy of image-potential states 7-64303
 Al, anodised, variation in polarised light intensity with grain orientation 7-54041
 AlGaAs/GaAs:Si heterostruct., MBE growth on polar surfaces 7-7863
 Co-Cr, continuously sputtered films, crystallographic orientation and mag. props. 7-27176
 Co-Cr films, sputter deposition and characterisation 7-27178
 CoCr double-layered film, sputter deposition 7-27177
 CoCr films, vacuum evaporation, thickness depend. of mag. props. 7-27576
 Cu (10,10) and (510), adsorption of Pb, faceting, LEED, AES studies 7-32828
 Cu films, sputter deposition, effect of ion bombardment of growing film 7-64009
 Cu, ion irradiation, sputtering and lattice damage, cryst. orientation effect 7-64843
 Cu, single crystals, with different orientations, strain localisation during high temp. deform. 7-13506
 Cu surface, binding energy of image-potential states 7-64303
 Cu surface, ion irradiation, sputtering and lattice damage, cascade simulation 7-59327
 Fe, single crystals, flow stress at 225, 250 and 273 K, orientation depend. 7-53832
 Fe-Si sheets, grain oriented, orientation of individual grains by means of Kossel patterns (*Japanese*) 7-22716
 Fe-Si sheets, grain oriented, generation of secondary nuclei (*Japanese*) 7-22717
 GaAlAs, MOVPE growth rate, orientation depend. 7-22556
 GaAs, MOVPE growth rate, orientation depend. 7-22556
 Ge, SHG, cryst. orientation depend. 7-50640
 KNbO₃, single domain cryst. prep., orientation and dielec. polarisation 7-45950
 LaB₆, crystals grown with Xe arc image furnace, subgrains 7-59411
 LaB₆, orientational effects of interactions of electrons in APS spectra 7-46243
 LaNi₅, anisotropic H migration, deposition potentials, hardness, brittleness meas. 7-6873
 LiNbO₃, degenerate acoustic elastic convolver, crystal orientation dependencies of figure of merit 7-62917
 MgWO₄·2H₂O, cryst. struct., topotactic dehydration, X-ray powder diffr. study 7-32393
 Mo single crystal, rolling, dynamic recovery rel. to deform. temp. (*Russian*) 7-65095
 Mo, single crystals, rolling, rel. between dynamic recovery and changes in orientation (*Russian*) 7-53759
 Mo single crystals, struct. changes during annealing after bending deform. (*Russian*) 7-44446
 Ni surface, adsorbed S, field electron emission props. 7-33529

crystal orientation continued

- Ni-base superalloy, single cryst., SRR99, creep behaviour 7-17587
 Ni-Fe film, ion beam sputter deposition, ion bombardment effect on preferred orientation 7-64010
 NiAl single crystal, surface oxide softening 7-39751
 NiAl₂O₃, spinel growth, thin film Al₂O₃ substrate, topotactic relationships 7-58717
 NiO-CaO eutectic, directionally solidified, struct. imperfections 7-65026
 Pd films, sputter deposition, effect of ion bombardment of growing film 7-64009
 PrO₂, fluorite prototype struct., interfaces and domain form. study 7-58498
 Pt films, sputter deposition, effect of ion bombardment of growing film 7-64009
 Rb_x(NH₄)_{1-x}AlF₆, ESR study of orientational order with Fe³⁺ probe 7-53119
 Si, SHG, cryst. orientation depend. 7-50640
 Si, thermal oxidation, cryst. orientation effects 7-3534
 Si:W⁺ layers, implanted and annealed, struct., TEM, electron diffr. studies 7-32858
 Si-alkaline earth fluoride structures, heteroepitaxial growth, struct., elec. props. 7-12567
 SiC single crystal, electron channelling patterns, lack of centrosymm. effects obs. and calcs. 7-51901
 TbO₂, fluorite prototype struct., interfaces and domain form. study 7-58498
 α -Ti, hexagonal, texturised sheet stock, orientation distrib. function 7-22714
 B-Ti-Mo, single crystals, age and quench hardening, effects of cryst. orientation and surface condition (*Japanese*) 7-22709
 (Ti_{1-x}V_x)₂Ni, orientation relationship between the icosahedral and crystal-line phases 7-16477
 V₂, orientational effects of interactions of electrons in APS spectra 7-46243
 V₃Si/V₂Si₃ interface, crystallography of matrix-precip. interface and elastic strain field (*French*) 7-65036
 Zn, electrodeposition kinetics on Zn single crystals, pot. step method, SEM anal. 7-27189
- crystal oscillators** *see crystal resonators*
- crystal properties**
see also crystal chemistry
 No entries
- crystal purification**
see also zone refining
 W monocrystals, with P impurities, removal during chem. and metallurgical treatments 7-6645
- crystal resonant gamma-ray interactions** *see Mossbauer effect*
- crystal resonators**
see also piezoelectric oscillations
 double-ended tuning fork quartz accelerometer, design and characts. 7-56230
 frequency control, conf., Philadelphia, PA, USA (May 1986) 7-55893
 high-quality quartz crystals, production developmental results 7-59823
 low-Q piezoelec. material constants, automated meas. system 7-328
 multifrequency SAW waveguide resonators, amplitude-freq. characts. anal. 7-16050
 quartz, growth and sweeping of high quality quartz 7-39369
 quartz bars, nonlinear electroelastic eqns. of wave propag. and vibr. 7-57625
 quartz crystal chemical polishing, use of surfactants, results 7-59655
 quartz crystal etched figures, expt. study and numerical simulation 7-59654
 quartz crystal irradiation effects study using low-temp. dielec. relax. 7-58334
 quartz crystal resonators radiation sensitivity with different Al impurity content 7-58335
 quartz fluid density sensor pressure transducer, design and characts. 7-56249
 quartz miniature resonator thermal detector 7-349
 quartz oscillator for density measurement of a-Si films 7-7079
 quartz piezoelectric resonators, electron and gamma radiation dosimetry appls. 7-15416
 quartz plate simple thickness modes, acoustic viscosities and time constants 7-1372
 quartz resonator temperature transducer with no activity dips, expt. and theoretical study 7-56268
 quartz resonators, contoured, nonlinear resonance analysis 7-31564
 quartz sensor for automatic dew-point hygrometry 7-61344
 quartz tuning fork resonator transducers 7-35512
 Rayleigh wave resonator and oscillator appls. 7-1347
 Rayleigh wave resonators and delay lines, 1/f noise 7-1348
 SAW resonators, continuous representations of mode shape 7-57663
 synthetic quartz growth, Brazilian lascar charact. for synthetic quartz growth, props. correlation 7-59394
 temperature sensor using quartz tuning fork resonator, design, fabrication and characts. 7-56269
 thickness monitor using four quartz crystal oscillators for evaporation system 7-61319
 ultrasonics conference, San Francisco, USA (Oct. 1985) 7-11
 x-ray machine for generally rotated blanks 7-37806
 AlPO₄ berlinite: characterization of crystals with a low water concentrations and design of bulk wave resonators 7-59396
 CuAl-quartz, SAW resonators, annealing behaviour and phase noise performance 7-11242
 ZnO/Y₂La_{0.2}Al_{0.2} SAW resonator struct., amplitude-freq. and phase-freq. characts. 7-16051
- crystal structure**
see also crystal atomic structure; crystal microstructure; crystal morphology; crystal orientation; crystal symmetry; crystallography; granular structure; polymorphism
 cubic lattices, regular and optimal subdivisions into sublattices 7-16456
 diffraction intensities from cylindrically curved crystallites with layer disorders 7-1810
 fatty acid Langmuir-Blodgett monolayers, structural study of conducting defects 7-52325
 quasicrystals, intermediate state between amorphous and crystalline 7-1888
 Mo, single crystals and polycrystals, high-angle boundaries of deformation origin 7-6712

crystal surface and interface vibrations

- acoustic phonon scatt. from atomically irregular surfaces, intensity reflection coeffs. 7-12446
- adlayer photostimulated phase transitions on semicond. surface, reson. conditions calcs. (*Russian*) 7-45016
- admolecular processes, laser induced, energy and phase relax. 7-21610
- adsorbed atoms, thermal relax. in an intense laser field 7-38330
- adsorbed layers, laser-induced photodesorption 7-52281
- adsorbed molecules, hindered rotations, energy levels and thermodynamic props. 7-27130
- adspecies, anharmonic, transient excitation by pulsed laser radiation 7-21611
- anharmonic crystal surface, statistical theory 7-32766
- atom scattering from surfaces, low energy, appl. in struct. anal. 7-33504
- atom-surface scattering thermal attenuation, multiphonon contrib. 7-39338
- bilayer systems, long-range surface phonon-polaritons, damping props. 7-12881
- chemisorbed atoms, vibration, electron-hole friction mechanism 7-38317
- coadsorption, promotion and poisoning effects, analytic modelling based on band-order conservation 7-27121
- conference, Oconomowoc, WI, USA (April-May 1985) 7-18468
- continuum model of a solid with a free surface, normal mode analysis 7-63939
- continuum model of solid with free surface, appl. to particle-surface interactions 7-64866
- diamond crystals, surface phonon modes and reconstructions, Green's function method calcs. 7-2339
- displacive surface reconstructions, incommensurate sandwiches 7-52223
- dynamical phenomena at surfaces, interfaces and superlattices, summer school, Erice, Italy, (July 1984) 7-1
- EXAFS, Debye-Waller factor, influence of adsorbed monolayer 7-39316
- formate ion incorporated into tunnel junction, quantitative analysis of inelastic tunnelling spectrum 7-38769
- gas-solid interface, photon-phonon conversion, laser-linewidth effects 7-58599
- graphite (001), surface phonon dispersion, inelastic atom scatt. study 7-52227
- graphite surface, adsorbed N₂ mol. zero-point energies, out-of-plane orientation, nucl. reson. photon scatt. study 7-32819
- graphite surface with adsorbed H₂, rotational states of physisorbed molecules 7-52278
- heterostructures, lattice theory, phonon propagation 7-58602
- incomplete crystals, surfaces, defects, interfaces and layered structures, theory 7-16926
- ionic cryst.-semicond. superlattice interface excitations, classical anal. 7-52845
- laser-stimulated desorption, desorption mode instability 7-21634
- material analysis, computer-based, conf., Boston, MA, USA (Dec. 1985) 7-14709
- metal particles, sintered, low freq. vibr. modes, Mossbauer study 7-45853
- metal surfaces, EELS studies of dynamics 7-3127
- metallic superlattices, elastic props., effect of strain 7-52376
- metallic surface, pseudopotentials and dynamical props. 7-2341
- metals, surface lattice dynamics of ordered overlayers 7-2342
- methane, physisorbed on NaCl (100), EELS spectra 7-13289
- modulated structures, lattice dynamics, appl. to superlattices 7-52220
- noble metal surfaces, high resolution inelastic He-atom scatt., surface phonon dispersion relations 7-3144
- nonequilibrium gas-solid system, transport processes, kinetic theory calcs. 7-16254
- nonequilibrium solid, SAW attenuation, gas-induced high freq. anomalies 7-52218
- one-dimensional atom-surface energy transfer, consistent quantum treatment 7-27840
- optical absorption lines, influence of exciton motion, appl. to surface vibrations 7-7317
- overlayers, mismatched, mol. dynamics study 7-2344
- phonon conc. catastrophes in cubic crystals 7-44714
- phonons at interfaces and superlattices, Green's function method 7-2340
- photodesorption, laser-induced, effect of resonant vibrational energy transfer 7-52293
- photodesorption via stimulated Raman emission of coherent surface phonons 7-16865
- polyatomic molecules colliding with nonrigid surfaces, quantum theory of energy exchange 7-64865
- semiconductor superlattices, dynamical screening, quasi-2D electron gas, electron-phonon interactions 7-45464
- semiconductor superlattices, phonons, acoustic and optic modes 7-12455
- semiconductor surfaces, interaction with H₂ 7-58632
- simple cubic lattice, inelastic scatt. and trapping of an atom 7-27122
- solid-solution interfaces, transition probability of reactive processes, contrib. of medium phonons 7-54181
- superlattices, bulk and surface phonons 7-2343
- superlattices, surface acoustic soliton, anal. 7-63938
- surface (001)(2×1), surface vibr. excitations 7-16854
- surface phonon conc. 7-2335
- surface phonons, EELS excitation cross section 7-16855
- surface science techniques, book 7-60888
- surface with adsorbed Ne, H₂, D₂ films, phonon scatt. 7-21609
- surfaces, atomic, electronic and vibronic props. 7-2307
- surfaces, conference, Jülich, Germany (April 1986) 7-55890
- surfaces, force sum rules, Hellmann-Feynman theory 7-44989
- techniques for surface studies, book 7-60911
- transition metal oxides, catalysts, laser Raman spectra 7-53295
- transition metal surfaces, He atom scattering potential energy surfaces, vibr. substrate relax. effects 7-53478
- vibrational spectroscopy, lineshapes and dissipative processes 7-45956
- Ag (110), clean and O₂ covered, adsorption and reaction of acetonitrile 7-28344
- Ag clusters, vibrational characteristics, SERS studies 7-22255
- Ag films, with surface adsorbed ethylene, adsorbate-substrate bonding 7-52292
- Ag, SERS, very low freq. mode 7-22264
- Ag surface, (111), one-phonon scatt. of He atoms 7-3143
- Ag surface, CO₂ molecules impact, quantum theory of energy exchange 7-64865
- Al, chemisorption, interaction of atoms and mols. with surfaces, cluster approx., total energy calcs. 7-52265
- AlAs-GaAs superlattices, lattice vibration, Raman spectra 7-63937

crystal surface and interface vibrations continued

- Au films, with surface adsorbed ethylene, adsorbate-substrate bonding 7-52292
- CN chemisorbed on Cu (100), field induced vibr. freq. shifts 7-45991
- CO, adsorbed, integral absorpt. coeff., IR vibr. spectroscopy 7-53323
- CO chemisorbed on Cu (100), field induced vibr. freq. shifts 7-45991
- CO monolayer on Cu (111), Debye-Waller factor anisotropy, SEXAFS study 7-63936
- Co, physisorbed multilayer, near-threshold electronic excitation, EELS spectra anal. 7-45001
- CoCl₂, electronic transitions, IETS 7-50099
- Cu (100), c(2×2)N overlayer, surface phonon dispersion, LEED, AES and EELS studies 7-12459
- Cu (100), cross-section anal. of surface and bulk phonons by electron scatt. 7-2336
- Cu (100), Rayleigh phonon dispersion, stress-induced freq. shift, EELS studies 7-27090
- Cu (110) and polycrystalline surfaces, UPS, XPS, AES, EELS, LEED studies of adsorbed O₂ 7-32820
- Cu (111), adsorption of TCNQ, vibr. spectra, EELS, work function meas. 7-52228
- Cu films, with surface adsorbed ethylene, adsorbate-substrate bonding 7-52292
- Cu layer on steel substrate, thickness meas. by transverse surface waves (*French*) 7-4815
- Cu particles, ZnO-supported, vibr. spectra of adsorbed species, operation of metal surface selection rule 7-53350
- Cu surface, Raman intensity of adsorbate vibr. cluster-model calc. 7-27089
- Fe-Pd multilayer structs., localised phonon modes 7-46061
- GaAs quantised inversion layers, hot 2D electron gas, spectral acoustic phonon emission intensity 7-52452
- GaAs/AlAs superlattice, optical phonons and interface thickness, Raman scatt. studies 7-7705
- GaAs/AlAs superlattices, folded acoustical Raman line intensities 7-46050
- GaAs/GaAlAs superlattice, optical phonons and interface thickness, Raman scatt. studies 7-7705
- GaAs-Al_xGa_{1-x}As multiple quantum well structs., nonequilib. LO phonons 7-12457
- GaAs-Al_xGa_{1-x}As quantum wells, doubly reson. LO phonon Raman scatt., photoluminescence spectra 7-53327
- GaAs-AlAs superlattices, Raman scattering finite size effects 7-39105
- GaAs-AlAs superlattices, lattice dynamics 7-52220
- GaAs-AlGaAs superlattice, surface and interface optical phonons, EELS studies 7-6955
- GaSe, surface phonons, inelastic electron tunnelling spectroscopy 7-63935
- Ge crystals, surface phonon modes and reconstructions, Green's function method calcs. 7-2339
- Ge-GaAs heterostructures, lattice theory, phonon propagation 7-58602
- In_{0.18}Al_{0.82}As-GaAs strained layer superlattices, Raman studies 7-12854
- InAs-superthin insulator-Au struct., inelastic electron tunnelling spectra 7-27436
- LiF(00), surface optical phonons, obs. by inelastic He scatt. 7-44987
- MgO barrier MIM structures, IETS study 7-12878
- MgO:Ca²⁺ (100), entropy of segregation calcs. 7-2323
- N₂, physisorbed multilayer, near-threshold electronic excitation, EELS spectra anal. 7-45001
- N₂, surface layer on graphite, motion investig. 7-32792
- Na-colloid in NaCl, low freq. surface enhanced Raman scatt. from NaCl-Na interface localized fractal vibrational modes 7-59195
- NaCl (001), deposited Au, elastic surface wave anomalies near cluster to layer transition 7-21606
- NaCl:CO₂²⁻ cryst. surface, localised intramol. vibrations, IR transmission spectra study 7-2132
- NaCl-type lattices, (100) surface, surface atomic vibr. modes 7-2337
- NbC (001), surface phonon dispersion, double shell-model anal. 7-21608
- Ni (100), adsorbed N₂, surface phonon dispersion, adsorbate induced reconstruction 7-52225
- Ni (100), adsorbed O₂, p(2×2) structures, surface phonons, bond-stretching interactions 7-21607
- Ni (100), chemisorbed H and D, vibr. motion, high resolution EELS 7-12458
- Ni (100), surface vibrs., EELS, surface and bulk phonon contribs. 7-44986
- Ni (111), coadsorbed CO and K, adsorbates electrostatic interaction, IR reflection-absorption spectra, TPD, LEED obs. 7-32824
- Ni (111), isothermal adsorption/desorption parameters of CO, EELS meas. 7-6971
- Ni, surface phonon generation and picosecond light pulse detection 7-12456
- Ni, surface phonons, HREELS study 7-13291
- O (2×1) overlayer on Cu (110), surface reconstruction, mean free path and Debye-Waller factor, SEXAFS study 7-46238
- P, black, surface acoustic props., Brillouin scatt. study 7-38316
- Pd (100), clean and S covered, adsorption and desorption of NO, surface reactions, TPD, EELS, LEED 7-58639
- Pd (100) and (111), surface resonances in vibr. spectroscopy 7-52229
- Pd (110) with chemisorbed N₂, EELS, LEED and AES 7-63960
- Pd (111), O₂ adsorpt., EELS and LEED studies 7-2378
- Pd, adsorbed CO, vibr. spectra 7-12475
- Pd/Al₂O₃ surfaces, ethylidyne covered, CO adsorpt., IR spectra studies 7-2371
- Pt (111), adsorbed O₂, p(2×2) structures, surface phonons, bond-stretching interactions 7-21607
- Pt (111), clean and O covered, surface phonon dispersion, inelastic atom scatt. meas., lattice dynamical calcs. 7-52226
- Pt (111), coadsorption of K and CO, structural and vibrational studies 7-52266
- Pt (111), O adsorbate-induced surface-phonon softening 7-58600
- Pt (111), studies of CO adsorbate vibr. modes, inelastic He atom scatt. obs. 7-32782
- Pt (111), with adsorbed CO, molecule-substrate vibr. mode, IR emission spectra study 7-57126
- Pt (111) with adsorbed Kr, adsorbate-substrate vibr. coupling 7-52221
- Pt (111) with coadsorbed CO and K, inverse photoemission 7-52726
- Pt, adsorbed CO, vibr. spectra 7-12475
- Pt stepped surfaces with adsorbed CO, coupled harmonic oscillator models 7-52230
- Pt surface, CO₂ molecules impact, quantum theory of energy exchange 7-64865

crystal surface and interface vibrations continued

- Pt-Rh alloys, surface composition, lattice vibrational entropy 7-52207
 Pt₃Ti (111), chemisorption of CO and O₂ 7-27131
 Ru (0001) with adsorbed H monolayer, adsorbate bonding and vibr. 7-52291
 Ru (001), vibr. dephasing of terminally bonded CO 7-17318
 Si (111), chemisorption of benzene, pyridine and thiophene, surface vibr. studies 7-21615
 Si (111) (2×1), π -bonded chain model, vibr. props. 7-16856
 Si (111) surface, H₂ dissociation, chemisorption dynamics 7-54169
 Si (111)/CaF₂ interface and surface phonons, high resolution EELS study 7-38319
 Si (111)2×1, pseudofunction slab calcs. 7-52727
 Si (111)2×1, thiophene adsorpt., annealing-induced mol. fragmentation, surface vibr. spectra, HREELS study 7-27088
 Si crystals, surface phonon modes and reconstructions, Green's function method calcs. 7-2339
 Si laser annealed surface, Au submonolayer coverage, Kapitza anomaly reentry obs. 7-38318
 Si quantised inversion layers, hot 2D electron gas, spectral acoustic phonon emission intensity 7-52452
 Si surface, (111)2×1, surface phonon and surface state excitations, EELS, polarisation depend. 7-2338
 Si surface, (111)(2×1), obs. of 10 meV Einstein oscillator mode 7-38320
 Si/Si_{1-x}Ge_x-strained layer superlattices, folded phonon dispersion 7-44718
 Si-Ge_{1-x}Si_x superlattices, Raman scatt. involving umklapp processes 7-3043
 Si(001), 2 × 1 surface relax. and vibr. excitations 7-6949
 α -Sn crystals, surface phonon modes and reconstructions, Green's function method calcs. 7-2339
 TaC (001), surface phonon dispersion, double shell-model anal. 7-21608
 TiC (100), surface phonon dispersion curves, EELS determ. 7-52224
 UO₂, single cryst., surface phonon struct., high resolution EELS 7-27087
 W (001), adsorbed H, displacive surface reconstructions, incommensurate sandwiches 7-52223
 W (100) reconstructed surface, vibrational props., force-constant model calcs. 7-44988
 W (110), adsorption of Cu, Ag and Au, calcs. based on nonadditive effective binding pot. 7-12483
 W (110), anisotropic surface atom vibrs., high energy He⁺ ion backscattering 7-58601
 W (211), activated chemisorption of methane 7-52279
 ZnSe-ZnTe strained-layer superlattices, lattice strain and lattice dynamics 7-58654

crystal symmetry

- see also crystallography; group theory; space groups*
 Al-Mn quasicrystal, struct. model with m35 symm. 7-6570
 alkali metal halide crystals, impurities, local and gap mode freq. calcs. 7-26888
 binary alloys, TEM study of precipitate growth mechanisms 7-52064
 binary cubic solid solns., structure factor determ. 7-16374
 boundary geometry determ. 7-16475
 charge, spin and momentum densities, conf., Sanga-Saby, Sweden (July, Aug 1985) 7-24258
 crystallographic and metacystallographic groups, book 7-18517
 dense sphere packings w.r.t. coordination number and symm. equivalence 7-58187
 FCC crystal, constrained and unconstrained deform., multiple slip 7-44657
 finite crystallographic symmetry, table of 32 types 7-44436
 fivefold symmetry, early proof and models 7-26688
 four-dimensional crystal classes, crypto-rotation planes, nomenclature and graphic representation 7-11979
 four-sublattice Jahn-Teller crysts., phase transitions, free energy and symm. props. calcs. 7-2544
 guanidinium aluminium pentafluoride dihydrate single crysts., struct. and symm. determ., X-ray diffr. study (French) 7-37960
 icosahedral and decagonal quasicrystals, twins of 820-atom cubic cryst. 7-58189
 icosahedral boron-rich solids 7-63537
 icosahedral crystals from cuts in six-dimensional space 7-1929
 icosahedral phases, discommensurations 7-44437
 icosahedral quasicrystals, elastic moduli and elastic instability, density-functional theory calcs. 7-44649
 icosahedral solids, third-order elastic constants 7-32543
 icosahedral structures and tiling, geometry and crystallography 7-1930
 incommensurate structure refinement using a least-squares algorithm 7-51558
 lattice relationships analysis program 7-11830
 mechanoluminescence studies of crystal structure 7-59268
 numerical vector representation 7-11978
 oxide crystals, TO₄ units, correl. of ang. and bond length distortions 7-32359
 periodic and quasiperiodic crystals 7-1928
 perovskite-related ABX₃ compounds, phonon-induced displacive transitions, octahedral librations, group anal. 7-12225
 phase transitions, appl. of group theory 7-55926
 polychromatic crystals, mag. props. 7-51683
 polycrystals with trigonal and tetragonal symmetry, effective elastic moduli, Hashin-Shtrikman bounds 7-32544
 polycrystals, X-ray elasticity const. calc. from elastic const. data of single cryst. of arbitrary cryst. symm. (German) 7-16668
 quasi-crystallinity, non-uniformity and nanocomposites 7-1926
 quasicrystal diffraction patterns, distortion and peak broadening 7-11981
 quasicrystal equilib. state of two-component 2D Lennard-Jones system, Monte Carlo simulations 7-58148
 quasicrystal transformations, topological constraints investig. 7-16472
 quasicrystals, diffr., geometric struct. factor 7-16473
 quasicrystals, phonons, phasons and dislocations 7-6732
 quasiperiodic tilings obtained by projection 7-1931
 SEM electron back scatter diffr. patterns for cryst. symmetry elements determ. 7-58107
 semiconductor alloys, band struct. and reduced local symm., virtual-cryst. approx. calcs. 7-38451
 semiconductors, polycrystalline, extended interfacial defects, geometrical character 7-6640
 space groups in reciprocal space, Euclidean normaliser implications 7-26687

crystal symmetry continued

- square matrices, symmetry, Bravais nets, point groups and plane groups 7-58183
 supersymmetry and symmetry 7-51684
 TEM, use in precip. morphology anal. 7-46489
 tetrahedral structure survey 7-6571
 tetramethylammonium hexachloroplatinate, crystal struct. and theoretical symmetry analysis of phase transition sequence 7-51739
 tris-(ethylenedithio) benzene salt, (TEDTB)₂BF₄, C₃ symmetry, synthesis and crystal struct. 7-63602
 two-dimensional Penrose lattice, distrib. of vertices and near neighborhoods, decorations 7-37915
 X-ray intensity statistics, non-ideal distributions 7-58185
 X-ray intensity statistics, significance of residuals 7-58186
 X-ray intensity statistics, symmetry and ideal distributions 7-58184
 Ag_{1/2}In_{1/2}PS₃ lamellar cpd., cryst. struct. refinement studies 7-58235
 Al-Fe-Ce, quasicrystalline decagonal phase, TEM 7-46492
 Al-Ge, TEM anal. of Ge precip. morphology 7-46489
 Al-Mn, pressure induced quasi-crystal to crystal transition for melt span alloys 7-16726
 Al-Mn alloy, decagonal phase, struct. model 7-63552
 Al-Mn alloys, icosahedral symmetry versus local icosahedral environments, NMR spectra meas. 7-63536
 Al-Mn periodic and aperiodic alloys, local atomic environments 7-44454
 Al-Mn quasicrystal, two-dimensional Patterson synthesis, optical method 7-11993
 Al-Mn quasicrystals, 1D translational periodicity and ten-fold rotation axis 7-26643
 Al-Mn system, quasicrystal form., metallurgy 7-3295
 Al₃Mn, diffraction approach to the structure of decagonal quasi-crystals 7-6586
 Ar, rapidly quenched, Voronoi polyhedron distrib. calc., mol. dynamics method 7-26636
 Ba₃(P₃O₉)₂·4H₂O, cryst. struct. 7-6610
 BaPb_{1-x}Bi_xO₃ soln.-grown single crystals, crystallographic symmetries, effect on supercond. props. 7-37916
 Bi₂O₃, ionic cond., w.r.t. lone pair separation and cryst. symm. 7-12361
 CaCO₃ crystal symmetry elements determ. by SEM 7-58107
 Cs_{1-x}Lu_xF_{10-x} cryst. struct., space group, least-squares refinement 7-6604
 Cs₂Ti_{2-x}O₄ phase struct. and stability, composition depend., X-ray studies 7-58229
 Cs₂V₂O₇, crystals, struct., cathodic reduction from melt, and elec. props. studies 7-58236
 Cu-Zn-Al (26.4 wt.%), shape memory alloy, crystallography of martensitic transform. (Chinese) 7-7995
 Fe₇₅B₂₅, polymorphous crystallisation into Fe₃B orthorhombic phase 7-37874
 Gd₂O₃·P₂O₅ phosphors, Eu³⁺ activated, luminesc. spectra, cryst. symm. 7-3080
 K₂Cr₂O₇ crystals grown from soln., enantiomorphism 7-51682
 K₂O-Fe₂O₃-TiO₂ system, cryst. growth of titanates, morphology, ionic cond. 7-53523
 KPbLaF₆ solid soln. twinned cryst. struct., lattice parameters and point group, X-ray diffr. studies (French) 7-58231
 Mg, transformation matrices for hexagonal and trigonal crystals 7-63541
 Na_{1-x}P_xW₁₀O₅₀ struct. refinement, single cryst. X-ray anal. study 7-58233
 Pd-U-Si glassy state, quasicrystalline phase form., X-ray and electron diffr. studies 7-26645
 Rb, rapidly quenched, Voronoi polyhedron distrib. calc., mol. dynamics method 7-26636
 RbCdF₃, struct. phase transition, ENDOR study 7-33298
 Rb₂KFeF₆, structural phase transition, Raman scatt. and group-theoretical studies 7-52045
 Rb₂KMF₆ (M=Al, Cr, Fe, Y, Br), structural phase transitions 7-52044
 Rb₂KYFe₆, structural phase transition, Raman scatt. and group-theoretical studies 7-52045
 RbV₂O₇ crystals, struct., cathodic reduction from melt, and elec. props. studies 7-58236
 Rb₂ZnCl₄, incommensurate transition, pot. energy and mol. dynamics ab initio calcs. 7-21435
 SiC single cryst., electron channelling patterns, lack of centrosymm. effects obs. and calcs. 7-51901
 Sn crystal symmetry elements determ. by SEM 7-58107
 Sr(BrO₃)₂·H₂O(D₂O), EFG parameters, H bonding, PMR, deuteron mag. reson. 7-27612
 Sr₆Nb₃O₉ single cryst., bronze-type struct., X-ray diffr. study (German) 7-37949
 Ti, oxides and silicates, Ti XANES study, site geometry, spectral features 7-59288
 TiNO₃, ferroelastic switching, mech. twinning, at. mechanism, symm. anal. 7-2186
 Y₂O₃-P₂O₅ phosphors, Eu³⁺ activated, luminesc. spectra, cryst. symm. 7-3080
 Zn(BrO₃)₂·6H₂O, H bonding, PMR study 7-33277
 ZrO₂, nondestructive phase transform. of single cryst. at high press. 7-59511
 ZrSiO₄ crystal symmetry elements determ. by SEM 7-58107

crystal vacancies *see vacancies (crystal)***crystal whiskers** *see whiskers (crystal)***crystalline-amorphous transformations** *see amorphisation***crystallisation**

- see also crystal growth; dendrites; heat of crystallisation; nucleation*
 alloys, amorphous, friction and wear behaviour rel. to microstruct. and surface chem. 7-8127
 alloys, electrochemical deposition, cryst. growth modelling 7-59386
 amorphous film, crystallisation kinetics, statistical model 7-16426
 amorphous matrix, cubic crystalline precipitate morphology, strain energy effects 7-26963
 amorphous metal alloy thin films, thermal stability 7-21761
 amorphous semiconductor films, laser-induced explosive crystallisation, Raman microprobe analysis 7-12430
 amorphous semiconductors, X-ray absorpt. studies, review 7-64756
 batch cooling crystalliser, microcomputer programming of temp. 7-53522
 bicyclooctene, mol. plastic cryst., muonium adduct radicals, temp. depend. 7-53207
 bisphenol A polycarbonate crystals, melting point rel. to vapour induced crystallisation and annealing treatment 7-32312

crystallisation continued

- chalcogenide thin films, glass-crystal transitions, photoacoustic studies 7-45073
- cholesterol acetylferulate, liq. cryst. transitions, glass transition and cold crystn., DSC study 7-63814
- column crystallisation, thermal countercurrent process (*German*) 7-52002
- crystal-melt interface, diffusional light scatt. 7-39137
- Czochralski method, controlled crystn. dynamics model anal. 7-27885
- Czochralski method, melt level variations effect on crystn. rate 7-3160
- deeply quenched liquids, crystalline nucleation 7-32607
- diamond, thermal cond., C-defect effects 7-27035
- diamond crystallisation, conf., Warsaw, Poland (June 1985) 7-18469
- diamond layers, crystallisation from gas phase, growth kinetics (*Russian*) 7-22505
- dicyclohexyl-18-crown-6, A and C isomers, struct., X-ray diffr. study 7-42799
- diffusion-controlled interfacial growth, dense branching morphology form. 7-21147
- domain growth from melt, temp. gradient, form. kinetics study 7-51681
- DSC crystallisation peaks, superimposed, nonlinear regression anal. 7-6514
- E-glass batch melting redox and its effect on specific glass properties 7-7947
- EBBA melting and crystn. processes, Raman spectroscopy, X-ray and thermal anal. 7-63777
- electrocrystallisation processes, excluded nucleation zones 7-32318
- epoxydiane oligomers, struct., X-ray diffr. and IR spectra (*Russian*) 7-11968
- epoxydiane polymers, struct., X-ray diffr. and IR spectra (*Russian*) 7-11968
- explosive crystallisation, instabilities and mode selection 7-26686
- faceting effects on cryst. shape at crystn. front 7-32335
- Fe-Ni-B metallic glasses, struct. and crystn. kinetics, DSC and X-ray diffr. meas. 7-16436
- fibre reinforced composites, fibre and matrix orientations 7-39478
- gelatin-water system mixed crystal formation and glassy solidification 7-16717
- glass, crystallisation and liquid-phase separation 7-26649
- glass ceramic materials, liq. phase separation, nucleation and crystn., book 7-24327
- glass ceramics, development in China, review 7-6527
- glass powders, calcia-aluminosilicate, sintering and crystn., kinetic processes 7-37877
- growth dislocations, in-situ detection using Seebeck effect 7-32451
- growth of crystalline and amorphous structures (*French*) 7-63526
- high polymers, spherulite crystallization and spherulitic morphology 7-11967
- high temp. crystallisation, flaw form., AE detection, automatic system 7-3557
- ice, formation of cubic phase from water aerosol droplets 7-60364
- inclined plane boundary with cooling and crystallisation 7-8942
- incomplete explosive crystn., linear stability anal. 7-1885
- inorganic crystals, atomic coordination numbers and defects, geometric estimate 7-63571
- interleukin-2, human recombinant, crystn. 7-65679
- ion beam modification of materials, conf., Catania, Italy (9-13 June 1986) 7-60865
- ion-implanted layers, crystallisation dynamics, during pulsed laser irradi. 7-44435
- isotactic polybutene-1, high press. crystallisation and melting 7-12242
- laser-induced phase transformations in semiconductor and metal surfaces, nonlinear optical diagnostics 7-2061
- Laval nozzle with equilibrium crystallisation of condensed particles, two-phase flow 7-31864
- (LuYBiPb)₃(FeGa)₂O₁₂, crystn. from soln. melt, component distrib. 7-21149
- magnetic materials, conference, Freudenstadt, Germany (April 1986) 7-48144
- mass crystallisation from solns., exact solutions of eqn. 7-21401
- metallic glasses, laser annealed struct. and magnetoelastic props., effects of surface charact. 7-45785
- metallic glasses, one-component, amorphisation and crystallisation (*Russian*) 7-32301
- metals, melting and crystallisation in EM crucible 7-52009
- mullite-alumina composites, sintering and charactn. 7-3252
- norbornene, mol. plastic cryst., muonium adduct radicals, temp. depend. 7-53207
- nuclear waste glass, devitrification, role of melt insolubles 7-6525
- nucleation and growth, crystal defects 7-58169
- nylon-6,6, crystallisation, supercooling, temp. depend. of fold length 7-21072
- nylon-6, crystallisation, supercooling, temp. depend. of fold length 7-21072
- oligocaprolactone glycol-PVC, amorphous matrix, crystallisation (*Russian*) 7-11969
- organic crystals, polymorphism and nonlinear optical activity 7-57400
- organic materials, crystal growth kinetics, tailor-made additives influence 7-58171
- paraffins, chain-folded crystn., time-resolved X-ray study 7-37902
- Pd(Fe,Cu,Ni)_{0.05-0.15}Si_{0.17} metallic glasses, crystallization kinetics, elec. resist. obs. (*Chinese*) 7-11919
- PEEK matrix for high performance composites, processing, struct. and props. 7-3262
- PET fibres, heat treatment kinetics 7-44407
- PET film, solvent induced crystallisation, morphology, SEM obs. 7-44406
- PET films, crystallisation induced by integral sorption of organic vapours 7-12473
- PET films, crystallisation under strain, annealing, morphology, mech. props. 7-44415
- PET films, quenched, crystallisation kinetics rel. to methylene chloride vapour sorption 7-44405
- phase transition temp. determ. in optical ovens for refractory materials 7-30014
- poly(ϵ -caprolactone), crystn. nucleation and spherulitic growth rates 7-37905
- poly(ethylene terephthalate), changes in molecular conformations produced by crystallization and drawing, neutron scatt. anal. 7-10799
- poly(vinylidene fluoride), α -polymorph, melting behaviour and isothermal lamellar thickening 7-12240

crystallisation continued

- poly(vinylidene fluoride)-poly(ethyl acrylate) blends, phase diagram and morphology 7-63538
- poly-3,3-diethyloxetane, spherulitic growth rates 7-1915
- poly- ϵ -caprolactone, crystallisation from melt, real-time pulse NMR meas. 7-27621
- poly-ether-ether-ketone crystallisation, investig. 7-6558
- polyaniline, doped, thermoplastic amorphous-crystalline conversion 7-32315
- cis-1,4 polybutadiene, crosslinked, anomalous thermal conductivity 7-27038
- polybutene-1-polypropylene blends, polybutene-1 crystallinity enhancement 7-63509
- polybutylene, crystallisation, electron microsc. obs. 7-32309
- polybutylene, crystallisation, X-ray scatt., differential scanning calorimetry and torsion pendulum investig. 7-32308
- polybutylene terephthalate fibres, heat treatment kinetics 7-44408
- polydimethylsiloxane, refr. index and thermal expansion coeff. variations with temp. 7-39060
- polyester-polycarbonate blend, crystallising crazes, probable source of solvent stress cracking resist. 7-13621
- polyester-polyether segmented copolymer, melt spinning, fibre form., struct., phase separation 7-46407
- polyesters, aromatic, conformational reorganisation viewed by Raman spectra 7-32311
- polyesters, cycloaliphatic, stress optical behaviour 7-45975
- polyetheretherketone, penetrant durability rel. to processing and struct. 7-65168
- polyethylene, interlamellar links, environmental stress cracking agent effect 7-53928
- polyethylene, linear, DSC, origins of endothermic peaks 7-11952
- polyethylene, low density, bulk crystallisation kinetics, morphology 7-37893
- polyethylene, low density, crosslinked, morphology, transmission electron microscopy 7-37894
- polyethylene, low density, crystallisation and melting behaviour 7-37892
- polyethylene, oriented, temp-induced crystallisation 7-11954
- polyethylene, oriented, temp-induced crystallisation 7-16446
- polyethylene, single cryst., regime II growth from dil. soln. in *n*-octane 7-21133
- polyethylene, soln. crystallisation kinetics and morphology 7-21148
- polyethylene blends, melting, crystallisation, DSC, X-ray diffr., Raman spectra 7-44411
- polyethylene blends, melting, crystallisation, relax., DSC, light scatt. 7-44412
- polyethylene blends, melting and crystallisation, small angle light scatt. 7-44413
- polyethylene crystals, twinned, nucleation controlled growth 7-44401
- polyethylene oxide-melaminoformaldehyde cocured copolymer, crystallisation and melting (*Russian*) 7-26923
- polyethylene single crystals, high temp. soln. growth rates, morphology 7-17402
- polyethylene terephthalate, glass transition and crystallisation studies positron annihilation meas. 7-46230
- polyethylene terephthalate glycol, films, uniaxially stretched, amorphous orientation and induced crystallisation 7-16448
- polyethylene terephthalate glycol, uniaxially stretched, amorphous orientation and induced crystallisation 7-11956
- polyethylene-tetrafluoroethylene, row crystallised film, deform. mechanism 7-44663
- polyethylenes, crosslinked, nucleation density, morphology, transmission electron microscopy 7-37895
- cis-polyisoprene films, crystallisation kinetics and morphology 7-6553
- polymer, thermotropic, structure and structure formation 7-11962
- polymer crystallisation, assoc. acoustic emission due to stress release 7-44704
- polymer melts, crystallisation, localised diffusion, reptation effect 7-44414
- polymer melts, rate-controlled solidification, zone model 7-1917
- polymers, nonequilibrium phenomena, real-time NMR measurement system 7-2944
- polyolefines, struct., dielec. props., crystallisation conditions effects (*Russian*) 7-64564
- polypropylene, isotactic, γ -phase morphology 7-6554
- polypropylene films, glass isotactic, crystallisation, struct., dynamic mech. props. 7-16445
- polypropylene-ethylene-propylene copolymer blends, isotactic, mechanical props. and morphology 7-63539
- polyvinylidene fluoride, struct., melting and crystn. (*Russian*) 7-6563
- profiled crystal growth, surface tension as an automatic control parameter 7-32324
- PVC, rigid, stabilised, crystallinity detection by hardness testing 7-8223
- rapidly condensed highly dispersed films and glasses, phase size effect 7-2149
- rare earth alloys, RNi₂ Laves phase (R=Y, La, Ce, Pr, Sm, Gd, Tb, Dy, Ho, Er), H induced amorphisation 7-51641
- rare earth mixed ligand crystals, temperature reduction and spontaneous crystallisation prep. 7-46294
- rubber, gel and mol. wt. influence on mech. props. 7-37904
- rubber, natural, low temp. crystallisation, shear and compressive strain 7-6559
- rubber blends, cryo-ground, rheology rel. to natural rubber matrix viscosity 7-59566
- SAW transducer, layered struct. tempering (*German*) 7-31615
- semiconductors, ion beam induced epitaxial crystn., kinetics, mechanisms and microstruct. 7-12171
- sialon ceramics, processing, Al ion redistrib., crystallisation EDX analysis 7-3237
- silicate systems, natural, crystallisation 7-8938
- solutions, saturation temperature determination, crystallisation 7-44429
- sphere crystallisation, thermoelastic stresses in weightless conditions 7-1424
- stearic acid soln., cryst. growth modelling 7-59386
- Stepanov crystallisation method, stationary state existence conditions 7-32323
- Stepanov method crystallisation on a rotating seed 7-33540
- supercooled melt, kinetics of crystal growth 7-1924
- Te elemental and alloy thin films, laser irradi. effects, refl. meas., optical data storage appl. 7-12144
- thin film pulsed heating, thermal and plasma models 7-26946

crystallisation continued

- transition metal-metalloid metallic glasses, struct. relax. and segregation (*Russian*) 7-32300
- zeolite, ZSM-5, crystallisation kinetics from organic solvent-water mixture 7-22457
- zeolite ZSM-5, hydrothermal synthesis, nucleation and growth 7-33537
- Zerodur, lightweight large mirror blanks prod. 7-37223
- Al-Mn, Al-rich alloy, rapidly solidified, crystn. of quasicryst. icosahedral phase 7-63472
- Al-Mn, pressure induced quasi-crystal to crystal transition for melt span alloys 7-16726
- Al-Zn eutectic, oriented crystallisation, buoyancy-driven convection effects 7-27887
- AlMn films, ion irradiation-induced amorphous to quasicryst. transform., comp. depend. study 7-16654
- Al_{0.8}Mn_{0.2}-Fe_x, rapidly quenched, crystn. process, high temp. X-ray studies 7-1922
- Al₂O₃ ceramics, microstruct.-mech. prop. relationship 7-65147
- Al₂O₃, cryst. growth from melt, phase boundary displacement mechanism, defect distrib. 7-32328
- α -Al₂O₃, hexagonal, plate-like, synthesis using hydrated Al₂(SO₄)₃ as starting material (*Japanese*) 7-22454
- α -Al₂O₃, ion implantation, crystallisation of amorphous surface layers 7-58304
- Al₂O₃-SiO₂:Cr mullite transparent glass ceramics, Cr³⁺ luminesc. 7-46102
- Al₂O₃-SiO₂-CaO glasses containing rare alkali oxides, struct. and elec. props 7-6528
- Al₂O₃-ZrO₂, Zr environment, EXAFS studies 7-63465
- Al₂O₃-ZrO₂-Y₂O₃ system, synthesis and props. 7-22614
- As-Sb-Se glasses, calorimetric meas. 7-26652
- (As₂Se₃)_{1-x}Tl_x, elec. and thermal transport props., effect of Tl addition 7-38200
- Au films, rapid crystn. kinetics under laser irradi., picosec. transient reflectance meas. 7-11915
- B₂O₃-Li₂O-LiCl-Al₂O₃, amorphous ionic conductor, crystallisation, position annihilation study (*Chinese*) 7-37872
- BaO-B₂O₃-Fe₂O₃ glasses, γ -irradiated and heat treated, elec. conductivity and crystn. 7-21510
- BaO-Fe₂O₃-B₂O₃-based glasses, crystallisation behaviour, nucleating agent effects 7-51650
- BaO-4B₂O₃ glasses, crystallisation 7-63490
- Ba(PO₃)₂-AlF₃-NaF system, glass form. and props. 7-11929
- a-C films, crystallisation, influence of residual stresses and density fluctuations 7-21750
- CaO-Al₂O₃ glass, 3-5 μ m transmission, rain erosion resist., surface crystallisation treatment 7-37070
- CaSO₄.1/2 H₂O: Cd, crystallisation from phosphoric acid 7-27882
- CaTiO₃, ion implantation, crystallisation of amorphous surface layers 7-58304
- CdGeAs₂, amorphous, superimposed DSC crystn. peaks, nonlinear regression anal. 7-6514
- CdS surfaces, electron-beam-stimulated processes, real-time atomic-resolution electron microscopy 7-7798
- Co-B amorphous alloys, ⁵⁹Co hyperfine field distrib., NMR spin echo studies 7-53174
- Co₂B₁₈ amorphous alloy, reminiscent devitrification, X-ray diffr. studies 7-6547
- (Co_{0.85}Fe_{0.06}Ni_{0.08}Nb_{0.01})₇₅Si₁₀B₁₅ amorphous alloys, structural relax. and crystn., positron annihilation studies 7-37869
- Co₆₈Fe₁₃Ni₁₇Si₂B₃, amorphous alloy, superplasticity 7-3368
- Co_{83.3}Fe_{5.7}Si_{7.5}Ge_{1.5}B_{2.5}, amorphous alloy, struct. changes after γ -irrad. (*Russian*) 7-58336
- CoP amorphous films, FMR spectra during crystallisation 7-53142
- Co₇₀Si₃₀ amorphous films, coercive force rel. to crystallisation (*Russian*) 7-59078
- Cr₂O₃, in transparent glass-ceramic, crystn. and spectroscopic props., melting conditions and heat treatment influence 7-7588
- Cr₇₅Si₂₅ thin films, microstruct. and resist., room temp. to 950°C 7-38410
- Cu, electrocrystallisation kinetics, surface ion conc. depend. on overvoltage in case of slow adatom surface diffusion (*Russian*) 7-2429
- Cu, electrocrystallisation processes, excluded nucleation zones 7-32318
- Cu electrocrystallisation on indifferent substrates, twinning 7-53639
- Cu films, rapid crystn. kinetics under laser irradi., picosec. transient reflectance meas. 7-11915
- CuInSe₂ epitaxial films deposited on GaAs and CdS, RHEED studies 7-12549
- Cu_{0.85}Si_{0.15}, amorphous melt-quenched alloys, crystn. (*Russian*) 7-37881
- Cu₄₈Fe₅₂, amorphous, crystallisation, intermediate long period superlattice phase form. 7-21098
- Cu₂Ti_{100-x}, x=50,66, metallic glasses, crystn., DTA, X-ray diffr., hardness meas. 7-63489
- Cu₆₀Zr₄₀, amorphous, isothermal crystallisation, nucleation activation energy, DSC obs. 7-11926
- DyIG:Ga,Bi, RF sputtered films for magneto-optical memory, mag. props. 7-64613
- Er-Cu (Ni) metallic glass form. by near-isothermal cold rolling 7-22610
- Fe garnet film, epitaxial growth from weakly dissolved molten soln. 7-64944
- Fe-B, amorphous alloys, crystallisation, morphology rel. to sample thickness (*Russian*) 7-37861
- Fe-B (15 at.%), amorphous powder and strip, struct., mag. props., thermal stability (*Russian*) 7-63470
- Fe-B amorphous sandwich films, concentration-dependent diffusion 7-45027
- Fe-B metallic glasses, struct. relax., Curie temp. meas. 7-21124
- Fe-based amorphous alloys, thermal devitrification kinetics 7-51651
- Fe-based amorphous alloys, secondary ion emission during heating (*Russian*) 7-51656
- Fe-Co-B films, phase transition, microstruct. 7-33568
- Fe-Cr-B, amorphous, Cr redistribution between phases during crystallisation, Mossbauer spectroscopy 7-21100
- Fe-Cr-Si-B metallic glass wires, corrosion rel. to crystallinity and comp. 7-46701
- Fe-M-B metallic glasses (M=Ti,V,Cr,Mn,Co,Ni,Cu,Pd,C,Si,Ge,Sn), formation kinetics, thermal stability 7-58474
- Fe-Ni-B, amorphous, shock loading, inclusions dissolving, domain struct. (*Russian*) 7-63487
- Fe-Ni-B metallic glasses, crystallisation, microhardness (*Russian*) 7-59617

crystallisation continued

- Fe-Ni-based amorphous alloys, relax. spectra, effect of pulse treatment 7-46536
- Fe-Si (33 at.%), amorphous films, mag. anisotropy, effect of crystn. and deform. (*Russian*) 7-53088
- Fe-Si-B, amorphous alloys, crystallisation, morphology rel. to sample thickness (*Russian*) 7-37861
- Fe-Si-B alloy glass, crystn., effect of solid-liq. interfacial energy 7-16437
- Fe-Si-B amorphous alloys, hypoeutectic, thermal stability and soft mag. props. 7-11928
- Fe-Sm amorphous alloys, crystn. behavior, DTA, magnetisation and X-ray diffr. meas. 7-44372
- Fe-Zr, mechanically alloyed, glass forming ability 7-21110
- Fe₂B₅, polymorphous crystallisation into Fe₂B orthorhombic phase 7-37874
- Fe₇₉B₂₁, amorphous alloy, elec. resist. and crystn. on hardening from different temps. 7-44380
- Fe₈₀B₂₀ ribbons, amorphous and crystallised, surface comp., electronic props., topography, AES, XPS, ion scatt. studies 7-27065
- Fe₈₄B₁₆ amorphous alloy, layer-by-layer phase anal., depth-selective conversion-electron Mossbauer spectroscopy 7-17255
- Fe₇₈B₁₃Si₉ amorphous and partially crystalline alloy, high resolution TEM studies 7-21127
- Fe₈₂B₁₂Si₆, amorphous, initial crystallisation 7-44387
- Fe₈₃B₁₂Si₅ metallic glasses, crystn., magnetisation, scaling, mag. relax. meas. 7-63496
- Fe₈₁B_{13.5}Si_{3.5}C₂, Metglass 2605 SC, surface crystn. behaviour 7-58154
- Fe₇₇B₁₆Si₅C₂, metallic glass, crystallisation, DSC and X-ray diffr. studies 7-11932
- Fe_{90-x}B₁₀Zr₁₀, amorphous, B addition effect on mag. props., elec. resistivity, crystallisation (*Chinese*) 7-7487
- Fe₇₀(CeNdPr)₂₀B₁₀, rapidly quenched ribbons, hard mag. props. 7-27562
- (Fe_{1-x}Co_x)₈₀B₂₀, amorphous alloy, crystallisation kinetics (*Korean*) 7-26638
- Fe₆₇Co₁₈B₁₄Si, amorphous mag. alloy, crystallisation, elec. resist., TEM obs. 7-11927
- Fe₇₄Co_{10-x}Cr₆B₁₆ amorphous alloys, form. and crystn. 7-11930
- Fe₇₄Co_{10-x}Cr₆B₁₆, amorphous, prep. by melt spinning, X-ray diffr., DSC, Mossbauer studies 7-46369
- Fe₄₃Cr₂₅Ni₂₀B₁₂ glass, devitrification, mag. meas. and X-ray diffr. studies 7-21128
- (Fe_{1-x}Mn_x)₇₈B₂₂, amorphous alloys, lattice parameters, annealing, X-ray diffr., elec. resist. 7-37878
- Fe₇₁Nd₁₅B₃-based melt spun ribbons, crystallisation and mag. props. 7-26662
- Fe₈₀Ni₄₀B₂₀, amorphous, positron annihilation studies 7-45859
- Fe₈₀Ni₄₀B₂₀, amorphous and crystalline, elec. resistivity, temp. dependence 7-21892
- Fe_{45.5}Ni_{44.5}B_{10.0}, amorphous, internal friction, thermo-EMF struct., annealing effect (*Russian*) 7-59560
- Fe₄₀Ni₃₈B₁₈Mo₄, Metglass 2826 MB, surface crystn. behaviour 7-58154
- Fe₄₀Ni₃₈Mo₄B₁₈, amorphous, positron annihilation studies 7-45859
- Fe₄₀Ni₃₈Mo₄B₁₈, amorphous alloys, thermal devitrification kinetics 7-51651
- Fe₄₀Ni₄₀P₁₄B₆, Metglass 2826, crystn. behaviour, influence of annealing atm. 7-53768
- Fe₇₀Ni₁₀P₁₃C₇, amorphous powder, crystallisation (*Russian*) 7-58162
- (Fe_{0.8}Ni_{0.4})₈₂Si₈B₁₀ amorphous alloys, structural relax. and crystn., positron annihilation studies 7-37869
- Fe₇₀Ni₈Si₁₀B₁₂, amorphous alloys, thermal devitrification kinetics 7-51651
- Fe_{0.44}Ni_{0.76}Si_{0.78}B_{14.56}C_{0.25}, amorphous filler metal, struct. props. (*Korean*) 7-32292
- FeOOH sols, crystallisation, Mossbauer study 7-38970
- Fe₈₀P₂₀, amorphous ribbons, structural relax., crystallisation, Mossbauer spectra (*Chinese*) 7-11918
- Fe₆₅Si₃₅ amorphous films, coercive force rel. to crystallisation (*Russian*) 7-59078
- Fe₇₈Si₉B₁₂ amorphous alloys, surface crystallisation and mag. props. 7-51649
- Fe_{90-x}Si₁₀ amorphous alloys, multistep-micro-crystallisation studies 7-21129
- Fe₈₀Si₁₀P_{20-x} amorphous alloys, struct., mag. and elec. props. (*Korean*) 7-2893
- Fe_{84-x}V_xB₁₆, amorphous alloys, crystn., products and kinetics 7-51677
- Fe₉₀Zr₁₀ glasses, crystallisation characteristics 7-51647
- Fe₉₀Zr₁₀ glasses, crystallisation characteristics 7-51648
- Ga film, vac. condensates, struct. and opt. characts. 7-2404
- Ga-SeTe₁, phase change optical recording, write erase characteristics 7-57491
- a-GaAs films, dynamics of laser annealing by transient grating method 7-12122
- GaAs-AlAs, solid soln., temp.- and current-controlled LPE, theoretical model 7-39447
- Ga₂₀Te₈₀, double glass transition and double stage crystn., X-ray diffr. studies 7-58157
- Gd₂Si_{1-x}Al_x, x=0.18, 0.59, 0.87, amorphous, thermal, elec. and mag. props. 7-53039
- Ge, amorphous and partially crystallised, X-ray absorpt. investig. of struct. (*German*) 7-46241
- Ge amorphous films, struct. and crystn., EXAFS study 7-64005
- a-Ge films, dynamics of laser annealing by transient grating method 7-12122
- a-Ge films, laser-induced phase transitions, time resolved TEM study 7-38056
- Ge microcrystals, gas-evaporated, thermal annealing, Raman and electron microscopic study 7-64635
- Ge, thermodynamic interrelation between amorphous, diamond cubic and liquid states 7-12245
- Ge-Sb-Se glasses, crystallisation ability, high energy electron irradi. effects (*Russian*) 7-32306
- Ge-transition metal eutectic alloys, cryst. growth by directional crystallisation 7-64887
- Ge_{80-x}Mn_xB₂₀ amorphous alloy, Curie point and crystallisation temp. 7-17173
- Ge₂₀S_{80-x}Bi_x, n-type amorphous semiconductors, morphological struct. 7-51652
- GeTe₂ amorphous films, struct. changes by annealing 7-63467
- a-Ge_{1-x}Te_x films, crystallisation behaviour and local order 7-44386
- Hf_{1-x}Cu_x, metallic glass, thermal stability and phase transformations 7-21125

crystallisation continued

- KAl(SO₄)₂ solutions, effect of impurities on props. 7-6495
 LiCl-Li₂O-B₂O₃-Al₂O₃, amorphous Li⁺ conductor, crystn. and phase separation, interface effect (*Chinese*) 7-38245
 LiFeP₂O₇, cryst. synthesis, at. struct., DTA, X-ray diffr. study 7-26708
 LiNbO₃ polycrystalline films, prep. by hydrolytic decomp. of metal alkoxide alcoholic solns., SEM obs. 7-7044
 LiNbO₃ powders obtained by the alkoxy method, crystallisation and ferroelectric props. 7-7648
 LiNbO₃, prod. by Czochralski and Stepanov methods, elec. phenomena accompanying growth 7-32332
 Li₂O-MgO(CaO)-Al₂O₃-SiO₂, multicomponent glasses, sequence of cryst. phases 7-26648
 Li₂O-SiO₂ glass, phase nucleation, melting temp. depend. 7-6549
 Li₂O-SiO₂ glass, Pt catalysed crystallisation 7-6524
 Li₂O.2SiO₂ sol-gel glass, prep. and devitrification behaviour 7-58158
 Mg-Sm-Zn system, phase equilib. 7-46413
 Mg-Zn metallic glasses, room temp. stability, crystallisation and precipitation 7-11931
 Mg-Zn rapidly solidified alloys, mech. props. 7-22711
 MgO, sinterability, prep. and charact. of sample powder 7-22623
 MgO-Al₂O₃-SiO₂ glass-ceramics, nucleation crystallisation, modulus of rupture, acousto-US obs. 7-59723
 Mg₇₂Zn₂₈, amorphous, crystn., X-ray small angle scatt. 7-11935
 Mo₄Ni_{100-x}, x=20, 28, 35, 48, 63, amorphous, struct., short range order, thermal stability 7-21107
 NaNO₂, single cryst. growth by Stepanov's method 7-32329
 NaNbO₃ polycrystalline films, prep. by hydrolytic decomp. of metal alkoxide alcoholic solns., SEM obs. 7-7044
 Na₂O-(MgO, NaO)-GeO₂-H₂O system, crystallisation of fibrous (Mg, Ni) germanates 7-2153
 Na₂O-V₂O₅-P₂O₅, crystallised glass, containing V bronze crystals, elec. cond. 7-21922
 Na_{1+x}Zr₂P_{3-x}O₁₂, NASICON, superionic cond. and glass-crystal transition 7-6870
 Nd-Hf-B system, phase equilib. in Nb corner 7-46415
 Nd-Fe-B, metastable amorphous alloys, crystn., thermal stability 7-39482
 Nd-Fe-B amorphous ribbons, effect of crystallisation conditions on hard mag. props. 7-27561
 Ni-Ag amorphous thin films, crystallisation and internal constraints (*French*) 7-2433
 Ni-B, implanted, mech. props., disorder and amorphicity 7-53819
 Ni-B alloy, electroless, heat induced struct. changes 7-13639
 Ni-B amorphous alloys, crystallisation produced by ion implantation, TDPAC study 7-32288
 Ni-based consolidated rapidly solidified alloys, strengthening mechanisms 7-22712
 Ni-P, amorphous electrodeposited alloys, short-range order (*Russian*) 7-32291
 Ni-P, implanted, mech. props., disorder and amorphicity 7-53819
 Ni-P electroless deposited amorphous coatings, wear resistance, crystallisation effects 7-53913
 Ni-P films, electroless deposited, struct., electron microscopy studies 7-7041
 Ni-P ion-implanted and melt spun amorphous alloys, crystn., TEM, RBS and DTA meas. 7-16439
 Ni-P metallic glasses, electronic struct., XPS study 7-39357
 Ni-Ta amorphous alloy, struct. changes and crystallization during heating (*Russian*) 7-16419
 Ni-Ti(Ta)(Cr), amorphous and cryst. reaction with Si studied by RBS and TEM 7-21704
 Ni₂Ag_{1-x} amorphous thin film, RF sputtered, real-time crystallization kinetics (*French*) 7-52349
 Ni₃B, amorphous, surface electronic struct. during crystallisation and O₂ and CO adsorption 7-7308
 Ni₃₀B₅₄C₁₆, B-rich amorphous alloy prep. by rapid quenching, crystn., hardness and elec. resist. 7-13441
 Ni₇₅B₁₅Si₁₀ amorphous alloy, metalloid redistribution, scanning Auger microprobe study 7-32655
 Ni₇₀Cr₇Fe₅Si₈B₁₂ ribbon, rapidly quenched from melt, struct. inhomogeneity and crystallised metastable phase (*Chinese*) 7-63477
 Ni₈₃Cr₇Fe₅Si₄B₃, amorphous alloy, crystallisation (*Chinese*) 7-6518
 NiFe₂O₄ films, crystn. kinetics 7-45090
 Ni₇₇P₂₃ amorphous alloy, struct. relax. and crystn., elec. resist. and X-ray diffr. obs. 7-1894
 Ni₄₅Pd₃₅P₂₀ metallic glass, decomposition, crystallisation and embrittlement, atom-probe FIM study 7-33639
 NiTa, quenched amorphous alloy, thermal stability and crystn. (*Russian*) 7-11911
 NiZr₂ metallic glasses, crystallisation, influence of O and other trace impurities 7-51633
 Ni_{100-x}Zr_x metallic glasses, low temp. sp. ht. study, density of states and Debye temp. determ. 7-2226
 Ni₆₁Zr₃₉, X-ray diffraction pattern, crystallization behaviour and magnetic props. 7-3219
 PZT films, crystn. kinetics 7-45090
 PbCl₂-Sb₂O₃ glass system, structural aspects 7-44389
 PbMoO₄, Czochralski grown, crystallisation front rel. to cryst. quality 7-59402
 PbO-B₂O₃ glass form., crystallisation 7-37875
 PbO-Fe₂O₃-B₂O₃ glass ceramics, mag. props. and EPR spectra of precipitated mag. phases 7-45748
 Pb₈₀Si₂₀, amorphous, thermal stability, Auger study 7-58577
 Pb_{0.8}Sn_{0.2} Te epitaxial films, vacuum deposition growth in a quasiclosed vol. 7-46329
 PbTiO₃, distorted cubic, crystn. and phase transform. 7-39548
 Pd film, vapour quenched, resistivity meas., indirect obs. of amorphous to crystalline transition 7-52864
 Pd-U-Si glassy alloys, glassy-to-icosahedral polymorphous crystn. transform., X-ray and electron diffr. studies 7-6515
 Pd_{77.5}Cu₆Si_{16.5} glass, cryst. nucleation and growth kinetics 7-11917
 Pd_{0.84}Si_{0.16} metallic glasses, crystallisation kinetics, elec. resist. obs. (*Chinese*) 7-11919
 Pd₇₇Si₂₃ metallic glasses, picosecond laser annealing 7-44613
 Pd₈₀Si₂₀, metallic glass, crystallisation 7-37882
 PdSiCu, amorphous, ultrasonic vel., mechanical props. (*Korean*) 7-26874
 Sb films, amorphous, vacuum-deposited, growth of hexagonal plate cryst. 7-51634
 Sb layers, amorphous phase stability rel. to metal overdeposits 7-52324
 Sb-Ge-Se-Mn, effect of Mn impurity on comp. and physicochemical props. 7-11922

crystallisation continued

- Sb-Sb₂Se₃-SbI₃ system, phase diagrams investig. 7-2212
 a-Sb₂S₃ films, thermally induced relax. of mechanical stresses 7-8032
 Se, amorphous, vitrification and crystallisation, thermal prehistory effects (*Russian*) 7-63479
 Se, amorphous films, crystn., kinetic study 7-21101
 Se, thin films, amorphous, crystn. 7-44371
 Se-Te, glass forming melts, nonisothermal crystn., DTA, crit. cooling rate 7-44394
 Si, amorphisation and crystallisation 7-11914
 Si, amorphous, ion implanted, picosecond laser induced crystn. 7-16621
 Si, amorphous layers, liq. phase crystallisation under pulsed heating 7-44773
 Si, amorphous to crystalline transformation, TEM in situ technique 7-44376
 Si CVD thin film, struct. and elec. props. 7-21730
 Si for solar cells, growth by horizontal supported web technique 7-17412
 Si growth by SOG method and Stepanov method, stability anal. 7-33602
 Si, ion implanted, amorphous phase transformation during rapid thermal annealing 7-16435
 Si, ion implanted, laser beam melting and resolidification 7-12126
 Si, ramp assisted foil casting and photovoltaic appls. 7-16609
 Si, single crystal, effects of shape of crystn. front, melting boundary 7-6566
 Si, solid-phase amorphous to crystalline transformation for shallow junction processing 7-32642
 Si, thermodynamic interrelation between amorphous, diamond cubic and liquid states 7-12245
 Si:As ion implanted, defect structs. generated by buried amorphous layer regrowth 7-38078
 Si:B film deposition in Si₂H₆-B₂H₆-He gas system, doping effect 7-27184
 Si:Cu, amorphous, explosive crystn., RBS and time-resolved reflectivity studies 7-21265
 a-Si:H, amorphous to microcrystalline structure transformation, phase stabilisation 7-63475
 Si:H binary alloys, crystallisation of polysilane 7-21105
 Si:In, amorphous, low temp. annealing, impurity diffusion, phase separation and crystn. studies 7-16808
 a-Si/Al films, laser-induced phase transitions, time resolved TEM study 7-38056
 a-Si/Au thin film bilayers, Si crystallisation study 7-21699
 SiC, single crystals, and polycrystals, oxidation kinetics in dry O₂ 7-39683
 SiO₂, tridymite, form. from colloidal silica, kinetics 7-23053
 SiO₂-Al₂O₃ system, charactn. of spinel phase from xerogels and form. process of mullite 7-39464
 SiO₂-GeO₂ system, gels and gel-glasses, struct. study using vibr. spectroscopy 7-44381
 SiO₂:P films, pure and doped, low press. CVD growth, structural, optical, elec. props. 7-27186
 Si_xTe_{100-x} glasses, crystallisation, DSC studies 7-6542
 SnO₂, amorphous film, vacuum prep., struct., crystallisation 7-53594
 SrTiO₃-SiO₂-Al₂O₃ glass-ceramics, anomalous crystn. behaviour obs. 7-44395
 Ta-Ir amorphous thin film thermal stability, crystallisation behaviour studies 7-63464
 Ta₃Ir₄₅ amorphous alloy, crystallisation study 7-58145
 Ta₂Cu_{1-x} amorphous thin-film diffusion barriers on GaAs, thermal and structural stabilities 7-52321
 Tb₂Si_{1-x}, x=0.18, 0.59, 0.87, amorphous, thermal, elec. and mag. props. 7-53039
 Te alloys for optical data storage, phase-change properties, transition metal elements effects 7-50662
 Te-based materials, reversible optical data storage appl. 7-37068
 Te-based thin films, crystn. rate, thermal stability, erasable optical recording appl. 7-37069
 Te-Ge alloy glass, isothermal surface crystallisation 7-58576
 Te_{1-x}Ge_x amorphous films as reversible phase-change optical data storage materials 7-1242
 TeO₂ films, nanosecond pulsed laser-induced segregation 7-44610
 TeO₂:Ge,Sn films, optical props., thermal stability 7-39207
 Ti electrodes, passivated, photoelectrochemical studies 7-12757
 Ti-Ni-Al rapidly quenched amorphous alloys, thermal stability studies 7-21123
 Ti-Pd, amorphous, differential thermal anal., obs. of exothermic crystallization 7-59479
 TiNi-TiCu amorphous alloy, thermal devitrification kinetics, DSC obs. 7-21116
 TiO₂ films, phase transitions, Raman spectra 7-12556
 TiO₂ films, pulse laser irradiated, Raman studies of phase transformations 7-12569
 TiO₂-GeO₂ glasses, crystallisation, ion coordination, X-ray diffr., IR spectra 7-6523
 TiO_x, amorphous, reactive ion beam deposition 7-45091
 (Ti_{1-x}V_x)₂Ni, orientation relationship between the icosahedral and crystalline phases 7-16477
 Ti-Ge-Se, bulk glass formation region, elec. and struct. characts. 7-58159
 Tm₂FeO₁₂, double phase transition, EXAFS studies 7-63799
 V₇₅Si₂₅ amorphous films, crystallisation and elec. props. 7-21102
 W CVD films, high temp. stress meas. 7-58718
 W, LPCVD from W(CO)₆ in hot-wall environment 7-17465
 W/C multilayer films, thermal stability, X-ray diffr. studies 7-27169
 W/C multilayer films for X-ray reflectors, thermal stability 7-32871
 W-Re amorphous thin film thermal stability, crystallisation behaviour studies 7-63464
 W-Ru amorphous thin film thermal stability, crystallisation behaviour studies 7-63464
 W-Si amorphous thin films, DC sputter deposited, crystn. temp., DTA 7-21720
 W-Si amorphous thin films, interfacial reactions with polycryst. metal overlayers 7-21763
 W-Ti-Si system, metallisation materials, amorphous phase form. and stability 7-22640
 W-Zr amorphous films as diffusion barriers between Al and Si 7-21504
 WO₃-Na₂O(NaF), nucleation and flux growth 7-44430
 WS₂, amorphous films, crystallisation, stacking faults and resistivity 7-21759
 WS₂, CVD films, high temp. stress meas. 7-58718
 YIG:Ga, Bi, RF sputtered films for magneto-optical memory, mag. props. 7-64613
 Y₂O₃-Al₂O₃-B₂O₃ system, glass formation, props. and struct. 7-2205
 Y₂O₃-TiO₂ system, fluoride type solid soln. crystallisation 7-1882

crystallisation continued

- $\text{Y}_2\text{O}_3\text{-ZnO-Al}_2\text{O}_3\text{-SiO}_2$, glass form. and crystn., effect of ZnO additions 7-44382
 Yb amorphous films, stability, effect of mag. field (*Russian*) 7-52319
 Zn_3P_2 thin films, amorphous-crystalline transitions, elec. cond., 100-300K 7-38560
 Zr-Ni metallic glass, crystallisation, metastable crystalline phase form. 7-21126
 $\text{ZrF}_4\text{-BaF}_2\text{-AlF}_3$ glass, viscous flow vs. phase separation, DSC study 7-44383
 $\text{ZrF}_4\text{-BaF}_2\text{-LaF}_3\text{-AlF}_3\text{-NaF}$ glass, crystal growth and microstruct. 7-1896
 $\text{ZrF}_4\text{-BaF}_2\text{-LaF}_3\text{-AlF}_3$, heavy metal fluoride glass system, viscosity and crystallisation 7-37883
 $\text{ZrF}_4\text{-BaF}_2\text{-NaF}$ glasses, crystallisation study 7-11933
 $\text{ZrF}_4\text{-BaF}_2\text{-NaF-AlF}_3$ glass, crystn. (*Japanese*) 7-26659
 $\text{ZrF}_4\text{-BaF}_2\text{-NaF-AlF}_3\text{-LaF}_3$ glasses, crystallisation study 7-63491
 ZrO_2 films, pulse laser irradiated, Raman studies of phase transformations 7-12569
 ZrO_2 gel, transparent, glass-like, thermal evolution 7-28356
 $\text{ZrO}_2\text{-CaO-P}_2\text{O}_5\text{-SiO}_2$ glass ceramics, prep. and mech. props. (*Japanese*) 7-7942
 $\text{ZrO}_2\text{-GeO}_2\text{-NaOH-H}_2\text{O}$ system, hydrothermal crystn. investig. 7-2152

crystallite texture *see texture*

crystallites

see also crystal microstructure

- 2D, crack growth, computer modelling 7-43787
 alkali metal halide crystals, impurities, local and gap mode freq. calcs. 7-26888
 alloys, amorphous, friction and wear behaviour rel. to microstruct. and surface chem. 7-8127
 epoxydian polymers, struct., X-ray diff. and IR spectra (*Russian*) 7-11968
 graphite surface, methane adsorption, incomplete wetting at low temps. 7-32798
 growth shape on substrate, Monte Carlo simulation 7-44426
 metal particles, size-dependent melting points 7-44771
 metal particles, ultra fine, ferromag., growth rel. to mag. field 7-53515
 MgO films, prep. by RF sputtering, orientation and microstruct. (*Japanese*) 7-22480
 nucleation and growth at high press., colloidal theory 7-46301
 polyoxymethylenes, low temp. dielec. relax., crystallite surface folds motion contrib. study (*Russian*) 7-17267
 polypropylene, high-oriented, struct. rel. to physico-mech. props. (*Russian*) 7-26672
 polypropylene, isotactic, crazing, energetic characts. (*Russian*) 7-12201
 powder diffractometry, preferred orientation, intensities correction, March model appl. 7-1808
 semiconductor clusters, zero-dimensional excitons, optical spectra and luminesc. 7-12615
 semiconductor microcrystallites, laser-excited, absorption blue shift 7-33409
 sputtered magnetic thin film, ion beam irradiat., struct. studies 7-22588
 X-ray diffractometer, four-crystal, crystallite mosaicity and perfection meas. 7-44302
 Ag (100), adsorption of Cl, Auger, LEED, XPS, thermal desorption studies 7-58635
 Al_2O_3 , cryst. growth from melt, phase boundary displacement mechanism, defect distrib. 7-32328
 $\text{As}_2\text{Ge}_{50}\text{-Se}_{50}$, amorphous struct. study, positron lifetime spectra meas. 7-37886
 Au crystallites, annealing, grain boundary untwisting and untilting, dislocation climb and glide 7-12076
 Au, diffusion process on (100) cleavage planes of KBr, KCl, NaCl 7-21590
 Be coatings, sputter deposited using confined ion beam cylinder technique, morphology TEM 7-53586
 $(\text{CdSe})_n$, polymerised, metallic and supercond. 7-7433
 $\text{CdSe}(\text{S})$ thin films, electrophys. props., electron irradiation effects study, solar cell appl. 7-16894
 Fe-Si, melt quenched, struct. formation 7-13480
 Fe-Si (3 wt.%), microstructure, change in stereological characteristics on secondary recrystallisation 7-13468
 $\text{Fe}_{78}\text{Si}_{22}$ amorphous alloys, surface crystallisation and mag. props. 7-51649
 HoMo_6S_8 ferromagnetic films, supercond. props., temp. and mag. field depend. 7-45538
 In crystallites, surface free energy anisotropy 7-27091
 LiNbO_3 powders obtained by the alkoxy method, crystallisation and ferroelectric props. 7-7648
 MnO_2 , crystallite size, strain, X-ray diff. study 7-2221
 Ni-P coating, electrolytic, electron microscope obs. of struct., P content depend., amorphous layer form. 7-8157
 Ni-Si interface, struct., RHEED, Rutherford backscattering spectrometry 7-27143
 PbI_2 aggregated microcrystallites, Raman scatt. 7-22233
 PbTe:O films, O diffusion to bulk and crystallite boundaries 7-63884
 Pt crystallites supported on C black, surface struct., TEM study 7-32778
 $\text{RuO}_2\text{-TiO}_2$ thin films, microheterogeneous struct. 7-12541
 Si:P(B) LPCVD films, amorphous and polycrystalline, struct., elec. resist. meas. 7-52870
 a-Si/c-Si interface, microcrystallites and orientational proximity effect, HREM image interpretation, comment and reply 7-45028
 $\beta\text{-Si}$ monocryst. thin films, ion implantation and annealing, amorphisation and recryst. processes study 7-16596
 SnO_2 , amorphous film, vacuum prep., struct., crystallisation 7-53594
 $\text{SrO}_{0.5}\text{Fe}_2\text{O}_3$, doped with kaolin and BaB_2O_4 , sintering temp., effect on structural and mag. parameters 7-7543
 Te-based thin films, crystn. rate, thermal stability, erasable optical recording appl. 7-37069
 Zn_3P_2 , vacuum deposited films, struct., transmission electron microscopy and X-ray diff. 7-52316
- crystallographic shear**
 (BEDT-TTF) $_2\text{X}$ salts struct., anion length depend., shear transform. anal. 7-37961
 rotational deformations role in spherical particles form. in fatigue fracture 7-17612
 shells, noncircular cylindrical, dynamic anal., thickness shear deformation theories 7-6141
 shells, shallow spherical sheared and twisted, stress conc. factors 7-43717

crystallographic shear continued

- shells of revolution, rubber-like, undergoing torsionless axisymmetric deformation, strain-energy density 7-43687
 Al steady-wave shock compression, thermoplastic shear 7-51937
 $\text{BaMn}_{1-x}\text{Ta}(\text{Zn})_x\text{O}_3$ phase struct. and transforms., high resolution electron microscopy obs. 7-58237
 $\text{K}_{1-x}\text{Rb}_x\text{AlF}_4$, shear structural phase transition, temp. behavior 7-63809
 Ni base superalloys, hot deformed, matrix dislocations, weak beam electron microscopy obs. (*French*) 7-21210
 V_2TiO_5 , valency distrib. determ., XANES 7-16509
- crystallography**
see also crystal atomic structure; electron diffraction crystallography; gamma-ray diffraction; isomorphism; lattice constants; neutron diffraction crystallography; space groups; X-ray crystallography
 3D intensity data from single crystal reflections, graphical display 7-11829
 alloys, disordered, multi-site correlations, at. size effect 7-16347
 anisotropic crystal, secondary extinction studies 7-32193
 Borie-Sparks method in diffuse scatt. 7-32195
 Bragg-peak location employing a maximum-entropy formalism 7-11827
 catalyst surfaces, characterisation by neutron inelastic scatt. from adsorbates 7-7000
 crystal density functions, program package for multipole anal. 7-58092
 difficult structures, modified MULTAN approaches 7-51559
 digital image processing techniques used in astronomy, appl. to diff. data 7-11828
 direct methods, trial and error procedures (*Chinese*) 7-37802
 DREAM data reduction and error anal. routines, appl. to single cryst. diff. intensity meas. 7-16348
 ESR crystallography, two/three circle ESR goniometers (*Japanese*) 7-44328
 grain boundary crystallography, practical approach to determ. 7-21224
 icosahedral structures and tiling, geometry and crystallography 7-1930
 incommensurate structure refinement using a least-squares algorithm 7-51558
 intensity distributions of sums and of ratios of sums of intensities 7-11821
 lattice relationships analysis program 7-11830
 macromolecules, direct method combination with isomorphous replacement and anomalous dispersion 7-58091
 periodic and quasiperiodic crystals 7-1928
 periodic point scatterer system, dynamical diffraction theory 7-32194
 phase inhomogeneity visualisation in holographic method (*Russian*) 7-16375
 phase refinement using partial structural information, SIR and SAS phase problems 7-11823
 position sensitive detectors, 2D detector data for crystallography, fast treatment using processor arrays 7-10354
 positional parameters obtained with anharmonic temperature factors 7-11822
 powder diffractometry, preferred orientation, intensities correction, March model appl. 7-1808
 protein crystallography, restrained least-squares procedure using Numerix MARS-432 array processor 7-34105
 radial distrib. calcs. using cubic spline 7-58116
 reciprocal lattice symmetry operators, representation in proper basis 7-16349
 single-crystal diffraction data, collection with area detectors 7-11825
 structure factors, joint probability distribution for triplet phase sum 7-11819
 structure refinement, peakiness test functions 7-11818
 surface electronic function props. charact. from defect heterogeneity dominated small-angle scatt. diff. pattern, static synergetics algorithm 7-21041
 weak intensities of reflexion, treatment 7-11826
 Widmanstätten crystallography in Fe meteorites, habit planes and lattice orientations 7-9448
- crystals**
see also bicrystals; crystal structure; crystallography; dendrites; epitaxial layers; liquid crystals; plastic crystals; whiskers (crystal)
 elastic moduli and nonaffine deformations, density-functional theory calcs. 7-44649
 nonmetallic, radiation-induced struct. changes, mechanisms and criteria 7-63651
 $\text{LaF}_3\text{:Pr}^{3+}$ crystal photon echo effect, use in contemporary electronics 7-15820
- CSP lasers** *see semiconductor junction lasers*
- Curie point** *see Curie temperature; ferroelectric Curie temperature*
- Curie point writing** *see thermomagnetic recording*
- Curie temperature**
see also ferroelectric Curie temperature
 Anderson model calcs., long range magnetic order and intermediate valence considerations 7-45247
 BCC ordered alloy, high temp. mag. states (*Russian*) 7-64466
 dilute ferromagnetic alloys, magnetisation and Curie temp. calcs., approximated Heisenberg model 7-7549
 ferromagnetic 4f-systems, Curie temp., valence instability effects calcs. 7-38865
 ferromagnetic superconductors, intermediate state 7-52915
 ferromagnets, insulating, surface and interface magnetisation changes with temp., Green's function calcs. (*Chinese*) 7-38869
 ferromagnets with low carrier densities, indirect exchange 7-33162
 Heisenberg ferromagnet, semi-infinite, Curie temp. calcs. 7-45603
 intermediate valence systems, Ferromagnetic order coexistence, mag. props 7-64187
 Ising ferromagnet, with biquadratic exchange interaction and uniaxial anisotropy 7-17189
 Ising model on Bethe lattice, critical temp., variation with bilinear exchange interactions 7-2877
 magnetic alloys, phase breakdown model, Curie temp., magnetisation (*Russian*) 7-45677
 metals, phase transitions, ion-induced secondary particle emission 7-39341
 organic polymer ferromagnet, prep., ESR and Mag. props. 7-64439
 photoinduced magnetism, effects on Curie point 7-52931
 rare earth alloys, $\text{R}_2(\text{Fe,Al,Co})_4\text{B}$, mag. props., composition depend. 7-53030
 rare earth alloys, R-Co-Fe system between 2:17 and 2:7 phase regions, phase equilibria, metallography, X-ray diff., thermomagnetic anal. 7-17511

Curie temperature continued

- rare earth aluminium AlAl_2 layered structural sintered composite, mag. entropy 7-59016
 single crystal, elastic scatt. of slow electrons over surface, effect of mag. transform. (Russian) 7-52549
 spin dynamics above the Curie temp. studied by neutron scatt. 7-45685
 steel, alloy, electrical resistivity and magnetisation, temp. depend. 7-38535
 steel, austenitic stainless, electrical resistivity and magnetisation, temp. depend. 7-38535
 steel, stainless, dual phase, phase transform. obs. using thermomag. analysis 7-53696
 steel, stainless, type 304, elec. resist. and magnetisation 7-45268
 superlattices, Heisenberg magnetism study (Chinese) 7-27485
 surface, electron capture spectroscopy 7-59368
 surface ferromagnetism in transition metals, Hubbard model 7-33139
 thermomagnetic engine, demonstration of Carnot principle 7-48233
 $\text{BaCo}_2\text{Fe}_{10}\text{O}_{27}$, Curie temp., magnetization, susceptibility, mag. anisotropy meas. (French) 7-27507
 $\text{Ba}_2\text{Fe}_2^{2+}\text{Fe}_{12}^{3+}\text{O}_{22}$ hexagonal ferrite, hydrothermal synthesis, elec., magnetic and structural characterisation 7-45637
 $\text{BaFe}_{12-x}\text{Mn}_x\text{O}_{19}$, magnetoplumbite system, transport props., influence of internal electric field 7-52662
 $\text{BaFe}_{12-x}\text{Mn}_x\text{O}_{19}$, Mn substitution effects on mag. props. (Chinese) 7-7486
 $\text{BaIn}_{1-x}\text{Fe}_{10.5}\text{O}_{19}$ single crystals, magnetocrystalline anisotropy consts., anomalous temp. depend. 7-45664
 $\text{BaMg}_2\text{Fe}_{16}\text{O}_{27}$, Curie temp., magnetization, susceptibility, mag. anisotropy meas. (French) 7-27507
 BaTiO_3 , Nd_2O_3 -modified, defect struct. and dielec. props 7-37968
 Bi-based metallic glasses, thermal relax. processes 7-51653
 Bi-Zn-Fe-O amorphous films, struct. and mag. props. 7-51645
 $\text{Bi}_3(\text{GaFe})_2\text{O}_{12}$, epitaxial films, mag. and magneto-optical props. 7-53102
 $\text{CdCr}_2(\text{Se}_{1-x}\text{S}_x)_4$ spinel, mag. prop. anomalies 7-64453
 $\text{Cd}(\text{Cu}_{1-x}\text{Ni}_x)_2$, mag. and cryst. props. 7-27506
 Ce-Fe-Co-B-Si system alloys, melt spun ribbons, mag. props. (Japanese) 7-53052
 CeMn(Fe)Si_2 , struct. and mag. props. studies (French) 7-37950
 $\text{CeNi}_{5-x}\text{Fe}_x$, mag. and cryst. props., effect of H absorpt. 7-33168
 $\text{CeNi}_{5-x}\text{Mn}_x$, mag. and cryst. props., effect of H absorpt. 7-33168
 $\text{CeRh}_3(\text{Bi}_{1-x}\text{Si}_x)_2$, 4f shell dehybridisation, Curie temp. and mag. moments 7-45679
 Co and its alloys, spin wave excitations and magnetisation temp. depend. 7-45642
 Co-P, amorphous, Curie temp. meas. 7-45669
 Co-Y amorphous alloys, mag. props. 7-58990
 Co_3Er noncrystalline alloy, local atomic order, magnetism 7-32286
 $(\text{Co}_{1-x}\text{Mn}_x)_2\text{B}$, crystalline and amorphous, mag. and elec. props. 7-2827
 $(\text{Co}_{0.6}\text{Ni}_{0.4})_{78}\text{Si}_{14}$, amorphous, itinerant electron charact., current induced reson. mag. field shift obs. 7-27590
 Co_3Ti , effect of plastic deformation on mag. props. 7-33259
 CrTe-CrSe system, mag. phase diagram 7-22105
 $\text{Cu-Cd}_{1-x}\text{Fe}_x\text{O}_4$ system, elec. resist. and cation distrib. 7-7256
 $\text{CuK}_2(\text{SO}_4)_2 \cdot 6\text{H}_2\text{O}$ - ^3He , thermal resist., surface mag. coupling, effect of ^4He addition 7-52173
 DyFe amorphous alloys, local mag. anisotropy energy estimation 7-7503
 DySe-UsSe system, mag. props. of solid solns. 7-22121
 $\text{Dy}_x\text{Y}_{1-x}\text{Al}_2$, intrinsic low field susceptibility studies 7-45633
 Er-H solid soln., mag. props., H addition effects 7-7510
 Fe (111) , electron capture spectroscopy 7-59368
 Fe and its alloys, spin wave excitations and magnetisation temp. depend. 7-45642
 Fe, BCC, mag. ordering and electronic struct. (Russian) 7-33170
 Fe epitaxial monolayers on the Au (100), surface magneto-optic Kerr effect 7-59080
 Fe ores, saturation magnetisation, temp. depend., Backer's chem. reaction (Korean) 7-33263
 Fe, static paramag. spin susceptibility at finite temps. 7-33138
 Fe, surface magnetism 7-27528
 Fe-B metallic glasses, struct. relax., Curie temp. meas. 7-21124
 Fe-Ce amorphous alloys, mag. props. and elec. resist. 7-59010
 Fe-cementite alloy castings, Young's modulus and thermal expansion 7-65068
 Fe-Co-Ni based alloys, crystalline and amorphous, magnetoresistance 7-38538
 Fe-Co-based ternary alloys, atomic and mag. moment mutual ordering (Russian) 7-33169
 Fe-Cr-B-Si, amorphous, annealing effects on Curie temp. 7-45675
 Fe-La amorphous alloys, high-field susceptibility and Curie temp. 7-58989
 Fe-Ni films, γ -phase low temp. precipitation investig. (Russian) 7-33666
 Fe-Sc alloys, struct. and mag. props. NMR and X-ray diffr. studies (Russian) 7-6578
 Fe-Sc amorphous alloys, Curie temp., mag. moment and magnetovolume effects 7-33172
 Fe-Tb amorphous alloys, film and bulk mag. props. and thermal expansion meas. 7-7540
 Fe-Zr-B, amorphous, meas. of Curie temp. 7-2853
 $\text{Fe}_{90-x}\text{B}_x\text{Zr}_{10}$, amorphous, B addition effect on mag. props., elec. resistivity, crystallisation (Chinese) 7-7487
 FeCoCrSi_8 , crystallographic and mag. props., Mossbauer study (Korean) 7-33310
 $\text{Fe}_2\text{Co}_{70-x}\text{Cr}_x\text{Si}_{10}\text{B}_{15}$, $x=0, 3, 6, 9$, amorphous ferromagnet, 180° domain wall (Korean) 7-33198
 $\text{Fe}_{75-x}\text{Cr}_x\text{Si}_{10}\text{B}_{15}$, $x=0, 2, 4, 6$, amorphous ferromagnet, 180° domain wall (Korean) 7-33198
 $\text{Fe}_{80-x}\text{Cr}_x(\text{SiB})_{20}$ amorphous alloy, induced anisotropy, melt spinning effects (Russian) 7-59004
 $\text{Fe}_2\text{Ni}_{80-x}\text{B}_{18}\text{Si}_2$, glassy alloys, variation of mag. inhomogeneity 7-45634
 $\text{Fe}_{5-x}\text{Ni}_x\text{C}_2$, prep. and characterisation 7-17490
 $\text{Fe}_{30}\text{Ni}_{36}\text{Cr}_{12}\text{Mo}_2\text{Si}_3\text{B}_{15}$, amorphous alloy, Curie temp., press. effect 7-52976
 $(\text{Fe}_{1-x}\text{Ni}_x)_7\text{Si}_{10}\text{B}_{13}$, amorphous, effective mag. moment, Curie temp. (Korean) 7-27503
 Fe_2O_3 nearly spherical particles in low mag. fields, mag. props. 7-27568
 FePga , amorphous, magnetoelastic props. 7-27591
 $\text{Fe(Pd}_{1-x}\text{Au}_x)_3$ disordered alloys, atomic and mag. structs., Mossbauer studies (Russian) 7-17247
 Fe_3Si , near-stoichiometric high temp. creep and struct. investig. 7-22762
 $\text{Fe}_{80}\text{Si}_{12}\text{P}_{20-x}$ amorphous alloys, struct., mag. and elec. props. (Korean) 7-2893

Curie temperature continued

- $(\text{Fe}_{1-x}\text{W}_x)_{84.5}\text{B}_{15.5}$ amorphous alloys, elec. and mag. props. (Chinese) 7-12969
 FeZr , amorphous and microcryst., exchange interaction and saturation magnetisation (Russian) 7-12963
 Gd Curie temp. press. depend., Fermi surface struct. effects 7-7509
 Gd equal magnetisation lines, effective field const., paramag. Curie temp. and magnetocaloric effect 7-7546
 Gd monolayer on W, ferromag. order and crit. exponent, ESR study 7-45680
 Gd, μSR studies, Knight shifts and relax. above Curie temp. 7-45877
 Gd surface, evidence for ferromag. order above bulk Curie temp. 7-33173
 Gd-Co, amorphous, influence of hydrogenation or mag. props. 7-2899
 Gd-Fe evaporated amorphous alloy films, mag. props. and FMR behaviour studies 7-45825
 $\text{Gd}_3(\text{Ga}_{1-x}\text{Fe}_x)_2\text{O}_{12}$ and $\text{Gd}_3[\text{Al}_3(\text{Ga}_{1-x}\text{Fe}_x)_2]\text{O}_{12}$, mag. solid soln. systems for regenerator materials 7-59015
 GdNi_3 , paramag. suscept. studies 7-52935
 $\text{Ge}_{80-x}\text{Mn}_x\text{B}_{20}$ amorphous alloy, Curie point and crystallisation temp. 7-17173
 ^3He , adsorbed on Grafoil, nuclear ferromagnetism and surface ferromagnetic effect 7-2296
 HgCr_2Se_4 , stoichiometry and phys. props. investig. 7-2218
 In equal magnetisation lines, effective field const., paramag. Curie temp. and magnetocaloric effect 7-7546
 $\text{La}(\text{Cr}_x\text{Mn}_{1-x})_2\text{Ge}_2$, layer struct. intermetallic cpd., mag. props. comp. depend. studies 7-7489
 LaMn(Fe)Si_2 , struct. and mag. props. studies (French) 7-37950
 Mn-Sn, homogenised, mag. props., thermal expansion 7-2900
 $\text{Mn}_{11}\text{Ge}_8$, intermetallic compound, mag. props. 7-52985
 $\text{Mn}_{0.97}\text{Ti}_{0.03}\text{As}$, mag. phase transitions, effect of Ti additions 7-27519
 Nd-Fe-B , metastable amorphous alloys, crystn., thermal stability 7-39482
 Nd-Fe-B permanent magnets, BCC phase mag. props. at grain boundaries 7-53044
 Nd-Fe-B-Co-Al based permanent magnets, mag. props. and temp. characts. 7-53045
 $\text{Nd-Fe-C(Si)(Ge)(Pb)(Sn)}$ ternary phase studies. X-ray anal. and Curie temp. meas. 7-7508
 Nd-Fe-Co , amorphous films, perpendicular magnetic, mag. and magneto-optical props. 7-64496
 $\text{Nd}_2(\text{Fe}_{0.67}\text{Al}_{0.33})_{14}\text{B}$, reduction of mag. hyperfine fields and Curie temp. on Al substitution, Mossbauer spectra 7-38859
 $\text{Nd}_2\text{Fe}_{14}\text{B}$, magnetic props., H_2 absorption effects 7-38906
 $\text{Nd}_2\text{Fe}_{23}\text{B}_3$, struct., Curie temp., X-ray diffraction anal. 7-11994
 NdFeBCoAl magnets, Curie temp., coercive force and magnetisation 7-52982
 $\text{Nd}_2\text{Fe}_{14-x-y}\text{Co}_x\text{Al}_y\text{B}$ alloys, permanent mag. props. 7-45755
 $\text{Nd}_2\text{Fe}_{14-x}\text{Co}_x\text{B}$ system, mag. phase transitions and anisotropy 7-27524
 $\text{Nd}_2\text{Fe}_{14-x}\text{M}_x\text{B}$, ($\text{M}=\text{Co}, \text{Ni}, \text{Cu}, \text{V}, \text{Al}, \text{Cr}, \text{Mn}$), crystallographic and mag. props. 7-27522
 $\text{Nd}_2\text{Fe}_{12-x}\text{Mn}_x\text{Co}_2\text{B}$, mag. props. 7-52946
 NdFe(Mn)Si_2 , struct. and mag. props. studies (French) 7-37950
 $\text{Nd}_2\text{Fe}_{14-x}\text{Ru}_x\text{B}$ alloys, mag. props., comp. depend. study 7-7547
 $\text{Nd}_2(\text{Fe}_{0.67}\text{Si}_{0.33})_{14}\text{B}$, reduction of mag. hyperfine fields and Curie temp. on Si substitution, Mossbauer spectra 7-38859
 $\text{Nd}_{2-x}\text{R}_x\text{Fe}_{12}\text{Co}_2\text{B}$, mag. characts. 7-45670
 $\text{Nd}_2(\text{Y}_{1-x}\text{Al}_x)_{14}\text{B}$, intrinsic and permanent mag. props. (Chinese) 7-13003
 Ni (111) , electron capture spectroscopy 7-59368
 Ni (111) , secondary ion emission, temp. depend., under Ne^+ bombardment 7-64856
 Ni and its alloys, spin wave excitations and magnetisation temp. depend. 7-45642
 Ni, cryst., anomalous ion-photon and secondary ion emission mean Curie pt. 7-39343
 Ni hydroxy-mica intercalation complexes, mag. props. 7-17162
 Ni, static paramag. spin susceptibility at finite temps. 7-33138
 Ni-Cu, heterodiffusion, effect of γ -rad. (Russian) 7-44617
 Ni-Mn disordered alloys, magnetic phase diagram near multicritical point 7-59024
 $\text{Ni}_{1-x}\text{Fe}_x\text{MnSb}$, half-metallic ferrimag., mag. and crystallographic props. 7-45672
 Ni_2MnM ($\text{M}=\text{Al}, \text{Ga}, \text{In}, \text{Sn}, \text{Sb}$), Heusler alloys, Curie temp., effect of hydrostatic press. 7-64455
 $\text{PbMn}_{2/3}\text{MO}_3$, perovskite-type cpds., ($\text{M}=\text{Mo}, \text{Te}, \text{Re}$), dielec. and mag. props. 7-7650
 $\text{Pb}_{1-x}\text{Mn}_x\text{Te}$, indirect exchange interaction between Mn^{2+} ions 7-27509
 PbTe:Gd , mag. props. EPR study 7-53126
 $\text{Pb(Zr}_{0.58}\text{Fe}_{0.20}\text{Nb}_{0.20}\text{Ti}_{0.02})_{0.995}\text{U}_{0.005}\text{O}_3$ ferroelec. ceramic, TEM study 7-17272
 Pr-Fe , amorphous films, perpendicular magnetic, mag. and magneto-optical props. 7-64496
 $\text{Pr}_2\text{Fe}_{14-x}\text{Co}_x\text{B}$ system, struct. and magnetism 7-45631
 $\text{PrCo}_{1-x}\text{Fe}_x\text{B}$, crystallographic and mag. props. 7-45671
 $\text{Pr}_2(\text{Fe}_{1-x}\text{Co}_x)_{14}\text{B}$, mag. props. 7-64549
 PrMn(Fe)Si_2 , struct. and mag. props. studies (French) 7-37950
 PrNi_3 , paramag.-ferromag. phase transition, external mag. field, spin ordering model 7-52988
 $\text{Pr}_{2-x}\text{R}_x\text{Fe}_{12}\text{Co}_2\text{B}$, ($\text{R}=\text{Dy}, \text{Tb}$), mag. characts. 7-45670
 PtMnGa , Curie temp., hydrostatic press. effect 7-27527
 $\text{R}_2\text{Fe}_{14-x}\text{Mn}_x\text{B}$ ($\text{R}=\text{Y}, \text{Nd}, \text{Pr}, \text{Gd}$), mag. characts. 7-27523
 $\text{R}_2\text{Fe}_{12-x}\text{Mn}_x\text{Co}_2\text{B}$ ($\text{R}=\text{Pr}, \text{Gd}$), mag. props. 7-27500
 $\text{Sc}(\text{CO}_{1-x}\text{Al}_x)_2$, pseudobinary system, weak itinerant ferromagnetism 7-2825
 Si-Fe BCC alloy , struct. and mag. props., order-disorder transition effects (Russian) 7-32346
 SmMnSi_2 , struct. and mag. props. studies (French) 7-37950
 TbAg amorphous alloys, local mag. anisotropy energy estimation 7-7503
 TbFe amorphous alloys, local mag. anisotropy energy estimation 7-7503
 TbFeCo -based amorphous films, magneto-optical recording apps. 7-53074
 $(\text{Tb}_x\text{Fe}_{1-x})_y\text{U}_y$, amorphous, magneto-optical effects 7-59187
 $\text{Tb}_2\text{Gd}_{1-x}\text{Al}_2$, intrinsic low field susceptibility studies 7-45633
 $(\text{Tb}_{1-x}\text{Y}_x)_2$ ferrimagnetic alloy, sp.-ht., Curie temp. and density of states comp. depend. meas. 7-7514
 Tm , polycrystalline, electrical resistivity, mag. struct. effect 7-52564
 TmNi_2 , singlet ground-state cpd., induced-moment ferromagnetic ordering meas. 7-38866
 U-Cu-P(As) , ternary particles, cryst. struct. and mag. props. 7-12955
 U-Ni-As(P) , ternary particles, cryst. struct. and mag. props. 7-12955

Curie temperature continued

- $U_2Gd_{1-x}Ga_x$ Curie temp., loss of ferromagnetism, comp. depend, competing exchange interactions 7-12970
 UNi_2 , polarised neutron diffraction study 7-12946
 $U_3Sb_2Cu_2$, crystal structure, mag. props. 7-38864
 $U_2Y_{1-x}Ga_x$, Curie temp., loss of ferromagnetism, comp. depend, competing exchange interactions 7-12970
V, surface (100)p(1×1), ferromagnetic order, electron capture spectra studies 7-27526
Y(Dy)(Er) $_{2-x}$ Th $_x$ Fe $_{14}$ B alloys, mag. props., comp. depend. study 7-7492
 $Y_2(Fe,Al,Co)_{14}B$, mag. props., composition depend. 7-53030
 $Y_2Fe_{14}B$, magnetic properties, H_2 absorption effects 7-38906
 $Y_2Fe_{14-x}Si_x(Cu)B$ alloys, mag. props. 7-45681
YIG, critical mag. relaxation, ESR linewidth 7-22106
 $Y_5Ni_{10}H_x$ amorphous thin films, mag. and elec. transport props., H content effect, 1.5 to 400K (Chinese) 7-38909
 $(Y_xZr_{1-x})Co_{2.9}$, crystal structure, mag. props. 7-51719

Curie-Weiss law *see* magnetic susceptibility; paramagnetic properties of substances; paramagnetism

Curium

see also nuclei with

- aqueous soln., reaction rate consts. of radiation-produced transients 7-60903
neutron-activation detectors with fissionable nuclides 7-56907
solid state and thermodynamic props., f-electron bonding and structure, review 7-12321
 $Ca_2Nd_3(SiO_4)_6O_2$:Cm, radiation effects, appl. for nuclear waste disposal 7-32522
 $Ca_2Nd_3(SiO_4)_6O_2$:Cm ceramic simulated nuclear waste forms, radiation effects on microstructure and fracture props. 7-58373
 $CaZrTi_2O_7$:Cm, radiation effects, appl. for nuclear waste disposal 7-32522
 ^{242}Cm , Curie quantity source preparation 7-19599
 ^{244}Cm and ^{239}Pu , lung clearance and translocation following inhalation, rat obs. 7-34290
 $Gd_2Ti_2O_7$:Cm, radiation effects, appl. for nuclear waste disposal 7-32522

Curium compounds

- CmO_2 , photoacoustic-spectroscopy 7-27731

Current (electric) *see* electric current

Current algebra

see also elementary particle theory; hadron current; light cones; quantum field theory

- Abelian gauge theories, systematic search in n-dimensions. Minkowski space 7-4973
axial vector current props., γ_5 and dimensional regularisation 7-61504
bound states and asymptotically free quarks, duality relations 7-5050
BRST analysis of super Kac-Moody and superconformal current algebras 7-4996
conformal and current algebras on a general Riemann surface 7-56475
conformal invariant field theory, current algebra, group theoretic anal. 7-35710
constituent quark model picture for non-leptonic hyperon decays 7-49139
electromagnetic and hadron radiation 7-10031
electroweak interactions with the nucleon and tests of the standard model 7-61513
Fermi decays, verification of conserved vector current and standard model predictions 7-19208
free fermionic currents, Jacobi identity failure, rel. to axial anomaly 7-56469
interacting field theory in 2D, Sugawara-Sommerfield construction 7-48986
Kac-Moody current algebras of 2D massless gauge theories 7-61505
lattice Monte Carlo simulation with Wilson fermions, current algebra, quark masses 7-15069
lattice QCD with Susskind fermions, current algebra relation 7-41730
locally supersymmetric string Jacobian 7-35383
model independent exchange current determ. in e^- scatt. and baryons as topological solitons 7-35743
N=1 super-Poincaré superspace current, model-independent improvement 7-49018
N=1 superspace translator tensor, improved Minkowski-space currents and residual shifts 7-5007
neutrinoless double β -decay without Majorana neutrinos in supersymmetric theories 7-61839
quark currents, complete bosonisation, quantum theory based on anomalies 7-30240
sigma model, geometrostatics and current algebra on supergroup manifolds 7-56411
sigma model, SU(2), Wess-Zumino term calcs., chiral currents, Kac-Moody algebraic props. 7-61427
singlet form factors and local observables in the Glashow-Weinberg-Salam model 7-5014
Skyrme model, expressions for various currents using gauge transformations 7-30162
Skyrme model, recent developments in context of QCD, review 7-414
standard six-quark model with hierarchical symmetry breaking, quark mixing, mass generation 7-5065
string propagation and affine Lie algebras on group manifolds 7-35814
string theory, energy-momentum tensor and conserved currents 7-35833
SU(3) current algebra, nonlocal 7-56470
super AKNS scheme and its infinite conserved currents, 3×3 eigenvalue problem 7-434
two-body relativistic systems, bound-state solns., invariant scalar products and conserved currents 7-48984
Ward identities and chiral anomalies in stochastic quantization 7-24774
weak axial nuclear exchange current and the many-body force 7-56614
Yang-Mills theory, covariant Lie variations and conformally conserved currents 7-48951
 $D^0 \rightarrow K^0 \phi$, dynamical enhancement from current algebra, hard meson techniques 7-49136
 $K \rightarrow \pi\pi$ amplitude, kaon-to-vacuum weak matrix element, soft pion techniques 7-49135
 $\mu^+ \rightarrow e^+ \gamma$, search for right-handed currents 7-15151
 $\nu(\bar{\nu})N \rightarrow \pi X$, diffractive PCAC dominated π -production 7-15143
 $\nu_\mu d \rightarrow \mu^+ pp$, pion exchange current effects 7-56559
dq plasma near equilibrium, kinetic coeffs., colour density matrix 7-10023
 $\gamma\gamma$ -pion pairs, comparison with current algebra 7-565

Current control, electric *see* electric current control

Current density

- see also* critical current density (superconductivity); electron density
arcs critical current density, V-I characts. 7-26553
chemisorbed atoms, electronic structure and tunnelling current 7-6962
conducting plate eddy current density and force on moving filament 7-62583
corona discharge, unipolar space charge flow 7-26567
corrosion rates determ., polarisation curves, mass transport effect 7-28191
DC ionised field quantities as influenced by coronating conductor surface gradient 7-58074
eddy currents in conducting slab under moving parallel circular current loop 7-62581
elliptic conductors, boundary-matching method 7-36849
Faraday cup to measure ion current in a strong magnetic field 7-19597
Frascati Tokamak, confinement and heating study 7-6438
ion beam generation and focusing from conical pinched electron beam diode 7-11806
linear particle transport theory, current density transients 7-56191
metals, nonlocal cond., microwave radiation transmission 7-13269
mirror-trapped collisional plasma, axial confinement, mirror ratio scaling 7-37727
molecular gas, beam-plasma discharge at retarding pot. 7-37705
monitor for intense relativistic electron beams 7-19595
one-dimensional disordered Hubbard chain, high-field dynamical theory far from equilib. 7-2447
p-n-p-n structures, on state spreading, diffusion and drift ratio 7-21937
quantum-box lasers, 3D, gain and threshold current density 7-10937
thyatron current and plasma quantities intrinsic relationships, thyatron plasma cond. 7-32121
tokamaks, natural current profiles 7-37721
toroidal plasma equilibria in an external magnetic multipole field 7-1726
trifluoromethanesulphonic acid electrolyte in fuel cells, O solubility, diffusion coeff., reduction rate, adsorption on Pt surface 7-28395
vacuum arcs, high current, anode discharge mode and cathode plasma state 7-44284
(AlGa)As-GaAs DQW-SCH lasers grown by MOCVD, design, fabrication and characterisation 7-36990
AlGa $_{1-x}$ As-GaAs LOC lasers for high power low threshold current density operation, optimisation 7-10934
GaAs-GaAlAs heterostructures, dissipationless quantum Hall effect, critical current density meas. 7-2696
GaInAsSb/AlGaAsSb injection lasers, threshold current density reduction 7-5886
H $^-$, D $^-$ vol. prod. ion source by sheet plasma, proton accelerator and thermonuclear fusion research applications (Japanese) 7-5511
H $_3$ PO $_4$ electrolyte in fuel cells, O solubility, diffusion coeff., reduction rate, adsorption on Pt surface 7-28395
 3He , superfluid B-phase, orbital ang. momentum in mag. field 7-38289
La $_0.7$ Sr $_0.3$ CoO $_3$ cathodes for CO $_2$ waveguide lasers, electrical and emission characts. 7-59383
Nd $_0.7$ Sr $_0.3$ CoO $_3$ cathodes for CO $_2$ waveguide lasers, electrical and emission characts. 7-59383
Pt anode in fuel cell, performance in presence of CO and CO $_2$, CO poisoning adsorption parameters calc. 7-13855

Current distribution

- see also* current density
gyrotropic media, scalar Hertz potentials for transversally oriented current density distrib. 7-57205
stratified media, current source in presence of insulating and conducting disks 7-25699
thick cylinder eddy current distrib. and losses due to exterior circular currents 7-62587
thick cylinder eddy current distrib. and losses due to interior circular currents 7-62586
two-electrode semiconductor systems, electric field, resistance and current distrib. calc. 7-38600

Current fluctuations

- see also* noise
1/f noise, carrier mobility fluctuation origin 7-38653
nonlinear conductors, current noise (French) 7-7298
tunnel junctions, prism coupled light emission 7-38770
Fe-Cr, passive current fluctuations, statistical anal. 7-28190

Current limiters *see* limiters

Current measurement, electric *see* electric current measurement

Current mirrors *see* amplifiers

Current transformers

- see also* electric current control; electric current measurement
50 kA current transformer intercomparison between China and West Germany 7-18815
educational applications 7-35177
S-1 spheromak, current transformer 7-32055
spheromak plasma, mag. flux injection through inductive transformer 7-32056

Current transients *see* transients

Currents algebra *see* current algebra

Curvature measurement

- drop curvature meas. by differential interferometry 7-41339

Curvature of field *see* aberrations

Curve fitting

- AC/DC transfer instruments comparison using digital bridge 7-18835
Cauvery River and its tributaries, India, flow data, fit of gamma probability distrib. 7-55093
cubic B-splines in least-squares smooth fitting for irregularly spaced data 7-47555
digital image input devices, resolution, curve-fitting method 7-57600
Fourier transform IF self-deconvolution for protein structure, determ. 7-54476
Kurosu's method for fitting curve to data (Japanese) 7-41084
metal surfaces, quantitative analysis using XPS or AES, data reduction techniques 7-28371
overlapped bands resolution by Fourier method 7-48885
peak-separation algorithm for personal computer, appl. to visible emission and IR absorpt. spectra (Japanese) 7-31015
radioimmunoassay data processing software 7-40284
solar cell I-V characteristics, parameter recovery, curve fitting error criteria 7-39995

curve fitting continued

- solar cell I-V characteristics 7-8411
- CaBr, pot. energy curves and dissociation energy, curve fitting procedure 7-36511

cutting

- see also machine tools; machining
- ceramics, abrasive wear, fine-scale, by plastic cutting process 7-3458
- ceramics and coated carbides for matching stainless steels, failure mechanisms 7-3432
- cornea cutting for implantation by microsurgery robot (*Japanese*) 7-14153
- optical fibre cutting tool, automatic, design and development 7-15998
- plasma appls. in industry (*French, English*) 7-20966
- steel, high speed, wear mechanisms and tool life rel. to microstruct. 7-8128
- tool materials, statistical wear model, appl. to machining 7-33804
- Si, cutting of single crystal, surface damage anisotropy 7-13664
- Si, layers damaged by cutting, struct., X-ray diff. obs. 7-2401
- Si₃N₄ based composites, design and wear resist. 7-3459
- Ti-N reactively ion plated coatings on high speed steel, turning performance, wear 7-46656

CVD see chemical vapour deposition**CVD coatings**

- borophosphosilicate glass film, rapid isothermal fusion 7-21425
- C thin films, RF discharge deposition, mech., elec. and optical props. 7-22509
- diamond, Raman and IR spectroscopy study 7-17428
- diamond crystallisation, conf., Warsaw, Poland (June 1985) 7-18469
- diamond films, microwave plasma CVD synthesised, thermal conductivity meas. 7-38417
- diamond layers, crystallisation from gas phase, growth kinetics (*Russian*) 7-22505
- metal nitride films, prep., props., microelectronics appls. 7-33557
- photoformation of dielectric materials, review 7-53633
- plasma-enhanced, plasma-surface interactions, book contrib. 7-27943
- polysilicon thin films for VLSI, elec. props. 7-38789
- polysilicon-SiO₂, surface texturing effect on SiO₂ cond. and breakdown 7-39773
- polyvinyl carbazole plasma CVD thin films, photoconductive props. study, IR and UV spectra meas., electrode effects 7-27367
- polyvinyl carbazole thin films, plasma-CVD polymerised, photoconduction props. 7-38628
- ring resonator fabricated in phosphosilicate glass films deposited by CVD 7-15968
- structural, mechanical and tribological props. and applications 7-53935
- transition metal amorphous alloy coatings, microindentation response, microstruct. and composition effects 7-46625
- Ag/AgCl electrodes fabricated with IC-compatible technologies, chemical sensor reference appl. 7-8343
- Al film, laser deposition for metallisation 7-53631
- AlAs-GaAs superlattice, Si⁺ implantation, depth dependent mixing 7-27032
- AlGaAs terrestrial solar cells, high-efficiency concepts 7-8390
- AlN amorphous film, plasma CVD from metal organic Al source 7-52368
- AlN-sapphire, low temp. epitaxial film growth 7-13387
- Al₂O₃, CVD, morphology rel. to growth conditions 7-17431
- α-Al₂O₃, CVD coating morphology, trace impurity effects 7-3191
- Al₂O₃ CVD coatings, high-temperature microhardness profiles 7-28181
- Al₂O₃ thin films, electron emission characts., continuous dynode appl. 7-17376
- Al₂O₃:C,S CVD layers, C and S distrib., SIMS anal. 7-6668
- Al₂O₃-TiC, on cemented carbides, diffusion of Co and W, TEM/AES study 7-27942
- BN films, microwave plasma CVD process 7-17435
- c-BN, phase diagram, p,T,E 7-17517
- Bi₂O₃ dielectric films, activated reactive evaporation using resistively heated sources 7-13383
- C films, diamond-like, microwave plasma CVD process 7-17435
- C insulating films for MIS struct., interfacial characts. 7-2732
- C layers, deposition, by RF plasma decomp., physical props. 7-22508
- a-C:H polymeric layers, plasma-activated CVD produced, spectroscopic investigations 7-22572
- a-C:H polymeric plasma-activated CVD films, tribological and mechanical props. studies 7-16920
- CdTe, polycryst., grown by UV-enhanced OMCVD, picosecond photocond. 7-52873
- CdTe thin film heterojunction solar cells 7-17914
- CdTe thin film solar cells, efficiency improvement 7-17883
- CoB layers and crystals, prep. by diffusion and CVD processes 7-17434
- CoSi layers, prep. by Co siliconisation using Si₃Cl₆ source by diffusion and CVD processes, microhardness meas. 7-17700
- Co₂Si layers, prep. by Co siliconisation using Si₃Cl₆ source by diffusion and CVD processes, microhardness meas. 7-17700
- CrC_x coatings, tribological props., comp. depend. studies 7-53914
- Fe thin films, formed by laser breakdown CVD, metastable phase form. 7-38377
- γ-Fe₂O₃ films, CVD deposited, uniaxial mag. anisotropy 7-33234
- Fe₂O₃ polycryst. photoactive MOCVD films, photocond. and time-resolved microwave cond. meas. 7-45386
- GaAlAs MOCVD layers, stoichiometry variation determ., pulsed laser atom probe anal. 7-12305
- GaAlAs-GaAs heterostructures grown by MOCVD, transition region, ellipsometric anal. 7-2388
- GaAlAsGaAs quantum well heterostructures, grown by MOCVD, props. 7-45479
- GaAs films on amorphous insulating substrates, laser recrystallisation 7-38397
- GaAs photoluminescence rel. to Si substrate orientation 7-53411
- GaAs single domain layer growth on Si wafers by MOCVD/MBE, heteroepitaxy 7-52357
- GaAs:Si,Se MOCVD epitaxial layer photolum. spectral shift and doping efficiency obs. (*Japanese*) 7-45076
- GaAs/AlAs:Mg/GaAs tunnel structs., current transport mechanisms 7-7357
- GaAs/AlAs/GaAs:Se heterojunctions, elec. behaviour, DLTS studies 7-7360
- GaAs-Si₃N₄ interface, multipolar plasma deposition, high resolution electron microscopy study 7-12499

CVD coatings continued

- GaAs_{1-x}Al_xAs MQW, MOCVD grown, excitons, photoluminescence spectra 7-38702
- GaAsP terrestrial solar cells, high-efficiency concepts 7-8390
- GaAsSb terrestrial solar cells, high-efficiency concepts 7-8390
- GaInAs terrestrial solar cells, high-efficiency concepts 7-8390
- GaInAs-InP double-barrier heterostructs., room temp. resonant tunnelling, neg. resist. effects 7-58814
- Ga_{0.47}In_{0.53}As-InP heterojunction, MOCVD grown, 2D hole gas 7-21992
- Ga_{0.47}In_{0.53}As-InP superlattices, MOCVD grown, room temp. excitons 7-21986
- In_{2-x}Sn_xO₃-γ-WO₃-MgF₂-Au, electrochromic coatings for solar windows 7-53621
- Mo CVD coating on graphite, struct., thermal resist. props. 7-52375
- Nb₂Ge, high supercond. transition temp., struct. instabilities and electronic props. 7-58943
- Nb₂Ge tape conductors, CVD deposited, compositional distrib. and superconducting props. 7-58936
- Ni, siliconised layer form. by diffusion and CVD, oxidation and corrosion resist. 7-59659
- Ni single crystal films, resistivity ratio and mean free path length 7-52857
- Ni thin films, formed by laser breakdown CVD, metastable phase form. 7-38377
- Ni-Zn ferrite and Ni ferrite films, prep., mag. props. 7-13378
- P₂O₅-B₂O₃-SiO₂ CVD glass films, components characterization 7-45085
- PbTe films and electrical contacts with Au, Al and Ag, photothermal deflection meas. 7-38784
- SAW device, coating responses, rel. to solubility and chem. struct., pattern recognition 7-54162
- Si, amorphous film, density-of-gap-states distrib. field effect meas. analytic determ. 7-52391
- Si, CVD in annular tubes, film thickness profiles in mixed convection-diffusion regime 7-27190
- Si CVD thin film, struct. and elec. props. 7-21730
- Si, CVD thin film backside gettering effectiveness 7-38217
- Si, deposition by photolytic or pyrolytic dissociation of SiH₄ under laser irradi. 7-13388
- Si doped, laser deposition for interconnections 7-53632
- Si films, structural changes due to annealing 7-52346
- Si polycrystalline CVD film, etch rate free carrier depend., doping level and grain size depend. meas. 7-28219
- Si polycrystalline films, optical props. 7-7782
- Si polycrystalline films on (100) Si substrate, epitaxial alignment using rapid thermal processing 7-38413
- Si, polycrystalline layers, TEM meas. of grain size 7-32672
- a-Si, prep. by low press. CVD, characts. 7-7884
- a-Si solar cells, conversion efficiency improvement 7-17879
- Si:B, amorphous, solar cell, roll-to-roll mass prod. process 7-17902
- a-Si:H, RF glow discharge prod., high deposition rate study 7-7889
- Si:H binary alloys, crystallisation of polysilane 7-21105
- a-Si:H CVD coating, high temp. elec. cond. meas. 7-45336
- a-Si:H CVD films, density of states distrib., I-V characts. meas. 7-45113
- a-Si:H film, photoenhanced deposition and characts. 7-53635
- a-Si:H films, annealing, compressive stress, H evolution 7-28059
- a-Si:H films, photocond. characts. stabilisation (*Japanese*) 7-45393
- a-Si:H films photo-CVD, photoelectric and structural props. 7-7869
- a-Si:H films preparation by CVD 7-17453
- a-Si:H photo-CVD coatings, characterisation using TFT structure 7-38561
- a-Si:H solar cell prep. by laser-induced CVD of SiH₄ 7-7890
- a-Si:H solar cells, photo-CVD prep. 7-17885
- a-Si:H solar cells prod. by positive-column glow-discharge method 7-8397
- Si:H(F)-Si:Ge:H(F) amorphous multilayer struct., fabrication and near IR photoconductivity characts. 7-52797
- Si:P polycrystalline films, segregation at grain boundaries, NMR study 7-38953
- Si:P(B) LPCVD films, amorphous and polycrystalline, struct., elec. resist. meas. 7-52870
- Si-SiC superlattice structs. prep. by photo-CVD, solar cell appl. 7-54326
- SiC, cubic, epitaxial films, compensation 7-7268
- SiC film, laser deposition for solar cell use 7-53634
- 3C-SiC, n- and p-type epitaxial CVD layers, elec. props. temp. depend. studies 7-58917
- SiC:H, amorphous CVD film, electron optical characterisation 7-52372
- a-SiC:H alloys for solar cells, electronic and optical props. 7-17899
- a-SiGe:H solar cells preparation by photo-CVD 7-17885
- SiN film CVD coatings, Al void form. suppression in MOS struct. 7-7406
- a-SiN_x:H CVD film, IR and ²⁹Si NMR studies 7-38952
- a-SiN_x:H plasma-enhanced CVD film props. rel. to SiH₄-N₂ gas vol. ratio, RF power and substrate temp. (*Korean*) 7-3201
- Si₃N₄ CVD film, prep. and props. 7-46337
- Si₃N₄, CVD from Si₃Cl₆-NH₃-H₂ gas mixture 7-22560
- Si₃N₄ CVD layers, etch rate modification by ion bombard. and annealing 7-28217
- Si₃N₄ films, IR charactn., optical dispersion induced freq. shifts 7-27709
- Si₃N₄ films in MIS structs., cond. characts. 7-38793
- Si₃N₄ films prep. by ECR plasma CVD, phys. and elec. props. 7-58716
- Si₃N₄ LPCVD films, bombardment induced H redistribution 7-38404
- Si₃N₄, plasma CVD on steel substrate (*Japanese*) 7-27939
- Si₃N₄, surface structure and chemisorption, XPS, AES and direct recoil studies 7-32790
- Si₃N₄ thin films, electronic conduction 7-58932
- Si₃N₄/GaAs buried interface, EXAFS studies in total reflection and dispersive modes 7-64765
- Si₃N₄-SiC film, hybrid material prepared by plasma CVD, microhardness and internal stress 7-13616
- Si₃N₄-SiC film, hybridisation by plasma CVD 7-13379
- Si₃N₄-H, films, synchrotron radiation excited CVD, deposition mechanisms and H content 7-52369
- SiO₂ CVD photox layers, Hg-sensitised, elec. props. 7-64379
- SiO₂ films, LPCVD from diacetoxymethylbutoxysilane in temp. range 450 to 600°C 7-53622
- SiO₂ films, low temp. CVD, dielec. const., dissipation factor 7-59149
- SiO₂ films, prod. by low temp. CVD, role of carrier gas in deposition kinetics 7-59452
- SiO₂, low temp.-CVD films, DC dielec. breakdown studies 7-22188
- SiO₂, plasma assisted vapour deposited and laser fused coatings, corrosion protective props. 7-28208

CVD coatings continued

SiO₂-P₂O₅ glass films, deposited by different CVD methods, phys. props. 7-27220
SiO_x thin films, plasma enhanced CVD deposited, Si chem. states, IR spectra, XPS, AES 7-21721
SiO_xP films, pure and doped, low press. CVD growth, structural, optical, elec. props. 7-27186
SiON-GaAs interface, plasma enhanced CVD deposited SiON, NH₃ plasma pretreatment effects 7-7874
SiO₂N_x films, PECVD deposited, props. as selective diffusion barrier 7-2440
SiO₂N_x films, plasma-enhanced CVD deposited, annealing 7-32861
SiO₂N_x plasma-enhanced CVD films as selective Zn diffusion barriers 7-12539
SiO_xN_y LPCVD layers, phys. and elec. charactn. 7-38792
SnO₂ films for solar cells, struct., elec., and optical props. 7-40003
SnO₂ pure and F doped CVD films, UV absorpt. props. study 7-22370
SnO₂:F thin film, uses for a-Si:H/a-Si_{1-x}C_xH solar cells 7-46952
SnO₂-Si (100), CVD coatings, X-ray studies 7-7886
TaSi₂, LPCVD process 7-59449
TiB₂, plasma-enhanced CVD films on Si, furnace annealing, metallisation appls. 7-38411
Ti(C, N) CVD coatings, morphology and struct. 7-58712
Ti(C,N) films on steel substrates, residual stress 7-52373
TiC, amorphous films, prep. and characts. 7-7885
TiC and TiB₂ coatings, effect of stoichiometry on D retention, thermal desorption study 7-6997
TiC CVD coatings, plasma exposure in mag. fusion devices 7-42193
TiC coated cemented carbide cutting tool inserts, performance and material props. 7-46712
TiC, on cemented carbides, diffusion of Co and W, TEM/AES study 7-27942
TiC_x coatings, tribological props., comp. depend. studies 7-53914
TiCN, TiC and TiN CVD coatings, high-temperature microhardness profiles 7-28181
TiN coated carbide indexable inserts, spalling resistance 7-53933
TiN coated WC-Co, residual stress and strength, X-ray diff. study (Japanese) 7-8101
TiN films on tool steel, plasma-assisted CVD deposited, interfacial composition 7-52303
TiN protective coatings on cemented carbides, adhesion and toughness 7-65159
TiSi₃, plasma-enhanced CVD films for interconnect appls. 7-52342
W CVD films, chem. charactn. 7-16915
W CVD films, high temp. stress meas. 7-58718
W CVD films, nucleation on insulators and surface reaction with Si 7-16911
W CVD films on Si substrate, growth kinetics and elec. props. 7-16909
W films, LPCVD deposition kinetics in single wafer vacuum reactor 7-59448
W films by selective LPCVD, struct. charactn., diffusion barrier appls. 7-17468
W films prep. by various deposition methods, effects on elec. resist. 7-52860
W LPCVD film struct., IC appls. 7-58692
W LPCVD film thickness depend. on native oxide thickness 7-17473
W LPCVD from W(CO)₆ in hot-wall environment 7-17465
W nonselective CVD films, adhesion to SiO₂ 7-17760
W selective CVD films, diffusion barrier props. 7-52155
W selective LPCVD films on Si substrate, characts. 7-38409
W selective LPCVD layers on Si substrate, interfacial struct. 7-16883
W, selective LPCVD on Si substrate, elec. and struct. props. 7-17467
W selective low press. CVD growth on Ti, TiSi₂ and PtNiSi, surface reactions, struct. 7-27183
W-Si interface, thermal behaviour rel. to silicide form. 7-16822
W-Si interfaces, microstruct. charactn. 7-16882
W-Si system, silicidation reaction suppression up to 1100°C 7-16821
WC_x coatings, tribological props., comp. depend. studies 7-53914
WSi_x CVD films, high temp. stress meas. 7-58718
WSi_x CVD films on Si and Si₃N₄ coated Si, excess Si redistribution upon annealing 7-21723
WSi_x films, CVD, resistivity and composition changes by annealing 7-2738
Zn_xCd_{1-x}Te thin film heterojunction solar cells 7-17914
ZnS, epitaxial film, TEM and photoelectron study 7-53408
ZnSe:Al, MOCVD growth, deep level characterisation 7-52519
ZnSe:As, MOCVD growth, exciton and deep emission bands 7-52367
ZnSe/GaAs interface, MOCVD grown, ZnSe film stoichiometry 7-39415
(ZnSe)_x(CdTe)_{1-x} films, CVD fabricated, phys. props. 7-7055

CVD epitaxial growth see vapour phase epitaxial growth

CVD thin films see CVD coatings

cyanogen, C₂N₂ see carbon compounds

cyclotron resonance

for ion cyclotron resonance spectroscopy see mass spectroscopy; for ion cyclotron resonance heating see plasma heating
see also diamagnetism; dopplers
CT-6B tokamak discharge, electron cyclotron resonance preionisation (Chinese) 7-58031
dirty semiconductors, parametric cyclotron resonance, inelastic electron scatt. from phonons 7-2466
electron beam acceleration by large amplitude Em wave in uniform mag. field 7-10308
electron gas, 2D, cyclotron resonance linewidth due to alloy scatt. 7-27399
free electron tunnelling transitions scale time determ. at cyclotron reson., semiclassical approx. calcs. 7-48446
ion beam, phase indication 7-22144
Landau level broadening, 2D electron gas in strong electric field 7-52455
metal plates, Doppler-shifted cyclotron resonance and skin effect 7-17224
metals, anomalous skin effect, Fermi surface curvature effects (Russian) 7-58827
multiphoton excitation of relativistic cyclotron resonance and phase bistability 7-62761
Plasma-Materials Interactions Test Facility electron cyclotron resonance microwave plasma system 7-51477
quasi 2D electron gas in quantum well, cyclotron reson. lineshape calcs. 7-27269
relativistic cyclotron resonance maser linear theory with resonant electrodynamic systems 7-62658
two-dimensional polaron, cyclotron reson. spectrum calc. 7-45175

cyclotron resonance continued

Al_{1-x}Ga_xAs heterostructures, 2D electron space charge layers, plasmon and magnetoplasmon excitation 7-38696
Bi, nonlinear cyclotron resonance, lineshape and mechanisms 7-32897
Bi, nonlinear size cyclotron resonance, second harmonic generation calcs. (Russian) 7-13036
GaAs 2D electron gas, dynamical cond., IR cyclotron reson. meas., electron interaction effects 7-45195
GaAs, electron scattering in quantum limit 7-38552
n-GaAs films, magneto-optical studies under high hydrostatic press. 7-13247
GaAs/GaAlAs 2D electron gas, cyclotron resonance study 7-2676
GaAs-Al_{1-x}Ga_xAs heterojunctions, subband Landau-level spectroscopy 7-21996
GaAs-GaAlAs heterojunctions, cyclotron resonance, screening effects 7-38706
GaAs-GaAlAs heterojunctions, electron-phonon interactions, cyclotron and magnetophonon reson. meas. 7-45463
GaInAs/InP heterojunction, 2D electron gas nonequilib. cyclotron reson. obs. 7-12845
Ga_{0.47}In_{0.53}As/InP heterojunction, chem. beam epitaxy grown, 2D electron gas 7-12803
Ge, electron irradi., hole effective mass parameters, cyclotron reson. 7-58730
Ge hot-hole cyclotron resonance maser with negative effective hole masses 7-15838
HgCdTe IR photodetectors, magnetoresist. and cyclotron resonance characterisation 7-64054
n-Hg_{0.8}Cd_{0.2}Te accumulation layer electrons, tilted field cyclotron resonance 7-7591
InAs/GaSb quantum well, 2D electron gas, cyclotron reson. oscills. meas. 7-38944
In_xGa_{1-x}As-In_yAl_{1-y}As heterojunction, cyclotron resonance linewidth due to alloy scatt. 7-27399
InSb, cyclotron resonance harmonics in conduction band, obs. 7-53136
InSb, electron inversion layers, cyclotron and electron spin resonance 7-38736
KCl, muonium to diamagnetic muon conversion, time-differential muon spin reson. meas. 7-13070
NaCl, muonium to diamagnetic muon conversion, time-differential muon spin reson. meas. 7-13070
Pb_{0.98}Yb_{0.02}Te, cyclotron resonance meas., k.p model calcs. 7-27605
Te, cyclotron reson. characts. of nonequilibrium carriers at low temps. 7-64532
W, electromagnetic absorption of ultrasound near Doppler-shifted cyclotron resonance 7-45402

cyclotrons

see also microtrons; synchrocyclotrons
beam extraction system and extracted beam emittance, transmission matrix calcs. (Chinese) 7-5522
pseudo-monoenergetic neutron beam course from 15 to 40 MeV for activation cross section measurements 7-30820
residual radioactivity in components and surroundings 7-8701
RIKEN Ring Cyclotron and its experimental program 7-36355
superconducting cyclotron at Chalk River, operation 7-62151
trim coils power supplies for the Milan Superconducting Cyclotron 7-25272
U-150 cyclotron neutron time of flight spectrometer 7-36376
¹⁴C, radiocarbon dating using low energy cyclotron 7-55310
H⁺ beam dynamics, mag. field studies in cyclotron 7-62168
H⁰ variable beam extraction from the Univ. of Manitoba Cyclotron 7-49764
²⁰Ne³⁺ and ²⁰Ne⁴⁺ ion acceleration at the U-120 cyclotron (German) 7-56887

cytology see cellular biophysics

Czochralski method see crystal growth from melt

D-layer see D-region

D mesons

exclusive decays, CP violation, phenomenology 7-41656
inclusive production, quark-gluon-string model 7-41750
lifetime meas. in NA27 expt. 7-61662
D → $\nu\ell(\omega\mu)$, branching ratios and $\nu\ell$ mass limits 7-24884
D → γX , helicity suppression and colour thaw problem 7-61590
D-mesons, vacuum insertion and nonperturbative effects 7-10057
D⁻ lifetime meas. from e⁺e⁻, 29 GeV 7-19098
D⁰ → K⁻π⁺ lifetime meas. 7-41795
D⁰ → K⁻π⁺π⁺ lifetime meas. 7-41795
D⁰ → K⁰φ, branching ratio meas. 7-61661
D⁰ → K⁰φ, dynamical enhancement from current algebra, hard meson techniques 7-49136
D⁰ → K⁺π⁻, search for wrong-sign decays 7-35860
D⁰ lifetime meas. 7-19106
D⁰ lifetime meas. from e⁺e⁻, 29 GeV 7-19098
D⁰ → φK⁰, anal. using algebraic method with hard-meson extrapolation 7-19103
D⁰ D⁰ system, partial decay rate asymmetries, CP violation 7-35864
D⁺ → K⁺π⁺π⁺ lifetime meas. 7-41795
D_s → KKπ, mean lifetime and mass meas. 7-61656
D_s → φπ⁺, lifetime meas. using TASSO 7-24882
D⁰*(2420), candidate for Qq bound state, semi-relativistic anal. 7-61545
e⁺e⁻ → mesons, D⁰ D⁰ mixing signature 7-24894
e⁺e⁻ → D⁰*X, production cross section meas. at 29 GeV 7-56561
e⁺e⁻ → D⁺*X, cross-section, fragmentation function and forward-backward asymmetry 7-15167
γγ → D⁰*X, inclusive production, event rate and topology 7-61782
pp → D(D⁰)X, inclusive cross-sections, comparison with fusion. model 7-49191
pp → X, charm particle prod., cross sections and characts. 7-5131
D⁺ → μ⁺ν_μ, R₁ = Γ($\bar{\nu}_e \rightarrow \gamma \gamma$) / Γ(D⁺ → μ⁺ν_μ) calcs. bound state quark model anal. 7-61582
D⁰ → K⁺π⁺γ, fragmentation function meas. 7-56561

D-region

charged particle fluctuations in lower ionosphere, assoc. scale times and scale lengths 7-29359
disturbance signatures during substorm growth phase and onset 7-29335
dynamical regime over E Siberia, meas. during quiet and disturbed conditions 7-47614
electron densities during auroral radio absorption events 7-29334
electron density at mid-latitude, seasonal behaviour 7-9291

D-region continued

- electron density profile determ. using antenna outputs of VLF waves (Japanese) 7-66394
 incoherent scatter radar probing 7-9211
 ion composition use for mesosphere H₂O estimation 7-60435
 long-distance 40 kHz signals propag., effects of geomag. storms on sunrise fading 7-55360
 negative-ion photodetachment at sunrise, radar obs. in auroral-zone mesosphere 7-66376
 radio waves absorpt. during solar eclipse, 1.8 and 2.2 MHz obs. 7-29361
 radiowave propagation, artificial periodic inhomogeneities formation, attachment and recombination processes 7-60443
 solar flare induced changes in total electron content, 24 April 1984 flare (Chinese) 7-4251
 winter anomaly of D-region, numerical calcs. 7-47620
 winter ionisation anomaly, effects on propag. of LF (40 kHz) radio waves 7-47611
 winter-time D-region, electron densities and wind vels. from partial refl. radar obs. 7-47612

D/A conversion *see digital-analogue conversion***dairying**

- milk pasteurization using solar pipe collectors 7-23218

damage, radiation *see radiation effects***damming** *see dams***damping***see also dislocation damping; internal friction*

- 1-D sound and vibration isolators based on periodic structures, connecting waveguide length optimization 7-62908
 acoustic wave, nonlinear damping in liq. with gas bubbles 7-20491
 active vibration absorber design 7-1472
 arterial occlusive disease, US, diagnosis, some failings of pulsatility index and damping factor 7-47187
 beam, two-layer cpd., damping characts., influence of quality of adhesion 7-50972
 beam structure, vibr. control using EM damper with vel. feedback, forced vibr. response 7-20618
 beam structure, vibr. control using EM damper with vel. feedback, shock response 7-20619
 beams, suppression of 1st and 2nd resonances by dynamic vibration absorbers 7-37370
 beams, symmetric laminated, optimal design considering damping 7-31639
 beating motion of a damped mechanical oscillator 7-26075
 buildings, noise and vibration control 7-6040
 car vibration isolation, optimal characts., jerk vs. acceleration 7-50980
 Collette torsion pendulum theory 7-14934
 constrained-layer model investigation based on exact elasticity theory 7-31674
 dissipative systems, Lagrangian and Hamiltonian formulation 7-18524
 dynamic reanalysis of weakly non-proportionally damped systems 7-31682
 elastic column having linear viscous internal damping, stability 7-6087
 elastodynamics with viscous damping, stress functions, axisymmetric problems 7-16064
 epoxy, Al particle filled, damping charactn., dynamic structural model appl. 7-33709
 epoxy-polyamide mixture, dynamic props. in wide temp.-freq. range 7-33721
 fibre reinforced composite, energy dissipation properties, anisotropy 7-6143
 fibre reinforced composites, damping by dry friction of dynamic loads 7-32563
 flexural wave damping, constrained-layer technique using exact elasticity theory 7-63050
 flexural wave power flow, active control 7-51009
 fluid-conveying pipe, effect of elastic foundation and dissipative forces on stability 7-1471
 galaxies spiral density waves, effects of cloud collisional damping 7-66755
 glass fibre reinforced polypropylene, damping characts. 7-59565
 glass fibre reinforced polypropylene, subjected to pure bending, dynamic tensile props. 7-46545
 harmonic oscillator, stragulation on damping, Kanai-Caldirola Hamiltonian energy dissipation anal. 7-24474
 hearing aid frequency response damping, effects on speech clarity and preferred listening level 7-8763
 hydroelastic viscous liquid system, coupled freq. 7-43674
 mammalian tissues and bones, shock-absorbing props. 7-3829
 metal-polymer composites, wear resist., damping device appl. 7-17657
 nonlinear vibration absorber, practical implementation 7-16138
 nonstationary random vibrs. of yielding multi-degree of freedom systems 7-6130
 optimum Lanchester damper for a non-linear main system 7-20631
 pendulum damping, mathematical model 7-18522
 piezoceramic-polymer-composites, damping props. 7-64575
 plate, damped elastic infinite, adjacent semi-infinite fluid, impulsive force effect study 7-63052
 plate, elliptical, oscillation problem soln. with allowance for energy dissipation 7-20641
 poly(acrylic acid)-ceramic filler composite, filler chem. influence on T_g behaviour, dynamic mech. spectroscopy 7-59559
 polyethylene, chlorinated, rutile-filled, 7-39573
 porous vibroisolator, vibration transmission analysis 7-63040
 railway brake squeal damping 7-57635
 rotors, autobalancing techniques 7-37371
 scanning tunnelling microscopy, design criteria 7-4920
 shells, axisymm., Miles' evolution eqns., simple strange attractors in struct. dynamics 7-35268
 shells, spherical, elastic, filled with compressible viscous liq., vibration damping 7-1477
 shells, spherical, orthotropic, shallow, on elastic foundation, nonlinear studies 7-37357
 steel, Cr-Ni type, temper hardened, strain rate effect on plastic deform. resist. and energy characts. 7-39601
 steel, stainless, martensitic and austenitic, amplitude depend. damping rel. to annealing and tempering (German) 7-13498
 steel sheet, hot-dipping into Al-Zn eutectoid base superplastic alloy (Japanese) 7-59664
 stochastic Korteweg-de Vries hierarchy, soliton eqns. 7-29766

damping continued

- structural elements with fibre reinforced composite coverings, dynamic stiffness and damping props. determ. method 7-31717
 synchronous vibration eliminator for an object having one degree of freedom 7-57723
 system sensitivity for a class of mechanical systems by the method of structural numbers 7-43656
 thin elasto-viscoplastic layers, wave propag. 7-1481
 transient mean square response of randomly damped linear systems 7-62971
 variable pressure meas., errors due to vibratory acceleration reduction 7-291
 viscoelastic bar, response to sudden axial loading 7-37345
 Al cylindrical tank, water-filled, damping characteristic determ. from vibration meas. 7-16200
 Al-Si, cold worked, damping characts. 7-28064
 BW alloy fibre, torsional pendulum, shear modulus and internal friction meas. 7-48232
 C fibre reinforced plastic, thermal fatigue, flexure strength (Japanese) 7-13568
 Cu-Al-Zn, β -phase stability, mech. props. rel. to quenching rate 7-33659
 Fe, Armco, mag. internal friction, cathodic charging effect 7-17212
 Fe, cast, vermicular graphite, elastic props. 7-13493
 Zr, internal friction due to grain boundary relax. 7-65076

dams*see also civil engineering; hydroelectric power stations*

- flood retarding structures evaluation 7-60280
 Histos network for hydrological and meteorological measurement for East-Scheldt storm surge barrier construction 7-47557
 hydropower station, Sanmen Gorge project, China, environmental impact of sedimentation in reservoir 7-29086
 Quebec, Canada, reservoir induced seismicity at several hydroelectric sites (French) 7-18118
 seepage flow through porous dam, free boundary problem soln. 7-66182
 seismicity induced at hydroelectric reservoirs in Canada (French) 7-18118
 ship-board echo location system accuracy and system for East-Scheldt storm barrier construction 7-47558
 site planning with enhanced satellite imagery 7-17848
 tidal power barrage sites in UK, environmental problems caused by schemes 7-33994

dark space *see discharges (electric)***DASD** *see magnetic disc storage***data abstraction** *see data structures***data acquisition***see also CAMAC; data handling; recorders*

- 7-4846
 acoustic Doppler current profiler, vessel-mounted, for use in rivers and estuaries 7-9262
 air pollution monitoring using Commodore 64 home computers 7-54418
 analytical software in laboratory research 7-24632
 ASDEX data acquisition system, local area network 7-19464
 bathymetric surveying data acquisition and processing system (SDS III) 7-66361
 bioacoustic, digital signal acquisition, analysis and synthesis, microcomputer based system, PAL 7-54817
 cardiac action potentials and twitches, real time acquisition and analysis 7-65737
 cerebral blood flow measurement, indicator elution curves analysis by microcomputer 7-40389
 Contronic P modular process control data acquisition system (German) 7-56247
 cooling device for operation at 10K, mounting without rot. seals on four-circle diffractometer 7-14954
 Coulter Counter Mod. TA II, automatic data acquisition system 7-40566
 crystallography, single-crystal diffraction data, collection with area detectors 7-11825
 D0 experiment at Fermilab, data acquisition system 7-19672
 DIII-D tokamak, data acquisition and control system 7-36252
 DIII-D Tokamak, physics analysis database 7-5429
 EPR, microcomputer-based data acquisition and analysis system 7-48794
 flow meas., multichannel time counter and data acquisition system 7-37571
 gamma-ray spectrometry system, data acquisition circuitry, long-term stability 7-19624
 heart, programmed stimulation, real time data collection 7-34329
 HERB high-rate CAMAC acquisition system 7-42444
 human gait data acquisition and processing using digital camera 7-65809
 ice slurry system for low temperature thermal energy storage, data acquisition and reduction system 7-65622
 Integrated Lake-Watershed Acidification Study database documentation 7-46976
 intelligent FASTBUS, 168/E data acquisition interface system for NA31 experiment 7-18769
 IR 2D detector array, microcomputer-based data acquisition 7-9382
 JFT-2M tokamak, data processing system 7-15405
 JFT-2M tokamak data acquisition system 7-15404
 laboratory information management, IBM PC package 7-24631
 LEED, automated high-speed data acquisition system 7-21589
 lightweight US data acquisition and graphic display system 7-1335
 low-earth-orbit satellite tracking and data acquisition, use of microcomputer systems 7-55425
 low-Q piezoelec. material constants, automated meas. system 7-328
 magnetic hysteresis, low freq. meas., well-defined time depend. of flux density, meas. system 7-29985
 metal-insulator-metal (semiconductor) structs., circuit anal., automated 7-27438
 MFTF ICRH system, control and data acquisition 7-15396
 MFTF-B, diagnostic control, data acquisition and data processing 7-5422
 MFTF-B data triggered data processing 7-15399
 microcomputer data-acquisition system for flow rate sensor 7-51349
 microcomputer-based solar and meteorological data acquisition and control system 7-4186
 microprocessor controlled high density multiwire proportional chambers, 2D angular correlation of positron annihilation 7-36422
 minicomputer appl. for radiocarbon anal. control and meas. 7-34682
 modular acquisition system for coincidence data 7-49850
 Mossbauer spectrometer and data anal. system, IBM PC-based 7-18959
 multi-ADC data acquisition and transfer system for nuclear physics expts. 7-25335

data acquisition continued

multichannel data acquisition suites with time-scale conversion and storage CRT, design 7-61321
neonates with low birth weight, data acquisition system for monitoring 7-3920
neurosurgical intensive care unit, computerised monitoring system 7-3420
neutron flux mapping data collection system for reactor core monitoring, personal computer based 7-42128
NMR spectra phase distortion spectral generation algorithm 7-24664
nuclear power plant operation simplification by reliability data collection 7-10276
nuclear systems, automatic fault monitoring system 7-833
nyquist frequency extension by interleaved data acquisition, Fourier transform NMR spectroscopy 7-24680
online FASTBUS processor for LEP 7-19590
parallel-pipelined data driven processor, development status 7-19671
particle beam fusion accelerator II (PBFA II) data acquisition system with waveform recorders 7-30753
particle beam fusion accelerator II (PBFA II) high speed multi-channel data acquisition system 7-30752
PDP-8 on-line computer for missing mass spectrometer data handling 7-9824
pellet injectors, control and data acquisition system, design 7-36254
photoelectron spectrometer interfacing to microcomputer for data acquisition and processing 7-48919
photogrammetric acquisition, graphical verification subsystem 7-40618
photon counting image acquisition system, performance analysis 7-30088
photovoltaic, solar plant, automatic data acquisition system 7-54273
piezoelectric crystals, frequency and electrochem. data collection and anal. 7-53239
plasma fluctuations meas., integrated data acquisition and handling system based on digital time series anal. 7-25231
polarisation spectrophotometer for meas. of polarised emission and excitation spectra 7-56318
pollution monitoring, automatic station and data telemetry system 7-59900
polyurethane foam, form., exotherm data acquisition using microcomputer 7-54118
potentiostat, modular microcomputer controlled for electrochemical meas. 7-59819
Princeton Large Torus data acquisition and analysis system 7-5424
Prognost-10, data acquisition adaptive principles 7-55417
prosthetic heart valve test apparatus, microcomputer-based data acquisition system 7-40364
protein crystallography, static and time-resolved, real-time reduction of area detector data by hardware 7-14170
quadrupole mass spectrometer based on low-performance RF generator 7-30111
quasi-elastic light scattering, data acquisition and evaluation 7-56239
radionuclide ventriculography, computer program 7-40289
Raman spectrometer for time resolved meas. in gaseous samples, computer-controlled 7-18886
rectilinear scanner, interfacing with a microcomputer 7-65858
remote sensing of environment, 19th international conf., Ann Arbor, MI, USA (Oct 1985) 7-15
respiratory pressure data analysis for detecting breathing circuit faults in ventilated patients 7-40330
RFX, data acquisition and anal. system design 7-15398
Romania geodynamic observatories, sensors and auxiliary apparatus characteristics for Earth tides obs. (Romanian) 7-9243
scanning laser acoustic microscope with digital data acquisition 7-50882
seismic reflection profiling, MIPEX data acquisition system using personal computer (Japanese) 7-55265
seismic shallow layer reflecting survey system for Japan Geographical Survey Office (Japanese) 7-23855
seismometer hydrophone array system on seafloor 7-23890
SEM, voltage contrast meas., data acquisition and processing techniques 7-24727
SEM images acquisition and enhancement, using microcomputer 7-377
SIMS, image depth profiling with high dynamic range, automated method 7-23086
SIMS, quadrupole, data acquisition and control system 7-24722
small-angle neutron scatt. spectrometer 7-32227
solid Earth tide recording, digital data acquisition system 7-29245
SPOT satellite series, characteristics, 7-47551
stereo real-time metrology with CCD cameras 7-47314
stereocomputer, three axis, for SEM photogrammetry 7-4934
strain gauge rosette data acquisition and analysis, microcomputer-data logger interfacing 7-29995
streak photography, two-dimensional transients acquisition and processing, using IBM personal computer 7-15025
TFTR CAMAC data-acquisition system 7-5426
TFTR computer support system, configuration and performance 7-36251
TFTR data management system 7-5425
thermal decomposition study instrument 7-59818
thermal diffusivity and propagation props. of thermal waves meas. 7-305
thermal variables meas., microcomputer data-acquisition and control system 7-4841
thermophysical meas. automation, software for a microcomputer data-acquisition and control system 7-4824
TMX-U data analysis, database tools 7-5428
TMX-U diagnostic computer system, improvements 7-36255
tomographic analysis of the evolution of plasma crosssections 7-1741
TOPAZ time projection chamber, FASTBUS digitizer system 7-62244
two-parameter data-acquisition system for slit-scan chromosome analysis 7-35501
UHF water-content meters for cotton materials 7-48758
UPS, XPS and Auger spectrometers, digital power supply and counting interface 7-9825
urodynamic data-acquisition and anal. system, microcomputer-aided 7-3914
VME/VMX parallel multiprocessor system for the data acquisition of the UA1 streamer tubes 7-19665
water-content measurement system appl. to apatite concentrates 7-55300
wave theoretical approach to acoustic currentprofiling 7-4821
X-ray diffr. data collection and processing, high press. study 7-3944
X-ray diffractometer for tensometry using SAPI 1 microcomputer and FORTH language (Czech) 7-56390
X-ray spectrometer, Apple IIe microcomputer controlled data acquisition 7-41571

data acquisition continued

X-ray time resolved expts., multiwire detector and data acquisition system, appl. to muscle 7-14169
Zeiss/Oberkochen PLANIMAP system extensions 7-40620
H beam probes, data acquisition storage and processing system (Chinese) 7-6449
U atomic vapour laser isotope separation data acquisition and control system 7-15735
data analysis
see also data reduction
advanced laboratory data analysis systems 7-18767
airborne microwave rain scatterometer/radiometer, DP software system (Japanese) 7-23908
airborne microwave rain scatterometer/radiometer system, rain meas. and data anal. (Japanese) 7-23909
audiological test data analysis by microcomputer 7-40176
biostatigraphic data collection and analysis 7-40435
cerebral blood flow measurement, multicompartment analysis of trace clearance 7-18010
chemometric analysis of multisensor arrays 7-8344
continuous observation data analysis using computer methods 7-60397
DIII-D tokamak, data acquisition and control system 7-36252
DLTS, modulating functions waveform analysis 7-52523
DLTS, multiexponential analysis, by CONTIN program 7-52524
ECG interpretation online system using Bonner program 7-40325
echelle spectrographs, scattered light background correction method 7-34874
electrophoretic separation of macromolecules, two-dimensional multivariate data analysis 7-54440
EPR, microcomputer-based data acquisition and analysis system 7-48794
equine ground reaction force data analysis 7-54650
film digitisation, low cost solutions implementation 7-18893
graphics display of 3-D analysis data 7-4826
lidar, range-height indication measurements, data anal. 7-57394
magnetic bubble domain devices, review 7-17209
median filtering of seismic data, response in high-freq. range 7-66357
Mekometer distance meas., statistical correction methods (German) 7-23519
model-independent method of data analysis 7-14930
modulated grid Faraday cup plasma instruments, response function 7-23972
Mossbauer spectrometer and data anal. system, IBM PC-based 7-18959
nuclear physics data, linear correlation coeffs., significance levels 7-49851
optimal estimation theory in data analysis and signal processing, Kalman filter appl. 7-35500
piezoelectric crystals, frequency and electrochem. data collection and anal. 7-53239
potentiostat, modular microcomputer controlled for electrochemical meas. 7-59819
Princeton Large Torus data acquisition and analysis system 7-5424
propagation of boundary effects in large systems on vectorprocessors 7-4989
raster graphics devices, display and anal. of geometry of molecular cpds. 7-56236
rectangular measuring signals, digital evaluation (German) 7-24636
remote sensing of environment, 19th international conf., Ann Arbor, MI, USA (Oct 1985) 7-15
respiratory pressure data analysis for detecting breathing circuit faults in ventilated patients 7-40330
solar insolation data analysis by means of Allan variance and Fourier transform 7-60371
strain gauge rosette data acquisition and analysis, microcomputer-data logger interfacing 7-29995
stratigraphically constrained cluster analysis, FORTRAN 77 program 7-66114
thermal decomposition study instrument 7-59818
thermal diffusivity in thin plates, remote meas. of in-plane components 7-62958
time and frequency transfer, NBS calibration service based on GPS common view data 7-14926
TK!Silver for students in Fluid Mechanics Laboratory 7-16260
TMX-U data analysis, database tools 7-5428
TMX-U diagnostic data base, evolution 7-5423
watershed acidification, computer simulation 7-14322
X-ray photoelectron spectroscopy, data analysis, factor anal. and curve fitting 7-35639
X-ray pulse height analyser data, probabilistic modelling, plasma electron temperature, enhancement factor calcs. 7-5566
data communication equipment
see also telemetering equipment
fibre optic transmitters and receivers for data communication, miniaturized modules 7-62847
fibre optics' advantages for computerised control systems, data highways and sensors 7-15988
optical directional couplers for LANs, parallel single-mode/multimode fibres config. wave coupling study 7-31486
weather satellite automatic picture transmission, design of grey scale test pattern generator 7-29292
data communication systems
Magellan mission to Venus, data transmission to Earth 7-55468
METEIS system for satellite broadcast of weather information; earth station config. 7-47522
rock mass stress data, acquisition and radio telemetry (Russian) 7-34681
data compression
see also information theory
ECG, data compression VCG anal., comparison of two algorithms 7-40356
event sampling by particle-number difference, using high-speed A/D processor 7-10365
flow, multi-point vector measurement by pulsed laser velocimetry with image compression 7-37610
human visual system models appl. to digital colour image compression 7-65744
image processing in cardiovascular radiology 7-65833
image processing technology, medical radiography appl., review 7-65856
portable continuous blood pressure monitor utilizing an M68705 microcomputer 7-28755
pure orientation filtering, scale invariant image processing tool for perception research and data compression 7-60005

- data compression** continued
 solar insolation data analysis by means of Allan variance and Fourier transform 7-60371
 use of Kalman filters in data compression of gastransmission pipeline data 7-11553
 Voyager-2 at Uranus, engineering aspects 7-55424
- data conversion**
see also analogue-digital conversion; digital-analogue conversion
 nuclear quadrupole resonance thermometers, freq.-temp. conversion (*Russian*) 7-41385
- data dictionaries** *see database management systems*
- data flow computing** *see parallel processing*
- data handling**
see also data analysis; data reduction
 cartography automation conf. London, England (Sept. 1986) 7-35105
 chemical analysis of igneous rocks and CIPW norm calculations, FORT-RAN listing 7-29263
 Fourier domain processing, mathematics of spectral treatment 7-48870
 Mossbauer unresolved spectra with multiple convolutions, FFT-based processing 7-38972
 PDP-8 on-line computer for missing mass spectrometer data handling 7-9824
 plasma fluctuations meas., integrated data acquisition and handling system based on digital time series anal. 7-25231
 position sensitive detectors, 2D detector data for crystallography, fast treatment using processor arrays 7-10354
 SCALE, nuclear waste cask analysis, critically safety analysis 7-15411
 soil survey, use of Landsat and digital elevation data 7-4233
 three-channel plasma diagnostic data handling system based on the VAX 11/780 and the LeCroy 3500 signal analyzer 7-26527
- data loggers**
 AC-DC difference meas. system establishment at NPL, Israel, using multi-junction thermal converters 7-18837
 geological data logger with 8085 microprocessor 7-9179
 Particle Beam Fusion Accelerator Marx generators 7-30767
 seismometer hydrophone array system on seafloor 7-23890
 sonic logging, 2D spectrum anal. 7-4203
 strain gauge rosette data acquisition and analysis, microcomputer-data logger interfacing 7-29995
 tethered current meter, ENDECO Type 174 model evolution 7-9253
 CO, personal exposure monitor with automatic data-logging 7-3943
- data preparation**
see also word processing
 USA geological survey, digital system development, MARK II 7-47320
- data processing (administrative)** *see administrative data processing*
- data reduction**
see also data analysis
 2D photoelastic shear-difference data, computer-assisted reduction 7-57775
 AES, instrumentation, data reduction, depth profiles 7-22390
 crystallography, 3D intensity data from single crystal reflections, graphical display 7-11829
 differential scanning calorimeters, standard operating procedures development 7-18786
 DREAM data reduction and error anal. routines, appl. to single cryst. diff. intensity meas. 7-16348
 IUE spectra, VIRIS-VAX interactive reduction 7-40720
 model-independent method of data analysis 7-14930
 multispectral imagery dimension reduction and interpretable, Chebyshev polynomials 7-4236
 peak-separation algorithm for personal computer, appl. to visible emission and IR absorpt. spectra (*Japanese*) 7-31015
 soft X-ray streak camera, absolute calibration 7-18963
 solar insolation data analysis by means of Allan variance and Fourier transform 7-60371
 spectroscopic data manipulation, UNIX based computer workstation 7-48859
 surface tension measurements, optimisation algorithm 7-14929
 FTIR computer support system, configuration and performance 7-36251
 FTIR data management system 7-5425
 video/computer technology role in exptl. mech. 7-63093
 U atomic vapour laser isotope separation data acquisition and control system 7-15735
- data reduction and analysis** *see data analysis; data reduction*
- data security** *see security of data*
- data structures**
 cartography automation conf. London, England (Sept. 1986) 7-35105
 crystal structures, nonconvex, polygonal mesh and quad-tree display algorithms 7-51672
 environmental change, remote detect., data struct. appls. 7-4240
 generalisation, cartographic, data types 7-47323
 Integrated Lake-Watershed Acidification Study database documentation 7-46976
 Zeiss/Oberkochen PLANIMAP system extensions 7-40620
- data tables** *see collections of physical data*
- data transmission equipment** *see data communication equipment*
- data transmission systems** *see data communication systems*
- database machines** *see database management systems; special purpose computers*
- database management systems**
see also relational databases
 aerometric database for field experiment, real-time display and development 7-54407
 archiving of X-rays: digital or analogue methods? (*German*) 7-62313
 biostratigraphic data collection and analysis 7-40435
 cartography automation conf. London, England (Sept. 1986) 7-35105
 collapse of MRL 38 mm shaped charge, database for computer modelling 7-63192
 DIII-D Tokamak, physics analysis database 7-5429
 geographic database, Minute Man National Historical Park, map input software 7-47319
 microcomputer-based relational database system for monitoring water quality for the Niagara Falls drinking water treatment plant 7-54419
 nuclear power plant Risk Management Query System 7-15291
 remote sensing, data base approach to Landsat data appls. 7-4223
 spectral line parameters database creation 7-50017
 TMX-U data analysis, database tools 7-5428
 TMX-U diagnostic data base, evolution 7-5423
- databases** *see database management systems; information services*
- dating, Earth** *see geochronology*
- dating, radioactive** *see radioactive dating*
- Davydov splitting**
 layer crystals dynamics, long wavelength vibrs., factor group anal. 7-58424
 CsCoCl₃·2H₂O, 1D antiferromagnet, exciton transfer, absorpt. spectra 7-27254
 β-HgI₂ crystals, phonon spectrum and vibr. mode symmetry, first-order Raman scatt. (*Russian*) 7-3056
- Davydov states** *see Davydov splitting*
- dawn chorus** *see atmospheric*
- dayglow** *see airglow*
- DBR lasers** *see distributed Bragg reflector lasers*
- DC motors**
 wheelchairs and prostheses, switching converters for efficient control of DC motors 7-34355
- DC sputter deposition** *see sputter deposition*
- DC sputtered coatings** *see sputtered coatings*
- DC sputtering** *see sputtering*
- DC to AC invertors** *see invertors*
- DDC** *see direct digital control*
- de Broglie waves** *see wave mechanics*
- de Haas-van Alphen effect**
see also diamagnetic properties of substances; diamagnetism
 graphite intercalation compounds, first stage, with heavy alkali metals, electronic props. 7-2463
 Au, Fermi surface curvature, de Haas-van Alphen effect meas. 7-2467
 CeCu₆, heavy-electron compound, de Haas-van Alphen effect 7-12587
 Co₉₂Fe_{0.08}, FCC, Fermi surface, de Haas-van Alphen studies 7-52406
 Cu dislocated single cryst., sub-grain misorientation, de Haas-van Alphen meas. 7-12300
 GaAs-GaAlAs superlattices, density of states of Landau levels, sp. ht., magnetisation meas. 7-52823
 Pb, self-consistent relativistic band struct., normal and high press. 7-52413
 Pb_{1-x}Sn_xTe quantum oscills. spectrum anal., two-window Fourier transform technique 7-52404
 Pd, Fermi surface curvature, de Haas-van Alphen effect meas. 7-2467
 Pd, X-pocket holes, anisotropy of conduction electron Zeeman splitting 7-32963
 Pd-Fe(Ni) dilute alloys, Fermi surface exchange splitting, de Haas-van Alphen effect studies 7-52405
 Pt, Fermi surface curvature, de Haas-van Alphen effect meas. 7-2467
 UPd₃ Fermi surface meas., de Haas-van Alphen effect study 7-12589
- Debye-Huckel theory**
 random fractals, Debye-Huckel theory 7-212
 short range forces between charged lipid bilayers, theoretical model 7-28478
 NH₄F in dioxane-methanol mixtures, assoc. constant. from cond. meas. 7-33939
- Debye-Scherrer cameras** *see cameras; X-ray crystallography apparatus*
- Debye temperature**
see also specific heat
 alkali halide mixed crystals, phys. props., review 7-37943
 β-(BEDT-TTF)₂I₃, organic superconductor, Debye temperature 7-64399
 α-brass, Mossbauer spectroscopy 7-59125
 heavy Fermi liquids and narrow band metals, characteristic temps. 7-45689
 HVEM, materials characterisation, critical voltage effect 7-37819
 insulators, Schottky defect form. enthalpy-Debye temp. correl. study 7-26742
 lattice thermal cond. reduction by point defects at intermediate temps., appl. to Ge-Si 7-52161
 metal nitrides, vibrational entropy 7-6745
 NaCl single cryst., high temp. elasticity meas., rectangular parallelepiped reson. method 7-63714
 nonmagnetic metallic glasses, negative TCR and electronic struct. studies 7-52562
 rare gas floating monolayers, dynamics in self-consistent phonon theory 7-2362
 TGS, crystalline samples, low temp. sp. ht. meas. 7-2225
 transition metals, lattice dynamics 7-51972
 AU clusters and bulk samples, Debye temps., EXAFS studies 7-2136
 (Ag_{0.5}Sn_{0.5})₁₂Ge₆ cluster cpd., elastic behaviour and vibr. anharmonicity 7-12223
 Au, metal and clusters, dynamical props., EXAFS studies 7-64805
 Au, temp. depend. of elec. resist. 7-58792
 BaTiO₃, crystalline samples, low temp. sp. ht. meas. 7-2225
 Bi-Pb, superconducting transition temp., effect of plastic deform. 7-52879
 Bi-Pb alloys, supercond. and normal state, thermal cond., effect of plastic deform., 1.5-300K 7-17132
 Bi-Tl, superconducting transition temp., effect of plastic deform. 7-52879
 Bi-Tl alloys, supercond. and normal state, thermal cond., effect of plastic deform., 1.5-300K 7-17132
 CdTe epitaxial layers on GaAs substrates, X-ray diff. 7-27201
 Co_{0.55}Cu_{0.45}Cr₂S_{4-x}Se_x spinels, X-ray diff. study 7-44475
 Cu, X-ray photoelectron diff., temp. depend., surface and bulk effects 7-39356
 Dy, mean square amplitude of vibr. and Debye temp. 7-21368
 Fe₃Si, near-stoichiometric high temp. creep and struct. investig. 7-22762
 Gd, mean square amplitude of vibr. and Debye temp. 7-21368
 Ge (111), adsorbed Pb monolayers, photoelectron scatt., temp. depend. 7-13328
 GeTe, valence and energy spectrum, supercond. state 7-45534
 KCl-KBr mixed crystals, cohesion, harmonic and anharmonic props. calcs. 7-51907
 LiNb(Ta)O₃, crystalline samples, low temp. sp. ht. meas. 7-2225
 Lu, mean square amplitude of vibr. and Debye temp. 7-21368
 NaBrO₃-NaClO₃ solid soln. single crystals, X-ray Debye temps. 7-58428
 NaNO₃, crystalline samples, low temp. sp. ht. meas. 7-2225
 NbC, elastic constants meas. 7-6703
 NbSe₂H_x, heat capacity, Debye temp., electron-phonon coupling, electronic contrib. meas. (*Russian*) 7-6820
 Nb₃Sn superconductor, sp. ht. meas. in mag. fields up to 19 T 7-17134
 Ni_{100-x}Zr_x metallic glasses, low temp. sp. ht. study, density of states and Debye temp. determ. 7-2226

Debye temperature continued

Pb, temp. depend. of elec. resist. 7-58792
Si, electron planar channelling radiation, temp. depend. 7-46172
Sn, superconducting transition temp., effect of plastic deform. 7-52879
TiC, effective and Debye temps. of Ti, gamma ray reson. scatt. meas. 7-44731
TiC-WC-TaC-Co hard metals, Ta conc. effect on comp. and physicochem. of carbide and Co phases 7-53708
TiH₂, effective and Debye temps. of Ti, gamma ray reson. scatt. meas. 7-44731
TiO₂, effective and Debye temps. of Ti, gamma ray reson. scatt. meas. 7-44731
TiCl₃Br₃, Debye temp., Debye-Waller factor and mean vibr. amplitude, X-ray determ. 7-26893
Y, mean square amplitude of vibr. and Debye temp. 7-21368
YAl nonmagnetic metallic glasses, negative TCR and electronic struct. studies 7-52562
Zn, Mossbauer spectroscopy 7-59125
Zr-Co; electronic struct., supercond. and magnetism 7-64398
Zr-Fe compounds, electronic, lattice and supercond. props., rel. to amorphous alloys 7-17133

Debye-Waller factors

see also lattice dynamics
alkali halide mixed crystals, phys. props., review 7-37943
alkali metal iodides, Debye-Waller factors of ¹²⁹I, Mossbauer study 7-2135
atom-surface scattering, general theory of scattering 7-59359
ferromagnet, Debye-Waller factor anomaly and diffuse scatt. studies (Russian) 7-12973
fine structure theory refinements 7-27819
perylene in microcryst. n-heptane, selectively laser excited in phonon side-band, stimulated emission 7-33415
Si, spherical wave EXAFS, Si K-edge anal. 7-64822
single crystal, elastic scatt. of slow electrons over surface, effect of mag. transform. (Russian) 7-52549
single crystals containing random distrib. of dislocations, integral characts. of X-ray diffr. (Russian) 7-51563
solid-liquid interface, self diffusion coeff., Debye-Waller factor calc. 7-16706
strong-absorbing single crysts., Laue X-ray diffr. thickness depend. anal. and interpretation (Russian) 7-44310
surface EXAFS, Debye-Waller factor, influence of adsorbed monolayer 7-39316
Au clusters and bulk samples, Debye temps., EXAFS studies 7-2136
Al, lattice dynamics and three-body forces, phonon freq. Debye-Waller factor calcs. 7-63760
As, amorphous, vibr. density of states, EXAFS, Debye-Waller factors 7-64820
Bi-Ge-S chalcogenide glasses doping mechanism and structural effects, EXAFS study 7-1909
Ca₅(PO₄)₃OH, EXAFS spectrum anal., spherical wave theory 7-33485
Cd single cryst., interatomic distance and thermal motion, K-shell EXAFS, temp. and orientation depend. 7-64814
CdS(Se), X-ray graphic elastic constants and lattice spectrum 7-32546
Co monolayer on Cu (111), Debye-Waller factor anisotropy, SEXAFS study 7-63936
Cu, X-ray photoelectron diffr., temp. depend., surface and bulk effects 7-39356
CuI, Debye-Waller factors of ¹²⁹I, Mossbauer study 7-2135
CuI, Debye-Waller factors, Mossbauer scatt. meas. 7-6746
Fe-Co(V) alloys 7-51708
GaAs, fundamental energy gap, temp. depend. 7-7115
GaAs, X-ray diffr., anomalous dispersion effects, thermal vibrs. and bonding changes 7-44733
Ge₂₀S₈₀Bi chalcogenide glasses, doping, coordination number and cond. transition, EXAFS study 7-64764
LiNbO₃:Fe²⁺, anomalous phase transitions, Mossbauer spectroscopy studies 7-2992
Mn-Cu single crystals, Debye-Waller coeff. behaviour, energy dispersive X-ray diffr. study (Russian) 7-51983
NaBrO₃-NaClO₃ solid soln. single crystals, X-ray Debye temps. 7-58428
O (2×1) overlayer on Cu (110), surface reconstruction, mean free path and Debye-Waller factor, SEXAFS study 7-46238
Pd-C solid solution, X-ray diffr. study 7-21383
RbC₈, 2D graphite intercalation cpds., bond angle determ, EXAFS study, Debye-Waller anisotropy. 7-59293
RbCl-RbBr mixed crystals, X-ray diffraction and color centres 7-58258
Si, crystalline, amorphous and H-doped, structural props., EXAFS study 7-64760
SnTe, Debye-Waller factors of ¹²⁹I, Mossbauer study 7-2135
TiCl₃Br₃, Debye temp., Debye-Waller factor and mean vibr. amplitude, X-ray determ. 7-26893
ZnO, X-ray graphic elastic constants and lattice spectrum 7-32546
ZnTe, Debye-Waller factors of ¹²⁹I, Mossbauer study 7-2135

decay periods (radioactive) see radioactive decay periods

decay schemes (radioactive) see radioactive decay schemes

decay theory (nuclear) see nuclear decay theory

decentralised control see distributed control; multivariable control systems

decision support systems

nuclear power plant, UNIRAM modelling for availability improvement 7-10274
nuclear power plant probabilistic risk assessment microcomputer software 7-10271

decision theory

see also Bayes methods; dynamic programming
nuclear power plants, reliability and risk allocation, decision theoretic anal. 7-36081
reliability estimate for multiparameter NDT 7-3562

decision theory and analysis see decision theory

decoding

see also demodulation
coding theoretic approach to cancer detection 7-47252
communications techniques in radio physics and astronomy 7-29411
fractal aggregates, imaging, in-line holograms, digital decoding 7-10884

decomposition

microstructure features and processes only; for other aspects see dissociation and pyrolysis
see also spinodal decomposition
bearing type, austenite transform. kinetics and internal stresses in bainitic hardening 7-39563
Ge_{1-x}Si_xCu, supersaturated solid solution, decomposition 7-32654
Iwasawa and triangle decomp. eval. for Lie algebra real forms 7-18552
metallic binary alloy solid solns. with retrograde solidus, decomposition 7-21457
multicomponent systems, pores filled with two-component molecular gas, coalescence (Russian) 7-59490
oxides, AM₂O₃(M₂O₄)_n derived from the rutile structure by chemical twinning, structural evolution and stability 7-16757
peritectic transformations, simple rate prediction 7-22635
polystyrene-polyvinylmethylether blends, phase decomp., small angle neutron scatt. 7-28021
semiconducting binary alloy solid solns. with retrograde solidus, decomposition 7-21457
steel, constructional, struct. and props. after high-temp thermomech. isothermal working 7-46522
steel, Cr-Ni-Mn, decomp., martensite struct. rel. to alloying comp. (Russian) 7-59531
steel, Cr-Ni-Mo type, austenitisation conditions effect on austenite decomp. kinetics and mech. characts. 7-39557
steel, duplex stainless, decomp. of deformed ferrite, TEM obs. 7-28091
steel, eutectoid, microstruct. obs. of bainite stars 7-53695
steel, hardening process modelling, stresses effect on struct. transform 7-39555
steel, high speed, peritectic transform., decomp., carbide precip. Nb alloying effect (German, English) 7-22677
steel, high-C, hardened, mech. prop. changes on tempering, martensite decomp. role 7-3375
steel, low-pearlite, rules of austenite decomp. in continuous cooling 7-3339
steel, Ni-Co-W, maraging, martensite isothermal aging, hardness, struct. and elec. resist. kinetic behaviour study 7-17553
steel, plain C, eutectoid, continuous cooling austenite-to-pearlite transform. kinetics, prediction using isothermal data 7-17524
two-sublattice crystals with spinel struct., crystal-chemical model of stability 7-16481
Ag-Cu (12 at.%), supersaturated solid soln., decomp. kinetics, effect of creep (Russian) 7-33748
AgN₃, elec. cond. under high press., decomp. by dielec. breakdown 7-27010
Al-Ag (5.9 at.%), precip., positron study 7-46485
Al-Co, melt spinning, microstruct., precip., microhardness (Korean) 7-46444
Al-Li-Si, cast, decomp., mech. props., struct. (Russian) 7-59532
Al-Mn (15 wt.%), melt spun ribbons, icosahedral struct., decomp. rel. to annealing 7-28030
Al-Zn, disintegration kinetics, hardening temp. effects 7-52055
Au-Ag-Cu-Pd, cast microstruct, segregation, TEM obs. 7-39495
Ce(Co,Cu,Fe)₆, magnetically hard, heat treatment effects on struct. and mag. characts. 7-27564
Co-Al alloys, magnetic hardening 7-33209
Co-Al solid solutions, porous decay, temp. conc. existence limits (Russian) 7-33680
Co-W, ageing, polymorphism, cellular mechanism (Russian) 7-59514
Co₂SiO₄, decomp., O₂ pot. gradient, stability investig. (German) 7-17767
Cu-Al-Zn, β-phase stability, mech. props. rel. to quenching rate 7-33659
Cu-Be (30 at.%), eutectoid decomp., spatial distrib. of α-phase (Russian) 7-53694
Cu-Co (2.7 at.%), decomp., atom probe FIM 7-3268
Cu-Co alloy decomposition, TEM, FIM and SANS studies 7-53749
Cu-Cr bronze, decomp. kinetics of supersaturated solid solns. 7-3320
Cu-Fe (0.6 to 2.2 at.%), solid solns., decomp. processes, effect of O₂ (Russian) 7-33681
Cu-Ni-Fe, alloy decomposition and periodic struct. coarsening 7-53735
Cu-Ni-Fe, irradi., stability of periodic decomp. struct. 7-58366
Cu-Ti (5.7 at.%), cellular decomp. (Russian) 7-53693
Cu-NiFe, electron irradi., decomposition kinetics and morphology 7-58491
Cu₄₈Ti₅₂, amorphous, crystallisation, intermediate long period superlattice phase form. 7-21098
Fe-Ag sputtered films, thermal stability, X-ray diffr. and Mossbauer studies 7-58679
Fe-Cu alloys, phase transformations, SANS studies 7-53747
Fe-Cu sputtered films, thermal stability, X-ray diffr. and Mossbauer studies 7-58679
Fe-Mn, FCC alloys, H-induced martensitic transform. (Japanese) 7-33655
Fe-Ni-Al-Co system, miscibility gap, phase decomp. in Alnico mag. alloys 7-17537
Gd-Sb, phase diagram, peritectic reactions, congruent melting, DTA, microstructural and X-ray anal. 7-39481
HgS-Ga₂S₃, phase diagram, incongruently melting compounds 7-13436
LaNi₅H₆O, dissociation press., O content depend. 7-63825
Mn-Ni alloys, γ-phase decomposition, annealing and quenching, X-ray phase anal. 7-17510
Ni alloy, heat-resisting, supersaturated solid soln., isothermal decomp. kinetics 7-33682
Ni-GaAs interfacial reactions, contact elec. props. 7-12504
Ni₄₅Pd₅₅P₂₀ metallic glass, decomposition, crystallisation and embrittlement, atom-probe FIM study 7-33639
Pd-Te, phase diagram, DTA, X-ray powder diffr. studies 7-39483
RbHSeO₄, optical birefr. meas., temp. depend. 7-27689
Si epitaxial films, low temp. growth by very low press. CVD 7-27936
Si-Ge-O, single crystal, thermoadsors. rel. to solubility of O 7-12648
Si₃Ge_{1-x}(C_x) semiconductor alloys, ordering and decomposition 7-6574
SiO₂ films thermally grown on Si, decomposition acceleration factors 7-63999
Te-As-S chalcogenide system, annealing, crystalline precipitate phase form., X-ray diffr. anal. 7-16751
Ti alloys, ordered structure form. during decomp. of metastable β-phase (Russian) 7-53725
Ti-Al-Cr-Mo alloy VT3-1 mech. props. depend. on decomp. product morphology for metastable phases 7-39655
Ti-Al-Mo-V-Cr alloy VT22, metallographic study of β-solid soln. decomp. 7-39523
U-Ti (4 at.%), quenching, decomp., TEM obs. 7-39527

decomposition continued

- V-N system, phase equilib., crystallography, thermodynamic props. 7-28011
 W-Fe-Co-Ni system, phase equil., peritectic transform. 7-53701
 ZnO films, elec. props., decomp., chemisorption of O², photocond. meas. 7-27445
 ZnS:Cu, solid solution, electroluminescent phosphor, compositional inhomogeneities 7-6800
 Zr-Nb (20 wt.%), ageing behaviour, effect of H 7-46527

decomposition, spinodal *see spinodal decomposition*decomposition, thermal *see pyrolysis*

decorative coatings

- Zn-Ni bright coatings deposited from weak acid electrolytes (*German*) 7-39441

dedicated computers *see special-purpose computers*deep level transient spectra *see deep level transient spectroscopy*

deep level transient spectroscopy

see also deep levels

- bicrystal boundaries, transient spectra of dislocation levels 7-52497
 capacitance methods used for the study of deep levels 7-45205
 computer controlled, capacitance transient characterisation 7-18805
 defect state generation, Si rapidly annealed with incoherent light 7-52504
 EL2 defect, identification 7-38502
 II-VI semiconductors, transient spectroscopy, deep level characterisation 7-58776
 lock-in amplifier appls. at freq. up to 2000 Hz 7-327
 metal-insulator-semiconduct. struct., interface state density profile determ., DLTS spectra interpretation 7-38733
 MIS structure, small-signal DLTS response from insulator semiconductor interfacial traps, model anal. 7-64147
 modulating functions waveform analysis, of multiexponential transients 7-52523
 MOS interface charge state transient spectroscopy 7-45506
 MOS structures, interface and bulk traps, effect of processing steps 7-38758
 multiexponential analysis, by CONTIN program 7-52524
 multiexponential capacitance transients, anal., refinements in method of moments 7-52505
 optical current, bipolar rectangular weighting function 7-52525
 p-type, undoped, electron irradiation, defect level annealing and DLTS 7-12660
 passivation of dislocations in Si at high H₂ press. 7-39763
 polysilicon for solar cell appls., DLTS study 7-38512
 selective detection of deep recomb. centres 7-7168
 semiconductor electrical characterisation, non-contacting methods, book contrib. 7-45335
 semiconductors, deep centres, nonsteady capacitive spectrosc. investig. 7-12665
 semiconductors, deep trap profiles determ. 7-58768
 semiconductors, DLTS for defect characterisation 7-52521
 Al-Si:Ar,H, ion implanted ultrahigh Schottky barriers, interfacial traps, DLTS study 7-45489
 AlGaAs, DX centres, DLTS signature anal. 7-45204
 AlGaAs superlattices, donor state instability, DLTS and Hall meas. 7-12663
 Al_{0.5}Ga_{0.5}As MBE layers, deep electron traps, flux ratio effects 7-12641
 Al_{0.5}Ga_{0.5}As p-n junction solar cell radiation-induced defects obs. using DLTS 7-13875
 CdS, with compensated i-layer, photosimulated deep level transient spectroscopy 7-7765
 CdSe:Cu, deep levels investigated by photoconductivity and space-charge region capacitance techniques 7-7148
 CdTe grown on Si by LPMOCVD, physical props., DLTS of defect levels 7-27181
 CdTe-AuCu, AC contact impedance, influence on high freq., low temp. on fast transient junction meas. 7-64311
 CoSi₂-Si heterostructures, MBE or solid phase epitaxially grown, Schottky barrier heights, DLTS spectra 7-12859
 GaAs, EL2 centre stability under electron-hole recomb. conditions 7-16978
 GaAs, EL2 defect profiling, DLTS 7-12652
 p-GaAs, electron irradiation-induced trap defects, DLTS study 7-12155
 GaAs, electron irradiated, defect profiling, DLTS 7-12652
 GaAs, electron irradiation induced defects, DLTS study 7-58338
 GaAs epitaxial layer, EL2 midgap electron trap prod. by rapid thermal annealing, DLTS study 7-64154
 GaAs epitaxial layers, native deep level defects 7-12888
 GaAs, hydride VPE layers, deep level incorporation and background doping 7-17120
 GaAs LEC substrates, EL2 deep donor kinetics under annealing, IR absorpt., DLTS, Hall effect meas. 7-32955
 GaAs MBE layers, bias-dependent capture-emission processes, DLTS anal. 7-64166
 GaAs, MBE layers, deep level defects, passivation by H₂ plasma exposure 7-21850
 GaAs MBE layers, deep level defects and impurities 7-22051
 GaAs, MOCVD layers on Si substrates with superlattice intermediate layers, DLTS studies 7-38501
 GaAs microwave absorption transient spectroscopy for investigation of deep levels in semiconductors 7-52520
 GaAs, plastically deformed, spatial distrib. of dominant electron and hole traps 7-7160
 GaAs, scanning DLTS study of deep level defects 7-21865
 GaAs, semi-insulating, deep levels, nondestructive microwave DLTS measurements 7-45210
 GaAs, semi-insulating, switching effect, deep level spectroscopy appl. 7-38630
 GaAs, semi-insulating bulk with thin conducting layer, optical DLTS distortions calcs. 7-58766
 GaAs, semi-insulating LEC crystals, thermal conversion, DLTS studies 7-7150
 GaAs, semi-insulating wafer, inhomogeneity characterization by scanning photo-induced current transient spectroscopy 7-7164
 GaAs, semiconducting/semi-insulating reversibility 7-21939
 GaAs, VPE growth in hydride system, elec. props. 7-2751
 GaAs:Cr, deep levels characterisation using photo-induced transient spectroscopy 7-16973
 GaAs:Ni, acceptor like electron trap, DLTS study 7-7166
 GaAs:Sb, deep level formed by Sb doping 7-52496

deep level transient spectroscopy continued

- GaAs:Sn epilayers, MOCVD using triethylgallium and tetraethyltin, characterisation 7-22515
 GaAs:Sn(Te)(Zn) surface layers, luminesc., electrophys. parameters, effect of annealing 7-64680
 GaAs/AlAs/GaAs:Se heterojunctions, elec. behaviour, DLTS studies 7-7360
 GaAs-Al junction, interface states, DLTS study 7-58892
 GaAs-AlGaAs heterostruct., band discontinuity determ., DLTS, interface charge density, trap conc. 7-12833
 GaAs-AlGaAs superlattice defects, DLTS study 7-21854
 GaAs-Au Schottky diodes, DLTS 7-58896
 GaAs-GaAs MOVPE epitaxially-grown interfaces, anomalous C-V carrier conc. profiles, model 7-52648
 GaAs-Mo Schottky diodes, elec. characts. and microstruct. study 7-22015
 GaAsP, DX centres, DLTS signature anal. 7-45204
 GaAs_{1-x}P_x crystals, electron-traps, DLTS study (*Japanese*) 7-7146
 GaAs_{1-x}P_x, EL2 level 7-21859
 GaAs_{1-x}Sb_x, alloy disorder broadening of defect energy levels 7-52516
 GaP, deep level centres at excited states, study by transient optical absorpt. spectroscopy 7-13188
 GaP:Zn, electron irradiation induced defects, DLTS study 7-52513
 Ge p-n junction solar cell radiation-induced defects obs. using DLTS 7-13875
 In_{0.5}Ga_{0.5}P layers, LPE, elec. and optical props. 7-17119
 InGaAs/InP superlattices, effective mass filtering obs. 7-12799
 InGaAs-GaAs MOVPE epitaxially-grown interfaces, anomalous C-V carrier conc. profiles, model 7-52648
 InP crystals and solar cells, radiation-induced defects, room-temperature annealing 7-39993
 p-InP, electron irradiat., atomic displacement threshold energy 7-2066
 InP, electron irradiat. damage, impurity effects 7-12154
 p-InP, γ -ray irradiated low temp., nonradiative-recomb.-enhanced defect struct. transformation 7-2062
 InP, microwave absorption transient spectroscopy for investigation of deep levels in semiconductors 7-52520
 Si bicrystals, grain boundaries, electronic states, transient capacitance spectroscopy meas. 7-7173
 Si crystals, low energy Ag⁺ implantation-induced deep centre depth distrib., DLTS study 7-26820
 Si, Czochralski, electron-irradiated, DLTS and photoluminesc. studies 7-7149
 Si, DLTS and MCTS spectra, charge-dependent defect traces 7-7161
 Si, DLTS spectrum of dislocations introduced by CW CO₂ laser (*Chinese*) 7-32939
 Si, diffusion length depend. on cooling rates and bulk resistivity 7-7266
 p-Si, electron irradiation induced defects, DLTS study 7-38500
 Si, laser induced defects, rapid and classical thermal processing, annealing kinetics 7-44609
 Si layers, electron irradiation-induced defect levels, annealing behaviour, DLTS studies 7-52493
 Si MBE layers, deep levels, DLTS meas. 7-12667
 Si MOS capacitor struct., defect profiling, DLTS 7-12652
 Si, neutron-irradiated, relax. space-charge-limited current spectroscopy 7-38493
 Si, precipitation induced microdefects, DLTS characts. 7-38511
 Si:As(BF₃), ion implanted, diffusion and defects, transient scanning electron beam annealing 7-38065
 Si:Au, deep levels, multiexponential anal. of deep level transient spectroscopy 7-52524
 Si:Au, supersaturated low-temp. substitutional impurities, annealing 7-6665
 Si:Au,Fe-SiO₂, MOS struct., trap centres 7-7388
 Si:B, electron-irradiated, AC hopping conductivity and DLTS 7-44624
 Si:B, ion implanted, transient annealing and residual defect DLTS study (*Chinese*) 7-12642
 Si:B,Fe, EBIC and DLTS meas., comparisons 7-7265
 Si:B plastically deformed crystals, dislocation struct. and elec. activity, annealing effects study 7-37998
 n-Si:B⁺(BF₃), ion implanted, rapid thermal annealing, DLTS 7-16619
 Si:B(Al)(Ga)(P)(Sb) thermal donor props., impurity effects, DLTS, Hall effect, and admittance spectra meas. 7-21851
 Si:Co, impurity energy levels, Hall and DLTS meas. 7-52509
 Si:H, B(Al)(Ga)(In), polishing, acceptor compensation by atomic H 7-33860
 a-Si:H, electronic density of states, DLTS and capacitance transient spectra anal. 7-45134
 a-Si:H, mobility gap state transitions, transient photocapacitance studies 7-12669
 Si:Li counterdoped n⁺p solar cells, proton-irradiated, DLTS studies 7-8376
 Si:O, electronic struct. and atomic symmetry of the thermal donor 7-16986
 Si:O Czochralski wafers, electron traps resulting from O precipitation 7-21866
 Si:O(O,H), heat treated, DLTS 7-16991
 n-Si:P,C, electron-irradiated and injection-annealed, vacancies, dislocations and C interstitials 7-51815
 Si:P,O,D, donor passivation and reactivation 7-17031
 Si:PF₆⁻ ion implanted, recrystallisation kinetics during fast thermal annealing 7-16618
 Si:Pt, deep levels and diffusion profiles 7-58767
 Si:Sb, pot. enhanced doping during MBE growth, elec., optical props., cryst. quality 7-12112
 Si:Ti, deep level transient spectroscopy, transient capacitance data anal. 7-52526
 Si:Ti, electron and hole energy levels, DLTS and DDLTS meas. 7-32941
 Si:Ti, ion implanted, deep level charact. 7-38513
 Si/NiSi₂ heterojunction, interface states, DLTS and hydrogenation studies 7-12777
 Si/SiO₂ interface, oxide trap capture cross section and tunnelling emission, DLTS study 7-12875
 Si-SiO₂-xN₂-xN₂/3-Al structures, interface states, DLTS study 7-45513
 SiO₂ CVD photox layers, Hg-sensitised, elec. props. 7-64379
 SiSe⁺, photothermal release of carriers, deep levels, capacitance spectroscopy 7-16968
 ZnSe:Al, MOCVD growth, deep level characterisation 7-52519

deep levels

- see also *deep level transient spectroscopy*
- dielectrics with deep traps, currents in strong elec. fields 7-33023
- DLTS method for selective detection of deep recomb. centres 7-7168
- double Schottky barrier, grain boundaries, elec. props. in presence of deep bulk traps, appl. to ZnO varistors 7-7334
- electric field enhanced carrier emission, spectroscopic study 7-45350
- III-V semiconductors, localised electron states of substantial transition metal impurities, review 7-27295
- photosensitive semiconductor, parametric instability due to a travelling illumination intensity grating 7-38614
- semiconductor heterostructures, band-edge discontinuities, heuristic approach 7-52815
- semiconductors, Auger recombination via deep double-charged centres (*Ukrainian*) 7-12732
- semiconductors, compensated, impurity photoconductivity, field and spectrum dependences, exclusion effect 7-38635
- semiconductors, deep centres, book 7-18510
- semiconductors, deep centres, nonsteady capacitive spectrosc. investig. 7-12665
- semiconductors, deep level carrier capture and emission press. depend. meas., lattice relax. determ. 7-21862
- semiconductors, deep trap profiles determ. 7-58768
- semiconductors, electroabsorption of light by deep impurity centres 7-45988
- semiconductors, extrinsic n-type, stochastic self-oscillations under intense illumination 7-2639
- semiconductors, fluorescence line shape anal. for free-to-bound transitions 7-46097
- semiconductors, unipolar injection in presence of deep centres with negative Hubbard energy 7-38568
- Al_xGa_{1-x} As-GaAs multiple quantum wells, photoluminescence studies, press. depend. (*Chinese*) 7-13194
- AlGaAs:Sb, MBE growth, Sb doping 7-2038
- AlGaAs/GaAs modulation-doped heterojunctions, 2D electron gas, DX centres 7-38694
- AlGaAs-GaAs superlattices, impurity electron states (*Japanese*) 7-12662
- Al_xGa_{1-x}As, hot-electron capture at DX centres 7-45344
- Al_xGa_{1-x}As crystals, DX centre props. 7-2534
- Al_xGa_{1-x}As, DX centre, theory 7-12654
- Al_xGa_{1-x}As films and multilayer structures, MOCVD growth and characterisation, review 7-33586
- Al_xGa_{1-x}As:Si, deep donor centres 7-45217
- Al_xGa_{1-x}As/GaAs photoexcited heterojunction, charge transfer calcs. 7-12688
- AlInAs-GaInAs superlattices, electronic transport and depletion by tunnelling 7-27395
- As₂Se_{100-x}, vitreous chalcogenide semicond. layers, deep trapping levels, photostimulated effects (*Russian*) 7-2754
- Bi₁₂GeO₂₀, photoelectric props., influence of deep trapping centres 7-7279
- CaSO₄:Dy, gamma radiation damage on thermolum. 7-38059
- CdIn₂S₄, electron trap characts., TSC meas. 7-27340
- CdS thin films, deep trap depth, TSC meas. 7-58774
- CdS, with compensated i-layer, photosimulated deep level transient spectroscopy 7-7765
- CdSe_xTe_{1-x} and CdSe_xTe_{1-x}:Cu films, deep local states, photosensitivity, spectral study 7-22371
- GaAs, deep level nonradiative carrier capture press. depend. calcs. 7-12735
- GaAs epitaxial films, growth by close-spaced vapour transport, unwanted doping, X-ray diff., SEM obs. 7-27187
- GaAs, high-resistivity semiconductor, deep centres, determ. by optical transient current spectroscopy 7-52498
- GaAs, hydride VPE layers, deep level incorporation and background doping 7-17120
- GaAs, LEC-grown wafer, EL2 conc., stress distrib., near-IR absorption mapping 7-52522
- GaAs microwave absorption transient spectroscopy for investigation of deep levels in semiconductors 7-52520
- GaAs, photoconductivity, slow-relaxation phenomena 7-58837
- GaAs, plastically deformed, Hall effect meas. 7-27351
- GaAs, scanning optical fibre microscope, laser beam induced current images 7-48846
- GaAs, semi-insulating, LEC grown, midgap native donor concentration 7-33547
- GaAs semiinsulating LEC substrate, elec. homogeneity evaluation, thermally stimulated drain conductance meas. 7-32954
- GaAs, undoped semi-insulating, dislocations, deep trap levels, FET meas. (*Chinese*) 7-12643
- GaAs, VPE grown, defect formation leading to deep levels, review 7-64151
- GaAs:B, ion implanted, near-intrinsic and extrinsic photocapacitance due to the EL2 level 7-7147
- GaAs:C, impurity levels determ. 7-32949
- p-GaAs:Cr, excited and metastable states of Cr-related double centres 7-7153
- GaAs:Cu, neutral state of deep acceptors, photoluminescence spectra, Jahn-Teller effect 7-64149
- GaAs:In, strain effects, electrorefl. and photocapacitance study 7-22224
- n-GaAs:O, semi-insulating, impurity centres, electron capture 7-52643
- GaAs:S₂Si epitaxial layers, close space vapour transport growth, photoluminescence and electrical props. 7-21776
- GaAs:S surface elec. props. modification by plasma exposure 7-27346
- GaAs:Sn, photolum. spectra, line shape anal., conduction band to deep acceptor transition 7-46098
- GaAs:V, electromodulation spectra, deep level energy positions 7-38496
- GaAs-GaAs:In epitaxial layers, dislocation reduction, device performance effects 7-7354
- GaAs_{0.6}P_{0.4} degraded LEDs, origin of nonradiative centres, photocapacitance, electrolum. spectra 7-53413
- GaAs_{1-x}P_x epitaxial struts., radiative characts., deep centres effects 7-45220
- n-Ga_{1-x}In_xSb:Se(S), impurity states, press. and comp. depend., Hall coeff. and elec. resist. meas. 7-2533
- GaP, epitaxial struts., radiative characts., deep centres effects 7-45220
- GaP single crystals., anisotropic deep centres, polarised photolum. and thermolum. studies (*Russian*) 7-21867
- GaP:Fe, deep levels formed by Fe complexes 7-12657
- n-GaSb impurity Auger hole recomb. via deep acceptor, electron density depend. calcs. 7-38573

deep levels continued

- Ge:Zn deep impurity, shallow positive acceptor, far IR photocond. meas. 7-7157
- HgGa₂Se₄, single cryst., deep levels, photocond. and photolum. spectra 7-7159
- In_{0.5}Ga_{0.5}P layers, LPE, elec. and optical props. 7-17119
- InP microwave absorption transient spectroscopy for investigation of deep levels in semiconductors 7-52520
- InP:Fe, deep levels formed by Fe complexes 7-12657
- InP:Fe, midgap impurity levels, isomer shift and charge state calcs. 7-2538
- InP:Fe, Si-implanted and rapid thermal annealed, photoluminesc. study 7-59243
- InP:Fe, transient photoconductive response 7-52681
- InP:Mn, deep acceptor level, props. 7-21853
- InP-InP:As epitaxial layers, dislocation reduction, device performance effects 7-7354
- InSb, Dember EMF contrib. to capacitor photo-EMF 7-38621
- Mg₂Cd_{1-x}Se single crystals., impurity photocurrent temp. activation meas. and calcs. (*Russian*) 7-45394
- Se vitreous chalcogenide semicond. layers, deep trapping levels, photostimulated effects (*Russian*) 7-2754
- a-Se:Te films, space-charge depletion studies of deep states 7-59148
- Si : BF₂ preamorphised implanted samples, defects and leakage currents abs. 7-38514
- Si, deep impurity centres, thermophysical studies 7-58765
- Si, divacancy levels in the band gap 7-12644
- a-Si films, ion implanted device structures, solid phase epitaxy, elec. props. 7-12564
- Si, group III acceptors, neutral and ionised states, deep dopant description 7-64155
- Si MBE films, deep level defects 7-12668
- Si MBE layers, deep levels, DLTS meas. 7-12667
- Si, radiation-induced deep centres due to fast neutrons (*Czech*) 7-12661
- Si: transition metals, solubilities, diffusivities and deep levels 7-32465
- Si:As, ion implanted defects, laser annealing 7-21869
- Si:Au, deep levels, multiexponential anal. of deep level transient spectroscopy 7-52524
- Si:C, electron irradiated, photolum. defect spectra, obs. of interstitial C 7-59253
- Si:Cu(Au), deep level position in forbidden gap, charactn. using ionisation Gibbs free energy (*Chinese*) 7-58760
- Si:Gd,C profiled single crystal., electronic parameters and SiC inclusions 7-32944
- a-Si:H, glow discharge prepared, steady-state photoconductivity 7-38632
- a-Si:H, photocond. response, light soaking effects 7-45396
- a-Si:H, surface deep hole trap, photocurrent studies 7-45424
- Si:H and near-surface damage of Si caused by H ions, review 7-16813
- a-Si:H films, deep levels in the mobility gap 7-12670
- a-Si:H/a-SiN_x:H interface, deep states and photoluminescence spectra, transistor characts. 7-39186
- Si:Mn, optical props. (*Chinese*) 7-33043
- Si:Mn, temperature-electric instability, elastic compression effect 7-64239
- Si:n, deep level generation and annihilation 7-16612
- Si:N(O), pseudo Jahn-Teller effect and chemical rebonding 7-16992
- Si:Ni, deep levels elec. props. study 7-64156
- Si:Ni, thermal cond., impurity effect 7-44929
- Si:Ni reverse-biased p⁺nn⁺ junctions, electron thermal emission rates 7-7169
- n-Si:O, donor states of O rel. to heat treatment 7-12647
- Si:Pd, deep levels electronic struct., Xα-SW study (*Chinese*) 7-58761
- Si_{1-x}Ge_x:S(Se)(Te) solid solns., deep levels investig. 7-2529
- SiO₂:Ge, impurity charge trapping props., EPR spectra 7-27290
- SiSe⁺, photothermal release of carriers, deep levels, capacitance spectroscopy 7-16968
- Zn_{0.25}Cd_{0.75}Se mixed crystals., electron and hole deep level traps 7-16980
- ZnO varistors, electroluminescence temp. depend. and conduction mechanisms 7-17349
- ZnSe:As, MOCVD growth, exciton and deep emission bands 7-52367
- ZnSe:Fe, impurity ion photoionisation, EPR, photoconductivity spectra 7-52495
- ZnTe:Cl(Al), crystals, vacancy-impurity complexes, ODMR studies 7-2530

defect electron energy states

- see also *colour centres; deep levels*
- 1/f² from single-energy-level defects 7-52712
- α phase, E_i centre, nonradiative charge transfer rate 7-12659
- alkali halide crystals., self-trapped exciton recomb. luminesc.-recomb. induced F-centre form. anticorrel. calcs. 7-13201
- alkali halides, colour centres, Hartree-Fock cluster computations 7-16985
- alkali halides, Schottky defect energy, effect of three-body forces 7-21864
- alkali metals, impurities and defects, electronic structure 7-27299
- alkali oxides with antifluorite structure, F⁺-centre absorption energy calcs. 7-12658
- alkaline earth oxides, colour centres, Hartree-Fock cluster computations 7-16985
- alloys and metals, packing defect energy rel. to electron density (*Russian*) 7-45212
- amorphous semicond. III-V and II-VI cpds., electronic struct. of bulk and defect sites, tight-binding recursion method 7-45222
- amorphous semiconductors, multiple trapping, effect of defect level 7-27237
- amorphous tetrahedrally bonded semiconds., dangling-bond and void-like struts., microscopic structural model 7-21803
- anthracene single crystals., structural imperfections as triplet exciton traps, defect recovery 7-64160
- bicrystal boundaries, transient spectra of dislocation levels 7-52497
- chalcogenide glasses, dangling-bond and void-like struts., microscopic structural model 7-21803
- chalcogenide glasses, field dependent negative U-model and switching 7-7252
- crystalline solar cells, conditions for high efficiency 7-23145
- deep levels study, capacitance methods 7-45205
- defect state generation, Si rapidly annealed with incoherent light 7-52504
- diamond, electron beam irradi., vacancies, photoluminescence, radiative decay time meas. 7-46107
- diamond, radiation damage prod. of 5RL centres, phonons, absorpt. spectra, cathodoluminescence studies 7-33461

defect electron energy states continued

- diamond anomalous muonium, vacancy-associated model 7-51758
 dislocation mobility in semiconductors under illumination 7-44545
 double Schottky barrier, grain boundaries, elec. props. in presence of deep bulk traps, appl. to ZnO varistors 7-7334
 EL2 defect, identification 7-38502
 electronic struct. of incoherent grain boundary, recursion approach 7-64161
 grain boundary trap occupancy and recomb. models anal. 7-64266
 graphite intercalation cpds., staging dislocation electronic struct., electron scatt. rates, residual resist. 7-52558
 III-V semiconductor surfaces, virtual gap states and Fermi level pinning by adsorbates 7-2654
 insulating halide crystals, exciton-defect conversion 7-7122
 ion-implanted polymers, fractal elec. cond., current transients, percolative transition calcs. 7-2645
 L1₂ intermetallics, localised grain-boundary electronic states and intergranular fracture calcs. 7-45215
 LEC wafers, cathodolum. mapping, IR absorpt., X-ray topography obs. 7-33462
 local electron centre config. instability, quasilocal modes interaction model calcs. 7-58772
 metals, electronic structures of lattice defects, tight binding recursion method 7-27289
 metals, EM wave interaction with dislocations, conduction electron density (Russian) 7-63615
 muonium energy profiles, unrestricted Hartree-Fock cluster calcs., comment and reply 7-45907
 nondegenerate semiconds., charged dislocation hole capture, hole thermal ionisation and free density calcs. 7-38574
 nonmetals, defect polarization and Haldane-Anderson model 7-21858
 optical polarisation of nuclear moments in Si with 1D defects 7-7602
 p-type, undoped, electron irradiation, defect level annealing and DLTS 7-12660
 passivation of dislocations in Si at high H₂ press. 7-39763
 polarisation of solids by point defects, multipole theory 7-13086
 quantum well controlled conductivity, new donors 7-38491
 quartz, E'₄-centres, conversion rate into E'₂-centres 7-52517
 quartz, exoemission centre with O vacancies, cluster model 7-12651
 recombination of dislocation excitons 7-38578
 semiconductors, calculational schemes for defects, review 7-48201
 semiconductors, complex neutral defects, bound hole states, mag. props. 7-64157
 semiconductors, cubic, phonon scatt. at electronically degenerate defect states 7-21827
 semiconductors, deep centres, book 7-18510
 semiconductors, DLTS for defect characterisation 7-52521
 semiconductors, muonium defect centres, muon spin resonance studies 7-52502
 semiconductors, neutral vacancy electron states, orbital removal method 7-64047
 transition metal aluminides (TAl, T=Fe, Co, Ni, V), electronic struct. of vacancies 7-16975
 transition metal oxides, impurity and defect electron struct., self-consistent local density theory 7-45208
 transition metal perovskite type oxides, electronic struct. of point defects 7-16979
 transition metals, impurity and defect electron struct., self-consistent local density theory 7-45208
 zincblende-structure semiconductors; muonium states, muon spin resonance studies 7-53206
 AgCl, electronic struct. of intrinsic interstitial defects 7-21852
 AlAs/GaAs:Si super-doped structs., short-period superlattice electrical and defect props. (Japanese) 7-7353
 Al_{1-x}Ga_xAs, Ga interstitial identification by ODMR 7-33302
 AlN formed by N ion implantation of Al, electronic struct. 7-58926
 Al₂O₃ surface electrocathodolum., defect state transitions under high voltage stress 7-39187
 Al₂O₃:Fe,Y, high temp. DC elec. cond. rel. to superalloy oxide scale adherence 7-52615
 Al₂O₃-B₂O₃-SiO₂-Cu₂O glass, Cu activated, photoconductivity, lumin., influence of radiation defects 7-45381
 As-Se glasses, defect levels and photoconductivities 7-12673
 Au-GaAs (110) interface, photoemission studies, temp. effects 7-33517
 BaTiO₃, elec. cond. rel. to point defects 7-6619
 a-C:H, props., review 7-51630
 CaO, self-trapped hole centres, ODMR and spin coherence studies 7-7612
 CdGa₂S₄, luminesc. associated with defect complexes 7-27757
 CdI₂-Ag interface, absorpt. and luminesc. spectra studies (Russian) 7-59224
 CdS, carrier transport, defect effects, photoacoustic and photocurrent spectra 7-38626
 CdS, luminesc. associated with defect complexes 7-27757
 CdS, nonradiative recombination, elec. transport, combined photoacoustic and photocurrent spectra 7-38582
 CdS, photolum., exciton scatt. from defects and impurities, depend. on exciting light intensity 7-39156
 CdS single crystals, nonequilib. high-temp. vacuum annealing effects, intrinsic defect transform. 7-58764
 CdTe/GaAs heterojunction, defect and impurity states, photovoltage meas. 7-17065
 CoAl, electronic struct. of antistructure Co atoms and Co-vacancies 7-7165
 CoGa(Al), electronic struct. of vacancies 7-16975
 CoSi₂-Si heterostructures, MBE or solid phase epitaxially grown, Schottky barrier heights, DLTS spectra 7-12859
 CsCl, F_H(OH⁻)-centre absorpt. bands, pseudopotential calc. 7-52512
 Cs₂O-SiO₂ glasses, intrinsic and recomb. luminesc. and fundamental absorpt. spectra 7-13195
 Cu, nearest-neighbour host site elec. field gradient, monovacancy effects, muffin tin pot. calcs. 7-2549
 CuInS₃, heterogeneous, VLS growth, electronic defects, photocurrent spectra, photolum., EBIC analysis 7-27288
 CuInSe₂ polycrystalline thin film solar cells, donor-acceptor pair luminescence 7-17890
 CuInSe₂-CdS solar cells and CuInSe₂ thin films, charge transport studies 7-12890
 Cu₂O films, annealing of Cu and O vacancies, cathodoluminescence study 7-59263
 Ga_{1-x}Al_xAs, DX centres, inner and outer crossing lattice relax. 7-45218

defect electron energy states continued

- GaAs (001), chemisorption of CF₃ radicals, RHEED, photoelectron spectra, HF SCF calcs. 7-53497
 GaAs, defect structure defect., US meas. 7-21363
 GaAs, EL2 and As antisite defect props., review (Japanese) 7-7152
 GaAs, EL2 centre stability under electron-hole recomb. conditions 7-16978
 p-GaAs, electron irradiation-induced trap defects, DLTS study 7-12155
 GaAs, electron irradiation induced defects, DLTS study 7-58338
 GaAs, electron-irradiated, relative density of levels of radiation defects 7-52500
 GaAs, FTIR spectra of acceptors, electronic intrasite transitions and local vibr. modes 7-53377
 GaAs, internal thermal conversion, material for integrated circuits 7-12767
 GaAs MBE layers, deep level defects and impurities 7-22051
 GaAs, monovacancy electronic struct. and positron states, self-consistent LMO calcs. 7-2536
 GaAs, n-type, electron-irradiated, photoionization cross sections of E levels 7-64152
 GaAs, photorefractive beam coupling with picosec. pulses 7-31386
 GaAs, plastically deformed, Hall effect meas. 7-27351
 GaAs, point defects, props. and processes, dislocation form. and characterisation (Japanese) 7-7151
 GaAs pure and Si, Mn or Cu doped crystals, impurity and defect props., heat treatment, photolum. studies 7-39163
 GaAs semi-insulating cryst. characts., IC substrate appls. (Japanese) 7-6622
 GaAs thin films, grain boundaries, electronic props. 7-7172
 GaAs, undoped semi-insulating, dislocations, deep trap levels, FET meas. (Chinese) 7-12643
 GaAs, VPE grown, defect formation leading to deep levels, review 7-64151
 GaAs, variation of EL2 with As press. during heat treatment 7-58770
 a-GaAs:H/F, electronic struct., dangling bonds, cluster-Bethe lattice method calcs. 7-12592
 GaAs:Sn(Te)(Zn) surface layers, luminesc., electrophys. parameters, effect of annealing 7-64680
 GaAs/GaNAs interface, EELS near a single misfit dislocation 7-33497
 GaAs-AlAs superlattices, folded acoustic branches, leakage-induced and disorder-activated modes 7-33389
 GaAs-AlGaAs superlattice defects, DLTS study 7-21854
 GaAs_{1-x}Sb_x, alloy disorder broadening of defect energy levels 7-52516
 GaInAs, Czochralski-grown, dislocation effects investig. 7-7261
 GaSb/AlSb single quantum wells, electroreflectance and photoluminescence studies 7-46136
 GaSe, gamma irradi., photoluminescence spectra, temp. depend. 7-17336
 Ge, anomalous muonium, vacancy-associated model 7-51758
 Ge, grain boundary energies, computer calcs. 7-6639
 Ge, muon channelling, evidence for pionium formation 7-51897
 Ge, quenched, SA₂ acceptor, uniaxial stress effects, far IR optical study 7-64673
 a-Ge:H, B, P, As, dopant incorporation and doping efficiency 7-44587
 GeTe, valence and energy spectrum, supercond. state 7-45534
 HgCr₂Se₄ spinel magnetic semicond., electronic struct., elec. props., defects and ferromag. anisotropy 7-38857
 HgGa₂Se₄, photocond., photoluminescence spectra, annealing and ion implantation effects 7-39152
 InP (110) cleaved surface and Schottky diodes 7-58850
 InP, luminesc. associated with defect complexes 7-27757
 InP-Au interface, Fermi level pinning, growth characts., photoemission spectra 7-22009
 InP-Au(Al) Schottky barriers, defects introduced by mech. polishing 7-39768
 In₂Se₃, layered semicond., photolum. studies 7-7746
 KCl, Frenkel defect recomb., thermally stimulated electron emission obs. 7-64869
 KCl X-ray and γ -irrad., F-centre destruction owing to subsequent laser light excitation, luminesc. spectral characts. 7-27772
 KCl:Ca²⁺, Z₂⁺-centres, axial config., pseudopotential perturbation calc. 7-32952
 K₂O-SiO₂ glasses, intrinsic and recomb. luminesc. and fundamental absorpt. spectra 7-13195
 LaF₃, spectral parameters, lattice defects effects, X α discrete-variation method calcs. 7-7170
 LiBr, lattice deform. around an F-centre 7-32435
 LiCl, lattice deform. around an F-centre 7-32435
 LiF, lattice deform. around an F-centre 7-32435
 LiI, lattice deform. around an F-centre 7-32435
 Li₂O, F⁺-centre absorption energy calcs. 7-12658
 Li₂O-SiO₂ glasses, intrinsic and recomb. luminesc. and fundamental absorpt. spectra 7-13195
 MgO, deformed and annealed, red cathodoluminescence spectrum 7-27792
 NaCl, X-ray and γ -irrad., F-centre destruction owing to subsequent laser light excitation, luminesc. spectral characts. 7-27772
 NaCl:Ag Frenkel defect recomb., thermally stimulated electron emission obs. 7-64869
 NaCl:Eu²⁺, gamma irradi., optical absorpt. spectra, TSC meas. 7-58337
 NaCl:Mg, X-ray irradi., exciton interactions with impurity-vacancy dipoles, absorpt. and luminesc. spectra 7-45162
 Na₂O-SiO₂ glasses, intrinsic and recomb. luminesc. and fundamental absorpt. spectra 7-13195
 NbC, vacancy electronic struct., muffin tin Green's function method calcs. 7-2531
 NiSi₂-Si, Schottky barrier, interfacial defect states 7-27428
 PbSe₂Te_{1-x} thin films, localised defect states and Hall effect 7-2752
 Pb_{1-x}Sn_xTe solid solns., intrinsic defect donor states characts. Hall effect temp. depend. meas. 7-58762
 Pb_{1-x}Sn_xTe:In, impurity levels, covalent defect theory 7-52515
 PbTe, impurity levels, covalent defect theory 7-52515
 Rb₂O-SiO₂ glasses, intrinsic and recomb. luminesc. and fundamental absorpt. spectra 7-13195
 a-Se, structural disorder model 7-26641
 Se:O, electrophotographic props., doping depend. (Japanese) 7-12752
 Si : BF₂ preamorphised implanted samples, defects and leakage currents abs. 7-38514
 Si (111), local density of states near ideal vacancies 7-27380
 p-Si, alpha-particle irradi., defect form. and thermal stability 7-38073
 Si, anomalous muonium, vacancy-associated model 7-51758

defect electron energy states continued

- Si bicrystals, grain boundaries, electronic states, transient capacitance spectroscopy meas. 7-7173
- Si bicrystals and thin films, grain boundaries, electronic props. 7-7172
- Si, crystallised thin films, electrical characterisation 7-33116
- Si, DLTS spectrum of dislocations introduced by CW CO₂ laser (*Chinese*) 7-32939
- Si, dangling bond defect polarization and Haldane-Anderson model 7-21858
- Si, defect states on the surface and in the bulk, H passivation 7-13665
- Si diffused p-n struts, recomb. props. of base region, effect of thermal and radiation defects 7-17089
- Si, dislocation luminescence lines, polarisation 7-39154
- Si, divacancy electronic struct. calc. (*Chinese*) 7-38490
- α-Si, EPR-active centres, floating bond defects 7-38506
- Si, electron irradi., obs. of IR bands during annealing, kinetic study 7-45214
- p-Si, electron irradiation induced defects, DLTS study 7-38500
- Si, grain boundary energies, computer calcs. 7-6639
- Si, Jahn-Teller vibronic state of the neutral vacancy 7-16705
- Si layers, electron irradiation-induced defect levels, annealing behaviour, DLTS studies 7-52493
- Si MBE layers, deep levels, DLTS meas. 7-12667
- Si MBE layers, defect characterisation, luminesc., TEM studies 7-13227
- Si, monovacancy electronic struct. and positron states, self-consistent LMO calcs. 7-2536
- Si, neutron irradi. induced IR absorpt. bands 7-46004
- Si, neutron transmutation doped, optical current deep level transient spectroscopy 7-52525
- Si, off-centre impurities and defects, local electronic struct. valence-bond theory calcs. 7-2532
- Si, optical props. of isolated dangling bond 7-38507
- Si, precipitation induced microdefects, DLTS characts. 7-38511
- Si, radiation defect thermal ionisation, effect of dislocations on activation energy 7-6680
- a-Si, recomb. via dangling bonds, occupation statistics 7-38515
- Si Schottky diodes with dislocations, tunnelling transitions 7-52831
- Si solar cells, H passivation of dislocations 7-54323
- a-Si technology, review of developments 7-38551
- Si, with stacking faults, electron and phonon spectra, recursion method 7-32945
- Si:B, B-vacancy complex, electronic and atomic struct., ENDOR studies 7-63649
- Si:B, ion implanted, transient annealing and residual defect DLTS study (*Chinese*) 7-12642
- Si:B plastically deformed crystals, dislocation struct. and elec. activity, annealing effects study 7-37998
- Si:B(Al)(Ga)(P)(Sb) thermal donor props., impurity effects, DLTS, Hall effect, and admittance spectra meas. 7-21851
- Si:C, electron irradiated, photolum. defect spectra, obs. of interstitial C 7-59253
- Si:Ga, electron irradiated and annealed, photoluminescence spectra 7-13206
- Si:Ge, irradiated, photoluminescence spectra 7-13207
- a-Si:H, B, P, As, dopant incorporation and doping efficiency 7-44587
- a-Si:H, broken bond local environment relax., g-factor, cluster calcs. 7-37876
- a-Si:H, bulk, surface state densities, Bethe lattice method, CPA calcs. 7-32898
- a-Si:H, defect structure, ab initio theory 7-32298
- a-Si:H, divacancy electron struct., semiempirical CNDO/2 cluster calcs. 7-38495
- a-Si:H, electronic struct., inadequacy of the conventional view 7-32961
- a-Si:H, electronic transport 7-33004
- a-Si:H, metastable defect states, capacitance studies 7-45225
- a-Si:H, neutral dangling bond defect, photocarrier processes 7-32962
- a-Si:H, photoconductivity and light-induced changes 7-2640
- a-Si:H, RF sputtered, dangling bond energies, ESR studies 7-45818
- a-Si:H, recomb. at dangling bonds and steady-state photocond. Fermi level depend. calcs. 7-12734
- a-Si:H, surface deep hole trap, photocurrent studies 7-45424
- a-Si:H films, electron irradi., photocond., absorpt. coeff. spectral depend. 7-64279
- a-Si:H solar cells, density of states asymmetry effects 7-46946
- Si:O, cluster computations related to thermal donors 7-16990
- Si:O, magnetic resonance of O-related defects 7-17223
- Si:O₂B, ab initio MO electronic struct. calcs. 7-38499
- Si:PF₆⁺ ion implanted, recrystallisation kinetics during fast thermal annealing 7-16618
- Si/NiSi₂ heterojunction, interface states, DLTS and hydrogenation studies 7-12777
- Si-SiO₂, E' centre in thermally grown SiO₂, bias depend. annealing 7-45503
- Si-SiO₂ (111) interface, dangling bonds, dipolar interactions investig. 7-17107
- Si-SiO₂ interface, chem. transition, density of states calcs. 7-7397
- Si-SiO₂, MOS capacitors, defect struct. and interface state generation 7-7399
- SiC, 6H polytype, defect lumin., due to excess C vacancies 7-53391
- SiC, paramag. muonium centres, hyperfine freqs. 7-52503
- a-Si_{1-x}C_xH, B(P) films, valence band localised holes, light-induced ESR spectra studies 7-53110
- Si_{1-x}Ge_x films, optical band gap, photocond. props. 7-52672
- Si₃N₄ thin films, reactively sputtered, hopping cond., defect states 7-52620
- SiO₂, amorphous, intrinsic defects, semiempirical mol. orbital studies 7-63474
- SiO₂ films, energy levels of electron traps (*Japanese*) 7-64148
- V-SiO₂ intrinsic defect electronic struct., optical transitions, cluster-Bethe lattice calcs. 7-2541
- SiO₂:OH, X-irrad. induced defect centres, EPR obs. 7-45221
- a-Si_{1-x}Sn_x:H films, electronic structure of divalent defects 7-32960
- SnO₂, mechanical activation, defect form. and struct. 7-16972
- TaC_x, defect states, core level binding energy and valence band struct., XPS meas. 7-27291
- TaC_x, stoichiometric, core-level binding energies and valence-band struct., XPS 7-22450
- TiC_x energy band struct., Fermi energy and density of states, vacancy states effects, LMO-ASA calcs. 7-64078
- VC_x energy band struct., Fermi energy and density of states, vacancy states effects, LMO-ASA calcs. 7-64078

defect electron energy states continued

- W, magnetoresistance, crystal with surface defects (*Russian*) 7-32988
- YAG:Ni (Ni, Zr) (Fe), defect and optical props. 7-59258
- YF₃, spectral parameters, lattice defects effects, X_α discrete-variation method calcs. 7-7170
- ZnS, single crystal, annealed in O, intrinsic defects rel. to elec. and luminesc. props. 7-12649
- ZnS:Al, Cr, Fe crystals, recomb. luminesc., EPR and photocond. meas. 7-3076
- ZnSe:Cu(Ag)(Au), cationic substitutional impurities and metal vacancy, microscopic models 7-27296
- ZrN_x (100), vacancy state, UPS obs. 7-52718
- defect-impurity interactions** *see* *impurity-defect interactions*
- defect-phonon interactions** *see* *phonon-defect interactions*
- defectoscopy** *see* *flaw detection*
- defects, crystal** *see* *crystal defects*
- defibrillators**
see also *patient treatment*
Bioengineering Program of the Universidad Nacional de Tucuman (Argentina, 1974-85), cardiac fibrillation, defibrillation research 7-4650
blood pressure sensor for fibrillation detect. method, implantable defibrillator output circuit evaluation (*Japanese*) 7-14160
cardiac defibrillators, safety and reliability (*Spanish*) 7-65892
cardiac defibrillators, technological development (*Spanish*) 7-3939
- deformation**
see also *bending; cold working; creep; drawing (mechanical); elastic deformation; elongation; ferroelasticity; plastic deformation; shape memory effects; thermomechanical treatment*
alloys and metals, packing defect energy rel. to electron density (*Russian*) 7-45212
amorphous alloys, isothermal compressibility, theoretical analysis (*Russian*) 7-58391
amorphous Lennard-Jones solid, shear deform.-induced orientational ordering, computer simulation 7-38155
arbitrary Eulerian-Lagrangian formulation 7-6105
bar, bending vibrs., amplitude-dependent internal friction, influence of non-uniformly stressed condition (*Russian*) 7-58410
beam element, curved isoparametric quadratic thick 7-4684
binary alloys, TEM study of precipitate growth mechanisms 7-52064
chemicothermal treatment conditions of metals, form. kinetics of irreversible deform. 7-17692
cholesteric liquid crystal, mechanical shear deformation, time-depend. behaviour 7-26631
composite systems with randomly oriented short fibres, mech. response, microstruct. approach 7-20593
conference on the safety and reliability of reactor pressure components, Stuttgart, Germany, (Oct. 1985) 7-9583
coupled plate linear problems 7-1406
crack flanks, deform. modes due to shear, paradoxes 7-57754
cracked bodies, effective elastic moduli in plane deform. 7-58395
crystals, elastic moduli and nonaffine deformations, density-functional theory calcs. 7-44649
cylinder, viscoelastic, finite deformations under rolling contact 7-6159
damage model, 3-D finite strain viscoelastic 7-50955
deformed cubic crystals, generalised set of elastic moduli and stability calcs. 7-51914
dynamical response of systems with localized nonlinearities, ultimate state method 7-10190
Earth crust, thermoelastic strain in half-space covered by unconsolidated material 7-29001
Earth crust deformation, appl. of two-layer model for biaxial extension of lower layer 7-8886
eigenstrains in regions bounded by ellipsoidal surfaces 7-92
ethylene-propylene-diene elastomer, sorption and swelling in water and humid media (*Russian*) 7-27139
FEM for elastic-plastic plane stress, appl. to anti-plane strain 7-14768
fibre reinforced composites, flexible, nonlinear elastic behaviour 7-39570
fluid mixtures, diffusion induced by nonhomogeneous shearing deform. field 7-14765
foils and films tensile testing, specimen-deformation machine for X-ray diffractometers 7-33874
graphite, contamination-mediated deformation, scanning tunnelling microscope study 7-44967
graphite, nucl. grade, polycryst., deform. under press., elastic moduli rel. to struct., neutron irradi. effect 7-28069
heat absorption demonstration using incorrectly installed bulb 7-48257
heat of solid deformation meas., by quick-response calorimetry 7-1522
high temperature reactor components, multiaxial loading tests 7-49541
Holocene sediments of Himalayan-Andaman Arc, deformational struts. (seismites) prod. by earthquakes 7-66120
holographic interferometry, computer-based fringe interpretation 7-31264
Hookean materials, nonlinear mode II crack tip fields 7-37392
icosahedral quasicrystals, elastic moduli and elastic instability, density-functional theory calcs. 7-44649
inelastic state-variable theory, large strain 7-4686
irregular surface simulation using spline fitting 7-43311
large deformation elasticity theory, nonlinear spectral characts. 7-6094
laser Doppler anemometer for measuring superlow velocities 7-43812
linear reversible, thermodynamics 7-32551
liquid droplet deformation in gas flow, anal. 7-51278
logarithmic strain, material time derivative 7-24421
Luders bands, phenomenological theory 7-21328
measurement using spatial frequency modulation of holographic interferometry, moire method (*Japanese*) 7-56218
membrane deformation under creep conditions 7-1449
metallic materials with ellipsoidal second-phase particles, high temp. deformation 7-17577
metals, nonelastic deformation, modelling internal stresses 7-51924
bis-methylammonium tetrachloro manganese antiferromag. crystals, struct. deform. by exciton self-localisation, luminesc. spectra fine struct. study (*Russian*) 7-27752
nematic liq. cryst., localised deform. near surface defects, birefringence study 7-45978
network polymers, deform. under compression, resistance, struct. factors (*Russian*) 7-13538
nonlinearity elastic solids, Volterra dislocations, large deformations, Weingarten theorem generalization 7-43669
nuclear power plant piping, technical and economical incentives behind strain limitation 7-10221

deformation continued

- optical method of measuring deformations using diffraction phenomenon (French) 7-6167
- paperboard, constitutive behaviour under uniaxial and biaxial loading 7-63019
- PET membranes, permeability and struct. in adsorpt.-active medium (Russian) 7-28347
- planar analysis using digital correlation method, optimised 7-26136
- plate, flexible, loaded by short press. pulse, deflection 7-57683
- plates, deformation and fracture under thermal shock 7-43763
- plates, shear deformable elastic, small finite deflections 7-26144
- plates and cylinders, surface-cracked, J-integral and HRR dominance under large-scale yielding 7-63080
- plates and shells, finite strain large deformation, nonlinear theory 7-20602
- plates and shells, surface-flawed, line-spring anal. using deform. theory 7-63021
- PMMA, temp. change during rapid compressive deform., thermoelastic coeffs. 7-13495
- polyethylene, high density, temp. change during rapid compressive deform., thermoelastic coeffs. 7-13495
- polyethylene terephthalate films, struct., effect of rolling (Russian) 7-13476
- polyethylene-tetrafluoroethylene, row crystallised film, deform. mechanism 7-44663
- polymers, deform. under impact, transient high temp. meas. 7-22802
- polymers, deformation isothermal conditions, dynamometric curves (Russian) 7-8073
- power plant mechanical components, stress and strain limitation 7-10187
- power station piping systems, dynamic test data, comparison with analytical methods 7-10191
- PVC, pure and plasticized, orientation, Fourier transform IR study 7-44661
- PWR fuel rods, power ramp data, FROST and THERMOST codes, cladding deform. rod elongation 7-62034
- reactor construction codes and engineering mechanics conf., Paris, France, Aug. 1985 7-48153
- reactor piping systems, strain limitation calcs. 7-10188
- refined transverse shear deformation theory form multilayered anisotropic plates 7-1434
- Reissner's theory of transversely isotropic plates, error bound 7-50963
- rock flow due to gravity, use of Newtonian and non-Newtonian fluid dynamics scaling without inertia 7-8939
- rocks, appl. of stream function and Gauss's principle of least constraint in structural geology 7-29009
- rocks, crack-seal mechanism as deform. factor in strike-slip faulting 7-29010
- rocks, effect of press. on elastic and strain-strength props. 7-47424
- rocks, Mohr diagram and 3D strain 7-40594
- rocks, plane strain kinematics 7-14270
- rocks, problems in extrapolation of laboratory rheological data to tectonic processes 7-66107
- rocks, relation between mag. susceptibility and strain in laboratory expts. 7-66109
- rocks, sectional strain ellipse during progressive coaxial deformations 7-40470
- RPHIN—a FORTRAN 77 program for acquiring axial ratios, long axis orientations and centroid positions of elliptical strain markers 7-17581
- rubber, crosslinked chain entanglement and orientational effect, form factor, deform. depend. 7-6711
- rubber-like solids, nonhomogeneous deform., appl. of generalised strain meas. 7-37328
- sedimentary rocks, straining of cross-bed populations 7-4034
- shear deformation plate continua of large double layered space structs. 7-43660
- shear moduli, positive/negative, for small and large deformations of elastic materials 7-6088
- shell elements, degenerated, implementation with transverse shear and membrane strains 7-50944
- shell with rigid inclusion, finite deformation 7-9667
- shells, noncircular cylindrical, deformation 7-11308
- shells, spherical, orthotropic, shallow, on elastic foundation, nonlinear studies 7-37357
- shells, spherical, with delaminations, bifurcation of equilb. 7-31669
- shells coaxial, orthotropic, cylindrical, with flowing fluids, axisymm. normal wave propag. 7-106
- shells of revolution, finite axisymmetric deflections, strain-displacement relations 7-57682
- short-chain network, orientation functions 7-6557
- solid deformable body mechanics, modern directions 7-1398
- steel, austenitic stainless, in-reactor deformation 7-56826
- steel, Mn-Mo-V, reactor piping material, strength, deformation and fracture behaviour 7-13578
- steel tubes, energy dissipation characts. 7-63034
- stochastic modified Korteweg-de Vries equation 7-29767
- strain concentration in inhomogeneous boundless thin plate with circular opening 7-29754
- strain estimation for external event loads 7-10189
- superalloys and ceramics, electron microscopy studies, symposium, Nantes France (July 1986) 7-18479
- surface deformation measurement by light speckle using optical fibre bundle 7-30078
- synchrotron radiation mirror, thermal distortion prediction with finite element analysis 7-43306
- thin plate, stretching deformation, method of generalized plane stress 7-29760
- velocity field equations and strain localisation 7-43672
- Zircaloy, claddings, creep deform., bulge growth, time to failure 7-59589
- Al, lattice sparing of interstitial solid solns. of B and C, deform. interaction, pseudopotential method (Russian) 7-58271
- Al sheet, dislocation relax. contrib. to deform., internal friction and dynamic modulus meas. during creep 7-63626
- Au, defect struct. evolution following DT neutron irradiation 7-58346
- CaF₂-Si interface, strains in MBE grown insulator films, MeV ion channeling meas. 7-7080
- CoO, deformed, dislocation struct., TEM study 7-21209
- CsMnCl₂ antiferromag. crystals, struct. deform. by exciton self-localisation, luminesc. spectra fine struct. study (Russian) 7-27752
- Cu-Al bronze, hot deform. and annealing, mechanical props. and softening kinetics 7-17552

deformation continued

- Fe-C system, elastic anal. of deform near spherical C particle embedded in Fe matrix 7-63709
- GaAs, seminsulating, electrophysical props., dislocation effects 7-16557
- GaAs single crystals, high temp. mechanical props., effects of doping and environment 7-21326
- GaAs single quantum well, doubly resonant LO-phonon Raman scatt. via deform. pot., polarisation obs. 7-39114
- Ge crystals, high temp. deform., fine slip band struct. (Russian) 7-44561
- Li₂SO₄H₂O, charge density at 80 and 298 K, X-ray and neutron diffraction 7-21166
- MnO, deformed, dislocation struct., TEM study 7-21209
- Ni, defect struct. evolution following DT neutron irradiation 7-58346
- Ni, mag. props., influence of low-temp. US deform. (Russian) 7-53878
- Pd membrane, diffusion of H₂, transport coeffs. and energetics 7-21533
- Si, recoil implantation of O₂, characterisation by double-crystal X-ray diffraction, TEM, Monte Carlo simulation 7-51807
- Si, self-implanted, strain 7-51918
- Si, twinning partial dislocations, velocity 7-63629
- TaC, high temp. hardness, stacking faults, hardening rel. to C diffusion 7-3369
- Ti-glass mirror, temp. deformation 7-20386
- (ZrO₂)_{0.9}(Y₂O₃)_{0.1} fiamite crystals, bending and compressive strength temp. depend. meas. 7-44653

deformation lines see Luders bands

degenerate semiconductor materials see degenerate semiconductors

degenerate semiconductors

- see also heavily doped semiconductors; superconducting semiconductors
- anisotropic hot carrier distrib., transport eqn. solns. anal. 7-58815
- diffusivity-mobility ratio, modified form of Einstein rel. in presence of electric and mag. field 7-45356
- runaway effect 7-52607
- GaAs-AlAs heterojunctions, asymmetrically doped, photoresponse under external bias 7-38692
- HgCr₂Se₄, magnetisation, temp. depend. 7-45629
- n-InAs, Kane-type semiconductors, Einstein relation, mag. quantisation effect 7-52603

dekstrons

No entries

delamination

- aramid fiber reinforced epoxy, delamination fracture toughness 7-53900
- composite laminates, with matrix cracking and interior delamination, stiffness props. 7-44669
- composite materials, mode I edge delamination, stress distrib. ahead of crack, thermal residual stress 7-6151
- composites, compressive failure modes 7-6717
- compression induced failure, surface delamination along macrocrack 7-6155
- cracked-lap shear specimen thickness for interlaminar fracture toughness determ., delamination vs. adherend failure 7-1510
- edge delamination, strain energy release rate anal., residual thermal and moisture influences 7-1508
- end-notch flexure specimen, mode II interlaminar fracture toughness, finite element anal. 7-1509
- fibre reinforced composites, delamination growth in angle-ply laminated composites 7-31701
- films, decohesion from ceramic or semiconductor substrates 7-21711
- flexure specimen, end-notched, for mode II testing, design and anal. 7-51005
- glass fibre reinforced epoxy, unidirectional, impact behaviour, temp. influence 7-3427
- glass fibre reinforced polyester, random short fibre SMC, interlaminar fatigue crack growth interlaminar fatigue crack growth 7-33772
- graphite fiber reinforced epoxy, delamination fracture toughness 7-53900
- graphite fibre reinforced epoxy, interlaminar fracture toughness, effects of rad. 7-33773
- graphite fibre reinforced epoxy laminates, fatigue damage mechanisms and residual props. 7-44671
- graphite fibre reinforced epoxy laminates, holographic investigation of stressing techniques for detecting flaws 7-59732
- graphite fibre reinforced epoxy laminates static or fatigue loading, fracture surface anal. (German) 7-22826
- layered materials, semitransparent, modulated photothermal radiometric anal. 7-54033
- mechanics of damage and fatigue, conf., Haifa, Israel (Jul. 1985) 7-48139
- multilayered plate, acoustic material signature calc. 7-37300
- panels, cylindrical, instability, effect of centrally located midplane delamination 7-63022
- poly-p-phenylene benzobisthiazole-epoxy composite, adhesive behaviour 7-65278
- polymer, composite structure, thermal and thermomech. response 7-8150
- shells, spherical, with delaminations, bifurcation of equilb. 7-31669
- C fibre reinforced plastic laminates, ply failure under moisture and temp. influences (German) 7-22744
- C fibre reinforced plastic laminate; impeding edge-delamination development effect on tension-tension loading (German) 7-22827
- C fibre reinforced plastic, damage states, US and acoustic emission study (German) 7-22828
- C fibre reinforced thermoplastic laminates, compressive strength 7-39580
- Fe, ductile and grey cast, laser surface hardened, sliding wear 7-17650

delay-differential systems

chaos, statistics and dimensions 7-48572

delay lines

see also acoustic delay lines

- acoustooptical delay line for optical distrib. processing 7-42977
- coherent optical fibre delay-line processor 7-31253
- large plotted circuit board production, delay lines for particle calorimeter 7-25330
- multicell detectors, delay-line readout method 7-831
- optical delay lines using active feedback, beam overlap 7-43293
- oscillator using interdigital transducer 7-11241
- Rayleigh wave resonators and delay lines, 1/f noise 7-1348
- SAW dispersive delay line design 7-20530
- AlN-sapphire, low temp. epitaxial film growth 7-13387
- AlPO₄ SAW delay lines, heat treated, IR meas., temp. coeff. of delay and insertion loss 7-13486

delayed neutrons

r-process, role of delayed neutrons in element production 7-60534

delayed neutrons continued

- Pu content of Mururoa Atoll coral samples, delayed neutron anal. 7-54415
⁴⁸Rb, A=94, 95, P_n values by β - γ spectroscopic method 7-30507
⁴⁸Rb, A=94, 95, P_n values measured by β - γ spectroscopic method 7-5194
²³⁵U(n,f), delayed neutron activity, few-group anal. 7-42084
²³⁵U(n,f) thermal fission, composite delayed neutron energy spectra 7-61932

delayed protons

- A=124-146, beta-delayed proton emission, ground state spins and rot. bands 7-49349
 heavy nuclei, Gamow-Teller resonance in β^+ decay and delayed proton emission 7-49327
⁶¹Ge, beta-delayed proton decay 7-41946
⁴⁰Sc decay, selected aspects in the structure of beta-delayed particle spectra 7-49346
¹⁵¹Yb, β -delayed proton spectrum structure, peaks from N=81 precursors 7-15202

delays

- see also distributed parameter systems*
 group delays meas. of guided modes, in optical fibre waveguides (Czech) 7-57596
 measurement for signal traversing dispersely inhomogeneous ionosphere layer, accuracy 7-23934
 respiratory gas exchange calc. using mass spectrometer, correction for instrument time constant and transport delay 7-60143

delta modulation

- ECG signal changes reconfiguration, using delta modulation (Czech) 7-60119

demagnetisation

- see also magnetisation*
 Bloch wall motion simulation 7-59049
 discharge equipment for rock AF demagnetization 7-55274
 ferromagnetic bodies of finite dimensions, mag. states rel. to elastic stresses in trans-Rayleigh region 7-27587
 magnetic thin films, demagnetising energy in imperfect films, directional depend., appl. for mag. storage media 7-45770
 NDT use, automatic demagnetisation system 7-65260
 superconductors and magnetic materials, internal fields 7-17131
 Ce(Co,Cu,Fe)₆, magnetically hard, heat treatment effects on struct. and mag. characts. 7-27564
 Co-Cr sputtered films, microstructural inhomogeneity, mag. props. 7-45768
 Co-Ni-P electroless plated thin films, microstructure, mag. props., mag. recording appl. 7-27581
 Co-P electroless plated thin films, microstructure, mag. props., mag. recording appl. 7-27581
 Fe-Cr-Co-Si-Ti, permanent mag. alloy, ductile, effect of heat treatment on mag. props. (Korean) 7-8137
 Nd-Fe-B rapidly solidified permanent magnet materials, magnetisation processes and domain wall motion 7-38902
 Nd-Fe-B rapidly solidified ribbons, magnetisation, quench rate depend. 7-53034
 (YSm)₃(FeGa)₃O₁₂ garnet film, demagnetisation, elongation of striped domain struct. 7-45737

demagnetisation, adiabatic *see magnetic cooling***demand assignment, telecommunications** *see multiplexing; switching theory***Dember effect**

- InSb, Dember EMF contrib. to capacitor photo-EMF 7-38621

demodulation

- see also demodulators; modulation*
 FIR heterodyne detectors, review 7-35596
 heterodyne detection, interferometric phase synchronisation of remote heterodynes 7-60570
 heterodyne interferometric temp. sensor using transverse He-Ne Zeeman laser and polarisation maintaining fibre 7-25991
 interferometric distance meas. by wavelength shift of laser diode light 7-4806
 Cd_{1-x}Hg_xTe IR heterodyne detectors, intermediate temp. operation 7-35594

demodulators

- see also demodulation*
 submm laser system for local oscillator use in heterodyne receiver, astron. appl. 7-34869
 TaS₂, quasi-1-dimens. conductor, dynamic behaviour, possible electronic apps. 7-38548

demography

- American astronomers, evolving demographics 7-35191

demonstrations

- includes student experiments*
see also student laboratory apparatus
 A-level physics (Nuffield) investigations, assessment criteria 7-29640
 acoustic diffraction expt., geometrical theory 7-35179
 adsorption calorimetry, beginners course (Japanese) 7-35182
 aerodynamic lifting force on aerofoil, companion of explanations 7-48234
 atmospheric diffraction rings, eclipses and lunar phases, appl. of Tensor lamp 7-48245
 balancing toy, centre of gravity, oscills. about equilb. 7-48243
 ball, bouncing, chaotic dynamics 7-35160
 Boltzmann constant meas. 7-14742
 carrier mobility meas., Haynes-Shockley expt. use for student laboratory 7-55933
 Curie point thermomagnetic engine, demonstration of Carnot principle 7-48233
 diffraction patterns display using electric razor 7-35168
 drift velocity, direct demonstration using the Hall effect 7-48229
 e/m experiment, magnetic field and electron trajectory calcs. 7-48228
 elasticity, nonideal experiment 7-14741
 electrical transients, multimeter obs. 7-41044
 electrophilic aromatic substitution, relative activating ability of ortho and para directors 7-9635
 Elihu Thomson expt., example of progressive modelling 7-55930
 equipotential plotting apparatus, for student laboratory 7-41040
 fluids, differential light scatt. expts. 7-29627
 general purpose correlator for introductory student demonstration expts. 7-18537
 glycerin, motion of sphere studied using videotapes, viscosity meas. 7-35149

demonstrations continued

- glycerine, use of Atwood machine to study Stokes' law and viscosity meas. 7-35150
 gravitational acceleration, meas. using bouncing rubber ball 7-48237
 guided inquiry laboratory at US Military Academy, West Point 7-9621
 heat absorption demonstration using incorrectly installed bulb 7-48257
 heat engine, pV cycle area rel. to work done 7-35170
 holography in high school science classroom 7-24342
 inertial moment, slip method determ. using functional force and impulse 7-41038
 internal assessment of practical coursework in GCSE 7-29613
 light wavelength in water 7-35167
 longitudinal standing waves in pipe 7-41039
 mechanics teaching using bubble-tube accelerometer 7-14739
 metal ring levitation, alternating mag. field, induced current demonstration 7-43
 moire fringes, transparencies 7-24336
 molecular models for overhead projector demonstrations 7-9637
 Newton's laws of rigid body mechanics, proof using stroboscopic photograph 7-55927
 nuclear track detector kit for use in teaching 7-18543
 optical systems, relative phase effects 7-57
 order to chaos transition, expt. 7-41
 pendulum interfacing to microcomputer 7-35166
 physics course practical work assessment, state-of-the-art 7-29612
 physics experimental and practical work assessment through OEA 7-29641
 Ranque-Hilsch tube, demonstration of second law of thermodynamics (Spanish) 7-14746
 retrograde motion demonstration model machine 7-18531
 school physics experiment, planning 7-14745
 solar constant measurement from snow melting from barn roof 7-48256
 solitons, demonstration of behaviour using nonlinear electrical transmission line 7-55932
 squeezeable junctions for electron tunnelling and surface electric field experiment 7-24344
 stability, of overhanging pile of heavy objects 7-48255
 Stimpfmer, for speed meas. of golf ball on putting green 7-24343
 two phase flow demonstration device for nuclear thermal hydraulics education 7-29647
 variable star, digitally synthesised light curve lecture demonstrations 7-18520
 visual, PLZT transparent ceramic modulator appl. 7-4647
 water waves in a ripple tank 7-18526
 Cu, rod, skin depth and complex mag. susceptibility, expt. 7-51
 Ge, band gap determ. method 7-35155
 Si, band gap determ. method 7-35155

dendrites

- see also crystal growth*
 axisymmetric needle crystals., 3-D, solvability condition at large undercooling 7-32337
 crystal growth, sidebranch generation mechanisms, nonlinear effects 7-64035
 crystallisation front morphology rel. to inclusions in melt (Russian) 7-64890
 dimethyl sulphoxide, dendritic solidification and surface-pressure-induced wetting transition in narrow gaps 7-27223
 electrodeposition, dendritic and fractal structures, diffusion and current fields 7-45102
 growth, geometrical model, small velocity limit 7-7081
 numerical finite difference model for steady state cellular array growth 7-21787
 polypyrrole, diffusion-controlled polymerisation, growth instability 7-28311
 pyrrole polymerisation, diffusion-controlled statics and dynamics, fractal and dendritic growth in electrochem. cell 7-59758
 Saffman-Taylor finger, sidebranching in interfacial dynamics, white noise effect 7-21627
 Saffman-Taylor instability, narrow fingers 7-37436
 snowflakes, solidification, pattern form. in structs. 7-34560
 stability of dendritic crystals 7-38422
 symmetric model of growth, boundary integral formulation 7-45103
 Ag-AgI-Ag 2D ionic cond. system, fractional dimensionality of Ag dendrites 7-45100
 Al-Cu-Mg, growth by Stepanov's method, macro- and microstructure, strength, plasticity meas. 7-33546
 Al₂O₃-ZrO₂, rapid solidification, alumina dendrite morphology 7-21424
 BiSeI, dendritic, growth from vapour, characteris. 7-21788
 Cd(OH)₂, dendritic structures in agar gel 7-58723
⁴He crystals, dendritic growth obs. 7-44948
⁴He dendritic growth, spatio-temporal coherence and chaos, conf. Los Alamos, USA, Jan. 1986 7-48158
 NH₄Cl, irregular fractal-like crystal growth, diffusion-limited aggregation model 7-2445
 Si, dendritic web cryst., solar cells and modules fabrication status 7-8391
 Si dendritic web ribbon, electrical and struct. props. 7-16922
 Si dendritic web ribbons, structural defect characterisation 7-12074
 Si-H, amorphous, dendritic web, Czochralski flat plate modules and concentrator module, price comparison 7-17904
 β -SiC dendrites, CVD, propag. mechanism 7-38423
 Tb_{0.27}Dy_{0.73}Fe₂, twinned [112] crystals, magnetostriction 7-53105
 Zn-NiOOH cells, KOH conc. effects on shape change and cycle life 7-28393
 ZnTe, chemical vapour transport and homoepitaxial growth in closed-tube system, thermodynamic analysis 7-33582

dendritic crystals *see dendrites***dendritic structure**

- alloy, heterogeneous, fusion kinetics 7-3280
 alloy melts, undercooled, dendritic growth, effect of growth rate dependent partition coeff. 7-65015
 alloys, binary, unidirectional solidification, cell-dendrite transition criterion (Chinese) 7-65018
 alloys, undercooled, rapid dendrite growth 7-65014
 growth is channel from supersaturated soln. 7-44433
 growth models, comparison of theory with expt. 7-22649
 microsegregation, effect of solidification rate 7-46480
 numerical finite difference model for steady state cellular array growth 7-21787
 pivalic acid directional solidification, metastable dendritic interface pattern obs. 7-63779

dendritic structure continued

- planar interface, cellular and dendritic struct. transitions during rapid solidification 7-22666
- steel, C, directional solidification, δ/γ transform., P and Mn solute distrib. in dendrites 7-65020
- steel, cast, nonmetallic inclusions influence on fracture character 7-3421
- steel, high speed, peritectic transform., decomp., carbide precip. Nb alloying effect (*German, English*) 7-22677
- steel, stainless, martensitic, cooling rate and heat treatment effect on chem. microinhomogeneity 7-3294
- Udimet 700, Ni-base alloy, solidified, dendrite arm spacing rel. to cooling rate 7-53713
- Ag-Sn hypoeutectic alloys, primary phase shape rel. to cooling rate and comp. 7-59509
- Al-Co, melt spinning, microstruct., precip., microhardness (*Korean*) 7-46444
- Al-Cu, solidification, microsegregation in coarsened dendritic microstruct. 7-28048
- Al-Cu (4.5 wt.%), laser treated, surface solidification with moving heat source 7-22648
- Al-Mg (9.8 wt.%), AlMgSi, AlZnCuMgZr, directional solidification, microstruct. (*German*) 7-46452
- Al-Si, chill-cast, heat flow and dendritic arm spacing during solidification 7-53714
- Al-Si-Mg (7, 0.3 wt.%), strength and ductility, effect of macroporosity 7-3386
- AlCuLi alloys, large quasicrystalline dendrites, triacontahedral solidification morphology 7-32345
- Al₂O₃-TiN powder composites, densification kinetics and struct. form. during sintering under high press. 7-53687
- Cu-Sn (11 wt.%), stir cast, torsion behaviour 7-46567
- Fe crystals, growth shape, effect of melt undercooling (*Russian*) 7-46308
- Fe-C-based alloys, high C, rapidly solidified, mech. props. 7-22673
- Fe₆₇Co₁₈B₁₅Si, amorphous mag. alloy, crystallisation, elec. resist., TEM obs. 7-11927
- Ge droplets, undercooled, microstruct. 7-65013
- K₂O-CaO-SiO₂ system, cryst. growth kinetics, morphology, melt comp. depend. 7-46303
- Nb₃Al superconducting tape prepared by CO₂ laser beam irradiation 7-17145
- Ni-base superalloy, cast, high Al-Ti, eutectic form. and σ -phase control (*Chinese*) 7-7983
- Ni-base superalloy powders, Ar atomised, dendritic struct. 7-46451
- Ni-base superalloys, cast, solidification behaviour w.r.t. Hf additions (*Chinese*) 7-7984
- Ni-Cr-Ti-Al-(Mo), dendritic single crystals, microsegregation 7-46477
- Ni-NbC eutectic, directed crystallisation, comp. growth laws (*Russian*) 7-65021
- Ni-Sn highly undercooled droplets, rapidly solidified, microstruct. studies 7-22670
- Ni-Ti-Nb, shape memory alloy, cast microstruct. 7-7988
- Pb-Bi system, peritectic crystallisation, cooling rate effect 7-46440
- Sb-Sn alloy, maximum microsegregation from peritectic phase systems 7-12286
- Si dendritic web solar cells, twin plane effects on minority carrier diffusion length 7-13868
- Si ribbons, dendritic web grown, high temp. mech. behaviour, strain rate and temp. depend. of yield stress 7-65099
- Sn-Bi alloy, heterogeneous, fusion kinetics 7-3280
- V-W single crystal alloys, directionally solidified, growth structs. 7-3159

dense fluids, theory see liquid theory**densification**

- see also density; powders; sintering*
- α -Al₂O₃ powders, high press. compaction, density, pore size, grain size 7-13413
- bronze BrAZh, elec. discharge sintering of powder from swarf, electrophys. and mech. props., microstruct. 7-27974
- carborundum refractory provisions with aluminium-chromium phosphate binder 7-46395
- ceramic composites, liq. phase sintered, hot isostatic pressing 7-64989
- ceramic composites, sintering, role of shear deform. 7-64988
- ceramic powders, green state, real-time US NDE during compaction 7-22955
- ceramic powders, tapping behaviour, numerical analysis 7-46360
- ceramic synthesis from molecular precursors, conf., Palo Alto, USA (Apr. 1986) 7-35113
- ceramics, powder compaction response diagrams, generation 7-39450
- compressible materials, complex math. model of plastic flow 7-64959
- explosive consolidation of powders into rods, computer simulations 7-64955
- graphite, powder, elec. resistivity, rel. to degree of comminution 7-45257
- isostatic pressing pressure rel. to relative compact density 7-7912
- metal, powders, hot isostatic pressing, empirical model 7-46365
- metallic glass reinforced Al composite fabrication by multi-lamina explosive compaction 7-59482
- mullite-alumina composites, sintering and charactn. 7-3252
- particles, ultrafine, consolidation kinetics, influence of interface irregularity (*Russian*) 7-53649
- porcelain, sintering kinetics, struct. evolution 7-28004
- porous body, deformability criterion based on continual model 7-64958
- porous materials, strain hardening, compaction eqns. 7-64953
- porous solids, kinetics of press. assisted final stage densification, pore size distrib., computer simulation 7-59477
- powder densification by interface-reaction controlled grain boundary diffusion 7-64950
- powder diffractometry, preferred orientation, intensities correction, March model appl. 7-1808
- powder metallurgical materials, plastic working in presence of free surface, math. modelling 7-53651
- powder plastically worked articles, annealing effect on behaviour in temp. jump and substruct. 7-27961
- powder sinterability characteristics linked with manuf. method, mech. processing and heat treatment effects 7-53652
- powder sintering, temp. jump behaviour, manufacture method and impurities effect 7-13402
- pressure sintering, computer simulation using finite element anal. 7-3214
- PVC, implosive compaction of powders 7-33630
- PVC based powder mixtures, shock consolidation, densification, industrial appls. 7-39473
- refractories, compactum under quadrilateral compacting press. 7-13397

densification continued

- refractory carbide powder, mech. treatment model, energy characts. 7-53653
- shock compression induced modification and synthesis, book contrib. 7-27957
- silica monolithic gels, autoclave prepared Raman studies 7-8314
- sintered materials, characts., influence of porosity 7-7910
- sintering, intermediate and final-stage, microstruct. development 7-64952
- soft soil consolidation model, integral methods for partial differential eqn. 7-66124
- steel, austenitic stainless, liq. phase sintering, effect of Si additions 7-53678
- steel, high-speed, powdered, struct. after sintering in presence of liq. phase 7-53677
- steel, high-speed, produced from machining waste, liq. phase forming during sintering 7-3226
- steel, stainless, Cr-Ni type, powder, force characts. of powder compaction process 7-7912
- zonal segregation in powder bodies, model analysis 7-27962
- Al alloys, liquid dynamic compaction, microstruct. and precipitation, TEM study 7-59529
- Al powders, cold sintering 7-64972
- Al-Cu compact, struct. form. during sintering 7-53675
- Al-Mg, rapidly solidified powders, effect of extrusion parameters on props. 7-39595
- Al-Ni-Fe-(Co) powders, cold sintering 7-64972
- Al-Zn-Mg-Cu, high-energy rate powder metallurgy processed, microstruct. evaluation 7-22607
- Al₂O₃ fine powders, high purity, props. and sinterability (*Japanese*) 7-22621
- Al₂O₃, neutron irradi., microstruct., mech. props. 7-51843
- Al₂O₃-MgO, diphasic xerogels, densification, sintering, isostructural seed, epitaxy 7-27987
- Al₂O₃-TiN composite, interfacial reaction and mass transport of components during sintering 7-3254
- Al₂O₃-TiN powder composites, densification kinetics and struct. form. during sintering under high press. 7-53687
- Al₂O₃-ZrO₂ ceramics, densification kinetics 7-27992
- B₂C ceramics, pressureless sintering with polycarbosilane addition 7-46389
- BN, cubic, polycryst., influence of sintering conditions on phys. props. 7-22618
- BN, graphite-like powder particles, shock compression effects 7-39453
- c-BN, high press. sintering 7-22615
- BN, wurtzite, sintered polycryst., texture form. during hot compacting at high press., sphalerite transition 7-53685
- Bi₄Ti₃O₁₂ ceramic fabrication, grain-oriented, by normal sintering, sintering mechanisms (*Japanese*) 7-22619
- C Cu powder, force characts. of powder compaction process 7-7912
- C, hard type, B-doped, prep., phys. and mech. props. 7-39571
- Co₇Si₁₀B₁₅, amorphous powder, static consolidation, mechanical and mag. props. 7-3217
- Cu powders, sintering, densification, grain growth (*Japanese*) 7-53662
- Cu spheres, 2D arrays, rearrangement during sintering 7-46361
- Cu-Al₂O₃, dispersion strengthened powder alloys struct. and mech. props. 7-53667
- Cu-Cr powders, sintering, densification rel. to Cr content 7-13405
- Cu-graphite contacts prep. using atomised Cu powder 7-27976
- Cu-Sn-Pb system, struct. form. during sintering 7-64967
- Fe powder, force characts. of powder compaction process 7-7912
- Fe powder, quality assessment method 7-53671
- Fe powder, ultrafine, and hot forged specimens, reduction temp. effect on struct. form. and props. 7-53670
- Fe powders, sintering, densification, grain growth (*Japanese*) 7-53662
- Fe-Cu, sintering, form. of Cu pockets in Fe grains 7-7922
- Fe-P system, sintering at atm. press. 7-64971
- Fe-P-Cu(Ni)(Mo), sintered atomised powder premixes, mech. props. 7-7931
- Fe₂O₃ reactivity, decomposition mechanism depend., reaction vol. and densification meas. 7-28308
- LaB₆ dispersed powders and compact specimens, struct. and morphology 7-64976
- Li₂SiO₃ pellets, sintering, density, struct., porosity 7-53682
- MgAl₂O₄, neutron irradi., microstruct., mech. props. 7-51843
- MgO compacts, sintering, densification and porosity rel. to Mg₃(PO₄)₂ additions 7-17505
- MgO-CaO, activated sintering, densification, microstruct. (*Chinese*) 7-13410
- Mg₂SiO₄, fosterite-based ceramic with BaO addition, synthesis, sintering, struct. and props. 7-46397
- Mo powder, sintering of porous bodies, rate growth and heredity phenomena 7-53652
- Na₆Al₆Si₆O₂₄·2xNaBr, bromosodalite powders, compaction kinetics 7-3215
- (Na_{0.5}K_{0.5})NbO₃, sintering, densification and elec. props., effect of Ba additions 7-46387
- Na₂O-B₂O₃-SiO₂ glass ceramic, prep., SiO₂ replacement, phase separation, struct. 7-13428
- Ni powder plastically worked articles, annealing effect on behaviour in temp. jump and substruct. 7-27961
- Ni-base alloys, microcryst. powders, shock consolidated, microshear bonding 7-22745
- Ni-Mo-Cr-B powders, amorphous and microcrystalline, shock consolidated, wear props. 7-46655
- Ni₃Al(B,Ti), rapidly solidified powders, struct. of consolidated products 7-3222
- NiTi alloy powder, shock compaction 7-59480
- PZT:Nb ceramics, sintering, pair doping, elec. characts. 7-39469
- α -SiC, sintered, occurrence and distrib. of B-containing phases 7-39466
- Si₃N₄ fine particles, aggregate struct. and compacting process (*Japanese*) 7-46393
- Si₃N₄, gas press. sintering, fracture toughness, fibre like struct., additions effect 7-13414
- Si₃N₄ powders, high press. not pressing, mech. props., thermal cond. temp. depend. 7-3231
- Si₃N₄, sintered, microstruct., mech. props., Pr₆O₁₁ additive effect 7-17506
- Si₃N₄-TiC composites, densification, matrix-dispersoid reaction, mech. props. microstruct., impurities effect 7-64994
- SiO₂, amorphous, densified, O diffusion kinetics, annealing, gamma-ray effects 7-52127

densification continued

- SiO₂, amorphous, thermal, UV irradiation induced compaction and photoetching 7-12146
 SiO₂ powder compacts, densification rel. to sintering atmosphere 7-13417
 SiO₂, spherical particles synthesis, thermal behaviour (*Japanese*) 7-7943
 SiO₂-Al₂O₃ powders, prep. by spray pyrolysis, sinterability, effect of chem. comp. (*Japanese*) 7-3246
 SiO₂-P₂O₅ system, glass-ceramic materials, compaction kinetics using centrifugal forces 7-27999
 SiO₂-N₂ films, deposited by plasma-enhanced CVD, charact. 7-2413
 Si₃ON₂, impure densification by liquid phase sintering 7-17494
 SmCo₅ powder magnet, texture form. in alternating and steady mag. fields 7-27977
 Sr(NO₃)₂, ionic cond. study as function of pelletizing press. 7-12358
 Ti filters, filters, hydrodynamic compaction and sintering 7-7915
 Ti parts prod. from TiH₄ powder by hot pressing 7-27973
 Ti-Fe-Mn, sintering, dilatometry, thermographic obs. 7-13404
 TiB₂ ceramics, pure and liq. phase sintered, processing and microstruct. development 7-3251
 TiC, ultrafine powder behaviour during annealing and sintering 7-3244
 TiC-Fe-Cr alloyed with Si, high-Cr, sinterability and mech. props. improvement 7-64986
 TiSi₂ ultrafine powder prep. and film charactn. 7-64975
 W monosized spherical powder, dynamic compaction 7-39458
 W-Cu compacted pseudoalloys, elastic props., deform. diagram and pores effect 7-33722
 WC, powder, sintering of porous bodies, rate growth and heredity phenomena 7-53652
 WC-Co compact, stereological analysis of struct. form. during consolidation of carbide powder 7-53688
 WC-Co powder mixtures, electrolytic Co plating effect on densification and strength props. 7-53686
 WC-TaC-Co, N contained cemented carbides, sinterability, mech. props. rel. to prep. 7-17507
 WC-TiC-Co TK type hard metal prod. using Ti alloy swarf 7-27996
 Y₂O₃ powders, agglomerate strength distrib., US meas. 7-46379
 Zn₃P₂ pellets, elec. cond., compacting press. depend. 7-58809

densimeters *see* **densitometry****densitometers** *see* **densitometry****densitometry**

- see also photometry*
 Compton scatter densitometry, multiple-and single-scatter fractions 7-56315
 coronary arteries densitometry in radiographs, improved phys. model 7-28689
 dyestuff, optical density determ. with multi-reflection, correction eqn. (*Japanese*) 7-35563
 hydrostatic densitometer, absolute meas. of temp. dependences of density and related variables 7-35496
 Lexan polycarbonate, automatic scanning of enlarged fission tracks 7-30881
 rock microstructure, image analysis of particles, FORTRAN V program 7-66311
 vibrating-rod densimeter theory 7-31894
 vibrodensitometric determination of percent stenosis, effect of beam hardening and scatt. 7-28686
 CdSe lattice defects, digital struct. anal. by ion beam thinning for high resolution electron microscopy 7-6616
 Ti film charactn. for LiNbO₃ integrated optic devices 7-57607

density

- see also atmospheric pressure and density; density measurement; density of gases; density of liquids; density of solids; plasma density*
 1D inverse problems of elasticity 7-41102
 Hugoniot values, calc. from atomic props. 7-44735
 isobutyric acid-H₂O, near-critical binary fluid mixture, refractive index, Lorentz-Lorenz rel. 7-7659
 C films, diamond-like, empirical categorization and naming 7-16919

density, atmospheric *see* **atmospheric pressure and density****density, vapour** *see* **density of gases****density functional theory**

- alkali metal clusters, structures, pseudopotential method, local density approx. 7-36840
 atomic exchange energy functionals, rational fn. representation, HF calcs. 7-49905
 atomic kinetic energy density, approx. functionals study, HF calcs. 7-36476
 atomic point transformation and one-electron density, many-electron energy-density-functional theory 7-62250
 atoms, microscopic stress tensors 7-42481
 atoms, molecules and solids, appls. 7-27225
 atoms and ions, closed shell, polarisability, local density approximation 7-56999
 BA's, structural and electronic props., pseudopotential method, local density approx. 7-32353
 charge, spin and momentum densities, conf., Sanga-Saby, Sweden (July, Aug 1985) 7-24258
 charged solid-liq., interfaces, dipolar hard spheres, density functional theory study 7-63414
 condensed matter calculations, alternative to extended Thomas-Fermi theory 7-27274
 conference, Marineland, Florida, USA (March 1986) 7-40985
 crystals, elastic moduli and nonaffine deformations, density-functional theory calcs. 7-44649
 d-band metals, binding force, effective interatomic pots., strong scatt. open shell metals 7-32262
 diamond, energy band gap calc., self-interaction correction to local density approx. 7-45144
 diamond, optical phonons and elasticity at megabar stresses 7-21375
 diatomic molecules, potential energy curves, numerical basis function calcs. 7-25438
 effective medium approach 7-45201
 electron correlation, band gaps and quasiparticle energies calcs. for semiconductors and insulators 7-27278
 electron gas, dielectric function, dynamical local-field factor 7-21840
 electron gas with uniform density, screened-exchange functional 7-64138
 exchange energies, exact, local density approx. calcs. 7-38481
 fluid interfaces, phase transitions, local density approx. and smoothed density approx. study 7-63912
 freezing and interfaces, appl. of density functional theories in 2D and 3D 7-32621

density functional theory continued

- generalised exchange local-spin-density-functional theory, 7-36499
 hard-sphere fluids, density functional models 7-58112
 Hohenberg-Kohn-Sham theory, formulation 7-38427
 icosahedral quasicrystals, elastic moduli and elastic instability, density-functional theory calcs. 7-44649
 III-V semiconductors, electronic struct. calcs. 7-12608
 inert gas, pair pot., energy density functionals, Thomas-Fermi theory 7-42485
 inert-gas atoms, hyperpolarizabilities, local-density approx. method 7-25630
 inhomogeneous electron gas pressure calc. (*German*) 7-64145
 ion distribution near charged electrode, local density functional approx. 7-54131
 kinetic energy, gradient expansion, graph approach 7-42463
 LCGTO X α method, appl. to photodissociation and conform. energy problems 7-25393
 local approximations, applications 7-27229
 many-fermion systems of arbitrary dimensionality and interparticle interaction, nonlocal exchange energy 7-38482
 metal surface, self-consistent image pot. 7-38662
 metal surfaces, jellium model, nonlocal exchange and correlation 7-52736
 metal-metal tunnelling electrons, barrier height, image-force effects 7-52747
 metal-solid electrolyte boundary, self-consistent electron theory, double layer, parametric instability, capacitance anomalies 7-52832
 metallic molecules and cpds., magnetic moment formation and mag. susceptibility 7-58995
 metals, nonuniform liq., in partially ionised states, density functional theory 7-6504
 microscopic optical pot., radial shape, real part modification by second order diagrams, appl. to ⁴⁰Ca 7-41926
 noninteracting electrons, nonequilibrium thermodynamic pot. functional, h⁴-order terms, gradient expansion 7-48667
 orbital systems, fractionally occupied, density functional theory, appl. to ionisation and transition energies 7-42451
 physical significance of eigenvalues, orbital electronegativity and ionisation pot. 7-62245
 plasmon dispersion relations, correl. and inhomogeneity corrections, local density approx. calcs. 7-21839
 quantum systems, microscopic stress tensors 7-41147
 recent advances, time depend. version 7-38426
 rigid particles in external field, density functional statistical mechs. 7-44332
 semiconductor heterojunctions, self-consistent density functional calcs. 7-17097
 semiconductor superlattices, dynamical screening, quasi-2D electron gas, electron-phonon interactions 7-45464
 semiconductor-alloy phase diagram, first-principles self-consistent local-density total-energy calcs. 7-44751
 semiconductors, transport phenomena in electron gas, correlation effects 7-38479
 shock Hugoniot eqn. of state, electron band theory approach 7-21392
 submonolayer adsorbed film, phase diagram, intrinsic and extrinsic ordering forces, density functional theory calcs. 7-63952
 submonolayer film, phase diagram, relax. mechanisms, density functional theory calcs. 7-63953
 superionic conductors, density functional theory, appl. to Ag₂S 7-32697
 thin metal films, power absorpt. due to electron-hole pair production, screening pot. at surface 7-52490
 transition metal oxides, impurity and defect electron struct., self-consistent local density theory 7-45208
 transition metal surfaces and interfaces, hyperfine fields 7-58847
 transition metals, fast electrons, energy loss spectra, microscopic anal. for 4d-systems 7-39329
 transition metals, impurity and defect electron struct., self-consistent local density theory 7-45208
 transition metals, resistivity and superconducting transition temp. 7-17013
 Al plasma, high density, high temp. at. pot., comparison with bremsstrahlung Gaunt factors, density functional theory 7-63254
 AlAs-GaAs superlattices, phase transitions under high press. 7-64016
 AlGaAs/GaAs heterostruct., quasicrystalline system, electronic struct. studies 7-38699
 Ar crystal, dielec. const., density depend., in-cryst. polarisability calc. 7-22175
 Ar fluid, positronium bubble and positron induced clusters, positron lifetime meas. 7-39246
 Ar, kinetic energy density, nonlocal correl. fn., CI wave fns. and HF calcs. 7-42496
 Ar-CO₂ interface, wetting transitions, density functional theory and modified hypernetted chain calcs. 7-63913
 As, structural calcs. 7-7143
 Au-Sd transition metal alloys, heat of form. and cryst. struct., linear augmented STO calcs. 7-51705
 Be, kinetic energy density, nonlocal correl. fn., CI wave fns. and HF calcs. 7-42496
 Be⁻, metastable ion, shape resons. scaled local density calcs. 7-42464
 Be₂, bonding, appl. of local spin density approx., comparison with other studies 7-25371
 C, single-particle excitations, dynamic correl. corrections, local density theory 7-45115
 C₂, Coulomb and exchange-correlation energies, local density functional calcs. 7-20087
 C₆CS, first stage intercalation cpd., self-consistent band struct. calc. 7-52395
 C₈K, first stage intercalation cpd., self-consistent band struct. calc. 7-52395
 CO, potential energy curves, numerical basis function calcs. 7-25438
 C₆₀Rb, first stage intercalation cpd., self-consistent band struct. calc. 7-52395
 Ce compounds, band description with localising orbitals 7-45121
 CeAl₃, quasiparticle band struct., local-density approx. anal. 7-27250
 CeBe₁₃, band struct. calc. 7-32905
 CeCu₂Si₂, quasiparticle band struct., local-density approx. anal. 7-27250
 CePb₃, heavy fermion material, magnetism and superconductivity 7-52880
 Co clusters, small, reactivity 7-15781
 Cr₂, bonding, appl. of local spin density approx., comparison with other studies 7-25371
 CsI, press. induced structural instability, ab initio pseudopotential techniques 7-52042

density functional theory continued

- CuNi, substitutionally disordered, electronic struct., LCAO-CPA calcs. 7-64067
- CuZn, work function, influence of ordering 7-33062
- Fe overlayers or sandwiches with Cu (001), electronic and mag. props. 7-64499
- Fe, paramagnetic ground state props. and pair potentials 7-32352
- Fe₁₃ clusters, icosahedral and cubo-octahedral coordination, electronic struct., first-principles method calcs. 7-45132
- Fe₂P, electronic struct., mag. props., KKR, LMTO methods, LSD approx. 7-64070
- GaAs, dielectric response and electronic states 7-33320
- GaAs, single-particle excitations, dynamic correl. corrections, local density theory 7-45115
- GaAs-AlAs superlattices, GaAs and AlAs, energy band gap calc., self-interaction correction to local density approx. 7-45144
- GaP, single-particle excitations, dynamic correl. corrections, local density theory 7-45115
- Ge, dielectric response and electronic states 7-33320
- Ge, single-particle excitations, dynamic correl. corrections, local density theory 7-45115
- Ge valence electron subsystem, local and exchange pot. approxs. calcs. 7-38477
- H₂O, correl. and Born-Oppenheimer energy eval. 7-62257
- H₂O, Coulomb and exchange-correlation energies, local density functional calcs. 7-20087
- H₂O, mol. struct., density functional anal. 7-62272
- He, Kohn-Sham time-depend. orbital density functional theory, hydrodynamic formulation 7-25678
- HPt, electronic struct. calcs. 7-45200
- In_{0.5}Ga_{0.5}As_{0.5}P_{0.5}-InP quantum well, 2D electron gas, self-consistent calcs. 7-58890
- Kr, kinetic energy density, nonlocal correl. fn., CI wave fns. and HF calcs. 7-42496
- LaBe₁₃, band struct. calc. 7-32905
- Li, simple local pseudopotential 7-32888
- Mg⁺, metastable ion, shape resons. scaled local density calcs. 7-42464
- Mg₂Si antiferroelectric semicond., electronic struct. calcs. 7-12608
- Mn₂P, electronic struct., mag. props., KKR, LMTO methods, LSD approx. 7-64070
- Mo (001), unoccupied surface states, inverse photoemission study 7-46171
- Mo, electronic struct. of mag. 3d impurities, local density approx. 7-64432
- N₂ crystals, molecular-to-nonmolecular transformation at high press., theory 7-21432
- N₂, potential energy curves, numerical basis function calcs. 7-25438
- Nb and its dihydride, Compton profiles 7-59281
- Nb, electronic struct. of mag. 3d impurities, local density approx. 7-64432
- Ne, electronic kinetic energy, energy-density functional calcs. 7-42465
- Ne impurity immersed in liq. metallic H, polarisation effects on core levels 7-64158
- Ne, kinetic energy density, nonlocal correl. fn., CI wave fns. and HF calcs. 7-42496
- Ni, paramagnetic ground state props. and pair potentials 7-32352
- Ni, spin polarised electronic struct., mag. and bonding props. 7-32904
- Ni:B(s), grain-boundary cohesion, impurity segregation effects, density-functional cluster model calcs. 7-44835
- Ni-H system, band structure calcs. 7-45140
- Ni₂Ga, momentum density distrib., Compton scatt., positron annihilation, symmetrised APW method 7-64069
- NiH, spin polarised electronic struct., mag. and bonding props. 7-32904
- Ni₄ clusters, charge distrib., Hartree-Fock SCF INDO calcs. 7-52411
- Ni₂P, electronic struct., mag. props., KKR, LMTO methods, LSD approx. 7-64070
- Pb, self-consistent relativistic band struct., normal and high press. 7-52413
- Si (100) with chemisorbed H₂, transition from the dihydride to the monohydride phase 7-58631
- Si, energy band gap calc., self-interaction correction to local density approx. 7-45144
- Si, energy calcs. using four-centre integrals 7-27227
- Si, single-particle excitations, dynamic correl. corrections, local density theory 7-45115
- a-Si:H, defect structure, ab initio theory 7-32298
- Si:Mg(Be) metastable impurity levels, self-consistent local-density total-energy calcs. 7-38503
- Si-Ge heterojunction, structural and electronic props. 7-21997
- SiC, single-particle excitations, dynamic correl. corrections, local density theory 7-45115
- (SiH₃)₂O mol. struct., hydrolysis of Si-O bonds, density functional anal. 7-62272
- SiH₃OH, mol. struct., density functional anal. 7-62272
- Sr, relativistic band struct., self-consistent calcs. under normal and high press. 7-64068
- Ta, Compton profiles, APW calcs. 7-27809
- TaIr, electronic struct. calcs. 7-45200
- ThBe₁₃, band struct. calc. 7-32905
- UBe₁₃, band struct. calc. 7-32905
- UPt₃, heavy fermion superconductivity and normal state props. 7-52412
- USi₃(Sn₃)(Ru₃), electronic struct. and f hybridisation 7-12600
- V and its dihydride, Compton profiles 7-59281
- W, Compton profiles, APW calcs. 7-27809
- WO₃, electronic struct. calcs. 7-45200
- W(001), unoccupied surface states, inverse photoemission study 7-46171
- Xe, two-photon one-electron ionisation cross sections, RPA, LDA HF calcs. 7-49912
- Yb, relativistic band struct., self-consistent calcs. under normal and high press. 7-64068
- ZnSe (110) surface atomic geometry and energy states, self-consistent pseudopot. calcs. 7-21582

density measurement

see also hydrometers

- 1:1-electrolyte, solns., apparent molar vol. calc. 7-32538
- air, using variable-volume aerometric body 7-4818
- alkali metal vapour number density, optical determ. using Faraday rotation 7-48696
- ceramics NDT by acoustic microscopy with single zoom lens 7-3570

density measurement continued

- column density meter, high precision technique for line-of-sight vapour densities meas. 7-48695
- fluidic volumetric-flow, mass-flow density and viscosity meter 7-26367
- gamma-source backscatter density gauges modelling 7-34716
- high pressure rolling-ball viscometer up to 1 GPa 7-1655
- hydrostatic densitometer, absolute meas. of temp. dependences of density and related variables 7-35496
- melt, high temp., density meas. method (Chinese) 7-4817
- methane, press., density and temp. meas. in crit. region 7-52000
- positron emission tomography meas. of regional lung density 7-14116
- precision densitometer which compensates for liquid viscosity 7-48697
- quartz oscillator for density measurement of a-Si films 7-7079
- real-time neutron radiography system, quantitative density meas. 7-33901
- soot particles formed from acetylene, density, optical meas. (German) 7-4819
- standard, 1-kg Si sphere, polishing 7-56224
- supersonic expansion, density meas. using beam-deflection optical tomography 7-44080
- trabecular bone density in proximal femur, quantitative CT assessment 7-14129
- ultrasonic levitators, appl. to density meas. 7-50874
- vibroscopes, electrostatic self-resonating, cct. design 7-56226
- density of gases**
- alkali metal vapour number density, optical determ. using Faraday rotation 7-48696
- bromotrifluoromethane, liq. and gaseous phases, compression factor, vapour press. meas. 7-51905
- column density meter, high precision technique for line-of-sight vapour densities meas. 7-48695
- dimethylether-Xe, vap. press. and density, excess molar enthalpy and entropy 7-12319
- ethane, ionisation by X-rays, effect of fluid density on energy absorpt. 7-31920
- ethane, thermal diffusivity around crit. point along liquid-gas coexistence curve, light scatt. meas. 7-52098
- gas/liquid critical points under reduced gravity, density distrib. 7-21426
- measurement of air density, using variable-volume aerometric body 7-4818
- methane, ionisation by X-rays, effect of fluid density on energy absorpt. 7-31920
- methane-H₂ mixture, isochoric meas. at temp. from 140 to 273.15K, eqn. of state, density 7-26377
- methanol, compressed gas and liq. PVT props. meas., pseudoisochores determ. 7-16713
- resistive transducer (Polish) 7-35507
- Ar-Ne mixture, density meas. up to 8000 bar, Lennard-Jones comparison 7-1669
- CO₂-ethane gaseous mixture, determ. of virial coeffs., ref. index meas. method 7-51362
- CO₂-n-hexadecane supercritical system, phase equilb. and vapour density meas., high-pressure multiproperty apparatus appl. 7-12249
- H₂O ordinary fluid, thermal cond., viscosity and density data 7-60898
- He-Ar mixture, density meas. up to 8000 bar, Lennard-Jones comparison 7-1669
- He-H₂ system, density inversions between fluid and solid phases at high pressures 7-58451
- K, density meas. 1500-2100K, 1.4-4.0 MPa 7-51371
- N₂O, thermal diffusivity around crit. point along liquid-gas coexistence curve, light scatt. meas. 7-52098
- Rb, density meas. 1450-2000K, 1.7-5.2 MPa 7-51371
- SF₆, thermal diffusivity around crit. point along liquid-gas coexistence curve, light scatt. meas. 7-52098
- Si, CVD, thermal diffusion effects, math. model 7-2410

density of liquids

see also hydrometers

- 1:1-electrolyte, solns., apparent molar vol. calc. 7-32538
- alcohol-water mixture, volumetric behaviour, high press. study 7-51904
- alkali halide solns. in water-acetamide mixtures, partial molal vol. meas. 7-58389
- n-alkanes C₆-C₂₀, nonpolar liqs., viscous flow, thermodynamic activation functions 7-6341
- 4-(trans-4'-n-alkylcyclohexyl) isothiocyanatobenzenes, mesogenic props. 7-1852
- benzene, acoustic and thermodynamic props., press. and temp. depend. 7-63745
- binary alloy in ID lattice, density oscillations model 7-9800
- bromotrifluoromethane, liq. and gaseous phases, compression factor, vapour press. meas. 7-51905
- butoxybenzylidene phenylazoaniline, liq. cryst. transitions, density and US vel. studies 7-32266
- t-butyl alcohol-H₂O mixtures, X-ray scatt., Kirkwood-Buff parameters 7-44337
- carbohydrate solns., aqs., molar vols., isobaric expansion coeffs. and compressibilities 7-12183
- carbohydrate solns., non-aqs., molar volumes, isobaric expansion coeffs., compressibility 7-12184
- classical one-component plasma, surface props. 7-6490
- clay suspensions, montmorillonite and kaolinite, viscosities and densities 7-28351
- crystal growth from melt, physical constants of melt determ. 7-13348
- cumene/1-butanol mixtures, US studies 7-58414
- cyclohexane, acoustic and thermodynamic props., press. and temp. depend. 7-63745
- cyclohexane-carbon tetrachloride-ethyl acetate, ultrasonic and rheological study 7-31727
- dense liq. departures from Joule's law near freezing w.r.t. vacancy props. of hot crysts. 7-63840
- 1,2-dibromoethane-alcohol mixtures, excess vol., comp. depend. meas. 7-63704
- dichloromethane-benzene(toluene) mixtures, US vel., densities and viscosities 7-6726
- 3,3-dimethylbutan-1-ol-n-hexane mixtures, excess molar enthalpy, heat capacity and molar vol. 7-44850
- 1:1 electrolytes, high-temp. thermodynamic props. 7-21481
- 1:1 electrolytes, specific heat and density meas. 7-6816
- equations of state, reference states for liquid density temp. dependence 7-26899
- ethane, thermal diffusivity around crit. point along liquid-gas coexistence curve, light scatt. meas. 7-52098

density of liquids continued

ethylbenzene-acetonitrile (butyronitrile) (nitromethane)(nitroethane), excess molar volumes 7-44640
gas/liquid critical points under reduced gravity, density distrib. 7-21426
hard discs and hyperspheres, freezing 7-44768
N-(p-n-heptyloxybenzylidene) p-n pentylaniline, liq. cryst. transitions, density meas. 7-26821
N-(p-n-heptyloxybenzylidene) p-n-pentylaniline, liq. cryst. phase transitions, density, US vel. meas. 7-1874
Lennard-Jones fluid, repulsive, sound dispersion, density depend. 7-12212
methanol, compressed gas and liq. PVT props. meas., pseudoisochores determ. 7-16713
methyl methacrylate-n-heptane, excess enthalpies and vols. at 298.15K 7-44824
methyl methacrylate-n-hexane, excess enthalpies and vols. at 298.15K 7-44824
octyloxycyanobiphenyl reentrant nematic, preferred density model, P-V-T test 7-12271
n-pentane-dichloromethane, excess thermodynamic props. 7-52079
p-n-pentyl-p'-cyanobiphenyl and dil. solns. with tetraethylmethane, nematic and isotropic phases, density meas. 7-2079
perturbed soft-chain theory, thermodynamic props. prediction, group-contrib. correlation 7-16711
polymer melt struct., nonperturbative integral eqn. theory calcs. 7-44345
polymer solns., conc., relax. of long wavelength density fluctuations 7-37838
polyol, in soln., US vel., density and viscosity meas. 7-32693
pyrene solubility in binary solvent systems, meas. and NIBS model calcs. 7-63829
smectic A-smectic A transitions, density dielec. and X-ray studies 7-2196
smectic mixtures of A₁ and A₂ phases, nematic gap obs. 7-6792
sulpholane-benzene (toluene)(p-xylene)(mesitylene), ultrasonic speeds, compressibility and excess molar quantity at 303.15K 7-26870
transition metals, liquid, thermodynamic props. 7-12323
water-2-propanol-nitromethane, US vel. at miscibility point 7-21355
AlNH₄(SO₄)₂ multicharged electrolyte soln. in water-tert butyl alcohol, viscosity and density studies 7-52104
Ba, liquid phase, density and surface tension 7-44957
CO₂ saturated liq., sp. ht. meas. 7-16783
Ca, liquid phase, density and surface tension 7-44957
Ca²⁺+D-ribose (D-arabinose), enthalpies, sp. heat and molal vols. at 25°C 7-8253
Co complexes and related cpds., aq. soln., densities, viscosities and electrolytic cond. (Japanese) 7-12347
DCl, molar vol., vapour press. meas. 7-44779
HCl, molar vol., vapour press. meas. 7-44779
H₂O ordinary fluid, thermal cond., viscosity and density data 7-60898
He-H₂ system, density inversions between fluid and solid phases at high pressures 7-58451
Hg-In liquid alloys, vol. and thermal expansion coeffs., higher-order correlation effects 7-12328
Hg-Sn liquid alloys, vol. and thermal expansion coeffs., higher-order correlation effects 7-12328
Hg_{1-x}Cd_xTe, pseudobinary melts, heat capacity, enthalpy of melting, thermal cond. 7-21477
KAl(SO₄)₂ multicharged electrolyte soln. in water-tert butyl alcohol, viscosity and density studies 7-52104
KAl(SO₄)₂ solutions, effect of impurities on props. 7-6495
Li-Pb, sp. ht. calc. from expt. density and temp depend. press. data 7-63839
LiNbO₃, crystal growth from liquid, physical consts. determ. 7-32322
N₂, liq., compressed, far IR absorpt. spectrum, density effects and rel. diffusion 7-39112
N₂, liquid, molecular dissociation and shock-induced cooling at high densities and temperatures 7-28307
N₂O, thermal diffusivity around crit. point along liquid-gas coexistence curve, light scatt. meas. 7-52098
SF₆, thermal diffusivity around crit. point along liquid-gas coexistence curve, light scatt. meas. 7-52098
Se-Te liquid mixtures, mass density at high temp. and press. 7-63701
Sr, liquid phase, density and surface tension 7-44957

density of solids

bronze, powder particle shape effect on stability props. 7-7927
coal, thermal charactn., piezoelectric photoacoustic microscopy 7-44643
1-difluoronitroacetyl-2,2-dimethylhydrazine, cryst. and mol. struct., X-ray diffr. anal. 7-26735
α-thoxyacrolein semicarbazone, cryst. and mol. struct., X-ray diffr. 7-26734
Furko glasses, quenched, isothermal relaxation of density and stresses 7-1893
glass, fused spots formed by laser radiation, interferometric study 7-2054
halide eutectic composites, growth, struct., mech., elec. and optical props. 7-33648
Indian upper mantle rocks, pressure-temp. studies for Gruneisen coeff. and specific heat 7-55267
ivory, tensile props. and fracture rel. to comp. and struct. 7-14032
metal and alloy temperature-conc.-density phase diagram calcs. 7-3282
(Na₂O)₂₅(Li₂O)₂₅(P₂O₅)₅₀ glass fibres, struct., birefringence, density and thermal shrinkage, drawing parameters depend. 7-6536
Ni, electron core states overlap at very high compressions 7-21849
polyacetylene films, polymerisation condition effect on morphology 7-37906
polypropylene films, isotactic, struct., quenching temp. effect 7-11950
polystyrene, tracer diffusion meas. using Si and the elastic recoil detect. 7-39337
PVC-polyvinyl butyral (phenolformaldehyde resin), thermophys. props. (Russian) 7-27040
α-quartz, neutron irradiated and annealed, positron annihilation and mag. susceptibility meas. 7-39274
shock waves, equation of state calcs. 7-21393
simple metals, physisorption interaction of H₂ 7-12480
steel, austenitic, Cr-Mn, thermal and mech. props., fusion reactor appl. 7-53795
steel, stainless, (Cr₂Fe₂)₂C₆ compact specimens, corrosion-electrochem. and phys. props. w.r.t. comp. 7-54000
ternary intermetallic compounds, single crystal, Czochralski growth, charactn. 7-53557
trabecular bone density in proximal femur, quantitative CT assessment 7-14129

density of solids continued

Ag₂O-Tl₂O-B₂O₃ glasses, physical props. and tandem monovalent ions effect 7-3013
Al₂O₃-MgO, diphasic xerogels, densification, sintering, isostructural seed, epitaxy 7-27987
B₂C ceramics, pressureless sintering with polycarbosilane addition 7-46389
BN, film, optical energy gap, density, hardness 7-39204
Ba₉Ge₂O₃₃(OH)₄, high press. phase, cryst. struct., X-ray diffr. study 7-32412
Bi₂Ge₂O₁₂ single cryst. growth, characterisation and appls. 7-33550
a-C:H, film, optical energy gap, density, hardness 7-39204
a-C:H films, plasma deposited, optical props. 7-27799
(CaO)₂₅(BaO)₂₅(P₂O₅)₅₀ glass fibres, struct., birefringence, density and thermal shrinkage, drawing parameters depend. 7-6536
CoO, sputtered thin, annealing effects on mag. props. and structure, Co-CoO layer separation 7-27180
Cu plating, grain density and cyclic stresses (Japanese) 7-7904
Cu-Ni-Fe-Mn, physical props. rel. to precip. and thermal treatment (German) 7-12698
EuRh_{1-x}Sn_{4-x}, anomalous mag. and elec. props. 7-64440
F₂ solid, high-press. behaviour at low temps. 7-37923
Fe powder, quality assessment method 7-53671
Fe₃B₁₇, metallic glass, struct. relax. X-ray and neutron diffr. study 7-6521
Fe₂SiO₄-Zn₂SiO₄, limited solid soln., cation ordering 7-51709
GaSb single crystals, intrinsic point defects and microdefects, TEM studies 7-44529
He-H₂ system, density inversions between fluid and solid phases at high pressures 7-58451
³He, BCC solid, nuclear magnetism, molar volume depend. 7-58565
K₂Pb₁₀Nb₁₀O₃₀-K₂Li₄Nb₁₀O₃₀ solid soln., density and struct. studies 7-1973
Li borate glasses, density w.r.t. atomic arrangements, comp. depend. 7-6533
LiF crystals, influence of deformation temp. on change in density 7-44655
LiFeP₂O₇, cryst. synthesis, at. struct., DTA, X-ray diffr. study 7-26708
LiNbO₃:MgO, melt growth and charactn. 7-58170
Li₂O-B₂O₃, ion conducting glass, effect of CaO substitutions on transport and physical props. 7-58535
Li₂SiO₃ pellets, sintering, density, struct., porosity 7-53682
Mo-ZrO₂, sintered composites, tetragonal to monoclinic transform. of ZrO₂ (Japanese) 7-13450
Mo_{3.25}Ir, cryst. struct., X-ray diffr. meas. at 293K and 12.5K 7-16491
MO₃ thin films, amorphous, vacuum deposited, struct. 7-51635
Na₂O-Al₂O₃-GeO₂ glasses, ionic transport meas., packing density depend. 7-32710
Na₂O-Fe₂O₃-SiO₂ systems, glass formation and props. 7-2203
Na₂O-FeO-SiO₂ systems, glass formation and props. 7-2203
Na₂O-TiO₂-GeO₂ glasses, refractive index, density 7-59170
Ni-Ti composite powder, prod. and processing props. 7-3230
Ni₄B₃₆, metallic glass, struct. relax. X-ray and neutron diffr. study 7-6521
PZT, shock-recovery expts. 7-38119
Pb_{1-x}Sn_xTe_{1-x}Se_x solid soln. single crystals, density, comp., lattice const. and galvanomag. props. (Russian) 7-44500
a-Si films, density measurement using quartz oscillator 7-7079
SiC powder compacts, formed by cold isostatic pressing, influence of shape and size on homogeneity (Japanese) 7-64981
Si₃N₄, gas press. sintering, fracture toughness, fibre like struct., additions effect 7-13414
SiO₂ film on Si produced by thermal oxidation 7-65228
SiO₂ films on Si produced by surface oxidation, stresses and defects 7-65230
SiO₂ powder/ceramic fibre composites, packing density model 7-13426
SiO₂, spherical particles synthesis, thermal behaviour (Japanese) 7-7943
SiO₂-P₂O₅ glass films, deposited by different CVD methods, phys. props. 7-27220
Si₃Se_{1-x} glasses, intermediate range order 7-11938
TbCo sputtered films, mag. and magneto-optic props., stability 7-53076
Te-As-S chalcogenide system, annealing, crystalline precipitate phase form., X-ray diffr. anal. 7-16751
TeO₂-based halide glasses, prep., thermal, mechanical, elec. and optical props. characterisation (French) 7-37884
TeO₂-ZnCl₂ system, glass prep. and composition 7-46403
Ti-Ge-Se, bulk glass formation region, elec. and struct. characts. 7-58159
V-Si-N system at reduced N press., phase relations at 1273K, absence of supercond. 7-17518
WC-TaC-Co, N contained cemented carbides, sinterability, mech. props. rel. to prep. 7-17507
Y₂O₃ powders, agglomerate strength distrib., US meas. 7-46379
Y₂O₃-ZnO-Al₂O₃-SiO₂, glass form. and crystn., effect of ZnO additions 7-44382
ZrO₂ single crystals, stabilised, growth by skull melting technique, charactn. 7-53560
Zr₂Pb₃, fusion blanket neutron multiplier, fabrication and props. 7-49656

density of states, electron see electronic density of states

deoxyribonucleic acids see DNA

depurmering see demagnetisation

desalination

feedwater composition and physical properties determ., experimental methods 7-28364
ion exchange installations, meas. and control 7-28339
reverse osmosis desalination meas. and controls 7-28338
solar desalination system selection for supply of water in remote arid zones 7-54339
solar distillation plants, instrumentation and control devices 7-28410
solar still, cascade, modified type for water desalination 7-23219
water desalination by electrochemical membrane process (German) 7-13819

desalting see desalination

describing functions

ferromagnetic substance magnetisation curve descriptive function 7-64490

design aids

see also design engineering; nomograms

No entries

design engineering

see also project engineering; systems engineering

- Particle Beam Fusion Accelerator II (PBFA II) engineering design of pulse forming system 7-30770
 plastic and advanced plastic composites, design methods and applics., book 7-4642
 scanning tunnelling microscopy, design criteria 7-4920
 Li-TiS₂, 35 Ah ambient temperature rechargeable cells, design options 7-34011

desk calculators see calculating apparatus

desk-top computers see microcomputers

desorption

- adsorbed molecules photodesorption by IR laser-adsorbate coupling 7-58616
 adsorption-desorption phenomena, macroscopic meas. and microscopic interpretation 7-27136
 alkali halides, electron and photon stimulated positive ion desorption dynamics calcs. 7-27141
 alkali halides, photon-surface interaction dynamics 7-27826
 alkali metal chlorides, electron-stimulated desorption, Coulombic ejection mechanism 7-59315
 alkali metal halides, desorption, UV-photon-stimulated, laser-synchrotron studies of dynamics 7-21612
 alkali metal iodides, electron-stimulated desorption, Coulombic ejection mechanism 7-59315
 angular scan-attenuated total reflection spectra, appl. to study of molecular adsorption and desorption 7-4901
 compound semiconductors, laser stimulated desorption, dimerisation enhanced phase transition 7-58619
 conference, Oconomowoc, WI, USA (April-May 1985) 7-18468
 diatomic mol. on substrate, reson. laser induced desorption, classical and quantum models 7-58618
 electrode surface contamination, desorpt., field and secondary emission, enhancement by electric fields 7-23033
 electron and photon-stimulated, probes of surface struct. and bonding 7-32817
 electron stimulated processes at surfaces, excitation anisotropy 7-13282
 electron-stimulated desorption ion angular distributions method, use for determ. structs. of surface molecules 7-7005
 electronic desorption and sputtering by energetic ions, incident angle depend. 7-53479
 electronic transition induces, workshop, Schloss Elmau, Bavaria, Germany (Oct. 1984) 7-20
 ESD, desorption cross-sections meas. 7-13283
 ESD and photoemission, extended core-hole Hamiltonian 7-52252
 ESD cross sections, electron beam inhomogeneity effects 7-13284
 fusion solid breeders, T recovery and inventory, surface desorption effect 7-49651
 graphite, He ion irradi., thermal desorpt. 7-52245
 graphite surface laser irradiation, ionic cluster desorption, time-of-flight meas. 7-12138
 heavy ion induced desorption from surfaces, thermal spike model 7-44996
 heavy-ion induced desorption, ion form. studies 7-46259
 heterocyclic aromatic polymers, laser desorption FT mass spectrosc. anal. 7-23085
 ice films, Kr⁺ bombardment, ion cluster desorption, TOF mass spectra study, astrophysical implications 7-26815
 Inconel GH39, thermal desorption study (Chinese) 7-52295
 insulators, fast heavy ion impact-induced secondary ion emission studies 7-27845
 insulators, radiation effects, conf., Guildford, England (July 1985) 7-29590
 ion bombardment of thin films, secondary emission yield, incident charge state depend. 7-59319
 ion emission from PVDF film, elec. field-induced, polarity effects 7-27872
 ionic desorption, Auger-induced, nonadiabatic effects 7-38326
 isothermal, Fokker-Planck eqn. for physiosorption kinetics 7-52257
 ketene adsorbed on Pt(III), surface chemistry, substrate temp. influence, EELS 7-46867
 Langmuir-Blodgett films, thermal desorption, quartz-crystal microbalance studies 7-63949
 laser-induced desorption from surfaces, nonequilib. infrequent events, mol. dynamics 7-38322
 laser-induced photodesorption 7-52281
 laser-stimulated desorption, desorption mode instability 7-21634
 laser-stimulated desorption of adsorbed molecules via electronic excitation 7-59309
 light induced desorption, bistability mechanism in integrated optical devices 7-57424
 linear chain of adsorption sites, desorption, kinetic ising model 7-21649
 liquid evaporation and quantum desorption processes (French) 7-38343
 matrix-assisted field desorption mass spectrometry, temp. effects 7-30108
 metal surface, field adsorbed He and Ne, atom-probe spectroscopy studies 7-32803
 metal surface, pulsed laser induced desorption 7-58617
 metallic films, growth by laser photolysis of carbonyls, C and O incorporation mechanisms 7-58685
 metals, adsorbed H₂, kinetics model of chemisorption layer (Korean) 7-32813
 metals, electrochemical desorption step, rel. to isotope effect 7-13782
 metals, H ion implants, trapping coefficients 7-6884
 noble metal surfaces, laser stimulated desorption during Cl₂ reactions 7-53453
 order-disorder phase transition of adsorbed layers, effect on rate of elementary processes 7-6976
 photodesorption, laser-induced, effect of resonant vibrational energy transfer 7-52293
 photodesorption via stimulated Raman emission of coherent surface phonons 7-16865
 poly-p-phenylene-1,3,4-oxadiazole, photoconduction, O₂ adsorption effects 7-52683
 polyaryl ether ether ketone, solubility and diffusion of water 7-44917
 polymers, conducting, laser desorption/Fourier transform mass spectral analysis 7-1920
 porous catalysts, temp.-programmed desorpt., modeling and expt. verifications 7-13799
 pulsed laser field desorption TOF spectroscopy, ultrafast ion reaction time meas. 7-20072

desorption continued

- scanning tunnelling microscopy, atom transfer mechanisms 7-4921
 semiconductor and metal surfaces, field-assisted photodesorption 7-32809
 semiconductor surface chemistry, adsorption and desorption kinetic meas. combined with Auger spectroscopy 7-65348
 silicate glass, Na desorption during X-ray microanalysis 7-23114
 single bubbles free rising in Newtonian liquids, gas desorption, mass transfer, drag coeffs. 7-16233
 SOS structures, SIMS depth profiling, electron stimulated desorption and charging effects 7-33501
 steel, austenitic, in fusion reactor first wall, gas thermal desorption by plasma streams 7-49616
 steel, austenitic, thermal desorption after high-energy d implantation 7-52232
 steel, stainless, CO and SO₂ adsorpt., kinetics and laser-stimulated surface oxidation 7-63958
 surface at. imaging by TEM 7-51594
 surface science, modern techniques, book 7-60911
 surface science, synchrotron radiation studies, review 7-33977
 surface science techniques, book 7-60888
 TDS of interacting molecules 7-21635
 TeV e⁺e⁻ linear collider, cathode life and gas desorpt. meas. (Japanese) 7-19587
 thermal desorpt. kinetics, surface phase transitions influence, compensation effect 7-13815
 thermal desorption expt., microcomputer-controlled mass spectroscopy 7-3619
 thermal desorption spectra, effect of adsorbate diffusion into the solid 7-52283
 thermal desorption spectra, simple rate eqn. derivation 7-21646
 thermopiezic analysis, gas absorption and desorption studies on milligram samples 7-16861
 transient dilation of bubbles and drops; theoretical basis for dynamic interfacial meas. 7-32757
 vacuum symposium, Tokyo, Japan (1985) (Japanese) 7-14698
 XPS, UPS, work function meas. 7-12485
 zirconia transparent gel-monomolith from Zr alkoxide, controlled hydrolysis prep. 7-8313
 (111), with adsorbed S, mass spectrometry of desorption products (German) 7-33953
 Ag (100), adsorption of Cl, Auger, LEED, XPS, thermal desorption studies 7-58635
 Ag (110), adsorption of ethylene oxide, surface interactions, XPS, TDS, AES, EELS studies 7-33963
 Ag (110), adsorption of ethylene and ethylene oxide, work function, LEED, UPS, TDS meas. 7-52270
 Ag (110), adsorption of NO₂ and surface nitrate formation 7-52286
 Ag (110), clean and O₂ covered, adsorption and reaction of acetonitrile 7-28344
 Ag film, adsorbed NH₃(ND₃)(Xe), IR laser photodesorption spectroscopy 7-17825
 Ag films, with surface adsorbed ethylene, adsorbate-substrate bonding 7-52292
 Ag surface, adsorbed pyridine, IR laser stimulated desorption mol. spectroscopy 7-58614
 Ag surface, O₂ chemisorption, flash desorption spectra (Chinese) 7-52294
 AgBr, desorption of gelatin by means of sodium polystyrene sulphate 7-15022
 Al (100), CO adsorption, EELS and thermal desorpt. 7-17815
 Al disks, He ion implanted, He re-emission ratios and surface obs. (Japanese) 7-12089
 Al:F, electron-stimulated desorption, Coulombic ejection mechanism 7-59315
 Al₂O₃, adsorbed butylamine, thermal desorption and IR study 7-39110
 Ar (111), of HCl, internal state depend. 7-6963
 Ar solid crystalline films, electron stimulated desorption, exciton mechanism calcs. (Russian) 7-27096
 Au films, with surface adsorbed ethylene, adsorbate-substrate bonding 7-52292
 BaF₂ (111), laser sputtering, layer-dependent 7-13274
 BaTiO₃:Ni ceramic, H defect diffusion 7-58545
 CO and K coadsorbed on Ni (111), adsorbates electrostatic interaction, IR reflection-absorption spectra, TPD, LEED obs. 7-32824
 CO, chemisorbed on Ni (111), mol. orientation, effect of adsorbed K, ESDIAD study 7-32825
 CaO, adsorbed butylamine, thermal desorption and IR study 7-39110
 Cd₃₀H₈₀Te, electron stimulated desorption of Hg 7-17378
 CdS surfaces, electron-beam-stimulated processes, real-time atomic-resolution electron microscopy 7-7798
 CdTe (001), of Cd and Te, surface stoichiometry and reaction kinetics, RHEED studies 7-21613
 Co catalyst, O₂ adsorpt. and oxidation of Si at CoSi (100) surfaces 7-46865
 Co surface, metal atom catalysed oxidation, UPS and AES studies 7-46865
 Cr (110) with chemisorbed CO, electron stimulated desorption 7-63965
 CsI, H₂⁺ cluster ion impact-induced Cs⁺ desorption, TOFS study 7-27843
 Cu, chlorinated surface, laser-induced desorption and etching processes 7-27092
 Cu films, with surface adsorbed ethylene, adsorbate-substrate bonding 7-52292
 Cu, O₂ chemisorption kinetics as function of ion bombardment and temp. (Russian) 7-58622
 Cu surface, physisorbed Xe, Ar O₂ and CO, laser-induced thermal desorption 7-17817
 Cu, Xe desorpt., surface temp. determ. using pyroelectric calorimeter 7-52233
 CuCl solid surface, laser-induced desorption and etching processes 7-27092
 D trapping and desorption during high fluence implantation in insulators and semiconds. 7-26781
 Fe (100) with surface C, gasification by O, CO desorption 7-6993
 Fe (111), CO₂ adsorption and dissociation, ARUPS 7-63961
 Fe, surface, H₂ and N₂ interactions, pulsed laser atom probe studies 7-32811
 Fe_{1-x}Nd_x(Y)(Ce)₂B, or H, fine particles prep., mag. props., recording appls. 7-53660
 GaAs, surface oxide desorption, temp. meas., Auger anal. 7-58608
 Gd₂Si₂H₇, H-D exchange, H desorption 7-28304

desorption continued

- Ge surface laser irradiation, ionic cluster desorption, time-of-flight meas. 7-12138
- H absorption and desorption on milligram samples 7-6981
- H₂ sorption, kinetic models and appls. to H₂-M systems 7-65646
- H₂ thermal absorption or desorption studies, microcomputer controlled apparatus 7-21668
- HeRh²⁺, cpd. ion, dissoc. in high elec. field, at. tunnelling, orientational and isotope effects 7-42777
- Ho₂Si₂H₂, H-D exchange, H desorption 7-28304
- In foils, ion bombarded, desorbed neutral energy distrib. studies 7-22406
- In monolayer and multilayer surface diffusion, growth mode and thermal stability on W (100), LEED, TDS and scanning AES studies 7-2386
- InP(As)(Sb) surfaces, oxidation processes studied by high-resolution electron microscopy 7-39766
- Ir, field evaporation rate, temp. depend. 7-33525
- Ir foil sample, Cs diffusion and surface ionisation studies 7-3138
- KCl (100), interaction of NaCl mol. beams with surface, desorption flux meas., SIMS obs. 7-33508
- KCl(Br), F-centre near-surface generation by synchrotron radiation 7-26744
- La_{2-x}Ca_xMg₁₇, H₂ storage appl. 7-40052
- α-LaNi₅-H, multiply cycled, inelastic neutron scatt. 7-32835
- LiAlO₂, surface adsorpt. isotherms, T inventory appl. 7-52246
- LiF, electron beam irradi., desorbed ground state Li atoms, signal time depend. 7-52260
- LiF, electron stimulated desorption of Li, role of F-centre diffusion 7-16864
- LiF₂ electron- and photon-stimulated desorption, threshold effects 7-58623
- LiF evaporated films, surface anal., electron stimulated desorption, XPS studies 7-27173
- LiF, of bromomethane, laser photofragmentation and photodesorpt. 7-50275
- LiF surface, Ar⁺ and Ar²⁺ bombarded, desorption of F⁺, secondary ion mass spectra study 7-21661
- Mg surface, air exposed, XPS after hydrogenation-dehydrogenation cycles 7-17923
- Mo (100), chemically modified, chemisorption bond energies of Lewis acids and bases 7-23056
- Mo (100), clean and with S or C overlayers, adsorption and reactions of hydrocarbons 7-28345
- Mo (110) chemically modified surface, Au thin film form. study 7-12489
- Mo single crystal, cold worked, He pipe diffusion along dislocation, thermal desorption spectra 7-52142
- Mo-Ni, adsorbed S, in acidic medium, destabilizing effect of Mo and passivation consequences (*French*) 7-16858
- MoS₂, powder and exfoliated samples, temp. programmed desorpt. of CO₂, CO and O₂, adsorpt. sites study 7-2385
- Na clusters, at. desorpt. energies determ. 7-15787
- Na₂CaAl₂Si₂O₁₂·6H₂O, zeolite, adsorption and desorption of ethylene, TPD study 7-32826
- NaCl, laser-induced vibr. predesorption of ethene 7-58615
- Na₂O-B₂O₃-SiO₂ glass, Na desorption during X-ray microanalysis 7-23114
- Nb, adsorbed H₂, kinetic model (*Korean*) 7-32814
- Nb:He⁺(H⁺) films, radiation defects produced by ion implantation 7-7059
- Ne solid crystalline films, electron stimulated desorption, exciton mechanism calcs. (*Russian*) 7-27096
- Ni (100), chemisorption and decomposition of ethylene 7-59785
- Ni (100), K treated, rare gas physisorption, wetting, photoemission spectra 7-32822
- Ni (100), S-covered, adsorption of NO 7-6990
- Ni (110), adsorption of D₂, LEED, TDS, RBS, nucl. reaction anal., work function meas. 7-58638
- Ni (110), adsorption of O, electron stimulated ion desorption O⁺ yield meas. 7-12487
- Ni (111), coadsorption of NH₃ and CO, multilayer formation studied by metastable quenching spectroscopy 7-21639
- Ni (111), desorption of CO and CO₂ molecules, Ni atom evaporation during laser bombardment 7-58628
- Ni (111), isothermal adsorption/desorption parameters of CO, EELS meas. 7-6971
- Ni (111), N₂ adsorption, XPS, UPS, work function and TPD studies 7-52272
- Ni (111), of H₂, ang. distrib., rel. to coverage 7-27103
- Ni, H permeation, diffusion and surface rate coeff., press.-modulated absorpt.-desorpt. 7-58612
- Ni, H trapping phenomena, meas. by desorption thermal anal. technique 7-6673
- Ni, polycryst., adsorption-desorption of CO, kinetics 7-16873
- Ni surface, ion desorbed D charge state fractions study 7-46268
- Ni surface, monolayer Au atoms, partial sputtering cross sections 7-59331
- NiZr-H₂, metallic glass, pressure-concentration isotherms 7-26665
- O adsorption and desorption on Sn-Sb₂O₃ catalyst kinetics 7-63944
- O₂, chemisorbed on MgO, photostimulated desorption 7-27107
- OH, radical, desorpt. on TiO₂(NaCl)(SrF₂) surfaces, kinetic and internal energy, determ., fluoresce. detect. 7-8298
- Pb electrodeposition from aq. HCl soln. onto Pt (111) 7-27954
- PbSe films, elec. cond. and thermoelec. power, dynamic behaviour 7-2750
- Pd (100), clean and S covered, adsorption and desorption of NO, surface reactions, TPD, EELS, LEED 7-58639
- Pd (111), CO and O co-adsorption, SIMS and TPD studies 7-27137
- Pd, H diffusion coeff., influence of subsurface layer on meas. 7-6892
- Pd, H permeation, diffusion and surface rate coeff., press.-modulated absorpt.-desorpt. 7-58612
- Pd polycrystalline surface, internal energy distrib. of recombinatively desorbing D₂ 7-2350
- Pd surface, H₂(D₂) desorption, rovibr. state distrib., VUV laser induced fluoresc. 7-17826
- Pt (110), water adsorption 7-21644
- Pt (111), adsorption and desorption of NO, CO or H₂ 7-21643
- Pt (111), adsorption of ethylene oxide, surface interactions, XPS, TDS, AES, EELS studies 7-33963
- Pt (111), contaminated with Si or oxidised Si, interaction with water 7-27134
- Pt (111), of CO, electronically stimulated adsorbate rotation studies 7-45006

desorption continued

- Pt (111), of NO, electronically stimulated adsorbate rotation 7-45006
- Pt (111), reaction of coadsorbed C₂N₂ and H₂ 7-54186
- Pt, adsorbed NO, high-speed ramped field desorption spectra 7-32810
- Pt, of previously adsorbed tracer amounts of Cs and K 7-58636
- Pt/Ti (111), chemisorption of CO and O₂ 7-27131
- Rh (100), diffusion of Rh adsorbed clusters, classically exact overlayer dynamics 7-38328
- Rh (111), clean and with adsorbed O, ion bombarded, desorbed atoms distributions 7-22420
- Rh foils, ion bombarded, desorbed neutral energy distrib. studies 7-22406
- Rh surfaces, adsorption and desorption of NO, effect of surface structure 7-6994
- Rh surfaces, clean and B contaminated, adsorption and dissociation of H₂O 7-27135
- Ru (001), alkali modified, adsorption of O, TDS, AES, EELS, work function meas. 7-58637
- Ru (001), chemisorption and rot. epitaxy of Li, LEED, TDS obs. 7-12479
- Ru (001), clean and O covered, adsorption of NO₂, EELS, thermal desorption mass spectrometry 7-52267
- Ru (001), coadsorption of H₂O and Li 7-21645
- Ru (001), H₂ chemisorption, effect of coadsorbed O₂, LEED spectra anal. 7-33959
- Si (100), adsorption of H₂O, photon stimulated ion desorption surface EXAFS 7-58633
- Si (100), adsorption of H₂O, surface struct., photon stimulated ion desorption SEXAFS determ. 7-64752
- Si (100), exposed to CO, CO₂, O₂, NO and SO₂, photodesorption 7-52290
- Si (100), nitridation kinetics in NH₃ by thermal activation or electron bombard., LEED, AES, and TDS study 7-39770
- Si (100), reaction with propylene, adsorption and desorption kinetic meas. combined with Auger spectroscopy 7-65348
- Si (100), reactivity, thermal desorption of propylene, defect- and electron-enhanced chemistry 7-21660
- Si (100), UV-stimulated interaction with Cl₂, reaction mechanisms for photon-enhanced etching 7-22926
- Si (100) surface, H desorption, reactivity enhancement by electronic excitation 7-2366
- Si (100) with chemisorbed H₂, transition from the dihydride to the monohydride phase 7-58631
- Si (111), adsorbed Mo(CO)₆, laser induced electronic excitation followed by CO desorption 7-12470
- Si (111), metal atom catalysed oxidation, UPS and AES studies 7-46865
- Si epitaxial films, low temp. growth by very low press. CVD 7-27936
- Si, ion-induced etching, surface processes 7-59702
- Si, MBE cryst. growth, dopant incorporation 7-12559
- Si surface, reaction with propylene, effect of addition of H 7-54187
- Si surface laser irradiation, ionic cluster desorption, time-of-flight meas. 7-12138
- Si wafer substrates, oxide removal, transient mass spectrometry, XPS studies 7-13670
- a-Si:H, photo-CVD deposition, initial processes (*Japanese*) 7-7053
- Si:H, polycrystalline, grain boundary interactions 7-12117
- SiO₂, adsorbed butylamine, thermal desorption and IR study 7-39110
- SiO₂, ion-induced etching, surface processes 7-59702
- SiO₂N₂ films, deposited by plasma-enhanced CVD, charact. 7-2413
- β-Sn surface laser irradiation, ionic cluster desorption, time-of-flight meas. 7-12138
- SrTiO₃ (100), adsorption of H₂O, surface struct., photon stimulated ion desorption SEXAFS determ. 7-64752
- SrTiO₃ single cryst., H defect diffusion 7-58545
- SrTiO₃ surface, adsorbed H₂O, photon stimulated ion desorption 7-52276
- TaD_x foils, D desorpt., Auger electron and thermal desorpt. spectra studies 7-32800
- TaH_x foils, of H, Auger electron and thermal desorpt. spectra studies 7-32800
- Ti surface, heavy-ion-induced D desorpt. meas. 7-44990
- TiC and TiB₂ coatings, effect of stoichiometry on D retention, thermal desorption study 7-6997
- TiO₂ (110), O deficient surfaces, electronic excitations, EELS 7-58853
- TiO₂ surface defect-struct., photon- and electron-stimulated desorption ion yield studies 7-44974
- UO₂ thin films, adsorption of H₂O vapour lumin. studies 7-22351
- W (100), adsorbed CO, electron-stimulated desorption, metastable particle production 7-21628
- W (100), NH₃ sat., two-photon reson. three-photon laser ionisation 7-10768
- W (100), Nd thermal desorption, anomalous kinetics 7-45010
- W (110), adsorption of Eu, Gd and Tb 7-27118
- W (110), field adsorption and desorption of H, atom probe FIM 7-21647
- W (110) with adsorbed Ni, Cu, Ag or Au, thermal desorption spectroscopy 7-27119
- W surface, desorption of Na atoms, resonance ionisation study 7-63966
- W surface, field adsorption of He 7-32816
- W surface, Hg absorption, field emission microscopy studies 7-32804
- W surface, high temp. field evaporation, desorption studies 7-64881
- W surface adsorbed F⁻ ions, photo- and electron-stimulated desorption 7-12465
- W surfaces, chemisorbed ²³Na, nuclear-spin-polarized thermal atom scattering 7-53476
- Zn (0001) with adsorbed H, thermal desorption spectra 7-21646
- Zr (0001) HCP to BCC phase transition He⁺ capture effects, AES, TDS and SIMS studies 7-58590
- Zr surface, chemisorption of Cl, neutral and negative ion thermal desorption spectroscopy 7-6988
- Zr₇₃Fe₂₅, hydrogenised, positron lifetime and Mossbauer study 7-46198

detection (demodulation) see demodulation**detectors**

- see also electric sensing devices; hydrophones; infrared detectors; microwave detectors; nonelectric sensing devices; particle detectors; photodetectors; ultraviolet detectors
- 1980s state and future development trends (*Slovak*) 7-24641
- amputee's stump, shape measuring probe-type system for prosthetics CAD 7-34349
- chemical sensors, research and development trends (*German*) 7-24645
- chemometric analysis of multisensor arrays 7-8344
- database of sensors maintained by Warren Spring Laboratories 7-14933

detectors continued

- fault detection procedure for faulty sensors, implementation 7-5368
- length measurement, improving sensitivity, noise removal (*Japanese*) 7-48690
- photoionisation detector for capillary column gas chromatography 7-48702
- pyromagnetic detector, pulsed-periodic radiation behavior (*Russian*) 7-35509
- SAW gas sensors, design aspects, review 7-48716
- sensor technology and appls., conf., Bad Nauheim, FRG (March 1986) (*German*) 7-24271
- sensors for intelligent processing of materials 7-41366
- temperature sensors (*French*) 7-303

determinants

- see also *matrix algebra*
- No entries

detonation

- see also *explosions; shock waves*
- air, gaseous charge explosion, blast wave propag. 7-57881
- converging detonation waves, temp. var. meas. (*German*) 7-51207
- gas-solid particle mixture, acceleration wave 7-11525
- gasdynamic flow form. for colliding plates at sharp angle 7-63169
- hydroelastic three-layer cylindrical shell reaction to internal explosion, elastic deform. 7-31692
- laser supported detonation waves, oblique incident beam on Al, computational study 7-63312
- laser-driven flyers backed by high impedance windows, vel. meas. 7-30029
- metals, asymmetric oblique supersonic collisions, shock polar method anal. 7-32572
- plane detonation wave at convex corner, diffr. 7-57880
- plane detonation wave in combustible gas mixture, direct initiation 7-31836
- polyvinylidene fluoride films, active gauge for initiation diagnostics 7-30000
- porous granular systems, convective combustion 7-13772
- porous multicomponent media, wave similarity problems 7-43740
- reacting shock waves, theoretical and num. structure 7-20759
- reaction zone measurements in high explosive detonation waves by means of shock-induced polarization 7-11558
- reactive granular materials, deflagration-to-detonation transition, two-phase mixture theory 7-37518
- self-sustaining, explosive gas bubble in liqs., compression wave effects 7-31839
- shell, spherical, thick-walled, under short pulse loading max. stresses eval. 7-20640
- solid particle acceleration by gaseous detonation products 7-20778
- time dependent 2D, interaction of edge rarefactions with finite length reaction zones 7-26363
- waves, spherical, attenuation under strong luminesc., num. soln. 7-63179
- waves, transonic flow behind wave front, stationarity conditions 7-63174
- weak disturbance velocity measurement, bulk density in porous media 7-31826
- Al particles, ignition, behind detonation and shock waves 7-8287
- Al plasma, laser-supported detonation waves in obliquely incident beam 7-11648
- H₂-air mixtures, 1-D tube combustion processes, numerical calc. 7-65647
- H₂-air detonations, large scale expts. review, reactor safety 7-36211
- HF, chem. laser, modeling based on standing detonation wave 7-62681

detonation spraying see *powder spraying***deuterium**

- adsorbed layers on Si, phonon scatt. at crystal surface 7-21609
- adsorpt. on Ni (100), diffusion, investig. 7-6960
- adsorption of H(D) on Rh(110), form. of high density chemisorbed phase, LEED investigations 7-27094
- adsorption on Ni (110), LEED, TDS, RBS, nucl. reaction anal., work function meas. 7-58638
- adsorption on Ni (111), isotope effects, kinetic investig. 7-21624
- upper atmosphere, D and H concentrations in daytime thermosphere 7-60437
- atom, Rydberg const. meas. via Balmer- α wavelength single-photon determ. 7-36516
- atomic scattering, from Cu, Au and Ni, energy spectrum, scattering trajectories 7-64854
- chemisorbed on Ni (100), vibr. motion, high resolution EELS 7-12458
- cosmic nucleosynthesis, relation between ³He, ⁴H and ⁴He prod. 7-40979
- desorption from Pd surface, rovibr. state distrib., VUV laser induced fluoresc. 7-17826
- diffusion in α - and β - phases of LaNi₅ 7-6874
- discharge, surface effects at very high E/n 7-21040
- doubly spin-polarized, observation by ESR 7-6915
- Fe-D formed by D ion implantation, multiple D occupancy of vacancies 7-63643
- fuel density-radius product of inertial confinement fusion targets, determ. using secondary nuclear fusion reactions 7-5405
- HCP solid, orientational ordering, NMR 7-38293
- heavy-ion-induced desorpt. from Ti surface 7-44990
- interstellar chemistry within broad model 7-35030
- ion desorbed and reflected charge state fractions from Ni surface 7-46268
- ion extraction from large magnetic multipole source 7-58037
- outer ionosphere, D⁺ concs. rel. to charact. freqs. of deuterium whistlers 7-18335
- molecular beam impact with Cu (100), resonant sticking coeff. 7-13308
- molecule, dissociative single and double photoionisation, photoion spectra anal. 7-19984
- molecule, doubly excited states, photodissoc. cross section 7-19980
- molecule, hyperpolarisabilities, vibr. contribs., CARS 7-57074
- molecule, rot. transition, Raman line position 7-62380
- molecule, triple-point measurements 7-60902
- molecules, recombinative desorption from polycrystalline Pd surfaces, internal energy distrib. 7-2350
- nuclear target, nuclear spin orientation enhancement by RF irradiation 7-15435
- ortho monolayers, physisorbed on graphite, specific heat studies 7-52271
- parametric Raman gain suppression 7-43232
- permeability in austenitic stainless steel, He irradiation effects 7-2267
- permeation of Ni rel. to surface impurities and Ar sputtering 7-52141
- plasma, H neutral beam heating in JET 7-6415

deuterium continued

- plasma chromatograph and mass spectrometer deuterium ion source 7-4909
- plasma pinch, particle acceleration and neutron prod. 7-63330
- quadrupole echo NMR spectroscopy, artifact suppression 7-48799
- radioisotope distribution in precipitation, surface and groundwaters in NW Yugoslavia 7-23254
- resonant IR two-photon ionisation 7-15573
- retention in TiC and TiB₂ coatings, effect of stoichiometry, thermal desorption study 7-6997
- solid, compressibility and pressure, LOCV calc. 7-52182
- solid, cubic phase, orientational ordering, NMR 7-38294
- solid, ground state energy in LOCV method 7-52181
- solubility in SrCe_{0.95}Yb_{0.05}O_{3- δ} proton conductor, SIMS study 7-12298
- spin polarised, nonequilib. props. within Fermi liquid theory 7-6913
- spin-polarized, ground state props. 7-27055
- stimulated rotational Raman scattering for high power emission at 11 to 14 μ m 7-15941
- stopping cross sections, in Ti-D and Zr-D, deviations from Bragg's rule 7-51903
- synthesis in stellar atm. in binary systems with accretion disks (*Russian*) 7-24218
- trapping and desorption during high fluence implantation in insulators and semiconds. 7-26781
- trapping in Nb:O, perturbed ang. correl. obs. 7-27641
- C_n⁺-D₂(O₂) cluster ions, ion+mol. reactions 7-50432
- CaF₂:Er³⁺, D⁺, IR excitation and absorpt. spectra anal. of sites 7-53306
- D, T-cube plasma, β -line central dip, ion dynamic effects anal. 7-36542
- D⁺, H⁺ vol. prod. ion source by sheet plasma, proton accelerator and thermonuclear fusion research applications (*Japanese*) 7-5511
- D⁺ ion trapping in Al, Mo, Nb and stainless steel 7-64857
- D⁺ JET tokamak plasma, ion cyclotron emission spectra meas. 7-58067
- D/H ratio in atmosphere of Uranus implications of methane-d₁ detect at 1.6 μ m wavelength 7-55529
- D-T mixture, plasma focus, inductive explosive magnetic generator current source study 7-44299
- D+D reaction, detection of occurrence during shock fracture of D₂O ice 7-39874
- D+Fe(Ti), thick target bombardment, X-ray production cross sections 7-20025
- D+H₂, collision theory thermal rate const., on SLTH pot. surface 7-54085
- D+H₂, mol. beam scatt. study, differential cross sections meas. 7-39860
- D+H₂-HD+H, quantum mech. reactive scatt. problem, L² soln. 7-62485
- D+methyl radical, rate const. determ., laser photolysis and reson. fluoresc. 7-8250
- D+Ne⁴⁺(Ar⁴⁺), collision parameters, energy-gain spectra meas., multi-channel Landau-Zener model anal. 7-36752
- D⁺+H₂(D₂) trajectory surface hopping calcs. 7-59747
- D₂ chemisorption on W (100), free carrier surface scatt., IR obs. of adsorbate induced changes 7-22268
- D₂⁺+Cs, dissociative charge exchange, D₂ predissociation spectra anal. 7-36753
- D₂⁺, nonadiabatic lower and upper bound calcs. 7-36469
- D₂-Ar spectrophotometric lamp, construction and material influence 7-41422
- D₂+C⁺(He⁺)(Ne⁺), rate const. determ. 7-17774
- D₂+Ca, collisional quenching, time-resolved emission spectra anal. 7-36528
- D₂+Cr⁺ 7-65293
- D₂+Cs⁺, low-energy collisions, absolute total cross section meas., curve-crossing model anal. 7-36749
- D₂+D⁺(H⁺), trajectory surface hopping calcs. 7-59747
- D₂+F, quantum reaction probabilities, hyperspherical coordinates 7-13754
- D₂+H, collision theory thermal rate const., on SLTH pot. surface 7-54085
- D₂+H⁺, charge transfer into 2S state, differential cross sections meas. 7-36750
- D₂+H₂-HD+D, product rot-state distrib., information-theoretic anal. using perturbation method 7-62495
- D₂+Kr⁺, spin-orbit state and isotope effects, pot. energy curve, cross sections meas. 7-39859
- D₂+Mu reaction, rate const., 480 to 675K 7-50412
- D₂+Ne⁴⁺(Ar⁴⁺), collision parameters, energy-gain spectra meas., multi-channel Landau-Zener model anal. 7-36752
- D₂+O, trajectory isotope effects, pot. energy surfaces 7-65296
- D₂+Rb, fine-structure transition cross-sections, quantum-mechanical calcs., importance of perturber rotational levels 7-57161
- D₂⁺+inert gas, high Rydberg fragments, kinetic energy spectra 7-42745
- D₂⁺, IR spectra, ab initio calcs. 7-30929
- D₂⁺, semiclassical vibr. eigenvalues, adiabatic switching method 7-57043
- DT, rot. transition, Raman line position 7-62380
- Fe:H(D), lattice strains, meas. 7-2268
- Gd₂Si₂H₇, H-D exchange, H desorption 7-28304
- a-Ge-D₂H, plasma deposited, deuteron magnetic resonance 7-27626
- a-GeSi₂D₂F, D NMR lineshapes and spin-lattice relax. studies 7-45836
- H⁺/D⁺ fractionation, NMR investig. with various probe nuclei 7-56312
- H-D exchange, fast atom bombardment mass spectrometric obs. 7-50392
- H₂-D₂ mixtures adsorbed on graphite, phase diagrams 7-52180
- H₂-D₂ system, CO₂ laser induced breakdown 7-6352
- Ho₂Si₃H₈, H-D exchange, H desorption 7-28304
- Mo-D, ion implanted, impurity trapping 7-38029
- Nb-D-O(N) system supercond., tunnelling of D trapped by O(N), anelastic relax. meas. 7-39572
- Nb-Ti-H(D), anomalous anelastic relax., statistical model 7-28065
- Nb-Ti-H(D), substitutional alloys, intermediate temp. relax., Fermi-Dirac model 7-26858
- Pd₉Ag_{0.1}D_{0.61}, lattice dynamics and phonon line shapes 7-2120
- ScD₂, D diffusion 7-52117
- Si:B:D Schottky and n⁺-p junction diodes, electrical transport of acceptor-compensating defect 7-16823
- Si:D, ion implanted, channelling meas. 7-16597
- a-Si:D, F, D NMR lineshapes and spin-lattice relax. studies 7-45836
- a-Si:D₂F, plasma deposited, deuteron magnetic resonance 7-27626
- a-Si:D(D,H), deuteron mag. resonance, annealing effects 7-33292
- a-Si:H,D, H abstraction from surface, HD formation 7-39914
- Si:P,O,D, donor passivation and reactivation 7-17031
- a-SiGe:D, F, vibr. modes, Fourier transform IR spectra studies 7-46053
- a-SiGe:D,F, plasma deposited, deuteron magnetic resonance 7-27626

deuteron continued

- SrTiO₃:D, O-D stretching vibr. under applied electric field and uniaxial stress 7-44723
 Ta:H(D)(T), heat of transport, isotope and temp. depend. 7-27024
 V-T-H(D), substitutional alloys, intermediate temp. relax., Fermi-Dirac model 7-26858
 Zr₂PolD_{2.9}, metallic glass, deuteron mag. resonance study 7-22159

deuteron compounds

- see also heavy water*
 CsH₉, D₂O, As₂O₃, melting pt., phase diagram 7-21417
 DBr⁺, X²Π_{3/2} ground state, mol. rot.-vibr., isotope shifts, double modulation Faraday LMR IR spectra 7-62369
 DCN, formation on Pd (111), and (100) by hydrogenation of adsorbed CN 7-6985
 DCN, metastable states, spectral quantisation appl. 7-25434
 DCO⁺+H₂→HCO⁺+D, ion reaction at interstellar cloud conditions 7-23008
 D₂CO + inert gas, Coriolis enhanced vibr. energy transfer theory and its appls. 7-31153
 D₂CP, ν₁+ν₂ vibr.-rot. band, Fermi reson. in (100,002) diad 7-5662
 DCl + OH (OD), reaction rates, vibr. excitation and isotopic substitution effect 7-22996
 DCl, molar vol., vapour press. meas. 7-44779
 DF chemical lasers, mixing enhancement using supersonic nozzle design 7-5878
 DF dimer+DF(HF), collisional vibr. relax., rate consts. meas. 7-50320
 DF pulsed laser performance, gas mixture composition depend. 7-62682
 DF-Ar₂, trimers, mol. rot., hyperfine struct., spectra anal. and calcs. 7-50060
 DF-CO₂ pulsed laser performance, gas mixture composition depend. 7-62682
 DF-methyl cyanide, hyperfine struct., rot. spectra 7-31012
 DI, Ar matrix, conc. effects, binary complexes with impurities, IR spectra anal. 7-31034
 DI in solid N₂, IR spectra in temp. range 9 to 30 K 7-50127
 DO₂, third-order anharmonic pot. consts. equilb. structure parameters, calc. procedure 7-10544
 D₂O, ¹⁸O isotopically labelled, reaction with SiO₂-Na₂O-CaO-MgO glass 7-26993
 D₂O, IR spectra, vibro.-rot. transitions, line intensity meas. 7-50109
 D₂O, ice, detection of D+D reactions during shock fracture 7-39874
 D₂O/KC₈, X-ray diffr., NMR, EPR and gas phase mass spectra anal. 7-46843
 D₂O⁺, electron impact dissoc. fragment cross sections 7-5777
 D₂OCl, FTIR spectrum, band origins 7-50140
 D₂Se, E, band, rot. contour analysis and predissoc. mechanisms, VUV spectra anal. 7-25537
 D₂Se, Rydberg series identification, VUV spectra anal. 7-25538
 D₂Te, E, band, rot. contour analysis and predissoc. mechanisms, VUV spectra anal. 7-25537
 D₂Te, Rydberg states, high resol. VUV spectra 7-50173
 HF-DF chemical laser, electrically initiated (*Chinese*) 7-5879

deuteron effects

- austenitic stainless steel, defects study by positron annihilation 7-39296
 metals, deuteron irradi., multiple fracture planes, bubble growth 7-58372
 metals, He production and long-term activation by protons and deuterons, fusion reactor appl. 7-58371
 steel, austenitic, thermal desorption after high-energy d implantation 7-52232
 steel, stainless, ion trapping of D⁺, mechanisms 7-64857
 Al, ion trapping of D⁺, mechanisms 7-64857
 C foils, charge equilb. of swift H beams 7-22409
 Dy, L subshell ionis. by deuteron impact, cross section determ. 7-51878
 Mo, ion trapping of D⁺, mechanisms 7-64857
 Nb, ion trapping of D⁺, mechanisms 7-64857
 Nb, radioactivation monitoring based on local activation by p,d,α 7-49726
 Ta, L-subshell ionis., proton deuteron and alpha impact induced, low-velocity effects 7-51879
 Ta, radioactivation monitoring based on local activation by p,d,α 7-49726
 Ti-D, D stopping cross sections, deviations from Bragg's rule 7-51903
 W, L-subshell ionis., proton deuteron and alpha impact induced, low-velocity effects 7-51879
 Yb, L subshell ionis. by deuteron impact, cross section determ. 7-51878
 Zr, radioactivation monitoring based on local activation by p,d,α 7-49726
 Zr-D D stopping cross sections, deviations from Bragg's rule 7-51903

deuteron interactions *see deuteron-nucleus reactions***deuteron-nucleus reactions**

- for inelastic deuteron-nucleus scattering, see 'deuteron-nucleus scattering'*
see also nuclear fusion
 multiestimating models, test of hadron-nucleus and nucleus-nucleus interactions 7-41771
 muon-catalysed fusion, physics and prospects for power prod. 7-62080
 (d,p), direct stripping anal. powers, DWBA anal., optical pots. 7-634
 (d,p), j=1-1/2 transfer reactions at intermediate energy, far-side dominance 7-638
 (d,pn), three body model using multiparticle scatt. theory, optical pot. 7-36015
 (d,r), hole state excitations in ¹⁵N and ³⁹K, correlations with (γ,γ') 7-61833
 (d,X), X-mesons, baryons, quark-gluon phase transition and strangeness anal. 7-49390
¹H(d,2pn), 95 MeV, tensor analysing power meas. 7-61898
¹⁹⁷Au(d,³He), E_d=108.4 MeV proton-hole response fns., low-lying level analysis 7-42028
¹⁹⁷Au(d,np), 9,10.5,12 MeV, sub-Coulomb breakup, tensor anal. power meas., DWBA comparisons 7-19261
¹B(d,n)¹²C, 4.44 MeV, finite-range calcs., anomalous anal. power 7-49367
²⁰⁹Bi(d,³He), ²⁰⁸Pb isoscalar 1⁺ state, proton and neutron contribs. constraints 7-19172
⁴C(d,³He)⁴B, A=12,13 analysing power meas. 7-49430
¹²C(d,⁶Li), ⁸Be, transitions to ground and excited states 7-19153
¹²C(d,⁶Li)³Be, vector analysing power meas. 7-49431
¹²C(d,⁶Li)³Be, ang. distribts. to ground and first excited states 7-30435
¹²C(d,p), 12 MeV, anal. powers for stripping reaction leading to bound and unbound states 7-630
¹²C(d,p), 56 MeV, polarisation transfer, anal. power ang. distribts. 7-636

deuteron-nucleus reactions continued

- ⁴⁰Ca(d,³He), analyzing powers, tensor pots. and D-state amplitudes 7-56662
⁴⁰Ca(d,α), analyzing powers, tensor pots. and D-state amplitudes 7-56662
⁴⁰Ca(d,t), analyzing powers, tensor pots. and D-state amplitudes 7-56662
 C(d,X), vector and tensor analysing power meas. 7-10158
 (d,N), 23 MeV on A=16-209, 1f_{7/2} transfer, DWBA problems 7-629
¹H(d,γ)³He, tensor analysing powers, anal. of ³He,⁴He wavefunction D-state components 7-30415
¹H(d,π⁰)³He, 500-2200 MeV, tensor anal. power and diffr. cross section 7-30406
²H(³H,X)³H, high resolution search for narrow dibaryons 7-5209
²H(d,π⁰X), √S_{NN}=31 GeV, invariant cross section meas. 7-61899
²H(d,X), √S_{NN}=31.2 GeV, nuclear stopping power, Lund model comparisons 7-10161
²H(d,X), many-particle rapidity correlations, cluster model framework 7-19220
²H(d,X), multiplicity dependence of transverse momentum spectra at ISR energies 7-56581
²H(d,X), singlet d intermediate state in four-body breakup reaction (*Chinese*) 7-24985
²H(d,απ⁰), charge symmetry breaking in the n-p system 7-30434
²H(d,γ)³He, cross-sections, tensor and vector analysing powers 7-61896
²H(d,γ)³He, M1, E1, M2, E2 transitions, ⁴He D state anal. 7-19262
²H(d,γ)³He, tensor analysing powers, anal. of ³He,⁴He wavefunction D-state components 7-30415
²H(d,γ)³He, tensor force effects 7-49433
²H(d,n)³He, E_{cm}=20-150 keV, polarized and unpolarized cross section calcs. DWBA anal. 7-10159
²H(d,nd)³H, complete breakup in four body AGS theory 7-693
²H(d,π⁰X), √S_{NN}=31 GeV, high p_T invariant cross section meas. 7-35907
²H(d,γ)³He, analysing powers and cross-sections 7-49427
³H(d,X), muon catalysed fusion, classical trajectory Monte Carlo method 7-61936
³H(d,n)⁴He, muon catalysed fusion, μα sticking probabilities 7-713
³H(d,X), muon catalysed fusion, muon sticking, low energy resonance effects 7-49488
³He(d,p), 18-22 MeV, forward angle cross sections and anal. powers 7-632
⁴He(d,pγ), A=202, 204, γ-ray and conversion electron meas., neutron hole states 7-49432
⁸⁰Kr(d,p)⁸¹Kr, Q-value determ. 7-49429
⁶Li(d,α)³He, 6.88-7.04 MeV, meas. of spin dependences for isospin forbidden decay ⁸Be=d+⁶Li 7-5204
⁷Li(d,γ)⁸Be, second T=3/2 state width, isospin mixing 7-30399
⁷Li(d,γ)⁸Be, 361 keV, T=3/2 state width anal., isospin mixing 7-41900
 Li(d,X), vector and tensor analysing power meas. 7-10158
¹⁴N(d,³He)¹⁴C, analysing power meas. 7-49430
 Ni(d,X), vector and tensor analysing power meas. 7-10158
¹⁶O(d,⁶Li)¹²C, vector analysing power meas. 7-49431
²⁰⁸Pb(d,np), 10.5,12 MeV, sub-Coulomb breakup, tensor anal. power meas., DWBA comparisons 7-19261
²⁰⁸Pb(d,p), 12.3, 15.0 MeV, ang. distribts. of anal. powers and diffr. cross section 7-631
²⁰⁸Pb(d,p), D-state to S-state ratio, tensor analysing power meas. 7-24986
 Pb(d,X), vector and tensor analysing power meas. 7-10158
⁴Pd(d,d), A=104-110, 22 MeV, ang. distribts. of cross sections and anal. powers 7-643
¹⁰⁸Pd(d,³He), proton-hole states and spectroscopic factors, DWBA comparison 7-41944
¹⁹⁶Pt(d,³He), E_d=108.4 MeV, proton-hole response fns., level analysis 7-42028
²⁸Si(d,p), distortion effects and binding energy calcs. 7-49229
²⁸Si(d,p), 18 MeV, polarisation transfer meas., d D-state effects 7-633
²⁸Si(d,p), 56 MeV, polarisation transfer, anal. power ang. distribts. 7-636
²⁹Si(d,α)²⁷Al, 12.3 MeV, microscopic DWBA anal. 7-19265
³⁰Si(d,α), 12.3 MeV, microscopic DWBA anal. 7-19265
¹⁴⁴Sm(d,p), 19 MeV, ¹⁴⁵Sm single particle config. splitting, J assignments 7-572
¹¹⁶Sn(d,p), 79 MeV, far-side dominance in large-l transfer, anal. powers, cross sections 7-640
¹¹⁶Sn(d,p), 79 MeV, vector and tensor anal. powers, j-depend., DWBA anal. 7-637
¹¹⁶Sn(d,p), 80 MeV, far-side dominance for spin-depend. observables, theoretical implications 7-639
¹¹⁶Sn(d,p), intermediate energy, l=0 reaction mech., DWBA anal., anal. powers 7-641
¹¹⁶Sn(d,p)¹¹⁷Sn, 79 MeV, antisymmetrization corrections with strong break-up 7-41963
 Sn(d,p), low energy, vector anal. power and pol., d D-state effects, DWBA anal. 7-635
⁸⁶Sr(d,p), level struct. and transition strength study 7-41899
⁸⁶Sr(d,p)⁸⁷Sr, DWBA anal., differential cross-sections and vector analysing powers 7-694
⁸⁷Sr(d,p), differential cross sections for transitions to particle-hole states 7-61897
²³⁰Th(d,d)²³⁰Th, nuclear struct. study and binding energy determ. 7-41902
⁴⁶Ti(d,α)⁴⁶Sc, 7-9.75 MeV, spin-parity meas. 7-19165
⁴⁸Ti(d,α)⁴⁶Sc, 7-9.75 MeV, spin-parity meas. 7-19165
¹³⁶Xe(d,p), D-state to S-state ratio, tensor analysing power meas. 7-24986

deuteron-nucleus scattering

- elastic high energy scatt., polarisation effects, multiple diffr. scatt. theory calcs. (*Russian*) 7-56686
 (d,d), 400 MeV, coupled channel anal., Woods-Saxon, optical potential comparisons 7-42029
 (d,d), existence of T₁ and T₂ tensor pots. 7-642
 (d,d), Fourier-Bessel anal. for optical pot. 7-648
 (d,d), polarizability and breakup model for heavy nuclei 7-15214
 (d,d), three body model using multiparticle scatt. theory, optical pot. 7-36015
 (d,d), three-body formalism with Coulomb interaction 7-42027
 (d,d), ultrarelativistic vector particles stopping ray differential cross section calcs. (*Russian*) 7-19263
¹²C(d,d)¹²C, cross-section meas., excitation functions (*German*) 7-30430
⁴⁰Ca(d,d), 22 MeV, ang. distribts. of cross sections and anal. powers 7-643

deuteron-nucleus scattering continued

- ⁴H(d,d), A=1,2, vector and tensor analysing power meas. 7-10158
- ⁴He(d,d), multi three-cluster coupling model anal., polarisation 7-588
- ²⁴Mg(d,d), 10-15 MeV, comp.-nucleus effects 7-36014
- ²⁶Mg(d,d), 52 MeV, elastic and inelastic scatt., struct. depend. of anal. powers 7-646
- ⁴⁰Mo(d,d), A=92, 100, 22 MeV, ang. distrib. of cross sections and anal. powers 7-643
- ⁵⁸Ni(d,d), A=58-64, 22 MeV, ang. distrib. of cross sections and anal. powers 7-643
- ²⁰⁸Pb(d,d), polarizability and breakup, cross section calcs. 7-15214
- ¹⁰⁴Ru(d,d), 23 MeV, neutron-proton moment differences in a triaxial nucleus 7-644
- ³²S(d,d), 52 MeV, effective interaction and mass distrib., Fourier-Bessel anal. 7-647
- ²⁸Si(d,d), distortion effects and binding energy calcs. 7-49229
- ²⁸Si(d,d), 52 MeV, elastic and inelastic scatt., struct. depend. of anal. powers 7-646
- ¹¹⁶Sn(d,d), 23 MeV, dynamical deuteron pol. pot., Fourier-Bessel anal. 7-645
- ⁹⁰Zr(d,d), 22 MeV, ang. distrib. of cross sections and anal. powers 7-643

deuteron photodisintegration

- 50-100 MeV by linearly polarised photons, differential cross section asymm. meas. 7-49374
- total cross section meas. between 15 and 75 MeV 7-5224
- γ d \rightarrow np, asymmetry and angular distribution of deuteron photodisintegration in the 20-60 MeV range 7-49376
- γ d \rightarrow pn, cross-section asymmetry, $E_{\gamma}=0.4-0.8$ GeV 7-5099
- H(γ ,pn), 300-500 MeV, photodisintegration by linearly pol. γ , pol. parameters 7-35991

deuteron polarisation

No entries

deuteron scattering *see deuteron-nucleus scattering***deuterons**

- asymptotic D/S state meas. from (d,p) tensor analyzing powers 7-24986
- axial magnetic field and azimuthally streaming medium energy deuterons in a plasma focus 7-63364
- charge form factor in perturbative QCD 7-41719
- 1-D-3,3-dimethyl-1-butene, acetylenic deuteron quadrupole coupling const. determ. 7-62410
- dynamical model for six-quark admixture 7-467
- magnetic moment, quark corrections using compound quark bag anal. 7-56523
- magnetic moments of multi-quark systems, chiral bag model 7-41816
- quadrupole moment, rms radius and form factors from local NN potential 7-5165
- wave function, large momentum components, Reid soft core and Paris pots. 7-35950
- π NN bound state problem, appl. to deuterons 7-19033
- ²H, electromagnetic structure of the deuteron in the Skyrme model 7-49235
- ²H, magnetic form factor, topological exchange current contrib. 7-35941
- ²H, NN pot. and phase shifts with quark degrees of freedom 7-41886
- ²H wave functions, exact rel. theory of two-body bound state wave functions 7-30353

developers (photographic) *see photographic materials***development, photographic** *see photographic process***development management** *see research and development management***DFB lasers** *see distributed feedback lasers***DH lasers** *see semiconductor junction lasers***diagnosis, patient** *see patient diagnosis***diagnostic radiography**

see also computerised tomography

- absolute kVp calibration using characteristic X-ray yields 7-40268
- absorption and scatt. props. of elemental filters for X-ray beams 7-23451
- angiographic images, anal. and interpolation by use of fractals 7-34271
- angiography and surgery, ideal marriage for managing massively traumatized patients 7-3872
- automatic exposure in peripheral angiography 7-14112
- automatic left ventricular cineangiograms analysing system 7-47258
- biplane fluorography: neuroangiographic appls. 7-18065
- biplane multidirectional angiocardiography with a new X-ray system 7-14111
- blood flow phase detection on digital subtraction angiography 7-47257
- blood flow velocity meas. in intraarterial digital subtraction angiography, pulsed-injection method 7-14128
- cardiac left-to-right shunts, quantitation using digital subtraction angiography 7-40285
- cardiac wall motion abnormality visualised in the 30° RAO and 60° LAO projections, comparison of magnitude 7-28688
- carotid angiograms abnormality detection using computerised syntactic pattern recognition 7-40354
- chest phantoms development 7-54725
- chest radiography, anatomical compensation filter evaluation 7-28659
- chest radiography, ANDS-V1 computer detect. of lung nodule 7-47249
- chest radiography, comparison of filters 7-47229
- chest radiography, digital image processing 7-23455
- chest radiography, effect of a multiple-scanning beam device and trough filter on scatt. 7-47228
- chest radiography, signal/noise and sensitometry limitations 7-47227
- chest radiography using patient-specific digitally-prepared compensating filters 7-47250
- compensation filter made of Pb loaded acrylic, perceived advantages 7-65854
- compression of radiological images with 512, 1024, and 2048 matrices 7-54738
- computed radiography system TCR 201 7-18067
- computed radiography system using an imaging plate as an X-ray sensor, TCR-201 7-40282
- computer processing of X-ray images 7-23435
- conference on medical imaging and instrumentation, Boston, MA, USA (April 1985) 7-40996
- conference on medical imaging and PACS, Newport Beach, CA, USA (Feb. 1986) 7-18490
- contact gel as a source of error in X-ray films of the skull (German) 7-65855
- convolution filtering technique for estimating scatt. distrib. 7-23457
- diagnostic radiography continued**
- coronary angiograms, digitised, computer anal. for assessment of changes in poststenotic coronary flow 7-28687
- coronary angiography, quantitative, accuracy of the catheter as a reference for arterial dimensions 7-28685
- coronary angiography, quantitative, improvement by exact calc. of radiological magnification factors 7-40288
- coronary arteries densitometry in radiographs, improved phys. model 7-28689
- coronary arteries skeleton from cineangiograms 7-18062
- coronary arteriography, quantitative, state of the art, book 7-54742
- coronary artery diameter meas. by angiography, Monte Carlo assessment of precision 7-47240
- coronary artery opacification improvement with gated injections and digital subtraction angiography 7-28690
- coronary artery quantification by digital radiography 7-28691
- coronary blood vel., phasic, clinical assessment using digital subtraction angiography 7-3873
- detective quantum efficiency of X-ray image intensifiers 7-23443
- digital diagnostic imaging, versatile image processor and its appl. in computed radiography 7-28673
- digital fluoroscopic image data, appl. to radiation dosimetry 7-23439
- digital fluoroscopy, medical imaging 7-47271
- digital image store, 1024 \times 1024 pixel, with pulsed progressive readout camera, appl. to gastro-intestinal radiology 7-28680
- digital imaging systems comparison: dedicated vs. add on 7-47237
- digital radiographic assessment of coronary arterial geometric diameter and videodensitometric cross-sectional area 7-28675
- digital radiographic imaging system with multiple-slit scanning X-ray beam 7-54737
- digital radiographic units comparison 7-23448
- digital slot radiography system based on a linear X-ray image intensifier and 2D image sensors 7-23450
- digital subtraction angiographic units, quality assurance protocol 7-65824
- digital subtraction angiography, automated tracking of the vascular tree using a double-square-box region-of-search algorithm 7-28674
- digital subtraction angiography, image quality evaluation 7-47238
- digital subtraction angiography, technique for automatic motion correction 7-23456
- digital subtraction angiography of the heart and coronary arteries 7-18064
- digital subtraction angiography system, high resolution 7-28679
- digital subtraction angiography systems, acceptance testing and calibration 7-47239
- digital subtraction radiography technology, equipment and techniques 7-40267
- digital unsharp masking, effect on detectability of interstitial infiltrates and pneumothoraces 7-47248
- digital videofluorography, clinical basis 7-28678
- digital X-ray imaging 7-60079
- dual energy imaging in projection radiography 7-23438
- dual energy subtraction in digital radiography (Japanese) 7-14120
- dual-energy projection radiography using condenser X-ray generator and digital radiography apparatus 7-54739
- dual-energy subtraction imaging, 1-shot 7-28684
- equivalent spectra as a meas. of beam quality 7-54724
- exposure and organ dose estimation in diagnostic radiology 7-54752
- film processing evaluation, comparison of freshly exposed and preexposed control films 7-47233
- fluoroscopic diagnostic exams., levels of radiation exposure 7-60090
- fractional Brownian motion, max. likelihood estimation rel. to image texture, radiography appl. 7-13945
- HF spatial filtration of X-ray images (Russian) 7-54730
- high stability developer for medical X-ray processing 7-47232
- high-resolution screen-film radiography, noise sources 7-23440
- hysterosalpingography, radiation dose reduction: an appl. of scanning-beam digital radiography 7-28714
- image evaluation using sequential dependency 7-8681
- image intensifier digital imaging systems, struct. mottle obs. 7-54721
- image intensifier TV digital systems, accurate meas. of charact. curves by Al stepwedge technique 7-54726
- image processing in cardiovascular radiology 7-65833
- image processing technology, medical radiography appl., review 7-65856
- image quality in Se-based digital radiography 7-23452
- imaging at medium energies using multilayer mirrors 7-47225
- imaging systems for digital radiography: present status and future prospects 7-8679
- kinesthetic charge detector for digital radiography, performance parameters 7-23449
- left ventricular contraction charactn., comparative study of quantitative methods 7-34261
- left ventricular function after heart transplantation, anal. from myocardial markers 7-34263
- left ventriculograms, digital subtraction, automated edge detect. method 7-34269
- line spread functions by the pre-exposure and multiple-exposure methods 7-23437
- liquid crystal light valves for medical imaging 7-14107
- loading myelography, functional exam. technique for lumbar spinal canal 7-18077
- mammographic systems, dose comparisons 7-40298
- mammography, absorbed breast dose rel. to radiographic modality, technique and breast thickness 7-28716
- mammography, comparative study of films and screens 7-54716
- mammography, image quality rel. to anti-scatt. grids and magnification technique 7-54714
- mammography, performance evaluation of a dedicated system 7-47235
- mammography, subtle microcalcifications detect., evaluation of digital unsharp-mask filtering 7-28677
- medical use of radioactive isotopes 7-47220
- multilayer mirrors as X-ray filters for slit scan radiography 7-34243
- neuroimaging interpretation, radiologic automated diagnosis. (RAD) 7-65857
- neuroradiology, conf., Amsterdam, Netherlands, (Sept. 1985) 7-14706
- neuroradiology, role of digital subtraction angiography, intra-venous and intra-arterial experiences 7-18078
- neuroradiology, transcranial Doppler sonography rel. to angiography 7-18035
- ocular lens, radiation dose in radiology of the orbit 7-40292
- optical centering unit adjustment device 7-28664

diagnostic radiography continued

patient doses and risks from diagnostic radiology in north-east Italy 7-60089
personnel exposure in interventional radiology, shielding method 7-47261
prenatal obstetric X-ray exam., unborn child cancer risk, Oxford survey analysis 7-8694
quantisation effect on digitised noise and detect. of low-contrast objects 7-23454
radiotherapy, external beam, on-line electronic portal imaging system 7-14110
radon transform data, reconstruction, resolution and ill-conditionedness 7-40280
rare earth tantalate phosphors for radiographic screens, fundamental props. 7-47231
renal images, digitally subtracted, diagnostic effects of edge sharpening filtration and magnification 7-54722
review of conventional X-ray imaging 7-60078
right ventricular regional wall motion, meas. from biplane contrast angiograms using the centerline method 7-34262
rotational panoramic radiography: comparison of radiation doses in the standard and reverse posns. 7-40293
scanned projection digital mammographic imaging 7-47251
scanning beam radiography using rot. aperture wheel device 7-47241
scanning equalisation radiography, beam geometry optimisation 7-65853
scanning equalisation radiography, efficacy in chest diagnosis 7-47226
scanning X-ray imaging system for quantitative arteriography and blood flow meas. 7-40266
scattered radiation reaching doors and windows of diagnostic X-ray rooms 7-60076
scattered radiation transfer prediction technique, expt. verification 7-54720
scintigram-standard radiograph superimposition, image processing system, ventilation index determ. 7-40259
scoliosis evaluation, radiation dose reduction, appl. of digital radiography 7-28715
screen-film evaluation, comparison of phys. autocorrel. and digital Wiener spectrum techniques 7-23441
screen-film images, computer simulation 7-23442
screen-film systems, logit model for MTF 7-54723
screen-film systems, MTF 7-60086
semi automatic computerised system for producing heart and coronary arteries images 7-3875
sharpness of definition and density in film screen systems (German) 7-23459
Shimadzu angiographic system PANGIOMAX-S (Japanese) 7-18075
signal processing model of diagnostic X-ray scatt. 7-54719
signal-to-noise-ratio obs. on 2 high-resolution screen-film systems 7-47230
skeletal maturity, fuzzy grammars for syntactic recognition from X-rays 7-34317
standardisation of X-ray examinations, engng. basis 7-28663
stomach and duodenum, radiographic mag. using computed radiography 7-14126
storage phosphor system for computed radiography: destructive scanning 7-23444
storage phosphor system for computed radiography: screen optics 7-23445
subtraction angiography: comparative performance and cost of digital vs. film subtraction methods 7-47247
subtraction radiography, use of image similarity for the selection or synthesis of projections 7-28671
synchrotron beam line critical elements, heat transfer studies 7-42255
telettransmission of radiographic images, digital system 7-14108
texture analysis by use of fractional Brownian motion, digital coronary angiograms, appl. 7-8474
tissue heterogeneity effect on operating regime selection of X-ray tube 7-40278
tomosynthesis using a digital radiographic system 7-23446
ventricular pressure-volume relationships, automated anal. by digital ventriculography 7-28692
ventriculograms, normal, curvature anal.: fundamental framework for assessment of shape changes in man 7-34260
vessel sizing wire: accurate vessel measurement using digital subtraction arteriography 7-54740
videodensitometric determination of percent stenosis, effect of beam hardening and scatt. 7-28686
visual perception of radiographs, correl. with meas. noise 7-23360
water phantoms in diagnostic radiology, photon scatt. props., Monte Carlo simulation study 7-54718
X-ray energy measurement 7-60083
X-ray image intensifier, with large input aperture and high resolution (Czech) 7-35650
X-ray imaging, Conf., San Diego, CA, USA (Aug 1986) 7-40995
X-ray spectra reconstruction by numerical anal. of transmission data 7-40272
X-ray tube anode, evolution 7-18066
X-ray tubes, half-value-layer increase owing to W buildup 7-14130
xeromammography, higher sensitivity, process studies 7-47236
Al equivalence of materials used in diagnostic radiology, dependence on beam quality 7-34242
Ge drift detector, tomographic device, for external analysis of tissue chemical props. 7-47273
diagnostics, particle beam *see particle beam diagnostics*
diagnostics, plasma *see plasma diagnostics*
diagrams
see also Bode diagrams; Feynman diagrams; flowcharting; nomograms; phase diagrams
No entries
diakoptics *see network topology*
dialogue systems *see interactive systems*
diamagnetic properties of substances
see also de Haas-van Alphen effect; diamagnetism
3d transition metals and alloys, induced diamag. form factor calcs. 7-2813
alkali metal vapour number density, optical determ. using Faraday rotation 7-48696
 β -(BEDT-TTF)₂I₃, supercond. transitions, diamag. suscept. study 7-52886
N-(p-n-butoxybenzylidene)p-n-ethylaniline, mag. susceptibility, anisotropy and order parameter 7-16416

diamagnetic properties of substances continued

graphite:B-Na intercalation cpd., Fermi level displacement, diamag. anisotropy and Hall effect meas. 7-16933
lyotropic nematic mesophase with benzenesulphonate solute, induced diamag. anisotropy sign reversal, PMR 7-21089
metal dithiolenes, struct., elec. and optical props. 7-44516
metals and binary alloys, diamag. susceptibility 7-45615
nematic liquid crystals, diamagnetic anisotropy meas. 7-38845
thiophene, in liq. crystals., variable angle spinning ¹H NMR 7-929
AgO, tetragonal, struct. and mag. props. 7-32399
Ag₃P₂I₃, solid electrolyte, prep., props. and cryst. struct. 7-32396
AgTlTe, molten, struct. factors and radial distrib. functions, X-ray diff. meas. 7-26617
Al-Pb disordered 3D normal metal-superconductor composite, elec. transport, magnetisation meas. 7-64383
An-In liq. alloys, magnetic and thermodynamic props. 7-2812
BaLaCuO, magnetic susceptibility meas., indication of high-T_c superconductivity, diamagnetic props. 7-58953
Cr-Ga intermetallic cpds., mag. suscept. meas. 7-12942
Cu, muon level crossing resonance, general considerations 7-53185
Cu-Rh, diamag. susceptibility calc. 7-45615
Cu₂P₂I₃, solid electrolyte, prep., props. and cryst. struct. 7-32396
Ge-Au(Pd) alloys, temp. and conc. depend. diamag. susceptibility 7-2811
E-glass, coord. of iron, ESR and mag. meas. 7-13021
Hg₂AsF₆, 1D BCS Hamiltonian 7-45558
KCu₄Cl₃(I₂) and KCu₄I₅ solid electrolytes, elec. conductivity and mag. susceptibility 7-12360
La_{1-x}Sn_{0.2}CuO₄, superconducting transition at 36.2 K 7-58947
MoS₂, high press. synthesis, characterisation 7-26716
NbH₄, mag. spin susceptibility and Knight shift 7-33141
Rh_{1-x}Ru_xS₂, prep., mag. and crystallographic props. 7-33154
Si (001), anomalous diamagnetic effect in highly excited surface subbands 7-64305
Ti-SbTiSe₃, liq., semicond., elec., mag. and thermoelec. props. 7-58825
Ti-SbTiTe₃, liq., semicond., elec., mag. and thermoelec. props. 7-58825
Y₇Co₆Sn₂₃ cryst. struct. and mag. suscept. studies (Russian) 7-21161
Yb_{1-x}Tm_xSe, anomalous Tm valence, lattice parameters, diamag. suscept. and Hall effect meas. 7-16998
Zn₃(P₂As_{1-x})₂ solid solutions, interatomic interaction, mag. susceptibility 7-52932
diamagnetic resonance *see cyclotron resonance*
diamagnetism
see also cyclotron resonance; de Haas-van Alphen effect; diamagnetic properties of substances
dirty superconductors, conductivity and diamag. susceptibility fluctuations near Anderson localisation 7-45563
electron gas, diamagnetic susceptibility at low temps., surface effects 7-21841
free-electron gas diamagnetic props. in external helical magnetic fields 7-45610
Landau diamagnetism, perimeter corrections for free electron gas 7-38843
magnetic field homogenisation by diamagnetic shields 7-42848
muon level crossing resonance, general considerations 7-53185
superconductivity with triplet pairing, diamagnetic limit, critical mag. field determ. 7-64395
H, diamagnetic Rydberg states, meas. and calcs. 7-5615
Li_{0.25}Co_{0.25}Zn_{0.5}Fe₂O₄, mixed ferrites, neutron diff. study 7-52943
diameter measurement
bubble diameter meas. by fringe method, using laser Doppler anemometer 7-16278
capillary holes meas., in 0.2 to 2 mm range 7-4807
coronary artery diameter meas. by angiography., Monte Carlo assessment of precision 7-47240
diffraction-schlieren image method of measuring hollow cylindrical objects 7-6024
digital radiographic assessment of coronary arterial geometric diameter and videodensitometric cross-sectional area 7-28675
Gaussian laser-beam-diameter measurement using sinusoidal and triangular rulings 7-43186
glass fibre, diff. pattern analysis, holography appl. 7-25762
laser beams of about 1 μ m diameter, meas. 7-5932
laser shadow method for transparent filament diameter meas. 7-29977
membranes with locatable single pores generation, obs. and testing 7-298
multilayer dielectric cylinder, diffraction meas. accuracy improvement 7-293
optical fibre, tolerance checking on diameters during drawing 7-62852
optical fibres, single-mode, mode field radius meas., harmonics detection appl. 7-37163
optical position sensing using Si photodetectors 7-48691
plant stem diameter contactless measurement apparatus using LED and photodetector (Japanese) 7-23506
precision selenoid diameter measurement, systematic error anal. (Japanese) 7-18740
single-mode fibres, mode field diameter meas., transmitted field pattern method (Japanese) 7-1266
X-ray mirror substrates, grazing incidence, precision machining/metrology facility 7-37222
diamond
abrasion by plasma deposited SiO₂ films 7-13608
abrasives, frictional behavior on hard materials 7-3461
aligned crystal, pion creation, coherent Primakoff effect 7-22389
anomalous muonium, vacancy-associated model 7-51758
axial channelling radiation from positrons, dislocation effects 7-12180
Borrmann-Lehmann interference patterns, synchrotron radiation obs. 7-32209
brown, vibronic coupling to nearly localised modes in luminescing bands 7-51980
channelling radiation spectra of high-energy electrons and positrons 7-27806
crystal, ultrarelativistic electron beam, parametric quasi-Cerenkov radiation 7-46174
crystallisation, conf., Warsaw, Poland (June 1985) 7-18469
crystals, band structure, LMTO calcs. 7-2477
crystals, surface phonon modes and reconstructions, Green's function method calcs. 7-2339
cut-off discs, example of positive effect of stress conc. 7-31642
CVD, Raman and IR spectroscopy study 7-17428
diamond, strain measurement in convergent beam electron diffraction 7-16562

diamond continued

- dust, thermal diffusivity, photoacoustic technique meas. 7-4837
electron beam irradi., vacancies, photoluminescence, radiative decay time meas. 7-46107
electron correlation, band gaps and quasiparticle energies 7-27278
electronic structure, STEM study 7-16939
energy band gap calc., self-interaction correction to local density approx. 7-45144
epitaxial growth in methane-H₂ plasma 7-12532
films, diamond like, prep. and props. 7-22472
films, microwave plasma CVD synthesised, thermal conductivity meas. 7-38417
films, plasma fluorination, surface structure determ. 7-27196
high pressure phase transitions total energy methods 7-63802
interstitial H or muonium, Hartree-Fock analysis 7-32947
ion implanted, struct. props., EPR and electron diff. studies 7-32363
IR absorption spectra, platelets in type Ia crystals 7-7723
knife edges, megavolt and cryo electron microscopy 7-41547
KVV Auger electron spectra calcs., band and cluster approx. methods 7-46252
large unit cell CNDO calculations 7-7106
layers, crystallisation from gas phase, growth kinetics (*Russian*) 7-22505
layers, elec. props. (*Russian*) 7-17124
layers, growth in laser heated substrate (*Russian*) 7-22507
layers, growth kinetics (*Russian*) 7-22506
layers deposited from C ion beams, struct. (*Russian*) 7-17475
Mu* hyperfine parameters, absolute sign, muon polarisation studies 7-53204
muonium, anomalous, model as body-centered interstitial muonium, HF calc. 7-45899
muonium defect energy profiles, unrestricted Hartree-Fock cluster calcs., comment and reply 7-45907
muonium-related paramagnetic centres, UHF calcs. 7-38980
normal muonium, lattice relax. calcs. 7-51789
nucleation and growth at high press., colloidal theory 7-46301
optical phonons and elasticity at megabar stresses 7-21375
planar channelled protons, breakthrough angles 7-21308
positron planar channelling radiation energy levels. variational calcs. 7-63696
powders, dynamically synthesised, polycrystal microstructure formation during sintering 7-22603
radiation damage prod. of 5RL centres, phonons, absorpt. spectra, cathodoluminescence studies 7-33461
relativistic electron beam, γ -ray emission, angular distribution 7-64722
semiconductors, synthesis and props. (*Russian*) 7-16588
Sierra Leone, diamond-source kimberlite paradox 7-34406
single crystals, relativistic positron channelling radiation, spectral density peak splitting studies (*Russian*) 7-21310
stimulated Raman measurements, time-resolved 7-15928
stopping cross section of ¹²C projectiles 7-51899
structure, determ. by radial distrib. function 7-16485
surface, (111), reconstruction, energy minimisation calculations 7-12434
surface graphitisation (*Russian*) 7-17667
surface with graphite layer, optical anisotropy of surface layer 7-53267
synthesis at low press., basic thermodynamics and kinetic conditions (*Russian*) 7-17486
synthesis by laser induced CVD, low press. 7-13371
synthesis of polycrystals using refractory metal catalysts, press. up to 13 GPa 7-53646
synthetic prod. from graphite 7-53647
thermal cond., C-defect effects 7-27035
tilt boundary struct., computer modelling 7-16579
type Ia, voidites, evidence for crystalline phase containing nitrogen, cell constant determ. 7-2011
type IaB, platelets, dislocation loops and voidites, TEM anal. 7-16560
type IIa, ion implanted, volume expansion 7-58298
ultradisperse, obtained from C plasma, energy spectrum 7-22384
voidites, electron microscopy study 7-32425
volume expansion during ion implantation, point defect creation and interactions 7-51890
wear behaviour, cathodolum. mode appl. in SEM 7-8228
X-ray radiation generated by transmitting electrons, ang. distrib. and energy depend. 7-26819
B doped, VPE, physicochem. basis of doping (*Russian*) 7-16587
B-doped, hopping photoconductivity 7-38617
K-Ar isochron dating of Zaire cubic diamonds, exptl. results 7-23612
P doped, VPE, physicochem. basis of doping (*Russian*) 7-16587

diaphragms

see also valves

- optically excited resonant diaphragm pressure sensor 7-56243
photoelectric devices, hollow mirror lightguide and diaphragms, optical system calcs. 7-43365
pressure transducer, strain gauge based, grid geom. influence on output 7-56250
Si pressure sensor diaphragm, displacement and slope analysis, holospeckle-shearing interferometry 7-29972

dibaryons see baryon resonances**dichroism**

see also magnetic circular dichroism; pleochroism

- benzenes, mono-substituted, biaxiality in nematic solutions, IR dichroism studies 7-36662
benzenes, mono-substituted, orientational order in nematic solutions, IR dichroism studies 7-36661
binaphthyls, near-IR triplet-triplet spectrum and circular dichroism as probes for electron delocalisation 7-31086
4,4'-bipyridyl radical cation- β -cyclodextrin inclusion complex, dichroism and MO calcs., ESR 7-25580
bisphenol-A polycarbonate, stressed, reversible mol. orientation, IR studies 7-50428
cholesterics, pretransition phenomena, circular dichroism method study 7-51628
chromophore, achiral, circular dichroism selection rules, symm.-adapted perturbation model 7-25579
cyanine dyes, Scheibe aggregate monolayers, without long alkyl chains, spectra, dichroism 7-59221
cyanobicyclohexyls, crystn. and liq. cryst. phase, IR, Raman and dichroic spectra 7-3051
diamagnetic molecular system, magneto-chiral birefringence and dichroism at longitudinal elec. saturation 7-42661

dichroism continued

- diamagnetic molecular system in DC electric field, magneto-spatial dispersive effect 7-31087
diamagnetic molecules, magneto-chiral birefringence and dichroism, reorientational processes influence 7-15812
12,2-dimethyl-1,3-dioxolane-4-methanol, OH stretching band, free and H bonded species equilb., dichroism and IR spectra 7-10641
trans-diphenylpolyenes in polymer film, transition moment, luminesc. 7-19943
DNA liquid cryst. microphases in water-organic solns., optical props. 7-65709
ethylenediamine ligands, vibr. circular dichroism, ion assoc., ring conform. and ring currents 7-31084
ferrofluid, near mm wavelength studies of refr. indices by dispersive Fourier transform spectra 7-53289
high-birefringence fibres, dichroism eval. using crosstalk meas. 7-20421
isolucine, homooligo peptide, conformational anal. by singlet-singlet energy transfer method 7-46998
cis-1,4-isoprene, mol. orientation, FT IR dichroism 7-17322
lanthanide (III) complexes, two-photon circular dichroism 7-27688
liquid crystals, orientational order parameters, IR dichroism of mol. groups 7-44358
magnetic dipole transition moments and rotational strengths of vibr. transitions 7-62453
matrix-isolated molecules, FTIR vibr. circular dichroism 7-50104
2-methyl oxetan, vibr. circular dichroism spectra, expt. and theoretical results 7-50208
2-methyl-4-nitroaniline, harmonic generation rel. to dichroism 7-43212
methylthiirane, vibr. spectra and ab initio calcs. 7-50147
modulation spectroscopy 7-48872
molecular alignment parameters, circular dichroic photoelectron angular distrib. meas. 7-36687
nematic liq. cryst. orientation and induction interaction effects on IR dichroism 7-39079
nematic liq. crystals, photoinduced chirality 7-44352
nematic liquid crystal-isotropic liquid phase transition, dimensional effects, UV dichroism (*Russian*) 7-2202
neutral molecules, C₂ symmetry, vibrational circular dichroism 7-31085
nonlinear mol., orientational ordering absorpt. dichroism 7-42659
1S,4R-norcamphor, circular dichroism, solvent effects and vibronic coupling perturbations calc. 7-42658
nucleic acids, liq. cryst. microphases, 'external chromophores' and intense bands in circular dichroism spectra 7-54459
orientational distribution coefficients, rel. to asym. orientational distrib. function 7-26621
poly-L-lysine, conform., in aq. soln., pH effects, vibr. circular dichroism effects 7-10783
poly-L-lysine, deuterated, Fourier transform vibr. circular dichroism in amide I bands 7-54475
polyacetylene:I films, liquid crystal polymerisation synthesis under mag. fields 7-65318
polyesteramideurethane, segmented, struct., polar low mol. wt. cpds. effects (*Russian*) 7-26673
cis-1,4-polyisoprene, mol. orientation, FT IR dichroism 7-13159
polymeric colloidal suspensions in polymeric suspending fluids, dichroism and birefringence meas. 7-11478
polypeptides, vibr. circular dichroism, 3_{10} -helix form., chain length depend., IR spectra, PMR 7-15633
purple membrane, circular dichroic spectrum of L form and blue light product of M form 7-54492
PVC: cholesteryl acetate, raw and moulded, crystallinity determ., positron lifetime studies 7-46228
rubber, natural, mol. orientation, FT IR dichroism 7-13159
rubber, natural, mol. orientation, FT IR dichroism 7-17322
tetraphenylmethane, vibr., dichroism, IR and Raman spectra 7-31042
thylakoid membranes and functional subunits, organisation, linear dichroism and fluoresc. polarisation obs. 7-59944
N-urethanyl- α -amino acids, Fourier transform vibr. circular dichroism of carbonyl stretching modes 7-50207
CoF₂, antiferromag. insulator, H-odd linear dichroism of exciton-magnon transitions 7-53282
Cu II complexes, interligand interaction, spectrosc. props. (*Japanese*) 7-57093
Er formate dihydrate, circular dichroism meas. 7-17301
Ho formate dihydrate, circular dichroism meas. 7-17301
K₂MAF₄, optical dichroism, spin forbidden *d-d* transitions, intensity prod. mechanisms 7-33360
LiIO₃ crystals, iron-group doped, impurity centres, circular dichroism studies 7-45976
LiYF₄:Tm³⁺ crystal, Tm optical spectrum, press. induced linear dichroism, electron-phonon interaction 7-3069
NO, excited state, circular dichroism in photoelectron ang. distrib. 7-19909
Rb₂MnCl₄, optical dichroism, spin forbidden *d-d* transitions, intensity prod. mechanisms 7-33360
Ru complex, circular dichroism spectra 7-33359
SiO, diffusivity and solubility of O review 7-16809
SiO, vacancy-enhanced O diffusion 7-16811
Tb₂Ge₂O₇, circular dichroism, chirality, UV spectra 7-33412
TeO₂, paratellurite, circular dichroism and weak absorption bands 7-45977
Tm₂Ge₂O₇, circular dichroism, chirality, UV spectra 7-33412

dictionaries see glossaries**die steel** see tool steel**dielectric breakdown** see electric breakdown**dielectric constant** see permittivity**dielectric depolarisation**

see also dielectric polarisation

- 1,2-diol solns. with water or electrolytes, dielectric props. 7-13080
disordered dielectrics, electret relax., persistent polarisation decay and injected charge cond. calcs. 7-39003
ellipsoidal homogeneous dielectric, depolarisation field 7-48241
polyethylene, polarisation and depolarisation currents superposition, time depend. meas. and calcs. 7-27652
polyethylene, space charge form., needle-plane arrangement, partial discharge and TSC meas. 7-39008
polyethylene film, TSC due to dipolar depolarisation in temp. gradient 7-59141
polyethylene terephthalate, polarisation and depolarisation currents superposition, time depend. meas. and calcs. 7-27652

dielectric depolarisation continued

- polypropylene, space charge form., needle-plane arrangement, partial discharge and TSC meas. 7-39008
 spherical particles, electromag. response, normal mode theory 7-17263
 $\text{Ti}_2\text{Cu}(\text{SO}_4)_2$, glassy γ -modification, structural and electronic props. studies 7-58161

dielectric devices

- see also capacitors; dielectric resonators; ferroelectric devices; insulators; piezoelectric devices; pyroelectric devices; space-charge limited devices
 No entries

dielectric dispersion see permittivity**dielectric-filled waveguides** see dielectric-loaded waveguides**dielectric function**

- amorphous and thermally annealed, optical props. (Russian) 7-17352
 amorphous semiconductors, optical absorpt., tight-binding model 7-45961
 binary charged fluids, screening lengths, thermodynamic stability 7-52480
 composite materials, dielec. function, momentum depend. effective medium approach 7-27281
 Coulombic systems, interacting, thermodynamic functions and self-energy 7-16963
 cubic metals, phonon spectra, dynamical pseudopot. shell model calcs. 7-51965
 disordered systems, activated processes, logarithmic scaling and $1/f$ noise power spectrum 7-61248
 electron gas, dielectric function, dynamical local-field factor 7-21840
 electron gas, one-dimensional inhomogeneity, dielec. matrix analytic inversion model calcs. 7-16964
 electron liquid at any degeneracy, thermodynamic and dielectric props. 7-7135
 glass, Fourier Transform Infrared spectra 7-53435
 interband absorpt. in disordered semiconductors, semiclassical approx. 7-53262
 metallic surfaces and small particles, relax. time effects in transverse dielectric fn., electromag. props. 7-38483
 metals, dielectric function, local-density-dependent 7-27285
 metals, liquid, dielectric function, neutron and X-ray scatt. methods 7-52481
 metals, phonon spectra, dynamical pseudopot. shell model calcs. 7-51964
 metals, plasmon linewidth, memory-function approach 7-45193
 metals, thermodynamics during high-pressure shock 7-21352
 p-doped semiconds., dielec. functions, band-gap narrowing anal. 7-52482
 periodic electron system, dielectric function, VAA theory, plasmon damping 7-32930
 polar semicond., carrier-carrier interaction and picosecond phenomena 7-45309
 polar semiconductors, phonon-plasmon coupling 7-33041
 trans-polyacetylene:Na, undoped and doped, momentum depend. dielec. functions, EELS study 7-64144
 trans-polyacetylene, momentum depend. dielec. function, EELS meas. 7-21843
 polychlorotrifluoroethylene-Au composite films, optical response in visible region, effective medium approach 7-53433
 quasi-one-dimensional electron gas, screened hydrogenic impurity, binding energy 7-52508
 quasi-one-dimensional semiconductor, electron mobility investig. 7-2616
 real-space inverse, derivation 7-32932
 semiconductor superlattices, dynamical screening, quasi-2D electron gas, electron-phonon interactions 7-45464
 semiconductors, ferromagnetic, dielectric function and reflectivity above T_c 7-7661
 semiconductors, plasmon linewidth, memory-function approach 7-45193
 semiconductors, Raman scatt. in the presence of photoexcited nonequilibrium carriers 7-27719
 small metallic spheres, effect of diffuse surface scatt. on electromag. props. 7-3042
 solids, optical spectra dimensionality, fractional calculus anal. 7-45958
 superlattices, inverse dielectric function, local field effects, spatial dispersion 7-52489
 surface polaritons, absorpt. by molecules near metallic surface 7-58749
 transition metals, low energy in elastic electron scatt. props. 7-63700
 transverse conductivity of nondegenerate two-dimensional electrons scattered from longitudinal optical phonons in a strong magnetic field 7-21885
 TTF-TCNQ, dielec. function in submillimetre range 7-27282
 two dimensional, electron gas, partially occupied Landau level, dielec. const. RPA calcs. 7-64139
 type II superlattice, dielectric function inversion, explicit analytic results 7-52772
 Ag, electron mean-free-path calculations using a model dielectric function 7-52583
 Al, electron mean-free-path calculations using a model dielectric function 7-52583
 Al, IR spectrum, intraband and interband processes 7-22256
 AlAs optical props., pseudodielec. function, spectroscopic ellipsometry meas. 7-52487
 As_2Se_3 , cryst., optical props., ab initio total energy calcs. 7-45965
 Au, electron mean-free-path calculations using a model dielectric function 7-52583
 Au film, optical props. 7-17296
 Bi, dielectric function, temp. depend. of band struct. parameters 7-7138
 $(\text{Bi}_{1-x}\text{Sb}_x)_2\text{Te}_3$ single crystal, optical constants, IR spectra study 7-46030
 C-W multilayers, sputtered, ellipsometry monitoring, X-ray refl., XPS 7-39376
 CdSe, dielectric fn. and interband crit. points. 7-2480
 CrCl_3 , ionic crystals, optical and electron energy loss studies 7-3066
 Cu, electron mean-free-path calculations using a model dielectric function 7-52583
 CuCl polycrystalline layers, nonlinear propagation of nanosecond laser pulses 7-53263
 GaAs-Ga $_{1-x}$ Al $_x$ As quantum well structures, energy spectra of donors and acceptors, spatially dependent screening effects 7-45459
 GaP thin films, optical props., meas. by surface plasmon excitation 7-46166
 Ge, pure and heavily doped, dielec. function, impurity conc. depend., spectroellipsometric meas. 7-2525
 Ge $_{1-x}$ Sn $_x$ amorphous films, structural changes on annealing 7-16422
 ^3He -He mixture films, surface superfluidity, vortex pair pot. energy (Chinese) 7-12391

dielectric function continued

- Hg $_{1-x}$ Cd $_x$ Se, reson. Raman Scatt. meas. 7-7701
 HgTe-CdTe superlattice, alloying, far IR study 7-13143
 $\text{In}_{1-x}\text{Ga}_x\text{As}_y\text{P}_{1-y}$ /InP heterojunctions, MOCVD grown, spectroscopic ellipsometry study 7-39195
 In_2O_3 :Sn evaporated films, optical props. and applications to energy-efficient windows 7-46157
 In_2O_3 :Sn films, theoretical model for optical props. in 0.3 to 50 μm range 7-39200
 KBr films, high temp. phonon anharmonicity, IR spectra study 7-33469
 $\text{K}_{1-x}\text{Rb}_x$ mixed crystals, FIR props., optical phonons 7-46011
 LaS, NaCl type lattice, current carriers and cond. 7-45346
 MnO, band struct., optical props. 7-32912
 $\text{NH}_4\text{H}_2\text{PO}_4$, temp. depend. IR active lattice modes in para- and antiferro-electric phase 7-46012
 NbSe $_3$, microwave harmonic mixing below threshold 7-64140
 Pd silicide formation, in situ ellipsometric studies 7-21694
 Sb-Se, thin films, amorphous and thermally annealed, optical props. (Russian) 7-17352
 ScN compensated semimetal single crystals, electronic struct., reflectivity and elec. props. meas. 7-27253
 Se, trigonal, optical props., local field effects 7-22204
 n-Si, complex dielectric fn., carrier interactions, Monte Carlo calcs. 7-33041
 Si transiently molten layers, dielec. function, picosec. laser pulse reflectivity meas. 7-52488
 a-Si:H,B(P) films, optical props. 7-64720
 a-Si:H films, glow-discharge-deposition, initial nucleation and growth 7-63997
 Si-Al $_2\text{O}_3$, SOS struct., UV reflectance meas., ellipsometry study 7-33414
 SiO_2/N_2 films, IR optical props. 7-7777
 Si(111), surface dielectric props., reflection high resolution electron energy loss study, azimuthal depend. 7-33498
 TaS $_2$, 1T, submillimetre conductivity, dielectric function 7-12749
 UO $_2$, single cryst., surface phonon struct., high resolution EELS 7-27087
 Zn $_x$ Hg $_{1-x}$ Se, far IR spectra study 7-22262
- dielectric hysteresis**
 DOBAMBC, ferroelec. chiral smectic C phase, crit. field, temp. depend. 7-26624
 ferroelectric hysteresis loop tracer, automatic 7-4865
 polyvinylidene fluoride, shock response, ferroelec. and piezoelec. props. meas. 7-32568
 tetramethylammonium tetrachlorocobaltate, ferroelec. incommensurate phase, thermal hysteresis, memory effect 7-33346
 TGS crystals, paraelec. phase, gamma irradiated, nonlinear dielec. props. studies 7-53214
 TGS-L- α -alanine admixture, dielec. props., influence of rejuvenation process 7-33339
 vinylidene fluoride-trifluoroethylene copolymer, shock response, ferroelec. and piezoelec. props. meas. 7-32568
 AgNO $_3$, metastable phase III, ferroelectricity 7-39052
 $\text{K}_2\text{BiCl}_6 \cdot 2\text{KCl} \cdot \text{KH}_2\text{F}_4$, improper ferroelectric phase transition, dielec. meas. 7-45943
 $\text{K}_{1-x}\text{Li}_x\text{TaO}_3$ single cryst., dielec. properties at 10^{-2} to 10^3 Hz 7-2997
 K_2ZnCl_4 , incommensurate phase, piezo-optical effects, birefr. meas. 7-45973
 NH $_4$ HSeO $_4$, X-ray irradi., existence of incommensurate phase, permitt. meas. 7-33338
 NaH $_2$ (SeO $_3$) $_2$, low temp. struct. phase transition 7-64580
 NaNO $_2$ thin films, ferroelectric and dielectric props. 7-39037
 PLZT ferroelectric ceramics, gamma, electron and neutron irradi. effects study 7-6677
 PLZT polarised ceramics, electroconductivity asymmetry obs. 7-7225
 PLZT-PZN electro-optic ceramics, elec., opt. and switching props. 7-7646
 (Pb $_x$ Ba $_{1-x}$)TiO $_3$, ferroelec. solid solns., dielectric and hysteresis props. 7-64588
 Pb $_{1-x}$ La $_x$ Ti $_{1-(x/4)}$ O $_3$ sputtered film struct., dielec., and pyroelec. props. studies 7-21724
 PbMg $_{1/3}$ Nb $_{2/3}$ O $_3$ -PbTiO $_3$, MnO doped, relaxor ferroelec. ceramics, dielec. ageing effects 7-22195
 Pb(SCo $_5$ Nb $_5$)O $_3$ ferroelectric ceramics, gamma, electron and neutron irradi. effects study 7-6677
 (Pb $_x$ Sr $_{1-x}$)TiO $_3$, ferroelec. solid solns., dielectric and hysteresis props. 7-64588
 PbTiO $_3$ based glass ceramics piezoelectricity, pyroelectricity and ferroelectricity 7-7654
 Rb $_2$ ZnCl $_4$, commensurate-incommensurate phase transition, X-ray and dielec. studies 7-63800
- dielectric-loaded waveguides**
 conducting spheres, FEM for scattering 7-15808
 six-port reflectometer for meas. complex dielectric constant 7-18821
- dielectric loss angle** see dielectric losses
- dielectric loss-angle measurement** see dielectric loss measurement
- dielectric loss measurement**
 see also dielectric losses
 capacitance bridge for low-temperature, high-resolution dielectric measurements 7-48778
 polymers, permittivity, loss tangent and refractive index meas., mm-wave technique 7-18820
 snow, dielectric properties meas. in 3 to 37 GHz range 7-23710
- dielectric losses**
 see also loss angle
 7-33321
 alcohols in glassy media, dielectric and IR spectral study 7-2968
 alumina, neutron irradi., permittivity and dielec. loss studies 7-33321
 aluminosilicate oxynitride glasses, dielectric studies 7-55917
 9,9'-bianthryl, n-hexane soln., excited states, dipole moments, transient dielectric loss results 7-13088
 calcium tartrate single crystals, dielectric props. rel. to X-ray on γ -ray irradi. 7-59161
 4-N,N-dimethylaminobenzonitrile, cyclohexane (1,5-dioxane) solns., excited states, dipole moments, transient dielectric loss results 7-13088
 epoxide resin-fatty monoepoxyesters, relax. props., struct. (Russian) 7-64565
 epoxy resins, cured, with perfluorobutenyloxy group, dielec. props. 7-53222
 glass ionic conductivity mechanism 7-44902
 glasses, dielectric losses in MM and subMM regions 7-39000

dielectric losses continued

- glucose, water mixtures, liq. and glassy states, dielectric relaxation study 7-33325
- hexamethyldisiloxane films, plasma polymerised, dielec. props., complex permitt. 7-33316
- internal friction in solids, review 7-6720
- laminated dielectric with losses, parameters determ. in broad freq. range, inspection method 7-65263
- marble, temp. effect on dielec. behaviour at 1 kHz 7-47434
- mica-epoxy composite dielectric strength obs. 7-64570
- oxide glass, relax. time and loss peak correl. with DC cond. 7-22181
- PET films, low frequency dielectric response 7-13091
- piezoceramic-polymer-composites, damping props. 7-64575
- PMMA, modified, γ -ray effects, dielec. props. 7-22185
- PMMA/polystyrene double layer system, dielec. const. and loss factor, temp. and freq. depend. 7-22190
- polar liquids, dielec. parameters at 9.2 GHz 7-13073
- poly (N-benzylidiphenylaminomethane) film, synthesis, elec. and optoelectronic props. 7-45384
- 1,2-polybutadiene, mol. motion, glass transition, loss curve, NMR, ^{13}C spin-lattice relax. 7-17234
- polyester resins, polymerisation kinetics, dielectric behaviour anal. (French) 7-46847
- polyethylene, high and low density, dielec. γ relaxation 7-39004
- polyethylene, spherulitic low density, dielec. relax. of dipolar aromatics, glass transition 7-45924
- polyethylene films, high field dielectric loss meas. 7-17264
- polyimide films, uniaxially-stretched, conductivity and dielec. losses 7-39005
- polymer-metallic filler systems, dielectric characts. (Russian) 7-39002
- polymerisation kinetics, dielectric behaviour anal. (French) 7-46847
- polyolefines, struct., dielec. props., crystallisation conditions effects (Russian) 7-64564
- polyoxy-(allyl)phenylene electrochemically prepared film, elec. props., permittivity and solubility 7-27665
- polypropylene oxide 4000, liq. and glassy states, dielec. props. 7-17266
- polypropylene oxide in toluene, dielec. relax. in liq. and glassy states 7-7638
- polystyrene blends, secondary relax. dielec. props., memory effect 7-53221
- polyvinyl formal, thermooxidation, dielec. props. rel. to chemical struct. 7-45927
- polyvinyl methyl ether, chain motions, dielec. props. 7-45928
- precision millimetre wave meas. in birefringent and ceramic materials 7-14978
- semiconductors, time-resolved dielectric loss meas. 7-64562
- siloxane nematogenic side chain polymer, director alignment, dielec. relax. spectra study 7-63457
- styrene-butadiene rubber, C-black loaded, elec. props., effect of gamma irradi., dosimetry appls. 7-33006
- p-terphenyl, dielec. response 7-22180
- triglycine sulphate, Cr doped, amplitude depend. of dielectric losses 7-64587
- XLPE, dielectric properties modification due to corona discharges, humidity effects 7-39022
- Al_2O_3 , electrical props., radiation effects 7-52617
- Al_2O_3 -CaO cement-glass microsphere composites, relative dielectric permittivity 7-33319
- Al_2O_3 - SiO_2 -CaO glasses containing rare alkali oxides, struct. and elec. props. 7-6528
- Ba ferrite filled styrene-isoprene-styrene composite, dynamic mech., elec. and mag. props. 7-13001
- $\text{Ba}_{1-x}\text{Gd}_x\text{F}_{2+x}$ defect struct., ionic thermocurrents, dielec. meas., EPR obs. 7-44907
- $\text{BaR}_2\text{Ti}_2\text{O}_{12}$ (R=La, Pr, Nd, Sm), dielectric props. at low temps. 7-45909
- BaTiO_3 ceramics, zone sintering, dielec. props. rel. to microstruct. 7-13078
- BaTiO_3 , dielectric, electrical and acoustic props. 7-53224
- $\text{Bi}_{1/2}\text{V}_{1/2}\text{TiO}_{3/4}$ layered cpd., crystal-chemical and dielectric props. 7-6595
- $\text{CaO-Al}_2\text{O}_3\text{-SiO}_2$ cement, macro-defect-free processing and low freq. dielec. response 7-13081
- $\text{Ca}_3\text{Y}_2(\text{PO}_4)_6(\text{OH})_{2-x}\text{O}_x$, synthesis, struct., dielec. props., AC elec. cond., IR spectra 7-3235
- H_2O , permittivity meas. by node-displacement method for open circuit 7-38981
- HgI_2 solution-grown crystals, X-ray and γ -ray irradi. effect on elec. props., radiation detector performance 7-58838
- K-Ca- NO_3 - H_2O glasses, low temp. dielectric study 7-38999
- KCl single crystals, laser excited dielec. props. and cond., X-ray irradi. effects study 7-27649
- KCl:Zn, elec. cond., dielec. loss meas., before and after X-irrad. 7-33324
- KNO_3 , dielectric props., effect of X-ray or γ -ray irradiation 7-53215
- KTaO_3 UHF dielectric resonators, mechanical pressure effects on permittivity and dielectric loss 7-7642
- $\text{La}_2\text{O}_3\text{:Sr}$, Er, Nd, mag. susceptibility, dielec. const. and dielec. losses 7-2810
- $\text{Li}_2\text{B}_4\text{O}_7\text{-WO}_3$ glasses, dielec. behaviour, space charge effects 7-45917
- LiD:Mg^{2+} , elec. props., X-irradiation effects, DC cond., dielec. loss and ionic thermocurrent meas. 7-27341
- LiF, quenched, dielectric props., effect of high AC field and X-ray irradiation 7-38985
- LiH:Ca^{++} , elec. props., X-irradiation effects, DC cond., dielec. loss and ionic thermocurrent meas. 7-27341
- LiTaO_3 low freq. dielec. response, charged point defect migration contrib. anal. 7-38984
- $\text{Mo}_0.3\text{-P}_2\text{O}_5$ glasses, permittivity, temp. depend., microwave meas. 7-45912
- Mg_2SiO_4 , fosterite-based ceramic with BaO addition, synthesis, sintering, struct. and props. 7-46397
- NH_4Cl , phase transitions, elec. props. study 7-17257
- NaCl:Ca , impurity dipoles, aggregation with dislocations under alternating elec. field 7-44598
- $\text{NaH}_2(\text{SeO}_3)_2$, low temp. struct. phase transition 7-64580
- PLZT ferroelectric ceramics, gamma, electron and neutron irradi. effects study 7-6677
- $\text{Pb,Cd}_{1-x}\text{F}_2$ phonon spectra, superionic props. 7-6735
- $\text{Pb}(\text{M}_{1/2}\text{Sb}_{1/2})\text{O}_3$, perovskite type antiferroelectrics, (M=Sc, Ho-Lu), X-ray and dielec. characts. 7-7649
- $\text{PbMg}_{1/3}\text{Nb}_{2/3}\text{O}_3\text{-PbTiO}_3$, MnO doped, relaxor ferroelec. ceramics, dielec. ageing effects 7-22195

dielectric losses continued

- $\text{Pb}(\text{Sc}_{0.5}\text{Nb}_{0.5})\text{O}_3$ ferroelectric ceramics, gamma, electron and neutron irradi. effects study 7-6677
- $\text{PbTi}_x\text{Zr}_{1-x}\text{O}_3$ piezoceramic, annealing in gaseous media with controllable comp., effect on electrophysical props. 7-8012
- PbZrO_3 -based piezoelectric ceramics containing $\text{Pb}(\text{Zn}_{1/3}\text{Nb}_{2/3})\text{O}_3$ 7-2984
- $\text{PbZr}_{1-x}\text{Ti}_x\text{O}_3$ polyethylene 3-0 connected composite, dielec. and piezoelec. props. 7-45937
- SiO-SnO_2 , vac. evaporated films, AC elec. props. 7-45528
- SiO_2 films, low temp. CVD, dielec. const., dissipation factor 7-59149
- SiO_2 fused, frequency dependent equation of state 7-51987
- SiO_2 glasses, prep. by sol-gel technique, dielec. props. 7-45918
- $\text{SiO}_2\text{-CaO-MgO-Na}_2\text{O}$ glass, frequency dependent equation of state 7-51987
- $\text{SrTiO}_3\text{-Al}_2\text{O}_3\text{-SiO}_2$ glass-ceramics, low temp. dielec. props. 7-7636
- TeO_2 -based halide glasses, prep., thermal, mechanical, elec. and optical props. characterisation (French) 7-37884
- YIG, multicomponent systems, synthesis, microwave characts., mathematical modelling 7-33626
- $\text{Y}_2\text{O}_3\text{:Sr}$, Er, Nd, mag. susceptibility, dielec. const. and dielec. losses 7-2810

dielectric materials

- see also antiferroelectric materials; dielectric thin films; electrets; ferroelectric materials; glass; insulating materials; insulation; piezoelectric materials
- composite electroceramics, book contrib. 7-27645
- contactless testing, RF method, linear antennas impedance meas. 7-54054
- new sensing materials (Japanese) 7-54142
- polymeric dielectric, in partial discharge, depression rel. to elec. ageing (Russian) 7-26577
- BaTiO_3 based ceramics for multilayer ceramic capacitors, chemical processing 7-46399

dielectric measurement

- see also dielectric loss measurement; permittivity measurement
- composite material, nondestructive meas. of dielec. permeability by non-steady frequency-phase method 7-33888
- fast measurement techniques for research in dielectrics 7-30034
- ferroelectric hysteresis loop tracer, automatic 7-4865
- H-plane sectoral waveguide as sensor for dielectric props. determ. 7-14977
- impedance spectroscopy applic. to materials sci., book contrib. 7-24659
- millimeter wave dielectric meas. of birefringent and ceramic materials 7-14978
- radiation diagnostics of electric potentials, sensitivity and resolution 7-8233
- relaxation measurement by lumped-capacitor time-domain spectroscopy (Japanese) 7-4862
- time domain spectroscopy using coaxial probe, human skin in vivo meas. appl. 7-14961
- wheat seeds, germinating, dielec. response meas. using resonant cavity 7-34127

dielectric phenomena

- see also dielectric hysteresis; dielectric losses; dielectric properties of substances; dielectric relaxation; dielectric resonance; electric strength; ferroelectricity; photodielectric effect; piezoelectricity; solvated electrons
- EM waves, freq. properties of dielectric scatterers in half-space 7-57215
- glassy phases, review 7-39054
- infinitesimal discontinuities in nonlinear dielectric media, wave front propagation 7-50627
- interfacial electrochemical processes, low freq. dispersion 7-39904
- piecewise homogeneous dielectric with general boundaries, plane fields computation (German) 7-62563
- satellites, electron-irradiated dielectric discharges, statistical behaviour 7-55423
- space charge effects, in HV stressed dielectric liquids 7-53235

dielectric polarisation

- see also Barkhausen effect; dielectric depolarisation
- automatic polarisation curve analyser, polarographic study appl. 7-24634
- diglycine nitrate, alanine-doped, dielectric props. 7-45908
- diglycine nitrate, dielec. const. and spontaneous polarisation anisotropy 7-45914
- diglycine nitrate, spontaneous polarisation and electrocaloric effect near the ferroelectric transition 7-17273
- disordered systems, nonexponential relaxations 7-64566
- dynamic thermopolarisation effects 7-45922
- ester type smectic C* liquid crystal, ferroelectric polarisation props. 7-13100
- ferroelectric crystal, first order ferroelec. transition in external mag. field 7-2994
- ferroelectric liquid crystals with high spontaneous polarisation 7-59159
- ferroelectrics with multi-domain layers, fabrication and SAW excitation 7-27676
- image charges and their influence on the growth and the nature of thin oxide films 7-64312
- incommensurate phases, phasons, dynamic pinning mechanisms 7-45941
- linear feedback models for polarisation and magnetisation of dielectric materials 7-22179
- lung, feline, dielec. polarisation at radio freqs. 7-59968
- magnetic ferroelectrics, inhomogeneous magnetoelectric effect 7-38920
- multipole theory of polarisation of solids by point defects 7-13086
- nonmetals, defect polarization and Haldane-Anderson model 7-21858
- nonpolar fluid, ellipsoid mols., induced birefringence and dielectric polarisation 7-33363
- onsager model modifications, mol. moment calcs. 7-53225
- oxides, rutile-type, dipole polarisabilities, cohesive energies and press. derivatives of bulk moduli 7-2967
- perovskites, nonferroelec. displacive phase transition to spontaneously polarised state 7-2169
- polyethylene, polarisation and depolarisation currents superposition, time depend. meas. and calcs. 7-27652
- polyethylene terephthalate, polarisation and depolarisation currents superposition, time depend. meas. and calcs. 7-27652
- polymer films, pyroelectric behaviour for IR detection 7-7644
- polymers, highly conjugated, giant anomalous polarisation investig. 7-7635
- polyvinylidene fluoride, shock response, ferroelec. and piezoelec. props. meas. 7-32568
- polyvinylidene fluoride films, active gauge for initiation diagnostics 7-30000

dielectric polarisation continued

- purple membrane, electric polarisability, electrooptic scatt. spectra anal. 7-54530
- PVDF films, thermal Barkhausen effect, spontaneous polarisation 7-59142
- PVDF pyroelectric film, improved poling conditions 7-64577
- PZT piezoceramics, reorientational polarization effects on stability and isotropy (French) 7-59153
- rigid dielectrics with polarisation inertia, wave propag. 7-7634
- semiconductor microcrystallites, laser-excited, absorption blue shift 7-33409
- Stockmayer fluid between Lennard-Jones plates, mol. dynamics study, electric field effect, polarisation 7-21060
- superdielectric polymers, nomadic polarisation 7-33323
- temperature modulation, effect on props. of ferroelectric materials 7-39044
- TGS, uniaxial ferroelec., transition under nonequilibrium conditions 7-13107
- TGS crystals, polarisation relax., defect effects 7-17265
- TGS-L- α -alanine admixture, dielec. props., influence of rejuvenation process 7-33339
- tris(trimethylammonium)Sb₂Cl₃ single crysts., dielec. and pyroelec. props. study 7-53210
- tris (dimethylammonium) nonachlorodiantimonate, ferroelectric phase transition 7-33345
- tris-sarcosine calcium chloride, deuterated, ferroelectric props. 7-39050
- two-level cryst., nonlinear dielectric response 7-7633
- twofold incommensurate phases, ferroelectricity, polarisation-wave condensation 7-53243
- vinylidene fluoride-trifluoroethylene copolymer, shock response, ferroelec. and piezoelec. props. meas. 7-32568
- weakly anisotropic media, elec. relax. theory 7-7640
- Al-Dy₂O₃-Al thin-film sandwiches, dielec. polarisation props. 7-38772
- Al-insulator-Si, optical and elec. charact. of (Al₂O₃)_{1-c}(AlN)_c 7-38766
- Al₂O₃, high field dielec. relax. effects 7-7641
- (Ba,Sr)TiO₃ film metal-dielec.-metal system, polarisation switching 7-52849
- Ba(Ca_{1/3}Nb_{2/3})O₃-PbZrO₃-PbTiO₃ ceramics, hot-pressed, ferroelectric phase transitions 7-7652
- Ba₂Sr_{1-x}Nb₂O₆ paraelec. phase, polarisation distrib. studies 7-38993
- Ba₂Sr_{1-x}Nb₂O₆, poly- and single-domain samples, integrated light scatt. and polarisation 7-53361
- BaTiO₃, ferroelectric, optical switching 7-37020
- Bi₂O₃-V₂O₅-CaO system, vitreous oxide semiconductor, polarisation processes 7-59139
- Cr₂BeO₄ multi-sublattice antiferromag., elec. polarisation, magnetoelec. effect calcs. (Russian) 7-7577
- K₂BiCl₆.2KCl.KH₂F₄, improper ferroelectric phase transition, dielec. meas. 7-45943
- K_{1-x}Li_xTaO₃ monocrys., polarisation jump, ferroelec. transition and domains study (Russian) 7-22200
- K_{1-x}Li_xTaO₃ single cryst., dielec. properties at 10⁻² to 10³ Hz 7-2997
- KNO₃, surface charge layer, spontaneous polarisation rel. to particle size (Korean) 7-27673
- KNbO₃, single-domain cryst. prep., orientation and dielec. polarisation 7-45950
- KTaO₃:Gd³⁺(Fe³⁺), ESR, effect of external electric field 7-38933
- Li₂Ge₂O₇, ferroelectric single crystals, pyroelectric props. 7-64576
- LiNbO₃:Fe cryst., Raman spectra, photo-induced refractive index change effects 7-53300
- NH₄Cl, spontaneous and field induced current peaks at order-disorder phase transition 7-45948
- NH₄HSeO₄ crystals, deuterated, pyroelectric props. 7-13098
- NaNO₂ thin films, ferroelectric and dielectric props. 7-39037
- PLZT ceramics, mechanical strength, composition and polarisation depend., microindentation meas. 7-6697
- PLZT-PZN electro-optic ceramics, elec., opt. and switching props. 7-7646
- PVDF films, elec. field-induced gas emission meas., ionic charge transport study 7-27872
- PZT ceramic, pressure induced ferroelectric-antiferroelectric transition 7-22201
- PZT solid solutions, p-t-x diagram 7-64581
- Pb₂Ge₂O₁₁:Gd³⁺, impurity ion reorientation kinetics 7-45940
- PbHPO₄, photostimulated luminescence near ferroelec. Curie temp. 7-64697
- Pb(M_{1/2}Sb_{1/2})O₃, perovskite type antiferroelectrics, (M=Sc, Ho-Lu), X-ray and dielec. characts. 7-7649
- PbMn_{2/3}MO₃, perovskite-type cpds., (M=Mo, Te, Re), dielec. and mag. props. 7-7650
- PbTiO₃, cryst. optical studies of precursor and spontaneous polarisation 7-45921
- PbZr_{1-x}Ti_xO₃-polyethylene 3-0 connected composite, dielec. and piezoelec. props. 7-45937
- Pt electrodes, porous, in solid-electrolyte cell, polarization 7-23027
- Sb_{1-x}Bi_xSI crystals, elec. props. at ferroelec. Curie point 7-2991
- SnO₂-n-Sb₂S₃-Al structures, polarization current relaxation and space charge 7-33090
- TiN reactively RF sputtered coatings, structural defects and porosity, electrochem. polarisation meas. 7-52333

dielectric properties of gases

No entries

dielectric properties of liquids and solutions

- acetone-benzophenone mixture, benzene solvent, dielectric relax. study 7-64563
- acetonitrile-cyclohexane-benzene, crit. solns., nonlinear dielec. effect obs. 7-53213
- alcohols in glassy media, dielectric and IR spectral study 7-2968
- alkali halides, aq. solns., ion hydration, dielec. props., microwave spectrosc. obs. (French) 7-54111
- alkaline earth halides, aq. solns., ion hydration, dielec. props., microwave spectrosc. obs. (French) 7-54111
- 4-4'-alkoxybenzoyloxy-4'-cyanoazobenzenes, monolayer smectic A₁-nematic transition, dielec. studies 7-21085
- N-alkyl aliphatic amide mixtures, dielec. constant 7-27648
- n-alkylamine-n-dodecane systems, static dielec. consts. and excess molar enthalpies 7-59134
- 4-(trans-4'-n-alkylcyclohexyl) isothiocyanatobenzenes, mesogenic props. 7-1852

dielectric properties of liquids and solutions continued

- ammonium hydrogen-DL-malate monohydrate, dielec. and pyroelec. props. 7-59138
- aromatic aldehydes in cyclohexane solvent, internal mobility study, far-IR and microwave Fourier transform spectra anal. 7-64631
- automatic polarisation curve analyser, polarographic study appl. 7-24634
- benzonitrile-hexane, binary solns., pseudospinodal curve, nonlinear dielec. effect 7-53212
- biphenyl ester series, ferroelectric liquid crystals, dielec. props. 7-37843
- Born equation electrostatic solvation energies, off-centre mol. charge distrib. corrections 7-33916
- bubbles, maximum size during nucleate boiling in elec. field 7-50918
- N-(p-n-butoxybenzylidene)p-n-butylaniline, nematic, mol. alignment, permitt. meas. 7-1875
- ditert-butyl malonate in dioxane-water media, acid-catalysed hydrolysis, kinetic and mechanistic studies 7-39884
- Carnauba wax, liq., complex impedance 7-17026
- CE8, liquid crystalline, chiral and racemic, audio frequency dielectric response 7-33318
- charged dielectric sphere, electron bound states 7-21960
- chlorobenzene-nitrobenzene mixtures, dielectric absorpt. meas. in microwave region 7-53211
- cholesteryl oleate, isotropic-blue phase transition, nonlinear dielectric effect meas. 7-12272
- di(tetraphenylphosphine) ammonium perchlorate, dielectric props., conc. depend. 7-38998
- 4,4'-di-n-pentyloxazobenzene, nematic and rotary phases, molecular reorientation 7-32278
- dielectric, field-stimulated isothermal diffusion calcs. 7-63855
- 1,2-diol solns. with water or electrolytes, dielectric props. 7-13080
- dioxans with dimethylene linking groups, liquid crystalline props. 7-1854
- dipolar hard sphere mixtures, dielectric const., Monte Carlo simulation 7-45911
- DNA liquid cryst. microphases in water-organic solns., optical props. 7-65709
- dye mols. in polar fluids, correl. between mol. reorientation and dielectric friction 7-22182
- electrical cond. and dielec. breakdown 7-45932
- electro-dilatometric effect in dielectric liq. 7-33335
- electrolyte, solutions, viscosity, dielec. function theory 7-44883
- ester type smectic C* liquid crystal, ferroelectric polarisation props. 7-13100
- ferroelectric liquid crystals, distortion free energy density, electrostatic screening 7-37844
- ferroelectric smectic C* liquid crystal, alignment and switching characteristics 7-64589
- fractal cluster form. by aq. nanodroplets in apolar media, dielec. 7-39921
- glucose, water mixtures, liq. and glassy states, dielectric relaxation study 7-33325
- insulating liquids, air bubbles attached to point electrodes 7-37779
- nematic liq. crystals, molecular association, influence on dielectric and electro-optic props. 7-16407
- nematic liquid crystal in switched DC electric field, time response 7-32271
- nitrobenzene-hexane, binary solns., pseudospinodal curve, nonlinear dielec. effect 7-53212
- n-nonane liq. dielectric, gas form. under particle discharge 7-51532
- nonpolar fluid, ellipsoid mols., induced birefringence and dielectric polarisation 7-33363
- nonpolar liquids, permittivity meas., mol. polarisability determ. (French) 7-53217
- octylcyanobiphenyl, liq. cryst., elastic consts., permitt., birefr. meas. 7-21314
- perfluoromethylcyclohexane-carbon tetrachloride, liq.-liq. critical point, dielectric const. 7-13079
- photoconductor-liq. crystal rectifier, liq. crystal dielectric anisotropy, low-freq. inversion effect 7-45395
- polar liquid dielectrics, mag. field effects 7-13072
- polar liquids, 1-parameter model of dielectric relax. 7-27653
- polar liquids, dielec. parameters at 9.2 GHz 7-13073
- polar liquids, dielec. permittivity, mol. shape and polaris. anisotropy 7-17258
- polar liquids, dielec. relax. parameters 7-2972
- poly(propylene oxide), glassy and liq. states, water effect on dielectric props. 7-38987
- polyatomic ions in soln., rot., Hubbard-Onsager-Felderhof's dielectric friction theory 7-17281
- polymer liq. cryst. solns., optical microscopy, Freedericksz transition, permitt. meas. 7-1864
- polyolefines, struct., dielec. props., crystallisation conditions effects (Russian) 7-64564
- polypropylene oxide 4000, liq. and glassy states, dielec. props. 7-17266
- polypropylene oxide 4000, liq. and glassy states, dielec. relax. and permittivity 7-13083
- polypropylene oxide in toluene, dielec. relax. in liq. and glassy states 7-7638
- prebreakdown phenomena in liq. dielectrics, effects of hydrostatic pressure (French) 7-33327
- 4H-pyran-4-one, derivatives and related S cpds. aromaticity, dipole moment anal. 7-22177
- pyrimidines with dimethylene linking groups, liquid crystalline props. 7-1854
- quadrupole glass with axial interaction, solvable model 7-64591
- rotators, 2D and 3D, with permanent elec. dipoles, dielec. function 7-2963
- smectic A-smectic A transitions, density dielec. and X-ray studies 7-2196
- smectic B phase in binary mixture, dielec. relax. 7-13089
- solutions, ionic props., mol. dynamics simulation 7-44331
- Stockmayer fluid between Lennard-Jones plates, mol. dynamics study, electric field effect, polarisation 7-21060
- surfactant-water-nonaqueous liq. systems, elec. cond. study 7-13789
- suspensions, dielectric properties, Maxwell mixture formula, Debye type contributions 7-13090
- tetraalkylammonium perchlorates, dielectric props., conc. depend. 7-38998
- tetraphenyl arsenic iodide, dielectric props., conc. depend. 7-38998
- thiophene, benzene solvent, dielectric relax. study 7-64563
- thiophene-benzophenone mixture, benzene solvent, dielectric relax. study 7-64563
- toluylaldehydes, mobilities, microwave and far IR complex permittivities meas. 7-53218

dielectric properties of liquids and solutions continued

- 4-C(trans-4'-n-hexylcyclohexyl)isothiocyanatobenzene, nematic and isotropic phases, dielec. relax. 7-53229
 urea and its derivatives, aq. soln., dielectric relax. 7-22183
 water, liquid network structure model 7-11878
 9H-xanthen-9-one derivatives and related S cpds. aromaticity, dipole moment anal. 7-22177
 H₂O imprecision of permittivity values for application to remote sensing 7-66331
 H₂O, permittivity meas. by node-displacement method for open circuit 7-38981
⁴He liq., electric permittivity, microwave meas. 7-13074
 4-n-hexyloxyphenyl 4'-n-decyloxybenzoate, liq. cryst. phases, dielec. relax. 7-53228
 KCl, organic liquid emulsions, dielectric props. meas. 7-22173
 Li⁺, in water, Stokes radius, Hubbard-Onsager's dielectric friction theory 7-33347
 Ru complex, outer sphere electron transfer, solvent relax. dynamics effect 7-65290
 TiO₂, nonaq. dispersion in petroleum, dielectric const. in electric field investig. 7-38982

dielectric properties of solids

- acetanilide, dielectric const. meas., effect on energy transport 7-59137
 alcohols in glassy media, dielectric and IR spectral study 7-2968
 alkali halides, refractive index, Szigeti charge, dielec. parameters ab initio calcs. 7-13082
 calcium tartrate single crystals, dielectric props. rel. to X-ray on γ -ray irradi. 7-59161
 composite dielectric materials, interface response theory of electromagnetism 7-62564
 composite piezoelectric sensors, elec. characts., hydrophone appl. 7-62943
 conference, Erlangen, W.Germany (July 86) 7-35099
 crack extension force in a dielectric medium 7-6152
 crystalline dielectrics, piezoelec. and flexoelec. responses, surface contris., unified approach 7-22193
 disaccharide maltose monohydrate, water binding modes, TSC meas. 7-38997
 double injection charge transport in dielectrics 7-33334
 elastic dielectric, conservation laws and material momentum tensor 7-6086
 epoxide resins, mech. and dielec. relax. rel. to spiro-ring struct. 7-17572
 ethylene-propylene rubber, dielectric props., water detection using photoacoustic spectroscopy 7-53298
 frequency distrib. function anal., dielec. and scatt. props., orthogonalised moments method 7-64633
 glasses, characterisation by electron bombardment 7-32506
 hexamethyldisiloxane films, plasma polymerised, dielec. breakdown 7-33328
 hexamethyldisiloxane films, plasma polymerised, dielec. props., complex permitt. 7-33316
 ice:RbOH, phase transition, dielec. studies 7-53220
 linear isotropic, lattice defects 7-26749
 linear magneto-optical effect anisotropy in dielectric cryst. 7-39092
 marble, temp. effect on dielec. behaviour at 1 kHz 7-47434
 metal-dielectric systems, adhesion calc. 7-7023
 PMMA/polystyrene double layer system, dielec. const. and loss factor, temp. and freq. depend. 7-22190
 poly(propylene oxide), glassy and liq. states, water effect on dielectric props. 7-38987
 polybis-benzimidazobenzisquinolinones, dielec. β -relax., -150 to 80°C 7-7637
 1,2-polybutadiene, mol. motion, glass transition, loss curve, NMR, ¹³C spin-lattice relax. 7-17234
 polyethylene, dielectric props., water detection using photoacoustic spectroscopy 7-53298
 polyethylene, spherulitic low density, dielec. relax. of dipolar aromatics, glass transition 7-45924
 polymer dielectrics, injection role in charge accumulation process 7-33026
 polymers, permittivity, loss tangent and refractive index meas., using Fourier transform technique 7-18820
 polypropylene films, morphology and dielec. props., impregnants effects 7-39024
 polystyrene blends, secondary relax. dielec. props., memory effect 7-53221
 polyurethane-CaCO₃ composites, segmented, dielec. relax., glass transition 7-45926
 polyvinyl alcohol-polyvinyl acetate blends, TSDC, effect of blending 7-13084
 polyvinyl formal, thermooxidation, dielec. props. rel. to chemical struct. 7-45927
 polyvinyl methyl ether, chain motions, dielec. props. 7-45928
 polyvinylidene fluoride/PZT, composites, dielec. behaviour 7-38992
 PVC, field induced thermally stimulated relax. 7-27654
 quantum paraelectric material with two types of impurity, structural phase transition, CPA calc. 7-44786
 styrene-butadiene rubber, C-black loaded, elec. props., effect of gamma irradi., dosimetry appls. 7-33006
 p-terphenyl, dielec. response 7-22180
 triphenylchloromethane-o-terphenyl, sp. ht. capacity and glass transition temp. meas., thermodynamic config. anal. 7-21446
 two-level cryst., nonlinear dielectric response 7-7633
 wave propagation in rigid dielectrics with polarisation inertia 7-7634
 Al₂O₃, electrical props., radiation effects 7-52617
 Al₂O₃, high field dielec. relax. effects 7-7641
 Al₂O₃-SiO₂-CaO glasses containing rare alkali oxides, struct. and elec. props. 7-6528
 α -AlPO₄, berlinite, piezoelec. and elastic props., effect off defects on phys. props. 7-51909
 AlPO₄, glass, dielectric, charge buildup, influence on charging electron beam motion 7-44294
 Ba(NO₃)₂· $\frac{1}{2}$ H₂O, cryst., phase transition at 211K, DTA and dielec. meas. 7-32633
 BaTiO₃ ceramics, zone sintering, dielec. props. rel. to microstruct. 7-13078
 BaTiO₃ composites, dielec. and elec. props., rel. to prep. and microstruct. 7-64559
 BaTiO₃, Nd₂O₃-modified, defect struct. and dielec. props 7-37968
 Bi films, IR and visible spectra, refractive index, extinction coeff. and dielectric const. 7-46156

dielectric properties of solids continued

- Ca₃Y₂(PO₄)₆(OH)₂-xO_x, synthesis, struct., dielec. props., AC elec. cond., IR spectra 7-3235
 Ge₂S_{1-x}, glass, ordered phases, effective microscopic cross charge 7-13077
 Ge₂Se_{1-x}, glass, ordered phases, effective microscopic cross charge 7-13077
 HgI₂, solution-grown crystals, X-ray and γ -ray irradi. effect on elec. props., radiation detector performance 7-58838
 Hg₂Se, dielec. parameters and mag. susceptibility (Russian) 7-53254
 Hg₂Te, dielec. parameters and mag. susceptibility (Russian) 7-53254
 LiCsSO₄, dielec. props., press. effect 7-64555
 LiF single cryst., dielectric, charge buildup, influence on charging electron beam motion 7-44294
 Mg₂O₃-P₂O₅ glasses, permittivity, temp. depend., microwave meas. 7-45912
 MgO, strain derivatives of dielec. constants 7-17259
 Mg₂SiO₄, fosterite-based ceramic with BaO addition, synthesis, sintering, struct. and props. 7-46397
 NH₄Cl, phase transitions, elec. props. study 7-17257
 PZT:Mn, dielec. dispersion 7-13076
 Pb(Mg_{1/3}Nb_{2/3})O₃ ceramics, dielec. props. 7-46382
 PbZrO₃-based piezoelectric ceramics containing Pb(Zn_{1/3}Nb_{2/3})O₃ 7-2984
 Rb_{1-x}(NH₄)_xH₂AsO₄, proton glassy state, dielec. props. 7-13075
 SiO₂ glasses, prep. by sol-gel technique, dielec. props. 7-45918
 Ta₂O₅ crystalline films, sputter deposited, phys. and elec. props. 7-2412
 TiBr₃, strain derivatives of dielec. constants 7-17259
 TiCl₃, strain derivatives of dielec. constants 7-17259
- dielectric properties of substances**
 see also antiferroelectricity; dielectric depolarisation; dielectric function; dielectric materials; dielectric measurement; dielectric phenomena; dielectric polarisation; dielectric properties of gases; dielectric properties of liquids and solutions; dielectric properties of solids; electric strength; optical susceptibility; permittivity; piezoelectricity; pyroelectricity
 bone materials used as US transducers, charactn. 7-60130
 electrical breakdown, physics, acoustic theory appl. 7-33329
 helical surface waves on a dielectric rod 7-62571
 multipolar lattice sums convergence and dielectric props., computer simulation 7-59163
 PMMA dielectric, sub-ohmic I-V characts. below glass transition temp. 7-27335
 polymer-metallic filler systems, dielectric characts. (Russian) 7-39002
 tumours, solid., dielec. props. during normothermia and hyperthermia 7-3778
 zwitterionic lipid bilayers, dielec. props. of polar head group region 7-8504
 β -radioactive dielectrics, space electric charge distrib. in surface layer 7-33326
- dielectric relaxation**
 see also dielectric resonance
 acetone-benzophenone mixture, benzene solvent, dielectric relax. study 7-64563
 acetonitrile, dielec. relax., inertia-corrected Budo theory calcs. 7-2969
 alcohols in glassy media, dielectric and IR spectral study 7-2968
 aromatic aldehydes in cyclohexane solvent, internal mobility study, far-IR and microwave Fourier transform spectra anal. 7-64631
 bisphenol-A-type epoxide resin, mech. and dielec. relax., alkyl side chains effect 7-45925
 Carnauba wax, liq., complex impedance 7-17026
 CE8, liquid crystalline, chiral and racemic, audio frequency dielectric response 7-33318
 chlorobenzene-nitrobenzene mixtures, dielectric absorpt. meas. in microwave region 7-53211
 4,4'-di-n-pentyloxazoxybenzene, nematic and rotary phases, molecular reorientation 7-32278
 1,2-diol solns. with water or electrolytes, dielectric props. 7-13080
 disaccharide maltose monohydrate, water binding modes, TSC meas. 7-38997
 disordered dielectrics, electret relax., persistent polarisation decay and injected charge cond. calcs. 7-39003
 disordered systems, nonexponential relaxations 7-64566
 dye mols. in polar fluids, correl. between mol. reorientation and dielectric friction 7-22182
 epoxide resin-fatty monoepoxesters, relax. props., struct. (Russian) 7-64565
 epoxide resins, mech. and dielec. relax. rel. to spiro-ring struct. 7-17572
 epoxide resins, spiro type, acid anhydride cured, mech. relax. props. 7-21349
 epoxy resins, polymerisation kinetics, dielectric behaviour anal. (French) 7-46847
 fractal cluster form. by aq. nanodroplets in apolar media, dielec. 7-39921
 glasses, dielectric relaxation studies, high-resolution laser techniques 7-39006
 glassy materials, relax. from Levy stable distribs. 7-32299
 glucose, water mixtures, liq. and glassy states, dielectric relaxation study 7-33325
 hexamethyldisiloxane films, plasma polymerised, dielec. props., complex permitt. 7-33316
 hexanone-2, dielec. relax., inertia-corrected Budo theory calcs. 7-2969
 ice:RbOH, phase transition, dielec. studies 7-53220
 ion-implanted polymers, fractal elec. cond., current transients, percolative transition calcs. 7-2645
 ITC spectrum analysis, role of background currents 7-38996
 measurement method by lumped-capacitor time-domain spectroscopy (Japanese) 7-4862
 MIS structures, nonequilibrium surface potential relax. under constant charge conditions 7-38732
 oxide glass, relax. time and loss peak correl. with DC cond. 7-22181
 plant leaves, binding modes of water, dielectric study 7-54839
 PMMA, charge motion and self-relaxation, pulsed electro-acoustic meas. 7-27655
 PMMA, noncryst., relax. phenomena and elec. fluctuations (Russian) 7-16454
 polar liquids, 1-parameter model 7-27653
 polar liquids, dielec. relax. parameters 7-2972
 poly(propylene oxide), glassy and liq. states, water effect on dielectric props. 7-38987
 poly(propylene oxide) elec. relax. time, high press. effects study 7-32703
 polyacrylate derivatives, liq. cryst., dielectric transitions eval. (Russian) 7-39001

dielectric relaxation continued

- polybis-benzimidazobenzosquinoxalones, dielec. β -relax., -150 to 80°C 7-7637
- polyester resins, polymerisation kinetics, dielectric behaviour anal. (*French*) 7-46847
- polyethylene, dielec. and mechanical relaxations, rate theory eqn. calcs. 7-26983
- polyethylene, high and low density, dielec. γ relaxation 7-39004
- polyethylene, polarisation and depolarisation currents superposition, time depend. meas. and calcs. 7-27652
- polyethylene, spherulitic low density, dielec. relax. of dipolar aromatics, glass transition 7-45924
- polyethylene terephthalate, polarisation and depolarisation currents superposition, time depend. meas. and calcs. 7-27652
- polymers, dielectric dispersions, complex plane, anal. methods 7-22176
- polyoxymethylenes, low temp. dielec. relax., crystallite surface folds motion contrib. study (*Russian*) 7-17267
- polypropylene oxide 4000, liq. and glassy states, dielec. props. 7-17266
- polypropylene oxide 4000, liq. and glassy states, dielec. relax. and permittivity 7-13083
- polypropylene oxide in toluene, dielec. relax. in liq. and glassy states 7-7638
- polystyrene, noncryst., relax. phenomena and elec. fluctuations (*Russian*) 7-16454
- polyurethane-CaCO₃ composites, segmented, dielec. relax., glass transition 7-45926
- polyvinyl alcohol-polyvinyl acetate blends, TSDC, effect of blending 7-13084
- polyvinyl formal, thermooxidation, dielec. props. rel. to chemical struct. 7-45927
- PVC, field induced thermally stimulated relax. 7-27654
- PVC, noncryst., relax. phenomena and elec. fluctuations (*Russian*) 7-16454
- rotators, 2D and 3D, with permanent elec. dipoles, dielec. function 7-2963
- semiconductors, minority carrier injection, boundary conditions effects, numerical computation 7-21935
- siloxane nematogenic side chain polymer, director alignment, dielec. relax. spectra study 7-63457
- sliding CDW systems, dielectric relax. freq. 7-45293
- smectic A-smectic A transitions, density dielec. and X-ray studies 7-2196
- smectic B phase in binary mixture, dielec. relax. 7-13089
- TGS crystals, polarisation relax., defect effects 7-17265
- thermal noise correl. anal. 7-22186
- thiophene, benzene solvent, dielectric relax. study 7-64563
- thiophene-benzophenone mixture, benzene solvent, dielectric relax. study 7-64563
- 4-C(trans-4'-n-hexylcyclohexyl)isothiocyanatobenzene, nematic and isotropic phases, dielec. relax. 7-53229
- triphenylchloromethane-o-terphenyl, sp. ht. capacity and glass transition temp. meas., thermodynamic config. anal. 7-21446
- urea and its derivatives, aq. soln., dielectric relax. 7-22183
- vinylidene cyanide-vinyl acetate alternate copolymer, dielec. relaxation 7-7639
- water, liquid network structure model 7-11878
- weakly anisotropic media, elec. relax. theory 7-7640
- Al₂O₃, high field dielec. relax. effects 7-7641
- Ba_{1-x}Gd_xF_{2+x} defect struct., ionic thermocurrents, dielec. meas., EPR obs. 7-44907
- Ba(NO₃)₂·1/2H₂O, cryst., phase transition at 211K, DTA and dielec. meas. 7-32633
- BaTiO₃ ceramics, Maxwell-Wagner relax. and degradation 7-2970
- CaH₂PO₄ ferroelec., dielec. relax. meas. in paraelec. and ferroelec. phases, time domain spectroscopy method (*Japanese*) 7-4862
- Dy₂O₃-CaO solid solutions, dipole complexes, dielectric relax. 7-53231
- Fe₃O₄ single cryst., dielec. and conducting props. study below Verwey point 7-53230
- H₂O, dielectric microwave and near-millimetre wavelength spectra 7-27646
- 4-n-hexyloxyphenyl 4'-n-decyloxybenzoate, liq. cryst. phases, dielec. relax. 7-53228
- (KBr)_{0.5}(KCN)_{0.5} small-signal freq. response relax., exponential and Gaussian activation energy distrib. models calcs. 7-59143
- KCl single crystals., laser excited dielec. props. and cond., X-ray irradi. effects study 7-27649
- KH₂PO₄, hydrostatic pressure effect on ferroelectric relaxational mode, light scatt. study 7-2971
- K_{0.3}MoO₃, CDW system, stretched exponential dielec. relax. 7-45929
- KTa_{0.991}Nb_{0.009}O₃, dipolar glass, cluster dynamics 7-22184
- α -LiO₃, cryst., elastic wave attenuation, freq. and temp. depend. (*Russian*) 7-21364
- N-HO bond complexes, association equilib. const. using dielectric relax. data 7-65291
- ND₄DSeO₄, deuterated AHSe, crystals, dielectric relax. 7-45930
- PZT:Mn, dielec. dispersion 7-13076
- PbMg_{1/3}Nb_{2/3}O₃-PbTiO₃, MnO doped, relaxor ferroelec. ceramics, dielec. ageing effects 7-22195
- Sb₂S₃ amorphous condensers, electroelectret state and local levels studies (*Russian*) 7-45923
- a-Si:H, charge transport and relax., luminesc. long-time tail distrib. anal. 7-39185
- a-Si:H pin solar cells, photocurrent, transient behaviour 7-46950
- SrTiO₃ ceramics, Maxwell-Wagner relax. and degradation 7-2970
- SrTiO₃-Al₂O₃-SiO₂ glass-ceramics, low temp. dielec. props. 7-7636

dielectric resonance

- see also dielectric relaxation; paraelectric resonance
- ErFeO₃, magnetodynamic resonance near low-temp. phase transition 7-38862
- RbCl:Ag⁺, hydrostatic press. depend. of tunnelling splitting 7-64590
- SrFe₂O₁₉, mm wave magnetic and dielec. resonances 7-53139

dielectric resonators

- complex permittivity meas. of semiconductors, TE₀₁₈ mode dielectric resonator appl. 7-14976
- ESR spectrometer sensitivity enhancement, using dielectric resonator 7-9865
- KTaO₃ UHF dielectric resonators, mechanical pressure effects on permittivity and dielectric loss 7-7642
- PZT piezoelectric ceramic prop. meas., applied compressive stress parallel to polar axis 7-45939

dielectric strength see electric strength**dielectric susceptibility** see optical susceptibility**dielectric thin films**

- see also ferroelectric thin films; insulating thin films; optical films; piezoelectric thin films
- beam combiner, design and development 7-5978
- characterisation, by Fourier Transform Infrared spectra 7-53435
- coatings, mol. struct. and phys. props. Raman studies 7-45063
- conf., Las Vegas, USA (Oct. 1985) 7-35108
- crystal, refl. and transmission coeffs., S-matrix method calcs. (*Russian*) 7-33473
- double layer dielec. films, X-ray irradi. effects 7-58332
- electron irradi., space-charge buildup, atomic number effect 7-33330
- electrostatic problems, integral eqns. for thin dielec or conducting layers 7-31209
- ethylene-vinyl acetate/polyethylene double layer dielec. films, TSC phenomena obs. 7-27663
- hexamethyldisiloxane films, plasma polymerised, dielec. breakdown 7-33328
- hexamethyldisiloxane films, plasma polymerised, dielec. props., complex permitt. 7-33316
- layered structures, Raman and IR spectroscopy 7-3059
- MBE growth, process monitoring and equipment 7-27909
- mirrors, low loss, high reflecting for high power laser appls. 7-5967
- multilayer dielec. coatings, spectral characts., reflection and transmission bands (*Russian*) 7-22374
- nondestructive inspection of cond. surfaces and dielec. coatings using radiowave diffract. 7-39820
- nonlinear, optical reflectivity and transmissivity power depend. calcs. 7-53429
- nylon films, thermally stimulated and pyroelectric currents, H bond struct. effects 7-27664
- overlayers, on GaAs, effect on surface depletion potential 7-38678
- oxide films, RF sputtered, high intensity electron beam irradi. effects 7-44626
- oxide thin films, dielec. breakdown, censored Weibull statistics 7-27656
- PMMA/polystyrene double layer system, dielec. const. and loss factor, temp. and freq. depend. 7-22190
- polybutadiene thin films, elec. cond. in sandwich config., I-V characts. meas., electrode effects 7-27449
- polycarbonate films, pure and N-isopropylcarbazole doped, low freq. relative permittivity temp. depend. meas. 7-27666
- polyethylene dielec. thin films, hot-electron-induced damage and charge storage, electron spectra studies 7-27662
- polyethylene films, charge storage lifetime, structural effects 7-27344
- polyethylene lightly doped films, breakdown strength meas., injected space charge effects study 7-39019
- polyethylene terephthalate/polyvinylidene fluoride double layer dielec. films, TSC phenomena obs. 7-27663
- polyoxy-(allyl)phenylene electrochemically prepared film, elec. props., permittivity and solubility 7-27665
- polypropylene films, charge storage lifetime, structural effects 7-27344
- PVDF, elec. field-induced gas emission meas., ionic charge transport study 7-27872
- pyrometric temperature measurement, effect of thin dielectric films on accuracy 7-18789
- refractive index and thickness meas. using waveguide props. 7-56323
- short-circuited, dispersive charge transport, space charge dynamics calcs. 7-39038
- stearic acid films, dielec. breakdown field meas. 7-27661
- TM-polarized nonlinear slab-guided waves in saturable media 7-31407
- TSC phenomena effects on double-layer dielectric films, carrier interaction and interface characts. 7-45934
- underlayer film, sputter etching treatment before TbCo film deposition 7-45767
- vacuum methods of film deposition (*Polish*) 7-64901
- AlN reactively evaporated encapsulating films, annealing, RBS and RHEED studies 7-21744
- AlN sputtered film, Kerr effect enhancement 7-64610
- Al₂O₃ anodic films, thickness depend. of dielectric breakdown voltage 7-39007
- Al₂O₃ insulating thin films, normal press. CVD (*German*) 7-59453
- Al₂O₃-Ta₂O₅ thin films, dielec. props. rel. to electrolum. display appls. 7-2975
- (Al₂O₃)_{1-x}(AlN)_x optical and elec. props., comp. depend. 7-38766
- BN, optical and compositional props. 7-39206
- Bi₂O₃, activated reactive evaporation using resistively heated sources 7-13383
- C, dielectric film growth, on GaAs and InP substrates 7-39420
- C thin films, electrophys. props., MIS struct. as tool for anal. 7-17268
- a-C:H, diamondlike, props. rel. to deposition parameters 7-39419
- a-C:H, optical and compositional props. 7-39206
- GaAs, dielectric protective coatings during heat treatment 7-33852
- GaAs-Al₂O₃, interface struct., dielectric film mol. beam epitaxial growth 7-38360
- GaAs-CaF₂, interface struct., dielectric film mol. beam epitaxial growth 7-38360
- In, granular films, metal-insulator transition, conducting props. study (*Russian*) 7-7116
- MgF₂-MF₂ mixtures, (M=Ca,Sr,Ba), films, prep., physicochemical and optical props. 7-3178
- a-Nb₂O₅, by alkoxide method on Nb and Al substrates 7-13394
- Pb_{1-x}La_xTi_{1-(x/4)}O₃ sputtered film struct., dielec., and pyroelec. props. studies 7-21724
- PbO-B₂O₃-SiO₂ glass dielec. thin films on anodised Al substrates 7-17269
- PbTiO₃ gels and films, hydrolysis conditions effect on characts. 7-46400
- Si-O, electrophysical parameters, laser oxidation of Si 7-17741
- a-SiN_x:H dielectric films with low defect density 7-39036
- Si₃N₄, low temperature photo-CVD, characterisation 7-13377
- Si₃N₄ thin films, growth by microwave-excited plasma 7-59458
- Si₃N₄, remote plasma enhanced CVD 7-39425
- SiO sputtered film, Kerr effect enhancement 7-64610
- SiO thin dielec. film, deposition on Kodial glass, optical props. 7-7872
- SiO-SnO₂, vac. evaporated films, AC elec. props. 7-45528
- SiO₂ CVD photox layers, Hg-sensitized, elec. props. 7-64379
- SiO₂ films, breakdown lifetime meas., defect density determ. 7-22189
- SiO₂, gate dielectric films, growth by rapid thermal processing, material and electrical props. 7-16906

dielectric thin films continued

- SiO₂ interference system, influence of normal nonhomogeneity of refractive index (*Czech*) 7-64712
- SiO₂ RF sputtered thin films, atomic defects and stresses, optical and elec props. 7-16898
- SiO₂ thin films, dielectric breakdown phenomenon, model 7-64567
- SiO₂ thin films, growth by microwave-excited plasma 7-59458
- SiO₂ thin films, production from glow discharge decomp. of NO-SiH₄ mixtures, elec. props. 7-22512
- SiO₂ ultrathin films, intrinsic breakdown characts. 7-64571
- Si₃O₄, remote plasma enhanced CVD 7-39425
- SiO₂N₂, high press. NH₃-nitrided, elec. characts. 7-39039
- Si₃O₄N₂, plasma enhanced CVD, characterisation 7-39426
- Si₃O₄N₂, remote plasma enhanced CVD 7-39425
- TbFeCo/dielectric interface, chemical stability, interdiffusion and oxidation, AES, XPS and RBS depth profile studies 7-12513
- TiO₂ films, phase transitions, Raman spectra 7-12556
- TiO₂ films, pulse laser irradiated, Raman studies of phase transformations 7-12569
- TiO₂ interference system, influence of normal nonhomogeneity of refractive index (*Czech*) 7-64712
- TiO₂ thin dielec. film, deposition on Kodial glass, optical props. 7-7872
- ZrO₂ films, pulse laser irradiated, Raman studies of phase transformations 7-12569
- ZrO₂ thin films, high index, optical const. in UV region 7-7775

dielectric triodes *see space-charge limited devices***dielectric waveguides**

- see also optical waveguides*
- dielectric surface-relativistic electron beam interaction, expt. investig. 7-44195
- doubly periodic dielectric guide, wave propag. 7-11109
- rod waveguides with flat cross-section, anal. 7-43383
- sensors for dielectric constants use 7-4863
- symmetric planar waveguide, degenerate nonlinear modes 7-57399
- SiO₂-SiC layer systems, waveguide polaritons 7-7126

dielectrics *see dielectric materials***diesel engines** *see internal combustion engines***difference amplifiers** *see differential amplifiers***difference equations**

- acoustic microscope, elastic wave propag., accurate field anal. 7-43472
- advection eqn., 1D, 3-pt. 2-level finite difference methods 7-16149
- advection eqn., 1D, improved 5 pt. implicit finite difference methods 7-16150
- advection-diffusion eqn., accurate finite difference methods and Pascal listing 7-16148
- air pollution modelling, num. method and computer simulation 7-54394
- astrophysical flows, initial value problems, simple adaptive grids in 1D 7-66457
- atmospheric convection, comparison of GR FEM models 7-18298
- axisymmetric flows in swirlers, difference method 7-51166
- boundary value problem, stability anal. using analytical calcs. 7-18568
- cavity flow, buoyancy effect, finite difference method (*Chinese*) 7-11429
- coastal flow, numerical modelling 7-55078
- composite shell of revolution, flexible, weakened by notches, stress-strain state, num. method 7-16075
- computational continuum dynamics, parallel algorithms 7-4683
- computational fluid dynamics, implicit soln. methods 7-51020
- conservative nonlinear operator difference scheme, correctness theorems 7-18567
- conservative uniformly accurate difference method for a singular perturbation problem in conservation form 7-48325
- continuous versus on-off heating 7-37310
- convection, linear 1D eqn., numerical dispersion by upwind differencing 7-26267
- convection in viscous fluid, finite difference methods 7-14784
- diffraction gratings, embedded in inhomogeneous lossy dielec., finite-difference coupling technique anal. 7-1256
- diffusion eqn., 1D lin., 5-pt. explicit finite difference method 7-14898
- diffusion theory, least squares principle to unify finite element, finite difference and nodal methods 7-56194
- discrete scatt. theory, eigenvalue problems and nonlinear differential-difference evolution eqns. 7-4725
- dispersive trap-controlled carrier transport, surface pot. decay, space charge effects, finite difference calcs. 7-38588
- driven flow in square cavity, Navier-Stokes eqns., finite difference scheme 7-20795
- duct flow, 3D laminar use of curvilinear coordinates 7-16269
- elastic waves computation, fourth-order accurate finite-difference scheme 7-3991
- electrode design for gas discharge laser using finite difference method 7-1178
- exponential separation, exponential dichotomy, and almost periodicity of linear difference equations 7-24379
- FEMSYN code for multiprop diffusion theory 7-10183
- ferromagnet EM field spatial-temporal distrib. calc. using small parameter method (*Polish*) 7-62580
- ferromagnetic chain systems, difference schemes (*Chinese*) 7-52923
- field transient phenomena duration numerical determ. (*Polish*) 7-31633
- finite difference and shooting methods for ODE eigenvalue problems, relationship 7-35250
- finite difference eigenvalues, asymptotic correction 7-18324
- flame, premixed, struct. and extinction limit, Lewis no. effects (*Chinese*) 7-11559
- fluid layer, finite difference method and spurious reflection of waves 7-51185
- Fokker-Planck equations, conservative finite difference schemes 7-61278
- FORTTRAN code automatic generation, in LISP, for finite difference method appl. to flow 7-37468
- gas dynamics in 1D, AZTEC software 7-26237
- heated plate, acoustically perturbed 2D separated flow 7-16195
- incompressible fluid flow, implicit finite difference method 7-37416
- integrated optical waveguides, finite difference anal. without spurious mode solns. 7-1262
- irregular saw-tooth shaped boundaries, normal mode analysis 7-6230
- isotropic gas dynamic eqns., simplified Godunov schemes for 2X2 systems of conservation laws 7-51229
- journal bearings, numerical modelling of thermal effects 7-51004
- laminar, duct flow, heat cond., numerical soln. 7-57790
- leap-frog finite difference schemes, nonlinear instabilities 7-29694
- difference equations continued
- ledge interphase boundaries, growth kinetics, computer modelling 7-65041
- ledged interphase boundaries, growth kinetics, computer modelling 7-65040
- linear difference eqns., criteria for right dislocality 7-24388
- linear nodal S_n calculations, acceleration using diffusion-synthetic method 7-36072
- linear transport equation, inner iteration convergence for finite difference approx. 7-35482
- local stability of nonautonomous difference equations in Rⁿ 7-61027
- low-dimensional lattice fermion field theories, finite element methods 7-4956
- magneto-optical thin films, under laser irradiation, thermal anal. 7-45995
- Maxwell's eqns. in inhomogeneous media, 2D finite-difference time-domain analysis 7-15809
- MHD laminar flow, vortex behaviour 7-63228
- MHD Stokes problem for vertical plate in dissipative fluid with const. heat flux, finite-difference analysis 7-26358
- multidimensional wave eqn., absorbing boundary conditions for difference approx. 7-48384
- multi-point total variation diminishing difference schemes, construction conditions 7-26317
- N waves, evolution and decay, Burgers eqn. anal. 7-43980
- neutron diffusion equation, modal expansion method, accuracy improvement using finite-difference scheme 7-15224
- nonlinear boundary value problems, difference schemes in L₂ net space 7-18565
- nonlinear difference equations, critical values 7-61003
- nonlinear maps with memory 7-41070
- numerical finite difference model for steady state cellular array growth 7-21787
- numerical solution of systems of 2nd order boundary value problems 7-35248
- numerical study of swirling flow field in a vortex device 7-20682
- oceans, depth-dependent channel flow modelling 7-18325
- optical bistability, dispersive, finite difference equations 7-50619
- orthogonal polynomials and oscillation criteria for second order linear difference eqns. 7-24381
- oscillations in a linear system of differential-difference equations of arbitrary order 7-24382
- oscillations of neutral differential difference equations with several retarded arguments 7-35235
- oscillatory second order linear difference equations and Riccati equations 7-61047
- periodic Lyapunov and Riccati difference equations, inertia theorems 7-48311
- phase change material, one-dimensional solidification, charact. dimensionless time 7-63781
- physics in terms of difference equations 7-49125
- pipe laminar thermal energy region, transient unsteady convective heat transfer 7-31775
- plate, short vertical, free convection heat transfer, Nusselt and Grashof numbers 7-6077
- plates, circular, elasto-plastic deflection analysis, full system vs. layered yield criteria prediction 7-1450
- plates, interlaminar shear stress determination using MSC/NASTRAN theory 7-20597
- plates, rectangular on linear elastic foundation, nonlinear dynamic response 7-20599
- plates and envelopes, nonlinear theory and net approx. 7-18597
- porous media, degenerate parabolic eqns., difference schemes 7-51306
- quasiperiodic differential difference equations, second order, Galerkin procedure soln. (*Japanese*) 7-18588
- reactor subchannel anal., numerical technique using finite difference method 7-10209
- Routh-Hurwitz problem, stability analysis of difference schemes 7-48301
- Schrodinger field on a Galileo lattice, explicit finite difference schemes 7-41609
- shell, cylindrical, axisymmetric dynamic problems soln. by num. methods 7-16105
- singularly perturbed linear two-point boundary value problem analysis 7-35246
- soil, infiltration from cavities, num. soln. 7-18254
- spectral properties of random and almost periodic differential and finite-difference operators 7-48329
- Stefan problems, multidimensional, efficient finite difference scheme 7-6069
- Stirling cycle simulation, globally-implicit finite-difference method 7-65553
- Stokes equations, soln. for incompressible fluid in multiconnected domain 7-20797
- Sturm-Liouville system, eigenvalues of boundary value problem from band matrix inverse 7-60959
- tensile test, numerical investig. using finite difference 1D elasto-viscoplastic code 7-46747
- thermal radiation, transfer eqns., implicit difference eqns. (*Russian*) 7-43642
- thin-walled sections under combined bending and torsion, nonlinear theory 7-57698
- Toda lattice eqn. from homogeneous realisation of A₁⁽¹⁾ basic representation 7-9795
- torus reactor, magnetic field calc. (*Russian*) 7-25157
- transonic flow, Euler equations, compressible, soln. by time-marching scheme 7-26311
- transonic full potential eqn., intermediate boundary condition in Holst AF2 scheme 7-26308
- tubular specimen under HF induction heating, temp. distrib. anal. 7-43650
- two-point masses joined by an elastic bar, difference eqns. (*Spanish*) 7-61094
- two-dimensional linear advection equation, high resolution schemes 7-37456
- two-point boundary value problems, stability of finite difference schemes 7-35244
- unsteady compressible viscous flow over airfoils, integro-differential and finite-difference methods 7-31821
- van der Waals fluid, Riemann problem, numerical integration 7-38153
- weather prediction model, semi-implicit semi-Lagrangian time integration scheme 7-47525

difference equations continued

BaTiO₃ capacitor material, elec. field distrib. around flaws, finite difference modelling 7-64574
 Cu, tensile test, numerical investig. using finite difference 1D elastoviscoplastic code 7-46747
 Fe cathode surface, plasma nitriding, N conc. profile modelling 7-54188
 Si:B, ion implanted, dopant redistrib. during rapid thermal annealing 7-38042
 Si:B, magnetic Czochralski growth, computer simulation of B transport 7-32344

difference frequency generation (optical) *see optical frequency conversion*

differential amplifiers

see also instrumentation amplifiers
 CMOS charge sensitive amplifier-cable driver, monolithic detector readout electronics 7-42438

differential calculus *see differentiation*

differential equations

see also boundary-value problems; difference equations; Green's function methods; integro-differential equations; linear differential equations; Navier-Stokes equations; nonlinear differential equations; partial differential equations

abstract delay-differential equation modelling size dependent cell growth and division 7-61049

air-water/steam-water jets, confined two phase, analytical entrainment model (*Chinese*) 7-1596

alloys, atomic diffusion via vacancies, quasielastic coherent scatt. studies 7-58527

approximate analytical solutions of general Lotka-Volterra equations 7-61029

autonomous ordinary differential eqns., periodic orbits of competitive and cooperative systems 7-29698

axisymmetrical magnetic devices, anal. using conjugated diff. eqns. 7-24660

beam, infinite periodic, bending wave propag. 7-57722

beams, finitely deformed 3-D, tangent-stiffness expression, use in space frame analysis 7-6104

beams, naturally twisted, rectilinear, theoretical anal. 7-96

beams/columns subjected to non-uniform axial loads, vibration and buckling 7-6140

Bessel functions, phase integral formulae and their relation to existing asymptotic formulae 7-35228

bifurcations in a piecewise linear system 7-9769

bifurcations in Lorenz's symmetric fourth-order system 7-18699

boundary-value problems, nonlinear, numerical soln., ordinary differential eqns. (*Russian*) 7-56005

buckling in beam-column problem for anisotropic cylindrical shells 7-16082

Cauchy problem, singularly perturbed with unstable spectrum 7-35222

Caudrey-Dodd-Gibson-Sawada-Kotera eqn., solitons and discrete eigenfunctions 7-35232

coal dust flame acceleration, feedback control model for unsteady flow 7-65326

complex eigenvalues of differential eqns., critical layer singularities, review 7-4714

computational techniques, conf., Melbourne, Vic., Australia (Aug. 1985) 7-14704

conference, Logan, UT, USA, (July 1984) 7-55889

coupled Langevin eqns., asymptotic props. 7-35406

coupled ordinary oscillatory differential eqns., appl. to simulation of Pc 1 mag. pulsations generation 7-66401

cubic differential delay equation, exact formulae for periodic solns. 7-29725

curved members, consistent discrete elements technique 7-50948

decomposition and control 7-61025

delay differential equations asymptotic expansions for midpoint rule 7-48326

delay differential equations with first integral, soln. asymptotic behaviour 7-61012

delay force systems, parametrically excited oscils. 7-11268

diffraction Raman scattering in focused geometry, coupled pump and Stokes differential eqns. 7-20339

discrete Hankel transform, simple algorithm 7-48300

distributional solutions of hypergeometric differential equation 7-61018

eigenvalue equations, second order, extension of renormalized Numerov method 7-29737

elliptic equations, local behaviour of solutions 7-55970

energy equipartition for hyperbolic systems and compatible forms (*French*) 7-60980

Enskog equation in two space variables 7-4799

explicit solution of the inverse periodic problem for Hill's equation 7-61046

finite difference and shooting methods for ODE eigenvalue problems, relationship 7-35250

finite difference eigenvalues, asymptotic correction 7-18324

flow, determinacy of degenerate equilibria 7-57782

flow problems, stiff ODE solver software, selection 7-26239

frame response to a harmonic excitation, taking intoaccount the effects of shear deformation and rotatoryinertia, Timoshenko beam theory 7-6132

Fredholm integral equations, solution using maximum entropy method 7-41064

frequency-domain approach to nonlinear oscillations of some third-order differential equations 7-48317

functional differential equations, retarded, heteroclinic orbits 7-18574

functional equations, exact soln. 7-73

G-asymptotic representation of differential operators 7-18570

Gelfand-Phillips space, existence of solns. involving dissipative and compact operators 7-24385

generalised Liouville-Green asymptotic approximations for second-order differential equations 7-24395

geophysical eigenvalues, efficient computation 7-18323

group analysis of some ordinary differential equations 7-9654

growth properties of solutions to a linear differential equation 7-61042

Hausdorff dimension inequalities for ordinary differential eqns., applications 7-56000

heat equation with absorption, singular soln. 7-37318

homoclinic and heteroclinic tangency, appl. of Melnikov's method, numerical study 7-61036

Hopf bifurcation problem, parameter functionization 7-55988

ice floes, interacting around an obstacle, simulation methodology 7-55081

differential equations continued

ideal MHD equations, Galerkin method for differential equations with regular singular points 7-11624

incompressible granular flow, instability in evolution eqns. 7-51283

initial-value problems, numerical integration for small-parameter system in presence of derivative (*Russian*) 7-61081

integrable multiwave interaction systems of ordinary differential equations 7-4671

interacting diffusions, fluctuation phenomena, tightness problem, stochastic evolution 7-211

inviscid fluids in channel under localised perturbations, steady flows 7-11546

isovectors of class of nonlinear diffusion equations 7-24603

Ito stochastic differential eqns., Lyapunov function method anal. (*Russian*) 7-35399

K-distributed noise, Fokker-Planck description, stochastic diff. eqns. 7-61236

Kadomtsev-Petviashvili eqn., infinite-dimensional symm. group and Backlund transforms. 7-24370

Kolmogorov flow, 2D turbulence, nonlinear chaotic eqn., asymptotic study (*French*) 7-37440

laminar boundary-layer flows, separation point determ. 7-31741

laminar forced convection inside ducts with temp. periodic variation 7-31736

Lane-Emden equation, 7-digit tables 7-18402

Langevin equation, derivation for systems interacting with a thermal bath 7-24613

Lienard equation, generalized, boundedness condition for solns. 7-18578

Lienard equations, forced, existence of periodic solns. 7-55996

linear filtration of cylindrical stochastic processes in normed spaces (*Russian*) 7-56017

linear stochastic difference eqns., matrix criteria, sufficient conditions (*Russian*) 7-35212

linear systems associated with discretised boundary value problems of ordinary diff. eqns. 7-35245

Liouville-type results for fourth order elliptic equations 7-24393

liquid-gas interface, linear stability of liq. film with counter-current gas flow (*French*) 7-1533

logistic equation with recruitment delays, stability and nonoscillation 7-55990

Lorenz attractor, effective noise, stochastic differential eqn. 7-223

Lorenz equations, second order dynamical system 7-4659

meromorphic differential equations, second order, reduction theory 7-48313

monotone semiflows generated by functional differential equations 7-61010

multiconductor transmission line, effect of pulse corona discharge on coupling coeffs. and wave impedances 7-63383

multivalued differential systems, integral equivalence 7-18564

N×N matrix differential operators, spectral problem on the line 7-56086

neutral delay differential eqns., oscillatory and nonoscillatory solns. 7-24384

neutral delay differential equation, necessary and sufficient condition for oscillations 7-61004

NMR spectroscopy, numerical treatment of models arising 7-14928

noise correlation function props. of Langevin-type eqns. 7-234

non-Newtonian films, dimpled, drainage 7-26321

nonautonomous rigid system of ordinary differential equations, difference schemes (*Russian*) 7-61062

nonlinear boundary value problems, numerical soln. methods (*Russian*) 7-61063

open magnetic field lines, differential eqns. 7-15799

optical fibres, birefringent, anal. 7-57587

ordinary and measure differential equations using fixed point theorems in lattice normed spaces 7-29710

ordinary differential equation, numerical soln. using interval methods 7-41079

ordinary differential equations, one-step form of linear multistep methods (*Russian*) 7-61061

ordinary differential equations, second-order, inverse problem 7-60998

ordinary differential equations in locally convex spaces, initial value problem 7-48316

oscillations in a linear system of differential-difference equations of arbitrary order 7-24382

oscillations of some retarded differential equations 7-61048

oscillatory property for second order linear delay differential equations 7-61020

Painleve property and integrability 7-41068

parabolic differential equations, bifurcation from a homoclinic orbit 7-24396

particle dynamics in Coulomb pot. anisotropic harmonic oscillator pots. 7-61163

periodic boundary value problem for differential equations with delay and monotone iterative method 7-61017

periodic competitive and cooperative systems, periodic solutions 7-40085

periodic orbits class in classical mech. 7-48349

plate, cracked, description using Lagrange method (*Polish*) 7-43793

plate, uniform and shear flows at high Reynolds numbers, boundary value technique appl. 7-63126

plates, circular, plastic limit load numerical evaluation using Mises yield criterion 7-20604

plates, sheardeformable elastic, small finite deflections 7-26144

Poisson differential equation, appl. to determ. of gravit. pot. of arbitrary mass distrib. 7-66447

polymer-dominated multi-material systems, hygrothermal process interdependence and elasto-viscoplastic behaviour 7-53785

polymers, deformation isothermal conditions, dynamometric curves (*Russian*) 7-8073

predator-prey eqns., global anal. 7-14757

PVC-styrene-butadiene rubber blends, bending in elastic range 7-39606

quadratic system with two cycles appearing in a homoclinic loop bifurcation 7-48305

quantum field theory, stochastic quantization and Langevin eqn. 7-41588

quantum fluctuations and the Lorenz equations 7-9696

quantum mechanical stochastic differential equations, observables and multiple Wiener integrals 7-48543

quantum mechanics, measurement theory, stochastic differential eqns. 7-126

quasilinear elliptical equation, second member distrib., relative rearrangement (*French*) 7-61009

differential equations continued

- quasiperiodic differential difference equations, second order, Galerkin procedure soln. (*Japanese*) 7-18588
 random differential inclusions in Banach spaces 7-29696
 real singularities of singular Sturm-Liouville expansions 7-61052
 reducibility of variational dynamic systems (*French*) 7-56026
 representation projections for polygonal Bazilevich functions 7-18559
 rotating harmonic, 3D, and doubly anharmonic oscillators, Schrödinger eqns., confinement pots. 7-35313
 scalar meromorphic differential equations of second order, reduction to special form 7-60995
 second order boundary value problems with nonlinear boundary conditions, upper and lower solns. 7-9650
 second order ordinary diff. eqns., one-sided existence and uniqueness for periodic solns. 7-9653
 second order ordinary differential equations related to free boundary problems, properties 7-55999
 second-order differential equations, integrals of soln. combinations 7-35231
 semi-boundedness of systems of differential operators 7-29701
 shells, hollow flexible multilayer orthotropic, nonlinear theory, Bubnov-Galerkin method 7-24430
 shells, shallow, of variable thickness, differential eqns. 7-11278
 singular boundary value problems 7-55967
 singularity perturbed differential equations, dichotomies and stability 7-55995
 singularly perturbed linear two-point boundary value problem analysis 7-35246
 sinh-Gordon equation, quantum and classical statistical mechanics 7-24535
 slabs, frequencies and modes of bending vibrations with allowance for propagating modes; 7-11338
 SO(3, 2) representation, special functions 7-35729
 solid bodies, motion in atmosphere, numerical study (*Russian*) 7-63172
 solution by group theoretical methods 7-61065
 sorption, nonequilibrium dynamics, soln. uniqueness for inverse problems 7-58647
 spectral properties of random and almost periodic differential and finite-difference operators 7-48329
 spline nodes for approximate soln. of differential equations 7-35219
 stability of a 1D delay-differential eqn. 7-24378
 stable attracting sets in dynamical systems and in their one-step discretizations 7-35417
 stable bifurcating periodic solns., simple criteria 7-61045
 steady flow problems, press.-vel. components, algorithm comparison 7-37417
 stochastic differential equations, comparison of solutions (*French*) 7-60988
 stochastic differential equations with variable diffusivity, numerical integration 7-35233
 stochastic evolution equation 7-61019
 Stokes equations, collocation method, variational problem (*French*) 7-55973
 strange attractor in a synergistic problem (*Russian*) 7-61252
 Sturm-Liouville equations with intermittently negative principle coeffs., limit points, limit circles 7-24394
 Sturm-Liouville system, eigenvalues of boundary value problem from band matrix inverse 7-60959
 Taylor-vortex flow, dynamical system 7-11434
 thin-walled sections under combined bending and torsion, nonlinear theory 7-57698
 time evolution of spectral discretizations of hyperbolic systems 7-48322
 time-dependent partial differential eqns., 2D mesh moving technique 7-18573
 unidirectional diffusion fields in a plane, transformations in stochastic space (*Russian*) 7-61277
 vector fields on three-manifolds, modulus of stability 7-29699
 viscoelasticity, absorbing boundary conditions for numerical soln. of problems (*Russian*) 7-63018
 Volterra equation, homogenization 7-35480
 XY model, accelerated stochastic algorithms near critical temp. 7-41296
 Be⁻ shape reson., complex-rotated HF method 7-842
 LiNbO₂:Fe photorefractive crystals, light-induced scattering 7-10887

differential geometry

- σ -models, momentum mapping construction for quaternionic Kahler manifold 7-48937
 angular coefficients in systems of bodies of revolution 7-41075
 Banach space valued dependent random variables, uniform bound in central limit theorem 7-29727
 bosonic string reparametrizations and the geometry of path space 7-35832
 BRS transformations and anomalies, differential geometric interpretation 7-56457
 compact connected 3D Riemannian manifolds, classification 7-61072
 conformal field theory, analytic fields on Riemannian surfaces 7-24788
 conformally invariant elliptic equation on R^n 7-24401
 cotangent bundle, Lie group characterisation 7-9991
 covariant quantum field theory of gravitation, scaling limit and space-time metric 7-56134
 diagonals group and lattice coverings in n-dimensional Euclidean space 7-56009
 dilaton β -function on a Kahler manifold 7-61208
 dimensional reduction via dimensional shadowing 7-35752
 divergence free Weyl conformal tensor and perfect fluid distributions 7-61171
 E₈ superstrings, calabi-Yau manifolds motivations and constructions 7-56109
 Einstein action, 3+1 Regge calculus with conserved momentum and Hamiltonian constraints 7-48465
 elliptic equations, local behaviour of solutions 7-55970
 functions similar to Lie functions, algebras 7-60941
 general relativity, conservation laws in spacetimes with boundary 7-29829
 geometric quantisation, modular reduction theory and coherent states 7-41132
 geometry of differential equations, secondary differential calculus and quantum field theory 7-56408
 global existence theorems for hyperbolic harmonic maps 7-61066
 gravitational interactions, path integral quantisation, local symmetry props. 7-24528

differential geometry continued

- Hadarnard factorization of Selberg zeta function on compact Riemann surface 7-24392
 Harry Dym eqn. in 2+1 dimensions, reciprocal link with Kadomtsev-Petviashvili eqn. 7-61037
 Henon map unstable manifold, functional equation for segment 7-4661
 hyperkahler manifolds and nonlinear supermultiplets 7-56403
 hyperkahler metrics, constructions and supersymmetry 7-56404
 immersion of (m-2)-disk bundle, generalisation of Boy's surface 7-18583
 Kaluza-Klein model, conversation laws and integrability conditions for gravitational and Yang-Mills field equations 7-56108
 Kaluza-Klein theories, scalar fields and dynamical torsion 7-4746
 Kaluza-Klein theory, harmonics and spectra on general coset manifolds 7-24520
 Kaluza-Klein theory in 11D, compactifications with SU(3)×SU(2)×U(1) symmetry 7-29840
 Kerr black hole, null geodesics in stationary Ernst-Wild space-time 7-61170
 Kerr-Newman black hole in mag. field, surface geometry 7-56103
 Lipschitz domain, comparison between internal and minimal thinness (*French*) 7-56011
 Lorenz equations, second order dynamical system 7-4659
 martensitic transition, Bonnet transformation and differential geometry 7-7997
 multidimensional space physics, Metagalaxy, review 7-4663
 multiplicative renormalisation of 2D chiral theories 7-30216
 N=2, d=2 supergravity and superconformal transformations 7-41654
 nonsymmetric Kaluza-Klein theory, numerical predictions 7-35371
 null vectors, spinors, and strings 7-35253
 one loop effective potential with spontaneous compactification, stability 7-61187
 passive gravitational mass and inertial mass inequality of extended body 7-9372
 planar convex sets containing many lattice points, van der Corput's theorem 7-56010
 polyadic structure, near-integrability 7-29726
 Proca field in a spacetime with curvature and torsion 7-29850
 Pryce's relative distance in R_{∞}^2 , geodesics, relative error for vectors 7-48336
 quantum gravity and cosmology, Kyoto, Japan (May 1985), conference 7-24295
 quantum topological geometrodynamics 7-30222
 quasi-Einsteinian manifolds, geometric and algebraic characts. 7-48474
 random central limit theorem for dependent random variables 7-29728
 regular hyperstrip, dual normal connections 7-35256
 rim-finite spaces and the property of universality 7-18584
 secondary invariants of flat bundles (*French*) 7-56012
 simple transversal polybundles 7-35255
 string theory, Dirac operator determinants, anomaly cancellation and torsion 7-35813
 SU(1,1) propagator as a path integral over noncompact groups 7-4994
 SU(2,2)N)XSU(N') supergravity, superspace for supergauge actions 7-29852
 SU(2,2)XSU(m), decomposition of manifold O₂(4,m) 7-19030
 submanifolds with finite type Gauss map 7-24400
 supergravity, graded exceptional algebras and symmetric spaces 7-35384
 supermanifold cohomology and the Wess-Zumino term of the covariant superstring action 7-61186
 supersymmetric nonlinear σ -models, construction and geometry of graded supermanifolds 7-61448
 symplectic manifolds with Lagrangian fibration 7-29745
 ultrametricity for physicists, elementary background 7-4664
 Wess-Zumino supermultiplet, Lagrangian constraint free theory 7-388
 Yang-Mills equations, thickenings and gauge fields on 4-manifold 7-30159
 Yang-Mills gravitational theory, geometrical content 7-56130
 Yang-Mills theories and instantons, Hamiltonian structure, differential geometric anal. 7-30193
- differential scanning calorimetry** *see thermal analysis*
differential thermal analysis *see thermal analysis*
- differentiation**
see also differential equations
 Banach spaces, optimisation and differentiation 7-55985
 decreasing rearrangement of functions 7-61026
 excess Gibbs free energy of binary liquid mixture, numerical differentiation appl. 7-14899
 multi-valued mappings approximation, marginal function differentiability (*Russian*) 7-60990
 operator theory, symposium, Athens, Greece (Aug. 1985) 7-55878
 optical image differentiation using an optical filter (*Japanese*) 7-5843
 second order differential operator equations, boundary value problems 7-29712
 Hg electrode-soln. interface, 2-anion simultaneous adsorpt., elec. double layer parameters algorithm 7-54132

diffraction

- see also acoustic wave diffraction; diffraction gratings; diffractometers; electromagnetic wave diffraction; electron diffraction; neutron diffraction*
 apertures, magnetic polarizability anal. 7-58096
 fluid, wave-diffraction, submerged cylinder of arbitrary shape, second-order num. soln. 7-51192
 gap between two breakwaters, long waves, matched asymptotic expansions soln. 7-47446
 Helmholtz-type eqns., weak-element method 7-24484
 limiting absorption and amplitude principles for diffraction problem with two unbounded media 7-14786
 surface analysis from scattering amplitude, inverse problem 7-61116
 Ge-As-Se chalcogenide glasses, structural models, medium range order and interference functions, first sharp diff. peak calcs. 7-6540
- diffraction gratings**
see also holographic gratings
 3D object repositioning using a projected grating and photographic enlarger 7-41456
 acoustic, finite-transmissivity strips 7-50798
 aplanatic grazing incidence, theory 7-11101
 auxiliary dispersing element for crossed-dispersion spectrograph 7-41484
 benzene dynamic gratings, self-diffraction and reflection in degenerate four-wave interaction 7-37050
 blazed grating fabricated by synchrotron radiation lithography 7-37125
 book, laser-induced dynamic gratings 7-9605

diffraction gratings continued

calibration facilities for Extreme Ultraviolet Explorer 7-24712
 chalcogenide glass grating couplers, fabrication using electron beam induced Ag doping (*Japanese*) 7-62817
 channel waveguides intersecting at right angle, Bragg grating coupling analysis 7-6023
 chiral smectic C periodic liquid crystals, light diffraction props. 7-59164
 cholesteric liq. crystals, photoinduced periodic grating obs. 7-37127
 classical grating and bigrating, light diff. 7-20129
 colour image recording, computer generated linear tricolour sampling pattern 7-42952
 combined resonator component; widening of CO₂ laser continuous tuning band 7-25847
 conference, diffraction phenomena in optical engineering appls., San Diego, CA, USA (Aug. 1985) 7-60870
 conical diffraction mounting, generalisation of rigorous differential method 7-5831
 correlator tracking nonlinearity 7-57249
 corrugated waveguide diffraction gratings in integrated optics, TE-TE and TM-TM coupling coeffs. 7-26035
 couplers, fabrication technology and characts. 7-20412
 cross-grating interferometer, fringe formation 7-35578
 crossbar interconnections using variable grating mode devices 7-42949
 cryptocyanine, degenerate four-wave mixing, in saturable absorber, effects of optical coherence (*Korean*) 7-25901
 deep metallic grating, light scatt., surface plasmon dispersion 7-20128
 degenerate four-wave and multiwave mixing, saturation behavior 7-11075
 desorption, light induced, bistability mechanism in integrated optical devices 7-57424
 dielectric gratings, coated, in conical diffraction mounting, diffraction anomalies 7-5985
 dielectric gratings, plane wave diff., finite element anal. (*Japanese*) 7-43342
 dielectric gratings, slanted and unslanted, total field formulation 7-5981
 dielectric gratings with losses, diffraction analysis 7-5982
 dielectric surface-relief gratings as antireflection coatings 7-43320
 diffraction radiation generator, electronic efficiency, microwave field distribution, phase nonuniformities effect 7-37124
 diffuse light in diffraction gratings and surfaceplasma oscillations 7-10847
 diverging beams, 3D bundle, generation using crossed diffraction gratings 7-35165
 double monochromator, prism-grating, apparatus function 7-20395
 double-channel planar BH multimode laser, 1.55 μm fibre grating external cavity, single-mode behaviour 7-15908
 dye laser DFB, achromatic pumping condition using grating 7-10999
 dye laser with diffraction grating in resonator for holographic interferometry 7-43159
 dye solutions, quantum efficiency of fluoresc., determ. by diffraction at laser induced phase grating 7-3081
 dynamic gratings induced by electrostrictive compression of critical microemulsions 7-11032
 echelle spectrograph, camera lens system design 7-55475
 efficiency measurement and automated scatter inspection system 7-62853
 electro-optic Bragg gratings for integrated optical combinatorial logic 7-26040
 EM plane wave scatt. by semi-infinite strip grating 7-42860
 EM scattering from finite strip grating; curvature effect 7-50474
 EM scattering from resistive strips complex periodic struct., anal. 7-50476
 embedded in inhomogeneous lossy dielec., finite-difference coupling technique anal. 7-1256
 engineering meas., conf., Cannes, France (Dec. 1985) 7-29586
 EXAFS surface structure studies, at Daresbury SRS, in 60 to 11100 eV range 7-33486
 fibre compensation, grating compressor with positive group velocity dispersion 7-57575
 formation of periodic surface structures on film coatings 7-38051
 four-beam mixed dynamic gratings, diffraction characts. in Na vapour (*Russian*) 7-57406
 four-wave mixing and dynamic gratings, basic considerations, review 7-11029
 four-wave mixing techniques for studying orientational relaxation, comparison 7-10779
 frequency modulation of optical beam using ultrasonic diffraction grating 7-20405
 fringe pattern analysis, holographic-moire technique 7-20164
 gas waveguide lasers with diffraction grating, frequency selectivity and resonator losses 7-43158
 Gaussian beam divergence meas. using SAW modulation 7-20297
 Gaussian laser-beam-diameter measurement using sinusoidal and triangular rulings 7-43186
 glass: CdSe gratings, darkening effect, optical phase conjugation 7-57476
 grating resonator, selective props., appl. to lasers 7-50596
 grating structs., determ. of surface polariton minigaps, const.-freq. and const.-angle scans 7-2506
 Henry Rowland and astronomical spectroscopy, conference, Baltimore, Maryland (June 1984) 7-18493
 Hipparcos astrometry mission, diffraction grid fabrication by electron beam lithography 7-24014
 holographic interferometer with monomode fibres, appl. to integrated optic grating device manufacture 7-25757
 III-V semiconductor, integrated optoelectronics, micrograting form. by HV electron beam lithography 7-31443
 integral grating coupler on optical fibre 7-26004
 integrated-intensity grating formation with pulsed light sources, fourth-order partial coherence effects 7-20403
 intensity-dependent guided wave phenomena 7-25872
 interferometer, grating shearing with variable shear and fringe orientation 7-35579
 inverse scattering and three-wave interaction in nonlinear optics, review 7-11030
 IR diffractive filters fabricated by electron beam lithography, spectral and polarising characts. 7-62816
 IR monochromator with concave diffraction grating, spread function determ. 7-50725
 lamellar transmission gratings in soft X-ray region, behaviour 7-20402
 laser Doppler velocimetry, multi-pt. system using phase diffraction grating 7-37605

diffraction gratings continued

laser image plotter for high-information-density images recording 7-26043
 laser-induced surface ripples, gratings written with single laser beam 7-20400
 Lau interferometer, coherence anal. 7-9879
 Lau interferometry and diffraction correlation (*Chinese*) 7-57247
 light induced grating formed by free charge carriers in external elec. field, dynamics 7-62819
 light scattering by diffraction gratings, false gratings and random rough surfaces, numerical comparison 7-5830
 linear grating sensors, moire signal quality rel. to light source coherence and grating gaps 7-31446
 low density transmission grating pitch meas. by moire deflectometry, hybrid Talbot effect 7-43337
 material surface deformation slope meas., reflection grating method, digital image processing 7-29974
 metal strip gratings as submillimetre laser output couplers, power transmission theory 7-43339
 metallic surface-relief gratings, rigorous coupled-wave anal. 7-31444
 moire deformation field quality and strain meas., effects of spatial coherence of light source and grating gap 7-61372
 moire interferometry, high sensitivity, for displacement meas., tutorial paper 7-56331
 monochromator wavelength automatic setting 7-37120
 multichannel grating phase-shift interferometers 7-30076
 multipass grating interferometer applied to line narrowing in excimer lasers 7-35573
 narrow-linewidth fibre laser with integral fibre grating 7-5904
 nematic liquid crystals, dynamic gratings, self diffractions and wavefront conjugation processes 7-11067
 nematic liquid crystals, dynamic self-diffraction effects 7-11033
 nonlinear guided-wave phenomena, review 7-57422
 nonstationary radiation diffraction, temporal-spatial radiation functional meas. 7-30060
 nontrivial grating possessing only specular characts., normal incidence 7-31445
 null correctors, diffractive, systems considerations, tight tolerances in fabrication 7-62820
 oppositely directed waves, self-diffraction in medium with nonlocal response 7-42907
 optical multiplexing techniques and equipment (*German*) 7-1286
 parametric oscillation with aid of dynamic gratings, threshold conditions 7-1228
 passive synthetic aperture imaging using achromatic grating interferometer 7-10867
 periodic 1D grating, free oscills. of EM field (*Russian*) 7-62822
 phase diff. grating parameter control, computational technique 7-43338
 phase grating detection, speckle correl., optical inverse scatt. 7-50495
 photoconductive insulators, diffusion length meas. using photocarrier gratings 7-12750
 photorefractive crystals, multi-grating phase conjugation 7-31403
 photorefractive crystals, multiple phase-conjugate beam coupling 7-25902
 photorefractive gratings and phase-conjugate waves, phase shifts 7-43341
 picosecond light pulses scattered by optically induced gratings in semiconductors, frequency shift and spectral changes 7-1024
 planar meshes with discrete loads, circuit modelling, equiv. mesh impedances 7-62600
 planar metal-grating free-electron lasers 7-10969
 planar waveguide, electro-optic light deflection, optimal parameters anal. 7-37154
 planar waveguide, grating element for entry and focusing of radiation 7-37126
 plane diff. grating, resolution and wavefront evaluation by FFT 7-31266
 radial grating meas. systems, accuracy improvement using fibre optic whole circumference sensor 7-31511
 reflecting grating, H-polarised inhomogeneous plane wave reson. scatt. (*Ukrainian*) 7-10823
 reflection grating, second-order, canonical equations 7-43340
 reflection gratings, grazing incidence, in high resolution scanning spectrometers 7-20401
 reflective, wave scatt., const. and dynamic phase effects 7-37128
 reflective grating with rectangular grooves, resonance props., finite cond. effects calcs. (*Russian*) 7-31448
 reflector-backed perfectly blazed strip gratings simulate corrugated reflector effects 7-42854
 rhodamine 6G dye laser, 580 nm, small line width, cavity arrangement 7-62728
 Ronchi test with daylight illum. for testing mirrors and lenses 7-11180
 scanning spectrometer design and props. 7-56353
 second-order reflection grating theory 7-25945
 sensor, moire signal modulation depth under incoherent illum. 7-31447
 soft X-ray, efficiency enhancement by multilayer coating 7-25946
 soft X-ray optical systems, book 7-55901
 spacing error testing using holographic interferometry 7-37216
 spectral measurement for wavelength regions 400 nm to 750 nm and 700 nm to 2500 nm (*Japanese*) 7-351
 stimulated Wood's anomalies on laser-illuminated surfaces 7-11040
 strain measurement using moire by shifting model grating, image processing (*Japanese*) 7-31715
 surface EM wave conversion by diff. grating on dielectric film 7-43345
 testing echelle gratings, simple method 7-43450
 TM wave diffraction by 3D phase grating 7-36856
 transducer for angular and linear displacements with separated gratings 7-4829
 tunable-laser-induced gratings for the measurement of ultrafast phenomena 7-11041
 UV normal incidence concave diffraction grating spectrometer for telescope, calibration 7-29400
 variably-spaced linear and circular gratings, fabrication, interferometrically controlled rotary ruling engine 7-62854
 varied line-space gratings: past, present and future 7-62821
 velocimetry in laminar and turbulent flows using the photothermal deflection effect with a transient grating 7-31901
 waveguide Bragg mirror with negative differential characteristic 7-43447
 waveguide diffraction gratings, Rouard's method and coupled mode theory 7-57530
 waveguide horn-grating demultiplexer circuit, single-mode operation 7-62846
 wavelength-tunable single-mode fibre grating reflector 7-31442
 wide-angle diffraction phenomena, finite beam size effects 7-62622

diffraction gratings continued

- Wood's anomaly effects on gratings of large amplitude 7-5986
 X-ray applications, prospects 7-24739
 X-ray Bragg optics 7-21043
 X-ray optics, theories to optimise high refl. of mirrors and gratings 7-30141
 Ag gratings of various groove depths, SHG study 7-57462
 Ag-AgCl-ZnS photoinduced periodic struct. for planar waveguide study 7-43371
 Al-ethyl alcohol interface, surface polaritons, four-wave mixing 7-43244
 BaTiO₃, photo-excited holes, photorefractive meas. of mobility anisotropy 7-21918
 Bi₁₂GeO₂₀ crystals, photorefractive parameters determ. using transient grating anal. 7-3004
 Bi₁₂SiO₂₀ crystal, phase conjugate signal at elevated temps. 7-43242
 Bi₁₂SiO₂₀ photorefr. crystals, moving grating erasure, expt. study 7-5940
 Bi₁₂SiO₂₀ photorefractive gratings, buildup and decay, effect of electric field 7-17306
 Bi₁₂SiO₂₀ photorefractive crystal, wave mixing with moving gratings, appl. to phase conjugation 7-20363
 CO₂ laser TE, tunable using near grazing incidence grating, performance 7-43052
 CdS excited state dynamics studied by transient grating techniques 7-12616
 CdS, refractive index nonlinearity due to excitonic molecule resonance state 7-11044
 CdS resonant self-diffraction from dynamic laser-induced gratings 7-11036
 CuCl excited state dynamics studied by transient grating techniques 7-12616
 GaAlAs laser, collinear nearly degenerate four-wave mixing in amplifying media 7-11071
 GaAs, direct maskless fabrication of submicrometre gratings 7-62855
 a-GaAs films, dynamics of laser annealing by transient grating method 7-12122
 GaAs Fresnel waveguide grating lenses, aberration corrected, simulation 7-26036
 n-GaAs, sawtooth gratings, photoelectrochemical fabrication 7-50726
 GaAs surface, formation of gratings in laser photoemission wet etching 7-8205
 GaAs:Cr, photorefractive behaviour using two-beam coupling 7-31387
 a-Ge films, dynamics of laser annealing by transient grating method 7-12122
 HgCdTe, ambipolar diffusion and free carrier recombination studied by transient grating technique 7-12731
 InGaAsP device fabrication using HBr-H₂O etching soln. 7-46728
 InP device fabrication using HBr-H₂O etching soln. 7-46728
 InP, submicron gratings, reactive ion beam etching and deformation-free LPE overgrowth 7-13659
 InSb, four-wave mixing, degenerate and nondegenerate 7-11069
 InSb, transient grating formation under two-photon excitation 7-11037
 KCl:Li; F₂-centre crystals, diffraction efficiency of photoinduced gratings 7-62818
 LaP₂O₇:Nd³⁺ degenerate four-wave mixing spectroscopy 7-11039
 LiNbO₃ blazed grating couplers and appl. to integrated optics 7-15969
 LiNbO₃, shallow gratings, leaky surface waves, trapping and temp. compensation 7-12449
 LiNbO₃:H waveguides, anomalous side-shifted multimode spectra 7-37140
 Li₂O-P₂O₅:Eu³⁺, laser-induced refractive-index gratings, four-wave-mixing techniques 7-11102
 Li₂TiO₃, shallow gratings, leaky surface waves, trapping and temp. compensation 7-12449
 Na₂, forward four-beam mixing, diffraction by dynamic gratings 7-15951
 Na₂O-SiO₂:Eu³⁺, laser-induced refractive-index gratings, four-wave-mixing techniques 7-11102
 Nd:glass laser system, appl. of diffraction grating to increase tuning range 7-5916
 NdP₂O₇ crystals, dynamics of population gratings studied by four-wave mixing 7-11038
 P₂O₅:Eu³⁺ laser-induced refractive-index gratings, four-wave-mixing techniques 7-11102
 Si, crystalline, ion-implanted and amorphous, light diffraction by transient gratings 7-11034
 Si, etching V-groove structures 7-26031
 Si monocrystalline, light-induced grating measurements 7-11035
 Si on sapphire, bistable optical device using guided mode excitation 7-57423
 W (100), IR surface-wave interferometry 7-44245
 ZnO resonant self-diffraction from dynamic laser-induced gratings 7-11036

diffraction instruments *see diffractometers***diffraction model**

- pp, single diffractive excitation to elastic scatt. ratio 7-5125
 pp (pp) elastic scatt., diff. cross sections, multiple-dip struct., diffractive limit 7-61725
 pp-ppp+ $\pi^+x\pi^0$, $x=0,1,2$, diffractive dissociation, 360 GeV/c quark-diquark fragmentation 7-553

diffractometers

- see also X-ray diffractometers*
 multilayer dielectric cylinder diameter determ., diffraction meas. accuracy improvement 7-293
 neutron double crystal diffractometer procedures 7-51580
 neutron flat-cone diffractometer, Bragg data collection 7-1818

diffusion

- see also bi-diffusion; diffusion in gases; diffusion in liquids; diffusion in solids; electromigration; membranes; osmosis; permeability; self-diffusion; surface diffusion; thermal diffusion; turbulent diffusion*
 2D fluid translational diffusion, spin relax, pair correl. fn. dynamic effects 7-50186
 advection diffusion systems, multidimensional, generalized streamline operator, FEM 7-26240
 advection transport algorithm, multidimensional positive definite, further development and appl. 7-29945
 advection-diffusion eqns., shock layer solns., stability 7-28314
 advection-diffusion systems, multidimensional, FEA formulation 7-26241
 aerosol particles with fractal structure, effect of coagulation on diffusive spread 7-18728
 aerosols, Brownian diffusion and particle coagulation 7-48564

diffusion continued

- anisotropic 2D square lattice, random hopping model, percolation, diffusion and conductivity 7-61282
 anisotropic particles, diffusion meas. using correlation spectroscopy 7-44088
 anomalous diffusion on fractal, first passage time problem 7-277
 asymptotic sufficiency for some partial observations of a diffusion process 7-56014
 axisymmetric vortices, momentum diffusion effects, appl. in tornado simulation 7-57850
 basal membranes, diffusion of organic cpds., continuous radioactivity method meas. (French) 7-65345
 Bernoulli-Laplace diffusion model, time to reach stationarity 7-61249
 biased tight-binding lattice, quantum tunnelling and thermally resisted motion 7-29946
 bimolecular fast reversible reactions diffusion influenced, kinetics study 7-65282
 bimolecular reactions, diffusion influenced, kinetics study 7-65283
 binary fluid mixtures, comparative anal. by extended irreversible thermodynamics and kinetic theory 7-16290
 binary mixture with diffusion, mass transfer across moving interface, boundary condition 7-58436
 boundary conditions at outflow for a problem with transport and diffusion 7-61109
 Brownian particle, diffusion in bistable potential, general inverse friction expansion 7-29950
 Chebyshev collocation methods for parabolic eqns., heat eqn., advection-diffusion eqn. 7-48649
 classical diffusion, intermittency and quantum particle motion in modulated or random media 7-137
 coefficient, coloured noise, projection approach calcs. 7-35412
 convection-diffusion eqn., smoothing of numerical soln. by central difference method (Japanese) 7-41312
 convection-diffusion equations, bracket formulation 7-6214
 convection-diffusion system, global existence 7-11420
 convection/diffusion phase change, enthalpy formulation anal. 7-51118
 correlated exponential random walks, linear Boltzmann transport formulation 7-35407
 correlated random walk on a BCC lattice with next-nearest-neighbour hops, self-consistent decoupling approx. 7-41259
 cosmological baryon diffusion and inhomogeneities in big-bang plasma 7-60848
 coupled viscous flow/transport problems, numerical computation 7-44065
 dense fluids, viscosity and mutual diffusion coeff. calcs. 7-26379
 diatomic molecules in flows with convective and diffusive particle transport, nonequilibrium, dissociation 7-20811
 diffusion controlled reactions, Monte Carlo study 7-22994
 diffusion eqn., 1D lin., 5-pt. explicit finite difference method 7-14898
 diffusion-controlled reactions among static reactive sinks, conc. depend. 7-39868
 diffusion-limited aggregation, anisotropic sticking probability on 2D square lattice, computer simulation 7-24590
 diffusion-limited aggregation, anomalous diffusion for regular and random models 7-239
 diffusion-limited aggregation, diverging length scales 7-254
 diffusion-limited aggregation, generalization and fractal dimensions 7-247
 diffusion-limited aggregation, singularities, asymptotics and scaling anal., comment and reply 7-44834
 diffusion-limited aggregation without branching, continuum approx. model 7-41287
 diffusion-limited aggregation without branching, Monte Carlo group anal. 7-61269
 diffusion-limited-aggregation in porous medium, effect of morphological disorder on viscous fingers 7-56173
 diffusion-reaction systems, fluctuations, adiabatic elimination of transport modes 7-39855
 disordered system, non-interacting quantum particle diffusion 7-41310
 dispersion and convection in periodic porous media 7-51140
 dissipative structures in an active diffusive medium with a spatially periodic source 7-35483
 double-diffusion convection in completely confined fluids 7-57835
 driven diffusive system, field theory of critical behaviour 7-29949
 driven diffusive systems, fast rate limit for lattice gas 7-29948
 driven flow in square cavity, Navier-Stokes eqns., finite difference scheme 7-20795
 droplet vaporisation, internal circulation integral eqn. formulation 7-37530
 dynamical processes in many-body systems, random motion approx. 7-48587
 dynamical systems and statistical physics conf., Koszeg, Hungary, Aug.-Sept. 1984 7-48194
 electrodeposition, dendritic and fractal structures, diffusion and current fields 7-45102
 electrolyte distribution inside and outside membrane, low freq. streaming pot. with overlap of diffusion layers 7-8291
 electron longitudinal diffusion in two-component magnetised plasma 7-20875
 electron swarm in a model gas, diffusion coeffs., Monte Carlo simulation 7-1662
 electron swarms, scatt. cross-sections, diffusion theory 7-20873
 equation soln. for particles with magnetic moments in inhomogeneous mag. field (Russian) 7-44893
 excitation transfer between donors and acceptors in fluid soln., donor fluorescence decay meas. (French) 7-59236
 excitation transfer between donors and acceptors in fluid soln., theoretical anal. (French) 7-59745
 Fermi multicomponent liq., transport props. 7-61220
 finite velocity of propag. in diffusional quantum theory 7-35323
 flow through porous media, diffusion, interfacial surface statistics 7-16236
 fluid mixtures, diffusion induced by nonhomogeneous shearing deform. field 7-14765
 fluids, enhanced heat diffusion by oscillation 7-51116
 fractal clusters and percolation clusters, diffusion noise 7-35415
 fractal pores, nucl. mag. relax. 7-27625
 fractals, combinatorial algebra 7-269
 fractals, mapping to hopping on hierarchical structures 7-24574
 fractional diffusion equation 7-35470
 gaseous mixture wrinkled flames, reactive-diffusive model 7-46849
 Gaussian polymer chain, translational diffusion coeff. 7-62551
 gradient percolation and diffusion fronts in 3D 7-41292

diffusion continued
 growth probability and harmonic measure, fractal struct., scaling props. 7-61268
 growth probability distribution in kinetic aggregation processes 7-2145
 heat source movement over heat conducting medium surface 7-1379
 heavy particle in 1D system, mass depend. in diffusive behaviour, numerical simulation 7-29947
 hierarchical structures, complexity and relax. 7-18702
 high flux, single solute mass transfer in spherical rigid drops 7-16217
 hindered diffusion across a membrane 7-29943
 Hopf bifurcation and symmetry, travelling and standing waves on circle, reaction-diffusion eqns. 7-56192
 hopping transport model, dynamics, phase transition 7-268
 incipient infinite percolation cluster, diffusion exponents nonuniversality, exact enumeration method 7-4794
 indefinite Sturm-Liouville problems, half-range solns. 7-55979
 interacting Brownian particles in hydrodynamical limit, bulk diffusion and equilibrium fluctuations 7-48585
 interacting diffusions, fluctuation phenomena, tightness problem, stochastic evolution 7-211
 interfacial growth, dense branching morphology form. 7-21147
 inverse problems and the Newton-Kantorovich method 7-62596
 isovectors of class of nonlinear diffusion equations 7-24603
 kinetic gelation clusters in 3D anomalous diffusion, random walks 7-61279
 lattice gas of diffusing interacting particles in concentration gradient, Monte Carlo simulation 7-48596
 least squares principle to unify finite element, finite difference and nodal methods 7-56194
 linear transport eqns. in a random medium, projection operator methods 7-61287
 liquid soln.-solid grain system, stability of steady states, diffusion effect 7-32622
 Ljapunov equation, appl. to 1D diffusion eqn. stabilisation 7-61283
 Marangoni convection, surface deformation, nonlinear diffusion eqn. 7-51130
 Markov jump processes, boundary behaviour of diffusion approximations 7-29897
 methane-air laminar counterflow diffusion flames, struct., CARS meas. 7-57939
 methane-air laminar diffusion flames, struct. 7-65327
 micelles, cylindrical, intramolecular fluoresc. quenching rate const. 7-54189
 mobility and Einstein relation for stationary nonequilibrium state 7-48651
 molecular diffusion, FT pulsed gradient spin echo investig. 7-22161
 molecular fluid, Brownian motion reaction kinetics, diffusion limited 7-56167
 monomolecular reactions, diffusion-induced, fluctuations and rotation 7-39864
 multi-component convection/diffusion/reaction systems, FEM 7-44063
 multicomponent mass transfer in spherical rigid drops 7-16218
 multifractality in diffusion-limited aggregation model, exptl. evidence 7-41264
 non-Newtonian fluid, buoyancy effects, magnetic field parameter, magnetisation 7-6257
 nondissipative quantum diffusion eqns., comment and reply 7-41309
 nonFickian mass transport through polymers, viscoelastic theory 7-61295
 nonideal systems, dynamic light scatt. and mutual diffusion 7-50485
 nonlinear diffusion eqns., spectral fn. methods 7-48640
 nonlinear heat and wave eqns., symmetries 7-14787
 nonlinear heat eqn. with absorption, regularity of solns. and interfaces 7-62959
 nonuniform 1D fluid model system, self-diffusion process calcs. 7-24607
 oblate ellipsoids, diffusion, shape effect on consumption in fluid-particle processes 7-33930
 ocean floor sediment as repository barrier, radionuclide diffusion 7-5481
 off lattice diffusion-limited aggregation with radial bias, liquid crystal fingering 7-63412
 one dimensional porous media, turbulent filtration eqn. 7-31879
 open quantum systems, Lindblad theory for collective mode damping 7-61138
 particle charging process, electric field depend. 7-20786
 particle diffusion and trapping, arbitrary trap size and conc. 7-9761
 particles, diffusion-controlled growth in supersat. soln. 7-8323
 pattern dynamics and optimization by reaction diffusion systems 7-54078
 pattern formation for a one dimensional evolution equation based on Thom's river basin model 7-24608
 percolation, thresholds and critical indices 7-29913
 phase separation on regular and fractal lattices in two dimensions 7-14887
 polymer membranes, sorption meas. using quartz cryst. microbalance 7-54171
 polymer microarchitecture formation, nonlinear diffusion equations 7-4795
 polyvinyltrimethylsilane membranes, modified by acrylonitrile, gas permeability and diffusion (Russian) 7-8301
 potential energy barrier, diffusive crossing with curved reaction path, simulation 7-270
 predator-prey populations with diffusion, persistence in models 7-9748
 quasiperiodic chain, diffusion analysis 7-48611
 radiative transfer, equilibrium diffusion theory initial and boundary conditions 7-4793
 radiative transfer, Levermore flux limited diffusion theory 7-35472
 radioactive waste, transient diffusional release in basalt repository 7-5482
 random process with infinitely many interacting particles 7-29894
 random walk and diffusion in a stochastic lattice gas model 7-41274
 reaction-diffusion eqn., numerical solns. asymptotic behaviour 7-61284
 reaction-diffusion eqns., semidiscrete approx. asymptotic behaviour 7-39880
 reaction-diffusion equation, microscopic selection principle 7-54079
 reaction-diffusion equations, pseudo-arclength continuation method for nonlinear eigenvalue problems 7-35481
 reaction-diffusion equations, stability of steady state solns. 7-29952
 reaction-diffusion equations for interacting particle systems 7-29924
 reaction-diffusion systems, scaling, renormalization group anal. 7-59744
 relative diffusion in stochastic fields, Monte Carlo simulation 7-271
 rock matrix, sorption and diffusion of radionuclides 7-5478
 rotational diffusion in cubic fields 7-275
 runaway phenomenon, diffusion with varying drag 7-57977
 scaling properties for the surfaces of fractal and nonfractal objects: an infinite hierarchy of critical exponents 7-18715

diffusion continued
 semilinear diffusion equations, time-periodic solutions to semilinear parabolic equations 7-56193
 Sierpinski gasket fractals, hierarchical model relaxation, diffusion generalisation 7-9784
 soil, infiltration from cavities, num. soln. 7-18254
 soil column with central hole, infiltration 7-18253
 solid fractal surfaces, diffusion, relation to observable diffusion 7-61280
 solvent, dissociation, isomerisation and diffusion in double-well potential 7-33922
 sorption-diffusion equations, singularly perturbed boundary-value problem, soln. asymptotics (Russian) 7-61297
 sparsely packed porous layer, double diffusive convection 7-11531
 sparsely packed porous medium, double diffusive convection, rot. effect 7-1553
 spatial dissipative structures, generated by diffusion and photochem. bistability 7-46111
 sphere, diffusion controlled growth from finite size, numerical solns. 7-44889
 spherical fluid inclusion, convective instability 7-43856
 steady-state chemical kinetics on fractals, segregation of reactants 7-41295
 stirred percolation, annealed disorder, diffusion, continuous time random walk 7-61266
 stress assisted diffusion in elastic and viscoelastic materials 7-50953
 structured media, diffusion, theory 7-17965
 survival probability for particle diffusing in a medium containing nonoverlapping or spatially correlated traps 7-48648
 ternary electrolyte systems, diffusion pot. in simple porous membranes 7-54170
 thin tubes, Knudsen flows, dynamics of test particle, diffusion approx. 7-11470
 transport theory conf., Montecatini Terme, Italy, June 1985 7-60874
 tubular flow chemical reactors, stochastic axial dispersion model 7-14864
 two component gas bubbles in fluid, diffusively driven oscillations 7-16235
 two-dimensional site-percolation model, diffusion and long-time tails, vel. autocorrel. function calcs. 7-24606
 two-sublattice systems, correlated random walks, Monte Carlo simulations 7-4783
 two-sublattice systems, correlated random walks 7-4782
 ultrafiltration, modelisation and structure modulus (French) 7-16245
 unidirectional diffusion fields in a plane, transformations in stochastic space (Russian) 7-61277
 vaporisation and dispersion from a surface to a turbulent boundary layer 7-52018
 CaCO₃ deep ocean sediment samples, distrib. and diffusion meas. of Np and Am radioisotopes 7-36273
 H swirling turbulent diffusion flames, turbulence intensity study 7-26287
 He-rich white dwarfs, C diffusion rel. to C conc. in stellar atmosphere 7-47850
 MgCl₂ diffusion through polycarbonate nucleopore membranes 7-3603
 Ne²¹ in Ar plasma afterglow, ambipolar diffusion coeff. meas. 7-20949
 Si materials science and technology, conf., Boston, MA, USA (May 1986) 7-29598
 a-Si:H, H₂ distrib., exodiffusion spectra 7-27026

diffusion coefficient *see diffusion*

diffusion creep
 grain boundary, unstable spreading of fluid inclusion under normal stress 7-26761
 grain boundary dislocation geometry during diffusional creep 7-38013
 Inconel 718, Ni-base superalloy, creep deform., back stress determ. 7-46564
 metals, FCC, creep activation energy (Russian) 7-46577
 phenylene, in H₂O, creep process, mathematical model (Russian) 7-8072
 superplastic deform. props. 7-65092
 Ag-Zn (50 wt.%), diffusion coeff., segregation, high temp. creep of β -phases (French) 7-32658
 Al₂O₃-MgO-TiO₂-Na₂O system, sintering and creep, Na₂O influence, Cable and Reijnen-Readley models (German, English) 7-7933
 Cu-Al (25 wt.%), diffusion coeff., segregation, high temp. creep of β -phases (French) 7-32658
 Cu-Sn (14.37 at.%) alloy, hypoeutectoid, diffusion coeff. governing high-temp. creep (French) 7-46572
 Cu-Sn (14.4 wt.%), diffusion coeff., segregation, high temp. creep of β -phases (French) 7-32658
 Cu-Zn (52 wt.%), diffusion coeff., segregation, high temp. creep of β -phases (French) 7-32658
 NiAl, slow plastic creep props. between 1200 and 1400 K, effect of comp. and grain size 7-65084
 Pb-Sn (9 wt.%), solid soln. alloy 7-8066

diffusion in gases

see also self-diffusion in gases; thermal diffusion in gases
 alkali-inert gas pair diffusion cross sections, light-induced drift 7-51366
 atmospheric air, fast response Langmuir probe 7-34724
 Boltzmann-Lorentz-Enskog equation, gas diffusion at moderate densities, anal. 7-37617
 crystal growth, closed-tube chem. vapour transport, interface kinetical limitations, semiempirical calcs. 7-27878
 CVD of Si in annular tubes, film thickness profiles in mixed convection-diffusion regime 7-27190
 dilute gases, binary diffusion coeff., mean free path theory 7-9624
 electrodes, gas diffusion type, diffusion resistances influence 7-26378
 III-V semiconductors, VPE, interplay between kinetics and diffusion in hot wall reactors 7-46330
 inert gas moderator, transient electron longitudinal and transverse diffusion coeffs., elec. field depend. 7-6347
 inhomogeneous fluid, tracer diffusion, kinetic theory 7-58111
 metal vapours and vapour-gas mixtures, atomic interactions and transport coeffs. 7-11575
 methyl bromide, thermal electron attachment and diffusion 7-20837
 non-Arrhenius rate constants involving diffusion and reaction 7-46797
 nonisothermal gas mixture, transport coeff. calc. 7-11574
 organic compounds, atmospheric, thermal desorpt./gas chromatographic anal. using hollow tube collectors 7-17928
 physical vapour transport in rectangular horizontal enclosures, surface reactions, convection 7-17398
 positron diffusion and annihilation rates 7-37621
 soil, laboratory samples, redox pot. and O₂ diffusion rate meas. using microcomputer controlled probe 7-8454

diffusion in gases continued

- tubular CVD reactor, deposition rate and uniformity, diffusion and convection effects, mathematical model 7-22559
 Ar, positron annihilation and diffusion, computer-based anal. 7-50378
 Ar, positron drift and diffusion in crossed elec. and mag. fields, simulation 7-36760
 CO, electron mobility to diffusion coeff. ratio meas. 7-20840
 Ca, metastable states energy pooling time-resolved emission spectra anal. 7-36519
 Cs, optically pumped, hyperfine relax. with Ar collisions 7-10511
 H₂, diffusion into Pd alloy tubes 7-20828
 H₂-CO₂ binary mixtures, H component fugacities, press. depend. 7-51367
 Hg, diffusion coeff. in Ar gas, interaction pot. determ. 7-6348
 Li⁺, in the, mobility and longit. diffusion 7-20834
 N₂ gas breakdown by 13.56 MHz electric field 7-1806
 N₂, lateral diffusion coefficient to electron mobility ratio meas. 7-20829
 Na diffusion coeffs. in He, Ne, N₂ and CO₂, fluoresc. detection 7-6346
 Na vapour in He, light-induced drift without physical adsorption on inner surface of cell 7-44089
 Sm vapour, vel. diffusion effects, RF-laser double reson., Raman heterodyne investig. 7-882
 Tl, interaction pot. diffusion coeffs. in inert gases 7-31913

diffusion in liquids

- see also electromigration; self-diffusion in liquids; thermal diffusion in liquids*
 n-alkane binary mixtures, Asfour Dullien eqn. modification, diffusivities depend. on conc. 7-6842
 n-alkane binary mixtures, liq.-phase diffusivity meas. 7-6843
 4-n-alkyl-4'-cyanobiphenyls, nCBs, methyl red binary mass diffusion consts., forced Rayleigh scatt. 7-64661
 alloys, binary, unidirectional solidification, cell-dendrite transition criterion (Chinese) 7-65018
 bidispersion, dil., sedimentation and diffusion, Onsager symmetry, kinetic coeffs. 7-26322
 binary liquid diffusion coeff. estimation using empirical correls. 7-38229
 boiling, heat and mass transfer 7-31627
 carbon tetrachloride, liq. rot. and translation, mol. dynamics simulation 7-2240
 carboxymethylcellulose, monosubstituted, cadoxene solns., diffusion, sedimentation and flow birefringence (Russian) 7-63859
 chloroform-methyl acetate, diffusion and activity coeff. 7-38232
 comb-like polymers, with mesogenic side fragments, conform. and optical anisotropy (Russian) 7-63516
 concentrated particle dispersions, diffusion coeffs. 7-44875
 dielectric, field-stimulated isothermal diffusion calcs. 7-63855
 dimethylzinc, Zn isotope separation by liq. phase thermal diffusion 7-15732
 dyes, determ. of progressive diffusion constants by method of fluorescence recovery after photobleaching (Russian) 7-3091
 emulsion liquid membrane, dicyclohexano-18-crown-6 mediated Tl⁺ transport 7-13814
 gas-bubble nucleation in supersaturated solns., gas diffusion into cavity 7-52095
 glass melts, nonisothermal, meas. of standard Seebeck coeffs. by means of ZrO₂ electrodes 7-3597
 glycine, diffusivity in conc. sat. and supersat. solns. 7-12335
 hydrodynamic flows, spatially periodic, diffusive transport 7-31801
 inhomogeneous fluid, tracer diffusion, kinetic theory 7-58111
 liquid membranes, macrocycle-mediated cation transport, halocarbon solvent effects 7-13813
 lyotropic liq. crystals, spin relax., local order with cylindrical interfaces, translational diffusion, continuous diffusion model 7-64540
 macromolecular diffusion coeffs. meas. using holographic interferometry, digital image processing 7-31272
 methanol-n-hexane near liquid-liquid critical point, mutual diffusion coeff. 7-44876
 micellar and hard sphere solutions, concentrated, diffusion 7-8316
 mixtures, transport processes, mutual diffusion, microscopic description 7-58514
 organic binary liquid mixtures, excess diffusion calc. 7-26991
 P6/6M-ACAP system, diffusion coeff., conc. depend 7-12339
 pair diffusion at close range 7-44878
 particle diffusion in fluctuating fluid with creeping flow 7-20788
 phospholipid monolayers, translational molecular diffusion, substrate coupling and phase transitions 7-8509
 poly-m-phenylenisophthalamide, in dimethyl acetamide; hydrodynamic props., conform. characts. (Russian) 7-11894
 polyamide 6, aq. solns., stationary diffusion of acids (Russian) 7-63433
 polyamidobenzimidazole solns., hydrodynamic and optical props. (Russian) 7-26619
 polybutadienes, high-temp. struct. transition obs. (Russian) 7-63820
 polyelectrolyte solns., spin relax., local order with cylindrical interfaces, translational diffusion, continuous diffusion model 7-64540
 polymer melts, crystallisation, localised diffusion, reptation effect 7-44414
 polymer melts, polymolecular, diffusional relax. of composition (Russian) 7-26618
 polypyrrole, diffusion-controlled polymerisation, growth instability 7-28311
 o-positronium diffusion controlled quenching reactions, influence of solvent dielec. constant 7-39852
 pyrrole polymerisation, diffusion-controlled statics and dynamics, fractal and dendritic growth in electrochem. cell 7-59758
 rigid particle suspensions, mass and entropy transport 7-32691
 rod-like particle fluid, transport props., mol. dynamics 7-42802
 salinity-temperature front, double-diffusive horizontal intrusions, linear stability theory 7-26250
 shock wave structure, liq. with bubbles, transient heat and mass transfer effect 7-6249
 solar ponds, concentration profile of salt in gradient zone 7-65583
 solidification, rapid, theory of eutectic growth 7-65016
 solution, diffusion coeff., hydrodynamic stability 7-63115
 steady flow dispersion, gently curving tube, low Dean number, Monte Carlo and num. solns. 7-44053
 supercooled liquids interacting with repulsive Yukawa pot., glass transition 7-63856
 supercritical fluid, diffusion and mass transfer 7-63106
 surfactant-water-nonaqueous liq. systems, elec. cond. study 7-13789
 tracer diffusion in concentrated colloidal dispersions 7-8303

diffusion in liquids continued

- tracer diffusion in dense ethanol, correl. for nonpolar and H-bonded solvents 7-32688
 trifluoromethanesulphonic acid electrolyte in fuel cells, O solubility, diffusion coeff., reduction rate, adsorption on Pt surface 7-28395
²²NaCl, aq. soln., adsorpt. and diffusion at low concs. 7-27106
 Ag-Cu (15 wt.%), rapidly solidified, microsegregation 7-59524
 Am, nuclear waste, leaching by salt solns. 7-36272
 Ar-Kr liquid mixtures, diffusion coeffs., simulation 7-44344
 Bi-Te-Ge, dissolution kinetics of Ge, diffusion controlled 7-44820
 CO dil. soln. in liq. Ar, linear biased correlated walk, general soln. 7-61237
 Co complexes, Co (II) hydroxo, in KOH solns., diffusion coeffs. determ. 7-52096
 HCl and NaOH interdiffusion meas. at 25°C in aq. soln. 7-6841
 H₃PO₄ electrolyte in fuel cells, O solubility, diffusion coeff., reduction rate, adsorption on Pt surface 7-28395
³He-⁴He superfluid soln., phonon-impurity system kinetics, review (Russian) 7-52179
 Kr diffusion in liquid Ar determ., cryogenic temp. controller 7-30020
 NaCl soln., salt vel. correl. functions, microscopic interpretation 7-12338
 NaNO₃-KNO₃:Ag⁺, diffusion coeffs. meas. by electrochem. methods 7-52097
 O₂, solubility in organic liqs., diffusion coeff. determ. (German) 7-52101
 Pb-Tl, Bridgman growth, pattern generation at solidification front, forbidden cells 7-22651
 Pu, nuclear waste, leaching by salt solns. 7-36272
 Si-B, impurity transport in mag. Czochralski growth, computer simulation 7-58182
 Zn isotopes, separation by liq. phase thermal diffusion 7-15732

diffusion in plasma *see plasma transport processes***diffusion in solids**

- see also electromigration; grain boundary diffusion; ionic conduction in solids; self-diffusion in solids; surface diffusion*
 2D diffusion kinetics, influence of point defects 7-38263
 acetone, mol. diffusion in C₂F₆, NMR 7-7598
 active C, organic compounds adsorption, intradiffusional kinetics model 7-32830
 aggregation, diffusion-limited, without branching 7-21146
 alkali halides, positron states, hopping- and tunnelling-diffusion calcs. 7-44921
 alloys, ion bombardment-induced segregation and redistribution 7-58381
 alloys, preferential sputtering, segregation, mixing and diffusion 7-59337
 alloys, solvent and solute diffusion enhancement, effect of non-random solute distrib. around vacancies 7-63868
 amorphous, gas transport, structural implications 7-63870
 amorphous polymers, microstruct., diffusion, positron annihilation investig. (Russian) 7-63524
 amorphous polymers, relax. of free vol., diffusional contrib. (Russian) 7-16453
 applied materials charact., conf., San Francisco, CA, USA (April 1985) 7-18495
 binary multiphase system, growth of layers, diffusion parameters 7-2249
 borosilicate glass leaching behaviour, mol. struct. effects 7-21530
 buried layer, three-layer sample, photothermal exam. 7-48724
 butadiene-styrene graft block copolymers, low-mol. cpds. diffusion (Russian) 7-36834
 camphorquinone, mass diffusion in polystyrene studied by holographic relax. studies 7-21529
 chalcogenide-metal contacts, interdiffusion, struct., comp., electron irradi. effects 7-21686
 channelling contrast microscopy, He⁺ microbeam, semiconductor impurity profiles 7-51587
 charged impurities in a semiconductor, anal. of diffusion 7-52137
 chemiothermal treatment conditions of metals, form. kinetics of irreversible deform. 7-17692
 coarsening, particle motion and diffusion interactions, in situ obs. 7-32652
 coating formation kinetics in metal solns. under isothermal conditions 7-17670
 coating-solid interface, nonlinear mechano diffusion 7-17669
 composite material, diffusion and heat transfer, practical eqns. 7-6855
 computer simulation of transport in solids, book contrib. 7-26994
 continuous two-level media, defects, motion and plastic fields (Russian) 7-58260
 crystalline rocks, nonsorbing species porosity and diffusivity 7-23639
 cubic lattices, diffusing atoms, Mossbauer spectrum studies 7-64552
 cubic lattices, long-range impurity diffusion, mono- and divacancy mechanisms 7-58526
 Darken diffusion eqns., corrections generalisation 7-52158
 defects, neutron and synchrotron radiation studies, comparisons 7-51754
 dichloromethane, sorpt. and diffusion on polypropylene films, isotactic, struct., quenching temp. effect 7-11950
 disordered systems, impurity diffusion (Russian) 7-52145
 dopant diffusion eqns., numerical soln., moving finite element method 7-12376
 dopant diffusion into Si, solar cell junction form. 7-28401
 dye, diffusion in polymer, time-depend. phenomena, impulse-response photoacoustic spectroscopy monitoring 7-42797
 edge dislocation, pipe diffusion, isotope separation 7-58521
 energy transfer, kinetics, many-particle effects (Russian) 7-28282
 epoxide networks, crosslinked, sorption and diffusion of chloroform vapours (Russian) 7-27021
 ethylene-propylene-diene elastomer, sorption and swelling in water and humid media (Russian) 7-27139
 eutectic solidification, fiber coarsening 7-59499
 Fe-Si multilayered thin films, stacking structs., magnetostatic coupling and layer boundary interdiffusion 7-7574
 ferrous laminated composite with unique microstruct., development by C diffusion control 7-17501
 fibre reinforced composite with barrier coatings on fibres, diffusional interaction of components effect on cond. 7-52167
 Fick equation, second, anal. of solns. for finite-size systems (Russian) 7-58524
 Fickian diffusion, uptake curves 7-17821
 fusion materials, gas diffusion and temperature dependence of bubble nucleation during irradiation 7-51874
 fusion reactor structural materials, irradiation, He effects control 7-51845

diffusion in solids continued

garnet bubble films, H_2^+ -implanted, H out-diffusion suppression of over-layers 7-38259
 gases, adsorbed, surface diffusion, connectivity effects 7-46864
 glass, activation enthalpy for diffusion 7-38236
 glass, dilation by field-assisted ion exchange 7-11188
 glass waveguides, Ag film diffused, diffusion process and optical props. 7-50737
 glasses, leached, analytical electron microscopy studies using ultramicro-tomic thin sections 7-6544
 glassy, non-Fickian sorption, effect of mol. size 7-38324
 grain boundary migration, diffusion induced misorientation depend. 7-21229
 graphite intercalation compound with HNO_3 , diffusion, charge transfer and strain fields, ESR study 7-53117
 hard metal parts, sintered, local alloying 7-27997
 heavy ion Rutherford backscattering spectrometry, metal-GaAs reactions 7-53488
 high temp. materials, carburisation, mathematical model, diffusion and precip. (*German*) 7-8193
 HT-9, stainless steel, tritium permeation props. 7-38239
 hydrothermal behaviour, mech. props. rel. to water absorpt. 7-46665
 ideal gas diffusion through porous plug, finite-time thermodynamics 7-31914
 III-V semiconductor quantum well structures, destruction mechanism due to impurity diffusion 7-63971
 III-V semiconductor-metal interface, reaction and interdiffusion, review 7-21544
 III-V semiconductors, modelling techniques for diffusion 7-58522
 impurity diffusion, with form. of segregation phases at dislocations (*Russian*) 7-52146
 impurity diffusion coeffs., calculation with aid of elastic constants 7-16797
 impurity profiling in mixed diffusion by neutron activation analysis 7-59810
 inert gases implanted in solids, model of diffusion and release behaviour (*Chinese*) 7-38257
 interdiffusion in coupled mag. layers, spin wave resonance approach 7-2278
 intermetallic cpds., diffusion layer at cathodes in ionic melts 7-52150
 interstitial atom motion and lattice dynamics, quantum mechanical model 7-58528
 interstitial diffusion and trapping, Monte Carlo simulations 7-32720
 interstitial diffusion and trapping, Monte Carlo simulations 7-32721
 interstitial diffusion in crystals, quantum theory 7-44916
 ion mixing, radiation-enhanced diffusion, cohesive energy correlation 7-32510
 ionic crystals, positronium dynamic props. calcs. 7-45233
 isophthalic acid-phenylene diamine-DMA-H₂O copolymer, diffusion kinetics, mass-thermal anal. method (*Russian*) 7-23096
 laminated membranes consisting of alloy and oxide layers, non-steady-state H permeation 7-6889
 layered solid, marker evolution on ion irradi., computer simulation 7-21302
 layered structures, growth kinetics in various diffusion couples 7-21678
 leaching processes, 3D diffusion eqn., numerical soln. 7-48638
 ledge interphase boundaries, growth kinetics, computer modelling 7-65041
 ledged interphase boundaries, growth kinetics, computer modelling 7-65040
 light interstitial quantum diffusion rate, strongly coupled vibrs. 7-52106
 marker evolution on ion irradi., computer simulation 7-21302
 mass transport in solids 7-26995
 measurement by analytical electron microscopy 7-39946
 membranes, diffusion under strain, thermodynamics 7-44886
 metal electrodes, H atom diffusion and trapping, meas. by potentiostatic double-step method 7-21524
 metal electrodes, H atom diffusion and trapping, meas. by potentiostatic double-step method 7-21525
 metal films, characterisation by SIMS, Auger spectroscopy and TEM 7-12550
 metal powder, superfine, mass transfer features 7-27963
 metal-gas interface, effect on diffusion layer growth kinetics 7-26911
 metal-semiconductor interfaces, epitaxial silicide technology 7-52835
 metal-semiconductor interfaces and Schottky barriers, microscopic and macroscopic props. 7-2721
 metal-Si (SiO_2), silicidation reactions, rapid thermal annealing/TEM technique 7-52156
 metallic glasses, atomic transport, diffusivity meas. 7-52144
 metallic glasses-H₂, prep., struct. and props. 7-26663
 metallic superlattices, mech. props. and diffusion 7-52377
 metallisation process study 7-12350
 metals, emission spectrochemical anal. using glow discharge, appl. to in-depth anal. (*Japanese*) 7-63886
 metals, H ion implants, trapping coefficients 7-6884
 metals, He bubble nucleation and growth under neutron and proton irradi., nonequilib. statistics 7-51848
 metals, heavy particle tunnelling, electronic polaron effects 7-52118
 metals, heavy particles diffusion coeff., Kubo formula calc. 7-6877
 metals, irradiated, internal stress, diffusion relaxation 7-58313
 metals, light interstitial motion, recent expts. 7-52114
 metals, light particle quantum tunnelling and diffusion 7-52113
 metals, neutron scattering studies, conf., Julich, Germany (Oct. 1985) 7-48178
 metals, positive muon diffusion and hopping rate 7-52111
 metals, positron self-trapping and adiabatic diffusion 7-45228
 metals, quantum diffusion, path integral approach 7-52112
 metals, radiation point defects, diffusion processes, defect drains 7-6894
 microelectronic materials, characterisation by SIMS, book contrib. 7-44976
 microelectronic materials processing, appl. of neutron depth profiling, book contrib. 7-44595
 mobile interstitial atom-substitutional impurity complex form. (*Russian*) 7-12372
 multiparticle diffusion, fractal kinetics 7-24604
 multiphase system, two-component, diffusion parameter calc. 7-2248
 muon spin resonance, conference, Uppsala, Sweden (June 1986) 7-48141
 Nb-Ti compositionally modulated films, low-temp. interdiffusion 7-38269
 nitrilebutadiene rubber, diffusion coeffs. of salt soln. and distilled water, solubility meas. 7-2269

diffusion in solids continued

noble metal film adhesion on sapphire, ion beam induced enhancement 7-21292
 nuclear fuels, diffusion processes, review 7-19350
 oxide growth by plasma anodisation, ionic transport processes 7-65162
 oxides, defect behaviour, computer-based atomistic simulation studies 7-16548
 particle diffusion and trapping, arbitrary trap size and conc. 7-9761
 PCA, austenitic steel, tritium permeation props. 7-38239
 PET films, crystallisation induced by integral sorption of organic vapours 7-12473
 planar microrelens fabrication by ion exchange/diffusion, distrib. index profile 7-31417
 PMMA, environmental stress cracking in methanol, mol. props. effects 7-65153
 point defect absorption by dislocations, preference parameter temp. depend. (*Russian*) 7-16607
 poly 2-hydroxy ethyl methacrylate films, swollen membranes, phenylalanine solute diffusion 7-28343
 polyacetylene: I₂ complexes, monosubstituted, isomerism, elec. cond., UV spectra 7-45289
 trans-polyacetylene, soliton diffusion, memory-function formalism 7-7128
 polyethylene film, low density, diffusion and sorption of liquids, IR ATR spectrosc. obs. (*German*) 7-53302
 polymers, gaseous diffusion, eqn. of state, free vol. concepts 7-21390
 polymers, solid, solvent swelling and noninvasive visualisation by ESR imaging 7-45797
 polystyrene, normal and deuterated blends, isotope effects on interdiffusion 7-27029
 polystyrene, tracer diffusion meas. using Si and the elastic recoil detect. 7-39337
 polystyrene diffusion in porous silica 7-12351
 polyvinyltrimethyl silane, plasticised, low-mol. cpd. translational and rot. mobility (*Russian*) 7-44818
 poly[bis(trifluoroethoxy)phosphazene] membranes, synthesis, casting, diffusion testing 7-13812
 porous material, diffusion and heat transfer, practical eqns. 7-6855
 positive muon diffusion, spin dynamics, strong collision model corrections 7-52107
 positron-phonon interaction and positron diffusion in solids, review 7-38240
 PTFE, bonding and surface struct., ESCA investigation, electron beam interactions 7-51662
 PVC-polycaprolactone interface, diffusion, temp. and time depend. 7-32723
 quantum theory of atomic diffusion in solids 7-44892
 quartz, H₂ diffusional uptake and hydrolytic weakening 7-40469
 α -quartz, muonium atoms, diffusion and quadrupole interactions, temp. depend. 7-52138
 radiation damage and defects, computer simulation studies 7-2048
 radiation effects in glasses 7-32518
 radiation-enhanced diffusion of implanted impurities in semiconductors, calc. 7-6883
 radiation-stimulated diffusion during ion etching 7-38261
 random alloy, phenomenological coeffs. for atom transport 7-38241
 rapid thermal processing, conf., Boston, MA, USA (Dec. 1985) 7-14713
 rare earth metals, thermophysical props. studied using mol. laser radiation 7-58555
 rare earth silicide epitaxial formation by rapid annealing 7-21768
 rare gas crystals, diffusion of vacancy complexes (*Russian*) 7-52149
 restricted hopping diffusion in cubic environment, Mossbauer spectra calc. 7-38964
 rheology, conf., Ann Arbor, MI, USA (Oct. 1985) 7-18481
 sapphire, implanted ions recrystallisation driven migration and oriented precipitation 7-2266
 semiconductor, dopant profiles modification due to surface and interface modifications 7-58306
 semiconductor and metal adatom overlayers, diffusion and interactions 7-7012
 semiconductor wafer, ion implanted dopant profile evolution during annealing, diffusion eqn., anal. 7-58536
 semiconductors, covalent, positron self-trapping and adiabatic diffusion 7-45228
 semiconductors, diffusion without vacancies and interstitials, concerted exchange mechanism 7-26997
 semiconductors, implanted ions diffusion redistribution, effect of radiation defects 7-51810
 semiconductors, impurity profile and concentration-dependent diffusion 7-51809
 semiconductors, processing and charactn. techniques, conf., Los Angeles, CA, USA (Jan. 1986) 7-18489
 silicide formation on Si, epitaxial nature, initial nucleation processes and effect 7-21767
 SOI buried layer form. by high dose implantation, mass transport studies 7-32479
 solid solution, two-component, joint diffusion 7-58520
 solid solution alloys, FCC and BCC lattice structs., H diffusion models 7-21532
 solid-fluid mixtures, boundary conditions 7-6854
 solid-solid interfaces, radiation-induced mixing 7-32516
 solidification, rapid, oscillatory morphological instabilities, role of diffusion in the solid. 7-12235
 solids, ion-implanted impurities, steady-state concs., ultimate retained doses, determ. 7-6658
 solubility and diffusion in polyaryl ether ether ketone 7-44917
 spinodal decomposition, nonlinear effects 7-39479
 square root diffusivity 7-12349
 steel, 4340, positron annihilation parameter and H behaviour, effects of tempering temps. 7-46205
 steel, alloy type, boronizing and alloying elements influence 7-59661
 steel, austenitic, martensite transform. start temp. increase in electrolytic H impregnation, internal microstresses role 7-17690
 steel, austenitic, thermal desorption after high-energy d implantation 7-52232
 steel, austenitic stainless, Cr₂₃C₆ precipitation kinetics (*German*) 7-46486
 steel, carbon and low-alloy, nitriding temperature in glow discharge effect on nitride zone thickness and comp. 7-8176
 steel, carburising process for dense and porous materials, math. model 7-39745
 steel, Cr-Mo, ferritic, effective H permeability 7-44918
 steel, dispersoid, H embrittlement, mechanical props. 7-33795

diffusion in solids continued

- steel, ferrite-perlite, H occlusivity and embrittlement, effect of C content 7-3417
- steel, H anomalous diffusion, nonlinear partial differential eqns., C^2 solns. 7-58525
- steel, H diffusivity from electropermeation transients under galvanostatic charging 7-6887
- steel, high strength, defect enhanced diffusion process and hydrogen delayed fracture 7-39673
- steel, HSLA, H-induced crack propag., method to evaluate crit. H conc. 7-65116
- steel, low C, Al-killed, H diffusion 7-6886
- steel, low C, H diffusion and trapping by TiC precipitates (*Chinese*) 7-7998
- steel, low C, vacuum carburising with methane 7-54009
- steel, migration-effect of N⁺ implantation, during wear (*Chinese*) 7-53998
- steel, mild, H diffusivity meas. using electropermeation transients 7-22903
- steel, nitrided layer, hardness distrib. prediction model 7-39746
- steel, stainless, ion trapping of D⁺, mechanisms 7-64857
- steel, stainless, surface corrosion products after exposure to liq. alkali metals, glow discharge optical spectroscopy, SIMS anal. 7-22896
- steel, structural, diffusion chromised, elevated temp. effect on comp., struct. and mech. props. 7-8178
- steel, tool, surface layers, Cr and V diffusion 7-46685
- steel 45, hardening coatings, electroerosion alloying 7-17722
- steel bimetallic plate, cold-clad, diffusion processes in preboundary zone 7-46708
- steels, C and austenite welded joint, microhardness, effect of C redistrib. 7-13571
- steels and weld metals for LWR press. vessels, brittle failure resist. 7-59636
- stress relaxation, dislocation-diffusion mechanisms, review (*Russian*) 7-32564
- substitutional impurity atoms uprise diffusion in cryst. near-surface layers (*Russian*) 7-44920
- thermal desorption spectra, effect of adsorbate diffusion into the solid 7-52283
- thin film pulsed heating, thermal and plasma models 7-26946
- thin films, interdiffusion, phase suppression in transient stages 7-16820
- tracer diffusion and ionic cond., correlation effects 7-6857
- transition metal-metalloid metallic glasses, struct. relax. and segregation (*Russian*) 7-32300
- transparent conducting oxides, uses in a-Si:H solar cells 7-46953
- X-ray diffr. meas. of diffusivity 7-44925
- Ag, H₂ permeability in metals at high-press. and high-temp. 7-27011
- Ag/amorphous chalcogenide, Ag photodiffusion, semiconductor heterojunction formation 7-45026
- Ag/In thin film couples, interface AgIn₂ cpd. form. and props., gamma ray spectra 7-21688
- Ag-Au, thin interface regions; EXAFS studies 7-59285
- Ag-Au bilayers, EXAFS and X-ray reflectivity meas. 7-27821
- Ag-brass, mixing layer, friction props., ion beam mixing (*Chinese*) 7-51888
- Ag-Pd alloys, H₂ permeability at 2 kbar press. and high temp. 7-27011
- Ag-Sn, internal oxidation kinetics, influence of oxide particles density 7-13722
- AgI-Ag₂O-B₂O₃ glasses, superionic, crossover freq. between phonon and fraction regimes, scaling behaviour 7-44728
- AgNO₃, countercurrent diffusion with HCl in cellulose and Nafion films 7-12377
- Ag_{0.25}Nb_{0.75}Li, Li diffusion and intercalation 7-16806
- (Al, Ga)As films, doped, Si migration during MBE growth 7-27171
- (Al, Ga)As/GaAs undoped quantum wells, Al and Ga interdiffusion, photoluminesc. study 7-2271
- Al diffusion annealing effects on Mo plates magnetoresist. (*Russian*) 7-7408
- Al, ion tapping of D⁺, mechanisms 7-64857
- Al, muon trapping and diffusion after electron irradiation, μ SR study 7-45864
- Al, surface oxidation, diffusion of Au atoms through oxide layers 7-8200
- Al/Si contacts, diffusion at room temp. (*German*) 7-32724
- Al/TiN/Si contacts for VLSI, analytical electron microscopy 7-58651
- Al-Cu, thin interface regions, EXAFS studies 7-59285
- Al-Cu interface, grazing incidence X-ray study of interfacial reactions 7-21543
- Al-Cu(Mg)(Ag) system, trapping and diffusion mechanism, μ SR study 7-45863
- Al-GaAs, pure and Si or Zn doped interfaces, composition depth profile, pulsed laser atom probe study 7-32842
- Al-GaAs Schottky barrier contacts, MBE grown, interface reactions, vacuum annealing effects 7-45022
- Al-GaSb interfacial chem. reactions, surface refl. Raman Scatt. study 7-2275
- Al-killed 1006 steel, H diffusion effect on enamelling 7-33816
- Al-Li (9.5 at.%), coarsening of δ -Al₃Li precipitates, var. of average Li content in Al matrix 7-3313
- Al-Mn, electron wind-induced muon drift 7-52115
- Al-Mo, rapid solidification processed, diffusion-induced dislocation migration 7-65047
- Al-Sb, Xe ion irradiated, intermixing rates, backscattering spectra, anal. by computer program 7-64840
- Al-Si(Ge)(Ga), low temp. diffusion and trapping of muons 7-45865
- Al-W/Ti(Ni) thin film reactions, W diffusion marker studies 7-2277
- AlAs/GaAs superlattice mixing induced by Si⁺ implantation 7-58649
- AlAs-GaAs superlattices, Si ion implantation, dose-dependent mixing 7-12500
- AlAs-GaAs superlattice, Si⁺ implantation, depth dependent mixing 7-27032
- AlAs-GaAs superlattice, compositional disordering control by Ar ion implantation 7-51806
- AlGaAs:Si(Zn), MOCVD, impurity induced disordering, quantum well laser fabrication and characts. 7-27934
- AlGaAs-GaAs superlattices, Si-Be co-doping, compositional disordering suppression, SIMS study 7-16878
- AlGaAs-GaAs superlattices, Se (Si)(Mg)(Be) ion implantation, intermixing, residual damage 7-26782
- AlGaAs-GaAs-Si, Be superlattices, correlation between Si diffusion and Si-induced disordering 7-38034
- Al₁Ga_{1-x}As:Si, Si diffusion from sputtered Si film 7-58537

diffusion in solids continued

- Al₁Ga_{1-x}As-GaAs stripe-geometry quantum well heterostructure lasers defined by defect diffusion 7-1181
- Al₁Ga_{1-x}As-GaAs superlattices, ion implanted, defect struct. 7-26783
- Al₂O₃, diffusion of ¹¹⁰Ag tracer, 627-1400°C 7-2270
- β -Al₂O₃, diffusion of implanted ions (*Chinese*) 7-51798
- Al₂O₃ refractory, ceramic, wettability and contact angle with Al melt, nitride additive effects (*Russian*) 7-12402
- Al₂O₃ scale growth on Fe-Cr-Al alloys, diffusion and transport props. 7-65214
- Al₂O₃-MgO-TiO₂-Na₂O system, sintering and creep, Na₂O influence, Cable and Reijnen-Readley models (*German, English*) 7-7933
- Al₂O₃-NiO thin-film reactions, NiAl₂O₄ form. investig. 7-16877
- Al₂O₃-Ti interface reactions studied by AES and UPS 7-21702
- Al₂O₃-TiC, CVD coating on cemented carbides, diffusion of Co and W, TEM/AES study 7-27942
- AlSi-Ti bilayer structs., effect of Si on reaction kinetics 7-58546
- Au dilute alloys, electron irradi., positron lifetime meas. 7-39250
- Au, H₂ permeability in metals at high-press. and high-temp. 7-27011
- Au layer plated on stainless steel, tritium permeation meas. 7-6852
- Au/In thin film couples, interface AuIn₂ cpd. form. and props., gamma-ray spectra 7-21688
- Au/Ni thin film diffusion couples (*French*) 7-12576
- Au-Ag sandwiches, grain boundary electron scatt. (*Russian*) 7-12883
- Au-Cu alloys, polycryst., room temp. interdiffusion 7-2274
- Au-Ge-GaAs, interfacial reactions, struct. after annealing 7-27154
- Au-InP, solid-state reactions, Au₂P₃ formation 7-58550
- Au-Ni-Cu, diffusion of Au and Cu through Ni layer, depend. on ambient 7-38266
- AuAl alloys, Al diffusion, NMR study 7-33287
- AuGe-GaAs, ion beam induced phenomena 7-12166
- AuNiGe-GaAs ohmic contacts, microstruct. anal. and contact resist. meas. 7-2393
- BaTiO₃/Ni ceramic, H defect diffusion 7-58545
- C diffusion in compound welds having intermediate layer 7-44887
- Cd₂Hg_{1-x}Te, abrupt interfaces using thermal and photo-MOVPE, Hall meas. 7-27917
- CdI₂-Ag interface, absorpt. and luminesc. spectra studies (*Russian*) 7-59224
- CdS/ZnS, multilayer structures, MOCVD, wide band gap, interdiffusion characts. 7-53610
- CdSe/ZnSe, multilayer structures, MOCVD, wide band gap, interdiffusion characts. 7-53610
- Co, diffusion of ⁴⁸V, mag. anomalies, quasi-chemical model 7-6862
- Co, silicisation using Si₂Cl₆ source by diffusion and CVD processes 7-17700
- Co-Al system, diffusion markers in thin films Co₂Al₃ formation 7-58549
- Co-Si, direct silicidation, on Si:B(As)(P), rapid thermal annealing 7-21546
- Co-Si bilayered films, chem., elec., and struct. charges upon annealing 7-22037
- Co-Si multilayers, amorphisation and interdiffusion, EXAFS and XANES studies 7-64812
- CoSi₂, self-aligned silicide technology using rapid thermal processing 7-52154
- CoTi-CoNb amorphous alternating layers, magnetic and diffusional props. study 7-7563
- Cr, metallic and surface-oxidised, H and D diffusion 7-6888
- Cr, zero field muon spin rotation study 7-45871
- Cr-Al system, diffusion markers in thin, film CrAl₇ formation 7-58549
- Cr-Ge thin film interface, interdiffusion, reaction and intermixing, soft X-ray photoemission study 7-27028
- Cr-Si, lateral growth of CrSi₂, role of Si transport 7-38272
- Cr₃C₂-Ni-P hard metal, Cr₃C₂ solution in Ni matrix, liq. phase influence 7-53689
- CrSi₂-Ar⁺ ion beam induced surface and subsurface modifications, AES study 7-64846
- Cr₃Si, Ar⁺ ion beam induced surface and subsurface modifications, AES study 7-64846
- Cu, diffusion bonding, strain-free mounting appl. 7-3572
- Cu, dislocation-diffusion mechanism of wear reduction in selective transfer 7-17658
- Cu films, interaction with Cl₂, bulk diffusion processes 7-21783
- Cu, ion mixing and thermochemical props. of markers 7-26805
- Cu, muon hopping rates, low longitudinal mag. field muon spin relax. studies 7-53198
- Cu, ultra-pure samples, diffusion of positive muons, detection by zero-field muon spin resonance 7-45862
- Cu/Au thin film systems, interdiffusive kinetics, EXAFS studies 7-16819
- Cu/In thin film couples, interface CuIn₂ cpd. form. and props., gamma ray spectra 7-21688
- Cu/Pb-Sn solder interfacial reactions, Cu₃Sn intermetallic formation 7-44924
- Cu-Al (111), S segregation, LEED and AES studies 7-2321
- Cu-CdTe interface form., effect of different cation-anion bond strengths 7-27149
- Cu-Hg_{0.75}Cd_{0.25}Te interface form., effect of different cation-anion bond strengths 7-27149
- Cu-Ni multilayer thin film system, low temp. mutual diffusion (*Russian*) 7-58551
- 2-Cu-Ni-Sn solid solutions, ternary diffusion and thermodynamic interactions 7-52159
- Cu-Sn thin film diffusion couple, reaction kinetics at room temp. 7-21536
- Cu-Ti (5.7 at.%), diffusion of products of cellular dissoln. (*Russian*) 7-58485
- Cu-Zn system, diffusion induced grain boundary migration 7-21227
- Cu-Zr, compositionally modulated amorphous films, sputter deposition prep. 7-22482
- CuInS₂ films, RF sputtering, struct. and elec. props. 7-3169
- CuZnAl alloys, β -phase, defects study by positron annihilation 7-39297
- Dy, positive muon diffusion in helicoidally-ordered antiferromagnets 7-45870
- Fe, Al diffusion, influence of mag. field, radioactive isotope study (*Russian*) 7-52157
- Fe, Armco, diffusion bonding, precip. of Fe carbides in ferrite 7-39521
- Fe, cast, diffusion interaction with steel in forging, explosive treatment and thermal cycling 7-28070
- Fe, diffusion of ⁵⁹Fe and ⁶⁰Co, mag. anomalies, quasi-chemical model 7-6862
- Fe, dilute alloys, electron irradi., positron lifetime meas. 7-39250

diffusion in solids continued

- Fe electrodes, H atom diffusion and trapping, meas. by potentiostatic double-step method 7-21525
 d-Fe, ferromag., positron spin polarisation relax. study 7-46203
 Fe, H pumping and compression by superpermeation 7-58543
 Fe, migration-effect of N^+ implantation, during wear (*Chinese*) 7-53998
 Fe, mono- and poly-crystalline, positive muon studies, low temp., dipolar fields, jump freqs. 7-45861
 Fe, permeation of H(D), oscill. press. effects 7-27025
 Fe, plastic deform., H permeation, dislocation traps 7-65082
 Fe, pure, diffusion of H, dislocation trapping, interstitial impurities effect (*Japanese*) 7-52140
 α -Fe single crystals, activation energy of S diffusion, surface segregation, AES obs. 7-39529
 Fe:H(D), lattice strains, meas. 7-2268
 Fe:He(C), distribution and migration of interstitial impurities in the field of a screw dislocation core 7-6669
 Fe/Fe-FeO/ Al_2O_3 systems, diffusion bonded, interface chemistry, bonding strength 7-28079
 Fe/FeZn₁₃/Fe-Si composite diffusion couples, effect of Si on stability and growth of Fe-Zn phases 7-54011
 Fe/Ni Reed blades, Au coated, AES/SEM study 7-44972
 Fe/Zn diffusion couple, anomalously fast diffusion 7-16818
 Fe-Al bilayered samples, ion beam induced atomic mixing 7-6689
 Fe-B amorphous sandwich films, concentration-dependent diffusion 7-45027
 Fe-C austenite, binary, C diffusivity, revised expression 7-38238
 Fe-Cr alloys, H diffusion and trapping 7-27018
 Fe-GaAs(001)-c(8×2) interface, simultaneous epitaxy and substrate out-diffusion 7-38355
 Fe-N, Snoek-Koster relax., dislocation effects (*Russian*) 7-44686
 Fe-Si, H-induced grain boundary migration 7-21230
 Fe-Si (3 wt.%), grain oriented, desulphurisation kinetics, 899-1171°C 7-8002
 Fe-Si thin films, silicide formation, AES and EELS studies 7-32862
 Fe-Si-B metallic glasses, struct. relax. (*Chinese*) 7-65070
 Fe-Ti compositionally modulated amorphous films, sputter deposition prep. 7-22482
 Fe-Zr alloy formation at Fe/Zr thin film interfaces, Mossbauer study 7-63975
 Fe₈₀B₂₀ ribbons, amorphous and crystallised, surface comp., electronic props., topography, AES, XPS, ion scatt. studies 7-27065
 Fe₈₀C₂₀-Si compositionally modulated amorphous struct., mag. and diffusional props. study 7-7564
 Fe₂O₃- γ , hematite, O activity depend., high temp. Mossbauer spectra 7-38978
 Fe₃- γ O₄, diffusion-controlled form. during reactions, defects effects 7-17768
 Fe₃- γ O₄, magnetite, O activity depend., Mossbauer spectra 7-38977
 Fe₃O₄, magnetite, Fe and impurity cations, migration enthalpies meas. 7-58541
 GaAs (100)-Ni interface, effect of O on diffusion and compounding 7-21539
 GaAs, diffusion coeff. of Fe, temp. depend. 7-6875
 GaAs epitaxial film shallow homojunction solar cells fabrication by Zn solid state diffusion method 7-17860
 GaAs substrates, laser-induced metal and alloy plating, silicide form. 7-39448
 GaAs:Ge,Se, diffused contact regions, rapid thermal annealing 7-17103
 GaAs:Zn, Zn diffusion by open-tube technique 7-38260
 GaAs:Zn,Si, selective double diffusion using sputtered Si masks 7-51805
 GaAs-Al_{0.65}Ga_{0.35}As, transverse junction stripe laser, lateral heterobarrier by diffusion enhanced alloy disordering 7-10929
 GaAs-AlAs superlattices, Se implantation, effect on compositional disordering 7-26784
 GaAs-GaAs:Cr(Te), VPE grown, photoluminescence study, effect of substrate doping 7-27771
 GaAs-Nb(NbN) Schottky barriers, interdiffusion obs. 7-58856
 GaAs-Pt reacted ohmic contact charactn., effect of Mg layer 7-7387
 GaInAs, pn junction formation by simultaneous implantation and diffusion annealing 7-38028
 GaInAs-SiO₂ system, annealing behaviour, SIMS and elec. meas. 7-38270
 Ga_{0.4}In_{0.53}As:Be epitaxial films, ion implanted, rapid thermal and furnace annealing 7-22729
 GdTbFe, corrosion resistance improvement by metal coatings 7-53952
 Ge, free exciton diffusion and decay, lumin. 7-32918
 Ge:Ga single crystals, tracer diffusion coeff. and isotope effect, SIMS meas. 7-27019
 Ge:H, H composition at surfaces and interfaces 7-27083
 a-Ge/au interfaces, atomic intermixing, asymmetries 7-21682
 Ge-Sb-Te system, diffusion of Fe, Cr and Ni impurities 7-21527
 Ge,Si_{1-x}-Si multilayers, MBE grown, thermally annealed, Ge diffusion, strain relax., ion channelling, backscattering anal. 7-6896
 H diffusion in long-range ordered alloys 7-21508
 H in Pd, molecular dynamics simulation model for mobility and thermotransport props. 7-58554
 H₂, adsorption rate at H₂-LaNi₅ interphase, diffusion coeff. eval. 7-32696
 H₂ diffusion in pure crystals, continuous-time correlated walk with unrestricted jumps model appl. 7-27015
 HCl, counter-current diffusion with AgNO₃ in cellulose and Nafion films 7-12377
 HfNi, amorphous phase form. by solid-state reaction, dominant moving species 7-21706
 HgCdTe, epitaxial film, interdiffusion profiling, microreflection spectroscopy 7-53369
 Hg_{1-x}Cd_xTe/Ag(Cu)(Al) interfaces, morphology, Hg bonding effects 7-7021
 HgTe based superlattice, MBE growth and props., interdiffusion 7-7345
 HgTe/ZnTe, isothermal interdiffusion expts. 7-52152
 In, muon trapping and diffusion after electron irradiation, μ SR study 7-45864
 In-GaAs reactions, interfacial native oxide layer effects 7-12501
 In-GaAs(110), interfacial chem. reaction, UPS study 7-2276
 InAs (110), surface electron states, effect of Al submonolayer coverage, soft XPS study 7-2653
 InGaAs, LPE diffusion-limited growth 7-21727
 In_{0.53}Ga_{0.47}As/In_{0.52}Al_{0.48}As quantum wells, lamp annealing interdiffusion and optical props. 7-12502

diffusion in solids continued

- In_{0.5}Ga_{0.5}As (100)-metal interfaces, Fermi level pinning and chem. interactions 7-2712
 InP, electron irradiation, damage, impurity effects 7-12154
 InP surface metal-p⁺-n enhanced Schottky barriers formed by open tube diffusion technique 7-2710
 InP:S, shallow n⁺ diffusion of S, open-tube diffusion technique, n⁺-p junction formation 7-44912
 n-InP:Zn, Zn diffusion 7-63882
 InP:Zn(Cd), interstitial-substitutional diffusion, doping effects 7-6878
 InP/InGaAs heterojunction bipolar transistors, open-tube Zn diffusion 7-44914
 InSb MOS interfaces, annealing, O diffusion and reaction 7-58665
 InSe-Ag intercalation cpd., prep. 7-54146
 In₂Se₃-Ag intercalation cpd., prep. 7-54146
 KCl (100), interaction of NaCl mol. beams with surface, desorption flux meas., SIMS obs. 7-33508
 KCl(Br):Cu²⁺, diffusion, nuclear spin-lattice relax. rate meas. (*German*) 7-6885
 K(NH₃)₂C₂₄, intercalation cpd., 2D diffusion-limited kinetics 7-58552
 KNO₃-glass, ion-exchange diffusion, planar waveguides 7-11108
 LaNi₅, anisotropic H migration, deposition potentials, hardness, brittleness meas. 7-6873
 LaNi₅, diffusion of H and D, temp. depend. 7-6874
 LaNi₄AlH_x and LaNi_{4.5}Al_{0.5}H_x, dynamical disorder of H, quasi-elastic neutron scatt. study 7-21535
 LaNi₄MH₂ (M=Mn, Cu), dynamical disorder of H, quasi-elastic neutron scatt. study 7-21535
 γ -LiAlO₂, fusion reactor breeder blanket, T transport modelling 7-49642
 LiAlO₂ spheres, T release, time depend., diffusion coeff. 7-49643
 LiF, electron beam irradiation, desorbed ground state Li atoms, signal time depend. 7-52260
 LiF, electron stimulated desorption of Li, role of F-centre diffusion 7-16864
 LiMnFe₂O₄ ferrite, solid solution form. in contact diffusion pairs 7-2273
 LiNbO₃:He⁺ optical waveguides, ion implanted, Li outdiffusion modelling 7-62832
 LiNbO₃:Ti, Ti in-diffusion, intermediate phase structure 7-44473
 LiNbO₃:Ti waveguides, Ti diffusion, model 7-21528
 LiO₂ spheres, T release, time depend., diffusion coeff. 7-49643
 LiTaO₃ low freq. dielec. response, charged point defect migration contrib. anal. 7-38984
 Li₂V₆O₁₃ single cryst., Li transport props. and partial molar entropy 7-6871
 MgO:H, C single crystals, ion implanted, C and H diffusion behaviour, SIMS studies 7-32714
 Mn_{1-x}O, manganosite, relax. kinetics in CO-CO₂ mixtures 7-58539
 Mo film ion beam mixing of marker atoms, heat of mixing effect 7-21304
 Mo film on Si, ion beam mixing, amorphous layer form. 7-21301
 Mo, He pipe diffusion along dislocations 7-58544
 Mo, ion trapping of D⁺, mechanisms 7-64857
 Mo, pion-decay channelling, high and low temps. 7-45866
 Mo single crystal, cold worked, He pipe diffusion along dislocation, thermal desorption spectra 7-52142
 Mo, thermodynamic stability in a fusion reactor environment, H, O and C implantation and diffusion 7-49658
 Mo/Al-Si interdiffusion kinetics and contact resistance study for VLSI appls. 7-21714
 Mo-Ag pseudoballoys, Ni and Co effect on interphase interaction 7-27975
 Mo-Al system, diffusion markers in thin film MoAl₁₂ formation 7-58549
 Mo-Pd-Si, thin film metallisation system, interdiffusion, cpd. formation 7-21538
 MoS₂, intercalated with Fe, Ni and Pd, AES, sputtering studies 7-63867
 Na₂CaAl₂Si₄O₁₂·6H₂O, zeolite, adsorption and desorption of ethylene, TPD study 7-32826
 Na₂O-CaO-SiO₂ glass, hydration, fluid flow effects 7-13758
 Na₂O-GeO₂ glasses, ionic transport studies 7-6864
 Na₂O-SnO₂-SiO₂ glass, diffusion of cations, 500-800°C 7-12371
 Na₂O·3SiO₂ glass, Na leaching rates in H₂O and D₂O, comparison 7-63885
 Nb, diffusion and trapping of H(T), NMR obs. 7-27616
 Nb, effective H permeability 7-44918
 Nb, ion trapping of D⁺, mechanisms 7-64857
 Nb single crystals, reverse lattice nodes form rel. to N diffusion (*Russian*) 7-58201
 Nb, ultra-pure type II superconductor, diffusivity of positive muons, μ SR study 7-45869
 Nb-Al thin film diffusion couples, Nb₃Al A15 phase form. during annealing, XPS and Auger studies 7-58548
 Nb-Al₂O₃, diffusion processes and interphase boundary morphology 7-16817
 Nb-C alloy, thermotransport of C 7-46479
 Nb-H system, electron irradiation, vacancy recovery, positron lifetime studies 7-37972
 Nb-H system 7-44919
 Nb-H systems, muon diffusion, μ SR study 7-45868
 Nb-Mo-Zr alloy, protective props. of thermomodification Mo-B-Si coating 7-8156
 Nb-Sn composite wires, effectiveness of V as diffusion barrier material 7-15353
 Nb-V-O system, solute atom trapping, O diffusivity, kinetics and thermodynamics 7-12368
 NbO_xH_y, H tunnelling and local diffusion 7-58529
 NbSe₂:Li, Li diffusion and intercalation 7-16806
 NbSi₂ film form. by scanning electron beam annealing 7-21285
 Nb₃Sn films, superconducting critical temp., effect of ion beam irradiation 7-7430
 Ni (100), adsorpt. of CO and D, diffusion, investig. 7-6960
 Ni and Ni-Cu, gamma-irradiated, point defect migration 7-6893
 Ni, D permeation rel. to surface impurities and Ar sputtering 7-52141
 Ni epitaxial growth on Fe (001), LEED and AES studies 7-64022
 Ni film on Cu, SIMS meas. of interdiffusion coeffs., SIMS analysing depth 7-27853
 Ni films on Mo or Cu surfaces, out-diffusion through Au overlayers 7-12511
 Ni, H permeation, diffusion and surface rate coeff., press.-modulated absorpt.-desorpt. 7-58612
 Ni, H trapping phenomena, meas. by desorption thermal anal. technique 7-6673

diffusion in solids continued

- Ni, ion implantation and pulsed laser melt quenching, metastable phase and defect struct. form. studies 7-16625
 Ni, ion irradiation-induced implant diffusion and segregation, synergistic effects, kinetic model calcs. 7-16658
 Ni, permeation of H(D), oscill. press. effects 7-27025
 Ni, silicised layer form. by diffusion and CVD, oxidation and corrosion resist. 7-59659
 Ni single crystal, amorphisation by Zr polycrystal bilayers 7-63463
 Ni:Bi, ion implanted, high temp. oxidation, defect diffusion 7-33846
 Ni:H, diffusivity, diffusion-elastic effect and Gorsky effect 7-27023
 Ni/Al/Si system, contact structure formation by rapid thermal melting 7-45019
 Ni/Zr thin film diffusion couples, amorphisation, DSC studies 7-26639
 Ni-Al system, diffusion markers in thin film Ni₃Al formation 7-58549
 Ni-Al₂O₃, diffusion processes and interphase boundary morphology 7-16817
 Ni-AuGe-GaAs, ion beam induced phenomena 7-12166
 Ni-AuGe-GaAs, ohmic contacts, interface reactions, elec. behaviour 7-27031
 Ni-C, C-vacancy binding 7-44601
 Ni-Cr, carburisation, kinetics, diffusion and precipitation (*German*) 7-8194
 Ni-Cr, high temp. alloys, carburisation, finite difference model of C diffusion 7-39712
 Ni-Cr (1 wt.%), internal oxidation, two-phase region form. kinetics in diffusion zone (*Russian*) 7-46497
 Ni-Cu, heterodiffusion, effect of γ -rad. (*Russian*) 7-44617
 Ni-GaAs, lateral reactions, hot-stage TEM 7-27030
 Ni-MgO, diffusion processes and interphase boundary morphology 7-16817
 Ni-Nb amorphous films, early stages of reaction with cryst. Au films 7-21703
 Ni-NiAl, formation of NiAl coatings by CVD, kinetics 7-59451
 Ni-P contacts, phase formation 7-63983
 Ni-Si bilayered films, chem., elec., and struct. charges upon annealing 7-22037
 Ni-Si interface reactions induced by pulsed incoherent light, silicide formation 7-32725
 Ni-Si thin film diffusion couples, lateral silicide formation 7-21540
 Ni-SnPBi system, crack form. in diffusion zone 7-3397
 Ni-TiC-Si, TiC as mixing barrier for Ni-Si ion beam mixing 7-44922
 Ni-Zr, amorphous phase formation by solid state reaction, evidence for nucleation barrier 7-58146
 Ni₃AlHfB/Ni couples, up-hill Hf interdiffusion studies 7-12378
 NiAl₂O₃, spinel growth, thin-film Al₂O₃ substrate, topotactic relationships 7-58717
 NiSi₂ formation by reaction of filament evaporated Ni with Si substrate 7-38268
 NiTa-GaAs, phase separation, cross-sectional TEM 7-27152
 Ni₃₅Ti₆₅, amorphous, internal friction of H 7-39577
²³⁹Np, diffusion in simulated high level waste glass 7-49684
 O₂ transport in dry rocks, exptl. study 7-54954
 Pb/PbSn, chem. diffusivity of Sn in Pb, expt. determ. 7-63887
 PbBi₄Te₇, synthesis and physicochemical props. 7-13349
 PbO₂, diffusion of H, electrochem. meas. 7-16807
 PbSe films, elec. cond. and thermoelec. power, dynamic behaviour 7-2750
 PbSe:Ag, electron irradi. stimulated impurity diffusion 7-63878
 Pb_{0.8}Sn_{0.2}Te:Ga solid solns., diffusion coeff., temp. depend. study 7-2254
 Pb_{0.8}Sn_{0.2}Te:In, impurity diffusion, thermoelec. probe meas. 7-63879
 PbTe:O films, O diffusion to bulk and crystallite boundaries 7-63884
 PbTe_{0.99}Se_{0.08}:Ga solid solns., diffusion coeff., temp. depend. study 7-2254
 Pd Frank-Van der Merwe growth on Ag (111), AES, surface reflectance spectra studies 7-32829
 Pd, H diffusion and segregation in grain boundaries 7-63632
 Pd, H diffusion coeff., influence of subsurface layer on meas. 7-6892
 Pd, H permeation, diffusion and surface rate coeff., press.-modulated absorpt.-desorpt. 7-58612
 Pd membrane, diffusion of H₂, transport coeffs. and energetics 7-21533
 Pd monolayers on Ta(110), morphology and struct. phase transitions 7-38374
 Pd/Si:B,As/Si:B, As ion implant redistribution during Pd₂Si formation using rapid thermal annealing 7-16816
 Pd-GaAs, phase formation sequence, morphology 7-27153
 Pd-H, and substitutional alloys, thermodynamics of dil. solns. 7-21480
 Pd-H, single particle dynamics, simulation model 7-27016
 Pd-H system, H transport coeffs. and energetics 7-6891
 Pd-H system, phase form., process (*Russian*) 7-33640
 Pd-PET membranes, H diffusivity and solubility, meas. by nonequilib. stripping potentiostatic method 7-6809
 Pd-Y-H ternary solid soln., H diffusivity 7-63866
 Pd₄₀Si₂₀H₃, metallic glass, H diffusion, quasielastic neutron scatt. study 7-21534
 PdFe ordered alloy, discontinuous domain coalescence (*Russian*) 7-2025
 PdH_x, H diffusion by tunnelling 7-6880
 PdSi, phase transform. to Pd₂Si, kinetics 7-16795
 Pd₂Si formation, dopant redistrib. in Si substrate 7-21255
 Pd₃₀Si₃₀, amorphous, H solubility and diffusion 7-26969
 Pt, H permeability in metals at high-press. and high-temp. 7-27011
 Pt-Si interfacial growth following Si chemisorption, intermixing, SEXAFS obs. 7-64772
 PtSi-Si, interfacial metallurgical interactions, elec. characts., effect of H 7-52834
 Rn, diffusion effects on tissue microdistribution, CR-39 autoradiography study 7-54731
 Rn, emanation into pores of solid material, recoil effect 7-49730
 Ru film, ion beam mixing of marker atoms, heat of mixing effect 7-21304
 Si (111) with oxidised Cr overlayer, CrSi₂ formation and reduction of Cr₂O₃ during annealing 7-58660
 Si (111)/Pt interface form. by interstitial chemisorpt. EXAFS and X-ray absorpt. resonance spectra studies 7-38336
 Si, amorphisation and crystallisation 7-11914
 Si, defect reactions and atomic diffusion 7-38264
 Si, diffusing metallic impurities, H implantation effects 7-12370
 Si, diffusion modelling, point defect interactions 7-32715
 Si, diffusion of ion-implanted impurities, modelling on IBM PC 7-38265
 Si, dopant diffusion under thermal nitridation conditions 7-32716
 Si epitaxial layers, autodoping effects 7-63635

diffusion in solids continued

- Si gettering, review of phenomenology 7-38215
 Si, implantation damaged, transient enhanced dopant diffusion 7-44910
 Si, ion implantation, interstitial trapping, dopant migration and epitaxial regrowth 7-12103
 Si ion implanted surface dopant cross-contamination, enhanced diffusion effects 7-32719
 Si materials science issues in IC processing 7-35115
 Si, nitridation treatments, review 7-17747
 Si, oxidation, kinetics of ultrathin SiO₂ growth 7-8204
 Si, oxidation, transport processes 7-65232
 Si, oxidation, transport processes 7-65233
 Si, polycrystalline, ¹²⁵Sb, ³²P, ⁷⁴(73)As donor elements, diffusion 7-12373
 Si, polycrystalline, for solar cell apps., photovoltaic props., effect of impurities and defects 7-38639
 Si, polycrystalline, H₂ passivation, grain boundaries, EBIC technique 7-26769
 Si, rapid thermal annealing of ion implanted layers, role of trapped interstitials 7-17568
 Si SOI structure, high-dose O₂⁺ implanted, dopant diffusion 7-52139
 Si, self-diffusion and impurity diffusion, review 7-32713
 Si solar cells, crystalline, metal grid optimisation and emitter tailoring, computer model extension 7-54292
 Si solar cells, polycrystalline, junction formation by light induced diffusion 7-13919
 Si substrates, laser-induced metal and alloy plating, silicide form. 7-39448
 Si, surface, laser beam melting and recrystallisation 7-12431
 Si, thermal nitridation in NH₃, atomic transport mechanisms 7-8201
 Si: transition metals, solubilities, diffusivities and deep levels 7-32465
 Si:As, dopant diffusion, finite element based simulation, quasilinear formulation with remeshing scheme 7-21526
 Si:As, highly doped, spinodal decomposition and clustering 7-52063
 Si:As, ion implanted, rapid thermal annealing 7-16615
 Si:As, laser annealed, Raman scatt. study 7-53325
 Si:As,Sb(P,Sb), Sb diffusion 7-44915
 Si:As porous layer, impurity diffusion under incoherent light exposure 7-38258
 Si:As⁺(As₂⁺), ion implanted, phys. props., spreading resist., TEM, Rutherford backscattering, SIMS 7-26775
 Si:As(BF₃), ion implanted, diffusion and defects, transient scanning electron beam annealing 7-38065
 Si:As(B), ion implant redistribution, diffusion modelling 7-16814
 Si:As(P)(B)-SiO₂ interface, segregation, transport coeffs. of impurities 7-63880
 Si:As(Sb)(In), heavily doped, laser induced oxidation 7-13672
 Si:Au, U- and W-shaped impurity diffusion profiles investigation 7-16805
 Si:B, diffused through narrow windows, doping profiles 7-12113
 Si:B, diffusion and activation of implanted B during rapid thermal annealing 7-16643
 Si:B, excimer laser-induced shallow diffusion, junction form. 7-38038
 Si:B, implant redistribution during high pressure oxidation, SIMS and C-V meas. 7-27020
 Si:B, impurity diffusion from BN sources, non-Fickian model 7-27012
 Si:B, ion implanted, B diffusion, rapid thermal annealing 7-58538
 Si:B, ion implanted, dopant redistrib. during rapid thermal annealing 7-38042
 Si:B, magnetic Czochralski growth, computer simulation of B transport 7-32344
 Si:B, preamorphised, B diffusion during rapid thermal annealing 7-32717
 Si:B (As) diffusion source, diffusion into single crystal Si 7-32727
 Si-Bi polycrystalline-single cryst. interface, impurity diffusion across boundary 7-27013
 Si:B(As)-Ti(Co), silicide formation using rapid thermal processing, defect behaviour 7-32726
 Si:B(Au), electron irradi. stimulated impurity diffusion 7-63878
 Si:B(Ga)(As)(Sb) 7-2040
 Si:B(P), lateral diffusion, modeling LOCOS effects 7-33865
 Si:B(P)(As)(Sb), retarded and enhanced dopant diffusion related to implantation-induced excess vacancies and interstitials 7-63881
 Si:C,O, solubility, segregation, diffusion and precipitation 7-16777
 Si:C,O,P, C precipitation after P junction diffusion 7-16779
 Si:C(C,P), C diffusion during annealing and P in-diffusion 7-16812
 Si:Co, supersaturated solid solution, annealing 7-63642
 Si:F, implanted, dry oxidation kinetics, impurity effects 7-13667
 Si:H, B(Al)(Ga)(In), polishing, acceptor compensation by atomic H 7-33860
 a-Si:H, charge transport and relax., luminesc. long-time tail distribns. anal. 7-39185
 Si:H, H composition at surfaces and interfaces 7-27083
 Si:H, polycrystalline, chemistry of grain boundary passivation 7-12375
 a-Si:H:B, effective p⁺ doping by plasma-assisted B diffusion 7-38036
 Si:H and near-surface damage of Si caused by H ions, review 7-16813
 Si:H films, ion implant redistribution 7-16921
 a-Si:H solar cells, p-layer doping by plasma assisted B diffusion 7-13898
 Si:In, amorphous, low temp. annealing, impurity diffusion, phase separation and crystn. studies 7-16808
 Si:N, N incorporation and behaviour 7-16598
 Si:Ni, diffusion of Ni under action of concentrated luminous flux 7-44913
 Si:O, C, low temp. precipitation, IR and SANS meas. 7-32666
 Si:O, C, thermal donor form., T<800K 7-27294
 Si:O, defects created by electron irradiation and subsequent thermal treatments, review 7-16642
 Si:O, diffusion of O during thermal donor form. 7-38262
 Si:O, diffusivity and diffusion mechanism of O 7-16810
 Si:O, diffusivity and solubility of O review 7-16809
 Si:O, enhanced diffusion at thermal donor formation temp. 7-44911
 Si:O, O precipitation, numerical models 7-16775
 Si:O, precipitation kinetics, interstitial diffusion 7-44837
 Si:O, self-interstitial migration, dislocation loops and elongated Frank dipoles 7-58300
 Si:O, vacancy-enhanced O diffusion 7-16811
 Si:O,C, intrinsic point defects and impurity interactions 7-16611
 Si:O/Si interfaces, MBE grown, O trapping effects 7-16881
 Si:P, heavily implanted, influence of precipitation on P diffusivity 7-6879
 Si:P, Ni⁺, ion implantation and annealing 7-21245
 Si:P, surface conc. manipulation for P diffusion using ambient control 7-6660
 Si:P, transient enhanced dopant diffusion 7-52136

diffusion in solids continued

- Si:P MOS source/drain struts., 2D P diffusion props. 7-32718
 Si:P solar cells, effects of P pre-diffusion on properties 7-3677
 Si:P solar cells, shallow junction formation by light-induced diffusion from spin-on source 7-8418
 Si:P thin films, surface energy-driven grain growth during rapid thermal annealing 7-63994
 Si:P/Ti, enhanced grain growth by silicide form. 7-27142
 Si:P(B), tail diffusion model 7-16815
 Si:Pt, deep levels and diffusion profiles 7-58767
 Si:S(Ti)(Ge)(P)/Pt system, impurity migration during silicide form. 7-6895
 Si:Sb, dry oxidation retarded impurity diffusion, SIMS meas. and numerical simulations 7-27014
 Si:transition metals, anomalous diffusion and gettering 7-2264
 a-Si/Au thin film bilayers, Si crystallisation study 7-21699
 Si/Ge amorphous multilayer films, interdiffusion, neutron scatt. meas. 7-32722
 Si/Ni system, silicide formation, ion beam induced, embedded markers and moving species 7-21298
 Si-Al structures, ion mixing, effect of interfacial oxide 7-21537
 Si-Au-Pt interfaces, PtSi formation, RBS studies 7-58547
 Si-binary alloy interfacial interactions, Rutherford backscattering spectrometry, TEM 7-12505
 Si-Co₅₀Mo₅₀-Au, amorphous Co₅₀Ta₅₀ alloys as diffusion barriers 7-44923
 Si-Co₅₀Ta₅₀-Al, amorphous Co₅₀Ta₅₀ alloys as diffusion barriers 7-44923
 Si-Co(Pt)(Au), high energy density pulsed ion beam irradiation, study of reacted layers 7-52151
 Si-Ge interface, solid phase epitaxy, intermixing, EXAFS, AES, LEED obs. 7-63973
 a-Si-Ge multilayer films, interdiffusion, modulation wavelength depend. 7-27033
 Si-M (M=In, Te, Re, Bi), metal implantation using pulsed electron beam 7-6882
 Si-P, dopant redistribution during high pressure oxidation, four-point probe meas. 7-27020
 Si-Pd, Pd₂Si formation, TEM study 7-38267
 Si-Pt, Pt₂Si formation, TEM study 7-38267
 Si-Si interfaces, MBE grown, sputter cleaned, microstructure, electron microscopy obs. 7-12512
 Si-Si surfaces, direct bonding, silanol group reactions and O diffusion mechanisms 7-21791
 Si-SiO₂ system, H₂ diffusion 7-21531
 Si-SiO₂-Ag(Cu)(Au)(Pd)(Ti) MOS structures, diffusion coeff. meas. in elec. fields, solid solubilities 7-2279
 Si-Ti interface, laser irradiated, silicide formation 7-45079
 Si-W, buried conductor formation, low press. CVD W deposition on porous Si 7-32877
 a-SiC:H,B, effective p⁺ doping by plasma-assisted B diffusion 7-38036
 SiO₂, diffusion of F, consts. and profiles meas. 7-58540
 SiO₂, dopant diffusion under thermal nitridation conditions 7-32716
 SiO₂ films, thermal growth kinetics 7-13663
 SiO₂, γ-ray induced defect centres, thermal bleaching 7-63659
 SiO₂, nitridation treatments, review 7-17747
 SiO₂-B, diffusion investig., H₂ annealing atmosphere effects 7-6876
 SiO₂(B/P), thermally grown, diffusion of ion-implanted dopants 7-38041
 SiO₂-F, P fibres, dopant materials behaviour in MCVD process 7-20462
 SiO₂-Sb, ion-implanted, diffusion 7-58542
 SiO₂-B₂O₃-K₂O-Na₂O-Al₂O₃-TiO₂-ZnO:Ti⁴⁺, diffusion 7-27022
 SiO₂-Na₂O-CaO-MgO glass, reaction in isotopically labeled water, D₂¹⁸O 7-26993
 SiO₂, corrosion protective coatings on Ni-Cr Inconel alloy 7-39754
 SiO₂N₃ films, PECVD deposited, props. as selective diffusion barrier 7-2440
 SiO₂N₃, plasma-enhanced CVD films as selective Zn diffusion barriers 7-12539
 Sm-Si Schottky barriers, elec. and struct. charact., 7-38675
 Sn-Ge interface form., growth mode, AES, RBS studies 7-58666
 SrTiO₃ single cryst., H defect diffusion 7-58545
 Ta, diffusion of H, internal friction 100-400K (Chinese) 7-6872
 Ta, electron irradi., transverse muon-spin relax. functions 7-53197
 Ta, pion-decay channelling, high and low temps. 7-45866
 Ta:H(D)(T), heat of transport, isotope and temp. depend. 7-27024
 Ta/W diffusion couples, analytical electron microscopy 7-39946
 Ta-Cu, multilayer systems, temp. depend. of ion beam mixing, 77-book (Chinese) 7-51884
 Ta-H system, electron irradi., vacancy recovery, positron lifetime studies 7-37972
 Ta-H system, T migration in Hall field, effect of temp. 7-6890
 Ta-Nb bimetal, accelerated mutual diffusion during thermal cycling (Russian) 7-44926
 TaCu_{1-x} amorphous thin-film diffusion barriers on GaAs, thermal and structural stabilities 7-52321
 TaSi₂ film form. by scanning electron beam annealing 7-21285
 TaSi₂-Si interface, ion implanted, dopant diffusion, SIMS anal. 7-38271
 TbCo sputtered films, mag. and magneto-optic props., stability 7-53076
 TbFeCo/dielectric interface, chemical stability, interdiffusion and oxidation, AES, XPS and RBS depth profile study 7-12513
 Th-Mo(Zr)(Re)(W), diffusion and electrotransport of transition metals in BCC Th 7-63888
 ThO₂-UO₂, polycryst., lattice and grain boundary diffusion 7-58519
 β-Ti alloys, metastable, effective H permeability 7-44918
 α-Ti, commercial purity, oxidation 7-17717
 α-Ti, mutual interactions of O and H during heat treatment, diffusion coeffs. meas. 7-39549
 Ti, nitriding in rarefied activated nitrogen 7-8181
 Ti thin films, dissolution and diffusion of O, resist., X-ray diffr., particle backscatt. and AES studies 7-58913
 α-Ti:Si, ion implanted, diffusion profiles, annealing behaviour 7-12369
 Ti/Si (111) interface, diffusion and silicide form. kinetics, XPS meas. 7-52308
 Ti/Si(B,As,Sb) interface, dopant redistrib. during silicide form. by rapid thermal processing 7-63641
 Ti-Al-V-Mo-Cr alloy, VT23, gas impregnation influence in heat treatment, rapid heating effect 7-17696
 Ti-Cu-Ti thin films, reaction kinetics, stress, and microstruct. 7-21764
 Ti-Si, native contamination layer effect on interface props. 7-17104
 Ti-Si, Schottky barrier heights, 175 to 295K, silicide form. 7-38679
 Ti-Si interface, nucleation and growth of TiSi₂, influence of O₂ 7-21541

diffusion in solids continued

- Ti-Si interface, self-aligned Ti silicide formed by rapid thermal annealing, RBS study 7-2391
 Ti-SiO₂-TiSi₂-Si, high temp. reaction between Ti and SiO₂, XPS, sputtering (Japanese) 7-7022
 Ti-TiN bilayers, diffusion barrier props. for low resistivity contacts, comparison with Zr-ZrN 7-38726
 TiC, CVD coating on cemented carbides, diffusion of Co and W, TEM/AES study 7-27942
 TiC-coated cemented carbide cutting tools, role of interface development during CVD 7-53930
 TiFe, oxidised, bulk and surface phase composition 7-46700
 TiH_x, sites and diffusion for muons and H 7-45867
 Ti₂Mo₂C₂-TiO₂-C black mixture, complex carbide interactions on heat treatment, homogenisation 7-53684
 TiN films as diffusion barriers in high temp. metallisation (Japanese) 7-46319
 TiN_{0.1}-TiSi₂, bilayer, formation by rapid thermal anneal in N₂ 7-21547
 TiSi₂ films on polysilicon, elec. resist., implications for low temp. appls. 7-58907
 TiSi₂ formation kinetics on Si (100) and Si (111) 7-38273
 TiSi₂(B(P)(As) films on Si, impurity diffusion 7-7077
 Ti_{1-x}W_x-Si, Schottky barrier heights, 175 to 295K, silicide form. 7-38679
 TiNO₃-glass, ion-exchange diffusion, planar waveguides fabrication 7-11108
 U/Nb diffusion couples, analytical electron microscopy 7-39946
 V/Si, silicide formation, comparison of SiO₂ and a-Si surface protection layers 7-58662
 V-Al system, diffusion markers in thin film VAl₃ formation 7-58549
 V-C alloy, thermotransport of C 7-46479
 V-Ge(111) interface, temp. depend. intermixing, core level photoemission study 7-21542
 VD_x, H distrib. and diffusion near impurities, Mossbauer and PAC obs 7-33314
 VH_x, H distrib. and diffusion near impurities, Mossbauer and PAC obs 7-33314
 V₂Si, muon diffusion and localisation, transverse field muon spin resonance studies 7-53194
 W CVD films, nucleation on insulators and surface reaction with Si 7-16911
 W CVD films on Si substrate, growth kinetics and elec. props. 7-16909
 W films by selective LPCVD, struct. charact., diffusion barrier appls. 7-17468
 W films CVD on Si by Si reduction of WF₆, effect of substrate dopants and crystal perfection 7-22576
 W LPCVD films by WF₆/Si reduction method, influence of deposition variables 7-17461
 W, pion-decay channelling, high and low temps. 7-45866
 W selective CVD films, diffusion barrier props. 7-52155
 W selective LPCVD films on Si substrate, charact. 7-38409
 W, thermodynamic stability in a fusion reactor environment, H, O and C implantation and diffusion 7-49658
 W-Ag pseud alloys, Ni and Co effect on interphase interaction 7-27975
 W-Cu, multilayer systems, temp. depend. of ion beam mixing, 77-book (Chinese) 7-51884
 W-GaAs diode system, Schottky barrier degradation after high temp. annealing 7-33089
 W-Si, sputter deposition on Si (100), rapid thermal annealing 7-21548
 W-Si amorphous thin films, interfacial reactions with polycryst. metal overlayers 7-21763
 W-Si interface, thermal behaviour rel. to silicide form. 7-16822
 W-Si interfaces, microstruct. charact. 7-16882
 W-Si system, selective deposition of W films on Si wafers, WSi₂ formation 7-21748
 W-Si system, silicidation reaction suppression up to 1100°C 7-16821
 W-Ti-Si interface, WSi₂ form. by rapid thermal annealing, growth kinetics, Ti film effects 7-63969
 W-Zr amorphous films as diffusion barriers between Al and Si 7-21504
 WC-Ni hard metal parts, sintered, local alloying 7-27997
 WSi₂, silicide formation by rapid thermal annealing, Raman scatt. study 7-59193
 WSi₂-TiSi₂, bilayer, on Si, rapid thermal annealing 7-21549
 WSi₂-GaAs interface, thermal stability 7-52302
 YIG:H, ion implanted, elastic recoil analysis using 44 MeV Cl ions 7-12107
 ZnS/ZnSe, multilayer structures, MOCVD, wide band gap, interdiffusion charact. 7-53610
 ZnSe:Al(Ca)(In), impurity diffusion coefficients, cathodoluminesc. study 7-27017
 ZnTe:Cu, impurity related neutral complex with bound exciton, photoluminescence, absorpt., Zeeman meas. 7-45165
 Zr cathode, material and structural changes during arc operation in N₂ 7-46866
 Zr-Co (2 at.%), Co fast diffusion, quasielastic neutron scatt. study 7-63883
 Zr-H system, T migration in Hall field, effect of temp. 7-6890
 Zr-ZrN bilayers, diffusion barrier props. for low resistivity contacts, comparison with Ti-TiN 7-38726
 ZrO₂-YO_{1.5}, thermal behaviour of ⁵⁶Fe implantations 7-27006
 ZrTi, ZrTi_{1.6}, ageing, TEM study 7-51773

diffusion pumps

- optical coating deposition, pump requirements 7-33570

diffusivity see diffusion

diffusivity, thermal see thermal diffusivity

digital-analogue conversion

- see also analogue-digital conversion
 bioacoustic, digital signal acquisition, analysis and synthesis, microcomputer based system, PAL 7-54817
 NMR spectrometer, computer control of magnetic field homogeneity 7-48795

digital arithmetic

- see also adders; counting circuits; dividing circuits
 linear analogue optical systems, digital multiplication by analogue convolution algorithm 7-10862
 optical adder based on spatial filtering 7-11099
 optical binary coded ternary arithmetic and logic 7-10863
 optical computing, medium accuracy, highly redundant number representation 7-10864

digital arithmetic continued

- optical matrix-matrix multiplier based on Kronecker product decomposition 7-57248
- optical single-instruction multiple-data array architectures for digital optical computing 7-42941
- symbolic substitution logic for digital optical computing 7-10859

digital audio discs *see video and audio discs***digital communication systems**

- atmospheric transmission losses use for interference resistant communications 7-34585
- eLF/VLF/LF propagation and system design 7-40642
- fiber-optic inverter repeater to cancel distortion 7-15993
- HF groundwave and skywave propagation 7-40643
- limits of dispersive optical fibre transmission for chirped pulses 7-31476
- optical fibre chromatic dispersion measurements and related system power penalties 7-43415
- weather pictures from space using Meteosat (*German*) 7-23970

digital control

- see also direct digital control*
- circular traveling wave motor, speed control characts. and digital servosystem 7-35511
- controller for magnetic suspension system 7-333
- magnetic suspension systems with digital controllers 7-332
- MOS device, microcomputer-based instrumentation system for carrier transport study 7-64350
- paralysed limbs, joint angle control by using functional electrical stimulation with digital PID control system (*Japanese*) 7-60128
- power supplies to magneto-optical elements of particle channels, digital remote control system 7-42268
- strained radiotelescope reflectors, phase distortions compensation, automatic control 7-60541
- TRR power regulating system, digital controller 7-49575

digital filters

- see also signal processing*
- acoustical communication in animals, digital signal processing 7-50854
- chest radiography using patient-specific digitally-prepared compensating filters 7-47250
- digital filter for electron instrumentation 7-47034
- ECG baseline wander reduction using linear phase filters 7-18086
- EELS data analysis, digital filters use and limitations 7-18944
- effect of digital lowpass filters on the maximum velocity of saccadic eye movements 7-13996
- finite impulse response digital filters, appl. to brainstem evoked pots. 7-23491
- FIR digital filter, hearing impaired subjects, speech discrimination assessment 7-37274
- Fourier transform spectrometer, Los Alamos design with microprocessor control 7-48860
- generalized median filters for biological signal processing 7-8785
- geosound signal detection, appl. of adaptive dig. filtering (*Chinese*) 7-20508
- hearing aids, prescription technique comparison using computerised filter adjustment for aid simulation 7-34163
- inverse digital filtering of radiographic pictures, tomographic props. 7-9930
- lattice filtering applications to earthquake observation 7-9248
- linear-phase FIR filters for ECG processing 7-34309
- nonlinear, for separating nonstationary and stationary EEG waves 7-47267
- room acoustics, inverse control using multiple loudspeakers and/or microphones 7-37252
- smoothing method for Earth tides obs. data (*Chinese*) 7-55271
- solar collector performance transient testing using digital filter 7-65582
- spline time varying digital filter, ventricular blood pressure meas. appl. 7-47268
- stochastic sound system, digital filter design for state estimation 7-6056

digital instrumentation

- see also digital readout; digital voltmeters*
- bridge for AC/DC transfer instruments comparison 7-18835
- contactless IR thermometer principle and digital operation (*Japanese*) 7-56266
- electronic hygrometer, cct. (*Spanish*) 7-34744
- IETS, digital and high resolution meas. (*Chinese*) 7-61402
- ions activity meas. 7-3614
- magnetic recorders, raising recording density 7-41365
- mass spectrum extremes meas., automatic digital recording system 7-30109
- microscopy for cellular/subcellular features identification 7-54821
- multichannel digital temperature meter using transistor sensor, design for medical appls. (*Spanish*) 7-30010
- multimeter sophistication and new applications 7-18771
- photometer, portable, digital display, for recording irradiance from near UV to near IR 7-61366
- portable temp. measuring instruments (*German*) 7-18776
- precision digital manometer, Model 2661, based on compound timing-fork pressure sensor (*Japanese*) 7-48719
- quartz temperature sensing device, output nonlinearity correction 7-41380
- radiation meter with counter tube or p-i-n-diode detector, design (*German*) 7-30900
- radiographic digital imaging systems comparison: dedicated vs. add on 7-47237
- rectangular measuring signals, digital evaluation (*German*) 7-24636
- reverberation time meter 7-20506
- solar collector, flat-plate type electronic, heat transfer coeff. digital meter 7-23220
- Tektronix 11000 Series of digitizing and analogue CROs 7-61324
- tunnelling spectrometer using IEEE-48 instrument bus and IBM PC-XT controller 7-56383
- X-ray image sensors based on optical time-delay-and-integration CCD imager 7-24753

digital instruments *see digital instrumentation***digital integrated circuits**

- see also cellular arrays; integrated logic circuits; microprocessor chips*
- FFT spectrum analyzer possessing high speed operation characts. 7-47710

digital modulation *see pulse modulation***digital radiography** *see radiography***digital radiography (medical)** *see diagnostic radiography***digital readout**

- see also digital instrumentation*
- photometer, portable, digital display, for recording irradiance from near UV to near IR 7-61366
- SGS digital strip readout electronics for streamer tubes 7-62238
- temperature indicator, low cost, with Chromel-Alumel thermocouple 7-14942

digital signal processing *see computerised signal processing; signal processing***digital signals**

- film digitisation, low cost solutions implementation 7-18893
- rectangular measuring signals, digital evaluation (*German*) 7-24636
- underground object imaging system with computerized reconstruction 7-47580

digital simulation

- see also circuit analysis computing; virtual machines*
- 7-22742
- 1D chain with random distribution of linear side branches and loops, electronic props. 7-64191
- 4-cylinder internal combustion engine, 2D intake manifold flow digital simulation 7-63170
- acceleration-dependent fluid forces 7-31907
- acid rain modelling, turbulent spiral boundary layer and thermal wind simulator 7-14370
- action potential propag. in septated nerve fibres, computerised numerical simulation 7-59960
- adaptive control of a solar central receiver: modelling and simulation 7-59877
- adsorption, random, sequential, on to surface of small spheres 7-44994
- adsorption dynamics, exchange reactions and defect form. at solid surfaces, computer simulations 7-32823
- advanced boiling water reactor core supervision and analysis using 3D-core simulator 7-61993
- aggregation, efficient algorithm for Brownian dynamics simulation 7-48552
- air pollution, CPU-time reduction for IFDM computer model 7-54399
- air pollution, Monte Carlo simulation of plume dispersion in turbulence 7-54396
- air pollution, plume rise and dispersion, Salford software model 7-54398
- air pollution chemistry, computer simulation 7-54393
- air pollution in Kuwait, modelling of Shuaiba Industrial Area 7-54400
- air pollution modelling, num. method and computer simulation 7-54394
- air pollution screening model, development of MICROGAUSS-I 7-54401
- air quality simulation models, computerized system for evaluation 7-54409
- air quality simulations, nonGaussian climatological model 7-55243
- alkali metal ions in inert gases, energy distribts. 7-20839
- alloy, solidification, differential thermal anal., modelling (*French*) 7-65024
- alloys, preferential sputtering, segregation, mixing and diffusion 7-59337
- alveolar flooding: a computer simulation 7-23379
- amorphous Lennard-Jones solid, shear deform.-induced orientational ordering, computer simulation 7-38155
- approximate dense liq. struct. theories, comparison using force correl. function 7-63420
- atmosphere sulphur deposition, spreadsheet-based model 7-54397
- atomic collision cascade mol. dynamics computer simulations in insulators 7-26793
- atomic solids, mol. dynamics simulation 7-51673
- atomic structure models, electron microscope images, computer simulation 7-16380
- batteries, Ni-Cd, Goddard model for aerospace appls., alterations using computer simulation 7-34017
- benzonitrile-Ar(Kr)(N₂O)(H₂O)(trifluoromethane) van der Waals complexes, LIF spectra 7-50222
- binary liquid mixtures, heat and mass transport 7-1559
- biomechanics models in manual work design 7-40209
- bioprosthetic heart valves, computer simulations of closing sounds 7-34343
- bipolaron formation, Monte Carlo computer simulation studies 7-27268
- Bloch line and Bloch wall dynamics, computer simulation using lumped-constant model 7-59090
- Bloch wall motion simulation 7-59049
- bond graph analysis of automatic guided vehicle dynamics 7-61096
- bounded plasma-electron beam system, nonlinear interaction, instability and oscills. (*Russian*) 7-58029
- BWR nuclear power plant simulation 7-49530
- carbon tetrachloride, liq. rot. and translation, mol. dynamics simulation 7-2240
- cardiac arrhythmia haemodynamics, simulation with a real-time computer model 7-3826
- cardiac rhythms and arrhythmias: a teaching program 7-48247
- cardiac tissue, anisotropic, electronic interactions 7-13989
- channel flow, rectangular turbulent promoters, computer generation 7-37549
- chromatography, computer simulation of physico-chemical stochastic processes 7-65379
- chromophore distrib. in solid determ. using impulse-response photoacoustic spectroscopy 7-51948
- clonogenic capacity of irradiated cells, factors influencing, computer simulation study (*Russian*) 7-14061
- combustion research, reaction rate constants computing, using Harris Super minicomputer 7-33912
- compensated electron flows, propag. in finite system, numerical simulation (*Russian*) 7-20125
- composite RF pulses, num. design for NMR spectroscopy appl. 7-24676
- conjugated systems, computer reaction simulation, hybrid model 7-49874
- coronary arteries microembolisation, computer simulation of hyperemic flow 7-18007
- cut model reconstructed from a three-dimensional data represented by Miller-Bravais indices and a simulation of Hirano bodies 7-6572
- detached flow around profiles with ang. points, computer modelling 7-43924
- developing simplified models of combustion chemistry by simulation with detailed chemical kinetics models 7-13779
- diamond, tilt boundary struct., computer modelling 7-16579

digital simulation continued

diesel engine with exhaust heat recovery, combustion chamber insulation effect 7-65599
diffusion-limited aggregation, anisotropic sticking probability on 2D square lattice, computer simulation 7-24590
dipolar fluids computer simulation, perturbation approach 7-10700
discrete Radon transform in a continuous space 7-56235
dislocation loops, small hexagonal, diffraction contrast images and lattice fringe patterns, computer simulation 7-44325
displacement in two phase flow in porous media, finite element simulation 7-51295
DNA-ligand interactions, groove binding, computer simulations 7-54447
drainage network simulation 7-55088
dye lasers, two-mode, first-passage-time problems 7-1097
electrolyte solutions, ionic props., mol. dynamics simulation 7-44331
electrostatic electron-beam deflectors, comparison of electron optics 7-18910
energy resources in energy crisis (*Japanese*) 7-23118
equipartition times among translational and vibr. degrees of freedom, exponential law 7-61213
explosive consolidation of powders into rods, computer simulations 7-64955
external counterpulsation in the presence of arrhythmias, computer simulation anal. 7-14156
fatigue crack propagation computer simulation (*Japanese*) 7-14772
FCC bicrystals, computer simulation of non-uniform multiple slip (*Japanese*) 7-51780
FCC crystal, vacancy jumps, self-correls., MD simulation 7-2015
feedback-stabilised actively mode-locked laser 7-25831
ferromagnets, static surface critical behaviour, scaling and renormalisation, book contrib. 7-33183
films, grain growth phenomena and microstructural evolution during deposition, Monte Carlo simulation 7-52336
films, grain structures and grain growth 7-16903
films grown from a partly ionised molecular beam, computer simulation of structure 7-7060
flat-plate and trough concentrators, transient models comparison 7-65412
floating zone imaging furnace, molten zone temp. distrib., calc. method 7-17416
flow, large-range, calibration by changeable water level system with computer simulation 7-37592
flow meas., hot-wire procedures and appraisal through simulation 7-44078
fluid in pore, phase behaviour modelling 7-2141
fluid-wall interface, wetting, computer simulation and statistical sum rules 7-32753
fusion physics, simulations 7-5307
fusion reactor T-cycle process modelling 7-62082
garnet film, strip domain stretching, computer simulation 7-59083
gas boilers, seasonal efficiency simulation and energy quality 7-65593
glass, low temp. sp. ht. calcs. 7-44846
glasses, tilting model, relax. behaviour, Monte Carlo simulation 7-44816
glycoprotein, proline-rich, from human parotid saliva, NMR and computer-simulated struct. anal. 7-59922
gradient time-shape measurement by NMR 7-14985
graphite basal plane, adsorbed N₂, computer simulation 7-52297
graphite surface, adsorbed Kr incommensurate phase, computer simulation studies 7-7009
groundwater flow, transport velocity representation, environmental apps. 7-55114
Group VB metal-H solid solutions, thermodynamic props., Monte Carlo calcs. 7-21487
heart's pathological sinus mode modelled by system of interconnected pacemaker cells 7-54518
heavy gas atoms, particle behaviour simulation 7-9749
Henon mapping with Pascal, dynamic systems simulation 7-34836
high energy ion scatt., struct. anal. of surfaces and interfaces 7-22410
hole distribution in Eden clusters, computer simulation 7-35450
ice floes, interacting around an obstacle, simulation methodology 7-55081
imaging bandpass electron energy analyser 7-375
incident control, simulation of man machine interaction 7-15287
inert gases, liquefied, inherent structure, thermal disruption, mol. dynamics computer simulation 7-26612
inherent viscoelasticity, simulation and soln. of dynamic problems (*Russian*) 7-29756
interaction-induced dipoles in dense media, translational correl. function 7-44335
interface and surface struct. characterization, ion scatt. and channelling, scanning tunnelling microscopy and computer simulation (*Japanese*) 7-7803
interfacial melting, 2D model, computer simulation 7-58448
ion backscattering from solids at oblique and grazing incidence, analytical calcs. and computer simulation 7-53466
ionic crystals, grain boundaries, review 7-6632
ions implanted into single crystals, depth distributions 7-6667
irradiated metals, isochronal annealing PAC monitored defect reactions anal. 7-44623
Ising model, simulation using microcanonical algorithm 7-29932
Jupiter, physical and visual simulation 7-34910
lake pollution, computer assessment of eutrophication countermeasures 7-55112
lakes and oceans, 1D models of thermal stratification 7-55076
laser-induced desorption from surfaces, nonequilib. infrequent events, mol. dynamics 7-38322
lattice gas model, Monte Carlo study of propagating fronts 7-48615
lattice models, parallel computations in physics 7-48593
layered solid, marker evolution on ion irradi., computer simulation 7-21302
left ventricle, ²⁰¹Tl perfusion imaging simulated by a dynamic model 7-34267
Lennard-Jones fluid, 2D, virial eqn. of state 7-6747
Lennard-Jones fluid mixtures, infinite-dilution activity coeffs., computer simulation 7-16383
light charged particles, equilibrium behaviour 7-9750
liquid crystals, hard-core models, computer simulation 7-58468
liquid-liquid dispersions, time- and event-driven Monte Carlo calcs. 7-54193
liquids, Lennard-Jones, wavevector-depend. shear viscosity 7-58518
LPCVD, film thickness distrib., 3D computer simulation 7-17451
Lyman-alpha profiles, ion dynamics effects, computer simulated study 7-10470

digital simulation continued

magnetic domain wall motion, computer simulation 7-53099
magnetic hysteresis, digital simulation, simplified 7-64489
manual materials handling task design using computerised biomechanical modelling 7-14040
Markov chain algorithms for canonical ensemble simulation 7-48520
martensitic transformations, 2D magnetic-analogue model 7-26905
material analysis, computer-based, conf., Boston, MA, USA (Dec. 1985) 7-14709
metals, grain boundary structure (*German*) 7-44571
metals, HCP, computer simulation of twin boundaries 7-38014
microprocessor based respirator digital simulation 7-14154
microwave reflectometry, frequency-domain, image reconstruction, parameter identification, simulation tools appl. 7-65834
molecular crystals, triplet exciton diffusion and capture, Monte Carlo modelling 7-12620
molecular design, computer-aided, conf., London, England (Oct. 1986) 7-50429
molecular solids, mol. dynamics simulation 7-51673
monatomic systems, liq. and dilute gas, thermodynamics and transport props., MSK pot. calcs. 7-6826
monolayer post-deposition cluster growth, nearest-neighbour model, computer simulation 7-58621
Monte Carlo simulations, autocorrels. and subservices average 7-41234
moving bodies, method for computing flow fields 7-65789
multi-level SOI recrystallization using a novel seed structure 7-53778
multilattice microcanonical simulation algorithm, 2D Ising model calcs. 7-24597
multiparticle diffusion, fractal kinetics 7-24604
multipolar lattice sums convergence and dielectric props., computer simulation 7-59163
multivane expander simulation, design and operation optimisation 7-3713
musculotendon actuator models for neuromuscular stimulation system CAD 7-28573
neural networks, computer simulation for perceptual psychology 7-60007
NMR, 2-dimens., simulation by numerical density matrix calcs. 7-35550
NMR imaging computer simulation, implementation and preliminary results 7-23430
NMR multipulse experiments, BOWMAN simulation program 7-35552
NMR spectra, two-dimensional, simulation 7-35544
NMR spectrometer, solid-state, tomographic expts. 7-30052
NMR spectroscopy, numerical treatment of models arising 7-14928
nonequilibrium processes, computer simulation 7-18688
nonideal fluid mixtures, phase diagrams, Monte Carlo calcs. 7-51989
nuclear power plant availability impact of limiting conditions for operation 7-10272
nuclear power station simulation, parallel-processing modular system 7-10197
numerical study of swirling flow field in a vortex device 7-20682
ocean wave modeling 7-34502
Olympic main coliseum, acoustic simulation (*Japanese*) 7-62915
one-dimensional degenerate Hubbard model, Monte Carlo simulations 7-45609
optical system design, 3D simulator appl. 7-62814
oxides, defect behaviour, computer-based atomistic simulation studies 7-16548
paramagnetic-ferromagnetic transitions, fluid system, internal quantum states, computer simulation 7-45678
Particle Beam Fusion Accelerator II (PBFA II), energy transport meas. and computer simulation 7-30764
particle physics experiments, design and simulation system 7-49194
phase diagrams, thermodynamic formalism, computer calcs. 7-3269
photodetection process in optical range finding 7-41467
photoelectron statistics effects on Thomson scattering meas. 7-11800
photophysical imaging processes, simulation algorithms 7-61398
photovoltaic array performance and life-cycle cost simulation 7-17913
photovoltaic cells, photoacoustic signal, computer simulation 7-43588
photovoltaic module fabrication and testing for bulk electric power production 7-23169
plasma dynamics, simulation using many particles 7-37736
pneumatic portable artificial heart drive system, design based on efficiency anal. 7-65893
polyacetylene, alkali metal doped, role of spin-orbit coupling in EPR spectra 7-64527
1,4-polybutadienes, thermodynamic flexibility, continuum model (*Russian*) 7-10802
polymerisation kinetics, simulation 7-54122
polypropylenes, thermodynamic flexibility, continuum model (*Russian*) 7-10802
polyunsaturated hydrocarbon chains, natural, temp. dependence of conformational characts. 7-28453
positronium, formation and inhibition in cyclohexane, model calcs. 7-17812
powder compact recovery fixtures, shock-induced temperature distributions 7-39454
precipitation hardening, creep and reverse mechanical aftereffect processes (*Russian*) 7-3317
pressure sintering, computer simulation using finite element anal. 7-3214
programmable simulator of photovoltaic generators 7-28404
projectile fragmentation, Monte Carlo simulations of anomalous expts. 7-614
proteins, conformational change mechanisms 7-54457
proteins in membranes, powder samples, label positions, determ. by neutron and anomalous X-ray diffr. 7-3755
proton beam deflection by bent Si cryst. 7-44632
quasicrystal equilb. state of two-component 2D Lennard-Jones system, Monte Carlo simulations 7-58148
quaternary gas diffusion between alveolar and blood compartments, simulation 7-54508
radiation damage and defects, computer simulation studies 7-2048
radiation-induced late effects, computer simulation by system dynamics 7-18024
radiographic screen-film images simulation 7-23442
radionuclide spills and discharge plumes, Lake Ontario, microcomputer-based model 7-13942
random magnetic materials, numerical simulations with a special purpose computer 7-17182
ring polymers, equilb. statistics and dynamics 7-25692
SAF: a sophisticated engineering simulator mainly devoted to emergency guidelines testing and crisis situation analysis 7-62056
sapphire, growing crystals, hot zone heat transfer simulation 7-32321

digital simulation continued

- seismic holography, computer simulation 7-18124
semiconductor lasers field spectra computing asymmetry due to noise obs. (Japanese) 7-15862
semiconductors, deep trap profiles determ. 7-58768
semiconductors, solid-phase epitaxial regrowth, amorphous-crystalline interface evolution 7-12568
semiflexible polymers, collapse transition, Monte Carlo simulation 7-10785
semiquinone cation radical, immobilised, EPR spectral simulation calcs. 7-50200
serrated yielding, computer simulation using negative resist. characts. 7-2089
shock waves, simulation in 3D 7-6247
simulation studies of tidal analysis using meteor echo returns 7-40623
soft-sphere crystal, shear flow, nonequilib. mol. dynamics calcs. 7-1526
soft-sphere fluid, shear flow, nonequilib. mol. dynamics calcs. 7-1526
SOI large area growth, pseudo-line electron beam technique with lateral seeded epitaxy (Japanese) 7-7842
solar cell array electrical output for flat plate tracking arrays 7-3690
solar cell array performance computer simulation models 7-54320
solar cell photoacoustic measurements, computer simulation 7-8422
solar pond simulation using upward flow through storage zone 7-65604
solar-heated farm buildings, short-term monitoring and computer aided performance 7-28413
solid, elastic wave propag., computer simulation of US 7-33890
solid bodies, motion in atmosphere, numerical study (Russian) 7-63172
solid state materials, computer modelling 7-51676
solid/melt interfaces, cryst. growth, computer simulation studies 7-16469
solids, sputtering and atomic collisions, computer simulations 7-59323
sonar system simulation design technique (Chinese) 7-11219
Space Station solar dynamic power system, simulation 7-65494
spin glasses, replica Monte Carlo simulation 7-45713
sputter induced surface topography, computer simulation 7-64867
sputtering, conference, Spitz an der Donau, Austria (June 1986) 7-55880
sputtering, energy distribts., Monte Carlo program calcs. 7-59324
SQUID, DC, noise effect on instabilities and chaotic solns. 7-52908
SQUID, DC, noise effect on instabilities and chaotic solns. 7-52909
stacking faults, X-ray diff. contrast images, computer simulation developments 7-1809
statistical mechanics systems, transputer array simulation 7-48519
steel, stainless, high velocity shock impact, numerical simulation of sample recovery fixture 7-38120
Stirling cycle simulation, globally-implicit finite-difference method 7-65553
strained radiotelescope reflectors, phase distortions compensation, automatic control 7-60541
supersonic flow interaction between moving bodies, moving grid FEM 7-26314
synthetic discriminant function filters, computer-generated and phase-only 7-20392
ternary electrolyte systems, diffusion pot. in simple porous membranes 7-54170
test simulator for computer controlled tensile tests (French) 7-33701
tetrachloromethane, induction spectra, mol. dynamics simulation 7-1830
thermal energy storage system performance, impact of operation and control, DOE2 simulation 7-65621
thin diaphragm capacitive pressure sensor simulator 7-61328
thiourea, paraelectric phase, mol. dynamics simulation 7-37920
tip shape evolution, capillarity induced matter transport by surface diffusion 7-58592
Topographic Air Pollution Analysis System 7-54395
TRNSYS/GROCS simulation of horizontal coil ground coupled heat pump 7-8427
turbulent flowfield visualisation, computer generated, for flow around cubic model 7-37447
twist boundary structure and interatomic pots., computer modelling studies 7-16578
two-line spectrum, meas. by photon correl. and multichannel anal. techniques 7-24705
underwater acoustics, finite element analysis appl. (French) 7-11209
URFOR, urban-scale computer model for short-term prediction of air pollution (Polish) 7-66205
vertical Bloch line propag. under pot. well by cond. current 7-59088
vertical Bloch line propagation at multiple stripe domain heads 7-59089
Vuilleumier cycle heat pump for domestic appl., computer simulation 7-65554
water, liq., three-body forces and single-molecule dynamics 7-11880
water, quenched to low temp., glassy state, Monte Carlo simulation 7-26633
water, shock wave propag., free surface reflection effects, computer simulation studies 7-32540
water, structure, quantum effects, gamma-ray diff. obs. 7-26609
water resource planning, geographic information systems for encoding soil information 7-47473
watershed acidification, computer simulation 7-14322
WODA—a modelling support system for BOD-DO assessment in rivers 7-9041
Wolff-Parkinson-White preexcitation syndrome, computer simulation with a modified Miller-Geselowitz heart model 7-3765
X-ray diff. phase anal., calibration-free, Monte Carlo error simulation 7-1812
X-ray fluoresc., energy dispersive, 2-variable cumulative distrib. functions, cubic spline representation 7-23073
X-ray spectra, energy dispersive, Monte Carlo simulation of backscattered peaks 7-23070
Zircaloy-2, cold worked, irradi. growth, point defect trapping, computer simulation 7-16613
Al (100), polycryst., single cryst. and amorphous, ballistic collision cascade anisotropies 7-58379
Al (110), Ar⁺ sputtered, vacancy-type defect distribts., variable energy positrons study, mol. dynamics simulations 7-12429
Al (110), Ar-induced Auger electron emission, Doppler broadening 7-59345
Al, explosively launched expanding ring test, computer simulation and anal. 7-33878
Al polycrystalline target, sputtering by 40 keV Ar⁺ ions, computer simulation 7-64848
Ar, on graphite, fluid-solid monolayer transition, simulation 7-32796
Ar+methane (methane-d₄)(SiH₄)(tetrafluoromethane), energy transfer, simulation 7-15690
- digital simulation continued**
Au (110), 180° enhancement of ion backscatt. surface peak yield 7-3131
BeCl₂, aq. soln., mol. dynamics, X-ray diff. study 7-21075
Br₂, inelastic scatt. from graphite surface, Monte Carlo classical trajectory calcs. 7-27837
CdS anodic film growth, initial stages, voltammetry and computer simulation studies 7-28216
Cl⁻, limiting ionic cond. in aq. soln., mol. dynamics simulation 7-44879
Co single crystal foils, α - and β -phase, ion transmission and sputtering 7-59322
Cu polycrystalline target, sputtering by 40 keV Ar⁺ ions, computer simulation 7-64848
Cu, recrystallisation texture, deformation temp. effects (Russian) 7-8007
Cu surface, Cu atom sticking and penetration, computer simulation studies 7-59326
Cu surface, ion irradi., sputtering and lattice damage, cascade simulation 7-59327
Cu surface, low energy O⁺ ion bombardment, atom and mol. ejection 7-59325
Cu₃Pd, long-period superstructures 7-21430
 α -Fe, edge dislocation, zones of spontaneous absorpt. of point defects 7-44599
Fe, low energy ⁴He ion range and damage distribts. 7-63674
Fe:He(C), distribution and migration of interstitial impurities in the field of a screw dislocation core 7-6669
Ga liquid surface, In monolayer, sputtering, computer simulation studies 7-17387
GaAs Fresnel waveguide grating lenses, aberration corrected, simulation 7-26036
GaAs, ion implant depth profiles, channelling, Monte Carlo simulation 7-51811
GaAs, surface recombination velocity and bulk minority carrier lifetime 7-17037
GaAs-AlGaAs superlattice, lattice images, high contrast TEM obs. 7-7027
Ge, tilt boundary struct., computer modelling 7-16579
H atom, positron annihilation, computer expt. 7-36791
H, line number to line intensity, logarithmic relationship 7-49977
H₂O, dissoci. and ion pair form., rate consts., computer simulation 7-28294
He gas, positron mobility edge, Monte Carlo simulation 7-44086
He-H mixtures, positron annihilation, simulation 7-36792
³He, superfluid B-phase, sound wave pulse propag. in reson. medium 7-44940
InP, surface recombination velocity and bulk minority carrier lifetime 7-17037
Li_{0.5}Pb_{0.5} liq. mixture, fast sound computer simulation, Mori-Zwanzig formalism 7-44696
LiCl-KCl, molten mixture, eutectic, isotope self-exchange vels., simulation 7-57187
LiCl.3H₂O, soln., struct., mol. dynamics simulation 7-58127
MgO(Al₂O₃)₂ spinel, first-order twin boundaries struct., TEM obs. and computer simulation studies 7-51782
MgO(Al₂O₃)₂ spinel, lateral twin boundaries struct., electron microscopy obs. and computer simulation studies 7-51783
Mo, low energy ⁴He ion range and damage distribts. 7-63674
N₂, surface layer on graphite, motion investig. 7-32792
N₂ surface semichannelling on Cu target, computer simulation 7-63697
N₂O downstream mixing gasdynamic laser, numerical simulation 7-36940
N₂O, in liq. SF₆, rot. self-correl. functions, mol. dynamics simulation 7-44343
Na⁺, limiting ionic cond. in aq. soln., mol. dynamics simulation 7-44879
NaF-AlF₃ cryolite melt, struct., computer simulation (Chinese) 7-6494
Na₂O-B₂O₃-Al₂O₃ glass struct., NMR and computer simulation 7-1898
Ni {100}, adsorption of I, surface phases, SEXAFS, multishell simulation anal. 7-59303
Ni close packed polytypic struct., stacking order, mol. dynamics computer simulation studies 7-51691
Ni, dislocation-impurity C interstitial interaction, computer simulation studies 7-2046
Ni, nucleation and growth of He platelets, computer simulation 7-58269
Ni polycrystalline target, sputtering by 40 keV Ar⁺ ions, computer simulation 7-64848
Ni-Al-Cr based alloy plasma-sprayed thermal barrier coatings, sp. ht. and thermal cond. meas. and 2D computer simulation 7-7076
Ni₃Al, computer simulation of grain boundaries, effect of comp. 7-21228
Ni₆₄B₃₆ amorphous alloy, struct., boundary effects, computer simulation study (Chinese) 7-11920
Pb-Sn-Ag solder alloys, phase equilibria 7-46426
Pd-H, single particle dynamics, simulation model 7-27016
S₈, liq., chem. reactions, mol. dynamics simulation 7-39862
SO₂ pollution forecasting around thermal power stations 7-55244
Si, amorphous, p-n solar cells, light-induced defects influence on performance 7-17910
Si, dislocation loops, generated by ion implantation and furnace annealing, depth profiles, RBS, X-ray diff., TEM anal. 7-51882
Si, self-implantation-induced temp. depend. amorphisation, TEM and Monte Carlo simulation studies 7-16595
Si, single cryst. temp. distrib. during czochralski growth, computer modelling 7-17414
Si, tilt boundary struct., computer modelling 7-16579
Si:B, impurity transport in mag. Czochralski growth, computer simulation 7-58182
a-Si:B(P)(As), implanted ion distrib., lateral spreading, theoretical predictions and computer simulation 7-16604
Si:P MOS source/drain structs., 2D P diffusion props. 7-32718
Si-SiO₂ interface, computer simulation of high-resolution TEM images 7-44318
 β -SiC CVD film growth and props., gas phase comp. depend. simulation and meas. 7-22516
 β -SiC monocryst. thin films, ion implantation and annealing, amorphisation and recrystn. processes study 7-16596
SiO₂ thin films, constant current stressed voltage-time characts., dynamic trapping effects 7-45529
SiO₂:OH, X-irrad. induced defect centres, EPR obs. 7-45221
Ta₂O₅, preferential sputtering, collisional processes 7-59338
Ti, HCP, ⁴⁷Ti and ⁴⁹Ti NMR studies, spin-echo profiles 7-7599
VSi₂, sputter yield, computer simulation technique 7-33505
W (100), glancing elastic relativistic electron scatt., computer simulation 7-64835

digital simulation continued

- Zn, dislocation motion across two-component forest dislocations and point obstacles (*Russian*) 7-58277
 ZnO-SiO₂ amorphous system, structure, mol. dynamics computer simulation studies 7-21114
 ZnSe epitaxial films, twin boundaries, high resolution TEM obs. and computer simulation studies 7-51784
 ZrO₂-Y₂O₃ plasma-sprayed thermal barrier coatings, sp. ht. and thermal cond. meas. and 2D computer simulation 7-7076

digital simulation of computers *see virtual machines***digital storage**

- see also content-addressable storage; cryotrons; magnetic storage; optical storage; random-access storage; semiconductor storage*
 liquid-crystal polymers as dielectrically variable materials as storage media 7-51618
 scanning electron microscopy, online digital recording system 7-4933

digital voltmeters

- automated DC meas. at NPL, India 7-18842

digitisers *see analogue-digital conversion***digraphs** *see directed graphs***dilatometers** *see extensometers***dilute alloys**

- see also impurity electron states; Kondo effect; magnetic properties of dilute systems*

- Ag-¹¹¹In, O agglomeration in presence of radiation defects 7-26791
 electron scatt., many-impurity effects (*Russian*) 7-45305
 ferromagnetic, magnetisation and Curie temp. calcs., approximated Heisenberg model 7-7549
 low-temperature resistivity, transport eqn. 7-21898
 thin films of diluted ferromag. alloys, mag. contrib. to elec. resistivity 7-22036
 transition metal impurities in host metals, magnetic nature, superconductivity studies, review 7-7437
 Ag alloys, dil., EFG, asymmetry parameter calcs. 7-2545
 Ag-based dilute alloys, low temp. elec. resist. 7-52565
 Ag-Mn, nonlinear dynamic suscept. meas. at spin-glass transition 7-45694
 Ag-Tb(Tm) dilute alloys, magnetoelastic coupling coeff., 5d virtual found state effects calcs. 7-53108
 Al dilute alloys, deviation from Matthiessen's Rule, three group model 7-12601
 Al disordered alloys, vacancy form. energy, comp. and temp. depend. calcs. 7-37983
 Al-Cd single crystals, Cd-vacancy complex disassociation under ion irradiation 7-26741
 Al-Cu (2.5 wt.%), electrical resistivity, effect of precipitation 7-12697
 Al-Ge, dilute alloys, quenched, formation and growth of vacancy type clusters, positron annihilation study 7-39294
 Al-H, H-point defect interactions, extended Huckel mol. orbital calcs. 7-44533
 Al-Hf dilute quenched cold-worked alloys, vacancy migration recovery processes, PAC and positron annihilation studies 7-39545
 Al-Mg(Ca)(Zn)(Si)(Ge) dilute alloys, divacancy effect, annihilation radiation Doppler broadening meas. 7-37982
 Al-Si, dilute alloys, quenched, formation and growth of vacancy type clusters, positron annihilation study 7-39294
 Al-W/Ti(Ni) thin film reactions, W diffusion marker studies 7-2277
 Al-Zn dilute alloy, mixed dumbbells orientational ordering transition (*Russian*) 7-51688
 Al-Zn dilute alloys, stress-induced mixed dumbbell tunnelling, sound prop. meas. (*Russian*) 7-51674
 AlZn dilute alloys, electron irradiation induced interstitial defects, EXAFS study 7-63661
 Au alloys, dil., EFG, asymmetry parameter calcs. 7-2545
 Au dilute alloys, electron irradi., positron lifetime meas. 7-39250
 Au-Fe, dil., Kondo system, mag. scatt. time of conduction electrons meas. 7-21902
 AuAl alloys, Al diffusion, NMR study 7-33287
 Cd-In alloys, vacancy-induced elec. field gradient temp. depend., PAC meas. 7-52541
 Cd₉₇Ag₃, Ag density of states, Auger and photoelectron spectra, Clogston-Wolff model calcs. 7-2451
 CdMg dilute alloys, muon Knight shift temp. depend. study 7-45892
 Cr-Al dilute alloys, mag. phase diagram, mag. susceptibility studies (*Russian*) 7-2840
 Cr-Ge dilute alloys, elec. resist. temp. and press. depend. studies 7-32980
 Cr-Mo dilute alloys, magnetoelasticity, antiferromagnetism disappearance effects 7-45789
 Cr-Si dilute alloys, magnetic phase diagram near tricritical point, neutron diff. meas. 7-2836
 Cu alloys with 3d elements, electronic struct., K-edge XAS study 7-64066
 Cu, with 3d impurities, X-ray absorpt. edges (*German*) 7-46241
 Cu-based binary dilute alloys, electron struct., X-ray L α emission spectra studies 7-12598
 Cu-based dilute alloys, low temp. elec. resist. 7-52565
 Cu-In alloys, vacancy-induced elec. field gradient temp. depend., PAC meas. 7-52541
 Cu-Mn dil. alloys, electronic struct. of mag. impurities 7-58771
 Cu-Mn dilute alloys, oxidized formation, Auger lines relative intensities 7-17726
 Cu-Ni alloys, dislocation vel. determ., stress pulse etch pit and slip line cinematography techniques 7-63627
 Cu-Rh, dilute alloy, surface composition, Auger electron spectroscopy 7-16845
 Cu-_{1-x}Pt_x disordered system, X-ray absorpt. edges (*German*) 7-46241
 CuSb(In), vacancy formation enthalpy, positron annihilation studies 7-7787
 Fe alloys with 3d elements, electronic struct., K-edge XAS study 7-64066
 Fe, dilute alloys, electron irradi., positron lifetime meas. 7-39250
 Fe, with 3d impurities, X-ray absorpt. edges (*German*) 7-46241
 Fe-Au(Sb)(Cu), dilute alloys, electron irradiated, vacancy-solute interaction, positron lifetime, muon spin rotation studies 7-39288
 Fe-Co dil. alloy, ^{56,57,60}Co isotopes, hyperfine anomalies, α -factors NMR/ON obs. 7-33278
 Fe-Pt, dilute alloys, ferromagnetic, internal mag. fields, impurity conc. dependence 7-38858
 FeSnSb dilute alloys, local lattice relax. around impurity, K-edge EXAFS study 7-64159

dilute alloys continued

- K-Rb dilute alloy, electron-electron and electron-phonon interactions, plastic deform. effects 7-12710
 Mg-Fe, dil., Kondo system, mag. scatt. time of conduction electrons meas. 7-21902
 Mg-Fe dilute thin film, mag. screening and Kondo-type behaviour 7-12944
 Mo-Fe dilute alloy, Fe solute atom-screw dislocation interaction force, modified tight-binding recursion method calcs. 7-51814
 Nb-Hf-Ta-O dilute alloy system, O-induced nonaxially symmetric elec. field gradient, TDPAC meas. 7-12686
 NbH_x, interstitial H total cross-section determ., localised modes and diffusion, neutron transmission meas. 7-12061
 Ni alloys with 3d elements, electronic struct., K-edge XAS study 7-64066
 Ni, with 3d impurities, X-ray absorpt. edges (*German*) 7-46241
 Ni-Al dilute alloys, oxide growth and microstruct. at high temp. 7-17735
 NiSnInSb dilute alloys, local lattice relax. around impurity, K-edge EXAFS study 7-64159
 Pb-Tl, Bridgman growth, pattern generation at solidification front, forbidden cells 7-22651
 Pd alloys, internal oxidation of impurities, XAS study 7-63633
 Pd-Ag-Fe (1 and 2 at.%), plastically deformed, elec. resist., short range order effects 7-27318
 Pd-Fe(Ni) dilute alloys, Fermi surface-exchange splitting, de Haas-van Alphen effect studies 7-52405
 Pd-H, dil., elec. resist. meas., 250-350 K 7-64233
 PdCe, Ce impurity, ground state studies, multiplet effects, near-edge XAS 7-64803
 PdH_x, dilute alloys, Pd substituted, interaction of H with impurities, EXAFS study 7-64806
 PdNi alloys, magnetic clusters interaction energy calcs. 7-45652
 Pd₂Th, impurity internal oxidation, EXAFS 7-17360
 PtMn dilute alloy, longitudinal magnetoresist. meas. 7-12700
 SbSn dilute alloys, muon Knight shift and trapping, comp. and temp. depend. 7-45889
 ScCe, Ce impurity, ground state studies, multiplet effects, near-edge XAS 7-64803
 Ta-Cf dilute alloy, Cf diffusion meas. 7-12353
 Ta-Es dilute alloy, Es diffusion meas. 7-12353
 Ta-Fm dilute alloy, Fm diffusion meas. 7-12353
 TbSc(V)(Cr)(Mn)(Co), dilute alloys, hyperfine fields and local moment form. 7-64433
 U-Ga dilute alloys, microstructure study 7-16780
 U-Ti dilute alloys, phase transformations 7-16730
 U_{1-x}Th_xRe₂, polymorphic transform., supercond. crit. temp., low temp. sp. ht. meas. 7-17125
 β -V-B, rhombohedral phase, struct. and solid solubility, X-ray single cryst. diff. study 7-1948
 W dilute binary alloys, resistivity contribution of solutes 7-32979
 W-Ni dilute alloy, Ni enrichment at screw dislocations, atomistic calcs. and atom probe FIM meas. 7-33638
 Y_{1-x}Dy_x dilute alloys, spin density wave antiferromagnetism 7-52947
 Zn-Ag dilute alloy single crystals, thermally activated and quantum creep, impurity effects (*Russian*) 7-26755
 Zn-Au dilute alloy single crystals, thermally activated and quantum creep, impurity effects (*Russian*) 7-26755
 Zn-In alloys, vacancy-induced elec. field gradient temp. depend., PAC meas. 7-52541
 Zr-Ni dil. alloy, Auger electron anal. of oxides 7-22907

diluted magnetic semiconductors *see semimagnetic semiconductors***dimensions**

- No entries

dimer lasers *see excimer lasers***dimerisation** *see association***dimers** *see molecules***dineutrons** *see neutrons***diode lasers** *see semiconductor junction lasers***diode sputter deposition** *see sputter deposition***diode sputtered coatings** *see sputtered coatings***diode sputtering** *see sputtering***diode tubes** *see diodes***diodes**

- see also plasma diodes; rectifier tubes; rectifiers; semiconductor diodes*
 ablative macroparticle accelerator using electron beam diodes for accelerating projectiles 7-36266
 Si diodes, radiation effects of 10-12 MeV electrons (*Chinese*) 7-6685

dipole antennas

- electric field meas., low frequency, antenna calibration 7-56233
 Hertzian dipole measurements with InP photoconductors 7-52690
 Hertzian dipole radiation in stratified uniaxial anisotropic media, computation 7-36860
 oscillating dipole EM radiation in chiral media using dyadic Green's function 7-1005
 reference field strength meters with dipole antennas, appl. of thermistors 7-56232
 spherically symmetric inhomogeneous isotropic media, fields of sources calcs. 7-37696

dipole moment, electric *see electric moments***dipole moments, magnetic** *see magnetic moments***dipole moments, molecular** *see molecular moments***Dirac electron theory** *see Dirac equation; electron theory***Dirac equation**

- see also relativistic quantum field theory*
 Abelian Higgs model, APS index for fermion-vortex system 7-19011
 Abelian monopole geometry in 6D, Dirac wave functions 7-19045
 anomalous positron peaks and Dirac eqn., comment and reply 7-56697
 antiparticle role in Dirac phenomenology for nuclei 7-19215
 atomic and mol. electronic struct., calcs., relativistic effects 7-36504
 atomic relativistic bound-state energies determ. extremum principles 7-868
 atoms, quasirelativistic theory, Dirac second-order eqn. 7-49958
 center-of-mass motion of a system of relativistic Dirac particles 7-48939
 chiral QCD, topological anomalies from Dirac equation 7-49051
 Clifford bundles and the Dirac operator, connections 7-61443
 coherency matrix description for electron 7-15811
 composite system in motion, structure in rel. quantum mech. 7-41150

Dirac equation continued

- constrained Hamiltonian dynamical system, path integral quantisation 7-18532
- Coulomb fields, quantum solns. and classical limits 7-30192
- Coulomb scattering for the Dirac equation, asymptotic observations 7-15085
- Dirac formalism, mathematical introduction, book 7-60896
- Dirac Hamiltonian, canonical transformation, comparison with Foldy-Wouthuysen analysis 7-48947
- Dirac Hamiltonian for fermion-solenoid interactions, vacuum charge, scatt. theory 7-35700
- Dirac operators, eta invariants and holonomy theorem for elliptic families 7-15049
- Dirac particle in four species 7-10016
- Dirac spinor orbits 7-56413
- Dirac-Coulomb eqn., relativistic perturbation soln. He-like atom appl. 7-24767
- Dirac-Coulomb Hamiltonian, relativistic many-bodies, Foldy-Wouthuysen type diagonalisation procedure 7-9698
- Dirac-like equations for gauge fields 7-4978
- electron hidden U(3) symmetry, Zitterbewegung and degrees of freedom, Dirac eqn., Lie algebra 7-19031
- electron pair production, fermion field operator expansion 7-9988
- exact parapositronium like solution to two-body Diracequations 7-5039
- exact solutions in constant chromomagnetic fields 7-61434
- fermion propag. on hypercubic lattice with random hopping parameters 7-4967
- fermion theories, causal phase-space approach, Clifford algebras 7-9752
- Fierz identities in Dirac gamma matrix algebra 7-9982
- fine-structure constant in plasma model of fluctuating vacuum substratum 7-30230
- generalisation admitting isospin and colour symmetries 7-9941
- geometrical unified theory of connection fields and frame fields 7-56121
- hydrodynamical description of the Dirac equation in curved spacetime 7-19014
- interacting field theory in 2D, Sugawara-Sommerfield construction 7-48986
- isospectral invariance for 1D Dirac operator 7-18987
- magnetic monopoles, electric currents, and Dirac strings 7-15070
- massive Yang-Mills field, exact solns. and Wong and Dirac eqn. solns. 7-61439
- matrices, in gravitational field, construction mode 7-56098
- maximal symmetry group, anal. using Lie's extended group method 7-24763
- Maxwell's eqns., soln. in curved space-time, Green's function adiabatic expansions 7-41183
- Maxwell-Dirac isomorphism 7-35777
- minimax principle for eigenvalue calcs. 7-419
- nonlinear, (1+1)-dimensional, existence of localized solutions with scalar self-interaction 7-24764
- nucleon motion in nuclei, use of Dirac eqn. and gluon condensate modification 7-49279
- nucleus as a source in Kerr-Newman geometry 7-48476
- numerical implementation of the boundary element method with point-source approximation of the potential 7-386
- photons and neutrinos, gauge transformations 7-46
- Plebanski metric perturbations in general relativity, fermion field perturbations 7-18645
- pseudoclassical spin 1/2 particle models, classical trajectory and spin precessions 7-18997
- quantum wave propagation near a black hole event horizon, QED scatt. 7-9505
- random lattice, doubling problem and chiral symm. breaking 7-394
- relativistic bound state wave, function solns., Wood-Saxon potentials, (γ , K^+) anal. 7-42073
- relativistic potential model for Dirac particle, bound state level ordering 7-61465
- relativistic scattering operators for Dirac particles, struct., symmetries and reconstruction 7-30394
- relativistic wave equations, invariance algebras and superalgebras 7-61440
- rotation, space reflection, time reversal and charge conjugation separable potential 7-9987
- Runge approximation theorems in complex Clifford anal. 7-55978
- self-interacting quantum electron, chaotic plane-wave solutions 7-41697
- SO(ν , ν) pure spinors, Dirac eqn. soln. 7-41574
- soliton solutions, existence conditions 7-24765
- space-time Dirac-Kahler spinors 7-41625
- square root in supersymmetry 7-35688
- string theory, Dirac operator determinants, anomaly cancellation and torsion 7-35813
- superspace mechanics as the classical limit of superfield theory 7-49012
- supersymmetry in nonabelian, chromomagnetic field 7-35726
- symmetry, with external nonAbelian gauge field 7-41589
- synchrotron radiation of relativistic magneton, classical and quantum theory 7-62603
- topological invariants and anomalies associated with Dirac operators 7-41613
- two-centre Dirac equation with separable potentials 7-61473
- vacuum polarisation and fractional fermion number 7-24759
- wave equations consistency of use in basis set variational solns. with Dirac hole theory 7-19692
- Weyl-Dirac equation for an SU(2) gauge theory with spherical symmetry 7-41622
- zero mode representations of Majorana fields and Klein transformations 7-9983
- NN scattering and bound state, Dirac eqn. with separable pot., rel. effects 7-30351
- (p,p), Dirac and Schrodinger approach, scatt. model 7-41988
- H atom, Dirac equation, separation and eigenvalue anal., hyperfine splitting in IS state, 2S state shift 7-36807
- H-like atoms, relativistic corrections to ground state energies, Dirac eqn. variation perturbation method 7-24766
- He isoelectronic series, binding energies and radiative lifetimes, Dirac Hamiltonian, relativistic variational soln. 7-25456
- PbTe-type narrow gap semicond., with antiphase boundary, physical realisation of parity anomaly 7-38432
- direct access storage devices** *see magnetic disc storage*
- direct current motors** *see DC motors*
- direct digital control**
see also control systems
JT-60 toroidal field coil power supply, DC output control 7-15319
semiconductor laser, digital control using microcomputer, freq. stabilisation (Japanese) 7-5912
- direct energy conversion**
see also bioenergy conversion; cells (electric); chemical energy conversion; magnetohydrodynamic conversion; photothermal conversion; plasma diodes; solar energy conversion; thermionic conversion; thermoelectric conversion
electrical to fluid kinetic energy conversion in electro-fluid-dynamics device 7-3712
electrodes, material effects on energy conversion efficiency, neutral beam injection system appl. (Japanese) 7-10277
electromechanical energy conversion, theory (Polish) 7-34071
insertion materials for energy conversion and storage, review 7-28391
photomotor for energy conversion from light to mechanical rotation 7-40047
power transmission by laser beam, direct energy converter and laser produced plasma confinement 7-3720
pulse combustion, characts., appls., and research needs 7-65594
technology breakout in energy conversion, conf., San Diego, CA, USA (Aug. 1986) 7-60875
 H^+ ion heat engine for direct conversion to electricity 7-28409
Ni-Ti, nitinol, shape memory alloy, phase transitions, thermal energy conversion appl. 7-39514
- direct memory access** *see file organisation*
- direct nuclear reactions and scattering**
see also pick-up reactions; stripping reactions
A=9-136, direct neutron capture, channel-capture formalism 7-42023
conf., Smolenice, Czechoslovakia, June 1985 7-41005
conference on nuclear scatt. data eval. methods, Berlin, Germany (June 1985) 7-21
continuum reactions, multistep direct reaction analysis 7-41966
critical energy deposition in nuclei, evaporation and percolation model, multifragmentation energy 7-19230
cross section fluctuations in direct reactions, statistical anal. 7-41965
differential cross-section, direct reaction contribution 7-621
dissipative nuclear collisions, Ericson fluctuations 7-49352
EMC effect in terms of knock out reactions 7-49150
exciton model and multistep compound reactions 7-41956
heavy ion incomplete fusion reactions, fragment emission, influence of projectile cluster props. 7-19315
heavy-ion reactions, quasiclassical DWBA anal. 7-56699
inclusive reactions, high-momentum component and short-range correlations 7-603
one-nucleon spectroscopic amplitudes for 1p-shell nuclei excited states 7-61795
(p,n), nuclear level density determ. 7-41905
particle decay of resonant state generated by direct reaction 7-49366
preequilibrium reaction theory 7-35990
semiempirical nuclear fragmentation model 7-56689
two nucleon effective interaction, direct reaction modelling, medium corrections 7-613
(d,d), polarizability and breakup model for heavy nuclei 7-15214
(e,e'p), quasi-free knockout, nucl. medium effects on photon-proton vertex 7-35997
(n, γ), fast n, expt. data review, direct-semidirect model anal. 7-42022
(\bar{n} , γ), j-dependence, direct-semidirect model study 7-49394
(p,p), radial sensitivity, direct reaction modelling, medium corrections 7-613
 $^{27}Al(^{16}O,\alpha)$, 62, 84.5 MeV, α energy spectra and ang. distrib., direct emission mech. 7-30440
(Au,X), 1 GeV/N in emulsion, multifragmentation, reaction mech., exclusive expt. results 7-36033
 $^7Be(p,\gamma)$, differential and total cross section calcs., direct capture model 7-42004
 $^9Be(n,2n)$, reaction mechanisms 7-42018
 $^9Be(n,\gamma)$, radiative transition and direct capture anal., optical pot. model 7-41996
 $^9Be(p,d)$, spectroscopic factors and nuclear vertex constants, DWBA calcs. 7-56603
 $^{12}C(n,\gamma)$, A=12, 13, radiative transition and direct capture anal., optical pot. model 7-41996
 $^{12}C(^4He,pp)$, differential cross sections and analysing powers 7-42032
 $^{12}C(^{16}Li,p)^{17}O$, energy level study and Hauser-Feshbach calcs. 7-15218
 $^{13}C(p,d)$, spectroscopic factors and nuclear vertex constants, DWBA calcs. 7-56603
 $^{40}Ca(\alpha,\alpha')$, quasifree knockout, DWIA calcs. and spectroscopic factors 7-42038
 $^{52}Cr(n,n')$, direct contributions, DWBA anal. 7-42014
 $^{63}Cu(p,\gamma)$, direct-semidirect capture in the giant dipole resonance region 7-49417
 $^{63}Cu(p,\gamma)^{64}Zn$, 6.5-11 MeV, capture cross section meas., excitation fn. anal. using CN/DSO models 7-10153
 $^{168}Er(n,n')$, cross section calcs., direct processes and compound nuclei 7-30420
 $^{56}Fe(n,n')$, direct contributions, DWBA anal. 7-42014
 $^2H(d,X)$, singlet d intermediate state in four-body breakup reaction (Chinese) 7-24985
 $^3He(e,e'd)^3H$, 500 MeV, 3He spectral fn. dependence on relative p-d energies, $^3He(e,e'p)$ comparisons 7-56672
 $^3He(e,e'p)^3H$, 500 MeV, 3He spectral fn. dependence on relative p-d energies, $^3He(e,e'd)$ comparisons 7-56672
 $^3He(p,2p)^3H$, knockout reactions, spectral function 7-61894
 $^3He(p,pd)^3H$, knockout reactions, spectral function 7-61894
 $^7Li(p,d)$, spectroscopic factors and nuclear vertex constants, DWBA calcs. 7-56603
 $Li(\alpha,\alpha')$, exchange processes and spin-orbit pot. effects 7-30437
 $^{14}N(^{28}Si,X)$, forward-angle yield, equilibration in orbiting reactions 7-5270
 $^{93}Nb(^{20}Ne,X)$, complete and incomplete fusion, inclusive fragment spectra meas. 7-42055
 $^{144}Nd(p,\alpha)^{141}Pr$, 25 MeV, level excitation, α -particle distrib., knock-on contributions 7-10154
 $^{58}Ni(n,n')$, direct contributions, DWBA anal. 7-42014
 $^{16}O(\alpha,\alpha')$, quasifree knockout, DWIA calcs. and spectroscopic factors 7-42038

direct nuclear reactions and scattering continued
¹⁶O(π^+ , π^0 p) cross section, coincidence meas. 7-42078
(p,X), very hot nuclei, decay processes, canonical Metropolis sampling of multifragmentation 7-61876
²⁰⁸Pb(α ,³He)²⁰⁹Pb, 183 MeV, neutron response fns., high-spin single particle strengths, DWBA anal. 7-19154
²⁰⁸Pb(d,d), polarizability and breakup, cross section calcs. 7-15214
²⁸Si(¹⁸O,¹⁶F), 19.6 MeV/N, one-step direct contrib., cross-sections, double folding DWA anal. 7-30401
²⁸Si(³⁸Ni, ⁵⁹Ni), transfer cross section meas., isotopic dependence, DWBA anal. 7-5256
²⁸Si(³²Ni, ⁶²Ni), transfer cross section meas., isotopic dependence, DWBA anal. 7-5256
²⁸Si(n,n')²⁸Si, excited states and direct reaction mechanism 7-36003
³⁰Si(⁴He, α), CCBA, DWBA anal. 7-42034
³⁰Si(i,g), CCBA, DWBA anal. 7-42034
¹³⁰Te(²⁸Si,X), transfer reactions, optimum Q-values (*Korean*) 7-24997
²³⁸U(p,X), decay of very hot nuclei, Microcanonical Metropolis sampling of multifragmentation 7-61877
⁶²Zn giant dipole resonances built on excited states, Brink hypothesis verification from ⁶²Cu(p, γ) 7-41959
⁷⁰Zn(⁴⁰Ar,X), inclusive variables, random walk model calcs. 7-42050
⁴Zr(n, α)⁴³Sr, A=90,91 α -spectrum meas., pick-up and knock-on theories 7-49408
⁹⁰Zr giant dipole resonances built on excited states, Brink hypothesis verification from ⁸⁹Y(p, γ) 7-41959
⁹⁰Zr(e,e'p), 2p proton knockout, momentum distrib., optical pot. anal. 7-61849

direct graphs
open-channel network flow model (*Japanese*) 7-35285

direction finders, radio see *radio direction-finding*

directional antennas see *directive antennas*

directional couplers
desorption, light induced, bistability mechanism in integrated optical devices 7-57424
electro-optic directional coupler switches, crosstalk due to reversed- $\Delta\beta$ electrode misalignment 7-20471
electrooptic modulators, digital and quasi-linear, synthesized from directional couplers 7-50727
fibre interferometer with 4X4 coupler quadrature outputs 7-31506
fibre optic directional coupler, polarisation preserving 7-25999
fibre optic directional couplers, biconical taper technology and device appls. 7-26008
fibre optic directional couplers, single-mode asymmetrical tunable wavelength-selective with intermediate layer 7-43396
fibre optic fused biconical monomode directional couplers, power transfer wavelength selectivity control 7-37159
fibre-optic directional coupler, polarisation-preserving, appls. 7-1279
nonlinear directional coupler, beam-propag. method anal. 7-37148
nonlinear guided-wave phenomena, review 7-57422
optical $\Delta\beta$ phase reversal directional coupler switches, crosstalk characts. 7-26037
optical couplers for LANs, parallel single-mode/multimode fibres config. wave coupling study 7-31486
optical couplers made of nonidentical asymmetric slabs 7-57548
optical directional coherent coupler, nonlinear, instabilities, all-optical phase-controlled switching 7-11027
optical directional couplers with gain or loss anal. and appl. to semiconductor slab dielectric guides 7-31457
optical fibre directional coupler splicing for duplex communication 7-50754
optical modal filter, highly selective evanescent, for two-mode optical fibres 7-5980
optical single-mode fibre resonant cavity calcs. (*French*) 7-50745
spatial sampler using integrated optic techniques, electrooptic directional couplers 7-31524
telecommunications using integrated optics including wave conductors and electro-optical couplers (*German*) 7-50790
GaAs-GaAlAs MQW waveguides, nonlinear propag. 7-26033
LiNbO₃:Ti 4X4 directional coupler switch with permanently attached polarisation maintaining fibre array, low crosstalk 7-31520
LiNbO₃:Ti 4X4 nonblocking interconnection network for test bed, video switching 7-26039
LiNbO₃:Ti directional couplers, appl. of coupled-mode theory to design with non-parallel sections 7-20410
LiNbO₃:Ti integrated optical devices, domain inversion effects 7-62849
LiNbO₃:Ti modified 1X2 directional coupler waveguide modulator 7-1259
LiNbO₃:Ti X- and Z-cut directional coupler and BOA switches, voltage-length product 7-43352
Ti:LiNbO₃ optical switch, three-electrode 7-15970

directional patterns see *antenna radiation patterns*

directional solidification
alloys, binary, unidirectional solidification, cell-dendrite transition criterion (*Chinese*) 7-65018
asymptotic eqns. and solid-liquid interface struct. 7-52010
binary alloy, directional solidification, buoyancy effects 7-6764
binary alloys, directional solidification, morphological and thermosolutal instabilities, perturbation anal. 7-58446
binary semiconductor alloys, directional solidification, convection, segregation, ampoule and furnace design 7-59501
ceramic eutectic composites, microstruct. and mech. props. 7-64991
dendritic growth models, comparison of theory with expt. 7-22649
domain growth from melt, temp. gradient, form. kinetics study 7-51681
halide eutectic composites, growth, struct., mech., elec. and optical props. 7-33648
IR optical materials, production 7-37075
morphological stability, weakly nonlinear, effect of latent heat 7-59497
moving symmetric model of solidification cells at low velocity 7-32618
pivalic acid directional solidification, metastable dendritic interface pattern obs. 7-63779
rapid solidification, steady and oscillatory cellular morphologies 7-2157
Rene 80, Ni-base superalloy, creep rupture props., influence of coating treatment and directional solidification 7-28116
solute distrib. coeff., numerical analysis 7-28027
steel, C, directional solidification, δ/γ transform., P and Mn solute distrib. in dendrites 7-65020
steel, Cr-Mo, normalised heavy section plate, weld cold cracking susceptibility (*Japanese*) 7-3425

directional solidification continued
steel, Cr-Mo, plate, directional solidification, rolling, strength, toughness, microstruct., weldability 7-59622
steel, high speed, peritectic transform., decomp., carbide precip. Nb alloying effect (*German, English*) 7-22677
superalloy single crystals, directional solidification, mech. anisotropy, fatigue, creep 7-3293
superalloys, oxide dispersion strengthened, manufacturing process developments 7-27979
tetrabromomethane:Br₂ dil. binary mixture, directional solidification, cellular instabilities 7-26921
transport processes, analytical modelling and expt. obs. 7-53541
water, initially superheated, solidification in horizontal cylinder study 7-58443
Al, directionally solidified, rolling, recrystallisation texture 7-33646
Al-Al₃Ni eutectic alloys, chill cast, directionally solidified, hot rolling microstruct. 7-46447
Al-Cu, directionally crystallised, crystallographic texture transform. during wear 7-17660
Al-Mg (9.8 wt.%), AlMgSi, AlZnCuMgZr, directional solidification, microstruct. (*German*) 7-46452
Al-Si (12.7 wt.%), eutectic microstruct., twinning and branching mechanisms 7-17521
Al-Si eutectic alloys, partial modification mechanism 7-59498
Al-Si-Sb, directionally solidified eutectics, inter-Si flake spacing rel. to Sb addition 7-53717
Al-Zn eutectic, oriented crystallisation, buoyancy-driven convection effects 7-27887
Bi-MnBi eutectic, pure and modified, growth 7-59500
Cu, with dispersed Al₂O₃ and Mo particles, directional solidification in reduced gravity (*German*) 7-22658
Fe, cast, graphite, directionally solidified, struct. transitions 7-13443
Fe, cast, graphite morphology and growth kinetics (*Chinese*) 7-65017
Fe, cast, white, Cr-Mo, unidirectionally solidified, sclerometric study 7-3455
Fe, grey cast, skin casting under microgravity conditions 7-22661
Ge-transition metal eutectic alloys, cryst. growth by directional crystallisation 7-64887
InSb-NiSb eutectic composite, rel. between metal fibre morphology and elec. props. 7-59644
MgO-Al₂O₃-SiO₂, leucosapphire, crystal growth by directional crystn., gas inclusions formation 7-33539
MnBi/Bi eutectic, freezing rates, convection effect on microstruct. 7-22652
Ni-Al-Co-Cr-Ta, polycrystalline superalloys, microstruct. rel. to Ta content 7-46446
Ni-Al-Mo eutectic high temp. alloy, directional solidification within ZrO₂ supporting skin (*German*) 7-22660
Ni-Cr-Ti-Al-(Mo), dendritic single crystals, microsegregation 7-46477
Ni-Mo₂C eutectic, directional solidification oriented struct., strength, hardening mechanism (*Russian*) 7-59507
Ni-Nb-C system, directionally solidified, phase equilb. and struct. 7-46416
Ni-NbC eutectic, directed crystallisation, comp. growth laws (*Russian*) 7-65021
NiO-based aligned eutectics, microstruct., crystallography and interfaces 7-65025
NiO-CaO eutectic, directionally solidified, struct. imperfections 7-65026
Pb-Sn eutectic, spiral structures, convection influence 7-22653
Pb-Tl, Bridgman growth, pattern generation at solidification front, forbidden cells 7-22651
Pd_{77.5}Cu₆Si_{16.5} glass, cryst. nucleation and growth kinetics 7-11917
Si, on carbon-fabric support 7-13350
Sn-Sb, dil., planar solid-liq. interface, morphological development and stability (*Korean*) 7-7985
Sn-Sb (2 at.%), morphological development of planar solid-liq. interface (*Korean*) 7-17523
Zn-Al, solidification, segregation, foundry procedure appl. 7-53712

directive antennas
see also *loop antennas*
horn antenna with low sidelobe response for observations of diffuse celestial radiation 7-47701
low-cost satellite image reception and analysis facility 7-66305
RF absorber horn test system 7-43605

dirty superconductors
(BEDT-TTF)₂I₃, organic superconductor, critical temp., randomness effects 7-52882
conduction electron inelastic lifetime, nonlocalisation method studies 7-64210
conductivity and diamag. susceptibility fluctuations near Anderson localisation 7-45563
quasi 2D, Kosterlitz's recursion relations and anisotropic XY model 7-64390
strong-coupling eqns., disorder effects 7-64393
strong-coupling theory, McMillan soln. and T_c degradation 7-64394
strongly disordered superfluids, quantum fluctuations, critical behavior 7-2288
thin films, superconducting transition temp., weakly localised regime 7-52883
(TMTSF)₂PF₆, organic superconductor, critical temp., randomness effects 7-52882
weak localisation and supercond. fluctuations 7-64403

disabled persons' aids see *handicapped aids*

disc storage see *magnetic disc storage; optical disc storage*

discharge lamps
see also *arc lamps; flash lamps; fluorescent lamps; metal vapour lamps*
heavy atom spectra sources for use with high resolution Fourier transform spectrometer 7-50403
hollow cathode lamp, LSP-1, emission lines intensities and contours 7-48863
hollow-cathode lamps, optogalvanic effect, electrical resonance effect 7-58079
Penning discharge source for extreme ultraviolet calibration 7-25919
solar insolation simulation by compact-source iodide lamps 7-23122
D₂-Ar spectrophotometric lamp, construction and material influence 7-41422
Xe lamp, double discharge, for Nd laser pumping 7-11002

discharge lasers *see gas lasers*

discharge tubes *see gas discharge tubes*

discharges (electric)

see also arcs (electric); electric breakdown; exploding wires and foils; flashover; glow discharges; high-frequency discharges; lightning; partial discharges; positive column; sparks; surface discharges; Townsend discharge

AC plasma displays, discharge development 7-21012
AC plasma displays, discharge ignition 7-21017
air, atmospheric, optical discharge plasma sustained by Nd laser radiation, diagnostics 7-63355
air, breakdown in discharges, emission study 7-26574
air, ionisation currents in cylindrical chambers 7-37778
airgap breakdown charact. obs., under ambient conditions of reduced air density 7-20978
anode spot formation, time determ., photoelec. method 7-11789
Boltzmann equation for electron distrib. function (*Russian*) 7-20995
carbon tetrafluoride, beam-plasma discharge for plasmachemical appls. 7-37706
cathode fall, optogalvanic diagnostics 7-32187
cathode layer dynamics, effect on externally sustained discharge current 7-21024
chemical sputtering of carbon in tokamak discharge 7-51537
composite discharge sustained by N₂ injection from capillary plasmatron 7-1798
conical discharge tube, striation excitation 7-6479
continuous optical discharge, electron distrib. function 7-21033
coordinate-sensitive gas discharge detectors, fibre optic readout system 7-30852
current sheet dynamics, coaxial plasma accelerator, atm. initial press., num. anal. 7-31945
difference resonance expt. with polarising prism 7-26385
diffuse discharge opening switches 7-37766
diffuse discharge switching appls., temp. depend. electron transport studies 7-32189
double impulse tests of long airgaps, pre-existing space charge effects 7-20977
double sawtooth oscillations in the text tokamak 7-20921
dynamical pinch discharges, power limits 7-32149
E×B type devices, discharge phenomena (*Japanese*) 7-51539
electric-explosion cavity development, dynamics 7-31824
electrode design for gas discharge laser using finite difference method 7-1178
electrolyte, pulsed discharge, plasma composition determ. 7-20991
electron beam controlled discharges, charactn. and switching performance 7-26533
electron collectors in gas discharges 7-44296
electron-beam-sustained, secondary electron thermalisation, attachment effects 7-58080
electronegative gases, beam-plasma discharge, physical props. 7-32001
electrostatic discharges from human body 7-34125
ESD current waves, classification vs. approach speed, voltage, electrode geometry and humidity 7-42841
ESD simulation difficulties and test procedures (*French*) 7-37787
ESD testing, rising slope reproducibility 7-42843
Eta-Beta II reversed field pinch, heating and confinement studies 7-26497
explosive electron emission in microwave fields, excitation and evolution 7-63310
filament structure in high-press. UHF discharge 7-11816
focus discharge, magnetically driven sheath, elec. signal simulation 7-44184
gas, low-pressure, electron beam injection, discharge time lag 7-37770
gas discharges, dynamical behaviour, relation to elementary processes 7-20999
gas laser, photo-initiated, electrically excited, electron density meas. 7-31335
gas lasers with high pressure volume discharges, review 7-36953
ground state, gas discharge, longit. nucl. relax. time, temp. depend. 7-20997
high voltage spark discharges, light scatt. diagnostics 7-20971
high-current, spot behaviour and local cathode heating 7-58089
high-current discharges, pinch current sheet near mag. separatrix surface, MHD eqn. soln. 7-51482
high-frequency discharges from plasma under pressure 7-1807
high-pressure, stability, electron dissociation attachment effects 7-51540
hollow and coaxial plasma, collisional drift instability 7-44164
hollow cathode effect, modelling 7-21006
hot cathode plasma discharge, role of filament orientation and limiter 7-32017
hot-cathode discharge, Langmuir oscils. self-excitation 7-37794
human ESD: the phenomena, their reproduction and some associated problems 7-42842
ignition voltage of spark gaps in technically important gases (*Czech*) 7-32144
inception voltage from free cond. particles in air 7-51544
inert gas, contracted discharge, ionisation waves, 2D theory 7-16343
inert gas atoms, anisotropic collisions with atoms and ions, intermultiplet mixing 7-57154
inert gas-O₂-(SF₆) discharges, charged particle induced, O₃ synthesis 7-3587
insulating liquids, air bubbles attached to point electrodes 7-37779
insulating material, inception voltage of discharges in voids 7-53236
integral model of discharge in rail accelerator with circumferential flow 7-32159
ion thruster, inert gas, plasma confinement by surface mag. fields 7-51486
ion-acoustic wave reflection from discharge-tube walls, expt. obs. 7-26411
ionisation wave front, diffusional-electrodynamical instability 7-20973
ionised gas physics, conf., Sibenik, Yugoslavia, (Sept. 1986) 7-24307
laser guided discharges and appls., pulsed power considerations 7-37801
laser plasma, supersonic turbulent propag. of optical discharge 7-63280
laser produced optical discharge in air of reduced density containing solid particles 7-26475
line profiles influenced by selective ionization in low pressure discharges 7-21002
linear thyatron in tetrode configuration, develop. 7-32120
liquid dielectrics prebreakdown phenomena 7-32146
liquid evaporation, low-current high-voltage discharge effect 7-58453

discharges (electric) continued

long gap discharges, electric field meas. using a Pockels device 7-4822
low-pressure discharge, hydrodynamic description, singularity removal 7-20882
magnetic fluctuations during current rise in divertor discharge 7-11689
metal vapour-inert gas mixture, low current steady state and periodic pulse discharge, props. 7-63379
methane, dissociative ionization and electron attachment 7-31182
methane, pulse discharge, a π_n radical form. and decay 7-23003
MHD channel, electric current fluctuations accompanying interelectrode breakdown 7-63248
MHD mode reconstruction from projections 7-1681
micropinch discharge with plasma point source, X-ray emission, anode material at. number effect 7-44233
microsecond discharges in flash lamps, elec. cct. matching 7-10978
microwave discharge ion source, Na⁺ ion production 7-15030
modified Penning discharge, edge turbulence studies 7-16331
molecular gas, beam-plasma discharge at retarding pot. 7-37705
molecular gas at moderate pressure, discharge impedance 7-32150
n-nonane liq. dielectric, gas form. under particle discharge 7-51532
opposed-targets sputtering system, unbalanced potential discharge characteristics 7-63393
optical discharge, laser dragon, breakdown along a beam in vapour of target 7-58086
optical gain meas. in discharges, spontaneous emission amplification obs. 7-14989
optical plasmatron, subsonic gas vortex motion 7-44264
optoacoustic effect in discharge plasmas, phenomenological approach 7-31987
parallel plate accelerator, time evolution of plasma column 7-19562
Penning discharge, electron plasma column, density diagnostics 7-37741
plasma armature voltage gradients using static discharge 7-26584
plasma diode, planar vacuum type effect of current rise time on maximum current 7-44270
plasma electric discharge production, plasma processing appls. (*Japanese*) 7-6405
plasma focus, inductive explosive magnetic generator current source study 7-44299
poloidal magnetic field in EXTRAP system, breakdown 7-63326
polyethylene, low-density, elec. discharges and tree channels under impulse voltages 7-27657
pulsed beam-driven discharge, cathode spots evolution 7-63378
pulsed power supplies, IEEE conf., Arlington, VA, USA (1985) 7-35110
radial electron distribution structure, meas. in high-current discharge, ion laser media appl. 7-44295
radial field discharge for high-flux ion extraction 7-41534
resonant wave scattering by magnetic fluctuations in Tokamak discharge, microwave diagnostic technique extension 7-58059
RF ion source, with metal discharge chamber 7-30114
RF plasma electron kinetics, attachment and ionis., self-consistent treatment 7-20850
RF plasma electron kinetics, current density 7-20849
RF solid-state oscillator for optogalvanic spectroscopy, NO detection using overtone transition 7-9904
self-sustained volume discharge initiation in lasers by radioisotopes 7-50534
semiconductors, crystal excitation by electric discharges, point defect ionisation 7-33331
short pulse, high power microwave air breakdown 7-26585
spark breakdown time-lag, negative ion effects in air 7-29233
spiral solitons and filamentation 7-44298
St. Elmo's fire mechanism explanation from liq. surface instability in external electric field 7-44293
steam, high density, initiation of electrical discharge 7-15324
stepwise discharge and ionisation, kinetic eqns. 7-32143
streamer develop. mechanism in nonuniform electric fields (*Russian*) 7-44276
streamer plasma polarisation behind an ionisation wavefront 7-1799
surface discharges as soft X-ray flashlamps 7-25236
surface wave discharge in conical plasma column 7-21019
tetrachloroethene discharges, radical reactions, spectrosc. investig. 7-20990
tetrachloroethene-O₂ discharges, radical reactions, spectrosc. investig. 7-20990
tetrachloromethane discharge, chloromethylidyne A²Δ-X²Σ⁺ emission investig. 7-31183
tetrafluoromethane-O₂ discharge, plasma etching, chem. processes 7-3475
thermal model, boundary-value problem soln. 7-20985
Titan tholins, production by d.c. discharge and form. of amino acids, implications for Titan atm. 7-34858
toroidal device, striking characteristics of plasma discharge, filament orientation depend. 7-20905
trigatron-triggered breakdown initiated by streamers, streak photographic studies 7-32191
unipole multipactoring discharge in the LHRF launcher 7-26440
vacuum arc centrifuge, ion and electron temp. meas., rotation vel. meas. 7-26582
vacuum breakdown in pulsed-power plasma expts., diode perveance 7-32184
very high resolution Doppler-free spectroscopy in a hollow-cathode discharge 7-15014
volume gap discharges with small interelectrode separation, high press. charact. 7-51533
vortex structures, pulsed plasma stream, snow-plow model calcs. 7-31953
XUV emission spectra, pulsed discharges through capillary in inert gas 7-44292
Z-discharge channel, ion beam pulse propagation in 2-D 7-6369
Z-discharge plasma, H atom density from H_α and H_β spectral line intensities 7-26512
AlPO₄, glass, dielectric, charge buildup, influence on charging electron beam motion 7-44294
Ar discharge, homogeneous longit. mag. field effects 7-21026
Ar discharge, nonequilibrium behaviour of electrons 7-21039
Ar discharge, pulsed electron beam injection, potential profile, temporal evolution 7-51534
Ar discharge, thermionic cathode double sheath-plasma interaction 7-1707
Ar, laser-induced discharges, electron distribution function, collision frequency effects 7-63387
Ar, metastable ions, optical pumping in hollow cathode discharge 7-30990

discharges (electric) continued

- Ar, plasma characts., study of high current discharges appl. to pulsed-power devices 7-32188
- Ar, RF discharge plasma, electron swarm, time-resolved spectroscopy 7-20959
- Ar surface wave discharges, influence of excitation frequency 7-63386
- Ar⁺, transition probabilities and radiative lifetimes, saturated fluoresc. spectra anal. 7-42543
- Ar-H₂O plasmas, dissociation processes, macroscopic kinetics 7-32173
- Ar-Ne discharge, steady-state cataphoretic density profile, collapse 7-44287
- Ar-tetrachloromethane, RF discharge, GaAs etching study 7-32167
- CO laser discharges, electron-beam-controlled, maximum input energy and field intensity 7-44285
- CO-Xe(NH₃) mixtures, photoionisation discharge, energy characts. 7-21027
- CO₂ gas laser, preionisation using α particles study 7-62508
- CO₂ laser, form. of self-maintained volume discharge using compact electrode system 7-63394
- CO₂ laser, TE CW, influence of electrical discharge homogeneity 7-50537
- CO₂ laser, transverse flow, elec. discharge parameters 7-20279
- CO₂ laser discharges, electron-beam-controlled, maximum input energy and field intensity 7-44285
- CO₂-He-N₂ laser glow discharge, influence of magnetic fields on instability growth 7-5868
- CO₂-Xe(NH₃) mixtures, photoionisation discharge, energy characts. 7-21027
- Cd⁺ recombination laser oscillation, obs. 7-43075
- CO₂-N₂-He laser mixture, beam-driven discharge, gasdynamic processes 7-50538
- Cs, laser initiation of discharge channels for pulsed ion beam research 7-25291
- Cu I plasma, at. quantities, diagnostic determ., capillary discharge technique 7-11787
- Cu vapour laser, structure and characts. (*Chinese*) 7-10994
- Cu vapour laser using metallic walls for discharge confinement 7-43146
- D₂ discharge, surface effects at very high E/n 7-21040
- Fe I, II, excited state level populations in ICP discharge 7-30963
- H discharge, at. and mol. meas. using reson. multiphoton ionisation 7-20955
- H⁻ discharge, atomic processes investig. 7-51527
- H⁺ beam, space charge compensation by pregenerated plasma 7-44200
- H₂ electron beam ionisation luminesc. in high-current discharge, vacuum-UV radiation props. 7-57183
- H₂, metastable, discharge rotational temp. and density determ., resonant multiphoton ionisation method 7-44105
- H₂-Ar, externally sustained discharge, instability mechanism 7-63381
- H₂ profiles at high electron densities from optical discharges 7-6447
- HCN, in discharged He flow, CN(B² Σ^+) form. 7-25476
- HCl/Xe/He gas mixture, kinetic model of discharge (*Russian*) 7-11577
- HCl-Xe-He self-sustained discharge, population dynamics of electronic states of atoms and ions 7-37781
- He, breakdown in discharges, emission study 7-26574
- He I excited states in He-Ne laser discharge, population density ratios determ. from Kirchhoff's law 7-58072
- He plasma, spatial resolved line-intensity meas., electron density determ. 7-36641
- He-Cd discharge in concentric hollow-cathode struct., spectrosc. obs. 7-20953
- He-Cd positive column discharge 441.6 nm laser level (*French*) 7-11811
- He-N₂ laser, pulsed electric-discharge, laser props. investig. 7-62675
- He-Xe pulsed discharge, Xe(P₂) radial distrib. 7-26573
- He-Xe-HCl excimer laser discharge growth dynamics 7-1086
- Hg, discharge, low-pressure, excited state pop. mechanisms determ. using pulsed optical pumping 7-26557
- Hg discharge, low-pressure, laser diagnostics 7-58085
- Hg-Ar, low pressure, electrical discharge, isotope effects, hyperfine struct. 7-37786
- Hg-Ar discharge, degenerate four-wave mixing 7-5958
- Hg-Ar discharge, Hg 6P₁ and 6P₂ reson. level population study 7-57011
- Hg-Ar mixtures, in discharge, current variations and plasma parameters 7-21011
- LaB₆ pulsed hot cathode discharge, for uniform plasma production 7-32006
- La_{0.9}Sr_{0.1}CoO₃ cathodes for CO₂ waveguide lasers, electrical and emission characts. 7-59383
- Li hollow cathode discharge, spectrosc. obs. 7-21008
- LiF single cryst., dielectric, charge buildup, influence on charging electron beam motion 7-44294
- N₂ discharges, electron-beam-controlled, maximum input energy and field intensity 7-44285
- N₂ flowing and post discharge, vibr. level, CARS spectroscopy (*French*) 7-11810
- N₂ high pressure, electron beam drives discharge, cathode sheath dynamics 7-1706
- N₂, in gas discharge, vibr. levels excitation, CARS obs. 7-20021
- N₂ metastable states in gas discharge, vibr. level population dynamics 7-37754
- N₂ nonequilibrium weakly ionised discharge, energy balance 7-10711
- N₂ photoionisation discharge plasma, decay characts. 7-21038
- N₂ plasma jet, post-discharge, radical spatial distrib. 7-20969
- N₂ streamers, 2D numerical simulation 7-32190
- N₂-CO, vibr. relax. in N₂ post discharge 7-20023
- NaCl, synthetic, microcrystalline powders, spontaneous colloid formation in electrodeless discharge 7-12065
- NaK discharge, laser excited, fluoresc. spectrum (*French*) 7-10646
- NaK, Stark effect, appl. to plasma local electric field determ. 7-26563
- Nd_{0.9}Sr_{0.1}CoO₃ cathodes for CO₂ waveguide lasers, electrical and emission characts. 7-59383
- Ne electric discharge degenerate four-wave and multiwave mixing, saturation behavior 7-11075
- Ne gas, optogalvanic effect, role of Ar impurity, kinetic eqns. anal. 7-30970
- Ne II, Stark parameters meas. 7-36538
- Ne, positive column, ionisation-diffusion waves, Kolmogorov entropy 7-44277
- Ne pulsed transverse discharge, population inversion, secondary process influence 7-58084
- O DC discharge, O, O₂(¹ Δ) and O₃ conc. meas. 7-20957
- O₂, b² Σ_g^+ state excitation in gas discharge plasma 7-19735
- O₂, microwave discharge, elementary processes investig. 7-32177

discharges (electric) continued

- O₂ RF discharge, charge carrier distrib., power and press. depend. 7-32096
- O₂ singlet form. kinetics in gas discharge plasma, expt. investig. 7-21037
- O₃, synthesis in charged particle induced inert gas-O₂(-SF₆) discharges 7-3587
- O₃, synthesis in electric discharge 7-32174
- SF₆ beam-plasma discharge for plasmachemical appls. 7-37706
- SF₆, discharge characts. and insulating props., review of Japanese research 7-44279
- SF₆ filled spark gap, high-power discharge, electrode erosion and breakdown voltage study 7-44300
- SF₆-O₂ discharges, etching of Si wafers, diagnostic meas. 7-28214
- SF₆-O₂ discharges, LF and RF, etching and surface modification of polyimide films 7-22858
- SF₆+CFCl₃, directional plasma etching of Si:P 7-39788
- SiCl₂, UV emission spectrum, vibr. anal. 7-31024
- SiF₄-O₂, microwave discharges, mass spectrometric study 7-32169
- SiH₄, RF discharge, electron props., Monte Carlo simulation 7-21036
- Ti vapour, heated cathode discharge prod. 7-21022
- U vapour, heated cathode discharge prod. 7-21022
- XeCl laser, UV-preionised, long optical pulse duration, preionisation and discharge stability 7-1080
- XeCl laser, X-ray preionised with small discharge volume, performance improvement 7-1081
- discharges (partial) see partial discharges**
- disclinations**
- amorphization of a disclination core 7-6624
- crystal symmetry and supersymmetry 7-51684
- epitaxial layer-substrate interface defects 7-21715
- ferroelectric liquid crystals, surface stabilised, disclination dynamics, switching process 7-58137
- helical biological polymers, liq. cryst. phases, columnar textures 7-34106
- helical instability of A χ +1 disclination line in a cholesteric (*French*) 7-16398
- liquid crystalline polymers, domains, are they disclination arrays 7-44359
- liquid crystals, structures, energies and interactions of defects, review 7-63441
- lyotropic nematic with discotic micelles, orientation in mag. field 7-44357
- nematic liq. cryst., line defect dynamics, viscous damping effects study 7-44365
- nematic liq. cryst. films, disinclinations, textures, four-state clock model description 7-257
- plastic distortion moments, disclinations and Somigliana dislocations 7-63611
- poly- γ -benzyl-L-glutamate, helical polymer, cholesteric liquid crystalline phases 7-6506
- S² blue phase, disclination, elastic energy calcs. 7-58135
- tobacco mosaic virus in water, freeze-fracture imaging of ordered phases 7-3751
- xanthan, helical polymer, cholesteric liquid crystalline phases 7-6506
- Ba₂NaNb₂O₇, incommensurate ferroelec. thin films, disinclinations, textures, four-state clock model description 7-257
- discontinuous metallic thin films**
- discontinuous films, charge carrier mobility, temp. depend. 7-22035
- enhanced IR absorption of adsorbed molecules, electromagnetic effect 7-27805
- granular films, electron localisation, transition from weak to strong 7-64083
- granular films, kinematic diffraction, numerical simulation 7-64025
- island films, optical props., Maxwell Garnett and Hampe-Shklyarevskii theories 7-3102
- locally discontinuous thin films, gas-sensitive electrical conduction 7-12882
- optical absorpt. continuous spectrum 7-22369
- Ag discontinuous films, large scale coalescence, post-deposition DC resistance increase 7-45069
- Ag films, electroplating in electrochemical cell, scanning tunneling microscopy studies 7-22589
- Ag island film, Si evaporated layer, surface-enhanced Raman scatt. study 7-13165
- Ag island films, crystal violet adsorbed layer, surface-enhanced reson. Raman scatt. 7-46022
- Ag island films, surface enhanced second harmonic generation 7-1232
- Ag island films, surface plasma emission, electron-photon spectra anal. 7-52491
- Ag, on amorphous and crystalline substrates, electron irradiation stimulated coalescence 7-2437
- Ag oxidised granular film, optical absorpt. calcs., Gaussian broadening model 7-27802
- Ag thin film form., nucleation and growth processes 7-2419
- Ag thin films, discontinuous, post-deposition resist., ageing studies 7-58909
- Ag-Si interfaces, micro-quantitative AES anal. using SEM-SAM apparatus 7-27147
- Al discontinuous films, large scale coalescence, post-deposition DC resistance increase 7-45069
- Al₂Mo precipitate microstruct. and orientation, implantation and annealing effects, electron microscopy study 7-16782
- Au, discontinuous films, percolation metal-insulator transition, nonlinear behaviour 7-45156
- Au films, surface plasmon modes 7-7316
- Au, on amorphous and crystalline substrates, electron irradiation stimulated coalescence 7-2437
- Au thin films, on Au (111), surface-diffusion-induced ageing processes 7-45080
- Cu and Cu/Ag composite discontinuous thin films, aging and field effect studies 7-7413
- Cu discontinuous films, aging, elec. field and temp. effects 7-64364
- Cu discontinuous films, large scale coalescence, post-deposition DC resistance increase 7-45069
- Cu thin films, discontinuous, post-deposition resist., ageing studies 7-58909
- Fe ultrathin films on Pd (111), photoemission, LEED and AES studies 7-45068
- In, growth on GaAs (110), RHEED study 7-2425
- In, on amorphous and crystalline substrates, electron irradiation stimulated coalescence 7-2437
- Mo low temperature growth on Al, electron spectra studies 7-12540

discontinuous metallic thin films continued

- Pb, superconducting granular film SAW attenuation, percolation model 7-2781
 Pt, sputtered films on ZrO_2 substrates, agglomeration and electrical conduction props. 7-52859
 Sn-GeO granular films, struct., resistivity and superconducting props. study 7-45082
 W growth kinetics on thermal oxide 7-16910

discophases see discotic liquid crystals**discotic liquid crystals**

- bis(1,3-di(p-n-alkoxyphenyl) propane-1,3-dionato) copper (II), discotic liq. cryst. props. 7-37846
 caesium pentadecafluorooctanoate-water discoid micelle solns., order-disorder transitions, X-ray scatt., elec. cond., NMR meas. 7-26949
 defects in liquid crystals, structures, energies and interactions, review 7-63441
 freely suspended strands, synchrotron X-ray scattering studies 7-1850
 lyotropic liquid crystal, smectic-nematic transition, electron-microscope obs. 7-32648
 lyotropic nematic with discotic micelles, orientation in mag. field 7-44357
 phase diagram for discotic liquid crystals 7-2197
 reentrant columnar mesophase and crystalline polymorphism (French) 7-63442
 strands, freely suspended, cross sectional shape 7-37845
 Rh complex, dirhodium tetradecanoate, discotic mesophase struct., optical microscopy, DSC and X-ray diffr. study 7-26627

discrete Fourier transforms see fast Fourier transforms**discrete symmetries**

- see also *C invariance; CP invariance; CPT invariance; P invariance; parity; T invariance*
 axially symmetric higher-dimensional gravity, Belinsky-Zakharov N-soliton transforms. 7-41207
 axially symmetric higher-dimensional gravity, Neugebauer-Kramer transforms. 7-41206
 conformal theories, discrete symmetries and twisted boundary conditions 7-250
 $E_8 \times E_8$ superstring theory, topology of the compactified manifold 7-41686
 L parity and ν_e masses in E_8 superstrings 7-19048
 lepton nonconservation in $^{48}Ti(\mu, e^-)$, experimental upper limits, anal. of generation problem 7-41979
 quark-gluon plasma in SU(2) $T=200-300$ MeV, reduction of degrees of freedom from T, Q, Y effects 7-5062
 standard model, softly broken SUSY extended, lepton number and lepton flavour violation 7-41671
 superstring models with intermediate scale breaking, inflation as cure for cosmological problems 7-56113
 three-generation superstring model, compactification and discrete symmetries 7-35818
 NN symmetric Lorentz invariant scatt. amplitude, Yukawa representation 7-41830
 τ neutrinoless decay, lepton-number and lepton-flavour violation search 7-61675
 $u-\bar{u}$, quark scattering on SU(5) colourless magnetic monopole, baryon nonconserved processes 7-30300

disinclinations see disclinations**disintegration (radioactive) see radioactivity****disintegration energies see radioactivity****dislocation anchoring see dislocation pinning****dislocation arrays**

- bicrystals, shear incompatible, approx. evaluation method for elastic stresses by virtual array of dislocations (Japanese) 7-32841
 boundary dislocations, extrinsic and intrinsic types 7-63616
 grain boundary theory based on dipolar array of dislocations 7-6635
 SOI technology by zone-melting recrystn. on quartz substrates 7-21736
 Cu-Si (6 at.%), secondary grain boundary dislocation nodes at junction of three grains 7-63648
 Si, polycrystalline, H_2 passivation, grain boundaries, EBIC technique 7-26769
 V_3Si/V_3Si_3 interface, crystallography of matrix-precip. interface and elastic strain field (French) 7-65036

dislocation breakaway, pinned see dislocation damping**dislocation climb**

- carbide/ α -Fe matrix interface, void nucleation mechanism 7-38354
 crack tip, image forces and pot. energy of dislocations 7-26758
 dislocation distribution growth by climb and glide over non-planar surfaces 7-16556
 edge dislocation, vacancy diffusion and capture calcs. (Russian) 7-44550
 grain boundary dislocation geometry during diffusional creep 7-38013
 grain boundary-slip interaction, role in cavity nucleation 7-21219
 Inconel 718, Ni-base superalloy, creep deform., back stress determ. 7-46564
 Inconel MA 6000, oxide-dispersion hardened superalloy, cyclic creep and anelastic relax anal. 7-17596
 metals, irradiated, creep mechanisms, dislocation climb and slip 7-12194
 metals, irradiated, deformation rate, radiation swelling and creep (Russian) 7-44597
 steel, austenitic stainless, creep and anelasticity at const. homogeneous dislocation struct. 7-17586
 steel, austenitic stainless, TiN dispersion hardened, creep below transition stress 7-65079
 superplastic deform. props. 7-65092
 Zircaloy-2, cold worked, irradi. growth, point defect trapping, computer simulation 7-16613
 AgCl, strain ageing, temp. depend. 7-65065
 Al, monocrystalline, Harper-Dorn creep, dislocation network theory 7-22749
 Al thin films, stress relax. mechanisms 7-21784
 Al-Cu (2.5 wt.%), creep deform., effect of θ precipitates 7-65088
 Al-Cu-In alloy, deformed, θ' -phase precipitation 7-22691
 Al-Mo, rapid solidification processed, diffusion-induced dislocation migration 7-65047
 Au crystallites, annealing, grain boundary untwisting and untilting, dislocation climb and glide 7-12076
 BaTiO₃, perovskite, TEM study of dislocations 7-38003
 CaTiO₃, perovskite, TEM study of dislocations 7-38003
 CdTe and CdZnTe, single-crystal substrates, struct. characterisation 7-32769

dislocation climb continued

- Cu, dislocation-diffusion mechanism of wear reduction in selective transfer 7-17658
 Cu-Al₂O₃ films, dispersion strengthened, flow stress, temp. depend. (Russian) 7-53815
 MgO(Al₂O₃)_n, electron beam irradi., point defect aggregation, screw dislocation climb 7-63662
 Mg₂SiO₄:V, forsterite, high temp. deform., creep study 7-21332
 Ni base superalloys, hot deformed, matrix dislocations, weak beam electron microscopy obs. (French) 7-21210
 Ni-SiO₂ films, dispersion strengthened, flow stress, temp. depend. (Russian) 7-53815
 Ni₃Al, dislocation line stability 7-21212
 Ni₃B₁₇Si₈, ultrafine fine-grained, prep. from amorphous ribbon, creep deform. 7-22748
 Pb-Sn (9 wt.%), solid soln. alloy 7-8066
 Pt-W, Pt diffusion and platelet defect form. (Russian) 7-44895

dislocation damping**see also Bordoni effect**

- BCC metals, Snoek-Koster relax. model investig. (Russian) 7-12115
 fluctuation unpinning from point defects, one-dimensional diffusion eqn. 7-26752
 ice, pure and doped, US absorpt., dislocation damping 7-26756
 steel, C, plane load wave, elastic precursor decay, eqn. of state 7-33751
 steel, Cr type, dislocation struct. after hydraulic pressing followed by austempering 7-3334
 steel, plain C, lower yield stress, strain rate depend. at high strain rates (Japanese) 7-53801
 Al sheet, dislocation relax. contrib. to deform., internal friction and dynamic modulus meas. during creep 7-63626
 Al-Ag (5 wt.%), anelastic effects, quench sensitivity, precip. and dissolution 7-53784
 Cu based alloys, internal friction, Young's modulus, amplitude relationship (Russian) 7-65075
 Fe-base alloys, interstitial impurity-dislocation binding energy (Russian) 7-58310
 Fe-N, Snoek-Koster relax., dislocation effects (Russian) 7-44686
 GaAs, dislocation core struct. 7-38007
 KCl:CaCl₂, internal friction 7-38114

dislocation density

- acoustoplastic effect during active deformation of crystal 7-44700
 alkali halide crystals, dislocation displacements distrib. characts., local dislocation density effects (Russian) 7-21214
 ammonium hydrogen tartrate, dislocation etch pits 7-37999
 austenitic stainless steels, fatigue props., time-depend modes, dislocation concepts appl. 7-28128
 brass, Naval, transgranular SCC, dislocation distrib. 7-17708
 creep, recovery-controlled, dislocation network model 7-2022
 crystals, interaction of excitations with dislocations 7-38553
 deformation at min. elastic strain energy 7-38097
 FCC bicrystals, computer simulation of non-uniform multiple slip (Japanese) 7-51780
 ferromagnet, spin wave excitation by acoustic fields, non-uniformly distrib. dislocations (Russian) 7-45646
 graphite fibre reinforced Al matrix composites, interface charactn., TEM obs. 7-44554
 highly deformed materials, low energy dislocation struct. 7-63614
 ice, pure and doped, US absorpt., dislocation damping 7-26756
 local strain hardening and nonuniformity of plastic deformation 7-22751
 low energy dislocation struct., props. and effects 7-63622
 metal, cold-deformed, microcrack development (Russian) 7-39652
 metals, BCC, ductile-brittle transition rel. to dislocation density 7-39668
 metals, deformed, heterogeneous dislocation distrib., two-parameter description 7-44547
 metals, dislocation assemblies, parameter linking change in internal energy and vol. in creation (Russian) 7-58279
 micrograph evaluation errors 7-16559
 monolayer films, equilibrium configurations, molecular dynamics simulations 7-21771
 serrated yielding, computer simulation using negative resist. characts. 7-2089
 shape memory alloys, ageing and thermal cycling effects 7-3336
 single crystals containing random distrib. of dislocations, integral characts. of X-ray diffr. (Russian) 7-51563
 steel, austenitic stainless, fusion reactor first wall, fast neutron irradi., microstruct. evolution model 7-51846
 steel, austenitic stainless, strain ageing and load relax. behaviour at room temp. 7-28092
 steel, austenitic stainless radiation damage process obs. using high voltage electron microscopy 7-51831
 steel, Cr-Mn(V), bainite transform. kinetics, austenitising and working conditions effect 7-22674
 steel, Cr-Ni-Ti-Al, cold-prestrained, length changes during annealing 7-65058
 steel, high Ni, reactor irradi., dislocation struct. and steady-state creep (Russian) 7-2068
 steel, Ni-Co-W, maraging, martensite isothermal aging, hardness, struct. and elec. resist. kinetic behaviour study 7-17553
 steel, Ni-Cr, deform. dislocation struct., fracture 7-33740
 strong-absorbing single crystals., Laue X-ray diffr. thickness depend. anal. and interpretation (Russian) 7-44310
 structural steels, coercivity and Barkhausen noise power spectrum, stress depend. meas. 7-7548
 Al alloy, high temp. creep, role of surface layer in power law breakdown 7-65089
 Al single crystals, cyclic deform. at low const. plastic strain amplitude 7-65114
 Al, US deform, modelling of reduced bandwidth distortion to wide-area electron channelling mapping 7-16694
 Al-Cu-Mg, Al-Mg, plastic deform., AE, X-ray obs. (Russian) 7-46579
 Al-Cu-Mg-Al₂O₃-Al₄C₃, IN 9021, mechanically alloyed precip. hardened, tensile behaviour 7-13525
 Al-Zn (11 wt.%), dislocation density in high temp. creep 7-39611
 Al₃Ni-Al eutectic alloy, Bauschinger effect, influence of Al₃Ni dispersion state (Japanese) 7-22761
 AlPO₄, berlinite, hydrothermal cryst., growth, X-ray topography, bulk acoustic wave device characts. 7-59391
 Al₂SiO₅ polymorphs, dislocation strain energy 7-16555
 CaF₂, cryst., defect struct., high temp. (German) 7-32449

dislocation density continued

CdTe and CdZnTe, single-crystal substrates, struct. characterisation 7-32769
CdTe, single crystal, structural perfection, X-ray topography 7-12070
Copper, extrusion, dislocation density determ. (Russian) 7-58285
Cr-Mo-Ni ferritic-martensitic steel, irradi. in RTNS-II, TEM study 7-58345
Cu, dislocation-diffusion mechanism of wear reduction in selective transfer 7-17658
Cu, polycrystalline, US and neutron irradi., struct. and mech. props. (Russian) 7-3402
Cu single crystals, corrosion fatigue in aq., oxide-forming environment, electrochem. response 7-65115
Cu, third-order elastic modulus, effect of plastic deform. (Russian) 7-46544
Cu-Ni-Al (7.5, 2.5 at.%), thermomech. treatment (Japanese) 7-8013
Cu-Zn (30 wt.%), anomalous instantaneous creep strain, obs. after stress change 7-46585
Cu-Zn-Al, dislocation density and mobility during reversible martensitic transforms. 7-26759
Fe alloys, high-temp. creep, rel. between dislocation density and internal stress 7-13524
Fe, edge and screw dislocation density determ., TEM, etching and positron lifetime meas. 7-38006
Fe-Mo (14.5 wt.%), ageing, discontinuous dislocational transform., coercivity obs. 7-3305
Fe-Ni (36 at.%), Invar, oxidation, effect of annealing conditions 7-28167
GaAs (001), rel. between etch pit density and dislocation density 7-51771
GaAs, crack form., quenching by dislocation ensembles (Russian) 7-44680
GaAs, crystals, liquid-phase electroepitaxial growth, dislocation density reduction 7-58681
GaAs, dislocation density reduction in crystal growth 7-2020
GaAs, dislocation network density determ., thermal wave microscopy 7-51778
GaAs, epitaxial layers, grown in temp.-gradient field, effects on dislocation density 7-13393
GaAs epitaxial layers and heterostructures grown on Si substrates, material props. 7-7046
GaAs FET arrays, electrical parameter mapping 7-32438
GaAs, LEC grown, threshold for dislocation form., role of cryst. dia. and impurity hardening 7-53551
GaAs, MBE growth, defect reduction using superlattice structures 7-13359
GaAs MOCVD growth on Si with superlattice intermediate layers, material props. 7-27923
GaAs, melt grown, theoretical and expt. fundamentals of decreasing dislocations 7-53547
GaAs, overlapping etch pits, density, evaluation technique 7-32443
GaAs, plastically deformed, Hall effect meas. 7-27351
GaAs, semi-insulating wafer, inhomogeneity characterization by scanning photo-induced current transient spectroscopy 7-7164
GaAs, semiinsulating, electrophysical props., dislocation effects 7-16557
GaAs:In, LEC growth, annealing, solid soln. hardening, dislocation density, elec. props. 7-17404
GaAs:In, strain effects, electrorefl. and photocapacitance study 7-22224
GaAs:Si(S), LEC grown, struct. defects, influence of Si and S doping 7-53550
Ga_{1-x}In_xAs, high-temperature hardness 7-44675
Ga_{1-x}In_xAs, solid soln. strengthening, mech. props. 7-32452
Ga_{1-x}In_xP, OMVPE growth and characterisation 7-3192
InAsSbP/InAs bent heterostructures, dislocation distribution 7-21673
InGaAsP film, defect struct. and strain anal., X-ray topography 7-52344
InP, dislocation density reduction in crystal growth 7-2020
InP, melt grown, theoretical and expt. fundamentals of decreasing dislocations 7-53547
InP thin film solar cells on Si substrate, high efficiency and high radiation resistance 7-59852
InP:Fe,Ga,Sb, LEC growth, dislocation density, resistivity, SIMS obs. 7-53552
InP:Ga,As,Sb single crystals, LEC growth, isoelectronic doping, dislocation density, X-ray topography 7-33549
InP:Ge,S, LEC-growth, dislocation-free 7-17409
InP:S,Ga,Sb, LEC growth, appl. mag. field method, dislocation etching 7-53553
InP:S substrate wafers for LPE growth of laser diode heterostructures, polarised IR and X-ray topographic evaluation 7-32453
KCl:Ca, γ -irrad., Z₁-centre growth, effect of dislocations, thermolum. study 7-32487
LaB₆ crystals, floating zone growth using Xe arc image furnace, dislocation density 7-33552
LiF, cryst., defect struct., high-temp. annealing effects (German) 7-32448
LiF plastic crystals, formation of cracks at cleavage fracture front 7-44674
MgO single crystals, high temp. creep and dislocation struct. at low stresses 7-21336
Mo, cyclic deformation, dislocation substructures and hardening 7-21330
Mo single crystal., rolling, dynamic recovery rel. to deform. temp. (Russian) 7-65095
Mo, single crystals, rolling, rel. between dynamic recovery and changes in orientation (Russian) 7-53759
NaCl, synthetic, microcrystalline powders, spontaneous colloid formation in electrodeless discharge 7-12065
Nb, polycrystalline, US excitation, critical current, dislocation struct., flow limit (Russian) 7-58966
Nb single crystals, reverse lattice nodes form rel. to N diffusion (Russian) 7-58201
NdP₂O₄ single crystals., growth from pyrophosphoric acid soln., cold finger technique, defect struct. 7-59389
Ni, dislocation structure after US deformation, physical props. (Russian) 7-44699
Ni, fatigue cycling, lattice defect characterisation 7-37978
Ni, substructure at accelerated high temp. creep (Russian) 7-65096
Ni thin strips, cryst. growth 7-53580
Pb, deforming stress and defect struct. in low temp. anomaly region (Russian) 7-38093
Pb, superconducting transition, deform. strengthening, dislocation density (Russian) 7-58939
PbTe films grown by hot-wall epitaxy on KCl and BaF₂, TEM anal. 7-59432

dislocation density continued

Si, charged defect states at grain boundaries 7-44564
Si dendritic web ribbons, structural defect characterisation 7-12074
Si, dislocation density reduction by thermal cyclic annealing 7-12072
Si, indentation dislocation rosettes length, influence of Vickers indenter edge orientation rel. to slip directions 7-58284
Si LPE layer form., depend. on Al₁₈M chem. reaction, M=refractory metal 7-7043
Si, polycrystalline p-type, Al and Cu diffusion effects on electronic properties 7-17038
Si, recombination channels, dislocations interaction with point defects, lumin. study 7-46094
Si ribbon growth, dislocation dynamics and thermal viscoplastic stresses 7-2017
Si, thermoplastic deformation, nondestructive ultrasonic detection 7-12215
Si tube, growth from shaped seed, struct. development 7-32326
Sn surface, plastic deformation, multiplied dislocations, density gradient 7-26757
Ti, hardened from β -region, fine struct. study (Russian) 7-32450
Ti, impact produced adiabatic shear bands, deform. twins, dislocation density, HVTEM obs. 7-22753
TiN (100) epitaxial film sputtering, defect density, ion irradi. effects, TEM study 7-58684
W-Ni, sintering, liq. phase and solid-state, influence of dislocation density 7-64969
YAG:Nd crystals, high quality, growth by temp. gradient technique 7-22464
Zn single crystals, creep, dislocation struct., high press. effect (Russian) 7-59578
Zn, deformation, action of series of elec. pulses 7-44659
Zn-Cd monocystals, dislocation struct. as function of Cd content (Russian) 7-44556

dislocation dipoles

alkali metal halides, hardening, effect of dislocation elec. charge 7-51816
metals, FCC, cyclic deform., dipolar wall spacings in dislocation struct. 7-53825
CuFeS₂, natural chalcopyrite single crystals, deformed, TEM study 7-38002
Fe-Si single crystals, deformed, dipole drift mechanism of early stages of dislocation pattern 7-38098
GaAs, undoped, thermal activation of plastic deform., 528-813K 7-6710
InGaAsP layers on InP (001), origin of grown-in dislocations 7-38415
KCl:CaCl₂, internal friction 7-38114
SiO₂, Czochralski grown, O-related defects after annealing, IR TEM and resistivity meas. 7-32466
V₃Si/V₅Si₃ interface, crystallography of matrix-precip. interface and elastic strain field (French) 7-65036

dislocation drag

magnetic material, dislocation drag by defects (Russian) 7-63623
metals, irradiated, creep mechanisms, dislocation climb and slip 7-12194
GaAs LEC wafers, cathodolum. mapping, IR absorpt., X-ray topography obs. 7-33462

dislocation energy

grain boundary theory based on dipolar array of dislocations 7-6635
mixed dislocations, dynamic annihilation study 7-44548
planar polygonal dislocation loop self-energy calcs. in elastically anisotropic media 7-26750
Al₂SiO₅ polymorphs, dislocation strain energy 7-16555
Ge, grain boundary energies, computer calcs. 7-6639
Ni-based superalloys, stiffness const., dislocation line energy and tension, ultrasonic vel. meas. 7-63719
Ni₃Al, stiffness const., dislocation line energy and tension, ultrasonic vel. meas. 7-63719
Si, grain boundary energies, computer calcs. 7-6639
Si, ramp assisted foil casting and photovoltaic appls. 7-16609

dislocation etching

ammonium hydrogen tartrate, dislocation etch pits 7-37999
ammonium hydrogen tartrate, ferroelectric, crystal growth and dislocation etching kinetics 7-51770
diglycine sulphate single crystals, anhydrous, elec. activated dislocation motion 7-12069
III-V semiconductors, selective photoetching studies of defects 7-32426
CdTe high-resistivity undoped crystals, defects, EBIC studies 7-21211
CoO, deformed, dislocation struct., TEM study 7-21209
Cu-Ni alloys, dislocation vel. determ., stress pulse etch pit and slip line cinematography techniques 7-63627
Fe, edge and screw dislocation density determ., TEM, etching and positron lifetime meas. 7-38006
GaAs (001), rel. between etch pit density and dislocation density 7-51771
GaAs (001) surface, etch pits, depend. on Burgers vectors of dislocations 7-39767
GaAs crystals, selective etching and photoetching of CrO₃-HF aq. solns. 7-32442
GaAs, dislocations, obs. by transmission IR microscopy 7-32447
GaAs, MBE growth, defect reduction using superlattice structures 7-13359
GaAs MOCVD growth on Si with superlattice intermediate layers, material props. 7-27923
GaAs, semiinsulating LEC substrates, defect etching 7-59694
GaAs, substrates, multi-technique approach to defect microstructure characterisation 7-52215
GaAs:In, LEC growth, annealing, solid soln. hardening, dislocation density, elec. props. 7-17404
GaAs:In LEC crystals, dislocation etch pits 7-38000
GaAs:Si wafer, failure, dislocation distrib., etching 7-12067
HgCdTe-CdZnTe heterojunctions, lattice matching 7-21717
InGaAsP (001), surface, dislocation etch pits, new etchant props. 7-59699
InP:S,Ga,Sb, LEC growth, appl. mag. field method, dislocation etching 7-53553
InSb, n-type, 60° dislocation motion, etching studies 7-63619
LiF, crack tip dislocation nucleation obs. in bulk specimens 7-37996
LiF, N ion implanted and X-irrad., microhardness response 7-21344
LiNbO₃ crystals, struct. defects and etch figures 7-44555
MgO single crystals, high temp. creep and dislocation struct. at low stresses 7-21336
MnO, deformed, dislocation struct., TEM study 7-21209

dislocation etching continued

- NdP₂O₁₄ single crystals, growth from pyrophosphoric acid soln., cold finger technique, defect struct. 7-59389
 Si, Czochralski grown, tensile props., 900-1200°C 7-51922
 Si dendritic web ribbons, structural defect characterisation 7-12074
 Si, indentation dislocation rosettes length, influence of Vickers indenter edge orientation rel. to slip directions 7-58284
 Si:As, high dose implanted, defect density reduction by low temp. oxidation 7-58297
 TiAsSe₃ crystals, Bridgman growth, dislocation etching, thermal stress distrib. 7-21208

dislocation glide *see slip***dislocation-impurity interactions** *see impurity-dislocation interactions***dislocation interactions**

see also impurity-dislocation interactions; vacancy-dislocation interactions

- alkali halide crystals, dislocation displacements distrib. characts., local dislocation density effects (*Russian*) 7-21214
 alkali metal halide microcrystalline powders, correl. between coloration stability and microhardness 7-32486
 alloys, dislocation glide during ageing, hardening phase particle interaction modelling (*Russian*) 7-38010
 alloys, FCC, internal friction, interaction between dislocation kinks and substitutional solute atoms 7-51935
 BCC metals, Snoek-Koster relax. model investig. (*Russian*) 7-12115
 crack tip, image forces and pot. energy of dislocations 7-26758
 crystals, interaction of excitations with dislocations 7-38553
 edge dislocation interaction with circular inclusions in infinite medium, elastic consts. 7-37989
 edge dislocation with included glide plane, interaction with semi-circular cut on straight boundary 7-6670
 edge dislocation-rigid elliptical inclusion interaction 7-12116
 elastic wave scattering at dislocation edges at low angles (*Russian*) 7-51959
 emission from crack tip, computer simulations 7-37994
 emission from cracks, electron microscope obs. 7-38005
 emission from cracks in crystals, or along cryst interfaces 7-37992
 emission into mode III crack tip plastic zone 7-37995
 ferromagnetics, multidomain, containing lattice dislocations, dynamics (*Russian*) 7-53144
 fusion reactor structural alloys, irradi., creep fracture by grain boundary cavitation, modelling 7-53859
 magnetic material, dislocation drag by defects (*Russian*) 7-63623
 mathematical modelling of dislocation-crack interactions 7-37993
 metals, FCC, quantitative assessment of forest hardening 7-65055
 metals, grain boundary interactions with dislocations (*Russian*) 7-63645
 metals, irradiated, deformation rate, impurity atmosphere effects (*Russian*) 7-33727
 microcrack behaviour near low angle grain boundary 7-2096
 mixed dislocations, dynamic annihilation study 7-44548
 nonactivation penetration into a random 2D array of point obstacles (*Russian*) 7-58278
 parallel screw dislocations, configurational force calcs. 7-26751
 pinning centre distrib., interaction force statistics (*Russian*) 7-58276
 radiation damage and defects, computer simulation studies 7-2048
 steel, austenitic stainless, low-cycle fatigue, 350 to 550°C, microstruct. developments, effect on cyclic strength and life 7-39646
 steel, austenitic stainless, strain hardening in powder metallurgy alloys 7-22721
 steel, Nb-V microalloyed, controlled rolled, yield strength rel. to microstruct. (*Chinese*) 7-13503
 strip, displacement loaded, semi-infinite crack, dislocation interaction, non-linear stress-strain law 7-44676
 unpinning from point defects, one-dimensional diffusion eqn. 7-26752
 AgBr-AgI crystals, strain-ageing 7-6627
 Al, fatigue, dislocation mobility (*French*) 7-13539
 Al-Li-Mn (Cu), precip.-hardened, cyclic stress response and deform. behaviour 7-22791
 Al-Zn, fatigue particle coarsening, vacancy creation 7-53895
 Bi, ultrasound absorption, amplitude and orientation dependences 7-26873
 Cd, twin crossing during dynamic loading, dislocation interactions (*Russian*) 7-6629
 Cu electrodeposits, decorated grain boundary dislocations, electron microscopy obs. 7-27185
 Cu-Co, age hardened, tensile deform., acoustic emission characts. 7-13536
 Cu-Fe-Al, cold rolled, γ to α transform. of fine α -Fe precipitates, mag. props. 7-3300
 Cu-Ni alloys, dislocation vel. determ., stress pulse etch pit and slip line cinematography techniques 7-63627
 Cu-Si (6 at.%), secondary grain boundary dislocation nodes at junction of three grains 7-63648
 α -Fe, cryst., point defect and edge dislocation interaction simulation and radiation creep rate estimation 7-21216
 α -Fe, edge dislocation, zones of spontaneous absorpt. of point defects 7-44599
 GaAs, dislocation-complex defect interactions, photoluminescence studies 7-16608
 GaAs epilayers grown on Ge or Ge/Si substrates, defects 7-21778
 GaAs FET arrays, electrical parameter mapping 7-32438
 GaAs LEC wafers, cathodolum. mapping, IR absorpt., X-ray topography obs. 7-33462
 GaAs, semiinsulating, electrophysical props., dislocation effects 7-16557
 Ge, dislocation transmission through $\Sigma=9$ symm. tilt boundaries, synchrotron X-ray topography, HVEM obs. 7-63646
 Ge, dislocation transmission through $\Sigma=9$ symm. tilt boundaries, dynamic and crystallographic anal. 7-63647
 InP, dislocation-complex defect interactions, photoluminescence studies 7-16608
 KBr microcrystalline powders, interstitial cluster stability 7-32485
 KCl, F-centre destruction at elevated temps. under elec. field 7-32488
 KCl:Ca, γ -irradi., Z₁-centre growth, effect of dislocations, thermolum. study 7-32487
 Kr monolayer adsorbed on graphite surface, dislocation interactions 7-2357
 MgO(Al₂O₃)_n, electron beam irradi., point defect aggregation, screw dislocation climb 7-63662
 Ni binary alloys, solid soln. hardening, flow stress, Young's modulus 7-13465

dislocation interactions continued

- Ni₃Al, solid soln. hardening with ternary additions, Young's modulus 7-13464
 Pb-Sn solder, deform. props. 7-46590
 Sb single crystals, dislocation thermoactivated amplitude-dependent internal friction (*Russian*) 7-51934
 Si, dislocation emission from cracks, X-ray topography obs. 7-38004
 Si, dislocation transmission through $\Sigma=9$ symm. tilt boundaries, synchrotron X-ray topography, HVEM obs. 7-63646
 Si, dislocation transmission through $\Sigma=9$ symm. tilt boundaries, dynamic and crystallographic anal. 7-63647
 Si, impurity gettering, defect-defect interaction mechanisms 7-16585
 Si, recombination channels, dislocations interaction with point defects, lumin. study 7-46094
 n-Si:P,C, electron-irradiated and injection-annealed, vacancies, dislocations and C interstitials 7-51815
 Xe monolayer on graphite, dislocation interactions 7-2357
 Zn, dislocation motion across two-component forest dislocations and point obstacles (*Russian*) 7-58277

dislocation jog motion *see dislocation jogs***dislocation jogs**

- point defect absorption by dislocations, preference parameter temp. depend. (*Russian*) 7-16607
 Al, neutron irradi., positron trapping rates, temp. depend. 7-46218
 Al-Hf dilute quenched cold-worked alloys, vacancy migration recovery processes, PAC and positron annihilation studies 7-39545
 α -Fe, dislocation pair jog, energy characts., mol. dynamics method anal. (*Russian*) 7-32440
 LiF crystals, influence of deformation temp. on change in density 7-44655
 Mg₂SiO₄:V, forsterite, high temp. deform., creep study 7-21332
 Mo, positron trapping by vacancies, loops and voids, positron annihilation studies 7-46216
 Ni, fatigued, crystal defects, positron annihilation studies 7-46213
 Zn, deformation recovery, positron annihilation spectroscopy 7-21329

dislocation locking

see also Cottrell atmospheres

- steel, low C, strain ageing, internal stress, Bauschinger effect 7-39612

dislocation loops

see also vacancy condensation loops

- 2D Frenkel-Kontorova model, dislocation generation at high stresses 7-32441
 B2 ordered alloy, edge dislocation, computation of core struct. 7-37991
 crystal with dislocations, first-order phase transitions 7-38178
 diamond, platelets, dislocation loops and voids, TEM anal. 7-16560
 dislocation motion modelling through complex dislocation ensembles in HCP cryst. lattice 7-63612
 ferromagnetic materials, defect and microstructural analyses using TEM 7-37817
 fibre reinforced metal, subjected to uniform temp. change, dislocations punched out around short fibre 7-21491
 first wall candidate alloys, HFIR irradi. microstruct. development 7-56824
 Frenkel-Kontorova model in 2D 7-44549
 fusion material, irradiation, model for interstitial dislocation loop nucleation and growth kinetics 7-51817
 hexaethylene glycol dodecyl ether, lyotropic liquid crystal, defect-mediated phase transition, electron-microscopy obs. 7-21439
 Inconel 718, Ni-base superalloy, creep deform., back stress determ. 7-46564
 metal tritides, disorder induced by aging 7-21199
 metals, FCC, cyclic deform., dipolar wall spacings in dislocation struct. 7-53825
 mobile interstitial atom-substitutional impurity complex form. (*Russian*) 7-12372
 planar polygonal dislocation loop self-energy calcs. in elastically anisotropic media 7-26750
 single crystals, defective structs., appl. of thickness dependencies for integrated intensities of X-ray scatt. (*Russian*) 7-51561
 small hexagonal loops, diffraction contrast images and lattice fringe patterns, computer simulation 7-44325
 SOS, double solid phase epitaxial regrowth, amorphous layer, self-implantation, ion energy, defect density 7-58691
 steel, austenitic stainless, swelling by electron irradi., influence of appl. stress (*Japanese*) 7-16632
 steel, austenitic stainless, TiN dispersion hardened, creep below transition stress 7-65079
 steel, austenitic stainless radiation damage process obs. using high voltage electron microscopy 7-51831
 steel, Cr-Ni-Mo-Nb, precipitates formation, effect of He 7-13460
 steel, ferritic, a/2 {111} dislocation loop formation 7-16565
 steel, ferritic stainless, He-doped, microstruct. evolution following 14 MeV Ni ion irradi. 7-58363
 steel, stainless and alloy, electron radiation damage in fusion reactor materials, voids 7-2064
 stress field of isolated subgrain 7-63613
 thin crystal with anisotropic distortion of cryst. lattice, X-ray beam Laue diff. (*Russian*) 7-58101
 Al, high purity samples, Doppler-broadened positron annihilation spectra, fast Fourier transform/power spectra deconvolution method 7-33481
 Al, neutron irradi., positron trapping rates, temp. depend. 7-46218
 Al, quenched, secondary defect form., isochronal annealing, positron lifetime study 7-39298
 Al single crystals, cyclic deform. at low const. plastic strain amplitude 7-65114
 Al-Cu-In alloy, deformed, θ' -phase precipitation 7-22691
 AlGaAs-GaAs superlattices, Se (Si)(Mg)(Be) ion implantation, intermixing, residual damage 7-26782
 Al₂O₃, neutron irradi., microstruct., mech. props. 7-51843
 CaSO₄:Dy, gamma radiation damage on thermolum. 7-38059
 CdS:Ri⁺(Kr⁺)(Ar⁺)(Ne⁺), ion implantation damage 7-26812
 CdTe, electron irradi., a (100) dislocation loops 7-6686
 CdTe, ion milling, TEM 7-39344
 Cr-Mo-Ni ferritic-martensitic steel, irradi. in RTNS-II, TEM study 7-58345
 Cu₂O(He) vacancy cluster stability calcs., void form., O and the impurity effects 7-51763
 Cu₃Au alloy, displacement cascade collapse at low temp. 7-51892
 CuFeS₂, natural chalcopyrite single crystals, deformed, TEM study 7-38002

dislocation loops continued

Fe, Armco, annealed and cold worked, neutron irradi. damage 7-2067
Fe-Cr-Ni, austenitic, electron irradi., conversion of stacking fault tetrahedra to voids 7-58342
Fe-Si, melt quenched, struct. formation 7-13480
GaAs, dislocation loops, TEM image profiles, electron diffr. two-beam dynamical theory 7-12071
GaAs, dislocation rosette generation round Vickers indentations, mobility and twinning, TEM study 7-63618
GaAs: Si(Si)(Zn)(Be), ion implanted, rapidly annealed, damage removal process 7-17043
GaAs:Be⁺, ion implanted, residual microstruct., TEM studies 7-32675
InGaAsP layers on InP (001), origin of grown-in dislocations 7-38415
InP:Fe, Czochralski-grown, stoichiometric-related faulted loops, struct. and lumin. props. 7-51772
MgAl₂O₄, neutron irradi., microstruct., mech. props. 7-51843
Mo, positron trapping by vacancies, loops and voids, positron annihilation studies 7-46216
Mo, radiation dislocation loops, clustering 7-12073
NaCl:Eu²⁺ crystals, γ -irradiated, colourability 7-12062
Ni and Ni-Cu, gamma-irradiated, point defect migration 7-6893
Ni-Al(Si), aged γ/γ' alloys, He²⁺ implantation studies 7-22690
Pd₂Si formation, dopant redistribution, in Si substrate 7-21255
Si 7-26753
Si, dislocation loops, generated by ion implantation and furnace annealing, depth profiles, RBS, X-ray diffr., TEM anal. 7-51882
Si, intrinsic gettering by butterfly-type defects 7-38047
Si, ion implantation, interstitial trapping, dopant migration and epitaxial regrowth 7-12103
Si photoelectrochemical and MIS solar cells, surface dislocation loops effect on J-V characts. 7-17862
Si ribbons, dendritic web grown, high temp. mech. behaviour, strain rate and temp. depend. of yield stress 7-65099
Si:Ar⁺, ion implanted thin film, defect form., dose depend. study 7-51793
Si:As, high dose implanted, defect density reduction by low temp. oxidation 7-58297
Si:As, implanted, supersaturated soln., defect struct., TEM obs. 7-58483
Si:As ion implanted, defect structs. generated by buried amorphous layer regrowth 7-38078
Si:As⁺, heavily doped, ion implant deactivation 7-17567
Si:Au, U- and W-shaped impurity diffusion profiles investigation 7-16805
Si:B layers, preamorphised and ion implanted, structural and elec. characterisation 7-52347
Si:B p⁺-n shallow junctions obtained by implantation into preamorphised Si, elec. charact. 7-38703
Si:BF₃⁺ (001), ion implanted, residual defects, cross-sectional TEM study 7-32471
Si:O, self-interstitial migration, dislocation loops and elongated Frank dipoles 7-58300
Si:O Czochralski wafers, electron traps resulting from O precipitation 7-21866
Si:P, pulsed laser processing via free carrier absorpt. 7-21273
n-Si:P,C, electron-irradiated and injection-annealed, vacancies, dislocations and C interstitials 7-51815
Si:PF₃⁺, ion implanted, recrystallisation kinetics during fast thermal annealing 7-16618
Si:Sn,B, shallow junction formation, preamorphisation by Sn implantation 7-7338
 β -SiC monocryst. thin films, ion implantation and annealing, amorphisation and recryst. processes study 7-16596
Ti, electron beam welded, neutron irradi. effects 7-56832
Ti-6Al-4V, electron beam welded, neutron irradi. effects 7-56832
TiN (100) epitaxial film sputtering, defect density, ion irradi. effects, TEM study 7-58684
VB, 14 MeV neutron irradi., TEM dislocation obs. 7-56819
W-H system, H-defect interactions, positron annihilation studies 7-38045
ZnS(Se), ion milling, TEM 7-39344
Zr₇₀Cu₃₀ melt spun ribbons, collective flux pinning dimensional crossover obs. 7-17143

dislocation motion

for dislocation relaxation see dislocation damping
see also dislocation climb; slip
2D Frenkel-Kontorova model, dislocation generation at high stresses 7-32441
alkali halide crysts., dislocation displacements distrib. characts., local dislocation density effects (Russian) 7-21214
alloys, FCC, internal friction, interaction between dislocation kinks and substitutional solute atoms 7-51935
alloys with periodic antiphase boundary struct., dislocation motion 7-63620
asymmetric radiation due to oscillating dislocations 7-44546
Au, internal friction background, low-frequency 7-38113
bias stress expts. using a two-wave acoustic method 7-63621
critical resolved shear stress for systems with general periodic stress fields 7-38085
diglycine sulphate single crystals, anhydrous, elec. activated dislocation motion 7-12069
disordered crystals with high Peierls barriers, dislocation dynamics 7-6625
dynamic kinks on dislocations 7-2016
edge dislocations, velocity in a crystalline solid, applied shear stress depend. 7-21206
grain boundary movement analogous to dislocation movement, anal. 7-6637
highly deformed materials, low energy dislocation struct. 7-63614
ledge interphase boundaries, growth kinetics, computer modelling 7-65041
metals, BCC, H-dislocation interaction mechanism, embrittlement and dislocation motion 7-44600
metals, dislocation mobility, damping by conduction electrons, kink model 7-51768
metals, steady state creep, strain response to complete unloading 7-59568
mismatched overlayers, dislocation depinning, mol. dynamics investig. 7-7011
moving dislocations in II-VI semiconductors, dislocations, effect on physical props. 7-7224
Nimonic 105, Ni-base superalloys, precip. and tensile deform. behaviour 7-65078

dislocation motion continued

nonequilibrium processes, computer simulation 7-18688
semiconductors under illumination, dislocation mobility 7-44545
serrated yielding, computer simulation using negative resist. characts. 7-2089
smectic A liquid crystals, screw dislocation dynamics 7-21090
steel, alloy, structure evolution during strong plastic deformation (Russian) 7-3358
steel, Cr-Ni-Ti-Al, cold-prestrained, length changes during annealing 7-65058
superplastic to non-superplastic deform., transition at high strain rates 7-46586
TEM, first recorded obs. of moving dislocations 7-32444
twinning in plastic deformation, simple model 7-38018
Zircaloy-4, cold worked, anelastic contrib. to high temp. stress relax., model 7-65072
Al, dislocation kinks, tunneling, acoustic study 7-2023
Al, fatigue, dislocation mobility (French) 7-13539
Al-Cu-MG, annealed, creep, 623-723 K 7-53802
Au crystals, small, surface twin form., high resolution electron microscopy 7-44566
Bi, ultrasound absorption, amplitude and orientation dependences 7-26873
CdS single crysts., acoustoelectronic interaction, ultrasonic attenuation and amplification, dislocation motion effects (Russian) 7-21953
Cr-base alloys, high-alloy, plasticity, effect of twinning (Russian) 7-46582
Cu based alloys, internal friction, Young's modulus, amplitude relationship (Russian) 7-65075
Cu, fatigue crack propagation rate model based on a dislocationmechanism 7-8093
Cu, structure evolution during strong plastic deformation (Russian) 7-3358
Cu-Zn (30 wt.%), anomalous instantaneous creep strain, obs. after stress change 7-46585
Cu-Zn-Al, dislocation density and mobility during reversible martensitic transforms. 7-26759
 α -Fe, moving edge dislocation, interaction with moving defects (Russian) 7-12114
GaAs, dislocation rosette generation round Vickers indentations, mobility and twinning, TEM study 7-63618
GaAs, undoped, thermal activation of plastic deform., 528-813K 7-6710
Ge, dislocation transmission through $\Sigma=9$ symm. tilt boundaries, synchrotron X-ray topography, HVEM obs. 7-63646
Ge, dislocation transmission through $\Sigma=9$ symm. tilt boundaries, dynamic and crystallographic anal. 7-63647
InSb, α dislocations, motion, small shear stresses 7-44553
InSb, n-type, 60° dislocation motion, etching studies 7-63619
KBr microcrystalline powders, interstitial cluster stability 7-32485
KCl, F-centre destruction at elevated temps. under elec. field 7-32488
KCl, γ -irradiated, influence of plastic deformation on colour centre conc. 7-44538
KCl microcrystalline powders, correl. between microhardness, dislocation mobility and coloration stability 7-32436
KCl:Ca, γ -irrad., Z₁-centre growth, effect of dislocations, thermolum. study 7-32487
LiF, γ -irradiated, influence of plastic deformation on colour centre conc. 7-44538
LiF, highly pure single crystals, dislocation mobility 7-26754
LiF shock-loaded single crysts., dislocation transport, impact surface sources effects calcs. 7-44543
NaCl, dislocation motion, flexible and reacting dislocation forest, simulation 7-44544
NaCl:Eu²⁺ crysts., mechanical strength, dopant distrib. and γ -irrad. effects study 7-26800
Ni, creep, electron bombardment effect, 200 to 500°C 7-8062
Ni, creep, T charging, He bubble migration and coalescence 7-65102
Ni, structure evolution during strong plastic deformation (Russian) 7-3358
Ni-base superalloys, creep resist. improvement, role of Re additions, APFIM study 7-22772
Si 7-26753
Si, dislocation transmission through $\Sigma=9$ symm. tilt boundaries, synchrotron X-ray topography, HVEM obs. 7-63646
Si, dislocation transmission through $\Sigma=9$ symm. tilt boundaries, dynamic and crystallographic anal. 7-63647
Si single cryst., dislocation line kink mobility and double kink form. kinetics 7-26760
Si, twinning partial dislocations, velocity 7-63629
SiC, CVD, microstruct. around indentation, TEM obs. (Japanese) 7-22822
W-Re, damage mechanisms, cold brittleness, dislocation motion (Russian) 7-59619
(ZrO₂)_{0.9}(Y₂O₃)_{0.1} fliantite crysts., bending and compressive strength temp. depend. meas. 7-44653

dislocation motion, nonconservative see dislocation climb

dislocation motion hindrance see dislocation drag

dislocation multiplication

austenitic stainless steels, fatigue props., time-depend modes, dislocation concepts appl. 7-28128
steel, low C, work hardening, softening and dislocation multiplication 7-3324
steel, Ni-Cr, deform. dislocation struct., fracture 7-33740
SiC, 6H single crysts., dislocation glide induced plasticity (Japanese) 7-21215
Sn surface, plastic deformation, multiplied dislocations, density gradient 7-26757

dislocation nucleation

2D Frenkel-Kontorova model, dislocation generation at high stresses 7-32441
cleavage fracture, ductile-brittle transition 7-21339
grain boundary sources for dislocations, analytical treatment 7-44568
stress relaxation, dislocation-diffusion mechanisms, review (Russian) 7-32564
Fe-Si, plasticity, influence of thermomechanical parameters 7-13512
LiF, crack tip dislocation nucleation obs. in bulk specimens 7-37996
Si, ion implantation, interstitial trapping, dopant migration and epitaxial regrowth 7-12103

dislocation nucleation continued

- Si LOCOS substrates, nucleation of dislocations at thin film edges 7-51597
- Si:Ge, Ge⁺ preamorphisation implants, effect on extended defect formation during subsequent solid phase epitaxy 7-16599

dislocation pile-ups

- crack emanating from circular hole in loaded plane 7-43775
- grain boundary-slip interaction, role in cavity nucleation 7-21219
- metallic crystals, twin boundary reversible shift dynamics, dislocation pile-up model (*Russian*) 7-16573
- steel, high strength, near threshold fatigue crack growth behaviour, effect of prior austenitic grain size 7-53906
- Cd, polycrystalline, work-hardening and recovery during steady-state creep 7-63734
- Ga_{0.94}Al_{0.06}Sb/GaSb epitaxial struct., misfit dislocations anomalous visibility, Bragg geometry X-ray topograms 7-2019
- Ge, dislocation transmission through $\Sigma=9$ symm. tilt boundaries, dynamic and crystallographic anal. 7-63647
- Si, dislocation transmission through $\Sigma=9$ symm. tilt boundaries, dynamic and crystallographic anal. 7-63647
- Si, indentation dislocation rosettes length, influence of Vickers indenter edge orientation rel. to slip directions 7-58284

dislocation pinning

- see also *dislocation damping*
- fluctuation unpinning from point defects, one-dimensional diffusion eqn. 7-26752
- ice, pure and doped, US absorpt., dislocation damping 7-26756
- metals, fatigued, dislocation patterning, labyrinth structures, rotational effects 7-38009
- mismatched overlayers, dislocation depinning, mol. dynamics investig. 7-7011
- pinning centre distrib., interaction force statistics (*Russian*) 7-58276
- steel, austenitic stainless, high cycle fatigue props., age hardening 7-13598
- steel, stainless, martensitic and austenitic, amplitude depend. damping rel. to annealing and tempering (*German*) 7-13498
- Al-Ag (5 wt.%), anelastic effects, quench sensitivity, precip. and dissolution 7-53784
- Cu, polycrystalline, US and neutron irradi., struct. and mech. props. (*Russian*) 7-3402
- Cu-based binary alloys, Young's modulus, microalloying effects (*Russian*) 7-33711
- KBr microcrystalline powders, interstitial cluster stability 7-32485
- KCl:CaCl₂, internal friction 7-38114
- Mg, dislocations, interaction with pinning centres, 4.2 to 295K 7-44558
- Ni and Ni-Cu, gamma-irradiated, point defect migration 7-6893
- W-Ni dilute alloy, Ni enrichment at screw dislocations, atomistic calcs. and atom probe FIM meas. 7-33638
- Zr, internal friction due to grain boundary relax. 7-65076

dislocation relaxation see *dislocation damping***dislocation scattering**

- used for carrier scattering by dislocations
- metals, transverse magnetoconductivity, dislocation scatt. effects (*Russian*) 7-52547
- Al, high purity, elec. cond., low-temp. plastic deform. effects (*Russian*) 7-17009
- K, electron-electron and electron-phonon interactions, plastic deform. effects 7-12710
- K-Rb dilute alloy, electron-electron and electron-phonon interactions, plastic deform. effects 7-12710

dislocation sources

- see also *Frank-Read sources*
- edge dislocation climb, vacancy diffusion and capture calcs. (*Russian*) 7-44550
- grain boundary sources for dislocations, analytical treatment 7-44568
- semiconductor crystals, Czochralski, growth, slip dislocation generation 7-22467
- LiF shock-loaded single crystals, dislocation transport, impact surface sources effects calcs. 7-44543
- Mo(100), pulsed laser irradiated, use of LEED for surface damage charact. 7-21592
- Si:As films, preannealed and As ion implanted, structural changes during transient post-annealing 7-16904
- Sn surface, plastic deformation, multiplied dislocations, density gradient 7-26757

dislocation structure

- alloys, dislocation glide during ageing, hardening phase particle interaction modelling (*Russian*) 7-38010
- alloys with periodic antiphase boundary struct., dislocation motion 7-63620
- austenitic stainless steels, fatigue props., time-depend modes, dislocation concepts appl. 7-28128
- BCC metals, polycrystalline, dislocation struct., strain hardening (*Russian*) 7-59545
- deformation at min. elastic strain energy 7-38097
- fatigue failure at stresses below fatigue limit 7-38102
- fracture, in-situ, TEM obs., influence of several parameters 7-6713
- high resolution electron microscopy in materials science (*German, English*) 7-39806
- highly deformed materials, low energy dislocation struct. 7-63614
- low energy, props. and effects 7-63622
- low energy dislocation structures in interfaces 7-63976
- Luders bands, phenomenological theory 7-21328
- metals, deformed, heterogeneous dislocation distrib., two-parameter description 7-44547
- metals, fatigued, dislocation patterning, labyrinth structures, rotational effects 7-38009
- metals, FCC, cyclic deform., dipolar wall spacings in dislocation struct. 7-53825
- metals, grain boundary structure (*German*) 7-44571
- metals, internal interfaces, grain boundary struct., intergranular fracture 7-26766
- metals, steady state creep, strain response to complete unloading 7-59568
- monolayer films, equilibrium configurations, molecular dynamics simulations 7-21771
- Nimonic 80, coupled plastic and creep damage at finite deform. (*Japanese*) 7-33736
- semiconductors, grain boundaries, at. struct. 7-6638
- semiconductors, optical beam induced current imaging of dislocations 7-58106

dislocation structure continued

- smectic A liquid crystals, screw dislocation dynamics 7-21090
- sphalerite single crystals, plastic behaviour between 473 and 873K, dislocation structure, TEM anal. 7-2093
- steel, austenitic stainless, creep and anelasticity at const. homogeneous dislocation struct. 7-17586
- steel, austenitic stainless, dislocation structure and secondary cyclic hardening at 600°C 7-33783
- steel, austenitic stainless, extrinsic grain boundary dislocations, spreading kinetics 7-44569
- steel, austenitic stainless, fusion reactor first wall, fast neutron irradi., microstruct. evolution model 7-51846
- steel, austenitic stainless, low-cycle fatigue, 350 to 550°C, microstruct. developments, effect on cyclic strength and life 7-39646
- steel, C, creep, glide plane stresses, yield point, dislocation theory (*Russian*) 7-59580
- steel, C, dislocation structure, rolling temp. effects (*Russian*) 7-44552
- steel, Cr type, dislocation struct. after hydraulic pressing followed by austempering 7-3334
- steel, Cr-Mo-V, nitrided, wear resist rel. to preliminary thermomech. treatment 7-17659
- steel, dislocation struct. rel. to cyclic bending strain 7-22760
- steel, ferritic stainless, He-doped, microstruct. evolution following 14 MeV Ni ion irradi. 7-58363
- steel, high Ni, reactor irradi., dislocation struct. and steady-state creep (*Russian*) 7-2068
- steel, HSLA, mech. props. rel. to ferrite substruct. and grain size. 7-13531
- steel, HSLA, Nb, ductile fracture, plastic deform. mechanisms 7-28115
- steel, low alloy, damaged surface, comp., displacement dislocations, Auger spectra (*Russian*) 7-59620
- steel, Ni-Cr, deform. dislocation struct., fracture 7-33740
- steel, Ni-Cr-Mo, phase transform., structural inheritance, dislocations effect (*Russian*) 7-39503
- steel, Si-Mn-Mo, austenitising, bainite transform., lump-like composite struct., mech. props. (*Chinese*) 7-13477
- steel, stainless, transition class, deform. method effect on microstruct. 7-3299
- strengthening diagram, relationship with dislocation kinetics (*Russian*) 7-53753
- US attenuation spectral analysis of grain size and dislocation content 7-65271
- Zircaloy-4, low cycle deform. at elevated temps. 7-22832
- Zircaloy-4, temp. depend. of elongation 7-65094
- Al, fatigue, dislocation mobility (*French*) 7-13539
- Al, monocrystalline, Harper-Dorn creep, dislocation network theory 7-22749
- Al, repeated cold rolling effect on recrystn. Vickers hardness obs. 7-59543
- Al-Cu (2 wt.%) single crystals, rolled, shear band form. rel. to θ' precipitates 7-3385
- Al-Cu (2 wt.%) single crystals, rolled, shear band form., θ precip. 7-28099
- Al-Cu-Mg, Al-Mg, plastic deform., AE, X-ray obs. (*Russian*) 7-46579
- Al-Cu-Mg, deformed, dislocation struct., AE obs., electron microscopy (*Russian*) 7-39832
- Al-Cu-Mg, hot workability, recrystallisation during torsional deform. (*Korean*) 7-46559
- Al-Li-Cu-Mg-Zr, yield stress, temp. and strain rate depend. (*Japanese*) 7-33734
- Al-Li-Cu-Zr, nucleation of precipitates 7-46476
- Al-Mg, creep, stress exponent, dynamic strain ageing, dislocation struct. 7-17591
- Al-Mg, deformed, dislocation struct., AE obs., electron microscopy (*Russian*) 7-39832
- Al-Mg (5 at.%), creep, interpretation of internal stress determ. from dip tests 7-65091
- Al-Si-Pb-Bi, duplex alloys, melt quenching, microstruct. supercond. props. 7-45593
- Al₃Ni-Al eutectic alloy, Bauschinger effect, influence of Al₃Ni dispersion state (*Japanese*) 7-22761
- Au, defects in multiply-twinned particles 7-16558
- CaF₂, cryst., defect struct., high temp. (*German*) 7-32449
- CdTe high-resistivity undoped crystals, defects, EBIC studies 7-21211
- CoO, deformed, dislocation struct., TEM study 7-21209
- Copper, extrusion, dislocation density determ. (*Russian*) 7-58285
- Cu alloys, irradi. in FFTF to 16 dpa at 450°C, microstruct. eval. 7-51837
- Cu alloys, rapidly solidified powder metallurgy, irradi. to 13.5 dpa with neutrons, microstruct. evolution and swelling 7-51840
- Cu, fatigue near surface indentations and pits, deform. 7-46628
- Cu, polycrystalline, high cycle fatigue behaviour, effect of grain size 7-46626
- Cu single crystal, deformed, lattice parameter changes through long-range internal stresses (*German*) 7-16673
- Cu single crystals, fatigue crack initiation mechanism, persistent slip band model 7-53869
- Cu, third-order elastic modulus, effect of plastic deform. (*Russian*) 7-46544
- Cu-Zn-Al, thermoelastic, two-way memory effect, dislocations origin 7-22754
- Fe, creep, glide plane stresses, yield point, dislocation theory (*Russian*) 7-59580
- Fe-Au, solute segregation, grain boundary structural transform. 7-22687
- Fe-Ni, austenitic, Mag. ordering and mech. props. (*Russian*) 7-58280
- Fe-Ni-C alloys, martensitic transform., effect of soln. strengthening of austenite 7-53728
- Fe-Si, melt quenched, struct. formation 7-13480
- Fe-Si, plasticity, influence of thermomechanical parameters 7-13512
- Fe-Si (3.2 wt.%), mag. props., influence of substructural features 7-12996
- Fe-Si single crystals, deformed, dipole drift mechanism of early stages of dislocation pattern 7-38098
- GaAs crystals, selective etching and photoetching of CrO₃-HF aq. solns. 7-32442
- GaAs dislocated and In-doped dislocation free, inhomogeneities obs. by video-enhanced IR topography 7-32446
- GaAs, dislocation core struct. 7-38007
- GaAs, dislocations, obs. by transmission IR microscopy 7-32447
- GaAs, dislocations, stereographic obs. by IR light scatt. 7-32235

dislocation structure continued

GaAs high quality layers grown on Si by MOCVD, misfit dislocations at interface 7-27922
GaAs LEC wafers, cathodolum. mapping, IR absorpt., X-ray topography obs. 7-33462
GaAs, semiconducting and semi-insulating LEC crystals, SEM-EBIC characterisation 7-51777
GaAs:In crystals, LEC growth, grown-in dislocation elimination 7-22465
GaAs:Si, dislocations, STEM and CTEM micrographs 7-1825
Ge crystals, high temp. deform., fine slip band struct. (Russian) 7-44561
GeSi-Si heterostructures, MBE grown, structural props., quality, electron diffr., imaging obs. 7-7036
In As_{1-x}Sb_x epitaxial layers, MOCVD, strained-layer superlattices 7-39407
InP:Ga,As,Sb single cryst., LEC growth, isoelectronic doping, dislocation density, X-ray topography 7-33549
KH₂PO₄ crystals grown at boiling point, surface microtopography 7-21581
LiF, cryst., defect struct., high-temp. annealing effects (German) 7-32448
MgO single crystals, high temp. creep and dislocation struct. at low stresses 7-21336
MgO:Fe, small angle [001] twist boundaries, Fe solute effect 7-32459
MnO, deformed, dislocation struct., TEM study 7-21209
Mo, cyclic deformation, dislocation substructures and hardening 7-21330
Mo single cryst., rolling, dynamic recovery rel. to deform. temp. (Russian) 7-65095
Mo, single crystals and polycrystals, high-angle boundaries of deformation origin 7-6712
Mo-base alloy, welded joint, strain hardening and fracture (Russian) 7-53877
NaCl filamentary crystals, yield stress and plastic flow 7-51917
Nb, polycrystalline, US excitation, critical current, dislocation struct., flow limit (Russian) 7-58966
Nb single crystals, cyclic deform., dislocation behaviour 7-63729
Nb-Zr, mixed dislocations, nuclei atomic configs., computer modelling (Russian) 7-58281
Ni base superalloys, hot deformed, matrix dislocations, weak beam electron microscopy obs. (French) 7-21210
Ni, dislocation structure after US deformation, physical props. (Russian) 7-44699
Ni dislocation structure evolution during creep, alternating mag. field effects study (Russian) 7-58286
Ni-base superalloy, single cyst., SRR99, creep behaviour 7-17587
Ni-CO, limitations of dynamic recovery as revealed by temp. change tests at large strains 7-22723
Ni-P coating, electrolytic, electron microscope obs. of struct., P content depend., amorphous layer form. 7-8157
Ni₃Al, dislocation bowing and partial separation during in situ straining, TEM obs. 7-63617
Ni₃Al, dislocation line stability 7-21212
Ni₃Ga, atomic ordering, strain disruption (Russian) 7-53808
Si, Czochralski grown, tensile props., 900-1200°C 7-51922
Si, dislocation density reduction by thermal cyclic annealing 7-12072
Si, dislocation luminescence lines, polarisation 7-39154
Si:B plastically deformed crystals, dislocation struct. and elec. activity, annealing effects study 7-37998
SiC, sintered, microstruct. and props., influence of fabrication method (Japanese) 7-22622
Ta-T system, distortion by He form. 7-51717
W, n (Russian) 7-51699
WC, high press. sintering, microstruct. 7-39470
WC-Co, high press, sintering, microstruct. 7-39470
WC-Co composites, plastic deform. mechanisms, dislocation struct., TEM obs. (French) 7-22765
ZN single crystals, creep, dislocation struct., high press. effect (Russian) 7-59578
Zn, amplitude-dependent internal friction, press. depend. (Russian) 7-58409
Zn-Cd monocrystals, dislocation struct. as function of Cd content (Russian) 7-44556
Zr, dislocation substruct. after hydrostatic extrusion (Chinese) 7-6626
ZrT, ZrT_{1.6}, ageing, TEM study 7-51773

dislocation translation see slip

dislocation-vacancy interactions see vacancy-dislocation interactions

dislocations

For pipe diffusion, see diffusion in solids. See also dislocation
see also Bordoni effect; Cottrell atmospheres; disclinations; edge dislocations; grain boundaries; prismatic dislocations; screw dislocations
A15 superconductors, mechanisms for martensitic transformations 7-38188
alloys, dislocation annihilation and strain hardening (Russian) 7-46500
anthracene single crystals, dislocation photolum. study, exciton scatt. effects (Russian) 7-22343
antiferromagnets, dislocation-generated domain walls at spin-reorientation phase transitions (Russian) 7-53023
Auger recomb. of dislocation excitons 7-38578
austenitic steels, small precip., moire imaging in TEM 7-46490
 β -brass, strength anomaly, effect of prestrain 7-38094
Burgers circuit about a dislocation, reanalysis 7-37990
coherent multilayer structures, damage by dislocation or crack injection 7-21674
continuous two-level media, defects, motion and plastic fields (Russian) 7-58260
continuum theory 7-51767
crack tip field, work-hardening, nonlinear dislocation model 7-43772
crystal with dislocations, first-order phase transitions 7-38178
crystallites, 2D, crack growth, computer modelling 7-43787
diamond, strain measurement in convergent beam electron diffraction 7-16562
diamond struct., axial channelling radiation from positrons, dislocation effects 7-12180
disordering transitions, nucleation mechanism, review 7-44743
dissociated dislocation in weak beam image, determ. of sign, electron microscope studies 7-44323
distributions, stochastic models 7-12066
electron-acoustic microscopic study on dislocation lines in the base region of npn Si-Tr 7-20538
epitaxial layer-substrate interface defects 7-21715
epitaxial structures, X-ray diffr. analysis 7-21047

dislocations continued

grain boundary dislocation form. by coincidence tilt boundary bulging 7-38015
graphite intercalation cpds., staging dislocation electronic struct., electron scatt. rates, residual resist. 7-52558
growth dislocations, in-situ detection using Seebeck effect 7-32451
III-V semiconductor laser, effect of LPE grown crystal defects on reliability 7-36960
III-V semiconductors, lattice defects detection using IR tomography 7-32234
impurity diffusion, with form. of segregation phases at dislocations (Russian) 7-52146
incommensurate structures, soliton line formation, kinetics 7-38157
insulators, high dose radiation damage, voids and dislocations 7-32502
kinetics behind shear shocks 7-26862
lattice damage due to dynamic loading, simulation 7-26835
low angle symmetric tilt boundary, thermal fluctuations 7-21220
magnetically ordered regions in crystals with dislocations, static susceptibility 7-38851
metallic filaments strongly anisotropic 2D system, weak localisation in magnetoresistance 7-45282
metals, BCC and FCC cryst. struct., H trapping, thermal anal. obs. 7-22830
metals, EM wave interaction with dislocations, conduction electron density (Russian) 7-63615
metals, polycrystalline BCC, work hardening scheme 7-33691
metals, radiation swelling, vacancy-interstitial and interstitial-impurity complex form. (Russian) 7-58309
micas, synthetic, growth spirals and complex polytypism, occurrence frequencies 7-37997
nondegenerate semiconds., charged dislocation hole capture, hole thermal ionisation and free density calcs. 7-38574
nonlinear continuous medium model for stress, strain and displacement fields 7-6623
nonlinearity elastic solids, Volterra dislocations, large deformations, Weingarten theorem generalization 7-43669
plastic distortion moments, disclinations and Somigliana dislocations 7-63611
plastic flow instabilities, dislocation models 7-38099
plastic solids, dislocation moment, classical and statistical thermodynamics 7-29958
positron trapping and annihilation and Peierls-Nabarro dislocation core model 7-39263
precipitation hardening, creep and reverse mechanical aftereffect processes (Russian) 7-3317
pyroxene, mineral lattice defects and crystalline plasticity, review (French) 7-34476
quasicrystal diffraction patterns, distortion and peak broadening 7-11981
quasicrystals, phonons, phasons and dislocations 7-6732
semiconductors, light absorption by dislocations, exciton effects 7-53371
SOI films, zone melting recrystallisation, subboundary structure 7-38388
SOI films scan-melted at low velocities, subboundary misalignment 7-38387
solid solution softening effect, kink nucleation on dislocations 7-44662
stainless steel, ion irradiated, X-ray microanalysis, of equilibrium and nonequilibrium segregation 7-46488
steel, growth under impact tension 7-28105
steel, structural, cleavage fracture toughness predictions 7-13544
superalloys and ceramics, electron microscopy studies, symposium, Nantes France (July 1986) 7-18479
superplastic deformation, boundary migration, grain growth 7-17600
surface features, thermal wave imaging studies in a SEM 7-44874
tribochemistry, chemical reaction increase by friction 7-46868
X-ray microanalysis, of equilibrium and nonequilibrium segregation 7-46488
YZ-LiNbO₃, domain structure and lattice defects, effects of piezoelectricity, TEM anal. 7-2999
Al, defect struct. during plastic deformation, periodic variation 7-44656
Al internal friction peak obs., dislocation configurations 7-38115
Al, polycrystalline, deformed, positron trapping and annihilation 7-39258
Al, shocked, polycryst. positron annihilation ang. correlation studies 7-46197
Al, surface damage, dislocation struct., TEM anal. 7-16564
Al thin films on Si substrates, plastic props., meas. by submicron indentation hardness, substrate curvature techniques 7-58720
Al under shock loading conditions, constitutive relation 7-26865
Al-Zn-Mg, serrated flow, second phase precip., dislocation ageing 7-22755
Al-Zn-Mg (4.5, 1.75 at.%), ageing, specific surface energy of Guinier-Preston zones 7-28046
Al₂O₃, bicrystals, high-purity, grain boundary structures 7-58668
AlPO₄, modulated phase, electron microscopy study 7-26937
BaF₂, phase transitions, influence of shear deformation 7-21429
Cd, positron lifetimes, prevacancy effect 7-37973
CdTe-GaAs heteroepitaxial interface, at. resolution HVEM study 7-2392
CsI dislocation study using US technique 7-21362
CsI single crystals, dislocation internal friction mechanisms study 7-63625
Cu dislocated single cryst., sub-grain misorientation, de Haas-van Alphen meas. 7-12300
Cu, dislocation mechanism based model for stage II fatigue crack propagation rate 7-21338
Cu, dislocation-mechanics-based constitutive relations for material dynamics calcs. 7-63706
Cu electrodeposits, decorated grain boundary dislocations, electron microscopy obs. 7-27185
Cu, near-threshold fatigue crack propag. and high cycle fatigue 7-13545
Cu-Zn alloy, cyclic BCC-9R martensitic transform.-induced dislocations Burgess vector, electron microscopy studies 7-51775
Cu-Zn-Al, thermoelastic, two way memory effect, dislocation form. model 7-22741
Cu₃Au ordered alloys, twin boundary structure, TEM anal. 7-2027
CuZnAl alloys, β -phase, defects study by positron annihilation 7-39297
Fe, dislocation-mechanics-based constitutive relations for material dynamics calcs. 7-63706
 α -Fe, plastic deformation, magnetoacoustic and Barkhausen emission study 7-45749
 α -Fe single crystals, plastically deformed, dislocation arrangement anal. using magnetic small-angle neutron scatt. 7-2021
Fe-C-H system, H charged, methane bubble form., positron studies 7-37967

dislocations continued

- Fe-Cr-C, martensite nucleation, dislocations, grain boundaries, plastic accommodation 7-28040
 Fe-Ni, martensitic transform., defect form., positron annihilation study (Chinese) 7-39213
 Fe-Ni alloys, martensitic transform., positron annihilation study of defects 7-39266
 Fe-Ni(-C), martensite nucleation, dislocations, grain boundaries, plastic accommodation 7-28040
 Fe-Si (5.8 at.%) bicrystals, plastic deform., coincident twin boundaries 7-13502
 FeNiCr, strain measurement in convergent beam electron diffraction 7-16562
 γ -Fe₂O₃ particles, pure and Co-modified, microstructural defects 7-58497
 Ga growth into supercooled melt, faceted solid-liq. interface kinetics, kinetic roughening 7-58172
 GaAlSb/GaSb (111) heterostructures, signs of misfit dislocations, X-ray topographic determ. 7-38349
 Ga_{0.94}Al_{0.06}Sb/GaSb epitaxial struct., misfit dislocations anomalous visibility, Bragg geometry X-ray topograms 7-2019
 GaAs, Czochralski grown, defect. conc., spatially resolved photoluminesc. 7-22341
 GaAs, dislocation containing, positron annihilation 7-39279
 GaAs, EL2 clusters, scattering and absorpt. of IR light 7-53382
 GaAs LEC substrates, EL2 deep donor kinetics under annealing, IR absorpt., DLTS, Hall effect meas. 7-32955
 GaAs, MOCVD growth on Si, band gap energy and stress 7-38368
 GaAs molecular beam epitaxial layers, defect density reduction by thermal annealing, TEM study 7-45041
 GaAs, point defects, props. and processes, dislocation form. and characterisation (Japanese) 7-7151
 GaAs, semi-insulating, IR light scattering from defect centres 7-64620
 GaAs, semi-insulating, photoluminescence imaging using laser scanning microscope 7-53384
 GaAs semi-insulating cryst. characts., IC substrate appls. (Japanese) 7-6622
 GaAs semi-insulating thin wafers, EL2 defect and dislocation mapping, near-IR transmittance meas. 7-63605
 GaAs seminsulating LE wafers, radiative centres, dislocations after plastic deform., local photoluminescence study 7-33458
 GaAs thin semi-insulating wafers, EL2 distrib., dislocation network correl., near IR absorpt. maps and X-ray topographs 7-21203
 GaAs, undoped semi-insulating, dislocations, deep trap levels, FET meas. (Chinese) 7-12643
 GaAs, X-ray topographic examination 7-32225
 GaAs:Cr semiinsulating LEC wafers, microhardness cartography 7-32886
 GaAs:In crystals, dislocations, in situ X-ray topographic studies 7-21207
 GaAs:In(Cr), doped and undoped, microdefects obs. by IR light scatt. topography 7-32662
 GaAs:Si, ion implanted, amorphisation and epitaxial regrowth, defect depth profiles 7-12088
 GaAs:Si, MBE growth, carrier concentration, dislocation effects 7-58682
 GaAs/AlGaAs heterostructs. on Si substrate, MOCVD and MBE growth 7-7883
 GaAs/GaNAs interface, EELS near a single misfit dislocation 7-33497
 GaAs-GaAlAs interface dislocations, stereographic obs. by IR light scatt. 7-32235
 GaAs-GaAs:In epitaxial layers, dislocation reduction, device performance effects 7-7354
 GaAs-In_{0.4}As strained layer superlattices, photolum. microimaging of dislocations 7-27161
 GaAs-Si heteroepitaxial interface, at. resolution HVEM study 7-2392
 GaInAs, Czochralski-grown, dislocation effects investg. 7-7261
 GaP films, MBE growth on Si(211), defects obs. 7-58695
 GaP-GaAs_{1-x} strained layer superlattices, photolum. microimaging of dislocations 7-27161
 GaSb/GaSb:Si (111) autoepitaxial structures, signs of misfit dislocations, X-ray topographic determ. 7-38349
 Ge, bicrystal boundaries, transient spectra of dislocation levels 7-52497
 Ge:Sb single cryst., extended defects, X-ray topography meas. 7-38020
 Ge-GeO₂, defect formation, during thermal oxidation 7-65237
 Ge, Si_{1-x} multilayers, MBE grown, thermally annealed, Ge diffusion, strain relax., ion channelling, backscattering anal. 7-6896
 HgCdTe, bulk melt growth and LPE, defect control 7-64940
 Hg_{1-x}Cd_xTe crystals, lattice defect imaging, high resolution electron microscopy obs. 7-51769
 In, positron lifetimes, prevacancy effect 7-37973
 InGaAs layers on InP, LPE growth 7-33608
 InGaAs/GaAs lattice-strained double heterojunction bipolar struct., comp., recomb. props. and device performance 7-64322
 In_{0.4}As-In_{0.6}Al_{0.4}As superlattices, lattice-matched and lattice-mismatched, dislocation filtering 7-21671
 InGaAsP, LPE growth on GaAs_{0.7}P_{0.3} substrate, crosshatch pattern 7-59472
 In_{1-x}Ga_xP epitaxial layers, LPE, surface morphology rel. to lattice mismatch 7-33604
 InP substrates, influence of inhomogeneities on quality of quaternary layers 7-32770
 InP-InP:As epitaxial layers, dislocation reduction, device performance effects 7-7354
 KCl:Ca, γ -irrad. Z₁ colour centres, mech. bleaching form. 7-6620
 KTaO₃ UHF dielectric resonators, appearance of dislocations during pressure 7-7642
 Kr, defect props. in condensed two-dimensional lattice 7-2018
 Kr monolayer adsorbed on graphite surface, dislocation interactions 7-2357
 YZ-LiNbO₃, dislocation electric fields and small-angle grain boundaries, ferroelectric domains 7-3000
 Mg, dislocations, interaction with pinning centres, 4.2 to 295K 7-44558
 NH₄H₂PO₄ crystals, kinetics of dislocation growth of dipyrmaid and prism faces 7-58578
 NaCl whisker crystals, strength, depend. on dislocation struct. 7-45101
 Ni, dislocation arrangements in single crystals fatigued at low temps. 7-12068
 Ni-base alloy, (Nimonic 75), creep-fatigue interaction, SEM and TEM studies (Chinese) 7-13543
 Ni₃B₂Si₃, ultrafine grained, creep deformation mechanisms 7-22781
 NiSi₂-Si (111) epitaxial interface, strain meas. by MeV ion channelling 7-27157
 Pt surface, graphite island form., FEM, SEM and AES studies 7-32805

dislocations continued

- Si, amorphous to crystalline transformation, TEM in situ technique 7-44376
 Si bicrystals and thin films, grain boundaries, electronic props. 7-7172
 Si, broken dislocation bonds, annealing effects, optical polarisation of nuclear moments study 7-38008
 Si, DLTS spectrum of dislocations introduced by CW CO₂ laser (Chinese) 7-32939
 Si, defect diagnostics for submicrometer VLSI, book contrib. 7-44562
 Si, dislocated, charge carrier recomb. processes 7-7264
 Si, dislocation photoluminescence, thermal quenching effects 7-39155
 Si, dislocations and electron-hole radiative recombination 7-13203
 Si, MBE grown, defect densities 7-12560
 Si MBE layers, defect characterisation, luminesc., TEM studies 7-13227
 Si MBE layers, defects 7-21772
 Si, neutron irradiated, recovery 7-39567
 Si, passivation of dislocations at high H₂ press. 7-39763
 Si, polycrystalline, for solar cell appls., photovoltaic props., effect of impurities and defects 7-38639
 Si, radiation defect thermal ionisation, effect of dislocations on activation energy 7-6680
 Si, recombination activity of dislocations 7-12733
 Si, ribbons, γ -irradiated, defect form., photoluminesc. investig. 7-46147
 Si solar cells, H passivation of dislocations 7-54323
 Si, strain measurement in convergent beam electron diffraction 7-16562
 Si, surface, laser beam melting and recrystallisation 7-12431
 Si, twinning partial dislocations, effective stresses, anal. 7-63630
 Si:As, implanted, supersaturated soln., defect struct., TEM obs. 7-58483
 Si:As(B)(P), impurities at dislocations and grain boundaries, high-resolution TEM imaging 7-37815
 Si:C,O,P, C precipitation after P junction diffusion 7-16779
 Si:Cu thin single crystals, decorated dislocations, X-ray Laue diff. and scatt. studies (Russian) 7-58282
 Si:O, ion implanted, octahedral oxide particle nucleation and growth 7-16776
 Si:O(H)(C)(N), conf., Boston, MA, USA (Dec. 1985) 7-14711
 Si:Ti(V)(Cr)(Fe)(Zr) polycrystalline solar cells, structural, elec., photovoltaic props., impurity effects 7-39990
 β -SiC films on substrates, CVD, X-ray topography 7-63998
 SiO₂, modulated phase, electron microscopy study 7-26937
 β -Sn, positron lifetimes, prevacancy effect 7-37973
 SrF₂, phase transitions, influence of shear deformation 7-21429
 W thin films on Si substrates, plastic props., meas. by submicron indentation hardness, substrate curvature techniques 7-58720
 Xe, defect props. in condensed two-dimensional lattice 7-2018
 Xe monolayer on graphite, dislocation interactions 7-2357
 ZnS:Cr²⁺, Fe³⁺ single crystals, impurity centre charge exchange, plastic deform. effects, ESR spectra studies 7-16984
- disordered systems, vibrational states** *see vibrational states in disordered systems*
- disperse systems**
see also aerosols; Brownian motion; colloids; dust; emulsions; foams; fog; gels; powders; smoke; sols; suspensions
 annular dispersed two-phase flow in vertical pipes 7-20781
 bidispersion, dil., sedimentation and diffusion, Onsager symmetry, kinetic coeffs. 7-26322
 clay soil, filtrational prop. form., adsorbed H₂O struct. role 7-51297
 coagulation of spatially nonuniform systems, kinetic Smoluchowski eqn. 7-46873
 coke dust, polydisperse, combustion kinetics 7-13776
 concentrated dispersions, phenomenological rheology, shear viscosity, phenomenological models, nonNewtonian behaviour 7-8309
 concentrated dispersions, shear viscosity discontinuities, structure transitions 7-8310
 concentrated particle dispersions, diffusion coeffs. 7-44875
 condensed dispersed phase plasma, ionisation equilb. shift 7-31929
 convective dispersion and interphase mass transfer 7-51269
 diffuse radiation reflection 7-42918
 diffusion-controlled growth of particles in supersat. soln. 7-8323
 diffusive transport in spatially periodic hydrodynamic flows 7-31801
 droplet coalescence in turbulent liquid-liquid dispersions 7-51272
 drops, motion and mass transfer in pulsed column 7-6290
 dynamics of disperse streams in presence of boundaries 7-43845
 flow with internal degree of freedom, nonequilb. gasdynamics, kinetics and catalysis 7-44019
 fluid phases, separation, and bubble dynamics in temp. gradient and microgravity conditions 7-20722
 fly ash and coal, radiative characts. 7-43640
 gas-liquid kinetics, meas. using press-response method 7-13821
 gas-particle mixture, supersonic two-phase flow around a wedge 7-1614
 heterogeneous media, spatial correlation functions from computer simulations 7-18692
 holography, far-field in-line, and diff. pattern analysis of particulates, filtering effects 7-31279
 light scatt., correl. radius estimate 7-42917
 liquid-liquid dispersions, time- and event-driven Monte Carlo calcs. 7-54193
 liquid-liquid systems with aqueous or organic dispersed phase, interfacial and binary coalescence time 7-6270
 methylated Aerosil R-972, organophilic, alcoholic dispersions, coagulation by additions of water and electrolytes 7-8325
 molar mass polydispersity index, dynamic rheological meas. 7-43830
 nonstationary heat transfer, internal heat source influence 7-63202
 particle motion study in concentrated dispersions, tracer diffusion method 7-51351
 particle shape and size determination, concurrent spatial harmonic and fractal analysis 7-31263
 particle size and velocity measurement using phase Doppler particle analyser 7-29968
 particle sizing and spray analysis, conf., San Diego, USA (Aug. 1985) 7-29583
 particle sizing interferometer nephelometry 7-30070
 particle velocity and displacement distrib. from double-exposure holograms using opt. and digital processing 7-31277
 particulates in three-dimensional sample, coherent imaging, meas. accuracy 7-31278
 Poiseuille flow stability, suspended particle effect 7-1613
 poly(tetrafluoroethylene) dispersions, high resolution electron microscopy 7-44341
 polydisperse Percus-Yevick fluid, struct. and scatt. function 7-63423

disperse systems continued

- polydisperse polymer solution, size distrib. fn. determ., light scatt. appl. (Russian) 7-5806
- polydispersed MHD flow in a cylindrical vessel 7-51285
- polyethylene, disperse, heating in gas-thermal spraying 7-26536
- polyhexazocyclane, solns., viscosity props. (Russian) 7-63864
- polymer melts, kinetic theory, polydispersity effects 7-51601
- polymer microdispersions, preparation 7-22631
- polystyrene, monodisperse lattices, He-Ne laser transmission, attenuation coeff., specific turbidity meas. 7-62617
- polystyrene spheres, monodispersed, microscope images, image processing algorithm 7-4888
- polystyrene-polybutadiene-toluene, mono- and polydisperse solns., interaction parameter determ. 7-10795
- random packing of identical particles, model development 7-3613
- salt-stratified fluid, turbulent boundary layers, mixing, mean circulation and transport rates 7-51086
- sandy rock, pore moisture thawing and freezing, aq.-phase press. influence 7-52004
- silica-stabilised ferrite particle dispersions, magnetic recording appls. 7-53057
- slurries, flow curve, rheological props. 7-43833
- solid electrolyte disperse systems, elec. cond., phenomenological classification 7-6858
- spherical and rodlike macromolecules binary mixture, photon correlation spectroscopy 7-42909
- spontaneous condensation of vapor in a nonequilibriumsupersonic monodisperse flow 7-6286
- supersonic jet, light amplification coefficient and intensity, spasmodic increase during metastable atom and mol. condensation (Russian) 7-50523
- toluene dispersed in water, transient behaviour of holdup in reciprocating plate extraction column 7-11497
- transient dispersed-film flows in channels containingfuel rod bundles 7-10236
- two-point distribution function for a dispersion of impenetrable spheres in a matrix 7-33969
- ultradisperse matrix mixture, optical props., struct. anisotropy effect 7-31250
- viscoelastic disperse mixture, effective rheological properties, calcs. 7-26233
- CaF₂-Al₂O₃ (ZrO₂) dispersions, single and polycrystalline, elec. conductivity 7-27005
- Fe aggregated particles fractal dimension meas. by electron microscopy 7-26598
- Ni ultradisperse powders, recrystallisation induced dilatation effect 7-39537
- Rh-Re/SiO₂ catalysts, metal dispersion 7-39918
- TiO₂, nonaq. dispersion in petroleum, dielectric const. in electric field investig. 7-38982

dispersion (wave)

- see also acoustic dispersion; optical dispersion
- dispersive long-wave equation, soln. using inverse spectral transform method 7-61118
- fibre acoustic and optical waveguides, similarities and differences 7-1298
- fibre reinforced laminate plate, wave propag. 7-63051
- liquid filled distensible tube systems, dissipation and dispersion exhibition, wave propag. and refl. 7-1627
- MHD waves, short-period, propagating in ionospheric ducts, dispersion and attenuation props. 7-66392
- ponderomotive effects for plane uniform EM waves in magnetoplasma 7-31986
- PSR 0809+74, average pulse profile and dispersion measure from decametric wavelength obs. (Russian) 7-55697
- Saturn ring system, nonlinear dispersion relation for Mimas 5:3 density wave 7-24057
- seismic waves, simultaneous smoothing of phase and group vels. from multi-event surface wave data 7-28865
- wave propagation in a weakly dispersive medium, 1D wave eqn. 7-31825
- whistler dispersion, semi-annual and annual vars. meas. 7-14410

dispersion hardening

- see also precipitation hardening
- alloys, binary, simultaneous external and internal oxidation, form. of two-phase regions in diffusion zone (Russian) 7-46704
- ceramics, transformation toughening, shear, shape and orientation effects 7-39626
- Inconel MA 6000, oxide dispersion strengthened superalloy, cyclic creep, HF effect, anelastic model 7-53827
- Inconel MA 6000, oxide-dispersion hardened superalloy, cyclic creep and anelastic relax anal. 7-17596
- mechanical alloying, development of strong alloys 7-39534
- metal-carbide composites, implantation modified, friction, surface chemistry 7-46660
- steel, austenitic stainless, TiN dispersion hardened, creep below transition stress 7-65079
- steel, dispersoid, H embrittlement, mechanical props. 7-33795
- steel, ferrite-pearlite and pearlite-free, microfracture resistance (Russian) 7-33765
- steel, low alloy, pearlite free, fracture energy, effect of microstruct. parameters (Russian) 7-33787
- steel, rapid solidification, fusion reactor appl. 7-49657
- steel, structural, diffusion chromised, elevated temp. effect on comp., struct. and mech. props. 7-8178
- stress relaxation, dislocation-diffusion mechanisms, review (Russian) 7-32564
- superalloys, oxide dispersion strengthened, manufacturing process developments 7-27979
- Al-Al₂O₃-MgO, cast particulate composites, microstruct. and mech. props. 7-65086
- Al-Cu-Mg-Al₂O₃-Al₂C₃, IN 9021, mechanically alloyed precip. hardened, tensile behaviour 7-13525
- Al-Fe-Si-TiO₂, dispersion hardened, strength props., effect of matrix particle size and oxide vol. fraction 7-17544
- Al-Li base system, solid-state phase transform. 7-46456
- Al-Ti, powder metallurgy alloys, mech. and thermal stability 7-64973
- Al-Ti, rapid solidification processed/mechanically alloyed, high temp. deform. 7-65100
- Al₃Ni-Al eutectic alloy, Bauschinger effect, influence of Al₃Ni dispersion state (Japanese) 7-22761
- Al₂O₃, strengthening, mech. props. and microstruct. (Japanese) 7-22820

dispersion hardening continued

- β -Al₂O₃-Na₂O, ZrO₂ toughened solid electrolyte, failure initiation, critical current density, AE obs. 7-38252
- B'-Al₂O₃-Na₂O-ZrO₂ ceramics, transform toughened, fabrication, mech. props. ionic resist. 7-65143
- Al₂O₃-SiC composites, microstruct. and mech. props. (Japanese) 7-22821
- Cu alloys, neutron damage microstructs. 7-58347
- Cu alloys, rapid solidification, fusion reactor appl. 7-49657
- Cu alloys, rapidly solidified powder metallurgy, irradi. to 13.5 dpa with neutrons, microstruct. evolution and swelling 7-51840
- Cu, dispersion hardened, melting and solidification in microgravity environment 7-22659
- Cu-Al₂O₃, dispersion strengthened powder alloys struct. and mech. props. 7-53667
- Cu-Al₂O₃ films, dispersion strengthened, flow stress, temp. depend. (Russian) 7-53815
- Cu-Cr bronze, decomp. kinetics of supersaturated solid solns. 7-3320
- Cu-Fe, thermomech. treatment, softening rel. to disperse α -Fe particle, size and orientation 7-28054
- Cu-GeO₂, dispersion hardened polycryst., intermediate temp. embrittlement 7-53903
- Fe-Ni, austenitic, Mag. ordering and mech. props. (Russian) 7-58280
- Fe-TiB, eutectic system, microhardness, modulus of elasticity (Russian) 7-39648
- MgO-ZrO₂, dispersed, phase transform., toughening 7-65034
- Mo-Nb-Zr-C, nitrided single crystals., effect of NbN ϵ to δ phase transition 7-28052
- Mo-Ti-Zr alloy, creep resistance, particle strengthening contribution 7-28073
- Mo-ZrO₂, sintered composites, tetragonal to monoclinic transform. of ZrO₂ (Japanese) 7-13450
- Mo-ZrO₂, sintered composites, mech. props, microstruct. (Japanese) 7-13558
- Ni-Cr (1 wt.%), internal oxidation, two-phase region form. kinetics in diffusion zone (Russian) 7-46497
- Ni-Cr superalloy, high-temp. material, microstruct. and mech. props. with high-temp. heating 7-3341
- Ni-SiO₂ films, dispersion strengthened, flow stress, temp. depend. (Russian) 7-53815
- Pt-Zr internally oxidised alloys, morphology, struct. and stability (Russian) 7-33687
- Si₃N₄-TiC composites, densification, matrix-dispersoid reaction, mech. props. microstruct., impurities effect 7-64994
- Si₃N₄-TiC composites, mech. props., wear resist., dispersoid-matrix interaction 7-65145
- TiC-steel hard alloys, abrasive and hydroabrasive wear 7-17656
- (U_{0.3}Pu_{0.7})C, hyperstoichiometric, hot hardness, 293-1573K 7-59608
- WC-Co cermet particle reinforced low alloy steel composite, elastic const., laser US technique 7-65268

dispersion power, rotatory see optical rotation

dispersion relations

- see also dispersion (wave); Kramers-Kronig relations; Mandelstam representation; N/D method; phonon dispersion relations; phonons; plasma instability; plasma waves; S-matrix theory
- Alfvén wave stimulated Brillouin scatt. in low-density plasmas in ionospheric conditions 7-44146
- convection, linear 1D eqn., numerical dispersion by upwind differencing 7-26267
- diatomic crystal, 1D relativistic model, transfer matrix and dispersion relation 7-52382
- electron beam, relativistic, self-pinch, propagation in dense plasma, transverse two stream instability, dispersion relations 7-32000
- EM form factors and $\pi\pi$ scattering, consistency in $\rho(1600)$ region, dispersion relation anal. 7-567
- hadron-hadron interactions, inclusion of quark-gluon degrees of freedom, dispersion approach 7-5008
- layer thickness, generalised linear inversion calcs. from phase vels. of Love waves (Russian) 7-24627
- liquid metals, capillary wave dispersion relation modifications due to electric charge, surface Green fn. matching method 7-21575
- metal inhomogeneous surface layer, Love waves (Russian) 7-16683
- metal-insulator superlattices, optical properties, plasma wave effects 7-64599
- metals, surface plasmon dispersion relation by ricochet photoemission 7-27280
- nuclear forward Compton amplitude in GDR and Δ regions, dispersion relation anal. 7-49377
- periodic envelope wave, 1D stability against 2D perturbations, nonlinear Schrodinger eqn. calcs. 7-41160
- plasma dispersion function, numerical computation 7-44103
- plasma waves, cold, wave and energy propag. directions 7-57999
- Saturn ring system, nonlinear dispersion relation for Mimas 5:3 density wave 7-24057
- turbulent plasma, renormalised dispersion eqn. calcs., correl. time effects on plasma waves 7-51450
- π -dispersion relation in nuclear matter, test using $(\gamma,\pi^+\pi^-)$ 7-56666
- $\pi N \rightarrow \pi N$, isospin-even forward scatt. amplitude as low-energy QCD test 7-56572
- $\pi\pi$ scattering, inclusion of quark-gluon degrees of freedom, dispersion anal. 7-5008
- Al/Ag layers, surface plasmon dispersion, plasma wave effects, reflectivity meas. 7-58848
- Al/Al₂O₃/Au tunnel junction, electromagnetic modes anal. 7-27439
- Be, polycrystalline, plasmon dispersion, EELS meas. 7-27283
- Bi, effective electron mass, quasi-1D systems, theoretical investig. 7-2468
- ⁴⁰Ca(p,p), optical pot., dispersion relation approach to extrapolation to negative energy 7-41958
- CdS inversion layers, carrier effective mass calcs. 7-64055
- GaAs-AlGaAs quantum wells, electron-phonon scatt. rate reduction by total spatial quantisation 7-45482
- ²⁰⁸Pb(N,N), optical pot., dispersion relation approach to extrapolation to negative energy 7-41958
- πN low energy scatt., isospin-even forward scatt. amplitude as QCD test 7-41835

dispersions see disperse systems

dispersoids see disperse systems

displacement measurement

- 3D displacement and strain meas., automated evaluation by quasi-heterodyne holographic interferometry 7-31287
- combined laser interference system for the meas. of motion 7-41443

displacement measurement continued

- composite plate, spectral analysis of natural grid features for surface analysis 7-63096
 cosmic and geophysical noise in measurements of small displacements 7-4757
 deformation meas. using spatial frequency modulation of holographic interferometry, moiré method (*Japanese*) 7-56218
 deformation measurement using holographic interferometry and moiré fringes 7-48685
 dilatometer based on electro-optical meas. technique 7-41338
 EM, error sources in dynamic appls. 7-48712
 fibre optic, displacement transducer, characts. meas. 7-25968
 fibre optic displacement sensor, based on Mach Zehnder interferometry 7-43432
 fibre optic reflective sensing technique employing GRIN rod lens 7-43387
 fibre optic sensors and their appls., conf., Cannes, France (Nov. 1985) 7-40999
 fibre-optic sensors, displacement measurements, loss-compensation technique 7-57561
 fringe contrast improvement in speckle photography, speckle reduction using vibr. optical fibre 7-9889
 fringe pattern analysis, holographic-moiré technique 7-20164
 fringe visibility in lateral displacement measurement from double-exposure laser photographs 7-41442
 gauge for rock mechanics laboratory 7-34695
 holographic interferometry, deformation and shape meas. 7-43817
 holospecklegram orthogonal polarisation props., in- and out-of-plane surface displacement meas. 7-24695
 interferometer combined arrangement for displacement meas. 7-48835
 interferometry, conjugate shear and moiré, appl. to obtaining out-of-plane displacements derivative 7-9880
 IR holographic interferometry, displacement meas. appl. 7-10882
 laser speckle strain gauge, using spatial filtering detector 7-43821
 linear displacement meas. using spatial phase detection of 1D periodic pattern (*Japanese*) 7-56217
 minute spatial displacement field determ. from multiple interferometric holograms, fast algorithm (*Chinese*) 7-56215
 moiré interferometry, high sensitivity, tutorial paper 7-56331
 moiré interferometry for out-of-plane displacement meas. 7-18871
 moiré technique using digital processing 7-43822
 monofrequency laser interferometer with fine resolution 7-18753
 optical method of angular displacement when the rotation axis steeply inclines 7-41333
 optical three-dimensional displacement meter 7-41343
 optron displacement sensor [geophysical application], geophysical equipment appl. 7-4809
 sandwich holospeckle interferometry for 3D displacement determination 7-50519
 sensor based on two-beam interferometry 7-13716
 sound freq. in resonant pipe, displacement meas. 7-24622
 speckle interferometer based remote electro-optic displacement sensor 7-48838
 speckle metrology techniques, displacement and strain meas. 7-42936
 speckle modulation methods, transverse rel. to longitudinal displacement (*Korean*) 7-29965
 speckle photography, photography, diffraction halo effect 7-35574
 speckle-shearing interferometry, compensation for rigid and deformational displacements 7-48841
 strain gauge displacement sensor for surface crack profile meas. 7-22939
 surface, 3D displacement meas. by white light speckle photography 7-29973
 surface deformation measurement by light speckle using optical fibre bundle 7-30078
 transducer for angular and linear displacements with separated gratings 7-4829
 ultrasonic measurement method using 40 kHz wave 7-18742
 US, using laser-speckle interferometry 7-24624
 US displacement meas. system, microcomputer controlled (*German*) 7-56222
 Si lattice spacing meas., NRLM work relating to precision meas. and fundamental constants 7-14915
 Si pressure sensor diaphragm, displacement and slope analysis, holospeckle-shearing interferometry 7-29972

displacive transformations

- see also martensitic transformations; polymorphic transformations; reverse martensitic transformations; soft modes*
 alkali feldspar, hypersolvus, Raman spectroscopic study of order parameter behaviour, displacive transform. and evidence for Na-K site ordering 7-22254
 chloranil soft mode driven displacive transition, Raman meas. using I cell 7-59204
 ferroelectric transitions, electric field perturbed NQR 7-17276
 ferroelectrics, structural phase transitions (*Japanese*) 7-27670
 incommensurate sandwiches in displacive surface reconstructions 7-52223
 mechanisms for soft mode formation and dispersion in displacive phase transformations 7-38150
 model Hamiltonian, continued fraction technique 7-44789
 perovskite-related ABX₃ compounds, phonon-induced displacive transitions, octahedral librations, group anal. 7-12225
 perovskites, nonferroelec. displacive phase transition to spontaneously polarised state 7-2169
 polypheyls, hydrogenated p-terphenyl and deuterated biphenyl, structural transitions (*French*) 7-12256
 Rochelle salt, phase transition dynamics 7-21367
 tris-sarcosine calcium chloride, dielectric dispersion 7-2965
 As₂O₃, structural phase transition, Raman scatt. 7-6785
 Ca₂OSiO₄, crystallochemistry of phases 7-1965
 Co-Al alloys, magnetic hardening 7-33209
 CsVF₄, layer cpd., struct. phase transitions 7-6788
 K₂OSCl₆, mode softening and phase transition, press. depend., NQR study 7-26896
 (NbSe₄)₃I, long-range order formation near the second-order phase transition temp. 7-44802
 (NbSe₄)₃I, phase transition props. 7-44803
 SnSe(Si), second order displacive transition and soft mode behaviour, neutron diff. study 7-26895
 W (001), adsorbed H, displacive surface reconstructions, incommensurate sandwiches 7-52223

displacive transformations continued

- W (001) clean surface, surface-reconstruction phase transition and high temp. phase 7-6934
 ZrO₂ ceramics, displacive transform. mechanism 7-65031
 ZrO₂, high press. phase, cryst. struct. 7-16523
 ZrO₂-Y₂O₃, displacive cubic to tetragonal phase transform. 7-65027
- display devices**
see also cathode-ray tube displays; electroluminescent displays; gas-discharge displays; liquid crystal displays
 amorphous semiconductors, conference, Palo Alto, CA, USA (April 1986) 7-29602
 attention and visual perception: the availability of features 7-47075
 diffractive diffusers for display applications 7-5977
 electrochromic materials, book contrib. 7-25913
 head-up displays, holographic diffractive optics progress 7-25749
 holographic optical elements, industrial appls. in display systems 7-25753
 legibility evaluation of a large-screen display system under medium ambient illumination 7-8576
 magnetometer for geophysical exploration, compensation display device (*Russian*) 7-30045
 sputtered transparent conductive coatings for display industry use 7-50663
 wide angle distortion free holographic head-up display 7-25766
- display equipment** *see display instrumentation*
- display instrumentation**
see also cathode-ray tube displays; display devices; oscilloscopes; screens (display)
 colour, direction and speed of motion, perceived relations 7-47078
 colour parameters modelling and algorithmic colour selection 7-28538
 colours description w.r.t. natural colour system 7-23356
 densitometer, precision with microprocessor-based display unit 7-48697
 image quality, human detection of undersampled gratings 7-14004
 modulation transfer function for the display engineer 7-25730
 peripheral information display 7-40162
 peripheral information extraction: cognitive load effects 7-40161
 programmable visual display for diagnosing, assessing and rehabilitating unilateral neglect 7-65880
 speckle stereograms for 3D display 7-20146
 visual perception of direct-view and collimated displays under vibration 7-54575
 wide angle high aperture projection system for passive display 7-43288
- display instruments** *see display instrumentation*
- display systems** *see display instrumentation*
- disruptive voltage** *see electric breakdown*
- dissipation (heat)** *see cooling*
- dissociation**
see also electrolytic dissociation; heat of dissociation; ionisation; molecular dissociation; molecular dissociation energies; photodissociation
 carbon tetrafluoride, beam-plasma discharge for plasmachemical appls. 7-37706
 carboxylated rubber, study of maleic acid residue and vinylic monomer on props. 7-39902
 palladium acetate films, decomposition with microfocused ion beam 7-52314
 pulsed laser field desorption TOF spectroscopy, ultrafast ion reaction time meas. 7-20072
 PVC surface, sputtered, AES, electron beam induced dissociation 7-20077
 solvent, dissociation, isomerisation and diffusion in double-well potential 7-33922
 AgNO₃, electrical resistance effects accompanying high pressure and temperature melting and decomposition 7-16719
 AgO cathode used in AgO/Zn batteries, decomposition kinetics 7-46827
 Au (110), clean and oxidised, adsorption of formic acid and formaldehyde, acid-base and nucleophilic reactions 7-59783
 Co(NO₃)₂·6H₂O, electrical resistance effects accompanying high pressure and temperature melting and decomposition 7-16719
 Eu₂TiSi₂ mixed valence intercalation cpd., low-temp. synthesis and mag. props. 7-17779
 InP-Au interface, Fermi level pinning, growth characts., photoemission spectra 7-22009
 KMnO₄, thermal stability changes upon adsorption of water vapour in an electric field 7-8262
 Li/MoX₂ and Li/WX₂ (X=S,Se,Te) electrochemical cells at low voltages, dichalcogenide decomposition 7-65436
 Li₂HfF₆, hyperfine interactions, temp. depend. 7-12679
 Li₂ZrF₆, hyperfine interactions, temp. depend. 7-12679
 Mg₂N²⁺ microparticles, fragmentation, density-functional calc. 7-5810
 (NH₄)₂MoO₄-Ni(NO₃)₂, interaction, effect of mechanical activation on NiO:MoO₄ ratio 7-8261
 Na₂N²⁺ microparticles, fragmentation, density-functional calc. 7-5810
 Pt (111), adsorption of ethylene oxide, surface interactions, XPS, TDS, AES, EELS studies 7-33963
 SF₆ beam-plasma discharge for plasmachemical appls. 7-37706
 SiO₂, electron induced dissociation, AES study 7-22392
 Sm₂O₃, aging in air 7-65160
 Th₃N₄ and ThN, prep. and oxidation behaviour 7-22600
 W selective low press. CVD growth on Ti, TiSi₂ and PtNiSi, surface reactions, struct. 7-27183
 Yb₂TiSi₂ mixed valence intercalation cpd., low-temp. synthesis and mag. props. 7-17779
- dissociative attachment** *see electron attachment; molecular dissociation*
- dissolution** *see dissolving*
- dissolving**
see also solubility; solutions; solvation
 borosilicate glass, dissolution method study using fission track method 7-53937
 borosilicate glass, durability, influence of Cs₂O(SrO) (U₃O₈) (ZnO) 7-8144
 brass, 63/37, electrochem. behaviour in binary mixtures of N,N-dimethylformamide and water 7-46677
 α-brass, SCC propagation after exposure to NaNO₂ soln. 7-65174
 cellulose, dissolution in N-methylmorpholine-N-oxide mixtures, calorimetric and viscometric study (*Russian*) 7-38214
 chemical dissolution, assoc. fractal patterns 7-44061
 defect mapping by in-water photocorrosion 7-59692
 fluorozirconate glass, chem. durability, reaction with water 7-39682
 liquid metal anodes, dissolution during low freq. current interruptions 7-12287

dissolving continued

liquid soln.-solid grain system, stability of steady states, diffusion effect 7-32622
metal, passive dissolution rate in halide solns., transitional complex form. 7-17681
molten steel, melting and dissolution of falling body (*Czech*) 7-63776
nonferrous metals and carbonates, chemical dissolution under conditions of gas form. 7-46820
nuclear waste glasses, water chemistry and dissolution kinetics in geological disposal site 7-59906
particle dissolution kinetics, size determ., DSC obs. 7-3309
cis-1,4-polybutadiene-poly(styrene-co-butadiene) blend, phase dissolution kinetics 7-63831
porous medium, chemical dissolution by reactive fluid 7-44062
rare earth Ga-Fe garnets, $R_2Fe_{3-x}Ga_xO_{12}$, dissoln. forms 7-58481
silicate glass, dissolution in closed glass/water system 7-63828
steel, austenitic stainless, corrosion in high temp. water containing both dissolved H and O 7-65177
steel, austenitic stainless, SCC at const. load in molten NaCl-CaCl₂ at 570°C 7-53944
steel, HSLA, carbonitride particle response to weld thermal cycle 7-33661
steel, soln. kinetics in molten Zn 7-16752
steel, stainless, polarisation behaviour and admittance response in NaCl soln. (*Japanese*) 7-22871
steel, stainless, soln. kinetics in molten Al 7-16753
thin film dissolution kinetics, meas. using quartz crystal microbalance 7-2439
water in benzene and some n-alkanes, heat of soln. at 298.15, 308.07 and 313.14K 7-26959
Al-Ag, anelastic effects due to precip. and dissoln. 7-13487
Al-Zn (15 at.%), precip. during ageing, interaction of continuous and cellular mechanism 7-13454
Al₂Ga_{1-x}As layers, form. by regrowth on surface of GaAs during contact with undersaturated liq. containing Al 7-46311
As₂S₃ thin films, dissolution investig., surfactant effects 7-6802
B₂O₃-SiO₂-Li₂O-Na₂O-ZnO glasses, chemical durability 7-8143
BaSO₄ powder, solubility in water containing strong acidic ion exchange resin 7-21468
CaCO₃, formation in cooling water, critical pH depend. 7-54158
Cd₂GeAs₄ semiconducting glass electrolytic dissolution in HCl and water 7-12289
CdSe electrodes, photoanodic dissolution in NaCl soln. (*Japanese*) 7-23026
Cr-rich oxides, dissolution using H₂SO₄-Ce(IV) soln., radiation decontamination appl. 7-6803
Cu, anodic oxidation in Br⁻ and SCN⁻ solns., mechanism 7-52052
Cu, SCC propagation after exposure to NaNO₂ soln. 7-65174
 α -Cu-Al, ordered domain charactn. from dissoln. kinetics study 7-22693
Cu-Ti (5.7 at.%), diffusion of products of cellular dissoln. (*Russian*) 7-58485
Fe electrodes, electrodisolution and passivation K₂CO₃-KHCO₃ solns., ionic comp. effect 7-17677
Fe, H pumping and compression by superpermeation 7-58543
Fe, passivation and spontaneous dissolution in presence of O₂ 7-22872
GaAs-Ga_{1-x}H₂, dissolution of GaAs, crystallographic characteristics 7-12415
Ge, diffusion controlled dissolution kinetics in Bi-Te liquid 7-44820
graphite overlayer dissolution into the substrate 7-26966
Ir, anodic dissolution in Cl⁻ melts, salt passivation 7-52053
K films, adsorption of H₂O, XPS, UPS, work function meas. 7-12485
KCl crystals, dissolution and dispersion characts. from batch dissolver size distrib. 7-16750
Mo-Ni, adsorbed S, in acidic medium, destabilizing effect of Mo and passivation consequences (*French*) 7-16858
Na₂O-B₂O₃-SiO₂ glass ceramic, prep., SiO₂ replacement, phase separation, struct. 7-13428
Na₂O-K₂O-CaO-SiO₂ glass, mixed alkali effect on chemical durability 7-8145
Nb-Ti-O ceramic coatings, synthesis by reactive ion plating and sputter deposition, struct., electrophysical props. 7-64031
Ni (111), adsorption of Te, adsorbate induced C segregation and dissolution 7-12477
Ni, dissolution in molten NaCl-KCl at 700°C, appl. of rotating ring disc electrode technique 7-23025
Ni-P, glassy, dissolution in H₂SO₄ and HCl electrolytes 7-28189
Pb, dissolution in HNO₃, thermometric obs. 7-8189
Pb-Sn, cellular transform., directional invariance of grain boundary migration 7-22695
Pd-H, and substitutional alloys, thermodynamics of dil. solns. 7-21480
Ru-Ti-O ceramic coatings, synthesis by reactive ion plating, struct., electrophysical props. 7-64031
 α -Ti, mutual interactions of O and H during heat treatment, diffusion coeffs. meas. 7-39549
Ti thin films, dissolution and diffusion of O, resist., X-ray diffr., particle backscatt. and AES studies 7-58913
UO₂ oxidative dissolution, thermodynamic approach, CANDU spent-fuel disposal appl. 7-49688
UO₂, in vitro dissolution characts. 7-14137
Zn₃(PO₄)₂ coating, deposited on cold rolled steel surface, Fe dissolution, X-ray fluoresc. anal. 7-28168
ZrO₂-containing glass fibres, alkali corrosion process, XPS study (*Japanese*) 7-3480

distance measurement

V1343 Aql (SS 433), distance estimate from extended radio struct. obs. with European VLBI Network 7-29478
best wave interferometer with Zeeman laser for measuring short range 7-18752
Carina dwarf galaxy, distance modulus from obs. of RR Lyr stars 7-4570
computer simulation of the photodetection process in optical range finding 7-41467
16 Cyg A and B, solar analogue candidates, distance determ. rel. to absolute magnitudes 7-24162
E2, LMC halo cluster, distance modulus and age from deep CCD photometry 7-66685
elliptical galaxies, more precise L σ distance indicator 7-9541
extragalactic distance scale, implications of surface brightness-luminosity relation for dwarf galaxies 7-60794

distance measurement continued

galaxies, nearby, distances determ. using nonlinear Virgocentric flow model 7-40723
geodetic deformation nets, distance and distance ratio meas. sensitivity (*German*) 7-23520
interference range finders design principles 7-4808
interferometric distance meas. by wavelength shift of laser diode light 7-4806
interferometric system for absolute distance meas., using continuously tunable light source 7-24621
intraocular distances, system for continuous high-resolution meas. based on A-scan US 7-40234
laser distance sensor (*Japanese*) 7-20313
laser ranging, extended Kalman filter for automatic target following of lunar reflectors (*German*) 7-23521
LHS 288, LHS 1070, new nearby faint red stars, parallaxes and photometry 7-4455
LMC, apparent distance modulus from magnitudes of RR Lyr stars 7-47924
Lynds 810, large interstellar globule, distance determ. rel. to membership of Vul OB1 complex 7-24178
Magellanic Clouds, distance moduli from IR photometry of Cepheid variables 7-14592
Mekometer distance meas., statistical correction methods (*German*) 7-23519
NGC 6649, galactic cluster containing Cepheid variable V367 Sct, distance modulus from CCD photometry 7-55747
NGC 7039, NGC 7063, northern open clusters, distance moduli from UV by β photometry of early-type stars 7-66687
optical range sensing method 7-29978
optical range sensing method for surface tracing 7-29979
optical ranging by wavelength multiplexed interferometry 7-4813
Per OB2 association, membership, distance and age rel. to props. of peculiar stars 7-66592
proper-motion stars, parallaxes from photographic astrometry 7-4296
quasars, luminosity-volume test rel. to local hypothesis 7-35064
ranging by optical method, precision, for long baseline meas., error of point approx. method for air integral refr. index 7-66342
satellite laser ranging, chord and relative height estimation from single data passes (*Chinese*) 7-3961
satellite laser ranging, observations smoothing via correction of orbital parameters and station coordinates 7-54844
stars of South Galactic Cap, astrometry, trigonometric parallaxes, proper motions and photometry 7-47734
stars of South Galactic Cap, parallaxes and proper motions rel. to stellar populations, density functions, and luminosity distrib. 7-47832
Stock 17, young open cluster, distance estimate from UVB photometry 7-4533
two-mode Zeeman laser system (*Japanese*) 7-24623
ultrasonic distance detector for industrial appls. (*Spanish*) 7-16043
US rangefinders with various types of cct., error estimation of standard channel 7-62930
visual double stars, dynamical parallaxes and masses for twenty-one pairs 7-18431
visual double stars, dynamical parallaxes from orbital elements (*French*) 7-18430
S Vul cluster (C 1947+272), UVB photometry rel. to reddening, distance and age 7-14620

distillation

see also isotope separation
binary batch distillation in tray or packed columns, optimal control 7-58450
deep-basin solar stills, nocturnal distillation factors 7-3715
heat pump assisted distillation system operating characteristics with R11 external working fluid 7-65513
low-order, nonlinear, dynamic models for distillation columns 7-6773
macromolecules, chem. inhomogeneous mixtures, fractionation efficiency anal. (*Russian*) 7-26928
solar distillation plants, instrumentation and control devices 7-28410
solar still, cascade, modified type for water desalination 7-23219
solar still mass transfer rate prediction from condensing surface mass fraction 7-28411
solar still performance synthesis and predictions 7-23217
solar stills, comparison of various designs using performance and tests of water 7-54340
D₂O distillation process, steady and unsteady state models 7-6340

distortion measurement, electric

see electric distortion measurement

distortive transformations

see solid-state phase transformations

distributed Bragg reflector lasers

DFB lasers, fibre-extended-cavity, oscillation frequency tuning 7-57381
nonsymmetrical five-layer LOC, DFB and DBR lasers, waveguiding props. 7-57319
waveguide lasers, anomalous modal spectrum 7-15888
AlGaAs integrated-hybrid Bragg heterostruct. laser thermal stability of distributed-refl. spectral bands 7-57393
AlGaAs/GaAs DBR laser with multiquantum well active/passive waveguides 7-57350
GaAlAs-GaAs multi-heterostructures, MOCVD growth for surface emitting lasers 7-59440
InGaAsP-InP, integrated external cavity laser 7-36993
p-InP substrate mass transport BH laser, narrow active stripe 7-31357

distributed control

Contronic P modulator process control data acquisition system (*German*) 7-56247

distributed feedback lasers

asymmetric quarter-wave-shifted DFB semiconductor lasers 7-10990
Bragg injection semiconductor laser with external mirror, distrib. feedback 7-36985
coupling coeff. determ. method 7-57314
deficiencies and proposed alternatives 7-1194
dye DFB picosecond freq.-tunable laser source for time-resolved meas. 7-50584
dye laser, DFB oscillation in slab-type optical waveguide 7-15904
dye laser, DFB producing tunable picosecond pulses, review 7-10992
dye laser, energy characteristics 7-25810
dye laser, picosecond, excimer laser pumped 7-43086
dye laser DFB, achromatic pumping condition using grating 7-10999
fibre optic technology advances 7-1193
fibre-extended-cavity, oscillation frequency tuning 7-57381
free-electron lasers with distributed feedback, dynamics 7-50588

distributed feedback lasers continued

- gain-switched laser diode, transform-limited 5.6 ps optical pulse generation using pulse compression technique 7-31367
 high frequency response characteristics of DFB-DC-PBH LDs 7-50593
 light-wave communication appl. 7-15903
 MQW DFB laser, theoretical anal. 7-20223
 multielectrode DFB laser, broad wavelength tuning under single-mode oscillation 7-20258
 nonsymmetrical five-layer LOC, DFB and DBR lasers, waveguiding props. 7-57319
 numerical matrix method for anal. of structure 7-57349
 phase tunable type, 1.5 μm operation, FM and spectral characts. study 7-43171
 semiconductor DFB laser, 1.5 μm , feedback effects on spectra 7-31321
 semiconductor DFB laser amplifiers, optical bistability 7-57324
 semiconductor DFB lasers, spectral chirping suppression 7-20220
 semiconductor diode, direct FM characts. meas. using delayed self-homodyne technique 7-11014
 semiconductor laser amplifier, optical freq., selective amplification 7-57311
 semiconductor lasers, external optical feedback 7-57332
 semiconductor lasers, single longitudinal-mode high-power type, design, theoretical aspects 7-10987
 semiconductor optical amplifiers, adjustable gain and bandwidth 7-57365
 single longitudinal mode operation considering light refl. from optical fibre facet (Japanese) 7-20284
 spectral linewidth meas. using fibre-optic gyroscope 7-1279
 stimulated scattering, nonstationary mechanism 7-5867
 thin film energy transfer dye laser with DFB oscillator-amplifier system (Japanese) 7-43088
 tunnelling distributed feedback in optical waveguide, theory 7-57550
 V-groove, 1.3 to 1.55 μm operation 7-20257
 waveguide lasers, anomalous modal spectrum 7-15888
 AlGaAs laser diodes, MBE grown, fabrication and characts. (Japanese) 7-20273
 AlGaAs/GaAs DFB laser diodes, MOCVD growth, CW operating characts. 7-25836
 AlGaAs/GaAs long cavity ridge waveguide DFB lasers, spectral linewidth reduction 7-11179
 AlGaAs-GaAs, DFB lasers, low threshold, 0.88 μm emission, MOCVD fabricated with ridge waveguide struct. 7-5906
 AlGaAs-GaAs DFB-TJS external-cavity laser with optical phase control loop, spectral linewidth 7-20222
 GaAlAs-GaAs DFB lasers with double channel planar buried heterostructure, low threshold operation 7-20256
 GaAlAs-GaAs DFB laser with double-channel planar BH 7-50594
 GaAlAs-GaAs ridge waveguide DFB lasers, lateral anal. 7-62686
 GaAs-AlGaAs DFB struct. with multiquantum well for surface emitting laser 7-10939
 GaInAsP DFB lasers, 1.3 μm , single-mode, realisation and characts. (German) 7-57357
 GaInAsP/InP entirely VPE-grown 1.5 μm DFB lasers with low threshold currents 7-50577
 InGaAsP 1.5 μm DFB laser diodes, optical communication appls. 7-37202
 InGaAsP DFB lasers, extremely low-noise facet-reflectivity-controlled 7-31320
 InGaAsP DFB laser, phase noise and linewidth 7-31322
 InGaAsP DFB laser for passive ring cavity-type fibre optic gyroscope 7-57562
 InGaAsP device fabrication using HBr-H₂O etching soln. 7-46728
 InGaAsP/InP DFB lasers, DFB mode oscillation, temp. range 7-5910
 InGaAsP-InP, heterolaser struct., distributed feedback conditions, luminesc. spectra anal. 7-50561
 InGaAsP-InP DFB laser with modified double-channel planar BH struct., 1.3 μm high-speed operation 7-15896
 InGaAsP-InP DFB lasers with monolithic external cavity, spectral characts. for 1.3 μm 7-20281
 InGaAsP-InP DFB laser monolithically integrated with tunable external cavity, linewidth and FM characts. 7-57316
 InGaAsP-InP distributed-feedback injection laser, fabrication by LPE and VPE 7-57337
 InGaAsP-InP Fabry-Perot and DFB lasers, VPE transport fabrication 7-20277
 InGaAsP-InP heterostruct. laser output characts., quantum size effect active layer thickness variation effects 7-31323
 In_{1-x}Ga_xAs_{1-y}P_y-InP quarter-wavelength-shifted DFB laser source for 1.55 μm underwater optical cable system (Japanese) 7-62720
 InP device fabrication using HBr-H₂O etching soln. 7-46728
 Nd³⁺:SiO₂ narrow-linewidth single-mode fibre laser 7-5904

distributed parameter systems

- 3D 2-phase immiscible flow displacement, finite element analysis and error analysis (Chinese) 7-16229
 heavy gas atoms, particle behaviour simulation 7-9749
 partial differential eqns. model with two-time and two-space scales 7-59474

distributed processing

- see also computer networks; multiprocessing systems
 qualification concepts for instrumentation and control systems of nuclear power plants 7-19419

distribution networks

- AC network transient anal., RFX fusion expt., Italy 7-30666

distributions, statistical see statistical analysis; statistics**district heating**

- domestic heating emissions reduction by using district heating (German) 7-46979
 nuclear district heating plants, thermal design, AST-500 plant appl. (German) 7-23127
 nuclear power station use in the German Democratic Republic (German) 7-23126
 solar district heating plant with rock cavern seasonal thermal storage 7-65609

divacancies see vacancies (crystal)**diversity reception**

- see also fading
 HF propagation problems in ionosphere 7-23943
 marine paths, correlation props. of signals in 10 cm band with angular diversity reception 7-23823

dividing circuits

- decade scaler with fractional variable division factor 7-10367

DLTS see deep level transient spectroscopy**DMOS integrated circuits** see field effect integrated circuits**DNA**

- A-form helices, Ru complex as chiral probe 7-34096
 aperiodic, electronic structure and cond. props. 7-23297
 aqueous soln., resonant microwave absorpt. model 7-23310
 B-DNA model segment, binding of water 7-34099
 base damage induced by ionising radiation, review of current aspects 7-47169
 book, annual review of biophysics and biophysical chemistry 7-30
 cell content, distrib. modelling problem 7-47303
 cleavage after UV-irrad., block by restriction endonucleases 7-18026
 conformation, rel. to economics in the hydration of phosphate groups 7-34109
 conformational state in aq. soln. of glycine, β -alanine and γ -aminobutyric acid, conformational transitions 7-28447
 conformational state in aq. solns., containing glycine, β -alanine and γ -aminobutyric acid 7-28446
 contour-clamped homogeneous elec. fields, method for large DNA mols. separation 7-65906
 DNA-Eco RI endonuclease recognition complex, struct. at 3 Å resolution 7-65698
 DNA-salt solutions, thermodynamic coeffs., Monte Carlo calcs. 7-54443
 double helices, electrostatic forces, Monte Carlo simulation 7-42803
 double helix, effect of base sequence on fine struct. 7-54454
 electric charge transfer phenomena, TSC investig. (Czech) 7-13948
 electrical conductivity, possible mechanisms of action of an external electrostatic field 7-54668
 electronic structure and cond. props., calcs. 7-23296
 flow cytometrically determined DNA distributions with abnormal stem-lines, automatic analysis 7-59949
 fragments, stability, stacking interactions, pseudo-polarisation tensor theory 7-997
 helical biological polymers, liq. cryst. phases, columnar textures 7-34106
 hepatoma cells, γ -irrad., change in initiation of DNA synthesis at a nuclear matrix and its DNA-protein content (Russian) 7-47174
 hybrid cell clone between xeroderma pigmentosum and Potorous tridactylis, DNA repair characts. 7-60045
 injury in continuous long term low-dose irrad., fluorometric obs. in rats, mice and men (Russian) 7-54506
 ionising radiation and Pt complexes, effect of combined treatment on DNA in vitro 7-40099
 laser induced interstrand covalent crosslink, fluoresc. obs. 7-8490
 lesions, role in form. of radiation damage in chromosomes (Russian) 7-47170
 ligand interactions, groove binding, computer simulations 7-54447
 liquid cryst. microphases in water-organic solns., optical props. 7-65709
 liquid crystal microphases, 'external chromophores' and intense bands in circular dichroism spectra 7-54459
 looped DNA, elastic model 7-5800
 luminescence, dependence on excitation energy (Russian) 7-28470
 mammalian cell culture, DNA single- and double-strand breaks by thermal neutrons 7-23392
 mesogenic helical polymer, cholesteric liquid crystalline phases 7-6506
 metals and DNA: molecular left-handed complements 7-17941
 methylation, 5-methylcytosine effect on interaction between stacked boxes 7-59920
 neutron-induced free radicals in oriented DNA 7-23391
 nucleoids, restoration of hyperthermia-associated protein to DNA ratio 7-65720
 oligo-DNA duplexes, sequence depend. struct., Raman spectra 7-31199
 plasmid damaged at a specific region by UV light, mutational DNA base sequence changes 7-59948
 platinated, site specifically, biological activity probe for anticancer drugs 7-34095
 polyelectrolyte solutions, extensive force, num. eval. 7-46853
 radiation damage to ϕ X174 DNA and biological effects 7-28617
 repair kinetics after exposure to X-irrad. and to internal β -rays in CHO cells 7-28619
 repair mechanisms and their pot. modification radiotherapy 7-23314
 satellite evolution, nonlinear phenomena 7-57193
 Simian Virus 40 assembly 7-34117
 soliton excitations, dynamical theory 7-47001
 spatial liquid crystal packing of 2-chain mols. for a different cation composition of the solvent 7-28448
 stable branched structures, junction design considerations 7-34101
 strand breaks induced by X-irrad. and internal β -rays, 3 classes 7-23408
 superhelical phenomena, math. basis, review 7-34102
 SV40 DNA, possible use for CETI 7-40090
 UV induced thymine dimers, bound serotonin effect 7-8489
 yeast cells, X-ray induction of DNA double-strand breaks 7-8657
 Mn-DNA binding modes, nuclear mag. relax. dispersion results 7-23271
 Pt complex, diamminodichloroplatinum(II), isomers orbital study, coordination with DNA, relativistic multiple scatt. Xa calcs. 7-56973
- document retrieval** see information retrieval
Doherty amplifiers see power amplifiers
domain boundaries
 for boundaries between magnetic domains and electric domains see magnetic domain walls and electric domain walls respectively
 see also antiphase boundaries
 3d- and 4f- metals, periodic spin structs., critical props. calcs. (Russian) 7-59031
 domain-wall interactions and spatially modulated phases 7-2146
 graphite intercalated with Br, struct. and phase transitions, review 7-52041
 icosahedral phases, discommensurations 7-44437
 kinetics, space-time complexity and nonlinear field eqns. 7-51996
 molecular struct. relaxation in flat channel, thermodynamics and kinetics 7-32583
 pinning centre distrib., interaction force statistics (Russian) 7-58276
 strain free coherent elastic domain boundaries, general conditions (French) 7-63838
 TTF-chloranil, neutral-ionic transition, phenomenological theory 7-26939
 urea inclusion cpds. with n-paraffins, phase transitions and ordering 7-32634
 α -Ag-Mg, annealed, twin like domain boundary, high resolution electron microscopy 7-26763
 GaAs epitaxial films, domain form., crystallographic analysis 7-58690

domain boundaries continued

- Kr monolayer adsorbed on graphite, dislocation interactions 7-2357
 $\text{NDP}_{0.14}$, ferroelastic domain walls, X-ray topography studies (*Chinese*) 7-58493
 PrO_x , fluorite prototype struct., interfaces and domain form. study 7-58498
 Re_2B_3 , inverse boundaries, rel. to defects in M_7C_3 carbides 7-12083
 Ru_2B_3 , inverse boundaries, rel. to defects in M_7C_3 carbides 7-12083
 TaSe_2 , 2H polytype, high resolution TEM study of triply incommensurate phase 7-6813
 TbO_x , fluorite prototype struct., interfaces and domain form. study 7-58498
 Xe monolayer on graphite, dislocation interactions 7-2357
 Xe monolayers on graphite, low temp. phase diagram, striped helical Potts model calcs. 7-38327
 YIG, γ -irradiated, amplification effects and nuclear relax. in domain walls 7-7603

domains

- see also antiphase domains; crystal microstructure; domain boundaries; electric domains; magnetic domains
 2D three-state chiral clock model, domain-growth kinetics 7-35460
 bistable cholesteric twist cell, anisotropic domain growth 7-1865
 crystal, nonlinear bleaching and domain formation, exciton part of spectra 7-45161
 ferroelastic film on deformable substrate, Love waves and domain struct. near phase transition 7-52216
 graphite intercalation cpds., staging dislocation electronic struct., electron scatt. rates, residual resist. 7-52558
 graphite-Br intercalation cpds., 2D stripe-domain system, melting transition 7-58449
 graphite-Cs, $\text{C}_{24}(\text{Cs})_{x/2}$, domain mobility and rot. tunnelling spectrum 7-63525
 heteroepitaxial systems, domain size determ. from LEED angular profiles 7-7075
 liquid crystalline polymers, domains, are they disclination arrays 7-44359
 polyarylate-polydimethylsiloxane rigid block copolymers, domain struct., electron microscopy (*Russian*) 7-63520
 polyesteramidourethane, segmented, struct., polar low mol. wt. cpds. effects (*Russian*) 7-26673
 smectic C phases, bistability and domain wall motion induced by strong elec. fields 7-63450
 Ag_2Te , domain struct. and phase transforms., electron diff. and microscopy studies 7-58194
 AlPO_4 , modulated phase, electron microscopy study 7-26937
 BaTiO_3 ceramics, grain struct. and phase anal. (*German*) 7-58496
 C graphite with Kr monolayers, domain wall modes 7-38333
 $\text{Ca}_2\text{Fe}_2\text{TiO}_{8+x}$, perovskites, microdomains, electron microscopy 7-16533
 $\text{Ca}_3\text{Mn}_{1.8}\text{Fe}_{1.2}\text{O}_{3+y}$, perovskites, microdomains, electron microscopy 7-16533
 $\text{Dy}(\text{As}_x\text{V}_{1-x})\text{O}_4$, random-field effects on Ising Jahn-Teller phase transition 7-58461
 Fe-Ni-B , amorphous, shock loading, inclusions dissolving, domain struct. (*Russian*) 7-63487
 GaAs, epitaxial film on (001) oriented Si and Ge substrates, structural props. 7-58687
 GaAs epitaxial films, domain form., crystallographic analysis 7-58690
 GaAs, epitaxial layers grown directly on Si (100) by low press. MOVPE 7-27924
 GaAs MOCVD growth on Ge (100) and Si (100) substrates, antiphase and single domains 7-27925
 LiKSO_4 , domain structures and phase transitions, SO_4^- EPR study 7-38937
 LiKSO_4 , phase transitions, domain form., optical birefr. meas. 7-3019
 SiO_2 , modulated phase, electron microscopy study 7-26937
 $\text{Sr}_2\text{Mn}_{2-x}\text{Ti}_x\text{O}_{5+x/2}$, struct. and defects 7-44490
 TiNO_3 , ferroelastic switching, mech. twinning, at. mechanism, symm. anal. 7-2186

domestic appliances

- see also ovens; refrigerators
 gas meter using coherently modulated US carrier 7-1659
 Vuilleumier cycle heat pump for domestic appl., computer simulation 7-65554

donor levels see impurity electron states**doping, semiconductors** see semiconductor doping**doping profiles**

- channelling contrast microscopy, He^+ microbeam, semiconductor impurity profiles 7-51587
 diffusion eqns., numerical soln., moving finite element method 7-12376
 grain boundaries, interaction with doping atoms (*Russian*) 7-51781
 impurity profiling in mixed diffusion by neutron activation analysis 7-59810
 InP:Si , ion implanted, rapid thermal annealing and solid phase epitaxy 7-21296
 microelectronic materials, characterisation by SIMS, book contrib. 7-44976
 microelectronic materials processing, appl. of neutron depth profiling, book contrib. 7-44595
 multilayer targets, models for implementation 7-26772
 phthalocyanine polymer films, I_2 implantation 7-26776
 redistribution of dopants during prebake and epitaxial deposition 7-38039
 semiconductor, dopant profiles modification due to surface and interface modifications 7-58306
 semiconductor device structures, Auger sputter depth profiling 7-21254
 semiconductor doping profiles, appls. and limitations of SIMS 7-35621
 semiconductor epitaxial layers, sharp doping profiles determ. 7-12111
 semiconductor microelectronic structures, depth profiling by SIMS and AES 7-26790
 semiconductor structures, MeV He^+ microbeam analysis 7-13315
 semiconductors, depth resolution of SIMS 7-54253
 semiconductors, implanted ions diffusion redistribution, effect of radiation defects 7-51810
 semiconductors, tandem accelerator secondary ion mass spectrometry 7-54252
 SOI buried layer form. by high dose implantation, mass transport studies 7-32479
 solar cell efficiency, doping gradient effects 7-8412
 solar cells, passivated, high efficiency, optimum surface dopant conc. 7-23190

doping profiles continued

- X-ray fluorescence, grazing incidence, for implantation profile tracing (*French*) 7-13834
 (Al, Ga)As films, doped, Si migration during MBE growth 7-27171
 AlGaAs:Sb , MBE growth, Sb doping 7-2038
 As-Se:Ag amorphous films, Ag doping profiles, ellipsometric studies 7-7779
 Cr carbonaceous films, prod. in situ in Tokamak TEXTOR, depth profiling 7-22893
 GaAlAs-GaAs superlattice, Auger sputter depth profiling 7-21254
 GaAs backwall Schottky barrier solar cells, minority carrier current collection, built-in elec. field enhancement limitations 7-54305
 GaAs, ion implant depth profiles, channelling, Monte Carlo simulation 7-51811
 GaAs sawtooth doping superlattices, photoluminescence, transport props. 7-52825
 GaAs:Al , surface layer, degree of disordering, effect of dopant 7-63929
 GaAs:Sn , epitaxial layers, carrier carrier distrib. 7-12530
 GaAs:Zn , Zn diffusion by open-tube technique 7-38260
 GaAs-AlGaAs heterojunctions, Be^+ , O^+ ion implantation, impurity profiles, elec. charact. meas., SIMS, annealing 7-12813
 GaAs-GaAlAs heterojunction bipolar transistors, ^{24}Mg and ^{64}Zn implanted profiles 7-44591
 $\text{Ga}_{0.47}\text{In}_{0.53}\text{As:Be}$ epitaxial films, ion implanted, rapid thermal and furnace annealing 7-22729
 $\text{GaSb:Te(Si)(Si)(Ge)}$ single crystals, Czochralski growth, carrier conc. rel. to dopant conc. 7-22462
 Ge, floating zone growth, lateral solute segregation rel. to gravity conditions 7-53576
 Ge:H , H composition at surfaces and interfaces 7-27083
 Ge:P crystals, seeded growth in soft lined crucible, dopant distrib. 7-53559
 Ge-Se:Ag amorphous films, Ag doping profiles, ellipsometric studies 7-7779
 $\text{Ge}_{30}\text{S}_{70}\text{:Ag}$ chalcogenide films, Ag photodoping, optical transmission spectra 7-59231
 HgCdTe epitaxial layers and structures, characterisation of intentional dopants 7-12552
 InP:Bi thin film, epitaxy, impurity distrib., photoluminesc. spectra anal. 7-53388
 InP:Fe , epitaxial layers, MOCVD, doping profiles, SIMS, resist., temp. depend. 7-21248
 InP:Fe,Ga,Sb , LEC growth, dislocation density, resistivity, SIMS obs. 7-53552
 InP:Sn substrate/epilayer interface, Sn depth profiling, AES and SIMS studies 7-27146
 n-InP:Zn , Zn diffusion 7-63882
 InSb:Te, Cd, Zn single crystals, Czochralski growth, solute distrib., mag. field effect on melt 7-3158
 $\text{LiNbO}_3\text{:MgO}$, melt growth and charactn. 7-58170
 $\text{MgAl}_2\text{O}_4\text{:Ni}^{2+}$, Czochralski growth and optical props., effective segregation coeff. 7-59406
 Ni carbonaceous films, prod. in situ in Tokamak TEXTOR, depth profiling 7-22893
 $\text{Pb}_{1-x}\text{Sn}_x\text{Te:}^{57}\text{Br}^+$, depth profiles, SIMS meas. and theoretical calcs. 7-6662
 Pd(Si:B,As/Si:B) , As ion implant redistribution during Pd_2Si formation using rapid thermal annealing 7-16816
 $\text{Sb}_2\text{Te}_3\text{:Sn, Ti}$, single crystals, X-ray spectral microanalysis 7-44590
 Si , acceptor neutralizing species, low temp. injection mechanisms 7-32482
 Si carbonaceous films, prod. in situ in Tokamak TEXTOR, depth profiling 7-22893
 Si, diffusion of ion-implanted impurities, modelling on IBM PC 7-38265
 Si, dopant profiles by the spreading resistance technique, book contrib. 7-44594
 Si, heavily doped crystals, behaviour of O and dopants 7-32483
 Si, implantation damaged, transient enhanced dopant diffusion 7-44910
 Si, implanted layers, short time annealing, light source comparisons 7-21263
 Si, impurity profiles, depth resolution of SIMS 7-54253
 Si ion implanted, epitaxy by thermal and laser processing, review 7-33706
 Si, MBE dopant profiling, electrochemical CV technique 7-12108
 Si, MBE grown, abrupt doping profiles, spreading resist. determ. 7-12110
 Si MBE grown layers, arbitrary doping profiles 7-12109
 Si MBE growth, conf., Toronto, Ont., Canada (May 1985) 7-9588
 Si MBE homoepitaxial growth, expt. considerations 7-13369
 Si MBE layers, spreading resist. anal. carrier spilling effects 7-2741
 Si MBE layers, spreading resist., etching, bevelling, staining characterisation techniques 7-12891
 Si materials and process charact. for VLSI, SIMS studies 7-33988
 Si, neutron doping in RBMK-1000 power reactors 7-38068
 p-Si, polycrystalline, ion implanted, resistivity modelling (*Korean*) 7-2608
 Si solar cells, crystalline, metal grid optimisation and emitter tailoring, computer model extension 7-54292
 Si, solid-phase amorphous to crystalline transformation for shallow junction processing 7-32642
 Si substrate, dopant redistrib. during Pd_2Si formation 7-21255
 Si:Al, atom and acceptor depth distributions of channelled Al as a function of ion energy and crystal orientation 7-21247
 Si:Al surfaces, SIMS anal. of contaminants 7-33989
 Si:Al(In), recrystallisation by pulsed electron beam, impurity profiles 7-16605
 Si:As, dopant diffusion, finite element based simulation, quasilinear formulation with remeshing scheme 7-21526
 Si:As, high dose implanted, defect density reduction by low temp. oxidation 7-58297
 Si:As, ion implanted, rapid thermal annealing 7-16615
 Si:As:P, double diffused shallow junctions, rapid thermal annealing 7-22006
 Si:As(BF_3), ion implanted, diffusion and defects, transient scanning electron beam annealing 7-38065
 Si:Au, U- and W-shaped impurity diffusion profiles investigation 7-16805
 Si:B, B ion dose identification, HF C-U meas. 7-6661
 Si:B, diffused through narrow windows, doping profiles 7-12113
 Si:B, ion implanted, defect and dopant depth profile studies 7-2045
 Si:B, ion implanted, dopant redistrib. during rapid thermal annealing 7-38042

doping profiles continued

- Si:B, MBE grown, coevaporation doping 7-12562
 Si:B, SIMS depth profiles in the near-surface region, correction for ion yield transients 7-22430
 Si:B, SIMS depth profiles, characterisation and removal of ion yield transients in the near surface region 7-65368
 Si:B layers, preamorphised and ion implanted, structural and elec. characterisation 7-52347
 Si:B⁺(BF₃)⁻ submicron p-n junctions, ion implanted, dopant distrib., Raman study 7-21252
 a-Si:B(P)(As), implanted ion distrib., lateral spreading, theoretical predictions and computer simulation 7-16604
 Si:H, B(Al)(Ga)(In), polishing, acceptor compensation by atomic H 7-33860
 Si:H, H composition at surfaces and interfaces 7-27083
 a-Si:H, H₂ distrib., exodiffusion spectra 7-27026
 a-Si:H,B p-n and n-i-p solar cells, doping profile effects 7-46947
 a-Si:H,B(P) films, dopant conc. meas. and depth profiling by means of (p,γ) resonant reactions 7-12555
 Si:P MOS source/drain struts., 2D P diffusion props. 7-32718
 Si:P(Al), random and channelled implantation profiles and range parameters of dopants 7-21246
 Si:P(B), tail diffusion model 7-16815
 Si:Sb MBE, electron irradi. effect on doping levels and profiles 7-63660
 Si:Sb MBE film, doped by electron impact ion source, improved doping characts. 7-12101
 Si:Sb(As)(P)(B) epitaxial films, low temp. deposited by low press. CVD, autodoping 7-27182
 Si:Sn, ion implanted, annealing behaviour, channelling and conversion electron Mössbauer spectroscopy 7-13485
 Si:Zn, amorphous-crystalline interface, backscattering and channelling study 7-6663
 Si-SiO₂, Si oxidation kinetics, interface width determ. 7-39764
 SiGe superlattice structures, Sb doped, MBE grown, comp., doping profiles, SIMS, Rutherford backscattering spectra 7-7035
 SiO₂:F, P fibres, dopant materials behaviour in MCVD process 7-20462
 Ta₂O₅:H films, NPL standard, distrib. of H, AES and SIMS 7-26789
 Ti/Si:B,As,Sb interface, dopant redistrib. during silicide form. by rapid thermal processing 7-63641
 TiSi₂:As(Sb) layers, dopant redistribution during silicidation by rapid thermal annealing, ion scatt. spectra study 7-21253

Doppler broadening *see Doppler effect***Doppler effect**

see also atomic spectra; red shift; spectral line breadth

- acoustic Doppler current profiler, vessel-mounted, for use in rivers and estuaries 7-9262
 acoustic Doppler profiler intercomparison expt., Delaware Bay (1984) 7-9263
 arterial occlusive disease, US, diagnosis, some failings of pulsatility index and damping factor 7-47187
 atmospheric wind meas., 405 MHz phased array antenna design 7-34752
 atomic excited fragment, Doppler profile analysis, optical instrument design and construction (*Japanese*) 7-31172
 blood flow parameters estimation using pulse Doppler US with corrections for spectral broadening 7-8671
 brachial artery, Doppler US vel. waveforms, vector based approach to age-related changes 7-65822
 bubble diameter meas. by fringe method, using laser Doppler anemometer 7-16278
 cardiac indices meas. from freq. transformed TAV Doppler US signals 7-28626
 carotid artery blood flow: single factor classification of Doppler waveforms 7-3844
 Coastal Ocean Dynamics Experiment, shipboard Doppler current profiling 7-9260
 CW Doppler US spectra, comparison with spectra derived from a flow visualisation model 7-14071
 cyclododecane, plastic cryst., positron annihilation study 7-39224
 diamond, stopping cross section of ¹²C projectiles 7-51899
 directional laser Doppler velocimeter, dual sinusoidal modulation 7-56228
 distant light source in Schwarzschild gravit. field, Doppler shift 7-4319
 droplet sizing techniques, laser interferometric, performance comparison 7-30071
 electron-molecule collision induced dissociative excitation as studied by Doppler profile analysis (*Japanese*) 7-985
 excitation of atomic nuclei and of atoms in single crystals by charged particles 7-7784
 fibre laser Doppler velocimeter, integrated optic device 7-6022
 flow velocity profile meas. by US Doppler shift method 7-51346
 flowmeter, velocity profile measurement by ultrasound Doppler shift method 7-37585
 formic acid, ν₃ band, sub-Doppler laser-stack and Fourier transform spectroscopy 7-62430
 four-level velocity-selective atomic model, nonstationary effects, time-dependent anal. 7-36555
 frequency standards based on stored ions 7-14924
 trans-glyoxal, photodissoc., photofragment excited state distrib., fluoresc. spectra anal. 7-50226
 graphite stopping cross section of ¹²C projectiles 7-51899
 graphite surface with physisorbed Ar, N₂ or O₂, positronium formation 7-33483
 graphite-K intercalation cpd., C₆K, anisotropic binding of K, nuclear resonance photon scatt. of bremsstrahlung 7-51695
 graphite-K intercalation cpd., C₆K, positron annihilation spectra, effect of H absorption 7-39270
 gravity waves, in atmosphere, effects of Doppler shifts on wave spectra observed by MST radar 7-47490
 inductivity coupled plasma, emitted lines, widths and shapes 7-54232
 injection locked magnetron, phase noise meas., Doppler weather radar system appl. 7-30042
 ion bombardment induced X-ray emission spectra 7-13310
 laser differential Doppler gauge for contactless meas. of speed and length 7-24628
 laser Doppler anemometer, two-colour four-beam system, two-phase mist flow meas. 7-37581
 laser Doppler flowmetry, appl. to quantification of heat-induced changes in skin and RIF-1 tumour of mice 7-65711
 laser Doppler interferometry methods for highly accurate flow meas. 7-44073
Doppler effect continued
 laser Doppler velocimetry for solid surfaces, using specular reflection (*Japanese*) 7-41359
 laser frequency standard accuracy improvement, based on saturation absorption method 7-18761
 laser-generated ultrasound, detect. using confocal Fabry-Perot interferometer 7-50893
 left ventricular assist device, pulsed US Doppler rel. obs. 7-8667
 magnetised plasma, HF wave propag., complex Doppler effect 7-51456
 medical US, algorithms for fast computation of the intensity weighted mean Doppler freq. 7-65820
 medical US Doppler flowmeter for use in theatre 7-47188
 metal plates, Doppler-shifted cyclotron resonance and skin effect 7-17224
 methyl nitrate, photodissoc. NO photofragment excited state distrib., fluoresc. spectra anal. 7-50225
 molecular saturated absorpt. resonances, transit time effects 7-25608
 neonatal haemodynamics assessment, use of Doppler US 7-28629
 neuroradiology, transcranial Doppler sonography rel. to angiography 7-18035
 oceanographic acoustic Doppler current profiler, intercomparison with conventional instruments and tidal flow model 7-9266
 oceanographic acoustic Doppler profile current meter, field evaluations 7-9264
 oceanographic acoustic Doppler profiles, surface wave kinetic energy influence 7-9274
 oceanographic current meas., Conf., Airlie, VA, USA (Jan. 1986) 7-4633
 oceanographic current meters standardisation problems and solutions 7-9272
 oceanographic current profiler, using pulse-to-pulse coherent Doppler technique 7-9268
 oceanographic mid-ocean acoustic current profiling from submerged buoys 7-9269
 optical autodyne detection, theory and experiment 7-41465
 optical frequency standard based on Ramsey excitation in Ca atomic beam 7-14925
 optically phase-locked electronic speckle pattern interferometer 7-56326
 particle sifting with phase Doppler spray analyser, nonspherical drops effect 7-29969
 particle size and velocity measurement using phase Doppler particle analyser 7-29968
 plasma, electric field measurement using atom beam-Doppler spectroscopy 7-11710
 plasma, optical characts. freq. depend. 7-32083
 plasma ion dynamics, anomalous Doppler reson., single-particle and collective descriptions 7-51438
 polyethylene, positron annihilation radiation lifetime, Doppler broadening 7-39217
 poststenotic flow disturbance in dog aorta as measured with Doppler US 7-8668
 proximity sensors, flow meas. with beam-scanning LDV 7-37604
 PS-3.5 spheromak, flow field study by C impurity spectral line shifts 7-26403
 α-quartz, neutron irradiated and annealed, positron annihilation and mag. susceptibility meas. 7-39274
 regurgitant flow through heart valves: hydraulic model applicable to US Doppler meas. 7-28563
 relativistic acoustic Doppler effect in the optical limit 7-55
 satellite remote sensing, Doppler props. of radars in circular orbits 7-4288
 scanning three-velocity-component laser Doppler anemometer 7-16277
 shipboard Doppler current profiler data merging with LORAN-C data, absolute current estimation 7-9267
 solar Doppler measurements, spatial smearing errors rel. to limb effect and large-scale vel. fields 7-66551
 solar spectrum, effects of finite spectral resolution on Stokes V profile and downflows meas. 7-47803
 solid-liquid two-phase flow, laser Doppler velocimeter meas. and turbulence props. 7-37533
 sonars for Doppler acoustic velocity profiling in the Arctic 7-9265
 steel, 4340, positron annihilation parameter and H behaviour, effects of tempering temps. 7-46205
 stenosis and bulb induced spectral changes in CW Doppler US, in vitro obs. 7-65821
 superior vena caval blood flow vels. in adults, Doppler echocardiographic study 7-8623
 symmetric heavy ion collisions, K X-ray prod., target thickness fn., X-ray spectra anal. 7-30978
 transcranial Doppler sonography, exam. technique and normal reference values 7-14070
 turbulent developing flow in U-bend of circular cross section 7-16267
 two-photon multiwave mixing Doppler broadening effects 7-15578
 ultrasound Doppler velocimeter signals anal. using personal computers 7-54687
 umbilical artery, Doppler US indices derived from max. vel. waveforms 7-47185
 umbilical artery, Doppler US indices derived from mean vel. and first moment waveforms 7-47186
 underwater optical probe for laser Doppler anemometry 7-16279
 US blood flow meas., error bounds 7-8672
 US Doppler signals of blood vel. and adaptive filtering 7-8670
 US signals, CW, statistical props. and speckle, simulation model 7-43538
 vapour, multiplet, spectral broadening, temp. depend. 7-42551
 VHF radar for ocean surface current and sea state remote sensing 7-60422
 wave theoretical approach to acoustic current profiling 7-4821
 Ag, resonant-like reabsorption in AC arc plasma 7-13842
 Al (110), Ar-induced Auger electron emission, Doppler broadening 7-59345
 Al, divacancy effect, annihilation radiation Doppler broadening meas. 7-37982
 Al, high purity samples, Doppler-broadened positron annihilation spectra, fast Fourier transform/power spectra deconvolution method 7-33481
 Al-Mg(Ca)(Zn)(Si)(Ge) dilute alloys, divacancy effect, annihilation radiation Doppler broadening meas. 7-37982
 Ar plasma, relativistic electron beam gas puff Z pinch, spectroscopic studies 7-58044
 Ba⁺, optical Lamb-Dicke confinement 7-19807
 C glassy state, stopping cross section of ¹²C projectiles 7-51899
 Ca, reson. photon emission quantum interference effect, fluoresc. 7-10486

Doppler effect continued

- Cl I, arc plasma, Stark broadening of spectral lines study 7-36536
 $\text{Co}_2\text{Si}_{1-x}\text{Ge}_x$ polycrystalline alloys, positron lifetime, Doppler studies 7-33480
 Cr vacancy formation enthalpy, positron annihilation studies 7-44536
 Cs, atomic beam frequency standard, NRLM-II, atomic vel. distrib. and second-order Doppler shift 7-14910
 Cs atomic clock, velocity distrib. determ. 7-18755
 Cs beam primary frequency standard, C-field setting, transitions and disturbances 7-18757
 Cs, stopping with diode laser beam 7-10507
 Cu, resonant-like reabsorption in AC arc plasma 7-13842
 Cu, vacancy formation enthalpy, positron annihilation studies 7-7787
 Cu-Al-Zn-Mn-Ni shape memory alloy, positron annihilation study 7-46206
 CuSb(In), vacancy formation enthalpy, positron annihilation studies 7-7787
 Fe, positron annihilation, high press. Doppler broadening expts. in diamond anvil 7-46189
 Fe-Si-B amorphous alloys, electron momentum distrib. and Fermi energy, Doppler broadening positron annihilation 7-39220
 $\text{Fe}_{40}\text{Ni}_{40}\text{Si}_{20}\text{B}_4$ metallic glass, positron trap depth distrib. determ., lifetime and Doppler effect meas. 7-39304
 GaAs, dislocation containing, positron annihilation 7-39279
 GaP, neutron irradiated and as-grown, vacancy defects, positron studies 7-2012
 H, excited state, translational energy distrib. in DC discharge, spectroscopic meas. 7-20946
 H, laser spectroscopy with relativistic beams 7-19778
 H^+ , laser spectroscopy with relativistic beams 7-19778
 H-like ion plasma, laser interaction, X-ray line emission self absorpt. and escape factors 7-37689
 HONO, laser induced chem. processes anisotropies, OH ejection 7-19973
 He plasma, spectral line Stark broadening for theta-pinch turbulent plasma parameter meas. 7-44255
 He-like ions, plasma, laser interaction, X-ray line emission self absorpt. and escape factors 7-37689
 In, monovacancy formation enthalpy, positron annihilation Doppler broadening studies 7-37976
 Mo, alpha-particle-induced defects, annealing, positron annihilation studies 7-44633
 Na, optical piston dynamics using light-induced drift 7-10508
 Na_2 , photodissoc., atomic fragment Doppler spectroscopy 7-10686
 Na_2 , photodissoc., Doppler photofragment spectroscopy 7-19972
 Nb, positron annihilation Doppler broadening studies 7-39255
 NiO, substoichiometric, positron annihilation meas. 7-37981
 OH photoproduct, momentum distrib. Doppler and polarisation spectra 7-13795
 Rb, vapor, wall-induced velocity changing collisions, laser optical pumping, complete Doppler coverage 7-962
 Si, neutron irradiated, recovery 7-39567
 Si:O, positron annihilation study 7-3105
 Sn, phase transitions, Doppler broadened positron annihilation studies 7-38190
 Sr, Rydberg states with $n/100$, laser spectroscopy 7-10461
 TaSe₂ crystals, ZH polytype, positron meas. 7-46202
 (TaSe₂)₂I, ID CDW system, positron annihilation 7-39272
 Ti vacuum arc characterisation and struct. of deposited Ti and TiN films 7-63392
 U, vacancy formation and phase transformations, positron annihilation studies 7-39248
 W, electromagnetic absorption of ultrasound near Doppler-shifted cyclotron resonance 7-45402
 W, vacancy formation enthalpy, positron annihilation studies 7-37974

Doppler shift see Doppler effect

dopplers

- metal plates, Doppler-shifted cyclotron resonance and skin effect 7-17224

dosimeters see dosimeters

dosimeters

see also dosimetry; thermoluminescent dosimeters

- A-150 plastic radiometric calorimeter for charged particles and other radiations 7-25264
 book, introduction to radiation detectors 7-33
 Bristol CR-39 neutron dosimeter, background track reduction 7-30724
 bubble damage polymer detector, low energy threshold 7-42233
 CR-39 electrochemically etched n dosimeters, pre-etching time effects on response characts. 7-30871
 CR-39 polymer dosimeters, electrochemical development of particle tracks 7-30873
 CR-39/radiator dosimeter, neutron response 7-30723
 cylindrical chamber dimensions and the corresponding values of A_{wall} and $N_{\text{gas}}/(N_{\text{e}}A_{\text{ion}})$ 7-40304
 Eberline RO2 ionisation chamber survey instrument, modifications for the quantities ambient and directional dose equiv. 7-54758
 energy dependence in γ -ray and X-ray dosimeters 7-30713
 exposure rate of a radioactive check device, calibration methods uncertainty 7-23464
 extrapolation chamber for β -ray detect., performance characts. 7-25302
 foil-type electret dosimeter for surface α -contamination monitor 7-36304
 FWT-60 and glutamine dosimeters, dose intercomparison for 400 to 500 keV electrons 7-28702
 high-level solid-state personnel dosimetry system, performance characts. in pulsed radiation meas. 7-3882
 high-pressure ionisation chamber to meas. mean neutron energy and γ -ray dose fraction 7-34281
 LWR pressure vessel surveillance using solid state track recorder neutron dosimetry 7-36199
 microprocessor use in (German) 7-25257
 multielement personal neutron track dosimeter 7-30722
 neutron, proton build-up calc. 7-65860
 neutron doses in nuclear power plants, need for personnel dosimeters 7-25263
 neutron dosimeter, radiator contribution to sensitivity 7-30716
 neutron dosimeters, evaluation and calibration for class F neutron spectra (Russian) 7-15419
 neutron dosimetry in high intensity fields, SSNTD limitations, review 7-42234
 parallel-plate chambers, determs. of N_{gas} and P_{repl} factors from 4 commercially available chambers 7-54751
 parallel-plate ion chamber, N_{gas} determ., dosimetry appl. 7-40299
 dosimeters continued
 phantom microdosimetric spectrometer, ionising radiation quality meas. 7-8692
 photon-radiation absorbed dose rates meas. by water calorimeter 7-5489
 pMOS dosimeters, long-term annealing and neutron response 7-56880
 polycarbonate detector, meas. of neutron dose equivalent of natural background 7-30720
 polycarbonate detectors, Rn/decay product dosimetry by electrochemical etching, calibration (German) 7-15418
 polymeric dosimeters, internal heating during electrochemical etching 7-30872
 quartz piezoelectric resonators, electron and gamma radiation dosimetry appls. 7-15416
 solid state nuclear track detectors, conference, Rome, Italy (Sept. 1985) 7-40991
 tissue equivalent radiochromic waveguide dosimeters for X, γ and fast neutron meas. 7-34279
 tissue-equivalent chambers, low press., performance and method for parameterising dose equiv. 7-3883
 track detectors for personnel neutron dosimetry, characteristics 7-30884
 $\text{CaF}_2:\text{Tm}$ Teflon TLD discs of different thicknesses, fast neutron responses 7-54757
 Mg/Ar ionisation chambers used as γ -ray dosimeters in mixed neutron-photon fields, characts. 7-34282
 Si photodiodes, use for dose depth distrib. meas. in oncology 7-60092
 dosimetry
 see also dosimeters; radiation detection and measurement; radiation monitoring
 airborne radioactive gases inside a nuclear reactor containment building, Monte Carlo program to calc. exposure rate 7-54766
 $\text{Al}_2\text{O}_3:\text{Fe}$, single cryst., thermoluminesc. response 7-27794
 alanine system sensitivity, fast neutron irradiation effects 7-34188
 beta radiation unit of absorbed dose rate to tissue, PTB National Primary Standard 7-28717
 biostack dose meas. on Spacelab 1 7-42406
 Bonner sphere dose equivalent determ. neutron spectra, fluence response data effect 7-30728
 brachytherapy, 'natural' vol-dose histogram 7-54749
 Bulgarian population radiation exposure from the gamma background (Russian) 7-54762
 Bulgarian radiation exposure from nuclear power facilities (Russian) 7-54763
 calibration of radon detectors 7-49823
 calibrators, accuracy testing 7-3879
 cellulose nitrate as Rn and daughter detectors for indoor meas. 7-49824
 cellulose nitrate films for miners personal dosimetry 7-49822
 chamber-dependent wall correction factors in dosimetry 7-23462
 Chernobyl fallout, monitoring and impact on UK 7-42229
 Chernobyl nuclear reactor accident, individual dose assessment at Berkeley, UK 7-3880
 Chernobyl reactor accident, UK aquatic environment, fisheries viewpoint 7-42230
 coal-fired power stations in India, radiation exposures 7-40309
 code system to compute radiation dose in human phantoms 7-34285
 conference on fission product behaviour and source term research, Snowbird, UT, USA (July 1984) 7-10
 conference on radiation protection physics, Bad Schandau, Germany (Feb. 1986) 7-24267
 cosmic ray induced ionisation intensity meas. 7-40308
 cosmic-ray muons, indoor exposure rate, effect of partition walls and neighboring buildings 7-34277
 CR39 proton detector in neutron dosimeter, etching times 7-829
 CR-39 fast neutron dosimeter, nearly flat dose equivalent response 7-42418
 CR-39 manufacture for neutron dosimetry appl. 7-42412
 CR-39 neutron dosimeters, electrochemically etched 7-42422
 CR-39 neutron recoil track etch dosimetry 7-42419
 CR-39 plastic, neutron response, background, ageing and fading props. 7-42417
 CR-39 polycarbonate, structure property correlation in dosimetry, track etching 7-32313
 cycloaliphatic epoxy resin, ageing, irradiation environmental conditions effect 7-33707
 deep geologic storage of spent nucl. fuel, radiation safety and personnel monitoring 7-36303
 depth-dose distributions, conversion from slab to spherical geometries for space-shielding appls. 7-56879
 deregulated solid biomedical radwaste incineration, dose assessment 7-30682
 digital fluoroscopic image data, appl. to radiation dosimetry 7-23439
 DIORIT research reactor, activation product distrib. in shielding materials (German) 7-49536
 discrepancies obtained using a guarded parallel-plate ion chamber with a high input impedance electrometer 7-14136
 dose calibrator ionisation chamber standards for radionuclide assay 7-40310
 DOSKMF2 code for gamma radiation field meas. on high dose rate radiation equipment 7-15417
 effective dose equivalent, H_E , use as risk parameter in CT 7-40294
 electron depth-dose curves calc. with EGS and ETRAN Monte Carlo codes, differences 7-40301
 energy dependence of dose equiv. on primary photon energy, comparison of CASIM and Moyer model calcs. 7-54747
 epidemiological evaluation of radiation risk using populations exposed at high doses 7-8687
 etched track Rn dosimeters, international intercomparisons 7-49737
 ethane, ionisation by X-rays, effect of fluid density on energy absorpt. 7-31920
 exposure and organ dose estimation in diagnostic radiology 7-54752
 fast neutron dosimetry using CR-39 with scintillator filled etched pit method 7-42410
 fluoroscopic diagnostic exams., levels of radiation exposure 7-60090
 fusion materials, neutron irradi., dosimetry and damage calcs. 7-51847
 gamma radiation in Swedish dwellings 7-3884
 gamma spectrometry, inexpensive and multipurpose calibration phantom for in-vivo measurements of internal contaminants 7-54746
 gamma-ray buildup factors, G-P method applicability 7-56883
 gamma-ray skyshine calcs., effects on nuclear facility design 7-42239
 gastroesophageal scintiscanning in a paediatric population: dosimetry 7-65843

dosimetry continued

genetically significant dose from diagnostic nuclear medicine exams, USA, 1980 7-8689
 ground level air radionuclide conc. 1984-1986, N. Germany and N. Norway 7-59896
 Gundremmingen power plant, operating experience with automatic dosage metering (*German*) 7-49725
 high energy electrons, influence of cylindrical air cavities on fluence distrib. 7-62097
 high-pressure ionisation chamber, appl. to meas. mean neutron energy or γ -ray dose fraction in a mixed neutron- γ field 7-34280
 hip joint meas. in children, radiation exposure and image quality in CT 7-23460
 HLW land disposal, radionuclide pathways to man, radiological impact, doses 7-5467
 homogeneous phantoms, effect of Pb attenuators on dose 7-54753
 hysterosalpingography, radiation dose reduction: an appl. of scanning-beam digital radiography 7-28714
 ICRU tissue sphere, effect of cross-section struct. on dosimetric response function for 0.4 to 10 MeV neutrons 7-8693
 individual and collective dose estimation method for subthreshold detection 7-28704
 inhomogeneous slabs in a ^{60}Co beam scatt. anal.: differential tissue-air ratio method 7-23436
 interface phenomena, Monte Carlo prediction 7-56878
 International Commission on Radiological Protection, principles of dose limitation system 7-54745
 interstitial radiation therapy, optimum schemes of placing radiation sources (*Russian*) 7-28662
 ionisation chamber collection efficiency in a pulsed swept beam: chamber size effects 7-14134
 ionisation chamber collection efficiency in a pulsed swept beam: collimator scatt. effects. 7-14135
 Karlsruhe radon diffusion chamber appl. in sub-surface U exploration 7-49820
 Krakow region, Poland, estimation of radiation effects from local industrial activity 7-25260
 La Crosse BWR, operational radiation protection for reducing cumulative exposure 7-42240
 Light Ion Beam Fusion Target Development Facilities, activation studies 7-49732
 logistic estimate of the final incidence of lateradiation effects 7-8653
 long term Rn monitor using polycarbonate foil 7-25265
 low radiation doses, effects and mechanisms, possible beneficial effects (*German*) 7-28577
 LR 115 track detector, neutron dosimetry and proton detection 7-30721
 LR-115-11 Kodak track film indoor Rn meas. 7-49738
 LWR surveillance dosimetry anal., changing source distrib. effects 7-62098
 lymphocytes, human, chromosome aberrations yield rel. to dose (*Russian*) 7-18027
 lymphocytes, human, lower limits of dose detect. after X-irrad. 7-34196
 Magnox reactors, ingestion dose study from postulated releases 7-42231
 mammographic systems, dose comparisons 7-40298
 mammography, absorbed breast dose rel. to radiographic modality, technique and breast thickness 7-28716
 maximum dose equivalent due to passing of spent fuel transport vehicle 7-10299
 medical beta source radiation charact. meas. 7-54748
 medical irradiation, effect of utilising age and sex dependent factors for detriment calc. 7-54734
 methane, ionisation by X-rays, effect of fluid density on energy absorpt. 7-31920
 mica track filters for Rn meas. 7-49734
 microdosimetric approach in radiation biology, correctness (*Russian*) 7-14063
 microdosimetric investigation of a fast neutron radiobiology facility utilising the $\text{d}(4)^9\text{Be}$ reaction 7-23463
 microdosimetric studies of ^{252}Cf 7-28709
 MICROSHIELD, microcomputer program for dose rate, gamma shielding anal. 7-42109
 microwave hyperthermia, thermal dosimetry method using microwave radiometry for temp. control 7-65859
 model for risk assessment of inhaled particles, factors to be considered 7-54756
 molecular fraction method for personnel radiation dose meas. 7-62096
 Monte Carlo dosimetry for ^{125}I and ^{60}Co in eye plaque therapy 7-40300
 multilayered devices, algorithm for dose profile calc. using personal computer 7-56877
 multiplicative correction factor for tissue heterogeneities, radiotherapy dosimetry appl., Monte Carlo calcs. 7-14124
 muscovite mica, effect of high γ -ray doses on thermal props. 7-8270
 natural Rn daughter exposure meas. in French houses 7-54414
 neutral beam injection duct concrete shield, differential gamma dose rate 7-36242
 neutron detector, moderated activation, photon sensitivity 7-40302
 neutron dose and energy spectrum outside a 20-MV accelerator treatment room 7-40303
 neutron doses in nuclear power plants, need for personnel dosimeters 7-25263
 neutron dosimetry in high intensity fields, SSNTD limitations, review 7-42234
 neutron dosimetry standard for fission track dating 7-36433
 neutron dosimetry system based on the chemical etch of CR-39 7-42411
 neutron quality factor for dosimetry and biological damage 7-25258
 neutron radiation fields set: dose equiv. conversion coeffs., instruments and dosimeter responses 7-54761
 neutron sources, dosimetric characteristics for biology and medicine 7-56894
 nuclear and space radiation effects in electronics, conf., Providence, RI, USA (July 1986) 7-55875
 nuclear medicine workshop. Chalk River, Ont., Canada (Aug. 1985) 7-24308
 nuclear power plant, neutron dosimetry using Kodak LR 115 II B 7-30718
 nuclear techniques in diagnostic medicine, book 7-24312
 nursing mothers, radionuclide administration, math. derived guidelines 7-14127
 ocular lens, radiation dose in radiology of the orbit 7-40292
 open track films for ^{222}Rn -meas. in dwellings 7-49825

dosimetry continued

ophthalmic applicators, B-particle, calibration of US National Bureau of Standards 7-47259
 Oyster Creek emergency off-site dose assessment, ocean breeze inclusion 7-30725
 patient doses and risks from diagnostic radiology in north-east Italy 7-60089
 personnel neutron dosimetry using hot, low-frequency electrochemical etching 7-42414
 Petten HFR, reactor vessel replacement, dismantling, segmentation, waste disposal, doses 7-5488
 photon beam dose calculation, density correction algorithms (*Korean*) 7-28707
 photon-radiation absorbed dose rates meas. by water calorimeter 7-5489
 picture-processing-based automated system 7-28713
 plant tissues exposed to γ -rays, dose distrib. patterns 7-34275
 polycarbonate detector, meas. of neutron dose equivalent of natural background 7-30720
 polymers solid state nuclear track detectors in high energy particle dosimetry 7-42405
 proton accelerators, high energy, estimation of radiation fields 7-813
 PWR containment, postaccident conditions, airborne dose rates/skyshine radiation calcs. 7-19554
 radiation detection for radiation protection meas., electrical effects use (*German*) 7-15420
 radiation detection in radiation protection meas., thermal. mag. and other effects (*German*) 7-19551
 radioactive cloud, dose reduction factors for large buildings, computer codes 7-54759
 radioactive dust sampling, entry characts. of dust samplers used in British nuclear industry 7-40079
 radiolabelled antibodies for tumour therapy, dosimetric aspects 7-40297
 radionuclide dose calibrator meas., evaluation 7-30891
 radiotherapy, CNS tumours, technique for delivering uniform dose at the junction of 2 spinal fields 7-3878
 radiotherapy, computerised treatment planning systems, comparison when calculating dose under shielding blocks 7-28706
 radiotherapy, dose distrib. of high-energy electron beam, chromosome aberration freqs. 7-14131
 radiotherapy, dosimetry of asymmetric X-ray collimators 7-54754
 radiotherapy, extension of Fourier methods to calc. of effective depths in heterogeneous media of arbitrary contour 7-54426
 radiotherapy, external, use of microcomputer for nonlinear optimisation of doses 7-34283
 radiotherapy, external beam treatment planning, analytic evaluation of heterogeneity locations 7-40275
 radiotherapy, fractionated, graphical method to simplify the appl. of the linear-quadratic dose-effect eqn. 7-28660
 radiotherapy, nominal accelerating pot. determ. 7-54729
 radiotherapy, photon beam peak-depth profile, description rel. to field size 7-54750
 radiotherapy, proton beam penumbra: effects of separation between patient and beam modifying devices 7-40276
 radiotherapy, source-surface distance and source-axis distance beam data acquisition 7-54755
 radiotherapy, total body irrad., practical approach to dose uniformity 7-65840
 reactor pressure vessel neutron dosimetry using solid-state track recorder 7-36305
 relative tissue kerma sensitivity of thermoluminescent materials to neutrons 7-54760
 relativistic charged particle beam dosimetry with solid state detectors. (*Czech*) 7-62091
 relativistic proton dosimetry with SSNTDs (*Czech*) 7-62094
 remote sensing neutron dosimetry using prompt γ -ray spectrometry 7-49727
 risk analysis and exposure meas., dose equivalent concepts 7-47260
 rotational panoramic radiography: comparison of radiation doses in the standard and reverse posns. 7-40293
 scoliosis evaluation, radiation dose reduction, appl. of digital radiography 7-28715
 SEFOR test reactor, gamma anal. of soil following decommissioning 7-30726
 sensitisers and radiation dose fractionation: results and interpretations 7-23461
 simulated basalt geological radwaste repository, SSNTD neutron dosimetry 7-42199
 single element neutron personal dosimeter using poly allyl diglycol carbonate 7-42415
 soft X-ray sources and instruments calibration, 1986 status 7-25322
 solid state nuclear track detector for dose assessment of heavy charged particles 7-19626
 source term composition effects on offsite doses after reactor accidents 7-782
 space radiation dosimetry, track detector appl. 7-42404
 spaceflight heavy-ion dosimetry data comparison with CREME model LET spectra 7-60107
 Spacelab D1 mission, dosimetric mapping inside Biorack 7-8713
 spent nuclear fuel, reprocessing and direct disposal, radiological comparison (*German*) 7-49683
 spent nuclear fuel shipping vessel, neutron dose rates, Monte-Carlo anal. 7-25267
 standard for unit of absorbed dose in water 7-60091
 styrene-butadiene rubber, C-black loaded, elec. props., effect of gamma irrad., dosimetry appls. 7-33006
 T-1 cells, human, inverse γ -ray dose rate effect in ^{252}Cf RBE expt. 7-28616
 thermal neutron dosimetry using CR-39 with scintillator etch pit method 7-42409
 tissue equivalent phantom materials for negative pions 7-65850
 tissue phantom for phototherapy, optical dosimetry study 7-34284
 TMI-2 reactor cavity, neutron dosimetry using solid-state track detectors 7-30717
 tumour phantom models, miniature TLD absorbed dose obs. 7-40296
 US cavitation, sonochemical reaction and local temp. determ. 7-3594
 whole-body uniform irrad. with 1000 MeV protons, dose-rate contrib. to effect (*Russian*) 7-14067
 worker dose distributions rel. to ICRP dose limitation recommendations 7-34276
 X-ray and electron dosimetry, clarification of the AAPM Task Group 21 protocol 7-40305

dosimetry continued

- X-ray examinations standardisation, engng. basis 7-28663
n- γ radiation field dosimetry using miniature Si photodiodes 7-25262
Au-Al interfaces, dose profiles for 100 to 1250 keV photons, ONETRAN calcs. 7-56874
BaSO₄-culture medium interface, phys. and biological dosimetry 7-28703
K, kerma factor for 18 and 20 MeV neutrons, exact meas. 7-36302
CaSO₄:Dy phosphor, thermoluminesc. props. of a new prep., dosimetry appl. 7-28701
²⁵²Cf irradiation, facilities, thermal neutron calibration curve meas. 7-30719
²⁵²Cf neutron calibration flux distrib., Monte Carlo simulation 7-30805
²⁵²Cf neutron therapy, time and dose considerations for clinical trials 7-28712
²⁵²Cf physics and dosimetry 7-28708
²⁵²Cf radiation, phys. and biological dosimetries 7-28711
²⁵²Cf radiation dosimetry, studies in the USSR 7-28710
⁶⁰Co irradiator at Hiroshima Univ., dose rate distrib. (Japanese) 7-40295
¹³⁷Cs, A=134,137, comparative pathway analysis in Hudson River estuary, dose assessment 7-8699
³H β -rays, radiation quality, microdosimetric distrib. for nm-size targets 7-8691
³H, environmental aspects, toxicity, metabolism and dosimetry: research at CRNL 7-54774
³H metabolism in newborn mice and estimation of accumulated dose 7-60100
³H, normal releases from fusion processes and environmental radiation doses 7-54775
¹³¹I treatment of thyroid cancer: absorbed dose calc. from post-therapy scans 7-65842
^{113m}In-indifer use, patient irradiation doses (Russian) 7-3881
¹⁹²Ir, accidental internal deposition, absorbed organ dose, γ -camera meas. 7-8688
¹⁹²Ir dosimetry, use of simulator-based CT 7-14132
LiF thermoluminescent dosimeter appl. in n- γ mixed field dosimetry in TRIGA reactors 7-49733
²¹⁰Pb concs. and states of equilib. with ²³⁸U, ²³⁴U and ²³⁰Th in U miners' lungs 7-28724
²²⁴Ra in mouse bone, dosimetry calcs. 7-8690
Rn concentration in Danish dwellings, CR-39 track detector meas. 7-49826
Rn dosimetry, rectangular geometry effects 7-42426
Rn dosimetry meas. by electrochemical etching of polycarbonate detectors (German) 7-15418
Rn, emanation into pores of solid material, recoil effect 7-49730
Rn personal dosimeter for miners 7-49736
²²²Rn, A=220, 222, progeny inhalation, lung cancer risk at low doses of α particles 7-28608
Si, energy deposited by mesons in 1- μ m sites, probability distrib. 7-58312
Si photodiodes, use for dose depth distrib. meas. in oncology 7-60092
Si-SiO₂-Si layered struct., dose calcs. for X-ray and X-ray irradiation 7-58333
¹⁵³Sm, accidental internal deposition, absorbed organ dose, γ -camera meas. 7-8688
^{99m}Tc-pyrphotech use, patient irradiation doses (Russian) 7-3881
U distribution in blood samples, fission track study 7-54771

double heterostructure lasers see semiconductor junction lasers

double layers (electric) see electrochemistry; liquid theory

double nuclear magnetic resonance

see also ENDOR

- amino group containing moles., double quadrupole reson., solid effect 7-59123
diglycine nitrate, ferroelec. transition mechanism, mol. reorientation, ¹⁴N and ¹⁷O quadrupole coupling meas. 7-53245
heteronuclear relayed coherence transfer NMR spectroscopy, 2D, sensitivity enhanced 7-9857
metal-phosphine complexes, stereodynamics, equilib. conformations, DNMR 7-31083
methylammonium mercury chloride, ferroelec. phase transition, proton-¹⁴N double reson. study 7-7653
Raman magnetic resonance spectroscopy, continuous coherence transfer method 7-41413
T4 lysozyme, ¹H amide resonance assignment, ¹³C, ¹⁵N DNMR spectra anal. 7-25572
4-thiacyclohexanones, 2,6-disubstituted, stereochemistry, ¹H and ¹³C NMR 7-57096
CaF₂:Eu³⁺, ¹⁵³Eu-¹⁵¹Eu quadrupole moment ratio, optically detected NMR studies 7-22164
²³Na ions, biexponential relax. detect. using double-quantum filtering 7-25446
a-Si:H, H clustering, multiple quantum NMR 7-32671

double refraction see birefringence

double refraction, electric see electro-optical effects

double refraction, magnetic see magneto-optical effects

double resonance, electron nuclear see ENDOR

doublet antennas see dipole antennas

DP management

- see also contracts; security of data; software selection
software engineering in physics, conf. Nove Mesto na Morave, Czechoslovakia (Sept. 1985) 7-18471

DPPH, diphenylpicrylhydrazyl see organic compounds

drag

see also drag reduction

- aerosol particles, gravitational settling, turbulent flow field 7-51284
aerosols gravitational settling in randomly orientated cellular flow fields 7-1616
airfoil with oscillating flap, unsteady wake meas. at transonic speed 7-51208
atmospheric gliding entry, heating, scaling relations 7-51200
automobile deceleration force by the coast-down method 7-18541
axisymmetric body, force in linearised time-depend. motion 7-26303
bird flight, calc. of lift, thrust and drag 7-18011
body rotating in viscous liquid, minimum moment acting on body 7-51160
Carreau fluid creeping flow past Newtonian drops 7-63188
circular cylinder in cross flow, tripping wire effect on boundary layer transition 7-43847
circular cylinder in turbulent boundary layer; fluid forces 7-6200
coefficient, Newton-Raphson calc. 7-31753

drag continued

- creeping flow around spherical gas-bubble in liquid, Oseen's eqn. soln. 7-37513
curved rectilinear channels, drag creeping flow, asymptotic soln. 7-37541
cylinder in cross flow of water with injection into boundary layer, heat transfer and drag 7-43888
duct, scalene triangular, rib-roughened, turbulent friction factors study 7-57812
fluid flow with free surface past bodies, hydraulic modelling of drag and friction resistance 7-31822
flycasting mechanics, flyline investig. 7-50
fuel-rod bundles model, hydraulic drag 7-10237
gas-liquid flow in film-type evaporators, fluid dynamics study 7-11503
Hookean dumbbells with anisotropic hydrodynamic drag and Brownian motion, Giesekus model 7-16216
hydraulic drag coefficient determination in Couette flow at high Re 7-43841
incompressible fluid, cylinder creeping motion study 7-20825
laminar flow past short, heated cylinder, finite element soln. 7-57789
liquid films, air-driven, interfacial instability 7-11513
liquid-gas flow through coarse particle beds, 1D model 7-57904
magnetic fluid, thin layer coating, hydrodynamic drag, num. investig. 7-51061
micropolar fluid, unsteady flow past flat plate 7-63113
neutrally stable atmospheric boundary layer flow, drag coeff. theory 7-14357
nonequilibrium linearised MHD flow over wavy wall 7-63226
Oldroyd fluid through circular pipe, unsteady flow 7-63112
Oseen flow past sphere as function of Reynolds number 7-51038
packed beds, flow, drag force, wall effect 7-51292
pipe flow, gas, permeable walls, turbulent flow, heat transfer, phys. props. temp. depend effect 7-63217
power law fluid, multiple drop slow motion, drag and mass transfer 7-11472
runaway phenomenon, diffusion with varying drag 7-57977
sphere in rot. and straining inviscid flow, virtual mass and lift force 7-57848
sphere motion in air flow through horizontal pipe 7-26344
sphere motion in rarefied gas, temp. variation 7-43984
spheres in beds in lengthwise flow, fluid friction and convective exchange 7-57917
spinning baseball, lateral force study 7-48231
Stokes flow past a slightly deformed fluid sphere 7-51032
subsonic bluff-body flows, wake periodicity 7-31807
supersonic gas flow past 3D bodies and wings of maximum lift-drag ratio 7-57874
supersonic wake past blunt body, heat transfer, and drag 7-51214
transient induced drag 7-6235
tube, cylindrical with perforated baffles, hydraulic drag 7-44046
twisted oval tube, heat transfer and hydraulic drag coeffs. 7-1631
two-dimensional flow past bluff flexible low porosity membranes 7-16241
two-phase wavy film flow, interfacial shear factor, interfacial mobility study 7-57899
undehated liquid, surface boiling, forced motion, Reynolds analogy appl. 7-31806
upward thin-film flow in desalination unit, drag, dynamics 7-11509
vertical entry of solids into water 7-31849
viscous flow, Stokes drag on falling hollow cylinders and conglomerates 7-51049
water, turbulent flow at supercritical press. in smooth channel, drag coeffs. determ. 7-43866
Mn, vapour, photoelectron ang. distrib. and drag current, nondipole part 7-15575

drag reduction

- channel, longitudinally grooved, drag reduction in flow 7-51060
curved pipes, dilute polymer soln. flow, drag reduction, pressure loss in 360° bends 7-16211
forced convection of drag reducing fluids in vertical pipes, buoyancy effect on heat transfer 7-26278
gas-liquid two-phase flow of drag reducing fluids, heat transfer 7-16175
ideal gas supersonic flow past blunt bodies with protruding spikes 7-57873
laminar boundary layers, active stabilisation, turbulence transition, drag reduction 7-20683
microbubble skin friction reduction on an axisymmetric body in turbulent boundary layer 7-31772
polymer solutions, cascade, theory of drag reduction 7-11474
polymeric additive effect on nucleate pool boiling 7-11512
surfactant systems, drag reduction, physico-chem. props., rheology 7-43992
Toms effect, reduction of turbulent diffusivity by addition of polymers (French) 7-16173
turbulent boundary layers, mean flow, drag reduction, review 7-16171
turbulent boundary-layer, surface drag reduction by riblet modification, visualisation study 7-11394
turbulent boundary-layer skin-friction drag reduction meas. 7-51081
viscous incompressible laminar flow, drag reduction, optimal control 7-57794

drawability see ductility

drawing (mechanical)

- glass fibre processing, spinning process in liq. state 7-3258
glass rod forming process, mathematical model construction 7-20476
glass technology, mixed transfer processes 7-7948
magnetic vortex field, 2D, with boundary conditions of 3rd kind, numerical determ. for tube drawing, inductive heating (German) 7-33811
metal, cold-deformed, microcrack development (Russian) 7-39652
optical fibre, tolerance checking on diameters during drawing 7-62852
optical fibre drawing, high speed and coating, review 7-11134
optical fibre transmission loss characteristics during drawing, continuous measurement 7-6004
PET, biaxially oriented sheets, orientation rel. to mech. compliance 7-53781
PET, drawn sheets, molecular orientation, Raman spectra, refractive index 7-53318
PET, high-modulus, cord prod. by microwave heat drawing 7-22735
PET, high-temp. viscoelasticity and heat-setting, strain recovery meas. 7-63721
PET films, one-way drawn, trichroic IR absorpt. spectra 7-33381
PMMA, drawn, filled with ultrafine SiO₂ particles, elastic and yield props. 7-3351

drawing (mechanical) continued

- poly(ethylene terephthalate), changes in molecular conformations produced by crystallization and drawing, neutron scatt. anal. 7-10799
 polyethylene, lin., deform. process, morphological study 7-13518
 polyethylene, ultra-high modulus, tensile strength, effect of mol. wt. 7-39590
 polyethylene films, drawing, mech. props. rel. to polymerisation temp. 7-59488
 polymers, neck propag., plane strain 7-44658
 polyoxymethylene, tubes, microwave heat drawing, tensile load and precursor size effects 7-22734
 polypropylene, oriented, thermal expansion behaviour 7-6839
 polypropylene, quenched, isotactic, glass transition, effect of drawing 7-12278
 silica optical fibres, defect struct. and drawing-induced absorption, drawing depend. 7-3071
 steel, deep drawing, recrystn. texture development, investig. by ODF anal. 7-13466
 steel, low C, struct. rel. to deform. method (*Russian*) 7-46580
 steel, stainless, wire, electroplastic drawing, struct. and physicom. studies (*Russian*) 7-8057
 stress anal. of wire drawing dies and boreholes, expt. study (*German*) 7-22769
 thermoplastic rubber/liquid crystal polyester dualcoextrusion coating system for optical fiber drawing 7-11190
 vapour axial deposited preform stretching, numerical model for internal distortion 7-11133
 zirconia induction furnace for high strength fibre production, design 7-11184
 CaO-BaO-P₂O₅ glass fibres, stress optical studies 7-7673
 Na₂O-Li₂O-P₂O₅ glass fibres, stress optical studies 7-7673
 Ni strip, drawing after annealing at various heating rates 7-28071
 PdFe, drawing effects on elec. resist. and mech. props. (*Russian*) 7-17584
 SiO₂-GeO₂ optical fibre, drawing- and radiation-induced paramagnetic defects 7-11084

drift chambers see *position sensitive particle detectors; proportional counters*

drives

- see also *clutches; electric drives; propulsion*
 refrigerator, Vuilleumier, with mag. linkage, test and analysis 7-56290

drop model (nuclear) see *nuclear liquid drop model*

droplets see *drops*

drops

- accelerated droplets in nonisothermal flow, heat transfer (*Russian*) 7-16179
 air flow with fine droplets, evaporative cooling heat transfer 7-11508
 annular flow, vertical, droplet entrainment and its contrib. to momentum transfer 7-11492
 atmosphere, aerosol conc. changes in drops due to particle scavenging and redistrib. by coagulation 7-55201
 atmosphere, large water droplets dispersion model 7-34583
 binary nematic systems, anisotropic droplet observation in phase separation 7-52054
 body entering liquid, splash formation, droplet size distn. 7-63195
 Carreau fluid creeping flow past Newtonian drops 7-63188
 cavitation damage impact erosion, continuum model 7-11479
 cloud condensation nuclei, conc., obs. and prediction discrepancies 7-4088
 cloud droplet size and critical supersaturation rel. to mixing processes 7-66225
 cloud drops, exposure by camera technique 7-55277
 cloud pt. and nucleation theory 7-26906
 clouds supercooled liq. water characts. at mountaintop sites in Colorado Rockies 7-29147
 clustering in microemulsions, electric birefringence study 7-28354
 condensation and evaporation of a drop in a vapour-gas mixture 7-52014
 condensation kinetics under ideal supersaturation conditions (*Russian*) 7-63787
 condensing droplet in high Reynolds no. flow, transport mechanism, stagnant surfactant cap effect 7-51271
 conference, Cambridge, England (March 1986) 7-40987
 convective vaporisation, of irradiated droplets, hydrodynamic description 7-31800
 crystal violet in ethanol, spreading layer, capillary convection 7-6925
 curvature meas. by differential interferometry 7-41339
 dense particle fields, laser diffraction meas. correction for multiple scatt. 7-1212
 diameter and hold-up variation in dense-packed dispersion 7-6270
 diffusion-convective vaporisation by intensive optical radiation, quasistationary soln. 7-50914
 dispersed drops, motion and mass transfer in pulsed column 7-6290
 droplet coalescence in turbulent liquid-liquid dispersions 7-51272
 dropwise condensation heat transfer on a horizontal tube 7-20704
 electrostatic charging of solid particles and liquid droplets 7-26586
 evaporation anal. taking account of variability of gas props. 7-44029
 evaporation under subatmospheric press. 7-44010
 exclusion process and droplet shape, isomorphism with stochastic Ising model 7-29922
 ferrofluid droplet shape stability in magnetic field 7-6324
 ferrofluid jet in mag. field, droplet form. using capillary nozzles 7-37553
 fluids confined between solid surfaces, wetting dynamics 7-12406
 formation from single nozzles under pulsed flow conditions 7-11496
 fractal cluster form. by aq. nanodroplets in apolar media, dielec. 7-39921
 freezing data anal. using mathematical technique 7-58444
 frontiers in fluid mechanics, book 7-4640
 fuel drop, liq., moving, combustion, thin-flame theory, variable density effect 7-26364
 fuel drop-air mixtures, flame propag. 7-23018
 fuel drops combustion, stability loss mechanism in stream of oxidising gas 7-31892
 fuel spray ignition by hot surface 7-51337
 generation from capillary streams 7-57913
 Great Dun Fell, England, meteorological conditions 7-34661
 Handlos-Baron model for simple drop extraction in turbulence, limitations 7-16219
 high flux, single solute mass transfer in spherical rigid drops 7-16217
 high pressure bubble growth in multicomponent liquid droplets in a flowing immiscible liquid stream 7-63785
 instability development in elec. field 7-31850
 drops continued
 interacting drops in 2-phase flow, fluid dynamics and mass transfer 7-63203
 intrinsic contact-angle hysteresis in Hg porosimetry 7-31872
 inviscid, with surface tension, 3D oscillations, quadratic reson. 7-11519
 inviscid drop in zero gravity environment, free and forced nonlinear oscils. (*German*) 7-20739
 laser beam in medium containing droplets, nonlinear refraction phase compensation 7-4183
 light scattering and microscopic video obs. of droplet patterns 7-56332
 liquid, breakup, rarefaction waves 7-20785
 liquid droplet deformation in gas flow, anal. 7-51278
 liquid drops, charged, instability of evap. 7-20091
 liquid in vibrating cylindrical container, liquid surface response, turbulence, waves 7-16196
 liquid jets, breakup and atomisation, transient behaviour 7-51249
 liquid metal drops, energy characts. 7-32762
 liquid metal turbulent jet, mixing and solidification in co-flowing stream 7-51250
 liquid spreading on solid, contact lines 7-6929
 liquid spreading on substrate, nonequilibrium thermodynamic appls. 7-6920
 liquid thread breakup in linear flow 7-57805
 many-body hydrodynamic interactions between spherical drops in an emulsion 7-16147
 mass-transfer rates from single drops and dropswarms 7-6274
 methanol particle sizing with phase Doppler spray analyser 7-29969
 microemulsions, viscosity peaks, percolation-like transitions, salinity variations, Krieger-type formula, modelling 7-8307
 modulated water jets, numerical modeling 7-63190
 motion in conducting liquid in variable elec. field 7-51326
 multicomponent droplet vaporization in a high temperature gas 7-57898
 multicomponent mass transfer in spherical rigid drops 7-16218
 nematic, light scatt. 7-22274
 nematic droplets, tangentially anchored, parity breaking transition 7-26626
 non-Newtonian films, dimpled, drainage 7-26321
 nonlinear optical processes in micron-size droplets 7-11063
 nonNewtonian flow, transient mass and heat transfer from drops or bubbles 7-11473
 oscillations, viscosity effect 7-37500
 particle shape and size variations from morphology-depend. reson. in fluorescence spectra 7-29970
 particle siting with phase Doppler spray analyser, nonspherical drops effect 7-29969
 particle sizing techniques, laser interferometric, performance comparison 7-30071
 particles, drops and bubbles, velocity calcs. 7-57896
 pendent drop, falling, surface tension, density, viscosity effects. (*Russian*) 7-16838
 pipe extraction column, operating with two-phase drops, design (*German*) 7-51311
 polar stratospheric cloud drops, heterogeneous chemical reactions rel. to Antarctic O₃ hole form. 7-55163
 polydimethylsiloxane, liq., spreading, existence and role of thin precursor film 7-44954
 power law fluid, multiple drop slow motion, drag and mass transfer 7-11472
 pressure pulse reflection at free surfaces of water 7-11480
 rain drops, capture of sulphate aerosol 7-40059
 raindrop size spectra from frontal convective clouds over Israel 7-66238
 raindrop splash, physically-based model of splash droplets dispersion 7-9036
 rapid reactions, microdroplet mixing technique investig. using Raman spectrosc. 7-54082
 rhodamine 590 droplet, micrometer size, high intensity laser interaction 7-43210
 rhodamine 590/water soln, droplet whispering-gallery-mode laser characts. 7-31310
 rotating in weightlessness, equilb. shapes 7-63198
 separation of droplets of lower channels, channel profile geometry effect 7-44017
 single capillaries, droplet formation in the jet regime of a liquid/liquid system (*German*) 7-16227
 solar cooling by direct evaporation from sprays 7-37532
 solid particulates and aerosol droplets at entrance of pore, hydrodynamic and mol. wall interaction effects 7-51270
 solid surface, dislodgment due to surrounding fluid motion 7-52190
 spherical droplets, semi-transparent, hologram structure 7-31281
 sprays, drop size distrib. function analysis (*Chinese*) 7-11517
 steam, dropwise condensation, heat transfer study, falling drops effect 7-43890
 steam-water dispersed flow heat transfer in vertical round tube, post-dryout regime (*Chinese*) 7-11419
 surface temperature meas. with IR technique (*Chinese*) 7-48733
 surface tension, pendent drop profile computer calcs. 7-2298
 surface tension dynamics, laser-induced modification 7-58570
 suspensions, gas-droplet, shock wave struct. 7-6252
 transient dilation of bubbles and drops, theoretical basis for dynamic interfacial meas. 7-32757
 transient dispersed-film flows in channels containing fuel rod bundles 7-10236
 two-phase flow, concentration and droplet size distrib., simultaneous and instantaneous meas. 7-37535
 US atomisation, drop particle size assessment 7-53654
 vaporisation, internal circulation integral eqn. formulation 7-37530
 vapour phase homogeneous nucleation, interfacial tension rel. to droplet size 7-58435
 vertical wind tunnel for water drop studies 7-6293
 viscous liq. drop breakup, capillary wave instabilities, transient effect 7-43954
 visualisation and meas. using digital image anal. 7-37577
 warm shallow convective clouds, large raindrops obs. 7-47479
 water drops in atmosphere, microdynamic mechanisms for airborne particles scavenging 7-55200
 water flow in capillary, surface and kinetic energy, laboratory exercise 7-18528
 water in atmospheric aerosol drops, activity calcs. 7-9110
 Au liquid metal ion source, focused droplet beam 7-30801
 H₂O droplet, vaporisation by laser beam, electrohydrodynamics self-similar study 7-1645

- drops continued**
H₂O droplets, laser-induced explosion, spatially resolved spectra 7-42632
³He and ⁴He liquid drops, ground states, variational Monte Carlo calcs. 7-12383
Sb liquid droplets, undercooling and crystallisation 7-39496
- drying**
ceramic synthesis from molecular precursors, conf., Palo Alto, USA (Apr. 1986) 7-35113
filtration process, hydrodynamics 7-57918
gels, drying induced shrinkage, liquid flow and chem. reactions 7-23069
gels, film and flat plate, drying behaviour, anal. 7-59794
granular solids, fluidised-bed drying, mathematical model 7-50917
heat-sensitive substances, drying using vibration- and air-fluidised beds, fluid dynamics 7-44036
hog fuel predrying by flue gas heat recovery 7-8356
licorice root drying using solar energy 7-33997
moist soil drying model, integral methods for partial differential eqn. 7-66187
pulse combustion, characts., appls., and research needs 7-65594
solar collector with heat pump for food and agricultural products drying 7-54344
solar dryer based on convective heat and mass transfer 7-54354
solar fruit-dryer-greenhouse, test results 7-33998
solar grain dryer, per performance tests and design 7-23221
solar kiln dryers for timber and agricultural produce 7-39965
solvent-dried coal liquefaction reactivity improvement by disposable catalyst 7-39953
- DSC** *see thermal analysis*
- DTA** *see thermal analysis*
- dual resonance model** *see duality and dual models*
- duality (mathematics)**
No entries
- duality and dual models**
see also string theory; Veneziano model
(2,2) SUSY σ -models, higher order counterterms, superstring effective action 7-15079
action principle for strings and superstrings 7-15134
axially symmetric higher-dimensional gravity, Belinsky-Zakharov N-soliton transforms. 7-41207
axially symmetric higher-dimensional gravity, Neugebauer-Kramer transforms. 7-41206
book, dual theory reprint 7-60893
bosonic σ -model, two-dimensional, defined on curved two-space, conformal anomaly anal. 7-9953
bosonic massless gauge fields with arbitrary spin and permutation symm. 7-4960
bosonic nonlinear σ -models, consistent string propag. 7-4977
bosonic open string, one-loop amplitudes, first quantised approach 7-10045
bosonic or SUSY minimal surfaces and strings in 4D, ambitwistor description 7-185
bosonic string field theories, gauge invariant action construction 7-10042
bosonic string theory, two- and three-loop vacuum amplitude calcs. 7-5025
bosonic strings, dilaton coupling-to σ -model and BRST 7-10040
bound states and asymptotically free quarks, duality relations 7-5050
decaying particles multiproduction in the central region of the soft hadronic interaction, dual parton model 7-61608
closed bosonic string, modular invariance and two-loop vacuum amplitude 7-24811
closed bosonic strings, two-loop analyses and modular forms 7-5019
closed bosonic strings in a covariant phase space 7-24809
compactified superstring, global symmetries and flat pots., D=4 supergravity 7-14851
composite string, Lorentz invariance and SUSY transformations, quantisation 7-5078
cosmic strings, baryon concentration in string wakes at $z \geq 200$ rel. to galaxy form. 7-14687
cosmic strings, gravit. effects and temp. discontinuity 7-14841
cosmic strings, gravit. radiation and microwave background 7-14838
cosmic strings from hidden-sector flux tubes 7-18658
covariant string field theory, gauge fixing, physical degrees of freedom 7-5072
dual description of a confined colour field 7-61565
E₈ superstrings, ν - ν' - γ decay rate calcs. 7-30266
E₈ superstrings, L parity and ν_e masses 7-19048
E₈ superstrings, phenomenology of exotic particles 7-169
fermionic string loop amplitudes with external bosons 7-5026
fermionic string models in 4D, construction 7-15136
free bosonic string fields, resolution of indefiniteness problem 7-5021
galaxy formation, cosmic string basis 7-14693
galaxy formation, recent developments in cosmic string theory 7-14694
gravitomeric pole and mass quantisation, comment 7-181
gravity as the limit of the type-II superstring theory, graviton-graviton scatt. 7-4751
heterotic string, Lorentz and gauge anomalies cancellation and world sheet SUSY 7-15094
heterotic string, vanishing vacuum amplitude, modular forms and cosmological constant 7-15091
heterotic string in d=10 supergravity background 7-5017
heterotic string in superspace 7-10048
heterotic string model, confusion mechanism as global modification 7-15093
heterotic string theory, anomaly cancellation and modular invariance 7-5024
heterotic string theory, gauge and gravitational anomalies, role of modular invariance 7-10002
heterotic string theory 7-9735
heterotic string theory low energy effective action 7-5036
heterotic superstring, compactifications 7-10046
heterotic-string anomalies in (1,0) superspace 7-24513
heterotic-string O(α') corrections to D=10, N=1 supergravity 7-24515
higher order corrections to supersymmetry and heterotic string compactifications 7-4997
inflation in the heterotic E₈×E₈ superstring model, reheating 7-4604
interacting field theory of open superstrings 7-5071
interacting string dynamics, gauge invariance over a group as the first principle 7-5074
intersecting string model, star-triangle eqn., inversion relation and exact soln. 7-14892
- duality and dual models continued**
invariant string field theory, gauge symmetry using light-cone gauge M⁻¹ generator 7-5020
loop amplitudes in the fermionic string 7-5035
Lorentz covariant string theories in D=10 and D=18 7-19038
lower dimensional heterotic strings, toroidal compactification 7-15137
magnetic monopoles, electric currents, and Dirac strings 7-15070
massless higher-spin fields, coupling and gauge algebra, rel. to string theories 7-177
matter coupled to D=2 simple unidexteroussupergravity, local (supersymmetry) and strings 7-184
N=1 conformal supergravity, 2D and 3D, constraints and actions, spinning strings, SUSY σ -models 7-4756
Neveu Schwarz model, scattering amplitude calcs. using supersheet functional integration 7-442
nonabelian bosonization, triality, and superstring theory 7-14852
O(16)×O(16) heterotic string theory compactification 7-15092
O(32) open superstrings, pentagon diagram evaluation 7-441
open bosonic strings, three-string vertex and conformal mappings 7-24810
open superstring theory, vector field effective action 7-5076
open superstrings, effective action for vector field 7-500
oriented closed boson string theory, two- and three-loop vacuum amplitudes 7-502
particles in the early universe, conference, Thessaloniki, Greece (June 1985) 7-9596
percolation in random fields on a plane, duality principle 7-35469
Polyakov's string theory on multi-loop computations 7-15133
quantum strings with a dynamic geometry 7-501
regulated string theories, critical dimensions 7-5015
relativistic string in Peres space-time 7-35354
rotating cosmic string surrounded by grav. radiation, Einstein eqns. solns. 7-18464
sigma-model superstring corrections to the Einstein-Hilbert action 7-4961
SO(10)×E₈ superstrings, phenomenology 7-9998
spin and lattice gauge models, topological excitations, mean field methods 7-9973
spin structures in string theory 7-5070
spinning cosmic strings and quantization of energy 7-170
string action, scale invariant term, σ -model 7-15095
string field theory, modular invariance 7-5018
string field theory, vertex function in Witten's representation 7-19037
string field theory action, group theoretic approach 7-5073
string field theory and conformal geometry 7-15135
string field theory and equations of motion 7-10044
string field theory candidates from C* algebra cohomology 7-19036
string Lorentz algebras, Veneziano, Neveu-Schwarz-Ramond model anal. 7-10043
string tension and plaquette-plaquette correlation from QCD sum rules 7-478
string tensions in SU(2) lattice gauge theory 7-417
string theories, compactifications and θ -structures 7-18659
string theory effective actions 7-15061
string theory on nonsimply-connected group manifolds, soliton structure 7-5077
string theory path integral, genus two and higher, for bosonic spectrum 7-10041
string theory with Majorana and Dirac fermions, modular invariance 7-19040
string-induced gravity and ghost-freedom 7-4743
SU(2) flux-tube model of quark deconfinement at hightemperature, effective string tension calcs. 7-473
superconducting cosmic strings, induced ang. momentum 7-9566
superconducting strings and membranes, heterotic string behaviour 7-9739
superstring compactification on Calabi-Yau manifolds, conformal invariance 7-10047
superstring fermion amplitudes, covariant, sum over fermionic surface 7-9999
superstring field theories, symmetry structs., rigid space-time supersymmetry 7-5075
superstring in 4D, evolution with temp. and possibility of inflation 7-9728
superstring low energy theory, spontaneous breakdown of E₈ 7-9736
superstring models, baryon-number nonconservation and neutrinos masses 7-453
superstring models, compactified, down-quark mixing 7-5022
superstring models, renormalisation group anal. 7-9737
superstring models, theory of everything 7-15087
superstring modifications of Einstein's equations 7-9727
superstring neutrino mass problem without high intermediate energy scale, soln. search 7-15096
superstring one-loop nonrenormalization theorem in covariant path-integral formalism 7-24514
superstrings, finite-temperature instability for compactification 7-9564
superstrings, fundamental quantum theory 7-455
superstrings, gaugino mass contributions in low-energy limits 7-24812
superstrings, problems for (2,0) compactifications 7-5023
superstrings and partially broken global supersymmetry 7-15077
superstrings and preons, uniqueness, parameterlessness and good quantum gravity 7-9738
superstrings with closed twisted boundary conditions, Green-Schwarz formalism, quantization 7-30231
supersymmetric Yang-Mills theory, self dual condition 7-35660
swelling nucleons in QCD, superconducting state, string tension 7-15124
tachyons in heterotic string models in 10D, removal by compactifications 7-171
ultrarelativistic nuclear collisions, stopping power in dual parton model 7-61780
Universe, large-scale structure, cosmic strings 7-14688
vacuum fluctuations outside cosmic strings 7-9565
Veneziano amplitude from interacting string field theory 7-19082
e⁺e⁻ \rightarrow ff, asymmetries and cross section, superstring gauge boson effects 7-499
e⁺e⁻ \rightarrow $\gamma\gamma\bar{\nu}\nu$, superstring effects, contrib. of ν and right handed neutrino to cross section 7-30263
e⁺e⁻ \rightarrow X, effects of Z'-bosons from superstring or nonlinear σ models 7-444
ep \rightarrow ep, scattering asymmetries, superstring gauge boson effects 7-499
 η mass in SU(3) lattice gauge theory, topology 7-429

ductility and dual models continued

- pp—KX, charged particle multiplicity, dual parton and quark fragmentation models 7-19135
pp— π X, charged particle multiplicity, dual parton and quark fragmentation models 7-19135

ductile-brittle transition

see also embrittlement

- amorphous alloys, cold shortness (Russian) 7-39649
brittle failure in compression, micromechanics, splitting, faulting and brittle-ductile transition 7-13590
cleavage fracture 7-21339
Cr-MoVW ferritic steel, ductile-brittle transition temp., irradiation flux depend. 7-56825
fracture toughness, size effect, Irwin β_{fc} adjustment 7-43780
glass fibre reinforced epoxy, unidirectional, impact behaviour, temp. influence 7-3427
kinetic model for ductile-brittle fracture mode transition behaviour 7-21337
low activation, tempering, toughness, ductile-brittle transition props. 7-53862
metals, BCC, ductile-brittle transition rel. to dislocation density 7-39668
miniature disc bend tests for ductile-brittle transition temp. determ. 7-54038
PEEK, fracture toughness, temp. and strain-rate effects 7-39660
PEEK glass fibre reinforced plastics, fracture toughness, temp. and strain-rate effects 7-39660
polycarbonate, fracture, effect of rolling orientation on ductile-brittle transition 7-46644
polypropylene, ductile-brittle transition and size effects 7-39634
PVC, unplasticised, satisfactory service life under static load 7-8219
steel, alloy, impact behaviour, influence of grain boundary carbide density 7-13574
steel, C, brittle fracture micromechanism in specimens containing intergranular cementite (Russian) 7-59621
steel, cast, nonmetallic inclusions influence on fracture character 7-3421
steel, constructional carbon type, original charge purity influence on microstruct. hardenability and mech. props. 7-46521
steel, Cr-Mo, toughness, impurity element effects 7-53856
steel, Cr-Mo ferritic-martensitic, fracture toughness precip. of Laves phases 7-53849
steel, CR-Mo-Ni, temper embrittlement, effect of V additions 7-13575
steel, dual phase, effective grain size, cleavage crack propag. 7-28118
steel, ferrite-pearlite, viscous-brittle transition model (Russian) 7-3401
steel, ferritic, unirradiated, low activation, microstructure and mechanical props. 7-53863
steel, ferritic, yielding and fracture in transition region of quasistatic to dynamic loading 7-13581
steel, ferritic stainless, 11 MeV proton irradiation behaviour 7-58369
steel, heat treatment method effect on struct. and mech. props. 7-39561
steel, HSLA, mech. props. rel. to ferrite substruct. and grain size. 7-13531
steel, low-alloy, H-beams, controlled rolling effect on mech. props. 7-39562
steel, low-C, Ni influence on struct., fracture resist. and fractographic features 7-3420
steel, Mn, lath martensite, embrittlement in specimens containing 6 to 10% Mn (Japanese) 7-33774
steel, Ni-Cr, anelastic props. of grain boundaries and transition temp., effect of temper embrittlement 7-22815
steel, Ni-Cr, ductile-to-brittle transition temp. shift due to temper embrittlement and neutron irradiation. evaluation by small-punch test 7-28114
steel, Ni-Cr-Mo, pressure vessel, crack tip opening displacement, stretch zone width correl. 7-39670
steel, plain C, peritectic reaction, temp. and comp., influence of alloying elements 7-13435
 Al_2O_3 , neutron irradiation, microstruct., mech. props. 7-51843
Fe-Al-Mn, austenitic, SCC in NaCl soln. 7-8195
Fe-Si alloy, high-Si, alloy elements influence on plasticity and mag. props. 7-8067
Fe-Si-Al(Ga)(Al)(Ni)(Co)(Cr)(Mn)(Nb), atomic ordering and mechanical props. 7-11990
Hf_{1-x}Cu_x, metallic glass, thermal stability and phase transformations 7-21125
MgAl₂O₄, neutron irradiation, microstruct., mech. props. 7-51843
Mo, arc melting, impurity content, mech. props. 7-27980
Mo-W (30 wt.%) alloy, temp. depend. of crack resist. 7-22808
Nb, H embrittlement, crack propag., 120-300K, hydride form. 7-33757
SiC, sintered, fracture after Li exposure 7-28103

ductile fracture

see also ductile-brittle transition; notch ductility

- Al-Zn-Mg-Cu, impact toughness improvement by intermediate thermomech. treatment 7-53907
brittle failure in compression, micromechanics, splitting, faulting and brittle-ductile transition 7-13590
cermets, structural materials, cyclic strength 7-59624
compact tension specimens, ductile instability prediction 7-37383
crack tip opening displacement, ductile and brittle fracture anal. of surface flaws 7-63078
defect and fracture mechanics, conf., Bad Honnef, Germany (Jan. 1985) 7-24260
disk, rotating, variable thickness, dynamic creep rupture 7-43781
dynamic fracture of ductile solids, internal state variable description 7-26844
instability phenomena in solids, conf., Trieste, Italy (Aug. 85) 7-55896
local approach of fracture, continuum damage mechanics 7-50988
metal tubes, ductile, no. of cracks in axial splitting 7-59597
metallic glasses, ductile and brittle fracture at low temp. (Russian) 7-39650
microvoid-damage model for ductile fracture 7-26843
plane stress, essential work of fracture vs. energy dissipation rate 7-20649
polycarbonate sheets, ductile fatigue crack propagation 7-11966
polymers, ductile fracture, essential work 7-53842
porous plastic solids, necking and failure, effect of yield surface curvature 7-43715
sheet metal forming limits under complex strain paths using void growth and coalescence model 7-13532
steel, austenitic stainless, ductile failure under biaxial loading, thermal transients, analytical model 7-59609

ductile fracture continued

- steel, bearing type, quenching temp. rel. to microstruct. and fracture surface morphology 7-8015
steel, high strength, control-rolled in two-phase region, ductile unstable failure (Japanese) 7-53865
steel, HSLA, Nb, ductile fracture, plastic deform. mechanisms 7-28115
steel, low-alloy construction, nonmetallic inclusions influence on impact strength and fracture type 7-8085
steel, low-C, Ni influence on struct., fracture resist. and fractographic features 7-3420
steel, martensitic stainless, precipitation hardened, impact toughness rel. to Mo content, AES obs. 7-39666
steel, Mn-Cr, case carburising, mech. props., influence of inclusion characters. 7-65135
steel, Mo-Ni-Mn, creep fracture mechanisms and rupture life 7-65137
steel, Ni, p/m type, fracture struct. features 7-33789
steel, rotor type, deformed, microcrack dimens. rel. to acoustic emission parameters and struct. 7-65258
steel, stainless, austenitic, valve type, heat treatment schedule effect on failure nature 7-3423
steel filaments, fatigue failure signs 7-46642
steels, stainless, α -particle irradiated, mech. props. and microstruct. 7-51872
three-point bend ductile fracture specimen, dynamically loaded, anal. 7-26206
Al alloy sheets, LY12CZ, fracture resist. characts., crack initiation, stable and unstable propagation. (Chinese) 7-46592
Al, ductile fracture rel. to heat treatment, vacancy conc. effect 7-8095
Al-Cu-Li, 2020, low-cycle fatigue, effect of environment and temp. 7-28117
Al-Cu-Li alloys, cyclic fracture, mechanisms 7-46634
Al-Cu-Mg, IN 9021, creep crack growth fracture morphology 7-53881
Al-Zn-Mg, 7090, fracture, stress intensity rel. to notch root radius 7-17635
Co₈₄Nb₁₀B₆ fully crystallised metallic glass, fracture processes 7-22841
Cu-Al-Ni-Ti-Zr, shape memory alloy, grain refinement, fracture mode, Ti and Zr additions effect 7-3301
Cu-Sn, ductility at elevated temps., effect of small amounts of B, P or Mg 7-53904
Cu-Sn-B(Mg)(P), ductility at high temp., alloying additions effect (Japanese) 7-13515
Cu-Zn-Al shape memory alloys, grain refinement 7-53774
Fe, cast, nodular graphite, fatigue crack propag. rel. to microstruct., SEM obs. (Chinese) 7-13542
Fe-Cr-Ni-Mn-N (18, 20, 5, 0.16 wt.%), weld metal, fully austenitic, tensile and fracture props. at 4K 7-53901
Mg-Y alloy, IMV6, fatigue crack growth and fracture microrelief, 293 and 140K 7-17614
Mo-base alloy, welded joint, strain hardening and fracture (Russian) 7-53877
Ni-Si, ductility, influence of rad.-induced segregation 7-53798
Ni₃Al-B, with and without Hf additions, dynamic embrittlement at 600°C 7-65112
Ni₃Al-Be, ductility, strength, grain boundary segregation, solid soln. strengthening, Be addition effect 7-39608
V-CR-Ti (15, 15 wt.%), mech. props., effect of heat treatment and impurity conc. 7-53857

ductility

see also ductile fracture; notch ductility

- brass sheet formability, grain struct. and stress raisers influence 7-3376
colliding bodies, penetration model accounting for ductile props. 7-58398
creep-fatigue life, long-term, prediction and evaluation 7-39796
cutting tool materials, mech. props., wear-resist. relations 7-3443
fibre reinforced Ti-base alloy, development of creep-resisting composites 7-3228
Inconel X-750, air environment/creep interactions, prior exposure times effect 7-13499
intermetallic phases, appl. as high temp. materials, review 7-22775
metals pure, new approach to creep 7-53805
PMMA based materials, craze resist., struct., water absorpt. 7-59602
polycarbonate-polystyrene-acrylonitrile, coextruded multilayer composites, tensile props. 7-59572
rocks, fracture anal. 7-66106
rubber toughened epoxy polymers, toughness rel. to dispersed rubber phase vol. fraction 7-65125
shape memory alloys, mech. props., polycrystal model (Japanese) 7-53789
steel, alloy, trace element precipitation and segregation, hot brittleness effects (French) 7-17608
steel, alloy type, low-C, tempering temp. effect on mech. props. and crack resist. 7-39654
steel, alloyed structural, struct. rel. to cold deformability, softening heat treatment methods development 7-39556
steel, austenitic, stainless, high temp. ductility, H and He effects 7-5406
steel, austenitic stainless, creep rupture properties of heavy section Type 304 forgings for LMFBRs 7-13582
steel, austenitic stainless, low activation, development, mechanical props., fusion reactor structural material 7-53799
steel, austenitic stainless, Mo-N alloyed, static recrystn. and hot ductility 7-3327
steel, austenitic stainless, single crystals, rolling texture and elastic consts. (Russian) 7-51912
steel, austenitic stainless, tensile and impact props., effect of grain boundary carbides 7-33785
steel, C and alloy, tensile ductility limit calc. (Russian) 7-39597
steel, C-Mn, hot ductility, influence of grain size 7-3374
steel, C-Mn and Nb treated, high temp. ductility loss, grain boundary segregation 7-46573
steel, Cr-Mo, mech. stability of retained austenite, absence of H influence 7-28125
steel, Cr-Mo, normalised, tempered, neutron irradiation, 390-550°C, tensile props. 7-17621
steel, Cr-Mo type, ageing effect on heat resist. props. after cold deform. and tempering 7-22813
steel, Cr-Mo type, temp. and deform. rate conditions influence on mech. props. 7-33752
steel, CR-Mo-Ni, temper embrittlement, effect of V additions 7-13575
steel, Cr-Mo-V, creep crack growth at 838K, const. load behaviour 7-17625

ductility continued
 steel, Cr-Mo-V, creep ductility, impurity and microstruct. effects 7-46587
 steel, Cr-Mo-V type, service props. in different struct. conditions 7-8107
 steel, Cr-Ni high-temp. type, N and heat treatment effect on struct. and mech. props. 7-33688
 steel, Cr-Ni-Co VKS6, struct. and mech. characts., effects of Ni, Co and heat treatment 7-8108
 steel, Cr-Ni-Mo, Ge and melting method influence on mech. props. at high temp. 7-8025
 steel, cryogenic, Al alloying effect on mech. and mag. props. 7-39679
 steel, dislocation struct. rel. to cyclic bending strain 7-22760
 steel, ferrite, low activation, correl. of hot microhardness with elevated temp. tensile props. 7-53797
 steel, ferrite-pearlite, H occlusivity and embrittlement, effect of C content 7-3417
 steel, heat treatment method effect on struct. and mech. props. 7-39561
 steel, high speed, TiN coated, ductility, impact testing 7-46569
 steel, high temp. ductility, effects of B 7-46588
 steel, high-C, hardened, mech. prop. changes on tempering, martensite decomp. role 7-3375
 steel, high-strength low-C weldable, C content effect on struct. and mech. props. 7-46583
 steel, linepipe weldments, ductility rel. to cathodic protection 7-39578
 steel, low-alloy, H-beams, controlled rolling effect on mech. props. 7-39562
 steel, low-alloy, high-temp. drop in plasticity 7-46640
 steel, low-C, wrought, thermal strengthening methods effectiveness 7-46524
 steel, low-pearlite, rules of austenite decomp. in continuous cooling 7-3339
 steel, managing, 18 Ni, erosion, effect of microstruct. and mech. props. 7-22849
 steel, microalloyed, hot ductility rel. to grain size and precip. 7-28088
 steel, mild and Cr, surface saturation with B by laser radiation 7-8172
 steel, Mn-Al-Nb, cryogenic, low temp. tensile props., effect of Al content 7-46576
 steel, Mn-Cr, case carburising, mech. props., influence of inclusion characts. 7-65135
 steel, Mn-V, low-pearlitic, normalized, struct. and mech. props., sheet thickness depend. 7-8006
 steel, Mo-Ni-Mn, creep fracture mechanisms and rupture life 7-65137
 steel, stainless, austenitic, low-activation, constitution, struct. and mech. props. 7-42195
 steel, stainless, ductility rel. to cold working 7-22759
 steel, stainless, superalloy, fracture toughness, tensile props., T and ³He effect 7-46616
 steel, structural, diffusion chromised, elevated temp. effect on comp., struct. and mech. props. 7-8178
 steel, took, Cr-Mo-V, hot working, ductility, C content, toughness, eutectic carbide segregation 7-59592
 steel, tool and struct., nitrided, prior heat treatment effect on mech. props. 7-46707
 strain estimation method for low cycle dynamic loads 7-26171
 superplastic alloys, plastic instabilities and uniaxial tensile ductilities, effect of grain growth 7-53820
 tensile tests, nonisothermal, anal. using measured temp. distrib. 7-65245
 Zircaloy-4, temp. depend. of elongation 7-65094
 Al alloys, heat treatment, prediction of start of exposure phase 7-33698
 Al alloys, medium strength, formability rel. to microstruct. 7-17592
 Al-Cu-Li-Mn-Cd alloy, 2020, micromechanisms governing elevated temp. fracture resist. 7-22803
 Al-Ge-X and Al-Si-X alloys, amorphous ductile, with two separate phases, form. range and props. for X=Mn, Fe, Co or Ni 7-59493
 Al-Li alloys, grain boundary fracture 7-39644
 Al-Li base alloys, deform. and fracture 7-39594
 Al-Li-Cu-(Mg), stress corrosion resist. and mech. props. 7-33833
 Al-Mg-Zn system, fracture viscosity rel. to surplus phase morphology 7-46610
 Al-Si-Mg (7, 0.3 wt.%), strength and ductility, effect of macroporosity 7-3386
 Al-Si-Zn-Mg-Ti-(Sr) system alloys, mech. props., Sr microalloying effect 7-3377
 Al-Ti, powder metallurgy alloys, mech. and thermal stability 7-64973
 Al-Ti, rapid solidification processed/mechanically alloyed, high temp. deform. 7-65100
 Al-Zn-Mg-Cu alloy, microalloying effect on struct. and mech. props. 7-53755
 Al-Zn-Mg-Cu-Ni-Zr, modified 7075, prod. by liq. dynamic compaction, struct. and props. 7-46437
 Al-Zn-Mg-Mn-Si, rapid solidification, superplasticity 7-53826
 Al₂O₃-TiO₂ system detonation coatings, struct. and phase characts., physico-mech. props. 7-65212
 Co-Cr surgical implant alloy, mech. props., effects of N additions 7-59573
 Cr-base alloys, high-alloy, plasticity, effect of twinning (*Russian*) 7-46582
 Cu alloys, neutron irradiat., 13 dpa, mech. prop. and elec. cond. changes 7-51839
 Cu alloys, rapidly solidified powder metallurgy, irradiat. to 13.5 dpa with neutrons, microstruct. evolution and swelling 7-51840
 Cu, creep, new approach 7-53805
 Cu, electroless deposits, ductility, effect of inclusions 7-58719
 Cu-Al-Zn, β -phase stability, mech. props. rel. to quenching rate 7-33659
 Cu-GeO₂, dispersion hardened polycrystals, intermediate temp. embrittlement 7-53903
 Cu-Sn-B(Mg)(P), ductility at high temp., alloying additions effect (*Japanese*) 7-13515
 (Fe,Ni)₃V, LRO alloys, mech. props., effects of strain rate and long-term ageing 7-53796
 Fe, cast, bainitic ductile, microstruct. rel. to comp. and heat treatment 7-39579
 Fe high temp. ductility, effects of B 7-46588
 Fe powder, ultrafine, and hot forged specimens, reduction temp. effect on struct. form. and props. 7-53670
 Fe-Al(Si) cold-rolled nonbrittle powder strip prep., texture and mag. props. 7-46370
 Fe-Cr-Co-Si-Ti, permanent mag. alloy, ductile, effect of heat treatment on mag. props. (*Korean*) 7-8137
 Fe-P-Cu(Ni)(Mo), sintered atomised powder premixes, mech. props. 7-7931

ductility continued
 Fe-Si alloy, high-Si, alloy elements influence on plasticity and mag. props. 7-8067
 Fe-Si alloy wires, rapidly solidified by in-rotating-water-spinning method, prod. and props. (*Japanese*) 7-22654
 Fe-Si-Al, electrical steel sheet, rollability, core losses (*German*) 7-59549
 Mo alloys, forging, crystallographic texture, X-ray diff. (*Russian*) 7-39538
 Ni alloy, heat-resisting, hot strain rate effect on microstruct. and mech. props. 7-39559
 Ni alloys, high temp. ductility, H and He effects 7-5406
 Ni base superalloys, pressure vessel performance, strength, ductility, comp., struct. 7-3365
 Ni-Al-Cr, melt spun ribbons, microstruct., mech. props., Cr conc. effect 7-28031
 Ni-base superalloy, IN 939, high Cr, effects of heat treatment on mech. props. 7-13526
 Ni-base superalloys and intermetallics, rapidly solidified, mech. props. 7-22839
 Ni-Co-Cr-Al-Y, plasma sprayed, high temp. tensile and creep behaviour 7-28083
 Ni-Cr alloy, wrought, Hf effect on struct. and mech. props. 7-33689
 Ni-Cr superalloy, heat-resistant, heat treatment effect on ductile props. in cold deform. 7-46584
 Ni-Cr superalloy, high-temp. material, microstruct. and mech. props. with high-temp. heating 7-3341
 Ni-Si, ductility, influence of rad.-induced segregation 7-53798
 Ni₃Al-B, elevated temp. ductility, effect of testing environment 7-39614
 Ni₃Al-B, with and without Hf additions, dynamic embrittlement at 600°C 7-65112
 Ni₃Al-B-Hf alloys, B and Hf grain boundary segregation, ductility, atom probe FIM study 7-33675
 Ni₃Al-Be, ductility, strength, grain boundary segregation, solid soln. strengthening, Be addition effect 7-39608
 NiCoCrAlY, plasma sprayed coatings, low cycle fatigue behaviour 7-22793
 Ni₆₀Nb₄₀ glass ribbons, H embrittlement susceptibility, effects of cold working 7-46503
 Ti alloy, two-phase, microstruct. and failure nature correl. 7-8110
 Ti-Al-Mo-Cr alloy, VT3-1, cooling regimes in heat treatment effect on mech. props. 7-8026
 Ti-Al-Mo-Cr alloy, VT3-1, vac. annealing of blanks after isothermal deform., hydrogen plasticising effect 7-8027
 Ti-Al-V (6, 4 wt.%) plates, rolling, heat treatment, microstruct., mech. props., turbine blade appl. 7-17644
 Ti-Al-V alloys, VT20 and VT6, annealing temp. effect on mech. props. of semifinished products 7-39558
 Ti-Cr, β -eutectoid, deform. behaviour of retained β phase 7-39589
 Ti-Mn, alpha and beta phases, yield and tensile strength, ductility, Bauschinger behaviour, fatigue life, crack propag. 7-8052
 Ti-Ni-Cu system metallic glasses, superplastic props. in vitrification temp. range 7-3356
 Ti-R (R=rare earth) alloys, rapidly solidified, tensile and creep props. 7-22778
 Ti₃Al-Nb alloys, ductility and fracture toughness, dispersoid modification effects 7-22779
 V-Cr-Ti (15, 15 wt.%), mech. props., effect of heat treatment and impurity conc. 7-53857
 W base heavy metal alloys, mech.-props., porosity, impurity effects 7-17495
 W-Cu pseudobinary, Si alloying effect on solute redistrib. and ductility characts. 7-53741
 W-Ni-Fe, sintered, ductility and precip. 7-17589
 W-Re alloys, annealed and sintered, elevated temp. softening, appl. for thermionic energy conversion 7-28077

Duralumin see aluminium alloys

dust

see also cosmic dust
 air quality-degrading substances and conditioning equipment (*German*) 7-40069
 atmosphere, entry characts. of dust samplers used in British nuclear industry 7-40079
 atmosphere, Saharan dust transport by atmosphere, review 7-9073
 atmosphere, wind erosion vulnerable areas, detection by satellite imaging of dust storms 7-8949
 atmosphere dust storm detection, satellite image processing method 7-66329
 atmosphere of Beijing, China, particulate dry deposition velocity (*Chinese*) 7-29219
 atmosphere sand and dust storms, MM wave propagation 7-47480
 El Chichon dust cloud and sunlight absorpt. over India 7-9126
 industrial workers, lung dust, inverse problem solution in magnetisation studies 7-54630
 Martian limb hazes, vertical struct. from scattered light profiles 7-55513
 mass flowmeter using heat transfer for dense phase solid-gas two-phase flow 7-37579
 microparticles from Antarctic Dome C ice core samples, TEM study 7-55228
 pulverised coal/air two-phase flowmeter 7-37580
 Quelccaya Ice Cap, Peru, dust stratigraphy rel. to Little Ice Age record 7-34670
 Saharan dust transport by atmosphere, observations and model 7-14343
 solid-gas two-phase flowmeter for blast furnace pulverized coal injection 7-37578
 stratosphere volcanic dust and atm. extinction 7-4177

dust storms see storms

DVM see digital voltmeters

dwarf novae

amplitude-period length relation 7-4472
 atmospheric vel. fields, conf., Trieste, Italy (August-September 1982) 7-35118
 SS Aur, energy distrib. and var., UBVRi obs. 7-40817
 SS Aur, U Gem star, spectroscopic orbit 7-14581
 OY Car, SU UMa-type dwarf nova, IUE obs. in superoutburst 7-55689
 HT Cas, U Gem star, mean cycle length determ. 7-66598
 Z Cha, eclipsing dwarf nova, white dwarf surface luminosity distrib. 7-4458
 SS Cyg, UV behaviour in quiescence and in outburst 7-55688
 EY Cyg, visual magnitude estimates (1986 August-September) 7-4480
 EY Cyg, visual magnitude estimates (1986 September) 7-9480

dwarf novae continued

- U Gem, evidence for prolonged quiescence and large-amplitude flickering from early obs. 7-66621
 U Gem stars, period lengths estimation methods (*German*) 7-9378
 AH Her, dwarf nova outburst, UBVR photometric obs. 7-34995
 AH Her, IR photometry of dwarf nova outburst 7-9485
 AH Her, primary and secondary spectral obs. 7-60668
 VW Hyi, SU UMa star, outbursts recurrent behaviour 7-60688
 IR photometry, evidence for ellipsoidal vars. in CW Mon, X Leo, IP Peg, and AF Cam 7-4471
 IUE-Voyager observations of luminous accretion disk systems 7-66623
 T Leo, new SU UMa star, superhumps characts. from photometric obs. (1987 January 24 to 27) 7-66605
 X Leo, U Gem star, spectroscopic orbit 7-14581
 V358 Lyr, fast nova or WZ Sge star, 1965 light curve 7-66613
 V2051 Oph, IR and optical photometry of eclipsing dwarf nova 7-55670
 V2051 Oph, structure and variability of cataclysmic binary 7-18423
 IP Peg, eclipsing dwarf nova, system parameters from high-speed photometry 7-14595
 IP Peg, near-IR spectroscopy and photometry 7-66619
 GK Per, 1986 November obs. of minor outburst 7-24147
 GK Per, outburst obs. (1986 Nov.-Dec.) 7-40836
 GK Per (=Nova Per 1901), IR magnitudes of outbursts 7-40844
 PHL 227, UX UMa star, orbital period determ. from periodic radial vel. vars. 7-55668
 BV Pup, X-ray, UV and optical obs. 7-47922
 TA observations (1986 August) 7-14588
 TA observations (1986 December) 7-55646
 TA observations (1986 July) 7-24143
 TA observations (1986 June) 7-14586
 TA observations (1986 November) 7-55644
 TA observations (1986 September) 7-34987
 BZ UMa, photometry of dwarf novae indicating low state 7-47908
 CH UMa, visual magnitude estimates (1986 Oct.-Nov.) 7-40838
 CH UMa, visual magnitude estimates rel. to rapid flickering during outburst 7-66608
 SU UMa, visual magnitudes during supermaximum (1986 October) 7-18410
 SU UMa stars, similarities to recurrent Population II X-ray transients 7-14604
 wind-formed resonance lines, inclination and orbital phase dependent resonance line profile calcs. 7-60692

dwarf stars

- see also *flare stars*; *white dwarfs*
 BD+13°3683, cool subdwarf, spectroscopic orbit and companion mass 7-40806
 binary systems among bright stars, comparison with systems with evolved primary components 7-29505
 CK Boo, W UMa star, photoelectric obs. rel. to light curve vars. 7-40870
 bright stars with solar-type UBVR-colours 7-40802
 brown dwarf stars, astrophysics, symposium, Fairfax, Virginia (October 1985) 7-18
 brown dwarf stars, evolution and IR spectra 7-29472
 α Cen binary system, non-resonance Ca I lines obs. in optical spectrum 7-4444
 BE Cep, contact binary star with components in poor thermal contact, light curves anal. 7-4521
 chemical composition determ. for late-type stars, accuracy from synthetic spectra 7-66566
 chromospheric Mg II emission lines, influence of interstellar Mg II absorpt. 7-47840
 cool dwarf stars, chromosphere emission, rot. modulation, IUE spectra obs. 7-55629
 16 Cyg A and B, solar analogue candidates, absolute magnitudes and luminosity-related parameters 7-24162
 dead stars as dark matter 7-60658
 AB Dor, fast H_α variations on a rapidly rotating spotted star 7-55627
 AB Dor (HD 36705), 8.4 GHz and photometric obs. of active radio star 7-55628
 AB Dor (HD 36705), active chromosphere star, evolutionary status from space vel. 7-24133
 BY Dra stars, photometry and spot models rel. to rot. modulation and flares 7-4467
 BY Dra stars, UBVR photometry of southern objects 7-40830
 dwarf novae, ellipsoidal modulation in secondaries of CW Mon, X Leo, IP Peg, and AF Cam 7-4471
 in elliptical and lenticular galaxies, near-IR spectra 7-60792
 ϵ Eri, spectral characts. 7-55629
 40 Eri A, gravit. lens effect during appulse to background star 7-47861
 evolving low-mass stars, activity-related characts. of convective envelopes 7-4440
 F to M-type dwarf stars, activity-rot. relationship from Mg II h and k flux 7-55624
 F-type subdwarfs used as spectrophotometric standards, photometric anal. 7-47851
 G5 to M-type stars at South Galactic Pole, density distrib. from spectroscopic and photometric surveys 7-4448
 G 64-12, population II dwarf, ^7Li abundance of metal-poor star 7-60642
 G and K type stars, large and kinematically unbiased samples 7-14572
 G and K-type dwarf stars in Pleiades, VBLUV photometry 7-66686
 G-type stars, general characts. 7-24135
 Gliese 268, M dwarf double-lined binary, Digicon obs. 7-40875
 Gliese 490A, BY Dra star, periodic var. 7-14582
 globular cluster main sequences, mass functions determ. from CCD photometry and stellar models 7-66586
 halo stars, Li abundances of metal deficient halo dwarfs 7-60641
 HD 152391, HD 154417, Ca II emission solar-type stars, Stromgren uvby-H β photometry 7-55622
 HD 27130, Hyades solar-type star, H-R diagram position rel. to solar models testing 7-66665
 HD 82558, chromospherically active single BY Dra star 7-34986
 AM Her stars, spectrophotometric detect. of secondary in three systems 7-9514
 K and M stars, BVRI photometry program 7-14571
 K-type stars, orange giants and dwarfs, review 7-4457
 late-type dwarf stars, radii determ. from IRAS 12 μm fluxes 7-60644
 late-type dwarfs, radial vel. meas. rel. to binary nature 7-9516

dwarf stars continued

- late-type Population I dwarf stars, Li abundances and $^7\text{Li}/^6\text{Li}$ ratios 7-14562
 LHS 288, LHS 1070, new nearby faint red stars, parallaxes and photometry 7-4455
 low-luminosity M-type dwarfs as possible solar neighbourhood missing mass 7-48079
 M67, old open cluster, dwarf stars Li abundance 7-55743
 M-type dwarf stars, photometry and spectra rel. to chromospheric activity, kinematics, and metallicities 7-9466
 M-type stars in SAO catalogue, luminosity classes 7-4435
 magnetic braking in cool dwarfs 7-34973
 main-sequence luminosity functions, effects of mass segregation 7-40884
 metal-poor field subdwarfs, age and temp. characts. 7-47865
 AU Mic, BY Dra star, IUE spectra of fluxes 7-47939
 nearby stars with possible planetary systems, catalogue 7-66480
 NSV 12040, W UMa star, first ephemeris from photoelectric and visual obs. 7-66669
 planetary systems habitability, 36th International Astronautical Congress, Stockholm, Sweden (October 1985) 7-2
 planets formation around stars, theory for 1 solar mass star 7-55497
 proper-motion stars, parallaxes from photographic astrometry 7-4296
 soft X-ray transients, relaxation to evolution of low-mass X-ray binaries 7-55707
 solar analogues along path of P/Comet Halley (1982i), photometry 7-9416
 V471 Tau, evidence for large-scale structs. in atmosphere of active K-dwarf component 7-47874
 PZ Tel (HD 174429), active chromosphere star, evolutionary status from space vel. 7-24133
 W UMa stars, light curves anal. for four objects 7-35006
 Van Biesbroeck 8, IR speckle interferometry rel. to binary nature 7-66587
 VB 8, comparison discovery and nature 7-55722
 very low mass stars, evolution characts. and processes 7-60648
 VM 10.1 in field of galaxy DDO 155, cool subdwarf radial vel. anal. 7-66588
 wide binary stars, theoretical implications of observational data 7-66664
 H I Lyman alpha profiles, correction for interstellar absorpt. and geocoronal emission 7-60637
 Na abundances, implications for Galaxy chemical enrichment 7-4446

dye lasers

- adsorbed dye laser molecules on optical surface, SHG and THG (*Chinese*) 7-57457
 aqueous cyanine solns., organic acid effect on spectral luminescent props. 7-46087
 aqueous micellar solns., flashlamp pumped, efficiency and photostability 7-43084
 azacoumarin dyes, fluorinated, laser dye stability, lifetimes, fluoresc. 7-59237
 birefringent filter design for CW dye laser resonator, spectral tuning band 7-50720
 1,4-bis(β -pyrazinyl-2-vinyl)-benzene, solns. and solid state, irradi. and solvent effects, visible fluoresc. anal. 7-36674
 blue-green, efficiency enhancement by spectrum converter 7-15927
 blue-green efficiency enhancement using spectrum converter dye 7-36956
 cavity construction for single-mode tunable pulsed ring dye laser 7-11006
 computer-controlled two-dye-laser heterodyne spectrometer of high precision 7-15012
 coumarin-4 laser efficiency under coaxial flash-lamp pumping 7-62684
 cryptocyanine, Q-switching of ruby laser, output characts. (*Korean*) 7-31332
 current density profile diagnostic system for Li beam spectroscopy in a tokamak 7-1760
 CW, with intracavity photorefractive element, mode selection 7-43167
 DCM dye laser, CW, passive mode locking 7-1202
 DFB, achromatic pumping condition using grating 7-10999
 DFB laser, energy characteristics 7-25810
 DFB oscillation in slab-type optical waveguide 7-15904
 DFB picosecond freq.-tunable laser source for time-resolved meas. 7-50584
 DFB producing tunable picosecond pulses, review 7-10992
 distributed feedback dye laser; picosecond, excimer laser pumped 7-43086
 dye laser radiation, frequency conversion and surface spectroscopy appl. 7-15931
 dye solutions, quantum efficiency of fluoresc., determ. by diffraction at laser induced phase grating 7-3081
 energy transfer processes, ratio of radiative to nonradiative 7-36957
 Fabry-Perot resonator, confocal 4.5 m long for storage of megawatt laser pulses 7-1200
 femtosecond streak camera 7-18895
 FM dye lasers for use in optical metrology 7-15860
 high power, synchronously pumped operating at 410 to 550 nm 7-25841
 high power subpicosecond UV dye laser system 7-20250
 holographic grating fabrication by tunable pulsed dye laser 7-5983
 hypocycloidal pinch device development for dye laser pumping (*Korean*) 7-62719
 infrared, contactless spatially resolved meas. of bulk free-carrier lifetime in Si 7-52650
 injection-locked dye lasers, generation of optical pulse sequences with phase control 7-43087
 intensity correlations; effective eigenvalue charactn. 7-50531
 IR, action in traveling-wave pumping geometry 7-25809
 jet laser, continuous, liquid-circulation systems 7-31312
 3-methoxybenzanthrone in soln., picosecond spectroscopy of intermolecular proton phototransfer 7-54150
 syn-(methyl,methyl)limane aq. soln., lasing action obs. under flashlamp excitation 7-43083
 4-methylumbelliferone-fluorescein laser dye mixture, stimulated emission, conc. depend. 7-1098
 mode-locked laser, amplification by KrF* laser 7-62724
 multicomponent solution tunable lasers, electronic excitation energy migration 7-31308
 multimode CW laser, dynamical instabilities, stimulated Brillouin scatt. 7-50552
 Nile blue, oxazine dye, luminesc. and H^+ phototransfer in solns. 7-13762
 optical analog signal amplification by backward Raman scattering 7-37042

dye lasers continued

- optogalvanic spectroscopy, system design and optimisation, use in discharge studies 7-61389
oxazine 1 laser CW, pumped by He-Ne laser 7-36958
performance in near UV range 7-5881
picosecond Raman studies using 5 kHz tunable dye laser system 7-18881
polarisation modulation using intracavity method 7-62740
polymethine grazing-incidence laser, construction (*Russian*) 7-50583
pulsed, expression for small signal gain 7-15889
pulsed, intracavity, absorpt. kinetics 7-50554
pulsed dye laser for KEK optically pumped polarized ion source (*Japanese*) 7-20280
pulsed dye laser with diffraction grating in resonator for holographic interferometry 7-43159
pumped by Cu vapour laser with unstable resonator, background radiation influence 7-25856
pumping by Cu vapour laser for U isotope separation 7-50553
pyridylaryloxazoles, spectral-luminesc. and lasing props. study 7-43089
Q-switching, output characts. (*Japanese*) 7-5926
Raman dye laser, Nd:YAG pumped, pulsed tunable for spectroscopy (*French*) 7-25814
rhodamine 110 dye laser, passive mode locking and dispersion compensation 7-62742
rhodamine 590 droplet, micrometer size, high intensity laser interaction 7-43210
rhodamine 590/water soln, droplet whispering-gallery-mode laser characts. 7-31310
rhodamine 6G, photodegradation in PMMA, kinetics 7-50555
rhodamine 6G, polymer matrix effect on spectral and lasing characts. 7-31309
rhodamine 6G and B CW dye lasers, three state pulse amplifier 7-31344
rhodamine 6G dye laser, 580 nm, small line width, cavity arrangement 7-62728
rhodamine 6G dye laser, Ar flashlamp pumping (*Korean*) 7-25813
rhodamine 6G laser, CW, combined mode locking using triphenylmethane dyes 7-37003
rhodamine 6G laser, synchronously pumped, characts. (*Chinese*) 7-5880
rhodamine 6G laser with Brewster prisms, hybridly mode-locked 7-15913
rhodamine 6G ring dye laser, flashlamp pumped, short pulse generation using colliding pulse mode locking 7-43170
rhodamine 6G ring dye laser with external retroreflecting mirror 7-50597
rhodamine 6G-DODCI femtosec. dye laser synchronously pumped by Nd:YAG laser, stabilisation 7-31346
rhodamine 6G-ethanol dye laser, Ar flashlamp pumping (*Korean*) 7-25812
rhodamine 6G-ethylene glycol, soln., dye laser light source for visible spectroscopy 7-20275
rhodamine 6G-sulphur rhodamine 101 laser, CW, passive mode locking 7-11015
rhodamine 6G/DTDCI laser dye mixtures, undamped relaxation oscillations due to self-gain-switching 7-1094
rhodamine B laser, femtosecond, synchronously mode locked, spectral optimisation 7-37004
rhodamine B laser, femtosecond hybrid mode locked 7-5927
rhodamine G, intracavity laser spectroscopy sensitivity enhancement, use of saturable filter 7-62794
rhodamines, aq. micellar solns., flash lamp excitation, photostability, lasing props. 7-57308
ring dye laser, CW multimode, spontaneous oscillations of emission spectrum 7-43085
ring dye laser, high resolution computer controlled 7-20249
ring dye laser for probing trapped ions, optical frequency standard appl. 7-20285
ring laser, 580 nm, CW, single-mode, dye circulation system 7-1201
short-cavity dye laser, tunable near IR picosec. pulse generation 7-50550
single-mode laser, coloured noise induced first-order phase transition 7-57309
spectral condensation in intracavity spectroscopy, steady-state. waves 7-50551
spectral evolution and relaxation oscillations 7-15859
spectrometer with ultra-high-resolution, using passive reference resonator 7-18889
surgical successes 7-34217
synchronously excited dye laser with additional ultrathin resonator, picosecond pulse generation 7-31365
synchronously pumped, generation of high-power tunable picosecond pulses (*Chinese*) 7-5923
synchronously pumped, picosecond pulse formation 7-25811
synchronously pumped dye laser, periodicity multiplication obs. with cavity length tuning 7-31311
synchronously pumped femtosecond CW, variable intracavity spectral windowing 7-36998
thin film energy transfer dye laser with DFB oscillator-amplifier system (*Japanese*) 7-43088
tissue-laser interaction, thermal and biological aspects of medical laser appl. 7-60037
transients, statistical fluctuations meas. 7-31297
travelling wave laser with two photon picosec. optical pumping, time characts. 7-62685
tunable, CW, Ar⁺ laser-pumped, spectral props. 7-1096
tunable with electro-optic Q-switching of coupled laser, characts. 7-1197
tuning by a cholesteric liquid crystal device 7-15858
two-mode, first-passage-time problems 7-1097
UV generation using FM dye laser 7-50644
VUV laser source for high-resolution spectroscopy, dye laser freq. mixing in Mg 7-24709
wide-range systems, development problems 7-31313
XUV radiation generated by resonant third- and fifth-order frequency conversion of dye laser radiation 7-20327
O₂, A band, line profiles study, IR spectra anal., dye laser excitation 7-50114
XeCl laser, dye laser pumped, single picosecond UV pulse generation by mode-locking 7-1095

dye penetrant tests *see* nondestructive testing

dyeing

- waste heat recovery heat pumps appl. (*Japanese*) 7-59867

dynamic nuclear polarisation

- see also* CIDNP; Overhauser effect; solid effect
solids, nuclear polarisation at optical transition saturation 7-45841

dynamic nuclear polarisation continued

- D target, dynamically polarized, nuclear spin orientation enhancement by RF irradiation 7-15435
Si, broken dislocation bonds, annealing effects, optical polarisation of nuclear moments study 7-38008

dynamic programming

- automatic labeling system using speaker-dependent phonetic unit references 7-43573
US kidney images recognition by 2D dynamic programming method 7-18034
Xe oscillations in load follow of large nuclear reactor, optimal control 7-30620

dynamic response

- optical bistable devices graphical anal. of dynamic response 7-15922

dynamic stability *see* stability

dynamic testing

- see also* fatigue testing
composite materials, columnar, subjected to impulsive loading, dynamic response testing 7-59708
composite panel, in situ testing of mech. props., flexural wave phase changes obs. 7-63095
conference on the safety and reliability of reactor pressure components, Stuttgart, Germany, (Oct. 1985) 7-9583
crack arrest specimen, dynamic anal. under reactor pressurised thermal shock conditions 7-13693
fatigue precracked Charpy-type specimens, crack initiation testing, reactor piping appl. 7-13579
high-speed mechanisms fabricated with composite laminates, mechanical tests 7-37404
industrial fans, vibration analysis 7-20675
integrated dynamic test/modelling system 7-26232
modal density meas. techniques 7-57771
snapback excitation of structures using multiple force inputs 7-57777
split Hopkinson pressure bar method use in dynamic testing, review 7-22944
thermocouples under field conditions, using online identification 7-4848
viscoelastic materials, dynamic parameters meas., vibr. transducer design 7-61326
Al, explosively launched expanding ring test, computer simulation and anal. 7-33878
Cu, dynamic elongation determ. expanding ring test, 2D hydro-plasto-dynamic code anal. 7-33755
Ta, dynamic elongation determ. expanding ring test, 2D hydro-plasto-dynamic code anal. 7-33755

dynamical symmetry

- charge-monopole interaction, O(3,1) symm. problem 7-48943
dynamical chiral symmetry breaking in Nambu-Jona-Lasinio model, pion props. 7-437
fermion mass generation in preon dynamics, relevance of Higgs field mass parameter variation 7-408
flavour symmetry, dynamical breaking and scalar exchange 7-30210
harmonic oscillator, dynamical supersymmetries 7-24801
IBM4, dynamical symmetry in light nuclei 7-56625
IBM, dynamical symmetries in non-U(6) formalism 7-41918
large-N QED₃, dynamical mass generation 7-19061
monopole asymptotic scatt., bound-state spectrum and dynamical symm. 7-56424
QCD, dynamical symmetry breaking 7-24843
SU₃ dynamical symmetry, interacting boson-fermion approximation, inertial parameters 7-41913
SU(2)×U(1) breaking, dynamical, doubly charged pseudo-Goldstone bosons 7-41659

dynamics

- see also* ballistics; fluid dynamics; force; friction; haemodynamics; impact (mechanical); kinematics; resonance; rotating bodies; rotation; vibrating bodies; vibrations
angular velocity concept 7-29632
balancing toy, centre of gravity, oscills. about equilb. 7-48243
bifurcation and chaotic behaviour of system with delayed feedback (*Chinese*) 7-35263
bond graph analysis of automatic guided vehicle dynamics 7-61096
chaos in classical dynamics, deterministic representation with appl. to turbulence 7-61091
Coma galaxy cluster, mass determ. from galaxies positions and vels. 7-40945
composite system, one dimens., with random parameters, dynamic processes 7-107
dynamics in bio-mathematical perspective 7-56030
galactic disks, perturbed models rel. to tidal triggering of Seyfert galaxies and quasars 7-9537
generalized dynamics, extension to unidimensional phase space 7-61093
gyroscopic systems, periodically perturbed linear, dynamic behaviour 7-11273
gyroscopic systems, undamped, eigenproblem soln. with Lanczos algorithm 7-4668
interstellar giant molecular clouds in galaxies, N-body simulation of random vel. generation and accel. 7-18445
Josephson effect for dynamic mag. susceptibility and ESR measurements 7-12917
modified Newtonian dynamics (MOND), appl. to shell system of elliptical galaxy (NGC 3923) 7-66749
nonlinear dynamical systems, decomposition method for modelling 7-24411
reducibility of variational dynamic systems (*French*) 7-56026
rigid body dynamics, general integrable cases for problems with no axial symmetry 7-24413
stellar dynamics, relaxation and dynamical friction in non-integrable stellar systems 7-4524
stellar dynamics, stochastic stellar orbits in galaxies 7-9519
two-frequency dynamical systems, rotation interval from a time series 7-61088

dynamometers

- see also* force measurement
adhesion strength measurement method for In-glass seals 7-59715
split point drills, TiN and ZrN coatings performance charact. meas. 7-65244
three-level standard system 7-302

dysprosium

see also nuclei with

- air pollution from diesel vehicles, use of Dy as tracer to study aerosol sources 7-59899
antiferromagnetic phase transition, second order, μ SR study 7-45880
atom, L subshell ionis. by deuteron impact, cross section determ. 7-51878
band struct., effect of nonspherical pot., warped muffin-tin approx., APW method 7-72746
magnetoheterogeneous state, H-T phase diagram 7-7507
mean square amplitude of vibr. and Debye temp. 7-21368
positive muon diffusion in helicoidally-ordered antiferromagnets 7-45870
thin films, conduction electron scattering on magnetic spin system 7-64362
thin films, influence of thickness on mag. phase transitions 7-38860
BaFCl:Dy, thermolum., X-irradiated at room temp. 7-53419
CaSO₄:Dy, gamma radiation damage on thermolum. 7-38059
CaSO₄:Dy phosphor, thermoluminesc. props. of a new prep., dosimetry appl. 7-28701
Dy + H⁺, L-subshell ionisation cross section, X-ray emission 7-50327
GdBO₃:Pr³⁺, Dy³⁺, host lattice sensitisation, energy transfer and photolum. 7-46113
KMgF₃:Dy³⁺, ligand hyperfine interaction of Dy³⁺, ENDOR 7-22163
LaF₃:Dy³⁺(Ho³⁺)(Er³⁺), surface temp. meas., fluoresc. appl. 7-19947
Pt-Dy contact, mag. order destruction by cold current 7-52980
Si:Dy, neutron irradi., Hall effect, elec. cond., IR absorpt. spectra 7-51834
ZnS:O, Dy, activator centres, spectrosc. investig. 7-13184

dysprosium alloys

- L_{III} X-ray absorption spectra 7-39312
ternary alloys, evaporation, thermodynamic props., Knudsen effusion method 7-32627
Cu-Dy, thermodynamic props. rel. to glass forming ability 7-38204
DgTb amorphous ferrimag. anisotropic films, Hall voltage polarity voltage and temp. depend. studies 7-7206
Dy_{0.73}Tb_{0.27}Fe₂ alloys, magnetomechanical coupling 7-45788
Dy-Re-Fe(Co)(Ni), intermetallic-based solid solns., phase equil. and mag. props. 7-22639
Dy-Y highly dil. alloys, mag. props. 7-7483
DyAg, antiferromag. crystalline and ferromag. amorphous alloys, spin dynamics, μ SR study 7-45873
DyAl₂, monocrystalline, longitudinal μ SR studies, ferromag. and paramag. phases 7-45876
DyAl₂, muon spin relax. in paramag. and ferromag. regimes 7-45879
DyAl₂ single crystals, low temp. heat capacity meas. in mag. field, mean field approx. calcs. 7-27530
Dy_{1-x}Al₂, intrinsic coercive field 7-45728
DyAuCu₄, cubic alloys, mag. props. 7-52936
DyCo₅, magnetocrystalline anisotropy, rare earth contribution 7-45659
Dy₂Co_{1-x} thin films, ferrimagnetic reson. in region of spin-reorientation transitions 7-45824
Dy₂Co₉Ni₂₃ cryst. struct. and mag. suscept. studies (Russian) 7-21161
DyFe alloys, amorphous thin films, thermomag. recording, magnetisation reversal, coercivity 7-64459
DyFe amorphous alloys, local mag. anisotropy energy estimation 7-7503
DyM₂ (M=Al, Ni), paramag. fluctuations, μ SR study 7-45878
a-DyNi, critical props. and universality class of disordered systems 7-2884
Dy_{2-x}Th_xFe₁₄B alloys, mag. props., comp. depend. study 7-7492
Dy₂Y_{1-x}Al₂, intrinsic low field susceptibility studies 7-45633
Dy₂Y_{1-x}Al₂, intrinsic coercive field 7-45728
Fe-Dy-C high coercivity permanent magnet materials 7-2903
Fe₁₄Nd₂B permanent magnet, Dy substituted positron annihilation studies 7-3108
Nd-Dy-Fe-B based sintered magnet, microstruct., heat treatment effects 7-53767
NdDyFe₁₄B spin orientation and preferential 4f site occupation, powder neutron diff. study 7-22100
Nd_{0.5}Dy_{0.5}Fe₁₂Co₂B, mag. characts. 7-45670
Nd₂HoDyFeB permanent magnets with zero temp. coeff. of induction 7-53047
Pd₂Y_{1-x}Dy_xSn, Heusler alloy system, field-induced reentrant superconductivity 7-2765
Pr_{2-x}Dy_xFe₁₂Co₂B, mag. characts. 7-45670
Sn_{1-x}Dy_xOs₈Sn₁₈, disordered II' phase, structural study, electron and X-ray diff. meas. 7-63549
Tb_{0.3}Dy_{0.7}Fe₂, spin reorientation, Mossbauer study 7-13068
Tb_{0.27}Dy_{0.73}Fe₂, Terfenol, polycrystalline, domain structures and magnetomech. coupling 7-53025
Tb_{0.27}Dy_{0.73}Fe₂, twinned [112] crystals, magnetostriction 7-53105
Y_{1-x}Dy_x dilute alloys, spin density wave antiferromagnetism 7-52947
Zr-Ti (Sn)(Dy)(Au), neutron irradiated, solute effects on damage production and recovery 7-51861

dysprosium compounds

see also dysprosium alloys

- L_{III} X-ray absorption spectra 7-39312
Al-Dy₂O₃-Al thin-film sandwiches, dielec. polarisation props. 7-38772
Bi₂Dy_{1-x}Fe_{3-8x}Al₁₂O₁₂ garnet films, magneto-optical props. 7-64614
(BiDySmLu)₃(FeAl)₃O₁₂ bubble garnet films, Bi-substituted, LPE growth rate reduction 7-45049
(BiDySmLuGd)₃(FeGa)₃O₁₂ bubble garnet films, Bi-substituted, LPE growth rate reduction 7-45049
CrDy₂S₇, synthesis, physicochemical props. 7-44470
Dy₃Al₅O₁₂, refrigerant characts. for Carnot mag. refrigerator 7-56286
Dy₃Al₅O₃, exchange metamagnetism 7-2841
Dy(As₂V_{1-x})O₄, random-field effects on Ising Jahn-Teller phase transition 7-58461
DyCl₃·6H₂O, quantum mechanical ground state 7-38839
DyFeO₃, interphase magnetic domain wall motion studies (Russian) 7-27543
DyIG:Ga,Bi, RF sputtered films for magneto-optical memory, mag. props. 7-64613
DyLiFeO₃, orthoferrite, mag. props. 7-2824
Dy₂(MoO₄)₃, improper ferroelectrics, energy spectrum and vacuum UV spectra 7-33413
Dy₂O₃-CaO solid solutions, dipole complexes, dielectric relax. 7-53231
Dy₂O₃-Er₂O₃-Ho₂O₃, mixtures, IR reflectance spectrum, wavelength standard 7-41330
Dy₂O₃-P₂O₅ glasses, struct., mag. and thermal props. 7-26658

dysprosium compounds continued

- Dy₂O₃·4H₂O, absorpt. spectra intensity parameters, fluoresc. radiative transition probabilities (Chinese) 7-39141
Dy₂(SO₄)₃·8H₂O, magnetic and hyperfine props., cryst. field effects calcs. 7-27305
DySe-USe system, mag. props. of solid solns. 7-22121
DySi_{2-x}Si, silicide thin films, phase composition, conductance, surface morphology 7-7072
KD₂(WO₄)₂, vibr. characts. of O bonds, IR and Raman spectra 7-32587
KDy(MoO₄)₂, elastic characts. near structural phase transition, sound vel. meas. (Russian) 7-26872
LiDyP₄O₁₂, and Li(Dy,Y)P₄O₁₂, flux cryst. growth 7-13345
PrO_x-DyO_{1.5} solid solutions, phase diagrams and variable valency 7-33642

E-layer see E-region**E-region**

see also sporadic-E layer

- auroral electrojet, rocket-borne interferometric phase vel. meas. 7-55364
auroral region, radar irregularities, propag. angle depend. 7-60447
double peak electron density profile near Peru, and new transport process 7-29345
E-layer height vars. and daytime valley 7-40625
ELF wave generation in lower ionosphere 7-9307
enhanced electron temperatures due to broadband plasma waves with large amplitude 7-60467
equatorial E-region, effect of electron temp. on electron number density and dynamics 7-66390
equatorial electrojet, drift speeds of irregularities of kilometre and metre sizes 7-4257
equatorial electrojets, small scale plasma motions, HF Doppler obs. 7-55361
equatorial irregularities, phase vel. depend. on polarisation elec. field 7-47628
equatorial scintillations, effect of mag activity 7-34762
ion-neutral collision frequency, EISCAT observations 7-29336
long-distance 40 kHz signals propag., effects of geomag. storms on sunrise fading 7-55360
plasma waves due to two-stream instability and elevated electron temps. 7-55357
plasma waves of 1 metre wavelength, Doppler velocity depend. on aspect angle 7-9309
radio waves absorpt. during solar eclipse, 1.8 and 2.2 MHz obs. 7-29361
radiowave heating experiment at Tromsø, 1-metre irregularity production 7-29353
radiowave modification of electron distrib. function, due to resonant HF absorpt. 7-60459
semi-diurnal tide, EISCAT obs. 7-34782
vertical velocity structures, SABRE obs. 7-4254
whistler dispersion, semi-annual and annual vars. meas. 7-14410

ear

see also hearing

- audiological investigations using microcomputer system 7-65882
auditory thresholds and cochlear mechanisms 7-47081
calibration of ear canals for audiometry at high frequencies 7-65774
chinchilla cochlea, basilar membrane mechanics: low freq. responses and microphonics and spike initiation 7-47093
Chorimac cochlear prosthesis, discrimination of elementary phonemes (French) 7-47288
cochlea, chinchilla, basilar membrane mechanics: input-output functions, tuning curves and response phases 7-47092
cochlea, equivalent cct. modelling 7-47085
cochlea computational model, expts. 7-47117
cochlea representation in primary auditory cortex of ferret 7-8585
Cochlear hydromechanics modelling 7-65762
cochlear mechanics and physiology, interrelationships (French) 7-47082
cochlear nonlinear 2-stage model with automatic gain control 7-47091
cochlear vibrations, model of effect of outer hair cell motility 7-8586
frequency discrimination in the mammalian cochlea: theory versus experiment 7-54599
hair cell damage produced by acoustic trauma in the chick cochlea 7-54597
hearing damage effects of noise 7-28541
interaural correlations in normal and traumatized cochleas: length and sensory cell loss 7-47158
matching impedance of a nonuniform transmission line: application to cochlear modeling 7-54605
middle-ear input admittance, changes during postnatal auditory development in chicks 7-40165
organ of Corti, computer-assisted morphometric anal. system 7-40373
organ of Corti, elec. coupling differences in vitro and in vivo 7-54593
otorhinolaryngology, low-power laser therapy using fiberoptic instruments 7-28648
pathological high impedance tympanograms, simulation 7-47115
phase effects in masking related to dispersion in the inner ear 7-47098
protectors, theory and tests (Spanish) 7-11215
Riccati equations describing impedance relations for forward and backward excitation in the one-dimensional cochlea model 7-65765
semi circular canal, mech. model (French) 7-3800
sound processing for cochlear implant 7-37276
speech processor with lateral inhibition, 8 channel cochlear implant, subject testing evaluation 7-37275
speech recognition using a cochlear model 7-43554
stereocilia, tip links, vulnerability to acoustic trauma in the guinea pig 7-54590
stereocilia micromechanics, changes following overstimulation in metabolically blocked hair cells 7-40164
stria vascularis, DC pots. in different cells, in vitro obs. 7-54586
stria vascularis potentials, in vivo electrophysiological obs. 7-54587
surgery, ENT, use of OPM-212F microscope 7-8755
surgery in general practice, OPM-110 microscope use 7-8757
threshold characteristics of the human auditory brain stem response 7-54600
tympanic membrane, fibrous dynamic continuum model 7-47107
wearable pocket-sized processor for digital hearing aid and hearing prostheses 7-37277

ear microphones see microphones**EAROM see PROM****earphones**

see also hearing aids

- active free-field equalizer for TDH-39 earphones 7-28768

Earth

- see also *Earth composition*; *Earth orbit*; *Earth rotation*; *Earth structure*
 accretion, implications of shock-induced volatile loss from Murchison carbonaceous chondrite 7-34949
 accretionary history 7-40390
 accumulation of Earth and initial state, dynamical model 7-34367
 core formation time, implications of high-press. metallisation of FeO 7-66101
 early evolution, accretion rel. to atmosphere form. and Earth thermal history 7-54840
 Earth-Moon system, origin 7-23509
 formation, metal-silicate fractionation in growing Earth as energy source for magma ocean 7-8888
 formation, planetary growth rate around 1 solar mass star 7-55497
 free oscillations, asymptotic normal modes of laterally heterogeneous Earth 7-40425
 free oscillations, generation by localised source in viscoelastic inhomogeneous Earth 7-28887
 free oscillations and surface waves of an aspherical Earth 7-60180
 free oscillations spectra, anomalous splitting rel. to inner core anisotropy 7-66025
 geoid shape in Sudan, by astrogeodetic and satellite observations 7-40394
 gravitational field, Earth-Moon system, momentum current picture 7-55934
 gravitational potential expansion, convergence improvement methods 7-47742
 gravity models, freq. windows and resonant solns. as test of accuracy 7-3966
 image from space, Giotto spacecraft observation and image processing method 7-9380
 lunar natural satellites collision orbits with Moon via method of surface of section 7-9387
 meteor flux, mean density hitting Earth 7-29438
 neutrino oscillations, buildup in Earth 7-10051
 origin of Earth-Moon system 7-47740
 passive gravitational mass and inertial mass inequality of extended body 7-9372
 planet Earth, processes, Conf., Orlando, FL, USA (October 1985) 7-41015
 planetary perturbations by Earth-Moon system, effects on motion of asteroids and comets 7-4297
 spaceborne imaging radars, Earth and planetary obs. 7-55334
 tidal torques, components determ. independently of Earth internal density distrib. 7-18107

earth (electric) see *earthing*

earth (soil) see *soil*

Earth age see *geochronology*

Earth atmosphere see *terrestrial atmosphere*

Earth composition

- 6th international conference on geochronology, cosmochronology and isotope geology, Cambridge, England (June-July 1986) 7-8
 Ackley Granite, SE Newfoundland, geochemical trends rel. to magmatic-metallogenic processes 7-8941
 Afro-Arabian dome, volcanic rocks comp. rel. to geological evolution 7-29027
 Aileu Formation, East Timor, Indonesia, interpretation of ⁴⁰Ar/³⁹Ar and K/Ar dating 7-28916
 Amitsoq gneisses (early Archaean) of Isukasia area, W Greenland, geochronology and isotopic var. 7-34485
 Late Archaean granites of Napier Complex, Enderby Land, Antarctica, Rb-Sr, Sm-Nd and U-Pb systematics 7-14231
 Archaean high-grade metasediments, rare earth element patterns and tectonic significance 7-34486
 Aurora U deposit, McDermitt Caldera Complex, Oregon, He soil gas survey 7-40441
 basalt melts, effect of comp. and struct. on viscoelastic props. 7-8933
 basalts, tectonic settings discrimination using trace element abundances 7-28957
 basalts from Reunion and Grand Comore Islands, Indian Ocean, noble gas systematics 7-29012
 basalts from S Atlantic hotspots, geochemical correl. with southern African kimberlites 7-34409
 Bir Safsaf-Aswan uplift, SW Egypt, petrology, geochemistry, and structural development 7-66118
 Cainozoic basalts of E China, Pb, Sr and Nd isotope systematics and chemical characts. 7-29011
 calc-alkaline volcanic rocks of Namaqua mobile belt, South Africa, evidence for Middle Proterozoic volcanic arc 7-34493
 California, groundwater Rm as earthquake fluid phase precursor 7-40424
 California, San Andreas and Calaveras faults, H₂ due to fault strips and earthquakes 7-40438
 carbonates in mantle-derived xenoliths in kimberlite pipes 7-34408
 chemical composition of rocks, relation to elec. parameters 7-18181
 China, fluids chem. comp. var. due to seismic activity 7-40421
 clay-mineraloid weathering products in Antarctic meteorites, mineralogy and comp. 7-34951
 continental crust, comp. and evol. (book) 7-60913
 outer core, effect of impurities on melting curve and temp. profile 7-23614
 inner core chemical composition density model indicating elements other than Fe 7-54958
 core composition, implications of high-press. metallisation of FeO 7-66101
 core composition, S and O contents rel. to inner core adcumulus growth and geomag. dynamo 7-66027
 core formation, effects of impact heating during Earth accumulation 7-34367
 core-mantle separation in accreting Earth, effects of atmosphere form. on thermal history 7-54840
 Devonian shales from Appalachian Basin, C and S relations as indicator of deposition environment 7-65988
 dunite nodule from Reunion Island, Indian Ocean, noble gas systematics 7-29012
 Eifel peridotite xenoliths, trace element and isotope geochemistry rel. to subcontinental lithosphere 7-34484
 glaciolacustrine sediments of Yukon Territory, stratigraphic, isotopic and micrological evidence for early Holocene thaw unconformity 7-9034
 granites of E Zambia, initial ⁸⁷Sr/⁸⁶Sr ratios and Rb-Sr ages 7-18147
 groundwater, Ra isotopes abundances from porous flow model for steady state transport 7-23725

Earth composition continued

- Hawaiian lavas, geochemical and geophysical constraints on origin 7-8943
 hornblende, Al content as empirical igneous barometer 7-55029
 igneous rocks, effects of convection and mixing in magma chambers 7-4028
 indochinite tektites, K, Rb and Li concs, rel. to selective volatilisation and imperfect mixing 7-34500
 isotopic data multidimensional treatment method 7-66315
 Jabal Tifl layered gabbro, SW Saudi Arabia, mineral chemistry rel. to magma origin 7-29015
 Johnson Camp, Arizona, Cu-Zn ore bodies determ. from soil and soil gas comp. anal. 7-40591
 Karelian granite-greenstone terrain, ages and comps. of volcanic rocks 7-34489
 kimberlites from southern Africa, geochemical correlation with S Atlantic hotspots 7-34409
 komatiites, role of spurious correl. in development of alteration model 7-55039
 Laurentian Trough sediments, Gulf of St. Lawrence, radionuclide profiles, sedimentation rates, and bioturbation 7-28995
 magnetite compositions in Holocene tephra, appl. of discriminant function and for tephra identification 7-8893
 mantle, chem. heterogeneities origin 7-66315
 upper mantle, geochemical implications of viscosity of partial melts 7-8934
 mantle composition, effects of chemical and phase transitions on intermediate mantle struct. (*Russian*) 7-66038
 mantle depletion, implications of partial melting for Archaean lithosphere stabilisation and heat loss 7-34398
 mantle dregs, interaction with convection rel. to lateral heterogeneity at core-mantle boundary 7-66022
 Mariana Trough basalt glasses, light noble gases comp. anal. 7-40436
 Mid-Atlantic Ridge, three-component isotropic heterogeneity near Oceanographer transform 7-54956
 mineralogy of deep-sea sediments, results from drillholes near East Pacific Rise 7-14260
 Muong Nong type tektites from moldavite and North American strewn fields, implications of element abundances 7-55050
 Nagano, Japan, ³He/⁴He ratio anomalies in hot spring gases, assoc. with 1984 September 14 earthquake 7-40422
 Nagano region, Japan, gas anomalies at mineral springs and fumarole before earthquake 7-40423
 Nevado del Ruiz volcano, Colombia 7-8897
 oceanic basalts, siderophile and chalcophile abundances rel. to Pb isotope evolution and growth of Earth's core 7-34397
 oceanic crust, O isotopic profile through upper kilometer at DSDP Hole 504B 7-34467
 Okinawa Trough, sediments chem. comp. and characts. (*Chinese*) 7-47420
 olivine in upper mantle rel. to 400-km seismic discontinuity 7-47404
 Onverwacht Group, Archaean flow-top alteration zones form. in low-temp. sulphate-rich environment 7-34488
 outer core composition, implications of Fe-H₂O reaction under high press. 7-8887
 Outer Hebrides, evidence for enriched lithospheric keel, mantle xenoliths comp. anal. 7-47407
 peridotitic upper mantle origin, implications of melting of dry peridotite up to 14 GPa 7-8937
 Phanerozoic, natural divisions, mass extinctions and chem. comp. anal. 7-47403
 early Precambrian Al₂O₃ rich rocks of Kaapvaal Craton, indicators of palaeosols 7-29020
 Precambrian continental crust, struct., comp. and evolution from deep drillholes in USSR 7-34413
 Precambrian ophiolites and basement in Central Asian foldbelt, Mongolia, structural-metamorphic evolution 7-34495
 Precambrian palaeosols of Dominion and Pongola Groups, Transvaal, chemistry and mineralogy 7-29018
 Precambrian palaeosols on basaltic and granitic parent materials, elemental concs. profiles 7-29019
 Precambrian rocks of Ural Mountains, petrochemistry rel. to geodynamic regimes 7-34494
 primary lavas from Okmok volcano, central Aleutians, geochemistry rel. to arc magmatogenesis 7-28949
 primitive mantle, chemical fractionation rel. to origin and early growth rate of continents 7-14229
 pristine mantle composition analysis, implications for Earth accretionary history 7-40390
 Early Proterozoic bimodal volcanic rocks in central Colorado, petrogenesis and tectonic setting 7-23645
 Proterozoic mafic volcanic rocks of Nagu-Korpo area, SW Finland, stratigraphy and geochemistry 7-14275
 Early Proterozoic supracrustal rocks of SW United States, geochemistry and tectonic setting 7-55037
 proto-mantle differentiation in accreting Earth, effects of atmosphere form. on thermal history 7-54840
 rare gases rel. to evolution and structure of mantle 7-60386
 Roberts Victor eclogites, ¹⁸O/¹⁶O ratios rel. to ancient oceanic crust hypothesis 7-55042
 Rockall Plateau, dipping-reflector passive margin struct., Pb isotopic evidence 7-66037
 sandstone-mudstone suites, tectonic setting determ. using SiO₂ content and K₂O/N₂O ratio 7-29014
 Saskatchewan, Canada, well water He and methane anomalies origin 7-40440
 Sea of Japan, U and Th contents as indicators of continental-type volcanism 7-14274
 sediments of Red Sea rift, mineral comp. of coarse aluritic fraction 7-14261
 Seychelles microcontinent, chem., comp. determ. 7-40452
 soil, gas composition analysis use for geochemical exploration for mineral resources 7-40590
 stable isotopes in high-temp. geological processes, book 7-35126
 Stillwater Complex, Montana, rare-earth element evidence for form. of Ultramafic Series 7-65987
 sulphate deposits in S Alberta fractured till, $\delta^{18}\text{O}$ and $\delta^{34}\text{S}$ anal. rel. to origin 7-23726
 tektites, F and Cl contents 7-34501
 till deposits in drumlins near Caledonia, S Ontario, geochemical characts. of inverse-graded units 7-9033

Earth composition continued

- Triassic megaporphyrized monzogranites of S California, modal and chemical comps. rel. to offset along San Andreas Fault 7-55043
 volatiles distribution in accreting Earth, implications of shock-induced volatile loss from Murchison carbonaceous chondrite 7-34949
 volcanic rocks from Yap-Mariana trenches intersection, petrology, geochemistry, and tectonic implications 7-34469
 Fe oxides mineralogy determ. in sediments, appl. of Kubelka-Munk colour theory 7-66098
 He isotopes in sedimentary basins, relation to form. mechanism 7-47405
 Hg dispersion patterns around El Sid-Fawakhir Gold Mine, Eastern Desert, Egypt, stream sediments meas. 7-18148
 Ir abundances across Ordovician-Silurian boundary stratotype, meas. 7-4014
 Ir anomalies, new discovery in Middle-Lower Jurassic of Venetian region, N Italy 7-55038
 K-rich lamprophyres of S Scotland, geochemistry rel. to primary magma origin 7-4032
⁴⁰K/³⁹K ratio in lower mantle, implications of K-Ar isochron dating of Zaire cubic diamonds 7-23612
 Mg₂SiO₄-MgSiO₃ system, melting and phase relations at 20 GPa under hydrous conditions 7-8935
 Mn fluxes from Juan de Fuca Ridge, regional perspective from hydrothermal plume meas. 7-66095
 Os, isotopic composition in terrestrial samples from accelerator mass spectrometry meas. 7-23611
 Pb isotope evolution rel. to Earth core growth, implications of siderophile and chalcophile abundances in oceanic basalts 7-34397
 Rn concentration variations in active volcanoes and seismic regions 7-54963
²²²Rn in Gulf Coast geopressured-geothermal reservoirs, United States 7-8881
²²²Rn transport from soil, role of channels 7-40442
 U concentration meas. in soil and rocks by γ -ray spectrometry 7-54373
²³⁴U/²³⁸U activity ratios in geological materials, determ. by α spectrometry 7-60255
²³⁸U decay series nuclides, evidence for recent migration in granite pluton 7-28917

Earth core

- 3D structure and free-oscillations spectra splitting 7-60187
 adcumulus growth of inner core, implications for geomag. dynamo 7-66027
 chemical composition of inner core, density model indicating elements other than Fe 7-54958
 composition of outer core, implications of high-pressure metallisation of FeO 7-66101
 core-mantle boundary, evidence against 2 to 50 km size corrugations from PeP amplitudes 7-66018
 core-mantle boundary, evidence for aspherical struct. from PKP' travel times 7-66017
 core-mantle boundary topography, determ. from geoid anomalies 7-66021
 dynamo problem and mag. fields turbulent transport 7-60511
 dynamo theory, role of fluctuations 7-60512
 fluid outer core, inertial waves identification 7-60225
 formation, effects of impact heating during Earth accumulation 7-34367
 formation, implications of Fe-H₂O reaction under high press. 7-8887
 formation, siderophile and chalcophile abundances in ocean basalts rel. to Pb isotope evolution 7-34397
 geodynamo and geomagnetic field morphology 7-54874
 geomagnetic dynamo, mag. fields fluctuations in coupled-disk dynamo models rel. to secular vars. 7-14187
 geomagnetic dynamo, models for mag. field reversals 7-23539
 geomagnetic dynamo coupling with mantle, thermal and topographic coupling models 7-65933
 geomagnetic field components, effects on magnetisation modelling in North and Equatorial Atlantic Ocean using Magsat data 7-40414
 geomagnetic main field anal. at core-mantle boundary, spherical harmonics compared with harmonic splines 7-65935
 geomagnetic variations, due to influence of Sun on Earth's liquid core 7-34382
 heat flux, lateral modulation by mantle convection and dregs 7-66022
 inner core, search for lateral heterogeneity from differential travel times near PKP-D and PKP-C 7-66026
 inner core anisotropy, evidence from free oscillations spectra 7-66025
 inner core anisotropy, evidence from PKIKP travel times 7-66024
 lateral variations of density and seismic velocity in outer core 7-47400
 liquid core lateral homogeneity, evidence from seismic travel-time residuals inversion 7-66036
 magnetic field at core-mantle boundary, models for fields of 1715, 1777 and 1842 AD 7-54870
 magnetic field reversals periodicity, rôle of mantle plumes 7-65934
 magnetic flux expulsion from Earth core, 2D model 7-23532
 mantle base (D'' region), seismic lateral heterogeneity and convection 7-8841
 mantle interface depression and Indian Ocean geopotential hours 7-47412
 metal-silicate fractionation in growing Earth, energy source for magma ocean 7-8888
 nonhydrostatic aspherical structure, contrib. to anomalous splitting of seismic multiplets 7-28892
 nutation of Earth core, possible detection 7-23513
 outer core temperatures, implications of physics of melting for Fe melting curves 7-23614
 Rikitake two-disk dynamo rel. to polarity intervals 7-65936
 rotation relative to mantle, rel. to C₂₁ and S₂₁ geodetic gravity coeffs. 7-47399
 seismic velocity struct. of core and mantle 7-54925
 seismic waves propagation, appl. to internal struct. determ. (French) 7-23588
 steady flows at top of core, determ. from geomag. field models 7-40444
 steady surficial core motions determ. from geomag. field models, alternate method 7-66023
 symmetrical fluid flow, MHD model for the Earth's magnetic field with spatially dependent electrical conductivity 7-60165
 thermal core-mantle interactions 7-54960
 westward drift motion of core and Earth rotation 7-23515
 Fe, phase diagram and Earth interior conditions 7-38179
 K content of Earth, possible incorporation in to Fe core 7-40437

Earth crust

see also oceanic crust

- 7-34495
 N Aegea, Greece, Oligocene formations palaeomag. data, tectonic implications 7-47417
 Afro-Arabian dome, geological evolution 7-29027
 Alai Range, USSR, mineral exposures and tectonic associations 7-8883
 W Alaska, earthquakes focal mechanisms and stress orientations from seismicity studies 7-28907
 S Alaska, USA, crust structure, seismic anal. 7-66033
 Albigeois, France, relict clinopyroxenes in Paleozoic metabasites, indication of extensive transitional-to-tholeiitic volcanism (French) 7-66003
 Aldanian shield, USSR, phlogopite and apatite deposits and tectonophysical environment 7-60222
 Alpine-Himalayan belt, tectonic implications of nonshear-type earthquakes 7-8854
 Western Alps, lithospheric sections assuming that the Sezia zone is not of South Alpine origin (French) 7-66004
 Amazonian foothills of Peruvian Andes, seismicity and tectonic activity 7-47373
 N America, deglaciation-induced vertical motion and transient lower mantle rheology 7-8912
 America-Eurasia plate boundary in eastern Asia and the opening of marginal basins 7-60236
 N American Cordillera, USA, deep seismic traverse and orogenic evolution 7-55000
 Andaman-Nicobar Islands, seismo-tectonics anal. 7-65962
 Anza, California, USA, seismicity and source parameters rel. to crustal stress 7-65951
 N Apennines, deformation phases dating using K-Ar and ⁴⁰Ar/³⁹Ar techniques 7-40459
 Appalachian Basin, USA, C and S relations in Devonian shales as indicator of depositional environment 7-65988
 Aquitaine shelf, crustal thinning, deep seismic data 7-54961
 W Arabian continental margin, S Red Sea, tectonic configuration 7-14276
 Archaean continent formation and anomalous sub-continental mantle link, mineralogical anal. 7-47408
 Archaean high-grade terrains, tectonic significance of REE patterns in metasediments 7-34486
 Archaean lithosphere stabilisation, effects of mantle melting 7-34398
 Armenia volcanic highland, USSR, Late Cainozoic volcanic geology, petrology etc. 7-8884
 aseismic crustal deformation at Hollister, California, dislocation model 7-40445
 Asia, crust struct. from teleseismic obs. 7-60170
 Asia (West-Central region), Kimmerian movements and structural development 7-60242
 Astrid Ridge off Queen Maud Land, Antarctica, fracture zone nature 7-66035
 Atlantic-type continental margins, thermo-mech. evolution, numerical models 7-54950
 Australia, underplated crustal material indicated by seismological evidence 7-8900
 Australia, unstable platform for tide-gauge meas. of changing sea levels 7-29049
 E Australia metallogeny and tectonics, conf., Sydney, Australia (August 1984) 7-55882
 Baijing-Beigezhuang profile, magnetotelluric data inversion via continuous resist. var. model (Chinese) 7-34375
 Baikalsk-Amur Main Line, USSR, elec. struct., mag. var. profiling anal. 7-23527
 Baltic Shield, 1.9-1.8 Gyr strike-slip megashears and plate tectonic implications 7-14284
 Baltic Shield, crustal struct. determ. from off-FENNOLORA refr. data 7-14232
 E Baltic Shield, polar wander path from palaeomagnetism of Archaean and Proterozoic basic intrusives 7-28828
 basalt formation, peridotite root zone beneath Grand Lagon Nord, New Caledonia (French) 7-66087
 basaltic volcanism, tectonic settings discrimination using trace element abundances 7-28957
 basins tectonic maps, principles of tectonic classification and structural units description 7-34435
 Bassaride Belt, Guinea-Senegal, evidence for Panafrican tectonics events (French) 7-66060
 Bay of Islands Ophiolite, 2D seismic reflection-modelling of fossil oceanic crust-mantle transition 7-40428
 Bir Salsaf-Aswan uplift, SW Egypt, petrology, geochemistry, and structural development 7-66118
 Bissau-Kidira-Kayes fault zone, extension in W Africa (French) 7-34434
 Black Sea trough, crust struct., geology and tectonics 7-60214
 Borah Peak, Idaho, USA, fault scarp shallow struct. by seismic profiling 7-23557
 borehole electropotential, influence of surface deposits on const. current field in anisotropic medium 7-28831
 Boso and Miura peninsulas, Japan, collision area, convergence changes tectonic record 7-66066
 Bridge River terrane, British Columbia, Canada, geology and tectonics 7-55001
 SW British Columbia, Canada, Hozameen fault system and Coquihalla serpentine belt 7-4009
 Bushveld Complex, S Africa, geoelectric struct. of arc-like bodies 7-60167
 Caledonian orogen collapse and 'Old Red Sandstone' characts. 7-4013
 S California, fault systems rel. to 1930 Santa Monica and 1979 Malibu earthquakes 7-54883
 California, Quaternary faults props. rel. to seismic hazard 7-40430
 California, San Andreas and Calaveras faults, H₂ due to fault strips and earthquakes 7-40438
 N California, USA, geology of Franciscan Complex and Coast range ophiolite 7-54969
 N California, USA, mantle struct. and teleseismic P-wave residuals azimuthal var. 7-66031
 N California Coast Ranges, 3-D vel. struct. from inversion of local earthquake arrival times 7-3987
 Cameroon Adamawa region, crust mantle seismic velocity structure 7-8839
 Campi Flegrei volcanic area, S Italy, Q_e from volcanic microearthquakes 7-3999

Earth crust continued

E Canada, continental rifting and diabase from Northumberland Strait 7-4018
Canadian Appalachian crust, thermal nature from heat flow meas. 7-66041
Canadian Cordillera, electrical conductivity structures of crust 7-60160
Canadian Cordillera, seismic refl. geometry of Columbia River fault zone and Shuswap metamorphic complex 7-14281
Cape Basin, sediment sound vel. provinces from multichannel seismic refl. profiles 7-55008
Cape Breton Highlands, Nova Scotia, geology of Cheticamp pluton 7-65989
carbonate platform stratigraphy as record of past earthquakes 7-8859
Carboniferous pre orogenic magmatism in Central Jebilet Morocco (French) 7-66007
Cariboo gold belt, BC, Canada, imbricated terrane geology and tectonics 7-23584
Carpathian Mountains, USSR, geomag. anomaly and geoelectric model 7-40411
E Carpathians Arc Bend, Romania, shallow vs. deep and old vs. recent tectonic movements 7-28987
Castle Mountain (Alaska) fault system, Sutton earthquake rel. to activity on Talkeetna segment 7-3984
SE Caucasus, USSR, north slope chaotic complexes, morphology and stratigraphy 7-29013
Cenozoic global plate motions, determ. relative to hot spot reference frame 7-40455
Charleston region, South Carolina, vertical crust movements, levelling data anal. 7-8911
Charlotte belt, N and S Carolina, USA, deformed composite batholith 7-18141
Charvak reservoir, USSR, isostatic state of Earth's crust rel. to induced seismicity 7-23576
Chile Ridge-Chile Trench interaction, mag., thermal and bathymetric characts. 7-66074
E China, continental lithosphere contrib. to isotope systematics and chemistry of Cainozoic basalts 7-29011
China, crustal stress state rel. to faulting and earthquakes (Chinese) 7-34396
China, SE coastal region, geomag. anomalies from deep crustal sources 7-47337
N China, seismic tomography (Chinese) 7-28912
China, tectonic activity anal., use of fluid-geochem. methods 7-40421
clastic dikes in Numidian Flysch, Tunisia and Sicily (French) 7-66006
coal deposits of USA, lignite deposits of Texas to Georgia region 7-18139
coal seams, tectonic disturbances and quality changes, geoelectric anal. method 7-34712
Colorado Plateau, palaeomag. data anal. rel. to tectonic rotation 7-14251
Colorado Plateau, palaeomag. evidence for tectonic rotation 7-14250
continent development and geothermal field 7-28930
continental, seismic reflectors, elec. cond., water and stress 7-4011
continental crust, comp. and evol. (book) 7-60913
continental crust, origin and early growth rate 7-14229
continental crust density rel. to seismic vel., relationship use in gravity data anal. 7-18144
continental rifting, thermomechanical models of active rifting 7-14247
Coso region, California, USA, crust seismic struct. 7-66032
cratonization and mantle thermal evolution 7-23622
Crete, geological linear features seen by satellite 7-47402
Crimea-Romania, lithosphere struct. along Geotraverse V 7-60207
crustal regions shallow sounding using EM surface waves 7-14193
crustal tilt anomaly patterns assoc. with earthquakes, features and classification (Chinese) 7-34388
Cuba, ophiolite assoc. struct. 7-28926
Cyprus, rot. and translation, palaeomagnetic timing 7-66067
Dakota (North and South), USA, Precambrian basement geology 7-23586
deep seated anisotropic oblique zones assoc. multiple elec. discontinuities mapping, magnetotelluric freq. sounding use 7-47573
deformation, appl. of stream function and Gauss's principle of least constraint in structural geology 7-29009
Derbyshire Dome, UK, Dinantian sedimentation and basement struct. 7-66012
diapiric structures, relation between initial conditions and late stage of Rayleigh-Taylor instabilities 7-66108
Dneiper-Donets trough and Donets folded struct. in USSR 7-60216
Donets Basin, USSR, Carboniferous deposits parting fractures 7-34403
Donets basin, USSR, principal faults and wrench faults 7-8908
earliest crust form. 7-60147
earthquake focal regions, physics and geodynamics of deform. processes, conf., Potsdam, East Germany (November 1985) 7-48140
earthquake instability rel. to frictional slip depth var. 7-14226
earthquake source mechanisms, behaviour of viscoelastic medium with microfractures under extension and shear 7-29003
earthquakes hazard and prediction, conf., Tokyo, Japan (1985) 7-60859
East African rift and northeast lineaments, possible continental spreading-transform system 7-66071
East European Platform seismic model of lithosphere beneath Baltic Sea-Black Sea profile 7-14236
East Germany, gravity var. and temporal heights, assoc. neotectonic characts. 7-14177
East Germany, tectonomagnetic field var. 7-14183
elastic characteristics, definition 7-54945
Elbe valley, lithospheric geochemistry and petrology in fault zone 7-54946
electrical parameters of rocks, relation to chemical comp. 7-18181
electrical prospecting, potential soln. for nonuniform thin vein with transverse conductance variability 7-28830
EM emission during seismic activity, crustal mechanical-electric convertors model 7-8856
SW England, Variscan strain pattern in Palaeozoic series at Lizard front 7-14279
Eromanga Basin, N Australia, seismic study of crust and Carboniferous orogeny 7-65960
N Eurasia, seismic velocity structure of lower lithosphere and asthenosphere 7-8857
Europe, combined geophysical-thermal models of crust and upper mantle 7-28933
NW Europe, contemporary seismicity and tectonics 7-28848
central Europe, earthquake props. and fault characts. 7-54911

Earth crust continued

E Europe and Middle East, lithosphere mag. suscept. anomalies 7-23535
East European platform, lithosphere struct. from geophysical data 7-60208
Faizabad earthquake prediction site, Tajikistan, USSR, tectonic lineaments seen from space 7-60245
fast tectonic wave theory, interaction at lithosphere-asthenosphere interface 7-4020
fault and geothermal anomaly remote sensing method 7-28920
fault geometries in basement-induced wrench faulting under different initial stress states 7-40458
fault rupture characts. for $ML \sim 3$ earthquakes near Anza, S California, tomographic source imaging results 7-40431
fault zones, internal struct. 7-54995
faulting associated with earthquakes (Japanese) 7-65980
Fergana intermontane basin, USSR, geology from remotely sensed images 7-66029
Finland, tectono-exogenic evolution of Precambrian supracrustal rocks 7-34490
S Florida Platform, seismic velocity struct. of crust 7-54930
Friuli area, Italy, crustal deform. and 1976 earthquakes 7-54948
W Ganga Basin, India, evidence for oceanic crustal block from shear vel. struct. 7-54939
Garm region, Central Asia, seismicity rel. to deform. in zone of continental convergence 7-28847
garnet amphibolites metamorphism, garnet-hornblende thermometry and min. press. limits 7-29005
geodynamics since Archaean, implications of previous higher mantle temp. 7-54994
W Germany, DEKORP 2-S seismic profile of crust deep struct. 7-40418
global displacement and stress fields due to tidal attraction (Chinese) 7-54841
global satellite laser ranging use for tectonic deform. anal. 7-55287
Gobles oil field (SW Ontario) microearthquakes, first motions rel. to fault plane solns. 7-28856
GPS baseline determ., bias fixing and water vapour radiometer correction 7-9228
graben subsidence, influences of crustal stress and temp. regimes 7-66083
granites and density loss in far E USSR 7-34402
gravity anomalies of sedimentary basin, basin depth estimation by anomaly inversion 7-3968
gravity anomalies of trapezoidal model with quadratic density function, appl. to San Jacinto graben 7-28819
gravity anomaly due to 2-D body with variable density contrast 7-54842
gravity sounding, uniqueness in inverse logarithmic potential problem 7-29280
S Great Basin, Nevada, local stress field determ. from earthquakes focal mechanism 7-54884
Great Britain, Moho seen on seismic refl. profiles, flatness as artefact of isostatic compensation 7-60176
Great Valley, California, 2D seismic vel. struct. along synclinal axis 7-28861
Great Valley, California, vel. and Q struct. from synthetic seismogram modelling of refr. data 7-3988
greenstone belts tectonic evolution, conf., Houston, USA (January 1986) 7-41017
Gulf of Genoa, location methods for underwater seismic shots and structural implications 7-14217
Gulf of Suez, tectonic interpretation of joint systems in extensional environment (French) 7-34432
heat flow estimation at lower boundary of Earth's crust, methods for 2D geothermal models 7-18155
Hebrides region, seismic struct. 7-65985
Higashi-Izu monogenetic volcano group, Japan, petrology and geochemistry 7-8892
NW Himalaya, palaeomag. evidence for rot. overthrusting from Riasi thrust sheet, India 7-34379
W Hoggar, Algeria, Pan-African crustal decoupling zone in Timagouine area 7-34439
Central Hoggar, Algeria, struct., geochronology and tectonic evolution 7-54997
Hyllingen Series, Norway, basal reversal in layered intrusion 7-18152
Iceland, accretionary volcanic processes rel. to crustal struct. 7-66081
Ile-Ife, Nigeria, possible fault zone, elec.-geomag. surveys and minerals existence 7-47330
Illinois Basin, tectonic subsidence anal. 7-54984
Illinois borehole UPH 3, USA, crust stress from stress relief microcracking 7-18150
Imperial fault, California, surface displacement triggered by Westmorland earthquake (1981 April 26) 7-3983
Imperial Valley, California, travel-time, time-term, and basement depth maps 7-28860
S India, magnetotelluric study of geoelectric anomalies 7-8804
India, super-mobility of hot lithosphere 7-14255
Indo-Antarctic metamorphic terrain, Late Proterozoic dates from India rel. to sapphirine granulites correl. 7-34414
Inuyama area, central Japan, Triassic paleolatit. from paleomag. study of red cherts 7-54872
W Ionian Sea, reflection data and deep seismic soundings 7-54877
W Ireland, Caledonides Palaeozoic terrane accretion 7-55004
N Italy, geophysical exploration of upper crust from Ligurian coast to N Po Valley 7-14240
Ivory coast-Ghana continental margin, evidence for transform margin evol. 7-66075
Jabal Tirt layered gabbro, SW Saudi Arabia, continental extension model for magma origin 7-29015
Central Japan, gravity and magnetotelluric study of Fossa Magna region 7-23609
SW Japan, Jurassic oblique collisional orogen 7-55003
NE Japan arc, 3D seismic velocity struct. of subduction zone 7-18128
NE Japan Arc, horizontal crustal strain and tectonics 7-18175
NE Japan arc, oceanic plate bending rel. to normal faulting events in deep seismic zone 7-14211
Japan Sea, U and Th contents of basalts as indicators of continental-type volcanism 7-14274
Japan Sea earthquake (1983 May 26), rupture process determ. via waveform inversion method 7-54889
Josephine ophiolite of Klamath Mountains, N California, timing and kinematics of emplacement 7-14282

Earth crust continued

- Kamchatka, increased elec. conductivity layer in crust and upper mantle 7-54868
 Kamchatka, USSR, tectonics and volcanism 7-28963
 N Kapuskasing uplift, Ontario, deep crustal struct. and tectonic history 7-14277
 Central Karelia, magnetotelluric sounding in 10^{-3} to 10^4 s period interval 7-28829
 Karelian granite-greenstone terrain, geological evolution 7-34489
 central Kazakhstan, USSR, lithosphere heat flow, struct. and evolution model 7-23608
 Kenya, failed Jurassic rift and triple junction, geomag. and gravity evidence 7-60197
 Kenya rift, crustal struct. from seismic refr. study 7-54957
 Kidal gneissic assemblage (Adrar des Iforas, Mali), tectonometamorphic evolution rel. to Pan-African thrust tectonics 7-66117
 Kiev-Gomel' DSS profile, struct. of deep crustal layers and sedimentary cover 7-47394
 Kinki district, Japan, crust seismic velocity struct. 7-65983
 Kinki district, SW Japan, crustal stress and lineaments 7-66086
 Kirishima Volcano, seismicity and stress field (1982-5) 7-8898
 E Klamath Mountain, California, island arc sedimentation in Middle Devonian Kennett Formation 7-29017
 Klamath Mts., California, USA, native terrane geology and evolution 7-54968
 Kodiak convergent margin, episodic growth of accretionary prism 7-54992
 Kola Peninsula, upper crustal struct. along Pechenga Bay-Kovdor-Alakurti profile from geophysical data 7-47395
 Korbalkha ore deposits, Rudnyi Altai, USSR, geologic-genetic model 7-14224
 central Krak Massif, USSR, struct. and petrology 7-28925
 Krivoi Rog superdeep hole site, Ukraine, seismic investigations 7-47343
 Kulyab, Tajikistan, USSR, earthquakes due to active salt doming 7-47372
 S Kuril Islands, space-time distrib. and focal mechanisms of lithospheric earthquakes 7-28885
 Kuznets basin, USSR, coal measure concentric folding 7-14222
 Kvamshesten, W Norway, tectonic implications of Solundian (Upper Devonian) magnetisation of Devonian rocks 7-34376
 L_g-waves propagation, effects of structural boundaries 7-3992
 La Grande-2 Reservoir, Quebec, crust vertical movement and gravity var. 7-8793
 lateral wave propagation in a three-layered medium 7-14192
 Ligurian Tethys, ultramafic and gabbroic sea-floor (*French*) 7-18160
 lineament imaging and identification using remotely sensed data 7-66333
 lithosphere in-plane stress, effects on sedimentary basin stratigraphy 7-14278
 lithosphere mag. field, origin and dynamics of long wavelength anomalies 7-47338
 lithosphere mineral matter, elastic props. var. with press. and temp., laboratory anal. 7-55015
 lithosphere structure and physical props. rel. to earthquake foci depths 7-54910
 lithosphere thermal characts. 7-54953
 lithosphere thinning under conditions of large heat flows, numerical study 7-28928
 lithospheric strain, temporal vars. 7-54949
 Long Valley, California, borehole seismograms anal. rel. to caldera struct. 7-40448
 Long Valley caldera, California, deep crustal struct. from extremal inversion of travel-time residuals 7-28862
 Los Angeles Basin, two-dimensional model of extension, subsidence and thermal evolution 7-66080
 Love waves propagation in irregular dry sandy layer, phase vels. determ. 7-8825
 low-pressure metamorphic belt form., role of plutonism 7-28975
 lower crust magnetic anomalies, conf., Prague, Czechoslovakia (August 1985) 7-40992
 magma ascent by porous flow, role of magmons 7-8928
 magma ascent in deformable vent, vent response to magma reservoir press. 7-8929
 magma chambers, magma convection and mixing 7-4028
 magmatic heat pumps, evidence from igneous cumulates 7-47406
 magnetic crust, bottom depth estimation method 7-47575
 magnetic field at core-mantle boundary, models for fields of 1715, 1777 and 1842 AD 7-54870
 mantle diapirs evolution, effects of comp. and thermal buoyancies 7-8890
 Marlboro Mts. Outlier, New York, USA, geology of arenite sequence 7-18142
 North Massif Central, gravimetry contribution to model of igneous intrusions emplacement (*French*) 7-18135
 Mediterranean geosynclinal belt, Carpathian and E Alps, segments, pre-Alpine evol. and main tectonic boundaries 7-34437
 Mediterranean-Asiatic seismic belt, earthquake foci and stress state 7-54915
 megathrust evolution, role of strain heating 7-40443
 Merida Andes, Venezuela, struct. and stratigraphy rel. to Neo-gene transcurrent motion 7-14283
 mesofractures anal. using space images, appl. to oil and gas exploration 7-66337
 Mesozoic Mogollon Highlands, Arizona, Early Cretaceous rift shoulder model 7-29016
 metamorphism, continents and subduction zones (*Russian*) 7-8945
 Miami Pliocene coral reefs, geomorphology and Atlantic coastal ridge in Florida 7-29028
 Mianwali re-entrant and W Salt Range, Pakistan, palaeomag. constraints on form. 7-34380
 Michigan Basin, USA, seismic refl. profiling study of crust 7-28894
 SW Michipicoten Greenstone Belt, Ontario, evidence for complex Archean deform. history 7-55040
 Mindoro Island, Philippines, allochthonous terrane evolution 7-14249
 Miramichi (New Brunswick) earthquake sequence, focal depth and fault dip from GRF broad-band array anal. 7-54921
 Mississippi Embayment, gravity field temporal var. due to crust elevation 7-8794
 Moho depth in and around Great Britain 7-54937
 Moho seen on seismic refl. profiles, flatness as artefact of isostatic compensation 7-60176
 Mongolia, ring structures and fractures, assoc. gravity and topographic characts. 7-28962

Earth crust continued

- Mongolia, tectono-magmatic devel., Late Palaeozoic and Early Mesozoic stages 7-28960
 Mongolia, Trans-Altai zone tectonics and struct. 7-28961
 Mono Craters area, E California, shallow magma chamber indicated by teleseismic obs. 7-54924
 Monte La Quaglia (Abruzzo, Central Italy), geophysical investigations of carbonate struct. 7-40477
 N Morocco, crustal structure (*French*) 7-60220
 Mount Hood, Oregon, USA, magnetotelluric investigations 7-28839
 Mount Hood area, Oregon, USA, seismic velocity struct. and extensive-dilatancy anisotropy 7-40432
 Muria volcano, Java, magmatic series (*French*) 7-66050
 Murmansk block, Kola Peninsula, magnetotelluric sounding in 10^{-3} to 10^4 s period interval 7-28829
 Mygdonian graben, Greece, struct., microearthquake data anal. 7-66010
 Nagano region, Japan, stress var. before earthquake causing gas anomalies in mineral springs and fumaroles 7-40423
 Nagano region, Japan, tectonic-seismic activity and $^3\text{He}/^4\text{He}$ anomalies in hot springs 7-40422
 Namaqua mobile belt, South Africa, calc-alkaline volcanism assoc. with Middle Proterozoic volcanic arc 7-34493
 Napier Complex, Enderby Land, Antarctica, Late Archaean tectonothermal evolution from Rb-Sr, Sm-Nd and U-Pb systematics 7-14231
 Near-Caspian basin, USSR, basement structures seen from space 7-60221
 Neogene continental crust structural devel., conf., Moscow, USSR (January 1985) 7-18474
 E Nepal, petro-structural study of ductile Himalayan layers (*French*) 7-23617
 SE New England, tectonic model for Late Palaeozoic history 7-4029
 New Madrid seismic zone, evidence for periodic energy release 7-3986
 New Madrid seismic zone, evidence for recurrent faulting, Mini-Sosie refl. data anal. 7-23626
 New Zealand, palaeomag. evidence for large tectonic rot. in last 5 Myr 7-34377
 New Zealand, seismicity, struct. and tectonics of Wellington region 7-23624
 SE Newfoundland, Avalon-Gander terranes boundary rel. to geochemical trends in Akeley Granite 7-8941
 North American-Pacific relative plate motion in S California, determ. from VLBI meas. 7-28978
 North Sea, tectonic models rel. to seismic risk anal. 7-4004
 Northumberland Trough magnetic anomaly in N England, interpretation using 2D current model 7-23530
 Norway, Caledonian thrust front and palinspastic restorations 7-40475
 S Norway and adjacent offshore areas, lineaments study 7-29026
 Ocoee Supergroup in eastern USA, origin of Late Precambrian sedimentary sequence 7-28915
 S Oklahoma aulacogen, appl. of quasi-ideal spatial filters to gravity anomalies mapping 7-28808
 Olary Block, South Australia, stratigraphic and structural constraints on Proterozoic tectonic history 7-55045
 Oregon, USA, fault patterns obs. and Cenozoic rot. characts 7-66068
 Oregon-Idaho seismic zone, fault-plane soln. for Powder River earthquakes (August-September 1984) 7-3985
 Orfordville Belt, New Hampshire, press., temp. and structural evolution 7-55044
 Oslo Graben, Norway, anatexis cumulates and residues 7-28951
 Osmansagar reservoir, Hyderabad, India, tectonic stresses rel. to microearthquakes 7-23573
 Outer Hebrides, evidence for enriched lithospheric keel, mantle xenoliths comp. anal. 7-47407
 P-wave travel times, estimation of slowness-dependent source and receiver corrections 7-54893
 Pacific Northwest, tectonic history from paleomagnetism of Tertiary Clarno Formation, Oregon 7-54871
 circum-Pacific region, subduction zone seismicity, review 7-54934
 East Pacific Rise, hydrothermal clay mineral formation from basalt 7-14256
 Palaeozoic continental reconstruction, appl. of cladistic methods 7-4019
 Panxi region, SW China, tectonic stress field and earthquake distrib. (*Chinese*) 7-54977
 Paris Basin, Variscan overthrusts characts. 7-4012
 partial melting process and biotite-sillimanite-spinel assemblages characts. anal. 7-40434
 E Pennsylvania, USA, Valley and Ridge Province geology 7-18140
 Perth region, Australia, Holocene sealevel var., crystal effects 7-47462
 S Peru, 3D P- and S-wave vel. structures rel. to tectonics 7-14227
 Pesterevskii and Malo-Salairka limestone geology, W Siberia, USSR 7-14221
 petroleum geology of USA Gulf Coast, Niger and Beaufort-Mackenzie area 7-18138
 Pharusian Range, Silet area, Hoggar, Algeria, stratigraphy and struct. (*French*) 7-60192
 Piedmontese Tertiary Basin in N Italy, mag. anomalies and geological struct. 7-54858
 Piton de la Fournaise, Reunion Island, discovery of old magmatic chamber, volcanological implications (*French*) 7-66048
 plate motions and mantle flows 7-18171
 plate tectonics, use of VLBI 7-55325
 plates motion and an expanding Earth, fossil data anal. 7-47418
 Poland, crustal seismic velocity struct. of E European Platform 7-14196
 post-glacial rebound and transient lower mantle rheology 7-18170
 postseismic viscoelastic relaxation following 1959 Hebgen Lake earthquake 7-14245
 Precambrian basinal and shelf sedimentation relation to Archaean-Proterozoic boundary 7-34492
 Precambrian continental crust, struct., comp. and evolution from deep drillholes in USSR 7-34413
 Precambrian geology, 27th IGG Congress, Moscow (August 1984) 7-29580
 precision geodesy and crustal deform. meas. instrument, hydrostatic levels 7-9229
 Priest River Complex, Washington-Idaho, mylonite zone metamorphism rel. to tectonic evolution 7-4033
 Proterozoic ophiolite preservation problem and prevailing plate tectonics, and Venus comparison 7-28980
 Provencal Basin (W Mediterranean), heat flow, heat prod., and fission track data from surrounding Hercynian basement 7-14239

Earth crust continued

- Provencal Basin (W Mediterranean Sea), thermal regime anal. from flumed heat flow surveys 7-14238
 N Pyrenees, tectonostratigraphic units rel. to apparent western termination of North Pyrenean fault 7-14280
 Pyrenees occidentales, France, cover and tilted fault blocks gliding (French) 7-66000
 Rajmahal Hills, E India, gravity field over Palaeo-Mesozoic continental margin 7-28820
 rheological properties, problems in extrapolation of laboratory data to tectonic processes 7-66107
 ring structures seen by remote sensing, due to jointing following earthquakes 7-54951
 rock deformation 7-47424
 Rocky Mountains, SW Alberta, Canada, duplex structures in Lewis thrust sheet 7-54989
 S Rocky Mts., USA, tectonic redefinition 7-34450
 Saint-Clement Subbrianconais Flysch, French Alps, dynamics of marine nummulitic deposits (French) 7-18182
 salt bearing formations during Palaeozoic, book 7-35137
 San Andreas fault, California, United States, fractal geometry and seismicity 7-66030
 San Andreas fault, reanal. of COCORP deep seismic refl. profile at Parkfield, California 7-54938
 San Andreas Fault, S California, evidence for 160 km offset from Triassic megaporphyritic monzogranites 7-55043
 San Andreas fault, United States, fault geometry, appl. of fractal anal. 7-66348
 San Andreas fault near Hollister, USA, electrical resistivity temporal variations 7-28840
 San Andreas fault system, S California, seismic evidence for conjugate slip and block rot. 7-14216
 S San Jacinto fault zone, California, rupture patterns and preshocks of large earthquakes 7-28854
 San Jacinto Graben, California, USA, gravity anomalies 7-54842
 San Jacinto graben California, gravity anomalies of trapezoidal model with quadratic density function 7-28819
 Saskatchewan, Canada, well water He and methane anomalies correl. with crust tectonic features 7-40440
 Saudi Arabia, ray path interpretation of crustal struct. 7-28956
 E Sayan, USSR, magmatic geology 7-23598
 S Scandinavia, seismic tomographical mapping of lithosphere and asthenosphere 7-14234
 Scotia arc, evol. and continental mag. anomalies 7-60155
 SW Scotland, Luger and other sills, age and geology 7-66013
 S Scotland, tectonic implications of Late Caledonian lamprophyre dyke swarms 7-4032
 sedimentary basin analysis (book) 7-35129
 sedimentary basins, form. mechanism rel. to He isotopic comps. 7-47405
 sedimentary basins development, heterogeneous stretching model with simple shear 7-34399
 sedimentary layer amplification of short period S-waves 7-8868
 seismic exploration, new approach to study of crustal and upper mantle struct. 7-47342
 seismic faulting, development of conjugate-shear fracture in marble (Chinese) 7-34474
 seismic faulting, tectonic stress evolution and earthquake rebound in anti-plane case 7-8821
 seismic inhomogeneities of fractal nature 7-28901
 seismic inversion of long-period regional body waves for crust struct. 7-8849
 seismic reflection surveys for deep crust anal. 7-14394
 seismic sounding, nonuniform waves propag. in space divided by thin fluid-filled fracture 7-28891
 seismic surface waves propag., phase speed perturbations and 3D scatt. effects due to topography 7-28866
 seismic velocity profiles use to determine mantle contrib. to ocean gravity field 7-54849
 seismic velocity structure, simultaneous estimation of hypocentres and velocity parameters for inclined-layer vel. model 7-14207
 seismic waves velocities mapping, resolution matrix calc. via tomographic inversion method 7-14212
 S Senegal basin, geoelectromagnetic meas. 7-47413
 Senegal basin, W Africa, geoelectric struct., MT and DGS study 7-18111
 Sette-Daban ridge, S Verkhoynay, USSR, Carboniferous basalt geology 7-23596
 shear crack in elastic medium, nonstationary radiation direction 7-54916
 shear zones in St. Barthelemy Massif, Cretaceous crustal stretching (French) 7-34433
 Shebandowan greenstone belt, Ontario, Canada, magmatism age and regional deformation 7-23585
 Shumagin Islands earthquake sequence, Alaska, 1983 February 14, focal mechanisms 7-54886
 Shumagin seismic gap, Alaska, vertical crust deform. detect. via sea level var. 7-9223
 NW Siberia, aerospace imagery of lineament zones rel. to presence of oil and gas 7-66335
 Siberia, modern dynamics of the main lithospheric tectonotypes 7-54979
 Siberia, the state of tectonic research 7-54978
 NE Siberia (Yakutia), USSR, crust evol. 7-23593
 W Siberian Plate, geology of Palaeozoic carbonate facies 7-23597
 Sierras Pampeanas of Argentina, modern analogue of Rocky Mountain foreland deformation 7-66113
 simultaneous correlation analysis of gravity, magnetic and seismic data, appl. to deep crust investigations 7-47552
 Skagerrak-Kattergat region, seismic refl. and refr. investigations 7-14233
 Solomon Islands arc, Neogene displacements rel. to geology and arc configuration 7-66082
 S Spain, crust seismic velocity struct. under Betic cordillera 7-8826
 NW Spain, seismic velocity struct. of crust 7-54936
 spatial problem soln. using repeated geodetic meas. 7-23623
 spherical shell tectonics and buckling of subducting lithosphere 7-47419
 spreading zones devel. in modern and palaeo-oceanic structures 7-34436
 Sredne-Tersa ultrabasic massif, deep structure and rock composition 7-14223
 Sri Lanka, seismicity anal. rel. to uplift of central highlands 7-23570
 S St. Helens seismic zone, Washington, earthquakes near Swift Reservoir (1958-63) 7-54885
 stable isotopes in high-temp. geological processes, book 7-35126
 strain and tilt rel. to earthquake occurrence in Kyoto, Japan 7-8864
 stress accumulation, creep and earthquake rebound 7-54914

Earth crust continued

- stress changes and fractures rel. to pre-earthquake subsurface gas comp. var. 7-8870
 stress determination from focal mechanisms 7-66072
 stress field due to faulting in presence of asperity, antiplane crack model 7-8822
 stress measurement by borehole deform. meas. using pre-pressed multi-probe unit (Chinese) 7-29259
 stress pattern in central Europe and adjacent areas 7-54947
 strike-slip duplexes 7-40457
 strike-slip faulting, role of crack-seal mechanism, in deform. process 7-29010
 subcontinental lithosphere evolution, implications of trace element and isotope geochemistry of Eifel periodotite xenoliths 7-34484
 subducting lithospheric slabs, thermal vel. models rel. to teleseismic mislocation of island arc earthquakes 7-14209
 subduction zones, dynamics of sediment subduction, melange formation, and prism accretion 7-28967
 submarine accretionary wedges, evidence from Barbados for origin of convex wedges 7-28992
 Sunda Arc, seismic history and seismotectonics 7-65952
 Superstition Hills fault, California, surface displacement triggered by Westmorland earthquake (1981 April 26) 7-3983
 surface faulting in Rainbow Mountain-Fairview Peak-Dixie Valley (Nevada) earthquakes, 1954-59, appl. to seismic processes anal. 7-40429
 Svecofennian fold belt of SW Finland, tectonic environment of Proterozoic mafic volcanic rocks 7-14275
 Taconic arc-continent collision, geological evidence for plate convergence rate 7-28966
 tangential tectonic and carboniferous thrusting in leucogranites, French Central Massif (French) 7-66055
 tectonic evolution of Earth's crust, evidence from new geological developments (Russian) 7-60254
 tectonic features and geomag. obs. from balloons 7-47574
 tectonic setting of sandstone-mudstone suites, determ. using SiO₂ content and K₂O/N₂O ratio 7-29014
 tectonic stratification, evidence from oceanic expeditions (Russian) 7-66076
 Tengchong geothermal field region, China, tectonics, thermal springs and active structures 7-60219
 Tengchong volcanic-geothermal region, China, crust thickness and stress charact. (Chinese) 7-54875
 S Texas, evolution of seismic barriers and asperities caused by fault planes depressing in oil and gas fields 7-3982
 thermoelastic strain in half-space covered by unconsolidated material, prediction technique 7-29001
 thickness determ. method using postglacial uplift data 7-34440
 thinning of lithosphere, thermomechanical destabilization models 7-34456
 Tibet, lower crust seismic velocity struct. 7-18120
 Tibetan Plateau, 1985 Chinese/British expedition results 7-8913
 Tibetan Plateau, rise, continental underplating model 7-40454
 tidal tilt, strain and displacement meas., effects of surface topography 7-54851
 S Tien Shan, greenschist metamorphism conditions and geotectonic evol. model 7-34401
 Tien-Shan region, isostatic gravity anomaly from isostatic compensation models 7-28965
 Tomioka, Fukushima, Japan, borehole logging of crust and seismic wave amplification (Japanese) 7-18115
 Tonga-Kermadec island arc, tectonic struct. from earthquake mechanisms 7-8823
 Tornquist-Teisseyre zone (Poland), deep crustal struct. in contact zone of Palaeozoic and Precambrian platforms 7-14235
 Transantarctic Mountains-Ross Embayment region, asymmetric extension and assoc. uplift and subsidence 7-40453
 Transbaikai, USSR, magnetovariational study of crust and upper mantle 7-14179
 Transylvanian Depression, struct. and morphology (Rumanian) 7-8891
 Troodos microplate, Cyprus, palaeorotation in Meso-Cenozoic plate tectonic framework of E Mediterranean 7-34441
 two-layer model, investigation of biaxial extension of lower layer 7-8886
 two-layer planet with Burgers-body mantle, moment of inertia, effect of faulting 7-14509
 Tyrmayaz ore field Front Range, N Caucasus, structural development 7-34438
 United States, crust struct., Magsat data anal. 7-47411
 SW United States, geochemistry and tectonic setting of Early Proterozoic supracrustal rocks 7-55037
 trans-Ural marginal downwarp, numerical interpretation of regional mag. anomaly 7-29279
 Ural Mountains, Precambrian geodynamic regimes 7-34494
 S Urals, USSR, lithosphere heat flow, struct. and evolution model 7-23608
 S Urals and N Caucasus, structure and tectonic evolution 7-8906
 central Urals region, USSR, crust struct. and ore prospecting multi-wave seismic obs. 7-23549
 USA, lignite deposits of Texas to Georgia region 7-18139
 USSR, ore deposits charact. (Russian) 7-40478
 Verkhoynay folded zone, eastern USSR, fault dislocations and petroleum prospect 7-28918
 Vermilion granitic complex, NE Minnesota, USA, multiple folding and pluton emplacement 7-65990
 vertical crust motion meas. by VLBI, effects of atm. water vapour 7-9227
 vertical crustal deformation assoc. with 1979 Imperial Valley (California) earthquake, implications for fault behaviour 7-54929
 vertical motion, use of GPS meas. 7-8795
 vertical motion meas. by mobile VLBI and GPS, effects of atm. water vapour 7-9226
 vertical motions, obs. with portable absolute gravimeter 7-9225
 Washington continental margin, crustal struct. from seismic refr. data 7-4006
 Western Australia, relations between Archaean high-grade gneiss and granite-greenstone terrain 7-34491
 Wopmay Orogen in Canada, geology of metamorphic internal zone 7-54998
 Xianshuihe Fault Zone, S China, seismic activity estimation via earthquake activity parameters (Chinese) 7-34387
 Xikang-Yunnan continental palaeorift zone, China, Curie isotherm depths determ. from geomag. obs. (Chinese) 7-28914

Earth crust continued

- Yakataga seismic gap, S Alaska, strain accumulation 7-14246
 Yinchuan graben, N China, seismicity rel. to fault scarps produced by AD 1739 earthquake 7-28859
 Yunnan Province, China, crustal struct., seismic refr. profiles anal. 7-40446
 Zabargad Island, struct. and Red Sea rifting 7-66034
 Zambia, provisional metamorphic maps and explanatory notes 7-18184
 E Zambia, Rb-Sr studies of metamorphic and igneous events 7-18147
 N Zeravshan faults, USSR, tectonic movements indicated by river drainage pattern 7-66070
 Zyoso Terrace, Japan, ELF magnetotelluric surveying (*Japanese*) 7-23604
 Au placer deposits in upper Yukon River, Alaska 7-66042
 O₂ transport in dry rocks, exptl. study 7-54954
 Os isotopic comp. of crustal material, determ. by accelerator mass spectrometry 7-23611

Earth electricity *see terrestrial electricity***Earth heat** *see terrestrial heat***Earth interior** *see Earth structure***Earth magnetic field** *see geomagnetism***Earth magnetic field variations** *see geomagnetic variations***Earth mantle**

- 3D structure and free-oscillations spectra splitting 7-60187
 N America, deglaciation-induced vertical motion and transient lower mantle rheology 7-8912
 anisotropic flow in layered asthenosphere 7-60209
 apatite, decomposition to dense polymorph of Ca₃(PO₄)₂ for mantle conditions 7-44796
 Archaean continent formation and anomalous sub-continental mantle link, mineralogical anal. 7-47408
 Archaean mantle, contrib. of melting to lithosphere stabilisation and heat loss 7-34398
 asthenosphere composition, geochemical correl. between southern African kimberlites and S Atlantic hotspots 7-34409
 N Atlantic, upper mantle seismic velocity inhomogeneities 7-54920
 N Atlantic Ocean, convective upwellings location rel. to residual geoid anomalies 7-28814
 Baijing-Beigzhuang profile, magnetotelluric data inversion via continuous resist. var. model (*Chinese*) 7-34375
 Baikal-Amur Main Line, USSR, elec. struct., mag. var. profiling anal. 7-23527
 basal dregs, interaction with convection rel. to lateral heterogeneity at core-mantle boundary 7-66022
 basalt magma sources, noble gas systematics for Reunion and Grand Comore Islands 7-29012
 brittle failure of upper mantle during continental lithosphere extension 7-18173
 N California, USA, mantle struct. and teleseismic P-wave residuals azimuthal var. 7-66031
 Cameroon Adamawa region, crust mantle seismic velocity structure 7-8839
 Cape Verde Rise, in N Atlantic, heat flow anomaly and geoid indicating mantle plume support 7-47396
 carbonates in mantle-derived xenoliths in kimberlite pipes 7-34408
 Carpathian Mountains, USSR, geomag. anomaly and geoelectric model 7-40411
 chemical heterogeneities origin 7-66315
 E China, continental lithosphere contrib. to isotope systematics and chemistry of Cretaceous basalts 7-29011
 SE China, high-conductivity layer depth determ. (*Chinese*) 7-34374
 N China, seismic tomography (*Chinese*) 7-28912
 continental rifting, thermomechanical models of active rifting 7-14247
 convection, geoid anomalies and topography 7-28971
 convection, rheology and struct. of olivine-basalt partial melts 7-8931
 convection in mantle, analytical soln. of 2D convection problems 7-8910
 convection in mantle and terrestrial heat flow, Nusselt number calc. 7-47398
 convection in spherical shell, onset of time-dependence 7-60212
 convection models, boundary condition effects, numerical study 7-23613
 convection under oceans and continents 7-54952
 convective mixing, effects of chemical density differences 7-28969
 core interface depression and Indian Ocean geopotential hours 7-47412
 core-mantle boundary, evidence against 2 to 50 km size corrugations from PcP amplitudes 7-66018
 core-mantle boundary, evidence for aspherical struct. from PKP' travel times 7-66017
 core-mantle boundary, mantle heterogeneity scales from ScS-S differential travel times 7-66019
 core-mantle boundary topography, determ. from geoid anomalies 7-66021
 core-mantle boundary topography and liq. core lateral heterogeneity, results from travel-time residuals 7-66036
 core-mantle separation, implications of Fe-H₂O reaction under high press. 7-8887
 coupling with core dynamo, thermal and topographic coupling models 7-65933
 cratonization and mantle thermal evolution 7-23622
 Crimea-Romania, lithosphere struct. along Geotraverse V 7-60207
 Crozet Plateau in Indian Ocean, anomalous heat flow and mantle convection 7-8879
 D'' layer stability 7-18143
 D'' zone (basal mantle layer), revised thermal cond. rel. to thermal boundary layer model 7-66020
 deep mantle seismic discontinuities, broadband records anal. 7-47401
 degassing and structure from basaltic glass N isotope geochemistry 7-60193
 diapiric structures, relation between initial conditions and late stage of Rayleigh-Taylor instabilities 7-66108
 diapirs evolution, effects of comp. and thermal buoyancies 7-8890
 diatreme phenomena responsible for volcanoes, fountains continental motion, etc. 7-34420
 East European Platform seismic model of lithosphere beneath Baltic Sea-Black Sea profile 7-14236
 electrical conductivity, effects of sample-electrode interface polarisation on props. of partially molten rock 7-8932
 electrical conductivity of olivine undergoing creep 7-18180
 equilibrium distrib. of two-phase system in grav. field 7-34404
 N Eurasia, seismic velocity structure of lower lithosphere and asthenosphere 7-8857
 Eurasia northern shield areas, mantle Q depth and freq. depend. 7-54906

Earth mantle continued

- Eurasia shield area, seismic quality factor freq. depend. 7-54904
 Europe, combined geophysical-thermal models of crust and upper mantle 7-28933
 W Europe, upper mantle vel. and density struct. from higher-mode surface-wave meas. 7-14237
 flows and plate motions 7-18171
 fluid dynamics, soln. of Rayleigh-Taylor problem 7-66084
 French Massif Central, inverse problem for bounds on mantle heat flow 7-28953
 geochemical heterogeneities and deep subduction 7-66039
 geochemical isotopic heterogeneity with different size scales 7-8889
 Hawaiian plume, melting model for origin of Hawaiian lavas 7-8943
 heat flow, inverse problem for limits determ. 7-28953
 heat flow estimation at lower boundary of Earth's crust, methods for 2D geothermal models 7-18155
 heat transfer, 2D model 7-54940
 homogenisation by convective mixing and diffusion 7-66009
 Indian Shield and Tibetan Plateau, mantle seismic velocities and tectonics 7-8838
 intermediate mantle zone structure, effects of chemical and phase transitions (*Russian*) 7-66038
 island arc magmagenesis, implications of geochemistry of lavas from Okmok volcano, central Aleutians 7-28949
 NE Japan arc, 3D seismic velocity struct. of subduction zone 7-18128
 NE Japan arc, oceanic plate bending rel. to normal faulting events in deep seismic zone 7-14211
 Japan-Arc area, upper mantle seismic velocity structure 7-8840
 Kamchatka, increased elec. conductivity layer in crust and upper mantle 7-54868
 Central Karelia, magnetotelluric sounding in 10⁻³ to 10⁴ s period interval 7-28829
 Kiev-Gomel' DSS profile, struct. of deep crustal layers and sedimentary cover 7-47394
 Liaohe Basin, China, mantle heat flow (*Chinese*) 7-28913
 lithosphere thinning under conditions of large heat flows, numerical study 7-28928
 low-pressure metamorphic belt form., role of plutonism 7-28975
 lower mantle velocity structure, evidence for shear vel. discontinuity in S and sS phases 7-66016
 lower mantle velocity structure, role of wave propag. effects in inhomogeneous mantle 7-66015
 lowermost mantle, seismic lateral heterogeneity and convection 7-8841
 magma ascent by porous flow, role of magmas 7-8928
 magma-rich zones, buoyancy-driven instabilities of low-viscosity zones 7-8930
 lowermost mantle, seismic velocity and Q-struct., teleseismic study 7-34392
 Mariana Trough region, mantle characts. determ. from basalt glass noble gases anal. 7-40436
 melt segregation driven by dynamic forcing 7-60210
 metal-silicate fractionation in growing Earth, energy source for magma ocean 7-8888
 Mid-Atlantic Ridge, seismic reflections below upper mantle discontinuities 7-60179
 Mid-Atlantic Ridge, three-component isotropic heterogeneity near Oceanographer transform 7-54956
 Moho seen on seismic refl. profiles, flatness as artefact of isostatic compensation 7-60176
 Murmansk block, Kola Peninsula, magnetotelluric sounding in 10⁻³ to 10⁴ s period interval 7-28829
 central New Hebrides Island Arc, seismicity patterns assoc. with asperity complex 7-40427
 ocean, gravity field, mantle component calc. from crust seismic vel. profiles anal. 7-54849
 oceanic crust-mantle boundary, 2D seismic refl. modelling of fossil transition in Bay of Islands Ophiolite 7-40428
 oceanic upper mantle, effective mag. suscept., Magsat data anal. 7-47331
 Okhotsk Sea, lower mantle slab penetration indicated by teleseismic data 7-54923
 Outer Hebrides, evidence for enriched lithospheric keel, mantle xenoliths comp. anal. 7-47407
 P-wave travel times, estimation of slowness-dependent source and receiver corrections 7-54893
 S Pacific, seismic anisotropy of oceanic lithosphere 7-47352
 Pacific Ocean, deep magnetovariation sounding curve determ. using continuum spectrum method 7-40569
 Pacific plate subduction beneath central Alaska, seismic evidence for down-dip tension 7-28855
 partial melting, connectivity of melt phase in partially molten peridotite 7-8924
 partial melting, effect of water saturation on partial melt distrib. in olivine-pyroxene-plagioclase system 7-8925
 partial melting phenomena in Earth and planetary evolution, conference, Eugene, Oregon (September 1984) 7-4625
 peridotite melting under ultrahigh pressure 7-34481
 peridotitic upper mantle origin, implications of melting of dry peridotite up to 14 GPa 7-8937
 S Peru, 3D P- and S-wave vel. structures rel. to tectonics 7-14227
 plate-scale flow, stirring and mixing, blobs and tendrils 7-60213
 plumes and origin of Samoa 7-60229
 plumes dynamics, relation to periodicity of mag. field reversals 7-65934
 pristine mantle composition analysis, implications for Earth accretionary history 7-40390
 proto-mantle differentiation in accreting Earth, effects of atmosphere form. on thermal history 7-54840
 Provencal Basin (W Mediterranean), mantle heat flow rel. to geothermal data from surrounding Hercynian basement 7-14239
 Provencal Basin (W Mediterranean Sea), effects of subcrustal heat flow distrib. on thermal regime 7-14238
 pyrope (Mg₃Al₂Si₂O₁₂), melting up to 10 GPa rel. to press.-induced struct. change in pyrope melt 7-8936
 rare gases rel. to evolution and structure 7-60386
 rheological properties, problems in extrapolation of laboratory data to tectonic processes 7-66107
 Roberts Victor eclogites, ¹⁸O/¹⁶O ratios rel. to ancient oceanic crust hypothesis 7-55042
 rotational variations and nutation of Earth rotation, influence of mantle anelasticity 7-23512
 S-wave velocity anomalies in lower mantle, evidence from SKS and SKKS waves from Tonga-Fiji events 7-65945

Earth mantle continued

- S Scandinavia, seismic tomographical mapping of lithosphere and asthenosphere 7-14234
 Scotland, Caledonian Pb isotope geochemistry and mantle source 7-23590
 Sea of Okhotsk, lower mantle slab penetration, broadband S-waves anal. 7-47416
 seismic anisotropy due to crystallite partial alignment 7-60175
 seismic anisotropy of upper mantle, mineral alignment model 7-28893
 seismic body wave amplitude fluctuations modelling, appl. of 3D slowness method 7-40426
 seismic discontinuity at 400 km and olivine in upper mantle 7-47404
 seismic exploration, new approach to study of crustal and upper mantle struct. 7-47342
 seismic quality factor of upper mantle beneath Eurasian shield 7-54905
 seismic velocity struct. of core and mantle 7-54925
 seismic waves in low-velocity layer of mantle 7-8851
 seismic waves propagation, appl. to internal struct. determ. (French) 7-23588
 seismic waves velocities mapping, resolution matrix calc. via tomographic inversion method 7-14212
 S Senegal basin, geoelectromagnetic meas. 7-47413
 Senegal basin, W africa, geoelectric struct., MT and DGS study 7-18111
 Seychelles microcontinent, mantle evolution and magma-crust interaction 7-40452
 Sierra Leone submarine Rise, Atlantic Ocean, sedimentary mantle and basement struct., seismic anal. 7-23607
 spherical Earth model mag. field, mantle appl. (German) 7-8796
 stable isotopes in high-temp. geological processes, book 7-35126
 subcontinental lithosphere evolution, implications of trace element and isotope geochemistry of Eifel peridotite xenoliths 7-34484
 subcontinental mantle, thermal evol., implications of eclogite equilibration temps. and origin depths 7-28955
 subducting lithospheric slabs, thermal vel. models rel. to teleseismic mislocation of island arc earthquakes 7-14209
 tectonic spread of anomalous mantle beneath lithosphere, causing topography changes 7-54982
 tectonics mantle transient rheology and glacial isostasy 7-28970
 thermal convection in Earth interior, review (French) 7-23618
 thermal core-mantle interactions 7-54960
 Tien-Shan region, isostatic gravity anomaly from isostatic compensation models 7-28965
 time-dependent layered mantle convection, high spatial resolution models 7-18145
 Tonga subduction zone, upper mantle P-wave vel. 7-65946
 Tonga subduction zone area, S-wave splitting in upper mantle wedge 7-47355
 Transbaikai, USSR, magnetovariational study of crust and upper mantle 7-14179
 transient lower mantle rheology and post-glacial rebound 7-18170
 two-component marble cake mantle 7-4010
 Tydemian fracture in N Atlantic seismic study of crust and mantle 7-8844
 Tyrrhenian Sea region, subduction zone geometry and stress patterns 7-28976
 Ultramafic Series of Stillwater Complex, Montana, rare earth element evidence for mantle magmas origin 7-65987
 velocity structure from Sp diffraction beneath Australian Shield 7-14206
 viscosity estimates for mantle 7-60237
 viscosity of mantle, transient creep calc. using generalized Maxwell bodies 7-54980
 viscosity of partial melts in upper mantle, exptl. and theoretical results 7-8934
 Wellington region, New Zealand, anal. of Sp and Ps phases from microearthquake survey 7-28863
 xenoliths, kinetics of partial melting and dissolution 7-8944
 young oceanic lithosphere, thermal model 7-18177
 He isotopes in sedimentary basins, mantle component rel. to basin form. mechanism 7-47405
 K-rich lamprophyres of S Scotland, mantle melting model and tectonic implications 7-4032
⁴⁰K/K ratio in lower mantle, implications of K-Ar isochron dating of Zaire cubic diamonds 7-23612
 Mg₂SiO₄-MgSiO₃ system, melting and phase relations at 20 GPa under hydrous conditions 7-8935
 O₂ transport in dry rocks, exptl. study 7-54954
 Pb isotope evolution rel. to Earth core growth, implications of siderophile and chalcophile abundances in oceanic basalts 7-34397

Earth orbit

- parameter changes, effect on climate simulations 7-29236
 secular perturbations due to polar flattening of Sun, theory 7-29452
 Venus/Earth orbital resonance, contrib. to recurrent phenomena of Venus 7-66489

Earth rotation

- acceleration determ. from anal. of lunar occultations of stars (AD 186-567) (Chinese) 7-3963
 angular velocity as function of orbital elements of Moon and Sun 7-3965
 atmosphere zonal tides, influence on Earth's rot. rate (Chinese) 7-4073
 S Australia, Precambrian perigial varivites, palaeomagnetism, palaeoaltitude and palaeoclimate 7-8798
 Chandler wobble, effects of oceanic pole tides on period 7-8969
 Chandler wobble dissipation by ocean pole tide resonances 7-47445
 chandler wobble excitation, role of global water storage 7-60151
 Chandler wobble quality factor (Chinese) 7-3962
 core rotation rel. to C₂₁ and S₂₁ geodetic gravity coeffs. 7-47399
 core westward drift and Earth rotation rel. to secular geomagnetic changes 7-23515
 day length (1657-1984) 7-23516
 day-length variations, correl. with spline representation of geomag. temporal change 7-14185
 day-length variations, effects of linear trend and mean value on maximum entropy spectral analysis 7-29305
 determination of Earth rotation parameters, appl. of lunar laser ranging data (Chinese) 7-3959
 determination of Earth rotation parameters, optimal conditions (Chinese) 7-3960
 diurnal rotation rate, source of nonlinear fluctuations 7-14176
 dynamical flattening, implications for normal density Earth models 7-18154
 dynamo problem and mag. fields turbulent transport 7-60511

Earth rotation continued

- dynamo theory, role of fluctuations 7-60512
 elastic deformation of lithosphere 7-54945
 extraterrestrial object impacts and triggering of geomagnetic reversals, mechanism involving Earth rotation changes 7-40413
 geomagnetic variations, due to influence of Sun on Earth's liquid core 7-34382
 global vorticity and rotation of deformable Earth 7-60152
 inner core rotation, implications of seismic anisotropy inferred from PKIKP travel times 7-66024
 intradiurnal nonuniformity, cosmic radiation effects 7-28809
 LAGEOS laser ranging and Earth rot. parameters derivation 7-14178
 LAGEOS satellite Earth rotation parameters meas. anal. 7-40398
 lunisolar precession-nutation with time-varying second zonal harmonic, dynamical theory 7-28810
 mantle anelasticity influence on nutation and rotational variations 7-23512
 moment of inertia determ., non-tidal angular acceleration 7-54853
 North Sea, pole tide dynamics 7-18195
 nutation of Earth core, possible detection 7-23513
 palaeorotation since Silurian period, and Earth shape and gravity field 7-23511
 parameters accuracy, estimation in different freq. bands 7-54843
 parameters determ. from six techniques, comparison (Chinese) 7-29247
 parameters determination, atm. limitations on accuracy 7-60412
 Paris Observatory APP 1985 meas. and time and latitude (French) 7-60509
 peculiarities and tidal effects (Russian) 7-40397
 proto-Earth contraction, implications for rot. and origin of Earth-moon system 7-23509
 shifting date line, interesting feature of solar calendar 7-9362
 techniques for determ. of rotation parameters, comparison (Chinese) 7-29246
 tidal deceleration of Earth rot. and lunar mean motion, theoretical estimates 7-18348
 tidal energy dissipation, comparison between astronomical and geophysical estimates 7-14301
 tidal torques, components determ. independently of Earth internal density distrib. 7-18107
 Tokyo Astronomical Obs., Time and Latitude Bulletins (April to June 1986) 7-23977
 Tokyo Astronomical Obs., Time and Latitude Bulletins (July-September 1986) 7-55433
 two-layer planet with Burgers-body mantle, moment of inertia, effect of faulting 7-14509
 universal time determination, current accuracy 7-56211
 variation measurement (French) 7-23518
 velocity variations, correl. with global activity of large earthquakes (Chinese) 7-34386
 VLBI obs. of Earth rot. parameters (Chinese) 7-29248
 wobble, VLBI obs. 7-55325

Earth structure

- see also *Earth core; Earth crust; Earth mantle*
 accumulation of Earth and initial state, dynamical model 7-34367
 aspherical structure, contrib. to anomalous splitting of seismic multiplets 7-28892
 core-mantle boundary, evidence against 2 to 50 km size corrugations from PCP amplitudes 7-66018
 core-mantle boundary, evidence for aspherical struct. from PKP' travel times 7-66017
 core-mantle boundary, lateral heterogeneity due to interaction of mantle dregs with convection 7-66022
 core-mantle boundary, mantle heterogeneity scales from ScS-S differential travel times 7-66019
 core-mantle boundary topography, determ. from geoid anomalies 7-66021
 core-mantle boundary topography and liq. core lateral heterogeneity, results from travel-time residuals 7-66036
 core-mantle separation in accreting Earth, effects of atmosphere form. on thermal history 7-54840
 D* zone (basal mantle layer), revised thermal cond. rel. to thermal boundary layer model 7-66020
 density distribution, choice of norm 7-18106
 expanding Earth and plates motion fossil data anal. 7-47418
 free oscillations, eigenfrequencies first order asymptotics 7-18116
 free oscillations, generation by localised source in viscoelastic inhomogeneous Earth 7-28887
 free oscillations of Earth, for slightly anisotropic Earth 7-23554
 free-oscillations spectra splitting and Earth 3D struct. 7-60187
 heat conduction within elastic Earth, temp. profile and radial deform. 7-23592
 inertial moments, evidence for decrease from tidal deceleration of Earth and Moon 7-18348
 inner core, search for lateral heterogeneity from differential travel times near PKP-D and PKP-C 7-66026
 internal structure, determ. by seismology, methods and results (French) 7-23588
 internal structure of Earth, evidence from new geological developments (Russian) 7-60254
 laterally heterogeneous Earth models, asymptotic normal modes 7-40425
 Love numbers of Earth tides, harmonic anal. of strain tidal data in Shanghai City (Chinese) 7-34368
 lower mantle velocity structure, evidence for shear vel. discontinuity in S and sS phases 7-66016
 magma ocean, energy source from metal-silicate fractionation in growing Earth 7-8888
 lower mantle S-velocity struct., evidence from anomalous difference travel times and amplitude ratios of SKS and SKKS waves 7-65945
 mantle velocity structure, modelling of body wave amplitude fluctuations via 3D slowness method 7-40426
 lower mantle velocity structure, role of wave propag. effects in inhomogeneous mantle 7-66015
 normal density Earth models, constraints of external gravit. field and dynamical flattening 7-18154
 palaeorotation since Silurian period, and Earth shape and gravity field 7-23511
 Precambrian continental crust, struct., comp. and evolution from deep drillholes in USSR 7-34413
 seismic velocity structure, effects of focusing on amplitudes at antipode 7-28864

Earth structure continued

- TeV neutrino beams, physical bases and geophysical appls., review 7-40587
- viscoelasticity, absorption effects on plane waves in layered media 7-28868
- wave reflectors and sources detection 7-23562

Earth surface processes *see geomorphology***earthring**

- escalating arcing ground fault phenomenon, effect of preventative solns. on equipment specifications 7-51530
- textile industry, conf., Charlotte, NC, USA (May 1986) 7-29594

earthquake recorders *see seismometers***earthquakes**

- 1977 global seismicity, centroid-moment tensor solutions 7-47379
- N Aegean, seismic activity as middle-term precursor of Calabrian earthquakes 7-23582
- West Africa, seismicity (1615-1984) 7-54878
- large aftershock prediction, based on prior aftershock activity 7-28850
- central Alaska, seismic evidence for down-dip tension in Pacific plate 7-28855
- W Alaska, seismicity studies synthesis 7-28907
- W Alps, prediction of places for strong earthquakes 7-65973
- Amazonian foothills of Peruvian Andes, seismicity and tectonic activity 7-47373
- Andaman-Nicobar Islands, earthquakes focal mechanisms rel. to plate tectonics 7-65962
- Andreanof Islands, 1986 May 7 source parameters 7-60178
- Annual Review of Earth and Planetary Sciences 7-9606
- Anza, California, USA, seismicity and source parameters rel. to crustal stress 7-65951
- Anza, S California, rupture characts. and tomographic source imaging of $M_1 \sim 3$ earthquakes 7-40431
- Arctic mid-ocean ridge, focal depths and mechanisms of large quakes 7-54926
- SE Asia, earthquake focal mechanisms and crustal stress 7-14197
- Central Asia, precursory seismicity to strongest earthquakes 7-65969
- atmospheric temperature anomaly for prediction 7-28897
- Bali Basin, tectonic origin, anal. of gravity, bathymetry and earthquake data 7-66073
- Banda Arc subduction zone structure from earthquake depths 7-54981
- Bhatsa reservoir, Maharashtra, India, induced seismicity anal. 7-23578
- NW Bohemia, Czechoslovakia, microseismicity 7-54912
- Bulgaria, electric potential anomalies as earthquake precursors 7-65930
- Caliente (Nevada), August 1966, regional data rel. to seismic discrimination capabilities of short-period phases 7-3989
- California, borehole seismograms from Long Valley rel. to caldera struct. 7-40448
- California, groundwater Rm as earthquake fluid phase precursor 7-40424
- S California, mechanisms for 1930 Santa Monica and 1979 Malibu earthquakes 7-54883
- California, San Andreas and Calaveras faults, H_2 due to fault strips and earthquakes 7-40438
- California, seismic hazard anal. from props. of Quaternary faults 7-40430
- California, seismic risk anal. and appl. to North Sea 7-4004
- S California, USA, forecast model for large and great earthquakes 7-54922
- S California, USA, prediction of strong earthquakes, probabilistic approach 7-3997
- N California Coast Ranges, local earthquake arrival times inversion for 3-D vel. struct. determ. 7-3987
- Campania, S Italy, 21 August 1962 earthquakes 7-47354
- carbonate platform stratigraphy as record of past earthquakes 7-8859
- E Carpathians Arc Bend, Romania, tectonic movements depth and age rel. to seismicity 7-28987
- catalogue of worldwide earthquakes, software for data bank 7-65975
- Great Caucasus, USSR, gravity anomalies for earthquake prediction 7-65971
- centroid-moment tensor solns. (for October-December 1985) 7-14213
- Centroid-moment tensor solutions (1986 January-March) 7-47378
- Chiba-Ibaraki, Japan, focal mechanism of 4 Oct. 1985 event 7-65984
- Chile, 1985 March 3, source characts. 7-47371
- central Chile, 3 March 1985 great earthquake and earthquake occurrence 7-4001
- Chile, interplate coupling rel. to temporal vars. of mechanisms of intermediate-depth earthquakes 7-54888
- Chilean earthquake of 3 March 1985, rupture process 7-8848
- N China, appl. of order clustering methods to seismogenic process of strong earthquakes (Chinese) 7-34384
- China, crustal stress state in epicentral area after earthquake (Chinese) 7-34396
- N China, hypocentres relocation (Chinese) 7-28912
- N China, implications for seismicity of magnetotelluric data inversion (Chinese) 7-34375
- China, seismic activity anal., use of fluid-geochem. methods 7-40421
- Colombia, 1979 December 12, aftershocks, source mechanisms using digital surface-wave data 7-54887
- crustal earthquake instability in relation to the depth variation of frictional slip properties 7-14226
- crustal tilt anomaly patterns assoc. with earthquakes, features and classification (Chinese) 7-34388
- crustal-strain sand tilt rel. to earthquake occurrence in Kyoto, Japan 7-8864
- damage to buildings, analysis by OR techniques 7-60169
- data acquisition system (MIPEX) for seismic reflection profiling (Japanese) 7-55265
- depth determination methods, review 7-54933
- detection and recording by small seismograph networks, results from SNARE system 7-28873
- Dunaharaszti, Hungary, 12 Jan. 1956 event near Budapest 7-28844
- eastern USA, earthquake source scaling relations, nuclear plant safety appl. 7-36236
- El Asnam, Algeria, 1980 October 10 rel. to Cheliff basin seismotectonics 7-28906
- EM emission during seismic activity, crustal mechanical-electric convertors model 7-8856
- NW Europe, contemporary seismicity and tectonics 7-28848
- central Europe, earthquake props. and fault characts. 7-54911
- fault formation mechanism in viscoelastic medium 7-23545

earthquakes continued

- fault rupture determ. method, by principal parameter analysis of aftershocks 7-8828
- fault rupture model, propagation of brittle failure 7-18121
- faulting predictability, slip events along a laboratory fault 7-40419
- faulting process, effect of gouge and surface roughness 7-65957
- focal depths dependence on lithosphere struct. and physical props. 7-54910
- focal mechanisms use for stress determination 7-66072
- focal regions, physics and geodynamics of deform. processes, conf., Potsdam, East Germany (November 1985) 7-48140
- forecasting earthquakes in Japan (French) 7-60188
- Fourier analysis for computation of focal mechanisms 7-18131
- fracture mechanics, for shear crack quasistatic extension in viscoelastic media 7-54902
- frequency-apparent magnitude relations 7-8827
- Friuli, Italy, focal parameter determ. from seismicity and geodetic data 7-8829
- Friuli area, Italy, crustal deform. and 1976 earthquakes 7-54948
- Friuli earthquake of 1977, Italy, fault rupture determ. from aftershocks 7-8828
- Garm region, Central Asia, seismicity rel. to deform. in zone of continental convergence 7-28847
- geodetic precursor, solid Earth tide tilt and strain near to dilatant region 7-3996
- geomagnetic pulsations excited during strong earthquakes 7-14417
- global activity of large earthquakes, statistical characts. (Chinese) 7-34386
- global seismic activity, correl. with Sun's motion around solar system barycentre 7-18127
- S Great Basin, Nevada, local stress field determ. from earthquakes focal mechanism 7-54884
- Greece, precursory seismic electric signals and source dynamic parameters 7-65961
- ground motion intensity, index for meas. of effects of topography 7-14201
- Guerrero gap, Mexico, seismic prognosis rel. to Michoacan earthquake (1985 September 19) 7-18126
- Gulf of Corinth (Greece), 1981 February 24 7-8824
- Hawaii, earthquakes of regular occurrence and earthquake prediction 7-65958
- hazard and prediction, conf., Tokyo, Japan (1985) 7-60859
- Hebgen Lake, 1959, postseismic viscoelastic relaxation 7-14245
- Hellenic Arc, prediction of strong shocks using Bayesian discrete distrib. 7-54935
- Himalayan-Andaman Arc, earthquakes rel. to deformational structs. (seismites) in Holocene sediments 7-66120
- hypocentre location errors appraisal, complete approach for single-event locations 7-54892
- hypocentres and velocity parameters, simultaneous estimation for inclined-layer velocity model 7-14207
- Imperial Valley (California), 1979, assoc. vertical crustal deform. and implications for fault behaviour 7-54929
- India region, earthquake return periods 7-28898
- SW Indian Ocean Ridge, seismic activity and faulting 7-47370
- Indonesia, 1977 August 19, focal process 7-54913
- induced earthquakes in Zhelin reservoir, E China, focal mechanisms 7-23571
- induced seismicity, IASPEI symposium, Hyderabad, India (1984) 7-18484
- induced seismicity near Charvak reservoir, USSR, statistical anal. and mathematical models 7-23576
- induced seismicity of Indian coal-mines, field investigations 7-23568
- Iran-Afghan region, precursory seismicity to strongest earthquakes 7-65968
- NE Iraq, earthquake activity in Lesser Zab region 7-14218
- island arc earthquakes, teleseismic mislocation determ. from 3D ray tracing 7-14209
- Israel, seismic activity (for 1984) 7-47382
- Japan, earthquake prediction research (1978 to 1986) 7-4000
- NE Japan, probability of future large earthquake based on current seismicity 7-8847
- Japan, seismicity changes assoc. with impounding of major artificial reservoirs 7-23569
- NE Japan arc, normal faulting events in upper plane of deep seismic zone 7-14211
- Japan Sea (1983 May 26), rupture process determ. via waveform inversion method 7-54889
- mid-Japan Sea earthquake, source characts. of 26 May 1983 event 7-18134
- Japan Sea earthquake of 1983, aftershock spatial distribution 7-65953
- Japan Sea earthquake of 1983, focal process (Japanese) 7-8831
- Japan Sea earthquake of 26 May 1983, anomalous aftershocks 7-65982
- Kinki district, Japan, shear wave splitting above earthquakes 7-47381
- Kisakata, Japan, seismic intensity and tsunami of AD 1804 earthquake (Japanese) 7-28852
- Konda fault, Osaka Plain, Japan, displacement caused by 1510 earthquake 7-8863
- Kulyab, Tajikistan, USSR, earthquakes due to active salt doming 7-47372
- S Kuril Islands, space-time distrib. and focal mechanisms of lithospheric earthquakes 7-28885
- Kyoto, Japan, earthquake occurrence possibility, from geodetic observations 7-65954
- Lake Oroville, California, reservoir-induced seismicity rel. to August 1975 earthquake sequence 7-23574
- lake sediments as method for determining occurrence of past earthquakes 7-3993
- Lesser Zab region, NE Iraq, earthquake activity 7-14218
- location method for earthquake hypocentres, using nonlinear inversion scheme 7-23859
- lunar periodicity in great earthquakes (1950-65) 7-60184
- magnitude frequency b-values for earthquakes, unbiased estimation 7-23565
- magnitude-frequency relation generalisation 7-8860
- magnitudes, seismicity and detectability, study using global network 7-54890
- mechanisms 7-60251
- Mediterranean-Asiatic seismic belt, earthquake foci and stress state 7-54915

earthquakes continued

- Mexico City, 19 Sept. 1985 earthquake and survey of damage to buildings (*Japanese*) 7-4002
- Mexico City, appl. of Bayes theorem to prediction of inter-arrival times of strong earthquakes 7-14210
- Mexico earthquake, 1985, building foundations and soil response characteristics (*Japanese*) 7-28904
- Michoacan (Mexico), 1985 September 19, strong ground motion anal. 7-18126
- microearthquakes of Gobles oil field area, SW Ontario, evidence for pumping-induced seismicity 7-28856
- microtremors, 1 to 5-second, in San Fernando Valley, California, 2D study of site effects 7-54898
- Miramichi (New Brunswick) earthquake sequence, January-March 1982, GRF broad-band array anal. 7-54921
- Multan (Pakistan), shear vel. struct. of W Ganga Basin (India) rel. to oceanic crustal block 7-54939
- Mygdonian graben, Greece, struct., microearthquake data anal. 7-66010
- Nagano, Japan, $^3\text{He}/^4\text{He}$ ratio anomalies in hot spring gases, assoc. with 1984 September 14 earthquake 7-40422
- W Nagano Prefecture, Japan, 1984, precursory Rn conc. increases 7-8866
- W Nagano Prefecture, Japan, 1984, precursory subsurface gas comp. var. 7-8870
- W Nagano Prefecture earthquake, 5 to 30 g accelerations and boulder ejection, 14 Sept. 1984 event 7-18129
- Multan Prefecture earthquake, Japan, geomagnetism in fault area (*Japanese*) 7-65942
- Nagano region, Japan, gas anomalies at mineral springs and fumarole before earthquake 7-40423
- Nahanni (Canada) earthquake aftershock, missing V-accelerograph peak rel. to vertical accel. exceeding 2 g 7-28871
- near-field ground motion synthesis, seismic radiation from kinematic fault models 7-54897
- central New Hebrides Island Arc, seismicity patterns assoc. with asperity complex 7-40427
- New Madrid seismic zone, evidence for periodic energy release 7-3986
- Ninghe, China, strong ground motion of Nov. 1976 earthquake 7-28851
- nonshear-type earthquakes of Alpine-Himalayan belt, evidence from P-wave first motions 7-8854
- North Sea, seismic hazard assessment 7-23579
- North Sea, seismicity characts. 7-47380
- North Sea peak ground accel. prediction from seismic risk anal. 7-4004
- nuclear plants, seismic hazard methodology for the central and eastern USA 7-15285
- occurrence simulation, numerical model (*Japanese*) 7-65980
- oceanic crust stress state inferred from intraplate earthquakes 7-34442
- Osmansagar reservoir, Hyderabad, India, microearthquakes obs. 7-23573
- circum-Pacific belt, prediction of strongest earthquakes 7-65970
- Panxi region, SW China, tectonic stress field and earthquake distrib. (*Chinese*) 7-54977
- Parkfield, California, USA, forecasting of future earthquake using geodetic obs. 7-28979
- Parma earthquake, N Italy, event of 9 Nov. 1983 and aftershock 7-54881
- Petalan region, Mexico, moment magnitude scale from recorded peak horizontal vel. 7-28857
- Poisson earthquake occurrence model, nuclear power plant site anal. 7-25150
- Powder River (Oregon) earthquakes, 1984, evidence for seismic zone on Oregon-Idaho border 7-3985
- precursory accelerated motions of dislocations of a fault (*Chinese*) 7-3979
- precursory changes in chemistry of emitted gases, review 7-34394
- precursory seismicity changes in New Zealand and California 7-8842
- prediction, radio technique appl. 7-60168
- Rainbow Mountain-Fairview Peak-Dixie Valley (Nevada) earthquakes, 1954-59, seismic processes anal. 7-40429
- rebound process, creep and stress accumulation 7-54914
- reservoir-induced seismicity in vicinity of Lake Bhatsa, Maharashtra, India 7-23567
- rigid block rocking on randomly shaking foundations, nuclear plant seismic response appl. 7-25132
- ring structures seen by remote sensing, due to jointing following earthquakes 7-54951
- RULISON nuclear explosion, effect of tectonic release on body-wave magnitude 7-3990
- rupture length and propag. speed, determ. from seismic and acoustic data 7-8855
- San Andreas fault, central branch, gravity anomalies and earthquake epicentres 7-65972
- San Andreas fault system, S California, seismic evidence for conjugate slip and block rot. 7-14216
- San Fernando (California), 1971 February 9, complex polarisation anal. of particle motion 7-28867
- S San Jacinto fault zone, California, rupture patterns and preshocks of large earthquakes 7-28854
- San Juan Bautista, California, 26 May 1984, near-source strain field 7-28895
- sand, liquefaction, initial static shear stresses effect 7-4037
- scaling relation between earthquake size and duration of faulting 7-23564
- Seattle (Washington), 1965 April 29, strong ground motion prediction in Puget Sound region 7-3980
- secondary subevents with different mechanisms, wave source characts. 7-14214
- seismic risk trend analysis, appl. of human-computer interaction method to real example (*Chinese*) 7-34385
- seismic source inversion, effect of strong-motion array configuration 7-28853
- seismic source mechanisms, relation to tectonic characts. of seismic region 7-8823
- seismic sources (2D) causing plane strain deformation, two representations 7-14195
- seismic sources imaging, 3D vector-wave field technique for anisotropic heterogeneous media 7-28872
- seismic-ionospheric electrical interaction, resonant phenomena 7-28890
- Shumagin Islands sequence, Alaska, 1983 February 14, focal mechanisms 7-54886
- Shumagin seismic gap, Alaska, searches for precursory crust motion 7-9223

earthquakes continued

- Sierras Pampeanas of Argentina, compressional earthquakes rel. to foreland deformation tectonics 7-66113
- SE Solomon Islands, earthquake multiplet characts. and tectonics 7-47377
- Sophades, Central Greece, 30 April 1954 earthquakes, field observations 7-47351
- source mechanisms, behaviour of viscoelastic medium with microfractures under extension and shear 7-29003
- source mechanisms, numerical modelling of nonplanar faults 7-28886
- source parameters estimation by waveform data inversion, appl. to global seismicity (1981-3) 7-54882
- source process modelling 7-8867
- sources, dynamic rupture process, numerical methods for simulation (*Chinese*) 7-54876
- spatial distrib. before and after large earthquakes 7-23580
- Sri Lanka, seismicity anal. 7-23570
- Sriramsagar reservoir, Andhra Pradesh State, India, microearthquake investigations 7-23575
- static shear crack with a zone of slip-weakening 7-47353
- stress field due to faulting in presence of asperity, antiplane crack model 7-8822
- strong motion records and A_{95} parameter 7-65943
- Sunda Arc, seismic history and seismotectonics 7-65952
- surface ground motion during earthquake, rot. components determ. 7-14202
- Surugu Bay, Japan, microearthquake activity (1981-3) 7-8869
- Sutton (Alaska), 1984 August 14, activity on Talkeetna segment of Castle Mountain fault system 7-3984
- Swift Reservoir, Washington, 1958-63, seismicity anal. along S St. Helens seismic zone 7-54885
- systematic errors determ. in magnitude estimates, anal. of data from Parkfield, California 7-54891
- T-waves, duration rel. to earthquake magnitudes and seismic motion and appl. to tsunami warning 7-14208
- Takase Dam, Japan, microearthquake activity before and after water impounding 7-23572
- tectonic feedback in earthquake cycle at plate boundaries 7-3998
- tectonic stress evolution and earthquake rebound, numerical solns. for antiplane case 7-8821
- Tengchong volcanic-geothermal region, China, microseismicity and hydrothermal activity (*Chinese*) 7-54875
- Tenmei Odawara earthquake of 23 Aug. 1782, magnitude and epicentre and tsunami 7-18133
- S Texas, evolution of seismic barriers and asperities caused by fault planes depressuring in oil and gas fields 7-3982
- Thien Dam, NW Himalayas, India, microearthquake obs. 7-23577
- Tokai District, Japan, earthquake precursory crustal deformation (*Japanese*) 7-8834
- Tokyo, Japan, 1887 January 15, epicentre determ. (*Japanese*) 7-65981
- Tonga-Fiji earthquakes, anomalous difference travel times and amplitude ratios of SKS and SKKS waves 7-65945
- tsunami warning, implications of T-wave duration rel. to earthquake magnitudes and seismic moment 7-14208
- underground explosions-earthquakes discrimination using discriminant functions, examples for Eurasia and North America 7-28849
- volcanic earthquakes, and stress-strain state of crust with magma inclusion 7-65967
- volcanic earthquakes, seismic radiation pattern theory 7-8843
- volcanic tremor at Mount St. Helens (April and May 1980) 7-3981
- Vrancea, Romania, 1985 August 1 seismic doublet source parameters (*Rumanian*) 7-8861
- Washington continental margin, earthquakes distrib. and stress orientation from crustal struct. anal. 7-4006
- waveform inversion method for rupture process 7-65955
- Wellington region, New Zealand, anal. of Sp and Ps phases from microearthquake survey 7-28863
- Westmorland (California), 1981 April 26, triggered surface displacement on Imperial and Superstition Hills faults 7-3983
- Xianshuihe Fault Zone, S China, seismic activity estimation via earthquake activity parameters (*Chinese*) 7-34387
- E Yamanashi earthquakes, Japan, source region P-wave vel. 7-8865
- Yamasaki earthquake, Japan, crustal movements observations 7-65926
- Yamasaki fault earthquake in Japan, associated crust resistivity changes (*Japanese*) 7-8835
- Yangbajing fault, isotopic depth 7-28973
- Yinchuan-Pingluo (China), 1739 January 3, surface fault scarps rel. to seismicity of Yinchuan graben 7-28859
- Rn concentration variations in active volcanoes and seismic regions 7-54963
- Rn outgassing related to geothermal faults 7-54964

EAS see cosmic ray showers and bursts

Eberhard effect see photographic materials

EBIC

- image interpretation using Monte Carlo simulations 7-35640
- organic semiconductors, electrical transport props., electron bombardment method 7-52641
- semiconductor materials characterisation techniques, review 7-51598
- semiconductors, polycrystalline, beam induced current characterisation, appl. to Si solar cells 7-7267
- semiconductors, polycrystalline, localised defects, EBIC studies 7-21933
- semiconductors, scanning electron microscope characterisation, book contrib. 7-41551
- solar cell, polycrystalline, grain boundary parameters determ. using EBIC signal derivative 7-8382
- AlGaAs-GaAs solar cells, fabrication on Si substrates 7-46937
- CdS-CuGaSe₂ solar cells, physical properties and photovoltaic potential of CuGaSe₂ thin films 7-12889
- CdS-CuInSe₂ thin-film solar cells, junction formation and O role, EBIC studies 7-17915
- CdTe high-resistivity undoped crystals, defects, EBIC studies 7-21211
- CuInSe₂, heterogeneous, VLS growth, electronic defects, photocurrent spectra, photolum., EBIC analysis 7-27288
- CuInSe₂, p-type, CdS induced homojunction formation 7-58867
- CuInSe₂/CdS solar cells, modelling and anal. 7-17893
- GaAlAs-GaAs laser diodes, catastrophic optical damage, electrolum., cathodolum., EBIC and TEM obs. 7-57329
- GaAs, MBE growth, defect reduction using superlattice structures 7-13359

EBIC continued

- GaAs polycrystalline solar cell, electron beam generated carriers in presence of grain boundaries 7-64262
 GaAs, scanning DLTS study of deep level defects 7-21865
 GaAs, semiconducting and semi-insulating LEC crystals, SEM-EBIC characterisation 7-51777
 GaAs, transport props., charge collection microscopy 7-52649
 GaAs/Au(Cr) Schottky barriers, hole diffusion length, photon and electron excitation studies 7-2707
 InP, electron irradi. damage, impurity effects 7-12154
 NiSi₂-Si Schottky barrier heights, study by electron beam induced current 7-27381
 Si, as-grown and annealed bicrystals, conductance of grain boundaries 7-64245
 Si bicrystals, grain boundary carrier recombination, chemical origin 7-17039
 Si, crystallised thin films, electrical characterisation 7-33116
 Si dendritic web ribbons, structural defect characterisation 7-12074
 Si dislocation-free single crystals, microdefect recomb. activity, electron irradi. and annealing effects, SEM study (*Russian*) 7-21287
 Si, polycrystalline, H₂ passivation, grain boundaries, EBIC technique 7-26769
 Si, polycrystalline p-type, Al and Cu diffusion effects on electronic properties 7-17038
 Si polycrystalline solar cell p-n junction, carrier lifetime, effective recomb. vel. and diffusion length, EBIC meas. 7-23138
 Si, ramp assisted foil casting and photovoltaic appls. 7-16609
 Si solar cells, heavily doped emitter and junction regions, EBIC studies 7-34039
 Si wafer, stacking and technological faults, elec. activities, SEM study (*Russian*) 7-21234
 Si:B,Fe, EBIC and DLTS meas., comparisons 7-7265
 Si/PtSi(CrSi₂) Schottky diodes, surface imperfection induced elec. leakage paths 7-2719
 SiO₂ layers, space charge distrib. meas., electron beam induced conduction method 7-27660
 ZnSe-ZnS electroluminescent MIS structures, MOCVD growth and charactn. 7-59443

ebullition *see boiling*

ECG *see electrocardiography*

echelles *see diffraction gratings*

echelons *see diffraction gratings*

echo

- see also anechoic chambers; architectural acoustics; reverberation; sonar*
 HF radar sea echoes, Bragg coherence 7-40588
 plasma, inhomogeneous, echoes hydrodynamic theory 7-44167
 US attenuation coeff. meas. by multifreq. echo technique 7-43591
 US pulse echo signals, processing for electro-acoustic conversion distortion removal (*Japanese*) 7-43540
 US vel. meas., dip point anal. from echo spectrum 7-43607
 RbD₂PO₄, ultrasonic propagation, pulse-echo method, anomalies 7-44703

echo cancellation *see echo suppression*

echo suppression

- acoustic echo canceller based on subjective assessment, echo return loss 7-37262
 acoustic echo canceller for teleconference systems 7-37263
 audioconference rooms and reverberators, modelling 7-37253
 high-quality loudspeaking system development with acoustic signal processing (*Japanese*) 7-57661
 subsurface imaging by scanning acoustic microscopy 7-3569

echocardiography *see biomedical ultrasonics; cardiology*

echolocation (physiological) *see bioacoustics; mechanoreception*

eclipses

- see also solar eclipses*
 asteroids, eclipse-type light curves rel. to possible binary asteroids 7-18367
 eclipses and lunar phases, demonstration using a Tensor lamp 7-48245
 Galilean satellite eclipse timings: 1983/5 report. I 7-18368
 Galilean satellite eclipse timings, for AD 1983 to 1985 period 7-55524
 Galilean satellites, photometric obs. of mutual events (Project Omega 1985/86) 7-18370
 Galilean satellites mutual phenomena, conf., Bagnères de Bigorre, France (April 1986) 7-60856
 ghosts's shadows and superluminal occultations 7-35154
 Jupiter, mutual satellite phenomena, longitude discrepancy resolution 7-40747
 Moon, total eclipse, 1982 July 6, ALPO obs. 7-18361
 Pluto-Charon 1987 mutual events 7-47760
 Pluto-Charon eclipse events, December 1986, photometric obs. rel. to radii and albedos 7-55530
 Pluto-Charon mutual eclipse events, first-order modelling 7-34925
 Pluto-Charon system, eclipse obs., April 1986, rel. to radii, orbital period, and orbital inclination 7-29424
 Pluto-Charon system, eclipses, diff. theory 7-55528
 Vel X-1 (4U 0900-403), X-ray probing of circumstellar matter during eclipse phase 7-55726

eclipsing binary stars

- Algol-type stars, evolution assuming ang. momentum loss via mag. winds 7-40864
 CN And, light curve anal., use of Wilson-Devinney method 7-14501
 V1343 Aql (=SS 433), stationary lines variable struct. 7-60689
 V1343 Aql (=SS 433), extended radio struct. obs. with European VLBI Network 7-29478
 V1343 Aql (SS 433), evidence for relativistic beaming from VLBI obs. 7-9476
 V1343 Aql (SS 433), Fe K X-ray line obs. 7-14594
 V1343 Aql (SS 433), no optical variability on time scale of 10⁻⁶ to 10 s 7-66596
 V1343 Aql (SS 433), quiescent and active flaring periods obs. at 408 MHz 7-9478
 RY Aqr, low-mass semi-detached eclipsing binary, photometric obs. 7-60713
 R Aqr, obs. of jet at UV and radio wavelengths 7-55686
 FF Aqr, RS CVn star, G-type giant star surface and atm. struct., IUE obs. 7-55730
 CX Aqr, semi-detached binary system, radial vels. and light curve anal. 7-47990
 R Aqr, UV variability and mass expulsion from IUE obs. 7-55651

eclipsing binary stars continued

- V1343 Aquilae (SS 433), Doppler-shifted X-ray line emission obs. 7-9493
 R Ara (=HD 149730), eclipsing binary star, UVB observations 7-35007
 UX Ari, H α line obs. of double-lined eclipsing RS CVn system 7-40873
 IM Aur, Algol-type eclipsing binary, UV spectrum 7-4509
 ϵ Aur, high-resolution spectroscopy during 1982-4 eclipse 7-4519
 IM Aur, light-time effect obs. 7-34999
 SX and TT Aur, simultaneous differential photometry with St. Andrews twin photometric telescope 7-60731
 SS Aur, U Gem star, spectroscopic orbit 7-14581
 \dagger Aur type detached binary systems, IUE obs. rel. to accretion shocks 7-55732
 TY Boo, BV photoelectric light curves 7-18435
 44=I Boo (ADS 9494B), BV photoelectric photometry of W UMa system 7-55718
 EM Car, radial vel. study of massive O-type system 7-9518
 OY Car, SU UMa-type dwarf nova, IUE obs. in superoutburst 7-55689
 V368 Cas, Algol-type binary, UBVR photometric studies 7-35009
 V373 Cas, early-type eclipsing binary, spectroscopic orbit and physical dimensions 7-55706
 XX Cas, period anal. 7-40876
 V641 Cas, photometry of VV Cep type star 7-18414
 V375 Cas, semi-detached binary, components radii, photometric obs. (*Chinese*) 7-4504
 HT Cas, U Gem star, mean cycle length determ. 7-66598
 V523 Cas, W UMa star, light curve soln. and derived mass ratios uniqueness 7-40868
 YZ Cassiopeiae, eclipsing binary star showing small out-of-eclipse changes 7-18434
 cataclysmic binaries, eclipsing fraction rel. to mass spectrum of white dwarfs 7-29476
 cataclysmic binary stars, observational selection in magnitude-limited sample 7-29479
 cataclysmic variable stars, resonance line profile calcs. during primary eclipse 7-60692
 V346 Cen, eccentric orbit eclipsing binary light curves from four-colour photometry 7-29507
 VW Cep, 1984-5 photoelectric times of minima 7-4514
 RS Cep, Algol type semidetached star with Be star component, system characts. 7-47972
 U Cep, classical Algol binary system, photometry rel. to accretion structs. 7-4512
 BE Cep, contact binary star with components in poor thermal contact, light curves anal. 7-4521
 CW Cep, early-type eclipsing binary star, apsidal motion determ. from min. light times 7-60729
 AH Cep, early-type eclipsing binary star, photometric and spectroscopic study 7-47987
 CQ Cep, eclipsing Wolf-Rayet star, spectrophotometric and spectroscopic studies 7-66618
 U Cep, interacting and eclipsing binary star 7-9482
 U Cep, photometric asymmetry of disturbed eclipses 7-47991
 XZ Cep, spectral characts. 7-4511
 Z Cha, eclipsing dwarf nova, white dwarf surface luminosity distrib. 7-4458
 YZ Cha, VRI photoelectric obs. of Algol-type system 7-40874
 AT Cnc, cataclysmic binary star behaviour in AD 1985/6 season 7-9486
 AC Cnc, UBVR obs. of eclipsing cataclysmic binary 7-29489
 contact binaries, EXOSAT and IUE obs. 7-60723
 contact binary star with one component having two surface spots, light curve 7-29512
 contact binary stars, equilib. solns. and stability 7-60716
 θ CrB, UBVR photometry, no eclipse in 1984-6 period 7-66610
 RV Crv, near-contact binary system, radial vels. and light curves anal. 7-47989
 60 Cyg, Be star and suspected eclipsing binary stars, UVB obs. 7-4484
 Y Cyg, early-type eclipsing binary star, apsidal motion determ. from min. light times 7-60729
 CG Cyg, eclipsing RS CVn star, photometry obs. 7-47896
 CH Cyg, eclipsing symbiotic star, photometry, spectra and radio flux characts. (*Russian*) 7-40846
 C Cyg, eclipsing symbiotic star, radio outburst characts. (*Russian*) 7-40847
 V444 Cyg, eclipsing Wolf-Rayet binary star, Doppler tomography of stellar wind from IUE obs. 7-47947
 V382 Cyg, period of eclipsing binary star 7-35008
 CH Cyg, possible end of shell spectrum phase and transition to real symbiotic star (1983-4), spectral characts. 7-4487
 V1329 Cyg, UBVRJHK photometry (1980-3) 7-29492
 AA Dor (LB 3459), sdOB-type eclipsing binary ephemeris from primary minima obs. 7-24167
 BV and BW Dra, contact binaries, combined photometric and spectroscopic solns. 7-14603
 UZ Dra, photometric light curve of eclipsing binary 7-55716
 BZ Eri, UBVR photometric study 7-14605
 evolution of interacting binary stars, implications of IUE obs. 7-47997
 TZ For, eclipsing Capella-like system observed with IUE, UV emission-line fluxes meas. 7-47996
 YY Gem, BY Dra star, components atm. activity, IUE and H β spectra anal. 7-55677
 U Gem, dwarf nova, evidence for prolonged quiescence and large-amplitude flickering from early obs. 7-66621
 gravity darkening of highly distorted components, determ. for detached main-sequence stars 7-4505
 HD 149779, B-type eclipsing binary uvby photometry and light curve anal. 7-24161
 HD 153919 (=4U 1700-37), massive X-ray binary star, orbital variability in stellar wind ionisation from IUE obs. 7-55737
 HD 164270, variable WC9 star, model of close binary with precessing disk 7-47925
 HD 17198A, spectroscopic binary, possible start of eclipses (on 1988 February 5) 7-55723
 HD 27130, Hyades solar-type star, H-R diagram position rel. to solar models testing 7-66665
 AM Her, 1985 light curve and colour indices characts. 7-66670
 u Her, eclipsing spectroscopic binary BV photometry 7-14606
 AM Her, optically variable X-ray binary star 7-4481
 HZ Her (=Her X-1), UV spectroscopy rel. to line emission site 7-55736
 AM Her stars, spectrophotometric detect. of secondary in three systems 7-9514

- eclipsing binary stars continued**
 Her X-1, 35 day cycle, clock mechanism characts. 7-60711
 Her X-1, γ -ray emission mechanism 7-47975
 Her X-1, companion-star beam steering of high-energy particles rel. to gamma-ray emission 7-14611
 HR 3527, new eclipsing binary star, photometric obs. 7-47854
 HR 6902, possibly eclipsing composite-spectrum star, spectral types, orbital elements, and masses 7-66674
 HV 12714, luminosity and possible LMC membership, spectral obs. 7-47981
 EV Lac, eclipsing UV Cet star, photometric obs. of flares 7-66614
 SW Lac, period change in W UMa system, UV photometry 7-55720
 AR Lac, RS CVn star, atm. active regions and lines rot. modulation, IUE obs. 7-55728
 EV Lac, UV Cet star, UV radiation rot. modulation 7-47933
 SW Lac, W UMa star, photoelectric light curves and elements 7-60718
 Lanning 10 (V363 Aur), eclipsing cataclysmic binary, component masses and spectrophotometric obs. 7-66602
 late-type contact binaries, chromospheric-coronal activity, UV obs. of Mg II lines 7-47994
 late-type supergiant eclipsing binaries, chromospheric ionisation and opacity, UV, spectra 7-40869
 β Lyr, search for secondary spectrum 7-55714
 β Lyr, UV spectrum, P Cyg lines anal. 7-55731
 mass anomalies of close binaries, due to metallicity and evolution and not to observational errors 7-40877
 mass ratio distrib. 7-18432
 minimum light epochs, determ. for 27 objects 7-4522
 RU Mon, physical parameters from 85-year study 7-55710
 V651 Mon in planetary nebula NGC 2346, light curve 7-4516
 NSV 12040, W UMa star, first ephemeris from photoelectric and visual obs. 7-66669
 V451 Oph, absolute dimensions from uvby light curves 7-29503
 V2051 Oph, IR and optical photometry of eclipsing dwarf nova 7-55670
 RZ Oph, long-period eclipsing binary, photometric and radial vel. study 7-29504
 V2051 Oph, possible low-field polar, high-speed photometric obs. 7-60694
 V566 Oph, UV light curve of A-type W UMa binary 7-40862
 ϵ Ori, orbital elements determ. rel. to stellar dimensions and tidally induced mass loss 7-55738
 VV Ori, UV obs. 7-35004
 AT Peg, BV photoelectric photometry and light elements 7-66673
 BO Peg, BV photometric and spectral obs. 7-66678
 IP Peg, eclipsing dwarf nova, system parameters from high-speed photometry 7-14595
 IP Peg, near-IR spectroscopy and photometry 7-66619
 RY Per, asynchronously rotating Algol binary study 7-35002
 AG Per, light curves anal. rel. to apsidal rot. 7-66658
 IZ Per, new period determ. and period trend from light min. times 7-66657
 β Per, VLBI astrometry 7-35055
 AG Per early-type eclipsing binary star, apsidal motion determ. from min. light times 7-60729
 AD Phe, W UMa star, photoelectric light minima obs. rel. to decreasing orbital period 7-4501
 photometry of eclipsing binaries, Cancer to Corona Borealis (1972 to 1984) 7-4517
 CF Pup, new ephemeris and V light curve 7-55719
 RT Scl, near-contact binary system, radial vels. and light curve anal. 7-47988
 EG Ser, spectroscopic orbits 7-66676
 U Sge, asynchronously rotating Algol binary study 7-35002
 U Sge, classical Algol binary system, photometry rel. to accretion structs. 7-4512
 RS Sgr, Algol-type system, fainter component lines 7-66679
 ν -Sgr, H-deficient binary star, evidence for pulsation from UVB light curves 7-14608
 ν Sgr, H-deficient star, mass loss and mass characts., UV spectra anal. 7-14579
 TA observations (1986 August) 7-14588
 TA observations (1986 July) 7-24143
 TA observations (1986 June) 7-14586
 V471 Tau, evidence for large-scale structs. in atmosphere of active K-dwarf component 7-47874
 AQ Tuc, contact binary system, radial vels. and light curve anal. 7-47988
 4U 1700-37, X-ray flux time var. and wind characts. 7-66655
 4U 1700-37 (HD 153919), EXOSAT search for X-ray periodicities 7-14610
 XY UMa, RS CVn star, photometric characts., contrib. of star spots 7-47976
 XY UMa, RS CVn star, X-ray light curve 7-47982
 DN UMa, spectroscopic orbits 7-66676
 W UMa stars, light curves anal. for four objects 7-35006
 W UMa stars, models with dissipative heating for light curves anal. 7-55705
 FY Vel (=HD 72754), satellite line system spectra of eclipsing binary 7-47983
 Vel X-1, neutron star orbit and rot. characts. 7-66659
 Vel X-1 (4U 0900-403), X-ray probing of circumstellar matter during eclipse phase 7-55726
 22 Vul, δ Aur star, mass loss and wind props., IUE obs. 7-14601
 QQ Vul, long-period AM Her star, period determ. using new minima from old plates 7-66672
 Wilson-Devinney method for light curves anal., soln.-convergence characts. 7-14501

- ecology**
 acidic precipitation, conf., Muskoka, Ontario, Canada (Sept. 1985) 7-48167
 aquatic organism acidification effects, data evaluation and compilation 7-40054
 chlorophyll fluorescence, appl. in ecophysiology 7-47299
 desertification, review and definitions of concept 7-9157
 downstream fish migration protection technologies for hydroelectric application 7-34075
 energy and environment 7-17924
 environmental change, remote detect., data struct. appls. 7-4240
 eutrophication process in coastal bay, 3D eco-hydrodynamic model 7-55082

- ecology continued**
 extraterrestrial solar radiation on inclined surfaces, FORTRAN program 7-55138
 forest decline, acid rain and other contributory factors, report 7-28419
 lake acidification meas., integrated palaeoecological approach 7-65658
 Lake Norman, NC (USA) application of ecosystem assessment model 7-65654
 Mount Kenya, origin and palaeoclimatic-ecological significance of sand dunes in Mutonga drainage 7-18186
 population governed by stochastic Verhulst eqn. 7-48559
 tidal barrage effects 7-33994
 water pollution by fertilisers and pesticides, book 7-24314
- economic and sociologic effects**
see also demography; personnel; social aspects of automation
 Arab Gulf states, climate effect on economic activity 7-9160
 health care technology evolution in USA, economic and ethical implications 7-4648
 Medicare's Prospective Payment System: paying for magnetic resonance imaging 7-4651
 water resource valuing, existence values and normative economics 7-29108
- economics**
 accounting treatment for nuclear fuel leasing 7-30540
 Alice Springs Solar Pond project, technical and economic viability 7-40045
 automotive long range highway vehicle propulsion system using fuel cells, R&D needs 7-65456
 biomass, alternate supply systems, cost anal. 7-65395
 CANDU reactors, economic threats from reduced cost enrichment processes 7-10306
 coal gasification-combined-cycle plant thermoeconomic anal. 7-23206
 dry sorbent injection technologies for SO₂ and simultaneous NO_x control 7-65667
 electric power industry Inter-RAM conference, Syracuse, NY, USA (June 1986) 7-9592
 Electricite de France, nuclear power development and economics 7-46928
 energy, environmental damage and environmental policy, economic anal. (German) 7-40055
 energy conservation, entropy-based regional approach 7-65381
 energy conservation investment, economic efficiency 7-65380
 energy consumption rel. to economic growth 7-65384
 ethanol fuel production from wheat, technico-economic aspect (French) 7-28385
 fibre optics' advantages for computerised control systems, data highways and sensors 7-15988
 finished lens moulding technology saving time and money 7-31535
 fission reactors, accelerated fuel depreciation as economic incentive for low-leakage fuel management 7-30512
 flat-plate solar cells economic payoff, 1975 to 1985 7-3687
 flue gas desulphurisation, NOXSO, SOXAL and limestone process evaluation 7-46983
 fusion machines, highpower density, MFAC report 7-15313
 heat exchanger design, thermoeconomic perspective 7-65516
 heat pump design, economic viability and performance estimates 7-8430
 heat pump system, thermoeconomic optimisation 7-23210
 hybrid heat pump appl. study 7-23213
 induction linac driver for inertial fusion, cost/performance analysis 7-25209
 industrial heat pumps, comparative economic evaluation 7-65529
 industrial heat pumps, novel approach to placement, sizing and selection 7-65527
 inertial fusion drivers, KrF laser appl., cost/performance anal. between different systems 7-25210
 laboratory robot, decision criteria for purchasing 7-24637
 Large Deployable Reflector, moderate cost, system concept 7-40711
 LLW volume reduction, economic incentives model 7-49689
 LWR fuel cycle, long-term analysis 7-30533
 magnetic fusion program, economic aspects 7-15426
 mild coal gasification yielding gaseous, liquid and solid products 7-28408
 mini-compressed air energy storage plant analysis and evaluation 7-23225
 nuclear decommissioning, financial recoverability and reliability problems 7-30641
 nuclear decommissioning, utility perspectives, accounting and funding, South Texas Project 7-30642
 nuclear fuel, financial and accounting issues FERC perspectives 7-30538
 nuclear fuel cost impacts of using constant cycle-based amortization rates 7-30541
 nuclear fuel plants, statistical sampling for holdup measurement 7-30584
 Nuclear Fuels-River Bend Nuclear Group accounting interface for reactor fuel 7-30539
 nuclear generating facilities, phase-in, load forecasting and utility regulation 7-39972
 nuclear generating unit incentive regulation program and its relationship with safety 7-49597
 nuclear plant prudence reviews for regulatory purposes 7-39976
 nuclear power, impact on world energy supply (German) 7-65416
 nuclear power, rate base treatment of large power plants 7-39974
 nuclear power, rate-of-return regulation 7-39973
 nuclear power, ratemaking and rate shock reduction 7-39971
 nuclear power, schedule reconciliation tests for management prudence determination 7-39979
 nuclear power industry in USSR, cost reduction of power (Russian) 7-25269
 nuclear power plant piping, technical and economical incentives behind strain limitation 7-10221
 nuclear power plants, in-service maintenance, economic aspects (German) 7-61987
 nuclear rate regulation 7-39978
 nuclear utility prudence issues 7-39980
 ocean energy extraction technology status and economic prospects 7-65403
 Ontario Hydro nuclear stations, innovations in design, operation, and construction 7-10194
 optical fibre cable laying methods (Japanese) 7-43436
 organic Rankine system for energy recovery, optimisation and economic evaluation strategy 7-40024
 photovoltaic array performance and life-cycle cost simulation 7-17913
 photovoltaic system tracking and concentrator collectors, linear and Fresnel optics, cost comparison 7-17853

economics continued

- primary paraboloid/secondary hyperboloid tandem solar concentrator, cost advantages 7-46924
- prudence concept for nuclear power regulation 7-39975
- Rankine cycles optimisation for low temp. heat recovery 7-65523
- Rocky Mountain I underground coal gasification project 7-28407
- solar kiln dryers for timber and agricultural produce 7-39965
- solar thermal dish appls., sensible and thermochemical energy transport systems, economics 7-65414
- solar-hydrogen project, dimensions, costs and timing (*German*) 7-46938
- Somalian energy trends and renewable resource potential 7-39949
- superconducting magnetic energy storage plant for electric utility load leveling, design and estimated costs 7-54369
- Thailand, energy planning case study 7-54259
- thermochemical energy transfer systems, direct work output 7-54334
- US economic activity, comparative roles of energy and money 7-65386
- H⁺ ion heat engine for direct conversion to electricity 7-28409
- H₂ production from coal and petroleum coke, technical and economical perspectives 7-40050
- Si, solar cell fabrication using laser groove technique, commercial viability 7-59862
- Si solar cells, terrestrial, production costs and conversion efficiency 7-17869
- Si:H, amorphous, dendritic web, Czochralski flat plate modules and concentrator module, price comparison 7-17904

eddy current losses

- hollow conducting cylinder eddy current calc. 7-62585
- irreversible Barkhausen jumps of sinusoidally moving 180° domain wall, induced losses, multidomain wall model 7-27555
- magneto-surface-acoustic-wave propagation, anal. considering micro-eddy current loss 7-27589
- multifilamentary superconducting conductors, AC eddy current losses caused by tangential magnetic field (*Slovak*) 7-58952
- sinusoidally time varying eddy currents in metallic structures, three-dimensional calc. 7-25702
- soft magnetic materials, specific magnetic loss meas. at remagnetisation freq. 50 Hz to 200 kHz 7-9850
- thick cylinder eddy current distrib. and losses due to exterior circular currents 7-62587
- thick cylinder eddy current distrib. and losses due to interior circular currents 7-62586
- Fe-Si, electrical steels and alloys, conf., Vladimir, USSR (Dec. 1984) 7-9576
- Fe-Si, rapidly quenched ribbons, grain growth, mag. props. 7-8017
- Fe-Si (3 wt.%), domain structure and mag. props., influence of plane tension and insulating coatings 7-12991
- Fe-Si (3 wt.%), mag. props. and domain struct., influence of laser treatment 7-12993
- Fe-Si (3 wt.%), specific magnetic loss meas. at remagnetisation freq. 50 Hz to 200 kHz 7-9850
- Fe-Si (3.2 wt.%), mag. props., influence of substructural features 7-12996

eddy current testing

- 3D NDT, surface impedance boundary condition 7-65267
- boiler tube NDT inspection systems 7-20549
- claddings measurements, eddy current impedance methods 7-33904
- coating thickness meas. 7-13703
- electrical cond. meter graduation without specimens 7-28243
- electrical cond. meters, inspection errors rel. to geometric parameters 7-28244
- electrically conducting half-space, analytic Green's dyads 7-10821
- EM field calculations in inspection problems of weakly cond. weakly mag. media 7-39821
- ferromagnetic metals, eddy current testing, mag. permeability effect 7-22958
- flaw detectors, impedance components for probe coils, standardisation prediction 7-33891
- flaw inversion algorithm, experimental verification 7-54059
- metallic materials, crack detection, structural inhomogeneities, multi-freq. eddy current testing 7-22954
- metallic sheets, conductivity and surface buckling meas. by eddy current testing 7-54058
- nondestructive, automatic classification and recognition of defects 7-39841
- PWR failed fuel rod, pellet-cladding interaction, in-pile eddy current test 7-19354
- steel, austenitic stainless, strain martensite determ., eddy current method 7-3559
- steel, C₄₂, inverse magnetostrictive effect and electromagnetic non-destructive testing methods 7-13714
- steel tubes, eddy current testing using electromagnet technique 7-39826
- surface flaw detection for hot steel slabs, eddy current method (*Japanese*) 7-53771
- surface-breaking structures, eddy current imaging 7-65266
- weld, NDT, elec. current methods modelling 7-3553
- Zircaloy tube sample eddy current testing 7-56762
- Al structures, corrosion damage depth meas., eddy current method (*German*) 7-13711
- Zr-Nb (2.5 wt.%) pressure tubes, remote field through wall EM inspection 7-46759

eddy currents

- see also induction heating
- 2D electrostatic and EM problems, general interactive finite element package 7-62569
- conducting plate eddy current density and force on moving filament 7-62583
- conducting slab under moving parallel circular current loop 7-62581
- conducting structures with pulsed excitation, time domain anal. of eddy current effects 7-62573
- electrically conducting half-space, analytic Green's dyads 7-10821
- EM half-space problems, anal. using Green's functions 7-62579
- flux reflection and flux conc. effects, 3D finite element anal. 7-42845
- high speed rotating disk, asymmetrical eddy currents and conc. effect of mag. flux 7-5814
- hollow conducting cylinder eddy current calc. 7-62585
- inductance standards, LF models comparison 7-18834
- magnetic field effects on biological and chem. processes 7-47135
- magnetic flaw detection of pipelines, eddy currents as interfering factor 7-39822

eddy currents continued

- magnetic shield with active compensation, improvement of props. 7-47192
- magnetic systems, multiply-excited, finite element soln. of transient eddy-current problem 7-62575
- magnetics conference, Phoenix, AZ, USA (April 1986) 7-29572
- metallic optical films, contactless thickness meas. using eddy currents (*German*) 7-24626
- modelling in three dimensions 7-31214
- multi-torus system, eddy current analysis, finite element circuit theory 7-58048
- parallel circular loop moving above conducting slab, analytical calc. 7-31213
- rectangular cavity for EPR in TE₁₀₂ mode 7-48823
- simple cubic lattice of conducting mag. spheres, mag. permeability 7-45742
- skin depth-independent finite element method for eddy current problems 7-62572
- solid yoke bending magnetic, eddy current effects during slow acceleration (*Chinese*) 7-25284
- thick cylinder eddy current distrib. and losses due to exterior circular currents 7-62587
- thick cylinder eddy current distrib. and losses due to interior circular currents 7-62586
- three-dimensional formulation, using multiply connected regions 7-42844
- tokamak structural components, 3D analysis of eddy currents using boundary element method 7-25199
- Cu, rod, skin depth and complex mag. susceptibility, expt. 7-51
- Cu_{1-x}Cd_xFe₂O₄, irreversible magnetisation, depend. on magnetising field 7-64487
- Fe₈₃Co_{17.15}Mo₂B₁Si₅, amorphous ribbons traversed by DC electric currents excess resistance, collective motion of ferromag. domain walls 7-32989
- Pt-Bi (22 wt.%), supercond. films, pinning in appl. mag. field (*Russian*) 7-64418

edge-defined film fed growth see crystal growth from melt**edge dislocations**

- alkali halide crystals, dislocation displacements distrib. characts., local dislocation density effects (*Russian*) 7-21214
- alkali metal halides, hardening, effect of dislocation elec. charge 7-51816
- anthracene single crystals, structural imperfections as triplet exciton traps, defect recovery 7-64160
- B2 ordered alloy, edge dislocation, computation of core struct. 7-37991
- climb, vacancy diffusion and capture calcs. (*Russian*) 7-44550
- dielectric materials, linear isotropic, lattice defects 7-26749
- ferromagnet, spin wave excitation by acoustic fields, non-uniformly distrib. dislocations (*Russian*) 7-45646
- grain boundary theory based on dipolar array of dislocations 7-6635
- interaction between edge dislocation and rigid elliptical inclusion 7-12116
- interaction with circular inclusions in infinite medium, elastic consts. 7-37989
- metals, BCC, H-dislocation interaction mechanism, embrittlement and dislocation motion 7-44600
- metals, FCC, cyclic deform., dipolar wall spacings in dislocation struct. 7-53825
- metals, irradiated, deformation, impurity atmosphere effects (*Russian*) 7-59569
- mixed dislocations, dynamic annihilation study 7-44548
- pipe diffusion, isotope separation 7-58521
- quantum crystals, linear defects, zero-phonon friction mechanism 7-52186
- quartz, synthetic, edge dislocations, optical contrast, birefringence topography studies (*Chinese*) 7-59176
- semi-circular cut on straight boundary, interaction with edge dislocation with inclined glide plane 7-6670
- smectic A liq. crystals, point-like impurity-dislocation interactions, Peach-Kocher formula calcs. 7-11903
- smectic C liquid crystals, twisted, textures 7-51626
- steel, low alloy, damaged surface, comp., displacement dislocations, Auger spectra (*Russian*) 7-59620
- velocity in a crystalline solid, applied shear stress depend. 7-21206
- Al, crystals with edge dislocations, 2D angular correlation of positron annihilation radiation 7-39242
- AlH₃, cryst. imperfection obs., TEM 7-32445
- Au crystallites, annealing, grain boundary untwisting and untilting, dislocation climb and glide 7-12076
- Cu, crystals with edge dislocations, 2D angular correlation of positron annihilation radiation 7-39242
- Cu-Ni alloys, dislocation vel. determ., stress pulse etch pit and slip line cinematography techniques 7-63627
- CuFeS₂, natural chalcopyrite single crystals, deformed, TEM study 7-38002
- α-Fe, cryst., point defect and edge dislocation interaction simulation and radiation creep rate estimation 7-21216
- α-Fe, dislocation pair jog, energy characts., mol. dynamics method anal. (*Russian*) 7-32440
- Fe, edge and screw dislocation density determ., TEM, etching and positron lifetime meas. 7-38006
- α-Fe, edge dislocation, zones of spontaneous absorpt. of point defects 7-44599
- α-Fe, moving edge dislocation, interaction with moving defects (*Russian*) 7-12114
- Fe-Al, B2-ordered alloys, dislocation energies and mobilities 7-58283
- Fe-H system, dislocated single crystals, positron trapping reduction on H charging 7-39262
- GaAs, dislocation-complex defect interactions, photoluminescence studies 7-16608
- GaAs faulted dislocation dipoles, electron diffr. and high-resolution TEM studies 7-44551
- GaAs, undoped, thermal activation of plastic deform., 528-813K 7-6710
- InP, dislocation-complex defect interactions, photoluminescence studies 7-16608
- Li hydrides, (LiAlH₄, LiH, LiBH₄), cryst. imperfection obs., TEM 7-32445
- LiF:Mg²⁺ doped, elec. charge of dislocations 7-6628
- MgH₂, cryst. imperfection obs., TEM 7-32445
- Na hydrides, (NaAlH₄, NaH, NaBH₄) cryst. imperfection obs., TEM 7-32445
- Ni binary alloys, solid soln. hardening, flow stress, Young's modulus 7-13465

edge dislocations continued

- Ni, dislocation-impurity C interstitial interaction, computer simulation studies 7-2046
 Ni-based superalloys, stiffness constns., dislocation line energy and tension, ultrasonic vel. meas. 7-63719
 Ni-Cu alloy, equilb. segregation, embedded atom simulation 7-17538
 Ni₃Al, solid soln. hardening with ternary additions, Young's modulus 7-13464
 Ni₃Al, stiffness constns., dislocation line energy and tension, ultrasonic vel. meas. 7-63719
 PbS-Bi₂S₃, chemically twinned phases, transformation to Galena struct. 7-12078
 Pt-W, Pt diffusion and platelet defect form. (*Russian*) 7-44895
 Si, optical polarisation of nuclear moments in Si with 1D defects 7-7602
 Si, reconstructed structures of symmetrical (011) tilt grain boundaries 7-51785

e.d.p. management *see DP management***education**

- see also computer science education; educational aids; educational courses; teaching; training*
 bioengineering, college-level programs in Indiana, Michigan, and Ohio 7-35144
 Bioengineering Program of the Universidad Nacional de Tucuman (Argentina, 1974-85), cardiac fibrillation, defibrillation research 7-4650
 chemical education in China (Lanzhou University) 7-29611
 cosmos, space education, conf., Copenhagen, Denmark (Aug. 1986) 7-48182
 fluid mechanics education, computer graphics techniques for flow pattern visualisation 7-55939
 grading of students and distributive justice 7-55925
 inverse sprinklers, conservation principle 7-40
 Kolb learning-style inventory system 7-55922
 LWR thermal-hydraulic issues in nuclear training 7-29618
 materials science education frontiers, conf., Boston, USA (Dec. 1985) 7-35112
 nuclear thermal-hydraulics education, Yankee Atomic/Univ. of Lowell experience 7-29615
 optical fibres, refractive indices and birefringence meas., interferometric methods 7-29644
 physics laboratory, undergraduate, computer management system 7-48223
 physics taught as service subject 7-29642
 polyatomic molecules, Franck-Condon factors, calc. for undergraduate quantum chem. 7-60919
 remote site instruction in physics: a test of the effectiveness of a new teaching technology 7-18518
 scanning camera with line CCD sensor for use in schools (*Slovak*) 7-29646
 school-university interface in West Germany 7-14730
 Schrodinger's cat paradox, orthodox soln. 7-29614
 solar water heating system design criteria for schools 7-8442
 space colonization, AIP conference, Geneva, NY, USA (October 1985) 7-4614
 TMI-2 technology transfer, progress report 7-25120
 undergraduates, teaching students to continue their education 7-55924

educational aids

- see also student laboratory apparatus*
 computer graphics techniques for flow pattern visualisation in fluid mechanics education 7-55939
 discontinuous flows, teaching using interactive techniques and windowing 7-60923
 molecular models for overhead projector demonstrations 7-9637
 molecules and ions, resonance, teaching approach using transparent overlays 7-9638
 Newton's laws of rigid body mechanics, proof using stroboscopic photograph 7-55927
 overhead projector, lens addition for image size reduction 7-48246
 SATIS project 7-14729
 Science Toolkit, software, with light and temperature probes, for Apple II 7-35180

educational computing

- see also computer-aided instruction*
 Air-track kinematics and ultrasonic ranging module interface for Apple IIe 7-35148
 cinema and lecture hall acoustic design by computer (*Hungarian*) 7-50850
 computational physics, undergraduate physics option at Univ. of Birmingham 7-29643
 convergence acceleration, computation 7-55938
 fluid mechanics education, computer graphics techniques for flow pattern visualisation 7-55939
 physics A-level teaching, modular microprocessor system 7-48248
 physics laboratory, undergraduate, computer management system 7-48223
 radiotherapy, microcomputer-based computing course 7-65888
 trajectory-plotting program for moving charges in static electric fields 7-29645

educational courses

- A-level physics (Nuffield) investigations, assessment criteria 7-29640
 adsorption calorimetry, beginners course (*Japanese*) 7-35182
 computational physics teaching 7-48226
 EM theory, teaching in one-course setting for undergraduates 7-55923
 energy for art and communication students 7-9620
 GCSE meteorology, course and examination 7-29619
 guided inquiry laboratory at US Military Academy, West Point 7-9621
 imaging science education in the 1980s at the polytechnic of Central London 7-37
 integrated college freshman natural science curriculum 7-48224
 internal assessment of practical coursework in GCSE 7-29613
 laboratory chemistry, students' attitudes 7-9641
 materials science education frontiers, conf., Boston, USA (Dec. 1985) 7-35112
 physics course practical work assessment, state-of-the-art 7-29612
 radiotherapy, microcomputer-based computing course 7-65888
 service chemistry courses, reports and examples 7-48225
 SPISE, Select Programme In Science and Engineering 7-14728
 summer program for high school physics teachers 7-35143

educational courses continued

- technical courses, utilising short writing assignments to improve student writing skills 7-55921
 thermal hydraulics in nuclear engineering courses at the Univ. of Illinois 7-29617
EEG *see electroencephalography*
EELS *see electron energy loss spectra*
EEPROM *see PROM*
effective mass (band structure)
 alkali halide crystals, positronium momentum distrib., effective mass determ., annihilation γ -rays ang. correl. meas. 7-45235
 Anderson model, transport props. at low temps. 7-27311
 binary compound polar semiconductors with nonparabolic energy bands, electronic struct. 7-2478
 d- and f-metals and alloys, anomalous props. due to charge density fluctuations 7-7132
 effective-mass superlattices, band struct. determ., comment 7-38442
 electron and electron-hole liquids, self-energy calculations, effective interactions 7-38473
 graphite intercalation compounds, first stage, with heavy alkali metals, electronic props. 7-2463
 heavy fermion metals, supercond. upper crit. field, temp. depend. 7-45587
 heterostructures with mass modulation in a magnetic field 7-7342
 hole subbands, 4×4 Luttinger-Kohn Hamiltonian, numerical soln. 7-38783
 II-VI semiconductors, shallow donor problem, pseudopot. approach 7-45216
 III-V semiconductor, strained layer superlattice research developments 7-52766
 insulating crystals, delocalised positronium momentum distrib., phonon interactions and apparent mass anal. 7-45236
 interstitial diffusion in crystals, quantum theory 7-44916
 ionic crystals, positronium dynamic props. calcs. 7-45233
 metal surfaces, effective masses, lifetimes, images potential induce states 7-52722
 metal surfaces, plasmon effects on image states 7-7309
 metals, EM generation of acoustic waves, theory 7-51945
 modulation mass superlattice, negative resistance, quantum mechanical reflection 7-52763
 multivalley semiconductors, excited states of shallow donors 7-52514
 narrow-gap cpd. semiconds., weak-coupling polarons, band nonparabolicity effects, comment 7-21830
 one-dimensional conductors, electron-phonon backscatt. and phonon dynamics calcs. 7-38468
 Peierls-CDW state, 1D, impurity distrib., $2k_F$ distortion 7-44593
 phonon-assisted tunnelling between two quantum wells, calc. 7-33073
 polarons, small radius, effective mass studies 7-38465
 polyacetylene:1, metallic, effective mass, magnetoreflexion studies 7-64056
 proximity systems, low-dimensional, Josephson current, field effect, appl. to Nb-InAs-Nb system 7-45573
 quantum well structures, localised states, strain depend. 7-7312
 semiconductor clusters, zero-dimensional excitons, optical spectra and luminesc. 7-12615
 semiconductor junction, size-quantised variable gap layer, 2D electron spectrum and optical transitions calcs. 7-38688
 simple metals, positron studies 7-64729
 superlattice band struct., nonparabolicity effects, Kane theory calcs. 7-2693
 superlattice band structures of group IV and III-V semicond., axial strain effects 7-2697
 superlattices, effective mass eigenfunctions, well capture 7-38704
 superlattices with complex unit cells, conduction band energy levels 7-27402
 transition metals, X-ray electron spectra asymmetry and Fermi level density of states (*Russian*) 7-3112
 two-dimensional electron systems, magnetoconductance, density and mag. field dependences 7-33033
 Ag (111) and (100), effective mass of image-potential states 7-64304
 β -Ag₂Se, high temp. phase, band parameters, energy struct. 7-12603
 AlAs/GaAs/AlAs quantum wells, eigenvalues calcs. 7-12820
 Al_xGa_{1-x}As/GaAs, multilayer and superlattice structs., electronic subbands 7-58877
 AlSb, hot electron luminesc. 7-46119
 As₂Se₃, crystalline, electronic and geometric struct., ab initio total-energy calcs. 7-12607
 Bi, effective electron mass, quasi-1D systems, theoretical investig. 7-2468
 Bi, ultrathin films, size quantization effect on effective electron mass 7-38778
 CdS inversion layers, carrier effective mass calcs. 7-64055
 CdTe, acceptor higher excited states calcs. 7-52511
 CeCu₆, heavy-electron compound, de Haas-van Alphen effect 7-12587
 Cu (100), effective mass of image-potential states 7-64304
 Cu surface states, simple, effective-mass theory 7-38661
 n-GaAs films, magneto-optical studies under high hydrostatic press. 7-13247
 GaAs heterostructures, valence subbands, excitons and luminescence 7-7321
 GaAs, phonon and plasmon deformation potentials, FIR spectra under uniaxial stress 7-26886
 GaAs, space-charge layer effective mass in parallel mag. field 7-2469
 GaAs/AlGaAs single and coupled double wells, energy depend. light hole mass, photolum. spectra anal. 7-38691
 GaAs/GaAlAs 2D electron gas, cyclotron resonance study 7-2676
 GaAs-(AlGa)As heterostructure, modulation-doped, valence band mixing, and optical emission 7-7344
 GaAs-Al_xGa_{1-x}As, modulation-doped quantum wells, photoabsorpt., electronic props. 7-64330
 GaAs-Al_xGa_{1-x}As type I superlattices, electronic struct., tight binding calcs. 7-45475
 GaAs-AlAs ultra-thin layer semicond. superlattices, energy band and stable structs. study 7-52789
 GaAs-AlGaAs-GaAs heterostructure barriers, quantum tunnelling 7-52816
 GaAs-Ga_{1-x}Al_xAs quantum wells, interband photocond. and excitonic Landau level transitions in mag. field 7-27390
 GaAs-Ga_{1-x}Al_xAs quantum well structures, energy spectra of donors and acceptors, spatially dependent screening effects 7-45459

effective mass (band structure) continued

- GaAs-Ga_{1-x}Al_xAs quantum well, hydrogenic donor low-lying excited states, reson. states, positions and widths 7-45460
 GaAs-Ga_{1-x}Al_xAs superlattice localised states in barrier 7-17079
 GaAs-GaAlAs heterojunctions, cyclotron resonance, screening effects 7-38706
 GaAs-GaAlAs-GaAs heterojunction barriers, single particle tunnelling, five level k.p theory 7-64341
 Ga_{0.47}In_{0.53}As/Al_{0.48}In_{0.52}As quantum well, interband magnetoabsorpt. meas., effective mass determ. 7-17088
 Ga_{0.47}In_{0.53}As-InP heterojunction, with three electron subbands, hydrostatic press. effect 7-2695
 Ga_{0.1}In_{0.9}As_{0.1}P_{0.9}, effective masses and alloy disorder effects, shallow donor photocond. 7-64289
 Ge, electron irradi., hole effective mass parameters, cyclotron reson. 7-58730
 Ge, holes optical effective mass, determ. by interf. method 7-17290
 Ge hot-hole cyclotron resonance maser with negative effective hole masses 7-15838
 Ge:H:Si:H amorphous superlattices, electrical transport 7-7336
 Ge_{0.5}Si_{0.5}-Si strained layer heterojunctions, selectively doped, hole mobilities, temp. depend. 7-7383
 HfTe₂, Fermi surface, effective masses, energy bands, determ. from Schubnikov-de Haas effect 7-64051
 HgCdTe IR photodetectors, magnetoresist. and cyclotron resonance characterisation 7-64054
 HgCr₂Se₄ spinel magnetic semicond., electronic struct., elec. props., defects and ferromag. anisotropy 7-38857
 Hg_{1-x}Mn_xTe, magnetoresist. meas., effect of valence band spectrum quantisation at low temps. 7-52653
 InAlAs-InGaAs resonant tunnelling barrier struct., MBE grown, NDR characts. 7-52796
 In_{0.1}Al_{0.9}As/GaAs strained-layer superlattices, effective mass reversal 7-17078
 InGaAs strained-layer superlattices, valence-band nonparabolicity and tailorable hole masses 7-12798
 InGaAs/InP superlattices, effective mass filtering obs. 7-12799
 InGaAs-GaAs and GaAs-GaPAs strained layer superlattices, press. depend. magneto-optic meas. at low temp. 7-27404
 In_{0.5}Ga_{0.5}As, magnetophonon resonance effect 7-21942
 In_{0.2}Ga_{0.8}Sn films, electron effective mass determ., refractive index carrier density depend. meas. 7-38440
 InP, acceptor higher excited states calcs. 7-52511
 InSb, density of states and effective mass determ. 7-38433
 LaS, NaCl type lattice, current carriers and cond. 7-45346
 MgF₂ single crystals, positronium effective mass and phonon interactions, annihilation γ -rays ang. correl. meas. 7-45234
 Na, Ward identity with nonlocal interaction, effective electron mass 7-45130
 PbS, density of states and effective mass determ. 7-38433
 Pd (111), high resolution inverse-photoemission study 7-17357
 Si, excitonic absorpt., MCD spectra, low mag. fields 7-27257
 Sn, valence band struct., angle resolved photoelectron spectra 7-52416
 UPd₃ Fermi surface meas., de Haas-van Alphen effect study 7-12589
 UPT₃ single crystals, electronic structure, low energy reflectivity study 7-45137
 YbAgCu₄, strong electronic correlations 7-45194
 YbAuCu₄, strong electronic correlations 7-45194
 YbPdCu₄, strong electronic correlations 7-45194
 Zn_{0.1}Hg_{0.9}Se, electrophysical props. and carrier scatt. mechanisms 7-17024
 ZnTe, acceptor higher excited states calcs. 7-52511
 ZrTe₃, optical props. 7-64667

effusion

- molecular beam source using multiholed plug effusion cell (*Japanese*) 7-18911

EFG see crystal growth from melt**EHD see electrohydrodynamics****EHT calculations**

- aluminosilicates, at. charges, SCF and semiempirical calcs. 7-2942
 cinnamide compounds, conform., MO calc. 7-56986
 decamethylcobaltocene, electronic struct. and dynamic Jahn-Teller effect EPR 7-59104
 decamethylnickelocenium, electronic struct. and dynamic Jahn-Teller effect EPR 7-59104
 one-dimensional systems, electronic stability and density of states on Fermi surface, topological effect 7-58728
 one-electron model for EHT MO calcs., embedded at. field linkages 7-30953
 polymer interaction with small mol., iterative transfer perturbation method 7-19709
 tetrakis(alkylthio)tetrathiafulvalenes, valence electronic struct., UPS, EHT calcs. 7-21810
 transition metal dithiolates and diselenolates, molecular and electronic structs. 7-52397
 Ag adsorbed layer on Si (111), geometric struct. and density of states, cluster model and charge self-consistent extended Huckel method calcs. 7-21619
 Al-H, H-point defect interactions, extended Huckel mol. orbital calcs. 7-44533
 Fe complex, nucleophilic attack, activation mechanism, EHT and INDO calcs. 7-39847
 α -Fe, H-H binding energy, lattice location and heat of formation 7-32361
 Fe sites in minerals, electronic struct., iterative EHT, multiple scatt. X α calcs. and Mossbauer meas. 7-17244
 I₂, solid, UPES and EHT calcs. 7-64870
 K, electronic band struct., interatomic distance, role of p-orbitals, EHT tight-binding calcs. 7-32906
 Li, electronic band struct., interatomic distance, role of p-orbitals, EHT tight-binding calcs. 7-32906
 Mo₆L₈L'₆, (L, L' = S, Se, Cl, Br), cluster compounds, electronic struct., 3-band model, tight-binding and extended Huckel method calcs. 7-32913
 N₂ on Fe and Re crystals, adsorpt. and dissoc., EHT calcs. 7-56988
 (NH₄)₂SO₄·Ti, mol. orbitals, EHT calc., rel. to absorption spectra 7-64181
 Na, electronic band struct., interatomic distance, role of p-orbitals, EHT tight-binding calcs. 7-32906
- EHT calculations continued**
 Pt₂(P₂O₅H₂)₄⁴⁻, electronic struct., bonding and spectra SCF EHT calcs. 7-42489
 Rb, electronic band struct., interatomic distance, role of p-orbitals, EHT tight-binding calcs. 7-32906
 Re₆L₈L'₆, (L, L' = S, Se, Cl, Br), cluster compounds, electronic struct., 3-band model, tight-binding and extended Huckel method calcs. 7-32913
 S₈, crown struct., pot. hypersurface, EHT calcs. 7-36483
 Sc₂Cl₂B(N) infinite chain phases, single cryst. struct. studies 7-32385
 Sc₂Cl₂B(N) metal-metal bonded cluster phases, single cryst. struct. studies 7-32385
- eigenfunctions see eigenvalues and eigenfunctions**
- eigenvalues and eigenfunctions**
 1D disordered system, random chains and complex transfer matrix attractors 7-61250
 air ducts, cylindrical, radial sound level variations and cross modes 7-50847
 alkyl cpds., vibr., high resol. spectra, effective Hamiltonians 7-31010
 anharmonic oscillator, $\kappa X^2 + \beta X^4$, nonperturbative method study 7-61164
 anharmonic oscillator, short-lived quasi-stationary states (*Russian*) 7-24462
 anharmonic oscillators, quartic and sextic, Schrodinger eqn., eigenvalues, lower bounds calc. 7-41126
 anisotropic materials, crack tip field evaluation, iterative soln. of eigenvalue problem 7-43776
 anomalous positron peaks and Dirac eqn., comment and reply 7-56697
 atomic configurations, energy expressions in L-S coupling scheme 7-49891
 bars, tensile, void coalescence, plastic localisation, failure modes 7-6108
 beam, oscillation eigenfrequencies, follower load effect 7-16110
 Benard-Marangoni's instability, nonuniform temp. gradient and Coriolis force effect 7-43886
 benzene derivatives, vibronic coupling in dimeric systems 7-25533
 Bethe method, thermodynamics and limit states 7-61307
 binary random harmonic chains, special freqs. and Lifshitz singularities 7-35404
 block-tridiagonal Hamiltonian, calc. method 7-18551
 Boltzmann equation, Fourier transform for Maxwell model (*Korean*) 7-24605
 bound-state energies of the generalized exponentialcosine-screened Coulomb potential 7-134
 bounded convergence compact operators, eigenvalue ascents 7-41053
 calculation of eigenvalues through recurrence relations 7-24449
 Caudrey-Dodd-Gibbon-Sawada-Kotera eqn., solitons and discrete eigenfunctions 7-35232
 chaotic repellers as eigenvalues, charact. exponents 7-41250
 chaotic systems, quantum description, complete integrability 7-9705
 complex domain, behaviour of eigenfunction expansion, pointwise convergence 7-61040
 complex eigenvalues of differential eqns., critical layer singularities, review 7-4714
 complex resonance eigenvalues by the Lanczos recursion method 7-10375
 convective dispersion and interphase mass transfer 7-51269
 Coulomb dipole matrix elements, nonvanishing 7-135
 Coulomb-like pot., bound and resonant state calcs. 7-48428
 critical point calculation with nonzero interaction parameters 7-32597
 criticality transport problems for spherical systems with specular boundary conditions 7-61292
 cubic crystalline field eigenstates and energies, group-theoretical computational approach 7-21877
 de Sitter space, integral transform in (4+1) dimens. 7-35666
 defective eigenvalues, simultaneous inverse iterations 7-48344
 dielectric closed shell quantum systems, SCF energy surface, catastrophe theory anal. (*Rumanian*) 7-14832
 differential eigenproblems, error estimation 7-61007
 differential eigenvalue equations, second order, extension of renormalized Numerov method 7-29737
 diheliumacetylene dication, metastable, C-He bond prediction 7-49888
 dilute dimple gas, equilibrium eigenmodes 7-16291
 Dirac's formalism generalised eigenfunctions in trajectory spaces 7-18637
 Dirac equation, minimax principle for eigenvalue calcs. 7-419
 Dirac operator in 0=3, 4, 7, 8 characterisation of round sphere by first eigenvalue 7-9687
 Dirichlet discontinuity factor analogue for non-self-adjoint extensions of a Laplace operator (*Russian*) 7-60991
 dirty superconductors, strong-coupling eqns., disorder effects 7-64393
 discrete scatt. theory, eigenvalue problems and nonlinear differential-difference evolution eqns. 7-4725
 discrete Schrodinger operator absence of localisation 7-48424
 disordered ultrametric models, relaxational dynamics, eigenvalue and eigenmode determ. 7-4789
 distortion analyticity and molecular resonance curves 7-57040
 double-sine-Gordon kink, eigenfunctions of small oscillations 7-18995
 eigenfunction methods and nonlinear hyperbolic boundary value problems at resonance, wave eqn. appl. 7-61121
 eigenvalues, sensitivity under elementary matrix perturbations 7-60955
 Einstein field eqns. without symmetries, perfect fluid solns. 7-41171
 elastic waves in a periodic band (*French*) 7-11336
 elasticity, dynamical theory, ray series method appl. to axisymmetric non-stationary problems 7-41114
 electron microscope image reconstruction, geometrical transformation groups for 3D object 7-371
 electron microscopic molecule images reconstitution, correspondence analysis, struct. interpret. tool 7-60138
 EM scattering and eigenvalue problems, numerical solution, hybrid technique 7-50478
 evolution equations, nonlinear, multisoliton solns. 7-48377
 Feigenbaum attractor, fractal dimension, calc., comments 7-35413
 Fermi systems, boson representation, composite particle theory 7-48541
 fermion field on a random lattice 7-35716
 Fibonacci chain eigenstates study 7-35459
 field-reversed mirrors, axisymm. eigenmodes calcs. 7-32046
 finite difference and shooting methods for ODE eigenvalue problems, relationship 7-35250
 finite difference eigenvalues, asymptotic correction 7-18324
 finite-size scaling in strips, log. corrections, Potts model appl. 7-35429
 force-deflection anal., eigenvalue convergence in the finite element method 7-24420

eigenvalues and eigenfunctions continued

Fourier transform ion cyclotron reson. spectra, residual spatial mag. field gradient effects 7-42550
Fredholm alternative generalisation for nonlinear diff. operators, boundary value problem 7-9652
functional equations, exact soln., differential eqn. approach 7-73
gas phase relaxation process, bulk props. at early times, anal. soln. 7-50319
geophysical eigenvalues, efficient computation 7-18323
ground-state energy, lower bound by Steiner pot. symmetrisation 7-48426
gyroscopic systems, undamped, eigenproblem soln. with Lanczos algorithm 7-4668
hard disks and spheres, power series expansions, critical point singularities 7-44333
harmonic oscillator, schrodinger equation and canonical perturbation theory 7-48401
Hausdorff dimension inequalities for ordinary differential eqns., applications 7-56000
heat conduction, boundary value problems, eigenvalues eval. 7-62949
Hermitian matrix linearisation using LINRZ program 7-48269
Hopf bifurcation and symmetry, traveling and standing waves on circle, reaction-diffusion eqns. 7-56192
hot QCD, nonAbelian Debye screening, singlet pot. and gauge symm. breaking 7-49075
hydrogenic atoms in potential $V(r)=gr+\lambda r^2$, exact solns., ground-state eigenvalue bounds, moment calcs. 7-49910
hyperbolic potential functions, energy eigenvalues 7-42725
III-V semiconductor surfaces (110), Sb p(1 × 1) overlayers, atomic and electronic struct. 7-7007
incommensurate systems, fractal spectra, Aubry model energy spectrum 7-12581
incomplete crystals, surfaces, defects, interfaces and layered structures, theory 7-16926
indefinite Sturm-Liouville problems, half-range solns. 7-55979
inequality properties of eigenfunctions and adjoint functions of an ordinary differential operators (*Russian*) 7-55976
inert gas, contracted discharge, ionisation waves, 2D theory 7-16343
infinite graphs with the least limiting eigenvalue greater than -2 7-24357
integrated optical waveguides, finite difference anal. without spurious mode solns. 7-1262
intermittent chaos, global spectral structs. for periodic laminar motions with turbulence 7-41271
interpolation of eigenvalues, integration scheme 7-32894
IR detector arrays, directions-of-arrival estimation, eigenstructure approach 7-56334
Ising model, quantum Hamiltonian rel. to one-spin transfer-matrix descriptions 7-56180
Jordan form, influence of marked reduced graph of nonnegative matrix 7-55956
Kadomtsev-Petviashvili eqn., recursion operator, Schrodinger operator, squared eigenfunctions 7-24478
Klein-Gordon eqn., large-N solution 7-4708
laminar channel flow with stepwise variations of wall temp., transient forced convection 7-37426
laminar duct flow subjected to axial variation of heat transfer coeff. 7-51111
Laplacian, eigenspaces on hyperbolic spaces, composition series and integral transforms 7-48333
large scale, conference, Oberlech, Austria (July 1985) 7-48189
laser modes, intensity correlations; effective eigenvalue charactn. 7-50531
Lie superalgebras, Casimir operators for infinite-dimens. representations 7-9647
liquid film downflow, Orr-Sommerfeld eqn. soln., optimal approach 7-51119
local density functional theory, physical significant of eigenvalues, orbital electronegativity and ionisation pot. 7-62245
locally perturbed XY model, return to equilibrium, one particle Hamiltonian 7-9791
low energy scattering theory for one-dimensional systems with $\int dx V(x)=0$ 7-61153
macroscopic system, quantum energy eigenvalues near separatrix energy 7-41152
many electron atom and ion systems, theoretical model 7-14815
many-electron atoms, relativistic HF and RPA calcs. 7-19675
many-fermion Hamiltonian, relationship among fermion pairs, pairons and natural spin geminals 7-41242
matrix polynomials, common multiples, divisors and eigenvalues 7-55955
minimax theory, radical simplification 7-56060
molecular spectra, program for symmetry-adapted rotational eigenfunctions and energy levels of asymmetric top molecules 7-4324
molecular systems, disordered, influence of noise on density of states and absorption 7-16949
molecular unit orbital approx., theory and numerical calc. method 7-25340
multichannel reaction matrix theory and CI in discrete and continuous spectrum 7-49873
multigroup linear transport in exponent half-space, exit distrib. problem 7-48644
multigroup linear transport in exponent half-space 7-48643
multiple-stripe-geometry laser arrays, chirped and unchirped, modal eigenfunctions 7-57335
multiplicity results for nonlinear elliptic equations involving a critical Sobolev exponent 7-24397
N×N matrix differential operators, spectral problem on the line 7-56086
non-negative irreducible matrix, spectrum localization using Holder norms 7-60937
nonlinear gravity-capillary waves, stability 7-16161
nonlinear Schrodinger equation with an external field, soliton studies 7-41121
nonlinear time evolution eqns., bifurcating periodic solns. 7-48562
nonrelativistic multichannel scatt., strong limit of operator values sequence 7-29818
nuclear matter, one-dimensional, simultaneous eigenstates of spin, isospin and energy 7-56631
one-dimensional incommensurate model, mobility edges and electronic density of states calcs. 7-21799
one-dimensional oscillators, two-step coherent state approx., modified operator method 7-35326
operator theory, symposium, Athens, Greece (Aug. 1985) 7-55878

eigenvalues and eigenfunctions continued

optical reflection from planetary surfaces, operator-eigenvalue theory 7-24032
optical waveguide arrays, nearly uniform coupled, perturbation anal. 7-5992
orbital systems, fractionally occupied, density functional theory, appl. to ionisation and transition energies 7-42451
orthogonal Waller-Hartree spin eigenfunctions 7-56142
oscillators, nonseparable systems, higher order resons., eigenvalues, semiclassical calc. 7-4705
particle dynamics in Coulomb pot. anisotropic harmonic oscillator pots. 7-61163
particle families as radial excitations, eigenstates of relativistic wave eqns. 7-30179
particle in a box, eigenvalues and eigenfunctions, Gaussian wavepacket dynamics anal. 7-118
particle moving in free space, eigenfunction normalisation 7-29638
Pearlstein-Berk mode of drift waves in slab geometry, variational anal. 7-26422
Peierls-Hubbard model, exact and approximate solns. 7-52383
pencils of matrices, lower eigenvalue bounds 7-48280
period doubling in four-dimensional symplectic maps 7-29721
periodic Lyapunov and Riccati difference equations, inertia theorems 7-48311
periodic potential, perturbation theory, level-splitting and large-order behaviour 7-61144
periodic trajectories for nonintegrable 2D Hamiltonians 7-48448
phase conjugate mirror, non-degenerate, for resonator system, mode selectivity and misalignment sensitivity 7-20356
phase space eigenfunctions of multidimensional quadratic Hamiltonians 7-144
phase space exploration, quantum localisation 7-61245
plasma diffusion and heat flow coupling, and anomalous transport 7-44106
plates, circular, plastic limit load numerical evaluation using Mises yield criterion 7-20604
plates, flat, clamped, expt. eigenvalues and mode shapes 7-63035
plates, flat clamped, vibration, eigenvalues and mode shapes 7-31670
plates, orthotropic, linear bending and buckling, eigenvalue problems 7-37352
potential scattering R matrix, Wigner infinite product representation 7-131
pyrazine $S_1(^1B_{3g})$ state, rot. induced vibr. energy redistrib. and K selectivity model 7-10710
quantum cusp, catastrophe pot. 7-132
quantum mechanical systems, U-matrix theory anal., eigenstates 7-61157
quantum optics, squeeze operator, eigenvalues and eigenfunctions 7-20172
quantum system, discrete energy spectra, time evolution 7-48398
quasi-lattices, two-dimensional, tight binding electron props. 7-27233
radial functions of non-self adjoint Laplace operator, inequalities (*Russian*) 7-48303
radiative transfer cylindrically symmetric infinite homogeneous medium, anisotropic scatt., orthogonal eigenfunctions determ. 7-41306
random Schrodinger equation, transition from pure point to continuous spectrum 7-48460
ray matrix method for analysis of opt. resonators with image rot. 7-50599
reaction-diffusion equations, pseudo-arclength continuation method for nonlinear eigenvalue problems 7-35481
rectangular elastic plate problem, bifurcations near a multiple eigenvalue 7-6098
resistive MHD, complex eigenvalue spectrum computations 7-51336
resonance energies and widths, comparison of theoretical methods for short-range potentials 7-14814
resonance state determ. using complex scaling method 7-36443
resonance states, wave function localisation using optical potential 7-14811
resonance wave functions, normalisation, reson. width calcs. 7-130
resonant classical motion, EBK quantisation, Fourier transform approach, semiclassical eigenvalues 7-42587
rotating compressible flow, nonself adjoint operator, eigenvalue problem 7-57861
rotating cylindrical cavity, inertial waves in fluid, time-depend. complex eigenfrequencies 7-57856
rotating harmonic, 3D, and doubly anharmonic oscillators, Schrodinger eqns., confinement pots. 7-35313
Rydberg atoms in uniform magnetic field, quantum stochasticity, eigenvalue spectra calcs. 7-42526
Schrodinger equation, eigenstate determination using large N method 7-61167
Schrodinger equation, Hill determinant method, false eigenvalues 7-9697
Schrodinger equation soln. for few-body systems, variational method 7-4701
Schrodinger equation with polynomial potential, soln. using numerical method 7-41125
seismology, asymptotic normal modes of laterally heterogeneous Earth 7-40425
self-adjoint operator, quasi-eigenfunctions 7-29658
shifted 1/N expansion for energy eigenvalues of the exponential cosine screened Coulomb potential 7-36442
shifted 1/N expansion for the Hulthen potential, atomic appl. 7-42453
Sierpinski carpets, classification and universal props., Potts model critical points 7-61259
simultaneous reduction of sets of matrices under similarity 7-55954
spin precession, classical adiabatic angle and geometrical phase 7-49882
spinning structure dynamic anal., free vibr. problem, numerical algorithms 7-37366
spontaneous emission by single atom in ideal cavity 7-31001
statistical spatial acoustics, reverberation time meas. for low density of eigenfrequencies (*German*) 7-57637
stellar pulsations, eigenfreqs. of low-frequency oscillations of uniformly rotating stars 7-60635
Stokes phenomena and monodromy deformation problem for nonlinear Schrodinger equation 7-24445
structure matrix of (0, 1)-matrices, rank, trace and eigenvalues 7-29671
Sturm-Liouville boundary value problems, sinc function computation of eigenvalues 7-61006
Sturm-Liouville system, eigenvalues of boundary value problem from band matrix inverse 7-60959
sudden approximation, classical limits 7-4704

eigenvalues and eigenfunctions continued

- sum-rules in resonance calculations with complex coordinates 7-42527
- super AKNS scheme and its infinite conserved currents, 3x3 eigenvalue problem 7-434
- superlattices, band theory 7-45124
- superlattices, effective mass eigenfunctions, well capture 7-38704
- surface energy term, particle in cube or square with infinite pot. walls 7-58604
- TDHF approximation for soluble models with large degeneracies 7-24944
- thermoelasticity, spectral theorems via eigenfunction expansions 7-26149
- transport in semi-infinite ducts, singular integral eqn. formulation 7-48641
- triatomics, closed shell configs. SINDO method calcs. 7-19705
- two-centre Dirac equation with separable potentials 7-61473
- two-electron atomic states with conserved angular momentum and parity, Schrödinger eqn. 7-5593
- unstable resonators with 90° beam rotation 7-5918
- upper convected Maxwell fluid, plane Couette flow, linear stability 7-16160
- viscous fluid in porous medium, stability criteria for convection, eigenvalue problems 7-44033
- von Neumann measurement postulate, generalised gauge independence and physical limitations 7-48406
- water waves, reson. freqs. in baffled container, linearised theory investig. 7-57867
- XXZ chain, conformal invariance and spectrum 7-63768
- AlAs/GaAs/AlAs quantum wells, eigenvalues calcs. 7-12820
- CS, singlet and triplet excitations, selective control, coherent multicolor laser spectroscopy 7-42629
- CS₂, dynamical model for lattice frequencies and cryst. field splittings 7-16699
- GaAs n⁺-n-n⁺ structs., quasi-elastic inter-Landau-level scattering processes 7-17086
- Ge, heavy holes, Landau level spectrum, optical gap form. 7-45191
- H atom, Dirac equation, separation and eigenvalue anal., hyperfine splitting in 1S state, 2S state shift 7-36807
- H, impurity in metals, electronic struct., higher order approx. 7-52518
- H⁺, free-free absorpt. coeff., R-matrix method 7-62524
- H₂ and isotopes, nonadiabatic eigenvalues and adiabatic matrix elements 7-62381
- H₃⁺, Born-Oppenheimer electronic polarisability, perturbational-variational Rayleigh-Ritz formalism appl. 7-10387
- H₃⁺ and isotopes, semiclassical vibr. eigenvalues, adiabatic switching method 7-57043
- H₂O, vibr.-rot. eigenvalues, calc. 7-31007
- Li, excited states, electron correlation calc. (Chinese) 7-10438
- Mg isoelectronic series, energy levels, multiconfig. optimised pot. model calcs. 7-19723
- Mg₂SiO₄ single cryst., ¹⁷O nuclear quadrupole coupling tensors determ. 7-13057
- Rh_x(CO)_y (x=4 to 7, y=12,15,16), metal cluster bonding topology, graph theory 7-42817
- SiF₄, stretching vibr. overtone and combination states, multiphoton processes 7-25488
- Si(001), 2 × 1 surface relax. and vibr. excitations 7-6949
- ²³²Th, space-dependent fast neutron spectra, eigenvalue and eigenfunction study 7-30532
- TmCu₂, ³H₆ multiplet splitting, cryst. field effect 7-52533

eigenvectors see eigenvalues and eigenfunctions**eightfold way see SU₃ theory****Einstein-de Haas effect**

- see also gyromagnetic ratio
- No entries

einsteinium

- see also nuclei with
- diffusion in Ta-Es dilute alloy 7-12353
- solid state and thermodynamic props., f-electron bonding and struct., review 7-12321

einsteinium compounds

- No entries

elastic aftereffect

- Nb, elastic aftereffect due to O, press. effect and clustering 7-32548

elastic constants**see also elastic moduli**

- alkali cyanides, multipole interaction effects on cohesive and anharmonic props. 7-1942
- alkali halide mixed crystals, phys. props., review 7-37943
- alkenyl esters, nematic liq. crystals, influence of rigid cores, side-chains and polarity on props. 7-16405
- alloys, two-phase, models of tensile behaviour from components 7-46570
- anisotropic crystals with chain structure, elastic Green tensor 7-6700
- cadmium arachidate Langmuir-Blodgett films, elastic props., Brillouin scatt. study 7-32885
- composite column, Euler load determ. by direct computation 7-62976
- corundum (α-Al₂O₃), elasticity and high pressure instabilities 7-66103
- crystals, form. of phonon-focusing caustics, rel. to catastrophe theory 7-2116
- cubic materials, textured, diff. elastic consts., Voigt model calcs., Hill approx. 7-51913
- diamond, optical phonons and elasticity at megabar stresses 7-21375
- disordered solids, 3rd order elastic constants, Green's function approach 7-38088
- edge dislocation interaction with circular inclusions in infinite medium, elastic consts. 7-37989
- ferroelectric liquid crystals, distortion free energy density, electrostatic screening 7-37844
- fibre reinforced composites, random short fibre, fatigue damage evolution assoc. with anisotropic elastic prop. changes 7-44673
- glasses, elastic properties, theory 7-12189
- glasses, photoelastic constants, evaluation method 7-39080
- grain boundary dislocations, elastic props. 7-21205
- graphite-K intercalation cpd., KC₂₄, 2D layer melting dynamics, neutron scatt. meas. 7-21420
- graphite-Rb intercalation cpd., RbC₂₄, 2D layer melting dynamics, neutron scatt. meas. 7-21420
- icosahedral solids, third-order elastic constants 7-32543
- III-V ternary alloy semiconductors, short-range order 7-44821
- N-isopropylcarbazole, phase transition, elastic props. 7-38087
- magnetic garnet films, stress induced optical anisotropy 7-53430

elastic constants continued

- material, homogeneous, isotropic, stiffness and strength reduction due to crack development 7-51927
- metal sheets with randomly drilled holes, nonuniversal critical behaviour meas. 7-45259
- metal superlattices, elastic and plastic props. 7-27085
- metallic superlattice elastic and acoustic props. 7-2086
- metallic superlattices, elastic props., effect of strain 7-52376
- metallic superlattices, mech. props. and diffusion 7-52377
- metals, BCC refractory, mag. susceptibility, elastic consts. and compressibility 7-33142
- misfitting cuboidal inhomogeneities, elastic interaction and stability, determ. 7-63713
- NaCl single cryst., high temp. elasticity meas., rectangular parallelepiped reson. method 7-63714
- nematic liquid crystal displays, multiplexed twisted, elastic constants of hybrid mixtures 7-2078
- nematic liquid crystals, supertwisted, hysteresis effect 7-16408
- nematic liquid-substrate interface, orientational transitions, wetting, Landau-de Gennes theory 7-63914
- nematic solutions of rod-like and semi-flexible polymers, elastic constants 7-32537
- nematics, disc-like mols. Frank consts. ratio meas. at mag. Frederiks transition to columnar phase 7-58136
- nematics, elastic constants calc. 7-63703
- octylcyanobiphenyl, liq. cryst., elastic consts., permitt., birefr. meas. 7-21314
- orthorhombic paramagnet, J=1, external field induced Jahn-Teller effect (Polish) 7-7179
- orthotopically damaged elastic solid, effective material consts., constitutive eqn. 7-1489
- paramagnets, tetragonal, magnetoelastic excitations and struct. phase transitions 7-27489
- perfect crystal tensile strength, anisotropy and interatomic pot. effect 7-12187
- PET, biaxially oriented sheets, orientation rel. to mech. compliance 7-53781
- piezoelectric media, finite, elec. and elastic multipole defects 7-43673
- PMMA, drawn, filled with ultrafine SiO₂ particles, elastic and yield props. 7-3351
- polycrystal average elastic consts., tensor invariants calcs., general formalism 7-63718
- polycrystalline aggregates with texture, thermal expansion coeffs. 7-52091
- polycrystals, elastic const. press. derivative, self-consistent T-matrix calcs. 7-26828
- polycrystals with trigonal crystal and orthorhombic specimen symmetry, elastic props. 7-44646
- polycrystals, X-ray elasticity consts. calc. from elastic const. data of single cryst. of arbitrary cryst. symm. (German) 7-16668
- polymer honeycomb filter, strength and stiffness in shearing determ. 7-17634
- polymer nematic-liquid-crystal cells, periodic Freedericks transition investig. 7-32282
- polymer spherulites, elastic deform., effect of spherical axis 7-33718
- polymers, piezoelectricity, elec. cond. effects, three-phase model calcs. 7-33336
- polyvinylidene fluoride sheet evaluation for large sonar arrays 7-2986
- α-quartz, electroelastic constants meas. 7-59151
- quartz plates, doubly rotated, thickness vibr., frequency-temperature behaviour 7-20624
- rare-gas solids, phonons, close to melting 7-63757
- rocks, dynamic elastic const. determ. (Japanese) 7-29312
- rough surfaces, elastoplastic deform. in real contact zones, friction coeffs. calc. 7-16136
- second order phase transition, wave vector depend. susceptibility, elastic coupling effects, mean field theory 7-32599
- self-diffusion and impurity diffusion coeffs., calculation with aid of elastic constants 7-16797
- steel, austenitic stainless, single crystals, rolling texture and elastic consts. (Russian) 7-51912
- stiffness calculations for superlight industrial robots 7-22743
- stishovite (SiO₂), elasticity and high pressure instabilities 7-66103
- stress field around interface crack 7-37378
- strongly anisotropic layer crystals, elastic Green tensor, calc. 7-44645
- superlattices, photoelastic, elastic and dielectric consts. in long wavelength regime 7-33361
- system sensitivity for a class of mechanical systems by the method of structural numbers 7-43656
- textured sheets, Young's modulus anisotropy, elastic consts. calc. 7-46535
- thin layered superlattices, effective dielectric and photoelastic constants, determ. 7-53268
- TMMC, pure and Cu doped, struct. phase transitions, Brillouin scatt., study 7-46055
- tobacco mosaic virus in water, freeze-fracture imaging of ordered phases 7-3751
- two-dimensional soap froth, shear elastic const. 7-3610
- ultrasound, anharmonic props. under intense excitation in diamond-like crystals and quartz plate 7-20488
- Ag, binding energies and elastic constants, one-parameter model pseudopotential calc. 7-44650
- (Ag₆Sn₂P₁₂)Ge₆ cluster cpd., elastic behaviour and vibr. anharmonicity 7-12223
- α-Al₂O₃, ceramic matrices, precip. morphology 7-65049
- Al₂O₃, trigonal crystal, elastic constants, rectangular parallelepiped resonance study 7-38090
- AlP(As)(Sb), elastic coefficients, pressure effects 7-63720
- α-AlPO₄, berlinite, elastic const., thermal behaviour (Chinese) 7-6699
- α-AlPO₄, berlinite, piezoelec. and elastic props., effect off defects on phys. props. 7-51909
- Au, binding energies and elastic constants, one-parameter model pseudopotential calc. 7-44650
- Ba(Ca_{1/3}Nb_{2/3})O₃-PbZrO₃-PbTiO₃ ceramics, hot-pressed, ferroelectric phase transitions 7-7652
- BaF₂, low temp. thermal expansion, calc. 7-44867
- BaTiO₃ single crystal, elastic and piezoelec. coeffs. 7-2979
- Bi₁₂Si(Ge)O₂₀ crystals, sillenite struct., dielec., elastic and piezoelec. props. calcs. 7-51714
- C fibre reinforced epoxy, laminates, quasi-isotropic, response to biaxial stress 7-33732
- Ca, cryst., FCC, generalised Morse pot. and mech. stability 7-6575

elastic constants continued

- Ca, FCC and BCC, lattice dynamics 7-38134
 CaCO₃, calcite, polycrystals, elastic props. 7-44646
 CaF₂, low temp. thermal expansion, calc. 7-44867
 CdS(Se), X-ray graphic elastic constants and lattice spectrum 7-32546
 Cr-Mo dilute alloys, magnetoelasticity, antiferromagnetism disappearance effects 7-45789
 Cs BCC single cryst., lattice dynamics, coherent inelastic neutron scatt. study 7-21376
 CsX (X=Cl,Br,I), low temp. thermal expansion, calc. 7-44867
 Cu, binding energies and elastic constants, one-parameter model pseudo-potential calc. 7-44650
 Cu, cubic polycrystals, elastic consts., Young's modulus rel. to axial texture (*Russian*) 7-59562
 Cu two-dimensional systems, lattice and continuum percolation transport exponents 7-45275
 β -Cu-Zn-Al alloys, elastic constants and lattice stability 7-13492
 CuGe₂P₃, semicond., elastic consts., anharmonic props. 7-26830
 Fe, cubic polycrystals, elastic consts., Young's modulus rel. to axial texture (*Russian*) 7-59562
 Fe-C system, elastic anal. of deform near spherical C particle embedded in Fe matrix 7-63709
 Fe-Ni-Cr-Ti-B, constant elastic alloy, torsion reson. freq. temp. coeff. rel. to B content (*Chinese*) 7-13488
 Fe-Pd multilayer structs., localised phonon modes 7-46061
 FeCl₃, magnetostriction, X-ray diff. meas. 7-33258
 FeTiO₃, ceramic matrices, precip. morphology 7-65049
 (Ga_{0.5}Al_{0.5})As, MBE grown, elastic consts., diffuse X-ray scatt. study 7-16918
 GaAs interatomic force consts. and normal modes, group theoretical method calcs. 7-32588
 GaAs third order elastic constants, US displacement interferometry 7-2087
 GaN, X-ray phase anal., elastic props. 7-45050
 Ge third order elastic constants, US displacement interferometry 7-2087
 Ge-Se-As glasses, elastic constants, rigidity percolation 7-44648
 HF solid, elastic and photoelastic anisotropy at high press. 7-2083
 In, crystallographic equivalence between BCT and FCT structs. 7-37924
 InGaAs/InP heteroepitaxial structs., misfit stress, elastic eqns., comment 7-21676
 (KBr)_{1-x}(KCN)_x mixed crystals, elastic shear const. and internal friction, torsion pendulum resonance meas. 7-26829
 KCl-KBr mixed crystals, cohesion, harmonic and anharmonic props. calcs. 7-51907
 KCl_xMn_{1-x}Ca(Mn), doped crystals, elastic constants, meas. using US pulse superposition method 7-26827
 La₂Ga₂SiO₁₄, elastic and piezoelectric consts., temp. depend. 7-53242
 LaNbO₄, single crystal, elastic props. 7-51915
 Li₂B₄O₇, temp. compensated piezoelectric cryst. SAW study 7-12452
 LiKSO₄, Brillouin light scatt. between 20 and 80°C, elastic constants meas. 7-7712
 LiKSO₄, phase transition, low temp. Brillouin studies 7-44806
 LiNaSO₄, trigonal, phys. props. 7-13099
 LiNbO₃, elastic and dielec. props. 7-63715
 LiNbO₃, γ -irradiated, elastic and piezoelectric props. 7-45935
 LiNbO₃, nonlinear elastic, piezoelectric, electrostrictive and dielectric consts. 7-64573
 LiNb_{0.1}Ta_{0.9}O₃ single cryst., piezoelec., pyroelec., dielec. and elastic consts. 7-53565
 ND₃, elastic consts. and elasto-optic coeffs., Brillouin spectra anal. 7-53359
 β -NH₄LiSO₄, elastic stiffness constants, ultrasonic pulse echo overlap meas. 7-12188
 NaBF₄, orthorhombic, cryst. growth and phys. props. 7-7834
 Na-Na₃, microscopic theory of elastic softening 7-16665
 NaN₃, trigonal-monoclinic phase transition, Brillouin scatt. studies 7-22275
 NbC, elastic constants, meas. 7-6703
 Nb₃Ir films, lattice-stiffness changes due to ion irradiation, Brillouin scatt. 7-52379
 Nb₃Sn_{1-x}Sb_x, A15 pseudobinary alloy, structural transitions and related anomalies 7-38182
 Ni-based superalloys, stiffness consts., dislocation line energy and tension, ultrasonic vel. meas. 7-63719
 Ni₃Al, stiffness consts., dislocation line energy and tension, ultrasonic vel. meas. 7-63719
 PZT piezoelectric ceramic prop. meas., applied compressive stress parallel to polar axis 7-45939
 Pb_{4.7}Ba_{0.3}O₁₁, rhombohedral, acoustic symmetry and vibr. anharmonicity 7-16695
 Pb₃Ge₃O₁₁, rhombohedral, acoustic symmetry and vibr. anharmonicity 7-16695
 PbSe and other IV-VI cpds., acoustic mode vibr. anharmonicity 7-63751
 Pd, single crystals, high temp. elastic props. 7-63710
 Pd-B-H alloys, internal friction, elastic consts. 7-26857
 RbI single cryst. high press. Brillouin scatt. meas. 7-3061
 α -S orthorhombic, elastic behaviour under pressure, lattice dynamics anal. 7-16667
 Sb alloys, polycrystalline, elastic consts. meas. 7-21319
 Si, elastic consts., mol. dynamic calcs., shear modulus 7-6705
 n-Si, ultraheavily doped, Rayleigh surface waves, Brillouin scatt. study 7-21605
 SiO₂, electroelastic consts. meas. (*Chinese*) 7-39040
 SnTe, acoustic mode vibr. anharmonicity 7-63751
 SrF₂, low temp. thermal expansion, calc. 7-44867
 TiNi, mono- and polycryst., elastic props. and internal friction, premartensitic anomalies (*Russian*) 7-59564
 V-H(D), elastic shear consts., temp. depend., effect of H and D 7-63711
 VD_x, force dipole tensor and elastic consts., diffuse X-ray scatt. obs. 7-26831
 WSi₂-WSi, effective elastic consts., surface acoustic wave anal. 7-58597
 Yb, cryst., FCC, generalised Morse pot. and mech. stability 7-6575
 ZnCl₂, pure glass, elastic consts. and struct. 7-63716
 ZnO, X-ray graphic elastic constants and lattice spectrum 7-32546
 Zr, α and β phases, differential heat of H absorption, isoperibol calorimetry studies 7-6967
 ZrO₂, ceramic matrices, precip. morphology 7-65049

elastic deformation

- see also bending; elasticity; electrostriction; stress-strain relations; torsion
 acoustoelastic effect, influence of plastic deformation, stress distrib. in slightly orthotropic materials 7-16069
 bar, hyperstatic nonlinear bending 7-6091
 beam theory, torsion, buckling and vibr. problems 7-1458
 beams, linear elastic in contact problems, moving FEM 7-20663
 beams and rods, small strain deformations including large deflections 7-1423
 biomechanics dynamic problems, deformable solid model with reaction 7-47140
 boundary element method for elastostatics with internal constraints 7-29758
 columns subjected to intermediate concentrated load, stability analysis, FEM 7-20608
 composites, binary elastic, effective transform. strain 7-44660
 contact problem, dual FEM for elastic bodies with enlarging contact zone 7-57763
 correction plate fabrication by elastic deformation method for free support of blank 7-43455
 curved beam elements with penalty relaxation 7-37335
 cylinders and spheres, hollow, internally pressurised, finite deform. for class of compressible elastic material 7-43676
 defective crystals, continuum theory 7-51767
 elastically deformable porous medium, gas filtration during dynamic expansion of cavity 7-16248
 elastoplastic bodies, Landau phase transitions, order parameter fluctuation effects calcs. 7-44739
 elastoplastic shells under finite deformation, general dynamic theory (*German*) 7-6116
 fibre reinforced composite, spatially reinforced, deform. props. eval., rigidity 7-6097
 fibrous material slender models 7-1407
 finite length straight pipe subject to waterhammer, wall elastic deform. 7-37544
 frame response to a harmonic excitation, taking into account the effects of shear deformation and rotary inertia, Timoshenko beam theory 7-6132
 grainy liquid saturated medium 7-1425
 granular materials, shear band analysis by Cosserat theory (*German*) 7-20598
 hydroelastic three-layer cylindrical shell reaction to internal explosion, elastic deform. 7-31692
 hyperelastic materials, elastostatic equilib., weak convergence of sets of constraints (*French*) 7-61100
 hyperelastic materials, localisation of deformation, gradient approach 7-16066
 impact test, stress strain relationships, elastic deformation, specimen connected with long bar (*Japanese*) 7-11290
 infinite plate, plane rectilinear crack, pot. method soln. 7-63070
 inhomogeneous theory of elasticity with deformations 7-9672
 lenses, cement contact, heat resistance depend. on construction parameters 7-43299
 mechanoluminescence studies of crystal structure 7-59268
 membrane, elastic, with rigid inclusion, finite deform. 7-57692
 membranes, cylindrical, unsymmetric solns. 7-37339
 metals, inhomogeneity of elastic and plastic deform. 7-58399
 minimum elastic strain energy, deform. 7-38097
 orthorhombic crystals, deformed, elastic moduli and stability 7-16666
 orthotropic spherical caps, nonlinear axisymmetric response under shear deform. 7-31644
 photodisplacement techniques for defect detection 7-44865
 plane elasticity, two-grid FEM method 7-6089
 plate, annular, elastic wrinkling under uniform tension on inner 7-50950
 plate, damped elastic infinite, adjacent semi-infinite fluid, impulsive force effect study 7-63052
 plate/shell element, field-consistent four-noded laminated anisotropic 7-62983
 plates, first-ply failure analysis of composite laminates 7-63053
 plates, laminated composite, 3D hybrid stress isoparametric element 7-56020
 plates, multilayered shear-deformable, finite elements 7-43667
 cis-1,4-polyisoprene networks, uniaxial extension, stress-strain relation 7-39605
 polymer solution flow, elastic deformation effects 7-43670
 polymer spherulites, elastic deform., effect of spherical axis 7-33718
 polymers, deformation, elastic and plastic, IR spectrosc. obs. (*Russian*) 7-64659
 polyoxypropylene, cross-linked model networks, swelling, elastic stress-strain props. 7-46540
 poroelastic medium deform. containing thin internal crack, approx. solns. 7-62990
 precipitates, inhomogeneous, elastic fields 7-39531
 PVC-styrene-butadiene rubber blends, bending in elastic range 7-39606
 rate-type finite elasticity constitutive law, elastic and elastic-plastic deformation 7-57700
 rigid line inhomogeneity tip under antiplane shear loading, stress singularity 7-6100
 shell, cylindrical, lateral loading, equilib. study 7-62998
 shells, cylindrical orthotropic, uniformly stressed, linear anal. 7-11295
 shells, elastic, spherical, with variable rigidity, nonaxisymm. deform., numerical soln. 7-62994
 shells, shallow, boundary/interior element method for quasi-static and transient response analyses 7-6090
 shells, statically loaded global stability, Berger's hypothesis 7-57719
 shells of revolution, rubber-like, undergoing torsionless axisymmetric deformation, strain-energy density 7-43687
 smectic liquid crystals. A-type, focal conic texture, continuum theory 7-1878
 solid, nonsimple elastic, yield function, constitutive eqn. 7-62980
 solid, simple elastic, constitutive eqn. limitations 7-62979
 solids, elastic, 2D inhomogeneities, minimum stress conc. 7-37342
 steel, Cr-Mo, friction pair, contact zone surface struct. and mech. props. (*Russian*) 7-59640
 steel, Cr-Mo, friction pair, surface layer structural modifications (*Russian*) 7-39678
 steel, notched specimens, cyclic deform., thermoelastic effect (*German*) 7-33746
 thin elastic shells, general concept in rotation shell theory, to torus appl. 7-6101

elastic deformation continued

- tobacco mosaic virus in water, freeze-fracture imaging of ordered phases 7-3751
 transversely isotropic elastic plate pressed between two rigid cylindrical surfaces, contact problem 7-16130
 transversely isotropic half-space indented by parabolic concave punch 7-48366
 whisker-type monocrystal, elastic limit rel. to phys. characts. 7-2443
 Ag specimen, contact resist. meas., deform., fretting effects 7-9848
 Ag-Ag₂RbI₃-Ag ionic conducting system, elec. current press. and relax. effects, plastic deform. obs. 7-52123
 C fibres, retorsional deform., annealing, acid treatment, struct., mech. props 7-22768
 a-C:H polymeric plasma-activated CVD films, tribological and mechanical props. studies 7-16920
 Ge-Si alloys, piezoresistance under uniaxial elastic deform. (*Russian*) 7-58813
 InGaAsP epitaxial films, strain mapping by an X-ray diffraction technique 7-21786
 KCl crystals, rolling friction, elastoplastic deform. 7-16681
 LiNbO₃/Ti, acousto-optical diff. elastic strain and electric field effects 7-45985
 NbC_{0.97}, single cryst., mechanical stresses, thermo-EMF 7-21944
 Si:P, transmutation doped, deform. pot. shear const. determ. 7-38086
 TiC_{0.98}, single cryst., mechanical stresses, thermo-EMF 7-21944
 V₃Si/V₂Si₃ interface, crystallography of matrix-precip. interface and elastic strain field (*French*) 7-65036
 (YEuTmCa)₃(FeGe)₂O₁₂ films, planar anisotropy and magnetisation, ion irr. effects study 7-2906
 ZrC_{0.95}, single cryst., mechanical stresses, thermo-EMF 7-21944

elastic hysteresis

- lung parenchymal and airways recoil hysteresis, time dependence 7-8625
 shape memory heat engine performance and optimum stress calc. 7-23207
 Pb(Mg_{1/3}Nb_{2/3})O₃ ceramics for microdisplacement actuators, electrostrictive characts. (*Japanese*) 7-17270

elastic limit

- Einvar alloys, dispersion hardening and softening, elastic limit studies (*Russian*) 7-59539
 whisker-type monocrystal, elastic limit rel. to phys. characts. 7-2443
 Tb, single crystals, plastic strain between 77 and 683 K 7-21327

elastic moduli

see also Poisson ratio; shear modulus; Young's modulus

- 1D inverse problems of elasticity 7-41102
 alloys, amorphous and crystalline, local atomic struct., computer simulation 7-58160
 anisotropic materials of different moduli, cylindrical shell theory 7-43684
 aspen fibre reinforced polyethylene, mech. props., effect of extreme conditions 7-39604
 BAs, structural and electronic props., pseudopotential method, local density approx. 7-32353
 beam, two-layer cpd., damping characts., influence of quality of adhesion 7-50972
 beryl, high press. cryst. struct. and compressibilities 7-16505
 β-barrel, elastic constants, phase stability, dynamic obs. 7-3347
 cancellous bone in canine proximal femur: elastic moduli, yield stress and ultimate stress 7-54657
 cellulose fibre reinforced polyester, prep., and props. 7-3265
 cellulose fibres, native and regenerated, chain modulus, intramolecular H bonding 7-17575
 chalcopyrite ternary compounds, bulk modulus-vol. relationship 7-6707
 coal, thermal charactn., piezoelectric photoacoustic microscopy 7-44643
 composite laminates, with matrix cracking and interior delamination, stiffness props. 7-44669
 composite micromechanics, simplified, 3D finite element anal. 7-31637
 composite system, design problems with allowance for interphase reactions 7-43661
 composites, fibre-reinforced, stress distribution, Raman spectrosc.-mech. anal. 7-21333
 composites, isotropic multicomponents, Walpole bounds on effective elastic moduli 7-6704
 composites, laminated, struct.-performance maps 7-17574
 composites, periodic, elastic and instantaneous elastoplastic and moduli, overall, bounds 7-37349
 composition modulated layered structs., elastic strain, X-ray diff. studies 7-27086
 cracked bodies, effective elastic moduli in plane deform. 7-58395
 crystals, elastic moduli and nonaffine deformations, density-functional theory calcs. 7-44649
 bis-cyclopentadienyl oligomers, optically active polymer form., moduli, photoelasticity (*Russian*) 7-63092
 d- and f-metals and alloys, anomalous props. due to charge density fluctuations 7-7132
 deformed cubic crystals, generalised set of elastic moduli and stability calcs. 7-51914
 electrorheological suspensions, viscoelastic behaviour 7-43826
 epoxide resins, particulate filled, parameters determining strength and toughness 7-65071
 epoxy composites, Fe powder reinforced, flexural props., water condition temp. depend. 7-59587
 epoxy composites, Fe-filled, elastic modulus evaluation using concept of mesophase 7-13496
 epoxy filled with Fe particles, dynamic mech. props., storage and loss moduli 7-3349
 epoxy resin, aminimide-cured, mica reinforced, improved mech. props. 7-59489
 epoxy resins, effects of epoxy number and hardener on properties (*German*) 7-22973
 epoxy-amine matrices, improvement of phys. and mech. props. 7-39574
 fibre reinforced polyester resin, glass sphere filled, Young's and flexural moduli 7-3350
 fibre-reinforced composites, bounds on properties 7-7301
 fibre-reinforced composites, effective properties, effects of polydispersity n fibre diameter 7-6702
 flexure specimen, end-notched, for mode II testing, design and anal. 7-51005
 fluorite struct. crystals, phys. props., effective pot. calcs. 7-26692
 forsterite, elastic props., theoretical modelling, polyhedral approach 7-38091
 fused quartz particulate composite, fracture behaviour (*Chinese*) 7-8079
- elastic moduli continued**
 glass fibre reinforced polypropylene, short-fibre, struct. and mech. props., effects of moulding geometry 7-3348
 glass fibre reinforced polypropylene, subjected to pure bending, dynamic tensile props. 7-46545
 graphite fibre reinforced Al-Mg-Fe, unidirectional and angle-ply, strength and fracture anal. 7-59605
 graphite fibre reinforced epoxy, thermomech. behaviour, space rad. effects 7-51828
 graphite fibre reinforced epoxy laminates, fatigue damage mechanisms and residual props. 7-44671
 icosahedral quasicrystals, elastic moduli and elastic instability, density-functional theory calcs. 7-44649
 ionic solids, overlap interactions and bonding 7-1940
 Kevlar 49-285 style fabric for space structures use, thermoelastic behaviour 7-37329
 lamellar composite materials, elastic properties (*Japanese*) 7-13489
 liquid crystals, blue phase, light scatt. and elastic moduli, Landau theory calcs. 7-2084
 liquids, rheometrical device for meas. shear wave speed and elastic moduli 7-26823
 liquids, shear wave speed and elastic moduli 7-26824
 low density materials, mechanics 7-38089
 mat-reinforced polymeric composite, thermal expansion and elastic characteristics 7-33631
 metal superlattices, elastic and plastic props. 7-27085
 metallic foil, comp. modulated, mech. props., book contrib. 7-27222
 metallic superlattices, mech. props. and diffusion 7-52377
 metals, bulk modulus and its press. derivative 7-21322
 metals, ferromagnetic, elastic moduli anomalies, thermodynamic theory (*Russian*) 7-2080
 metals, ferromagnetic, sound propagation, velocity and absorption 7-38919
 multiphase materials, elastic moduli calc. (*Russian*) 7-2081
 nylon-6,6, fatigue crack propag., temp. and absorbed water effect 7-39662
 one-dimensional model, elastic props., boundary effects 7-6706
 optimal thermoelastic designs in case of fixed stress and deform. fields. 7-1417
 ordered substitution alloys, lattice parameters, elasticity modulus (*Russian*) 7-46542
 oriented polymers, elasticity modulus, temp.-time depend. (*Russian*) 7-21324
 orthorhombic crystals, deformed, elastic moduli and stability 7-16666
 oxides, rutile-type, dipole polarisabilities, cohesive energies and press. derivatives of bulk moduli 7-2967
 PEEK and C fibre reinforced PEEK materials potential as bioimplants 7-60126
 PET, high-modulus, rod prod. by microwave heat drawing 7-22735
 PET fibres, sonic modulus, peculiarities (*Japanese*) 7-33715
 plastic foams, stress relax. curves, charactn. 7-44688
 plate, epoxy, subjected to rapid cooling on both surfaces, residual stress anal. 7-63007
 plates, sectorial, laminar, orthotropic, flexure anal. on basis of finite-shear theory 7-63014
 PMMA based materials, craze resist., struct., water absorpt. 7-59602
 poly(ether sulphone)-poly(dimethylsiloxane)-poly(ether sulphone), elastic modulus in glass transition range 7-63722
 poly(vinyl acetate), network, mechanical and swelling behaviour investig. 7-12185
 poly(vinyl alcohol), network, mechanical and swelling behaviour investig. 7-12185
 poly ether ether ketone film, zone annealing prep., dynamic modulus, tensile strength 7-8038
 polybutadiene acrylates, UV-curable optical fibre coating material, low-temp. modulus 7-51911
 polychloroprene, tear strength, crosslinking, viscoelastic loss mechanisms 7-39632
 polycrystals, high temp. internal friction, rel. to grain boundary diffusion 7-63743
 polycrystals with trigonal and tetragonal symmetry, effective elastic moduli, Hashin-Shtrikman bounds 7-32544
 polydimethylsiloxane, swelling by phenylmethylsiloxane, modulus, stress-strain isotherms 7-8039
 polyethylene, chlorinated, prep., mech. and thermal props. 7-28006
 polyethylene, chlorinated, rutile-filled, 7-39573
 polyethylene, high density, struct. and props. (*Russian*) 7-44421
 polyethylene, oriented films, oxidation effects on dynamic and struct. parameters (*Russian*) 7-17823
 polyethylene, ultra-high modulus, tensile strength, effect of mol. wt. 7-39590
 polyimide thin films, friction and wear rel. to struct. 7-8130
 polymer composites, elastic characts., effect of aggregation of dispersed rigid filler 7-32547
 polymer melts, mol. wt. and mol. wt. distrib. from dynamic meas. 7-43829
 polymers, semicrystalline, EPR, elastic modulus data, mol. mobility phenomena 7-37900
 polymers elastic moduli, semiempirical method calc. 7-51908
 polymers films, high modulus, fabrication by solid-state rolling 7-46525
 polyolefines, oriented, mech. props. and mol. mobilities (*Russian*) 7-63723
 polyoxymethylene, tubes, microwave heat drawing, tensile load and precursor size effects 7-22734
 polyphosphazene 7-39632
 polypropylene, microindentation hardness and dynamic mech. moduli near glass transition 7-13564
 polypropylene, quenched, isotactic, glass transition, effect of drawing 7-12278
 polypropylene-cryo-ground rubber blends melt flow, dynamic mech. props. 7-12346
 polystyrene, glass bead filled, sonic modulus, peculiarities (*Japanese*) 7-33715
 polystyrene latex spheres, colloidal dispersion, high freq. elastic moduli calc. 7-38083
 polystyrene melts, tensile stress, recoverable strain, rubberlike elasticity 7-44884
 polytrimellitamideimide films, dynamic mech. props., glass transition, molecular aggregation effect 7-53782
 polytrimethylene, terephthalate, elastic moduli of cryst. region (*Japanese*) 7-33714

elastic moduli continued

polyurethanes, molecular struct., morphology, phase mixing, mech. props. 7-51664
 precipitation hardening, creep and reverse mechanical aftereffect processes (*Russian*) 7-3317
 PVC, mech. props. in β -transition region (*Russian*) 7-63724
 PVC-chlorinated PVC, miscible blends, rheological and mech. props. 7-8040
 rare earth metals, ground and excited state props., local density total energy calcs. 7-7141
 rocks, elastic moduli changes during thermal cycling between 110 and 370K (*Japanese*) 7-47432
 rubber, particle reinforced, with distributed damage, micromech. model for nonlinear viscoelastic behaviour 7-43698
 semiconductors, insulators and metals, structural, electronic and vibr. props., pseudopotential calcs. 7-16484
 shear moduli, positive/negative, for small and large deformations of elastic materials 7-6088
 solid struct. calcs. 7-51932
 sp-bonded nonmetal solids, cryst. stability and structural transition press., total-energy minimisation, tight-binding calcs. 7-2190
 steel, dual-phase, strength differential effect 7-46547
 strain-space plasticity formulation for hardening-softening materials with elastoplastic coupling 7-26164
 styrene-butadiene rubber, tear strength, crosslinking, viscoelastic loss mechanisms 7-39632
 tetrafluoroethylene-perfluoroethylene copolymers, composition-props. correls. (*Russian*) 7-16746
 textile structural composites, 3D, fibre inclination model 7-32545
 thermoplastic materials, erosion resistance, angular particle impingement at normal incidence 7-3442
 type II superconductors, flux-line lattice, elastic and plastic props. 7-27481
 universal eqn. of state of solids, temp. effects 7-44736
 wall theorem, elastic moduli of classical system 7-29867
 Al-Ag, anelastic effects due to precip. and dissoln. 7-13487
 Al-Ag (5 wt.%), anelastic effects, quench sensitivity, precip. and dissolution 7-53784
 Al-Li-Cu-Mg-Zr powder alloy, superplastic, high modulus and hardness 7-53816
 Al-Mg (5 at.%), creep, interpretation of internal stress determ. from dip tests 7-65091
 Al-Zn dilute alloy, mixed dumbbells orientational ordering transition (*Russian*) 7-51688
 AlN, electronic struct., first principles LCAO calc. 7-21813
 Ba ferrite filled styrene-isoprene-styrene composite, dynamic mech., elec. and mag. props. 7-13001
 BaO, self-consistent electronic structs. 7-32910
 BeAlSiO₄OH, euclase, high press. cryst. struct. and compressibilities 7-16505
 C fibre reinforced plastic laminates, ply failure under moisture and temp. influences (*German*) 7-22744
 C fibres, Celion, elec. resist., temp. depend. 7-65073
 C fibres, Celion, mechanical and fracture behaviour 7-22786
 C layers, arc plasma deposition, struct., mech. props. (*Russian*) 7-22581
 CaO, self-consistent electronic structs. 7-32910
 CaTiO₃ (perovskite), bulk modulus determ. 7-14269
 Cs, continuous valence transition under high press. 7-32965
 Co_{0.55}Cu_{0.45}Cr₂S₄-ySe₂ spinels, X-ray diffr. study 7-44475
 Cr alloys, charge and spin density waves (*Russian*) 7-2514
 Cr thin films, intrinsic stress, elasticity modulus, thermal expansion and struct. 7-16889
 Cr-base alloys, high-alloy, plasticity, effect of twinning (*Russian*) 7-46582
 Cr-Mo dilute alloys, magnetoelasticity, antiferromagnetism disappearance effects 7-45789
 CsI, Hugoniot overtake sound-rel. meas. 7-44705
 CsI, shock wave overtake meas. 7-21353
 Cu, ion irradiated, mech. prop. meas. 7-51873
 Cu, third-order elastic modulus, effect of plastic deform. (*Russian*) 7-46544
 Cu-Zr, ion irradiated, mech. prop. meas. 7-51873
 Fe, amorphous, elastic constants, relax. effects 7-51910
 Fe-Ni-Cr-Ti-B, constant elastic alloy, torsion reson. freq. temp. coeff. rel. to B content (*Chinese*) 7-13488
 Fe-TiB₂ eutectic system, microhardness, modulus of elasticity (*Russian*) 7-39648
 α -Fe₂O₃, hematite, magnetoelastic wave, parametric amplification in reversal of wavefront 7-7578
 Fe₃O₄, magnetite, cryst. struct. under press. 7-16524
 Fe₃O₄, magnetite, high press. cryst. chemistry 7-16521
 Ge-As-S, glasses, elastic properties 7-21323
 K, compression and polymorphism, up to 400 kbar 7-32632
 KCl-KBr mixed crystals, cohesion, harmonic and anharmonic props. calcs. 7-51907
 K₂SeO₄ incommensurate ferroelectric, ultrasonic rel. and elastic moduli meas., phason obs. 7-51956
 K₂ZnCl₄ incommensurate ferroelectric, ultrasonic rel. and elastic moduli meas., phason obs. 7-51956
 LaMgAl₁₁O₁₉, elastic and anharmonic props., acoustic meas. 7-44706
 LaNiO₃ crystals, US studies (*Chinese*) 7-58417
 Lu₂IrSi₁₀, superconducting, electronic phase transition and partially gapped Fermi surface 7-12902
 MgAl₂O₄ spinel, high press. cryst. chemistry 7-16521
 beta-NaN₃, elastic moduli, softening, microscopic theory 7-21320
 NbH, β - and γ -phases, electronic struct. and phonon anharmonicity 7-45199
 Nb₃Sn, phonon spectrum, temp. depend. (*Chinese*) 7-64413
 Ni-Fe-Cr, Inconel 600 and Incoloy 800, fracture toughness 7-59596
 NiAl₂, high press. studies 7-16689
 NiO₂, high press. studies 7-16689
 PbMg_{1/3}Nb_{2/3}O₃ ceramic, elastic moduli and diffuse ferroelec. phase transition, press. depend. 7-63717
 PbMg_{1/3}Nb_{2/3}O₃, single cryst. and ceramic samples, isotropic elastic moduli 7-6701
 Pd, single crystals, high temp. elastic props. 7-63710
 Rb₂ZnCl₄ incommensurate ferroelectric, ultrasonic rel. and elastic moduli meas., phason obs. 7-51956
 Ru, electronic, structural and cohesive props., theoretical study 7-37922
 Si, self-consistent band struct. and total energy, Shaw pot. calcs. 7-32909
 a-Si-H, elastic properties 7-21323

elastic moduli continued

SiC, cubic, ab initio calc. of ground state props. 7-6751
 SiC whisker or particle reinforced Al composites, deform. thermal expansion, strengthening mechanisms 7-3373
 SiO₂, fused, frequency dependent equation of state 7-51987
 SiO₂-CaO-MgO-Na₂O glass, frequency dependent equation of state 7-51987
 TaH_{0.19}, degenerate excited H states, Jahn-Teller effects calcs. 7-52535
 Tb₂Ti₂O₇, elastic modulus, low temp. anomalies 7-44651
 ThC powders, structural stability, eqn. of state, press. up to 36 GPa 7-16688
 β -Ti alloy, springs, design and mech. props. 7-46630
 α -Ti, elastic constants, phase stability, dynamic obs. 7-3347
 Ti-Al-Fe, mech. props., investig. as implant material (*German*) 7-46647
 TiNi, mono- and polycryst., elastic props. and internal friction, premartensitic anomalies (*Russian*) 7-59564
 UP(Sb), bulk moduli and phase transforms., high press. X-ray diffr. study 7-12206
 W fibre reinforced Fe-Cr-Al superalloy, surface cladding and matrix deform., thermomech. loading 7-46568

elastic moduli measurement

ceramics, green and sintered, elasticity calc. from US velocity meas. 7-2085
 composite panel, in situ testing of mech. props., flexural wave phase changes obs. 7-63095
 dentin, human and supporting bone, elastic modulus meas. by laser speckle photography 7-34183
 glass fibre reinforced polypropylene, damping characts. 7-59565
 plastic film covered steel plates, thermoelastic props. meas. 7-33713
 PMMA, Fe filled, techniques and models for elastic moduli, US evaluation 7-39833
 polyethylene, semicrystalline, elastic modulus meas. method 7-13683
 polymer films, strain measurement with laser speckle gauge, Poisson ratio evaluation 7-43821
 polymers, stress/strain coupled diffusion studied by vibrational time-delay technique 7-51012
 PVC, dynamic mechanical props., structure-regulating additives effect (*Russian*) 7-37344
 structural elements with fibre reinforced composite coverings, dynamic stiffness and damping props. determ. method 7-31717
 thin films, mechanical properties meas., depth-sensing indentation instruments 7-8211
 ultrasound meas. method for high temps. 7-43813
 underwater polymer composition rel. to acoustic props., Young's and longitudinal bulk modulus meas. 7-1304
 viscoelastic materials, dynamic parameters meas., vibr. transducer design 7-61326
 viscoelastic test block dynamic rigidity form factor for complex Young's modulus meas. (*Hungarian*) 7-51010
 WC-Co cermet particle reinforced low alloy steel composite, elastic constants, laser US technique 7-65268

elastic scattering of atoms and molecules

atomic vapour collision kernels, use of classical transport theory 7-36725
 atoms, RF optical resonance line; effect of elastic collisions 7-57148
 cross sections calcs., forward and inverse functional variations 7-50295
 differential cross section, depolarisation interference struct. 7-5740
 forward and inverse elastic scatt., cross section/potential surface dependence anal. 7-20000
 monatomic gases, large angle neutron scatt., collisions effect on dynamical form factor 7-50296
 rainbow scatt. study in mol. and nucl. physics, and surface science 7-62482
 H⁺ + H in solar wind, elastic collision cross sections 7-47654
 H⁺ + He in solar wind, elastic collision cross sections 7-47654
 H⁺ muonic H, low energy collisions, isotopic derivatives, cross sections, electron screening effect 7-31143
 H+He(H₂(N₂)(O₂), differential scatt. cross-sections for neutral particle precipitation 7-5739
 H₂⁺ + He, electron screening effects 7-5741
 H₂⁺ + He, elastic and inelastic scatt. mechanisms, energy loss spectra 7-15671
 HBr+K(Li), elastic scatt., complex Lennard-Jones pot., WKB calcs., Regge Pole anal. 7-36724
 He⁺ + H₂, elastic and inelastic scatt. mechanisms, energy loss spectra 7-15671
 Li+HBr, complex optical pots., large angle elastic scatt. calcs. using WKB theories 7-42728
 Na, optical piston dynamics using light-induced drift 7-10508
 O+He, van der Waals interaction, mol. beam study 7-20001

elastic scattering of electrons by atoms and molecules

see also gas phase electron diffraction
 absolute cross sections 7-20040
 atom-electron (positron) interactions, semiempirical polaris. pots. calcs. 7-974
 atomic clusters, multiple-scatt. theory, appl. of a non-muffin-tin pot. general pot. develop. 7-36839
 atomic electron scattering, nonreson., in low-freq. laser field 7-20050
 benzene, electron momentum transfer cross-section calcs. 7-20039
 charge deformation maps, molecular moments, and high-energy electron scattering 7-36723
 complex scaling methods 7-46819
 electron+H₂, scatt., polarisation pot. calcs. 7-15716
 electron-atom scatt., two-photon exchange, Coulomb-gauge electrodynamics anal. 7-24829
 ethane, positron and electron collisions, cross section meas., time-of-flight spectra anal. 7-36799
 ethylene, positron and electron collisions, cross section meas., time-of-flight spectra anal. 7-36799
 inert gas atoms small angle differential cross sections for electron elastic scatt. 7-15713
 inert-gas atoms, elastic scatt. of electrons, phaseshifts and differential cross sections, local-density approx. 7-19695
 inversion of molecular scattering data 7-42731
 Kroll-Watson formula, electron-atom collisions in presence of strong laser field 7-5638
 laser assisted atomic physics studies at Griffith University 7-20073
 laser modified elastic scatt. from Yukawa pot. modelled atom 7-25654
 local frequency redistribution in reson. line photons, elastic collisions effects 7-10757

elastic scattering of electrons by atoms and molecules continued

- methane, elastic electron scatt., multiple scattering method cross section calcs., anal. of method 7-25370
 methane, electron elastic scatt., differential cross sections meas. 7-25653
 methane, electron scatt. cross sections, 0.1 to 500 eV, complex optical pot. calcs. 7-25382
 methane, positron and electron collisions, cross section meas., time-of-flight spectra anal. 7-36799
 molecular ions, electron capture, rot.-vibr. transitions in autoionisation, CF method anal. 7-20036
 molecular solids, electron elastic scatt., reson. absence 7-31169
 molecule, electron angular scatt., electron vel. distrib. shaping 7-981
 polyatomic molecules, electron scatt. theory, review 7-36765
 positron-gas system, EM wave irradi., positron distrib. 7-36761
 positronium negative ion, photodetachment and electron elastic scatt., variational techniques calc. 7-50363
 resonant EM radiation absorption 7-50353
 scattering factors 7-20041
 Ar, elastic electron scatt., multiple scattering method cross section calcs., anal. of method 7-25370
 Ar, electron (positron) elastic scatt., calcs. 7-977
 Ar, electron (positron) elastic scatt. 7-36768
 Ar, electron scattering length 7-20049
 Ar, positron annihilation and elastic scatt. cross sections 7-42763
 Ar, positron annihilation and diffusion, computer-based anal. 7-50378
 Ar, positron differential elastic scattering cross-section meas. 7-25656
 Ar, positron drift and diffusion in crossed elec. and mag. fields, simulation 7-36760
 Bi, elastic scatt. of electrons, spin polarisation meas. 7-50364
 Bi, low-energy electron elastic scatt. calcs. 7-50362
 Cs, elastic positron scatt., integral eqn. approach 7-42762
 H, elastic electron scatt., reson. struct. study 7-20045
 H, electron and positron scatt., exact eikonal approx. 7-50360
 H, electron elastic scatt., second-order eikonal exchange amplitudes, Glauber approx. 7-25655
 H, electron scatt. in chaotic laser field 7-10703
 H forward-angle dispersion relation 7-15712
 H, laser-assisted electron. elastic scatt., differential cross sections, exchange and dressing study 7-20046
 H, lepton (antilepton) scattering, field theoretic calcs. 7-36769
 H, mesic 2 s state, elastic and inelastic slow electron scatt. 7-10781
 H non-ideal plasma, effect of electron scatt. on conductivity 7-44109
 H, positron elastic scatt., continued-fraction approach to optical pot. calcs. 7-20048
 H, positron elastic scattering, empirical correl. pot. calcs. 7-36770
 H, positron scatt., superelastic and inelastic processes 7-15711
 H⁻, free-free absorpt. coeff., R-matrix method 7-62524
 H₂, electron scatt., elastic and vibr. excitation differential cross section calcs. 7-25652
 H₂, fixed nuclei, elastic electron scatt., cross sections calcs. 7-15717
 H₂ formulation of ab initio optical potential for electron elastic scatt. 7-15714
 H₂, high energy electron scatt. cross sections calcs., revised Bethe theory 7-42507
 H₂, low energy elastic positron collisions, R-matrix method 7-50361
 H₂, low-energy electron scatt., static exchange calcs. 7-988
 H₂, low-energy positron scatt., Z_{eff} calcs. 7-50384
 H₂O, electron elastic scatt., 100 to 1000 eV 7-5768
 H₂O, electron scatt., small-angle, meas. and calcs. 7-50346
 H₂O, electron scatt. at intermediate energies, total absolute cross sections 7-62523
 H₂S, electron scatt., low energy, absolute total cross-sections meas. 7-25650
 He electron scatt. below excitation threshold, phase shift anal. 7-15715
 He, positron annihilation and elastic scatt. cross sections 7-42763
 He, positron elastic scatt., 2-pot. calcs. 7-36766
 He, positron elastic scattering, empirical correl. pot. calcs. 7-36770
 He, positron scatt., superelastic and inelastic processes 7-15711
 Hg, elastic scatt. of electrons, spin polarisation meas. 7-50364
 Hg, electron elastic scatt., electron spin polarisation, electron spectra study 7-25651
 Hg, low-energy electron elastic scatt. calcs. 7-50362
 K, elastic positron scatt., integral eqn. approach 7-42762
 Kr, electron scatt., intermediate energy, elastic and inelastic, differential cross-sections 7-25648
 Kr, relativistic electron (positron) elastic scatt. 7-36767
 Li, electron elastic scatt., spin dependence meas. 7-15718
 liq. Ar, effective momentum transfer cross section for excess electrons 7-21956
 N₂, electron and photon collision cross section 7-18513
 N₂, electron elastic scatt. and vibr. excitation, differential cross section meas. 7-36798
 N₂, high energy electron scatt. cross sections calcs., revised Bethe theory 7-42507
 N₂, low energy elastic positron collisions, R-matrix method 7-50361
 N₂, low-energy electron scatt., static exchange calcs. 7-988
 NO, low-energy electron scatt., R-matrix method, close-coupling expansion study 7-36490
 Na, elastic positron scatt., integral eqn. approach 7-42762
 Ne, electron (positron) elastic scatt., calcs. 7-977
 O₂, electron scatt. cross section meas., 0.2 to 100 eV impact energy 7-20047
 O₂, high energy electron scatt. cross sections calcs., revised Bethe theory 7-42507
 O₂-electron scattering at intermediate and high energies 7-5769
 Pb, elastic scatt. of electrons, spin polarisation meas. 7-50364
 Pb, low-energy electron elastic scatt. calcs. 7-50362
 Rb, elastic positron scatt., integral eqn. approach 7-42762
 SO₂, electron scatt., low energy, absolute total cross-sections meas. 7-25650
 SiH₄, electron impact cross sections, spherical-complex-optical pot., ab initio HF calcs. 7-49904
 SiH₄+e⁺, optical pot. approach 7-30933
 TiCl₄, electron attachment, scatt. cross section, multiple scatt. Xalpha continuum calcs. 7-62483
 Ti, elastic scatt. of electrons, spin polarisation meas. 7-50364
 Ti, low-energy electron elastic scatt. calcs. 7-50362
 Xe, elastic electron scattering, differential cross section meas. 7-62525
 Xe, electron elastic scatt., electron spin polarisation, HF calcs. 7-25369

elastic scattering of electrons by atoms and molecules continued

- Xe, electron elastic scatt., electron spin polarisation, electron spectra study, scattering and amplitude anal. 7-25651
 Xe, electron scatt., rel. differential cross-sections 7-25661
- elastic waves**
see also acoustic waves; Love waves; magnetoelastic waves; Rayleigh waves; seismic waves; vibrations
 acceleration wave propagation and evolution in thermoelastic solids (*Italian*) 7-20616
 acoustic microscope, elastic wave propag., accurate field anal. 7-43472
 acoustic microscope, elastic wave propag. focusing props. of small-aperture lenses 7-43473
 acoustoelastic effect, influence of plastic deformation, stress distrib. in slightly orthotropic materials 7-16069
 arbitrary Lagrangian-Eulerian finite element method for path-dependent materials 7-14766
 attenuation in rocks containing fluids 7-6718
 axisymmetric nonstationary problems of dynamic elasticity, ray series method appl. 7-41114
 bar, propag. velocity determ. of elastic-plastic boundaries (*Chinese*) 7-43732
 beam, infinite periodic, bending wave propag. 7-57722
 boundary element method for 3D problems transient elastodynamic anal. 7-34694
 composite media, thermoelastic waves, photothermal generation 7-44685
 composite panel, in situ testing of mech. props., flexural wave phase changes obs. 7-63095
 cracked solid, propag. const., higher order approx. 7-16091
 curvilinear cylindrical cavity, harmonic elastic wave propag., geometrical optics methods 7-1479
 cylinder, hollow, fluid-filled, initial stresses effect on wave speed 7-43749
 cylinder, thermoelastic, longitudinal wave propag. 7-1474
 cylindrical cavity of arbitrary cross section, elastic surface wave propag. (*French*) 7-63033
 diffraction in layered-inhomogeneous solid media 7-16028
 diffraction tomography, quantitative, with pulsed waves 7-50878
 dynamic photoelastic of wave propagation and energy transfer across contacts 7-16139
 elastic solids with microstruct. having a symmetric stress tensor, wave propag. 7-63032
 elastodynamics with viscous damping, stress functions, axisymmetric problems 7-16064
 EM radiation on collision of solids 7-42890
 equations of motion of elastic medium of different moduli, general theory of solns. 7-1475
 flexural wave damping, constrained-layer technique using exact elasticity theory 7-63050
 fourth-order accurate finite-difference scheme for elastic waves computation, examples 7-3991
 half-space, elastic with voids, surface wave propag. 7-63027
 heavily loaded semi-infinite cylindrical elastic shell, vibr., boundary value problem 7-31690
 hyperelastic solid, finite amplitude shear wave propag. 7-6146
 impact test, stress strain relationships, elastic deformation, specimen connected with long bar (*Japanese*) 7-11290
 inextensible transversely isotropic elastic body, surface wave propag. 7-1483
 inhomogeneous anisotropic bodies, elastodynamic anal 7-43675
 ion implantation, mechanical stresses 7-12094
 Lamb's initial and boundary value problem, elastic medium with memory 7-41103
 Lamb's plane problem in thermoelastic solid 7-6128
 linear viscoelastic materials, dynamic props. by wave propagation testing, PMMA appl. 7-16090
 longitudinal elastic-plastic waves with radial effects, numerical anal. for circular rods 7-31691
 longitudinal shock wave reflection from plane rigid boundary 7-1484
 longitudinal wave velocity and amplitude in rocks, effect of press. 7-47424
 metals, compression pulses, nanosecond, attenuation 7-58413
 micropolar elastic crystals, solitary waves 7-6135
 modeling of elastic wave phenomena near a plane interface 7-31566
 multilayered elastic half-space, distribution of energy from a harmonic surface load 7-43735
 nonlinear elastic solid, parametrically excited Gaussian wave beam form. (*Ukrainian*) 7-11325
 nonlinear properties in wave propag. in solids with initial stresses 7-11337
 nonlinear waves of different physicommechanical nature in finite continua 7-18604
 nonuniform waves propag. in space divided by thin fluid-filled fracture, theory 7-28891
 one-dimensional acoustic pulse propagation in linear layered hereditary medium (*Russian*) 7-20644
 orthotropic materials, stress measurement using vertically polarized shear waves 7-57699
 penny-shaped cracks, time-harmonic elastic wave HF scatt. 7-57759
 periodic band, behaviour of elastic waves (*French*) 7-11336
 periodic waveguides, finite element anal. (*Japanese*) 7-6148
 phonon concentrating, catastrophe theory for caustic behaviour 7-2113
 piezoceramic shell, applied theory modification 7-43750
 plane waves, elliptically polarised, propag. along acoustic or optical axes 7-56057
 plate, infinite monoclinic crystal, shear waves 7-26192
 porous media, liquid and/or gas saturated, compressional wave propagation 7-31677
 pressure pulse reflection at free surfaces of water 7-11480
 pressure wave, stepped, plane, reflection from convex cylindrical cavity 7-61127
 propagation in media with thin rigid inclusions 7-50832
 propagation in perfect cond. due to mag. field 7-56038
 resonance theory for elastic wave scattering 7-48222
 rocks, elastic wave velocity determ. methods (*Japanese*) 7-29312
 rods, elastic, solitary wave interactions 7-26199
 rods, nonlinear propagation of elasto-plastic waves 7-26200
 scattering by rigid elliptic fibre 7-26195
 scattering by spherical inclusions, with appl. to low frequency wave propag. in composites 7-6719
 scattering from interface crack in layered half space submerged in water, applied tractions at interface 7-11340

lastic waves continued

- scattering from interface crack in layered half space submerged in water 7-11341
- seismic tomography for 3D struct. and vel. determ. 7-29268
- shear wave bundles in nonlin. hereditary medium, quasioptical approx. 7-31654
- shell, cylindrical, axisymmetric dynamic problems soln. by num. methods 7-16105
- shell, sectional, with holes, wave fields 7-16106
- shell, structural, initially stressed, vibrs. and freq. characts. 7-16104
- shells, cylindrical, stability and design optimisation during stress wave propag. (Ukrainian) 7-11326
- slabs, frequencies and modes of bending vibrations with allowance for propagating modes; 7-11338
- slowness surfaces of incompressible and nearly incompressible elastic materials 7-16092
- solid, elastic wave propag., computer simulation of US 7-33890
- strain gauge, bonded resistance type, dynamic characts. exam. method 7-18772
- stress field calc. under action of 1D compressive wave after reflections (Chinese) 7-11335
- strip, infinite, transient field under point force 7-11339
- surface elastic wave in point group 6 7-21600
- surface waves guided by exterior of rectangular elastic solid 7-11342
- thermoelasticity, anisotropic, generalised, plane harmonic wave propag. 7-6093
- TM polarisation waves, diffraction on rectangular wedge struct; (Russian) 7-18605
- torsional dispersion relations in a radially dual elastic medium 7-50820
- transient generalized thermoelastic waves in a transversely isotropic half-space 7-63031
- two-dimensional wave propagation in a thermoelastic layer; couple stress effects 7-63030
- velocity anisotropy in piezoelectric, theoretical study 7-44684
- volume elastic waves in ferroelectrics, theoretical study 7-44684
- Cu, halides, photochromic glasses, elastic props., 20-500 °C (Russian) 7-21365
- Cu layer on steel substrate, thickness meas. by transverse surface waves (French) 7-4815
- GaAs, ion implantation, H^+ , He^+ , Ar^+ 7-12094
- α - $LiIO_3$, cryst., elastic wave attenuation, freq. and temp. depend. (Russian) 7-21364
- $LiNbO_3$, ion implantation, H^+ , He^+ , Ar^+ 7-12094
- $Na_2O-Al_2O_3-SiO_2$ glasses, elastic props., annealing and Al substitution effects 7-8035
- PLZT, electrically excitable mechanical resonant mode shapes 7-26854
- PZT ceramics, pulsed TEA CO_2 laser irradi., signal generation 7-16623
- Si, ion implantation, H^+ , He^+ , Ar^+ 7-12094

asticity

- for crack problems in elasticity see crack-edge stress field analysis
- see also elastic constants; elastic moduli; elasticity of liquids; elastoplasticity; photoelasticity; rheology; thermoelasticity
- 2D elastostatics, stress computation by BEM 7-37330
- 3D elastic bodies, contact problems, mathematical models of friction 7-51002
- acoustoelastic effect, influence of plastic deformation, stress distrib. in slightly orthotropic materials 7-16069
- acoustoelastic effects caused by plastic anisotropy growth 7-62991
- analogy between elastic and EM fields (Polish) 7-20095
- anisotropic elastic strip, elastodynamic crack, complex variable approach 7-37389
- anisotropic elasticity for string sources, 1D inverse problem 7-35280
- anisotropic half-plane, elasticity, mixed problem soln. (Ukrainian) 7-11284
- anisotropic Hertz problem in 2-dimens., complex variable anal. 7-57765
- anisotropic materials of different moduli, cylindrical shell theory 7-43684
- anisotropic media and composites, linear-elastic, lateral press. coeff. 7-1416
- aorta, circumferential variation in stiffness in large animals 7-8643
- aortic valve tissues, relative vols. of struct. components rel. to biochem. components 7-34182
- arterial elasticity in human fingers and rabbit forelegs, noninvasive automatic meas. using photoelec. plethysmography 7-28794
- arterial flow at a 90° bifurcation, effects of nonNewtonian viscoelasticity and wall elasticity 7-3812
- articular cartilage in canine knee, indentation study of biomech. props. 7-54651
- asperity pair elastic joints, friction resistance 7-11363
- asymptotic behaviour of an elastic body with a surface having small adhered regions (French) 7-61104
- asymptotic solution of three-dimensional elasticity problems of elongated plane tensile cracks 7-1502
- axisymmetric problems solution using triangular three-node nonconforming elements 7-56042
- bar, circular, weakened by rectilinear cut, torsion problem 7-11288
- bar, prestressed, on elastic foundation with initial stresses, contact problem soln. 7-43809
- bars, continuous, lying on elastic supports, nonlinear and buckling anal., theory of elastica (German) 7-20609
- bars, thin walled, torsion with annulus cross-section of variable size 7-26137
- beam on elastic base, optimal design 7-4690
- beam theory, material forces 7-43686
- beam vibration, nonlinear constitutive eqn. 7-57736
- beam-point mass system, stability of 1D unbounded elastic systems 7-26185
- beams, elastic, positive deflections, fourth-order boundary value problems 7-37338
- beams, free vibr., nonlinear elastic foundation effects 7-6147
- beams, thin-walled open, elastic nonlinear static analysis 7-62984
- beams and rods, small strain deformations including large deflections 7-1423
- blood vessels, nonlinear elasticity (Chinese) 7-18009
- body collision between elastic half-planes, mixed problem soln. 7-43738
- body with plane crack, elasticity theory three-dimens. problem, variational soln. method 7-63072
- boundary element method for 3D problems transient elastodynamic anal. 7-34694
- boundary elements for elastostatics, conforming versus nonconforming 7-14760

elasticity continued

- boundary problems, solution using Vinner-Hopf system and inversion of integral transforms 7-4692
- boundary separating two media, elasticity theory for cracks, singular problems 7-1515
- boundary-integral-equation and finite-element methods, combined scheme for elasticity theory problems 7-56041
- cantilever beam, large deflection anal. with end rotational load 7-29761
- cantilever beam, large deflections with vertical load at free end (Japanese) 7-11294
- CDW elasticity model 7-52472
- circular hollow cylinder, coupled thermal stresses due to thermal and mech. loads 7-16063
- circular ring under internal pressure, stress distrib. in 2nd order elasticity 7-57693
- classical shell theory, accuracy-loss effect, proof 7-31647
- coherent phase transformations, asymptotic form of small density differences 7-24615
- columns, cantilever resting on elastic foundation, dynamic stability 7-50965
- columns, thick-faced sandwich, buckling under distributed axial loads 7-26176
- columns, thin-faced sandwich, buckling under distributed normal loads 7-26175
- columns with elastic axial restraint, FEM-based stability analysis 7-50964
- composite materials, linear elasticity rel. to homogenisation and optimal bounds 7-31645
- conservation laws in nonconservative linear elastodynamics 7-1408
- contact problems with nonlinear friction laws, existence of local uniqueness of solns. 7-37397
- coupled axial-torsional oscillator with neo-Hookean spring 7-35265
- crack extension force in a dielectric medium 7-6152
- critical flutter parameters of orthotropic rectangular flat panels with in-plane loads 7-37368
- cubic crystals, impurity centre-phonon interaction energy calcs. 7-32586
- curved members, consistent discrete elements technique 7-50948
- cylinder, elastic circular containing cavity or penny-shaped crack, thermal stresses 7-26202
- cylinder, hollow, with nonplanar end-faces, stressed state, approx. method 7-16067
- cylinder, hollow isotropic, free axisymm. vibr. freqs. 7-11327
- cylinder, inhomogeneous, axially symmetric problem of elasticity theory 7-9671
- cylinder, isotropic, spatial stressed state, mixed problem of elasticity theory (Ukrainian) 7-11282
- cylinder, nonlinear elastic thick-walled, multi-parameter equations solution 7-26143
- cylinders, free hollow circular, vibrations 7-43758
- cylinders, uniformly loaded, relaxed Almansi-Michell problem soln. 7-43679
- cylindrical shell, thin walled with winding, ultimate press. rel. to prestressing 7-31650
- dielectric, elastic, conservation laws and material momentum tensor 7-6086
- Dirichlet problem for Lamé's equations (French) 7-62985
- Dirichlet problem in crescent-shaped domain, solution 7-57670
- disc in contact with liquid, natural freq. disc and liq. props. effects 7-26189
- discs with fluctuating radii, simulation of elastic response 7-56040
- displacement problem in homogeneous linear elastostatics in exterior domains 7-50954
- dynamics of elastic body containing moving crack 7-43788
- edge dislocation-rigid elliptical inclusion, elastic field created 7-12116
- elastic inclusions, stress distrib., 2D soln. 7-62989
- elastic layer on rigid foundation with annular hole, torsion study 7-37332
- elastic-plastic shrink fit with supercritical interference 7-43662
- elastodynamics with viscous damping, stress functions, axisymmetric problems 7-16064
- elastoelctromagnetic Neumann boundary value problems, self-consistent theory 7-26145
- epitaxial films, multilayer, X-ray diffr. determ. of elastic stresses and misalignment (Russian) 7-38371
- equations of motion of elastic medium of different moduli, general theory of solns. 7-1475
- fatigue crack propagation computer simulation (Japanese) 7-14772
- FEMs in linear elasticity, post-processing procedures 7-14777
- fibre reinforced composites, fatigue damage and degradation mechanics 7-11353
- fibre reinforced composites, mechanical properties, statistical and deterministic approach comparison 7-11287
- fibre reinforced plastic hollow cylinder, 3D stress state 7-37333
- fibres in elastic matrix with finite strains, stability 7-11322
- fibrous composites with weak bonding, elastic response 7-31646
- finite plane isotropic elastic medium, straight crack, complex path independent integrals 7-43792
- flexible cylinder array, fluidelastic in stability in cross-flow 7-16089
- flexural wave damping, constrained-layer technique using exact elasticity theory 7-63050
- flight vehicle aeroelasticity, 3D motion, nonlinear integrodifferential eqns. 7-43737
- fluidelastic instability of rectangular plates under shearing load in subsonic flow 7-51057
- four-point bending, large deflections, fundamental theory (Japanese) 7-11293
- frame, two-bar, nonlinear stability anal., elastic type approach appl., buckling behaviour 7-43720
- functional transformations of variational principles 7-35282
- graphite-Li intercalation cpd., Li_xC_6 , elastic effects, comp. depend. staging studies 7-63707
- Green matrix construction for stratified elastic half-space (Russian) 7-61106
- Griffith's crack, interaction with rigid inclusions in elastic space 7-57741
- gypsum, initial hardening with cement, pulse rheometry investig. 7-37411
- half-plane with system of rectilinear thin elastic inclusions, stress-strain state 7-11285
- half-planes interface, stress conc. at tip of hard inclusion 7-16065
- half-space, elastic with voids, surface wave propag. 7-63027
- half-space, prestressed elastic, general spatial static contact problem 7-1516

elasticity continued

- half-space with initial stresses, contact interaction with a finite elastic cylinder 7-63084
 heavily loaded semi-infinite cylindrical elastic shell, vibr., boundary value problem 7-31690
 heavy elastica, critical review 7-11286
 Hexsny rubber, high-flex ozone resistant, prep. and appl. 7-13767
 hydraulic fracturing mechanics, explicit approx. solns. 7-6158
 hydroelastic viscous liquid system, coupled freq. 7-43674
 hydroelasticity of slender bodies in an unbounded fluid in the medium frequency range (French) 7-20643
 hydroxypropyl cellulose, lyotropic liq. crystals, capillary rheometry 7-63099
 hyperbolic conservation laws with relaxation 7-48373
 hyperelastic materials, elastostatic equilb., weak convergence of sets of constraints (French) 7-61100
 hyperelastic materials, localisation of deformation, gradient approach 7-16066
 hyperelastic multilayered bodies, micromorphic effects, nonstandard anal. 7-56037
 hyperelastic solid, finite amplitude shear wave propag. 7-6146
 II-V semiconds., cryst. growth, characterisation and appls., review 7-26685
 inclusions and voids, stress distrib. calc. 7-43685
 inextensible transversely isotropic elastic body, surface wave propag. 7-1483
 inf-sup conditions, equivalent forms and applications 7-1431
 infinite elastic body, stresses around two cylindrical inclusions under tension 7-37343
 infinite plate, plane rectilinear crack, pot. method soln. 7-63070
 inhomogeneous anisotropic bodies, elastodynamic anal 7-43675
 inhomogeneous elastic media, Green's tensor and its potentials 7-62997
 inhomogeneous materials, effective elastic moduli 7-1426
 inhomogeneous theory of elasticity with deformations 7-9672
 integro-differential eqns., nonlinear, method of freezing for appl. to elasticity problems 7-48359
 isotropic medium with almost spherical reinforced cavity, axisymm. stress state 7-1421
 isotropic solid, elliptical cracks under shear loading, polynomial solns. 7-57758
 knee, effect of muscular activity on valgus/varus laxity and stiffness 7-3819
 Lagrangian, second-order, duality under dependency inversion and Noether theory 7-24426
 Lamb's initial and boundary value problem, elastic medium with memory 7-41103
 Lamé equations, nonlinear Galilean invariant generalization 7-48360
 lamellar inclusion problem in plane elasticity 7-1422
 laminated thick composite plates, buckling, hygrothermal effects 7-11321
 laminates, elastic, twinned crystal, linear response 7-43665
 large deformation elasticity theory, nonlinear spectral characts. 7-6094
 layer, elastic with nonconvex stored energy function, plane nonlinear shear 7-35283
 layered elastic systems, boundary element transfer matrix analysis 7-35281
 linear, class of conservation rules assoc. with sensitivity anal. 7-26146
 linear elastic beam elements of MODULEF library (French) 7-31655
 linear elastic body covered by thin shell, Ventcel problem (French) 7-61103
 linear elastic fracture mechanics, computerised R-functions method 7-63066
 linear elasticity equations, perturbation of invariant subspaces, spectral theory 7-48363
 linearised elastostatics, existence and uniqueness theorems for boundary integral equations 7-61102
 local approach of fracture, continuum damage mechanics 7-50988
 machining centre design improvements to give enhanced stiffness 7-21318
 materials with small viscosity and capillarity, elasticity as asymptotic theory 7-6099
 mechanics of deformable media, book 7-35135
 membrane, transversely loaded, geometrically nonlinear analysis 7-6095
 membrane spargers, elastic and flow mechanics 7-31877
 membrane/plate equilibrium finite element models 7-1429
 membranes, nonlinear elastic constitutive model, strain stiffening behaviour 7-13497
 metals, hot oxidation, solute-elastic effect in interstitial solid solns. (French) 7-58478
 microcracked elastic solid, 1D constitutive model 7-1488
 microelastic continuum theories, relationships and appl. possibilities 7-24423
 micropolar cylinders, generalised twist for torsion 7-93
 minimization in incompressible nonlinear elasticity theory 7-14769
 mode II fatigue crack test specimen, elastic analysis 7-1505
 multidimensional discrete mech. system, freq. spectrum depend. on elasticity parameters 7-1395
 multiple and maximal periodicity in linear elastostatics 7-41105
 multipolar rod model, virtual power method appl. 7-57684
 nonhomogeneous and transversely isotropic media, fundamental soln. 7-57690
 nonideal experiment 7-14741
 nonlinear 3D fracture dynamics, path-independent integrals 7-63069
 nonlinear elastic solid, parametrically excited Gaussian wave beam form. (Ukrainian) 7-11325
 nonlinear elasticity, spherically symm. problems, regular and singular equilibria 7-41100
 nonlinear elastostatics, principal stress and strain trajectories 7-35284
 nonlinear problems, error estimates for mixed finite element approximations 7-4691
 nonlinearity elastic solids, Volterra dislocations, large deformations, Weingarten theorem generalization 7-43669
 null Lagrangians, admissible tractions, and finiteelement methods 7-4693
 orthotropic elastic contact, plane problem 7-6165
 orthotropically damaged elastic solid, effective material constns., constitutive eqn. 7-1489
 oscillating cascades, unsteady flow, asymptotic solns. 7-37437
 penny-shaped crack embedded in transversely isotropic elastic half-space 7-43760
 periodontal ligament, human, mech. props. of tooth and root sections 7-3824

elasticity continued

- permittivity and resistivity meas. of elastic, fibrous and porous materials (Czech) 7-61355
 phase transitions in elastic and viscoelastic bodies, state of stress and strain 7-29961
 piezoceramic shell, applied theory modification 7-43750
 piezoelectric layer with periodic system of electrodes, plane problem of electroelasticity 7-2983
 piezoelectric media, finite, elec. and elastic multipole defects 7-43673
 plane, elastic, hole-defect interaction, stress distrib., integral eqn. method 7-37964
 plane elastic stresses in an adhesive single-lap bonded joint in tension loading (French) 7-62987
 plant vegetative tissue, cell wall elastic constitutive laws and stress-strain behaviour 7-40184
 plastic medium, semi-infinite, with hollow spherical inclusion, stress conc. 7-31651
 plate, bending anal. using fourth order eqn. finite element algorithm 7-29759
 plate, damped elastic infinite, adjacent semi-infinite fluid, impulsive force effect study 7-63052
 plate, elastic, containing two collinear transverse edge cracks, stress distrib. 7-43761
 plate, large square, central circular hole, uniaxial loading, elastic stress concs., photoelastic models 7-43682
 plate, periodically ribbed, bounded sound wave scattering 7-1297
 plate, thick, contact interaction with thick elastic layer 7-11361
 plate, trapezoidal, on elastic base, vibration and buckling 7-48365
 plate theory, matched asymptotic expansions, clamped edge (French) 7-1412
 plate with line crack subject to varying shear load, nonlinear elasticity anal. 7-48367
 plate with thin regions, stress conc., theoretical and photoelastic studies 7-57697
 plate/shell element, field-consistent four-noded laminated anisotropic 7-62983
 plate/shell error indicators and accuracy improvement of finite element solutions 7-1430
 plate/shell problems, effect of asymptotic error estimate studies 7-1428
 plates, anisotropic laminated elastic, finite deflections 7-37336
 plates, bent, strain energy upper and lower bounds 7-26138
 plates, biharmonic eqn. general soln., generalised Levy's method 7-1396
 plates, elastic, shape optimisation, sufficient conditions for extremum 7-26150
 plates, elastic annular, connected by elastic rods, stress analysis 7-62992
 plates, elastic sandwich, use of boundary value problems solutions 7-26141
 plates, elastic with variable flexural rigidity, inverse problems 7-26148
 plates, flexible, rectangular, on nonlinearly elastic base, optimal design 7-62995
 plates, orthotropic folded, elasticity versus finite strip analysis 7-1427
 plates, polygon-shaped bent, strain energy inequalities 7-26139
 plates, shallow anchor, calc. 7-9673
 plates, sheardeformable elastic, small finite deflections 7-26144
 plates, thick composite, loading, nonlinear finite element anal. using cubic spline functions 7-31643
 plates, vibr. studied using Berger's dynamic field eqns. 7-43731
 plates and shells, perforated, with system of attached masses, eqns. of motion 7-1393
 Poisson ratio independence in elastostatics with generalised boundary conditions 7-14771
 poly(vinyl alcohol) hydrogels, elastodynamics, Brillouin scatt. meas. 7-39136
 polybutadiene networks, mechanical and swelling behaviour 7-11965
 polymer chain, eqn. of state, entropy spring model 7-21394
 polymer fluids, nonlinear, elastic props, convective transfer processes 7-43824
 porous, anisotropic and variable strength media, applied theories of plasticity 7-16072
 porous media, wave features of nonlinear theory 7-56054
 pressure wave, stepped, plane, reflection from convex cylindrical cavity 7-61127
 psos fibres, skinned, rabbit, stiffness in MgATP and MgPP_i soln. 7-23377
 punches, elliptical, on elastic half space, general theorem 7-6164
 quasilinear hyperbolic systems with involutions 7-29755
 rate-type finite elasticity constitutive law, elastic and elastic-plastic deformation 7-57700
 Rayleigh-Ritz method, initial postbuckling of columns 7-48361
 rectangle, elastic, compressible object, contact interaction of two stressed half-planes 7-1518
 rectangular elastic plate problem, bifurcations near a multiple eigenvalue 7-6098
 rectangular elastic-plastic cantilever, deflection anal. (Chinese) 7-48358
 rectangular parallelepipeds, vibr. 7-43736
 regularized integral equations for a two-dimensional body containing a crack of an arbitrary form (French) 7-62988
 reinforcement problems, formulation in terms of boundary integral equations 7-1410
 Reissner plates, simply supported, integral equation system 7-94
 reissner-Sagoci problem for a non-homogeneous elastic solid 7-43680
 residual stresses in elastic body 7-14770
 rigid line inhomogeneity tip under antiplane shear loading, stress singularity 7-6100
 rocks, effect of press. on elastic and strain-strength props. 7-47424
 rocks, fracture anal. 7-66106
 rocks and concretes, failure process, dynamic description 7-57738
 rods, elastic, stationarity for non-selfadjoint problems 7-26178
 rotary-wing aerelasticity, time-domain unsteady aerodynamics appls. 7-20686
 rotating elastic-plastic shrink fit with hardening 7-43663
 rotating nonlinearly elastic rods, multiple steady state, buckled and unbuckled states 7-11291
 rubber, natural, nonlinear elastic constitutive model, strain stiffening behaviour 7-13497
 semiplate weakened by holes and cracks, elasticity theory 7-11347
 separating inclusion in an elastic half-space 7-43678
 shell, bifurcational stability problems soln. using finite element method 7-16087
 shell, cylindrical, hinged compressed, connected to elastic filler, axisymmetric stability, boundary conditions 7-43730

elasticity continued

- shell, cylindrical, lateral loading, equilib. study 7-62998
 shell, cylindrical, on absolutely solid bed, contact problem, stress-strain state (*Ukrainian*) 7-11357
 shell, cylindrical four-layer coiled, stress state 7-11292
 shell, cylindrical leaning on rigid support, stress-deformed state 7-16132
 shell, flat, multiply, nonlinear variant of elasticity theory 7-1414
 shell, inclined Timoshenko-type, triangular finite element construct. 7-1415
 shell, laminated composite, applied theory development 7-1413
 shell, spherical, in contact with elastic filler, natural oscils., asymptotic analysis 7-11328
 shell, spherical, transversely isotropic, thick-walled, transient response, ray theory determ. 7-26142
 shell, stresses under local loads, calc. using Timoshenko method 7-57696
 shells, cylindrical, thick-walled, nonlinear cross section, stress state anal. 7-62993
 shells, cylindrical orthotropic, uniformly stressed, linear anal. 7-11295
 shells, elastic, spherical, vibration anal. 7-26193
 shells, elastic, spherical, with variable rigidity, nonaxisymm. deform., numerical soln. 7-62994
 shells, elastic-viscoelastic layered, multi-director formulation 7-37347
 shells, hollow flexible multilayer orthotropic, nonlinear theory, Bubnov-Galerkin method 7-24430
 shells, nonlinear elastic-viscoelastic layered, multi-director FEM formulation 7-43695
 shells, shallow saddle-shaped hypar, initial post-buckling behaviour 7-26177
 shells, shallow spherical on Winkler foundation, static and dynamic behaviour 7-57767
 shells, single-layer reticulated, stress function and its relation to continuous membrane shells 7-26140
 shells, spherical, and circular membranes, flexure theory, stochastic bifurcation 7-26151
 shells, spherical, elastic, filled with compressible viscous liq., vibration damping 7-1477
 shells, thin elastic, variational formulation for large deflections 7-43671
 simple layer of arbitrary anisotropy, stress operator limiting values from elastic pot. 7-43668
 slowness surfaces of incompressible and nearly incompressible elastic materials 7-16092
 small-strain problems, geometrically nonlinear discretization, convergence at infinitesimal element division 7-48362
 solid, elastic transversely isotropic semiinfinite, torsional loading 7-43664
 solid, nonsimple elastic, yield function, constitutive eqn. 7-62980
 solid, simple elastic, constitutive eqn. limitations 7-62979
 space with two hyperboloidal cuts under the action of a uniformly distributed pressure 7-97
 sphere, elastic, above critical strains 7-11289
 sphere, elastic isotropic, of compressible material, dynamics under cubic initial loading 7-1480
 spherical cavity in infinite elastic dielectric, nonlinear oscillations 7-31672
 spherical cavity in isotropic micropolar elastic medium, anal. 7-57691
 spherical inclusions in periodic array, elastic coeffs. 7-50952
 spine, method for identification of in vivo segmental stiffness props. 7-65801
 spiral longitudinal systems, tensioning and twisting 7-50949
 square lattice, site percolation and elastic props. 7-261
 stability of cantilever elastic column having linear viscous internal damping 7-6087
 stainless steel plate, thermoviscoelastic stress analysis 7-2092
 steady-state shock wave parameters in porous compressible materials, approximate calcs. 7-31653
 stress assisted diffusion in elastic and viscoelastic materials 7-50953
 stress functions for plane problem of couple elasticity theory (*Ukrainian*) 7-11283
 stress functions in a problem of elasticity theory (*French*) 7-62986
 submicrosecond elastic loading, material relax. phenomena 7-12186
 superconducting elastic crystals, constitutive theory 7-26826
 superelement method soln. (*Russian*) 7-43688
 T-junctions, stamped, thick walled, stress-strain state anal. (*Russian*) 7-1409
 tendon stiffness: methods of meas. and significance for movement control, review 7-54825
 tensile strip with large circular hole, stress analysis using nonlinear FEM 7-20596
 thermal stresses, theoretical aspects, book 7-9607
 thin elastic shells, general concept in rotation shell theory, to torus appl. 7-6101
 thin-walled sections under combined bending and torsion, nonlinear theory 7-57698
 three-dimensional body, asymptotics of stress-strain state in vicinity of pointed inclusion 7-6096
 Timoshenko beam on elastic foundation under moving spring-mass system, stability 7-43719
 torsional axially symmetric finite element model for problems in elasticity 7-57701
 trabecular bone specimens, stiffness behaviour obs. 7-54660
 transversely isotropic elastic plate pressed between two rigid cylindrical surfaces, contact problem 7-16130
 transversely isotropic half-space indented by parabolic concave punch 7-48366
 turbulent flows-elastic shell interaction, finite element anal. 7-43874
 two-component medium model dynamics, interaction of parallel elastic rods 7-1460
 unbounded bodies without strain energy function, uniqueness in finite elastodynamics 7-62982
 unbounded body, cracks, 3D loading, stress intensity factor history 7-50998
 unilateral boundary value problems, numerical approx. solutions 7-61105
 unilateral BVPs, num. methods 7-24427
 variational problems, with small parameter 7-24428
 vascular compliance of canine lung, longit. distrib. 7-8624
 vascular prostheses, validity of some methods of estimating circumferential elastance 7-8761
 velocity field equations and strain localisation 7-43672
 Au mechanical resonance spectra 7-21712
 Bi₂Ge₃O₁₂ single cryst. growth, characterisation and appls. 7-33550
 C fibre reinforced plastics, cylindrical interface crack study 7-26201

elasticity continued

- Fe₇₈Si₂₂B₁₃, amorphous, tensile strength, elastic stiffness (*Japanese*) 7-3346
 GaAs, dislocation loops, TEM image profiles, electron diffr. two-beam dynamical theory 7-12071
⁴H, liq. and solid, elastic props., and density up to 20 GPa 7-32733
 KDy(MoO₄)₂, elastic characts. near structural phase transition, sound vel. meas. (*Russian*) 7-26872
 Li₂TiSi₂, intercalation cpd., elastic effects, comp. depend. staging studies 7-63707
 Ni film on sapphire substrate, adhesion, mechanical resonance spectra 7-21712
 Ni₃Al, dislocation line stability 7-21212
 Ni₇₇Si₂₃B₁₅, amorphous, tensile strength, elastic stiffness (*Japanese*) 7-3346
 No₂O.nSiO₂+propylene carbonate, gels form., comp. of phases and rheological props. meas. 7-39875
 PLZT, electrically excitable mechanical resonant mode shapes 7-26854
 TiNi shape memory alloys, wear resist. and hardness, influence of heat treatment (*Korean*) 7-17647
- elasticity of liquids**
see also compressibility of liquids
 fibre suspensions in Newtonian fluids and polymer solns., capillary flow 7-6318
 fluorobiphenylalkane nematics, physical and mol. props. 7-38983
 glass bead and glass fibre suspensions, flow through flat orifices, elastic props. influence (*German*) 7-6296
 interfacial monolayer between surfactants, rheological anal. of the Marangoni effect. 7-38233
 interfacial turbulence and mass transfer, importance of surface compression elasticity modulus and Reynolds number 7-63128
 linear polyester, mainchain nematic polymer, viscoelastic coeffs., meas. by NMR 7-17231
 liquids, shear wave speed and elastic moduli 7-26824
 magnetic liquid, water-based, elastic parameters 7-54198
 nematic liq. cryst., parallel-aligned, phase retardation depend. optical response time 7-3018
 nematic liq. crystals., generalised Freedericksz transition, weak anchoring effects 7-32273
 nematic liquid crystal displays, multiplexed twisted, elastic constants of hybrid mixtures 7-2078
 nematic liquid crystals, biaxial, elastic continuum theory 7-1877
 nematic liquid crystals, Frank constants, effects of compression 7-63702
 nematic liquid crystals, heterocycles, NCS-polar groups and double bonds effects on material props. 7-1838
 nematic liquid crystals, supertwisted, hysteresis effect 7-16408
 nematic solutions of rod-like and semi-flexible polymers, elastic constants 7-32537
 nematics, elastic constants calc. 7-63703
 octylcyanobiphenyl, liq. cryst., elastic constns., permitt., birefr. meas. 7-21314
 polymer liq. cryst. solns., optical microscopy, Freedericksz transition, permitt. meas. 7-1864
 polymer nets, high elasticity, mol. theory with allowance for topological constraints 7-37839
 rheometrical device for meas. shear wave speed and elastic moduli 7-26823
 S³ blue phase, disclination, elastic energy calcs. 7-58135
 slender body, motion in quiescent polymer solns. 7-11523
 smectic C chiral liquid crystals, elastic free energy 7-11900
 smectic material props. modulated and cubic phase form. model 7-58133
 surfaces, effective bending rigidity calcs., integration meas. 7-58571
 TBBA, smectic-C phase, abnormal ultrasonic damping, anharmonic effects, ang. depend. 7-44697
 tobacco mosaic virus in water, freeze-fracture imaging of ordered phases 7-3751
- elasto-optical effects** *see photoelasticity; piezo-optical effects*
- elastomers**
see also rubber
 adherence, study by cyclic unloading expt. 7-33909
 butadiene elastomers, soot-filled, struct., IR spectra 7-39127
 ethylene-propylene-diene elastomer, sorption and swelling in water and humid media (*Russian*) 7-27139
 fluoroelastomer copolymers and terpolymers, glass transition temps. 7-12280
 fluoroelastomer copolymers and terpolymers, glass transition temps. calcs. 7-16745
 gels, swollen cis-trans isomerisation, network density effects 7-8273
 impact wear 7-22844
 impurity containing, exposed to laser pulses, thermooptic lenses, form. kinetics 7-51671
 low-molecular ingredients, migration in elastomer compositions (*Russian*) 7-39942
 Neoprene/styrene-butadiene rubber laminates, water permeation study 7-12374
 poly(propylene oxide) elec. relax. time, high press. effects study 7-32703
 poly(propylene oxide)-Li salt complexes, ionic cond., high press. effects study 7-32703
 polybutadiene, sequence distribs., polymerisation kinetics, IR spectra, NMR 7-16444
 polybutadiene networks, mechanical and swelling behaviour 7-11965
 polychloroprene, tear strength, crosslinking, viscoelastic loss mechanisms 7-39632
 polydimethyl siloxane, stress relax rig for use in γ -irrad. environments 7-8224
 polydimethylsiloxane, swelling by phenylmethylsiloxane, modulus, stress-strain isotherms 7-8039
 polyisoprene, sequence distribs., polymerisation kinetics, IR spectra, NMR 7-16444
 cis-polyisoprene films, crystallisation kinetics and morphology 7-6553
 cis-1,4-polyisoprene networks, uniaxial extension, stress-strain relation 7-39605
 polyisoprene vulcanizate, double step retraction, molecular models comparison 7-16685
 polyphosphazene, tear strength, crosslinking, viscoelastic loss mechanisms 7-39632
 polypropylene-EPDM elastomer multicomponent blend, CaCO₃ filled, mech. and rheological props. 7-3381
 polyurethane biomaterials, hydrolytic stability in model biological media, surface morphology changes 7-17673

elastomers continued

- polyurethane elastomer deformation heat meas., by quick-response calorimetry 7-1522
 polyurethanes, molecular struct., morphology, phase mixing, mech. props. 7-51664
 positron lifetime and annihilation radiation ang. correl. meas. 7-46229
 PVC-thermoplastic copolyester elastomer blends, γ -irrad., mech. props., fractography 7-21317
 rigid probe mobility in bulk elastomer, stationary fluorescence depolarisation obs. 7-7744
 silicone materials for optical fibre protection 7-15992
 silk fibre filled thermoplastic elastomer, tensile rupture 7-39635
 sliding friction mechanics, asperities adhesion fracture 7-53922
 underwater polymer composition rel. to acoustic props., Young's and longitudinal bulk modulus meas. 7-1304
 viscoelasticity meas. by electronic speckle pattern interferometry 7-33877

elastoplasticity

- acoustoelastic effect, influence of plastic deformation, stress distrib. in slightly orthotropic materials 7-16069
 alloys, fracture, deform., porosity effect 7-22750
 anisotropic media, necking and forming limit diagrams, instability problem (French) 7-31665
 anisotropic plastic hardening, FEM 7-26156
 antiplane parallel periodical crack field, elastic-perfect plastic soln. 7-57744
 axisymmetric elastoplastic torsion problem, num. soln. (Chinese) 7-14775
 bar, propag. velocity determ. of elastic-plastic boundaries (Chinese) 7-43732
 bars, initially curved, dynamic elastoplastic buckling 7-63024
 bars, tensile, void coalescence, plastic localisation, failure modes 7-6108
 beams, cold-bent, flowchart for overbend prediction 7-6103
 beams, elastoplastic, biaxial dynamic bending 7-62999
 beams and frames, elastic-plastic with unilateral boundary conditions 7-1442
 bifurcation by shear band localisation, incrementally nonlinear constitutive eqns. (French) 7-1441
 body under stamp action, unloading process for contact interaction 7-1517
 boundary element method applied to some inverse problems 7-1436
 cohesive-frictional material, approx. statistical soln. of elastoplastic interface for Galin problem 7-43707
 composite crack profile model for CTOD determ., theoretical anal. 7-63058
 composite with biperiodic system of circular fibers in an elastoplastic matrix, stability anal. 7-63026
 composites, periodic, elastic and instantaneous elastoplastic and moduli, overall, bounds 7-37349
 constitutive equations of hardening, analytical integration, elastic-plastic finite element analysis 7-63016
 contact, elasto-plastic under large deformation, finite element based quadratic programming 7-43805
 contour integration around crack tips in elastic plastic material, mixed mode loading 7-50994
 convergent bounding principle for a class of elastoplastic strain-hardening solids 7-43704
 crack tip elastoplastic stresses, experimental-analytical hybrid model 7-63065
 crack-containing body, elastoplastic problem of antiplanar deform., discontinuous solns. 7-11343
 crack-tip field parameters for large and small fatigue cracks 7-11356
 cyclic plasticity and creep, constitutive modelling using internal time concept 7-1437
 cylinder, non-homogeneous, elastic-plastic and limit soln. under internal pressure (Chinese) 7-43693
 discontinuous crack model, constitutive eqn. 7-26223
 displacement fields for mixed mode elastic-plastic cracks 7-16111
 dynamic deform. processes in elastoplastic solids, computation with allowance for continual failure 7-43696
 dynamic elastic-plastic fracture toughness parameters by instrumented Charpy test, accuracy of meas. 7-59705
 elastic-plastic eqn. analysis and numerical soln. (French) 7-41101
 elastic-plastic state of a wedge with limiting resistance to shear and separation 7-31662
 elastic-viscoplastic constitutive eqns., modelling of continuum damage 7-43764
 elastico-plastic flow in a rot. annulus, non-homogeneity effects 7-57710
 elastoplastic analysis of structures and linear complementarity 7-6117
 elementary localized potentials, stability loss for internally unstable elastic-plastic material 7-41104
 fatigue crack growth at notch root in elastic-plastic region (Japanese) 7-58404
 FEM for elastic-plastic plane stress, appl. to anti-plane strain 7-14768
 FEM solution of elastoplastic problems at finite strain 7-43694
 fibre reinforced metals, plastification, numerical and expt. investig. (German) 7-26172
 finite element analysis, precision and efficiency increase (Chinese) 7-43691
 finite element method for solving elasto-plastic and elasto-viscoplastic problems 7-26155
 finitely deforming rigid-plastic materials, Lagrangian strain space formulation 7-6109
 fluid-and-gas-filled elasto-plastic solids, anal. 7-43657
 fracture toughness, J-integral, under modes I, II and III, effect of notch root radius 7-63060
 Galerkin approach to boundary element elastoplastic analysis 7-50956
 Hertz contact, elastoplastic axisymmetric problems, FEM solution 7-20662
 indentation of elasto-plastic half-space by rigid circular cylinder 7-26226
 infinite elastoplastic medium with point source of heat, plastic zone generation 7-1443
 J-integral, estimation using FEM, simplified eqns. (Japanese) 7-50999
 J-integral estimates for cracks in infinite bodies 7-63056
 layered media with dissimilar materials, elastoplastic anal. 7-26160
 linearly strengthened systems, extremum principles and optimisation problems 7-63015
 longitudinal elastic-plastic waves with radial effects, numerical anal. for circular rods 7-31691
 mechanics of solids—equivalent response of structure under cyclic loadings (French) 7-63006

elastoplasticity continued

- metal-polymer two-layer plates under bending load, strength and stiffness calc. 7-57713
 metals, elastoplastic problems, numerical methods, double exposure speckle photography 7-57714
 nonlinear 3D fracture dynamics, path-independent integrals 7-63069
 nonlinear hardening materials, constitutive model of cyclic plasticity 7-6113
 nonlinear hardening model for elasto-plastic materials (Chinese) 7-26154
 nonlinear materials, energy release rate for crack growth, multiaxial loadings formula (Japanese) 7-11346
 nonlinear waves of different physicochemical nature in finite continua 7-18604
 notch root stress/strain prediction 7-63017
 panels, tensile, elastic-plastic models of surface cracks 7-63077
 perfect elastoplasticity, dynamic problem, generalized solns. 7-24429
 plane load wave, elastic precursor decay, eqn. of state 7-33751
 plastic potential theory in large strain elastoplasticity 7-4687
 plastic rupture during compression along near-surface fractures 7-43795
 plate, crack growth rel. to geometry and material props. 7-16112
 plate, elastoplastic, bending anal. by BEM 7-43705
 plate, stiffened tension, with eccentric crack, elastic-plastic finite element analysis (Chinese) 7-16119
 plate bending, finite element model with limit analysis capacity 7-63013
 plate with incremental constitutive relation, buckling (French) 7-26179
 plates, circular, elasto-plastic deflection analysis, full system vs. layered yield criteria prediction 7-1450
 plates, elastico-plastic stability at combined loading (Russian) 7-63025
 plates, orthogonally stiffened, under lateral and axial loads, nonlinear analysis 7-37360
 polycrystals, rate-dependent, finite elasto-plastic deformation 7-16671
 polyester thermoelastoplastics, softening, thermodynamics (Russian) 7-63847
 polymer-dominated multi-material systems, hygrothermal process interdependence and elasto-viscoplastic behaviour 7-53785
 porous, anisotropic and variable strength media, applied theories of plasticity 7-16072
 porous body, deformability criterion based on continual model 7-64958
 power station piping systems, dynamic test data, comparison with analytical methods 7-10191
 Prandtl-Reuss Law, generalised Norton-Hoff model 7-31658
 pressure vessel, elastic-plastic J-anal. for inner surface flaw 7-63076
 rate-type finite elasticity constitutive law, elastic and elastic-plastic deformation 7-57700
 reactor pressure vessel, thermoplastic stress calcs. from stress-relief up to thermal shock 7-10216
 reactor pressure vessels, fracture mechanics of cracks under cyclic thermal shock 7-10218
 reliability considerations in the numerical solution of elasto-plastic, viscoplastic and flow problems 7-1452
 rocks, elastoplastic dilatation model 7-14272
 rotating disc with jump-like nonhomogeneity, elastic, limit and decohesive carrying capacities 7-63001
 rough surfaces, elastoplastic deform. in real contact zones, friction coeffs. calc. 7-16136
 row of circular fibres in elastic-plastic matrix, stability 7-1455
 shakedown of elastic-plastic bodies, influence of geometrical nonlinearities 7-1438
 sheet metals with complex strain bending histories, elastic-plastic springback 7-37348
 shell, cylindrical, dynamic stability under nonaxisymmetry loading 7-57720
 shell, open sandwich conical, elastic-plastic, critical loads and stability loss (Polish) 7-43728
 shell of revolution with hole, elastic-plastic axisymmetric state under concentric loading 7-16078
 shells, axisymmetric sandwich, numerical shakedown anal. 7-26161
 shells, cylindrical, elastic-plastic buckling anal. 7-26181
 shells under finite deformation, general dynamic theory (German) 7-6116
 small strains quasistatic elastoviscoplasticity 7-50960
 soap-mineral oil lubricating grease, 12 Li-hydroxystearate greases, thick film, ambient pressure, shear flow transient tests (French) 7-6169
 solid deformable body mechanics, configurational forces 7-26167
 steady stress cycle construction for elastic-plastic structures 7-57706
 steel, austenitic stainless, pipe weldments, toughness at LWR operating temps. 7-13599
 steel, Cr, high C, notched rods, breaking by heating process, elastic-plastic stress analysis (Japanese) 7-33777
 steel, high strength, strength meas., anal. of elastic-plastic ball indentation method 7-63088
 steel, low-tensile, crack resist. in elastoplastic region under static loading 7-33793
 steel, quenched, high hardenability, thermal stress and strain generation 7-8071
 steel, stainless, LWR piping systems, LBB feasibility eval., fracture criteria 7-61968
 steel structure, biaxially-loaded connections, fracture condition (Japanese) 7-58403
 steel/composite, double-lap joints, stress anal. and failure props. 7-33769
 steels, deformation steel, model taking into account inhomogeneous microscopic behaviour (French) 7-63725
 stepped circular tubes, collapse under impact axial load (Japanese) 7-11310
 strain fields under low-cycle loading, use of isoparametric elements 7-26222
 strain hardening of material, elastic-plastic problem soln. 7-11304
 strain-space plasticity formulation for hardening-softening materials with elastoplastic coupling 7-26164
 stress-strain state in contact zone and rolling resist. in repetitive rolling 7-26229
 strip, elastic-plastic, contact problems under complex loading 7-43808
 strip, infinitesimal and large strain in rolling contact problems 7-11359
 structural metallic elements, elastic-plastic response, to irregular cyclic loadings 7-1445
 surface crack configurations, crack tip opening displacement, expt. investig. 7-63079
 thermoplasticity with simple loading processes, 3D problems soln. 7-31641
 thin elasto-viscoplastic layers, wave propag. 7-1481
 thin-walled frames, large elastoplastic deform., geometrically and materially nonlinear finite element anal. 7-1447

elastoplasticity continued

- torispherical heads, elastic-plastic state 7-26162
- total stability for elastic-plastic systems (*German*) 7-6115
- truss, three-bar, elastic/perfectly plastic, nonuniqueness, causes and consequences 7-11276
- yield surface, influence of plastic deformation (*Russian*) 7-63011
- Al alloy, Duralumin type, stability of struts in compression in elastoplastic range 7-22771
- Al alloy sheets, LY12CZ, fracture resist. characts., crack initiation, stable and unstable propag. (*Chinese*) 7-46592
- B fibre reinforced Al tube under multi-axial loadings, elastic-plastic deformation 7-46548
- PLZT, elastic-plastic contact damage 7-39627
- Ti, plate, fatigue crack initiation in orthotropic materials, effect of stress freq. (*Japanese*) 7-53867

elastoresistance

No entries

ELDOR

- platelets, human, lateral diffusion of lipid probes in surface membrane, ELDOR obs. 7-8526
- slow molecular motions, anisotropy, ELDOR obs. 7-62426

electrets

- see also *dielectric devices; electrostatics; photoelectrets; thermoelectrets*
- caruba wax, magneto-electret, surface charge density and dielec. const. 7-22126
- disordered dielectrics, electret relax., persistent polarisation decay and injected charge cond. calcs. 7-39003
- polyethylene films, charge storage lifetime, structural effects 7-27344
- polypropylene, electret and mechanical props., supermolecular structure effects (*Russian*) 7-64560
- polypropylene film electrets, corona-charge mechanism 7-53227
- polypropylene films, charge storage lifetime, structural effects 7-27344
- PVDF/PMMA blends, electret props., effects of structure, open-circuit thermally stimulated current anal. 7-13087
- Teflon-FEP electrets, stability, stretching effects 7-27650
- GaSe layered intercalated crystals, formation of electretic state 7-38994
- Sb₂S₃ amorphous condensers, electroelectret state and local levels studies (*Russian*) 7-45923

electric actuators

- piezoelectric actuators for scanning tunnelling microscopy, behaviour and calibration 7-18926
- Pb(Mg_{1/3}Nb_{2/3})O₃ ceramics for microdisplacement actuators, electrostrictive characts. (*Japanese*) 7-17270

electric admittance

- inhomogeneous transmission lines, supersymmetry and signal propagation 7-1011
- liquid thin film, with and without Al substrate, refl. coeffs., admittance method investig. 7-64711
- steel, stainless, polarisation behaviour and admittance response in NaCl soln. (*Japanese*) 7-22871
- CuInSe₂ photovoltaic devices, analysis using admittance spectroscopy 7-7171
- InP MIS structures, prep. by RF plasma oxidation, interface elec. props. 7-2731
- Si metal tunnel-thin insulator-semiconductor structures, effects of high field corners 7-64348
- Si:B(Al)(Ga)(P)(Sb) thermal donor props., impurity effects, DLTS, Hall effect, and admittance spectra meas. 7-21851
- Si/SiO₂, two-step oxidation of thin gate oxides, trapping characts., hot electron effect study 7-64351
- n-Si/SiO₂/Al struct., inductive admittance meas. 7-17108
- SiO₂/SiC interface. elec. characts., MOS conductance technique meas. 7-12873
- α -ZrP-propylamine, intercalation cpd., amine loading, protonic cond., admittance meas. 7-44909

electric admittance measurement

- Si solar cells, SILSO, grain boundary charact., meas./test techniques 7-13858

electric amplifiers see *amplifiers***electric arc furnaces** see *arc furnaces***electric arc welding** see *arc welding***electric arcs** see *arcs (electric)***electric birefringence** see *electro-optical effects***electric breakdown**

- see also *electric breakdown of gases; electric breakdown of liquids; electric breakdown of solids*
- dielectrics, electrical breakdown, physics, acoustic theory appl. 7-33329
- ion accelerator electrodes, energy dissipation during HV vacuum breakdown 7-30777
- trigatron-triggered breakdown initiated by streamers, streak photographic studies 7-32191
- vacuum breakdown in pulsed-power plasma expts., diode perveance 7-32184
- vacuum prebreakdown currents, anode oxidation effects 7-37780

electric breakdown of gases

- see also *electron avalanches; plasma production*
- air, atmospheric, optical breakdown during axicon laser focusing 7-44288
- air, breakdown due to rock fracture, light emission (*Chinese*) 7-29000
- air, breakdown in discharges, emission study 7-26574
- air, impulse breakdown voltage of slightly nonuniform field gaps, wave-front effect 7-32145
- air, optical breakdown near solid rough surface, time of appearance 7-26386
- airgap breakdown characts. obs., under ambient conditions of reduced air density 7-20978
- alpha-particle corona streamer counter 7-55333
- binary gas mixtures, electron transport, collision cross-section and dielectric strength 7-63244
- composite material, organically based, breakdown in high-temperature gas flow 7-26383
- dusty weak ionised gas, phys. and physicochem. props. 7-20841
- electrostatic precipitators back-corona initiation, anal. 7-51555
- hexane, gas, high density, Townsend ionis. coeff. and breakdown voltage 7-20842
- ignition voltage of spark gaps in technically important gases (*Czech*) 7-32144
- impulse surface discharge in compressed air in nonuniform field, characts. 7-51550
- interelectrode breakdown in MHD ducts 7-37765

electric breakdown of gases continued

- laser-triggered electrical breakdown of gases, unconventional geometries 7-44095
- lightning, physical process and effects 7-34662
- magnetic switches, formative time lags, extension of Davidson's theory 7-51547
- metal vapor formed by laser irradiation, breakdown 7-63316
- MHD channel, electric current fluctuations accompanying interelectrode breakdown 7-63248
- optical discharge, laser dragon, breakdown along a beam in vapour of target 7-58086
- plasma optical breakdown, supersonic turbulent propag. regime 7-20836
- plasma sheath develop., Mather's type plasma focus geometry, geometrical conditions anal. 7-32182
- reentrant cavity as a low-power plasma source 7-44199
- rod-plane gap, corona, breakdown and humidity effects 7-20979
- spark breakdown time-lag, negative ion effects in air 7-29233
- streamer develop. mechanism in nonuniform electric fields (*Russian*) 7-44276
- strongly electronegative gases; figure of merit meas. 7-51553
- Ar, breakdown, ruby laser induced 7-11579
- Ar-CF₄ mixtures in corona discharges in diffuse discharge switch appls., decomposition 7-37799
- H⁺ beam, space charge compensation by pregenerated plasma 7-44200
- H₂-D₂ system, CO₂ laser induced breakdown 7-6352
- He, breakdown in discharges, emission study 7-26574
- He-Ar(Ne) lasers, pumping by CO₂-laser induced optical breakdown 7-62668
- Kr, primary and secondary ionisation coeffs. meas. 7-1668
- N₂, breakdown voltage distribution meas. 7-31922
- N₂, flashover at dielectric interfaces: the interaction of surface and volume processes 7-51549
- N₂ gas breakdown by 13.56 MHz electric field 7-1806
- N₂, impulse breakdown voltage of slightly nonuniform field gaps, wave-front effect 7-32145
- Ne atoms, IS₂ metastable states, non-radiative lifetimes 7-37772
- SF₆ and air, impulse breakdown voltage for nonuniform field gaps with different wavefronts 7-51546
- SF₆ and SF₆ mixtures, streamer to leader transition under positive impulse 7-37774
- SF₆, breakdown and corona, electrode surface processing effect 7-51557
- SF₆ conditioning under repetitive positive HV conditions 7-51552
- SF₆, discharge characts. and insulating props., review of Japanese research 7-44279
- SF₆ filled spark gap, high-power discharge, electrode erosion and breakdown voltage study 7-44300
- SF₆ gas, Paschen's law, impurity effects 7-37771
- SF₆, impulse breakdown voltage of slightly nonuniform field gaps, wave-front effect 7-32145
- SF₆, RF breakdown and discharges, continuum modelling 7-37798
- SF₆ under DC stress, potential distortion from change on solid insulators 7-51554
- SF₆+Freon 113 mixtures in nonuniform field gaps, breakdown 7-51551
- SF₆+O₂, decomp. rate of SF₆, influence of O₂ in corona 7-51548
- UF₆, laser induced breakdown and appl. to flow diagnostics 7-20832
- Xe, primary and secondary ionisation coeffs. meas. 7-1668

electric breakdown of liquids

- aerosols, laser-induced breakdown, droplet size effects 7-44272
- dielectrics, elec. cond. and dielec. breakdown 7-45932
- electrokinetic phenomena in dielectric liquids 7-51542
- electrolytic solns. for processing metals, elect. discharges (*German*) 7-51528
- fast discharges in thin liquid layers 7-51541
- insulating oils, gamma-ray effects on elec. props. 7-48829
- n-hexane, DC-induced prebreakdown events 7-32147
- n-hexane, effect at press. on streamer initiation 7-53234
- n-nonane liq. dielectric, gas form. under particle discharge 7-51532
- prebreakdown phenomena in liq. dielectrics, effects of hydrostatic pressure (*French*) 7-33327
- prebreakdown phenomena in liquid dielectrics 7-32146
- prebreakdown phenomena observations of cryogenic and hydrocarbon liquids 7-58075
- St. Elmos's fire mechanism explanation from liq. surface instability in external electric field 7-44293
- Supermite accelerator water-plastic-vacuum interface design 7-30748
- transformer oil streamer mechanisms under AC voltage conditions 7-51543
- vaporization and breakdown of thin columns of water 7-59145
- H₂O and H₂O mixtures, effects of alloys and surface treatments on elec. breakdown strength 7-32185
- H₂O, deionized, for capacitor insulation, partial discharge and electric breakdown 7-32186
- N-liquid, mobility of positive ion 7-26576
- N₂, liq., electrical breakdown in presence of thermally induced bubbles 7-63377

electric breakdown of solids

- see also *impact ionisation; partial discharges; Zener effect*
- bipolar electric field flashover of vacuum interfaces in accelerator cavities 7-30750
- CR-39, electric breakdown model for particle registration sensitivity in electrochemical etching 7-30876
- dielectric, optical breakdown, equilb and nonequilb. absorpt. mechanisms in steady wave 7-45933
- dielectrics, breakdown and prebreakdown phenomena, charge transport and dielectric aging 7-39014
- dielectrics, conference, Erlangen, W.Germany (July 86) 7-35099
- electrical treeing, breakdown lifetime and microstruct. sequence 7-13092
- electrothermal breakdown, dielectric between electrodes, thermal resistance in electrodes, model 7-64568
- ethylene copolymers, electric breakdown and high-field conduction meas. 7-39011
- ethylene-aromatic monomer copolymers, elec. props. and breakdown voltages, new insulating materials 7-39010
- gate oxide defect localisation by tunnelling current microscopy and dielec. breakdown meas. 7-26601
- glass, laser exposure, repeated, absence of below-threshold ionisation and cumulation effect 7-63653
- glass fibre reinforced epoxy resin insulator, interface treeing phenomena study 7-39012

electric breakdown of solids continued

- hexamethyldisiloxane films, plasma polymerised, dielec. breakdown 7-33328
- insulating films on semiconductors, conf., Toulouse, France (April 1985) 7-35103
- insulating material, inception voltage of discharges in voids 7-53236
- insulating polymers, elec. cond. and breakdown phenomena 7-45306
- insulating thin layers, specific breakdown field concept 7-39035
- insulators, electric and mechanical breakdown, space environment effects simulation 7-39013
- insulators, laser breakdown due to nonequilibrium changes in their optical charact. near absorbing inclusions 7-53233
- metal foil plasma form., rail gun operation 7-32115
- micaplast materials with inorganic binders, electrical properties at temps. up to 900°C 7-12714
- MoS capacitors, breakdown by charge injection 7-38757
- MOSFET, substrate hole current, oxide breakdown 7-12863
- NMR preamplifier protection at UHF 7-9866
- organic insulating materials tracking breakdown, associated discharge light emission charact. 7-44274
- oxide thin films, dielec. breakdown, censored Weibull statistics 7-27656
- polyester fibre-epoxy resin insulator, prebreakdown space charge injection meas. 7-39017
- polyethylene, low density, electric breakdown and high-field conduction meas. 7-39011
- polyethylene, low density semicrystalline, elec. strength temp. depend. meas. and calcs. 7-39015
- polyethylene, low-density, AC elec. treeing phenomena, ramp voltage effects 7-39009
- polyethylene, low-density, elec. discharges and tree channels under impulse voltages 7-27657
- polyethylene, low-density, near-UV emission obs. during electrical-tree initiation 7-59259
- polyethylene, water tree growth, anion penetration 7-39030
- polyethylene, water treeing under DC and AC voltages 7-39028
- polyethylene, water-treeing, chemical structure and additives effects 7-39032
- polyethylene film, low density, elec. props. rel. to nuclear irradi., 5K 7-53232
- polyethylene films, electrical conduction, breakdown charact., effects of gamma radiation 7-27658
- polyethylene lightly doped films, breakdown strength meas., injected space charge effects study 7-39019
- polyethylenes, dielectric breakdown, threshold field meas. 7-39018
- polymeric insulating material, dielec. breakdown strength rel. to lamella struct. 7-53237
- polymeric insulation, water treeing, failure and growth mechanisms 7-39034
- polymeric insulation, water treeing, ion penetration 7-39031
- polymeric insulation, water treeing and morphology 7-39029
- polyolefin insulating materials, bow-tie and vented-tree formation 7-39033
- polypropylene film, DC, AC and impulse breakdown strength temp. depend. meas. 7-39016
- polysilicon oxidation, appl. to double polysilicon devices 7-39774
- polysilicon-SiO₂, surface texturing effect on SiO₂ cond. and breakdown 7-39773
- polysilicon-SiO₂ interfaces, textured, electronic props. 7-38754
- polyurethane insulation, thermal and elec. aging, prebreakdown phenomena, FTIR spectra study 7-39568
- prebreakdown and dielec. breakdown, fractal model anal. 7-2973
- Proto II accelerator, low inductance diode design for imploding plasma loads, insulator breakdown 7-30760
- quantized Hall effect, impurity bound state ionisation 7-12742
- quenched random media, size effects of electric breakdown 7-2974
- review of Japanese research 7-45931
- semiconductors, intrinsic, solid-state plasma, local impact ionisation regions form. 7-52663
- silane XLPE, electrical breakdown study 7-27659
- soil, breakdown initiation rel. to gaseous ambient 7-59883
- stearic acid films, dielec. breakdown field meas. 7-27661
- surface flashover in insulator with reduced E-field 7-64569
- surface topography, electric breakdown effects obs. using nematic liquid crystals 7-18744
- voltage measurement method 7-48771
- XLPE, cable insulation, water treeing, microstructural effects 7-39027
- XLPE insulation, water treeing 7-39026
- AgN₃, elec. cond. under high press., decomp. by dielec. breakdown 7-27010
- Al₂O₃ anodic films, thickness depend. of dielectric breakdown voltage 7-39007
- Al₂O₃-Ta₂O₅ thin films, dielec. props. rel. to electrolum. display appls. 7-2975
- BaTiO₃ ceramics, Maxwell-Wagner relax. and degradation 7-2970
- BaTiO₃, polycrystalline, dielec. breakdown, microstructural effects 7-39021
- Bi_{1-x}Sb_x narrow-gap semicond., intraband breakdown, current-voltage charact., size effect conditions 7-52624
- CaF₂-Si, MBE of CaF₂ on Si and overgrowth with Si or Ge charact. 7-22495
- CaF₂-Si interface, with epitaxially grown insulator, post-growth annealing treatments 7-7074
- CaF₂-Si structure with epitaxial CaF₂, electronic characteris. 7-22026
- Ga_{1-x}Al_xAs MIS and SIS structures, prep. by metallorganic chem. hydride method, electrophysical props. 7-22018
- GaAs current limiters, impact ionisation breakdown 7-52639
- p-Ge, electric avalanche breakdown, chaotic and hyperchaotic states 7-52630
- LiF, electric breakdown due to injected electron beam. 7-64837
- PbO-B₂O₃-SiO₂ glass dielec. thin films on anodised Al substrates 7-17269
- Si MOS structures, anodically and thermally grown, breakdown field strengths 7-17113
- Si, plasma assisted oxidation below 800°C 7-39783
- Si, plasma etching, oxide breakdown due to charge accumulation 7-17743
- Si, pyrogenic oxides, carrier trapping and breakdown, rel. to H₂O partial press. 7-64267
- Si/PtSi(CrSi₂) Schottky diodes, surface imperfection induced elec. leakage paths 7-2719

electric breakdown of solids continued

- Si/SiO₂, two-step oxidation of thin gate oxides, trapping charact., hot electron effect study 7-64351
- Si/SiO₂ system, dielec., elec. and struct. props. 7-7040
- Si/SiO₂ system, two-step oxidation and interface structs. 7-3542
- Si-SiO₂, oxide breakdown, high field and current stress, thickness depend. 7-59144
- Si₃N₄ films, plasma deposited, bonds and defects 7-17437
- Si₃N₄ films prep. by ECR plasma CVD, phys. and elec. props. 7-58716
- a-Si₃N₄:H films deposited by plasma enhanced CVD, optical and elec. props. 7-39205
- SiO₂, behaviour under high elec. field/current stress conditions 7-7254
- SiO₂, CVD photox layers, Hg-sensitised, elec. props. 7-64379
- SiO₂ films, breakdown lifetime meas., defect density determ. 7-22189
- SiO₂ layers, electrical properties 7-58931
- SiO₂ low temp.-CVD films, DC dielec. breakdown studies 7-22188
- SiO₂ on polysilicon, thermally grown, elec. cond. and breakdown props. 7-45508
- SiO₂ thermal oxide films on Si substrate, ramp-voltage-stressed I-V charact. 7-17112
- SiO₂ thermally grown on Si substrates, breakdown and defects studies 7-33104
- SiO₂, thin film growth, on Si, annealing by lamp heating 7-22930
- SiO₂ thin films, constant current stressed voltage-time charact., dynamic trapping effects 7-45529
- SiO₂ thin films, dielectric breakdown phenomenon, model 7-64567
- SiO₂ thin films in MOS capacitors, wear-out charact., processing depend. 7-38756
- SiO₂, thin thermal dielectric, breakdown susceptibility, correlation with process dependent charge trapping 7-33333
- SiO₂ ultrathin films, intrinsic breakdown charact. 7-64571
- SiO₂ ultrathin gate oxide films, breakdown props., post-oxidation annealing effects 7-22187
- SiO₂N_y, high press. NH₃-nitrided, elec. charact. 7-39039
- SrTiO₃ ceramics, Maxwell-Wagner relax. and degradation 7-2970
- SrTiO₃-based SPBT ceramics, DC conduction and breakdown at high temps. 7-39020
- ZnS:Mn thin films, DC electrolum. and local destructive dielec. breakdown model calcs. 7-59147
- ZnS:Mn thin films, local destructive breakdown and DC electrolum., film prep. and test conditions depend. 7-59146
- electric cables** *see cables (electric)*
- electric capacity** *see capacitance*
- electric cells** *see cells (electric)*
- electric charge**
see also space charge
black holes, bosonic instability effects on elec. charge (Russian) 7-55702
collision of solids, EM radiation 7-42890
conference on natural and man-made ions in atm., London, England (October 1985) 7-24304
electrostatic charging of solid particles and liquid droplets 7-26586
Giotto spacecraft, charging effects in cometary environment of P/Halley (1982i) 7-14473
ISIS-II spacecraft, discharge of RF-induced DC potential by positive ions 7-66427
plasma, charge distrib. in elec. sheath region, math. expression 7-51462
steel, mild, H diffusivity meas. using electropermeation transients 7-22903
stratified media, current source in presence of insulating and conducting disks 7-25699
Fe, cathodic charging, H trapping 7-21256
Li-SO₂ commercial cells, impedance meas. at various states of charge 7-54281
- electric coils** *see coils*
- electric condensers** *see capacitors*
- electric conductance** *see electric admittance*
- electric conductance measurement** *see electric admittance measurement*
- electric conduction processes** *see electrical conductivity*
- electric conductors** *see conductors (electric)*
- electric connectors**
see also cable jointing
interfacing fibres with equipment, optical to electrical connection concept 7-37151
piezoelectric transducers, thickness mode, back-face only elec. connections 7-43619
solar cell interconnector fatigue simulation testing, satellite appl. 7-13873
GaAs with Al honeycomb substrate, flat-plate space solar panels interconnector design 7-13879
Pd-Ag alloy electroplated coating contact and corrosion resistance and wear 7-3509
- electric current**
see also arcs (electric); corona; critical currents; current density; current distribution; current fluctuations; eddy currents; fault currents; leakage currents; overcurrent; short-circuit currents; sparks
ampere reproduction from proton gyromag. ratio and quantum magneto resonance phenomena 7-61309
conductor motion through magnetoplasma, assoc. Alfvén wings struct. 7-23989
EM edge wave, current point source, conducting wedge presence 7-15801
EM field coupling, lightning discharge, current induced in aerial on buried telecom. line (French) 7-10817
EM waves, auxiliary currents method and wave potentials, diffraction field anal. 7-50469
lightning, physical process and effects 7-34662
plane wave diffraction by dielectric cylinder, oblique incidence 7-50461
pulsar magnetospheres, pair creation rel. to return-current mode changes and normal-null transitions 7-14598
radar cross-sections calc., equivalent currents, flat plates with surface impedance coatings anal. 7-42867
shocks, injury by electric current passing through acupuncture points (Russian) 7-28493
solar atmosphere, current sheets form. model 7-66539
solar corona, 3D model of preflare energy build-up in filament oct. 7-66558
solar corona, elec. currents-mag. field interaction set to form. of coronal transients with forerunners 7-66538
solar quiescent prominences, static current-sheet models 7-66540

electric current continued

- stellar atmospheres, effect of Hall currents on thermal-convective instability of composite plasma 7-4437
 Vega-1 spacecraft, impact-induced secondary electron currents meas. during Comet Halley flyby 7-14521

electric current control

- JT-2M poloidal field coils, power supply and control system 7-15323
 JT-60 toroidal field coil power supply, DC output control 7-15319
 microwave spectrometer, electromagnet power system improvement using dual control 7-30057
 photography, waste fixing solution electrolysis, programmed current control system (*Russian*) 7-35616
 plasma spray deposition process parameters control, math. model 7-3477
 power supplies to magneto-optical elements of particle channels, digital remote control system 7-42268
 wideband power regulation system for Ar ion laser 7-31347

electric current measurement

- see also ammeters; galvanometers*
 10 mA LF AC current standard using single-junction type thermal AC-DC transfer converters (*Japanese*) 7-9842
 50 kA current transformer intercomparison between China and West Germany 7-18815
 AC/DC transfer instruments comparison using digital bridge 7-18835
 Faraday cup for intense electron beam pulses 7-51515
 fibre optic current sensors using highly birefringent bow-tie fibres 7-15976
 LED current sensor for electrostatic double probes 7-63357
 NBS absolute ampere experiment 7-18827
 NBS primary AC-DC transfer standards, using multijunction thermal converters 7-18836
 optical fibre calibrated Faraday rotation current and mag. field sensor 7-25980
 optical fibre sensor, calibrated, as Faraday rotation current and magnetic field sensor 7-31515
 phenol-formaldehyde novolac resin, thermally stimulated depolarisation current meas. using blocked electrodes 7-17261
 photovoltaic array I-V characteristic measurement error 7-3688
 relativistic electron beam current and position monitor 7-19596
 SI ampere and volt units, electrical metrology example 7-18807
 solar cell short-circuit current meas. as method for efficiency calc. 7-13872
 solar cells, large area, spectral response meas., microcomputer controlled apparatus 7-3642
 solar simulators and I-V meas. methods 7-54310
 toroid-amplifier system for mag. meas. of current in biological tissue, capabilities 7-23493
 twisted optical fibre, Faraday rotation meas. using rotating polarisation and analogue phase detect. 7-25981
 GaAs solar cells with varying junction depths, spectral mismatch correction 7-65475
 a-Si alloy tandem solar cells, spectral response and I-V characts. 7-54315
 Si:B(P) solar cell emitter saturation current meas. by contactless photoconductivity decay method 7-13866

electric discharge machining *see spark machining***electric discharges** *see discharges (electric)***electric distortion measurement**

- GaAlAs laser diodes under microwave intensity modulation, linearity charactn. 7-10944

electric domain walls

- A_2BX_4 -type crystals, incommensurate phase, zig-zag domain wall structure 7-33342
 bistable cholesteric twist cell, anisotropic domain growth 7-1865
 ferroelectric crystals, domain memory studies, sound generation method 7-39053
 ferroelectrics, unstable point domains 7-17280
 graphite, intercalation cpds., staging walls charge profile, Thomas-Fermi description 7-12687
 triglycine sulphate, Cr doped, amplitude depend. of dielectric losses 7-64587
 YZ-LiNbO₃, domain structure and lattice defects, effects of piezoelectricity, TEM anal. 7-2999
 BaTiO₃:Nb(Ca), ferroelec. domains, SEM and TEM obs. 7-2998

electric domains

see also electric domain walls; ferroelectric materials

- calcium tartrate single crystals, dielectric props. rel. to X-ray on γ -ray irradi. 7-59161
 ferroelectric liquid crystals, surface stabilised, disclination dynamics, switching process 7-58137
 ferroelectric smectic C* liquid crystal, alignment and switching characteristics 7-64589
 ferroelectrics with multi-domain layers, fabrication and SAW excitation 7-27676
 high accuracy universal polarimeter 7-17300
 MBBA liq. cryst., Williams domain evolution process, Fourier spectrum anal. 7-32274
 polyvinylidene fluoride, Form I, ferroelectric switching characts., microdomain nucleation and growth model 7-22197
 tetramethylammonium tetrachlorozincate, ferroelec., optical activity in incommensurate phase 7-64602
 TGS single crystal solution growth with modulated struct. 7-59388
 BaSrNb₂O₆, ferroelectric thin films, pyroelec. props 7-59154
 BaSrNb₂O₁₂, chaotic states, high resolution electron microscope study 7-3001
 Ba₂Sr_{1-x}Nb₂O₆, poly- and single-domain samples, integrated light scatt. and polarisation 7-53361
 n-GaAs films, electron-hole plasma stratification and blue luminesc. near static domain 7-52666
 K_{1-x}Li_xTaO₃ monocrysts., polarisation jump, ferroelec. transition and domains study (*Russian*) 7-22200
 KNbO₃, single domain cryst. prep., orientation and dielec. polarisation 7-45950
 LiKSO₄ single crystals, optical activity, ferroelec. and ferroelastic props. 7-27687
 LiND₄SO₄, ferroelastic and ferroelectric domain struct., SEM obs. 7-27675
 LiNH₄SO₄, ferroelastic and ferroelectric domain struct., SEM obs. 7-27675
 YZ-LiNbO₃, dislocation electric fields and small-angle grain boundaries, ferroelectric domains 7-3000

electric domains continued

- LiNbO₃, profiled cryst. growth by Stepanov's method, regular domain struct. prod. 7-32330
 LiNbO₃ single crystal fibres, ferroelec. domain structs. 7-22202
 LiNbO₃:Ti integrated optical devices, domain inversion effects 7-62849
 Li₂O-Nb₂O₅-(TiO₂)₂ system, vicinity of LiNbO₃, solid solns., crystal chemical and ferroelectric props. 7-6805
 Li₂O-Ta₂O₅-(SnO₂)₂ system, vicinity of LiTaO₃, solid solns., crystal chemical and ferroelectric props. 7-6805
 LiTaO₃, Czochralski grown with modulated struct., periodic laminar ferroelec. domains, SHG 7-59405
 PZT, shock-recovery expts. 7-38119
 PbGeO₃, ferroelec. domain struct. and diffuse phase transition, permittivity meas. 7-13108
 Pb₂Ge₃O₁₁, acoustic devices, appl. of regular domain structs. 7-20567
 Pb₂Ge₃O₁₁, ferroelec. domain-struct. dynamics visualisation using a nematic liq. cryst. 7-53250
 Pb₂Ge₃O₁₁:Gd³⁺, impurity ion reorientation kinetics 7-45940
 Pb(Sc_{1/2}Ta_{1/2})O₃, single crystals, and hot pressed ceramics, ordering, domain struct., TEM obs. 7-26936
 PbTiO₃ based glass ceramics piezoelectricity, pyroelectricity and ferroelectricity 7-7654

electric double layers *see electrochemistry; liquid theory***electric double refraction** *see electro-optical effects***electric drives**

see also clutches

- electrodynamical drive of Mossbauer spectrometer, controller design 7-35508
 Kinor film camera, crystal controlled electric drive use (*Russian*) 7-35617
 tensile testing machine modification to perform simultaneous tensile and torsion tests 7-22948
 VVER 440 reactor, control element drives, diagnostics 7-36239

electric field effects

- see also acoustoelectric effects; discharges (electric); electrical conductivity; electro-optical effects; electrochemistry; electrodynamics; electrohydrodynamics; electrokinetic effects; electroluminescence; electromechanical effects; electromigration; electron field emission; electrophoresis; field emission ion microscopy; field evaporation; field ion emission; field ionisation; high field effects; magnetoelectric effects; particle optics*
 2D nucleation in elec. field, form. free energy 7-58434
 airway smooth muscle responsiveness to elec. field stimulation, K⁺-induced alterations 7-8548
 alkali metal atom-He system, Rydberg energy levels, Coulomb and Coulomb-Stark-Green fn. 7-42476
 blue phase I-cholesteric transition, electric field-induced, kinetic hindrance 7-58465
 Brownian motion, obs. in laser 7-57293
 bubbles, maximum size during nucleate boiling in elec. field 7-50918
 cation-exchange resin, granulated, ionic composition, pulsed elec. field effects 7-54134
 chemical electric field effects in biological macromols., review 7-54444
 crystal growth in high electric fields, review 7-32338
 dielectronic recombination, electric field enhancement over Rydberg spectrum 7-5618
 differential heating of tissues by UHF field, decrease of effect of ionising radiation (*Russian*) 7-28610
 diglycine sulphate single crystals, anhydrous, elec. activated dislocation motion 7-12069
 dipole polarisability of atoms and ions, ionis. pot. correl. 7-42529
 dipole transitions induced from pulsed electric field on molecular beams (*French*) 7-62452
 DNA, elec. cond., possible mechanisms of action of an external electrostatic field 7-54668
 dusty weak ionised gas, phys. and physicochem. props. 7-20841
 electrorheological suspensions, viscoelastic behaviour 7-43826
 ELF electric fields, effects on neuronal activity in rat brain 7-28583
 ELF-LF electric fields, quantification of interaction with human bodies 7-3836
 evaporation, phase transition kinetics, electric field effect 7-52020
 external electric field, first-order perturbed wave fn. 7-36465
 gyrotopical plasma, semibounded, parametric excitation of surface cyclotron waves 7-51432
 HCL, condensation on charged CO₂ walls, Stockmayer model calcs. 7-63784
 ice, nucleation mechanism under elec. effect 7-52005
 incommensurate phase transitions, electric field induced, Landau-type thermodynamic pot. 7-63766
 ionic mass transport through homogeneous membrane in uniform elec. field 7-54173
 linear particle transport theory, current density transients 7-56191
 liquid crystal blue phase, frustrated, Kassel diagrams show elec. field-induced cubic-tetragonal struct. transition 7-32649
 liquid crystal capillary cell, orientational and struct. effects in conical elec. field 7-44370
 liquid crystal mesophases, orientational optical nonlinearity, review 7-1880
 liquid crystalline polymers, cross linked, shape variation by elec. fields 7-32280
 living cell model for electric field and overvoltage effects (*Polish*) 7-60031
 magnetised plasma subjected to external EM radiation in lower hybrid reson. region, temp. relax. 7-44100
 maintenance and operations personnel at 750 kV installations, effects of intense electric fields (*Rumanian*) 7-28585
 metal surfaces, field adsorption of rare gases 7-21648
 methane, gas, positron annihilation, density and elec. field effects 7-36825
 molecular dynamics, noninertial accelerations, statistical correlations study, electromagnetic field effect 7-62344
 nematic and cholesteric to isotropic phase transitions, dynamic effects of elec. fields 7-16740
 nematic liq. crystals, Fredericksz effect in crossed elec. and mag. fields 7-63446
 neurons, polarisation by extrinsically applied elec. fields, model 7-40132
 one-dimensional lattice, charged particle motion, dynamic localisation in elec. field 7-16924
 particle charging process, electric field depend. 7-20786
 plasmasphere structure, effect of field vars. 7-66399

electric field effects continued

- poly- γ -benzyl-L-glutamate, cholesteric soln., elec. field effects (*Russian*) 7-11909
- polymer liquid crystals, synthesis, characterisation and applications 7-17508
- polysiloxane, liq. cryst., with side chains, elec. field effects 7-11883
- porous solid-liquid systems, mass exchange in elec. field 7-12398
- rigid molecule, orientation in nematic liq. cryst., NMR study 7-62414
- rotating electric fields, cell behaviour rel. to surface charges and cell structs. 7-28584
- semiconducting crystals, surface reconstruction model calcs. 7-32780
- semiconductor and metal surfaces, field-assisted photodesorption 7-32809
- sensory receptors of cat's hindlimb, response to a transient, step-function DC elec. field 7-28581
- smectic C phases, bistability and domain wall motion induced by strong elec. fields 7-63450
- solid materials, bonding, external electrostatic field effects 7-26693
- spin 3/2 2D-dimensional wave equation with definite charge, propag. in external elec. field 7-110
- steel, quenching, elec. field enhancement 7-46517
- (TMTF)₂Mo₆Cl₁₄, prep. by electrocrystallisation, struct. and spectroscopic characterisation 7-46295
- triglycine sulphate, single cryst., neutron irradiat., elec. cond. 7-7227
- Al-Si (1.14 at.%) alloy, supersaturated, anomalous solute conc. fluctuation under elec. current influence 7-13457
- Ar, positron annihilation and diffusion, computer-based anal. 7-50378
- Ar, positron drift and diffusion in crossed elec. and mag. fields, simulation 7-36760
- CO, electron mobility to diffusion coeff. ratio meas. 7-20840
- ¹³³Cs, ⁷²P_{3/2} state, level crossing in elec. and mag. fields 7-50003
- Fe electrodes, electrodisolution and passivation K₂CO₃-KHCO₃ solns., ionic comp. effect 7-17677
- Gd, autoionising states, electric field effects, UV spectra anal. 7-42531
- H atom, positron annihilation, computer expt. 7-36791
- H EM energy density distrib., van der Waals forces 7-50048
- H electric field effects, Feynman path-integral formalism 7-42547
- H excited states, 1D atom construction using external electric fields 7-19730
- H, laser spectroscopy with relativistic beams 7-19778
- H⁺, laser spectroscopy with relativistic beams 7-19778
- He, n¹D₂ levels, alignment and orientation in elec. field 7-865
- HeRh²⁺ adsorbed compound ion, field dissociation by atomic tunneling 7-33919
- HeRh²⁺, cpd. ion, dissoc. in high elec. field, at. tunnelling, orientational and isotope effects 7-42777
- InSb MOS structures, electric field effects on characteristics 7-38738
- KBr single crystals, F-band absorpt., X-irrad., thermolum., mag. and elec. field effects 7-59230
- KCl doped crystals, impurity centres, form. processes and thermoactivation solution 7-44576
- KCl, F-centre destruction at elevated temps. under elec. field 7-32488
- KMnO₄, thermal stability changes upon adsorption of water vapour in an electric field 7-8262
- KTaO₃:Gd³⁺(Fe³⁺), ESR, effect of external electric field 7-38933
- Li + He(Ne), electric field effect, fluoresc. and radiative decay rate determ. 7-20009
- Mg, multiphoton ionisation, DC elec. field effects 7-62337
- NaK discharge, laser excited, fluoresc. spectrum (*French*) 7-10646
- NbSe₃, CDW conductor, interference effects with AC+DC excitations 7-52475
- NbSe₃, CDW conductors, mode locking phenomena and routes to chaos 7-52474
- Pt, adsorbed NO, high-speed ramped field desorption spectra 7-32810
- Si single crystals, defect struct., high DC elec. fields, X-ray diffr. 7-44530
- Si:B p-n⁺ junction, injection annealing of radiation defects 7-12161
- TaS₃, CDW conductors, mode locking phenomena and routes to chaos 7-52474
- W (110), field adsorption and desorption of H, atom probe FIM 7-21647
- W, He field adsorption and evaporation 7-32802
- W surface, He fluid adsorption and diffusion, atom-probe field ion microscopy studies 7-32808

electric field gradient (condensed matter) *see crystal hyperfine field interactions; hyperfine field interactions (condensed matter)*

electric field measurement

- see also field plotting*
- 1 to 20 MHz lightning radiation fields, amplitude spectra meas. 7-40549
- antenna directional patterns measurement using extended radio sources 7-56234
- C fibre composite tubular struct., induced EM fields, 2D model prediction 7-25703
- DC electric field meter with fiber-optic readout 7-30040
- dielectric material, radiation diagnostics of electric potentials, sensitivity and resolution 7-8233
- ELF, at human body surface 7-18840
- Fabry-Perot fibre optic sensor and its appls. 7-43424
- fibre optic sensors, piezoelectric copolymer jacketed single-mode fibers forelectric-field sensor application 7-6011
- laser pulse spatial modes, direct measurement 7-5931
- long gap discharges, electric field meas. using a Pockels device 7-4822
- low frequency, antenna calibration 7-56233
- mill sensor for use on aircraft, to study clouds 7-55213
- plasma, electric field measurement using atom beam-Doppler spectroscopy 7-11710
- reference field strength meters with dipole antennas, appl. of thermistors 7-56232
- rod-plane gap, space-charge behaviour evaluation using Pockels' cells 7-20980
- sensor, miniature two-component, design calc. 7-56231
- NaK, Stark effect, appl. to plasma local electric field determ. 7-26563

electric field strength measurement *see electric field measurement*

electric fields

- see also electric field effects; electric field measurement; electromagnetic fields; electromagnetic waves; field plotting*
- 3D Laplacian finite element formulation 7-50453
- accelerator energy level upgrade, electrostatic field calcs. 7-25273
- alternating electric field, model for action on a human 7-34187
- asymmetric strip line segments, cross coupling, electrodynamic theory 7-36848

electric fields continued

- auroral ionosphere, electric field and electron flux effects on SW radio signals 7-40630
- bipolar electric field flashover of vacuum interfaces in accelerator cavities 7-30750
- centrosymmetrical dielectric, Rayleigh waves on surface excited by external periodic electric field 7-31614
- charge simulation method with boundary shape taken into account 7-15797
- charged particle, cyclotron motion in spherical microwave cavity 7-15810
- collision of solids, EM radiation 7-42890
- P/Comet Halley (1982i), Vega APV-V electric field and plasma meas. (*Russian*) 7-14538
- computation, finite-element and boundary-element methods combined (*Chinese*) 7-10822
- crossed-field analyzer, aberration anal., elec. and mag. field expressions 7-10841
- DC ionised field quantities as influenced by coronating conductor surface gradient 7-58074
- dielectric and magnetic materials, linear feedback models for polarisation and magnetisation 7-22179
- dielectrics, elec. fields, computer calc. 7-42837
- diffraction magnetodielectrics, integral equation 7-36846
- discharge inception voltage from free cond. particles in air 7-51544
- dyadic Green's function as an inverse operator 7-36851
- dyadic Green's function expansions in spherical coordinates 7-62570
- electron gun, electrostatic field problem, Poisson equation, numer. soln. 7-29774
- electrostatic discs with parallel and intersecting axes, mean potentials and potential coeffs. (*Russian*) 7-42835
- electrostatic field and capacitance calcs. for spheroidal shells (*Russian*) 7-42836
- electrostatic field measurements and the mechanism of intracloud discharges 7-55121
- electrostatic problems, integral eqns. for thin dielec or conducting layers 7-31209
- electrothermal processes, one-dimensional, boundary-value problems (*German*) 7-31623
- gas lasers, multimode, total electric field strength, temporal evolution 7-15848
- global geometry of polyphase structures fed by complex current systems (*Italian*) 7-31207
- glow discharge switches and electrode design, electric field calculations using the ELF codes 7-32134
- heterogeneous environments, potential fields anal. (*Polish*) 7-20093
- hybrid type infinite element, finite element approach to unbounded Poisson and Helmholtz problems 7-1003
- implicit method for solving Maxwell's equation 7-57206
- insulating material, inception voltage of discharges in voids 7-53236
- interelectrode gap strength calc., Kilpatrick's criterion approximation 7-10815
- interplanetary medium, plasma wave meas. in environment of Periodic Comet Halley (1982i) 7-14524
- ionosphere, EM disturbances, IKB-1300 meas. at auroral latitudes 7-66389
- ionosphere, perturbed reflection layer, electric field calc. 7-40637
- ionospheric inhomogeneities and field disturbances 7-40626
- magnetosphere, reconnection model, magnetic and electric field behaviour 7-14414
- Maxwell's eqns. in inhomogeneous media, 2D finite-difference time-domain analysis 7-15809
- metal cluster ions, stored, spectroscopy in Penning trap 7-15779
- multiwire drift chamber, electric field calcs. (*Chinese*) 7-25319
- near-Earth shocks, microstructure 7-55410
- oscillating electric fields in low temperature plasmas, mol. fluoresc. meas. 7-20958
- Penning trap confinement of electron appl. to ion spectroscopy 7-10834
- piecewise homogeneous dielectric with general boundaries, plane fields computation (*German*) 7-62563
- piezoelectric layer with periodic system of electrodes, plane problem of electroelasticity 7-2983
- plasma deflagration gun, simple model including self-consistent electric and magnetic field 7-32138
- plasma jet injection into ionosphere elec. field eqns. 7-51416
- polysilicon oxide, elec. cond. model 7-45526
- polysilicon-SiO₂ interface, enhanced electron injection 7-38755
- pulsar magnetospheres, pair creation rel. to return-current mode changes and normal-null transitions 7-14598
- radar cross-sections of polygonal cylinders and flat plates, TGD calc. 7-42864
- solar wind, elec. fields rel. to plasma concentration vars. in main ionospheric trough during mag. storm 7-34780
- solar wind, mag. and elec. fields meas. near Periodic Comet Halley (1982i) 7-14522
- streamer develop. mechanism in nonuniform electric fields (*Russian*) 7-44276
- Sun, flare elec. fields 7-24105
- turbulent medium, coherent and incoherent sources 7-15807
- vector diffraction theory, plane wave and spread function decompositions 7-62599
- Venus, lightning evidence 7-47746
- wire, long, back electric field 7-35162
- N-liquid, mobility of positive ion 7-26576
- Si junctions very shallow, elec. field anal. 7-21989

electric filters *see filters*

electric furnaces

see also arc furnaces

- glass furnace, 3D model for glass flow and Joule heat release calc. 7-20707
- glass melting tank, electrically boasted 3D model for flow simulation and heat transfer 7-20805
- heat storage furnace, low-cost electric, using crushed rock for storage, residential use 7-65635
- molten metal flow pattern calc. in induction furnace (*German*) 7-31729
- zirconia induction furnace for high strength fibre production, design 7-11184
- NbC heaters use in α -SiC single cryst. growth 7-27881

electric fuses

- characteristics for multi-megajoule capacitor bank appl. 7-30792

electric fuses continued
 exploding metallic foils time-dependent behaviour and hydrodynamic expansion, computer model 7-32036
 pulsed power supplies, IEEE conf., Arlington, VA, USA (1985) 7-35110
 Al electrically exploded foil opening switches, high performance 7-32034

electric generators
see also magnetohydrodynamic converters; standby generators; turbogenerators; Van de Graaff generators
 lighting generators for commercial vehicles, oil cooled, heat transfer coefficients comparison (*German*) 7-37312
 overheating, early diagnostics using data for release of aerosols in insulation (*Russian*) 7-59787
 overheating faults in insulation, detection by gas and capillary chromatography 7-28382

electric glow *see corona*

electric heaters *see electric heating*

electric heating
see also domestic appliances; drying; electric furnaces; induction heating; ovens; radiofrequency heating; space heating
 periodic-heating method development for meas. thermophysical props. of liquids 7-4844
 powder materials, electric contact sintering method 7-13401
 space heating of occupied houses, solar and electric heating contributions, regression model 7-28389
 wind-driven DC shunt-generator for resistance heating, power output optimisation 7-65400

electric ignition
 No entries

electric immittance
see also electric admittance; electric impedance
 ionic conduction, small-signal AC frequency response functions 7-63869

electric impedance
see also electric reactance; electric resistance
 asymmetric strip line segments, cross coupling, electrodynamic theory 7-36848
 bipolar batteries with common electrolyte paths, leakage currents 7-28392
 cardiac tissue, impedance meas., tissue struct. model 7-13985
 current distribution in conductors with arbitrary cross sections Biringier, P.P. (Dept. of Electr. Eng., Toronto Univ., Ont., Canada) 7-62576
 eddy current 3D NDT, surface impedance boundary condition 7-65267
 elliptic conductors, boundary-matching method 7-36849
 EM wave scattering by a thick impedance half plane 7-42868
 Faraday impedance, connections for impedance elements (*German*) 7-17803
 flat plate steel conductor impedance to earth fault currents 7-62582
 inhomogeneous transmission lines, supersymmetry and signal propagation 7-1011
 large impedance coated bodies of revolution hybrid EM scatt. solns. 7-20107
 magnetic coaxial pipe, impedance 7-5815
 materials science application of impedance spectroscopy, book contrib. 7-24659
 multiconductor transmission line, effect of pulse corona discharge on coupling coeffs. and wave impedances 7-63383
 PTFE, chem. modified, humidity sensor appls. 7-9839
 radar cross-sections calc., equivalent currents, flat plates with surface impedance coatings anal. 7-42867
 shock safety criteria, conf., Toronto, Ontario, Canada (Sept. 1983) 7-18500
 three-layer Earth model with thin intermediate conducting layer, surface impedance determ. 7-60166
 trifluorochloromethane-Ar discharges, for plasma etching of Si:P, parametric modelling and impedance anal. 7-28221
 trifluorochloromethane-Ar discharges, for plasma etching of Si:P. modelling of ion bombard. energy distrib. 7-28222
 yeast, elec. impedance charge during growth and fermentation (*Japanese*) 7-47021
 Al, anodic polarisation in NaCl soln., instantaneous impedance study 7-23032
 Al-FeS₂, secondary cell, positive electrode reaction kinetics, AC impedance study 7-8372
 (CF₃)₂-Li battery, complex impedance plots (*Japanese*) 7-23129
 CoFeMoB amorphous thin films, prep. and high-freq. impedance studies 7-53585
 GaAs-AlGaAs heterostructures, equipotential distrib. in quantum Hall effect 7-21994
 Li electrodes, semicond. passivating film, impedance meas. 7-33111
 Li/MoS₂ cell, spirally wound, inductive impedance 7-46931
 Nb, thin film, microstrip line, parameter change during superconducting to normal conducting state switching 7-22075
 Si-aqueous electrolyte interfaces, impedance spectra, freq. dispersion 7-27414
 Zn passive electrodes, space charge effects 7-28315
 ZrSiO₄, burnt zircon with alkali hardeners, humidity sensitivity 7-18793

electric impedance measurement
see also electric reactance measurement; electric resistance measurement
 dielectric materials, contactless testing, RF method, linear antennas impedance meas. 7-54054
 electrode impedance, freq. meas. equipment 7-9823
 fruit quality measurement by microwave impedance tomography (*Japanese*) 7-28800
 ionic conductors, solid, impedance studies, bridge balance conditions and error corrections (*German*) 7-30033
 low-Q piezoelec. material constants, automated meas. system 7-328
 materials science application of impedance spectroscopy, book contrib. 7-24659
 medical impedance cardiography, motion artifact from spot and band electrodes 7-28732
 polyetherimide, RF elec. props., 10 kHz to 1 MHz 7-48779
 polyethylene, terephthalate, RF elec. props., 10 kHz to 1 MHz 7-48779
 polyimides, RF elec. props., 10 kHz to 1 MHz 7-48779
 rheography method for quantitative eval. of pulse blood flow of limbs 7-40352
 solid ionic conductors, impedance meas. 7-9843
 stabilised cct. for equivalent parallel resistance and capacitance and small changes meas. 7-18804
 Li-SO₂, commercial cells, impedance meas. at various states of charge 7-54281

electric load *see load (electric)*

electric machine analysis computing
 2D magnetic field problems, boundary and finite element methods combined 7-62584

electric machine testing *see machine testing*

electric machine theory *see machine theory*

electric machines
see also AC machines; electric generators; electric motors; machine bearings; machine insulation; machine testing; machine theory; machine windings; rotors; superconducting machines
 steel, wear resistant, for cutout dies of electric machine manufacture 7-13719

electric moments
see also atomic electric moment; elementary particle electric moment; molecular moments; nuclear electric moment
 covalent solids, lattice dynamics, quadrupolar charge deform., adiabatic formulation 7-26879
 dipole moments of conducting particle chains 7-20092
 equipotential surface around electrical dipole, field lines diagram 7-59
 ferroelectric ceramic bar, normal mode responses, influences of domain switching and dipole dynamics 7-45945
 2-methoxyethylamine, H bonded config. mol. rot., rot. isomerism barrier, quadrupole coupling const., microwave spectra 7-50093
 molecular elec. dipole moments, dielec. meas. 7-31185
 oscillator strengths, transition energies and probabilities, CI STO calcs. 7-25423
 purple membrane, electric polarisability, electrooptic scatt. spectra anal. 7-54530
 two-level cryst., nonlinear dielectric response 7-7633
 Vavilov-Cherenkov radiation, elec., mag. and toroidal dipole moments in thin channels 7-56059
 RbCl(Br)(I):Ag⁺(OH⁻) crystals, paraelec. centres, elec. dipole moment temp. depend., dielec. meas. 7-38508

electric motors
see also AC motors; DC motors; linear motors; stepping motors
 escalating arcing ground fault phenomenon, effect of preventative solns. on equipment specifications 7-51530

electric networks *see networks (circuits)*

electric noise measurement
 injection locked magnetron, phase noise meas., Doppler weather radar system appl. 7-30042
 IR imager performance meas., objective meas. of minimum resolvable temp. difference 7-30092
 photon counting photomultipliers, noise power spectrum 7-40716
 primary broadbanded coaxial thermal noise standard, watt unit realisation 7-18819
 radioastronomy appl. (*Spanish*) 7-4336
 two-dimensional electron gas, using SQUID flux-transformer-coupled instrument 7-18830
 Si solar cells, polycrystalline, interface state characterization by electric noise meas. 7-13920

electric potential
see also contact potential; overvoltage; surface potential; voltage control; voltage measurement
 charge simulation method with boundary shape taken into account 7-15797
 dielectric material, radiation diagnostics of electric potentials, sensitivity and resolution 7-8233
 EM field problems, polynomial distribution over curved triangular domain, potential integral 7-36847
 EM waves, auxiliary currents method and wave potentials, diffraction field anal. 7-50469
 equipotential plotting apparatus, for student laboratory 7-41040
 global geometry of polyphase structures fed by complex current systems (*Italian*) 7-31207
 heterogeneous environments, potential fields anal. (*Polish*) 7-20093
 inhomogeneous electron gas pressure calc. (*German*) 7-64145
 metal target, elec. charged, pot. change under laser irradi. 7-44616
 multipole, constraint relations among partial harmonic potentials 7-57203
 photoemf measurement in semiconductor, by two-capacitors method 7-30037
 piezoelectric layer with periodic system of electrodes, plane problem of electroelasticity 7-2983
 RF plasma potential meas. using emitting probes 7-20941
 SCC electrochemical potential profile models 7-46717
 Schottky p-type polycryst. junction 7-7331
 solar wind, electrostatic potential jump at Earth bow shock from ion components meas. 7-34821
 standard cells, SO_x sensor using Ag⁺- β -alumina solid electrolyte 7-326
 thermionic converters, internal parameter determ. from current-voltage characts. 7-34051
 vector diffraction theory, plane wave and spread function decompositions 7-62599
 α -Ag₂S, energy gap, EMF const. determ. by SALS program (*Japanese*) 7-16943
 AlCl₃/1-butylpyridinium chloride electrolyte for Al-FeS₂ secondary cell, phys. and elec. characts. (*Japanese*) 7-8371
 HCl-SrCl₂ mixed electrolyte, thermodynamic study, appl. of Pitzer's eqns. 7-33940
 K-Pb liquid alloys, excess stability, entropy 7-26975
 LiNbO₃, prod. by Czochralski and Stepanov methods, elec. phenomena accompanying growth 7-32332

electric power generation
see also cogeneration; direct energy conversion; ocean thermal energy conversion; power stations; wave power generation
 antiproton technology, potential develop. of advanced power sources 7-62102
 conference, ANS winter meeting, Washington, DC, USA, (Nov. 1986) 7-29591
 cost-effectiveness of utility sponsored energy conservation programs 7-34004
 least cost utility planning, Michigan Electric Options Study 7-34001
 peak-power crisis, residential energy storage systems 7-34005
 Seabrook power station, supply-side alternative 7-34003
 solar pond research and appls., organic Rankine cycle engines compared to diesels 7-46971
 thermal energy storage for space solar power system, phase change materials compatibility 7-65628

- electric power generation continued**
 thermal storage sizing methodology for solar cooling/power generation systems 7-65617
 Virginia Power's alternative energy study 7-34002
 Ti in power generation industry 7-46283
- electric reactance**
see also capacitance; inductance
 No entries
- electric reactance measurement**
see also capacitance measurement; inductance measurement
 No entries
- electric resistance**
 EM scattering from resistive strips complex periodic struct., anal. 7-50476
 paraxial cylinders, resistance and capacitance, undergraduate laboratory expt. 7-44
 photovoltaic cell, diffused top layer resistance calc. 7-59845
 shock safety criteria, conf., Toronto, Ontario, Canada (Sept. 1983) 7-18500
 Ag/AgCl electrodes fabricated with IC-compatible technologies, chemical sensor reference appl. 7-8343
 Ni-Cd cell, electrode kinetics and failure-mode prediction, internal short equiv. resist. estimation 7-54288
 Ti-Al-Nb-Zr, plastic deform., elect. resist. oscills. 7-20605
- electric resistance measurement**
see also ohmmeters
 $2e/h$ and h/e^2 determ. from volt and quantised Hall resist. meas. in SI units 7-41332
 AC bridge for precision resistance meas., computer-controlled 7-18832
 AC resistance divider 7-18831
 automated cryogenic current comparator resistance bridge 7-18829
 auxiliary electrode method for determination of ohmic resistance 7-35536
 computerised instruments interfaces standardisation, for low-temp. meas. 7-4857
 contact resist., four-terminal meas. techniques 7-35537
 Hamon type resistance standards and appl. (Czech) 7-61358
 hydrostatic pressure electric resistance cell, for 30 kbars (Korean) 7-24656
 ionic conducting ceramics, elec. resist. meas. by impedance spectroscopy 7-9844
 laboratory unit determ., using quantum Hall effect 7-18812
 magnetometers for simultaneous magnetic and resistive meas. at low temp. high magnetic field 7-48788
 photothermal radiometry appl. using IR scanners 7-33898
 quantised Hall resistance meas. at LCIE, using quadrature bridge 7-14909
 quantized Hall resistance measurement at the National Measurement Laboratory, Australia, using GaAs/GaAlAs heterostructure 7-14965
 quantum Hall effect appl., US legal unit monitoring 7-18808
 quantum Hall resistance, fine structure constant determ. at PTB 7-14966
 quantum Hall resistance meas., from 4K to 20mK 7-14969
 quantum Hall resistance meas., using improved Josephson potentiometer 7-18810
 quantum Hall resistance standard realisation at BIPM 7-18811
 quantum Hall resistance value determ., using calculable capacitor at ETL 7-14968
 self-balancing resistance bridge 7-35539
 sheet resistance low dose monitoring using the double implant technique 7-21244
 SI ohm determ., Australia's contribution 7-14975
 solar cell serial resistance meas. (Slovenian) 7-65473
 SQUID flux-transformer-coupled instrument appl., optimum DC current resolution 7-18830
 standard, precise comparisons of quantized Hall resistances 7-18809
 transfer standard, theory and design 7-18828
 voltage and resistance, US legal units 7-41329
 Ag specimen, contact resist. meas., deform., fretting effects 7-9848
 Al-Ti (CoSi₂)-Si contacts, four-terminal resistor structs. for contact resist. determ. from end resist. meas. 7-38730
 Pb acid battery initial short-circuit current prediction and obs. 7-3634
 a-Si:H, contact resist. meas. technique 7-24658
- electric resistors** *see resistors*
- electric sensing devices**
see also instruments; measurement
 amorphous semiconductors for microelectronics appls., conf., Los Angeles, CA, USA (Jan. 1986) 7-24282
 capacitive pressure sensor IC, micropower ccts. design for implantable device, biomedical appl. 7-34316
 CMOS magnetosensitive square wave oscillator 7-61360
 composite ceramics, multiphase interaction, sensor appls. 7-64996
 composite piezoelectric sensors, elec. characts., hydrophone appl. 7-62943
 conductometry of turbulent flows, sensors with hydrodynamic smoothing 7-57961
 conference on semiconductors, Jevnaker, Norway (June 1986) 7-14705
 current density monitor for intense relativistic electron beams 7-19595
 debris flows, noncontact speed sensors 7-40615
 dilatometer based on electro-optical meas. technique 7-41338
 diode-bridge temperature sensor 7-18783
 displacement sensor, error sources in dynamic appls. 7-48712
 double-ended tuning fork quartz accelerometer 7-56230
 electric field sensor, miniature two-component, design calc. 7-56231
 ELF electric field meas., at human body surface 7-18840
 EM flowmeters, noise reduction 7-37599
 environment monitoring system for multiphase and porous media, modelling 7-59904
 eye internal pressure meas., using electric sensors (Slovak) 7-60112
 field mill sensor for use on aircraft, to study clouds 7-55213
 field-effect chemical microsensors, advances, review 7-48710
 flowmeter, mW power consumption EM type 7-37600
 flowmeter, vortex shedding type with piezoelectric sensor 7-37602
 H-plane sectoral waveguide as sensor for dielectric props. determ. 7-14977
 IC microtransducer for air flow and differential pressure sensing 7-61329
 integrated semiconductor magnetic field sensors, features, appls. 7-331
 ion-selective electrodes for ion conc. measurement, operation in nonlinear suboptimal response range 7-56246
 LED current sensor for electrostatic double probes 7-63357
 magnetic monopole detector, with sensitivity to extremely small magnetic charge 7-18844
- electric sensing devices continued**
 magnetoresistive elements, Barkhausen noise meas., magnetoresistive suscept. method 7-48785
 magnetoresistive sensors, highly sensitive, characts. 7-4872
 metal-metal oxide-based sensors for cyclovoltammetric meas. of pH value 7-17838
 MOSFET, Pt-gate, ammonia sensitivity, dependence on gate electrode morphology 7-61330
 multichannel digital temperature meter using transistor sensor, design for medical appls. (Spanish) 7-30010
 multipackage induction sensing units, multifrequency, choice of package number and ang. displacement (Russian) 7-14962
 new sensing materials (Japanese) 7-54142
 odour sensing (Japanese) 7-54623
 oxides, elec. props. under conditions of oxidation, reduction and catalysis, gas sensors appl. 7-7250
 parametric sensor, appl. in clamp-type ammeter 7-4864
 peak amplitude and time detector for narrow pulse signals 7-48903
 Peltier probe flowmeter, performance analysis 7-44083
 pH sensor, hybrid, microelectronic, fabrication 7-46891
 plant stem diameter contactless measurement apparatus using LED and photodiode (Japanese) 7-23506
 polyvinylidene fluoride films, active gauge for initiation diagnostics 7-30000
 quartz fluid density sensor pressure transducer, design and characts. 7-56249
 quartz resonator temperature transducer with no activity dips, expt. and theoretical study 7-56268
 quartz sensor for automatic dew-point hygrometry 7-61344
 quartz tuning fork resonator transducers 7-35512
 rotation frequency sensing units, white longitudinal mag. flux pulsations (Russian) 7-14983
 SAW chemosensor, processes involved at chemical interface 7-65376
 software for real-time acoustic remote sensing instrumentation and atmospheric pollution control 7-54403
 solid-state gas sensors, role of catalysis, review 7-48718
 solid-state resistive and electrochemical sensors in gas anal., review (Spanish) 7-39936
 solid-state sensors, classification 7-48714
 spaceborne synthetic aperture radar sensor technology 7-4234
 split-drain MOS magnetic field sensor 7-4875
 SQUID, DC, cooled to 4.2 K with hybrid closed-cycle cryocooler, operation 7-56278
 steel flatpack soil stress gauge, shock loading, elec. noise anal. 7-30001
 taste sensing system (Japanese) 7-54622
 temperature measurement, thermocouples and resistance temperature devices comparison 7-4852
 temperature sensor using quartz tuning fork resonator, design, fabrication and characts. 7-56269
 temperature sensors, principles and signal processing aspects (German) 7-18777
 thermal sensors based on transistors and ICs review 7-48743
 thermometric characts. of planar semiconductor diodes correction (Czech) 7-61334
 thick film resistors with high TCR 7-48735
 thick film sensors, review 7-48717
 thick-film sensors, design and fabrication 7-48704
 vacuum deposition, Wheatstone bridge with two thin film arms, dynamic balancing 7-22491
 Ag/AgCl electrodes fabricated with IC-compatible technologies, chemical sensor reference appl. 7-8343
 γ -Fe₂O₃ superfine powder, prep. and gas sensitive props. (Chinese) 7-59484
 K⁺ selective electrodes on valinomycin/PVC overlayered substrates 7-65375
 NA vapour sensor using Au and Sb intermetallic compounds 7-18774
 Ni, thin film temperature sensors 7-35519
 NiFe/SiO₂/CoPt multilayer magnetoresistors sensitivity anal. 7-48786
 SO₂ sensor using β -Al₂O₃-Na₂O-Ag₂O solid electrolyte 7-326
 a-Si based integrated type X-ray sensor (Japanese) 7-15456
 Si colour image sensor, based on wavelength dependence of radiation adsorption 7-4892
 Si IC sensor technology and applications (German) 7-24644
 Si monolithic gas flow sensor with polyimide athermal insulator 7-6332
 Si vibrating sensor, optical activation 7-9826
 Si-based sensors, deposition methods and appls., review 7-48715
 SnO₂-Pd-Sb H₂ gas sensor insensitive to alcohol (Japanese) 7-56242
 ZnO-SiO₂-Si SAW chemosensor for NO₂ gas concentration meas. 7-3621
 ZrSiO₄, burned, humidity sensor with H₃PO₄, sensitivity rel. to acidic groups 7-9838
- electric sheet** *see iron alloys; silicon alloys*
- electric shielding, nuclear** *see nuclear screening*
- electric shocks**
see also electrical faults; protection; safety
 effects on the human body 7-24337
 heart muscles effect (German) 7-3776
 injury by electric current passing through acupuncture points (Russian) 7-28493
 safety against electrical shock, criteria, conf., Toronto, Ontario, Canada (Sept. 1983) 7-18500
- electric spark machining** *see spark machining*
- electric sparks** *see sparks*
- electric steel** *see iron alloys; silicon alloys*
- electric strain gauges** *see strain gauges*
- electric strength**
see also electric breakdown
 dielectrics, electrical breakdown, physics, acoustic theory appl. 7-33329
 gas mixtures, electron transport, collision cross section and dielectric strength 7-63244
 hexamethyldisiloxane films, plasma polymerised, dielec. breakdown 7-33328
 insulating oils, gamma-ray effects on elec. props. 7-48829
 interelectrode gap strength calc., Kilpatrick's criterion approximation 7-10815
 mica-epoxy composite dielectric strength obs. 7-64570
 poly(ethylene terephthalate), irradiated, phys. and dielec. props. 7-33332
 polymeric insulating material, dielec. breakdown strength rel. to lamella struct. 7-53237

electric strength continued

- polypropylene, electret and mechanical props., supermolecular structure effects (*Russian*) 7-64560
- polypropylene, irradiated, phys. and dielec. props. 7-33332
- strongly electronegative gases; figure of merit meas. 7-51553
- surface flashover in insulator with reduced E-field 7-64569
- XLPE, dielectric properties modification due to corona discharges, humidity effects 7-39022
- XLPE insulation, water treeing 7-39026
- BaTiO₃, polycrystalline, dielec. breakdown, microstructural effects 7-39021
- PbTiO₃ gels and films, hydrolysis conditions effect on characts. 7-46400
- Si-O, film, electrophysical parameters, laser oxidation of Si 7-17741
- SiO₂ thermal oxide films on Si substrate, ramp-voltage-stressed I-V characts. 7-17112
- SrTiO₃-based SPBT ceramics, DC conduction and breakdown at high temps. 7-39020

electric susceptance *see* **electric admittance**

electric susceptibility *see* **optical susceptibility**

electric switchgear *see* **switchgear**

electric transformers *see* **transformers**

electric utilities *see* **electricity supply industry**

electric variables measurement

- see also* **attenuation measurement**; **capacitance measurement**; **charge measurement**; **dielectric measurement**; **electric admittance measurement**; **electric current measurement**; **electric distortion measurement**; **electric field measurement**; **electric impedance measurement**; **electric noise measurement**; **electric reactance measurement**; **electric resistance measurement**; **electrical conductivity measurement**; **frequency measurement**; **gain measurement**; **inductance measurement**; **phase measurement**; **power factor measurement**; **power measurement**; **Q-factor measurement**; **voltage measurement**
- calibration, Italian (SIT) services 7-18738
- contactless measurement of carrier mobility and concentration in semiconductors 7-30036
- EM precision meas., conf., Gaithersburg, MD, USA (June 1986) 7-14710
- Hall effect measurement in the diamond anvil high-pressure cell 7-30041
- lightning surge and transient protection and warning systems 7-34663
- measurement methods, conf., Prague, Czechoslovakia (April 1985) 7-48169
- MIS structures, minority carrier lifetime meas. (*German*) 7-56306
- photoemf measurement in semiconductor, by two-capacitors method 7-30037
- photon detector devices, local investig. by scanning laser microprobe 7-30083
- semiconductor bicrystal, diffusion length and grain boundary recomb. vel. determ. by laser excitation 7-41402
- semiconductor materials, electrophysical parameters, local monitoring non-destructive contactless UHF cavity methods 7-48768
- solar cell optical and electrical characts., meas. systems 7-13906
- solar cell volt-ampere characts. meas., generator of intense millisecond light pulses 7-34042
- solar cells volt-ampere characts. meas. (*Slovak*) 7-39994
- Si, minority carrier lifetime and resist. mapping, flying-spot scanning method 7-4867
- Si, polycrystalline, grain boundary recomb. vel. eval. from spectral response of solar cells 7-41403

electric vehicles

- see also* **electric drives**
- automotive long range highway vehicle propulsion system using fuel cells, R&D needs 7-65456
- DC motors in wheelchairs and prostheses, switching converters for efficient control 7-34355
- electricity and modern techniques, conf., Bordeaux, France (Oct. 1985) 7-14708
- MEV 1 electric vehicle prototype with additional solar cells (*German*) 7-3644
- solar vehicles, electrical networks (*German*) 7-3643
- Al-air battery with crystallizer to extend electrolyte lifetime, traction appls. 7-65441
- N/s 14 kWh/21 kW batteries for electric vehicles, performance testing 7-65438

electric welding

- see also* **welding**; **electron beam welding**; **resistance welding**
- No entries

electrical conduction in condensed matter

- see also* **carrier density**; **carrier lifetime**; **carrier mean free path**; **carrier mobility**; **carrier relaxation time**; **dislocation scattering**; **electrical conductivity of liquids**; **electrical conductivity of solids**; **electrical conductivity transitions**; **electron density (metals)**; **electron mean free path (metals)**; **electron mobility (metals)**; **electron-phonon interactions**; **electron relaxation time (metals)**; **high field effects**; **hopping conduction**; **impurity scattering**; **Lorenz number**; **minimum metallic conductivity**; **minority carriers**; **mixed conductivity**; **negative resistance effects**; **one-dimensional conductivity**; **photoconductivity**; **point defect scattering**; **size effect**; **skin effect**; **small polaron conduction**; **space-charge-limited conduction**; **spin disorder resistivity**; **surface conductivity**; **surface scattering**; **thermally stimulated currents**; **tunnelling**
- agar phantom electrically adaptable for tissue simulation in 5-40 MHz range, hyperthermia cancer treatment 7-65713
- a periodic linear atomic arrays, electron propag. 7-21891
- disordered conductors, low temp. current spatial fluctuations, size depend. and coherent length 7-17003
- disordered media, electrical cond. and incoherent excitation transport, self-consistent mode-coupling theory 7-52548
- Equivalence of the Meyer-Neldel rule and the Schweidler relaxation function for kinetic behavior 7-7194
- excess Johnson noise, thermal noise voltage modulation effects 7-17058
- Kubo formula extension for elec. cond. tensor, to arbitrary polarisations of elec. field 7-38528
- Onsager reciprocal relations, symmetries of magnetoconductivity tensor 7-193
- porous media with charges, electrolytic conduction 7-63858
- quantum transport equation for electric and magnetic fields 7-52550
- quasicrystals, 1D, electron transmission 7-45254
- Ramo's theorem generalisation, electric charge motion, induced currents, energy balance and noise calcs. 7-21889

electrical conduction in condensed matter continued

- random impenetrable spheres suspension, effective elec. cond., general Beran bounds calcs. 7-38527
- random resistor-capacitor networks, anomalous transport, appl. to composite materials 7-27312
- solid solutions, non-uniform, elec. resist. (*Russian*) 7-32968
- thin films, electron diffusion, scattering-act correl. effects 7-32972
- unitary transformations in solid state physics, book 7-24310
- waiting time distrib. function, asymptotic solns. of continuous time random walk problems (*Chinese*) 7-35398

electrical conductivity

- see also* **electrical conduction in condensed matter**; **electrical conductivity of gases**; **electron mobility**; **ion mobility**; **space-charge-limited conduction**
- Aharonov-Bohm effect with integer and half-integer flux quanta, cond. oscills. 7-52552
- anil brown, anisotropy in elec. cond. induced by external field 7-39924
- binary mixture of isotropic materials, effective conductivity, exact estimates 7-62961
- cellular foams, fn. between aeration ratio and electric cond. ratio. 7-39922
- disordered conductor, mesoscopic fluctuations distrib. function, renormalisation-group anal., statistical props. 7-272
- electron gas, localisation effects, Keldysh representation 7-52529
- ion exchange membranes in organic salts, molar conductance, viscosity model 7-13801
- ion-selective membranes, with chelating agents, stoichiometry of current-carrying complexes 7-33955
- macroscopically inhomogeneous anisotropic media, kinetic phenomena, review (*Russian*) 7-56195
- mesoscopic systems, transport props., book contrib. 7-52553
- quantum adiabatic particle transport 7-18729
- Sierpinski gasket, hierarchy of current cumulants 7-52551
- two-dimensional site-percolation model, diffusion and long-time tails, vel. autocorrel. function calcs. 7-24606

electrical conductivity measurement

- anil brown, anisotropy in elec. cond. induced by external field 7-39924
- chemical reaction rates meas. at high pressure 7-33913
- eddy current electrical cond. meter graduation without specimens 7-28243
- eddy current electrical cond. meters, inspection errors rel. to geometric parameters 7-28244
- elastic, fibrous and porous materials, meas. of permittivity and resistivity (*Czech*) 7-61355
- galvanomagnetic studies of organic metals, at high pressures and low temp. 7-30035
- high pressure, in diamond anvil cells at cryogenic temp. 7-56299
- ionic conducting ceramics, elec. resist. meas. by impedance spectroscopy 7-9844
- MA 5964 laboratory microprocessor-controlled conductivity meter (*Slovenian*) 7-18803
- metallic sheets, conductivity and surface buckling meas. by eddy current testing 7-54058
- nondestructive inspection of case hardened parts using resistivity 7-39842
- resistivity, four-point probe, ultrahigh vacuum compatibility 7-61357
- seawater effective salinity determ., conductivity comparator 7-4209
- soil, radiation-induced conductivity meas. 7-59882
- solar cell substrate charactn. techniques 7-40004
- surface resistivity measurement methods and standards 7-61356
- transient photoconductivity measurements of amorphous semiconductors by subnanosecond nitrogen lasers 7-18806
- ZrO₂-MgO electrolyte mixed ionic and electronic conduction obs. 7-2644
- FeCO colloids, anisotropy in elec. cond. induced by external field 7-39924
- GaP electrical conductivity meas., high pressure, in diamond anvil cells at cryogenic temp. 7-56299
- KOH aq. soln., highly conductive, electrolytic conductivity meas. 7-3595
- Pb electrical conductivity meas., high pressure, in diamond anvil cells at cryogenic temp. 7-56299
- RbAg₄I₃ ionic conductivity meas., electrodeless meas. method 7-48777
- Si electrical conductivity meas., high pressure, in diamond anvil cells at cryogenic temp. 7-56299
- Si, minority carrier lifetime and resist. mapping, flying-spot scanning method 7-4867
- Si resistivity meas, using TE₀₁₄ mode dielectric resonator 7-14976

electrical conductivity of amorphous metals and alloys

- see also* **dislocation scattering**; **electron density (metals)**; **electron mean free path (metals)**; **electron mobility (metals)**; **electron relaxation time (metals)**; **electronic conduction in metallic thin films**; **impurity scattering**; **point defect scattering**; **surface scattering**
- alloys, modified mag. Kondo theory 7-33000
- ferrite ceramics, AC and DC cond. (*Spanish*) 7-52560
- low temp. resistivity meas., temp. depend. (*Spanish*) 7-52561
- metallic glasses, elec. cond. temp. and mag. field depend., localisation and electron interaction effect calcs. 7-2568
- metallic glasses, low temp. resist. anomaly, two-level systems, incipient localisation and electron correl. effects 7-2570
- metals, disordered, temp. coeff. of elec. resist., Mooij correlation nonuniversality 7-21893
- metals, multiple scattering effects, cluster calcs. 7-7100
- nonmagnetic metallic glasses, negative TCR and electronic struct. studies 7-52562
- normal metal, Aharonov-Bohm effect, quantum coherence and transport, review 7-52559
- Pd(Fe,Co,Ni)_{0.05-0.15}Si_{0.17} metallic glasses, crystallization kinetics, elec. resist. obs. (*Chinese*) 7-11919
- Ag-Pd, random alloys, resistive electrical resistivity, first-principles calc. 7-2569
- Al-Am, quasicrystalline and crystalline alloys, temp. dependence of elec. resistivity 7-2574
- Al-base icosahedral alloys, elec. resist. and Hall coeff. studies 7-27316
- Al-Co icosahedral alloys, struct., elec. and mag. props. 7-6583
- Al-Cr, quasicrystalline and crystalline alloys, temp. dependence of elec. resistivity 7-2574
- Al-Ge-X and Al-Si-X alloys, amorphous ductile, with two separate phases, form. range and props. for X=Mn, Fe, Co or Ni 7-59493
- Al-Mn alloy icosahedral quasicryst., mag. and elec. props. studies 7-2858
- Al-Nb amorphous films, elec. props. and charactn. (*Japanese*) 7-32977
- Ca-Al-Ga metallic glasses, electron transport 7-45264
- Ce-Cu amorphous alloys, mag. and transport props., Ce-derived anomalies 7-52601

electrical conductivity of amorphous metals and alloys continued

- CoFeSiB inhomogeneous magnetic alloys, anomalous Hall effect—magnetic polarisation corrls. 7-7208
 $(\text{Co}_{1-x}\text{Mn}_x)_2\text{B}$, crystalline and amorphous, mag. and elec. props. 7-2827
 $\text{Co}_{55}\text{Ni}_{10}\text{Fe}_5\text{B}_{10}\text{Si}_{10}$, metallic glass, reversible struct. transformation, resistivity meas. 7-1907
 $\text{Cr}_{75}\text{Si}_{25}$ thin films, microstruct. and resist., room temp. to 950°C 7-38410
Cu-Ga, random alloys, residual electrical resistivity, first-principles calc. 7-2569
Cu-Ge, random alloys, residual electrical resistivity, first-principles calc. 7-2569
Cu-Zn, random alloys, residual electrical resistivity, first-principles calc. 7-2569
Cu-Zr metallic glass, elec. cond., annealing effects 7-7198
Fe-Ce amorphous alloys, mag. props. and elec. resist. 7-59010
Fe-Ni based metallic glasses, quenched-in excess vol. and structural relax. 7-6531
Fe-Te amorphous thin films, RF sputtered, struct. and elec. meas. 7-12534
 $\text{Fe}_{100-x}\text{B}_x$ amorphous alloy, temp. depend. of the resistivity (Chinese) 7-27314
 $\text{Fe}_{100-x}\text{B}_x$ metallic glass system, elec. resist. under press. 7-7200
 $\text{Fe}_{79}\text{B}_{21}$, amorphous alloy, elec. resist. and crystn. on hardening from different temps. 7-44380
 $\text{Fe}_{85}\text{B}_{15}$, high energy heavy-ion irradiation, electrical resistance meas., evidence for electronic energy loss effect 7-58353
 $\text{Fe}_{90-x}\text{B}_{10}\text{Zr}_{10}$, amorphous, B addition effect on mag. props., elec. resistivity, crystallisation (Chinese) 7-7487
 $(\text{Fe}_{1-x}\text{Co}_x)_{84}\text{B}_{16}$ amorphous alloy, temp. depend. of the resistivity (Chinese) 7-27314
 $\text{Fe}_{67}\text{Co}_{18}\text{B}_{14}\text{Si}_4$ amorphous mag. alloy, crystallisation, elec. resist., TEM obs. 7-11927
 $\text{Fe}_{80-x}\text{Cr}_x\text{B}_{20}$ metallic glasses, electron transport props., disorder and mag. effects 7-52563
 $\text{Fe}_{85-x}\text{Cr}_x\text{B}_{15}(\text{Ni}_x\text{B}_{15})$ metallic glasses, mag. and elec. props. 7-13002
 $(\text{Fe}_{1-x}\text{Mn}_x)_{78}\text{B}_{22}$, amorphous alloys, lattice parameters, annealing, X-ray diff., elec. resist. 7-37878
 $(\text{Fe}_{1-x}\text{Mn}_x)_{84}\text{B}_{16}$, amorphous, Mn content effect on elec. resistivity (Chinese) 7-12692
 $(\text{Fe}_{1-x}\text{Ni}_x)_{84}\text{B}_{16}$, amorphous alloy, temp. depend. of the resistivity (Chinese) 7-27314
 $\text{Fe}_{40}\text{Ni}_{40}\text{B}_{20}$, amorphous and crystalline, elec. resistivity, temp. dependence 7-21892
 $\text{Fe}_{75}\text{Ni}_{30-x}\text{B}_{20}$ amorphous ferromagnets, elec. resist. and thermopower meas., comp. and temp. depend. 7-45263
 $\text{Fe}_{0.44}\text{Ni}_{0.57}\text{Si}_{0.78}\text{B}_{14.56}\text{C}_{0.25}$, amorphous filler metal, struct. props. (Korean) 7-32292
 $\text{Fe}_{77}\text{Si}_{10}\text{B}_{13}$, as-quenched and cold-rolled amorphous alloy, mag. props. 7-33219
 $\text{Fe}_{80}\text{Si}_{10}\text{P}_{20-x}$ amorphous alloys, struct., mag. and elec. props. (Korean) 7-2893
 $(\text{Fe}_{1-x}\text{V}_x)_{84}\text{B}_{16}$, amorphous, low temp. resistivity anomaly (Chinese) 7-64198
 $(\text{Fe}_{1-x}\text{W}_x)_{84.5}\text{B}_{15.5}$ amorphous alloys, elec. and mag. props. (Chinese) 7-12969
 $\text{Fe}_{92}\text{Zr}_8$, mag. susceptibility, elec. resist., magnetoresistance meas. 7-52954
 $\text{Hf}_{1-x}\text{Cu}_x$ metallic glass, thermal stability and phase transformations 7-21125
 $\text{La}_{100-x}\text{Al}_x$ metallic glasses, electron transport 7-45265
Mg-based amorphous alloys, elec. resist., press. depend. 7-7199
Mn-Ga, amorphous film, prep. by ionised cluster beam deposition 7-3205
Mo-Si amorphous alloys, cluster formation and percolation 7-27455
 $\text{Nb}_{100-x}\text{B}_x$ alloy films, sputtered, elec. cond., hardness, amorphous and crystal struct. 7-13354
Ni-B alloy with transition metal additives, amorphous, mag. scatt. influence on transport props. 7-33001
Ni-based metallic glasses, quenched-in excess vol. and structural relax. 7-6531
Ni-Cr-Al films, thin film resistor appl., struct., temp. coeff. of resist. props. 7-58912
Ni-Mo, random alloys, residual electrical resistivity, first-principles calc. 7-2569
Ni-Si-B amorphous alloy films, electrical resistance and activation energy 7-27315
 $\text{Ni}_{30}\text{B}_{40}\text{C}_{16}$, B-rich amorphous alloy prep. by rapid quenching, crystn., hardness and elec. resist. 7-13441
 $\text{Ni}_{77}\text{P}_{23}$ amorphous alloy, struct. relax. and crystn., elec. resist. and X-ray diff. obs. 7-1894
 $\text{Ni}_{82}\text{P}_{18}$, amorphous state, electrical resistance meas. in gaseous H_2 7-32978
 $\text{Ni}_{64}\text{Zr}_{36}$, amorphous state, electrical resistance meas. in gaseous H_2 7-32978
Pd-Si alloys, H absorption, structural disorder effects 7-52249
 $\text{Pd}_{0.67}\text{B}_{0.33}$, amorphous, prep. by low temp. ion beam mixing (Chinese) 7-51887
 $\text{Pd}_{82-y}\text{Ni}_y\text{Si}_{18}$, ($y = 10, 20, 32$), amorphous alloy, electrical resistance meas. in gaseous H_2 7-32978
 $\text{Pd}_{0.84}\text{Si}_{0.16}$ metallic glasses, crystallisation kinetics, elec. resist. obs. (Chinese) 7-11919
 $\text{Pd}_{100-x}\text{Si}_x$ ($x = 15, 17, 18$), amorphous alloy, electrical resistance meas. in gaseous H_2 7-32978
PdSiCo inhomogeneous magnetic alloys, anomalous Hall effect—magnetic polarisation corrls. 7-7208
 $\text{V}_{75}\text{Si}_{25}$ amorphous films, crystallisation and elec. props. 7-21102
W films, amorphous and finely cryst., elec. props. (Russian) 7-38776
YAl nonmagnetic metallic glasses, negative TCR and electronic struct. studies 7-52562
 Y_2Ni_{19} , sputtered amorphous film, Hall effect (Chinese) 7-64202
 $\text{Y}_2\text{Ni}_{19}\text{H}_x$ amorphous thin films, mag. and elec. transport props., H content effect, 1.5 to 400K (Chinese) 7-38909
Zr-Co amorphous alloys, superconductivity, normal-state resistivity and mag. susceptibility 7-12900
Zr-Ni(V) amorphous superconductors, struct. and supercond. props. 7-27482

electrical conductivity of amorphous semiconductors and insulators

see also carrier density; carrier lifetime; carrier mean free path; carrier mobility; carrier relaxation time; dislocation scattering; electrical conductivity transitions; electronic conduction in insulating thin films; high

electrical conductivity of amorphous semiconductors and insulators continued

- field effects; hopping conduction; impurity scattering; minority carriers; negative resistance effects; photoconductivity; point defect scattering; small polaron conduction; surface scattering
aerospace polymers, electron irradi. effects on AC and DC elec. props. and unpaired electron densities 7-58339
aluminosilicate oxynitride glasses, dielectric studies 7-55917
amorphous, low temp. electron transport near mobility edge 7-38562
amorphous, obliquely deposited film, elec. and optical props. 7-12529
amorphous, sputtered, response to intense ion bombardment 7-27447
amorphous semiconductor films, photo-assisted CVD and opto-electronic characterisation 7-33595
amorphous-crystalline mixture, electrical conductivity formula, anal. 7-58804
carrier mobility measurement techniques 7-58800
ceramics, low thermal expansion dec. insulators 7-2237
chalcogenide glasses, AC conduction, theoretical models and expt. data, review 7-64252
disorder, electronic states, transport 7-27239
electronic and transport props., coherent potential approx. 7-27241
ethylene copolymers, electric breakdown and high-field conduction meas. 7-39011
graphite fibres, galvanomag. props., weak localisation and carrier interaction effects calc. (Russian) 7-27347
low alkali borosilicate glasses, electrical resistivity, depend. on composition 7-58806
oxide glass, relax. time and loss peak corrl. with DC cond. 7-22181
phthalocyanine polymer films, I_2 implantation, RBS studies 7-26776
PMMA, charge motion and self-relaxation, pulsed electro-acoustic meas. 7-27655
PMMA dielectric, sub-ohmic I-V charact., below glass transition temp. 7-27335
poly (N-benzylidiphenylaminomethane) film, synthesis, elec. and optoelectronic props. 7-45384
poly-4(3-pyridyl)-8-methyl-2,3,6,7-quinolino ladder polymer, electronic props., I doping effects 7-64526
poly-p-phenylenevinylene film, opt. and elec. props., band gap 7-46161
polyacetylene:Br(I), polarised EXAFS and near edge spectra studies 7-64778
polyacetylene, doped, DC elec. cond. studies 7-33018
polyanthracene:1, charged elementary excitations, EPR study 7-7246
polyethylene, low density, electric breakdown and high-field conduction meas. 7-39011
polyethylene film, low density, elec. props. rel. to nuclear irradi., 5K 7-53232
polyethylene naphthalate, electrolum. and electronic conduction in high DC fields 7-27788
polyimide films, uniaxially-stretched, conductivity and dielec. losses 7-39005
polymers, elec. cond. and breakdown phenomena 7-45306
polyphenylenesulphide:As conducting polymers, ion implantation techniques 7-21923
polypropylene evaporated films, SCL currents 7-21924
polyvinyl alcohol films, elec. cond., 293 to 353K 7-45530
rare earth borides, RB_{60} , elec., optical and thermal cond. props. 7-21910
solid dielectrics, breakdown and prebreakdown phenomena, charge transport and dielectric aging 7-39014
styrene-butadiene rubber, C-black loaded, elec. props., effect of gamma irradi., dosimetry appls. 7-33006
Ag-As-Se glasses, electrical conductivity studies 7-27369
 $\text{Ag}_{0.15}\text{As}_{0.425}\text{Se}_{0.425-x}\text{Te}_x$ chalcogenide glasses, ionic and electronic cond., comp. depend. study 7-12768
 $(\text{Ag}_2\text{O})_x(\text{B}_2\text{O}_3)_{100-x}$ glasses, microstruct. and electronic cond. studies 7-6534
 $\text{Ag}_2\text{S}(\text{Se})\text{-Ag}_2\text{Te}(\text{Se})$ liq. and glassy semicond., activation energy of carrier thermal generation, elec. meas. 7-17035
 $\text{Ag}_2\text{S}(\text{Se})(\text{Te})\text{-Cu}_2\text{S}(\text{Se})(\text{Te})$ liq. and glassy semicond., activation energy of carrier thermal generation, elec. meas. 7-17035
AlN, hot pressed ceramic, porosity effect on elec. cond. 7-7223
As-Te-based glasses, small polaron hopping and transport props. 7-21911
 $\text{As}_2\text{Se}_3/\text{Ni}$ films, electronic struct. and transport props. 7-12595
 $(\text{As}_2\text{Se}_3)_{1-x}\text{Te}_x$, elec. and thermal transport props., effect of TI addition 7-38200
 $\text{As}_{2-x}\text{Te}_x\text{-In}_{2x}$ and $\text{As}_{20-x}\text{Te}_{80-x}\text{-In}_{2x}$ systems, chalcogenides, thin films, optical and electrical props. 7-27446
B, amorphous, elec., optical and thermal cond. props. 7-21910
 $\text{BaO-V}_2\text{O}_5\text{-Fe}_2\text{O}_3$ semiconducting glasses, elec. props., Mossbauer, EPR and X-ray diff. studies 7-7236
 $\text{Bi}_2\text{O}_3\text{-V}_2\text{O}_5\text{-CaO}$ system, vitreous oxide semiconductor, polarisation processes 7-59139
C black filled polymer composites, elec. resist. rel. to curing temp. 7-65001
a-C:H, props., review 7-51630
 $\text{CdGeAs}_2/\text{Ni}$ amorphous films, elec. cond., low temp. impurity breakdown, high field effects 7-52625
CdTe amorphous thin films, electrical and optical props. 7-22045
CdTe layers, electrochemical deposition, struct. and elec. props. 7-12526
 CuInTe_2 film, flash evap., DC cond. mechanisms, density of states 7-22041
 $\text{CuO-P}_2\text{O}_5$ glasses containing NiO or CoO, elec. cond. 7-17025
 Fe_2Se_3 and $\text{As}_2\text{Se}_3\text{-Fe}_x$ films, electronic props. 7-58922
GaAs:H amorphous sputtered films, AC cond. studies 7-21947
GaSe amorphous film, high field kinetics of photocurrent 7-2748
a-Ge:H, elec. props., effect of H plasma press. (Korean) 7-27332
Ge:H films, post-deposition hydrogenated, electrical props. 7-32296
Ge:H-Si:H amorphous superlattices, electrical transport 7-7336
 $\text{GeN}_x\text{-H}$, amorphous, reactively sputtered, optical and electronic props. 7-58830
 $\text{GeO}_2\text{-PrCl}_3$ glasses, elec. props., effect of PrCl_3 content 7-21907
 $\text{Ge}_{20}\text{S}_{80-x}\text{Bi}_x$, amorphous, electronic cond. props. under high press. 7-45328
a- $\text{Ge}_{20}\text{Se}_{80-x}\text{Bi}_x$ films, n-type, electron transport props. studies 7-7422
 $\text{Ge}_{20-x}\text{Se}_{80-x}\text{In}_{2x}$ system, chalcogenides, thin films, optical and electrical props. 7-27446
 $\text{Ge}_4\text{Se}_6\text{-Te}_x$ amorphous chalcogenide, elec. cond., prep. technique effects 7-7237
 $\text{Ge}_4\text{Se}_6\text{-Te}_x$ amorphous chalcogenide, elec. cond., bulk and thin film effects 7-7238
 $\text{Ge}_{1-x}\text{Sn}_x\text{Se}_2$ glasses, elec. cond. rel. to Mossbauer and Raman spectra 7-64250
a- $\text{Ge}_{1-x}\text{Te}_x$ films, crystallisation behaviour and local order 7-44386

electrical conductivity of amorphous semiconductors and insulators continued
a-HgSe films, elec. conductivity, thermoelectric power, optical absorpt. 7-22050
In₂O₃/Sn films, prep. by thermal decomposition of organometallic cpds., optical and electrical props. 7-17483
La₂O₃ film, DC cond. mechanism 7-22055
Li₄TeO₄ glassy electrolyte, vibrational, thermal and elec. characts. study 7-6866
Mo group glasses, anomalously high bulk cond. meas. in metal-glass structs. 7-17029
MoSe₃S cathode for secondary Li batteries, prep. and characterisation 7-64948
Na₂B₂O₇-Pb₂O₇-CuO glasses, elec. props., effect of added CuO 7-2605
Na₂O-V₂O₅-P₂O₅, crystallised glass, containing V bronze crystals, elec. cond. 7-21922
Na₂O-WO₃-B₂O₃ glass ceramics, containing W bronze, prep. and elec. props. (Japanese) 7-3261
PdO-CdO-B₂O₃ glasses, elec. cond. and density meas. 7-1895
Pt group glasses, anomalously high bulk cond. meas. in metal-glass structs. 7-17029
Sb₂S₃, amorphous thin films, electrical resistivity 7-45523
Sb₂S₃ thin films, vacuum deposited, elec. and photoconductive props. (Korean) 7-52682
Se, amorphous, elec. resist. and Hugoniot shock wave vel. meas. 7-32567
Se, amorphous films, crystn., kinetic study 7-21101
Se_{1-x}Te_x-Se photoreceptor, amorphous, xerographic time of flight technique for drift mobility determ. 7-58807
Si alloys, amorphous, CVD, electrical and optical props. 7-33596
a-Si, lamellate structure 7-21740
a-Si, prep. by low press. CVD, characts. 7-7884
a-Si technology, review of developments 7-38551
Si:As⁺(As₂⁺), ion implanted, phys. props., spreading resist., TEM, Rutherford backscattering, SIMS 7-26775
Si:B, F implanted amorphous layers, struct. and elec. props., ESR and Hall effect meas. 7-26634
a-Si:H, B, P-type, increased elec. cond. studies 7-45337
a-Si:H, B Films, photoinduced changes in elec. props. 7-38634
a-Si:H, charge transport and relax., luminesc. long-time tail distrib. anal. 7-39185
a-Si:H, conductivity, fundamental pre-exponential factor, Meyer-Neldel rule 7-7249
a-Si:H, doped, electronic transport 7-21916
a-Si:H, evaporated samples, post-hydrogenation, characts. 7-59103
a-Si:H, gas-phase and ion-implantation doped, doping efficiencies 7-51790
a-Si:H, influence of H on defects and instabilities 7-26647
a-Si:H, thermal-equilib. processes, electronic transport 7-64167
a-Si:H,B, effective p⁺ doping by plasma-assisted B diffusion 7-38036
Si:H,F by thermal CVD, photosensitivity, spin density, conductivity and p-n type 7-17454
a-Si:H,F films, dark discharge mechanism of surface potential (Japanese) 7-17034
a-Si:H,F films, H-radical-assisted CVD, hole transport 7-64264
a-Si:H,P multilayer films, plasma CVD and elec. cond. studies 7-39428
a-Si:H,P(B) films, ion implanted, photoelectric and optical props. 7-38615
a-Si:H biased activated reactive layer evaporation and charactn. 7-59428
a-Si:H CVD coating, high temp. elec. cond. meas. 7-45336
a-Si:H CVD films, density of states distrib., I-V characts. meas. 7-45113
a-Si:H film, photo-assisted plasma CVD 7-33593
a-Si:H films, CVD using microwave excited Ar plasma stream 7-64918
a-Si:H films, contact potential difference, surface photovoltage and conductivity 7-58855
a-Si:H films, high rate deposition and impurity doping effects (Japanese) 7-13385
a-Si:H films, high rate deposition by RF planar magnetron sputtering (Japanese) 7-39373
a-Si:H films, illumination effects on conductivity 7-7291
a-Si:H films, photo-enhanced CVD 7-33594
a-Si:H films, RF glow discharge deposition, optical and electrical props. 7-33598
a-Si:H films deposited by dual ion beam sputtering, characterisation 7-32882
a-Si:H films preparation by CVD 7-17453
a-Si:H material and p-i-n cell, light-induced charge 7-17055
Si:H microcrystalline films, glow discharge prep., elec. and optical props. 7-7415
Si:H solar cells, p-layer doping by plasma assisted B diffusion 7-13898
a-Si:H thin films, elec. and optical props., thickness depend. 7-46168
Si:P, Ni⁺, ion implantation and annealing 7-21245
Si:P(B) LPCVD films, amorphous and polycrystalline, struct., elec. resist. meas. 7-52870
Si-Te-As-Ge chalcogenide glass film, electronic processes in strong elec. field 7-45524
a-SiC:H, elec., optical and local structure props. 7-45089
a-SiC:H,B, effective p⁺ doping by plasma-assisted B diffusion 7-38036
SiC:H,F amorphous films, struct., elec. and optical props. 7-22360
a-SiC:H film prepared by magnetron sputtering, elec. and optical props. (Japanese) 7-12887
a-SiC:H(B), thin film, solar cells fabricated by plasma deposition (Korean) 7-33585
a-Si_{1-x}C_x-x:H films, adsorbates influence on conductance, surface state 7-33115
a-SiGe:H, F glow discharge films, elec. and optical props. 7-46169
a-SiGe:H,F glow discharge films, electronic transport and density of states 7-45114
Si_{1-x}Ge_x films, optical band gap, photocond. props. 7-52672
a-Si_{1-x}Ge_x:H, F, light-induced degradation meas. 7-45397
Si₃Ge_{1-x}:H,F amorphous films, struct., elec. and optical props. 7-22360
α-SiGeH, electronic and transport props., coherent potential approx. 7-72741
α-SiH, electronic and transport props., coherent potential approx. 7-72741
a-SiN:H, electrical behaviour 7-2627
a-SiN:H plasma-enhanced CVD film props. rel. to SiH₄-N₂ gas vol. ratio, RF power and substrate temp. (Korean) 7-3201
Si₃N₄, amorphous hopping cond. in high elec. and mag. fields 7-64257
Si₃N₄ thin films, reactively sputtered, hopping cond., defect states 7-52620
a-Si_{1-x}N_{1-x}-x:H,B films, DC sputtered, photoelectronic and optical props. 7-27361

electrical conductivity of amorphous semiconductors and insulators continued
a-SiSn:Cl,H glow discharge films, elec. and optical props. (Chinese) 7-58805
a-Si_{1-x}Te_x amorphous alloys, electronic and optical props. 7-7234
TeO₂-based halide glasses, prep., thermal, mechanical, elec. and optical props. characterisation (French) 7-37884
Ti-Ge-Se, bulk glass formation region, elec. and struct. characts. 7-58159
Ti₂Cu(SO₄)₂, glassy γ-modification, structural and electronic props. studies 7-58161
Ti_{1-x}Se_{100-x} glasses, glass transition, melting, recrystallisation, elec. transport 7-64246
V₂O₅ and Li₂V₂O₅, amorphous thin films, electrical conductivity 7-58921
V₂O₅-As₂O₅-B₂O₃, vitreous, elec. cond., semiconducting props. 7-2620
V₂O₅-P₂O₅-Bi₂O₃(Sb₂O₃) glasses, DC conductivity 7-45316
V₂O₅-TeO₂ glasses, memory switching 7-27370
V₂O₅-TeO₂-PbO, glass, elec. and optical props. (Korean) 7-27330
WO₃ amorphous evaporated film, complex cond., temp. and freq. depend. studies 7-2756
ZnO-V₂O₅ glasses, DC conductivity 7-27327
Zn₃P₂ thin films, amorphous-crystalline transitions, elec. cond., 100-300K 7-38560

electrical conductivity of crystalline metals and alloys
see also dislocation scattering; electron density (metals); electron mean free path (metals); electron mobility (metals); electron relaxation time (metals); electronic conduction in metallic thin films; impurity scattering; point defect scattering; surface scattering
actinides bulk magnetic and transport props. 7-12953
Aharonov-Bohm effect, influence of electron-phonon interaction 7-21895
alloys, binary, short range order, coherent pot. approx. 7-7142
alloys, substitutionally random, electron localisation and metal-insulator transition, CPA calcs. 7-27302
bronze, powder particle shape effect on stability props. 7-7927
bronze BRAZh, elec. discharge sintering of powder from swarf, electro-phys. and mech. props., microstruct. 7-27974
DC transport in metals 7-17010
dilute alloys, low-temperature resistivity, transport eqn. 7-21898
electrical resistivity and magnetisation, temp. depend. 7-38535
existence and electrical props. (French) 7-17008
ferromagnetic metal near reorientation phase transition point, resistivity 7-33180
ferromagnets, randomly inhomogeneous, elec. resist., temp. depend. (Russian) 7-58791
induction-heated conductor, relax. temp.-electric self-oscillations (Russian) 7-52665
low temp. resistivity meas., temp. depend. (Spanish) 7-52561
magnetic alloys, dilute, negative magnetoresistance; coupling pair model 7-32987
metal, quasi-2D conductivity, high freq. effects (Russian) 7-33038
metal ring, conductance oscillation and Aharonov-Bohm effect 7-2566
metals, impure, localisation, interactions and transport phenomena 7-64169
metals, nonlocal cond., microwave radiation transmission 7-13269
metals, strongly coupled, universal disorder-induced resistivity behaviour 7-21954
noble metals, residual resist. calc. (Russian) 7-45274
particle mixture, mixing model with particles of different elec. resist. (Japanese) 7-44831
polycrystalline, DC conductivity 7-52566
quantum transport equation for electric and magnetic fields 7-52550
quasicrystals, electron localisation 7-21901
resistivity saturation in metals with structural instabilities 7-45277
saturation of elec. resist., 1D Kronig-Penney model 7-38533
shock Hugoniot eqn. of state, electron band theory approach 7-21392
small metallic wires, conductance fluctuation 7-64201
steel, alloy, electrical resistivity and magnetisation, temp. depend. 7-38535
steel, austenitic stainless, electrical resistivity and magnetisation, temp. depend. 7-38535
steel, Cr, ferritic, neutron irradi., isochronal annealing, elec. resist. recovery 7-58348
steel, cryogenic, Al alloying effect on mech. and mag. props. 7-39679
steel, Ni-Co-W, maraging, martensite isothermal aging, hardness, struct. and elec. resist. kinetic behaviour study 7-17553
steel, stainless, (Cr_xFe_{1-x})₂₃C₆ compact specimens, corrosion-electrochem. and phys. props. w.r.t. comp. 7-54000
steel, stainless, type 304, elec. resist. and magnetisation 7-45268
steel, stainless, wire, electroplastic drawing, struct. and physicochem. studies (Russian) 7-8057
thin metal wire, galvanomagnetic effects, effect of shape of cross section 7-17015
transition metals, resistivity and superconducting transition temp. 7-17013
Zircaloy-2, phase transition temp., resist. obs. 7-59512
Ag, proton and ion irradi., self-interstitial atom interactions with defect clusters, elec. resist. meas. 7-58384
Ag strained samples, Matthiessen's rule, sign of deviations 7-7201
Ag-based dilute alloys, low temp. elec. resist. 7-52565
Ag-Mn-Al, beta to zeta reversible transformation, elec. resist. meas. (Russian) 7-16728
Ag-Zn, dynamics of β' to ζ transform., elec. resist. obs. (Japanese) 7-53720
AgAl concentrated alloys, vacancy activation enthalpies 7-32431
AgAl, short-range order-induced equilib. resist. conc. depend. meas. 7-26700
AgCd, martensite transformation and shape memory effect, resistivity and thermoelectric power meas. 7-53729
Al dilute alloys, deviation from Matthiessen's Rule, three group model 7-12601
Al, disordered films, density of states, electron-electron interactions tunnel conductance meas. 7-52393
Al, high purity, elec. cond., low-temp. plastic deform. effects (Russian) 7-17009
Al, high purity samples, cryoconductivity investig. (Russian) 7-12695
Al-Am, quasicrystalline and crystalline alloys, temp. dependence of elec. resistivity 7-2574
Al-Cr, quasicrystalline and crystalline alloys, temp. dependence of elec. resistivity 7-2574
Al-Cu (2.5 wt.%), electrical resistivity, effect of precipitation 7-12697
Al-Mn (15 wt.%), melt spun ribbons, icosahedral struct., decomp. rel. to annealing 7-28030

electrical conductivity of crystalline metals and alloys continued

- Al-Si (1.14 at.%) alloy, supersaturated, anomalous solute conc. fluctuation under elec. current influence 7-13457
 Al-Zn alloys, quenching effect on growth of Guinier-Preston zones, resistivity 7-22733
 AlMn, quasicrystalline phases, plasmon electron energy loss spectroscopy and electrical resistivity 7-3123
 AlMnSi, quasicrystalline phases, plasmon electron energy loss spectroscopy and electrical resistivity 7-3123
 Au, temp. depend. of elec. resist. 7-58792
 Au-Cr superlattices, electrical resistivity 7-27384
 Bi₂Ni, α -irrad. and H implanted, elec. resist. and superconducting T_c 7-7202
 Ce (Fe_{1-x}Al_x)₂, Fe-rich intermetallics, mag. and elec. props. 7-45621
 Ce cpds. and alloys, kondo effect versus crystal field 7-2602
 Ce Kondo systems, thermopower, elec. resist. and cryst. field effects 7-21900
 CeCu_{2-x}Ni_xSi₂, Kondo-lattice system, resist. anomalies 7-58799
 CeGe_{1-x}Si_x, nearly ferromag. props., temp. and comp. depend. study 7-7493
 Ce(Rh_{1-x}Co_x)₃B₂ ferromag. Kondo system, anomalous elec. resist. temp. depend. 7-2601
 CeZn₂, Kondo anomaly and metamagnetism 7-64234
 Co, optical props., electronic struct. depend. (Russian) 7-33356
 (Co_{1-x}Mn_x)₂B, crystalline and amorphous, mag. and elec. props. 7-2827
 Copper, extrusion, dislocation density determ. (Russian) 7-58285
 Cr alloys, charge and spin density waves (Russian) 7-2514
 Cr single crystals, thermoelec. power near the Neel temp., precursor behaviour 7-64209
 Cr-Ge dilute alloys, elec. resist. temp. and press. depend. studies 7-32980
 (Cr_{1-x}Al_x)₂Mo₃, antiferromagnetism disappearance, comp. depend., elec. resist. and sound rel. meas. 7-2843
 Cu alloys, candidate materials for high heat load appl. in neutron environments 7-49636
 Cu alloys, neutron irrad., cond. changes, porosity swelling and transmutation contrib. 7-51838
 Cu alloys, neutron irrad., 13 dpa, mech. prop. and elec. cond. changes 7-51839
 Cu alloys, rapidly solidified powder metallurgy, irrad. to 13.5 dpa with neutrons, microstruct. evolution and swelling 7-51840
 Cu and alloys, neutron irrad. effects, elec. cond., fusion reactor appl. 7-51835
 Cu cable, electrical conduction, comparison with light transmission 7-57594
 Cu elec. resist., strain-induced changes in temp. depend. component, magnetic impurity effects 7-52567
 Cu fibre, porous, physicochem. props. and model prediction 7-3353
 Cu rod, skin depth and complex mag. susceptibility, expt. 7-51
 Cu stabiliser, supercond. mag. material, fusion reactor conditions simulation 7-52922
 Cu thin polycryst. wires, elec. resist. meas., surface induced deviations from Matthiessen's rule 7-27319
 Cu two-dimensional systems, lattice and continuum percolation transport exponents 7-45275
 Cu, whiskers, derivation from Matthiessen's rule, effect of surface condition 7-45276
 Cu wire, size effect of DC resistance (Chinese) 7-12694
 Cu-based dilute alloys, low temp. elec. resist. 7-52565
 Cu-Be-Co, elec. resist., decomposition and coarsening effects 7-2573
 Cu-Ni-Fe-Mn, physical props. rel. to precip. and thermal treatment (German) 7-12698
 Cu-Pt (48.1 at.%), elec. resist. var. during ordering under press. (Russian) 7-33810
 Cu-Zn alloys, electron irradiation, interstitial cluster form., diffusion rates, resistivity 7-2013
 CuAl, short-range order-induced equilib. resist. conc. depend. meas. 7-26700
 Cu₃Au, irradiation disordering and reordering by fusion neutrons, electrical resistivity meas. 7-51864
 Cu₃Au, quenched, vacancies, ordering and annealing, positron lifetime and elec. resist. meas. 7-39544
 CuBe, scatt. anisotropy of conduction electrons 7-38536
 CuMn, short-range order-induced equilib. resist. conc. depend. meas. 7-26700
 Cu₂MnAl, high press. phase transition, elec. resist., saturation magnetisation, lattice parameters (Russian) 7-46457
 CuZn, short-range order-induced equilib. resist. conc. depend. meas. 7-26700
 Er₃Ir₂Si₁₃, existence and electrical props. (French) 7-17008
 Er₃Os₂Si₁₃, existence and electrical props. (French) 7-17008
 Eu-Yb, high press. mag. and elec. props. studies 7-7541
 EuRh_{1-x}Sn_x, anomalous mag. and elec. props. 7-64440
 Fe, alpha phase, high energy proton and alpha-particle irrad., radiation defects (Russian) 7-16645
 Fe, electrical resistivity, high temp. and press. 7-38534
 α -Fe, electron irradiated, residual resistivity recovery and mag. after-effect 7-27570
 Fe, Fermi surface change near the mag. transition 7-16935
 Fe-Al bilayered samples, ion beam induced atomic mixing 7-6689
 Fe-Cr-Mn, may susceptibility and elec. resist. (Russian) 7-52952
 Fe-Cr-Ni alloys, local ordering, neutron irrad. effects, elec. resist. meas. 7-2070
 Fe-Mo (14.5 wt.%), ageing, discontinuous dislocational transform., coercivity obs. 7-3305
 FeAl, short-range order-induced equilib. resist. conc. depend. meas. 7-26700
 Fe₄₀Ni₄₀B₂₀, amorphous and crystalline, elec. resistivity, temp. dependence 7-21892
 Fe₈₄-V₂B₁₆, amorphous alloys, crystn., products and kinetics 7-51677
 Gd(Al_{1-x}Ga_x)₂, cryst. struct., paramag. susceptibility, elec. resist. meas. 7-16492
 Gd₂In, mag. transitions under press. 7-59013
 Ho₃Ir₂Si₁₃, existence and electrical props. (French) 7-17008
 Ho₃Os₂Si₁₃, existence and electrical props. (French) 7-17008
 Ho_{1-x}Y_xCo₃, orientational phase transitions and elec. resist. (Russian) 7-7506
 K, electron-electron and electron-phonon interactions, plastic deform. effects 7-12710
 K-Rb dilute alloy, electron-electron and electron-phonon interactions, plastic deform. effects 7-12710
 LaAg, nonmag. cpds., transport props. and electronic struct. 7-2575

electrical conductivity of crystalline metals and alloys continued

- La_{1-x}Ce_xNi, Kondo lattice form., elec. resist. and susceptibility meas. 7-21899
 Li, electron-electron scatt., elec. resistivity meas. 7-32981
 LiMg, electron-electron scatt., elec. resistivity meas. 7-32981
 Li_{0.9}Mo_{0.1}W₂O₁₇, W substitutional effects on elec. resistivity and transport props. 7-45260
 LuAg, nonmag. cpds., transport props. and electronic struct. 7-2575
 α -LuD₂ single crystals, anisotropic ordering, resistivity and heat capacity studies 7-21894
 Lu₃Os₂Si₁₃, existence and electrical props. (French) 7-17008
 Mo-Ce alloy point contacts, low temp. I-V charact., thermoelec. effects obs. 7-27382
 (Na_{1-x}Li_x)_{0.9}Mo_{0.1}O₁₇, Na substitutional effects on elec. resistivity and transport props. 7-45260
 Ni, dislocation structure after US deformation, physical props. (Russian) 7-44699
 Ni, electrical resistivity, high temp. and press. 7-38534
 Ni, fatigue cycling, lattice defect characterisation 7-37978
 Ni, fatigue life in const. mag. field and ultrasonic field, 4.2-273K (Russian) 7-46639
 Ni, Fermi surface change near the mag. transition 7-16935
 Ni fibre, porous, physicochem. props. and model prediction 7-3353
 Ni, irrad. with energetic ions, defect prod. and recovery 7-58370
 Ni-Cr fibre, porous, physicochem. props. and model prediction 7-3353
 Ni-Fe-Cu, mag. props., hardness, elec. resist., V, Nb and Ta additions effect (Japanese) 7-12998
 Ni₃Al, thermal and elec. cond., temp. and comp. depends. 7-64200
 Ni₂MnIn(Sn)(Sb) Heusler alloys, galvanomag. props. and magnetisation meas., fermi level shift effects 7-7207
 NiTi alloy powder, shock compaction 7-59480
 Pb, deforming stress and defect struct. in low temp. anomaly region (Russian) 7-38093
 Pb, temp. depend. of elec. resist. 7-58792
 Pd-Ag-Fe (1 and 2 at.%), plastically deformed, elec. resist., short range order effects 7-27318
 Pd-Ce-H, electrical resistance meas. 7-32984
 Pd-Er alloys, elec. resist., temp. depend., Matthiessen's rule deviations 7-45269
 Pd-H, dil., elec. resist. meas., 250-350 K 7-64233
 Pd-Si alloys, H absorption, structural disorder effects 7-52249
 Pd_{100-x}Ag_x, plastically deformed, elec. resist., short range order effects 7-27318
 PdFe, drawing effects on elec. resist. and mech. props. (Russian) 7-17584
 Pd_{58.8}U_{20.6}Si_{20.6} alloys, glassy to icosahedral quasicrystalline phase transition, elec. and mag. props. 7-37863
 Re, anisotropy of thermoelectric power and electrical resistivity 7-17017
 Sm, phase transitions at high pressures 7-64457
 Sn alloys, surface and interphase phenomena, grain boundaries and growth 7-13431
 Ta-H system, elec. resist., phase transition (Russian) 7-46458
 α -Ti, mag. suscept. and elec. resist. meas., itinerant antiferromagnetism, comment 7-33151
 Ti, oxidation, Rutherford backscattering spectrometry, AES, X-ray diff., elec. resist. meas. 7-22894
 TiNiFe, premartensitic state investig., Mossbauer effect studies (Russian) 7-3298
 TiSi₂, oxidation, Rutherford backscattering spectrometry, AES, X-ray diff., elec. resist. meas. 7-22894
 Tm intermediate valence systems, dynamics, self-consistent perturbation theory studies 7-27309
 Tm, polycrystalline, electrical resistivity, mag. struct. effect 7-52564
 TmCu₂, magnetic phase transitions, suscept., sp. ht., elec. resist. and magnetisation meas. 7-2857
 U alloys, optical and elec. transport props., review 7-13119
 UAl(Ga)(Sn)Ni(Co)(Ru) ternary alloys, magnetic behaviour, elec. resist. and sp. ht. meas., 5f electron effects 7-12999
 U₂La_{1-x}Te single crystals, elec. resist. temp. depend. Kondo effect and ferromagnetic ordering 7-13119
 UPdSn, heavy electron behaviour, elec. resist., mag. susceptibility, sp. ht. meas. 7-32679
 U(Pt,Pd)₃₁, heavy-fermion alloys, resistivity 7-17012
 UPt₃ Kondo lattice, low-temp. sp. ht., suscept. and resist. meas., press. depend. anal. 7-7220
 UPt₃ single crystals, electronic structure, low energy reflectivity study 7-45137
 URu₂Si₂, heavy electron system, competing electronic correlations, press. effect 7-45539
 URu₂Si₂ single crystal, Czochralski growth, charactn. 7-53557
 V₃Ga(Au)(Pt), superconducting A15 cpds., resistivity and magnetoresistance 7-32982
 V₃Ge solid solns. of Fe, Cr and Co, elec. resist. (Russian) 7-45273
 V₃Si solid solns. of Fe, Cr and Co, elec. resist. (Russian) 7-45273
 W dilute binary alloys, resistivity contribution of solutes 7-32979
 W films, amorphous and finely cryst., elec. props. (Russian) 7-38776
 W-Cu-Ni contact materials, elec. props., particle size effect 7-2672
 W-Cu-Ti(Zr), saturation rate of porous W with Cu, effect of Ti and Zr 7-3220
 W-Ni powder compact, activated sintering process, electrical resistance meas. 7-27969
 YAg, nonmag. cpds., transport props. and electronic struct. 7-2575
 Y₆Co₇, resistivity and Hall effect temp. depend. meas. 7-52568
 YbAgCu₄, strong electronic correlations 7-45194
 YbAuCu₄, strong electronic correlations 7-45194
 YbPdCu₄, strong electronic correlations 7-45194
 Zn, electrical conductivity, Harrison's method appl. 7-7203
 Zr, doped with O, mech. props. and elec. resist. at 4.2 K influence of annealing (French) 7-59554

electrical conductivity of crystalline semiconductors and insulators

- see also carrier density; carrier lifetime; carrier mean free path; carrier mobility; carrier relaxation time; dislocation scattering; electronic conduction in crystalline semiconductor thin films; electronic conduction in insulating thin films; high field effects; hopping conduction; impurity scattering; minority carriers; negative resistance effects; photoconductivity; point defect scattering; small polaron conduction; surface scattering
 = 7-1986
 alkali halides, powdered, electrophysical investigation during molding 7-7232

electrical conductivity of crystalline semiconductors and insulators continued
alumina, polycrystalline, X-ray and proton irradi., elec. cond. studies 7-33014
anisotropic semiconductors, electrical conductivity, inhomogeneous electric field depend. 7-52606
anthracene: acridine crystals, conduction mechanism and trap levels, TSC meas. 7-27342
bicrystals, as-grown and annealed, conductance of grain boundaries 7-64245
bis-5,6-diseleno-11,12-ditellurotetracene bromide (chloride), struct. and elec. cond. 7-44512
15-15' cis β -carotene crystal, electrical conduction, compensation effect 7-58810
ceramic semiconductors, granular: struct. and elec. props. (German) 7-58495
compositionally graded semiconductors and device applics., book contrib. 7-27323
DC conductivity, surface conductivity 7-21919
defects produced by electron and X-ray irradiation, surface effects 7-6687
electron-electron scatt. in nondegenerate semiconductors, anisotropic electron distrib., displaced Maxwellian 7-2624
3-ethyl-5-[2-(3-ethyl-2-benzothiazolylidene)-ethylidene]-rhodanine, polymorphism and electronic props. 7-37959
extrinsic, freq. locking, quasiperiodicity and chaos 7-2618
fast-neutron irradiated, electrical behaviour during thermal recovery 7-13029
ferrous spinel, oxidation kinetics and mechanism, elec. cond., thermogravimetry 7-27326
field-effect capacitor, carrier ambipolar drift vel., field control study 7-52840
halide eutectic composites, growth, struct., mech., elec. and optical props. 7-33648
HfTe₂, electronic props. 7-2610
highly excited, nonequilibrium Green's functions and kinetic equations 7-32889
II-V semiconds., cryst. growth, characterisation and appls., review 7-26685
In_{0.53}Ga_{0.47}As:Fe metalorganic CVD epitaxial growth and elec. props. 7-63993
inversion band bending at surface, generation-recombination noise 7-17067
ion radical salt, (AsPh₄)_{0.25}(Ni(dmit)₂), synthesis, elec. cond. and cryst. struct. 7-37958
local field-enhanced electronic conduction, activation energy and Poole-Frenkel const. calcs. 7-38570
LPCVD production, anal and solar cell appls. 7-17452
many-valley semiconductor crystals, interaction of excitations with dislocations 7-38553
metal dithiolenes, struct., elec. and optical props. 7-44516
metal phthalocyanines, elec. and photocond., props., coordination metal effects (Japanese) 7-12753
Meyer-Neldel rule, phenomenological model 7-21904
micaplast materials with inorganic binders, electrical properties at temps. up to 900°C 7-12714
moving dislocations in II-VI semiconductors, dislocations, effect on physical props. 7-7224
multi-S π donor and π -acceptor charge transfer complexes, struct., elec. and optical props. 7-44513
n-type, electron heating and intervalley redistribution in strong electric fields 7-27336
n-type, oscillations and chaotic current fluctuations 7-64253
nondegenerate semiconductor, resistivity, impurity depend. 7-7240
oxides, elec. props. under conditions of oxidation, reduction and catalysis 7-7250
perovskite-like ferroelectrics, optical and electrophysical props. 7-3002
phenyl-2,4-dinitrophenyl polycryst. substituted ether, elec. cond. meas. 7-17022
piezoelectric semiconductors, small-signal conductivity, diffusion of electrons, system with nonequilib. phonons 7-45313
polar semiconductors, doped, conductivity tensor, interference effects 7-12711
resonant scatt. of carriers, effect on transport coeffs. 7-38602
SAW transducer, layered struct. tempering (German) 7-31615
scheelite structure crystals, optical and elec. props. 7-33431
semiconducting materials, cryst., and device appls., book 7-60894
semiconductor electrical characterisation, non-contacting methods, book contrib. 7-45335
semiconductors, doped, crit. transport props. 7-64248
semiconductors, extrinsic, thermal gradient magnetoc. effect 7-52659
semiconductors, photothermal spectroscopy, review 7-48732
semiconductors, polycrystalline, grain-boundary barrier heights, grain curvature effects 7-2607
semiconductors, singular perturbation anal. (French) 7-21905
shock Hugoniot eqn. of state, electron band theory approach 7-21392
TCNQ salt, N-n-propyl phthalazinium 7,7,8,8 TCNQ₂, struct., elec., mag. props., EPR meas. 7-33005
TCNQ salts, semiconducting, dielec. response in submillimetre range 7-45916
TGS crystals, polarisation relax., defect effects 7-17265
transition metal chalcogenides, ternary and quaternary, struct. and substitutional chem. 7-32384
triglycine sulphate, single cryst., neutron irradi., elec. cond. 7-7227
two-electron semiconductor systems, electric field, resistance and current distrib. calc. 7-38600
two-phase mixture, effect of dispersoid on elec. transport 7-2621
[α -]Mn₂S antiferromag. semicond., elec. and mag. props. 7-7244
AgNO₃, electrical resistance effects accompanying high pressure and temperature melting and decomposition 7-16719
Ag₂O-Al₂O₃ ceramics and single crystals, cond. fluctuations and contact noise meas. 7-58840
Ag₂Te-Ag₂SSe, thermoelectrical props. 7-45364
AlN, hot pressed, elec. cond. rel. to CaO addition 7-38559
Al₂O₃, electrical props., radiation effects 7-52617
Al₂O₃ porous ceramics, elec. cond. and fluid flow permeability corrls. 7-38566
Al₂O₃:Fe, Y, high temp. DC elec. cond. rel. to superalloy oxide scale adherence 7-52615
B, defects produced by electron and X-ray irradiation, surface effects 7-6687

electrical conductivity of crystalline semiconductors and insulators continued
Ba(Bi,Pb)O₃, semiconducting props., X-ray powder diff. and transport meas. (Japanese) 7-64237
Ba₂Fe₂²⁺Fe₁₂³⁺O₂₂ hexagonal ferrite, hydrothermal synthesis, elec., magnetic and structural characterisation 7-45637
BaFe_{12-x}Mn_xO₁₉, magnetoplumbite system, transport props., influence of internal electric field 7-52662
BaLn₂O₄:TiO₂, (Ln=La,Nd), phase props., X-ray and elec. meas. 7-2220
Ba₂NaNb₂O₁₅ cryst., elec. cond. small signal amplification 7-27333
Ba₂NaNb₂O₁₅ single crystals, spatio-temporal electrical instabilities 7-52632
BaPb_{1-x}Bi_xO₃, supercond., struct. and elec. props. 7-58247
Ba_{0.93}Sr_{0.07}TiO₃, single crystal, electronic transport behaviour 7-33011
Ba_{0.9}Sr_{0.1}TiO₃:Sb, positive temp. coeff. of resist., synthesis method depend. 7-45324
BaTiO₃, acceptor state behaviour, influence of impurities and lattice defects 7-2539
BaTiO₃, dielectric, electrical and acoustic props. 7-53224
BaTiO₃, elec. cond. rel. to point defects 7-6619
BaTiO₃:Mn, Mn oxidation state change near phase transitions 7-16974
BaTiO₃:Y₂O₃(La₂O₃)(Ce₂O₃), semiconductor props., influence of dopant oxides 7-6650
Bi₂(MoO₄)₃, Czochralski growth, monoclinic unit cell (Korean) 7-27890
BiVO₄, pure and CaO doped polycryst. samples, scheelite struct., elec. cond., anion vacancy motion investigation 7-32712
C fibres, Celion, elec. resist., temp. depend. 7-65073
C fibres, high electrical conductivity intercalation treatment (French) 7-59646
C films, CK α spectra and interatomic bonding (Russian) 7-58705
C, hard type, B-doped, prep., phys. and mech. props. 7-39571
Ca₃Y₂(PO₄)₆(OH)_{2-x}O_x, synthesis, struct., dielec. props., AC elec. cond., IR spectra 7-3235
(CdBi)(M_{1/2}Sb_{1/2})O₇, (M=Cr, Ga, V, Mn, Fe, Rh, Sc, In), pyrochlores, struct. and characterisation 7-1986
CdF₂, field enhanced electronic transport 7-45329
Cd_{1-x}Hg_xTe crystals, impurity band elec. conduction, Fermi glass model anal. 7-27328
Cd₂Hg_{1-x}Te, LPE and MOVPE grown, elec. props. and annealing 7-53512
CdS, single crystal, US wave absorption, impurity distrib. effect., electron-probe X-ray anal. 7-53241
CdS single crystals, nonequilib. high-temp. vacuum annealing effects, intrinsic defect transform. 7-58764
CdS-CuGaSe₂ solar cells, physical properties and photovoltaic potential of CuGaSe₂ thin films 7-12889
CdSe, single crystal, US wave absorption, impurity distrib. effect., electron-probe X-ray anal. 7-53241
CdTe, polycrystalline, grain boundaries elec. and optical characts. 7-38012
CdTe:Sn, impurity compensation effect on elec. resist. and mobility 7-52614
CdTe-HgTe superlattices, IR material characterisation, transport phenomena anal. 7-64338
Ce_{1-x}Bi_xO₃F_{3-2x} solid solns., O substitution, influence on struct. and elec. props. (French) 7-12019
Ce₂Mo₆S₈, crystal growth and struct., susceptibility and transport props. 7-64889
Co(NO₃)₂.6H₂O, electrical resistance effects accompanying high pressure and temperature melting and decomposition 7-16719
CrNbO₄-VO₂-MoO₂ system, rutile phases, prep. and props. 7-6806
CrTe-CrSe system, mag. phase diagram 7-22105
CsV₃O₇, crystals, struct., cathodic reduction from melt, and elec. props. studies 7-58236
Cu_xAg_{1-x}InSe₂, liquid-encapsulated Bridgman-Stockbarger melt growth, p-type cond. 7-59403
Cu_xCd_{1-x}Fe₂O₄ system, elec. resist. and cation distrib. 7-7256
CuInGa_{1-x}Se₂, liquid-encapsulated Bridgman-Stockbarger melt growth, p-type cond. 7-59403
CuInS₂, chem. diffusion, 20-100°C 7-16799
Cu_{2-x}Se, electrical resistivity, temp. and carrier density dependences 7-38556
Eu-Bi-S, synthesis and props. 7-44471
Eu-Bi-Se(Te), synthesis and props. 7-44471
Eu-Sb-S, synthesis and props. 7-44471
Eu-Sb-Se(Te), synthesis and props. 7-44471
Fe-Ge-Te, compound formation, microstructure, X-ray diffraction, dilatometry studies 7-7980
FeO, wustite, defect agglomeration at high temps., elec. conduction model 7-21197
Fe_{0.94}O, metallisation at elevated press. and temp., shock wave elec. resist. meas. 7-7297
Fe₂O₄ single cryst., dielec. and conducting props. study below Verwey point 7-53230
Fe₂O:Li₂O(CaO)(Al₂O₃)(SiO₂), synthetic wustite, elec. cond., doping elements effect (Korean) 7-2609
Fe₃(1- δ)O₄, magnetite, synthesis, crystal growth and characterisation 7-2647
GaAs diode, active layer <1 μ m, low temp. current flow 7-52757
GaAs, horizontal Bridgman growth, semi-insulating props. characts. 7-64896
GaAs, ion irradi. high-resistivity layer, thickness and resistance, free carrier density and cryst. orientation dependence 7-58354
GaAs LEC semi-insulating crystals, pure and In-doped, IR absorpt. WRT resistivity 7-64629
GaAs, mixed electron-hole conductivity 7-58808
GaAs, neutron transmutation doped, variable range hopping studies 7-33012
GaAs, phonon-plasmon coupling in electron transport 7-33041
GaAs, semi-insulating LEC crystals, thermal conversion, DLTS studies 7-7150
GaAs, semiinsulating, electrophysical props., dislocation effects 7-16557
GaAs: Si(Se)(Zn)(Be), ion implanted, rapidly annealed, damage removal process 7-17043
n-GaAs:Co, impurity double acceptor state, Hall effect and resistivity meas., temp. and press. depend. 7-12656
GaAs:Ho, electroluminescence and injection currents 7-13232
GaAs:In, B, electrical props., role of residual B impurity, liquid encapsulated Czochralski growth 7-45312
GaAs:Si, electrical props. of p-type layer 7-12722
GaAs:Si, ion implanted, rapid thermal annealing effects 7-21259

electrical conductivity of crystalline semiconductors and insulators continued

- n-GaAs_{1-x}Sb_x epitaxial film, impurity distrib., cond. and Hall mobility study 7-51808
 n-Ga_{1-x}In_xSb:Se(S), impurity states, press. and comp. depend., Hall coeff. and elec. resist. meas. 7-2533
 GaN:Zn n-i structures 7-38565
 GaSb+GaV₃Sb₅, eutectic alloys, elec. props., anisotropy 7-12717
 GaSb+V₂Ga₃, eutectic alloys, elec. props., anisotropy 7-12717
 GaSe-Li, intercalated layer compounds, conc. depend. of electrode potential 7-7230
 Ge crystal, carrier mobility meas. using Haynes-Shockley expt. for student laboratory 7-55933
 Ge deformed single cryst., AC conductivity at 4.2K 7-7245
 Ge, drag thermoelec. power, anisotropy parameter, carrier density depend. 7-38603
 Ge, extrinsic photoconductors, nonlinear dynamics and chaos 7-52685
 Ge, n-type and ultrapure samples, electron transport and press. coeffs. 7-2615
 p-Ge, nonlinear I-V characts. and spontaneous current oscillations 7-52631
 Ge point contacts, nonlinear elec. cond. effects due to electron-phonon interactions (*Russian*) 7-52628
 p-Ge, spatio-temporal coherence and chaos, conf. Los Alamos, USA, Jan. 1986 7-48158
 p-Ge:As, Hall effect and electrical conductivity, temp. corrections 7-38592
 p-Ge:Ga, resistivity at low temp. appl. to bolometers 7-41471
 Ge:P crystals, seeded growth in soft lined crucible, dopant distrib. 7-53559
 Ge:Sb(Al)(Ga)(In), heavily doped, charge carrier scatt., elec. cond., Hall effect meas. 7-7228
 Ge-Si alloys, piezoresistance under uniaxial elastic deform. (*Russian*) 7-58813
 GeTe-GeSe₂, polythermal section of Ge-Te-Se, effects of deviations from stoichiometry 7-7977
 GeTe-PbSe, phase transformations, cation-anion substitution, electrophysical props. 7-7978
 HgI₂, solution-grown crystals, X-ray and γ -ray irradiation effect on elec. props., radiation detector performance 7-58838
 α -HgS:Ti single cryst., elec. relax. current 7-64241
 InAs:Sb(Ga)(Mn), single crystal, elec. inhomogeneity, effects of isovalent impurities 7-7229
 InP:Fe,Ga,Sb, LEC growth, dislocation density, resistivity, SIMS obs. 7-53552
 InP:Fe wafer, semi-insulating, elec. characteristics 7-45323
 InP:Yb LPE layers, luminesc. and elec. props. 7-59464
 InSb, Czochralski growth rate and spreading resist. relations (*Japanese*) 7-26679
 InSe-Li, intercalated layer compounds, conc. depend. of electrode potential 7-7230
 In₂Se₃:S(Li), electrical transport props. 7-21917
 In₂Te₃:Fe, Fe²⁺ elec. inactivity study, mag. suscept., Mossbauer spectra and XPS anal. 7-52494
 Ir complex, (Ir(CO)₂4,4',5,5'-tetracyano-2,2'-biimidazole)⁻, anisotropic conductor, phys. props. 7-7242
 KCl:Zn, elec. cond., dielec. loss meas., before and after X-irrad. 7-33324
 K_{12-x}Nb_{8+x}O₁₇, mixed-valence rutile structures 7-27329
 KTAWO₆.H₂O, pyrochlore-type cpd., characterisation 7-1989
 (La,Ca)(Co,Mn)O₃, sinterability, phase composition and microstructure 7-33622
 La_{1-x}Ca_xCr_{1-y}Ni_yO₃, production and elec. parameters 7-33007
 La₂NiO₄, struct. characterisation of orthorhombic form 7-1990
 La_{0.6}Pb_{0.4}Co_{0.5}Mn_{0.5}O₃, elec. conductivity, influence of Co ion substitution for Mn 7-45314
 LaS, NaCl type lattice, current carriers and cond. 7-45346
 La₂TiMo₆ (M=Fe, Ni, Cu, Zn), synthesis, struct. and elec. props. 7-2619
 LiD:Mg²⁺, elec. props., X-irradiation effects, DC cond., dielec. loss and ionic thermocurrent meas. 7-27341
 Li₂GaSe intercalation cpd., elec. resist. and Hall effect meas. 7-12719
 LiH:Ca²⁺, elec. props., X-irradiation effects, DC cond., dielec. loss and ionic thermocurrent meas. 7-27341
 LiMO₂, M=Sc, Ti, V, Cr, Mn, Fe, Co, Ni, Cu props., review 7-64437
 (Li_{1-x}Na_x)K_{0.9}Mo₆O₁₇, anomalous transport props., resist., mag. suscept., sp. ht., struct. and supercond. transition temp. meas. 7-21913
 Li₂O-Al₂O₃-TiO₂, synthesis and props. 7-33643
 Li₂SO₄-Li₂CO₃ system, phase diagram and elec. cond. meas. 7-32612
 Li₂Sn_{1-x}Y_{2x}O₄, metal-insulator transition, Seebeck coeff. and elec. resist. studies 7-21817
 Li₂TiGaSe₂, ion intercalated, dark current and photocurrent relax. meas. 7-38622
 Li_{1-x}V_{0.13+x}, nonstoichiometric intercalation cpd., phase stability and elec. cond. studies 7-12723
 (Mg,Fe)₂SiO₄, olivine, electrical conductivity changes due to creep at Earth mantle conditions 7-18180
 Mg,Cd_{1-x}Se single crystals, impurity photocurrent temp. activation meas. and calcs. (*Russian*) 7-45394
 MgFe₂O₄, photoelectrochemical props., effect of defects and doping 7-45385
 Mg₂NiH₄, struct., thermal and elec. props., rel. to covalent bonding 7-21184
 MgO:Fe, gamma-ray and electron radiation-induced conductivity 7-33015
 Mg₂Si₂O₆-CaMgSi₂O₆ system, solid solutions, dilatometry and elec. conductivity meas. 7-2175
 Mn_{1-x}O, manganosite, relax. kinetics in CO-CO₂ mixtures 7-58539
 α -Mn₂S₃, antiferromag. semiconductors, elec. conductivity 7-64240
 Mn_{0.61}Zn_{0.26}Fe_{2.13}O₄, ferrite, conductivity study 7-21909
 MoI₂, preparation, elec. and optical props. 7-64946
 Na₂O-V₂O₅-P₂O₅, crystallised glass, containing V bronze crystals, elec. cond. 7-21922
 Na₂O-WO₃-B₂O₃ glass ceramics, containing W bronze, prep. and elec. props. (*Japanese*) 7-3261
 NbO₃, semicond., AC cond. meas., 4-196K, 5-92 kHz 7-45327
 (NbSe₄)₃I, phase transition props. 7-44803
 Nd_{2-x}Cu_xRu_{2-y}O_{7-y}, pyrochlore type phases, elec. and cryst. characts., X-ray fluoresc. anal. (*French*) 7-45325
 NiCuNbO₄, cryst. data and conductance investigation 7-38550
 NiMn₂O₄, elec. cond. and cation distrib. 7-33009
 NiO, two-phase mixture, effect of dispersoid on elec. transport 7-2621
 PLZT polarised ceramics, electroconductivity asymmetry obs. 7-7225

electrical conductivity of crystalline semiconductors and insulators continued

- Pb chalcogenides, mechanisms of electron scatt. 7-52611
 Pb-Sn-G solid solns., elec. transport props. and defect form. studies (*French*) 7-33017
 PbBi₄Te₇, synthesis and physicochemical props. 7-13349
 Pb_{1-x}Cr_xTe, prep. and electrical props. 7-12721
 Pb_{1-x}Zn_x single crystals, growth and semicond. behaviour 7-53577
 PbLiInSe, intercalation-layer compound, dielectric-metal cond. transition 7-7230
 SPbS₂Sb₂S₃, boulangerite, elec. cond. (*Korean*) 7-27331
 Pb_{0.75}Sn_{0.25}Te:In, Ge(Si)(Se), elec. resist., photocond., Hall effect meas. 7-17050
 PbTe:Ti, Na, carrier reson. scatt., effect on transport coeffs. 7-38602
 PbTe-Gd₂Te₃ system, solid solns., synthesis and props. 7-21458
 PbTe-MnTe₂ system, phase diagram, conductivity and thermoelectromotive force 7-63824
 PbTe-Tb₂Te₃, solid solns., physicochemical anal. 7-21456
 PbTe_{1-x}S_x, free carrier scatt. near a phase transition 7-38557
 PrRuO₃, perovskite phase, effects of high press. 7-2103
 RbNO₃ cryst., AC cond. near first-order phase transition points 7-21948
 RbVO₃ crystals, struct., cathodic reduction from melt, and elec. props. studies 7-58236
 ReS₂, single cryst. growth by chem. vapour transport, elec. resist., Hall mobility meas. 7-64251
 ReSe₂, single cryst. growth by chem. vapour transport, elec. resist., Hall mobility meas. 7-64251
 Sb_{1-x}Bi_xSI crystals, elec. props. at ferroelec. Curie point 7-2991
 SbSI, elec. charactn. of crystals grown from melt by temp. fluctuation technique 7-13104
 SbSI, elec. cond., ferroelec., phase transition temp. 7-45326
 SbSI, SbSOI, cryst. growth and elec. charactn. 7-53564
 Sb₂Te₃ crystal, semimetallic, semicond. behaviour at low temps. 7-12716
 Sb₂Te₃ crystals, pure and Cd-doped, point defects, reflectivity and elec. props. room temp. meas. 7-33008
 ScN compensated semimetal single crystals, electronic struct., reflectivity and elec. props. meas. 7-27253
 Se₂S₃, solid, elec. cond. (*Japanese*) 7-33002
 Si (111)-7 \times 7, temp.-depend. surface resistivity, electron energy loss meas. anal. 7-21973
 Si, charged defect states at grain boundaries 7-44564
 Si, circular wafer, edge effects on bulk resistance 7-58811
 p-Si conductivity and Hall mobility calcs., impurity scatt., anisotropic-nonparabolic effects 7-12720
 Si defect annealing and impurity activation during high-intensity As⁺ implantation doping 7-58295
 Si, defects produced by electron and X-ray irradiation, surface effects 7-6687
 Si, diffusion length depend. on cooling rates and bulk resistivity 7-7266
 Si, dopant profiles by the spreading resistance technique, book contrib. 7-44594
 n-Si, gamma-irrad., intrinsic defects, Hall effect and elec. cond. meas. 7-6615
 Si, gamma-ray effects on micro defects and electrophysical props. 7-16629
 Si, high purity, charge carrier lifetime meas. 7-45351
 Si microstrip detector structures with implanted p-n junctions, functional props. 7-42325
 Si, minority carrier lifetime and resist. mapping, flying-spot scanning method 7-4867
 Si, neutron-transmutation-doped, elec. resist. inhomogeneity form. characts. estimation 7-38026
 Si polycrystalline, gap state density determ., field-effect conductance anal. calcs. 7-21794
 p-Si, polycrystalline, ion implanted, resistivity modelling (*Korean*) 7-2608
 Si, polycrystalline p-type, Al and Cu diffusion effects on electronic properties 7-17038
 Si self-doping using Stepanov method, elec. resist. meas. 7-32470
 Si single cryst. wafer, charge carrier kinetics, excess microwave cond. meas. 7-38580
 Si strips, grown by Stepanov's reversed method, strength, struct., electrophysical props., effects of thermal conditions during growth, photocell appl. 7-32325
 Si:Al, Mg transmutation doping by proton irradiation 7-38027
 Si:As, high dose implanted, defect density reduction by low temp. oxidation 7-58297
 Si:As, ion implanted, electronic transport props. 7-7233
 Si:As, ion implanted, rapid thermal annealing 7-16615
 Si:As, ion implanted, rapid thermal annealing, metastable activation 7-16616
 Si:As, precipitation and cluster form., elec. resist., backscatt. and TEM studies (*Chinese*) 7-12285
 Si:As on sapphire, ion beam recrystallised and laser annealed, elec. props. 7-16649
 Si:As⁺, heavily doped, ion implant deactivation 7-17567
 Si:Au, supersaturated low-temp. substitutional impurities, annealing 7-6665
 Si:B, diffusion and activation of implanted B during rapid thermal annealing 7-16643
 Si:B,O, thermal donor formation, bending stress effects 7-17563
 Si:Er(Dy)(Yb)(Ho)(Gd), neutron irradiation, Hall effect, elec. cond., IR absorpt. spectra 7-51834
 Si:H, polycrystalline, chemistry of grain boundary passivation 7-12375
 Si:N, deep level generation and annihilation 7-16612
 Si:O, Czochralski grown, O-related defects after annealing, IR TEM and resistivity meas. 7-32466
 Si:O, IR absorption spectra of thermal donors 7-17326
 Si:O, influence of growth microdefects on microdefect formation during heat treatment 7-17559
 Si:O²⁺, ion implanted, reverse annealing 7-16617
 Si:P, Ni⁺, ion implantation and annealing 7-21245
 Si:P, transmutation doped, deform. pot. shear const. determ. 7-38086
 Si:P,O,D, donor passivation and reactivation 7-17031
 Si:P,Sb, mixing of P and Sb ions by recoil implantation, sheet resist., annealing temp. depend. 7-21291
 n-Si:Sb, resistivity at low temp. appl. to bolometers 7-41471
 SiC-Si₃N₄ fibres, prep. by polycarbosilazane precursors pyrolysis 7-27988
 Si₂Ge_{1-x}Ga_x, resistivity and Hall constant, temp. depend. 7-7231
 Si₃N₄, hot pressed, elec. cond., microstruct., fusion reactor insulator appl. 7-52619
 SiO films, field enhanced electronic transport 7-45329

electrical conductivity of crystalline semiconductors and insulators continued
 SiO_2 layers, space charge distrib. meas., electron beam induced conduction method 7-27660
 $\text{Sm}(\text{NO}_3)_3 \cdot 6\text{H}_2\text{O}$, electrical and optical props. 7-59223
 $\text{Sn}_{1-x}\text{Mn}_x\text{Te}$, degenerate ferro-spin-glass, transport props. and spin disorder 7-45330
 SnO_2 , nonstoichiometry and defect equilib. rel. to cond. props. 7-52069
 SnS_2 - TiS_2 phases, ^{119}Sn Mossbauer study (*French*) 7-27639
 $(\text{SnSe})_{1-x}\text{Sb}_x$ solid solns., phase diagrams and elec. props., comp. depend. 7-2172
 SnTe , conc. depend. props. in region of homogeneity 7-45366
 SrO-UO_2 system, elec. cond. of uranates, 550-1300K 7-45321
 SrTiO_3 , acceptor state behaviour, influence of impurities and lattice defects 7-2539
 $\text{SrTiO}_3\text{:Mn}$, Mn oxidation state change near phase transitions 7-16974
 SrTiO_3 -based SPBT ceramics, DC conduction and breakdown at high temps. 7-39020
 $\text{SrTi}_{0.97}\text{Zr}_{0.03}\text{O}_3$ ceramics, superconducting transitions from states with low normal conductivity 7-27452
 $\text{SrTi}_{0.97}\text{Zr}_{0.03}\text{O}_3$, superconductivity at low carrier conc. and indications of charged Bose gas 7-27453
 TaSe_3 , transport props., uniaxial stress effect 7-38801
 Te-Sc , whisker crystals, growth and elec. props. 7-12578
 TiB_2 , neutron bombardment, nature of rad. damage (*Russian*) 7-38067
 TiC_x , order-disorder transition 7-63796
 TiO_{2-x} , rutile, H reduced, elec. cond. 7-21912
 TiS_2 , intercalation cpd. with Mn, Fe, Co, Ni elec. resist. and thermopower studies 7-45331
 $\text{Ti}_{1.17}\text{S}_2$ crystals, metal-insulator transition investig. 7-7296
 p-TiInSe_2 single cryst., impurity photocond. studies 7-2642
 TiPrSe_2 (Se_2)(Te_2), elec. cond., Hall effect and thermoelec. studies 7-2606
 UO_{2+x} , pure and cation doped, elec. conductivity, O potentials, defect structures 7-12718
 $\text{V}_{3-x}\text{Mo}_x\text{S}_4$, struct. and phase relations, comp. depend., X-ray powder diff. study 7-1978
 WO_2 , resistivity anomaly 7-38567
 WO_3 electrochromic films, obliquely deposited, elec. props. and morphology 7-7781
 WS_{2+x} elec. cond. and permittivity, temp. and freq. depend. studies 7-7235
 YAG:Ni (Ni, Zr) (Fe), defect and optical props. 7-59258
 YFe_2O_4 , elec. resist. and Seebeck coeff. studies 7-21914
 $\text{Y}_{1-x}\text{M}_x\text{CrO}_3$, (M=Mg, Ca, Sr, Ba), electrical and thermal transport props 7-45319
 Y_2O_3 , DC cond. as function of water vap. press. 7-45317
 Y_2O_3 , elec. cond. as function of O_2 partial press. in wet and dry atm. 7-45405
 Yb-Sb-S(Se) , synthesis and props. 7-44471
 YbBiS(Te) , synthesis and props. 7-44471
 $\text{Yb}_{1-x}\text{In}_x\text{Se}$, anomalous Tm valence, lattice parameters, diamag. suscept. and Hall effect meas. 7-16998
 $\text{Zn}_{1-x}\text{Ge}_x\text{Fe}_2\text{O}_4$, ferrites, atomic, mag. and electronic disorder (*French*) 7-44477
 ZnGeP_2 , Hall effect and conductivity in zinc vapours, high temp. meas. 7-27350
 $\text{Zn}_x\text{Hg}_{1-x}\text{Se}$, electrophysical props. and carrier scatt. mechanisms 7-17024
 ZnO ceramic, grain growth kinetics during synthesis, optimum elec. props. 7-46398
 ZnO varistors, electroluminescence temp. depend. and conduction mechanisms 7-17349
 Zn_3P_2 pellets, elec. cond., compacting press. depend. 7-58809
 ZnS , cryst., p-type cond., luminesc. 7-13226
 ZnS , single crystal, annealed in O_2 , intrinsic defects rel. to elec. and luminesc. props. 7-12649
 ZnS , ZnSe , crystal growth by chem. transport using NH_4Cl transport agent 7-59385
 n-ZnSe , heavily doped strongly compensated crystals, electron mobility 7-7247
 ZnSe layer growth by plasma-assisted epitaxy 7-52365
 ZnSiP_2 and ZnGeP_2 , single crystals, prep. and characterisation 7-2612
 ZrO_2 , partially stabilised, phase stability, elec. cond., fusion reactor elec. insulator appl. 7-52618

electrical conductivity of electrolytic liquids

see also electrochemical analysis; electrolytic ion mobility; Wien effect
alkali chlorides, molten, ionic diffusion coeffs. calcs. 7-32689
ammonium perfluorononanoate- H_2O system, micellar nematic phase, conductivity, relax. times 7-38230
electrolyte solution, elec. cond., ionic trace effects, mobility determ. 7-21497
electrolyte solutions, ionic transport, space-charge density, Nernst-Planck and Poisson eqn. calcs. 7-26989
lead II 9,10-dihydroxyoctadecanoate, and binary mixtures, molten elec. cond. 7-38231
lithium trifluoromethyl sulphite, in polymer electrolytes, ion pairs triplet form., conductance meas. 7-32690
porous media with charges, electrolytic conduction 7-63858
surfactant-water-nonaqueous liq. systems, elec. cond. study 7-13789
 AgCl-KCl(CsCl) , binary molten mixtures, elec. cond. 7-12340
 AgI-CsI(KI)(NaI) , binary molten mixtures, elec. cond. 7-12340
 $\text{AlCl}_3/1\text{-butylpyridinium chloride}$ electrolyte for Al-FeS_2 secondary cell, phys. and elec. characts. (*Japanese*) 7-8371
 $\text{BaCl}_2\text{-HCl}$, cond. meas. at 298.15 K, anal. using Lee and Wheaton eqn. 7-16792
 $\text{Ca(AlCl}_2)_2\text{-SOCl}_2$ cells, cond., C cathode performance improvement 7-13851
 CdCl_2 , aqs., cond. meas. at 298.15 K, anal. using Lee and Wheaton eqn. 7-16792
 CdCl_2 solns., aqs., dil., transport nos. determ. at 298.15 K 7-16793
 Cl^- , limiting ionic cond. in aq. soln., mol. dynamics simulation 7-44879
Co complexes and related cpds., aq. soln., densities, viscosities and electrolytic cond. (*Japanese*) 7-12347
 HCl-SrCl_2 mixed electrolyte, thermodynamic study, appl. of Pitzer's eqns. 7-33940
 K-Cl melts metal-nonmetal transition, elec. cond. and optical reflectivity study 7-38457
 KBr-AgBr , binary molten mixtures, elec. cond. 7-12340
 $\text{K}_2\text{O-SiO}_2\text{-NaCl}$ melts, alkali cation dissociation determ., solidification temp., elec. cond. and cryoscopic meas. 7-12288

electrical conductivity of electrolytic liquids continued

KOH aq. soln., highly conductive, electrolytic conductivity meas. 7-3595
(Li, K)Cl, molten, internal cation mobilities 7-2243
 LiClO_4 , in polymer electrolytes, ion pairs triplet form., conductance meas. 7-32690
 $\text{Li}_2\text{O-SiO}_2\text{-NaCl}$ melts, alkali cation dissociation determ., solidification temp., elec. cond. and cryoscopic meas. 7-12288
 NH_4F in dioxane-methanol mixtures, assoc. constant. from cond. meas. 7-33939
 Na^+ , limiting ionic cond. in aq. soln., mol. dynamics simulation 7-44879
 $\text{Na}_2\text{O-SiO}_2\text{-KCl}$ melts, alkali cation dissociation determ., solidification temp., elec. cond. and cryoscopic meas. 7-12288
 Rb-RbCl melts, metal-nonmetal transition, elec. cond. and optical reflectivity study 7-38457
electrical conductivity of gases
see also space-charge-limited conduction
electric conductivity, freq. depend., of slightly nonideal plasmas 7-20872
electron swarms, electron diffusion tensors, conservation inelastic collisions effects 7-37618
high-temperature chamber elements, evaporation, effect on electrophys. props. of gases 7-44777
partially ionized gases, scalar DC electrical conductivity 7-51381
post-arc cond., circuit breaker arc, plasma parameters meas. 7-32183
tetrafluoromethane, electron conduction pulses, shortening by electron attachers 7-51382
tetrafluoromethane, electron conduction pulses, shortening by electron attachers 7-51383
Ar, electron swarms, collision cross sections 7-37619
 HCl-Ar gas mixtures, electron irradi., negative differential conductivity 7-63243
K, plasma, electron collisions, momentum transfer cross sections, expt. data fit 7-20845
Na, vapour, light-induced current calcs. and meas. 7-44096
 SF_6 , electronegative gas, electron beam transmission anomalies study 7-44094
Xe plasma, Cs additive, conc. depend. anal. 7-51399

electrical conductivity of liquids

see also electrical conductivity of electrolytic liquids
alkali metal atomic fluids, thermodynamic and electronic props. 7-45157
alloys, liquid, binary, high order perturbative effects 7-52085
atomic liquids with mol. impurities, similarity law for kinetic coefficients of hot electrons 7-16999
caesium pentadecafluorooctanoate-water discoid micelle solns., order-disorder transitions, X-ray scatt., elec. cond., NMR meas. 7-26949
Carnauba wax, liq., complex impedance 7-17026
crown ether-anion radical salt complexation, electrical cond. investig. 7-58842
dielectric liquids, charging current and conductivity 7-57202
dielectrics, elec. cond. and dielec. breakdown 7-45932
2-(2-hydroxy-4-alkoxybenzylideneamino)-9-methylcarbazoles, photocond. props. 7-38631
liquid methane, mobility of injected electrons, calc. 7-38564
metals, multiple scattering effects, cluster calcs. 7-7100
metals and alloys, electrical resistivity and finite mean free paths 7-45266
pentacyanobiphenyl, ionic mobility, viscosity, Walden's rule 7-21498
polymer solns., scaling laws for charge transport 7-17002
 Ag-Ge liq. eutectic alloys, elec. resist. and struct., 600 to 900 K (*German*) 7-45334
 $\text{AgI-Ag}_2\text{MoO}_4$ system, conductivity in the liquid and glassy states 7-44881
 AgNO_3 , electrical resistance effects accompanying high pressure and temperature melting and decomposition 7-16719
 $\text{Ag}_3\text{S-Ag}_2\text{Se-Ag}_2\text{Te}$, quasi-binary systems, elec. conductivity, thermoEMF 7-21908
 $\text{Ag}_2\text{S(Se)-Ag}_2\text{Te(Se)}$ liq. and glassy semicond., activation energy of carrier thermal generation, elec. meas. 7-17035
 $\text{Ag}_3\text{S(Se)(Te)-Cu}_3\text{S(Se)(Te)}$ liq. and glassy semicond., activation energy of carrier thermal generation, elec. meas. 7-17035
 AgTiTe , molten, struct. factors and radial distrib. functions, X-ray diff. meas. 7-26617
 Al-Mg , liq., excess entropy of mixing, resist. calcs. 7-2571
 Bi , liq., elec. resist. meas. 7-38532
 Bi-Ga , liq., elec. resist. meas. 7-38532
 Co-Ce(Pr) liquid alloys, variable valency investig. 7-7192
 $\text{Co(NO}_3)_2 \cdot 6\text{H}_2\text{O}$, electrical resistance effects accompanying high pressure and temperature melting and decomposition 7-16719
 Fe-Ce(Pr) liquid alloys, variable valency investig. 7-7192
 FeCO colloids, anisotropy in elec. cond. induced by external field 7-39924
 Ga , liq., elec. resist. meas. 7-38532
 Ge-Te liq. eutectic alloys, elec. resist. and struct., 600 to 900 K (*German*) 7-45334
 H_2O , Raman spectroscopy during the passage of strong shock waves 7-22271
 $\text{I}_2\text{-KI-S}_8$ melts, percolative cond. calcs. 7-6845
 KH_2PO_4 solution, elec. cond., temp. and conc. depend., 10 to 70°C 7-2242
 Kr , liquid, electron mobility meas. 7-2614
 Li-Mg , liq., excess entropy of mixing, resist. calcs. 7-2571
 N , shock compressed, elec. cond. meas. 7-33019
 N_2 , liquid, molecular dissociation and shock-induced cooling at high densities and temperatures 7-28307
 Na-Ga , liq., phase diagram and electrical resistivity 7-21408
 Na-Pb liq. alloy, thermodynamic prop. and transport coeff. 7-64199
 Ni-Ce(Pr) liquid alloys, variable valency investig. 7-7192
 Se-Te-Au(Ag) liq. mixtures, electronic props. 7-64247
 $\text{TiS}_2\text{-Cu}_2\text{S}$ melts, ionic-electronic conductivity 7-33057

electrical conductivity of one-dimensional systems *see one-dimensional conductivity*

electrical conductivity of plasmas *see plasma transport processes*

electrical conductivity of solids

see also electrical conductivity of amorphous metals and alloys; electrical conductivity of amorphous semiconductors and insulators; electrical conductivity of crystalline metals and alloys; electrical conductivity of crystalline semiconductors and insulators; electronic conduction in crystalline semiconductor thin films; electronic conduction in insulating thin films; electronic conduction in metallic thin films; ionic conduction in solids; recovery; superconductivity

electrical conductivity of solids continued

- 1D chain with random distribution of linear side branches and loops, electronic props. 7-64191
- 3D continuum percolation systems, nonuniversal behaviour of conductivity exponent, exptl. obs. 7-38656
- aniline, substituted, polymerisation and characterisation 7-33929
- $\text{Au}_x(\text{TeO}_2)_{1-x}$ thin films, nanosecond laser annealing, Au cluster redistribution, growth and coalescence 7-12145
- (BEDT-TTF) $_2\text{BrI}_2$, synthesis, structure and electrical props. 7-46296
- β -(BEDT-TTF) $_2\text{AuBr}_2$, conducting charge transfer salt, struct. and props. 7-58259
- β -(BEDT-TTF) $_2\text{I}_3$, high T_c superconducting state, effect of high-temp. phase transitions, c^* resistivity study 7-58934
- BEDT-TTF radical cation salts, synthesis, conducting and superconducting props. 7-64855
- (BMDT-TTF) $_2\text{Au}(\text{CN})_2$ organic metal, synthesis, struct. and props. 7-32420
- brine-saturated fractured rock, elec. cond. for various confirming press. 7-29002
- ceramic oxides, cond., for use as molten carbonate fuel cell electrodes 7-13854
- compact tension specimens, crack length measurement by pot. drop method, improved anal. 7-31695
- composites, quantitative microstruct. effects (German) 7-17666
- continuum percolating systems, transport exponents, ϵ expansion 7-4786
- cylinders, pairs and square array, transport props., multiple coeffs. 7-32973
- cylindrical electrical conductor, heat transfer eqn. soln. using optimal linearization method 7-57672
- dielectrics, conference, Erlangen, W.Germany (July 86) 7-35099
- disordered electronic systems, scaling theory for freq. depend. conductivity 7-58790
- disordered metal-nonmetal mixtures, percolation, anisotropic conductivity, Hall effect, thermopower 7-52555
- disordered systems, activated processes, logarithmic scaling and 1/f noise power spectrum 7-61248
- disordered two-dimensional system in strong magnetic field and random potential, conductivity calcs. 7-58788
- electron-electron interaction effects on Aharonov-Bohm effect 7-12689
- extended s-f model, elec. cond. calc. 7-64194
- fibre reinforced composite with barrier coatings on fibres, diffusional interaction of components effect on cond. 7-52167
- fibre-reinforced composites, effective properties, effects of polydispersity in fibre diameter 7-6702
- granular metals with potential disorder, conduction 7-52554
- graphite, powder, elec. resistivity, rel. to degree of comminution 7-45257
- graphite, resistivity at high temp. calc., anisotropy, temp. depend. 7-52556
- graphite fibre, benzene-derived, exfoliation and characters. 7-46663
- graphite intercalation compound, C_{1-x}F_x , resistivity and ESR study 7-64197
- graphite intercalation cpds., staging dislocation electronic struct., electron scatt. rates, residual resist. 7-52558
- graphite-Br intercalation compound, electromech. effect on heating 7-45414
- graphite-CuCl $_2$ intercalation cpd., ideal resistivity studies 7-32976
- graphite-K intercalation cpd., KC_{24} , kinetically-hindered low-temp. staging transition, P-T phase diagram, resist. anomaly meas. 7-6786
- HMTTeF-TCNQF $_4$ solid complex, partial charge transfer, Raman and XPS studies 7-32967
- incident carrier flux consequences in electric transport 7-64195
- inhomogeneous material, resistive breakdown 7-52714
- ion-implanted polymers, fractal elec. cond., current transients, percolative transition calcs. 7-2645
- many channel disordered system, transmission, localization length distrib. and one parameter scaling 7-2563
- metal, universal conductance fluctuations, effects of finite temp., interactions and mag. field 7-64196
- metal matrix composites, transverse elec. cond. model 7-45415
- metal sheets with randomly drilled holes, nonuniversal critical behaviour meas. 7-45259
- metal-insulator composite mean-field theories, DC cond. and percolation threshold calcs. 7-45253
- normalised conductance scaling functions forteperature-dependent systems 7-7197
- one-dimensional disordered system, elec. resist., statistical props. 7-27310
- organic charge transfer solids; review 7-7222
- penanthrene-TCNQ complex, physical props. 7-52622
- Penrose lattice, 2D, DC cond., recursion method calcs. for tight-binding Hamiltonian 7-64192
- periodic composite materials, effective transport props., multipole coeffs. 7-32974
- periodic solid, one-dimensional, Schrodinger eqn. soln. for electron in uniform electric field 7-56078
- poly(p-phenylene) films, elec. cond. enhancement by heat treatment 7-64361
- poly(p-phenylene) films, heat treated, electrical conductivity, thermoelectric power 7-52557
- poly m-phenylene sulphide, SbF_6^- doping, elec. cond., IR spectra 7-17006
- poly-p-phenylene:K, heavily doped, elec. cond., chain length depend. 7-32975
- polyacetylene: K(Rb)(Cs), elec. cond. temp. depend. meas. 7-17030
- polycarbonate-C black composites, TEM obs. of percolation threshold 7-12771
- polydiacetylene, conductivity enhancement by chemical doping and ion implantation 7-21957
- polydiacetylene Langmuir-Blodgett films, ion beam irradiation 7-6690
- polyethylene, exfoliated graphite filled, elec. props. 7-38986
- polymer films, I-doped, prep. by glow discharge polymerisation, elec. conductivity 7-22584
- polymeric materials, electrical conductivity mechanisms (Korean) 7-52604
- polynaphthylene films, elec. cond. enhancement by heat treatment 7-64361
- polypropylene, electrical cond., temp. and thickness depend. 7-38655
- polypropylene films, Cu-filled, struct. and elec. cond. 7-64301
- polyvinylidene fluoride/PZT, composites, dielec. behaviour 7-38992
- PVC, metal-filled, compensation effect 7-64300
- quasi-one-dimensional wire, cond., thermopower, effect of lifetime broadening 7-45252

electrical conductivity of solids continued

- α -quinqueithiophene-stearic acid: I Langmuir-Blodgett films, elec. cond. 7-33106
- random Hubbard alloys, localisation-affected conductivity, numerical studies 7-45223
- random resistor and random supercond. networks, multiscaling approach 7-17000
- rheology, conf., Ann Arbor, MI, USA (Oct. 1985) 7-18481
- semiconductors, processing and charactn. techniques, conf., Los Angeles, CA, USA (Jan. 1986) 7-18489
- silicone rubber, vulcanised, elec. props. 7-7302
- strongly disordered systems, conductor-insulator transition 7-64087
- synthetic sulphide bearing rocks, complex resist. 7-8918
- textured materials, effective transport coeffs. 7-45251
- thermal and electrical conductivity investigation in solids at high temp. 7-32730
- TTF-TCNQ complexes, intramolecular charge transfer 7-7241
- two-component composite, elec. and thermal cond., Bergman-Milton theory of bounds appl. 7-23635
- $\text{Al}_2\text{O}_3\text{-TiO}_2\text{-NaO}_{1/2}$ system, elec. cond. meas. to detect suspected liq. phase 7-39467
- Au complex, $\text{Au}_{55}(\text{PPh}_3)_{12}\text{Cl}_6$, high-nuclearity cpd., DC conductivity 7-33016
- Au-polymer composite thin films, elec. behaviour 7-52856
- Ba ferrite filled styrene-isoprene-styrene composite, dynamic mech., elec. and mag. props. 7-13001
- Br_3^- , electrical cond. mechanism, tight-binding and ab initio pseudopot. calc. 7-52546
- C sputtered films, ion enhancement, struct. prop. relationships studies 7-52332
- C-Sn composite sputtered films, ion enhancement, struct. prop. relationships studies 7-52332
- C-Ti composite sputtered films, ion enhancement, struct. prop. relationships studies 7-52332
- $\text{C}_3\text{S}_2\text{F}_6$ fibre intercalation cpds., enhanced elec. cond. 7-33927
- (CSe) $_n$, polymerised, metallic and supercond. 7-7433
- I_3^- , electrical cond. mechanism, tight-binding and ab initio pseudopot. calc. 7-52546
- InSb-NiSb eutectic composite, rel. between metal fibre morphology and elec. props. 7-59644
- $\text{In}_{2-x}\text{Sn}_x\text{O}_{3-y}/\text{Ag}/\text{In}_{2-x}\text{Sn}_x\text{O}_{3-y}$ magnetron sputtered transparent heat-reflective films, thermal stability study 7-53426
- $\text{K}_3\text{Cu}_2\text{S}_6$, mixed valence 2D metal, CDW 7-45294
- $\text{Li}_{0.33}\text{MoO}_3$, stoichiometric triclinic bronze, cryst. struct. 7-6600
- Mo_4Se_8 , superconductivity and metal-insulator transition (Russian) 7-58742
- SbCl_5 intercalated graphite, stage 2, basal plane resistivity and phase diagram 7-45258
- SnO_2 :glass, thick film, elec. resistance, effect of struct. 7-7300
- TiC-WC-TaC-Co hard metals, Ta conc. effect on comp. and physicochem. of carbide and Co phases 7-53708
- TiO_2 , elec. resist. meas., 1023-1323K 7-38531
- VO_2 , elec. resist., Seebeck coeff. meas., 1023-1323K 7-38531
- ZnO , glass-doped, prep., elec. props. and degradation phenomena 7-13425
- $\text{ZnO}/\text{Ag}/\text{ZnO}$ magnetron sputtered transparent heat-reflective films, thermal stability study 7-53426
- electrical conductivity transitions**
see also metal-insulator transition
- amorphous chalcogenide alloy, multicomponent, threshold switching phenomena 7-52709
- anisotropic composites, kinetic Hall and seebeck coeffs., critical behaviour calcs. 7-45411
- β -(BEDT-TTF) $_2\text{I}_3$ organic conductor, high resolution thermal expansion meas. 7-26986
- (BEDT-TTF) charge transfer complex, phase transition 7-52703
- α -(BPDT-TTF)(Ni(dmit) $_2$) $_2$ struct. phase transition accompanied by change of electronic struct. 7-52704
- charge transfer complexes, one-dimensional conductors, nonlinear conduction, electrical switching 7-2648
- conducting polymer films produced by Ar^+ irradiation of HPR-204, physical and elec. props. 7-26808
- disordered 2D system, AC cond., anomalous permitt. 7-45406
- fluoranthrene radical cation salts, mag. resonance anal. of phase transition 7-52705
- (fluoranthenyl) $_2\text{AsF}_6$, metal-semiconductor transition, anisotropic diffusion and electron spin relaxation 7-52598
- ion-implanted polymers, fractal elec. cond., current transients, percolative transition calcs. 7-2645
- metal-insulator transition, critical conductance 7-64084
- metals, strongly coupled, universal disorder-induced resistivity behaviour 7-21954
- narrow energy band-systems, insulator-metal transition 7-38455
- one-dimensional incommensurate systems, DC cond., metal-insulator phase diagram 7-21818
- one-dimensional metals, Peierls problem solns. (Russian) 7-45304
- poly(p-phenylene vinylene) films, highly graphitisable, elec. conductivity, thermoelectric power 7-32916
- polythiophene film in electrochem. color switching cells, cycle life, stability and characters. 7-62815
- rare earth cpd. intermediate valence systems, charge ordering 7-7189
- switching, phase-slip model 7-52700
- (TMTSF) $_2\text{ClO}_4(\text{PF}_6)$, high field magnetoresist., quantum effects and phase transitions 7-45301
- (TMTSF) $_2\text{PF}_6$, unified phase diagram, magnetotransport data anal. 7-45410
- (TMTSF) $_2\text{X}$ Bechgaard salts, field-induced phase transitions 7-45409
- TTF-chloranil mixed-stack charge transfer crystal, domain wall dynamics 7-52702
- ultrasmall tunnel junctions, transition to ohmic conduction 7-2673
- Ag_2HgI_4 , photosensitivity near a superionic phase transition 7-41522
- $\text{As}_{0.45}\text{Se}_{0.55}\text{Te}_{0.45}$ glassy alloy, struct. model and switching props. 7-1904
- $\text{BaPb}_{1-x}\text{Bi}_x\text{O}_3$, supercond., struct. and elec. props. 7-58247
- Bi-Ge-S chalcogenide glasses doping mechanism and structural effects, EXAFS study 7-1909
- $\text{Bi}_{12}\text{Si}(\text{Ge})\text{O}_{20}$, light-induced field redistrib., photocond. studies 7-38623
- CdGeAs_2 :Ni amorphous films, elec. cond., low temp. impurity breakdown, high field effects 7-52625
- Cu-SiO_2 -Cu sandwich struct., thermal voltage memory effect, time depend. 7-45527

electrical conductivity transitions continued

- Fe₂Mn_{1-x}S, high temp. metal-nonmetal transition 7-7117
 Fe_{0.94}O, metallisation at elevated press. and temp., shock wave elec. resist. meas. 7-7297
 GaAs, electron beam irradi., carrier density, anomalous temp. depend. 7-52610
 GaAs, internal thermal conversion, material for integrated circuits 7-12767
 GaAs, semi-insulating, switching effect, deep level spectroscopy appl. 7-38630
 GaAs/Langmuir-Blodgett MISS devices, switching characts. 7-38751
 GaSb:Se, resist. and thermoelec. power meas. at metal-insulator transition 7-45403
 Gd₂Si_{1-x}, x=0.18, 0.59, 0.87, amorphous, thermal, elec. and mag. props. 7-53039
 Ge, electron irradi., annealing kinetics, impurity effects 7-16630
 Ge, n-type and ultrapure samples, electron transport and press. coeffs. 7-2615
 p-Ge, threshold switching and microwave-induced spontaneous emission in static magnetic field 7-52707
 Ge₂₀S₈₀:Bi chalcogenide glasses, doping, coordination number and cond. transition, EXAFS study 7-64764
 a-Ge₂₀Se₇₀:Bi films, n-type, electron transport props. studies 7-7422
 HgCdTe, 0⁻ giant oscillation near semimetal-semiconductor transition 7-64053
 Hg_{0.79}Cd_{0.21}Te, metal-insulator transition, mag. field induced, low temps. 7-45158
 Hg_{1-x}Cd_xTe with metallic donor clusters, anomalous Hall effect below mag. field induced metal insulator transition 7-2485
 In₂O₃ 3-D disordered samples, Anderson transition, finite temperature aspects 7-7118
 InSb amorphous films, metal-semicond. transitions, superconductivity 7-64085
 InSb, metal-insulator transition, mag. field induced, low temps. 7-45158
 InSb with metallic donor cluster, anomalous Hall effect below mag. field induced metal insulator transition 7-2485
 K_{0.3}MoO₃, switching, intermittent oscillations 7-52699
 La₂Mo₂O₇, quasi-2D single cryst. struct. and electronic props. studies 7-58238
 Mo₃O₂₃, low-dimensional conductors, inelastic neutron scatt. study 7-52701
 Mo_{0.9}-W_{0.1}O_{3n-1}, electrical conductivity, mag. susceptibility and IR spectra 7-38546
 Nb, thin film, microstrip line, parameter change during superconducting to normal conducting state switching 7-22075
 (NbSe₄)_{10/31}, AC conductivity, dielectric constant 7-52591
 (NbSe₄)₂, lattice vibrs. at CDW transitions 7-51973
 Ni₂Fe_{3-x}O₄, elec. cond., thermoelec. power meas., 10-300K 7-38648
 NiSi_{1-x}Se_x, effect of Se substitution on mag. and electrical transition 7-2846
 PbLiInSe, intercalation-layer compound, dielectric-metal cond. transition 7-7230
 SbI₃ film, photosensitive, heating effect on elec. cond., switching behaviour 7-58920
 Si, superconducting high-press. phases, occurrence and props. 7-2646
 Si-Te-As-Ge chalcogenide glass film, electronic processes in strong elec. field 7-45524
 SmSe, thermoelec. power, elec. resist., meas. near semiconductor-metal transition, press. up to 12 GPa 7-45404
 β-Sn, superconducting high-press. phases, occurrence and props. 7-2646
 (TaSe₄)₂I, AC conductivity, dielectric constant 7-52591
 (TaSe₄)₂I, chain-like conductor, Peierls gap, optical study 7-52469
 (TaSe₄)₂I, lattice vibrs. at CDW transitions 7-51973
 (TaSe₄)₂I, low-dimensional conductors, inelastic neutron scatt. study 7-52701
 Tb₂Si_{1-x}, x=0.18, 0.59, 0.87, amorphous, thermal, elec. and mag. props. 7-53039
 V₂O₅-TeO₂ glasses, memory switching 7-27370

electrical contacts

- see also contact potential; contact resistance; ohmic contacts; point contacts*
 surface, two-dimens. FTIR mapping 7-48882
 Ag contacts, transparent, for a-Si solar cells with ITO antireflection coating 7-65478
 Ag specimen, contact resist. meas., deform., fretting effects 7-9848
 Al/Si contacts, diffusion at room temp. (German) 7-32724
 Cu-composite material contact, sliding characts. and contact resistance (Japanese) 7-8120
 Cu-Cu contact, sliding characts. and contact resistance (Japanese) 7-8120
 Cu-graphite contacts prep. using atomised Cu powder 7-27976
 Mo-Ag, pseudoalloys, Ni and Co effect on interphase interaction 7-27975
 Pd and alloy contact finish performance and cost 7-3508
 Pd-Ag alloy electroplated coating contact and corrosion resistance and wear 7-3509
 TaIr-GaAs Schottky barrier contacts 7-17102
 W-Ag pseudoalloys, Ni and Co effect on interphase interaction 7-27975
 W-Cu-Ni contact materials, elec. props., particle size effect 7-2672

electrical double layers *see electrochemistry; liquid theory***electrical engineering**

- see also high-voltage engineering*
 seismic support of electronic and computer equipment, design of raised floor systems 7-4003

electrical engineering applications of computers *see electrical engineering computing***electrical engineering computing**

- see also computerised control; computerised instrumentation; electric machine analysis computing; power system analysis computing*
 2D electrostatic and EM problems, general interactive finite element package 7-62569
 batteries, Ni-Cd, Goddard model for aerospace apps., alterations using computer simulation 7-34017
 dielectrics, elec. fields, computer calc. 7-42837
 exploding metallic foils time-dependent behaviour and hydrodynamic expansion, computer model 7-32036
 field computation, finite-element and boundary-element methods combined (Chinese) 7-10822
 solar photovoltaic and thermal collector, theoretical anal. and design 7-54347

electrical engineering computing continued

- thermal power stations, SO₂ pollution forecasting 7-55244
 GaAs solar cells with corrugated surface, computer code for performance eval. 7-3667
 Si:H, amorphous, dendritic web, Czochozalski flat plate modules and concentrator module, price comparison 7-17904
electrical fault location *see fault location*
electrical faults
see also accidents; discharges (electric); fault currents; fault location; flashover; insulation; losses; overvoltage; protection; testing; transients
 escalating arcing ground fault phenomenon, effect of preventative solns. on equipment specifications 7-51530
 RFX fusion expt., Italy, power supply protection against plasma disruption and fault conditions 7-30668
electrical forming *see electroforming*
electrical insulation *see insulation*
electrical noise *see noise*
electrical power systems *see power systems*
electrical properties of substances
see also dielectric properties of substances; discharges (electric); electrical conductivity; flexoelectricity; thermoelectricity
 actinide metal, compound and alloy props., conference, Aix en Provence, France (Sept. 1985) 7-9579
 inorganic layered cpds., reactivity, conf., New York, NY, USA (Apr. 1986) 7-41003
 magnetic materials, conference, Freudenstadt, Germany (April 1986) 7-48144
electrical resistance measurement *see electric resistance measurement*
electrical resistivity *see electrical conductivity*
electrical transport processes *see electrical conductivity*
electricity
see also atmospheric electricity; electric charge; electric current; electrical properties of substances; electromagnetism; terrestrial electricity
 development of theory of electricity 7-35151
electricity supply industry
 cloud-to-ground Lightning Position and Tracking System for electric utility weather problems 7-14371
 Inter-RAM conference, Syracuse, NY, USA (June 1986) 7-9592
electro-oculography *see bioelectric potentials; eye*
electro-optical devices
see also electrochromic devices; liquid crystal devices; optical modulation
 acoustoelectrooptic multichannel spectrum analyzer 7-50714
 bistable devices, graphical anal. of dynamic response 7-15922
 CW laser power stabilisation, using electrooptic modulator 7-1203
 developments in integrated optical components (German) 7-50789
 digital and quasi-linear electrooptic modulators synthesized from directional couplers 7-50727
 dilatometer based on electro-optical meas. technique 7-41338
 directional coupler switches, Δφ phase reversal, crosstalk characts. 7-26037
 directional coupler switches, crosstalk due to reversed-Δφ electrode misalignment 7-20471
 dye laser, tunable, with electro-optic Q-switching of coupled laser, characts. 7-1197
 fast measurement techniques for research in dielectrics 7-30034
 fibre optic sensors, piezoelectric copolymer jacketed single-mode fibers forelectric-field sensor application 7-6011
 fibre-optic sensors, developments and A/D signal conversion problems (German) 7-26019
 frequency shifters appl. in heterodyne interferometric systems 7-18866
 guided-wave optical devices, electro-optic materials 7-37134
 hybrid bistable systems, periodic states with fractional freqs. 7-57398
 III-V semiconductor electrooptic waveguide modulator, microwave performance prediction 7-43349
 integrated optical combinatorial logic using electro-optic Bragg gratings 7-26040
 integrated optical devices, review (Spanish) 7-37208
 integrated quantum well self-electro-optic effect device using 2X2 array of optically bistable switches 7-11176
 Kerr effect voltage measurements on multi-megavolt pulsed power accelerators 7-25286
 laser double-pulsed velocimetry, image shifting technique to resolve directional ambiguity 7-37559
 logic gate using spatial light modulator and interference fringe shifting 7-43351
 long gap discharges, electric field meas. using a Pockels device 7-4822
 meteor observation systems, techniques and results of electro-optical obs. 7-47716
 microchannel spatial light modulator with improved resolution and contrast ratio 7-25954
 microwave pulse photonic meas. using electro-optic and fibre-optic components 7-25983
 modulators, total internal reflection, with multimode strip lightguides 7-43355
 multichannel optoelectronic processor with correlation-function processing 7-25740
 multilayer interference laser light modulator, optical bistability 7-25950
 nematic twisted configurations with nonzero pretilt angles, director patterns, numerical calcs. 7-11898
 notch filter, narrow-band electro-optic tunable 7-37114
 optical computing, bistable devices, fast response/low-energy 7-25941
 optical parallel logic operation with microchannel spatial light modulator 7-25731
 parallel logic gate using Pockels effect modulators, fundamental components for optical digital computing 7-43347
 photo-emitter membrane spatial light modulator 7-37135
 planar waveguide, electro-optic light deflection, optimal parameters anal. 7-37154
 polymer film, laser beam modulator and pulse former using electro-optic spectral hole burning 7-20288
 quantum well structures, electro-optic props., device applications (Japanese) 7-22223
 quantum well structures, linear optical props. elec. field depend. waveguide electroabsorpt. and sum rules 7-13133
 radiometry and the military 7-48826
 relativistic electron beams, time-resolved studies with subnanosecond Cerenkov electro-optic shutter 7-49757
 review of electro-optic devices, Pockels cell 7-50729

electro-optical devices continued

- rod-plane gap, space-charge behaviour evaluation using Pockels' cells 7-20980
 SAW acousto-electron-optic device, Raman-Nath regime meas. and calcs. 7-20550
 scanning polarisation/interference contrast microscopy, linear imaging 7-9895
 SDI driving optics development 7-48824
 semiconductor quantum wells, optical modulators and bistable devices using self-electro-optic effect 7-5990
 SHG, critically phase matched, electrooptic tuning 7-43213
 shutter, large-aperture, with liquid electrodes 7-20248
 solid-state ring and linear lasers with electro-optic Q-switching, numerical modelling 7-36999
 spatial light modulator, electron beam addressed 7-25955
 spatial light modulator, high-gamma, for nonlinear optical processing 7-25959
 spatial sampler using integrated optic techniques, electrooptic directional couplers 7-31524
 speckle interferometer based remote electro-optic displacement sensor 7-48838
 switch for providing active feedback to solid laser 7-1205
 telecommunications using integrated optics including wave conductors and electro-optical couplers (*German*) 7-50790
 travelling-wave modulators, ultrafast, with reduced vel. mismatch 7-50730
 tunable filters, active guided wave devices, coupled mode anal. 7-62829
 waveguides, electrooptic light modulation by fringing field of Gunn domain 7-57534
 AlGaAs-GaAs MQW CCD spatial light modulators using electroabsorption effects 7-20407
 CO₂ laser pumping source for CH₂F₂ laser, Stark cell stabilisation 7-43134
 CdS_xSe_{1-x} crystal waveguide Bragg light modulators 7-1288
 FeSi₂ thin films, appl. to electro-optic VLSI interconnects 7-53427
 GaAs biased semi-insulating, cross modulation effect 7-50731
 GaAs inverted rib, phase modulators grown by VPE, optical and electro-optical anal. 7-31450
 GaAs PIN electro-optic travelling-wave modulator at 1.3 μ m 7-1287
 GaAs/GaAlAs double-well superlattice, ultra-fast optical modulator 7-52801
 GaAs-AlGaAs MQW electroabsorpt. modulator for non-resonant optoelectronic logic gate 7-37139
 GaInAsP strip-loaded planar waveguide for high-speed electroabsorpt. modulator 7-31449
 InGaAs-InAlAs MQW structure, anisotropic electroabsorpt. and optical modulation 7-13134
 InGaAs-InAlAs multiple quantum wells, long wavelength optical modulation, electro-optical effects 7-7677
 InGaAsP/InP multiple quantum well waveguide phase modulator 7-57531
 LiNbO₃ electro-optic freq. translators for coherent optical fibre systems 7-25953
 LiNbO₃ integrated optical components for optical communication appls. (*German*) 7-37210
 LiNbO₃ waveguide electro-optic freq. translators, appl. to coherent optical fibre systems 7-20468
 LiNbO₃ waveguide mode extinction modulators, design 7-26030
 LiNbO₃:Ti 4×4 directional coupler switch with permanently attached polarisation maintaining fibre array, low crosstalk 7-31520
 LiNbO₃:Ti 4×4 nonblocking interconnection network for test bed, video switching 7-26039
 LiNbO₃:Ti channel waveguide electro-optic cutoff modulator 7-43353
 LiNbO₃:Ti electro-optic Mach-Zehnder waveguide modulators, 1.51 μ m operation, optically induced drift effects 7-20404
 LiNbO₃:Ti integrated electro-optic devices, modelling and beam propag. anal. 7-11177
 LiNbO₃:Ti integrated optical devices, domain inversion effects 7-62849
 LiNbO₃:Ti modified 1×2 directional coupler waveguide modulator 7-1259
 LiNbO₃:Ti X- and Z-cut directional coupler and BOA switches, voltage-length product 7-43352
 PLZT light shutter for color viewfinder and video projector appl. (*Japanese*) 7-20398
 PLZT transparent ceramic modulator, visual classroom demonstrations appl. 7-4647
 Ti:LiNbO₃ optical switch, three-electrode 7-15970

electro-optical effects

- see also electroabsorption; electrochromism; electroluminescence; electroreflectance; Kerr electro-optical effect; photorefractive effect; Pockels effect; Stark effect
 bicyclo(2.2.2)octane esters, mesogenic, transition temps., viscosity, birefr., electro-optical characts. 7-1863
 Cherenkov radiation generation by femtosecond optical pulses in electro-optic media 7-27808
 chiral smectic liquid crystal cells, bistability and switching 7-37842
 chiral smectic-C liq. cryst., light diff. props. in external elec. field 7-64604
 cholesteric-nematic transition, electrooptic characteristics, control (*Russian*) 7-16741
 crystalline donor-acceptor complexes, vibronic coupling in charge-transfer states 7-52542
 diatomic polar molecules, radiation spectrum, plasma elec. field effects 7-19956
 electrogyratory communication device 7-25951
 ester type smectic C* liquid crystal, ferroelectric polarisation props. 7-13100
 ferroelectric ceramics, electromagnetic wave scatt. from dielec. permittivity tensor inhomogeneities 7-7629
 ferroelectric liquid crystal with negative dielec. anisotropy, switching behaviour 7-39084
 ferroelectric liquid crystals, electro-optics 7-39087
 ferroelectric liquid crystals, surface stabilised, disclination dynamics, switching process 7-58137
 holographic gains in electro-optic crystals with bipolar conductivity 7-20162
 liquid cryst. display, SBE type, fundamental characteristics (*Japanese*) 7-7670
 liquid cryst. display, SBE type, supertwisted nematic, display characts., effects of various parameters (*Japanese*) 7-7669

electro-optical effects continued

- liquid crystal cells, thin nematic, electro-optic behaviour 7-25957
 liquid crystal display, supertwisted transitions, theory 7-16410
 liquids, non-polarised IR spectra, electric field effects, transparent capacitor spectroscopic cell 7-35607
 material advances, book contrib. 7-25914
 MBBA, liquid crystal, electric field effects, cell for optical studies 7-44360
 molecular electro-optical materials, orbital symmetries 7-39086
 molecular fluid, elec. field induced second harmonic generation, orientational effects 7-50638
 molecular gases, absorpt. spectra, elec. modulation method 7-10553
 molecules, electrooptical anharmonism, parametric reson. generation 7-42660
 nematic liq. cryst. cell with cholesteric additive, electro-optic twist effect, structural effects 7-63449
 nematic liq. cryst. orientation and induction interaction effects on IR dichroism 7-39079
 nematic liq. crystals, molecular association, influence on dielectric and electro-optic props. 7-16407
 nematic liquid crystal, light scattering in elec. field 7-1843
 nematic liquid crystal film, quasi-static elec. field enhanced optical propag. effects 7-27702
 nematic liquid crystal films, laser-induced distortion, cavityless optical bistability due to thermal effects 7-57441
 nematic liquid crystals, negative dielec. anisotropy, near IR light scatt. 7-1844
 nematic liquid crystals, optical modulation, high-speed 7-37131
 nematic liquid crystals, torsional anchoring on substrates, birefringence study 7-1858
 nematic liquid crystals, diamagnetic anisotropy meas. 7-38845
 nematocholesteric mixtures with two-freq. control, electro-optical props. 7-59183
 nonpolar fluid, ellipsoid mols., induced birefringence and dielectric polarisation 7-33363
 nonrigid molecules, elec. birefringence, field strength depend. 7-45989
 nucleic acid purine bases, electrooptical props., finite perturbations CNDO/S3 calcs. (*Russian*) 7-25407
 organic molecules as nonlinear electro-optical materials 7-37024
 picosecond electro-optic sampling 7-53278
 polyatomic molecules, electrooptic parameters, valence optical theory 7-31088
 polydiacetylene pTS-FBS single crystal, electric field induced SHG 7-43214
 polyelectrolytes, transient elec. birefringence of rod-like polyions 7-39083
 polyethylene, low density, IR spectroscopy under high elec. stresses 7-39129
 polypropylene, IR spectroscopy under high elec. stresses 7-39129
 polysiloxane, liq. cryst., with side chains, elec. field effects 7-11883
 polysiloxane side chain liq. crystals, optical and electro-optical props. 7-16387
 purple membrane, electric polarisability, electrooptic scatt. spectra anal. 7-54530
 quantum well structures, electro-optic props., device applications (*Japanese*) 7-22223
 rigid molecules, elec. birefringence, field strength depend. 7-45989
 semiconductors, intermediate valence, theory 7-38526
 thin films, conference, India (Jan. 1985) 7-4619
 thin noncentrosymmetric crystals, Rayleigh scatt. of light 7-7710
 toroidal mag. materials, magneto- and electro-optical effects 7-45994
 transparent ferroelectric ceramics, cryst. chem. and struct. props. and modifications 7-6590
 TTF-chloranil mixed-stack charge transfer crystal, domain wall dynamics 7-27202
 ultrafast optical electronics from femtoseconds to tetrahertz 7-45993
 waveguides, electrooptic light modulation by fringing field of Gunn domain 7-57534
 Al_{0.3}Ga_{0.7}As-GaAs quantum well structure, electric-field-induced optical modulation, theory using Monte Carlo approach 7-17077
 Ba_{2-x}Sr_xK_{1-y}Na_yNb₂O₇, ferroelectric tungsten bronzes, crystal growth and optical appl. 7-39085
 BaTiO₃, electro-optic props. 7-39088
 BaTiO₃, ferroelectric, optical switching 7-37020
 Bi₁₂GeO₂₀, electrogyratory and electrooptic coupling 7-27701
 Bi₂GeO₁₂ single cryst. growth, characterisation and appls. 7-33550
 Bi₁₂SiO₂₀ crystals, electrooptic consts. dispersion determ., linear approx. calcs. 7-53270
 Bi₁₂SiO₂₀, electrogyratory and electrooptic coupling 7-27701
 Bi₁₂SiO₂₀ photorefractive gratings, buildup and decay, effect of electric field 7-17306
 Cd₂Nb₂O₇, ferroelectric, electrooptic props. 7-59180
 CsH₂AsO₄ crystals, electrogyration effects investig. 7-3022
 CuInSe₂ large grain (112) oriented thin films grown by RF sputtering, solar cell applications 7-17422
 GaAs p-n junction, space charge region, electrooptic effect investig. 7-52756
 GaAs-Al_{0.3}Ga_{0.3}As SQW structure, photolum. switching by pulsed elec. field 7-13197
 GaAs-Al_{0.3}Ga_{1-x}As, p-n junction waveguide, phase modulation, orientation depend. 7-57536
 GaAs-GaAlAs quantum wells, nonlinear optics and electro-optics 7-52809
 Ge light hole Landau level inversion, light amplification in crossed elec. and mag. fields 7-31293
 H-like atoms, spectral restructuring in magnetised plasma in quasimonochromatic elec. field 7-19776
 HCl, vibr. transition probabilities, reactive field effect 7-36584
 HF, vibr. transition probabilities, reactive field effect 7-36584
 HI, vibr. transition probabilities, reactive field effect 7-36584
 KCl doped crystals, impurity centres, form. processes and thermoactivation solution 7-44576
 K(H_{1-x}D_x)₂PO₄ crystals, electrogyration effects investig. 7-3022
 KTiOPO₄, electro-optic and dielectric props. 7-13129
 LiNbO₃ piezoelectric photorefractive crystal, hologram writing and reconstruction 7-57268
 LiNbO₃ proton-exchanged single cryst. optical waveguides, electro-optic effects, lattice const. and refractive index changes meas. 7-22220
 LiNbO₃:Fe, linear electro-optic effect, optical damage by He-Ne laser (*Korean*) 7-27698
 LiNbO₃:T surface, acousto-optic interaction, photoelastic and electro-optic contribs. 7-45982

electro-optical effects continued

- LiNbO₃:Ti, acousto-optical diffr. elastic strain and electric field effects 7-45985
- Nd laser with positive electro-optic feedback, mode-locked generation of transverse modes 7-1204
- PLZT ceramics (*Japanese*) 7-2981
- PLZT electro-optical ceramics, electron pulse irradiation-induced transient optical absorpt. study 7-6682
- PLZT ferroelec. ceramics, IR optical and electrooptical props. studies 7-7675
- PLZT, ferroelectric films, properties and applications 7-59156
- PLZT transparencies contrast increase, using electrically controlled light scattering 7-25909
- PLZT-PZN electro-optic ceramics, elec., opt. and switching props. 7-7646
- PbMg_{1/3}Nb_{2/3}O₃, ferroelectric, electrooptic props. 7-59180
- Pb(Se_{1-x}Nb_x)O₃, ferroelec. ceramics, IR optical and electrooptical props. studies 7-7675
- PbSnEuTe, superlattices, prep. by hot wall epitaxy, props. (*Japanese*) 7-12546
- PbTiO₃, ferroelectric films, properties and applications 7-59156
- RbH₂PO₄ crystals, electrogyration effects investig. 7-3022
- Si, electrooptical effects 7-59182
- Si:B p⁺-n-n⁺ solar cells fabricated using masked ion implantation, electro-optical characts. 7-23143
- Sr_{0.6}Ba_{0.39}Nb_{0.01}O₃:Ce crystals, light emission obs. during freq.-degenerate laser pumping 7-15947
- Sr_{1-x}Ba_xNb₂O₆, ferroelectric tungsten bronzes, crystal growth and optical appl. 7-39085
- Sr(La_{1/2}Nb_{1/2})O₃-PbZrO₃-PbTiO₃, hot-pressed ceramics, dielectric, piezoelectric and optical props. 7-64583
- SrTiO₃:H(D), O-H and O-D stretching vibrs. under applied electric field and uniaxial stress 7-44723
- ZnTeSeS, superlattices, prep. by hot wall epitaxy, props. (*Japanese*) 7-12546

electroabsorption

- anthracene, cryst., electroabsorpt. spectra resolution, nonlin. least-squares procedure 7-59181
- metal phthalocyanine films, electro-absorpt. spectra, charge transfer excitation 7-27695
- quantum well structures, linear optical props. elec. field depend. waveguide electroabsorpt. and sum rules 7-13133
- semiconductor quantum wells, optical modulators and bistable devices using self-electro-optic effect 7-5990
- semiconductors, electroabsorption of light by deep impurity centres 7-45988
- semiconductors, many-photon Franz-Keldysh effect in the field of two electromagnetic waves 7-45987
- semiconductors subjected to the fields of two interacting strong optical waves, Franz-Keldysh effect 7-53269
- AlGaAs-GaAs MQW CCD spatial light modulators using electroabsorption effects 7-20407
- GaAs:V, electromodulation spectra, deep level energy positions 7-38496
- GaAs/GaAlAs double-well superlattice, ultra-fast optical modulator 7-52801
- GaAs-AlGaAs MQW electroabsorpt. modulator for non-resonant optoelectronic logic gate 7-37139
- GaAs-AlGaAs quantum wells in waveguides, physics and appls. 7-26034
- GaAs-Ga_{1-x}Al_xAs superlattices, in appl. elec. field, interband optical transitions 7-53274
- GaInAsP strip-loaded planar waveguide for high-speed electroabsorpt. modulator 7-31449
- InGaAs-InAlAs MQW structure, anisotropic electroabsorpt. and optical modulation 7-13134
- InGaAs-InAlAs multiple quantum wells, long wavelength optical modulation, electro-optical effects 7-7677
- Li₂WO₃ films, free-electron electrochromic modulation 7-22359
- PbTe, interband absorption in a mag. field, exciton states 7-22227
- PbTe, low-voltage electroabsorpt., exciton states, magnetabsorpt. spectra 7-2501
- a-Si:H/a-SiN_x:H superlattices, interface defects and disorder 7-52306
- a-Si:H/a-SiO(N)_x:H multilayer films, interface electroabsorpt. meas. 7-2689

electroacoustic effects see acoustoelectric effects

electroacoustic generators see acoustic generators

electrocaloric effects see pyroelectricity

electrocardiogram see electrocardiography

electrocardiography

- see also bioelectric potentials; biomagnetism; cardiology
- ambulatory arrhythmia analysis: a dual-channel, Bayesian approach 7-40332
- ambulatory recordings, performance evaluation of algorithms for QT interval meas. 7-40343
- analysis, long term automated system, low cost microprocessor based implementation 7-40350
- arrhythmia detect. in Holter records: reliability of multi-lead vs. single-lead anal. 7-40355
- arrhythmia detector performance, confidence limits estimation 7-40335
- arrhythmia typification in a real-time anal. system for monitoring geriatric patients during exercises 7-40337
- automated arrhythmia anal. combined with ST anal. for exercise monitoring 7-34326
- baseline wander reduction using linear phase filters 7-18086
- body surface mapping, Nijmegen, Netherlands (June 1985) 7-48192
- chronic disease detection from EKG tracings, computer-aided technique 7-14151
- computer program for anal. of 12 simultaneous leads during an exercise test, precision and accuracy 7-40342
- computerised ECG interpretation, of right ventricular hypertrophy 7-65878
- computerised pattern recognition, Hilbert transforms and Wigner-Ville distributions 7-47265
- computerised system for 24 hr simultaneous recording and anal. of walking and ECG 7-40347
- coronary dilation, ECG-mapping: improvement of diagnosis and therapy control 7-28758
- data compression VCG anal., comparison of two algorithms 7-40356
- databases, software interface for arrhythmia detector evaluation 7-40336
- digital filter for electron instrumentation 7-47034

electrocardiography continued

- digital sampling of cardiac Purkinje fiber action potentials, maximum frequency components 7-18085
- dynamic arrhythmia filtration for gated blood-pool imaging: validation against list mode technique 7-40260
- ECG, dedicated cardiac signal processor 7-34303
- ECG interpretation online system using Bonner program 7-40325
- electrodes, recording and stimulating, for biological research 7-47306
- epicardial array ECG signals, myocardial ischaemia studies 7-14149
- epicardial array ECG signals, myocardial ischaemia studies 7-14150
- epicardial electric activation, knowledge based classification from array ECG signals 7-8752
- exercise ECG anal., versatile computer system 7-28743
- exercise ECG system, computerised, for phys. working capacity meas. 7-40339
- exercise ECG-testing, computerised, and ²⁰¹Tl scintigraphy: relative diagnostic accuracy 7-28757
- fibrillation waveform from normothermic and hypothermic myocardium, meas. and spectral anal. 7-28494
- filtering of vector signals based on the singularvalue decomposition 7-3916
- foetal ECG signal processing for implementation of foetal monitoring (*Chinese*) 7-18089
- frequency-domain QRS classification algorithm using an annotated ECG database 7-34307
- heart rate monitor, design, operation and construction (*Spanish*) 7-40327
- heart rate variability signal processing, diagnostic aid in cardiovascular pathologies 7-54800
- heart rate variations and EEG changes during nocturnal monitoring of ischaemic patients 7-34315
- HF, microcomputer-based analyser 7-54787
- Hilbert transform, appl. to ECG display and QRS detect. 7-40344
- Holter analysis, fourth generation computer aided system: Mk4 7-40331
- Holter ECG processing, distrib. 2-channel system 7-40349
- Holter ECG processing, improvement of morphology clustering through directed search techniques 7-40334
- Holter monitoring: indication, anal. quality and clinical satisfaction 7-40333
- Holter monitoring, computer-aided, use for S-T changes detect. 7-40348
- lead selection problem for measuring body surface maps of heart pots., parameter soln. 7-40345
- left ventricular diastolic function, scintigraphic meas., effects of ECG gating 7-34265
- linear phase filtering for distortion-free ECGs 7-34310
- linear-phase FIR filters for ECG processing 7-34309
- mapping, simulation in an analog heart-thorax model (*German*) 7-40083
- Markov-chain analysis of RR intervals 7-28498
- micropotentials recovery, advanced digital techniques 7-34304
- multi-lead ECG, respiratory signals derivation 7-28745
- multivariate characterisation of normal ST response derived from a computerised exercise ECG system 7-34325
- noise-dependent QRS delineation in exercise testing 7-34306
- nonlinear selective filter for electrocardiograph 7-60108
- oesophageal electrodes for recording His-Purkinje activity based on signal variance, evaluation 7-23469
- optimal averaging of cardiac signals, criteria 7-23471
- P wave recognition, CSE database in the development of a new algorithm 7-40340
- P-wave, algorithm for automatic detect. in single or multiple lead signals 7-28746
- portable continuous blood pressure monitor utilizing an M68705 microcomputer 7-28755
- power line interference estimation and removal 7-65863
- power spectral anal. of heart rate variability in sudden cardiac death 7-54788
- preexcitation syndromes, book 7-41020
- QRS complex detection under strong noise, real-time method 7-47266
- QRS detection rules, quantitative investigation using MIT/BIH arrhythmia database 7-54789
- respiratory information extraction by detect. of elec. axis variation 7-40346
- respiratory waveforms from ECG traces 7-18084
- rhythm analysis of arterial blood press, and ECG 7-54653
- RR-intervals during atrial fibrillation, heart rate stratified anal. from ambulatory tape recordings 7-34314
- RT interval in the 1st month of life, heart rate dependence 7-40133
- signal changes reconfiguration, using delta modulation (*Czech*) 7-60119
- signal processing methods for microcomputer-based automatic diagnostic system 7-47284
- spectral analysis of heart rate variability 7-3906
- ST segment shape recognition, automatic method 7-23476
- ST-T segment anal., template matching algorithm 7-34327
- subtle alternating ECG morphology as an indicator of decreased elec. stability, dog expts. 7-28497
- torsades de pointes: a characteristic spectral pattern in sudden cardiac death 7-3905
- vectorcardiography, continuous, in acute myocardial infarction 7-34302
- vectorcardiography, high quality system 7-34322
- ventricular ectopy, level changes in long-term recordings, detect. method 7-28744
- ventricular fibrillation, automatic detect. 7-18082
- ventricular fibrillation waveform characts. 7-34308
- whole-body γ -irrad., changes in ECG and haemodynamics (*Russian*) 7-8659
- Wolff-Parkinson-White anomaly, computerised ECG diagnosis 7-34323

electrocataphoresis see electrophoresis

electrochemical analysis

- see also electrochemistry; polarography; voltammetry (chemical analysis)
- α -aminoalkyl radicals, electrochemical detection, bond dissociation energies determ. using oxidation pots. 7-28286
- automatic polarisation curve analyser, polarographic study appl. 7-24634
- conductometer, microprocessor HF contactless, design 7-59808
- electroactive species, Fourier transform IR reflectron absorpt. spectra 7-23093
- microprocessor implementation 7-8353
- pyridine-l₂ complex, ionic dissociation, electrochem. investig. 7-54209
- solid-state resistive and electrochemical sensors in gas anal., review (*Spanish*) 7-39936

electrochemical analysis continued

- stainless steel, 304, strain effects on sensitisation developments, STEM/EDS and electrochemical potentiokinetic reactivation methods 7-54014
- surface analysis using XPS and electrochemistry 7-28370
- α -AgI ion-exchange reaction with β'' - Al_2O_3 - Na_2O , potentiometric study 7-54230
- Al complexes, Al (III)-amino acid complexes, stability const. determ., ionophoretic technique investig. 7-28381
- β'' - Al_2O_3 - Na_2O , ion-exchange reaction with α -AgI, potentiometric study 7-54230
- CO , personal exposure monitor with automatic data-logging 7-3943
- Ca^{2+} , ion-selective electrode, subnanomolar range detection limit 7-17833
- CdTe electrochemical sensor, sensitivity 7-65363
- Cr complex, Cr (III)-amino acid complexes, stability const. determ., ionophoretic technique investig. 7-28381
- Cu, anodic oxidation in KOH soln., in situ spectroelectrochemical anal. 7-28192
- Fe-tetrasulphonated phthalocyanines, photography, SERS and electrochemical studies 7-13155
- Fe_3O_4 - ZnFe_2O_4 system, thermodynamic props., EMF obs., X-ray diff. 7-22646
- H ion neutral carriers, for solvent polymeric membrane electrodes 7-17834
- InP, electrochemical C-V profiling 7-27325
- InP electrodes, surface modified, time resolved photoelectrochemical meas. 7-27415
- K^+ selective electrodes on valinomycin/PVC overlayers substrates 7-65375
- $\text{Na}_x\text{Mo}_6\text{O}_{24}$ intercalation cpd., struct., mag. suscept., X-ray diff. and electrochemical anal. 7-46842
- O_2 measurement with membrane-covered electrochemical Clark cell sensor 7-65367
- Si, MBE dopant profiling, electrochemical CV technique 7-12108
- Si MBE grown layers, arbitrary doping profiles 7-12109
- Si:Sb, pot. enhanced doping during MBE growth, elec., optical props., cryst. quality 7-12112
- Th complex, Th (IV)-amino acid complexes, stability const. determ., ionophoretic technique investig. 7-28381
- Zn, electrodeposition kinetics on Zn single crystals, pot. step method, SEM anal. 7-27189

electrochemical batteries *see cells (electric)***electrochemical electrodes***see also electrochemistry*

- accumulators, examination of graphite additive to electrodes 7-39984
- auxiliary electrode method for determination of ohmic resistance 7-35536
- Bi-Pb-Sn-Cd alloy negative electrode for secondary Li batteries (*Japanese*) 7-65435
- biological research, recording and stimulating electrodes 7-47306
- bipolar batteries with common electrolyte paths, leakage currents 7-28392
- corrosion rates determ., polarisation curves, mass transport effect 7-28191
- electrically conductive laser waveguide for in-situ spectroscopic study of rotating electrochem. electrode 7-5994
- Faraday impedance, connections for impedance elements (*German*) 7-17803
- fluidised bed, electrodes, mass transport 7-20789
- gas diffusion electrodes, diffusion resistances influence 7-26378
- glycol/air fuel cells, electrode catalyst and fuel electrolyte soln. 7-39987
- impedance, freq. meas. equipment 7-9823
- Matsumita molten carbonate fuel cell development (*Japanese*) 7-65455
- piezoelectric crystal electrode substrates Fe electrodeposition and corrosion obs. 7-39707
- poly(2,6-naphthoquinone) deposited film, time-separated two-step oxidation and electrochem. props. 7-22855
- polymers, electroactive, electrode appls. for nonaqueous secondary batteries 7-65437
- rotating ring disc electrode technique, appl. to study of Ni dissolution in molten NaCl-KCl at 700°C 7-23025
- rotating ring-disc electrodes, metal and semicond. types, appl. of redox contacts 7-39982
- semiconductor electrodes, adsorption, review 7-16867
- semiconductor polymer electrode kinetics in Li cells 7-54285
- surface analysis using XPS and electrochemistry 7-28370
- Ag, adsorpt. of pyridine, electrode pot. and Raman line intensities 7-19865
- Ag electrode, 4-cyanopyridine adsorpt. and electrochem. reduction, SERS 7-54165
- Ag electrode in NaClO_4 soln., capacitance, pH depend. 7-54135
- Ag electrodes, galvanostatic oxidation, relax. spectrum anal. 7-13788
- Ag electrodes, interfacial water surface-enhanced Raman scatt. using halide solns. 7-17311
- Ag/AgCl electrodes fabricated with IC-compatible technologies, chemical sensor reference appl. 7-8343
- Ag-Ag₂S, reference electrode, high temp. behaviour in aq. alkaline sulphide solns. 7-39714
- Ag-Zn intermetallic phase, reversible electrode 7-17802
- AgInSe₄ photoelectrodes, thermodynamic stability in electrolytes 7-54330
- AgO cathode used in AgO/Zn batteries, decomposition kinetics 7-46827
- Al-FeS₂, secondary cell, positive electrode reaction kinetics, AC impedance study 7-8372
- Al-FeS₂ secondary cell performance develop. using AlCl_3 /1-butylpyridinium chloride electrolyte 7-8370
- Al-FeS₂ secondary cell with basic AlCl_3 -NaCl melt, cell performance and positive electrode reaction (*Japanese*) 7-13852
- Bi_2CdS_4 thin film photoelectrodes, electrochemical photovoltaic cell appls. 7-17918
- C cathode performance improvement in $\text{Ca}(\text{AlCl}_4)_2$ - SOCl_2 cells 7-13851
- C electrodes in Li-SO₂ rechargeable cell 7-65443
- C, glassy, anodic oxidation of surfaces 7-46850
- Ca^{2+} , ion-selective electrode, subnanomolar range detection limit 7-17833
- CdSe electrodes, photoanodic dissolution in NaCl soln. (*Japanese*) 7-23026
- CdTe electrochemical sensor, sensitivity 7-65363
- Cl_2 -H₂ cells containing PbCl₂ solid electrolyte, cathodic characts; effect of vac. deposited FeCl₃ (*Japanese*) 7-13850
- electrochemical electrodes continued**
- Cr electrode, interaction with Li_2S_3 , cyclic voltammetry study 7-13786
- Cu, adsorpt. of halide ions, electroreflectance obs. 7-13132
- Cu, anodic oxidation in KOH soln., in situ spectroelectrochemical anal. 7-28192
- Cu bright plating electrodeposition kinetics, adsorption on cathode surface (*Russian*) 7-33942
- Cu electrode-electrolyte interface, surface anal., XPS, ion scatt. spectra 7-22895
- p-CuCNS photocathode, dye-sensitized, stabilisation by Pt deposition 7-27416
- p-CuCNS photocathode sensitized with Acridine Orange, photocurrent quantum efficiency 7-33944
- CuInS_4 photoelectrodes, thermodynamic stability in electrolytes 7-54330
- CuMo_6S_8 -y porous film, prep. on Cu₂S by solid-gas reaction; secondary battery appl. 7-27897
- Cu_2O electrodeposited film electrodes in photoelectrochemical cells, n-type photocond. obs. 7-17917
- Fe electrode in NaOH, pot. modulated reflectance spectra 7-28316
- Fe electrode surface, second harmonic generation study using a picosecond laser 7-23030
- Fe-Zn, intermetallic phase, reversible electrode 7-17802
- Fe_2O_3 /o-toluidine photoelectrochemical imaging system (*Japanese*) 7-35590
- H ion neutral carriers, for solvent polymeric membrane electrodes 7-17834
- Hg, dropping type, coumarin adsorpt., Cd^{2+} (In^{3+}) reduction retardation 7-58609
- Hg electrode-soln. interface, 2-anion simultaneous adsorpt., elec. double layer parameters algorithm 7-54132
- Hg film electrode, square wave voltammetry, theory 7-54204
- Hg, organic substance adsorpt., electromag.-radiation study 7-13805
- InP electrodes, surface modified, time resolved photoelectrochemical meas. 7-27415
- InP-aqueous electrolyte interfaces, laser induced photoelectrochemistry 7-27412
- Ir, anodic dissolution in Cl^- melts, salt passivation 7-52053
- Ir electrodes, deposition and stripping props. of Hg 7-45058
- $\text{La}_{0.9}\text{Nd}_{0.2}\text{Ni}_{1.5}\text{Co}_{2.5}\text{Si}_{1.1}$ electrode, storage capacity investig. 7-33946
- Li solvated electron electrode for secondary batteries 7-23130
- Li-LiNO₃ thermal battery cell discharge lifetime with soluble cathode materials 7-3630
- $\text{Li}_x\text{Cr}(\text{Mn})(\text{Fe})(\text{Co})(\text{Ni})\text{O}_2$ electrode materials, electronic and electrochemical props., ion intercalation, electronic model 7-33945
- Mo electrode, interaction with Li_2S_3 , cyclic voltammetry study 7-13786
- Mo electrodes, porous, role of O in alkali metal thermoelec. convertor 7-13925
- Mo porous electrodes for alkali metal thermoelec. convertor, voltammetric studies 7-28405
- MoSe₃S cathode for secondary Li batteries, prep. and characterisation 7-64948
- $\text{Na}_x\text{Cr}(\text{Mn})(\text{Fe})(\text{Co})(\text{Ni})\text{O}_2$ electrode materials, electronic and electrochemical props., ion intercalation, electronic model 7-33945
- Ni, anode, electrochemical behaviour in H₂SO₄ solns., halide ions effect 7-39758
- Ni, anodic polarisation, film identification by Raman spectra 7-28194
- Ni-Cd aerospace cells, flood starved design 7-34015
- Ni-Cd cell, electrode kinetics and failure-mode prediction, internal short equiv. resist. estimation 7-54288
- Ni-Cd cells, O₂ recombination rate on plastic-bonded Cd electrode doped with Ni(OH)₂ 7-54287
- Ni-Cd high-capacity battery (*Japanese*) 7-65433
- Ni-Cd high-performance battery (*Japanese*) 7-65434
- Ni-Cd storage batteries, structural features and additives effects on elec. props. of Ni active materials (*Hungarian*) 7-17857
- Ni-hydride cell, hermetically sealed rechargeable battery with stable electrode material, expt. study 7-54290
- Ni-Zn, intermetallic phase, reversible electrode 7-17802
- $\text{NiFe}_{1.96}\text{O}_{4+}$, electrodes in aq. electrolytes, photoelectrochem. characts. meas. 7-46854
- NiO porous cathode model for molten carbonate fuel cell 7-3640
- Pb-acid storage batteries, role of transport phenomena (*Hungarian*) 7-17856
- Pd alloy electrode surface, H overpotentials 7-23031
- Pd electrode surface, H overpotentials 7-23031
- Pd electrodes, surface hydride formation 7-23067
- $\text{Pt}_2\text{O}_3(\text{g})$ /stabilised ZrO_2 interfaces, electrode reactions, theory 7-65329
- $\text{Pt}_2\text{O}_3(\text{g})$ /stabilised ZrO_2 interfaces, electrode reactions, electrochem. anal. 7-65330
- Pt anode in phosphoric acid fuel cell electrolyte, H₂S poisoning 7-46933
- Pt, CN⁻ oxidation, polarisation modulation IRRAS 7-17836
- Pt electrochemical electrode surface struct. existence of electro-faceting 7-16841
- Pt electrode, in anhydrous methanol solns., added water effects 7-33936
- Pt electrodes, porous, in solid-electrolyte cell, polarization 7-23027
- Sb₂S₃-electrolyte interfaces, electrochemical photovoltaic cell fabrication appl. 7-40016
- n-Si-MnO photoanodes, photoelectrochemical and struct. behaviour 7-54329
- SnO_2 :F electrodes, surface modification by underpotential deposition of noble metals 7-44998
- Ti electrodes, passivated, photoelectrochemical studies 7-12757
- TiNb oxide electrodes, photoelectrochemical characts., zero point of charge effect on flat band potential and O₂ evolution 7-33943
- TiO₂ films, sol-gel method prep., appl. to photoelectrochem. electrodes 7-7903
- TiO₂ photoanode thickness effect on quantum yield of photoelectrolytical cells 7-40018
- V Redox cell, eval. of electrode materials 7-54286
- V_2O_5 -P₂O amorphous cathode Li secondary batteries, ethylene carbonate/2-methyltetrahydrofuran electrolyte 7-3635
- Zn, electrochem. and corrosion props. in mixed aq.-ethanolic media 7-54140
- Zn passive electrodes, space charge effects 7-28315
- Zn-air button type battery for hearing aids (*Japanese*) 7-65890
- Zn-NiOOH cells, KOH conc. effects on shape change and cycle life 7-28393
- ZnO-electrolyte interface, electrochem. under cathodic and anodic pulsed polarisation 7-13235
- ZrO_2 electrodes used for measuring standard Seebeck coeffs. of nonisothermal glass melts 7-3597

electrochemical machining *see electrolytic machining*

electrochemical polishing *see electrolytic polishing*

electrochemistry

see also Debye-Huckel theory; electrical conductivity of electrolytic liquids; electrochemical analysis; electrochemical electrodes; electrolysis; electrolytic devices; electrophoresis

airborne particles, photoelectric charging, implications for ion comp. and chem. reactions 7-28326

alkali metal cations, half-wave pots., solvent effects 7-23029

(BEDT-TTF)₂Br₂, synthesis, structure and electrical props. 7-46296

BEDT-TTF complexes with linear chain anions, crystal growth 7-46297

BEDT-TTF derivative (DIMET) radical cation salts, synthesis, conducting and superconducting props. 7-46855

BEDT-TTF radical cation salts, synthesis, conducting and superconducting props. 7-46855

(BMDT-TTF)₂Au(CN)₂ organic metal, synthesis, struct. and props. 7-32420

(BPDT-TTF)₂IBr₂, synthesis by electrochemical oxidation, struct. and ESR spectra 7-46856

brass, 63/37, electrochem. behaviour in binary mixtures of N,N-dimethylformamide and water 7-46677

charge-transfer reactions, electrode pot. effects 7-13784

charged particles, spatial correl., turbulence influence 7-8324

chemical potentials and activities, electrochem. introduction 7-9632

4-cyanopyridine, electrochem. reduction, SERS 7-54165

double layer capacity and corrosion rate, relax. technique meas. 7-39680

double-layer interaction between curved surfaces bearing pot., Derjaguin approx. 7-17819

electric double layer, thermodynamic consistency of the modified Poisson-Boltzmann eqn. 7-33941

electrochemical tests for sensitization detection 7-33894

electrodes, Fourier transform IR techniques, in-situ spectroelectrochemistry 7-54144

electrolytes near charged hard wall, local HNC/HNC approx. 7-8290

equilibrium diagrams, atlas prep. 7-24324

ferrocene, electrochemical response, orientation effect 7-26622

III-V semiconds., ion beam damage-induced masking for photoelectrochem. etching 7-44628

impedance spectroscopy applic. to materials sci., book contrib. 7-24659

interfacial electrochemical processes, low freq. dispersion 7-39904

IR spectroscopy, Ottawa, Ont., Canada (June 1985) 7-48160

lipid bilayers and thin films, phase transition kinetics, lifetimes distrib. function 7-8510

matrix-type diaphragms, electrochem. parameters and electroosmotic permeabilities 7-13800

MBBA, nematic, electrochemistry, orientational effects 7-26622

metal-solid electrolyte boundary, self-consistent electron theory, double layer, parametric instability, capacitance anomalies 7-52832

metallic glasses-H₂, prep., struct. and props. 7-26663

metals, electrochemical desorption step, rel. to isotope effect 7-13782

methoxybutyl azobenzene, nematic, electrochemistry, orientational effects 7-26622

MPB5 diffuse layer pot. drop 7-13785

optical materials for energy efficiency and solar energy conversion, conf., San Diego, CA, USA (Aug. 1985) 7-48159

4-pentyl-4'-cyanobiphenyl, nematic, electrochemistry, orientational effects 7-26622

phthalocyanine metallomacrocyclic assemblies, [Si(Pc)O]_n, molecular metals, conduction props. 7-2585

piezoelectric crystals, frequency and electrochem. data collection and anal. 7-53239

polyacetylene, electrochemical oxidation, additive effects 7-65331

polyacetylene copolymers and composites, physical props., electrochemistry and environmental stability 7-2587

polyaniline, conducting polymer, electronic and electrochem. props., MNDO calc. 7-2462

polyaniline, geometries, bond struct., electrochemistry, MNDO calcs. 7-15750

polyaniline films, electrochemical switching mechanism 7-64710

polyazulene, electrochem. and mag. props. 7-52929

polybis(pyrrolyl)phosphazene, synthesis and electrochemical oxidation 7-65315

polymers and related cpds., electronic props., Winter School, Kirchberg, Austria (March 1985) 7-4613

polypyrrole, diffusion-controlled polymerisation, growth instability 7-28311

polypyrrole electronically conductive polymer, fibrillar/microporous morphology control 7-26667

polypyrrole-phthalocyanine conducting complexes, spectroelectrochemical props. 7-3023

polythiophene, polymerisation from mono-, bi- and trithiophene oligomers, electronic props. 7-2597

polythiophene films, electrochemically polymerised, optical studies 7-51670

polythiophene films, photolum. quenching by electrochemical doping 7-59254

reactor steam generator pitting, electrochemical effects on Ni-base alloys 7-10228

restricted primitive model for electrical double layers: modified HNC theory of density profiles and Monte Carlo study of differential capacitance 7-11868

SCC electrochemical potential profile models 7-46717

semiconductor-electrolyte interface photoelectrochemical system, quantum yield interpretation and surface state model calcs. 7-23036

sodium tetraethylaluminate with NaH, thermodynamic characterisation using phase diagrams and electrochemical meas. for H₂ storage 7-54366

solid/liquid interface struct. and elec. props. (Japanese) 7-63941

stainless steel, type 304L, electrochemical tests for sensitization detection 7-33894

steel, high strength, modified HY 130, corrosion fatigue and electrochem. reactions 7-65201

steel, stainless, (Cr₂Fe)₂₃C₆, compact specimens, corrosion-electrochem. and phys. props. w.r.t. comp. 7-54000

steel, stainless, polarisation behaviour and admittance response in NaCl soln. (Japanese) 7-22871

surfactant-water-nonaqueous liq. systems, elec. cond. study 7-13789

TCNE, electrochemical response, orientation effect 7-26622

TCNQ, electrochemical response, orientation effect 7-26622

transition metal phosphorous trisulphides, electronic, structural and mag. props., intercalation cpds. and chemical props. 7-44499

electrochemistry continued

water desalination by electrochemical membrane process (German) 7-13819

n-WSe₂-electrolyte interface, microwave photoelectrochemistry studies 7-27413

zinc tetra-2,3-pyridino porphyrine, photoreduction, photochemical, electrochemical and spectroscopic study 7-33949

Ag electrode, SHG as surface probe 7-57463

Ag, normal potentials in liq. NH₃ 7-39903

AgCl-Ag clusters on Ag electrode surface, optical second harmonic generation, SERS, luminesc. 7-11057

AlN corrosion protective coating for TbFe magneto-optical media 7-53953

Au-HCl₄.5H₂O electrode-electrolyte interface, double layer capacity, temp. and freq. depend. 7-59769

CN⁻, oxidation at Pt electrode, polarisation modulation IRRAS 7-17836

CO adsorbed on Pt, vibr. spectrum, electrochemical pot., stark tuning rate 7-10570

CdGeAs₂, glassy, optoelectronic props., photoelectrochemical investigation 7-45382

Cd₃GeAs₄ semiconducting glass electrolytic dissolution in HCl and water 7-12289

CdGeP₂, glassy, optoelectronic props., photoelectrochemical investigation 7-45382

CdSe-polysulphide photoelectrochem. system. corrosion reactions, thermodynamic stability calcs. 7-28320

CdTe, cathodic electrochemical surface modifications, Cd layer form. 7-65239

CoCr films, corrosion in H₂SO₄, electrochemical study 7-33824

Cu single crystals, corrosion fatigue in aq., oxide-forming environment, electrochem. response 7-65115

Cu-Si₃N₄, effect of Si₃N₄ on deposition of Cu chemical coatings 7-3207

CuCrO₂:Ca, semiconductor, prep., opto-electronic props. 7-2705

Fe in strongly alkaline soln., electrochem. behaviour, Mossbauer resonance (French) 7-59768

Fe, surface, H₂ and N₂ interactions, pulsed laser atom probe studies 7-32811

FeCN ion, mass transfer of submerged jet impinging on cylindrical surface 7-26325

n-GaAs, photoelectrochemical etching, orientational depend. 7-65224

H₂ production, electrocatalytic materials comparison and eval. 7-65645

H₂ production by TiO₂ thin film electrodes of photoelectrolysis solar cells 7-3725

Hg electrode-soln. interface, 2-anion simultaneous adsorpt., elec. double layer parameters algorithm 7-54132

HgCdTe, electrochemical and electrolyte electroreflectance studies 7-64607

HgZnTe, electrochemical and electrolyte electroreflectance studies 7-64607

n-InP, minority carrier diffusion length meas. using a photoelectrochemical technique 7-33030

InSe-Ag intercalation cpd., prep. 7-54146

In₂Se₃-Ag intercalation cpd., prep. 7-54146

Ir surface, oxidised, in acidic solns., zero charge points 7-13783

Li spinel insertion compounds, reactions, mag. and elec. props. 7-33920

Li/SOCl₂ cell, corrosion, calorimetric study 7-46929

Li-In-Sb, ternary phase diagram, electrochem. investig. 7-58441

Li₂Cr(Mn)(Fe)(Co)(Ni)O₂ electrode materials, electronic and electrochemical props., ion intercalation, electronic model 7-33945

LiMoS₃, synthesis, electrochemistry and struct. 7-33619

Li₂Mo₂Se₃ intercalation cpd., entropy, electrochem. cell calorimetry studies 7-6833

Li₂Mo₂Se₃-I₂, Li electrochemical insertion, struct. studies 7-37947

Li₂Na₂TiS₂ intercalated dichalcogenides, struct., electrochem. and thermodynamic props. studies 7-21167

MgFe₂O₄, photoelectrochemical props., effect of defects and doping 7-45385

Mn₂O₄, electrolytic preparation, phase transitions and ion exchange 7-33921

MoS₂ single crystals, grown in presence of Co, photoelectrochemical props. 7-8294

MoSe₂, melt grown layered crystals, optoelectronic props. 7-21946

Na₂Cr(Mn)(Fe)(Co)(Ni)O₂ electrode materials, electronic and electrochemical props., ion intercalation, electronic model 7-33945

NaH, thermodynamic characterisation using phase diagrams and electrochemical meas. for H₂ storage 7-54366

Na₂Mo₂O₄ intercalation cpd., struct., mag. suscept., X-ray diffr. and electrochemical anal. 7-46842

NaNO₃-KNO₃:Ag⁺, diffusion coeffs. meas. by electrochem. methods 7-52097

Ni, dissolution in molten NaCl-KCl at 700°C, appl. of rotating ring disc electrode technique 7-23025

O₂, electroreduction, cobalt porphyrin effect, cyclic voltammetry and UV-absorpt. spectroscopy 7-59778

Pb, normal potentials in liq. NH₃ 7-39903

PbO₂, diffusion of H, electrochem. meas. 7-16807

Pb₃O₄ thin film, electronic props., electrochem. technique characterisation 7-7416

Pd surface, oxidised, in acidic solns., zero charge points 7-13783

Rh surface, oxidised, in acidic solns., zero charge points 7-13783

Si, impurity and carrier conc. profiles, electrochem. C-V method (Chinese) 7-12105

a-Si:H solar cells, leakage currents, electrochem. treatment effects 7-65467

Si-SiO₂-Cu(Ni), light induced deposition of metal films on SOI substrates 7-66354

TaS₂, electrochem. intercalation reactions with Li, K, H, In, Ga, In_{0.17}Ga_{0.83}, nucl. quadrupole interactions, TDPAC meas. 7-17245

TiN reactively RF sputtered coatings, structural defects and porosity, electrochem. polarisation meas. 7-52333

TiNb oxide electrodes, photoelectrochemical characts., zero point of charge effect on flat band potential and O₂ evolution 7-33943

TiO₂ sputtered thin film electrodes with low donor densities, photoelectrochemical behaviour 7-27359

TiO₂-redox polymer detector junctions, flatband pot. meas. 7-13787

TiO₂-RuO₂ in chloride solns., corrosion and electrochem. props. 7-53951

Tl, normal potentials in liq. NH₃ 7-39903

V₂O₅ electrodes, prep. by electrolytic reduction of molten salts 7-3211

WSe₂, melt grown layered crystals, optoelectronic props. 7-21946

electrochemistry continued

- n-WSe₂ single crystal, growth, struct. and photoelectrochem. props. 7-27879
 Zn, normal potentials in liq. NH₃ 7-39903
 ZnO, solubility product const. determ. 7-13790

electrochromic devices

- materials developments, book contrib. 7-25913
 polythiophene film in electrochem. color switching cells, cycle life, stability and characts. 7-62815
 In_{2-x}Sn_xO_{3-y}WO₃-MgF₂-Au, electrochromic coatings for solar windows 7-53621
 Li₂WO₃, crystalline and amorphous, electrochromic solar attenuation 7-39090
 Li₂WO₃-LiClO₄-Nb₂O₅ electrochromic cells, electrochromic window development, materials and devices 7-50664
 WO₃ based electrochromic windows, recent R&D 7-37122
 WO₃ electrochromic films on SnO₂:F, spray deposition and props., window appl. 7-3204

electrochromism

- display device materials, book contrib. 7-25913
 molecular fluid, molecular, electromag. radiation absorpt., electrochromic effect 7-13130
 polyaniline films, electrochemical switching mechanism 7-64710
 polyaniline films on platinized n-Si, photo-assisted electrochromic behaviour 7-27697
 polypyrrole films on platinized n-Si, photo-assisted electrochromic behaviour 7-27697
 polypyrrole-phthalocyanine conducting complexes, spectroelectrochemical props. 7-3023
 Au-WO₃-LiF-Au, solid state electrochromic struct. study 7-53275
 GaAs-AlGaAs quantum wells in waveguides, physics and appls. 7-26034
 In_{2-x}Sn_xO_{3-y}WO₃-MgF₂-Au, electrochromic coatings for solar windows 7-53621
 KTiOPO₄ crystals, electrochromic effects obs. (Russian) 7-33367
 Li-W-O films, electrochromic props., UV radiation effects study 7-22222
 Li₂-WO₃-Nb₂O₅ sputtered amorphous films, electrochromic props. study 7-22221
 Li₂WO₃, crystalline and amorphous, electrochromic solar attenuation 7-39090
 Li₂WO₃ films, free-electron electrochromic modulation 7-22359
 MoO₃, amorphous electrochromic films, plasma enhanced CVD 7-22561
 NiO thin films, electrochromic switching props determ. 7-39089
 NiO_x electrochromic hydrated coatings for energy efficient windows 7-45986
 WO₃, amorphous electrochromic films, plasma enhanced CVD 7-22561
 WO₃ based electrochromic windows, recent R&D 7-37122
 WO₃ electrochromic films, obliquely deposited, elec. props. and morphology 7-7781
 a-WO₃ films, electrochromic effect kinetics 7-45992
 WO₃ thin films, transparent, amorphous, prep. by dip-coating method 7-53644
 WO₃-Nb₂O₅ sputtered amorphous films, electrochromic props. study 7-22221

electrodeposited coatings *see electrodeposits***electrodeposited films** *see electrodeposits***electrodeposited layers** *see electrodeposits***electrodeposition**

- see also electrodeposits; electroplating*
 alloys, electrochemical deposition, cryst. growth modelling 7-59386
 dendritic and fractal structures, diffusion and current fields 7-45102
 electrocrystallisation, kinetics, computer simulation studies 7-58173
 II-VI semiconductor films, prep., electronic props., solar cell appl. (Japanese) 7-54299
 intermetallic cpds., diffusion layer at cathodes in ionic melts 7-52150
 laboratory scale, practice and appls. 7-48252
 layer formation with two-dimens. nucleation and growth 7-22590
 pyrrole polymerisation, diffusion-controlled statics and dynamics, fractal and dendritic growth in electrochem. cell 7-59758
 semiconductor compounds, liquid phase electroepitaxy 7-33607
 (TMTSF)₂X salt, isolated single cryst. growth, electrochemical technique 7-59393
 transition metals, electrodeposition from aromatic solvents 7-33611
 Ag, electrodeposition, electrode impedance, brightening and levelling agents effect 7-33612
²⁴¹Am electrodeposition geometry in the assay of environmental samples 7-28718
 CdS anodic film growth, initial stages, voltammetry and computer simulation studies 7-28216
 CdS thin films, electrochem. bath deposition, photovoltaic cell props. 7-7900
 CdSe thin films, electrodeposited from SeSO₃²⁻ soln., comp. performance, polarography, RBS, cyclic voltammetry, power meas. 7-2411
 n-CdSe thin films grown from low purity materials for solar cell appls. 7-65480
 CdTe, electrodeposition from acidic aq. solns., voltammetry 7-27188
 CdTe film in a photovoltaic cell, electrodeposition and props. 7-64938
 CdTe layers, electrochemical deposition, struct. and elec. props. 7-12526
 Co powder, very fine, electrodeposition from electrolytes of various anion comps. 7-3224
 Cr films, acoustic emission during electrodeposition 7-52329
 Cr-Ni, electrodeposition, role of Cr(II) 7-33614
 Cu, electrocrystallisation kinetics, surface ion conc. depend. on overvoltage in case of slow adatom surface diffusion (Russian) 7-2429
 Cu electrocrystallisation on indifferent substrates, twinning 7-53639
 Cu-Ni electrodeposition, comp. modulated alloy form. 7-59468
 Cu-Si₃N₄, effect of Si₃N₄ on deposition of Cu chemical coatings 7-3207
 Cu-Zn, electrodeposits, comp. rel. to deposition pot. (Japanese) 7-27951
 (Fe,Co,Ni)-P layers, electrochemical deposition, struct. (Chinese) 7-7037
 Fe film, electrodeposition and corrosion, piezoelec. cryst. substrate obs. 7-39707
 Fe-P, amorphous alloys, electrodeposition and melt spinning prep., struct. anal. 7-11934
 Ge coated circular metallic hollow waveguides for IR radiation, electrodeposition prep. (Japanese) 7-31463
 Hg deposition and stripping props. on Ir electrodes 7-45058
 Ni, electrodeposition from aromatic solvents 7-33611
 Ni/Ni-P compositionally modulated films, electrodeposition 7-3209
 Ni-P amorphous alloy electrodeposition and corrosion obs. 7-27953
 Ni-P coating, electrolytic, electron microscope obs. of struct., P content depend., amorphous layer form. 7-8157

electrodeposition continued

- Ni-Ti, electrodeposition from aq. (NH₄)₂ TiF₆ bath 7-7902
 NiSn-SiC composite coatings, electrodeposition, wear resist., hardness, porosity 7-33613
 Pb electrodeposition from aq. HCl soln. onto Pt (111) 7-27954
 Pd electrodeposition assisted by laser beam (German) 7-39440
 Pd, pulsed current electrodeposition, pulse parameters effect on deposit morphology, H content 7-59473
 Pd-Ag alloy electrodeposition assisted by laser beam (German) 7-39440
 Rn, electrodeposition from sulphate solns., grain growth, additive effect (Japanese) 7-17481
 a-Si, cathodic deposition from organic solvents (Japanese) 7-64947
 a-Si:H solar cells, leakage currents, electrochem. treatment effects 7-65467
 Si-SiO₂-Cu(Ni), light induced deposition of metal films on SOI substrates 7-46354
 TiB₂-Mo electrospray coatings on steel, form. kinetics and high-temp. oxidation 7-65210
⁴⁴Ti, radioactive target preparation by high yield electrodeposition 7-819
 V₆O₁₃ electrodes, prep. by electrolytic reduction of molten salts 7-3211
 Zn, electrodeposition, macromorphology, impurity effects, pot. sweep analysis 7-22595
 Zn electrodeposition, struct. rel. to inhibition conditions 7-22593
 Zn, electrodeposition kinetics on Zn single crystals, pot. step method, SEM anal. 7-27189
 ZnSe films, electrochemical co-deposition, photoelec. conversion characts. 7-46959

electrodeposits

- see also electroplated coatings*
 electrodeposits for high temp. oxidation and corrosion resistance, appl. for gas turbines 7-46358
 hardening coatings, electroerosion alloying, of steel 45 7-17722
 polyoxy-(allyl)phenylene electrochemically prepared film, elec. props., permittivity and solubility 7-27665
 Al, electrodeposition from nonaq. solns. (Japanese) 7-64964
 C fibres, tensile strength distrib., statistical model, electrodeposited coating effect 7-39585
 CdS anodic film growth, initial stages, voltammetry and computer simulation studies 7-28216
 CdSe thin film liquid-junction photovoltaic cell, photoelectrochem. charactn. 7-54331
 CdTe films, electrochemically deposited, resistivity, carrier conc. and carrier mobility 7-7419
 CdTe films, electrochemically deposited, comp., struct., AES, electron probe anal., X-ray diffr. spectroscopy 7-58694
 Co-P, amorphous, Curie temp. meas. 7-45669
 CoP amorphous films, FMR spectra during crystallisation 7-53142
 Co₉₀P₁₀, amorphous films, electrodeposited, optical and NMR spectra, annealing effect (Russian) 7-45831
 Cr, electrodeposited, groove adhesion tests 7-46789
 Cr-Cr₂O₃/Zn multilayer electrogalvanised coating on steel, XPS analysis 7-22890
 Cu current collecting grid on Si solar cells, oxidation and spalling 7-22910
 Cu, decorated grain boundary dislocations, electron microscopy obs. 7-27185
 Cu electrocrystallisation on indifferent substrates, twinning 7-53639
 Cu metal leaves, electrodeposited, Hausdorff dimension or fractal nature 7-12523
 Cu, ultrapure, electrorefining, vacuum switch electrode appl. 7-27966
 Cu-Ni electrodeposition, comp. modulated alloy form. 7-59468
 Cu-Zn, electrodeposits, comp. rel. to deposition pot. (Japanese) 7-27951
 CuInSe₂, electrodeposited films, photoelectrochem. solar cells fabrication 7-3710
 Cu₂O electrodeposited film electrodes in photoelectrochemical cells, n-type photocond. obs. 7-17917
 Cu₂S thin films, form. by electrochem. procedure 7-39445
 (Fe,Co,Ni)-P layers, electrochemical deposition, struct. (Chinese) 7-7037
 Fe, electrodeposited, grain struct. and size, positron lifetime study 7-46209
 Fe film, electrodeposition and corrosion, piezoelec. cryst. substrate obs. 7-39707
 Fe-P, amorphous alloys, electrodeposition and melt spinning prep., struct. anal. 7-11934
 Hg₂Cl₂ thin films, morphology and growth on Hg surface, electron beam damage 7-59469
 Mo, smooth electrodeposits in KF-Na₂B₄O₇-Na₂MoO₄ fused salt melts 7-27950
 Ni electrodeposit on steel turbine disc, pot.-pH diagram 7-39699
 Ni, electrodeposited films, occurrence of multiply twinned particles 7-38373
 Ni-B based electrochemical coatings, heat resistance, oxidation 7-3499
 Ni-Mo-Cd electrocoated cathodes for water electrolysis, H₂ evolution kinetics 7-3728
 Ni-P, amorphous electrodeposited alloys, short-range order (Russian) 7-32291
 Ni-P coating, electrolytic, electron microscope obs. of struct., P content depend., amorphous layer form. 7-8157
 Ni-P electrodeposited amorphous alloy, prep. and characterisation 7-22598
 Ni-ZnO/ZnS, selective Ni black coating, struct. and optical response 7-58697
 NiSn-SiC composite coatings, electrodeposition, wear resist., hardness, porosity 7-33613
 Pd and alloy contact finish performance and cost 7-3508
 Pd, pulsed current electrodeposition, pulse parameters effect on deposit morphology, H content 7-59473
 Rn, electrodeposition from sulphate solns., grain growth, additive effect (Japanese) 7-17481
 Ta₂Si electrodeposited coatings, composition, morphology and hardness meas. 7-27191
 TiB₂-Mo electrospray coatings on steel, form. kinetics and high-temp. oxidation 7-65210
 Zn, electrodeposition, macromorphology, impurity effects, pot. sweep analysis 7-22595
 Zn electrodeposition, struct. rel. to inhibition conditions 7-22593
 ZnSe films, electrochemical co-deposition, photoelec. conversion characts. 7-46959

electrodes

- see also anodes; cathodes; electrochemical electrodes; microelectrodes
- accumulators, examination of graphite additive to electrodes 7-39984
- advanced high energy density battery with NaAlCl_4 and β -alumina solid electrolyte 7-39981
- alkaline fuel cells, low cost, development and hydrogen economy appls. 7-39950
- batteries, discharge capacity dependence on electrode fractality 7-3631
- biomedical US transducer design for uniform insonation 7-3847
- broadband light modulators, quasi-matched-velocity travelling-wave type electrodes (Japanese) 7-43354
- coaxial electrode system, steep wavefront discharges 7-51545
- design for gas discharge laser using finite difference method 7-1178
- electric field calculations using the ELF codes glow discharge switches and electrode design 7-32134
- extracochlear electrode, temporary, use in preoperative testing of permanent implant candidates 7-54611
- Fourier transform IR techniques, in-situ spectroelectrochemistry 7-54144
- inter-electrode gap strength calc., Kilpatrick's criterion approximation 7-10815
- ion accelerator electrodes, energy dissipation during HV vacuum breakdown 7-30777
- ion source, plasma boundary-extractor electrode distance, erosion effects 7-18918
- ion-selective electrodes for ion conc. measurement, operation in nonlinear suboptimal response range 7-56246
- lead-off electrode systems, concept of local resolution 7-28738
- medical electrodes, optimal design for electrosurgery, defibrillation, and external cardiac pacing: finite-element computer model 7-3928
- medical impedance cardiography, motion artifact from spot and band electrodes 7-28732
- metals, H atom diffusion and trapping, meas. by potentiostatic double-step method 7-21524
- metals, H atom diffusion and trapping, meas. by potentiostatic double-step method 7-21525
- monopolar electrodes used in EMG automatic analysis with ANOPS computer 7-8738
- multiplexed implantable, for monitoring evoked responses in cerebral cortex, design 7-47305
- oesophageal electrodes for recording His-Purkinje activity based on signal variance, evaluation 7-23469
- organic-type Geiger-Muller tube with third electrode, design and performance 7-19627
- polarographic O_2 (Chinese) 7-18083
- polymer-based in vivo reference electrodes, functional mechanisms 7-40318
- PTCR, high temp., interaction with O models 7-58861
- relativistic electron beam diodes, electrode design and appls. 7-20967
- spark gap, SF_6 filled, high-power discharge, electrode erosion and breakdown voltage study 7-44300
- stainless steel electrode surface damage anal. in high energy spark gaps 7-33991
- steel, stainless, microelectrodes, pitting dissolution in NaCl solns., nitrate passivation 7-39703
- surface, organic surfactant coverage and polarographic maxima of the third kind 7-13838
- surface contamination, desorpt., field and secondary emission, enhancement by electric fields 7-23033
- ventricular fibrillation, 60 Hz, thresholds for large-surface-area electrodes, animal expts. 7-3931
- venturi suction electrode array for clinical bodysurface mapping 7-3904
- Ag electrodes, adsorbed layers of azide, cyanate and thiocyanate, pot. difference IR spectra, coverage depend. orientation 7-22252
- Ag, SHG as surface probe 7-57463
- Al direct conversion electrodes, material effects on energy conversion efficiency, neutral beam injection system appl. (Japanese) 7-10277
- Al-Si-Cu sputtered electrode for VLSI, Cu distributions meas. by RBS 7-2415
- Au, adsorbed halide and pseudohalide, SERs, metal-adsorbate vibr. freqs., surface bonding 7-12468
- Au- HCl_4 .5 H_2O electrode-electrolyte interface, double layer capacity, temp. and freq. depend. 7-59769
- Bi electrode, single cryst., adsorpt. of butyl acetate 7-52239
- Bi, polycrystalline, adsorpt. of cyclohexanol 7-32785
- C, adsorption of Cl, theory 7-12462
- Cd electrodes, electrochemical aspects and alkaline battery appls., review 7-3638
- CdSe thin films, electrodeposited from SeSO_3^{2-} soln., comp. performance, polarography, RBS, cyclic voltammetry, power meas. 7-2411
- Cd_3SnO_4 transparent thin film electrodes prepared by DC reactive sputtering from Cd-Sn alloy targets 7-22477
- Cu, vacuum switch electrode, electrorefining prep. 7-27966
- Fe, H atom diffusion and trapping, meas. by potentiostatic double-step method 7-21525
- H_2 evolving electrode with superimposed electrolyte flow, mass transfer 7-46852
- K^+ selective electrodes on valinomycin/PVC overlaid substrates 7-65375
- $\text{La}_{1-x}\text{Sr}_x\text{MO}_3$ (M=Cr, Mn, Fe, Co), electrodes for high temp. oxide fuel cells 7-54291
- Li electrodes, semicond. passivating film, impedance meas. 7-33111
- Li three electrode secondary cells, electrode processes at Li-polymer electrolyte interface 7-3639
- Ni-Cd cells, additive effects on anodic behaviour of negative Cd electrode in KOH solutions 7-3637
- Pb-acid batteries, mass transport during plate formation 7-39985
- SF_6 , corona and glow discharges, electrode-F reaction influence 7-26565
- (Ti,Cr)B₂ sintered electrode exposed to liq. Al, degradation, effect of segregated Cr 7-28045
- Ti direct conversion electrodes, material effects on energy conversion efficiency, neutral beam injection system appl. (Japanese) 7-10277
- TiO_2 , illum., elementary steps in charge transfer mediated by surface states 7-12780
- TiO_2 sputtered thin film electrodes with low donor densities, photoelectrochemical behaviour 7-27359

electrodynamics

- see also electron beams; electron optics; electron tubes; ion beams; ion optics; ion sources; quantum electrodynamics
- 2D media, polarisable and magnetisable, forces in EM field 7-50459
- Ampere-Neumann electrodynamics of metallic conductors 7-20115

electrodynamics continued

- asymmetric strip line segments, cross coupling, electrodynamic theory 7-36848
- axial toroidal moments in electrodynamics and solid-state physics 7-31232
- black hole electrodynamics (Russian) 7-9507
- Bloch density matrix for oscillator in electric and mag. field, path integral formulation 7-62605
- Born-Infeld electrodynamics, motion of gravitationally interacting particles 7-48479
- brachistochrone, relativistic, anal. using Bernoulli's method 7-56032
- charged particle, cyclotron motion in spherical microwave cavity 7-15810
- charged particle in mag. field, alternative lagrangians 7-42873
- charged particle motion in EM field, guiding centre motion problem 7-1016
- charged particle moving parallel to current, stable oscillating orbits 7-35164
- charged particle trajectories between charged surfaces 7-25708
- charged particles, relativistic trajectory eqns. in orthogonal curvilinear coordinates 7-10830
- charged-particle system, elementary theory of transport phenomena under elec. field 7-62607
- classical bremsstrahlung ang. distrib. in Coulomb case 7-62606
- collective excitations of electrons by intense wave in magnetic field 7-20116
- diffraction problems and threshold (Ukrainian) 7-10831
- electric quadrupoles, minimal EM coupling 7-10833
- electrodynamic potential propagation, Carl Neumann vs. Rudolf Clausius 7-63
- electron stored in Penning trap appl. to ion spectroscopy 7-10834
- fluorescence spectrometer for a single electrostatically levitated micro-particle 7-9905
- Galilean-kinematic electrodynamics, proposal for Lorentz force test. 7-5823
- infinite-order Lagrangians, order-two reduction 7-18608
- iterative method of problem soln. (Russian) 7-62609
- jump conditions in relativistic electrodynamics 7-18609
- laminar space-charge flow form., relativistic theory 7-51040
- Lorentz-force-induced motion of a solid object with a fixed point 7-41086
- Maxwell-Dirac isomorphism 7-61
- Maxwell-Dirac isomorphism 7-35777
- metal-electrolyte interface electrodynamics, surface soliton form. 7-21958
- nonlinear electrodynamics generated via gravitational nonminimal coupling 7-24512
- nonrelativistic particle in blackbody radiation field, Lorentz-Dirac equation soln., stationary states 7-36864
- ocean, electrodynamics of slowly-moving medium rel. to elec. field meas. 7-47444
- parametric resonance in magnetically (electrically) anisotropic systems 7-42874
- point charge, photon density radiation limits 7-62608
- polarizable vacuum, confining classical potential, two-particle case 7-42870
- radiation from point charges 7-41033
- relativistic charged particles, coherent curvature radiation pulse duration 7-1015
- resonant transformation of electrostatic energy in ExBfield system 7-6367
- stirrers and induction pumps, liquid metal velocity distrib. effects on electrodynamic forces (Polish) 7-63231
- superconducting oscillatory ccts., influence of time-depend. gravit. fields 7-41181
- synchrotron radiation, coherent, spectrum and angular distrib. 7-5824
- young stars, accretion-driven jets, electrodynamic processes 7-60643
- electrodynamometers see dynamometers
- electroencephalograms see electroencephalography
- electroencephalography
- see also bioelectric potentials; biomagnetism; brain
- adaptive techniques for signal enhancement in human EEG 7-34319
- alpha rhythm in normal state, generation model 7-8536
- ambulatory monitoring, 24 hr. development and appls. 7-23472
- auditory evoked responses during NREM sleep stage 2 in man, late component variants 7-23370
- automatic classification based on syntactical pattern recognition, ARMA model 7-40328
- autoregressive EEG modelling, best AR model order 7-54539
- background activity stages identification for drug effects detect. 7-54781
- classifier-directed signal processing in brain research, EEG and magnetoencephalogram appl. 7-54820
- cognitive dysfunction diagnosis, multimicroprocessor-based real-time EEG analyser 7-23475
- coherence and cortico-cortical associations, 2-compartmental model 7-13987
- comatose patients, long-lasting reactions after repetitive stimulation 7-65864
- correlated EEG-like data, testing for normality using a modified Kolmogorov-Smirnov statistic 7-54536
- epileptic, structural anal., multi-channel Kalman filter algorithm 7-54793
- epileptic electroencephalogram, syntactic analysis 7-34126
- epileptogenic sharp transients detect., multichannel signal processor 7-54786
- event related potentials, component and interval detection algorithms 7-34139
- evoked potential analysis using crosscorrelation and dynamic time-warping 7-8551
- evoked potential components, mid and long latency, law of 3.5 c/sec 7-3771
- evoked potentials processing with tactile and thermal stimulation; prototype system (Spanish) 7-34318
- extracellular neural recording with multichannel microelectrodes 7-8780
- filter transient response to EEG waveforms 7-54792
- focal epileptic spikes, computer-based technique for averaging, spatio-temporal mapping and dipole modelling 7-23473
- frequency analysis, filtering and aliasing of muscle activity 7-3894
- head-injured patients, computer assessment of neurological status using EEG power spectrum anal. 7-34128
- heart rate variations and EEG changes during nocturnal monitoring of ischaemic patients 7-34315

electroencephalography continued

- hippocampal EEG, centre of spectral mass as meas. of EEG ontogeny, rat obs. 7-8553
- human, correl. dimension estimation, mental activity, recording site and signal length effects 7-13988
- ignorance-based signal estimation given multiple noisy realizations 7-47264
- infant EEG, spectral anal. rel. to behavioural outcome at age 5 7-3769
- intraoperative EEG monitoring, comparison of a set of power distrib. parameters 7-3927
- inverse solutions based on magnetoencephalograms and EEGs, appl. to vol. cond. anal. 7-54637
- large-scale neuron-glia network dynamics, rel. to brain functions 7-23327
- magnetoencephalogram and EEG, method for combining to determ. sources 7-54635
- magnetoencephalogram topography and source model of abnormal neural activities associated with lesions 7-47032
- maximum likelihood method for estimating EEG evoked pots. 7-54421
- monitoring brain electrical and magnetic activity 7-8743
- multisensory activity anal. of cortical and subcortical structs. in photosensitive baboons 7-65748
- neural computation, sigmoid nonlinearly, rat olfactory bulb obs. 7-54619
- noise generated in digitising or analogue recording, reduction method 7-54784
- nonlinear digital filter for separating nonstationary and stationary EEG waves 7-47267
- power spectral density, efficient formula for estimating generalized moments, EEG appl. 7-54423
- power spectral density rel. to sleep duration 7-13986
- quantification of EEG and unit activity 7-65740
- Rett syndrome, EEG findings 7-65738
- SAMICOS, sleep analysing microcomputer system using multichannel EEG 7-23470
- segmentation algorithms (*Spanish*) 7-8549
- sleep EEG and EMG, computer program for automatic anal. 7-54783
- sleep EEG in the rat as a function of prior waking 7-3770
- spatial patterns classification with a tree-structured methodology, rabbit olfaction appl. 7-54420
- spectral power and phase, averaging via vector diagram best fits 7-54782
- subcortical dementia, EEG changes, Steele-Richardson-Olszewski syndrome patient obs. 7-54531
- task difficulty effects on steady state visual evoked response 7-54544
- tourrette syndrome patients, unmedicated and neurologically and intellectually intact, EEG findings 7-3892
- visual evoked potentials, anal. through Wiener filtering applied to a small no. of sweeps 7-40142

electroendosmosis *see* **electrophoresis****electroerosive machining** *see* **spark machining****electrofluidynamics** *see* **electrohydrodynamics****electrofluorescence** *see* **electroluminescence****electroforming**

- Cu-SiO₂-Cu sandwich struct., thermal voltage memory effect, time depend. 7-45527
- Ni plating basics, electroforming, surface prep. and quality control procedures 7-13638

electrofluidynamics *see* **electrohydrodynamics****electrogyration** *see* **electro-optical effects**; **optical rotation****electrohydrodynamics**

- 3D tuft corona and EHD, num. simulation 7-20983
- adiabatic multiphase fluids, hydrodynamics and EHD 7-1611
- aerosols, electrohydrodynamic equations with dispersed phase particles with diffusion charging 7-1642
- atomiser electrostatic spray nozzle, aerodynamically shaped for insecticide selective deposition 7-51262
- axisymmetric Bennett pinch stability, two fluid approx., relativistic electro-magnetic hydrodynamic calcs. 7-44232
- axisymmetric electrovortical flows for alternating current in a cylindrical container 7-51331
- bubbles, maximum size during nucleate boiling in elec. field 7-50918
- canonical equations, variational principle appls. (*Russian*) 7-26360
- condensation, turbulent gas jets, elec. field control 7-11485
- convection in hemispherical shell due to radial electrostatic forces, simulation of planets and stars 7-29393
- convective heat transfer in an electric field 7-63133
- defect motion in EHD cell with two free lateral side-walls 7-63444
- dielectric liquid, stationary instabilities, unipolar injection and thermal gradient effects 7-26357
- dielectric liquids, stressed, transient EHD motion, computer simulation 7-1643
- direct conversion from electrical to fluid kinetic energy in electro-fluid-dynamics device 7-3712
- drag anemometry for measuring velocities in electromagnetically driven flows 7-44076
- drops, motion in conducting liquid in variable elec. field 7-51326
- electrically boosted glass melting tank, 3D model for flow simulation and heat transfer 7-20805
- electrified menisci, cone-like shapes, emitted charge effects 7-31888
- electro-dilatometric effect in dielectric liq. 7-33335
- electrostatic dynamic effect on small perturbation development in the boundary layer on a thin airfoil 7-1641
- electrokinetic phenomena in dielectric liquids 7-51542
- electrolyte solution surfaces, hydrodynamic instabilities caused by elec. forces. 7-51322
- exploding metallic foils time-dependent behaviour and hydrodynamic expansion, computer model 7-32036
- fluid layer, EHD stability, effect of tangential periodic field 7-26359
- fluidized beds, electric behaviour, capacitor model 7-6305
- heat transfer in unsteady MHD Couette flow of electrically conducting viscous incompressible rarefied gas, theory 7-66448
- jets, current-carrying, deformation by nonviscous elec. cond. liquid 7-51257
- linear array of forced vortices, instability 7-63227
- liquid drop, instability development in elec. field 7-31850
- MBBA liq. cryst., Williams domain evolution process, Fourier spectrum anal. 7-32274
- nematic liquid crystal, EHD oscillatory instability (*Russian*) 7-6323
- nematic liquid crystals, EHD instabilities (*Japanese*) 7-1879
- nematic liquid crystals, electrohydrodynamics, director oscill. process, scaling props. 7-58139

electrohydrodynamics continued

- nematic liquid layers, convective flow, multiple spatial periodicities, EHD instability 7-43909
- particle charging process, electric field depend. 7-20786
- polymeric nematics, electrohydrodynamic instabilities, comment 7-11557
- self-similarity in electrohydrodynamics with spherical symm. 7-1645
- stirrers and induction pumps, liquid metal velocity distrib. effects on electrodynamic forces (*Polish*) 7-63231
- Ga, liquid, electrohydrodynamics, ion source appls. 7-31887
- Li, liquid ion-source, nonlinear behaviour of liq. surface in electric fields 7-42259
- Li⁺, in water, Stokes radius, Hubbard-Onsager's dielectric friction theory 7-33347
- Si drift chambers, electron dynamics 7-42329

electrojets

- auroral electrojet, rocket-borne interferometric phase vel. meas. 7-55364
- counter electrojet generation, role of tidal winds 7-66378
- E-region, equatorial irregularities phase vel. var. with electrojet electron drift 7-47628
- electric fields and currents during substorms, modelling study 7-29350
- electric fields determ. from VHF radar meas. 7-60414
- equatorial counter electrojet, soln. of some dilemmas 7-34769
- equatorial electrojet, drift speeds of irregularities of kilometre and metre sizes 7-4257
- equatorial electrojet, effect of source-field geometry on EM induction Earth 7-28821
- equatorial electrojet, irregularities phase vel. height profiles, elec. fields determ. 7-60453
- equatorial electrojet, relation to VHF scintillations increase during mag. activity 7-34762
- equatorial electrojet, type II irregularities modification by finite amplitude type I waves 7-34778
- equatorial electrojet, type II irregularities phase vel., elec. fields determ. 7-60454
- equatorial electrojet effect of electron temp. on electron number density and dynamics of E-region 7-66390
- equatorial electrojets, small scale plasma motions, HF Doppler obs. 7-55361
- oil pipeline, induced EM fields due to electrojet current sources 7-8814

electrokinetic effects*see also* **electrodynamics**; **electrophoresis**

- dielectric liquids, electrokinetic phenomena 7-51542
- mixed-lipid membranes, electrokinetic effects, nonequilibrium thermodynamics 7-54495
- Teflon, wetting, effect of diphilic polyelectrolytes conc. 7-38302
- Ag₂SI-potential forming ions-solution interface, potentials calcs. (*Russian*) 7-27138

electroless deposited coatings

- Co-Ni-P electroless plated thin films, microstructure, mag. props., mag. recording appl. 7-27581
- Co-P electroless plated thin films, microstructure, mag. props., mag. recording appl. 7-27581
- CoNiReP alloy films for perpendicular mag. recording, thickness depend. of perpendicular coercivity 7-59066
- Cu, electroless deposits, ductility, effect of inclusions 7-58719
- Cu, electroless plating, microdistrib., soln agitation, temp. and pH depend. 7-7907
- Ni electroless plated mirrors, diamond-turned, surface finish meas. 7-37218
- Ni, electroless plating, outdoor exposure, accelerated atmospheric corrosion (*Japanese*) 7-13633
- Ni-B alloys heat induced struct. changes 7-13639
- Ni-Mo-P, electroless plating prep., film props. 7-13392
- Ni-P, electroless coating on ultrahigh strength maraging steels, H embrittlement 7-28136
- Ni-P, electroless coatings, wear rel. to counterface materials and heat treatment 7-33802
- Ni-P alloy electroless deposits, hardening by baking treatments (*Japanese*) 7-33759
- Ni-P electroless coatings, electronics components, thickness meas. 7-14920
- Ni-P electroless coatings, corrosion resistance 7-17484
- Ni-P electroless deposited amorphous coatings, wear resistance, crystallisation effects 7-53913
- Ni-P films, electroless deposited, struct., electron microscopy studies 7-7041
- Ni-P-B, prep. and deposit characts. 7-59671

electroless deposition

- metal plating process, photograph analogy 7-56361
- metallic thin films, electroless deposition, appl. for ⁶⁰Co radiation control in BWR 7-49590
- Co-Ni-Re-P films for perpendicular mag. recording media, electroless deposition and mag. props. 7-27580
- Cu, electroless plating, microdistrib., soln agitation, temp. and pH depend. 7-7907
- Cu, electroless plating rate rel. to K₃Fe(CN)₆ in bath 7-22594
- Ni anodes for molten carbonate fuel cells, stabilisation 7-39988
- Ni-B alloys heat induced struct. changes 7-13639
- Ni-Mo-P, electroless plating prep., film props. 7-13392
- Ni-P-B, prep. and deposit characts. 7-59671

electroluminescence*see also* **phosphors**

- conference, Rovno, USSR (Nov. 1984) 7-24263
- copper phthalocyanine thin films, thermoelectroluminescence studies 7-7770
- MIM electroluminescent device structs., impurity centre electron impact-induced luminesc. mechanism 7-59260
- perylene films, electroluminescence with conducting polymer anodes 7-22349
- photovoltaic effect, related bulk electrolum. 7-38638
- polyethylene, low-density, near-UV emission obs. during electrical-tree initiation 7-59259
- polyethylene film, electrolum. meas., electrode work function effects 7-27789
- polyethylene naphthalate, electrolum. and electronic conduction in high DC fields 7-27788
- polystyrene film, electrolum. meas., electrode work function effects 7-27789
- quantum well structs., electric field effect for luminescence (*Japanese*) 7-13236

electroluminescence continued

- semiconductor doping superlattices, physics and applications 7-52826
 zinc phthalocyanine thin films, thermoelectroluminescence studies 7-7770
 Al:Eu³⁺, ion implanted, anodization, electroluminesc. obs. 7-7761
 Al-Al₂O₃-Ag MIM struts. biased near breakdown voltage, optical emission 7-52853
 Al-Al₂O₃-Au MIM struts. biased near breakdown voltage, optical emission 7-52853
 Al₂O₃ surface electrocathodolum., defect state transitions under high voltage stress 7-39187
 Au/Cd stearate/n-GaP electroluminescent device struct., electron-hole recomb. luminesc., minority carrier injection mechanism 7-59260
 Au/i-ZnS/n-ZnS electroluminescent device struct., electron-hole recomb. luminesc., minority carrier injection mechanism 7-59260
 CdF₂:Eu³⁺ electrolum. studies 7-27785
 CdSb, optical energy gap and light emission (*Japanese*) 7-53264
 GaAlAs-GaAs laser diodes, catastrophic optical damage, electrolum., cathodolum., EBIC and TEM obs. 7-57329
 GaAs doping superlattices, efficient room temp. electroluminescence, tunability 7-27782
 n-GaAs films, electron-hole plasma stratification and blue luminesc. near static domain 7-52666
 GaAs n-i-p-i doping superlattices, selective contacts, MBE growth through shadow mask 7-13356
 GaAs:Ho, electroluminescence and injection currents 7-13232
 GaAs/AlAs MQW structures, life-time-free switching of luminescence by elec. fields 7-52791
 GaAs-(Al,Ga)As double heterojunction lasers, dislocation control, electroluminescence 7-7046
 GaAs_{0.6}PO₄ degraded LEDs, origin of nonradiative centres, photocapacitance, electrolum. spectra 7-53413
 GaAs_{1-x}P_x solid solns., indirect band gap temp. depend., electrolum. spectra studies 7-38448
 GaInAsP-InP BH laser fabrication, MOCVD epitaxy, validation by photoluminescence imaging 7-31360
 GaP and GaP:N diodes, electroluminescence, high press. effects 7-27787
 InGaAs:Si LED, electrical and luminesc. props., ultrasonically-induced changes 7-22350
 In_{1-x}Ga_xP solid solns., indirect band gap temp. depend., electrolum. spectra studies 7-38448
 InP:Yb LPE layers, luminesc. and elec. props. 7-59464
 α -SiC:Al₂O₃ crystals, photolum. and electrolum. studies (*Russian*) 7-22344
 ZnO varistors, electroluminescence temp. depend. and conduction mechanisms 7-17349
 ZnO:Cu(Bi), phosphor electroluminescence mechanism, spectral energy distrib. 7-7760
 ZnO-electrolyte interface, electrolum. under cathodic and anodic pulsed polarisation 7-13235
 ZnS, rare earth impurities, electrolum. of Schottky barriers, photolum., charge compensation, and impurity electron states 7-64700
 ZnS:Cu, electrophosphors, aging phenomena 7-27791
 ZnS:Cu, Mn (H), electroluminesc., simultaneous action of AC and DC fields 7-64699
 ZnS:Cu, solid solution, electroluminescent phosphor, compositional inhomogeneities 7-6800
 ZnS:Cu,Mn films, vacuum deposition and DC electroluminescence 7-7868
 ZnS:Cu,Yb phosphor, AC electrolum. study 7-13233
 ZnS:Er, impact cross section of Er³⁺ in luminesc. spectra 7-46150
 ZnS:Mn, electrolum. study 7-13234
 ZnS:Mn, impact excitation and Auger quenching 7-27827
 ZnS:Mn, thin film electroluminesc. capacitors, trapping level spectra 7-12666
 ZnS:Mn electrolum. thin film-based struts., native memory formation, supersound effects study (*Russian*) 7-3020
 ZnS:Mn electroluminescent thin films, photothermal deflection spectroscopy 7-27804
 ZnS:Mn films, struct. and electroluminescence props. (*Japanese*) 7-27783
 ZnS:Mn heavily doped phosphors, mechano and electroluminesc. 7-13240
 ZnS:Mn thin films, DC electrolum. and local destructive dielec. breakdown model calcs. 7-59147
 ZnS:Mn thin films, electrolum., review 7-27784
 ZnS:Mn thin films, local destructive breakdown and DC electrolum., film prep. and test conditions depend. 7-59146
 ZnS:TbF thin-film electroluminescent devices, excitation mechanism 7-46149
 ZnS:TbF_x sputtered thin films, electrolum. and photolum. 7-7727
 ZnS-based electroluminescent phosphor, influence of surface Cu₂S 7-7759
 ZnSe-ZnS electroluminescent MIS structures, MOCVD growth and charactn. 7-59443

electroluminescent devices *see electroluminescent displays; luminescent devices*

electroluminescent displays

- Al₂O₃-Ta₂O₅ thin films, dielec. props. rel. to electrolum. display appls. 7-2975
 ZnS, polycrystalline, AC driven thin film electrolum. displays 7-7762
 ZnS:Cu,Mn films, vacuum deposition and DC electroluminescence 7-7868
 ZnS:TbF thin-film electroluminescent devices, excitation mechanism 7-46149

electrolysis

- see also anodisation; electrical conductivity of electrolytic liquids; electrodeposition; electroforming; electrolytic dissociation; electrolytic ion mobility; electrolytic machining; electrolytic polishing*
 alkali metal chloride melts, anodic Cl evolution, galvanostatic transient anal. 7-33938
 alkaline earth orthovanadates, solid solns., defect struct. and electrochem. changes of O 7-32787
 alkaline earth orthovanadates, surface electrochem. of O, cyclic voltammetric obs. 7-33957
 cation-exchange resin, granulated, ionic composition, pulsed elec. field effects 7-54134
 cyanocobalt (III) phthalocyanine, conductive crystals prepared by electrolysis 7-2590
 electrochemical H₂ production, electrocatalytic materials comparison and eval. 7-65645
 gas-bubble nucleation in supersaturated solns. during electrolysis, electrode surface effects 7-54139

electrolysis continued

- liquid metal anodes, dissolution during low freq. current interruptions 7-12287
 ozone generation by membrane electrolysis for treating ultra-pure water 7-23024
 photoelectrochemical cell for H₂ production, photoelectrolysis of H₂S using n-CdSe photoanode 7-54328
 photography, waste fixing solution electrolysis, programmed current control system (*Russian*) 7-35616
 solar H₂ production, S-I₂ cycle versus water vapour electrolysis 7-65651
 solar H₂ technology, water electrolysis (*German*) 7-65642
 solid oxide electrolytes, electroreduction, galvanostatic process kinetics 7-21505
 solid state electrolyte, δ -transfer and diffusion (*French*) 7-17801
 Titan tholins, production by d.c. discharge and form. of amino acids, implications for Titan atm. 7-34858
 tritiated water, enrichment and vol. reduction using an electrolysis cell with a permeable cathode 7-49668
 water electrolyser for H₂ production, membrane electrolysis 7-23230
 water electrolysis and the use in electrolytic H₂ and NH₃ production 7-23231
 Ag, electrolytic recovery from fixing solutions, modern commercial equipment (*Russian*) 7-35612
 Al, anodic oxidation coatings, electrolytic colouring, mag. field effects (*Japanese*) 7-59662
 Cr-rich oxides, dissolution using H₂SO₄-Ce(IV) soln., radiation decontamination appl. 7-6803
 Cu, reduction, electrochem., autocatalytic, by formaldehyde 7-54138
 Fe electrodes, electroreduction and passivation K₂CO₃-KHCO₃ solns., ionic comp. effect 7-17677
 Fe, passivation and spontaneous dissolution in presence of O₂ 7-22872
 Ge:Na(K), impurity addition by electrolysis 7-44578
 H overpotentials on Pd(Pd alloy) electrode surfaces 7-23031
 H₂ as energy carrier, H₂ production using alkaline water electrolysis cell (*German*) 7-65641
 H₂ energy storage using alkaline type ion exchange membrane water electrolysis 7-3727
 H₂ evolution kinetics for water electrolysis at Ni-Mo-Cd electrocoated cathodes 7-3728
 H₂ production by solar photovoltaic convertor and electrolyser 7-3721
 H₂ production by TiO₂ thin film electrodes of photoelectrolysis solar cells 7-3725
 H₂ production from water electrolysis (*French*) 7-59879
 H₂ production processes, thermodynamic perform. anal. and comparison 7-65650
 H₂ production using electricity from 500 kW solar energy generating facility (*German*) 7-28417
 H₂ production using photovoltaic solar energy electrolysis, review 7-3726
 H₂O electrolysis for H₂ production using photovoltaic power unit 7-46973
 H₂S electrolysis in aqueous alkaline solutions 7-65649
 H₂SO₄ and H₂ production from electrolysis of aqueous S slurry 7-3724
 In surface, electrochem. H evolution in US field 7-11231
 Mn-NH₄ solutions, electrolysis, pH rise at cathode 7-33937
 NaCl solns., electrolysis, alkali conc., filtering diaphragms effects 7-54136
 Rh-Ru alloys, electroreduction, electrocatalytic activity 7-54137
 Si:Na(K), impurity addition by electrolysis 7-44578
 n-Si-MnO photoanodes, photoelectrochemical and struct. behaviour 7-54329
 SrCeO₃ based proton conductive solid electrolyte in high temp steam electrolysis for H₂ production 7-54364
 T₂O water decomposition using ZrO₂-Pt cell for H₂ production 7-3581
 V complex, vanadium(III)bis(2,2'-bipyridyl) chloride-Fe(III) system, photogalvanic effect 7-54145

electrolytes

- for solid electrolytes see superionic conducting materials*
see also electrolysis; superionic conducting materials
 1,1-electrolyte, solns., apparent molar vol. calc. 7-32538
 absorbed in charged surface, mean spans calcs. 7-44995
 advanced high energy density battery with NaAlCl₄ and β -alumina solid electrolyte 7-39981
 alkali halide solns. in water-acetamide mixtures, partial molal vol. meas. 7-58389
 alkali metal perchlorate vitrified dil. solns., IR spectra anal. 7-19857
 alkali metal poly(styrenesulphonate)s, enthalpy of dilution, large dielectric constant solvent 7-21483
 alkaline batteries, thermodynamic framework for efficiency estimation 7-3636
 aqueous solutions, activation energy for viscous flow, temp. depend. 7-6846
 aqueous solutions, single and mixed, vap. press. prediction at 25°C. 7-38176
 binary mixtures, US studies 7-26869
 bipolar batteries with common electrolyte paths, leakage currents 7-28392
 carboxylated rubber, study of maleic acid residue and vinyl monomer on props. 7-39902
 1,2-diol solns. with water or electrolytes, dielectric props. 7-13080
 diphilic polyelectrolytes, conc. effect on wetting of Teflon 7-38302
 distribution inside and outside membrane, low freq. streaming pot. with overlap of diffusion layers 7-8291
 double layer, local HNC/HNC approx. 7-8290
 electric double layer, thermodynamic consistency of the modified Poisson-Boltzmann eqn. 7-33941
 electrochromic materials, book contrib. 7-25913
 electrolyte-metal rough interface, AC response, inverse-Cantor-bar model anal. 7-22012
 1:1 electrolytes, high-temp. thermodynamic props. 7-21481
 four component mixtures, phase diagrams 7-12274
 interface in electrolyte near critical point elec. struct., elec. double layer 7-33063
 ion distribution near charged electrode, local density functional approx. 7-54131
 lithium trifluoromethyl sulphite, in polymer electrolytes, ion pairs triplet form., conductance meas. 7-32690
 magnesium poly(styrenesulphonate)s, enthalpy of dilution, large dielectric constant solvent 7-21483
 Matsushita molten carbonate fuel cell development (*Japanese*) 7-65455

electrolytes continued

- mean spherical approximation, chem. ion assoc. and dipolar dumbbells 7-54141
- methylated Aerosil R-972, organophilic, alcoholic dispersions, coagulation by additions of water and electrolytes 7-8325
- microprocessor measurement of electrolyte concentration by a conductometric method (Polish) 7-54143
- molten carbonate fuel cell electrolyte structures, fabrication techniques 7-46934
- molten carbonate fuel cells, fabrication of bubble press. barriers 7-13856
- molten carbonate fuel cells with low press. electrolyte, effect of carbonate content on cell performance (Japanese) 7-17858
- MPB5 diffuse layer pot. drop 7-13785
- new sensing materials (Japanese) 7-54142
- osmotic coefficients for polyelectrolyte solutions with ionic mixtures from Poisson-Boltzmann eqn. 7-13806
- plasma-electrolyte metal heating mechanism 7-46857
- polyacrylic acid, pyrene substituted, solns., fluoresc. quenching, polyelectrolyte effects 7-62446
- polyanion-polycation complexes, charge density and side-chain branching struct. effects 7-21136
- polyelectrolyte, weakly charged, in poor solvent, struct. phase transitions 7-51600
- polyelectrolyte chain in soln. containing counterions, size study 7-58122
- polyelectrolyte solns., small-angle scatt. 7-44338
- polyelectrolyte solns., spin relax., local order with cylindrical interfaces, translational diffusion, continuous diffusion model 7-64540
- polyelectrolyte solutions, extensive force, num. eval. 7-46853
- polyelectrolyte solutions, small angle X-ray scatt. 7-11886
- polyelectrolytes, counterion condensation, Poisson-Boltzmann eqn. sol. 7-52029
- polyelectrolytes, highly asymmetrical, spinodal curve 7-21466
- polyelectrolytes, transient elec. birefringence of rod-like polyions 7-39083
- polyions, charged spherical, time depend. electrolyte friction calc. 7-21067
- polymethacrylic acid, solns., chain dimens., small-angle scatt. obs. 7-16389
- pulsed discharge, plasma composition determ. 7-20991
- salt/water/aprotic solvent mixtures, alkali cation influence, IR spectra anal. 7-19856
- short range forces between charged lipid bilayers, theoretical model 7-28478
- solution, elec. cond., ionic trace effects, mobility determ. 7-21497
- solution surfaces, hydrodynamic instabilities caused by elec. forces. 7-51322
- solutions, ionic props., mol. dynamics simulation 7-44331
- solutions, ionic transport, space-charge density, Nernst-Planck and Poisson eqn. calcs. 7-26989
- solutions, viscosity, dielec. function theory 7-44883
- solutions for processing metals, elec. discharges (German) 7-51528
- specific heat and density meas. of several 1:1 electrolytes 7-6816
- strong, equations of state 7-6750
- sulphobetaine polymers, phase behaviour and soln. props. 7-38164
- symmetric problems, field theoretic approach 7-11874
- ternary electrolyte systems, diffusion pot. in simple porous membranes 7-54170
- tetrabutylammonium iodide in formamide, surface segregation phenomena, angle resolved electron spectroscopy 7-52058
- trifluoromethanesulphonic acid electrolyte in fuel cells, O solubility, diffusion coeff., reduction rate, adsorption on Pt surface 7-28395
- unassociated, ionic activities, hydration model 7-54081
- vitryfied dil. alkali metal nitrate solns., IR spectra anal. 7-19857
- ²²NaCl, aq. soln., adsorpt. and diffusion at low concs. 7-27106
- Ag, electrodeposit structure rel. to plating from complex electrolytes 7-2406
- Al-air battery with crystallizer to extend electrolyte lifetime, traction appls. 7-65441
- Al-FeS₂ secondary cell performance develop. using AlCl₃/1-butylpyridinium chloride electrolyte 7-8370
- AlCl₃/1-butylpyridinium chloride electrolyte for Al-FeS₂ secondary cell, phys. and elec. characts. (Japanese) 7-8371
- AlNH₄(SO₄)₂ multicharged electrolyte soln. in water-tert butyl alcohol, viscosity and density studies 7-52104
- β -Al₂O₃-Na₂O, solid electrolytes, Debye-Huckel-type relax. processes 7-17800
- Ca(AlCl₄)₂-SOCl₂ cells, cond., C cathode performance improvement 7-13851
- Ca(AlCl₄)₂-SOCl₂ electrolytes in Ca-SOCl₂ cells, performance improvement using C cathodes 7-65444
- H₂ evolving electrode with superimposed electrolyte flow, mass transfer 7-46852
- H₂ production using WC cathodes in acid electrolytes 7-3729
- HCl-SrCl₂ mixed electrolyte, thermodynamic study, appl. of Pitzer's eqns. 7-33940
- HCl₅.5H₂O-Au electrolyte-electrode interface, double layer capacity, temp. and freq. depend. 7-59769
- H₃PO₄ electrolyte in fuel cells, O solubility, diffusion coeff., reduction rate, adsorption on Pt surface 7-28395
- H₂SO₄, 1-1 electrolyte theory 7-9631
- KAl(SO₄)₂ multicharged electrolyte soln. in water-tert butyl alcohol, viscosity and density studies 7-52104
- KOH, conc. effects on Zn-NiOOH cell shape change and cycle life 7-28393
- Li three electrode secondary cells, electrode processes at Li-polymer electrolyte interface 7-3639
- Li-(CF)_n cells, improved discharge characts. at low temp. using mixed organic electrolytes 7-8368
- LiCl-LiBr-KBr molten electrolyte in Li-Al/FeS₂ secondary cell 7-65439
- LiClO₄, in polymer electrolytes, ion pairs triplet form., conductance meas. 7-32690
- Li(SO₃)₃AlCl₄ electrolyte in Li-SO₂ rechargeable cell 7-65443
- NH₄F in dioxane-methanol mixtures, assoc. constant. from cond. meas. 7-33939
- NaCl, aq. soln., transport across membrane, hydrated species interactions 7-33968
- NaCl soln., salt vel. correl. functions, microscopic interpretation 7-12338
- NaSCN, NH₃ soln., IR spectra study 7-46901
- Ni-Cd aerospace cells, flood starved design 7-34015
- Ni-Cd high-performance battery (Japanese) 7-65434
- Pb-acid batteries, mass transport during plate formation 7-39985

electrolytes continued

- Pb-acid storage batteries, role of transport phenomena (Hungarian) 7-17856
- α -RuCl₃, intercalation reactions, hydrated phases 7-46837
- SiO₂ in aqs. solns. of cetylpyridinium bromide and inorganic salts, coagulation, thermodynamic stability 7-8326
- SrCeO₃ based proton conductive solid electrolyte in high temp steam electrolysis for H₂ production 7-54364
- Ta-Ta₂O₅-electrolyte system, conduction processes 7-38725
- Zn-air battery with flowing alkaline electrolyte 7-65442
- Zn-Br cells, selection of quaternary ammonium bromides as electrolyte 7-39986
- ZnO:Co, pulsed-laser induced photopots., time evolution, electron-hole recombination 7-45379
- electrolytes, solid** *see superionic conducting materials*
- electrolytic capacitors**
Zr/ZrO₂/Na₂SO₄ soln., charge storage props. study 7-58930
- electrolytic conductivity of liquids** *see electrical conductivity of electrolytic liquids*
- electrolytic deposition** *see electrodeposition*
- electrolytic devices**
No entries
- electrolytic dissociation**
see also electrolytic ions
K₂O-SiO₂-NaCl melts, alkali cation dissociation determ., solidification temp., elec. cond. and cryoscopic meas. 7-12288
Li₂O-SiO₂-NaCl melts, alkali cation dissociation determ., solidification temp., elec. cond. and cryoscopic meas. 7-12288
Na₂O-SiO₂-KCl melts, alkali cation dissociation determ., solidification temp., elec. cond. and cryoscopic meas. 7-12288
- electrolytic ion mobility**
see also electrophoresis
electrolyte solution, elec. cond., ionic trace effects, mobility determ. 7-21497
- electrolytic ions**
see also electrical conductivity of electrolytic liquids; electrolytic dissociation; electrolytic ion mobility
microprocessor measurement of electrolyte concentration by a conductometric method (Polish) 7-54143
- electrolytic machining**
see also electrolytic polishing
W, scrap processing into powders by electroerosion disintegration 7-3225
- electrolytic polishing**
see also electrolytic machining
jet electropolishing method for optical metallography 7-59653
Al-In, monotectic alloy, section prep., micromilling, polishing (German, English) 7-22937
Al-Pb, monotectic alloy, section prep., micromilling, polishing (German, English) 7-22937
Cu, fatigue near surface indentations and pits, deform. 7-46628
Cu₃₃Zr₆₇ metallic glasses, flux pinning and critical current peak effect studies 7-22079
Fe₇₈B₁₃Si₉ amorphous ribbons, ferromag. resonance 7-27606
Ni₃₃Zr₆₇ metallic glasses, flux pinning and critical current peak effect studies 7-22079
Zn-Pb, monotectic alloy, section prep., micromilling, polishing (German, English) 7-22937
- electromagnetic absorption** *see electromagnetic wave absorption*
- electromagnetic compatibility**
see also electromagnetic pulse; frequency allocation
RF anechoic room absorbers eval. in 30 to 1000 MHz range 7-43604
- electromagnetic corrections**
"electromagnetic corrections" is distinguished in use from "radiative corrections" by application to elementary particle and nuclear interactions
see also radiative corrections
de Sitter symm., spontaneous breaking by radiative effects 7-35373
E₈-SU (3)_CXSU (2)_LXU (1)_XU (1)_YXU (1)₁' GUT, bounds on Z masses and couplings from electroweak corrections 7-61527
electroweak radiative corrections, renormalization scheme dependence 7-35774
electroweak standard model, 1-loop renormalisation, leptonic processes appl. 7-61512
finite temperature QED at one loop level, renormalisation and radiative corrections 7-19056
gaugino masses from radiative corrections in superstring models 7-24864
heavy leptonium, radiative corrections to one-photon annihilation leptonic decays 7-35871
Kobayashi-Maskawa-Cabibbo matrix, standard model test of O(α) radiative corrections 7-41785
neutrino indices of refraction, quantum loop corrections 7-41680
optical experiments for electroweak theory, atomic mirror symmetry breaking, Z⁰ exchanges 7-61534
pseudo-Dirac ν as possible explanation of solar ν puzzle 7-56481
quantum effects of elementary particle interaction with intense EM field 7-49045
radiative corrections to vector boson masses for heavy Higgs bosons 7-30272
SO₃ gauge field interacting with isovector Higgs field, radiative corrections, monopole model 7-15090
SO (10)-SU (3)_CXSU (2)_LXU (1)_XU (1)_Y GUT, bounds on Z masses and couplings from electroweak corrections 7-61527
solar ν problem, Mikheyev-Smirnov-Wolfenstein mechanism and pseudo-Dirac ν 7-24819
SU(2)XSU(1) radiative corrections, nonstandard Higgs bosons 7-10005
SU(2) gauge theory, topological mass induced by radiative corrections 7-420
e⁺e⁻ \rightarrow hadrons, asymmetries, electroweak radiative corrections, Z₀ resonance 7-15166
e⁺e⁻ \rightarrow $\gamma\gamma$, electroweak radiative corrections 7-35848
e⁺e⁻ \rightarrow $\mu^+\mu^-$, radiative corrections to charge asymmetry in supersymmetric theories 7-5081
e⁺e⁻ \rightarrow tt, polarization asymmetries, one-loop electroweak corrections 7-534
e⁺e⁻ \rightarrow Z γ , QED radiative corrections 7-535
e⁺e⁻ \rightarrow Z γ , renormalised Zec vertex function 7-536
Z⁰ \rightarrow $\nu\bar{\nu}$, electron energy spectrum calcs. with radiative corrections 7-61670

electromagnetic corrections continued

tt resonance, one-loop electroweak radiative corrections 7-41819
 W- ν_μ ($\bar{\nu}_\mu$)($\bar{\nu}_\mu$), electroweak one-loop corrections, form factor, calc. scheme 7-5091

electromagnetic decays

hyperon radiative decays, Skyrme model predictions 7-61696
 leptonic-decay and E1 transition rates, instantaneous BS eqn./confining force anal. 7-5053
 low energy meson physics in the superconducting quark model 7-35811
 photinos stability and primordial nucleosynthesis 7-66793
 quantum effects of elementary particle interaction with intense EM field 7-49045
 single electron search expt., sparticle mass limits 7-49142
 vector meson radiative decay in lattice QCD 7-35879
 $A_2 \rightarrow \gamma\gamma$, radiative width meas. from $e^+e^- \rightarrow e^+e^- A_2(1320)$ 7-526
 $B \rightarrow \gamma X$, helicity suppression and colour thaw problem 7-61590
 $B \rightarrow K^{*0}(K^{*+})\gamma$, branching fraction upper limits 7-61655
 B_b , mass spectra, leptonic-decay and E1 transition rates, instantaneous BS eqn./confining force anal. 7-5053
 cc states, radiative angular distribns. 7-15162
 $\chi_c \rightarrow \psi\gamma$, mass, width, branching ratios from $p\bar{p}$ annihilation (French) 7-56542
 $D \rightarrow \gamma X$, helicity suppression and colour thaw problem 7-61590
 $\eta \rightarrow \gamma\gamma$, meson-quark coupling constants, one-loop quark model 7-61695
 $\eta' \rightarrow \pi\pi^0\pi^0$, radiative width meas. 7-61717
 $\eta' \rightarrow \omega\gamma$, branching ratio meas. 7-61654
 F^* charmed strange pseudovector meson, cascade radiative decay obs. 7-49137
 $\iota(1466) \rightarrow \gamma\gamma(0\gamma)$, radiative decays and SU(3) flavour structure 7-15161
 $\iota \rightarrow \gamma\gamma$, constraints due to topological susceptibility and chiral Ward identities 7-5097
 J/ψ decays, rare phenomena, comparison of hadronic and radiative processes 7-61666
 $K^- \rightarrow \pi^0\gamma e\bar{\nu}$, decay probability, dependence on γ -detection threshold, T violation asymmetry 7-56538
 $K_L^0 \rightarrow \gamma\gamma$, chiral perturbation theory corrections to SU(3) terms 7-15160
 $K_S^0 \rightarrow \gamma\gamma$, branching ratio upper limit determ. 7-35878
 K^0 decay, CP violation, experimental anal. 7-41786
 $\mu \rightarrow e\gamma$, and heavy exotic fermions in E_6 models 7-15153
 $\mu \rightarrow e\gamma$, lepto-quark effects in E_6 superstring models 7-61651
 $\mu^+ \rightarrow e^+\gamma$, branching ratios, experimental upper limits 7-41802
 $\mu^+ \rightarrow e^+\gamma\gamma$, branching ratios, experimental upper limits 7-41802
 $\nu \rightarrow \gamma X$, heavy ν , lifetime constraints from primordial light-element photodestruction anal. 7-10059
 $\nu \rightarrow \nu\gamma$, lifetime in left-right models 7-35764
 $O \rightarrow \pi^+\pi^-$, radiative decays of 1^- quarkonia to $O^0, 1^+, 2^\pm$ states 7-525
 $\phi \rightarrow \pi^+\pi^- \gamma$, rare decay mode anal. 7-5086
 $\pi \rightarrow \gamma\gamma$, partial decay widths in QCD with coloured light scalars 7-19105
 $\pi^0 \rightarrow \gamma\gamma$, branching ratio, experimental limitations 7-15163
 $\pi^0 \rightarrow e^+e^- \gamma$, two-photon-exchange contribution calcs. 7-61653
 $\pi^0 \rightarrow e\bar{e}\gamma$, form factor information 7-15145
 $\pi^0 \rightarrow \gamma\gamma$, meson-quark coupling constants, one-loop quark model 7-61695
 $\pi^+ \rightarrow e^+\gamma$, axial vector to vector weak π^+ form factor meas. 7-10055
 $\pi^+ \rightarrow e^+\nu_e\gamma$, pion axial-vector to vector form factor ratio meas. 7-41802
 $\pi \rightarrow \eta\gamma(\eta'\gamma)$, gluonium content in phenomenological limits for SU(3) breaking 7-19108
 $\psi \rightarrow \gamma H$, Higgs production, comparison with phenomenological limits for $K \rightarrow e\bar{\nu}H$ and $\psi \rightarrow \nu\bar{\nu}H$ 7-513
 $\psi \rightarrow \gamma X$, MARK III results 7-41791
 $\psi \rightarrow \eta\pi_0, \eta_c \rightarrow \phi\phi, \eta_c$ search, branching ratio meas. 7-24878
 $\psi \rightarrow \gamma\phi\phi \rightarrow \gamma K^+K^-K^+K^-$, glueball search 7-24879
 $\psi \rightarrow \gamma\phi$, helicity amplitudes, glueball picture of $\theta(1700)$ 7-41818
 $\rho \rightarrow \pi\gamma$, partial decay widths in QCD with coloured light scalars 7-19105
 $\rho \rightarrow \pi\pi\gamma$, pseudoscalar coupling constant, relativistic confinement calcs. 7-515
 $S(V_1V_2) \rightarrow \gamma\gamma(\gamma Z^0), V_L = W^\pm, Z^0$, branching ratios, nonrelativistic bound-state calcs. 7-49154
 $\Sigma^0 \rightarrow \Delta\gamma$, transition magnetic moment meas. 7-524
 $\Sigma^+ \rightarrow p\gamma$ asymmetry, W-exchange dominance in SU(6) broken quark-diquark model 7-49153
 $\tilde{t} \rightarrow \gamma H$, minimal and two-doublet Higgs prod., standard model 7-35762
 $\tau \rightarrow \nu\gamma\tau(\rho)$, radiative 3-body decays 7-15152
 $T(1S)$, decay spectrum, α_s determ. 7-61663
 $T(1S)$, exotic decay modes search at ARGUS 7-24890
 $T(2S) \rightarrow \gamma\chi_{b0}, \chi_{b0} \rightarrow \gamma T(1S) \rightarrow e^+e^- (\mu^+\mu^-)$, branching ratio meas. 7-19102
 $V \rightarrow H^0\gamma$ radiative decay, relativistic effects calcs. 7-49094
 $V \rightarrow p\gamma$, decay amplitude calcs., lattice QCD anal. 7-35801
 $V(t) \rightarrow \gamma$, investigation of weak neutral currents in $h_1h_2 \rightarrow V(t)\bar{t})X$ 7-5098
 $\tilde{W} \rightarrow \mu\gamma$, supersymmetric signals in leptonic decays 7-41808
 $W \rightarrow \gamma l \bar{\nu}_l, \mu\bar{\nu}_\mu$ meas. proposals as electroweak model test 7-15156
 $Z \rightarrow \gamma\gamma(HH\gamma)$, composite model study 7-24886
 $Z \rightarrow \bar{\nu}\nu\gamma$, composite model study 7-24886
 $Z^0 \rightarrow \mu\gamma$, Stokes parameter calcs. and anomalous mag. moment 7-41807
 $Z^0 \rightarrow q\bar{q}\gamma$, Stokes parameter calcs. and anomalous mag. moment 7-41807
 $D^{*0} \rightarrow K^-\pi^+\gamma$, fragmentation function meas. 7-56561
 $\eta_c \rightarrow \gamma\gamma, R_1 = \Gamma(\eta_c \rightarrow \gamma\gamma)/\Gamma(D^{*+} \rightarrow \mu^+\nu_\mu)$ calcs. bound state quark model anal. 7-61582
 $H \rightarrow W^+W^-\gamma$, decay width determ. 7-15155
 $\nu \rightarrow \nu'\gamma$, decay rate calc. in E_6 superstrings 7-30266

electromagnetic energy see electromagnetic waves**electromagnetic field theory**

see also *electromagnetic waves; electromagnetism*
 2D electrostatic and EM problems, general interactive finite element package 7-62569
 Bloch transform as scattering problem, inversion problem 7-61131
 charged particles motion, bounded systems with collisions 7-48521
 curl $a = ka$, solutions 7-48392
 Debye scalar potentials for the electromagnetic fields, mag. monopoles 7-36850
 dipole EM radiation in chiral media using dyadic Green's function 7-1005
 dyadic Green's function, improper integrals evaluation 7-31216
 edge wave, current point source, conducting wedge presence 7-15801
 electric source problem in Hermite-symmetric Einstein field theory 7-29838
 finite element study (French) 7-15796
 force-free EM fields, cylindrical oscillations 7-34857
 generalised field theory, EM field eqns. using gauge structs. 7-9720
 geometric optics, Riemann-Cartan space-time 7-1010

electromagnetic field theory continued

gyrotropic media, scalar Hertz potentials for transversally oriented current density distribns. 7-57205
 half-rhombic EMP simulator, pulse excitation EM fields anal. (French) 7-10816
 Helmholtz equation semi-infinite medium, inverse problem 7-61132
 Hertz vectors, role in description of source free EM fields in vacuo 7-42847
 Hertzian dipole radiation in stratified uniaxial anisotropic media, computation 7-36860
 HF field expression, reflector caustic region, Maslov method appl. 7-36852
 HF multiple diffraction by flat strip, higher order asymptotics 7-15800
 Hodge-deRham theory, appl. to Maxwell's eqns. for transverse electromagnetic wave 7-48391
 inverse source problem comparison for quasihomogeneous, partially coherent sources in two and three dimens. 7-62597
 ionosphere, perturbed reflection layer, electric field calc. 7-40637
 Killing vectors and Maxwell collineations in general relativity 7-48486
 Laplace eqn. in open geometry, approx. soln., variational calculus appl. (Hungarian) 7-50442
 lightning discharge, current induced in aerial on buried telecom. line (French) 7-10817
 linear response theory, gauge invariance 7-25707
 macroscopic EM field in nonlinear or time-variant media, energy and momentum theorems 7-25701
 magnetised plasma far field, minimum distance determ. 7-37694
 Maxwell's eqns., soln. in curved space-time, Green's function adiabatic expansions 7-41183
 Maxwell's equations, extended Lorentz invariant formulation 7-5812
 Maxwell eqns. independency (Hungarian) 7-50441
 monochromatic EM radiation, wave structure 7-50466
 multilayer X-ray reflectivity calcs., lossy transmission line theory 7-37103
 near-zone field transmitted through an electrically small aperture in a perfectly conducting plane screen 7-5817
 open boundary problems, differential and integral methods 7-50454
 particle in cell codes, vectorising interpolation routines 7-50462
 physical optics, fields, perfectly conducting screen aperture, line integrals 7-15802
 polynomial distribution over curved triangular domain, potential integral 7-36847
 Poynting vector, electromagnetic momentum, and Abraham-Minkowski controversy (Japanese) 7-31215
 Proca equation and electromagnetic fields, connection in orthochronous Lorentz group framework 7-24439
 propagators for quantum systems with electromagnetic fields, constructive representations 7-48420
 scattering, dielectric cylinder partially covered by conductor, anal. 7-50473
 scattering by large conducting cylinders, moment method 7-50475
 scattering by two multilayered dielectric cylinders, asymptotic solution 7-42869
 scattering from finite strip grating; curvature effect 7-50474
 scattering from resistive strips complex periodic struct., anal. 7-50476
 shield topology, EM interaction with large systems 7-10820
 squeezed states generation by parametric down conversion, noise level reductions 7-25790
 teaching EM theory in one-course setting for undergraduates 7-55923
 three-dimensional scalar potentials, hybrid finite-element/boundary-element solutions 7-50455
 three-dimensional state space model 7-50456
 unsaturated ferromagnet, EM field eqns., reduction to Burgers eqn. and exact analytic soln. 7-33216
 Vavilov-Cherenkov radiation, elec., mag. and toroidal dipole moments in thin channels 7-56059
 vector-spinor space and field equations 7-56092
 virial theorem generalisation for EM fields 7-20098
 wedge diffraction problem, path integral Riemann space approach 7-4699
 C fibre composite tubular struct., induced EM fields, 2D model prediction 7-25703

electromagnetic fields

2D media, polarisable and magnetisable, forces in EM field 7-50459
 analogy between elastic and EM fields (Polish) 7-20095
 analysis and synthesis based on modified approx. of vector lines (Russian) 7-5816
 atomic photon-dressed discrete states in the continuum 7-19813
 auxiliary currents method and wave potentials, diffraction field anal. 7-50469
 biological membranes, microwave effects, rel. to crit. phase transition 7-40114
 boundary Neumann's problem described by the integral equation-problems of analysis and synthesis (Polish) 7-20094
 bounded nonlocal media, EM field, with several resons. 7-10819
 cavities with current normal to walls, monochromatic solns. 7-42849
 conducting structures with pulsed excitation, time domain anal. of eddy current effects 7-62573
 current distribution in conductors with arbitrary cross sections Biringier, P.P. (Dept. of Electr. Eng., Toronto Univ., Ont., Canada) 7-62576
 dielectric targets composed of continuous assembly of circular discs, light scatt. 7-50482
 E polarisation, thin wire loop, backscattered field anal. 7-36861
 eddy current 3D NDT, surface impedance boundary condition 7-65267
 eddy current inspection problems of weakly cond. weakly mag. media, EM field calcs. 7-39821
 eddy currents three-dimensional formulation, using multiply connected regions 7-42844
 elastoelectromagnetic Neumann boundary value problems, self-consistent theory 7-26145
 EM field production by shock wave propag. in condensed medium 7-32565
 explosive buildup at plasma boundary, surface waves and whispering-gallery modes interaction 7-50457
 ferromagnet EM field spatial-temporal distrib. calc. using small parameter method (Polish) 7-62580
 Feynman's disk paradox, field ang. momentum 7-35163
 flow-rate meter for electrically conducting fluid (Russian) 7-11571
 geophysics, EM modelling program for 2D structures 7-34714
 helical surface waves on a dielectric rod 7-62571

electromagnetic fields continued

- hyperthermia, unbounded electromagnetic problems, hybrid element method 7-18037
- infrared measurements of scattering and electromagnetic penetration through apertures 7-56336
- inhomogeneous systems, EM phenomena, path-integral approach 7-57207
- lateral EM field of vertical dipole, props. and appl. 7-23537
- Leontovich boundary condition calcs. of EM radiation from gamma-ray source 7-31233
- macroscopic EM field in nonlinear or time-variant media, energy and momentum theorems 7-25701
- magnetic dipole-emission during uniform motion in homogeneous medium (*Russian*) 7-20120
- magnetic systems, multiply-excited, finite element soln. of transient eddy-current problem 7-62575
- magnetised compressible media, spatial mapping and time reversal 7-20097
- nuclear field-enhanced internal conversion, appl. to γ -ray laser 7-10125
- open boundary problems solution using finite element method 7-31212
- particle motion in field of two rotating mag. dipoles, equilb. points stability 7-34839
- pulsars, protons and electrons accel. in EM field of rot. orthogonal mag. dipole 7-9339
- relativistic electron beam and spatially inhomogeneous field, energy exchange peculiarities 7-50481
- relativistic orotron with sinusoidal HF distribution along electron trajectories, theory 7-50458
- semiconductor laser in small loop antenna as sensitive HF EM field probe 7-24657
- short magnetic cylinder in transverse time-harmonic mag. field, 7-62574
- smoothly irregular layer, plane wave refl. 7-50488
- three-dimensional exterior field problems, finite-element soln., inversion transformation 7-20096
- two parallel conducting strips, arbitrarily oriented, EM plane wave scattering study (*Japanese*) 7-42859
- vacuum energy of electromagnetic field in rotating system 7-24779
- wave field, rough surface with high Rayleigh parameter scattered, intensity correlation 7-57209
- wedges, structure of Meixner's series 7-62578
- C fibre composite tubular struct., induced EM fields, 2D model prediction 7-25703

electromagnetic induction*see also inductance*

- cylindrical induction pump with inductors producing travelling mag. field, anal. of liquid metal flow (*German*) 7-63107
- DC magnetic field stabiliser based on NMR (*Slovak*) 7-24662
- Earth, dipole induction profiling above sphere buried in homogeneous half-space 7-28827
- Earth, effect of source-field geometry on EM induction India 7-28821
- Elihu Thomson expt., example of progressive modelling 7-55930
- Green's function, determ. for induction equation in spherical region with boundary 7-66445
- lightning discharge, current induced in aerial on buried telecom. line (*French*) 7-10817
- magnetic fields, variable, meas. under cryogenic conditions 7-48787
- power lines, transient behaviour, real ground presence (*French*) 7-10818
- scattering problems, hybrid iterative method 7-20099
- SEM type-1 magnetic contrast, rel. to mag. field vector pot. 7-56378
- time-dependent current, induced electric field 7-41037
- transducers for Barkhausen jump detection, computation and design problems 7-39823
- wires and loops, inductance, upper and lower bounds 7-42850
- C fibre composite tubular struct., induced EM fields, 2D model prediction 7-25703
- NdHoDyFeB permanent magnets with zero temp. coeff. of induction 7-53047

electromagnetic interference*see also electromagnetic pulse; radiofrequency interference*

- magnetic vortex field, 2D, with boundary conditions of 3rd kind, numerical determ. for tube drawing, inductive heating (*German*) 7-33811
- satellites, electron-irradiated dielectric discharges, statistical behaviour 7-55423
- shield topology, EM interaction with large systems 7-10820

electromagnetic launchers

- ablative macroparticle accelerator using electron beam diodes for accelerating projectiles 7-36266
- discharge in rail accelerator with circumferential flow, integral model 7-32159
- unipole multipactoring discharge in the LHRF launcher 7-26440

electromagnetic lenses *see magnetic lenses***electromagnetic oscillations***see also cavity resonators; lasers; masers; ring lasers*

- cylindrical oscillations of force-free EM fields, freq. spectrum prediction 7-34857
- monochromatic EM radiation, wave structure 7-50466

electromagnetic pulse

- electron beam produced, calcs. 7-20118
- half-rhombic simulator, pulse excitation EM fields anal. (*French*) 7-10816
- impulsive atmospheric noise, hourly APDs, semitropical location and evening transition period 7-47483
- lightning storms intensity determ. using centimetre and metre-wave radar (*Russian*) 7-47549
- near-zone field transmitted through an electrically small aperture in a perfectly conducting plane screen 7-5817
- power lines, transient behaviour, real ground presence (*French*) 7-10818
- pulse power radial transmission line, matching problems 7-32075

electromagnetic radiation *see electromagnetic waves***electromagnetic theory of light**

No entries

electromagnetic wave absorption

- see also electromagnetic wave propagation in plasma; gamma-ray absorption; light absorption; spectra; X-ray absorption*
- 1-350 GHz sea level attenuation, dry air and water vapour effects determ. algorithms 7-40548
- atmospheric, estimation of partitioned set of parameters 7-40554
- atoms, electron impact, resonant EM radiation absorption 7-50353
- cm and mm wave propagation, tropical raindrop size characts. and effects 7-66280

electromagnetic wave absorption continued

- conductors, comparison between exactly and approximated boundary conditions 7-42858
- dielectric slab lossy, absorpt., effect of surface texture 7-42851
- ionosphere, absorption of cosmic radio noise at high latitudes, spectrum 7-14405
- microwave communication, equatorial and tropical regions, rain effects 7-66281
- polar molecules in nonlinear interaction with radiation, resonant variation of energy 7-19992
- semiconductors, high frequency EM surface heating wave attenuation calcs. (*Russian*) 7-59307
- soil, photon attenuation, particle size effects 7-21279
- superconducting films, nonequilibrium dynamic quasi-particle distrib., high freq. EM field effects calcs. (*Russian*) 7-27467
- TM wave resonance absorption in inhomogeneous plasma 7-58018
- Cr, surface EM wave absorpt., 4-350K 7-33354
- Ge IR absorpt. coeff. meas. with compensating calorimeter 7-56270
- InSb:Te, resonance absorpt. of electromag. wave due to impurity band 7-52499
- Si, amorphous, IR absorpt., local phonon-induced bond angle distortion model 7-26642

electromagnetic wave attenuation *see electromagnetic wave absorption; electromagnetic wave scattering***electromagnetic wave diffraction***see also electromagnetic wave propagation in plasma; gamma-ray diffraction; light diffraction; X-ray diffraction*

- antennas and propagation, conf. Philadelphia, PA, USA (June 1986) 7-41011
- array of strips with small random fluctuations of dimensions 7-36863
- auxiliary currents method and wave potentials, diffraction field anal. 7-50469
- backscattering from triangular cylinder and hexahedron 7-42865
- conducting polygonal cylinder, 2D wave diffraction theory 7-36853
- cylinder, circular, diff. pattern behind cylinder in penumbral region 7-50465
- dielectric gratings, slanted and unslanted, total field formulation 7-5981
- dielectric gratings with losses, diffraction analysis 7-5982
- dielectric scatterers in half-space, freq. properties 7-57215
- grating, reflective, wave scatt., const. and dynamic phase effects 7-37128
- gratings, embedded in inhomogeneous lossy dielec., finite-difference coupling technique anal. 7-1256
- gyrotropic medium, half-plane, Wiener-Hopf eqns. soln. 7-50460
- HF field expression, reflector caustic region, Maslov method appl. 7-36852
- HF multiple diffraction by flat strip, higher order asymptotics 7-15800
- interstellar medium, refractive and diffractive scatt. of radio waves 7-55759
- Maxwell's eqns. in inhomogeneous media, 2D finite-difference time-domain analysis 7-15809
- multiple reflector antennas, diffraction losses calc., asymptotic transition region theory 7-50471
- optical waveguide interdigital circuit struct., waveguide mode diffraction, gap effects 7-57543
- perfectly conducting flat strip, pulsed signal scattering, deemphasizing LF defects in GTD anal. 7-20104
- perfectly conducting half-plane screen, EM diff. problem 7-20105
- perfectly conducting semicircular cylinder, hybrid UTD-MM anal. of scattering 7-20103
- periodic boundaries between isotopic dielectrics, EM waves diff. 7-57212
- physical optics, fields, perfectly conducting screen aperture, line integrals 7-15802
- plane monochromatic wave incident upon a lattice, diff. 7-41109
- plane wave diffraction, impedance cylinder with arbitrary cross section, quasiwave asymptotic form 7-50467
- plane wave diffraction by array of perfectly conducting cylinders of circular cross section 7-31220
- plane wave diffraction by dielectric cylinder, oblique incidence 7-50461
- plane wave diffraction from circularly symmetric aperture 7-15804
- radar cross-sections, higher order diffractions from a circular disk 7-42866
- radar cross-sections, physical theory of diffraction, double reflections anal. 7-42863
- radar cross-sections calc., equivalent currents, flat plates with surface impedance coatings anal. 7-42867
- radar cross-sections of polygonal cylinders and flat plates, TGD calc. 7-42864
- radiowave diffraction method of complex quality control of cond. surfaces and dielec. coatings 7-39820
- rectangular wedge structure, electromag. wave diffraction (*Russian*) 7-62601
- surface EM wave conversion by diff. grating on dielectric film 7-43345
- thermal radio emission at sea surface 7-60268
- TM wave diffraction by 3D phase grating 7-36856
- two-dimensional diff. problems, adaptive collocation method 7-57211
- vector diffraction theory, plane wave and spread function decompositions 7-62599
- wedge diffraction problem, path integral Riemann space approach 7-4699

electromagnetic wave diffusion *see electromagnetic wave scattering***electromagnetic wave interference**

- see also atmospheric; electromagnetic wave interferometers; electromagnetic wave interferometry; electromagnetic wave propagation in plasma; light interference; moire fringes*
- synchrotron X-ray fluorescence, diffraction interference 7-17830
- X-ray polarisation technique (*Russian*) 7-56393
- X-ray spherical wave diff. on wedge-shaped gap of bicryst. interferometer, interference effects calcs. 7-63398
- Si bent oxidised cryst. wafers, X-ray spherical wave diff., interference phenomena 7-63402

electromagnetic wave interferometers

- see also electromagnetic wave interferometry; light interferometers; radiowave interferometers*
- chaos in a superconducting quantum interferometer 7-18873
- Fabry-Perot, conc. determ. in plasmas using absorpt. method 7-11790
- Fabry-Perot interferometers with three mirrors for submillimeter wave region 7-35577
- JET microwave interferometer, plasma electron density meas. 7-44242
- MERLIN systems, observational performance and potential for radioastronomical research 7-24010

electromagnetic wave interferometers continued

- scanning X-ray interferometer translation stage 7-56240
 Simeiz-Pushchino interferometer obs. baseline determ. 7-4334
 TARA tandem mirror, ECE diagnostic using fast scanning Michelson interferometer 7-11744
 FTIR, optically thin electron cyclotron emission meas. using Michelson interferometer 7-11755
 tokamak plasma, multichannel submillimeter wave interferometer 7-37749
 X-ray dual crystal interferometer, spherical X-ray diffraction 7-63396
 X-ray interferometer for surface roughness transducers calibration 7-35649

electromagnetic wave interferometry

- see also light interferometry; moire fringes; radiowave interferometry*
 V1343 Aql (=SS 433), extended radio struct. obs. with European VLBI Network 7-29478
 V1343 Aql (SS 433), evidence for relativistic beaming from VLBI obs. 7-9476
 element complex X-ray atomic scatt. factors, X-ray interferometry studies 7-32208
 environmental effects in nanometer-range precision meas. (Japanese) 7-48689
 film thickness meas. by autocorrelation function 7-41336
 geodetic radio interferometric surveying for sea-level monitoring 7-18312
 low frequency variable radio sources, two-epoch VLBI obs. 7-4579
 mobile VLBI for vertical crust motion anal. 7-9226
 multiple-beam collimation of X-rays 7-18958
 plasma, in Tokamak, temp. meas. 7-60922
 polymers, permittivity, loss tangent and refractive index meas., using Fourier transform technique 7-18820
 quartz, complex dielec. const. meas. at 245 GHz using double-beam interferometer 7-7632
 QUASAT, scientific and industrial appls. for Australia 7-4340
 radio interferometry, representation of time delay and interference freq. in coordinate-independent form 7-60571
 radiointerferometric sounding of ionosphere, appl. to gravity waves obs. 7-4253
 Raman spectroscopy, interferometric observation, photomultiplier and avalanche diode detectors appls. 7-61379
 satellite VLBI, appl. of orbits with periodic flights around Moon 7-34833
 soft X-ray interferometry and holography 7-18950
 TEXT diagnostics, digital complex demodulation applied to interferometry 7-11752
 VLBI, appl. to North American-Pacific relative plate motion meas. in S California 7-28978
 VLBI, interferometric phase synchronisation of remote heterodynes 7-60570
 VLBI, possible appls. of acousto-optical correlators 7-60569
 VLBI for atomic clocks (French) 7-30068
 VLBI for vertical crust motion meas., effects of atm. water vapour 7-9227
 VLBI fringe-fitting with antenna-based residuals, algorithm 7-34885
 X-ray interferometer for surface roughness transducers calibration 7-35649
 X-ray interferometry image of deform. field around dislocation cluster (Russian) 7-51575
 X-ray Laue-Laue interferometry 7-11831
 BN, complex dielec. const. meas. at 245 GHz using double-beam interferometer 7-7632
 BeO, complex dielec. const. meas. at 245 GHz using double-beam interferometer 7-7632
 H active masers for VLBI appls. 7-43042
 NiFe₂O₄, Trans-Tech 2-111, complex dielec. const. meas. at 245 GHz using double-beam interferometer 7-7632
 SiO₂, complex dielec. const. meas. at 245 GHz using double-beam interferometer 7-7632

electromagnetic wave polarisation

- see also light polarisation*
 0133+476, 0235+164, 1749+096, 2131-021, variable quasars, multifreq. radio polarisation obs. 7-40955
 0634-20, radiogalaxy, linear polarisation and total radio power maps anal. 7-35038
 1759+211, nearby radio galaxy, polarisation and mag. field of oscillating radio galaxy 7-55820
 Abell galaxy clusters, linear polarisation maps at 11.1 cm wavelength 7-18454
 active galaxies, radio cores polarisation props. 7-60803
 astronomical hard γ -ray sources, possibilities for polarisation meas. 7-4593
 atmospheric precipitation preferred orientation relationship with dual polarisation radar echo characts. 7-60367
 B2 1320+299, quasar with asymmetric radio struct., mag. field lines distrib. 7-35065
 3C 219, radiogalaxy, jets collimation and polarisation 7-14647
 3C 2, compact steep-spectrum quasar, radio characts. 7-60833
 3C 428, neglected 3C radio source, spectral index and polarisation distrib. from VLA obs. 7-14672
 3C 445, radiogalaxy, linear polarisation and total radio power maps anal. 7-35038
 correlation (balanced) polarimeter for RATAN-600 radio telescope, polarisation characts. 7-66465
 E polarisation, thin wire loop, backscattered field anal. 7-36861
 FIR and MM wave polarisation transforming reflectors 7-36854
 first year sea ice in tank, multifreq. passive SHF and EHF obs. 7-23659
 G7.7-3.7, highly-polarised radio supernova remnant, total power and polarisation meas. 7-48045
 galactic centre radio arc, 4.8 GHz polarisation obs. rel. to nonthermal radio emission 7-55844
 galactic centre region, prominent polarised plumes and their mag. field, linear polarisation obs. 7-14656
 liquid thin film, with and without Al substrate, refl. coeffs., admittance method investig. 7-64711
 Lyman- α radiation, polarisation analyser 7-57526
 M81, spiral galaxy, radiowave polarisation meas. 7-55798
 monochromatic EM radiation, wave structure 7-50466
 Muller matrices of polarisation systems, general props. 7-66464
 multilayer X-ray polarizers 7-30142
 OMC-1, NH₃ line emission, search for linear polarisation 7-48011
 Orion 8 km s⁻¹ H₂O maser source, time behaviour 7-24233
 plane wave diffraction by dielectric cylinder, oblique incidence 7-50461

electromagnetic wave polarisation continued

- plane wave diffraction from circularly symmetric aperture 7-15804
 polymers, permittivity, loss tangent and refractive index meas., using Fourier transform technique 7-18820
 radio galaxies, 0.6 GHz intensity and linear polarisation mapping of edge-brightened double sources 7-66737
 radio sources, extragalactic, rot. measure vars. rel. to small-scale variations in galactic mag. field 7-29524
 randomly distributed finitely conducting particles, polarised wave scattering and depolarization 7-5818
 reflecting grating, H-polarised inhomogeneous plane wave reson. scatt. (Ukrainian) 7-10823
 solar flare gamma-rays, linear polarisations as indicators of particle directions 7-66563
 Sun, O VI 103.2 nm line polarisation use for coronal mag. field determ. 7-34958
 transitional scattering at a charged filament of spiral sinusoidal form, polarization anal. 7-5822
 VHF-FM broadcast Es propagated signal polarisation obs. 7-60468
 VHF/UHF vertically and horizontally polarised waves, propag. in 3-100 m range (Japanese) 7-14367
 whistler at low latitudes, automatic obs. of polarisation, meas. and tracking equipment (Japanese) 7-34749
 whistlers, nonlinear wavenumber shifts of circularly polarised waves in ionosphere 7-66380
 X-ray polarisation technique (Russian) 7-56393
 Fe, circularly polarised X-ray absorpt. 7-59302
 K, direct EM ultrasound generation, polarisation dependence expt. 7-2110
 Si X-ray phase plate, optimisation for circular polarisation 7-24742

electromagnetic wave propagation

- see also atmospheric electromagnetic wave propagation; atmospheric light propagation; backscatter; electromagnetic wave absorption; electromagnetic wave diffraction; electromagnetic wave interference; electromagnetic wave propagation in plasma; electromagnetic wave reflection; electromagnetic wave refraction; electromagnetic wave scattering; guided electromagnetic wave propagation; light propagation; radiowave propagation*
 anomalous propagation effects on microwave systems 7-1012
 anomalous propagation effects on the performance of a modern 3-D radar 7-1013
 antennas and propagation, conf. Philadelphia, PA, USA (June 1986) 7-41011
 asymmetric waves in a highly nonlinear symmetric layered structure 7-50470
 atmospheric near-mm wave propag., instrumentation for study 7-4219
 book 7-24329
 cermet topology, electromagnetic wave propag., multiple scatt. approach 7-1031
 charged particle acceleration by transverse EM wave in static mag. field (Japanese) 7-20119
 crustal regions shallow sounding using EM surface waves 7-14193
 cylindrical waveguides, aperiodic EM wave processes 7-50464
 cylindrical waveguides, resonance phenomena and aperiodic wave processes 7-50463
 edge wave, current point source, conducting wedge presence 7-15801
 ferrite slab with domain struct., EM waves (Russian) 7-2920
 fourth moment of waves propagating in random media, solution 7-36862
 Gaussian beams at large distances, anal. 7-57210
 ID random medium, minimum wave-localisation length 7-15805
 infinitesimal discontinuities in nonlinear dielectric media, wave front propagation 7-50627
 inhomogeneous media with smooth spatial-temporal inhomogeneities quadratic characts. of waves 7-62625
 intensity cross spectrum, two frequency 7-10826
 lateral wave propagation in a three-layered medium 7-14192
 layered medium propagation, dyadic Green's function formulation 7-62589
 liquid crystals, screw-like orientated, EM wave propag. calc. 7-20113
 magnetosphere whistlers, polarisation of half-gyrofrequency waves in two-component plasma 7-34803
 Maxwell's eqns. in inhomogeneous media, 2D finite-difference time-domain analysis 7-15809
 metal particles, randomly distributed in a dielectric medium, Anderson localisation of EM waves 7-31218
 metals, EM wave interaction with dislocations, conduction electron density (Russian) 7-63615
 metals, nonlinear magnetic Landau damping 7-64277
 model studies for observed increase in delay spread and strength during thunderstorms in Tropo links 7-1014
 monochromatic EM radiation, wave structure 7-50466
 multiple scattering noise in 1D, universality through localisation length scaling 7-1315
 network of wave guides, strong localisation 7-61115
 nonlinear media, propagation of TM modes 7-20110
 nonlinear random waves, evolution of higher order spectra 7-62886
 nonlocal metal optics, screened electromagnetic propagators, Green's function calcs. 7-27260
 periodic 1D grating, free oscills. of EM field (Russian) 7-62822
 phase change meas. of wave propag. through free-electron laser 7-62715
 plane waves, elliptically polarised, propag. along acoustic or optical axes 7-56057
 pulse transmission propagation effects 7-15806
 rough surface bounding layered medium, equiv. impedance, appl. to integrated optical waveguide 7-57239
 singular dispersive medium, wave propag., absorpt. theorem 7-56056
 strongly scattering particles, high density medium, integral equations for first two statistical moments of field 7-10828
 surface electromagnetic waves on the flat interface of moving mediums 7-62591
 teaching EM theory in one-course setting for undergraduates 7-55923
 turbulent medium, coherent and incoherent sources 7-15807

electromagnetic wave propagation in plasma

- see also ionospheric electromagnetic wave propagation; light propagation in plasma; magnetospheric electromagnetic wave propagation*
 Alfvén wave stimulated Brillouin scatt. in low-density plasmas in ionospheric conditions 7-44146
 amplification of electromagnetic waves by a ring-beam distribution of moderately relativistic electrons 7-51503
 atoms, electron impact, resonant EM radiation absorption 7-50353

electromagnetic wave propagation in plasma continued

- beat waves in hot magnetised plasma, decay 7-1692
 charged particle trapping in mag. neutral sheet by mag. field and EM wave 7-11690
 collisional plasma column, whistler waves, dispersion and damping meas. 7-51455
 collisionless electron plasma, plane EM wave propag., solitary wave solns. 7-16309
 degenerate four-wave mixing and phase conjugation in collisional plasma 7-25899
 diatomic polar mol. plasma, quasimonochromatic electric field influence on spectral line shift 7-37757
 double freq. laser irradi. plasma, density profile, elec. field struct. (Chinese) 7-6394
 double stimulated Brillouin scattering in a nonuniform laser plasma 7-6396
 electron cyclotron fluctuations in magnetised plasma, quasi-linear relativistic treatment 7-37690
 EM wakefields for axisymmetric charge distrib. moving through cold uniform plasma, 2D dynamics 7-44263
 envelope solitons of electromagnetic waves in a magnetized plasma 7-44176
 explosive electron emission in microwave fields, excitation and evolution 7-63310
 field patterns of microstrip antenna in two component plasma 7-6397
 filamentation instability of relativistic-intensity EM waves 7-63284
 flat waveguide, potential wave propag., strictional nonlinearity effect 7-20898
 forward Raman scattering obs. in laser-produced plasma 7-11712
 Gaussian EM beam nonlinear interaction with electrostatic upper hybrid wave 7-26436
 Gaussian ripple growth on beam in collisionless magnetosphere 7-26437
 geometric optics at lower hybrid frequencies 7-37693
 inhomogeneous magnetoactive plasma, particle heating by low-amplitude wave 7-32009
 inhomogeneous plasma, particle heating in upper hybrid resonance region 7-32004
 ion-acoustic wave parametric excitation by electron-cyclotron wave 7-37672
 ionosphere, electron beam expts. 7-55354
 ionosphere, HF modification, small scale plasma density depletions form. 7-4263
 JET plasma, ICRF waves anal. 7-1723
 Langmuir turbulence, electron probe beam study 7-1699
 laser plasma, fast electron prod., absorpt. coeff. 7-63282
 laser-plasma interactions, density profile steepening, self-consistent treatment 7-26438
 line-focused laser-irradiated target experiments 7-26439
 linear resonant EM wave absorpt., collisional and thermal effects, numerical anal. 7-26435
 lossy plasma, electromagnetic pulse propagation, shape-dependent effects 7-44177
 low-temp. plasma, low freq. electric field parameters, mol. fluoresc. diagnostics 7-37756
 magnetic pumping by magnetosonic waves in the presence of noncompressive electromagnetic fluctuations 7-26449
 magnetically insulated gaps, obliquely propag. EM wave linear stability 7-44260
 magnetised plasma, HF wave propag., complex Doppler effect 7-51456
 magnetised plasma, intrinsic EM solitary vortices 7-11630
 magnetised plasma far field, minimum distance determ. 7-37694
 magnetised plasma subjected to external EM radiation in lower hybrid reson. region, temp. relax. 7-44100
 magnetospheric waves, whistler waves and ion-cyclotron waves interaction 7-60482
 microwave plasma interaction, reson. absorpt. 7-44178
 nonlinear space-charge and transverse mag. waves with longitudinal wiggler, stimulated Raman scatt. 7-44182
 plane plasma waveguide with random density inhomogeneities, parametric interaction of waves 7-58023
 plasma, convection amplification of wave beams in nonuniform plasma during stimulated Brillouin scatt. 7-63286
 plasma, upper hybrid resonance and turbulence excitation by intense radio wave 7-55362
 plasma-beat wave accelerator, pump depletion 7-32103
 polyformaldehyde plasma, optical and thermodynamic props. 7-11592
 ponderomotive effects for plane uniform EM waves in magnetoplasma 7-31986
 ponderomotive interactions in collisionless plasma, hydrodynamics 7-44113
 quasistationary plasma, reflectometry, freq. modulated EM waves 7-63257
 rarefied magnetised plasma, external source field nonlinear modifications calcs. 7-44180
 regeneration of the electromagnetic wave in an inhomogeneous magnetized plasma 7-31988
 relativistic electron beam interaction, static transverse periodic mag. field generation 7-44185
 resonant electrons in monochromatic EM wave, relativistic motion and damping during transverse propag. 7-26444
 resonant wave scattering by magnetic fluctuations in Tokamak discharge, microwave diagnostic technique extension 7-58059
 RF fields, focused, for local control of plasmas 7-6398
 satellite double stimulated Brillouin scattering 7-51453
 scattering by electrons in weak laser field 7-1691
 singular dispersive medium, wave propag., absorpt. theorem 7-56056
 skin-layer problem, numerical simulation 7-63283
 spectral line splitting in plasmas interacting with strong EM wave 7-20951
 stimulated radio emission of the ionospheric plasma at the second harmonic of the pump wave frequency 7-29331
 surface wave excitation during total transmission through plasma slabs 7-1704
 surface waves excitation by intense EM pump wave 7-1694
 time resolved second harmonic emission from laser produced plasmas, cut off, retardation characts. 7-37695
 time-dependent line transport calcs., Monte Carlo scheme 7-20897
 TM wave resonance absorption in inhomogeneous plasma 7-58018
 toroidal magnetised plasma, fast wave excitation 7-26414
 transient reflection, Lorentz medium half-space, TM polarisation, closed-form soln. 7-31989

electromagnetic wave propagation in plasma continued

- warm plasma, plasma wave transformation at ionisation front 7-58017
 whistler nonneutral envelope solitons, charge separation effects 7-37692
 whistler wave, EM filamentation instability 7-37691
 whistler waves, stimulated Brillouin scattering in low-density collisionless plasmas 7-58019
 whistlers propagation in ionosphere, nonlinear shift of wave parameters 7-66380
 Ar-N₂ laser pumping by plasma focus generated charged particle beams, num. calcs. 7-63367
 Au plasma, atomic processes, collisional-radiative and average-ion hybrid models 7-51387
 Cs, surface-ionised plasma in hot cavity, power-shifted microwave reson. 7-58020
 K, surface-ionised plasma in hot cavity, power-shifted microwave reson. 7-58020
- electromagnetic wave reflection**
see also electromagnetic wave propagation in plasma; light reflection; X-ray reflection
 anthracene crystal monolayer, photodimer disorder effects, UV reflection spectra anal. 7-53362
 Bloch transform as scattering problem, inversion problem 7-61131
 coherent combination-frequency reflection of electromagnetic waves from a rough interface exposed to acoustic radiation 7-43494
 convex cylinder, EM wave scattering, anal. using multiple Laplace transform 7-5819
 film-substrate system, magneto-optical longit. Kerr effect 7-13136
 FIR and MM wave polarisation transforming reflectors 7-36854
 HF propagation problems in ionosphere 7-23943
 HF radar sea echoes, Bragg coherence 7-40588
 ionosphere, winter anomaly effects on propag. of LF (40 kHz) radio waves 7-47611
 liquid thin film, with and without Al substrate, refl. coeffs., admittance method investig. 7-64711
 magnetic film-magnetic substrate system, magneto-optical transverse Kerr effect 7-22226
 Maxwell's eqns. in inhomogeneous media, 2D finite-difference time-domain analysis 7-15809
 ocean surface, whitecap and foam effects on wind speed extraction with pulse-limited radar altimeter 7-29306
 radar cross-sections, physical theory of diffraction, double reflections anal. 7-42863
 radiative-transfer problems with reflective boundary conditions, modified spherical-harmonic method 7-34853
 reflector-backed perfectly blazed strip gratings simulate corrugated reflector effects 7-42854
 RF absorber horn test system 7-43605
 semi-infinite inhomogeneous atm., radiation refl. for case of general laws of incoherent scatt. 7-4310
 slab with periodically varying surfaces, reflection and transmission characts. 7-15803
 TV VHF signal propagation, far beyond primary service zone 7-34768
 uniaxial media, reflection optical activity 7-27679
 US parametric modulation of EM wave at water-air boundary 7-37308
 In₂O₃/Sn evaporated films, optical props. and applications to energy-efficient windows 7-46157
 Si diffusion layers with high charge carrier densities, IR radiation refl. 7-13123
- electromagnetic wave refraction**
see also electromagnetic wave propagation in plasma; light refraction
 interstellar medium, refr. scintillation obs. in quasar (1741-038) 7-55845
 interstellar medium, refractive and diffractive scatt. of radio waves 7-55759
 radio waves refraction at altitudes above 1 km, effective Earth radius method 7-18274
 satellite communications, amplitude scintillations, meas. and preliminary effects (Italian) 7-23821
 total electromagnetic momentum, homogeneous and inhomogeneous media (Korean) 7-25704
 tropospheric waveguide, modal equation, roots instability 7-60368
- electromagnetic wave scattering**
see also backscatter; electromagnetic wave propagation in plasma; gamma-ray scattering; light scattering; X-ray scattering
 1-350 GHz sea level attenuation, dry air and water vapour effects determ. algorithms 7-40548
 2D anisotropic rod scatt., plane-wave integral eqn. 7-57219
 2D scattering by homogeneous anisotropic rod 7-20102
 airborne scatterers, multi-(bi)-static HF (PO/GO) radar target imaging 7-25706
 antenna far field pattern, reflector support boom effect 7-50472
 antennas and propagation, conf. Philadelphia, PA, USA (June 1986) 7-41011
 aperture antenna radiation, arbitrary scatterers presence, excited field calc. 7-50468
 artificial Kerr medium, microspheres suspension, moving electromag. gratings, response study, Planck-Nernst eqn. 7-64605
 atmosphere, effect of meteorological conditions on satellite radar images of Earth's surface 7-66217
 backscattering from triangular cylinder and hexahedron 7-42865
 Born vs. Rytov approximations, is the debate over? 7-62593
 boundary operator in EM scatt., soln. to time harmonic Maxwell eqns. 7-5820
 cm and mm wave propagation, tropical raindrop size characts. and effects 7-66280
 complex structure backscatter, flat-plate physical optics approximation 7-57217
 convex cylinder, EM wave scattering, anal. using multiple Laplace transform 7-5819
 cyclotron wave in relativistic electron beam, EM wave scatt. 7-42861
 cylindrical noncontiguous screens of arbitrary profile with Dirichlet boundary conditions, wave scatt. 7-42852
 cylindrical object buried in dielectric half-space, asymptotic solns. for plane wave scatt. 7-20106
 cylindrical screens of arbitrary profile with Dirichlet boundary conditions wave scatt. 7-42853
 cylindrical-wave spectrum anal., multiple bodies scattering 7-42855
 D-region, winter-time, scatt. irregularities scale from partial refl. radar meas. 7-47612
 dielectric cylinder partially covered by conductor, anal. 7-50473

electromagnetic wave scattering continued

dielectric cylinders embedded in two-layer lossy medium, EM scatt. anal. 7-1009
 dielectric scatterers in half-space, freq. properties 7-57215
 dielectric slab lossy, absorpt., effect of surface texture 7-42851
 dielectric sphere buried in lossy medium, scatt. Sommerfeld integral computation 7-57218
 dielectrically-loaded conducting spheres, FEM for scattering 7-15808
 dipole scattering from a conducting sphere coated with a lossy dielectric 7-20111
 ELF radio wave scattering on global inhomogeneities of earth-ionosphere cavity 7-29332
 F-region parameters determ., resonance scattering method 7-55356
 finite wire-structures (*German*) 7-1007
 H-plane sectoral waveguide as sensor for dielectric props. determ. 7-14977
 Hermite-Gaussian beam mode, high freq. scatt. by perfectly conducting cylinder 7-57208
 HF multiple diffraction by flat strip, higher order asymptotics 7-15800
 HF radar sea echoes, Bragg coherence 7-40588
 high voltage spark discharges, light scatt. diagnostics 7-20971
 hybrid iterative method 7-20099
 impenetrable object tomographic reconstruction 7-62592
 incoherent scatter radar probing 7-9211
 infrared measurements of scattering and electromagnetic penetration through apertures 7-56336
 inhomogeneous ice layer with rough surfaces 7-29044
 interstellar medium, refractive and diffractive scatt. of radio waves 7-55759
 inverse methods, review 7-42857
 inverse optics, conf., San Diego, CA, USA (Aug. 1985) 7-60869
 inverse problems and the Newton-Kantorovich method 7-62596
 inverse scattering, inverse source approach 7-62594
 inverse scattering analysis using renormalisation techniques 7-62598
 inverse scattering problem soln. using null field method 7-62595
 lower ionosphere, appl. of radio waves resonance scattering to ionospheric diagnostics 7-47613
 ionosphere, SABRE backscatter meas. rel. to E-region vertical velocity structures 7-4254
 Kennaugh's physical optics impulse response. for slightly bistatic case 7-42862
 Kirchhoff approximation, variational divergence 7-42856
 large impedance coated bodies of revolution hybrid EM scatt. solns. 7-20107
 layered medium propagation, dyadic Green's function formulation 7-62589
 Maxwell and integral eqn. equivalency for 3D and 7D scatt. problems 7-57220
 metal particles, randomly distributed in a dielectric medium, Anderson localisation of EM waves 7-31218
 meteor burst propagation and system design 7-40644
 microwave communication, equatorial and tropical regions, rain effects 7-66281
 Mie scattering coefficients algorithm 7-50479
 multiple conducting and lossy dielectric cylinders, E-field soln. of TM-scattering 7-10824
 multiple scattering noise in 1D, universality through localisation length scaling 7-1315
 mutual scattering effects between spheres, microwave open resonator meas. 7-1008
 nonlinear problem of incoherent anisotropic scatt., soln. 7-4309
 parallel thin dielec. cylinders of finite length, scattering study 7-31217
 particle effects eval. using turbulence scattering theories 7-20100
 passive microwave remote sensing, scatt. from layered medium connected with rough interfaces 7-20109
 perfectly conducting flat strip, pulsed signal scattering, deemphasizing LF defects in GTD anal. 7-20104
 perfectly conducting rectangular cylinders, EM wave scattering study (*Japanese*) 7-5821
 perfectly conducting semicircular cylinder, hybrid UTD-MM anal. of scattering 7-20103
 periodic array of conductors with arbitrary shape, thickness and resist., scatt. props. 7-20108
 periodic screens, scattering general screens 7-1006
 planar meshes with discrete loads, circuit modelling, equiv. mesh impedances 7-62600
 plane EM waves far field scattering, time domain Born approx. by penetrable object 7-10827
 plane wave diffraction, impedance cylinder with arbitrary cross section, quasiwave asymptotic form 7-50467
 plane wave diffraction by dielectric cylinder, oblique incidence 7-50461
 plane wave scatt. by semi-infinite strip grating 7-42860
 prolate spheroidal vector-wave functions, translation addition theorem 7-36858
 radiative-transfer problems with reflective boundary conditions, modified spherical-harmonic method 7-34853
 radio waves scattering from underdense meteor trains, electron volume density formulae 7-4383
 randomly distributed finitely conducting particles, polarised wave scattering and depolarization 7-5818
 reflecting grating, H-polarised inhomogeneous plane wave reson. scatt. (*Ukrainian*) 7-10823
 reflector-backed perfectly blazed strip gratings simulate corrugated reflector effects 7-42854
 SAR data from dynamic ocean surfaces, multi-look processing 7-40606
 scattering and eigenvalue problems, numerical solution, hybrid technique 7-50478
 scattering by a thick impedance half plane 7-42868
 scattering by large conducting cylinders, moment method 7-50475
 scattering by two multilayered dielectric cylinders, asymptotic solution 7-42869
 scattering from finite strip grating; curvature effect 7-50474
 scattering from resistive strips complex periodic struct., anal. 7-50476
 scattering problems, time matching problems instabilities 7-62588
 semi-infinite inhomogeneous atm., radiation refl. for case of general laws of incoherent scatt. 7-4310
 short radiowave multiple scattering in ionosphere, effect on fluctuations 7-60444
 sparse matrix solution, algorithms comparison 7-50477
 spectral iterative technique appls. 7-62590

electromagnetic wave scattering continued

strongly scattering particles, high density medium, integral equations for first two statistical moments of field 7-10828
 three-body scattering produces precipitation signature of special diagnostic value 7-60369
 transitional scattering at a charged filament of spiralar sinusoidal form, polarization anal. 7-5822
 TV VHF signal propagation, far beyond primary service zone 7-34768
 two parallel conducting strips, arbitrarily oriented, EM plane wave scattering study (*Japanese*) 7-42859
 wave field, rough surface with high Rayleigh parameter scattered, intensity correlation. 7-57209
 wavefront and resonance analysis of scattering by a perfectly conducting flat strip 7-20101

electromagnetic wave transmission

see also light transmission
 book 7-24329
 Maxwell's eqns. in inhomogeneous media, 2D finite-difference time-domain analysis 7-15809
 metals, nonlocal cond., microwave radiation transmission 7-13269
 slab with periodically varying surfaces, reflection and transmission characts. 7-15803
 NbSe₃, harmonic mixing at large microwave power levels 7-64141
 NbSe₃, microwave harmonic mixing below threshold 7-64140

electromagnetic waves

see also bremsstrahlung; channelling radiation; Cherenkov radiation; electromagnetic field theory; electromagnetism; gamma-rays; heat radiation; light; microwaves; solar radiofrequency radiation; synchrotron radiation; transition radiation; undulator radiation; whistlers; X-rays
 Babinet's principle for an anisotropic resistive surface using different approaches 7-36857
 charged particle with uniform motion, radiation, angular and spectral distrib. 7-10832
 collective excitations of electrons by intense wave in magnetic field 7-20116
 condensed media, powerful surface EM wave generation role in intense light effect 7-33348
 dipole EM radiation in chiral media using dyadic Green's function 7-1005
 ferromagnets, nonlinear EM waves 7-17201
 FFT with conjugate gradient method for soln. of EM problems 7-10812
 ionosphere, near-field radiation from pulsed electron beams in space 7-66391
 Kerr geometry, electric and mag. multipole analogues for EM waves 7-31219
 linear resonant absorpt. in inhomogeneous plasmas, validity of Denisov's anal. 7-26400
 magnetic dipole-emission during uniform motion in homogeneous medium (*Russian*) 7-20120
 Maxwell eqns., solitary EM wave solns., focus wave modes 7-20112
 nonlinear singular integral eqns. arising in physical problems 7-36859
 plane-wave frequency operator in a dispersive anisotropic medium 7-57216
 radiation sources for IR to γ -rays, developments 7-42877
 relativistic charged particles, coherent curvature radiation pulse duration 7-1015
 semiconductor spectrum, exciton region, optical nonlinearity 7-52433
 shield topology, EM interaction with large systems 7-10820
 stimulated-Cerenkov free electron laser, multiple scatt. effect 7-25832
 superheterodyne amplification and generation of electromagnetic waves in electron beams 7-36855
 Takagi equations for sliding angles of incidence, matrix analogue (*Russian*) 7-57213
 teaching EM theory in one-course setting for undergraduates 7-55923
 TEM standing waves with E||B 7-57214

electromagnetism

see also electric fields; electrodynamics; electromagnetic field theory; electromagnetic induction; electromagnetic oscillations; electromagnetic waves; magnetic fields; magnetism
 capacitance between perpendicular conducting planes separated by gap, comments and reply 7-42832
 composite dielectric materials, interface response theory of electromagnetism 7-62564
 conductor, mech. deform. under EM stresses 7-42833
 deformable electromagnetic solids, variational approach to Maxwell's eqns. 7-42828
 electric and gravitational forces, and the ballistic theory of light 7-29836
 electric quadrupoles, minimal EM coupling 7-10833
 energy methods, book 7-55902
 excitonic polaritons, relationship between microscopic theory and phenomenological Maxwell eqns. 7-38462
 FFT with conjugate gradient method for soln. of EM problems 7-10812
 generalised field theory, EM field eqns. using gauge structs. 7-9720
 graph theory, alternative labeling schemes 7-10810
 gravitation and electromagnetism, contributions to theories 7-36845
 gravitational analogies. rel. between electromagnetism and gravitation 7-41187
 implicit method for solving Maxwell's equation 7-57206
 magnetic dipoles suspended above line charge, dynamic origin 7-18536
 Maxwell's eqns. in inhomogeneous media, 2D finite-difference time-domain analysis 7-15809
 Maxwell's equations, advanced solns. 7-42834
 Maxwell's equations, correction for signals, and comments and replies 7-42829
 Maxwell's equations, correction for signals, magnetic current density addition, and comments and replies 7-42830
 Maxwell's equations, physical interpretation 7-10813
 Maxwell's equations near the edge of a half-plane with impedance type two-sided boundary conditions 7-4118
 Maxwell's mechanical model of electromagnetic phenomena, heuristics role 7-48393
 Maxwell's theory, transient front, initial conditions 7-61133
 Maxwell eqns. independency (*Hungarian*) 7-50441
 metal ring levitation, alternating mag. field, induced current demonstration 7-43
 particle in cell codes, Maxwell's equations 7-50443
 Petrov type D and type III space-times, conformally invariant scalar wave eqn., Maxwell's eqns. and Weyl's neutrino eqn. 7-24499
 scattering matrices, bounds and norms 7-10811
 signals, propagation velocity 7-42831

electromagnetism continued

- system theory, conf., Knoxville, TN, USA (Apr. 1986) 7-14714
- Takagi equations for sliding angles of incidence, matrix analogue (*Russian*) 7-57213
- trajectory-plotting program for moving charges in static electric fields 7-29645
- Vislov-Maxwell equation, initial value problem, local solns. 7-9683

electromagnets

see also coils; superconducting magnets

- CANDU nuclear reactor, EM pulse power coils for coolant tube spacer repositioning 7-49566
- coercive force meter with U-shaped electromagnet, operation rel. to test piece cross-section area 7-329
- DC magnetic field stabiliser based on NMR (*Slovak*) 7-24662
- finite element study (*French*) 7-15796
- geometric parameter optimization of high field magnets (*Chinese*) 7-9851
- HHIRF tandem accelerator energy analysing magnet, calibration 7-49765
- high resolution analysing magnet with aberration correction, 2D field mapping and field correction 7-25283
- jets, current-carrying, deformation by nonviscous elec. cond. liquid 7-51257
- microwave spectrometer, electromagnet power system improvement using dual control 7-30057
- optimum mathematical design of electromagnet systems, appl. to charged-particle beam transport 7-49758
- poloidal field coils for DIII-D, fabrication 7-19460
- powder and granule fabrication by EM pulveriser (*French*) 7-3218
- pulsed power systems for modified betatron accelerator 7-30793
- stellarator reactor, modular coils, field distribution, stresses and strains 7-20968

electromechanical effects

- chiral smectic C* liq. cryst., electromech. effect 7-2978
- conductor, mech. deform. under EM stresses 7-42833
- ferroelectric ceramic bar, normal mode responses, influences of domain switching and dipole dynamics 7-45945
- graphite-Br intercalation compound, electromech. effect on heating 7-45414
- macroscopic body couple, elec. and mech. induced, electromechanical interaction 7-59152
- metals, plastic deformation, high density current action 7-46550
- nonlinear electro-magneto-thermo-elasticity, steady-state problems 7-37331
- α -quartz, electroelastic constants meas. 7-59151
- spherical cavity in infinite elastic dielectric, nonlinear oscillations 7-31672
- steel, stainless, cryogenic structural material, low-temp. strength under action of elec. current pulses 7-22814
- Ag-Ag₂RbI₃-Ag ionic conducting system, elec. current press. and relax. effects, plastic deform. obs. 7-52123
- KAl(SO₄)₂·12H₂O, cubic, second order electroelastic tensor studies 7-27668
- LiNbO₃, leakage SAW propag. characs. for new cut (*Japanese*) 7-44985
- PLZT, electrically excitable mechanical resonant mode shapes 7-26854
- PZT ceramic, pressure induced ferroelectric-antiferroelectric transition 7-22201

electromechanical filters

- BaTiO₃ piezoelectric ceramics, studies for appl. in electromechanical filters 7-20558

electrometers

see also charge measurement

- Bayard-Alpert vacuum gauge controller with logarithmic response 7-14959
- Kelvin type electrometer for absolute determ. of volt 7-14973
- rotor electrometer for bulk matter quark search expts. 7-30913
- rotor electrometer for fractional charge searches 7-14964

electrometry see electrometers**electromigration**

- electron wind force in electromigration in jellium metal 7-32728
- glass, electromigration and charging effects during Auger and XPS analysis of insulators 7-17393
- isotope separation 7-58521
- planar microlens, fabrication by transverse electromigration method 7-62811
- quartz, as-grown or Li-, Na-, Cu- electrodiffused, radiation-induced conductivity 7-6691
- surface diffusivity variation on surface morphology and electromigration 7-63920
- Ag-AgI-Ag 2D ionic cond. system, fractional dimensionality of Ag dendrites 7-45100
- Al-Si/Ti/Al-Si VLSI metallisation, electromigration and microstruct. props. 7-21550
- Al-Ti-based homogeneous alloy films, elec. resist., microstruct., electromigration, comp. effects 7-21765
- AlSi-Ti multilayer interconnects on oxidised Si substrates, electromigration resistance 7-21713
- AlSi-Ti(Ta) layered films, compound formation and Si behavior 7-21762
- CO dil. soln. in liq. Ar, linear biased correlated walk, general soln. 7-61237
- CdSb-In crystal, In atom electrodiffusion study 7-63890
- CdTe crystals, resistive element defect electromigration, flicker noise enhancement 7-63889
- GaAs, semi-insulating, AL metallisation, electromigration failure anal. 7-44927
- La epitaxial layer on W field emitter, surface self-diffusion studies 7-32702
- LiNO₃, molten, ⁶Li enrichment by electromigration 7-2244
- ⁶Li, enrichment by electromigration in molten LiNO₃ 7-2244
- Si surface, electromigration of Ag, In, Sb, and Sn ultrathin films, scanning AES study 7-63891
- Si:As,Sb(P,Sb), Sb diffusion 7-44915
- Si:B(H,D) Schottky and n⁺-p junction diodes, electrical transport of acceptor-compensating defect 7-16823
- Si:H and near-surface damage of Si caused by H ions, review 7-16813
- Si-SiO₂-Ag(Cu)(Au)(Pd)(Ti) MOS structures, diffusion coeff. meas. in elec. fields, solid solubilities 7-2279
- SiO₂-Na₂O-CaO-MgO-Al₂O₃-BaO-FeO₃ glass, elec. field stimulated Na depletion 7-6897
- TaH_{0.015}, ³H migration in a Hall field, temp. effect 7-32729

electromigration continued

- Th-Mo(Zr)(Re)(W), diffusion and electrotransport of transition metals in BCC Th 7-63888
 - ZnS:Cu, electrophosphors, aging phenomena 7-27791
 - ZrH_{0.015}, ³H migration in Hall field, temp. effect 7-32729
- electromotive force** see electric potential
- electromyography** see bioelectric potentials; muscle
- electron absorption**
- see also beta-ray absorption
- No entries
- electron accelerators**
- see also betatrons; electron ring accelerators; microtrons
- 18 MeV electron linac for picosecond and nanosecond beam prod. 7-49747
 - Advanced Test Accelerator, electron beams, laser guiding 7-10327
 - beam brightness from a relativistic, field-emission diode with a velvet-covered cathode 7-1121
 - beam energy measurement technique 7-36362
 - capture and retention of ions by an electron bunch circulating in a storage ring 7-15430
 - CEBAF cavity cryostat 7-62183
 - CEBAF cryogenic system 7-62184
 - CEBAF facility, design, few-body research program 7-62105
 - collider constraints in the choices for wavelength and gradient scaling 7-5502
 - compact and high efficient electron beam accelerator 7-30740
 - constant impedance structures, raising the beam blow up threshold current (*Chinese*) 7-5496
 - CW injector linac for 35 MeV double sided microtron (*Japanese*) 7-19557
 - cyclotron resonance laser acceleration of electron beam by a large amplitude EM wave in a uniform magnetic field 7-10308
 - Electron Test Accelerator, beam injector, chopper and buncher system 7-25271
 - ELSA, future expts. in few-body physics 7-61860
 - FEL intense low emittance beams prod. in electron linacs 7-1116
 - FEL spiking mode operation for a uniform-period wiggler 7-1109
 - grid pulse generator for KEK PF linac (*Japanese*) 7-56903
 - HERMES III, passive control of high-energy high-current beam 7-30809
 - high brightness electron injector for FEL driven by RF linacs 7-1117
 - High Brightness Test Stand 7-1114
 - IKONET, distributed accelerator and experiment control application 7-19560
 - image processing system for electron linac beam diagnosis (*Japanese*) 7-19621
 - injector linac design (*Japanese*) 7-19584
 - IR laser particle accelerators with oversized DBR and HFB waveguide 7-10309
 - KEK e⁺ generator, magnet power supply control system (*Japanese*) 7-19580
 - KEK e⁺ injection system, beam characs. (*Japanese*) 7-19613
 - Kharkov electron linac as injector for stretcher ring 7-62104
 - laser acceleration of particles, strong internal elec. fields in nonlinear force produced cavitons 7-11662
 - laser acceleration using inverse noncollinear Compton laser 7-49744
 - laser plasma beat-wave accelerator 7-62141
 - laser-irradiated plasma, electron acceleration 7-11651
 - LEP collider, refrigeration system of superconducting accelerating cavities 7-49780
 - linac, control system for Photon Factory 7-5498
 - linac, operation in short-beam mode 7-62143
 - linac, upgrade to high duty factor machine 7-62147
 - linac beam post-acceleration in chain of passive cavity structures 7-62141
 - linac laboratory, modification to applied radiation facility 7-62142
 - linac modifications to produce short, intense beam pulses 7-62139
 - linac with feedback, self-oscillatory mode 7-62144
 - linacs, high-current beam dynamics and transport, theory and experiment review 7-62117
 - linacs for medical and industrial applications 7-62110
 - linear colliders, beam-beam effects 7-62194
 - linear induction accelerator, ion focused, design and operation 7-36344
 - linear induction accelerators 7-62107
 - Los Alamos FEL, electron micropulse diagnostics 7-1108
 - Los Alamos FEL, oscillator expt. 7-1107
 - Los Alamos FEL, status 7-1106
 - MEDEA II two-pulse electron beam accelerator to study electron beam propagation 7-30743
 - multipass multisection linac, feedback system anal. for beam breakup 7-62145
 - neutron TOF spectrometer at KURRI electron linac 7-30831
 - NIKHEF-K, future exptl. developments for few body physics 7-61859
 - Orsay storage ring FEL, operating point modifications 7-1110
 - plasma beat-wave accelerator, collinear optical mixing of relativistic electron plasma waves 7-11614
 - radiometric standards comparison cryogenic radiometer vs. electron storage ring BESSY 7-18861
 - RF drive system for the CEBAF superconducting cavities 7-62182
 - RF structs. for excitation of electrooptic transducer by beam in picosecond electron linac 7-15428
 - RF superconducting linac structures for heavy ions and electron 7-62119
 - SLAC Linear Collider, linac developments 7-62123
 - SLAC Linear Collider, progress report 7-62122
 - slow positron production by the use of the ETL linac (*Japanese*) 7-1956
 - standing wave and travelling wave structures comparison for linacs 7-62121
 - Stanford Mark III infrared free electron laser 7-1112
 - stellartron electron accelerator 7-30791
 - storage rings, beam-beam limit, solvable model 7-42266
 - storage rings, current-lifetime product, Touschek limit 7-36352
 - storage rings, transverse mode coupling instability due to localized structures 7-5506
 - synchrotron, vertical electron oscillations, dynamics control 7-56889
 - TeV e⁺e⁻ linear collider, cathode life and gas desorpt. meas. (*Japanese*) 7-19587
 - TeV e⁺e⁻ linear collider, high power test of accelerating cavity (*Japanese*) 7-19586
 - TeV e⁺e⁻ linear collider, lasertron design studies (*Japanese*) 7-19589
 - Tohoku 300 MeV e⁻ linac cooling system, trouble and warning systems 7-19579

electron accelerators continued

- transients study of Neva-01 electron accelerator 7-30797
 TRISTAN positron generator beam transport system (*Japanese*) 7-19568
 UCSB FEL 400 μm expt., spectral characteristics 7-1111
 UVSOR storage ring, ion-clearing system 7-36353
 Van de Graaff 3 MV accelerator, using laser photoelectron emission from cold Y_2O_3 cathode 7-10314
 wake field acceleration by proton bunches 7-62140
 XUV FEL, high-gain, storage-ring design 7-1115
 XUV FEL oscillator at Stanford X-ray Centre Storage Ring 7-1138

electron affinity

- alkali metal atoms in rare gas matrices, Rydberg states, model pot. 7-5737
 alkali metal hydroxides, electron affinity, mass spectrometric determ. 7-15740
 alkali metal oxides, electron affinity, mass spectrometric determ. 7-15740
 aqueous soln., free energies of hydration, ionisation pots., electron affinities 7-65292
 atomic ionisation energy and electron affinity, correl. energy estimation by local approx. 7-56991
 benzene and azabenzene adsorbed on Cu(111) and Au(110), electron affinity levels studied by inverse photoemission 7-44991
 benzenes, soln. electron affinities, isotope enrichments 7-10770
 benzenes, substituted, ionisation pots., electron affinity, HAM/3 study 7-19710
 chlorophyll- H_2O system, ab initio LCAO SCF MO calcs., ionisation pot., electron affinity, intermol. mechanics 7-8520
 cyanobenzenes, electron affinity, electron transfer equilibria 7-10741
 dicyanoethylene electron affinity, electron transfer equilibria 7-10741
 ethyl, ethenyl and ethynyl anions, structs. and rearrangement processes, ab initio MO calcs. 7-59757
 flavins, struct. and REDOX props., electron distrib., MINDO/3 calcs. 7-56977
 hydrocarbons, temporary negative ion states, electron transmission 7-42586
 molecular electron affinities evaluation 7-5591
 polyaniline, conducting polymer, electronic and electrochem. props., MNDO calc. 7-2462
 polyaniline, geometries, bond struct., electrochemistry, MNDO calcs. 7-15750
 trans-polyenes, electronic struct., DVM- $X\alpha$ calcs. 7-25392
 polyfuran and copolymers, electronic struct., cond. props., ab initio cryst. orbital calcs. 7-52410
 polypyrrole and copolymers, electronic struct., cond. props., ab initio cryst. orbital calcs. 7-52410
 polythiophene and copolymers, electronic struct., cond. props., ab initio cryst. orbital calcs. 7-52410
 semiconductor heterojunctions, breakdown of electron affinity rule, photoemission tests 7-2690
 tetracyanoethylene, electron affinity, electron transfer equilibria 7-10741
 transition metal complexes, spin and charge densities calcs. 7-27491
 tribromomethyl radical, geometry and electronic struct., SW $X\alpha$ calcs., ab initio UHF calcs. 7-19703
 trichloromethyl radical, struct. and electronic states, ab initio UHF SW $X\alpha$ calcs. 7-30949
 CN^- , electron affinity calc. with fourth order many body perturbation theory 7-42471
 Cl^- , electron affinity calc. with fourth order many body perturbation theory 7-42471
 Cu_n ($n=1-10$), cluster, photoelectron spectra 7-62561
 F^- , electron affinity calc. with fourth order many body perturbation theory 7-42471
 FeF_2 - FeF_3 , ion-molecule equilibria, mass spectra, heat of form., electron affinity 7-46862
 GaAs (110), O_2 adsorption, electronic props., contact pot. meas. 7-2353
 H_2Si_2 , electronic struct., MC SCF CI and CEPA calcs. 7-56992
 K^+ , electron affinity and photodetachment cross sections, ab initio multi-channel calcs. 7-36463
 Li ion affinities of O_2 and N_2 bases, basis set and correl. effects 7-5610
 LiH, ground and first excited state electron affinities, extended-Koopman's-theorem, ab initio calcs. 7-25352
 $^{15}\text{NH}_3$, $X^2\Pi$ state, IR rot.-vibr. spectrum, isotopic shifts and equilib. consts. 7-50107
 NH_2^- , electron affinity calc. with fourth order many body perturbation theory 7-42471
 O , electron affinity, CI STO calcs. 7-5606
 OH^- , electron affinity calc. with fourth order many body perturbation theory 7-42471
 PH_2^- , electron affinity calc. with fourth order many body perturbation theory 7-42471
 PX , PX^+ and PX^- where $X = \text{H}, \text{F}$ and Cl , low-lying electronic states, ab initio calcs. 7-30937
 SF_6 , electron affinity, HF SCF calcs. 7-49907
 SH^- , electron affinity calc. with fourth order many body perturbation theory 7-42471
 a-SiGe:H alloys for solar cells, electronic and optical props. 7-17899
 $\text{SiH}_3(\text{D}_3)$, ions and radicals, pot. energy curves and electron affinities determ., photoelectron spectra anal. 7-25603
 TeF_6 , electron affinity calcs. 7-36453
 TiCl_4 , electron attachment, scatt. cross section, multiple scatt. Xalpha continuum calcs. 7-62483

electron annihilation *see electron-positron inclusive interactions***electron-atom collisions** *see atomic electron impact excitation; atomic electron impact ionisation; elastic scattering of electrons by atoms and molecules***electron attachment**

- acrylonitriles, ion form. by dissoc. electron attachment, mechanism 7-42754
 allyl chloride, dissoc. attachment cross sections 7-28290
 benzonitrile, ion form. by dissoc. electron attachment, mechanism 7-42754
 benzyl chloride, dissoc. attachment cross sections 7-28290
 chlorobenzene, dissoc. attachment cross sections 7-28290
 decafluorobutane, electron attachment rate const. 7-62534
 dichlorodifluoromethane, electron attachment lineshapes and cross sections at ultra-low electron energies 7-62522
 diffuse discharge switching appls., temp. depend. electron transport studies 7-32189
 discharge, electron-beam-sustained, secondary electron thermalisation, attachment effects 7-58080

electron attachment continued

- electronegative molecules, gaseous, electron attachment and detachment processes 7-19967
 fluoroethylene radical anions, dissoc. electron attachment 7-50349
 gas mixtures, electron transport, collision cross section and dielectric strength 7-63244
 halocarbons, electron attachment influence on zero-field electron mobility in Ar 7-20833
 hexafluoroethane-Ar mixture, electron drift velocity, attachment, ionization coeff. 7-31181
 hexafluoroethane-methane mixture, electron drift velocity, attachment, ionization coeff. 7-31181
 ionised gases, atomic and mol. physics, conf. Greifswald, Germany (Aug. 1986) 7-18499
 methane, dissociative ionization and electron attachment 7-31182
 methyl bromide, thermal electron attachment and diffusion 7-20038
 methyl bromide, thermal electron attachment and diffusion 7-20837
 nitriles, sat., ion form. by dissoc. electron attachment, mechanism 7-42754
 perfluoroalkanes, electron attachment and ionisation processes 7-50348
 perfluorocyclobutane, electron attachment lineshapes and cross sections at ultra-low electron energies 7-62522
 perfluorocyclobutene, electron attachment lineshapes and cross sections at ultra-low electron energies 7-62522
 perfluoromethylcyclohexane, electron attachment lineshapes and cross sections at ultra-low electron energies 7-62522
 RF plasma electron kinetics, attachment and ionis., self-consistent treatment 7-20850
 spectroscopy using modified electron capture detector 7-18947
 tetrachloromethane, dissoc. in RF plasma, probe diagnostic and relative emission intensity meas. 7-32095
 tetrafluoromethane, electron conduction pulses, shortening by electron attachers 7-51382
 tetrafluoromethane, electron conduction pulses, shortening by electron attachers 7-51383
 trifluoroacetonitrile, isomers, anion form. and dissoc., electron attachment 7-10740
 trifluoroiodomethane, dissociative electron attachment, unbalanced excess energy distrib. 7-25676
 trifluoroisocyanide, isomers, anion form. and dissoc., electron attachment 7-10740
 van der Waals clusters, electron attachment 7-20090
 vinyl chloride, dissoc. attachment cross sections 7-28290
 CO , dissociative electron attachment, ang. distrib. of O^- 7-25674
 CS_2 , dissociative attachment bands, impact electron and fragment ion energy spectra anal. 7-50386
 H_2 , negative ion generation, atomic processes investig. 7-51527
 HCl , low-energy electron collisions, inelastic processes, R matrix theory anal. 7-31180
 H_2O , electron attachment cross-sections meas. 7-25649
 $\text{NH}_3(\text{ND}_3)$, predissociation, dissoc. attachment cross section 7-50279
 NO_2 , electron attachment temp. depend. 7-10755
 N_2O , negative ion form., thermal electron attachment 7-15704
 O_2 , electron impact, vibr. excitation, three-body electron attachment, isotope effect 7-57185
 O_2 , form. and resonant vibr. levels of O_2^- , spectra anal., cross sections calc. 7-15730
 O_2 , negative ion mobilities meas. 7-20838
 O_3 , admixture in air influence on Trichel pulse characts., electron attachment rate determ. 7-20034
 SF_6 , charge transfer, time-resolved study 7-10748
 SF_6 , electron swarm kinetics with attachment and ionis., higher-order Boltzmann eqn. calcs. 7-20854
 SF_6 , RF breakdown and discharges, continuum modelling 7-37798
 SF_6 , thermal attachment rate constants, 200-600K 7-975
 SOCl_2 , in $\text{Ar}(\text{N}_2)$ (methane), electron attachment rate consts. 7-36758
 SiH_4 and Si_2H_6 , ionisation and attachment coeffs. meas. 7-1667
 TiCl_4 , electron attachment, scatt. cross section, multiple scatt. Xalpha continuum calcs. 7-62483
 XeF lasers, electron beam pumped, N_2 production from Ne/Xe/NF_3 mixtures 7-43063

electron avalanches

- air, breakdown by laser radiation, mechanism modelling 7-20996
 air, ionisation currents in cylindrical chambers 7-37778
 gas discharge, electron multiplication, primary and secondary ionisation processes 7-51535
 image convertor, gas discharge, operating in avalanche mode, intrinsic blurring and freq. contrast characts. 7-4937
 linear thyatron in tetrode configuration, develop. 7-32120
 short pulse, high power microwave air breakdown 7-26585
 Ar, ionis. behind normal plasma shock waves, conservation eqns. 7-31980
 N, electron avalanche simulating using Monte Carlo technique and renormalisation anal. 7-29731

electron beam absorption *see electron absorption***electron beam annealing**

- rare earth silicide epitaxial formation by rapid annealing 7-21768
 SOI films, recrystallisation by obliquely scanned pseudoline electron beam 7-58686
 SOI large area growth, pseudo-line electron beam technique with lateral seeded epitaxy (*Japanese*) 7-7842
 SOI laterally seeded epitaxial films recrystallised by electron beam, sub-grain boundaries charact. 7-53779
 SOI structures, lateral epitaxy formation, melting and resolidification 7-38386
 SOS films, regrowth rates of amorphous layers created by self-implantation 7-16661
 thermal anal., 2D finite element method (*Japanese*) 7-32507
 Cu:Ar(Ne)(C), single crystal, ion implantation, damage profile anal. using Auger electron spectroscopy 7-51802
 Cu-Zr amorphous alloy, induced recrystallisation by electron and laser beam irradiation 7-12152
 CuInS_2 :P, ion implanted, pulsed electron beam annealing 7-16644
 n-GaAs/AuGe-Ni, ohmic contact fabrication RBS anal. 7-32840
 Ge, ionisation-stimulated annealing of Frenkel pairs under electron or gamma irradiation 7-38061
 KBr crystal, radiation defects destruction by electron beam generated pulsed stresses 7-63663
 NbSi $_2$ film form. by scanning electron beam annealing 7-21285
 NiSi $_2$ -Si, epitaxial growth of silicide layers by electron beam annealing 7-27213

electron beam annealing continued

- Si, ionisation-stimulated annealing of Frenkel pairs under electron or gamma irradiation 7-38061
 Si, surface structure, pulsed electron-beam annealing 7-21284
 Si:Al(In), recrystallisation by pulsed electron beam, impurity profiles 7-16605
 Si:As(BF₃), ion implanted, diffusion and defects, transient scanning electron beam annealing 7-38065
 Si:B, diffusion and activation of implanted B during rapid thermal annealing 7-16643
 Si:B, preamorphised, B diffusion during rapid thermal annealing 7-32717
 TaSi₂ film form. by scanning electron beam annealing 7-21285

electron beam applications

- see also electron beam annealing; electron beam deposition; electron beam lithography; electron beam machining; electron beam welding; radiation therapy*
 dielectric material, radiation diagnostics of electric potentials, sensitivity and resolution 7-8233
 discharge, electron-beam-sustained, secondary electron thermalisation, attachment effects 7-58080
 excimer laser excitation, using low impedance electron beam system 7-36989
 excimer lasers, electron beam pumped, multiwavelength, studies 7-15847
 high-current relativistic electron beam, ionisation wavefront struct. and propag. vel. 7-51469
 holography using local reference beam 7-20159
 microwave power standard, using electron beam 7-14967
 organic semiconductors, electrical transport props., electron bombardment method 7-52641
 radiotherapy, dose distrib. of high-energy electron beam, chromosome aberration freqs. 7-14131
 semiconductor laser electron-beam-pumped, single longitudinal mode operation 7-10938
 spatial light modulator, electron beam addressed 7-25955
 vacuum, electron and ion technologies, conf., Sozopol, Bulgaria (Oct. 1985) 7-35098
 Ar ion lasers excited by low-energy electron beams 7-20186
 Ar-Xe laser at 1.73 μ m, electron beam and electric field pumped 7-1077
 Ar-Xe pulse-periodic large-volume electron beam-controlled laser, IR transitions in Xe atom 7-43059
 ArF excimer laser, electron-beam pumped, using low-pressure Ar-Rich mixture 7-36945
 ArH* exciplex laser, pumped by electron or proton beam, active medium modelling 7-62672
 CO₂ high power laser, pumping by self-sustained volume discharge, electron beam initiated 7-57297
 CO₂ laser, short pulse cold-cathode glow-discharge electron beam pumped 7-43150
 CdS and Zn_xCd_{1-x}S, electron-pumped, high-efficiency semiconductor laser 7-5884
 CdS laser excited with several electron beams, light pulse formation 7-43098
 GaAs laser excited with several electron beams, light pulse formation 7-43098
 KrF e-beam sustained discharge laser, efficiency 7-31307
 KrF electron beam pumped laser mixtures, electron density meas. 7-57300
 Ne laser based on 3p-3s transitions with electron beam excitation 7-20185
 XeCl laser mixtures, electron beam, pumped, electron density meas. 7-43064
 XeF electron beam pumped laser mixtures, electron density meas. 7-57300
 XeF lasers, electron beam pumped, N₂ production from Ne/Xe/NF₃ mixtures 7-43063
 Zn_xCd_{1-x}S and ZnS_xSe_{1-x}, electron-pumped, high-efficiency semiconductor laser 7-5884
 ZnCdSe, electron beam pumped, cathodolum., gain and stimulated emission 7-64701
 ZnSe/GaAs, electron beam pumped lasing action obs. 7-43093

electron beam deposition

- metal-polyethylene, adhesion of metal films, effects of Ar⁺ bombardment 7-28267
 multilayer soft X-ray coatings, automatic electron-beam deposition 7-3184
 multilayer soft X-ray coatings, electron beam evaporated, anal. with Cu-K α radiation 7-30145
 multilayer soft X-ray reflection coatings, automatic electron beam deposition 7-33571
 polymer film deposition, electron beam induced polymerisation 7-27898
 Al film deposition on amorphous substrates 7-21770
 Al, reactively evap., morphology and opt. props. 7-59272
 Be-Ti multilayer interference system, struct. and phase composition, electron microscopy, X-ray and neutron diff. meas. 7-63984
 CoSi₂-Si, solid phase epitaxial growth of CoSi₂, nonultrahigh vacuum method 7-45043
 Cu films on MgO, epitaxial and electronic structures, LEED, AES, and EELS studies 7-52352
 CuInSe₂, thin film, electron beam evaporation optical props. (Korean) 7-27801
 GaAs-Ge crystal growth on Ta₂O₅-coated Si substrates, zone melting and MOCVD 7-53579
 Ge polycrystalline film, preferred orientation control by two-step growth method 7-21728
 HfO₂-MgO system massive vacuum condensates, structure (Ukrainian) 7-12527
 In₂O₃:Sn transparent conducting films, electr., optical props., appls. (Korean) 7-59842
 Mo epilayers on MBE GaAs, RHEED study of struct. 7-21755
 Nb films, epitaxial growth and superconducting props. 7-3181
 Nb films, oriented, electron beam evaporation in ultrahigh vacuum onto GaAs 7-3175
 Nb-Si multilayers, electron beam deposited, characts. 7-27456
 Nb-V sinusoidally modulated superlattice, growth and charact. 7-21741
 NbC, amorphous films, prep. and characts. 7-7885
 Ni-Co-Cr-Al-Y coatings, electron beam deposition, oxidation rel. to pretreatment 7-46702
 Ru and Os layers by electron-beam decomposition of carbonyls 7-53597
 Si thin film, doped, electron beam evaporation, elec. props. 7-2743
 a-Si:H,N thin films, activated reactive evaporation 7-13355

electron beam deposition continued

- Si-Ti thin-film superlattices, structure 7-38350
 SiN_x films, phase separated structures, Ar⁺ ion bombardment effects, ZPS studies 7-22439
 Si₃N₄ film synthesis by ion-assisted deposition, antireflection coating use 7-37213
 Si_xN_{1-x} amorphous thin films grown by ion beam assisted deposition, IR and ion beam anal. 7-39209
 Si₃N₄ film form. and charact., ion and vapour deposition method 7-13370
 SiO₂ film synthesis by ion-assisted deposition, antireflection coating use 7-37213
 SiO_x evaporated thin films, struct. study 7-58699
 TiC, amorphous films, prep. and characts. 7-7885
 TiO₂ thin dielec. film, deposition on Kodial glass, optical props. 7-7872
 TiO₂-SiO₂ dielec. multilayer reflector for surface emitting lasers, electron beam evaporation 7-59427
 TiSi₂ vacuum electron beam evaporation, annealing effects, Auger and electron diff. anal. 7-22492
 W film on MBE GaAs, RHEED study of struct. 7-21755
 ZrO₂, Y₂O₃ stabilised thermal barrier coatings, ionisation assisted physical vapour deposition 7-46349
 ZrO₂-SiO₂ optical films, struct. modification by coevaporation 7-45064

electron beam effects

- see also beta-ray effects; cathodochromism; cathodoluminescence; electron beam annealing; electron impact; plasma-beam interactions*
 aerospace polymers, electron irradi. effects on AC and DC elec. props. and unpaired electron densities 7-58339
 alkali halides, electron and photon stimulated positive ion desorption dynamics calcs. 7-27141
 alkali metal chlorides, electron-stimulated desorption, Coulombic ejection mechanism 7-59315
 alkali metal iodides, electron-stimulated desorption, Coulombic ejection mechanism 7-59315
 alkanes, long-chain, cryst. and molten, low energy electron transmission and secondary electron emission expts. 7-33492
 alloys, electron irradi. induced transforms. 7-2065
 atomic displacements detection using channelled electron induced X-ray emission 7-21311
 bladder urothelium, mouse, electron irradi. effects, SEM obs. 7-60058
 bounded plasma-electron beam system, nonlinear interaction, instability and oscills. (Russian) 7-58029
 ceramics, cation-conductive, lattice imperfections, 1 MV HRTEM obs. 7-2258
 ceramics, electron irradi. induced transforms. 7-2065
 Cerenkov radiation and electromagnetic pulse produced by electron beams traversing a finite path in air 7-20118
 chalco-genide glass grating couplers, fabrication using electron beam induced Ag doping (Japanese) 7-62817
 chalco-genide-metal contacts, interdiffusion, struct., comp., electron irradi. effects 7-21686
 channelling of charged particles in solids 7-38081
 channelling patterns, many beam effects and phase information 7-32534
 contaminated optical solar reflectors, simulated synchronous altitude environment effects 7-34040
 cordierite, electron beam induced phase decomposition 7-13796
 current enhancement for hose-unstable electron beams 7-11598
 damage estimation in microscopy 7-16634
 defects produced by electron and X-ray irradiation, surface effects 7-6687
 dense plasma channel, large scale resistive instability of relativistic electron beam 7-51431
 depth-dose distributions, conversion from slab to spherical geometries for space-shielding appls. 7-56879
 desorption, electron and photon-stimulated, probes of surface struct. and bonding 7-32817
 diamond, electron beam irradi., vacancies, photoluminescence, radiative decay time meas. 7-46107
 diamond, radiation damage prod. of 5RL centres, phonons, absorpt. spectra, cathodoluminescence studies 7-33461
 diamond crystal, X-ray radiation generated by transmitting electrons, ang. distrib. and energy depend. 7-26819
 diamond single crystals, relativistic positron channelling radiation, spectral density peak splitting studies (Russian) 7-21310
 dielectric film, electron irradi., space-charge buildup, atomic number effect 7-33330
 dielectric surface-relativistic electron beam interaction, expt. investig. 7-44195
 discontinuous metallic thin films, on amorphous and crystalline substrates, electron irradiation stimulated coalescence 7-2437
 divertor materials, heat load expts. with electron beam facility 7-49638
 electron small angle incidence on cryst., radiation processes, incoherent multiple scatt. effects calcs. 7-44625
 emission spectrum of hyperchannelled positrons 7-21309
 energy deposition by X-rays and electrons, microscopy implications 7-38064
 enstatite, electron beam induced phase decomposition 7-13796
 fluorapatite, relative defect-production efficiency for fission fragments, alpha decay and electron irradiation 7-12167
 French Metallurgy Society meeting, Paris, France (Oct. 1986) (French) 7-29579
 Frenkel defect recombination zone, influence of uniaxial tension (Russian) 7-37970
 gas, low-pressure, electron beam injection, discharge time lag 7-37770
 glass, K-208, electrification effects in radiation optical props. 7-64592
 glass specimens, brittle fracture threshold under effect of pulsed electron beam, effect of geometrical dimensions 7-3399
 glasses, characterisation by electron bombardment 7-32506
 graphite, tokamak limiter material, high heat load tests using 120 kW electron beam 7-26803
 graphite fibre reinforced epoxy, thermomech. behaviour, space rad. effects 7-51828
 heavy target, boundary layers arising when intermediate energy beam is stopped 7-16292
 hydrides, amorphous and crystalline, comparative studies via incoherent scatt. 7-21798
 insulators, electrostatics, in electron microscope 7-41540
 insulators, high dose radiation damage, voids and dislocations 7-32502
 ionosphere, electron beam expts. 7-55354

electron beam effects continued

ionosphere, near-field radiation from pulsed electron beams in space 7-66391
 liquid metal ion source, residual gas and secondary electron bombardment effects 7-30800
 metal films, etching, kinetic model, electron flux activation 7-3492
 metal particles, electron beam irradiated, structural instability (*Japanese*) 7-21286
 metallic glasses, metastable struct., surface melting, by plasma, laser or electron beams 7-63495
 metals, isochronal annealing PAC monitored defect reactions anal. 7-44623
 Monte Carlo transport, PRESTA algorithm 7-49854
 MOS capacitors, radiation-induced interface state generation 7-58899
 MOS samples, radiation effects of 10-12 MeV electrons (*Chinese*) 7-6685
 optical materials for interferometric devices 7-44618
 organic conducting single crystals, electron irradi., Bragg spot fading 7-12158
 oxide films, RF sputtered, high intensity electron beam irradi. effects 7-44626
 oxide surfaces, structure and rearrangements, atomic imaging 7-27078
 paragonite mica, characteristic beam damage in TEM images 7-12159
 particle beam fusion accelerator II (PBFA II), vacuum insulator stack failure mechanisms 7-30749
 PEEK, cryst., mech. relax., electron beam irradi. effects 7-16686
 phthalocyanines, halogenated, radiation damage and structural studies 7-6688
 poly(ethylene terephthalate), irradiated, phys. and dielec. props. 7-33332
 polyaryl-ether-ether-ketone, semicryst., mech. relax., electron beam irradi. effects 7-12204
 polyethylene, electron beam charged, space charge decay currents 7-27338
 polyethylene dielec. thin films, hot-electron-induced damage and charge storage, electron spectra studies 7-27662
 polymer, radiation-induced stress change during electron irradi. 7-16631
 polymer sheets, beam charged, ion spot phenomenon anal. 7-58356
 polypropylene, irradiated, phys. and dielec. props. 7-33332
 polypropylene films, electron irradiated, structural study by X-ray diffr. 7-44422
 polyvinylidene fluoride, modifications under high energy heavy ion, X-ray and electron irradi., XPS study 7-38076
 positron continuous slowing down approx. range 7-44638
 PTFE, amorphous and cryst., irradiated, thermal characts. (*Russian*) 7-6681
 PTFE, bonding and surface struct., ESCA investigation, electron beam interactions 7-51662
 PTFE and PVDF, aging, irradiation by X-rays, electron and ion beams, XPS study 7-32498
 PTFE surface chemical struct. and adhesive props., effects of low-energy electron bombardment 7-44963
 pulsed power technique research at IAE in Beijing 7-11693
 PVC surface, sputtered, AES, electron beam induced dissociation 7-20077
 quartz, crystalline, neutron and electron irradi., glassy props. 7-63664
 radiation effects in glasses 7-32518
 radiotherapy, dose distrib. of high-energy electron beam, chromosome aberration freqs. 7-14131
 satellites, electron-irradiated dielectric discharges, statistical behaviour 7-55423
 solar cells, microscopic defect structures and equivalent electron fluence concepts 7-23179
 stainless steel, electron beam heating, vaporisation and melting meas. 7-26929
 steel, austenitic stainless, electron beam welded, void swelling under electron irradi. 7-51830
 steel, austenitic stainless, electron irradi., cold working, vacancy swelling, void form., carbide precip., electron microscopy 7-21282
 steel, austenitic stainless, swelling by electron irradi., influence of appl. stress (*Japanese*) 7-16632
 steel, austenitic stainless, Ti addition effect on swelling under HVEM conditions 7-58343
 steel, austenitic stainless radiation damage process obs. using high voltage electron microscopy 7-51831
 steel, ferritic, a/2 {111} dislocation loop formation 7-16565
 steel, ferritic stainless, cavity form., effect of electron/He dual beam irradi. 7-58341
 steel, low C, alloying using high-intensity sources 7-28179
 steel, stainless, ferritic, irradi., grain boundary segregation, STEM microanalysis 7-22701
 steel, stainless and alloy, electron radiation damage in fusion reactor materials, voids 7-2064
 STEM use in electron damage meas. 7-16635
 surface engineering for corrosion protection, electron beam and laser glazing 7-3478
 surface helicons, electron beam interactions, energy exchange and magnetic damping calcs. (*Russian*) 7-21949
 thin crystals, electron irradi., Pendellosung radiation and coherent Bremsstrahlung 7-33476
 thin short-circuited dielec. films, dispersive charge transport, space charge dynamics calcs. 7-39038
 total stopping power, semiempirical eqn. 7-6696
 transition metals, low energy in elastic electron scatt. props. 7-63700
 X-ray spectra, K_{α} satellites during electron bombardment (*Russian*) 7-53449
 X-ray tubes, microfocus, electron beam melting of anodes 7-35646
 yeast cells, photoreactivable damage rel. to O_2 effect in radio- and UV-sensitive mutants (*Russian*) 7-14053
 Ag film, pure transition radiation following electron irradi. (*French*) 7-64708
 Al film, low energy electron transmission, inelastic and elastic scattering cross section calcs. 7-63698
 Al, muon trapping and diffusion after electron irradiation, μ SR study 7-45864
 Al:Fe, electron-stimulated desorption, Coulombic ejection mechanism 7-59315
 Al-Cu-Mg system, D16 alloy, struct. changes during electron bombardment 7-8005
 Al-Mn icosahedral alloy form. by pulsed electron beam and laser beam surface melting 7-26924

electron beam effects continued

Al-Mn(-Si) rapidly solidified alloys, quasicrystal form. by electron beam melting 7-26915
 Al-V alloy, amorphous and quasicrystalline state, electron diffr. study 7-63562
 Al-V alloys, phase transitions between amorphous, quasicrystalline and crystalline phases 7-63807
 Al-Zn (1.95 wt.%), X-ray microanal. in medium voltage electron microscope, radiation effects 7-46902
 Al-Zn dilute alloys, stress-induced mixed dumbbell tunnelling, sound propag. meas. (*Russian*) 7-51674
 AlGaAs/GaAs/Ge multijunction solar cell, model for calc. of displacement damage by radiation 7-13878
 AlGaAs/GaAs/InGaAs multijunction solar cell, model for calc. of displacement damage by radiation 7-13878
 AlGaAs-GaAs solar cell fabrication, elec. characts. and space appl. 7-54307
 $Al_{1-x}Ga_x$ -As p-n junction solar cell radiation-induced defects obs. using DLTS 7-13875
 Al_2O_3 , lattice relaxation induced by electronic relax. 7-44622
 Al_2O_3 , leucosapphire single crystals, transformation of colour centres 7-37986
 Al_2O_3 - B_2O_3 - SiO_2 - Cu_2O glass, Cu activated, photoconductivity, lumin., influence of radiation defects 7-45381
 $AlPO_4$, glass, dielectric, charge buildup, influence on charging electron beam motion 7-44294
 AlZn dilute alloys, electron irradiation induced interstitial defects, EXAFS study 7-63661
 Ar discharge, pulsed electron beam injection, potential profile, temporal evolution 7-51534
 Ar gas, electron beam deposition 7-5771
 Ar solid crystalline films, electron stimulated desorption, exciton mechanism calcs. (*Russian*) 7-27096
 As_2X_3 , X=S,Se,Te, thin film, electron irradi. effect 7-16636
 Au dilute alloys, electron irradi., positron lifetime meas. 7-39250
 B, defects produced by electron and X-ray irradiation, surface effects 7-6687
 BaF_2 - ThF_4 - YbF_4 glass, electron irradiation effects, Yb^{3+} optical transitions 7-27764
 $BaMn_{1-x}Ta_x(Zn)O_3$ phase struct. and transforms., high resolution electron microscopy obs. 7-58237
 $Be_3Al_2Si_6O_{18}$, beryl, electron-irradiation induced amorphism 7-32505
 CO, physisorbed multilayer, near-threshold electronic excitation, EELS spectra anal. 7-45001
 $Ca_2Nd_6(SiO_4)_6O_2$:Cm ceramic simulated nuclear waste forms, radiation effects on microstruct. and fracture props. 7-58373
 $CdCr_2Se_4$, band structure characteristics and props. of nonequilibrium carriers, cathodoabsorption 7-46064
 CdS, electron beam irradiated, red flash-like luminescent centres, annealing 7-7740
 CdSe(S) thin films, electrophys. props., electron irradiation effects study, solar cell appl. 7-16894
 CdTe, electron irradi., a {100} dislocation loops 7-6686
 Co, single crystal and polycrystalline, mag. relax. following electron irradiation 7-53067
 Cr (110) with chemisorbed CO, electron stimulated desorption 7-63965
 CsBr, two-halogen self-trapped excitons, metastable optical absorpt. 7-53365
 CsH_2AsO_4 and $CsH_2D_2(1-x)AsO_4$, ferroelectric, optical props., radiation effects 7-33406
 CsI, surface stoichiometry, changes under electron and laser radiation 7-44961
 Cu, electron beam heating, vaporisation and melting meas. 7-26929
 Cu-Ti, amorphisation, high resolution electron microscopy 7-44377
 Cu-Ti alloy system, electron irradi.-induced amorphisation, chemical disordering effects study 7-16640
 Cu-Zn alloys, electron irradiation, interstitial cluster form., diffusion rates, resistivity 7-2013
 Cu_3Au , electron irradiation, long range ordering, recovery, vacancy migration and clustering, positron lifetime study 7-39543
 CuNiFe, electron irradi., decomposition kinetics and morphology 7-58491
 Cu_4Ti_3 , electron irradiation induced amorphisation, high resolution electron microscopy 7-44373
 Fe, dilute alloys, electron irradi., positron lifetime meas. 7-39250
 α -Fe, electron irradiated, residual resistivity recovery and mag. after-effect 7-27570
 Fe-Al (40 at.%), electron irradi., Huang scatt. from interstitials 7-58272
 Fe-Au(Sb)(Cu), dilute alloys, electron irradiated, vacancy-solute interaction, positron lifetime, muon spin rotation studies 7-39288
 Fe-Cr-Ni, austenitic, electron irradi., conversion of stacking fault tetrahedra to voids 7-58342
 Fe-H system, electron and neutron irradi., positron lifetime meas. 7-44603
 Fe-Ni, electron irradi., low temp. phase transitions (*Russian*) 7-51832
 Fe-Ni-Cr, high-purity, irradi., void swelling and nucl.-induced phase transforms. 7-58340
 GaAs CCD, high resistivity gate struct., radiation effects 7-6683
 GaAs, defect structure charactn., US meas. 7-21363
 GaAs, electron beam irradi., carrier density, anomalous temp. depend. 7-52610
 p-GaAs, electron irradi.-induced trap defects, DLTS study 7-12155
 GaAs, electron irradiated, defect profiling, DLTS 7-12652
 GaAs, electron irradiation induced defects, DLTS study 7-58338
 GaAs, electron-irradiated, relative density of levels of radiation defects 7-52500
 GaAs, n-type, electron-irradiated, photoionization cross sections of E levels 7-64152
 GaAs, plastically deformed or electron or neutron irradiated, antisite defects 7-37987
 GaAs polycrystalline solar cell, electron beam generated carriers in presence of grain boundaries 7-64262
 GaAs, positron lifetime, electron beam effects and temp. depend. 7-39280
 GaAs solar cells, depletion layer recombination effects on radiation damage hardness 7-13888
 GaAs solar cells, sequential irradiation effects of electrons and protons 7-13877
 GaAs solar concentrator cells, perform. under 1 MeV electron irradiation 7-3704
 GaAs, surface potential barrier in ion-etched (100) surface, electron-voltaic effect 7-7819

electron beam effects continued

- GaAs-Si thin film solar cells, radiation damage 7-65465
 GaP:Zn, electron irradiation induced defects, DLTS study 7-52513
 Ge, channeling effects in radiative emission of electrons 7-2074
 Ge, electron irradi., annealing kinetics, impurity effects 7-16630
 Ge, electron irradi., hole effective mass parameters, cyclotron reson. 7-58730
 Ge p-n junction solar cell radiation-induced defects obs. using DLTS 7-13875
 p-Ge, undoped, deep level defects produced by electron irradiation, annealing 7-12660
 Ge, volume capture effect for relativistic electrons, computer simulation 7-12156
 p-Ge:B(Al)(Ga)(In), annealing kinetics of radiation defects, influence of impurity binding energy 7-39547
 Ge-Sb-Se glasses, crystallisation ability, high energy electron irradi. effects (Russian) 7-32306
 Ge-Si, p-n junctions, photoelectric props., effects of electron bombardment 7-7351
 Ge-Si solar cells, electron radiation effects 7-34031
 GeX, X=S,Se,Te, thin film, electron irradi. effect 7-16636
 HCl-Ar gas mixtures, electron irradi., negative differential conductivity 7-63243
 Hg_{1-x}Cd_xTe, electron-irradiated, positron annihilation 7-38060
 Hg₂Cl₂ thin films, morphology and growth on Hg surface, electron beam damage 7-59469
 HgTe, electron-irradiated, positron annihilation 7-38060
 In, muon trapping and diffusion after electron irradiation, μ SR study 7-45864
 In_{0.9}Ga_{0.1}As, atomic displacements detection using channelled electron induced X-ray emission 7-21311
 InP crystals and solar cells, radiation-induced defects, room-temperature annealing 7-39993
 p-InP, electron irradi., atomic displacement threshold energy 7-2066
 InP, electron irradi. damage, impurity effects 7-12154
 InP solar cells, potential for use in space radiation environment 7-23181
 InP solar cells, radiation resistant characters. 7-8413
 InP solar cells in space radiation environment, comparison with GaAs and Si cells 7-65484
 InP(As)(Sb) surfaces, oxidation processes studied by high-resolution electron microscopy 7-39766
 In₂-Sn₂O₃- γ protective coatings for Galileo spacecraft, radiation testing 7-59647
 Ir (111) with graphite monolayer, adsorbed Cs atoms, photo- and electron-stimulated deformation of monolayer 7-58627
 KBr crystal, radiation defects destruction by electron beam generated pulsed stresses 7-63663
 KBr, stable hole defect formation by ionizing radiation 7-63669
 KFe₁₇O₂₅, ceramic, radiation induced products STEM microanalysis 7-16639
 KH₂PO₄ and KH₂D_{2(1-x)}PO₄, ferroelectric, optical props., radiation effects 7-33406
 Kr gas, electron beam deposition 7-5771
 Li, electron scatt., charge polarisation effect 7-63685
 LiF, electrification mechanism during cleaving 7-44621
 LiF, electron beam irradi., desorbed ground state Li atoms, signal time depend. 7-52260
 LiF, electron stimulated desorption of Li, role of F-centre diffusion 7-16864
 LiF, electron- and photon-stimulated desorption, threshold effects 7-58623
 LiF single cryst., dielectric, charge buildup, influence on charging electron beam motion 7-44294
 LiIO₃, ferroelectric, optical props., radiation effects 7-33406
 MgAl₂O₄ spinel, electron irradiation, Mg depletion, cubic γ -alumina form. and microcracking 7-26802
 MgAl₂O₄ stoichiometric spinel, electron beam-induced diffusion, cracking and phase separation 7-16641
 MgAl₂O₄:He spinel, implanted, high temp. electron irradi., structural damage 7-51829
 Mg₂Al₂Si₂O₁₈, cordierite, electron-irradiation induced amorphism 7-32505
 MgO, deformed and annealed, red cathodoluminescence spectrum 7-27792
 MgO, electron irradi., stored energy, differential thermal anal. studies 7-32503
 MgO:C, single crystals, solute C and C segregation, SIMS study 7-16759
 MgO:Fe, gamma-ray and electron radiation-induced conductivity 7-33015
 MgO(Al₂O₃)_n, electron beam irradi., point defect aggregation, screw dislocation climb 7-63662
 Mo, positron trapping by vacancies, loops and voids, positron annihilation studies 7-46216
 Mo, radiation dislocation loops, clustering 7-12073
 Mo, tokamak limiter material, high heat load tests using 120 kW electron beam 7-26803
 N₂, electron beam induced lasing at atmospheric pressures 7-15845
 N₂, physisorbed multilayer, near-threshold electronic excitation, EELS spectra anal. 7-45001
 NaCl crystals, electron-coloured, transmission and holographic props. 7-43001
 NaCl, intense nanosecond electron beam irradi., periodic damage struct. form. 7-12157
 NaCl, pure and Mg doped, electron range vel. to heat treatment 7-21283
 NaF:Mg, doped and undoped, electron beam irradiated, thermoluminescence and thermally stimulated conductivity 7-7771
 Na₂O-SiO₂ glass, relative defect-production efficiency for fission fragments, alpha decay and electron irradiation 7-12167
 Nb, electron beam heating, vaporisation and melting meas. 7-26929
 Nb-H system, electron irradi., vacancy recovery, positron lifetime studies 7-37972
 NbN(C) sputtered films on Nb substrates, surface props. 7-64833
 Ne gas, electron beam deposition 7-5771
 Ne solid crystalline films, electron stimulated desorption, exciton mechanism calcs. (Russian) 7-27096
 Ni, creep, electron bombardment effect, 200 to 500°C 7-8062
 Ni, electron irradi., H-defect interactions, positron annihilation study 7-6674

electron beam effects continued

- Ni-Ag overlayers, pulsed electron beam irradiation, heat flow model 7-38062
 Ni-Al-B-based alloys, site occupations, APFIM and channelling studies 7-32367
 Ni-Si alloy, Ni₃Si precipitation during electron and ion irradiation 7-51876
 Ni₃Al and NiAl, positron annihilation and DSC studies of diffusion mechanisms 7-46204
 Ni₃Fe, order-disorder transformation, positron annihilation study 7-39509
 (Ni₃Fe)_{1-x}Cr_x alloys, ordering study, comp. depend., electron diff. and Mossbauer meas. 7-51690
 PLZT electro-optical ceramics, electron pulse irradiation-induced transient optical absorpt. study 7-6682
 PLZT ferroelectric ceramics, gamma, electron and neutron irradi. effects study 7-6677
 PLZT, transparent ferroelectric ceramic, irradiation effects 7-59157
 Pb(Sr_{0.5}Nb_{0.5})O₃ ferroelectric ceramics, gamma, electron and neutron irradi. effects study 7-6677
 Pb(Sr_{0.5}Nb_{0.5})O₃, transparent ferroelectric ceramic, irradiation effects 7-59157
 PbSe:Ag, electron irradi. stimulated impurity diffusion 7-63878
 Pt (110), water adsorption 7-21644
 Pt microcrystals, charact. using high resolution electron microscopy 7-32676
 Pt small crystals, atomic-resolution study of struct. rearrangements 7-32243
 Ru (001), coadsorption of H₂O and Li 7-21645
 SF₆, electronegative gas, electron beam transmission anomalies study 7-44094
 Si (100), exposed to CO, CO₂, O₂, NO and SO₂, photodesorption 7-52290
 Si (100), nitridation kinetics in NH₃ by thermal activation or electron bombard., LEED, AES, and TDS study 7-39770
 Si (100), reactivity, thermal desorption of propylene, defect- and electron-enhanced chemistry 7-21660
 Si, bifacial solar cell for space solar generators 7-8388
 Si, Czochralski, electron-irradiated, DLTS and photoluminesc. studies 7-7149
 Si, Czochralski grown, electron irradi., thermal donor form. 7-21868
 Si, DLTS and MCTS spectra, charge-dependent defect traces 7-7161
 Si, defects produced by electron and X-ray irradiation, surface effects 7-6687
 Si diodes, radiation effects of 10-12 MeV electrons (Chinese) 7-6685
 Si dislocation-free single crystals, microdefect recomb. activity, electron irradi. and annealing effects, SEM study (Russian) 7-21287
 Si, electron and ion irradiation induced amorphisation, point defect dispersion and mobility 7-11916
 Si, electron beam irradiated at different temps., formation of complexes 7-12153
 Si, electron irradi., Mu to Mu* transition, strain field induced 7-53205
 Si, electron irradi., obs. of IR bands during annealing, kinetic study 7-45214
 p-Si, electron irradiation induced defects, DLTS study 7-38500
 Si, electron planar channelling radiation, temp. depend. 7-46172
 Si layers, electron irradiation-induced defect levels, annealing behaviour, DLTS studies 7-52493
 Si MINP solar cells, electron beam radiation effects 7-13876
 Si MINP solar cells, radiation damaged, conduction mechanism 7-65463
 Si, neutron transmutation doped p-n-p-n structs., fast electron irradiated, minority carrier lifetime variations 7-45352
 Si single crystals, relativistic positron channelling radiation, spectral density peak splitting studies (Russian) 7-21310
 Si solar cells, metal insulator n on p, radiation damage 7-3703
 Si solar cells, sequential irradiation effects of electrons and protons 7-13877
 Si solar concentrator cells, perform. under 1 MeV electron irradiation 7-3704
 Si space solar cells, damage coeffs. of 1 MeV electron fluences 7-13880
 Si triodes, radiation effects of 10-12 MeV electrons (Chinese) 7-6685
 Si, volume capture effect for relativistic electrons, computer simulation 7-12156
 Si:Al implanted crystals, amorphous surface regions with crystalline impurity grains, TEM study 7-58579
 Si:B, electron-irradiated, AC hopping conductivity and DLTS 7-44624
 Si:B(Au), electron irradi. stimulated impurity diffusion 7-63878
 Si:C, electron irradiated, photolum. defect spectra, obs. of interstitial C 7-59253
 Si:Ga, electron irradiated and annealed, photoluminescence spectra 7-13206
 a-Si:H films, electron irradi., photocond., absorpt. coeff. spectral depend. 7-64279
 Si:In, substitutional ion implanted dopants, electron and positron channelling studies 7-26778
 Si:O, Czochralski grown, electron irradiated, thermal donor formation 7-44619
 Si:O, defects created by electron irradiation and subsequent thermal treatments, review 7-16642
 Si:O, electron irradi. on varying O content, defect anal. 7-16637
 Si:O, magnetic resonance of O-related defects 7-17223
 Si:O, vacancy-enhanced O diffusion 7-16811
 n-Si:P,C, electron-irradiated and injection-annealed, vacancies, dislocations and C interstitials 7-51815
 Si:Sb MBE, electron irradi. effect on doping levels and profiles 7-63660
 Si-M (M=In, Te, Re, Bi), metal implantation using pulsed electron beam 7-6882
 SiC single cryst., electron channelling patterns, lack of centrosymm. effects obs. and calcs. 7-51901
 SiO₂, electron induced disloc., AES study 7-22392
 SiO₂, electron ionisation tracks, cluster anal. 7-58387
 SiO₂ layers, space charge distrib. meas., electron beam induced conduction method 7-27660
 SiO₂ native oxide, ion and electron bombardment induced surface modifications studies 7-12175
 SrTiO₃ cryst., electron pulse irradiation-induced transient optical absorpt. study 7-6682
 Ta, electron irradi., transverse muon-spin relax. functions 7-53197
 Ta-H system, electron irradi., vacancy recovery, positron lifetime studies 7-37972
 β -TbH(D)_{1.9+x}, defect study 7-37971
 α -TeO₂:Al single crystals, electron irradi., colour centre ESR obs. 7-33271

electron beam effects continued

- Ti epitaxial films, electron beam bombardment, oxidation, structural and phase transforms. 7-21746
- Ti polycrystalline films, electron beam bombardment, recrystallisation, oxidation and phase transforms. 7-21746
- Ti vapour, heated cathode discharge prod. 7-21022
- Ti-Nb alloys, struct. and precipitation under high energy electron irradi. (Russian) 7-44620
- Ti-Ni, crystalline to amorphous transitions, struct. anal. 7-44375
- TiN(C) sputtered films on Nb substrates, surface props. 7-64833
- TiO₂ (110), O deficient surfaces, electronic excitations, EELS 7-58853
- U vapour, heated cathode discharge prod. 7-21022
- VC precipitates in steel, radiation damage influence 7-16638
- W, electron and proton irradi., thermal annealing, positron annihilation studies 7-46214
- Zn, electron irradiated, positron lifetime spectra, temp. depend. 7-39249
- Zn₃P₂, vacuum deposited films, struct., transmission electron microscopy and X-ray diffr. 7-52316
- ZnS thin films, radiation enhanced adhesion to SiO₂ substrates 7-32504

electron beam impact *see electron impact***electron beam induced conductivity** *see EBIC***electron beam induced currents** *see EBIC***electron beam lithography***see also electron resists*

- Aharonov-Bohm magnetoconductance oscills. study using nm-scale lithography 7-52836
- electron matrix lens, aberrations reduction using offset apertures 7-20122
- electron-beam decomposition of carbonyls on Si 7-53597
- electrostatic electron-beam deflectors, comparison of electron optics 7-18910
- Hipparcos astrometry mission, diffraction grid fabrication by electron beam lithography 7-24014
- Hipparcos project, grid pattern calibration by e-beam 7-29403
- III-V semiconductor, integrated optoelectronics, micrograting form. by HV electron beam lithography 7-31443
- IR diffractive filters fabricated by electron beam lithography, spectral and polarising characts. 7-62816
- micro-Fresnel lens arrays, rectangular-apertured, fabrication by electron beam lithography 7-57505
- nanometre-scale electron beam lithography 7-16663
- zone plate fabrication 7-18957
- GaAs-AlAs superlattice struct., lithographic fabrication of TEM cross-sections 7-370

electron beam machining

- oxide films, RF sputtered, high intensity electron beam irradi. effects 7-44626

electron beam welding

- steel, austenitic stainless, electron beam welded, void swelling under electron irradi. 7-51830

electron beams*see also electron impact; electron optics; Schwarz-Hora effect*

- aberration theory, relativistic for electron beam in combined electromagnetic focusing-deflection system with spherical cathode 7-62613
- aberration theory for electron beams combined in focusing system with spherical cathode 7-62612
- aberrations in combined electromagnetic focusing spherical cathode lens, theory (Chinese) 7-36868
- abnormal glow discharge creation, energy spectrum 7-26564
- acceleration of electrons in vacuum by two laser beams 7-50480
- BESSY multipole magnet, electron opt. props. and electron trajectories 7-42254
- bombarded plate, backscatter, transmission and energy release 7-36872
- Buneman instability in neutral gas, ion collective acceleration 7-49749
- cathodes, electron beam quality, surface roughness effects 7-57225
- centrifugal electrostatic focusing system, bunching mechanism and kinetic anal. of relativistic electron beam 7-36871
- charged-particle beams, trajectory based phase-space anal. 7-42886
- charged-particle beams in cylindrical waveguide, ponderomotive confinement 7-35624
- compensated electron flows, propag. in finite system, numerical simulation (Russian) 7-20125
- Compton scattering free electron laser system, electron beam trapping expt. 7-1136
- current density monitor for intense relativistic electron beams 7-19595
- drift space, expt. study 7-36873
- e/m experiment, magnetic field and electron trajectory calcs. 7-48228
- electromagnetic wave scattering by a slow cyclotron wave in a relativistic electron beam 7-42861
- electrostatic blanking system for electron beams (Slovak) 7-61399
- energy broadening in thermal field emission electron beams 7-25710
- excitation using glass foils 7-35627
- extended high permeance beams investig. fixed node approx. 7-36874
- Faraday cup for intense electron beam pulses 7-51515
- free electron laser, gain degradation and electron beam quality 7-43128
- free electron laser, wiggler and alternating-gradient quadrupole field, electron beam envelopes and matching conditions 7-1128
- free electron laser EUV, three-dimens. simulation 7-43131
- free electron laser by relativistic electron beam, quantum-kinetic theory 7-43124
- free-electron laser amplification and phase shift meas. 7-36973
- gas, laser beam configs. for cumulative interaction with electrons 7-11584
- gate, limiting currents taking secondary electron emission into consideration 7-31237
- generation by cold cathode plasma guns, appl. to laser excitation 7-26534
- generation in duoplasmatron ion source 7-32114
- guiding from RF accelerator by laser-ionized channel 7-56891
- high current e⁻ beam injected into air, expt. study 7-30808
- high current electron beam equilibrium with anisotropic transverse temp. 7-36866
- high voltage pulser for beam pulsing of e⁺ linac (Japanese) 7-19611
- high-current strip electron beam, low-frequency stability 7-57227
- high-power, modulation in corrugated waveguide 7-10839
- hollow cathode arc, beam electron relax. 7-21005
- insertion device beam line optics, review 7-43305
- insertion device Beam Line Wunder design at SSRL 7-42256
- insertion device performance in ESRF 7-42251
- insertion devices, future developments, limitations 7-42257
- insertion devices, variational theory 7-42879

electron beams continued

- instabilities, wake field anal. by boundary element method (Japanese) 7-19616
- ion motion in autoresonant accelerator with hollow electron beam, num. simulation 7-37620
- ion-focused transport of relativistic electron beams 7-30813
- Marx bank, low jitter, for cold cathode electron beam sources (Chinese) 7-4912
- MFTF-B mag. field alignment diagnostic, electron-beam source development 7-25222
- nanosecond electron injector 7-36367
- nonrelativistic, high-current, vacuum dielectric channel, external mag. field 7-62175
- optical klystron, effects of finite electron beam emittance, energy spread and wiggler errors 7-1127
- plasma channel, axisymmetric erosion of relativistic electron beam 7-31998
- plasma channel, ion hose instability of relativistic electron beam 7-31999
- plasma channel, relativistic electron beam propagation, ion density model, Langmuir probe and beam transport meas. 7-31997
- plasma focus device as beam source rms beam emittance 7-30807
- position monitor using slot antennas (Japanese) 7-19618
- positron beams, low-energy, field-assisted moderator 7-62152
- pulse width selecting system for e⁺ beam transport line (Japanese) 7-19609
- pulsed metastable atomic beam source for time-of-flight applications 7-41533
- radial focusing in biperiodic slow-wave struct. with high accel. rate 7-41550
- relativistic, propagation at sub-Torr pressures 7-42262
- relativistic aberrations in combined electromagnetic focusing-deflection system, theory (Chinese) 7-36869
- relativistic electron beam, high-intensity, bending in circular dielectric structs. 7-18909
- relativistic electron beam, self-pinch, propagation in dense plasma, transverse two stream instability, dispersion relations 7-32000
- relativistic electron beam, tubular, current convective instability 7-5826
- relativistic electron beam and spatially inhomogeneous field, energy exchange peculiarities 7-50481
- relativistic electron beam current and position monitor 7-19596
- relativistic electron beam generation in laser-based foilless diode 7-42267
- relativistic electron beam in beam-induced ion channel, transverse instability 7-58027
- relativistic electron beams, periodic permanent magnet field-transport 7-57226
- relativistic electron beams, time-resolved studies with subnanosecond Cerenkov electro-optic shutter 7-49757
- RF ion source, ion energy distrib., radial extraction, injected electron beam 7-30118
- self-consistent equilibrium states of electron beam in longitudinal magnetic field 7-57224
- self-pinch hollow, filamentation instability 7-11642
- solar corona, electron beam injection angle from obs. of type III radio bursts 7-66562
- solar corona, lower limit to type III burst brightness temps. rel. to metre-wave microbursts obs. 7-66561
- stimulated-Cerenkov free electron laser, multiple scatt. effect 7-25832
- superheterodyne amplification and generation of electromagnetic waves in electron beams 7-36855
- synchrotron beam line critical elements, heat transfer studies 7-42255
- trapping into gyro magnetic autoresonance, Coulomb field effects 7-42887
- UK free electron laser project, beam transport and diagnostics 7-1134
- undulator, linear, variable gap permanent magnet, for ENEA free electron laser expt 7-43151
- undulator, long, evolution of radiation beam system 7-42880
- undulator, microwave, theory construct, and exptl. results 7-42878
- undulator, short period, design and performance 7-42252
- undulator, soft X-ray, performance predictions 7-42876
- vacuum photorecorder, grid shutter anal. 7-18914
- wiggler, NdFe-steel hybrid permanent magnet, development for insertion in SPEAR ring 7-42250
- wiggler design, 3 Tesla, with supercond. windings, for ESRF 7-42253
- X-ray source using low energy electron beams traversing superlattice 7-20114
- Young's double hole interference experiments with hairpin cathode electron gun 7-1020

electron capture*see also charge exchange; electron attachment*

- acrylic acid, electron capture gas chromatographic determ. 7-33974
- atom-ion collisions, electron capture, symmetric eikonal theory 7-31144
- atom-ion collisions, electron capture, off-shell Coulomb radial wavefunctions soln. 7-62520
- atom-ion collisions, first order Born perturbation theory 7-10746
- atom-ion collisions, K shell charge transfer cross sections, symmetric eikonal theory 7-50328
- charge exchange cross section meas. (Chinese) 7-5765
- eikonal approximation, extension 7-20035
- glassy media, irradiated, excess electron capture, radiative and nonradiative mechanisms 7-27339
- highly charged ions, multiple-electron capture, classical over-barrier model 7-10744
- hydrogenic states of arbitrary ang. momentum, amplitude evaluation method 7-62514
- iodomethane+NO⁺, charge exchange, ground state radiative lifetimes, ion cyclotron reson. spectra anal. 7-31114
- molecular ion-partially stripped ion collisions, Oppenheimer-Brinkman-Kramers approx. calcs. (Russian) 7-57169
- molecular ions, rot.-vibr. transitions in autoionisation, CF method anal. 7-20036
- nitroaromatic radical anions in aqs. solns., electron transfer kinetics, temp. and steric configuration effect 7-39872
- relativistic symmetric eikonal approximation for electron capture 7-31161
- Rydberg states, high-lying, generation and decay in beam-foil encounters 7-49965
- trans-stilbene-fumarionitrile ion pair, back-electron transfer, solvent effects 7-39873
- symmetric heavy ion collisions, K X-ray prod., target thickness fn., X-ray spectra anal. 7-30978
- three-body rearrangement and break-up, critical angle second-order scattering 7-5747

electron capture continued

- Al (110), H_2^+ scatt., charge exchange 7-3133
 $Al^{3+}H$, charge-transfer reaction, mol. representation, CI calcs. 7-36485
 $Ar^+ + N_2$, charge transfer collision, Franck-Condon principle at low collision energies study 7-62511
 $Ar^{q+} + D_2(D)$, collision parameters, energy-gain spectra meas., multichannel Landau-Zener model anal. 7-36752
Be, determ. in natural water, by electron capture detect. gas chromatography 7-13932
 $Be^{4+} + He$, charge exchange cross sections, quasimolecule Feshbach method calcs. 7-36754
 $C^{4+} + He$, two-electron capture cross sections, comparison of calc. methods 7-15703
 $C^{4+} + He(H_2)(Ar)(Xe)$, one-step double electron capture 7-50344
 $CS^{q+} + \text{atom}(\text{molecule})$, ($q=2, 3$), electron capture 7-5763
 Ca^{4+} , reson. transfer and excitation, charge state and electron momentum distrib. depend. 7-970
CdS particles deposited on porous vycor glass electron transfer and photoluminesc. dynamics 7-64678
 Cs^- , low-energy collisions with atoms and mols., absolute total cross section meas., curve-crossing model anal. 7-36749
 $Cs + HeH^+$, HeH bound excited state form., predissoc. and radiative disoc. 7-20033
H atoms, proton collisions, higher-order electron capture processes 7-25647
H, electron capture by bare ions, coupled-state calcs., convergence 7-31166
H plasma, ion collisions, low-energy charge exchange, XUV spectra 7-20032
H+fully stripped ion collision, electron capture, travelling MO expansion study 7-50341
H+H, ion-pair form. reaction, mol. treatment 7-50340
 $H + H^+$, electron capture, strong pot. Born approx. calcs. 7-972
 $H + H^+$, reson. electron capture from excited 2 s states, cross section calcs. 7-36747
 $H + He(Ar)(Ne)(Kr)(Xe)(H_2)$, electron capture cross sections 7-10747
 $H^+ + Cs$ charge transfer collisions, laser radiation influence 7-25646
 $H^+ + H$, electron capture at intermediate energies from 1 to 200 keV 7-62515
 $H^+ + H_2$ double capture, collisions, H^+ ion excitation energy meas., Franck-Condon calcs. 7-36751
 $H^+ + H_2(D_2)$, charge transfer into 2S state, differential cross sections meas. 7-36750
 $H^+ + H_2(He)(N_2)(Ne)(Ar)$, 20-100 keV, charge exchange cross section meas. (Chinese) 7-5765
 $H^+ + H(Ar)$, capture theory, first-order Born approx. Coulomb boundary conditions 7-10745
 $H^+ + H(Ar)$, electron capture, K-shell cross sections 7-10752
 $H^+ + H(He)$, 2l-electron capture, first-Born-type approximation, cross sections 7-10743
 $H^+ + K$, ionisation and charge transfer collisions, cross section meas. 7-20031
 $H^+ + K$ charge transfer collisions, laser radiation influence 7-25646
 $H^+ + Na$ charge transfer collisions, laser radiation influence 7-25646
 $H^+ + Ne(Na)(Mg)$, multiple ionisation, charge transfer cross sections 7-15706
 $H^+ + Ru$ charge transfer collisions, laser radiation influence 7-25646
 $H_2 + Ar^{q+} (q^+=)$, total one-electron capture cross sections 7-10754
 H_2 +fully stripped ion collision, electron capture, travelling MO expansion study 7-50341
 $H_2^+ + Ar$ collisions, dissociation and electron capture cross section meas. 7-31156
 $H_2^+ + He$ collisions, dissociation and electron capture cross section meas. 7-31156
 $H_2^+ + Ne$ collisions, dissociation and electron capture cross section meas. 7-31156
He, collisions with fast, highly charged ions, electron capture to the continuum meas. 7-20026
He, ground state, one-electron loss cross section in H_2 gas 7-50338
He, multiply charged ions collisions, semiclassical model, double electron transitions 7-10733
He plasma, ion collisions, low-energy charge exchange, XUV spectra 7-20032
 He^{2+} , charge exchange collisions, multiply charged closed K shell targets, exponential model study 7-25426
 $He + (He^{2+})(C^{6+})(O^{8+})$, electron capture cross section calc. by distorted-wave perturbation theory 7-50336
 $He + Ar^{q+} (q^+=)$, total one-electron capture cross sections 7-10754
 $He + B^{3+}(O^{8+})(Si^{12+})$, double- and single-electron capture and loss cross section meas., OBK scaling calcs. 7-42756
 $He + C^{6+}(Ne^{10+})$, electron capture, bound and continuum states, impulse approx. 7-50329
 $He + C^{6+}(O^{8+})$, intermediate energy collisions, electron capture cross sections, AO expansion method calcs. 7-25381
 $He + H^+$, simultaneous single-electron capture, H^{2+} production, existence of critical scatt. angle 7-10750
 $He + Li^{3+}(C^{6+})(O^{8+})$, electron capture, Coulomb integral eval. 7-15679
 $He^+ + He^+$, electron capture cross sections, SCF-CI calcs. 7-15526
 $He^+ + Ne(Na)(Mg)$, multiple ionisation, charge transfer cross sections 7-15706
 $He^{2+} + K$, ionisation and charge transfer collisions, cross section meas. 7-20031
 $HeH^+ + C$, fast mol. ion dissoc., charged fragment wake effects (French) 7-50345
 $^3He^{2+}$ electron capture and stripping cross section in Al, Ni, Ag and Au targets 7-10753
 $^{111}InCl$ and ^{111}InI , ion-molecule collisions in gaseous forms, cross sections 7-20006
 Kr^{36+} , emerging from solid foils, anomalous population of deep capture states 7-42758
 $Kr^{4+} + He(Ne)$, state-selective electron capture, translational energy spectra 7-50337
 $Li + Cs$, ion pair prod. cross sections, beam-gas study 7-39871
 $Li + He^{2+}$, electron capture, Coulomb integral eval. 7-15679
 $N^{2+} + Kr(Xe)$, energy loss spectra 7-50334
 $N_2 + N_2$, charge transfer reaction, calc. of vibr. levels for neutral mols. 7-42759
 $NH^+ + C$, fast mol. ion dissoc., charged fragment wake effects (French) 7-50345
 N_2O , negative ion form., thermal electron attachment 7-15704

electron capture continued

- $Na + He^{2+}$, charge transfer, excitation processes coupled state impact parameter model 7-62518
 $Na + Li^{2+}$, charge exchange collisions, cross sections calcs., atomic-orbital expansions method 7-36460
 $Na + Ne^+(Ar^+)(Xe^+)$, Rydberg electrons removal, cross section meas. 7-36742
 $Na^+ + Li$, charge exchange collisions, cross sections calcs., atomic-orbital expansions method 7-36460
NaCl, excess electron localisation, QUPID calcs. 7-20029
 $Ne + H^+$, electron capture probabilities at large scatt. angles 7-62517
 $Ne^{q+} + H_2$ charge exchange collisions, Ne^{6+} excited states, VUV spectra anal. 7-20030
 $Ne^{q+} + He$, transfer excitation in low-energy collisions, spectroscopic meas. 7-15696
 $Ne^{q+} + D_2(D)$, collision parameters, energy-gain spectra meas., multichannel Landau-Zener model anal. 7-36752
 Ne^+ , excess electron localisation, QUPID calcs. 7-20029
 ^{16}O , collisions with wide range of targets, K-shell ionisation, polarisation and binding effects 7-31165
 $O^{6+} + He(H_2)(Ar)(Xe)$, one-step double electron capture 7-50344
 $Pb^{26+} + Sn(Xe)$, impact parameter depend. target K X-ray emission, XES spectra anal. 7-62314
 $Pb^{4+} + Ag$, electron capture, K X-ray emission spectra study 7-36524
 $Rb + Rb$, collisional ion-pair form., Coulomb pot. 7-15698
 ^{32}S , collisions with wide range of targets, K-shell ionisation, polarisation and binding effects 7-31165
 SE^- , negative ionis. source for quadrupole mass analyser 7-35620
 Si^+ , transversing Fe and Gd foils transient mag. fields 7-10537
 $Sm^{q+} + Xe$ collisions, $q=34$ to 52, resonant electron transfer and L-shell excitation, X-ray spectra study 7-30979
 $Sr^+ + Ba$, laser-induced charge exchange, quasi-mol. model, fluores. anal. 7-36748
 $U^{q+} + Al(C)(Be)(Mylar)$, electron stripping, cross section meas. 7-64849
 $U^{q+} + Sn$, electron capture, K X-ray emission spectra study 7-36524
 $Xe^{45+} + Al(C)(Be)(Mylar)$, electron stripping, cross section meas. 7-64849
- electron capture, nuclear see nuclear electron capture
electron capture in solids see electron traps
electron density
see also carrier density; current density; electron density (metals); plasma density
aperture limiter shadow of T-10 tokamak, Langmuir probe meas. 7-51394
atoms, closed-shells, s-state and total electron density, convolution relation, HF calcs. 7-42475
XZ Cep, eclipsing binary, shell electron density characts. 7-4511
FK Com stars, outer atm. characts., UV spectral obs. 7-47936
P/Comet Halley (1982i) plasma tail, electron density irregularities from radio source scintillation obs. 7-66516
covalent bonds, electron density accumulation 7-15470
D-region, electron density profile determ. using antenna outputs of VLF waves (Japanese) 7-66394
D-region, winter-time, electron densities and wind vels. from partial refl. radar obs. 7-47612
discharge, constricted, charged particles, radial distribution 7-63382
discharge laser, photo-initiated, electrically excited, electron density meas. 7-31335
Earth magnetosheath, power spectra of electron density and mag field fluctuations 7-34786
electron momentum density, near HF limit analytic wave fns., atoms and mols. 7-49884
equatorial electrojet, drift speeds of irregularities of kilometre and metre sizes 7-4257
F₂-layer, noon bite-out phenomenon at Waltair 7-66385
F-region parameters determ., resonance scattering method 7-55356
flash lamp, low-pressure, background radiation from ablation phenomena 7-43282
graphite, electron momenta, Hartree-Fock-Roothaan calc. 7-42466
interstellar electron density determ. from pulsars interstellar scintillation 7-40856
interstellar medium, electron density power spectrum determ. from refractive and diffractive scatt. 7-55759
interstellar medium, limits on 'local fluff' from IUE Mg I data 7-55782
ionised interstellar gas towards galactic centre, electron density from low-freq. radio recomb. lines 7-66719
ionosphere, effect of electron temp. on electron number density and dynamics of equatorial E-region 7-66390
lower ionosphere, electron density determ. via radio waves resonance scattering method 7-47613
ionosphere, plasma parameters meas. in vicinity of Space Shuttle 7-29360
ionosphere, variations at VLF signals refl. height 7-60448
ionosphere, VHF transionospheric signal time delay at subauroral latitudes anal. 7-23933
ionosphere, whistler (Chinese) 7-29258
ionosphere electron content, solar flare effects (Chinese) 7-18394
AD Leo, UV Cet star, giant flare, atm. characts. 7-55676
local interstellar medium, Voyager heliospheric shock obs. (Russian) 7-14634
low Z impurity behaviour in TFTR 7-20919
meteor trains, theory for radio waves scatt. from underdense trains 7-4383
methane, electron momenta, Hartree-Fock-Roothaan calc. 7-42466
pharmacologically active cpds., similarity meas. calcs. 7-49890
plasmopause, electron density var., GEOS-2 obs. 7-60449
plasmaphere, electron temp. vars. along geomag. field lines rel. to electron density profiles and VLF paths 7-4258
polyacetylene, electron momenta, Hartree-Fock-Roothaan calc. 7-42466
radial electron distribution structure, meas. in high-current discharge, ion laser media appl. 7-44295
reversed field pinch, electron temp. and density meas. 7-20922
solar corona, density, temp. and expansion vel. meas. during eclipse (1980 February 16) 7-29449
sub-auroral ionosphere, height-latitude distrib. 7-40624
Sun, eruptive prominence at several solar radii, physical conditions 7-4426
tetrafluoroterephthalonitrile, electron distrib. calc. 7-42454
travelling ionospheric disturbances and daylight mid-latitude spread-F 7-60451

electron density continued

- vacuum arcs, high current, anode discharge mode and cathode plasma state 7-44284
- WC stars, C and O abundances rel. to electron densities and mass loss rates 7-29480
- Ar gas, surface-wave produced microwave discharges 7-63389
- B(OH)₃, electron density, X-ray diffr. determ. at 105 K, ab initio calcs. 7-44458
- CO₂ waveguide laser, anomalous refr. indices of amplifying medium 7-36933
- Cu-like heavy positive ions, binding energy and electron density, relativistic Thomas-Fermi theory 7-49923
- H-like Balmer alpha lines, recomb. and photo-pumping mechanisms for gain prod. 7-20212
- H₂, b³Σ_u⁺, excited states, mag. effects, ab initio calcs. 7-10413

electron density (crystallography) *see crystallography***electron density (metals)**

- heavy fermion systems, hydrodynamic fluctuations 7-44708
- metal surface, pot. change with charge, Thomas-Fermi-Dirac-jellium model 7-52715
- metals, grain boundary energies from local-electron-density distributions 7-6634
- polyacetylene:I, metallic, effective mass, magnetoreflexion studies 7-64056
- thermal conductivity theory, Lorenz ratio 7-45272
- Al, grain boundary energies from local-electron-density distributions 7-6634
- CePd₃ mixed valence system, conduction carrier density, energy and temp. depend. 7-21882
- Nb/Cu artificial superconductive metallic superlattices, electron density, pair tunnelling studies 7-58959

electron density (semiconductors and insulators) *see carrier density***electron density of states** *see electronic density of states***electron density of states (condensed matter)** *see electronic density of states***electron detachment**

- atomic negative ions, autodetaching states, electron correl. effects 7-19789
- atomic negative ions, electron detachment, overview 7-15563
- electronegative molecules, gaseous, electron attachment and detachment processes 7-19967
- PIG, ion source for negative ions 7-36704
- positronium negative ion, photodetachment 7-36818
- Cl⁻ laser photodetachment spectroscopy 7-19790
- Cs⁻, low-energy collisions with atoms and mols., absolute total cross section meas., curve-crossing model anal. 7-36749
- FeO⁻, rot., autodetachment spectroscopy 7-62462
- GaAs_n⁻ semicond. cluster anions, photodetachment and photofragmentation 7-36837
- Ge_n⁻ semicond. cluster anions, photodetachment and photofragmentation 7-36837
- H⁻, positron impact electron detachment, with excitation, threshold law calcs. 7-25668
- H⁻+He, single-electron detachment, time correlated electron spectrum study. 7-36741
- H₂⁻, autodetaching states, Feshbach-type formalism 7-15705
- He+H⁻, electron detachment, energy and ang. distrib. 7-20013
- K⁻, electron affinity and photodetachment cross sections, ab initio multichannel calcs. 7-36463
- KrF electron beam sustained discharge excimer lasers, discharge constriction, photodetachment, ionisation instabilities 7-10920
- O₃⁻, photodetachment cross sections Franck-Condon anal. 7-57139
- Pd⁻, core size role in photoelectron spectra 7-15571
- Sc⁻, core size role in photoelectron spectra 7-15571
- Se⁻, resolved Zeeman thresholds in photodetachment in mag. field 7-42549
- Si_n⁻, semicond. cluster anions, photodetachment and photofragmentation 7-36837
- Y⁻, core size role in photoelectron spectra 7-15571

electron detection and measurement

- analyser with position sensitive detector, scattered electrons influence 7-36377
- BGO calorimeter, performance in electron beam 7-62224
- current density monitor for intense relativistic electron beams 7-19595
- DELPHI forward EM calorimeter, edge effects (*Spanish*) 7-49789
- dosimetry, clarification of the AAPM Task Group 21 protocol 7-40305
- electron yield detectors for near surface EXAFS 7-61414
- FEU-130 photomultiplier characts. meas. 7-30889
- FWT-60 and glutamine dosimeters, dose intercomparison for 400 to 500 keV electrons 7-28702
- gas phase X-ray absorption spectroscopy with an electron yield detector 7-62311
- gas-scintillator detection of low-energy electrons 7-5536
- high energy electrons, influence of cylindrical air cavities on fluence distributions. 7-62097
- high pressure Xe gas time projection chamber, electron trajectories, Monte Carlo simulation 7-49801
- high spatial resolution positron emission tomograph 7-36421
- large area transition radiation detectors for electron identification at CERN UA6 expt. 7-42291
- LEED with position-sensitive detection, comparison with positron diffr. 7-26597
- low pressure multistep detectors, high energy particle identification appl. 7-42290
- MD-1 detector, proportional chambers with delay line readout 7-36386
- microchannel plate chevron as position sensitive detector for β-spectrometers 7-25313
- NE104 and NE110 aged large vol. scintillators, response to fast n, p and e 7-5538
- polarised electron sources and detectors, surface studies appls., book contrib. 7-30806
- position sensitive LSI detector for low energy ESCA electrons 7-19668
- positron camera for industrial appl. 7-42320
- positron imaging, electron gamma shower for Monte Carlo calcs. 7-36424
- quartz piezoelectric resonators, electron and gamma radiation dosimetry appls. 7-15416
- surface topography meas. using SEM with two secondary electron detectors 7-295
- transition radiation detector for electron identification in a high energy experiment 7-49797

electron detection and measurement continued

- transition radiation detectors for electron identification up to 100 GeV 7-42289
- tridial plasma devices, system for mapping magnetic field errors 7-51500
- wire chamber advances for Mossbauer spectroscopy expts. 7-36384
- He-filled proportional counter for low temps. and appl. to cryogenic resonance-electron Mossbauer spectroscopy 7-62234
- Pb scintillation calorimeter for electron and pion detection, radiation damage props. 7-15451
- Si photodiodes, use for dose depth distrib. meas. in oncology 7-60092
- Si(Li)-W 4 inch sandwich calorimeter for pp collider expts. 7-5548
- U gas sampling hadron calorimeter, performance 7-5547

electron device noise

- 1/f noise, carrier mobility fluctuation origin 7-38653
- microstructures, noise effects, device sensitivity 7-52713
- photodiodes, 1/f noise, extended Burgess' variance theorem 7-45412
- photomultipliers, photon counting, 1/f noise 7-40716
- semiconductor laser, mode locked, suppression of timing and energy fluctuations by CW injection 7-50609
- spacial solar panels, LF noise as nondestructive inspection test 7-39996
- UV radiometers, detector elec. characteristics 7-41417
- Cd_{1-x}Hg_xTe IR heterodyne detectors, intermediate temp. operation 7-35594
- CuAl-quartz, SAW resonators, annealing behaviour and phase noise performance 7-11242
- GaAs devices, 1/f fluctuation, surface states effects (*Japanese*) 7-21955
- InGaAsP DFB lasers, extremely low-noise facet-reflectivity-controlled 7-31320
- INSb array IR imaging camera, for astronomical appls. 7-34865
- Nb-In point contact, observation of chaotic noise 7-7445

electron diffraction

- see also electron diffraction crystallography; electron diffraction examination of materials; gas phase electron diffraction; high energy electron diffraction; low energy electron diffraction*
- ion-induced secondary electrons emitted from foil, diffraction obs. 7-13307
- X-ray photoelectron diffraction, submonolayer interface struct. determ. appls. (*Japanese*) 7-11852

electron diffraction crystallography

- see also crystal atomic structure; Debye-Waller factors; electron diffraction examination of materials*
- atomic imaging of semiconductors, using JEOL 4000 EX TEM 7-32230
- Bloch wave treatment of electron transmission 7-16366
- channelling patterns, many beam effects and phase information 7-32534
- Compton profiles, dynamical scatt. effects in electron scatt. meas. 7-51585
- computer aided analysis of electron channelling patterns 7-16664
- contrast due to large cryst. inclusions, modified Bloch wave theory calcs. 7-51583
- convergent beam diffr. in the transmission electron microscope 7-37808
- convergent beam electron diffraction, meas. lattice parameter changes in semiconductor device structures 7-52371
- convergent beam electron diffraction from organic crystals 7-16371
- convergent-beam, simultaneous obs. of zone-axis pattern and ±G dark-field patterns 7-32231
- convergent-beam electron diffr., zone-axis pattern and ±G dark-field pattern simultaneous obs. 7-1821
- dark field imaging as paired complements to bright 7-16367
- diffuse satellites in electron diffr. patterns of Pb orthovanadates and orthophosphates 7-26595
- dynamical diffraction from modulated structures 7-16364
- Ewald dispersion surface, review in electron diffraction cases 7-32228
- granular films, kinematic diffraction, numerical simulation 7-64025
- hemicyanine Langmuir-Blodgett films, optically nonlinear 7-51584
- Holz patterns, anal. and appls. of dynamical effects 7-44314
- image formation by plasmon loss electrons in small spheres 7-16369
- interface structural eval., matrix reflection fall-off, interference effects and coherence conditions depend. 7-11855
- interface structure determination by CB diffraction from epitaxial crystals 7-16899
- Kukuchi lines, contrast reversal near reflex points with same indices in crystals. with defects (*Russian*) 7-51582
- line analysis of electron diffraction information 7-16365
- metallic materials, electron diffr. anal., appl. of theoretical diffr. patterns 7-11853
- morphology of small particles under weak beam conditions 7-44313
- phase diagrams, determination by analytical electron microscopy 7-37820
- quasi-periodic lattice structures, dynamical calcs. 7-16370
- rubredoxin thin microcrystal, electron diffr. data, elastic bend distortion effects 7-13956
- scattering in crystals with distortions of second class, basic eqns. of dynamic theory (*Russian*) 7-32204
- TEM, precip. growth at atomic level 7-46491
- tilted illumination studies of crystalline polymers 7-16372
- transmission electron microscopy, convergent beam electron diffr. techniques 7-4915
- Al alloys, quasicrystals, electron diffraction structure anal. (*German*) 7-37930
- TiO₂, rutile, dynamical thermal diffuse scatt. of fast electrons, crystal struct. 7-32229

electron diffraction examination of materials

- see also gas phase electron diffraction; high energy electron diffraction; low energy electron diffraction; reflection high energy electron diffraction*
- 7-32363
- p-acetoxybenzoic acid, tetramer, topotactic transitions 7-12264
- alkali metal layered Mo bronzes, (A⁺(H₂O)_n)_xMoO₃^{x-}, (A=Li, Na, K, Rb, Cs), composition and struct. 7-16518
- bacteriorhodopsin M₄₁₂ intermediate, electron diffr. anal. 7-28463
- binary alloys, crystal-amorphous transformation, thermodynamics and kinetics 7-21108
- clusters, molecular beam studies 7-24724
- conference, electron microscopy and anal. Newcastle-upon-Tyne, England, (Sept. 1985) 7-14707
- diamond, strain measurement in convergent beam electron diffraction 7-16562
- diamond, synthesis by laser induced CVD, low press. 7-13371
- diamond, type Ia, voidites, evidence for crystalline phase containing nitrogen, cell constant determ. 7-2011

electron diffraction examination of materials continued

- didymium tartrate crystals, gel grown, charactn., thermal behaviour 7-39367
- grain boundary struct., annealing above 1800K in W wire 7-6636
- imperfect surfaces and adsorbates, short range order and correlations 7-6953
- interface, internal, interphase, diff. effects 7-12496
- interfaces, internal, diff. effects, general considerations and grain boundary effects 7-12495
- long chain molecules, epitaxial crystallisation, morphological, structural study 7-16901
- metal clusters, dispersed in polymeric matrices, synthesis and props. 7-17370
- metallic fine particles, surface free energy anisotropy determ. 7-32783
- morphology of small particles under weak beam conditions 7-44313
- organic conducting single crysts., electron irr., Bragg spot fading 7-12158
- oxides, $\text{Al}_2\text{O}_3(\text{M}_2\text{O}_4)_n$, derived from the rutile structure by chemical twinning, structural evolution and stability 7-16757
- paraffins, direct lattice imaging 7-16542
- n-paraffins, electron crystallography 7-16541
- poly(p-phenylene terephthalamide), single cryst. and spherulites, morphology and struct. investig. 7-11949
- poly-p-phenylene sulphide, solution-grown crystals and crystalline thin films, morphology 7-16441
- poly-p-phenylene vinylene films, electron diff. struct. investig. 7-44409
- polyacetylene films, synthesised via Durham precursor route, struct. and morphological study 7-37897
- polymer microcrystals, natural, diff. data from electron diff. patterns 7-11862
- polyparaphenylene: Na, electron and cryst. struct., EELS and electron diff. studies 7-63514
- p-polyphenyls, electron microscopical studies 7-16440
- polypropylene, isotactic, γ -phase morphology 7-6554
- polypropylene films, Cu-filled, struct. and elec. cond. 7-64301
- polystyrene films, craze microstruct., low angle electron diff., Fourier transforms of TEM images 7-13560
- quasicrystal diffraction patterns, distortion and peak broadening 7-11981
- quasicrystals, alloy quasiperiodic structures, diffraction pattern simulations 7-6585
- reactive dyes, water soluble, lyotropic liq. cryst. mesophases and solid physical form 7-32276
- semiconductor superlattices, synthesis by MBE (*Japanese*) 7-12544
- steel, austenitic stainless, N-bearing, Nitronic 60, fretting wear at temps. up to 600°C 7-17653
- steel, austenitic stainless, streaking effects of H induced ϵ martensite phase, TEM obs. 7-28038
- steel, Cr-Mo, friction pair, surface layer structural modifications (*Russian*) 7-39678
- steel, dual-phase, Mn-partitioning, austenite form. 7-39552
- steel, stainless, austenitic, pre-precipitation phenomena associated with γ' form. 7-22696
- steel, stainless, ferritic-martensitic, high-Cr, fast reactor irr., phosphide phases 7-22700
- steel, stainless, Type 316, microstruct. exam. around weldments 7-22697
- steel, stainless FCC 7-63409
- superalloys, crystalline struct. and growth twin of Cr_7C_3 , electron diff. (*Chinese*) 7-12077
- superalloys, topologically close packed phases, domain struct. (*Chinese*) 7-11989
- surface and epitaxial overlayer structures from X-ray photoelectron diff. 7-27862
- surface science techniques, book 7-60888
- surfaces and overlayers, struct. determ. with diff. methods 7-2324
- techniques for surface studies, book 7-60911
- thin films, struct. and compositional characts, electron diff. patterns 7-21752
- transition metal amorphous alloy coatings, microindentation response, microstruct. and composition effects 7-46625
- ultra-thin foil thickness determination from large-angle convergent beam electron diffraction patterns 7-63406
- Xe monolayers on graphite, low temp. struct. and incommensurate-commensurate transition, electron diff. study 7-38335
- zeolite theta-1, structural TEM studies 7-16534
- zirconia transparent gel-monolith from Zr alkoxide, controlled hydrolysis prep. 7-8313
- Ag-Ag, thin film system, phase growth, electron microscope obs. 7-58488
- AgCu thin epitaxial films, struct. investig. (*Russian*) 7-12528
- $(\text{Ag}_2\text{O})_x(\text{B}_2\text{O}_3)_{100-x}$ glasses, microstruct. and electronic cond. studies 7-6534
- Ag_2Te , domain struct. and phase transforms., electron diff. and microscopy studies 7-58194
- Al coating on Rene 80 and pure Ni, high temp. oxidation, TEM obs. 7-28202
- Al:Ar, solid Ar bubble, diffraction anal. 7-16547
- Al/a-SiC films, RF sputtered, interfacial struct. and reactions, 573-773K (*Japanese*) 7-53583
- Al-Ag, γ' precip. growth, TEM studies at atomic level 7-46491
- Al-Ag alloys, γ' precipitates, convergent-beam electron diff. studies, space-group anal. 7-11854
- Al-Cr(Mn)(Fe) amorphous films, quasicrystalline transformation by ion irradiation 7-2071
- Al-Fe-Si, dil., solidification, intermetallic cpd. form. 7-13442
- Al-GaAs interfaces, convergent beam electron diff. patterns 7-27156
- Al-Mn, rapidly solidified, decagonal phase morphology 7-39499
- Al-Mn (15 wt.%), melt spun ribbons, icosahedral struct., decomp. rel. to annealing 7-28030
- Al-Mn-Zr (7.1 wt.%), rapidly solidified, quasicrystalline phase precip. 7-3310
- Al-Nb amorphous films, elec. props. and charactn. (*Japanese*) 7-32977
- Al-Pd, rapidly solidified, decagonal phase morphology 7-39499
- Al-Si (12.7 wt.%), eutectic microstruct., twinning and branching mechanisms 7-17521
- Al-Ti-Gd, rapidly solidified ribbons, aged, ternary phase precipitate identification 7-3311
- Al-V alloy, amorphous and quasicrystalline state, electron diff. study 7-63562
- AlMn icosahedral phase, atomic struct., electron diff., studies 7-32366
- Al_xMn alloy, decagonal and icosahedral phase coexistence, electron diff. studies 7-11991

electron diffraction examination of materials continued

- Al_xMn , icosahedral, fine line struct. in convergent beam electron diff. 7-63560
- $\text{Al}_{88}\text{Mn}_{12}\text{Fe}_2$, $\text{Al}_{88}\text{Mn}_{14}$, icosahedral alloys, obs. of mirror-related grains 7-37867
- Al_2O_3 , profiled, plastic flow in surface layers during diffusion welding 7-33730
- $\alpha\text{-Al}_2\text{O}_3$, surface structure, identification by electron diff. 7-27069
- AlPO_4 , modulated phase, electron microscopy study 7-26937
- Au, twin boundary struct. determ. of twinned bicrystals, convergent-beam electron diffraction study 7-51786
- Au-Fe (10 to 35 at.%), early stage clustering struct. 7-59536
- Au-Mn (15 at.%), disordered phase, high resolution electron microscopy study 7-63834
- BN, ion-plated, prep. and charact. 7-17477
- c-BN, phase diagram, p,T,E 7-17517
- BN, pyrolytic, macrodefects study 7-44523
- BaPb β (II)-alumina, superstructure, high resolution electron microscopy study 7-12021
- $\text{BaTiO}_3\text{:Nb(Ca)}$, ferroelec. domains, SEM and TEM obs. 7-2998
- $\text{Ca}_{1-x}\text{Ba}_x\text{F}_2$ epitaxial layer growth and struct., electron microscopy studies 7-27174
- $\text{Ca}_3\text{Fe}_2\text{TiO}_{8+x}$, perovskites, microdomains, electron microscopy 7-16533
- $\text{Ca}_3\text{Mn}_{1.8}\text{Fe}_{1.2}\text{O}_{3+y}$, perovskites, microdomains, electron microscopy 7-16533
- $\text{Ca}_3(\text{PO}_4)_2\text{CaF}_2$, apatite, carbonated crystallites, high resolution TEM study 7-6643
- $\text{Cd}_{1-x}\text{Mn}_x\text{Te}$ films, hot wall vacuum growth, twinned struct. 7-53593
- $\text{Cd}_{1-x}\text{Mn}_x\text{Te}$ - $\text{Cd}_{1-x}\text{Mn}_x\text{Te}$ superlattices, electron diff. using partially coherent illumination 7-37807
- CdF_2 , crystal structures and microphases, devil's staircase 7-11982
- Co-Al alloys, magnetic hardening 7-33209
- CoCr films, texture formation, appl. for perpendicular mag. recording 7-39539
- CoNi sputtered films on Cr and polyimide, mag. props., relation to struct. 7-33228
- Cr films, thin polycrystalline sputtered, oxidation by CW CO_2 laser irradiation 7-13642
- Cr, thin films, crystallographic props., electron diff. patterns 7-21751
- Cr, vacuum-deposited, hardness and struct. studies 7-33761
- Cr, zone-axis critical voltages in HEED, accidental Bloch wave degeneracies obs. 7-63409
- Cr, zone-axis critical-voltage effect obs. 7-63408
- Cr-Ni (45 wt.%) amorphous free-standing thin films, struct. transformations, pulse laser irradiation 7-38382
- Cu epitaxial film struct. and surface purity on MgO single cryst. substrates 7-16896
- Cu, thin films, crystallographic props., electron diff. patterns 7-21751
- Cu-Al-Mg alloys, complex oxide form. and precipitate morphology (*Russian*) 7-33664
- Cu-Be, explosive cladding, martensitic transform., electron diff. 7-46468
- Cu-Pt (25.7 at.%), transform. from short-range order to L_{12} and L_{12} , ordered states 7-53726
- Cu-Sn thin film diffusion couple, reaction kinetics at room temp. 7-21536
- Cu_{3+x}Pd , long-period superstructures 7-21430
- Cu_2S thin films, form. by electrochem. procedure 7-39445
- Fe and alloys, alloying with N under high press. 7-3266
- Fe, magnetic films, MBE growth on GaAs, interface effects 7-27584
- Fe/Cu multilayered samples, ion beam mixing-induced metastable phases 7-58377
- Fe-C martensite, struct. in transition state from first to third stage of tempering, electron microscopy and diff. study 7-46528
- Fe-GaAs(001)-c(8 \times 2) interface, simultaneous epitaxy and substrate out-diffusion 7-38355
- Fe-Si sheets, grain oriented, orientation of individual grains by means of Kossel patterns (*Japanese*) 7-22716
- Fe-Si sheets, grain oriented, generation of secondary nuclei (*Japanese*) 7-22717
- $\text{Fe}_{81}\text{B}_{13}\text{Si}_{3}\text{C}_2$, Metglass 2605 SC, surface crystn. behaviour 7-58154
- $\text{Fe}_{40}\text{Ni}_{18}\text{B}_{18}\text{Mo}_4$, Metglass 2826 MB, surface crystn. behaviour 7-58154
- FeNiCr, strain measurement in convergent beam electron diffraction 7-16562
- $\gamma\text{-Fe}_2\text{O}_3$ reactive RF sputter deposition, struct., elec. and mag. props. studies 7-17421
- GaAs, crystal polarity, convergent beam electron diff. study 7-21162
- GaAs faulted dislocation dipoles, electron diff. and high-resolution TEM studies 7-44551
- GaAs films on oxidised Si, zone melting recrystallisation 7-38396
- GaAs-InAs superlattice, reflection electron diffraction intensity oscillation 7-7030
- $\text{Ga}_{1-x}\text{In}_x\text{As}$, heterostruct., local composition, CBED anal. 7-16529
- GaP films, MBE grown on Si, antiphase domain structures 7-64014
- $\text{GaSb}_{1-x}\text{As}_x$, 7-16529
- $\text{Ge}_{20}\text{S}_{80-x}\text{Bi}_x$, n-type amorphous semiconductors, morphological struct. 7-51652
- GeSi thermally evaporated epitaxial heterolayers on GaAs substrate, Si distrib. (*Russian*) 7-63988
- GeSi-Si heterostructures, MBE grown, structural props., quality, electron diff., imaging obs. 7-7036
- $\text{Hg}_{1-x}\text{Cd}_x\text{Te}$ /CdTe superlattices, MBE growth and props. 7-53602
- Hg_2Cl_2 thin films, morphology and growth on Hg surface, electron beam damage 7-59469
- InGaAsP, layers on InP, rel. lattice parameter meas., convergent beam electron diffraction 7-52371
- InP films on oxidised Si substrate, laser recrystallisation 7-38398
- InSe crystals, melt-grown, electron diff. study 7-1994
- Mg_2NiH_4 , twinning at unit cell level, low temp. phase, electron microscopy study 7-26762
- $\delta\text{-Mn}_2\text{Ge}_2$, high temp. phase structs., electron microscopy obs. 7-26697
- $\text{Mn}_3\text{Ni}_2\text{Si}$, rapidly solidified, Friauf-Laves phase related quasicrystal, TEM obs. 7-51706
- Mo:Cu(Re), pulsed ion implantation, surface struct. 7-51867
- Mo/Ni superlattice, sputtered, struct. anal. 7-45030
- Mo-Si amorphous alloys, cluster formation and percolation 7-27455
- MoO_3 crysts., surface structure, implications for catalytic oxidation of hydrocarbons 7-6942
- MoO_3 , interaction, of reduction products with C to form Mo_2C 7-8260
- Nb film microstruct., nonnormal incidence ion bombardment effects 7-12174
- NbC, amorphous films, prep. and characts. 7-7885

electron diffraction examination of materials continued
NbTe₄, discommensurate distortion waves, struct. changes on cooling 7-1996
NbTe₄, discommensurate state microstruct., electron diffr. pattern obs. 7-6598
Ni, defects created by low-energy ion bombardment, investig. by slow electron diffr. (*Russian*) 7-58374
Ni superalloy, MAR M002, borides analysis using convergent beam electron diffr. 7-22699
Ni-Al alloy phase transforms. during ion beam mixing, electron diffr. and microscopy studies 7-16655
Ni-Al-Mo, precip. in Ni-base superalloys 7-53745
Ni-Mn, microtwinning, β - θ martensitic transform 7-32455
Ni-Mo-Fe-Cr alloy, transient phase obs during long range ordering to Ni₃Mo, electron diffr. study 7-63806
Ni-P films, electroless deposited, struct., electron microscopy studies 7-7041
(Ni₃Fe)_{1-x}Cr_x alloys, ordering study, comp. depend., electron diffr. and Mossbauer meas. 7-51690
NiO-CaO eutectic, directionally solidified, struct. imperfections 7-65026
NiO-CuO solid solutions, tweed microstruct., investig. using TEM 7-44756
NiSi₂-Si, epitaxial growth of silicide layers by electron beam annealing 7-27213
NiSi₂-Si interfaces, convergent beam electron diffr. patterns 7-27156
Pb orthovanadates and orthophosphates, diffuse satellites in electron diffr. patterns 7-26595
Pb(Si_{1/2}Ta_{1/2})₂O₃, single crystals, and hot pressed ceramics, ordering, domain struct., TEM obs. 7-26936
Pb_{1-x}Sn_xS films, phase composition, fast-electron diffr. 7-63990
Pb_{1-x}Sn_xTe surfaces, AES, LEED and Kikuchi pattern obs. 7-52200
Pb₃(VO₄)₂, β - γ transition, intermediate modulated struct. 7-2183
Pd-U-Si, growth of quasicrystalline phase from glassy state 7-58144
Pd-U-Si glassy alloys, glassy-to-icosahedral polymorphous crystn. transform., X-ray and electron diffr. studies 7-6515
Pd-U-Si glassy state, quasicrystalline phase form., X-ray and electron diffr. studies 7-26645
Pd₃Si₂₀, metallic glass, crystallisation 7-37882
Pt-Sr internally oxidised alloys, morphology, struct. and stability (*Russian*) 7-33687
PtSi/p-Si thin Schottky diodes, TEM, TED, I-V curve and photoemission characts. 7-12861
Rh epitaxial film struct. and surface purity on clean and Cu-covered MgO single cryst. substrates 7-16896
Si (111) with adsorbed Ga, X-ray photoelectron and Auger electron diffr. 7-27116
Si film, amorphous, small-angle scatt. of electrons in STEM obs. of defects and voids 7-21754
Si SOI structures, O₂⁺ implanted, oxide precipitates, ordering 7-21449
Si, strain measurement in convergent beam electron diffraction 7-16562
Si, twin boundary struct. determ. of twinned bicrystals, convergent-beam electron diffraction study 7-51786
Si, zone-axis critical voltages in HEED, accidental Bloch wave degeneracies obs. 7-63409
Si:B-Mo interface, specimen preparation by chemical etching and polishing, for electron studies 7-29989
Si:H binary alloys, crystallisation of polysilane 7-21105
a-Si:H/Ti/Al system, solid state reactions, TEM and SAD studies 7-3602
Si:O, microcrystalline precipitates, electron microdiffraction studies 7-16769
Si:P, pulsed laser annealing, molten phase local nucleation study 7-63655
Si:S(Tl)(Ge)(P)/Pt system, impurity migration during silicide form. 7-6895
Si:W⁺ layers, implanted and annealed, struct., TEM, electron diffr. studies 7-32858
Si/Ge_{1-x}Si_x, convergent beam electron diffraction and imaging of strained-layer superlattices 7-17095
 α -SiC, 6H polytype, Kikuchi map 7-58225
 β -SiC epitaxial layers, cubic cryst. struct., electron diffr. and microscopy studies 7-27199
a-Si_{1-x}C_x films, RF sputtered, IR absorpt., X-ray diffr., RHEED (*Japanese*) 7-53584
a-Si_{1-x}C_xH thin films, struct. investig., electron diffr. studies 7-2430
Si₃C_{1-x}H_x, amorphous, local atomic arrangement, EELS and electron diffraction 7-44378
 α -Si₃N₄ whiskers, microstruct. investig. by TEM (*Japanese*) 7-21789
Si₃N₄-Ti, reaction under rapid thermal annealing 7-39334
SiO₂, modulated phase, electron microscopy study 7-26937
Si_{1-x}Sn_xO_{1+x} amorphous thin films, optical and structural studies 7-64714
Sn, graphoeptitaxial growth on monatomic steps, TEM, electron diffr. studies 7-58714
Sn/SnTe bilayers, electron diffr. pattern fine struct., influence of angular misorientation 7-16885
Sn_{1-x}Dy_{4+x}Os₈Sn₁₈, disordered II' phase, structural study, electron and X-ray diffr. meas. 7-63549
SnO₂, amorphous film, vacuum prep., struct., crystallisation 7-53594
Sn_{1-x}Tb_{4+x}Rh₆Sn₁₈, disordered II' phase, structural study, electron and X-ray diffr. meas. 7-63549
Sr_{0.5}Ba_{0.5}Nb₂O₆, incommensurate superstructures, phase transition, electron diffr. study 7-63792
Sr₂Mn_{2-x}Ti₂O_{5+x/2}, struct. and defects 7-44490
Sr₂SiO₄, β to α to β transformation, electron microscope study 7-16723
Ti binary alloys, reduced technological plasticity and struct. (*Russian*) 7-17583
Ti, heat treated, softening, in situ HVEM obs. 7-17548
Ti, implantation-induced textures, electron diffr. and microscopy studies 7-46507
Ti-Al-Mo-Fe, struct. changes during phase transitions (*Russian*) 7-53721
Ti-Al-Sn, silicide precipitates struct. 7-63561
Ti-Cr, β -eutectoid, deform. behaviour of retained β phase 7-39589
Ti-Ni, crystalline to amorphous transitions, struct. anal. 7-44375
TiC, amorphous films, prep. and characts. 7-7885
TiC film ion plated on austenitic stainless steel, adherence rel. to ionisation (*Japanese*) 7-53636
Ti₃₀Ni₄₀Au₁₀, martensitic transform., TEM study 7-59522
Ti₃₀Ni₄₅Au₅, martensite, interstitial H-induced extra reflection, TEM and electron diffr. study 7-59521
TiO₂, rutile, dynamical thermal diffuse scatt. of fast electrons, crystal struct. 7-32229

electron diffraction examination of materials continued
TiSe₃, prep. in presence of Sb, struct. studies 7-33616
Ti_{1.17}S₂ crystals, metal-insulator transition investig. 7-7296
TiSi₂ vacuum electron beam evaporation, annealing effects, Auger and electron diffr. anal. 7-22492
U-Ti (4 at.%), quenching, decomp., TEM obs. 7-39527
V₄₁Ni₃₆Si₂₃, rapidly solidified, quasicrystalline and Frank-Kasper phases, tenfold electron diffr. pattern obs. 7-65022
V₇O₁₃, metallic, electron state, electron diffr. determ. 7-37921
VSe₂-1T, distorted struct., convergent beam diffraction study 7-16528
W selective low press. CVD growth on Ti, TiSi₂ and PtNiSi, surface reactions, struct. 7-27183
Zn_{1-x}Cd_xS thin films, struct. and electrical props. 7-64372
ZnF₂, crystal structures and microphases, devil's staircase 7-11982
Zr-Cr-Fe, polytype structures, TEM, electron diffr. obs. 7-37925
Zr-Ni(V) amorphous superconductors, struct. and supercond. props. 7-27482
ZrO₂ based films, composition and struct., X-ray emission and ESCA studies 7-22385
ZrO₂, Y₂O₃ partially stabilised, microstruct. after ageing at high temp. 7-65061
ZrO₂-Y₂O₃, Y-TZP, toughened, microstruct., TEM and electron diffr. study (*Japanese*) 7-22634
electron-electron double resonance *see* ELDOR
electron-electron interactions
see also electron-electron scattering
ee-ee $\gamma\gamma$, Feynman diagrams representing partial helicity amplitudes, substitution rules 7-49023
electron-electron scattering
see also electron-electron interactions
No entries
electron emission
see also cathodes; electron field emission; exoelectron emission; photoemission; secondary electron emission; spin polarised electron emission; thermionic electron emission; work function
emission electronics, conf., Tashkent, USSR (Oct. 1984) 7-9575
electron energy bands *see* band structure
electron energy loss spectra
acetaldehyde, electronic struct. and decay channels, negative ion mass and electron impact spectroscopy 7-50383
acetylene, on Si (111), rehybridisation, vibr. investig., EELS 7-17816
adsorbate orientation, electronic excitation by electron beam, differential cross-section meas. 7-27101
adsorbed states on Pd (110), EELS and LEED study 7-27115
adsorption and thermal decomposition on Ni (110), isolation and identification of NH₂ and NH 7-6986
adsorption of O₂ on Pd (110) at 300K, LEED and EELS studies 7-27093
adsorption on Ge (100), high resolution energy loss spectra study 7-38331
alkali metal adsorbed layers on solid surfaces (*Japanese*) 7-21966
alkanes, linear and branched, C K-shell excitation, electron energy loss spectra 7-57172
amorphous films, laser generated, struct. and bonding, Raman and electron energy loss spectra study 7-27800
analyser with position sensitive detector, scattered electrons influence 7-36377
analytical electron microscopy of thin films, review (*Czech*) 7-59261
analytical TEM, MV, with JEOL 4000FX 7-30129
(BEDT-TTF)₂I₃, alpha and beta phases, electronic struct., EELS studies 7-45118
benzene, chemisorbed on Pt {110}, influence of orientation on H-D exchange reactions 7-59781
benzene, solid, electron scatt., mean free paths determ. 7-39328
benzene gas, K-shell EXAFS studied by EELS 7-62403
bound state existence confirmation for atomic and mol. projectiles inside solid targets, expt. investig. (*French*) 7-22427
brass, two-phase, Al-B Masteralloy addition, B redistrib. during solidification, grain refining effect 7-22664
trans-1,3-butadiene, vibr. struct., EELS 7-5767
carbon tetrafluoride gas, K-shell EXAFS studied by EELS 7-62403
characteristic signals from complex spectra, single-stage technique for separation 7-18945
chemical analysis in electron microscope, book 7-55903
coincidence counting techniques in analytical electron microscopy 7-23104
conference, electron microscopy and anal. Newcastle-upon-Tyne, England, (Sept. 1985) 7-14707
core-excitation spectra, multiple scatt. artifact removal 7-13290
cyclohexane gas, K-shell EXAFS studied by EELS 7-62403
diatomic molecules, dissociative single and double photoionisation, photoion spectra anal. 7-19984
digital filters use and limitations in data analysis 7-18944
double-pass high-resolution electron energy loss spectrometer, design and performance 7-374
electronics and vacuum physics, conf., Bratislava, Czechoslovakia (Sept. 1985) 7-24292
ethane, positron and electron collisions, cross section meas., time-of-flight spectra anal. 7-36799
ethylene, adsorption on Si(111), vibr. study 7-45012
ethylene, positron and electron collisions, cross section meas., time-of-flight spectra anal. 7-36799
ferromagnets, electron energy loss spectrum in the near-specular regime, electron-hole excitations 7-33496
ferromagnets, inelastic electron scatt., spin-depend. energy loss processes, book contrib. 7-33500
graphite, secondary-electron emission and electron-energy loss spectra 7-33491
graphite surface with adsorbed H₂, rotational states of physisorbed molecules 7-52278
hexafluorobenzene gas, K-shell EXAFS studied by EELS 7-62403
HSLA steel, precip. anal., EDX and EELS 7-46495
HV STEM and EELS at 1000 kV 7-1825
HV use for electron energy loss analysis 7-22403
hydrocarbons, cyclic, k-shell excitation, EELS 7-20037
interfaces, TEM imaging using inner potential differences 7-52299
ionic crystals, surface excitons, EELS obs. 7-12781
k-factor approach to EELS analysis 7-18946
ketene adsorbed on Pt(111), surface chemistry, substrate temp. influence, EELS 7-46867

electron energy loss spectra continued

- light elements, electron impact K-shell ionisation cross-sections, anal. appls. 7-25666
- magnetic shielding CAD for EELS spectrometer 7-48923
- materials characterisation at subnanometer spatial resolution using finely focussed electron beams 7-21058
- metal foils, surface loss intensity of incident electrons, angular distribution 7-64836
- metal surfaces, EELS studies of dynamics 7-3127
- metallic, electron scatt. by plasmons 7-32931
- metallic films, growth by laser photolysis of carbonyls, C and O incorporation mechanisms 7-58685
- metals, surface lattice dynamics of ordered overlayers 7-2342
- methane, physisorbed on NaCl (100), EELS spectra 7-13289
- methane, positron and electron collisions, cross section meas., time-of-flight spectra anal. 7-36799
- methyl radical, pyrolytic precursors, electronic spectrum, EELS anal. 7-42760
- molecular adsorbates, structure determ. using dynamic LEED and HREELS 7-12493
- nanometre-scale electron beam lithography 7-16663
- nondestructive depth profiling using secondary emission spectroscopy 7-27836
- overlayers on Si, Schottky barrier formation, local electronic struct., EELS study 7-21975
- oxide scales, chem. mapping using electron energy loss imaging microscope 7-37812
- parallel detection setups 7-18943
- perylene, vapour, electron scatt., energy loss spectra 7-31168
- polarised electrons in surface physics, book 7-29607
- trans-polyacetylene:Na, undoped and doped, momentum depend. dielec. functions, EELS study 7-64144
- trans-polyacetylene, momentum depend. dielec. function, EELS meas. 7-21843
- polyimide films, vibr., EELS and UPS study 7-46257
- polyparaphenylene: Na, electron and cryst. struct., EELS and electron diff. studies 7-63514
- pyrazine, adsorbed on Ag (111), affinity level, EELS, inverse and direct photoemission spectra studies 7-52724
- pyridine, chemisorbed on Pt {110}, influence of orientation on H-D exchange reactions 7-59781
- scanning CTEM image technique in energy filtered imaging 7-22404
- semiconductor superlattices, plasmons, Raman spectra, EELS and finite-size effects 7-27392
- semiconductor surfaces, interaction with H₂ 7-58632
- small metallic spheres, plasmon excitations, EELS study in STEM 7-32937
- small particle or interface charact., appl. of parallel detection EELS 7-33499
- solid surfaces, ferromagnetic and nonmagnetic, spin-dependent electron scatt., photoemission and inverse photoemission calcs., book contrib. 7-33493
- spectrometer, double-pass, high-resolution 7-61404
- spectrometer, dual parallel and serial detection, design 7-18942
- steel, HSLA C/N ratio in (TiNb)(CN) precip., EELS obs. 7-22698
- STEM of surfaces and interfaces, dielec. theory and verification 7-18935
- surface (111), dielectric props., reflection high resolution electron energy loss study, azimuthal depend. 7-33498
- surface chemical bonds, electron spectroscopy methods 7-39364
- surface electron energy loss fine struct. spectroscopy, EXAFS-like anal. 7-64834
- surface phonons, EELS excitation cross section 7-16855
- surface plasmon excitation of small supported particles, EELS study 7-45197
- surfaces (100) and (110), Stoner excitation spectrum, spin-polarised electron energy loss spectroscopy 7-53463
- surfaces and adsorbates, EELS studies 7-3128
- tetracene, film, secondary electron emission (*Russian*) 7-17375
- thin crystals, electron irradi., Pendellosung radiation and coherent Bremsstrahlung 7-33476
- thiolane, gas, solid and monolayers, EELS and XPS study 7-19949
- thiophene, gas, solid and monolayers, EELS and XPS study 7-19949
- time-resolved electron energy loss spectroscopy, position-sensitive detector performance 7-373
- transition metal nitrides and carbides, hard wear-resistant coatings, microstructural and microchemical characterisation 7-52328
- transition metals, fast electrons, energy loss spectra, microscopic anal. for 4d-systems 7-39329
- transmission electron microscope, EELS 7-35644
- twin crystals, orientational depend. of fast electron energy loss, determ. 7-7799
- X-ray photoelectron loss spectroscopy, characterisation of Al-N, Al-O compounds 7-59382
- (110), O₂ dissociative chemisorpt. studies 7-2377
- Ag (110), adsorption of ethylene oxide, surface interactions, XPS, TDS, AES, EELS studies 7-33963
- Ag (110), adsorption of NO₂ and surface nitrate formation 7-52286
- Ag (110), clean and O₂ covered, adsorption and reaction of acetonitrile 7-28344
- Al, bremsstrahlung isochromat spectra, electron-energy losses 7-22377
- Al film, low energy electron transmission, inelastic and elastic scattering cross section calcs. 7-63698
- Al foils, electron absorpt. and scatt. energy spectra, Monte Carlo calcs. 7-22399
- Al, surface plasmons, electron energy loss peaks 7-7305
- Al-N, sputter deposited, characterisation 7-59382
- Al-O, sputter deposited, characterisation 7-59382
- AlMn, quasicrystalline phases, plasmon electron energy loss spectroscopy and electrical resistivity 7-3123
- AlMnSi, quasicrystalline phases, plasmon electron energy loss spectroscopy and electrical resistivity 7-3123
- AlN formed by N ion implantation of Al, electronic struct. 7-58926
- AlN thin crystalline stoichiometric film, electronic struct., electron spectra studies 7-58916
- Al₂O₃ thin films, spectral ellipsometric TEM and electron spectra studies 7-27208
- AuGa₂-GaAs (001), chemically unreactive interfaces formation 7-7050
- B, inner shell excitation profiles visibility 7-22403
- BF₃·H₂O, electronic struct., EEL and UV photoelectron spectra, ab initio MO STO calcs. 7-36449
- BN, inner shell excitation profiles visibility 7-22403

electron energy loss spectra continued

- Be, polycrystalline, plasmon dispersion, EELS meas. 7-27283
- C foils, electron absorpt. and scatt. energy spectra, Monte Carlo calcs. 7-22399
- C, inner shell excitation profiles visibility 7-22403
- a-C thin films, bonding core-EELS and ¹³C NMR studies 7-21099
- a-C:H, props., review 7-51630
- a-C:H films, glow discharge deposited, valence electron props., electron energy loss spectra study 7-13288
- C₆K, intercalation cpd., density of states, interlayer band occurrence 7-2454
- CO adsorbed on Pt, vibr. spectrum, electrochemical pot., stark tuning rate 7-10570
- CO, adsorption on Al (100), EELS and thermal desorpt. 7-17815
- CO, adsorption on Ni (111), well defined gas-solid interphase, statistical rate theory approach 7-21655
- CO gas, K-shell EXAFS studied by EELS 7-62403
- CO, physisorbed multilayer, near-threshold electronic excitation, EELS spectra anal. 7-45001
- CO₂ gas, K-shell EXAFS studied by EELS 7-62403
- CS₂, dissociative attachment bands, impact electron and fragment ion energy spectra anal. 7-50386
- Ca, near-trace-element concs. in organic matrix 7-46903
- Ce (001), H₂ adsorption, initial stages of hydride form., UPS, LEED and EELS studies 7-21629
- CoSi₂, MBE growth, struct. props. and device appls. 7-21738
- Cr (110), chemisorption of O₂ 7-21662
- Cr and Cr-compounds, Auger and absorpt. spectra involving M_{2,3} levels, atomic effects 7-59311
- Cr, EELS studies of Cr-L_{2,3} core levels 7-46258
- Cr, surface extended energy loss fine structure above L_{2,3} edge 7-17377
- Cr-Fe-C system, EELS fine struct. 7-39333
- CrCl₃, ionic crystals, optical and electron energy loss studies 7-3066
- CrSi₃, EELS studies of Cr-L_{2,3} core levels 7-46258
- CSi, surface stoichiometry, changes under electron and laser radiation 7-44961
- Cu (001), adsorbed K, valence-electronic struct., work function changes and EELS 7-45002
- Cu (100), c(2×2)N overlayer, surface phonon dispersion, LEED, AES and EELS studies 7-12459
- Cu (100), cross-section anal. of surface and bulk phonons by electron scatt. 7-2336
- Cu (100), Rayleigh phonon dispersion, stress-induced freq. shift, EELS studies 7-27090
- Cu (110) surface, K doped, CO adsorption, EELS study 7-7006
- Cu (111), adsorption of TCNQ, vibr. spectra, EELS, work function meas. 7-52228
- Cu based alloy, EELS at 1000 kV 7-1825
- Cu films on MgO, epitaxial and electronic structures, LEED, AES, and EELS studies 7-52352
- Cu foils, electron absorpt. and scatt. energy spectra, Monte Carlo calcs. 7-22399
- CuZr metallic glass, blistering under He implantation, EELS anal. 7-16593
- D adsorbed on Rh (111), delocalised quantum behaviour, EELS study 7-38666
- DCN, formation on Pd (111), and (100) by hydrogenation of adsorbed CN 7-6985
- ErSi₂, behaviour under ion bombard. and O exposure, AES, EELS 7-33506
- Fe (III) surface, K precovered, promotion of surface reactions with N₂ 7-13807
- Fe (110), clean and O-covered, struct., surface extended energy loss fine struct., spectra obs. 7-12481
- Fe particles on planar Al₂O₃ supports, low rate growth 7-32779
- Fe, Stoner excitations, free-electronlike, spin-polarised EELS 7-45648
- Fe surface, polycryst., interaction with O₂(N₂), electron spectrosc. obs. 7-7794
- Fe-Cu, epitaxially grown Fe films, electronic and crystallographic struct. 7-27214
- Fe-Si thin films, silicide formation, AES and EELS studies 7-32862
- Fe₃Ge_{1-x} amorphous magnetic alloys, d-band occupancy, EELS study 7-64059
- Fe₃Si_{1-x} amorphous magnetic alloys, d-band occupancy, EELS study 7-64059
- Ga small metallic clusters, vol. and surface plasmons, EELS studies 7-27271
- GaAs (511) and (711) surfaces, struct. studies using LEED AES, and EELS 7-2312
- GaAs/GaInAs interface, EELS near a single misfit dislocation 7-33497
- GaAs-AlGaAs superlattice, surface and interface optical phonons, EELS studies 7-6955
- GaN, band struct., pseudopotential method anal. 7-52421
- Ge, electron mean free path needed for excitation of volume and surface plasmons 7-21838
- Ge, surface plasmons, electron energy loss peaks 7-7305
- H adsorbed on Rh (111), delocalised quantum behaviour, EELS study 7-38666
- H₂ on TiO₂ (110) stoichiometric and defective surfaces 7-6983
- InAs (110), oxidation, correlated changes of electronic surface props. 7-2354
- InN, band struct., pseudopotential method anal. 7-52421
- InP (100), prep. by P deposition and annealing, surface reconstruction, LEED, EELS studies 7-38311
- K film, clean and contaminated, CDW search using EELS 7-53462
- Kr, adsorbate, excited states assignment 7-52725
- Kr⁴⁺+He(Ne), state-selective electron capture, translational energy spectra 7-50337
- Mg, bremsstrahlung isochromat spectra, electron-energy losses 7-22377
- MgO (001), initial stages of Cu deposition, EELS 7-63959
- MgO smoke particles, energy filtered imaging by scanning CTEM technique 7-22404
- MoO₃, oxidic standard for EELS quantification of M edge in MoSi₂ 7-46904
- MoS₂(0001), Ar⁺-sputtered, adsorption props., LEED, AES, EELS, and work function studies 7-52275
- MoSe₂-MoS₂ ultrasharp interfaces grown with van der Waals epitaxy 7-13367
- N₂, electron scatt., high energy, X-ray incoherent scatt. factor 7-36757
- N₂, physisorbed multilayer, near-threshold electronic excitation, EELS spectra anal. 7-45001

electron energy loss spectra continued

NO, adsorpt. on Rh (111), dissoci., EELS and LEED study 7-16859
NO, coadsorbed on Rh (111) with CO and O, EELS 7-16860
N₂O, energy loss spectra, window reson., momentum transfer depend. 7-57173
Nb(100) surface, H₂ chemisorption, LEED, EELS and work function meas. 7-32815
Ni (100), adsorbed N, surface phonon dispersion, adsorbate induced reconstruction 7-52225
Ni (100), chemisorbed H and D, vibr. motion, high resolution EELS 7-12458
Ni (100), chemisorption and decomposition of ethylene 7-59785
Ni (100), coadsorption of H₂ and CO 7-27117
Ni (100), surface vibr., EELS, surface and bulk phonon contribs. 7-44986
Ni (110), adsorption and reaction of CO₂ and CO₂/O co-adsorption 7-52289
Ni (110), coadsorption of O and water, EELS study 7-32821
Ni (111), isothermal adsorption/desorption parameters of CO, EELS meas. 7-6971
Ni (111), ordering of acetylene and ethylene, LEED, EELS 7-52269
Ni surface, with adsorbed N₂ or coadsorbed N₂ and Al or Ba, N(1s) spectrum 7-21968
Ni, surface phonons, HREELS study 7-13291
Ni-Al alloy phase transforms. during ion beam mixing, electron diffr. and microscopy studies 7-16655
NiSi₂, MBE growth, struct. props. and device appls. 7-21738
Ni₂Si, L_{2,3} absorpt. edges, EELS study 7-3125
O₂, adsorbed on Cu (110) and polycrystalline surfaces, UPS, XPS, AES, EELS, LEED studies 7-32820
OH groups chemisorbed on Ge₂Si_{1-x} (100), shape resonances 7-6998
Pb foils, electron absorpt. and scatt. energy spectra, Monte Carlo calcs. 7-22399
Pd (100), clean and S covered, adsorption and desorption of NO, surface reactions, TPD, EELS, LEED 7-58639
Pd (100) and (111), surface resonances in vibr. spectroscopy 7-52229
Pd (110) with chemisorbed N₂, EELS, LEED and AES 7-63960
Pd (111), O₂ adsorpt., EELS and LEED studies 7-2378
Pt (111), adsorption of ethylene oxide, surface interactions, XPS, TDS, AES, EELS studies 7-33963
Pt (111), coadsorption of K and CO, structural and vibrational studies 7-52266
Pt (111), reaction of coadsorbed C₂N₂ and H₂ 7-54186
Pt, surface (110), deuteration of adsorbed pyridine, EELS study 7-7006
Rh (100), coadsorption of CO and H₂, adsorbate-adsorbate interactions effects 7-44997
Rh surfaces, clean and B contaminated, adsorption and dissociation of H₂O 7-27135
Ru (001), alkali modified, adsorption of O, TDS, AES, EELS, work function meas. 7-58637
Ru (001), clean and O covered, adsorption of NO₂, EELS, thermal desorption mass spectrometry 7-52267
Ru, adsorpt. of ethylene, on (001) surface, H₂(CO₂) coadsorpt. effects 7-32789
SF₆, inner- and valence-shell excitation, X-ray and EELS study 7-57171
Si (111)/CaF₂, interface and surface phonons, high resolution EELS study 7-38319
Si (111)-2×1, dipole scatt., inelastic electron cross sections 7-3126
Si (111)-7×7, temp.-depend. surface resistivity, electron energy loss meas. anal. 7-21973
Si (111)2×1, thiophene adsorpt., annealing-induced mol. fragmentation, surface vibr. spectra, HREELS study 7-27088
Si, bremsstrahlung isochromat spectra, electron-energy losses 7-22377
Si, cleaved surface, ethylene adsorption, high-resolution EELS study 7-63951
Si single cryst., electron axial and planar channelling, gamma-ray emission studies 7-44636
Si surface, (111)-2×1, surface phonon and surface state excitations, EELS, polarisation depend. 7-2338
Si surface, RIE, Si₃N₄ CVD 7-59691
Si surface layers characterisation after annealing in an RF H plasma 7-58630
Si surfaces, (7×7)-Ge and (5×5)-Ge superstructures, angle-resolved EELS studies 7-21583
Si₃N₄, small particles, elemental and chem. anal., EELS method 7-17379
SiC (0001) and (000 $\bar{1}$) surface segregation, electron spectroscopy 7-21459
SiC:H, amorphous CVD film, electron optical characterisation 7-52372
a-Si_{1-x}C_x:H thin films, struct. investig., electron diffr. studies 7-2430
Si₂C_{1-x}H_x, amorphous, local atomic arrangement, EELS and electron diffraction 7-44378
Sn small metallic clusters, vol. and surface plasmons, EELS studies 7-27271
 α -Sn, thin film quantization studies using high resolution electron energy loss spectroscopy 7-27448
Ti, heat treated, softening, in situ HVEM obs. 7-17548
Ti, plasmon spectra and energy, high energy EELS studies 7-12635
Ti-N-C system, EELS fine struct. 7-39333
TiC (100), surface phonon dispersion curves, EELS determ. 7-52224
TiC plasma sprayed coatings, microstruct., composition 7-16902
TiC_x, reactively sputtered film, characterisation by TEM 7-45092
TiH₂, plasmon spectra and energy, high energy EELS studies 7-12635
TiO₂ (110), O deficient surfaces, electronic excitations, EELS 7-58853
UO₂, single cryst., surface phonon struct., high resolution EELS 7-27087
VC precipitates in steel, radiation damage influence 7-16638
Xe, adsorbate, excited states assignment 7-52725
ZnO (10 $\bar{1}$ 0), initial stages of Cu deposition, EELS 7-63959

electron energy states (condensed matter)

see also band structure; band theory models and calculation methods; deep levels; defect electron energy states; dopplers; electron energy states of amorphous solids; electron energy states of liquid metals; electron energy states of liquid semiconductors; electron gas; electron traps; electronic density of states; exchange interactions (electron); excitons; Fermi level; Fermi surface; field interactions (condensed matter); heli-cons; hole traps; impurity electron states; Landau levels; localised electron states; magnetic breakdown; magnons; metal-insulator transition; metal theory; plasmons; polar semiconductors; polarons; positron states; ripplons; spin-orbit interactions; spin-phonon interactions; surface electron states; triplet state

electron energy states (condensed matter) continued

α -(BEDT-TTF)₂(NO₃)₂, electronic excitations, optical study 7-53367
charged particle scatt., energy-level oscillations accompanying the shadow effect (Russian) 7-38082
continuous composite materials, interface response theory 7-64039
dichalcogenides, low-dimens., as secondary cathodic materials, book contrib. 7-28394
disordered alternant structures, electron energy spectrum 7-38436
disordered alternant structures, electron energy spectrum 7-42458
electronic structure change in solids, high press. effect 7-44788
metallic fine particles, energy level statistics 7-38431
MOS capacitors, interface trap charge effect on C-V and I-V characts. 7-27437
polyacetylene, self-consistent calc. of solitons 7-64105
polydiacetylene fragments, extended Pariser-Parr-Pople model, 2¹A and 1³B states 7-52486
quasi-1D infinite linear atomic chain, Hartree-Fock eqns., numerical soln. 7-21793
quasicrystals, 1D, acoustic and electronic props. 7-6730
rare earth hydrides, core level shifts, adiabatic excitation, sudden core excitation 7-53502
semiconductors, fluorescence line shape anal. for free-to-bound transitions 7-46097
solid electronic structure change, high press. appl., review (Czech) 7-58411
theoretical aspects, conference, San Francisco, CA, USA (Aug. 1985) 7-24301
transition metal dithiolates and diselenolates, molecular and electronic structs. 7-52397
transition metal hydrides, core level shifts, adiabatic excitation, sudden core excitation 7-53502
Fe sites in minerals, electronic struct., iterative EHT, multiple scatt. X α calcs. and Mossbauer meas. 7-17244
Fe-V superlattices and alloys, magnetism study 7-64436
La, crystal electronic struct., electron-phonon interactions and superconducting transition temp. calcs. (Chinese) 7-27261
LaNiAl₁₀O₁₉, magnetoplumbite type cpd., synthesis, cryst. growth and struct., electronic spectra 7-44476
Li₂Si, electronic struct., INDO calcs. 7-38437
Pt clusters in Y-zeolite, atomic and electronic struct. and chemical reactivity 7-32677
Tb oxides, TbO₂, Tb₄O₇, Tb₂O₃, X-ray absorpt. study of 4f electrons 7-64795

electron energy states of amorphous solids

see also Anderson model
amorphous semiconductors, conference, Palo Alto, CA, USA (April 1986) 7-29602
amorphous semiconductors, multiple trapping, effect of defect level 7-27237
amorphous superlattices, mean free path and size quantisation 7-22003
amorphous tetrahedrally bonded semiconds., dangling-bond and void-like structs., microscopic structural model 7-21803
binary non-crystalline alloys, electronic density of states calc. 7-45112
bonding and struct., conf., Reston, VA, USA (May 1983) 7-60879
chalcogenide glasses, dangling-bond and void-like structs., microscopic structural model 7-21803
chalcogenide glasses, electrons in mobility gap, spectra and thermodynamic props. 7-2471
conjugated polymers, impurities, nonlinear dynamics 7-64115
conjugated polymers, self-localised excitations 7-64168
disordered alloys, density of states approx., overlapping Lorentzian functions calcs. 7-38435
disordered systems, single particle energy spectrum, local density of states 7-12593
disordered systems, single-particle energy spectrum, state vectors, total density of states 7-12594
electronic and transport props., coherent potential approx. 7-27241
glasses, critical behaviour of double-well potentials, two-level systems model 7-32305
iterative transfer perturbation method, appl. to interaction between polymer and small molecules 7-64049
metal alloy hydrides, disordered, theory of electronic states 7-27243
metallic glasses, weak localisation, magnetoresistance meas. 7-52574
metals, disordered, temp. coeff. of elec. resist., Mooij correlation nonuniversality 7-21893
metals, multiple scattering effects, cluster calcs. 7-7100
nonmagnetic metallic glasses, negative TCR and electronic struct. studies 7-52562
one-dimensional conductors, conf., Kyoto, Japan (June 1986) 7-60872
polaroid K, reson. Raman scatt., absorpt. spectra, amplitude mode model anal. 7-64658
poly-p-phenylenevinylene film, opt. and elec. props., band gap 7-46161
polyacetylene, alkaline metal doped, ab initio SCF MO calc. of electronic struct. 7-64048
polyacetylene, cond., fast FTIR and IR intensity spectra, struct. and electronic props. 7-53335
polyacetylene, Coulomb correlations, optical gap 7-64142
polyacetylene, electron-electron interactions, optical gap, negative spin density 7-2473
polyacetylene, electrons and phonons, semi-continuum model 7-64112
trans-polyacetylene, equivalent orbital theory, electronic struct. study 7-64062
polyacetylene, ground, excited, polaronic, solitonic and impurity states calcs., doping effects 7-45131
trans-polyacetylene, momentum depend. dielec. function, EELS meas. 7-21843
trans-polyacetylene, optical absorpt. due to soliton lattice 7-64109
trans-polyacetylene, random soliton distrib., localisation and density of states calcs., renormalised virtual cryst. method 7-52453
trans-polyacetylene, reson. Raman scatt. from amplitude modes, temp. effects 7-64654
trans-polyacetylene, third order optical susceptibility, 2A_g excited state obs. 7-62782
trans-polyacetylene, within the extended tight-binding picture, interband transitions, hopping processes 7-27678
trans-polyacetylene(-d), ns time resolved photoinduced absorption spectrum 7-64668
trans-polyacetylene chain, bipolaron form. and desorpt., Su-Schrieffer-Heeger model calcs. 7-52454

electron energy states of amorphous solids continued

- polyacetylene films, doped, electronic struct., elec. cond. and thermopower 7-64065
- polyacetylene thin films, photoexcited states, ps relax. 7-64291
- polyaniline, geometries, bond struct., electrochemistry, MNDO calcs. 7-15750
- polyfuran and copolymers, electronic struct., cond. props., ab initio cryst. orbital calcs. 7-52410
- polyisothianaphthene and derivatives, valence effective Hamiltonian band struct. calcs. 7-16936
- polymers, electronic struct. and orientation on Pt, XANES studies 7-64058
- polymers, highly conducting, electronic structure, correlation effects 7-64064
- polymers and related cpds., electronic props., Winter School, Kirchberg, Austria (March 1985) 7-4613
- polyparaphenylene: Na, electron and cryst. struct., EELS and electron diff. studies 7-63514
- polypyrrole and copolymers, electronic struct., cond. props., ab initio cryst. orbital calcs. 7-52410
- polyselenophene, electronic and struct. modifications during doping, EXAFS and XANES studies 7-63507
- polysilane model compounds, struct., electronic props., MNDO calc. 7-44403
- polythiophene and copolymers, electronic struct., cond. props., ab initio cryst. orbital calcs. 7-52410
- polythiophene derivatives, bandgaps, conductivities 7-64061
- polyvinylene, reson. Raman scatt., absorpt. spectra, amplitude mode model anal. 7-64658
- polyyne infinite chain, solitons, polarons and phonon spectrum calcs. 7-12626
- random systems, electron density of states 7-27230
- semiconductor III-V and II-VI cpds., electronic struct. of bulk and defect sites, tight-binding recursion method 7-45222
- semiconductors, amorphous, optical absorpt., tight-binding model 7-45961
- semiconductors, amorphous, prepared by fast glass transition, localised states 7-63818
- semiconductors, cryst. and amorphous, and heterojunctions, electronic struct. using bremsstrahlung isochromat spectroscopy 7-52795
- semiconductors, electronic states, transport, theory 7-27239
- a-Si:H, structural characterisation, hyperfine interaction, ESR, ENDOR 7-53135
- structurally disordered systems, electron localisation, $2k_F$ scatt. theory anal. 7-7174
- transition metal alloys, amorphous, short-range order, approx. to coherent locator (*Russian*) 7-58731
- transition metal alloys, disordered, electron struct. and positron annihilation (*Russian*) 7-45133
- transition metal alloys, liquid and amorphous, chemical short-range order, electronic theory 7-44349
- transition metal-metalloid metallic glasses, glass formability and electronic struct. 7-21804
- two dimensional quasi-periodic Penrose lattice, electronic and vibr. modes, localised states and band struct. 7-27300
- $Ag_2S(Se)-Ag_2Te(Se)$ liq. and glassy semicond., activation energy of carrier thermal generation, elec. meas. 7-17035
- $Ag_2S(Se)(Te)-Cu_2S(Se)(Te)$ liq. and glassy semicond., activation energy of carrier thermal generation, elec. meas. 7-17035
- As- Te_{30} based glasses, small polaron hopping and transport props. 7-21911
- $As_{40}Se_{60}$ glasses, surface pot. relax., TSC meas. 7-64261
- As_2Se_3 -Ni films, electronic struct. and transport props. 7-12595
- $(As_2Se_3)_{1-x}Ti_x$, elec. and thermal transport props., effect of Ti addition 7-38200
- $\alpha-As_2Te_3$ films, hole transport investigation by transient field-effect and time-of-flight methods 7-22040
- a-C:H, props., review 7-51630
- a-C:H films, plasma deposited, optical props. 7-27799
- a-C:H polymeric layers, plasma-activated CVD produced, spectroscopic investigations 7-22572
- p-crystalline Si/n-amorphous Si heterojunction, electrostatic pot. barrier distrib. calcs. 7-58881
- Cu, amorphous, density of states calc. cluster embedding in effective shell 7-2457
- Cu-Mg amorphous alloys, 2D weak localisation effects 7-21871
- $Cu_{1-x}Pt_x$ disordered system, X-ray absorpt. edges (*German*) 7-46241
- Cu_xY_{1-x} amorphous alloys, empty and occupied electronic states, inverse and direct photoemission spectroscopies study 7-32899
- Er_2Co glasses, electronic struct., photoemission and magnetism 7-64060
- Fe-B, metallic glasses, photoemission investig. (*Slovak*) 7-59369
- Fe-Ge amorphous and cryst. layers, short range order and valence bands 7-13266
- Fe-Si-B amorphous alloys, electron momentum distrib. and Fermi energy, Doppler broadening positron annihilation 7-39220
- Fe_{13} clusters, icosahedral and cubo-octahedral coordination, electronic struct., first-principles method calcs. 7-45132
- Fe_xGe_{1-x} amorphous magnetic alloys, d-band occupancy, EELS study 7-64059
- $Fe_{40}Ni_{60}P_{20}$ amorphous alloy, electron struct. and surface struct., XPS and UPS studies 7-27238
- Fe_xSi_{1-x} amorphous magnetic alloys, d-band occupancy, EELS study 7-64059
- GaAs, L near-edge structure, X-ray photoabsorpt. spectra 7-64766
- a-GaAs:H:F, electronic struct., dangling bonds, cluster-Bethe lattice method calcs. 7-12592
- Gd_2Co glasses, electronic struct., photoemission and magnetism 7-64060
- a-Ge:H, B, P, As, dopant incorporation and doping efficiency 7-44587
- $Ge_{28.5}Pb_{1.5}Se_{6.5}$ glasses, surface pot. relax., TSC meas. 7-64261
- a- $Ge_{27}Se_{68}Bi_5$ thin film, photoconductivity 7-17052
- $GeSe_6-xTe_x$ amorphous chalcogenide, elec. cond., bulk and thin film effects 7-7238
- $Ge_{1-x}Sn_xSe_2$ glasses, elec. cond. rel. to Mossbauer and Raman spectra 7-64250
- Ni-Ge amorphous and cryst. layers, short range order and valence bands 7-13266
- Ni-P metallic glasses, electronic struct., XPS study 7-39357
- Ni_3B , amorphous, surface electronic struct. during crystallisation and O_2 and CO adsorption 7-7308
- $(Ni_{1-x}Cu_x)_{77}B_{13}Si_{10}$ pseudobinary metallic glass, low-temp. sp. ht. studies 7-12309

electron energy states of amorphous solids continued

- $(Ni_{1-x}Cu_x)_{80}P_{20}$ pseudobinary metallic glass, low-temp. sp. ht. studies 7-12309
- $Ni_{1-x}P_x$ amorphous glasses, electronic structure, calcs. 7-7101
- $Ni_{1-x}P_x$ metallic glass, electronic struct. and props., LMTO calcs. 7-52409
- $Ni_{100-x}Zr_x$ metallic glasses, low temp. sp. ht. study, density of states and Debye temp. determ. 7-2226
- Pd-Si, metallic glasses, photoemission investig. (*Slovak*) 7-59369
- S, polymeric, energy surface struct. and electronic props. 7-2472
- a-Se, structural disorder model 7-26641
- Si, amorphous film, density-of-gap-states distrib. field effect meas. analytic determ. 7-52391
- a-Si, density of states, spectral function, calcs. using eqn. of motion method in k-space 7-27236
- a-Si, electron and hole concentration modelling 7-64269
- a-Si, recomb. via dangling bonds, occupation statistics 7-38515
- α -Si:H, amorphous, coherent potential approx., potential well analogy 7-7240
- a-Si:H, B, P, As, dopant incorporation and doping efficiency 7-44587
- a-Si:H, bulk, surface state densities, Bethe lattice method, CPA calcs. 7-32898
- a-Si:H, density of states, SCLC meas., effect of injection electrodes 7-64265
- a-Si:H, distrib. of states study by capacitance-voltage method 7-7089
- a-Si:H, divacancy electron struct., semiempirical CNDO/2 cluster calcs. 7-38495
- a-Si:H, electronic density of states, DLTS and capacitance transient spectra anal. 7-45134
- a-Si:H, electronic struct. modelling with small clusters 7-64057
- a-Si:H, fluctuation induced gap states 7-27242
- a-Si:H, metastable defect states, capacitance studies 7-45225
- a-Si:H, photocond. response, light soaking effects 7-45396
- a-Si:H, picosecond photoinduced absorption and transmission 7-3006
- a-Si:H, SCL currents, step-by-step anal., density of states determ. 7-2623
- a-Si:H, surface deep hole trap, photocurrent studies 7-45424
- a-Si:H, thermal-equilib. processes, electronic transport 7-64167
- a-Si:H:P multilayer films, plasma CVD and elec. cond. studies 7-39428
- a-Si:H biased activated reactive layer evaporation and charactn. 7-59428
- a-Si:H CVD films, density of states distrib., I-V characts. meas. 7-45113
- a-Si:H films, density of states and photoconductivity 7-45392
- a-Si:H n^+-i-n^+ struct., freq.-depend. noise studies 7-45484
- a-Si:H solar cells, density of states asymmetry effects 7-46946
- a-Si:H solar cells, impurities and metastable centres 7-40010
- a-Si:H/ SiO_2 /metallic gate struct., capacitance-volt. characts. 7-45515
- a-Si:H/a-SiN_x:H interface system, struct. and electronic props. 7-38361
- a-Si:H(F), mobility edge, density of states and carrier activation energy calcs., random Bethe lattice approach 7-16937
- Si/Sb,As, cryst. and amorphous, impurity band form., X-ray spectra studies 7-12650
- a-Si_{1-x}C_x:H, valence band, UPS studies (*Chinese*) 7-38443
- a-SiGe:H,F glow discharge films, electronic transport and density of states 7-45114
- a-SiGe:H glow discharge films, field effect density of states determ. 7-21796
- Si_{1-x}Ge_x films, optical band gap, photocond. props. 7-52672
- Si_{1-x}Ge_x:H amorphous alloys, electronic struct., soft X-ray and photoelectron spectra studies 7-27857
- α -SiGe:H, electronic and transport props., coherent potential approx. 7-27241
- α -SiH, electronic and transport props., coherent potential approx. 7-27241
- SiO₂, amorphous, intrinsic defects, semiempirical mol. orbital studies 7-63474
- SiO₂, cluster approx. of electron struct. 7-12591
- SiO₂, cryst. and amorphous, point defects and electronic props. 7-64082
- SiO₂-related materials, cryst. and amorphous, electronic struct. calcs. 7-64081
- U glasses, unoccupied 5f states, XANES study 7-39318
- YAl nonmagnetic metallic glasses, negative TCR and electronic struct. studies 7-52562
- Zr-based transition metal glasses, local densities of states 7-7086
- electron energy states of glassy solids** see *electron energy states of amorphous solids*
- electron energy states of liquid metals**
- capillary wave dispersion relation modifications due to electric charge, surface Green fn. matching method 7-21575
- density functional theory for a model of nonuniformliquid metal in partially ionized states 7-6504
- liquid metal films, wedging press. 7-12410
- multiple scattering effects, cluster calcs. 7-7100
- sd metals, liq., variational thermodynamic calcs. 7-12590
- simple liquid metals, pseudoclassical approach to electron and ion density correlations 7-6503
- transition metal alloys, liquid and amorphous, chemical short-range order, electronic theory 7-44349
- Ag-Ge liquid alloy, structural phase transitions, photoemission studies 7-1836
- electron energy states of liquid semiconductors**
- Ge liquid, structural phase transitions, photoemission studies 7-1836
- Si, amorphous fol, time-resolved X-ray absorption during pulsed laser irradiation 7-12128
- Si, liquid, electronic props., tight binding-mol. dynamics calcs. 7-16931
- electron field emission**
- Boersch effect meas. in pulsed field emission gun, cross-over points 7-13338
- electrode surface contamination, desorpt., field and secondary emission, enhancement by electric fields 7-23033
- electron gun, extremely high vac. design and operation (*Japanese*) 7-64879
- HV regulator for field emission 7-30039
- metal surfaces, ion-electron emission mechanism 7-7825
- metal-insulator, composite microemitters, hot electron emission 7-33532
- MIM cathodes, emissivity, temperature and area effects 7-13336
- MIM structures, explosive electron emission 7-13335
- photofield emission, current versus reciprocal field curves, semiquantitative anal. 7-33536
- plasma double probe measurements, electron emission effects, continuum theory 7-51508

electron field emission continued

probe design, miniature variable energy, for nanometric analysis, electron opt. parameters 7-18939
size quantization near semiconductor surface (*Russian*) 7-64882
TiC (100) field emitter, surface-processed, field emission props. (*Japanese*) 7-64880
vacuum gauge, field-emission cold cathode for oscillator gauge (*Chinese*) 7-48767
BaO films on W, field emission spectroscopy 7-13334
C field emission cathodes, effect of forming on structure 7-39365
Fe₇₀Cr₃₀Si₁₀B₁₅ metallic glass, field electron emission 7-33530
Ga-In-Sn liquid alloy, electron field emission studies 7-33535
Ge (001), field emission flicker noise and electron states 7-33533
K-Ni coadsorbed layer on W (110), field emission flicker noise 7-32807
LaB₆ space-charge-limited electron gun analysis 7-56380
La_{0.7}Sr_{0.3}CoO₃ cathodes for CO₂ waveguide lasers, electrical and emission characts. 7-59383
Nb surface, enhanced field emission sites during heat treatment 7-33531
Nd_{0.7}Sr_{0.3}CoO₃ cathodes for CO₂ waveguide lasers, electrical and emission characts. 7-59383
Ni surface, adsorbed S, field electron emission props. 7-33529
Si:P, polycrystal. thin film, carrier transport, temp. depend. study 7-22043
Si₃N₄ MIS struct., electron transport and heating, vacuum emission studies 7-2723
SiO₂ MOS structures, electron heating for low fields and thick films 7-2722
SiO₂N_x MIS struct., electron transport and heating, vacuum emission studies 7-2723
TiC tip, surface-processed, field emission stability (*Japanese*) 7-64879
W (011) plane, edge atoms surface migration activation energy, emission current meas. 7-32887
W (110), thermal field emission and thermal photofield emission 7-7826
W (112), K adatoms, density fluctuation simulation 7-32806
W point single crystal, Lu and Ba adsorption, field emission characteristics 7-12466
W tip, field emission noise (*French*) 7-13337

electron gas

see also cathode ray tubes; electron optics
2D, cyclotron resonance linewidth due to alloy scatt. 7-27399
2D, density of states for high Landau levels and random potential 7-58753
2D, fractional quantum Hall effect, density-density response function 7-52740
alkali metal atomic fluids, thermodynamic and electronic props. 7-45157
antiferromagnet, anisotropic electron fluid, magnon spectrum and attenuation 7-59000
atom-atom potentials via electron gas theory 7-36720
binary charged fluids, screening lengths, thermodynamic stability 7-52480
charged particle energy loss in solids, confined-atom model calcs. 7-44634
condensation to incompressible Fermi liq., Coulomb gap size determ., spectroscopic method 7-61223
coupled 2D electron systems, field theoretical treatment of plasma modes 7-58758
deformable jellium model, electronic density of states calcs. 7-64044
degenerate, electronic stopping power, local-field corrections calcs. 7-48533
degenerate, tunnelling atom interactions, low temp. behaviour 7-27270
diamagnetic props. in external helical magnetic fields 7-45610
diamagnetic susceptibility at low temps., surface effects 7-21841
dielectric function, dynamical local-field factor 7-21840
disordered, interacting, quasi-2D; plasmon dispersion relations calcs. 7-38485
dynamic struct. factor, particle self-energy contributions 7-45182
electron-electron scatt., energy loss to phonons, integral eqn. 7-52478
exchange and correlation potential for a two-dimensional electron gas at finite temperatures 7-38480
exchange energies, exact, local density approx. calcs. 7-38481
fluctuation phenomena, low freq. results near metal-dielectric transition point 7-38654
fractional quantum Hall states, hierarchy termination and impurity effect scaling 7-21978
fractional quantum Hall states, size depend. in small system calcs. 7-2517
galvanomagnetic props., interaction effects, applied electric and mag. fields 7-52477
generalised exchange local-spin-density-functional theory, 7-36499
glass, surface recomb. of electrons and ions, kinetic theory 7-46263
heavy particle one-dimensional hopping motion, phonon and electron gas interactions, localisation, scaling eqn. calcs. 7-12634
homogeneous electron gas, ground state energy as function of potential energy, extended Thomas-Fermi calcs. 7-56974
homogeneous electron gas, para- and ferromagnetic states, correlation energy interpolation fn. 7-45196
inhomogeneous electron gas pressure calc. (*German*) 7-64145
interacting electron gas system, U-matrix theory 7-29878
kinetic energy density functional 7-48535
Landau diamagnetism, perimeter corrections for free electron gas 7-38843
Landau level broadening, 2D electron gas in strong electric field 7-52455
light quantum particle motion in metallic environment, path-integral formalism calcs. 7-52459
localisation effects, Keldysh representation 7-52529
localized electron. system with electron-phonon interactions, U-matrix theory anal. 7-61157
magnetoresistance of 2D electron in lateral superlattice 7-38599
many-fermion systems of arbitrary dimensionality and interparticle interaction, nonlocal exchange energy 7-38482
metal foils, surface loss intensity of incident electrons, angular distribution 7-64836
metal surface, low energy positron interactions, elastic and inelastic scatt. calcs. 7-39330
metal-insulator-semicond. struct., 2D electron gas, skin effect and nonuniform states obs. 7-64353
metals, grain boundary energies from local-electron-density distributions 7-6634
metals, quantum diffusion, path integral approach 7-52112
metals, thermodynamics during high-pressure shock 7-21352

electron gas continued

modulation doped heterostructures, 2D electron gas, transport coeffs., parallel conduction effects 7-2677
multipair excitations and sum rules 7-45183
one-dimensional inhomogeneity, dielec. matrix analytic inversion model calcs. 7-16964
organic conductors, IR absorption spectra and electron-electron interactions 7-46032
orthogonal Waller-Hartree spin eigenfunctions 7-56142
particle coupled to fermionic environment, ground state static props. 7-45107
periodic electron system, dielectric function, VAA theory, plasmon damping 7-32930
positron annihilation, momentum-dependent enhancement factors for an electron gas of high density 7-46192
proximity systems, low-dimensional, Josephson current, field effect, appl. to Nb-InAs-Nb system 7-45573
quantised Hall effect in 2D 7-7271
quantum well structures, metal-insulator transition due to surface roughness scatt. 7-27400
quasi 2D electron gas in quantum well, cyclotron reson. lineshape calcs. 7-27269
quasi-1D conductors, quantum Hall effect 7-64273
quasi-one-dimensional conductors, coherent polaron superlattices and long-range Coulomb forces 7-45184
quasi-one-dimensional electron gas, screened hydrogenic impurity, binding energy 7-52508
radiative transfer relativistic Compton scatt. kernel 7-35471
sandwich type complexes, electron-gas model modification 7-7137
screened-exchange functional 7-64138
self-energy calculations, effective interactions 7-38473
selfconsistent screening effect, Coulomb interactions 7-29889
semiconductor heterojunctions, nonequilibrium electron-phonon scatt. 7-45457
semiconductor structures, 2D localisation and interaction effects 7-52531
semiconductor superlattices, dynamical screening, quasi-2D electron gas, electron-phonon interactions 7-45464
semiconductor superlattices, layered electron gas plasmons, Raman scatt., Green's functions calcs. 7-17313
semiconductor thin films and wires, hot electrons under quantum size effect conditions 7-38780
semiconductors, transport phenomena in electron gas, correlation effects 7-38479
Si-SiGe strained superlattices on Si substrates, MBE growth, characterisation, appl. for HEMT 7-27218
SIS layered structures with metallised surfaces, interface excitations 7-22031
slow ions, nonlin. energy-loss straggling, in solids 7-2075
stopping power calculation due to Green's functionmethod 7-4758
superconducting electron pairing, exchange and correl. contributions 7-45574
superlattice of a 2D electron gas, local plasma oscillations 7-64120
tetrafluoromethane-O₂ mixtures, electron gas investig. 7-20861
thermodynamic and dielectric props. at any degeneracy 7-7135
(TMTSF)₂(ClO₄)_{1-x}(ReO₄)_x, supercond. ground state, role of anions 7-45555
(TMTSF)₂X salts, quasi-1D, cascade of field-induced SDW phases 7-45701
tunnelling, heavy particle in a metal, electronic polaron effects 7-52118
two dimensional, Condon domains, dynamical effects 7-12631
two dimensional, Condon domains, electrical charging effects 7-12630
two dimensional, nonlinear cond. in quantising mag. field, electron-acoustic phonon scatt. (*Russian*) 7-17004
two dimensional, partially occupied Landau level, dielec. const. RPA calcs. 7-64139
two dimensional, spatially periodic charge density, magnetoplasma mode dispersion calcs. 7-12638
two dimensional, thermodynamic props., interaction and disorder effects, HF approx. calcs. 7-2516
two-dimensional, background density of states between Landau levels 7-2456
two-dimensional, Condon domains, transition to vortex state 7-12629
two-dimensional, correlation functions and Laughlin quasiparticle operators 7-16965
two-dimensional, in GaAs heterostructure, meas. using SQUID flux-transformer-coupled instrument 7-18830
two-dimensional, spatially periodic charge density, magnetoplasma modes study 7-12637
two-dimensional electron layer, Wigner liq. magnetisation, collective motion model calcs. 7-58757
Al, thermodynamics during high-pressure shock 7-21352
AlGaAs:Sb, MBE growth, Sb doping 7-2038
AlGaAs:Si-GaAs 2D electron gas structure, scatt. mechanisms 7-38718
AlGaAs/GaAs modulation-doped heterojunctions, 2D electron gas, DX centres 7-38694
AlGaAs-GaAs 2D electron gas structs., scatt. mechanisms 7-52783
AlGaAs-GaAs heterointerface, ballistic transport of quasi-2D electron gas 7-52788
AlGaAs-GaAs heterostructures, organometallic VPE grown, galvanomagnetic effect 7-12800
AlGaAs-GeAs n-n heterojunction, thermionic current and capacitance, effect of subband quantisation in 2D electron gas 7-17090
Al_{0.26}Ga_{0.74}As/GaAs heterojunction, high mobility 2-D hole gas 7-2679
Al_xGa_{1-x}As-GaAs heterointerface, 2D electron gas density 7-45448
Be, polycrystalline. plasmon dispersion, EELS meas. 7-27283
GaAs 2D electron gas, dynamical cond., IR cyclotron reson. meas., electron interaction effects 7-45195
GaAs, inversion layers, hot free electron gas, intraband absorpt. coeff. calc. 7-33083
GaAs MESFET and JFET devices, elec. resist., Hall effect, influence of electronic subband mag. depopulation 7-38740
GaAs quantised inversion layers, hot 2D electron gas, spectral acoustic phonon emission intensity 7-52452
GaAs:Si/Al_xGa_{1-x}As quantum wells, photolum. studies 7-39178
GaAs/Al_{1-x}Ga_xAs modulation-doped heterostrcuts., 2D electron gas mobility meas. and calcs. 7-12840
GaAs/Al_xGa_{1-x}As heterostrcut., 2-D density of states in extreme quantum limit 7-2455
GaAs/Al_xGa_{1-x}As heterostrcuts., 2D electron gas, polaron screening effects, optical absorpt. calcs. 7-2511

electron gas continued

- GaAs/Al_xGa_{1-x}As heterostruct. localisation and interaction in a strong mag. field 7-64343
 GaAs/Al_xGa_{1-x}As modulation doped heterostruct., high temp. annealing effects (*Chinese*) 7-12805
 GaAs/AlGaAs 2D electron gas MBE structures, carrier mobility and density meas. 7-64321
 GaAs/AlGaAs modulation doped heterostructs., transport props. studies 7-52752
 GaAs/AlGaAs single heterojunction quantum well struct., photolum. characts. 7-46085
 GaAs/GaAlAs 2D electron gas, cyclotron resonance study 7-2676
 GaAs/n-AlGaAs MBE-grown selectively doped heterostructs., 2D electron gas, transport props. 7-21988
 GaAs-Al_xGa_{1-x}As heterojunctions, subband Landau-level spectroscopy 7-21996
 GaAs-Al_xGa_{1-x}As heterostructures, voltage-controlled dissipation in the quantum Hall effect 7-27393
 GaAs-Al_xGa_{1-x}As junction, 2D electron gas, plasmons, radiation absorpt. and emission 7-2686
 GaAs-Al_xGa_{1-x}As multiple quantum well, electron-phonon interaction 7-2684
 GaAs-AlGaAs heterojunction, narrow 2D electron gas, mag. depopulation of 1D subband 7-17080
 GaAs-AlGaAs heterostructures, transport props. of 2D electron and hole gases 7-52812
 GaAs-AlGaAs modulation-doped heterointerface, photoluminescence spectra studies 7-46137
 GaAs-Ga_{1-x}Al_xAs superlattice, plasmon propagation across layers 7-27276
 GaAs-Ga_{1-x}Al_xAs superlattices, in appl. elec. field, interband optical transitions 7-53274
 GaAs-Ga_{1-x}Al_x heterojunction, nonequilibrium electron-phonon scatt. 7-45457
 GaAs-Al_xGa_{1-x}As, 2D electron gas, edge depletion width 7-58866
 GaInAs/GaAs single quantum well pseudomorphic struct., high electron mobility meas. 7-12841
 GaInAs/InP heterojunction, 2D electron gas nonequil. cyclotron reson. obs. 7-12845
 Ga_{0.47}In_{0.53}As/InP heterojunction, chem. beam epitaxy grown, 2D electron gas 7-12803
 Ga_{0.47}In_{0.53}As-InP heterojunction, MOCVD grown, 2D hole gas 7-21992
 HgCr₂Se₄, magnetisation, temp. depend. 7-45629
 InAlAs/InGaAs modulation-doped heterostructs., 2D electron gas mobility meas. 7-12842
 InAs/GaSb quantum well, 2D electron gas, cyclotron reson. oscills. meas. 7-38944
 In_xGa_{1-x}As_yP_{1-y}InP quantum well, 2D electron gas, self-consistent calcs. 7-58890
 In₂O₃:Sn films, theoretical model for optical props. in 0.3 to 50 μ m range 7-39200
 InP-AlGaAs, 2D electron gas, persistent photoconductivity 7-33046
 InSb/CdTe interface, quasi-2D electron gas obs. 7-21987
 n-InSe layered crystals, 2D electron gas regions, magnetoresist. meas. 7-45359
 Mg, local density of states region, determ. by core-core-valence Auger transitions 7-39325
 Si (001) inversion layers in parallel mag. fields, electronic g-factor 7-12783
 Si (100) surface, electron delocalisation in 2D electron gas 7-12779
 Si (111) in MIS struct., Hall resistivity of 2D electron gas in strong mag. fields 7-7391
 Si inversion layer, localisation and interaction in a strong mag. field 7-64343
 Si MOS struct., phonon emission spectroscopy of 2D electron gas 7-27435
 Si MOSFETs, weak localisation in isotropic and anisotropic 2D electron gases 7-64172
 Si n-type (100) inversion layers, valley splitting enhancement by lossless edge currents 7-7395
 Si quantised inversion layers, hot 2D electron gas, spectral acoustic phonon emission intensity 7-52452
 Si quantum well struct., 2D electron gas, transport props. 7-52774
 Si-Si_{0.55}Ge_{0.45} modulation doped superlattice, MBE grown, electron mobility enhancement, Hall meas. 7-7382
 Si-SiGe strained-layer superlattices, optical and electronic props. 7-53353

electron guns

- Aurora KrF laser system, design and performance of large area monolithic electron guns 7-36987
 beam emittance measurement on electron gun 7-62193
 Boersch effect meas. in pulsed field emission gun, cross-over points 7-13338
 continuous-operation sectional microtron, calc. and expt. meas. 7-56888
 electrostatic field problem, Poisson equation, numer. soln. 7-29774
 energy broadening in thermal field emission electron beams 7-25710
 field emission electron gun extremely high vac., design and operation (*Japanese*) 7-64879
 grid pulse generator for KEK PF linac (*Japanese*) 7-56903
 grid pulser for short pulse e⁻ gun, design and simulation (*Japanese*) 7-19610
 hairpin cathode electron gun, Young's double hole interf. expts. 7-1020
 high performance avalanche pulse generator for e⁻ gun appl. (*Japanese*) 7-19612
 high performance two-electrode electron gun lens, microscopy appls. 7-5827
 magnetron ring system, ultrasoft X-rays generation 7-30115
 positron gun, modified Soa immersion lens 7-61401
 predispersive electron gun for an electron monochromator 7-15034
 scanning electron microscopy, ultra-high vacuum techniques with field emission gun, surface studies 7-24725
 short pulse grid pulser for positron generator gun (*Japanese*) 7-19607
 spatial light modulator, electron beam addressed 7-25955
 spherical aberration elimination using aspherical mesh lenses 7-20121
 thermionic gridded e⁻ gun for KEK e⁺ linac, characts. (*Japanese*) 7-19608
 toroidal plasma devices, system for mapping magnetic field errors 7-51500
 AlGaAs surface cleaning using ECR radical beam gun 7-54028
 GaAs surface cleaning using ECR radical beam gun 7-54028
 He-Zn metal vapor mixture, laser excitation by electron guns 7-26534
 LaB₆ space-charge-limited electron gun analysis 7-56380

electron-hole avalanches *see impact ionisation***electron-hole drops**

- self-energy calculations, effective interactions 7-38473
 semiconductors, electron-hole liq., general props., review 7-7121
 GaS, layered, high temp. e-h liq., radiative recomb., luminesc. spectra study 7-17343
 Ge crystal, exciton gas-electron-hole liq. interactions, phase diagram, nuclei drift effects 7-2488
 Ge electron-hole liq., ultrasonic attenuation calcs., intraband collision effects 7-12214
 Ge, strongly excited, nonequilibrium carrier recomb., electron-hole drops 7-38461
 Ge:Zn, electron-hole droplet transport, suppression by deep impurities 7-58746
 Ge:Zn, large electron-hole drop, Alfvén wave dimensional reson., impurity scatt. effects 7-16950
 Si electron-hole liq., ultrasonic attenuation calcs., intraband collision effects 7-12214
 Si, electron-hole plasma, second condensed phase 7-27357
 Si:C,O, photoluminescence of C-O related complex defects 7-22346
 Si:O, new donors, bound exciton recomb., photolum. study 7-22300

electron-hole liquid *see electron-hole drops***electron-hole plasma** *see solid-state plasma***electron-hole recombination***see also carrier mobility*

- alkali halide crystals, self-trapped exciton recomb. luminesc.-recomb. induced F-centre form. anticorrel. calcs. 7-13201
 ambipolar photoconductors with surface states, photoelec. amplification 7-38620
 amorphous semiconductors, photoconductivity behaviour during the approach to steady state 7-38637
 Auger recomb. of dislocation excitons 7-38578
 direct-gap semiconductor, reversible picosecond brightening during interband absorpt. of intense light pulses 7-12761
 DLTS method for selective detection of deep recomb. centres 7-7168
 double heterostructures, microcathodoluminescence studies 7-39189
 grain boundary trap occupancy and recomb. models anal. 7-64266
 InP:Cu, band-edge photolum. quenching, impurity recomb. centre effects study 7-39177
 MNOS struct., bipolar injection and recombination, calc. 7-2726
 optical bistability in semiconductor laser amplifiers, switching speed 7-50564
 optically bistable semiconductor devices, carrier surface recombination 7-57401
 organic semiconductors, electrical transport props., electron bombardment method 7-52641
 p-n structures, electron-probe analysis using the dependence of the induced current on the acceleration voltage 7-38348
 poly-p-phenylenevinylene films, photoconduction 7-12760
 polydiacetylene-toluene-sulphonate, single crystal, transient photoinduced reflectance change study 7-53257
 quartz, luminescence of pure and Ge-activated samples 7-46152
 radiationless carrier surface recomb. model calcs. 7-52646
 semiconductor, inversion band bending at surface, generation-recombination noise 7-17067
 semiconductor, surface recombination vel. calc. 7-38587
 semiconductor bicrystal, diffusion length and grain boundary recomb. vel. determ. by laser excitation 7-41402
 semiconductor electron-hole plasma, noise spectrum calcs. near slow recomb. wave excitation threshold 7-38649
 semiconductor epitaxial layers, recombination lifetime profiles meas., injection level depend. 7-52874
 semiconductor grain boundary photovoltaic effect, scanning laser beam obs. anal. 7-12766
 semiconductor superlattices, amorphous, carrier relax. processes (*Chinese*) 7-58864
 semiconductor thin film, band population inversion under strong alternating elec. field 7-64371
 semiconductors, Auger recombination via deep double-charged centres (*Ukrainian*) 7-12732
 semiconductors, deep centres, book 7-18510
 semiconductors, electrical breakdown at grain boundaries 7-45339
 semiconductors, electron-hole recombination, coherent effects due to Coulomb interaction 7-7255
 semiconductors, extrinsic, thermal gradient magnetoconc. effect 7-52659
 semiconductors, narrow gap, spontaneous oscills. under plasma resonance conditions 7-38605
 semiconductors, nonequilibrium carrier recomb. processes, plasmon effects, luminesc. spectra calcs. 7-58818
 semiconductors, optical beam induced minority carrier distrib. 7-17036
 semiconductors, polycrystalline, beam induced current characterisation, appl. to Si solar cells 7-7267
 semiconductors, polycrystalline, localised defects, EBIC studies 7-21933
 semiconductors, Rayleigh wave excitation during optical pulse absorption 7-38314
 semiconductors with parabolic density of states, activity coeffs. of electrons and holes 7-27324
 solar cells, recombination and transport parameters, advanced measurement techniques 7-54316
 surface junction solar cells, illumination and surface recombination effects on currents, anal. 7-34046
 AlGaAs/AlAs multiquantum-well struct., staggered band alignments 7-7361
 AlGaAs/GaAs solar cells, proton irradiated, defect production 7-46936
 AlSb, hot electron luminesc. 7-46119
 As₂Se₃ glasses, defect levels and photoconductivities 7-12673
 As₂S₃ amorphous films, persistent photocurrent 7-45389
 As₂Se₃ amorphous films, persistent photocurrent 7-45389
 As₂Se₃, non-exponential photocurrent decay, anal. 7-38633
 As₂Se₃ single crystals, geminate pair recomb., photocond., photoluminescence meas. 7-38581
 Au/Cd stearate/n-GaP electroluminescent device struct., electron-hole recomb. luminesc., minority carrier injection mechanism 7-59260
 Au/I-ZnS/n-ZnS electroluminescent device struct., electron-hole recomb. luminesc., minority carrier injection mechanism 7-59260
 Bi₁₂SiO₂₀ photorefractive gratings, buildup and decay, effect of electric field 7-17306
 CdCr₂Se₄, band structure characteristics and props. of nonequilibrium carriers, cathodoabsorption 7-46064
 n-Cd_xHg_{1-x}Te, doped and undoped, minority-carrier lifetime 7-21932

electron-hole recombination continued

p-Cd_{1-x}Hg_xTe, doped and undoped, minority carrier lifetime 7-45353
Cd_{1-x}Mn_xTe(Se), mag. field-induced exchange effects, photolum. meas. 7-27705
CdS, carrier transport, defect effects, photoacoustic and photocurrent spectra 7-38626
CdS, electron-hole exchange interaction for donor-acceptor pairs as a function of separation distance 7-52537
CdS, nonradiative recombination, elec. transport, combined photoacoustic and photocurrent spectra 7-38582
CdS, nonradiative recomb., elec. transport, combined photoacoustic and photoconductive spectra, theory 7-38583
CdS single crystals, nonequilib. high-temp. vacuum annealing effects, intrinsic defect transform. 7-58764
CdS-CuInSe₃ backwall solar cells, intrinsic loss mechanisms calc. 7-23187
CdSe, photogenerated high density electron-hole plasma, energy relax., rapid expansion 7-33039
CdSe:Cu films, radiative recomb. centres form., photolum. spectra studies (Russian) 7-33453
CdTe, polycrystalline, grain boundaries elec. and optical characts. 7-38012
CdTe, Schottky-barrier height determ. including electron-hole recomb. and electron trapping effects 7-2720
CdTe:P-CdS solar cells, control of open circuit voltage by carrier density variation 7-17887
n-CdZnS/p-CuInSe₂ polycrystalline solar cells, open circuit voltage 7-17889
CsI, two-photon induced luminesc. 7-64696
Cs₂O-SiO₂ glasses, intrinsic and recomb. luminesc. and fundamental absorpt. spectra 7-13195
p-CuInS₂, strongly sublinear photocond. 7-52667
Cu₂O, long-lived strain-confined paraexciton thermodynamics, recomb. luminesc. and thermalisation 7-2492
GaAs (100) unpinned surface, picosecond transient reflectivity 7-59168
GaAs device structures, γ -ray effects, surface generation-recombination processes 7-64349
GaAs doping superlattices, pulsed and CW photoluminescence obs. 7-46138
GaAs, EL2 centre stability under electron-hole recomb. conditions 7-16978
GaAs, highly doped, polarised hot electron photoluminescence 7-46121
GaAs, photoconductivity and Hall voltage kinetics, recombination and scattering centre recharging 7-27364
GaAs, photoholes in the spin-split band, energy relax. and spin depolarisation 7-22301
GaAs polycrystalline solar cell, electron beam generated carriers in presence of grain boundaries 7-64262
GaAs solar cells, depletion layer recombination effects on radiation damage hardness 7-13888
GaAs, surface recombination velocity and bulk minority carrier lifetime 7-17037
GaAs-(AlGa)As heterostructure, modulation-doped, valence band mixing, and optical emission 7-7344
GaAs-Al_{0.4}Ga_{0.6}As, intrabarrier recomb., luminesc. spectra anal. 7-53387
GaAs-Al_{0.7}Ga_{0.3}As SQW structure, photolum. switching by pulsed elec. field 7-13197
GaAs-Al_{1-x}Ga_x-As, superlattices, carrier behaviour, mag. field effect 7-45449
GaAs-Al_{1-x}Ga_x-As quantum well structure, recomb. dynamics, photolum. obs. 7-12809
GaAs-Al_{1-x}Ga_x-As solar cell, operation with band-gap gradient in space charge region 7-54295
GaAs-AlAs short period superlattice, photoexcited carriers, dynamics 7-53402
GaAs-AlGaAs quantum wells, field-induced lifetime enhancements, ionisation of excitons 7-39181
GaAs-Ga_{0.7}Al_{0.3}As heterojunction, donor-acceptor radiative recomb. mechanism, photolum. spectra study 7-17083
GaAs-GaAlAs heterostructure, LPE grown, interface photoluminescence spectra 7-53390
GaAs-GaAlAs quantum well structs., recomb. dynamics of carriers 7-12830
GaAs_{0.12}P_{0.88}N, Te and GaP:N, Si(Te) epitaxial layers, minority carrier lifetimes, surface and interface recombination effects 7-7424
GaS, layered, high temp. e-h liq., radiative recomb., luminesc. spectra study 7-17343
n-GaSb impurity Auger hole recomb. via deep acceptor, electron density depend. calcs. 7-38573
GaSe, photoexcited localised excitons thermalisation, stacking disorder effects, photolum. study 7-27770
GaSe, spontaneous and stimulated photoluminescence studies 7-22315
Ge, carrier conc., mag. gradient effect (Russian) 7-17040
Ge, laser irradiated, electron-hole plasma dynamics investigated by time-resolved spectroscopy 7-13276
n-Ge:Ni, photocond., spontaneous oscills. in an electric field 7-52670
GeS₂ amorphous films, persistent photocurrent 7-45389
GeSe amorphous films, persistent photocurrent 7-45389
GeSe₂ amorphous films, persistent photocurrent 7-45389
HgCdTe, ambipolar diffusion and free carrier recombination studied by transient grating technique 7-12731
HgI₂ single crystals., photoconduction, carrier surface generation and recombination 7-33045
In/GaAs:Cu/In struct., I-V characts., carrier recomb. and generation, impurity thermionic field ionisation effects (Russian) 7-22030
InAs surface on InP, epitaxial regrowth, surface states and recomb. velocity 7-2431
InGaAs/GaAs lattice-strained double heterojunction bipolar structs., comp., recomb. props. and device performance 7-64322
InGaAsP/InP heterostructures, carrier lifetimes and quantum efficiencies, photoluminesc. studies 7-64675
InGaAsP-GaAs double heterostructures, luminescence efficiency and surface recombination velocity 7-13196
InGaAsP-InP, quantum well wire, Auger recombination 7-7374
InGaAsP-InP double heterostructures, luminescence efficiency and surface recombination velocity 7-13196
p-InP, γ -ray irradiated low temp., nonradiative-recomb.-enhanced defect struct. transformation 7-2062
InP room temp. band edge photolum. intensity interpretation 7-27762
InP, surface recombination velocity and bulk minority carrier lifetime 7-17037

electron-hole recombination continued

InP:Fe, transient photoconductive response 7-52681
InP-GaInAs, 2D electron gas, persistent photoconductivity 7-33046
InSb, carrier lifetime, pressure depend. 7-52644
InSb, coherent spontaneous oscills. under transverse breakdown conditions, high frequencies 7-17046
KCl, Frenkel defect recomb., thermally stimulated electron emission obs. 7-64869
K₂O-SiO₂ glasses, intrinsic and recomb. luminesc. and fundamental absorpt. spectra 7-13195
K₂ZnCl₄, X-ray induced luminesc. and thermoluminesc. spectra anal. 7-46132
Li₂O-SiO₂ glasses, intrinsic and recomb. luminesc. and fundamental absorpt. spectra 7-13195
Mg₂Cd_{1-x}Se single cryst. solid solns., local centres parameters determ. (Russian) 7-32953
NaCl:Ag Frenkel defect recomb., thermally stimulated electron emission obs. 7-64869
Na₂O-SiO₂ glasses, intrinsic and recomb. luminesc. and fundamental absorpt. spectra 7-13195
P, amorphous, radiative recomb., time-resolved photolum. study 7-13212
PbTe single-cryst. films, negative photocond., slow relax. and photomeas. 7-58832
PbTe-PbEuTeSe multiquantum wells, electron-hole recomb., photolum. 7-13216
trans-polyacetylene, inter-chain versus intra-chain electron-hole photogeneration 7-27362
RbCu₂Cl₃, luminesc. band profile, localised carrier tunnel recomb. effects calcs. 7-3075
Rb₂O-SiO₂ glasses, intrinsic and recomb. luminesc. and fundamental absorpt. spectra 7-13195
Rb₂ZnCl₄, X-ray induced luminesc. and thermoluminesc. spectra anal. 7-46132
Si (100), magnetoconductivity of nonequilibrium electron-hole pairs associated with surface charge layer 7-38671
Si (100) MIS structs., state density of 2D electrons in transverse mag. field 7-12870
Si, Auger recombination at low carrier densities 7-7328
Si BSF solar cells, Rose-Weaver meas. technique 7-8423
Si bicrystals, grain boundary carrier recombination, chemical origin 7-17039
Si bifacial solar cells, minority carrier diffusion length and surface recomb. vel. determ. 7-8407
Si concentrator solar cells, efficiency limits 7-8384
Si crystalline solar cells, conditions for high efficiency 7-23145
Si diffused p-n structs., recomb. props. of base region, effect of thermal and radiation defects 7-17089
Si, dislocated, charge carrier recomb. processes 7-7264
Si, dislocations and electron-hole radiative recombination 7-13203
Si, fast ionisation waves due to absorpt. and reemission of luminesc. 7-52627
a-Si, generation-recombination rate 7-33032
Si high-low junction emitter solar cell, quantum efficiency improvement 7-3681
Si, laser irradiated, electron-hole plasma dynamics investigated by time-resolved spectroscopy 7-13276
Si MINP solar cells, high efficiency, performance, fabrication, characts. 7-23153
Si MINP solar cells, radiation damaged, conduction mechanism 7-65463
Si MIS device diffusion length meas. by spectral response 7-8424
p-Si n⁺pp⁺ solar cell structs., quasisurface recomb. vel. determ. in contact layers 7-58875
Si n-n⁺ epitaxial layers, recomb. parameters anal. by moving light strip method 7-21930
Si, neutron-transmutation doped, spatially resolved carrier lifetime meas. 7-7257
Si, polycrystalline, grain boundary recomb. vel. eval. from spectral response of solar cells 7-41403
Si, polycrystalline, H₂ passivation, grain boundaries, EBIC technique 7-26769
Si polycrystalline layers, elec. props. and grain boundary carrier dynamics under solar illumination 7-38625
Si polycrystalline solar cell p-n junction, carrier lifetime, effective recomb. vel. and diffusion length, EBIC meas. 7-23138
Si, ramp assisted foil casting and photovoltaic appls. 7-16609
a-Si, recomb. via dangling bonds, occupation statistics 7-38515
Si, recombination activity of dislocations 7-12733
Si solar cell, improved determ. of lifetime and surface recomb. vel. by transient methods 7-13870
Si solar cell efficiency improvement simulation analysis 7-13865
Si solar cell performance, influence of heavy doping 7-23147
Si solar cells, heavy doping effects 7-3653
Si solar cells, high efficiency, identification of key parameters limiting perform. 7-59846
Si solar cells, low recombination p⁺ and n⁺ regions for high performance 7-3655
Si solar cells, passivation using ZnS_{0.9}Se_{0.1} and GaP semiconductor coatings 7-65479
Si solar cells, performance anal. 7-65466
Si solar cells systematic design theory using optimisation techniques 7-23146
Si space solar cells, damage coeffs. of 1 MeV electron fluences 7-13880
Si, spin-dependent recombination and low-freq. ESR studies 7-38577
Si surface recomb. vel. determ. using solar cell struct. 7-21938
Si thin film solar cells, high performance considerations 7-23152
Si, transmutation-doped, carrier recomb. props. at gamma-irrad. defects, transport meas. 7-38575
Si wafers, doped by neutron transmutation, minority carrier lifetime, photocond., annealing 7-38785
Si:B, carrier lifetime meas., capture and recombination 7-38585
Si:B(P) solar cell emitter saturation current meas. by contactless photoconductivity decay method 7-13866
Si:C,O, photoluminescence of C-O related complex defects 7-22346
a-Si:H, carrier trapping and recombination, IR enhancement spectra of photoconductivity 7-33052
a-Si:H, charge transport and relax., luminesc. long-time tail distribns. anal. 7-39185
a-Si:H, glow discharge prepared, steady-state photoconductivity 7-38632
a-Si:H, neutral dangling bond defect, photocarrier processes 7-32962
a-Si:H, non-exponential photocurrent decay, anal. 7-38633

electron-hole recombination continued

- a-Si:H, photoconductivity exponent for recombination at dangling bonds 7-33054
- a-Si:H, photocurrent, surface recombination effects 7-33048
- a-Si:H, recomb. at dangling bonds and steady-state photocond. Fermi level depend. calcs. 7-12734
- a-Si:H,B p-i-n and n-i-p solar cells, doping profile effects 7-46947
- Si:H amorphous, recombination-enhanced defect reactions, reversibility 7-45343
- a-Si:H based alloys for solar cells, elec. props. and degradation behaviour 7-52642
- a-Si:H films, electronic props., effects of γ -irradiation 7-38584
- a-Si:H solar cells, optically induced degradation 7-59848
- a-Si:H thin film solar cells, device properties 7-13897
- Si:O, new donors, bound exciton recomb., photolum. study 7-22300
- Si:P, meas. of heavy doping parameters 7-12855
- Si-SiO₂ interface properties in the 10^{17} - 10^{19} cm⁻³ doping range 7-38762
- α -SiC:N, single carrier SCL flow, computer calcs. 7-21925
- SiO₂ thermal oxide films on Si substrate, ramp-voltage-stressed I-V characts. 7-17112
- SiO₂ thin films, constant current stressed voltage-time characts., dynamic trapping effects 7-45529
- ZnIn₂S₄, recombination kinetics, photoconductivity and photoluminesc. studies 7-2637
- ZnO-electrolyte interface, electrolum. under cathodic and anodic pulsed polarisation 7-13235
- ZnS:Al, temp. depend. of visible photolum., ESR studies 7-46099
- ZnS:Fe,Cu, three-centre Auger recombination, EPR study 7-45806
- ZnTe:O, red cathodolum. kinetics, two-step electron capture model calcs. 7-59262

electron impact

- see also atomic electron impact excitation; atomic electron impact ionisation; molecular electron impact dissociation; molecular electron impact excitation; molecular electron impact ionisation; secondary electron emission*
- alkali halides, electron bombardment, excited-atom production 7-22400
- alkali halides, electron- and ion-induced sputtering, atomic excitation 7-59348
- backscatter loss calcs. in electron probe microanalysis 7-8342
- backscattered electron signal at edges and surface steps, depend. on surface tilt and take-off direction 7-7800
- electron scatt. by Al atoms in solids, polarisation and exchange 7-22401
- electron scatt. by Li atoms in solids, polarisation and exchange 7-22401
- electron stimulated processes at surfaces, excitation anisotropy 7-13282
- energy losses for a charged particle moving through a layer of plates 7-58388
- ESD, desorption cross-sections meas. 7-13283
- ESD and photoemission, extended core-hole Hamiltonian 7-52252
- ESD cross sections, electron beam inhomogeneity effects 7-13284
- low-energy electron surface diagnostics and shaping of electron energy distributions at low exciting-beamenergies 7-13286
- luminescent centres in crystals, impact excitation and Auger quenching, appl. to ZnS:Mn 7-27827
- mean free path, effective backscatt. and differential scatt. cross-sections, 5-40 keV 7-53461
- metal surface, low energy positron interactions, elastic and inelastic scatt. calcs. 7-39330
- metal surfaces, disordered, elastic reflection of medium-energy electrons 7-13285
- metal surfaces, low energy positron diffr. pattern calcs., scatt. processes anal. 7-39331
- MIM electroluminescent device structs., impurity centre electron impact-induced luminesc. mechanism 7-59260
- solid surface exam. by ion and electron spectroscopy, with angular resolution 2-6° 7-32773
- solid surfaces, chemistry and physics, book 7-60891
- solid surfaces, ferromagnetic and nonmagnetic, spin-dependent electron scatt., photoemission and inverse photoemission calcs., book contrib. 7-33493
- solid surfaces, positronium refl. and diffr. coeff. meas. method 7-39332
- SOS structures, SIMS depth profiling, electron stimulated desorption and charging effects 7-33501
- thick-target bremsstrahlung spectra generated by the β particles of ⁹⁰Sr-⁹⁰Y and ⁹⁹Tc 7-39212
- threshold spectrometer, double cylindrical mirror analyser 7-24735
- transition metals, low energy in elastic electron scatt. props. 7-63700
- VUV spectrometer-detector system calibration using synchrotron radiation 7-24710
- Al surface, O₂ adsorption, electron beam effects, AES and secondary electron emission studies 7-27835
- Cd_{0.2}Hg_{0.8}Te, electron stimulated desorption of Hg 7-17378
- CdS surfaces, electron-beam-stimulated processes, real-time atomic-resolution electron microscopy 7-7798
- LiF, electric breakdown due to injected electron beam. 7-64837
- N₂ film, solid, quasielastic hot-electron transport 7-39327
- Ne, solid films, erosion by keV electrons 7-3124
- Ni (100) with adsorbed O₂ overlayers, elastic diffuse and inelastic electron scatt. 7-22402
- Ni (110), adsorption of O, electron stimulated ion desorption O⁺ yield meas. 7-12487
- Ni magnetic surfaces, elastic spin-polarised low-energy electron scatt., book contrib. 7-33494
- Pd (100) and (111), surface resonances in vibr. spectroscopy 7-52229
- Pt (111), NO and CO electronically stimulated adsorbate rotation and desorpt. studies 7-45006
- Pt, electron stimulated adsorption, of vapour 7-63955
- Si, chemical sputtering by ions, electrons and photons 7-59355
- SiO₂, chemical sputtering by ions, electrons and photons 7-59355
- TiO₂, surface defect-struct., photon- and electron-stimulated desorption ion yield studies 7-44974
- W (100), adsorbed CO, electron-stimulated desorption, metastable particle production 7-21628
- W (100), glancing elastic relativistic electron scatt., computer simulation 7-64835
- W surface adsorbed F⁻ ions, photo- and electron-stimulated desorption 7-12465

electron interactions *see elastic scattering of electrons by atoms and molecules; electron attachment; electron-electron interactions; electron-nucleon interactions; electron-nucleus reactions; electron-positron interactions; electron spectra; hadron electroproduction; secondary emission*

electron ionisation *see electron impact*

electron lenses

- see also aberrations; electron microscopes; electron optics; electrostatic lenses; magnetic lenses*
- aberration shift relations, matrix derivation 7-18938
- asymmetrical unsaturated magnetic electron lenses, focal props. calc. 7-31236
- centrifugal electrostatic focusing system, bunching mechanism and kinetic anal. of relativistic electron beam 7-36871
- combined electrostatic focusing-deflection systems, asymptotic aberrations 7-10835
- electron beams, aberrations in combined electromagnetic focusing spherical cathode lens, theory (Chinese) 7-36868
- electron beams, relativistic aberrations in combined electromagnetic focusing-deflection system, theory (Chinese) 7-36869
- electron guns, spherical aberration elimination using aspherical mesh lenses 7-20121
- high performance two-electrode electron gun lens, microscopy appls. 7-5827
- matrix lens, aberrations reduction using offset apertures 7-20122
- misalignment of electron lenses, influence on image quality 7-20123
- probe design, miniature variable energy, for nanometric analysis, electron opt. parameters 7-18939
- probe-forming lens, axial geometrical aberrations meas. by means of shadow image of fine particles 7-42882
- saturated objective, electron opt. parameters computation 7-18937
- STEM objective lens, high excitation, Munro programs data variations effect on predicted opt. props. 7-18933
- TEM lens shape with min. spherical aberration coeff., computation method 7-18936

electron lifetime (metals) *see electron relaxation time (metals)*

electron lifetime (semiconductors) *see carrier lifetime*

electron lithography *see electron beam lithography*

electron mean free path (metals)

- Aharonov-Bohm effect, influence of electron-phonon interaction 7-21895
- alloys, substitutionally random, electron localisation and metal-insulator transition, CPA calcs. 7-27302
- ferromagnets, inelastic electron scatt., spin-depend. energy loss processes, book contrib. 7-33500
- film, average electron mean free path calc. using stat. model 7-58911
- liquid metals and alloys, electrical resistivity and finite mean free paths 7-45266
- metal wire, size effect, analytical expression w.r.t. Cotter mean free path 7-12885
- metallic alloys and cpds., phonon point contact spectroscopy, review (Russian) 7-12788
- quasicrystals, electron localisation 7-21901
- transition metals, low energy in elastic electron scatt. props. 7-63700
- Ag, electron mean-free-path calculations using a model dielectric function 7-52583
- Al, electron mean-free-path calculations using a model dielectric function 7-52583
- Al, ultrasonic attenuation in a transverse mag. field, electron mean free path 7-64296
- Au, electron mean-free-path calculations using a model dielectric function 7-52583
- Au-Au point contacts, electronic thermal cond. temp. depend. study (Russian) 7-12789
- Bi-Ga, liq., elec. resist. meas. 7-38532
- Cu, electron mean-free-path calculations using a model dielectric function 7-52583
- Cu thin polycryst. wires, elec. resist. meas., surface induced deviations from Matthiessen's rule 7-27319
- Cu-Be-Co, elec. resist., decomposition and coarsening effects 7-2573
- Ga, liq., elec. resist. meas. 7-38532
- Na, carrier scattering, photo- and secondary electron emission studies 7-13324
- Ni single crystal films, resistivity ratio and mean free path length 7-52857
- Rh polycrystalline films, electrical size effects 7-7412
- V-Si films, electrical transport props. 7-33108
- V₂Ge, solid solns. of Fe, Cr and Co, elec. resist. (Russian) 7-45273
- V₃Si, solid solns. of Fe, Cr and Co, elec. resist. (Russian) 7-45273

electron mean free path (semiconductors) *see carrier mean free path*

electron micrographs *see electron microscope examination of materials; electron microscopy*

electron microprobe analysers *see electron probe analysis*

electron microprobes *see electron probes*

electron microscope applications *see electron microscopy*

electron microscope examination of materials

- see also electron microscopy; scanning electron microscope examination of materials; scanning-transmission electron microscope examination of materials; transmission electron microscope examination of materials*
- alloys, amorphous, struct. features, HREM 7-1883
- alloys, dislocation glide during ageing, hardening phase particle interaction modelling (Russian) 7-38010
- amorphous films, ferromag., induced mag. anisotropy (Russian) 7-52974
- analytical electron microscopy of thin films, review (Czech) 7-59261
- bacteriorhodopsin, cryst., radiation-sensitive specimens, high resolution image quality achieved in electron diffr. pattern 7-47302
- bicrystal, grain boundary dislocations, struct., steps, HREM study 7-16488
- biological cryo-electron microscopy, cryst. size and cooling rate 7-3949
- biological materials, surface relief of thin sections rel. to image quality 7-65904
- biological specimen etching, ion beam sputtering appl. 7-7850
- butadiene-styrene graft block copolymers, low-mol. cpds. diffusion (Russian) 7-36834
- carbon, electron microscopy, past, present, future 7-16379
- cell components, computer environment for 3D shaded perspective display 7-65905
- cellulose acetate, membranes, osmosedimentation, performance, morphology 7-13816
- ceramics, ion implantation and near surface microstructures, analytical electron microscopy 7-37816

electron microscope examination of materials continued

- coke, metallurgical, microstruct. analysis and intercalated species 7-28008
- collection of airborne pollution particles for analytical electron microscopy 7-17935
- compound semiconductor/metal contacts, interfacial microstruct., elec. props., phase diagrams 7-45495
- conference, electron microscopy and anal. Newcastle-upon-Tyne, England, (Sept. 1985) 7-14707
- defects at surfaces, microscopy and diffr. studies 7-2325
- deinococcus radiodurans, surface protein projected struct. determ. by cryomicroscopy 7-47003
- diamond, voidites, electron microscopy study 7-32425
- diamond knife edges, megavolt and cryo electron microscopy 7-41547
- dislocation density, micrograph evaluation errors 7-16559
- dislocation emission from cracks, electron microscope obs. 7-38005
- dislocation loops, small hexagonal, diffraction contrast images and lattice fringe patterns, computer simulation 7-44325
- dissociated dislocation in weak beam image, determ. of sign, electron microscope studies 7-44323
- epoxy matrices, microstruct. 7-33632
- ethylene copolymers, crystalline struct., electron microscopy 7-44404
- FCC crystals, overlapping and intrinsic faults, electron microscope images 7-12084
- grain boundaries, electron microscope analysis 7-37818
- hexaethylene glycol dodecyl ether, lyotropic liquid crystal, defect-mediated phase transition, electron-microscopy obs. 7-21439
- high resolution electron microscopy in materials science (*German, English*) 7-39806
- highly oriented pyrolytic graphite, surface with deposited Ag(Au) clusters, scanning tunnelling microscopy study 7-12413
- HSLA steel, precip. anal., EDX and EELS 7-46495
- Inconel 718, Ni-base superalloy, creep deform., back stress determ. 7-46564
- inert gas bubble precipitate solid in Al, defects, high resolution electron microscopy studies 7-32424
- interface and surface struct. characterization, ion scatt. and channelling, scanning tunnelling microscopy and computer simulation (*Japanese*) 7-7803
- internal friction peak obs., dislocation configurations 7-38115
- Langmuir-Blodgett films, surface study using electron microscopy and X-ray reflectivity 7-58677
- local autoepitaxial layers, packing defect density, depend. on crystallographic orientation of side boundaries 7-58701
- low-molecular ingredients, migration in elastomer compositions (*Russian*) 7-39942
- lyotropic liquid crystal, lamellar phase, electron microscope observations (*French*) 7-32269
- lyotropic liquid crystal, smectic-nematic transition, electron-microscope obs. 7-32648
- metal particles, ultra fine, ferromag., growth rel. to mag. field 7-53515
- metallic glasses, superplastic deform. (*Russian*) 7-39599
- metallic materials, ion implantation and near surface microstructures, analytical electron microscopy 7-37816
- metallic thin films, prep. by vacuum and electroless deposition methods, island growth 7-49590
- metallurgical appl. of electron microscope in Cambridge 7-4927
- metals, grain boundary structure (*German*) 7-44571
- metals, struct. changes under action of thermal cycling (*Russian*) 7-53752
- mono-AZO pigment, electron microscope studies 7-16543
- neuron tracing system, CARTOS-ACE, 3D reconstruction of electron micrographs 7-23502
- organic Langmuir-Blodgett films, molecular design (*Japanese*) 7-21742
- oxide scales, chem. mapping using electron energy loss imaging microscope 7-37812
- oxide surfaces, structure and rearrangements, atomic imaging 7-27078
- oxynitride ceramics, anal. by electron microscopy 7-16428
- paraffin, thin crystals, radiation-sensitive specimens, high resolution image quality achieved in electron diffr. pattern 7-47302
- phthalocyanines, halogenated, radiation damage and structural studies 7-6688
- phthalocyanines, polymeric structural arrangements 7-16544
- poly(tetrafluoroethylene) dispersions, high resolution electron microscopy 7-44341
- poly-p-phenylene sulphide, solution-grown crystals and crystalline thin films, morphology 7-16441
- polyamide acid, supermol. struct. change in thermal imidisation (*Russian*) 7-42809
- polyarylate-polydimethylsiloxane rigid block copolymers, domain struct., electron microscopy (*Russian*) 7-63520
- polybutylene, crystallisation, electron microsc. obs. 7-32309
- polyethylene, lin., deform. process, morphological study 7-13518
- polyethylene, soln. crystallisation kinetics and morphology 7-21148
- polymer microcrystals, natural, diffr. data from electron diffr. patterns 7-11862
- p-polyphenyls, electron microscopical studies 7-16440
- polypropylene, isotactic, γ -phase morphology 7-6554
- polypropylene films, Cu-filled, struct. and elec. cond. 7-64301
- polypropylene films, glass isotactic, crystallisation, struct., dynamic mech. props. 7-16445
- proteins in membranes, powder samples, label positions, determ. by neutron and anomalous X-ray diffr. 7-3755
- PTFE single-crystal, lattice imaging studies 7-11951
- quartz, intermediate phase between α and β phases 7-1937
- quasicrystal diffraction patterns, distortion and peak broadening 7-11981
- quasiperiodic tiling in two and three dimensions 7-35432
- rhodopsin molecules in disc membrane of frog rod outer segments, 3D electron microscopical investigation 7-65690
- D-ribulose-1,5-bisphosphate carboxylase/oxygenase from *Alcaligenes eutrophus* H16, struct. obs. 7-65691
- semiconductors, grain boundaries, at. struct. 7-6638
- semiconductors, ion implantation and near surface microstructures, analytical electron microscopy 7-37816
- Si, intrinsic faults, weak beam contrast study 7-16377
- skeletal muscle fibres, frog, quick-freezing following electrical stimulation 7-28798
- small particles, atomic struct. and props., conf., Wickenburg, AZ, USA (Jan. 1986) 7-29592
- steel, analytical electron microscopy, developments and trends 7-22949
- electron microscope examination of materials continued**
- steel, austenitic, Mn-Cr, hardening characts. and hydroextrusion parameters (*Russian*) 7-59540
- steel, austenitic stainless, corrosion and grain boundary Cr depletion, comparison in modified Strauss test 7-39728
- steel, austenitic stainless, electron irradi., cold working, vacancy swelling, void form., carbide precip., electron microscopy 7-21282
- steel, austenitic stainless, heavy ion bombarded, η -phase precipitate form., electron microscopy studies 7-13459
- steel, austenitic stainless, swelling by electron irradi., influence of appl. stress (*Japanese*) 7-16632
- steel, austenitic stainless radiation damage process obs. using high voltage electron microscopy 7-51831
- steel, C, dislocation structure, rolling temp. effects (*Russian*) 7-44552
- steel, Cr-Mo, friction pair, surface layer structural modifications (*Russian*) 7-39678
- steel, Cr-Ni-Mo-Nb, precipitates formation, effect of He 7-13460
- steel, dislocation struct. rel. to cyclic bending strain 7-22760
- steel, ferritic stainless, cavity form., effect of electron/He dual beam irradi. 7-58341
- steel, high C, quenched, structural changes, tempering effects (*Russian*) 7-17556
- steel, high-speed, produced from machining waste, liq. phase forming during sintering 7-3226
- steel, low C, low alloy, tempering investig., epitaxial ferrite stability studies (*Russian*) 7-13479
- steel, maraging, sintered, ageing process, precip. phases investig. 7-3322
- steel, mild, brittle fracture, microcracks effect (*Russian*) 7-59618
- steel, Mo-base high speed, carbide chem. composition, electron microscopy studies 7-22671
- steel, Ni, bainite transform. kinetics, influence of grain size 7-65030
- steel, Ni maraging, austenite form. characts. (*Russian*) 7-46466
- steel, packet martensite deformation, struct. and crystal geometry (*Russian*) 7-3357
- steel, stainless, austenitic, pre-precipitation phenomena associated with γ' form. 7-22696
- steel, stainless, ferritic-martensitic, high-Cr, fast reactor irradi., phosphide phases 7-22700
- steel, stainless, films, sputter deposited, vacuum annealing-induced solute depletion 7-64012
- steel, stainless, microstruct., aging effects, atom probe FIM, optical and analytic electron microscopy studies 7-33700
- steel, stainless, neutron irradiated, microstruct. and swelling, Si and N impurity effects (*Russian*) 7-2217
- steel, stainless FCC 7-63409
- superalloy L1₂ structures, high temp. deform. mechanisms (*French*) 7-22766
- superalloys, topologically close packed phases, domain struct. (*Chinese*) 7-11989
- surface (111), reconstruction study 7-2315
- surfaces, crystal lattice termination, reflection electron microscopy studies 7-12437
- tobacco mosaic virus in water, freeze-fracture imaging of ordered phases 7-3751
- transition metal silicide layers, electron microscope exam. (*German*) 7-45081
- twinned apatite bicrystals, theoretical detect. of a dark contrast line, rel. to chem. props. of human dentin and enamel 7-40097
- Ag₂Te, domain struct. and phase transforms., electron diffr. and microscopy studies 7-58194
- Al alloy surface, UV laser pulse irradi., microscopic crater form. 7-12124
- Al alloys, icosahedral quasicrystals, high resolution electron microscopy 7-16497
- Al two phase alloys, high temp. deformation, microtexture 7-16563
- Al-Cu-Mg, deformed, dislocation struct., AE obs., electron microscopy (*Russian*) 7-39832
- Al-Li (9.5 at.%), coarsening of δ -Al₃Li precipitates, var. of average Li content in Al matrix 7-3313
- Al-Mg, deformed, dislocation struct., AE obs., electron microscopy (*Russian*) 7-39832
- Al-Mn, icosahedral-glass and icosahedral quasicrystal models distinguished via high-resolution lattice imaging 7-32295
- Al-Mn, lattice model of quasicrystalline phase, high resolution electron microscope images 7-37866
- Al-Ti alloys, 1D antiphase domain structures 7-63557
- Al-V alloys, phase transitions between amorphous, quasicrystalline and crystalline phases 7-63807
- Al-Zn, fatigue particle coarsening, vacancy creation 7-53895
- Al-Zn, Guinier-Preston zones, size distrib., small angle X-ray scatt. studies 7-28043
- Al-Zn (1.95 wt.%), X-ray microanal. in medium voltage electron microscope, radiation effects 7-46902
- Al-Zr-Mg (Cu), grain boundary struct. and superplasticity, electron microscopy studies (*Russian*) 7-6630
- Al₂Mn alloy, decagonal and icosahedral phase coexistence, electron diffr. studies 7-11991
- Al₈₆Mn₁₄, atomic level interpretation of quasicrystal microstructure 7-16498
- (Al₆Mn)₂-Si₂, icosahedral phase transform., electron microscope study 7-2187
- Al₂Mo precipitate microstruct. and orientation, implantation and annealing effects, electron microscopy study 7-16782
- Al₂O₃ anodic film, barrier layer, surface imaging using scanning tunneling microscope 7-17706
- Al₂O₃ ceramic, grain boundaries, microanal. 7-16577
- Al₂O₃-ZrO₂ composites, high temp. behaviour and microstruct. study with HVEM (*Japanese*) 7-22819
- AlPO₄, modulated phase, electron microscopy study 7-26937
- Au crystals, small, surface twin form., high resolution electron microscopy 7-44566
- Au films, surface plasmon modes 7-7316
- Au, small metallic particles, surface fractal dimension 7-38308
- Au small particles on amorphous substrates, dynamic atomic-level rearrangements 7-12542
- Au, structural rearrangements in small metal particles at atomic resolution 7-16576
- Au-Mn (15 at.%), disordered phase, high resolution electron microscopy study 7-63834
- Au₇₇Mg₂₃, atom sublattices, selective high resolution electron microscopy 7-6486

electron microscope examination of materials continued

- Au₂Mn, atom sublattices, selective high resolution electron microscopy 7-6486
- Au₂Zn, non-periodic antiphase boundaries, obs. by HREM 7-63550
- B, crystal growth in solar furnace 7-33538
- B thin film preparation, ion beam sputtering appl. 7-7850
- BN, wurtzite, sintered polycryst., texture form. during hot compacting at high press., sphalerite transition 7-53685
- BaFe₁₂O₁₉, defects created by Kr ion bombardment, HREM study 7-12168
- BaFe₂S₄ and Ba₁₃(Fe₂S₄)₁₂, vernier struct. series, high resolution electron microscope study 7-6603
- BaMn_{1-x}Ta(Zn)_xO₃ phase struct. and transforms., high resolution electron microscopy obs. 7-58237
- Ba₂NaNb₅O₁₂, atom sublattices, selective high resolution electron microscope study 7-6486
- BaO.Nd₂O₃.5TiO₂, ceramics, matrix phase struct. 7-39488
- BaPb β(II)-alumina, superstructure, high resolution electron microscopy study 7-12021
- BaSO₄ powder, solubility in water containing strong acidic ion exchange resin 7-21468
- BaSrNb₄O₁₂, chaotic states, high resolution electron microscope study 7-3001
- Be, superplastic flow, electron microscopy studies (*Russian*) 7-3360
- Be-Ti multilayer interference system, struct. and phase composition, electron microscopy, X-ray and neutron diffr. meas. 7-63984
- C, amorphous film, modification by inert gas ion irradiation 7-64018
- C black, in styrene-butadiene rubber soln. relax. properties 7-8317
- C, fractographic studies 7-17645
- Ca-SiAlON ceramic system, A'≡B' transition study 7-16738
- CdP₂, crystal structures and microphases, devil's staircase 7-11982
- CdS surfaces, electron-beam-stimulated processes, real-time atomic-resolution electron microscopy 7-7798
- CdSe-Cu₂Se heterojunction solar cell, dry formation, electron microscope study 7-17916
- CdTe, epitaxial growth on GaAs (100) 7-21779
- CdTe-Cd_{0.6}Mn_{0.4}Te superlattices, high resolution electron microscope study 7-27162
- CdTe-GaAs heteroepitaxial interface, at. resolution HVEM study 7-2392
- Co particles, magnetic structure and thickness distrib., holographic interference electron microscopy appl. 7-5860
- Co-Al, precipitation product dissolution (*Russian*) 7-58479
- Co-Al (10.9 at.%), cellular prep. from supersaturated solid soln. (*Russian*) 7-65045
- Co-Cr thin films prepared by fracture, microtome and ion-beam thinning methods, microstructure obs. 7-2427
- CoCr films, texture formation, appl. for perpendicular mag. recording 7-39539
- Co₉₀M₁₀ (M=Cr,Sm) sputtered thin film recording media, micromag. and struct. studies 7-33243
- Co₉₀M₁₀ (M=Pt,Re) sputtered thin film recording media, micromag. and struct. studies 7-33243
- Cr evaporated and ion assisted deposited coatings, microstruct., electron microscope obs. 7-52335
- Cr, zone-axis critical voltages in HEED, accidental Bloch wave degeneracies obs. 7-63409
- Cr, zone-axis critical-voltage effect obs. 7-63408
- Cr-Ta-C, ageing, hardening processes, carbide separation and dissolving (*Russian*) 7-59541
- Cu alloys, high-strength, rad.-enhanced recrystn. 7-51871
- Cu, dislocation-diffusion mechanism of wear reduction in selective transfer 7-17658
- Cu, recrystallisation texture, deformation temp. effects (*Russian*) 7-8007
- Cu single crystals., low temp. recrystallisation characts. (*Russian*) 7-17546
- Cu-Al long-period superlattice, interface struct., TEM and HREM study 7-16499
- Cu-Al-Mg alloys, complex oxide form. and precipitate morphology (*Russian*) 7-33664
- Cu-based alloys, rapid solidified and ion implanted, struct. studies 7-21130
- Cu-Mn-Sn, phase conc. nonuniformities rel. to annealing (*Russian*) 7-59494
- Cu-Pd bimetallic system, electron microscopy 7-16504
- Cu-Pt (25.7 at.%), transform. from short-range order to L₁₂ and L₁₂-₂ ordered states 7-53726
- Cu-Ru bimetallic system, electron microscopy 7-16504
- Cu-Ti, amorphisation, high resolution electron microscopy 7-44377
- Cu-Ti-Al single crystals., strain hardening due to multiple twinning (*Russian*) 7-46501
- Cu-Zn alloy, cyclic BCC-9R martensitic transform.-induced dislocations Burgess vector, electron microscopy studies 7-51775
- CuAu I and II, initial ordering stages, twinning, periodic antiphase boundaries, electron microscopy 7-28032
- Cu₂O, use of dynamic electron scatt. for studying O atom position 7-44501
- Cu_{3-x}Pd, long-period superstructures 7-21430
- Cu₃Ti, electron irradiation induced amorphisation, high resolution electron microscopy 7-44373
- Fe aggregated particles fractal dimension meas. by electron microscopy 7-26598
- Fe, Armo, annealed and cold worked, neutron irradi. damage 7-2067
- Fe-B-based amorphous alloys, struct. evolution during heating (*Russian*) 7-16418
- Fe-C martensite, struct. in transition state from first to third stage of tempering, electron microscopy and diffr. study 7-46528
- Fe-Cr-Ni, austenitic, electron, irradi., conversion of stacking fault tetrahedra to voids 7-58342
- Fe-Ni, austenite form. during continuous heating (*Russian*) 7-17557
- Fe_{2-x}Al_{1-x}O₃ 1-8 H₂O substituted ferrihydride, Mossbauer, X-ray diffr. and electron microscopy studies 7-7617
- FeCl₃-graphite intercalates, high resolution electron microscopy 7-16433
- FeH₃(PO₄).2.5H₂O, pyrite-phosphate mixtures, X-ray phase and electron microscopy studies 7-33652
- FeNiCr, grain boundary solute segregation 7-56833
- Fe₂O₃, haematite, prep. from δ-FeOOH by thermal decomp. on grinding, X-ray diffr. line broadening 7-46390
- GaAs film on NaCl, heteroepitaxial growth and composition 7-7052
- GaAs, ion implanted, stoichiometry violation, electron microscopy studies 7-12303
- GaAs, substrates, multi-technique approach to defect microstructure characterisation 7-52215

electron microscope examination of materials continued

- GaAs/Au contacts, interface morphology 7-45020
- GaAs-Si heteroepitaxial interface, at. resolution HVEM study 7-2392
- GaAs-Si₃N₄ interface, multipolar plasma deposition, high resolution electron microscopy study 7-12499
- Ge, dislocation transmission through Σ=9 symm. tilt boundaries, synchrotron X-ray topography, HVEM obs. 7-63646
- Ge microcrystals, gas-evaporated, thermal annealing, Raman and electron microscopic study 7-64635
- Ge₂₀Sn_{80-x}Bi_x, n-type amorphous semiconductors, morphological struct. 7-51652
- GeSi-Si heterostructures, MBE grown, structural props., quality, electron diffr., imaging obs. 7-7036
- Hg_{1-x}Cd_xTe crystals., lattice defect imaging, high resolution electron microscopy obs. 7-51769
- Hg₂Cl₂ thin films, morphology and growth on Hg surface, electron beam damage 7-59469
- InP(As)(Sb) surfaces, oxidation processes studied by high-resolution electron microscopy 7-39766
- KCl (100), interaction of NaCl mol. beams with surface, desorption flux meas., SIMS obs. 7-33508
- KCl(Br), radiation defects created by decay of electronic excitations 7-16626
- La_{2-x}Ca_xMg₁₇, H₂ storage appl. 7-40052
- Mg-Gd supersaturated solid soln., precipitate cryst. struct. (*Russian*) 7-33665
- MgGa₂O₄-Mg₂GeO₄ system, spineloid phases charact. 7-37946
- MgO (100), atomic-level surface features studied by an electron-microscopic technique 7-6939
- MgO:Na, ion implanted single crystals, HREM obs. 7-12292
- MgO(Al₂O₃)₂ spinel, lateral twin boundaries struct., electron microscopy obs. and computer simulation studies 7-51783
- γ-Mn₂Ge₂, high temp. phase structs., electron microscopy obs. 7-26697
- Mo permalloy films, mag. domain walls stability, external mag. field, Lorentz microscopy 7-45780
- Mo/C multilayered structs., high resolution electron microscopy studies 7-63968
- Mo/Si multilayered structs., high resolution electron microscopy studies 7-63968
- MoO₃ thin films, amorphous, vacuum deposited, struct. 7-51635
- NaCl, crystal growth from vap., 2D nucleation 7-16467
- NaY zeolite, Au impregnated, positron lifetime spectra 7-17358
- Nb:He⁺(H⁺) films, radiation defects produced by ion implantation 7-7059
- 2H-NbSe₂ surface, atomic image, scanning tunneling microscopy study 7-12423
- Nb₂Sn, heat treatment for in-situ processing, Cu, Nb, Sn, distrib. (*Chinese*) 7-12924
- NbTe₄, incommensurate state microstruct., electron diffr. pattern obs. 7-6598
- Ni base superalloys, hot deformed, matrix dislocations, weak beam electron microscopy obs. (*French*) 7-21210
- Ni, dislocation structure after US deformation, physical props. (*Russian*) 7-44699
- Ni powder metallurgical superalloy, intermetallic phase 7-16503
- Ni single crystals., low temp. recrystallisation characts. (*Russian*) 7-17546
- Ni, substructure at accelerated high temp. creep (*Russian*) 7-65096
- Ni superalloy, MAR M002, borides analysis using convergent beam electron diffr. 7-22699
- Ni-Al alloy phase transforms. during ion beam mixing, electron diffr. and microscopy studies 7-16655
- Ni-Al alloys, premartensitic behaviour, neutron scatt. study 7-44717
- Ni-Al dilute alloys, oxide growth and microstruct. at high temp. 7-17735
- Ni-Al synthesis by shock compression of composite particles 7-39462
- Ni-Al₂O₃ composites, small metal particles, high resolution electron microscopy and X-ray diffr. meas. 7-46376
- Ni-Al-B-based alloys, site occupations, APFIM and channelling studies 7-32367
- Ni-base superalloys, age hardening, ordered strengthening phase characts., electron microscopy (*French*) 7-22710
- Ni-Mn, microtwinning, β-θ martensitic transform 7-32455
- Ni-P coating, electrolytic, electron microscope obs. of struct., P content depend., amorphous layer form. 7-8157
- Ni-P films, electroless deposited, struct., electron microscopy studies 7-7041
- Ni₃Al, dislocation line stability 7-21212
- Ni₃B/Ni eutectic, SEM and HREM struct. and chem. anal. 7-17515
- Pb thin films, surface plasmon detection, attenuated total refl. meas. 7-16961
- Pb₂Ca₄(PO₄)₆(OH)₂, apatite struct., Pb substitution, HREM study 7-16530
- Pb₂Ca₄(Si₂O₇)Cl₂, apatite struct., Pb substitution, HREM study 7-16530
- PbSe films, photosensitivity mechanism 7-58923
- Pb₃(VO₄)₂, β-γ transition, intermediate modulated struct. 7-2183
- Pd (100), surface topographies, SEM and scanning tunnelling microscopy studies 7-12436
- Pd particles, multiply-twinned, direct atomic imaging 7-44565
- Pd, small metallic particles, surface fractal dimension 7-38308
- Pd-Y system, obs. of order 7-58456
- PdFe, drawing effects on elec. resist. and mech. props. (*Russian*) 7-17584
- PdFe ordered alloy, discontinuous domain coalescence (*Russian*) 7-2025
- Pd₈₁Si₁₉, glassy, surface topographies, SEM and scanning tunnelling microscopy studies 7-12436
- Pr₂O₃, related structs., in HREM study 7-16531
- Pt (100) surface, defect struct. rel. to catalytic behaviour, scanning tunnelling microscopy study 7-6930
- Pt microcrystals, charact. using high resolution electron microscopy 7-32676
- Pt small crystals, atomic-resolution study of struct. rearrangements 7-32243
- Pt, small metallic particles, surface fractal dimension 7-38308
- Pt-Al₂O₃ composites, small metal particles, high resolution electron microscopy and X-ray diffr. meas. 7-46376
- Pt-W, Pt diffusion and platelet defect form. (*Russian*) 7-44895
- Pt-Zr internally oxidised alloys, morphology, struct. and stability (*Russian*) 7-33687
- Re₂B₃, inverse boundaries, rel. to defects in M₇C₃ carbides 7-12083
- Ru₂B₃, inverse boundaries, rel. to defects in M₇C₃ carbides 7-12083
- Sb layers, amorphous phase stability rel. to metal overdeposits 7-52324

electron microscope examination of materials continued

- Sb₂S₃-PbS systems, non-stoichiometric phases close to Sb₂S₃, structure 7-32674
- Si (100) surface, atomic terraces and steps, refl. electron microscopy obs. 7-52211
- Si (111), Ar ion bombardment, RHEED and REM studies 7-32511
- Si (111), atomic-level surface features studied by an electron-microscopic technique 7-6939
- Si bicrystals obtained by solid-phase intergrowth, interface region struct., electron microscopy 7-45023
- Si crystal, electron microdiffraction patterns, image reconstruction 7-6487
- Si, dislocation transmission through $\Sigma=9$ symm. tilt boundaries, synchrotron X-ray topography, HVEM obs. 7-63646
- Si films, structural changes due to annealing 7-52346
- Si, lattice images, screening effect 7-51592
- Si, ramp assisted foil casting and photovoltaic appls. 7-16609
- Si, self-implanted, defects and amorphisation 7-2041
- Si, zone-axis critical voltages in HEED, accidental Bloch wave degeneracies obs. 7-63409
- Si-Au, U- and W-shaped impurity diffusion profiles investigation 7-16805
- Si-B plastically deformed crysts., dislocation struct. and elec. activity, annealing effects study 7-37998
- Si-B-Mo interface, specimen preparation by chemical etching and polishing, for electron studies 7-29989
- Si-H binary alloys, crystallisation of polysilane 7-21105
- a-Si:H/ α -SiN_x:H superlattice interface struct. charactn. 7-58652
- Si-O, ion implanted, octahedral oxide particle nucleation and growth 7-16776
- Si-O, self-interstitial migration, dislocation loops and elongated Frank dipoles 7-58300
- Si-Tl ion implanted layers, defect form. and precipitation, electron microscopy studies 7-12097
- a-Si/c-Si interface, microcrystallites and orientational proximity effect, HREM image interpretation, comment and reply 7-45028
- Si-Si interfaces, MBE grown, sputter cleaned, microstructure, electron microscopy obs. 7-12512
- SiAlON composites, interfacial microstruct. 7-16429
- β -SiC epitaxial layers, cubic cryst. struct., electron diffr. and microscopy studies 7-27199
- SiC polytypes, lattice imaging studies on struct. and disorder 7-37933
- β -SiC powder, sintering, phase transform. rel. to additives (*Japanese*) 7-17527
- SiC short fibre filamentary crystals., phase comp. and morphology 7-65010
- a-SiN_x:H-Si:H, multilayer struct. study using HREM 7-16879
- Si₃N₄, grain boundary phases, EM anal. 7-16569
- Si₃N₄, nanostruct. defects, high-resolution electron microscopy studies 7-12302
- Si₃N₄:AlN, grain boundary phases, EM anal. 7-16569
- Si₃N₄:Y₂Al₂O₇, grain boundary phases, EM anal. 7-16569
- a-SiO₂, electron microdiffraction patterns, image reconstruction 7-6487
- SiO₂ evaporated and ion assisted deposited coatings, microstruct., electron microscope obs. 7-52335
- SiO₂, modulated phase, electron microscopy study 7-26937
- Sn-In-S ternary system, cryst. growth and charact. (*French*) 7-33645
- SnO₂, amorphous film, vacuum prep., struct., crystallisation 7-53594
- Sr₂Mn_{2-x}Ti_{1+x/2}O_{5+x/2}, struct. and defects 7-44490
- Sr₂SiO₄, β to α' to β transformation, electron microscope study 7-16723
- SiO₂ evaporated and ion assisted deposited coatings, microstruct., electron microscope obs. 7-52335
- TbFe films, micron-size laser-written mag. domains, Lorentz microscopy 7-2913
- TbO₂, anion deficient, surface topography, atomic imaging 7-27079
- TeO₂-ZnCl₂ system, glass prep. and composition 7-46403
- Ti alloys, ω -phase, special features of twinning (*Russian*) 7-44570
- Ti, implantation-induced textures, electron diffr. and microscopy studies 7-46507
- Ti, pure, plate, yield strength, H content depend. (*Chinese*) 7-8044
- Ti-Al-V, pseudo-alpha alloys, BCC lattice hydrides (*Russian*) 7-53751
- Ti-Mo, omega transition anal. 7-16737
- Ti-Ni (51 at.%), aged shape memory alloy, precip. morphology, comp., cryst. struct. 7-28049
- Ti_{1-x}Al_{3-x}, long period struct. 7-16500
- Ti₃Al-Nb-Er rapidly solidified alloy, microstruct. effects and dispersoid stability 7-22669
- TiC, ultrafine powder behaviour during annealing and sintering 7-3244
- TiN powders, fine, prep. by vap. phase reaction (*Korean*) 7-7938
- TiN(C) hard reactively sputtered and evaporated coatings, composition and microstruct. studies 7-52331
- TiNi alloy, amorphisation by high press. shear deform. (*Russian*) 7-8053
- TiNi-Ge, premartensitic effects (*Russian*) 7-53692
- TiNi-X, X=Fe, Ge, Re or Ni, struct. transitions in premartensitic range (*Russian*) 7-39504
- TiO₂ evaporated and ion assisted deposited coatings, microstruct., electron microscope obs. 7-52335
- TiO₂, amorphous reactive ion beam deposition, crystallisation 7-45091
- (Ti_{1-x}V_x)₂Ni, orientation relationship between the icosahedral and crystalline phases 7-16477
- U₃O₈, superstructure and surface images 7-16532
- V film, B ion implementation, phase changes, electron microscopy study 7-12169
- V₃Si/V₂Si₃ interface, crystallography of matrix-precip. interface and elastic strain field (*French*) 7-65036
- W/C multilayered structs., high resolution electron microscopy studies 7-63968
- W/Si multilayered structs., high resolution electron microscopy studies 7-63968
- WC-Co composite, grain boundary films, mean inner pot. determ. by Fresnel technique 7-16431
- WO₃ electrochromic films, obliquely deposited, elec. props. and morphology 7-7781
- Zn_{1-x}Fe_{2+x}O₄, shock synthesised, electron microscopy 7-37955
- ZnP₂, crystal structures and microphases, devil's staircase 7-11982
- ZrN(C) hard reactively sputtered and evaporated coatings, composition and microstruct. studies 7-52331
- ZrO₂ ceramic, grain boundaries, microanal. 7-16577
- ZrO₂/Al₂O₃ ceramic incoherent interface struct. 7-16430
- ZrO₂/mullite composite ceramic, grain boundary HREM study 7-16427
- ZrTe₅, struct. polytypes 7-51718

electron microscopes

- see also *electron microscopy; field emission electron microscopes; scanning electron microscopes; scanning-transmission electron microscopes; transmission electron microscopes*
- 400 kV high resolution analytical electron microscope, advantages, appl. 7-15037
- aberration shift relations, matrix derivation 7-18938
- astigmatism in electron microscope, detection using radon transform (*Japanese*) 7-18931
- asymmetrical unsaturated magnetic electron lenses, focal props. calc. 7-31236
- development and electron optics 7-41049
- high resolution 400 kV electron microscope 7-15038
- imaging bandpass electron energy analyser 7-375
- lens, saturated objective, electron opt. parameters computation 7-18937
- electron microscopy**
- see also *electron microscope examination of materials; electron microscopes; field emission electron microscopy; metallography; scanning electron microscopy; scanning-transmission electron microscopy; scanning tunnelling microscopy; specimen preparation; transmission electron microscopy*
- 3D reconstructions of individual particles 7-41546
- AEI contribution in UK 7-4926
- atomic resolution electron microscopy in perspective 7-15036
- atomic structure models, electron microscope images, computer simulation 7-16380
- Australian historical background 7-4928
- automatic image binarisation in electron microscopy (*French*) 7-36900
- autoradiography, quantitative, multiple linear regression analysis application 7-60141
- autoradiography intensification by enhancer ENLIGHTNING 7-368
- biological, beam damage, contrast, noise 7-8783
- biological macromolecules, anomalous member identification of noisy image set 7-13957
- biological specimen visualisation by cryoHVEM 7-40380
- carbon, electron microscopy, past, present, future 7-16379
- Cliff-Lorimer k_{AB} factors at zero foil thickness, extrapolation method 7-39935
- coincidence counting techniques in analytical electron microscopy 7-23104
- conference, electron microscopy and anal. Newcastle-upon-Tyne, England, (Sept. 1985) 7-14707
- contrast of electron microscopic images, enhancement by optical shadow method 7-48916
- curved filamentous structures, image straightening algorithm 7-11865
- defocused images, atomic-level surface features 7-11863
- dynamical diffr. calcs., surface struct. anal. 7-32232
- EELS, chemical analysis in electron microscope, book 7-55903
- electron beam damage estimation in microscopy 7-16634
- electron holography approaching atomic resolution 7-43018
- electron-acoustic microscopic study on dislocation lines in the base region of n-pn Si-Tr 7-20538
- electrostatics, of insulators charged by electron beams 7-41540
- energy deposition by X-rays and electrons, microscopy implications 7-38064
- energy dissipation processes in scanning tunneling microscopy 7-1827
- energy loss probability, fast electron self energy 7-63411
- fine-particle beam experiments 7-30133
- heat sensitive materials, C coating for heat damage prevention 7-22864
- high contrast phase electron microscopy, improved method 7-35643
- high performance two-electrode electron gun lens, microscopy appls. 7-5827
- high resolution, ion beam sputtering characts. 7-4930
- high resolution, study of amorphisation of intermetallic compounds 7-44377
- high resolution electron microscopy in materials science (*German, English*) 7-39806
- high resolution electron microscopy of small particles 7-1824
- high-resolution, image deconvolution using direct method 7-11860
- holographic interferometry, quantitative phase anal. and magnetic field meas. appl. 7-41538
- HVEM, materials characterisation, critical voltage effect 7-37819
- image reconstruction, geometrical transformation groups for 3D object 7-371
- low-temperature embedding of biological tissue 7-23496
- mammalian tissues, particulate radiation damage, electron microscopy appls. 7-28623
- materials science, use of high resolution electron microscopy 7-35641
- materials science appls. of electron microscopy 7-44324
- medium voltage analytical electron microscopy, radiation damage effects 7-15039
- membranes with locatable single pores generation, obs. and testing 7-298
- metallurgical appl. of electron microscope in Cambridge 7-4927
- molecule images reconstitution, correspondence analysis, struct. interpret. tool 7-60138
- multibeam effects in convergent beam (*French*) 7-44322
- oxide scales, chem. mapping using electron energy loss imaging microscope 7-37812
- photoelectron microscopy, applications to biological surfaces 7-8773
- point-contact imaging, atomic resolution 7-21048
- probe-forming lens, axial geometrical aberrations meas. by means of shadow image of fine particles 7-42882
- quasi-periodic lattice structures, dynamical calcs. 7-16370
- quasi-real space image simulation in high resolution electron microscopy (*Chinese*) 7-37810
- radioactive effluent monitor sample lines, radioactive and electron microscopy analysis 7-42116
- real colour microscopy 7-35642
- scanning tunneling microscope, development and operation 7-372
- scanning tunneling microscopy applied to optical surfaces 7-4929
- scanning tunnelling microscopy, current saturation through image surface states 7-7320
- solid surfaces, chemistry and physics, book 7-60891
- specimen thickness determination in electron microscopy 7-9928
- squeezable tunnelling junctions 7-7447
- stereoscopic photograph quality improvement 7-18928
- styrene-isoprene block copolymers, mol. architecture effect, phase separation 7-38212
- submicron techniques, conf., Nova Scotia, Canada (July-Aug. 1984) 7-35104

electron microscopy continued

- successive generations of electron microscopists 7-41045
- surface anal. methods (*Japanese*) 7-63921
- surface structure, electron microscopy, review 7-51593
- three-dimensional morphometric cytology, pictorial pattern recognition 7-28801
- three-dimensional reconstruction of objects characterised by linear elements 7-56377
- three-dimensional scanner for scanning tunnelling microscopy 7-376
- UK involvement in development 7-4925

electron mobility

- see also carrier mobility; electron mobility (metals)*
- diffuse discharge switching appls., temp. depend. electron transport studies 7-32189
- electron swarms in gases, vel. distrib. function and transport coeffs. 7-1663
- gases, dense, electron mobility, Ioffe-Regel and Mott criteria 7-26382
- gases, positron diffusion and annihilation rates 7-37621
- halocarbons, electron attachment influence on zero-field electron mobility in Ar 7-20833
- methane ($-d_4$), gas, electron swarm characteristic energies 7-63388
- methyl bromide, thermal electron attachment and diffusion 7-20837
- pentane isomers, ionis. and electron thermalisation distances, mol. shape and density effects 7-50347
- plasma, laser prod., magnetised electron transport, bifurcation 7-44208
- Ar-perfluorocarbon systems, time-dependent electron mobilities calcs. 7-20835
- CO, electron mobility to diffusion coeff. ratio meas. 7-20840
- H_2S , gas, electron swarm characteristic energies 7-63388
- He gas, positron mobility edge, Monte Carlo simulation 7-44086
- He, positron thermalisation and annihilation 7-63245
- N_2 , lateral diffusion coefficient to electron mobility ratio meas. 7-20829
- Ne positron thermalisation and annihilation 7-63245
- $SiH_4(D_4)$, gas, electron swarm characteristic energies 7-63388

electron mobility (metals)

- metals, plasmon linewidth, memory-function approach 7-45193

electron mobility (semiconductors and insulators) *see carrier mobility***electron-molecule collisions *see elastic scattering of electrons by atoms and molecules; molecular electron impact dissociation; molecular electron impact excitation; molecular electron impact ionisation*****electron multipliers**

- soft X-ray imaging with high-gain MCP detector systems 7-41564
- $(CO_2)_n^+$ cluster ions, recording by secondary electron multiplier 7-42827

electron nuclear double resonance *see ENDOR***electron-nucleon interactions**

- see also electron-nucleon scattering; electron-proton interactions*
- ed interactions, nonperturbative QCD corrections to $R=\sigma_L/\sigma_T$, use of MIT bag model 7-481
- $eN \rightarrow axion$, production in heavy targets 7-49155
- $eN \rightarrow e\Delta$, high Q^2 , $N-\Delta$ form factors, perturbative QCD anal. 7-19119
- $eN \rightarrow eN + axion$, search for axion-like particles in electron bremsstrahlung 7-24891
- $e^-N \rightarrow X$, axion bremsstrahlung 7-530
- ep interactions, nonperturbative QCD corrections to $R=\sigma_L/\sigma_T$, use of MIT bag model 7-481

electron-nucleon scattering

- see also electron-nucleon interactions; electron-proton scattering*
- 2N, 0.1-1.0 GeV^2/c^2 , nucleon magnetic moment and effective hadronic degrees of freedom 7-24973
- $\bar{e}N \rightarrow eN$, polarization expts. at CEBAF 7-35999

electron-nucleus reactions

- for inelastic electron-nucleus scattering, see "electron-nucleus scattering"*
- see also electron-nucleon interactions; nuclear electron capture*
- conf., Leningrad, USSR, April 1985 7-29574
- conf., Washington, DC, USA, April 1986 7-60881
- deep inelastic scatt., vector meson dominance and EMC effect 7-30317
- NIKHEF-K, future exptl. developments for few body physics 7-61859
- scattering of electrons, nucleons, and pions as probes of nuclear structure, review 7-56593
- Δ production in nuclei by electrons and photons 7-49358
- (e^- , axion), stellar axion production mechanism 7-24974
- (\bar{e}, e^+), many-body theory calcs. 7-41983
- (e, e^+), quasi-free knockout, nucl. medium effects on photon-proton vertex 7-35997
- (e, e^+), deep inelastic scatt., nuclear binding and Fermi motion effects on $R_A=\sigma_L/\sigma_T$ 7-49232
- $^{209}Bi(e, f)$, absolute cross section meas. in 43-250 MeV range 7-5301
- $Bi(e, fission)$, fragment activity from delayed fission 7-42092
- $^2H(e, e^+N)$, nucleon momentum distrib. using y-scaling 7-5226
- $^2H(\bar{e}, e^+N)$, d disintegration by pol e^- , neutron electric form factor 7-61862
- $^2H(\bar{e}, e^+n)^1H$, neutron electric form factor 7-35880
- $^2H(\bar{e}, e^+pn)$, proton polarisation and neutron electric form factor (*Russian*) 7-15212
- $^2H(e, epn)$, final state interaction effects 7-5100
- $^2H(e, p n)$, hybrid-quark-hadron model anal. 7-56673
- $^3H(e, X)$, inclusive electron scatt. expts. 7-61867
- $^3H(e, 2np)$, longitudinal and transverse response fn. meas. 7-61863
- $^2He(e, e^+n)$ cross section calcs., six-quark cluster effects 7-655
- $^3He(e, e^+2p)$, role of correlations, final state interactions and meson exchange 7-56668
- $^3He(e, X)$, inclusive electron scatt. expts. 7-61867
- $^3He(e, X)$, many-body effects in inclusive and exclusive scatt. 7-61866
- $^2He(e, 2pn)$, longitudinal and transverse response fn. meas. 7-61863
- $^3He(e, e^+N)$, nucleon momentum distrib. using y-scaling 7-5226
- $^3He(e, e^+N)$, electrodisintegration coincidence cross section, final state interaction anal. 7-36000
- $^3He(e, e^+X)$, electrodisintegration, PWIA 7-61865
- $^3He(e, e^+d)^1H$, 500 MeV, 3He spectral fn. dependence on relative p-d energies, $^3He(e, e^+p)$ comparisons 7-56672
- $^3He(e, e^+p)^1H$, 500 MeV, 3He spectral fn. dependence on relative p-d energies, $^3He(e, e^+d)$ comparisons 7-56672
- $^AIn(e, X)$, $A=113, 115$ cross-sections for deep-spallation reactions 7-41976
- $^6Li(e, e^+d)$, 480 MeV, 6Li ground state, α -d momentum distrib. 7-24975
- $^6Li(e, \pi^+ e^+)e^+He$, elastic pion electroproduction, differential cross section 7-41980

electron-nucleus reactions continued

- $^{93}Nb(e, X)$, spallation cross section meas. using activation methods 7-30412
- $^{28}Si(e, e^+p)$, coincidence studies in the giant resonance region 7-49384
- $^{28}Si(e, e^+n)$, coincidence studies in the giant resonance region 7-49384
- $Ta(e^+, e^+)$, 1.9 MeV, peak structure in kinetic energy spectra 7-30414
- $^{238}Th(e^+, e^+)$, 1.9 MeV, peak structure in kinetic energy spectra 7-30414
- $^{238}U(e, e^+f)$, 5-23 MeV, coincidence cross section meas. 7-19240
- $U(e, e^+f)$, fission decay of giant multipole resonances, coincidence study 7-49360
- $^{51}V(e, e^+p)^{50}Ti$, spectroscopic strength of $1f_{7/2}$ transitions 7-15211
- $^{90}Zr(e, e^+p)$, 2p proton knockout, momentum distrib., optical pot. anal. 7-61849

electron-nucleus scattering

- see also electron-nucleon scattering*
- $^AO(e, e^+)$, $A=16, 18$, form factors and transition charge densities 7-35942
- conference on nuclear scatt. data eval. methods, Berlin, Germany (June 1985) 7-21
- electronuclear structure functions and quark deconfinement in nuclear matter 7-5177
- longitudinal response quenching in nuclei due to gluon condensate modification 7-49279
- model independent exchange current determ. for few nucleon systems 7-35743
- quasielastic scatt., probe of three body structure 7-61869
- (e, e), inverse problem for data eval., max. entropy method 7-618
- (e, e), model independent densities from scatt. data, form factors 7-657
- (e, e^+), 0.1-1.0 GeV^2/c^2 , nucleon magnetic moment and effective hadronic degrees of freedom 7-24973
- (e, e^+), many quark effects, phenomenological anal. 7-49387
- (e, e^+), model independent DWBA anal., recoil corrections 7-658
- (e, e^+), new M1 mode, properties 7-49299
- (e, e^+), nuclear medium effects on nucleon size 7-56599
- (\bar{e}, e^+), polarization expts. at CEBAF 7-35999
- (\bar{e}, e^+), Y-scaling, FSI and scaling variables 7-56560
- $^3Be(e, e^+)$, parity violation meas. in quasielastic electroweak scattering 7-49388
- $^{12}C(e, e^+)$, longitudinal charge response, RPA calcs. 7-56669
- $^{12}C(e, e^+)$, longitudinal charge response in quasielastic region, RPA approach 7-61861
- $^{12}C(e, e^+)$, relativistic RPA response function for quasielastic scatt. in local density approx. 7-41984
- $^{12}C(e, e^+)m$ nuclear structure fns., anal. using multiple scatt. theory 7-24972
- $^{12}C(e, e)$, dispersive effects in form factor meas. 7-5227
- $^{13}C(e, e^+)$, 78-338 MeV, M4 excitations, cross section meas., shell model anal. 7-19195
- $^{14}C(e, e^+)$, form factors and stretched M4 configurations, shell model comparisons 7-41981
- $^{A}Ca(e, e^+)$, $A=40, 48$, relativistic RPA response function for quasielastic scatt. in local density approx. 7-41984
- $^{40}Ca(e, e^+)$, longitudinal charge response, RPA calcs. 7-56669
- $^{40}Ca(e, e^+)$, longitudinal charge response in quasielastic region, RPA approach 7-61861
- $^{19}F(e, e^+)$, form factor calcs. using projected Hartree-Fock function 7-30413
- $^{56}Fe(e, e^+)$, longitudinal charge response, RPA calcs. 7-56669
- $^{56}Fe(e, e^+)$, longitudinal charge response in quasielastic region, RPA approach 7-61861
- $^{150}Gd(e, e^+)$, diff. cross section, $K^*=1^+$ mode structure from DWBA anal. 7-41876
- $^{150}Gd(e, e^+)$, orbital mag. dipole strength distrib., resonance fluoresc. meas. 7-10104
- $^2H(e, e^+)^2H$, transverse quasielastic scattering, cross-sections 7-49379
- $^2H(e, e^+)$, nucleon momentum distrib. using y-scaling 7-5226
- $^2H(e, e^+)$, future experiment at ELSA stretcher ring 7-61860
- $^2H(e, e^+)^3He$, EM radii determ., tensor polarisation meas. 7-49383
- $^2H(e, e^+)^-$, tensor polarisation and spin observables as perturbative QCD test 7-35998
- $^3H(e, e^+)$, EMC effect and high Q^2 three body physics at SLAC 7-56674
- $^3H(e, e^+)$, NN interactions for bound state wave function calcs. 7-5162
- $^3H(e, e^+)$, cross section meas. 7-61863
- $^3He(e, e^+)$, EMC effect and high Q^2 three body physics at SLAC 7-56674
- $^3He(e, e^+)$, longitudinal spectra in the low-energy scheme 7-41986
- $^3He(e, e^+)$, M1, M2 transition strength search using 180° scattering 7-61864
- $^3He(e, e^+)$, NN interactions for bound state wave function calcs. 7-5162
- $^3He(e, e^+)$, nucleon momentum distrib. using y-scaling 7-5226
- $^3He(e, e^+)^3He$, quasielastic scatt., y-scaling function from PWIA 7-61868
- $^3He(e, e^+)$, cross section meas. 7-61863
- $^AHe(e, e^+)^AHe$, $A=3, 4$ effect of hidden colour 7-49382
- $^6Li(e, e^+)Li$, cluster distortion effects on EM props. 7-49381
- $^{14}N(e, e^+)$, 2.313 MeV state, transverse scatt. form factors and phenomenological wave fn. 7-41982
- $^{14}N(e, e^+)$, form factors and stretched M4 configurations, shell model comparisons 7-41981
- $^{14}N(e, e^+)$, ground state, transverse scatt. form factors and phenomenological wave fn. 7-41982
- $^{40}O(e, e^+)$, $A=17, 18, 15-23$ MeV, excitation of M4 transitions, form factor meas. 7-19238
- $^{A}Pb(e, e^+)$, $A=204, 206-208, 502$ MeV, charge density differences meas. 7-41890
- $^{208}Pb(e, e^+)$, high spin state form factor calcs. 7-49218
- $^{208}Pb(e, e^+)$, isoscalar quadrupole giant resonance, electron spectra statistical anal. 7-49380
- $^ASe(e, e^+)$, $A=78, 80$, differential cross section meas. and phase shift anal. 7-41985
- $Ta(e^+, e^+)$, 1.9 MeV, peak structure in kinetic energy spectra 7-30414
- $^{238}Th(e^+, e^+)$, 1.9 MeV, peak structure in kinetic energy spectra 7-30414
- $^{238}U(e, e^+)$, 280-500 MeV/c, response fns., Rosenbluth separations 7-19239

electron optics

- see also beta-ray spectrometers; electron beams; electrostatic lenses; ion optics; magnetic lenses; particle optics*
- aberration corrector 7-20124
- aberration shift relations, matrix derivation 7-18938
- aberration theory, relativistic for electron beam in combined electromagnetic focusing-deflection system with spherical cathode 7-62613

electron optics continued

- aberration theory for electron beams combined in focusing system with spherical cathode 7-62612
- aberration theory for electrostatic round lenses, multipole lenses and deflectors 7-1021
- asymmetrical unsaturated magnetic electron lenses, focal props. calc. 7-31236
- BESSY multipole magnet, electron opt. props. and electron trajectories 7-42254
- cathode lenses, design, Pontryagin's max. principle 7-42885
- charged-particle beams, trajectory based phase-space anal. 7-42886
- combined electric-magnetic focusing-deflection system, relativistic fifth order geom. aberration eqn. 7-10838
- combined electrostatic focusing-deflection systems, asymptotic aberrations 7-10835
- dynamics, in plane travelling wave in steady mag. field (*Russian*) 7-62614
- electron holography approaching atomic resolution 7-43018
- electron microscope development and electron optics 7-41049
- electron microscopes astigmatism detection using radon transform (*Japanese*) 7-18931
- electrostatic cathode lenses, design, Pontryagin's max. principle 7-42884
- electrostatic electron-beam deflectors, comparison of electron optics 7-18910
- electrostatic systems, fast charge-simulation procedure for electron-optical props. determ. 7-42881
- grid shutter in a vacuum photorecorder 7-18914
- heavy-current cathode for X-ray tubes with electrostatic focusing (*German*) 7-24740
- imaging bandpass electron energy analyser 7-375
- lens, saturated objective, electron opt. parameters computation 7-18937
- magnetic focusing and deflection systems of camera tubes (*Chinese*) 7-10837
- matrix lens, aberrations reduction using offset apertures 7-20122
- misalignment of electron lenses, influence on image quality 7-20123
- positron optics and expts. with electrostatically focused positron beams 7-62615
- post-acceleration systems in electron-beam devices, props. calc., approximate method 7-42888
- probe design, miniature variable energy, for nanometric analysis, electron opt. parameters 7-18939
- probe-forming lens, axial geometrical aberrations meas. by means of shadow image of fine particles 7-42882
- resolution function of CMA systems used for Auger signal measurements 7-30119
- STEM objective lens, high excitation, Munro programs data variations effect on predicted opt. props. 7-18933
- TEM image quality criteria, appl. on thin phase objects (*German*) 7-56379
- TEM lens shape with min. spherical aberration coeff., computation method 7-18936
- variable-aperture systems, field calcs. 7-42883
- Young's double hole interference experiments with ahairpin cathode electron gun 7-1020

electron pair annihilation *see electron-positron inclusive interactions***electron pair production**

- Cyg. X-1 and related sources, electron pair prod. rel. to bimodal spectral behaviour 7-9510
- fermion field operator expansion 7-9988
- heavy leptonium, radiative corrections to one-photon annihilation leptonic decays 7-35871
- nuclear internal-pair-transitions, restrictions on 1.7 MeV axion production 7-19200
- oriented crystals, electron-positron pair production by high energy photons 7-46173
- QED, intense external field intensity problems 7-49046
- quantum effects of elementary particle interaction with intense EM field 7-49045
- radio pulsars, pair creation rel. to return-current mode changes and normal-null transitions 7-14598
- relativistic heavy ion collisions, EM processes, giant resonances, π and e^+e^- prod. 7-19270
- resonant prod. in heavy ion collisions, QED external field problem 7-5038
- stellar interiors, pair creation instability in massive high-luminosity stars 7-29461
- supernovae, element abundances from pair creation supernova in massive Wolf-Rayet star 7-29462
- X-ray binary systems, pair prod. rel. to ultra-high-energy gamma-ray emission 7-47971
- X-ray sources, effects of one-generation pair production in synchrotron self-Compton sources 7-55452
- e^+e^- peaks, constraints on nuclear transitions, axions and particle interpretation 7-35776
- γ -monopole \rightarrow monopole $+e^+e^-$, energy spectrum calcs. 7-56582
- NN \rightarrow X EM production of spinless neutral particles 7-544
- $\pi^0 \rightarrow e^+e^- \gamma$, two-photon-exchange contribution calcs. 7-61653
- $\Psi \rightarrow e^+e^-$, $R_2 = \Gamma(T \rightarrow e^+e^-) / \Gamma(\Psi \rightarrow e^+e^-)$ calcs. bound state quark model anal. 7-61582
- $T(2S) \rightarrow \gamma \chi_b$, $\chi_b \rightarrow \gamma T(1S) \rightarrow e^+e^- (\mu^+\mu^-)$, branching ratio meas. 7-19102
- $T \rightarrow e^+e^-$, $R_2 = \Gamma(T \rightarrow e^+e^-) / \Gamma(\Psi \rightarrow e^+e^-)$ calcs., bound state quark model anal. 7-61582
- $\gamma\gamma \rightarrow e^+e^-$, cross section oscills., external field effects 7-30302

electron pairs

- see also electron pair production; positronium*
- two-temperature plasma cloud, electron-positron pair equilibria, stability analysis 7-40677

electron paramagnetic resonance *see paramagnetic resonance***electron-phonon interactions**

- see also phonon drag; strong-coupling superconductors; tunnelling spectra; tunnelling spectroscopy; Umklapp process*
- 1D, with commensurability 3, numerical study of fractionally charged states 7-52445
- 1D electron-phonon systems, nearly quarter-filled, CDW struct. 7-45186
- 1D electron-phonon systems, quarter-filled, solitons 7-45179
- 4d x Pb, phonon density of states from heat capacity temp. depend., inverse problem 7-6736
- A15 cpds., normal, long-wavelength static spin suscept., temp. depend., electron-phonon interaction effects 7-64103

electron-phonon interactions continued

- A_2B_{1-x} BCC alloys, low temp. props., spin fluctuations, alloying effects 7-52402
- Aharonov-Bohm effect, influence of electron-phonon interaction 7-21895
- β -(BEDT-TTF) $_2I_3$ /Cu point contact spectra 7-27383
- bipolaron formation, Monte Carlo computer simulation studies 7-27268
- Chatterjee-Mitra transform., appl. to electron-phonon interaction 7-7131
- cohesion of solids under very high electronic excitation 7-51696
- conductive thin films, Nernst-Ettinghausen effect, nonmonotonous behaviour in strong transverse mag. field 7-2632
- conjugated polymers, impurities, nonlinear dynamics 7-64115
- degenerate semiconds., anisotropic hot carrier distrib., transport eqn. solns. anal. 7-58815
- dense Kondo heavy fermion systems, Cooper pairs attractive interactions freq. depend. 7-58951
- diamond, brown, vibronic coupling to nearly localised modes in luminescing bands 7-51980
- dimer-lattice phonon interaction, lattice relax., exciton and electron condition terms 7-7130
- dirty metals, conduction electron inelastic lifetime, nonlocalisation method studies 7-64210
- dirty semiconductors, parametric cyclotron resonance, inelastic electron scatt. from phonons 7-2466
- disordered media, small polaron charge transport model, density-matrix formalism calcs. 7-52612
- disordered metals, 1D, thermal effects in spatial dispersion of conductivity 7-38549
- DMTCF salts, electronic and vibr. absorption spectra, electronic correlations 7-46034
- doped crystals, phonon mechanism of phase relax. of electron excitation 7-38464
- double quantum well structs., parallel electron transport studies 7-45474
- electron excitations, energy transport, luminesc. of impurity pairs, modelling 7-2508
- electron gas, galvanomag. props., interaction effects, applied electric and mag. fields 7-52477
- electron gas, localisation effects, Keldysh representation 7-52529
- electron-electron scatt., energy loss to phonons, integral eqn. 7-52478
- electronic relaxation, infinite order effects and non-Markovian theory 7-51974
- ferroelectrics, nonequilibrium state, phase transitions in electromagnetic fields 7-33340
- ferromagnetic semicond., donor state, thermally induced abrupt shrinking 7-52510
- ferromagnetic semiconductors, hot magnons 7-22099
- field theoretical approach to solid state physics 7-12934
- fractionally charged states in quarter-filled electron-phonon systems 7-52446
- free electron distrib., parabolic band, Landau level population inversion in crossed elec. and quantising mag. fields 7-38472
- graphite, relax. time, parametrisation 7-2513
- heavy electron coupling to lattice, US attenuation meas. 7-2129
- heavy fermion systems, Gruneisen parameter electron-phonon coupling 7-2138
- heavy fermion systems, itinerant f-electron model 7-38808
- II-VI semiconductors, shallow donor problem, pseudopot. approach 7-45216
- III-V semiconductors, negative magnetoresistance and nonequilib. electron cooling 7-17042
- impure metals and superconductors, electron-phonon interaction 7-38143
- insulating crystals, weakly coupled electron-phonon systems, nonequilibrium phonons, quantum mech. Boltzmann eqn. 7-2128
- laser interactions with condensed matter, review 7-12125
- layer inhomogeneous semiconds., hot electron effects, N-type current-voltage characts. calcs. 7-38689
- liquid methane, mobility of injected electrons, calc. 7-38564
- magneto-optical absorpt. of polarons 7-39094
- mean field approx. for fermion or pseudo-spin boson interaction 7-32590
- metallic alloys and cpds., phonon point contact spectroscopy, review (*Russian*) 7-12788
- metallic thin films, electron scatt. times, magnetoresist. studies 7-64369
- metals, DC transport 7-17010
- metals, dirty, electron-phonon scatt., collision rates 7-64235
- metals, electronic sp. ht., finite conduction electron lifetime correction calcs. 7-16784
- metals, sound attenuation by electrons 7-63747
- metals, strongly coupled, universal disorder-induced resistivity behaviour 7-21954
- metals and alloys, thermal conductivity theory, Lorenz ratio 7-45272
- mixed stack charge transfer crystals, regular dimerized stack, neutral ionic instability 7-51698
- mixed-stack cpds., electronic states, soliton structs. 7-52451
- mixed-stack organic charge-transfer crystals, regular-dimerised stack and neutral-ionic interfaces 7-7216
- molecular polaron with q^2 coupling, mean-field approx. 7-16958
- molecular system, complete vibronic Hamiltonian, hidden superconductivity 7-52887
- narrow energy band systems, insulator-metal transition 7-38455
- nondegenerate semiconds., charged dislocation hole capture, hole thermal ionisation and free density calcs. 7-38574
- nonlinear problem, Schrodinger eqn. and fractal dims. 7-7129
- nonradiative multi-phonon transition rate from different electronic bases, numerical evaluation 7-22326
- one-dimensional CDW states, self-similar band structure and electron-phonon coupling 7-21833
- one-dimensional conductors, electron-phonon backscatt. and phonon dynamics calcs. 7-38468
- one-dimensional electron-phonon Peierls condensate, amplitude solitons 7-52449
- one-dimensional electron-phonon system, CDW structure 7-52444
- one-dimensional electron-phonon system (*Rumanian*) 7-16960
- one-dimensional Peierls system, Eilenberger equation studies 7-64040
- one-dimensional polaron model, collective excitation spectrum, quantum inverse scatt. method calcs. 7-12625
- ordered binary alloys of isovalent metals, superconducting transition temp., conc. depend. (*Russian*) 7-64386
- organic mixed crystals, impurities optical dephasing temp. and freq. depend. 7-22286
- Peierls-Hubbard model, exact and approximate solns. 7-52383
- perylene in microcryst. n-heptane, selectively laser excited in phonon side-band, stimulated emission 7-33415

electron-phonon interactions continued

- phonon-assisted hopping, higher-order memory effects 7-16956
 piezo-electric polaron, mobility at low temps. 7-7127
 polar semicond., carrier-carrier interaction and picosecond phenomena 7-45309
 polar semiconductors, negative momentum relaxation rate and transport 7-12712
 polar semiconductors, quasi-2D, hot carriers 7-12807
 polaronic states in a slab of a polar crystal 7-2512
 polyacenic skeletons, low temp. ordered states, superconductivity 7-64396
 polyacetylene, CDW, interaction and disorder 7-64136
 polyacetylene, Coulomb correlations, optical gap 7-64142
 polyacetylene, ground, excited, polaronic, solitonic and impurity states calcs., doping effects 7-45131
 polyacetylene, Raman scatt. from CDW, ab initio calcs. 7-46015
 trans-polyacetylene, soliton-lattice to polaron-lattice transition 7-64117
 polyacetylene, solitons and IR-active localised vibrational states, Su-Schrieffer-Heeger model calcs. 7-2134
 polydihalogenoacetylene, bond alternation and solitons 7-63511
 polyyne infinite chain, solitons, polarons and phonon spectrum calcs. 7-12626
 pyrene-biphenyl mixed crystals., local heating, phonon modes and Dicke optical superradiance (*Russian*) 7-13178
 quantum well ground state, 2D gas; electron temp. and energy losses 7-17092
 quarter filled band systems, 1D, solitons 7-45181
 quasi 2D electron gas in quantum well, cyclotron reson. lineshape calcs. 7-27269
 quasi 2D electron system, spin relax. 7-64101
 quasi 2D quantum wells, linear and nonlinear electrical conduction 7-64331
 quasi-2D strongly-coupled electron-phonon systems, CDW and superconductivity, polaron theory 7-58750
 quasi-one-dimensional conductors, coherent polaron superlattices and long-range Coulomb forces 7-45184
 random Kronig-Penney pots., resist. and phase-disrupting collisions 7-7095
 resistivity saturation in metals with structural instabilities 7-45277
 ruby, impurities optical dephasing temp. and freq. depend. 7-22286
 scanning tunnelling microscopy, phonon detection appl. 7-51588
 self-consistent calculation of electron-phonon couplings 7-21377
 semiconducting quantum well wires, hot electron transport 7-7356
 semiconductor film, electron scattering by charged impurities 7-21886
 semiconductor films and wires, cond., carrier quasielastic scatt. by acoustic phonons under size quantization conditions 7-38781
 semiconductor heterojunctions, 2D hot electron time-depend. energy relax., nonequilib. optical phonon effects 7-64102
 semiconductor heterojunctions, nonequilibrium electron-phonon scatt. 7-45457
 semiconductor n-i heterojunction, time depend. tunnelling and coherent Zener oscils. 7-17087
 semiconductor quantum well struct., exciton linewidth calcs., polar optical phonon scatt. 7-2491
 semiconductor quantum well structs., 2-D thermopower studies 7-33081
 semiconductor structures, electrons and phonons in 1D and 2D 7-2734
 semiconductor superlattices, dynamical screening, quasi-2D electron gas, electron-phonon interactions 7-45464
 semiconductor superlattices, electron-phonon scatt., Fohlich coupling 7-2681
 semiconductor thin films and wires, hot electrons under quantum size effect conditions 7-38780
 semiconductors, cubic, phonon scatt. at electronically degenerate defect states 7-21827
 semiconductors, electrical breakdown at grain boundaries 7-45339
 semiconductors, electron-phonon weak scatt. in high elec. fields, Boltzmann eqn. 7-2625
 semiconductors, highly doped and excited, electron-phonon mobility variation with carrier density 7-64249
 semiconductors, insulators and metals, structural, electronic and vibr. props., pseudopotential calcs. 7-16484
 semiconductors, intrinsic, solid-state plasma, local impact ionisation regions form. 7-52663
 semiconductors, magnetic two-phonon resonance involving acoustic phonons 7-45355
 semiconductors, magnetophonon resonance of short-wave phonons, anisotropy 7-12744
 semiconductors, negative differential resistance, scattering-induced, plasmon-phonon coupling and phonon reabsorption effects 7-2626
 semiconductors, tunnel delocalisation of electrons 7-33022
 semiconductors, Umlklapp 1/f noise, Hooge parameter, relativistic correction, appl. to $Hg_{1-x}Cd_xTe$ resistors 7-2649
 single-electron excitation energies, electron-phonon interaction effects, pseudopot. calcs. 7-27264
 small polaron form., path-integral and scaling theories 7-2510
 strong-coupling superconductors, energy gap eqn. inversion, electron tunnelling spectrum temp. corrections, phonon spectrum determ. 7-52900
 strong-coupling superconductors, specific heat difference functional derivative 7-38815
 strongly coupled electron-phonon systems, 1D and 2D, BCS pairing versus bipolaron crystallisation 7-45552
 subsystem interaction with boson field, kinetics, appl. to weak electron-phonon interaction 7-32591
 superconducting electron pairing, exchange and correl. contributions 7-45574
 superconducting film, resistive state, high freq. nonJosephson vibrations and quasi-particle interaction calcs. (*Russian*) 7-27263
 superconducting tunnel junction, quasi-particle current jump at gap voltage 7-12918
 superconductors, disordered and amorphous nontransition metals and alloys, electron-phonon coupling strength and phonon spectrum calcs. 7-52889
 TCNQ salts, quasi 1D molecular crystals, optical props., Hubbard model generalization, cond. calc. 7-45952
 ternary semicond. alloy ultrathin wires, alloy scatt. limited mobility calcs. 7-12724
 tetracene in ethanol glass, appl. of hole-burning spectroscopy as a tool to eliminate inhomogeneous broadening 7-46104
 tetramethyl-phenylene-diamine chloranil, mixed-stack cpds., spectroscopy of dimerisation 7-22260
 thermal Green's function generating functional from functional integrals with one-sided boundary conditions 7-52447

electron-phonon interactions continued

- thermoelectric power singularity at topological Lifshitz transition, electron-phonon scatt. effect 7-45285
 thermopower, electron-phonon enhancement effect calcs. 7-38542
 TMTCT salts, electronic and vibr. absorption spectra, electronic correlations 7-46034
 transition metal dichalcogenides, CDW transition effects of lattice fluctuations 7-21831
 transition metals, resistivity and superconducting transition temp. 7-17013
 transition metals, X-ray electron spectra asymmetry and Fermi level density of states (*Russian*) 7-3112
 transverse conductivity of nondegenerate two-dimensional electrons scattered from longitudinal optical phonons in a strong magnetic field 7-21885
 two dimensional electron gas, nonlinear cond. in quantising mag. field, electron-acoustic phonon scatt. (*Russian*) 7-17004
 two-dimensional polaron, cyclotron reson. spectrum calc. 7-45175
 uncommensurate charge density wave system, phenomenological Lagrangian 7-38474
 unitary transformations in solid state physics, book 7-24310
 Ag-based dilute alloys, low temp. elec. resist. 7-52565
 Ag-D films, implanted, elec. resist. meas., vibr. props. 7-38775
 Al dilute alloys, deviation from Matthiessen's Rule, three group model 7-12601
 Al films and wires, fluctuation and localisation effects 7-64176
 Al, phonon density of states from heat capacity temp. depend., inverse problem 7-6736
 Al, superconducting transition temperature, press. depend. 7-22058
 Al, ultrasonic attenuation in a transverse mag. field, electron mean free path 7-64296
 AlGaAs:Si-GaAs 2D electron gas structure, scatt. mechanisms 7-38718
 $Al_{0.28}Ga_{0.72}As$, photoluminescence half-width and intensity, temp. depend. 7-39179
 $Al_xGa_{1-x}As$ heterojunction, tunnelling current modulation by optical phonons 7-27394
 $Al_xGa_{1-x}As:Si$, deep donor centres 7-45217
 $AlNbO_4:Cr^{3+}$ tunable IR laser crystals, fluorescent spectra 7-43110
 $Al_2O_3:Cr^{4+}$, V^{3+} , electron-phonon interaction and impurity energy levels, APR and EPR studies (*Russian*) 7-45814
 $AlTaO_4:Cr^{3+}$ tunable IR laser crystals, fluorescent spectra 7-43110
 $Al_2(WO_4)_3:Cr^{3+}$, tunable IR laser crystals, fluorescent spectra 7-43110
 Au-SiO₂-Bi, low temp. hot electron energy relaxation and inelastic collisions in thin metal films 7-27441
 $Au_{60}Pd_{40}$ thin films, warm electron energy loss meas. 7-2739
 $BaPb_{1-x}Bi_xO_3$, electron-phonon interaction and superconductivity 7-27463
 $BaPb_{1-x}Bi_xO_3$, semicond. phase, CDW gap, optical meas. 7-53328
 $BaPb_{1-x}Bi_xO_3$, superconductivity and metal-semicond. transition 7-58940
 C-AsF₆ intercalation cpd., Raman scatt., coupled electron-phonon excitation 7-46045
 Ca, phonon density of states from heat capacity temp. depend., inverse problem 7-6736
 CdF₂, field enhanced electronic transport 7-45329
 p-CdGeAs₂ semicond., hole mobility and scatt., temp. depend. study 7-52609
 CdSe, dielectric fn. and interband crit. points. 7-2480
 CdSe, optimally annealed in molten Cd, DC galvanomagnetic props. 7-27352
 CdSe, photogenerated high density electron-hole plasma, energy relax., rapid expansion 7-33039
 CdSe, strongly excited, electron-phonon interaction screening, luminesc. meas. 7-38606
 CeAl₃, heavy fermion system, fluctuating bands 7-58736
 CePb₃, heavy fermion material, magnetism and superconductivity 7-52880
 CeRu₂Si₂, heavy-fermion system, magnetoacoustic effects in high mag. fields 7-64506
 $(Co_{0.6}Ni_{0.4})_{78}Si_{14}$, amorphous, itinerant electron charact., current induced reson. mag. field shift obs. 7-27590
 Cu-based dilute alloys, low temp. elec. resist. 7-52565
 CuBe, scatt. anisotropy of conduction electrons 7-38536
 CuInS₂ films, RF sputtering, struct. and elec. props. 7-3169
 $Cu_{2-x}Se$, electrical resistivity, temp. and carrier density dependences 7-38556
 $EuGa_2S_4$, optical props. near fundamental absorption edge 7-17295
 $(Fe_{1-x}W_x)_{84.5}B_{15.5}$ amorphous alloys, elec. and mag. props. (*Chinese*) 7-12969
 GaAs, deep level nonradiative carrier capture press. depend. calcs. 7-12735
 GaAs, electron scattering in quantum limit 7-38552
 GaAs, electron-LO phonon dynamics, subpicosecond Raman spectroscopy 7-46052
 GaAs, electron-electron interactions, appl. for hot electron decay 7-32934
 GaAs, electron-hole plasma dynamics under subpicosecond optical excitation, optical absorption saturation 7-27356
 n-GaAs, free carrier IR absorpt. spectra, scattering mechanisms, RPA calcs. 7-2604
 GaAs, fundamental energy gap, temp. depend. 7-7115
 n-GaAs, Hall factor calcs. 7-52657
 n-GaAs, intervalley processes, nonequilib. phonon spectroscopy and hydrostatic compression, Monte Carlo study 7-58425
 GaAs, inversion layers, hot free electron gas, intraband absorpt. coeff. calc. 7-33083
 GaAs, lattice dynamics and electron-phonon interactions, quasi-ion approach calcs. 7-58422
 GaAs quantised inversion layers, hot 2D electron gas, spectral acoustic phonon emission intensity 7-52452
 GaAs quantum wells, 2D hot-electron mobility 7-45470
 GaAs quantum wells, hot-carrier phonon interactions, steady-state and picosecond meas. 7-12837
 GaAs:Sn, photolum. spectra, line shape anal., conduction band to deep acceptor transition 7-46098
 GaAs/Al_{1-x}Ga_xAs modulation-doped heterostructs., 2D electron gas mobility meas. and calcs. 7-12840
 GaAs/Al_{1-x}Ga_xAs heterostructs., 2D electron gas; polaron screening effects, optical absorpt. calcs. 7-2511
 GaAs/Al_{1-x}Ga_xAs superlattices, magnetophonon oscils. damping, polar-optical phonon contrib. calcs. 7-27391
 GaAs-(Ca,Sr)F₂ heterostructure interfaces, twinning, Raman spectra 7-13148

electron-phonon interactions continued

- GaAs-Al_xGa_{1-x} multiple quantum well, electron-phonon interaction 7-2684
- GaAs-Al_xGa_{1-x} multiple quantum well structs., nonequilib. LO phonons 7-12457
- GaAs-AlGaAs multiple quantum well structs., photolum. under high laser excitation 7-13213
- GaAs-AlGaAs quantum wells, electron-phonon scatt. rate reduction by total spatial quantisation 7-45482
- GaAs-Ga_xAl_{1-x} heterojunction, nonequilibrium electron-phonon scatt. 7-45457
- GaAs-GaAlAs heterojunctions, cyclotron resonance, screening effects 7-38706
- GaAs-GaAlAs heterojunctions, electron-phonon interactions, cyclotron and magnetophonon reson. meas. 7-45463
- GaAs-GaAlAs modulation doped quantum wells, hot carrier energy relax., time resolved photoluminescence spectra 7-52828
- GaAs-GaAlAs superlattice, electronic struct., envelope function approx., phonon limited mobility, Boltzmann eqn. 7-2698
- GaAs-GaAlAs/Si modulation doped quantum wells, electron mobility, temp. depend. 7-45473
- Ge, drag thermoelec. power, anisotropy parameter, carrier density depend. 7-38603
- Ge, electron-hole plasma transport 7-7272
- p-Ge, Hall effect, mag. field and temp. depend., transport eqn. soln. 7-52651
- p-Ge, hot electron transport, perturbed acoustic phonon distrib. effects, Monte Carlo anal. 7-64254
- Ge, lattice dynamics and electron-phonon interactions, quasi-ion approach calcs. 7-58422
- Ge, n-type and ultrapure samples, electron transport and press. coeffs. 7-2615
- Ge point contacts, nonlinear elec. cond. effects due to electron-phonon interactions (Russian) 7-52628
- Ge, superconductivity and electron-phonon interactions 7-12899
- Ge, tubular hole distrib. under streaming conditions, scatt. anisotropy effects calcs. 7-58802
- GeTe, ferroelec. phase transition, electron-phonon interaction 7-13106
- Hg_{1-x}AsF₆, 1D BCS Hamiltonian 7-45558
- Hg_{0.8}Cd_{0.2}Te, low temp. hot electron energy relax. time in extreme quantum limit mag. fields 7-33035
- In nonequilibrium superconductor, Bernoulli effect meas. (Russian) 7-7455
- In superconducting film, temp. dependent order parameter relax. time determ., critical DC current meas. 7-17147
- In type I supercond. granule metastable state destruction by external 7-27475
- p-InP, γ -ray irradiated low temp., nonradiative-recomb.-enhanced defect struct. transformation 7-2062
- n-InP, Hall factor calcs. 7-52657
- InSb, conduction band, deformation potential constant 7-7112
- n-InSb, magnetic two-phonon resonance involving acoustic phonons 7-45355
- K, electron-electron and electron-phonon interactions, plastic deform. effects 7-12710
- K-Rb dilute alloy, electron-electron and electron-phonon interactions, plastic deform. effects 7-12710
- KAl(MoO₄)₂·C₂H₅³⁺ tunable IR laser crystals, fluorescent spectra 7-43110
- La, crystal electronic struct., electron-phonon interactions and superconducting transition temp. calcs. (Chinese) 7-27261
- LaAg, nonmag. cpds., transport props. and electronic struct. 7-2575
- LiYF₄Tm³⁺ crystal, Tm optical spectrum, press. induced linear dichroism, electron-phonon interaction 7-3069
- LuAg, nonmag. cpds., transport props. and electronic struct. 7-2575
- Mo_{1-x}Re_x, enhanced superconductivity by electron renormalization of directly obs. Brout-Visscher local phonon 7-38824
- Mo₂Si, Al₅ cpd., phonon dispersion and density of states, inelastic neutron spectra, electron-phonon coupling effects 7-2121
- NO₂⁻ molecular luminescence centre in nitrites and nitrates, struct. and electron-phonon interaction 7-3088
- NaCl, electron-phonon scatt. in XUV induced electron emission, Monte Carlo simulation 7-27861
- Nb, Fermi surface, Fermi vel., many-body enhancement and supercond. energy gap anisotropies calcs. 7-58729
- Nb₃(Al-Ge), high T_c supercond., Raman spectra studies 7-7699
- NbSe₃, CDW gap, tunnel junction spectra 7-21897
- NbSe₃-I-Pb, tunnel junctions under press. 7-52594
- NbSe₂H₂, heat capacity, Debye temp., electron-phonon coupling, electronic contrib. meas. (Russian) 7-6820
- Ni_{100-x}Zr_x metallic glasses, low temp. sp. ht. study, density of states and Debye temp. determ. 7-2226
- P, black, interplanar forces caused by electron-lattice interaction 7-63547
- Pb-Pb and Pb-Sn, superconducting point microcontacts, electron-phonon interaction 7-2509
- Pb_{0.93}Sn_{0.07}Se, ferroelec. phase transition, electron-phonon interaction 7-13106
- PbTe, ferroelec. phase transition, electron-phonon interaction 7-13106
- PbTe-PbEuTeSe multiquantum wells, electron-hole recomb., photolum. 7-13216
- Pd-H, dil., elec. resist. meas., 250-350 K 7-64233
- Pd₇₀T₃₀, quasiharmonic phonon dispersion relation, coherent neutron scatt. study 7-38141
- Si, charge carrier-lattice interaction, X-ray diffr. study 7-51975
- p-Si conductivity and Hall mobility calcs., impurity scatt., anisotropic-nonparabolic effects 7-12720
- Si exciton transport, optical time-of-flight investigation 7-64244
- Si, lattice dynamics and electron-phonon interactions, quasi-ion approach calcs. 7-58422
- Si MOS struct., phonon emission spectroscopy of 2D electron gas 7-27435
- Si quantised inversion layers, hot 2D electron gas, spectral acoustic phonon emission intensity 7-52452
- Si, superconductivity and electron-phonon interactions 7-12899
- Si, tubular hole distrib. under streaming conditions, scatt. anisotropy effects calcs. 7-58802
- 3C-SiC, n- and p-type epitaxial CVD layers, elec. props. temp. depend. studies 7-58917
- 6H-SiC neutron-radiated crystals, green luminesc., electron-vibrational interaction study (Russian) 7-59255
- SiO films, field enhanced electronic transport 7-45329
- SiO₂ films, ballistic electron transport 7-45531

electron-phonon interactions continued

- SiO₂, high field electron transport, rel. to positive charge generation at Si-SiO₂ interface 7-38571
- Si(111), surface structure, temp. depend. polaron shifts 7-7325
- Sn superconductivity and electron-phonon interactions 7-12899
- Tc-Ag point contacts, current-voltage characts., temp. depend. studies (Russian) 7-7335
- Th, phonon density of states from heat capacity temp. depend., inverse problem 7-6736
- ThSiO₄ single crystal, low temp. Raman and room temp. IR spectra 7-13158
- TiS₂ intercalation cpd. with Mn, Fe, Co, Ni elec. resist. and thermopower studies 7-45331
- UBi₃, electron-phonon coupling calcs., unconventional superconductivity mechanism 7-38811
- UPt₃, anisotropic superconductivity 7-7461
- UPt₃, heavy fermion superconductivity and normal state props. 7-52412
- UPt₃, heavy-fermion system, magnetoacoustic effects in high mag. fields 7-64506
- V-Si films, electrical transport props. 7-33108
- V₃Ga films, supercond. electron-phonon interaction spatial function, electron tunnelling spectra study 7-45578
- V₂Si, high T_c supercond., Raman spectra studies 7-7699
- W single crystals, galvanomagnetic props., low temp. Fermi surface local features effects (Russian) 7-27320
- W, valence bands, angle resolved XPS spectra 7-22441
- Xe, liquid, thermal electron mobility calc. 7-17027
- Y electronic struct., electron-phonon matrix and superconductivity, high press. effects, KKR calcs. 7-21805
- YAG:Yb, electron-phonon relax. in ³D₄ of Tb³⁺ 7-2130
- YAG, nonmag. cpds., transport props. and electronic struct. 7-2575
- YAlO₃:Nd³⁺, sub-levels R₁ and R₂, thermal shifts 7-32940
- Y₂O₃:Eu³⁺, impurities optical dephasing temp. and freq. depend. 7-22286
- Y₂Ti₂O₇, small-polaron conduction 7-21915
- Zn, phonon spectrum fine structure 7-16702
- ZnTe:O, hot luminesc., reson. Raman scatt. studies 7-64695
- Zr-Co amorphous alloys, superconductivity, normal-state resistivity and mag. susceptibility 7-12900
- ZrN superconducting thin films, electron tunnelling, phonon coupling effects 7-45580

electron-positron inclusive interactions

- baryon production and parton fragmentation at PEP, TPC studies 7-61714
- charged particle multiplications at 29 GeV in central rapidity regions 7-61713
- conference on nuclear scatt. data eval. methods, Berlin, Germany (June 1985) 7-21
- galactic centre, common origin for gamma-ray lines at 0.51 and 1.81 MeV 7-24238
- HEP computing in US, future plans for pp and e⁺e⁻ colliders 7-19146
- multijet production in e⁺e⁻ annihilation at PETRA energies 7-61715
- polarised electron-positron pairs annihilation in strong mag. fields, one-quantum annihilation cross-section 7-47674
- signatures of new particles at high energy colliders 7-56520
- strong coupling const. determ. from e⁺e⁻ annihilation hadron events 7-61716
- X-ray binary systems, relation between annihilation line and ultra-high-energy gamma-ray emission 7-47971
- e⁺e⁻→X, observation of scalar and tensor meson prod. at 29 GeV 7-19122
- e⁺e⁻→W⁺L⁺ν_e test for γW⁺W⁻, Z⁰W⁺W⁻ structure, W-magnetic moment anal. 7-24870
- e⁺e⁻→X, E₈×E₈ superstring theory, extra U(1) phenomenology 7-41688
- e⁺e⁻→Z⁰X, inclusive prod. at 29 GeV 7-56562
- e⁺e⁻→W⁺e⁺ν_e test for γW⁺W⁻, Z⁰W⁺W⁻ structure, W-magnetic moment anal. 7-24870
- e⁺e⁻→46.8 GeV, excited quarks search at CELLO, final state topologies 7-30276
- e⁺e⁻, √s=34.6 GeV, semi-muonic branching ratio determ. and heavy quark fragmentation function calcs 7-61710
- e⁺e⁻→hadrons, asymmetries, electroweak radiative corrections, Z₀ resonance 7-15166
- e⁺e⁻→mesons, D⁰-D⁰^{*} mixing signature 7-24894
- e⁺e⁻→neutralinos, production and decay anal. 7-15140
- e⁺e⁻→3 jets, average hadron multiplicities, total multiplicity formula 7-5105
- e⁺e⁻ annihilation, 29 GeV, p-Λ correls., local baryon number conservation 7-49163
- e⁺e⁻ annihilation, P_T dependence of π[±], K[±], p and p̄ prod. in central rapidity region 7-61757
- e⁺e⁻→D⁺(D⁰)X, 29 GeV, lifetime meas. 7-19098
- e⁺e⁻→D⁰X, production cross section meas. at 29 GeV 7-56561
- e⁺e⁻→D⁺X, cross-section, fragmentation function and forward-backward asymmetry 7-15167
- e⁺e⁻→e⁺e⁻A₂(1320), A₂→π⁺π⁻π⁰ decay obs. 7-526
- e⁺e⁻→e⁺e⁻X, scaling of photon structure function at low Q² 7-41825
- e⁺e⁻→e⁺e⁻+hadrons, 7-70 (GeV/c)², photon structure fn. meas. QCD, parton model comparisons 7-540
- e⁺e⁻→e⁺e⁻γγ, longitudinally polarized beams, longitudinal and P-violating asymmetries, supergravity GUT calcs. 7-5082
- e⁺e⁻→f(1270)X, status on f-meson data 7-56576
- e⁺e⁻→ff, f≠e, ν, τ, forward-backward and polarization asymmetries for SU(2)_L×U(1)_Y×U(1)_V and SU(2)_L×SU(2)_R×U(1)_{B-L} 7-61708
- e⁺e⁻→γ+2 jets, quark charge test 7-61706
- e⁺e⁻→γ+nothing, ν_e², Z² contributions, superstring calcs. 7-30263
- e⁺e⁻→γγ, γγγ, γγγγ, √s=29 GeV, QED tests 7-61642
- e⁺e⁻→γγν, superstring effects, contrib. of ν and right handed neutrino to cross section 7-30263
- e⁺e⁻→hadrons, strong coupling constant meas. 7-24897
- e⁺e⁻→hadrons, washing out final state interactions for longit. pol. asymmetry 7-24896
- e⁺e⁻→heavy baryons, perturbative QCD anal. 7-35887
- e⁺e⁻→Hγ(μ⁺μ⁻), helicity amplitudes, cross section calcs. 7-61641
- e⁺e⁻ high energy annihilation, quark and gluon fragmentation, Feynman diagrams 7-24901
- e⁺e⁻→jets, geometric struct. anal. review, QED tests, review 7-541
- e⁺e⁻→jets, hadronic final states, QCD and string model comparisons, review 7-30274

electron-positron inclusive interactions continued

- e^+e^- \rightarrow jets, pion and kaon multiplicities 7-61705
- e^+e^- \rightarrow light scalars, $E \leq 2$ TeV, expl. constraints on detection, extended technicolour model anal. 7-484
- e^+e^- \rightarrow $llVV$ ($l=e,\mu$; $V=W,Z^0$), TeV energies, longitudinal gauge boson scatt. anal. 7-61639
- e^+e^- \rightarrow AX , inclusive production, angular distribution asymmetry 7-35885
- e^+e^- \rightarrow MM , search for magnetically charged particles 7-41777
- e^+e^- \rightarrow neutralinos, CP violation effect, SUSY electroweak model anal. 7-10065
- e^+e^- \rightarrow $\pi^0 X$, angular distrib., differential cross-sections and mean multiplicity 7-35890
- e^+e^- \rightarrow $\pi^+\pi^-$, $2\pi^+2\pi^-$, $\pi^+\pi^-\pi^0$, observation of $\rho'(1600)$ 7-61711
- e^+e^- \rightarrow $q\bar{q}g$, three-jet event cross-section, transverse momentum distribution, first order QCD calcs. 7-24895
- e^+e^- \rightarrow $q\bar{q}g(\gamma)$, $E_{cm}=29$ GeV, charged particle flow comparisons 7-10066
- e^+e^- \rightarrow $q\bar{q}g(q\bar{q}\gamma)$, particle flow in annihilation events 7-539
- e^+e^- \rightarrow $q\bar{q}\gamma\gamma$, scalar quark production, Monte Carlo QCD simulation 7-35888
- e^+e^- \rightarrow $S(V_L V_L)X$, $V_L=W^\pm$, Z^0 , cross section calcs. 7-49154
- e^+e^- \rightarrow it , polarization asymmetries, one-loop electroweak corrections 7-534
- e^+e^- \rightarrow $t\bar{t}$, t -quark detection at high energy colliders 7-24899
- e^+e^- \rightarrow W^+W^- , anal. using rank-5 Wilson-loop-broken E_8 model 7-61646
- e^+e^- \rightarrow W^+W^- , cross sections, angular distrib. using W^\pm , Z^0 self-interaction Lagrangian 7-61515
- e^+e^- \rightarrow W^+W^- , Monte Carlo simulation of multiboson production processes, two and three jet decays 7-30268
- e^+e^- \rightarrow $W^+W^-WZ,W\gamma,ZZ$, tri-boson gauge coupling effects, standard model calcs. 7-24868
- e^+e^- \rightarrow W^+W^+ \rightarrow four fermions, beam polarization effects, γWW , ZWW vertex meas. analysis 7-61640
- e^+e^- \rightarrow X , asymmetries from E_8 GUTs 7-448
- e^+e^- \rightarrow X , Bose-Einstein correlations, string model predictions and Monte Carlo calcs. 7-24898
- e^+e^- \rightarrow X , CP nonconservation search using jet variables 7-41665
- e^+e^- \rightarrow X , hadronic contributions to electroweak parameter shifts 7-10068
- e^+e^- \rightarrow X , modifications in neutrino counting due to additional gauge bosons 7-35889
- e^+e^- \rightarrow X , multijet production studies 7-35891
- e^+e^- \rightarrow X , quark fragmentation, charged particle multiplicity 7-35886
- e^+e^- \rightarrow X , rapidity dependence of multiplicity distrib., KNO scaling 7-532
- e^+e^- \rightarrow X , single photon search and supersymmetric particle mass limits 7-533
- e^+e^- \rightarrow $Z^0 Z^0$, effects of E_8 -charged lepton mixing 7-61645
- e^+e^- \rightarrow $Z^0 \rightarrow H(\rightarrow q\bar{q})\nu\bar{\nu}$, minimal standard model anal. 7-19120
- e^+e^- \rightarrow $Z^0 \rightarrow b\bar{b}$, $t\bar{t}$, unpolarized and polarized forward-backward asymmetries, properties 7-538
- e^+e^- \rightarrow Z^0 , $\sqrt{s}=M(Z^0)$, asymmetry meas., Z^0 - Z' mixing, Z' mass constraints 7-49129
- e^+e^- $\rightarrow e^+e^-H$, $\sqrt{s}=90-130$ GeV, problems related to Higgs detection, resolution, mass 7-56534
- H_2 gas, galactic environment, direct positron annihilation, laboratory simulation 7-14426

electron-positron interactions

- see also *electron-positron inclusive interactions; electron-positron scattering*
- electroweak standard model, 1-loop renormalisation, leptonic processes appl. 7-61512
- mirror fermion production near Z^0 peak in e^+e^- collisions 7-49128
- ultra-heavy quarks, prod. and decay props., quarkonia prod. in hh and e^+e^- 7-30242
- e^+e^- \rightarrow ff , asymmetries and cross section, superstring gauge boson effects 7-499
- e^+e^- \rightarrow $\tau^+\tau^-$, cross section determ. from 14 to 465.8 GeV 7-15142
- e^+e^- , absence of forward-backward multiplicity correlations 7-24910
- e^+e^- , $4 \leq E_{cm} \leq 34$ GeV, unified multiplicity scaling, quantum statistical analysis 7-61709
- e^+e^- \rightarrow $\nu\bar{\nu}$, ν counting effects from light ν 's and gauge bosons in E_8 models 7-19094
- e^+e^- \rightarrow 2 mesons $+\gamma$, high energies, QCD perturbation theory anal., cross sections, wave functions 7-19123
- e^+e^- annihilations, joint quarkonium and neutral Higgs boson production anal. 7-15168
- e^+e^- \rightarrow $b\bar{b}$, forward-backward asymmetry, electroweak interference in new model 7-41824
- e^+e^- $\rightarrow e^+e^-$, $\mu^+\mu^-$, two photon muon pair process, QED comparison (Chinese) 7-10050
- e^+e^- $\rightarrow e^+e^-K_S^0 K^\pm \pi^\mp$, two photon spin-1 meson production obs. 7-24900
- e^+e^- $\rightarrow e^+e^-e^+e^-$ ($\mu^+\mu^-$), noncollinear two charged particle events 7-35847
- e^+e^- $\rightarrow e^+e^- \gamma$, radiative width meas. 7-61717
- e^+e^- $\rightarrow e^+e^- \gamma$, bremsstrahlung amplitude calcs. 7-61712
- e^+e^- $\rightarrow e^+e^- \gamma^* \gamma^* \rightarrow e^+e^- R$, virtual photon-photon interactions, search for high-mass narrow resonances 7-41866
- e^+e^- \rightarrow $ff\gamma$, bremsstrahlung amplitude calcs. 7-61712
- e^+e^- \rightarrow γX , identification of missing neutrals using long. pol., ν , $\bar{\nu}$, $\tilde{\gamma}$ and H^0 7-49127
- e^+e^- \rightarrow $\gamma\gamma$, differential cross-sections, QED predictions 7-35846
- e^+e^- \rightarrow $\gamma\gamma$, electroweak radiative corrections 7-35848
- e^+e^- \rightarrow $\gamma\gamma\gamma$, ang. distrib. meas., QED comparison 7-5080
- e^+e^- \rightarrow $\gamma\gamma\gamma$, heavy flavor production with gluon bremsstrahlung 7-15125
- e^+e^- \rightarrow $H^\pm tb$, Higgs boson prod. cross sections, standard model comparison 7-19124
- e^+e^- \rightarrow hadrons, sub-Poissonian hadronic multiplicity distrib. 7-19121
- e^+e^- \rightarrow hadrons, superclusters and hadronic multiplicity distribution 7-19132
- e^+e^- \rightarrow heavy Majorana fermions $\rightarrow I^{1+}$, cross sections, tests for Majorana nature, CP, CPT-invariance 7-61702
- e^+e^- \rightarrow leptons, electroweak interference effects 7-506
- e^+e^- \rightarrow leptons, strong interaction contributions to four-lepton processes in electroweak $SU(2) \times U(1)$ 7-61644
- e^+e^- \rightarrow ll , forward-backward asymmetry as E_8 model probe 7-19093

electron-positron interactions continued

- e^+e^- $\rightarrow \mu^+\mu^-$, radiative corrections to charge asymmetry in supersymmetric theories 7-5081
- e^+e^- $\rightarrow \nu\bar{\nu}$, mag. field effects, Glashow-Weinberg-Salam model study 7-41778
- e^+e^- $\rightarrow \pi^0 \pi^0$, π^0 EM properties in dominance model of quark-loop anomalies 7-19147
- e^+e^- $\rightarrow \pi^+\pi^-\pi^0$ reaction cross section up to 1.40 GeV 7-49164
- e^+e^- $\rightarrow \pi X$, Bose-Einstein correlations among identical pions, Fourier transform technique, string model comparisons 7-61707
- e^+e^- $\rightarrow \pi\pi\pi\pi$, cross sections, N/D model anal. 7-61739
- e^+e^- $\rightarrow q\bar{q}g$, invariant amplitudes in QCD 7-537
- e^+e^- $\rightarrow q\bar{q}g$, parity violating structure function calcs. 7-10067
- e^+e^- $\rightarrow \tau^+\tau^-$ 7-41824
- e^+e^- $\rightarrow \tau^+\tau^- \rightarrow \pi^-\pi^+\pi^0\nu_\tau$, branching ratio determ., evidence for $\tau \rightarrow \omega\pi\nu_\tau$, branching ratio meas. 7-61674
- e^+e^- $\rightarrow W^+W^-$, factorization of helicity amplitudes and angular correlations for electroweak processes 7-41775
- e^+e^- $\rightarrow W^+W^-$, probing the weak boson sector, anomalous couplings search, helicity amps. 7-56533
- e^+e^- $\rightarrow X$, effects of Z' -bosons from superstring or nonlinear σ models 7-444
- e^+e^- $\rightarrow Z'X$, phenomenology of extra neutral gauge boson 7-41776
- e^+e^- $\rightarrow Z\gamma$, QED radiative corrections 7-535
- e^+e^- $\rightarrow Z\gamma$, renormalised Zee vertex function 7-536
- e^+e^- $0 \rightarrow X$, sparticle pair prod. with polarized beams 7-61493
- e^+e^- annihilation, cross section of prod. of arbitrary number of photons 7-15141

electron-positron scattering

- see also *electron-positron interactions*
- e^+e^- $\rightarrow e^+e^-$, $\sqrt{s}=29$ GeV, differential cross section meas., electroweak effects 7-61643
- e^+e^- $\rightarrow e^+e^-$, differential cross-sections, QED predictions 7-35846

electron probe analysers see *electron probe analysis***electron probe analysis**

- alloy conc. determ. in energy dispersive system, ZAF factor approx. 7-28369
- atomic displacements detection using channelled electron induced X-ray emission 7-21311
- Auger elemental depth profiling, preferential sputtering 7-54247
- backscatter loss calcs. in X-ray microanalysis 7-8342
- biological electron probe X-ray microanal., current status, history 7-8782
- brass, two-phase, Al-B Masteralloy addition, B redistrib. during solidification, grain refining effect 7-22664
- butadiene-styrene graft block copolymers, low-mol. cpds. diffusion (Russian) 7-36834
- Cliff-Lorimer k_{AB} factors at zero foil thickness, extrapolation method 7-39935
- coincidence counting techniques in analytical electron microscopy 7-23104
- correction procedure, universal, development 7-23108
- crystal orientation effects in X-ray and Auger electron microanalysis 7-23109
- diffusion meas. by analytical electron microscopy 7-39946
- digital image analysis with Camebax equipment (French) 7-46746
- EDX analysis in a 400 keV electron microscope 7-39945
- EELS analysis, HV use 7-22403
- EELS analysis, k-factor approach 7-18946
- EELS complex spectra, separation of charact. signals 7-18945
- EELS data analysis, digital filters use and limitations 7-18944
- EELS in STEM of surfaces and interfaces, dielec. theory and verification 7-18935
- EELS parallel detection setups 7-18943
- EELS spectrometer, dual parallel and serial detection, design 7-18942
- electrostatics, of insulators charged by electron beams 7-41540
- energy dispersive analysis accuracy and sensitivity for light element microanalysis 7-23101
- energy filtered imaging by scanning CTM technique 7-22404
- energy-dispersive X-ray detector, mineral standards for calibration 7-23105
- energy-dispersive X-ray detector performance, contamination influence 7-23106
- fatigue apparatus for testing in UHV and controlled environments, computer-controlled 7-39811
- grain boundaries, electron microscope analysis 7-37818
- Incoloy 800 H, oxidation, EMPA profiles in depletion zone 7-17727
- incomplete charge collection and X-ray microanalysis 7-23100
- Inconel 617, oxidation, EMPA profiles in depletion zone 7-17727
- low-molecular ingredients, migration in elastomer compositions (Russian) 7-39942
- miniature variable energy probe design for nanometric analysis, electron opt. parameters 7-18939
- multi-job, multi-user electron probe X-ray microanalyser, JXA-8600 series 7-33978
- multispectral scanning Auger imaging technique 7-23110
- p-n structures, electron-probe analysis using the dependence of the induced current on the acceleration voltage 7-38348
- peridotite melting under ultrahigh pressure, SEM and EMPA analysis appl. 7-34481
- phase diagrams, determination by analytical electron microscopy 7-37820
- quantitative compositional mapping on an electron microprobe 7-23107
- scanning Auger microscopy, high resolution, for mineral surfaces 7-60426
- scanning Auger microscopy, quantitative multi-element analysis 7-23112
- scanning Auger microscopy and AES, effects of peak to background ratios 7-23111
- scanning electron microscopy and microanalysis, conf., Leuven, Belgium (May, 1986) 7-40988
- semiconductor materials characterisation techniques, review 7-51598
- semiconductors, scanning electron microscope characterisation, book contrib. 7-41551
- silicate glass, Na desorption during X-ray microanalysis 7-23114
- small particles and thin films, quantitative electron probe microanal. 7-8327
- sputtered films, electron-induced X-ray emission for chemical composition anal. 7-3166
- steel, analytical electron microscopy, developments and trends 7-22949
- steel, austenitic stainless, sensitisation resistance improvement, application of analytical electron microscopy 7-39762
- steel, C analysis in case-hardened parts, software (French) 7-46889

electron probe analysis continued

steel, case-hardened, C profile, automatic quantitative meas. 7-17728
 steel, eutectoid, 1.3 wt.% Cr, specimen prep. technique influence on analytical TEM obs. of partitioning 7-22950
 steel, ferritic, energy-dispersive X-ray analysis, contamination influence on P meas. in presence of Mo 7-23106
 steel, HSLA C/N ratio in (TiNb)(CN) precip., EELS obs. 7-22698
 steel, stainless, ferritic, irradi., grain boundary segregation, STEM microanalysis 7-22701
 steel, stainless, ferritic-martensitic, high-Cr, fast reactor irradi., phosphide phases 7-22700
 steel, stainless, Type 316, microstruct. exam. around weldments 7-22697
 steel, structural, STEM-EDS X-ray microanalysis of grain boundary segregation 7-22702
 steel, surface characterization, EPMA, XPS, GDOS anal. 7-17372
 steel fibre reinforced Cu composites 7-13595
 steels, C microanalysis, statistical method of brief countings (French) 7-46888
 submicron backscattered electron microanalysis in SEM 7-23113
 TEM, conference, Boston, MA, USA (Dec. 1985) 7-35119
 TEM light element analysis using windowless X-ray detectors 7-23099
 ternary intermetallic compounds, single crystal, Czochralski growth, charactn. 7-53557
 wedge shaped specimen, simulation of charact. fluoresc. behaviour 7-23102
 X-ray fluorescence analysis in SEM, at. number depend., detection limits improvement 7-23103
 X-ray image acquisition using an IBM-PC, SEM based energy dispersive spectroscopy 7-4942
 X-ray microanalysis, of equilibrium and nonequilibrium segregation 7-46488
 Al two phase alloys, high temp. deformation, microtexture 7-16563
 Al-Fe-Si system, intermetallic phases, electron probe microanalysis, X-ray diffr. 7-59491
 Al-Mg-Ce system, liquidus, intermetallic compound (Chinese) 7-7960
 Al-Zr-V, rapid solidification, age hardening, solid soln. form. (Korean) 7-46475
 AlGaAs, low press. MOCVD grown, surface morphology and defects 7-64023
 B, inner shell excitation profiles visibility 7-22403
 BN, quantitative, Area/Peak Factor concept 7-46886
 BN, inner shell excitation profiles visibility 7-22403
 BaO-La₂O₃-Nd₂O₃-Al₂O₃ systems, synthesis, characterisation and spectroscopic investigations of mixed hexa-aluminates 7-63827
 BaTiO₃ ceramics, grain struct. and phase anal. (German) 7-58496
 Bi₁₂GeO₂₀ Czochralski-grown crystals, comp. anal., holographic storage props., stoichiometry depend. 7-63837
 C, inner shell excitation profiles visibility 7-22403
 C, quantitative, Area/Peak Factor concept 7-46886
 CdS, single crystal, US wave absorption, impurity distrib. effect., electron-probe X-ray anal. 7-53241
 CdSe, single crystal, US wave absorption, impurity distrib. effect., electron-probe X-ray anal. 7-53241
 CdTe, D plasma etching, surface comp. 7-46730
 CdTe films, electrochemically deposited, comp., struct., AES, electron probe anal., X-ray diffr. spectroscopy 7-58694
 CdCo_{1-x}Si_{2+x}, cryst. struct., homogeneity range, X-ray diffr., electron probe anal. 7-37939
 Cu tubes, pitting pot. in hot water, oxidising agents effect 7-28207
 Cu₂Ag_{1-x}InSe₂, liquid-encapsulated Bridgman-Stockbarger melt growth and props. 7-59403
 CuIn_{1-x}Se₂, liquid-encapsulated Bridgman-Stockbarger melt growth and props. 7-59403
 (Fe,Co,Ni)-P layers, electrochemical deposition, struct. (Chinese) 7-7037
 Fe surface layers under toluene, laser irradiated, supersaturation with C 7-51820
 Fe/Fe-FeO/Al₂O₃ systems, diffusion bonded, interface chemistry, bonding strength 7-28079
 Fe-Cr-Al-Ce, microstruct., high temp. corrosion rel. to Ce additions 7-13648
 Fe-Cr-Co-(Si), permanent magnet alloys, microstruct., mag. props., Si content effect 7-22117
 Fe-Pd-S system, phase equilib. 7-3272
 GaAs, impurity atom site location using channelling enhanced microanalysis 7-38023
 GaSb/Gd₂Ho crystal grown by horizontal zone melting, precipitate identification 7-21462
 In_xGa_{1-x}As, atomic displacements detection using channelled electron induced X-ray emission 7-21311
 InP, impurity atom site location using channelling enhanced microanalysis 7-38023
 LuCo_{1-x}Si₂, cryst. struct., homogeneity range, X-ray diffr., electron probe anal. 7-37939
 MgO smoke particles, energy filtered imaging by scanning CTM technique 7-22404
 Mo fibre reinforced Cu or Fe composites, extruded, struct. and fractography 7-13595
 MoS₂ coatings, thickness meas., nondestructive methods performance 7-18751
 Na₂O-B₂O₃-SiO₂ glass, Na desorption during X-ray microanalysis 7-23114
 Ni superalloy, MAR M002, borides analysis using convergent beam electron diffr. 7-22699
 Ni-Al-Fe system, phase equilibria in the Ni-rich region 7-39487
 Ni-Al-Mo-W system, constitution of Ni₃Al-Ni₃Mo-Ni₃W section 7-13434
 Ni-base superalloys, accuracy evaluation without standard materials 7-33979
 Ni₃Al produced by shock compaction, TEM 7-39480
 PbSe/Cd, crystal growth and impurity distrib., electron probe X-ray microanal. studies 7-63639
 PbTe-EuTe short period superlattices, props., appl. to laser diodes 7-52785
 Pd/C model catalyst supported on TEM grids, in-situ heating and microanalysis expts. 7-23098
 Pd-Pt, mixed layers, electroplated on stainless steel support, oxidation catalyst appl. 7-22596
 Pd-Te system, phase diagram study 7-26934
 PdRhPSi(SiNi), amorphous laser processed surface alloy on cryst. Ni in NaOH soln., anodic characts. 7-28317

electron probe analysis continued

SiAlON-YAG ceramics, Auger electron microscopic quantification of phase comp. 7-22951
 SiC:H, amorphous CVD film, electron optical characterisation 7-52372
 Ta/W diffusion couples, analytical electron microscopy 7-39946
 TeO₂-ZnCl₂ system, glass prep. and composition 7-46403
 Ti-Al-V, ternary phase diagram 7-28017
 TiC film ion plated on austenitic stainless steel, adherence rel. to ionisation (Japanese) 7-53636
 TiC/Fe multicomponent films on steel, sputter deposition and characterisation (Japanese) 7-3167
 U/Nb diffusion couples, analytical electron microscopy 7-39946
 ZrF₄-BaF₂-NaF-AlF₃-LaF₃ glasses, crystallisation study 7-63491
 ZrO₂ single crystals, stabilised, growth by skull melting technique, charactn. 7-53560
 ZrO₂-CaO-P₂O₅-SiO₂ glass-ceramics, prep. and mech. props. (Japanese) 7-7942
 electron probe microanalysis see electron probe analysis
 electron probe microscopy see electron probe analysis
 electron probes
 see also electron probe analysis
 miniature variable energy design for nanometric analysis, electron opt. parameters 7-18939
 scanning Auger electron microprobe, spatial resolution improvement to ultimate values 7-30131
 STEM focused electron probes, Fourier analysis 7-18934
 electron-proton interactions
 see also electron-proton scattering
 e(ē)p, nucleon structure fns., SUSYQCD anal. 7-61689
 ep → hadrons + jets, cross sections, perturbative QCD calcs. 7-24869
 electron-proton scattering
 see also electron-proton interactions
 ep → ep, scattering-asymmetries, superstring gauge boson effects 7-499
 electron radiation
 atoms, Z=6 to 92, bremsstrahlung double differential cross section, photon energy depend. 7-42569
 cyclotron maser emission from pulsed electron beams 7-25791
 diamond crystal, relativistic electron beam, γ-ray emission, angular distribution 7-64722
 diamond crystal, ultrarelativistic electron beam, parametric quasi-Cerenkov radiation 7-46174
 point charge, photon density radiation limits 7-62608
 spontaneous radiation of an electron beam in a free-electron laser with a quadrupole wiggler 7-5898
 undulator radiation, effect of inclination of electron transit 7-62602
 X-ray source using low energy electron beams traversing superlattice 7-20114
 electron relaxation time (metals)
 bulk and thin film samples, polycrystalline, DC conductivity 7-52566
 dirty metals, conduction electron inelastic lifetime, nonlocalisation method studies 7-64210
 electroconductivity in const. mag. field, electron relax. time and interactions (Russian) 7-32994
 metals, electronic sp. ht., finite conduction electron lifetime correction calcs. 7-16784
 plasmon linewidth, memory-function approach 7-45193
 polyacetylene:I, metallic, effective mass, magnetoreflexion studies 7-64056
 transverse magnetoconductivity, dislocation scatt. effects (Russian) 7-52547
 Au-Pd films, electron scatt. times, weak localisation studies 7-64367
 Au-Pd thin films and wires, localisation and electron-electron interaction effects, magnetoresist. meas. 7-52863
 Au-SiO₂-Bi, low temp. hot electron energy relaxation and inelastic collision times in thin metal films 7-27441
 Au₆₀Pd₄₀ thin films, warm electron energy loss meas. 7-2739
 Ce Kondo systems, thermopower, elec. resist. and cryst. field effects 7-21900
 Cu_{1-x}Ti_x metallic glasses, magnetoresist., quantum interference and electron interaction effects 7-2576
 Mg quasi-two-dimensional films, electron localisation and interaction effects 7-7411
 electron relaxation time (semiconductors) see carrier relaxation time
 electron resists
 molecular electronics materials, Langmuir-Blodgett technique, microlithography resist appls. (Japanese) 7-6964
 electron ring accelerators
 atomic physics expts. appls. 7-19561
 electron scattering see elastic scattering of electrons by atoms and molecules; electron-electron scattering; electron-nucleon scattering; electron-nucleus scattering; electron-positron scattering; electron spectra; hadron electroproduction; secondary emission
 electron solvation see solvation
 electron sources
 4πβ sources for 4πβ-γ coincidence counting, thin source preparation 7-36439
 beam brightness from a relativistic, field-emission diode with a velvet covered cathode 7-1121
 beam emittance measurement on electron gun 7-62193
 cold electron beam sources for Raman FEL 7-1118
 compact and high efficient electron beam accelerator 7-30740
 conf., Saskatoon, Canada, May 1986 7-29595
 glow-discharge, high-power, production and appl. (Czech) 7-56373
 high current electron guns, brightness enhancement 7-1119
 laser-driven metal-photoelectron electron source 7-9921
 linear acceleration, conf., Tsukuba, Japan, (Sept. 1986) 7-18504
 low current density nanosec. electron beam diode 7-36369
 Marx bank, low jitter, for cold cathode electron beam sources (Chinese) 7-4912
 MFTF-B mag. field alignment diagnostic, electron-beam source development 7-25222
 photoelectronic source for swarm expts. in high-density gases 7-9925
 plasma focus device, rms beam emittance 7-30807
 plasma focus particle beams, RMS emittance meas. 7-32113
 polarised electron sources and detectors, surface studies appls., book contrib. 7-30806
 positron gun, modified Soa immersion lens 7-61401
 pulsed metastable atomic beam source for time-of-flight applications 7-41533

electron sources continued

- slow positron production by the use of the ETL linac (*Japanese*) 7-19569
 slow positrons, solid Ne moderator 7-18908
 thermionic gridded e^- gun for KEK e^+ linac, characts. (*Japanese*) 7-19608
 thin 4π β -sources for absolute meas., preparation method 7-5519
 $CS_2O-Al_2O_3-SiO_2$ thermionic cathode as efficient electron source 7-9923
 Ga-In-Sn liquid alloy, electron field emission studies 7-33535
 GaAs photoemission electron source, operating experience 7-41535
 SF_6^- , negative ionis. source for quadrupole mass analyser 7-35620

electron spectra

- see also Auger effect; conversion electron spectra; electron energy loss spectra; electron impact; electron spectroscopy; photoelectron spectra
 atom-ion collisions, emission-angle depend. post collision interaction 7-25644
 attenuation of isotropically emitted electron beams 7-13272
 borate minerals, unoccupied mol. orbitals of B-O bond mol. orbital calcs., XANES, NMR and electron transmission spectra 7-33281
 final-state effects in above-threshold ionisation 7-31167
 gas causing inelastic backscattering of electrons, analytical calculation 7-50350
 highly charged ions, multiple-electron capture, classical over-barrier model 7-10744
 inert gas atoms small angle differential cross sections for electron elastic scatt. 7-15713
 Langmuir-Blodgett monolayer films, exposed mol. ends, Penning ionis. electron spectrosc. 7-63991
 mean free path, effective backscatt. and differential scatt. cross-sections, 5-40 keV 7-53461
 methane, electron elastic scatt., differential cross sections meas. 7-25653
 multiple core holes, electronic system response and spectra prod., many-body theory 7-42477
 organic compounds, Feshbach resons. auto-detachment, electron spectra 7-57181
 propene, electronic states, electron impact spectrosc. and ab initio CI calcs. 7-25417
 PTFE, bonding and surface struct., ESCA investigation, electron beam interactions 7-51662
 sulphone rings, four-membered, photoelectron and electron transmission spectra, sulphone effect 7-50253
 thietane 1,1-dioxide, photoelectron and electron transmission spectra, sulphone effect 7-50253
 thiote 1,1-dioxide, photoelectron and electron transmission spectra, sulphone effect 7-50253
 Ar, electron impact ionisation, cross sections, fast-neutral beam method, TOF spectra 7-42769
 Ar, photoionis. with synchrotron radiation, angle-resolved electron spectra 7-905
 Ar, photoionisation, photoelectron and electron momentum spectroscopy 7-36560
 atom, electron elastic scatt., electron spin polarisation, electron spectra study 7-25651
 Ba, superelastic collisions with electrons (*French*) 7-10758
 CO, free and adsorbed mol., valence wavefunctions, deexcitation electron spectroscopy 7-36756
 CS_2^{2+} + atom(molecule), ($q=2, 3$), electron capture 7-5763
 Cu (111), epitaxial FCC γ -Fe (111)p(1 \times 1) films, surface ferromagnetic order electron capture spectroscopy 7-45773
 Fe phthalocyanine, local electron distrib., Penning ionis. electron spectrosc. 7-62521
 FeO $^-$, rot., autodetachment spectroscopy 7-62462
 Ga, resonant state, autoionis., electron spectra 7-900
 H $^+$, elastic electron scatt., reson. struct. study 7-20045
 H $^+$ + inert gas, electron transfer and ionis., δ -electron spectrosc. 7-42685
 H $_2$, vibrational excitation by electrons, electron spectra 7-57181
 H $_2^+$ + He(Ne)(Ar)(H $_2$) electron loss to the continuum, absolute cross sections 7-50304
 He, collisions with fast, highly charged ions, electron capture to the continuum meas. 7-20026
 He, electron impact ionisation, cross sections, fast-neutral beam method, TOF spectra 7-42769
 He+H $^+$, electron ejection, double differential cross section meas. 7-20024
 He+Li(Na)(K)(Rb)(Cs), Penning ionisation, pot. well depth calcs., electron energy spectra anal. 7-62510
 He $^+$ + He(Ne)(Ar)(H $_2$), electron loss to the continuum, absolute cross sections 7-50304
 I, X-ray photoelectron and Auger electron spectrosc. 7-5647
 In, resonant state, autoionis., electron spectra 7-900
 Kr, electron impact ionisation, cross sections, fast-neutral beam method, TOF spectra 7-42769
 N $_2$, vibrational excitation by electrons, electron spectra 7-57181
 NH $_3$ (ND $_3$), predissociation, dissociation, attachment cross section 7-50279
 N $_2O$, threshold electron impact spectrum 7-50385
 Na, 3 P state, electron impact excitation, differential cross section and alignment parameter meas. 7-20052
 Ne, electron impact ionisation, cross sections, fast-neutral beam method, TOF spectra 7-42769
 Ne, photoionis. with synchrotron radiation, angle-resolved electron spectra 7-905
 Ni (100) with adsorbed O $_2$ overlayers, elastic diffuse and inelastic electron scatt. 7-22402
 Ni (111), coadsorption of NH $_3$ and CO, multilayer formation studied by metastable quenching spectroscopy 7-21639
 Ni magnetic surfaces, elastic spin-polarised low-energy electron scatt., book contrib. 7-33494
 O $_2$, electron scatt. cross section meas., 0.2 to 100 eV impact energy 7-20047
 O $_2$, form. and resonant vibr. levels of O $_2^-$, spectra anal., cross sections calc. 7-15730
 Pb, electron momentum spectra, multiconfiguration DF wavefunction 7-50351
 Pb, resonant state, autoionis., electron spectra 7-900
 Sn complexes, ESCA, Mossbauer and IR spectrosc. investig. 7-5678
 TlI, X-ray photoelectron and Auger electron spectrosc. 7-5647
 Xe, electron elastic scatt., electron spin polarisation, electron spectra study, scattering and amplitude anal. 7-25651

electron spectra continued

- Xe, photoionis. with synchrotron radiation, angle-resolved electron spectra 7-905
 Xe photoionisation, photoelectron and electron momentum spectroscopy 7-36560
- electron spectrometers**
 see also beta-ray spectrometers
 Auger electron spectroscopy and X-ray photoelectron spectroscopy in surface anal. 7-24732
 calibration and quantitative Auger anal. 7-24729
 double-pass high-resolution electron energy loss spectrometer, design and performance 7-374
 double-pass high-resolution vibrational electron energy loss spectrometer 7-61404
 EELS, dual parallel and serial detection, design 7-18942
 EELS parallel detection setups 7-18943
 EELS spectrometer, magnetic shielding CAD 7-48923
 in-lens spectrometer for electron beam testing, secondary electron trajectories and fields calc. 7-61405
 magnetic scintillation electron spectrometer for cosmic radiation meas. 7-40715
 photoelectron spectrometer for vapour-phase species studies >2000K 7-35522
 positron beam surface anal. spectrometer, design features 7-36378
 threshold spectrometer, double cylindrical mirror analyser 7-24735
 trochoidal spectrometer, appl. to electron-molecule collisions study 7-57181
 tunnelling spectrometer using IEEE-48 instrument bus and IBM PC-XT controller 7-56383
 UV photoelectron spectrometer modification using pulsed free jets 7-36685
 Si:Li electron spectrometer for in-beam internal pair spectroscopy 7-49788
- electron spectroscopy**
 see also electron spectra; photoelectron spectroscopy
 AES and ISS, sputter depth profile analysis, hybrid electron-ion gun and CMA spectrometer 7-39941
 analyser with position sensitive detector, scattered electrons influence 7-36377
 angle resolved of gases and solid surface, UHV instrument 7-24730
 atoms, electronic struct. and dynamics study by electron spectrometry 7-36755
 attachment spectroscopy using modified electron capture detector 7-18947
 depth profiling, resolution improvement by superposition of original signals 7-54219
 depth profiling by lineshape anal. for XPS and AES 7-28380
 digital power supply and counting interface for UPS, XPS and Auger spectrometers 7-9825
 double-pass cylindrical-mirror analyzer, imaging props. charact. 7-24731
 EELS in a 400 kV transmission electron microscope 7-35644
 elastic peak electron spectroscopy 7-59314
 HV STEM and EELS at 1000 kV 7-1825
 inert gas atoms small angle differential cross sections for electron elastic scatt. 7-15713
 integral secondary electron spectroscopy (*Russian*) 7-61406
 laser plasma, stimulated Raman scatt. Thomson scatt., electron spectroscopy and IR diagnostics 7-37745
 momentum spectroscopy, differential cross section 7-36771
 optical surface contaminants identification, using electron spectroscopy and SEM techniques 7-4935
 poly-N $^+$ -trifluoroacetyl-L-lysine-polysarcosine diblock copolymers, ESCA of surfaces 7-21588
 polymer flashover potential, surface anal. using ESCA 7-33990
 predispersive electron gun for an electron monochromator 7-15034
 resolution function of CMA systems used for Auger signal measurements 7-30119
 resonant tunnelling electron spectroscopy, technique for hot electron energy distrib. determ. in semiconductors 7-45447
 secondary electron imaging, high resolution, in VG HB501 STEM 7-18932
 solid surface exam. by ion and electron spectroscopy, with angular resolution 2-6 $^\circ$ 7-32773
 submicron techniques, conf., Nova Scotia, Canada (July-Aug. 1984) 7-35104
 surface science, modern techniques, book 7-60911
 tetrabutylammonium iodide in formamide, surface segregation phenomena, angle resolved electron spectroscopy 7-52058
 time-resolved electron energy loss spectroscopy, position-sensitive detector performance 7-373
 transmission electron spectrometry for void detection in solids 7-39827
 UHV apparatus for heavy ion induced electron spectroscopy (*Japanese*) 7-56381
 CuBe, oxidised, secondary electron emitters, AES and ESCA studies (*Chinese*) 7-54238
 GaAs-oxide interfaces, defect stabilised electronic properties 7-38748
 NbC, amorphous films, prep. and characts. 7-7885
 TiC, amorphous films, prep. and characts. 7-7885
- electron spin**
 No entries
- electron spin echo** see spin echo (EPR)
- electron spin-lattice relaxation**
 anthraquinone anion radicals, frozen soln., ENDOR spectra, temp. depend. 7-7610
 p-benzosemiquinone radical anion, halogenated, mol. motion, electron spin relax. 7-45796
 dichlorobenzene-dibromobenzene mixed cryst., triplet electron spin dephasing, ODMR spectra study 7-33300
 disordered systems, spin-lattice relax. and vibr. mode localisation 7-64541
 electron relaxation studies, review 7-22158
 ethylsulphate:Nd $^{3+}$, high press. spin-lattice relax. and ground state 7-38934
 ferromagnets, electron and nuclear spin wave attenuation coeffs., scatt. by two-level systems (*Russian*) 7-27508
 (fluoranthenyl) $_2$ AsF $_6$, metal-semiconductor transition, anisotropic diffusion and electron spin relaxation 7-52598
 fractal structures, electron spin-lattice relaxation 7-45802
 III-V semiconductors, conduction electrons, spin relaxation, strain effects 7-38942

electron spin-lattice relaxation continued
laser pulse heated ferromagnets 7-64460
naphthazarine anion radicals in a glassy matrix of N,N-dimethylformamide, spin-lattice relax. 7-45823
poly-4(3-pyridyl)-8-methyl-2,3,6,7-quinolino ladder polymer, electronic props., I doping effects 7-64526
trans-polyacetylene: I, electron spin-lattice relax. and phase memory time, spin echo studies 7-64512
trans-polyacetylene, neutral soliton diffusion, EPR, PMR meas. 7-64513
trans-polyacetylene, pristine, neutral soliton dynamics, anisotropic ESR T₁ and line width 7-7585
quartz, neutron irradi., electron spin-lattice relax., effect of exchange interaction 7-45794
quartz spin-lattice relax. of AlO⁻ centres, EPR studies 7-38936
quasi 2D electron system, spin relax. 7-64101
Raman spin-lattice relax. rates, long wave approx. 7-33378
semiconductors, induced spin orientation and polarisation of paramagnetic centres interacting with photocarriers 7-7583
semiconductors with zinc-blende structure, electron spin relax. in a quantising mag. field 7-45822
X-band time-domain EPR spectrometer, computer-controlled 7-30054
Ag particles, electron spin-lattice relax. freezing-in, spin echo obs. 7-2921
K particles, electron spin-lattice relax. freezing-in, spin echo obs. 7-2921
Li particles, electron spin-lattice relax. freezing-in, spin echo obs. 7-2921
(Mg,Fe)SiO₃, hyperthene, Mossbauer spectra of Fe²⁺, electronic spin relax. 7-33307
Mg particles, electron spin-lattice relax. freezing-in, spin echo obs. 7-2921
MnSi, amorphous, concentrated spin glass, ESR study 7-13022
Na particles, electron spin-lattice relax. freezing-in, spin echo obs. 7-2921
PbTiO₃:Cr⁵⁺, ceramic, EPR, ENDOR, ESE investigs. 7-13020
a-Si:H, RF sputtered, dangling bond electron spin-lattice relaxation 7-22141
a-SiC:H, RF sputtered, dangling bond electron spin-lattice relaxation 7-22141
Ta complex, (BEDT-TTF)₂Ta₂F₁₁, optically enhanced phase transition, EPR investig. 7-64454
ZnTiF₆:Cu²⁺.6H₂O, Jahn-Teller effect and phase transitions, powder EPR study 7-13023

electron spin polarisation

see also CIDEP; spin polarised atomic hydrogen; spin polarised electron emission
alkali metal atoms, interaction with dichlorodimethylsilane coated reson. cells wall relax. 7-59317
clean and adsorbate surfaces, nonmagnetic, elastic spin-polarised LEED studies, book contrib. 7-32233
electron capture spectroscopy as a probe of surface electron-spin polarisation 7-59368
ferromagnets, inelastic electron scatt., spin-depend. energy loss processes, book contrib. 7-33500
LEED, spin polarised, dynamical theory 7-44316
magnetic films, Neel surface domain wall structures, spin-polarized SEM studies 7-13010
magnetic surfaces, electron scatt. and emission 7-59379
magnetic surfaces, polarised electron probes 7-33264
photoelectron spin-polarisation spectroscopy, appl. in adsorbate physics 7-3145
polarised electrons in surface physics, book 7-29607
polyatomic mols., stretching force consts., inner-shell polarisation effect, HFD calcs. 7-15588
s-f model with antiferromag. s-f exchange 7-45653
SEM, spin polarised, for mag. domains obs. 7-17197
surface and solid state physics based on spin polarised electrons (German) 7-64045
surface magnetism, spin-polarised electron diff. and photoemission 7-59380
surface magnetism, study by spin polarised electrons 7-2901
transition metal magnetism, singular volume dependence, spin-polarised band structure calcs. 7-22108
Xe, electron elastic scatt., electron spin polarisation, electron spectra study 7-25651
Bi, elastic scatt. of electrons, spin polarisation meas. 7-50364
Bi, low-energy electron elastic scatt. calcs. 7-50362
Cu (111), epitaxial FCC γ -Fe (111)p(1 \times 1) films, surface ferromagnetic order electron capture spectroscopy 7-45773
Fe epitaxial films, mag. size effects 7-59081
Fe itinerant ferromagnets, electronic struct. determ., spin depend. inverse photoemission studies, book contrib. 7-33479
Fe, Stoner excitations, free-electronlike, spin-polarised EELS 7-45648
Gd surface, evidence for ferromag. order above bulk Curie temp. 7-33173
He, electron impact excitation, fine-struct. effect, electron spin polarisation fn. 7-50374
He, liquid, spin-polarized, evidence for viscosity reduction 7-6909
He, spin-polarised, general model for steady-state melting 7-52184
Hg, elastic scatt. of electrons, spin polarisation meas. 7-50364
Hg, electron elastic scatt., electron spin polarisation, electron spectra study 7-25651
Hg, low-energy electron elastic scatt. calcs. 7-50362
Ir (111), spin-resolved photoemission meas. of transitions to secondary unoccupied bands 7-53501
Ni (110) with chemisorbed O₂ or CO, mag. props. investigated by spin-polarised electron beams 7-58994
Ni epitaxial films and interfaces with Cu and Pd, mag. size effects 7-59081
Ni itinerant ferromagnets, electronic struct. determ., spin depend. inverse photoemission studies, book contrib. 7-33479
Ni magnetic surfaces, elastic spin-polarised low-energy electron scatt., book contrib. 7-33494
Pb, elastic scatt. of electrons, spin polarisation meas. 7-50364
Pb, low-energy electron elastic scatt. calcs. 7-50362
Rb-Xe laser-enhanced spin-exchange collisions 7-10453
Ti, elastic scatt. of electrons, spin polarisation meas. 7-50364
Ti, low-energy electron elastic scatt. calcs. 7-50362
V, surface (100)p(1 \times 1), ferromag. order, electron capture spectra studies 7-27526
Xe, electron elastic scatt., electron spin polarisation, HF calcs. 7-25369

electron spin relaxation see electron spin-lattice relaxation
electron spin resonance see paramagnetic resonance
electron states, impurity see impurity electron states
electron states, surface see surface electron states
electron streams see electron beams
electron structure of solids (crystallography) see crystallography
electron structure of solids and liquids (energy structure) see electron energy states (condensed matter)
electron theory
see also quantum electrodynamics
atomic relativistic bound-state energies determ. extremum principles 7-868
relativistic self-interacting quantum electron, chaotic plane-wave solutions 7-41697
electron theory of metals see metal theory
electron traps
see also colour centres; hole traps; impurity electron states
amorphous semiconductors, multiple trapping, effect of defect level 7-27237
amorphous semiconductors, photoconductivity behaviour during the approach to steady state 7-38637
anthracene: acridine crystals, conduction mechanism and trap levels, TSC meas. 7-27342
anthracene single crystals, structural imperfections as triplet exciton traps, defect recovery 7-64160
chlorophyll *a*, pigment in diolephosphatidylcholine monolayer, fluoresc. conc. quenching master eqn. 7-50219
copper phthalocyanine evaporated thin films, mobility and trap concentration 7-2746
deep levels, electric field enhanced carrier emission, spectroscopic study 7-45350
dielectrics with deep traps, currents in strong elec. fields 7-33023
disordered solids, dispersive hopping and trapping transport, mean field theory 7-38554
dispersive trap-controlled carrier transport, surface pot. decay, space charge effects, finite difference calcs. 7-38588
double Schottky barrier, grain boundaries, elec. props. in presence of deep bulk traps, appl. to ZnO varistors 7-7334
glassy media, irradiated, excess electron capture, radiative and nonradiative mechanisms 7-27339
grain boundary trap occupancy and recomb. models anal. 7-64266
insulating films on semiconductors, conf., Toulouse, France (April 1985) 7-35103
ion-implanted polymers, fractal elec. cond., current transients, percolative transition calcs. 7-2645
metal-insulator-semicond. structs., interface state density profile determ., DLTS spectra interpretation 7-38733
methylmethacrylate-dimethacrylate oxymethylantracene polymer blend, γ -irrad., recomb. luminesc. spectra anal. 7-46145
MIS structure, small-signal DLTS response from insulator semiconductor interfacial traps, model anal. 7-64147
MNOS struct., bipolar injection and recombination, calc. 7-2726
molecular crystals, trapped electron Fermi distrib. 7-27286
MOS structure, X-ray irradi., interface trap annealing, two-reaction model 7-58901
MOS structures, interface and bulk traps, effect of processing steps 7-38758
MOS systems, interface state generation upon carrier injection 7-38759
multivalent traps, capture to emission ratios 7-7260
naphthalene crystals, indole admixture trap form., thermolum. study (Russian) 7-22357
polyethylene, electron beam charged, space charge decay currents 7-27338
polyethylene, thermally stimulated luminesc. and depolarisation, electron trapping studies 7-27651
polyethylene dielec. thin films, hot-electron-induced damage and charge storage, electron spectra studies 7-27662
polyethylene films, charge storage lifetime, structural effects 7-27344
polyphenylacetylene, plasma-polymerised, carrier traps 7-7263
polypropylene films, charge storage lifetime, structural effects 7-27344
polysilicon for solar cell appls., DLTS study 7-38512
polysilicon oxide, elec. cond. model 7-45526
polysilicon-SiO₂ interface, enhanced electron injection 7-38755
polystyrene film, electron thermalisation and trapping 7-27343
preexisting traps for electrons in polar liquids, model 7-21855
quartz, luminescence of pure and Ge-activated samples 7-46152
 α -quartz, synthetic, defects 7-63603
semiconductor fast surface state parameter meas. using SAWs 7-11230
semiconductor thin film, steady-state photoresponse under subbandgap illum., effect of surface states 7-64290
semiconductor thin films, bulk trap spectroscopy by temp.-modulated space-charge-limited current meas. 7-45338
semiconductors, compensated, impurity photoconductivity, field and spectrum dependences, exclusion effect 7-38635
semiconductors, deep level carrier capture and emission press. depend. meas., lattice relax. determ. 7-21862
tight-binding solids, theory of electron trapping by micropores 7-21870
TLD electron trap level determ. by two temperature annealing 7-16970
AlGaAs/GaAs modulation-doped heterojunctions, 2D electron gas, DX centres 7-38694
Al_{0.5}Ga_{0.5}As, hot-electron capture at DX centres 7-45344
Al_{0.5}Ga_{0.5}As MBE layers, deep electron traps, flux ratio effects 7-12641
As₂Se_{100-x}, vitreous chalcogenide semicond. layers, deep trapping levels, photostimulated effects (Russian) 7-2754
Au-GaAs, Schottky contact, interface states, trap characterisation 7-27421
Au-TiO₂:Nb diodes, trapping states, admittance spectra study 7-45494
Ba(PO₃)₂-LiF gamma irradiated activated glasses, optical absorpt. and ESR spectra corrls. 7-13030
Bi₂SO₂₀, trapping levels, obs. using photorefractive effect 7-12639
Bi₂SiO₂₀ photorefractive gratings, buildup and decay, effect of electric field 7-17306
CdInGaS₄ in MSM surface-barrier structs., photovoltaic effect and SCL currents 7-52687
CdIn₂S₄, electron trap characts., TSC meas. 7-27340
CdIn₂Se₄, energy spectra of local centres (Russian) 7-64150
CdSe:Cu, deep levels investigated by photoconductivity and space-charge region capacitance techniques 7-7148

electron traps continued

- CdTe, Schottky-barrier height determ. including electron-hole recomb. and electron trapping effects 7-2720
 Ga_{1-x}Al_xAs MIS and SIS structures, prep. by metallorganic chem. hydride method, electrophysical props. 7-22018
 GaAs, deep level nonradiative carrier capture press. depend. calcs. 7-12735
 GaAs, EL2 clusters, scattering and absorpt. of IR light 7-53382
 p-GaAs, electron irradiation-induced trap defects, DLTS study 7-12155
 GaAs epitaxial layer, EL2 midgap electron trap prod. by rapid thermal annealing, DLTS study 7-64154
 GaAs FET arrays, electrical parameter mapping 7-32438
 GaAs, hydride VPE layers, deep level incorporation and background doping 7-17120
 GaAs, IR imaging 7-32238
 GaAs, LEC-grown wafer, EL2 conc., stress distrib., near-IR absorption mapping 7-52522
 GaAs MBE layers, bias-dependent capture-emission processes, DLTS anal. 7-64166
 GaAs, MOCVD layers on Si substrates with superlattice intermediate layers, DLTS studies 7-38501
 GaAs, metastable defects, electronic Raman scatt. of nonequilibrium holes 7-26748
 GaAs, metastable state annealing 7-27297
 GaAs, midgap levels, quenching and recovery spectra measured by double-beam photoconductivity 7-58769
 GaAs, plastically deformed, spatial distrib. of dominant electron and hole traps 7-7160
 GaAs, semi-insulating bulk with thin conducting layer, optical DLTS distortions calcs. 7-58766
 GaAs, semi-insulating wafer, inhomogeneity characterization by scanning photo-induced current transient spectroscopy 7-7164
 GaAs, uniformity imaging 7-32481
 GaAs, vapour etching, buried interface, carrier traps 7-28213
 GaAs, variation of EL2 with As press. during heat treatment 7-58770
 GaAs:In, doped and undoped, EL2 maps from computer based IR image analysis 7-32237
 GaAs:In, strain effects, electrorefl. and photocapacitance study 7-22224
 GaAs:In MBE layers, defect density reduction by isoelectronic In doping 7-3176
 GaAs:Ni, acceptor like electron trap, DLTS study 7-7166
 n-GaAs:O, semi-insulating, impurity centres, electron capture 7-52643
 GaAs:Sn, epitaxial layers, current carrier distrib. 7-12530
 GaAs:Sn epilayers, MOCVD using triethylgallium and tetraethyltin, characterisation 7-22515
 GaAs-Al_{1-x}Ga_xAs quantum well structure, recomb. dynamics, photolum. obs. 7-12809
 GaAs-AlGaAs-GaAs large area graded gap diodes, discrete resistance levels obs. at low temps. 7-52749
 GaAs-Au Schottky diodes, DLTS 7-58896
 GaAs-Mo Schottky diodes, elec. characts. and microstruct. study 7-22015
 GaAs_{1-x}P_x crystals, electron-traps, DLTS study (Japanese) 7-7146
 GaAs_{1-x}P_x, EL2 level 7-21859
 GaP single crystals, anisotropic deep centres, polarised photolum. and thermolum. studies (Russian) 7-21867
 p-Ge, undoped, deep level defects produced by electron irradiation, annealing 7-12660
 HgCr₂Se₄ spinel magnetic semicond., electronic struct., elec. props., defects and ferromag. anisotropy 7-38857
 HgI₂ crystals, AC photoconductivity, temp. depend. 7-64278
 InP:Fe, transient photoconductive response 7-52681
 InP/Al UHV-cleaved and laser annealed interface, acceptor-like electron traps 7-7310
 InP-SiO₂ MISFET, electron tunnelling into oxide traps 7-38764
 K₂Cd₂(SO₄)₃:Sm, doped and undoped, thermoluminescence 7-39191
 Li-Al₂O₃-P₂O₅:Ag glasses, Ag⁰ centre thermal and photochemical conversion, spectroscopic consequences 7-39906
 LiNbO₃, pure and Mg, Fe doped crystals, photoconductivity props. studies 7-38624
 Mg₂Cd_{1-x}Se single cryst. solid solns., local centres parameters determ. (Russian) 7-32953
 MgO:Fe, gamma-ray and electron radiation-induced conductivity 7-33015
 a-Se, residual potential, dark discharge 7-27360
 Se vitreous chalcogenide semicond. layers, deep trapping levels, photostimulated effects (Russian) 7-2754
 Si, charged defect states at grain boundaries 7-44564
 a-Si, generation-recombination rate 7-33032
 Si layers, electron irradiation-induced defect levels, annealing behaviour, DLTS studies 7-52493
 Si, neutron-irradiated, relax. space-charge-limited current spectroscopy 7-38493
 Si, oxidation, trap generation by avalanche electron injection, HCl effects 7-3531
 Si p-amorphous/n-cryst. anisotype heterojunction characts., acceptor doping level depend. 7-7355
 Si, polycrystalline, H₂ passivation, grain boundaries, EBIC technique 7-26769
 Si polycrystalline layers, elec. props. and grain boundary carrier dynamics under solar illumination 7-38625
 Si, pyrogenic oxides, carrier trapping and breakdown, rel. to H₂O partial press. 7-64267
 Si, radiation-induced deep centres due to fast neutrons (Czech) 7-12661
 Si, recombination activity of dislocations 7-12733
 Si thin films, polycrystalline, elec. props. 7-33117
 Si:B, carrier lifetime meas., capture and recombination 7-38585
 Si:B, electron-irradiated, AC hopping conductivity and DLTS 7-44624
 n-Si:B⁺(BF₃)₂, ion implanted, rapid thermal annealing, DLTS 7-16619
 Si:C:O, heat-treated, photoconductivity relax., α traps 7-52677
 a-Si:H, carrier trapping and recombination, IR enhancement spectra of photoconductivity 7-33052
 a-Si:H, deep trapping, transient photocurrent saturation 7-21952
 a-Si:H, electron traps, telegraph noise spectroscopy 7-21928
 a-Si:H, neutral dangling bond defect, photocarrier processes 7-32962
 a-Si:H, photoconductivity exponent for recombination at dangling bonds 7-33054
 a-Si:H:F films, initial carrier trapping stages observed by femtosecond spectroscopy 7-27301
 Si:O, energy levels and capture cross-sections of thermal donors 7-16988
 Si:O, new donors, bound exciton recomb., photolum. study 7-22300

electron traps continued

- Si:O Czochralski wafers, electron traps resulting from O precipitation 7-21866
 Si:P, polycrystal. thin film, carrier transport, temp. depend. study 7-22043
 Si:Ti, deep level transient spectroscopy, transient capacitance data anal. 7-52526
 Si:Ti, ion implanted, deep level charactn. 7-38513
 Si/SiO₂, ion implantation-induced interface states generation and charge trapping study 7-12874
 Si/SiO₂, two-step oxidation of thin gate oxides, trapping characts., hot electron effect study 7-64351
 Si/SiO₂ interface, oxide trap capture cross section and tunnelling emission, DLTS study 7-12875
 Si/SiO₂/TiSi₂(WSi₂) MOS capacitors, radiation-induced interface traps 7-58897
 Si-SiO₂ interface, electrically active defects 7-33102
 Si-SiO₂ interface properties in the 10¹⁷-10¹⁹ cm⁻³ doping range 7-38762
 Si-SiO₂ MOS capacitors, defect struct. and interface state generation 7-7399
 α -SiC:N, single carrier SCL flow, computer calcs. 7-21925
 a-Si:N:H, electrical behaviour 7-2627
 Si₃N₄ MNOS structures, degradation, thermoactivation spectroscopic study 7-12872
 Si₃N₄ thin films, electronic conduction 7-58932
 SiO₂:N ultrathin films, carrier conduction, nitriding effects obs. 7-38790
 SiO₂, behaviour under high elec. field/current stress conditions 7-7254
 SiO₂ film MOSFET, excimer laser beam irradiation and RIE, radiation damage 7-2056
 SiO₂ films, energy levels of electron traps (Japanese) 7-64148
 SiO₂ films in MOS capacitors, ion implantation induced electron traps 7-38589
 SiO₂, hot carrier trapping characts., effect of post-oxidation annealing 7-64268
 SiO₂ MIS structures, trap generation under charge injection stress 7-7392
 α -SiO₂, quartz, E' centre, nonradiative charge transfer rate 7-12659
 SiO₂ thermal oxide films on Si substrate, ramp-voltage-stressed I-V characts. 7-17112
 SiO₂ thin films, constant current stressed voltage-time characts., dynamic trapping effects 7-45529
 SiO₂:Ge, impurity charge trapping props., EPR spectra 7-27290
 SiO₂:V amorphous films, Rf-sputtered, SCL conduction 7-64380
 SiO₂-Si interface, electronic state charactn. 7-38747
 Zn_{0.25}Cd_{0.75}Se mixed crystals, electron and hole deep level traps 7-16980
 ZnO varistors, bulk electron traps 7-45348
 ZnO:In films, microstruct., elec. and optical props., film thickness depend. study 7-16895
 ZnS:Al, Cr, Fe crystals, recomb. luminesc., EPR and photocond. meas. 7-3076
 ZnS:Al, electron capture processes, role of donors, transient ESR meas. 7-45347
 ZnS:Mn, thin film electroluminesc. capacitors, trapping level spectra 7-12666
 ZnSe:Al, MOCVD growth, deep level characterisation 7-52519
 ZnTe:O, red cathodolum. kinetics, two-step electron capture model calcs. 7-59262
- electron tube diodes** *see diodes*
electron tube rectifiers *see rectifier tubes*
electron tube testing
 proximity image intensifier persistence improvements with Y₂O₃:Tb phosphor 7-57598
- electron tubes**
see also cold-cathode tubes; diodes; electron emission; microwave tubes; relativistic electron beam tubes; tetrodes; thermionic tubes; triodes; ultra-high frequency tubes; vacuum tubes; X-ray tubes
 inverted coaxial diode with magnetic insulation, operating characts. 7-51523
- electron tunnelling** *see tunnelling*
electron valves *see electron tubes*
electron-wave tubes
see also klystrons; magnetrons; travelling-wave-tubes
 conf., Saskatoon, Canada, May 1986 7-29595
- electronegativity**
 acetylenes, substituted, spin-spin coupling consts., 7-31074
 actinide metals, solid state and thermodynamic props., f-electron bonding and struct., review 7-12321
 aqueous soln., free energies of hydration, ionisation pots., electron affinities 7-65292
 atomic ionisation pot. and orbital electronegativity, physical significance of local density functional theory eigenvalues 7-62245
 atoms and groups, relationship between charge capacity and hardness 7-49972
 bond form., atomic orbital deform., energy effects 7-25439
 main group elements, electronegativities and hardnesses, bond hybridisation effects 7-36446
 metal complexes, co-ordinates stoichiometry, K-absorption edge shifts and effective nucl. charge 7-5697
 reduced electronegativities and atompolarizabilities of certain elements 7-5784
 semiconductor heterojunction band discontinuities, dielec. electronegativity anal. 7-2699
 tetrahedral molecules, hybrid orbitals with d-character 7-56940
 transition metal complex, charge distrib. calc. (Chinese) 7-15534
 tribromomethyl radical, geometry and electronic struct., SWX α calcs., ab initio UHF calcs. 7-19703
 AsS, realgar, X-ray chemical shift, K absorpt. spectra anal. 7-46239
 As₂S₃, orpiment, X-ray chemical shift, K absorpt. spectra anal. 7-46239
 Au-Ni-Cu, diffusion of Au and Cu through Ni layer, depend. on ambient 7-38266
 CoAs₃, smaltite, X-ray chemical shift, K absorpt. spectra anal. 7-46239
 Cs halides, low energy electron collisions, cross section-electronegativity relation 7-20061
 FeAsS, arsenopyrite, X-ray chemical shift, K absorpt. spectra anal. 7-46239
 Mo (100), chemically modified, chemisorption bond energies of Lewis acids and bases 7-23056

Electronegativity continued

- Mo (100), chemically modified by adsorption of B, C, O, CO, surface atom oxidation states, ESCA meas. 7-28333
 Ni (100), adsorption of CO, poisoning in heterogeneous catalysis, role of electronegativity 7-13818
 SF₆, electronegative gas, electron beam transmission anomalies study 7-44094
 SO₂-containing cpds., Cl effect on ³³S and ¹⁷O NMR 7-36646

Electronic conduction in crystalline semiconductor thin films

- for electronic conduction in amorphous thin films, see "electrical conductivity of amorphous semiconductors and insulators"
 see also electrical conductivity of amorphous semiconductors and insulators; electrical conductivity of crystalline semiconductors and insulators; electrical conductivity transitions
 aromatic hydrocarbons, semicond., nondispersive transport, model of difficult jumps 7-58812
 copper phthalocyanine evaporated thin films, mobility and trap concentration 7-2746
 diamond:P(B) (Russian) 7-16587
 epitaxial layers, recombination lifetime profiles meas., injection level depend. 7-52874
 films, plasma deposited from methane, elec. conductivity, optical absorpt. 7-38786
 hot electrons under quantum size effect conditions 7-38780
 In_{0.33}Ga_{0.67}As:Fe metalorganic CVD epitaxial growth and elec. props. 7-63993
 ion implantation in Si polycrystalline films, annealing, sheet resistance 7-12886
 lead phthalocyanine, electrical props., influence of I impurity 7-58927
 lutetium bisphthalocyanine, doped p- and n-type thin films, cond., visible spectra anal. 7-52865
 organic layers, carrier drift mobility, anomalous field depend. 7-58928
 phthalocyanine thin films, gas-surface reactions, elec. cond. meas., ESCA 7-52262
 polysilicon thin films for VLSI, elec. props. 7-38789
 semi-insulating polycrystalline films, electrical conduction mechanism 7-52869
 semiconductor epitaxial layers, sharp doping profiles determ. 7-12111
 size quantised films and wires, cond., carrier quasielastic scatt. by acoustic phonons 7-38781
 TCNQ salt, conducting Langmuir-Blodgett film, electronic transport props. 7-38782
 zinc phthalocyanine thin films, electrical, structural and gas sensing props. 7-38787
 n-Al_{1-x}Ga_{1-x}As epitaxial layers, graded-gap, resistance, press. dependence 7-33113
 Al_{1-x}Ga_{1-x}N MOVPE growth, struct. and elec. props. 7-21729
 Bi thin films, lattice thermal cond. meas., modified Mayadas-Shatzkes model 7-21554
 Bi-Sb:Te(Sn) thin films, elec. props. 7-64376
 Bi_{2-x}As_xS₃ thin films, solution-gas interface deposition technique 7-7901
 Cd_{0.8}Hg_{0.2}Te MOVPE layers, elec. props. and Hall effect behaviour 7-27444
 CdIn₂O₄ RF sputtered films, transparent heat mirror characts., elec. and optical meas. 7-39199
 CdS films in CdS/CdTe solar cells, film thickness effects on photovoltaic props. 7-65468
 CdS photoconductive thin films, optimum spray pyrolysis preparation conditions 7-17418
 CdS polycrystalline films, temp. variation in thermoelectric power 7-22048
 CdS thin films, deep trap depth, TSC meas. 7-58774
 CdSe_{1-x}Te_x inhomogeneous solid soln., semicond. films, Hall effect temp. depend. meas. 7-58915
 CdSnO₄:PbO highly conducting films, characterisation 7-22049
 Cd₂SnO₄ CVD, struct., elec. and optical props. (Korean) 7-27940
 Cd₂SnO₄ transparent thin film electrodes prepared by DC reactive sputtering from Cd-Sn alloy targets 7-22477
 CdTe films, electrochemically deposited, resistivity, carrier conc. and carrier mobility 7-7419
 CdTe grown on Si by LPMOCVD, physical props., Hall meas. 7-27181
 CdTe layers, electrochemical deposition, struct. and elec. props. 7-12526
 p-CdTe RF sputtered thin films, resistivity, forbidden gap, optical and X-ray diff. spectra studies 7-21747
 CdTe, very high conductivity films, formation and props. 7-45522
 CuBiS₂ thin films, spray pyrolytic deposition, elec. and optical props. 7-7894
 CuGaSe₂ thin films, flash evaporated, optical and elec. props. 7-7417
 CuGaSe₂ thin films, physical props. and photovoltaic potential 7-22047
 CuGaTe₂ thin films, elec. cond., 100-300K 7-22042
 CuInSe thin films, flash evaporation prep. and characterisation 7-7893
 CuInSe₂, flash evaporation, elec. and optical props. 7-7892
 CuInSn₂ thin films, flash evaporated, electrical cond. and optical absorpt. spectrum 7-33112
 CuInSe₂ thin films, polycrystalline, elec. props., effect of excess Cu 7-52871
 CuInSe₂-CdS solar cells and CuInSe₂ thin films, charge transport studies 7-12890
 CuInTe₂ thin films, flash evaporated, elec. conductivity, optical absorption 7-7428
 Cu₂S films, flash-evaporated, optical props. and solar selectivity 7-64719
 n-GaAs compensated samples, MOVPE grown, Hall effect meas. 7-27348
 GaAs epitaxial layers, vacancy doping 7-6656
 GaAs epitaxial layers grown directly on Si (100) by low press. MOVPE 7-27924
 GaAs high quality layers grown on Si by MOCVD, high electron mobility 7-27922
 GaAs, MOCVD, plasma stimulation, growth kinetics, elec. props. 7-22548
 GaAs thin films, grain boundaries, electronic props. 7-7172
 GaAs thin films, on glass substrates, transport props. 7-2742
 GaAsS layers obtained by gas-phase epitaxy, electrophysical props. 7-7418
 GaAs:Si heteroepitaxial growth on sapphire, low press. MOCVD three-step method 7-27927
 GaAs:Sn, epitaxial layers, current carrier distrib. 7-12530
 GaAs:Sn epilayers, MOCVD using triethylgallium and tetraethyltin, characterisation 7-22515
 GaAs:Te films, flash evaporation, annealing, elec. props. 7-64373

Electronic conduction in crystalline semiconductor thin films continued

- GaN films, epitaxial growth by reactive ion plating, elec. props. 7-3206
 GaN:Zn films, MOVPE, electron cyclotron resonance plasma excitation, low temp. growth, elec. props. 7-22549
 Ge polycrystalline films, photoassisted CVD prep. 7-3200
 HgCdTe epitaxial layers, Hall effect and elec. resist. characterisation 7-64375
 p-Hg_{0.78}Cd_{0.22}Te:Sb LPE films, elec. props. 7-7426
 HoH₂ films, H annealing, elec. resist. 7-64000
 InGaAlP epilayers, MOCVD, laser appl. 7-39404
 In₂O₃:Sn, sputtered films prep. and optical props. 7-53587
 In₂O₃:Sn evaporated films, optical props. and applications to energy-efficient windows 7-46157
 In₂O₃:Sn films, prep. by thermal decomposition of organometallic cpds., optical and electrical props. 7-17483
 In₂O₃:Sn vapour deposited films, growth, struct., electronic props. 7-12535
 In₂O₃:Sn(In)(Cd) films, optical and elec. props. 7-22365
 In₂O₃Sn thin films, prep. by pyrolysis, props. 7-2749
 n-InP compensated samples, MOVPE grown, Hall effect meas. 7-27348
 InP pure and Er doped liquid phase epitaxial films, elec. props. in strong elec. fields 7-38779
 InP, undoped and Zn(Cd) doped thin films, prep. and characts., appl. for solar cells 7-17895
 InP:Fe, epitaxial layers, MOCVD, doping profiles, SIMS, resist., temp. depend. 7-21248
 InP:Fe, OMVPE grown, electronic and optical props. 7-52868
 InP:Fe semi-insulating layers, MOVPE growth and elec. characts. 7-22511
 InSe and γ -In₂Se₃ films, formation by double source evaporation 7-59436
 γ -In₂Se₃ bound layer, elec. props. and surface states (Japanese) 7-22038
 In_{2-x}Sn_xO_{3-y} films, reactive RF magnetron sputtering prep., elec. and optical props. 7-46324
 In_{2-x}Sn_xO_{3-y} sputter deposited, elec. cond., oxidation resistant coatings for spacecraft applic. 7-22866
 In_{2-x}Sn_xO_{3-y} thin films, RF reactive sputtering prep., elec. and optical props. 7-39378
 MoS₂ films, RF magnetron sputtered, elec. and optical props. 7-2747
 NiS thin films, deposition by soln. growth techniques, X-ray diff., optical, elec. meas. 7-32870
 NiSe thin films, deposition by soln. growth techniques, X-ray diff., optical, elec. meas. 7-32870
 PbSe films, elec. cond. and thermoelec. power, dynamic behaviour 7-2750
 PbSe films, photosensitivity mechanism 7-58923
 Pb_{1-x}Sn_xTe films prepared by MOCVD, elec. props. 7-27919
 PbTe films and electrical contacts with Au, Al and Ag, photothermal deflection meas. 7-38784
 PbTe films prepared by MOCVD, elec. props. 7-27919
 PbTe:Ti(Ti,Na) films, superconducting transition 7-38797
 SbI₃, photosensitive, heating effect on elec. cond., switching behaviour 7-58920
 Si bicrystals and thin films, grain boundaries, electronic props. 7-7172
 Si CVD thin film, struct. and elec. props. 7-21730
 Si, crystallised thin films, electrical characterisation 7-33116
 Si, epitaxial growth using photochem. vapour deposition at 200°C 7-39431
 Si epitaxial layers, VPE growth, charactn. (Japanese) 7-63986
 Si, heteroepitaxial growth on ZrO₂-Y₂O₃ substrates 7-21735
 Si, MBE dopant profiling, electrochemical CV technique 7-12108
 Si, MBE grown, abrupt doping profiles, spreading resist. determ. 7-12110
 Si MBE layers, spreading resist. anal. carrier spilling effects 7-2741
 Si MBE layers, spreading resist., etching, bevelling, staining characterisation techniques 7-12891
 Si, microcrystalline films, carrier lifetime from transient photoconductivity meas. 7-7290
 Si polycrystalline film, mobility temp. depend. (Chinese) 7-2744
 Si, polycrystalline films, undoped, nonlinear I-V characteristics 7-22039
 Si thin film, doped, electron beam evaporation, elec. props. 7-2743
 Si thin films, polycrystalline, elec. props. 7-33117
 Si:As, ion implanted polycrystalline films, electrical activation by rapid thermal annealing 7-58914
 Si:As films, preannealed and As ion implanted, structural changes during transient post-annealing 7-16904
 Si:As(B) polycrystalline films, rapid thermal processing before and after ion implantation, effect on cond. 7-22046
 Si:Ga MBE layers, ion implantation doping using liq. metal ion source, carrier conc., spreading resist., SIMS profiles 7-12563
 Si:H,Ge single junction and tandem solar cells, thin film properties and corollary plasma diagnostics 7-13893
 Si:H films, ion implant redistribution 7-16921
 Si:P, polycrystal. thin film, carrier transport, temp. depend. study 7-22043
 Si:P films, CVD and electrical props. 7-64913
 Si:P(B) LPCVD films, amorphous and polycrystalline, struct., elec. resist. meas. 7-52870
 Si:Sb, pot. enhanced doping during MBE growth, elec., optical props., cryst. quality 7-12112
 Si:Sb(As)(P)(B) epitaxial films, low temp. deposited by low press. CVD, autodoping 7-27182
 β -SiC CVD film growth and props., gas phase comp. depend. simulation and meas. 7-22516
 SiC, growth, struct., and elec. props. 7-52354
 β -SiC:Al⁺(P⁺) epitaxial films, ion implanted, rapid thermal annealing 7-16905
 β -SiC:B(N) films, ion implanted, rapid thermal annealing 7-17569
 Si_{1-x}Ge_x, epitaxial growth, struct., and elec. props. 7-52354
 SiN_x:H,B microcrystalline, wide-gap, RF glow discharge deposition 7-22503
 SiN_x:H,B microcrystalline films, B doping 7-44586
 SnO₂ films for solar cells, struct., elec., and optical props. 7-40003
 SnO₂, oriented thin films, elec. props. 7-17123
 SnO₂:Cl coatings, electrical and optical props. 7-58925
 SnO₂:F thin films, CVD deposition, elec. and optical props. 7-7425
 SnO₂:Sb spray deposited coatings, comp., elec. props. thermal treatments, AES study 7-22393
 SnO₂:Sb thin films, doped and undoped, prep. by photolysis, phys. props. 7-22368
 Zn_xCd_{1-x}Sn thin films, struct. and electrical props. 7-64372

electronic conduction in crystalline semiconductor thin films continued

- ZnO films, elec. props., decomp., chemisorption of O^- , photocond. meas. 7-27445
 ZnO films, with high elec. resistance, conductivity-controlled preparation 7-17122
 ZnO films with high resistance, electrical conductivity, press. and temp. depend. 7-22044
 ZnO thin film preparation by spray pyrolysis for photoelectrochemical solar cells 7-23166
 ZnO:Al films, RF reactive sputter deposition, struct., elec. and optical props. (Japanese) 7-27900
 ZnO:Ga thin films, temp. depend. of conductivity, effect of H_2O vapour chemisorbed states 7-7427
 ZnO:Si thin films, RF magnetron sputtered, conductive and transparent props. 7-22476
 Zn_3P_2 polycrystalline films, hot-wall deposited, elec. and optical props. 7-22487
 Zn_3P_2 thin films, amorphous-crystalline transitions, elec. cond., 100-300K 7-38560
 ZnS:Al, low resistivity, grown by MOVPE 7-27921
 ZnSe epitaxial layers, MOVPE grown, elec. and photolum. props. 7-7420
 $(ZnTe)_x(CdTe)_{1-x}$ films, CVD fabricated, phys. props. 7-7055
 ZnTe films, vacuum deposition, elec. resist. and photocond. meas. 7-3179

electronic conduction in insulating thin films

- see also *electrical conductivity of amorphous semiconductors and insulators; electrical conductivity of crystalline semiconductors and insulators*
 amorphous thin films, elec. resist. meas. at high temps. (German) 7-33118
 C thin films, RF discharge deposition, mech., elec. and optical props. 7-22509
 diamond layers, elec. props. (Russian) 7-17124
 films, plasma deposited from methane, elec. conductivity, optical absorpt. 7-38786
 polybutadiene thin films, elec. cond. in sandwich config., I-V characts. meas., electrode effects 7-27449
 polychlorophenylacetylene, elec. cond., carrier mobility, doping effect 7-52875
 polyoxy-(allyl)phenylene electrochemically prepared film, elec. props., permittivity and solubility 7-27665
 polyphenylacetylene, elec. cond., carrier mobility, doping effect 7-52875
 polypyrrole salt films, conductivities, acid and base effects 7-12893
 polysilicon oxide, elec. cond. model 7-45526
 polysilicon- SiO_2 surface texturing effect on SiO_2 cond. and breakdown 7-39773
 polythiophene film, photoinduced effects 7-52876
 polyvinyl alcohol films, elec. cond., 293 to 353K 7-45530
 PTFE, chem. modified, humidity sensor appls. 7-9839
 steel, austenitic stainless, passive layers, elec. cond. rel. to W alloying 7-17676
 transparent conducting oxides, uses in a-Si:H solar cells 7-46953
 $AgInTe_2$ polycrystalline thin films, elec. and optical props. study 7-58924
 AlN_x nonstoichiometric sputtered films, electron localisation, transport props. 7-58929
 Al_2O_3 insulating thin films, normal press. CVD (German) 7-59453
 C diamondlike coatings, ion beam induced conductivity and structural changes 7-22053
 C films, transparent, sputter- and plasma-deposition 7-22474
 C layers, deposition, by RF plasma decomp., physical props. 7-22508
 CaF_2 , crack-free epitaxial film, on GaAs (100), surface morphology, elec. props. 7-39392
 $\gamma-Fe_2O_3$ reactive RF sputter deposition, struct., elec. and mag. props. studies 7-17421
 $GeO-BaO$ thin films between metallic electrodes, elec. props. 7-22054
 Mn/SiO_2 thin cermet films, electroformed characts. in dielec. range 7-12892
 MoS_2 , amorphous thin films, elec. resist. meas. at high temps. (German) 7-33118
 Nb-Ti-O ceramic coatings, synthesis by reactive ion plating and sputter deposition, struct., electrophysical props. 7-64031
 PbO chemically deposited layers, electrical props. 7-64377
 Ru-Ti-O ceramic coatings, synthesis by reactive ion plating, struct., electrophysical props. 7-64031
 Si/SiO_2 system, dielec., elec. and struct. props. 7-7040
 Si-N-H glow-discharge films, elec. and optical props., comp. depend. 7-58933
 Si_3N_4 films in MIS structs., cond. characts. 7-38793
 Si_3N_4 films prep. by ECR plasma CVD, phys. and elec. props. 7-58716
 Si_3N_4 MIS struct., electron transport and heating, vacuum emission studies 7-2723
 Si_3N_4 thin films, electronic conduction 7-58932
 Si_3N_4 thin films, growth by microwave-excited plasma 7-59458
 Si_3N_4 thin films, reactively sputtered, hopping cond., defect states 7-52620
 Si_3N_4 thin films in MNOS structs., charge transport in elec. fields 7-12730
 a- $Si_3N_4:H$ films deposited by plasma enhanced CVD, optical and elec. props. 7-39205
 $SiO-SnO_2$ vac. evaporated films, AC elec. props. 7-45528
 SiO_2 :N ultrathin films, carrier conduction, nitriding effects obs. 7-38790
 SiO_2 CVD photox layers, Hg-sensitised, elec. props. 7-64379
 SiO_2 deposition by photo-initiation 7-59454
 SiO_2 films, LPCVD from diacetoxymethyltrimethoxysilane in temp. range 450 to 600°C 7-53622
 SiO_2 layers, electrical properties 7-58931
 SiO_2 layers, thermally nitrided, charge transport 7-38791
 SiO_2 on polysilicon, thermally grown, elec. cond. and breakdown props. 7-45508
 SiO_2 RF sputtered thin films, atomic defects and stresses, optical and elec. props. 7-16898
 SiO_2 thermal oxide films on Si substrate, ramp-voltage-stressed I-V characts. 7-17112
 SiO_2 thin films, growth by microwave-excited plasma 7-59458
 SiO_2 thin films, production from glow discharge decomp. of NO-SiH₄ mixtures, elec. props. 7-22512
 $SiO_2:V$ amorphous films, RF-sputtered, SCL conduction 7-64380
 SiO_x films in MIM struct., thermal voltage memory effect, time depend. 7-45527
 $SiO_x:P$ films, pure and doped, low press. CVD growth, structural, optical, elec. props. 7-27186

electronic conduction in insulating thin films continued

- SiO_xN_y , high press. NH_3 -nitrided, elec. characts. 7-39039
 SiO_xN_y MIS struct., electron transport and heating, vacuum emission studies 7-2723
 SiO_xNy LPCVD layers, phys. and elec. charactn. 7-38792
 SnO_2 films, CVD deposition, elec. and optical props. 7-7429
 $SnO_2:F$ thin film, uses for a-Si:H/a- $Si_{1-x}C_x$:H solar cells 7-46952
 Ta_2O_5 film, photocurrent and elec. cond. mechanism, electrode interface effects studies 7-27366
 TiN_x epitaxial layers, atomic and electronic struct., growth, physical props. 7-32854
 $TiSi_2$ ultrafine powder prep. and film charactn. 7-64975
 VO_2 film, cond., magnetoresist. and nonlinear resist. in strong elec. field, metal-insulator transition study 7-52706
- electronic conduction in metallic thin films**
 see also *discontinuous metallic thin films; electrical conductivity of amorphous metals and alloys; electrical conductivity of crystalline metals and alloys*
 cylindrical films, magnetoresist. in weakly localised regime 7-7414
 discontinuous films, charge carrier mobility, temp. depend. 7-22035
 electron localisation and size effect in single-crystal films 7-17118
 electron mean free path, average, stat. model calc. 7-58911
 evaporated films, elec. resist., influence of surface roughness (German) 7-64368
 fine wires, quantum transport effects 7-52767
 locally discontinuous thin films, gas-sensitive electrical conduction 7-12882
 plasma-enhanced CVD for metallisation appls. 7-17459
 polycrystalline, DC conductivity 7-52566
 polycrystalline multi-layered thin films, elec. transport props. 7-64363
 size effect in thin wires, analytical expression w.r.t. Cotey mean free path 7-12885
 specular reflection coefficient of polycryst. thin metal films, effect of ageing 7-12884
 thin films of diluted ferromag. alloys, mag. contrib. to elec. resistivity 7-22036
 transition metal disilicide films, electrical transport props. 7-58908
 vapour quenched films, resistivity meas., indirect obs. of amorphous to crystalline transition 7-52864
 Ag contacts, transparent, for a-Si solar cells with ITO antireflection coating 7-65478
 Ag discontinuous films, large scale coalescence, post-deposition DC resistance increase 7-45069
 Ag films, vapour-quenched, elec. resistivity (Japanese) 7-33107
 Ag, resist. increase during O_2 adsorpt., surface roughness effects calcs. 7-45519
 Ag, thin films, chemisorption of O, electrical resistivity meas. 7-33110
 Ag thin films, discontinuous, post-deposition resist., ageing studies 7-58909
 Ag ultrathin films, elec. cond., size effects (Russian) 7-45520
 Ag-D films, implanted, elec. resist. meas., vibr. props. 7-38775
 Al discontinuous films, large scale coalescence, post-deposition DC resistance increase 7-45069
 Al film resistivity depend. on thickness and annealing time 7-11242
 Al foils, alumina form. by O_2^+ implantation, sheet resistance and XPS meas. 7-26780
 Al thin films, elec. cond. quantum size effect, Kubo formalism study 7-22034
 Al thin films, pulsed laser melting, transient elec. resist. and reflectance meas. 7-12141
 Al-Mo multilayered films, struct., elec. props. 7-58863
 Al-Nb amorphous films, elec. props. and charactn. (Japanese) 7-32977
 Al-Ni multilayered films, struct., elec. props. 7-58863
 Al-Ti-based homogeneous alloy films, elec. resist., microstruct., electromigration, comp. effects 7-21765
 Au, discontinuous films, percolation metal-insulator transition, nonlinear behaviour 7-45156
 Au films, sputtered, optical and elec. props., influence of surface scatt. of electrons 7-52858
 Au, temp. depend. of elec. resist. 7-58792
 Au-Ag sandwiches, grain boundary electron scatt. (Russian) 7-12883
 Au-Fe, dil., Kondo system, mag. scatt. time of conduction electrons meas. 7-21902
 Au-Pd thin films and wires, localisation and electron-electron interaction effects, magnetoresist. meas. 7-52863
 Au- SiO_2 -Bi, low temp. hot electron energy relaxation and inelastic collision times in thin metal films 7-27441
 $AuIn_{2+3}$ thin films, resistivity 7-7410
 Bi films, elec. resistivity, 1600-4500 angstroms 7-2737
 a-C-Ag thin multilayer struct., vacuum condensation, interface development, sheet cond., thickness 7-21681
 a-C-Au thin multilayer struct., vacuum condensation, interface development, sheet cond., thickness 7-21681
 Co-Si bilayered films, chem., elec., and struct. charges upon annealing 7-22037
 $CoSi_2$, electrical transport props. 7-27442
 Cr_7Si_{15} thin films, microstruct. and resist., room temp. to 950°C 7-38410
 Cu and Cu/Ag composite discontinuous thin films, aging and field effect studies 7-7413
 Cu discontinuous films, aging, elec. field and temp. effects 7-64364
 Cu discontinuous films, large scale coalescence, post-deposition DC resistance increase 7-45069
 Cu films, vapour-quenched, elec. resistivity (Japanese) 7-33107
 Cu thin films, discontinuous, post-deposition resist., ageing studies 7-58909
 Cu thin films, elec. cond. quantum size effect, Kubo formalism study 7-22034
 Cu-Al film resistivity depend. on thickness and annealing time 7-11242
 Cu-Mg amorphous alloys, 2D weak localisation effects 7-21871
 Dy thin films, conduction electron scattering on magnetic spin system 7-64362
 Dy thin films, influence of thickness on mag. phase transitions 7-38860
 Fe, films, ethane and ethylene adsorpt. and reaction, mass spectra, XPS, UPS, electrical resistance and work function meas. 7-32837
 Fe-Ti amorphous thin films, RF sputtered, struct. and elec. meas. 7-12534
 $Fe_{1-x}Si_x$ amorphous films, Hall effect and mag. anisotropy 7-2911
 Ga crystalline film amorphisation by pulsed excimer laser irradi., residual resist. and T_c meas. 7-12140

electronic conduction in metallic thin films continued

- GdFe and GdCo amorphous thin films, electrical conductivity, influence of mag. order 7-7409
 HoH, films, H annealing, elec. resist 7-64000
 In film, irreversible resistivities during annealing process 7-64365
 LaNi₅H films, resist. rel. to hydrogenation 7-58910
 Mg-Fe, dil., Kondo system, mag. scatt. time of conduction electrons meas. 7-21902
 Nb:He⁺ (H⁺) films, radiation defects produced by ion implantation 7-7059
 Nb-Si films, superconducting fluctuations weak localisation and electron interactions 7-2783
 Nb_{100-x}B_x alloy films, sputtered, elec. cond., hardness, amorphous and crystal struct. 7-13354
 Ni, films, ethane and ethylene adsorpt. and reaction, mass spectra, XPS, UPS, electrical resistance and work function meas. 7-32837
 Ni single crystal films, resistivity ratio and mean free path length 7-52857
 Ni-B amorphous films, ion implanted and sputtered, elec. props. 7-22032
 Ni-Cr vacuum deposition for reproducible thin film resistors, book contrib. 7-46332
 Ni-Cr-Al films, thin film resistor appl., struct., temp. coeff. of resist. props. 7-58912
 Ni-Cr-Si thin films, influence of Si on props. 7-22493
 Ni-Si bilayered films, chem., elec., and struct. charges upon annealing 7-22037
 NiAl thin films, ion irradi. induced amorphisation studies rel. to cascade parameters 7-63671
 NiSi₂, electrical transport props. 7-27442
 Pb, temp. depend. of elec. resist. 7-58792
 Pd films, vapour-quenched, elec. resistivity (*Japanese*) 7-33107
 PdH, thin film thickness depend. resistivity changes meas. 7-33109
 Pt, sputtered films on ZrO₂ substrates, agglomeration and electrical conduction props. 7-52859
 Rh polycrystalline films, electrical size effects 7-7412
 Sn-GeO granular films, struct., resistivity and superconducting props. study 7-45082
 TaSi₂, electrical transport props. 7-27442
 Te crystalline thin films, laser-induced transform., transient conductance and optical meas. 7-12142
 Ti film on Si, heat treatment in O₂, N₂ or O₂/N₂, Ti silicides, TiO and TiN formation 7-65191
 Ti thin films, dissolution and diffusion of O, resist., X-ray diffr., particle backscatt. and AES studies 7-58913
 TiB₂ plasma-enhanced CVD films on Si, furnace annealing, metallisation appls. 7-38411
 TiSi₂, electrical transport props. 7-27442
 TiSi₂ films on polysilicon, elec. resist., implications for low temp. appls. 7-58907
 TiSi₂ formation on Si by rapid thermal annealing 7-21707
 TiSi₂ thin films, production by LPCVD, charact. (*French*) 7-7888
 V polycrystalline films, struct. defect disappearance, activation energy, elec. resist. meas. 7-26740
 V-Si films, electrical transport props. 7-33108
 VO₂ film, cond., magnetoresist. and nonlinear resist. in strong elec. field, metal-insulator transition study 7-52706
 W and refractory metals, VLSI appls., conf., Albuquerque, NM, USA (Nov. 1984 and Oct. 1985) 7-14715
 W CVD films on Si substrate, growth kinetics and elec. props. 7-16909
 W film deposition by photolytic dissoc., charact. 7-17466
 W films, amorphous and finely cryst., elec. props. (*Russian*) 7-38776
 W films, LPCVD deposition kinetics in single wafer vacuum reactor 7-59448
 W films, magnetron sputtering prep., elec. and mech. props. 7-16913
 W films on GaAs substrates, electrical resistivity after high temp. annealing 7-64366
 W films prep. by various deposition methods, effects on elec. resist. 7-52860
 W LPCVD films by WF₆/Si reduction method, influence of deposition variables 7-17461
 W, LPCVD from W(CO)₆ in hot-wall environment 7-17465
 W reactively sputtered films, elec. resist., microstructure, effects of N or O partial press. 7-52861
 W selective LPCVD films on Si substrate, characts. 7-38409
 W, selective LPCVD on Si substrate, elec. and struct. props. 7-17467
 W sputter deposited films, impurity effects on elec. props. 7-52862
 W-Si system, selective deposition of W films on Si wafers, WSi₂ formation 7-21748
 WSi₂ amorphous films, crystallisation, stacking faults and resistivity 7-21759
 WSi_x films, CVD, resistivity and composition changes by annealing 7-2738
 WSi_x films, sputter deposited from cold pressed, vacuum sintered composite target, annealing, comp., resist. meas. 7-21719
 Y₃Ni₁₅, sputtered amorphous film, Hall effect (*Chinese*) 7-64202
 ZrN reactively sputtered films, elec. charact. rel. to submicron gate electrode appls. 7-38777

electronic density of states

- 7-27867
 1D chain with random distribution of linear side branches and loops, electronic props. 7-64191
 1D disordered systems, relativistic electronic states 7-12584
 2D systems, proceedings of Winter School, Mauterndorf, Austria (Feb. 1986) 7-48131
³He-A superfluid, chiral anomaly, finite fermion vacuum current calcs. 7-44945
 A15 cpds., normal, long-wavelength static spin suscept., temp. depend., electron-phonon interaction effects 7-64103
 A15 superconductors, anomalous ultrasound absorption 7-17135
 A₂B_{1-x}BCC alloys, low temp. props., spin fluctuations, alloying effects 7-52402
 alloys, binary, short range order, coherent pot. approx. 7-7142
 alloys and metals, packing defect energy rel. to electron density (*Russian*) 7-45212
 amorphous semicond. III-V and II-VI cpds., electronic struct. of bulk and defect sites, tight-binding recursion method 7-45222
 amorphous semiconductors, multiple trapping, effect of defect level 7-27237
 amorphous semiconductors, optical absorpt., tight-binding model 7-45961

electronic density of states continued

- analytic-quadratic method of determ., singular integrals over Brillouin zones 7-7085
 Anderson model, transport props. at low temps. 7-27311
 apparent atom size w.r.t. density of states in scanning tunnelling microscope, bias voltage depend. 7-44321
 β -(BEDT-TTF)₂I₃, electronic and struct. props., ¹H NMR meas. 7-53170
 binary compound polar semiconductors with nonparabolic energy bands, electronic struct. 7-2478
 binary non-crystalline alloys, electronic density of states calc. 7-45112
 bremsstrahlung isochromat spectroscopy for electronic struct. of semiconductors and heterojunctions 7-52795
 C* algebras, K-theory for density of states, Shubin's formula 7-58725
 chalcogenide glasses, electrons in mobility gap, spectra and thermodynamic props. 7-2471
 composite superconductors, density of states of normal section calc. 7-52386
 d- and f-metals and alloys, anomalous props. due to charge density fluctuations 7-7132
 deformable jellium model, electronic density of states calcs. 7-64044
 diamond, KVV Auger electron spectra calcs., band and cluster approx. methods 7-46252
 disordered 1D systems of localised states, single-particle density of states Coulomb gap calcs. 7-58777
 disordered alloy surfaces, density of states calc. 7-21961
 disordered alloys, density of states approx., overlapping Lorentzian functions calcs. 7-38435
 disordered interfaces, electronic struct. calcs., Lloyd model 7-2657
 disordered multilayered systems, local density of states determ., recursion method 7-52528
 disordered oxide-semiconductor interface, inversion layer electronic density of states 7-58852
 disordered systems, localised electron Coulomb gap, quantum hopping effects 7-2540
 disordered systems, single particle energy spectrum, local density of states 7-12593
 disordered systems, single-particle energy spectrum, state vectors, total density of states 7-12594
 disordered systems with statistical correlations electronic states, self-consistent Born approx. 7-2542
 DNA, aperiodic, electronic structure and cond. props. 7-23297
 electron closed shells, bare Coulomb pot., density matrices 7-27226
 electron gas, 2-D, background density of states between Landau levels 7-2456
 electron gas, 2D, density of states for high Landau levels and random potential 7-58753
 electron gas with uniform density, screened-exchange functional 7-64138
 ethylene-vinylacetate-Ag copolymer-metal contact, pot. barrier electronic props., photocurrent spectra meas. 7-27419
 ethylene-vinylacetate-Au copolymer-metal contact, pot. barrier electronic props., photocurrent spectra meas. 7-27419
 fractional quantum Hall effect, energy gaps 7-27272
 gapless semiconductor, low temp. density of states near Fermi surface 7-64042
 glass, two-level systems, density of states and distrib. functions derivation 7-12583
 graphite-HNO₃ intercalation cpds., absolute Pauli spin suscept. meas., Fermi level density of states determ., ESR/NMR method 7-12940
 heavy-fermion metals, electronic spectral density, periodic Anderson model 7-7087
 interfacial diffusion effect on superlattice electronic structure (*Chinese*) 7-7303
 Landau diamagnetism, perimeter corrections for free electron gas 7-38843
 local density for semiconductor surface narrow channels (*Chinese*) 7-7084
 metal hydrides, electronic density of states from press.-composition isotherms 7-7088
 metal-insulator-semicond. structs., interface state density profile determ., DLTS spectra interpretation 7-38733
 metallic films, electron states calc., allowance for transition layer in construction of pot. (*Russian*) 7-58733
 metals, dielec. const. giant quantum oscills. under coherent magnetic breakdown (*Russian*) 7-53216
 metals, electronic sp. ht., finite conduction electron lifetime correction calcs. 7-16784
 metals, granular, hopping conduction 7-17007
 mixed valent compounds, electronic properties, theory 7-21880
 mixed valent compounds, static susceptibility of the periodic Anderson hamiltonian 7-22096
 molecular crystals, trapped electron Fermi distrib. 7-27286
 molecular systems, disordered, influence of noise on density of states and absorption 7-16949
 Nb₃Ir films, supercond. transition temp., effect of radiation induced disordering 7-45540
 noble metal alloys, Al-K_α XPS intensities 7-27870
 one-dimensional incommensurate model, mobility edges and electronic density of states calcs. 7-21799
 one-dimensional periodic Anderson Hamiltonian, effect of disordered conc. nonmagnetic impurities 7-27517
 one-dimensional systems, electronic stability and density of states on Fermi surface, topological effect 7-58728
 Penrose lattice, electronic structure, local-environment depend. 7-52392
 periodic Anderson model, interatomic hybridisation, singular density of states, narrow band limit anal. 7-16927
 periodic polypeptides, band struct. ab initio HF cryst. orbital calcs. 7-23298
 polyacetylene, continuum model, random disorder, supersymmetric treatment 7-45111
 polyfuran and copolymers, electronic struct., cond. props., ab initio cryst. orbital calcs. 7-52410
 polymer, band struct., direct space exchange lattice sums, convergence props. 7-21797
 polyparaphenylene, disorder doped, electron density of states 7-58726
 polypyrrole and copolymers, electronic struct., cond. props., ab initio cryst. orbital calcs. 7-52410
 polythiophene and copolymers, electronic struct., cond. props., ab initio cryst. orbital calcs. 7-52410
 positionally disordered systems, weak electron-ion pot., density of states cutoff, path-integral formulation 7-52389
 quantized Hall effect, impurity bound state ionisation 7-12742

electronic density of states continued

- quantum wells, electronic struct., interface disorder effects 7-45476
 quasi-one-dimensional density-wave systems, electronic struct., high mag. field effects 7-58754
 quasi-one-dimensional wire, cond., thermopower, effect of lifetime broadening 7-45252
 quasicrystalline chain, vibr. and electronic spectral props., perturbative approach 7-45116
 quasicrystals, 1D tight-binding model, critical wave functions and Cantor-set spectrum 7-64189
 quasiperiodic and periodic lattices in 2 and 3D, electronic props. 7-32891
 random binary alloys, electronic props., max. entropy method 7-16929
 random systems, universality 7-27230
 randomly dil. Cayley tree, electronic density of states determ. 7-32890
 rare earth semiconductors, valence changes, many-impurity Anderson model 7-1816
 s-dimensional semiconds., Fermi energy, relativistic corrections, free-Fermi-gas model calcs. 7-2465
 semiconductors, disordered, with dispersive transport, elec. transient process 7-17074
 semiconductors, zinc-blende and diamond struct., recursion calcs., K space method 7-2453
 semiconductors with parabolic density of states, activity coeffs. of electrons and holes 7-27324
 spectroscopy of single atoms in the scanning tunneling microscope 7-33060
 strong-coupling superconductors, energy gap eqn. inversion, electron tunneling spectrum temp. corrections, phonon spectrum determ. 7-52900
 sulphide minerals, interpretation of AES 7-22391
 superconducting bilayer composite excitation spectrum, density of states, Bogoliubov eqns. 7-52892
 superconducting films, nonequilibrium dynamic quasi-particle distribns., high freq. EM field effects calcs. (Russian) 7-27467
 TCNQ, valence band density-of-states 7-38434
 thin films, electron state density in longitudinal mag. field 7-27440
 transition metal aluminides (TAl, T=Fe, Co, Ni, V), electronic struct. of vacancies 7-16975
 transition metal surfaces, metastable noble-gas atom interactions 7-64852
 transition metals, X-ray electron spectra asymmetry and Fermi level density of states (Russian) 7-3112
 two dimensional quasi-periodic Penrose lattice, electronic and vibr. modes, localised states and band struct. 7-27300
 two-dimensional electron systems, magnetoconductance, density and mag. field dependences 7-33033
 Urbach optical absorpt. edge, electron band tails 7-16930
 Ag adsorbed layer on Si (111), geometric struct. and density of states, cluster model and charge self-consistent extended Huckel method calcs. 7-21619
 Al, bremsstrahlung isochromat spectra, electron-energy losses 7-22377
 Al clusters, electron energy spectra, size effects 7-7103
 Al, disordered films, density of states, electron-electron interactions tunnel conductance meas. 7-52393
 Al film, quantum size effects and dimensionality 7-45521
 AlN formed by N ion implantation of Al, electronic struct. 7-58926
 AlN thin crystalline stoichiometric film, electronic struct., electron spectra studies 7-58916
 AlN_x nonstoichiometric sputtered films, electron localisation, transport props. 7-58929
 As₂Se₃, crystalline, electronic and geometric struct., ab initio total-energy calcs. 7-12607
 α-As₂Te₃ films, hole transport investigation by transient field-effect and time-of-flight methods 7-22040
 BaPb_{1-x}Bi_xO₃, electronic struct., photoemission studies 7-59375
 Bi-Pb, superconducting transition temp., effect of plastic deform. 7-52879
 Bi-Tl, superconducting transition temp., effect of plastic deform. 7-52879
 a-C:H films, plasma deposited, optical props. 7-27799
 C₆K, intercalation cpd., density of states, interlayer band occurrence 7-2454
 Cd₂Ag₂, Ag density of states, Auger and photoelectron spectra, Clogston-Wolf model calcs. 7-2451
 CdCr₂Se₄, band structure characteristics and props. of nonequilibrium carriers, cathodoabsorption 7-46064
 CdCr₂Se₄ thin films, ferromagnetic semicond., multielectron energy struct., absorpt. spectrum, temp. and doping depend. 7-38488
 CdTe amorphous thin films, electrical and optical props. 7-22045
 CdTe, d-core transitions, reflectivity spectra 7-53364
 Ce, photoelectron and bremsstrahlung isochromat spectra 7-7817
 CeB₆, optical props. and band struct., spectroscopic ellipsometry meas. 7-13157
 Ce₂La_{1-x}Cu₆, electronic states, resonant photoemission study 7-53496
 Co-Y alloys, low temp. sp. ht. study, crystalline and amorphous phases 7-52995
 CoAl, electronic struct. of antistructure Co atoms and Co-vacancies 7-7165
 CoGa(Al), electronic struct. of vacancies 7-16975
 Co(001), metastable BCC phase, electronic struct. and magnetism 7-45418
 Cr, EELS studies of Cr-L_{2,3} core levels 7-46258
 CrSi₃, EELS studies of Cr-L_{2,3} core levels 7-46258
 Cr_xTiS₂, intercalated dichalcogenide, electronic struct. 7-52387
 Cu:Mn(Cr) matrix, electronic struct. calcs. 7-16976
 Cu-Fe alloys, electronic structure and impurity states, optical investigations (Russian) 7-32943
 CuInTe₂ film, amorphous, flash evap., DC cond. mechanisms, density of states 7-22041
 CuNi, substitutionally disordered, electronic struct., LCAO-CPA calcs. 7-64067
 Cu₂O, electronic struct. and binding mech. 7-2482
 Cu₇₅Pd₂₅, partial densities of states determ., valence band photoelectron spectra meas. 7-52390
 Cu_xY_{1-x} amorphous alloys, empty and occupied electronic states, inverse and direct photoemission spectroscopies study 7-32899
 Er-H solid soln., mag. props., H addition effects 7-7510
 Fe (110) and (100) surfaces, Stoner excitation spectrum, spin polarised electron energy loss spectroscopy 7-53463
 Fe, BCC, mag. ordering and electronic struct. (Russian) 7-33170
 Fe dilute alloys with 3d elements, electronic struct., K-edge XAS study 7-64066
 Fe, ferromagnetic, band struct. and optical props. 7-2476
 Fe-based liq. alloys, density of electron states, calc. (Russian) 7-45110

electronic density of states continued

- Fe-Te cluster, localised props., multiple scatt. Xα SCF method 7-21848
 (Fe_{1-x}Co_x)₇₈Si₉B_{12.5} amorphous alloys, density of states, XPS studies (Chinese) 7-13320
 Fe_{1-x}O, wustite, electronic struct. and X-ray absorption spectra 7-2479
 Fe₂Si, transition metal impurities, electronic struct. and site preference 7-12653
 Fe₂TiS₂, intercalated dichalcogenide, electronic struct. 7-52387
 GaAs, electron-irradiated, relative density of levels of radiation defects 7-52500
 GaAs, heavily doped, carrier-carrier and carrier-dopant interactions 7-21903
 n-GaAs impurity bands and band tailing 7-21809
 GaAs LPE layers, heavily doped and compensated, hopping cond., density of states at Fermi level, carrier conc. determ. 7-2753
 GaAs MESFET and JFET devices, elec. resist., Hall effect, influence of electronic subband mag. depopulation 7-38740
 GaAs thin films, grain boundaries, electronic props. 7-7172
 GaAs/Al_xGa_{1-x}As heterostruct., 2-D density of states in extreme quantum limit 7-2455
 GaAs-AlGaAs DH injection laser, optical and transport props., emission energy shift, threshold current meas. 7-1101
 GaAs-AlGaAs heterostructures, density of states of Landau levels 7-52822
 GaAs-GaAlAs superlattices, density of states of Landau levels, sp. ht., magnetisation meas. 7-52823
 GaP finite cluster, local electronic struct., recursion method calcs. 7-2464
 GaSb:Se, resist. and thermoelec. power meas. at metal-insulator transition 7-45403
 Gd, ferromagnetic, electronic quasiparticle struct., temp. depend. 7-32908
 GeTe, valence and energy spectrum, supercond. state 7-45534
³He films, gapless superfluidity, diffuse boundary scatt. effects 7-44939
 HfFe₂, electronic struct. and mag. props., tight-binding approx. calcs. 7-2475
 HgCdTe, 0⁻ giant oscillation near semimetal-semiconductor transition 7-64053
 HgTe, d-core transitions, reflectivity spectra 7-53364
 InSb, density of states and effective mass determ. 7-38433
 InSb, impurity bands and their conductivity in strong mag. fields 7-45152
 KCl (100), sand gap photoemission yield spectroscopy 7-22445
 KHg-graphite intercalation cpd., supercond. props., density of states model 7-27457
 LaAg, nonmag. cpds., transport props. and electronic struct. 7-2575
 LaB₆, optical props. and band struct., spectroscopic ellipsometry meas. 7-13157
 La_{1.8}Sr_{0.2}CuO₄, superconducting transition at 36.2 K 7-58947
 LuAg, nonmag. cpds., transport props. and electronic struct. 7-2575
 LuFe₂, electronic struct. and mag. props., tight-binding approx. calcs. 7-2475
 Lu₂Ir₄Si₁₀, superconducting, electronic phase transition and partially gapped Fermi surface 7-12902
 Mg, bremsstrahlung isochromat spectra, electron-energy losses 7-22377
 Mg, local density of states region, determ. by core-core-valence Auger transitions 7-39325
 MnO, band struct., optical props. 7-32912
 Mo dislocated lattice, local density of states calcs. in tight binding model, modified recursion method 7-52401
 Mo-Re alloys, electron struct., X-ray spectra studies (Russian) 7-45135
 MoN Bi phase sputtered films, mag. susceptibility and defect struct. 7-53087
 2H-MoS₂, photoionisation cross-sections for whole valence band, synchrotron radiation obs. 7-7812
 Mo₂SiB₂, supercond, investig. 7-22082
 Mo₂Si(Ge), neutron irr., NMR and mag. suscept. studies (Russian) 7-13051
 Mo₂(SiRe), neutron irr., supercond. investig. (Russian) 7-12926
 N₂ film, solid, quasielastic hot-electron transport 7-39327
 NaCl (100), sand gap photoemission yield spectroscopy 7-22445
 NaNO₂, Fermi level and relative density of states, temp. dependence 7-21795
 Nb_{3-x}Ge_x and Nb₂Ge₃, superconducting alloys, thermoreflection spectra, electron struct. 7-33370
 NbC, vacancy electronic struct., muffin tin Green's function method calcs. 7-2531
 NbC₂N₂, nonstoichiometric, supercond. transition temp. and band struct. (Russian) 7-58935
 Nb₂Ir films, lattice-stiffness changes due to ion irradiation, Brillouin scatt. 7-52379
 NbSe₂, 2H polymorph, electronic density of states, phase matching of CDWs, NMR study 7-64538
 Ni (100), (111) and (110), N₂ chemisorption, molecular cluster calcs. 7-52280
 Ni clusters with surface adsorbed CO, surface electronic and mag. struct. 7-21969
 Ni dilute alloys with 3d elements, electronic struct., K-edge XAS study 7-64066
 Ni-H system, band structure calcs. 7-45140
 Ni-P metallic glasses, electronic struct., XPS study 7-39357
 Ni_{1-x}P_x amorphous glasses, electronic structure, calcs. 7-7101
 Ni₂Si, L_{2,3} absorpt. edges, EELS study 7-3125
 NiTe₂, electronic struct. determ. by self-consistent LMTO-ASA method 7-7111
 NiTi, electronic phase diagram for B2-R transition 7-52388
 Os single cryst., energy band struct. and optical absorpt. studies 7-16938
 a-P, sputtered, response to intense ion bombardment 7-27447
 Pb, self-consistent relativistic band struct., normal and high press. 7-52413
 Pb-Pt composite films oxidation, KPS 7-27867
 PbS, density of states and effective mass determ. 7-38433
 PbTe:Ti(Tl,Na) films, superconducting transition 7-38797
 PbTe clusters in C matrix, electronic and struct. studies by EXAFS and XANES 7-17363
 Pd-Si alloys, H absorption, structural disorder effects 7-52249
 Pd₂Fe, electronic struct. 7-52415
 Pd₂Fe, electronic density of states, recursion method 7-64043
 PdH_x, H-induced lattice expansion and effective H-H interaction 7-52247
 PdH_x, nonstoichiometric, electron density of states, analytic CPA model calcs. 7-52400

electronic density of states continued

- PdTe₂, electronic struct. determ. by self-consistent LMTO-ASA method 7-7111
- Pt-Pb bimetallic systems, Fermi level density of states, XPS studies 7-46278
- Pt-Sn bimetallic systems, Fermi level density of states, XPS studies 7-46278
- PtTe₂, electronic struct. determ. by self-consistent LMTO-ASA method 7-7111
- Si (100) MIS struts., state density of 2D electrons in transverse mag. field 7-12870
- Si (111), disordered adsorption of H, electronic struct. calcs. 7-27377
- Si (111), local density of states near ideal vacancies 7-27380
- Si bicrystals and thin films, grain boundaries, electronic props. 7-7172
- Si, bremsstrahlung isochromat spectra, electron-energy losses 7-22377
- Si, density of states, spectral function, calcs. using eqn. of motion method in k-space 7-27236
- Si polycrystalline, gap state density determ., field-effect conductance anal. calcs. 7-21794
- a-Si, tetrahedrally bonded, bond angle disorder 7-32297
- Si, with stacking faults, electron and phonon spectra, recursion method 7-32945
- Si:Ar laminated structure formed by Ar ion doping, electroreflectance 7-7676
- a-Si:H, B₂H₆(PH₃), localised density of states, electrophotography study 7-32957
- a-Si:H, deep trapping, transient photocurrent saturation 7-21952
- a-Si:H, density of states, SCLC meas., effect of injection electrodes 7-64265
- a-Si:H, distrib. of states study by capacitance-voltage method 7-7089
- a-Si:H, localised electronic state, light soaking and current injection 7-16994
- a-Si:H based alloys for solar cells, elec. props. and degradation behaviour 7-52642
- a-Si:H films, CVD, optical and electronic props. 7-33597
- a-Si:H films, deep levels in the mobility gap 7-12670
- a-Si:H films, metal-semiconductor contacts, characterisation 7-38724
- a-Si:H films preparation by CVD 7-17453
- a-Si:H/metal junction, pot. profile determ. 7-2715
- SiO, thermal donor impurity density of states, formalism and appl. 7-12655
- Si/SiO₂, ion implantation-induced interface states generation and charge trapping study 7-12874
- Si-SiO₂ interface, chem. transition, density of states calcs. 7-7397
- Si-SiO₂-xN₂-xN₂/3-Al structures, interface states, DLTS study 7-45513
- Si-SiO₂ interface density of localised states, C-V and G-V characts. meas. 7-38734
- SiC:H (F), amorphous, electronic and structural props. 7-17054
- a-SiGe:F solar cells, chemical basis for high efficiency 7-17884
- SiGe:H, amorphous, electronic and structural props. 7-17054
- a-SiGe:H glow discharge films, field effect density of states determ. 7-21796
- Si_{1-x}Ge_x films, optical band gap, photocond. props. 7-52672
- SiO₂ films, interface states, charge trapping (*Spanish*) 7-17110
- SiO₂/SiC interface. elec. characts., MOS conductance technique meas. 7-12873
- Si(111), energy minimisation calc. for dimer-adatom-stacking fault model 7-63940
- Sn, superconducting transition temp., effect of plastic deform. 7-52879
- Sn, white, (100) surface, electronic props. 7-12772
- (Tb_{1-x}Y_x)Co₂ ferrimagnetic alloy, sp. ht., Curie temp. and density of states comp. depend. meas. 7-7514
- TiC_x energy band struct., Fermi energy and density of states, vacancy states effects, LMTO-ASA calcs. 7-64078
- TiC_x, KVV Auger electron spectra and band struct. (*Russian*) 7-17371
- TiH_x, X-ray diffr., lattice parameter change, density of states 7-44469
- TiSe₂, IT polytype, CDW transition effects of lattice fluctuations 7-21831
- Ti_{1-x}V_x quench condensed thin films, supercond. crit. field and fluctuation cond. meas. 7-64415
- U cpds., metallic and nonmetallic, X-ray absorpt. at various thresholds 7-64793
- UF₆, spin-polarised energy bands, density of states and eqn. of state 7-58734
- URu₃ (Rh₃) (Pd₃) (Ir₃) (Pt₃), hybridisation, electronic struct. and props. 7-45136
- URu₂Si₂, heavy electron system, competing electronic correlations, press. effect 7-45539
- VC_x energy band struct., Fermi energy and density of states, vacancy states effects, LMTO-ASA calcs. 7-64078
- VC_x, KVV Auger electron spectra and band struct. (*Russian*) 7-17371
- (VCr)₃Si, neutron irradi., supercond. investig. (*Russian*) 7-12926
- (VMo)₃Si, neutron irradi., supercond. investig. (*Russian*) 7-12926
- WO₃, carburized, surface composition at catalytic activity 7-21594
- Y electronic struct., electron-phonon matrix and superconductivity, high press. effects, KKR calcs. 7-21805
- YAg, nonmag. cpds., transport props. and electronic struct. 7-2575
- Y₂Co₇, electronic struct. and mag. props. 7-7104
- Y₂Co₇B intermetallic cpd., electronic struct. and mag. props., tight-binding calcs. 7-2450
- Y₂Fe₁₄B, electronic struct. and mag. props. recursion method calcs. 7-2452
- YH₃ system, mag. susceptibility and electronic struct. (*Russian*) 7-58988
- ZnS:Cu²⁺, multimode Jahn-Teller effect in the luminescence spectrum 7-12675
- ZnTe, d-core transitions, reflectivity spectra 7-53364
- ZrFe₂, electronic struct. and mag. props., tight-binding approx. calcs. 7-2475
- ZrN, electronic struct., metal vacancy effects, KKR-CPA method anal. 7-12606

electronic density of states of amorphous solids see electron energy states of amorphous solids

electronic density of states of liquid semiconductors see electron energy states of liquid semiconductors

electronic engineering computing

- see also circuit analysis computing; circuit CAD; computerised instrumentation
- pyroelectric detector signals analysis by analogue technique 7-348
- semiconductor lasers field spectra computing asymmetry due to noise obs. (*Japanese*) 7-15862

electronic engineering computing continued

- sensor database maintained by Warren Spring Laboratories 7-14933
- six-port reflectometer for meas. complex dielectric constant 7-18821
- Si, diffusion of ion-implanted impurities, modelling on IBM PC 7-38265
- Si solar cells, crystalline, metal grid optimisation and emitter tailoring, computer model extension 7-54292
- electronic equipment manufacture
- see also printed circuit manufacture
- photochemical machining of etch-resistant metals 7-22909
- electronic equipment testing
- see also printed circuit testing
- biomedical, Electrotechnical Testing Institute practices (*Czech*) 7-18090
- CCDs for ROSAT star sensors, testing and characterisation 7-29401
- ESD simulation difficulties and test procedures (*French*) 7-37787
- ESD testing, rising slope reproducibility 7-42843
- Magellan SAR, system test and calibration 7-48681
- optoelectronic components stress meas., photoelasticity determ. with aid of computer 7-31725
- photon counting imaging microchannel plate detectors calibration, for EUV astronomy 7-29404
- picosecond semiconductor lasers for characterizing high-speed image shutters 7-20466
- picture transmission recorder, using grey scale test pattern generator 7-29292
- SAW resonators, 600 MHz band, driving current dependence of aging drift 7-20553
- thermal imager performance meas., objective meas. of minimum resolvable temp. difference 7-30092
- thermal imaging system performance assessment 7-30091
- to-and-fro zone plate method for 3D frequency characts. obs. 7-20393
- US diagnostic devices, USA Food and Drug Administration guidelines 7-3851
- electronic music
- see also musical acoustics; musical instruments
- aesthetic appeal in computer music 7-26093
- organ sound synthesis expts. (*Hungarian*) 7-50868
- source separation and note identification in polyphonic music 7-37261
- electronic office see office automation
- electronic structure, atomic see atomic structure
- electronic structure, molecular see molecular electronic states
- electronics applications of computers see electronic engineering computing electronics
- see also beta-rays; cosmic ray electrons; positrons
- anomalous magnetic moment, constraint on composite weak-interaction bosons 7-523
- anomalous magnetic moment at finite temperature, mass shift, QED anal. 7-5096
- coherency matrix description for electron 7-15811
- double wave description of a single relativistic free electron 7-9695
- dyon-electron bounds system, energy levels, wave functions 7-24460
- electric dipole moment anal. in E_g superlattice models 7-61651
- electric dipole moment bounds in a wide class of models 7-41815
- electric dipole moment in SUSY electroweak model anal. 7-10065
- electron, radiative mass and g-2, QED between conducting plates 7-457
- energy-momentum vector of the classical electron 7-24498
- fermion fields in the soliton background of Kaluza-Klein theories 7-41202
- fermion mass determination, Weinberg model 7-49021
- hidden U(3) symmetry, Zitterbewegung and degrees of freedom, Dirac eqn., Lie algebra 7-19031
- large-N QED, dynamical mass generation 7-19061
- magnetosphere, auroral zone, permanent flare activity during magnetically quiet periods 7-55379
- mass, gauge field theory 7-61433
- Plebanski metric perturbations in general relativity, fermion field perturbations 7-18645
- W value re-evaluation for electrons in dry air 7-62242
- weak neutral current coupling constant meas. from e⁻ν_e→e⁻ν_μ 7-56438
- ē-cν̄, single electron search expt., sparticle mass limits 7-49142
- ē mass limits in sparticle production expt. 7-49142
- electrooptics see electro-optical effects
- electroosmosis see osmosis
- electrophoresis
- see also electrophoretic coating techniques
- bovine serum albumin, photoinduced ionisation by holographic relax. method 7-14046
- continuous flow, hydrodynamics (*French*) 7-39901
- dielectrophoretic capture of a particle on a rod, sinusoidal field freq. effects 7-13791
- dielectrophoretic levitation, active feedback-controlled 7-3596
- dielectrophoretic levitation, dipole moments of conducting particle chains 7-20092
- DNA, large mols., separation by contour-clamped homogeneous elec. fields 7-65906
- macromolecule separation, two-dimensional, data analysis 7-54440
- mitochondria from bovine heart, electrophoretic behaviour of H⁺+ATPase proteolipid 7-59946
- Pa-Ne discharge, steady-state cataphoretic density profile, collapse 7-44287
- Cd⁺, ion drift velocity in He glow discharge, meas. using AlGaAs laser (*Japanese*) 7-20294
- electrophoretic coating techniques
- ceramic engine component fabrication techniques 7-3243
- β-Al₂O₃-Na₂O, ceramics, electrophoretic deposition 7-13390
- electrophoretic coatings
- Al powder-steel composite coatings, prod. by compacting electrophoretic and electrostatic deposits protective props. 7-3491
- β-Al₂O₃-Na₂O, ceramics, electrophoretic deposition 7-13390
- MgO coating on amorphous Co_{70.4}Fe_{4.6}Si₁₅B₁₀ alloy, mag. props. 7-22123
- PbO-B₂O₃-SiO₂ glass dielec. thin films on anodised Al substrates 7-17269
- WC-Co-B system, formation mechanism of composite coating, electrophoresis 7-3208
- electrophotography
- cellulose acetate, corona charged, electrothermographic characteristics 7-61391
- charge/mass particle spectrometer for electrophotographic toner 7-4910
- color printing using elliptical laser beam scanning 7-56362

electrophotography continued

- colour process, tone reproduction improvement by dot pattern erasing (Japanese) 7-9910
 donor-acceptor system, photoeffect injection sensitisation 7-45388
 electroradiography inspection method for castings 7-65262
 films, small charge drift current characteristics 7-33047
 fluorenone bisazo pigments, electrophotographic sensitivity (Japanese) 7-38611
 high resistivity semiconductors, xerographic time of flight technique for drift mobility determ. 7-58807
 image quality characts (Japanese) 7-356
 migration imaging, photographic technologies XDM and AMEN 7-24717
 polyporphazene photoconductive films as electrophotographic photoreceptors 7-57499
 polyvinylcarbazole film based photoreceptor, photoinduced memory effect, appl. to laser recording (Japanese) 7-37076
 xerographic developer, materials design (Japanese) 7-56359
 Ba-Zn ferrite carriers for electrophotography, charactn. 7-4903
 CdS, fine activated, prep. and props. for electrophotographic appl. 7-41514
 Se:O, electrophotographic props., doping depend. (Japanese) 7-12752
 a-Si:H, B₂H₆(PH₃), localised density of states, electrophotography study 7-32957
 a-Si:H:F films, dark discharge mechanism of surface potential (Japanese) 7-17034
 n⁺-a-Si:H/a-Si:H/a-SiC:H heterostructures, electrophotographic props. 7-45485
 Si₃N₄ layers, electrophotographic effect 7-46675
 ZnCdS:Ag/Cd(S,Se):Cu mixed photoconductor system for electrophotography 7-2636
 ZnO powder-polyvinyl butyral films, dark discharge props. 7-58919

electrophotoluminescence *see electroluminescence; photoluminescence***electrophysiology** *see bioelectric phenomena***electroplated coatings**

- Ag, electrodeposit structure rel. to plating from complex electrolytes 7-2406
 Au, from acidic plating paths, minute amounts of metal ions effect (Japanese) 7-3503
 Cd-Zn coatings on steel, extrusion, deform. force rel. to comp. and struct. 7-3367
 Co on WC, plating effect on WC-Co powder mixture props. 7-53686
 Co-P, amorphous, pulse plated, electrochemical props., corrosion resist. (Japanese) 7-53954
 Co-W-P electroplated alloys, struct. and mag. props. (Russian) 7-2428
 Cr, electrodeposits from Cr₂(SO₄)₃-potassium formate baths, hardness (Japanese) 7-59471
 Cr, electroplated deposits, hardness rel. to C content, heat treatment, bath comp. (Japanese) 7-17480
 Cr surface alloyed layer on steel, form. by CO₂ laser (Korean) 7-28196
 Cr coating on ultrahigh strength maraging steels, H embrittlement 7-28137
 Cu electroplated coating on ultrahigh strength maraging steel, H embrittlement 7-28136
 Cu/Ni/Cr, multilayer deposits, corrosion protective props. 7-8187
 Cu-Ni-CoW-Cr system, Cr plating, roughness and wear (Russian) 7-33801
 CuIn_{1-x}Ga_xSe₂ absorber materials, electroplating prep. 7-17894
 CuInSe₂/CdS, thin film chalcopyrite solar cells, electroplating prep. 7-17894
 Cu₂S films, field assisted chemiplating for CdS/Cu₂S heterostruct., growth mechanism 7-59470
 Ni coating on ultrahigh strength maraging steels, H embrittlement 7-28137
 Ni, electroplated coating on ultrahigh strength maraging steel, H embrittlement 7-28136
 Ni plating basics, electroforming, surface prep. and quality control procedures 7-13638
 Ni-Fe-In ternary Permalloy electroplated films, mag. props. and thermal stability 7-33236
 Ni-P, electrodeposition, pulse plating, corrosion resist. (Japanese) 7-53643
 Pd-Ag alloy electroplated coating contact and corrosion resistance and wear 7-3509
 Pd-Pt, mixed layers, electroplated on stainless steel support, oxidation catalyst appl. 7-22596
 Sn plated on cast Fe, heat diffusion method, corrosion resist in H₂SO₄ (Japanese) 7-53956
 Zn, acidic bath, corrosion resist. improvement with Co and Cr additions 7-13640
 Zn electroplates, whisker formations 7-17482
 Zn, whisker growth on electroplates, crystallographic texture 7-64034
 Zn-Ni bright coatings deposited from weak acid electrolytes (German) 7-39441

electroplating

- high tensile steel electroplating, H₂ embrittlement fracture prevention (German) 7-33767
 Hull cell with rotating cone agitation 7-46851
 laboratory scale, practice and appls. 7-48252
 laser enhanced plating and etching using photothermal effects 7-59651
 surface engineering for corrosion protection 7-3478
 Ag films, electroplating in electrochemical cell, scanning tunneling microscopy studies 7-22589
 Au, acoustic-jet plating of 7.5 MHz 7-59462
 Au, from acidic plating paths, minute amounts of metal ions effect (Japanese) 7-3503
 Au layer on stainless steel, tritium permeation meas. 7-6852
 Co-P, amorphous, pulse plated, electrochemical props., corrosion resist. (Japanese) 7-53954
 Cu, acoustic-jet plating of 7.5 MHz 7-59462
 Cu bright plating electrodeposition kinetics, adsorption on cathode surface (Russian) 7-33942
 Cu plating, grain density and cyclic stresses (Japanese) 7-7904
 Cu₂S films, field assisted chemiplating for CdS/Cu₂S heterostruct., growth mechanism 7-59470
 Fe, cast, Sn plating, heat diffusion method, corrosion resist in H₂SO₄ (Japanese) 7-53956
 Fe-P amorphous alloy preparation by electroplating 7-17489
 GaAs substrates, laser-induced metal and alloy plating, silicide form. 7-39448

electroplating continued

- Ni electrodeposition on Pt microelectrodes in the Watts bath, role of boric acid 7-46357
 Ni high-speed plating on Cu substrates, deposition rate rel. to temp. and flow 7-27952
 Ni plating basics, electroforming, surface prep. and quality control procedures 7-13638
 Ni-P, electrodeposition, pulse plating, corrosion resist. (Japanese) 7-53643
 Os thick targets prod. for electron scatt. expts., electroplating 7-25282
 Pb, electrodeposition kinetics, stripping voltammetric technique 7-27949
 Pd-Pt, mixed layers, electroplated on stainless steel support, oxidation catalyst appl. 7-22596
 Si substrates, laser-induced metal and alloy plating, silicide form. 7-39448
 Sn, electrodeposition kinetics, stripping voltammetric technique 7-27949
 Sn-Pb, electrodeposition kinetics, stripping voltammetric technique 7-27949
 Zn, acidic bath, corrosion resist. improvement with Co and Cr additions 7-13640
 Zn alloy films on Al, growth and adhesion rel. to application technique 7-13396
 Zn-Fe alloys, high-current density electroplating 7-17485
 Zn-Ni alloys, high-current density electroplating 7-17485

electropolishing *see electrolytic polishing***electrorefraction**

- 2,9-dimethyl-1,10-phenanthroline intercalated into α -Zr(HPO₄)₂, ion exchange with Co²⁺, Ni²⁺ and Cu²⁺, dimer formation 7-65305
 halide ions, adsorbed on Cu electrode, electrorefraction obs. 7-13132
 MIM structures, electrorefraction spectra, interface contribs. 7-53276
 semiconductors, defects, electrorefraction characterisation 7-64606
 Al-AnS-Al MIM structures, electrorefraction, props. 7-38773
 Al_{0.5}Ga_{0.5}As bandgap determ. by Schottky barrier spectral response meas. 7-2667
 Ga_{0.8}Al_{0.2}As-GaAs-Ga_{0.8}Al_{0.2}As quantum well structs., electrorefraction spectra, model 7-33365
 GaAs, MOCVD growth on Si, band gap energy and stress 7-38368
 GaAs:In, strain effects, electrorefl. and photocapacitance study 7-22224
 GaAs/AlAs MQW structure, exciton-induced dispersion of electrorefraction at room temp. 7-53277
 GaAs/AlAs quantum well structures, electrorefraction spectra and field-induced refractive index modulation 7-13135
 GaSb/AlSb single quantum wells, electrorefraction and photoluminescence studies 7-46136
 Ge-Si superlattices, structurally induced optical transitions, electrorefraction spectra 7-59184
 HgCdTe, electrochemical and electrolyte electrorefraction studies 7-64607
 HgCdTe in MIS struct., electrorefraction at 77K 7-13128
 HgZnTe, electrochemical and electrolyte electrorefraction studies 7-64607
 In₂O₃:Sn(In)(Cd) films, optical and elec. props. 7-22365
 Li₂WO₄ films, free-electron electrochromic modulation 7-22359
 Si:Ar laminated structure formed by Ar ion doping, electrorefraction 7-7676

electroretinography *see bioelectric potentials; eye***electrospark machining** *see spark machining***electrostatic accelerators***see also Van de Graaff accelerators*

- Cockcroft-Walton neutron generator research 7-30783
 conference heavy ion reaction, nuclear chemistry, with tandem accelerators, Tokai, Japan (Jan. 1986) 7-35116
 energy scanning system for van de Graaff or tandem accelerator 7-62172
 inductive acceleration of plane bodies 7-30739
 interelectrode gap strength calc., Kilpatrick's criterion approximation 7-10815
 KALIF ion accelerator, beam comp. investig. in anode plasma 7-30742
 magnetically insulated transmission line in PROTO II accelerator, anode and cathode joints, gap closure 7-30756
 MEDEA II two-pulse electron beam accelerator to study electron beam propagation 7-30743
 Mite accelerator, injector losses of magnetically insulated transmission line 7-30757
 Mite accelerator, kinetic loss expts., power flow in magnetically insulated power feed 7-30758
 Pelletron 3.2 MV accelerator for neutron cross section meas. 7-30782
 Proto II accelerator, low inductance diode design for imploding plasma loads, insulator breakdown 7-30760
 PROTO II accelerator power flow modification in insulator stack 7-30669
 PROTO II crossover network, time domain reflectometry meas. 7-30759
 Pulselac induction accelerator, post-acceleration gap operation 7-30810
 Rikkyo University fast-neutron facility 7-30781
 superconducting post accelerator linac for JAERI tandem 7-36371
 tandem fast neutron TOF facility 7-30780
 UCSB FEL 400 μ m expt., spectral characteristics 7-1111

electrostatic coatings

- Al powder-steel composite coatings, prod. by compacting electrophoretic and electrostatic deposits protective props. 7-3491

electrostatic devices

- see also capacitors; dielectric devices; electrostatic accelerators; electrostatic lenses; electrostatic precipitators*
 bed, static charge sensitive, for automatic anal. of sleep records 7-3896
 membrane mirror, configuring by least-squares fitting 7-31422
 multielectrode energy analyzers with electrically controlled characteristics 7-42271
 prism, decelerating, electric, test dispersion meas. 7-57229
 vibrosopes, electrostatic self-resonating, cct. design 7-56226

electrostatic discharge *see discharges (electric); electrostatics***electrostatic fields** *see electric fields***electrostatic lenses***see also aberrations; focusing; particle beams*

- aberration theory for electrostatic round lenses, multipole lenses and deflectors 7-1021
 cathode lenses, design, Pontryagin's max. principle 7-42884
 cathode lenses, design, Pontryagin's max. principle 7-42885
 combined electric-magnetic focusing-deflection system, relativistic fifth order geom. aberration eqn. 7-10838

electrostatic lenses continued

- combined electrostatic focusing-deflection systems, asymptotic aberrations 7-10835
- design, multiobjective optimisation techniques 7-25709
- electron matrix lens, aberrations reduction using offset apertures 7-20122
- focusing of multiply charged energetic ions using solenoidal B and radial E lenses 7-56899
- focusing property investigation 7-36870
- geometrical aberrations, comment and reply 7-62611
- heavy-current cathode for X-ray tubes with electrostatic focusing (*German*) 7-24740
- misalignment of electron lenses, influence on image quality 7-20123
- positron gun, modified Soa immersion lens 7-61401
- projection system with electrostatic lenses, aberrations calc. 7-57517
- projector image aberrations, illumination system collimator effect 7-57516
- projector with electrostatic lenses, chromatic aberrations anal. 7-57518
- scanning ion beam systems, in-lens deflection 7-42889
- spherical aberration reduction 7-10836
- STEM objective lens, high excitation, Munro programs data variations effect on predicted opt. props. 7-18933
- transfer matrix subroutines for common tube lenses 7-62616
- tube lenses, finite length, geometrical aberrations 7-31234

electrostatic microphones *see microphones***electrostatic precipitation** *see electrostatic precipitators; precipitation (physical chemistry)***electrostatic precipitators**

- back corona, effect in laboratory scale electrostatic precipitator 7-20981
- back-corona discharge, laboratory analysis 7-58083
- back-corona initiation, anal. 7-51555
- corona discharges, laboratory analyses 7-58082
- ground testing of fighter aircraft, p-static discharge effects 7-50452
- parallel-plate electrodes, corona wire, repulsive forces 7-58081
- particulate control technology transfer and utilisation, 6th symposium, New Orleans, LA, USA (Feb. 1986) 7-65668

electrostatics

- see also electrets; electric charge; electric fields; electrostatic devices; static electrification; triboelectricity*
- 2D electrostatic and EM problems, general interactive finite element package 7-62569
- atomiser electrostatic spray nozzle, aerodynamically shaped for insecticide selective deposition 7-51262
- carboxylate-imidazolium diad in *Streptomyces Griseus* protease A, electrostatic environment 7-59936
- charge generation in transformer insulation systems (*Polish*) 7-37431
- charging of solid particles and liquid droplets 7-26586
- P/Comet Halley, 1910 and 1986 apparitions, electrostatic charging effect on dust distrib. 7-66507
- conducting circular torus with dielectric sleeve, electrostatic problem 7-57204
- convection in hemispherical shell due to radial electrostatic forces, simulation of planets and stars 7-29393
- cyclopentene, adsorpt. on stepped (221) Ag surface, mol. orientation 7-27099
- diatomic molecules, Hellmann-Feynman electrostatic theorem (*Russian*) 7-62280
- dielectric liquids, charging current and conductivity 7-57202
- dipole moments of conducting particle chains 7-20092
- Dirichlet problem in crescent-shaped domain, solution 7-57670
- discharges from human body 7-34125
- discs with parallel and intersecting axes, mean potentials and potential coeffs. (*Russian*) 7-42835
- double-layer interaction between curved surfaces bearing pot., Derjaguin approx. 7-17819
- electron gun, electrostatic field problem, Poisson equation, numer. soln. 7-29774
- electron-optical props. of electrostatic systems, fast charge-simulation procedure 7-42881
- ESD current waves, classification vs. approach speed, voltage, electrode geometry and humidity 7-42841
- ESD simulation difficulties and test procedures (*French*) 7-37787
- ESD testing, rising slope reproducibility 7-42843
- flat laminae, capacity anal. 7-62565
- grid, electrostatic field calcs. 7-42840
- ground testing of fighter aircraft, p-static discharge effects 7-50452
- Helmholtz theorem, symbolic proof 7-48236
- human ESD: the phenomena, their reproduction and some associated problems 7-42842
- inhomogeneous systems, EM phenomena, path-integral approach 7-57207
- insulators, charged by electron beams in electron microscope 7-41540
- isoperimetric inequalities for capacity, polarisation and virtual mass 7-31208
- liquid drops, charged, instability of evap. 7-20091
- magnetic dipoles suspended above line charge, dynamic origin 7-18536
- metal-metal and metal-dielectric systems, adhesion calc. 7-7023
- multipole, constraint relations among partial harmonic potentials 7-57203
- nonlinear media, electrostatic problems 7-18529
- open boundary problems, differential and integral methods 7-50454
- parallel disc capacitors, fringing fields and total capacitance calc. 7-10814
- phospholipid bilayers, solvent-mediated interaction, nonlocal electrostatic theory of hydration force 7-17958
- plasma magnetoelectrostatic confinement, limitations 7-51484
- plate, thin conducting, arbitrary circular lune shape, charge distrib. 7-50451
- potential coefficient equations for non-parallel, non-orthogonal cells 7-15798
- potential energy surfaces, simulated annealing study 7-31211
- quasi-images and surface geometry 7-62568
- scanning tunnelling microscopy, multiple image potential effects 7-58108
- spheroidal shells, electrostatic field and capacitance calcs. (*Russian*) 7-42836
- stratified media, current source in presence of insulating and conducting disks 7-25699
- Supermite accelerator water-plastic-vacuum interface design 7-30748
- VX model compound, reactive props., electrostatic pot. calcs. 7-56954

electrostriction

- see also piezoelectric materials; piezoelectricity*
- binary charged fluids, screening lengths, thermodynamic stability 7-52480

electrostriction continued

- diglycine nitrate crystal, electrostriction determ. 7-45936
 - dynamic gratings induced by electrostrictive compression of critical microemulsions 7-11032
 - ferroelectric ceramics, elec. field-excited acoustic waves parametric instability, wave eqn. calcs. 7-6727
 - inverse scattering and three-wave interaction in nonlinear optics appl. to sound wave generation 7-11030
 - ($\text{Ba}_{1-x}\text{La}_x$)($\text{Ti}_{1-y}\text{Zr}_y$) $_{1-x/4}\text{O}_3$ ceramics, electrostrictive effect 7-53240
 - BaTiO_3 -based ceramic, nonlin. electromechanical parameter meas. 7-13094
 - $\text{CsH}_2(\text{D}_2)\text{PO}_4$, ferroelectrics, electrostrictive corrections to pseudo 1D Ising model 7-59158
 - Li_2GeO_3 , single cryst., nonlin. electromechanical parameter meas. 7-13094
 - LiKSO_4 single crystals, optical activity, ferroelec. and ferroelastic props. 7-27687
 - LiNbO_3 , elastic and dielec. props. 7-63715
 - LiNbO_3 , nonlinear elastic, piezoelectric, electrostrictive and dielectric consts. 7-64573
 - $\text{Na}_2\text{O-SiO}_2$ glass, longitudinal electrostriction tensor component 7-2982
 - $\text{Na}_2\text{O-SiO}_2\text{-Al}_2\text{O}_3$, glass, longitudinal electrostriction tensor component 7-2982
 - $\text{PbLaZrO}_3\text{TiO}_3$, electrostrictive ceramics, SAW transduction, electronic control 7-12450
 - $\text{Pb}(\text{Mg}_{1/3}\text{Nb}_{2/3})\text{O}_3$ ceramics for microdisplacement actuators, electrostrictive characts. (*Japanese*) 7-17270
 - $\text{PbMgO}_3\text{NbO}_3$, electrostrictive ceramics, SAW transduction, electronic control 7-12450
 - SbSI , single cryst., nonlin. electromechanical parameter meas. 7-13094
- electrosynchronisation** *see synchronisation*
- electroviscous effect**
see also colloids; viscosity
electrorheological fluids, optimisation for electrical control of viscosity and torque 7-44641
- electroweak model** *see unified field theories*
- element origin**
Blanchi cosmologies, He production, time scale arguments 7-40972
conf., Erice, Italy (April 1986) 7-41001
cosmic nucleosynthesis, relation between ^4He , ^2H and ^3He prod. 7-40979
cosmological nucleosynthesis, effects of quark-hadron transition 7-47677
Galaxy age and chemical evolution, general constraints 7-55809
light nuclide origin from various processes 7-47836
mass 22 nuclei, gamma-ray-imposed constraint on origin in astrophysical environments 7-35069
metals in Population II stars, 'dirty' Population III stars model 7-29470
primordial and stellar nucleosynthesis, nuclear reactions, laboratory analyses 7-47696
 ^{26}Al production by Wolf-Rayet stars, galactic yield and gamma-ray line emissivity 7-47830
He primordial abundance, implications of collisional effects in He I triplets 7-55446
- element relative abundance**
see also isotope relative abundance
Antarctic ureilites, petrology of four specimens rel. to ureilite petrogenesis 7-9447
Apollo 16 highland breccia, komatiite component, abundance characts. 7-60583
Apollo 16 subregolith basement, comp., struct. and age 7-55500
Apollo-16 impact melt splashes, petrography and major element comp. 7-55498
Archaean high-grade metasediments, rare earth element patterns and tectonic significance 7-34486
asymptotic giant branch stars, intermediate-mass, effects of connective overshooting on He and N abundances 7-40797
Barberton Mt. Land, S Africa, U and Th content of Archaean granitoids 7-18153
basalts, tectonic settings discrimination using trace element abundances 7-28957
basalts from S Atlantic hotspots, geochemical correl. with southern African kimberlites 7-34409
basalts of mid-ocean ridges, inert gas abundances 7-60198
Blanchi cosmologies, He production, time scale arguments 7-40972
blue compact galaxies, abundance characts. 7-40920
Cainozoic basalts of E China, Pb, Sr and Nd isotope systematics and chemical characts. 7-29011
Camel Donga meteorite, new eucrite from Nullarbor Plain, mineralogy and comp. 7-34953
Cayley Formation, Moon, comp. determ. from Apollo 16 impact melt splashes 7-55499
chondritic meteorites, comp. rel. to solid materials form. in preplanetary nebula 7-24024
chondritic meteorites, unequilibrated, elemental comps. of major silicic phases in chondrules 7-34954
clay-mineraloid weathering products in Antarctic meteorites, mineralogy and comp. 7-34951
P/comet Giacobini-Zinner (1984e), alkali metals abundances rel. to metal ions in coma 7-9415
compact blue dwarf galaxies, N and O conc. 7-48078
compact H II regions, S and N abundances 7-66695
cosmic dust grains in blue ice lakes of Greenland, electron microprobe anal. 7-14548
cosmic nucleosynthesis, relation between ^4He , ^2H and ^3He prod. 7-40979
Crab Nebula, element abundances in filaments from photoionisation models 7-40904
DDDM-1, C-poor halo planetary nebula, element abundances from optical and UV obs. 7-60766
dense molecular clouds, elemental abundances, influence of initial conditions 7-35029
dwarf irregular galaxies, CNO abundances determ. 7-40939
early A-type stars, C abundances 7-40815
East Pacific Rise and Guaymas Basin, hot springs U-Th-Pb systematics 7-40462
Eifel periodotite xenoliths, trace element and isotope geochemistry rel. to subcontinental lithosphere 7-34484
emission nebulae, implications of atomic data for astrophysics for element abundances 7-40689
enstatite (EH3, EH4.5 and EL6) chondrites, comps. and implications for form. 7-34950
eucrites, rare earth element patterns, genetic implications 7-40787

element relative abundance continued

- extragalactic H II regions, He abundance and dY/dZ meas. 7-40937
faint blue stars at high galactic latits., He/H ratios from UV and visual spectra 7-47878
galactic corona, IUE obs. rel. to kinematics, ionisation, and abundances 7-48054
galactic disk, metallicity variance of K-type giant stars 7-60640
galaxies effect of metallicity on optical and IR colour-luminosity relations 7-24213
galaxies metallicity vars. rel. to opacity-driven form. of interstellar mol. clouds 7-40908
Galaxy, chemical evolution rel. to Type I supernova rate in solar neighbourhood 7-24155
globular cluster system of M87, metallicity determ. from spectroscopic obs. 7-48001
Hedjaz meteorite, L-group chondrite, comp. and petrography rel. to metamorphic status 7-9446
indochinite tektites, K, Rb and Li concs, rel. to selective volatilisation and imperfect mixing 7-34500
inert gases, systematics in basalts and dunite from Reunion and Grand Comore 7-29012
interstellar C abundance, determ. toward ρ Oph and β^1 Sco. 7-9531
interstellar dust grains, heavy element abundances rel. to polarisation parameters 7-48015
interstellar matter, heavy element abundances 7-66725
interstellar medium, element depletions rel. to identification of astronomically important silicates 7-48017
interstellar medium, He and heavy-element enrichment 7-40905
intervening galaxy towards QSO B2 1225+317, high-resolution spectroscopy of $z=1.79$ absorpt. line system 7-66782
IRAS 1912+172P09, new binary planetary nebula, He/H ratio 7-48046
kimberlites from southern Africa, geochemical correlation with S Atlantic hotspots 7-34409
Laurentian Trough sediments, Gulf of St. Lawrence, radionuclide profiles, sedimentation rates, and bioturbation 7-28995
lunar highland breccias, 60018, 67435 and 67455, inert gases comp. anal. 7-55501
M81, O and N abundance gradients from spectrophotometry of H II regions 7-40941
Mariana Trough basalt glasses, light noble gases comp. anal. 7-40436
Markarian 306, double nucleus galaxy, element abundances from emission-line spectra 7-24199
meteorite, refractory trace elements in Allende 7-9440
meteorites, carbonaceous chondrite C isotopes and element abundances 7-24086
Moon, solar cosmic ray inert gases in regolith minerals 7-14507
Muong Nong type tektites from moldavite and North American strewn fields, implications of element abundances 7-55050
Murchison carbonaceous chondrite, shock-induced volatile loss and implications for planetary accretion 7-34949
NGC 1566, barred spiral galaxy, metal-abundance indices distrib. from imaging spectroscopy of spiral arm 7-24214
NGC 2403, spiral galaxy, chemical comp. gradient and stellar mass limit 7-40940
NGC 4151, Seyfert galaxy, Fe abundance in nucleus from Fe line emission at 6.4 keV 7-18452
NGC 4922, binary galaxy, chemical comp. from spectrophotometric investigation 7-24200
NGC 7492, globular cluster, metal and He primordial abundances 7-60738
Nova Vul 1984 No.1 (PW Vul) slow nova, abundances, visible and IR obs. 7-40850
ocean water, statistical anal. of relative ionic composition data 7-14315
oceanic basalts, siderophile and chalcophile abundances rel. to Pb isotope evolution and growth of Earth's core 7-34397
Orion A, He abundance, spectral obs. (Russian) 7-40951
Orion Nebula, element abundance detems. from IUE lines 7-55784
SW Pacific islands, Pb, Sr, Nd isotope and element abundances study 7-8874
planetary nebulae in LMC and SMC, element abundances from IUE survey 7-48055
Precambrian palaeosols on basaltic and granitic parent materials, elemental concs. profiles 7-29019
primary lavas from Okmok volcano, central Aleutians, geochemistry rel. to arc magmagenesis 7-28949
primordial He abundance determ. from metal-poor galaxies 7-40978
radioactive nuclide pairs, general constraints on age and chemical evolution of Galaxy 7-55809
Ragland meteorite, LL 3.4 chondrite find from New Mexico, chemical and isotopic anal. 7-9450
rare earth elements in Stillwater Complex, Montana, evidence for form. of Ultramafic Series 7-65987
Sea of Japan, U and Th contents as indicators of continental-type volcanism 7-14274
solar flare particles, element abundances rel. to temp. of energetic particle emission regions 7-66532
solar wind C, N and O ions in magnetosheath of Earth 7-9318
supernovae, element abundances from pair creation supernova in massive Wolf-Rayet star 7-29462
time-varying coupling constants and primordialnucleosynthesis 7-4607
Venus surface, rock comp. at Vega 2 landing site 7-55510
volcanic rocks from Yap-Mariana trenches intersection, petrology, geochemistry, and tectonic implications 7-34469
Wethersfield (1982) chondrite, abundances of cosmogenic radionuclides and noble gases 7-34952
Al in River Esk and River Duddon and tributaries, Cumbria 7-13933
Al/Mg in interstellar medium rel. to ^{26}Mg excess in meteorites 7-48036
C abundance in P/Comet Halley (1982i), rocket-borne UV spectroscopy 7-47784
C/N ratio in Lake Karewa sediment, India, palaeoclimate characts. determ. 7-4175
CNO abundances evol. in galaxies 7-40934
CNO abundances in field horizontal-branch and A-type stars 7-9472
Ca-Ti-Cr isotopic anomalies in Allende meteorite, correlation with solar $^{48}\text{Ca}/^{46}\text{Ca}$ abundance 7-55586
D, synthesis in stellar atm. in binary systems with accretion disks (Russian) 7-24218
Ga to Sr abundances in Sun, anal. of s-process and r-process contribs. 7-23990
Ga/H in Si star HD 25823, spectrum synthesis of UV Ga II and Ga III lines compared with IUE obs. 7-47943

element relative abundance continued

- H II regions, extragalactic, line ratios modelling rel. to element abundances 7-40903
H II regions, photoionisation models rel. to abundances and ionising star temp. determ. 7-40907
He in metal-poor H II regions of dwarf irregular galaxies 7-55804
He primordial abundance, implications of collisional effects in He I triplets 7-55446
He/H ratio in globular cluster NGC 6752, determ. from photographic photometry 7-29520
He/H ratio in H II region complexes, implications of He ionisation struct. models 7-40906
He/H ratio in Hyades, implications of H-R diagram position of eclipsing binary star (HD 27130) 7-66665
He/H ratios in B-type stars, determ. for members of open clusters and associations (Russian) 7-55626
Mg abundance gradient in planetary nebula NGC 7027, implications of ionization impact excitation rate coeffs. for Mg^{++} and Mg^{+} 7-55455
O/Fe in metal-poor late-type stars 7-40803
P depletion in interstellar mol. clouds, evidence from upper limits to PO abundances 7-66713
Pb in Antarctic ice during Wisconsin/Holocene transition 7-40074
Pb in river sediments, Christchurch, New Zealand 7-13934
Rn in soil, anomalous increases as earthquake precursor 7-8866
 ^{232}Th concentrations in seawater, meas. techniques and results 7-34554
U and Th, concentrations in geological samples, plastic track detector study 7-40596
 ^{238}U (A=238, 234) ratios in seawater, meas. techniques and results 7-34554
 ^{238}U decay series nuclides, evidence for recent migration in granite pluton 7-28917

elemental semiconductors

- 7-27150
Si:O, heavily doped, SIMS meas. of O conc. 7-17388
bicrystal, grain boundary dislocations, struct., steps, HREM study 7-16488
channelling contrast microscopy, He⁺ microbeam, semiconductor impurity profiles 7-51587
conduction-band-edge charge density, empirical pseudopot. calcs. 7-64046
CVD, adsorption on Si (111) of Si-H system species, rel. to temp., supersaturation, bond strength and press. 7-33583
deep centres in semiconductors, book 7-18510
defects produced by electron and X-ray irradiation, surface effects 7-6687
dendritic web Si solar cells 7-40005
diamond:B, hopping photoconductivity 7-38617
diamond, electron beam irradi., vacancies, photoluminescence, radiative decay time meas. 7-46107
diamond, electronic structure, STEM study 7-16939
diamond, energy band gap calc., self-interaction correction to local density approx. 7-45144
diamond, KVV Auger electron spectra calcs., band and cluster approx. methods 7-46252
diamond, large unit cell CNDO calculations 7-7106
diamond, Mu^* hyperfine parameters, absolute sign, muon polarisation studies 7-53204
diamond, muonium defect energy profiles, unrestricted Hartree-Fock cluster calcs., comment and reply 7-45907
diamond, normal muonium, lattice relax. calcs. 7-51789
diamond, optical phonons and elasticity at megabar stresses 7-21375
diamond, planar channelled protons, breakthrough angles 7-21308
diamond, positron planar channelling radiation energy levels, variational calcs. 7-63696
diamond, synthesis and props. (Russian) 7-16588
diamond, type Ia, voidites, evidence for crystalline phase containing nitrogen, cell constant determ. 7-2011
diamond, volume expansion during ion implantation, point defect creation and interactions 7-51890
diamond anomalous muonium, vacancy-associated model 7-51758
diamond crystals, band structure, LMTO calcs. 7-2477
diamond crystals, surface phonon modes and reconstructions, Green's function method calcs. 7-2339
diamond single crystals, relativistic positron channelling radiation, spectral density peak splitting studies (Russian) 7-21310
diamond structure, muonium states, muon spin resonance studies 7-53206
diamond-like structure semiconductors vibrational spectra of interstitials (Chinese) 7-32592
doped, preparation and thermal conductivity, review 7-38279
n-Ge, many-valley semicond., surface photogalvanic effect calcs. 7-52679
hierarchical lattices, phase transition universality sputtered, photoelec. props. 7-35486
highly doped and excited, electron-phonon mobility variation with carrier density 7-64249
LPCVD production, anal and solar cell appls. 7-17452
magnetothermoelectric power meas. in quantising mag. fields 7-45362
marker evolution on ion irradi., computer simulation 7-21302
MOS structures, anodically and thermally grown; breakdown field strengths 7-17113
muonium defect centres, muon spin resonance studies 7-52502
optical polarisation of nuclear moments in Si with 1D defects 7-7602
polysilicon, plasma etching in single slice planar reactor (German) 7-46736
polysilicon films, etching in parallel plate plasma reactor, freq. depend. 7-17744
polysilicon for solar cell appls., DLTS study 7-38512
polysilicon oxidation, appl. to double polysilicon devices 7-39774
polysilicon-thin films for VLSI, elec. props. 7-38789
polysilicon-SiO₂, surface texturing effect on SiO₂ cond. and breakdown 7-39773
polysilicon-SiO₂ interface, enhanced electron injection 7-38755
polysilicon-SiO₂ interfaces, textured, electronic props. 7-38754
Si:B polycrystalline solar cell substrates, B conc. meas. using IR spectroscopy 7-23176
a-Si:H, structural characterisation, hyperfine interaction, ESR, ENDOR 7-53135
a-Si:H solar cells stability, role of Si-H bonds studied by Fourier transform infrared spectroscopy 7-13896
Si, intrinsic faults, weak beam contrast study 7-16377
Si, spherical wave EXAFS, Si K-edge anal. 7-64822

elemental semiconductors continued

- Si MOSFET, resistance laboratory unit determ., using quantum Hall effect 7-18812
- Si solar cells, SILSO, grain boundary charact., meas./test techniques 7-13858
- Si solar cells in high concentration photovoltaic module 7-17874
- Si solar cells used in photovoltaic 22.5X linear Fresnel lens concentrator module 7-17873
- Si-Al Schottky barriers, Ar ion implantation damage, thermal anneal recovery 7-17101
- Si-Cu, Auger electron emission (*Russian*) 7-17100
- Si-Ni thin film diffusion couples, lateral silicide formation 7-21540
- Si-SiGe strained superlattices on Si substrates, MBE growth, characterisation, appl. for HEMT 7-27218
- Si/SrO/Si heteroepitaxial structure formation by molecular beam epitaxy 7-53600
- SIPOS, AES and XPS studies (*Chinese*) 7-33511
- SIPOS-Si heterojunction current flow props. 7-38713
- SOI, conf., Boston, MA, USA (Dec. 1985) 7-35101
- SOI, films lamp zone melting recrystallisation, effect of plasma nitrided SiO₂ encapsulant 7-38391
- SOI buried layer form. by high dose implantation, mass transport studies 7-32479
- SOI film, two-beam laser recrystallisation 7-38393
- SOI films, halogen lamp recrystallisation 7-38394
- SOI films, inhomogeneous carrier transport props., influence of temp. 7-33094
- SOI films, lamp zone melting recrystallisation, liquid-solid interface 7-38419
- SOI films, laser recrystallisation, agglomeration, surface roughness and crystal imperfection 7-38389
- SOI films, recrystallisation by obliquely scanned pseudoline electron beam 7-58686
- SOI films, thermal stresses during zone melting recrystallisation, sub-boundaries, in-plane orientation 7-33554
- SOI films, twin stabilised planar growth 7-38392
- SOI films, zone melting recrystallisation, subboundary structure 7-38388
- SOI films, zone-melting recrystallisation, capping techniques 7-38390
- SOI films scan-melted at low velocities, subboundary misalignment 7-38387
- SOI formation, high dose O⁺ ion implantation, lamp annealing 7-32527
- SOI heterostructure technology 7-38750
- SOI large area growth, pseudo-line electron beam technique with lateral seeded epitaxy (*Japanese*) 7-7842
- SOI struct., implanted buried oxide elec. props., high temp. annealing effects 7-58904
- SOI structures, ion beam synthesised, carrier lifetime increase 7-12865
- SOI structures, ion implanted, defect EPR spectra studies 7-27603
- SOI structures, lateral epitaxy formation, melting and resolidification 7-38386
- SOI structures, thickness determ. using optical interf. method 7-18743
- SOI technology by zone-melting recrystn. on quartz substrates 7-21736
- SOI thin films, props. after laser focused beam processing 7-32497
- SOI wafers, O implantation prep., background doping effects 7-32478
- Solar cells, recombination and transport parameters, advanced measurement techniques 7-54316
- SOS, crystalline quality improvement by ion beam technique 7-16651
- SOS, double solid phase epitaxial regrowth, amorphous layer, self-implantation, ion energy, defect density 7-58691
- SOS, ion beam improved, elec. characts. 7-17114
- SOS, submicron-gap photocond. switching 7-52689
- SOS epitaxial layers, strain meas., using X-ray diffr. 7-44305
- SOS films, pulsed laser beam excitation, femtosecond dynamics 7-13249
- SOS films, regrowth rates of amorphous layers created by self-implantation 7-16661
- Triotron sputtering equipment for the production of mixed Ta/Si layers (*German*) 7-33564
- vacancies, hyperfine interactions, ENDOR and EPR studies 7-63609
- Si, low energy ion beam damage, ellipsometric characterisation, two-film optical model 7-27680
- Al/Pt/Si structures, PtSi formation 7-63972
- Al/Si contacts, diffusion at room temp. (*German*) 7-32724
- Al/SiO₂/Si₃N₄/Si illuminated struct., nonlinear capacitance props. study 7-38731
- Al/TiN/Si contacts for VLSI, analytical electron microscopy 7-58651
- Al-As₂S₃-n-Si, I-V characteristics 7-7390
- Al-Ge-Si, heterojunction ohmic contacts 7-27432
- Al-insulator-Si, optical and elec. charact. of (Al₂O₃)_{1-c}(AlN)_c 7-38766
- Al-Si:Ar,H, ion implanted ultrahigh Schottky barriers, interfacial traps, DLTS study 7-45489
- AlGaAs/GaAs/Ge multijunction solar cell, model for calc. of displacement damage by radiation 7-13878
- AlGaAs-Si mechanically stacked multijunction solar cells, optical effects of thin film adhesives 7-3670
- As magnetothermoelectric power meas. in quantising mag. fields 7-45362
- B, defects produced by electron and X-ray irradiation, surface effects 7-6687
- Bi, liq., elec. resist. meas. 7-38532
- C films, plasma deposited from methane, elec. conductivity, optical absorpt. 7-38786
- C, single-particle excitations, dynamic correl. corrections, local density theory 7-45115
- CaF₂-Si (111) interface, electronic struct. 7-38737
- CaF₂-Si(111), tensile strain, interfacial disorder, reordering 7-27163
- CdS-Si heterojunctions, struct., elec. and photoelectric props. 7-22001
- CoSi₂-Si, mesotaxy, single crystal growth of buried CoSi₂ layers 7-58671
- CoSi₂-Si epitaxial heterostructures, growth and characterisation 7-27212
- Cr/SiO₂/Si structs., Fowler-Nordheim tunnelling oscils., I-V characts. meas. 7-38745
- Cr-Ge thin film interface, interdiffusion, reaction and intermixing, soft X-ray photoemission study 7-27028
- p-crystalline Si/n-amorphous Si heterojunction, electrostatic pot. barrier distrib. calcs. 7-58881
- Fe₈₀C₂₀-Si compositionally modulated amorphous struct., mag. and diffusional props. study 7-7564
- Ga, electron impact ionisation function meas. 7-50367
- Ga melting and triple points realisation, comparison of sealed cells 7-61333
- GaAs-Ge crystal growth on Ta₂O₃-coated Si substrates, zone melting and MOCVD 7-53579

elemental semiconductors continued

- GaAs-Ge-SiO₂, semiconductor MBE layers on Ge islands on insulator, photolum. study 7-33455
- GaAs-Si, nucleation and growth of GaAs 7-45038
- a-GaAs-Si (100), epitaxial regrowth by excimer laser annealing, FET fabrication 7-32875
- GaAs-Si cells, photovoltaic 7-17903
- GaAs-Si mechanically stacked multijunction solar cell 7-8402
- GaAs-Si p-n heterojunctions, interface charge polarity 7-38686
- GaAs-Si thin film solar cells, radiation damage 7-65465
- Ga_{1-x}P_x-GaP-Si mechanically stacked multijunction solar cells, p-n junction model 7-3668
- Ge (001), field emission flicker noise and electron states 7-33533
- Ge (001) (2×1), electronic struct., first principles self-consistent calc. 7-12778
- Ge (100), H adsorption, high resolution energy loss spectra study 7-38331
- Ge (100) substrate for ZnSe layers, MBE growth and photoluminesc. 7-7858
- Ge (110), electron states calc., tight-binding muffin-tin orbital Green's function method 7-52721
- Ge (111), adsorbed Pb, atomic geometry, surface X-ray diffr. 7-52277
- Ge (111), adsorbed Pb monolayers, photoelectron scatt., temp. depend. 7-13328
- Ge (111), chemisorption of atomic H, nonempirical cluster-model study 7-38332
- Ge (111), Sn adsorbate geometry determ., X-ray photoelectron diffr. study (*Japanese*) 7-11852
- Ge (111), stability and struct. of 7×7 reconstruction 7-2310
- Ge (111) and Ge (220), EXAFS surface structure studies at Daresbury SRS, in 60 to 11100 eV range 7-33486
- Ge (111) cleaved surface, optical props. and atomic struct. 7-58595
- Ge (111) pure and As doped, surface electronic struct., photoemission studies 7-2658
- Ge, (111) surface structure, lattice gas model anal., DAS structure 7-2309
- Ge (111), dynamical recovery 7-13475
- Ge, amorphous and partially crystallised, X-ray absorpt. investig. of struct. (*German*) 7-46241
- Ge, amorphous films, laser induced image storage 7-11078
- Ge amorphous films, struct. and crystn., EXAFS study 7-64005
- Ge, amorphous layers on GaAs, solid phase epitaxial Growth during annealing 7-21777
- Ge, anharmonic props. of ultrasound under intense excitation 7-20488
- Ge, anomalous muonium, vacancy-associated model 7-51758
- Ge, anomalous photovoltage films X-ray irradiation effects studies 7-58834
- Ge, atomic-scale surface modifications by scanning tunnelling microscope 7-58583
- Ge, avalanche photomultiplication in the far infrared 7-45375
- Ge, band gap determ. method 7-35155
- Ge, bicrystal boundaries, transient spectra of dislocation levels 7-52497
- Ge, carrier conc., mag. gradient effect (*Russian*) 7-17040
- Ge, cathode sputtering process statistical modelling, optical layer deposition 7-39375
- Ge cleaved surface in liquid He, photo-EMF production, quasi-2D carrier diffusion in surface cond. gradient 7-38636
- Ge clusters, TOF mass spectra 7-20084
- Ge, coincidence spectrometer with scintillation and planar detectors, time characts. 7-36438
- p-Ge, correlation between deep-level parameters and energy resolution in γ -detectors, trapped hole re-emission effects 7-15454
- Ge crystal, carrier mobility meas. using Haynes-Shockley expt. for student laboratory 7-55933
- Ge crystal, disordered surface layer, standing X-ray wave excited photoelectron emission, energy dispersion meas. 7-366
- Ge crystal, exciton gas-electron-hole liq. interactions, phase diagram, nuclei drift effects 7-2488
- Ge crystal, laser irradiated, thermal excitation 7-38137
- Ge crystals, band structure, LMT0 calcs. 7-2477
- Ge crystals, surface phonon modes and reconstructions, Green's function method calcs. 7-2339
- p-Ge, cubic crystals, magnetic field-induced circular photocurrent drag effect calcs. 7-58833
- Ge cubic crystals, electron struct., cluster approx., X α calcs. 7-38445
- Ge, curved cryst X-ray optics, inelastic scatt. expts., X-ray spectrometer design parameters 7-16354
- Ge, Czochralski growth, cryst. wt. rel to melt temp. variation 7-7841
- Ge deformed single cryst., AC conductivity at 4.2K 7-7245
- Ge detector, solder natural radioactivity effects in low background expts. 7-62220
- Ge, dielectric response and electronic states 7-33320
- Ge, dislocation transmission through $\Sigma=9$ symm. tilt boundaries, synchrotron X-ray topography, HVEM obs. 7-63646
- Ge, dislocation transmission through $\Sigma=9$ symm. tilt boundaries, dynamic and crystallographic anal. 7-63647
- Ge, dopant profiles modification due to surface and interface modifications 7-58306
- Ge, drag thermoelec. power, anisotropy parameter, carrier density depend. 7-38603
- p-Ge, electric avalanche breakdown, chaotic and hyperchaotic states 7-52630
- Ge, electron channelling 7-21305
- Ge, electron correlation, band gaps and quasiparticle energies 7-27278
- Ge, electron escape fns., determ. by methods of calibrated amorphous layers and total external reflection 7-39362
- Ge, electron irradi., annealing kinetics, impurity effects 7-16630
- Ge, electron irradi., hole effective mass parameters, cyclotron reson. 7-58730
- Ge, electron mean free path needed for excitation of volume and surface plasmons 7-21838
- Ge electron-hole liq., ultrasonic attenuation calcs., intraband collision effects 7-12214
- Ge, electron-hole plasma transport 7-7272
- Ge, electronic struct. of incoherent grain boundary, recursion approach 7-64161
- Ge, energy gap, indirect meas. 7-7107
- Ge epitaxial films, CVD growth on Ge substrates, surface morphology 7-53618
- Ge, epitaxial films, remote plasma-enhanced CVD 7-39395

elemental semiconductors continued

- Ge epitaxial growth on CaF_2/Si (111), film quality improvement by Ge predeposition 7-7070
 Ge, extrinsic, freq. locking, quasiperiodicity and chaos 7-2618
 p-Ge, far IR multiphoton absorption 7-27723
 Ge film growth on (HgCd)Te substrates, surface preparation effects 7-45037
 a-Ge films, dynamics of laser annealing by transient grating method 7-12122
 a-Ge films, laser-induced phase transitions, time resolved TEM study 7-38056
 Ge films on amorphous substrates, prep. by surface-energy-driven grain growth 7-38385
 Ge, floating zone growth, lateral solute segregation rel. to gravity conditions 7-53576
 Ge, for MOCVD growth of AlGaAs and GaAs, tandem solar cell appl. 7-3671
 Ge, fourth-order thermal expansion coeff. fn. 7-44868
 Ge, free exciton diffusion and decay, lumin. 7-32918
 Ge, grain boundary energies, computer calcs. 7-6639
 Ge, growth surface optical characts. oscills. during MBE, automatic reflection ellipsometry meas. 7-64715
 p-Ge, Hall effect, mag. field and temp. depend., transport eqn. soln. 7-52651
 Ge, heavy holes, Landau level spectrum, optical gap form. 7-45191
 Ge, heteroepitaxy on CaF_2/Si (111) 7-22497
 Ge heteroepitaxy on CaF_2/Si structures, planarised growth by electron beam exposure to predeposited layers 7-52855
 Ge highly ionised atoms injected into PLT and TFTR discharges, spectra 7-19748
 Ge, holes optical effective mass, determ. by interf. method 7-17290
 p-Ge, hot electron transport, perturbed acoustic phonon distrib. effects, Monte Carlo anal. 7-64254
 Ge, hot hole FIR laser action investig. 7-57341
 p-Ge, hot hole intersubband transitions, stimulated emission and gain, quantum oscills. 7-1052
 Ge hot-hole cyclotron resonance maser with negative effective hole masses 7-15838
 Ge IR absorpt. coeff. meas. with compensating calorimeter 7-56270
 Ge, impurity doping by photonuclear reactions 7-16589
 Ge ion beam deposition on (100) single cryst. substrate, interface, thin film and damage form. 7-17423
 Ge ion cluster beam deposition substrates for MOCVD GaAs solar cells 7-23182
 Ge, ionisation-stimulated annealing of Frenkel pairs under electron or gamma irradiation 7-38061
 Ge large crystal growth by Stepanov method 7-33543
 Ge, laser heated, time-dependent X-ray reflectivity 7-26796
 Ge, laser irradiated, electron-hole plasma dynamics investigated by time-resolved spectroscopy 7-13276
 Ge, lattice dynamics, real-space force consts., adiabatic bond-charge model 7-32589
 Ge, lattice dynamics and electron-phonon interactions, quasi-ion approach calcs. 7-58422
 Ge Lege-type detector, time props. 7-62216
 Ge lenses, diamond-machine for IR, quality and performance 7-25932
 Ge light hole Landau level inversion, light amplification in crossed elec. and mag. fields 7-31293
 Ge liquid, structural phase transitions, photoemission studies 7-1836
 Ge, MBE growth on CaF_2/Si (111), structural and electrical characteristics 7-45051
 Ge, MBE on Si, role of surface reconstruction, LEED, Rutherford back-scattering, channelling meas. 7-7034
 Ge, metastable phases, vibr. props. 7-2126
 Ge, microcrystals, amorphous-like Raman signals 7-53349
 Ge microcrystals, gas-evaporated, thermal annealing, Raman and electron microscopic study 7-64635
 Ge, mixed group III and group V ion implantation 7-21243
 a-Ge, molecular dynamics simulation, struct. of solid phases 7-32293
 Ge, multibeam streaming of heavy holes 7-12728
 Ge, multipoint field photocathodes, fabrication and emission characteristics 7-13323
 Ge, muon channelling, evidence for pionium formation 7-51897
 Ge, n-type and ultrapure samples, electron transport and press. coeffs. 7-2615
 n-Ge, Nernst-Ettingshausen coeff. in the case of scatt. by impurities in quantising mag. fields 7-12745
 p-Ge, nonlinear I-V characts. and spontaneous current oscillations 7-52631
 p-Ge, nonlinear light absorpt. coeff., IR intensity study 7-53258
 Ge, nonlinear transport, morphogenetic reaction-diffusion model 7-27337
 Ge, nuclear radiation detector, spherical coaxial structure, elec. field distrib. 7-5562
 Ge p-n junction solar cell radiation-induced defects obs. using DLTS 7-13875
 Ge, p-type, photon drag effect (*Chinese*) 7-33042
 Ge, p-type, stimulated submillimetre emission props. 7-46074
 Ge, periodic surface microrelief, determ. optical constants of laser-irradiated material 7-63926
 Ge photodiode, pyrometer for 60 to 1400°C range (*Rumanian*) 7-4856
 Ge photodiodes, temperature and uniformity effects 7-61378
 Ge point contacts, nonlinear elec. cond. effects due to electron-phonon interactions (*Russian*) 7-52628
 Ge polycrystalline film, preferred orientation control by two-step growth method 7-21728
 Ge polycrystalline films, photoassisted CVD prep. 7-3200
 Ge, positron planar channelling radiation energy levels, variational calcs. 7-63696
 Ge profiled crystals, growth by Stepanov's method, appl. for optical components 7-31409
 Ge, pulsed laser melting, time-resolved reflectivity meas. 7-2158
 Ge, pure and heavily doped, dielec. function, impurity conc. depend., spectroellipsometric meas. 7-2525
 Ge, quenched, SA_2 acceptor, uniaxial stress effects, far IR optical study 7-64673
 Ge, reflectivity meas. during pulsed laser irradiation 7-12132
 Ge, reverse recovery experiments, diode geometry effect 7-34038
 n-Ge, room temp. anomalous Hall effect 7-38595
 Ge, SHG, cryst. orientation depend. 7-50640
 Ge, scattering inhomogeneities, two-wavelength probe meas. 7-46063

elemental semiconductors continued

- Ge semiconductor plasma, laser produced, ultrafast switching simulation 7-11020
 Ge, semiconductor surfaces, atomic, electronic and vibronic props. 7-2307
 Ge shallow donor levels, valley-orbit splitting in mag. field, zero-radius central cell model calcs. 7-58763
 Ge single cryst., native oxide and nitride insulator layers, microstruct. and props. 7-12574
 Ge single crystals., plasticity meas. near yield peak (*Russian*) 7-44664
 Ge, single-particle excitations, dynamic correl. corrections, local density theory 7-45115
 Ge, six-beam X-ray spherical wave diff., intensity distrib. 7-32198
 Ge solar cell parameters, theoretical temp. depend. 7-23161
 Ge solar cells for thermophotovoltaic appls. theoretical efficiency 7-59855
 p-Ge, solid-state radiation source for submillimeter and far IR waves 7-37079
 p-Ge, spatial correlations of chaotic oscillations in post-breakdown regime 7-64255
 p-Ge, spatio-temporal coherence and chaos, conf. Los Alamos, USA, Jan. 1986 7-48158
 Ge, spin-orbit splitting, determ. from ab initio pseudopotential 7-2547
 Ge sputtered (100) textured film, TEM grain growth obs. 7-45040
 Ge, strongly excited, nonequilibrium carrier recomb., electron-hole drops 7-38461
 Ge, structural props., ab initio pseudopotential calcs. 7-44797
 Ge substrate (001) oriented, with GaAs epitaxial film, structural props. 7-58687
 Ge substrate for single-domain epitaxial growth of GaAs 7-22578
 Ge surface, evanescent X-ray diffraction during total external reflection, struct. studies 7-26590
 Ge surface, GeO stabilisation on laser irradi., X-ray photoelectron spectra anal. 7-46723
 Ge surface, H_2S adsorption, orientation and temp. depend. 7-58634
 Ge surface, NO scattering, energy distributions, state-resolved measurements 7-53477
 Ge surface laser irradiation, ionic cluster desorption, time-of-flight meas. 7-12138
 a-Ge, surface phonon generation and picosecond light pulse detection 7-12456
 Ge, surface plasmons, electron energy loss peaks 7-7305
 Ge, surface potential, photomemory effects 7-12775
 Ge surface state characts., surface struct. and low temp. annealing effects 7-45426
 Ge, surface structure, optical transitions 7-12439
 Ge, swirl defects formation 7-51753
 Ge, thermal donor states 7-7155
 Ge, thermally scattered X-rays, anomalous transmission obs. 7-51573
 Ge, thermodynamic interrelation between amorphous, diamond cubic and liquid states 7-12245
 Ge thin film bolometer with fast response 7-56261
 Ge third order elastic constants, US displacement interferometry 7-2087
 p-Ge, threshold switching and microwave-induced spontaneous emission in static magnetic field 7-52707
 Ge, tilt boundary struct., computer modelling 7-16579
 Ge, tubular hole distrib. under streaming conditions, scatt. anisotropy effects calcs. 7-58802
 Ge ultra-thin films, self-implantation, grain growth enhancement, TEM study 7-12173
 Ge, ultrafine particles, Raman and X-ray scatt. study 7-64627
 p-Ge, undoped, deep level defects produced by electron irradiation, annealing 7-12660
 Ge, uniaxially stressed, internal strain parameters, surface effects 7-44980
 Ge valence electron subsystem, local and exchange pot. approxs. calcs. 7-38477
 Ge, vapour phase growth on Ge substrates, influence of p and n doping 7-3198
 Ge, vibrational correlation functions 7-51966
 Ge, volume capture effect for relativistic electrons, computer simulation 7-12156
 Ge with a-C:H diamond-like coating rain erosion resistance improvement obs. 7-31435
 Ge, X-ray phase determination using multiple-beam effects 7-32210
 Ge X-ray resonators tuned to the spectral interval wavelength $\text{CoK}_{\alpha 1}$ 7-24736
 p-Ge:As, Hall effect and electrical conductivity, temp. corrections 7-38592
 Ge:As(Sb)(Te)(Bi), implanted, heavy ion damage, TEM, annealing studies 7-63676
 n-Ge:As, electron heating, photocond., photo-Hall effect 7-12765
 p-Ge:B(Al)(Ga)(In), annealing kinetics of radiation defects, influence of impurity binding energy 7-39547
 Ge:CuH(D) $_2$, acceptor electronic state symm., isotope effects study 7-21863
 a-Ge:D,H, plasma deposited, deuteron magnetic resonance 7-27626
 Ge:Ga, impurity g-factor determ. piezo-Zeeman spectra obs. 7-16982
 p-Ge:Ga, resistivity at low temp. appl. to bolometers 7-41471
 Ge:Ga single crystals., tracer diffusion coeff. and isotope effect, SIMS meas. 7-27019
 Ge:Ga(Be)(Zn) extrinsic photoconductor material, cryst. growth and characterisation 7-64893
 a-Ge:H, B, P, As, dopant incorporation and doping efficiency 7-44587
 a-Ge:H, elec. props., effect of H plasma press. (*Korean*) 7-27332
 Ge:H, H composition at surfaces and interfaces 7-27083
 Ge:H,Be(Zn), shallow acceptor complexes 7-45219
 Ge:H films, post-deposition hydrogenated, electrical props. 7-32296
 a-Ge:H glow discharge deposited thin films, H content determ., spectroscopic ellipsometry study 7-38365
 a-Ge:H/Si:H superlattice struct., light absorption and photocond. studies 7-38715
 Ge:H-Si:H amorphous superlattices, electrical transport 7-7336
 Ge:Na(K), impurity addition by electrolysis 7-44578
 Ge:Ni, inhomogeneously photoexcited, cond. random spontaneous oscills. 7-52675
 n-Ge:Ni, photocond., spontaneous oscills. in an electric field 7-52670
 Ge:O, γ -irrad., majority carrier mobility meas. 7-27334
 Ge:O, Li, IR absorption spectra and bands, Li-O complexes 7-33375
 Ge:O, thermal donor binding energies 7-16989

emental semiconductors continued

- Ge:P crystals, seeded growth in soft lined crucible, dopant distrib. 7-53559
 Ge:Sb, Cu, impurity photoconductivity, field and spectrum dependences, exclusion effect 7-38635
 n-Ge:Sb, electron heating, photocond., photo-Hall effect 7-12765
 Ge:Sb, mobility anisotropy coeff. determ. 7-12715
 Ge:Sb single cryst., extended defects, X-ray topography meas. 7-38020
 Ge:Sb(Al)(Ga)(In), heavily doped, charge carrier scatt., elec. cond., Hall effect meas. 7-7228
 Ge:Si, ion-implanted amorphous surface layers, EXAFS 7-27823
 Ge:Zn, electron-hole droplet transport, suppression by deep impurities 7-58746
 Ge:Zn, large electron-hole drop, Alfven wave dimensional reson., impurity scatt. effects 7-16950
 Ge:Zn, photolum. spectrum, effect of (001) uniaxial stress 7-33450
 Ge:Zn deep impurity, shallow positive acceptor, far IR photocond. meas. 7-7157
 a-Ge/au interfaces, atomic intermixing, asymmetries 7-21682
 Ge/GaAs heterojunction interfaces, cyclic behaviour of band discontinuities 7-7365
 Ge/GaAs multijunction monolithic cascade solar cells with patterned Ge tunnel junctions 7-13863
 a-Ge/Pb/a-Ge trilayers, melting transition of Pb 7-32884
 Ge/Si ion cluster beam deposition substrates for MOVCD GaAs solar cells 7-23182
 Ge-Al₂O₃/Cr, layer-substrate structs., ESR, line-shape, nondestructive contactless meas. of layer conductivity 7-38924
 Ge-AlPO₄ MIS structures, inversion layers obs. 7-45502
 Ge-CaF₂-Si epitaxial structures, growth, structural and electrical props. 7-38356
 Ge-CaF₂-Si heteroepitaxial structures, MBE grown, twinning, topography, channelling, TEM, SEM 7-12566
 Ge-Fe interface electronic struct. calc., mag. effects 7-45496
 Ge-GaAs, epitaxial film on GaAs, extrinsic photoeffect obs. with X-ray diffraction apparatus 7-32221
 Ge-GaAs epitaxial interface, extended defects, geometrical character 7-6640
 Ge-GaAs heteroepitaxy on Si substrates, recrystallised Ge-on-insulator intermediate layers 7-52358
 Ge-GaAs heterostructures, lattice theory, phonon propagation 7-58602
 Ge-GeO₂, defect formation, during thermal oxidation 7-65237
 Ge-GeO₂, symmetry forbidden Raman scatt. from (100) oxidised surfaces 7-46002
 Ge-metal interfacial atomic struct. and cpd. form., FIM studies 7-32846
 Ge-Pb multilayers, cumulative disorder and X-ray line broadening 7-32847
 Ge-Si superlattices, structurally induced optical transitions, electroluminescence spectra 7-59184
 Ge-Si(111) interface, geometrical struct. 7-38310
 Ge-Sn heterostructure, MBE growth in ultra-high vac. system 7-2423
 Ge-Sn interface form., growth mode, AES, RBS studies 7-58666
 Ge_n⁻ semicond. cluster anions, photodetachment and photofragmentation 7-36837
 GeSi thermoelectric devices, fabrication, materials and properties 7-65499
 GeSi-Si strained superlattices, order-disorder transitions, obs. 7-27166
 Ge_{1-x}Si_x-GaAs-Si, multispectral high efficiency solar cells, semicond. selection criterion 7-8399
 Ge₂Si_{1-x}-Si strained layer superlattices, bandgap meas. 7-27408
 Ge₂Si_{1-x}-Si strained-layer superlattice, zone folding induced quasi-direct gap, optical absorpt. probability 7-27409
 In, electron impact ionisation function meas. 7-50367
 In₂-Sn₂O₃-SnO₂-Pt-Si:H solar cells 7-8395
 Mo/Si multilayered structs., high resolution electron microscopy studies 7-63968
 MoSi₂-As-poly Si struct., redistribution of As by silicidation tempering 7-51812
 Nb/a-Si/Nb structures, AC Josephson effect 7-12919
 Nb-a-Si-Nb Josephson junctions, for IR laser radiation response near plasma reson. freq. 7-58958
 Nb-Si multilayers, electron beam deposited, characts. 7-27456
 Ni-Si, interphase contact and interaction 7-16880
 Ni-Si interface reactions induced by pulsed incoherent light, silicide formation 7-32725
 Ni-TiC-Si, TiC as mixing barrier for Ni-Si ion beam mixing 7-44922
 Ni-ZnSe-SiO₂-Si struct., energy barriers for photocharging of trapping sights in ZnSe layer 7-52844
 NiSi₂-Si, epitaxial growth of silicide layers by electron beam annealing 7-27213
 NiSi₂-Si, interface states, barrier height, Fermi level 7-27430
 NiSi₂-Si, Schottky barrier, interfacial defect states 7-27428
 NiSi₂-Si, Schottky barrier height, structural characterisation 7-27429
 NiSi₂-Si, stability of MBE grown thin NiSi₂ layers on Si (111) 7-38380
 NiSi₂-Si (111), Schottky barrier height, rel. to Fermi level positions 7-27427
 NiSi₂-Si (111) epitaxial interface, strain meas. by MeV ion channelling 7-27157
 NiSi₂-Si interfaces, convergent beam electron diff. patterns 7-27156
 NiSi₂-Si Schottky barrier heights, study by electron beam induced current 7-27381
 NiSi₂-Si:B(BF₃), epitaxial growth of NiSi₂, influence of dopant atoms 7-45039
 P, amorphous, radiative recomb., time-resolved photolum. study 7-13212
 P, black, interplanar forces caused by electron-lattice interaction 7-63547
 P, black, surface acoustic props., Brillouin scatt. study 7-38316
 a-P, sputtered, response to intense ion bombardment 7-27447
 p-Si:As oxidation in HCl ambient, impurity pile-up, bubble pattern form. and local oxide bowing 7-13675
 Pd/Si interface composition and silicide form., atom probe FIM study 7-32845
 Pd/Si:B,As/Si:B, As ion implant redistribution during PdSi formation using rapid thermal annealing 7-16816
 PdSi₂-Si, interface states, barrier height, Fermi level 7-27430
 Pt/SiN/Si structure, nucleation kinetics and spatial distribution of spherulitic PtSi clusters 7-21675
 Pt-Si interface, PtSi formation and passivation 7-21709
 PtSi/p-Si thin Schottky diodes, TEM, TED, I-V curve and photoemission characts. 7-12861
 PtSi/Si heterogeneous interface struct., defects, and coherency, HRTEM meas. (Japanese) 7-7019

elemental semiconductors continued

- RSi_{2-x}-Si (R=Sc, Y, Gd, Ho, Tb, Dy, Er, Tm, Yb, Lu), silicide thin films, phase composition, conductance, surface morphology 7-7072
 SOI films, halogen lamp recrystallised, minority carrier lifetime studies 7-33101
 SOI, zone melting recrystallisation 7-2414
 Se, amorphous, elec. resist. and Hugoniot shock wave vel. meas. 7-32567
 Se, amorphous, vitrification and crystallisation, thermal prehistory effects (Russian) 7-63479
 Se, amorphous films, crystn., kinetic study 7-21101
 Se, amorphous-crystalline mixture, electrical conductivity formula, anal. 7-58804
 Se anti-Stokes Raman laser, high-power, radiating at 169 and 146 nm 7-43076
 Se film grown by hot wall epitaxy, XPS 7-7821
 Se film waveguide effects on quartz SAW resonator, amplitude-freq. characts. anal. 7-16050
 Se, glassy state, phys. props., chem. bonds and defects 7-6530
 Se highly ionised atoms injected into PLT and TFTR discharges, spectra 7-19748
 Se, multilayered structure, piezoelectric effect (Russian) 7-64572
 a-Se, residual potential, dark discharge 7-27360
 a-Se, structural disorder model 7-26641
 Se, thin film formation by pulsed laser evaporation 7-59426
 Se, thin films, amorphous, crystn. 7-44371
 Se, trigonal, optical props., local field effects 7-22204
 Se vitreous chalcogenide semicond. layers, deep trapping levels, photostimulated effects (Russian) 7-2754
 Se-O, electrophotographic props., doping depend. (Japanese) 7-12752
 Se-Se_{1-x}Te_x photoreceptors, amorphous, xerographic time of flight technique for drift mobility determ. 7-58807
 Si 7-17871
 Si 7-26753
 Si 7-51938
 Si : BF₂ preamorphised implanted samples, defects and leakage currents abs. 7-38514
 Si (001), anomalous diamagnetic effect in highly excited surface subbands 7-64305
 Si (001), clean and with adsorbed H, RHEED intensities 7-27123
 Si (001), scanning tunnelling microscopy 7-27072
 Si (001), step related surface states angle resolved photoelectron spectra 7-52716
 Si (001), surface order-disorder transition 7-52209
 Si (001) (2×1), electronic struct., first principles self-consistent calc. 7-12778
 Si (001) inversion layers in parallel mag. fields, electronic g-factor 7-12783
 Si (001)-(2×8), clean and Ni contaminated, ordered-defect model 7-21586
 Si (100), adsorption of H₂O, photon stimulated ion desorption surface EXAFS 7-58633
 Si (100), adsorption of H₂O, surface struct., photon stimulated ion desorption SEXAFS determ. 7-64752
 Si (100), bonding coordination photoemission studies 7-45071
 p-Si (100), chemical etching with aq. K₂Cr₂O₇, XPS, UPS, LEED and TRMC meas. 7-46719
 Si (100), chemisorption of water, MNDO calcs. 7-63963
 Si (100), exposed to CO, CO₂, O₂, NO and SO₂, photodesorption 7-52290
 Si (100), laser irradi., matrix atomic losses and impurity incorporation 7-2058
 Si (100), magnetoconductivity of nonequib. electron-hole pairs associated with surface charge layer 7-38671
 Si (100), nitridation kinetics in NH₃ by thermal activation or electron bombard., LEED, AES, and TDS study 7-39770
 Si (100), oxidation enhancement by Ce overlayers, CeSiO₃ formation 7-28226
 Si (100), propylene chemisorption, reaction chemistry, active-site manipulation 7-39916
 Si (100), reaction with propylene, adsorption and desorption kinetic meas. combined with Auger spectroscopy 7-65348
 Si (100), reactivity, thermal desorption of propylene, defect- and electron-enhanced chemistry 7-21660
 Si (100), static mode ion sputtering, bond breaking and atom ionisation 7-13306
 Si (100), surface reconstruction 7-16850
 Si (100), UV-stimulated interaction with Cl₂, reaction mechanisms for photon-enhanced etching 7-22926
 Si (100) 2 × 1, adsorbed alkali metals, anisotropic plasmons (Japanese) 7-21967
 Si (100) and (111), adsorption of K, AES, work function meas. 7-32818
 Si (100) MIS structs., state density of 2D electrons in transverse mag. field 7-12870
 Si (100) surface, atomic terraces and steps, refl. electron microscopy obs. 7-52211
 Si (100) surface, chemisorption of H₂O (Chinese) 7-33954
 Si (100) surface, electron delocalisation in 2D electron gas 7-12779
 Si (100) with chemisorbed H₂, transition from the dihydride to the monohydride phase 7-58631
 Si (100) with periodic MOS microstructures, dynamic magnetoconductivity of inversion electrons 7-38743
 Si (100)-(2×1), adsorption kinetics of propylene, propane and methane, chemical activity of C=C double bond 7-27127
 Si (100)2×1, adsorbed H, surface structure, high resolution, IR spectroscopy 7-13169
 Si (100)2×1, interaction with O₂ and N₂O 7-63962
 Si (111), adsorbed Ag, structure, scanning tunnelling microscopy studies 7-58625
 Si (111), acetylene adsorpt., rehybridisation, vibr. investig., EELS 7-17816
 Si (111), adsorbed Ag, geometry and local electron states 7-58626
 Si (111), adsorbed H, generalised Bethe lattices, chemisorpt. theory 7-7318
 Si (111), adsorbed Mo(CO)₆, laser induced electronic excitation followed by CO desorption 7-12470
 Si (111), Ag adsorbate geometry determ., X-ray photoelectron diff. study (Japanese) 7-11852
 Si (111), Ag adsorbed layer, geometric struct. and density of states, cluster model and charge self-consistent extended Huckel method calcs. 7-21619

elemental semiconductors continued

- Si (111), Ag and Au overlayers, room temp. oxidation behaviour, XPS study 7-13676
- Si (111), Ar ion bombardment, RHEED and REM studies 7-32511
- Si (111), atomic-level surface features studied by an electron-microscopic technique 7-6939
- Si (111), Br chemisorption, SCF HF cluster calculation 7-52251
- Si (111), CO monolayer, electronic props., pseudofunction method calcs. 7-2659
- Si (111), chemisorption of benzene, pyridine and thiophene, surface vibr. studies 7-21615
- Si (111), chemisorption of atomic H, nonempirical cluster-model study 7-38332
- Si (111), clean and Au covered, SEM, LEED and scanning Auger microscopy obs. 7-21056
- Si (111), convergent beam RHEED studies 7-32764
- Si (111), disordered adsorption of H, electronic struct. calcs. 7-27377
- Si (111), Ge adsorption, $\sqrt{3} \times \sqrt{3}$ adatom models 7-7008
- Si (111), local density of states near ideal vacancies 7-27380
- Si (111), MBE, ordered and disordered growth modes 7-12558
- Si (111), metal atom catalysed oxidation, UPS and AES studies 7-46865
- Si (111), ordered Au, Ag, Cu overlayers, surface states, inverse photoemission studies 7-2660
- Si (111), Pt chemisorption and interface form., EXAFS and X-ray absorpt. resonance spectra studies 7-38336
- Si (111), single crystal, interaction with HCl, 190-720K 7-13817
- Si (111), stability and struct. of 5×5 reconstruction 7-2310
- Si (111), surface bonding configuration, triangle-dimer stacking fault model 7-6946
- Si (111), surface reconstruction, benzene-like ring model 7-16851
- Si (111), surface reconstructions, X-ray standing-wave study 7-44968
- Si (111), surface ripples, depend. on laser pulse width 7-12445
- Si (111), surface struct., LEED data 7-6947
- Si (111), symmetry and order, SHG 7-15948
- Si (111), thermal oxidation, initial stages, AES, LEED and photoelectron spectra studies 7-3543
- Si (111) 7×7 , surface struct. study using scanning tunnelling microscope 7-4919
- Si (111) (2×1) , π -bonded chain model, vibr. props. 7-16856
- Si (111) anal., charge and current corrugation corrs. in scanning tunnelling microscopy 7-63410
- Si (111) cleaved 2×1 reconstruction, time-resolved VUV photoemission spectroscopy 7-18919
- Si (111) cleaved surface, optical props. and atomic struct. 7-58595
- Si (111) substrates with epitaxial CaF_2 - BaF_2 epitaxial bilayers, characterisation 7-12521
- Si (111) surface, study using an MBE system with automatic ellipsometer, nondestructive anal. 7-7058
- Si (111) surface structure, lattice gas model anal., DAS structure 7-2309
- Si (111) surfaces, reconstruction study 7-2315
- Si (111) with adsorbed Cs or Na, oxidation 7-54025
- Si (111) with adsorbed Ga, X-ray photoelectron and Auger electron diff. 7-27116
- Si (111) with adsorbed Ge, X-ray standing wave studies 7-58629
- Si (111) with ordered Cu, Ag and Au overlayers, inverse photoemission spectroscopy 7-59280
- Si (111) with oxidised Cr overlayer, CrSi_2 formation and reduction of Cr_2O_3 during annealing 7-58660
- Si (111)/Au interfaces, structural and electronic props., annealing effects 7-21679
- Si (111)/ CaF_2 , interface and surface phonons, high resolution EELS study 7-38319
- Si (111)- CaF_2 , MBE grown, electronic struct. 7-2725
- Si (111)- CaF_2 , UV irradiation-induced ordered struct., photoelectron spectroscopy study 7-7396
- Si (111)- 2×1 , dipole scatt., inelastic electron cross sections 7-3126
- Si (111)- 7×7 , temp.-depend. surface resistivity, electron energy loss meas. anal. 7-21973
- Si (111)- (7×7) , interface formation during W deposition 7-58710
- Si (111) 2×1 , electronic struct., scanning tunnelling microscopy studies 7-38668
- Si (111) 2×1 , pseudofunction slab calcs. 7-52727
- Si (111) 7×7 , surface structure, X-ray diff. studies 7-12438
- Si (111) 7×7 surface, total-energy calcs. for Takayanagi model 7-2345
- Si (211), twin boundary, rigid body translation 7-21223
- Si (5×5) surface reconstruction, stability against native oxide form. obs. 7-2318
- Si, acceptor neutralizing species, low temp. injection mechanisms 7-32482
- Si, accumulation layers, quasi-1D transport, strong localisation 7-64359
- a-Si alloy tandem solar cells, spectral response and I-V characts. 7-54315
- p-Si, alpha-particle irradi., defect form. and thermal stability 7-38073
- Si, amorphisation and crystallisation 7-11914
- Si, amorphised and rapidly thermally annealed, extended defects 7-16660
- Si, amorphised films, solid phase epitaxial regrowth, TEM characterisation 7-32883
- Si, amorphous, bibliography, 1985 update 7-24331
- Si, amorphous, deposition system, Si_2H_6 generation device 7-22501
- Si, amorphous, IR absorpt., local phonon-induced bond angle distortion model 7-26642
- Si, amorphous, ion implanted, picosecond laser induced crystn. 7-16621
- Si, amorphous, p-n solar cells, light-induced defects influence on performance 7-17910
- Si, amorphous, pulsed laser irradi., time-resolved X-ray absorption studies 7-3115
- Si, amorphous, single-junction and multijunction solar cells, US DOE/SERI research project 7-8392
- Si, amorphous and crystalline, light reflection, optical third-harmonic generation 7-11059
- Si, amorphous and single cryst., etching rate, ion backscatt. and channelling meas. 7-28231
- Si, amorphous film, density-of-gap-states distrib. field effect meas. analytic determ. 7-52391
- Si, amorphous film, Rutherford backscattering, depth resolution, modelling of noise sources 7-53487
- Si, amorphous foil, time-resolved X-ray absorption during pulsed laser irradiation 7-12128
- Si, amorphous layer radiation detector development 7-30858

elemental semiconductors continued

- Si, amorphous layers, liq. phase crystallisation under pulsed heating 7-44773
- Si, amorphous thin film solar modules, excitation intensity effects on photo-current response 7-40000
- Si, amorphous to crystalline transformation, TEM in situ technique 7-44376
- Si, anisotropic etching, micropylar inhibition method (Japanese) 7-3541
- Si, anisotropic etching with EDP 7-46725
- Si, anodic oxidation in pure water, appl. to MOS structs. 7-39776
- Si, anomalous muonium, vacancy-associated model 7-51758
- Si, anomalous photovoltaic films X-ray irradiation effects studies 7-58834
- Si, as-grown and annealed bicrystals, conductance of grain boundaries 7-64245
- Si, as-grown float-zone crysts., self-disorder vacancy associates, positron annihilation meas. 7-46232
- Si atomic imaging using JEOL4000 EX TEM 7-32230
- Si, Auger electron spectroscopy, sensitivity, contamination levels 7-54245
- Si, Auger recombination at low carrier densities 7-7328
- Si avalanche photodiode for photon correlation meas., passive quenching 7-41463
- Si, axial magnetic Czochralski growth 7-32343
- Si BSF solar cells, Rose-Weaver meas. technique 7-8423
- Si, band gap determ. method 7-35155
- Si barrier detectors for charged particle detection (Czech) 7-62204
- a-Si based integrated type X-ray sensor (Japanese) 7-15456
- Si bent oxidised cryst. wafers, X-ray spherical wave diff., interference phenomena 7-63402
- Si bicrystals, Czochralski growth, tilt boundaries 7-53558
- Si bicrystals, grain boundaries, electronic states, transient capacitance spectroscopy meas. 7-7173
- Si bicrystals, grain boundary carrier recombination, chemical origin 7-17039
- Si bicrystals and thin films, grain boundaries, electronic props. 7-7172
- Si bicrystals obtained by solid-phase intergrowth, interface region struct., electron microscopy 7-45023
- Si, bifacial solar cell for space solar generators 7-8388
- Si bifacial solar cells, minority carrier diffusion length and surface recomb. vel. determ. 7-8407
- a-Si, Bragg diff. from cryst. clusters 7-44374
- Si, bremsstrahlung isochromat spectra, electron-energy losses 7-22377
- Si, broken dislocation bonds, annealing effects, optical polarisation of nuclear moments study 7-38008
- Si, bulk free-carrier lifetime, IR absorpt., contactless spatially resolved meas. 7-52650
- Si buried oxide form. mechanisms by ion implantation 7-44580
- Si buried oxide structure formed by O ion implantation 7-12099
- Si, CVD, thermal diffusion effects, math. model 7-2410
- Si, CVD in annular tubes, film thickness profiles in mixed convection-diffusion regime 7-27190
- Si CVD thin film, struct. and elec. props. 7-21730
- Si, CVD thin film backside gettering effectiveness 7-38217
- Si, CaF_2 coated surfaces, influence of metal films on optical scatter and microroughness 7-13242
- Si carbonaceous films, prod. in situ in Tokamak TEXTOR, depth profiling 7-2893
- Si, carrier transport theory, picosecond processes 7-45342
- Si cascade branching, Monte Carlo simulation 7-58376
- a-Si, cathodic deposition from organic solvents (Japanese) 7-64947
- Si cells, crossed-lens photovoltaic concentrator appl. 7-17905
- Si ceramics, SIMS 7-9919
- Si, channelling radiation spectra of high-energy electrons and positrons 7-27806
- Si, characterisation by a microwave photoconductance technique 7-7281
- Si, charge carrier-lattice interaction, X-ray diff. study 7-51975
- Si, charge density, compact orbitals, LMTO tight binding representation 7-21806
- Si, charged defect states at grain boundaries 7-44564
- Si charged particle detector, large-area 7-25326
- Si, chemical sputtering by ions, electrons and photons 7-59355
- Si, chemically assisted ion beam etching using low energy Kaufman source 7-22931
- Si, chemisorbed on Pt, Pt-Si interfacial growth, intermixing, SEXAFS obs. 7-64772
- Si, circular wafer, edge effects on bulk resistance 7-58811
- Si cleaved semiconductor surfaces, scanning tunnelling microscopy 7-21051
- Si cleaved surface, ethylene adsorption, high resolution EELS study 7-63951
- Si clusters, TOF mass spectra 7-20084
- Si cold cathode for high current densities 7-12816
- Si, colloidal, prep., photochem. expts. 7-65332
- Si colour image sensor, based on wavelength dependence of radiation adsorption 7-4892
- n-Si, complex dielectric fn., carrier interactions, Monte Carlo calcs. 7-33041
- Si, complex permittivity meas. using TE_{016} mode dielectric resonator 7-14976
- Si, complex refractive index meas. during pulsed laser annealing 7-45970
- Si concentrator cell multifactorial experimental evaluation 7-13867
- Si concentrator solar cells, efficiency limits 7-8384
- Si concentrator solar cells, 27.5% efficiency 7-23135
- Si concentrator solar cells, low resistivity, 25% efficiency 7-23136
- p-Si conductivity and Hall mobility calcs., impurity scatt., anisotropic-nonparabolic effects 7-12720
- Si, cryst. growth, solid state photovoltaic research status at SERI 7-8389
- Si crystal, electron microdiffraction patterns, image reconstruction 7-6487
- Si, crystal data for high-pressure phases 7-16486
- Si, crystal growth, impurity effect on formation of microdefects 7-32340
- Si crystal growth, mould shaping, spinning, method 7-53568
- Si, crystal growth, semiconductor industry needs 7-53540
- Si crystal growth and epitaxial layer deposition for VLSI devices 7-46299
- Si, crystal growth and solidification, high speed laser heating technique 7-53566
- Si, crystalline, amorphous and H-doped, structural props., EXAFS study 7-64760

elemental semiconductors continued

- Si, crystalline, ion-implanted and amorphous, light diffraction by transient gratings 7-11034
- Si, crystalline, solar cell arrays, reliability lessons for thin film modules 7-13910
- Si, crystalline and amorphous, Monte Carlo growth simulation models 7-16470
- Si crystalline solar cells, conditions for high efficiency 7-23145
- Si, crystallised thin films, electrical characterisation 7-33116
- Si crystals, band structure, LMTO calcs. 7-2477
- Si crystals, low energy Ag⁺ implantation-induced deep centre depth distrib., DLTS study 7-26820
- Si crystals, radiation defect stabilisation and annealing kinetics study (*Russian*) 7-44608
- Si crystals, surface phonon modes and reconstructions, Green's function method calcs. 7-2339
- Si cubic crystals, electron struct., cluster approx., Xalpha calcs. 7-38445
- Si, curved cryst X-ray optics, inelastic scatt. expts., X-ray spectrometer design parameters 7-16354
- Si, cutting of single crystal, surface damage anisotropy 7-13664
- Si, Czochralski, electron-irradiated, DLTS and photoluminesc. studies 7-7149
- Si, Czochralski grown, electron irradi., thermal donor form. 7-21868
- Si, Czochralski grown, tensile props., 900-1200°C 7-51922
- Si, Czochralski grown crystals, octahedral crystalline inclusions, TEM obs. 7-16581
- Si, Czochralski growth, large diameter crystals, under horizontal or vertical mag. field 7-32342
- Si, Czochralski growth, relax. in point defects system 7-16468
- Si, Czochralski growth of high quality crystals. 7-53548
- Si, DC plasma etching in SF₆/O₂ mixtures, mass spectrometric transient study 7-8203
- Si, DLTS and MCTS spectra, charge-dependent defect traces 7-7161
- Si, DLTS spectrum of dislocations introduced by CW CO₂ laser (*Chinese*) 7-32939
- Si, dangling bond defect polarization and Haldane-Anderson model 7-21858
- Si, dangling-bond surface states, orientation depend. (*Chinese*) 7-58844
- Si, deep impurity centres, thermophysical studies 7-58765
- Si, deep level carrier capture and emission press. depend. meas., lattice relax. determ. 7-21862
- Si defect annealing and impurity activation during high-intensity As⁺ implantation doping 7-58295
- Si, defect diagnostics for submicrometer VLSI, book contrib. 7-44562
- Si, defect free zone, non-destructive microwave reflection decay meas. 7-51755
- Si, defect reactions and atomic diffusion 7-38264
- Si, defect states on the surface and in the bulk, H passivation 7-13665
- Si, defects and device processing, achievements and limitations 7-32428
- Si, defects produced by electron and X-ray irradiation, surface effects 7-6687
- Si, dendritic web cryst., solar cells and modules fabrication status 7-8391
- Si dendritic web ribbon, electrical and struct. props. 7-16922
- Si dendritic web ribbons, structural defect characterisation 7-12074
- Si dendritic web solar cells, twin plane effects on minority carrier diffusion length 7-13868
- a-Si, density of states, spectral function, calcs. using eqn. of motion method in k-space 7-27236
- Si deposition from SiH₄-Ar-H₂ system 7-23011
- Si detector with 2D pad readout, performance 7-30857
- Si detectors, high UV sensitivity and scintillator readout appls. 7-19666
- Si diffused p-n structs, recomb. props. of base region, effect of thermal and radiation defects 7-17089
- Si diffused-junction solar cells, shunt resist. and soft reverse characts. 7-17863
- Si, diffusing metallic impurities, H implantation effects 7-12370
- Si diffusion layers with high charge carrier densities, IR radiation refl. 7-13123
- Si, diffusion length depend. on cooling rates and bulk resistivity 7-7266
- Si, diffusion modelling, point defect interactions 7-32715
- Si, diffusion of ion-implanted impurities, modelling on IBM PC 7-38265
- Si, directional crystallisation, carbon-fabric support 7-13350
- Si, dislocated, charge carrier recomb. processes 7-7264
- Si, dislocation density reduction by thermal cyclic annealing 7-12072
- Si, dislocation loops, generated by ion implantation and furnace annealing, depth profiles, RBS, X-ray diff., TEM anal. 7-51882
- Si, dislocation luminescence lines, polarisation 7-39154
- Si, dislocation photoluminescence, thermal quenching effects 7-39155
- Si, dislocation transmission through Σ=9 symm. tilt boundaries, synchrotron X-ray topography, HVEM obs. 7-63646
- Si, dislocation transmission through Σ=9 symm. tilt boundaries, dynamic and crystallographic anal. 7-63647
- Si dislocation-free single crystals, microdefect recomb. activity, electron irradi. and annealing effects, SEM study (*Russian*) 7-21287
- Si, dislocations and electron-hole radiative recombination 7-13203
- Si, disorder generation by Ar⁺ implantation, Rutherford backscatt.-channelling meas. 7-63680
- Si, divacancy electronic struct. calc. (*Chinese*) 7-38490
- Si, divacancy levels in the band gap 7-12644
- Si, dopant diffusion under thermal nitridation conditions 7-32716
- Si, dopant profiles by the spreading resistance technique, book contrib. 7-44594
- Si, dopant profiles modification due to surface and interface modifications 7-58306
- Si doped, laser deposition for interconnections 7-53632
- a-Si, doped, thermal equilibration struct. 7-1887
- Si, doped layers, IR transmission spectra 7-59208
- Si doping superlattices, anomalous mobility enhancement 7-7381
- Si dot junction solar cells, fabrication and anal. 7-3708
- Si drift chamber for two-dimensional particle detection 7-25324
- Si, dry etching, radiation damage 7-54024
- a-Si, EPR-active centres, floating bond defects 7-38506
- Si, elastic const., mol. dynamic calcs., shear modulus 7-6705
- Si electrical conductivity meas., high pressure, in diamond anvil cells at cryogenic temp. 7-56299
- a-Si, electron and hole concentration modelling 7-64269
- Si, electron and ion irradiation induced amorphisation, point defect dispersion and mobility 7-11916
- Si, electron beam irradiated at different temps., formation of complexes 7-12153
- Si, electron channelling 7-21305

elemental semiconductors continued

- Si, electron correlation, band gaps and quasiparticle energies 7-27278
- n-Si, electron heating and intervalley redistribution in strong electric fields 7-27336
- Si, electron irradi., Mu to Mu⁺ transition, strain field induced 7-53205
- Si, electron irradi., obs. of IR bands during annealing, kinetic study 7-45214
- p-Si, electron irradiation induced defects, DLTS study 7-38500
- Si, electron planar channelling radiation, temp. depend. 7-46172
- Si, electron stimulated oxidation, surface effects, macroscopic continuum model 7-65236
- Si electron-hole liq., ultrasonic attenuation calcs., intraband collision effects 7-12214
- Si, electron-hole plasma, second condensed phase 7-27357
- Si, electrooptical effects 7-59182
- Si, element analysis, neutron activation and capture method 7-17846
- Si, energy band gap calc., self-interaction correction to local density approx. 7-45144
- Si, energy calcs. using four-centre integrals 7-27227
- Si, energy deposited by mesons in 1-μm sites, probability distrib. 7-58312
- Si, energy gap, indirect meas. 7-7107
- Si epitaxial film, with current filament radiation temp. coordinate distrib. 7-38650
- Si epitaxial films, low temp. growth by very low press. CVD 7-27936
- Si, epitaxial growth of FeSi₂, effects of thin interposing layers 7-22471
- Si, epitaxial growth of transition metal silicide, progress review 7-21766
- Si, epitaxial growth using dual heating, slip dislocations and radial temp. gradient 7-38366
- Si, epitaxial growth using photochem. vapour deposition at 200°C 7-39431
- Si epitaxial layers, autoping effects 7-63635
- Si epitaxial layers, free carrier conc., optical interference determ. 7-2745
- Si epitaxial layers, impurity anal. by photoluminescence spectroscopy 7-7057
- Si epitaxial layers, selective, surface morphology 7-32880
- Si epitaxial layers, selectively grown, lattice strain 7-64920
- Si epitaxial layers, ultrahigh-purity, photoluminesc. studies 7-45033
- Si epitaxial layers, VPE growth, charactn. (*Japanese*) 7-63986
- Si, epitaxial low temp. growth by hot wall UHV/low press. CVD techniques, surface optimisation 7-3194
- Si, epitaxial overgrowth on SiO₂ surface 7-21737
- Si, epitaxial rare earth silicide form. by rapid annealing 7-21768
- Si, epitaxial silicide form., initial nucleation processes and effects 7-21767
- Si, epitaxial wafers and films, temporal behaviour of modulated optical reflectance 7-53422
- Si, etch mechanism modelling, CF₄+O₂ 7-39785
- Si, etch products in XeF₂, doping and pressure effects 7-33855
- Si, etch rate, NF₃ plasma, kinetic model 7-39786
- Si, etch rates and reaction products study in NF₃-O₂ discharge 7-28218
- Si etched and polished (111) surfaces, LEED spot profile anal. 7-11859
- Si, etching by carbon tetrafluoride ion beams, mechanism, mass spectra obs. 7-3493
- Si, etching by HF-CrO₃-H₂O solns., selective dissolution studies 7-3530
- Si, etching in CF₄ discharge, SiF₂ and CF₂ radicals, laser-induced fluorescence study 7-46727
- Si, etching in CF₄ plasma, chemistry, model 7-3544
- Si, etching rates in CF₄/O₂ plasmas, effect of photoresist or Al masking 7-65222
- Si, etching V-groove structures 7-26031
- Si evaporated film on Ag island film, surface-enhanced Raman scatt. study 7-13165
- Si, excimer laser photoablation, spectroscopic characts. of plasma 7-54019
- Si exciton transport, optical time-of-flight investigation 7-64244
- Si, excitonic absorpt., MCD spectra, low mag. fields 7-27257
- n-Si, excitons bound to pairs of shallow impurities 7-45169
- Si, external photoelectric effect, Laue diff., anomalous X-ray transmission 7-7811
- Si FEL, possibility of obtaining coherent short wave radiation 7-20237
- Si, fast ionisation waves due to absorpt. and reemission of luminesc. 7-52627
- Si field ion imaging, Au shank overlayer effects, photoillumination and field-induced image-size effects 7-33534
- Si film, amorphous, small-angle scatt. of electrons in STEM obs. of defects and voids 7-21754
- Si film, deposition by photolytic or pyrolytic dissoc. of SiH₄ under laser irradi. 7-13388
- Si, film deposition by radical jet laser-induced CVD 7-59457
- Si film growth for MOS-VLSI, Ti and Pt silicide form. 7-7870
- Si film photoelements with drift field in solar cells, production and investigation 7-34030
- Si film solar cells on steel substrates 7-13921
- Si film thickness meas. by autocorrelation function 7-41336
- Si films, amorphous-crystalline mixtures, annealing effect on optical props. 7-59273
- a-Si films, density measurement using quartz oscillator 7-7079
- Si films, grain size and texture enhancement by seed selection through ion channelling 7-38401
- a-Si films, ion implanted device structures, solid phase epitaxy, elec. props. 7-12564
- Si films, laser beam melted, facet formation at solid-melt interface 7-38418
- Si films, laser-induced melting and recrystn., heat transfer algorithm 7-21269
- Si films, low-temperature growth by reactive ion beam deposition 7-59459
- Si films, n-channel inversion layers, piezoresist. effect studies 7-45318
- Si films, phase diagram of laser induced melt morphologies 7-12131
- Si films, plasma-enhanced chemical vapour deposition model anal. 7-27937
- a-Si films, preparation in separated ultra-high vacuum reaction chamber 7-59434
- Si films, processed and unprocessed, Raman microscopy of solid surfaces after laser irradiation 7-21264
- Si films, solid epitaxial regrowth, structural and electrical characteristics 7-38403
- Si films, solid phase epitaxial regrowth on epitaxially grown MgO·Al₂O₃ 7-38399
- Si films, structural changes due to annealing 7-52346

elemental semiconductors continued

- a-Si films, superlattice structure, photo-CVD deposition; solar cell fabrication 7-59450
 a-Si films, surface passivation, study by photothermal deflection spectroscopy 7-59689
 Si films on amorphous substrates, prep. by zone melting recrystallisation and surface-energy-driven grain growth 7-38385
 Si films on fused quartz, laser annealing and Raman spectra 7-58708
 Si films on glass substrates, laser recrystallisation 7-38395
 Si films on insulator, lamp zone melting, defect entrapment 7-53642
 Si float zone wafers, interstitial form. during thermal oxidation, effect of HCl 7-39789
 a-Si foils, pulsed laser irradi., clusters and plasmas, time resolved X-ray absorpt. meas. 7-64755
 Si for solar cells, characterisation by electrolyte-semiconductor interphase and SERS investigation 7-13887
 Si for solar cells, growth by horizontal supported web technique 7-17412
 Si, Fourier transform photoluminescence analysis 7-53412
 Si, fourth-order thermal expansion coeff. fn. 7-44868
 n-Si, gamma-irrad., intrinsic defects, Hall effect and elec. cond. meas. 7-6615
 Si, gamma-ray effects on micro defects and electrophysical props. 7-16629
 p-Si, gamma-ray irradi., recombination centres, p-n junction meas. 7-37985
 a-Si, generation-recombination rate 7-33032
 Si gettering, review of phenomenology 7-38215
 Si, grain boundary energies, computer calcs. 7-6639
 Si grain boundary photovoltaic effect, scanning laser beam obs. anal. 7-12766
 Si, grain boundary pot. barrier and role of distorted bonds 7-46080
 p-Si grating solar cells, 2D collection and injection 7-23163
 Si, group III acceptors, neutral and ionised states, deep dopant description 7-64155
 Si growth by SOG method and Stepanov method, stability anal. 7-33602
 Si growth for electronic industry 7-33590
 Si, HCP-FCC transition, at 78 GPa and studies to 100 GPa 7-63804
 Si, HF passivated, surface chemistry, XPS and ion scatt. spectra 7-33857
 Si, heavily doped, band-gap narrowing 7-7108
 n-Si, heavily doped, carrier conc. and activation energy, Lee-McGill model calcs. 7-58819
 Si, heavily doped, thermoreflectance, study 7-45999
 Si, heavily doped crystals, behaviour of O and dopants 7-32483
 Si, heteroepitaxial film, on Ge, Al-Mg spinel and sapphire substrates, resonance Raman scattering 7-64017
 Si, heteroepitaxial growth on ZrO_2 - Y_2O_3 substrates 7-21735
 Si, heteroepitaxy on CaF_2 -Si (111) 7-22497
 Si heteroepitaxy using BaF_2 epitaxial buffer layers 7-12522
 Si, high dose implantation, with Co, Ni, Fe ions struct. and phase modifications 7-12095
 Si high fluence D implantation, trapping and desorption, saturation conc. studies 7-26781
 Si, high purity, charge carrier lifetime meas. 7-45351
 a-Si high quality films and superlattice solar cells, prep. method 7-46346
 Si, high temp. drift mobility, determ. 7-52621
 Si high-low junction emitter solar cell, quantum efficiency improvement 7-3681
 Si homoepitaxial thin film growth by ultrahigh vacuum ion beam sputter deposition 7-22582
 Si homogeneous amorphisation, ion implantation energy depend. study 7-63638
 Si, hot hole dispersion laws 7-52629
 Si, hot-electron 1/f noise 7-21927
 a-Si hybrid photovoltaic and thermal solar collector 7-59856
 Si IC sensor technology and applications (German) 7-24644
 Si IGFET, quantum Hall resistance meas., using improved Josephson potentiometer 7-18810
 Si IGFET, quantum Hall resistance standard realisation at BIPM 7-18811
 Si, IR pyrometer for thermodynamic temp. meas. between 683K and 933K 7-18788
 a-Si, IR spectra calcs., static charge effects 7-3040
 Si image sensors and their appls., conf., Cannes, France (Nov. 1985) 7-24288
 Si, impact ionisation coeffs., lucky drift model including soft threshold energy 7-64258
 Si, implantation damaged, transient enhanced dopant diffusion 7-44910
 Si, implanted layers, short time annealing, light source comparisons 7-21263
 Si, impurity and carrier conc. profiles, electrochem. C-V method (Chinese) 7-12105
 Si, impurity and defect props., processes and characterisation (Japanese) 7-7151
 Si, impurity doping by photonuclear reactions 7-16589
 Si, impurity gettering, defect-defect interaction mechanisms 7-16585
 Si, impurity ionisation, doping conc. and temp. depend. 7-38509
 p-Si, impurity photocond. type inversion by fundamental absorpt. band illumination 7-64287
 Si, impurity profiles, depth resolution of SIMS 7-54253
 Si, in SF_6+O_2 and NF_3+O_2 mixtures, kinetic model 7-39787
 Si, indentation dislocation rosettes length, influence of Vickers indenter edge orientation rel. to slip directions 7-58284
 Si, ingot and foil casting 7-53711
 Si interdigital Schottky diode structure with fast UV response 7-24701
 Si interdigitated back contact solar cells development 7-8386
 Si, interstitial-based intrinsic gettering process appl. to multilevel defects structs. 7-38048
 Si, intrinsic gettering by butterfly-type defects 7-38047
 Si inversion layer, electrons and phonons in 1D and 2D 7-2734
 Si inversion layer, localisation and interaction in a strong mag. field 7-64343
 Si ion beam deposition on (100) single cryst. substrate, interface, thin film and damage form. 7-17423
 Si, ion beam induced recrystn., channelling effect 7-16650
 Si, ion bombard., damage accumulation, flux depend., RBS 7-51891
 Si, ion bombarded with H ions, refractive index variations in the near-surface region 7-17299
 Si, ion implantation, damage profile studies, multilayer model (Chinese) 7-6648

elemental semiconductors continued

- Si, ion implantation, interstitial trapping, dopant migration and epitaxial regrowth 7-12103
 Si, ion implantation-induced amorphous layer, temp. and dose depend. model calcs. 7-16594
 a-Si, ion implanted, 2D model of nucleation and regrowth 7-38408
 Si, ion implanted, amorphous phase transformation during rapid thermal annealing 7-16435
 Si, ion implanted, damage profiles, multilayer anal. by optical spectra (Chinese) 7-58294
 Si ion implanted, epitaxy by thermal and laser processing, review 7-33706
 Si, ion implanted, laser beam melting and resolidification 7-12126
 Si, ion implanted, mech. stresses, laser interferometer studies 7-6657
 Si ion implanted surface dopant cross-contamination, enhanced diffusion effects 7-32719
 Si, ion implanted with Ar^+ , H_2 passivation, polycrystalline phase formation 7-12087
 Si ion-implanted with MeV energy B^+ , P^+ and As^+ ions, annealing behaviour 7-51776
 Si, ion-induced etching, surface processes 7-59702
 Si, ionisation-stimulated annealing of Frenkel pairs under electron or gamma irradiation 7-38061
 Si islands, selective epitaxial deposition on SiO_2 , morphology 7-38402
 Si, isoelectronic bound exciton states, spin splitting, photolum. excitation spectra study 7-2493
 Si, isoelectronic structurally bistable defect configs. study 7-16546
 Si, Jahn-Teller vibronic state of the neutral vacancy 7-16705
 Si junction detector, characterisation by automatic system 7-19663
 Si junctions very shallow, elec. field anal. 7-21989
 Si, kinetic model, SF_6+O_2+Ar in plasma etch mode 7-39784
 Si, kinetics of growth of SiO_2 layer, optical props. 7-17740
 Si LOCOS substrates, nucleation of dislocations at thin film edges 7-51597
 Si LPCVD films properties when formed from SiH_4 in vertical flow reactor 7-22563
 Si LPE layer form., depend. on Al_M chem. reaction, M=refractory metal 7-7043
 Si, LPE on patterned substrates, growth and characters 7-22599
 a-Si, lamellate structure 7-21740
 a-Si, large are uniform thin films, production by scanning plasma method (Japanese) 7-17449
 Si, large unit cell CNDO calculations 7-7106
 Si, laser ablation, cluster and plasma formation, time-resolved X-ray monitoring 7-37710
 Si laser annealed surface, Au submonolayer coverage, Kapitza anomaly reentry obs. 7-38318
 Si, laser induced defects, rapid and classical thermal processing, annealing kinetics 7-44609
 Si, laser irradi., nonequilib. melting and solidification, computational modeling 7-2059
 Si, laser irradiated, electron-hole plasma dynamics investigated by time-resolved spectroscopy 7-13276
 Si, laser irradiated, surface morphology and phase transitions 7-12121
 Si, laser oxidation, electrophysical parameters of films produced 7-17741
 Si, laser-induced CVD for direct writing of Si lines 7-64921
 Si, laser-induced etching with Cl_2 7-22915
 Si, lattice distortions and vibr. modes of substitutional impurities 7-51979
 Si, lattice dynamics, real-space force consts., adiabatic bond-charge model 7-32589
 Si, lattice dynamics and electron-phonon interactions, quasi-ion approach calcs. 7-58422
 Si, lattice images, screening effect 7-51592
 Si lattice spacing meas., NRLM work relating to precision meas. and fundamental constants 7-14915
 Si layers, electron irradiation-induced defect levels, annealing behaviour, DLTS studies 7-52493
 Si, layers damaged by cutting, struct., X-ray diffr. obs. 7-2401
 Si light-enhanced oxidation, hot electron injection, electron population depend. study 7-46720
 Si, liq. and solid, solubility of O 7-26961
 Si, liquid, electronic props., tight binding-mol. dynamics calcs. 7-16931
 Si liquid crystal spatial light modulator 7-37130
 Si, local autoepitaxial layers, packing defect density, depend. on crystallographic orientation of side boundaries 7-58701
 Si, low pressure epitaxial growth, appl. to dielec. isolation technology 7-53624
 Si, low pressure epitaxy using Si_2H_6 7-53623
 Si, low resistivity dendritic web ribbon for high efficiency solar cells 7-3656
 a-Si, low temp. electron transport near mobility edge 7-38562
 Si, low temp. oxidation studies, internal stress 7-33864
 Si, low-angle silicon sheet (LASS) material, microstructure exam. 7-21231
 Si, low-energy ion beam oxidation, appl. to n-channel MOSFET fabrication 7-3529
 Si, low-temp. plasma nitridation process, props. and appls. 7-33867
 Si MBE, impurity sticking coeffs., substrate orientation depend. 7-52355
 Si MBE, review 7-33573
 Si, MBE cryst. growth, dopant incorporation 7-12559
 Si, MBE dopant profiling, electrochemical CV technique 7-12108
 Si MBE films, deep level defects 7-12668
 Si, MBE grown, abrupt doping profiles, spreading resist. determ. 7-12110
 Si, MBE grown, defect densities 7-12560
 Si MBE grown layers, arbitrary doping profiles 7-12109
 Si MBE growth, conf., Toronto, Ont., Canada (May 1985) 7-9588
 Si, MBE growth, RHEED intensity oscillations 7-7068
 Si, MBE growth, Radclean surface cleaning process 7-12557
 Si, MBE growth, selective diminution in RHEED pattern from (001)- 2×1 reconstructed surface 7-7069
 Si, MBE growth on CaF_2/Si (111), structural and electrical characteristics 7-45051
 Si MBE growth on Si (100) and (111), interface formation 7-21773
 Si MBE homoepitaxial growth, expt. considerations 7-13369
 Si MBE layers, deep levels, DLTS meas. 7-12667
 Si MBE layers, defect characterisation, luminesc., TEM studies 7-13227
 Si MBE layers, defects 7-21772
 Si MBE layers, spreading resist. anal. carrier spilling effects 7-2741

elemental semiconductors continued

- Si MBE layers, spreading resist., etching, bevelling, staining characterisation techniques 7-12891
- Si, MBE on Si, role of surface reconstruction, LEED, Rutherford back-scattering, channelling meas. 7-7034
- Si, MBE on Si substrates, stacking fault tetrahedra form. 7-21769
- Si, MBE simultaneous growth on multiple substrates, apparatus 7-7867
- Si MINP solar cells, electron beam radiation effects 7-13876
- Si MINP solar cells, high efficiency, performance, fabrication, characts. 7-23153
- Si MINP solar cells, I-V characteristics meas. 7-8408
- Si MINP solar cells, radiation damaged, conduction mechanism 7-65463
- Si MIS device diffusion length meas. by spectral response 7-8424
- Si MIS photodiode integrated arrays of photodetectors in spectral instruments 7-56335
- Si MIS solar cells, sputter deposition of barrier metal 7-17866
- Si MIS struct., quantum Hall resistance, localised and mobile electron states 7-38744
- Si MOS capacitor elec. parameters, effects of process chemical purity 7-33103
- Si MOS capacitor struct., defect profiling, DLTS 7-12652
- Si MOS inversion layers, high field low temp. transport props. (*Chinese*) 7-12862
- Si MOS inversion layers, quantum transport effects 7-52767
- Si MOS struct., phonon emission spectroscopy of 2D electron gas 7-27435
- Si MOS structure, space charge layer capacitance, quantisation effects 7-7398
- Si MOS structures, high field stressing, ESR study 7-33091
- Si MOSFETs, weak localisation magnetoresist. in almost quantising mag. fields 7-22024
- Si MOSFETs, weak localisation in isotropic and anisotropic 2D electron gases 7-64172
- Si, mag.-field Czochralski-grown neutron transmutation doped, thermal behaviour 7-53574
- Si, magnetic Czochralski growth, at high pulling rates 7-33551
- Si, magnetic-field-applied Czochralski growth (*Chinese*) 7-59401
- Si masked ion-implanted devices for solar cell and optical sensor appls. 7-40006
- Si materials and process charact. for VLSI, SIMS studies 7-33988
- Si materials for solar cells, nondestructive assessment using electrolyte-semiconductor boundary 7-13886
- Si materials science and technology, conf., Boston, MA, USA (May 1986) 7-29598
- Si materials science issues in IC processing 7-35115
- Si, melting induced by picosecond laser pulses 7-38166
- Si membrane (suspended), base carrier accumulation solar cell, fabrication 7-3664
- Si metal tunnel-thin insulator-semiconductor structures, effects of high field corners 7-64348
- a-Si, metallic state, prep., characts., appl. in devices (*Japanese*) 7-52697
- Si, metastable phases, vibr. props. 7-2126
- Si, microarea stress study by microprobe Raman spectroscopy 7-63708
- Si, microcrystalline films, carrier lifetime from transient photoconductivity meas. 7-7290
- Si, microcrystals, amorphous-like Raman signals 7-53349
- Si, microdefects, X-ray absorpt. during Laue diffr. study 7-2009
- a-Si, microelectronics appls., conf., Los Angeles, CA, USA (Jan. 1986) 7-24282
- Si micromechanic techniques for batch processed optical scanner 7-20473
- Si microstrip detector structures with implanted p-n junctions, functional props. 7-42325
- Si microstrip particle detector, low leakage current 7-19667
- Si, minority carrier lifetime and resist. mapping, flying-spot scanning method 7-4867
- p-Si, minority carrier transport TOF study 7-45310
- Si, mixed group III and group V ion implantation 7-21243
- Si molar volume results Avogadro constant determ. 7-14913
- Si, molecular dynamics, classical two and three-body interatomic potentials 7-16966
- Si monocrystalline, light-induced grating measurements 7-11035
- Si, monocrystalline, polycrystalline and amorphous solar cells, circulation meas. and spectral error reduction 7-13903
- Si monolithic gas flow sensor with polyimide athermal insulator 7-6332
- a-Si monolithically interconnected photovoltaic panels, single chamber glow discharge manufacturing process 7-13892
- Si, monovacancy electronic struct. and positron states, self-consistent LMTO calcs. 7-2536
- Si, multibeam X-ray diffr., scattering perturbation theory anal. 7-32200
- Si monocrystalline solar cells, fabrication using polyx technology (*French, English*) 7-23142
- Si multilayers, LPE growth, DEM, TEM obs. 7-12565
- Si, muonium, anomalous, model as body-centered interstitial muonium, HF calc. 7-45899
- Si n^+ -p-p $^+$ solar cells, superlinear behaviour of short circuit current 7-23192
- p-Si n^+ -pp $^+$ solar cell struct., quasisurface recomb. vel. determ. in contact layers 7-58875
- Si n^+ -epitaxial layers, recomb. parameters anal. by moving light strip method 7-21930
- Si n-type (100) inversion layers, valley splitting enhancement by lossless edge currents 7-7395
- Si, neutron irradi. induced IR absorpt. bands 7-46004
- Si, neutron irradiated, EPR study on C_2 symmetry defect 7-27602
- Si, neutron irradiated, recovery 7-39567
- Si neutron irradiated float zone crystals., triclinic symm. defect, EPR study 7-53134
- Si, neutron transmutation doped p-n-p-n struct., fast electron irradiated, minority carrier lifetime variations 7-45352
- Si, neutron transmutation doped, optical current deep level transient spectroscopy 7-52525
- Si, neutron-irradiated, photoluminescence study of annealing process 7-51833
- Si, neutron-irradiated, relax. space-charge-limited current spectroscopy 7-38493
- Si, neutron-transmutation doped, spatially resolved carrier lifetime meas. 7-7257
- Si, neutron-transmutation-doped, elec. resist. inhomogeneity form. characts. estimation 7-38026
- Si, nitridation treatments, review 7-17747

elemental semiconductors continued

- Si, nondegenerate, minority carrier diffusion length and doping density 7-33031
- Si, normal muonium, location and hyperfine props., Hartree-Fock cluster calcs. 7-52539
- a-Si, obliquely deposited film, elec. and optical props. 7-12529
- Si, off-centre impurities and defects, local electronic struct. valence-bond theory calcs. 7-2532
- Si on sapphire, bistable optical device using guided mode excitation 7-57423
- Si optical phonon spectrum transform. obs. under laser pulse bombardment, CARS study 7-51967
- Si, optical props. of isolated dangling bond 7-38507
- Si, optical reflection anisotropy due to surface band bending 7-39062
- Si, overheating during pulsed laser irradiation 7-12127
- Si, oxidation, catalytic effect of near-noble metal 7-3545
- Si, oxidation, conference, Paris, France (May 1986) 7-60866
- Si, oxidation, dissolved oxygen concentration effects 7-54016
- Si, oxidation, growth mechanism of thin oxide films 7-65235
- Si, oxidation, kinetics of ultrathin SiO_2 growth 7-8204
- Si, oxidation, linear regime analysis, film thickness 7-46729
- Si oxidation, $Si/oxide$ interface struct. 7-65231
- Si, oxidation, stress relax. model 7-65229
- Si, oxidation, stresses and defects 7-65230
- Si, oxidation, surface layer defect formation 7-46733
- Si, oxidation, thermal SiO_2 growth kinetics model 7-8207
- Si, oxidation, transport processes 7-65232
- Si, oxidation, transport processes 7-65233
- Si, oxidation, trap generation by avalanche electron injection, HCl effects 7-3531
- Si, oxidation, UV laser-induced 7-65234
- Si, oxidation 7-65227
- Si, oxidation and epitaxy, limited reaction processing 7-22577
- Si, oxidation in Cl containing ambients, impurity distrib. in resultant SiO_2/Cl films 7-26787
- Si, oxidation kinetics, quantitative model 7-33863
- Si oxidation models calcs., oxide thickness time depend. and stress effects 7-22916
- Si, oxidation of damaged surfaces, precipitation at stacking faults 7-38313
- Si, oxidation stacking faults, shrinkage during O_2/NF_3 oxidation 7-22913
- Si, oxidative packing defect form. during high temp. annealing 7-44522
- Si, oxide growth, rapid thermal processing 7-22929
- Si, oxide growth by plasma anodisation, current efficiency and temp. depend. 7-39777
- Si, oxide growth by rapid thermal oxidation 7-22922
- Si oxidised substrates with AlSi-Ti multilayer interconnects 7-21713
- Si p^+ - i - n^+ diodes, gamma irradi., capacitance detected mag. resonance 7-17243
- Si p^+ - n junction, superlinear response in IR spectral region (*Chinese*) 7-52751
- Si p-amorphous/n-cryst. anisotype heterojunction characts., acceptor doping level depend. 7-7355
- Si p-i-n diode, spectral information coding by IR photoreceptors, colour vision analogue 7-35593
- Si p-i-n diodes, potential distribution 7-58817
- a-Si p-i-n solar cells, CVD deposition from Si_2H_6 7-59841
- a-Si p-i-n solar cells with graded interface 7-23133
- Si p-n structures, induced current pot., temp. depend., impurity levels, SEM 7-17073
- Si passivated emitter solar cell, efficiency improvement 7-23149
- Si, passivation of dislocations at high H_2 press. 7-39763
- Si, Pendellosung intensity beat meas. with γ -radiation 7-46170
- Si periodic epitaxial structures, intraband IR absorpt., photocond. meas. 7-52674
- Si, periodic surface microrief, determ. optical constants of laser-irradiated material 7-63926
- Si, photo-oxidation under ArF excimer laser irradiation in O_2+NF_3 gas mixture 7-13658
- Si, photochemical CVD at 200°C 7-59456
- Si, photochemical etching in NF_3 gas, surface processes 7-59704
- a-Si photoconductor for liquid crystal spatial light modulator 7-43350
- Si photodetectors for optical position sensing 7-48691
- Si photodiode, edge illumination at UV wavelengths to improve quantum efficiency 7-41464
- Si photodiode quantum efficiency as absolute radiometric standard 7-14991
- Si photodiode transfer-standard monochromatic comparator pyrometer 7-14947
- Si photoelectrochemical and MIS solar cells, surface dislocation loops effect on J-V characts. 7-17862
- Si, photon enhanced oxidation mechanisms 7-54032
- Si, photothermostimulated exoelectron emission 7-22452
- Si, photovoltaic concentrator research progress 7-17903
- a-Si photovoltaic module performance 7-3684
- a-Si photovoltaic modules, electrochemical degradation 7-17870
- n-Si, piezoresistance associated with bending of the energy relief at the bottom of the conduction band 7-13095
- Si, piezoresistance sensitivity, shear stress effects (*Chinese*) 7-12713
- p-Si, piezoresistivity investig., nonlinear effects 7-7248
- Si, planar channelled protons, breakthrough angles 7-21308
- Si, plasma assisted oxidation below 800°C 7-39783
- Si, plasma etching, oxide breakdown due to charge accumulation 7-17743
- Si, plasma etching in Ar-tetrafluoromethane glow discharge 7-32170
- Si, plasma etching in H glow discharge 7-32168
- Si, plasma etching selectivity using negative DC biasing 7-39769
- Si, plasma etching with tetrafluoromethane and N_2O , role of O_2 in etching 7-3535
- Si, plasma passivated, subsurface H barrier layer obs. after surface adsorption of Al 7-17745
- Si point contact concentrator-solar cells, characts. 7-3658
- Si point contact solar cells, modelling and expt. results 7-13869
- Si point-contact solar cells for high conc. appls., modelling and expt. 7-23150
- Si, polished plate, kinetics of oxidation in air 7-13666
- Si, polycrystalline, ^{125}Sb , ^{32}P , ^{74}Tb as donor elements, diffusion 7-12373
- Si, polycrystalline, as strain gauge material 7-45322
- Si, polycrystalline, chemistry of plasma etching with H_2 and Cl_2 7-54021
- Si, polycrystalline, conf., Erice, Italy (July 1984) 7-4632

elemental semiconductors continued

- Si, polycrystalline, fabrication and use, overview 7-32879
 Si, polycrystalline, for solar cell appls., photovoltaic props., effect of impurities and defects 7-38639
 Si polycrystalline, gap state density determ., field-effect conductance anal. calcs. 7-21794
 Si, polycrystalline, grain boundary recomb. vel. eval. from spectral response of solar cells 7-41403
 Si, polycrystalline, H_2 passivation, grain boundaries, EBIC technique 7-26769
 p-Si, polycrystalline, ion implanted, resistivity modelling (Korean) 7-2608
 Si, polycrystalline, photolytic etching in SF_6 atmosphere 7-46732
 Si polycrystalline CVD film, etch rate free carrier depend., doping level and grain size depend. meas. 7-28219
 Si, polycrystalline cast ingots, bulk free-carrier lifetime, contactless meas. 7-7258
 Si, polycrystalline columnar crystals, acoustic visualisation 7-8242
 Si polycrystalline film, mobility temp. depend. (Chinese) 7-2744
 Si, polycrystalline film SOI structures, recrystn. by laser irradiation 7-32856
 Si, polycrystalline films, low press. CVD growth and annealing, morphology obs. 7-3187
 Si polycrystalline films, optical props. 7-7782
 Si polycrystalline films, sheet resistance, rapid thermal annealing prior to and post As ion implantation 7-12886
 Si, polycrystalline films, undoped, nonlinear I-V characteristics 7-22039
 Si, polycrystalline films, laser-recrystallized, grain boundary location using antireflection cap 7-46312
 Si polycrystalline films on (100) Si substrate, epitaxial alignment using rapid thermal processing 7-38413
 Si, polycrystalline layers, growth shape and struct. investig. 7-2405
 Si, polycrystalline layers, TEM meas. of grain size 7-32672
 Si polycrystalline layers, elec. props. and grain boundary carrier dynamics under solar illumination 7-38625
 Si, polycrystalline p-type, Al and Cu diffusion effects on electronic properties 7-17038
 Si polycrystalline ribbons stress meas., photoelasticity determ. with aid of computer 7-31725
 Si, polycrystalline solar cells (Japanese) 7-13861
 Si polycrystalline solar cell p-n junction, carrier lifetime, effective recomb. vel. and diffusion length, EBIC meas. 7-23138
 Si polycrystalline solar cells, passivation by low-energy H^+ ion implantation 7-23157
 Si polycrystalline thin film strain resistance model (German) 7-64033
 Si, porous, oxidation, 2D model 7-39791
 Si, porous, W deposition for buried conductor formation 7-3189
 Si porous amorphous sputtered films, oxidation, IR spectra studies 7-3532
 n-Si porous electrodes, photoelectrochem. behaviour 7-3711
 Si porous films, IR absorpt. study 7-39149
 Si porous layers on p-substrates, oxide form. rel. to SOI struct. realisation 7-39771
 Si position sensitive detector, photon counting image acquisition system, performance analysis 7-30088
 Si position sensitive detector, Tevatron beam tube tests 7-30856
 a-Si position sensitive photodetector (Japanese) 7-30093
 Si, positive ion yields of impurities in amorphous and crystalline samples 7-17381
 Si, positron diffusion 7-39281
 Si, positron planar channelling radiation energy levels, variational calcs. 7-63696
 Si powder layers, melt recrystallisation for solar cell fabrication 7-17492
 Si powders, prod. from laser-heated silane, cryst. struct. 7-46362
 Si, precipitation induced microdefects, DLTS characts. 7-38511
 a-Si, prep. by low press. CVD, characts. 7-7884
 a-Si protection layer on the surface of V/Si during silicide formation 7-58662
 Si, proton channelling, energy loss and straggling, inner shell electron collision calcs. 7-63699
 Si, proton-induced displacement damage, energy depend. 7-58355
 Si, pulsed laser melting, time-resolved reflectivity meas. 7-2158
 Si pure and As-doped single-domain reconstructed (100) surface state dispersion and struct., LEED and photoemission studies 7-38667
 a-Si pure and H doped films, defects and microvoids, positron annihilation study 7-45086
 Si, pure and heavily doped, X-ray fluorescence, strength of $K\alpha_{3,4}$ satellites 7-22386
 Si, pyrogenic oxides, carrier trapping and breakdown, rel. to H_2O partial press. 7-64267
 Si quantised inversion layers, hot 2D electron gas, spectral acoustic phonon emission intensity 7-52452
 Si, quantum well controlled conductivity, new donors 7-38491
 Si quantum well struct., 2D electron gas, transport props. 7-52774
 Si, radiation defect thermal ionisation, effect of dislocations on activation energy 7-6680
 Si, radiation-induced deep centres due to fast neutrons (Czech) 7-12661
 Si, Raman mode, anharmonic damping and freq. shift 7-27718
 Si, ramp assisted foil casting and photovoltaic appls. 7-16609
 Si, rapid thermal and furnace oxide growth, meas. and modelling studies 7-13677
 Si, rapid thermal annealing of ion implanted layers, role of trapped interstitials 7-17568
 Si, rapid thermal oxidation and nitridation 7-33861
 Si, rapid thermal processing, conf., Boston, MA, USA (Dec. 1985) 7-14713
 Si, rapidly annealed with incoherent light, defect state generation 7-52504
 Si, reactive ion etching, near-surface disorder, surface residues 7-16846
 Si, reactive ion etching using collimated beam prod. by 10^{-3} Torr magnetron discharge 7-54027
 Si, reactive sputter etching, damage removal methods 7-17742
 Si, recoil implantation of O_2 , characterisation by double-crystal X-ray diffraction, TEM, Monte Carlo simulation 7-51807
 a-Si, recomb. via dangling bonds, occupation statistics 7-38515
 Si, recombination activity of dislocations 7-12733
 Si, recombination channels, dislocations interaction with point defects, lumin. study 7-46094
 Si, reconstructed structures of symmetrical (011) tilt grain boundaries 7-51785
 Si, reduced-pressure low temp. epitaxy, photochem. effects 7-59455
 Si, reflectivity meas. during pulsed laser irradiation 7-12132

elemental semiconductors continued

- Si ribbon casting for solar cell fabrication 7-13907
 Si ribbon growth, dislocation dynamics and thermal viscoplastic stresses 7-2017
 Si ribbons, dendritic web grown, high temp. mech. behaviour, strain rate and temp. depend. of yield stress 7-65099
 Si, ribbons, γ -irradiated, defect form., photoluminesc. investig. 7-46147
 Si rough surfaces, ellipsometry spectra, Ohlidal-Lukes model anal. (Chinese) 7-13109
 Si, SAW generation by optical irradiation 7-63933
 Si SEM determ. of surface structure 7-56387
 a-Si, SERI Amorphous Silicon. Measurements Task Force results 7-54308
 Si, SHG, cryst. orientation depend. 7-50640
 Si, SIPOS and polysilicon films for low minority carrier current saturation point contact solar cells 7-8416
 Si SIS struct. photoresponse kinetics, current flow mechanism 7-52854
 Si SOI, buried oxide structures, ion implanted, ESR studies 7-59111
 Si, SOI lateral solid phase epitaxy, selective P ion implantation 7-52359
 Si SOI structure, high-dose O_2^+ implanted, dopant diffusion 7-52139
 Si SOI structure, O^+ implantation and high temp. annealing 7-44579
 Si SOI structures, implanted buried oxide, high-temp. annealing 7-6654
 Si SOI structures, O_2^+ implanted, oxide precipitates, ordering 7-21449
 Si SOI structures, polycrystalline Si films, seeding laser recrystn. 7-58706
 Si SOI technology, two-step oxidation technique on MBE film 7-22912
 Si, scanning optical fibre microscope, laser beam induced current images 7-48846
 Si, scanning tunneling microscopy of surface microstructure on rough surfaces 7-21580
 Si, scattering inhomogeneities, two-wavelength probe meas. 7-46063
 p-Si Schottky barriers, N_2 and Ar ion beam etching effects (Korean) 7-12858
 Si Schottky diodes, H_2^+ bombarded, elec. props. 7-38677
 Si Schottky diodes with dislocations, tunnelling transitions 7-52831
 Si, selective epitaxial growth by reduced press. CVD 7-53625
 Si, selectively epitaxial, origin of lattice defects 7-32881
 Si, self-consistent band struct. and total energy, Shaw pot. calcs. 7-32909
 Si, self-consistent Hartree-Fock and screened exchange calcs. 7-12585
 Si, self-diffusion and impurity diffusion, review 7-32713
 Si, self-diffusion without vacancies and interstitials, concerted exchange mechanism 7-26997
 Si self-doping using Stepanov method, elec. resist. meas. 7-32470
 Si, self-implantation, damage production kinetics 7-21239
 Si, self-implantation-induced temp. depend. amorphisation, TEM and Monte Carlo simulation studies 7-16595
 Si, self-implanted, defects and amorphisation 7-2041
 Si, self-implanted, strain 7-51918
 Si, semi-insulating polycrystalline films, electrical conduction mechanism 7-52869
 Si, semiconductor surfaces, atomic, electronic and vibronic props. 7-2307
 Si semiconductor-insulator-semiconductor structures, photocurrent amplification 7-64360
 Si shallow p-n junctions, reactive ion etching damage, defects and leakage current studies 7-27411
 Si, shallow thermal donor series, electronic struct. 7-7154
 Si sheet, growth by horizontal supported web technique, solar cell efficiency 7-53567
 Si, SiC microdefect generation, melt-interface mechanism 7-53710
 Si single cryst., dislocation line kink mobility and double kink form. kinetics 7-26760
 Si single cryst., electron axial and planar channelling, gamma-ray emission studies 7-44636
 Si single cryst., laser-driven shock induced damage study 7-64829
 Si single cryst., transition metal ion implantation, silicide form., RBS and X-ray diffr. studies 7-16656
 Si, single cryst., ultimate strength, surface treatment effect 7-2090
 Si, single cryst. temp. distrib. during czochralski growth, computer modelling 7-17414
 Si single cryst. wafer, charge carrier kinetics, excess microwave cond. meas. 7-38580
 Si, single crystal, effects of shape of crystn. front, melting boundary 7-6566
 Si single crystal, reactive ion etching-induced damage, nondestructive thermal wave monitoring 7-28230
 Si, single crystal, transient photoconductivity characterisation 7-52692
 Si, single crystal wafer, oxidation, rapid thermal processing 7-22928
 Si single crystals, defect struct., high DC elec. fields, X-ray diffr. 7-44530
 Si single crystals, dislocation-free, nature of microdefects 7-44528
 Si single crystals, insulating cpd. form. by ion beam synthesis, RBS, SIMS and cross-sectional TEM studies 7-26779
 Si single crystals, relativistic positron channelling radiation, spectral density peak splitting studies (Russian) 7-21310
 Si, single-particle excitations, dynamic correl. corrections, local density theory 7-45115
 Si, slow surface state determ. by SAW technique 7-21959
 Si small particles, Raman depolarisation ratio 7-64652
 Si solar arrays for low Earth orbit space stations, advanced module concept 7-3659
 Si solar cell, improved determ. of lifetime and surface recomb. vel. by transient methods 7-13870
 a-Si solar cell, light induced degradation, quantitative anal. 7-17911
 Si solar cell, planar, antireflection coatings effects 7-54303
 Si solar cell array, 30 kW, for space appls. 7-3660
 Si solar cell array module, 50 microns thick, space flight ready 7-65491
 Si solar cell arrays for EURECA space vehicle 7-3661
 a-Si solar cell characteristics improvement for indoor consumer electronics (Japanese) 7-65471
 Si solar cell efficiency improvements 7-3654
 Si solar cell efficiency improvement simulation analysis 7-13865
 Si solar cell fabrication by sheet casting 7-17868
 Si solar cell fabrication using masked ion implantation using SiO_2 7-23165
 Si, solar cell fabrication using laser groove technique, commercial viability 7-59862
 Si solar cell junction form., dopant diffusion process 7-28401
 a-Si solar cell modules fabricated with single-chamber load-lock deposition system 7-59860
 Si solar cell parameters, theoretical temp. depend. 7-23161
 Si solar cell parameters evaluation method 7-23159

elemental semiconductors continued

- Si solar cell perform. under global irradiance, atmospheric parameters effect 7-59850
- Si solar cell performance, influence of heavy doping 7-23147
- Si solar cell performance eval. 7-13864
- Si solar cell photovoltaics, edge-defined film fed growth 7-17413
- Si solar cell simulation by Monte Carlo modelling 7-8405
- a-Si solar cell submodules, integrated type, laser patterning method 7-65470
- Si solar cell with Al_2O_3 surface passivation 7-23191
- Si solar cells, alloyed inversion layer, with n-type substrates and TiO_2 antireflection coatings 7-17864
- Si solar cells, comparison with GaAs and InP cells in space 7-65484
- a-Si solar cells, conversion efficiency improvement 7-17879
- Si solar cells, crystalline, metal grid optimisation and emitter tailoring, computer model extension 7-54292
- Si solar cells, diffused junction single and polycrystal series resist., temp. depend., illum. level effect 7-39991
- a-Si solar cells, dynamic inner collection efficiency 7-39992
- Si solar cells, eval. of density of grain boundary states 7-34028
- a-Si solar cells, fabrication and characts. 7-13891
- a-Si solar cells, fabrication methods using UHV reaction chamber system, high conversion efficiency 7-54293
- Si, solar cells, front and back polycrystalline Si contacted 7-13908
- Si solar cells, grain boundary and intragrain recomb., beam induced current characterisation 7-7267
- Si solar cells, H passivation by ion beams 7-17867
- Si solar cells, H passivation of dislocations 7-54323
- Si solar cells, heavily doped emitter and junction regions, EBIC studies 7-34039
- Si solar cells, heavy doping effects 7-3653
- Si solar cells, high efficiency devices, review 7-3649
- Si solar cells, high efficiency 7-23148
- Si solar cells, high efficiency, design, process and material considerations 7-23151
- Si solar cells, high efficiency, identification of key parameters limiting perform. 7-59846
- a-Si solar cells, insulator-semiconductor interface properties 7-13901
- Si solar cells, loss reduction by ion implantation, laser radiation, protective coatings (*Dutch*) 7-23134
- Si solar cells, low recombination p^+ and n^+ regions for high performance 7-3655
- Si solar cells, metal insulator n on p, radiation damage 7-3703
- Si solar cells, multicrystalline, thermal annealing for fabrication 7-17865
- a-Si solar cells, open circuit voltage 7-46935
- Si solar cells, oxidation and spalling of Cu current collecting grid 7-22910
- Si solar cells, p^+n-n^+ , high efficiency, develop. 7-34047
- Si solar cells, passivated, laser processed, 18% efficiency 7-59837
- Si solar cells, passivation using $\text{ZnS}_0.9\text{Se}_{0.1}$ and GaP semiconductor coatings 7-65479
- Si solar cells, perform. and temp. dependencies of proton irradiated n-p cells 7-3702
- Si solar cells, performance anal. 7-65466
- Si solar cells, polycrystalline, efficiency improvement using plasma treatments 7-13909
- Si solar cells, polycrystalline, junction formation by light induced diffusion 7-13919
- Si solar cells, polycrystalline, interface state characterization by electric noise meas. 7-13920
- Si solar cells, sequential irradiation effects of electrons and protons 7-13877
- Si solar cells, spinning method for Si sheet mass production 7-13918
- Si solar cells, terrestrial, production costs and conversion efficiency 7-17869
- a-Si solar cells, vidicon mode characterisation 7-8421
- a-Si solar cells and modules, hot spot durability testing 7-13915
- Si solar cells for space appls., efficiency improvements 7-65487
- Si solar cells for spacecraft power, Advanced Photovoltaic Solar Array Program 7-65489
- Si solar cells for thermophotovoltaic appls. theoretical efficiency 7-59855
- Si solar cells in concentrators, performance meas. methods 7-54313
- Si solar cells in tandem with GaAsP on GaP, design, fabrication 7-3674
- a-Si solar cells on textured Al substrate, prep. by chemical etching 7-23156
- a-Si solar cells prepared by thermal evap. 7-23140
- Si solar cells systematic design theory using optimisation techniques 7-23146
- Si solar cells with internal reflection, fabrication by solution growth on steel substrates 7-3683
- a-Si solar cells with spectral response shift, applicability of reference cell method to perform. meas. 7-59858
- Si solar concentrator cells, perform. under 1 MeV electron irradiation 7-3704
- Si, solid-phase amorphous to crystalline transformation for shallow junction processing 7-32642
- Si space solar cells, damage coeffs. of 1 MeV electron fluences 7-13880
- Si, spherical wave EXAFS and multiple scatt. effects in XANES 7-64742
- Si, spin-dependent recombination and low-freq. ESR studies 7-38577
- Si, sputtering by multiply charged Ar ions 7-33507
- Si, Stepanov reverse method cryst. growth, thermal and capillary conditions 7-33545
- Si, strain measurement in convergent beam electron diffraction 7-16562
- Si strips, grown by Stepanov's reversed method, strength, struct., electro-physical props., effects of thermal conditions during growth, photocell appl. 7-32325
- Si, structural changes produced by one micron picosecond laser pulses, TEM characterisation 7-12133
- Si structural EXAFS study 7-64762
- Si, structures, 2D localisation and interaction effects 7-52531
- Si, substrate, (001) oriented, with GaAs epitaxial film, structural props. 7-58687
- Si substrate, anisotropic dry etching effects on surface props., XPS, ion channelling and Raman scatt. studies 7-28229
- Si substrate, dopant redistrib. during Pd_2Si formation 7-21255
- Si substrate, insulator growth by rapid thermal processing 7-22921
- Si, substrate for CVD of W, effects of dopants and cryst. perfection 7-16912
- Si substrate for thin film InP solar cells 7-59852

elemental semiconductors continued

- Si substrate for W CVD, effect of dopants and crystal perfection 7-22576
- Si substrate reaction with amorphous and cryst. Ni-refractory metal alloys 7-21704
- Si substrates, curved for multilayer X-ray reflective lenses 7-41566
- Si substrates, laser-induced metal and alloy plating, silicide form. 7-39448
- Si substrates, superlattices, props. (*Dutch*) 7-52755
- Si substrates for GaAs solar cells fabrication by MOCVD 7-23183
- Si, superconducting high-pressure phases, occurrence and props. 7-2646
- Si, superconducting transition temp., press. depend. 7-33121
- Si superlattice structs. using MBE (*German*) 7-64317
- Si surface, 100, in situ anal. of H, C, N and O using direct recoil time-of-flight technique 7-54242
- Si surface, (111) $\sqrt{3}\times\sqrt{3}$ -Sn, angle resolved UPS, rel. to other Si-metal overlayer surfaces 7-3149
- Si surface, (111)- 2×1 , surface phonon and surface state excitations, EELS, polarisation depend. 7-2338
- Si surface, (111) 2×1 , electronic surface transitions studied by polarised light 7-2664
- Si surface, (111)(2×1), obs. of 10 meV Einstein oscillator mode 7-38320
- Si surface, air exposed, air-resolved X-ray photoelectron spectroscopy 7-27863
- Si surface, Ar^+ ion impact, LMM and LVV Auger electron emission 7-59320
- Si surface, atomic and mol. F reactions, XPS studies 7-28350
- Si surface, cellular structures formation due to interaction with picosecond light pulses 7-44960
- Si surface, Cs migration and equilibrium in strong elec. field 7-2351
- Si surface, effect of preoxidation annealing, ion implantation and sputtering on oxide film decomposition 7-63999
- Si surface, electromigration of Ag, In, Sb, and Sn ultrathin films, scanning AES study 7-63891
- Si surface, electronic inversion layer, positive magnetoresist. obs. 7-38596
- Si surface, etching by HCl/H_2 mixtures, low pressure gas composition 7-65221
- Si surface, Fe-promoted nitridation, kinetics 7-59698
- Si surface, interaction with H_2 7-58632
- Si, surface, laser beam melting and recrystallisation 7-12431
- Si surface, O adsorpt., orientation depend., AES and photoelectron spectra 7-52237
- Si, surface, quantum states and atomic struct. 7-32775
- Si surface, RIE, Si_3N_4 CVD 7-59691
- Si surface, reaction probability with CF_2 radical from tetrafluoromethane plasma 7-23059
- Si surface, reaction with propylene, effect of addition of H 7-54187
- Si surface, residue form. in trifluoromethane discharge environment 7-54020
- Si surface, thermal cleaning in ultrahigh vacuum 7-13671
- Si surface, thermal oxides, X-ray scattering studies 7-52326
- Si surface barrier detector radiation spectrometer with 6 keV resolution 7-10349
- Si surface barrier detector, annular transmission, fabrication and characts. 7-19661
- Si surface barrier telescope for solar particles, characts. and calibration 7-62217
- Si, surface contamination during reactive ion beam etching with Cl_2 7-3539
- Si, surface damage induced by low energy ion sputtering (*Chinese*) 7-6693
- Si surface epitaxial growth of Pt-group epitaxial growth on Si (111) 7-21760
- Si, surface etching by COF_2 , thermal and photochemical promotion 7-33853
- Si surface etching by HCl/H_2 gas mixtures 7-65220
- Si surface laser irradiation, ionic cluster desorption, time-of-flight meas. 7-12138
- Si, surface layers, local mechanical stresses relaxation 7-21604
- Si surface layers characterisation after annealing in an RF H plasma 7-58630
- Si, surface nitridation, current status 7-33866
- Si surface passivation, angular dependent X-ray photoelectron spectroscopy 7-27864
- Si surface polishing strain-free and flat to better than $\lambda/20$ 7-11179
- n-Si, surface potential, stabilisation by ion bombardment 7-12782
- Si, surface reaction with XeF_2 , rel. to etching mechanism 7-17738
- Si surface recomb. vel. determ. using solar cell struct. 7-21938
- Si surface relief, 3D cellular struct. formed by picosec. light pulse irradi. 7-32772
- Si surface roughening by reactive ion etching, mech. 7-65240
- Si surface state after plasma etching in a diode type system 7-6940
- Si, surface structural phase identification, use of specular beam in LEED 7-58589
- Si, surface structure, optical transitions 7-12439
- Si, surface structure, pulsed electron-beam annealing 7-21284
- Si, surface structure, UHV scanning tunnelling microscope studies 7-18923
- Si surface studies with a high resolution transmission electron microscope 7-21595
- Si surface study after Ar ion-assisted Cl_2 etching 7-3538
- Si surface study using metal-vacuum-semiconductor structs. 7-38749
- Si surface with adsorbed Ne, H_2 , D_2 films, phonon scatt. 7-21609
- Si surface with deposited SiO_2 films, low temp. annealing 7-46526
- Si surface with Rh overlayers, FIM 7-52284
- Si surface-barrier detector as source of slow protons 7-49777
- Si surfaces, (100) and (111), XeF_2 exposure, F coverage, XPS studies 7-2379
- Si surfaces, (110), clean and hydrogenated, atomic configuration, LEED studies 7-2314
- Si surfaces, (111) and (100), chemisorption of halogen atoms 7-6979
- Si surfaces, (111) 7×7 -Ge and (111) 5×5 -Ge, angle-resolved photoelectron spectra 7-3150
- Si surfaces, (7 $\times 7$)-Ge and (5 $\times 5$)-Ge superstructures, angle-resolved EELS studies 7-21583
- Si surfaces, adsorbed C, annealing behaviour, XPS and AES studies 7-27108
- Si surfaces, conference, Julich, Germany (April 1986) 7-55890
- Si surfaces, passivated by H/hydrogen mixtures, surface dielectric layers characterisation 7-17746

elemental semiconductors continued

- Si, swirl defects formation 7-51753
 Si tandem junction solar cells, cryst. and polycryst., efficiency advantages 7-39997
 Si target, ion beam sputtering, heavy particle angular distrib. 7-59343
 a-Si technology, review of developments 7-38551
 Si, technology and electronic materials (*Japanese*) 7-22466
 Si, temperature depend. of $1/f$ noise 7-33058
 a-Si, tetrahedrally bonded, bond angle disorder 7-32297
 Si, thermal and electronic transport, photothermal deflection spectroscopy 7-32731
 Si, thermal donor states 7-7155
 Si, thermal donor-related isoelectronic centres, exciton binding, photoluminescence studies 7-21861
 Si, thermal donors, alignment by uniaxial stress, EPR and optical studies 7-59227
 Si, thermal nitridation in NH_3 , atomic transport mechanisms 7-8201
 Si, thermal oxidation, cryst. orientation effects 7-3534
 Si, thermal oxidation, effects of GeCl_4 7-65238
 Si, thermal oxidation, growth of very thin films 7-33850
 Si, thermal oxidation, low-temperature 7-39765
 Si, thermal oxidation, point defect kinetics modelling 7-13673
 Si, thermal oxidation, UV light stimulated 7-59687
 Si, thermal oxidation 7-65228
 Si, thermal oxidation in dry O_2 , 2D anal. (*Japanese*) 7-33859
 Si, thermal oxide growth conditions 7-39790
 Si, thermodynamic interrelation between amorphous, diamond cubic and liquid states 7-12245
 Si, thermoplastic deformation, nondestructive ultrasonic detection 7-12215
 Si, thin crystals, grinding, surface defect struct., X-ray diff. (*Russian*) 7-38304
 Si thin film, doped, electron beam evaporation, elec. props. 7-2743
 Si thin film, laser-irradiated melt morphology and order-disorder transitions studies 7-44614
 Si, thin film, Raman spectroscopy, characterisation 7-53354
 Si thin film solar cells, high performance considerations 7-23152
 Si thin films, polycrystalline, elec. props. 7-33117
 Si, thin sheets, EFG, thermal capillary mechanism for growth limit 7-17407
 Si thin wafers, photoacoustic pulses, optical detect. 7-54050
 Si, tilt boundary struct., computer modelling 7-16579
 Si, tilt grain boundaries, symmetrical (011), struct. and energies 7-16570
 Si, total energy and superconductivity, pseudopotential method 7-32358
 Si transiently molten layers, dielec. function, picosec. laser pulse reflectivity meas. 7-52488
 Si, transition metal dopant complexes photolum., review 7-45203
 Si, transmutation doped, carrier lifetime and hall effect, high temp. processing effects 7-33027
 Si, transmutation-doped, carrier recomb. props. at gamma-irrad. defects, transport meas. 7-38575
 Si, transverse photovoltaic effect due to intervalley diffusion of electrons under laser excitation conditions 7-38613
 Si, trench etching technique, ultrafine, using multi-step processing 7-54030
 Si tube, growth from shaped seed, struct. development 7-32326
 Si, tubular hole distrib. under streaming conditions, scatt. anisotropy effects calcs. 7-58802
 Si, twin boundary struct. determ. of twinned bicrystals, convergent-beam electron diffraction study 7-51786
 Si, twinning partial dislocations, velocity 7-63629
 Si, twinning partial dislocations, effective stresses, anal. 7-63630
 n-Si, ultraheavily doped, Rayleigh surface waves, Brillouin scatt. study 7-21605
 Si, ultrasonic shaping during pulling cryst. growth 7-33541
 Si, uniaxially stressed, internal strain parameters, surface effects 7-44980
 Si VPE using $\text{SiCl}_4\text{-SiH}_4\text{-H}_2$ system (*Chinese*) 7-33578
 Si, vacancies, hyperfine interactions, ENDOR and EPR studies 7-63609
 Si vertical junction and planar solar cells, proton radiation damage 7-13885
 Si vibrating sensor, optical activation 7-9826
 Si, vibrational correlation functions 7-51966
 Si, vibronic band, 1018 meV, W or I, band 7-51977
 Si, visualisation of microdefects by X-ray topography 7-1811
 Si, volume capture effect for relativistic electrons, computer simulation 7-12156
 Si wafer, laser and energy-beam annealing of mechanical damage, melting and recrystallisation 7-46516
 p-Si wafer, minority-carrier diffusion length determ., photocurrent generation method 7-38579
 Si wafer, stacking and technological faults, elec. activities, SEM study (*Russian*) 7-21234
 Si, wafer aqueous cleaning, chemical action, book contrib. 7-46737
 Si wafer substrates, oxide removal, transient mass spectrometry, XPS studies 7-13670
 Si wafers, doped by neutron transmutation, minority carrier lifetime, photocond., annealing 7-38785
 Si wafers, etching by NF_3 , plasma and reagent pulse induced transients 7-3533
 Si wafers, etching in SF_6 RF discharges, diagnostic meas. 7-28214
 Si wafers, pre-oxidation treatment, appl. of UV radiation 7-33862
 Si wafers, self and ion beam annealing, epitaxial growth and damage layer, TEM study 7-12172
 Si wafers, striation prod. by grazing ion incidence 7-63684
 Si wafers, surface contaminants, identification, depth distrib., SIMS 7-22418
 Si, wettability and adhesion with Sn-Si(Sb)(As) melts 7-21576
 Si, with Mo film, ion beam mixing, amorphous layer form. 7-21301
 Si, with stacking faults, electron and phonon spectra, recursion method 7-32945
 Si, with transition metal impurities, detect. using rapid thermal annealing 7-2044
 Si, X-ray electron charge density distrib. 7-26695
 Si, X-ray structure factor, Pendellosung method meas. 7-32362
 Si, transition metals, solubilities, diffusivities and deep levels 7-32465
 Si^{111}Cd , hyperfine interactions, temp. depend., gamma-ray spectra studies 7-64553
 Si:Ag, implantation damage regrowth studied via Ag depth profiling 7-22730

elemental semiconductors continued

- Si:Ag-Ag, formation of Schottky junctions by Ag implantation in Si 7-12784
 Si:Al, atom and acceptor depth distributions of channelled Al as a function of ion energy and crystal orientation 7-21247
 Si:Al, depth profiles, redistrib. of annealed Al implants 7-63640
 Si:Al, ion implanted and annealed, Al precipitation, TEM studies 7-21238
 Si:Al, Mg transmutation doping by proton irradiation 7-38027
 Si:Al films, LPE in a temperature-gradient field 7-64936
 Si:Al implanted crystals, amorphous surface regions with crystalline impurity grains, TEM study 7-58579
 Si:Al surfaces, SIMS anal. of contaminants 7-33989
 Si:Al(In), recrystallisation by pulsed electron beam, impurity profiles 7-16605
 Si:Ar, high dose implanted, thermal regrowth, RHEED studies 7-21734
 Si:Ar laminated structure formed by Ar ion doping, electroreflectance 7-7676
 Si:Ar⁺, ion implanted thin film, defect form, dose depend. study 7-51793
 Si:As, deep level spectra, ion implanted defects, laser annealing 7-21869
 Si:As, dopant diffusion, finite element based simulation, quasilinear formulation with remeshing scheme 7-21526
 Si:As, high dose implanted, defect density reduction by low temp. oxidation 7-58297
 Si:As, highly doped, spinodal decomposition and clustering 7-52063
 Si:As, implanted, supersaturated soln., defect struct., TEM obs. 7-58483
 Si:As, ion implantation, damage profiles determ. by spectroscopic ellipsometry and stripping (*Chinese*) 7-32468
 Si:As, ion implantation-induced defects 7-32433
 Si:As, ion implanted, diffusion and defects, transient scanning electron beam annealing 7-38065
 Si:As, ion implanted, electronic transport props. 7-7233
 Si:As, ion implanted, rapid thermal annealing 7-16615
 Si:As, ion implanted polycrystalline films, electrical activation by rapid thermal annealing 7-58914
 Si:As, laser annealed, Raman scatt. study 7-53325
 Si:As, precipitation and cluster form., elec. resist., backscatt. and TEM studies (*Chinese*) 7-12285
 Si:As, Rutherford backscattering-particle induced X-ray emission analysis 7-54251
 Si:As,In, formation of In-As complexes, perturbed angular correlation technique obs. 7-17254
 Si:As,P, double diffused shallow junctions, rapid thermal annealing 7-22006
 Si:As,Sb(P,Sb), Sb diffusion 7-44915
 Si:As (B)(BF₂)⁺, p-n junction diode, rapid thermal annealing 7-22005
 Si:As films, heavily doped, grown by partially ionised MBE, phys. and elec. characts. 7-12561
 Si:As films, preannealed and As ion implanted, structural changes during transient post-annealing 7-16904
 Si:As ion implanted, defect structs. generated by buried amorphous layer regrowth 7-38078
 Si:As ion implanted films, defects charactn. by AC Hall effect meas. 7-38601
 Si:As on sapphire, ion beam recrystallised and laser annealed, elec. props. 7-16649
 Si:As polycrystalline films, rapid thermal processing before and after ion implantation, effect on cond. 7-22046
 Si:As porous layer, impurity diffusion under incoherent light exposure 7-38258
 Si:As substrate, dopant effects on formation kinetics of Pt silicides 7-21697
 Si:As surface, TiSi_2 formation 7-12551
 Si:As⁺, epitaxial regrowth, CW Ar laser annealing (*Korean*) 7-27197
 Si:As⁺, heavily doped, ion implant deactivation 7-17567
 Si:As⁺(As₂)⁺, ion implanted, phys. props., spreading resist., TEM, Rutherford backscattering, SIMS 7-26775
 Si:As(B), ion implant redistribution, diffusion modelling 7-16814
 Si:As(B), ion implanted, pulsed laser annealing, optical reflection kinetics 7-58323
 Si:As(B)(P), impurities at dislocations and grain boundaries, high-resolution TEM imaging 7-37815
 Si:As(P)(B)-SiO₂ interface, segregation, transport coeffs. of impurities 7-63880
 Si:As(Sb)(Bi), implanted, heavy ion damage, TEM, annealing studies 7-63676
 Si:As(Sb)(In), heavily doped, laser induced oxidation 7-13672
 Si:As, deep level position in forbidden gap, charactn. using ionisation Gibbs free energy (*Chinese*) 7-58760
 Si:As, deep levels, multiexponential anal. of deep level transient spectroscopy 7-52524
 Si:As, laser radiation effects on impurity levels 7-12645
 Si:As, Li, Au-Si pair paramagnetic state, EPR studies 7-45817
 Si:As, supersaturated low-temp. substitutional impurities, annealing 7-6665
 Si:As,Fe-SiO₂, MOS struct., trap centres 7-7388
 Si:As n-n⁺ isotype junction, enhanced magnetosensitivity 7-7370
 Si:As, U- and W-shaped impurity diffusion profiles investigation 7-16805
 Si:B, amorphisation by ion implantation 7-38080
 Si:B, amorphous, solar cell, roll-to-roll mass prod. process 7-17902
 Si:B, B ion dose identification, HF C-U meas. 7-6661
 Si:B, B-vacancy complex, electronic and atomic struct., ENDOR studies 7-63643
 Si:B, BF₂⁺ ion implantation and rapid thermal annealing 7-21241
 Si:B, carrier lifetime meas., capture and recombination 7-38585
 Si:B, critical supercond. current induced by proximity effect, mag. field depend. 7-22069
 Si:B, diffused through narrow windows, doping profiles 7-12113
 Si:B, diffusion and activation of implanted B during rapid thermal annealing 7-16643
 Si:B, doping by XeCl excimer laser irradiation, ultra-shallow junction fabrication 7-58303
 Si:B, electron-irradiated, AC hopping conductivity and DLTS 7-44624
 Si:B, excimer laser-induced shallow diffusion, junction form. 7-38038
 Si:B, F implanted amorphous layers, struct. and elec. props., ESR and Hall effect meas. 7-26634
 Si:B, H, hydrogenation of B acceptor during electron injection by Fowler-Nordheim tunnelling 7-45504

elemental semiconductors continued

- Si:B, implant redistribution during high pressure oxidation, SIMS and C-V meas. 7-27020
 Si:B, impurity diffusion from BN sources, non-Fickian model 7-27012
 Si:B, impurity transport in mag. Czochralski growth, computer simulation 7-58182
 Si:B, ion implanted, amorphous layer thickness, SIMS profiling 7-51794
 Si:B, ion implanted, B diffusion, rapid thermal annealing 7-58538
 Si:B, ion implanted, defect and dopant depth profile studies 7-2045
 Si:B, ion implanted, dopant redistrib. during rapid thermal annealing 7-38042
 Si:B, ion implanted, strain profile, double cryst. X-ray rocking curve simulation 7-2060
 Si:B, ion implanted, transient annealing and residual defect DLTS study (*Chinese*) 7-12642
 Si:B, laser microprobe mass analysis, quantitative 7-54250
 Si:B, low temp. epitaxial films, nonequilibrium doping effects 7-58672
 Si:B, MBE grown, coevaporation doping 7-12562
 Si:B, mag. props. of the acceptor system 7-27496
 Si:B, magnetic Czochralski growth, computer simulation of B transport 7-32344
 Si:B, O, heavily doped, O precipitation, diffuse X-ray scatt. studies 7-32669
 Si:B, O epitaxial wafers, effect of pre- and postdeposition annealing on O precipitation 7-45060
 Si:B, preamorphised, B diffusion during rapid thermal annealing 7-32717
 Si:B, SIMS depth profiles in the near-surface region, correction for ion yield transients 7-22430
 Si:B, SIMS depth profiles, characterisation and removal of ion yield transients in the near surface region 7-65368
 Si:B,C,O, O clustering and thermal donor formation kinetics 7-17566
 Si:B,Fe, EBIC and DLTS meas., comparisons 7-7265
 Si:B,H(D) Schottky and n⁺-p junction diodes, electrical transport of acceptor-compensating defect 7-16823
 Si:B,O, thermal donor formation, bending stress effects 7-17563
 Si:B,O epitaxial wafers, internal gettering heat treatments and O precipitation 7-45059
 Si:B,O(Sb,O), heavily doped Czochralski wafers, O precipitation, 450°C thermal annealing 7-58477
 Si:B,P highly doped epitaxial layers, growth by low press. VPE 7-39432
 Si:B,P solar cells produced by pulsed excimer laser annealing of ion-implanted junctions 7-8419
 Si:B (As) diffusion source, diffusion into single crystal Si 7-32727
 Si:B film deposition in Si₂H₆-B₂H₆-He gas system, doping effect 7-27184
 Si:B layers, preamorphised and ion implanted, structural and elec. characterisation 7-52347
 Si:B MBE layers, shallow states, photoluminescence spectra, doping level depend. 7-13228
 Si:B p⁺-n-n⁺ solar cells fabricated using masked ion implantation, electro-optical charact. 7-23143
 Si:B p⁺-n shallow junctions obtained by implantation into preamorphised Si, elec. charact. 7-38703
 Si:B p-n⁺ junction, injection annealing of radiation defects 7-12161
 Si:B plastically deformed crystals, dislocation struct. and elec. activity, annealing effects study 7-37998
 Si:B polycrystalline films, rapid thermal processing before and after ion implantation, effect on cond. 7-22046
 Si:B-Mo interface, specimen preparation by chemical etching and polishing, for electron studies 7-29989
 Si:B-Si polycrystal-single cryst. interface, impurity diffusion across boundary 7-27013
 Si:B⁺ submicron p-n junctions, ion implanted, dopant distrib., Raman study 7-21252
 n-Si:B⁺(BF₃⁺), ion implanted, rapid thermal annealing, DLTS 7-16619
 Si:B⁺(BF₃⁺), ion implanted, characterisation by IR attenuated total reflection spectroscopy 7-17327
 Si:BF₂, ion implanted, diffusion and defects, transient scanning electron beam annealing 7-38065
 Si:BF₂⁺, ion implanted, solid phase epitaxial growth, cross-sectional TEM study 7-38364
 Si:BF₃⁺ (001), ion implanted, residual defects, cross-sectional TEM study 7-32471
 Si:BF₃⁺ p⁺-n diodes, BF₃⁺-implanted and rapid thermal annealed, junction leakage currents meas. 7-12814
 Si:BF₂⁺ submicron p-n junctions, ion implanted, dopant distrib., Raman study 7-21252
 Si:BF₃⁺(PF₃⁺), ion implantation damage, backscattering channelling meas. 7-63675
 Si:B(Al), hydrogenation and annealing kinetics 7-2527
 Si:B(Al)(Ga)(P)(Sb) thermal donor props., impurity effects, DLTS, Hall effect, and admittance spectra meas. 7-21851
 Si:B(Ar)-Ti(Co), silicide formation using rapid thermal processing, defect behaviour 7-32726
 Si:B(Au), electron irradi. stimulated impurity diffusion 7-63878
 Si:B(BF₂) wafers, activated carrier density profile and scatt. rate meas., nondestructive IR attenuated total refl. technique 7-22207
 Si:B(Ga)(As)(Sb) 7-2040
 Si:B(P), lateral diffusion, modeling LOCOS effects 7-33865
 Si:B(P) solar cell emitter saturation current meas. by contactless photoconductivity decay method 7-13866
 a-Si:B(P)(As), implanted ion distrib., lateral spreading, theoretical predictions and computer simulation 7-16604
 Si:B(P)(As)(Sb), retarded and enhanced dopant diffusion related to implantation-induced excess vacancies and interstitials 7-63881
 Si:Bi, solute trapping by lateral motion of {111} ledges 7-44592
 Si:C, carbide form. in Stepanov cryst. growth 7-33544
 Si:C, Czochralski grown, incorporation and disposition of C 7-32484
 Si:C, electron irradiated, photolum. defect spectra, obs. of interstitial C 7-59253
 Si:C, impurity concentration determ. by photoluminesc. method 7-46084
 Si:C, impurity content determ. IR absorpt.-charged particle activation anal. conversion factor 7-26788
 Si:C, photolum. detection of impurities introduced by dry etching processes 7-27748
 Si:C, polycrystalline, electrical and structural properties 7-12106
 Si:C,N, ion implanted, C surface contamination, AES and XPS studies 7-38312
 Si:C,O, heat-treated, photoconductivity relax., α traps 7-52677
 Si:C,O, luminescence props. of shallow donor centre 7-17347
 Si:C,O, photoluminescence of C-O related complex defects 7-22346
 Si:C,O, solubility, segregation, diffusion and precipitation 7-16777

elemental semiconductors continued

- Si:C,O,P, C precipitation after P junction diffusion 7-16779
 Si:C,O grown by gas-assisted solidification, impurities determination 7-16586
 Si:C,O wafers, C and O contents, Fourier transform IR spectra studies, book contrib. 7-44596
 Si:C,O wafers, defect generation, O precipitation effects (*Chinese*) 7-12058
 Si:C crystals, Stepanov method growth, defect structs. 7-32421
 Si:C(C,P), C diffusion during annealing and P in-diffusion 7-16812
 Si:Co, impurity energy levels, Hall and DLTS meas. 7-52509
 Si:Co, supersaturated solid solution, annealing 7-63642
 Si:Cr,B, optically-induced spin orientation, EPR study 7-2927
 Si:Cu, amorphous, explosive crystn., RBS and time-resolved reflectivity studies 7-21265
 Si:Cu, deep level position in forbidden gap, charactn. using ionisation Gibbs free energy (*Chinese*) 7-58760
 Si:Cu, ion implantation-amorphised, direct imaging of pulsed laser-induced buried molten layers 7-12130
 Si:Cu thin single crystals, decorated dislocations, X-ray Laue diff. and scatt. studies (*Russian*) 7-58282
 Si:D, ion implanted, channelling meas. 7-16597
 a-Si:D,F, D NMR lineshapes and spin-lattice relax. studies 7-45836
 a-Si:D,F, plasma deposited, deuteron magnetic resonance 7-27626
 a-Si:D(D,H), deuteron mag. resonance, annealing effects 7-33292
 Si:Er(Dy)(Yb)(Ho)(Gd), neutron irradi., Hall effect, elec. cond., IR absorpt. spectra 7-51834
 Si:F, implanted, dry oxidation kinetics, impurity effects 7-13667
 Si:F,H, amorphous, high efficiency solar cells fabrication and props. 7-17901
 a-Si:F,H films, glow discharge deposition, B doping efficiency 7-17436
 Si:Fe, interstitial Fe, spin delocalisation 7-13059
 Si:Fe, interstitial impurity, superhyperfine interaction and spin-lattice relax. 7-53178
 Si:Fe, intrinsic gettering, EPR and TEM study 7-38216
 Si:Fe, low damage surface anal., sputtered atom resonance ionisation method 7-58584
 Si:Fe, silicides obtained by Fe⁺ implantation 7-6655
 Si:Fe,O, Fe intrinsic gettering, EPR studies 7-16553
 Si:Ga, electron irradiated and annealed, photoluminescence spectra 7-13206
 Si:Ga, highly cond. shallow junction layer form. by ion implantation 7-38037
 Si:Ga epitaxial layers, growth induced planar defects 7-38414
 Si:Ga MBE layers, ion implantation doping using liq. metal ion source, carrier conc., spreading resist., SIMS profiles 7-12563
 Si:Gd, grown from melt, electrical and optical props., residual impurities 7-63636
 Si:Gd,C profiled single cryst., electronic parameters and SiC inclusions 7-32944
 Si:Ge, Ge⁺ preamorphisation implants, effect on extended defect formation during subsequent solid phase epitaxy 7-16599
 Si:Ge, irradiated, photoluminescence spectra 7-13207
 Si:Ge,P(B), IR absorpt. band broadening 7-64669
 Si:Ge⁺, ion implanted and annealed, crystalline to amorphous transformation, TEM study 7-32643
 a-Si:H, ²⁹Si and ¹H NMR spectra, peak position and line shape 7-2934
 a-Si:H, ambipolar drift length meas. using steady-state photocarrier grating technique 7-45390
 α -Si:H, amorphous, coherent potential approx., potential well analogy 7-27240
 Si:H, amorphous, dendritic web, Czochralski flat plate modules and concentrator module, price comparison 7-17904
 Si:H, amorphous, p-i-n solar cells, stability behaviour, impurities and doping residues effect 7-17912
 Si:H, amorphous, solar cells, current-induced and light-induced degradation, non-equivalence 7-17908
 Si:H, amorphous, transient photoconductivity characterisation 7-52692
 a-Si:H, amorphous to microcrystalline structure transformation, phase stabilisation 7-63475
 a-Si:H, B, P, As, dopant incorporation and doping efficiency 7-44587
 a-Si:H, B, P-type, increased elec. cond. studies 7-45337
 a-Si:H, B₂H₆(PH₃), localised density of states, electrophotography study 7-32957
 Si:H, B(Al)(Ga)(In), polishing, acceptor compensation by atomic H 7-33860
 a-Si:H, broken bond local environment relax., g-factor, cluster calcs. 7-37876
 a-Si:H, bulk, surface state densities, Bethe lattice method, CPA calcs. 7-32898
 a-Si:H, C superlattice struct., solar cell performance 7-46945
 a-Si:H, carrier trapping and recombination, IR enhancement spectra of photoconductivity 7-33052
 a-Si:H, charge transport and relax., luminesc. long-time tail distrib. anal. 7-39185
 a-Si:H, conductivity, fundamental pre-exponential factor, Meyer-Neldel rule 7-7249
 a-Si:H, configurational models and adiabatic potentials of H 7-51632
 a-Si:H, contact resist. meas. technique 7-24658
 α -Si:H, cross-polarisation dynamics, NMR 7-53151
 a-Si:H, deep trapping, transient photocurrent saturation 7-21952
 a-Si:H, defect structure, ab initio theory 7-32298
 a-Si:H, density of states, SCLC meas., effect of injection electrodes 7-64265
 a-Si:H, deposition rates in diode and triode discharges 7-3193
 a-Si:H, distrib. of states study by capacitance-voltage method 7-7089
 a-Si:H, divacancy electron struct., semiempirical CNDO/2 cluster calcs. 7-38495
 a-Si:H, doped, electronic transport 7-21916
 a-Si:H, EXAFS, spherical wave anal. and multiple scatt. effects 7-64740
 a-Si:H, elastic properties 7-21323
 a-Si:H, electron traps, telegraph noise spectroscopy 7-21928
 a-Si:H, electronic density of states, DLTS and capacitance transient spectra anal. 7-45134
 a-Si:H, electronic struct., inadequacy of the conventional view 7-32961
 a-Si:H, electronic struct. modelling with small clusters 7-64057
 a-Si:H, electronic transport 7-33004
 a-Si:H, evaporated samples, post-hydrogenation, charact. 7-59103
 a-Si:H, extended state mobility and tail-state distrib. 7-2617
 a-Si:H, fluctuation induced gap states 7-27242

elemental semiconductors continued

- a-Si:H, form. by ion flux control under toroidal mag. field (*Japanese*) 7-17446
- a-Si:H, gas-phase and ion-implantation doped, doping efficiencies 7-51790
- a-Si:H, glow discharge deposited, nucleation, substrate temp. effects 7-22504
- a-Si:H, glow discharge deposited, light soaking effects 7-52872
- a-Si:H, glow discharge deposition, surface roughness evolution 7-64933
- a-Si:H, glow discharge prepared, steady-state photoconductivity 7-38632
- a-Si:H, glow discharge thin films, deposition rate, optical props., influence of substrate temp. 7-59460
- a-Si:H, glow-discharge deposition, growth kinetics, radical separation technique 7-22513
- a-Si:H, H clustering, multiple quantum NMR 7-32671
- Si:H, H composition at surfaces and interfaces 7-27083
- a-Si:H, H₂ distrib., exodiffusion spectra 7-27026
- Si:H, impurity clustering, hydride form. on dislocations, TEM study 7-26964
- Si:H, impurity effects on IR absorpt. bands of Si-H centres, irradi. and unirrad. crystals 7-53379
- a-Si:H, influence of H on defects and instabilities 7-26647
- a-Si:H, intrinsic glow-discharge, elec. noise meas. 7-64297
- Si:H, ion implanted and annealed, H depth distrib. 7-26785
- a-Si:H, laser-assisted CVD growth, optical props. 7-22210
- a-Si:H, light induced degradation at high illum., inverse Staebler-Wronski effect 7-23195
- a-Si:H, light soaked, dangling bond creation 7-12150
- a-Si:H, light-induced dangling bonds, annealing behaviour 7-12119
- a-Si:H, light-induced degradation 7-2047
- a-Si:H, light-induced electron spin resonance 7-33274
- a-Si:H, light-induced metastable dangling bonds, annealing 7-12118
- a-Si:H, localised electronic state, light soaking and current injection 7-16994
- a-Si:H, metastable defect states, capacitance studies 7-45225
- Si:H, microcrystalline, photo-CVD growth 7-13382
- a-Si:H, mobility gap state transitions, transient photocapacitance studies 7-12669
- a-Si:H, NMR props. of ortho-H₂ centres 7-2935
- a-Si:H, neutral dangling bond defect, photocarrier processes 7-32962
- a-Si:H, non-exponential photocurrent decay, anal. 7-38633
- a-Si:H, optical dispersion relations, determ. 7-33353
- a-Si:H, photo-CVD deposition, initial processes (*Japanese*) 7-7053
- a-Si:H, photocond. response, light soaking effects 7-45396
- a-Si:H, photoconductivity and light-induced changes 7-2640
- a-Si:H, photoconductivity exponent for recombination at dangling bonds 7-33054
- a-Si:H, photocurrent, surface recombination effects 7-33048
- a-Si:H, photoinduced absorpt., ps decay 7-27684
- a-Si:H, photolum. and photoconductivity studies 7-33456
- a-Si:H, photoluminescence, high temp. annealing effects 7-7745
- a-Si:H, photoluminescence, thermal quenching 7-53389
- a-Si:H, picosecond photoinduced absorption and transmission 7-3006
- a-Si:H, picosecond photoinduced absorption decays, interference effects 7-3012
- a-Si:H, plasma deposited NMR, Pake doublet 7-27617
- a-Si:H, plasma enhanced CVD, integrated model 7-39423
- Si:H, polycrystalline, chemistry of grain boundary passivation 7-12375
- Si:H, polycrystalline, grain boundary interactions 7-12117
- Si:H, polycrystalline, plasma hydrogenation, ESR study 7-45819
- a-Si:H, prep. in rotary plasma isolated reactor and props. 7-7891
- a-Si:H, RF glow discharge prod., high deposition rate study 7-7889
- a-Si:H, RF sputtered, dangling bond electron spin-lattice relaxation 7-22141
- a-Si:H, RF sputtered, dangling bond energies, ESR studies 7-45818
- a-Si:H, recomb. at dangling bonds and steady-state photocond. Fermi level depend. calcs. 7-12734
- a-Si:H, SCL currents, step-by-step anal. 7-2623
- Si:H, Si-H IR stretching bands, models, CNDO calc. 7-53314
- a-Si:H, Si-H-Si three centre bonds IR spectra, LCAO-MO-SCF-STO-3G calcs. 7-6741
- a-Si:H, Staebler-Wronski effect and metastable light-induced defect creation kinetics model 7-64284
- Si:H, summary of present state of research 7-16584
- a-Si:H, surface deep hole trap, photocurrent studies 7-45424
- a-Si:H, surface structure, inert gas plasma exposure effects 7-21584
- a-Si:H, thermal-equilib. processes, electronic transport 7-64167
- a-Si:H, triplet exciton recomb., ODMR studies 7-2490
- a-Si:H,B, effective p⁺ doping by plasma-assisted B diffusion 7-38036
- a-Si:H,B, RF sputtered films, optical and electrical props. 7-33470
- a-Si:H,B, thin films, thermoelectric power 7-58826
- a-Si:H,B films, hole transport, time-of-flight meas. 7-45320
- a-Si:H,B p-i-n and n-i-p solar cells, doping profile effects 7-46947
- a-Si:H,B/a-Si:H,P doping modulated superlattice, photo-induced excess conductivity 7-17051
- a-Si:H,B(As) RF sputtered coatings, gas-phase doping efficiency 7-63471
- a-Si:H,B(P) films, dopant conc. meas. and depth profiling by means of (p,γ) resonant reactions 7-12555
- a-Si:H,B(P) films, optical props. 7-64720
- a-Si:H,Cl glow discharge films, Raman scatt. 7-39116
- a-Si:H,D, H abstraction from surface, HD formation 7-39914
- a-Si:H,F by thermal CVD, photosensitivity, spin density, conductivity and p-n type 7-17454
- a-Si:H,F films, dark discharge mechanism of surface potential (*Japanese*) 7-17034
- a-Si:H,F films, glow discharge decomposition from Si₂F₆ 7-64924
- a-Si:H,F films, H-radical-assisted CVD, hole transport 7-64264
- a-Si:H,F films, initial carrier trapping stages observed by femtosecond spectroscopy 7-27301
- a-Si:H,F films, prep. using H radical assisted CVD (*Japanese*) 7-17430
- a-Si:H,F multijunction solar cells, performance data 7-40011
- a-Si:H,F solar cells, radiation hardness to 1 MeV protons 7-23180
- a-Si:H,F/a-Si:Ge:H,F superlattices, elec. transport studies 7-38716
- a-Si:H,F/a-Si:H,Ge multiple junction solar cells on stainless steel substrates 7-13902
- a-Si:H,F/a-SiGe₂:H,F multiple layered films for enhancement in photoreponse in near IR spectrum 7-52668
- a-Si:H,F,Si_{0.4}Ge_{0.6}:H,F superlattices, carrier scatt., optical absorpt. study 7-38711
- a-Si:H,Ge single junction and tandem solar cells, thin film properties and corollary plasma diagnostics 7-13893

elemental semiconductors continued

- a-Si:H,N thin films, activated reactive evaporation 7-13355
- a-Si:H,O films, RF sputtered, photoelec. props. 7-38627
- a-Si:H,P, electron lifetime, excitation energy depend. 7-45349
- a-Si:H,P multilayer films, plasma CVD and elec. cond. studies 7-39428
- a-Si:H,P(B) films, ion implanted, photoelectric and optical props. 7-38615
- a-Si:H,P(B) p-i-n solar cells, open-circuit volt., wavelength depend. 7-46948
- a-Si:H (C,H) (O,H) (N,H), annealing of metastable defects 7-3343
- Si:H (100) proton bombarded surface, complex refractive index profile, ellipsometry study 7-22216
- Si:H amorphous, recombination-enhanced defect reactions, reversibility 7-45343
- a-Si:H and a-Si films, electrical conductivity and struct. 7-52866
- a-Si:H and a-Si:H, B films, photoinduced changes in elec. props. 7-38634
- a-Si:H and a-Si:H,P, electron nuclear double resonance expts. 7-2950
- Si:H and near-surface damage of Si caused by H ions, review 7-16813
- Si:H based alloy thin films, optical constants determ., device modelling appl. 7-7666
- a-Si:H based alloys for solar cells, elec. props. and degradation behaviour 7-52642
- a-Si:H biased activated reactive layer evaporation and charactn. 7-59428
- Si:H binary alloys, crystallisation of polysilane 7-21105
- a-Si:H CVD coating, high temp. elec. cond. meas. 7-45336
- a-Si:H CVD films, density of states distrib., I-V characts. meas. 7-45113
- a-Si:H doping modulated films, photocond., carrier separation effects 7-38641
- a-Si:H doping modulated multilayers, light-induced excess conductivity 7-38643
- a-Si:H doping modulated superlattices, light-induced excess cond., deposition effects 7-27410
- a-Si:H doping superlattice interface struct. charactn. 7-58652
- a-Si:H evaporated layer production from RF discharge, growth mechanism and props. 7-64898
- a-Si:H film, photo-assisted plasma CVD 7-33593
- a-Si:H film, photoenhanced deposition and characts. 7-53635
- a-Si:H film prep. by compressed mag. field magnetron sputtering (*Japanese*) 7-46323
- a-Si:H films, annealed, structural changes, PMR studies 7-7596
- a-Si:H films, annealing, compressive stress, H evolution 7-28059
- a-Si:H films, bond angle distortions, substrate temp. effects, Raman study 7-7882
- a-Si:H films, CVD, electrical and optical props. 7-33596
- a-Si:H films, CVD, optical and electronic props. 7-33597
- a-Si:H films, CVD using microwave excited Ar plasma stream 7-64918
- a-Si:H films, carrier transport 7-17023
- a-Si:H films, charge carrier dynamics, influence of preparation conditions 7-33053
- a-Si:H films, columnar morphology, evolution of vibr. spectra 7-64646
- a-Si:H films, contact potential difference, surface photovoltage and conductivity 7-58855
- a-Si:H films, deep levels in the mobility gap 7-12670
- a-Si:H films, density of states and photoconductivity 7-45392
- a-Si:H films, depth profiling of constituents and impurities, elastic proton scatt. 7-45044
- a-Si:H films, discharge and CVD deposition, surface reactions 7-33601
- a-Si:H films, electron irradi., photocond., absorpt. coeff. spectral depend. 7-64279
- a-Si:H films, electronic props., effects of γ-irradiation 7-38584
- a-Si:H films, glow discharge deposited, persistent photoconductivity 7-58835
- a-Si:H films, glow discharge deposition 7-65325
- a-Si:H films, glow-discharge-deposition, initial nucleation and growth 7-63997
- a-Si:H films, growth and photovoltaic appls. 7-64236
- a-Si:H films, growth habit, influence of substrate struct., ellipsometry study 7-45055
- Si:H films, H content meas. 7-12553
- a-Si:H films, high rate deposition and impurity doping effects (*Japanese*) 7-13385
- a-Si:H films, high rate deposition by RF planar magnetron sputtering (*Japanese*) 7-39373
- a-Si:H films, illumination effects on conductivity 7-7291
- Si:H films, ion implant redistribution 7-16921
- a-Si:H films, laser induced CVD using SiH₄ photodecomposition 7-13376
- a-Si:H films, light-induced bond breaking 7-12517
- a-Si:H films, light-induced defects and internal stresses 7-12751
- a-Si:H films, metal-semiconductor contacts, characterisation 7-38724
- a-Si:H films, metastable optically induced ESR, time depend. 7-45800
- a-Si:H films, photo-CVD from SiH₄-H₂ 7-39394
- a-Si:H films, photo-enhanced CVD 7-33594
- a-Si:H films, photochemical vapour deposition from SiH₄-H₂ 7-64916
- a-Si:H films, photocond. characts. stabilisation (*Japanese*) 7-45393
- a-Si:H films, photoconductivity, thermal quenching obs. 7-52686
- a-Si:H films, plasma CVD, deposition kinetics (*Japanese*) 7-17450
- a-Si:H films, RF glow discharge deposition, optical and electrical props. 7-33598
- a-Si:H films, reactive deposition 7-33592
- a-Si:H films, sputter deposition, optical and ESR props. 7-33565
- a-Si:H films, thermal-equilibrium defect processes 7-26640
- a-Si:H films and p-i-n solar cells, photo-assisted CVD and opto-electronic characterisation 7-33595
- a-Si:H films and solar cells, light induced effects 7-46954
- a-Si:H films deposited by dual ion beam sputtering, characterisation 7-32882
- a-Si:H films deposited in He atmosphere, characts. 7-45056
- a-Si:H films high-rate deposition by RF planar magnetron sputtering (*Japanese*) 7-17419
- a-Si:H films photo-CVD, photoelectric and structural props. 7-7869
- a-Si:H films preparation by CVD 7-17453
- a-Si:H films with columnar morphology, Raman scatt. study 7-64644
- Si:H floating zone single crystals, neutron irradi., isochronal annealing behaviour, positron annihilation studies 7-21288
- a-Si:H heterojunction solar cell modules, fabrication by laser scribing 7-13900
- a-Si:H high efficiency p-i-n solar cells using superlattice p-layers 7-23177
- a-Si:H junction position sensitive photodetector 7-56343
- a-Si:H large area integrated solar cells, fabrication 7-40013

elemental semiconductors continued

- a-Si:H material and p-i-n cell, light-induced charge 7-17055
 a-Si:H material and solar cells, light induced effects 7-23139
 Si:H microcrystalline films, glow discharge prep., elec. and optical props. 7-7415
 a-Si:H modulation doped multilayers, persistent photocond. studies 7-38642
 a-Si:H modulation doped multilayers, planar and perpendicular cond. meas. 7-38717
 a-Si:H multijunctions, charge carrier transport, theoretical anal. 7-38690
 a-Si:H multilayer films, charge transfer doping, cond., photocond. meas. 7-38735
 a-Si:H $n^+ - i - n^+$ struct., freq.-depend. noise studies 7-45484
 a-Si:H $p^+ - n - i$ structs., memory switching, transient current instability study 7-52762
 a-Si:H p-i-n solar cells, behaviour after light soaks through p-layer and n-layer 7-8398
 a-Si:H p-i-n solar cells, light induced degradation, effects of impurities and temp. 7-17886
 a-Si:H photo-CVD coatings, characterisation using TFT structure 7-38561
 a-Si:H pin solar cells, open-circuit volt., temp. and light intensity depend. 7-46949
 a-Si:H pin solar cells, photocurrent, transient behaviour 7-46950
 a-Si:H semiconductor-metal system, field effect problems, I-V meas. 7-38728
 a-Si:H short range order, impurity distrib. effects, EXAFS study 7-64761
 a-Si:H solar cell characts. change due to long term temp. stresses 7-8393
 a-Si:H solar cell on polymer substrate, roll-to-roll prep. 7-59861
 a-Si:H solar cell prep. by laser-induced CVD of SiH_4 7-7890
 a-Si:H solar cell technology in Japan, recent advances 7-40009
 a-Si:H solar cells, density of states asymmetry effects 7-46946
 a-Si:H solar cells, dynamic equilibrium dangling bond density 7-17878
 a-Si:H solar cells, effect of texturing 7-13857
 a-Si:H solar cells, hydrogenated microvoids and light-induced degradation 7-54294
 a-Si:H solar cells, i-layer stability thickness dependency 7-17880
 a-Si:H solar cells, impurities and metastable centres 7-40010
 a-Si:H solar cells, integrated series connection 7-40015
 a-Si:H solar cells, kinetics of light-induced degradation and thermal annealing 7-17909
 a-Si:H solar cells, leakage currents, electrochem. treatment effects 7-65467
 a-Si:H solar cells, optically induced degradation 7-59848
 a-Si:H solar cells, p-layer doping by plasma assisted B diffusion 7-13898
 a-Si:H solar cells, photo-CVD prep. 7-17885
 a-Si:H solar cells, photoconductivity-open cct. voltage relation 7-8396
 a-Si:H solar cells, radiation damage by 12 MeV protons and annealing 7-13895
 a-Si:H solar cells, turn-off character, wavelength depend. 7-46951
 a-Si:H solar cells, uses of transparent conducting oxides 7-46953
 a-Si:H solar cells deposited from disilane, blue response and efficiency improvement 7-17877
 a-Si:H solar cells eval., quantum efficiency meas. techniques 7-54314
 a-Si:H solar cells on textured glass substrate with SiO_2 film 7-13899
 a-Si:H solar cells prod. by positive-column glow-discharge method 7-8397
 a-Si:H sputtered film, low-temp. optical props. 7-3101
 a-Si:H sputtered films, intrinsic stress, H effects 7-7078
 a-Si:H stable heterojunction solar cells develop., thermal degradation phenomenon 7-65477
 a-Si:H surfaces and interfaces, microstruct., ellipsometry studies 7-38362
 a-Si:H thin film photovoltaic production, safety and industrial engineering 7-13894
 Si:H thin film solar cell technology, design and appls. 7-17872
 a-Si:H thin film solar cells, device properties 7-13897
 Si:H thin film solar cells, transparent module development 7-13911
 a-Si:H thin film solar cells, repeatable meas. system for accelerated stress testing 7-23174
 a-Si:H thin film solar cells, accelerated stress testing using photodiode array 7-28403
 a-Si:H thin film solar cells, light soaking condition effects 7-46956
 a-Si:H thin films, bulk and interface struct., in situ ellipsometry study 7-27200
 a-Si:H thin films, elec. and optical props., thickness depend. 7-46168
 a-Si:H thin films, ohmic and quasi-ohmic contacts 7-38729
 a-Si:H two-junction, two-terminal tandem solar cells, stability and efficiency 7-46957
 a-Si:H ultrathin layers, CW photoluminescence, layer thickness depend. 7-13202
 a-Si:H ultrathin layers, photoluminescence characts., layer thickness depend. in variety of sample configurations 7-46123
 a-Si:H/CdTe heterojunction, X-ray image sensor fabrication 7-41557
 a-Si:H/CuInS₂ heterojunctions, photovoltaic behaviour, c-v meas. 7-7340
 a-Si:H/Ge:H superlattice struct., light absorption and photocond. studies 7-38715
 a-Si:H/Pd system, silicide form., struct. and electronic props. 7-38363
 a-Si:H/SiC tandem solar cell, thermal and light-induced degradation 7-46955
 a-Si:H/SiN_x interface, slow states, transient photoconductivity studies 7-38670
 a-Si:H/SiN_x:H (a-SiC:H) double-barrier structs., resonant tunnelling coeffs. 7-45467
 a-Si:H/SiO₂/N₂H heterostruct., transport props 7-38768
 a-Si:H/SiO₂/metallic gate struct., capacitance-volt. characts. 7-45515
 a-Si:H/Ti/Al system, solid state reactions, TEM and SAD studies 7-3602
 a-Si:H/a-Ge:H multilayer films, photoconductivity enhancement 7-27443
 n⁺-a-Si:H/a-Si:H/a-SiC:H heterostructures, electrophotographic props. 7-45485
 a-Si:H/a-SiO₂C_{0.8}H superstructures, hot electron conduction 7-45453
 a-Si:H/a-Si_{1-x}C_xH solar cells, light trapping on SnO₂F 7-46952
 a-Si:H/a-Si_{1-x}C_xH superlattices, glow-discharge deposition 7-7879
 a-Si:H/a-Si₃N₄H superlattices, plasma deposition methods 7-39439
 a-Si:H/a-SiC:H heterojunction, valence-band discontinuity, photocurrent-voltage measurements 7-58868
 a-Si:H/a-SiGe:H multilayers, reactive deposition 7-33592
 a-Si:H/a-SiN_x:H, amorphous multilayer structures, optical props. 7-3014
 a-Si:H/a-SiN_x:H heterostructures, interface formation and microstructural evolution 7-2389

elemental semiconductors continued

- a-Si:H/a-SiN_x:H interface system, struct. and electronic props. 7-38361
 a-Si:H/a-SiN_x:H interface, deep states and photoluminescence spectra, transistor characts. 7-39186
 a-Si:H/a-SiN_x:H multilayer films, coplanar conductance, voltage-induced anomalies study 7-2729
 a-Si:H/a-SiN_x:H superlattices, interface struct., optical reflectance determ. 7-12497
 a-Si:H/a-SiN_x:H superlattices, interface defects and disorder 7-52306
 a-Si:H/a-SiN_x:H superlattice interface struct. charactn. 7-58652
 a-Si:H/a-SiN_x:H superlattice films, prep., struct., and optical props. (Chinese) 7-58676
 a-Si:H/a-SiO₂:H superlattice micropores, pyrene molecules adsorption and confinement 7-27112
 a-Si:H/a-SiO(N)_x:H multilayer films, interface electroabsorpt. meas. 7-2689
 a-Si:H/c-Si heterojunctions, energy-band discontinuities, internal photoemission studies 7-58869
 a-Si:H/c-Si heterojunctions, reverse current characteristics 7-58887
 a-Si:H/crystalline Si heterojunction, photosensitivity studies 7-38714
 a-Si:H/metal junction, pot. profile determ. 7-2715
 Si:H-CuInSe₂ tandem modules, thin film design and fabrication 7-13913
 Si:H-CuInSe₂ thin film tandem solar cells, energy based perform. and eval. 7-13890
 a-Si:H-Pt Schottky barrier contact, photocurrent excitation nonadditivity effects 7-17099
 Si:H-SiC:H heterojunction, amorphous solar cell anal. (Chinese) 7-34029
 a-Si:H-SiN_x:H, multilayer struct. study using HREM 7-16879
 a-Si:H-SiN_x:H interface, compositional profile, Rutherford backscatt. study 7-13292
 a-Si:H-SiN_x:H layered structures, effect of a-SiN_x:H composition on band bending near interface 7-45510
 a-Si:H-based films, photochemical vapour deposition, review 7-46345
 a-Si:H-based heterojunction stacked solar cells, design and fabrication 7-40012
 a-Si:H(F), mobility edge, density of states and carrier activation energy calcs., random Bethe lattice approach 7-16937
 Si:H(F)-SiGe:H(F) amorphous multilayer struct., fabrication and near IR photoconductivity characts. 7-52797
 Si:H(Ne)(Ar), ground state one-electron energies, SCF MS X_n calcs. 7-44582
 Si:H(Sn,H)(C,H), amorphous alloy fabrication and characterisation 7-8389
 Si:Hg⁺, ion implant range distributions, Rutherford backscatt. studies 7-2073
 Si:Hg(Au)(Pt)(Ir)(Os)(Re)(W), self-consistent one-electron states of 5d transition-atom impurities 7-32950
 Si:In, amorphous, low temp. annealing, impurity diffusion, phase separation and crystn. studies 7-16808
 Si:In, nucleation of internal melt during pulsed laser irradiation 7-12129
 Si:In, substitutional ion implanted dopants, electron and positron channelling studies 7-26778
 Si:In⁺, ion implanted, damage prod., incidence angle depend. 7-65242
 Si:Li, ion implanted, impurity redistribution under pulsed laser radiation 7-12098
 Si:Li counterdoped n⁺p solar cells, proton-irradiated, DLTS studies 7-8376
 Si:Li detector, TESLA BS 613 TEM for thin films composition determ. (Czech) 7-65371
 Si:Mg, photothermal ionisation spectroscopy 7-45374
 Si:Mg(Be) metastable impurity levels, self-consistent local-density total-energy calcs. 7-38503
 Si:Mn, optical props. (Chinese) 7-33043
 Si:Mn, temperature-electric instability, elastic compression effect 7-64239
 Si:N, deep level generation and annihilation 7-16612
 Si:N, high dose implanted, swelling, saturation, and sputtering effects 7-16648
 Si:N, host-impurity interactions, transferability of tight-binding parameters 7-58773
 Si:N, N incorporation and behaviour 7-16598
 Si:N, O, impurity complexes as shallow donors, optical absorpt. study 7-39147
 Si:N, oxidation-inhibiting behaviour after N implantation, thermogravimetric anal. 7-59697
 Si:N₂O, impurity interactions in optical defects 7-17348
 Si:N₂⁺, N₂⁺ implantation, local inhibition of oxidation 7-59688
 Si:N⁺, dose and dose rate of ion implantation, Si₃N₄ formation 7-32533
 Si:N(O), pseudo Jahn-Teller effect and chemical rebonding 7-16992
 Si:Na MOSFET struct., hopping cond. in 2D impurity band 7-45512
 Si:Na(K), impurity addition by electrolysis 7-44578
 Si:Ne⁺, ion implantation in elemental solids, range profile, gamma-ray spectra 7-2959
 Si:Ni, deep levels elec. props. study 7-64156
 Si:Ni, diffusion of Ni under action of concentrated luminous flux 7-44913
 Si:Ni, thermal cond., impurity effect 7-44929
 Si:Ni reverse-biased p⁺nn⁺ junctions, electron thermal emission rates 7-7169
 Si:O, C, low temp. precipitation, IR and SANS meas. 7-32666
 Si:O, C, precipitation, microstructures, TEM studies 7-32668
 Si:O, C, thermal donor form., T<800K 7-27294
 Si:O, cluster computations related to thermal donors 7-16990
 Si:O, Czochralski cryst. growth, impurity segregation, high axial mag. field effect 7-26960
 Si:O, Czochralski crystals, O precipitates, small-angle neutron scattering 7-58484
 Si:O, Czochralski grown, exigent-accommodation-volume factor associated with O precipitation 7-32670
 Si:O, Czochralski grown, electron irradiated, thermal donor formation 7-44619
 Si:O, Czochralski grown, O-related defects after annealing, IR TEM and resistivity meas. 7-32466
 Si:O, Czochralski-grown wafers, growth striations, X-ray topography study 7-59400
 Si:O, defects created by electron irradiation and subsequent thermal treatments, review 7-16642
 Si:O, dendritic web growth, plastic flow, O effects 7-16471
 Si:O, deposition from SiH₄-N₂O, role of adsorption stages 7-17447
 Si:O, diffusion of O during thermal donor form. 7-38262
 Si:O, diffusivity and diffusion mechanism of O 7-16810
 Si:O, diffusivity and solubility of O review 7-16809

elemental semiconductors continued

- n-Si:O, donor states of O rel. to heat treatment 7-12647
 Si:O, electron irradi. on varying O content, defect anal. 7-16637
 Si:O, electronic struct. and atomic symmetry of the thermal donor 7-16986
 Si:O, energy levels and capture cross-sections of thermal donors 7-16988
 Si:O, enhanced diffusion at thermal donor formation temp. 7-44911
 Si:O, Fourier transform IR spectroscopy and SIMS calibrations for O conc. meas. 7-16606
 Si:O, γ -irrad., majority carrier mobility meas. 7-27334
 Si:O, IR absorption meas. of interstitial O conc., calibration 7-33401
 Si:O, IR absorption spectra of thermal donors 7-17326
 Si:O, IR spectra of interstitial O 7-17325
 Si:O, influence of growth microdefects on microdefect formation during heat treatment 7-17559
 Si:O, ion implanted, octahedral oxide particle nucleation and growth 7-16776
 Si:O, ion implanted, structure before and after heat-pulse annealing 7-16600
 Si:O, low thermal donor conc. layer formation during annealing 7-17564
 Si:O, low thermal donor conc. layer formation during annealing 7-17565
 Si:O, magnetic resonance of O-related defects 7-17223
 Si:O, microcrystalline precipitates, electron microdiffraction studies 7-16769
 Si:O, new donors, bound exciton recomb., photolum. study 7-22300
 Si:O, O precipitate sintering, shaping, and shrinking, precursor oxide phase roles 7-16772
 Si:O, O precipitation, exigent-accommodation-volume factor 7-16771
 Si:O, O precipitation, numerical models 7-16775
 Si:O, O precipitation ad thermal donors 7-16767
 n⁺-Si:O, O precipitation and minority carrier generation lifetimes 7-16774
 Si:O, off-centre, impurities, theory 7-21251
 Si:O, optical transition at thermal donors 7-17346
 Si:O, oxide precipitate nucleation, thermal donor formation kinetics 7-32667
 Si:O, P, Sb wafers, O precipitation during simulated CMOS cycles 7-38218
 Si:O, positron annihilation study 7-3105
 Si:O, precipitates, X-ray diffuse scatt. study (*Japanese*) 7-63399
 Si:O, precipitation kinetics, interstitial diffusion 7-44837
 Si:O, precipitation phenomena, growth law for disc precipitates 7-16770
 Si:O, review 7-16583
 Si:O, self-interstitial migration, dislocation loops and elongated Frank dipoles 7-58300
 Si:O, structure and props. of the thermal donor 7-16766
 Si:O, thermal donor binding energies 7-16989
 Si:O, thermal donor formation, kinetics 7-6664
 Si:O, thermal donor impurity density of states, formalism and appl. 7-12655
 Si:O, thermal donors, photothermal ionisation spectroscopy and IR transmission meas. 7-16987
 Si:O, vacancy-enhanced O diffusion 7-16811
 Si:O, B⁺ ion implanted, reverse annealing 7-16617
 Si:O, C, intrinsic point defects and impurity interactions 7-16611
 Si:O, C, O precipitation, thermal donor generation and annihilation effects 7-16773
 Si:O, C, yield stress, impurities and O precipitate morphology effects 7-16674
 Si:O, C, N, precipitation phenomena, TEM studies 7-16768
 Si:O, N, small particles, elemental and chem. anal., EELS method 7-17379
 Si:O, CZ gram, O precipitation enhanced with vacancies 7-32664
 Si:O, Czochralski wafers, electron traps resulting from O precipitation 7-21866
 Si:O epitaxial films for hetero-bipolar transistors 7-53599
 Si:O epitaxial wafers, preanneal heat treatment effect on precipitation 7-38219
 Si:O substrate materials, heavily doped, control of O and precipitation behaviour 7-32665
 Si:O/Si interfaces, MBE grown, O trapping effects 7-16881
 Si:O, thermal donor formation and structure, review 7-17562
 Si:O₂⁺, Si on insulator structs., amorphous and crystalline oxide precipitates 7-13655
 Si:O₂, ab initio MO electronic struct. calcs. 7-38499
 Si:O(H)(C)(N), conf., Boston, MA, USA (Dec. 1985) 7-14711
 Si:O(N), impurity-dislocation interactions, review 7-16610
 Si:O(O,C), impurity aggregation, SIMS 7-16778
 Si:O(O,H), heat treated, DLTS 7-16991
 Si:P, directional plasma etching, in SF₆+CFCl₃ discharge 7-39788
 Si:P, EPR temp. depend. g-shifts obs. 7-27600
 Si:P, heavily doped, plasma etching with trifluorochloromethane-Ar discharges, modelling of ion bombard. energy distrib. 7-28222
 Si:P, heavily doped, plasma etching with trifluorochloromethane-Ar discharges, modelling of etching rate and directionality 7-28223
 Si:P, heavily implanted, influence of precipitation on P diffusivity 7-6879
 Si:P, interactions and localisation problems, review 7-64178
 Si:P, ion implanted, dynamic annealing, dose rate effects 7-12093
 Si:P, ion implanted defect structs. rel. to implant energy 7-38079
 Si:P, localisation theory 7-64170
 Si:P, MBE grown, coevaporation P doping 7-26773
 Si:P, many-valley semicond., electron intervalley scatt., optical pumping study 7-52608
 Si:P, meas. of heavy doping parameters 7-12855
 Si:P, Ni⁺ ion implantation and annealing 7-21245
 n-Si:P, nonlinear optics near metal-insulator transition 7-20322
 Si:P, polycrystal. thin film, carrier transport, temp. depend. study 7-22043
 Si:P, polycrystalline, excimer laser photochemical directional etching 7-65226
 Si:P, polycrystalline, high pressure reactive ion etching with HCl 7-28224
 Si:P, polycrystalline films, LPCVD, charactn. 7-53615
 Si:P, pulsed laser annealing, molten phase local nucleation study 7-63655
 Si:P, pulsed laser processing via free carrier absorpt. 7-21273
 Si:P, quenching thermodefect prod. Hall effect, EPR meas. 7-27293
 a-Si:P, selective doping and solid phase epitaxial growth, MOSFET apps. 7-27893
 Si:P, self-consistent multi-ion screening formalism 7-38505
 Si:P, surface conc. manipulation for P diffusion using ambient control 7-6660

elemental semiconductors continued

- Si:P, transient enhanced dopant diffusion 7-52136
 Si:P, transmutation doped, deform. pot. shear const. determ. 7-38086
 Si:P,B, SiO₂ coated cryst., floating zone growth under microgravity 7-53575
 n-Si:P,C, electron-irradiated and injection-annealed, vacancies, dislocations and C interstitials 7-51815
 Si:P,O,D, donor passivation and reactivation 7-17031
 Si:P,Sb, mixing of P and Sb ions by recoil implantation, sheet resist., annealing temp. depend. 7-21291
 Si:P films, CVD and electrical props. 7-64913
 Si:P heavily doped, plasma etching with trifluorochloromethane-Ar discharges, parametric modelling and impedance anal. 7-28221
 Si:P MOS source/drain structs., 2D P diffusion props. 7-32718
 Si:P polycrystalline films, segregation at grain boundaries, NMR study 7-38953
 Si:P slotted surface, IR emission showing organ pipe resonant modes 7-44873
 Si:P solar cells, effects of P prediffusion on properties 7-3677
 Si:P solar cells, shallow junction formation by light-induced diffusion from spin-on source 7-8418
 Si:P thin films, surface energy-driven grain growth during rapid thermal annealing 7-63994
 Si:P/Ti, enhanced grain growth by silicide form. 7-27142
 Si:P⁺(PF₃)⁺, ion implanted, rapid thermal annealing, solar cell apps. 7-23193
 Si:PF₃⁺ ion implanted, recrystallisation kinetics during fast thermal annealing 7-16618
 Si:P(Al), random and channelled implantation profiles and range parameters of dopants 7-21246
 Si:P(As)/SiO₂ interface, oxidation rates and oxide props., dopant effects determ. 7-12514
 Si:P(As)(P,B)(As,B) films, surface energy driven secondary grain growth 7-22740
 Si:P(B), tail diffusion model 7-16815
 Si:P(B) LPCVD films, amorphous and polycrystalline, struct., elec. resist. meas. 7-52870
 Si:Pd, deep levels electronic struct., X α -SW study (*Chinese*) 7-58761
 Si:Pd, inelastic relax., neutron irradi. effects 7-44689
 Si:Pt, deep levels and diffusion profiles 7-58767
 Si:S(Se)(Te), chalcogenide pairs, electronic structs., Green's function calc. (*Chinese*) 7-58759
 Si:S(Tl)(Ge)(P)/Pt system, impurity migration during silicide form. 7-6895
 Si:Sb, dry oxidation retarded impurity diffusion, SIMS meas. and numerical simulations 7-27014
 Si:Sb, local lattice relax. around impurity, K-edge EXAFS study 7-64159
 Si:Sb, pot. enhanced doping during MBE growth, elec., optical props., cryst. quality 7-12112
 n-Si:Sb, resistivity at low temp. appl. to bolometers 7-41471
 Si:Sb,As, cryst. aid amorphous, impurity band form., X-ray spectra studies 7-12650
 Si:Sb MBE, electron irradi. effect on doping levels and profiles 7-63660
 Si:Sb MBE film, doped by electron impact ion source, improved doping charact. 7-12101
 Si:Sb MBE layers, doping by secondary implantation 7-12102
 Si:Sb-SiGe modulation doped superlattices, growth and props. 7-7379
 Si:Sb(As)(P)(B) epitaxial films, low temp. deposited by low press. CVD, autodoping 7-27182
 a-Si:Se(Te) thermally evaporated films, photoelectronic props. 7-38640
 Si:Sn, ion implanted, annealing behaviour, channelling and conversion electron Mössbauer spectroscopy 7-13485
 Si:Sn,B, shallow junction formation, preamorphisation by Sn implantation 7-7338
 Si:Ti, deep level transient spectroscopy, transient capacitance data anal. 7-52526
 Si:Ti, electron and hole energy levels, DLTS and DDLTS meas. 7-32941
 Si:Ti, ion implanted, deep level charactn. 7-38513
 Si:Ti(V)(Cr)(Fe)(Zr) polycrystalline solar cells, structural, elec., photovoltaic props., impurity effects 7-39990
 Si:Tl ion implanted layers, defect form. and precipitation, electron microscopy studies 7-12097
 Si:transition metals, anomalous diffusion and gettering 7-2264
 Si:V, impurity self-ENDOR spectrum 7-64545
 Si:W⁺ layers, implanted and annealed, struct., TEM, electron diff. studies 7-32858
 Si:Zn, amorphous-crystalline interface, backscattering and channelling study 7-6663
 n-Si/a-CdS heterojunctions, elec. props. 7-64342
 Si/a-SiO₂/ZrO₂-Y₂O₃, SOI system fabrication, charact. 7-22025
 Si/Al, oxidation by microwave excited O₂+N₂ mixture plasma (*Japanese*) 7-65198
 a-Si/Al films, laser-induced phase transitions, time resolved TEM study 7-38056
 p-Si/Al Schottky barriers, Ar⁺ implantation damage, oxidation, etching and elec. props. 7-21290
 Si/Al/Ni system, contact structure formation by rapid thermal melting 7-45019
 Si/Au buried interface struct. determ., optical second harmonic generation studies 7-63982
 a-Si/Au thin film bilayers, Si crystallisation study 7-21699
 a-Si/c-Si interface, microcrystallites and orientational proximity effect, HREM image interpretation, comment and reply 7-45028
 Si/CoSi₂/Si structs., parallel and perpendicular transport, supercond. props. 7-45518
 Si/Ge amorphous layered system, implanted ion depth distrib. 7-21250
 Si/Ge amorphous multilayer films, interdiffusion, neutron scatt. meas. 7-37222
 Si/Ge_{1-x}Si_x superlattices, conduction band interactions and splitting, envelope-function approx. calcs. 7-64332
 Si/Ge_{1-x}Si_x, convergent beam electron diffraction and imaging of strained-layer superlattices 7-17095
 Si/GeSi strained layer superlattices, electronic and optical props. 7-7359
 Si/metal film interface, silicide nucleation, kinetic model 7-63970
 Si/metal interfaces, silicide form. kinetics during thermal annealing 7-16897
 n-Si/methanol junction device performance improvement 7-17098
 Si/Nb, proximity effect, superconducting transition temp. meas. 7-45566
 Si/Ni system, silicide formation, ion beam induced, embedded markers and moving species 7-21298

elemental semiconductors continued

Si/NiSi₂ heterojunction, interface states, DLTS and hydrogenation studies 7-12777
Si/NiSi₂(111), intrinsic interface states and defect states 7-22011
Si/oxide interfaces, native and thermal, stoichiometry and interface transition layer, atom probe FIM study 7-32844
Si/PLZT spatial light modulators, technology 7-20408
Si/PtSi₃/V/Al Schottky barrier diode metallisation system 7-2666
Si/PtSi(CrSi₂) Schottky diodes, surface imperfection induced elec. leakage paths 7-2719
a-Si/Si(111) interface ordering, X-ray diffr. 7-32848
Si/Si_{0.5}Ge_{0.5} strained layer superlattices, 2D electron systems 7-7380
Si/Si₃N₄ interfaces, phase separated structures, Ar⁺ ion bombardment effects, ZPS studies 7-22439
Si/Si_{0.5}Ge_{0.5} strained layer superlattices, folded phonon dispersion 7-44718
Si/Si_{0.5}Ge_{0.5} superlattices, strain induced confined electron states 7-7311
Si/SiO₂, ion implantation-induced interface states generation and charge trapping study 7-12874
Si/SiO₂, two-step oxidation of thin gate oxides, trapping characts., hot electron effect study 7-64351
Si/SiO₂ interface, digital control of avalanche injection method for studying carrier transport 7-64350
Si/SiO₂ interface, oxide trap capture cross section and tunnelling emission, DLTS study 7-12875
Si/SiO₂ interface band discontinuities, Cs and H intralayer effects obs. 7-22020
Si/SiO₂ interface struct., suboxide states, localisation and crystallographic depend., XPS study 7-58653
Si/SiO₂ system, dielec., elec. and struct. props. 7-7040
Si/SiO₂ system, two-step oxidation and interface structures. 7-3542
n-Si/SiO₂/Al struct., inductive admittance meas. 7-17108
Si/SiO₂/TiSi_x(WSi_x) MOS capacitors, radiation-induced interface traps 7-58897
Si/Ti amorphous superlattices, high resolution photovoltaic position sensing 7-48847
Si/Ti selectively sputter deposited interface, Auger and Rutherford backscatt. studies 7-21690
Si-Ag interfaces, micro-quantitative AES anal. using SEM-SAM apparatus 7-27147
Si-Al, P, defect struct. and dynamics 7-16552
Si-Al optically excited diaphragms, reson. freq., temp. depend. 7-18971
Si-Al Schottky barrier diodes, ion implant modification 7-45498
Si-Al Schottky barrier formation, local electronic struct., EELS study 7-21975
Si-Al struct., cond., transverse elec. field depend. 7-27417
Si-Al structures, ion mixing, effect of interfacial oxide 7-21537
Si-Al₂O₃, SOS struct., UV reflectance meas., ellipsometry study 7-33414
Si-alkaline earth fluoride structures, heteroepitaxial growth, struct., elec. props. 7-12567
Si-aqueous electrolyte interfaces, impedance spectra, freq. dispersion 7-27414
Si-Au interface, atomic bonding 7-58663
Si-Au-Pt interfaces, PtSi formation, RBS studies 7-58547
Si-B₂O₃ interaction during Si MBE, Auger spectra study 7-13277
Si-B⁺, Ge⁺, preamorphised shallow junctions, end-of-range and mask edge lateral damage 7-38071
Si-binary alloy interfacial interactions, Rutherford backscattering spectrometry, TEM 7-12505
Si-C based MIS struct., interfacial characts. 7-2732
Si-CaF₂ interface struct., high resolution TEM study 7-2394
Si-CaF₂, MBE of CaF₂ on Si and overgrowth with Si or Ge, characteris. 7-22495
Si-CaF₂ interface, strains in MBE grown insulator films, MeV ion channelling meas. 7-7080
Si-CaF₂ interface, with epitaxially grown insulator, post-growth annealing treatments 7-7074
Si-CaF₂ interface, with MBE grown insulator, trap states, I-V, C-V meas. 7-7407
Si-CaF₂ SOI technology by heteroepitaxial growth 7-22022
Si-CaF₂-Ge heteroepitaxial structures, MBE grown, twinning, topography, channelling, TEM, SEM 7-12566
Si-CaF₂-Si heteroepitaxial structures, MBE grown, twinning, topography, channelling, TEM, SEM 7-12566
Si-CaF₂-Si MOSFET structures, heteroepitaxial growth, struct., elec. props. 7-12567
Si-CaF₂-Si structure, reduction of Ca and F surface segregation by solid phase epitaxy of Si 7-38357
Si-Co₅₀Mo₅₀-Au, amorphous Co₅₀Ta₅₀ alloys as diffusion barriers 7-44923
Si-Co₅₀Ta₅₀-Al, amorphous Co₅₀Ta₅₀ alloys as diffusion barriers 7-44923
Si-CoSi₂, solid phase epitaxial growth of CoSi₂, nonultrahigh vacuum method 7-45043
Si-CoSi₂ heterostructures, MBE or solid phase epitaxially grown, Schottky barrier heights, DLTS spectra 7-12859
Si-CoSi₂ Schottky barriers, epitaxially grown, supercond. below 1.05K, tunnelling spectra 7-12860
Si-CoSi₂-CaF₂, MBE growth of epitaxial insulator-metal-semicond. struct. 7-22496
Si-CoSi₂-Si, transistor current modulation (French) 7-58894
Si-Co(Ni) bilayered films, chem., elec., and struct. charges upon annealing 7-22037
Si-Co(Pt)(Au), high energy density pulsed ion beam irradiation, study of reacted layers 7-52151
Si-Cr, lateral growth of CrSi₂, role of Si transport 7-38272
Si-Cu interface, atomic bonding 7-58663
Si-Cu interface, surface struct., angle resolved Auger electron emission determ. 7-21672
Si-Cu-Au layered struct. reflectivity and EXAFS study 7-59292
Si-electrolyte interface, Fourier transform IR spectroscopy 7-27124
Si-Fe, ion implanted, channelling/RBS studies 7-2039
Si-GaAs heteroepitaxial interface, at. resolution HVEM study 7-2392
Si-GaAs_{0.7}P_{0.3} multijunction solar cell, solid state photovoltaic research status at SERI 7-8389
Si-GaAsP-GaP solar cell, high efficiency mech. stack, performance meas. 7-8401
Si-GaF₃-Si epitaxial structures, growth, structural and electrical props. 7-38356
Si-Ge, epitaxial growth of Ge, study using an MBE system with automatic ellipsometer, nondestructive anal. 7-7058
Si-Ge heterojunction, structural and electronic props. 7-21997

elemental semiconductors continued

Si-Ge interface, solid phase epitaxy, intermixing, EXAFS, AES, LEED obs. 7-63973
a-Si-Ge multilayer films, interdiffusion, modulation wavelength depend. 7-27033
a-Si-Ge multilayer interfaces, Raman scatt., X-ray diffr. characterisation 7-27167
Si-Ge multilayered structures, Bi ion implanted, projected range distrib., glancing angle RBS anal. 7-63689
Si-Ge_{0.5}Si_{1-x} multilayers, MBE grown, thermally annealed, Ge diffusion, strain relax., ion channelling, backscattering anal. 7-6896
Si-Ge_{0.5}Si_{1-x} strained layer heterojunctions, selectively doped, hole mobilities, temp. depend. 7-7383
Si-Ge_{0.5}Si_{1-x} strained-layer heterostructure, transport, optical props. and appls. 7-7349
Si-Ge_{0.5}Si_{1-x} superlattices, Raman scatt. involving umklapp processes 7-3043
Si-Ge-Si epitaxial layer structs., particle channelling study, statistical equil. 7-58386
Si-GeSi heterostructures, MBE grown, structural props., quality, electron diffr., imaging obs. 7-7036
Si-InP (110) heterojunction, characterisation 7-33079
Si-InSb heterojunction, spectral characts. and detection props. 7-38712
Si-M (M=In, Te, Re, Bi), metal implantation using pulsed electron beam 7-6882
Si-metal, silicidation reactions, rapid thermal annealing/TEM technique 7-52156
Si-metal interfacial atomic struct. and cpd. form., FIM studies 7-32846
Si-metal-Si multilayers, backscattering contribution to Auger line intensity 7-28379
a-Si-metal-Si structures, rapid thermal sintering and annealing 7-21700
n-Si-MnO photoanodes, photoelectrochemical and struct. behaviour 7-54329
Si-Ni interface, silicide formation, backscattering spectrometry and TEM studies 7-21696
Si-Ni interface, struct., RHEED, Rutherford backscattering spectrometry 7-27143
Si-NiSi₂ epitaxial interface, extended defects, geometrical character 7-6640
Si-NiSi₂ interface struct., X-ray standing-wave analysis 7-58661
Si-NiSi₂(PdSi)(PtSi), interface electronic states (Chinese) 7-58845
Si-on-fused-SiO₂, cryst. quality improvement by zone melting recrystn. (Japanese) 7-33553
Si-P, dopant redistribution during high pressure oxidation, four-point probe meas. 7-27020
Si-Pd, Pd₂Si formation, TEM study 7-38267
Si-Pd interface, silicide formation, in situ ellipsometric studies 7-21694
Si-PdSi interface, at. struct., TEM obs. 7-63977
Si-polyethersulphone, amorphous, solar cell development 7-8394
Si-polymer contact solar cell fabrication 7-23168
Si-Pt, Pt₂Si formation, TEM study 7-38267
Si-PtSi, interfacial metallurgical interactions, elec. characts., effect of H 7-52834
Si-PtSi thin film Schottky diodes, barrier height meas. 7-64308
Si-pyrex, irreversibility of anodic bonding 7-33910
Si-Si homoepitaxial interfaces, MBE grown, oxygen trapping 7-32855
Si-Si interfaces, MBE grown, sputter cleaned, microstructure, electron microscopy obs. 7-12512
Si-Si surfaces, direct bonding, silanol group reactions and O diffusion mechanisms 7-21791
Si-Si_{0.55}Ge_{0.45} modulation doped superlattice, MBE grown, electron mobility enhancement, Hall meas. 7-7382
Si-Si_{1-x}Ge_x strained layer superlattices, electronic struct. 7-38707
Si-Si_{1-x}Sn_x strained layer superlattices, electronic struct. 7-38707
Si-Si₃N₄, nitridation of Si (100) by RF plasma, XPS study 7-33515
Si-Si₃N₄, SOI, N⁺ implanted, microstructural characterisation 7-52300
Si-Si₃N₄, SOI structs. formed by N⁺ implantation EPR of defects 7-33273
Si-Si₃N₄ and Si-Si₃N₄-SiO₂ SOI structures, laser recrystallisation, effects of different capping layers, characterisation 7-45511
Si-Si₃N₄ buried nitride SOI structs., N⁺ ion implantation, elec. and physical props. 7-33100
Si-Si₃N₄ SOI structs., formation by N⁺ implantation 7-32532
Si-SiGe strained layer superlattices, electronic subbands 7-2700
Si-SiGe strained-layer superlattices, optical and electronic props. 7-53535
poly-Si-SiO₂, Ar⁺ laser recrystallised interface characts., effects of technological parameters (Chinese) 7-33092
Si-SiO₂, buried layer SOI structs., elevated temp. high dose O⁺ implantation, effect of annealing 7-32530
Si-SiO₂, buried oxide formation by O⁺ implantation, donor creation, enhanced conductivity 7-32529
Si-SiO₂, buried oxide SOI struct., effects of annealing temp. on characts. 7-33099
Si-SiO₂, buried SiO₂ formation, high dose O⁺ implantation at room and liquid N₂ temp. 7-32528
Si-SiO₂, E' centre in thermally grown SiO₂, bias depend. annealing 7-45503
Si-SiO₂, interface trap annealing, rapid thermal processing 7-22027
Si-SiO₂, lateral solid phase epitaxial growth, SOI transistors fabrication 7-2399
Si-SiO₂, MBE SOI formation, Auger study 7-32876
Si-SiO₂, MIS struct., temp. stress influence (Slovak) 7-7389
Si-SiO₂, new donors effect, interface effect due to internal oxidation 7-33093
Si-SiO₂, oxide breakdown, high field and current stress, thickness depend. 7-59144
Si-SiO₂, SIMOX wafers, epitaxial growth 7-32878
Si-SiO₂, SOI struct., deep O⁺ implantation, strain and damage in Si 7-32531
Si-SiO₂, SOI structs. formed by O⁺ implantation, EPR of defects 7-33272
Si-SiO₂, Si oxidation kinetics, interface width determ. 7-39764
Si-SiO₂, symmetry forbidden Raman scatt. from (100) oxidised surfaces 7-46002
Si-SiO₂ (111) interface, dangling bonds, dipolar interactions investig. 7-17107
Si-SiO₂ interface, AES depth profiling during sample rotation 7-27829
Si-SiO₂ interface, chem. transition, density of states calcs. 7-7397
Si-SiO₂ interface, chem. struct., XPS determ., suboxide distrib. and interface state form. 7-38358

elemental semiconductors continued

- Si-SiO₂ interface, computer simulation of high-resolution TEM images 7-44318
- Si-SiO₂ interface, ESR signal from P_{b0} centres, anisotropic props. 7-38940
- Si-SiO₂ interface, electrically active defects 7-33102
- Si-SiO₂ interface, electronic state charactn. 7-38747
- Si-SiO₂ interface, insulator props. after exposure to H₂+N₂ and NH₃. 7-59693
- Si-SiO₂ interface, MOS capacitance derivative freq. depend., surface state densities and capture cross section 7-45507
- Si-SiO₂ interface, microchemistry 7-32850
- Si-SiO₂ interface, positive charge generation; rel. to high field electron transport in SiO₂ 7-38571
- Si-SiO₂ interface, roughening induced during AES depth profiling 7-21685
- Si-SiO₂ interface, struct. models 7-58658
- Si-SiO₂ interface, study using variable energy positron beam 7-38063
- Si-SiO₂ interface, wet oxidised, RF plasma annealing effects 7-54026
- Si-SiO₂ interface formation by catalytic oxidation using adsorbed alkali metals 7-54017
- Si-SiO₂ interface properties in the 10¹⁷-10¹⁹ cm⁻³ doping range 7-38762
- Si-SiO₂ interface relief study using scanning tunnelling microscopy 7-63978
- Si-SiO₂ interface roughness, evolution, characterisation 7-32852
- Si-SiO₂ interface state density effect on elec. props. of Pt-diffused MOS struct. (Japanese) 7-7404
- Si-SiO₂ interface struct., ellipsometric charactn., rel. to elec. props. 7-63985
- Si-SiO₂ interfaces, microstruct. and electronic props. 7-38359
- Si-SiO₂ interfaces, surface roughness and elec. cond. 7-2724
- Si-SiO₂ MOS capacitors, defect struct. and interface state generation 7-7399
- Si-SiO₂ SOI struct. formed by high dose ion implantation, high resolution TEM study 7-59690
- Si-SiO₂ SOI structure, lateral solid phase epitaxial growth, TEM study 7-38369
- Si-SiO₂ SOI structures using buried layers of oxidised porous Si 7-13660
- Si-SiO₂ struct., interfacial charged centres, low temp. RF plasma treatment 7-2661
- Si-SiO₂ structs., low and high temp. oxidised, inversion electron mobility study 7-22019
- Si-SiO₂ structures, prod. by recrystallisation, subgrain boundaries, barrier effects 7-52305
- Si-SiO₂ system, H₂ diffusion 7-21531
- Si-SiO₂ system, interface state generation by nonionizing UV radiation 7-38760
- Si-SiO₂-Cs MOS, semicond. flatband voltage depend. on impurity distrib. 7-27433
- Si-SiO₂-S, effect of S on the oxide charge 7-7024
- Si-SiO₂-N₂-N₂/3-Al structures, interface states, DLTS study 7-45513
- Si-SiO₂-Ag(Cu)(Au)(Pd)(Ti) MOS structures, diffusion coeff. meas. in elec. fields, solid solubilities 7-2279
- Si-SiO₂-Cu(Ni), light induced deposition of metal films on SOI substrates 7-46354
- Si-SiO₂-InSb hybrid struct. spectral characts. and detection props. 7-38712
- Si-SiO₂-Si layered struct., dose calcs. for X-ray and X-ray irradi. 7-58333
- Si-SiO₂-SiO_x-N_y-metal system, plasma oxynitride effect on interface charge 7-38761
- Si-SiO₂ interface density of localised states, C-V and G-V characts. meas. 7-38734
- Si-silicide interface, Schottky barrier heights, size effect 7-52837
- Si-Sm Schottky barriers, elec. and struct. characts. 7-38675
- a-Si-SnO₂ interface, solid state reaction, XPS study 7-22449
- Si-Ta interface, depth profile, Ar⁺ ion bombard., Auger electron spectra anal. 7-46261
- Si-Ti, native contamination layer effect on interface props. 7-17104
- Si-Ti, Schottky barrier heights, 175 to 295K, silicide form. 7-38679
- Si-Ti amorphous superlattices, electronic and photoelectronic props. 7-12795
- Si-Ti amorphous superlattice films, lateral photoeffect 7-45487
- Si-Ti amorphous superlattice films, lateral photovoltage, wavelength dependence 7-45488
- Si-Ti interface, laser irradiated, silicide formation 7-45079
- Si-Ti interface, nucleation and growth of TiSi₂, influence of O₂ 7-21541
- Si-Ti interface, silicide phase formation 7-21695
- Si-Ti thin-film superlattices, structure 7-38350
- Si-Ti_{1-x}W_x, Schottky barrier heights, 175 to 295K, silicide form. 7-38679
- Si-TiO₂ MIS structures, low temp. CVD of TiO₂ films 7-17105
- Si-TiO₂ electrolyte system, charge-transfer processes 7-22007
- Si-TiSi₂, TiSi₂ local epitaxial growth on Si (111), rapid thermal annealing, annealing ambient 7-33856
- Si-TiSi₂-B(P)(As) interface, impurity diffusion 7-7077
- Si-Ti(CoSi₂)-Al contacts, four-terminal resistor structs. for contact resist. determ. from end resist. meas. 7-38730
- Si-Ti(TiSi₂), Schottky barrier height investig. 7-2716
- Si-transition metal interfaces, competing initial chemical reactions 7-21693
- Si-W, buried conductor formation, low press. CVD W deposition on porous Si 7-32877
- Si-W CVD film interaction, annealing, silicide formation 7-2390
- Si-W interface, thermal behaviour rel. to silicide form. 7-16822
- Si-W interfaces, microstruct. charactn. 7-16882
- Si-W system, silicidation reaction suppression up to 1100°C 7-16821
- Si-Yb interfaces, mixed valence of Yb, synchrotron radiation photoemission spectra, metal coverage and annealing temp. depend. 7-32966
- Si_n (n=10 to 32), clusters, growth and struct., solid-liq. transform., mol. dynamics simulation 7-26682
- Si_n⁺, semicond. cluster anions, photodetachment and photofragmentation 7-36837
- Si_n⁺, clusters, mass resolution, photofragmentation and photodetachment spectroscopy 7-15795
- Si-C-Si, interface struct. study 7-45021
- SiGe-Si structures, MBE growth mode and interface structure 7-52311
- a-Si_xGe_{1-x}/a-Si:H/Al Schottky barrier form. and characts. 7-12787
- Si₃N₄ amorphous alloy films, microstructure, XPS study 7-22436
- SiO₂/Si (111) interface ordering, X-ray diffr. 7-32848

elemental semiconductors continued

- SiP, doping by XeCl excimer laser irradi., ultra-shallow junction fabrication 7-58303
- SiSe⁺, photothermal release of carriers, deep levels, capacitance spectroscopy 7-16968
- Si(001), 2 × 1 surface relax. and vibr. excitations 7-6949
- Si(001), biatomic steps 7-38309
- Si(001) surface, refinement of buckled-dimer model 7-6948
- Si(001)(2×1), surface vibr. excitations 7-16854
- Si(111) (7×7), geometrical struct. 7-38310
- Si(111), adsorption of ethylene, vibr. study 7-45012
- Si(111), energy minimisation calc. for dimer-adatom-stacking fault model 7-63940
- Si(111), H₂ chemisorption, dihydride phases, TDS studies (Chinese) 7-38321
- Si(111) initial stages of epitaxy of Cu, Ag, Au, UHV microscopy study 7-27210
- Si(111) substrates, MBE growth of non-lattice-matched (Ba,Ca)F₂, (Pb,Sn)Se-(Ba,Ca)F₂ and CdTe-(Ba,Ca)F₂ layers 7-27216
- Si(111), surface dielectric props., reflection high resolution electron energy loss study, azimuthal depend. 7-33498
- Si(111), surface structure, temp. depend. polaron shifts 7-7325
- Si(111) with adsorbed Ag layers, struct. anal. by impact collision ion scatt. spectroscopy 7-6999
- Si(111) with As overlayer, removal of surface reconstruction 7-21587
- Si(111) with evaporated Al film, wire bondability 7-21710
- Si(111)-CaF₂ interface form., photoemission study 7-2395
- α-Sn crystals, surface phonon modes and reconstructions, Green's function method calcs. 7-2339
- α-Sn, thin film quantization studies using high resolution electron energy loss spectroscopy 7-27448
- SnO₂:F-n-Si(poly) solar cells fabricated by CVD, characterisation 7-59859
- SnO₂-Si (100), CVD coatings, X-ray studies 7-7886
- SnO₂-SiO_x-Si surface barrier solar cells, optimisation of fabrication process 7-23154
- a-Si solar cells, transparent Ag contacts and ITO antireflection coating 7-65478
- TaSi₂/polycrystalline Si structures, oxidation, dopant effects 7-39686
- Te (0001), conductivity of size-quantised holes, hydrostatic pressure effects 7-45428
- Te (1010), He atom scatt. 7-64863
- Te, cyclotron reson. characts. of nonequilibrium carriers at low temps. 7-64532
- Te, gyrotropic crystals, transient photocurrent 7-38618
- Ti/Si (111) interface, diffusion and silicide form. kinetics, XPS meas. 7-52308
- Ti/Si interface, TiSi₂ formation by rapid thermal annealing 7-21707
- Ti/Si structure, heat treatment in O₂, N₂ or O₂/N₂, Ti silicides, TiO and TiN formation 7-65191
- Ti/Si,B,As,Sb interface, dopant redistrib. during silicide form. by rapid thermal processing 7-63641
- Ti-Si interface, self-aligned Ti silicide formed by rapid thermal annealing 7-2391
- Ti-Si interface, silicide form., Auger and appearance pot. spectra studies 7-45031
- Ti-Si:As⁺(P⁺)(BF₄⁺), TiSi₂ formation, ion implantation doping and masking oxide film effects 7-21708
- V/Si, silicide formation, comparison of SiO₂ and a-Si surface protection layers 7-58662
- W/Si multilayered structs., high resolution electron microscopy studies 7-63968
- W-Si multilayer structures, Auger depth profiles using a dual ion gun system 7-22429
- W-Si system, selective deposition of W films on Si wafers, WSi₂ formation 7-21748
- W-Ti-Si interface, WSi₂ form. by rapid thermal annealing, growth kinetics, Ti film effects 7-63969
- WSi₂-WSi, effective elastic constns., surface acoustic wave anal. 7-58597
- Yb-Si (111) interface mixed valence behaviour, angle-integrated photoemission study 7-13327
- ZnO-Cu-SiO₂-Si composite membrane, interdigital transducer generated US Lamb waves 7-11241
- ZnO-Si structures, transverse acoustoelectric effect 7-45398

elementary particle coupling constants

- λ_φ⁴ theory triviality problem in time-dependent space-time 7-18998
- φ₄⁴ model with negative coupling constant, necessity-sufficiency problem of renormalisation 7-56455
- φ₄⁴ theory with negative coupling 7-49005
- φ₄⁴ quantum field theory, coupling constant bound violation 7-9980
- φ₄⁴ theory, stochastic quantization simulation, renormalisation theory for bare couplings 7-48960
- axial vector coupling constant and quark confinement 7-24835
- baryons, effective chiral Lagrangian construction, coupling constant calcs. 7-49084
- chiral bag plus Skyrmin model, axial coupling g_A at large bag radius 7-10035
- chiral field theory, low momentum penguin loop contribs. and ΔI=1/2 rule 7-41647
- closed strings in open-string field theory 7-56529
- cloudy bag model, renormalised πNN coupling constant and P-wave phase shifts 7-5067
- Coleman-Weinberg transition on a lattice, mean field anal., gauge, φ⁴ coupling effects 7-35705
- confined Yang-Mills field, propag. props. and condensate form. 7-48991
- cosmic strings, radiation of Goldstone bosons 7-56129
- CSP⁻¹ model, deconfinement by minimally coupled massless fermions 7-56516
- Edwards Hamiltonian of polymer physics, stochastic quantisation study 7-48945
- effective coupling constant, finite temp., one-loop approximation calcs. 7-41577
- embeddings of generating functionals, generalized perturbation theory 7-30181
- Eotvos anomaly, gauge field coupled to fermion number interpretation 7-18682
- fine-structure constant in plasma model of fluctuating vacuum substratum 7-30230
- finite temperature deconfinement transition, Monte Carlo renormalisation group calcs. of critical exponent 7-49054

elementary particle coupling constants continued

Friedberg-Lee soliton bag model, chromomagnetic field anal., α_s calc. 7-494
 g_A and quark confinement in nucleons 7-56517
 g_{KN}^2 , bounds from $K^-p \rightarrow K^0n$, K^-n data 7-61738
 G_V , weak vector coupling constant, determ. from isospin-mixing corrections to Fermi matrix element in β -decay 7-56648
heavy quark meson decay constant calcs., nonrelativistic QCD potential model anal. 7-10054
heavy quarkonium pot. models, Green's function Schrodinger eqn. calcs. 7-15121
interacting gauge-covariant bosonic string, symm. and transformations 7-35684
Kaluza-Klein theory with multiply connected extra space, gauge field coupling constants (*French*) 7-41672
KSFR relation and strength of the nonSkyrme term 7-4968
lattice gauge theory, continuum limit and renormalized trajectory, weak coupling expansions 7-19009
lattice Gross-Neveu model, recovery of chiral symm. 7-19010
lattice QCD, chiral symm. breaking in strong coupling limit 7-56514
lattice $SU(N) \times SU(N)$ chiral models, two-loop coupling constant renormalization 7-424
lattice theory, weak coupling perturbation theory for QED 7-19001
long-range NN force, search at highly relativistic velocities 7-498
Majoron- ν coupling limits from ^{76}Ge beta-decay meas. 7-49340
mass dependence of coupling constants in relativistic mean field models 7-4990
mesons, micrononcausal Euclidean wave functions assuming Yukawa type couplings 7-41596
multiflavour QCD, nonAbelian bosonization and baryon mass formulae 7-61579
 $N=2$ harmonic superspace with central charges, appl. to self-interacting massive hypermultiplets 7-19020
 $N=2$ supergravity model with a light graviphoton 7-41227
neutral weak currents, universality of ν_e and ν_μ coupling 7-24830
nuclei, weak and EM interactions, conference, Heidelberg, Germany (July 1986) 7-48172
nucleon size, density dependence of f_π in nuclear medium, QCD sum rule anal. 7-480
particle families as radial excitations, eigenstates of relativistic wave eqns. 7-30179
propagating modes in gauge field gravit. theory 7-24523
QED₂, discretized light-cone quantization, bound-state problem 7-56497
QED, threshold effects in spontaneously broken theories, gauge and scheme depend. 7-5041
quantum field theory, progress, book 7-9602
random lattice gauge systems and interacting gaussian surfaces, strong coupling expansion 7-48958
relativistic bound-state problems, running coupling constant 7-399
renormalisation group approach to thermodynamical variables 7-18733
renormalisation in curved space-time and nonminimal gravit. coupling 7-35665
scalar field theory and gauge theory, renormalized coupling constants by Monte Carlo methods 7-41618
strong coupling const. determ. from e^+e^- annihilation hadron events 7-61716
strongly coupled QED, variational calc. of bound-state wavefunction 7-459
 SU_2 lattice gauge theory, strong-coupling anal. of space-time critical dimensionality 7-56430
 $SU(2)$ Yang-Mills lattice theory, correlation lengths and finite size effects 7-56426
superstring theory, classical symmetries in the low-energy limit 7-24804
superstring theory, time variation of Newton's gravit. constant 7-18661
supersymmetric nonAbelian gauge models, exact β -function from one-loop perturbation theory 7-41644
SUSY O(N) model, coupling constant behavior at high temp. 7-41664
Thirring model, derivative coupling model equivalence and fermionic Green's fns. 7-48993
variation of coupling constants, evidence 7-41670
Wess-Zumino model, coupling constant behavior at high temp. 7-41664
Yang-Mills theory, nonperturbative approach to strong-coupling confinement 7-56433
Yang-Mills theory, nonperturbative calcs. away from strong coupling 7-56434
 $Z(2)$ lattice gauge theory, Polyakov loop effective couplings, Monte Carlo calc. 7-41619
 $B^- \rightarrow FD^0(\bar{l}^-\nu D^0)$, $l^- = e, \mu$, decay rate calcs. f_F, f_D decay constant determ. 7-61660
 e^- weak neutral current coupling constant meas. from $e^- \nu_\mu \rightarrow e^- \nu_\mu$ 7-56438
 e^+e^- , 46.8 GeV, excited quarks search at CELLO, final state topologies 7-30276
 e^+e^- annihilations, joint quarkonium and neutral Higgs boson production anal. 7-15168
 $e^+e^- \rightarrow$ hadrons, 35 GeV, α_s determ., corrections to corrected data, second-order QCD anal. 7-30275
 $e^+e^- \rightarrow$ hadrons, strong coupling constant meas. 7-24897
 $e^+e^- \rightarrow$ hadrons, total hadronic cross sections, $\alpha_s, \sin^2\theta_W$ 7-61703
 $e^+e^- \rightarrow W^+W^-, WZ, W\gamma, ZZ$, tri-boson gauge coupling effects, standard model calcs. 7-24868
 $e^+e^- \rightarrow W^+W^-$ four fermions, beam polarization effects, $\gamma WW, ZWW$ vertex meas. analysis 7-61640
 $\eta \rightarrow \gamma\gamma$, meson-quark coupling constants, one-loop quark model 7-61695
 $n \rightarrow p\nu_e, g_A/g_V$ meas. from beta-asymmetry meas. 7-35866
 $NN\pi$ vertex function, influence on meson radial structure (*Chinese*) 7-10039
 $\nu(P)$, 400 GeV, neutral to charged current cross section ratios 7-15144
 ν_e, ν_μ coupling to charged weak currents, universality test 7-24872
 $pp \rightarrow pn\pi^+$ at 800 MeV, one-pion exchange model and Faddeev eqn. 7-41846
 $pp \rightarrow X$, three-jet prod. due to QCD fragmentation process 7-19141
 ϕ , light pseudoscalar boson, nucleon coupling, QED calcs. 7-36022
 π decay constant calcs. and dynamical symmetry breaking in QCD 7-24843
 $\pi^0 \rightarrow \gamma\gamma$, meson-quark coupling constants, one-loop quark model 7-61695
 πN parity-violating coupling constant, determination from nonleptonic Hamiltonians 7-4993
 $q\bar{q}$ realistic pot. with running coupling constant, fine and hyperfine splitting 7-19068

elementary particle coupling constants continued

$\rho^- \rightarrow \pi^- \gamma$, pseudoscalar coupling constant, relativistic confinement calcs. 7-515
 $\rho^- \rightarrow \pi^- \pi^0$, pseudoscalar coupling constant, relativistic confinement calcs. 7-515
 $Sff, S\gamma\gamma, S\gamma Z^0$ couplings, $S = V_L V_L, V_L = W^\pm, Z^0$, nonrelativistic bound state calcs. 7-49154
 $T(1S)$, decay spectrum, α_s determ. 7-61663
 $W \rightarrow e\mu(\mu\nu)(\tau\nu)$, $e\mu\tau$ universality test of weak couplings, $g_\tau/g_e, g_\mu/g_e$ meas. large missing energy events 7-61679
 Z masses and couplings, bounds in $SO(10)$, E_6 GUTs from electroweak corrections 7-61527
 $Z^0\gamma\gamma$ and $Z^0Z^0\gamma$ Green's functions, Ward identity derivation 7-41817
 $^9\text{Be}(e,e')$, parity violation meas. in quasielastic electroweak scattering $\tilde{\beta}, \tilde{\delta}$ coupling constant calcs. 7-49388
 K^+N channel coupling, quark pot. model with resonating group method 7-41705
 π field around static source, chiral invariant model 7-10034
 W^\pm, Z^0 self interactions, Lagrangian containing quadrupole terms, $e^+e^- \rightarrow W^+W^-$ anal. 7-61515

elementary particle decay
see also electromagnetic decays; elementary particle coupling constants; hadron decay; intermediate boson decay; lepton decay; leptonic decays; nonleptonic decays; semileptonic decays
boson resonance decay width calcs., Reggeon anal. 7-5009
fourth generation quark decays from $pp \rightarrow Q$ in grand unified model with 10^{12} GeV unification scale 7-4745
heavy flavour lifetimes, review 7-61548
neutralino decay in $e^+e^- \rightarrow$ neutralinos 7-15140
ultra-heavy quarks, prod. and decay props., quarkonia prod. in hh and e^+e^- 7-30242
 $b(c)$ -quark $\rightarrow \mu\nu, X$, semi-muonic branching ratio determ. and heavy quark fragmentation function calcs. e^+e^- , $\sqrt{s}=34.6$ GeV 7-61710
 $b \rightarrow s\gamma$, hard γ emission, Higgs boson doublet model 7-15179
 $b' \rightarrow \psi X$, detection possibilities of fourth generation b' quarks 7-510
 $D \rightarrow dg$, exotic quark decay in E_6 theories 7-19047
 q -decay ($q=c,b$) and CP violation, electroweak theory status 7-56486
 $s \rightarrow d + \text{gluon}$, h , quark scalar boson interactions and strangeness-changing weak vertex, heterotic ring anal. 7-30301
 ν quarks, possible signatures at e^+e^- colliders 7-5032

elementary particle electric moment
see also baryon electric moment; lepton electric moment; meson electric moment
semileptonic decay, bremsstrahlung, integration of photon quadrupole moment (*Spanish*) 7-61672
 $Z^0\gamma\gamma$ and $Z^0Z^0\gamma$ Green's functions, Ward identity derivation 7-41817

elementary particle electromagnetic interactions
low energy meson physics in the superconducting quark model 7-35811
massive spin 3/2 particle with EM and gravit. interactions by Kaluza-Klein reduction, theory 7-49024
parity invariance, strong and electromagnetic interactions 7-9995

elementary particle gravitational interactions
see also supergravity
massive spin 3/2 particle with EM and gravit. interactions by Kaluza-Klein reduction, theory 7-49024

elementary particle inclusive interactions
see also electron-positron inclusive interactions; elementary particle large momentum transfer interactions; pion-proton inclusive interactions; proton-proton inclusive interactions
backwards evolved initial state parton showers, Monte Carlo model 7-15128
fire balls stochastic decay, limiting fragmentation hypothesis (*Chinese*) 7-49103
hadron-hadron inclusive reactions, numerical results from quasi-nuclear quark model 7-24922
hadronic low transverse momentum transfer reactions, colour superconducting treatment 7-41738
hadronic systems eqn. of state, S-matrix statistical mechanics formulation, many-particle process effects (*Russian*) 7-41772
hadronization of quarks and gluons into hadron jets at high energies 7-41749
hard processes involving two quarks and four gluons, cross section, QCD tree approx. calcs. 7-49083
hyperon polarization in hadronic collisions 7-35908
initial state radiation effects on W and W production 7-5064
jet calculus, inclusion of coherence effects 7-61764
lepton-lepton and lepton-jet correlations at Z resonance, new particles vs. standard model 7-56476
multipomeron exchange processes, improved Regge-eikonal model and multiplicity distribts. 7-19089
nucleus-nucleus interactions, cosmic ray results from the JACEE experiments 7-60499
perturbative QCD and jets 7-61600
QCD light cone gauge, integral equation for multiplicity distribution 7-15115
quark-gluon plasma formation, pre-equilibrium plasma dynamics 7-56578
short-range rapidity fluctuations in high energy collisions 7-61781
squeezed coherent states and hadronic multiplicity distributions, quantum optical model 7-35843
ultrarelativistic heavy-ion collisions, flavour composition in scaling hydrodynamics 7-15178
ultrarelativistic nuclear collisions, initial temp. 7-61918
ultrarelativistic nuclear collisions, stopping power in dual parton model 7-61780
unequal nuclei collisions at high energy, rapidity distribts. and hydrodynamic model 7-9350
 $2N, 0.1-1.0$ GeV²/c², nucleon magnetic moment and effective hadronic degrees of freedom 7-24973
 $\alpha\alpha \rightarrow \pi^0 X, \sqrt{s_{NN}}=31$ GeV, high p_T invariant cross section meas. 7-35907
 $dd \rightarrow \pi^0 X, \sqrt{s_{NN}}=31$ GeV, high p_T invariant cross section meas. 7-35907
 $\gamma\gamma \rightarrow D^{\pm} X$, inclusive production, event rate and topology 7-61782
 $\gamma\gamma$ -jets, recent results on two-photon processes from DESY 7-61786
 $\gamma\gamma$ reactions, inclusive and exclusive final states, jets and total cross sections 7-61783
 $\gamma\gamma^*$ collisions, P_T and Q^2 depend. of multijet prod., 2, 3, and 4 jets 7-5137
 $\gamma p \rightarrow \Delta p X$, diffractive production meas., cross-sections and distribts. 7-41823

elementary particle inclusive interactions continued

- $\gamma p \rightarrow \pi^+ X$, diffractive production meas., cross-sections and distrib. 7-41823
 $hd \rightarrow pX$, π rescattering contrib. to p cumulative prod. 7-41861
 $hh \rightarrow X$, approach to chaos in high energy collisions 7-49187
 $hh \rightarrow X$, central fireball, momentum and mass distrib. 7-41851
 $h_1 h_2 \rightarrow V(t)X$, $V(t) \rightarrow \gamma$, Z^0 , $Z^0 \rightarrow ll$, weak neutral currents, expt. possibilities, lepton longitudinal polarization 7-5098
 $hN \rightarrow \gamma \gamma_{\text{opp}} + X$, $q\bar{q} \rightarrow \gamma\gamma$, $gg \rightarrow \gamma\gamma$, $qg \rightarrow q\gamma\gamma$ mechanisms, perturbative QCD anal. 7-61592
 $K^+ d \rightarrow \eta X$, $\eta \rightarrow 2\gamma$, 10 GeV, differential cross section meas., quark-fusion model anal. 7-5124
 $L \rightarrow \bar{u}d\bar{c}(s\nu)$ (L =heavy lepton), event search at CERN collider 7-61680
 $lN \rightarrow X$, deep inelastic scatt., two-photon collisions 7-19115
 $NK \rightarrow \phi X$, joint hadron prod., parton model comparison 7-19143
 $NK^+ \rightarrow \phi X$, low p_T interactions, Lund model comparison 7-19142
 NN in rel. nuclear collisions, charged particle multiplicity distrib., correl. characts. 7-19140
 $nn \rightarrow X$, 6.1 GeV/c, charged particle multiplicity characts. 7-30282
 $nn \rightarrow X$, high energy cosmic rays, particle production, multiplicity 7-47652
 $NN \rightarrow X$, multiplicity and transverse energy flux 7-61758
 $NN \rightarrow X$, quark-gluon dynamics and selection rules 7-30277
 $NN \rightarrow X$, quark-gluon plasma formation 7-56579
 $Np(\bar{p}) \rightarrow \phi X$, joint hadron prod., parton model comparison 7-19143
 $Np(\bar{p}) \rightarrow \phi X$, low p_T interactions, Lund model comparison 7-19142
 $\bar{n}p \rightarrow X$, inclusive ρ^0 and f^0 cross-sections 7-10072
 $np \rightarrow X$, multiplicity of γ -rays and π^0 , additive quark model comparison 7-42010
 $N\pi^+ \rightarrow \phi X$, low p_T interactions, Lund model comparison 7-19142
 $\bar{\nu}e \rightarrow \text{gaugino} + X$, poss. μ prod. from Cyg X-3 7-23962
 $\nu N \rightarrow X$, multiplicity of charmed mesons and baryons, quark parton model 7-41783
 (p,X) , X =hadrons, inclusive process, multi-quark configurations in nuclei 7-61882
 $pd \rightarrow K^+ X$, low-energy annihilation, cross section meas. 7-15169
 $pd \rightarrow \Delta X$, low-energy annihilation, cross section meas. 7-15169
 $pN \rightarrow \Delta X$, 13, 18 GeV/c, polarization transfer meas. 7-30294
 $pN \rightarrow X$, inclusive charged particle differential cross-section 7-35911
 $pN \rightarrow X$, primary energy estimation 7-5128
 $pp \rightarrow \pi^0 X$, $\sqrt{s_{NN}}=31$ GeV, high p_T invariant cross section meas. 7-35907
 ϕ production in heavy ion collisions (light pseudoscalar boson), QED calcs. 7-36022
 $\pi^+ d \rightarrow \eta X$, 10.5 GeV/c, A-dependence of η inclusive production 7-30296
 $\pi^+ d \rightarrow \eta X$, $\eta \rightarrow 2\gamma$, 10 GeV, differential cross section meas., quark-fusion model anal. 7-5124
 $\pi N \rightarrow \phi X$, joint hadron prod., parton model comparison 7-19143
 $\pi^- N$ -charged mesons, search results 7-61765
 $\pi^- N \rightarrow \mu^+ \mu^-$, 194 GeV/c, $\mu^+ \mu^-$ angular distrib. meas., QCD comparisons 7-563
 $\pi^- N \rightarrow p_{\text{back}} X$, on nuclear targets, 40 GeV/c, invariant cross sections 7-35914
 $\pi^- N \rightarrow \pi X$, 4 GeV/c in ^{12}C , multiplicity of charged and neutral particles 7-19131
 $\pi^+ N \rightarrow \mu^+ \mu^- X$, 80, 225 GeV, pion struct expt. 7-61693
 $\pi^+ N \rightarrow pX$, inclusive distributions, isospin subtraction technique 7-35916
 $\pi^- p \rightarrow \text{charm hadrons}$, 360 GeV/c, hadron decay props. 7-562
 $\pi^+ p \rightarrow X$, rapidity depend. of negative and all-charged multiplicities 7-558
 $W^\pm \rightarrow L \bar{\nu}$ (L =heavy lepton), event search at CERN collider 7-61680
 $Wg \rightarrow U\bar{D}$, heavy quark production, cross section calcs. in effective W approximation 7-61771
 $Wg \rightarrow U\bar{D}^*$, heavy squark production, cross section calcs. in effective W approximation 7-61771
 $Z^0 \rightarrow \nu\bar{\nu}$ (ν =new neutrino species), event search at CERN collider 7-61680
 $pN \rightarrow \Lambda^0 X$, polarisation in inclusive production, A dependence 7-15177
 $pN \rightarrow X$, inclusive spectra of secondary particles in quark-gluon string model 7-41859
 $\pi^+ N \rightarrow \pi^- X$, role of coherent diffraction in inclusive production of particles on nuclei 7-41860
 $\pi^+ \rho \rightarrow \rho^{\pm 0} \omega$, 250 GeV/c, inclusive cross section meas. 7-61755

elementary particle interaction models

- see also bootstrapping; composite models of hadrons; diffraction model; duality and dual models; peripheral models; statistical models; vector meson dominance model*
 annihilation reactions, spatial and temporal asymptotic behaviour 7-49123
 baryon mass spectrum, convexity props. in pot. models with flavour independence 7-503
 baryon spectroscopy effective intermediate range quark-quark interaction (*Chinese*) 7-49070
 conference on nuclear scatt. data eval. methods, Berlin, Germany (June 1985) 7-21
 dibaryons, positive parity, strangeness -1 potential model anal. 7-24846
 experiment and theory in high energy physics 7-35845
 form factors and static props. in relativistic potential model 7-15157
 four-quark states in heavy quark systems, pot. model study 7-41706
 heavy quark meson decay constant calcs., nonrelativistic QCD potential model anal. 7-10054
 heavy quarkonium pot. models, Green's function Schrodinger eqn. calcs. 7-15121
 light quark pair prod. in heavy quarkonia, pot. model study 7-41720
 light quark systems, potential models 7-61634
 meson-exchange currents in time-like axial-charge transitions, review 7-56532
 multi-quark systems, flux tubes and many-body props. 7-41704
 nonrelativistic interaction models with infinities, renormalisation, Green's function 7-30171
 Pamir expt. data, comparison with strong interaction model with weak scaling violation 7-10038
 quark matter, conference, Pacific Grove, CA, USA (April 1986) 7-55881
 relativistic potential model, center of mass corrections 7-15138
 relativistic potential model for Dirac particle, bound state level ordering 7-61465
 resonances and surface waves in nuclear and particle physics 7-608
 Schrodinger equation, local equivalent, with relativistic kinematics, WKB approximation 7-56406

elementary particle interaction models continued

- short-range repulsion and parameters of the NN interaction (*Chinese*) 7-49175
 squeezed coherent states and hadronic multiplicity distributions, quantum optical model 7-35843
 supersymmetric models of particle physics and their phenomenology, review 7-56467
 two-particle potential in: $\lambda(\phi^6 - \phi^4)$: field theory 7-49120
 ultra-relativistic hadronic collisions, pion interferometry 7-56565
 $\bar{c}c$ mass shift near deconfining temp., $c\bar{c}$ potential model anal. 7-19077
 $hd \rightarrow pX$, π rescattering contrib. to p cumulative prod. 7-41861
 $hh \rightarrow X$, central fireball, momentum and mass distrib. 7-41851
 $K^+ N$, elastic scattering, partial wave anal., SAID computer package 7-550
 NN , elastic scattering, partial wave anal., SAID computer package 7-550
 $NN \rightarrow NN\pi$, model depend. of unitary isobar model treatments at intermediate energy 7-5116
 NN phase shift anal., optimum polynomial expansions 7-548
 pp , high energy elastic scatt., Chou-Yang conjecture 7-61743
 pp , low energy scatt., phase shift anal. 7-547
 pp elastic scattering, 10-100 GeV, impact-parameter representation anal., comparison with pp 7-35906
 $pp \rightarrow K_L K_S(K_S K_S)(K^- K^+)$, baryon exchange model anal., cross sections, resonances 7-30287
 $pp \rightarrow p\pi^+ \pi^+$, 800 MeV, unitary meson-exchange calc., spline function method 7-30288
 $pp \rightarrow pp\gamma$, cross sections and analyzing power, pot. model calcs. 7-5115
 πN , elastic scattering, partial wave anal., SAID computer package 7-550
 $q\bar{q}$ pair condensation, 3P_0 , QCD anal. using Coulomb plus Breit potential 7-61597
 $q\bar{q}$, nonsingular potential calc., quasistatic approximation 7-61607
 $K^+ N$ channel coupling, quark pot. model with resonating group method 7-41705

elementary particle interactions

- see also elementary particle coupling constants; elementary particle electromagnetic interactions; elementary particle gravitational interactions; elementary particle inclusive interactions; elementary particle large momentum transfer interactions; elementary particle scattering; elementary particle strong interactions; elementary particle weak interactions; hadron-deuteron interactions; hadron-hadron interactions; high-energy cosmic ray interactions; lepton-deuteron interactions; lepton-hadron interactions; lepton-lepton interactions; photon-deuteron interactions; photon-hadron interactions; photon-lepton interactions; photon-photon interactions; polarisation in elementary particle interactions; quantum field theory of interactions; unified field theories; vertex functions*
 dyon(Kaluza-Klein)-fermion interactions 7-56583
 experiment and theory in high energy physics 7-35845
 experimental design and simulation system 7-49194
 fifth force, anal. of Eotvos experiments 7-35385
 high energy physics event processing on vector computer 7-15180
 monopole-fermion interactions, SU(5) anal., Abelian and nonAbelian anomalies 7-9996

elementary particle large momentum transfer interactions

- see also elementary particle inclusive interactions*
 deep inelastic QED Compton scatt., topological isolation, inclusive cross sections 7-49157
 direct photon production, nuclear depend. for large p_T , parton distrib., gluon distrib. 7-5063
 $\gamma\gamma^*$ collisions, P_T and Q^2 depend. of multijet prod., 2, 3, and 4 jets 7-5137

elementary particle magnetic moment

- see also baryon magnetic moment; lepton magnetic moment; meson magnetic moment*
 fermion-scalar system, potential model anal. of magnetic moment and form factors 7-61691
 W bosons, anomalous magnetic moment, new bound 7-41814
 $\gamma e \rightarrow W\nu_e$, W prod. and decay diff. cross sections, beam pol. and anomalous mag. moment effects (*Russian*) 7-30299
 W, anomalous magnetic moment anal. in polarized e^+e^- collisions 7-24870
 W, composite particle, magnetic moment calcs. 7-49149
 W^\pm , Z^0 self interactions, Lagrangian containing quadrupole terms and anomalous magnetic moments 7-61515
 $Z^0 \rightarrow ll\gamma$, Stokes parameter calcs. and anomalous mag. moment 7-41807
 $Z^0 \rightarrow q\bar{q}\gamma$, Stokes parameter calcs. and anomalous mag. moment 7-41807
 $Z^0 \gamma\gamma$ and $Z^0 Z^0 \gamma$ Green's functions, Ward identity derivation 7-41817
 W^\pm , μ_W meas. proposals as electroweak model test 7-15156

elementary particle mass

- see also hadron mass; lepton mass; mass differences; mass formulae*
 axions, rest mass and Universe dark matter 7-60524
 confined Yang-Mills field, propag. props. and condensate form. 7-48991
 constituent quark mass and nucleon properties in nuclei 7-49088
 dynamical quark mass, mass-shell props. 7-24834
 $E_8 \times E_8$ superstring theory, extra U(1) phenomenology, Z boson mass constraints 7-41688
 $E_8 \times E_8$ superstring theory, quark mass generation constraints 7-41686
 electroweak Glashow-Weinberg-Salam theory, one-loop effects 7-61509
 fermion mass determination, Weinberg model 7-49021
 fermion mass matrices in unified models 7-446
 fermion masses in E_7 unified model 7-61536
 gauge hierarchy problem, mass generation by nonperturbative quantum effects 7-19007
 gaugino mass contributions in low-energy limit of superstrings 7-24812
 glueball mass in SU(2), effect of dynamical quarks 7-61501
 gluon, magnetic mass in QCD, two loop approx. 7-61563
 gluon mass in quenched Eguchi-Kawai model, momentum-space Monte Carlo method 7-19065
 Goldstone-Higgs particle mass, internal subgroup prediction 7-35756
 heat-kernel regularization of gauge theory, vanishing gluon mass 7-41624
 heavy quark dynamical mass, electroweak symmetric breaking, extended technicolour sector simplification 7-24837
 hierarchical quark-lepton masses and intermediate massscale in GUT 7-5016
 Higgs boson mass upper bounds in electroweak interaction models 7-19054
 Higgs doublet models, bounds on masses 7-61537
 Higgs field mass parameter, perturbative evolution in SUSY gauge theory 7-408

elementary particle mass continued

Higgs-boson doublets, model, with no increase in parameters 7-15110
inflationary cosmology in supergravity framework, fermion masses 7-48514
Kaluza-Klein theory, symm. breaking and vector boson masses 7-41192
Kobayashi-Maskawa matrix elements, expt. determination 7-56487
lattice Monte Carlo simulation with Wilson fermions, current algebra, quark masses 7-15069
lattice QCD, light hadron and quark masses, large lattice results 7-15139
lattice QCD, quenched SU(2) simulation, quark mass behaviour 7-61602
N=1 supergravity, SU(3)×SU(2)×U(1) models, superparticle and t-quark masses 7-41228
nonAbelian family symm., origin of fermion masses and mixing angles 7-19041
photinos, cosmological constraints 7-66793
quark mass and spin effects in meson wave functions 7-41744
quark mass effect on colour ferromagnet model of QCD vacuum 7-24842
quark mass matrices in standard electroweak model, maximal CP violation, anal. for many quark generations 7-30215
quark mass matrix under S₄ symmetry 7-61510
quark weak-interaction flavour mixing 7-61530
quarks, four generation mass fixing 7-61511
quarks, upper mass limits in model analysis 7-19006
radiative corrections to vector boson masses for heavy Higgs bosons 7-30272
shadow matter mass/charge constraints, from beam-dump expts. 7-49186
squark and gluino mass limits from CERN pp collider 7-56464
Stech mass matrix with fourth-generation quarks 7-462
symmetry tests in particle masses, review 7-30205
d quark-D fermion mixing, D=E_c fermion, KM mixing angle, SU (5) mass relation study 7-61528
e⁺e⁻, 46.8 GeV, excited quarks search at CELLO, final state topologies 7-30276
e⁺e⁻→X, single photon search and supersymmetric particle mass limits 7-533
pp → gluinos, squarks, search at Tevatron collider energies 7-24921
pp in standard model, m_t<m_W 7-49031
q mass matrices and symmetry props. of electroweak model 7-61529
q masses from preon model with three SU₃ hypercolours and three SU₅ hyperflavours 7-49026
q masses in Fritsch-Stech quark model in SO(10) 7-61547
W, astrophysical bound 7-5005
W mass limits from W, Z decays, SUSY signal 7-61682
W[±], effects of SU(2)_L×U(1)_Y×U(1)_{Y*} and SU(2)_L×SU(2)_R×U(1)_{B-L} gauge structures 7-61708
Z, mass limits from W, Z decays, SUSY signal 7-61682
Z masses and couplings, bounds in SO (10), E₆ GUTs from electroweak corrections 7-61527
Z', effects of SU(2)_L×U(1)_Y×U(1)_{Y*} and SU(2)_L×SU(2)_R×U(1)_{B-L} gauge structures 7-61708

elementary particle scattering

see also bootstrapping; elementary particle interactions; hadron-deuteron scattering; hadron-hadron scattering; lepton-deuteron scattering; lepton-hadron scattering; lepton-lepton scattering; Mandelstam representation; photon-deuteron scattering; photon-hadron scattering; photon-lepton scattering; photon-photon scattering; polarisation in elementary particle scattering; Pomeronchuk poles and trajectories; quantum field theory of elastic scattering; Regge poles and trajectories; relativistic scattering theory; S-matrix theory
charge-monopole scattering, Green fn. calc. 7-56584
resonances and surface waves in nuclear and particlephysics 7-608
Schrödinger inverse scattering problems, 3D anal. using differential and integral methods 7-18638
three particle bound state, use of bicubic splines for solving the Faddeev integro-differential equations 7-41757
γq Compton scatt., NA14 expt. results 7-61785
qq→qq, (q=u,d,s), low-energy amplitudes, meson masses, N/D dispersion method anal. 7-61549
u→ū, quark scattering on SU(5) colourless magnetic monopole 7-30300

elementary particle spin and parity

see also hadron spin and parity; lepton spin and parity
basis states for relativistic three-body calculations of particles with spin 7-19032
high energy spin physics and QCD tests 7-30236
interacting bosonic gauge fields of any spin and parity 7-15071
pseudoclassical spin 1/2 particle models, classical trajectory and spin precessions 7-18997

elementary particle strong interactions

see also composite models of hadrons; duality and dual models; hadron classification schemes; peripheral models; quantum field theory of strong interactions
conference, strong interactions and gauge theories, Les Arcs, Savoie, France (March 1986) 7-60876
light mesons, strong decays of radial excitations, relativistic model 7-19107
long-range NN force, search at highly relativistic velocities 7-498
multiquark states in QCD-like pot. model 7-41718
Pamir expt. data, comparison with strong interaction model with weak scaling violation 7-10038
parity invariance, strong and electromagnetic interactions 7-9995
QCD, implications of nucleon struct. determ. by deep inelastic lepton scatt. 7-10028
strongly interacting Higgs sector, σ-model simulation 7-48975
pp elastic scattering, 198.5 MeV, time reversal invariance test in strong interaction, polarization-analyzing power comparisons 7-5110

elementary particle symmetry

see also chiral symmetries; conservation laws; discrete symmetries; dynamical symmetry; helicity (elementary particles); isotopic spin (elementary particles); nonlinear symmetries; spontaneous symmetry breaking; SU_n theory; supersymmetry
bosonic massless gauge fields with arbitrary spin and permutation symm. 7-4960
Dirac equation symmetry, with external nonAbelian gauge field 7-41589
E₇ unified model based on coset space dimensional reduction scheme, fermion masses 7-61536
electron hidden U(3) symmetry, Zitterbewegung and degrees of freedom, Dirac eqn., Lie algebra 7-19031

elementary particle symmetry continued

flavour symmetries, realization in large N lattice QCD with Susskind fermions 7-15123
flavour symmetry, dynamical breaking and scalar exchange 7-30210
interacting bosonic gauge fields of any spin and parity 7-15071
nonperturbative BRS invariance and the Gribov problem 7-61454
Sp(2N), N fermion generation gauge group, existence of Z⁰ for N=4 7-9994
staggered fermion symmetry group, irreducible representations 7-19024
U(1) gauge symmetry, existence of paraton 7-9992
elementary particle theory
see also Bethe-Salpeter equation; complex angular momentum plane; current algebra; dispersion relations; electron theory; elementary particle interaction models; elementary particle symmetry; Feynman diagrams; form factors (elementary particles); group theoretical schemes; helicity (elementary particles); isotopic spin (elementary particles); Lee model; mass formulae; O groups; quantum field theory; S-matrix theory; scaling phenomena; SO groups; structure functions; sum rules; vertex functions
antiparticle representations in local observables theory 7-56472
book field theory in particle physics. Vol.1 7-4641
conference, Japanese Physical Soc., Kobe, Japan (Oct. 1986) (Japanese) 7-55897
cosmology and particle physics 7-48117
fine structure constant, numerical value explanation (German) 7-49122
future trends 7-49124
graph theoretical particle model 7-10049
hadron spectroscopy, particle and nucl. physics intersections conf., Lake Louise, Canada, May 1986 7-29569
hermitean oscillator-like realisations of classical algebras and superalgebras in Hilbert space 7-41655
lepton spectrum derivation using the TLVP EM model 7-61638
magnetic flux linking and enclosure 7-35844
mass parameters in renormalized perturbation theory, absence of log., growths 7-41641
nomenclature and basic concepts (Italian) 7-505
physics in terms of difference equations 7-49125
quantised fibre-bundled space, charged particle motion and charge density 7-41584
quantum mechanics from general relativity, theory of inertia, book 7-48215
stability, catastrophe theory on the space-time manifold 7-24808
statistical physics and field theory conf., Groningen, Netherlands, Aug. 1985 7-55899
transformation of elementary particle physics into many-body physics 7-49042
two-particle potential in: λ(φ⁶-φ⁴): field theory 7-49120

elementary particle weak interactions

see also charged currents; intermediate bosons; neutral currents; quantum field theory of weak interactions
charged leptonic weak interaction data from muon decays 7-56535
evolution and history 7-18548
generalized covariant field theory of electrodynamics, flat space-time limit 7-41694
hypernuclei, weak decay, exptl. review 7-49282
hypernuclei, weak decays 7-49283
left-right symmetric models of weak interactions 7-56498
nuclei, weak and EM interactions, conference, Heidelberg, Germany (July 1986) 7-48172
oriented nuclei far from stability, weak interaction studies 7-56601
shell model anal. weak and EM data, many body and single nucleonic features 7-49255
SU(4)×SU(4) composite model of weak interactions (Chinese) 7-10037
virtual meson flow in weak interaction, HFR exptl. program (Dutch) 7-19175
weakly decaying charmed baryon lifetime differences due to preasymptotic bound state effects 7-41801
NN interactions in nuclei, time-reversal symmetry test using (n,n') 7-30347
ν_e mass, weak forces and oscillations (Danish) 7-440
νN→νN, abnormally large coherent cross-section 7-49130
Wg→UD, heavy quark production, cross section calcs. in effective W approximation 7-61771
Wg→UD*, heavy squark production, cross section calcs. in effective W approximation 7-61771
¹¹B_Λ, hypernuclear lifetimes, neutron stimulated fraction meas., weak decay 7-41932
¹²C_Λ, hypernuclear lifetimes, neutron stimulated fraction meas., weak decay 7-41932
^AHe_Λ, A=4,5, hypernuclear lifetimes, neutron stimulated fraction meas., weak decay 7-41932

elementary particles

see also bosons; charm particles; fermions; gamma-rays; hadrons; hypothetical particles; leptons; quantum field theory; strange particles
electrodynamics, field theory on R×S³ topology 7-30271
nomenclature and basic concepts (Italian) 7-505

elements (chemical)

for specific metals and non-metals see appropriate chemical names
see also element relative abundance; periodic system of elements
charge distrib. in ion beam produced from RF-spark ion source 7-46883
medium-Z elements, Ka^x satellite, transition assignment, nonrelativistic single configuration HF calcs. 7-30941
single, element, ionisation equilib. theory, approximate soln. 7-19787
superheavy atoms, fractional charges, optical searches 7-10782
Cr and Cr-compounds, Auger and absorpt. spectra involving M_{2,3} levels, atomic effects 7-59311

Eliashberg strong-coupling model see strong-coupling superconductors

Elinvar

dispersion hardening and softening, elastic limit studies (Russian) 7-59539
Co-Fe-Ni-V alloys, Invar props. and mag. field distrib. (Russian) 7-45733

ellipsometers

see also ellipsometry
adjustment method allowing for compensator's optical activity 7-41429
automatic, birefringent components and systems meas. (German) 7-24687
IR automatic ellipsometer operation, optimum setting (Chinese) 7-48827
modulator, magneto-optic, highly efficient low field (French) 7-5989
nonlinear for polarisation meas. in ellipsometer optical nonlinear media 7-14993

ellipsometers continued

- polarisation state control, using fibre optics or Bragg cells 7-14992
- rotating-detector ellipsometer, response to partially polarised light 7-41427
- spectrometer, ellipsometric IR reflection absorption, design and performance 7-41494

ellipsometry

see also *ellipsometers; polarimetry*

- 7X GaAs, sputtered films, optical props., effective medium models (Chinese) 7-7774
- absorbing crystals, wave propagation, polaris. and rel. 7-10852
- arachidic acid, adsorbed layer on Ag, form. and struct., IR spectra, optical ellipsometry 7-44992
- birefringence meas. in single mode optical fibres 7-43428
- computer-based high resolution transmission ellipsometry 7-41428
- diphenyl cryst., surface melting, ellipsometry studies 7-32613
- eye, corneal polarisation, biaxial model for living human eye 7-59973
- fluorocarbon films plasma deposited on Si, ellipsometry studies 7-22373
- glass surface after ion-beam cleaning, ellipsometric investig. 7-43453
- inhomogeneous struts., ellipsometric data anal., complex refl. coeffs. determ. method 7-41430
- insulating oils, gamma-ray effects on elec. props. 7-48829
- magnetooptic multilayer films, permittivity tensor, photoelastic modulated ellipsometry 7-41426
- microstructure, visible-near UV spectroellipsometry and spectrophotometry studies 7-46758
- 4'-n-pentyl-4-cyanobiphenyl, well induced orientational order in isotropic phase, evanescent wave ellipsometry study 7-37857
- phase shifts of light wave on reflection, method for absolute values determ. 7-50490
- polished optical glasses, secondary ion mass spectroscopy and ellipsometric investig., correlation of results 7-43458
- poly-vinylacetate-Cu, thin polymer films, Fourier transform IR ellipsometry 7-53334
- rough surfaces, ellipsometry, depolarisation and cross polarisation 7-9873
- semiconductor multilayer structures, variable angle of incidence spectroscopic ellipsometric study 7-48830
- semiconductor wafers, surface temperature meas., non-contact method 7-41382
- spatially resolved ellipsometry, convergent beam approach 7-9874
- speckle polarisation analysis by ellipsometric method 7-42938
- spectroscopic ellipsometry, Al film surface roughness characterisation 7-9819
- thin films, optical constants and thickness meas. by two-incident angle ellipsometry (Chinese) 7-48828
- thin films, thickness and optical constants determ. from photometric and ellipsometric data 7-41419
- thin films and interfaces, characterisation by optical reflectance and ellipsometry 7-45084
- thin uniaxial nonabsorbing films, multiple-wavelength ellipsometry 7-33468
- ultrathin films, ellipsometric metrology using dual incidence angle meas., error anal., optimum angle determ. 7-24686
- vapour layer on liquid surface, mathematical model 7-20843
- Si, low energy ion beam damage, ellipsometric characterisation, two-film optical model 7-27680
- Al vacuum-deposited films, topography charactn. by ellipsometry 7-9817
- AlAs optical props., pseudodielec. function, spectroscopic ellipsometry meas. 7-52487
- Al₂O₃ thin films, spectral ellipsometric TEM and electron spectra studies 7-27208
- As-Se:Ag amorphous films, Ag doping profiles, ellipsometric studies 7-7779
- Au film, optical props. 7-17296
- Au films, optical thickness and filling factor determ. 7-39197
- a-C:H films, plasma deposited, optical props. 7-27799
- C-W multilayers, sputtered, ellipsometry monitoring, X-ray refl., XPS 7-39376
- C-W ultrathin layered stacks, sputtering techniques, in situ ellipsometry control system 7-1292
- CeB₆, optical props. and band struct., spectroscopic ellipsometry meas. 7-13157
- Co optical props., refl. and spectroscopic ellipsometry meas., hybridisation effects 7-39073
- CoSi₂ optical props., refl. and spectroscopic ellipsometry meas., hybridisation effects 7-39073
- Cu (111)-Fe crystal, CO adsorption 7-21616
- Cu (111)-Fe surface alloys, prep. and oxidation 7-22870
- Cu, polished surface, ellipsometric study of reflection 7-13121
- CuCl, giant two-photon excitation of excitonic molecules, nonlinear depolarisation effects 7-64594
- Fe (100) 7-8154
- Fe surface oxide layer, reduction by H adsorption, AES and LEED studies 7-8297
- GaAlAs-GaAs heterostructures grown by MOCVD, transition region, ellipsometric anal. 7-2388
- GaAs surface oxidation, AES, XPS and ellipsometry studies 7-22927
- GaAs-Al_{0.5}Ga_{0.5}As multiple heterostructures, variable angle of incidence spectroscopic ellipsometry 7-39055
- Ge, growth surface optical characts. oscills. during MBE, automatic reflection ellipsometry meas. 7-64715
- Ge, single crystal, optical constants, surface polishing effects 7-59175
- a-Ge:H glow discharge deposited thin films, H content determ., spectroscopic ellipsometry study 7-38365
- Ge-Se:Ag amorphous films, Ag doping profiles, ellipsometric studies 7-7779
- In_{1-x}Ga_xAs_{1-y}P_y/InP heterojunctions, MOCVD grown, spectroscopic ellipsometry study 7-39195
- LaB₆, optical props. and band struct., spectroscopic ellipsometry meas. 7-13157
- MgF₂ films deposited on fused SiO₂ with ion beam assistance, adhesion, internal stresses 7-21749
- Ni (111), CO adsorption, well defined gas-solid interphase, statistical rate theory approach 7-21655
- Ni, oxidation, oxide epitaxy depend. on growth temp., LEED, AES, ellipsometry studies 7-22869
- NiSi₂-Si, epitaxy of NiSi₂, study using an MBE system with automatic ellipsometer, nondestructive anal. 7-7058
- Pb thin film, optical constns. in visible region 7-7662
- Pd silicide formation, in situ ellipsometric studies 7-21694

ellipsometry continued

- Si (111) surface, study using an MBE system with automatic ellipsometer, nondestructive anal. 7-7058
- Si, complex refractive index meas. during pulsed laser annealing 7-45970
- Si, ion implantation, damage profile studies, multilayer model (Chinese) 7-6648
- Si, ion implanted, damage profiles, multilayer anal. by optical spectra (Chinese) 7-58294
- Si polycrystalline films, optical props. 7-7782
- Si rough surfaces, ellipsometry spectra, Ohlidal-Lukes model anal. (Chinese) 7-13109
- Si:As, ion implantation, damage profiles determ. by spectroscopic ellipsometry and stripping (Chinese) 7-32468
- a-Si:H, glow discharge deposited, nucleation, substrate temp. effects 7-22504
- a-Si:H, glow discharge deposition, surface roughness evolution 7-64933
- a-Si:H, surface structure, inert gas plasma exposure effects 7-21584
- Si:H (100) proton bombarded surface, complex refractive index profile, ellipsometry study 7-22216
- a-Si:H films, growth habit, influence of substrate struct., ellipsometry study 7-45055
- a-Si:H surfaces and interfaces, microstruct., ellipsometry studies 7-38362
- a-Si:H thin films, bulk and interface struct., in situ ellipsometry study 7-27200
- a-Si:H/a-Si₃N₄ heterostructures, interface formation and microstructural evolution 7-2389
- Si-Al₂O₃, SOS struct., UV reflectance meas., ellipsometry study 7-33414
- Si-Ge, epitaxial growth of Ge, study using an MBE system with automatic ellipsometer, nondestructive anal. 7-7058
- Si-SiO₂, interface props., ellipsometry (Russian) 7-17293
- Si-SiO₂, interface struct., ellipsometric charactn., rel. to elec. props. 7-63985
- SiO₂, gate dielectric films, growth by rapid thermal processing, material and electrical props. 7-16906
- SiO₂, optical waveguides, low-loss planar, fabrication using thermal nitridation and charactn. 7-26032
- SiO₂-Si₃N₄, multilayer nonabsorbing systems, multiple angle of incidence ellipsometric anal. 7-39203
- SiO₂-Si₃N₄-MgF₂, multilayer nonabsorbing systems, multiple angle of incidence ellipsometric anal. 7-39203
- SiO₂N₂, high press. NH₃-nitrided, elec. characts. 7-39039
- Ti surface oxide films, anodic and cathodic polarisation, ellipsometric anal. (Japanese) 7-33828
- W LPCVD film thickness depend. on native oxide thickness 7-17473
- ZnS film, ellipsometric in situ studies of growth 7-39196

elliptical polarisation see *polarisation***ELNES** see *electron energy loss spectra***elongation**

see also *deformation; thermal expansion*

- brass plated steel cords, mech. and cohesion props. in sulphurising environment 7-39740
- fibre reinforced composites, flexible, nonlinear elastic behaviour 7-39570
- fibres, natural, fracture behaviour, empirical evaluation of struct.-prop. relationships 7-39633
- glass fibre, softening point determ., numerical method, calculator program (Czech) 7-6796
- Li₂ ordered alloys, grain boundary strength and fracture, electronic and struct. studies 7-33756
- lignocellulosic fibres, phys. and mech. props. 7-53883
- necking development under uniaxial tensile deform., strain hardening, geometric defects, elongation to failure 7-33742
- nylon 6 composites, formed by in situ polymerisation of caprolactam, mech. performance 7-39575
- pineapple leaf fibre reinforced rubber, phys. and mech. props. 7-3378
- poly ether ether ketone film, zone annealing prep., dynamic modulus, tensile strength 7-8038
- polydimethylsiloxane melt, molecular orientation induced by elongational and shearing strains 7-44347
- polyesters, cycloaliphatic, stress optical behaviour 7-45975
- polyimide films, uniaxially-stretched, conductivity and dielec. losses 7-39005
- polyisoprene, cis- and trans-, blends, props., meas. 7-13517
- polymer solutions, phase changes during elongational flow 7-51237
- polypropylene mica filled composites, struct.-mech. props. relations 7-1919
- PVC-thermoplastic copolyester elastomer blends, γ -irrad., mech. props., fractography 7-21317
- PWR fuel rods, power ramp data, FROST and THERMOST codes, cladding deform. rod elongation 7-62034
- rubber, electroconductive, for flexible electrogoniometer, clinical use (Japanese) 7-14139
- steel, Al-killed, flow behaviour after tensile prestraining and strain ageing 7-17595
- steel, austenitic, Al-Mn, mech. props., oxidation and corrosion behaviour 7-65218
- steel, austenitic stainless, Mo-ion plated, corrosion resist. in flowing Na environment 7-59667
- steel, austenitic stainless, tensile, creep and low-cycle fatigue props., effect of prestrain (Japanese) 7-46621
- steel, C-Mn and Nb treated, high temp. ductility loss, grain boundary segregation 7-46573
- steel, CrMoV, cold rolled, effects of ageing on mechanical properties (Russian) 7-13478
- steel, dual-phase, micro alloyed, mech. props. and struct., effect of process variables 7-65108
- steel, ferrite, low activation, correl. of hot microhardness with elevated temp. tensile props. 7-53797
- steel, HSLA, TM-rolling, role of reverse temper embrittlement 7-8112
- steel, Mn-Al-Nb, cryogenic, low temp. tensile props., effect of Al content 7-46576
- steel, Ni-Cr, tensile flake form., H damage, dislocation transportation (Chinese) 7-8077
- steel, stainless, ductility rel. to cold working 7-22759
- steel, stainless, transition class, deform. method effect on microstruct. 7-3299
- steels, stainless, α -particle irradiated, mech. props. and microstruct. 7-51872
- thermoplastic materials, erosion resistance, angular particle impingement at normal incidence 7-3442
- viscoelastic fluids, kernel function for constitutive eqn. 7-6172

elongation continued

- whisker-type monocrystal, elastic limit rel. to phys. characts. 7-2443
 wollastonite reinforced polyamide 6, strength props., depend. on humidity and temp. 7-39636
 Zircaloy-4, temp. depend. of elongation 7-65094
 Al-Al₂O₃-MgO, cast particulate composites, microstruct. and mech. props. 7-65086
 Al-Fe-Si-TiO₂, dispersion hardened, strength props., effect of matrix particle size and oxide vol. fraction 7-17544
 Al-Li-Cu-Mg-Zr die forgings, mech. props., microstruct. 7-46636
 Al-Li-Cu-Mg-Zr powder alloy, superplastic, high modulus and hardness 7-53816
 Al-Zn-Mg-Mn-Si, rapid solidification, superplasticity 7-53826
 Au wires, very thin, fatigue 7-39671
 Co-Cr surgical implant alloy, mech. props., effects of N additions 7-59573
 Co-Si-B, change of elongation, rel. to conditions for hot working 7-3384
 Cu, dynamic elongation determ. expanding ring test, 2D hydro-plasto-dynamic code anal. 7-33755
 Cu wires, very thin, fatigue 7-39671
 Cu-Al-Fe, Al bronze, superplasticity, effect of Fe content 7-65109
 Cu-GeO₂, dispersion hardened polycrystals, intermediate temp. embrittlement 7-53903
 Cu-Ti-Al single crystals, strain hardening due to multiple twinning (*Russian*) 7-46501
 Cu-Zr (0.5 wt.%), high strength, high cond., prod. by rapid solidification technology 7-28029
 Fe, cast, bainitic ductile, microstruct. rel. to comp. and heat treatment 7-39579
 Fe-Cu, pore form. during sintering, effect on mech. props. 7-64970
 Fe-graphite compacts, sintering, alloying, mech. props. 7-39455
 Fe-Ni, austenitic, Mag. ordering and mech. props. (*Russian*) 7-58280
 Fe-Ni austenitic alloys, martensitic transformations, grain size effects (*Russian*) 7-46465
 Fe-P-Cu(Ni)(Mo), sintered atomised powder premixes, mech. props. 7-7931
 Fe-Si alloy wires, rapidly solidified by in-rotating-water-spinning method, prod. and props. (*Japanese*) 7-22654
 Fe-Ti-N, mech. props. rel. to cold working 7-28089
 Nb-D, implanted, lattice distortion, channelling method 7-58382
 Nb₃Sn tape, Cu-coated, effect on crit. bending diameter (*Russian*) 7-33747
 Ni alloys, struct.-sensitive props., effect of external thermal action 7-46558
 Ni-Cr-W superalloy, experimental, tensile props., effect of carburisation and aging 7-59576
 Ni₃Al-B, elevated temp. ductility, effect of testing environment 7-39614
 Ni₃Al-Be, ductility, strength, grain boundary segregation, solid soln. strengthening, Be addition effect 7-39608
 NiCoCrAlY, plasma sprayed coatings, low cycle fatigue behaviour 7-22793
 Pb-Al-Mg-Sn-Li, strength and microstruct. 7-8047
 Pb-Bi-Sn(In), alloy filaments, prod. by glass-coated melt spinning, enhancement of supercond. 7-58937
 Pb-Li, strength and microstruct. 7-8047
 PbTiO₃, spontaneous strain, anomalous press. depend. 7-26833
 Pt alloys, fast-quenched, struct. and props. (*Russian*) 7-59555
 Ta, dynamic elongation determ. expanding ring test, 2D hydro-plasto-dynamic code anal. 7-33755
 Ti-Al-Sn, weld metal, cryogenic toughness (*Japanese*) 7-46620
 Ti-Ni-Cu system metallic glasses, superplastic props. in vitrification temp. range 7-3356
 V and alloys, dispersion hardened, strength changes and recrystn. 7-17545
 W base heavy metal alloys, mech.-props., porosity, impurity effects 7-17495
 Zn-Al-Cu (ZZ,0.5%), superplastic behaviour 7-28093

EM waves see *electromagnetic waves*

embrittlement

- see also *ductile-brittle transition; hydrogen embrittlement; liquid metal embrittlement*
 Cr-MoVW ferritic steel, ductile-brittle transition temp., irradi. flux depend. 7-56825
 fusion materials, gas diffusion and temperature dependence of bubble nucleation during irradiation 7-51874
 fusion reactor structural alloys, irradi., creep fracture by grain boundary cavitation, modelling 7-53859
 fusion reactor structural materials, irradiation, He effects control 7-51845
 LWR pressure vessel surveillance using solid state track recorder neutron dosimetry 7-36199
 nuclear plant irradiated steel handbook 7-38069
 polyaminobismaleimide resin, dynamic recovery and embrittlement 7-38108
 rubber toughened plastic, surface embrittlement, fracture mechanics 7-28161
 steel, austenitic stainless, cold-worked, irradi. and unirradi., liq. Cs, Te-induced fatigue embrittlement 7-46637
 steel, austenitic stainless, grain boundary microstruct., He embrittlement resistance 7-56829
 steel, austenitic stainless, He-induced creep ductility loss, prediction and anal. 7-53854
 steel, austenitic stainless, in-beam creep rupture props. at 873K 7-53851
 steel, austenitic stainless, Ti-stabilised, high temp. embrittlement modification of rad. induced He distrib. by thermo mech. pretreatment (*German*) 7-17643
 steel, C-Mn and Nb treated, high temp. ductility loss, grain boundary segregation 7-46573
 steel, Cr-Mo, toughness, impurity element effects 7-53856
 steel, Cr-Mo-V type, heat resistant, impurities effect on temper embrittlement susceptibility 7-3419
 steel, Cr-Ni, microsegregation phenomena in long-term holding at 400°C 7-13458
 steel, Cr-Ni-Mo, fracture toughness rel. to austenitising temp. (*Japanese*) 7-33778
 steel, ferritic-pearlitic, welded joints, hot embrittlement proneness 7-39658
 steel, high temp. ductility, effects of B 7-46588
 steel, HSLA, TM-rolling, role of reverse temper embrittlement 7-8112

embrittlement continued

- steel, low alloy, rare earth-containing, temper embrittlement susceptibility, effect of S 7-65131
 steel, low-alloy, high-temp. drop in plasticity 7-46640
 steel, managing, precip. and notch toughness, effect of Cr (*Japanese*) 7-22798
 steel, Mn, lath martensite, embrittlement in specimens containing 6 to 10% Mn (*Japanese*) 7-33774
 steel, Ni-Cr, anelastic props. of grain boundaries and transition temp., effect of temper embrittlement 7-22815
 steel, Ni-Cr, ductile-to-brittle transition temp. shift due to temper embrittlement and neutron irradi. evaluation by small-punch test 7-28114
 steel, radiation embrittlement effects of P and Cu impurities 7-49535
 steel, reactor pressure vessel, neutron irradi. effect on mechanical and physical props. (*German*) 7-19358
 steel, secondary-hardening, bainitic embrittlement 7-3405
 steel, simulated void-box-capsule charpy impact test results, neutron irradi. effects 7-10231
 steel, stainless, austenitic-pearlitic, N effect on phase comp. and props. 7-53754
 steel, stainless, clad fuel rod, failure behaviour 7-61965
 steel, stainless, Cr type, chem. microinhomogeneity of solid solns. effect on brittleness 7-3422
 steel, stainless, powder compacts, props., influence of sintering conditions (*Korean*) 7-17496
 steel, stainless, repair welds, neutron irradiation embrittlement 7-5328
 steel, structural, temper embrittlement, preferential segregation, Auger spectra 7-53737
 Zircaloy oxidation and embrittlement criteria for emergency core cooling system acceptance, safety margins 7-36154
 Zircaloy-4 PWR fuel cladding, deformation, embrittlement and oxidation during LOCA 7-25036
 Al-Mg and Al-Zn-Mg alloys, plasma-coated, heat treatment effect on fine struct. and failure mechanism 7-3496
 Cr-base alloys, high-alloy, plasticity, effect of twinning (*Russian*) 7-46582
 Cu-Al-Ni, β -phase alloys, fracture rel. to grain boundary precip. and Ni content 7-59604
 Cu-GeO₂, dispersion hardened polycrystals, intermediate temp. embrittlement 7-53903
 Cu-Sn, ductility at elevated temps., effect of small amounts of B, P or Mg 7-53904
 Cu-Sn-B(Mg)(P), ductility at high temp., alloying additions effect (*Japanese*) 7-13515
 Cu-Zn, embrittlement in solidification process 7-3435
 Fe high temp. ductility, effects of B 7-46588
 Fe-B based metallic glasses, embrittlement, formation of B-rich zones 7-59598
 Fe-B-Ce-based metallic glasses, mag. domain structs. and annealing embrittlement 7-27586
 Fe-based metallic glasses, retardation of annealing embrittlement by Ce microadditions 7-65118
 Fe-Ni-Cr (25.15 wt.%), MC stabilized, fatigue life, effects of implanted He 7-53852
 Fe-Ni-Cr-Mo-Ti-C, JPCA, He injected and creep ruptured, microstruct. obs. 7-53853
 Fe-P-C system, ferritic, grain boundary segregation of P and C 7-39530
 Fe-Si alloy, high-Si, alloy elements influence on plasticity and mag. props. 7-8067
 Fe-Ti-N, mech. props. rel. to cold working 7-28089
 Fe₄₀Ni₄₀B₂₀ metallic glass ribbon, failure mechanics and atom probe study correlations 7-28139
 MgAl₂O₄/He spinel, implanted, high temp. electron irradi., structural damage 7-51829
 Mo and alloys, containing pores, segregation effects (*Russian*) 7-59533
 Mo single crystals, neutron irradiation embrittlement, yield strength 7-51854
 Mo-Ti-C system, embrittlement of ingots, role of phase stresses 7-3398
 Ni(B(s)), grain-boundary cohesion, impurity segregation effects, density-functional cluster model calcs. 7-44835
 Ni-Si, ductility, influence of rad.-induced segregation 7-53798
 Ni₃Al-B, with and without Hf additions, dynamic embrittlement at 600°C 7-65112
 Ni₄₅Pd₃₅P₂₀ metallic glass, decomposition, crystallisation and embrittlement, atom-probe FIM study 7-33639
 Ti-Al alloy, amorphous, rapidly solidified, high temp. oxidation 7-33841
 Ti-Al-Nb (6.2 wt.%), fusion weld, defect regions, cracking, porosity, interstitial analysis 7-28109
 U-Nb-Zr (7.5, 2.5 wt.%), SCC in gaseous O₂ and H₂ (*French*) 7-17619
 V alloys, neutron irradiation effects 7-53750
 W-Re alloys, mech. props., conc. depend. in different struct. conditions (*Russian*) 7-53876
 ZrNb1, fuel cladding, radiation induced embrittlement (*German*) 7-19359

EMC see *electromagnetic compatibility*

EMC effect

- colour dielectric model for nuclear binding and quark confinement 7-35936
 constituent quark mass and nucleon properties in nuclei 7-49088
 Drell-Yan processes, EMC effect (*Chinese*) 7-10070
 experimental status of the EMC effect 7-49151
 gluon condensate modification in nuclei and EMC effect 7-49279
 hadron-nucleus interactions, breaking of additivity of nucleons 7-24984
 hadrons flux tube model in nucl. matter, EMC effect 7-49272
 heretic model of confinement, EMC effect 7-49147
 nuclear dependence of structure functions 7-56602
 nuclear spectral function normalization and the EMC effect 7-56596
 nucleon structure functions in nuclei, EMC-SLAC effect calcs. (*Russian*) 7-30323
 (p,p'), spin-isospin response in nuclei 7-56682
 Q² dependence, nuclear binding and dynamical rescaling model anal. 7-19111
 QCD and Fermi gas model interpretations 7-49086
 QCD and higher twist, anal. of xF₃ 7-35793
 QCD evolution of structure functions, EMC effect study 7-61601
 quark and antiquark distrib., Q² rescaling approach 7-30316
 quark exchange in nuclei and the EMC effect, A=3 nuclei 7-61791
 quark-gluon plasma and EMC effect studies at CERN 7-49273
 review of the EMC effect 7-49146
 simple relativistic phenomena theory 7-61694

EMC effect continued

- SLAC data reanalysis and x rescaling 7-49233
 (e, e'), 0.1-1.0 GeV $^2/c^2$, nucleon magnetic moment and effective hadronic degrees of freedom 7-24973
 ($e, e'X$), deep inelastic scatt., nuclear binding and Fermi motion effects on $R_A = \sigma_L/\sigma_T$ 7-49232
 (e, X), deep inelastic scatt., vector meson dominance and EMC effect 7-30317
 (l, l'), deep inelastic process, nuclear binding, two body short range correlation effects 7-49386
 (l, eX), nuclear enhancement effect, colour oscillation mechanism 7-41987
 LN-X, deep inelastic scatt., direct interaction hypothesis 7-49160
 LN-X, EMC effect in terms of knock out reactions 7-49150
 μ N deep inelastic scatt., struct. function nucl. effects, EMC effect 7-30269
 μ N-X, quark-gluon structure study 7-49156
 N magnetic moment, scaling limits in nuclei 7-56554
 N quark structure changes, reanalysis 7-61688
 N size, nuclear medium effects 7-56599
 N size increase in nuclei 7-49152
 ^{12}C , dynamic and static longitudinal structure factors, RPA anal. 7-41884
 ^{40}Ca , dynamic and static longitudinal structure factors, RPA anal. 7-41884
 ^{56}Fe , dynamic and static longitudinal structure factors, RPA anal. 7-41884
 $^3\text{He}(e, e')$, EMC effect and high Q^2 three body physics at SLAC 7-56674
 $^3\text{He}(e, e')$, EMC effect and high Q^2 three body physics at SLAC 7-56674

emergency power generators see standby generators**emergency power supply**

- emergency diesel generator reliability at US nuclear power plants 7-42183
 nuclear power stations, safety equipment and emergency power supply (Hungarian) 7-25126

EMF see electric potential**EMI see electromagnetic interference****emission nebulae see nebulae****emission spectra see spectra****emissivity****see also brightness**

- alloys, spectral emissivity, 2-13 μm , 700-900K 7-44872
 black-body radiation, photon radiant and radiant exitance, analytic expression (Chinese) 7-50922
 blackbody radiant source, low temp. large area, with heat pipe (Chinese) 7-50923
 broadband pyrometer calibration, bandwidth effective emissivities of nonisothermal blackbody furnace 7-56271
 cylindro-inner cones, freezing point, radiant emission characts. 7-56254
 droplet surface temperature meas. with IR technique (Chinese) 7-48733
 earth surface, emissive props. model for radiometric meas. 7-66125
 glass fibres, Al coated, extinction props., thermal cond. meas. 7-52162
 graphite, laser heated, optical characts. 7-32686
 heat radiation, IR methods of temp. and process control 7-6082
 measuring apparatus, vac. high-temp. system 7-56272
 nonuniform materials spatial distrib. meas., NPL thermal imaging facility 7-4849
 pyrometric temperature measurement, effect of thin dielectric films on accuracy 7-18789
 quartz, emittance, blackbody comparison method meas. 7-58513
 refractory materials specific heat, resistivity and integral emissivity meas., automatic system 7-4842
 solar cell coverglass thermal characts., improvements by thin film coatings 7-13884
 solar heating units, paint coat thickness effects on radiation characts. 7-46968
 standards use in calibrating IR vision systems for biomed. use 7-60117
 steel, spectral emissivity, 2-13 μm , 700-900K 7-44872
 surface oxide films, on metals, spectral polarised directional emissivity meas., stratified media theory interpretation 7-17291
 surface temp. meas. of poor heat conducting materials radiation technique accuracy 7-26133
 transparent materials, spectral emissivity exam., using fast automatic system 7-4855
 B_2O_3 , melt, emissivity, nodal analysis (French) 7-63854
 Cu_2S films, chemically sprayed, optical and solar selective props. 7-54350
 Cu_2S films, flash-evaporated, optical props. and solar selectivity 7-64719
 KNO_3 , molten salt, emissivity, nodal analysis (French) 7-63854
 Si:P slotted surface, IR emission showing organ pipe resonant modes 7-44873
 W, oxidation, normal spectral emissivity meas., 800-1000K 7-26988
 WO_3 thin films, refractive indices, emissivity studies (French) 7-64718
 ZnO multilayers for solar collector coatings 7-3717

emitrons see television camera tubes**EMP see electromagnetic pulse****employees see personnel****employment****see also personnel**

No entries

emulsions**see also nuclear track emulsions; photographic emulsions**

- Aerosol-OT, stabilised microemulsion, X-ray scatt. data, fractal anal. 7-54190
 brine-toluene-n-butanol-Na-dodecyl sulphate system, diffuse interface in oil-in-water microemulsions 7-59788
 coalescent stratification intensity in turbulent flow 7-6266
 droplet clustering in microemulsions, electric birefringence study 7-28354
 dynamic gratings induced by electrostrictive compression of critical microemulsions 7-11032
 fractal cluster form. by aq. nanodroplets in apolar media, dielec. 7-39921
 liquid membrane, dicyclohexano-18-crown-6 mediated Ti^+ transport 7-13814
 many-body hydrodynamic interactions between spherical drops in an emulsion 7-16147
 micellar and microemulsion globules solvent induced attractions 7-54195
 microemulsions, interfacial phase transitions 7-33970
 microemulsions, interfacial props., critical roughening composition, disordered struct. 7-11893

emulsions continued

- microemulsions, rheological modelling salinity variations, viscosity properties, microstructural changes, Krieger-type formula 7-8307
 microemulsions and liquid crystals 7-1871
 model microemulsion, phase equilibria and critical endpoints 7-17828
 multilayer fluid membrane system in the lyotropic phase of quaternary microemulsion system, steric interactions 7-34116
 oil-water three component microemulsion, interfacial curvature studies 7-39930
 solvent-extraction systems, regularities in interfacial tension and emulsion unmixing 7-63903
 stirred percolation, annealed disorder, diffusion, continuous time random walk 7-61266
 styrene-n-butyl acrylate emulsion copolymers, microstruct., ^{13}C NMR 7-16390
 ternary microemulsion system, phase electric birefringence meas. 7-27699
 Tween 81-hexadecane- H_2O , props. in low-temp. region, struct., ^1H , ^2H and ^{13}C NMR 7-8318
 n-undecane, emulsion in sodium oleate stabilised water, conc. effect on aggregation 7-39926
 water-in-oil emulsions, adsorbed-solvated layers, optical obs. 7-59798
 water-in-oil microemulsion, exptl. evidence for interphasal water, scanning calorimetry anal. 7-3609
 water-oil microemulsion, critical dielectric behaviour of micellar water below cloud point 7-2964
 water-oil microemulsion, small-angle scatt., excess surfactant effect 7-59795
 water-oil-tenside microemulsion, three-phase regime 7-13826
 water-surfactant-oil microemulsion, spin-1 model 7-3612
 Ag halide emulsion microcrystals, Maxwell-Wagner effect 7-16800
 KCl, organic liquid emulsions, dielectric props. meas. 7-22173

emulsions (nuclear track) see nuclear track emulsions**emulsoids see emulsions****encapsulation****see also packaging**

- laser induced etching of polyimide encapsulants in IC evaluation 7-53941
 photovoltaic encapsulant, properties of new SSP system, comparative study 7-13914
 polyimide encapsulants, laser induced etching 7-53941
 SOI, films lamp zone melting recrystallisation, effect of plasma nitrided SiO_2 encapsulant 7-38391
 SOI films, laser recrystallisation, agglomeration, surface roughness and crystal imperfection 7-38389
 spacecraft HV solar cell array glass encapsulation for protection against plasma 7-65490
 CaF_2 TLDs, Al- or Ta-encapsulated, non-equilibrated bremsstrahlung dosimetry for 0.75 MeV electrons 7-56876
 $\text{Hg}_{1-x}\text{Cd}_x\text{Te}$:B, ion implanted, annealing, nature oxide encapsulation 7-2036
 InP:Si, substrate, encapsulated annealing, using SiN encapsulant 7-39779
 Si_3N_4 films on GaAs:Te, annealing-encapsulation props. investigated by nuclear analysis techniques 7-8030
 $\text{Si}_3\text{N}_4/\text{O}_2$ films on GaAs:Te, annealing-encapsulation props. investigated by nuclear analysis techniques 7-8030
 SiO_2 films on GaAs:Te, annealing-encapsulation props. investigated by nuclear analysis techniques 7-8030

enclosures see packaging**encoding****see also codes; decoding**

- acoustical communication in animals, digital signal processing 7-50854
 acoustics, speech and signal processing, conf., Tokyo, Japan (April '86) 7-35100
 adaptive image transform coding techniques, review 7-1036
 angular encoder automatic calibration system (Japanese) 7-56213
 binary phase coding of spatial-frequency filters 7-37112
 coding theoretic approach to cancer detection 7-47252
 digital optical adder based on spatial filtering 7-11099
 functional neuromuscular stimulated hand orthoses, sensory feedback using electrodes fitted to shoulder 7-34354
 human visual image coding, important obs. 7-65754
 human visual system models appl. to digital colour image compression 7-65744
 optical binary coded ternary arithmetic and logic 7-10863
 optical computing using hybrid encoded shadow casting 7-1032
 optical fibre sensors, wavelength encoded, for practical industrial meas. 7-50766
 optical parallel array logic system, architecture without memory elements 7-20144
 quasi interferometric set up, pseudocolour encoding, spatial frequency domain 7-62640
 self similar hierarchical transforms, block transform coding and human visual system model bridge 7-62641
 symbolic substitution logic, optical implementation using polarisation for coding 7-10860
 Wigner distribution function from single object transparency, optical system for efficient display, polarisation encoding 7-31259
 LiNbO_3/Fe crystal, white-light information processing, coupled wave theory 7-25728
 Si p-i-n diode, spectral information coding by IR photoreceptors, colour vision analogue 7-35593

end-fire antennas see antenna arrays**ENDOR**

- alkali halides, trapped atomic H and muonium 7-45900
 anthraquinone anion radicals, frozen soln., ENDOR spectra, temp. depend. 7-7610
 bacteriochlorophyll a radical cations, hyperfine interactions with ^{15}N nuclei, calcs. for ENDOR and EPR methods 7-15594
 biologically significant solids, irradiated, ESR and ENDOR studies, review 7-23309
 bis(chlorophyll)cyclophane, radical cations, ENDOR and TRIPLE reson. 7-42655
 chlorophyll a, radical cations, ENDOR and TRIPLE reson. 7-42655
 diacetylene oligomers, carbene and dicarbene triplet state, ENDOR and EPR study 7-7608
 disordered systems, ESEM and ENDOR spectra, model calcs. 7-53176
 electron spin echo resonator, variable temp., for single-crystal studies 7-30059
 gadolinium triacetate, frozen soln., coordination environment investig., ENDOR 7-25576

ENDOR continued

- gadolinium tripropanate, frozen soln., coordination environment investig., ENDOR 7-25576
 imaging, in aq. solns. of nitroxides, viscosity or O₂ conc. 7-24673
 α-phenyl-N-tert-butyl nitronite, deuterated, conform. of spin adducts, ENDOR investig. 7-50204
 α-quartz: AlO₄, hyperfine and quadrupole interactions, ENDOR study 7-2951
 α-Si:H, structural characterisation, hyperfine interaction, ESR, ENDOR 7-53135
 4,4'-terphenylenebisgalvinoxyl biradical, nematic liquid crystal, ENDOR and EPR spectra anal. 7-19908
 Ar solid matrix with methyl radical, ENDOR/TRIPLE spectra of matrix-isolated molecules 7-30058
 CaF₂:Ce³⁺, impurity ion-ligand nuclei interactions, ENDOR meas. and operator method calcs. 7-52538
 CaF₂:Tm²⁺ crystal, dynamic nuclear polarisation, strong hyperfine interaction, ENDOR study 7-45840
 Co complexes, bis(dimethylglyoximate)cobalt(II), frozen soln., EPR and ENDOR investig. 7-57097
 CsCaF₃:Gd³⁺, transferred hyperfine interaction of impurity centres, ENDOR, EPR meas. 7-32946
 CsMF₃:Gd³⁺ (M=Cd,Ca), transferred hyperfine interactions, ¹⁹F ENDOR studies 7-53177
 GdCl₃, frozen soln., coordination environment investig., ENDOR 7-25576
 KMgF₃:Dy³⁺, ligand hyperfine interaction of Dy³⁺, ENDOR 7-22163
 K[(OH)₂PO₂], irradiated single crystal struct. study, ESR and ENDOR anal. 7-38962
 LuPO₄:Gd³⁺, mag. hyperfine interactions, ³¹P and ⁵¹V ENDOR spectra 7-27630
 LuVO₄:Gd³⁺, mag. hyperfine interactions, ³¹P and ⁵¹V ENDOR spectra 7-27630
 Mn, in Ar solid, ENDOR/ESR spectra 7-5710
 MnH₂ in Ar solid, ENDOR/ESR spectra 7-5710
 N₂H₄⁺, radical ion, trapping site geometry, ENDOR and EPR spectra of hydrazinium hydrogen oxalate 7-7609
 Ni complex, tetraphenylarsonium-bis(maleonitriledithiolato)nickel(II), Rh complex dopant, hyperfine interactions, EPR-ENDOR study 7-53124
 PbTiO₃:Cr³⁺, ceramic, EPR, ENDOR, ESE investigations. 7-13020
 RbCdF₃, struct. phase transition, ENDOR study 7-33298
 RbCdF₃:Cr³⁺, tetragonal phase, ENDOR study 7-2952
 Si, vacancies, hyperfine interactions, ENDOR and EPR studies 7-63609
 Si:B, B-vacancy complex, electronic and atomic struct., ENDOR studies 7-63649
 Si:Fe, interstitial Fe, spin delocalisation 7-13059
 Si:Fe, interstitial impurity, superhyperfine interaction and spin-lattice relax. 7-53178
 α-Si:H and α-Si:H:P, electron nuclear double resonance expts. 7-2950
 Si:O, magnetic resonance of O-related defects 7-17223
 Si:V, impurity self-ENDOR spectrum 7-64545
 VO(II) complexes, ENDOR spectra, struct., hyperfine tensors 7-33299
 YVO₄:Gd³⁺, mag. hyperfine interactions, ³¹P and ⁵¹V ENDOR spectra 7-27630

energies, molecular dissociation see molecular dissociation energies

energy, binding see binding energy

energy, lattice see lattice energy

energy, surface see surface energy

energy bands see band structure

energy bands, electron see band structure

energy control see power control

energy conversion, direct see direct energy conversion

energy dispersive X-ray analysis see X-ray chemical analysis

energy gap

see also superconducting energy gap

7X GaAs, sputtered films, optical props., effective medium models (Chinese) 7-7774

alkali metal halide crystals, impurities, local and gap mode freq. calcs. 7-26888

amorphous semicond. III-V and II-VI cpds., electronic struct. of bulk and defect sites, tight-binding recursion method 7-45222

Anderson-Hubbard model, real-space renormalisation group method 7-38842

band offsets at pseudo-ternary semiconductor-alloy heterojunctions 7-12835

α-(BEDT-TTF)₂I₃, struct. charact. and band electronic struct. below metal-insulator transition 7-2007

binary crystals, structural stability, chem. trends 7-21153

α-(BPDT-TTF)(Ni(dmit)₂)₂, struct. phase transition accompanied by change of electronic struct. 7-52704

chalcogenide glasses, electrons in mobility gap, spectra and thermodynamic props. 7-2471

compositionally graded semiconductors and device applics., book contrib. 7-27323

Cu₂PS₂Br(Cl), superionic cryst., refractive indices, optical-refractometric correlation (Russian) 7-3016

diamond, electron correlation, band gaps and quasiparticle energies 7-27278

diamond, energy band gap calc., self-interaction correction to local density approx. 7-45144

diamond, optical phonons and elasticity at megabar stresses 7-21375

disordered alternant structures, electron energy spectrum 7-38436

disordered alternant structures, electron energy spectrum 7-42458

fractional quantum Hall effect, energy gaps 7-27272

incompressible Fermi liq. of 2D electrons, Coulomb gap size determ., spectroscopic method 7-61223

insulators, nonlocal exchange and correlation contributions to band gap 7-2458

lattice electronic wave functions, localisation due to local topology 7-21847

narrow energy band systems, insulator-metal transition 7-38455

one-dimensional electron-phonon Peierls condensate, amplitude solitons 7-52449

optical nonlinearity near the bandgap in semiconductors, review 7-62747

p-doped semiconds., dielec. functions, band-gap narrowing anal. 7-52482

p-type semiconductors, heavily doped, band-gap shifts 7-22333

parabolic semiconducting quantum wells, electrical and optical props. 7-22002

Peierls-CDW state, 1D, impurity distrib., 2k_F distortion 7-44593

energy gap continued

- penanthrene-TCNQ complex, physical props. 7-52622
 phenazine-tetracyanoquinodimethane, photoconductivity and optical absorpt. coeffs. near band edge 7-2641
 polar materials, band gap determ. from absorpt. spectra 7-45960
 polaroid K, reson. Raman scatt., absorpt. spectra, amplitude mode model anal. 7-64658
 poly-p-phenylene vinylene, conducting polymer with electron donating side-chains 7-2588
 poly-p-phenylenevinylene film, opt. and elec. props., band gap 7-46161
 polyacene, one-dimensional graphite series, electronic props. 7-64063
 polyacetylene:I, photoexcitation spectra 7-64657
 trans-polyacetylene:Na, undoped and doped, momentum depend. dielec. functions, EELS study 7-64144
 polyacetylene, CDW, interaction and disorder 7-64136
 polyacetylene, Coulomb correlations, optical gap 7-64142
 polyacetylene, electron-electron interactions, optical gap, negative spin density 7-2473
 trans-polyacetylene, equivalent orbital theory, electronic struct. study 7-64062
 polyacetylene, ground, excited, polaronic, solitonic and impurity states calcs., doping effects 7-45131
 polyacetylene, growth, struct., optical props. and photo-induced spin states 7-16455
 polyacetylene, Raman scatt. from CDW, ab initio calcs. 7-46015
 trans-polyacetylene, reson. Raman scatt. from amplitude modes, temp. effects 7-64654
 trans-polyacetylene, third order optical susceptibility, 2A_g excited state obs. 7-62782
 trans-polyacetylene, triplet solitonic excitations, optical gap 7-2496
 trans-polyacetylene(-d), ns time resolved photoinduced absorption spectrum 7-64668
 polyaniline, conducting polymer, electronic and electrochem. props., MNDO calc. 7-2462
 polyfuran and copolymers, electronic struct., cond. props., ab initio cryst. orbital calcs. 7-52410
 polyisothianaphthene, electronic struct. and conduction properties 7-45119
 polyisothianaphthene and derivatives, valence effective Hamiltonian band struct. calcs. 7-16936
 polyphenanthrene, one-dimensional graphite series, electronic props. 7-64063
 polypyrrole and copolymers, electronic struct., cond. props., ab initio cryst. orbital calcs. 7-52410
 polythiophene and copolymers, electronic struct., cond. props., ab initio cryst. orbital calcs. 7-52410
 polythiophene derivatives, bandgaps, conductivities 7-64061
 polyvinylene, reson. Raman scatt., absorpt. spectra, amplitude mode model anal. 7-64658
 quasicrystalline chain, vibr. and electronic spectral props., perturbative approach 7-45116
 semiconductor cpds., relation between energy gap data and periodic table 7-12609
 semiconductor doping superlattices, n-i-p-i crystals 7-7348
 semiconductor films, heavily doped, optical absorption band shift 7-7776
 semiconductor narrow and wide bandgap materials, refractive indices 7-13118
 semiconductors, charged defects, reaction rates 7-38497
 semiconductors, disordered, with dispersive transport, elec. transient process 7-17074
 semiconductors, intermediate valence, theory 7-38526
 semiconductors, nonlocal exchange and correlation contributions to band gap 7-2458
 semiconductors, zinc-blende and diamond struct., recursion calcs., K space method 7-2453
 semiconductors with parabolic density of states, activity coeffs. of electrons and holes 7-27324
 superlattice band struct., nonparabolicity effects, Kane theory calcs. 7-2693
 surface states in one dimension, effective range approx. 7-21963
 TGS:Cr³⁺ single crystals, valence bands and impurity levels, absorpt. edge meas. 7-33350
 (TMTSF)₂AsF₆ and (TMTSF)₂SbF₆, SDW state, far IR spectra 7-33388
 transition metal alloys, disordered, localised and extended state coexistence 7-7175
 two dimensional electron gas, thermodynamic props., interaction and disorder effects, HF approx. calcs. 7-2516
 two dimensional quasi-periodic Penrose lattice, electronic and vibr. modes, localised states and band struct. 7-27300
 zero gap semiconductors near inversion point, solitons 7-64100
 zero-gap type I state, spontaneous destruction in quantising mag. field 7-2460
 zincblende crystals, homopolar and heteropolar energy gaps 7-21811
 [Ag₆Ge₄P₁₂](Ge(Si)₆), bonding relationships and electronic struct. calcs. 7-16941
 [Ag₆Sn₄P₁₂](Ge(Si)₆), bonding relationships and electronic struct. calcs. 7-16941
 Ag₃As₃, proustite, energy band struct. at phase transitions 7-2167
 AgGa_{1-x}In_xS₂, solid solns., conc. depend. of band gap 7-52423
 AgGa_{1-x}In_xSe₂, thin films, evaporated, photosensitivity and optical props. study (Korean) 7-53423
 AgGaSe₂, cryst. field and spin-orbit interactions at fundamental gap, reflectivity meas. 7-16997
 AgInTe₂, polycrystalline thin films, elec. and optical props. study 7-58924
 AgNO₃ crystals, band structure calc. 7-21807
 α-Ag₂S, energy gap, EMF const. determ. by SALS program (Japanese) 7-16943
 Ag₂S(Se)-Ag₂Te(Se) liq. and glassy semicond., activation energy of carrier thermal generation, elec. meas. 7-17035
 Ag₂S(Se)(Te)-Cu₂S(Se)(Te) liq. and glassy semicond., activation energy of carrier thermal generation, elec. meas. 7-17035
 AlGaAs, MOCVD growth, refractive indices meas. by in situ reflectometry 7-59270
 AlGaAs superlattices, donor state instability, DLTS and Hall meas. 7-12663
 AlGaAs-GaAs, band-gap discontinuity, determ. by quantum oscillations of photolum. intensity 7-13217
 AlGaAs-GaAs heteroface solar cells, role of window layer 7-3695
 AlGa_{1-x}As bandgap determ. by Schottky barrier spectral response meas. 7-2667

energy gap continued

- AlGaInAs layers on InP, LPE growth 7-33608
 $\text{Al}_x\text{Ga}_{1-x}\text{N}$, photoluminescence in the edge emission region 7-27778
 AlN thin crystalline stoichiometric film, electronic struct., electron spectra studies 7-58916
 $\text{As}_2\text{Se}_3/\text{Ni}$ films, electronic struct. and transport props. 7-12595
 $(\text{As}_2\text{Se}_3)_{1-x}\text{Te}_x$, elec. and thermal transport props., effect of Te addition 7-38200
 $\text{As}_{2-x}\text{Te}_x\text{-xIn}_x$ and $\text{As}_{20-x}\text{Te}_{80-x}\text{In}_x$ systems, chalcogenides, thin films, optical and electrical props. 7-27446
 Au-GaAs, interface state meas. at Schottky contacts, admittance characterisation technique 7-2718
 BN, film, optical energy gap, density, hardness 7-39204
 $\text{BaPb}_{1-x}\text{Bi}_x\text{O}_3$, semicond. phase, CDW gap, optical meas. 7-53328
 Bi chalcogenides, binding energies, chem. shifts XPS and diffuse refl. spectra (*German*) 7-1943
 $\text{Bi}_4\text{Ge}_3\text{O}_{12}$, luminescence excitation and reflection spectra 7-46090
 $(\text{Bi}_{1-x}\text{Sb}_x)_2\text{Te}_3$ single crystal, optical constants, IR spectra study 7-46030
 C, dielectric film growth, on GaAs and InP substrates 7-39420
 C films, plasma deposited from methane, elec. conductivity, optical absorpt. 7-38786
 C, single-particle excitations, dynamic correl. corrections, local density theory 7-45115
 a-C:H, film, optical and compositional props. 7-39206
 a-C:H, film, optical and electronic props. rel. to deposition parameters 7-38406
 a-C:H, film, optical energy gap, density, hardness 7-39204
 a-C:H films, plasma deposited, optical props. 7-27799
 a-C:H plasma grown films, struct., physical props. 7-58713
 CaF_2 , film, on GaAs films, optical parameters 7-39204
 CaF_2 -Si interface, with MBE grown insulator, trap states, I-V, C-V meas. 7-7407
 $\text{CdGa}_2(\text{Se})_4$ defect chalcopyrite struct. crystals., linear optical response, atomic core electron contrib. calcs. 7-39061
 $\text{Cd}_x\text{Hg}_{1-x}\text{Te}$, band gap collapse, effects of Hg 5d electrons 7-64075
 CdI_2 , interband two-photon absorpt., freq. depend. 7-33451
 $\text{Cd}_{0.8}\text{Mn}_{0.2}\text{Te}/\text{Cd}_{0.7}\text{Mn}_{0.3}\text{Te}$ semimagnetic superlattices, electronic props., theory 7-45445
 $\text{CdO-B}_2\text{O}_3\text{-SiO}_2$ glasses, photochromism, photocond. and ESR (*Japanese*) 7-22282
 CdS/polymer composites, degenerate four-wave mixing 7-62795
 CdS-CuGaSe_2 solar cells, physical properties and photovoltaic potential of CuGaSe_2 thin films 7-12889
 CdSb , optical energy gap and light emission (*Japanese*) 7-53264
 $\text{CdSe}_{1-x}\text{Te}_x$ and $\text{CdSe}_{1-x}\text{Cu}_x\text{Te}$ films, deep local states, photosensitivity, spectral study 7-22371
 $\text{CdSe}_{1-x}\text{Te}_x$, bound excitons, thermal dissoc., photoluminescence, reflectivity meas. 7-46122
 $\text{CdSe}_{1-x}\text{Te}_x$, bowing parameter of direct band gap, press. depend. 7-38453
 $\text{CdSnO}_4/\text{PbO}$ highly conducting films, characterisation 7-22049
 Cd_2SnO_4 , CVD, struct., elec. and optical props. (*Korean*) 7-27940
 CdTe film in a photovoltaic cell, electrodeposition and props. 7-64938
 p-CdTe RF sputtered thin films, resistivity, forbidden gap, optical and X-ray diff. spectra studies 7-21747
 CeIn_3 antiferromagnetic alloys, thermolec. power meas., band gap form. 7-38543
 $(\text{Ce}_{1-x}\text{La}_x)\text{In}_3$ antiferromagnetic alloys, thermolec. power meas., band gap form. 7-38543
 CeO_2 films, optical absorption edge and energy gap 7-33471
 $\text{Co}_{0.2}\text{Ga}_{0.8}\text{S}_{2.2}$ single crystals., optical props. and impurity energy levels meas. 7-13122
 $\text{Co}_x\text{In}_{3-x}$ thin films, spray pyrolysis deposited, structural and optical props. 7-22468
 Cr, surface EM wave absorpt., 4-350K 7-33354
 CrCl_3 , ionic crystals, optical and electron energy loss studies 7-3066
 $\text{p-crystalline Si/n-amorphous Si}$ heterojunction, electrostatic pot. barrier distrib. calcs. 7-58881
 Cu (111), K doped, anomalous surface-state penetration near band edge, photoemission studies 7-39361
 Cu (111) surface electronic struct., perturbations induced by adsorption of K 7-52720
 Cu-Sb-S cpds., valence bands and semiconducting gaps, nonstoichiometry and phase separation 7-16941
 $\text{Cu}_{2-x}\text{Cd}_x\text{Te-Zn}_{39-x}\text{Cd}_{60-x}\text{Te:1}$, heterojunction solar cells, fabrication and characterisation (*Korean*) 7-28402
 CuCrO_2/Ca , semiconductor, prep., opto-electronic props. 7-2705
 $\text{CuGa}_{1-x}\text{In}_x\text{S}_2$, solid solns., conc. depend. of band gap 7-52423
 $\text{CuGaIn}_{1-x}\text{S}_2$ mixed chalcopyrite local struct., K-edge EXAFS meas. 7-63574
 CuGaSe_2 thin films, physical props. and photovoltaic potential 7-22047
 CuInSe thin films, flash evaporation prep. and characterisation 7-7893
 CuInSe_2 , flash evaporation, elec. and optical props. 7-7892
 CuInSe_2 , thin film, electron beam evaporation optical props. (*Korean*) 7-27801
 CuInSe_2 , thin films, flash evaporated, electrical cond. and optical absorpt. spectrum 7-33112
 CuInTe_2 thin films, flash evaporated, elec. conductivity, optical absorption 7-7428
 $\text{CuO-P}_2\text{O}_5$ glass, containing Pr_6O_{11} , optical props. 7-17292
 Cu_2S films, chemically sprayed, optical and solar selective props. 7-54350
 $\text{Cu}_3\text{SnP}_{10}$, bonding and electronic struct. studies 7-26694
 $\text{Fe}_x\text{Mn}_{1-x}\text{S}_2$, high temp. metal-nonmetal transition 7-7117
 Fe_2Se_3 and $\text{As}_2\text{Se}_3\text{-xFe}_x$ films, electronic props. 7-58922
 Ga-In-As-P system, ternary alloys, E_1 energy gap, CPA calc. 7-58740
 GaAlAs-GaAs MQW, optical bistability due to induced absorpt., model 7-5943
 GaAs, band-gap shifts 7-22333
 GaAs concentrator cells, design options and constraints 7-3698
 GaAs, fundamental energy gap, temp. depend. 7-7115
 n-GaAs impurity bands and band tailing 7-21809
 GaAs MOCVD growth on Si with superlattice intermediate layers, material props. 7-27923
 GaAs, MOCVD growth on Si, band gap energy and stress 7-38368
 GaAs, neutron transmutation doped, variable range hopping studies 7-33012
 GaAs, plastically deformed, Hall effect meas. 7-27351
 GaAs, Raman scatt. by LO phonons, interference effects 7-59213
 GaAs sawtooth doping superlattices, prep., LED and laser appls. 7-7372

energy gap continued

- GaAs sawtooth doping superlattices, photoluminescence, transport props. 7-52825
 GaAs, single-particle excitations, dynamic correl. corrections, local density theory 7-45115
 GaAs:In annealed substrates, In distribution in surface region 7-44959
 GaAs:Si/ $\text{Al}_x\text{Ga}_{1-x}\text{As}$ quantum wells, photolum. studies 7-39178
 GaAs/GaAlAs single and coupled double wells, energy depend. light hole mass, photolum. spectra anal. 7-38691
 $\text{GaAs/Ga}_{1-x}\text{Al}_x\text{As}$ graded interface superlattice band struct. calcs. 7-58879
 $\text{GaAs-Al}_x\text{Ga}_{1-x}\text{As}$, internal photoemission method for determ. of band offsets 7-12832
 $\text{GaAs-Al}_x\text{Ga}_{1-x}\text{As}$ quantum wells, parabolic, light scatt. studies 7-64651
 $\text{GaAs-Al}_x\text{Ga}_{1-x}\text{As}$ solar cell, operation with band-gap gradient in space charge region 7-54295
 $\text{GaAs-Al}_x\text{Ga}_{1-x}\text{As}$ type-I superlattices, electronic struct., tight binding calcs. 7-45475
 GaAs-AlAs multiple quantum wells, photoconductivity, photoreflectance and photolum. meas. 7-27368
 GaAs-AlAs superlattices, GaAs and AlAs, energy band gap calc., self-interaction correction to local density approx. 7-45144
 GaAs-AlAs-GaAs heterostructure, tunnelling transmission probability, many-band pseudopotential model 7-38701
 GaAs-AlGaAs quantum wells, high electric field, interband transitions, photocurrent spectra obs. 7-7289
 $\text{GaAs-Ga}_{1-x}\text{Al}_x\text{As}$ modulation-doped quantum well, photoluminesc. studies 7-2687
 GaAs-GaAlAs multiple quantum well structs., quasi-2D electron-hole plasma, band-filling effects, band gap renormalisation 7-7754
 GaAs-GaAlAs multiple quantum well structs., band-gap renormalisation 7-58888
 GaAs-Ge-SiO₂, semiconductor MBE layers on Ge islands on insulator, photolum. study 7-33455
 $\text{GaAs}_{0.75}\text{P}_{0.25}$ solar cells, high efficiency, grown by one atmosphere MOCVD 7-3697
 $\text{GaAs}_{1-x}\text{Py}_x$ solid solns., indirect band gap temp. depend., electrolum. spectra studies 7-38448
 $\text{Ga}_{0.47}\text{In}_{0.53}\text{As-InP}$ heterojunction, with three electron subbands, hydrostatic press. effect 7-2695
 GaInAsP-InP laser, anisotropic deform. influence on radiative characts., spectral characts. 7-43101
 GaInAsSb , MOVPE, band gap rel. to growth temp. 7-39409
 GaP, single-particle excitations, dynamic correl. corrections, local density theory 7-45115
 GaP: Te(Zn), doping superlattices, growth and props. 7-64684
 $\text{GaS}_2\text{Se}_{1-x}$ crystals, phase transitions under press., exciton-phonon interaction 7-44785
 GaSb-AlSb multiple quantum well structs., size-induced direct to indirect gap transition 7-7373
 GaSb-AlSb quantum wells, optical transitions, obs. 7-46086
 GdIn_3 antiferromagnetic alloys, thermolec. power meas., band gap form. 7-38543
 Ge, band gap determ. method 7-35155
 Ge, electron correlation, band gaps and quasiparticle energies 7-27278
 Ge, energy gap, indirect meas. 7-7107
 Ge, single-particle excitations, dynamic correl. corrections, local density theory 7-45115
 Ge-Sb-S glasses, bulk and thin film samples, optical and photo-acoustic props. study 7-22211
 GeN_xH , amorphous, reactively sputtered, optical and electronic props. 7-38830
 $\text{GeO}_2\text{-PrCl}_3$ glasses, optical props. rel. to comp. 7-13150
 GeSi single cryst., absorpt. coeff. meas., optical energy gap determ., 2D and 3D model anal. 7-17289
 $\text{a-Ge}_{30}\text{S}_{70}$ films, irreversible photobleaching 7-17353
 $\text{a-Ge}_{20}\text{Se}_{80}\text{Bi}$ films, n-type, electron transport props. studies 7-7422
 $\text{Ge}_{20-x}\text{Se}_{80-x}\text{In}_x$ system, chalcogenides, thin films, optical and electrical props. 7-27446
 $\text{Ge}_2\text{Se}_6\text{-xTe}_x$ amorphous chalcogenide, elec. cond., bulk and thin film effects 7-7238
 $\text{Ge}_{1-x}\text{Si}_x$ -Si strained layer superlattices, bandgap meas. 7-27408
 $\text{Ge}_{1-x}\text{Si}_x$ -Si strained-layer heterostructure, transport, optical props. and appls. 7-7349
 $\text{Ge}_{1-x}\text{Si}_x$ -Si strained-layer superlattice, zone folding induced quasi-direct gap, optical absorpt. probability 7-27409
 GeTe, energy bands, relativistic empirical tight binding theory 7-45149
 HgCdTe , electronic struct., alloying effects, ETBM calc. method 7-64080
 HgCdTe , IR nonlinear absorpt., dynamic Burstein-Moss effect (*Chinese*) 7-50615
 HgCr_2Se_4 spinel magnetic semicond., electronic struct., elec. props., defects and ferromag. anisotropy 7-38857
 a-HgSe films, elec. conductivity, thermoelectric power, optical absorpt. 7-22050
 HgTe-CdTe superlattices, growth of GaAs (100) substrates by MBE 7-12520
 HgTe-CdTe superlattices, IR optical props. 7-13166
 $\text{Hg}_{1-x}\text{Zn}_x\text{Te}$ solid solns. band gap, temp. and comp. depend. 7-58738
 I_2 , solid, UPES and EHT calcs. 7-64870
 In-Ga-As-P films highly excited, ps band filling 7-43261
 In-Ga-P-As, gap width, temp. depend. 7-12602
 $\text{In}_{0.18}\text{Al}_{0.82}\text{As-GaAs}$ strained layer superlattices, Raman studies 7-12854
 $\text{In}_{1-x}\text{Al}_x\text{Sb/Au}$ Schottky barrier heights, composition dependence 7-45431
 InAs-GaSb superlattices, transient photovoltaic effect 7-12764
 InGaAs-GaAs and GaAs-GaPAs strained layer superlattices, press. depend. magneto-optic meas. at low temp. 7-27404
 $\text{In}_{0.69}\text{Ga}_{0.31}\text{As-InP}$ strained-layer effective-mass superlattices 7-7378
 $\text{In}_x\text{Ga}_{1-x}\text{As}$, photoluminescence determ. of effects due to In alloying 7-46096
 $\text{In}_{1-x}\text{Ga}_x\text{Sb}_{1-x}$ cpd. semicond. alloys, lattice and band struct. props., review (*Japanese*) 7-7109
 $\text{In}_{1-x}\text{Ga}_x\text{P}$ solid solns., indirect band gap temp. depend., electrolum. spectra studies 7-38448
 $\text{In}_2\text{O}_3/\text{Sn}$ evaporated films, optical props. and applications to energy-efficient windows 7-46157
 InP-Au interface, Fermi level pinning, growth characts., photoemission spectra 7-22009
 $\beta\text{-In}_2\text{S}_3$ thin films, spray pyrolysis grown, optical energy gaps 7-33467
 InSb, density of excited electron-hole plasma 7-38608

energy gap continued

InSb, four-wave mixing, degenerate and nondegenerate 7-11069
InSe and γ -In₂Se₃ films, formation by double source evaporation 7-59436
KCl(Br) γ -irrad. single crystals, piezolum. and thermolum. spectral shift meas. 7-27796
K₂CuX₃, (X=Cl, Br), energy band struct., fundamental optical absorption 7-7093
LiCl, electron correlation, band gaps and quasiparticle energies 7-27278
LiF ionic crystals, band-gap-energy positron emission, comment 7-45227
Mg₂Si(Ge)(Sn)(Pb), Hall effect in solid and liq. states 7-38647
Mn₂Zn_{1-x}Se, energy gap comp. depend., photocond. and absorpt. edge meas. 7-38454
MoS₂ films, RF magnetron sputtered, elec. and optical props. 7-2747
MoS₂, high press. synthesis, characterisation 7-26716
NaF ionic crystals, band-gap-energy positron emission, comment 7-45227
NdIn₃ antiferromagnetic alloys, thermoelec. power meas., band gap form. 7-38543
NiFe_{1.96}O_{4+x} electrodes in aq. electrolytes, photoelectrochem. characts. meas. 7-46854
P, black, interplanar forces caused by electron-lattice interaction 7-63547
Pb_{1-x}Eu_xSe, MBE growth for IR device appls. 7-64908
Pb₂O₃ thin film, electronic props., electrochem. technique characterisation 7-7416
5PbS.2Sb₂S₃, boulangierite, elec. cond. (Korean) 7-27331
PbSe_{1-x}S_x epitaxial films, absorpt. edge, band gap, comp. depend., 77-300K 7-39063
Pb_{1-x}Sn_xTe narrow-gap semicond., electron-electron interaction, effect on permitt., two-band model 7-52420
Pb_{1-x}Sn_xTe_{1-y}Se_y solid soln. single crystals, density, comp., lattice const. and galvanomag. props. (Russian) 7-44500
PbTe, narrow gap semiconductors, Knight shift 7-53166
PbTe-EuTe short period superlattices, props., appl. to laser diodes 7-52785
PbTe_{1-x}S_x epitaxial films, absorpt. edge, band gap, comp. depend., 77-300K 7-39063
PbTe(Se)(S), energy bands, relativistic empirical tight binding theory 7-45149
trans-polyacetylene, inter-chain versus intra-chain electron-hole photogeneration 7-27362
Rb₂AgI₃, energy band struct., fundamental optical absorption 7-7093
Rb₂CuX₃, (X=Cl, Br, I), energy band struct., fundamental optical absorption 7-7093
a-Se, structural disorder model 7-26641
Si alloys, amorphous, CVD, electrical and optical props. 7-33596
Si, band gap determ. method 7-35155
a-Si, density of states, spectral function, calcs. using eqn. of motion method in k-space 7-27236
Si, electron correlation, band gaps and quasiparticle energies 7-27278
Si, energy band gap calc., self-interaction correction to local density approx. 7-45144
Si, energy gap, indirect meas. 7-7107
a-Si films, surface passivation, study by photothermal deflection spectroscopy 7-59689
Si, heavily doped, band-gap narrowing 7-7108
Si, single-particle excitations, dynamic correl. corrections, local density theory 7-45115
Si solar cells, heavy doping effects 7-3653
Si thin film, doped, electron beam evaporation, elec. props. 7-2743
Si:Cu(Au), deep level position in forbidden gap, charactn. using ionisation Gibbs free energy (Chinese) 7-58760
Si:H, amorphous film, optical absorption and bandgap rel. to temp. (Korean) 7-59228
a-Si:H, C superlattice struct., solar cell performance 7-46945
a-Si:H, fluctuation induced gap states 7-27242
a-Si:H, glow discharge thin films, deposition rate, optical props., influence of substrate temp. 7-59460
a-Si:H, laser-assisted CVD growth, optical props. 7-22210
a-Si:H, optical dispersion relations, determ. 7-33353
a-Si:H,B, RF sputtered films, optical and electrical props. 7-33470
a-Si:H,B, thin films, thermoelectric power 7-58826
a-Si:H,Ge single junction and tandem solar cells, thin film properties and corollary plasma diagnostics 7-13893
a-Si:H and a-Si:H, B films, photoinduced changes in elec. props. 7-38634
a-Si:H evaporated layer production from RF discharge, growth mechanism and films. 7-64898
a-Si:H film, photo-assisted plasma CVD 7-33593
a-Si:H films, CVD, optical and electronic props. 7-33597
a-Si:H films, RF glow discharge deposition, optical and electrical props. 7-33598
a-Si:H films, sputter deposition, optical and ESR props. 7-33565
a-Si:H sputtered film, low-temp. optical props. 7-3101
a-Si:H thin films, elec. and optical props., thickness depend. 7-46168
a-Si:H/Ge:H superlattice struct., light absorption and photocond. studies 7-38715
a-Si:H/a-SiN_x:H, amorphous multilayer structures, optical props. 7-3014
a-Si:H-Si₃N₄:H double barrier structs., resonant tunnelling 7-52848
a-Si:H-SiN_x:H, multilayer struct. study using HREM 7-16879
Si:Hg(Au)(Pt)(Ir)(Os)(Re)(W), self-consistent one-electron states of 5d transition-atom impurities 7-32950
a-Si:Se(Te) thermally evaporated films, photoelectronic props. 7-38640
Si-O amorphous films, structure and defects 7-58700
Si-PtSi thin film Schottky diodes, barrier height meas. 7-64308
Si-Ti(TiSi₂), Schottky barrier height investig. 7-2716
SiC, single-particle excitations, dynamic correl. corrections, local density theory 7-45115
a-SiC:H, elec., optical and local structure props. 7-45089
a-SiC:H,B, thin films, thermoelectric power 7-58826
SiC:H,F amorphous films, struct., elec. and optical props. 7-22360
a-SiC:H film prepared by magnetron sputtering, elec. and optical props. (Japanese) 7-12887
a-SiC:H thin films, glow discharge deposition, energy gap and activation energy 7-46352
Si_{1-x}Ge_x films, optical band gap, photocond. props. 7-52672
Si₂Ge_{1-x} coherently strained bulk alloys on Ge (001) substrate, indirect band gap and band alignment calcs. 7-2481
Si₃Ge_{1-x}H₂F amorphous films, struct., elec. and optical props. 7-22360
a-SiN_xH films, optical absorption const. evaluation by photothermal deflection spectroscopy 7-22361

energy gap continued

a-SiN_x, amorphous glow discharge films, gap state distrib., photocurrent phase shift anal. 7-7421
SiN_x:H,B, microcrystalline, wide-gap, RF glow discharge deposition 7-22503
a-SiN_x:H dielectric films with low defect density 7-39036
a-SiN_x:H plasma-enhanced CVD film props. rel. to SiH₄-N₂ gas vol. ratio, RF power and substrate temp. (Korean) 7-3201
Si₃N₄, amorphous, optical dispersion relations, determ. 7-33353
SiO₂, crystalline, optical activity and Faraday rotation comparison, band gap determ. 7-3017
SiO₂ thin films, dielectric breakdown phenomenon, model 7-64567
a-Si_{1-x}Sn_x:H films, electronic structure of divalent defects 7-32960
Si_{1-x}Sn_xO_{1+x} amorphous thin films, optical and structural studies 7-64714
SmB₆:Eu²⁺ energy gap temp. depend., impurity ESR study 7-45151
SmB₆:Er³⁺ energy gap temp. depend., impurity ESR study 7-45151
SmB₆:Gd³⁺ energy gap temp. depend., impurity ESR study 7-45151
SmIn₃ antiferromagnetic alloys, thermoelec. power meas., band gap form. 7-38543
SmS, golden phase, f-d hybridisation gap 7-27231
 α -Sn, thin film quantization studies using high resolution electron energy loss spectroscopy 7-27448
SnO₂/Sb thin films, doped and undoped, prep. by photolysis, phys. props. 7-22368
SnS₂-TiS₂ phases, ¹¹⁹Su Mossbauer study (French) 7-27639
SnS₂(Se₂), polytypes, electronic behaviour, rel. to energy conversion 7-38447
SnTe, energy bands, relativistic empirical tight binding theory 7-45149
Ta complex, (BEDT-TTF)₃Ta₂F₁₁, optically enhanced phase transition, EPR investig. 7-64454
Ta-Ta₂O₃-electrolyte system, conduction processes 7-38725
Te-Ag point contacts, current-voltage characts., temp. depend. studies (Russian) 7-7335
TiO₂, amorphous, optical dispersion relations, determ. 7-33353
p-TlInSe₂ single cryst., impurity photocond. studies 7-2642
TiSbS₂, near band gap optical props. 7-7715
UPt₃ single crystals, electronic structure, low energy reflectivity study 7-45137
URu₂Si₂, heavy electron system, competing electronic correlations, press. effect 7-45539
V₂O₅-TeO₂-PbO, glass, elec. and optical props. (Korean) 7-27330
Y₂Ti₂O₇, small-polaron conduction 7-21915
YbFeO₃, spontaneous spin reversal, magnetic reson. soft modes and energy gaps obs. 7-52964
ZnCdSe, electron beam pumped, cathodolum., gain and stimulated emission 7-64701
Zn_xHg_{1-x}Se, electrophysical, props. and carrier scatt. mechanisms 7-17024
ZnO:In films, microstruct., elec. and optical props., film thickness depend. study 7-16895
ZnS, interband two-photon absorpt., freq. depend. 7-33451
ZnSe, heteroepitaxial growth on GaAs, energy band gap, elastic strain effects 7-59242
ZnSe:Si, single crystal growth, chem. transport method (Korean) 7-27880
ZnSe-ZnMnSe strained layer superlattices, quantum confinement effects 7-27403
(ZnSe)_x(CdTe)_{1-x} films, CVD fabricated, phys. props. 7-7055
ZnSiP₂ cryst., exciton absorpt. spectrum, energy gap and exciton binding energy determ. 7-2500
ZrTe₃, optical props. 7-64667
energy gap, superconducting see *superconducting energy gap*
energy level crossing
see also *Hanle effect*
diamagnetic systems, muon level crossing resonance, general considerations 7-53185
energy transfer between Ce and Tb ions in LaOBr:Ce,Tb 7-5644
muon level crossing resonance, muon polarisation function for longitudinal fields 7-53187
organic free radicals, avoided level crossing muon spin rotation 7-42789
paramagnetic systems involving a muon, level crossing resonance 7-45905
¹³Cs, ⁷P_{3/2} state, level crossing in elec. and mag. fields 7-50003
H, microwave ionisation below classical chaos border 7-57142
He, 1 s4d config. fine struct., Zeeman sublevels crossing fields 7-50015
He⁺ low energy ion-surface scatt., reionisation process theory 7-22413
He-like ions, radiative corrections, multiconfigurational DF study 7-62299
He+H⁺ united atom rot. coupling collisions 7-958
He+Ne²⁺, collisional transition probabilities, avoided crossing, nonadiabatic effects (French) 7-10727
I₂, mag. predissoc., photoacoustics using RF laser optogalvanic detection 7-50273
K, Rydberg state, avoided crossings in elec. field using blackbody radiation 7-15558
LiNbO₃:Fe³⁺, Mossbauer spectroscopic evidence of angle-depend. intersystem crossing 7-33312
MnF₂, antiferromag., muon level crossing resonance 7-53186
NH, collision-induced intersystem crossing investigated using ArF laser photolysis 7-42692
NS, low-lying valence and Rydberg states obtained by CI studies 7-49947
SR + inert gases, collisional energy transfer, time resolved fluoresc. meas., quenching cross sections 7-62497
Xe, radiative collisions, curve crossing, two-photon laser excitation 7-19810
energy level transitions, atomic see *atomic spectra*
energy level transitions, molecular see *molecular spectra*
energy level transitions, nuclear see *nuclear energy level transitions*
energy levels see *energy states*
energy levels, atomic see *atomic structure*
energy levels, molecular see *molecular energy levels*
energy levels, nuclear see *nuclear energy levels*
energy levels in solids and liquids see *electron energy states (condensed matter)*
energy loss of particles
see also *channelling; electron energy loss spectra; radiation effects*
alkanes, long-chain, cryst. and molten, low energy electron transmission and secondary electron emission expts. 7-33492

energy loss of particles continued

amorphous solids, mean scatt. angle, first moments of longit. distrib., elastic losses of ion energy 7-26806
 atomic beams, stopping with laser light, entropy prod. 7-42556
 atomic cooling, stopping and trapping 7-10504
 beta particle energy distrib., stable moles (*Russian*) 7-49859
 borate minerals, unoccupied mol. orbitals of B-O bond mol. orbital calcs., XANES, NMR and electron transmission spectra 7-33281
 charged nuclear particles, energy loss in heat plasma 7-36436
 charged particle bremsstrahlung by barrier penetration in 1D 7-29775
 charged particle channelling in solids 7-38081
 charged particle energy loss in solids, confined-atom model calcs. 7-44634
 charged particle scatt., energy-level oscillations accompanying the shadow effect (*Russian*) 7-38082
 charged particles moving through layers of plates, anal. 7-58388
 charged particles stopping power 7-32003
 collision cascades, linear, variance calc. 7-63686
 collisional mixing, magnitude and mechanism 7-63677
 conversion electron Mossbauer spectra, backscattered electron intensities calc. 7-53181
 curved cryst., vol. capture of particles to channelling, reversibility principle calcs. 7-51900
 diamond, stopping cross section of ^{12}C projectiles 7-51899
 electron and positron small angle incidence on cryst., radiation processes, incoherent multiple scatt. effects calcs. 7-44625
 electron energy loss in thin films, Monte Carlo program MCSDA 7-51894
 electron gas, degenerate, electronic stopping power, local-field corrections calcs. 7-48533
 electron mean free path, effective backscatt. and differential scatt. cross-sections, 5-40 keV 7-53461
 electron Monte Carlo transport, PRESTA algorithm 7-49854
 electrons, total stopping power, semiempirical eqn. 7-6696
 electrons in dry air, W value re-eval. 7-62242
 energetic ions, flux and range distrib. calcs. appl. of Boltzmann transport eqn. 7-63692
 energy deposition by X-rays and electrons, microscopy implications 7-38064
 energy straggling of fast proton beams, energy and target atomic number dependences 7-2076
 fast ion dechannelling, electronic diffusion coeff. calc. 7-44635
 graphite stopping cross section of ^{12}C projectiles 7-51899
 hadron shower characteristics in iron and muon identification 7-15466
 heavy target, boundary layers arising when intermediate energy beam is stopped 7-16292
 high energy ion scatt., struct. anal. of surfaces and interfaces 7-22410
 inhomogeneous materials, implanted ion depth distrib. 7-21250
 ion backscattering from solids at oblique and grazing incidence, analytical calcs. and computer simulation 7-53466
 ion beam channelling, in semiconductor superlattices, review 7-51902
 ion beam modification of materials, conf., Catania, Italy (9-13 June 1986) 7-60865
 ion implantation depth profiles for high fluence implantations, method of equivalent at. stopping 7-51795
 ion implantation range distributions, moment calcs. 7-2072
 ion irradiation of solids, collision cascades, ionization, spikes and energy-transfer 7-12170
 ion range and damage 3D distrib. including recoil transport 7-63691
 Kapton foil, N ion energy loss meas. and calcs. 7-63694
 kinetics of implanting accelerated gas ions in crystalline solids 7-6649
 lost muon polarisation, longit. spin decoupling and muon spin reson. investigation. 7-17369
 Melinex, energy straggling and stopping power of 4 and 5.486 MeV α -particles 7-34199
 metal displacement cascade damage computer simulation using binary collision approx. code (*Japanese*) 7-32535
 metallic glasses, ion irradi., inelastic deform. induced by fast ion electronic energy loss 7-63688
 Mylar foil, N ion energy loss meas. and calcs. 7-63694
 plasma, charged particle stopping power 7-37625
 positive particle thermalisation, reaction and kinetics 7-51896
 positron continuous slowing down approx. range 7-44638
 proton build-up calculation for fast neutrons 7-65860
 radiative energy loss by relativistic electrons and positrons in crystals 7-21306
 radiative energy loss of relativistic electrons and positrons in crystals during channelling, temp. depend. 7-21307
 range and damage profile parameter predictions on a microcomputer, analytical approx. 7-62241
 recoil number fluctuations, power cross section approx. 7-36432
 slow ions, nonlin. energy-loss straggling, in solids 7-2075
 small metal particles, surface excitations by fast electron scatt. 7-7140
 solid surfaces, fast dust particle impact and related techniques, ion form. studies 7-46259
 solids, interaction of GeV heavy ions, GANIL results 7-63678
 stimulated collective inelastic stopping effect 7-36781
 stopping powers for ion bombardment using EDEP1 program 7-51895
 stopping powers for protons and He ions in various types of matter 7-12179
 surface (111), energy distrib. of reemitted nonthermalised positrons 7-16662
 temperature field evolution on ion beam irradiated absorber 7-63670
 tissue equivalent materials, energy straggling and stopping power of 4 and 5.486 MeV α -particles 7-34199
 transition metals, low energy in elastic electron scatt. props. 7-63700
 uniform ion doping, beam energy calc. program 7-32477
 variance reduction under exponential and scatt. angle biasing 7-62099
 β -particle transmission in LiF, acrylic, mylar, Teflon and PVC 7-25266
 (K^+), stopped-K hypernuclear expt. at KEK 7-41930
 Ar gas, electron beam deposition 7-5771
 $\text{Ar}^+ + \text{H}_2(\text{N}_2)$ collisions, ion energy-loss spectroscopy 7-50324
 $\text{Ar}^{q+} + \text{D}_2(\text{D})$, collision parameters, energy-gain spectra meas., multichannel Landau-Zener model anal. 7-36752
 Au, energy loss straggling of protons and He ions, 0.1 to 1.0 MeV/u 7-12182
 Au ion beam, residual ranges in various media, time of flight spectra and adsorption meas. 7-25333
 C foil, secondary electron emission from fast ion bombardment 7-53459
 C glassy state, stopping cross section of ^{12}C projectiles 7-51899

energy loss of particles continued

C:Au(Bi) films, ion implanted, projected ranges and range straggling, RBS anal. 7-63690
 CO, chemisorbed on Pt (111), adsorbate vibr. modes, inelastic He atom scatt. obs. 7-32782
 Cs, stopping with diode laser beam 7-10507
 Cu surface, Cu atom sticking and penetration, computer simulation studies 7-59326
 Cu surface, ion irradi., sputtering and lattice damage, cascade simulation 7-59327
 Cu^{q+} , effective charge, around 4 MeV per nucleon 7-50297
 Cu-He system, closed swelling layer, internal stress distrib. (*Russian*) 7-59571
 Fe, low energy ^4He ion range and damage distrib. 7-63674
 Fe_3B_{15} , high energy heavy-ion irradiation, electrical resistance meas. evidence for electronic energy loss effect 7-58353
 Ge, volume capture effect for relativistic electrons, computer simulation 7-12156
 $\text{H}_2^+ + \text{He}$, elastic and inelastic scatt. mechanisms, energy loss spectra 7-15671
 $\text{He}^+ +$ light target atoms ($28 \leq Z \leq 46$), L shell X-ray prod. cross sections meas., first Born approx. and ECPSSR theory anal. 7-36526
 $\text{He}^+ + \text{H}_2$, elastic and inelastic scatt. mechanisms, energy loss spectra 7-15671
 Kr gas, electron beam deposition 7-5771
 Kr^{q+} , effective charge, around 4 MeV per nucleon 7-50297
 Li, electron scatt., charge polarisation effect 7-63685
 Mo, low energy ^4He ion range and damage distrib. 7-63674
 NaCl, pure and Mg doped, electron range vel. to heat treatment 7-21283
 Ne gas, electron beam deposition 7-5771
 Ni foil, N ion energy loss meas. and calcs. 7-63694
 Pb (110), surface initiated melting, ion shadowing and blocking meas., RHEED 7-44769
 Pb surface, anomalous thermal expansion, ion shadowing meas. 7-58512
 SF₆, breakdown and corona, electrode surface processing effect 7-51557
 Si, dislocation loops, generated by ion implantation and furnace annealing, depth profiles, RBS, X-ray diffr., TEM anal. 7-51882
 Si, proton channelling, energy loss and straggling, inner shell electron collision calcs. 7-63699
 Si, volume capture effect for relativistic electrons, computer simulation 7-12156
 Si:Al, atom and acceptor depth distributions of channelled Al as a function of ion energy and crystal orientation 7-21247
 Si:As⁺(As₂⁺), ion implanted, phys. props., spreading resist., TEM, Rutherford backscattering, SIMS 7-26775
 Si:Hg⁺, ion implant range distributions, Rutherford backscatt. studies 7-2073
 Si:In, substitutional ion implanted dopants, electron and positron channelling studies 7-26778
 Si:P(Al), random and channelled implantation profiles and range parameters of dopants 7-21246
 Si:Ar:Hg⁺, ion implant range distributions, Rutherford backscatt. studies 7-2073
 Si-Ge multilayered structures, Bi ion implanted, projected range distrib., glancing angle RBS anal. 7-63689
 SiO₂, electron ionisation tracks, cluster anal. 7-58387
 SiO₂:Au(Bi), ion implanted, projected ranges and range straggling, RBS anal. 7-63690
 Ti-D, D stopping cross sections, deviations from Bragg's rule 7-51903
 YIG, irradiation by high energy heavy ions, electronic stopping power effects on damage rate 7-58352
 Zr-D D stopping cross sections, deviations from Bragg's rule 7-51903

energy measurement *see* power measurementenergy-range relations *see* energy loss of particles

energy resources

see also fuel; geothermal power; hydrogen economy; solar energy concentrators; solar power; wind power
 Arctic Ocean crust, seafloor geology and petroleum potential 7-18146
 Beijing area, China, geothermal resource of hot water aquifer 7-3622
 Canadian fusion research 7-10305
 Cauvery River and its tributaries, India, flow data, fit of gamma probability distrib. 7-55093
 coal deposits of USA, lignite deposits of Texas to Georgia region 7-18139
 cogeneration, oil, gas, coal gasification, issues in various countries, book 7-48200
 computer simulation model in energy crisis (*Japanese*) 7-23118
 conservation measures in industry, priority criterion 7-65385
 consumption rel. to economic growth 7-65384
 Dakongbeng geothermal area, SW China, hot spring activity 7-4064
 economic efficiency of energy conservation investment 7-65380
 energy supply without nuclear power (*German*) 7-59825
 environmental aspects 7-17924
 environmental aspects of energy consumption, climatic changes (*German*) 7-59881
 Gabcikovo-Nagymaros hydroelectric power scheme 7-29087
 global energy shortages, forecast energy consumption compared to world supplies (*German*) 7-59826
 hydro resources identification using enhanced satellite imagery, example from Peninsular Malaysia 7-17848
 Lena-Tunguska oil and gas province in eastern USSR 7-54942
 S Mangyshlak, Kazakhstan, USSR, oil and gas deposits 7-66028
 materials for energy utilization 7-28384
 national energy system, mathematical model for optimal functioning 7-65383
 oil and gas exploration, anal. of mesofractures visible in space images 7-66337
 oil fields of Los Angeles Basin, maturation age from 2D model of thermal evolution 7-66080
 oil/gas presence prediction, appl. of aerospace imagery 7-66335
 organic waste value enhancement through biometanization 7-17919
 recovery from wastewater treatment sludge 7-8355
 Regina, Saskatchewan, Canada, geothermal reservoir numerical model 7-18156
 regional approach to energy conservation based on entropy 7-65381
 solar and wind energy resources eval. in Jordan 7-54261
 Somalian energy trends and renewable resource potential 7-39949
 technologies of energy, mathematical models of substitution 7-65382

energy resources continued

- technology breakout in energy conversion, conf., San Diego, CA, USA (Aug. 1986) 7-60875
- Thailand, energy planning case study 7-54259
- USA economic activity, comparative roles of energy and money 7-65386
- USA, lignite deposits of Texas to Georgia region 7-18139
- USA wind power usage expansion prospects and requirements, workshop, Dallas, TX (March 1986) 7-65399
- Verkhoyansk folded zone, eastern USSR, fault dislocations and petroleum prospect 7-28918
- willow biomass production and utilisation 7-28406

energy states

- see also atomic structure; electron energy states (condensed matter); energy level crossing; molecular energy levels; nuclear energy levels; population inversion
- No entries

energy states in solids and liquids see electron energy states (condensed matter)

energy storage

- see also capacitor storage; direct energy conversion; energy storage devices
- Alice Springs Solar Pond project, technical and economic viability 7-40045
- alkali metal/halide thermal energy storage systems performance evaluation 7-65629
- aquifer seasonal thermal energy storage 7-65610
- aquifer thermal energy storage experiments, long and short term, Minnesota, USA 7-65612
- aquifer thermal energy storage for Canada Centre 12-storey office building 7-65607
- built-in type solar water heater performance analysis 7-3719
- chemical storage of solar energy, kinetics of H_2SO_4 and NH_3 reactions 7-40048
- chemical systems for seasonal medium and high-temp. thermal storage 7-65611
- convection coefficient effects on thermal energy storage in interior partition walls of buildings 7-28416
- convective layers solar ponds, sloping walls, shadow graph technique investigation 7-40046
- deep-basin solar stills, nocturnal distillation factors 7-3715
- dual temperature thermal storage with complex compounds 7-65620
- greenhouse solar system, transient response of latent heat storage 7-23227
- heat storage, high temp., using molten nitrate salt in insulated hot tank 7-65632
- heat storage from cogeneration processes, basin construction and measuring concept, west Berlin 7-65614
- hot water storage in aquifer, underground heat and fluid flow models 7-65600
- hydrated inorganic salts found in concrete, thermal energy storage appls. 7-17922
- ice slurry system for low temperature thermal energy storage 7-65622
- insertion materials for energy conversion and storage, review 7-28391
- integrated heat pipe-thermal storage design for a solar receiver, design anal. 7-65626
- large-scale heat accumulation at low temp. for domestic, industrial and farm heating (Portuguese) 7-13931
- latent thermal storage using pentaerythritol slurry, storage systems eval. 7-65616
- low temperature thermal storage using latent heat and direct contact heat transfer 7-65618
- low-temperature heat storage in unsaturated soils, design study 7-65606
- magnetic energy storage in vacuum, plasma opening switches at Pollux pulse power generator 7-32127
- main storage techniques (French) 7-59878
- MEATGRINDER circuit for enhanced energy transfer of inductive energy to imploding plasma loads 7-32131
- membrane stratified thermal storage system performance 7-65624
- mini-compressed air energy storage plant analysis and evaluation 7-23225
- nuclear power plant molten salt latent thermal energy storage for load following generation 7-65633
- Particle Beam Fusion Accelerator II (PBFA II), energy storage system 7-30765
- Particle Beam Fusion Accelerator II (PBFA II) Marx generator engineering and assembly line technology 7-30768
- PBFA II vacuum magnetically insulated transmission line redesign to inductive energy store 7-30755
- phase change material, one-dimensional solidification, charact. dimensionless time 7-63781
- phase-change material storage design for passive solar heating 7-8447
- photosynthetic bacteria reaction centre, electron transfer mechanism 7-23315
- plasma flow opening switch for magnetic energy storage 7-32124
- plasma flow switches, transmission line code modelling 7-32141
- plasma focus drivers, efficiency parameters for reactor conditions 7-63373
- polyethylene, form-stable high density, latent thermal storage unit performance 7-65602
- polyethylene, high density, latent thermal storage unit, heat transfer, numerical anal. 7-65603
- polytypes, electronic behaviour, rel. to energy conversion 7-38447
- pulsed power accelerators, low-jitter Marx generators for reliability 7-30766
- pulsed power supplies, IEEE conf., Arlington, VA, USA (1985) 7-35110
- semiconductor solar electric station-storage battery-solar stand, testing 7-34033
- small scale salt gradient solar ponds, parametric study 7-40035
- solar air heating systems, analytic model for performance prediction 7-59875
- solar collector water heater using sand for heat storage, transient anal. 7-23216
- solar district heating plant with rock cavern seasonal thermal storage 7-65609
- solar heated house, Jordan, thermal load reduction 7-54276
- solar hot water systems, control strategy and flow rate, comment and reply 7-8435
- solar methane reforming reactor for chemical energy transport 7-65589
- solar pond geometric mean temp. meas., digital meter design 7-54356
- solar pond simulation using upward flow through storage zone 7-65604

energy storage continued

- solar ponds, performance eval. and optimal control (French) 7-59869
 - solar receiver/reactors for thermochemical transport of solar energy 7-65591
 - solar shed greenhouses, storage of heat by forced air circulation 7-54270
 - solar thermal dish appls., sensible and thermochemical energy transport systems, economics 7-65414
 - switching problems, inductive storage plasma focus device, num. calc. 7-63368
 - technology breakout in energy conversion, conf., San Diego, CA, USA (Aug. 1986) 7-60875
 - thermal dynamics of a block-filled underground hot water store 7-46972
 - thermal energy storage, eval. of dual medium storage tank 7-65630
 - thermal energy storage, optimisation of packed bed of encapsulated phase-change material 7-65615
 - thermal energy storage, phase change materials testing, space appls. 7-65627
 - thermal energy storage, seasonal, in peat bogs, Motala, Sweden 7-65613
 - thermal energy storage at high temperatures, rapid charge and discharge rates 7-23226
 - thermal energy storage by thermochemical energy conversion and heat pumps 7-65568
 - thermal energy storage for organic Rankine cycle solar dynamic space power systems 7-65625
 - thermal energy storage for space solar power system, phase change materials compatibility 7-65628
 - thermal energy storage in deep sandstone aquifer, field observations, energy-transport model 7-65608
 - thermal energy storage in solar house, heat pump coupled to solar collector 7-65619
 - thermal energy storage system performance, impact of operation and control, DOE2 simulation 7-65621
 - thermal energy transportation from solar collector field to energy conversion facility 7-65590
 - thermal storage, phase change material melting process 7-65623
 - thermal storage, seasonal, choice of aquifer by numerical simulation 7-65605
 - thermal storage sizing methodology for solar cooling/power generation systems 7-65617
 - thermochemical energy transport for a large heat utility 7-65638
 - thermohaline system with mixed layer circulation, gradient layer entrainment 7-65601
 - transport of solar thermal energy by steam reforming of methane 7-65637
 - $Ba(OH)_2 \cdot 8H_2O$ latent heat storage unit, power range 2-6 kW, 25 kWh 7-8446
 - CO_2 -methane thermochemical energy transport system, closed-loop mode 7-65640
 - H_2 storage systems using thermochemical compression for transportation appl. 7-34072
 - H_2SO_4 decomposition and synthesis for chemical energy storage and transportation system 7-65639
 - H_2SO_4 , kinetics of heterogeneous reactions for chemical storage of energy 7-23229
 - Hg_2Cl_2 , photocatalytic props., O_2 photogeneration from water 7-54151
 - $K_2S_2O_8$ for chemical storage of solar energy 7-23228
 - $LaNi_{4.7}Al_{0.22}$ - $LaNi_5$, hydride chem. heat pump, thermodynamics 7-13926
 - Li-Na-K- CO_3 /MgO salt/ceramic phase change material for high temp. thermal storage, thermoanalytic investigation 7-65631
 - NH_3 , kinetics of heterogeneous reactions for chemical storage of energy 7-23229
 - $Na_2S_2O_8$ for chemical storage of solar energy 7-23228
 - Ni-Cd aerospace cells, study of long term storage effects 7-34018
- # energy storage devices
- composite thermal energy storage systems, high temp., for industrial appls. 7-65636
 - heat storage furnace, low-cost electric, using crushed rock for storage, residential use 7-65635
 - superconducting magnetic energy storage plant for electric utility load leveling, design and estimated costs 7-54369
 - superconducting solenoids appl., 1985 state and future potential (Czech) 7-59880
 - thermal energy storage using high temp. molten salt in hot tank 7-65634
- # energy transfer collisions, molecular see molecular inelastic collisions
- # engineering applications of computers see engineering computing
- # engineering computing
- see also aerospace computing; chemical engineering computing; civil engineering computing; control engineering computing; electrical engineering computing; electronic engineering computing; engineering graphics; mechanical engineering computing; nuclear engineering computing; telecommunications computing; virtual machines
 - compound parabolic concentrator collector, solar irradiance calc. using computer program 7-39964
 - droplet field visualization and characterization via digital image analysis 7-37577
 - laser Doppler velocimetry, multi-pt. system using phase diffraction grating 7-37605
 - numerical methods, innovative, in engineering, conf., Atlanta, GA, USA (March 1986) 7-12
 - optical system design, interactive ray-tracing program integrated with solid-modelling CAD system 7-50679
 - program for combining sound pressure levels in noise, BASIC 7-62909
 - solar cell array electrical output for flat plate tracking arrays 7-3690
 - solar still performance synthesis and predictions 7-23217
 - solar-heated farm buildings, short-term monitoring and computer aided performance 7-28413
 - water resources engineering, research projects, computer support 7-18215
- # engineering graphics
- 3D flow obs. by interferometry and image processing 7-37576
 - fluid mechanics education, computer graphics techniques for flow pattern visualisation 7-55939
 - metal-insulator-metal (semiconductor) structs., circuit anal., automated 7-27438
 - optical system design, interactive ray-tracing program integrated with solid-modelling CAD system 7-50679
- # engineering societies see societies
- # engineering workstations
- CAE-nuclear engineering analysis on 32-bit work-station computers 7-36083

engineering workstations continued

- nuclear power station simulation, parallel-processing modular system 7-10197
- reactor neutronic and thermal-hydraulic problems, solns. using engineering workstation 7-36084

engines

- see also *aerospace engines; heat engines; internal combustion engines; ion engines; propulsion*
- ceramic engine component fabrication techniques 7-3243
- ceramics, engine appl., conf., London, England (Nov. 1985) 7-5

entertainment

- cinema and lecture hall acoustic design by computer (*Hungarian*) 7-50850

enthalpy

- see also *heat of*
- alkali metal poly(styrenesulphonate)s, enthalpy of dilution, large dielectric constant solvent 7-21483
- alkali metals, condensed phase, thermodynamic props. study 7-32684
- 1-alkanols, vapour press. and thermal data simultaneous correls. 7-6767
- alkyl nitrites gas and liquid phases, syn-anti conformer equilib., MR chem. shift study 7-19895
- n-alkylamine-n-dodecane systems, static dielec. consts. and excess molar enthalpies 7-59134
- alkyne isomer groups, chemical thermodynamic props. data 7-60901
- alloy, solidification, differential thermal anal., modelling (*French*) 7-65024
- benzonitriles, substituted, thermodynamic functions 7-52082
- chlorocyclohexane, conformational enthalpy and vol. changes, Raman spectroscopy determ. 7-62383
- 2-(chloromethyl)-2-methyl-1,3-dichloropropane, conformational equilib., Raman and IR spectra study 7-46018
- compositional two-phase flow behaviour in pipelines, press. and temp. profiles prediction 7-20800
- condensation of flowing vapour on horizontal elliptic cylinder 7-58452
- convection/diffusion phase change, enthalpy formulation anal. 7-51118
- cyclohexane-methanol, liq.-liq. critical point, eqn. of state 7-12230
- 1-cyclohexyl-phenyl-2-methyl ethylenes, synthesis and phys. props. 7-1870
- 1,2-dichloroethane-n-alkane or -2,2,4-trimethylpentane liq. mixtures, excess enthalpy meas. and calcs. 7-6827
- dimethylether-Xe, vap. press. and density, excess molar enthalpy and entropy 7-12319
- glass, activation enthalpy for diffusion 7-38236
- graphite fibre reinforced epoxy, reflectance and thermal response during high-power CO₂ laser irradi. 7-32496
- hexamethylbenzene, phase transition, calorimetric obs. (*Japanese*) 7-16733
- II-VI-III-V systems, thermodynamics and reactivity 7-16790
- insulators, Schottky defect form. enthalpy-Debye temp. correl. study 7-26742
- laminar heat transfer and flow in curved square channels, elliptic nature, numerical visualisation 7-37432
- liquid crystals, monomers and polymers, mesophase behaviour, mol. structural effects study 7-63458
- magnesium poly(styrenesulphonate)s, enthalpy of dilution, large dielectric constant solvent 7-21483
- metals, thermodynamic functions of relative temps. 7-38225
- methyl methacrylate-n-heptane, excess enthalpies and vols. at 298.15K 7-44824
- methyl methacrylate-n-hexane, excess enthalpies and vols. at 298.15K 7-44824
- organic O O contrary comps. in C₁ to C₄ range, ideal gas thermodynamic props. 7-60904
- polymer mixtures, H bonding, enthalpy-IR freq. shift correl., acid-base interaction 7-51667
- polymeric glasses, enthalpy relax. determ. (*Japanese*) 7-38197
- polyvinyl methyl ether, ageing, enthalpy relax. meas. 7-8029
- pseudobinary alloys, tetrahedrally coordinated, Coulomb energy calcs. 7-1941
- smectic A₁ binary mixture, nematic phase creation, phase diagram, transition enthalpy comp. depend. study 7-12269
- solar cooling by direct evaporation from sprays 7-37532
- sphalerite single crystals, plastic behaviour between 473 and 873K, enthalpy calcs. from creep and stress relaxation tests 7-2093
- Stefan type problems, numerical methods 7-35489
- two-fluid corresponding states principle for prediction of enthalpy and entropy departures 7-51372
- Ag-Au-Zn ternary system, liq., thermodynamic functions (*German*) 7-44856
- Ag-Sn-Te system, ternary, enthalpy of mixing (*German*) 7-21469
- AgAl concentrated alloys, vacancy activation enthalpies 7-32431
- Al binary alloys liq., thermodynamic props. (*Korean*) 7-26978
- Al-Zn-Mg, serrated flow, second phase precip., dislocation ageing 7-22755
- α -Al₂O₃, cation solute segregation to surface 7-21593
- Co-B alloy, amorphous, thermodynamic, thermomag. and struct. studies (*French*) 7-16438
- Cu, pion decay site spectroscopy, interstitial sites 7-53191
- Fe-Co-Mo alloys, liq., H solubility meas. and estimates (*German*) 7-58487
- Fe_{1-x}O, wustite, defect clustering 7-51787
- Ge-Ba, liq. alloys, enthalpy of form. 7-23050
- Ge-Sr, liq. alloys, enthalpy of form. 7-23050
- Ge₂₀Te₈₀ glasses, heat capacity, relax. and thermodynamic kinetics during annealing 7-44843
- H₂O-CO₂(H₂S)(NH₃)(H₂SO₄)(H₃PO₄)(ZnCl₂)(CuCl₂), thermodynamic meas., bibliography of data sources 7-52070
- H₂O-LiBr absorption heat pumps, thermodynamic design data, heating 7-23209
- Hg_{1-x}Cd_xTe, pseudobinary melts, heat capacity, enthalpy of melting, thermal cond. 7-21477
- In-Bi, liq., heat of mixing, calorimetric study 7-12283
- Li₂SO₄-H₂O, supercooled melts, cryst. and mol. struct., thermal stability 7-21170
- Mg-Cu alloys, vap. press. meas. by boiling temp. method, thermodynamic props. 7-44778
- Mg(I), vap. press. meas. by boiling temp. method, thermodynamic props. 7-44778
- MgO, cation solute segregation to surface 7-21593
- Ni-C, C-vacancy binding 7-44601

enthalpy continued

- Ni-Pt, surface segregation, composition anal., AES studies 7-7999
- NO, physicochemical props. 7-21488
- NpO_{2-x}, hypostoichiometric, O dissociation press., partial thermodynamic functions 7-17520
- O₂-N₂ equimolar liq. mixture, excess props. and struct., mol. dynamics simulation 7-32246
- Pa vapour press. meas., form. enthalpy and bond dissociation energy calcs. 7-10765
- PaO₂ and PaO vapour press. meas., form. enthalpy and bond dissociation energy calcs. 7-10765
- Pb-Bi system, heat of fusion (*Russian*) 7-44766
- PdH₂, H-induced lattice expansion and effective H-H interaction 7-52247
- PdTi, enthalpy of form. by high temp. calorimetry 7-21410
- Sb-Ge-Zn system, thermodynamic investig. (*German*) 7-53703
- Se-Bi alloys, thermodynamic props. and phase equilib. 7-3276
- SiO₂-Al₂O₃, glassy system, thermal capacity, thermodynamic props. 7-12307
- SiO₂-TiO₂, glassy system, thermal capacity, thermodynamic props. 7-12307
- Si(001), biatomic steps 7-38309
- Sn-Bi system, heat of fusion (*Russian*) 7-44766
- U-Si-Fe, β to α phase transform., dilatometry, metallography 7-28036
- UO₂, Frenkel disorder, estimate of enthalpy contributions 7-6618
- UO₂, heat capacity, enthalpy, critical review 7-16787
- V-N system, phase equilib., crystallography, thermodynamic props. 7-28011
- VO, vaporisation study, mass-spectrometric anal. 7-6771
- VO-V mixture, vaporisation study, mass-spectrometric anal. 7-6771
- YrC_x (x=1,2) equilib. reaction, thermodynamic parameters evaluation, Knudsen effusion mass spectrometry 7-23054
- Zn-Ho alloy, two-phase, partial thermodynamic props., 690 to 1020K 7-7963
- Zr, α and β phases, differential heat of H absorption, isoperibol calorimetry studies 7-6967
- Zr-Ni metallic glasses, cryst. 7-21111
- ZrS₂, thermodynamic props., 298 to 1600K 7-28022

entropy*see also entropy of substances*

- λ -additive fuzzy measures, entropy 7-60947
- amorphous materials, structural anal., maximum entropy method 7-32285
- anisotropic honeycomb domain wall networks in uniaxial systems 7-26900
- big bang as the collapse of an ordered spin system 7-66798
- binary fluid mixtures, comparative anal. by extended irreversible thermodynamics and kinetic theory 7-16290
- black hole (quantised), spectrum and entropy 7-55703
- black hole accretion MHD, entropy accretion rate and moving black hole accretion 7-14599
- black hole entropy, classical derivation 7-47969
- Bragg-peak location employing a maximum-entropy formalism 7-11827
- chaos, ergodic theory 7-62657
- chaos, metric entropy estimation 7-61244
- chaotic dynamic system, temporal intermittency as multifractality in history space 7-24549
- chaotic systems, intermittency and Renyi entropies 7-24550
- cosmic microwave background, entropy of perturbed background radiation 7-66791
- cosmological particle creation, intrinsic measures of field entropy 7-35077
- CT methods use for nondestructive inspection under conditions of insufficient data 7-39818
- decoupling entropy and disorder, definitions 7-24616
- dimer model on square, bathroom tile lattices, entropy calcs. 7-61262
- disequilibrium and self-organisation, book 7-24328
- distribution and entropy of clusters in growth models 7-29915
- dynamic systems, generalized Caratheodory's construction, for dimens. char. acts. 7-48633
- energy conservation, entropy-based regional approach 7-65381
- entropy functions for symmetric systems of conservation laws 7-61300
- finite quantum systems, quasi-entropies, convexity props. 7-41157
- Fredholm integral equations, solution using maximum entropy method 7-41064
- freezing, density wave theory, thermodynamic consistency and entropy change calcs. 7-63845
- frustration models, two-dimensional, ordering and phase transitions due to entropy gains 7-246
- gas dynamics eqns., min. entropy principle 7-26235
- generalized dimensions and entropies from a measured time series 7-41256
- heat and power system long-term thermodynamic performance 7-3716
- heat conduction, variational techniques for nonlinear problems 7-62953
- heavy ion-nucleus collisions, relativistic, impact parameter dependence of specific entropy and fragment yield 7-19280
- heavy-ion collisions, entropy production, information and measurement theory 7-61901
- homogeneous chem. system. entropy prod. rate 7-13721
- ideal gas, classical statistical mechs. study 7-11578
- image reconstruction, maximum entropy data analysis 7-10874
- ion-molecule association and clustering form., thermochemical data 7-18514
- irreversible processes, general governing principles, entropy prod. 7-61301
- irreversible processes formulated in a superspace, quantum theory, variation principle 7-14869
- Ising antiferromagnet, ground-state entropies in two and three dimensions 7-45717
- ising antiferromagnets in maximum critical fields 7-17185
- Ising model, 3D thermodynamic functions at T>T_c (*Ukrainian*) 7-9781
- Ising model, multispin correls., multiparticle entropy method calcs. 7-45708
- Ising spin glass, three-dimensional, entropy and free energy, Monte Carlo simulation 7-17184
- isolated system, H-theorem and entropy production 7-41237
- kinetic theory of liquids, maximum entropy ensembles and equilib. soln. 7-26605
- kink solitons, activated generation, quantum theory 7-41123
- lattice spin system, microscopic anisotropy, influence on phase boundary, macroscopic behaviour 7-18730

- entropy continued
- Lebwohl-Lasher lattice model, inhomogeneous, Monte Carlo simulation 7-61261
- Liouville eqn., entropy evolution 7-29869
- low temperature thermal engines, problems with entropy 7-24618
- massive Schwarzschild black hole, entropy in stable thermal equilib. 7-24502
- maximum entropy distributions, existence criteria for prescribed first three moments 7-9809
- Measures of entropy and divergence 7-56200
- metals, twin-boundary energies and entropies, const. press. Monte Carlo calc. 7-2028
- micellar aggregates, packing of semi-flexible chains, statistical thermodynamics approach 7-28357
- multicomponent fluids, eqns. of motion, thermodynamical derivation 7-48653
- multicomponent systems, thermodynamics props., pairwise fluctuations 7-14900
- NMR spectroscopy, maximum entropy method calcs. 7-48797
- nonequilibrium ensemble dynamics 7-61214
- nonlinear irreversible processes, variational principle for entropy prod. 7-41324
- one-dimensional modal maps, topological entropy (*Chinese*) 7-35397
- ordered energy fluxes and exception to law of increasing entropy 7-24611
- Pacific Ocean, chaotic behaviour in large and mesoscale motions of Kuroshio current 7-55073
- phase-sensitive spectral analysis by maximum entropy extrapolation 7-48809
- phyllotaxis, universal model considering entropy and hierarchical primordia 7-65676
- plasma relaxation, entropy prod. 7-57980
- production during an early Universe isothermal phase transform. 7-4598
- radiative entropy production 7-31628
- redshift of distant objects and entropy 7-9544
- relative entropy, new characterization for normal states, appl. to quantum meas. problem 7-48659
- Rényi entropies, incompleteness 7-14857
- rigid particle suspensions, mass and entropy transport 7-32691
- self-diffusion and impurity diffusion coeffs., calculation with aid of elastic constants 7-16797
- space-time entropy of infinite classical systems 7-48669
- Stefan problem, two-phase, with interfacial energy and entropy 7-43633
- superstring model, baryogenesis and entropy generation 7-66801
- theory, Rudolf Clausius's contribution 7-35190
- thin spherical matter shell, gravitational entropy, beyond black holes 7-4750
- topological entropy and chaos of interval maps 7-56158
- transport theory connection with extended thermodynamics 7-29953
- two dimensional electron gas, thermodynamic props., interaction and disorder effects, HF approx. calcs. 7-2516
- two-fluid corresponding states principle for prediction of enthalpy and entropy departures 7-51372
- van der Waals fluid with entropy rate admissibility criterion, Riemann problem for nonisothermal system 7-18600
- variational principle, classical thermodynamics, second law formulation 7-48242
- viscoelastic bodies forced time-harmonic vibr. propag., acoustic scatt. inverse problem 7-62901
- Fe-Co, liq., thermodynamic mixing functions, Knudsen cell mass spectrometry (*German*) 7-21470
- No, physicochemical props. 7-21488
- VO solid solution, vaporisation study by mass spectrometric method, fusion reactor material 7-52027
- VO, vaporisation study, mass-spectrometric anal. 7-6771
- VO-V mixture, vaporisation study, mass-spectrometric anal. 7-6771
- entropy of substances
- actinide ions in aq. soln., thermodynamic props., oxidation states, coordination number and struct., review 7-12322
- adsorbed molecules, hindered rotations, energy levels and thermodynamic props. 7-27130
- air isentropic charge eqns. 7-31919
- alkyl nitrates gas and liquid phases, syn-anti conformer equilib., MR chem. shift study 7-19895
- alloys, order-disorder phenomena, Ising model calcs. allowing for atomic vibrations 7-21400
- ammonium hexafluorometallates, phase transitions 7-6787
- binary alloys, Monte Carlo calc. of configurational entropy and combinatorial factor 7-63846
- chain model, Edwards' continuous two-parameter, critical amplitudes 7-26616
- 1-cyclohexyl-phenyl-2-methyl ethylenes, synthesis and phys. props. 7-1870
- cyclosilanes, plastic and condit. crysts., thermal anal. 7-37910
- diffusion, isotope effect, quasi-harmonic calcs., appl. to CoO and NiO 7-26996
- difluorodichloromethane, mol. const., force field study, thermodynamics props. 7-19814
- dimethylether-Xe, vap. press. and density, excess molar enthalpy and entropy 7-12319
- gases, hard and Maxwellian mols., shock wave struct., local entropy balance, bimodal approach 7-26320
- glasses, surface singularities, topological origin 7-12444
- group IIB-VA liquid metal systems, Gibbs energy, composition depend. 7-52080
- III-V semiconductor-metal interface, thermodynamic stability considerations 7-21490
- lanthanide ions in aq. soln., thermodynamic props., oxidation states, coordination number and struct., review 7-12322
- liquid crysts., monomers and polymers, mesophase behaviour, mol. structural effects study 7-63458
- liquids, entropy changes and fluctuations near tensile instability 7-6830
- liquids, free volume, entropy, and relaxation phenomena 7-21484
- melting lines of simple substances, thermodynamic similarity and thermal props. calcs. 7-6762
- metal hydrides, thermodynamics of hysteresis at high pressures 7-39911
- metal nitrides, vibrational entropy 7-6745
- metals, electronic sp. ht., finite conduction electron lifetime correction calcs. 7-16784
- metals, liq., entropy, charged hard sphere model 7-21485
- metals, thermodynamic functions of relative temps. 7-38225
- entropy of substances continued
- methylammonium iodide, phase transitions, calorimetric and dilatometric studies 7-12261
- organic O O contrary comps. in C₁ to C₄ range, ideal gas thermodynamic props. 7-60904
- 4-(4-n-pentyloxybenzylideneamino)azobenzene, liq. cryst. transitions 7-63812
- physisorbed atoms on anisotropic rectangular lattice, struct. factor of incommensurate phases 7-52250
- point defect absorption by dislocations, preference parameter temp. depend. (*Russian*) 7-16607
- poly 4-methyl pentene-1, heat of fusion calc., PVT meas., X-ray diffr. 7-52007
- polybutene-1, heat of fusion, X-ray diffr. obs. 7-52008
- polymer, thermotropic, structure and structure formation, transition enthalpy/entropy 7-11962
- polymer chain, eqn. of state, entropy spring model 7-21394
- polymer gel in pure and mixed solvent media, phase transition 7-63431
- polymethylenes, melting characts., continuum model (*Russian*) 7-63782
- polystyrene, solid, liq., p-substituted, and crosslinked, heat capacity 7-44844
- rare earth aluminium Al₂ layered structural sintered composite, mag. entropy 7-59016
- simple gas, free expansion anal. by use of first law of thermodynamics 7-16293
- AgI-AgPO₃ glasses, thermoelec. power 7-6867
- Ag₄P₂O₇, glassy and cryst. states, thermal props., IR spectra 7-44845
- Al binary alloys liq., thermodynamic props. (*Korean*) 7-26978
- Al-Mg, liq., excess entropy of mixing, resist. calcs. 7-2571
- BaO-CeO₂, phase relations, thermodynamic parameters 7-6829
- BaTe, vaporisation thermodynamics and formation enthalpies (*German*) 7-26930
- Ca(OH)₂Zn(OH)₂·2H₂O, chem. comp., solubility in KOH, thermodynamic props., reaction equilib. const. 7-26962
- CaTe, vaporisation thermodynamics and formation enthalpies (*German*) 7-26930
- CeCu₂Si₂, lattice gas heavy fermion-boson model anal. of specific heat, entropy and magnetic susceptibility 7-58505
- Co-Sb system, α -solid soln., interdiffusion (*Japanese*) 7-6861
- CoO, defect processes, calc. using SHEOL code 7-58267
- Co-Si alloys, thermodynamic props. determ. by Knudsen cell mass spectrometry 7-26976
- Cu_{1-x}Ni_xCr₂O₄, heat capacity anomalies, cooperative Jahn-Teller effect 7-6823
- Dy₃Al₂O₁₂, refrigerant characts. for Carnot mag. refrigerator 7-56286
- EuS, refrigerant capacity and use in mag. cooling 7-56285
- Fe thermodynamic props., data tables and reviews 7-18512
- Fe-Co-Mo alloys, liq., H solubility meas. and estimates (*German*) 7-54847
- Fe_{1-x}O, wustite, defect clustering 7-51787
- FeSb₂O₄, thermodynamics studies, 10 to 300K 7-2231
- Gd₃Ga₅O₁₂, refrigerant characts. for Carnot mag. refrigerator 7-56286
- (GeSe₂)₇₀(GeTe)₁₅(Sb₂Te₃)₁₅, glass transition, thermodynamic and thermokinetic characts. 7-26953
- Ge₂₀Te₈₀ glasses, heat capacity, relax. and thermodynamic kinetics during annealing 7-44843
- In-Pb, liq., activities, temp. depend., EMF obs. (*Japanese*) 7-12320
- In-Tl, liq., activities, temp. depend., EMF obs. (*Japanese*) 7-12320
- In-Tl (23 at.%) alloy, FCC, thermodynamics of ferroelastic phase transition 7-2189
- K-Pb liquid alloys, excess stability, entropy 7-26975
- Li cpds., energy stability, struct., vibr. spectra, MO LCAO SCF calcs. 7-15512
- Li-Mg, liq., excess entropy of mixing, resist. calcs. 7-2571
- Li₂Mo₂Se₈ intercalation cpd., entropy and struct. transition, lattice gas model 7-6832
- Li₂Mo₂Se₈ intercalation cpd., entropy, electrochem. cell calorimetry studies 7-6833
- Li₂V₆O₁₃ single cryst., Li transport props. and partial molar entropy 7-6871
- Mg-Cu alloys, vap. press. meas. by boiling temp. method, thermodynamic props. 7-44778
- Mg(I), vap. press. meas. by boiling temp. method, thermodynamic props. 7-44778
- Mn_{0.63}Cr_{0.37}As, thermal, mag. and struct. props. of transitions, thermodynamics, 10 to 350 K 7-64463
- Na-Pb liq. alloy, thermodynamic prop. and transport coeff. 7-64199
- NbC_{1-x}, thermodynamic props., 1200-2500 K 7-44849
- Nb₂Sn_{1-x}Sb_x Al₁₅ pseudobinary alloy, structural transitions and related anomalies 7-38182
- NiSb₂O₄, thermodynamics studies, 10 to 300K 7-2231
- NpO_{2-x}, hypostoichiometric, O dissociation press., partial thermodynamic functions 7-17520
- O₂ liquid, SRO, thermal and mag. props. (*Russian*) 7-32253
- Pb-Bi system, heat of fusion (*Russian*) 7-44766
- Pb₃Cr₃F₁₉, nonlinear optic, lattice const., ferroelec. Curie temp., phase transition obs. at 555K 7-17275
- Pd-T system, solubility meas., comparison with Pd-D and PdH systems 7-21474
- Pd_{0.8}Ag_{0.2}-T systems, solubility meas., comparison with Pd_{0.8}Ag_{0.2}-D and Pd_{0.8}Ag_{0.2}-H systems 7-21474
- PdH, films, H absorption, press.-composition isotherm studies 7-52248
- Pd-Rh alloys, surface composition, lattice vibrational entropy 7-52207
- PuSb, heat capacity meas. 7-12975
- Sb-Ge-Zn system, thermodynamic investig. (*German*) 7-53703
- Si, thermodynamic props., data tables and reviews 7-18512
- SiO₂-Al₂O₃, glassy system, thermal capacity, thermodynamic props. 7-12307
- SiO₂-TiO₂, glassy system, thermal capacity, thermodynamic props. 7-12307
- Sn-Bi system, heat of fusion (*Russian*) 7-44766
- SrTe, vaporisation thermodynamics and formation enthalpies (*German*) 7-26930
- Ta-C_{1-x}, thermodynamic props., 1200-2500 K 7-44849
- Ti-Co, liq. alloys, thermodynamic props., mass spectrometry (*Japanese*) 7-52084
- TiCl₂, crystn. heat of form. and entropies data base 7-18511
- TiCl₃, crystn. heat of form. and entropies data base 7-18511
- TiCl₄, heat of form. and entropies data base 7-18511
- UB₂, lattice gas heavy fermion-boson model anal. of specific heat, entropy and magnetic susceptibility 7-58505

entropy of substances continued

- VC_{1-x}, thermodynamic props., 1200-2500 K 7-44849
 Zr-Sn, diffusion, chem. activity, modified evaporation method 7-38243
 Zr-Ti, diffusion, chem. activity, modified evaporation method 7-38243
 ZrO₂, high press. phase, cryst. struct. 7-16523
 ZrS₂, thermodynamic props., 298 to 1600K 7-28022

environmental degradation

- see also corrosion; stress corrosion cracking*
 asbestos-brucite-polyphenylene sulphide composites 7-53925
 bisphenol-A-polycarbonates, outdoor lifetime depend. on terrestrial UV irradiance spectrum 7-54357
 brass plated steel cords, mech. and cohesion props. in sulphurising environment 7-39740
 Cibachrome materials, permanence improvements under adverse display conditions 7-355
 composite materials, hygrothermal behaviour, new prediction methods 7-21492
 composites, response in adverse environment, reliable modelling, implication of 7-65169
 conference, tribology and lubrication, Tokyo, Japan (July 1985) 7-4631
 corrosion-related aspects of the chemistry and freq. of occurrence of atmospheric precipitation 7-46664
 cycloaliphatic epoxy resin, ageing, irradiation environmental conditions effect 7-33707
 epoxy composites, Fe powder reinforced, flexural props., water condition temp. depend. 7-59587
 fluorozirconate glass, chem. durability, reaction with water 7-39682
 fusion devices, plasma interactive components, neutron damage, sputter erosion 7-49623
 fusion reactor materials selection 7-49626
 glass fibre reinforced polyester laminate, hydrothermal ageing, degradation, US obs. 7-13708
 glass fibre reinforced polymers, hydrothermal behaviour, mech. props. rel. to water absorpt. 7-46665
 graphite, intercalated fibre elec. conductors, passivating coatings 7-8140
 graphite fibre reinforced epoxy, interface modified, moisture effects 7-3476
 graphite fibre reinforced epoxy, thermomech. behaviour, space rad. effects 7-51828
 Hexsyn rubber, high-flex ozone resistant, prep. and appl. 7-13767
 implanted cardiostimulators, polymeric insulation degradation (Czech) 7-23487
 Inconel X-750, air environment/creep interactions, prior exposure times effect 7-13499
 IR materials erosion due to rain, optical damage characterisation 7-31411
 laminated thick composite plates, buckling, hygrothermal effects 7-11321
 marble tombstone weathering due to air pollution, Philadelphia, USA 7-59886
 metal matrix composites, fatigue crack propag., effect of aq. environments 7-17624
 metals and alloys, environmentally assisted cracking at high vel. 7-65213
 natural fibre reinforced polyester composites, fabrication, mech. props., weathering 7-7956
 nylon 6 and 66, impact strength in dry and moist states 7-3414
 optical fibres, silicone-coated, influence of pH solns. on strength and dynamic fatigue 7-6006
 PMMA, environmental stress cracking in methanol, mol. props. effects 7-65153
 polyetheretherketone, penetrant durability rel. to processing and struct. 7-65168
 polyethylene, interlamellar links, environmental stress cracking agent effect 7-53928
 polyethylene, low density, environmental stress cracking in methanol, heat treatment effect 7-8146
 polymer. composite structure, thermal and thermomech. response 7-8150
 polysulphide rubber-butadiene-acrylonitrile copolymer/PVC blend, mech. props., ageing and solvent resist. 7-39593
 polysulphones, degradation and stabilisation, review 7-59652
 polyvinyl alcohol films, heat treatment, light irradiat., polyene mixtures, absorpt. spectra 7-53432
 rubber toughened plastic, surface embrittlement, fracture mechanics 7-28161
 rubber vulcanizates, natural and styrene butadiene, environment effect on friction and wear 7-8131
 steel, austenitic stainless type 316, unlubricated wear at room temp., environment influence 7-8121
 steel, Ni-Cr-Mo, pressure vessel, environmentally assisted fatigue crack growth 7-17638
 wollastonite reinforced polyamide 6, strength props., depend. on humidity and temp. 7-39636
 B⁺-Al₂O₃-Na₂O solid electrolytes, degradation in Na-S batteries 7-3466
 As-S glass IR fibre, Teflon clad, optical loss due to water diffusion 7-57556
 B fibre reinforced Al matrix composites, transverse mech. props., isothermal exposure effect 7-39688
 C fibre reinforced plastic laminates, ply failure under moisture and temp. influences (German) 7-22744
 C fibre reinforced plastics, strength, thermomech. props. thermal spiking and moisture absorpt. effect 7-28085
 C fibre reinforced polymer cracks, lightweight construction appl. (German) 7-22825
 a-C:H diamond-like coating on Ge, rain erosion resistance improvement obs. 7-31435
 C/glass fibre reinforced hybrid composites, aligned short fibres, SCC prop. 7-13615
 CoCr Permalloy films, weather resistance 7-28183
 Fe-Ni-Cr alloys, internal carburisation, effect of S 7-33839
 Mo, thermodynamic stability in a fusion reactor environment, H, O and C implantation and diffusion 7-49658
 Ni-Cr, high temp. alloys, carburisation, finite difference model of C diffusion 7-39712
 SiC, sintered, fracture after Li exposure 7-28103
 Sm₂O₃, aging in air 7-65160
 W, thermodynamic stability in a fusion reactor environment, H, O and C implantation and diffusion 7-49658
 ZnO ceramics ageing under AC voltage (French) 7-39564
 ZrO₂, Y₂O₃ stabilised, amorphous second phase, sintering, grain morphology, fracture roughness, surface degradation 7-46612

environmental engineering

- see also air conditioning; cooling; ergonomics; lighting; safety; space heating; temperature control; ventilation*
 acid rain deposition modelling for policy anal. 7-13944
 appropriate technology (AT) (Japanese) 7-23234
 Clyde River pollution control and cleaning 7-13941
 computers in environmental science, conf., Los Angeles, CA, USA (Nov. 1986) 7-48175
 environmental information software, waste management case study 7-8472
 flooding due to urbanization 7-54384
 flow visualisation, laser light sheet method for building environmental engineering 7-37570
 groundwater flow, transport velocity representation, environmental appls. 7-55114
 microcomputer-based relational database system for monitoring water quality for the Niagara Falls drinking water treatment plant 7-54419
 running averages, an efficient algorithm 7-8465
environmental requirements *see environmental engineering*
environmental stress cracking *see environmental degradation; stress corrosion cracking*
environmental testing
see also corrosion testing
 CCDs for ROSAT star sensors, testing and characterisation 7-29401
 fibre optic coupler, fused biconic taper, environmental performance 7-26003
 LMFBR, 316SS fuel cladding tube, stress-loaded corrosion tests in I₂ or Te (Japanese) 7-61958
 Nevada desert test site heat pump strategy 7-8429
 optical fibre cable integrated OTDR/throughput loss meas. system for environmental testing 7-43460
 optical particle counters, method for cross calibration 7-56398
 photon counting imaging microchannel plate detectors calibration, for EUV astronomy 7-29404
 polymer glazings for Ag mirror protection, evaluation and modification 7-37094
 solar cell array, hot-spot testing and analysis 7-34041
 splice, mechanical, for permanent fibre optic installation 7-26006
 CdS/CdTe screen-printed thin-film solar cell for indoor consumer electronics (Japanese) 7-65472
enzymes *see proteins*
ephemerides *see astronomical ephemerides*
epitaxial growth
see also liquid phase epitaxial growth; vapour phase epitaxial growth
 2D systems, proceedings of Winter School, Mauterndorf, Austria (Feb. 1986) 7-48131
 3D ICs, selection rule for epitaxial growth techniques, LPE, MOVPE and MBE 7-46326
 atomically controlled growth in 2, 1 and OD, and applications 7-52370
 conference, Boston, MA, USA (Dec. 1985) 7-18508
 ferromagnetic monolayers 7-2909
 growing crystal, correl. between chemoeptaxial temp. and thermodynamic characts. (Russian) 7-58704
 ice formation on substrates, crystallographic config., cooling rate and direction (Japanese) 7-6569
 laser direct writing and laser-assisted CVD of III-V cpds. on GaAs 7-13373
 long chain molecules, epitaxial crystallisation, morphological, structural study 7-16901
 Monte Carlo simulation of continuous-space crystal growth 7-6568
 rare earth silicide epitaxial formation by rapid annealing 7-21768
 sapphire, implanted ions recrystallisation driven migration and oriented precipitation 7-2266
 semiconductor, interaction of high power pulsed ion beams, solid phase epitaxy 7-12096
 semiconductor infrared detectors, conf., Innsbruck, Austria (April 1986) 7-60871
 semiconductor quantum well and 2D electron gas structures, epitaxial growth 7-52310
 semiconductors, doped, prep. and thermal cond., review 7-38279
 semiconductors, ion beam induced epitaxial crystn., kinetics, mechanisms and microstruct. 7-12171
 semiconductors, solid-phase epitaxial regrowth, amorphous-crystalline interface evolution 7-12568
 silicide formation on Si, epitaxial nature, initial nucleation processes and effect 7-21767
 SOI, conf., Boston, MA, USA (Dec. 1985) 7-35101
 SOI films, halogen lamp recrystallisation 7-38394
 SOI large area growth, pseudo-line electron beam technique with lateral seeded epitaxy (Japanese) 7-7842
 SOI lateral solid phase epitaxy, selective P ion implantation 7-52359
 SOI structures, lateral epitaxy formation, melting and resolidification 7-38386
 solid-state devices and materials, conf., Tokyo, Japan (Aug. 1986) 7-48173
 SOS, crystalline quality improvement by ion beam technique 7-16651
 SOS, double solid phase epitaxial regrowth, amorphous layer, self-implantation, ion energy, defect density 7-58691
 SOS, ion beam improved, elec. characts. 7-17114
 strained layer superlattices, symposium, Annandale, NJ, USA (June 1986) 7-48150
 structural transitions in epitaxial overlayers 7-27194
 transition metal silicide, on Si, progress review 7-21766
 transition metals, metallic epitaxy on semiconductors 7-27211
 Al₂Ga_{1-x}As layers, form. by regrowth on surface of GaAs during contact with undersaturated liq. containing Al 7-46311
 Al₂O₃-MgO, diphasic xerogels, densification, sintering, isostructural seed, epitaxy 7-27987
 As (0001), laser pulsed oxidation modification 7-58320
 Au, epitaxial growth on W (100), adsorbate props. 7-38329
 Au-Ge-Ni-GaAs, non-alloyed ohmic contact, solid phase epitaxy 7-27423
 Ca_{1-x}Ba_xF₂ epitaxial layer growth and struct., electron microscopy studies 7-27174
 CaF₂, epitaxial growth, conf., Toronto, Ont., Canada (May 1985) 7-9588
 CaTiO₃, ion implantation, crystallisation of amorphous surface layers 7-58304
 CoSi₂, epitaxial growth, conf., Toronto, Ont., Canada (May 1985) 7-9588
 CoSi₂-Si, mesotaxy, single crystal growth of buried CoSi₂ layers 7-58671

epitaxial growth continued

- CoSi₂-Si, solid phase epitaxial growth of CoSi₂, nonultrahigh vacuum method 7-45043
- CoSi₂-Si epitaxial heterostructures, growth and characterisation 7-27212
- CoSi₂-Si heterostructures, MBE or solid phase epitaxially grown, Schottky barrier heights, DLTS spectra 7-12859
- FeSi₂, on Si, effects of thin interposing layers 7-22471
- GaAs layers, effect of impurities on solid phase epitaxial growth 7-16907
- GaAs, ohmic contact, form. using ion beam mixing 7-21299
- GaAs, solid-phase-epitaxy, interface structure and impurity effects 7-2407
- GaAs-Si, ion implanted, amorphisation and epitaxial regrowth, defect depth profiles 7-12088
- a-GaAs-Si (100), epitaxial regrowth by excimer laser annealing, FET fabrication 7-32875
- Ge, amorphous layers on GaAs, solid phase epitaxial Growth during annealing 7-21777
- Ge heteroepitaxy on CaF₂-Si structures, planarised growth by electron beam exposure to predeposited layers 7-52855
- Ge-CaF₂-Si epitaxial structures, growth, structural and electrical props. 7-38356
- Ge₂Si₃, epitaxial growth, conf., Toronto, Ont., Canada (May 1985) 7-9588
- InAs surface on InP, epitaxial regrowth 7-2431
- InP-Si, ion implanted, rapid thermal annealing and solid phase epitaxy 7-21296
- Mo (100), pulsed laser irradiated, use of LEED for surface damage charact. 7-21592
- NbSe₂, thin film fabrication on MoS₂ by van der Waals epitaxy (*Japanese*) 7-12547
- Ni, oxidation, oxide epitaxy depend. on growth temp., LEED, AES, ellipsometry studies 7-22869
- Ni-GaAs, interphase contact and interaction 7-16880
- Ni-GaAs interfacial reactions, contact elec. props. 7-12504
- Ni-Si, interphase contact and interaction 7-16880
- NiSi layer on Si (111), solid phase epitaxial growth from Si/Ni multilayer structure 7-7071
- NiSi₂, epitaxial growth on Si (111) inside miniature size oxide openings 7-58673
- NiSi₂-Si, epitaxial growth of silicide layers by electron beam annealing 7-27213
- NiSi₂-Si:B(BF₃), epitaxial growth of NiSi₂, influence of dopant atoms 7-45039
- Pd-Ge ohmic contacts to InGaAsP-InP, solid-phase epitaxial growth 7-2706
- Pt-group metal silicides epitaxial growth on Si (111) 7-21760
- Si, amorphisation and crystallisation 7-11914
- Si, amorphised films, solid phase epitaxial regrowth, TEM characterisation 7-32883
- Si, atomic imaging using JEOL 4000 EX TEM 7-32230
- Si, crystalline and amorphous, Monte Carlo growth simulation models 7-16470
- Si, epitaxial growth, conf., Toronto, Ont., Canada (May 1985) 7-9588
- Si, epitaxial growth using dual heating, slip dislocations and radial temp. gradient 7-38366
- Si epitaxial layers, autoping effects 7-63635
- Si films, solid epitaxial regrowth, structural and electrical characteristics 7-38403
- Si films, solid phase epitaxial regrowth on epitaxially grown MgO:Al₂O₃ 7-38399
- Si, ion implantation, interstitial trapping, dopant migration and epitaxial regrowth 7-12103
- a-Si, ion implanted, 2D model of nucleation and regrowth 7-38408
- Si materials science issues in IC processing 7-35115
- Si on insulating substrates, zone melting recrystallisation 7-2414
- Si polycrystalline films on (100) Si substrate, epitaxial alignment using rapid thermal processing 7-38413
- Si, self-implanted, defects and amorphisation 7-2041
- Si, solid-phase amorphous to crystalline transformation for shallow junction processing 7-32642
- Si wafers, self and ion beam annealing, epitaxial growth and damage layer, TEM study 7-12172
- Si:Ar, high dose implanted, thermal regrowth, RHEED studies 7-21734
- Si:Ar⁺, ion implanted thin film, defect form., dose depend. study 7-51793
- Si:As ion implanted, defect structs. generated by buried amorphous layer regrowth 7-38078
- Si:B, ion implanted, transient annealing and residual defect DLTS study (*Chinese*) 7-12642
- Si:B, O epitaxial wafers, effect of pre- and postdeposition annealing on O precipitation 7-45060
- Si:BF₃⁺, ion implanted, solid phase epitaxial growth, cross-sectional TEM study 7-38364
- Si:Ge⁺, ion implanted and annealed, crystalline to amorphous transformation, TEM study 7-32643
- a-Si:P, selective doping and solid phase epitaxial growth, MOSFET appls. 7-27893
- Si-CaF₂-Si structure, reduction of Ca and F surface segregation by solid phase epitaxy of Si 7-38357
- Si-GaF₂-Si epitaxial structures, growth, structural and electrical props. 7-38356
- Si-Ge interface, solid phase epitaxy, intermixing, EXAFS, AES, LEED obs. 7-63973
- Si-SiO₂, buried layer SOI structs., elevated temp. high dose O⁺ implantation, effect of annealing 7-32530
- Si-SiO₂, lateral solid phase epitaxial growth, SOI transistors fabrication 7-2399
- Si-SiO₂, SIMOX wafers, epitaxial growth 7-32878
- Si-SiO₂, SOI structure, lateral solid phase epitaxial growth, TEM study 7-38369
- Si-TiSi₂, TiSi₂ local epitaxial growth on Si (111); rapid thermal annealing, annealing ambient 7-33856
- SiC polytype heteroepitaxial growth, and identification by Raman scatt. study 7-63992
- Sn, graphoepitaxial growth on monatomic steps, TEM, electron diffr. studies 7-58714
- Te-based thin films, crystn. rate, thermal stability, erasable optical recording appl. 7-37069
- Ti Si₂ epitaxial growth kinetics on (111)Si, TEM study 7-58683

epitaxial growth continued

- TiN_x epitaxial layers, atomic and electronic struct., growth, physical props. 7-32854
- ZnSe laser-induced epitaxial growth on GaAs using organic compounds 7-52366
- epitaxial layers**
see also *magnetic epitaxial layers; metallic epitaxial layers; semiconductor epitaxial layers*
- defects at epitaxial layer-substrate interface 7-21715
- epitaxial films, MOCVD growth on Si substrates, substrate offset angle effects 7-22567
- heteroepitaxial systems, domain size determ. from LEED angular profiles 7-7075
- interface structure determination by CB diffraction from epitaxial crystals 7-16899
- ion beam sputtering deposition growth technique 7-64030
- multilayer epitaxial films, X-ray diffr. determ. of elastic stresses and misalignment (*Russian*) 7-38371
- structural transitions in epitaxial overlayers 7-27194
- structure charactn. by Burger precession camera 7-58099
- thin films, interfaces and phenomena, conf., Boston, MA, USA (Dec 1985) 7-18502
- X-ray photoelectron diffr. studies of surface and epitaxial overlayer structures, review 7-27862
- BaF₂ epitaxial buffer layers for semiconductor heteroepitaxy 7-12522
- Ca_{1-x}Ba_xF₂ epitaxial layer growth and struct., electron microscopy studies 7-27174
- CaF₂ epitaxial films on Si, structural and electrical props. improvement by rapid thermal annealing 7-38400
- CaF₂, MBE growth of epitaxial insulator-metal-semicond. struct., CaF₂-CoSi₂-Si 7-22496
- CaF₂, MBE on Si and overgrowth with Si or Ge, characts. 7-22495
- CaF₂/GaAs (100) 7-64902
- CaF₂-BaF₂ epitaxial bilayers on Si (111), characterisation 7-12521
- CaF₂-Si, heteroepitaxy of Si and Ge 7-22497
- CaF₂-Si, interface struct., high resolution TEM study 7-2394
- CaF₂-Si (111), interface form., photoemission study 7-2395
- CaF₂-Si (111), MBE grown, electronic struct. 7-2725
- Ca₂Sr_{1-x}F₂ layers, epitaxial growth on CaF₂ by vac. evap. 7-22498
- Kr, physisorbed films on Pt (111), impurity-quenched orientational epitaxy 7-45003
- NiSi₂-Si, Schottky barrier, interfacial defect states 7-27428
- NiSi₂-Si, Schottky barrier height, structural characterisation 7-27429
- NiSi₂-Si (111), Schottky barrier height, rel. to Fermi level positions 7-27427
- PLZT, ferroelectric films, properties and applications 7-59156
- PbTiO₃, ferroelectric films, properties and applications 7-59156
- Si (111)/CaF₂, interface and surface phonons; high resolution EELS study 7-38319
- TiN (100) epitaxial film sputtering, defect density, ion irradiat. effects, TEM study 7-58684
- TiN_x epitaxial layers, atomic and electronic struct., growth, physical props. 7-32854
- (YEuTmCa)₂(FeGe)₂O₁₂, epitaxial films, O ion adsorpt. bubble diameter variation effect 7-22125
- ZnSe interference filters, thermally deposited and molecular-beam-grown, CW laser pumped bistability 7-25861
- epitaxy** see *epitaxial growth*
- EPR** see *paramagnetic resonance*
- EPR line breadth**
alkali metal tetrafluorotetracyanoquinodimethan(TCNFQ₄), charge transfer salts, comparative EPR studies 7-53114
- amorphous systems, spin Hamiltonian, resonance 7-2922
- ascorbic acid radical anion, Ca²⁺ exchange, ESR line broadening meas. of rate const. 7-28270
- β-(BEDT-TTF)₂AuBr₂, conducting charge transfer salt, struct. and props. 7-58259
- (BEDT-TTF)₂I₃, α and β phases, CESR 7-2930
- p-benzosemiquinone radical anion, halogenated, mol. motion, electron spin relax. 7-45796
- N-(4-butoxybenzylidene)-4'-butylaniline smectic G liq. cryst., orientational order 7-37847
- copper phthalocyanine iodide, anomalies in proton NMR spin-lattice relaxation 7-2815
- decamethylcobaltocene, electronic struct. and dynamic Jahn-Teller effect EPR 7-59104
- decamethylnickelocenium, electronic struct. and dynamic Jahn-Teller effect EPR 7-59104
- diluted magnetic systems, single ion and pair EPR lineshape 7-7587
- disordered metals with nuclear-spin impurities, ESR study 7-22135
- disordered systems, ESEEM and ENDOR spectra, model calcs. 7-53176
- double modulation EPR spectra, nonlinear behaviour 7-33267
- electron relaxation studies, review 7-22158
- ferroelectric phase, dipole impurity-induced ESR line broadening calcs. 7-53131
- fluorene-1,2,4,5-tetracyanobenzene, charge transfer cryst., triplet excitons, ODMR and ESR 7-7611
- graphite, ultrafine, heats of combustion, ESR meas., depend. on exposure to air 7-33266
- ion-implanted polymers, fractal elec. cond., current transients, percolative transition calcs. 7-2645
- MBBA, paramagnetic dopant mol. slow tumbling motion, EPR shift and broadening meas. 7-16458
- MEM(TCNQ)₂ spin-Peierls compounds, far IR ESR studies 7-22133
- perylene salt, organic conductor, spin transport props., pulsed ESR study 7-59105
- poly-4(3-pyridyl),8-methyl,2,3,6,7-quinolino ladder polymer, electronic props., I doping effects 7-64526
- polyacetylene, alkali metal doped, role of spin-orbit coupling in EPR spectra 7-64527
- polyacetylene, alkali metal doped, semiconductor-metal transition, EPR study 7-64528
- trans-polyacetylene, neutral soliton diffusion, EPR, PMR meas. 7-64513
- polyacetylene, prepared by Durham route, EPR meas. 7-64529
- trans-polyacetylene, pristine, neutral soliton dynamics, anisotropic ESR T₁ and line width 7-7585
- trans-polyacetylene, spin photogeneration, light-induced ESR studies 7-64514
- trans-polyacetylene, vibronic states of bond alteration defect, ESR spectrum 7-64511

EPR line breadth continued

- polyazulene, in situ optical and ESR studies during electrochemical doping 7-26670
 polymers, solid, solvent swelling and noninvasive visualisation by ESR imaging 7-45797
 polythiophene film, photoinduced effects 7-52876
 powdered systems, spin Hamiltonian, resonance 7-2922
 rare earth adsorbates on metal surfaces, EPR line shapes 7-53129
 semiconductors, n-doped insulating phase, ESR line shape studies 7-22134
 spectral calc., Fokker-Planck forms, Lanczos algorithm, conjugate gradient method 7-53111
 spin glasses, amorphous transition metal-metalloid, EPR linewidth, theory 7-45805
 TCNQ salt, N-n-propyl phthalazinium 7,7,8,8 TCNQ₂, struct., elec., mag. props., EPR meas. 7-33005
 BaMnF₄, 2D Heisenberg magnet, spin dynamics and EPR linewidth 7-38932
 Cd_{1-x}Mn_xTe semimag. semicond., ESR line shape meas., comp. and temp. depend. 7-7584
 Cd_{1-x}Mn_xTe_{1-y}Se_y, magnetic suscept. and ESR meas., temp. depend. study 7-45636
 CsH₂AsO₄ ferroelec. cryst., EPR studies of AsO₄⁴⁻ centres 7-45816
 CsH₂PO₄·Cu²⁺ pseudo-1D ferroelectric, 3D correl., EPR meas. 7-38931
 CsMnCl₃·2H₂O, 1D Heisenberg magnet, spin dynamics and EPR linewidth 7-38932
 Cu complex, aliphatic polyamine Cu (II), ESR hyperfine line width 7-19891
 Cu complex, bis(diisopropylsalicylato)copper(II) pyridyl nitronyl nitroxide, mol. conform., ESR study 7-57103
 Cu complexes, L-phenylalanine salt, EPR study 7-59106
 Cu(NO₃)₂·2.5 H₂O, EPR and magneto-microwave birefringence powder spectra 7-45810
 Cu₂S, stoichiometry and phase transitions, Cu²⁺ EPR studies 7-17219
 GaAs:Ti³⁺, EPR 7-45811
 Ge-Al₂O₃:Cr, layer-substrate structs., ESR, line-shape, nondestructive contactless meas. of layer conductivity 7-38924
 KFeS₂, hydrogenated, ESR meas. in 100 to 320K range 7-13016
 KH₂PO₄:Ti²⁺, impurity centres, ESR line width studies 7-38498
 K₂MoO₃, CDW state, metastable EPR study 7-53125
 MnPS₃, layered cpd., mag. props. 7-52951
 MnSi, amorphous, concentrated spin glass, ESR study 7-13022
 (NH₄)₂H(SO₄)₂·Cu²⁺ single crystals, EPR study 7-53118
 (NH₄)₂SO₄, phase transitions, appl. of NH₃⁺ paramag. probe to mol. motion 7-27604
 Ni(BF₄)₂·6H₂O, EPR lineshape function 7-38930
 Ni(ClO₄)₂·6H₂O, EPR lineshape function 7-38930
 RbH₂PO₄:Ti²⁺, impurity centres, ESR line width studies 7-38498
 Si:P, metallic, nearly-localised electron spin dynamics, EPR linewidth study 7-22110
 Si-SiO₂, SOI structs. formed by O⁺ implantation, EPR of defects 7-33272
 Si-SiO₂ interface, ESR signal from P_{bo} centres, anisotropic props. 7-38940
 SiH₃ radical in Xe matrix, EPR line shape 7-10632
 SiO₂-Al₂O₃-MgO-Cr₂O₃ glass, magnetism of spinel microcrystals, ESR study 7-27594
 U_{1-x}Gd_xO₂, solid soln., microcharacterisation by ESR, XPS and mag. susceptibility meas. 7-12957
 Zn_{1-x}Mn_xTe semimag. semicond., ESR line shape meas., comp. and temp. depend. 7-7584
 ZnTiF₆·Cu²⁺·6H₂O, Jahn-Teller effect and phase transitions, powder EPR study 7-13023

EPR spin echo *see spin echo (EPR)*

EPROM *see PROM*

E²PROM *see PROM*

epsilon meson resonances *see eta meson resonances*

equalisers

- active free-field equalizer for TDH-39 earphones 7-28768

equations

- for equations used in specific subjects, *see the specific indexing heading*
see also Bethe-Salpeter equation; differential equations; equations of state; functional equations; integral equations; nonlinear equations
 degenerate operator equations, solutions, optimization of regularization methods 7-35224

equations of state

- see also* equations of state of gases; equations of state of liquids; equations of state of solids; phase transformations; thermodynamics
 n-vector model and polymers, parametric eqn. of state 7-51986
 alternative binary system, two-dimensional, critical state 7-63783
 binary fluid mixtures, eqn. of state, high temp. and high press. 7-21385
 binary mixtures, eqn. of state, radial distrib. functions 7-32595
 Cauchy problem for linearised Navier-Stokes eqns. with allowance for compressibility 7-43964
 computational continuum dynamics, introduction 7-4800
 constitutive eqns., free energy functions, statistical and continuum mechanics 7-21389
 diatomic mols., quantum mechanical virial theorem, electronic kinetic energy and pot. energy representations 7-49872
 driven diffusive system, critical behaviour, field theoretic renormalisation group study 7-9811
 Grueneisen parameter, measurement from shock attenuation in a strongly decaying shock wave 7-21384
 hadronic systems eqn. of state, S-matrix statistical mechanics formulation, many-particle process effects (*Russian*) 7-41772
 hard ellipsoids of revolution, phase diagrams calcs. 7-2192
 hard sphere diameter, temp. depend. 7-16382
 homogeneous spinodal phase, stability boundaries, thermodynamic functions homogeneity (*Russian*) 7-41325
 Hugoniot values, calc. from atomic props. 7-44735
 infinite-pressure excess functions and VLE K values from liquid-phase activity coefficients 7-16708
 interaction third virial coefficients 7-44734
 linear scaling theory model and eqn. of state comparison 7-41316
 local pressure in quantum system, virial expansion 7-41129
 multicritical phenomena and critical dynamics, differential renormalisation group generators 7-38159
 neutron stars, magnetic moments of stars with different eqns. of state 7-40857

equations of state continued

- nuclear matter equation of state, relationship to relativistic heavy ion collisions 7-35969
 parametric, metastable fluid phase, thermodynamic props. at stability boundary, linear scaling theory model calcs. (*Russian*) 7-2140
 particles adsorbed on spherical surface, statistical thermodynamics, canonical ensemble 7-41231
 plasma, role of Planck-Larkin partition function in occupation numbers for reacting plasmas 7-55440
 pure-compound vapour pressures, direct calc. through cubic equations of state 7-16709
 quantum second virial coefficient paradox 7-24614
 rheology, conf., Ann Arbor, MI, USA (Oct. 1985) 7-18481
 scaling pressures and nonequilibrium props. 7-21391
 second virial coeffs., semi-theoretical correl., temp. depend. Lennard-Jones pot. calcs. 7-6749
 shock release adiabat approx. using the Hugoniot 7-21354
 shock waves, stability in media with arbitrary eqn. of state, quasi 1D anal. and numerical modelling 7-63180
 statistical mechanics of small systems, virial expansion calcs. 7-29863
 thermodynamical mechanical work, discussion on use of conventions (*Spanish*) 7-61306
 two-fluid corresponding states principle for prediction of enthalpy and entropy departures 7-51372
 Universe, depend. of baryon asymmetry on eqn. of state 7-24243
 van der Waals fluid, Riemann problem, numerical integration 7-38153
 van der Waals potentials, clustering, mol. dynamics and Monte Carlo calcs. 7-37829
 vapour-liquid equilibria calcs., cubic equation of state 7-38174
 N-vinyl carbazole-alkyl methacrylate random copolymers, thermodynamic props. (*Russian*) 7-26982
 visual theorem, applications 7-35174
 H₂+Ar(Kr)(Xe), pot. energy surfaces calcs. 7-50301
 HF, intermol. pot. model including polarisability 7-25623

equations of state of gases

- binary hard sphere mixtures eqns. of state, van der Waals perturbation term calcs. 7-12226
 binary-gas mixtures, phys. props. prediction, SSR-MPA and MSK pots. 7-51361
 Boltzmann gas, semi-relativistic, fitting formulae for eqn. of state 7-40685
 bromotrifluoromethane, liq. and gaseous phases, compression factor, vapour press. meas. 7-51905
 chain molecules, eqn. of state, Flory theory, continuous-space analog 7-12229
 ethane dilute gas thermophysical props. correl. and extrapolation, SSR-MPA pot. model calcs. 7-16294
 laboratory plasmas, weakly and strongly coupled, unified eqn. of state 7-11576
 metastable phase, parametric eqn. of state, use of linear model 7-58439
 methane-H₂ mixture, isochoric meas. at temp. from 140 to 273.15K, eqn. of state, density 7-26377
 methanol, compressed gas and liq. PVT props. meas., pseudoisochores determ. 7-16713
 mixtures with supercritical gases, vapour-liq. equilb. calcs., excess Gibbs energy method 7-6768
 molecular gases, second virial coeffs., nonspherical mol. interaction contribs. calc., improved numerical tables 7-16284
 monatomic gases and their mixtures, dilute gas props. 3 parameter MSK pot. calcs. 7-16285
 normal fluid chain-like molecule mixtures, quartic hard chain eqn. of state calcs. 7-12227
 P-V-T isotherms of real gases 7-9623
 n-pentane, vol. ratios, compressibilities, 278-338K, pressures up to 280 MPa 7-51906
 perturbed soft-chain theory, thermodynamic props. prediction, group-contrib. correlation 7-16711
 polar fluid, Soave-Redlich-Kwong equation of state 7-16710
 primary gas thermometry, harmful volume influence elimination, electro-physical method 7-310
 real fluid in critical region, eqn. of state, thermodynamic props. 7-58430
 refrigerants and mixtures, eqn. of state, hard sphere calc. 7-56273
 second virial coeff., kinetic theory derivation 7-29633
 second virial coefficient, reduced representation by straight lines 7-20830
 spherically symmetric pair-pot. energy fn., second acoustic virial coeff. method calc. 7-62481
 vapour-liquid equilibria, group contrib. eqn. of state calcs. 7-51985
 CO₂-ethane gaseous mixture, determ. of virial coeffs., ref. index meas. method 7-51362
 H₂-containing mixtures, interaction parameter in Peng-Robinson eqn. of state 7-16712
 H₂-hydrocarbon vapour-liquid equilibria and saturated densities at high press. and temp. 7-16707
 N₂ dilute gas thermophysical props. correl. and extrapolation, SSR-MPA pot. model calcs. 7-16294
 O₂ dilute gas thermophysical props. correl. and extrapolation, SSR-MPA pot. model calcs. 7-16294
 SO₂ vapour, second virial coeff., intermol. pair pots., mol. dynamics simulation method study 7-31908
 Xe, equation of state behind strong shock waves, fluid integral eqn. approach 7-20827

equations of state of liquids

- alcohol-water mixture, volumetric behaviour, high press. study 7-51904
 (n-1) alkane-butanone-polydimethylsiloxane solns., total and preferential sorption coeffs. 7-6499
 alloys, amorphous and liquid, internal press. kinetic component, eqn. of state calc. (*Russian*) 7-2139
 binary hard sphere mixtures eqns. of state, van der Waals perturbation term calcs. 7-12226
 bromotrifluoromethane, liq. and gaseous phases, compression factor, vapour press. meas. 7-51905
 chain molecules, eqn. of state, Flory theory, continuous-space analog 7-12229
 cyclohexane-methanol, liq.-liq. critical point, eqn. of state 7-12230
 discontinuous potentials, mol. dynamics of hard dumbbells and vibr. hard dumbbells 7-41249
 electrolytes, strong, equations of state 7-6750
 fluids containing small or large mols., thermodynamics, low-density and high-density contrib. 7-52077
 glass and melt, relaxational processes, eqn. of state 7-21386

equations of state of liquids continued

- hard sphere and disphere fluid mixtures, investig. 7-11867
- heavy water, equation of state, international standard 7-51988
- Lennard-Jones fluid, 2D, virial eqn. of state 7-6747
- metastable phase, parametric eqn. of state, use of linear model 7-58439
- methanol, compressed gas and liq. PVT props. meas., pseudoschores determ. 7-16713
- mixtures, pressure-volume-temperature behaviour correl. to zero-shear viscosity 7-21501
- mixtures with supercritical gases, vapour-liq. equilb. calcs., excess Gibbs energy method 7-6768
- nonelectrolyte liquids and their mixtures, eqns. of state and struct. 7-26898
- normal fluid chain-like molecule mixtures, quartic hard chain eqn. of state calcs. 7-12227
- octyloxycyanobiphenyl reentrant nematic, preferred density model, P-V-T test 7-12271
- n-pentane, vol. ratios, compressibilities, 278-338K, pressures up to 280 MPa 7-51906
- perturbed soft-chain theory, thermodynamic props. prediction, group-contrib. correlation 7-16711
- polar fluid, Soave-Redlich-Kwong equation of state 7-16710
- polymer soln. mixtures, vapour-liq. equilb., quartic hard chain eqn. of state calcs. 7-12228
- polymeric fluids, nonequilibrium extensions of Simha-Somcynsky equilb. theory 7-21387
- polymeric liquids and glasses, equations of state, multiple hole energy model 7-21388
- polystyrene mixtures in benzene solns. light scatt. virial coeffs. 7-44737
- polystyrene solns., integrated intensity light scatt., conc., temp., mol. wt. depend. 7-46056
- polystyrene-poly 2-chlorostyrene blend system, miscibility, vol. changes 7-44830
- real fluid in critical region, eqn. of state, thermodynamic props. 7-58430
- reference states for liquid density temp. dependence 7-26899
- refrigerants and mixtures, eqn. of state, hard sphere calc. 7-56273
- rheology, conf., Ann Arbor, MI, USA (Oct. 1985) 7-18481
- seawater, equation of state using UNESCO formula (Russian) 7-40488
- statistical methods, conf., Oaxtepec, Mexico, Jan. 1986 7-24268
- 1,3,5-trimethylbenzene, melting point meas., liq. self-diffusion study, hard-spheres method 7-52003
- vapour-liquid equilibria, group contrib. eqn. of state calcs. 7-51985
- water, supercritical, heat transfer and turbulent flow in vertical tube 7-51142
- CO₂ saturated liq., sp. ht. meas. 7-16783
- CO₂-Ne soln. thermodynamic props. near CO₂ vaporisation crit. point 7-12316
- H₂, cryogenic, high press. eqn. of state, laser interferometric meas. method 7-30027
- H₂-containing mixtures, interaction parameter in Peng-Robinson eqn. of state 7-16712
- H₂-hydrocarbon vapour-liquid equilibria and saturated densities at high press. and temp. 7-16707
- N₂ fluid, eqn. of state and vibron freq. thermodynamics, Monte Carlo, calcs. 7-12231
- N₂, liquid, molecular dissociation and shock-induced cooling at high densities and temperatures 7-28307
- N₂, shock-induced molecular dissociation 7-23022
- O₂, shock-induced molecular dissociation 7-23022

equations of state of solids

- alloys, amorphous and liquid, internal press. kinetic component, eqn. of state calc. (Russian) 7-2139
- amorphous solid polymers, yield prediction, nonlinear viscoelastic constitutive eqn. 7-22767
- ferroelectrics, and low temp. renormalisation group 7-64585
- glass and melt, relaxational processes, eqn. of state 7-21386
- graphite, adsorption of N₂, second surface virial coefficient 7-6970
- metals, thermodynamics during high-pressure shock 7-21352
- NaCl single cryst., high temp. elasticity meas., rectangular parallelepiped reson. method 7-63714
- P-T-X phase diagrams calc. using FORTRAN 77 programs PT-SYSTEM, TX-SYSTEM and PX-SYSTEM 7-38161
- polyepoxide co sulphide, elec. cond., press. and temp. depend. 7-21516
- polyethylene, monoclinic form, hydrostatic compression effect 7-44690
- polyethylenoxide, cryst., eqn. of state, anharmonic theory calcs. 7-32596
- polymer chain, eqn. of state, entropy spring model 7-21394
- polymeric liquids and glasses, equations of state, multiple hole energy model 7-21388
- polymers, gaseous diffusion, eqn. of state, free vol. concepts 7-21390
- polyoxymethylene, cryst., eqn. of state, anharmonic theory calcs. 7-32596
- polytetrahydrofuran, cryst., eqn. of state, anharmonic theory calcs. 7-32596
- rheology, conf., Ann Arbor, MI, USA (Oct. 1985) 7-18481
- shock Hugoniot eqn. of state, electron band theory approach 7-21392
- shock wave compression, review 7-21351
- shock waves, equation of state calcs. 7-21393
- spherical shock wave propagation and Hugoniot 7-32574
- steel, C, plane load wave, elastic precursor decay, eqn. of state 7-33751
- temperature effects on universal eqn. of state of solids 7-44736
- Zircalloy, mech. eqns. of state of material irradi. at 573K in deform. in working direction 7-8064
- Al, fourth-order thermal expansion coeff. fn. 7-44868
- Al, Hugoniot meas. to 420 GPa using a two-stage light-gas gun 7-21397
- Al, thermodynamics during high-pressure shock 7-21352
- Ar, high press. eqn. of state, interatomic pots. 7-58431
- Ar, solid, high press. eqn. of state 7-21396
- Au, static compression, basis for ruby pressure scale calibration 7-18802
- Au thermodynamic props., universal eqn. of state of solids 7-44736
- CaSiO₃, perovskite type, cryst. struct., lattice dynamics and eqn. of state 7-58248
- CsI, shock wave overtake meas. 7-21353
- Cu, fourth-order thermal expansion coeff. fn. 7-44868
- Cu, shock Hugoniot, ab initio interatomic pot. calcs. 7-21395
- Cu, static compression, basis for ruby pressure scale calibration 7-18802
- Ge, fourth-order thermal expansion coeff. fn. 7-44868
- Ge, structural props., ab initio pseudopotential calcs. 7-44797
- H₂, cryogenic, high press. eqn. of state, laser interferometric meas. method 7-30027
- H₂, dynamic isentropic loading, high press. eqn. of state, computational simulations 7-32747

equations of state of solids continued

- He, high density props., exponential-six pot. 7-32742
- MgSiO₃, perovskite type, cryst. struct., lattice dynamics and eqn. of state 7-58248
- NH₃, cryogenic, high press. shock temp. meas. 7-32566
- NaCl, thermodynamic props., universal eqn. of state of solids 7-44736
- Ni-Ti, Nitinol, thermodynamics 7-58506
- Si, fourth-order thermal expansion coeff. fn. 7-44868
- SiC, cubic, ab initio calc. of ground state props. 7-6751
- SiO₂, fused, frequency dependent equation of state 7-51987
- SiO₂-CaO-MgO-Na₂O glass, frequency dependent equation of state 7-51987
- ThC powders, structural stability, eqn. of state, press. up to 36 GPa 7-16688
- UFe₂, spin-polarised energy bands, density of states and eqn. of state 7-58734
- W monosized spherical powder, dynamic compaction 7-39458
- W, shock Hugoniot meas. 7-21398
- Xe, thermodynamic props., universal eqn. of state of solids 7-44736

equilibrium, chemical see chemical equilibrium

equilibrium, phase see phase equilibrium

equilibrium constants see chemical equilibrium

equilibrium diagrams see phase diagrams

equivalence classes

see also automata theory

quantum logics, Gudder conjecture and joint distrib. 7-18625

equivalent circuits

see also network analysis; network synthesis

- broadband analysis of a coaxial discontinuity used for dielectric measurements: solutions of direct and inverse problems 7-35540
- cable theory applied to blowfly receptor cells and large monopolar cells 7-47038
- DC arcs, equivalent circuits synthesis, math. modelling based on MHD description of plasma (Russian) 7-57986
- fibre optics, transmission line circuit model description 7-62833
- inductance standards, LF models comparison 7-18834
- nonlinear LC circuit, coupled Toda lattice with mass interface, soliton propag. study 7-29920
- nonlinear LC circuit, Toda lattice soliton scatt. with mass interface study 7-29919
- piezoelectric ceramics, thickness mode (French) 7-2976
- piezoelectric ceramics with low Q coeff. (French) 7-2977
- quartz, crystal growth, pragmatic model for simulation of self-induced striations 7-11973
- RF plasma reactors, plasma sheaths, modelling 7-31991
- SAW interdigital transducers, equiv. oct. taking propag. loss into account 7-20565
- SAW metallic gratings, equivalent network analysis 7-20563
- semiconductor-dielectric boundary, surface state density spectrum determ. using equivalent three element circuit (Russian) 7-27434
- semiconductor-electrolyte interface, equivalent circuit model, Mott-Schottky data dispersion 7-22008
- solar cells volt-ampere characts. meas. (Slovak) 7-39994
- tail thin piezoelectric bar, two-dimensional equivalent circuit 7-1366
- ultrasonic transducer bodies and matching stubs construction (Rumanian) 7-20552
- Al/Al₂O₃/Au thin film struct., dielec. props. meas. and equivalent circuit anal. 7-17115
- GaAlAs laser diodes, stripe geometry, directly modulated in microwave range, freq. response study 7-11017
- Zn passive electrodes, space charge effects 7-28315

erbium

see also nuclei with

- atom, low-lying states electronic density, ab initio multiconfiguration DF calcs. 7-15486
- fluoride glass:Er³⁺, impurity luminesc. and absorpt. spectra studies 7-53386
- fluorophosphate glass:Er³⁺, impurity luminesc. and absorpt. spectra studies 7-53386
- glass:Er³⁺, lasing props. 7-43109
- magnetic struct., synchrotron X-ray scatt. studies 7-45625
- VPE growth on W substrate, field electron emission microscopy 7-64029
- BaFCl:Er³⁺, charge transfer excitation and emission spectra 7-64688
- BaYb₂F₈:Er, energy levels Stark struct., crystn. field interactions 7-58782
- CaF₂:Er³⁺, H⁻(D⁻), IR excitation and absorpt. spectra anal. of sites 7-53306
- Er II, hyperfine struct. meas. by collinear fast beam laser and RF laser double reson. spectra 7-49957
- Er:BaYb₂F₈ active medium optimisation, lasing parameters at 1.96 μ m 7-31330
- Er:YAG laser, quasistationary generation, cross-relax. mechanisms 7-57339
- Er³⁺:CaF₂ IR laser, Q-switched, CW operation 7-43107
- Er³⁺:CaF₂ IR lasers, upconversion pumping 7-43111
- GaAs:Er MBE layer, dopant trapping level, photolum. obs. 7-44581
- GaInAsP:Er semiconductor injection laser, single longitudinal mode operation at 1.5 μ m 7-50558
- InP:Er liquid phase epitaxial films, elec. props. in strong elec. fields 7-38779
- K(Y, R)₂W₂O₈:Er³⁺ (R=Gd, Er, Lu) single crystals, stimulated emission spectra 7-7716
- LaF₃:Dy³⁺(Ho³⁺)(Er³⁺), surface temp. meas., fluoresc. appl. 7-19947
- La₂O₃S:Er, Nd, mag. susceptibility, dielec. const. and dielec. losses 7-2810
- LiLuF₄:Er³⁺, stimulated emission spectroscopy 7-13179
- LiNbO₃:Er laser-induced grating characteristics 7-62746
- LiYF₄:Ho³⁺, Er³⁺, Tm³⁺, excited-state absorpt., energy transfer, fluoresc. study 7-22322
- LiYbF₄:Er, energy levels Stark struct., crystn. field interactions 7-58782
- Si:Er, neutron irradi., Hall effect, elec. cond., IR absorpt. spectra 7-51834
- SmB₆:Er³⁺, Jahn-Teller phenomena in valency-mixing surroundings 7-45240
- SmB₆:Er³⁺ energy gap temp. depend., impurity ESR study 7-45151
- SrF₂:2YF₃:Er³⁺, interionic interaction, occupation kinetics, stimulated emission 7-46072
- (Y, R)₃Al₂O₁₂:Er³⁺ (R=Er, Lu) single crystals, stimulated emission spectra 7-7716

erbium continued

- (Y,Sc)₃Ga₂O₁₂:Cr³⁺,Er³⁺, spectral, luminesc. and lasing props., Stark sublevel lifetimes 7-25827
 YBO₃:Er³⁺, nonradiative energy transfer, activator ion interactions, laser-excited luminesc. study (*Russian*) 7-22345
 YOCl:Er, Yb, antiStokes luminesc., 1.5 μ m region 7-13223
 Y₂O₃:Er, Nd, mag. susceptibility, dielec. const. and dielec. losses 7-2810
 ZnSe:Er, impact cross section of Er³⁺ in luminesc. spectra 7-46150
 ZnSe:Er³⁺, ion implanted, identification of cathodolum. centres 7-53417

erbium alloys

- Au-Er dilute alloys, Er³⁺ crystalline electric fields, screening effects 7-27307
 Co₃Er noncrystalline alloy, local atomic order, magnetism 7-32286
 Cu-Er, thermodynamic props. rel. to glass forming ability 7-38204
 Cu-Er metallic glass, ion beam mixing, diffusion and phase separation meas. 7-16659
 Er-Cu (Ni) metallic glass form. by near-isothermal cold rolling 7-22610
 Er-H solid soln., mag. props., H addition effects 7-7510
 ErAg, sp. ht. meas. 0.5 to 21 K 7-52994
 ErAl₂, intrinsic coercive field 7-45729
 ErAl₂ single crystals, low temp. heat capacity meas. in mag. field, mean field approx. calcs. 7-27530
 ErAuCu₄, cubic alloys, mag. props. 7-52936
 ErCo₅, magnetocrystalline anisotropy, rare earth contribution 7-45659
 ErCo glasses, electronic struct., photoemission and magnetism 7-64060
 ErCo₂Ni₂, ferrimag. cpds., mag. anisotropy, temp. depend. 7-64450
 ErCo₅Sn₂₃ cryst. struct. and mag. suscep. studies (*Russian*) 7-21161
 Er₂(Fe,Co)₁₄B, struct., composition depend. 7-51701
 Er₂(Fe,Mn)₁₄B, struct., composition depend. 7-51701
 Er_{0.135}Fe_{0.813}Bo_{0.052} melt spun ribbons, mag. and struct. props. 7-59059
 Er₂Fe₁₄B alloys, magnetic anisotropy and spin reorientations 7-38855
 Er₂Fe₁₄-Co₂B, spin reorientations 7-64484
 Er₂-Th₂Fe₁₄B alloys, mag. props., comp. depend. study 7-7492
 Pd-Er alloys, elec. resist., temp. depend., Matthiessen's rule deviations 7-45269
 Sn-Er binary system, phase diagram and equilib. 7-7961
 Ti₃Al-Nb-Er rapidly solidified alloy, microstruct. effects and dispersoid stability 7-22669

erbium compounds

- see also erbium alloys*
 concentrated crystals, interionic interaction, stimulated emission 7-27744
 formate dihydrate, circular dichroism meas. 7-17301
 silicides, electronic struct., X-ray emission spectra studies 7-52419
 Ca₂ErF₇, fluorites, superlattice structs. 7-44485
 CrEr₂S₇, synthesis, physicochemical props. 7-44470
 Dy₂O₃-Er₂O₃-Ho₂O₃, mixtures, IR reflectance spectrum, wavelength standard 7-41330
 Er complexes, (tricarbamidotriacetato)erbium(III) monocarbamide, cryst. struct. 7-12029
 Er-Cr-B system, phase equilib., isothermal section at 1270°C 7-22647
 ErCl₃-GaCl₃-SOCl₂ system, solution viscosity 7-21500
 ErFeO₃, antiferromag. domain struct., spin reorientation region 7-45723
 ErFeO₃, low temperature phase transition, soft mode 7-38867
 ErFeO₃, magnetodynamic resonance near low-temp. phase transition 7-38862
 ErFeO₃, muon bonding sites, muon spin rot. study 7-45896
 Er_{0.187}Ho_{0.813}Rh₄B₄ re-entrant superconductor US attenuation obs. 7-2782
 Er_{0.705}Ho_{0.295}Rh₄B₄ re-entrant superconductor US attenuation obs. 7-2782
 ErIG, mag. prop. calc. 7-52977
 Er₂Ir₂Si₃, existence and electrical props. (*French*) 7-17008
 Er₂Os₂Si₃, existence and electrical props. (*French*) 7-17008
 ErRh₄B₄, body-centred tetragonal, cryst. struct., X-ray diffr. study 7-26704
 ErRh₄B₄ ferromagnetic supercond., coexistence phase, spin-orbit scatt. effects 7-22077
 ErRh₄B₄, magnetic transition temps., RKKY interaction studies 7-22107
 ErRh₄B₄, superconducting and ferromagnetic transitions 7-64385
 Er₂(SO₄)₃·8H₂O, magnetic and hyperfine props., cryst. field effects calcs. 7-27305
 ErSi₃, behaviour under ion bombard. and O exposure, AES, EELS 7-33506
 ErSi_{2-x}Si, silicide thin films, phase composition, conductance, surface morphology 7-7072
 HfO₂-Er₂O₃, solid soln. single crystals, physicochem. props. 7-2097
 HfO₂-Er₂O₃, solid solution single crystal growth 7-7838
 Li(Er,Y)P₄O₁₂ and Li(Ho,Er,Tm)P₄O₁₂, flux cryst. growth 7-13345
 SrF₂-2(Y_{1-x}Er_x)F₃ intracentre transition probabilities and luminesc. self-quenching 7-22332
 (UO)₂Er₂S₃, crystal struct. and oxidation state (*French*) 7-11999
 (Y,Er)₃Al₂O₁₂:Er³⁺ single crystals, stimulated emission spectra 7-7716
 Y_{1-x}Er_xF₃ and Y_{1-x}Er_xTm_{1-x}F₃, 1.5 μ m IR excitation of visible lum. via resonant energy transfer 7-46100

ergodic theorem *see statistical mechanics***ergonomics**

- see also human factors; man machine systems*
 VDU image polarity, ergonomic aspects 7-54571
 Zeiss/Oberkochen PLANIMAP system extensions 7-40620

erosion

- alluvial river channel, modelling of channel development 7-18234
 Antarctic meteorites, clay-mineraloid weathering products 7-34951
 Bangladesh ship scrapping area on Chittagong coast, pollution study 7-18212
 bare arable soils in E Shropshire, England, rainfall, runoff and erosion 7-9039
 Cape Shoalwater, Washington, USA, rapid coastal erosion 7-28991
 cliff erosion at Chesapeake Bay, Maryland, USA, due to groundwater 7-66123
 coastal wetland erosion accompanying coastal submergence 7-29029
 conference, Durham, England (Jan. 1984) 7-48138
 continental denudation balanced by accretion of oceanic crust 7-4021
 Deccan upland region, India, late Quaternary alluvial history and climate 7-60287
 Delaware Bay, USA, coastal wetland erosion accompanying sea level rise 7-29029
 desertification indicators 7-8452
 desertification process, importance of drought in intensification of desert conditions 7-8453

erosion continued

- desertification processes responsible for land degradation 7-8449
 England, Carboniferous sandstones origin, role of erosion 7-47409
 eroding surface profile during ion sputtering, Huygens' construction study 7-27842
 S Europe, desertification processes 7-8451
 geomorphology, book 7-48211
 hillslope failure due to groundwater seepage 7-29112
 ice thin films, ion irradiation erosion effects meas., astrophysical discussion 7-26814
 SW Idaho batholith, USA, erosional and chemical denudation rates meas. 7-9038
 IR materials erosion due to rain, optical damage characterisation 7-31411
 Japan, river flooding and land-slides during July 1985 in Noto area (*Japanese*) 7-18226
 Kavaratti atoll, sandy beach sediment transport processes (in India Ocean) 7-14257
 Port Lianyangang, muddy beach geology and erosion on Yellow Sea coast (*Chinese*) 7-55013
 Loess Hills region of Iowa, USA, Quaternary geology and geomorphology 7-47441
 Louisiana coast, USA, coastal changes accompanying rapid land subsidence 7-4023
 measurement of rock erosion rates, by cosmogenic ³He content analysis 7-60500
 Mississippi delta barrier islands, geomorphic recovery after hurricane erosion 7-4024
 Norwegian Channel, in Skagerrak-Kattegat region, seismic evidence for glacial erosion model 7-14233
 ocean bottom boundary layer with suspended sediments, model including turbulence 7-34470
 W Oregon, USA, rain-on-snow runoff and erosion 7-23788
 Pamlico Sound, USA, coastal wetland erosion accompanying sea level rise 7-29029
 rain splash erosion beneath tropical forest canopy, study of rain throughfall 7-34561
 rill erosion, transporting capacity of overland flow on plane and irregular beds 7-14317
 river with sandy bed, bridge pier scouring and dune migration (*Japanese*) 7-18225
 rivers, conf., Jackson, MS, USA (March to April 1986) 7-41008
 Rouge River, Quebec, migration patterns of asymmetric meandering river rel. to erosion and sediment transport 7-23765
 salt marsh creek, River Esk, Cumbria, seasonal changes in surface level 7-8914
 shore wave field, numerical modelling by boundary element method 7-55079
 soil degradation in drylands 7-8455
 soil erosion, model of dispersion of splash droplets from water drop impact 7-9036
 soil erosion by lahars following Nevado del Ruiz, Colombia, 1985 November 13 eruption 7-34431
 soil erosion planning, vectorization of Landsat TM land cover classification data 7-47443
 soil erosion planning in Dane County, Wisconsin 7-47442
 Solar Max samples, erosion studies 7-46743
 tektites, Australasian Muong Nong-type, buried crazed layers 7-8954
 E Texas, storm flow and sediment losses from site-prepared forestland 7-23768
 turbulent jet flow perpendicular to flat plate, shear stress meas. by erosion technique 7-31898
 E USA, agriculture impact on soil erosion in Chesapeake Bay area 7-23707
 valleys morphology on Hawaii, evidence for groundwater sapping and comparison with Martian valleys 7-55095
 wind erosion, measurement apparatus, book 7-35136
 wind erosion climatic factor, theory 7-8948
 wind erosion vulnerable areas, detection by satellite remote sensing of dust storms 7-8949
 a-C:H diamond-like coating on Ge, rain erosion resistance improvement obs. 7-31435
 S thin films, MeV He⁺ beam erosion, temp. depend. yield meas. 7-27847

error analysis

- see also error correction*
 3D 2-phase incompressible flow displacement, finite element analysis and error analysis (*Chinese*) 7-16229
 compressible flow, accuracy of nonuniform-mesh schemes 7-51202
 convection, linear 1D eqn., numerical dispersion by upwind differencing 7-26267
 DIAL meas. of O₃ in stratosphere from Space Shuttle 7-40560
 DREAM data reduction and error anal. routines, appl. to single cryst. diffr. intensity meas. 7-16348
 ellipsometric characterisation of single mode fibres 7-43428
 finite element viscoelastic analysis, integration error controls 7-20601
 flow, inviscid compressible, mesh refinement, for adaptive FEM 7-37485
 free convection near wall, random method with creation of vorticity 7-20728
 irradiance calc. in D* determ., precision improvement (*Chinese*) 7-48825
 linear elasticity, post-processing procedures for FEMs 7-14777
 membrane/plate equilibrium finite element models 7-1429
 Navier-Stokes eqns., arbitrarily convex quadrilateral elements (*Chinese*) 7-16144
 neutron spectra, error analysis for iterative algorithm 7-49493
 parabolic troughs, comprehensive optical anal., universal error parameters derivation 7-65411
 plate/shell error indicators and accuracy improvement of finite element solutions 7-1430
 plate/shell problems, effect of asymptotic error estimate studies 7-1428
 point projection onto a linear manifold, computing algorithm error anal. 7-24405
 random geostrophic modes and first-guess errors, spatial statistics 7-4162
 relative error minimisation, associated nonlinear integral eqn., harmonic mean 7-61014
 solar cell I-V characteristics, parameter recovery, curve fitting error criteria 7-39995
 time constant determination in kinetic studies involving radiolabelled tracer molecules 7-34236

error analysis continued

- visual double stars, obs. by 'old generation' observers, errors statistical anal. 7-14602
- vortex filament method, convergence 7-51179

error compensation

- see also error correction
- ellipsometer for birefringent components and systems meas. (*German*) 7-24687
- hot-wire anemometer compensated for ambient temperature variations 7-16275
- laser Doppler anemometer meas. corrections for curved channel flow 7-37608
- optical real-time matrix multiplier, operational error and compensation 7-10866
- precision machining/metrology facility for X-ray mirror substrates fabrication 7-37222
- refractive index meas., environmental conditions induced errors correction 7-340

error correction

- 1986 TN, time correction for astrometric obs. (1986 October 6) 7-24044
- 1986 TO, Aten-type asteroid, astrometric obs. correction, orbital elements, and ephemeris 7-24044
- dense particle fields, laser diffraction meas. correction for multiple scatt. 7-1212
- echelle spectrographs, scattered light background correction method 7-34874
- FTIR photoacoustic spectra, phase analysis 7-48878
- ionic conductors, solid, impedance studies, bridge balance conditions and error corrections (*German*) 7-30033
- land-cover mapping from synthetic aperture radar obs., importance of radiometric correction 7-4200
- laser Doppler anemometer meas. corrections for curved channel flow 7-37608
- sweep-nonlinearity correction procedures in picosecond streak camera measurements 7-15024

error statistics

- anti-multipath modulation technique, bit error rate improvement using variable decision threshold reception (*Japanese*) 7-47039
- fibre optic links, bit error rate, noise meas. on laser diodes single modes 7-37230
- free-space laser communications system design, SNR impact 7-34676
- mapping problems, smoothing error dynamics 7-8788

errors

- see also measurement errors
- atmospheric pressure gradient force in sigma coord. models, error reduction methods 7-34729
- atmospheric surface layer structure, errors in similarity scales evaluation 7-40514
- P/Comet Halley (1982i), a priori position prediction error from terrestrial and space-probe meas. 7-4370
- differential eigenproblems, error estimation 7-61007
- FTIR photoacoustic spectra, phase analysis 7-48878
- FTIR spectroscopy, quantitative, ADC errors 7-48877
- interplanetary Alfvénic fluctuations propagation direction determ., systematic errors 7-47659
- kinofilm lens fabrication errors, effect on pupil function 7-25739
- soil water extractor for minimising CO₂ degassing and pH errors 7-23916
- weather forecasts, diagnostic study of first year of Model Output Statistics forecasts in Australia 7-55125

erythema see biological effects of ultraviolet radiation**erythrocytes** see blood; cellular biophysics**Esaki diodes** see tunnel diodes**Esaki effect** see tunnelling**ESCA** see electron spectroscopy; spectrochemical analysis; ultraviolet photoelectron spectra; X-ray photoelectron spectra**ESD** see discharges (electric); electrostatics**ESPRIT** see research initiatives**ESR** see paramagnetic resonance**estimation theory**

- see also information theory
- disjunctive kriging, estimation and conditional probability 7-23754
- DNA content of cells, distrib. modelling problem 7-47303
- gamma-ray light curves analysis, appl. of kernel density estimators 7-47718
- linear struct. vibration model with nonGaussian noisy power obs., state estimation 7-37243
- mapping problems, smoothing error dynamics 7-8788
- optimal estimation theory in data analysis and signal processing, Kalman filter appl. 7-35500
- precision instrument calibration, criteria for neglect of small errors 7-290
- sensory thresholds, efficient estimation 7-59986
- two-point pressure-velocity correlations, conditional average and linear estimation in a round jet flow 7-26329
- unbiased estimators based on, incomplete sufficient statistics (*Japanese*) 7-35258

eta meson resonances

- production and decay processes involving pseudoscalar gluonium particles 7-41717
- η' mass and topology in SU(3) lattice gauge theory 7-24783
- $\eta_c=00$, η_c search, branching ratio meas. in $\psi \rightarrow \eta_c \gamma$ 7-24878
- $\eta \rightarrow \gamma\gamma$, meson-quark coupling constants, one-loop quark model 7-61695
- $\eta \rightarrow 3\pi^0$, electromagnetic mixing calcs. in η' and η decay 7-19104
- η effects and instanton physics in low energy axion dynamics 7-30191
- $\eta' \rightarrow \eta\pi^0\pi^0$, electromagnetic mixing calcs. in η' and η decay 7-19104
- $\eta' \rightarrow \eta\pi^0\pi^0$, radiative width meas. 7-61717
- η' mass in SU(3) lattice gauge theory, topology 7-429
- $\eta' \rightarrow \omega\gamma$, branching ratio meas. 7-61654
- $\gamma\gamma \rightarrow \eta_c(2980)$, recent results on two-photon processes from DESY 7-61786
- $pp \rightarrow \eta X$, inclusive production at low transverse momentum 7-10081
- $\pi^- p \rightarrow \pi^+ \pi^- \eta$ isobar-model partial wave anal., pseudoscalar reson. detection 7-549
- $\eta_c \rightarrow \gamma\gamma$, $R_1 = \Gamma(\eta_c \rightarrow \gamma\gamma) / \Gamma(D^+ \rightarrow \mu^+ \nu_\mu)$ calcs. bound state quark model anal. 7-61582

eta mesons

- U(1) problem on a lattice, massless π^0 and massive η 7-48996
- $\eta \rightarrow 3\pi^0$, electromagnetic mixing calcs. in η' and η decay 7-19104

eta mesons continued

- $\eta \rightarrow \gamma\gamma$, meson-quark coupling constants, one-loop quark model 7-61695
- $\eta \rightarrow H^+ X$, production mechanism, differential characteristics 7-41796
- η -mesic nuclei, experimental signatures 7-41925
- $K^+ d \rightarrow \eta X$, $\eta \rightarrow 2\gamma$, 10 GeV, differential cross section meas., quark-fusion model anal. 7-5124
- $M^0 \rightarrow \eta\eta$, 1750 MeV narrow meson observation 7-35861
- $\omega\eta$ resonance, evidence for four-quark states 7-15127
- π - η mass difference in lattice QCD, U(1) problem, strong coupling expansion 7-41810
- $\pi^+ d \rightarrow \eta X$, $\eta \rightarrow 2\gamma$, 10 GeV, differential cross section meas., quark-fusion model anal. 7-5124
- $\pi^- p \rightarrow \eta^0 \Delta^0(1232)$, 3.3 GeV/c, differential cross section and total cross section 7-35904

etalons see interferometers**etchants** see etching**etching**

- see also crystal defects; dislocation etching; sputter etching
- apatite, track etch anisotropy study 7-36403
- biological specimen etching, ion beam sputtering appl. 7-7850
- borosilicate glasses, fission track etching using deionized water 7-53938
- CR39 proton detector in neutron dosimeter, etching times 7-829
- CR-39, α -spectrometry using chemical and electrochemical etching 7-30829
- CR-39, α -track registration energy range broadening using electrochemical etching 7-30870
- CR-39, automated image anal. of α and p etched tracks 7-30880
- CR-39, bulk etch meas., standard method 7-19658
- CR-39, electric breakdown model for particle registration sensitivity in electrochemical etching 7-30876
- CR-39, modified microfilter study 7-36409
- CR-39, study of electrochemically etched α and p tracks as function of energy 7-30869
- CR-39 electrochemically etched n dosimeters, pre-etching time effects on response characts. 7-30871
- CR-39 neutron recoil track detectors, etching optimization up to 1 MHz 7-30874
- CR-39 plastic track detector, etched track anal. technique 7-30879
- CR-39 polycarbonate, structure property correlation in dosimetry, track etching 7-32313
- CR-39 polymer dosimeters, electrochemical development of particle tracks 7-30873
- CR-39 track detector, treeing during electrochemical etching, fracture mech. study 7-30877
- excimer laser applications in imaging technology (*Japanese*) 7-56367
- fission tracks, chemical etching and length distrib. model 7-49857
- III-V semiconductors, patterning using photoelectrochem. etching and focused ion beams 7-22924
- III-V semiconductors, selective photoetching studies of defects 7-32426
- ion beam modification of materials, conf., Catania, Italy (9-13 June 1986) 7-60865
- laser enhanced plating and etching using photothermal effects 7-59651
- laser etching and deposition, basic mechanisms, review 7-53923
- laser induced etching of polyimide encapsulants in IC evaluation 7-53941
- laser processing of materials, conf., London, England (Dec. 1986) 7-48185
- laser-assisted etching of electronic materials 7-28162
- LR-115 Kodak SSNTD, α -counting efficiency and thermoluminescence dating appl. 7-36401
- LR-115 track detector, change of etching condition after high n flux irradiation 7-30867
- LR-115 use in heavy ion scatt. expts. 7-19274
- Makrofol E, nuclear track profiles and chem. etching 7-828
- Makrofol E, particle registration studies and etching techniques 7-30875
- Makrofol E α -tracks, relationship between pre-etched track length and track spot size 7-30878
- Makrofol-E neutron recoil track detectors, etching optimization up to 1 MHz 7-30874
- mass removal in formation of internal cavities in metals by chemical etching 7-28186
- metal films, etching, kinetic model, electron flux activation 7-3492
- minerals, heavy ion track etching, implications for α -recoil track dating 7-36434
- noble metal surfaces, laser stimulated desorption during Cl₂ reactions 7-53453
- phosphate glass spectrometric detector, optimum etching for fission fragments 7-42429
- photochemical machining of etch-resistant metals 7-22909
- PMMA, photoetching, by UV radiation 7-65165
- poly(p-phenylene sulphide), etching technique for enhancement of morphological textures 7-44417
- polyacetylene films, glow discharge polymerisation and photoablation study 7-63650
- polyarylate, track effects on chemical etching 7-36380
- polycarbonate track detectors, electron spin resonance studies 7-33276
- polyethylene, linear, quantitative permanganic etching 7-8148
- polyimide, XeCl laser ablated, conical structures obs. 7-3467
- polyimide encapsulants, laser induced etching 7-53941
- polyimide films, laser ablation in pressurized gas ambients 7-46661
- polyimide films, UV laser ablation 7-59648
- polymer film, excimer laser micromachining and surface microstruct. modification 7-53940
- polymer film, photoetching, action of vacuum UV radiation 7-13622
- polymer films, photoetching using soft X-rays 7-22859
- polymer films, X-ray photoetching 7-7792
- polymer films patterning by dry photoetching technique involving UV laser 7-34232
- polymer surfaces, UV laser ablation dynamics 7-39684
- polymeric dosimeters, internal heating during electrochemical etching 7-30872
- powder, internal structure of solidified aerosol droplets, etching method 7-7920
- quartz, topography of etched rhombohedral faces, evidence for orientation effects 7-16840
- quartz crystal chemical polishing, use of surfactants, results 7-59655
- quartz crystal etched figures, expt. study and numerical simulation 7-59654
- quartz tuning fork resonator type temp. sensor, design, fabrication and characts. 7-56269

etching continued

- semiconductors, photoelectrochemical etching of holographic gratings 7-26051
 soda lime glass detectors, chemical etching characts. 7-30868
 solid-state devices and materials, conf., Tokyo, Japan (Aug. 1986) 7-48173
 SSNTD, radiographic imaging performance, image quality factors 7-36405
 steel, eutectoid, 1.3 wt.% Cr, specimen prep. technique influence on analytical TEM obs. of partitioning 7-22950
 Al foil, anodic etching, influence of activators and passivators in electrolyte on surface area increase (Polish) 7-22889
 Al thin films, corrective trimming by laser controlled wet chem. etching 7-28195
 Al-Si-Cu sputtered electrode for VLSI, Cu distributions meas. by RBS 7-2415
 Al_xGa_{1-x}As, low press. OMVPE, selective growth embedding in etched grooves on GaAs 7-22554
 Au-10% high-speed internal photoemission detectors enhanced by grating coupling to surface plasma waves 7-52688
 BN, cubic, aggregate tools, microstruct. and wear 7-3462
 a-C:H, film, optical and compositional props. 7-39206
 CdSe thin film liquid-junction photovoltaic cell, photoelectrochem. charactn. 7-54331
 CdTe and CdZnTe, single-crystal substrates, struct. characterisation 7-32769
 p-CdTe, single crystal and thin film, chemical etching study 7-46724
 Cu, chlorinated surface, laser-induced desorption and etching processes 7-27092
 Cu foil, excimer laser assisted gas phase etching 7-54015
 CuCl solid surface, laser-induced desorption and etching processes 7-27092
 Fe garnet films containing Bi, comp. study, and chemical etching anal. 7-45083
 Fe-Cr, thin oxide film form., XPS study 7-22898
 Fe-Ni, thin oxide film form., XPS study 7-22898
 (GaAl)As monolithic composite-cavity laser, chem. etching technique 7-50579
 GaAs (100), chemical etching and oxidation, XPS characterisation 7-21591
 GaAs chemical etching by Cl, thermodynamically predicted depend. on press. and temp. 7-22919
 GaAs, dielectric protective coatings during heat treatment 7-33852
 GaAs epitaxial films, growth by close-spaced vapour transport, unwanted doping, X-ray diff., SEM obs. 7-27187
 GaAs epitaxial layers and heterostructures grown on Si substrates, material props. 7-7046
 GaAs laser induced etching in carbon tetrachloride atm., fluoresc. 7-59700
 GaAs MOCVD growth on Ge (100) and Si (100) substrates, antiphase and single domains 7-27925
 GaAs, overlapping etch pits, density, evaluation technique 7-32443
 n-GaAs, photoelectrochemical etching, orientational depend. 7-65224
 n-GaAs, sawtooth gratings, photoelectrochemical fabrication 7-50726
 GaAs substrate for MBE growth, thermal etching 7-7861
 GaAs surface, anisotropically etched, p-n junction formation by MOCVD 7-13374
 GaAs surface, formation of gratings in laser photoemission wet etching 7-8205
 GaAs, surface morphology, in HNO₃-HF-H₂O etching system (Korean) 7-28225
 GaAs, vapour etching, buried interface, carrier traps 7-28213
 GaAs:In, VPE growth, isoelectronic In doping, etch pit densities 7-46340
 GaAs:In (B)(Si), dislocation free crystals, LEC grown, microscopic defects, eutectic etching 7-16545
 GaAs/Ca₂Si₂F₂ (100) SOI structures, epitaxial GaAs films, antiphase disorder 7-52315
 GaInAs, anodic oxides, growth and composition 7-39781
 GaInAs/InP heterostructures, VPE, homogeneity, mobilities 7-58882
 GaInAsP-InP etched mirror laser, passivation with angled sputtering 7-57358
 GaSb-based wafers, determ. of (110) and (-110) directions by etching 7-59696
 Ge substrate for single-domain epitaxial growth of GaAs 7-22578
 Ge-GeO₂, defect formation, during thermal oxidation 7-65237
 Hg_{1-x}Cd_xTe MBE layers, plasma oxidation, oxide growth, comp. and surface struct. 7-54018
 InGaAsP device fabrication using HBr-H₂O etching soln. 7-46728
 InGaAsP-InP high-performance 1.3 μm laser structures with both facets etched 7-20259
 In₂O₃:Sn(Te), thin films, etching, comparison of solns. dilute HCl and H₃PO₄ 7-8208
 InP (111), chemically polished and etched, characterisation of native oxide layer, ion scatt. spectra, AES, ESCA 7-22925
 InP {001} surfaces, chem. etch cleaning procedure 7-13668
 InP chemical etching by Cl, thermodynamically predicted depend. on press. and temp. 7-22919
 InP device fabrication using HBr-H₂O etching soln. 7-46728
 InP, electrochemical C-V profiling 7-27325
 InP films, hydride VPE, impurity incorporation, defect charactn. 7-53614
 InP, ion enhanced chem. etching in Cl₂, thermal pulse model 7-54029
 InP, MOVPE on SiO₂ masked substrates at reduced press., vapour etching 7-39398
 InP:Si, substrate, encapsulated annealing, using SiN encapsulant 7-39779
 InP-aqueous electrolyte interfaces, laser induced photoelectrochemistry 7-27412
 InSb surface, oxidation at room temp. 7-46734
 InSb surface damage layer refl. spectra and thickness meas. 7-22209
 KNbO₃, single domain cryst. prep., orientation and dielec. polarisation 7-45950
 LiNbO₃ blazed grating couplers and appl. to integrated optics 7-15969
 LiNbO₃, etching, laser-driven chem. reactions 7-3468
 Li₂O-SiO₂ based photosensitive glass, machining without photoresist 7-2865
 Mn_{0.52}Zn_{0.35}Fe_{2.12}O₄, single cryst. surface damage depth meas. 7-52979
 Mo, etching, new method 7-39749
 Mo, laser photochemical etching by surface halogenation 7-46676
 Ni-Mo (6 at.%), oxidation, ESCA study 7-22897
 Ni₅₀Fe₅₀ (100) alloy, segregation and adsorption of S 7-21617
 Si (100), UV-stimulated interaction with Cl₂, reaction mechanisms for photon-enhanced etching 7-22926

etching continued

- Si, anisotropic etching, micropylramid inhibition method (Japanese) 7-35101
 Si, anisotropic etching with EDP 7-46725
 Si, chemically assisted ion beam etching using low energy Kaufman source 7-22931
 Si, DC plasma etching in SF₆/O₂ mixtures, mass spectrometric transient study 7-8203
 Si, epitaxial low temp. growth by hot wall UHV/low press. CVD techniques, surface optimisation 7-3194
 Si, etch products in XeF₂, doping and pressure effects 7-33855
 Si, etching by HF-CrO₃-H₂O solns., selective dissolution studies 7-3530
 Si, etching V-groove structures 7-26031
 Si MBE layers, defects 7-21772
 Si MBE layers, spreading resist., etching, bevelling, staining characterisation techniques 7-12891
 Si, photochemical etching in NF₃ gas, surface processes 7-59704
 Si, polycrystalline, photolytic etching in SF₆ atmosphere 7-46732
 a-Si solar cells on textured Al substrate, prep. by chemical etching 7-23156
 Si surface, etching by HCl/H₂ mixtures, low pressure gas composition 7-65221
 Si surface etching by HCl/H₂ gas mixtures 7-65220
 Si:Ar laminated structure formed by Ar ion doping, electroreflectance 7-7676
 Si:B-Mo interface, specimen preparation by chemical etching and polishing, for electron studies 7-29989
 a-Si:H films, columnar morphology, evolution of vibr. spectra 7-64646
 a-Si:H/a-SiO₂:H superlattice micropores, pyrene molecules adsorption and confinement 7-27112
 β-SiC, epitaxially grown, antiphase boundaries 7-46722
 SiN films, plasma CVD deposition and props. (Japanese) 7-13381
 SiN, microwave plasma deposition, fabrication and characterisation 7-39421
 Si₃N₄ amorphous insulator thin films, defect-enhanced UV etching damage studies 7-26797
 Si₃N₄ films, plasma-enhanced CVD deposition from SiH₄/NH₃/N₂ mixtures 7-39414
 Si₃N₄ LPCVD films, bombardment induced H redistrib. 7-38404
 SiO₂, amorphous, thermal, UV irradiation induced compaction and photoetching 7-12146
 SiO₂, ion activated chem. etching, laser interferometer studies 7-6657
 SiO₂ layers on Si, patterning of fine structs. by ion beam exposure and wet chemical etching 7-13656
 SiO₂ silica fibre mechanical strength determ. (French) 7-11157
 SiO₂-P₂O₅ glass films, deposited by different CVD methods, phys. props. 7-27220
 SiO₂ amorphous insulator thin films, defect-enhanced UV etching damage studies 7-26797
 SiO₂N₂ films, deposited by plasma-enhanced CVD, charact. 7-2413
 SnO₂-SiO₂-Si surface barrier solar cells, optimisation of fabrication process 7-23154
 Ti sheet, grain orientation distrib. meas. by etch pit method 7-46510
 U contamination in Al foils, CR-39 track detector study 7-54218
 W, laser photochemical etching by surface halogenation 7-46676
 ZnO-Cu-SiO₂-Si composite membrane, interdigital transducer generated UV Lamb waves 7-11241
 ZnP glass detectors, chemical etching characts. 7-30868
 ZrF₄-BaF₂-LaF₃-AlF₃ glass, etching method for prep. of IR fibres with high tensile strength 7-1243

Ettingshausen effect see thermomagnetic effects

europium

- see also nuclei with
 adsorption on W (110) 7-27118
 atom, photoemission, orbital-collapse effects 7-15572
 carboxylate, luminescence props. calcs. 7-42667
 glass:Eu³⁺, erasable holographic grating obs. at room temp. 7-31276
 glass:Eu, stable and metastable impurity valence states, spectral props. (Russian) 7-27747
 impurity in garnets, compositional shift of spectral lines 7-53252
 Ly₂₃ satellite, X-ray emission spectra anal. 7-36523
 lanthanide oxysulphides (oxysulphides), Eu³⁺-doped, vibronic spectra 7-51968
 Al:Eu³⁺ ion implanted, anodization, electroluminesc. obs. 7-7761
 BaFCl:Eu³⁺, charge transfer excitation and emission spectra 7-64688
 Ba₃LaNb₃Nd³⁺(Eu³⁺) single crystals, spectral-luminesc. props. 7-39169
 BaO:Al₂O₃:Eu³⁺, Mn²⁺ phosphor, luminesc. props. 7-46112
 BaO:Al₂O₃:Eu³⁺ phosphor, luminesc. props. 7-46112
 CaF₂:Eu, X-ray luminesc., spectral-kinetic props. 7-39184
 CaF₂:Eu³⁺, ¹⁵¹Eu-¹⁵¹Eu quadrupole moment ratio, optically detected NMR studies 7-22164
 CaF₂:Eu³⁺, hyperfine coupling in ⁷F₀ and ⁵D₀ states, ODMR meas., optical hole burning 7-45842
 CaF₂:Eu³⁺, O₂⁻, quadrupole coupling and crystal-field shielding under hydrostatic press. 7-2551
 CaO-TiO₂-SiO₂:Eu³⁺ sphere ceramic, impurity laser-excited site-selective fluorescence line-narrowing spectra 7-13200
 Ca(PO₃)₂:Duo³⁺ glass, highly doped, fluorescence spectral width of ⁷D₀-⁷F₀ transition 7-13189
 CdF₂:Eu crystals, local field-enhanced electronic conduction, activation energy and Poole-Frenkel const. calcs. 7-38570
 CdF₂:Eu³⁺, electrolum. studies 7-27785
 CdF₂:Eu³⁺, hyperfine coupling in ⁷F₀ and ⁵D₀ states, ODMR meas., optical hole burning 7-45842
 Eu³⁺ + He (Ne), collisional lasers, high specific output energy 7-43078
 Eu³⁺, Eu, laser mechanism and energy characts., relax. processes of metastable states 7-62673
 Eu²⁺ in crystals, covalency and EPR hyperfine struct. const. 7-45815
 Eu³⁺ in soln., ⁷D₀-⁷F₀ luminesc. line shift and broadening, temp. depend. meas. (Russian) 7-17345
 Eu³⁺ ions in liquid solution, luminescence, selective excitation 7-3089
 Gd₂(MoO₄)₃:Eu³⁺, nonresonant energy transfer between two different Eu³⁺ ion sites 7-46125
 Gd₂O₃-P₂O₅ phosphors, Eu³⁺ activated, luminesc. spectra, cryst. symm. 7-3080
 KBr:Eu²⁺, impurity precipitates, Raman spectra meas. during annealing 7-64634
 KCl:Eu²⁺, f to f transitions, two-photon spectra studies 7-3068
 KCl:Eu²⁺, impurity precipitates, Raman spectra meas. during annealing 7-64634

europium continued

- KCl:F²⁺-Eu³⁺, optical absorpt., excitation and luminesc. spectra 7-59250
 KI:Eu²⁺, impurity precipitates, Raman spectra meas. during annealing 7-64634
 KX:Sr,Eu (X=Br,Cl), Sr precipitation, study using Eu³⁺ ions 7-53127
 LaMgAl₁₁O₁₉:Nd(Eu), single cryst., phys. chem. and spectrosc. props. 7-13185
 Li₂O-P₂O₅:Eu³⁺, laser-induced refractive-index gratings, four-wave-mixing techniques 7-11102
 NaCl:Eu single cryst., EuCl₂ phase precipitation, fluoresc. and X-ray diffr. studies 7-46108
 NaCl:Eu²⁺, gamma irradi., optical absorpt. spectra, TSC meas. 7-58337
 NaCl:Eu²⁺ crystals, γ -irradiated, colourability 7-12062
 NaCl:Eu²⁺ crystals, mechanical strength, dopant distrib. and γ -irrad. effects study 7-26800
 NaGdF₄:Ce, Eu, UV ⁵H₃ and visible ⁵D₃ luminesc. 7-64676
 Na₂O-Al₂O₃-SiO₂:Eu³⁺ glass, impurity laser-excited site-selective fluorescence line-narrowing spectra 7-13200
 Na₂O-CaO-Al₂O₃-TiO₂-SiO₂:Eu³⁺ glass ceramic, impurity laser-excited site-selective fluorescence line-narrowing spectra 7-13200
 Na₂O-SiO₂:Eu³⁺, laser-induced refractive-index gratings, four-wave-mixing techniques 7-11102
 Na₂O₃SiO₂:Eu³⁺, UV-irradiated glass, formation of colour centres 7-12063
 P₂O₅:Eu³⁺, laser-induced refractive-index gratings, four-wave-mixing techniques 7-11102
 RbBr:Eu²⁺, Z₂ colour centres, picosecond relax., nonstationary spectra 7-59233
 SmB₆:Eu²⁺ energy gap temp. depend., impurity ESR study 7-45151
 SrCl₂:Eu, defect equilibria, site selective laser spectrosc. 7-46078
 YAlO₃:Eu³⁺, Van Vleck paramagnet, low field Raman heterodyne study 7-53179
 YAlO₃:Eu³⁺ lattice and electronic contributions to the quadrupole interaction of trivalent Eu 7-2550
 Y₂O₃:Eu³⁺, impurities optical dephasing temp. and freq. depend. 7-22286
 Y₂O₃-P₂O₅ phosphors, Eu³⁺ activated, luminesc. spectra, cryst. symm. 7-3080
 YVO₄:Eu,Ga(Sc)(La), optical props. and electronic struct. 7-33423

europium alloys

- Eu-Yb, high press. mag. and elec. props. studies 7-7541
 Eu-Ce_{1-x}Cu₂Si₂ cryst., mixed valence state and Kondo system coexistence (Russian) 7-7185
 EuCu₂Si₂, Eu valency, effect of Cu or Si replacement by other ions 7-58787
 EuCu₂Si₂, mixed valence system, interconfiguration fluctuation model 7-64188
 EuIr₂Si₂, Eu intermediate valence 7-7188
 EuMo₈-₉Se₉, mag. field induced supercond. under pressure 7-64414
 EuNi₂P₂, 4f-magnetism study by susceptibility and NMR 7-22154
 EuNi₂P₂, mixed valence system, interconfiguration fluctuation model 7-64188
 Eu₂Pd_{1-x}, amorphous mixed valent alloys, X-ray absorpt. spectra 7-64802
 EuPd₂Si₂, mixed valence system, interconfiguration fluctuation model 7-64188
 EuRh_{1.5}Sn_{4.2}, anomalous mag. and elec. props. 7-64440
 Tb_{0.3}Dy_{0.5}Er_{0.2}Fe₂, spin reorientation, Mossbauer study 7-13068

europium compounds

- see also europium alloys
 chalcogenides, IR optical parameters, rel. to chemical bonds 7-53291
 chelate complexes, luminesc., photophys. 7-36669
 cleaved surface, struct. and comp. 7-12426
 complexes, in soln., spectral line width, temp. depend. 7-31025
 silicides, electronic struct., X-ray emission spectra studies 7-52419
 (Eu, Lu, La)₂Fe₂O₁₂ films, gyromagnetic ratio, damping parameter and mag. anisotropy 7-45777
 Eu complexes, Eu(II)ethylenediamine tetraacetate and Eu(III)bis-citric acid, polarised luminescence studies 7-22313
 Eu complexes, Eu(NO₃)₃(triphenylphosphine oxide)₃ systems, cryst. and mol. structs. 7-51723
 Eu-Bi-S, synthesis and props. 7-44471
 Eu-Bi-Se(Te), synthesis and props. 7-44471
 Eu-In-Te systems, phase equilib. investigations 7-2173
 Eu-Sb-S, synthesis and props. 7-44471
 Eu-Sb-Se(Te), synthesis and props. 7-44471
 EuAsO₄ crystal, vibr. spectra and optical absorption studies 7-13145
 Eu(As_{1-x}P_x)₃, mag. phase transitions, strip line transmission spectra studies 7-64458
 EuCrO₃, coexistence of mag. and electric dipole ordering after optical pumping 7-17171
 Eu(Cu_{1-x}M_x)₂Si₂ (M=Au, Ag, Ru, Ni), substitution effects on mixed valence behaviour, Mossbauer and XANES studies 7-64183
 EuCu₂(Si_{1-x}Sn_x)₂, substitution effects on mixed valence behaviour, Mossbauer and XANES studies 7-64183
 EuGa₂S₄, optical props. near fundamental absorption edge 7-17295
 Eu(II)- β -alumina, luminescence, order-disorder effects, optical, structural and ion transport props. 7-46114
 EuLiGe₃ crystal structure (Ukrainian) 7-12009
 Eu₂(MoO₄)₃, improper ferroelectrics, energy spectrum and vacuum UV spectra 7-33413
 Eu₂(MoO₄)₃, nonresonant energy transfer between two different Eu³⁺ ion sites 7-46125
 Eu(NO₃)₃·6H₂O, soln., anomalous temp. depend. of luminesc. decay 7-46116
 EuO (100), cleaved surface, struct. and comp. 7-12426
 Eu₂PCl(Br)(I), prep., mag. props. and cryst. struct. (German) 7-32379
 EuPd_{2-x}Au_xSi₂, valence determ., Mossbauer and X-ray absorpt. studies 7-64800
 Eu₂RuO₇, crystal struct. determ. 7-16520
 EuS (100), cleaved surface, struct. and comp. 7-12426
 EuS ferromagnetic single cryst., elec. field gradient and magnetic hyperfine interaction, NMR meas. 7-52540
 EuS ferromagnetic superlattices with magnetisation perpendicular to surface, collective excitations, magnetostatic theory 7-45647
 EuS Heisenberg ferromagnet, diverging and finite suscept. below T_c 7-7444
 EuS, mag. ordered and paramag. phases, Raman scatt. 7-22246
 EuS, mag. props. under high press., competing magnetic interactions 7-7542

europium compounds continued

- EuS, refrigerant capacity and use in mag. cooling 7-56285
 Eu-SrS mag. superlattices grown on Si(111), strain, study by He ion channelling 7-27215
 EuSe ferromagnet, ¹⁵¹Eu and ¹⁵³Eu NMR lineshape, mag. field depend. 7-22151
 EuSe, mag. phases, press., alloying effects, NMR and mag. studies 7-2847
 Eu_{0.4}Sr_{0.6}S spin glass, activated dynamic scaling relation for susceptibility 7-38878
 Eu_{1-x}Sr_xS solid soln., X-ray absorpt. spectra d-f exchange interactions effects study, comp. depend. 7-3114
 Eu₂Sr_{1-x}S₂ mag. sp. ht., field and temp. depend., numerical simulation 7-2883
 Eu₂Sr_{1-x}Te, dilute antiferromag., phase diagram, spin glass props. (German) 7-12981
 EuTe (100), cleaved surface, struct. and comp. 7-12426
 EuTe, bound magnetic polarons, spin dynamics 7-7502
 Eu₂TiS₂ mixed valence intercalation cpd., low-temp. synthesis and mag. props. 7-17779
 EuXO_n (X=Group, IV, V or IVA element), gaseous, stability 7-38224
 Eu₂Y_{2-x}Fe_{2-x}Ga₂O₁₂ LPE garnet films, ferromagnetic relax. meas. 7-38911
 HgTe-EuTe system, interactivity 7-6801
 KCl-Eu solid soln. crystals, thermal and radiation induced decay, impurity aggregation study (Russian) 7-2216
 LiEuP₄O₁₂, flux cryst. growth 7-13345
 Pb_{1-x}Eu_xSe, MBE growth for IR device appls. 7-64908
 PbEuSeTe/PbTe single quantum well diode laser with side optical cavity 7-43105
 Pb_{1-x}Eu_xTe epitaxial layers, mag. props. 7-45772
 PbSe-PbS(Pb_{1-x}Sn_xSe)(Pb_{1-x}Eu_xSe) DH lasers with remote p-n junctions 7-57333
 PbSnEuTe, superlattices, prep. by hot wall epitaxy, props. (Japanese) 7-12546
 PbTe-EuTe short period superlattices, props., appl. to laser diodes 7-52785
 PbTe-PbEuSeTe, compositional and doping superlattices, struct., electronic, optical and magnetooptical studies 7-53290
 PbTe-PbEuSeTe multiquantum wells, electron-hole recomb., photolum. 7-13216
 Sm_{1-x}Eu_xS(Se) solid solns., X-ray absorpt. spectra d-f exchange interactions effects study, comp. depend. 7-3114
 (UPuEu)O₂, reactor fuels, thermal conductivity 7-19352
 (YEuLuCa)₃(GeFe)₂O₁₂ films, mag. bubble motion in the presence of a modulated bias field 7-53098
 (YEuTmCa)₃(FeGe)₂O₁₂ films, planar anisotropy and magnetisation, ion irrad. effects study 7-2906
 (YEuTmCa)₃(FeGe)₂O₁₂, epitaxial films, O ion adsorpt. bubble diameter variation effect 7-22125
 (YEuTmCa)₃(FeGe)₂O₁₂(YLa)₃Fe₂O₁₂ ferrite/garnet layered structs., domain wall and ferromag. reson. props. (Russian) 7-45828
 (YEuTmCa)₃(FeGe)₂O₁₂ films, double layer, mag. bubbles, translational velocity 7-45781
 Yb_{1-2-x}Eu_xMo₈S₈, superconductivity and mag. interactions 7-38826
 (Yb_{0.95}Eu_{0.05})₂O₃, luminophor, granulometric composition 7-22715

eutectic alloys

- coatings on steel, wear resist. in corrosive medium 7-17694
 simple, latent heat of fusion, temp. and conc. relationships (Russian) 7-38170
 solidification, fiber coarsening 7-59499
 solidification, lamellar spacing, influence of convection 7-17522
 Ag-Ge liq. eutectic alloys, elec. resist. and struct., 600 to 900 K (German) 7-45334
 Ag-Sn hypoeutectic alloys, primary phase shape rel-to cooling rate and comp. 7-59509
 Al-Al₃Cu eutectic alloys, chill cast, directionally solidified, hot rolling microstruct. 7-46447
 Al-Al₃Ni eutectic alloys, chill cast, directionally solidified, hot rolling microstruct. 7-46447
 Al-Fe system, phase diagram, DTA obs. 7-39485
 Al-Ge eutectic alloy, interaction with SiC whisker reinforced Al matrix composite 7-46689
 Al-In, monotectic alloy, section prep., micromilling, polishing (German, English) 7-22937
 Al-Mg-Ce system, liquidus, intermetallic compound (Chinese) 7-7960
 Al-Pb, monotectic alloy, section prep., micromilling, polishing (German, English) 7-22937
 Al-Si (12.7 wt.%), eutectic microstruct., twinning and branching mechanisms 7-17521
 Al-Si eutectic, Sr-modified, fibrous Si cryst. morphology, TEM study 7-28015
 Al-Si eutectic, unmodified, Al grain struct. 7-65012
 Al-Si eutectic alloy, interaction with SiC whisker reinforced Al matrix composite 7-46689
 Al-Si eutectic alloys, partial modification mechanism 7-59498
 Al-Si-Sb, directionally solidified eutectics, inter-Si flake spacing rel. to Sb addition 7-53717
 Al-Zn eutectic, oriented crystallisation, buoyancy-driven convection effects 7-27887
 Al₃Ni-Al eutectic alloy, Bauschinger effect, influence of Al₃Ni dispersion state (Japanese) 7-22761
 Bi-MnBi eutectic, pure and modified, growth 7-59500
 Co-Te system, phase diagram, DTA 7-46425
 Fe based eutectic alloy powder, plasma coatings with interstitial phases, tribotechnical props. 7-17731
 Fe cast, Cr-type, duplex nature of eutectic carbides 7-13440
 Fe-C base ternary and multicomponent alloys, eutectic temp. and comp., theoretical calc. 7-59504
 Fe-C hypoeutectic melt struct., temp. and holding time depend., X-ray studies (Russian) 7-16396
 Fe-Pd-S system, phase equilib. 7-3272
 Fe-TiB₂ eutectic system, microhardness, modulus of elasticity (Russian) 7-39648
 Ga-Te system, phase diagram, DTA 7-46425
 GaSb+GaV₂Sb₃, elec. props., anisotropy 7-12717
 GaSb+V₂Ga₃, elec. props., anisotropy 7-12717
 Gd₂Si_{1-x}As_{2x}, x=0.18, 0.59, 0.87, amorphous, thermal, elec. and mag. props. 7-53039
 Ge-Au(Pd) alloys, temp. and conc. depend. diamag. susceptibility 7-2811

eutectic alloys continued

- Ge-Te liq. eutectic alloys, elec. resist. and struct., 600 to 900 K (*German*) 7-45334
 Ge-transition metal eutectic alloys, cryst. growth by directional crystallisation 7-64887
 InSb-NiSb eutectic composite, rel. between metal fibre morphology and elec. props. 7-59644
 Li-Pb, liq. fusion reactor blanket, mass transfer in dynamic environment, corrosion damage 7-49659
 Mn-C system, fusibility diagram in ϵ -solid soln. and carbide Mn_7C_3 region 7-7964
 MnBi/Bi eutectic, freezing rates, convection effect on microstruct. 7-22652
 Mo-TiC eutectic composites, yield strength in temp. range 285 to 2270 K 7-53831
 Na-K eutectic mixture in fusion-fission pebble bed blanket, magnetohydrodynamic flow 7-15366
 Nb-B-C system, struct. and phase equil. of Nb 7-22638
 Nb-Hf-B system, phase equil. in Nb corner 7-46415
 Ni-Al-Mo eutectic high temp. alloy, directional solidification within ZrO_2 supporting skin (*German*) 7-22660
 Ni-Mo₂C eutectic, directional solidification oriented struct., strength, hardening mechanism (*Russian*) 7-59507
 Ni-Nb-C system, directionally solidified, phase equil. and struct. 7-46416
 Ni-NbC eutectic, directed crystallisation, comp. growth laws (*Russian*) 7-65021
 Ni-P, solution of Cr_3C_2 , liq. phase influence 7-53689
 Ni₃B/Ni eutectic, SEM and HREM struct. and chem. anal. 7-17515
 Pb-Sn eutectic, spiral structures, convection influence 7-22653
 Pb-Sn eutectic, superplasticity, investig. by impression creep testing 7-3372
 Pb-Sn-Ag system, eutectic temp. rel. to Ag content, phase diagram, thermodynamic props. 7-65005
 PbLi eutectic, flowing, corrosion of stainless steel 7-53958
 Sn-R binary systems (R=La, Nd, Gd, Er, Lu), phase diagrams and equil. 7-7961
 Tb₂Si_{1-x}, x=0.18, 0.59, 0.87, amorphous, thermal, elec. and mag. props. 7-53039
 Zn-Al eutectic alloy, interaction with SiC whisker reinforced Al matrix composite 7-46689
 Zn-Ho, two-phase, partial thermodynamic props., 690 to 1020K 7-7963
 Zn-Pb, monotectic alloy, section prep., micromilling, polishing (*German, English*) 7-22937
 Zr-Ni metallic glass, crystallisation, metastable crystalline phase form. 7-21126

eutectic structure

- alloys, morphological analysis of eutectic structures 7-7987
 ceramic eutectic composites, microstruct. and mech. props. 7-64991
 crystal growth, conf., York, England (Jul. 1986) 7-48142
 halide eutectic composites, growth, struct., mech., elec. and optical props. 7-33648
 metallic glasses, atomic radial distrib. functions, ultradispersed eutectic structural model 7-11923
 microsegregation, effect of solidification rate 7-46480
 Nimonic 80A, crack growth under sulphidising conditions, metallography 7-59680
 solidification, lamellar spacing, influence of convection 7-17522
 solidification, rapid, theory of eutectic growth 7-65016
 steel, high speed, peritectic transform., decomp., carbide precip. Nb alloying effect (*German, English*) 7-22677
 steel, stainless, pulsed and continuous laser welded, solidification behaviour and microstruct. characts. 7-13444
 steel, took, Cr-Mo-V, hot working, ductility, C content, toughness, eutectic carbide segregation 7-59592
 Ag-Sn hypoeutectic alloys, primary phase shape rel-to cooling rate and comp. 7-59509
 Al-Al₂Cu eutectic alloys, chill cast, directionally solidified, hot rolling microstruct. 7-46447
 Al-Al₃Ni eutectic alloys, chill cast, directionally solidified, hot rolling microstruct. 7-46447
 Al-Co, melt spinning, microstruct., precip., microhardness (*Korean*) 7-46444
 Al-Fe system, phase diagram, DTA obs. 7-39485
 Al-Li-Be alloys, arc-melted, microstruct. evaluation 7-22655
 Al-Mn, rapid solidification, extended solid soln. and eutectic growth 7-33647
 Al-R (R=Er,Nd,Gd) rapidly solidified alloys, microstruct. and thermal props. 7-22667
 Al-Si, hypereutectic alloys, primary Si particles 7-33649
 Al-Si (12.7 wt.%), eutectic microstruct., twinning and branching mechanisms 7-17521
 Al-Si eutectic, Sr-modified, fibrous Si cryst. morphology, TEM study 7-28015
 Al-Si-Sb, directionally solidified eutectics, inter-Si flake spacing rel. to Sb addition 7-53717
 Al₂O₃-TiO₂-NaO_{1/2} system, elec. cond. meas. to detect suspected liq. phase 7-39467
 Au-Ag-Cu-Pd, cast microstruct. segregation, TEM obs. 7-39495
 BaTiO₃ ceramics, sintering, liq. phase enhanced discontinuous grain growth control 7-46384
 Bi-In-Sn alloys system, phase relationships 7-13433
 Bi-MnBi eutectic, pure and modified, growth 7-59500
 Fe cast, Cr-type, duplex nature of eutectic carbides 7-13440
 Fe, cast, white, Cr-Mo, unidirectionally solidified, sclerometric study 7-3455
 Fe-C-based alloys, high C, rapidly solidified, mech. props. 7-22673
 Fe-Si-B amorphous alloys, hypoeutectic, thermal stability and soft mag. props. 7-11928
 InSb-NiSb eutectic composite, rel. between metal fibre morphology and elec. props. 7-59644
 Li₂O-MgO(CaO)-Al₂O₃-SiO₂, multicomponent glasses, sequence of cryst. phases 7-26648
 MnBi/Bi eutectic, freezing rates, convection effect on microstruct. 7-22652
 Ni-base superalloy, cast, high Al-Ti, eutectic form. and σ -phase control (*Chinese*) 7-7983
 Ni-Mo₂C eutectic, directional solidification oriented struct., strength, hardening mechanism (*Russian*) 7-59507

eutectic structure continued

- Ni-NbC eutectic, directed crystallisation, comp. growth laws (*Russian*) 7-65021
 Ni-Sn highly undercooled droplets, rapidly solidified, microstruct. studies 7-22670
 Ni-Ti-Nb, shape memory alloy, cast microstruct. 7-7988
 NiO-based aligned eutectics, microstruct., crystallography and interfaces 7-65025
 NiO-CaO eutectic, directionally solidified, struct. imperfections 7-65026
 Pb-Sn eutectic, spiral structures, convection influence 7-22653
 Pt-Pd-Cu₂S-Ni₃S system, annealing, phase comp., DTA 7-46412
 Pt-PtS system, phase equil. 7-22644
 Ru-Cu₂S system, annealing, phase comp., DTA 7-46412
 Zr-Ni metallic glasses, crystn. 7-21111
eutectic transformations see phase diagrams; phase equilibrium
eutectoid steel see carbon steel
eutectoid transformations see solid-state phase transformations
evaporated layer production see vapour deposition
evaporation
 see also drying; field evaporation
 7-44029
 air flow with fine droplets, evaporative cooling heat transfer 7-11508
 Australian class A pan evaporation network, evaporation reduction due to bird screen 7-4193
 Bangladesh, evaporation rates, water pan observations 7-29092
 bare soil surface, moisture and energy fluxes, event-based simulation model 7-55107
 Brazil, estimation of global solar radiation and evap. from precip. data 7-66272
 Brazil coast, mean sea-level var. with atm. temp., press., precipitation and evaporation 7-18194
 P/Comet Giacobini-Zinner (1984e), evaporation rel. to origin of metal ions in cometary coma 7-9415
 cryogenic liquids, evaporative loss during vibration and transport 7-44776
 crystal violet in ethanol, spreading layer, capillary convection 7-6925
 droplet evaporation under subatmospheric press. 7-44010
 droplet shape and size variations from morphology-depend. reson. in fluorescence spectra 7-29970
 droplets, accelerated, in nonisothermal flow, heat transfer (*Russian*) 7-16179
 East Germany, evaporation height rel. to air temp., global radiation and saturation deficit (*German*) 7-9055
 evapotranspiration, thermal IR remote sensing 7-34696
 evapotranspiration, var. correl. with ground self pot. var. 7-29275
 falling liq. film, vapour generation nucleate boiling, acoustic diagnostic technique 7-11502
 filler evaporation from porous body with plane surface 7-51230
 fluid interfaces, phase transitions, local density approx. and smoothed density approx. study 7-63912
 fractionating condensation and evaporation in plate-fin devices 7-43644
 freons, liquid-vapour system, shock wave compression 7-31874
 fuel drop, liq., moving, combustion, thin-flame theory, variable density effect 7-26364
 graphite surface pulsed laser melting, cluster form. and evaporative loss, nanosecond time resolved reflectivity meas. 7-12137
 heat pump utilisation in process industry evaporators 7-65420
 high-temperature chamber elements, evaporation, effect on electrophys. props. of gases 7-44777
 Hodder catchment evaporation model 7-40589
 hydrology, catchment-scale evaporation and atmos. boundary layer 7-18231
 hydrology, evaporation from water surface in humid tropical area of India 7-29090
 III-V semiconductor-Au system, heat treatment, gaseous species evolution, mass spectra studies 7-39881
 Indian Ocean, evaporation from equatorial regions 7-23791
 kinetic theory, temp. paradox 7-48660
 laser interactions with condensed matter, review 7-12125
 laser surface treatment, recent developments 7-21274
 liquid drops, charged, instability of evap. 7-20091
 liquid evaporation, low-current high-voltage discharge effect 7-58453
 liquid evaporation and quantum desorption processes (*French*) 7-38343
 liquid metals, light scattering during evaporation under monochromatic radiation 7-13172
 noncondensable gas behaviour in vapour, macroscopic eqns., boundary conditions and Knudsen layer corrections calcs. 7-31840
 nonNewtonian laminar falling liquid film, thermal entrance region, heating and evaporation 7-51235
 oblate ellipsoids, diffusion, shape effect on consumption in fluid-particle processes 7-33930
 W equatorial Pacific, evaporative cooling by anomalous winds 7-9023
 Persian Gulf, evaporation from coastal water of central pt. 7-66127
 phase transition kinetics, electric field effect 7-50200
 polymer microdispersions, preparation 7-22631
 potential evapotranspiration calc. for East Germany (*German*) 7-4071
 Priestley-Taylor evaporation formula performance, effect of synoptic-scale advection 7-4093
 rainfall-runoff-percolation model using programmable spreadsheet 7-55116
 refractory substances, apparatus for examining sublimation and evaporation 7-41374
 refrigerant-12 evaporator, swirl flow press. drop calcs. 7-51162
 sapphire, filaments, CO₂ laser heating, evaporation and chlorination 7-58331
 snow-covered surface, evaporated water vapour flux driving convection 7-4089
 solid surface in vacuum, vaporisation, transition from free mol. to collisional flow, test particle method appl. 7-58447
 Stepanov method growth, dopant evaporation effects 7-32319
 TGS group crystals, thermal anomalies, evaporation products mass spectra study (*Russian*) 7-44781
 thermal calculation of bubbling-type evaporators 7-50929
 tip shape evolution, capillarity induced matter transport by surface diffusion 7-58592
 two-dimensional growth models, interface dynamics, time-reversal invariance and universality 7-63532
 vapour flow in low temp. heat pipes, effect of evaporation and condensation zones 7-63136
 vapour-gas mixture, condensation and evaporation of a drop 7-52014
 water aerosol, light scattering, evaporation effect study 7-62626

evaporation continued

- CdS-InP solar cells, high efficiency, with thermally evaporated window layers 7-3701
- Cu ionic clusters, evaporation, evaporation ensemble approach, unimol. rate consts. effects 7-62562
- Cu, vapour press. and heat of sublimation 7-58454
- Dy-Tb-Pd(Pt) ternary alloys, evaporation, thermodynamic props., Knudsen effusion method 7-32627
- GaAs, decomposition during rapid thermal annealing 7-13657
- GaAs, laser evaporation, spectroscopic study 7-58324
- GaAs, superheating during picosecond laser melting 7-12246
- GaAs surfaces, picosecond laser melting and evaporation 7-12120
- HgI₂, evaporation studies and phase stability 7-52025
- InSb, pulsed laser evaporation, neutral and charged particle emission 7-3120
- Ir single crystals, bulk self-diffusion, radiometric anal. (*Russian*) 7-58530
- KCl (100), interaction of NaCl mol. beams with surface, desorption flux meas., SIMS obs. 7-33508
- Ni (111), desorption of CO and CO₂ molecules, Ni atom evaporation during laser bombardment 7-58628
- Si thin film, doped, electron beam evaporation, elec. props. 7-2743
- SiO₂-K₂O-CaO-MgO-CdO glass melts, evaporation 7-2160
- SiO₂-K₂O-PbO glass melts, evaporation 7-2160
- UO₂, vaporisation, transition from free mol. to collisional flow, test particle method appl. 7-58447
- Zr-Sn, diffusion, chem. activity, modified evaporation method 7-38243
- Zr-Ti, diffusion, chem. activity, modified evaporation method 7-38243

Evershed effect see sunspots

evoked potentials see bioelectric potentials

evolution (biological)

- 1986 ISSOL meeting, Berkeley, CA, USA (1986) 7-24274
- conf., Los Alamos, New Mexico, USA (May 1985) 7-48157
- Cretaceous-Tertiary boundary extinctions, evidence at DSDP site 577, Shatsky Rise, Pacific Ocean 7-23706
- Cretaceous-Tertiary boundary extinctions, relation to Deccan flood basalts 7-34417
- Cretaceous-Tertiary boundary in N America, vegetation, climate and floral changes 7-29031
- Cretaceous-Tertiary extinction event, palaeoceanography charact., isotopic and geochem. anal. 7-18104
- Cretaceous-Tertiary extinctions 7-8953
- evolutionary ecosystems, sources of diversity, EVOLVE III model anal. 7-54431
- evolutionary game theory 7-54430
- flora devastation at Cretaceous/Tertiary boundary in E Hokkaido 7-40476
- fossils and climate, conf., Glasgow, Scotland (Sept. 1982) 7-35121
- intra-neuronal as a substrate for evolutionary learning 7-54434
- mass extinctions, relation to mantle plumes and periodicity of mag. field reversals 7-65934
- molecular evolution, dynamics 7-54432
- (neo)⁴-Darwinism 7-54428
- Ordovician-Silurian boundary extinction event, Ir abundances across stratotype section 7-4014
- origin of life, evidence from new geological developments (*Russian*) 7-60254
- Phanerozoic, natural divisions, mass extinctions and chem. comp. anal. 7-47403
- pulsations, correl. with seafloor spreading rates 7-18174
- rates of evolutionary processes, numerical modelling 7-54427
- taxonomic hierarchy, diversity trends 7-54429
- test of phylogenical predictions using combinatorial optimisation 7-40084
- three-dimensional protein struct., amino acid residue changes, mol. evolution (*Japanese*) 7-13955
- vertebrate hearing, evolution rel. to noise 7-54588

EXAFS

- 4f mixed valence cpds. X-ray absorpt. spectroscopy 7-59301
- acetylene, chemisorbed state on noble metal surfaces 7-52261
- adsorbed overlayer, specularly reflected X-rays, surface EXAFS meas. 7-3117
- backscattering amplitude and phase shift functions 7-64739
- benzene gas, K-shell EXAFS studied by EELS 7-62403
- biological calcification, appl. of X-ray absorpt. spectroscopy 7-65706
- biological systems, EXAFS charact. of poorly cryst. deposits in the presence of highly cryst. mineral 7-65900
- borosilicate glasses, corrosion studies, conventional and glancing angle EXAFS 7-59284
- borosilicate glasses, leached, containing U nuclear waste, EXAFS with grazing incidence 7-3116
- carbon tetrafluoride gas, K-shell EXAFS studied by EELS 7-62403
- chemisorbed molecules, NEXAFS and SEXAFS, studies 7-13261
- conference, Abbaye Royale de Fontevraud, France, (July 1986) 7-60862
- cyclohexane gas, K-shell EXAFS studied by EELS 7-62403
- cytochrome c and b₂ cores in oxidised and reduced states, EXAFS and XANES obs. 7-65683
- Daresbury Laboratory Synchrotron Radiation Source, selected activities 7-35651
- double crystal high resolution EXAFS-XANES spectrometer 7-61409
- double crystal monochromator for soft X-ray beam line, XANES and EXAFS spectra 7-61411
- double crystal X-ray monochromator for EXAFS and XANES 7-61410
- electron focusing processes, spherical wave approach 7-64745
- element complex X-ray atomic scatt. factors, X-ray interferometry studies 7-32208
- ethane chemisorbed state on noble metal surfaces 7-52261
- ethylene, chemisorbed state on noble metal surfaces 7-52261
- ethylene, hydroformylation, in situ IR and EXAFS 7-59755
- Fe-Mo-S systems of biological relevance, X-ray absorpt. spectroscopy 7-65703
- ferritin, Fe core: form., struct. and dissolution, X-ray absorpt. spectroscopy obs. 7-65685
- fine structure in ionisation cross sections, surface science appl., review 7-27074
- fluorescence detection systems for EXAFS meas. 7-61415
- fluorescence EXAFS meas. from 2 to 25 keV using Si photodiode array detector 7-61413
- formate on Cu surfaces, adsorpt. site symm. and bond lengths, SEXAFS data, multishell simulation anal. 7-63947
- graphite-Fe intercalation cpd., atomic structure, EXAFS studies 7-12011

EXAFS continued

- haeme enzymes and model compounds, EXAFS study of active intermediates 7-65684
- harmonic effect on amplitude in poly-element systems (*Chinese*) 7-5696
- hexafluorobenzene gas, K-shell EXAFS studied by EELS 7-62403
- horseradish peroxidase, struct. charact. of high valent intermediates, EXAFS and XANES obs. 7-65682
- II-VI and III-V semicond. solid solns., short range order and free energy of mixing, EXAFS meas. 7-63573
- inelastic processes, semiclassical treatment 7-64741
- interstellar dust, appl. of EXAFS studies 7-24185
- laboratory ReflEXAFS spectrometer 7-61408
- Lamellar cpds., X-ray absorpt. studies 7-59286
- linear detector for time-resolved EXAFS in dispersive mode 7-61412
- liver alcohol dehydrogenase, horse, EXAFS investigation of struct. site 7-65704
- metallisation of superhard material powders, X-ray method for determ. of degree of metallisation 7-54043
- metalloporphyrin stacked polymeric structs., difference EXAFS spectra studies 7-63508
- metals, FCC, EXAFS spectra, backscattering amplitude and phase shift functions 7-27820
- model compounds, scatt. amplitude and phase transferability 7-64743
- multicomponent systems, bond length determ. from EXAFS data 7-63553
- near surface EXAFS using electron yield detectors 7-61414
- ovotransferrin, chicken, Fe binding-sites, EXAFS and XANES obs. 7-65688
- oxide anodic films on Al, struct., surface EXAFS, magic angle spinning NMR studies 7-22382
- phosphate glasses, corrosion studies, conventional and glancing angle EXAFS 7-59284
- photosynthetic O₂ evolving Mn complex, X-ray edge and EXAFS studies 7-65722
- polyacetylene:Br(I), polarised EXAFS and near edge spectra studies 7-64778
- polyselenophene, electronic and struct. modifications during doping, EXAFS and XANES studies 7-63507
- quartz, structural EXAFS study 7-64762
- related phenomena, expt. calibration and calcs. for struct. determ. 7-64735
- semiconductor superlattices and heterostructures, structure, EXAFS studies 7-12509
- SEXAFS technique overview, evolution, accomplishments and impact 7-64767
- Si, spherical wave EXAFS, Si K-edge anal. 7-64822
- silicate glasses, cation environments, EXAFS and NEXAFS studies 7-63482
- silicate minerals and glasses, Fe K-edge EXAFS studies, Fe coordination 7-59287
- superoxide dismutase, EXAFS and XANES obs. 7-65681
- surface EXAFS, Debye-Waller factor, influence of adsorbed monolayer 7-39316
- surface layer struct., study using depth controlled EXAFS, near edge spectroscopy 7-59297
- surface studies at Daresbury SRS, in 60 to 1100 eV range 7-33486
- surfaces, clean and chemisorbed, SEXAFS studies 7-13262
- thermionic emission cathodes, surface struct., EXAFS study 7-44970
- transferrin, human, N-terminal fragment containing a single Fe binding site, EXAFS obs. 7-65707
- two phase systems, phase content and atomic struct. determ. 7-7788
- X-ray and electron spectroscopy, conf., Irkutsk, USSR (Sept. 1984) 7-9574
- AU clusters and bulk samples, Debye temps., EXAFS studies 7-2136
- Ag (111), adsorbed Cl, weakly ordered and disordered, struct. studies 7-2365
- Ag thin films, surface sensitivity of fluoresc. EXAFS in refl. conditions 7-64750
- Ag, with adsorbed Cl, adsorbate-substrate bond lengths, coverage depend., SEXAFS 7-63948
- Ag, with adsorbed Cs, adsorbate-substrate bond lengths, coverage depend., SEXAFS 7-63948
- Ag-Au, thin interface regions, EXAFS studies 7-59285
- Ag-Au bilayers, EXAFS and X-ray reflectivity meas. 7-27821
- AgBr₂-xI₂ rock-salt solid solns., local struct., X-ray studies 7-63586
- Al films, chemisorption of O, Al-O bond lengths, photoemission EXAFS meas. 7-64871
- Al-Cu, thin interface regions, EXAFS studies 7-59285
- Al-Cu interface, grazing incidence X-ray study of interfacial reactions 7-21543
- Al-Mn alloys, icosahedral, amorphous and cryst. local struct., EXAFS study 7-63466
- Al-Mn quasicrystals, local struct., EXAFS and XANES studies 7-6582
- Al-Mn-Ru-Si icosahedral alloys, EXAFS study 7-39317
- Al₈₆M₁₄ (M=Mn,Cr), quasicrystals, EXAFS studies 7-64804
- AlMn, icosahedral struct., EXAFS 7-26701
- Al₈₅Mn₁₅, quasicrystals, EXAFS studies 7-64804
- AlMnSi, icosahedral and α -phase structs., EXAFS anal. 7-63554
- AlMnSi, icosahedral struct., EXAFS 7-26701
- Al₂O₃-Fe particle dispersed system, cosputtered films, EXAFS study 7-64810
- Al₂O₃-ZrO₂, Zr environment, EXAFS studies 7-63465
- AlZn dilute alloys, electron irradiation induced interstitial defects, EXAFS study 7-63661
- As, amorphous, vibr. density of states, EXAFS, Debye-Waller factors 7-64820
- As, amorphous and crystalline, bond strength anal., EXAFS temp. depend. study 7-64763
- As-Se, amorphous, short range structures, EXAFS studies (*Chinese*) 7-37871
- As_{1-x}S_x:Ag film, coordination distance determ., EXAFS study 7-64004
- As₂S₃, amorphous, bulk glass and thin films, photostructural changes, EXAFS meas. 7-39314
- As₂S₃ glass, photostructural effects, EXAFS study 7-64758
- a-As₂S₃ vapour deposited films, thermostructural and photostructural changes, EXAFS study 7-64003
- As₂S₃, crystalline and glassy, bond strength anal., EXAFS temp. depend. study 7-64763
- Au, metal and clusters, dynamical props., EXAFS studies 7-64805
- Au₃Cu short range order, EXAFS study 7-63555
- BaF₂-ZrF₄ glass, Zr local environment, EXAFS studies 7-63485

EXAFS continued

- Bi, electronic structure, effect of ion implantation 7-45143
 Bi oxides, small distortions, EXAFS transmission studies 7-63580
 Bi-Zn-Fe-O amorphous films, struct. and mag. props. 7-51645
 Br₂ solid, high press. X-ray absorpt. study, energy dispersive mode 7-59299
 CO gas, K-shell EXAFS studied by EELS 7-62403
 CO gas phase molecules, O K-edge absorption spectra 7-62405
 CO₂ gas, K-shell EXAFS studied by EELS 7-62403
 CO₂ gas phase molecules, O K-edge absorption spectra 7-62405
 CaF₂-Si (111), MBE grown, electronic struct. 7-2725
 CaF₂-Si (111) interface, electronic struct. 7-38737
 CaMgSi₂O₆ - CaFeSi₂O₆, solid solns. short range order parameters, determ. from EXAFS pair distrib. fns. 7-59289
 CaO-ZrO₂, defect struct., EXAFS studies 7-63608
 CaPO₃, EXAFS, multiple scatt. processes 7-64777
 Ca₃(PO₄)₂OH, EXAFS spectrum anal., spherical wave theory 7-33485
 CaZrTi₂O₇, zirconolite, alpha-recoil damage 7-6692
 Cd single cryst., interatomic distance and thermal motion, K-shell EXAFS, temp. and orientation depend. 7-64814
 Cd single crystals, anisotropic thermal effect, first shell distance and thermal motion, EXAFS study 7-63753
 CeMRu₂Si₂ (M=La,Y), high energy EXAFS and XPS studies 7-64801
 CeNi₂Hx, stoichiometry deviation and structural disorder, H content depend., EXAFS study 7-64815
 CeO₂, bond lengths, Ce K-edge EXAFS meas. 7-64753
 Cl, chemisorption, on Cu (111), site info. from EXAFS and photoelectron diffraction 7-32788
 Co, Auger spectra, extended fine structures 7-64831
 Co monolayer on Cu (111), Debye-Waller factor anisotropy, SEXAFS study 7-63936
 Co-Au-Fe, dil., local structural and mag. environments of Fe 7-26965
 Co-Sn multilayers, amorphisation and interdiffusion, EXAFS and XANES studies 7-64812
 Cr film on polyimide, interface chemistry 7-46871
 Cu (100) and (110), formate adsorption, bonding, EXAFS studies 7-38341
 Cu (111), Co adsorbed layer, surface EXAFS investig. (French) 7-6957
 Cu, Auger spectra, extended fine structures 7-64831
 Cu complex, Cu (II) α,ω -dicarboxylato polybutadiene, microstruct. obs. 7-13259
 Cu complex, Cu (II) α,ω -dicarboxylato polybutadiene, microstruct. investig. 7-16450
 Cu complexes, glutamic acid, struct., EXAFS study 7-19882
 Cu monolayer on Au (111), fluoresc. detected surface EXAFS 7-46235
 Cu/Au thin film systems, interdiffusive kinetics, EXAFS studies 7-16819
 Cu-Al bilayers, EXAFS and X-ray reflectivity meas. 7-27821
 Cu-albumin complex, local struct., EPR and EXAFS obs. 7-65689
 Cu-Fe, dil., local structural and mag. environments of Fe 7-26965
 Cu-Hf multilayers, interface EXAFS study 7-64811
 Cu-Mo-S systems of biological relevance, X-ray absorpt. spectroscopy 7-65703
 Cu_{70-x}Au₃₀Fe_x, ferromagnetic interactions, EXAFS and XANES anal. of Fe atom environment and clustering 7-64808
 CuBr, X-ray absorption study at higher press. 7-17362
 Cu₂Cr₂Sn_{2-x}S₄ spinels, Cu-Cu distances, EXAFS studies 7-63585
 Cu₉₈Fe₂, antiferromagnetic interactions, EXAFS and XANES anal. of Fe atom environment and clustering 7-64808
 CuFeS₂, electronic struct., K-edge EXAFS study 7-64079
 CuFe₂S₃, EXAFS meas. under high press. by diamond anvil cell 7-64754
 CuGaIn_{1-x}Se₂ mixed chalcopyrite local struct., K-edge EXAFS meas. 7-63574
 Cu_{0.26}Mn_{0.87}PS₃, crystalline lamellar cpds. EXAFS studies of disorder 7-59295
 Cu₇₀Ti₃₀ metallic glass, atomic neighbouring struct., EXAFS study (Chinese) 7-6519
 CuZn brass alloys, local disorder and premartensitic phenomena, EXAFS study 7-64817
 Dy compounds, L_{III} X-ray absorption spectra 7-39312
 Eu₂Pd_{1-x}, amorphous mixed valent alloys, X-ray absorpt. spectra 7-64802
 EuPd_{2-x}Au_xSi₂, valence determ., Mossbauer and X-ray absorpt. studies 7-64800
 Fe, Auger spectra, extended fine structures 7-64831
 Fe-B, amorphous, structural characterisation by laboratory EXAFS spectrometer 7-1911
 Fe-Cr oxide film struct., in- and ex-situ fluorescence EXAFS study 7-64007
 Fe-Pt Invar alloys, premartensitic transform., local structural change, EXAFS study 7-63556
 Fe₈₀B₂₀ amorphous alloys, EXAFS meas. at B k-edge 7-64807
 FeCo oxides, oxidation state and site symmetry, EXAFS and XANES studies 7-63584
 Fe₄₀Ni₄₀P₁₄B₆ metallic glass, heterogeneous struct., EXAFS study 7-27816
 FeO-PbO-P₂O₅ glasses, atomic environments, EXAFS studies 7-64787
 Fe₂O₃-P₂O₅-K₂O glasses, mixed valence, EXAFS studies 7-64786
 FeOOH, poorly-ordered precursors, local struct., EXAFS studies 7-63577
 FeSnSb dilute alloys, local lattice relax. around impurity, K-edge EXAFS study 7-64159
 GaAs:Te, struct. environment of dopant, study by EXAFS in fluorescence mode 7-59300
 GaAs:Zn, ion damage and recrystn. annealing, conversion electron EXAFS meas. 7-64821
 GaAsSb_{1-y} relaxed zinc-blende lattice, EXAFS study 7-64759
 Gd_{1-x}Sr_xCrO₃, coordination number and elec. cond., EXAFS and XANES studies 7-64785
 Ge, amorphous and partially crystallised, X-ray absorpt. investig. of struct. (German) 7-46241
 Ge amorphous films, struct. and crystn., EXAFS study 7-64005
 Ge:Si, ion-implanted amorphous surface layers, EXAFS 7-27823
 GeO₂ glass, high resolution EXAFS and XANES studies 7-27817
 GeS₂ glass, photostructural effects, EXAFS study 7-64758
 GeS₂, amorphous system, struct. anal. by X-ray spectroscopy 7-26653
 Ge₂₀S₈₀Bi chalcogenide glasses, doping, coordination number and cond. transition, EXAFS study 7-64764
 GeSe₂ glass, photostructural effects, EXAFS study 7-64758
 InGaAsP local struct., EXAFS and near-edge struct. studies 7-64006
 In_{1-x}Ga_xAs_{1-y}P_{1-y} cpd. semicond. alloys, lattice and band struct. props., review (Japanese) 7-7109

EXAFS continued

- K₂O-P₂O₅-WO_{3-x} mixed valence glasses, local order, EXAFS and X-ray diffusion studies 7-1903
 K(Ta_{0.91}Nb_{0.09})O₃, ferroelec. transitions, EXAFS studies 7-64780
 KTaO₃, Fourier transformed EXAFS spectra, comparison with NaTaO₃ 7-64749
 Kr, Fourier transform EXAFS spectra, nonstructural low-R peak 7-64744
 LaNi₂H_x, stoichiometry deviation and structural disorder, H content depend., EXAFS study 7-64815
 La₂S₃-La₂O₃-Ga₂O₃-Ga₂S₃ glassy and crystalline chalcogenides, EXAFS structural study 7-63481
 La_{1-x}Sr_xCoO₃, local struct., EXAFS and XANES studies 7-63582
 Mg_{0.98}Na_{0.02}Fe₂O₄, spinel struct., EXAFS and XANES studies, humidity sensor appls. 7-64784
 MgO-FeO, solid solns. short range order parameters, determ. from EXAFS pair distrib. fns. 7-59289
 MgO-LiFeO₂, solid solns. short range order parameters, determ. from EXAFS pair distrib. fns. 7-59289
 Mn oxides, oxides, Ni- and Co-containing, structural chemistry, EXAFS studies 7-63578
 Mn-Al icosahedral quasicrystals, local structure 7-11997
 MnAlSi and MnAl icosahedral crystals, structure, EXAFS studies 7-11996
 (Mn(H₂O)₆)²⁺ complexes in aqueous solutions, X-ray absorption spectra studies 7-22381
 (MnO₄)⁻ complexes in aqueous solutions, X-ray absorption spectra studies 7-22381
 Mn₂Sn_{1-x}Mo_xS₈, Mn dopant props., supercond. transition temp., EXAFS, XANES, photoemission studies 7-46236
 Mo-one-dimensional amorphous organic systems, EXAFS and X-ray scatt. studies 7-64779
 ND, mixed valent clusters, X-ray absorpt. studies 7-64791
 NaCl:Cu⁺, lattice relax. around cuprous ion, EXAFS studies 7-64788
 (Na₂O.2SiO₂)_{1-x}(Fe₂O₃)_x glasses, Fe ions, ionic state and coordination geometry 7-63492
 NaTaO₃, Fourier transformed EXAFS spectra, comparison with KTaO₃ 7-64749
 NbS₂(Se₂)-transition metal intercalation cpds., EXAFS 7-53446
 Ni (110) and (111), adsorbed S, surface struct., SEXAFS, XANES studies 7-64770
 Ni (111), adsorption of Cl, surface struct., SEXAFS, photoelectron diff. studies 7-64775
 Ni {100}, adsorption of I, surface phases, SEXAFS, multishell simulation anal. 7-59303
 Ni {100}, adsorption of I, surface phases, SEXAFS, breakdown of Fourier filtering single shell anal. 7-59304
 Ni, Auger spectra, extended fine structures 7-64831
 Ni complex, bis(dimethylglyoximate)nickel(II), EXAFS meas. under high press. by diamond anvil cell 7-64754
 Ni-Fe (100), layered struct. reflectivity and EXAFS study 7-59292
 Ni-P glasses, local atomic struct., NMR and EXAFS studies 7-63504
 Ni₄Cd_{1-x}PS₃, crystalline lamellar cpds. EXAFS studies of disorder 7-59295
 Ni(OH)₂, EXAFS spectra, vacant cationic site model (French) 7-64783
 NiSnInSb dilute alloys, local lattice relax. around impurity, K-edge EXAFS study 7-64159
 Ni₆₄Zr₃₆, amorphous, short range order, EXAFS 7-44388
 Ni₆₄Zr₃₆ amorphous alloy, local struct., EXAFS and neutron diff. studies 7-64813
 O (2×1) chemisorbed layer on Ni (110), SAXAFS study 7-64768
 O (2×1) overlayer on Cu (110), surface reconstruction, mean free path and Debye-Waller factor, SEXAFS study 7-46238
 O₂ gas phase molecules, O K-edge absorption spectra 7-62405
 OCS gas phase molecules, O K-edge absorption spectra 7-62405
 Os clusters and complexes, Al₂O₃ supported, struct., EXAFS 7-62560
 Pb glaze glass system, local coordination EXAFS studies 7-63484
 Pd clusters in C matrix, electronic and struct. studies by EXAFS and XANES 7-17363
 PdH_x, dilute alloys, Pd substituted, interaction of H with impurities, EXAFS study 7-64806
 Pd₃Th, impurity internal oxidation, EXAFS 7-17360
 Pr, mixed valent clusters, X-ray absorpt. studies 7-64791
 Pt-Si interfacial growth following Si chemisorption, intermixing, SEXAFS obs. 7-64772
 RbC₈, 2D graphite intercalation cpds., bond angle determ., EXAFS study, Debye-Waller anisotropy. 7-59293
 ReO₃, bridging angle, high press. EXAFS studies 7-64781
 Ru-one-dimensional amorphous organic systems, EXAFS and X-ray scatt. studies 7-64779
 β -Sb₂O₄V(Mo), struct. characterisation, X-ray, neutron, and electron microscopy studies 7-32383
 Si (100), adsorption of H₂O, photon stimulated ion desorption surface EXAFS 7-58633
 Si (100), adsorption of H₂O, surface struct., photon stimulated ion desorption SEXAFS determ. 7-64752
 Si (111), Pt chemisorption and interface form., EXAFS and X-ray absorpt. resonance spectra studies 7-38336
 Si, amorphous, pulsed laser irradi., time-resolved X-ray absorption studies 7-3115
 Si, amorphous foil, time-resolved X-ray absorption during pulsed laser irradiation 7-12128
 Si, crystalline, amorphous and H-doped, structural props., EXAFS study 7-64760
 Si, spherical wave EXAFS and multiple scatt. effects in XANES 7-64742
 Si structural EXAFS study 7-64762
 a-Si:H, EXAFS, spherical wave anal. and multiple scatt. effects 7-64740
 Si:H binary alloys, crystallisation of polysilane 7-21105
 a-Si:H short range order, impurity distrib. effects, EXAFS study 7-64761
 Si:Sb, local lattice relax. around impurity, K-edge EXAFS study 7-64159
 Si-Cu-Au layered struct. reflectivity and EXAFS study 7-59292
 Si-Ge interface, solid phase epitaxy, intermixing, EXAFS, AES, LEED obs. 7-63973
 SiC fibre composites, structural EXAFS study 7-64762
 SiC, structural EXAFS study 7-64762
 Si_{1-x}C_xH films, amorphous, bond lengths, comp. depend., EXAFS study 7-64757

EXAFS continued

- $\text{Si}_{1-x}\text{Ge}_x$:H films, amorphous, bond lengths, comp. depend., EXAFS study 7-64757
 SiN_x :H films, amorphous, bond lengths, comp. depend., EXAFS study 7-64757
 $\text{Si}_3\text{N}_4/\text{GaAs}$ buried interface, EXAFS studies in total reflection and dispersive modes 7-64765
 SiO_2 glass, structural EXAFS study 7-64762
 $\text{SiO}_2\text{-B}_2\text{O}_3\text{-Na}_2\text{O-Al}_2\text{O}_3$ glasses, corroded, grazing incidence fluorescence EXAFS, near edge spectroscopy 7-59296
 $\text{SiO}_2\text{-B}_2\text{O}_3\text{-ThO}_2$ based glasses, local struct. around actinide, EXAFS and optical spectral studies, appl. for nuclear waste glasses 7-59290
 $\text{SiO}_2\text{-B}_2\text{O}_3\text{-UO}_{2.66}$ based glasses, local struct. around actinide, EXAFS and optical spectral studies, appl. for nuclear waste glasses 7-59290
 SiO_x evaporated thin films, struct. study 7-58699
 $\alpha\text{-SiO}_2$:H films, local struct. EXAFS study 7-59291
 $\text{Si}_x\text{Se}_{1-x}$ glasses, intermediate range order 7-11938
 Sm , mixed valent clusters, X-ray absorpt. studies 7-64791
 Sm small clusters, matrix isolated, mixed valence, critical cluster size 7-64186
 $\text{Sm}_{1-x}\text{Sc}_x$ alloys, intermediate valence, X-ray absorption study 7-7789
 SmSe , high press. EXAFS studies at 77 K 7-64799
 $\text{SnFe}_{0.05}\text{MoS}_8$, Chevrel-phase superconductor, collinear ordering, EXAFS studies 7-13258
 SrTiO_3 (100), adsorption of H_2O , surface struct., photon stimulated ion desorption SEXAFS determ. 7-64752
 $(\text{Ti,Ta})\text{O}_2$ solid solns., chem. shift and cryst. field splitting rel. to valence charge, EXAFS 7-27818
 $\text{Tm}_3\text{Fe}_2\text{O}_{12}$, double phase transition, EXAFS studies 7-63799
 Tm_2Se , mixed valent systems, atomic relax., determ. from EXAFS spectra 7-64797
 U cpds., metallic and nonmetallic, X-ray absorpt. at various thresholds 7-64793
 UBe_{13} , heavy fermion cpd., lattice dynamics, EXAFS study 7-64792
 $(\text{U,Ce}_{1-y})\text{O}_{2-x}$, struct. determ., EXAFS studies 7-63581
 UO_2 , struct. determ., EXAFS studies 7-63581
 U_4O_9 , struct. determ., EXAFS studies 7-63581
 V_2O_5 gel, V site struct., polarised EXAFS and XANES studies 7-65355
 W polycrystalline surfaces of thermionic cathodes, SEXAFS of absorbed Ba 7-64774
 W-Os polycrystalline surfaces of thermionic cathodes, SEXAFS of absorbed Ba 7-64774
 $\text{Y}_2\text{O}_3\text{-Bi}_2\text{O}_3$, local interactions and environments, EXAFS studies 7-63575
 $\text{Y}_2\text{O}_3\text{-ZrO}_2$, local interactions and environments, EXAFS studies 7-63575
 $\text{Y}_2\text{Pd}_{1-x}$, amorphous mixed valent alloys, X-ray absorpt. spectra 7-64802
 Zn enzymes, metal coordination, EXAFS obs. 7-65686
 $\text{Zn}_{0.98}\text{Na}_{0.02}\text{Fe}_2\text{O}_4$, spinel struct., EXAFS and XANES studies, humidity sensor appls. 7-64784
 ZnS:Fe electronic struct., K-edge EXAFS study 7-64079
 ZnS-ZnSe mixed powders, site selective EXAFS via optical de-excitation 7-53443
 ZnX_2 ($\text{X}=\text{Cl, Br, I}$), aqueous halide solns., EXAFS study of Zn^{2+} coordination 7-59282
 Zr , Fourier transform EXAFS spectra, nonstructural low-R peak 7-64744
 Zr-Ni(V) amorphous superconductors, struct. and supercond. props. 7-27482

exchange forces in nucleus see nuclear forces

exchange interactions (electron)

see also antiferromagnetism; ferromagnetism; RKKY interaction; superexchange interactions

3d- and 4f- metals, periodic spin structs., critical props. calcs. (Russian) 7-59031

- $\text{Al}_2\text{O}_3\text{:Cr,Ga}$, Cr-Ga complexes, energy transfer 7-22321
 actinide-transition metal alloys, AM_2 , $\text{A}=\text{U-Np}$, $\text{M}=\text{Fe-Ni}$, magnetism and electronic props. 7-27505
 actinides, elastic neutron scatt. and diff. studies, review 7-12945
 Anderson model, Coulomb repulsion between localised and extended states 7-17157
 anisotropic cubic spin-1 Ising model, linear chain approx. 7-2876
 anisotropic spin chain, magnon bound state energy and wave functions, Dzyaloshinskii interactions (Russian) 7-7500
 antiferromagnetic films, dipole-exchange spin-wave modes 7-45771
 antiferromagnetic quantum spin chains, random exchange effects, Monte Carlo study 7-64475
 antiferromagnetic semiconductor, bound magnetic polarons, spin dynamics 7-7502
 bound magnetic polarons, variational model in adiabatic approx. 7-12624
 charge transfer compounds, thermodynamic and dynamic props. 7-59048
 classical spin clusters, integrability criteria and analytic struct. of invariants 7-45720
 cryocrystal: O_2 , thermodynamic props., impurity mol. exchange interaction effects calcs. (Russian) 7-12308
 crystalline solids, electrostatic Madelung and cohesive energies 7-44442
 cubic metals, phonon spectra, dynamical pseudopot. shell model calcs. 7-51965
 disordered systems, ferromagnetism, Arrott-plot criterion 7-7521
 electron correlation, band gaps and quasiparticle energies calcs. for semiconductors and insulators 7-27278
 electron gas with uniform density, screened-exchange functional 7-64138
 electron scatt. by Al atoms in solids, polarisation and exchange 7-22401
 electron scatt. by Li atoms in solids, polarisation and exchange 7-22401
 exact exchange energies, local density approx. calcs. 7-38481
 exciton-exciton interaction, wave fn. normalised coeff., exchange effect role 7-52431
 ferrite film structure, layered, anisotropic, dipole exchange spin waves 7-64494
 ferromagnetic 4f-systems, Curie temp., valence instability effects calcs. 7-38865
 ferromagnetic antisymmetric exchange chain, sine-Gordon soliton stability 7-38889
 ferromagnetic film, with mixed exchange boundary conditions, theory of dipole-exchange spin wave spectrum 7-45644
 ferromagnetic Heisenberg spin chain, compressible, static π -kink 7-53020
 ferromagnetic semicond., donor state, thermally induced abrupt shrinking 7-52510
 ferromagnetic single-domain films with inclined anisotropy axis, magnetostatic spectrum 7-53092

exchange interactions (electron) continued

- ferromagnetic superconductors, mixed state, surface tension 7-52919
 ferromagnetic thin overlayer, exchange-coupled, on ferromag. substrate, FMR study 7-38946
 ferromagnets, electron energy loss spectrum in the near-specular regime, electron-hole excitations 7-33496
 ferromagnets, non-Heisenberg systems, random phase approx. and Green's function anal. (Russian) 7-45597
 ferromagnets, randomly inhomogeneous, elec. resist., temp. depend. (Russian) 7-58791
 ferromagnets with low carrier densities, indirect exchange 7-33162
 four-lattice rhombic antiferromagnet, reson. props., exchange, and high freq. suscept. calcs. (Russian) 7-13037
 graphite, pyrolytic, neutron irradi., ESR studies, exchange coupling model 7-7590
 Heisenberg antiferromagnets, multicritical points 7-27541
 Heisenberg ferromagnet, anharmonic spin-one, order of phase transitions, effect of press. 7-53018
 Heisenberg ferromagnet, anisotropic, with biquadratic exchange 7-12987
 Heisenberg models with competing interactions, quantum fluctuations and phase diagram 7-38895
 Hubbard model, 3-D, d-wave pairing near a spin-density-wave instability 7-45608
 Hubbard model with degeneracy, phase transitions 7-64041
 inhomogeneous electron gas pressure calc. (German) 7-64145
 insulators with spiral mag. struct., sound absorption 7-38918
 intermediate valence systems, Ferromagnetic order coexistence, mag. props 7-64187
 intermediate-valence systems, magnetic-nonmagnetic transitions 7-12965
 intersubband s-d exchange absorption of spinwaves in ferromagnetic conductors 7-7499
 iron porphyrin complexes, mag. moment susceptibility, Mossbauer study 7-22168
 Ising chains, spin-S, cryst. field effect on transverse susceptibility 7-45601
 Ising ferromagnet, magnetism at site-bond diluted anisotropic free surface 7-2800
 Ising ferromagnet, with biquadratic exchange interaction and uniaxial anisotropy 7-17189
 Ising model, 2D half-plane with layered exchange interactions and alternate surface magnetic fields 7-2836
 Ising model, multispin correls., multiparticle entropy method calcs. 7-45708
 Ising model on Bethe lattice, bilinear exchange interactions 7-2877
 Ising spin-1 model, with bilinear and biquadratic exchange interactions, renormalisation group calcs. 7-53010
 Ising systems, semi-infinite, critical and multicritical phenomena 7-59044
 itinerant electron model with crystalline or mag. long-range order 7-17152
 low symm. magnets, domain boundaries struct. and energy calcs. (Russian) 7-33200
 magnetic bubbles, translational motion, exchange relax. effects (Russian) 7-17206
 magnetic chains, anisotropic, of arbitrary spin, Bethe ansatz for two-magnon bound states 7-53015
 many-fermion systems of arbitrary dimensionality and interparticle interaction, nonlocal exchange energy 7-38482
 metal-metal tunnelling electrons, barrier height, image-force effects 7-52747
 metallic molecules and cpds., magnetic moment formation and mag. susceptibility 7-58995
 metals, indirect-exchange interaction, realistic calc. 7-38854
 metals, magnetic impurity spin coupling, s-d mixing interaction envelope function calcs. 7-2814
 metals, phonon spectra, dynamical pseudopot. shell model calcs. 7-51964
 one-dimensional Hubbard model, one- and two-hole excitation spectra 7-22088
 one-dimensional spin-1-bilinear-biquadratic exchange Hamiltonian, crossover effects 7-7464
 permanent magnet materials, props., struct., exchange interactions 7-53053
 planar magnetic materials with biquadratic exchange, nonlinear magnetisation waves 7-17165
 polyparaphenylene, conducting polymer, non-Curie like susceptibility, exchange-coupled pair model 7-52930
 polypyrrole, conducting polymer, non-Curie like susceptibility, exchange-coupled pair model 7-52930
 quartz, neutron irradi., electron spin-lattice relax., effect of exchange interaction 7-45794
 quasi-one-dimensional systems, spin-Peierls transition 7-59047
 random field models with long range exchange, scaling theory, $1/n$ expansion 7-24553
 rare earth-Al alloys, RAl_2 , paramagnetic fluctuations, muon spin rotation studies 7-12941
 s-f model with antiferromag. s-f exchange 7-45653
 semiconductors and insulators, local density band structure, self-energy corrections 7-7097
 spin systems, disordered, pair approx. to describe mag. props. 7-45655
 spin-1 Ising model, two and three dimensional, biquadratic exchange interactions, reentrant behaviour, Monte Carlo study 7-12986
 spin-1/2 Heisenberg antiferromagnet, triangular lattice, Ising-like exchange anisotropy, magnetisation process 7-53021
 superconducting electron pairing, exchange and correl. contributions 7-45574
 superconducting transition temp., electron exchange interaction influence (Chinese) 7-27450
 surface magnetism, study by spin polarised electrons 7-2901
 tight-binding itinerant ferromagnet, spin wave anal. 7-2833
 tunnelling exchange integral calc. using a variational formalism based on supersymmetry 7-32964
 valence fluctuating lattice systems, self-consistent perturbation theory 7-2561
 vertical Bloch line pair, lumped const. model 7-59093
 weakly localised regime, effect of mag. impurity on conductivity 7-2839
 XY model, one-dimensional, transverse auto-correlation function, short time behaviour 7-64430
 B clusters, magnetic properties, Heisenberg Hamiltonian 7-57199
 $\text{Ba}_2\text{CaCu}_2\text{Fe}_2\text{F}_{14}$, heteronuclear trimers with ferrimag. behavior (French) 7-64448
 $\text{Ba}_2\text{CaCu}_2\text{Fe}_2\text{F}_{14}$, exchange interactions, mag. susceptibility meas. 7-45654

exchange interactions (electron) continued

- BaMnAlF₄, exchange interactions, mag. susceptibility meas. 7-45654
 BaMnF₄, 2D Heisenberg magnet, spin dynamics and EPR linewidth 7-38932
 BaMnGaF₇, exchange interactions, mag. susceptibility meas. 7-45654
 CdCr₂Se₄ thin films, ferromagnetic semicond., multielectron energy struct., absorpt. spectrum, temp. and doping depend. 7-38488
 CdCr₂(Se_{1-x}S_x)₄ spinel, mag. prop. anomalies 7-64453
 Cd_{1-x}Mn_xS, antiferromag. exchange constants between nearest-neighbour Mn²⁺ ions 7-64449
 n-Cd_{1-x}Mn_xSe, magnetoresist. and Hall effect meas. near metal-insulator transition 7-12741
 Cd_{0.8}Mn_{0.2}Te/Cd_{0.7}Mn_{0.3}Te semimagnetic superlattices, electronic props., theory 7-45445
 Cd_{1-x}Mn_xTe, interband Faraday rot. meas. 7-39093
 Cd_{1-x}Mn_xTe, photoluminescence position and lifetime 7-13205
 Cd_{1-x}Mn_xTe(Se), mag. field-induced exchange effects, photolum. meas. 7-27705
 Cd_{1-x}Mn_xTe_{1-x}Sc_y, magnetic suscept. and ESR meas., temp. depend. study 7-45636
 Cd_{1-x}Mn_xTe_{1-x}Sc_y pseudoternary semimag. semicond., mag. suscept. and exchange interaction data anal. 7-7501
 (CdSe)_{1-x}(MnS)_x crystals, semimag. semiconductors, magnetooptic studies 7-64609
 Cd₂Zn_{1-x}Mn_xTe(Se) pseudoternary semimag. semicond., mag. suscept. and exchange interaction data anal. 7-7501
 Ce-Cu amorphous alloys, mag. and transport props., Ce-derived anomalies 7-52601
 CeAs, antiferromag., anisotropic exchange and spin dynamics, neutron study 7-33147
 CeSb, antiferromag., anisotropic exchange and spin dynamics, neutron study 7-33147
 Co (II) complexes, spin-exchange processes 7-12677
 Co, diffusion of ⁴⁸V, mag. anomalies, quasi-chemical model 7-6862
 Co-CoO multilayered films, exchange anisotropy 7-27579
 CoCl₂ dipyrindine quasi-1D Ising system, far IR magnetic excitation spectrum 7-59040
 CoCl₂-graphite intercalation cpds., mag. susceptibility meas. 7-45638
 Co₈₈Fe₁₂Ni₁₀Si₁₁B₁₆, metallic glasses, multiplet splitting, XPS study 7-27858
 Co₈₈Ni₁₀Fe₂B₁₆Si₁₁ amorphous ferromag. alloy struct., shock loading effects, mag. struct. anal. 7-2100
 Cr (001), near-surface antiferromagnetism and surface ferromagnetism, photoelectron spectroscopy 7-59381
 Cr complex, luminescence line narrowing, exchange parameter evaluation 7-64677
 Cr impurity ions, d-p electronic energy, coord. sphere radius depend. 7-16971
 Cr, magnetovolume, thermal expansion and Gruneisen parameters 7-33260
 Cr-V alloy, magnetovolume, thermal expansion and Gruneisen parameters 7-33260
 Cr₂BeO₄ multi-sublattice antiferromag., elec. polarisation, magnetoelec. effect calcs. (Russian) 7-7577
 Cr₂BeO₄ orthorhombic antiferromagnet, double exchange long-period magnetic struct. calcs. 7-2818
 Cr_{1/3}NbS₂, long-period helical spin struct. (Japanese) 7-45626
 CsCoCl₃·2H₂O, 1D antiferromagnet, exciton transfer, absorpt. spectra 7-27254
 Cs₃Cr₂I₉ critical singlet ground-state magnet, dimer excitations, inelastic neutron scatt. study 7-7477
 CsFeCl₃, quasi-one-dimensional ferromag., mag. field effects on optical spectrum 7-3026
 Cs₂FeCl₅·H₂O, antiferromagnet, mag. phase diagram, spin wave excitations, Mossbauer spectra 7-45676
 CsMnCl₃·2H₂O, 1D Heisenberg magnet, spin dynamics and EPR linewidth 7-38932
 Cu complex, CuBr₂·2DMSO, linear chain antiferromag., optical birefringence 7-7679
 Cu-Mn dil. alloys, electronic struct. of mag. impurities 7-58771
 CuCl₂·2DMSO, paramagnetic susceptibility of antiferromagnetic quantum chain 7-52997
 Dy-Y highly dil. alloys, mag. props. 7-7483
 DyAl₂ single crystals., low temp. heat capacity meas. in mag. field, mean field approx. calcs. 7-27530
 Dy₃Al₂O₃, exchange metamagnetism 7-2841
 ErAl₂ single crystals., low temp. heat capacity meas. in mag. field, mean field approx. calcs. 7-27530
 EuS, mag. props. under high press., competing magnetic interactions 7-7542
 Eu_{1-x}Sr_xS solid soln., X-ray absorpt. spectra d-f exchange interactions effects study, comp. depend. 7-3114
 EuTe, bound magnetic polarons, spin dynamics 7-7502
 Eu₂Y₃Fe₅Ga₂O₁₂ LPE garnet films, ferromagnetic relax. meas. 7-38911
 Fe (II) complexes, spin-exchange processes 7-12677
 Fe (II) complexes, spin-exchange processes 7-12677
 Fe (110) and (100) surfaces, Stoner excitation spectrum, spin polarised electron energy loss spectroscopy 7-53463
 Fe, diffusion of ⁵⁹Fe and ⁶⁰Co, mag. anomalies, quasi-chemical model 7-6862
 Fe, FCC metastable phase epitaxial films on Cu local mag. moment, XPS study 7-53504
 Fe-Al disordered alloys, mag. props., site-diluted Ising model calcs. 7-2873
 Fe-Au-Fe double layers, exchange coupling 7-27510
 Fe-Cr-Fe double layers, exchange coupling 7-27510
 Fe-Zr, amorphous and microcrystalline, exchange interaction and saturation magnetisation 7-45651
 Fe₈₉B₂₀, metallic glasses, multiplet splitting, XPS study 7-27858
 FeCO₃, antiferromag., magnetooptical determ. of exchange parameters (Russian) 7-53283
 FeCl₃ metamagnet, spin-lattice coupling and tricritical behaviour 7-2849
 Fe(NH₄)₂(SO₄)₂·6H₂O, EPR of Mn²⁺, Mn²⁺-Fe²⁺ exchange interaction 7-2924
 Fe₉₀Ni₁₀P₁₄B₆, metallic glasses, multiplet splitting, XPS study 7-27858
 (Fe_{1-x}Ni_x)₇₀Si₁₀B₁₃, amorphous, effective mag. moment, Curie temp. (Korean) 7-27503
 Fe_{1-x}O, double electron exchange, Mossbauer spectroscopy 7-17168
 Fe₂P, mag. props. under high press., competing magnetic interactions 7-7542

exchange interactions (electron) continued

- FeZr, amorphous and microcryst., exchange interaction and saturation magnetisation (Russian) 7-12963
 Fe₉₂Zr₈, mag. susceptibility, elec. resist., magnetoresistance meas. 7-52954
 Fe_{1-x}Cr_xBO₃, weak ferrimagnetism, antisymmetric exchange 7-45741
 GaAs 2D electron gas, dynamical cond., IR cyclotron reson. meas., electron interaction effects 7-45195
 GaAs, heavily doped, carrier-carrier and carrier-dopant interactions 7-21903
 GaAs-Al_xGa_{1-x}As heterostructures, voltage-controlled dissipation in the quantum Hall effect 7-27393
 Gd surface, evidence for ferromag. order above bulk Curie temp. 7-33173
 Gd-Co, anisotropic ferrimagnets in high mag. fields 7-17200
 GdFe_{1-x}Mn_xO₃, orthoferrite, mag. behaviour characts. 7-45657
 GdNi₃, paramag. suscep. studies 7-52935
 H, ortho-para conversion, new channel 7-36502
 n-Hg_{1-x}Cr_xCd_{1-x}Mn_xTe high field magnetoresist. and magnetisation, Mn-Mn exchange interaction effects 7-12964
 Hg_{1-x}Mn_xSe, zero gap semimag. semiconductor, inversion asymmetry spin level splitting 7-58784
 Hg_{1-x}Mn_xTe, Hall coeff., magnetoresist. meas., exchange interaction, field, temp. effects 7-64270
 Ho₂Co₁₇, intersublattice mol. field calc. 7-27511
 Ho₂(CoFe)₁₇ intermetallics, high field magnetisation studies 7-53038
 In₂O₃/Sn films, theoretical model for optical props. in 0.3 to 50 μm range 7-39200
 KCl(Br), longitudinal field quenching studies, precursor muonium state 7-53199
 KNi₂Mg_{1-x}F₃, nuclear spin-lattice relax., NMR studies 7-64542
 La₂Ce_{1-x}B₆, Zeeman splitting, thermodynamics of Coqblin-Schrieffer model 7-58783
 LiAl(Ga)(In)(Zn)(Cd) B32-type Zintl phases, mag. props., exchange enhancement, APW calcs. 7-27504
 Mg(NH₄)₂(SO₄)₂·6H₂O, EPR of Mn²⁺, Mn²⁺-Fe²⁺ exchange interaction 7-2924
 MnCl₂-graphite intercalation cpds., mag. susceptibility meas. 7-45638
 MnF₂ films, antiferromagnetic, dipole-exchange spin-wave modes 7-45771
 MnPS₃, layered cpd., mag. props. 7-52951
 MnTiO₃, quasi-2D antiferromag., spin dynamics 7-52987
 Ni(CH₃)₂VOF₃·H₂O, V⁴⁺-V⁴⁺ pair, mag. interaction (French) 7-58987
 NaIn B32-type Zintl phases, mag. props., exchange enhancement, APW calcs. 7-27504
 Nd₂Fe₁₄B, magnetic props., H₂ absorption effects 7-38906
 Ni cpds., ionic, ground state studies, multiplet effects, near-edge XAS 7-64803
 Ni magnetic surfaces, elastic spin-polarised low-energy electron scatt., book contrib. 7-33494
 Ni, photoemission above Curie temp., cluster calcs. 7-7814
 Ni-H system, band structure calcs. 7-45140
 Ni₂MnM (M=Al,Ga,In,Sb), Heusler alloys, Curie temp., effect of hydrostatic press. 7-64455
 Pb_{1-x}Eu_xTe epitaxial layers, mag. props. 7-45772
 Pb_{0.95}Gd_{0.05}Te, antiferromag. exchange constant between nearest-neighbour Gd³⁺ ions 7-59002
 Pb_{1-x}Mn_xTe, indirect exchange interaction between Mn²⁺ ions 7-27509
 Pb_{1-x}Sn_xTe narrow-gap semicond., electron-electron interaction, effect on permitt., two-band model 7-52420
 Pd-Fe(Ni) dilute alloys, Fermi surface exchange splitting, de Haas-van Alphen effect studies 7-52405
 Pd₂Fe disordered alloy, low-energy spin-wave excitations, Heisenberg model calcs. 7-2829
 PdNi alloys, magnetic clusters interaction energy calcs. 7-45652
 Pr₂Fe₁₄x Co₂ B system, struct. and magnetism 7-45631
 PtMnGa, Curie temp., hydrostatic press. effect 7-27527
 RCo₅ (R=Tb,Dy,Ho, Pr,Nd,Ce,Sm,Gd,Er,Tm,Yb), magnetocrystalline anisotropy, rare earth contribution 7-45659
 Rb_{1-x}Cs_xFeCl₃, random singlet-magnetic ground state system, mag. ordering effects 7-33167
 RbCuCl₃ single crystals., mag. suscept. meas., exchange interactions, magnetic and crystallographic transitions studies 7-52950
 Rb₂Mn_{0.7}Cr_{0.3}Cl₄, randomly disordered mag. system, mag. cluster excitations and wave-like magnons 7-38881
 Rb₂Mn₂Cr_{1-x}Cl₄ mixed crystals, mag. props. 7-2897
 Si, energy calcs. using four-centre integrals 7-27227
 Si, isoelectronic bound exciton states, spin splitting, photolum. excitation spectra study 7-2493
 Si, self-consistent Hartree-Fock and screened exchange calcs. 7-12585
 SiO₂-Al₂O₃-MgO-Cr₂O₃ glass, magnetism of spinel microcrystals, ESR study 7-27594
 Sm_{1-x}Eu_xS(Se) solid solns., X-ray absorpt. spectra d-f exchange interactions effects study, comp. depend. 7-3114
 Sn_{1-x}Mn_xTe, degenerate ferro-spin-glass, transport props. and spin disorder 7-45330
 a-Tb-Fe(Ni-Fe-Mo) bilayer films, unidirectional anisotropy 7-59065
 TbAl₂ single crystals., low temp. heat capacity meas. in mag. field, mean field approx. calcs. 7-27530
 TmAl₂ polycrystals., low temp. heat capacity meas. in mag. field, mean field approx. calcs. 7-27530
 U cpds., metallic and nonmetallic, X-ray absorpt. at various thresholds 7-64793
 U-based mag. alloys, mag. props. and electronic struct. (Russian) 7-12967
 UBr(Cl)(I), magnetic transitions, antiferromag. order and cryst. field splitting, neutron scatt. study 7-12974
 U₂Gd_{1-x}Ga_x Curie temp., loss of ferromagnetism, comp. depend, competing exchange interactions 7-12970
 USB, antiferromag., anisotropic exchange and spin dynamics, neutron study 7-33147
 U₂Y_{1-x}Ga_x, Curie temp., loss of ferromagnetism, comp. depend, competing exchange interactions 7-12970
 (VO)₂P₂O₇, 1D spin 1/2 Heisenberg antiferromagnet, mag. susceptibility meas. 7-45639
 Y(Dy)(Er)_{2-x}Th_{1-x}Fe₁₄B alloys, mag. props., comp. depend. study 7-7492
 Y₂Fe₁₄B, magnetic props., H₂ absorption effects 7-38906
 YIG films, ferromag. resonance absorpt., influence of exchange interaction, weak surface pinning 7-2931
 Yb₂Fe₁₄B, exchange and cryst. field interactions 7-27512

exchange interactions (electron) continued

- $Zn_{1-x}Mn_xSe$, antiferromag. exchange constants between nearest-neighbour Mn^{2+} ions 7-64449
- $Zn_{0.95}Mn_{0.05}Te$, antiferromag. exchange const. determ., free exciton Zeeman splitting meas. 7-22229
- $Zn_{1-x}Mn_xTe$, $x=0.25-0.71$, free exciton state exchange splitting, magnetoreflectance, magnetisation meas. 7-53288
- $Zn_{1-x}Mn_xTe$, interband Faraday rot. meas. 7-39093
- $Zn_{1-x}Mn_xTe$, photoluminescence position and lifetime 7-13205
- $Zn(NH_4)_2(SO_4)_2 \cdot 6H_2O$, EPR of Mn^{2+} , $Mn^{2+}-Fe^{2+}$ exchange interaction 7-2924
- $ZnS:Mn$, impact excitation and Auger quenching 7-27827
- $ZnTe:Cu$, impurity related neutral complex with bound exciton, photoluminescence, absorpt., Zeeman meas. 7-45165

exchange models see peripheral models

exchanges (chemical) see chemical exchanges

excimer lasers

- amplifiers, scalability, double-pass and expanding beam geometries calcs. 7-43143
- applications in imaging technology (*Japanese*) 7-56367
- Aurora KrF laser system, design and performance of large area monolithic electron guns 7-36987
- chemiluminescence based F_2 detector, excimer laser monitor appl. 7-20216
- condensed- and compressed-gas lasers, review 7-36952
- conf., Rochester, NY, USA 7-9595
- conference, laser science advances, Dallas, TX, USA (Nov. 1985) 7-9573
- dye DFB picosec. laser source, excimer laser pumped, for time resolved meas. 7-50584
- electro-optic voltage measurement in a high-power excimer laser 7-10977
- electron beam system, low impedance, for excimer laser excitation 7-36989
- etching of Cu foils 7-54015
- inert gas halide cryogenic solns., UV excitation and stimulated emission 7-10645
- medical and surgical appls. 7-60073
- micromachining of polymer films 7-53940
- multilayer coatings, for excimer laser, reflectivity calcs. 7-57521
- multipass grating interferometer applied to line narrowing in excimer lasers 7-35573
- multiwavelength excimer lasers, electron beam pumped, studies 7-15847
- oscillator-amplifier designs 7-62723
- physics, props. and appls. 7-50544
- synchronized ruby/ N_2 laser system for plasma prod. and diagnostics 7-31356
- technology developments and appls. 7-25840
- water dielectric pulse power driver for inert-gas halide lasers 7-36988
- X-ray lasers, excimer laser travelling-wave pumping 7-20268
- AF discharge excimer laser, capacitor-transfer-type with automatic preionisation, efficiency 7-20201
- Ar- N_2 laser, energy and efficiency, effect of Ne and He impurities 7-50545
- Ar₂ excimer laser, tunable intense coherent radiation generation around 126 nm, stimulated Raman scatt. in H_2 7-20328
- ArF excimer laser, electron-beam pumped, using low-pressure Ar-Rich mixture 7-36945
- ArF, excimer laser amplifiers VUV anti-Stokes Raman line generation 7-57450
- ArF laser, electron-beam-excited, investig. 7-43074
- ArH* exciplex laser, active medium modelling 7-62672
- Ca^+Eu^+ collisional lasers, high specific output energy 7-43078
- HCl-Xe-He self-sustained discharge, population dynamics of electronic states of atoms and ions 7-37781
- He- N_2 laser, pulsed electric-discharge, laser props. investig. 7-62675
- He-Xe-HCl excimer laser discharge growth dynamics 7-1086
- Hg halide photodissociation laser pumped by wide-band optical radiation, three-colour emission 7-50548
- HgBr laser, UV to green conversion 7-19877
- HgCl laser pumped by wide-band optical radiation emitting at 558 and 559 nm; 7-36955
- I_2 optically pumped molecular beam lasers 7-10916
- IF pulsed laser, flow parameters optimisation, intracavity gain detect. 7-10914
- KrCl laser spectrum, absorption lines and spontaneous emission 7-36947
- KrCl-XeCl, double laser oscill., quenching effect 7-57304
- KrCl* discharge laser, 0.6J output energy 7-43079
- KrF amplifiers, dynamic absorption effects 7-43062
- KrF discharge excimer laser, capacitor-transfer-type with automatic preionisation, efficiency 7-20201
- KrF e-beam sustained discharge laser, efficiency 7-31307
- KrF electron beam pumped laser mixtures, electron density meas. 7-57300
- KrF electron beam sustained discharge excimer lasers, discharge constriction, photodetachment, ionisation instabilities 7-10920
- KrF, excimer laser amplifiers VUV anti-Stokes Raman line generation 7-57450
- KrF laser, O_3 scalable effective saturable absorber 7-20369
- KrF laser as plasma source of soft X-rays 7-20909
- KrF laser cavity, multipass grating interferometer appl. to line narrowing 7-35573
- KrF laser gain meas. system 7-62717
- KrF laser optical-multiplexer pulse-compression system, Raman amplifier design 7-20337
- KrF laser system, Aurora, for inertial confinement fusion studies 7-15894
- KrF lasers, inertial confinement fusion appl. 7-10288
- KrF lasers at inertial fusion drivers, cost/performance anal. between different systems 7-25210
- KrF multibeam laser, pump for high-power forward Raman amplifiers 7-20344
- KrF multicomponent laser operating above atm. press. 7-31302
- KrF, picosecond high power laser system characts. 7-62676
- KrF* amplifiers for UV laser system 7-62724
- KrF*, high power subpicosecond laser system 7-62677
- N_2 , design and optimisation for pumping of dye lasers for optogalvanic spectroscopy 7-61389
- N_2 laser, atmospheric pressure, asynchronous progress of excitation across glow 7-44286
- N_2 laser, four-channel TEA, for interferometric meas. on plasma focus 7-43188

excimer lasers continued

- N_2 laser at 337.1 nm, design 7-36979
- N_2 TEA laser, traveling wave excited, investig. 7-20200
- N_2 -He-SF₆ laser, high power, UV preionised, characts. 7-25805
- Na_2 , optically pumped excimer laser action, expt. obs. 7-57305
- Na_2 , optically pumped molecular beam lasers 7-10916
- XeCl, design and optimisation for pumping of dye lasers for optogalvanic spectroscopy 7-61389
- XeCl discharge excimer laser, capacitor-transfer-type with automatic preionisation, efficiency 7-20201
- XeCl discharge laser, high pressure with UV pre-ionisation 7-43144
- XeCl electric-discharge laser, stimulated Raman scatt. conversion in compressed gases 7-50639
- XeCl excimer laser, amplification of UV ultrashort light pulses 7-62674
- XeCl excimer laser, discharge-pumped, electron density, H β line Stark broadening meas. 7-5873
- XeCl excimer laser, generation and amplification of sub-ps UV pulses 7-62722
- XeCl excimer laser with UV preionise capacitor-transfer oct. (*Japanese*) 7-5914
- XeCl laser, laser snow in active medium 7-43070
- XeCl laser, UV-preionised, long optical pulse duration, preionisation and discharge stability 7-1080
- XeCl laser, X-ray preionised with small discharge volume, performance improvement 7-1081
- XeCl laser mixtures, electron beam, pumped, electron density meas. 7-43064
- XeCl lasers, use of low-power ionisers in the excitation of active media 7-1184
- XeCl low divergence laser, excitation of stimulated Raman scatt. in compressed H_2 7-57468
- XeF electron beam pumped laser mixtures, electron density meas. 7-57300
- XeF laser, electron-beam-excited, injection-controlled tuning at 435 to 535 nm 7-20199
- XeF laser, gain of $^3He/Xe/NF_3$ mixtures pumped by $^3He(n,p)^3H$ reaction 7-1083
- XeF laser, spectra anal. over wide range of press. (*Russian*) 7-50543
- XeF laser mixtures, NF_3 fueled, N_2 excited state absorpt. 7-10918
- XeF laser pumped methane, Stokes generation, beam parameters 7-20346
- XeF laser pumped methane, high-efficiency first-Stokes generation 7-20347
- XeF lasers, electron beam pumped, N_2 production from Ne/Xe/ NF_3 mixtures 7-43063
- XeF lasers, use of low-power ionisers in the excitation of active media 7-1184
- XeF two-line laser sources, Raman beam combination in H_2 7-20336
- XeF* laser pumping by Xe₂* excimer emission, photoionisation cross section determ. 7-31306
- XeF* pumped by excimer radiation, near UV lasing on electronic-vibr. transitions 7-62671
- XrF nuclear pumped lasers 7-25794

excimers

see also excimer lasers

- alkali, atom-inert gas atom complexes, optical pumping, polaris. effects 7-15536
- alkylcyanobiphenyl-phenylcyclohexanecarboxylate mesomorphic mixtures, binary phase diagrams, fluoresc. spectral determ. 7-27765
- anthracene-NH₃, jet-cooled clusters, van der Waals complexes, exciplexes, visible fluoresc. spectra 7-19936
- anthracenes, aq.-micellar soln., dimethylaniline fluoresc. quenching and exciplex form. 7-36683
- 1,4-bis(β -pyrazinyl-2-vinyl)-benzene, solns. and solid state, irradi. and solvent effects, visible fluoresc. anal. 7-36674
- 1,3-di(1-pyrenyl)propane, intramolecular excimer formation, viscosity dependence, anal. study 7-19729
- 1-(N,N-dimethylaniline)-3-(anthryl)propane bichromophore, intramolecular exciplex, luminesc. 7-5716
- fuel sprays, exciplex-based diagnostics 7-23077
- inert gas-halide excimers, interaction with simple cryogenic liquids 7-42776
- 4-octyloxy-4'-heptyl-a-cyanostilbene, excimer fluorescence (*Russian*) 7-3093
- (perylene-Ag⁺)^{*} exciplex fluoresc., solvent influence 7-57113
- perylene-NH₃, jet-cooled clusters, van der Waals complexes, exciplexes, visible fluoresc. spectra 7-19936
- poly(2-vinylpyridine), protonated, dil. soln. with trifluoroacetic acid, excimer emission, fluoresc. anal. 7-31196
- poly(4-vinylpyridine), protonated, dil. soln. with trifluoroacetic acid, excimer emission, fluoresc. anal. 7-31196
- poly-N-vinylcarbazole; solns., nonexponential picosec trapping, electronic energy transport 7-13198
- polystyrene solns., excimer fluoresc., conc. depend. 7-7743
- (10-(3-pyrenyl)decyl)dimethylmonochlorosilane, chemically bonded to silica surfaces, solvent effects on config., excimer decay profiles 7-22329
- scintillator dye solutions, excited state absorpt. measurements 7-42516
- tryptophan, jet-cooled, excited state conformers and intramol. exciplex form., dispersed fluoresc. 7-36671
- Ar, solid, energy transfer during ion bombard. 7-64842
- Ar₂ excimer states, photoionisation cross sections 7-57137
- Ar₂, radiative lifetimes, time-resolved fluorescence study 7-5619
- Ca+He, saturated two-photon absorpt. in perturber bath 7-888
- Hg+NH₃, photosensitised reaction, complex form., luminesc. spectra 7-8256
- Hg₃, excimer, laser-induced fluoresc. spectroscopy 7-938
- Kr₂, excimer states, photoionisation cross sections 7-57137
- KrF-SF₆ mixtures, excimer mol. excitation in steady-state plasma jet 7-58070
- KrF* and Kr₂F*, formation kinetics in He/Ar/Kr/F₂ mixtures (*Chinese*) 7-39892
- Ne₂, excimer states, photoionisation cross sections 7-57137
- Xe₂ excimers, two-photon fluoresc. appl. to subpicosecond pulse duration meas. 7-43187
- XeF-SF₆ mixtures, excimer mol. excitation in steady-state plasma jet 7-58070

exciplex lasers *see* excimer lasers

exciplexes *see* excimers

exciters

superconducting turbogenerator rotors, stress-strain state investigation 7-13511

exciton-phonon interactions *see* phonon-exciton interactions

excitonic molecules

binding energies 7-16947

binding energy, adiabatic method 7-52437

solids, excitonic mols., book chapters 7-29610

CdS, refractive index nonlinearity due to excitonic molecule resonance state 7-11044

CuCl, giant two-photon excitation of excitonic molecules, nonlinear depolarisation effects 7-64594

CuCl polycrystalline layers, nonlinear propagation of nanosecond laser pulses 7-53263

CuCl single cryst. thin films, resonant two-photon absorption and emission 7-22310

excitons

see also excitonic molecules; phonon-exciton interactions

1D system, bound states of two soliton-type quasi-particles (*Russian*) 7-2502

absorption effects of spatial dispersion and damping 7-45164

alkali doped inert gas solids, matrix-bound systems, dipolar excitonic insulator transitions, mean field theory 7-45163

alkali halide crystals, charge transfer excitons, perturbation method anal. (*Chinese*) 7-12611

alkali halide crystals, self-trapped exciton recomb. luminesc.-recomb. induced F-centre form. anticorrel. calcs. 7-13201

alkali halides, RbCl, KCl, KBr, CsBr, luminescing solids, nonradiative decay channels of electronic excitations 7-27760

alkali halides with Tl^+ impurities, excitons, optical absorpt. D band study 7-64096

alkali iodide crystals, luminesc. induced by photo-generated excitons, excitation spectra struct. 7-46103

anthracene-Ag struct., charge carrier photogeneration (*Japanese*) 7-38610

anthracene crystal monolayer, photodimer disorder effects, UV reflection spectra anal. 7-53362

anthracene crystals, polaritons, picosecond secondary emission studies 7-21825

anthracene single crystals, dislocation photolum. study, exciton scatt. effects (*Russian*) 7-22343

anthracene single crystals, structural imperfections as triplet exciton traps, defect recovery 7-64160

anthracene-pyromellitic N,N' -dimethyldiimide, triplet exciton contact pairs 7-64093

Auger recomb. of dislocation excitons 7-38578

biphenylene-1,2,4,5-tetracyanobenzene charge transfer complex, cryst. struct. and photoexcited triplet excitons EPR study 7-63600

bounded crystals, exciton polarisation, spatial dispersion effects 7-17286

charge transfer excitons, crystallisation under strong excitation conditions 7-45160

charge transfer excitons, spatial ordering during intensive excitation 7-64097

chlorophyll in vivo, exciton states and exciton interaction processes, nonlinear transmission effects 7-59931

covalent semiconductor, intermediate radius exciton, orbital model (*Russian*) 7-16951

crystal, nonlinear bleaching and domain formation, exciton part of spectra 7-45161

crystal optics with spatial dispersion 7-45954

crystal phosphor, quantum yield, electron-hole pair hot escape effects 7-33433

current-current interaction, influence of quasiparticle nonconservation 7-12619

4,4'-dibromobenzophenone-1,4-dibromonaphthalene in polymer films, phosphoresc. study 7-59244

β -9,10-dichloroanthracene, triplet excitons, zero field DF ODMR 7-27631

9,10-dichloroanthracene monocrystals, alpha scintillations, decay kinetics 7-7769

4,4'-dichlorobenzophenone single crystals, spin polarised triplet exciton mutual annihilation characts. (*Russian*) 7-12614

dimer-lattice phonon interaction, lattice relax., exciton and electron condition terms 7-7130

direct-gap semiconds., coherent polariton waves, anti-Stokes scatt. props. 7-16955

disordered 2D and anisotropic 3D systems, excitation transfer, time-resolved obs., spatial geometry effect 7-15642

disordered media, electrical cond. and incoherent excitation transport, self-consistent mode-coupling theory 7-52548

disordered systems, excitation diffusion and energy relax. 7-21792

energy transfer and lattice phonons, mutual influence 7-16977

exciton absorption tails in one-dimensional systems 7-2495

exciton-exciton interaction, wave fn. normalised coeff., exchange effect role 7-52431

Fabry-Perot resonator, M-band cryst. luminesc., exciton-photon system, optical bistability phenomenon (*Russian*) 7-20323

fluids, topologically disordered systems Frenkel excitons, electronic absorpt. spectra 7-17287

fluorene-1,2,4,5-tetracyanobenzene, charge transfer cryst., triplet excitons, ODMR and ESR 7-7611

fractional quantum Hall effect, large-scale config.-interaction calcs., Haldane's spherical model 7-2628

2,4-hexadiyne-1,6-diol-bis (p-toluene sulphonate), phase transitions, piezomodulated reflection spectroscopy 7-27691

II-VI semiconductor solid solutions, luminescence, exciton localisation 7-33429

inert gas crystals, surface or bulk location of self-trapped excitons, luminesc. 7-46129

insulating halide crystals, exciton-defect conversion 7-7122

ionic crystals, surface excitons, EELS obs. 7-12781

ionic solids, radiation effects, review 7-26792

layer semiconductors, low binding energy exciton impurity complexes (*Russian*) 7-16952

linear macromolecules, quantum theory of quasi-particle motion, thermal vibrs. 7-52461

luminescence, conference, Rovno, USSR (Nov. 1984) 7-24263

excitons continued

magnetic insulators, light absorpt. by intersublattice charge transfer 7-46065

bis-methylammonium tetrachloro manganese antiferromag. crystals, struct. deform. by exciton self-localisation, luminesc. spectra fine struct. study (*Russian*) 7-27752

modulated semicond. structs., conf., Kyoto, Japan (Sept. 1985) 7-4630

molecular chains, solitary excitations, intramol. vibrs. anharmonicity 7-44712

molecular cryst. thin films, surface exciton calcs. 7-52429

molecular crystal, temp. depend. of reson. splittings of mol. pairs 7-16700

molecular crystals, triplet exciton diffusion and capture, Monte Carlo modelling 7-12620

molecular polymer chain, exciton-lattice interactions, bisoliton creation continuum approx. calcs. 7-2499

molecular systems, disordered, influence of noise on density of states and absorption 7-16949

multiple quantum wells and superlattices, refractive index, exciton effects 7-13115

naphthalene:pyrene, triplet excitons, prompt and delayed fluoresc. 7-22298

naphthalene with α -bromonaphthalene or α -chloronaphthalene impurities, intercombination conversion during exciton capture 7-46091

naphthalene-tetrachlorophthalic anhydride charge transfer complex, triplet excitons, phosphorescence 7-39159

nickel (II) tetra (p-vinylphenyl) porphyrin, benzene soln., aggregation and luminesc. props., visible spectra anal. 7-42635

one-dimensional cryst. with impurity, coherent exciton motion propagator and capture prob. calcs. 7-52436

one-dimensional mol. chain, electron transfer kinetic coeff., donors and acceptors perturbative influence, Davydov solitons 7-27266

optical absorption lines, influence of exciton motion, appl. to surface vibrations 7-7317

optical nonlinearity near the bandgap in semiconductors, review 7-62747

α -perylene, crystals, excitons, hydrostatic press. effects 7-52430

phonon-exciton system, quantum chaos model 7-61231

photoinduced phase transition in magnets 7-38923

picolytricyanoquinodimethane, mol. cryst., charge transfer transitions, electronic spectra 7-22279

polar semiconductors, polaritons, secondary emission spectra, energy relax. 7-27755

poly(N-vinylcarbazole) films and solns., localised exciton hopping, fluoresc. studies 7-52435

trans-polyacetylene, momentum depend. dielec. function, EELS meas. 7-21843

trans-polyacetylene, photogenerated exciton-breather state 7-21823

trans-polyacetylene, triplet solitonic excitations, optical gap 7-2496

polyaniline, localised mol. excitons, UV absorpt. spectra 7-31192

polymers, isolated flexible chains, tagged with chromophores, electronic excitation transport 7-15751

propanol-2 radical + CdS, photochemistry and radiation chemistry, nonlinear optical effects 7-46858

quantum well, optical absorpt. due to excitonic unbound states 7-64593

quantum well structures, linear optical props. elec. field depend. waveguide electroabsorpt. and sum rules 7-13133

quantum wells, oscillator strengths of excitons 7-7375

quartz, luminescence of pure and Ge-activated samples 7-46152

rhodamine 6G, aggregated, in PMMA matrix, polarisation props. in transmitted light, simple exciton theory 7-31060

self-localisation in randomly inhomogeneous media 7-7123

self-trapping on a dimer, discrete nonlinear Schrodinger eqn., time-depend. solns. 7-18721

semiconducting plane-parallel slabs, normal-incidence exciton transmission and refl. spectra 7-39058

semiconductor, excitonic trions, Landau level oscills., mag. field effect study 7-21820

semiconductor, two-photon-biexciton resonance, polarisation instability 7-3005

semiconductor clusters, zero-dimensional excitons, optical spectra and luminesc. 7-12615

semiconductor cubic crystals, magneto-optic anisotropy induced by spatial dispersion 7-17307

semiconductor microcrystallites, laser-excited, absorption blue shift 7-33409

semiconductor quantum well struct., exciton linewidth calcs., polar optical phonon scatt. 7-2491

semiconductor quantum-well structures, excitation diffusion and energy relax. 7-21792

semiconductor spectrum, exciton region, optical nonlinearity 7-52433

semiconductor superlattices, excitons, optical props., size effect (*Japanese*) 7-12621

semiconductor superlattices, I-type, intersubband collective excitations (*Chinese*) 7-12804

semiconductors, coherently driven exciton system, collective excitations and the dynamical stark effect 7-32919

semiconductors, complex neutral defects, bound hole states, mag. props. 7-64157

semiconductors, dynamic Stark effect in interacting electron-hole systems, light-enhanced excitons 7-33366

semiconductors, electron-hole liq., general props., review 7-7121

semiconductors, FIR absorption and near-IR photoluminescence spectroscopy of bound excitons 7-39122

semiconductors, highly excited nonlinear optical and transport props. of many-exciton system 7-32920

semiconductors, intermediate valence, theory 7-38526

semiconductors, light absorption by dislocations, exciton effects 7-53371

semiconductors and insulators, charge transfer electron-exciton complexes 7-27258

semimetals, effect of interband transitions on acoustic spectra 7-38478

solids, excitonic processes, book 7-29610

spatial dispersion medium, optical SHG in exciton reson. region 7-37034

strong coupling electron systems, CDW, supercond., effect of randomness 7-27459

superconducting films, nonequilibrium dynamic quasi-particle distribns., high freq. EM field effects calcs. (*Russian*) 7-27467

superlattices, microstructures and microdevices, conf., Goteborg, Sweden (Aug. 1986) 7-35097

TCNQ salt, N-n-propyl phthalazinium 7,7,8,8 TCNQ₂ struct., elec., mag. props., EPR meas. 7-33005

TCNQ salts, quarter-filled band, optical absorption studies 7-46033

excitons continued

- p-terphenyl aggregates, pure and doped, excitation energy transfer, spectral props. 7-2504
- p-terphenyl single crystals, singlet excitons, transient photoabsorpt. spectrum 7-27729
- tetraalkylammonium iodides, exciton absorpt. spectra 7-59165
- tetraalkylphosphonium iodides, exciton absorpt. spectra 7-59165
- tetramethylammonium manganese (II) trichloride 1D antiferromagnet, exciton trapping, luminesc. investig. 7-52434
- tetramethylammonium manganese tribromide:Cu²⁺, emission dynamics, exciton trapping 7-39164
- tetramethylammonium manganese tribromide, photoexcited crystals, exciton annihilation, luminesc. decay curves 7-53385
- tetramethylammonium manganese trichloride, photoexcited crystals, exciton annihilation, luminesc. decay curves 7-53385
- thin crystals, incoherent exciton migration, detector luminesc. decay rate (*Russian*) 7-2503
- (TMN)₃X₂ (X=ClO₄, AsF₆), cation radical salts of tetramethoxynaphthalene, EPR, optical absorpt. and conductivity studies 7-53113
- Wannier-Mott excitons, distrib. fn., secondary radiation of light 7-64090
- X-ray exciton, transfer model 7-64091
- zinc (II) tetra (p-vinylphenyl) porphyrin, benzene soln., aggregation and luminesc. props., visible spectra anal. 7-42635
- Ag₃As₂S₃ undoped proustite crystals, photolum. obs., exciton-impurity complexes 7-33445
- AgGaSe₂, cryst. field and spin-orbit interactions at fundamental gap, reflectivity meas. 7-16997
- AgNa(NO₂)₂, low temp. triplet exciton decay, photolum. decay temp. depend. meas. 7-21821
- AlAs/GaAs superlattices, X-point excitons 7-33069
- Al_{1-x}Ga_xAs-GaAs multiple quantum wells, photoluminescence studies, press. depend. (*Chinese*) 7-13194
- AlGaAs-GaAs single quantum well, MBE growth interruption, well width fluctuations 7-7865
- AlGaAs-GaAs single quantum wells with growth interrupted heterointerfaces, photoluminesc. 7-39168
- Al_{0.25}Ga_{0.75}As, photoluminescence half-width and intensity, temp. depend. 7-39179
- Al_{0.3}Ga_{0.7}As-GaAs quantum well structure, electric-field-induced optical modulation, theory using Monte Carlo approach 7-17077
- Al_{1-x}Ga_xAs-AlAs quantum well, magneto-optical absorpt. study 7-7681
- Al₂O₃, lattice relaxation induced by electronic relax. 7-44622
- Ar cryogenic crystals, exciton diffusion and energy transport studies 7-52438
- Ar, solid, energy transfer during ion bombard. 7-64842
- Ar solid crystalline films, electron stimulated desorption, exciton mechanism calcs. (*Russian*) 7-27096
- As₂Se₃ single crystals, geminate pair recomb., photocond., photoluminescence meas. 7-38581
- Bi₂Ge₂O₁₂, luminescence excitation and reflection spectra 7-46090
- Cd_{1-x}Br, indirect excitons, isoelectronic impurity effects, luminesc. spectra 7-27255
- Cd_{1-x}Mn_xTe exciton localisation, time resolved photolum. study 7-46106
- Cd_{1-x}Mn_xTe(Se), mag. field-induced exchange effects, photolum. meas. 7-27705
- CdS, A-exciton, normal-incidence exciton transmission and refl. spectra 7-39058
- CdS, bound-exciton states, resonant Brillouin scatt. 7-46062
- CdS excited state dynamics studied by transient grating techniques 7-12616
- CdS, excitonic polaritons, transmission and damping 7-58748
- CdS, integral exciton absorpt. coeff., temp. depend. characts. 7-45959
- CdS, photoconductivity spectrum, surface excitons, localised hole in quantum inversion layer 7-12762
- CdS, photolum., exciton scatt. from defects and impurities, depend. on exciting light intensity 7-39156
- CdS platelet, nonlinear optical and transport props. of many exciton system 7-32920
- CdS platelets, fast all-optical switching 7-57430
- CdS, semicond. crystallite, quantum size effects, energy spectrum calc. 7-12613
- CdS, transmission and damping of excitonic polaritons 7-58747
- CdSe, dielectric fn. and interband crit. points. 7-2480
- CdSe, exciton luminesc., polarisation depend. 7-59248
- CdSe, highly excited, exciton dynamics, picosec. time-resolved gain-absorpt. spectra study 7-2494
- CdSe, photogenerated high density electron-hole plasma, energy relax., rapid expansion 7-33039
- (CdSe)_{1-x}(MnS)_x crystals, semimag. semiconductors, magneto-optic studies 7-64609
- CdSe_{0.9}Te_{0.1}, bound excitons, thermal dissoc., photoluminescence, reflectivity meas. 7-46122
- CdTe (001) films, MBE grown on InSb substrates, low temp. photolum. studies 7-22317
- CdTe epitaxial layers, MBE growth on GaAs substrates, photoluminesc. 7-46083
- CdTe grown on Si by LPMOCVD, physical props., photolum., exciton related emission peak 7-27181
- CdTe, optical anisotropy due to spatial dispersion 7-53266
- CdTe/(Cd,Mn)Te superlattice, optical props. heterointerface effects 7-7736
- CdTe/ZnTe superlattice, quasi-2-D excitons in strongly localised regime 7-12617
- CdTe-(Cd,Mn)Te MQW, optical and magneto-optical props. 7-13137
- CdTe-CdMnTe, quantum wells, excitons and kinetics 7-12622
- CdTe-CdMnTe superlattices, photoluminesc. props. 7-13218
- Cd₂Zn_{1-x}Te, second-order optical process, transient behavior, luminesc., Raman scatt. 7-64689
- CoF₂, antiferromag. insulator, H-odd linear dichroism of exciton-magnon transitions 7-53282
- CrCl₃, ionic crystals, optical and electron energy loss studies 7-3066
- CsBr, two-halogen self-trapped excitons, metastable optical absorpt. 7-53365
- CsCoCl₂·2H₂O, 1D antiferromagnet, exciton transfer, absorpt. spectra 7-27254
- CsI, excitons, three-photon magnetoabsorpt. meas., g-value determ. 7-2498
- CsMnBr₃, photoexcited crystals, exciton annihilation, luminesc. decay curves 7-53385
- CsMnCl₃ antiferromag. crystals, struct. deform. by exciton self-localisation, luminesc. spectra fine struct. study (*Russian*) 7-27752

excitons continued

- CsMnCl₃, photoexcited crystals, exciton annihilation, luminesc. decay curves 7-53385
- CuCl excited state dynamics studied by transient grating techniques 7-12616
- CuCl, excitonic particle study by laser spectroscopy 7-16953
- CuCl microcrystals, excitons, size quantisation effects, luminesc. spectra anal. 7-53409
- CuCl, photo-induced optical activity, nonlinear ellipsometric studies 7-14993
- CuCl single cryst. thin films, resonant two-photon absorption and emission 7-22310
- CuCl, time-resolved degenerate four-wave mixing under nanosecond pulsed excitation 7-43206
- CuCl₂Br_{1-x} colloids in glasses, x=0-1, exciton spectrum (*Chinese*) 7-38459
- CuO_x crystals, diamagnetic excitons, valence band corrugation 7-64546
- Cu₂O, long-lived strain-confined paraexciton thermodynamics, recomb. luminesc. and thermalisation 7-2492
- Ga_{0.65}Al_{0.35}As-GaAs quantum wells, elect. field-induced decrease of exciton lifetimes 7-45481
- Ga_{0.8}Al_{0.2}As-GaAs-Ga_{0.8}Al_{0.2}As quantum well structs., electroreflectance spectra, model 7-33365
- Ga_{1-x}Al_xAs quantum-well wires, Wannier excitons, binding energies 7-64092
- Ga_{1-x}Al_xAs-GaAs quantum wells, diamag. shift of exciton energy levels 7-21824
- Ga_{1-x}Al_xAs-GaAs superlattice, exciton CW-photoluminesc., excitation intensity depend. 7-59252
- GaAs, exciton-exciton and exciton-electron collisions, ultrafast phase relaxation 7-12618
- p-GaAs, excitons bound to pairs of shallow impurities 7-45169
- GaAs, giant exciton resonance in nonlinear optical activity 7-45167
- GaAs heterostructures, valence subbands, excitons and luminescence 7-7321
- GaAs, magneto-optical photoluminescent spectra studies 7-46148
- GaAs photoluminescence rel. to Si substrate orientation 7-53411
- GaAs, picosecond phase coherence, orientational relax. of excitons 7-16948
- GaAs quantum wells, optical Stark effect on excitons 7-31384
- GaAs quantum-well wire hydrogenic impurity state binding energy and lowest exciton state lum. efficiency calc. 7-2683
- GaAs single quantum well, doubly resonant LO-phonon Raman scatt. via deform. pot., polarisation obs. 7-39114
- GaAs single quantum wells, free excitons, phase coherence and line broadening 7-45170
- GaAs:In MBE layers, defect density reduction by isoelectronic In doping 7-3176
- GaAs:Si/Al_{1-x}Ga_xAs quantum wells, photolum. studies 7-39178
- GaAs/Al_{1-x}Ga_xAs quantum wells, excitonic transitions, photocurrent spectra studies 7-7816
- GaAs/AlAs MQW structure, exciton-induced dispersion of electroreflectance at room temp. 7-53277
- GaAs/AlAs quantum wells, photoexcited transport 7-2674
- GaAs/AlAs quantum well structures, electroreflectance spectra and field-induced refractive index modulation 7-13135
- GaAs/AlGaAs quantum wells, MBE growth, interface disorder studies 7-7026
- GaAs/AlGaAs quantum wells and double heterostruct. lasers, chemical beam epitaxy, photolum. 7-22523
- GaAs/AlGaAs single heterojunction quantum well structs., photolum. characts. 7-46085
- GaAs-Al_{0.37}Ga_{0.63}As quantum wells, photolum. studies, MBE growth, effect of interruption 7-39150
- GaAs-Al_{0.44}Ga_{0.56}As quantum wells, MBE grown, tunnelling assisted photon emission, photoluminescence meas. 7-46120
- GaAs-Al_{1-x}Ga_xAs, modulation-doped quantum wells, photoabsorpt., electronic props. 7-64330
- GaAs-Al_{1-x}Ga_xAs quantum wells, doubly resonant LO-phonon Raman scatt. obs. 7-27722
- GaAs-Al_{1-x}Ga_xAs quantum wells, homogeneously broadened 2D excitonic transitions, optical depasing 7-45461
- GaAs-Al_{1-x}Ga_xAs quantum wells, doubly reson. LO phonon Raman scatt., photoluminescence spectra 7-53327
- GaAs-Al_{1-x}Ga_xAs semicond. superlattice, exciton transitions study 7-52432
- GaAs-Al_{1-x}Ga_xAs-Al_{1-x}As-AlAs, multi quantum well structs., picosecond spectra. 2D excitons 7-13215
- GaAs-AlAs superlattices, 2D excitons, magneto-optical study (*Japanese*) 7-13139
- GaAs-AlGaAs, high quality MOVPE quantum wells, optical props. 7-53406
- GaAs-AlGaAs, multiple quantum well structs., 2s state, excitons, luminesc. study 7-22337
- GaAs-AlGaAs MQW optical NOR gate, exciton and carrier dynamics, time resolved obs. 7-50628
- GaAs-AlGaAs modulation-doped heterointerface, photoluminescence spectra studies 7-46137
- GaAs-AlGaAs multiple quantum well lasers, voltage-controlled optical bistability, 2D exciton 7-5883
- GaAs-AlGaAs multiple quantum wells, temp. depend. of photoreflectance 7-7753
- GaAs-AlGaAs quantum wells, high electric field, interband transitions, photocurrent spectra obs. 7-7289
- GaAs-AlGaAs quantum well heterostructures, spectroscopy of excitons and phonons 7-7706
- GaAs-AlGaAs quantum well structs., luminesc. from 2s heavy hole exciton, low temp. 7-22338
- GaAs-AlGaAs quantum wells, field-induced lifetime enhancements, ionisation of excitons 7-39181
- GaAs-Ga_{0.3}Al_{0.7}As quantum wells, uniaxial stress depend. of spatially confined excitons 7-33078
- GaAs-Ga_{1-x}Al_xAs quantum wells, interband photocond. and excitonic Landau level transitions in mag. field 7-27390
- GaAs-Ga_{1-x}Al_xAs quantum well structures, electronic props. 7-52817
- GaAs-Ga_{1-x}Al_xAs undoped quantum wells, excitonic spectrum, valence band coupling and Fano resonance effects calcs. 7-27256
- GaAs-GaAlAs MQW structures, exciton-exciton interaction 7-52439
- GaAs-GaAlAs quantum wells, exciton binding energy, magneto-optical determ. 7-7752

excitons continued

- GaAs-GaAlAs quantum well excitons, interface disorder and mobility 7-52808
 GaAs-GaAlAs quantum wells, excitonic coupling in elec. field, photolum. spectra 7-64094
 GaAs_{1-x}Al_xAs MQW, MOCVD grown, excitons, photoluminescence spectra 7-38702
 GaAs_{1-x}P_xN, bound excitons, energy spectrum, optical absorpt. cross section, two-band model 7-16945
 GaAs_{1-x}P_xN, cathodoluminesc. efficiency, N-bound excitons influence 7-7768
 GaInAs/InP quantum wells, atmospheric organometallic vapour phase epitaxial growth 7-27912
 Ga_{0.47}In_{0.53}As-InP superlattices, MOCVD grown, room temp. excitons 7-21986
 Ga_{1-x}In_xAs/InP heterostructures, MOVPE, electron mobility, exciton peak, magnetotransport 7-58883
 Ga_{0.7}In_{0.3}As, photoluminescence line shape of excitons 7-3087
 Ga_{0.1}In_{0.9}As-GaAs strained layer superlattices, low temp. photolum. 7-53407
 GaN crystals, polarisation props. of band-edge emission, dispersion theory appl. 7-64694
 GaP and GaP:N diodes, electroluminescence, high press. effects 7-27787
 GaP: Te(Zn), doping superlattices, growth and props. 7-64684
 GaSb/AlSb single quantum wells, electroreflectance and photoluminescence studies 7-46136
 GaSb-Al_{0.5}Ga_{0.5}Sb multi quantum wells, excitons, electric field effect, photocurrent spectra obs. 7-7288
 GaSb_{0.5}AlSb quantum wells, nonparabolic behaviour under hydrostatic press. 7-64328
 GaSe, evidence of exciton-plasma transition in emission spectra 7-59249
 GaSe, excitons, room temp. self screening 7-45166
 GaSe, photoexcited localised excitons thermalisation, stacking disorder effects, photolum. study 7-27770
 GaSe, screening of excitons by free carriers, transmission, reflection and luminescence spectra 7-38460
 GaSe, spontaneous and stimulated photoluminescence studies 7-22315
 GdBO₃:Pr³⁺, Tb³⁺(Sm³⁺)(Dy³⁺), host lattice sensitisation, energy transfer and photolum. 7-46113
 Ge crystal, exciton gas-electron-hole liq. interactions, phase diagram, nuclei drift effects 7-2488
 Ge, free exciton diffusion and decay, lumin. 7-32918
 Ge:Zn, electron-hole droplet transport, suppression by deep impurities 7-58746
 Ge:Zn, photolum. spectrum, effect of (001) uniaxial stress 7-33450
 H-like systems in arbitrary mag. fields, ground and excited states wave functions expansion calcs. 7-2519
 HgGa₂Se₄, optical props. in fundamental absorption region 7-39065
 In_{0.53}Ga_{0.47}As-InP, epitaxial single quantum wells, spectroscopy of excited states 7-46126
 InGaAs/InAlAs multiple quantum well structs., nonlinear spectroscopy 7-1236
 InGaAs/InP quantum wires and boxes, low temp. photoluminesc. 7-59238
 InGaAs-InAlAs strained-layer superlattices, MBE grown, optical characterisation 7-13142
 In_{0.1}Ga_{0.9}As, photoluminescence determ. of effects due to In alloying 7-46096
 InGaP-InGaAlP MQW structs., room temp. excitons 7-58745
 InP single crystal (100) surface, atomic scatt., electron-hole pair creation 7-27841
 InSb, narrow-gap semiconductor, bound excitons, magneto-absorption studies 7-45168
 InSe, excitonic luminescence, influence of macroscopic inclusions 7-13204
 In₂Se₃, layered semicond., photolum. studies 7-7746
 K atoms in Ar matrix, site modification by X-ray and light irradiation 7-51819
 KBr:Sn²⁺, impurity localised excitons, form. energy calcs., UV spectra anal. 7-64095
 KBr:Ti(In), defect creation by excitons, room temp. (Russian) 7-16946
 KCl crystals, luminescent, detection of radiation shake 7-27761
 KCl, vibronic mechanisms of excitation decay, defect formation 7-39158
 KCl:Sn²⁺, impurity localised excitons, form. energy calcs., UV spectra anal. 7-64095
 KCoF₃ antiferromagnetic cryst., electronic Raman scatt. by high-energy magnetic excitons 7-46016
 KI crystal, dispersion curves near 1s and 2s exciton resonances 7-53260
 KI, exciton self-localisation, radiation defects, lumin. studies 7-64681
 K_{0.3}MoO₃, IR reflectivity and Raman scatt. from midgap-state exciton-polaritons 7-33386
 KX (X=Cl,Br), H-interstitials, struct. and crowding mechanism 7-38939
 Kr cryogenic crystals, exciton diffusion and energy transport studies 7-52438
 LaP₂O₁₄:Nd³⁺ degenerate four-wave mixing spectroscopy 7-11039
 LiF crystal, X-ray spectra rel. to electronic struct. (Russian) 7-39319
 LiH:Al(Mg)(Zn) single crystals, secondary emission, exciton luminesc. and reson. Raman scatt. studies 7-3038
 LiNbO₃, exciton lumin., ion beam induced 7-53418
 MnF₂, thermal behaviour of two-exciton bands 7-2497
 NaCl:Mg, X-ray irradiat., exciton interactions with impurity-vacancy dipoles, absorpt. and luminesc. spectra 7-45162
 NaCl:Sn²⁺, impurity localised excitons, form. energy calcs., UV spectra anal. 7-64095
 NaI crystals, bound excitation X-ray induced luminesc. spectra 7-53400
 NaMnCl₃ quasi 2D antiferromagnet, deforming magnetic exciton and light absorpt. characts. 7-53284
 NdP₂O₁₄ crystals, dynamics of population gratings studied by four-wave mixing 7-11038
 Ne solid crystalline films, electron stimulated desorption, exciton mechanism calcs. (Russian) 7-27096
 Ne, solid films, erosion by keV electrons 7-3124
 PbTe, interband absorption in a mag. field, exciton states 7-22227
 PbTe, low-voltage electroabsorpt., exciton states, magnetoabsorpt. spectra 7-2501
 RbCl, self-trapped excitons, excitation-induced atomic motion 7-21822
 RbCl:I, relaxed exciton states, optical conversion 7-53397
 RbI crystal, dispersion curves near 1s and 2s exciton resonances 7-53260
 RbI crystals, bound excitation X-ray induced luminesc. spectra 7-53400
 RbI, exciton self-localisation, radiation defects, lumin. studies 7-64681
 RbI, piezoreflectance of excitons in fundamental absorpt. region 7-22219

excitons continued

- RbMnCl₃, photoexcited crystals, exciton annihilation, luminesc. decay curves 7-53385
 Rb₂MnCl₄, photoexcited crystals, exciton annihilation, luminesc. decay curves 7-53385
 RbMnF₃, thermal behaviour of two-exciton bands 7-2497
 Rb₃MoO₃, IR reflectivity and Raman scatt. from midgap-state exciton-polaritons 7-33386
 RbX (X=Cl, Br), H-interstitials, struct. and crowding mechanism 7-38939
 Ru complex, circular dichroism spectra 7-33359
 Se, trigonal, optical props., local field effects 7-22204
 Si, electron-hole plasma, second condensed phase 7-27357
 Si exciton transport, optical time-of-flight investigation 7-64244
 Si, excitonic absorpt., MCD spectra, low mag. fields 7-27257
 n-Si, excitons bound to pairs of shallow impurities 7-45169
 Si, isoelectronic bound exciton states, spin splitting, photolum. excitation spectra study 7-2493
 Si, thermal donor-related isoelectronic centres, exciton binding, photoluminescence studies 7-21861
 Si, transition metal dopant complexes photolum., review 7-45203
 Si:C, O, photoluminescence of C-O related complex defects 7-22346
 Si:Ga, electron irradiated and annealed, photoluminescence spectra 7-13206
 Si:Ge, irradiated, photoluminescence spectra 7-13207
 a-Si:H, triplet exciton recomb., ODMR studies 7-2490
 Si:O, new donors, bound exciton recomb., photolum. study 7-22300
 SiC:Te, N, 6H polytype, ESR of (TiN)⁰ impurity pairs 7-2926
 SnTe, optical anisotropy due to spatial dispersion 7-53266
 (Ti,M)O₂ (M=V, Nb, Ta) rutile solid solns., charge transfer and ligand fields, XANES studies 7-64782
 (Ti,Ta)O₂ solid solns., chem. shift and cryst. field splitting rel. to valence charge, EXAFS 7-27818
 TiBr:I indirect exciton transition, effects of disorder 7-2489
 TiGaS₂, exciton states, absorpt. and refl. spectra 7-46066
 TiGaSe₂ crystals, exciton spectrum, phase transitions 7-7124
 TlI, excitons, band struct., polarised refl. spectra 7-27738
 TiSbS₂, near band gap optical props. 7-7715
 Xe cryogenic crystals, exciton diffusion and energy transport studies 7-52438
 Xe, solid, luminescence of trapped excitons, press. effects 7-64690
 Zn_{0.95}Mn_{0.05}Te, antiferromag. exchange const. determ., free exciton Zeeman splitting meas. 7-22229
 Zn_{1-x}Mn_xTe, x=0.25-0.71, free exciton state exchange splitting, magnetoreflection, magnetisation meas. 7-53288
 ZnO-electrolyte interface, photoconductivity and photocurrent spectra, influence of exciton absorption 7-45486
 ZnP₂, excitonic reflection and absorption spectra, optical anisotropy 7-45159
 ZnS, hexagonal, four-photon spectroscopy 7-5948
 ZnS_{0.95}Se_{0.05}, single crystals, growth, exciton luminesc. 7-22453
 ZnSe cryst., low press. melt growth technique, photolum., laser appl. 7-33548
 ZnSe epitaxial layers, MOVPE grown, elec. and photolum. props. 7-7420
 ZnSe, heteroepitaxial growth on GaAs, energy band gap, elastic strain effects 7-59242
 ZnSe MBE layers on GaAs, lattice mismatch effects, TEM, photolum. and X-ray diffr. studies 7-45042
 ZnSe, optical anisotropy due to spatial dispersion 7-53266
 ZnSe, single crystals, growth, exciton luminesc. 7-22453
 ZnSe:As, MOCVD growth, exciton and deep emission bands 7-52367
 ZnSe:N, MBE growth and doping, photoluminescence studies 7-27749
 ZnSe/(Zn,Mn)Se superlattice, optical props. heterointerface effects 7-7736
 ZnSe/Zn_{1-x}Mn_xSe strained layer superlattices, electronic energy states and relax. 7-45425
 ZnSe-ZnMnSe, quantum wells, excitons and kinetics 7-12622
 ZnSe-ZnMnSe superlattices, photoluminesc. props. 7-13218
 ZnSiP₂ cryst., exciton absorpt. spectrum, energy gap and exciton binding energy determ. 7-2500
 ZnTe, obs. of time evolution from reson. Raman scatt. to excitonic-polariton luminesc. 7-33390
 ZnTe:Cl(Al), crystals, vacancy-impurity complexes, ODMR studies 7-2530
 ZnTe:Cu, impurity related neutral complex with bound exciton, photoluminescence, absorpt., Zeeman meas. 7-45165
 ZnTe:O, red cathodolum. kinetics, two-step electron capture model calcs. 7-59262

EXELFS see electron energy loss spectra

exhibitions

No entries

exobiology see extraterrestrial life

exoelectron emission

- metals, fatigue deformed, stimulated electron emission kinetics (Russian) 7-3156
 models and critical experiment design 7-13339
 polyethylene, charged particle exoemission rel. to deform. and fracture 7-7827
 polyethylene dielec. thin films, hot-electron-induced damage and charge storage, electron spectra studies 7-27662
 quartz, exoemission centre with O vacancies, cluster model 7-12651
 BeO, TSEE, pyroelectric properties influence 7-13340
 CaSO₄, exoelectron spectroscopy under photon and low energy electron excitation 7-27873
 CdS, exoelectron emission, phonon drag, inhomogeneous energy distrib. 7-39366
 CsI:Na, exoelectron emission, phonon drag, inhomogeneous energy distrib. 7-39366
 Li₂B₄O₇:CuCl₂ crystallised glasses, pure and doped, thermally stimulated exoelectron emission, thermolum. 7-27874
 NaCl crystal, surface optical breakdown, exoelectronic emission with laser irradiation, impurity effects 7-59384
 Si, photothermostimulated exoelectron emission 7-22452

exosphere

- geocorona, Dynamics Explorer observations from 1981 to 1985 AD 7-55337
 solar cycle influence on H concentrations, Monte Carlo model 7-55338
 H dissipation flux, density meas. rel. to thermosphere temp. 7-23922

exotic atoms

- see also *hadronic atoms; muonic atoms*
- fermionium production in electron-atom collisions 7-36811
- positronic complexes with atoms and molecules, chem. stability calcs. 7-36827
- recent developments and expt. techniques 7-5787
- superheavy atoms, fractional charges, optical searches 7-10782

expanding Universe see cosmology

expansion, thermal see thermal expansion

expansion chambers see cloud chambers

expert systems

- see also *artificial intelligence; decision support systems*
- aerogeophysical prospecting, knowledge-based analysis system 7-29308
- alarm-filtering system for advanced test reactor 7-62054
- ALPA, diagnosis expert system for nuclear reactor supervision 7-25153
- APEX, aerogeophysical prospecting expert system (*Chinese*) 7-55268
- APHODEX, acoustic-phonetic decoding expert system 7-37289
- cartographic data generalisation from large to medium and small scale
- Ordnance Survey maps using expert systems techniques 7-47324
- cartography automation conf. London, England (Sept. 1986) 7-35105
- chemical graph theory 7-30916
- coastal flow, numerical modelling 7-55078
- computer vision system for automatic seismic wave-field movement anal. 7-23902
- corrosion, knowledge 7-3470
- corrosion knowledge, computer modelling, expert systems, decision tree 7-3469
- cosmic ray track analysis by expert system using distributed problem solving 7-55388
- emergency classification system at nuclear power plants, expert system application 7-15265
- expert systems and compiler techniques for intelligent implantable cardiac pacemakers 7-14162
- fault identification systems, model-based, development, nuclear reactor appl. 7-19412
- fusion energy experiment controlled by an expert system 7-5437
- IR spectra evaluation, expert systems for chemical analysis (*French*) 7-54227
- manual lifting, risks of overexertion, expert system, LIFTAN 7-40210
- Material Characterisation Expert System (MCES) for US materials testing 7-22964
- molecular modelling expert system, WIZARD-II 7-49877
- nuclear power plant accident management expert system, AMES 7-62055
- nuclear power plants, enhanced inspection using expert systems 7-36087
- oceanographic image anal. expert system, knowledge-based, features 7-23901
- optical relational-graph rule-based processor for structural-attribute knowledge bases 7-10861
- pacemakers, dual chamber, expert system and diagram for troubleshooting 7-28775
- reactor safety assessment system, expert system for US Nuclear Regulatory Commission 7-62053
- real-time photogrammetric input versus digitised maps: accuracy, timeliness and cost 7-40406
- signal image interpretation system, rule-based, seismic data anal. appl. 7-23903
- transformation of scientific objectives into spacecraft activities 7-66462
- two expert systems used in weather forecasting 7-66284
- water quality model, parameter estimation using prototype expert system 7-55111
- watershed acidification, computer simulation 7-14322

exploding foils see exploding wires and foils

exploding wires and foils

- see also *discharges (electric); plasma production*
- asymmetrically driven coaxial line, field asymmetry calc. 7-32076
- exploding cathode whiskers, plasma form., mass spectrometric diagnostics 7-44269
- imploding plasma experiments, diagnostics for Pioneer I 7-32038
- impulsive pressure meas. of thin metal wire explosion and electric discharge in H₂O 7-44275
- laser heated exploding foils, hydrodynamics, appl. to soft X-ray laser design 7-44209
- opening switches, 1-D MHD plasma simulations using MAGPIE code 7-32035
- Pioneer I experiments, foil implosion system design 7-32137
- Pioneer I foil implosion experiments 7-32037
- plasma expts., optical, and UV/X-ray imaging diagnostics 7-11784
- plasma flow driven implosion, 'quick-fire' experiments 7-32139
- pulsed power systems, exploding metallic foil candidates for switching elements 7-26539
- soft X-ray laser program at Livermore 7-20202
- time-dependent behaviour and hydrodynamic expansion, computer model 7-32036
- Al electrically exploded foil opening switches, high performance 7-32034
- Se X-ray laser targets, hydrodynamic aspects 7-20208

explosion bubbles see bubbles

explosions

- see also *accidents; detonation; nuclear explosions; safety; shock waves*
- adiabatic thermal explosion in small systems, stochastic theory, numerical results 7-9764
- air, gaseous charge explosion, blast wave propag. 7-57881
- droplets, laser-induced explosion, spatially resolved spectra 7-42632
- electric-explosion cavity development, dynamics 7-31824
- electron emission in microwave fields, excitation and evolution 7-63310
- explosive containment with spherically tamped powders 7-35535
- fibrous composites, influence of thermal effects of struct. and props. during explosive welding 7-17793
- flames, behaviour during cylindrical vessel explosions 7-59760
- foil implosion system design for Pioneer I experiments 7-32137
- hydroelastic three-layer cylindrical shell reaction to internal explosion, elastic deform. 7-31692
- hydromagnetic explosions, implications for volcanic hazard in Italy 7-66053
- imploding cylindrical plasmas as X-ray laser media 7-63322
- imploding plasma experiments, diagnostics for Pioneer I 7-32038
- imploding shell during coasting phase, inner surface perturbations, amplitude variation 7-56844
- invariant shock wave system, similarity transform. (*Russian*) 7-43983

explosions continued

- laser-fusion pellet, essential features 7-26468
- magnetically insulated transmission line in PROTO II accelerator, anode and cathode joints, gap closure 7-30756
- magnetogasdynamic cylindrical shock wave in isothermal gas 7-16270
- MEATRINDER circuit for enhanced energy transfer of inductive energy to imploding plasma loads 7-32131
- metallic glass reinforced Al composite fabrication by multi-lamina explosive compaction 7-59482
- MHD generators, assessment 7-65497
- molecules, explosive absorption of finite-diameter laser beam 7-50269
- ocean waveguide explosive source energy determ. 7-50827
- plane detonation wave in combustible gas mixture, direct initiation 7-31836
- propane-air flames, explosion venting, 2D Navier-Stokes eqns. 7-51340
- PROTO II accelerator power flow modification in insulator stack 7-30669
- radiative ignition in propagation of large explosions 7-54127
- reactive shear bands, dimensional anal., numerical integration 7-33931
- satellite explosions and space debris, mass distrib. 7-66420
- seismic explosions, layered elastic medium response to explosive point source using leaking modes 7-54895
- seismic radiation pattern from explosion in axisymmetric cavity 7-8843
- seismic water gun cavity collapse behaviour and far-field pattern 7-55282
- self similar cylindrical shock wave in radiating magnetodynamics, astro-physical appl. 7-34847
- shear flow, explosive processes, multidimensional and self-similar props. 7-37434
- shock waves from point-sources in a heat-conducting gas 7-34849
- shock waves in condensed matter, conference, Spokane, WA, USA (July 1985) 7-18501
- slab with spatially varying surface temp., thermal explosion 7-54129
- spherically symmetric scalar waves, backward energy flux 7-39897
- suspensions, gas-solid, explosion wave damping 7-6236
- thermal explosion and times to ignition in systems with distributed temps., behaviour at criticality and transition 7-54128
- thermal explosion by intense light, criticality dependence 7-65323
- thermal explosion critical conditions, turbulent natural convection effects 7-63122
- vapour explosions with a mass of grains, fuel-coolant interaction in reactor accident 7-19405
- weak disturbance velocity measurement, bulk density in porous media 7-31826
- Ar gas puff Z-pinch implosions, X-ray emission, appl. to X-ray lasers 7-26483
- Fe-Al₂O₃ melt, steam explosion suppression by coolant viscosity increase 7-8284
- H₂-air detonations, large scale expts. review, reactor safety 7-36211
- Li-SO₂ primary cells, safety hazards during charging 7-34007
- Ne gas puff Z-pinch implosions, X-ray emission, appl. to X-ray lasers 7-26483
- Ne, imploding Z pinch for X-ray laser research 7-20918
- Sn melt, steam explosion suppression by coolant viscosity increase 7-8284

exposure meters see photometers

extended Huckel theory calculations see EHT calculations

extended X-ray absorption fine structure see EXAFS

extensive air showers see cosmic ray showers and bursts

extensometers

- cryocrystal thermal expansion meas. automation 7-4845
- dilatometer based on electro-optical meas. technique 7-41338
- space-flight dilatometer/reactor development and testing, polymerisation kinetics obs. 7-13770

external flows

- active suppression of flow-excited cavity oscillations (*French, English*) 7-31774
- air crossflow, tube surface press. fluctuations, statistical anal. 7-44048
- arbitrary obstacle, 3-D boundary layer calc. (*French*) 7-11382
- axisymmetric free convection boundary layer flow of water at 4°C past slender bodies 7-20709
- axisymmetric wakes, stagnation point flow study 7-51152
- baroclinic instability over topography, nonlinear evolution 7-57804
- boundary integral equation method for solving stationary Stokes problem (*Chinese*) 7-14779
- boundary-layer transition, roughness trips with rows of spherical elements 7-51050
- coherent structures in the far field of a turbulent wake 7-31773
- cone in external stream, boundary layer eqns., FORTRAN code 7-37468
- convergent air intake with plane walls, flow study 7-11465
- cylinder circular, with slat devices, meas. in wake flow 7-20731
- electrically conducting body, electron dynamics in near wake 7-58052
- electrogasdynamic effect on small perturbation development in the boundary layer on thin airfoil 7-1641
- entropy layer absorption effect on supersonic flow heat transfer of submerged circular cone 7-43975
- falling water films on vertical cylinder with downward step 7-6334
- film, gravitational flow, initial velocity field 7-57784
- finite element formulation of stagnation flows 7-37423
- flow visualisation, laser light sheet method for building environmental engineering 7-37570
- free-convection boundary layer at heated vertical plate, heat transfer and temp. profiles 7-31795
- gas turbine CAD system with Denton scheme for flow program, comparison with expt. results 7-63177
- gas turbine computer-aided interactive design system, Denton scheme for flow program 7-63176
- gas-particle mixture, supersonic two-phase flow around a wedge 7-1614
- gravity influenced free surface flows, iteration method for integral equations (*Chinese*) 7-26246
- heat transfer, simulation for separated and reattached flow on flat plate 7-51107
- hydromagnetic free convection flow along porous plate with mass transfer, Hall effects 7-63141
- inertial settling of polydispersed particles at critical point of sphere 7-1620
- infinite Froude numbers cusped free surface flows 7-51028
- inviscid barotropic flow over topography, nonlin. stability and statistical mechanics 7-57806
- inviscid compressible fluid, flow past cylinder (*Chinese*) 7-26306
- laminar boundary-layer flows, separation point determ. 7-31741

external flows continued

- liquid film, laminar downflow over cylindrical surface, thermal entry region, heat transfer 7-51096
 liquid film downflow, Orr-Sommerfeld eqn. soln., optimal approach 7-51119
 liquid film on a rotating disk, slip effect 7-57849
 liquid films, plane, with free rims, dynamics 7-32763
 liquid thread breakup in linear flow 7-57805
 longitudinal flow past plates with blunt trailing edges, wake investig. (*German*) 7-20824
 magnetic fluid, thin layer coating, hydrodynamic drag, num. investig. 7-51061
 magnetic liquid, film flow stability 7-51329
 mass transfer, surface geometry meas. by projected moire fringes 7-31903
 moving bodies, method for computing flow fields 7-65789
 multilayer ideal incompressible heavy fluid flow past body 7-1601
 oscillating flow past infinite vertical plate, suction and free convection effects 7-1555
 perfect fluid flow past body with conical singularity 7-56044
 perturbed flows in a longitudinal gravity field 7-1594
 pipe laminar thermal energy region, transient unsteady convective heat transfer 7-31775
 plane Stokes flow around circular cylinder, necessary condition for existence 7-1527
 potential flow, 2D with separation in unsymmetrical bends 7-11538
 potential flow past a sinusoidal wall by direct variation 7-57786
 radiative heat fluxes in supersonic flow of inviscid gas over 3D bodies 7-43972
 roughness trips, effect on boundary layer transition 7-16167
 separation structures on cylindrical wings (*French*) 7-11451
 shear stress calculation for axial flow over rod bundle 7-43859
 stagnant zone, form. at different Bernoulli numbers, nonlin. num. soln. 7-51241
 Stokes flow past a slightly deformed fluid sphere 7-51032
 stratified stream flow over obstacle, formation of two-soliton internal wave 7-51264
 supersonic flow, asymptotic behaviour, determ., num. soln. 7-43976
 supersonic flow around wedge, Lavrentiev-Bitsadze approximations calcs. (*Russian*) 7-57879
 symmetry planes of differently shaped bodies, heat and mass transfer characts. 7-11447
 tube bundles, single- and multi-row, vibrations in crossflow 7-1630
 turbulent boundary layers, barriers, flow and heat transfer 7-51100
 turbulent flowfield visualisation, computer generated, for flow around cubic model 7-37447
 turbulent liquid film, freely-falling, momentum and heat transfer 7-20712
 turbulent wakes, press.-gradient effects and curvature 7-57843
 two-dimensional flow past bluff flexible low porosity membranes 7-16241
 two-dimensional slow viscous flows past obstacles in a half-plane 7-57788
 unsteady incompressible viscous flow over circular cylinder, body-fitted coordinates 7-43851
 unsteady laminar forced convection from impulsively started sphere, temp. field 7-43852
 vibrating-rod densimeter theory 7-31894
 viscous flow past right circular cylinder on β -plane 7-57847
 wake analysis, physical and schematic viscosity influence 7-26281
 wall-turbulence hypothesis, refinement 7-57814
 wave forces on vertical circular cylinder, num. investig. 7-57866
 P_2O_5 - SiO_2 glass in multilayer struct., laser-induced flow modelling 7-38057

external modes (crystals) *see lattice dynamics***extraordinary ray** *see birefringence***extrapolation**

- boundary-integral-equation and finite-element methods, combined scheme for elasticity theory problems 7-56041
 Cliff-Lorimer k_{AB} factors at zero foil thickness, extrapolation method 7-39935
 creep strength characteristics extrapolation, parametric methods suitability 7-22942
 creep strength rapid prediction, thermoactivation analysis basis, residual life eval. after TMT 7-22941
 seismic wavefield extrapolation by linearly transformed wave eqn. 7-28878

extraterrestrial life

- 1986 ISSOL meeting, Berkeley, CA, USA (1986) 7-24274
 bacterial dust grain model, appl. to 2 to 4 μm spectrum of P/Comet Halley (1982i) 7-34937
 intelligence and societies 7-35125
 radio aspects (book) 7-55914
 SETI, laser signals search from nearby stars 7-34889
 SETI, time and space acousto-optic folded spectrum processing 7-26080
 SETI, ultranarrowband searches with dedicated signal processing hardware 7-24013
 SETI at JPL, Caltech and Ames Research Centre (*French*) 7-60580
 SV40 DNA, possible use for CETI 7-40090
 terrestrial-like scientific-technical civilisations, possible existence in Galaxy 7-29416

extraterrestrial radiofrequency radiation *see radiofrequency cosmic radiation***extremum control** *see optimal control***extrusion**

- ceramic engine component fabrication techniques 7-3243
 glass fibre processing, spinning process in liq. state 7-3258
 graphite particle dispersed Al-Si alloys, powder extruded, wear characts. (*Japanese*) 7-53909
 liquid crystal polymer rods, thermotropic, flow and orientation behaviour during extrusion 7-57887
 natural rubber/polybutadiene elastomers, C black distrib., flow behaviour depend. 7-43832
 nonhardening material, plane strain, axisymmetric extrusion, viscoplastic FEM 7-63009
 optical fibre cables, sheath retraction 7-11165
 polycarbonate-polystyrene-acrylonitrile, coextruded multilayer composites, tensile props. 7-59572
 polyethylene, continuous melt extrusion, morphology, strength 7-39472
 polypropylene melt, $CaCO_3$ filled, on-line US monitoring of extrusion 7-59725
 quasi-steady state isochoric plane flow meas., noisy data anal. 7-63727

extrusion continued

- steel, austenitic, Mn-Cr, hardening characts. and hydroextrusion parameters (*Russian*) 7-59540
 steel, ferritic-martensitic stainless, warm forming (*Polish*) 7-13507
 thermoplastic rubber/liquid crystal polyester dualcoextrusion coating system for optical fiber drawing 7-11190
 Al alloys, liquid dynamic compaction, microstruct. and precipitation, TEM study 7-59529
 Al-Mg, rapidly solidified powders, effect of extrusion parameters on props. 7-39595
 Al-Mg-Si, squarely extruded, texture and mech. props. (*Japanese*) 7-33694
 Al-Si, graphitic, hot extruded powders, sintering, antifriction props. 7-13409
 Al-Zn-Mg-Cu-Ni-Zr, modified 7075, prod. by liq. dynamic compaction, struct. and props. 7-46437
 Cd-Zn electroplated steel, extrusion, deform. force rel. to comp. and struct. 7-3367
 Copper, extrusion, dislocation density determ. (*Russian*) 7-58285
 Fe-C-based alloys, high C, rapidly solidified, mech. props. 7-22673
 Mn-Al-C ferromag. alloys, phase, transformations, and struct. defects, positron annihilation study 7-46461
 Mo, hydroextruded single crystals, nonuniformity of texture deform. (*Russian*) 7-33695
 Mo, single cryst., recrystallised after hydraulic extrusion, wide-angle boundaries of anomalous grain 7-44563
 Nb-Zr (1 wt.%) alloy, hydroextruded, optimum degree of deform., microstruct. 7-3325
 Ni-Cu diffusion contact, mass transfer at grain boundaries in fields of diffusion-concentration stresses 7-2272
 Zr, extrusion substruct. after hydrostatic extrusion (*Chinese*) 7-6626

eye*see also contact lenses; vision*

- 3D rigid structure computation from fixed-axis motion 7-23354
 accommodation, natural, in the growing chicken, IR photoretinoscopy obs. 7-54551
 accommodation in chickens: corneal vs. lenticular accommodation and effect of age 7-23336
 accommodation response, effect of stimulus contrast 7-65745
 accommodation response to sinusoidal gratings, modulation dependence 7-17974
 accommodative system, human, computational model of error detector 7-54548
 achromatopsia, light induced oscills. of standing pot. 7-28505
 adaptive regulation of accommodative vergence and vergence accommodation 7-4612
 afterimage movement during saccades in the dark 7-47070
 age-related accommodative loss in human eye, mathematical model 7-54556
 amblyopia assessment: use of computerised contrast sensitivity, Arden gratings and low contrast letter charts 7-65751
 aperture pupil of single photoreceptors, linear behaviour 7-54549
 area centralis and visual streak, development in the grey kangaroo *Macropus fuliginosus* 7-47051
 astigmatism, influence of lid posn. 7-54547
 binocular fixation misalignment, objective meas. 7-8565
 blood circulation measurement use in ophthalmic diagnosis 7-8746
 children, differential effects of various causes of deafness on eyes, refr. errors, and vision 7-8555
 chromatic adaptation rel. to central binocular mechanism 7-59993
 colour defects rel. to eye disease 7-17994
 complementary projector system for contrast sensitivity meas. 7-8748
 cone dark adaptation, temporal modulation sensitivity 7-17989
 cone photoreceptors, human, spectral sensitivity obs. 7-59991
 cones, long- and middle-wavelength, spatial and chromatic antagonism in long-wavelength flashes detect. 7-54567
 cones in walleye, ultrastruct. obs. 7-59989
 convergence insufficiency, fixation disparity, and control systems anal. 7-8567
 cornea, effect-of epithelial and stromal oedema on light scatt. props. 7-34132
 cornea, effects of fibril orientations on light scattering 7-34134
 cornea, rabbit and human, mech. props. obs. 7-28556
 cornea, transmission of linearly polarised light 7-54550
 cornea cutting for implantation by microsurgery robot (*Japanese*) 7-14153
 corneal curvature changes during accommodation in chicks 7-47042
 corneal incisions induced by pulsed UV or IR lasers, comparative study on dogs 7-34193
 corneal iridescence in fish, light-induced changes 7-47044
 corneal polarisation, biaxial model for living human eye 7-59973
 corneal thickness and diameter in the domestic cat 7-23333
 crystalline lens, excised, computer assisted scanning laser monitor for optical quality meas. 7-23507
 d-amino Acid in irradiated and aged mouse, skin and lens obs. 7-18021
 dental photopolymerisation sources, curing efficiency and ocular hazards 7-60064
 diagnostics, internal pressure meas., using electric sensors (*Slovak*) 7-60112
 disparity vergence dynamics and fixation disparity 7-8563
 effect of digital lowpass filters on the maximum velocity of saccadic eye movements 7-13996
 electrooculogram and colour vision, effects of ethyl alcohol 7-28501
 electrooculographic control system, discrete, for severely handicapped persons 7-8736
 electroretinogram, single flash, electronic simulation model (*Japanese*) 7-59979
 ERG, local macular, in patients with Best's disease 7-28504
 ERG, oscill. pots. (*Italian*) 7-23337
 ERG, progress over 25 yrs. 7-17980
 ERG and visual evoked pot. abnormalities in myotonic dystrophy 7-23341
 ERG b-wave, rel. to outer segment disc shedding in rabbit retina 7-59982
 ERG components: a reappraisal 7-28506
 ERG of intact cat eye, mechanisms of azide induced increases in c-wave and standing pot. 7-40144
 ERGs of albino rabbits, simultaneously recorded, effects of intraocular perfusion with 2 alternating irrigation solns. 7-28507

eye continued
event-related pots. estimation improvement using statistical pattern classification, visuo-motor appl. 7-14002
examination setup, OAP-311, rational refraction system 7-8747
excimer lasers in medicine, ophthalmic appls. 7-60073
excursion tests of ocular motility 7-65750
extraocular muscle sideslip and orbital geometry in monkeys 7-59975
fatigue caused by reflected under intense illumination from fluorescent lamps (*Japanese*) 7-34130
fibre optic probes for ophthalmology 7-47206
fixation disparity, combined effects of spatial freq. and retinal eccentricity 7-8564
fixation disparity, computerised meas. 7-8726
fixation disparity, conf., Atlanta, GA, USA (Dec. 1985) 7-4615
fixation disparity clinical meas., rel. to use of central fusion stimulus on the dispartometer 7-8725
fixation disparity in binocular stress 7-65760
fixational eye movements, macaque and human, effects of light and dark environments 7-59984
flicker adaptation in the peripheral retina 7-47062
ganglion cells, constant dendritic coverage with growth of goldfish's retina 7-40145
gazing point definition for picture anal., appls. (*Japanese*) 7-34140
HDTV and 525-line viewing, sight-line displacements, eye movements eval. 7-59992
horizontal cells, c-type, in bowfin retina, response props. 7-47053
horizontal cells in eyecup and isolated retina, differing effects of excitatory amino acids 7-47056
horizontal forced vergence fixation disparity curve, effect of nearpoint stress 7-34136
3-hydroxyretinoids, separation and identification of geometric isomers and occurrence in eyes of insects 7-23348
interstitial retinol-binding protein, bovine, isolation and sequence anal. of cDNA clones 7-17983
intraocular distances, system for continuous high-resolution meas. based on A-scan US 7-40234
intraocular pressure, monitoring under μ G conditions (*German*) 7-8722
intraocular pressure meas., noncontact tonometry through soft contact lenses 7-54780
invertebrate photoreceptors, involvement of cyclic GMP in excitation 7-47059
laser coagulator, argon type, use in ophthalmic therapy 7-8674
laser coagulator, LAK argon type, for ophthalmic therapy 7-8673
laser hazard analysis, nominal hazard zone 7-60094
lens, mouse, X-ray acute radiation injury quantitative assessment, cataract development (*Russian*) 7-8658
lens, rabbit, ageing, in vivo quasielastic light scatt. obs. 7-28500
lens, radiation dose in radiology of the orbit 7-40292
lenses, human, diagnostic evaluation using quasi-elastic light scatt. spectroscopy 7-34230
lenses, human, in vivo meas. using quasielastic light scatt. 7-34231
light-dependent synaptic delay between photoreceptors and horizontal cells in the tiger salamander retina 7-59983
macular ERGs and contrast sensitivity as sensitive detectors of early maculopathy 7-28511
macular laser lesions, image anal. 7-34229
macular pigment density, human, rel. to aging 7-47043
magnetic field associated with eye movement (*Japanese*) 7-14031
Monte Carlo dosimetry for ¹²⁵I and ⁶⁰Co in eye plaque therapy 7-40300
motion perception and eye movement (*Japanese*) 7-28528
movement tracking, target brightness feedback (*Japanese*) 7-47049
myopic eye of the Black Moor goldfish 7-23335
nonlinear forced vertical vergence fixation disparity curves and their clinical significance 7-34137
nystagmus induced by off vertical axis rotation, three-dimensional model 7-47047
ocular-hypertensive subjects, muscular and intraocular press. responses 7-54553
ocular-motor quantitative indicator of visual fatigue 7-59977
oculomotor and skeletal motor systems, sharing of 1 visual space map 7-59972
ophthalmic applicators, B-particle, calibration of US National Bureau of Standards 7-47259
ophthalmic combined Ar YAG-laser system 7-47197
ophthalmic laser interferometry 7-47204
ophthalmological laser slit lamp 7-47202
ophthalmology, ultrasonic therapy and imaging 7-28632
perception model of curves in dot figures, role of virtual lines 7-65758
photoreceptor cells from retina of domestic pig, comparison of size as determ. by light and scanning electron microscopy 7-13999
photoreceptor membrane, Fourier transform IR difference spectroscopy for elucidating biomolecular mechanisms 7-54832
photoreceptor membranes, light-depend. nucleotide exchange, catalysis by rhodopsin (*German*) 7-8495
polymorphism of the long-wavelength cone in normal human colour vision 7-17990
presaccadic spike pot., rel. to eye movement direction 7-23340
presbyopia, forced vergence fixation disparity curves 7-34135
primary visual cortex and hypercolumn math. model 7-23339
protective eyewear for fluorescent dye penetrant inspection, UV radiation safety and visual enhancement 7-40311
pupil diameter and defocus effects on contrast sensitivity 7-65747
rapid-eye-movement brain state optimal monitor 7-23323
retina, central part, distrib. of sensitivity to coloured light (*Japanese*) 7-65755
retina; digital image correlation methodology use for deform. quantification 7-59718
retina, functional architecture 7-59974
retina, rabbit, double-label anal. of GAD- and GABA-like immunoreactivity 7-40146
retina, whole mount method for sequential anal. of photoreceptor and ganglion cell topography 7-40382
retina display and reconstruction 7-14000
retina of human and rabbit eyes, Ganzfeld light distribution 7-47041
retina of pigeon, projection of visual field 7-40141
retinal adaptation to non-uniform fields: average luminance or symbol luminance? 7-54562
retinal blood flow visualisation and meas. by laser speckle photography 7-47212
retinal camera, wide-angle RCS-310, prototype experience 7-8745
retinal camera, wide-angle RCS-310 design 7-8744

eye continued
retinal circuitry, retrospective review 7-17976
retinal electrical activity imbalance rel. to ocular dominance shift in kitten visual cortex 7-28517
retinal functions, simulation with Gaussian derivative model 7-3786
retinal ganglion cell processing of spatial information in cats 7-54560
retinal ganglion cells, turtle, photoreceptor input and temporal summation 7-17984
retinal glial cells, higher density of ion channels that mediate K⁺ buffering in endfeet 7-47048
retinal horizontal cells, changes in response waveform during dark and light adaptation 7-47060
retinal image movements, psychophysically perfect image stabilisation 7-60010
retinal ischaemia, rod-cone differences, rabbit obs. 7-28508
retinal optical intensity profile model for computer-aided visual acuity assessment 7-59976
retinal pigment epithelial cells, acetazolamide-induced changes of membrane pots. 7-28509
retinal rod outer segment suspensions, effect of sonication on nucleotide-dependent light scatt. changes 7-23398
retinal therapy, preselectable intensity distrib. in large-area laser coagulation by electronically controlled beam deflection 7-47207
retinitis pigmentosa, stimulus investigative range, preliminary findings 7-34143
retinol in insect photoreceptors, sensitising function 7-23352
review of human eye movement research 7-17978
rhodopsin molecules in disc membrane of frog rod outer segments, 3D electron microscopical investigation 7-65690
rod and cone signals in retina of goldfish, separation and light adaptation 7-17987
rod-cone interaction in monocular but not binocular pathways 7-59985
Roman crystalline lens, cataract development, water state, NMR spin echo obs. 7-8557
rotational movement anal. using template matching, IR image processing (*Japanese*) 7-60111
saccade accuracy, reduction of non-target stimuli influence: predictability and latency effects 7-47057
saccade and blink amplitudes rel. to visual suppression 7-23346
saccadic eye movement effect on threshold perception, model study 7-65757
saccadic eye movements, time-optimal control 7-59978
saccadic retraction and cyclotorsion, aftermath of horizontal saccades 7-23345
schematic eye predictions of relative spectacle magnification in unilateral aphakia 7-34131
short-wavelength-sensitive cone photoreceptors, isolation in 4-6-week-old human infants 7-59994
smooth pursuit eye movement, control characts., model (*Japanese*) 7-47040
solar radiation and the eye, review of knowledge relevant to eye care 7-8649
spatial pattern perception, visual mechanism commodity 7-40158
spatio-temporal model of ganglion cell receptive field in the cat retina 7-23338
spatio-temporal vision of macaques, with severe loss of P _{β} retinal ganglion cells 7-23344
static accommodation and the minimum angle of resolution 7-34133
stereo visual displays 7-17972
strabismus, visual localisation after surgery, compatibility with outflow theory 7-23367
striate cortex of cat, directional and orientational tuning for contrast and textured stimuli 7-34141
surgery, using OPS-330 Slitlamp Surgiscope 7-8758
surgery in general practice, OPM-110 microscope use 7-8757
targ film, struct. during blinking 7-65753
therapeutic laser instrument for ophthalmology, the VISULAS YAG 7-54709
threshold perception and saccadic eye movements 7-65756
tonic accommodation interocular equality and consensuality of accommodative hysteresis 7-65746
tracking of periodic square wave target motion 7-54554
ultrasonic A-scan ophthalmoscope, eye abnormality diagnosis 7-40233
vergence adaptation, review 7-34138
vergence eye movement system, dual-mode dynamic model 7-28513
vertebrate retina, physiological and morphological differences between On- and Off-centre bipolar cells 7-47050
vertical fixation disparity studies 7-8566
visual adaptation measurement using computer controlled device 7-34144
wetting value of tears, reliability 7-65752
Zeiss Gradal HS progressive addition lens, designs using splines, max. wearing comfort 7-50712
⁶⁰Co γ -source, accidental irradi. of technician, long-term follow-up: eye, skin and blood effects 7-34195
Nd:YAG Q-switched laser for ophthalmology, obs. on optical construction 7-47203

F-centre lasers see colour centre lasers

F-centres

see also A-centres; M-centres; R-centres; Z-centres
alkali halide crystals, F-centre formation threshold by two-photon absorpt. 7-32437
alkali halide crystals, self-trapped exciton recomb. luminesc.-recomb. induced F-centre form. anticorrel. calcs. 7-13201
alkali halides, F-centre production, impurity aggregate effects 7-21202
alkali halides, F-F' conversion, polaron theory 7-21201
alkali metal halide microcrystalline powders, correl. between coloration stability and microhardness 7-32486
alkali oxides with antiferroite structure, F⁺-centre absorption energy calcs. 7-12658
Al₂O₃, γ -irradiated, thermoluminescence from F and F⁺ centres (*Korean*) 7-27795
Al₂O₃ surface electrocathodolum., defect state transitions under high voltage stress 7-39187
BaF₂ crystals, γ -irrad., optical absorpt. 7-58275
BaFCl:Dy(Cu), thermolum., X-irradiated at room temp. 7-53419
BeO, optical props. of F⁺ centres 7-7717
CaF₂:Mn, gamma irradiation-induced defects, absorpt. and excitation spectra studies 7-26801
CaF₂-Si (111), UV irradiation-induced ordered struct., surface F-centres 7-7396

F-centres continued

- CaO, self-trapped hole centres, ODMR and spin coherence studies 7-7612
 CsCl, $F_2(\text{OH}^-)$ -centre absorpt. bands, pseudopotential calc. 7-52512
 CsCl:CN $^-$, $F_H(\text{CN}^-)$ -centre absorption bands, pseudopotential method calcs. 7-22292
 CsCl(Br)(I), luminescence quenching in F centers under pressure 7-22334
 KBr crystal, radiation defects destruction by electron beam generated pulsed stresses 7-63663
 KBr crystals, resonant secondary luminescence and vibr. F-centre relax. 7-33434
 KBr, F centre spin mixing parameters in optical pumping cycle 7-7181
 KBr microcrystalline powders, interstitial cluster stability 7-32485
 KBr single crystals, X-ray irradi., F-band absorpt. and thermolum., effect of laser excitation 7-21277
 KBr single crystals, F-band absorpt., X-irradi., thermolum., mag. and elec. field effects 7-59230
 KCl, F-centre destruction at elevated temps. under elec. field 7-32488
 KCl, heat treated, alpha particle dechanneling, range meas. by F-coloration depth determ. 7-32512
 KCl microcrystalline powders, additive coloration 7-32434
 KCl microcrystalline powders, correl. between microhardness, dislocation mobility and coloration stability 7-32436
 KCl, vibronic mechanisms of excitation decay, defect formation 7-39158
 KCl X-ray and γ -irradi., F-centre destruction owing to subsequent laser light excitation, luminesc. spectral characts. 7-27772
 KCl:H, F-centre accumulation during proton irradiation 7-46076
 KCl:O $^-$, F_H centre ionisation energy calc. 7-44539
 KCl(Br), F-centre near-surface generation by synchrotron radiation 7-26744
 KCl(Br)(I), luminescence quenching in F centers under pressure 7-22334
 KI, F centre spin mixing parameters in optical pumping cycle 7-7181
 KX:O $^-$ (X=Cl, Br), tunable CW laser operation in 1.45 to 2.16 μm range 7-62707
 LiBr, lattice deform. around an F-centre 7-32435
 LiCl, lattice deform. around an F-centre 7-32435
 LiF, electron beam irradi., desorbed ground state Li atoms, signal time depend. 7-52260
 LiF, electron stimulated desorption of Li, role of F-centre diffusion 7-16864
 LiF, F- and F_2 -centres induced by ion implantation 7-26747
 LiF γ -irradiated crystals, F-centres, positron annihilation and optical absorpt. meas. 7-44542
 LiF, lattice deform. around an F-centre 7-32435
 LiI, lattice deform. around an F-centre 7-32435
 LiNbO $_3$, F^+ centre wave function calc. 7-44540
 Li $_2$ O, F^+ centre absorption energy calcs. 7-12658
 Li $_2$ O, neutron and ion irradi. damage, ESR and optical absorption studies 7-32509
 MgF $_2$ cryst., electronic colour centres, UV absorpt. and luminesc. study 7-39174
 NaCl crystals, electron-coloured, transmission and holographic props. 7-43001
 NaCl, pure and doped, irradi. defect, thermoluminesc. 7-3098
 NaCl, pure and Mg doped, electron range vel. to heat treatment 7-21283
 NaCl, synthetic, microcrystalline powders, spontaneous colloid formation in electrodeless discharge 7-12065
 NaCl, X-ray and γ -irradi., F-centre destruction owing to subsequent laser light excitation, luminesc. spectral characts. 7-27772
 NaCl:Mg, X-ray irradi., exciton interactions with impurity-vacancy dipoles, absorpt. and luminesc. spectra 7-45162
 NaCl:O $_2^-$, tunable CW laser operation in 1.45 to 2.16 μm range 7-62707
 RbCl crystals, resonant secondary luminescence and vibr. F-centre relax. 7-33434
 RbCl, self-trapped excitons, excitation-induced atomic motion 7-21822
 RbCl-RbBr mixed crystals, X-ray diffraction and color centres 7-58258
 Si:C, O, luminescence props. of shallow donor centre 7-17347
 UO $_2$ thin films form by oxidation, luminesc. studies 7-22351
- F $_2$ -centres** *see* M-centres
F $_3$ -centres *see* R-centres
F $_A$ -centres *see* A-centres
F-layer *see* F-region
F-region
 collisional ion cyclotron instability, effect of finite current channel width 7-47630
 convection electric field large scale structures 7-29342
 decametric propagation, large-scale inhomogeneities effect 7-40629
 zonal electric field, prereversal enhancement due to F-region dynamo 7-55359
 electron concentration profile near max. of ionosphere, analytic extrapolation 7-9293
 electron drift velocity in vertical direction, radar observations 7-9310
 electron temperature enhancement in subauroral zone, DE 2 satellite obs. 7-29351
 EM ion drifts, relationship between meridional and longit. components at mid and low latits. 7-9315
 equatorial American sector, vertical plasma drifts 7-34773
 equatorial scintillations, effect of mag. activity 7-34762
 equatorial spread-F, effect of mag. activity during high and low solar activity 7-66377
 F $_2$ -layer, elec. dipole field in inhomogeneous ionospheric plasma 7-29330
 F $_2$ -layer, hourly variability estimation at low latitude station 7-60472
 F $_2$ -layer, ionisation response to solar 10.7 cm flux 7-14408
 F $_2$ -layer, MHD waveguide oscills., excitation by geoelectric currents 7-14407
 F $_2$ -layer, noon bite-out phenomenon at Waltair 7-66385
 F $_2$ -layer, semi-annual and annual vars. in whistler dispersion 7-14410
 F $_2$ -layer at equator, magnetic storm effects 7-23936
 F $_2$ -layer basic parameters during daytime, theoretical calcs. 7-9292
 F $_2$ -layer nighttime penetration freq. rel. to cold front passage (Chinese) 7-18331
 F $_2$ -layer peak electron density reduction due to N $_2$ vibrational excitation in summer 7-29355
 F $_2$ -layer visualisation, eleven years of ionospheric chronograms 7-23848
 HF-enhanced plasma line temporal evol. 7-34776
 high-latitude, electron temp. during solar max and winter conditions 7-34772

F-region continued

- ion temperature anisotropy in auroral region, EISCAT obs. 7-29341
 irregularities of small-scale, HF backscattering study indicating strong sub-auroral ion flow 7-23937
 irregularity obs. of SAR arc event 7-60470
 mid-latitude spread-F occurrence during daylight hours 7-60451
 nighttime irregularities, mid-latitude rocket-borne obs. 7-40639
 nonlinear wave structures in high-latit. F-region, generation by plasma instabilities 7-66386
 parameters determ., resonance scattering method 7-55356
 Pc 4 responsible for large fluctuating elec. fields 7-29339
 photoelectric lines at 22.2 to 27.2 eV, energy spectra depend. on ionospheric parameters 7-9290
 plasma convection patterns at high latitude, empirical models 7-60457
 plasma parameters measurements in vicinity of Space Shuttle, Langmuir probe results 7-29360
 plasma trough at high latitude, study of plasma flow 7-29338
 plasmopause and F-region and mid-latitude trough, simultaneous observations 7-47618
 polar cap F-region, plasma patches dynamics 7-34779
 poleward edge of mid-latitude trough, formation orientation and dynamics 7-23938
 radiowave heating expts., ionosphere response involving plasma instabilities 7-29344
 radiowave incoherent scatter sounding for temperature and ion composition 7-29284
 radiowave modification of electron distrib. function, due to resonant HF absorpt. 7-60459
 radiowave scintillation due to equatorial F-region irregularities, for trans-ionospheric 140 MHz signals 7-29357
 radiowave sounding using EISCAT incoherent scatter, deconvolution of altitude smearing 7-29283
 solar flare induced changes in total electron content, 24 April 1984 flare (Chinese) 7-4251
 spread-F, zonal drift variability observations 7-40635
 spread-F occurrence in equatorial region during evening, rel. to elec. field reversal 7-23935
 spread-F occurrence influenced by geomagnetic activity 7-47616
 storm disturbances of F $_2$ -layer, review 7-9288
 storm-time disturbance of F $_2$ -layer, positive phase 7-9295
 SF $_6$ release expt. at F-region altitudes, excitation of O permitted lines 7-9282
- f-values** *see* oscillator strengths
faces (crystal) *see* crystal faces
facility location *see* operations research
facsimile document reproduction *see* photocopying
facsimile equipment
 weather satellite automatic picture transmission, design of grey scale test pattern generator 7-29292
facsimile signals *see* video signals
factory automation
for general papers only
see also manufacturing computer control
 flowmeter calibration, computer-aided test system 7-37591
faculae *see* photosphere; solar activity
fading
see also radiowave propagation
 HF groundwave and skywave propagation 7-40643
 long-distance 40 kHz signals, effects of geomag. storms on sunrise fading 7-55360
 microwave fading, geographical distrib. prediction from ground based climatological meas. 7-55241
 microwave line-of-sight links, elevated atmospheric duct, multipath fading anal. 7-47482
 microwave links, seasonal variation of multipath parameters in Egypt 7-66282
 multipath fading, annual and seasonal variability 7-55242
 radiowave absorption fading at 18 GHz rel. to radio path direction (German) 7-66273
 radiowave propagation and acoustic sounding developments 7-34607
 sinusoidal pulse evolution in nonlinear medium with fading memory 7-16024
 terrestrial radio relay lines, wave propagation above 10 GHz, investig. 7-29214
 tropospheric propagation at low latitude areas 7-66283
 tropospheric radio links, fast signal fades rate distrib. 7-34658
- failure, electrical** *see* electrical faults
failure (mechanical)
see also fracture; mechanical strength; plastic deformation
 composite, failure criteria, tensor-polynomial type, expl. verification of efficiency 7-22812
 composite material failure under compression, complex stressed state case, continuous theory 7-62974
 composites, compressive failure modes 7-6717
 damage cumulation, self-similarity for different loading conditions 7-20658
 granular composites, failure anal. in conditions of adverse medium 7-33686
 NDT, fault tree anal. 7-17756
 plates, first-ply failure analysis of composite laminates 7-63053
 pulp fibres longitudinal compression device 7-13697
 refractory brick in rotary kiln burning zones, failure mode anal. 7-28140
 rock failure during uniaxial loading, 2D computer model 7-8922
 rock joints, shear failure constraints for empirical relations 7-55018
 rocks and concretes, failure process, dynamic description 7-57738
 steel, stainless, reactor pipe integrity prediction using R6 procedures 7-49542
 C fibre reinforced epoxy, laminates, quasi-isotropic, response to biaxial stress 7-33732
 SiO $_2$ -polyimide interface, locus of failure, XPS study 7-28261
- failure analysis**
see also electrical faults; wear
 electronic materials and devices corrosion 7-33815
 fault identification systems, model-based, development, nuclear reactor appl. 7-19412
 implantable electronic devices reliability, case studies 7-60122
 nuclear power plant dependent event data classification system 7-15290
 optical component reliability, effects of solder creep 7-15997
 PWR plant-specific availability modelling 7-10198

failure analysis continued

- secondary cells failure mechanism and rate, reliability studies using Weibull statistics 7-6540
- GaAs, semi-insulating, AL metallisation, electromigration failure anal. 7-44927
- Ni-H₂ secondary cells for low-Earth-orbit satellites, reliability and life testing 7-65451

fallout

see also air pollution

- ¹⁴C seasonal variations in atmosphere caused by bomb tests 7-23256
- Algeria, fallout during 1985 at two sites (French) 7-65665
- Chernobyl fallout, detecting and meas. in Nordic countries 7-30715
- Chernobyl fallout, monitoring and impact on UK 7-42229
- Chernobyl reactor accident, UK aquatic environment, fisheries viewpoint 7-42230
- nuclear winter, smoke scavenging by atmospheric ozone 7-9109
- radioactive fallout on west Algerian coast, early 1985 (French) 7-59895
- Tsjeernobyl radioactive fallout, appl. of two-dimensional trajectory model to radioactivity transport 7-59894
- Virgin Islands, Pu fallout and natural radioactivity of coral 7-60274
- Yala Glacier, Nepal, tritium vertical profile in glacier ice 7-40082
- ¹⁴C activity of atmosphere, response of hydrological systems 7-23253
- ¹³Cs, A=134,137, comparative pathway analysis in Hudson River estuary, dose assessment 7-8699
- ¹³⁷Cs, 1977 survey of conc. in British soil 7-34076
- ¹³⁷Cs in soil of W Germany field, fallout spatial variability 7-65655
- ³H fallout detection in tree ring records, short term precipitation 7-23255
- ³H, organically bound, distrib. in vegetation exposed to fallout 7-60096
- ²³⁹Np from global fallout after atm. testing, human tissue sample obs. 7-34291
- Pu content of Mururoa Atoll coral samples, nucl. techniques 7-54415
- Pu fallout, food ingestion in Japan 7-28723
- T from nuclear bombs, distrib. in oceans 7-66169
- U, fallout from nuclear powered satellites and volcanic eruptions, detect. in rain 7-3740
- UO₂ emissions from Windscale 1954-7, environmental impact 7-34293

Faraday effect

- alkali metal vapour number density, optical determ. using Faraday rotation 7-48696
- crystals, birefringence, Faraday effect, conversion of linear into circular light polarisation 7-59189
- current and mag. field sensor, calibrated optical fibre Faraday rot. 7-25980
- dielectric cryst., linear magneto-optical effect anisotropy 7-39092
- dielectric crystals, Faraday effect 7-17309
- fibre optic current sensors using highly birefringent bow-tie fibres 7-15976
- glass:Tb₂O₃ Faraday rotator low loss single mode fibres, MCVD fabrication 7-25993
- isolator, simple compact high performance permanent magnet 7-31437
- modulated grid Faraday cup plasma instruments, response function 7-23972
- modulator, magneto-optic, highly efficient low field (French) 7-5989
- multimode optical fibre probe in Z-pinch plasma expt., Faraday rotation 7-11785
- optical fibre sensor, calibrated, as Faraday rotation current and magnetic field sensor 7-31515
- plasma diagnostics appl. of optically pumped FIR lasers 7-5877
- pulsars, Faraday rotation meas. on 163 objects 7-66648
- radio sources, extragalactic, rot. measure vars. rel. to small-scale variations in galactic mag. field 7-29524
- twisted optical fibre, Faraday rotation meas. using rotating polarisation and analogue phase detect. 7-25981
- two-dimensional electron system, Faraday rotation, quantisation 7-3027
- waveguide-type optical isolator using the Faraday and Cotton-Mouton effects 7-31464
- YIG:Ca films, magneto-optical props., reducing treatment effects 7-64617
- Bi_{3-2x}Ca_{2x}Fe_{3-2x}V_{2x}O₁₂, sublattice magnetisation and Faraday rotation (Chinese) 7-17308
- Bi₃(GaFe)₂O₁₂, epitaxial films, mag. and magneto-optical props. 7-53102
- Bi₂Lu₂Y_{3-2x}Fe_{2x}O₁₂, ferrimagnetic garnets characterisation for MSW optical diffr. 7-13040
- Cd_{1-x}Mn_xTe, frequency-dependent Faraday rotation 7-22225
- Cd_{1-x}Mn_xTe, interband Faraday rot. meas. 7-39093
- DyIG:Ga,Bi, RF sputtered films for magneto-optical memory, mag. props. 7-64613
- FeCO₃, antiferromag., magneto-optical determ. of exchange parameters (Russian) 7-53283
- Fe₄₀Ni₄₀B₂₀ amorphous thin films, coercive field, annealing effects 7-7553
- Fe₂O₃ films, mag. anisotropy and magneto-optical props. 7-2910
- Gd-Co(Fe)(CoFe) alloys, amorphous thin films, Faraday rotation 7-64612
- Gd_{3-x}Bi_xFe₂O₁₂ crystal growth for 0.8 μm optical isolator 7-57605
- GdIG, Faraday effect meas. 7-64616
- Hg_{1-x}Mn_xTe, semimag. semicond., magneto-optical study of spin freezing 7-7678
- K₂O-Al₂O₃-B₂O₃-Fe₂O₃-Gd₂O₃ glasses, mag. props., composition dependences 7-2823
- SiO₂, crystalline, optical activity and Faraday rotation comparison, band gap determ. 7-3017
- SmIG, low temp. evolution of Faraday rotation 7-64615
- StF₂:Tm²⁺, optically detected low-field ESR, cross-relaxation effects 7-33301
- Tb-Co amorphous films, magneto-optic props. 7-64611
- TbCo sputtered films, mag. and magneto-optic props., stability 7-53076
- YIG, epitaxial layers, Faraday rot. meas., Bi and Pb ion contribs. 7-53071
- YIG, FZ growth for magneto-optic devices in fibre-optic communication systems 7-27892
- YIG, ferrimagnetic garnets characterisation for MSW optical diffr. 7-13040
- YIG:Ga, Bi, RF sputtered films for magneto-optical memory, mag. props. 7-64613
- (YSmLuCa)₃(FeGe)₂O₁₂, epitaxial films, Faraday rot., Sm³⁺ conc. effect. 7-53070
- Zn_{1-x}Mn_xTe, interband Faraday rot. meas. 7-39093

Faraday rotation see Faraday effect

farming

- large-scale heat accumulation at low temp. for domestic, industrial and farm heating (Portuguese) 7-13931
- solar-heated farm buildings, short-term monitoring and computer aided performance 7-28413

fast Fourier transforms

- astronomical radiotelescope patrol instrument using FFT processor as a 'digital lens' 7-47709
- composite plate, spectral analysis of natural grid features for surface analysis 7-63096
- DLTS, computer-controlled capacitance transient characterisation 7-18805
- dynamic stress intensity factors, meas. using FFT analyser, appl. to drop weight impact three-point bend testing (Japanese) 7-59712
- EM problems soln. using FFT with conjugate gradient method 7-10812
- EMG, real-time FFT to monitor muscle fatigue 7-28734
- EMG from human first dorsal interosseous muscles, Fourier and factor analysis 7-8545
- magnetotelluric sounding of Earth struct., Rayleigh-fast Fourier transform method 7-9181
- Mossbauer unresolved spectra with multiple convolutions, FFT-based processing 7-38972
- multiple-stripe-geometry laser arrays, chirped and unchirped, modal eigenfunctions 7-57335
- optical crossbar signal processor 7-25722
- optical wavefront estimation from difference meas. using discrete Fourier transform 7-31255
- protein structure, restrained least-squares refinement, incorporation of fast Fourier transforms 7-54451
- radio astronomy, wideband very fast FFT spectrum analyzer 7-47710
- seabed topography meas. by multibeam sonar 7-66327
- stellar spectroscopy, image processing by FFT (French) 7-14499
- STEM focused electron probes, Fourier analysis 7-18934
- thermal imager performance meas., objective meas. of minimum resolvable temp. difference 7-30092
- third heart sound in children, spectral anal., comparative study of max. entropy method and FFT 7-65818
- transient heat transfer in porous media—a two-temperature model 7-16181
- US 3D C-scan imaging using holographic reconstruction 7-43546
- US pulse diffraction in lossless media, Fourier domain calc. 7-1306
- wind scatterometer antenna release shock loads 7-23976
- Al, high purity samples, Doppler-broadened positron annihilation spectra, fast Fourier transform/power spectra deconvolution method 7-33481

fast ion conductors see superionic conducting materials

fast-response computer systems

- nuclear power plant emergency response and security system 7-42141

fastening see joining processes

fatigue

for thermal fatigue see "thermal stress cracking"

see also corrosion fatigue; fatigue cracks; fatigue testing

- Alloy 800 H, high temp. fatigue, damage mechanism (German) 7-17604
- austenitic stainless steels, fatigue props., time-depend modes, dislocation concepts appl. 7-28128
- brittle materials, contact flaws, strength, lateral crack growth effects 7-8091
- brittle materials fatigue data statistical analysis 7-17636
- ceramics, bending fatigue, room temp. (Japanese) 7-13597
- ceramics, microfracture prediction via microcontact model 7-16678
- ceramics, static and dynamic fatigue (Japanese) 7-46619
- ceramics, static-fatigue limit of materials containing small flaws 7-39620
- cermets, structural materials, cyclic strength 7-59624
- composite materials, fatigue life and residual strength, lognormal distribution model 7-17616
- crack growth rate dispersion rules 7-17615
- cumulative fatigue damage analysis re-examination 7-53836
- damage cumulation, self-similarity for different loading conditions 7-20658
- damage detection by position-sensitive detector, X-ray diffr. profile singularity change (Japanese) 7-8236
- damage process, thermometric investig. (German) 7-3439
- defects, stress- and fatigue-induced, small angle neutron scatt. studies 7-58273
- epoxide resin composites, particulate filled, static fatigue, time to failure predictions 7-13562
- failure at stresses below fatigue limit 7-38102
- failure criterion of mixed model 7-57750
- failure model, crack initiation and propag. 7-1499
- fibre reinforced composites, random short fibre, fatigue damage evolution assoc. with anisotropic elastic prop. changes 7-44673
- fibre reinforced plastics, fatigue (Japanese) 7-46619
- frequency dependence of fatigue strength criterion 7-22810
- glass fibre reinforced epoxy, fatigue life and static strength, statistical study 7-39618
- glass fibre reinforced polyester laminates, fatigue tests 7-3428
- graphite fibre reinforced epoxy laminates, fatigue damage mechanisms and residual props. 7-44671
- hard alloy, cyclic cracking resist. determ. method 7-13682
- IN738LC, Ni base superalloy, low cycle and thermal fatigue, small crack initiation and growth (Japanese) 7-13567
- laminates, centrally notched, residual strength determ. (Chinese) 7-13557
- life prediction, new method, high temp. low cycle conditions 7-39797
- life prediction accuracy for various loading spectra, improvement by use of correction factors 7-22788
- life prediction and crack initiation assessment of concepts 7-46649
- life prediction for Gaussian random loads at design stage 7-39623
- LMFBR, French creep-fatigue design rules 7-49522
- LMFBR class 1 components, design rules and elastic creep-fatigue damage evaluation 7-49540
- local approach of fracture, continuum damage mechanics 7-50988
- macrocrack initiation at stress raisers 7-13547
- Markovian processes for examining fatigue life, appl. of theory 7-32560
- materials fatigue behaviour, influencing factors (Japanese) 7-39642
- mechanics of damage and fatigue, conf., Haifa, Israel (Jul. 1985) 7-48139
- mechanics of solids—equivalent response of structure under cyclic loadings (French) 7-63006
- metal, cyclic hardening, hardening law and fatigue damage 7-58400
- metal surfaces, ion implanted, durability 7-53918

fatigue continued

metallic materials, high strength, life time prediction in creep-fatigue interaction regime (*German*) 7-53905
 metallic sliding friction, fatigue wear mechanism 7-8135
 metals, fatigue deformed, stimulated electron emission kinetics (*Russian*) 7-3156
 metals, fatigued, dislocation patterning, labyrinth structures, rotational effects 7-38009
 metals, FCC, cyclic deform., dipolar wall spacings in dislocation struct. 7-53825
 nonequilibrium statistical theory, microscopic mechanism 7-57760
 nonequilibrium statistical theory of fatigue fracture 7-63737
 notched specimens, fatigue threshold 7-20652
 notches, non-damaging 7-38103
 notches, permissible, size calc. for cyclically loaded bodies 7-8103
 optical fibre strength, dynamic and static fatigue 7-50769
 optical fibres, strength and fatigue, Weibull probability function 7-62842
 phenolic resin composites, optimisation for friction materials 7-39475
 plastic strains in stress conc. zone under static and cyclic loading 7-26846
 plate, elliptically notched semi-infinite, fatigue limits of crack initiation and propag. 7-1500
 polyaminobismaleimide resin, dynamic recovery and embrittlement 7-38108
 polyester fibres, fatigue and creep failure under cyclic loading 7-28110
 polyethersulphone, temp.-dependent mech. behaviour, use as matrices for short fibre reinforced laminates 7-17620
 polyimide, temp.-dependent mech. behaviour, use as matrices for short fibre reinforced laminates 7-17620
 pressure vessels, high temperature life prediction, computer modelling anal. 7-3391
 reactor construction codes and engineering mechanics conf., Paris, France, Aug. 1985 7-48153
 resinoid bonded abrasive materials, cyclic fatigue and reliability 7-17630
 rubber, containing inhomogeneous inclusions, tensile and fatigue fracture surfaces, fractographic investig. 7-13565
 shape memory alloys, ageing and thermal cycling effects 7-3336
 sialon, commercial, static fatigue and creep resist. 7-59601
 solids with microcracks, fatigue failure self-similarity, static thermodynamics 7-31706
 steel, alloy type, low-C, tempering temp. effect on mech. props. and crack resist. 7-39654
 steel, austenitic stainless, cold-worked, irradi. and unirradi., liq. Cs, Te-induced fatigue embrittlement 7-46637
 steel, austenitic stainless, dislocation structure and secondary cyclic hardening at 600°C 7-33783
 steel, austenitic stainless, FBR material, crack propag. under creep-fatigue interaction condition 7-22837
 steel, austenitic stainless, high cycle fatigue props., age hardening 7-13598
 steel, austenitic stainless, low cycle fatigue damage, crack initiation (*Japanese*) 7-33780
 steel, austenitic stainless, low-cycle fatigue, 350 to 550°C, microstruct. developments, effect on cyclic strength and life 7-39646
 steel, C, laser treatment on fatigue and wear resistance 7-39672
 steel, C, low-cycle fatigue, expt. and anal. (*Chinese*) 7-13556
 steel, C and alloy, rolling contact fatigue, asperity interacting frequency effect 7-39616
 steel, case hardened, struct. and contact endurance after plastic surface deform. tempering effect 7-46706
 steel, constructional carbon type, original charge purity influence on microstruct. hardenability and mech. props. 7-46521
 steel, Cr-Mo, cyclic softening, creep and fatigue, fusion reactor appls. 7-53757
 steel, Cr-Mo, cyclic stress-strain response at elevated temps. 7-39624
 steel, Cr-Mo-V, bainitic, high strain amplitude fatigue, cyclic stress and diametral strain response 7-39643
 steel, Cr-Mo-V, multistep cycling and cycling with compression hold at elevated temps. 7-13576
 steel, Cr-Mo-V, porosity assoc. with insoluble carbides, probable effect on rolling contact fatigue 7-17639
 steel, CR-Mo-V, thermal fatigue resist., effect of initial struct. 7-28132
 steel, Cr-Ni-Co VKS6, struct. and mech. characts., effects of Ni, Co and heat treatment 7-8108
 steel, cyclic fracture toughness, evaluated by use of concept of specific fracture work 7-28129
 steel, fatigue, criterion for omission of variable amplitude loading histories 7-22794
 steel, fatigue, microstruct. changes, thermometric assessment (*German*) 7-17641
 steel, fatigue fracture surface at elevated temps., X-ray fractographic study (*Japanese*) 7-8098
 steel, fatigue lifetime measurements for random loading in very high cycle range 7-22790
 steel, fatigue resistance under combined effect of cyclic bending and cyclic torsion 7-28131
 steel, fatigue threshold, effective, influencing factors 7-46607
 steel, finite-pearlite and austenitic, fractographic characts. of fatigue crack development 7-46643
 steel, hardened and tempered, struct. aspects of cyclic crack resist. 7-17613
 steel, heat-resistant, N and V influence on mech. and service props. 7-8105
 steel, high-speed, cast and wrought, impact-fatigue strength 7-39656
 steel, HSLA, electron channelling line width degradation, dependence on deform. mode 7-39613
 steel, low C, fatigue fracture surface, plastic deform., X-ray diffr. study (*Japanese*) 7-8097
 steel, low-C, cost, failure micromechanism in fatigue crack propag. after different heat treatments 7-46641
 steel, martensitic, tempering after surface plastic deform. effect on damageability in cyclic loading 7-46705
 steel, mild, cold-form-rolled, rotary bending fatigue behaviour (*Japanese*) 7-53866
 steel, Mn, fatigue resist., effect of Mo and V alloying, carbide precip. 7-8109
 steel, Mn, medium carbon, gas cylinder, fatigue behaviour (*Chinese*) 7-3411
 steel, Mn-Cr, case carburising, mech. props., influence of inclusion characts. 7-65135
 steel, N alloyed, mech. prop.-struct. relationship 7-3316

fatigue continued

steel, Ni-Cr A286, crack initiation and propag. characts. under high-temp. fatigue 7-22834
 steel, Ni-Cr A286, high-temp. fatigue strength characts. 7-22835
 steel, Ni-Cr-Mo-V, for turbine disc, fracture mechanics anal. 7-13589
 steel, pressure vessel with surface fatigue cracks, leak-before-break failures analysis 7-65141
 steel, roll type, crack resist. as criterion of effectiveness, alloying and heat treatment parameters influence 7-53884
 steel, Si-Mn, sintered, mech. props. (*German*) 7-22831
 steel, spring, residual stress meas., effect of decarburisation, shot peening and cyclic torsion loading (*German*) 7-22904
 steel, stainless, austenitic, low-activation, constitution, struct. and mech. props. 7-42195
 steel, stainless, type 316, neutron damage USA-Japan studies 7-56834
 steel, stainless, type 316L, fatigue in simulated fast reactor environments 7-39759
 steel, structural, micromechanisms of near-threshold fatigue crack propag. 7-13551
 steel, tool, heat treatment cycles, original struct. and deform. influence on mech. props. 7-39560
 steel beams, H-shaped, hysteretic and low cycle characts. under static and dynamic loadings (*Japanese*) 7-31694
 steel filaments, fatigue failure signs 7-46642
 steel weld joint, austenitic surfacing-pearlitic transition zone, cyclic crack resist. 7-17691
 steels, C, Cr, Cr-Mo, fatigue, statistical anal. of pooled S-N data 7-65136
 steels, Cr-Mo-Al, plasma-nitrided, fretting fatigue strength (*German*) 7-33848
 steels, creep-fatigue cracks, high temp., strain range partitioning anal. (*Japanese*) 7-33781
 strain criterion of fatigue failure 7-22943
 strain fields under low-cycle loading, use of isoparametric elements 7-26222
 strip with hole, fatigue resist., effect of multiple local plastic deform. 7-59625
 superalloy single crystals, directional solidification, mech. anisotropy, fatigue, creep 7-3293
 surface roughening of fatigued metals by random irreversible slip 7-2313
 TDF reaction chamber, fatigue lifetime analysis 7-25200
 Zircaloy-4, low cycle deform. at elevated temps. 7-22832
 Al alloy, crack growth rate dispersion rules 7-17615
 Al alloy, fatigue life predictions under complex loading (*Chinese*) 7-46594
 Al Alloy, fatigue macrocrack initiation at stress raisers 7-13547
 Al alloys, liquid dynamic compaction, microstruct. and precipitation, TEM study 7-59529
 Al, fatigue, dislocation mobility (*French*) 7-13539
 Al, fatigue cycling, oscillatory variation of half-width of X-ray diff. line profiles 7-46645
 Al single crystals, cyclic deform. at low const. plastic strain amplitude 7-65114
 Al-Cu-Li, 2020, low-cycle fatigue, effect of environment and temp. 7-28117
 Al-Cu-Li alloys, cyclic fracture, mechanisms 7-46634
 Al-Cu-Mg alloy D16T, endurance over wide range of stress variation 7-22811
 Al-Li-Mn (Cu), precip.-hardened, cyclic stress response and deform. behaviour 7-22791
 Al-Mg-Mn, fatigue, criterion for omission of variable amplitude loading histories 7-22794
 Al-Si-Cu castings, fatigue strength improvement by shot peening (*Japanese*) 7-8100
 Al-Zn, fatigue particle coarsening, vacancy creation 7-53895
 Al-Zn-Mg-Cu-Ni-Zr, modified 7075, prod. by liq. dynamic compaction, struct. and props. 7-46437
 Al₂O₃ ceramics, microstruct.-mech. prop. relationship 7-65147
 Au wires, very thin, fatigue 7-39671
 C fibre reinforced epoxy, failure in static and fatigue loading 7-17632
 C fibre reinforced plastic laminate; impeding edge-delamination development effect on tension-tension loading (*German*) 7-22827
 C steel, environmental fatigue stress rules appl. to reactor piping 7-13600
 Co-Cr surgical implant alloy, mech. props., effects of N additions 7-59573
 CrMoV ferritic steels, He containing, fatigue behaviour in fusion reactor 7-56828
 Cu bicrystals, fatigued at high temp., microstruct. obs. in vicinity of cavitated grain boundaries 7-38019
 Cu, cyclic stress-strain behavior of single- and {111} multiple-slip-oriented single crystals 7-26845
 Cu, fatigue near surface indentations and pits, deform. 7-46628
 Cu, near-threshold fatigue crack propag. and high cycle fatigue 7-13545
 Cu, polycrystalline, high cycle fatigue behaviour, effect of grain size 7-46626
 Cu wires, very thin, fatigue 7-39671
 Cu-Al-Ni, shape memory alloys, polycrystalline, cyclic deform., fatigue above transform temp. 7-3434
 Cu-Al-Ni shape memory alloys, polycrystalline, cyclic deform. and fatigue above transform temp. 7-3433
 Cu-Co (2 at.%), age-hardened, fatigue behaviour 7-33786
 Cu-Co (2 at.%), underaged, fatigue props., comparison of single crystals and polycrystals. (*German*) 7-46648
 Cu-Sn, low cycle fatigue damage, crack initiation (*Japanese*) 7-33780
 Fe, cast, alloyed, pearlite, flake graphite, thermal fatigue resist. 7-46606
 Fe-Ni-Cr (25.15 wt.%), MC stabilized, fatigue life, effects of implanted He 7-53852
 Mg-Y alloy, IMV6, fatigue crack growth and fracture microrelief, 293 and 140K 7-17614
 Mo, TiC coated, low cycle fatigue behaviour 7-53848
 Na₂O-CaO-SiO₂ glass, dynamic fatigue, indentation flaws, surface treatment 7-46629
 Nb single crystals, cyclic deform., dislocation behaviour 7-63729
 Ni alloy, surface plastic deformation by microballs, low-cycle damage 7-17698
 Ni, dislocation arrangements in single crystals fatigued at low temps. 7-12068
 Ni, faceted fatigue fractures, occurrence 7-53879
 Ni, fatigue cycling, lattice defect characterisation 7-37978

fatigue continued

Ni, fatigue life in const. mag. field and ultrasonic field, 4.2-273K (*Russian*) 7-46639
Ni, fatigued, crystal defects, positron annihilation studies 7-46213
Ni, mag. props., influence of low-temp. US deform. (*Russian*) 7-53878
Ni superalloy, Mar-M247, high-temp. fatigue crack propag. characts. 7-22736
Ni-base alloy, (Nimonic 75), creep-fatigue interaction, SEM and TEM studies (*Chinese*) 7-13543
Ni-base superalloy, single cryst., MAR-M200, with bimodal γ' distrib., low cycle fatigue at 750 and 870°C 7-17627
Ni-base superalloys, fatigue endurance at high temps., influence of struct. and surface oxidation 7-59626
Ni-base wrought superalloy, thermal fatigue resist. improvement by laser-glaze 7-22840
NiCoCrAlV, plasma sprayed coatings, low cycle fatigue behaviour 7-22793
Pb-Sn (2 wt.%), high temp. fatigue, dynamic recrystallisation 7-39667
 α -SiC, static fatigue limit at elevated temps., thermodynamics 7-17629
SiC whisker reinforced Al alloy, fabrication and props. 7-53680
Si₃N₄ ceramics, hot pressed, fatigue test with Knoop indentation, residual stress effects (*Japanese*) 7-17640
Si₃N₄, sintered, fatigue strength under rotary bending 7-65128
Si₃N₄, sintering, under rotary bending, mirrorlike region of fractured surface (*Japanese*) 7-3436
 β -Ti alloy, springs, design and mech. props. 7-46630
Ti-Al-Cr-Mo alloy VT3-1 mech. props. depend. on decomp. product morphology for metastable phases 7-39655
Ti-Al-Fe, mech. props., investg. as implant material (*German*) 7-46647
Ti-Al-Mo-Cr alloy, VT3-1, cooling regimes in heat treatment effect on mech. props. 7-8026
Ti-Al-Mo-Cr alloy, VT3-1, vac. annealing of blanks after isothermal deform., hydrogen plasticising effect 7-8027
Ti-Al-Mo-V, fatigue failure resist., appl. of high-freq. loading methods 7-59627
Ti-Al-V (6, 4 wt.%), powder metallurgy, fatigue props. rel. to microstruct. 7-8096
Ti-Al-V PT3V pseudo- α -alloy, fatigue resist. at increased temps. 7-17611
Ti-Al-Zr, IMI 829, low cycle fatigue 7-22792
Ti-Al-base alloys, fatigue failure resist., appl. of high-freq. loading methods 7-59628
Ti-base alloys, high-cycle fatigue damage, predicting onset, engng. appl. for long crack fatigue threshold data 7-22789
Ti-Mn, alpha and beta phases, yield and tensile strength, ductility, Bauschinger behaviour, fatigue life, crack propag. 7-8052
W-Cu bond, mechanical properties, fusion reactor divertor plate appl. 7-26848

fatigue cracks

Alloy 718, Ni-base superalloy, fatigue crack propag. under hold-time cycling, effect of grain size 7-28106
Astroloy, fatigue crack growth, closure anomalies 7-3403
bars, cylindrical, fatigue crack propag. 7-21346
closure behaviour, S-shaped unloading curve method (*Japanese*) 7-13684
closure behaviour, simulation by extended-body force, method (*Japanese*) 7-12199
compact tension specimen, J-integral functions for fracture and fatigue anal. 7-63055
composite laminates, fatigue and residual strength 7-44672
composite variability model for fatigue crack propag. rate (*Japanese*) 7-44677
computerized test system for thermal-mechanical fatigue crack growth 7-39801
crack growth life under random loads (*Chinese*) 7-1511
crack-tip field parameters for large and small fatigue cracks 7-11356
cyclic loading, crack growth rate, effect of different singularity fields 7-37381
cylinder, hollow, surface compression strengthened, stable crack growth 7-37385
elevated temperature fatigue crack growth under displacement control conditions 7-46608
epoxy polymers, compact tension specimen casting, fatigue crack growth rate testing 7-13681
estimation of fatigue crack length and closure/opening stress 7-43811
fibre reinforced composites, fatigue damage and degradation mechanics 7-11352
fibre reinforced composites, fatigue damage and degradation mechanics 7-11353
fleet tracking of fatigue damage, development of side-grooved crack gauge 7-57772
fracture life and fatigue crack growth rate under mixed mode loading (*Japanese*) 7-58406
fretting, spherical particle form., role of contact interaction of fatigue crack sides 7-3447
glass fibre reinforced polyester, random short fibre SMC, interlaminar fatigue crack growth interlaminar fatigue crack growth 7-33772
grain boundary oxidation and fatigue crack growth at elevated temps. 7-6714
graphite fibre reinforced epoxy laminates static or fatigue loading, fracture surface anal. (*German*) 7-22826
growth, dynamics factors (*Japanese*) 7-20657
growth, two element structural rheological model 7-16128
growth rate dispersion rules 7-17615
growth under general-yielding cyclic loading 7-11355
IN738LC, Ni base superalloy, low cycle and thermal fatigue, small crack initiation and growth (*Japanese*) 7-13567
incremental loading tests, effect of step size 7-39798
initiation at grain-boundary triple points in high-temp. deform., continuum mech. model 7-28104
intra-specimen variability model for fatigue crack propag. (*Japanese*) 7-51930
life prediction and crack initiation assessment of concepts 7-46649
local crack-tip strain approach to fatigue crack propag. 7-63057
macrocrack initiation at stress raisers 7-13547
mechanics of damage and fatigue, conf., Haifa, Israel (Jul. 1985) 7-48139
metal matrix composites, fatigue crack propag., effect of aq. environments 7-17624
metallic elements, cyclic local stress-strain and fatigue crack initiation life (*Chinese*) 7-46593
mode II fatigue crack test specimen, elastic analysis 7-1505

fatigue cracks continued

moire interferometry, crack tip displacement anal. 7-11367
nonequilibrium statistical theory of fatigue fracture, fatigue crack growth 7-39665
nylon-6,6, fatigue crack propag., temp. and absorbed water effect 7-39662
plastic strains in stress conc. zone under static and cyclic loading 7-26846
plasticity-induced crack closure, under plane strain conditions, finite element anal. 7-37379
PMMA, environmental fatigue, initiation of wavy striation (*Japanese*) 7-33814
polycarbonate, fatigue crack propag. and fracture toughness, specimen thickness and geometry influence (*German*) 7-3438
polycarbonate sheets, ductile fatigue crack propagation 7-11966
propagation for defects near free surface 7-57743
propagation model for random loading, stress ratio effect (*Japanese*) 7-12198
propagation rate, plastic deform. effect 7-13561
propagation site, determ. 7-58408
propagation under biaxial loading, anal. using inclined strip yield zone model of crack tip plasticity 7-43771
reactor bend pipes containing surface flaws, fatigue test results (*Japanese*) 7-56755
reactor pressure vessels, fracture mechanics of cracks under cyclic thermal shock 7-10218
scatter of fatigue crack growth rate, new model 7-43777
slow fatigue crack growth under step and random loading 7-17642
small, statement of problem and pot. soln. 7-32558
small fatigue crack growth at notch root in elastic-plastic region (*Japanese*) 7-58404
spherical particles formation, rot. deforms. role 7-17612
stage II fatigue crack growth behaviour of granular bainitic microstructures 7-28134
statistical analysis of growth data 7-16115
steel, 0.45% C, surface fatigue cracks, growth and threshold characts. 7-17607
steel, 18 Ni maraging, corrosion fatigue crack initiation and growth 7-3413
steel, austenitic, Mn-Cr, fatigue crack growth behaviour 7-59593
steel, austenitic stainless, crack tip cyclic plastic work, load ratio, frictional work 7-53897
steel, austenitic stainless, creep rupture, fatigue cracking in flowing liq. Na 7-53843
steel, austenitic stainless, fatigue crack growth in FBR castings and weldments, fast neutron irradiation effects 7-28127
steel, austenitic stainless, FBR material, crack propag. under creep-fatigue interaction condition 7-22837
steel, austenitic stainless, low cycle fatigue damage, crack initiation (*Japanese*) 7-33780
steel, austenitic stainless, near-threshold fatigue crack growth and crack closure under creep conditions (*Japanese*) 7-59616
steel, austenitic stainless, notch effect in low-cycle fatigue at elevated temps., life prediction 7-53899
steel, austenitic stainless, small fatigue cracks, threshold behaviour at notch root 7-3395
steel, austenitic stainless, tensile, creep and low-cycle fatigue props., effect of prestrain (*Japanese*) 7-46621
steel, C, fatigue crack growth behaviour at US freq., influence of temp. 7-39622
steel, C, fretting fatigue, crack propag. behaviour 7-39615
steel, corrosion fatigue, crack initiation determ. (*German*) 7-3527
steel, Cr-Mo, tube, fatigue crack growth at high temp. 7-59632
steel, Cr-Mo, tube, high temp. press. fatigue testing 7-65246
steel, Cr-Mo-V, rail, fatigue crack growth 7-8114
steel, Cr-Ni-W, fatigue striation, macrocrack propag. (*Chinese*) 7-8074
steel, fatigue crack growth, influence of ambient environment 7-28107
steel, fatigue crack propagation rate, effect of overloads 7-59623
steel, ferritic, fatigue crack growth, transients due to change in ΔK or R 7-46646
steel, finite-pearlite and austenitic, fractographic characts. of fatigue crack development 7-46643
steel, heterogeneous microstruct., near-threshold fatigue crack propag. 7-46602
steel, high strength, modified HY 130, corrosion fatigue and electrochem. reactions 7-65201
steel, high strength, near threshold fatigue crack growth behaviour, effect of prior austenitic grain size 7-53906
steel, high tensile, HT55, ΔK_{th} testing method for plastic zone size at fatigue crack tip 7-17748
steel, low alloy, B-containing, near-threshold fatigue cracks 7-46605
steel, low alloy, fatigue fracture in air and 3.5% NaCl soln., X-ray fractography (*Japanese*) 7-8099
steel, low alloy, surface crack growth under axisymm. cyclic bending 7-28130
steel, low C, small fatigue crack growth, effects of microstruct. and limitations of linear elastic fracture mechanics 7-39625
steel, maraging, fatigue at low growth rates 7-39621
steel, microalloyed, fatigue crack propag., effect of short-term static overload 7-13573
steel, Ni-Cr A286, crack initiation and propag. characts. under high-temp. fatigue 7-22834
steel, Ni-Cr-Mo, ΔK_{th} testing method for plastic zone size at fatigue crack tip 7-17748
steel, Ni-Cr-Mo, pressure vessel, environmentally assisted fatigue crack growth 7-17638
steel, Ni-Cr-Mo, weldments, dynamic fracture toughness, split Hopkinson bar technique 7-13685
steel, pressure vessel, fatigue crack growth rates under various conditions of loading and environment 7-28203
steel, Si-Mn-Mo, austenitising, bainite transform., lump-like composite struct., mech. props. (*Chinese*) 7-13477
steel, small surface crack propag. 7-65142
steel, stainless, pipe, detection of configuration of surface fatigue crack by DC pot. drop method (*Japanese*) 7-59726
steel, took, Cr-Mo-V, hot working, ductility, C content, toughness, eutectic carbide segregation 7-59592
steel, welded, corrosion fatigue testing, NaCl conc. and test freq. effects (*German*) 7-8230
steel weldment defects, quantification techniques by US normal beam testing 7-16044

fatigue cracks continued

- steels, fatigue crack resistance, influence of stress conc. 7-33792
- stochastic loading and material inhomogeneity in fatigue crack propagation 7-43768
- stochastic modelling of crack growth based on damage accumulation 7-6715
- surface crack growth with regular and random loading processes 7-43785
- surface flaw, stress intensity distrib. and fatigue crack growth predictions 7-63075
- wear in rolling contact 7-22845
- Al alloy, corrosion effects on fatigue crack propagation 7-39628
- Al alloy, crack growth rate dispersion rules 7-17615
- Al Alloy, fatigue macrocrack initiation at stress raisers 7-13547
- Al alloy, life prediction for corrosion fatigue 7-39629
- Al alloy, small surface crack propag. 7-65142
- Al alloy A5083-0, ΔK_{th} testing method for plastic zone size at fatigue crack tip 7-17748
- Al alloys, fretting, fatigue crack growth, spherical particle form. 7-3445
- Al alloys, IN9021 and 7090, powder metallurgy, fatigue crack growth, influence of load ratio 7-28124
- Al-base alloy, IN-9021, fatigue morphology 7-39653
- Al-Cu-Mg, fatigue crack growth, closure anomalies 7-3403
- Al-Cu-Mg, fatigue crack propagation rate, effect of overloads 7-59623
- Al-Li-Cu-Zr, 2090, small fatigue crack growth 7-22817
- Al-Zn, 7075, fatigue life, size effect in randomly loaded specimens 7-22795
- Al-Zn-Mg, small fatigue crack growth from a keyhole notch 7-65133
- Al-Zn-Mg-Cu, fatigue crack propag., influence of microstruct. (German) 7-22833
- BE prototype limiter for JET, thermal fatigue tests, microcracking 7-5415
- CoCrAlY, sputter ion plated coatings for gas turbines 7-53971
- Cu, dislocation mechanism based model for stage II fatigue crack propagation rate 7-21338
- Cu, fatigue crack propagation rate model based on a dislocation mechanism 7-8093
- Cu, near-threshold fatigue crack propag. and high cycle fatigue 7-13545
- Cu, polycrystalline, multiaxial low cycle fatigue, crack initiation, slip bands, damage mechanics 7-53840
- Cu single crystals, fatigue crack size distrib. 7-38101
- Cu single crystals, fatigue crack initiation mechanism, persistent slip band model 7-53869
- Cu-Sn, low cycle fatigue damage, crack initiation (Japanese) 7-33780
- Fe, cast, nodular graphite, fatigue crack propag. rel. to microstruct., SEM obs. (Chinese) 7-13542
- Fe-Al-Mn, fatigue crack growth 7-65130
- Fe-Si (3 at.%), grain-oriented, fatigue crack growth, direct, real-time obs. (Japanese) 7-59615
- Na₂O-CaO-SiO₂ glass with subthreshold flaws, dynamic fatigue 7-8111
- Ni superalloy, Mar-M247, high-temp. fatigue crack propag. characts. 7-22836
- Ni-base wrought superalloy, thermal fatigue resist. improvement by laser-glaze 7-22840
- Ni-W-Co-Cr superalloy single crystals, fatigue crack propag. under multiaxial cyclic loads 7-28122
- NiCrAlTi, sputter ion plated coatings for gas turbines 7-53971
- SiO₂ silica fibre mechanical strength determ. (French) 7-11157
- Ti, plate, fatigue crack initiation in orthotropic materials, effect of stress freq. (Japanese) 7-53867
- Ti-Al-V (6, 4 wt.%), powder metallurgy, fatigue props. rel. to microstruct. 7-8096
- Ti-Al-V (6, 4 wt.%) plates, rolling, heat treatment, microstruct., mech. props., turbine blade appl. 7-17644
- Ti-Al-V (6, 4 wt.%), annealed fatigue crack growth in water, SEM fractography (Chinese) 7-8076
- Ti-Al-V (6, 4 wt.%), powder metallurgy, thermomechanically treated, deform. behaviour 7-53908
- TiC/TiN double layer coated cemented carbide milling tools, wear mechanisms 7-53932
- TiC(N) coated cemented carbide milling tools, wear mechanisms 7-53932
- WC-Co cemented carbides, compression fatigue crack growth 7-28119

fatigue failure *see* **fatigue**

fatigue fracture *see* **fatigue**

fatigue life *see* **fatigue**

fatigue testing

- for corrosion fatigue testing, see corrosion testing*
- acoustic emission use for investig. of regularities of unstable crack development 7-22962
- computer-controlled fatigue apparatus for testing in UHV and controlled environments 7-39811
- computerized test system for thermal-mechanical fatigue crack growth 7-39801
- crack closure behaviour, S-shaped unloading curve method (Japanese) 7-13684
- creep-fatigue life, long-term, prediction and evaluation 7-39796
- cumulative fatigue damage analysis re-examination 7-53836
- endurance of specimens with small cracks, method and calibration 7-22946
- epoxy polymers, compact tension specimen casting, fatigue crack growth rate testing 7-13681
- frequency dependence of fatigue strength criterion 7-22810
- glass, dynamic fatigue limit, determ. method 7-8221
- hard alloy, cyclic cracking resist. determ. method 7-13682
- incremental loading tests, effect of step size 7-39798
- metal fatigue testing system, microcomputer based 7-46749
- optical fibre strength, break detect. in mandrel static fatigue process 7-50769
- plastic strain-limit control in cyclic deformation testing using servohydraulic testing machine 7-28233
- R-curve, effect of initial fatigue crack applic. conditions and crack length meas. method 7-22945
- reactor piping systems, cycle-dependent material props. 7-10222
- solar cell interconnector fatigue simulation testing, satellite appl. 7-13873
- steel, Cr-Mo, tube, high temp. press. fatigue testing 7-65246
- steel, welded, corrosion fatigue testing, NaCl conc. and test freq. effects (German) 7-8230
- strain criterion of fatigue failure 7-22943
- Al-Zn, 7075, fatigue life, size effect in randomly loaded specimens 7-22795

fatigue testing continued

- C steel, S45C, fretting fatigue damage accumulation, cycle and stress ratio effect 7-28232
- Si₃N₄ ceramics, hot pressed, fatigue test with Knoop indentation, residual stress effects (Japanese) 7-17640
- fault currents**
see also **flashover**; **leakage currents**; **overcurrent**; **short-circuit currents**
- flat plate steel conductor impedance to earth fault currents 7-62582
- fault location**
NDT of materials, subsurface control by photothermal radiometry 7-33898
- optical components microscopic inclusions location, automatic inspection device using Q-switched YAG laser 7-31544
- optical fibre fault location using He-Ne laser 7-31545
- optical fibre OTDR, range and accuracy in backscatter measurements 7-15999
- optical fibres, fault location using step frequency method 7-57558
- OTDR for single-mode fibre using P₂O₅ doped fibre Raman laser 7-31517
- fault tree analysis** *see* **failure analysis**; **reliability theory**
- faults, electrical** *see* **electrical faults**
- FDM** *see* **frequency division multiplexing**
- feature extraction** *see* **pattern recognition**
- feedback**
see also **control systems**
- air boundary layer, active transition fixing and control 7-31740
- artificial limbs, feedback in design 7-34345
- asymmetric quarter-wave-shifted DFB semiconductor lasers 7-10990
- automatic focus control for head alignment 7-5968
- bond graph model of a pool-type nuclear reactor 7-5438
- chemical kinetics, time delay effects in rate processes 7-39849
- coal dust flame acceleration, feedback control model for unsteady flow 7-65326
- delay-differential systems, chaos, statistics and dimensions 7-48572
- dielectrophoretic levitation, active feedback-controlled 7-3596
- double-channel planar BH multimode laser, 1.55 μ m fibre grating external cavity, single-mode behaviour 7-15908
- dynamical system with delayed feedback (Chinese) 7-35263
- electrodynamical drive of Mossbauer spectrometer, controller design 7-35508
- functional neuromuscular stimulated hand orthoses, sensory feedback using electrodes fitted to shoulder 7-34354
- grasp control during functional neuromuscular stimulation, force/position feedback 7-28764
- haemodynamic control systems, closed loop identification 7-60027
- inertial clock based on computer controlled servo-driven corotation system 7-14927
- jet flowmeter, medical instrumentation appl. (Bulgarian) 7-28740
- joint angle sensors for closed-loop control of movements in paraplegics 7-28766
- katharometer bridge circuit with linearising feedback 7-17840
- multichannel bolometer for radiation measurements on the TCA tokamak 7-20943
- nuclear power plant cascaded state feedback control 7-56776
- optical all fibre magnetometer with mag. feedback compensation 7-25989
- optical components manufacture, temperature control techniques 7-31541
- optical figure generation using feedback from IR phase-shifting interferometer 7-37219
- optical gain meas. in discharges, spontaneous emission amplification obs. 7-14989
- passive underwater tracking with nonlinear feedback, convergence anal. 7-31557
- pictorial nonlinear feedback, chaos, cooperation and quantised feedback 7-42947
- pictorial nonlinear feedback, chaos, cooperation and stability 7-42946
- pictorial nonlinear feedback, chaos and cooperation 7-42945
- planar musculoskeletal model for studying posture induced by functional neuromuscular stimulation 7-28574
- prosthetic sensory feedback system, open- and closed-loop models 7-54814
- self-balancing resistance bridge 7-35539
- sensory feedback in upper limb prostheses, robotics perspective 7-34347
- shoulder position evaluation for quadriplegics using neural prosthetic devices 7-28779
- solar collector/heat exchanger system, differential game control 7-65578
- soliton laser stabilisation, feedback from pulse-shaping fibre 7-50602
- Space Infrared Telescope Facility, Space Shuttle-based, active image stabilization 7-9377
- Tokamak device, feedback control, stable region (Chinese) 7-37714
- upper extremity prostheses with sensory feedback 7-34346
- Nd:YAG mode locked laser, timing fluctuations reduction by electronic feedback 7-31371

feeds, antenna *see* **antenna feeders**

FEL *see* **free electron lasers**

FEM *see* **field emission electron microscopy**

Fermi-Dirac statistics *see* **quantum statistical mechanics**

Fermi energy *see* **Fermi level**

Fermi gas *see* **fermion systems**

Fermi level

- alloys and metals, packing defect energy rel. to electron density (Russian) 7-45212
- binary compound polar semiconductors with nonparabolic energy bands, electronic struct. 7-2478
- chalcogenide glasses, electrons in mobility gap, spectra and thermodynamic props. 7-2471
- chemisorption, substrate impurity effects 7-63964
- crystal lattice, internal pot. w.r.t. electron work function 7-63545
- Curie temp. calcs. long range magnetic order and intermediate valence, Anderson model 7-45247
- d- and f-metals and alloys, anomalous props. due to charge density fluctuations 7-7132
- deformable jellium model, electronic density of states calcs. 7-64044
- disordered 1D systems of localised states, single-particle density of states Coulomb gap calcs. 7-58777
- grain boundary trap occupancy and recomb. models anal. 7-64266
- graphite:B-Na intercalation cpd., Fermi level displacement, diamag. anisotropy and Hall effect meas. 7-16933
- graphite intercalation compounds, first stage, with heavy alkali metals, electronic props. 7-2463

Fermi level continued

graphite-HNO₃ intercalation cpds., absolute Pauli spin suscept. meas., Fermi level density of states determ., ESR/NMR method 7-12940
heavy electron superconductors, normal impurity effects; excitation spectrum 7-27462
heavy-fermion metals, electronic spectral density, periodic Anderson model 7-7087
hierarchical lattices, phase transition universality sputtered, photoelec. props. 7-35486
III-V semiconductor quantum well structures, destruction mechanism due to impurity diffusion 7-63971
III-V semiconductor surfaces, virtual gap states and Fermi level pinning by adsorbates 7-2654
metal, universal conductance fluctuations, effects of finite temp., interactions and mag. field 7-64196
metal hydrides, electronic density of states from press.-composition isotherms 7-7088
metal-semiconductor interface, unified disorder induced gap state model 7-2656
mixed valent compounds, electronic properties, theory 7-21880
nonmagnetic metallic glasses, negative TCR and electronic struct. studies 7-52562
one-dimensional periodic Anderson Hamiltonian, effect of disordered conc. nonmagnetic impurities 7-27517
p-n junction, boundary conditions at high injection level in space charge region 7-17091
trans-polyacetylene, random soliton distrib., localisation and density of states calcs., renormalised virtual cryst. method 7-52453
s-dimensional semiconds., Fermi energy, relativistic corrections, free-Fermi-gas model calcs. 7-2465
semiconductor epitaxial layers, sharp doping profiles determ. 7-12111
semiconductors, ionised resonant donor and acceptor superlattice form., screened Coulomb interaction, carrier scatt. effects 7-16981
semiconductors, zero-gap, carrier temp. and density, nonequilib. fluctuations 7-38576
semimetals, high temp. kinetic coeffs. oscills., band struct. and magnetoresist. temp. depend. studies (*Russian*) 7-12738
transition metal alloys, disordered, localised and extended state coexistence 7-7175
transition metals, X-ray electron spectra asymmetry and Fermi level density of states (*Russian*) 7-3112
zero gap semiconductors near inversion point, solitons 7-64100
Ag-CdTe (100) interface, photoemission studies, surface struct., growth behaviour, Schottky barrier and surface photovoltage 7-39352
As₂Se₃/Ni films, electronic struct. and transport props. 7-12595
 α -As₂Te₃ films, hole transport investigation by transient field-effect and time-of-flight methods 7-22040
As_{2-x}Te_{3-x}In_{2x} and As_{20-x}Te_{80-x}In_{2x} systems, chalcogenides, thin films, optical and electrical props. 7-27446
Au-GaAs, Schottky contact, interface states, trap characterisation 7-27421
Au-GaAs (110) interface; photoemission studies, temp. effects 7-33517
BaPb_{1-x}Bi_xO₃, electronic struct., photoemission studies 7-59375
Bi, effective electron mass, quasi-1D systems, theoretical investig. 7-2468
Bi, ultrathin films, size quantization effect on effective electron mass 7-38778
Bi-Ge-S chalcogenide glasses doping mechanism and structural effects, EXAFS study 7-1909
C films, plasma deposited from methane, elec. conductivity, optical absorpt. 7-38786
Cd_{1-x}Hg_x alloys, electronic structure dependence on crystal lattice parameters 7-45141
CdS inversion layers, carrier effective mass calcs. 7-64055
CdSe, photogenerated high density electron-hole plasma, energy relax., rapid expansion 7-33039
Ce, core and valence photoemission, calc. 7-33516
Ce metallic systems, valence band photoemission spectra anal. 7-13332
CeCu₆ heavy fermion system, photoemission and inverse photoemission studies 7-3148
Co clusters, small, reactivity 7-15781
Co-Y alloys, low temp. sp. ht. study, crystalline and amorphous phases 7-52995
p-crystalline Si/n-amorphous Si heterojunction, electrostatic pot. barrier distrib. calcs. 7-58881
Cu:Mn(Cr) matrix, electronic struct. calcs. 7-16976
CuNi, substitutionally disordered, electronic struct., LCAO-CPA calcs. 7-64067
Fe-based liq. alloys, density of electron states, calc. (*Russian*) 7-45110
Fe-W (110), spin-resolved photoemission spectra of epitaxial Fe layers 7-46276
Fe₂P, electronic struct., mag. props., KKR, LMTO methods, LSD approx. 7-64070
GaAs (100), surface Fermi level unpinning in air using photochem. 7-2655
GaAs (110), O₂ adsorption, electronic props., contact pot. meas. 7-2353
GaAs (110), substrate for In growth, RHEED study 7-2425
GaAs LPE layers, heavily doped and compensated, hopping cond., density of states at Fermi level, carrier conc. determ. 7-2753
GaAs, MISS, common anion rule, density distrib., photoionisation 7-38765
GaAs Schottky-barrier formation and microscopic metal clusters 7-45497
GaAs, seminsulating LEC substrates, defect etching 7-59694
GaAs surface, Fermi level unpinning by flowing water 7-58843
GaAs-AuGeNi contacts, interface composition and barrier heights 7-58891
GaAs-metal interfaces, Fermi level pinning 7-2714
GaAs-Mn(V), extrinsic surface states, core level UPS study 7-2713
GaAs(110)-Al, Schottky barrier form., effect of surface and interface kinetics 7-2668
GaP, MISS, common anion rule, density distrib., photoionisation 7-38765
GaSb:Se, resist. and thermoelec. power meas. at metal-insulator transition 7-45403
Ge_{20-x}Se_{80-x}In_{2x} system, chalcogenides, thin films, optical and electrical props. 7-27446
HgCdTe, 0⁺ giant oscillation near semimetal-semiconductor transition 7-64053
Hg_{1-x}Cd_xTe, sputtered and cleaved surfaces, deposition of In and Al reactive metals, UPS study 7-33513
Hg_{1-x}Cd_xTe/Pt interface, overlayer-cation reaction, XPS, UPS and LEED studies 7-65349

Fermi level continued

Hg_{1-x}Mn_xTe, magnetoresist. meas., effect of valence band spectrum quantisation at low temps. 7-52653
HgTe-based solid solns., low temp. electron mobility, resonance scatt. 7-38558
I₂, solid, UPES and EHT calcs. 7-64870
InGaAs, MISS, common anion rule, density distrib., photoionisation 7-38765
In_{0.9}Ga_{0.1}As (100)-metal interfaces, Fermi level pinning and chem. interactions 7-2712
In_{1-x}Ga_xAs_{1-y}P_yTe films, Fermi energy, dopant conc. depend. 7-52867
InP (110) cleaved surface and Schottky diodes 7-58850
InP MIS structures, thermal treatment in P overpressure 7-7394
InP, MISS, common anion rule, density distrib., photoionisation 7-38765
InP surfaces, sputter etched, optoelectronic and structural props. 7-13661
InP:Ge, Fermi level, determ. from phase diagram data of InP-Ge system 7-21808
InP/Pd (110) interface, chem. reactions, overlayer morphology and Fermi level pinning 7-7020
InP-Au interface, Fermi level pinning, growth characts., photoemission spectra 7-22009
InP-metal interfaces, Fermi level pinning 7-2714
InP(110), P- and In-rich, electronic states, semi-empirical tight binding calcs. (*Chinese*) 7-12773
In_{1-x}Sn_x alloys, electronic structure dependence on crystal lattice parameters 7-45141
In₂Te₃Fe, Fe²⁺ elec. inactivity study, mag. suscept., Mossbauer spectra and XPS anal. 7-52494
KC₈ intercalation cpd., polarisation depend. XANES study 7-59298
KH_{0.8}C_x, polarisation depend. XANES study 7-59298
LaAg, nonmag. cpds., transport props. and electronic struct. 7-2575
Li₂Cr(Mn)(Fe)(Co)(Ni)O₂ electrode materials, electronic and electrochemical props., ion intercalation, electronic model 7-33945
LuAg, nonmag. cpds., transport props. and electronic struct. 7-2575
Mn₂P, electronic struct., mag. props., KKR, LMTO methods, LSD approx. 7-64070
MoN B1 phase sputtered films, mag. susceptibility and defect struct. 7-53087
MoS₂-Co catalyst-promotor interaction, UPS, XPS, LEED studies (*Chinese*) 7-39913
MoSi₂, band structure 7-27248
Mo₅SiB₂, supercond, investig. 7-22082
Na₂Cr(Mn)(Fe)(Co)(Ni)O₂ electrode materials, electronic and electrochemical props., ion intercalation, electronic model 7-33945
NaNO₂, Fermi level and relative density of states, temp. dependence 7-21795
NbC₂N_y, nonstoichiometric, supercond. transition temp. and band struct. (*Russian*) 7-58935
Nb₃Ir films, lattice-stiffness changes due to ion irradiation, Brillouin scatt. 7-52379
NbSe₂, 2H polymorph, electronic density of states, phase matching of CDWs, NMR study 7-64538
NbSe₂H_x, heat capacity, Debye temp., electron-phonon coupling, electronic contrib. meas. (*Russian*) 7-6820
Ni (100), adsorption of CO, poisoning in heterogeneous catalysis, role of electronegativity 7-13818
Ni, quasi-particle and band-calc. spectra, w.r.t. valence band photoemission meas. 7-2474
Ni-H system, band structure calcs. 7-45140
Ni_n (n=1 to 6) clusters, electronic struct., ab initio SCF and CI calcs. 7-10446
Ni₂MnIn(Sn)(Sb) Heusler alloys, galvanomag. props. and magnetisation meas., fermi level shift effects 7-7207
Ni_{1-x}P_x, amorphous glasses, electronic structure, calcs. 7-7101
Ni₂P, electronic struct., mag. props., KKR, LMTO methods, LSD approx. 7-64070
NiSi₂-Si, interface states, barrier height, Fermi level 7-27430
NiSi₂-Si, Schottky barrier, interfacial defect states 7-27428
NiSi₂-Si (111), Schottky barrier height, rel. to Fermi level positions 7-27427
NpO₂, radioactive layers, bremsstrahlen isochromat spectroscopy 7-39210
Pb₃O₄ thin film, electronic props., electrochem. technique characterisation 7-7416
Pb_{1-x}Sn_xTe:In, impurity levels, covalent defect theory 7-52515
PbTe, impurity levels, covalent defect theory 7-52515
PbTe:Ti(Ti,Na) films, superconducting transition 7-38797
Pd-B-H dilute solutions, statistical mechanics 7-21669
Pd-Si alloys, H absorption, structural disorder effects 7-52249
PdH_x, H-induced lattice expansion and effective H-H interaction 7-52247
PdSi₂-Si, interface states, barrier height, Fermi level 7-27430
Pt-Pb bimetallic systems, Fermi level density of states, XPS studies 7-46278
Pt-Sn bimetallic systems, Fermi level density of states, XPS studies 7-46278
Pt₃Ti (111), chemisorption induced surface core level shifts 7-22448
Si (111), ordered Au, Ag, Cu overlayers, surface states, inverse photoemission studies 7-2660
a-Si:H, glow discharge deposited, light soaking effects 7-52872
a-Si:H, recomb. at dangling bonds and steady-state photocond. Fermi level depend. calcs. 7-12734
a-Si:H/O films, RF sputtered, photoelec. props. 7-38627
a-Si:H CVD films, density of states distrib., I-V characts. meas. 7-45113
a-Si:H doping modulated multilayers, light-induced excess conductivity 7-38643
a-Si:H films, contact potential difference, surface photovoltage and conductivity 7-58855
a-Si:H films, metal-semiconductor contacts, characterisation 7-38724
a-Si:H multilayer films, charge transfer doping, cond., photocond. meas. 7-38735
Si:Mg(Be) metastable impurity levels, self-consistent local-density total-energy calcs. 7-38503
Si-Al Schottky barrier formation, local electronic struct., EELS study 7-21975
Si-InP (110) heterojunction, characterisation 7-33079
Si-polymer contact solar cell fabrication 7-23168
a-SiGe:H alloys for solar cells, electronic and optical props. 7-17899
Si_{1-x}Ge_xH amorphous alloys, electronic struct., soft X-ray and photoelectron spectra studies 7-27857
SiO₂, electronic structure, direct and inverse photoemission and soft X-ray emission spectra (*French*) 7-59374

Fermi level continued

- SiON-GaAs interface, plasma enhanced CVD deposited SiON, NH₃ plasma pretreatment effects 7-7874
 SnO₂ (110), O deficient surface, photoemission study, comparison with TiO₂ (110) 7-46277
 TaC_x, defect states, core level binding energy and valence band struct., XPS meas. 7-27291
 TiC, energy band struct., Fermi energy and density of states, vacancy states effects, LMTO-ASA calcs. 7-64078
 TiH_x, X-ray diffr., lattice parameter change, density of states 7-44469
 TiO₂ (110), O deficient surface, photoemission study, comparison with SnO₂ (110) 7-46277
 UBe₁₃, heavy fermion cpd., lattice dynamics, EXAFS study 7-64792
 URu₂Si₂, heavy fermion system, core levels and band struct., electron spectra studies 7-52418
 VC_x, energy band struct., Fermi energy and density of states, vacancy states effects, LMTO-ASA calcs. 7-64078
 W (110), thermal field emission and thermal photofield emission 7-7826
 YAg, nonmag. cpds., transport props. and electronic struct. 7-2575
 YAl nonmagnetic metallic glasses, negative TCR and electronic struct. studies 7-52562
 Y₂Co₇, electronic struct. and mag. props. 7-7104
 Y₂Hf₁₀, system, mag. susceptibility and electronic struct. (Russian) 7-58988
 Zn₂Hg_{1-x}Se, electrophysical props. and carrier scatt. mechanisms 7-17024
 Zr, α and β phases, differential heat of H absorption, isoperibol calorimetry studies 7-6967
 ZrN, electronic struct., metal vacancy effects, KKR-CPA method anal. 7-12606

Fermi liquid *see fermion systems***Fermi resonance**

- acetonitrile, anharmonic force consts., Fermi coupling, IR and Raman spectra 7-920
 acetylene, Fermi perturbation study, UV absorpt. and fluoresc. excitation spectra anal. 7-36638
 DPPC bilayers, aqueous assemblies, high press. IR studies 7-54501
 ethane and derivatives, vibr. Raman Stokes spectrum 7-57072
 fluoroform, mol. vibr., triidagonal Fermi reson. Hamiltonian, visible spectral anal. 7-50154
 formic acid-d₁, stretching vibr. Raman spectra 7-19866
 glyoxal, S₁-S₀ vibr. transitions, Fermi reson., visible fluoresc. spectra anal. 7-50230
 iodomethane, ν_4 band, high resolution IR spectra 7-5681
 phase space structure calcs. from experimental spectra 7-42585
 propanes, ¹H labelled, IR and Raman spectra, vibr. analysis, D substitution effect 7-50141
 propyne, $2\nu_3$ band study, Fourier transform IR spectra anal. 7-50119
 propyne, ν_3 and $2\nu_3$ bands study, Fermi reson., IR spectra anal. 7-50120
 trimethylchlorogermane, liq., vibr. anal., isotope effects, Raman bandshape anal. 7-33371
 CO₂, intramode and Fermi relax. influence on multiple-pass short pulse energy extraction 7-57156
 CO₂ mixtures, gas density effect on Q branch in IR spectra 7-42612
 D¹³CP, $\nu_1 + \nu_2$ vibr.-rot. band, Fermi reson. in (100,002) diad 7-5662
 HDO, $\nu_1 + \nu_2$ and $3\nu_2$ bands, energy level and intensity calcs. 7-5654
 ZnS_{1-x}Se_x polariton dispersion with Fermi reson., Raman scatt. cross-section (Ukrainian) 7-12623

Fermi surface

- ³He-A superfluid, chiral anomaly, finite fermion vacuum current calcs. 7-44945
 Anderson Kondo lattices, heavy-fermion superconductivity 7-2775
 band occupancy determ. using Fourier-transformed Compton profile 7-21801
 (BEDT-TTF)₂, superconducting and mag. instabilities 7-45697
 β -(BEDT-TTF)₂X salts (X=I₃, IBr₂, AuI₂), magnetoresistance, superconductivity 7-52884
 (BMDT-TTF)TCNQ, molecular conductor, dimensionality, struct. and electrical props. 7-52595
 composite superconductors, density of states of normal section calc. 7-52386
 conduction-electron spin-flip under mag. breakthrough conditions, model 7-38438
 degenerate Kondo lattice, magnetic instability and sp. ht. calcs. 7-58977
 gapless semiconductor, low temp. density of states near Fermi surface 7-64042
 \hbar/m_e determ., using rotating, superconducting ring 7-14914
 incommensurate CDW systems, long-range Coulomb effects 7-45189
 magnetoresistance of 2D electron in lateral superlattice 7-38599
 metal, Fermi surface, pseudopotential calcs., program set review (Russian) 7-64050
 metal, quasi-2D conductivity, high freq. effects (Russian) 7-33038
 metallic filaments strongly anisotropic 2D system, weak localisation in magnetoresistance 7-45282
 metals, anomalous skin effect, Fermi surface curvature effects (Russian) 7-58827
 metals, electronic topological transitions, tunnelling studies 7-64052
 metals, nonlocal cond., microwave radiation transmission 7-13269
 metals, positron annihilation studies, review 7-46180
 metals and alloys, electronic structure, positron annihilation studies, review 7-45126
 metals and alloys, electronic structure, positron studies 7-64730
 morpholinium TCNQ₂ salts, optical phonon mediated charge transport 7-52596
 one-dimensional systems, electronic stability and density of states on Fermi surface, topological effect 7-58728
 quasi-one-dimensional electron systems, phase transitions, theory 7-52408
 rare earth dihydrides, Fermi surface nesting 7-52398
 strongly coupled electron-phonon systems, 1D and 2D, BCS pairing versus bipolaron crystallisation 7-45552
 (TMTCF)₂X salts (C=S,Se), crystal struct., press. and temp. depend. 7-44520
 (TMTSF)₂ PF₆, field induced quantum oscillations, Hall effect studies 7-45280
 (TMTSF)₂PF₆(ClO₄), nesting vector, SDW amplitude and anisotropy 7-45125
 (TMTSF)₂X, superconducting and mag. instabilities 7-45697
 (TMTSF)₂X quasi-1D conductors, SDW transition temperature, superconductivity 7-45705
 (TMTSF)₂X salts, phase diagram, importance of 1D correlations 7-45190

Fermi surface continued

- (TMTSF)₂X salts, quasi-1D, cascade of field-induced SDW phases 7-45701
 Ag-Mg, commensuration and discommensuration characteristics, modulation periods 7-46463
 Al, crystals with edge dislocations, 2D angular correlation of positron annihilation radiation 7-39242
 Al dilute alloys, deviation from Matthiessen's Rule, three group model 7-12601
 Al single cryst., transverse conduction electron focusing and specular reflection 7-52407
 As, Fermi surface characts., hydrostatic press. depends. (Russian) 7-32896
 As-Sb alloys, magnetoresist., thermomag. power and Fermi surface quantum oscills. meas. 7-2578
 Au, Fermi surface curvature, de Haas-van Alphen effect meas. 7-2467
 Bi, nonlinear cyclotron resonance, lineshape and mechanisms 7-32897
 Cd, high pressure magnetoresist. near electronic topological transition (Russian) 7-7204
 Ce alloy cubic Laves phases, electronic struct., self-consistent APW calcs. 7-12599
 CeB₆, Fermi surface, 2D angular correlation of positron annihilation radiation 7-39241
 CeCuSi₂, heavy fermion superconductors, Fermi surface and cooperative phenomena 7-2771
 Co₉₂Fe₀₈, FCC, Fermi surface, de Haas-van Alphen studies 7-52406
 Cr, Fermi surface, 2D angular correlation studies 7-39236
 Cr, paramagnetic, two-photon momentum distrib. 7-45128
 Cr₃Si, A15 cpds., 2D angular correlation of positron annihilation radiation 7-39238
 Cu, crystals with edge dislocations, 2D angular correlation of positron annihilation radiation 7-39242
 Cu, electronic props., spectrosc. investig. 7-59216
 Cu-Ge (15.0 wt.%), Fermi surface, 2D angular correlation of positron annihilation radiation 7-39243
 CuBe, scatt. anisotropy of conduction electrons 7-38536
 CuNi, substitutionally disordered, electronic struct., LCAO-CPA calcs. 7-64067
 Fe, Fermi surface change near the mag. transition 7-16935
 (Fe_{1-x}Co_x)₇₅Si₂₅B₁₂₅ amorphous alloys, density of states, XPS studies (Chinese) 7-13320
 Ga, sound attenuation oscillatory deviation in weak mag. field, Fermi surface cross section and electron rel. determ. 7-2106
 Gd Curie temp. press. depend., Fermi surface struct. effects 7-7509
³He superfluid, A-phase, dynamic intrinsic orbital momentum (Russian) 7-32737
³He, superfluid B-phase, orbital ang. momentum in mag. field 7-38289
³He-A, orbital dynamics, Wess-Zumino function 7-63899
 HfTe₃, Fermi surface, effective masses, energy bands, determ. from Schubnikov-de Haas effect 7-64051
 In single crystal, Hall coeff. anisotropy, Fermi surface effects 7-12701
 Ir, itinerant electron Zeeman splitting anisotropy meas. 7-52536
 LaB₆, Fermi surface, 2D angular correlation of positron annihilation radiation 7-39241
 Lu₅Ir₃Si₁₀, superconducting, electronic phase transition and partially gapped Fermi surface 7-12902
 Mo_{1-x}Re_x system, thermal EMF and topological electronic transition 7-45286
 N₂ crystals, molecular-to-nonmolecular transformation at high press., theory 7-21432
 Na, induced torque and CDW ground state 7-2838
 Nb, Fermi surface, Fermi vel., many-body enhancement and supercond. energy gap anisotropies calcs. 7-58729
 Nb, Fourier transform of 2D angular correlation 7-38439
 Nb₃Ir, A15 cpds., 2D angular correlation of positron annihilation radiation 7-39238
 Nb₃Mb_{1-x} alloys and elemental metals, 2D angular correlation spectra studies, band struct. 7-39235
 NbSe₃, CDW and magnetotransport, mag. field effects to 230 kG 7-64215
 NbSe₃ CDW conductor, magnetothermopower studies 7-64226
 NdB₆, Fermi surface, 2D angular correlation of positron annihilation radiation 7-39241
 Ni, Fermi surface change near the mag. transition 7-16935
 Ni, spin polarised positron annihilation 7-46187
 Ni₃Ga, 2D electron-positron momentum density and Fermi surface 7-45127
 Ni₃Ga, momentum density distrib., Compton scatt., positron annihilation, symmetrised APW method 7-64069
 NiMnSb, half-metallic ferromagnet, positron-annihilation study 7-21802
 Pb, self-consistent relativistic band struct., normal and high press. 7-52413
 Pb_{1-x}Sn_xTe narrow-gap semicond., electron-electron interaction, effect on permitt., two-band model 7-52420
 Pb_{1-x}Sn_xTe quantum oscills. spectrum anal., two-window Fourier transform technique 7-52404
 Pd, Fermi surface curvature, de Haas-van Alphen effect meas. 7-2467
 Pd-Fe(Ni) dilute alloys, Fermi surface exchange splitting, de Haas-van Alphen effect studies 7-52405
 Pd₃Fe, electronic struct. 7-52415
 PrB₆, Fermi surface, 2D angular correlation of positron annihilation radiation 7-39241
 Pt, Fermi surface curvature, de Haas-van Alphen effect meas. 7-2467
 Re, Fermi surface, 2D angular correlation of positron annihilation radiation 7-39240
 Ru, Fermi surface, 2D angular correlation of positron annihilation radiation 7-39240
 SmCu₂ single cryst., high field transverse magnetoresist. meas., Fermi surface determ. 7-52576
 Sn, optical properties in 2.5 to 40 μ m range 7-59271
 Ta, Compton profiles, APW calcs. 7-27809
 TaSe₃, transport props., uniaxial stress effect 7-38801
 (TaSe₄)₂I, electronic struct., positron annihilation and UPS study 7-53500
 (TaSe₄)₂I, 1D CDW system, positron annihilation 7-39272
 Ti, Fermi surface, 2D angular correlation of positron annihilation radiation 7-39240
 UBe₁₃, heavy fermion superconductors, Fermi surface and cooperative phenomena 7-2771
 UPd₃, Fermi surface meas., de Haas-van Alphen effect study 7-12589
 UPt₃, anisotropic superconductivity 7-7461

Fermi surface continued

UPt₃, heavy fermion superconductors, Fermi surface and cooperative phenomena 7-2771
URu₃ (Rh₃) (Pd₃) (Ir₃) (Pt₃), hybridisation, electronic struct. and props. 7-45136
URu₂Si₂, heavy electron system, competing electronic correlations, press. effect 7-45539
V, 2D angular correlation studies 7-39237
V, Fourier transform of 2D angular correlation 7-38439
V-Mo disordered alloy electron-positron pair momentum density and Fermi surface calc. 7-45129
W, Compton profiles, APW calcs. 7-27809
W single crystals., galvanomagnetic props., low temp. Fermi surface local features effects (Russian) 7-27320
Yb, relativistic band struct., self-consistent calcs. under normal and high press. 7-64068
ZrTe₅, thermal and mag. meas. 7-44932

Fermi-Thomas model see Thomas-Fermi model

fermion systems

see also electron gas; heavy fermion systems; liquid helium-3
anyon statistics with single-valued wave functions 7-29879
Bloch equation, anal. using coupled-cluster method, N-fermion system appl. 7-61219
Bogolyubov generating functions, quantum method, current Lie algebra, representations, functional eqns. 7-41240
boson representation, composite particle theory 7-48541
bosonisation of the many-electron problem 7-41241
causal phase-space approach, Clifford algebras 7-9752
charged quantum fluids in 2D, ground state energy 7-29881
constrained fermionic system, equivalence with free parafermionic and sigma models 7-19018
correlation functions of order-parameter fluctuations in a Fermi system 7-56145
density matrices geometry, superoperators and unitary invariance 7-201
Dyson boson mapping, physical and spurious states, algebraic anal. 7-56628
extended fermion matter, single particle widths induced by axially symmetric vibrations 7-30360
extended thermodynamics of ideal gases with 14 fields 7-56197
Fermi gas, 1D, Bethe-ansatz soln., simple approx. 7-61221
Fermi gas, collisional evolution in 1D 7-203
Fermi liquid, normal, thermodynamics, nonlinear corrections 7-48534
Fermi liquid, strongly correlated, props. in valence fluctuation system, variational Monte Carlo anal. 7-2524
Fermi-Dirac functions, high-precision analytic approx. by elementary fns. 7-29880
fluctuating valence heavy fermion systems, impurity resistivity temp. depend. calcs. 7-2565
fractional quantum Hall effect of a multicomponent fermion system, collective excitations 7-21835
ground-state kinetic energies, explicit procedures 7-14827
heavy electron Fermi liquids, Hubbard model anal., similarities to ³He 7-2522
heavy electron superconductors, p-wave pairing consequences 7-2772
heavy fermion liquids, superconductivity, microscopic and phenomenological aspects 7-2773
heavy fermion superconductivity, tight binding picture and Cooper pairs 7-2776
heavy fermions and valence fluctuations, conf., Shima Kanko, Japan (April 1985) 7-23
hierarchical fermion model, renormalisation on square lattice in 2D 7-56153
incompressible 2D electrons, Coulomb gap size determ., spectroscopic method 7-61223
infinite systems, canonical anticommutation relations in Fermi-Dirac statistics 7-56152
interacting boson-fermion systems, functional integrals, holomorphic representation 7-14860
kinetic energy density functionals compatible with differential virial theorem 7-48540
Kondo lattice, heavy-fermion state form. calcs. 7-206
Landau theory of Fermi liquids reformulated 7-29882
magnetic properties of Fermi liq. systems 7-12387
many-electron systems, U(n₁) × U(n₂) reduced matrix elements and reduced Wigner coeffs. 7-4654
many-electron systems, U(n) matrix element evaluation in composite basis 7-5604
many-fermion Hamiltonian, relationship among fermion pairs, pairons and natural spin geminals 7-41242
Monte Carlo simulations 7-204
multicomponent liq., transport props. 7-61220
noninteraction spinless fermions, density functional theory 7-9753
normal, thermodynamics, quasi-particle occupation number functional calcs. 7-32741
polarised Fermi gases, flow through narrow channels 7-32739
probability density for Bose-Einstein and Fermi-Dirac particles, Slater-Kahn functions 7-48537
quantum adiabatic approximation to interacting boson-fermion systems 7-41243
quantum many-body systems, Monte Carlo studies of dynamical response 7-14862
relativistic many-fermion systems, vacuum-induced Friedel-type oscillations 7-29887
resonance splitting and broadening, dynamics 7-205
self-energy calculations, effective interactions 7-35395
semiconductors, electron-hole liq., general props., review 7-7121
spin 1/2 particles, spin props. from quantum theory, hidden-variables represent refutation 7-41120
spinless solvable 1D two-band model calcs., renormalisation-group eqns. 7-208
strongly correlated, Gutzwiller saddle-point approx., functional integral approach 7-207
superfluid, spin singlet triplet states in presence of strong mag. fields 7-38286
superfluid Fermi liquid in strong mag. fields, vertex eqn. 7-27046
TDHF extension with Grassmann variables, canonical invariance and coordinate system specification 7-56630
TDHF extension with Grassmann variables, formulation using Dirac's canonical theory of constraints 7-56629

fermion systems continued

two component, fractional quantum Hall effect, excitation spectrum 7-52656
ff system with $\mu^{\text{PC}}=0^{++}, 1^{--}, 1^{+-}, 0^{++}, 1^{++}$, Bethe-Salpeter wave fn. calcs. 7-48976
Ce intermetallic cpds., Hall effect meas. 7-12702
CeCu₆ heavy fermion system, photoemission and inverse photoemission studies 7-3148
CeCu₂Si₂, heavy fermion superconductors, Fermi surface and cooperative phenomena 7-2771
CeCu₂Si₂ Kondo lattice heavy fermion system, quasi-particle-phonon interactions 7-2521
D, spin polarised, nonequilib. props. within Fermi liquid theory 7-6913
UBe₃, heavy fermion superconductors, Fermi surface and cooperative phenomena 7-2771
UPt₃, heavy fermion superconductors, Fermi surface and cooperative phenomena 7-2771
U_{1-x}Th_xPt₃, Fermi surface instability modification by Th substitution in UPt₃ 7-2766

fermions

see also baryons; fermion systems; leptons
t Hooft-Polyakov monopole, charge-exchange and helicity-flip scattering 7-19043
bosons and fermions, fundamental problems 7-14858
chiral fermion propagation on 2D fractal structs. 7-48981
Clifford bundles and the Dirac operator, connections 7-61443
coherent effects in fermion emission, quantum mechanical description 7-14834
CP^{N-1} model, deconfinement by minimally coupled massless fermions 7-56516
Dirac fermion, chiral anomalies, dimensional regularisation 7-9990
Dirac fermion propag. on hypercubic lattice with random hopping parameters 7-4967
Dirac Hamiltonian for fermion-solenoid interactions, vacuum charge, scatt. theory 7-35700
dynamical props. of charged fermion in 6D Abelian monopole geometry 7-19045
E₈×E₈ superstring theory, extra U(1) phenomenology, fermion mass spectra 7-41688
Eotvos anomaly, gauge field coupled to fermion number interpretation 7-18682
Euclidean supersymmetric quantum theory, stochastic representation of arbitrary fermion sectors 7-18630
existence of physical charged fermions 7-35754
fermion + fermion → fermion + fermion + W⁺ + W⁻, charged current sector calc., effective W approx. comparison 7-24822
fermion-gauge field interactions, regularized determinants and non-perturbative definition of chiral anomalies 7-30176
fermionic strings, gauge invariant Liouville action 7-35771
fermionic/scalar field theories on Riemann surfaces of arbitrary topology, equivalence 7-9954
free fermionic currents, Jacobi identity failure, rel. to axial anomaly 7-56469
functional determinant of massless fermions in nonAbelian gauge pot., perturbative derivation 7-30169
gauge theory, dimensional reduction, spontaneous symm. breaking and absence of chiral fermions 7-41594
global gauge anomalies and scattering theory 7-35701
gravitons, matter-induced topological mass term, fermion and gauge field contrib. 7-18669
heterotic string theory in 4D with families of chiral fermions and standard gauge symm. 7-49033
inflationary cosmology in supergravity framework, fermion masses 7-48514
Kaluza-Klein theory, torsion and chiral fermions on topologically nontrivial Yang-Mills fields 7-48994
lattice fermion derivative formulation, locality and chirality without spectrum doubling 7-41632
lattice field theories with fermion degrees of freedom, near algorithm for numerical simulation 7-41602
lattice gauge theory, fermionic algorithms, conf., Wuppertal, Germany, Nov. 1985 7-60883
lattice gauge theory with Wilson fermions, hadron mass calcs. 7-61483
lattice QCD, quenched SU(2) simulation with staggered fermions, chiral limit 7-61602
lattice QCD, strongly coupled, fermions in Euclidean formulation 7-30247
lattice QCD with staggered fermions, chiral props. 7-61576
lattice QCD with Susskind fermions, current algebra relation 7-41730
lattice QCD with Wilson fermions, fast fermionic algorithms 7-61572
lattice QED, parity-violating fermionic vacuum currents, numerical study 7-19058
lattice theories of chiral fermions 7-19001
Lorentz, conformal and gauge anomalies in external fields 7-41219
mass calcs. from abelian generation group symm. breaking 7-61636
mass matrices in unified models 7-446
mass upper limits in model analysis 7-19006
masses and mixings in SU(3)_C×SU(2)_L×U(1)_Y six-dimensional model 7-30228
masses in E₇ unified model 7-61536
massive Schwinger model with Wilson fermions, chiral condensate calcs. 7-61541
metastable vacuum decay, presence of soliton localized soft fermionic and bosonic modes 7-4986
nonAbelian family symm., origin of fermion masses and mixing angles 7-19041
one-plaquette U(N) gauge model with fermions, leading order topological expansion 7-35721
quantization of gauge theories with Weyl fermions 7-4965
quantum cosmology, fermionic perturbations and wavefunction of the Universe 7-56128
quantum field theory with fundamental mass, stochastic quantisation 7-30199
quantum symmetries from quantum phases, fermions from bosons, a Z₂ anomaly and Galilean invariance 7-48970
scalar field theories, fermions and Gaussian effective pot. 7-35699
Sp(2N), N fermion generation gauge group, existence of Z₀ for N=4 7-9994
staggered fermion symmetry group, irreducible representations 7-19024

fermions continued

- string theory with Majorana and Dirac fermions, modular invariance 7-19040
- SU(2) lattice gauge theory with dynamical fermions, static quark pot. 7-61478
- superstring fermion amplitudes, covariant, sum over fermionic surface 7-9999
- superstrings, fermion emission vertex and space-time supersymmetry 7-35770
- Thirring model, derivative coupling model equivalence and fermionic Green's fns. 7-48993
- Ward identities on the lattice for Wilson fermions 7-56419
- Weyl-Dirac equation for an SU(2) gauge theory with spherical symmetry 7-41622
- zero-energy boundary state of superheavy fermion and SO(10) monopole (Chinese) 7-24777

fermion

- see also nuclei with
- diffusion in Ta-Fm dilute alloys 7-12353

fermium compounds

No entries

ferrimagnetic properties of substances

- see also ferrimagnetism; ferrites; garnets; magnetic semiconductors
- alloys, amorphous, role of single-ion anisotropy 7-45661
- garnets, ferrimagnetic, vertical Bloch line motion, memory appls. 7-53024
- magnetic insulators, light absorpt. by intersublattice charge transfer 7-46065
- Ba ferrite filled styrene-isoprene-styrene composite, dynamic mech., elec. and mag. props. 7-13001
- Ba₂CaCuFe₂F₁₄, heteronuclear trimers with ferrimag. behavior (French) 7-64448
- BaCo₂Fe₁₆O₂₇, hexagonal ferrites, neutron diff. studies 7-45622
- BaFe₂O₁₉, hexagonal ferrites, neutron diff. studies 7-45622
- BaIn_{1.5}Fe_{10.5}O₁₉ single crystals, magnetocrystalline anisotropy consts., anomalous temp. depend. 7-45664
- BaMg₂Fe₁₆O₂₇, hexagonal ferrites, neutron diff. studies 7-45622
- (Ba_{1-x}Sr_x)₂Zn₂Fe₁₂O₂₂ helimagnet single cryst., neutron diff. study 7-52942
- Bi_xLu_{1-x-y}Y_{3-x-y}Fe₅O₁₂, ferrimagnetic garnets characterisation for MSW optical diff. 7-13040
- Co_{0.55}Cu_{0.45}Cr₂S_{4-x}Se_x, high field susceptibility 7-45630
- Cu₂MnAl, Heusler alloy, heat and press. processed, changes in phys. props. during heating (Russian) 7-59645
- DgTb amorphous ferrimag. anisotropic films, Hall voltage polarity voltage and temp. depend. studies 7-7206
- Dy₂Co_{1-x} thin films, ferrimagnetic reson. in region of spin-reorientation transitions 7-45824
- DyFe amorphous alloys, local mag. anisotropy energy estimation 7-7503
- ErCo₃Ni₂, ferrimag. cpds., mag. anisotropy, temp. depend. 7-64450
- Fe-Tb amorphous alloys, film and bulk mag. props. and thermal expansion meas. 7-7540
- γ-Fe₂O₃ films, CVD deposited, uniaxial mag. anisotropy 7-33234
- γ-Fe₂O₃ thin films, mag. props. 7-33233
- γ-Fe₂O₃:H, H content, DTA, mag. anal. and Mossbauer studies (Chinese) 7-12104
- Fe₂O₄-CaO-SiO₂ amorphous oxides, magnetic props. and struct., Mossbauer spectra study 7-7538
- Fe_{2.4}Al_{0.6}O₄, magnetisation in 1 to 30 microns particle size range 7-47425
- Gd-Co, anisotropic ferrimagnets in high mag. fields 7-17200
- Gd-Co(Fe)(CoFe) alloys, amorphous thin films, Faraday rotation 7-64612
- Gd₂Co glasses, electronic struct., photoemission and magnetism 7-64060
- GdCo(Fe) amorphous films with perpendicular anisotropy, Hall loop meas., mag. struct. studies 7-7205
- Gd_{1.45-x}La_{0.55-x}Co_{2.5}B₁₀ mixed glasses, mag. props., phase transitions, microstruct. effects 7-64465
- GdNi amorphous ferrimag. anisotropic films, Hall voltage polarity voltage and temp. depend. studies 7-7206
- HoCo₃Cu₂, ferrimag. cpds., mag. anisotropy, temp. depend. 7-64450
- Ho₂Fe₄B spin reorientation, NQR meas. 7-52960
- HoNi amorphous ferrimag. anisotropic films, Hall voltage polarity voltage and temp. depend. studies 7-7206
- Li_{0.5}Ga_{1.5}Fe_{2.5-x}O₄, dilute ferrimagnetics, cluster spin glass state 7-38884
- Mg_{1-x}Cr_xFe₂O₄, Barkhausen noise parameters correl. with strength 7-22963
- Mn-Sn, homogenised, mag. props., thermal expansion 7-2900
- MnFeF₃(H₂O)₂, ferrimag., mag. and Mossbauer study 7-45845
- Mn₂Si₂Te₆ ferrimag. semicond., cryst. struct., X-ray diff. study 7-1977
- Ni-Zn ferrite films, prep., mag. props. 7-13378
- NiFeAlO₄, cation distrib. and canted spin alignment, Mossbauer obs. 7-22169
- PbMn_{2/3}MO₃, perovskite-type cpds., (M=Mo, Te, Re), dielec. and mag. props. 7-7650
- Tb-Co amorphous films, magneto-optic props. 7-64611
- a-Tb-Fe/Ni-Fe-Mo bilayer films, unidirectional anisotropy 7-59065
- TbAg amorphous alloys, local mag. anisotropy energy estimation 7-7503
- TbCo film, optical disc memory struct., mag. props., underlayer film treatment effect 7-45767
- TbCo sputtered films, compositionally modulated, mag. props., magneto-optical storage appl. 7-64495
- TbCo sputtered films, stability of mag. and magneto-optical props. (Japanese) 7-33241
- Tb₃Dy_{0.5}Er_{0.2}Fe₂, spin reorientation, Mossbauer study 7-13068
- TbFe amorphous alloys, local mag. anisotropy energy estimation 7-7503
- TbFe films, micron-size laser-written mag. domains, Lorentz microscopy 7-2913
- Tb₃Fe₉ amorphous films, mag. props. and domains, substrate temp. effects 7-13011
- TbNi amorphous ferrimag. anisotropic films, Hall voltage polarity voltage and temp. depend. studies 7-7206
- (Tb_{1-x}Y_x)Co₂ ferrimagnetic alloy, sp. ht., Curie temp. and density of states comp. depend. meas. 7-7514
- (TmBi)₃(FeGa)₅O₁₂ indicator film, visualisation of mag. field profile of thin-film magnetic heads 7-61359
- YFeO₃, orthoferrite, Dzyaloshinskii-Moriya electron-nuclear interaction, NMR data anal. 7-53162
- YIG, critical mag. relaxation, ESR linewidth 7-22106

ferrimagnetic properties of substances continued

- YIG, ferrimagnetic garnets characterisation for MSW optical diff. 7-13040
- YIG:Ho³⁺, laser mag. reson. study, quasi-Ising model 7-53147

ferrimagnetic resonance

- Bi_xLu_{1-x-y}Y_{3-x-y}Fe₅O₁₂, ferrimagnetic garnets characterisation for MSW optical diff. 7-13040
- Dy₂Co_{1-x} thin films, ferrimagnetic reson. in region of spin-reorientation transitions 7-45824
- YIG, ferrimagnetic garnets characterisation for MSW optical diff. 7-13040
- YIG:Ho³⁺, laser mag. reson. study, quasi-Ising model 7-53147

ferrimagnetism

- see also ferrimagnetic properties of substances
- bond-diluted Heisenberg ferrimagnet, spin damping near percolation threshold 7-17194
- polycrystalline ferrimagnets, shape of grains influence on magnetisation curve and hysteresis loop 7-45746
- spin waves, derivation 7-52956
- structural and magnetic instabilities in low-dimensional systems 7-59034

ferrite applications

- see also ferrite devices
- No entries

ferrite devices

- see also ferrite applications; magnetostatic wave devices
- thermal detector of optical radiation based on ferromagnetic resonance 7-61375

ferrites

- see also ferrimagnetic properties of substances; ferrimagnetism; ferrite applications; ferrite devices
- ceramics, AC and DC cond. (Spanish) 7-52560
- crystal, normal lattice vibr. modes determ., nuclear site group anal. 7-16701
- domain structure near the compensation temp. 7-7534
- EM waves in ferrite slab with domain struct. (Russian) 7-2920
- film, coplanar transducer excitation of magnetostatic surface wave 7-22102
- hexaferrite film growth, LPE on Ba₃(VO₄)₂ and CoGa₂O₄ substrates 7-52320
- magnetostatic wave excitation and propagation 7-33156
- nonlinear magnetisation components calc. 7-45743
- orthoferrites, mag. and dielec. props. at submillimetre wavelengths 7-38990
- powders, RF echoes investig. (Russian) 7-22162
- steel, low C, low alloy, tempering-investig., epitaxial ferrite stability studies (Russian) 7-13479
- surface magnetostatic wave, space-frequency dependence of energy flux 7-33158
- synthesis and sintering kinetics and mechanisms 7-13423
- thin film structure, resonant interaction between magnetostatic waves and volume elastic waves, effect of ideally conducting metal 7-22129
- YIG single-crystal ferrites, relation between biasing magnetic field and linewidth 7-4868
- Ba ferrite filled styrene-isoprene-styrene composite, dynamic mech., elec. and mag. props. 7-13001
- Ba-Zn ferrite carriers for electrophotography, charactn. 7-4903
- BaCo₂Fe₁₆O₂₇, Curie temp., magnetization, susceptibility, mag. anisotropy meas. (French) 7-27507
- BaCo₂Fe₁₆O₂₇, W-type hexagonal ferrite, cryst. struct. and Co location 7-6605
- BaCuFe₁₇O₂₇ W-type hexagonal ferrite, intermediate valency, oxidation annealing, magnetisation and neutron diff. studies 7-7187
- BaFe_{12-2x}Co_{2x}Ti₆O₁₉ superline particles, coercivity conc. and aspect ratio depend. meas. 7-53054
- Ba₂Fe₂²⁺Fe₁₃³⁺O₂₂ hexagonal ferrite, hydrothermal synthesis, elec., magnetic and structural characterisation 7-45637
- Ba_{1.06}Fe_{10.92}Mn_{1.02}O₁₉ and Ba_{1.03}Fe_{11.97}O₁₉ single crystals, white synchrotron radiation topography 7-6606
- BaFe₂O₁₉, acicular media for perp. mag. recording, dynamic props. 7-59061
- BaFe₂O₁₉, Bloch domain boundary, Neel boundary transition in mag. field, NMR study (Russian) 7-33195
- BaFe₂O₁₉, dispersion and particle packing of mag. oxide powders 7-3233
- BaFe₂O₁₉, FMR linewidth, temp. and freq. dependence 7-53140
- BaFe₂O₁₉ films, RF diode sputtering prep. and mag. props. (Japanese) 7-7852
- BaFe₂O₁₉ fine powder for particulate perp. mag. recording media, coercivity meas. method 7-59062
- BaFe₂O₁₉ hexaferrite, cryst. struct. formation and transformations 7-44489
- BaFe₂O₁₉ particulate media, magnetisation props, temp. effects study 7-53055
- BaFe₂O₁₉ particulate coatings, pigment-to-binder loading effects 7-53056
- BaFe₂O₁₉ powders, coprecipitated, magnetisation reversal, mag. dilution effects 7-53062
- BaMg₂Fe₁₆O₂₇, Curie temp., magnetization, susceptibility, mag. anisotropy meas. (French) 7-27507
- Ba₂S₂Mn(Ni)(Co)Fe_{10-x}Ga_xO₂₂ hexagonal ferrites, cryst. and magnetic struct. studies 7-44474
- Ba_{0.8}Sr_{1.2}Ca_{0.8}Fe₁₂O₁₉-La₂O₃ hexagonal ferrites, influence of electric field on struct. and props., Mossbauer study 7-7616
- Ba_{0.4}Sr_{0.4}Ca_{0.2}Fe₁₂O₁₉ hexagonal ferrites, influence of electric field on struct. and props., Mossbauer study 7-7616
- BaZn_{1.1}Co_{0.9}Fe₁₆O₂₇ hexaferrite, competing anisotropies, first order magnetisation processes and spin transitions obs. 7-38856
- Ca₂Co_{1-x}Fe₂O₄ substituted ferrite system, mag. props., comp. depend., Mossbauer study 7-7618
- CaFe₂Mn_{1-x}O_{3-y} ferrites, microdomains, role in oxidation, reduction and annealing 7-46830
- CaFe₂O₇, crystal struct. (French) 7-16519
- CaO-Fe₂O₃ system, solid state reactions, ferrite growth and morphology 7-3236
- Cd₂Cu_{1-x}Fe₂O₄, canted spin arrangements 7-45618
- Co_{1-x}Ca_xFe₂O₄, single domain-superparamagnet transition 7-17203
- CoFe₂O₄ (100)-textured thin films, anisotropy study 7-7568
- CoFe₂O₄ ferrite epitaxial layers, high coercivity (Chinese) 7-38908
- Co_xFe_{3-x}O₄ ferrites, polycrystalline, Verwey transition 7-7120

ferrites continued

- $\text{Cu}_{1-x}\text{Cd}_x\text{Fe}_2\text{O}_4$, irreversible magnetisation. depend. on magnetising field 7-64487
 $\text{Cu}_x\text{Cd}_{1-x}\text{Fe}_2\text{O}_4$ system, elec. resist. and cation distrib. 7-7256
 $\text{CuFe}_{2-x}\text{Al}_x\text{O}_4$ system, mag. props. 7-45740
 DyLiFeO_3 , orthoferrite, mag. props. 7-2824
 ErFeO_3 , muon bonding sites, muon spin rot. study 7-45896
 $\text{Fe}_{3-x}\text{M}_x\text{O}_4$ ($\text{M}=\text{Ti}, \text{Cr}, \text{Mn}, \text{Al}$), substituted magnetite, reactivity in O_2 , relation with cation distrib. (French) 7-46829
 $\gamma\text{-Fe}_2\text{O}_3$ particles, microstructure, X-ray diff., magnetisation props. 7-45757
 $\gamma\text{-Fe}_2\text{O}_3$ preparation by mechanochem. transform. of $\gamma\text{-FeOOH}$ in presence of Li_2CO_3 7-59478
 Fe_2O_3 silica coated particle dispersions, magnetic recording appls. 7-53057
 $\text{Fe}_2\text{O}_3/\text{Co}$ particles, coercivity time-scale depend., magnetic switching units vol. determ. 7-53059
 $\text{Fe}_2\text{O}_3\text{-PbO}$, binary phase diagram, DTA, X-ray diff. meas. 7-46434
 Fe_3O_4 film form. on Fe alloys, XPS study 7-22898
 Fe_3O_4 , magnetite, hysteresis props. rel. to particle size 7-14268
 Fe_3O_4 , magnetite, mag. after-effects at room temp. 7-64493
 Fe_3O_4 nearly spherical particles in low mag. fields, mag. props. 7-27568
 Fe_3O_4 , surface magnetism, ion bombardment effects 7-12949
 $\text{GdFe}_{1-x}\text{Mn}_x\text{O}_3$, orthoferrite, mag. behaviour characts. 7-45657
 GdFeO_3 orthoferrite crysts., RF mag. props. and frozen rare earth sublattice 7-17225
 $\text{LaZnFe}_{11}\text{O}_{19}$, cation distribution and random spin canting 7-37945
Li ferrites, microstruct. effects on mag. props. (German) 7-59052
 $\text{Li}_{0.25}\text{Co}_{0.25}\text{Zn}_{0.5}\text{Fe}_2\text{O}_4$, mixed ferrites, neutron diff. study 7-52943
 $\text{LiFe}_{0.5}\text{Al}_{0.5}\text{Ga}_{0.5}\text{O}_4$, magnetisation and lattice parameter, role of Al and Ga ions 7-22097
 $\text{LiMnFe}_2\text{O}_4$ ferrite, solid solution form. in contact diffusion pairs 7-2273
 $\text{Li}_{0.5+0.5x}\text{Ti}_x\text{Fe}_{2.5-1.5x}\text{O}_4$, dilute ferrite spinels, spontaneous magnetisation, anomalous temp. depend. 7-45739
 $\text{Li}_{1-x}\text{Zn}_x\text{Fe}_2\text{O}_4$, outside spin wave manifold effective linewidth values, effect of dimensional reson. 7-53146
 $\text{Mg}_{1-x}\text{Cr}_x\text{Fe}_2\text{O}_4$, Barkhausen noise parameters correl. with strength 7-22963
 MgFe_2O_4 , mag. props. depend. on preparation method 7-13066
 MgFe_2O_4 , photoelectrochemical props., effect of defects and doping 7-45385
 $\text{Mg}_{1-x}\text{Mn}_x\text{Fe}_2\text{O}_4$, outside spin wave manifold effective linewidth values, effect of dimensional reson. 7-53146
Mn-Zn ferrite US scatt. loss evaluation by line-focus-beam acoustic microscope 7-2331
 $\text{MnZnFe}_2\text{O}_4$, struct., Mossbauer, X-ray, and mag. meas. 7-1971
 $\text{Mn}_{0.61}\text{Zn}_{0.26}\text{Fe}_{2.13}\text{O}_4$ ferrite, conductivity study 7-21909
 $\text{Mn}_{1-x}\text{Zn}_x\text{Fe}_2\text{O}_4$ ferrite cores, hysteresis losses 7-33210
 $\text{Mn}_x\text{Zn}_{1-x}\text{Fe}_2\text{O}_4$ ferrites, magnetoacoustic props. (Russian) 7-22131
Ni finite films, sputtered, struct. and compositional studies 7-64024
Ni-Zn ferrite and Ni ferrite films, prep., mag. props. 7-13378
 $\text{Ni}_{1-x}\text{Co}_x\text{Fe}_2\text{O}_4$ polycryst. magnetostrictive ferrite, long-term bulk acoustic wave memory 7-59099
 $\text{Ni}_{0.97}\text{Cu}_{0.03}\text{Fe}_2\text{O}_3$, ferrite, domain-acoustic echo 7-13014
 NiFeAlO_4 , cation distrib. and canted spin alignment, Mossbauer obs. 7-22169
 $\text{NiFe}_{0.96}\text{O}_{4+y}$ electrodes in aq. electrolytes, photoelectrochem. characts. meas. 7-46854
 NiFe_2O_4 films, amorphous, uniaxial perp. mag. anisotropy, substrate temp. depend; 100 to 573K (Japanese) 7-53091
 NiFe_2O_4 films, crystn. kinetics 7-45090
 NiFe_2O_4 sputtered films, struct., comp., AES study 7-22478
 NiFe_2O_4 , Trans-Tech 2-111, complex dielec. const. meas. at 245 GHz using double-beam interferometer 7-7632
 $\text{NiFe}_2\text{O}_4\text{-MgO}$ sputtered films, struct., comp., AES study 7-22478
 $\text{Ni}_2\text{Fe}_{2-x}\text{O}_4$, elec. cond., thermoelec. power meas., 10-300K 7-38648
 $\text{Ni}_3\text{-xGe}_x\text{Fe}_2\text{O}_4$ spinel ferrite, AC susceptibility and Mossbauer studies 7-64441
 $\text{Ni}_{0.3}\text{Zn}_{0.5}\text{Fe}_2\text{O}_4$ ferrites, mag. spectra with temp. dependent mag. permeability (Russian) 7-27554
 $\text{PbO-Fe}_2\text{O}_3\text{-B}_2\text{O}_3$ glass ceramics, mag. props. and EPR spectra of precipitated mag. phases 7-45748
 SmFeO_3 , muon bonding sites, muon spin rot. study 7-45896
Sr ferrite fine particles, prep., mag. props. (Japanese) 7-53065
 SrFe_2O_9 , mm wave magnetic and dielec. resonances 7-53139
 $\text{SrO.5Fe}_2\text{O}_3$, doped with kaolin and BaB_2O_4 , sintering temp., effect on structural and mag. parameters 7-7543
 $\text{SrZn}_2\text{Fe}_{16}\text{O}_{27}$, cryst. struct. refinement, X-ray diff. study 7-32413
 $(\text{YEuTmCa})_3(\text{FeGe})_5\text{O}_{12}$, epitaxial films, O ion adsorpt. bubble diameter variation effect 7-22125
 $(\text{YEuTmCa})_3(\text{FeGe})_5\text{O}_{12}/(\text{YLa})_3\text{Fe}_5\text{O}_{12}$ ferrite/garnet layered struct., domain wall and ferromag. reson. props. (Russian) 7-45828
 $\text{Y}_3\text{Fe}_5\text{-xGa}_x\text{O}_{12}$ epitaxial film, high freq. threshold props. studies (Russian) 7-45775
 YFeO_3 , muon bonding sites, muon spin rot. study 7-45896
 YFeO_3 , orthoferrite, Dzyaloshinskii-Morié electron-nuclear interaction, NMR data anal. 7-53162
YIG film tangentially magnetised dielec. layered struct., nonlinear magneto-static wave mixing (Russian) 7-45649
YIG single crysts., FMR linewidth, parametrically excited spin wave effects 7-2828
YIG:Ho³⁺, laser mag. reson. study, quasi-Ising model 7-53147
YIG:Ne³⁺ ferrite films, surface magnetostatic wave damping, ion implantation effects (Russian) 7-33242
 YLiFeO_3 , orthoferrite, mag. props. 7-2824
 YLiFeO_3 , spontaneous spin reversal, magnetic reson. soft modes and energy gaps obs. 7-52964
Zn ferrite, shock-synthesised or furnace-reacted, mag. props. 7-38904
Zn ferrite, shock-synthesised, Mossbauer spectroscopy 7-38979
 $\text{Zn}_{1-x}\text{Fe}_x\text{Fe}_2\text{O}_4$, shock synthesised, X-ray diff. 7-39899
 $\text{Zn}_{1-x}\text{Fe}_{2-x}\text{O}_4$, shock synthesised, electron microscopy 7-37955
 $\text{Zn}_{1-x}\text{Ge}_x\text{Fe}_2\text{O}_4$ ferrites, atomic, mag. and electronic disorder (French) 7-44477

ferritic steel see steel

ferroacoustic resonance

No entries

ferroelastic domains see domains; ferroelasticity

ferroelastic transitions

critical dynamics in external field 7-38189

ferroelastic transitions continued

- ferroelastic film on deformable substrate, Love waves and domain struct. near phase transition 7-52216
mean-field theory of structural phase transitions in the $A'A''BX_4$ -type compounds 7-16734
rare earth cpds., RP_2O_4 , $\text{R}=\text{La-Nd}, \text{Sm-Tb}$, ferroelastic transitions, soft modes, Raman spectra (Chinese) 7-38177
 $\text{BiVO}_4\text{Gd}^{3+}(\text{Mn}^{3+})$, ESR spectra, temp. depend. 7-22137
In-Tl (23 at.%) alloy, FCC, thermodynamics of ferroelastic phase transition 7-2189
 $\text{K}_2\text{Hg}(\text{CN})_4$, cryst. struct. and phase transition 7-26933
 KMnF_3 , 2D order parameter fluctuations at antiferrodistortion phase transition, dielec. const. meas. 7-16735
 $\text{KSc}(\text{MoO}_4)_2$, first-order ferroelastic transition 7-58460
 LiCsSO_4 , dielec. props., press. effect 7-64555
 $\text{Na}_2\text{MoO}_4\text{F}_3$, ferroelastic and ferroelectric behaviour 7-44792
 NaN_3 , trigonal-monoclinic phase transition, Brillouin scatt. studies 7-22275
NaOH, struct. phase transition to lower symm. phase with increasing temp. 7-44805
 RbHSeO_4 , optical birefr. meas., temp. depend. 7-27689
 TiNO_3 , ferroelastic switching, mech. twinning, at. mechanism, symm. anal. 7-2186
 $\text{ZrO}_2\text{-Y}_2\text{O}_3$ partially stabilised, phase diagram, microstruct. (Japanese) 7-53707

ferroelasticity

- see also shape memory effects
noncentrosymmetric laser crystals, struct. and props. study review 7-62709
plastic slip in ferroelastic material 7-12190
unitary transformations in solid state physics, book 7-24310
 $\text{BaSrNb}_2\text{O}_{12}$, chaotic states, high resolution electron microscope study 7-3001
 BiVO_4 , ferroelastic, optical soft mode, quantum nature, EPR and Raman spectra study 7-45795
 $(\text{KBr})_{1-x}(\text{KCN})_x$ mixed crysts., elastic shear const. and internal friction, torsion pendulum resonance meas. 7-26829
 $\text{KTaO}_3\text{-Li}$, quadrupole ferroelastic phase 7-6778
 LiKSO_4 single crysts., optical activity, ferroelec. and ferroelastic props. 7-27687
 LiNd_2SO_4 , ferroelastic and ferroelectric domain struct., SEM obs. 7-27675
 LiNH_2SO_4 , ferroelastic and ferroelectric domain struct., SEM obs. 7-27675
 NdP_2O_4 , ferroelastic domain walls, X-ray topography studies (Chinese) 7-58493
 $\text{Pb}_{2-x}\text{K}_x\text{Li}_x\text{Nb}_2\text{O}_{15}$, tetragonal tungsten bronzes, ferroelastic-ferroelectric coupling (French) 7-27674
 $\text{Pb}_3(\text{VO}_4)_2$, $\beta\text{-}\gamma$ transition, intermediate modulated struct. 7-2183
 Sr_2SiO_4 , β to α transition, modulated struct. 7-16724
 ZrO_2 , tetragonal, ferroelastic domain switching as toughening mechanism 7-33712

ferroelectric Curie temperature

- TGS-L- α -alanine admixture, dielec. props., influence of rejuvenation process 7-33339
 $\text{VF}_2\text{-TrFE}$ random copolymers, Curie point meas., thermal and processing history depend. 7-33341
 $\text{Ag}_2\text{Pb}_2\text{Nb}_2\text{O}_{10}$, ferroelectric with tetragonal W-bronze struct., first-order transition 7-39048
 $(\text{Ba,Sr})\text{TiO}_3$ film metal-dielec-metal system, polarisation switching 7-52849
 $(\text{Ba}_{1-x}\text{La}_x)(\text{Ti}_{1-y}\text{Zr}_y)_{1-x/4}\text{O}_3$ ceramics, electrostrictive effect 7-53240
 BaTiO_3 ceramics, zone sintering, dielec. props. rel. to microstruct. 7-13078
 BaTiO_3 , ferroelectric solid, microwave absorpt., Curie temp. and ultrasonic attenuation 7-39049
 $\text{K}_2\text{BiCl}_6\cdot 2\text{KCl}\cdot \text{KH}_2\text{F}_4$, improper ferroelectric phase transition, dielec. meas. 7-45943
 KNO_3 , dielectric props., effect of X-ray or γ -ray irradiation 7-53215
 $\text{K}_2\text{Pb}_2\text{Nb}_2\text{O}_{10}$, ferroelectric with tetragonal W-bronze struct., first-order transition 7-39048
 $\text{LiNbO}_3\text{-MgO}$, melt growth and charactn. 7-58170
 $\text{Li}_2\text{O-Nb}_2\text{O}_5\text{-(TiO}_2)_2$ system, vicinity of LiNbO_3 , solid solns., crystal chemical and ferroelectric props. 7-6805
 $\text{Li}_2\text{O-Ta}_2\text{O}_5\text{-(SnO}_2)_2$ system, vicinity of LiTaO_3 , solid solns., crystal chemical and ferroelectric props. 7-6805
 $\text{LiTa}_{1-x}\text{Mg}_x\text{O}_{3-3x}\text{F}_{3x}$, prep., ferroelec. Curie temp., effect of cationic substitution 7-45946
 $\text{LiTa}_{1-x}\text{Zn}_x\text{O}_{3-3x}\text{F}_{3x}$, prep., ferroelec. Curie temp., effect of cationic substitution 7-45946
 $\text{NH}_4\text{H}_2\text{PO}_4\cdot \text{SeO}_4$, partially deuterated, D concentrations in H_2PO_4^- and NH_4^+ radicals, ESR spectra 7-27671
PZT:Nb ceramics, sintering, pair doping, elec. characts. 7-39469
 $(\text{Pb,Ba})_{1-x}\text{TiO}_3$, ferroelec. solid solns., dielectric and hysteresis props. 7-64588
 $\text{Pb}_3\text{Cr}_2\text{F}_{19}$, nonlinear optic, lattice constns., ferroelec. Curie temp., phase transition obs. at 555K 7-17275
 PbHPO_4 , photostimulated luminescence near ferroelec. Curie temp. 7-64697
 $\text{PbIn}_{1/3}\text{Nb}_{2/3}\text{O}_3$, antiferroelec., phase transition, B-site cation order effects 7-7651
 $\text{Pb}_{2-x}\text{K}_{1+x}\text{Li}_x\text{Nb}_2\text{O}_{15}$, tetragonal tungsten bronzes, ferroelastic-ferroelectric coupling (French) 7-27674
 $\text{Pb}_{1-x}\text{La}_x\text{Ti}_{1-x/4}\text{O}_3$ sputtered film struct., dielec., and pyroelec. props. studies 7-21724
 $\text{Pb}(\text{M}_{1/2}\text{Sb}_{1/2})\text{O}_3$, perovskite type antiferroelectrics, ($\text{M}=\text{Sc}, \text{Ho-Lu}$), X-ray and dielec. characts. 7-7649
 $\text{Pb}(\text{M}_{1/3}\text{Nb}_{2/3})\text{O}_3\text{-Pb}(\text{Zn}_{1/3}\text{Nb}_{2/3})\text{O}_3$, ferroelec. powder, prep., solid solubility, Curie point (Japanese) 7-7945
 $\text{PbO-K}_2\text{O-Nb}_2\text{O}_5$, polymorphism, DTA, X-ray phase anal. 7-6782
 $(\text{Pb,Sr})_{1-x}\text{TiO}_3$, ferroelec. solid solns., dielectric and hysteresis props. 7-64588
 $\text{Rb}_2\text{Pb}_2\text{Nb}_{10}\text{O}_{30}$, ferroelectric with tetragonal W-bronze struct., first-order transition 7-39048
 $\text{Sb}_{1-x}\text{Bi}_x\text{SI}$ crystals, elec. props. at ferroelec. Curie point 7-2991
 SbSI , elec. charactn. of crysts. grown from melt by temp. fluctuation technique 7-13104
 $\text{SbSI}, \text{SbSOI}$, cryst. growth and elec. charactn. 7-53564

ferroelectric devices

liquid crystals and devices 7-21094

ferroelectric domains *see electric domains*

ferroelectric-filled waveguides *see dielectric-loaded waveguides*

ferroelectric hysteresis *see dielectric hysteresis*

ferroelectric materials

see also antiferroelectric materials; electric domain walls; ferroelectric semiconductors; ferroelectric thin films; ferroelectric transitions; lattice dynamics of ferroelectric crystals
 ammonium hydrogen tartrate, dislocation etch pits 7-37999
 ammonium hydrogen tartrate, ferroelectric, crystal growth and dislocation etching kinetics 7-51770
 biphenyl ester series, ferroelectric liquid crystals, dielec. props. 7-37843
 calcium tartrate single crystals, dielectric props. rel. to X-ray on γ -ray irradi. 7-59161
 CE8, liquid crystalline, chiral and racemic, audio frequency dielectric response 7-33318
 ceramic bar, normal mode responses, influences of domain switching and dipole dynamics 7-45945
 ceramics, elec. field-excited acoustic waves parametric instability, wave eqn. calcs. 7-6727
 ceramics, electromagnetic wave scatt. from dielec. permittivity tensor inhomogeneities 7-7629
 chiral smectic C liq. crystals, mol. theory 7-1867
 crystals, domain memory studies, sound generation method 7-39053
 dipole impurity-induced ESR line broadening calcs. 7-53131
 DOBAMBC, ferroelec. chiral smectic C phase, crit. field, temp. depend. 7-26624
 DOBAMBC ferroelec. chiral smectic C liq. cryst., helical pitch free value meas. 7-26632
 electro-optic materials for data storage and processing 7-43021
 ester type smectic C* liquid crystal, ferroelectric polarisation props. 7-13100
 glass ceramics, development in China, review 7-6527
 incommensurate phase, impurity-order parameter and -soft modes interactions 7-64584
 IV-VI narrow gap vibronic ferroelec., correl. length estimate (*Russian*) 7-17277
 liquid crystal cell, surface stabilised ferroelec., homogeneous-twist transitions study 7-51620
 liquid crystal with negative dielec. anisotropy, switching behaviour 7-39084
 liquid crystals, distortion free energy density, electrostatic screening 7-37844
 liquid crystals, electro-optics 7-39087
 liquid crystals, solitary waves, mol. reorientation dynamics 7-21092
 liquid crystals, surface stabilised, disclination dynamics, switching process 7-58137
 liquid crystals with high spontaneous polarisation 7-59159
 methylammonium mercury chloride, ^{35}Cl NQR study of low temp. phase transition 7-22160
 methylammonium mercury chloride, ferroelec. phase transition, proton- ^{14}N double reson. study 7-7653
 noncentrosymmetric laser crystals, struct. and props. study review 7-62709
 perovskite-like ferroelectrics, optical and electrophysical props. 7-3002
 photorefractive ferroelectric crystals, polarisation reversal of light beam wavefronts 7-1235
 piezomaterials, ferroelectric, thermal stability of the resonance freq. 7-64579
 polyvinylidene fluoride, shock response, ferroelec. and piezoelec. props. meas. 7-32568
 powder, dynamics of polar gas mols., in strong surface fields 7-12786
 quartz, imperfect crystal, structural phase transition, elastic breakdown 7-2165
 rare earth molybdates, improper ferroelectrics, energy spectrum and vacuum UV spectra 7-33413
 smectic C* liquid crystal, alignment and switching characteristics 7-64589
 smectics, alignment technique for displays 7-63454
 temperature modulation, effect on props. of ferroelectric materials 7-39044
 terpenoid derivatives, ferroelec. spontaneous polarisation, steric hindrance of free rotation, optical rot. and transition temp. meas. 7-13101
 tetraethyl ammonium MX₄ compounds (MzCo,Zn,Mn;X=Cl,Br), structural phase transitions 7-44801
 tetramethyl ammonium tetrachlorozincate, internal motions and phase transitions, PMR studies 7-2993
 tetramethylammonium tetrachlorocobaltate, ferroelec. incommensurate phase, thermal hysteresis, memory effect 7-33346
 tetramethylammonium tetrachlorozincate, ferroelec., optical activity, high accuracy universal polarimeter meas. 7-17300
 tetramethylammonium tetrachlorozincate, ferroelec., optical activity in incommensurate phase 7-64602
 TGS:Fe³⁺ crystals, spatially distributed defects, luminescence studies 7-26770
 TGS, crystalline samples, low temp. sp. ht. meas. 7-2225
 TGS, unstable point domains in ferroelectrics 7-17280
 TGS crystals, nitro-aniline doped, dielec. and piezoelec. props. 7-22192
 TGS crystals, polarisation relax., defect effects 7-17265
 TGS single crystal solution growth with modulated struct. 7-59388
 TGS-L- α -alanine admixture, dielec. props., influence of rejuvenation process 7-33339
 thermodynamic equilib. critical exponents and stability 7-12237
 thiourea, paraelectric phase, mol. dynamics simulation 7-37920
 transparent ceramics, appl., theory and props., conference, Latvian State University, Latvian SSR (April 1985) 7-4622
 transparent ceramics, comp., struct. and props. characts. anal. 7-7647
 transparent ceramics, cryst. chem. and struct. props. and modifications 7-6590
 tris-sarcosine calcium chloride, deuterated, ferroelectric props. 7-39050
 uniaxial systems with strong dipolar interaction, nonasymptotic crit. behaviour 7-64467
 vibr. spectroscopic study 7-39115
 vinylidene fluoride-trifluoroethylene copolymer, shock response, ferroelec. and piezoelec. props. meas. 7-32568
 vinylidene-trifluoroethylene copolymer, ferroelec. phase transition, X-ray diff. investig. 7-53249
 YZ-LiNbO₃, domain structure and lattice defects, effects of piezoelectricity, TEM anal. 7-2999
 AgNa(NO₂)₂, low temp. triplet exciton decay, photolum. decay temp. depend. meas. 7-21821

ferroelectric materials continued

Ba(Ca_{1/3}Nb_{2/3})O₃-PbZrO₃-PbTiO₃ ceramics, hot-pressed, ferroelectric phase transitions 7-7652
 Ba₂NaNb₅O₁₅ single crystals, spatio-temporal electrical instabilities 7-52632
 Ba₂NaNb₅O₁₅, X-ray irradiated ferroelectrics, radioluminesc. and thermolum. 7-27797
 Ba_{2-x}Sr_xK_{1-y}Nb₂O₇, ferroelectric tungsten bronzes, crystal growth and optical appl. 7-39085
 BaSrNb₂O₆, ferroelectric thin films, pyroelec. props 7-59154
 BaSrNb₂O₁₂, chaotic states, high resolution electron microscope study 7-3001
 Ba₂Sr_{1-x}Nb₂O₆, poly- and single-domain samples, integrated light scatt. and polarisation 7-53361
 Ba_{0.5}Sr_{0.5}TiO₃ polycryst. films, SAW scatt. and ferroelec. transitions 7-44984
 BaTiO₃ ceramics, Maxwell-Wagner relax. and degradation 7-2970
 BaTiO₃, cryst. dynamics near T_c, Mossbauer diff. study 7-6733
 BaTiO₃, crystalline samples, low temp. sp. ht. meas. 7-2225
 BaTiO₃, dielectric, electrical and acoustic props. 7-53224
 BaTiO₃, electro-optic props. 7-39088
 BaTiO₃, ferroelectric, optical switching 7-37020
 BaTiO₃, ferroelectric solid, microwave absorpt., Curie temp. and ultrasonic attenuation 7-39049
 BaTiO₃, polycryst., glasslike behaviour at very low temp. 7-27647
 BaTiO₃ single cryst., elastic and piezoelec. coeffs. 7-2979
 BaTiO₃, submillimetre dispersion of permittivity 7-64556
 BaTiO₃, vibronic ferroelec., correl. length estimate (*Russian*) 7-17277
 BaTiO₃:⁵⁷Fe, multiphonon transitions from modulated hyperfine electric field gradients 7-27633
 BaTiO₃:Nb(Ca), ferroelec. domains, SEM and TEM obs. 7-2998
 BaTiO₃-based ceramic, nonlin. electromechanical parameter meas. 7-13094
 BaZnGeO₄, phase transitions, X-ray study 7-52036
 Bi_{1/3}V_{2/3}TiO₃, layered cpd., crystal-chemical and dielectric props. 7-6595
 Cd₂Nb₂O₇, Fe³⁺ ESR study 7-64516
 Cd₂Nb₂O₇, ferroelectric, electrooptic props. 7-59180
 CsCaF₃, fluoroperovskites, IR refl. spectra, temp. depend. 7-22248
 CsH₂AsO₄ and CsH₂D_{21-x}AsO₄, ferroelectric, optical props., radiation effects 7-33406
 CsH₂AsO₄ crystals, electrogyration effects investig. 7-3022
 CsH₂AsO₄ ferroelec. cryst., EPR studies of AsO₄³⁻ centres 7-45816
 CsH₂(D₂)PO₄, ferroelectrics, electrostrictive corrections to pseudo ID Ising model 7-59158
 CsH₂PO₄ ferroelec., dielec. relax. meas. in paraelec. and ferroelec. phases, time domain spectroscopy method (*Japanese*) 7-4862
 CsH₂PO₄:Cu²⁺ pseudo-1D ferroelectric, 3D correls., EPR meas. 7-38931
 EuAsO₄ crystal, vibr. spectra and optical absorption studies 7-13145
 Hg₂Cl₂, imperfect crystal, structural phase transition, elastic breakdown 7-2165
 K₃BiCl₆.2KCl.KH₃F₄, improper ferroelectric phase transition, dielec. meas. 7-45943
 KD₂PO₄-type ferroelectrics, central peak, deuteration effects 7-64586
 KH₂AsO₄, paraelectric, cluster distrib., proton spin-lattice relax. time 7-2946
 KH₂AsO₄, paraelectric, cluster distrib., ⁷⁵As spin-spin and spin-latt. relax. 7-2947
 K(H_{1-x}D_x)₂PO₄ crystals, electrogyration effects investig. 7-3022
 K(H_{1-x}D_x)₂PO₄, imperfect crystal, structural phase transition, elastic breakdown 7-2165
 KH₂PO₄, hydrostatic pressure effect on ferroelectric relaxational mode, light scatt. study 7-2971
 KH₂PO₄:Ti²⁺, impurity centres, ESR line width studies 7-38498
 K_{1-x}Li_xTaO₃ single cryst., dielec. properties at 10⁻² to 10³ Hz 7-2997
 KNO₃, surface charge layer, spontaneous polarisation rel. to particle size (*Korean*) 7-27673
 KNbO₃, single domain cryst. prep., orientation and dielec. polarisation 7-45950
 KNbO₃, unstable point domains in ferroelectrics 7-17280
 K₂SeO₄ incommensurate ferroelectric, ultrasonic rel. and elastic moduli meas., phason obs. 7-51956
 K(Ta_{0.9}Nb_{0.1})O₃, ferroelec. transitions, EXAFS studies 7-64780
 KTa_{1-x}Nb_xO₃, lattice dynamics, nonlinear shell model 7-51971
 KTaO₃, soft mode damping, determ. by submillimeter backward wave spectroscopy 7-45910
 KTaO₃:Fe³⁺, EPR of Fe³⁺ centres, electric field effect 7-38926
 KTaO₃:Li, time depend. phase transform., neutron diff. meas. 7-44799
 K₂ZnCl₄, incommensurate phase, piezo-optical effects, birefr. meas. 7-45973
 K₂ZnCl₄ incommensurate ferroelectric, ultrasonic rel. and elastic moduli meas., phason obs. 7-51956
 KZnF₃, fluoroperovskites, IR refl. spectra, temp. depend. 7-22248
 Li₃GeO₅, single cryst., nonlin. electromechanical parameter meas. 7-13094
 Li₃GeO₅ ferroelectric single crystals, pyroelectric props. 7-64576
 LiIO₃, ferroelectric, optical props., radiation effects 7-33406
 LiND₄SO₄, ferroelastic and ferroelectric domain struct., SEM obs. 7-27675
 LiNH₄SO₄, ferroelastic and ferroelectric domain struct., SEM obs. 7-27675
 LiNbO₃ crystals, struct. defects and etch figures 7-44555
 YZ-LiNbO₃, dislocation electric fields and small-angle grain boundaries, ferroelectric domains 7-3000
 LiNbO₃, elastic and dielec. props. 7-63715
 LiNbO₃, ferroelec. single crystals with multi-domain layers, fabrication and SAW excitations 7-27676
 LiNbO₃, ilmenite modifications, vibr. spectra 7-22243
 LiNbO₃ polycrystalline films, prep. by hydrolytic decomp. of metal alkoxide alcoholic solns., SEM obs. 7-7044
 LiNbO₃ powders obtained by the alkoxy method, crystallisation and ferroelectric props. 7-7648
 LiNbO₃, prod. by Czochralski and Stepanov methods, elec. phenomena accompanying growth 7-32332
 LiNbO₃, profiled cryst. growth by Stepanov's method, regular domain struct. prod. 7-32330
 LiNbO₃ single crystal fibres, ferroelec. domain structs. 7-22202
 LiNbO₃, z-cut interferometers, thermal instability, electrostatic mechanism 7-37207
 LiNbO₃:Cr³⁺ (Fe³⁺) (Mn²⁺), EPR of axial and low-symmetry paramagnetic centres 7-38925

ferroelectric materials continued

LiNbO₃:Fe³⁺, anomalous phase transitions, Mossbauer spectroscopy studies 7-2992
LiNbO₃:MgO, melt growth and charactn. 7-58170
LiNb(Ta)O₃, crystalline samples, low temp. sp. ht. meas. 7-2225
Li₂O-Nb₂O₅-(TiO₂)₂ system, vicinity of LiNbO₃, solid solns., crystal chemical and ferroelectric props. 7-6805
Li₂O-Ta₂O₅-(SnO₂)₂ system, vicinity of LiTaO₃, solid solns., crystal chemical and ferroelectric props. 7-6805
LiTa_{1-x}Mg_xO_{3-3x}F_{3x}, prep., ferroelec. Curie temp., effect of cationic substitution 7-45946
LiTaO₃, cryst. strip growth and quality, prod. by Stepanov's method 7-32331
LiTaO₃ crystals, parametric holographic-type light scatt. processes 7-1215
LiTaO₃, Czochralski grown with modulated struct., periodic laminar ferroelec. domains, SHG 7-59405
LiTaO₃ single crystals, synthesis and recrystallisation under hydrothermal conditions 7-3157
LiTa_{1-x}Zn_xO_{3-3x}F_{3x}, prep., ferroelec. Curie temp., effect of cationic substitution 7-45946
LiXO₃ (X=Nb,Ta,II), X-ray irradiated ferroelectrics, radioluminesc. and thermolum. 7-27797
NH₄HSeO₄, X-ray irr., existence of incommensurate phase, permitt. meas. 7-33338
(NH₄)₂SO₄, partially deuterated, phase transition, heat of transition 7-53246
(NH₄)₂SO₄, phase transitions, appl. of NH₃⁺ paramag. probe to mol. motion 7-27604
(NH₄)₂ZnCl₄, internal motions and phase transitions, PMR studies 7-2993
Na_{0.5}Bi_{0.5}TiO₃, Raman spectra study 7-53303
NaH₃(SeO₃)₂, low temp. struct. phase transition 7-64580
(Na_{0.5}K_{0.5})NbO₃, sintering, densification and elec. props., effect of Ba additions 7-46387
NaNO₂, cryst., piezoelec. strain const., calcs. 7-53238
NaNO₂, crystalline samples, low temp. sp. ht. meas. 7-2225
NaNO₂, incommensurate ferroelec., in transverse elec. field, virtual Lifshitz point 7-45947
NaNO₂, single cryst. growth by Stepanov's method 7-32329
NaNO₂, solid ferroelectric and paraelectric phases, lattice vibrs., Raman and IR spectra anal., mol. dynamics calcs. 7-21373
NaNbO₃, ilmenite modifications, vibr. spectra 7-22243
Nb₂O₅ and Nb oxide cpds., synthesis of fine particles, struct. studies 7-59212
PLZT ceramics, mechanical strength, composition and polarisation depend., microindentation meas. 7-6697
PLZT ceramics, optical second harmonics, temp. and elec. field depend. meas. 7-5952
PLZT electro-optical ceramics, electron pulse irradiation-induced transient optical absorpt. study 7-6682
PLZT ferroelec. ceramics, IR optical and electrooptical props. studies 7-7675
PLZT, ferroelec. ceramic, laser-induced surface metallisation 7-53924
PLZT ferroelec. polycrystalline oxides, controllable powder synthesis, HP and PHP methods 7-7935
PLZT ferroelectric ceramics, gamma, electron and neutron irr., effects study 7-6677
PLZT, ferroelectric films, properties and applications 7-59156
PLZT polarised ceramics, electroconductivity asymmetry obs. 7-7225
PLZT transparent ceramic modulator, visual classroom demonstrations appl. 7-4647
PLZT transparent ferroelec. ceramic, hologram recording energy transfer, light scatt. effects study 7-5855
PLZT transparent ceramics, laser beam self-deflection and self-focusing meas. 7-5960
PLZT transparent ferroelec. ceramics, low freq. dielec. props. study 7-7630
PLZT, transparent ferroelectric ceramic, surface composition and structure 7-32765
PLZT, transparent ferroelectric ceramic, irradiation effects 7-59157
PLZT-PZN electro-optic ceramics, elec., opt. and switching props. 7-7646
PZT 65/35 DISC, partially and fully poled, mechanical reson. associated with electrical reson. 7-59162
PZT:Nb ceramics, sintering, pair doping, elec. characts. 7-39469
Pb₄Ba_{0.9}Ge₂O₁₁, rhombohedral, acoustic symmetry and vibr. anharmonicity 7-16695
(Pb,Ba)_{1-x}TiO₃, ferroelec. solid solns., dielectric and hysteresis props. 7-64588
Pb₅Cr₂F₁₉, nonlinear optic, lattice const., ferroelec. Curie temp., phase transition obs. at 555K 7-17275
PbGeO₃, ferroelec. domain struct. and diffuse phase transition, permittivity meas. 7-13108
Pb₅Ge₂O₁₁, Mn²⁺ ESR study, pulsed saturation effects 7-64515
Pb₅Ge₂O₁₁, rhombohedral, acoustic symmetry and vibr. anharmonicity 7-16695
Pb₅Ge₂O₁₁, surface segregation of Pb upon heating to the melting pt. 7-6931
Pb₅Ge₂O₁₁:Gd³⁺, impurity ion reorientation kinetics 7-45940
PbHPO₄, phase transition, thermal expansion meas. 7-44861
PbHPO₄, photostimulated luminescence near ferroelec. Curie temp. 7-64697
Pb_{2-x}K_{1+x}Li₂Nb₂O₁₅, tetragonal tungsten bronzes, ferroelastic-ferroelectric coupling (French) 7-27674
Pb(Mg_{1/3}Nb_{2/3})O₃ ceramics, dielec. props. 7-46382
PbMg_{1/3}Nb_{2/3}O₃, ferroelectric, electrooptic props. 7-59180
PbMg_{1/3}Nb_{2/3}O₃, thermal expansion, effect of Mg and Nb substitution by divalent, trivalent, tetravalent and W⁶⁺ ions 7-63851
PbMg_{1/3}Nb_{2/3}O₃-PbTiO₃, MnO doped, relaxor ferroelec. ceramics, dielec. ageing effects 7-22195
Pb(Mg_{1/3}Nb_{2/3})O₃-Pb(Zn_{1/3}Nb_{2/3})O₃, ferroelec. powder, prep., solid solubility, Curie point (Japanese) 7-7945
PbNb₂O₆, unstable point domains in ferroelectrics 7-17280
PbO-K₂O-Nb₂O₅, polymorphism, DTA, X-ray phase anal. 7-6782
PbO-Nb₂O₅ oxide mixture transparent ferroelec. ceramics, phase form. during solid state reaction 7-6591
PbO-Nb₂O₅-Sc₂O₃ oxide mixture transparent ferroelec. ceramics, phase form. during solid state reaction 7-6591
Pb(Sc_{0.5}Nb_{0.5})O₃ ferroelectric ceramics, gamma, electron and neutron irr., effects study 7-6677

ferroelectric materials continued

Pb(Sc_{0.5}Nb_{0.5})O₃ transparent ferroelec. ceramic production by hot pressing and props. 7-7934
Pb(Sc_{0.5}Nb_{0.5})O₃, transparent ferroelectric ceramic, irradiation effects 7-59157
Pb(Sc_{1-x}Nb_x)O₃ ferroelec. ceramics, IR optical and electrooptical props. studies 7-7675
Pb(Sc_{1/2}Ta_{1/2})O₃, single crystals and hot pressed ceramics, ordering, domain struct., TEM obs. 7-26936
(Pb,Sr)_{1-x}TiO₃, ferroelec. solid solns., dielectric and hysteresis props. 7-64588
PbTiO₃, amorphous, with 10 mol.% B₂O₃, radial distrib. function determ., energy dispersive X-ray diff. method 7-16420
PbTiO₃ based glass ceramics piezoelectricity, pyroelectricity and ferroelectricity 7-7654
PbTiO₃, cryst. optical studies of precursor and spontaneous polarisation 7-45921
PbTiO₃ crystals, ferroelec. transition, phase boundary kinetics 7-2990
PbTiO₃, ferroelectric films, properties and applications 7-59156
PbTiO₃, spontaneous strain, anomalous press. depend. 7-26833
PbTiO₃:Fe³⁺, F⁻ charge compensating cluster form., EPR spectra studies 7-64518
Pb₂(VO₄)₂, β-γ transition, intermediate modulated struct. 7-2183
Pb(Zr_{0.5}Nb_{0.5})₂ piezoelectric ceramics containing Pb(Zn_{1/3}Nb_{2/3})O₃ 7-2984
Pb[(Mg,Zn)_{1/3}Nb_{2/3}]O₃, prep. and ferroelec. props. (Japanese) 7-27993
Rb_{1-x}(ND₄)_xD₂PO₄ structural glass phase, X-ray scatt. meas. 7-26660
RbCaF₃, fluoroperovskites, IR refl. spectra, temp. depend. 7-22248
RbH₂PO₄ crystals, electrogyration effects investig. 7-3022
RbH₂PO₄:Ti³⁺, impurity centres, ESR line width studies 7-38498
RbHSeO₄, optical birefr. meas., temp. depend. 7-27689
RbHSeO₄ single cryst. ferroelec., H bond vibr., polarised IR spectra studies 7-27707
Rb_{0.61}(NH₄)_{0.39}H₂PO₄, mixed crystal, dielec. study of ferroelec. transition 7-53248
Rb₂ZnCl₄ incommensurate ferroelectric, ultrasonic rel. and elastic moduli meas., phason obs. 7-51956
Sb_{1-x}Bi_xSI crystals, elec. props. at ferroelec. Curie point 7-2991
SbSI, elec. cond., ferroelec., phase transition temp. 7-45326
SbSI, single crystal, nonlin. electromechanical parameter meas. 7-13094
Sr_{0.5}Ba_{0.5}Nb₂O₆, incommensurate superstructures, phase transition, electron diff. study 7-63792
Sr_{0.61}Ba_{0.39}Nb₂O₆:Ce crystals, light emission obs. during freq.-degenerate laser pumping 7-15947
Sr_{1-x}Ba_xNb₂O₆, ferroelectric tungsten bronzes, crystal growth and optical appl. 7-39085
Sr(La_{1/2}Nb_{1/2})O₃-PbZrO₃-PbTiO₃, hot-pressed ceramics, dielectric, piezoelectric and optical props. 7-64583
SrTiO₃ (100), adsorption of H₂O, surface struct., photon stimulated ion desorption SEXAFS determ. 7-64752
SrTiO₃ ceramics, Maxwell-Wagner relax. and degradation 7-2970
TiD₂PO₄, cryst. struct., X-ray diff. study 7-32414
YIG/ferroelec. struct., surface magnetostatic wave propag. charact. meas. 7-52965

ferroelectric phenomena *see ferroelectricity*
ferroelectric semiconductor materials *see ferroelectric semiconductors*
ferroelectric semiconductors
IV-VI compounds, dipole-dipole interactions and ferroelectric props. 7-39046
(Ba_{1-x}La_x)TiO₃ semiconducting ceramic props., grain boundary and dopant effects (Japanese) 7-6631
Ba_{0.93}Sr_{0.07}TiO₃, single crystal, electronic transport behaviour 7-33011
BaTiO₃, acceptor state behaviour, influence of impurities and lattice defects 7-2539
BaTiO₃, elec. cond. rel. to point defects 7-6619
BaTiO₃, grain boundary inhomogeneity phenomena, microcontact meas. (German) 7-58893
BaTiO₃:Ce, Mg, Ga(Cr)(Cu), double doping study 7-2037
BaTiO₃:Y₂O₃(La₂O₃)(Ce₂O₃), semiconductor props., influence of dopant oxides 7-6650
BiSel, dendritic, growth from vapour, characteris. 7-21788
GeTe, ferroelec. phase transition, electron-phonon interaction 7-13106
Pb₂Ge₂O₁₁, ferroelec. domain-struct. dynamics visualisation using a nematic liq. cryst. 7-53250
Pb_{0.93}Sn_{0.07}Se, ferroelec. phase transition, electron-phonon interaction 7-13106
PbTe, ferroelec. phase transition, electron-phonon interaction 7-13106
SbSBr, ferroelec. semicond., band struct., X-ray spectral studies 7-58739
SbSI, crystals, grown from melt, microhardness study 7-12196
SbSI, elec. charactn. of crystals, grown from melt by temp. fluctuation technique 7-13104
SbSI, ferroelectric semiconductor, photoacoustic spectroscopy 7-16696
SbSI, hollow cryst. growth from vap. 7-53520
SbSI, SbSOI, cryst. growth and elec. charactn. 7-53564
SbSI single crystals, vapour growth, morphology rel. to temp. gradients 7-46287
SbSeI, crystals, grown from melt, microhardness study 7-12196
SrTiO₃, acceptor state behaviour, influence of impurities and lattice defects 7-2539

ferroelectric switching
ceramic bar, normal mode responses, influences of domain switching and dipole dynamics 7-45945
ferroelectric liquid crystal with negative dielec. anisotropy, switching behaviour 7-39084
liquid crystals, ferroelectric, molecular orientation structures of surface stabilised states and their switching processes 7-16406
polyvinylidene fluoride, Form I, ferroelectric switching characts., microdomain nucleation and growth model 7-22197
smectic C* liquid crystal, alignment and switching characteristics 7-64589
BaSrNb₂O₆, ferroelectric thin films, pyroelec. props 7-59154
PLZT hot pressed ceramic, polarisation reversal studies under hydrostatic press. 7-59160
PLZT-PZN electro-optic ceramics, elec., opt. and switching props. 7-7646
Pb₅Ge₂O₁₁, ferroelec. domain-struct. dynamics visualisation using a nematic liq. cryst. 7-53250
Pb₅Ge₂O₁₁:Gd³⁺, impurity ion reorientation kinetics 7-45940

ferroelectric thin films
polyvinylidene fluoride films, active gauge for initiation diagnostics 7-30000

ferroelectric thin films continued

- (Ba,Sr)TiO₃ film metal-dielec.-metal system, polarisation switching 7-52849
 Ba₂NbNb₂O₁₅ incommensurate ferroelec. thin films, disinclinations, textures, four-state clock model description 7-257
 BaSrNb₂O₆, ferroelectric thin films, pyroelec. props 7-59154
 Ba_{0.5}Sr_{0.5}TiO₃ polycryst. films, SAW scatt. and ferroelec. transitions 7-44984
 LiNbO₃ polycrystalline films, prep. by hydrolytic decomp. of metal alkoxide alcoholic solns., SEM obs. 7-7044
 NaNO₂ thin films, ferroelectric and dielectric props. 7-39037
 PLZT, ferroelectric films, properties and applications 7-59156
 PZT films, crystn. kinetics 7-45090
 PbTiO₃, ferroelectric films, properties and applications 7-59156

ferroelectric transitions

- see also critical fluctuations; displacive transformations; ferroelectric Curie temperature; order-disorder transformations*
 A₂BX₄-type crystals, incommensurate phase, zig-zag domain wall structure 7-33342
 atomic occupancies, in order-disorder and displacive transformations (Japanese) 7-27670
 crystal, first order ferroelec. transition in external mag. field 7-2994
 diglycine nitrate, alanine-doped, dielectric props. 7-45908
 diglycine nitrate, ferroelec. transition mechanism, mol. reorientation, ¹⁴N and ¹⁷O quadrupole coupling meas. 7-53245
 diglycine nitrate, spontaneous polarisation and electrocaloric effect near the ferroelectric transition 7-17273
 double-well potential model 7-45949
 dynamic mechanism, electron-ion interaction 7-22199
 electric field perturbed NQR 7-17276
 ferromagnetic ferroelectrics, dynamic characteristics, soft modes saturation (Russian) 7-27672
 IV-VI compounds, dipole-dipole interactions and ferroelectric props. 7-39046
 IV-VI narrow gap vibronic ferroelec., correl. length estimate (Russian) 7-17277
 low temperature renormalization group and ferroelectrics 7-64585
 magnetic ferroelectrics, inhomogeneous magnetoelectric effect 7-38920
 mean-field theory of structural phase transitions in the A'A''BX₄-type compounds 7-16734
 methylammonium mercury chloride, ³⁵Cl NQR study of low temp. phase transition 7-22160
 methylammonium mercury chloride, ferroelec. phase transition, proton-¹⁴N double reson. study 7-7653
 non-polar crystals, antiferroelectric ordering, 1D mechanism 7-33344
 nonequilibrium state, phase transitions in electromagnet fields 7-33340
 polytrifluoroethylene, ferroelec. order and phase transition 7-13105
 quasi-1-D, soft mode and central peak studies 7-13103
 Rochelle salt, phase transition dynamics 7-21367
 Rochelle salt crystals, low temp. relaxational soft mode transforms., dielec. spectra meas. 7-17279
 sequential antiferroelectric-ferroelectric phase transitions, phase diagrams 7-2988
 tetraethyl ammonium MX₄ compounds (M=Co,Zn,Mn;X=Cl,Br), structural phase transitions 7-44801
 tetramethyl ammonium tetrachlorozincate, internal motions and phase transitions, PMR studies 7-2993
 bis(tetramethylammonium) bromochlorocuprate single cryst. solid solns., phase diagram study 7-26944
 TGS, uniaxial ferroelec., transition under nonequilibrium conditions 7-13107
 triglycine sulphate:Ti⁴⁺, X-ray effects, changes in physical props. 7-22198
 trimethylammonium nanochlorodiantimonate, high freq. dielectric dispersion 7-53223
 tris(trimethylammonium)Sb₂Cl₆ single crystals, dielec. and pyroelec. props. study 7-53210
 tris (dimethylammonium) nonachlorodiantimonate, ferroelectric phase transition 7-33345
 tris-sarcosine calcium chloride: Mn²⁺ crystals, ferroelec. phase transition 7-2995
 tris-sarcosine calcium chloride, deuterated, ferroelectric props. 7-39050
 tris-sarcosine calcium chloride, dielectric dispersion 7-2965
 vinylidene-trifluoroethylene copolymer, ferroelec. phase transition, X-ray diff. investig. 7-53249
 AgNO₃, metastable phase III, ferroelectricity 7-39052
 Ag₂Pb₄Nb₁₀O₃₀, ferroelectric with tetragonal W-bronze struct., first-order transition 7-39048
 Ag₂Sb₂, ferroelectric transition, electric field perturbed NQR 7-17276
 Ba(Ca_{1/3}Nb_{2/3})O₃-PbZrO₃-PbTiO₃ ceramics, hot-pressed, ferroelectric phase transitions 7-7652
 Ba_{0.5}Sr_{0.5}TiO₃ polycryst. films, SAW scatt. and ferroelec. transitions 7-44984
 Ba_{1-x}Sr_xTiO₃ system, ferroelectric, weakly broadened phase transition 7-45944
 BaTiO₃, cryst. dynamics near T_c, Mossbauer diff. study 7-6733
 BaTiO₃, ferroelectric transition dynamics 7-26904
 BaTiO₃, Nd₂O₃-modified, defect struct. and dielec. props 7-37968
 BaTiO₃, vibronic ferroelec., correl. length estimate (Russian) 7-17277
 BaTiO₃:Fe³⁺, ferroelectric transition, EPR 7-33343
 BaZnGeO₄, phase transitions, X-ray study 7-52036
 Cd₂Nb₂O₇, ferroelectric, electrooptic props. 7-59180
 CsH₂AsO₄ crystals, electrogyration effects investig. 7-3022
 CsLiCrO₄, ferroelectric phase transition 7-39047
 EuCrO₃, coexistence of mag. and electric dipole ordering after optical pumping 7-17171
 GeTe, ferroelec. phase transition, electron-phonon interaction 7-13106
 K₂Ba(NO₂)₄, successive phase transitions, dipolar frustration 7-53247
 K(H_{1-x}D_x)₂PO₄ crystals, electrogyration effects investig. 7-3022
 KH₂PO₄ crystal, bifurcation response near ferroelectric transition 7-39051
 KH₂PO₄ type crystals, improper ferroelec., phase transition, quadratic electrogyration coeff. temp. anomalies study (Russian) 7-2996
 KH₂PO₄, ultrasonic attenuation oscils. near phase transition 7-38128
 KH₂PO₄:Ti²⁺, impurity centres, ESR line width studies 7-38498
 K_{1-x}Li_xTaO₃ monocrys., polarisation jump, ferroelec. transition and domains study (Russian) 7-22200
 K_{1-x}Li_xTaO₃ single cryst., dielec. properties at 10⁻² to 10³ Hz 7-2997
 KNbO₃, surface charge layer, spontaneous polarisation rel. to particle size (Korean) 7-27673

ferroelectric transitions continued

- K₂Pb₄Nb₁₀O₃₀, ferroelectric with tetragonal W-bronze struct., first-order transition 7-39048
 K₂SeO₄, β to α to β transition, modulated struct. 7-16724
 K(Ta_{0.91}Nb_{0.09})O₃, ferroelec. transitions, EXAFS studies 7-64780
 KTaO₃:Gd³⁺ (Fe³⁺), ESR, effect of external electric field 7-38933
 LiN(H₂D_{1-x})₂SO₄ crystals, vibr. spectra and ferroelec. transition, Raman scatt. study 7-53304
 LiNbO₃, elastic and dielec. props. 7-63715
 LiNbO₃:Fe²⁺ anomalous phase transitions, Mossbauer spectroscopy studies 7-2992
 NH₄Cl, spontaneous and field induced current peaks at order-disorder phase transition 7-45948
 NH₄H₂PO₄, antiferroelectricity, role of H bonds 7-64582
 NH₄H₂PO₄:SeO₃²⁻, partially deuterated, D concentrations in H₂PO₄⁻ and NH₄⁺ radicals, ESR spectra 7-27671
 NH₄HSeO₄ crystals, deuterated, pyroelectric props. 7-13098
 NH₄HSeO₄, X-ray irradi., existence of incommensurate phase, permitt. meas. 7-33338
 β-NH₄LiSO₄, elastic stiffness constants, ultrasonic pulse echo overlap meas. 7-12188
 (NH₄)₂SO₄, partially deuterated, phase transition, heat of transition 7-53246
 (NH₄)₂SO₄, phase transitions, appl. of NH₄⁺ paramag. probe to mol. motion 7-27604
 (NH₄)₂ZnCl₄, internal motions and phase transitions, PMR studies 7-2993
 NaH₃(SeO₃)₂, low temp. struct. phase transition 7-64580
 (Na_{0.5}K_{0.5})NbO₃, sintering, densification and elec. props., effect of Ba additions 7-46387
 Na₂MoO₄F₃, ferroelastic and ferroelectric behaviour 7-44792
 NaNO₂, incommensurate ferroelec., in transverse elec. field, virtual Lifshitz point 7-45947
 NaNO₂, solid ferroelectric and paraelectric phases, lattice vibrs., Raman and IR spectra anal., mol. dynamics calcs. 7-21373
 NaNbO₃ crystals, antiferroelec. transition, phase boundary kinetics 7-2990
 NaOD, ²³Na critical longitudinal relax. time near antiferroelec. transition 7-17235
 NaOD, low temp. phase transform., heat capacity, calorimetric study 7-16785
 PLZT rhombohedral ceramics, electrocaloric effect study, diffuse phase transition intermediate state 7-7645
 PZT ceramic, pressure induced ferroelectric-antiferroelectric transition 7-22201
 PZT, paraelectric phase transition broadening due to coexistence of ferroelectric and antiferroelectric phases 7-45942
 PZT solid solutions, p-t-x diagram 7-64581
 Pb₂CrF₉, nonlinear optic, lattice const., ferroelec. Curie temp., phase transition obs. at 555K 7-17275
 PbGeO₃, ferroelec. domain struct. and diffuse phase transition, permittivity meas. 7-13108
 Pb₂GeO₁₁, high pressure Raman scatt., phonon modes and Gruneisen parameters 7-33391
 Pb₂GeO₁₁, sound velocity discontinuities at the phase transition 7-17274
 PbHAsO₄, ferroelec. phase transitions, proton tunnelling effect, NQR study 7-53172
 PbHPO₄, phase transition, thermal expansion meas. 7-44861
 PbIn_{1/3}Nb_{1/2}O₃, antiferroelec., phase transition, B-site cation order effects 7-7651
 Pb(M_{1/2}Sb_{1/2})O₃, perovskite type antiferroelectrics, (M=Sc, Ho-Lu), X-ray and dielec. characts. 7-7649
 PbMg_{1/3}Nb_{2/3}O₃ ceramic, elastic moduli and diffuse ferroelec. phase transition, press. depend. 7-63717
 PbMg_{1/3}Nb_{2/3}O₃, cryst. struct., electrocaloric effect, diffuse phase transition 7-22194
 PbMg_{1/3}Nb_{2/3}O₃, ferroelectric, electrooptic props. 7-59180
 PbMn_{2/3}MO₃, perovskite-type cpds., (M=Mo, Te, Re), dielec. and mag. props. 7-7650
 PbO-K₂O-Nb₂O₅, polymorphism, DTA, X-ray phase anal. 7-6782
 Pb_{0.93}Sn_{0.07}Se, ferroelec. phase transition, electron-phonon interaction 7-13106
 PbTe, ferroelec. phase transition, electron-phonon interaction 7-13106
 PbTiO₃ based glass ceramics piezoelectricity, pyroelectricity and ferroelectricity 7-7654
 PbTiO₃ crystals, ferroelec. transition, phase boundary kinetics 7-2990
 Pb(Ti_{0.58}Fe_{0.20}Nb_{0.20}Ti_{0.02})_{0.995}O_{0.005}O₃ ferroelec. ceramic, TEM study 7-17272
 RBH₂PO₄ crystals, electrogyration effects investig. 7-3022
 RBH₂PO₄:Ti²⁺, impurity centres, ESR line width studies 7-38498
 RBHSeO₄, optical birefr. meas., temp. depend. 7-27689
 Rb_{0.61}(NH₄)_{0.39}H₂PO₄, mixed crystal, dielec. study of ferroelec. transition 7-53248
 Rb₂Pb₄Nb₁₀O₃₀, ferroelectric with tetragonal W-bronze struct., first-order transition 7-39048
 Rb₂ZnCl₄, cryst., incommensurate modulation, light propag. 7-22196
 Sb_{1-x}Bi_xSI crystals, elec. props. at ferroelec. Curie point 7-2991
 SbSI, elec. cond., ferroelec., phase transition temp. 7-45326
 Sn₂P₂(Se₂S_{1-x})₂, ferroelec., phase p, T, x diagram (Russian) 7-17278
 VDF/TrFE copolymer ferroelectric phase transition, observation using US spectroscopic system 7-20521

ferroelectricity

- see also antiferroelectricity; ferroelectric devices; ferroelectric materials; ferroelectric switching; ferroelectric transitions*
 crystals, toroidal ordering and impurity scattering 7-38838
 dielectric and magnetic materials, linear feedback models for polarisation and magnetisation 7-22179
 fabrication and SAW excitation of ferroelectric single crystals with multi-domain layers 7-27676
 ferroelectric antiferromagnet, resonance interaction of spin waves with polarisation waves 7-7579
 IEEE standard definitions of primary ferroelectric terms 7-39045
 imperfect crystal, structural phase transition, elastic breakdown 7-2165
 imperfect crystals, generation of second harmonic near struct. phase transitions 7-2168
 incommensurate phases, phasons, dynamic pinning mechanisms 7-45941
 liquid crystals and devices 7-21094
 magnetic ferroelectrics, inhomogeneous magnetoelectric effect 7-38920
 relaxation ferroelectrics, dielectric and thermal props. at low temps. 7-13102

ferroelectricity continued

- smectic liquid crystals, ferroelectric, helical twist and spontaneous polarisation direction, tilt orientation struct. 7-16401
smectic liquid crystals, ferroelectric, helical twist sense and spontaneous polarisation 7-16400
toroidal collective excitations and the optical properties of crystals 7-39059
twofold incommensurate phases, ferroelectricity, polarisation-wave condensation 7-53243
uniaxial ferroelectrics, background dielec. suscept. investig. 7-2987
unstable point domains in ferroelectrics 7-17280
H-bonded ferroelectrics, one-dimensional Schrodinger eqn. with double-well pot. 7-29807
KH₂PO₄, hydrostatic pressure effect on ferroelectric relaxational mode, light scatt. study 7-2971
LiKSO₄ single crystals, optical activity, ferroelec. and ferroelastic props. 7-27687

ferrofluids see magnetic fluids

ferromagnetic-antiferromagnetic transitions

- see also metamagnetism; Morin temperature
mixed phase transition for hierarchical Ising spin glass model 7-38886
Cd(Cu_{1-x}Ni_x)₂ mag. and cryst. props. 7-27506
Dy, magnetoheterogeneous state, H-T phase diagram 7-7507
Fe₂Ni_{85-x}Mn₁₅, low temp. sp. ht. near ferromag.-antiferromag. transition (Russian) 7-7512
La(Fe₂Al_{1-x})₁₃, mag. props. determined by neutron scatt. and Mossbauer spectroscopy 7-2820
Mn-Al-C system, mag. and struct. transform. (Russian) 7-59014
Mn₁₁Ge₈, intermetallic compound, mag. props. 7-52985
NpAs₂, single crystals, Hall resistivity 7-12739
RAlCu₄ (R=Gd, Tb, Dy, Ho, Er), cubic alloys, mag. props. 7-52936

ferromagnetic Curie temperature see Curie temperature

ferromagnetic-paramagnetic transitions

- see also Curie temperature
fluid system, internal quantum states, computer simulation 7-45678
semi-infinite ferromagnetic q-state Potts bulks separated by bond diluted interface, criticality 7-33179
steel, stainless, dual phase, phase transform. obs. using thermomag. analysis 7-53696
surface magnetism, spin-polarised electron diff. and photoemission 7-59380
Au-Fe, mag. hyperfine field, temp. and composition depend. 7-45243
CeSi₃, galvanomag. and thermoelec. props. 7-38537
Eu-Yb, high press. mag. and elec. props. studies 7-7541
Fe-Ni-Ti(Al)(Cr), nitrided layers, struct. investig. using Mossbauer spectroscopy (Russian) 7-53992
Gd₃(Ga_{1-x}Fe_x)₂O₁₂ and Gd₃[Al₃(Ga_{1-x}Fe_x)₂O₁₂], mag. solid soln. systems for regenerator materials 7-59015
MnAs, paramagnetic-ferromagnetic transition, nucleation model calcs. 7-52992
Mn₉₇Ti_{0.03}As, mag. phase transitions, effect of Ti additions 7-27519
Ni, Fermi surface change near the mag. transition 7-16935
Pd-Fe:B(O), mag. susceptibility, impurity effects 7-27520
PrNi₅, paramag.-ferromag. phase transition, external mag. field, spin ordering model 7-52988
Ta complex, (BEDT-TTF)₃Ta₂F₁₁, optically enhanced phase transition, EPR investig. 7-64454
YCo₃H_x, mag. props. meas. 7-33217
YCo₅H_x, mag. props. meas. 7-33217
Y₂Co₇H_x, mag. props. meas. 7-33217

ferromagnetic properties of substances

- see also ferromagnetic relaxation; ferromagnetic resonance; ferromagnetism; magnetic semiconductors
actinide-transition metal alloys, AM₂, A=U-Np, M=Fe-Ni, magnetism and electronic props. 7-27505
amorphous films, ferromag., induced mag. anisotropy (Russian) 7-52974
BCC ordered alloy, high temp. mag. states (Russian) 7-64466
bis(methylammonium) copper tetrachloride, ferromag., parallel-pumped magnons, deterministic chaos obs. 7-52962
Curie point thermomagnetic engine, demonstration of Carnot principle 7-48233
cyclohexyl ammonium copper tribromide-d₁₄, S=1/2 ferromag. chain system, short and long range correlations 7-17159
defect and microstructural analyses using TEM in ferromagnetic materials 7-37817
electrical steels, physical metallurgy, conf., New York, USA (Feb. 1985) 7-4626
FCC metastable phase epitaxial films on Cu local mag. moment, XPS study 7-53504
(Fe_{1-x}Ni_x)₉₂C₈ pseudobinary FCC alloys, magnetic phase diagram studies 7-2844
Fe-Si multilayered thin films, stacking structs., magnetostatic coupling and layer boundary interdiffusion 7-7574
ferromagnetic, electronic quasiparticle struct., temp. depend. 7-32908
ferromagnetic-nonferromagnetic supercond. superlattices, vortex pinning 7-45591
garnets, magneto-optical effects and appls. (French) 7-59190
graphite, nonmagnetic samples, ferromag. behaviour 7-53040
hexenylammonium copper tribromide, easy-plane ferromagnetic chains, sp. ht. and spin Hamiltonians, quantum statistics calcs. 7-64469
hexylammonium copper bromide, 1D easy plane ferromag., quantum Monte Carlo and transfer matrix calcs. 7-7468
insulating ferromagnets, surface and interface magnetisation changes with temp., Green's function calcs. (Chinese) 7-38869
magnetoplasma, fluctuations control by using shaped ferromag. material 7-31961
metal particles, ultra fine, ferromag., growth rel. to mag. field 7-53515
metallic glasses, defects, SANS studies 7-51659
metals, eddy current testing, mag. permeability effect 7-22958
misc metal-Fe-B melt-spun magnets, mag. and structural props. 7-53032
multilayer ferromag. thin films, NMR freq. anisotropy (Russian) 7-45830
Ni₃Al₈-based alloys, magnetic and structural props. studies 7-45635
organic polymer ferromagnet, prep., ESR and Mag. props. 7-64439
permalloy films, domain motions and instabilities, magneto-optic observation 7-53095
Permalloy films, field induced uniaxial anisotropy, thickness depend. 7-53086
Permalloy thin films heads, RF sputtered, mag. props. 7-33235

ferromagnetic properties of substances continued

- permanent magnet materials, props., struct., exchange interactions 7-53053
phase analysis, porosity, mag. meas. methods 7-28240
PMMA, nonmagnetic samples, ferromag. behaviour 7-53040
polymers, conjugated, ferromagnetic, polaron spins by doping, PPP model struct. anal. 7-52944
rare earth alloys, R₂(Fe,Al,Co)₁₄B, mag. props., composition depend. 7-53030
rare earth alloys, R₂Fe₁₄B, R=La-Nd, Sm, Gd-Tm, Lu and Y, ⁵⁷Fe Mossbauer spectra 7-64551
rare earth alloys, R-Co-Fe system between 2:17 and 2:7 phase regions, phase equilibria, metallography, X-ray diff., thermomagnetic anal. 7-17511
rare earth alloys, RMn₂, R=heavy rare earth, mag. state, spin echo NMR spectra 7-27629
rare earth aluminium RAl₂ layered structural sintered composite, mag. entropy 7-59016
rare earth high energy product permanent magnets, magnetising and B/H hysteresis loop meas. 7-53046
rare earth-Fe-B alloys, sintered permanent magnets, depend. of coercivity on anisotropy field 7-45744
rare earth-iron-boron permanent magnet materials, prep. and props., book contrib. 7-27981
semiconductor, donor state, thermally induced abrupt shrinking 7-52510
semiconductors, ferromagnetic, dielectric function and reflectivity above T_c 7-7661
soft magnetic materials, specific magnetic loss meas. at remagnetisation freq. 50 Hz to 200 kHz 7-9850
steel, alloy, electrical resistivity and magnetisation, temp. depend. 7-38535
steel, austenitic, cold deformed, mag. props. (Russian) 7-45734
steel, austenitic, Mn-Cr, hardening characts. and hydroextrusion parameters (Russian) 7-59540
steel, austenitic stainless, electrical resistivity and magnetisation, temp. depend. 7-38535
steel, C, inverse magnetostrictive effect and electromagnetic non-destructive testing methods 7-13714
steel, C, particles in superconducting samples critical current enhancement 7-2796
steel, Cr-Si type parts, mag. characts. after isothermal hardening, heat treatment quality inspection method 7-65261
steel, cryogenic, Al alloying effect on mech. and mag. props. 7-39679
steel, low C, cold rolled lamination, mag. props., Mn and S contents effect 7-7550
steel, magnetic state inspection, elastic stresses in trans-Rayleigh region 7-3558
steel, Ni-Cr-Mn, ferromag., mag. hysteresis loops, effects of grain size, hardness and stress 7-64482
steel, stainless, dual phase, phase transform. obs. using thermomag. analysis 7-53696
steel, stainless, ferromag., mag. hysteresis loops, effects of grain size, hardness and stress 7-64482
steel, structural, heat treated, coercivity in various remanent magnetization states, NDT method development 7-65259
superconductor films, mixed states 7-27478
superconductors, mixed state, surface tension 7-52919
surfaces (100) and (110), Stoner excitation spectrum, spin-polarised electron energy loss spectroscopy 7-53463
teflon, nonmagnetic samples, ferromag. behaviour 7-53040
transition metal surfaces and interfaces, hyperfine fields 7-58847
transition metal thin films, ferromagnetic, surface spin waves, multiband model 7-2834
transition metals, finite temp. ferromagnetism, review, book contrib. 7-33149
trimethylammonium copper decachloride, mag. suscept., linear tetramer with ferromag. coupling 7-7491
uniaxial systems with strong dipolar interaction, nonasymptotic crit. behaviour 7-64467
Al, nonmagnetic samples, ferromag. behaviour 7-53040
AuFe re-entrant spin glass, magnetoresist. and AC susceptibility studies 7-7518
Bi-based metallic glasses, thermal relax. processes 7-51653
Bi-Zn-Fe-O amorphous films, struct. and mag. props. 7-51645
CdCr₂Se₄, ferromag. semiconducting thin films, influence of electric field on magnetisation 7-45738
CdCr₂Se₄ thin films, ferromagnetic semicond., multielectron energy struct., absorpt. spectrum, temp. and doping depend. 7-38488
CdCr₂Se₄-Ga, lightly doped, ferromag., photoconductivity, band struct. 7-7278
Cd(Cu_{1-x}Ni_x)₂, mag. and cryst. props. 7-27506
Ce-(Fe,Co)-(B,Si) system alloys, melt spun ribbons, mag. props. (Japanese) 7-53052
Ce(Co,Cu,Fe)₆, magnetically hard, heat treatment effects on struct. and mag. characts. 7-27564
Ce₂Fe₁₄B, anisotropy constants, temp. depend. (Chinese) 7-59003
CeGe_{1-x}Si_x nearly ferromag. props., temp. and comp. depend. study 7-7493
CeMn(Fe)Si₂, struct. and mag. props. studies (French) 7-37950
CeNi_{5-x}Fe_x, mag. and cryst. props., effect of H absorpt. 7-33168
CeNi_{5-x}Mn_x, mag. and cryst. props., effect of H absorpt. 7-33168
CeRh₂(Bi_{1-x}Si_x)₂, 4f shell dehybridisation, Curie temp. and mag. moments 7-45679
Ce(Rh_{1-x}Co_x)₂B₂ ferromag. Kondo system, anomalous elec. resist. temp. depend. 7-2601
CeRh₂Si₂ Neel temp., chem. press. effects, partial substitution depend. meas. 7-59011
CeRu₂Si₂, heavy fermion, magnetism and spin fluctuation effects induced by partial substitution 7-38850
Co and its alloys, spin wave excitations and magnetisation temp. depend. 7-45642
Co, BCC and FCC forms, ferromag. phases investig. 7-2851
Co, diffusion of ⁴⁸V, mag. anomalies, quasi-chemical model 7-6862
Co ferromagnetic thin layer on Au(111), cryst. struct., TEM study 7-64015
Co, magnetic phase location, total energy spin polarised band calcs. 7-17176
Co, thermal equilibrium vacancies, muon spin resonance studies 7-51757
Co thin films, nucl. spin echo, effect of nonresonance pulsed mag. field 7-45839
Co-Al alloys, magnetic hardening 7-33209

ferromagnetic properties of substances continued

- Co-B alloy, amorphous, thermodynamic, thermomag. and struct. studies (French) 7-16438
 Co-based amorphous alloys, anisotropic electrical magnetoresistivity at 295 K 7-58796
 Co-based metallic glasses, magnetic aftereffect and magnetostriction studies 7-27571
 Co-based metallic glasses, flash annealing under stress 7-52971
 Co-CoO multilayered films, exchange anisotropy 7-27579
 Co-Cr, continuously sputtered films, crystallographic orientation and mag. props. 7-27176
 Co-Cr films, continuous fabrication by sputtering, substrate degassing effects 7-27904
 Co-Cr films, film growth and magnetisation reversal mechanism 7-27585
 Co-Cr films, mag. parameters, Brillouin light scattering study 7-53357
 Co-Cr films, sputter deposition and characterisation 7-27178
 Co-Cr films, sputter deposition, microstructure and its growth mechanism 7-27179
 Co-Cr films, sputter deposited, effects of additive gases on mag. props. 7-27575
 Co-Cr films for perpendicular mag. recording media, deposition in facing targets sputtering system 7-64899
 Co-Cr magnetic thin films, facing targets sputter deposition, microstruct. model 7-27905
 Co-Cr perpendicular recording media, props., effect of impurity gases 7-59069
 Co-Cr sputtered films, microstructural inhomogeneity, mag. props. 7-45768
 Co-Cr thin films, DC magnetron sputtered, mag. props., effect of substrate and deposition rate 7-59067
 Co-Cr thin films, sputter etching and annealing, FMR study 7-59112
 Co-Cr thin films for mag. recording, by facing targets sputtering, C-axis orientation 7-59418
 Co-Fe-Ni-V alloys, Invar props. and mag. field distrib. (Russian) 7-45733
 Co-Gd-Tb-based thin films, properties and stability for magneto-optic recording 7-53075
 Co-Ni-Fe underlayer for double-layer perpendicular media, vacuum deposition and mag. props. 7-27577
 Co-Ni-P electroless plated thin films, microstructure, mag. props., mag. recording appl. 7-27581
 Co-Ni-Re-P films for perpendicular mag. recording media, electroless deposition and mag. props. 7-27580
 Co-P, amorphous, Curie temp. meas. 7-45669
 Co-P electroless plated thin films, microstructure, mag. props., mag. recording appl. 7-27581
 Co-rich amorphous ferromag. alloys, aftereffect of mag. permeability 7-33223
 Co-rich metallic glasses, magnetostriction, anomalous temp. depend., single ion model 7-33261
 Co-Si-B amorphous alloys, mag. props., annealing effects 7-27513
 Co-W-P electroplated alloys, struct. and mag. props. (Russian) 7-2428
 Co-Y alloys, low temp. sp. ht. study, crystalline and amorphous phases 7-52995
 Co-Y amorphous alloys, high-field susceptibility, spin wave stiffness const. 7-33150
 Co-Y amorphous alloys, mag. props. 7-58990
 Co_{100-x}B_x amorphous sputtered thin films, magnetic anisotropy origins 7-27583
 CoCl₂-graphite intercalation cpds., mag. susceptibility meas. 7-45638
 CoCr evaporated films, mag. props. 7-33225
 CoCr films, magnetisation reversal mechanisms 7-59068
 CoCr films, sputter deposition, mag. characteristics of initial deposition layer 7-27574
 CoCr films, vacuum evaporation, thickness depend. of mag. props. 7-27576
 CoCr layers, domain obs. with digitally enhanced Kerr-microscope 7-45726
 CoCr sputtered films, struct. and mag. props., role of atomic mobility during film growth 7-33224
 CoCr-based thin films, growth and mag. props., nucleation layer effects 7-45065
 Co₉₂Fe₀₈, FCC, Fermi surface, de Haas-van Alphen studies 7-52406
 Co₇₄Fe₂₆B₂₀ amorphous sputtered thin films, magnetic anisotropy origins 7-27583
 CoFeCr sputtered films, struct. and mag. props. 7-27175
 Co_{70.4}Fe₄Si₁₅B₁₀, amorphous alloy, mag. props. rel. to mag. coating 7-27123
 (Co_{1-x}Mn_x)₂B, crystalline and amorphous, mag. and elec. props. 7-2827
 CoNi equiatomic ferromag. alloy, local mag. form factor determ., neutron scatt. study 7-38849
 Co₅₉Ni₄₁Fe₅B₁₆Si₁₁, amorphous ferromag. alloy struct., shock loading effects, mag. struct. anal. 7-2100
 Co₅₈Ni₄₂Fe₅B₁₆Si₁₁, amorphous ferromagnet, prep. and struct. 7-22605
 γ-CoNiMn alloys, mag. phase diagram, neutron diff. methods (Russian) 7-45667
 (Co₆₀Ni₄₀)₇₈Si₈B₁₄, amorphous, itinerant electron charact., current induced reson. mag. field shift obs. 7-27590
 (Co_{1-x}Ni_x)₇₅Si₁₅B₁₀ amorphous alloys, magnetostriction and other mag. props. 7-45787
 Co_{1-x}Rh_x(Ru₂)S₂, prep., mag. and crystallographic props. 7-33154
 Co₉₀Si₁₀ amorphous films, coercive force rel. to crystallisation (Russian) 7-59078
 CoTi soft ferromagnetic thin films, structure-related induced anisotropy 7-45663
 Cr (001), near-surface antiferromagnetism and surface ferromagnetism, photoelectron spectroscopy 7-59381
 Cr (100), electronic struct. and surface magnetism at finite temps. 7-12776
 Cr_{1-x}Mn_xGe, cryst. and amorphous, mag. characts., substitution effects 7-59009
 Cr_{1/3}NbS₂, long-period helical spin struct. (Japanese) 7-45626
 CrO₂, half-metallic ferromagnet, band struct. calcs. 7-7091
 CsFeCl₃, quasi-one-dimensional ferromag., mag. field effects on optical spectrum 7-3026
 Cs₂Fe₂F₉, precise struct. determ. and ferromag. props. anal. 7-1981
 CsNiF₃, 1D easy plane ferromag., quantum Monte Carlo and transfer matrix calcs. 7-7468
 CsNiF₃, easy-plane ferromag. chain, quantum sp. ht. 7-7522
 CsNiF₃, easy-plane ferromagnetic chains, sp. ht. and spin Hamiltonians, quantum statistics calcs. 7-64469

ferromagnetic properties of substances continued

- Cu complex, (C₆H₁₁NH₃)CuBr₃, easy-plane ferromag. chain, quantum sp. ht. 7-7522
 Cu, nonmagnetic samples, ferromag. behaviour 7-53040
 Cu-based binary dilute alloys, electron struct., X-ray L_α emission spectra studies 7-12598
 Cu-Ni-Fe-Mn, physical props. rel. to precip. and thermal treatment (German) 7-12698
 Cu_{70-x}Al₃₀Fe_x, ferromagnetic interactions, EXAFS and XANES anal. of Fe atom environment and clustering 7-64808
 DyAg, antiferromag. crystalline and ferromag. amorphous alloys, spin dynamics, μSR study 7-45873
 DyAl₂, monocrystalline, longitudinal μSR studies, ferromag. and paramag. phases 7-45876
 DyAl₂, muon spin relax. in paramag. and ferromag. regimes 7-45879
 Dy_{1-x}Al_x, intrinsic coercive field 7-45728
 DyCl₃·6H₂O, quantum mechanical ground state 7-38839
 DySe-USe system, mag. props. of solid solns. 7-22121
 Dy_xY_{1-x}Al₂, intrinsic low field susceptibility studies 7-45633
 Dy_xY_{1-x}Al₂, intrinsic coercive field 7-45728
 Er, magnetic struct., synchrotron X-ray scatt. studies 7-45625
 Er-H solid soln., mag. props., H addition effects 7-7510
 ErAl₂, intrinsic coercive field 7-45729
 ErRh₄B₄, body-centred tetragonal, cryst. struct., X-ray diff. study 7-26704
 ErRh₄B₄, ferromagnetic supercond., coexistence phase, spin-orbit scatt. effects 7-22077
 ErRh₄B₄, magnetic transition temps., RKKY interaction studies 7-22107
 ErRh₄B₄, superconducting and ferromagnetic transitions 7-64385
 Eu-Yb, high press. mag. and elec. props. studies 7-7541
 EuS ferromagnetic single cryst., elec. field gradient and magnetic hyperfine interaction, NMR meas. 7-52540
 EuS ferromagnetic superlattices with magnetisation perpendicular to surface, collective excitations, magnetostatic theory 7-45647
 EuS Heisenberg ferromagnet, diverging and finite suscept. below T_c 7-7444
 EuS, refrigerant capacity and use in mag. cooling 7-56285
 EuSe ferromagnet, ¹⁵¹Eu and ¹⁵³Eu NMR lineshape, mag. field depend. 7-22151
 EuSe, mag. phases, press., alloying effects, NMR and mag. studies 7-2847
 Fe (111), electron capture spectroscopy 7-59368
 Fe alloy ferromagnets, magnetic texture and inhomogeneity, muon polarisation and spin relax. rate meas. 7-45895
 Fe and Fe-Co-Ni fine powders, corrosion resist. and mag. prop. changes, surface-active agent use in prep. 7-54001
 Fe and its alloys, spin wave excitations and magnetisation temp. depend. 7-45642
 Fe, BCC, mag. ordering and electronic struct. (Russian) 7-33170
 Fe, BCC and FCC forms, ferromag. phases investig. 7-2851
 Fe, circularly polarised X-ray absorpt. 7-59302
 Fe, diffusion of ⁵⁹Fe and ⁶⁰Co, mag. anomalies, quasi-chemical model 7-6862
 Fe, electrical resistivity, high temp. and press. 7-38534
 α-Fe, electron irradiated, residual resistivity recovery and mag. after-effect 7-27570
 Fe epitaxial films, mag. size effects 7-59081
 Fe epitaxial monolayers on the Au (100), surface magneto-optic Kerr effect 7-59080
 Fe, Fermi surface change near the mag. transition 7-16935
 d-Fe, ferromag., positron spin polarisation relax. study 7-46203
 Fe, ferromagnetic, band struct. and optical props. 7-2476
 Fe, ferromagnetic, spin depend. Compton profile, circularly polarised synchrotron radiation study 7-33477
 Fe, ferromagnetic sp. ht. meas. by pulse-heating technique 7-7513
 Fe ferromagnetic superlattices with magnetisation perpendicular to surface, collective excitations, magnetostatic theory 7-45647
 Fe ferromagnets, spin-resolved photoemission and bremsstrahlung calcs. and data anal., book contrib. 7-33523
 Fe, Hall effect, anomalous, and energy band struct. (Russian) 7-52414
 Fe, itinerant electron ferromagnetism, mag. susceptibility, Curie-Weiss law, temp. depend. 7-27501
 Fe itinerant ferromagnets, electronic struct. determ., spin depend. inverse photoemission studies, book contrib. 7-33479
 Fe, liq. and solid, mag. susceptibility effect of O content (Russian) 7-52953
 Fe, mag. props., of different phases, modelling using Monte Carlo method (Russian) 7-58992
 Fe, magnetic domain walls, low freq. internal friction (Chinese) 7-38898
 Fe, magnetic domains, spin-polarised SEM studies 7-56376
 Fe, magnetic field effect on wear 7-7582
 Fe, magnetic films, MBE growth on GaAs, interface effects 7-27584
 Fe, negative muon spin precession and hyperfine field anomaly study 7-45894
 Fe overlayers or sandwiches with Cu (001), electronic and mag. props. 7-64499
 Fe oxide layer on Fe acicular particles morphology and mag. props. 7-52067
 α-Fe, paramag. and ferromag., critical mag. phenomena, results from μSR studies 7-45872
 α-Fe single crystals, plastically deformed, dislocation arrangement anal. using magnetic small-angle neutron scatt. 7-2021
 Fe, Stoner excitations, free-electronlike, spin-polarised EELS 7-45648
 Fe, surface ferromagnetic order 7-45773
 Fe, surface magnetism 7-27528
 Fe, thermal equilibrium vacancies, muon spin resonance studies 7-51757
 Fe, thermal expansion, electron correl. effects 7-2238
 Fe thin films, sputter deposited at oblique incidence, microstruct. and mag. props. (Japanese) 7-33560
 Fe ultra thin films, Brillouin scatt. 7-27728
 Fe ultrathin films on Pd (111), photoemission, LEED and AES studies 7-45068
 Fe whisker, ferromag. domain struct. obs. 7-7536
 Fe whiskers, (011), Neel's domain struct. in weak and zero applied fields 7-2888
 Fe-Al disordered alloys, electronic struct., mag. props. and Mossbauer spectra 7-64073
 Fe-Al-Si, Sendust, magnetocrystalline anisotropy 7-33165
 Fe-Al(Si) cold-rolled nonbrittle powder strip prep., texture and mag. props. 7-46370
 Fe-Au-Fe double layers, exchange coupling 7-27510

ferromagnetic properties of substances continued

- Fe-B metallic glasses, struct. relax., Curie temp. meas. 7-21124
Fe-B-Ce-based metallic glasses, mag. domain struct. and annealing embrittlement 7-27586
Fe-based metallic glasses, magnetic aftereffect and magnetostriction studies 7-27571
Fe-Ce amorphous alloys, mag. props. and elec. resist. 7-59010
Fe-Co, thermal equilibrium vacancies, muon spin resonance studies 7-51757
Fe-Co alloys, powder metallurgy produced, mag. props. 7-33211
Fe-Co-Cr-Mo alloys, electronic struct. and mag. props., X-ray spectra studies (Russian) 7-32902
Fe-Co-Mn(V) films, ion beam sputtered, soft mag. props. 7-33237
Fe-Co-Ni amorphous alloys, anisotropic magnetoresist. studies 7-58793
Fe-Co-Ni based alloys, crystalline and amorphous, magnetoresistance 7-38538
Fe-Co-Ni cryst. alloys, anisotropic magnetoresist. studies 7-58794
Fe-Co-Si-B and Fe-Ni-Si-B glass, liq.-quenched, cooling condition depend. of saturated mag. flux density 7-58991
Fe-Co-based ternary alloys, atomic and mag. moment mutual ordering (Russian) 7-33169
Fe-Cr-B-Si, amorphous, annealing effects on Curie temp. 7-45675
Fe-Cr-Co permanent magnetic alloys, casting 7-53051
Fe-Cr-Co solid soln., uniaxial tensile stress in spinodal decomp. effect on coercive force, thermomag. treatment effects 7-7555
Fe-Cr-Co-Mo permanent magnet ribbons, mag. props., influence of modulated structure 7-53043
Fe-Cr-Co-Si, permanent magnet alloys, microstruct., mag. props., Si content effect 7-22117
Fe-Cr-Co-Si-Ti, permanent mag. alloy, ductile, effect of heat treatment on mag. props. (Korean) 7-8137
Fe-Cr-Fe double layers, exchange coupling 7-27510
Fe-Cr-Mn, mag. susceptibility and elec. resist. (Russian) 7-52952
Fe-Cr-Ni, low temp. mag. susceptibility and mag. transitions (Russian) 7-45628
Fe-Cu-Ni, FCC ternary alloys, mag. props. 7-22852
Fe-Dy-C high coercivity permanent magnet materials 7-2903
Fe-La amorphous alloys, high-field susceptibility and Curie temp. 7-58989
Fe-Mn-Al alloy, mag. props., struct. and deform. texture 7-2892
Fe-Mo (14.5 wt.%), ageing, discontinuous dislocation transform., coercivity obs. 7-3305
Fe-N alloys, phase state and precipitation, plastic deformation effects (Russian) 7-46551
Fe-Nd-B magnets, microstructure and mag. props. 7-53049
Fe-Nd-B permanent magnets, prep. by liquid dynamic compaction 7-53661
Fe-Ni, austenitic, Mag. ordering and mech. props. (Russian) 7-58280
Fe-Ni, hyperfine mag. fields, temp. dependence 7-12683
Fe-Ni alloy, mag. remanence at low-temperature 7-24088
Fe-Ni evaporated films for a back layer of perpendicular mag. recording media, origin of high coercivity 7-27578
Fe-Ni films, γ -phase low temp. precipitation investig. (Russian) 7-33666
Fe-Ni Invar, high-field hysteresis and ferromag.-antiferromag. coexistence 7-22122
Fe-Ni soft magnetic film single-pole readout head, induced RF permeability variation 7-53072
Fe-Ni system, liq., phase equilib., above 1200K, mag. contrib., thermodynamic analysis 7-7966
Fe-Ni system, phase equilibria, mag. contrib. to thermodynamic functions, below 1200K 7-7965
Fe-Ni-based alloys, amorphous and crystalline, mag. phase transitions 7-52983
Fe-Pt, dilute alloys, ferromagnetic, internal mag. fields, impurity conc. dependence 7-38858
Fe-Pt (36 at.%), cryst. struct., permanent mag. props. (Japanese) 7-53036
Fe-R-B (R=rare earth) metallic glass permanent magnets, TEM studies 7-26661
Fe-Sc alloys, struct. and mag. props., NMR and X-ray diff. studies (Russian) 7-6578
Fe-Si, electrical steels and alloys, conf., Vladimir, USSR (Dec. 1984) 7-9576
Fe-Si, polycrystalline, magnetisation, domain struct. and magnetostriction (Russian) 7-59051
Fe-Si, rapidly quenched ribbons, grain growth, mag. props. 7-8017
Fe-Si, structure, texture and mag. props. 7-12995
Fe-Si (3 wt.%), domain structure and mag. props., influence of plane tension and insulating coatings 7-12991
Fe-Si (3 wt.%), dynamic remagnetisation, structural depend. of losses 7-12994
Fe-Si (3 wt.%), mag. props., influence of elastic-stress state produced by coatings 7-12990
Fe-Si (3 wt.%), mag. props. and domain struct., influence of laser treatment 7-12993
Fe-Si (3 wt.%), mag. texture of surface layers 7-13062
Fe-Si (3 wt.%), secondary recrystallisation grains, subboundaries formation and their influence on mag. domain struct. 7-13471
Fe-Si (3 wt.%), specific magnetic loss meas. at remagnetisation freq. 50 Hz to 200 kHz 7-9850
Fe-Si (3 wt.%) bicrystals, domain struct. and magnetisation 7-12992
Fe-Si (3.2 wt.%), mag. props., influence of substructural features 7-12996
Fe-Si alloy, high-Si, alloy elements influence on plasticity and mag. props. 7-8067
Fe-Si electrical sheet steel, magnetostriction variations meas., ponderomotive force influence 7-13012
Fe-Si electrical steels, anisotropic cold-rolled, magnetisation characts. 7-12966
Fe-Si-Al, carbide precip. kinetics, core loss 7-8001
Fe-Si-Al, electrical steel sheet, rollability, core losses (German) 7-59549
Fe-Si-Al, Sendust films, DC opposite sputtered, mag. and crystallographic characteristics 7-7847
Fe-Si-Al alloy single crystals, mag. props. (Japanese) 7-22104
Fe-Si-Al films, magnetoelastic effect and anisotropy fields 7-59071
Fe-Si-B, normalising, decarburisation, secondary recrystallisation, mag. induction obs. 7-8020
Fe-Si-B mag. film, magnetoelastic wave generation and detection 7-59070
Fe-W (110), spin-resolved photoemission spectra of epitaxial Fe layers 7-46276

ferromagnetic properties of substances continued

- Fe-W-based alloys, amorphous and crystalline, mag. phase transitions 7-52983
Fe-X, X=Al, Si, Nb, Ti, Zr, coercive field measurements 7-64491
Fe-Zn alloys, sputtered, X-ray diff., magnetisation and Mossbauer studies 7-59075
Fe-Zr, amorphous, high-field magnetisation hysteresis, spin glass clusters 7-2898
Fe-Zr, amorphous and microcrystalline, exchange interaction and saturation magnetisation 7-45651
Fe-Zr-B, amorphous, meas. of Curie temp. 7-2853
(Fe-B)₈₅Nd₁₅ amorphous films, soft mag. props. 7-53077
Fe₈₁B₁₉ amorphous alloy, thermally activated time fluctuations of nucl. spin orientation 7-7622
Fe₈₁B₁₉ amorphous ribbon, averaged spin orientation under uniaxial compression, Mossbauer spectra study 7-45792
FeBO₃, NMR of ⁵⁷Fe domains and domain walls 7-7593
Fe₇₈Si₂₂Si₉, amorphous alloys, mag. losses, aging kinetics 7-59056
Fe₈₀B₁₄Si₆ amorphous ribbons, anisotropy of losses 7-45658
Fe₈₁Si₁₄Si₅Si₄, amorphous, mag. hyperfine fields under stress, Mossbauer study 7-22166
Fe₈₃B₁₇Si₃ metallic glasses, crystn., magnetisation, scaling, mag. relax. meas. 7-63496
Fe₈₁Si₁₃Si₅Si₃C₂, amorphous ferromag. alloy, acoustic waves, mag. field induced changes 7-2917
Fe₈₁Be₁₃Si₅Si₃C₂ soft ferromag. metallic glasses, domain wall motion and energy dissipation studies 7-64478
FeCo alloys, critical mag. phenomena, results from μ SR studies 7-45872
Fe_{1-x}Co_x, spin-polarised positron annihilation and mag. moments 7-53439
(FeCo)₈₀B₂₀ amorphous ultrafine particles, mag. props. 7-53063
Fe₆₇Co₁₈B₁₄S metallic glass, magnetic aftereffect, thermal treatment, positron lifetime study 7-38907
Fe₇₄Co_{10-x}Cr_xB₁₆, amorphous, prep. by melt spinning, X-ray diff., DSC, Mossbauer studies 7-46369
Fe₂Co_{70-x}Cr_xSi₁₀B₁₅, x=0, 3, 6, 9, amorphous ferromagnet, 180° domain wall (Korean) 7-33198
Fe₈₅Co_{72.5}Mo_{2.5}Si₁₅ amorphous ribbons traversed by DC electric currents excess resistance, collective motion of ferromag. domain walls 7-32989
Fe₈₅-Cr₂B₁₅(Ni₂B₁₅) metallic glasses, mag. and elec. props. 7-13002
Fe₄₃Cr₂₅Ni₂₀B₁₂ glass, devitrification, mag. meas. and X-ray diff. studies 7-21128
Fe₇₆Cr₄P₈C₁₂, amorphous alloy, mag. short range order above T_c, paramag. phase 7-45623
Fe_{75-x}Cr_xSi₁₀B₁₅, x=0, 2, 4, 6, amorphous ferromagnet, 180° domain wall (Korean) 7-33198
Fe_{90-x}Cr_x(SiB)₂₀ amorphous alloy, induced anisotropy, melt spinning effects (Russian) 7-59004
FeGe₂ single cryst., magnetisation, temp. depend. (Russian) 7-2891
(FeM)₈₀B₁₄Si₆, M=Mn, Mo, V, glass, magnetoresistance 7-64203
(FeMn)₈₀B₁₄Si₆ glass, magnetoresistance and magnetisation 7-45354
(FeMo)₈₀B₁₄Si₆ glass, magnetoresistance and magnetisation 7-45354
Fe₇₅Mo₃Si₉B₁₃, amorphous, structural relax. and quasi-texture 7-11925
Fe₁₆N₂, high-dose ion implantation prep., mag. props. 7-59055
Fe_{3-x}N film, hexagonal, prep. by plasma reaction, mag. characts. 7-13380
Fe₁₄Nd₂B magnets, high-field magnetostriction 7-53104
Fe₁₄Nd₂B permanent magnet, Dy substituted positron annihilation studies 7-3108
Fe₇₇Nd₁₅B₈, sintered permanent magnets, domain wall obs. 7-27544
Fe₇₇Nd₁₅B₈-based melt spun ribbons, crystallisation and mag. props. 7-26662
Fe₅₀Ni₅₀, Deltamax, magnetic ribbons, inverse Wiedemann effect for very low torsions 7-45786
(Fe₆₅Ni₃₅)_{1-x}(Fe₈₄Mn₁₆)_x alloys, low field magnetisation and Mossbauer effect studies 7-33311
(Fe_{1-x}Ni_x)₈₀B₂₀, amorphous, contribution of Ni to hyperfine fields (Korean) 7-27636
Fe₄₀Ni₄₀B₂₀ amorphous thin films, coercive field, annealing effects 7-7553
Fe₄₀Ni₄₀B₂₀, concentration dependence of surface insulating coating, influence on magnetic props. 7-64479
Fe₂Ni_{80-x}B₂₀ amorphous ferromagnets, elec. resist. and thermopower meas., comp. and temp. depend. 7-45263
Fe₂Ni_{80-x}B₁₈Si₂, glassy alloys, variation of mag. inhomogeneity 7-45634
Fe₂-Ni₂C₂, prep. and characterisation 7-17490
Fe₂Ni_{85-x}Mn₁₅, low temp. sp. ht. near ferromag.-antiferromag. transition (Russian) 7-7512
Fe₄₀Ni₃₈Mo₄B₁₈, metallic glass, conversion electron Mossbauer spectra 7-48926
Fe₄₀Ni₃₈Mo₄B₁₈ soft ferromag. metallic glasses, domain wall motion and energy dissipation studies 7-64478
Fe₄₀Ni₃₈Mo₄B₁₈Si₂, ferromag. amorphous ribbons by field quenching technique, mag. anisotropy 7-33164
Fe_{48.5}Ni₃₄P_{17.5}, small-angle polarized neutron scattering study 7-52939
Fe₄₀Ni₄₀B₂₀, ferromag. amorphous alloy, struct. relax., effect of surface 7-28062
Fe₄₀Ni₄₀P₁₄Fe, Metglas 2826, magnetic ribbons, inverse Wiedemann effect for very low torsions 7-45786
(Fe_{1-x}Ni_x)₇₇Si₁₀B₁₃, amorphous, effective mag. moment, Curie temp. (Korean) 7-27503
Fe₇₅Ni₅Si₁₃, amorphous, structural relax. and quasi-texture 7-11925
 γ -Fe₂O₃ particles, colloidal suspension, mag. props. of ionic ferrofluids 7-45758
Fe₂O₃:Co sputtered films, X-ray diffraction anal. 7-58675
Fe₂O₄ nearly spherical particles in low mag. fields, mag. props. 7-27568
Fe₂P, electronic struct., mag. props., KKR, LMTO methods, LSD approx. 7-64070
Fe₈₂P₁₁B₇ metallic glass, mag. anisotropy and correlated hyperfine interactions 7-7505
Fe(Pd_{1-x}Au_x)₃ disordered alloys, atomic and mag. structs., Mossbauer studies (Russian) 7-17247
FeRh, X-ray emission and absorpt., ab initio self-consistent band struct. calcs., LMTO method 7-64826
Fe_{1-x}Si_x amorphous films, Hall effect and mag. anisotropy 7-2911
Fe₈₉Si₁₃ (Russian) 7-59078
Fe₉₃Si₃, magnetoelastic acoustic emission 7-33257
Fe₇₈Si₆B₁₂ amorphous alloys, surface crystallisation and mag. props. 7-51649

ferromagnetic properties of substances continued

- Fe₈₀Si_{20-x} amorphous alloys, struct., mag. and elec. props. (Korean) 7-2893
- Fe_{0.458}Sn_{0.088}O_{0.454} film, mag. props., appl. in perpendicular mag. recording 7-59005
- (FeV)₈₀B₁₀Si₆ glass, magnetoresistance and magnetisation 7-45354
- (Fe_{1-x}W_x)_{84.5}B_{15.5} amorphous alloys, elec. and mag. props. (Chinese) 7-12969
- Fe₉₁Zr₉, amorphous, long-range mag. order, neutron scatt. and AC susceptibility studies 7-58979
- Fe₉₁Zr₉, amorphous, long-range mag. order, small-angle neutron scatt. 7-58980
- Fe₉₂Zr₈, mag. susceptibility, elec. resist., magnetoresistance meas. 7-52954
- Fe₂Zr_{100-x} amorphous alloys, Kohlrausch thermal relax., sp. ht. meas. 7-59027
- Fe_{0.65}Si_{0.35} thin films, amorphous and crystalline, magnetisation rotational processes 7-53085
- Gd monolayer on W, ferromag. order and crit. exponent, ESR study 7-45680
- Gd, spin-polarised Auger electron spectroscopy 7-33489
- Gd surface, evidence for ferromag. order above bulk Curie temp. 7-33173
- Gd-Co, amorphous, influence of hydrogenation or mag. props. 7-2899
- Gd₂(Co_{1-x}Mn_x)₁₇, Co contribution to magnetocrystalline anisotropy, point charge model 7-45665
- Gd₃Fe₂O₁₂ ferrogarnets, heat of crystallisation, scanning calorimetry obs. 7-2154
- GdNi₃, paramag. suscept. studies 7-52935
- Ge_{80-x}Mn_xB₂₀ amorphous alloy, Curie point and crystallisation temp. 7-17173
- ³He, adsorbed on Grafoil, nuclear ferromagnetism and surface ferromagnetic effect 7-2296
- ³He, adsorbed on solid surface, magnetism (Japanese) 7-21564
- ³He spins on exfoliated graphite surface, detection of ferromag. domains 7-38291
- ³He, superfluid A₁-phase, magnetically generated superflow, nonlinear effect obs. 7-27047
- HfCo₂₊₅ C15 Laves phase system, ferromag. props., comp. depend. study 7-7490
- HfFe₂, electronic struct. and mag. props., tight-binding approx. calcs. 7-2475
- HfU₂S₃, mag. props. 7-22120
- HgCr₂Se₄, ferromag. semiconductor, sp. ht. 7-45684
- HgCr₂Se₄, magnetisation, temp. depend. 7-45629
- HgCr₂Se₄ spinel magnetic semicond., electronic struct., elec. props., defects and ferromag. anisotropy 7-38857
- HgCr₂Se₄, stoichiometry and phys. props. investig. 7-2218
- Ho₂Fe₁₄B single crystals, mag. anisotropy and magnetisation 7-27547
- Ho₃Fe₂O₁₂ ferrogarnets, heat of crystallisation, scanning calorimetry obs. 7-2154
- HoMo₅S₈ ferromagnetic supercond., coexistence phase, spin-orbit scatt. effects 7-22077
- HoMo₅S₈ ferromagnetic films, supercond. props., temp. and mag. field depend. 7-45538
- K₂CuF₄, 2D ferromagnet, polarised neutron studies of forbidden magnons 7-45693
- K₂CuMn_{1-x}F₄, quasi-two-dimensional mixed ferromagnetic-antiferromag. system, mag. phase transitions, intermediate spin glass phase 7-27525
- K₂O-Al₂O₃-B₂O₃-Fe₂O₃-Gd₂O₃ glasses, mag. props., composition dependences 7-2823
- La(Fe_{1-x}Al_x)₁₃, mag. props. determined via neutron scatt. and Mossbauer spectroscopy 7-2820
- LaMn(Fe)Si₂, struct. and mag. props. studies (French) 7-37950
- LaNi_{1-x}Fe_x, spin freezing props. 7-64464
- LiMo₅Li_{1-x}F₄, dilute dipolar-coupled magnet, ferromagnetism, glassiness, metastability 7-22098
- LuFe₂, electronic struct. and mag. props., tight-binding approx. calcs. 7-2475
- Mn-Al-C, anisotropic permanent magnet, rotational hysteresis 7-53050
- Mn-Al-C ferromag. alloys, phase, transformations, and struct. defects, positron annihilation study 7-46461
- MnAs, crystal struct. and mag. props. 7-6592
- MnBi ferromag. thin films, reversed micro-domain growth, magnitude-anisotropic dispersion 7-17205
- Mn_{0.615}Cr_{0.385}As, press-induced helimagnetic-ferromagnetic transition 7-52984
- MnCl₂-graphite intercalation cpds., mag. susceptibility meas. 7-45638
- Mn_{1-x}Fe_x, sputtered films, mag. props. 7-38915
- MnSb, epitaxial growth of ferromagnetic monolayers 7-2909
- MnTe, electronic struct. in magnetically ordered and disordered phases, tight-binding calcs. 7-45145
- Mn_{0.97}Ti_{0.03}As, mag. phase transitions, effect of Ti additions 7-27519
- Mo permalloy films, mag. domain walls stability, external mag. field, Lorentz microscopy 7-45780
- (Nd,Tb)_{16.7}Fe_{75.5}B_{7.8}, magnetisation meas., spin reorientation temp. 7-17161
- Nd-Fe-B, metastable amorphous alloys, crystn., thermal stability 7-39482
- Nd-Fe-B based permanent magnets, hysteresis loop and mag. anisotropy 7-53031
- Nd-Fe-B permanent magnet, microstructure and coercivity 7-27559
- Nd-Fe-B permanent magnets, BCC phase mag. props. at grain boundaries 7-53044
- Nd-Fe-B rapidly solidified ribbons, magnetisation, quench rate depend. 7-53034
- Nd-Fe-B system, permanent magnet, mag. props. (Korean) 7-7554
- Nd-Fe-B system, temp. depend. of coercive force, effect of annealing, aging and sintering 7-27560
- Nd-Fe-B-Co-Al based permanent magnets, mag. props. and temp. characts. 7-53045
- Nd-Fe-Co, amorphous films, perpendicular magnetic, mag. and magneto-optical props. 7-64496
- NdFe alloys, magnetic moment irreversibility from temperature cycling 7-33194
- Nd₂(Fe_{0.67}Al_{0.33})₁₄B, reduction of mag. hyperfine fields and Curie temp. on Al substitution, Mossbauer spectra 7-38859
- Nd₃Fe₇B₈ permanent mag., rotational hysteresis energy and magnetisation reversal 7-64492
- Nd₂Fe₁₄B, EFG tensor for interpretation of Mossbauer effect meas. near spin reorientation temp. 7-38968
- Nd₂Fe₁₄B, elastic props. between 120 to 300K 7-27529

ferromagnetic properties of substances continued

- Nd₂Fe₁₄B, magnetic props., H₂ absorption effects 7-38906
- Nd₂Fe₁₄B single crystals, mag. anisotropy and magnetisation 7-27547
- Nd₂Fe₁₄B sputtered films, perpendicular anisotropy 7-53073
- Nd₂Fe₂₃B₃, struct., Curie temp., X-ray diffraction anal. 7-11994
- NdFeCoAl magnets, Curie temp., coercive force and magnetisation 7-52982
- Nd₂Fe_{14-x}Co_xAl₂B alloys, permanent mag. props. 7-45755
- Nd₂Fe_{14-x}M_xB₃ (M=Co,Ni,Cu,V,Al,Cr,Mn), crystallographic and mag. props. 7-27522
- Nd₂Fe_{12-x}Mn_xCo₂B, mag. props. 7-52946
- NdFe(Mn)Si₂, struct. and mag. props. studies (French) 7-37950
- Nd₂(Fe_{0.67}Si_{0.33})₁₄B, reduction of mag. hyperfine fields and Curie temp. on Si substitution, Mossbauer spectra 7-38859
- NdHoDyFeB permanent magnets with zero temp. coeff. of induction 7-53047
- Nd_{2-x}R_xFe₁₂Co₂B, mag. characts. 7-45670
- Nd₂(Y₂)(Fe_{1-x}Al_x)₁₄B, intrinsic and permanent mag. props. (Chinese) 7-13003
- Ni (110) with chemisorbed O₂ or CO, mag. props. investigated by spin-polarised electron beams 7-58994
- Ni and its alloys, spin wave excitations and magnetisation temp. depend. 7-45642
- Ni, BCC and FCC forms, ferromag. phases investig. 7-2851
- Ni, dislocation structure after US deformation, physical props. (Russian) 7-44699
- Ni, electrical resistivity, high temp. and press. 7-38534
- Ni epitaxial films and interfaces with Cu and Pd, mag. size effects 7-59081
- Ni, Fermi surface change near the mag. transition 7-16935
- Ni, ferromag., magneto optical effects and band struct. (Russian) 7-59188
- Ni ferromagnets, spin-resolved photoemission and bremsstrahlung calcs. and data anal., book contrib. 7-33523
- Ni, Hall effect, anomalous, and energy band struct. (Russian) 7-52414
- Ni hydroxy-mica intercalation complexes, mag. props. 7-17162
- Ni, itinerant electron ferromagnetism, mag. susceptibility, Curie-Weiss law, temp. depend. 7-27501
- Ni itinerant ferromagnets, electronic struct. determ., spin depend. inverse photoemission studies, book contrib. 7-33479
- Ni, mag. props., influence of low-temp. US deform. (Russian) 7-53878
- Ni, magnetic biaxial anisotropy induced by plastic deformation 7-59006
- Ni, magnetic field effect on wear 7-7582
- Ni, magnetic phase location, total energy spin polarised band calcs. 7-17176
- Ni, magnetic props., Hubbard model 7-2806
- Ni, photoemission above Curie temp., cluster calcs. 7-7814
- Ni, spin polarised electronic struct., mag. and bonding props. 7-32904
- Ni, spin polarised positron annihilation 7-46187
- Ni, thermal expansion, electron correl. effects 7-2238
- Ni-Fe-Cu, mag. props., hardness, elec. resist., V, Nb and Ta additions effect (Japanese) 7-12998
- Ni-Fe-In ternary Permalloy electroplated films, mag. props. and thermal stability 7-33236
- Ni-Mn disordered alloys, ferro-spin-glass domain model calcs. 7-59025
- Ni-Mn disordered alloys, magnetic phase diagram near multicritical point 7-59024
- Ni-Mo metallic superlattices, macromag. and micromag. props. 7-2826
- Ni₂(Fe,M) (M=Cr, Mn, W, Mo), atom pair interaction energy and Kurnakov temp. (Russian) 7-1938
- Ni₂Fe, ordered and disordered, mag. permeability studies 7-59053
- Ni_{1-x}Fe_xMnSb, half-metallic ferrimag., mag. and crystallographic props. 7-45672
- NiMnSb, half-metallic ferromagnet, positron-annihilation study 7-21802
- NpAs₂, single crystals, Hall resistivity 7-12739
- PbMn_{2/3}Mo₃, perovskite-type cpds., (M=Mo, Te, Re), dielec. and mag. props. 7-7650
- Pb_{1-x}Mn_xTe, indirect exchange interaction between Mn²⁺ ions 7-27509
- Pd-Fe:B(O), mag. susceptibility, impurity effects 7-27520
- Pd₃Fe disordered alloy, low-energy spin-wave excitations, Heisenberg model calcs. 7-2829
- Pd₃Fe, disordered phase, electronic struct. anal. 7-58735
- Pd₃Fe, electronic struct. 7-52415
- Pd₃Fe hydrated ordered alloy, mag. behaviour, Mossbauer studies (Russian) 7-2890
- PdFeMn₂, reentrant alloy, ferromagnetism investig. 7-2860
- Pd₃MnSn, cubic ferromagnet, high temp. spin dynamics 7-2881
- Pr-Fe, amorphous films, perpendicular magnetic, mag. and magneto-optical props. 7-64496
- Pr₂Fe_{14-x}Co_xB system, struct. and magnetism 7-45631
- PrCo₅, microstructure and coercivity, effect of annealing, 650-850°C 7-38905
- PrCo_{4-x}Fe_xB, crystallographic and mag. props. 7-45671
- PrMn(Fe)Si₂, struct. and mag. props. studies (French) 7-37950
- PrNi₅, paramag.-ferromag. phase transition, external mag. field, spin ordering model 7-52988
- Pr_{2-x}R_xFe₁₂Co₂B (R=Dy, Tb), mag. characts. 7-45670
- PtMnGa, Curie temp., hydrostatic press. effect 7-27527
- PuSb, hybridisation-mediated anisotropic mag. behaviour 7-2850
- R-Co alloys, magnetic moment irreversibility from temperature cycling 7-33194
- Rb₂Mn₂Cr_{1-x}Cl₄ mixed crystals, mag. props. 7-2897
- Si-Fe BCC alloy, struct. and mag. props., order-disorder transition effects (Russian) 7-32346
- Sm-Co amorphous thin films, low temp. mag. props. (Chinese) 7-38910
- Sm-Co-Fe-transition metal permanent magnets, magnetisation 7-53033
- Sm₂(Co, Fe, Cu, Zr)₁₇ sintered compact permanent magnet, mag. props., comp. and heat treatment effects (Korean) 7-2894
- SmCo permanent magnet linear undulator for ENEA free electron laser expt., dipole moment meas 7-43151
- SmCo₅ fine particles, produced by ball milling, strain and domain wall energy (Japanese) 7-7556
- SmCo₅ powder magnet, texture form. in alternating and steady mag. fields 7-27977
- SmMnSi₂, struct. and mag. props. studies (French) 7-37950
- Sn_{1-x}Mn_xTe, degenerate ferro-spin-glass, transport props. and spin disorder 7-45330
- SrFe_{1-x}Co_xO₃ ferromag. cpd., mag. props., comp. depend., Mossbauer spectra and neutron diff. studies 7-7539
- Tb_{0.27}Dy_{0.73}Fe₂, Terfenol, polycrystalline, domain structures and magnetomech. coupling 7-53025

ferromagnetic properties of substances continued

- TbFeCo-based amorphous films, magneto-optical recording appls. 7-53074
 Tb(Fe_{1-x}Co_x)₃, struct. and mag. props. 7-1950
 Tb₃Fe₂O₁₂ ferrogarnets, heat of crystallisation, scanning calorimetry obs. 7-2154
 Tb₃Gd_{1-x}Al_x, intrinsic low field susceptibility studies 7-45633
 Tb₃Gd_{1-x}Al_x, intrinsic coercive field 7-45729
 Ti-N-Permalloy ferromag. multilayers, prep. and props. 7-64497
 TiCoSn ferromagnet, magnetisation, mag. suscept. and cryst. struct. determ. (*Russian*) 7-1952
 Tm₃Fe₂O₁₂ ferrogarnets, heat of crystallisation, scanning calorimetry obs. 7-2154
 U-based mag. alloys, mag. props. and electronic struct. (*Russian*) 7-12967
 U-Cu-P(As), ternary particles, cryst. struct. and mag. props. 7-12955
 U-Ni-As(P), ternary particles, cryst. struct. and mag. props. 7-12955
 UFe₂Al_{12-x}, ferromagnetic suscept. meas. 7-12954
 U₂Gd_{1-x}Ga_x, Curie temp., loss of ferromagnetism, comp. depend, competing exchange interactions 7-12970
 U₂La_{1-x}Te single crystals, elect. resist. temp. depend. Kondo effect and ferromagnetic ordering 7-13119
 U₃Sb₃Cu₂, cryst. struct., mag. props. 7-38864
 U₃Y_{1-x}Ga_x, Curie temp., loss of ferromagnetism, comp. depend, competing exchange interactions 7-12970
 V (100), electron capture spectroscopy 7-59368
 V, surface (100)p(1×1), ferromag. order, electron capture spectra studies 7-27526
 Y-Fe sputtered amorphous films, mag. props. 7-53083
 Y₂(Co_{1-x}Mn_x)₁₇, Co contribution to magnetocrystalline anisotropy, point charge model 7-45665
 YCo₅, ferromag. resonance, local Co anisotropy effects 7-53143
 Y(Co₂Ni_{1-x})₅, magnetocrystalline anisotropy studies (*Russian*) 7-45656
 Y₂(Fe,Al,Co)₁₄B, mag. props., composition depend. 7-53030
 Y₂Fe₁₄B, magnetic props., H₂ absorption effects 7-38906
 Y₂Fe_{14-x}(Si,Cu)B alloys, mag. props. 7-45681
 YIG, ferromagnet, domain struct., transform. in alternating mag. fields 7-53027
 YIG, ferromagnetic hysteresis loop, grain size distrib. effect 7-27556
 Y₃Ni₉H_x amorphous thin films, mag. and elec. transport props., H content effect, 1.5 to 400K (*Chinese*) 7-38909
 Yb₂Fe₁₄B, exchange and cryst. field interactions 7-27512
 Zr-Co, electronic struct., supercond. and magnetism 7-64398
 ZrFe₂, electronic struct. and mag. props., tight-binding approx. calcs. 7-2475
 ZrU₂S₅, mag. props. 7-22120

ferromagnetic relaxation

- see also *ferromagnetic resonance*
 multidomain ferromagnetics, containing lattice dislocations, dynamics (*Russian*) 7-53144
 Eu₃Y₃Fe_{5-x}Ga_xO₁₂ LPE garnet films, ferromagnetic relax. meas. 7-38911
 Fe₃B₁₂Si₅ metallic glasses, crystn., magnetisation, scaling, mag. relax. meas. 7-63496

ferromagnetic resonance

- see also *ferromagnetic relaxation*
 bis(methylammonium) copper tetrachloride, ferromag., parallel-pumped magnons, deterministic chaos obs. 7-52962
 bistability and strange nonlinear neutral curve inferromagnetic resonance 7-13038
 ferromagnetic thin overlayer, exchange-coupled, on ferromag. substrate, FMR study 7-38946
 ferromagnets, magnetic susceptibility of system with 360° domain walls (*Russian*) 7-7488
 Galerkin method and describing function method, appls. in ferroresonant systems (*French*) 7-22145
 garnet epitaxial thin film, FMR investig. 7-53069
 garnet films, He⁺(H₂⁺) implanted, magnetisation and uniaxial anisotropy meas. 7-7576
 high power resonance, spatial and temporal patterns 7-13039
 interdiffusion in coupled mag. layers, spin wave resonance approach 7-2278
 Landau-Lifshitz equation and a generalized two-level system 7-38945
 magnetic materials, nondestructive eval., FMR photothermal-deflection spectroscopy 7-53137
 magnetics, conf., Japan (Nov.1985) 7-24259
 one-dimensional magnet, breather gas, collision-free pumping field energy absorpt. calcs. (*Russian*) 7-7592
 parallel pumping in ferromagnets, nonlin. dynamics 7-53145
 parametric magnons, effect on spectra of other quasi-particles 7-52967
 Permalloy thin films, mag. anisotropy, angular spatial dispersion (*Russian*) 7-2905
 substrate, ferromag. resonance of thin Co films 7-2932
 thermal detector of optical radiation based on ferromagnetic resonance 7-61375
 BaFe₁₂O₁₉, FMR linewidth, temp. and freq. dependence 7-53140
 BaIn_{1.5}Fe_{10.5}O₁₉ single crystals, magnetocrystalline anisotropy consts., anomalous temp. depend. 7-45664
 Bi₃(GaFe)₅O₁₂, epitaxial films, mag. and magneto-optical props. 7-53102
 Co/Ag, compositionally modulated layered films, saturation magnetisation and FMR, thickness depend. 7-7565
 Co/Cr compositionally modulated layered films, saturation magnetisation and FMR, thickness depend. 7-7565
 Co-Cr thin films, sputter etching and annealing, FMR study 7-59112
 Co-Mg coevaporated films, prep. and mag. props. 7-53082
 CoFe₂O₄ ferrite epitaxial layers, high coercivity (*Chinese*) 7-38908
 (Co₉Ni_{0.4})₇₈Si₈B₁₄, amorphous, itinerant electron charact., current induced reson. mag. field shift obs. 7-27590
 CoP amorphous films, FMR spectra during crystallisation 7-53142
 (Eu, Lu, La)₃Fe₅O₁₂ films, gyromagnetic ratio, damping parameter and mag. anisotropy 7-45777
 Fe, magnetic films, MBE growth on GaAs, interface effects 7-27584
 Fe-Ni soft magnetic film single-pole readout head, induced RF permeability variation 7-53072
 FeB amorphous magnetic thin films, spin wave mode linewidth meas. 7-45826
 Fe₇₈B₁₃Si₉ amorphous ribbons, ferromag. resonance 7-27606
 Fe₇₈Si₁₀B₁₂ amorphous ribbons, X-band ferromag. resonance, transmission of microwaves 7-27607
ferromagnetic resonance continued
 Gd-Co-Mo amorphous magnetic thin films, spin wave mode linewidth meas. 7-45826
 Gd-Fe evaporated amorphous alloy films, mag. props. and FMR behaviour studies 7-45825
 Li_{1-x}Zn_xFe₂O₄, outside spin wave manifold effective linewidth values, effect of dimensional reson. 7-53146
 Mg_{1-x}Mn_xFe₂O₄, outside spin wave manifold effective linewidth values, effect of dimensional reson. 7-53146
 NdIG, mag. props. 7-45662
 Ni single cryst. films, quasi-localised spin-wave modes obs. 7-2830
 Ni-Ag multilayer films, magnetisation and FMR studies 7-22147
 PrIG, mag. props. 7-45662
 SrFe₁₂O₁₉, mm wave magnetic and dielec. resonances 7-53139
 W (110) with Gd monolayer, magnetic resonance 7-59113
 (Y,Gd)₃Fe₅O₁₂:Mn, thin films, noncubic mag. anisotropy origin 7-53068
 YCo₅, ferromag. resonance, local Co anisotropy effects 7-53143
 (YEuTmCa)₃(FeGe)₅O₁₂ films, planar anisotropy and magnetisation, ion irradi. effects study 7-2906
 (YEuTmCa)₃(FeGe)₅O₁₂/(YLa)₃Fe₅O₁₂ ferrite/garnet layered structs., domain wall and ferromag. reson. props. (*Russian*) 7-45828
 YIG, charact. of chaotic states of parallel-pumped magnons 7-52961
 YIG double-layered films, thermal detection of FMR, microwave freq. appls. 7-45766
 YIG films, ferromag. resonance absorpt., influence of exchange interaction, weak surface pinning 7-2931
 YIG powder, FMR line shape, test of independent powder particle model 7-64533
 YIG single crystal films, FMR foldover, Suhl instability 7-53141
 YIG single crystals, FMR linewidth, parametrically excited spin wave effects 7-2828
 YIG:Si epitaxial films, mag. anisotropy and spin reorientation under unpolarised white light irradi. (*Russian*) 7-33246
- ferromagnetism**
 see also *ferromagnetic properties of substances; ferromagnetic relaxation; ferromagnetic resonance; Ising model; spin waves*
 1D chain with ferromag. interactions, infinite susceptibility without long-range order 7-64426
 1D Ising ferromagnet, multi-spin flip critical dynamics 7-38888
 4f-systems, Curie temp., valence instability effects calcs. 7-38865
 amorphous, microscopic frozen spins model calcs. (*Russian*) 7-52945
 amorphous and crystalline, magnetostriction theory 7-13013
 amorphous ferromag. alloys, effects of stress on mag. permeability aftereffect 7-33221
 amorphous Ising ferromagnet, transverse suscept. investig. 7-2870
 amorphous ribbons, melt spinning prep. in external fields 7-22608
 anisotropic Heisenberg ferromagnet, low temp. props., spectral density method 7-2803
 anisotropic Heisenberg ferromagnet with biquadratic exchange 7-12987
 antisymmetric exchange chain, sine-Gordon soliton stability 7-38889
 biaxial, spin wave excitation with moving domain wall 7-45650
 Blume-Capel model, effective field theory 7-33134
 Blume-Capel model, ferromag. and antiferromag. props. 7-2867
 bodies of finite dimensions, mag. states rel. to elastic stresses in trans-Rayleigh region 7-27587
 bond-diluted Heisenberg ferromagnets, spin wave damping near percolation threshold, Green's function calcs. 7-17193
 Cayley tree, S=1, generalization of Falk's theorem and i-δ relations 7-7466
 chain systems, difference schemes (*Chinese*) 7-52923
 classical anisotropic Heisenberg ferromagnet, dynamical props., stereographic representation 7-2882
 classical spin chains, dil., effects of mag. field on thermodynamics 7-38840
 continuous symmetry ferromagnet, Monte Carlo simulations 7-2871
 continuum fluid, phase transition existence using correlation inequalities 7-17174
 cores, magnetisation, odd harmonics and secondary EMF 7-2889
 critical point phenomenology and neglect of irrelevant variables, renormalisation group results anal. 7-64468
 Curie-Weiss-Ising model, limit Gibbs states 7-7467
 cylindrical ferromag. specimen, surface slit, open circuit remagnetisation, cavity mag. field meas. 7-54051
 Debye-Waller factor anomaly and diffuse scatt. studies (*Russian*) 7-12973
 dilute ferromagnetic alloys, magnetisation and Curie temp. calcs., approximated Heisenberg model 7-7549
 dilute ferromagnets, lines and domain walls 7-33199
 dipolar waves in ferromagnetic systems with linear magnetoelectric properties 7-45645
 disorder points in d-dimensional mag. systems with competing interactions, RPA calcs. 7-7516
 disordered spin systems, effective susceptibility exponent, nonmonotonic temp. depend. 7-64461
 disordered systems, ferromagnetism, Arrott-plot criterion 7-7521
 domain structure induced by acoustic waves in easy-plane magnetic materials 7-2918
 easy-axis ferromagnet, 1D Bloch wall stability analysis 7-45731
 easy-plane ferromagnets, different-ion anisotropy, arbitrary site spin, low temp. props. 7-33193
 electron and nuclear spin wave attenuation coeffs., scatt. by two-level systems (*Russian*) 7-27508
 electron energy loss spectrum in the near-specular regime, electron-hole excitations 7-33496
 electronic struct. determ. by spin- and angle-resolved photoemission, book contrib. 7-33522
 EM field spatial-temporal distrib. calc. using small parameter method (*Polish*) 7-62580
 EM subsurface radar using transient field radiated by wire antenna 7-23866
 extended s-f model, elec. cond. calc. 7-64194
 ferroelectrics, dynamic characteristics, soft modes saturation (*Russian*) 7-27672
 ferromagnet-antiferromagnet superlattice struct., mag. props. 7-2831
 ferromagnetic hysteresis, domain wall pinning, mathematical model anal. 7-7544
 ferromagnetic thin films, density of energy for localised retarded modes 7-7569
 ferromagnetic thin films, magnetisation calcs., differential operator method 7-45774

ferromagnetism continued

- field theoretical approach to solid state physics 7-12934
 film, ferromag., backward bulk magnetostatic wave propag. by grating formed by ion implantation 7-53093
 film, ferromag. with mixed exchange boundary conditions, theory of dipole-exchange spin wave spectrum 7-45644
 films, surface and guided magnetic polariton dispersion relations 7-38463
 finite slab, nonlinear spin wave dynamics and surface magnetostatic wave dispersion, averaged Lagrangian method (*Russian*) 7-17181
 FMR in system of ferromag. substrate and exchange-coupled thin ferromag. overlayer 7-38946
 free energy, anisotropy and rotational invariance 7-59007
 frustrated spin clusters, dynamical susceptibility anal. 7-7526
 Gutzwiller-Hubbard-Kanamori model, crystallization props. 7-58974
 Heisenberg antiferromagnets, multicritical points 7-27541
 Heisenberg classical easy-plane models, 2D, Monte Carlo studies 7-27542
 Heisenberg ferromagnet, 3D, susceptibility, correl. length, free energy, twelfth order series study 7-27488
 Heisenberg ferromagnet, anharmonic spin-one, order of phase transitions, effect of press. 7-53018
 Heisenberg ferromagnet, anisotropic, thermodynamic props., Monte Carlo Method calcs. 7-38894
 Heisenberg ferromagnet, diagram technique for Green functions 7-17150
 Heisenberg ferromagnet, interaction anisotropy influence on surface magnetism 7-52970
 Heisenberg ferromagnet, semi-infinite, Curie temp. calcs. 7-45603
 Heisenberg ferromagnet, thermal boson expansion at finite temp. 7-2885
 Heisenberg ferromagnetic chain, bound states, correl. functions 7-64474
 Heisenberg ferromagnetic chains, classical and quantum, momentum and cryst. momentum 7-12932
 Heisenberg model, one- and two-dimensional, free energy and susceptibility 7-45722
 Heisenberg model, paramagnetic neutron scatt. temp. depend. anal. 7-38848
 Heisenberg models with competing interactions, quantum fluctuations and phase diagram 7-38895
 Heisenberg spin chain, compressible, static π -kink 7-53020
 homogeneous electron gas, para- and ferromagnetic states, correlation energy interpolation fn. 7-45196
 Hopfield model near saturation, mean field theory 7-52989
 impedance of magnetic coaxial pipe 7-5815
 incommensurate crystals and mag. crystals, 2D topological vortex-type defects 7-7462
 indirect exchange in ferromagnets with low carrier densities 7-33162
 insulating ferromagnets, surface and interface magnetisation changes with temp., Green's function calcs. (*Chinese*) 7-38869
 intermediate valence systems, Ferromagnetic order coexistence, mag. props 7-64187
 intermediate-valence systems, magnetic-nonmagnetic transitions 7-12965
 intersubband s - d exchange absorption of spinwaves in ferromagnetic conductors 7-7499
 Ising ferromagnet, fixed spin influence on thermodynamic behaviour 7-38887
 Ising ferromagnet, magnetism at site-bond diluted anisotropic free surface 7-2800
 Ising ferromagnet, surface effects, mean field renormalisation group study 7-12982
 Ising ferromagnet, with biquadratic exchange interaction and uniaxial anisotropy 7-17189
 Ising ferromagnets on triangular lattice, bond- and site-diluted model, critical props. 7-12983
 Ising model, 2D with layered quenched bond randomness, free energy and specific heat calcs. 7-7531
 Ising model, ferromagnetic, 3 D, with quenched random nonmagnetic impurities 7-17190
 Ising model, ground state magnetic struct., antiferromag. impurity effects (*Russian*) 7-22086
 Ising model, transverse mag. field effects, Monte Carlo simulation 7-64473
 Ising model, upper bounds on critical temp. 7-17183
 Ising model disordered ferromag. binary system, phase diagram 7-59041
 Ising random-field systems, integer optimization and zero-temperature fixed point 7-7530
 Ising system, transverse susceptibility, direct calc. from local mag. field distrib. 7-17149
 itinerant electron ferromagnetism, mag. susceptibility, Curie-Weiss law 7-27501
 itinerant ferromagnets, electron and magnon spectra, spin fluctuation effects, dynamical suscept. calcs. (*Russian*) 7-12960
 itinerant ferromagnets, heavy fermion superconductivity (*Chinese*) 7-38805
 laser pulse heated ferromagnets 7-64460
 low symm. magnets, domain boundaries struct. and energy calcs. (*Russian*) 7-33200
 magnetic alloys, phase breakdown model, Curie temp., magnetisation (*Russian*) 7-45677
 magnetic superconductor, coexistent states of ferro- and antiferromagnetism 7-58950
 magnetic susceptibility of system with 360° domain walls (*Russian*) 7-7488
 magnetism, conf., Japan (Nov.1985) 7-24259
 magnetisation, permeability and hysteresis loss in unidirectional field (*Russian*) 7-12997
 magnetisation curve descriptive function 7-64490
 magnetisation of thin ferromag. film, Ising approx. 7-64425
 magnetoacoustic and Barkhausen emission study for NDT of ferromagnetic materials 7-45749
 magnets in paramag. range, zero-field susceptibility 7-45612
 metallic superlattices, long wavelength bulk and surface spin waves 7-2835
 metals, ferromagnetic, elastic moduli anomalies, thermodynamic theory (*Russian*) 7-2080
 metals, ferromagnetic, spin fluctuations above T_c (*Japanese*) 7-22113
 metals, long-wavelength magnon relax. 7-64446
 metals, nonlocal cond., microwave radiation transmission 7-13269
 metals, sound propagation, velocity and absorption 7-38919
 metals, structural defects studies muon depolarisation method calcs. 7-45898
 microscopically inhomogeneous systems, NMR echo decay, moment description 7-2949

ferromagnetism continued

- mixed valent compounds, static susceptibility of the periodic Anderson hamiltonian 7-22096
 monochromatic spin wave, stability under parallel pumping conditions 7-45641
 multilayers, propagating spin waves 7-52959
 non-Heisenberg systems, random phase approx. and Green's function anal. (*Russian*) 7-45597
 nonlinear EM waves in ferromagnets 7-17201
 nuclear spin-lattice relax., one-magnon process effects (*Russian*) 7-33284
 one-dimensional classical anisotropic Heisenberg ferromagnet, numerical study 7-12933
 one-dimensional degenerate Hubbard model, Monte Carlo simulations 7-45609
 one-dimensional easy plane, quantum Monte Carlo and transfer-matrix calcs. 7-7468
 one-dimensional ferromag. $1/n^2$ Ising chain, crit. temp. 7-7527
 one-dimensional Hubbard model, one- and two-hole excitation spectra 7-22088
 planar Ising ferromagnet, Yang-Lee zeros 7-52924
 plasma filament instability in presence of ferromagnetic 7-44166
 positron spin polarisation relax. study in ferromag. materials 7-46203
 quantum spin model on triangular lattice, zero-temp. props. 7-27486
 quasicrystals, magnetic phase structure on the Penrose lattice 7-53013
 quasistatic magnetic permeability of an amorphous ferromagnet 7-33214
 randomly inhomogeneous, elec. resist., temp. depend. (*Russian*) 7-58791
 resistivity of ferromagnetic metal near the reorientation phase transition point 7-33180
 retarded modes in layered magnetic structures 7-64502
 rigid body in magnetic field, rotation problem 7-41087
 semi-infinite ferromagnetic q -state Potts bulks separated by bond diluted interface, criticality 7-33179
 semiconductor, ferromag., spin-depend. phonon Raman scatt., theory 7-46013
 semiconductors, hot magnons 7-22099
 single-domain films with inclined anisotropy axis, magnetostatic spectrum 7-53092
 soliton dynamics in a planar ferromagnetic chain 7-52999
 solitons in arbitrary anisotropy systems (*Russian*) 7-45682
 spherical model, fluctuation effects and phase transitions 7-33192
 spin polarised secondary electron emission, book contrib. 7-33495
 spin system, ferromagnetic, 1D driven damped, solitary waves, stationary motion 7-59028
 spin wave excitation by acoustic fields, non-uniformly distrib. dislocations (*Russian*) 7-45646
 static surface critical behaviour, scaling and renormalisation, book contrib. 7-33183
 statistical mechanical systems, critical behaviour and random walk representations 7-48532
 strongly correlated Fermi systems, Gutzwiller saddle-point approx., functional integral approach 7-207
 superconductor, ferromag., phase diagrams and order parameters 7-17127
 superconductor films, mixed states 7-27478
 superconductors, ferromagnetic, intermediate state and easy-axis mag. anisotropy 7-38831
 superconductors, ferromagnetic, intermediate state and easy-plane magnetic anisotropy 7-38832
 superconductors, intermediate state 7-52915
 superconductors, self-organising auto-wave regimes 7-17129
 superconductors, surfaces and thin films, mag. and superconducting props. 7-58986
 superlattices with magnetisation perpendicular to surface, collective excitations, magnetostatic theory 7-45647
 surface ferromagnetism in transition metals, Hubbard model 7-33139
 surface magnetism, spin-polarised electron diff. and photoemission 7-59380
 thin absorbing film on reflecting struct., equatorial Kerr effect 7-53287
 thin film, precession soliton, nonlinear integro-differential eqn. soln. 7-64500
 thin films of diluted ferromag. alloys, mag. contrib. to elec. resistivity 7-22036
 tight-binding itinerant ferromagnet, spin wave anal. 7-2833
 transition metal magnetism, singular volume dependence 7-22108
 transition metal surface, H_2 chemisorpt., self-consistent model 7-16862
 two-dimens. ferromagnets, domain struct. 7-53028
 two-dimensional Hubbard model, mag. props., mean-field phase diagram and spin-spin corrs. 7-64429
 two-layer films, surface magnetostatic waves 7-13009
 uniaxial ferromagnets, magnetic moment kinetics, magnetic anisotropy, spin wave decay and dispersion calcs. (*Russian*) 7-17166
 uniaxial ferromagnets, spin wave damping at orientational phase transition 7-52963
 unsaturated ferromagnet, EM field eqns., reduction to Burgers eqn. and exact analytic soln. 7-33216
 weak random anisotropy, wandering moments and resonances, perturbation calcs. 7-64451
 weakly itinerant ferromagnetic systems, magnetoelastic anomalies due to spin fluctuations 7-53106
 Winter oscillations, parametric excitation, in domain walls 7-22119
 Zener theory 7-7504
 ferromagnets see ferromagnetic properties of substances; ferromagnetism
 ferrous alloys see iron alloys
 Feshbach resonances see atomic resonant states; molecular resonant states
 FET see field effect transistors
 few-nucleon reactions see nuclear reactions involving few nucleon systems
 few-nucleon scattering see nuclear scattering involving few nucleon systems
 few-nucleon systems see nuclei with mass number 1 to 5
 Feynman diagrams
 Abelian theories, gauge-invariant regularizations 7-61471
 anomalous high-energy behaviour in boson fusion 7-35761
 bound electron in Coulomb field, self-energy, momentum space method 7-42511
 chiral field theory, low momentum penguin loop contribs. and $\Delta I=1/2$ rule 7-41647
 conformal invariant field theory, Green's functions and Feynman rules on $S^3 \times S^1$ hypertorus 7-41597
 Coulomb-gauge QED, one-loop vertex function in parametric integral form 7-19059

Feynman diagrams continued

- covariant light front perturbation theory and three-particle equations 7-41651
- critical phenomena, field theory applications 7-41578
- diatomic molecules, Hellmann-Feynman electrostatic theorem (*Russian*) 7-62280
- electron-atom scatt., two-photon exchange, Coulomb-gauge electrodynamics anal. 7-24829
- finite temperature field theory, renormalisability 7-30161
- Lewis structures and Feynman diagrams, treatment of germinal correl. in Fock space 7-41127
- massive vector field, EM interaction with mag. moment, Feynman rules 7-4946
- massless light-cone gauge Feynman diagrams, cut-off and dimens. regularization methods 7-41645
- nonAbelian gauge theory, scalar formalism using Klein-Gordon-type wave eqn. 7-4952
- O(32) open superstrings, pentagon diagram evaluation 7-441
- QCD in 2D, chiral symm. breaking and condensate calcs. 7-49073
- QED, Feynman graphs and amplitudes, automatic generation using GRAND program 7-49043
- QED, superfield formalism using loop functionals 7-61539
- scalar field theory, path integral approach to dissipative processes 7-19012
- substitution rules for Feynman diagrams representing partial helicity amplitudes 7-49023
- temporal-gauge finite-time Feynman rules and Gauss's law 7-19000
- thermo field dynamics, development and generalization 7-9984
- two loop diagram, 1440-fold symmetry 7-9977
- ed- \rightarrow epn, quantum field theory, projecting properties on the light front and suppression of loop diagrams 7-41669
- ed- \rightarrow epn, final state interaction effects, vertex fns., Feynman diagram anal. 7-5100
- e⁺e⁻ high energy annihilation, quark and gluon fragmentation, Feynman diagrams 7-24901
- e⁺e⁻ \rightarrow q \bar{q} g, invariant amplitudes in QCD 7-537
- s-d+gluon, h, quark scalar boson interactions and strangeness-changing weak vertex, heterotic string anal. 7-30301
- H atom in molecule, polarisability change calcs. (*Russian*) 7-62279

FFT see fast Fourier transforms

FGD see air pollution detection and control

fibre optic cables see optical cables

fibre optic gyroscopes see fibre optic sensors; gyroscopes

Fibre optic sensors

- acoustic and optical waveguides, similarities and differences 7-1298
- active and passive types, signal processing aspects and appls. (*German*) 7-20422
- adjacent optical fibre sensors in Raman spectrometry, simulation and optimisation (*French*) 7-31469
- advantages for computerised control systems, data highways and sensors 7-15988
- astronomical instruments and techniques, conf., Tucson, AZ, USA (March 1986) 7-48162
- bent birefringent fibre, compensated sensing based on retardation characts. 7-50752
- birefringent fibre polarisation components for sensor applications 7-20450
- birefringent stress location sensor 7-43420
- boilup heat transfer obs. 7-50778
- Cartesian oval fibre-optic lens as linear to angular position converter 7-43407
- chemical industry appls., industrial meas. of press., temp., and level 7-57579
- chemical sensing, particularly in biomedical field, areas for use and techniques 7-31472
- chemical sensors based on oxygen detection by optical methods 7-43426
- communication, control and sensing appls. of optical fibres (*French*) 7-6009
- composite structure analysis using optical fibre modal sensing techniques 7-28259
- conference on fibre optic sensors and their appls., Cannes, France (Nov. 1985) 7-40999
- conference San Diego, CA, USA (Aug. 1985) 7-18485
- configurations, operation and characts. (*Spanish*) 7-37169
- crossstalk sensors accuracies improvement, compensation method 7-43434
- cryothermometer using molecular luminesc. 7-48740
- current and mag. field sensor, calibrated optical fibre Faraday rot. 7-25980
- current sensors using highly birefringent bow-tie fibres 7-15976
- depolarisation of light in irregular anisotropic single mode fibres 7-62841
- design and construction for temp., vibration and pressure meas. (*German*) 7-11158
- development, configs., and appls., review 7-31485
- developments and A/D signal conversion problems (*German*) 7-26019
- displacement measurements, loss-compensation technique 7-57561
- displacement sensor, based on Mach Zehnder interferometry 7-43432
- displacement sensor with two-beam interferometry, US nondestructive evaluation of composite materials 7-13716
- displacement transducer, characts. meas. 7-25968
- distributed, review 7-37166
- distributed fibre optic sensors, review 7-20434
- distributed sensors, intrinsic and extrinsic 7-25984
- Doppler flowmeters, differential, with single-mode fibre waveguides 7-44079
- dynamic materials testing appl. 7-46778
- electricity supply, communications and meas. appls. of optical fibres 7-57578
- electro-optical Kerr effect voltage measurements on multi-megavolt pulsed power accelerators 7-25286
- ellipsometric characterisation of single mode fibres 7-43428
- embedded fibres in graphite fibre reinforced epoxy, NDT by OTDR 7-28255
- endoscope for optical fibre holography 7-25769
- endoscopes, fibre optics, diagnostic and surgical appl. 7-40243
- evanescent-wave coupling force transducer, using He-Ne laser 7-41367
- extrinsic, for remote meas., impact on meas. techniques 7-11154
- Fabry-Perot fibre optic sensor and its appls. 7-43424
- Faraday rotation current and magnetic field sensor 7-31515
- Faraday rotation in multimode optical fibre probe, Z-pinch plasma expt. 7-11785
- FDM using FM laser source 7-15986

fibre optic sensors continued

- fibrescopes and principles of fibre optics (*Spanish*) 7-6002
- fluid level sensor 7-20447
- fracture testing appl. (*German*) 7-11162
- frequency domain reflectometry for fibre/integrated optic systems, high resolution distrib. fibre optic sensing 7-25987
- functional principles and appl. 7-1276
- glass:Nd absorption thermometer with fluorescent referencing, fibre optic sensor 7-25996
- glass:Tb₂O₃ Faraday rotator low loss single mode fibres, MCVD fabrication 7-25993
- gyroscope, passive resonant ring laser, progress 7-20440
- gyroscope, passive ring cavity-type, 1.5- μ m DFB InGaAsP laser appl. 7-57562
- gyroscope, phase modulated, coherent backscatter analysis 7-43427
- gyroscope, self-pumped phase-conjugate 7-31509
- gyroscope technology, state-of-the-art, review 7-20441
- gyroscopes, fibre optic, noise problems 7-20439
- gyroscopes, fibre optic closed loop, performance 7-20438
- gyroscopes, solid state, optical, review 7-20437
- heterodyne interferometric temp. sensor using transverse He-Ne Zeeman laser and polarisation maintaining fibre 7-25991
- high-bandwidth fibre optic system using laser diode transmitters 7-25978
- holographic endoscopy with gradient-index optical imaging systems and optical fibres 7-31271
- hybrid integrated components for optical fibre communication and instrumentation systems 7-25997
- hydrophone with dual in-line resonant cavity 7-43600
- imaging techniques utilizing optical fibres and tomography 7-25977
- integrated optical components for fibre sensors 7-26042
- intensity modulated, RF phase detection 7-43422
- interferometer, rotating ring, nonreciprocal effects 7-37171
- interferometer and appl. to photographic materials testing 7-30077
- interferometer using FM laser diodes 7-31470
- interferometric detection of slow phenomena 7-43423
- interferometric pressure sensor, single-fibre, aperture stop influence on S/N ratio 7-43388
- interferometric sensor system, optically multiplexed 7-25986
- interferometric sensors multiplexed using partially coherent light, expected noise levels 7-25982
- interferometric strain meas. 7-43433
- intermodal interference appl., fringe counting meas. technique 7-31499
- intrinsic and extrinsic distributed optical-fibre sensors 7-50768
- laser Doppler anemometer and boundary-layer meas. appl. 7-37609
- laser Doppler velocimetry, fibre optics use 7-50771
- laser pulse spatial modes, direct measurement 7-5931
- level transducers, review 7-43405
- liquid film sensor for 2-phase annular and stratified flow 7-37611
- liquid mixtures, refractive index meas. using speckle based fibre optic sensor 7-11124
- Mach-Zehnder interferometric sensors, review 7-20432
- magnetic field sensor, all single mode fibre 7-25990
- magnetic field sensor, wideband optical fibre, using Cd_{1-x}Mn_xTe sensing element 7-25979
- magnetic field sensor utilizing fibre optics and magnetostrictive effect (*Japanese*) 7-334
- magnetometer, all-fibre, with mag. feedback compensation 7-25989
- magnetometer, polarimetric DC using composite metallic glass resonator 7-14981
- magnetometer fibre optic using Mach-Zehnder interferometer 7-18843
- magnetometer with magnetic feedback compensation 7-41411
- medical application, biochem. and physical parameters meas. 7-60072
- micro-bend dark-field sensor 7-43431
- microbend, principle and appls. (*Slovak*) 7-11123
- microbend-induced birefringence in optical fibres, temp. dependence 7-43425
- microwave power detection by optical fibre arrangement 7-18865
- microwave pulse photonic meas. using electro-optic and fibre-optic components 7-25983
- modulating techniques, review 7-57580
- monomode sensors, optical processing schemes for phase and polarisation state information recovery 7-50763
- multicore optical fibres for sensors 7-25988
- multimode fibre-optic sensors with frequency output 7-57581
- multiport fibre optic refractive index sensors 7-43419
- new designs and fabrication techniques, sensors and laser action 7-50744
- NMR imaging, optical detection of respiration and heart beats 7-47277
- noise due to birefringence modulation 7-31479
- nonlinear, synchronous sampling demodulation scheme 7-31508
- particle concentration sensor 7-20443
- particle size measurement by light scattering detection with fibre optic sensor 7-37160
- passive ring resonator gyro, reson. characts. of backscatt. 7-50753
- petal flowmeter for low gas pipe flows 7-44081
- photoelastic, for force, pressure, acceleration and sound meas. (*German*) 7-11159
- photoelastic fibre optic sensor response, spectral linewidth depend. 7-20446
- photoelastic pressure sensor, using low-birefringence fibre 7-43429
- photoelastic probe for high speed material diagnostics 7-65250
- photonics, high bandwidth appls., review 7-20433
- piezoelectric copolymer jacketed single-mode fibers forelectric-field sensor application 7-6011
- polar nephelometer, fibre array, scattered light phase functions meas. for atmospheric particles 7-23896
- position verification device, radiation therapy appl. 7-47213
- power industry appl. (*French, English*) 7-15972
- precision fiber optic sensor market forecast 7-20442
- pressure sensor, frequency-coded 7-6014
- pressure sensor based on fibre macrobending 7-43386
- pressure sensors, all-passive fibre-optic, operating principles 7-61325
- pyrometric sensor for high-temp. meas. 7-41393
- radial grating meas. systems, accuracy improvement using fibre optic whole circumference sensor 7-31511
- radiation sensors, high bandwidth, review 7-20449
- Raman temp. sensor, based on signal backscattering from multimode fibre 7-41387
- reflective sensing technique employing GRIN rod lens 7-43387
- reflectometer configured to sense temp. 7-25994
- reflectometer to monitor refr. index changes in fluids 7-25995
- reflectometric fibre optic hydrophones improvement 7-43601

fibre optic sensors continued

- remote, fibre optic absolute sensors, problems and approaches 7-20435
- remote measurement appls. 7-43394
- review of fibre optic sensors and their appls. 7-20431
- review of optical waveguide sensors 7-50779
- rotation rate meas. appl. (*German*) 7-11161
- sapphire blackbody design, temp. limits extension 7-30012
- SAW filters, acoustic field investig. using fibre optic homodyne laser probe 7-1358
- self referenced fibre optic glass absorption thermometer 7-41388
- semiconductor laser and integrated optics for optical fibre sensors 7-25998
- sensing methods and advantages 7-31471
- shocked optical fibres, spectral transmission characts., remote optical sensor component 7-31466
- single-mode fibre, two modes, polarisation state preservation 7-6015
- single-mode fibre coupler, fabrication and appls. (*Japanese*) 7-6018
- speckle detection based fibre line sensor 7-31514
- strain monitoring system, marine appl. 7-57597
- strain sensor using concentric core fibre 7-26020
- streak camera system to monitor X-ray refl. changes in metal multilayers 7-30135
- temperature distribution measurement using Raman ratio thermometry 7-25985
- temperature measurement using intrinsic optical fibre sensors 7-50762
- temperature sensing developments 7-18785
- temperature sensor, all-fibre, based on light amplitude modulation 7-50767
- temperature sensor, fibre optic thin film, for temp. meas. in mag. fields 7-25992
- temperature sensor using biconical fused taper low-loss coupler config. and characts. 7-43439
- temperatures near ambient, measurement using infrared fibre-optic cable system 7-14945
- thermometer for medical appl., using thermochromic transducer and TDM technique 7-47276
- thermometer using temp. depend. absorpt., broadband detect. and time domain referencing 7-50751
- thermometry, advantages and appls. 7-9835
- transducers application 7-6003
- twin-core or polarimetric sensors for nondestructive evaluation of composite materials 7-20448
- twisted optical fibre, Faraday rotation meas. using rotating polarisation and analogue phase detect. 7-25981
- two-mode fibre interferometer/amplitude modulator 7-50750
- two-wavelength fibre gyroscope with wide dynamic range 7-1270
- U-shaped curved multimode fibre sensor for process refractometry and temp. meas. (*German*) 7-11160
- US sensor, single-mode fibre config. with resonance tuning 7-6010
- velocimeter, fibre optic, low cost 7-20444
- vibration monitoring and maintaining system 7-43402
- vibration sensor using single-mode fibre 7-20445
- void fraction meas. in two-phase flow 7-43430
- waveguide couplers, fabrication by ion exchange 7-57583
- wavelength encoded optical fibre sensors for practical industrial meas. 7-50766
- X-ray remote detect., coupling between plastic scintillators and light fibres 7-25320
- LiNbO₃ integrated optical components for fibre gyroscopes 7-20472
- SO₂ analyzer, fibre optic 7-23090
- ZrF₄ glass fibre, IR temperature measurements, 60 to 150 °C 7-56262

fibre optical waveguides *see optical fibres***fibre optics**

- For fibre optical waveguides used in telecommunications, see optical fibres*
- see also fibre optic sensors*
- acoustic sensors, state of the art 7-11243
- acousto-optic tunable filter 7-5979
- angioplasty with a laser and fibre optics at 2.94 μm 7-34221
- beam splitters, fibre-optic polarising, anal. 7-15980
- biomedical fibre optical and video monitor stimulators, comparison in normals and multiple sclerosis patients 7-65865
- birefringent fibre waveguide with elliptic borosilicate cladding, polarisation characts. study 7-62835
- blood O₂ saturation, in vivo meas. using quartz fibre optics and an optical multichannel analyser (*German*) 7-23423
- cable for CO₂ laser scalpel 7-14086
- chemical measurements in industry (*French*) 7-46894
- chromatic dispersion meas. of multimode optical fibre waveguides (*Czech*) 7-11122
- CID-MCP detectors for scientific appls., fibre optic coupled 7-30087
- coil of single-mode fibre, birefringence and polarisation mode dispersion 7-31498
- communication systems technology 7-15971
- comparison and calibration lamp illumination system for Multiple Mirror Telescope, fibre optical system 7-4342
- comparison of optical and acoustical signalprocessing techniques 7-1317
- components, in-line filter, switch and in-line attenuator 7-26002
- conference, fibre optics, short-haul and long-haul meas. and appls., San Diego, CA, USA (Aug. 1985) 7-40998
- connector, epoxyless polishless plastic, for multimode fibres 7-26015
- connector, low loss single-mode 7-26005
- construction technology, materials, technique and future prospects (*Italian*) 7-1274
- coordinate-sensitive gas discharge detectors, fibre optic readout system 7-30852
- coupler, fused biconic taper, environmental performance 7-26003
- couplers, appl. to diagnostic expt. at Nevada Test Site 7-26001
- couplers, connectors and splices, conf., San Diego, CA, USA (Aug. 1985) 7-24277
- couplers, fused, mass production 7-26050
- couplers, single-mode fused tapered, simplified design equation 7-26009
- couplers, single-mode polarisation maintaining 7-26011
- cross-talk meas. on high birefringence fibres 7-57566
- data communication system for ocean bottom surveys using remotely operated vehicle 7-9200
- DC electric field meter with fiber-optic readout 7-30040
- design for specialist appls. 7-11147
- DFB laser, single longitudinal mode operation considering light refl. from optical fibre facet (*Japanese*) 7-20284

fibre optics continued

- DFB lasers, fibre optic technology advances 7-1193
- digital correlator, fibre-optic, proposed topologies 7-42988
- directional coupler, polarisation preserving 7-25999
- directional coupler, polarisation-preserving, appls. 7-1279
- directional couplers, biconical taper technology and device appls. 7-26008
- double-channel planar BH multimode laser, 1.55 μm fibre grating external cavity, single-mode behaviour 7-15908
- element for digital information storage 7-42995
- endarterectomy of expt. atheromas, fibre optic laser delivery 7-34220
- endoscope for optical fibre holography 7-25769
- engineering meas., conf., Cannes, France (Dec. 1985) 7-29586
- Fabry-Perot resonator, transversely coupled fiber device 7-56325
- fiberscope using SiO₂ image fiber, picture image transmission system 7-31482
- fibre option for image transmission, historical and present perspectives 7-50775
- fused D-fibre couplers 7-26010
- Gaussian beam focusing through hemispherical microlens 7-11090
- hard clad silica fibres for data and power transmission 7-50765
- holder, zero-birefringence V groove, for fibres 7-43401
- Holocoupler-Selfoc fibre system, coherent transfer matrix description 7-26016
- holographic applications 7-25773
- holographic endoscopy with gradient-index optical imaging systems and optical fibres 7-31271
- holographic interferometer with monomode fibres, appl. to integrated optic grating device manufacture 7-25757
- holographic systems with HOE and optical fibres 7-25772
- hybrid device, all-fiber 90° optical hybrid for coherent communications 7-57603
- integrated optic device for fibre laser Doppler velocimeter 7-6022
- interference-type optical fibre hydrophone, effect of fibre length 7-43611
- interferometer with 4X4 coupler quadrature output 7-31506
- IR fibre optic device for cardiac cycle timing and photoplethysmography 7-3856
- Landauer-type localization of light in randomly 'broken' optical fibres 7-62838
- laser beam delivery system for medical appls. 7-47200
- laser diode, dynamic spectra and propag. in single model fibres 7-20225
- laser Doppler velocimetry, fibre optics use 7-50771
- laser surgery, high power, fibre optic beam delivery systems 7-47201
- lasers, fibre, superfluorescent, anal. 7-31329
- lasers and optical fibres, technology, theory, propagation and nonlinear optical phenomena, review 7-43437
- LED pulse distortion in single-mode fibres near zero-dispersion wavelength 7-6005
- light amplification due to nonlinear interaction of counterpropagating waves in a single-mode optical fiber 7-50646
- linearly polarised light, topological phase using optical fibre 7-1281
- liquid-crystal spatial light modulator, coupled to image converter, expt. investig. 7-43440
- logic elements 7-57564
- logical inverter, stimulated Raman scatt. in optical fibre 7-57466
- Mach-Zehnder interferometer with multimode fibers using the double phase-conjugate mirror 7-48834
- Mach-Zehner interferometer, stabilisation as intensity modulator 7-20425
- matrix of gradient microlenses fabricated by electrostimulated diffusion, optical connectors development 7-25967
- medical fibreoptic laser probe for treatment of occlusive vessel disease 7-34227
- microbend-induced birefringence in optical fibres, temp. dependence 7-43425
- microoptic components formed by local modification of the structure of porous glasses 7-43451
- military service aspects of fibre optic technology 7-50774
- mirror, fibre-optic, fabrication 7-37214
- modulator and logic gate using nonlinear refr. and absorpt. 7-37174
- multimode dispersing fibre coupler to phase conjugator for polarisation recovery 7-43250
- multisoliton pulse interaction, FM influence 7-43390
- narrow-linewidth fibre laser with integral fibre grating 7-5904
- new designs and fabrication techniques, sensors and laser action 7-50744
- nonlinear optics for fibre meas. and special device functions 7-11139
- ophthalmology, fibre optic probes 7-47206
- optical fibre reliability, review 7-20455
- optical nondestructive evaluation at the National Bureau of Standards 7-39835
- otorhinolaryngology, low-power laser therapy using fibreoptic instruments 7-28648
- particle size measurement using fibre-optic dual-beam laser interferometer 7-35494
- passive components, differential mode loss and mode conversion 7-31496
- passive-loop resonator, optical multistability 7-1278
- phase noise anal. of system using laser source with arbitrary coherence time 7-15979
- photodetectors for optical fiber communication in the 1-1.6 μm wavelength range 7-43443
- polarisation preserving fibres, discharge fusion splice optimum method 7-31529
- polarisation spectrophotometer for meas. of polarised emission and excitation spectra 7-56318
- polarisation state control of optical instruments, using fibre optics or Bragg cells 7-14992
- polarisation state control using fibre optic techniques 7-43421
- polarisation-maintaining fibres and their appls., review 7-11136
- polariser, fibre optic, single-mode, in-line, design, testing and performance 7-20453
- polymer solutions cloud points meas., using pressurised apparatus 7-9871
- practical holography, conf., Los Angeles, CA, USA (Jan. 1986) 7-24281
- principles and fiberscope appls. (*Spanish*) 7-6002
- Raman laser, fibre, synchronously pumped, anal. 7-15873
- review of optical fibre technology 7-20436
- ring Raman laser, all-fibre low-threshold synchronously pumped 7-57375
- ring resonator with wavelength-selective input refl. coeff. 7-1273
- ring resonators for stabilisation of spectral linewidth and oscill. freq. of external-cavity laser diodes (*Japanese*) 7-5921
- scanning optical fibre microscope, laser beam induced current images, of semiconductor materials 7-48846
- signal phase meas. error when passed through multimode optical fibre 7-37013

fibre optics continued

- single mode fibres, picosec. stimulated Raman generation, pump pulse fragmentation and fragment compression 7-50635
- single model fibres elliptical, polarisation maintaining, effect of coatings 7-20454
- single-mode connector, high performance, development 7-26014
- single-mode cutoff wavelength meas. errors 7-43403
- single-mode fibre, polarisation retaining with improved coil performance 7-20451
- single-mode fibre ends, polished, reflections 7-26012
- single-mode fibre resonant cavity calcs. (*French*) 7-50745
- single-mode fibre with wide acceptance angle, design using flat disc lens 7-43406
- soliton laser stabilisation, feedback from pulse-shaping fibre 7-50602
- spatial filtering in spectrometry using coherently excited fibre (*German*) 7-43393
- speckle reduction in laser microscope images using rotating optical fibre 7-1038
- splice, mechanical, for permanent fibre optic installation 7-26006
- surface deformation measurement by light speckle using optical fibre bundle 7-30078
- taper, multimode, mode behaviour 7-26000
- testing by power meter 7-31510
- twisted birefringent fibres, intensity discrimination 7-31503
- two-dimensional optical beam switching techniques using dynamic holography 7-25755
- two-mode fibre interferometer/amplitude modulator 7-50750
- ultrasonic sensor using optical fibres (*French*) 7-62935
- vibration monitoring and maintaining system 7-43402
- wavelength filter from successive biconical tapers 7-31504
- AlGaAs-GaAs narrow spectral linewidth semiconductor optical-fiber ring laser 7-25817
- Ar fibre laser, stimulated Brillouin scattering, single-mode and multimode pumped, spontaneous mode locking 7-1079
- Hg liq. interface, optoacoustic effect study 7-44698
- InP dual-wavelength channelled-substrate BH laser light source 7-62726
- LiNbO₃:Ti guided-wave optical switch, 1×16, polarisation-independent 7-31525
- Nd doped Z 7-62713
- Nd:YAG fibre lasers, superfluorescent, anal. 7-31329
- Nd:YAG laser pulse compression in optical fibre 7-50643
- Nd³⁺:silica fibre laser, tunable CW at 0.900 to 0.945 and 1.070 to 1.135 μ m 7-36983

fibre reinforced composites

see also carbon fibre reinforced composites; glass fibre reinforced composites

- advanced composite developments 7-27956
- anisotropic materials of different moduli, cylindrical shell theory 7-43684
- aramid fiber reinforced epoxy, delamination fracture toughness 7-53900
- Aramid fibre reinforced composite beams, viscoelastic-plastic anal. in flexure 7-33717
- aspen fibre reinforced polyethylene, mech. props., effect of extreme conditions 7-39604
- barrier coatings on unidirectional fibres, diffusional interaction of components effect on cond. 7-52167
- beam with step, finite three point bending 7-43689
- beams, symmetric laminated, optimal design considering damping 7-31639
- bounds on properties 7-7301
- brittle composites, Weibull statistical distrib. of strength 7-3429
- brittle-matrix, fibre-reinforced composites, matrix cracking mechanics 7-65129
- cellulose fibre reinforced polyester, prep., and props. 7-3265
- cellulose/asbestos fibre reinforced mortar, strain softening, crack growth resist. curves 7-39640
- ceramic matrix, test techniques for mech. props. 7-13698
- ceramic matrix composite frictional stress evaluation along fibre-matrix interface 7-28143
- ceramics, multiphase, sintering 7-64963
- ceramics, multiphase and composite, conf., University Park, PA, USA (July 1985) 7-60880
- coated short fibre composite, thermal stresses 7-37327
- continuous fibre composites, compression moulded, tensile strength, fibre misorientation effect 7-3379
- cotton fibre reinforced polyester composites, friction and wear 7-13610
- crack-resistant planar composite in tension, optimum design 7-16126
- cross-ply laminates, cracked, stiffness reduction anal. 7-44644
- damage constitutive relations 7-43765
- damping by dry friction of dynamic loads 7-32563
- delamination growth in angle-ply laminated composites 7-31701
- design problems with allowance for interphase reactions 7-43661
- directional reinforced composites, flash method for thermal diffusivity meas. (*French*) 7-4835
- duplex fibre reinforced materials, fracture toughness development 7-22804
- effective properties, effects of polydispersity n fibre diameter 7-6702
- elastic matrix with finite strains, stability of fibres 7-11322
- electronics and electric technology appls. (*French*) 7-17540
- end-notch flexure specimen, mode II interlaminar fracture toughness, finite element anal. 7-1509
- energy dissipation properties, anisotropy 7-6143
- epoxy-amine matrices, improvement of phys. and mech. props. 7-39574
- failure criteria, tensor-polynomial type, expl. verification of efficiency 7-22812
- failure in compression, surface delamination along macrocrack 7-6155
- fatigue damage and degradation mechanics 7-11352
- fatigue damage and degradation mechanics 7-11353
- fibre reinforced concrete, shear test specimen geometry 7-46738
- finite crack impact response 7-63082
- flexible, nonlinear elastic behaviour 7-39570
- fracture, micromechanical and macromech. criterion 7-17609
- hybrid, tensile, compressive, flexural and shear props., review 7-39532
- inextensible transversely isotropic elastic body, surface wave propag. 7-1483
- jute fibre reinforced polyester resin with fillers, fibre matrix interactions, absorbed water influence 7-3263
- Kevlar 29 fibre reinforced bone and dental cements, mech. props. 7-28080
- Kevlar 49-285 style fabric for space structures use, thermoelastic behaviour 7-37329

fibre reinforced composites continued

- Kevlar fibre reinforced epoxy, average stress-strain curves 7-33733
- Kevlar fibre reinforced epoxy, energy absorpt. capability, effect of specimen geometry 7-3315
- Kevlar fibre reinforced epoxy resin composite strands, tensile props. rel. to fibre vol. fraction 7-65087
- Kevlar fibre reinforced polymer, flexible, nonlinear elastic behaviour 7-39570
- Kevlar fibres, epoxy reinforced, failure, lifetime distrib., kinetic approach 7-39533
- lamine, stress state analysis using orthotropic photoelasticity 7-57778
- lamine plate, wave propag. 7-63051
- laminated, strength of pin loaded holes, effect of pin load distrib. 7-1403
- laminated, struct.-performance maps 7-17574
- laminated cross-ply plates, micromech. initial failure anal. 7-62975
- laminates, 7-39637
- laminates, compressive failure modes 7-6717
- laminates, fatigue and residual strength 7-44672
- laminates, first ply failure anal. 7-44670
- laminates, strain energy release rate of edge delamination, residual thermal and moisture influences 7-1508
- laminates, stress singularity by FEM 7-1401
- laminates, with matrix cracking and interior delamination, stiffness props. 7-44669
- laminates, yield and ultimate strengths 7-22785
- lateral pressure coefficient of linear-elastic anisotropic media and composites 7-1416
- mat-reinforced polymeric composite, thermal expansion and elastic characteristics 7-33631
- materials definition, class and elaboration (*French*) 7-17539
- mechanical effects of Nd:glass laser 7-6676
- mechanical properties, statistical and deterministic approach comparison 7-11287
- mechanical response of composite systems with randomly oriented short fibres, microstructure, approach 7-20593
- metal matrix composites, transverse elec. cond. model 7-45415
- metallic matrix, plastification, numerical and expt. investig. (*German*) 7-26172
- natural fibre reinforced polyester composites, fabrication, mech. props., weathering 7-7956
- NDT techniques for fibre reinforced plastic composites 7-17752
- oriented, compressive-fluxural/shear failure mode transition, interface strength 7-39586
- orthogonally reinforced, fracture criteria 7-1494
- PEEK matrix, high performance, processing, struct. and props. 7-3262
- periodic structure, coupled problems of thermoviscoelasticity 7-16074
- permeable fibre materials, thin sheets, determ. of ave. pore size by optical method 7-22961
- pineapple leaf fibre reinforced rubber, phys. and mech. props. 7-3378
- plastic, advanced, design methods and appls., book 7-4642
- plastic matrix, fatigue (*Japanese*) 7-46619
- plastic matrix hollow cylinder, 3D stress state 7-37333
- plate, multilayer reinforced, with through crack, stress state and limiting equi. 7-11344
- plates, thick, vibr., effect of fibre orientation 7-20620
- plates and curved panels, fibre reinforced, post-buckling behaviour under compression and shear (*German*) 7-20615
- polydiacetylene single crystal fibres in composites, stress-induced twinning 7-16567
- polyester matrix, stress state analysis using orthotropic photoelasticity 7-57778
- polymer base, binder content in impregnated reinforcement, contactless US inspection use 7-3565
- polymeric, cracked orthotropic, long-time strength under constant tensile load 7-6156
- polypropylene fibre reinforced concrete, compact shear test specimens 7-39793
- polypropylene fibre reinforced concrete, shear test specimen geometry 7-46738
- random short fibre composites, fatigue damage evolution assoc. with anisotropic elastic prop. changes 7-44673
- relaxation property anisotropy 7-46534
- row of circular fibres in elastic-plastic matrix, stability 7-1455
- short fibre reinforced metal, subjected to uniform temp. change, dislocations punched-out around fibre 7-21491
- short fibre reinforced polymer composites, fibre orientation developments in moulding 7-3264
- silk fibre filled thermoplastic elastomer, tensile rupture 7-39635
- simplified composite micromechanics, 3D finite element anal. 7-31637
- single fibre composites, stress transfer, critical fibre length, Young's modulus ratio 7-59558
- spatially reinforced, deform. props. eval., rigidity 7-6097
- stability analysis of composite with biperiodic system of circular fibers in an elastoplastic matrix 7-63026
- steel fibre reinforced concrete, compact shear test specimens 7-39793
- steel fibre reinforced Cu composites, extruded, struct. and fractography 7-13595
- stress distribution, Raman spectrosc. mech. anal. 7-21333
- stress transfer in single fibre-resin tensile tests 7-28074
- structural elements with fibre reinforced composite coverings, dynamic stiffness and damping props. determ. method 7-31717
- sunhemp fibre reinforced polyester composites, tensile and impact props. 7-39592
- textile structural composites, 3D, fibre inclination model 7-32545
- thermal conductivity calc. using boundary collocation method (*Polish*) 7-44931
- tubes, radial impact strength 7-59709
- unidirectional composite, interfacial zone shear modulus (*French*) 7-63712
- unidirectional fibre composites, two in-plane fracture toughnesses relationship 7-53844
- unidirectional reinforcing elements, scale effect of strength in tensile loading 7-31640
- vibrations of laminate plates, flexural waves 7-43742
- viscoelastic matrix, stress state of isolated fibre 7-16079
- viscoelastic plate, circular hole or inclusion, stress, conc. calc. 7-1446
- wetting of solids, metal matrix composites prep. 7-46372
- wood pulp fibre-cement paste composites, fibre-matrix interface, SEM obs. 7-64985
- Al alloy matrix, fabrication process 7-46377
- AlCuSiC composite, shock response 7-26867

fibres reinforced composites continued

- Al₂O₃ fibre reinforced Al, fatigue crack propag., effect of aq. environments 7-17624
 Al₂O₃ fibre reinforced Al composites, compressive failure modes, dead weight or machine loading 7-39663
 B fibre reinforced Al, bond form. between alitized B fibres and matrix in rolling 7-3331
 B fibre reinforced Al, strength characts. 7-33768
 B fibre reinforced Al alloy, corrosive media influence on crack resist. 7-17668
 B fibre reinforced Al matrix composite, TiB₂ coated, prep. using liq. phase infiltration 7-3229
 B fibre reinforced Al matrix composites, transverse mech. props., isothermal exposure effect 7-39688
 B fibre reinforced Al tube under multi-axial loadings, elastic-plastic deformation 7-46548
 B fibre reinforced epoxy, cross-ply plates, micromech. initial failure anal. 7-62975
 C fibre reinforced C composites, tensile props. and fracture toughness at high temps. up to 2400°C (Japanese) 7-53864
 Mo fibre reinforced Fe and Cu composites, extruded, struct. and fractography 7-13595
 SiC fibre composites, structural EXAFS study 7-64762
 SiC fibre reinforced Al, corrosion protection to NaCl soln. exposure 7-3488
 SiC fibre reinforced Al alloys, whisker or particulate hybrids, mech. props. 7-13537
 SiC fibre reinforced Al, fatigue crack propag., effect of aq. environments 7-17624
 SiC fibre reinforced Al composite wires, neutron irradi., mech. props., fusion reactor appl. 7-49628
 SiC fibre reinforced Al wires, neutron irradi., mech. props., fusion reactor appl. 7-53794
 SiC fibre reinforced Al(-Si), wettability of SiC 7-58569
 SiC fibre reinforced Al-Mg, thermal residual stress 7-63848
 SiC fibre reinforced Li₂O-Al₂O₃-SiO₂ glass ceramics, tensile and flexural strength 7-13520
 SiC fibre reinforced Li₂O-Al₂O₃-SiO₂ glass ceramic composite, thermomech. mismatch 7-46538
 SiC fibre reinforced SiC, high heat flux, low activation struct. materials 7-49635
 SiC whisker or particle reinforced Al composites, deform. thermal expansion, strengthening mechanisms 7-3373
 SiC whisker reinforced Si₃N₄, microstruct. and props. 7-22824
 SiC whisker reinforced Al₂O₃, ZrO₂ or glass, microwave sintering, microstruct. 7-27995
 SiC whisker reinforced Si₃N₄ ceramics, fracture toughness (Japanese) 7-28138
 SiC whisker reinforced Al matrix composites, interaction, with eutectic brazing alloys 7-46689
 SiC whisker reinforced Al alloy, fabrication and props. 7-53680
 SiC whisker reinforced Al, flame spraying fabrication and forging, whisker distrib. and strengths 7-59483
 SiC whisker reinforced Al alloy, powder metallurgy, corrosion susceptibility, influence of metallurgical variables 7-65152
 SiC-Al composites, heat treatment and neutron irradi. effects on mech. props. 7-65081
 Si₃N₄ whisker reinforced Al₂O₃ or ZrO₂, microwave sintering, microstruct. 7-27995
 SiO₂ powder/ceramic fibre composites, packing density model 7-13426
 Ti-base alloy, development of creep-resisting composition 7-3228
 W fibre reinforced Fe-Cr-Al superalloy, surface cladding and matrix deform., thermomech. loading 7-46568
 W wire reinforced amorphous Ni₇₃Bi₇Si₈ matrix composite ribbons, melt spinning prep. 7-46373

fibres

- see also carbon fibres; composite materials; fibre reinforced composites; glass fibres; optical fibres; polymer fibres*
 aortic valve tissues, relative vols. of struct. components rel. to biochem. components 7-34182
 dralon fibres of kidney cross-sectional shape, double refr. meas. 7-4882
 formation, nonsteady regimes, heat removal effect 7-44025
 inextensible cloth or cable networks with bending stiffness, continuum theory 7-1400
 lignocellulosic fibres, phys. and mech. props. 7-53883
 natural, fracture behaviour, empirical evaluation of struct.-prop. relationships 7-39633
 paperboard, constitutive behaviour under uniaxial and biaxial loading 7-63019
 polycarbosilane powders and fibres, prep. by fluid soln. rapid expansion 7-13399
 pulp fibres longitudinal compression device 7-13697
 slender fibrous material models 7-1407
 steel filaments, fatigue failure signs 7-46642
 weakly guiding acoustic fibre longitudinal modes 7-1299
 yarn deformation during pulling from fabric 7-54074
 Al₂O₃ fibres, strength distrib., multi-model Weibull distrib. 7-28081
 C fibre, laser produced plasma, XUV expansion coded recombination lasers 7-62679
 Cu, porous, physicomech. props. and model prediction 7-3353
 LiAlO₂ battery separator felt, prep. by sol-gel technique, phase transitions in gels 7-22601
 LiNbO₃ single crystal fibres, ferroelec. domain structs. 7-22202
 MnBi/Bi eutectic, freezing rates, convection effect on microstruct. 7-22652
 Ni, porous, physicomech. props. and model prediction 7-3353
 Ni-Cr, porous, physicomech. props. and model prediction 7-3353
 PbTiO₃ piezoelectric fibres, synthesis by hydrothermal reaction (Japanese) 7-64974
 β-SiC fibres, chem. and phys. props. (Russian) 7-46284
 SiC fibres, continuous, synthesis from polycarbosilane 7-22616
 SiC fibres, neutron irradi., mech. props., fusion reactor appl. 7-53794
 SiC fibres, prep. from polycarbosilane, heat treatment, Raman study 7-65062
 SiC fibres, stability, thermomechanical analysis 7-33627
 SiC fibres, strength distrib., multi-model Weibull distrib. 7-28081
 SiC short-fibred filamentary crystals, phase comp. and morphology 7-65010
 SiC-Si₃N₄ fibres, prep. by polycarbosilane precursors pyrolysis 7-27988

fibrinogen *see* proteins**field, crystal internal *see* crystal field interactions****field effect devices**

- see also field effect integrated circuits; field effect transistors; metal-insulator-semiconductor devices*
 capacitor, carrier ambipolar drift vel., field control study 7-52840
 n-InSb MOS structures, heterogeneity of generation processes, expt. 7-17106

field effect integrated circuits

- see also charge-coupled device circuits; CMOS integrated circuits*
 blood rate detector, one chip VLSI implementation using PPL 7-65881
 blood-rate detector, one-chip VLSI implementation using PPL 7-28756
 implantable multielectrode array with on-chip signal processing, neural prostheses/biopotential recording appls. 7-34338
 NMOS multielectrode array chip, multiplexed implantable type, cerebral cortex evoked response monitoring appl. 7-47305
 SOI lateral solid phase epitaxy, selective P ion implantation 7-52359
 systolic architectures for connected speech recognition 7-6059
 GaAs semi-insulating cryst. characts., IC substrate appls. (Japanese) 7-6622
 Ta₂O₅ films for MOS DRAMs using ultra-high purity Ta sputtering target 7-59423
 W, selective LPCVD for MOS VLSI appls. 7-17456

field effect transistor circuits

- Used for general papers and papers where the use of field effect transistors is significant*
 MOSFET chopper amplifier based signal source, brain voltage changes meas. appl. 7-23480

field effect transistors

- see also field effect integrated circuits; high electron mobility transistors; insulated gate field effect transistors; junction gate field effect transistors; Schottky gate field effect transistors*
 chemical microensors, advances, review 7-48710
 HJFET 7-52811
 optoelectronic components, high performance, long wavelength, MOVPE, atm. press. growth, operating characts. 7-27930
 AlGaAs-GaAs split gate heterojunction FET, elec. resist., Hall effect, influence of electronic subband mag. depopulation 7-38740
 GaAs, electron drift vel.-elec. field characts. 7-38569
 GaAs FET arrays, electrical parameter mapping 7-32438
 GaAs high quality layers grown on Si by MOCVD, FET and LED appls. 7-27922
 GaAs, undoped semi-insulating, dislocations, deep trap levels, FET meas. (Chinese) 7-12643
 GaAs:Si, FET structs., rapid optical annealing for improved uniformity 7-16620
 a-GaAs-Si (100), epitaxial regrowth by excimer laser annealing, FET fabrication 7-32875
 K⁺ selective electrodes on valinomycin/PVC overlayers substrates 7-65375
 a-Si FET addressed liquid crystal spatial light modulator 7-37132
 a-Si technology, review of developments 7-38551

field electron microscopy *see* field emission electron microscopy**field emission, electron *see* electron field emission****field emission, ion *see* field ion emission****field emission electron microscopes**

- see also field emission electron microscopy*
 field emission gun scanning electron microscope columns, computer modelling 7-41548

field emission electron microscopy

- see also field emission electron microscopes*
 compact tension specimen, crack tip interaction with void, numerical analysis using J₂ corner theory (Japanese) 7-31703
 composites, laminated, strength of pin loaded holes, effect of pin load distrib. 7-1403
 emitter remodelling, microprocessor controlled 7-29987
 metal insulator-metal structures, field-induced hot-electron emission, energy anal. 7-30121
 metal-insulator, composite microemitters, hot electron emission 7-33532
 refractory metals, crystal growth and surface self-diffusion in high elec. fields, FEM studies 7-37914
 solid surfaces, chemistry and physics, book 7-60891
 steel, Cr, high C, notched rods, breaking by heating process, elastic-plastic stress analysis (Japanese) 7-33777
 surface science techniques, book 7-60888
 vibration shape function optimization appls. 7-43743
 Er, VPE growth on W substrate, field electron emission microscopy 7-64029
 La epitaxial layer on W field emitter, surface self-diffusion studies 7-32702
 Ni, grain boundaries in very clean tips, SEM, FEM obs. 7-52148
 Pd-Cu-Ag, ordering and precipitation, field emission microscopy studies (Russian) 7-46472
 Pt (110), nucleation and orientation of adsorbed graphite layers 7-21664
 Pt surface, graphite island form., FEM, SEM and AES studies 7-32805
 Pt-Rh surfaces, N₂ and CO adsorption, temp. depend. and work function studies 7-33960
 Rh surfaces, adsorption and desorption of NO, effect of surface structure 7-6994
 Ta, grain boundaries in very clean tips, SEM, FEM obs. 7-52148
 W, grain boundaries in very clean tips, SEM, FEM obs. 7-52148
 W surface, Hg absorption, field emission microscopy studies 7-32804

field emission ion microscopes

- see also field emission ion microscopy*
 resolution, thermal accommodation effects 7-48920
 surface (110) and (100), reconstruction, obs. in field ion microscope 7-1828
 temperature distribution of tip and loop under influence of gas mols. (Japanese) 7-18927

field emission ion microscopy

- see also atom probe field ion microscopy; field emission ion microscopes*
 conference, Berlin, Germany (July 1986) 7-29577
 field evaporation rate, temp. depend. 7-33525
 image processing, video digitiser and frame memory system 7-30122
 negative ion imaging using organic image gases 7-30120
 Nimonic superalloy, PE16, decomposition kinetics, TEM, FIM and SANS studies 7-53748
 optimal conditions, grain boundary studies in W and Ta 7-32461
 solid surfaces, chemistry and physics, book 7-60891

field emission ion microscopy continued

- specimen preparation technique, combined TEM/FIM examination 7-29988
specimens, sharpening and polishing method 7-29986
surface science, modern techniques, book 7-60911
surface science techniques, book 7-60888
Al-Mn quasicrystals, field ion images, computer simulation studies 7-32368
AlMn icosahedral phase, atomic struct., electron diff., studies 7-32366
CdSe, ordered structures, field ion microscopy studies 7-32768
Cu-Co alloy decomposition, TEM, FIM and SANS studies 7-33749
Cu-Fe alloy, BCC and FCC Fe particles, field ion microscopy studies 7-33667
Fe, field evaporation in Ne and H, temp. and field depend. 7-33526
Fe₇₀Cr₅Si₁₀B₁₅, metallic glass, field electron emission 7-33530
Ge-metal interfacial atomic struct. and cpd. form., FIM studies 7-32846
Ir (100), low temp. field evaporation of clusters, surface reconstruction, field ion microscopy studies 7-44973
Ir (100) surface reconstruction by field-ion microscopy 7-2316
Ir surfaces, reconstructed, direct imaging using field ion microscopy 7-32767
Mo surface, high-field corrosion, field-ion microscopy studies 7-33830
Nb, field evaporation in Ne and H, temp. and field depend. 7-33526
NiAlTi, decomposition kinetics, TEM, FIM and SANS studies 7-53748
Pt (100), low temp. field evaporation of clusters, surface reconstruction, field ion microscopy studies 7-44973
Re surface, high-field corrosion, field-ion microscopy studies 7-33830
Rh overlayers on Si surfaces, FIM 7-52284
Si field ion imaging, Au shank overlayer effects, photoillumination and field-induced image-size effects 7-33534
Si-metal complexes on W(110), atomic interactions, FIM study 7-21691
Si-metal interfacial atomic struct. and cpd. form., FIM studies 7-32846
W (011), pulsed field evaporation, impurity distrib. 7-63956
W mono-atomic tips for scanning tunnelling microscopy 7-21050
W surface, high-field corrosion, field-ion microscopy studies 7-33830
W surface single atom sites in He gas, field ionisation processes 7-33527
W/polyethylene interface struct. and defects, FIM obs. 7-27151
ZnO, ordered structures, field ion microscopy studies 7-32768

field evaporation

- activation energy formula, charge draining mechanism 7-33528
conference, Berlin, Germany (July 1986) 7-29577
ion sources, liq. metal, mech. 7-25275
scanning tunnelling microscopy, atom transfer mechanisms 7-4921
CdSe, ordered structures, field ion microscopy studies 7-32768
Fe, field evaporation in Ne and H, temp. and field depend. 7-33526
Fe₇₀Cr₅Si₁₀B₁₅, metallic glass, field electron emission 7-33530
Ir (100), low temp. field evaporation of clusters, surface reconstruction, field ion microscopy studies 7-44973
Ir, field evaporation rate, temp. depend. 7-33525
LaB₆ (001), field evaporation in the presence of H₂, atom probe FIM 7-21652
Mo ions, energy distrib. obs. and evidence for post field ionisation 7-46281
Mo²⁺, post fluid ionisation and evaporated ion energy distrib. 7-33524
Nb, field evaporation in Ne and H, temp. and field depend. 7-33526
Pt (100), low temp. field evaporation of clusters, surface reconstruction, field ion microscopy studies 7-44973
Ru, surfaces, CO reactions, Ru(CO)_xⁿ⁺¹ formation, field desorption study 7-54183
W (011), pulsed field evaporation, impurity distrib. 7-63956
W, He field adsorption and evaporation 7-32802
W surface, field adsorption of He 7-32816
W surface, high temp. field evaporation, desorption studies 7-64881
ZnO, ordered structures, field ion microscopy studies 7-32768

field intensity patterns (antenna) see antenna radiation patterns**field interactions (condensed matter)**

- see also *crystal field interactions; hyperfine field interactions (condensed matter)*
glass, transition metal doped, optical absorb. and luminesc. spectra 7-13186
Ca(PO₃)₂Du_{0.3}³⁺ glass, highly doped, fluorescence spectral width of ⁵D₂-F₃ transition 7-13189
Ce-Cu amorphous alloys, mag. and transport props., Ce-derived anomalies 7-52601

field ion emission

- electrified menisci, cone-like shapes, emitted charge effects 7-31888
liquid metal ion sources, field and temp. depend. of ion emission 7-7824
metal surfaces, field adsorption of rare gases 7-21648
Cu-P alloy liquid metal ion sources, ion formation 7-64878
Ga liquid metal ion source, influence of substrate geometry on emission props. 7-53508
Ni-B-Si alloy liquid metal ion sources, ion formation 7-64878
PVDF films, elec. field-induced gas emission meas., ionic charge transport study 7-27872
Pt-P alloy liquid metal ion sources, ion formation 7-64878
W surface, high temp. field evaporation, desorption studies 7-64881

field ion microscopy, atom-probe see atom probe field ion microscopy**field ionisation**

- atom, by strong elec. fields, 1D model 7-36804
conference, Berlin, Germany (July 1986) 7-29577
homoadamantane, ionised, methyl elimination, field ionisation kinetics and ²H and ¹³C labelling 7-42775
ionising solitary waves of elec. field, propag. along dielec. surface 7-21025
laser field ionisation, quantum model calcs. 7-50032
liquid metal ion sources, field and temp. depend. of ion emission 7-7824
polymeric dielectric, in partial discharge, depression rel. to elec. ageing (Russian) 7-26577
H, 1D atom, ionis. by reson. elec. field 7-5780
H, Stark effect and field ionis. 7-5628
He, atom, with turbulent flow, two electron group model for RF ionisation 7-31921
In/GaAs/Cu/In struct., I-V characts., carrier recomb. and generation, impurity thermionic field ionisation effects (Russian) 7-22030
Mo field evaporated ions, energy distrib. obs. and evidence for post field ionisation 7-46281
Mo²⁺, post fluid ionisation and evaporated ion energy distrib. 7-33524
Na ion beam generation, field ionisation of laser-excited Rydberg atoms 7-57186

field ionisation continued

- Si field ion imaging, Au shank overlayer effects, photoillumination and field-induced image-size effects 7-33534
W surface single atom sites in He gas, field ionisation processes 7-33527
field measurement, electric see *electric field measurement*
field measurement, magnetic see *magnetic field measurement*
field plotting
see also *field strength measurement*
ECG body surface mapping, Nijmegen, Netherlands (June 1985) 7-48192
high resolution analysing magnet with aberration correction, 2D field mapping and field correction 7-25283
TOPAZ magnet, field mapping device 7-14984

field strength measurement

- see also *electric field measurement; magnetic field measurement*
calibration of meters using loop antenna, conductive objects effect determ. 7-18822
RF field strengths and proton multiplicities, determ. by 2D NMR pulse techniques 7-24677
VHF-FM broadcast Es propagated signal polarisation obs. 7-60468

field theories, unified see unified field theories**field theory, classical see classical field theory****field theory, crystal see crystal field interactions****field theory, electromagnetic see electromagnetic field theory****field theory, meson see meson field theory****field theory, quantum see quantum field theory****fields, electric see electric fields****fields, magnetic see magnetic fields****filament lamps**

- heat absorption demonstration using incorrectly installed bulb 7-48257
schlieren optics methods, comparison of light sources 7-57503
sealed pulse lamp for underwater photography (Russian) 7-61396
spiral filament radiation approx. by radiation from cylindrical surface 7-37082
W lamp, temperature and pressure profiles, high-resolution CARS measurements 7-41377

filament reinforced composites see fibre reinforced composites**file management see file organisation****file organisation**

- see also *data handling; data structures; database management systems*
SCALE, nuclear waste cask analysis, critically safety analysis 7-15411

filled polymers

- asbopolymer material, friction and wear characts. vs. metal friction pairs 7-28153
biomedical US probe and array using PZT-polymer 1:3 composite 7-3848
biomedical US transducer array performance with PZT-polymer composite piezoceramic 7-3850
biomedical US transducers, PZT rod-polymer composite piezoelec. plate tailoring 7-3849
butadiene elastomers, soot-filled, struct., IR spectra 7-39127
ceramic filled poly(acrylic acid) composite, filler chem. influence on T_g behaviour, dynamic mech. spectroscopy 7-59559
composites, porous and dense, prep. from sol-gel 7-65002
composites containing anisometric particles, flow and flow orientation 7-37498
dimethacrylate paste with silanated silicate particles, photopolymerised, filler influence on fracture 7-3426
elastic characteristics, effect of aggregation of dispersed rigid filler 7-32547
epoxide resin composites, particulate filled, static fatigue, time to failure predictions 7-13562
epoxide resins, particulate filled, parameters determining strength and toughness 7-65071
epoxy, Al particle filled, damping charactn., dynamic structural model appl. 7-33709
epoxy composites, Fe powder reinforced, flexural props., water condition temp. depend. 7-59587
epoxy filled with Al₂O₃ in SF₆ under DC stress, potential distortion from change on solid insulators 7-51554
epoxy filled with Fe particles, dynamic mech. props., storage and loss moduli 7-3349
epoxy resin, aminimide-cured, mica reinforced, improved mech. props. 7-59489
ferrite-filled, highly loaded, melt rheology 7-12345
honeycomb filler, strength and stiffness in shearing determ. 7-17634
jute fibre reinforced polyester resin with fillers, fibre matrix interactions, absorbed water influence 7-3263
melt, matrix, mol. wt. effect on rheological props. 7-16141
metal embedded polymer film, plasma deposition, negative ion form. 7-7887
metal-polymer composites, wear resist., damping device appl. 7-17657
mica-epoxy composite dielectric strength obs. 7-64570
natural rubber/polybutadiene elastomers, C black distrib., flow behaviour depend. 7-43832
nylon 6 composites, formed by in situ polymerisation of caprolactam, mech. performance 7-39575
PEEK matrix for high performance composites, processing, struct. and props. 7-3262
phenolic resin composites, optimisation for friction materials 7-39475
piezoceramic-polymer-composites, damping props. 7-64575
plastics, conductive, continuous milling (Japanese) 7-46408
PMMA, drawn, filled with ultrafine SiO₂ particles, elastic and yield props. 7-3351
PMMA, Fe filled, techniques and models for elastic moduli, US evaluation 7-39833
PMMA-3-nitroaniline composite films, SHG obs. 7-62771
poly(acrylic acid)-ceramic filler composite, filler chem. influence on T_g behaviour, dynamic mech. spectroscopy 7-59559
polybutadiene, C filled elastomer, positron lifetime and annihilation radiation ang. correl. meas. 7-46229
polycarbonate, mica filled, determ. of mica orientation 7-39477
polycarbonate-C black composites, TEM obs. of percolation threshold 7-12771
polydiphenylborosiloxane/aminimide-cured epoxy resin composites, friction and abrasion props. 7-39677
polyester, clay-filled, tensile behaviour 7-3382

filled polymers continued

- polyester resin, glass sphere filled aligned fibre reinforced, Young's and flexural moduli 7-3350
- polyethylene, CaCO_3 filled, light scattering, struct. aspects of dichromatic laser speckle patterns 7-42931
- polyethylene, CaCO_3 filled, optically heterogeneous materials, light scatt., struct. aspects of dichromatic laser speckle patterns 7-31248
- polyethylene, chlorinated, rutile-filled, 7-39573
- polyethylene, cross-linked, C black composites, permittivity, percolative model 7-45913
- polyethylene, exfoliated graphite filled, elec. props. 7-38986
- polypropylene, glass-flake reinforced, impact fracture 7-39659
- polypropylene, mica-reinforced, fracture behaviour, effect of coupling agent, flake orientation and degradation 7-13593
- polypropylene films, Cu-filled, struct. and elec. cond. 7-64301
- polypropylene melt, CaCO_3 filled, on-line US monitoring of extrusion 7-59725
- polypropylene melts, fibre filled, rheological behaviour under steady and oscillatory shear 7-37413
- polypropylene mica filled composites, struct.-mech. props. relations 7-1919
- polypropylene-EPDM elastomer multicomponent blend, CaCO_3 filled, mech. and rheological props. 7-3381
- polystyrene, glass bead filled, sonic modulus, peculiarities (*Japanese*) 7-33715
- polystyrene, mica filled, determ. of mica orientation 7-39477
- polystyrene-3-nitroaniline composite films, SHG obs. 7-62771
- polyurethane- CaCO_3 composites, segmented, dielec. relax., glass transition 7-45926
- polyvinyl alcohol/polyvinyl acetate/carbon black composites, thermal currents meas. 7-45920
- propylene- Al_2O_3 system, mixing and flow props. (*Japanese*) 7-44832
- PVC, metal-filled, compensation effect 7-64300
- PVC, mica filled, determ. of mica orientation 7-39477
- PVC, rubber modified or filled, damage kinetics, AE analysis 7-54063
- PVC coating on polymerisation-modified fillers, morphological struct. (*Russian*) 7-63517
- rigid matrix particulate polymer composites, mechanical strength/filler content relationship 7-13594
- rubber, particle reinforced, with distributed damage, micromech. model for nonlinear viscoelastic behaviour 7-43698
- rubber-epoxy materials exhibiting increased crack resistance 7-17509
- silk fibre filled thermoplastic elastomer, tensile rupture 7-39635
- styrene-butadiene rubber, C-black loaded, elec. props., effect of gamma irradi., dosimetry appls. 7-33006
- styrene-isoprene-styrene block copolymer system, ferrite-filled, matrix-filler interactions 7-3352
- thermally conductive polymer compositions 7-2284
- underwater polymer composition rel. to acoustic props., Young's and longitudinal bulk modulus meas. 7-1304
- wollastonite reinforced polyamide 6, strength props., depend. on humidity and temp. 7-39636
- Au-polymer composite thin films, elec. behaviour 7-52856
- Ba ferrite filled styrene-isoprene-styrene composite, dynamic mech., elec. and mag. props. 7-13001
- C black filled polymer composites, elec. resist. rel. to curing temp. 7-65001

film badges *see dosimeters***films**

- see also adsorbed layers; coatings; foils; helium films; Langmuir-Blodgett films; liquid films; monolayers; optical films; polymer films; replicas; thick films; thin films*
- soap-film networks, 2D, mean-field theory 7-28361
- tensile testing of foils and films, specimen-deformation machine for X-ray diffractometers 7-33874

filtering and prediction theory

- see also information theory; Kalman filters; random processes; Walsh functions*
- acoustic signals, time series modelling by generalized adaptive function, appl. to random noise data 7-37268
- adaptive lattice noise canceller and optimal step size 7-43528
- adaptive noise cancellation, variable length lattice filter use 7-43527
- Brownian motions, absorbing and reflecting, filtering problems 7-48579
- cartography, quasi-ideal spatial filters for large maps 7-28808
- CT methods use for nondestructive inspection under conditions of insufficient data 7-39818
- digital tomography synthesis, 3D reconstructing algorithm 7-47254
- ECG, power line interference estimation and removal 7-65863
- frequency domain acoustic noise canceller, frequency bin adaptive filtering 7-37247
- Gabor filters applied to electronic speckle pattern interferometer images 7-9892
- geosound signal detection, appl. of adaptive dig. filtering (*Chinese*) 7-20508
- holography, far-field in-line, and diff. pattern analysis of particulates, filtering effects 7-31279
- L_1 deconvolution and its application to seismic signal processing 7-34717
- laminated materials, flaw detection, signal recognition automation using linear prediction model 7-3561
- mapping problems, smoothing error dynamics 7-8788
- medical images, edge enhancement by 3D processing 7-54803
- multi-channel Kalman filter algorithm in epileptic EEG structural anal. 7-54793
- noisy speech anal. using speech and electroglottal signals 7-28545
- nonlinear digital filter for separating nonstationary and stationary EEG waves 7-47267
- nuclear hyperfine interactions, appl. of digital filtering techniques 7-38523
- oceanographic data analysis, least-squares method as filter and related power in spectrometry 7-40575
- pathological voice acoustic anal., adaptive comb filtering method 7-37283
- programmable spatial filtering function using CCD technology (*Japanese*) 7-25715
- pure orientation filtering, scale invariant image processing tool for perception research and data compression 7-60005
- QRS complex detection under strong noise, real-time, medical appl. 7-47266
- radioastronomical data, optimum nonlinear filtering method 7-47721
- REDMASK noise reduction filtering for the hearing-impaired 7-34162
- resistivity logs, appl. of digital filter technique (*Chinese*) 7-29261

filtering and prediction theory continued

- retinal ganglion cell processing of spatial information in cats 7-54560
- smoothing method for Earth tides obs. data (*Chinese*) 7-55271
- speaker-independent isolated word recognition based on emphasized spectral dynamics 7-43556
- stereo vision algorithm using difference of recursive filters to obtain binary Laplacian image 7-28535
- stochastic sound system, digital filter design for state estimation 7-6056
- stratigraphic filter theory in seismology, effects of parallel bedding and random inhomogeneities 7-28877
- tomographic reconstruction consistency by iterative methods 7-47253
- underwater acoustic exploration, appl. of array processing for parallel linear recursive Kalman filtering 7-65986
- US tomography; resolution improvement using adaptive filtering (*Japanese*) 7-34202
- vocal tract source-filter model 7-37294

filters

- see also band-pass filters; crystal filters; digital filters; electromechanical filters; high-pass filters; Kalman filters; low-pass filters; matched filters; microwave filters; optical filters; passive filters; spatial filters*
- air filters, industrial, for particle sizes in submicron range, retention efficiency 7-59903
- EEG waveforms, filter transient response 7-54792
- EM flowmeters, noise reduction 7-37599
- fibre optic interferometric electrically tunable filter using the thermo-optic effect 7-37113
- median filtering of seismic data, response in high-freq. range 7-66357
- microphone arrays, adaptive optimisation under nonlinear constraint 7-37306
- multilayer mirrors as X-ray filters for slit scan radiography 7-34243
- nonlinear, threshold signal shaper for detector operating under increased loads 7-10363
- Nuclear Track Filters, development for liquid phases and gases 7-25098
- Ag, soft X-ray filter for plasma diagnostics 7-63353

filters, optical *see optical filters***filtration**

- blood filtration rates, review 7-54654
- brinkman equation, fractal model for porous media, and viscosity renormalization 7-44042
- cake filtration, formulation 7-11528
- circular orifice, 3-D hydrodynamic interaction of a finite sphere, num. soln. 7-51303
- clay soil, filtration prop. form., adsorbed H_2O struct. role 7-51297
- CR-39, modified microfilter study 7-36409
- deep bed filtration, stochastic compartmental model 7-6301
- drying, filtration process, hydrodynamics 7-57918
- flow rates for compressible and immiscible viscous filtration fluids 7-98
- fluid inertia and fibre proximity of airflow through fibrous filter 7-11535
- gas-liquid foam, fluid flow model 7-51301
- granular filters from loosely poured metal powders, operating characts. 7-28383
- hollow-fibre modules, flow distrib. study 7-65783
- macromolecules, ultrafiltration, transfer limiting phenomena 7-54167
- membranes transport process meas. techniques 7-28337
- mica nuclear track microfilter cascade fractionator, industrial appl. 7-36408
- mica nuclear track microfilter props. for industrial aerosol meas. instrument 7-36407
- Netherlands nuclear power plant air filter testing and monitoring 7-3741
- nuclear track microfilters, recent developments and appls. 7-65659
- paper filtration props., gamma irradiation effects 7-32499
- plasmapheresis, increase of filtration by pulsatile blood flow (*French*) 7-3930
- polyoxy-2,6-dimethyl-1,4-phenylene, sulphonated, ultrafiltration membrane prep. 7-54174
- porous medium with crack, elastic-hydrodynamic problem of fluid inflow 7-11534
- radioactive areas ventilation, filter testing, aerosol mixing 7-30727
- synthetic membranes, conf., Alcabi-deche, Portugal (June-July 1983) 7-24306
- ultrafiltration, membrane-solute interactions effects on pure solvent transfer 7-54177
- ultrafiltration, modelisation and structure modulus (*French*) 7-16245
- NaCl , solns., electrolysis, alkali conc., filtering diaphragms effects 7-54136

FIM *see field emission ion microscopy***FIM, atom-probe** *see atom probe field ion microscopy***fine structure, atomic** *see atomic fine structure***fine structure, molecular** *see molecular fine structure***finite automata**

- 1/f spectra in nonlinear dynamics, noise-induced trapping at attractor boundaries 7-48557
- cellular automata, Langevin equations, and unstable states 7-18703
- cellular automata for 2D hydrodynamic flow simulation (*French*) 7-16158
- cellular automata method for phase unwrapping 7-42976
- cellular automaton fluid models, continuum eqns. for large-scale behaviour 7-35286
- cellular automaton, long-range effects 7-29926
- inhomogeneous cellular automata, annealed and quenched, phase transitions 7-48613
- Kauffman cellular automata, two-dimens., phase transitions 7-35400
- pattern formation in reversible cellular automata 7-18712
- seismic P-wave modelling with cellular automata 7-66320
- self-generated complexity, quantitative theory 7-29690
- spatio-temporal coherence and chaos, conf. Los Alamos, USA, Jan. 1986 7-48158
- triangular lattice gas automaton, nature of turbulence 7-41302

finite difference methods *see difference equations***finite element analysis**

- 2D electrostatic and EM problems, general interactive finite element package 7-62569
- 2D magnetic field problems, boundary and finite element methods combined 7-62584
- 2D topographic responses in magnetotellurics, finite element modelling 7-47333
- 2D viscous flows, time-dependent, incompressible, anal. 7-26165
- 3D 2-phase immiscible flow displacement, finite element analysis and error analysis (*Chinese*) 7-16229

finite element analysis continued

3D contact problems with friction, mathematical programming approach 7-16131
3D cracked anisotropic bodies, stress intensity factors, singular isoparametric elements 7-1501
3D electrostatic fields, Laplacian finite element formulation 7-50453
3D FEM of mag. field intensity, computer verification 7-25700
3D structures, largely yielded, J-dominance of crack-tip fields 7-26210
(ϕ)₂ field theory, mass gap and mass renormalisation using finite elements method 7-35702
acoustic finite elements and their industrial applications 7-16014
acoustic microscope, elastic wave propag., accurate field anal. 7-43472
ADINA program use in nuclear plant CAD appls. 7-49505
advection equation, linearised, 2D, finite element approximations, stability and phase speed 7-37455
aerodynamics, mesh generation by a sequence of transformations 7-51201
AGR helically wound heat exchangers, vibration props. 7-56788
air, laminar flow and heat transfer in tube bank, finite element calcs. 7-51313
airfoil cascades, hybrid aerodynamic problems, variational principles 7-43963
alloys, fracture, deform., porosity effect 7-22750
alloys, two-phase, models of tensile behaviour from components 7-46570
amputee's stump, shape measuring probe-type system for prosthetics CAD 7-34349
analysis of structures produced from visco-elastic materials by the aid of ADINA-program 7-1453
anisotropic plastic hardening, FEM 7-26156
annular thermal entry problem, num. solns. 7-16180
aquifer contaminant transport, orthogonal-upstream finite element modelling 7-23780
arbitrary Eulerian-Lagrangian formulation for simulation of forming processes 7-6105
arbitrary Lagrangian-Eulerian finite element method for path-dependent materials 7-14766
arterial system, human, under periodic body accel., finite element anal. of blood flow through model 7-34178
Atlantic Ocean, M₂ tide, FEM 7-47464
Atlantic-type continental margins, thermo-mech. evolution, numerical models 7-54950
atmospheric convection, comparison of GR FEM models 7-18298
axisymmetric elastoplastic torsion problem, num. soln. (Chinese) 7-14775
azimuthally-periodic current distrib., mag. field calcs. 7-50446
Babuska-Brezzi conditions for two kinds of rectangular elements (Chinese) 7-51029
beam element, curved isoparametric quadratic thick 7-4684
beam theory, torsion, buckling and vibr. problems 7-1458
beams, finitely deformed 3-D, tangent-stiffness expression, use in space frame analysis 7-6104
beams, linear elastic in contact problems, moving FEM 7-20663
beams, thin-walled open, elastic nonlinear static analysis 7-62984
beams, vibrating, holographic and finite element studies 7-31718
beams/columns subjected to non-uniform axial loads, vibration and buckling 7-6140
beams/plates under combined loading, finite element dynamic inelastic analysis 7-63002
Benard convection, two-dimens., finite element numerical calcs. 7-37454
Bernard convection in finite cavity, two-dimensional, use of symmetry in bifurcation calcs. 7-31798
beveled diamond anvil cells design, finite element analyses 7-41398
binary semiconductor alloys, directional solidification, convection, segregation, ampoule and furnace design 7-59501
bioprosthetic valves, closed, influence of stent height upon stresses on cusps, finite element model 7-23387
bioprosthetic valves, porcine, leaflet stiffening effect on leaflet stresses 7-65889
boundary layer flow and frictional resistance of uniformly accelerating or decelerating flat plate 7-1544
CAE, embedding of finite elements, prerequisites for software 7-15231
cardiac conduction, time dependent anatomically detailed model 7-40130
ceramic matrix composite frictional stress evaluation along fibre-matrix interface 7-28143
ceramic/metal jointed interface, strain distrib. determ., laser speckle photography (Japanese) 7-54037
charged particle transport calcs., finite element method, ICF appl. 7-36244
columns, cantilever resting on elastic foundation, dynamic stability 7-50965
columns subjected to intermediate concentrated load, stability analysis, FEM 7-20608
columns subjected to intermediate concentrated load with axially restrained ends, FEM stability analysis 7-57718
columns with elastic axial restraint, FEM-based stability analysis 7-50964
combustion, flow simulation in vortex struct., variational entropy method (French) 7-44064
composite laminates, stress singularity by FEM 7-1401
composite micromechanics, simplified, 3D finite element anal. 7-31637
compressible flow, moving finite-element modelling 7-51222
compressible flows, vectorised finite element codes 7-37488
compressible turbulent flows, 2D, Navier Stokes eqns. solved using finite element method 7-43960
concrete, inelastic behaviour, damage mechanics constitutive theory, FEM model 7-53833
conductor, mech. deform. under EM stresses 7-42833
conf., London, England (September 1985) 7-18492
considerations in the numerical solution of elastoplastic, viscoplastic and flow problems 7-1452
constitutive equations of hardening, analytical integration, elastic-plastic finite element analysis 7-63016
contact, elasto-plastic under large deformation, finite element based quadratic programming 7-43805
contact layer modelling in solving tribotechnical problems by numerical methods 7-26230
contact problem, dual FEM for elastic bodies with enlarging contact zone 7-57763
contact problems, finite element analogy of Coulomb friction law 7-31711
convection-diffusion eqn., smoothing of numerical soln. by central difference method (Japanese) 7-41312

finite element analysis continued

convection-dominated linear and nonlinear parabolic problems, Petrov-Galerkin method 7-18726
corona discharge, unipolar space charge flow 7-26567
correction procedure use in multi-level finite element solution algorithms 7-35261
coupled natural convection and radiation in an axisymmetric cavity, finite element soln. 7-37311
coupled plate linear problems 7-1406
coupled viscous flow/transport problems, numerical computation 7-44065
crack arrest specimen, dynamic anal. under reactor pressurised thermal shock conditions 7-13693
crack closure integral method with quarter point elements 7-16121
crack parameter, finite element modelling of grinding residual stress effects 7-16113
creep crack growth parameters, finite element and exptl. investigations comparison 7-39674
creeping viscous flows followed by finite element meshes using pseudo-concentrations 7-43987
crystal growth, Czochralski furnace, numerical calc. of heat transfer 7-53543
curved members, consistent discrete elements technique 7-50948
cyclic loading, constitutive model and analytical integration method (Chinese) 7-14773
cyclic loading, creep plasticity problem 7-63003
cylinder, nonlinear elastic thick-walled, multi-parameter equations solution 7-26143
cylinder, viscoelastic, finite deformations under rolling contact 7-6159
cylinders, anisotropic, geometrically nonlinear pre-buckling state 7-1456
cylinders, hollow, axial through cracks, stress intensity factors, opening areas, internal press. loading 7-1496
Czochralski growth, global finite element calc. 7-39370
defence hole systems, for reduction of stress conc. in uniaxially loaded plate with two coaxial loads 7-37324
degenerate two-wave and four-wave mixing, nonlinear coupled wave eqn. soln. with FEM 7-43191
detached flow problems, soln. using finite element method 7-18599
dielectric gratings, plane wave diff., finite element anal. (Japanese) 7-43342
dielectrically-loaded conducting spheres, FEM for scattering 7-15808
dielectrics, elec. fields, computer calc. 7-42837
diffusion theory, least squares principle to unify finite element, finite difference and nodal methods 7-56194
displacement in two phase flow in porous media, finite element simulation 7-51295
dopant diffusion eqns., numerical soln., moving finite element method 7-12376
dynamic analysis of saturated porous media, higher order, mixed, and Hermitean finite element procedures 7-14263
dynamic response of saturated porous media, evaluation of u-w and u- π finite element methods 7-14262
dynamic three-point bending test, finite element anal. considering contact and frictional effects (Japanese) 7-57776
eddy current problems, skin depth-independent finite element method 7-62572
eddy currents, flux reflection and flux conc. effects, 3D finite element anal. 7-42845
elastic film on rigid substrate, contact stress and strain, zero friction, finite element anal. 7-57768
elastic film on rigid substrate, contact stress and strain with friction, finite element anal. 7-57769
elastic wave, periodic waveguides, finite element anal. (Japanese) 7-6148
elastic-plastic J-anal. for inner surface flaw in press. vessel 7-63076
elastic-plastic plane stress FEM appl. to anti-phase strain 7-14768
elasticity axisymmetric problems solution using triangular three-node non-conforming elements 7-56042
elasticity theory problems, combined scheme using boundary-integral-eqn. and finite-element methods 7-56041
elastoplastic and elastoviscoplastic problems 7-26155
elastoplastic finite element analysis, precision and efficiency increase (Chinese) 7-43691
elastoplastic problems at finite strain, FEM solution 7-43694
elastostatics null Lagrangians, admissible tractions, and finite element methods 7-4693
elbow, stress anal. before and after radial head resection (German) 7-23376
elbow, stresses after joint replacement, finite element method calcs. and expt. obs. (German) 7-54809
electric field computation, finite-element and boundary-element methods combined (Chinese) 7-10822
electromagnet, finite element study (French) 7-15796
electron beam annealing, pseudo-line, thermal anal., 2D finite element method (Japanese) 7-32507
elliptic finite element problems on regions partitioned into substructures, iterative methods 7-48341
EM field, open boundary problems solution using finite element method 7-31212
end-notch flexure specimen, mode II interlaminar fracture toughness, finite element anal. 7-1509
energy dependent neutron transport eqn., numerical soln., finite element approach 7-716
epiphyseal-based designs for tibial plateau components, stress anal. in frontal plane 7-3934
epiphyseal-based designs for tibial plateau components, stress anal. in sagittal plane 7-3935
equal order velocity-pressure formulation 7-16142
ERM thermal anal., heat radiation case study using finite element method 7-20588
errors in FEA of soil masses which incorporate pseudo-elastic soil models 7-3730
Euler and Navier-Stokes eqns., finite element flux corrected transport algorithm 7-43959
Euler equations, time depend., soln. using Taylor-Galerkin finite element method 7-43968
Euler transonic lifting flow, 2D/3D finite element soln., stream vector correction 7-43967
evolving discrete systems, calc. method (Russian) 7-56025
fatigue crack propagation computer simulation (Japanese) 7-14772
FBR above-core structures, finite element anal. using SAFE/RAS program 7-15230

finite element analysis continued

- FCC bicrystals, computer simulation of non-uniform multiple slip (Japanese) 7-51780
- FELTRAN finite element code, appl. to multigroup neutron transport 7-19345
- femoral stem of cemented total hip replacements, role of collar rel. to bone stresses and resorption 7-8760
- femoral stress anal., 3D, using CT scans and P-version FEM 7-8613
- FEMSYN code for multigroup diffusion theory 7-10183
- fibre reinforced composites, delamination growth in angle-ply laminated composites 7-31701
- fibre reinforced composites, fracture, micromechanical and macromech. criterion 7-17609
- fibre reinforced metals, plastification, numerical and expt. investig. (German) 7-26172
- field consistency in FEM, penalty function approach 7-57687
- field-consistent finite elements 7-4666
- finite element reactor calculations, improved algorithm 7-19340
- finite strain rod model, 3D, computational aspects 7-6119
- first order neutron transport eqn., finite element response matrix method 7-36075
- flooding due to urbanization 7-54384
- flow, inviscid compressible, mesh refinement, for adaptive FEM 7-37485
- flow interaction, finite element methods, adaptive and moving mesh 7-37493
- flow pattern anal. using observed data and numerical anal., appl. to air deflecting device 7-37420
- flow problems, finite element methods 7-41009
- flows through cascades of profiles in variable thickness layer, finite element solution 7-26307
- fluid dynamics, discontinuity-capturing operator for multidimensional advection-diffusion systems 7-26241
- fluid dynamics, generalized streamline operator for multidimensional advective diffusion systems 7-26240
- fluid flow in channel, nonsteady heat transfer calc. method 7-63223
- force-deflection anal., eigenvalue convergence in the finite element method 7-24420
- forced-convection heat transfer, 2D transient anal. 7-20724
- fourth order partial diff. eqns., soln. using finite element method 7-29759
- fracture, post-yield, 3D finite element simulation 7-26216
- fracture mechanics, linear elastic, singular nine-noded distorted isoparametric elements 7-63054
- free and forced convective heat transfer, FEM 7-51117
- free surface flow anal., 3D, FEM 7-43839
- FTU tokamak machine, vacuum vessel thermal and mechanical problems 7-25179
- Galerkin finite element analysis of complex viscoelastic flows 7-16143
- garnet epitaxial layers, Bloch line behaviour in an in-plane field 7-53101
- geophysics 2D structures, resist. modelling by finite element method (Chinese) 7-55270
- groundwater systems management, coupling of finite element and optimisation methods 7-60278
- hard spheres with Yukawa tail, critical behaviour, mean spherical approx., finite element solns. 7-12251
- heat conduction, 2D, isoparametric line and transition finite elements 7-43628
- heat conduction, axisymmetric, FEM analysis with temperature and temperature gradients as primary variables 7-6071
- heat transfer, 2-dimens., with melting and freezing, finite element soln. algorithm 7-1381
- Hertz contact, elastoplastic axisymmetric problems, FEM solution 7-20662
- hexagons, finite element diffusion program, trial function 7-49491
- hip endoprostheses, effects of stem design and material props. on stresses 7-40361
- hybrid type infinite element, finite element approach to unbounded Poisson and Helmholtz problems 7-1003
- hyperthermia, unbounded electromagnetic problems, hybrid element method 7-18037
- I-beams, inelastic distortional buckling analysis using FEM 7-43722
- ICF target implosion, moving finite element method 7-5439
- ideal MHD equations, Galerkin method for differential equations with regular singular points 7-11624
- IGNITOR structural evaluations, finite element models 7-15348
- implantable telemetry systems mag. field 7-28754
- incompatible singular elastic element for two- and three-dimensional problems 7-1503
- incompressible flow problems, finite element stability anal. 7-31730
- incompressible fluid, cylinder creeping motion study 7-20825
- incompressible fluid flow, 3D Navier-Stokes eqn. FEM 7-63103
- incompressible Navier-Stokes eqn., finite element stream function-vorticity solns. 7-63104
- indentation of elasto-plastic half-space by rigid circular cylinder 7-26226
- industrial turbulent flow, 3D, computation by FEM 7-43876
- inf-sup conditions, equivalent forms and applications 7-1431
- integrated optical waveguides, modelling 7-43362
- integration error controls for a finite element viscoelastic analysis 7-20601
- interface cracks, finite element approach 7-43801
- isovolumic contraction, left ventricular wall stresses determination using FEM 7-23378
- J-integral, estimation using FEM, simplified eqns. (Japanese) 7-50999
- Kirchhoff plate bending, C^1 finite element family 7-24418
- Kirchhoff-plate bending using C^1 finite elements (Spanish) 7-18598
- lagrangian finite element method, velocity correction technique 7-6232
- laminar flow past short, heated cylinder, finite element soln. 7-57789
- laminar flow through abrupt expansions, planar and axisymm., finite element anal. 7-37428
- laminar natural convection in square channel, penalty FEM 7-51132
- laminated composite plates, sound transmission characts. 7-57633
- laminated thick composite plates, buckling, hygrothermal effects 7-11321
- laminates, centrally notched, residual strength determ. (Chinese) 7-13557
- laminates, strain energy release rate of edge delamination, residual thermal and moisture influences 7-1508
- laminates, two-layered, subjected to impact load, dynamic response (Japanese) 7-50946
- large coil program, General Electric coil, engineering problems 7-19456
- lifting bodies, 2D and 3D Euler computations, finite element method 7-43961
- linear elasticity, post-processing procedures for FEMs 7-14777

finite element analysis continued

- linear stress analysis, comparison of boundary element and finite element methods 7-1390
- linearised compressible and resistive MHD equations, finite element semi-discretisation 7-11623
- longitudinal elastic-plastic waves with radial effects, numerical anal. for circular rods 7-31691
- low-dimensional lattice fermion field theories, finite element methods 7-4956
- lumbar intervertebral segment study, nonlinear finite element model 7-65792
- magnetic field computation, C^1 quadratic interpolant 7-50445
- magnetic field computation using locally orthogonal discretization 7-50447
- magnetic systems, multiply-excited, finite element soln. of transient eddy-current problem 7-62575
- magnetostatics, inverse nonlinear finite element problems 7-42838
- magnetron sputtering cathode, CAD using finite-element program 7-46316
- Maxwell fluid between eccentric rot. cylinders, spectral/finite element calcs. 7-51176
- medical electrodes, optimal design for electrosurgery, defibrillation, and external cardiac pacing: finite-element computer model 7-3928
- membrane/plate equilibrium finite element models 7-1429
- metallic materials, with elliptic inclusions, plastic deform. 7-28067
- metallic mould/casting thermal response characts., transient temp. field anal. 7-65019
- metals, elastoplastic problems, numerical methods, double exposure speckle photography 7-57714
- MFTF-B, structural mechanics methods for design optimisation 7-5411
- MOCVD, horizontal reactors, complex flow phenomena 7-22530
- MOCVD in inverted stagnation point flow 7-22531
- modal synthesis method considering rotational effects (Chinese) 7-11270
- mode II fatigue crack test specimen, elastic analysis 7-1505
- molecules and ions, vibr. energy wavefunctions, variational methods 7-36574
- multi-component convection/diffusion/reaction systems, FEM 7-44063
- multi-torus system, eddy current analysis, finite element circuit theory 7-58048
- multigroup finite element neutron transport, inclusion of anisotropic scattering in FELICIT code 7-19324
- multigroup neutron diffusion equation, 3D, soln. using finite element method 7-19344
- multigroup neutron transport with anisotropic scatt., finite element method anal. 7-19333
- multiphase flow in porous media, nonlinear conservation law, FEM (French) 7-44031
- multiphase interface and interaction problems, probabilistic modelling and simulation 7-52219
- multiple-stripe-geometry laser arrays, chirped and unchirped, modal eigenfunctions 7-57335
- myocardial electrical propag., 3D anisotropic model 7-40131
- Navier-Stokes eqns., arbitrarily convex quadrilateral elements (Chinese) 7-16144
- Navier-Stokes equations, penalty FEM, iterative methods convergence 7-51024
- near-incompressible material, FEM 7-11279
- net finite element schemes for Poisson eqn., rapid iteration methods 7-18571
- neutron diffusion, finite element method including nodal and difference methods 7-19317
- neutron transport, anal. using finite element, nodal and response matrix methods 7-19322
- neutron transport, inclusion of voids in finite element methods 7-19323
- neutron transport eqn. in X-Y, R-Z geometry, soln. using phase space finite element method 7-19319
- neutron transport equation, multigroup finite element soln., scatt. anisotropy 7-5308
- neutron transport equation, soln. using finite element analysis 7-19320
- neutron transport equation, soln. using finite element response matrix method 7-19334
- neutron transport theory, finite element methods, relation to nodal methods 7-19318
- nonhardening material, plane strain, axisymmetric extrusion, viscoplastic FEM 7-63009
- nonlinear coupled problems of Schrodinger eqn. and Klein-Gordon eqn. (Chinese) 7-101
- nonlinear fracture problems, path-independent integral 7-63068
- nonlinear problems, error estimates for mixed finite element approximations 7-4691
- nuclear fuel element transient heat transfer and using FEA 7-19362
- numerical methods, innovative, in engineering, conf., Atlanta, GA, USA (March 1986) 7-12
- numerical simulation of viscous flows in hydraulic turbomachinery by the finite element method 7-26256
- open boundary problems, differential and integral methods 7-50454
- optical fibre, stress-applied, with inhomogeneous core (Japanese) 7-50780
- optical fibres, weakly guiding with arbitrary refractive index distrib., anal. 7-11126
- optical fibres side-tunnel type, polarisation-maintaining, vectorial wave anal. by variational finite elements 7-11137
- optical storage, digital media, transient thermal conduction 7-57490
- orthotropic materials, fracture propag., finite element modelling 7-57751
- panel with uniformly spaced holes, crack stress intensity factors 7-57755
- panels, damped stiffened with viscoelastic damping, FEM free vibration analysis 7-20621
- paperboard, constitutive behaviour under uniaxial and biaxial loading 7-63019
- penalty finite-element analysis of coupled fluid flow and heat transfer for in-line bundle of cylinders in cross flow 7-31792
- phase change problems, curved interface straightening, isoparametric finite elements 7-62963
- photoacoustic-thermal signal generation, finite element simulation 7-51947
- photogrammetry, non-metric cameras calibration via finite-element method 7-3969
- planar optical waveguide, Si-clad, numerical anal. (Japanese) 7-6000
- plane elasticity, two-grid FEM method 7-6089
- plane elasticity theory, superelement method soln. (Russian) 7-43688
- plane layered media, global matrix formulation of wave phenomena 7-61125

finite element analysis continued

planetary boundary layer eqns. soln. by finite element technique 7-9232
 plasticity-induced crack closure, under plane strain conditions, finite element anal. 7-37379
 plate, annular, with cyclically symm. curvilinear notches, stress state anal. 7-1420
 plate, center cracked with singularity, finite element mesh 7-20645
 plate, circular, influence of annular stiffening rib on stress distrib. (*Rumanian*) 7-20594
 plate, crack growth rel. to geometry and material props. 7-16112
 plate, cracked, bending, stress intensity factor computation via path-independent integral 7-37380
 plate, stiffened tension, with eccentric crack, elastic-plastic finite element analysis (*Chinese*) 7-16119
 plate bending, finite element model with limit analysis capacity 7-63013
 plate bending element, bilinear, force evaluation 7-57707
 plate bending elements, nonconforming shape functions (*Chinese*) 7-50958
 plate bending using new hybrid element method 7-16070
 plate elements, geometric stiffness matrix formulation 7-43723
 plate/shell element, field-consistent four-noded laminated anisotropic 7-62983
 plate/shell error indicators and accuracy improvement of finite element solutions 7-1430
 plate/shell problems, effect of asymptotic error estimate studies 7-1428
 plates, bimodulus thick circular, axisymmetric buckling analysis using FEM 7-57716
 plates, circular, FEM for nonlinear forced vibrations 7-6139
 plates, first-ply failure analysis of composite laminates 7-63053
 plates, laminated composite, 3D hybrid stress isoparametric element 7-56020
 plates, multilayered shear-deformable, finite elements 7-43667
 plates, prismatic, folding, instability by finite strip method (*Spanish*) 7-20611
 plates, rectangular laminated composite, dynamic stability analysis using finite strip method 7-6118
 plates, rectangular thin laminated composites, bending analysis using FEM 7-57708
 plates, thick composite, loading, nonlinear finite element anal. using cubic spline functions 7-31643
 plates, weakened by cracks, tensile and compressive buckling 7-6124
 plates and cylinders, surface-cracked, J-integral and HRR dominance under large-scale yielding 7-63080
 plates and shells, finite strain large deformation, nonlinear theory 7-20602
 plates and shells, hybrid strain technique for FEA 7-20603
 plates/shells, two-dimensional FEM model for buckling analysis 7-57717
 plunger pump piston, numerical and expt. stress systems, math. representation (*German*) 7-18596
 PMMA, craze zone micromechanics at stationary crack tip 7-33775
 powder metallurgical materials, plastic working in presence of free surface, math. modelling 7-53651
 power law materials, neck form. invariance to strength and strain rate 7-17597
 power-law fluid, flow anal., finite element formulations (*Japanese*) 7-51238
 pressure sintering, computer simulation using finite element anal. 7-3214
 pressure variation in coaxial plasma experiments with low inductance drivers 7-32077
 propagation weak variational formulation 7-8853
 PVC sheets, biaxial tensile behaviour 7-17579
 pyramid finite elements, basis functions and numerical integration 7-24406
 quadratic shear flexible beam element 7-24425
 Radon transform inversion with finite elements, exact reconstruction filters 7-24380
 reactor pressure vessel and piping design, stress indices for nonradial branch connections 7-49520
 reluctivity characts. of magnetostatic fields, nonlinear finite element anal. 7-42846
 resistive MHD, complex eigenvalue spectrum computations 7-51336
 RFX vacuum vessel, structural and thermal anal. using FEM 7-25178
 rigid body-viscous flow interaction, finite element anal. 7-37424
 rotating beams, high order elements 7-16103
 rotating nonaligned straight tube, finite element soln. 7-43930
 rotational inviscid flows, 3D, finite element method 7-43940
 rotor bearing systems, analysis using modal transformation matrix 7-37372
 second-order fluid flow between two porous coaxial circular cylinders, finite element method 7-11530
 semiconductors, Hall effect, finite element simulation 7-21940
 shallow water calculations 7-47463
 shallow water eqns., two-stage FEM Fortran program, FEUDX 7-55080
 shallow water flow, boundary element soln. 7-40502
 sheet metals, planar anisotropic, deformation anal. using rigid-plastic FEM 7-43701
 shell, bifurcational stability problems soln. using finite element method 7-16087
 shell, inclined Timoshenko-type, triangular finite element construct. 7-1415
 shell analysis using a simple flat hybrid stress element 7-16081
 shell element, curved C^0 , based on assumed natural-coordinate strains 7-11313
 shell elements, 3-node triangular, improvements 7-4685
 shell elements, degenerated, implementation with transverse shear and membrane strains 7-50944
 shells, axisymmetric sandwich, numerical shakedown anal. 7-26161
 shells, cylindrical, calc. by finite-element method 7-95
 shells, elastic-viscoelastic layered, multi-director formulation 7-37347
 shells, nonlinear aperiodic vibrs., incremental Hamilton's principle with multiple time scales 7-6144
 shells, nonlinear elastic-viscoelastic layered, multi-director FEM formulation 7-43695
 sine-Gordon field theory, mass gap and mass renormalisation using finite elements method 7-35702
 sintering, thermal stress anal. using moving grid 7-53648
 sinusoidally time varying eddy currents in metallic structures, three-dimensional calc. 7-25702
 slab-heating square inductor vibration and acoustic analysis (*Russian*) 7-62905
 slightly viscous flows, FEMs 7-14785

finite element analysis continued

slow viscous flows, FEM for moving interface problems 7-16157
 small strains quasistatic elastoviscoplasticity 7-50960
 small-strain problems, geometrically nonlinear discretization, convergence at infinitesimal element division 7-48362
 solidification problems, comparison of FEMs 7-14759
 solidification processes with natural convection, FEM anal. 7-14758
 sphere in cylindrical tube, fluid flow and heat transfer 7-20706
 spiral motion segments, human, internal displacements from in vitro loading, expt. results and finite element model predictions 7-3833
 spinning structure dynamic anal., free vibr. problem, numerical algorithms 7-37366
 stagnation flows, finite element formulation 7-37423
 steel, Al killed, tensile testing, deform. heating 7-65105
 steel, dual phase, work hardening, accommodation strains in ferrite phase, finite element analysis 7-17550
 steel, structural, δ_1 and J_1 values, effect of a/W ratio 7-57753
 steel cylinders, thick-walled, stress intensity factors for large arrays of radial cracks 7-26207
 steel structure, biaxially-loaded connections, fracture condition (*Japanese*) 7-58403
 Stokes problem, stationary, boundary integral eqn. method (*Chinese*) 7-14779
 Stokes problems in multiple connected domains, press. pot. formulation 7-63105
 strain fields under low-cycle loading, use of isoparametric elements 7-26222
 stratified flows, incompressible, finite element anal. 7-37512
 stress, FEA using microcomputer 7-48357
 stress analysis, assumed stress hybrid finite element method 7-1451
 stress analysis combining speckle metrology with finite element modelling 7-43820
 stress intensity factor calculations, biaxial loading effects 7-63074
 stress intensity factors calc. by quarter-point quadrilateral method 7-50995
 stressed materials, magnetostriction, finite element anal. 7-59098
 strip, elastic-plastic, contact problems under complex loading 7-43808
 strip, infinitesimal and large strain in rolling contact problems 7-11359
 supersonic flow interaction between moving bodies, moving grid FEM 7-26314
 surface crack, stress intensity factor variation and back surface displacement 7-57762
 synchrotron radiation mirror, thermal distortion prediction with finite element analysis 7-43306
 T-junctions, stamped, thick walled, stress-strain state anal. (*Russian*) 7-1409
 temperature fields, finite elements nonlinear anal. 7-50924
 tensile flow stress beyond necking, determ. at very high strain rate 7-63726
 tensile strip with large circular hole, stress analysis using nonlinear FEM 7-20596
 tensile tests, nonisothermal, anal. using measured temp. distrib. 7-65245
 TFTR poloidal field coil, finite element modeling 7-15343
 thermal problems, time integration, least-squares schemes 7-50908
 thin-walled frames, large elastoplastic deforms., geometrically and materially nonlinear finite element anal. 7-1447
 three-dimensional exterior field problems, finite-element soln., inversion transformation 7-20096
 three-dimensional scalar potentials, hybrid finite-element/boundary-element solutions 7-50455
 tibial components, bone stresses beneath, effect of interface, finite element modelling 7-40188
 time-dependent partial differential eqns., 2D mesh moving technique 7-18573
 toroidal solenoid, thermomech. loaded, optimal design 7-57695
 torsional axially symmetric finite element model for problems in elasticity 7-57701
 transonic flows, least squares FEM for simulation 7-26309
 transonic potential flow, numerical solution, multigrid technique 7-6240
 transport equation, convective, finite element soln., determ. of optimal upstream weighting parameter 7-29764
 triangular and tetrahedral space-time finite elements in vibration analysis 7-24431
 TRISM, finite element transport code, spatial and angular flux approximations and accelerations 7-19342
 tubes, hollow, axisymmetric external projections, axial loading, stress conc. factors 7-43681
 turbulent boundary layers, finite element anal. 7-31771
 turbulent flow in 2D labyrinth, simulation 7-43873
 turbulent flows in complex geometries, finite element calcs. 7-43878
 turbulent flows-elastic shell interaction, finite element anal. 7-43874
 turbulent fully developed flows, prediction using control-vol. FEM and Reynolds stress model 7-43875
 turbulent thermally compressible fluid, finite element simulation 7-43877
 two dimensional line element for glacier flow problems 7-4063
 two-phase solid, cyclically loaded, residual stresses 7-63010
 undercooled melt, finite element simulation of planar instabilities during solidification 7-63774
 underwater acoustics, finite element analysis appl. (*French*) 7-11209
 uniform bar vibration, finite element space models 7-50981
 universal optimum quarter point element, fracture mechanics appl. 7-16117
 unsaturated flow of liquids in porous media, free boundary problem 7-37538
 unsteady compressible cascade flows anal. using boundary element and free vortex method 7-43962
 US hyperthermia simulation using finite element model 7-47181
 US levitation simulation, boundary- and finite-element approaches 7-1360
 variable explicit finite element methods for unsteady heat conduction equations 7-26118
 viscoelastic flow, finite element calc. 7-37499
 viscoelastic flow problems, integral constitutive models 7-16213
 viscoelastic rectangular body excited by rectangular waveguide, vibrs. and heating 7-16109
 viscoplastic finite element analysis of rapid fracture 7-63061
 viscoplasticity, nonlinear FEM anal. 7-63008
 wave load on body with arbitrary shape, coupled element anal. (*Chinese*) 7-26298
 weather prediction, energy conserving FEM 7-47524

finite element analysis continued

- weather prediction model, semi-implicit semi-Lagrangian time integration scheme 7-47525
 wiggler beam monochromator, distortion from synchrotron radiation thermal loading, finite element analysis 7-42269
 wind scatterometer antenna release shock loads 7-23976
 wind-driven circulation 7-9046
 Al-Zn-Mg, small fatigue crack growth from a keyhole notch 7-65133
 B fibre reinforced Al tube under multi-axial loadings, elastic-plastic deformation 7-46548
 C fibre reinforced plastic, cemented lap joint, stress-strain state and strength 7-33794
 Nb, shock-synthesised superconductor, characterisation 7-38116
 PZT composites, hydrostatic piezoelec. response, finite element modelling 7-64574
 Si, epitaxial growth using dual heating, slip dislocations and radial temp. gradient 7-38366
 Si, microarea stress study by microprobe Raman spectroscopy 7-63708
 Si, thin sheets, EFG, thermal capillary mechanism for growth limit 7-17407
 Si:As, dopant diffusion, finite element based simulation, quasilinear formulation with remeshing scheme 7-21526
 Ti_3AsSe_3 crystals, Bridgman growth, dislocation etching, thermal stress distrib. 7-21208

finite impulse response filters *see digital filters***finite state automata** *see finite automata***Finlay-Freundlich red-shift hypothesis** *see gravitational red shift***FIR filters** *see digital filters***fires**

- see also accidents; combustion; flames; safety*
 N Amazon Basin, Holocene fires as climatic indicators, dating 7-47531
 biomedical electronic instruments safety and testing Electrotechnical Testing Institute practices (Czech) 7-18090
 flameless peat fires, low temp., kinetic characts. 7-13774
 nuclear power plants, fire detection and suppression anal. 7-36213
 nuclear power station fire protection, Germany (German) 7-25146
 nuclear power station fire protection, licensing comparisons between USA and BRD (German) 7-10266
 peat bog fires, simulation and control 7-13773
 smoke plumes above large-scale fires, nuclear winter simulations 7-65662

fission*see also fission of plutonium; fission of uranium; photofission; spontaneous fission*

- absolute measurements of fission cross sections 7-30408
 angular and mass distribution of fission fragments 7-35993
 asymmetric nuclear shapes in structure, fission and cluster radioactivity, unified description 7-49228
 charge distribution yields, fine structure, coupling of charge asymmetry coordinates and relative motion 7-24967
 compound nucleus fission, tilting mode dynamics 7-5274
 compound nucleus formation, fast fission phenomena and deep inelastic reactions 7-19227
 conf., Copper Mountain, Colorado, USA (Feb. 1986) 7-4634
 conf., Smolenice, Czechoslovakia, June 1985 7-41005
 deep inelastic reactions and fast fission phenomena, statistical fluctuations and quantal diffractive effects 7-19228
 dissipation in fission and heavy-ion reactions 7-5221
 dissipation-fluctuation dynamics of the formation of fission-fragment mass distributions 7-42090
 evolution of fission decay at high temp. 7-35994
 fission in a narrow J-window and J-dependent fission barriers 7-19231
 fragment mass distribution for nuclei lighter than Th 7-42089
 independent fission yield measurements, review 7-61948
 Kolmogorov eqn. for fission chain-reacting system, approx. soln. 7-35992
 local-scale point transformations within the generator coordinate method 7-56623
 neutron induced fission rate meas. at high fluence and temp. by SSNTD 7-42081
 nuclear dissipation, fission probability and neutron multiplicity prior to fission 7-10174
 nuclear-charge distribution near symmetry for low-energy fission reactions 7-19232
 orientation spin tensors of fissioning compound nuclei produced through neutron capture 7-42095
 quasifission, tilting mode dynamics 7-5274
 radiochemical studies on fission 7-19312
 Rayleigh criterion for neck stability 7-5268
 rotating finite range fission barriers from nonrotating nuclei 7-49369
 scission, fragment-separation barrier, liquid-drop model anal. 7-5220
 self-consistent transport coefficients for damped large scale collective motion 7-35934
 sub-barrier fusion-fission reactions, anomalously broad spin distrib., comment with reply 7-10178
 (n,f), ternary fission, thermal and resonance n, meas. and appls., review 7-42026
 (p,f), $E_p=190$ MeV, target nuclei Nb, Ag, La, Ce, Pr, Nd, Dy, fission mass distrib. 7-5304
 180 W (^3He , fission), mass distributions of fission fragments from heated nuclei and the drop model 7-42041
 ^{240}Pu , bimodal symmetric fission observed in the heaviest elements 7-25012
 Ag(^{132}Xe , X), 14 MeV/N, multipronged events, fission and quasi-fission contribs., SSNTD use 7-19273
 ^{241}Am (n,f), cross section meas. at 14.7 MeV 7-30458
 Au(^{132}Xe , X), 14 MeV/N, multipronged events, fission and quasi-fission contribs., SSNTD use 7-19273
 ^{197}Au , fission, α and p-induced, ang. anisotropy and critical ang. momentum 7-42094
 ^{197}Au (^{12}C , f), ang. distrib. and excitation functions (Chinese) 7-25013
 ^{197}Au (^{40}Ar , X), 27 MeV/nucleon, nuclei deexcitation near nuclear matter instability temp. 7-19279
 ^{184}Ba (^{2}Mg , nf), 180 MeV, neutron emission prior to fission 7-5273
 ^{209}Bi , fission, α and p-induced, ang. anisotropy and critical ang. momentum 7-42094
 ^{209}Bi (^{12}C , f), ang. distrib. and excitation functions (Chinese) 7-25013
 ^{209}Bi (e,f), absolute cross section meas. in 43-250 MeV range 7-5301
 Bi(e, fission), fragment activity from delayed fission 7-42092
 ^{54}Ca (^{16}O , X), 69.3-87.3 MeV, A=40, 44 fission-like yields, fusion-fission reaction mech. 7-36038

fission continued

- ^{252}Cf , ternary fission, neutron and γ -ray emission, kinetic energy correlations 7-19311
 ^{248}Cm (n,f), 0.1 eV-100 keV, fission cross section meas. for reactor appls. 7-42083
 ^{160}Dy (^3He , fission), mass distributions of fission fragments from heated nuclei and the drop model 7-42041
 ^{258}Fm , fission channels, rel. to fragment kinetic energies and mass asymmetry 7-19310
 (^3He , f), $E=270$ MeV, target nuclei Nb, Ag, La, Ce, Pr, Nd, Dy, fission mass distrib. 7-5304
 ^{178}Hf (^3He , fission), mass distributions of fission fragments from heated nuclei and the drop model 7-42041
 ^{163}Ho (^{40}Ar , X), 27 MeV/nucleon, nuclei deexcitation near nuclear matter instability temp. 7-19279
 ^{173}Lu (^{12}C , f) (Chinese) 7-25013
 ^{24}Mg , symmetric fission following inelastic scatt. of $^{12}\text{C}+^{12}\text{C}$ 7-36031
 ^{24}Mg (p,p'), excitation of $^{12}\text{C}+^{12}\text{C}$ quasimolecular resonances by symmetric fission 7-42002
 ^{142}Nd (^{16}O , nf), 207 MeV, neutron emission prior to fission 7-5273
 ^{142}Nd (^{16}O , nf), 207 MeV, neutron emission prior to fission 7-5300
 ^{236}Np (n,X), fission cross-section for thermal neutrons 7-25010
 ^{236}Np (n,f), isomer thermal neutron-induced fission cross sections, spin depend. 7-42100
 ^{237}Np (γ , X), photonuclear cross-sections, branching 7-49483
 ^{237}Np (n,f), cross section meas. at 14.7 MeV 7-30458
 ^{237}Np (n,h,f), cross section, resonant fission integral meas. 7-61929
 Pb(^{12}C , f), ang. distrib. and excitation functions (Chinese) 7-25013
 ^{208}Pb , fission, α and p-induced, ang. anisotropy and critical ang. momentum 7-42094
 ^{208}Pb (^{16}O , f), 76.8, 77.3, 80.2 MeV, fragment angular distrib. 7-19286
 ^{108}Pd (^{50}Ti , nf), 216 MeV, neutron emission prior to fission 7-5273
 Pr(^{12}C , f), ang. distrib. and excitation functions (Chinese) 7-25013
 ^{239}Pu (n,f), resolved resonance region, multilevel parameter calcs. 7-61930
 ^{240}Pu , compound nucleus, enhanced neutron emission, fission calcs., diffusion model anal. 7-61903
 Re(^{12}C , f), ang. distrib. and excitation functions (Chinese) 7-25013
 ^{187}Re , fission, α and p-induced, ang. anisotropy and critical ang. momentum 7-42094
 ^{118}Sn (^{64}Ni , X), compound nucleus angular distrib. and fission cross sections, elastic fusion model comparisons 7-56694
 ^{124}Sn (^{38}Ni , f), cross sections and compound nucleus angular distrib., elastic fusion model comparisons 7-56694
 ^{181}Ta (^3He , fission), mass distributions of fission fragments from heated nuclei and the drop model 7-42041
 ^{181}Ta (^{12}C , f), ang. distrib. and excitation functions (Chinese) 7-25013
 ^{181}Ta (^{22}Ne , α), DWBA anal., exptl. comparisons 7-56699
 ^{126}Te (^{32}S , nf), 180 MeV, neutron emission prior to fission 7-5273
 ^{232}Th , photofission, fragment angular and mass distrib. 7-49486
 ^{232}Th (^{16}O , f), 77-86 MeV, ^{248}Cf compound nucleus spin determ. from fragment angular distrib. 7-19286
 ^{232}Th (n, f), fission cross section meas. relative to ^{235}U (n, f) 7-61928
 ^{232}Th (n,f), fission mass distrib. from degraded fission spectrum neutrons 7-61934
 ^{205}Tl , fission, α and p-induced, ang. anisotropy and critical ang. momentum 7-42094
 ^{169}Tm (^3He , fission), mass distributions of fission fragments from heated nuclei and the drop model 7-42041
 ^{169}Tm (^{12}C , f), ang. distrib. and excitation functions (Chinese) 7-25013
 ^{236}U (^{12}C , f), 60-68 MeV, ^{248}Cf compound nucleus spin determ. from fragment angular distrib. 7-19286
 ^{238}U (e,e'), 5-23 MeV, coincidence cross section meas. 7-19240
 W(^{12}C , f), ang. distrib. and excitation functions (Chinese) 7-25013
 W(fission, α and p-induced, ang. anisotropy and critical ang. momentum 7-42094
 ^{232}Yb (n,f), 14.7 MeV, Rh, Ag, In, Sb yield charge distrib. 7-19313

fission counters

No entries

fission of plutonium

- nuclear data evaluation for heavy nuclides 7-30461
 prompt neutron emission, energy depend. 7-61933
 volatile fission products, thermochemical approximation (Dutch) 7-36208
 ^{240}Pu , A=23, 241, reactor parameters, uncertainties in scientific measurements 7-42085
 ^{240}Pu (n,f), A=239, 241, fragment energy and mass characts., shell effects, static scission point model anal. 7-42099
 ^{240}Pu (n,f), A=240-2, 244, cross section meas. at 14.7 MeV 7-30458
 ^{240}Pu (sf), A=238, 240, 242 7-42099
 ^{239}Pu (γ , X), photonuclear cross-sections, branching 7-49483
 ^{239}Pu (n,f), fission product sum beta spectra, absolute meas. 7-56707
 ^{240}Pu (n,f), neutron width and level distance distrib., resonance width calcs. (Russian) 7-5161

fission of uranium

- effective σ_f^8/σ_f^5 cross section ratio meas. in BTS-4 critical assembly (Russian) 7-5302
 integral test for heavy nuclides 7-30509
 nuclear data evaluation for heavy nuclides 7-30461
 volatile fission products, thermochemical approximation (Dutch) 7-36208
 U(^3He , pf), 21.3 to 90 MeV, backward angle proton emission in central collisions 7-5305
 U(^6Li , pf), backward angle proton emission in central collisions 7-5305
 U, A=233, 235, reactor parameters, uncertainties in scientific measurements 7-42085
 U, A=234, 236 Coulomb effects in low energy fission 7-30460
 U, A=236, 238 7-49486
 U(γ , X), A=233, 234 photonuclear cross-sections, branching 7-49483
 U(μ , f), A=235, 238, muon induced fission yields, fission lifetimes, muon capture 7-5298
 U(n, f), A=234, 236, fission cross section meas. relative to ^{235}U (n, f) 7-61928
 U(n,f), A=233, 235, prompt neutron emission, energy depend. 7-61933
 ^{234}U (n,f), 0.8 MeV, mean kinetic energy depend. of fission fragments, vibr. resonance 7-42097
 ^{234}U (n,f), $E_n \sim 0.8$ MeV, fission fragment average kinetic energy meas., effect of vibrational state in second potential well 7-61935
 ^{235}U (n,f), <200 keV, fission of oriented nuclei, spin depend. 7-36063
 ^{235}U (n,f), average cross section meas. 7-30417
 ^{235}U (n,f), delayed neutron activity, few-group anal. 7-42084
 ^{235}U (n,f), fission product sum beta spectra, absolute meas. 7-56707
 ^{235}U (n,f), fragment mass, kinetic energy and ang. distrib. meas. 7-61931

fission of uranium continued

- ²³⁵U(n,f), γ -multiplicity and total energy meas. 7-10176
- ²³⁵U(n,f), international fission foil mass intercomparison, α -decay rates 7-42086
- ²³⁵U(n,f), neutron width and level distance distrib., resonance width calcs. (Russian) 7-5161
- ²³⁵U(n,f), prompt fission neutron spectrum tail 7-30457
- ²³⁵U(n,f), thermal-6 MeV, fragments mass, kinetic energy and ang. distrib. 7-42101
- ²³⁵U(n,f) thermal fission, composite delayed neutron energy spectra 7-61932
- ²³⁵U(n,f), 2-4 MeV, sub-Coulomb cross section meas. using SSNTD 7-19308
- ²³⁵U, fission charge distribution yields, fine structure, coupling of charge asymmetry coordinates and relative motion 7-24967
- ²³⁸U(¹²C,f), 81, 90 MeV, fragment angular distrib. 7-5303
- ²³⁸U(²²Ne,f), 125, 143, 175 MeV, fragment angular distrib. 7-5303
- ²³⁸U(⁴He,f), 25, 35 MeV, fragment angular distrib. 7-5303
- ²³⁸U(μ , ν), p, d, t and α emission obs. ang. and energy distrib. 7-10138
- ²³⁸U(p,X), heavy hypernuclei production 7-49284
- ²³⁸U(p,f), delayed fission observation, non-meson hypernuclear decay interpretation 7-42082
- U(α ,p), 20, 40 MeV, backward angle proton emission in central collisions 7-5305
- U(e,e'), fission decay of giant multipole resonances, coincidence study 7-49360
- U(μ , X), muon absorption, emission of charged particles 7-42087
- U(p,f), 19 MeV, A=110-118 fission product obs. 7-49487

fission products

- A=110-118 fission products from ^{nat}U(p,f) 19 MeV 7-49487
- actinide migration and sorption in conc. salt soln. in geological material 7-19546
- aerosol source terms in nuclear reactor accidents, ex-vessel fission product releases 7-36219
- angular and mass distribution of fission fragments 7-35993
- artificially perforated Zr barrier fuel rods, fission product release in test loop 7-783
- axial fission gas transport in power ramping expts. 7-15284
- BWR core meltdown condition, estimate of fission product release 7-777
- BWR fuel rod, pellet-cladding interaction, rod failure, fission product release (Japanese) 7-15242
- CANDU 600 MW(e) reactor, defective fuel detection in operating plant 7-784
- charge distribution yields, fine structure, coupling of charge asymmetry coordinates and relative motion 7-24967
- charge state of material sputtered by fission fragments from ultradisperse gold targets 7-7802
- conf., Copper Mountain, Colorado, USA (Feb. 1986) 7-4634
- conference on fission product behaviour and source term research, Snowbird, UT, USA (July 1984) 7-10
- decay energies for fission products in JNDC FP Decay Data File 7-15236
- decay heat calculation problems 7-30506
- dissipation-fluctuation dynamics of the formation of fission-fragment mass distributions 7-42090
- EBR-II, nonrecoil fission product release phenomena using multifreq. source perturbation expts. 7-5326
- FBR irradiated MOX fuel, transient fission gas release during direct heating expts. 7-778
- ITEMAXI-III calculations for the D-COM blind problem 7-717
- fission track age determination, neutron dosimetry, neutron energy effects 7-47570
- fission track annealing in apatite, track length and Arrhenius plot, comments 7-42431
- fission-product cross section evaluation, integral tests and adjustment based on integral data 7-30504
- ground level air radionuclide conc. 1984-1986, N. Germany and N. Norway 7-59896
- independent fission yield measurements, review 7-61948
- isomeric yields 7-19157
- JENDL-2 fission product file, resonance parameters 7-15235
- Lexan polycarbonate, automatic scanning of enlarged fission tracks 7-30881
- low volatility fission product release expts., surface vaporisation role, fuel debris bed appl. 7-25137
- LWR accident source term expts. deposition samples 7-62047
- LWR degraded cores, fission product release and retention phenomena 7-776
- LWR fuel rods, simple model for predicting fission gas release 7-789
- LWR fuel under degraded core conditions, fission gas release prediction, FASTGRASS-VFP model 7-790
- LWR irradiated fuel under accident conditions, fission product release 7-773
- LWR severe fuel damage events, burnup effects on fission product release 7-787
- Makrofol E, particle registration studies and etching techniques 7-30875
- mass distribution for nuclei lighter than Th 7-42089
- neutron capture transformation effects on decay power after reactor LOCA 7-49587
- nuclear reactor accidents, fission product release expts. overview 7-772
- nuclear-charge distribution near symmetry for low-energy fission reactions 7-19232
- phosphate glass spectrometric detector, optimum etching for fission fragments 7-42429
- PNP-500 HTGR, Cs release during a heat-up accident, fission product transport 7-15286
- polycarbonate detector use for fission fragment spectrometry 7-19659
- radiochemical studies on fission 7-19312
- reactor containment integrity and radionuclide behaviour during severe accidents, review of R&D 7-779
- reactor postulated severe accident, hot gas bubbles discharged into water, dynamic and thermal behavior 7-5377
- release mechanism, estimation of failed fuel rods (Korean) 7-30517
- retention of radionuclides in halite and anhydrite 7-36270
- SASCHA programme on fission product release under reactor core melting conditions, review 7-774
- scission, fragment-separation barrier, liquid-drop model anal. 7-5220
- source term composition effects on offsite doses after reactor accidents 7-782

fission products continued

- source term research implications for ex-plant reactor accident consequences modelling 7-780
- thin film detectors, response characts. for fission fragments 7-5544
- volatile fission products, thermochemical approximation (Dutch) 7-36208
- worst case reactor accidents, fission product source term methodology 7-781
- Zircaloy clad UO₂ fuel elements, fission product release, deposition behaviour 7-25149
- ²²Fr, thermodynamic method of calculating yields of light nuclei in spontaneous decay 7-42091
- (p,f), E_p=190 MeV, target nuclei Nb, Ag, La, Ce, Pr, Nd, Dy, fission mass distrib. 7-5304
- 180 W (²He, fission), mass distributions of fission fragments from heated nuclei and the drop model 7-42041
- ^{242m}Am, spontaneous-fission half-life meas., α -spectra, fission fragment spectra 7-61927
- ¹⁹⁷Au(⁴⁰Ar,X), 27 MeV/nucleon, nuclei deexcitation near nuclear matter instability temp. 7-19279
- ¹¹⁴Cd, A=123-130, strongly neutron rich fusion products, decay props 7-19210
- ²⁵²Cf, nucl. fission channels, Strutinsky-type calcs. 7-49484
- ²⁵²Cf, spontaneous fission, prompt fission neutron spectrum tail 7-30457
- ²⁴²Cm, spontaneous-fission half-life meas., α -spectra, fission fragment spectra 7-61927
- Cs and I source terms of irradiated UO₂ reactor fuel 7-775
- ¹³⁷Cs, 1977 survey of conc. in British soil 7-34076
- ¹¹⁴Cu, A=74-78, strongly neutron rich fusion products, decay props 7-19210
- ¹⁶⁵Dy (²He, fission), mass distributions of fission fragments from heated nuclei and the drop model 7-42041
- ²⁵⁸Fm, fission channels, rel. to fragment kinetic energies and mass asymmetry 7-19310
- ¹⁴⁶Ga, A=77-81, strongly neutron rich fusion products, decay props 7-19210
- ³H, chemistry in fission and fusion reactors 7-25234
- He-jet fed ISOL facility KUR-ISOL at the Kyoto University reactor 7-30822
- (²He,f), E=270 MeV, target nuclei Nb, Ag, La, Ce, Pr, Nd, Dy, fission mass distrib. 7-5304
- ¹⁷⁶Hf (²He, fission), mass distributions of fission fragments from heated nuclei and the drop model 7-42041
- ¹⁶⁵Ho(⁴⁰Ar,X), 27 MeV/nucleon, nuclei deexcitation near nuclear matter instability temp. 7-19279
- ¹⁶⁵Ho(²⁶Fe,X), SOS MeV, fragment analysis 7-5275
- I retention by Fe surface, role in source term reduction, reactor accident anal. 7-33961
- ¹¹⁴In, A=123,131, strongly neutron rich fusion products, decay props 7-19210
- ⁹⁹Mo and U separation in H₂SO₄ medium by D2EHPA in kerosene, solvent extraction study 7-25043
- Na cooled reactors, radionuclide behaviour 7-25038
- ²³⁷Np(γ ,f), 5.60-8.61 MeV, fragment ang. distrib., ang. anisotropies 7-49482
- ²⁰⁸Pb(¹⁶O,f), 76.8, 77.3, 80.2 MeV, fragment angular distrib. 7-19286
- ¹⁴⁶Pu(n,f), A=239, 241, fragment energy and mass characts., shell effects, static scission point model anal. 7-42099
- ¹⁴⁶Pu(sf), A=238, 240, 242 7-42099
- ²³⁹Pu(n,f), fission product sum beta spectra, absolute meas. 7-56707
- ²²¹Ra, A=221-224, 226 thermodynamic method of calculating yields of light nuclei in spontaneous decay 7-42091
- ¹⁴⁶Rb, A=94, 95, P_n values by β - γ spectroscopic method 7-30507
- Ru, behaviour, restraint in pot vitrification process 7-25251
- ⁹⁰Sr, removal from acidic nuclear waste solns. 7-25051
- ⁹⁰Sr retention mechanisms in synthetic ion-exchange resins 7-36269
- ¹⁸¹Ta (²He, fission), mass distributions of fission fragments from heated nuclei and the drop model 7-42041
- ⁹⁹Tc, nuclear fuel cycle chemistry 7-19384
- ²³²Th(¹⁶O,f), 77-86 MeV, ²⁴⁸Cf compound nucleus spin determ. from fragment angular distrib. 7-19286
- ²³²Th(n,f), fission mass distrib. from degraded fission spectrum neutrons 7-61934
- ¹⁶⁹Tm (²He, fission), mass distributions of fission fragments from heated nuclei and the drop model 7-42041
- U based intermetallic compounds, fission gas swelling, cryst. struct. stability 7-42115
- UC, fission gas bubble destruction by radiation re-solution 7-42114
- UO₂, fission gas bubble destruction by radiation re-solution 7-42114
- UO₂ fuel, irradi., fission products chemical state 7-724
- UO₂ irradiated fuel, ¹³⁷Cs and ¹²⁹I leaching, rel. with fuel element power 7-786
- UO₂ operating fuel elements, short-lived fission product release under oxidising conditions 7-785
- UO₂ trace irradiated pellets, volatile fission product release 7-788
- ²³⁴U(n,f), 0.8 MeV, mean kinetic energy depend. of fission fragments, vibr. resonance 7-42097
- ²³⁴U(n,f), E_n~0.8 MeV, fission fragment average kinetic energy meas., effect of vibrational state in second potential well 7-61935
- ²³⁵U(n,f), fission product sum beta spectra, absolute meas. 7-56707
- ²³⁵U(n,f), prompt fission neutron spectrum tail 7-30457
- ²³⁵U(n,f), thermal-6 MeV, fragments mass, kinetic energy and ang. distrib. 7-42101
- ²³⁶U, fission charge distribution yields, fine structure, coupling of charge asymmetry coordinates and relative motion 7-24967
- ²³⁶U(¹²C,f), 60-68 MeV, ²⁴⁸Cf compound nucleus spin determ. from fragment angular distrib. 7-19286
- ²³⁸U(¹²C,f), 81, 90 MeV, fragment angular distrib. 7-5303
- ²³⁸U(²²Ne,f), 125, 143, 175 MeV, fragment angular distrib. 7-5303
- ²³⁸U(⁴He,f), 25, 35 MeV, fragment angular distrib. 7-5303
- ¹³³U(e,e'), 5-23 MeV, coincidence cross section meas. 7-19240
- ¹³³Xe, activity determination by γ -ray spectrometry, nuclear plant effluent air check 7-25298
- ²³²Yh(n,f), 14.7 MeV, Rh, Ag, In, Sb yield charge distrib. 7-19313
- ¹¹⁴Zn, A=75-80, strongly neutron rich fusion products, decay props 7-19210

fission reactor cooling and heat recovery

- see also cooling: fission reactor core control and monitoring
- 3x6 fuel rod bundles, anisotropic turbulent flow in subchannels, numerical anal. 7-15272
- acoustic boiling noise in a sodium-water steam generator 7-36183

fission reactor cooling and heat recovery continued

- AGR, low temperature carbonaceous deposition, models and theory 7-42108
- AGR boilers, Heysham I and II and Hartlepool II modifications 7-15253
- AGR fuel handling, temp. and gas flows modelling 7-56745
- AGR helically wound heat exchanger, impacting phenomena anal. for Heysham 7-56790
- AGR helically wound heat exchanger, resonance tests at Heysham I 7-56789
- AGR helically wound heat exchangers, vibration props. 7-56788
- Alloy 600, steam generator material, properties and performance 7-30556
- alloy 600 nuclear steam generator tubes, local pitting conditions using Pourbaix diagrams 7-46716
- Alloy 600 PWR steam generator tubing, intergranular attack and SCC remedial methods 7-8199
- Alloy 690, thermally treated nuclear steam generator tubes 7-5334
- annular two-phase flow with liquid entrainment, improved mixing length model 7-5390
- ASME code for nuclear plant component in-service inspection, 1984-5 revisions 7-5404
- auxiliary feedwater system, common cause failures, defensive tactics for branched events 7-36232
- axial flow in square lattice rectangular rod bundle, wall shear stress meas. 7-16282
- Beaver Valley PWR, water chemistry control with morpholine 7-5362
- boiling heat transfer, anal. using hot ball quenching method (*Chinese*) 7-49596
- bowing of elements and changes in radial coolant temperature profile over subassembly lifetime 7-61997
- BR-10 reactor first circuit pipelines, radioisotope distrib. 7-30590
- BRIG-300 FBR, gas channel study program (*Russian*) 7-5361
- bubbling flow, local volume gas fraction, time history meas. (*German*) 7-25108
- BWR, assessment of the heat transfer models in the TRACBO2 code 7-62006
- BWR, correlation for predicting reactor power during ATWS 7-62038
- BWR, density wave oscills. in boiling water system, two-fluid model simulation 7-36192
- BWR, gravity-driven core cooling system for inherent safety 7-36201
- BWR, inherently safe design, passive steam-driven ECCS injectors 7-36226
- BWR, linear and nonlinear density wave instability modes, anal. modelling 7-5375
- BWR, mass transfer anal. of corrosion products in water circuit 7-61980
- BWR, MSIV-ATWS events, power level and pressure suppression pool temp. 7-42155
- BWR, new scenario for intersystem LOCAs 7-42162
- BWR, TRACBO4 study on suppression pool swelling during containment venting 7-42156
- BWR at Gundremmingen nuclear power station with twin 1300 MW units, corrosion products (*German*) 7-10241
- BWR broken recirculation line, two-phase flow phenomena 7-61989
- BWR feedwater systems, hydrogen water chemistry effects on radiation fields 7-771
- BWR LOCA, two bundle loop tests, SAFER03 and TRAC-BD1 anals. 7-36210
- BWR LOCA research and development of SAFER code (*Japanese*) 7-56711
- BWR piping, fracture mech. research in Japan 7-53891
- BWR piping research in Italy, IGSCC tests, fracture and cracks 7-53890
- BWR primary coolant system, radiochemical studies 7-25123
- BWR simulation, countercurrent gas/liquid flow in parallel channels 7-5380
- BWR stability anal., dual loop jet pump model 7-62005
- BWR suction line break LOCA, ROSA III RUNs 942 and 943, initial fluid condition effects 7-19416
- BWR/6 DBA analysis with limited ECC 7-42154
- Calder Hall, water chemistry control, corrosion prevention 7-56796
- Calder Hall and Chapelcross reactor pressure circuits, in-service inspection 7-56810
- Calvert Cliffs Unit 1 tube examination 7-61970
- CANDU, header void distrib. effects on fuel channel flow following inlet header stratification 7-15298
- CANDU, modeling of drift effects 7-61952
- CANDU, turbulent moderator flow, numerical modelling 3D 7-10259
- CANDU coolant pump seals, improved performance 7-36101
- CANDU fuel bearing pad, algorithm for nonlinear thermal anal. 7-15273
- CANDU fuel bearing pad thermal design, FEAT3D code 7-15274
- CANDU fuel channels, calculation of steam flow 7-10262
- CANDU fuel channels, subchannel flow distrib. following deformations 7-10210
- CANDU header manifold, flow stratification under small-break LOCA 7-62041
- CANDU heat transport system, stability criterion for flow oscillations 7-10205
- CANDU horizontal subchannels, numerical simulation of two-phase flow 7-10207
- CANDU LOCA, radial heat transfer from fuel to moderator, RAMA and CHAN II codes 7-15297
- CANDU thermohydraulic codes, transient two-phase velocity difference model for drift calcs. 7-36068
- CANDU-600 heat transport system flow stability 7-36067
- CEGB single-phase erosion-corrosion research programme for AGR boilers 7-59679
- centrifugal separators for PWR power stations (*French*) 7-25102
- Chernobyl accident, causes and effect in Spain/Italy (*Spanish*) 7-5373
- Chernobyl accident; event sequence, consequences, anal. (*German*) 7-25147
- Chernobyl accident, RBMK construction and operational features, accident causes (*German*) 7-56803
- COBRA-NC code anal. of steam line break 7-61954
- COBRA-OSU improved numerical method for subchannel cross-flow calculations 7-30497
- computer aided PWR power plant operation, control and meas. (*German*) 7-19394
- conduction-controlled rewetting with internal heat generation, 2D anal. 7-10254
- conf., Dresden, Germany (March 1985) 7-24266

fission reactor cooling and heat recovery continued

- conference on iodine chemistry in reactor safety, Harwell, England (Sept. 1985) 7-48176
- conference on nuclear engineering, Zittau, Germany (Apr. 1985) 7-18483
- conference on the safety and reliability of reactor pressure components, Stuttgart, Germany, (Oct. 1985) 7-9583
- conference on two-phase flow dynamics, Lake Placid, NY, USA (Aug. 1984) 7-4627
- conference on water reactor safety, Gaithersburg, MD, USA, (Oct. 1985) 7-48152
- confined Bernard problem, nonlinear phenomena, numerical parametric anal. 7-30482
- continuous longitudinal-transverse motion of liq. in annular heat generating layer (*Russian*) 7-49578
- convection-diffusion problems in irregular geometries, finite difference soln. 7-30493
- coolant boiling in research reactors, expts. in WWR-SM facility (*German*) 7-56781
- coolant energetic physical state, prediction using partial coherence functions (*Russian*) 7-49528
- coolant pumps, vibr. monitoring and diagnostic techniques 7-36203
- core coolant channels, coherent blockages, statistical thermodynamics, percolation anal. 7-36194
- core cooling and system behaviour following PWR LOCA 7-49563
- countercurrent flow and flooding with abrupt area changes 7-61999
- counterflow steam generator, water-sodium leaks, fault processes 7-5344
- Courant limit violating numerical method in RELAP5/MOD2 calcs. 7-30495
- CRBR fuel subassembly, 2D flow in partially blocked parallel plates, soln. using electrical network 7-36188
- degraded core coolability study 7-62046
- density wave oscillations, stability map construction method, reactor appls. 7-5378
- dissociating coolant reactors, core active zone thermotechnical reliability (*Russian*) 7-49525
- dNB prediction in assemblies with mixing vanes and unheated tubes 7-62040
- DNBR limit, prediction of transient axial power distrib. 7-62039
- DNBR studies, streamlined one-pass modeling 7-62004
- dryout heat flux for core debris bed, particle size mixing and coolant flow effects 7-30623
- dynamically loaded pipes with circumferential flaws, behaviour under internal pressure and external loads 7-13577
- EBR II, superheater SU-712, duplex-tube performance, statistical anal. of data 7-19395
- EBR II intermediate heat exchanger, real time anal. 7-30492
- EBR-II, delineations of power and power-to-flow feedback components 7-42132
- EBR-II, LOF transients without scram, primary pump coastdown characteristics, effects 7-15278
- EFWS, bus configurations, four-train versus two-train support 7-42161
- Experimental Steam Generating Facility, PWR secondary water chemistry study (*German*) 7-25116
- expert systems for PWR diagnostics 7-56798
- fast reactor HCDA anal., two phase flow aspects, ANEXDI code 7-15302
- FBR, horizontal gas jet submerged in liq., penetration study 7-62052
- feedwater system evaluation for reactor scram reduction 7-36229
- feedwater temperature measurement using sound 7-61994
- flow and heat-transfer at the intake of a radially symmetrical longitudinal flow heat exchanger (*German*) 7-30619
- flow induced valve operation and pressure wave propag. in single and two-phase flows 7-10239
- flow modelling in 3-D fracture networks 7-56799
- flow-induced vibration of fuel rods, review (*Japanese*) 7-25034
- fuel element, transient heat transfer and using FEA 7-19362
- fuel element bundles, 3D heat-carrier flow, numerical modelling 7-61981
- fuel-rod bundles model, hydraulic drag 7-10237
- fully developed axial turbulent flow in fuel rod bundles, finite vol. calc. 7-36189
- fundamental aspects of thermal hydraulics 7-61998
- gas cooled rod bundles, pressure drop and heat transfer, fuel design 7-36190
- German BWRs, experience in exchanging recirculation, class 1 piping systems 7-49574
- Hartlepool/Heysham I AGRs, re-ferruling of pod boilers, boiler performance effects 7-56792
- heat exchanger tubes, cyclic temperature transient influence on creep behaviour 7-10186
- heat exchangers, computer-aided tube fretting-wear predictions 7-10261
- heat generating fluid in horizontal cylinder, natural convection 7-20702
- heated gas flow in circular tube, friction factor studies (*Japanese*) 7-57924
- homogeneous flow model, validity for instability anal., steam generators 7-5379
- horizontal annular flow measurements using pulsedphoton activation and film thickness distributionmodelling 7-5357
- HTGR, adsorpt. removal of CO₂ from He coolant 7-30514
- HTR, reactor protection building anal. for He release (*German*) 7-30639
- Incoloy 800 H, permeability of ³H and H in heat exchanger tubes (*German*) 7-56759
- inverted annular flow in post-dryout region, flow regime transition and interfacial characts. 7-5386
- irradiated fuel disposal facilities, fuel cooling, concept to commissioning 7-56868
- JAERI reactor engineering dept 1985-6 annual report 7-56725
- JMTR OWL-1 loop water, crud behaviour, ⁶⁰Co chemical form 7-19390
- KMRr, thermal safety margin using hot-spot-factor approach 7-61996
- KNU1 plant transient simulation using RELAP5/MOD1/NSC 7-5374
- large steam-line break LOCAs, similarity study for ROSA-III, FIST and BWR-6 7-49593
- LaSalle-1 BWR, water chemistry, corrosion products and radiation-field buildup 7-36206
- liquid metal flow rate measurement using EM flowmeter, error in correl. method 7-57954
- liquid solid phase change front-prediction method 7-62002
- LMFBR, accelerated two-phase flow through perforated plates during core-disruptive accident 7-30609
- LMFBR, hot N submerged impinging jets study in molten NaOH 7-62051

fission reactor cooling and heat recovery continued

LMFBR, hypothetical core meltdown accident, pressure depend. of particle bed dryout heat flux 7-5393
LMFBR 37-pin bundle, low heat flux Na boiling test using SABENA code 7-25110
LMFBR HCDA, particle phase size effects in disassembly accident transient 7-25142
LMFBR plenum, thermal hydraulic anal. 7-10258
LMFBR steam generator design and experience in the UK 7-56791
LMFBR steam generator large leak accident, heat transfer into module shell tube 7-62016
LMFBR steam generators, thermohydraulic instabilities, expt. results 7-5382
LMFBR steam generators, thermohydraulic instabilities, nonlinear and linear anal. models 7-5381
LMFBR wire-wrapped fuel bundle, local heat transfer anal., HEATRAN program 7-15271
LOCA, air-water two-phase cross flow resistance in rod bundle 7-5356
LOCA, critical flow of initially subcooled flashing liquids, homogeneous equilib. model 7-5388
LOCA, ECCS, operation, active cavity model for flashing 7-5387
LOCA, peak cladding temp. calcs., LOFT anal. 7-42158
LOCA, pressure surge prediction in one-component two-phase bubbly flow 7-5398
LOCA, transition boiling heat transfer studies using the hot cylinder quenching method 7-25112
LOCA, uncertainty anal. using Fourier amplitude sensitivity test 7-42160
LOCA, very small cold-leg break, RELAP5/MOD1 predictions, ROSA IV expt. 7-19410
LOFT facility, rewet, NCC, stratified flow and plant recovery procedure studies 7-49564
LOFT pressurizer, on-line instrument failure detection, Kalman gain approach 7-5354
loop flow reactor plant for coolants with known technological characteristics (Russian) 7-5325
looped channel with natural circulation of dissociated N₂O₄ coolant, reactor tests (Russian) 7-5360
LWR, application of a direct-heating model to the Sandia SURTSEY tests 7-62042
LWR, Chen boiling heat transfer correlation 7-42153
LWR, corium droplet size in direct containment heating 7-62007
LWR, drift-flux model for void fraction prediction 7-25121
LWR, fuel rod performance during fission product release into coolant, validity limits of calcs. 7-56757
LWR, heat radiation through steam in direct containment heating 7-62008
LWR, heat transfer model for volumetrically heated nuclear debris beds 7-49591
LWR, hypothetical core meltdown accident, pressure depend. of particle bed dryout heat flux 7-5393
LWR, rapid thermal transients, fuel response to ECCS quenching 7-15252
LWR, reflooding, bubbly-slug interfacial shear, effect on liquid carryover using RELAP5/MOD2 7-62001
LWR, rewetting correlations, modifications and assessment 7-62000
LWR, severe accident containment load calculations using HMC code 7-62044
LWR degraded core coolability, two-phase flow through porous media 7-5394
LWR ECCS, steam-water interactions in a vertical tube, flooding 7-5383
LWR ECCS injection, fluid and pressure oscils. during direct contact condensation 7-5376
LWR LOCA, jets formed by high pressure subcooled water and steam-water mixtures 7-5391
LWR LOCA, phase separation mechanisms in branching conduits, review 7-5384
LWR LOCA, pressure transient and two-phase swelling due to small top break 7-5389
LWR LOCA, reflood simulation, numerical anal. based on KREWET code 7-15299
LWR LOCA, two-phase flow in unbounded two-phase critical flows 7-25131
LWR meltdown accident, fuel-coolant mixing, unsteady 1D 2-fluid model, PHOENICS code 7-5395
LWR neutronics and thermal-hydraulics, NTHAD code for scoping appls. 7-36086
LWR safety anal., steam direct contact condensation on slowly moving water 7-5358
LWR severe core damage accident, uncovered core thermal-hydraulics, model dev. 7-30624
LWR small break LOCA expts. at LOFT, RETRAN-03 anal. of LP-SB-1 and LP-SB-2 7-36237
LWR steam generator U-tube rupture transient anal. using DRUFAN-02 code 7-49562
LWR thermal hydraulics, SEFDAN code for severe core damage accidents 7-49503
LWR thermal-hydraulic issues in nuclear training 7-29618
LWR thermal-hydraulics after a severe accident, Power Burst Facility anal. with SEFDAN code 7-49586
LWR thermohydraulic core anal. methods 7-49499
LWRs, fuel rod failure/coolant activity relationship, data formatting and collection 7-36235
LWRs, thermal hydraulics research, history and present status 7-29653
MARS reactor plant, an inherently safe, small/medium multipurpose nuclear plant 7-25022
McGuire Nuclear Station, reliability centred maintenance of feedwater system 7-36207
mixture drift-flux eqns. soln. algorithm on multi-CPU pipeline machines 7-30494
modular HTGR plant, steam generator design considerations 7-62014
motor-operated valve, operability verification, reactor appl. 7-42178
Muhleberg BWR, extra decay heat removal, back-up protection system 7-30626
Mutsu, ship propulsion reactor, thermal-hydraulic transient characts. from safety anal. (Japanese) 7-25128
nonequilibrium film boiling in rod bundle geometries, post-CHF test 7-42151
nonlinear dynamics of two-phase flow 7-30617
NRC Degraded Piping Programme, LWR piping fracture research, Phase II progress 7-53889
nuclear piping systems, research overview 7-49595

fission reactor cooling and heat recovery continued

nuclear power plant neutral oxygenated water conditions appl. efficiency for corrosion protection (Russian) 7-765
nuclear power station two-stage coolant system, hydraulic and mechanical transients (Russian) 7-5351
nuclear power station with single loop, saturated steam characts. over variable part of load curve (Russian) 7-25103
nuclear steam generators, heat flux effects on concentration factor in crevices 7-19397
nuclear thermal-hydraulics education, Yankee Atomic/Univ. of Lowell experience 7-29615
numerical stability of upwinding calc. schemes 7-30496
Oconee steam generators, secondary-side chemical cleaning 7-42173
Paks coolant flowrate, gate valve effects (Hungarian) 7-62013
Paks Unit 2, noise meas. using in-core self-powered neutron detector strings 7-62012
Palo Verde full-range feedwater control system operating experience 7-36230
PAT loop for AGR fuel testing, flow meters for coolant 7-26370
PGN-200M loop steam generators, noise level measurements 7-61982
PKZh-902 instrument for solid phase monitoring in organic reactor coolants 7-49560
PNP-500, dynamic modeling and simulation of a high-temperature gas cooled pebble-bed reactor 7-10212
post accident heat removed, inclination effect on downfacing burnout heat flux 7-62022
post dryout heat transfer prediction using mechanistic model 7-5397
post-dryout boiling, dispersed flow heat transfer, review 7-5400
postulated severe accident, hot gas bubbles discharged into water, dynamic and thermal behavior 7-5377
precursory cooling effects on rewetting rate 7-49561
pressure vessels, thermal mixing and wall loads for emergency core cooling expts. 7-10217
primary coolant circuit parameters, control design and dynamical performance (German) 7-56785
pulsations in parallel steam-generating channels 7-5346
pump data correlation for single- and two-phase 7-61995
purification resins in reactor circuits as source for organic tritium, expts. on algae 7-49545
PWR, adequacy of automatic plant protection system 7-25152
PWR, characteristics of releases from TREAT source-term experiment STEP-1 7-42170
PWR, direct heating containment vessel interaction code DHCVIC 7-62043
PWR, flow distrib. calcs. in heated parallel channels (German) 7-25107
PWR, fluid and thermal mixing in model cold leg and downcomer, COM-MIX-1A anal. 7-15268
PWR, fuel rod vibration induced by baffle jet flow 7-25134
PWR, heat transfer during LOCA 7-25151
PWR, improved water chemistry controls for minimizing degradation of materials 7-30615
PWR, large break LOCA, dispersed flow heat transfer during reflood 7-42150
PWR, LOCA, film boiling heat transfer coefficient during reflood phase 7-10250
PWR, LOCA, simulation using TREAT source term expt. 7-42169
PWR, local coolant boiling monitoring by neutron noise anal. (German) 7-15259
PWR, multi-loop, power plant accident anal., digital simulator for transients and accidents 7-15301
PWR, natural convection heat transfer 7-31784
PWR, primary loop modelling, appl. of cascaded state feedback control 7-56776
PWR, solubility of simulated primary circuit corrosion products 7-19401
PWR, steam generator tube bundle flow, turbulence force correlation 7-62003
PWR, turbine trip transient, effect of pressurizer sizing 7-30604
PWR, water chemistry guidelines 7-25029
PWR, Westinghouse design, leak-before-break eval. of pressuriser surge line 7-56813
PWR boiler pipework, effect of feedwater conditioning on corrosion (German) 7-25115
PWR CHF predictions, EPRI-1 correlation effects under normal and abnormal fuel conditions 7-36198
PWR circulation piping, water chemistry and radiation field buildup 7-15251
PWR condenser improvements for corrosion impurity protection 7-15250
PWR coolant flow field in above-core region, approx. calcs. (German) 7-56783
PWR coolant pump flywheel radial crack testing, caustic curve method 7-15266
PWR coolant pump trip criteria, transient identification technique 7-62048
PWR feedwater, Cu oxides, acid chlorides, steam generator denting 7-5333
PWR hot leg, two-phase flow during natural circulation in once through steam generators 7-49579
PWR hot leg, two-phase natural circulation flows, literature survey for SBLOCA 7-49580
PWR leak detection studies, dew point, dry bulb temp. and flow rate monitoring 7-42157
PWR LOCA, best estimate anal. with thermal hydraulic codes 7-49502
PWR LOCA, FLECHT and FLECHT-SEASET reflood tests anal. with RELAP5/MOD2 7-25025
PWR LOCA, two-phase flow during bottom reflooding, computer modelling 7-49599
PWR LOCA licensing anal., expt. and best-estimate calc. comparison 7-49582
PWR power plant, auxiliary feedwater system anal. using dynamic logical analytical methodology 7-25114
PWR power plants, analytical control of hydrazine conc. in cooling circuits (German) 7-15262
PWR pressuriser, on-line instrument failure detection using improved likelihood ratio method and suboptimal control 7-25139
PWR pressurizer, accident and transient anal., nonequilibrium three-region model 7-36195
PWR primary coolant analytical and sampling problems, supplement IV 7-25119
PWR scram reduction by steam generator level control improvements 7-36228

fission reactor cooling and heat recovery continued

PWR secondary coolant circuits, sidestream condensate polishing 7-10243
 PWR secondary coolant system, deaeration of makeup water 7-10242
 PWR secondary system, automated derivation of failure symptoms for diagnosis 7-5370
 PWR secondary water chemistry, corrosion reduction (*German*) 7-62010
 PWR secondary water chemistry, corrosion reduction (*German*) 7-62011
 PWR secondary water systems, eval. of pH control agents 7-5363
 PWR steam generator sludge piles, chemical cleaning 7-10227
 PWR steam generator thermohydraulic anal., ATHOS3 code 7-10244
 PWR steam generator tube rupture transients, thermal-hydraulics in simulated 4-loop facility 7-49571
 PWR steam generator tubing sampling, feasibility study 7-5364
 PWR steam generators, correlation of tube support struct. studies, corrosion 7-10246
 PWR steam generators, depressurisation procedures for tubesheet crevice flushing 7-10248
 PWR steam generators, in-service cleaning (*German*) 7-15261
 PWR steam generators, review of secondary side tube degradation processes 7-30616
 PWR steam generators, tubesheet crevice-flushing effectiveness 7-56797
 PWR steam recirculation systems using brackish water, condensate polishers 7-19400
 PWR steam turbine secondary side SCC, remedial actions 7-61969
 PWR steam-generator simulation with non-equilibrium two-phase flow models 7-42122
 PWR turbulence modeling during high pressure coolant injection, COM-MIX-1B code 7-10255
 PWR U-tube steam generator, FAUST 3D 2-fluid code for thermal design anal. 7-36082
 PWR water chemistry control with morpholine, USA and foreign experience 7-10245
 PWR water systems, organics identity and concentration survey, corrosion reduction 7-19399
 PWRs, activity build-up in primary circuit, review (*German*) 7-19408
 PWRs, seawater cooled steam generators, tube support corrosion, chlorides effects 7-46715
 PWRs with once-through steam generators, radiation field build-up, coolant pH 7-36234
 random-walk boronimeter, experience in PWR plants 7-42129
 RAS III, modular noise diagnostics system for reactor primary circuit monitoring (*German*) 7-56787
 RBMK-1000/LWR comparison, differences in fuel coolant and moderator, Chernobyl accident (*Dutch*) 7-10213
 reactivity temp. coeff. meas. by noise method 7-5366
 Reactor Analysis Support Package, guidelines for LWR thermohydraulic safety anal. 7-42190
 reactor core debris bed, dryout heat flux, effects of system pressure and particle size 7-19406
 reactor neutronic and thermal-hydraulic problems, solns. using engineering workstation 7-36084
 rewetting phenomena, expt. investigation using round tubes and pressured Freon-12 7-25109
 Rheinsberg reactor, coolant flow rate determ. during coolant pump failures (*German*) 7-25106
 rod bundle wall sub-channels, turbulence structure 7-61985
 ROSA III SBLOCA tests, split break test RUN 921, 931 7-10267
 ROSA-III, break location effects on thermal-hydraulics during intermediate break LOCA expts. 7-49589
 Rossendorf research reactor, coolant boiling expts. (*German*) 7-56786
 safety relief valve position indication systems for reactor appl. 7-42179
 separated flow effect modelling in horizontal heated channel refill 7-10202
 shell-and-tube heat exchangers, velocity distrib. comparison for expt. and predictions 7-15275
 Sizewell B PWR, steam generator design for nondestructive exam. requirements 7-56793
 SLOWPOKE III, comparison of thermalhydraulic computer codes 7-10260
 spatial components of energy release functions in two-dimens. heat cond. problems (*Russian*) 7-51147
 spectral method of flow-velocity measurement 7-36182
 stability tests, limit cycles and bifurcations in nuclear systems 7-30618
 stainless steel, exposure to high temp. OWL-1 loop water, corrosion layer characterization 7-8167
 steam generator materials, properties and performance 7-30556
 steam generator submerged perforated screens, hydrodynamics (*Russian*) 7-5352
 steam generator tubing, primary side stress corrosion cracking, remedial measures 7-30613
 steam generator vessel and feedwater line integrity issues 7-30614
 steam generators, crevice hideout return testing, H_3BO_3 and $Ca(OH)_2$ effects 7-10247
 steam supply system, microcomputer data base 7-36093
 steam turbine condenser leakage detectors (*Czech*) 7-61988
 steam-water mixtures, thermodynamic equilibrium during loss from reactor 7-49577
 steam-water void fraction for vertical upflow in 73.9 nm pipe 7-1609
 steel, mild, erosion-corrosion control using O_2 - NH_4 -hydrazine dosed feed-water in reactor boilers 7-59675
 steel, X8CrNiTi18.10, corrosion product layers in PWRs at pH 7 (*German*) 7-19356
 steel LWR piping fracture mechanics database 7-53892
 stratified two-phase flow in horizontal circular tubes, mechanistic model of slugging onset 7-30596
 stress corrosion cracking test of expanded steam generator tubes 7-56764
 subchannel anal., numerical technique using finite difference method 7-10209
 subchannel void fraction predictions using drift-flux anal. 7-30605
 subcooled boiling flow in vertical eccentric annular channel, heat transfer study 7-51310
 supercritical heat transfer in an annular channel with bilateral heating 7-36179
 Superphenix reactor heat exchanger and pump development (*French*) 7-769
 Surry steam generator, examination and eval., nondestructive testing 7-54065
 temporary reverse osmosis makeup water systems 7-36205
 Terry turbine equipment and procedure modification for reliability improvements 7-36202

fission reactor cooling and heat recovery continued

thermal hydraulic anal. on mini- and microcomputers 7-30500
 thermal hydraulic analysis, boundary-fitted coordinate transform., BODYFIT codes 7-15240
 thermal hydraulics in nuclear engineering courses at the Univ. of Illinois 7-29617
 thermal hydraulics in undergraduate nuclear engineering education 7-29616
 thermal stratification predictions due to high-pressure injection in circulating reactor loop 7-30602
 thermal-hydraulic process expt. facilities, contrib. to reactor safety 7-19393
 thermalhydraulic aspects of natural circulation loop 7-10195
 thermalhydraulics, numerical methods conf., Montreal, Canada, Sept. 1983 7-9600
 thermoelectric temp. sensors., data anal. (*Czech*) 7-61991
 thermohydraulic explosions, spinodal lines and eqns. of state, review 7-5396
 time-dependent Nodal Integral Methods in linear and nonlinear heat conduction 7-30491
 TPTF, high pressure boiloff in rod bundle, slug-to-annular flow transition 7-49572
 TRAC analysis of upper plenum thermal-hydraulic phenomena in the Slab Core Test Facility 7-42152
 TRAC-PFI/MOD1 code assessment for annular, annular-mist, stratified flow 7-15234
 TRANS7 algorithm for transient anal. in reactor loops 7-30589
 transient 3D 3-phase 3-component nonequilib. flow in porous bodies by 3-velocity fields, 7-56782
 transient dispersed-film flows in channels containing fuel rod bundles 7-10236
 tubesheet sample removal from Point Beech 1 steam generator 7-56763
 TUF two-phase flow code for reactor thermal-hydraulics anal. 7-15237
 turbine rotor and disk stress corrosion cracking characteristics 7-33849
 turbulent diffusion in rod arrays with sodium coolant 7-36178
 two component flow stresses near walls 7-36184
 two phase flow demonstration device for nuclear thermal hydraulics education 7-29647
 two-fluid models, virtual mass term formulation, momentum transfer, reactor appl. 7-5385
 two-phase bubbly flow in a pipe, turbulence meas. reactor safety appl. 7-5392
 two-phase flow in bundle of fuel rods, volumetric vapour content 7-49576
 two-phase flow through breaks in horizontal pipe, stratified flow 7-770
 uncovered-bundle heat transfer under high-pressure boil-off conditions 7-5359
 UPTF PWR LOCA expt. program 7-49583
 valve stem packing improvements and gland adjustment for leakage reduction 7-10265
 very high temperature gas cooled reactor, control system design and dynamics 7-768
 VHTR steam generator, dryout and flow of gas-water flow in U and inverted U bends 7-5399
 void fraction determination in liquid flow systems by radiation attenuation, dynamic bias 7-61986
 VVER 440 and VVER 1000 nuclear power plants, coolant compensation processes (*Czech*) 7-766
 VVER in-reactor monitoring system, improvement of accuracy and reliability 7-30593
 VVER-1000 reactor, pre-operational cleaning, acidic and hydrazino-ammonium flushing (*Russian*) 7-56774
 VVER-440 reactor, heat removal from active zone, reliability anal. (*Russian*) 7-763
 water cooled reactors, steam generator tube performance during 1983 and 1984 7-25118
 water cooling circulation system thermal conditions anal. at Leningrad nuclear power station (*Russian*) 7-30595
 water level and pressure perturbations using Oyster Creek RETRAN model 7-62037
 water moderated reactor, oscillating control element, damping and added mass (*German*) 7-56779
 water-level measuring system for drum separators in nuclear power-plant with RBMK-1000 reactor (*Russian*) 7-764
 water-level monitor, ex-core, LOFT calculation comparisons 7-42127
 WWER, fuel assembly outlet temperatures (*German*) 7-15257
 WWER 440, primary coolant system, pressure ratios during positive reactivity insertion transients (*Czech*) 7-62024
 WWER core boiling crisis props. (*Czech*) 7-56777
 WWER temp. meas. reliability checking method (*Russian*) 7-30594
 WWER-40, primary coolant circuit pressure oscillations (*German*) 7-19392
 WWER-440, cold leg break LOCA, fuel rod thermomech. eval. under blowdown conditions (*Russian*) 7-49598
 WWER-440 nuclear power station, model of secondary circuit, computer program (*German*) 7-19388
 WWER-70, axial dependence of coolant temp. noise (*German*) 7-15258
 WWER-70, experimental fuel assemblies 7-15255
 WWER-70, measurement of spectral neutron flux density at boiling conditions (*German*) 7-15260
 WWER-70, unsteady boiling with expt. fuel assemblies, computer anal. (*German*) 7-15256
 Zircaloy clad UO_2 fuel elements, fission product release, deposition behaviour 7-25149
 Zircaloy oxidation and embrittlement criteria for emergency core cooling system acceptance, safety margins 7-36154
 Zircaloy-2, exposure to high temp. OWL-1 loop water, corrosion layer characterization 7-8167
 Cs, boiling liquid metal, critical heat flux (*German*) 7-49565
 H_2O_2 behaviour in RBMK-1000 BWR safety control system coolant circuit 7-30631
 He corrosion effect on high temp alloy (*German*) 7-30567
 I_2 volatility from evaporating PWR primary coolant films in accidents 7-49603
 K, boiling liquid metal, critical heat flux (*German*) 7-49565
 N_2O formation in irreversible dissociation of nitrite coolant (*Russian*) 7-49549
 N_2O_4 condensation in equilibrium maintaining chemical reaction, heat and mass transfer (*Russian*) 7-51341
 Na, boiling liquid metal, critical heat flux (*German*) 7-49565
 Na cooled reactors, radionuclide behaviour 7-25038
 Na ionization detector for FBR sodium leak detection system 7-5355

fission reactor cooling and heat recovery continued

- Na, liq. flow in FBR core sub-assemblies 7-767
- Na, rate limited molten fuel coolant interaction model 7-36102
- Na/steel system, NaCrO₂, form. threshold O level, LMFBF operation 7-42113
- NaOH, molten, wastage simulation with submerged impinging hot N jet 7-62050
- Rb, boiling liquid metal, critical heat flux (*German*) 7-49565
- UO₂ debris beds in pressurised water pools, coolability, DCC-1 and DCC-2 results 7-15279

fission reactor core control and monitoring

- see also fission reactor instrumentation; fission reactor safety; fission research reactors; nuclear engineering
- adaptive control methods, appl. to PWR power plants 7-36191
- advanced boiling water reactor core supervision and analysis using 3D-core simulator 7-61993
- AGR, Xe and temp. transients, 3D model anal. 7-15300
- AGR fuel handling, temp. and gas flows modelling 7-56745
- AGR fuel height stringer drop tests, damage estimates 7-56814
- AGR fuelling machine design, seismic constraints 7-56730
- AGR fuelling machine hoist system, single component failure mode deletion 7-56731
- AGR on-load refuelling, component vibr. problems 7-56732
- AGR refuelling approach at Hinkley Point B 7-56746
- AGR refuelling machine designs 7-56729
- automatic fuel shuffling 7-56744
- axial neutron distribution inertialess monitoring in reactors using triaxial gamma chambers 7-61979
- baffle/reflector region homogenisation calc. 7-30487
- Browns Ferry Unit 1 BWR, stability tests under single-loop operating conditions 7-25135
- burnable absorber modeling for PWR core reload design appl. 7-36080
- BWR, ADMIX reactor control system from Toshiba 7-36200
- BWR, heterogeneous model, detector field of view 7-36186
- BWR, heterogeneous model, neutron noise decomposition into local and global components 7-36187
- BWR, power distribution minimum variance estimation 7-5369
- BWR core stability estimation, applicability of multivariable autoregressive method 7-25140
- BWR fuel assemblies, pin-to-detector γ -ray transmission function by adjoint Monte Carlo methods (*German*) 7-61984
- cable-type thermoelectric converters, pulsed method for thermal inertia estimates 7-30592
- CAGR-on-load refuelling, safety case development 7-56815
- CANDU 600 MW(e) reactor, defective fuel detection in operating plant 7-784
- CANDU neutronics analysis, alternative approach using GAM, GATHER and CITATION 7-15269
- cell parameters, sensitivity coeffs., calc. method, neutronic props. 7-19389
- central control rod worth calculations in the multigroup approximation 7-25111
- Chernobyl, power excursion event anal. 7-62023
- Chernobyl accident, RBMK construction and operational features, accident causes (*German*) 7-56803
- colour graphic display systems for power station control rooms 7-56811
- computerised core refuelling 7-56743
- coolant energetic physical state, prediction using partial coherence functions (*Russian*) 7-49528
- cooling and system behaviour following PWR LOCA 7-49563
- core thermalhydraulics, numerical methods conf., Montreal, Canada, Sept. 1983 7-9600
- criticality calculation code SIMCRI 7-10192
- criticality problems, 3-dimensional, soln. by simplified response matrix technique 7-49531
- Darlington generating station fuel handling system 7-56733
- Diablo Canyon PWR plant, integrated control and communications system 7-42130
- digital upgrades for nuclear plant control and instrumentation 7-30597
- dissociating coolant reactors, core active zone thermotechnical reliability (*Russian*) 7-49525
- double heterogeneity effects, narrow resonance calcs. 7-30485
- EBR-II, delineations of power and power-to-flow feedback components 7-42132
- EBR-II, ramped power transients, feedback simulation using transfer functions in EROS code 7-42188
- engineering aspects of the Hartlepool and Heysham 1 fuelling machines 7-56735
- ESCORE code for LWR steady-state core reload eval. 7-25027
- expert systems for PWR diagnostics 7-56798
- extended burnup, ex-core and accident considerations 7-30547
- fast reactor core analysis, 3D transport anal., TRITAC and TWOT-RAN-II calcs. 7-49569
- FBR energy independent adjoint flux method, SEG-V configuration perfection 7-19337
- feedwater system evaluation for reactor scram reduction 7-36229
- FFTE, fuel rotation or reorientation for extended burnup 7-30546
- FFTE, reactivity worth of gas expansion modules 7-42131
- fluidised bed power reactor, transient neutron flux modelling 7-62017
- flux mapping, driving device for activated wire counting 7-30606
- fuel assembly subcriticality determ. by the Mihalcz method (*Japanese*) 7-25104
- fuel element load/unload machine for the Italian PEC reactor 7-56736
- fuel handling, microprocessor appl. 7-56741
- fuel handling machinery, control equipment 7-56740
- fuel handling options for commercial fast breeder reactors 7-56726
- fuel handling prototype machines, design and test methodology 7-56727
- fuel reinsertion strategies for out-of-core fuel management, OCEON code 7-30542
- fuel utilisation time factor, power plant discrete mode of consumption 7-61963
- fuelling machines, high integrity control system, design and development 7-56742
- Fugen, refuelling machine experience 7-56737
- Greifswald PWR plant, use of high burnup fuel assemblies at core edge (*German*) 7-15264
- GRENADE, coarse mesh program for static neutron diffusion eqns., flux and power distrib. 7-42107
- Hanford N Reactor, core simulation, development and appls., DELPHI code 7-42112

fission reactor core control and monitoring continued

- Hanford N Reactor, flux flattening programme, core physics calcs. 7-42133
- high conversion PWR, B₂C control rod worth calc. 7-19391
- in-core flux data, rational mapping technique 7-10256
- in-core management calculations for the EWA research reactor 7-49523
- independent fission yield measurements, review 7-61948
- integral fuel burnable absorber experience in two- and three-loop cores 7-30611
- IRT-2000 reactor, α -quantity meas. at thermal point by multiplicity spectroscopy (*Russian*) 7-42123
- JAERI reactor engineering dept 1985-6 annual report 7-56725
- LMFBR, 1000 MWe axially heterogeneous design, neutronics performance (*Japanese*) 7-15228
- LMFBR calculations in hexagonal geometry, nodal expansion method 7-56709
- LMFBR flux group const. generation Doppler effect calcs. 7-19336
- LMFBR ultra long life cores 7-61957
- LMFBRs, angular depend. of neutron-noise transmission through shields 7-42139
- LWHCR lattices, effects of WIMS data library changes on calc. results 7-5316
- LWR, generalised transient fuel-cycle model convergence 7-5327
- LWR, in-core gamma effects, power distrib., detector response 7-42137
- LWR in-core fuel management using CASMO-3 and SIMULATE-3 7-5323
- LWR lattice problems, 2D neutron transport, ang. current approx. choices, RICANT program 7-15270
- LWR neutronics and thermal-hydraulics, NTHAD code for scoping appls. 7-36086
- LWR pressure vessel mock-ups, fission rate meas. using SSNTD 7-42124
- LWR thermohydraulic core anal. methods 7-49499
- Magnox on-load refuelling grabheads, engineering design and development 7-56734
- monitoring system for nuclear reactors, reliability improvements (*Russian*) 7-25101
- MORSE-CG code for pulsed fast reactor problems, Monte Carlo anal. 7-15229
- neutron flux mapping data collection system for reactor core monitoring, personal computer based 7-42128
- neutron flux wave excitation in reactor core transients, Green's fn. anal. 7-30601
- neutron monitor for reactor startup range, design parameters 7-42126
- NF-6 program complex for multigroup diffusion network calcs. (*Russian*) 7-49526
- noise diagnosis techniques for nuclear power station fault detection (*German*) 7-19403
- noise monitoring, digital generation of stochastic signals of arbitrary spectral shape 7-5341
- nonsymmetric slabs, environment independ. homogenised parameters for neutron diffusion 7-15223
- nuclear fuel systems of the Pake NPP 7-56728
- nuclear reactor control information, provision in presence of instrument failures 7-5367
- Ontario Hydro CANDU fuel handling and storage facilities 7-56747
- Ontario Hydro Pickering generating station fuel handling system performance 7-56748
- optimal xenon control in heterogeneous reactors 7-56775
- optimum discharge burnup, advantages and disadvantages 7-30548
- Paks Unit 2, noise meas. using in-core self-powered neutron detector strings 7-62012
- Palo Verde full-range feedwater control system operating experience 7-36230
- passive high-integrity lifting equipment 7-56738
- PFR, core guide tube exchanges, experience 7-56751
- PFR Downreay, fuel handling, maintenance experience 7-56750
- PHWR fuel cluster geometry, interface current method, CLUB code 7-15238
- pin power predictions in the Westinghouse Advanced Nodal Code 7-30486
- power range monitoring systems and neutron channels, in situ detection of channel degradation 7-36214
- primary coolant circuit parameters, control design and dynamical performance (*German*) 7-56785
- prompt self-powered neutron detectors, reactor noise anal., REND code calcs. 7-36193
- pulsed source experiments, use of ex-core epithermal detectors, kinetic distortion 7-56771
- PUMA adjustments to core parameters and rational flux mapping procedure 7-10257
- PWR, core loading patterns to maximise beginning of cycle reactivity, automatic determ. 7-25113
- PWR, fuel element vibration effects on neutron flux fluctuations 7-25019
- PWR, high conversion, core performance parameters, sensitivity anal. 7-49524
- PWR, primary loop modelling, appl. of cascaded state feedback control 7-56776
- PWR, reactivity control of first cycle using Gd burnable poison system 7-56773
- PWR, reactivity temperature coeff. meas. by noise method, theory 7-25117
- PWR, soluble B reactivity control system substitution by Gd burnable poisons, BGUCORE anal. 7-36197
- PWR assembly, B and Gd burnable poisons effects on hot-to-cold reactivity swing 7-36196
- PWR core monitoring, backfit appl. of advanced technology 7-36204
- PWR load following operation control 7-5353
- PWR refuelling using revolving cylinder manipulator crane 7-56739
- PWR safety anal. using B1K 1D neutron kinetics program 7-5319
- PWR scram reduction by steam generator level control improvements 7-36228
- PWRs, neutronic aspects of different moderator-to-fuel volume ratios (*German*) 7-36185
- random-walk boronimeter, experience in PWR plants 7-42129
- RAS III, modular noise diagnostics system for reactor primary circuit monitoring (*German*) 7-56787
- RBMK, simulation of regulation system under power reduction conditions 7-25099
- RBMK-1500, fuel pin assemblies, critical power determ. 7-36076
- reactivity temp. coeff. meas. by noise method 7-5366

fission reactor core control and monitoring continued

- reactor burnup and heavy nuclide nuclear data 7-30510
 reactor core cal. code, 3D simulating Xe transient state, develop. (Japanese) 7-56778
 reactor neutronic and thermal-hydraulic problems, solns. using engineering workstation 7-36084
 reactor refuelling, conf.; Newcastle-upon-Tyne, England (May 1985) 7-55891
 research reactors, computer codes for operational control 7-15232
 RKFB, reactor kinetic code with feedback for materials testing reactors 7-36099
 ROSA-III, break location effects on thermal-hydraulics during intermediate break LOCA expts. 7-49589
 Rossendorf research reactor, coolant boiling expts. (German) 7-56786
 RP-10 reactor trip module, availability anal. 7-10238
 SCOPERS-2 program for LWRs, static core performance simulator, user's manual 7-19347
 seed/blanket core, power-sharing formula 7-30603
 Sequoyah PWR, low leakage fuel management 7-30543
 spectral disturbance influence on macroscopic few-group parameters (German) 7-56713
 system state monitoring method using state space trajectory patterns 7-49570
 two-dimensional space-time kinetics benchmarks, ADEP code 7-15239
 very high temperature gas cooled reactor, control system design and dynamics 7-768
 void fraction determination in liquid flow systems by radiation attenuation, dynamic bias 7-61986
 VVER, in-reactor monitoring systems 7-5343
 VVER 440 reactor, control element drives, diagnostics 7-36239
 VVER in-reactor monitoring system, improvement of accuracy and reliability 7-30593
 VVER-1000, external detector sensitivities to core power distribution changes 7-61983
 water moderated reactor, oscillating control element, damping and added mass (German) 7-56779
 water-level monitor, ex-core, LOFT calculation comparisons 7-42127
 Westinghouse fifteen years of reactor refuelling experience 7-56749
 WWER 440, primary coolant system, pressure ratios during positive reactivity insertion transients (Czech) 7-62024
 WWER fuel, burnup calc. verification, nuclide concs., expt. and theoretical data (German) 7-15245
 WWER-440, fast neutron dose meas. for pressure vessel using $^{93}\text{Nb}(n,n')^{93}\text{Nb}^m$ 7-56780
 WWER-440, increased burnup for optimum fuel utilisation (German) 7-15244
 $^{10}\text{B}/^{11}\text{B}$ ratio, determ. in nucl. reactor moderator 7-56753
 B_4C , neutron irradiation, damage effect 7-36104
 Cd plates, reactivity worth in MTR-fuel-type reactor 7-56772
 $^{252}\text{Cf}(\text{SF})$, noise equivalent source for freq. domain meas. 7-42135
 U-H₂O lattice assemblies, temp. effect of reactivity, subcriticality meas. methods 7-30591
 ^{232}U and ^{236}U effects on U recycling in BWRs, simultaneous eval. using TGBLA 7-36155
 Xe oscillations in load follow of large reactor, optimal control 7-30620

fission reactor decommissioning

- see also *fission reactor safety; radiation protection; radioactive waste*
 CADD/CAE use for remote vehicle system mission planning at nuclear facilities 7-49608
 chemical decontamination process for reactor decontamination and decommissioning 7-36238
 conference on radiation protection physics, Bad Schandau, Germany (Feb. 1986) 7-24267
 costs and radiological impacts with off-site waste disposal 7-62057
 financial recoverability a reliability problems 7-30641
 mobile robot use in nuclear power plants, TMI-2, Hope Creek, Salem 7-49613
 nuclear power plants, removal from operation (Russian) 7-56816
 occupational exposure reduction during nuclear facility decommissioning, IAEA review 7-25259
 remote equipment operators in nuclear facilities, training programme requirements 7-49607
 remote handling systems for reprocessing plant maintenance and reactor dismantling, testing and design 7-49614
 remote reconnaissance vehicle for core-bore sampling, operational experience at TMI-2 7-49612
 research reactor and fuel facility, technology and experience 7-30644
 robotic inspection of irradiated components from decommissioned nuclear plant 7-19420
 SEFOR test reactor, gamma anal. of soil following decommissioning 7-30726
 TMI-2, accident and recovery, defuelling and reactor inspection 7-42191
 TMI-2, integrated defuelling system, remote tools and support equipment 7-49610
 TMI-2 auxiliary building elevator shaft and pit decontamination 7-49606
 TMI-2 operations, robotics development, remote reconnaissance vehicle 7-49611
 TMI-2 sludge separation and packaging, anal. and conceptual designs 7-56863
 tools for decontamination and decommissioning of nuclear facilities 7-49609
 Triga facility, decontamination and decommissioning plan 7-30643
 utility perspectives, accounting and funding, South Texas Project 7-30642
 Windscale AGR, decommissioning, review 7-49605

fission reactor fuel

- see also *fission of plutonium; fission of uranium; fission reactor fuel claddings; fission reactor fuel preparation and reprocessing; isotope separation; nuclear materials safeguards; radioactive waste*
 accelerated fuel depreciation as economic incentive for low-leakage fuel management 7-30512
 accounting treatment for nuclear fuel leasing 7-30540
 actinide chemistry, Mossbauer spectroscopy appl. 7-22172
 actinide coordination chemistry, ligand site matching 7-19366
 actinides, physics and chemistry, handbook 7-24317
 AGR, Stage 2 fuel design, performance improvement 7-49543
 AGR fuel handling, temp. and gas flows modelling 7-56745
 AGR fuel height stringer drop tests, damage estimates 7-56814
 AGR fuelling machine design, seismic constraints 7-56730

fission reactor fuel continued

- AGR fuelling machine hoist system, single component failure mode deletion 7-56731
 AGR on-load refuelling, component vibr. problems 7-56732
 AGR refuelling approach at Hinkley Point B 7-56746
 AGR refuelling machine designs 7-56729
 AGR spent fuel handling in long term dry store 7-56869
 artificially perforated Zr barrier fuel rods, fission product release in test loop 7-783
 Bilibinsk reactor, fuel recharging modes with varying fraction of unloaded fuel assemblies 7-61959
 breached LMR fuel element, thermal effects of $\text{Na}_3(\text{U}_{1-y}\text{Pu}_y)\text{O}_4$ formation 7-30558
 breached spent-fuel rods, behaviour in flowing air atmosphere between 250 and 360°C 7-30534
 burnable absorber modeling for PWR core reload design appl. 7-36080
 BWR, commercial load following operation with KWU design 7-5347
 BWR fuel, criticality safety anal., burnable poisons effects 7-740
 BWR fuel, performance of lead test assemblies up to 35 MWd/kg 7-30545
 BWR fuel assemblies, pin-to-detector γ -ray transmission function by adjoint Monte Carlo methods (German) 7-61984
 BWR fuel design for load following 7-30561
 BWR fuel rod, pellet-cladding interaction, rod failure, fission product release (Japanese) 7-15242
 BWRs, TVO 1 and TVO 2 in Finland, retrofitting to increase output (German) 7-10240
 CAGR dismantled fuel, criticality safety, BNFL storage 7-739
 CAGR-on-load refuelling, safety case development 7-56815
 Calder Hall fuel elements, 30 years of metallurgical experience 7-56758
 CANDU 600 MW(e) reactor, defective fuel detection in operating plant 7-784
 CANDU reactor, fuel channel replacement program 7-10269
 CANDU/GCR clusters, collision probability calcs. using interface current method 7-19332
 ceramic cylindrical nuclear fuels, computer modelling, review 7-720
 ceramic materials and technology survey 7-10215
 ceramics, props. meas., conf., Soverato, Italy (Sept. 1986) 7-9582
 COMTA code for fuel performance, convergence behaviour of nonlinear eqn. solvers 7-15241
 conf., Dresden, Germany (March 1985) 7-24266
 conference, ANS winter meeting, Washington, DC, USA, (Nov. 1986) 7-29591
 conference on fission product behaviour and source term research, Snowbird, UT, USA (July 1984) 7-10
 criticality problems, 3-dimensional, soln. by simplified response matrix technique 7-49531
 criticality safety, American National Standards 7-761
 criticality safety, density-analog storage criteria 7-760
 criticality safety, DOE/ONS safety projects overview 7-758
 criticality safety, Monte Carlo code analysis problems 7-750
 criticality safety, Prescott interaction problem, MONK 6.4 anal. 7-751
 criticality safety, replacing aged professionals 7-759
 criticality safety, storage, transport, Limiting Surface Density Method 7-757
 criticality safety, US/Japan data development program plan 7-752
 criticality safety, validation 7-756
 criticality safety in fissile material storage, conf., Jackson, WY, USA, (Sept. 1985) 7-13
 criticality safety in low enriched U storage arrays in commercial plant 7-732
 criticality safety of Hanford fuel storage facilities 7-742
 damaged fuel assemblies, neutron tomography 7-30555
 damaged fuel assembly repair 7-56767
 Darlington generating station fuel handling system 7-56733
 decay energies for fission products in JNDC FP Decay Data File 7-15236
 densification and swelling, burn-up induced dimensional changes 7-5332
 diffusion processes, review 7-19350
 EBR-II, nonrecoil fission product release phenomena using multifreq. source perturbation expts. 7-5326
 effective resonance levels 7-36077
 engineering aspects of the Hartlepool and Heysham 1 fuelling machines 7-56735
 ESCORE code for LWR steady-state core reload eval. 7-25027
 extended burnup, ex-core and accident considerations 7-30547
 extended fuel burnup, criticality safety implications 7-733
 fast reactor fuel-rod bundle flow resistance anal. 7-49534
 FBR irradiated MOX fuel, transient fission gas release during direct heating expts. 7-778
 FEMAXI-III calculations for the D-COM blind problem 7-717
 FFTF, fuel rotation or reorientation for extended burnup 7-30546
 FFTF, IEM cell fuel pin weighing system, remote maintenance design considerations 7-49548
 FFTF interim examination and maintenance cell, remote tool development 7-49547
 financial and accounting issues FERC perspectives 7-30538
 fissile material storage, criticality safety, efficiency improvements 7-747
 fissile materials, criticality safety ANSI/ANS standards 7-745
 fissile solution storage criticality safety, Poisoned Tube Tank 7-735
 fission products release mechanism, estimation of failed fuel rods (Korean) 7-30517
 flow-induced vibration of fuel rods, review (Japanese) 7-25034
 French nuclear fuel manufacturing, criticality safety 7-731
 fuel assembly subcriticality determ. by the Mihalczko method (Japanese) 7-25104
 fuel cost impacts of using constant cycle-based amortization rates 7-30541
 fuel element load/unload machine for the Italian PEC reactor 7-56736
 fuel evolution and shuffling studies, generalized perturbation theory anal. 7-30490
 fuel handling options for commercial fast breeder reactors 7-56726
 fuel handling prototype machines, design and test methodology 7-56727
 fuel management for the RWE nuclear power plants (German) 7-36103
 fuel pin, dimensions determ. by neutron radiography, moments anal. method 7-25035
 fuel reinsertion strategies for out-of-core fuel management, OCEON code 7-30542
 fuel/cladding chemical interaction correlation for mixed-oxide fuel pins 7-30557
 Fugen, refuelling machine experience 7-56737

fission reactor fuel continued

FUTURE code for fuel cycle variables calc. 7-30480
 gas cooled rod bundles, pressure drop and heat transfer, fuel design 7-36190
 German nuclear fuel cycle, overview 7-49544
 Greifswald PWR plant, use of high burnup fuel assemblies at core edge (*German*) 7-15264
 Hanford N Reactor, core simulation, development and appls., DELPHI code 7-42112
 Hanford N Reactor, flux flattening programme, core physics calcs. 7-42133
 heat-carrier flow in fuel bundles, three-dimensional, numerical modelling 7-61981
 high burnup experience, appl. to consolidation equipment design 7-30552
 high-temperature pebble-bed reactor development and inherent safety 7-10273
 HTGR fuel behaviour at very high temps., TRISO-coated LEU particles 7-19364
 in-core management calculations for the EWA research reactor 7-49523
 inspection and repair of fuel assemblies 7-56766
 integral fuel burnable absorber experience in two- and three-loop cores 7-30611
 integral test for heavy nuclides 7-30509
 irradiated fuel disposal facilities, fuel cooling, concept to commissioning 7-56868
 JAERI criticality safety facilities and expts. 7-734
 JAERI Dept. of Chem. Jan. 1984-Dec. 1985 progress report 7-10233
 JENDL-2 fission product file, resonance parameters 7-15235
 laboratory assays for Pu and U for Savannah River purification and finishing 7-30519
 large scale enriched uranium soln. handling, criticality safety 7-736
 lattice homogenization procedure using the nodal expansion method and equivalence theory for LWR 7-49533
 LEU fuel conversion of test and research reactors, related problems 7-36106
 liquid metal fast breeder reactor fuels, swelling 7-19351
 LMFBR, voided cores, fuel vapour pressure buildup dynamics during transient heating 7-36215
 LMFBR calculations in hexagonal geometry, nodal expansion method 7-56709
 LMFBR long-life core designs, physics considerations 7-42111
 LMFBR sub-assemblies, mech. response under local accident conditions, state-of-the-art review 7-25129
 low volatility fission product release expts., surface vaporisation role, fuel debris bed appl. 7-25137
 LWBR, measured proof of breeding 7-42118
 LWBR irradiated fuel assay gauge, qualification 7-42117
 LWR, fuel rod performance during fission product release into coolant, validity limits of calcs. 7-56757
 LWR, generalised transient fuel-cycle model convergence 7-5327
 LWR, rapid thermal transients, fuel response to ECCS quenching 7-15252
 LWR fuel cycle, long-term analysis 7-30533
 LWR fuel failure detection using the grip slipping method 7-30544
 LWR fuel rods, simple model for predicting fission gas release 7-789
 LWR fuel under degraded core conditions, fission gas release prediction, FASTGRASS-VFP model 7-790
 LWR in-core fuel management using CASMO-3 and SIMULATE-3 7-5323
 LWR irradiated fuel under accident conditions, fission product release 7-773
 LWR load-following operation, fuel performance aspects, pellet-clad interactions 7-5350
 LWR MOX fuel performance, building a database 7-61967
 LWR severe fuel damage events, burnup effects on fission product release 7-787
 LWRs, fuel rod failure/coolant activity relationship, data formatting and collection 7-36235
 Magnox on-load refuelling grabheads, engineering design and development 7-56734
 Maple Research Reactor, core and fuel selection 7-5335
 materials management conf. New Orleans, LA, USA, (June 1986) 7-35087
 NFCIS, IAEA's directory of nuclear fuel cycle facilities 7-62101
 nuclear data evaluation for heavy nuclides 7-30461
 nuclear fuel systems of the Pake NPP 7-56728
 Nuclear Fuels-River Bend Nuclear Group accounting interface for reactor fuel 7-30539
 nucleate pool boiling using heated multirod, pressure effects 7-56715
 Ontario Hydro CANDU fuel handling and storage facilities 7-56747
 Ontario Hydro Pickering generating station fuel handling system performance 7-56748
 optimum discharge burnup, advantages and disadvantages 7-30548
 P₃ approximation for gas-cooled reactor fuel pins 7-49492
 pebble-bed reactor, physical behaviour and design (*German*) 7-49529
 PEC reactor core fuel element, structural verification criteria 7-49539
 pellet surface grooves for gas storage volume design 7-30559
 pellet-cladding interaction, bamboo ridge deformation, FEMAXI-III code anal. 7-36108
 pellet/cladding interaction, effects of fuel design and burnup, in-core diameter meas. 7-19361
 PFR, core guide tube exchanges, experience 7-56751
 PFR Dounreay, fuel handling, maintenance experience 7-56750
 PHWR fuel cluster geometry, interface current method, CLUB code 7-15238
 PWR, fuel element vibration effects on neutron flux fluctuations 7-25019
 PWR, fuel rod vibration induced by baffle jet flow 7-25134
 PWR, key radionuclide calcs. for failed fuel analysis 7-42176
 PWR, reactivity control of first cycle using Gd burnable poison system 7-56773
 PWR assembly, B and Gd burnable poisons effects on hot-to-cold reactivity swing 7-36196
 PWR CHF predictions, EPRI-I correlation effects under normal and abnormal fuel conditions 7-36198
 PWR failed fuel rod, pellet-cladding interaction, in-pile eddy current test 7-19354
 PWR fuel in spent fuel storage racks, criticality safety, Generic Reactivity Equivalence 7-743
 PWR fuel rod, pellet-cladding interaction study (*Japanese*) 7-5330
 PWR fuel rods, power ramp data, FROST and THERMOST codes, cladding deform. rod elongation 7-62034

fission reactor fuel continued

PWR LOCA fuel deformation and rupture simulation, PYTHONS code 7-56720
 PWR source term inventory and decay power, sensitivity to core management parameters 7-30630
 PWRs, neutronic aspects of different moderator-to-fuel volume ratios (*German*) 7-36185
 PYTHIA code for global burnup and flux calcs. in WWER-type reactors (*German*) 7-56714
 RBMK reactors, neutron physics considerations for fuel use efficiency improvements 7-30513
 RBMK-1000/LWR comparison, differences in fuel coolant and moderator, Chernobyl accident (*Dutch*) 7-10213
 reactor burnup and heavy nuclide nuclear data 7-30510
 reactor refuelling, conf., Newcastle-upon-Tyne, England (May 1985) 7-55891
 remote weighing of irradiated fuel pins at FFTF 7-49546
 research reactor fuel, in-storage criticality safety during manufacturing 7-730
 research reactors, computer codes for operational control 7-15232
 Rheinsberg Nuclear Power Plant, operating experience, expt. fuel assemblies (*German*) 7-15254
 rod bundle wall sub-channels, turbulence structure 7-61985
 rod steady state thermal behaviour, uncertainty analysis, probabilistic response surface method 7-729
 Sequoyah PWR, low leakage fuel management 7-30543
 simulated consolidated BWR fuel, thermal performance predictions using COBRA-SFS code 7-10229
 simulated LMFBR fuel pin, FCCI and I-assisted mass transfer 7-49537
 spent fuel, international safeguards, containment and surveillance 7-36112
 spent fuel casks, effects of high burnup 7-30551
 spent fuel criticality safety in large tanks 7-737
 spent fuel rods, accelerated high-temperature tests under dry storage conditions 7-36153
 spent fuel storage equipment, optimisation 7-30549
 sphere-pac fuels for LWRs and LMFBRs, analytical and expt. performance, review 7-36158
 SSYST-3 fuel rod behaviour analysis program (*Hungarian*) 7-56724
 storage systems, impact of high-burnup fuel cycles 7-30550
 time-dependent net core breeding gain of fusion-fissionsymbiotic systems 7-804
 TMI-2 boron dilution, criticality safety, operational considerations 7-753
 TMI-2 defueling criticality safety 7-754
 TMI-2 reactor cavity, fuel estimation from neutron dosimetry meas. 7-30717
 transient heat transfer and using FEA 7-19362
 TREAT transient overpower tests, behaviour of metallic U-fission fuel 7-36225
 utilisation time factor, power plant discrete mode of consumption 7-61963
 VVER reactors, neutron physics considerations for fuel use efficiency improvements 7-30513
 VVR-M5, thin-walled fuel elements 7-25031
 water reactor fuel performance code PROFESS, D-Com blind problem 7-721
 Westinghouse fifteen years of reactor refuelling experience 7-56749
 WWER fuel, burnup calc. verification, nuclide concs., expt. and theoretical data (*German*) 7-15245
 WWER fuel, power ramping performance using STOFFEL-1 code (*German*) 7-15246
 WWER fuel assemblies, fresh and irradiated, neutron spectrum estimation (*Russian*) 7-49550
 WWER-1000 fuel element performance, model computations. (*German*) 7-19355
 WWER-440, cold leg break LOCA, fuel rod thermomech. eval. under blowdown conditions (*Russian*) 7-49598
 WWER-440, increased burnup for optimum fuel utilisation (*German*) 7-15244
 WWER-70, experimental fuel assemblies 7-15255
 WWR-SM type fuel assemblies, γ -spectrometric burn-up study method 7-49552
 Zircaloy clad UO₂ fuel elements, fission product release, deposition behaviour 7-25149
 ZPPR fuel storage, borated concrete medium, criticality safety 7-746
²⁴²Cm(n,f), 0.1 eV-100 keV, fission cross section meas. for reactor appls. 7-42083
 Cs and I source terms of irradiated UO₂ reactor fuel 7-775
 Gd₂O₃ UO₂ nuclear fuel, interdiffusion coeff. study using autoradiographic technique 7-36157
 NpO_{2-x}, hypostoichiometric, O dissociation press., partial thermodynamic functions 7-17520
 Pb reflected UO₂ fuel pumps, criticality safety, expt. benchmark anal. 7-749
 (Pu, R)O₂, (R=Nd, Y), reactor fuels, thermal conductivity 7-19352
 (Pu,U)O₂ MOX fuel pins, ANSI standard criticality limits extension to heterogeneous systems 7-36156
 Pu soln. storage in 6 inch pipes, criticality safety 7-738
 Pu storage, criticality safety benchmarks 7-755
 Pu-containing fuel, models for estimation of spontaneous decay rate 7-15249
 Pu-fuelled high converter LWR test lattices, fuel enrichment effects on characteristics 7-19396
 Pu-O system, phase equilib., thermodynamics, 1400-1610 K 7-59496
²⁴¹Pu, A=23, 241, reactor parameters, uncertainties in scientific measurements 7-42085
²³⁹Pu, ²⁴⁰Pu and ²⁴²Pu, conc. determ. by isotope dilution-thermal ionisation mass spectrometry 7-10769
 T, post-irradiation recovery from Li₂O and LiAlO₂ ceramic breeder materials 7-49647
 (Th,U)O₂, irradiation induced dimensional changes 7-5331
 Th fuel resources and reprocessing for HTGRs (*Japanese*) 7-5329
 ThO₂-UO₂, polycryst., lattice and grain boundary diffusion 7-58519
²³²Th, space-dependent fast neutron spectra, eigenvalue and eigenfunction study 7-30532
 (U,Gd)O₂ solid solns., O/M ratio, gravimetry meas. 7-30560
 (U, R)O₂, (R=Nd, Sm, Eu, Gd, Y), reactor fuels, thermal conductivity 7-19352
 U accountancy in atomic vapour laser isotope separation 7-30520
 U based intermetallic compounds, fission gas swelling, cryst. struct. stability 7-42115

fission reactor fuel continued

- U, chemistry, laser appl. 7-19365
- U, enriched, storage in steel tubes in concrete, criticality safety 7-748
- U-H₂O lattice assemblies, temp. effect of reactivity, subcriticality meas. methods 7-30591
- UC, fission gas bubble destruction by radiation re-solution 7-42114
- UC, molten, pouring in Na, interactions and debris 7-36107
- U_{0.86}Gd_{0.14}O_{2+x} pellets, reaction with Cs fission product, annealing, diametral expansion 7-56756
- UO₂ and FISSION behaviour in Na vapour at temps. up to 2850°C 7-25041
- UO₂, electron emission studies using laser and conventional heating techniques 7-7810
- UO₂, fission gas bubble destruction by radiation re-solution 7-42114
- UO₂ fuel, irradiat., fission products chemical state 7-724
- UO₂ fuel improved burnup stability, microstruct. effects (German) 7-19357
- UO₂, heat capacity, enthalpy, critical review 7-16787
- UO₂, irradiated fuel, ¹³⁷Cs and ¹²⁹I leaching, rel. with fuel element power 7-786
- UO₂, molten, pouring in Na, interactions and debris 7-36107
- UO₂ operating fuel elements, short-lived fission product release under oxidising conditions 7-785
- UO₂, oxidation by high pressure steam, H₂ source in reactor accidents 7-25143
- UO₂, PWR power plants, load following operation, PCI failure criterion 7-25145
- UO₂, parametric studies in groundwater 7-25253
- UO₂ pins in boron-steel CAGR skip, criticality safety for long term storage 7-744
- UO₂ trace irradiated pellets, volatile fission product release 7-788
- UO₂, U₄O₉, U₃O₈, U₃O₇, charactn. by micro-Raman spectroscopy 7-59203
- UO₂-Gd₂O₃, solid solution, lattice parameters, O/U thermal conductivity meas. 7-21180
- UO₂-Gd₂O₃ fuel pellets, thermal expansion meas. at 293-1973K 7-49538
- UO₂-Na fuel-coolant interaction, thermodynamic bounds, LMFBR appl. 7-42138
- UO₂-PuO₂ solid soln. form. simulation 7-3289
- UO₂²⁺-humate interactions in soft, acid, humate-rich waters 7-13939
- UO_{2+x} pellets, reaction with Cs fission product, annealing, diametral expansion 7-56756
- UO_{2+x}, stoichiometry, thermodynamic analysis of point defects, 600-1400°C 7-16550
- (U_{0.3}Pu_{0.7})C, hyperstoichiometric, hot hardness, 293-1573K 7-59608
- (UPu)O₂, (R=Nd, Eu), reactor fuels, thermal conductivity 7-19352
- U₃Si, U₃Si₂ powders dispersed in Al matrix; heat of reaction, DTA 7-719
- AU, A=233, 235, reactor parameters, uncertainties in scientific measurements 7-42085
- ²³²U and ²³⁶U effects on U recycling in BWRs, simultaneous eval. using TGBLA 7-36155
- ²³³U fuel for naval and space reactors produced in a fusion reactor blanket 7-61964
- ²³⁵U, aqueous critical assemblies, Monte Carlo anal. with ENDF/B-V data 7-30476
- ²³⁵U fuel units, criticality safety in underwater rack storage 7-741
- ²³⁵U(n,f), delayed neutron activity, few-group anal. 7-42084
- ²³⁵U(n,f), international fission foil mass intercomparison, α -decay rates 7-42086

fission reactor fuel claddings

- artificially perforated Zr barrier fuel rods, fission product release in test loop 7-783
- breached spent-fuel rods, behaviour in flowing air atmosphere between 250 and 360°C 7-30534
- BWR fuel rod, pellet-cladding interaction, rod failure, fission product release (Japanese) 7-15242
- Calder Hall fuel elements, 30 years of metallurgical experience 7-56758
- decladding, bundle shear cold test 7-30554
- eddy current impedance methods for thickness meas. 7-33904
- ferritic alloy claddings for LMFBR mixed oxide fuel pins 7-30562
- fuel/cladding chemical interaction correlation for mixed-oxide fuel pins 7-30557
- HTGR, fines behaviour and recycling during fluidised bed operation 7-19363
- LMFBR, 316SS fuel cladding tube, stress-loaded corrosion tests in I₂ or Te (Japanese) 7-61958
- LWR load-following operation, fuel performance aspects, pellet-clad interactions 7-5350
- pellet-cladding gap, axial fission gas transport in power ramping expts. 7-15284
- pellet-cladding interaction, bamboo ridge deformation, FEMAXI-III code anal. 7-36108
- pellet/cladding interaction, effects of fuel design and burnup, in-core diameter meas. 7-19361
- PWR failed fuel rod, pellet-cladding interaction, in-pile eddy current test 7-19354
- PWR fuel cladding, plastic deformation behaviour for Zircaloy and Zr-Nb, EPSI-MOD2 code (German) 7-19339
- PWR fuel element, activation of end section using WIMS-E program (German) 7-56752
- PWR fuel rods, power ramp data, FROST and THERMOST codes, cladding deform. rod elongation 7-62034
- repair using CO₂ laser welding (Japanese) 7-15243
- SASCHA programme on fission product release under reactor core melting conditions, review 7-774
- simulated LMFBR fuel pin, FCCI and I-assisted mass transfer 7-49537
- spent fuel rods, accelerated high-temperature tests under dry storage conditions 7-36153
- stainless steel, dynamic reliability model for damage accumulation processes 7-30535
- steel, austenitic stainless, LWR cladding, oxidation in high temp. steam, LOCA appl. 7-727
- steel, stainless, clad fuel rod, failure behaviour 7-61965
- steel, stainless, corrosion in Na loop system, downstream effects 7-3504
- steel, stainless, nuclear fuel pin cladding, C distrib., SIMS study 7-19360
- Zircaloy, mech. eqns. of state of material irradiat. at 573K in deform. in working direction 7-8064
- Zircaloy, claddings, creep deform., bulge growth, time to failure 7-59589

fission reactor fuel claddings continued

- Zircaloy, corrosion resistance, precipitation of second phase particles effect 7-30564
- Zircaloy, PWR power plants, load following operation, PCI failure criterion 7-25145
- Zircaloy clad UO₂ fuel elements, fission product release, deposition behaviour 7-25149
- Zircaloy cladding, oxidation in air, 350-500°C 7-725
- Zircaloy oxidation and embrittlement criteria for emergency core cooling system acceptance, safety margins 7-36154
- Zircaloy-2, exposure to high temp. OWL-1 loop water, corrosion layer characterization 7-8167
- Zircaloy-2, irradiat. growth under temp. cycling, solute-interstitial complex mechanism 7-44607
- Zircaloy-2, low cycle corrosion fatigue in I₂ atmosphere 7-17705
- Zircaloy-2, nodular corrosion behaviour 7-8168
- Zircaloy-4, α -phase, burst data, CANSWEL-2 code anal. 7-36159
- Zircaloy-4, high temperature corrosion in flowing steam 7-28204
- Zircaloy-4, oxidation under limited steam supply from 1000-1400°C, LWR accident anal. 7-53968
- Zircaloy-4 fuel sheaths, failure model, circumferential temp. effect 7-728
- Zircaloy-4 PWR fuel cladding, deformation, embrittlement and oxidation during LOCA 7-25036
- AINiFe_{0.5}, corrosion resistance, rupture strength, neutron irradiation effects testing 7-59670
- AlSi₃Ni, corrosion resistance, rupture strength, neutron irradiation effects testing 7-59670
- Zr barrier fuel, operating experience 7-30563
- ZrNbI, fuel cladding, radiation induced embrittlement (German) 7-19359
- ZrO₂ fuel claddings, SEFDAN code for severe core damage accidents 7-49503

fission reactor fuel preparation and reprocessing

- see also isotope separation; radioactive waste
- accelerator breeder reactor, vortex flow target system, temp. distrib. for proton irradiation 7-19526
- actinide equilibrium constns. in soln. using analytical ultracentrifuge 7-25255
- actinide extraction using N-N'-di-alkyl aliphatic amides 7-25061
- actinide recovery using multi-purpose unit 7-25042
- advanced NDA workstation for integrated safeguards 7-36132
- AGR spent fuel handling in long term dry store 7-56869
- air cooled dry store performance for irradiated fuel 7-56867
- alkoxide-derived sol-gel coatings 7-30588
- Argonne Bulk Calorimeter, Pu assay, safeguards tool 7-36167
- AUC thermal decomposition by nonisothermal method, kinetics 7-25076
- authentication method for safeguards instruments securing data transmission 7-36136
- back-end of fuel cycle, reprocessing and intermediate radwaste storage (German) 7-25240
- BWR fuel, criticality safety anal., burnable poisons effects 7-740
- BWR spent fuel, heat generation rate, meas. and ORIGEN2 code anal. 7-812
- CAGR dismantled fuel, criticality safety, BNFL storage 7-739
- CANDU reactors, economic threats from reduced cost enrichment processes 7-10306
- CASMO-2 spent-fuel-rack criticality analysis 7-36176
- Castor V/21 PWR spent fuel storage cask, testing and analyses 7-56864
- China, R&D in fuel cycle 7-19374
- close-fitting shield doors with sculptured edges for nuclear fuel reprocessing plant 7-49739
- computer-assisted instruction for nuclear criticality safety 7-35186
- conference, nuclear and radiochemistry, Beijing, China (Sept. 1986) 7-18494
- criticality accident detection at nuclear reprocessing plants, CEA developments 7-36174
- criticality excursions in fissile solutions using CRITEX program 7-19373
- criticality safety, US/Japan data development program plan 7-752
- criticality safety in fissile material storage, conf., Jackson, WY, USA, (Sept. 1985) 7-13
- criticality safety in low enriched U storage arrays in commercial plant 7-732
- criticality safety of Hanford fuel storage facilities 7-742
- density meter algorithm and system for estimating sampling/mixing uncertainty 7-30528
- density meters for sample validation at Savannah River Plant 7-30527
- dissolver off-gas treatment, use of mineral zeolite as nitrogen oxides adsorbent 7-30575
- distribution ratios for U and P cons in TBP, paraffin and nitric acid 7-25046
- dry storage to provide flexibility in spent fuel and vitrified waste management 7-10291
- dye laser pumping by Cu vapour laser for U isotope separation 7-50553
- error propagation as a tool for evaluating process performance 7-30524
- extended fuel burnup, criticality safety implications 7-733
- extraction of actinides in PUREX process, ultracentrifuge anal. 7-25050
- fabrication and reprocessing at fuel, research and develop. (French, English) 7-19372
- facility model for the Los Alamos Plutonium Facility 7-30572
- FAID/SPAR fuel integrity seal tests 7-36138
- fast-fission tokamak breeder reactors 7-62067
- FBR reprocessing plant using remote maintenance, Japanese design 7-61977
- ferritic spent fuel casks, predrop test anal., stresses and fracture toughness 7-46651
- fissile material, critical soln., heating-up, nucleation and boiling 7-19368
- fissile material storage, criticality safety, efficiency improvements 7-747
- fissile solution storage criticality safety, Poisoned Tube Tank 7-735
- fluorinel nuclear fuel dissolution process, soluble B for criticality control, calc. validation 7-36172
- French nuclear fuel manufacturing, criticality safety 7-731
- FRG nuclear fuel reprocessing plant, remote maintenance aspects, manufacturer's viewpoint 7-49559
- fuel assembly identification in French reprocessing plants 7-36169
- fuel fabrication facilities, criticality safety training among NRC licensees 7-35184
- fuel facilities, criticality safety, performance based training and education 7-35183
- Fuel Processing Facility, Idaho, design and construction status 7-30580
- FUTURE code for fuel cycle variables calc. 7-30480

fission reactor fuel preparation and reprocessing continued

geochemistry of uranium and daughters in tailings from the milling of uranium ores 7-25256
German nuclear fuel cycle, overview 7-49544
glove boxes and enclosures, computer-aided design 7-30578
Hanford PUREX facility, input Pu accountability meas. 7-36165
Hefei Tokamak Hybrid Reactor, physics conceptual design 7-25238
high burnup LWR and FBR fuel reprocessing, solvent development 7-19381
high density spent-fuel storage racks, neutron absorbing materials performance 7-19543
HLW, high SO_4^{2-} content, glass formulation for vitrification 7-25091
HMBA, eluent for cation-exchange chromatographic separation of Am and Cm 7-25083
holdup materials accounting and control problems 7-36125
hydrocyclone and centrifuge as emulsion separators in the $\text{HNO}_3\text{-H}_2\text{O-TBP}$ -Mepasine system 7-36171
ion beam transport enrichment process, review 7-55920
irradiated fast breeder fuel, transportation preparation 7-56872
irradiated fuel, dry storage at reactor site 7-56866
JAERI criticality safety facilities and expts. 7-734
JAERI Dept. of Chem. Jan. 1984-Dec. 1985 progress report 7-10233
joint motion clusters in servomanipulator operations 7-36177
knowledge-based system for estimating physical inventories in MBA's involving complex chemical processes 7-36124
laboratory assays for Pu and U for Savannah River purification and finishing 7-30519
lanthanide chelate formation constant sequence for separation in cation exchange solutions 7-25080
large scale enriched uranium soln. handling, criticality safety 7-736
large-scale reprocessing plant, near real-time material accountancy, computer simulation 7-25044
laser cutting system for fuel disassembly 7-10235
liquid radwaste, particle size reduction using indirect fired rotary kiln 7-10294
LMFBR operational and fuel cycle experience worldwide (German) 7-5342
Load-Cell-Based Weighing System for weighing 9.1- and 12.7-tonne UF_6 cylinders 7-36120
low Enriched Uranium Fabrication Plant, physical inventory verification 7-36118
LWR, generalised transient fuel-cycle model convergence 7-5327
Manipulator Comparative Testing Program for nuclear fuel reprocessing appls. 7-49556
methodology for NDA performance assessment 7-30530
MINISTAR Surveillance System, Cobra Optical Fibre Seal System, EURATOM full experience 7-36127
mobile nondestructive assay and examination instruments 7-36283
modeling response variation for radiometric calorimeters 7-30573
monitor for characterization of leached hulls and dissolver sludges 7-36163
MOX fuel, co-conversion process, commercial plant design 7-61976
multi-camera multiplexed CCTV system for safeguards surveillance 7-36128
neutron induced fission rate meas. at high fluence and temp. by SSNTD 7-42081
NFCIS, IAEA's directory of nuclear fuel cycle facilities 7-62101
noble gas retention in German reprocessing plant (German) 7-56768
noble metal recovery from fuel reprocessing wastes 7-19383
nuclear criticality safety training, interactive computer-based simulator 7-35188
nuclear energy system model with requirements for elec. and thermal energy 7-65418
nuclear fuel plant, use of portable counter for in-plant fuel inventory verification 7-30587
nuclear fuel plants, holdup measurement 7-30583
nuclear fuel plants, statistical sampling for holdup measurement 7-30584
nuclear fuel plants, uranium holdup in concrete floors, comparison of non-destructive methods 7-30586
nuclear fuel reprocessing, fluid flow meas., microcomputer-based multi-channel polarity cross-correlator 7-42121
nuclear fuel systems having a free surface, reactivity effects from surface waves 7-30571
nuclear industry commitments to criticality safety performance based training 7-35185
Nuclear Track Filters, development for liquid phases and gases 7-25098
Ontario Hydro CANDU fuel handling and storage facilities 7-56747
organic acid ion exchange and spectrophotometric techniques, stability constant determ. for Am, Ce and Cm 7-25093
Portsmouth Gaseous Diffusion Plant, process holdup material characterisation 7-36161
preventive safety at nuclear facilities, criticality accident prevention 7-36175
Process Facility Modification Project for PUREX plant 7-30582
process monitoring concepts for safeguards and demonstrations at an Oak Ridge National Laboratory Test Facility 7-30522
program plan for the Modular Integrated Video System 7-36129
proton window for a spallation breeder with 300 MW beam power 7-19527
PUMA model for conc. profiles in the Purex process 7-36170
Purex and Thorex processes, crud formation 7-30576
PUREX process, improvements 7-19380
Purex process, product refining concept using crystallisation 7-36160
PUREX process, ranges of chemical parameters 7-19376
PUREX process behaviour of hydrazoic acid 7-25062
Purex process in pulsed sieve plate column, solvent extraction calc. model, PULCO code 7-49554
PWR fuel in spent fuel storage racks, criticality safety, Generic Reactivity Equivalence 7-743
radioactive solution level gauging, meas. system resolving power, γ -detection 7-24741
reactor refuelling, conf., Newcastle-upon-Tyne, England (May 1985) 7-35891
reinforced concrete pads for spent nuclear fuel casks, hardness effects on design 7-49700
remote handling in hot cells, state of the art and future view 7-49555
remote handling systems for reprocessing plant maintenance and reactor dismantling, testing and design 7-49614
remote maintenance using servomanipulator based system 7-5338
remote vacuum cleaner for PUREX cells 7-49557
reprocessed LWR fuel, α -waste assay 7-36164

fission reactor fuel preparation and reprocessing continued

reprocessing input analytical meas., NDA technology demonstration 7-36166
reprocessing plants near-real-time material accounting 7-36119
research reactor fuel, in-storage criticality safety during manufacturing 7-730
retention of radionuclides in halite and anhydrite 7-36270
safeguards data acquisition system for reprocessing facility process monitoring 7-36162
safeguards sealing system for multi-element fuel casks 7-36139
Sellafield nuclear reprocessing plant, computer-based training for criticality safety 7-35187
simulated spent fuel, dissolution behaviour in 3M HNO_3 7-25065
SNM soln. standards, preparation techniques 7-30529
sol-gel process for ceramic fuel, colloid chemistry 7-5340
spent fuel, international safeguards, containment and surveillance 7-36112
spent fuel criticality safety in large tanks 7-737
spent fuel shipping casks, surface dose to determine fuel loading pattern (Japanese) 7-25242
spent fuel transportation, safety criteria and accident anal. 7-42241
spent nuclear fuel, reprocessing and direct disposal, radiological comparison (German) 7-49683
spent nuclear fuel assemblies, nondestructive burnup meas. at reprocessing plant (Japanese) 7-17753
sphere-pac fuels for LWRs and LMFBRS, analytical and expt. performance, review 7-36158
steel, stainless, corrosion by Pu in PUREX reprocessing environment 7-25096
storage tank holdup measurements to reduce ion exchange process inventory differences 7-36123
strong base resins for U recovery, standard test methods 7-25045
systems engineering applications 7-30577
TBP hydrolytic and radiolytic degradation in dodecane/ $\text{H}_2\text{O-HNO}_3\text{-UO}_2(\text{NO}_3)_2$ systems 7-19382
thermal diffusion column for isotope separation, cut and feed rate effects on circulating flow 7-50393
tri-n-butylphosphate, radiolytic decomposition kinetics 7-39856
TRU waste, assay for (α ,n) sources 7-36282
TRU process for liquid TRU waste management and disposal 7-19379
TURF Californium Facility at ORNL 7-30581
U, elution from DB18C6-formaldehyde condensation polymer, adsorption behaviour 7-25077
ultracentrifuge enrichment plants, flow induced vibrations in gas tube assembly 7-30570
US arc seal signatures from NPD fuel bay demonstration 7-36140
user-friendly Interactive Control Module for safeguards equipment 7-36130
VAK III sealing system for LWR fuel assemblies 7-36137
ventilation duct in reprocessing plant shield, neutron streaming, numerical comparisons 7-19555
WAK reprocessing plant, in-service testing of techniques and components (German) 7-61973
ZPPR fuel storage, borated concrete medium, criticality safety 7-746
Am III extraction in presence of lanthanides 7-19385
Am, in Arctic waters, North Sea, Scottish and Irish coastal zones 7-13937
Am removal from HLW by TRPO extraction 7-25048
²⁴¹Am, processing chemistry 7-19375
⁶⁰Co, processing, flask positioner location sensing system 7-61978
¹³⁷Cs, immobilization using hydrous TiO_2 and zeolite 7-10295
Cu vapour laser for U isotope separation 7-50546
³H, chemistry in fission and fusion reactors 7-25234
³H inventory differences, sampling, U-getter pump holdup 7-36121
³H inventory differences, molecular sieve holdup 7-36122
⁹⁹Mo and U separation in H_2SO_4 medium by D2EHPA in kerosene, solvent extraction study 7-25043
Nb extraction from HNO_3 , Mo conc. effect 7-25064
Np (V,VI) electrolytic oxidation-reduction in HNO_3 7-25073
Np, valence state adjustment using laser photochem. in nucl. fuel reprocessing (Japanese) 7-61971
Np-Am removal from HLW, ALAS process 7-19377
²³⁷Np, nuclear fuel cycle chemistry 7-19384
(Pu,U) O_2 MOX fuel pins, ANSI standard criticality limits extension to heterogeneous systems 7-36156
Pu (IV) nitrate, third phase formation in extraction with TBP 7-25074
Pu combustibles processing at Cadarache (French) 7-19369
Pu, in Arctic waters, North Sea, Scottish and Irish coastal zones 7-13937
Pu isotopic γ -ray system measurement control program 7-30531
Pu processing facility, holdup measurements 7-30585
Pu pyrochemical research at Los Alamos 7-25047
Pu role in degradation of TBP in PUREX process 7-25066
Pu soln. storage in 6 inch pipes, criticality safety 7-738
Pu storage, criticality safety benchmarks 7-755
Pu traces in U after reprocessing, isotopic comp. 7-25095
Pu(III) oxalate precipitation 7-25060
Pu(III)- $\text{Fe}^{2+}\text{-N}_2\text{H}_5^+\text{-HNO}_3$, aqueous soln. photochemical reaction 7-25063
Pu(IV) extraction by neutral phosphorous based organic compounds 7-25052
Pu(NO_3) $_2\cdot 2\text{H}_2\text{O}$, Pu mass transfer rate coefficients 7-56770
PuO $_2$, reduction solvent salts, regeneration and recycle 7-25082
RuNO complexes, extraction behaviour with γ -irradiated TBP-kerosene 7-25072
RuNO(NO_3) $_3$, photodissociation in nitric acid soln. 7-25057
Sr, fixation on antimonite and phosphoantimonite acids 7-25089
⁹⁰Sr, immobilization using hydrous TiO_2 and zeolite 7-10295
⁹⁰Sr, removal from acidic nuclear waste solns. 7-25051
⁹⁰Sr retention mechanisms in synthetic ion-exchange resins 7-36269
T handling at CRNL, glove boxes, pumping systems 7-5339
Tc conc. in spent fuel soln., determ. by X-ray fluorescence 7-5337
Tc role in irradiated fuel technology, oxidation-reduction process 7-5336
Tc, nuclear fuel cycle chemistry 7-19384
⁹⁹TcO $_2$ microspheres with 0-35% U, prod. using sol-gel process in CCl_4 7-30569
Th fuel resources and reprocessing for HTGRs (Japanese) 7-5329
Th once-through fuel cycle for CANDU reactors, feasibility anal. 7-19371
Th(IV) stability consts. of complexes with α -amino-acids 7-25049

fission reactor fuel preparation and reprocessing continued

- Th₃N₄ and ThN, prep. and oxidation behaviour 7-22600
 Th(NO₃)₃, synergistic extraction by mixture of DMHMP+HTTA in benzene 7-25086
 Th(NO₃)₃, synergistic extraction mechanism for DMHMP and HEHEHP 7-25088
 Th(NO₃)₃-HNO₃-H₂O system, diffusion coeff., partition coeff., extraction kinetics 7-25097
 ThO₂-UO₃ sol preparation for gelation into microspheres in CCl₄-NH₃ media 7-19370
 U accountancy in atomic vapour laser isotope separation 7-30520
 U adsorption in amidoxime-polyacrylonitrile ion-exchange fibre 7-25069
 U control and accountability at Savannah River Plant 7-30526
 U, enriched, storage in steel tubes in concrete, criticality safety 7-748
 U enrichment, theoretical and expt. basis 7-19378
 U enrichment in gas centrifuge piping, NDA meas. 7-36168
 U enrichment using atomic vapour laser isotope separation 7-19367
 U, extraction from sea-water with titanate gel 7-25085
 U isotope chromatographic chemical separation, fission criticality 7-25059
 U laser isotope separation in the UK, development and policy implications 7-49553
 U, reaction rate with water vapour, 30-80 °C 7-42119
 U synergistic extraction by chelate-chelate-neutral extractant 7-25056
 U synergistic extraction with D2EHFA-TRPO-TBP mixed extractant 7-25070
 U/Pu assay in reprocessing input solns. using isotope dilution mass spectrometry 7-30574
 U-Th-Sn, liq. N-nitride equilb. 7-46417
 UF₄, fluorination kinetics, catalysts and impurities effect 7-42120
 U(III) stability and absorption spectra in HCl 7-25055
 U(IV) preparation by photochemical process, TBP degradation products 7-25075
 UO₂ extraction, ligand exchange and the synergistic effect 7-25092
 UO₂ extraction, synergistic effects in β -diketone/ligand 7-25094
 UO₂ fuel, phase behaviour of solid fission products 7-25090
 UO₂, lixiviation, effect of long term contact with groundwater 7-25079
 UO₂, oxidative dissolution, thermodynamic approach, CANDU spent-fuel disposal appl. 7-49688
 UO₂, oxidative sintering, microstruct. 7-3239
 UO₂ pins in boron-steel CAGR skip, criticality safety for long term storage 7-744
 UO₂²⁺ ion fluorometry in nitric acid soln. 7-61974
 UO₂²⁺-humate interactions in soft, acid, humate-rich waters 7-13939
 UO₂²⁺+2RH=R₂UO₂+2H⁺, ion exchange equilibria and kinetics 7-25071
 U₂O₃ powder, prep. by cation exchange resin calcination 7-762
 UO₂Cl₂-KCl-NaCl-NiCl₂, fusibility, differential thermal anal. study 7-61972
 UO₂(ClO₄)₂, synergistic extraction by TTA-PMBP-(C₆H₅)₄AsCl 7-25067
 UO₂Cl₂-2TBP, IR spectra, complex effect, isotope shift, extraction anal. 7-25058
 UO₂(NO₃)₂ solidification facility operation 7-30579
 UO₂(NO₃)₂ solution, criticality in slab geometry, benchmark expts. 7-36173
 UO₂(NO₃)₂, synergistic extraction by mixture of DMHMP+HTTA in benzene 7-25086
 UO₂(NO₃)₂, synergistic extraction by DMHMP, HDEHP, HEHEHP, HPMBP 7-25087
 UO₂(NO₃)₂-2TBP, uranium mass transfer rate coefficients 7-56769
 UO₂(SO₄)₂ solution, adsorption equilibrium study 7-25084
 U_{1-x}Pu_xC, mixed carbide fuel, thermodynamic props., effect of O and N impurities 7-58507
 U₃Si₂ fuel, production and characterisation of MTR fuel 7-25078
 U(VI), electro-reduction rates, component conc. depend. 7-25068
 U(VI) extraction by dicyclohexano-18-crown-6 isomer A 7-25053
 U(VI) extraction by neutral phosphorous based organic compounds 7-25052
 U(VI) extraction from phosphoric acid solns. with HDEHP and TOPO 7-25054
 U(VI) stability consts. of complexes with α -amino-acids 7-25049
²³²U and ²³⁶U effects on U recycling in BWRs, simultaneous eval. using TGBLA 7-36155
²³⁵U fuel units, criticality safety in underwater rack storage 7-741
²³⁵UO₂²⁺, ion exchange processes 7-25081

fission reactor instrumentation

- see also fission reactor core control and monitoring; fission reactor safety; fission research reactors; fission reactor instrumentation
 acoustic boiling noise in a sodium-water steam generator 7-36183
 BWR, heterogeneous model, detector field of view 7-36186
 BWR, heterogeneous model, neutron noise decomposition into local and global components 7-36187
 BWR fuel assemblies, pin-to-detector γ -ray transmission function by adjoint Monte Carlo methods (German) 7-61984
 BWR-4 Mark I containment, severe accident, survivability of electrical equipment 7-42180
 cable-type thermoelectric converters, pulsed method for thermal inertia estimates 7-30592
 colour graphics display system 7-25122
 digital upgrades for nuclear plant control and instrumentation 7-30597
 disturbance analysis using artificial intelligence, SAAP-2 system 7-19338
 emergency classification system at nuclear power plants, expert system application 7-15265
 error analysis in reactor-core neutron beam density measurements by gold-foil activation 7-36181
 flowmeter, EM, for liq. metal flow rate meas., error in correl. method 7-57954
 flux mapping, driving device for activated wire counting 7-30606
 horizontal annular flow measurements using pulsed photon activation and film thickness distribution modelling 7-5357
 LWR, in-core gamma effects, power distribs., detector response 7-42137
 LWR fuel failure detection using the grip slipping method 7-30544
 LWR pressure vessel mock-ups, fission rate meas. using SSNTD 7-42124
 LWR pressure vessel surveillance using solid state track recorder neutron dosimetry 7-36199
 LWR surveillance dosimetry anal., changing source distrib. effects 7-62098
 motor-operated valve, operability verification 7-42178

fission reactor instrumentation continued

- neutron flux mapping data collection system for reactor core monitoring, personal computer based 7-42128
 neutron monitor for reactor startup range, design parameters 7-42126
 noise diagnosis techniques for nuclear power station fault detection (German) 7-19403
 nuclear power stations, diagnostic subsystems in Czechoslovakia (Czech) 7-19386
 OSIRIS instrumentation for fusion reactor material irradiation tests; 7-49568
 Paks Unit 2, noise meas. using in-core self-powered neutron detector strings 7-62012
 PKZh-902 instrument for solid phase monitoring in organic reactor coolants 7-49560
 plant life extension, baseline characterization of electrical circuits 7-36096
 prompt self-powered neutron detectors, reactor noise anal., REND code calcs. 7-36193
 pulsed source experiments, use of ex-core epithermal detectors, kinetic distortion 7-56771
 PWR, instrument failure detection, nonlinear filtering appl. 7-25141
 PWR pressurizer, on-line instrument failure detection using improved likelihood ratio method and suboptimal control 7-25139
 random-walk boronimeter, experience in PWR plants 7-42129
 RAS III, modular noise diagnostics system for reactor primary circuit monitoring (German) 7-56787
 safety relief valve position indication systems 7-42179
 Santa Maria de Garona BWR, upgrade modifications to safety equipment 7-30625
 spectral method of flow-velocity measurement 7-36182
 thermoelectric temp. sensors., data anal. (Czech) 7-61991
 threshold-type neutron detector with hydrogen-containing scatterer 7-36180
 triaxial gamma chambers for axial neutron distribution inertialless monitoring 7-61979
 TRR power regulating system, digital controller 7-49575
 void fraction determination in liquid flow systems by radiation attenuation, dynamic bias 7-61986
 water-level monitor, ex-core, LOFT calculation comparisons 7-42127
²⁵²Cf(SF), noise equivalent source for freq. domain meas. 7-42135
 Xe-filled compensated ionisation chamber, transient anal. to quantify sensor degradation 7-42134

fission reactor materials

- see also fission reactor fuel; fission reactor fuel claddings; materials handling; moderators; radioactive waste
 advanced instrumented impact testing facility for characterization of dynamic fracture behavior 7-13692
 Alloy 600, steam generator material, properties and performance 7-30556
 alloy 600 nuclear steam generator tubes, local pitting conditions using Pourbaix diagrams 7-46716
 alloy 600 tubes, intergranular attack, cause evaluation 7-59685
 alloy 600 tubes, stress corrosion cracking in aggressive chemical environments 7-10230
 alloy 600 tubes in PWR steam generators, localised electrochem. corrosion 7-39760
 alloy 600 tubing in nuclear steam generators, intergranular attack, environmental effects eval. 7-39761
 Alloy 690, thermally treated nuclear steam generator tubes 7-5334
 ASME Boiler and Pressure Vessel Code, design developments 7-49506
 ASME Code Section XI US testing techniques assessment 7-56761
 bend pipes containing surface flaws, fatigue test results (Japanese) 7-56755
 BIBLIS-B reactor pressure vessel, fracture mech. anal. for thermal shock transients 7-10220
 BWR piping, fracture mech. research in Japan 7-53891
 BWR piping, use of Mechanical Stress Improvement Process to inhibit IGSCC 7-33836
 BWR piping research in Italy, IGSCC tests, fracture and cracks 7-53890
 BWR primary coolant system, radiochemical studies 7-25123
 BWR steel, CITROX decontamination solvent, corrosive effects 7-10232
 BWR top-guide structure, integrity eval., irradiation induced SCC 7-54012
 Calvert Cliffs Unit 1 tube examination 7-61970
 CANDU coolant pump seals, improved performance 7-36101
 CEGB single-phase erosion-corrosion research programme for AGR boilers 7-59679
 ceramic materials and technology survey 7-10215
 ceramics, props. meas., conf., Soverato, Italy (Sept. 1986) 7-9582
 components, asymptotic and reference stresses for design by anal. 7-49518
 components, design, construction and safety codes 7-49512
 components under complex loading, stress anal. incorporating fracture mech. and materials aspects 7-13584
 concrete, microplane model for progressive fracture, microcracking 7-15248
 concrete shield, heat-resistant, in nuclear reactor, capture γ -ray refl. and transmission 7-49532
 conference on the safety and reliability of reactor pressure components, Stuttgart, Germany, (Oct. 1985) 7-9583
 conference on water reactor safety, Gaithersburg, MD, USA, (Oct. 1985) 7-48152
 construction codes and engineering mechanics conf., Paris, France, Aug. 1985 7-48153
 coolant impurity anal., organic acids, organic carbon, anions 7-30566
 crack arrest specimen, dynamic anal. under reactor pressurised thermal shock conditions 7-13693
 DIORIT research reactor, activation product distrib. in shielding materials (German) 7-49536
 effective neutron absorption cross section determ. 7-56708
 EPRI, NDE Center, 1985 annual report 7-10226
 FACSIMILE code for void swelling calc. 7-25037
 fatigue precracked Charpy-type specimens, crack initiation testing, reactor piping appl. 7-13579
 FR2 research reactors, chemical and radiochemical meas. 7-25040
 graphite, reactor, thermal expansion, effect of rad. 7-26804
 graphite, siliconized, property variation during neutron irradiation 7-36105
 graphite isotropic, fine grained, oxidation effect on crack extension rate (Japanese) 7-56754

fission reactor materials continued

Hastelloy X, H₂ permeation in high temp. alloys, oxide layer effects (*German*) 7-30568
 heat exchanger tubes, cyclic temperature transient influence on creep behaviour 7-10186
 heavy water physical verification in power plants 7-30523
 high temperature reactor components, multiaxial loading tests 7-49541
 HTGR, adsorpt. removal of CO₂ from He coolant 7-30514
 HTR, reactor protection building anal. for He release (*German*) 7-30639
 HTR alloys, carburisation behaviour 7-10234
 hybrid reactor pebble bed blanket, magnetohydraulic flow in Na-K eutectic mixture 7-15366
 Incoley 800 H, permeability of ³H and H in heat exchanger tubes (*German*) 7-56759
 Inconel 617, H₂ permeation in high temp. alloys, oxide layer effects (*German*) 7-30568
 Inconel welds joining dissimilar metals, radiographic evaluation 7-39828
 JAERI Dept. of Chem. Jan. 1984-Dec. 1985 progress report 7-10233
 KEK Na coolant, radiochemical surveillance 7-25039
 liquid-metal-cooled nuclear reactors, applications of electrospray deposition coating technique 7-53978
 LMFBR, French creep-fatigue design rules 7-49522
 LMFBR class 1 components, design rules and elastic creep-fatigue damage evaluation 7-49540
 LMFBR components, RCC-MR code for design and construction 7-49511
 LMFBR high temp. components, UK research and design methods 7-49513
 LMFBR materials, buckling anal. and design rules 7-49517
 LWR, corrosion product release, radiation build-up effects 7-10225
 LWR, pressure vessel materials, environmental sensitive cracking (*German*) 7-10214
 LWR accident source term expts. deposition samples 7-62047
 LWR heavy section steel technology, crack arrest studies overview, reactor pressure vessels 7-53885
 LWR piping, flaw detection by US systems, digital techniques 7-46782
 metal housings for water-cooled power reactors, reliability improvement (*Russian*) 7-722
 metallic nuclear power plant components, German codes and standards 7-49508
 Millstone-2 PWR, wear and neutron activation of positioning pins, ⁶⁰Co buildup 7-15247
 Monju FBR, anal. and design for elevated temp. components 7-56717
 MPA thermoshock expt. anal. using TRAC PF 1 code, PTS in reactor ECC conditions 7-13588
 natural versus artificial aging of nuclear power plant components 7-56765
 neutral/oxygen water treatment 7-30537
 notched and precracked ISO-V specimens, loading rate effects on fracture resistance 7-13580
 NRC Degraded Piping Programme, LWR piping fracture research, Phase II progress 7-53889
 nuclear piping systems, research overview 7-49595
 nuclear plant irradiated steel handbook 7-38069
 online acoustic emission monitoring of cracks in nuclear systems, review 7-54066
 perforated plates, simplified creep anal. for steady creep conditions 7-28094
 piping, technical and economical incentives behind strain limitation 7-10221
 piping cracks, EPRI estimation formulas 7-56760
 piping criteria and construction costs 7-61953
 piping systems, cycle-dependent material props. 7-10222
 piping systems, strain limitation calcs. 7-10188
 power plant mechanical components, stress and strain limitation 7-10187
 pressure vessel, crack propag. under cyclic thermal loading, NDT results 7-10219
 pressure vessel, thermoplastic stress calcs. from stress-relief up to thermal shock 7-10216
 pressure vessel and piping design, stress indices for nonradial branch connections 7-49520
 pressure vessels, fracture mechanics of cracks under cyclic thermal shock 7-10218
 pressure vessels, thermal mixing and wall loads for emergency core cooling expts. 7-10217
 pump casings, sizing rules for pressure design 7-49519
 purification resins in reactor circuits as source for organic tritium, expts. on algae 7-49545
 PWR, improved water chemistry controls for minimizing degradation of materials 7-30615
 PWR, reactivity control of first cycle using Gd burnable poison system 7-56773
 PWR boiler pipework, effect of feedwater conditioning on corrosion (*German*) 7-25115
 PWR circulation piping, water chemistry and radiation field buildup 7-15251
 PWR condenser improvements for corrosion impurity protection 7-15250
 PWR feedwater, Cu oxides, acid chlorides, steam generator denting 7-5333
 PWR pressure vessels, fast neutron fluxes using Monte Carlo methods 7-36097
 PWR steam generator sludge piles, chemical cleaning 7-10227
 PWR steam turbine secondary side SCC, remedial actions 7-61969
 PWRs, seawater cooled steam generators, tube support corrosion, chlorides effects 7-46715
 radiation effects on lubricants 7-10224
 RBMK-1000/LWR comparison, differences in fuel coolant and moderator, Chernobyl accident (*Dutch*) 7-10213
 RCC-M code for design and development of PWR components 7-49507
 reactor components, dynamic reliability model for damage accumulation processes 7-30535
 SNR-300 LMFBR, design, erection and testing of steel containment 7-25024
 steam generator materials, properties and performance 7-30556
 steam generator pitting, electrochemical effects on Ni-base alloys 7-10228
 steel, alloy, crack arrest toughness, moment modified compact tension specimen, PTS conditions 7-13695
 steel, austenitic stainless, BWR pipe welds, toughness and tensile props. 7-46650

fission reactor materials continued

steel, austenitic stainless, cold-worked, irradi. and unirradi., liq. Cs, Te-induced fatigue embrittlement 7-46637
 steel, austenitic stainless, corrosion product release in lithiated high temp. water, mechanism and kinetics 7-65172
 steel, austenitic stainless, creep rupture properties of heavy section Type 304 forgings for LMFBRs 7-13582
 steel, austenitic stainless, fatigue crack growth in FBR castings and weldments, fast neutron irradiation effects 7-28127
 steel, austenitic stainless, FBR material, crack propag. under creep-fatigue interaction condition 7-22837
 steel, austenitic stainless, intergranular SCC resist., influence of Si 7-46681
 steel, austenitic stainless, LWR piping, ASME code for flaw eval. 7-13601
 steel, austenitic stainless, Mo-ion plated, corrosion resist. in flowing Na environment 7-59667
 steel, austenitic stainless, nuclear grade, SCC in simulated BWR environments 7-46682
 steel, austenitic stainless, pipe weldments, toughness at LWR operating temps. 7-13599
 steel, austenitic stainless, sensitised, SCC, re-anal. of results from constant extension rate tests 7-39723
 steel, austenitic stainless, Ti modified, void swelling and precipitation, aging effects 7-33685
 steel, C, LWR piping, flaw evaluation 7-46652
 steel, carbon and stainless, pipe fracture safety analysis using limit load and J-integral techniques 7-13585
 steel, Cr-Mo, elevated temp. strength, H attack resistivity and stress relief cracking suscept. improvements 7-13583
 steel, ferritic, reactor material, neutron irradi., positron annihilation studies 7-46215
 steel, ferritic, yielding and fracture in transition region of quasistatic to dynamic loading 7-13581
 steel, heavy section, Ni-Mo, elastodynamic fracture analysis of large crack-arrest experiments 7-53887
 steel, interface oxide growth in Magnox and AGR plant, assessment methods 7-59678
 steel, low alloy, oxides on fracture surfaces, failure anal. examination 7-13586
 steel, low alloy ferritic, strain induced corrosion cracking prevention for BWR piping 7-13641
 steel, mild, erosion-corrosion control using O₂-NH₄-hydrazine dosed feed-water in reactor boilers 7-59675
 steel, mild and austenitic stainless, on-site oxidation monitoring in AGRs 7-59677
 steel, Mn-Mo-V, reactor piping material, strength, deformation and fracture behaviour 7-13578
 steel, Ni-Cr-Mo, pressure vessel, environmentally assisted fatigue crack growth 7-17638
 steel, Ni-Mo, LWR pressure vessel cladding, irradiation effects and flow structures 7-53888
 steel, Ni-Mo, wide plate crack arrest testing using acoustic emission, reactor pressure vessel appl. 7-53886
 steel, nuclear pressure vessel, dynamic fracture toughness, crack tip strain behaviour, EM force appl. 7-28126
 steel, pressure vessel, fatigue crack growth rates under various conditions of loading and environment 7-28203
 steel, pressure vessel, neutron irradi. effect on mechanical and physical props. (*German*) 7-19358
 steel, pressure vessel with surface fatigue cracks, leak-before-break failures analysis 7-65141
 steel, radiation embrittlement effects of P and Cu impurities 7-49535
 steel, simulated void-box-capsule charpy impact test results, neutron irradi. effects 7-10231
 steel, stainless, crack growth in BWR piping, meas. techniques 7-39839
 steel, stainless, ferritic, irradi., grain boundary segregation, STEM microanalysis 7-22701
 steel, stainless, ferritic-martensitic, high-Cr, fast reactor irradi., phosphide phases 7-22700
 steel, stainless, heavy section, fracture studies, welds, neutron irradiation, crack arrest 7-13587
 steel, stainless, LWR piping systems, LBB feasibility eval., fracture criteria 7-61968
 steel, stainless, oxide growth mechanisms and corrosion rate for types 405 and 409 7-13649
 steel, stainless, pressure vessel, stress relief cracking, reactor safety 7-8117
 steel, stainless, reactor pipe integrity prediction using R6 procedures 7-49542
 steel, stainless, repair welds, neutron irradiation embrittlement 7-5328
 steel, stainless, Type 304 IGSCC, BWR plant life extension, materials aspects 7-53995
 steel, stainless, type 316L, fatigue in simulated fast reactor environments 7-39759
 steel, X8CrNiTi18.10, corrosion product layers in PWRs at pH 7 (*German*) 7-19356
 steel component surface treatment, detonation-deposition method (*Russian*) 7-39736
 steel LWR piping fracture mechanics database 7-53892
 steel nuclear containment building, buckling, expt. and anal. programme 7-53818
 steel pressure vessel, thermal transient, crack arrest in K-gradient 7-46617
 steels, alloy, crack arrest toughness, proposed ASTM test method, European experience 7-13694
 steels, oxidation performance of Magnox and AGR boiler materials in high press. CO₂ 7-59676
 steels and weld metals for LWR press. vessels, brittle failure resist. 7-59636
 strain estimation for external event loads 7-10189
 stress corrosion cracking test of expanded steam generator tubes 7-56764
 Surry steam generator, examination and eval., nondestructive testing 7-54065
 temporary reverse osmosis makeup water systems 7-36205
 thermal shock loadings in PTS accidents, J-integral concept appl. 7-13696
 tubesheet sample removal from Point Beech 1 steam generator 7-56763
 turbine rotor and disk stress corrosion cracking characteristics 7-33849
 vessel meth through by molten core materials, time calcs. (*Czech*) 7-62025

fission reactor materials continued

- vitrified colemanite and impregnated polymer, nuclear shielding materials 7-726
 VK-50 BWR, coolant radiolysis study 7-30515
 water cooled reactors, steam generator tube performance during 1983 and 1984 7-25118
 Zircaloy, corrosion resistance, precipitation of second phase particles effect 7-30564
 Zircaloy tube sample eddy current testing 7-56762
 Zircaloy-2, irradiation growth under temp. cycling, solute-interstitial complex mechanism 7-44607
 AlMgSc first wall materials, sputtering and radiation induced segregation 7-38072
 Al₂O₃, molten, pouring in Na, interactions and debris 7-36107
 C steel, environmental fatigue stress rules appl. to reactor piping 7-13600
 Cd plates, reactivity worth in MTR-fuel-type reactor 7-56772
 Cr-Mo ferritic steel, rust chemical reduction 7-30565
 CuZr metallic glass, blistering under He implantation, EELS anal. 7-16593
 Fe-based, Co-free alloys for valve hard facings in nuclear plants, 1985 progress 7-49551
 Fe-Ni-Cr, reactor bolting material A-286, failure analysis 7-30536
⁵⁴Fe(n,X), few MeV range, total, scatt., and γ -prod. cross sections, reactor appl. 7-41993
⁵⁶Fe(n, γ), capture in 1.15 keV resonance using Moxon-Rae detectors, reactor appl. 7-36004
 He corrosion effect on high temp alloy (*German*) 7-30567
 LiAlO₂ spheres, T release, time depend., diffusion coeff. 7-49643
 Li₂O spheres, T release, time depend., diffusion coeff. 7-49643
 NO₂ coolant, for loop flow reactor, radiation and thermal stability (*Russian*) 7-5325
 N₂O formation in irreversible dissociation of nitrite coolant (*Russian*) 7-49549
 N₂O₄ condensation in equilibrium maintaining chemical reaction, heat and mass transfer (*Russian*) 7-51341
 N₂O₄ coolant in looped channel, reactor tests (*Russian*) 7-5360
 Na circuit materials corrosion, electrochemical potentiokinetic reactivation method (*Czech*) 7-61966
 Na, rate limited molten fuel coolant interaction model 7-36102
 Na/salt system, NaCrO₂, form. threshold O level, LMFBR operation 7-42113
 NaOH, molten, hot N submerged impinging jets study 7-62051
 NaOH, molten, wastage simulation with submerged impinging hot N jet 7-62050
 Ni alloys, thin oxide films for H barriers, growth study 7-2434
 Ni base high temp. alloys, corrosion in simulated HTGR He environments 7-17703
 Ni-base weld metals, SCC in simulated BWR environments 7-46682
 Ni-Cr-W superalloy, experimental, tensile props., effect of carburisation and aging 7-59576
 Ni-Fe-Cr, age hardenable, SCC in PWR coolant water, heat treatment and Zr additions effect 7-39708
 Ti(n,X), X=p, np, 2n, threshold-20 MeV, cross sections, hybrid and Hauser-Feshbach anal. 7-61870
 Zr, doped with O, mech. props. and elec. resist. at 4.2 K influence of annealing (*French*) 7-59554
 Zr-Nb (2.5 wt.%) H and D profiling at surface, effect of surface prep. 7-59668
 Zr-Nb (2.5 wt.%) pressure tubes, remote field through wall EM inspection 7-46759

fission reactor operation

- see also *fission reactor cooling and heat recovery; fission reactor core control and monitoring; fission reactor safety*
 AMB-200 reactor, neutron flux control algorithms and monitoring system 7-49497
 automatic software generation and validation for nuclear power plant status monitoring 7-42136
 Bechtel automated control of design document data 7-36092
 Bohunice V-1 power plant, safety related operational features (*Czech*) 7-56805
 Browns Ferry Unit 1 BWR, stability tests under single-loop operating conditions 7-25135
 BWR, commercial load following operation with KWU design 7-5347
 BWR, reduced-order model of linear dynamics 7-30478
 BWR plant longevity, General Electric's approach 7-30598
 BWRs, TVO 1 and TVO 2 in Finland, retrofitting to increase output (*German*) 7-10240
 Calder Hall, 30 years of operation, design, procedures and requirements 7-56795
 Calder Hall, 30 years of operation, overview 7-56794
 CANDU nuclear reactor, EM pulse power coils for coolant tube spacer repositioning 7-49566
 centrifugal separators for PWR power stations (*French*) 7-25102
 colour graphics display system 7-25122
 computer aided PWR power plant operation, control and meas. (*German*) 7-19394
 conf., Toronto, Ont., Canada (1986) 7-9587
 conference on nuclear engineering, Zittau, Germany (Apr. 1985) 7-18483
 control rooms, appl. of embedded training 7-34006
 development research of nuclear reactors in France (*French, English*) 7-19398
 Embalse power station, weekend cycling performed during 1985, data collection program 7-10252
 French nuclear power plants, adaption for grid requirements 7-5348
 German LWRs, load following capability and experience 7-49573
 Greifswald PWR plant, use of high burnup fuel assemblies at core edge (*German*) 7-15264
 HTGR, fines behaviour and recycling during fluidised bed operation 7-19363
 human approach to process control and predictive information 7-30612
 human factors reliability (*Czech*) 7-61990
 in-service maintenance, economic aspects (*German*) 7-61987
 large scale fast breeder nuclear power stations, Superphenix description 7-19387
 Lepreau nuclear power station, innovative measures in operation, maintenance, commissioning and staffing 7-10251
 LMFBR, methodology for validation of measurements, plant state verification, and fault identification 7-61992

fission reactor operation continued

- LMFBR operational and fuel cycle experience worldwide (*German*) 7-5342
 LWBR, measured proof of breeding 7-42118
 LWR load-following operation, fuel performance aspects, pellet-clad interactions 7-5350
 Monticello BWR, technical feasibility of life extension, preventative maintenance 7-30599
 NRU, early innovation during operation 7-10253
 NRX, early innovation during operation 7-10253
 nuclear power plant availability impact of limiting conditions for operation 7-10272
 nuclear power plant availability improvement by reactor trip prediction software 7-10275
 nuclear power plant operation simplification by reliability data collection 7-10276
 plant life extension, baseline characterization of electrical circuits 7-36096
 PWR, probabilistic analysis of allowed outage times relaxation 7-42125
 PWR power plants, load following operation, PCI failure criterion 7-25145
 Rheinsberg Nuclear Power Plant, operating experience, expt. fuel assemblies (*German*) 7-15254
 safety principles during operation and accidents (*Dutch*) 7-10263
 special events in nuclear power plants, exchange of experience (*German*) 7-25100
 steady state operation of nuclear reactor, contributions to control design (*German*) 7-25105
 steam supply system, microcomputer data base 7-36093
 Surry 1 PWR, life extension study, near-term benefits from better reliability 7-30600
 THTR-300, operating experiences (*German*) 7-62009
 TMI-2 technology transfer, progress report 7-25120
 Unterweser nuclear power plant, performance under grid control (*German*) 7-5349
 water-level measuring system for drum separators in nuclear power-plant with RBMK-1000 reactor (*Russian*) 7-764
 WWR-440 reactor, permissible power determ., review (*German*) 7-15263
 WWR-440 type pressure vessel, manual and mechanized inspection (*German*) 7-56784
- fission reactor safety**
 see also *fission reactor cooling and heat recovery; fission reactor core control and monitoring; fission reactor instrumentation*
 accident confinement systems, vapour condensation in underheated non-flowing liquid 7-30621
 advanced thermohydraulic codes, development, validation and appl. 7-49500
 AEROSIM-S code for dry aerosols, FBR containment appls., user manual 7-56723
 aerosol behaviour, effect of hygroscopicity 7-42166
 aerosol source terms in nuclear reactor accidents, ex-vessel fission product releases 7-36219
 AGR, Xe and temp. transients, 3D model anal. 7-15300
 AGR fuel height stringer drop tests, damage estimates 7-56814
 AGR fuelling machine hoist system, single component failure mode detection 7-56731
 AGR helically wound heat exchanger, impacting phenomena anal. for Heysham 7-56790
 AGR helically wound heat exchanger, resonance tests at Heysham I 7-56789
 AGR helically wound heat exchangers, vibration props. 7-56788
 alarm-filtering system for advanced test reactor 7-62054
 ALPA, diagnosis expert system for nuclear reactor supervision 7-25153
 annular two-phase flow with liquid entrainment, improved mixing length model 7-5390
 apparatus for ⁸⁵Kr and ¹³³Xe meas. in fission reactor emergency situations 7-28439
 artificially perforated Zr barrier fuel rods, fission product release in test loop 7-783
 ASME Boiler and Pressure Vessel Code, design developments 7-49506
 ASME code for nuclear plant component in-service inspection, 1984-5 revisions 7-5404
 axial fission gas transport in power ramping expts. 7-15284
 Bechtel automated control of design document data 7-36092
 BIBLIS-B reactor pressure vessel, fracture mech. anal. for thermal shock transients 7-10220
 Bohunice V1, dose measurements in operation and overhead situations (*Czech*) 7-62093
 Bohunice V-1 power plant, safety related operational features (*Czech*) 7-56805
 boiling heat transfer, anal. using hot ball quenching method (*Chinese*) 7-49596
 BR-10 reactor first circuit pipelines, radioisotope distrib. 7-30590
 British Standard 5500 for pressure vessel design and construction, appl. to AGRs 7-49510
 Browns Ferry Unit 1 BWR, stability tests under single-loop operating conditions 7-25135
 Bulgarian radiation exposure from nuclear power facilities (*Russian*) 7-54763
 BWR, ⁶⁰Co radiation control using thin film coatings 7-49590
 BWR, correlation for predicting reactor power during ATWS 7-62038
 BWR, gravity-driven core cooling system for inherent safety 7-36201
 BWR, inherently safe design, passive steam-driven ECCS injectors 7-36226
 BWR, linear and nonlinear density wave instability modes, anal. modelling 7-5375
 BWR, MSIV-ATWS events, power level and pressure suppression pool temp. 7-42155
 BWR, new scenario for intersystem LOCAs 7-42162
 BWR, TRACB04 study on suppression pool swelling during containment venting 7-42156
 BWR at Gundremmingen nuclear power station with twin 1300 MW units, corrosion products (*German*) 7-10241
 BWR broken recirculation line, two-phase flow phenomena 7-61989
 BWR core meltdown accident, estimate of fission product release 7-777
 BWR core stability estimation, applicability of multivariable autoregressive method 7-25140
 BWR feedwater systems, hydrogen water chemistry effects on radiation fields 7-771

fission reactor safety continued

- BWR fuel rod, pellet-cladding interaction, rod failure, fission product release (*Japanese*) 7-15242
 BWR LOCA, two bundle loop tests, SAFER03 and TRAC-BD1 anal. 7-36210
 BWR LOCA research and development of SAFER code (*Japanese*) 7-56711
 BWR piping, fracture mech. research in Japan 7-53891
 BWR piping research in Italy, IGSCC tests, fracture and cracks 7-53890
 BWR plant longevity, General Electric's approach 7-30598
 BWR simulation, countercurrent gas/liquid flow in parallel channels 7-5380
 BWR simulations at high speed using parallel processors 7-36085
 BWR stability anal., dual loop jet pump model 7-62005
 BWR suction line break LOCA, ROSA III RUNs 942 and 943, initial fluid condition effects 7-19416
 BWR top-guide structure, integrity eval., irradiation induced SCC 7-54012
 BWR/6 DBA analysis with limited ECC 7-42154
 BWRs, methods for dose rate reduction, $^{58,60}\text{Co}$ concs. in coolant 7-42187
 CAGR-on-load refuelling, safety case development 7-56815
 Calder Hall, safety, inspection and maintenance 1956-86, review 7-56809
 Calder Hall and Chapelcross reactor pressure circuits, in-service inspection 7-56810
 Calvert Cliffs Unit 1 tube examination 7-61970
 CANDU, header void distrib. effects on fuel channel flow following inlet header stratification 7-15298
 CANDU 600 MW(e) reactor, defective fuel detection in operating plant 7-784
 CANDU fuel channels, calculation of steam flow 7-10262
 CANDU fuel channels, subchannel flow distrib. following deformations 7-10210
 CANDU header manifold, flow stratification under small-break LOCA 7-62041
 CANDU LOCA, radial heat transfer from fuel to moderator, RAMA and CHAN II codes 7-15297
 CANDU reactor, fuel channel replacement program 7-10269
 CFT displays of plant operation 7-49567
 Chernobyl, lessons for Western Europe 7-30628
 Chernobyl, power excursion event anal. 7-62023
 Chernobyl, Soviet information evaluation 7-30627
 Chernobyl, technical appraisal 7-62015
 Chernobyl accident, causes and consequences (*French*) 7-62035
 Chernobyl accident, causes and effect in Spain/Italy (*Spanish*) 7-5373
 Chernobyl accident, event sequence, consequences, anal. (*German*) 7-25147
 Chernobyl accident, first evaluation of Soviet report (*German*) 7-25125
 Chernobyl accident, RBMK construction and operational features, accident causes (*German*) 7-56803
 Chernobyl accident, thermal hydraulic characteristics and follow up calcs. (*Japanese*) 7-62021
 Chernobyl fallout, detecting and meas. in Nordic countries 7-30715
 Chernobyl nuclear reactor accident, individual dose assessment at Berkeley, UK 7-3880
 Chernobyl power station, nuclear accident and comparison with Daya Bay power station design 7-15277
 Chernobyl safety design comparisons with Ontario Hydro reactors 7-10270
 COBRA-NC code anal. of steam line break 7-61954
 colour graphic display systems for power station control rooms 7-56811
 commercial HTGR, safety concepts, probabilistic safety anal. expensive 7-25136
 common cause failures, defensive tactics for branched events 7-36232
 components, design, construction and safety codes 7-49512
 components, dynamic materials testing using fibre optic sensors 7-46778
 computational continuum dynamics, parallel algorithms 7-4683
 computerised core refuelling 7-56743
 computerised information processing for control room staff in FRG nuclear power plants 7-19407
 concrete, microplane model for progressive fracture, microcracking 7-15248
 concrete shield, fast neutron albedo calcs. 7-30622
 concrete shield, heat-resistant, in nuclear reactor, capture γ -ray refl. and transmission 7-49532
 conf., London, England (September 1985) 7-18492
 conference on fission product behaviour and source term research, Snowbird, UT, USA (July 1984) 7-10
 conference on iodine chemistry in reactor safety, Harwell, England (Sept. 1985) 7-48176
 conference on nuclear engineering, Zittau, Germany (Apr. 1985) 7-18483
 conference on the safety and reliability of reactor pressure components, Stuttgart, Germany, (Oct. 1985) 7-9583
 conference on two-phase flow dynamics, Lake Placid, NY, USA (Aug. 1984) 7-4627
 conference on water reactor safety, Gaithersburg, MD, USA, (Oct. 1985) 7-48152
 construction codes and engineering mechanics conf., Paris, France, Aug. 1985 7-48153
 containment integrity and radionuclide behaviour during severe accidents, review of R&D 7-779
 containment thermohydraulics in major accidents (*German*) 7-56802
 controlling principles for prior probability assignments in nuclear risk assessment 7-36212
 coolant boiling in research reactors, expts. in WWR-SM facility (*German*) 7-56781
 coolant pumps, vibr. monitoring and diagnostic techniques 7-36203
 core coolant channels, coherent blockages, statistical thermodynamics, percolation anal. 7-36194
 core cooling and system behaviour following PWR LOCA 7-49563
 core debris bed, dryout heat flux, effects of system pressure and particle size 7-19406
 counterflow steam generator, water-sodium leaks, fault processes 7-5344
 crack arrest specimen, dynamic anal. under reactor pressurised thermal shock conditions 7-13693
 CRACUK code, dosimetric models modifications 7-19349
 CRACUK user's guide (appendix to the CRAC2 user guide) 7-19348
 CRBR fuel subassembly, 2D flow in partially blocked parallel plates, soln. using electrical network 7-36188

fission reactor safety continued

- Creys-Malville (France) nuclear power station maintenance QA (*French*) 7-25127
 Crystal River-3, time-line technique for station blackout core-melt anal. 7-42181
 degraded core coolability study 7-62046
 density wave oscillations, stability map construction method, reactor appls. 7-5378
 dependent event data classification system 7-15290
 design of safe reactors 7-15276
 diffusion critical problem, two-dimensional, soln. using SIXTUS-2 code 7-19327
 dissociating coolant reactors, core active zone thermotechnical reliability (*Russian*) 7-49525
 disturbance analysis using artificial intelligence, SAAP-2 system 7-19338
 dNB prediction in assemblies with mixing vanes and unheated tubes 7-62040
 DNBR limit, prediction of transient axial power distrib. 7-62039
 DNBR studies, streamlined one-pass modeling 7-62004
 dryout heat flux for core debris bed, particle size mixing and coolant flow effects 7-30623
 dynamical response of systems with localized nonlinearities, ultimate state method 7-10190
 dynamically loaded pipes with circumferential flaws, behaviour under internal pressure and external loads 7-13577
 earthquake resistance by design, seismic research 7-36209
 eastern USA, earthquake source scaling relations, nuclear plant safety appl. 7-36236
 EBR-II, LOF transients without scram, primary pump coastdown characts. effects 7-15278
 EBR-II, nonrecirc fission product release phenomena using multifreq. source perturbation expts. 7-5326
 EBR-II, ramped power transients, feedback simulation using transfer functions in EROS code 7-42188
 EFWS, bus configurations, four-train versus two-train support 7-42161
 emergency classification system at nuclear power plants, expert system application 7-15265
 emergency diesel generator reliability at US nuclear power plants 7-42183
 emergency procedures and remote monitoring of nuclear power stations (*German*) 7-25148
 engineering aspects of the Hartlepool and Heysham 1 fuelling machines 7-56735
 enhanced inspection using expert systems 7-36087
 equipment-structure systems, eigenproperties, perturbation anal. 7-25130
 evaluating the safety of nuclear plant changes 7-42242
 expert system for USNRC emergency response 7-62053
 expert systems and accident management 7-62055
 expert systems for PWR diagnostics 7-56798
 Farmer's line, probability density functions, and overall risk 7-25144
 fast gas-cooled reactors, accident analysis methods (*Russian*) 7-5403
 fast reactor HCDA anal., two phase flow aspects, ANEXDI code 7-15302
 FBR, horizontal gas jet submerged in liq., penetration study 7-62052
 FBR irradiated MOX fuel, transient fission gas release during direct heating expts. 7-778
 feedwater system evaluation for reactor scram reduction 7-36229
 FEMAXI-III calculations for the D-COM blind problem 7-717
 FFTF, GEM shutdown device appl., use in unprotected LOF events 7-36227
 FFTF, reactivity worth of gas expansion modules 7-42131
 filters venting system for mitigating consequences of core-melt accidents 7-19409
 fire detection and suppression anal. 7-36213
 fire protection at German nuclear power stations (*German*) 7-25146
 fission product neutron capture transformation effects on decay power after reactor LOCA 7-49587
 fission product release expts. overview 7-772
 fission products release mechanism, estimation of failed fuel rods (*Korean*) 7-30517
 flow induced valve operation and pressure wave propag. in single and two-phase flows 7-10239
 flow-induced vibration of fuel rods, review (*Japanese*) 7-25034
 fluidised bed power reactor, transient neutron flux modelling 7-62017
 Forsmark-2 PWR, preventive maintenance during operation 7-15282
 fuel assembly subcriticality determ. by the Mihalcz method (*Japanese*) 7-25104
 fuel rod steady state thermal behaviour, uncertainty analysis, probabilistic response surface method 7-729
 GEMS environmental monitoring system for γ -ray emissions 7-10298
 German BWRs, experience in exchanging recirculation, class 1 piping systems 7-49574
 graphite moderated reactors, stored Wigner energy 7-42142
 Hanford N Reactor, flux flattening programme, core physics calcs. 7-42133
 health physics aspects of nuclear issues in NewZealand over the last decade 7-8697
 heat exchanger tubes, cyclic temperature transient influence on creep behaviour 7-10186
 high temperature reactor components, multiaxial loading tests 7-49541
 high temperature structures in reactors, creep curve variation effects on creep behaviour 7-39602
 high-temperature pebble-bed reactor development and inherent safety 7-10273
 high-temperature reactors, Germany design codes and standards 7-49514
 homogeneous flow model, validity for instability anal., steam generators 7-5379
 horizontal annular flow measurements using pulsedphoton activation and film thickness distributionmodelling 7-5357
 HTGR fuel behaviour at very high temps., TRISO coated LEU particles 7-19364
 HTGR severe air ingress accident, graphite/ O_2 reaction kinetics for various graphites 7-19415
 HTR, reactor protection building anal. for He release (*German*) 7-30639
 human approach to process control and predictive information 7-30612
 human factors in risk assessment 7-30637
 IAEA-SPE-1, pre-test calcs. for the PMK-NVH standard problem exercise 7-62045
 improbable nuclear reactor accidents, source-term containment anal. recent progress review 7-36218
 in-service inspection and reliability programme 7-15292

fission reactor safety continued

incentive regulation program and its relationship with safety 7-49597
 incident control, simulation of man machine interaction 7-15287
 inherently safe power reactor DYONISOS 7-49496
 inverted annular flow in post-dryout region, flow regime transition and interfacial characts. 7-5386
 JAERI reactor engineering dept 1985-6 annual report 7-56725
 jet discharge tests results under BWR and PWR LOCA conditions 7-5401
 JOYO radiation streaming, energy-space dependent error propagation in Monte Carlo coupling calculations 7-19335
 KNU1 plant transient simulation using RELAP5/MOD1/NSC 7-5374
 La Crosse BWR, 1986 viewpoint of emergency preparedness in USA 7-30632
 large size LMFBRs, designs for inherent safety capability, accident anal. 7-36223
 large steam-line break LOCAs, similarity study for ROSA-III, FIST and BWR-6 7-49593
 LaSalle-1 BWR, water chemistry, corrosion products and radiation-field buildup 7-36206
 learning curve estimation techniques for nuclear industry 7-15296
 licenced radioactivity release levels from French nuclear facilities (*German*) 7-56873
 Limerick PRA, transient response implementation plan procedures 7-30635
 liquid solid phase change front-prediction method 7-62002
 LMFBR, 1000 MWe axially heterogeneous design, neutronics performance (*Japanese*) 7-15228
 LMFBR, French creep-fatigue design rules 7-49522
 LMFBR, hot N submerged impinging jets study in molten NaOH 7-62051
 LMFBR, hypothetical core meltdown accident, pressure depend. of particle bed dryout heat flux 7-5393
 LMFBR, reactivity effects of hydrocarbon, effect of group constant generation method 7-56808
 LMFBR, smoke release behaviour of burning liquid Na pools, safety anal. 7-49592
 LMFBR, voided cores, fuel vapour pressure buildup dynamics during transient heating 7-36215
 LMFBR 37-pin bundle, low heat flux NA boiling test using SABENA code 7-25110
 LMFBR components, RCC-MR code for design and construction 7-49511
 LMFBR HCDA, particle phase size effects in disassembly accident transient 7-25142
 LMFBR steam generator large leak accident, heat transfer into module shell tube 7-62016
 LMFBR steam generators, thermohydraulic instabilities, expt. results 7-5382
 LMFBR steam generators, thermohydraulic instabilities, nonlinear and linear anal. models 7-5381
 LMFBR sub-assemblies, mech. response under local accident conditions, state-of-the-art review 7-25129
 LMFBR ultra long life cores 7-61957
 LMFBRs, angular depend. of neutron-noise transmission through shields 7-42139
 LMR, ATWS and LOF events, reactivity feedback uncertainties effects on inherent shutdown 7-36224
 LMR, ATWS calc. using SASSYS/SAS4A, effects of radial core expansion reactivity feedback model 7-36222
 LOCA, critical flow of initially subcooled flashing liquids, homogeneous equilib. model 7-5388
 LOCA, ECCS, operation, active cavity model for flashing 7-5387
 LOCA, peak cladding temp. calcs, LOFT anal. 7-42158
 LOCA, pressure surge prediction in one-component two-phase bubbly flow 7-5398
 LOCA, transition boiling heat transfer studies using the hot cylinder quenching method 7-25112
 LOCA, uncertainty anal. using Fourier amplitude sensitivity test 7-42160
 LOCA with severe fuel damage, radiation heat transfer model for SCDAP code 7-36216
 low probability event treatment, appl. to nuclear power plant incidents 7-36217
 low volatility fission product release expts., surface vaporisation role, fuel debris bed appl. 7-25137
 LWHCR lattices, effects of WIMS data library changes on calc. results 7-5316
 LWR, application of a direct-heating model to the Sandia SURTSEY tests 7-62042
 LWR, Chen boiling heat transfer correlation 7-42153
 LWR, coarse-mesh method for 1-D reactor kinetics, accident anal. 7-42140
 LWR, core damage frequency from internal initiators, PRA at Peach Bottom 7-42146
 LWR, core damage frequency from internal initiators, PRA level-1 study 7-42145
 LWR, core damage frequency from internal initiators in Grand Gulf 7-42148
 LWR, core damage frequency from internal initiators of Sequoyah 7-42147
 LWR, corium droplet size in direct containment heating 7-62007
 LWR, corrosion product release, radiation build-up effects 7-10225
 LWR, effects of water in film boiling over liquid-metal melts 7-42171
 LWR, heat radiation through steam in direct containment heating 7-62008
 LWR, heat transfer model for volumetrically heated nuclear debris beds 7-49591
 LWR, hypothetical core meltdown accident, pressure depend. of particle bed dryout heat flux 7-5393
 LWR, rapid thermal transients, fuel response to ECCS quenching 7-15252
 LWR, severe accident containment load calculations using HMC code 7-62044
 LWR, severe core damage, PRA methodology 7-42149
 LWR accident source term expts, deposition samples 7-62047
 LWR accidents, empirical aerosol correlations using MAAP 2.0 and 3.0 7-56722
 LWR decontamination, chemical and electrochemical processes 7-5372
 LWR degraded core coolability, two-phase flow through porous media 7-5394

fission reactor safety continued

LWR degraded cores, fission product release and retention phenomena 7-776
 LWR ECCS, steam-water interactions in a vertical tube, flooding 7-5383
 LWR ECCS injection, fluid and pressure oscils. during direct contact condensation 7-5376
 LWR engineered safety features in severe accident conditions 7-10268
 LWR fuel failure detection using the grip sipping method 7-30544
 LWR fuel rods, simple model for predicting fission gas release 7-789
 LWR fuel under degraded core conditions, fission gas release prediction, FASTGRASS-VFP model 7-790
 LWR heavy section steel technology, crack arrest studies overview, reactor pressure vessels 7-53885
 LWR irradiated fuel under accident conditions, fission product release 7-773
 LWR life extension, records requirement review 7-56721
 LWR load-following operation, fuel performance aspects, pellet-clad interactions 7-5350
 LWR LOCA, jets formed by high pressure subcooled water and steam-water mixtures 7-5391
 LWR LOCA, phase separation mechanisms in branching conduits, review 7-5384
 LWR LOCA, pressure transient and two-phase swelling due to small top break 7-5389
 LWR LOCA, reflood simulation, numerical anal. based on KREWET code 7-15299
 LWR LOCA, two-phase flow in unbounded two-phase critical flows 7-25131
 LWR meltdown accident, fuel-coolant mixing, unsteady 1D 2-fluid model, PHOENICS code 7-5395
 LWR piping, flaw detection by US systems, digital techniques 7-46782
 LWR piping systems, LBB feasibility eval. fracture criteria 7-61968
 LWR pressure vessel surveillance using solid state track recorder neutron dosimetry 7-36199
 LWR safety, main contributions to the KfK Nuclear Safety Project, review 7-36221
 LWR safety anal., steam direct contact condensation on slowly moving water 7-5358
 LWR severe core damage accident, uncovered core thermal-hydraulics, model dev. 7-30624
 LWR severe fuel damage events, burnup effects on fission product release 7-787
 LWR small break LOCA expts. at LOFT, RETRAN-03 anal. of LP-SB-1 and LP-SB-2 7-36237
 LWR steam generator U-tube rupture transient anal. using DRUFAN-02 code 7-49562
 LWR structured sensitivity anal. for severe accidents using MAAP 2.0 code 7-42189
 LWR surveillance dosimetry anal., changing source distrib. effects 7-62098
 LWR System Analysis and Risk Assessment system 7-15289
 LWR thermal hydraulics, SEFDAN code for severe core damage accidents 7-49503
 LWR thermal-hydraulic issues in nuclear training 7-29618
 LWR thermal-hydraulics after a severe accident, Power Burst Facility anal. with SEFDAN code 7-49586
 LWR thermohydraulic core anal. methods 7-49499
 LWRs, fuel rod failure/coolant activity relationship, data formatting and collection 7-36235
 LWRs, thermal hydraulics research, history and present status 7-29653
 MAEROS model for multicomponent aerosol dynamics, uncertainty and sensitivity anal. 7-19411
 MARS reactor plant, an inherently safe, small/medium multipurpose nuclear plant 7-25022
 materials management conf. New Orleans, LA, USA, (June 1986) 7-35087
 metallic nuclear power plant components, German codes and standards 7-49508
 MHTGR confinement radiation releases, aerosol removal rates 7-42172
 MICROSHIELD, microcomputer program for dose rate, gamma shielding anal. 7-42109
 Millstone-2 PWR, wear and neutron activation of positioning pins, ⁶⁰Co buildup 7-15247
 mobile robot use in nuclear power plants, TMI-2, Hope Creek, Salem 7-49613
 molten reactor core/concrete interactions in HCDA, mass and heat transfer simulation 7-25138
 monitoring system for nuclear reactors, reliability improvements (*Russian*) 7-25101
 Monju, prototype FBR, construction codes and safety evaluation 7-49509
 Monju FBR, anal. and design for elevated temp. components 7-56717
 Monte Carlo electron interface studies, incorporation into photon cavity theory 7-36079
 motor-operated valve, operability verification, reactor appl. 7-42178
 MPA thermoshock expt. anal. using TRAC PF 1 code, PTS in reactor ECC conditions 7-13588
 Muhleberg BWR, extra decay heat removal, back-up protection system 7-30626
 multicomponent aerosol modelling, numerical implementation for reactor accident mitigation 7-56800
 Mutsu, ship propulsion reactor, thermal-hydraulic transient characts. from safety anal. (*Japanese*) 7-25128
 NDT development at Harwell, review 7-65270
 neutron doses in nuclear power plants, need for personnel dosimeters 7-25263
 neutron dynamics transport codes, analytical benchmarks 7-61943
 neutron monitor for reactor startup range, design parameters 7-42126
 noise diagnosis techniques for nuclear power station fault detection (*German*) 7-19403
 noise monitoring, digital generation of stochastic signals of arbitrary spectral shape 7-5341
 nonequilibrium film boiling in rod bundle geometries, post-CHF test 7-42151
 NRC Degraded Piping Programme, LWR piping fracture research, Phase II progress 7-53889
 NUCLARR program for reactor risk assessment 7-30636
 nuclear class 1 pressure boundary components, requalification status 7-56812
 nuclear piping systems, research overview 7-49595
 nuclear power plant advanced concepts reviews, Chernobyl accident implications 7-62049

fission reactor safety continued

- nuclear power plant availability impact of limiting conditions for operation 7-10272
- nuclear power plant emergency response and security system 7-42141
- nuclear power plant probabilistic risk assessment microcomputer software 7-10271
- nuclear power plant Risk Management Query System 7-15291
- nuclear power plant siting criterion, social radiation risk in presence of large pop. centre 7-49584
- nuclear power renunciation consequences and arguments (*German*) 7-39968
- nuclear power station design and seismic ground motion in Central Europe (*German*) 7-19404
- nuclear power station fire protection, licensing comparisons between USA and BRD (*German*) 7-10266
- nuclear power stations, diagnostic subsystems in Czechoslovakia (*Czech*) 7-19386
- nuclear power stations, safety equipment and emergency power supply (*Hungarian*) 7-25126
- nuclear reactor control information, provision in presence of instrument failures 7-5367
- nuclear research, summary of recent papers (*Dutch*) 7-54670
- nuclear safety after Chernobyl 7-34000
- nuclear thermal-hydraulics education, Yankee Atomic/Univ. of Lowell experience 7-29615
- numerical methods in nuclear engineering, conf., Montreal, Canada, Sept. 1983 7-9600
- Oconee steam generators, secondary-side chemical cleaning 7-42173
- online acoustic emission monitoring of cracks in nuclear systems, review 7-54066
- operator diagnosis failure probabilities 7-42164
- organic iodides formation under reactor accident conditions 7-49604
- Oyster Creek emergency off-site dose assessment, ocean breeze inclusion 7-30725
- Palo Verde full-range feedwater control system operating experience 7-36230
- passive high-integrity lifting equipment 7-56738
- Peach Bottom 3 BWR, creviced safe ends, US inspection for cracks 7-46781
- PEC reactor core fuel element, structural verification criteria 7-49539
- Petten HFR, reactor vessel replacement, dismantling, segmentation, waste disposal, doses 7-5488
- piping, technical and economical incentives behind strain limitation 7-10221
- piping criteria and construction costs 7-61953
- piping systems, dynamic test data, comparison with analytical methods 7-10191
- piping systems, strain limitation calcs. 7-10188
- PNP-500 HTGR, Cs release during a heat-up accident, fission product transport 7-15286
- PNP-500 pebble bed reactor, massive water ingress accidents, computer anal., graphite corrosion (*German*) 7-5371
- Poisson earthquake occurrence model, nuclear power plant site anal. 7-25150
- post accident heat removed, inclination effect on downfacing burnout heat flux 7-62022
- post dryout heat transfer prediction using mechanistic model 7-5397
- post-dryout boiling, dispersed flow heat transfer, review 7-5400
- postulated severe accident, hot gas bubbles discharged into water, dynamic and thermal behavior 7-5377
- power plants, safety prediction technique 7-19414
- power range monitoring systems and neutron channels, in situ detection of channel degradation 7-36214
- PRA, continuous Bayes theorem updating 7-42159
- PRA, level-1, smart approach 7-42144
- PRA, methodology for plant upgrade integration 7-36233
- probabilistic risk assessment, accuracy and efficiency of the Monte Carlo method 7-15294
- PROCESS, source term calculation program for personal computers, results 7-42175
- PWR, adequacy of automatic plant protection system 7-25152
- PWR, characteristics of releases from TREAT source-term experiment STEP-1 7-42170
- PWR, direct heating containment vessel interaction code DHCVIC 7-62043
- PWR, fluid and thermal mixing in model cold leg and downcomer, COM-MIX-1A anal. 7-15268
- PWR, fuel rod vibration induced by baffle jet flow 7-25134
- PWR, heat transfer during LOCA 7-25151
- PWR, improved water chemistry controls for minimizing degradation of materials 7-30615
- PWR, instrument failure detection, nonlinear filtering appl. 7-25141
- PWR, key radionuclide calcs. for failed fuel analysis 7-42176
- PWR, large break LOCA, dispersed flow heat transfer during reflood 7-42150
- PWR, LOCA, film boiling heat transfer coefficient during reflood phase 7-10250
- PWR, LOCA, simulation using TREAT source term expt. 7-42169
- PWR, loss of pressurizer water level during station blackout 7-42182
- PWR, multi-loop, power plant accident anal., digital simulator for transients and accidents 7-15301
- PWR, n- γ shielding designs in France 7-25133
- PWR, thermal hydraulic behaviour during loss of offsite power transient without scram (*Japanese*) 7-56712
- PWR, turbine trip transient, effect of pressurizer sizing 7-30604
- PWR, Westinghouse design, leak-before-break eval. of pressuriser surge line 7-56813
- PWR accident, source term determ. and expt. verification methods (*German*) 7-56801
- PWR boiler pipework, effect of feedwater conditioning on corrosion (*German*) 7-25115
- PWR CHF predictions, EPRI-1 correlation effects under normal and abnormal fuel conditions 7-36198
- PWR coolant pump trip criteria, transient identification technique 7-62048
- PWR fault identification systems, model-based, development, nuclear reactor appl. 7-19412
- PWR fuel rods, power ramp data, FROST and THERMOST codes, clad-ding deform. rod elongation 7-62034
- PWR hot leg, two-phase flow during natural circulation in once through steam generators 7-49579

fission reactor safety continued

- PWR hot leg, two-phase natural circulation flows, literature survey for SBLOCA 7-49580
- PWR leak detection studies, dew point, dry bulb temp. and flow rate monitoring 7-42157
- PWR LOCA, best estimate anal. with thermal hydraulic codes 7-49502
- PWR LOCA, FLECHT and FLECHT-SEASET reflood tests anal. with RELAP5/MOD2 7-25025
- PWR LOCA, two-phase flow during bottom reflooding, computer modelling 7-49599
- PWR LOCA fuel deformation and rupture simulation, PYTHONS code 7-56720
- PWR LOCA licensing anal., expt. and best-estimate calc. comparison 7-49582
- PWR power plant, auxiliary feedwater system anal. using dynamic logical analytical methodology 7-25114
- PWR power plant design for optimum load following capability 7-5317
- PWR power plants, load following operation, PCI failure criterion 7-25145
- PWR pressuriser, on-line instrument failure detection using improved likelihood ratio method and suboptimal control 7-25139
- PWR pressurizer, accident and transient anal., nonequilibrium three-region model 7-36195
- PWR prestressed containments, response to earthquakes, gas cloud explosions and aircraft impact 7-10264
- PWR refuelling using revolving cylinder manipulator crane 7-56739
- PWR scram reduction by steam generator level control improvements 7-36228
- PWR secondary system, automated derivation of failure symptoms for diagnosis 7-5370
- PWR source term inventory and decay power, sensitivity to core management parameters 7-30630
- PWR steam generator sludge piles, chemical cleaning 7-10227
- PWR steam generator tube rupture transients, thermal-hydraulics in simulated 4-loop facility 7-49571
- PWR steam generators, review of secondary side tube degradation processes 7-30616
- PWR steam-generator simulation with non-equilibrium two-phase flow models 7-42122
- PWRs, activity build-up in primary circuit, review (*German*) 7-19408
- PWRs with once-through steam generators, radiation field build-up, coolant pH 7-36234
- radiation impact of Chernobyl in Western Europe 7-30714
- radiation streaming in duct, anal. using FENDER diffusion code 7-19331
- radioactivity, contamination, damage and risks (*Italian*) 7-47262
- radiological emergencies, mobilisation of robotic and teleoperated mobile vehicles at accidents 7-30633
- RAS III, modular noise diagnostics system for reactor primary circuit monitoring (*German*) 7-56787
- RBMK, simulation of regulation system under power reduction conditions 7-25099
- RBMK-1000/LWR comparison, differences in fuel coolant and moderator, Chernobyl accident (*Dutch*) 7-10213
- RCC-M code for design and development of PWR components 7-49507
- reactor accident consequences, effects of rain and snow on contamination 7-42143
- Reactor Analysis Support Package, guidelines for LWR thermohydraulic safety anal. 7-42190
- reactor components, dynamic reliability model for damage accumulation processes 7-30535
- reactor core cal. code, 3D simulating Xe transient state, develop. (*Japanese*) 7-56778
- reactor pressure vessel manipulators, functions and basic concepts (*German*) 7-56807
- reactor trips involving balance of plant failures 7-42163
- reduced source terms for ex-plant consequence modeling and emergency planning 7-62031
- reinforced concrete shear walls in nuclear power plants, probab.-based design criteria 7-36078
- reinspection methods implemented for quality 7-36231
- RELAP5/MOD2 code for PWR transient anal. 7-10201
- relaxed core stress in ratcheting evaluation for elevated temp. design 7-49521
- reliability and risk allocation in nuclear power plants, decision theoretic anal. 7-36081
- rewetting phenomena, expt. investigation using round tubes and pressured Freon-12 7-25109
- rigid block rocking on randomly shaking foundations, nuclear plant seismic response appl. 7-25132
- risk assessment application to NRC inspection 7-49594
- risk studies of accidents (*German*) 7-62018
- ROSA III SBLOCA tests, split break test RUN 921, 931 7-10267
- ROSA-III, break location effects on thermal-hydraulics during intermediate break LOCA expts. 7-49589
- Rosendorf Research Reactor, computer-based γ -ray area monitoring system (*German*) 7-19552
- SAF: a sophisticated engineering simulator mainly devoted to emergency guidelines testing and crisis situation analysis 7-62056
- safety principles during operation and accidents (*Dutch*) 7-10263
- safety related systems, basis for setting technical specs. and limiting conditions of operation 7-42185
- safety relief valve position indication systems for reactor appl. 7-42179
- SAFR, 350 MWe inherently safe fast reactor, design and development in USA 7-30472
- San Onofre Unit 1, problems of material aging and reliability 7-42177
- Santa Maria de Garona BWR, upgrade modifications to safety equipment 7-30625
- SASCHA programme on fission product release under reactor core melting conditions, review 7-774
- seismic hazard methodology for central and eastern USA, EQHAZARD code 7-19417
- seismic hazard methodology for the central and eastern USA 7-15285
- seismic risk quantification for design and construction errors 7-15280
- separated flow effect modelling in horizontal heated channel refill 7-10202
- severe accident source terms, methodology for quantification of uncertainties 7-42165
- severe core damage accidents, containment response, integrated phenomenological anal., CONTAIN code 7-36220
- severe reactor accidents, sequences and consequences 7-30629

fission reactor safety continued

SIPA, French simulator for PWR post-accident training and anal. 7-42110
 sizewell B PWR, degraded core anal., accident risks 7-62033
 SNR 2 fast breeder reactor development project (*German*) 7-15303
 SNR-300 LMFBFR, design, erection and testing of steel containment 7-25024
 SOLNAS, online noise surveillance and analysis system 7-15283
 source term composition effects on offsite doses after reactor accidents 7-782
 source term research implications for ex-plant reactor accident consequences modelling 7-780
 spherical concrete-walled room, gamma radiation reflection calcs. 7-42237
 SSYST-3 fuel rod behaviour analysis program (*Hungarian*) 7-56724
 stability-enhancing two-step method for Transient Reactor Analysis Code 7-10200
 standardisation from a risk concept 7-25124
 station blackout events, determ. of frequency/duration relationships 7-42184
 station blackout rule, effects on nuclear plants 7-62032
 steam generator materials, properties and performance 7-30556
 steam generator tubing, primary side stress corrosion cracking, remedial measures 7-30613
 steam generator vessel and feedwater line integrity issues 7-30614
 steam-water mixtures, thermodynamic equilibrium during loss from reactor 7-49577
 steel, alloy, crack arrest toughness, moment modified compact tension specimen, PTS conditions 7-13695
 steel, austenitic stainless, LWR cladding, oxidation in high temp. steam, LOCA appl. 7-727
 steel, austenitic stainless, LWR piping, ASME code for flaw eval. 7-13601
 steel, austenitic stainless, pipe weldments, toughness at LWR operating temps. 7-13599
 steel, carbon and stainless, pipe fracture safety analysis using limit load and J-integral techniques 7-13585
 steel, heavy section, Ni-Mo, elastodynamic fracture analysis of large crack-arrest experiments 7-53887
 steel, interface oxide growth in Magnox and AGR plant, assessment methods 7-59678
 steel, low alloy ferritic, strain induced corrosion cracking prevention for BWR piping 7-13641
 steel, Mn-Mo-V, reactor piping material, strength, deformation and fracture behaviour 7-13578
 steel, Ni-Mo, LWR pressure vessel cladding, irradiation effects and flaw struts. 7-53888
 steel, Ni-Mo, wide plate crack arrest testing using acoustic emission, reactor pressure vessel appl. 7-53886
 steel, stainless, clad fuel rod, failure behaviour 7-61965
 steel, stainless, heavy section, fracture studies, welds, neutron irradiation, crack arrest 7-13587
 steel, stainless, pressure vessel, stress relief cracking, reactor safety 7-8117
 steel, stainless, reactor pipe integrity prediction using R6 procedures 7-49542
 steel, stainless, Type 304 IGSCC, BWR plant life extension, materials aspects 7-53995
 steel LWR piping fracture mechanics database 7-53892
 steel nuclear containment building, buckling, expt. and anal. programme 7-53818
 steel pressure vessel, thermal transient, crack arrest in K-gradient 7-46617
 strain estimation for external event loads 7-10189
 stratified two-phase flow in horizontal circular tubes, mechanistic model of slugging onset 7-30596
 Surry steam generator, examination and eval., nondestructive testing 7-54065
 system design and anal. 7-15288
 system reliability, design stage quantitative anal. 7-62020
 systematic human action reliability procedure, benchmark process 7-30634
 technical specification optimisation programme for nuclear plant engineered safety features 7-42186
 technical systems reliability investigation for 440 MW nuclear power stations (*German*) 7-19402
 Terry turbine equipment and procedure modification for reliability improvements 7-36202
 testing strategies and testing environment for reactor safety system software 7-19418
 thermal hydraulics in nuclear engineering courses at the Univ. of Illinois 7-29617
 thermal hydraulics in undergraduate nuclear engineering education 7-29616
 thermal shock loadings in PTS accidents, J-integral concept appl. 7-13696
 thermal-hydraulic process expt. facilities, contrib. to reactor safety 7-19393
 thermohydraulic explosions, spinodal lines and eqns. of state, review 7-5396
 TMI-2, accident and recovery, defuelling and reactor inspection 7-42191
 TMI-2 boron dilution, criticality safety, operational considerations 7-753
 TMI-2 defueling criticality safety 7-754
 tornado missile hazard to nuclear plants, numerical methods for risk assessment 7-15293
 TPTF, high pressure boiloff in rod bundle, slug-to-annular flow transition 7-49572
 TRAC analysis of upper plenum thermal-hydraulic phenomena in the Slab Core Test Facility 7-42152
 TRANS7 algorithm for transient anal. in reactor loops 7-30589
 transient 3D 3-phase 3-component nonequilibrium flow in porous bodies by 3-velocity fields. 7-56782
 transient analysis, safety aspects of improved plant behaviour 7-49581
 TRANSLOOP code for PWR transients 7-49501
 TREAT transient overpower tests, behaviour of metallic U-fission fuel 7-36225
 Tsjernobyl accident, appl. of two-dimensional trajectory model to radioactivity transport 7-59894
 TUF two-phase flow code for reactor thermal-hydraulics anal. 7-15237
 two phase flow demonstration device for nuclear thermal hydraulics education 7-29647

fission reactor safety continued

two-fluid models, virtual mass term formulation, momentum transfer, reactor appl. 7-5385
 two-phase bubbly flow in a pipe, turbulence meas. reactor safety appl. 7-5392
 two-phase flow through breaks in horizontal pipe, stratified flow 7-770
 TWOLAY program for heat transfer in stratified molten pools after PWR or LMFBFR accidents 7-30501
 uncertainty propag. in fault trees, quantile arithmetic methodology 7-36095
 uncovered-bundle heat transfer under high-pressure boil-off conditions 7-5359
 UPTF PWR LOCA expt. program 7-49583
 valve manufacture in Czechoslovakia, design criteria 7-56804
 valve stem packing improvements and gland adjustment for leakage reduction 7-10265
 vapour explosions with a mass of grains, fuel-coolant interaction in reactor accident 7-19405
 vessel melt through by molten core materials, time calcs. (*Czech*) 7-62025
 VHTR steam generator, dryout and flow of gas-water flow in U and inverted U bends 7-5399
 vital area determination techniques at nuclear power plants 7-30640
 vitrified colemanite and impregnated polymer, nuclear shielding materials 7-726
 volatile fission products, thermochemical approximation (*Dutch*) 7-36208
 VVER, in-reactor monitoring systems 7-5343
 WAM-E code for reactor safety fault tree anal. and risk assessment, user's manual 7-19346
 water level and pressure perturbations using Oyster Creek RETRAN model 7-62037
 water-level monitor, ex-core, LOFT calculation comparisons 7-42127
 welding advances in nuclear plants 7-30638
 worst case reactor accidents, fission product source term methodology 7-781
 WWER 440, bubbling depressurisation containment, reliability anal. (*Czech*) 7-62026
 WWER 440, hermetic zone leakage tests, CSSR program and methods (*Czech*) 7-62027
 WWER 440, primary coolant system, pressure ratios during positive reactivity insertion transients (*Czech*) 7-62024
 WWER core boiling crisis props. (*Czech*) 7-56777
 WWER pressure vessel safety analyses by SKODA Plzen (*Czech*) 7-56806
 WWER-440, cold leg break LOCA, fuel rod thermomech. eval. under blowdown conditions (*Russian*) 7-49598
 WWER-440, fast neutron dose meas. for pressure vessel using $^{93}\text{Nb}(n,n')^{93}\text{Nb}^m$ 7-56780
 Zarnowiec nuclear power station, safety system eval. (*Polish*) 7-19413
 Zion Probabilistic Safety Study, methodology for PRA reviews 7-15295
 Zircaloy, claddings, creep deform., bulge growth, time to failure 7-59589
 Zircaloy clad UO_2 fuel elements, fission product release, deposition behaviour 7-25149
 Zircaloy oxidation and embrittlement criteria for emergency core cooling system acceptance, safety margins 7-36154
 Zircaloy-4, oxidation under limited steam supply from 1000-1400°C, LWR accident anal. 7-53968
 Zircaloy-4 fuel sheaths, failure model, circumferential temp. effect 7-728
 Zircaloy-4 PWR fuel cladding, deformation, embrittlement and oxidation during LOCA 7-25036
 $^{252}\text{Cf}(n, X)$, spectral investigations for biological shield labyrinth calc. 7-36298
 ^{60}Co ion adsorption on hematite particles, BWR radiation field build-up 7-49588
 Cs and I source terms of irradiated UO_2 reactor fuel 7-775
 CsI aerosol particles growth in steam environment, effects on removal 7-15281
 CsI solution radiolysis in conditions related to a PWR severe accident 7-49600
 H_2 -air detonations, large scale expts. review, reactor safety 7-36211
 H_2O_2 behaviour in RBMK-1000 BWR safety control system coolant circuit 7-30631
 I, source term calcs., effect of organic impurities 7-42168
 I, source term evaluations 7-42167
 I_2 gas phase radiation chemistry in reactor post-accident environments 7-49601
 I_2 volatility from evaporating PWR primary coolant films in accidents 7-49603
 $\text{I}_2\text{-H}_2\text{O}$ vapour partitioning under severe reactor accident conditions 7-49602
 Na ionization detector for FBR sodium leak detection system 7-5355
 Na removal from reactor components, test program 7-42174
 NaOH, molten, wastage simulation with submerged impinging hot N₂ jet 7-62050
 UO_2 debris beds in pressurised water pools, coolability, DCC-1 and DCC-2 results 7-15279
 UO_2 heat capacity, enthalpy, critical review 7-16787
 UO_2 irradiated fuel, ^{137}Cs and ^{129}I leaching, rel. with fuel element power 7-786
 UO_2 operating fuel elements, short-lived fission product release under oxidising conditions 7-785
 UO_2 oxidation by high pressure steam, H_2 source in reactor accidents 7-25143
 UO_2 trace irradiated pellets, volatile fission product release 7-788
 UO_2 -Na fuel-coolant interaction, thermodynamic bounds, LMFBFR appl. 7-42138
 Xe-filled compensated ionisation chamber, transient anal. to quantify sensor degradation 7-42134
 ^{135}Xe , activity determination by γ -ray spectrometry, nuclear plant effluent air check 7-25298
 Zr-Nb (2.5 wt.%) pressure tubes, remote field through wall EM inspection 7-46759

fission reactor theory and design

see also *fission reactors; fission research reactors; neutron transport theory*
 1D homogeneous plane slab, spectral anal. of multigroup neutron transport operator 7-715
 3×6 fuel rod bundles, anisotropic turbulent flow in subchannels, numerical anal. 7-15272

fission reactor theory and design continued

3D general geometry Monte Carlo calcs., vectorisation, reactor transport appls. 7-36088
 acceleration signal characteristics for loose part impact 7-49504
 advanced thermohydraulic codes, development, validation and appl. 7-49500
 aerosol source terms in nuclear reactor accidents, ex-vessel fission product releases 7-36219
 AGR, low temperature carbonaceous deposition, models and theory 7-42108
 AGR, Stage 2 fuel design, performance improvement 7-49543
 AGR boilers, Heysham I and II and Hartlepool II modifications 7-15253
 AGR fuel handling, temp. and gas flows modelling 7-56745
 AGR fuel height stringer drop tests, damage estimates 7-56814
 AGR fuelling machine design, seismic constraints 7-56730
 AGR fuelling machine hoist system, single component failure mode deletion 7-56731
 AGR on-load refuelling, component vibr. problems 7-56732
 AGR refuelling approach at Hinkley Point B 7-56746
 AGR refuelling machine designs 7-56729
 AGR spent fuel handling in long term dry store 7-56869
 AMB-200 reactor, neutron flux control algorithms and monitoring system 7-49497
 ASME Boiler and Pressure Vessel Code, design developments 7-49506
 ASME Code, Section III, subsection NB, revision suggestions 7-56719
 ASSERT and COBRA codes for flow distrib. in vertical bundles 7-10208
 automatic fuel shuffling 7-56744
 baffle/reflector region homogenisation calc. 7-30487
 Bechtel automated control of design document data 7-36092
 BIBLIS-B reactor pressure vessel, fracture mech. anal. for thermal shock transients 7-10220
 bifurcation, nonlinear dynamics, chaos 7-30481
 BRIG-300 FBR, gas channel study program (*Russian*) 7-5361
 British Standard 5500 for pressure vessel design and construction, appl. to AGRs 7-49510
 Brunswick Steam Electric Plant, visual weld acceptance criteria 7-36098
 burnable absorber modeling for PWR core reload design appl. 7-36080
 BWR, assessment of the heat transfer models in the TRACBO2 code 7-62006
 BWR, commercial load following operation with KWU design 7-5347
 BWR, correlation for predicting reactor power during ATWS 7-62038
 BWR, density wave oscills. in boiling water system, two-fluid model simulation 7-36192
 BWR, heterogeneous model, detector field of view 7-36186
 BWR, heterogeneous model, neutron noise decomposition into local and global components 7-36187
 BWR, linear and nonlinear density wave instability modes, anal. modelling 7-5375
 BWR, MSIV-ATWS events, power level and pressure suppression pool temp. 7-42155
 BWR, new scenario for intersystem LOCAs 7-42162
 BWR, reduced-order model of linear dynamics 7-30478
 BWR, TRACBO4 study on suppression pool swelling during containment venting 7-42156
 BWR broken recirculation line, two-phase flow phenomena 7-61989
 BWR core stability estimation, applicability of multivariable autoregressive method 7-25140
 BWR dynamics identification, dynamic data system methodology 7-30474
 BWR fuel design for load following 7-30561
 BWR LOCA research and development of SAFER code (*Japanese*) 7-56711
 BWR nuclear power plant simulation 7-49530
 BWR simulations at high speed using parallel processors 7-36085
 BWR stability anal., dual loop jet pump model 7-62005
 BWR/6 DBA analysis with limited ECC 7-42154
 CAE-nuclear engineering analysis on 32-bit work-station computers 7-36083
 CAGR-on-load refuelling, safety case development 7-56815
 Calder Hall, 30 years of operation, design, procedures and requirements 7-56795
 CANDU, header void distrib. effects on fuel channel flow following inlet header stratification 7-15298
 CANDU, modeling of drift effects 7-61952
 CANDU, turbulent moderator flow, numerical modelling 3D 7-10259
 CANDU coolant pump seals, improved performance 7-36101
 CANDU design improvements 7-10193
 CANDU fuel bearing pad, algorithm for nonlinear thermal anal. 7-15273
 CANDU fuel bearing pad thermal design, FEAT3D code 7-15274
 CANDU fuel channels, calculation of steam flow 7-10262
 CANDU fuel channels, subchannel flow distrib. following deformations 7-10210
 CANDU header manifold, flow stratification under small-break LOCA 7-62041
 CANDU heat transport system, stability criterion for flow oscillations 7-10205
 CANDU horizontal subchannels, numerical simulation of two-phase flow 7-10207
 CANDU neutronics analysis, alternative approach using GAM, GATHER and CITATION 7-15269
 CANDU thermohydraulic codes, transient two-phase velocity difference model for drift calcs. 7-30608
 CANDU-600 heat transport system flow stability 7-30607
 CANDU/GCR clusters, collision probability calcs. using interface current method 7-19332
 cell parameters, sensitivity coeffs., calc. method, neutronic props. 7-19389
 central control rod worth calculations in the multigroup approximation 7-25111
 Chernobyl, technical appraisal 7-62015
 Chernobyl accident, event sequence, consequences, anal. (*German*) 7-25147
 Chernobyl accident, RBMK construction and operational features, accident causes (*German*) 7-56803
 Chernobyl accident, thermal hydraulic characteristics and follow up calcs. (*Japanese*) 7-62021
 Chernobyl RBMK-1000 reactor, computer simulation of accident initiation (*German*) 7-62019

fission reactor theory and design continued

Chernobyl safety design comparisons with Ontario Hydro reactors 7-10270
 Chinese Atomic Energy Institute nuclear data work 7-30502
 classical slowing down problem, anal. soln. 7-42103
 coarse-mesh nodal methods for n diffusion and transport neutron diffusion reviews 7-5314
 COBRA-NC code anal. of steam line break 7-61954
 COBRA-OSU improved numerical method for subchannel cross-flow calculations 7-30497
 code writing organizations, coordination of industry, government and university research 7-49515
 colour graphics display system 7-25122
 common cause failures, defensive tactics for branched events 7-36232
 components, asymptotic and reference stresses for design by anal. 7-49518
 components, design, construction and safety codes 7-49512
 computational continuum dynamics, parallel algorithms 7-4683
 computer-graphic visualization of dynamics 7-30484
 computerised core refuelling 7-56743
 concrete shield, fast neutron albedo calcs. 7-30622
 conduction-controlled rewetting with internal heat generation, 2D anal. 7-10254
 conf., Dresden, Germany (March 1985) 7-24266
 conf., London, England (September 1985) 7-18492
 conf., Toronto, Ont., Canada (1986) 7-9587
 conference on two-phase flow dynamics, Lake Placid, NY, USA (Aug. 1984) 7-4627
 confined Bernard problem, nonlinear phenomena, numerical parametric anal. 7-30482
 construction codes and engineering mechanics conf., Paris, France, Aug. 1985 7-48153
 containment thermohydraulics in major accidents (*German*) 7-56802
 convection-diffusion problems in irregular geometries, finite difference soln. 7-30493
 coolant energetic physical state, prediction using partial coherence functions (*Russian*) 7-49528
 core coolant channels, coherent blockages, statistical thermodynamics, percolation anal. 7-36194
 core physics parameter calcs. using CELL2 code 7-25030
 cores, spectral disturbance influence on macroscopic few-group parameters (*German*) 7-56713
 countercurrent flow and flooding with abrupt area changes 7-61999
 Courant limit violating numerical method in RELAPS/MOD2 calcs. 7-30495
 CRACUK code, dosimetric models modifications 7-19349
 CRACUK user's guide (appendix to the CRAC2 user guide) 7-19348
 critical slabs, P_N approx., modified boundary conditions, neutron conservation 7-5310
 critical slabs, P_N approx., neutron conservation and conservation eqn. rel. 7-5309
 criticality calculation code SIMCRI 7-10192
 criticality problems, 3-dimensional, soln. by simplified response matrix technique 7-49531
 cylinder of finite height, neutron transport problems with anisotropic scatt., integral transform method 7-15225
 Czubek's method for neutron cross section meas., accuracy 7-36065
 damaged fuel assembly repair 7-56767
 Darlington generating station fuel handling system 7-56733
 decay energies for fission products in JNDC FP Decay Data File 7-15236
 degraded core coolability study 7-62046
 density wave oscillations, stability map construction method, reactor appls. 7-5378
 Diablo Canyon PWR plant, integrated control and communications system 7-42130
 diffusion critical problem, two-dimensional, soln. using SIXTUS-2 code 7-19327
 dimensional analysis, use in neutron transport theory 7-36066
 discrete ordinates transport methods, 3D, synthetic acceleration, interface current approach 7-36073
 dissociating coolant reactors, core active zone thermotechnical reliability (*Russian*) 7-49525
 distributed data base systems, control and application 7-36091
 DNBR limit, prediction of transient axial power distrib. 7-62039
 DNBR studies, streamlined one-pass modeling 7-62004
 double heterogeneity effects, narrow resonance calcs. 7-30485
 dynamical response of systems with localized nonlinearities, ultimate state method 7-10190
 EBR II intermediate heat exchanger, real time anal. 7-30492
 EBR-II, delineations of power and power-to-flow feedback components 7-42132
 effective resonance levels 7-36077
 EFWS, bus configurations, four-train versus two-train support 7-42161
 engineering aspects of the Hartlepool and Heysham I fuelling machines 7-56735
 equipment-structure systems, eigenproperties, perturbation anal. 7-25130
 ESCORE code for LWR steady-state core reload eval. 7-25027
 evaluation of threshold reaction data 7-30505
 extended burnup, ex-core and accident considerations 7-30547
 FACSIMILE code for void swelling calcs. 7-25037
 Farmer's line, probability density functions, and overall risk 7-25144
 fast reactor, appl. of hexagonal geometry nodal expansion diffusion method 7-19326
 fast reactor core analysis, 3D transport anal., TRITAC and TWOT-RAN-II calcs. 7-49569
 fast reactor critical expt., anal. using nodal diffusion and transport methods 7-19325
 FBR above-core structures, finite element anal. using SAFE/RAS program 7-15230
 FBR energy independent adjoint flux method, SEG-V configuration perfection 7-19337
 FBRs, safety assessment of severe accidents 7-62029
 fEMAXI-III calculations for the D-COM blind problem 7-717
 FFTF, reactivity worth of gas expansion modules 7-42131
 finite element reactor calculations, improved algorithm 7-19340
 first order neutron transport eqn., finite element response matrix method 7-36075
 fission product, decay heat calculation problems 7-30506
 fission product neutron capture transformation effects on decay power after reactor LOCA 7-49587

fission reactor theory and design continued

fission-product cross section evaluation, integral tests and adjustment based on integral data 7-30504
 flow modelling in 3-D fracture networks 7-56799
 fluidised bed power reactor, transient neutron flux modelling 7-62017
 FRJ-2 reactor, design developments (*German*) 7-61945
 fuel assembly subcriticality determ. by the Mihalcz method (*Japanese*) 7-25104
 fuel element load/unload machine for the Italian PEC reactor 7-56736
 fuel evolution and shuffling studies, generalized perturbation theory anal. 7-30490
 fuel handling, microprocessor appl. 7-56741
 fuel handling machinery, control equipment 7-56740
 fuel handling options for commercial fast breeder reactors 7-56726
 fuel handling prototype machines, design and test methodology 7-56727
 fuel rod steady state thermal behaviour, uncertainty analysis, probabilistic response surface method 7-729
 fuelling machines, high integrity control system, design and development 7-56742
 Fugen, refuelling machine experience 7-56737
 fully developed axial turbulent flow in fuel rod bundles, finite vol. calc. 7-36189
 fundamental aspects of thermal hydraulics 7-61998
 gas cooled rod bundles, pressure drop and heat transfer, fuel design 7-36190
 gas-cooled reactors for advanced terrestrial appl. 7-61956
 general next event surface crossing estimators for Monte Carlo methods 7-30470
 geometric progression formula for γ -ray buildup factor approx. 7-30475
 graphite moderated reactors, stored Wigner energy 7-42142
 Hamilton-Jacobi approach to neutron diffusion reactor theory 7-61937
 heat exchanger tubes, cyclic temperature transient influence on creep behaviour 7-10186
 heat exchangers, computer-aided tube fretting-wear predictions 7-10261
 heated gas flow in circular tube, friction factor studies (*Japanese*) 7-57924
 heterogeneous reactor, refined finite-difference equations 7-25021
 heterogeneous reactor polycell, fuel multirod cluster, neutron flux 7-61950
 high temperature reactor components, multiaxial loading tests 7-49541
 high temperature structures in reactors, creep curve variation effects on creep behaviour 7-39602
 high-temperature reactors, Germany design codes and standards 7-49514
 homogenization techniques in reactor lattices 7-10182
 HTGR, fracture criteria of reactor graphite under multi-axial stress (*Japanese*) 7-61946
 HTR, reactor protection building anal. for He release (*German*) 7-30639
 hybrid reactor pebble bed blanket, magnetohydraulic flow in Na-K eutectic mixture 7-15366
 hydraulic network, large-scale, nonlinear conservation laws 7-10196
 implicit Kalman filter algorithm for nuclear reactor analysis 7-30488
 in-core management calculations for the EWA research reactor 7-49523
 incident control, simulation of man machine interaction 7-15287
 independent fission yield measurements, review 7-61948
 Indonesian nuclear data activities 7-30503
 inherently safe power reactor DYONISOS 7-49496
 inspection and repair of fuel assemblies 7-56766
 integral test for heavy nuclides 7-30509
 irradiated fuel disposal facilities, fuel cooling, concept to commissioning 7-56868
 IRT-2000 reactor, α -quantity meas. at thermal point by multiplicity spectroscopy (*Russian*) 7-42123
 JAERI reactor engineering dept 1985-6 annual report 7-56725
 JENDL-2 fission product file, resonance parameters 7-15235
 KNU1 plant transient simulation using RELAP5/MOD1/NSC 7-5374
 KQCS-2 code for multigroup const. calc. for fast reactors 7-30511
 large size LMFBRs, designs for inherent safety capability, accident anal. 7-36223
 lattice homogenization procedure using the nodal expansion method and equivalence theory for LWR 7-49533
 learning curve estimation techniques for nuclear industry 7-15296
 linear nodal S_8 calculations, acceleration using diffusion-synthetic method 7-36072
 linear particle transport eqns., duality in transport theory 7-56710
 liquid solid phase change front-prediction method 7-62002
 LMFBR, 1000 MWe axially heterogeneous design, neutronics performance (*Japanese*) 7-15228
 LMFBR, development and evolution (*German*) 7-56716
 LMFBR, French creep-fatigue design rules 7-49522
 LMFBR, reactivity effects of hydrocarbon, effect of group constant generation method 7-56808
 LMFBR calculations in hexagonal geometry, nodal expansion method 7-56709
 LMFBR class 1 components, design rules and elastic creep-fatigue damage evaluation 7-49540
 LMFBR codes and standards EEC activities 7-49516
 LMFBR components, RCC-MR code for design and construction 7-49511
 LMFBR core, mechanical analysis using ARKAS code 7-30479
 LMFBR flux group const. generation Doppler effect calcs. 7-19336
 LMFBR high temp. components, UK research and design methods 7-49513
 LMFBR long-life core designs, physics considerations 7-42111
 LMFBR materials, buckling anal. and design rules 7-49517
 LMFBR plenum, thermal hydraulic anal. 7-10258
 LMFBR steam generator design and experience in the UK 7-56791
 LMFBR ultra long life cores 7-61957
 LOCA, peak cladding temp. calcs., LOFT anal. 7-42158
 LOCA, uncertainty anal. using Fourier amplitude sensitivity test 7-42160
 loop flow reactor plant for coolants with knowntechnological characteristics (*Russian*) 7-5325
 LWHCR lattices, effects of WIMS data library changes on calc. results 7-5316
 LWR, application of a direct-heating model to the Sandia SURTSEY tests 7-62042
 LWR, Chen boiling heat transfer correlation 7-42153
 LWR, coarse-mesh method for 1-D reactor kinetics, accident anal. 7-42140
 LWR, corium droplet size in direct containment heating 7-62007
 LWR, drift-flux model for void fraction prediction 7-25121
 LWR, generalised transient fuel-cycle model convergence 7-5327

fission reactor theory and design continued

LWR, heat radiation through steam in direct containment heating 7-62008
 LWR, in-core gamma effects, power distrib., detector response 7-42137
 LWR, reflooding, bubbly-slug interfacial shear, effect on liquid carryover using RELAP5/MOD2 7-62001
 LWR, rewetting correlations, modifications and assessment 7-62000
 LWR, severe accident containment load calculations using HMC code 7-62044
 LWR accident source term expts. deposition samples 7-62047
 LWR analysis, assembly homogenization techniques, review 7-5324
 LWR engineered safety features in severe accident conditions 7-10268
 LWR lattice problems, 2D neutron transport, ang. current approx. choices, RICANT program 7-15270
 LWR life extension, records requirement review 7-56721
 LWR severe core damage accident, uncovered core thermal-hydraulics, model dev. 7-30624
 LWR steam generator U-tube rupture transient anal. using DRUFAN-02 code 7-49562
 LWR thermal hydraulics, SEFDAN code for severe core damage accidents 7-49503
 LWR thermohydraulic core anal. methods 7-49499
 Magnox on-load refuelling grabheads, engineering design and development 7-56734
 Maple Research Reactor, core and fuel selection 7-5335
 MARS reactor plant, an inherently safe, small/medium multipurpose nuclear plant 7-25022
 metallic nuclear power plant components, German codes and standards 7-49508
 microcomputer appl. in nuclear engineering 7-30499
 mixture drift-flux eqns. soln. algorithm on multi-CPU pipeline machines 7-30494
 modular HTGR, very high temp. capability exploitation 7-61955
 modular HTGR plant, steam generator design considerations 7-62014
 Monju, prototype FBR, construction codes and safety evaluation 7-49509
 Monju FBR, anal. and design for elevated temp. components 7-56717
 monoenergetic integral transport eqn. across a plane boundary, improved soln. 7-15226
 monoenergetic neutron fluence standards 7-30508
 Monte Carlo electron interface studies, incorporation into photon cavity theory 7-36079
 Monte Carlo source biasing, choice of biasing fn. 7-36070
 multidimensional thermal hydraulic anal. of reactor components, computer codes 7-10199
 multiply connected secondary systems, instructure response spectrum for seismic anal. 7-5322
 multivariable control system design using CAD package 7-10211
 neutron diffusion equation, modal expansion method, accuracy improvement using finite-difference scheme 7-15224
 neutron dynamics transport codes, analytical benchmarks 7-61943
 neutron flux calcs., interface flux nodal method 7-10184
 neutron transport eqns., modified diffusion synthetic acceleration algorithms 7-36067
 neutron transport equation, multigroup finite element soln., scatt. anisotropy 7-5308
 NF-6 program complex for multigroup diffusion network calcs. (*Russian*) 7-49526
 nodal transport theory in hexagonal geometry for fast reactor appl. 7-19329
 noise monitoring, digital generation of stochastic signals of arbitrary spectral shape 7-5341
 nonlinear dynamics of multispecies Boltzmann equations 7-30483
 nonlinear dynamics of two-phase flow 7-30617
 nonsymmetric slabs, environment independ. homogenised parameters for neutron diffusion 7-15223
 NUCLARR program for reactor risk assessment 7-30636
 nuclear data conference, Tokai, Ibaraki, Japan (Nov. 1985) 7-29600
 nuclear data evaluation for heavy nuclides 7-30461
 nuclear engineering, heterogeneous dispersed data bases, organization and management 7-36090
 nuclear engineering documentation, archival and retrieval 7-36094
 nuclear fuel systems of the Pake NPP 7-56728
 nuclear piping systems, research overview 7-49595
 nuclear power station design and seismic ground motion is Central Europe (*German*) 7-19404
 nuclear reactor control information, provision in presence of instrument failures 7-5367
 nucleate pool boiling using heated multirod, pressure effects 7-56715
 numerical methods in nuclear engineering, conf., Montreal, Canada, Sept. 1983 7-9600
 numerical stability of upwinding calc. schemes 7-30496
 Ontario Hydro CANDU fuel handling and storage facilities 7-56747
 Ontario Hydro nuclear stations, innovations in design, operation, and construction 7-10194
 Ontario Hydro Pickering generating station fuel handling system performance 7-56748
 optimal xenon control in heterogeneous reactors 7-56775
 optimum discharge burnup, advantages and disadvantages 7-30548
 Paks coolant flowrate, gate valve effects (*Hungarian*) 7-62013
 parity simulation for nuclear plant analysis 7-30489
 passive high-integrity lifting equipment 7-56738
 pebble-bed reactor, physical behaviour and design (*German*) 7-49529
 PEC reactor core fuel element, structural verification criteria 7-49539
 perforated plates, simplified creep anal. for steady creep conditions 7-28094
 perturbation theory appl. to critical parameters and fundamental mode 7-718
 perturbation-based sensitivity anal. 7-5320
 PFR, core guide tube exchanges, experience 7-56751
 PFR Dounreay, fuel handling, maintenance experience 7-56750
 PHWR fuel cluster geometry, interface current method, CLUB code 7-15238
 pin power predictions in the Westinghouse Advanced Nodal Code 7-30486
 piping, technical and economical incentives behind strain limitation 7-10221
 piping criteria and construction costs 7-61953
 piping systems, cycle-dependent material props. 7-10222
 piping systems, dynamic test data, comparison with analytical methods 7-10191
 piping systems, strain limitation calcs. 7-10188

fission reactor theory and design continued

plant life extension, baseline characterization of electrical circuits 7-36096

PNP-500, dynamic modeling and simulation of a high-temperature gas cooled pebble-bed reactor 7-10212

point reactor model from diffusion theory 7-61951

Poisson earthquake occurrence model, nuclear power plant site anal. 7-25150

power plant mechanical components, stress and strain limitation 7-10187

power plants, safety prediction technique 7-19414

PRA, methodology for plant upgrade integration 7-36233

preconditioning techniques for the power method of reactor calcs. 7-30473

precursory cooling effects on rewetting rate 7-49561

pressure vessel and piping design, stress indices for nonradial branch connections 7-49520

primary coolant circuit parameters, control design and dynamical performance (German) 7-56785

PUMA adjustments to core parameters and rational flux mapping procedure 7-10257

pump casings, sizing rules for pressure design 7-49519

pump data correlation for single- and two-phase 7-61995

PWR, adequacy of automatic plant protection system 7-25152

PWR, characteristics of releases from TREAT source-term experiment STEP-1.7-42170

PWR, core loading patterns to maximise beginning of cycle reactivity, automatic determ. 7-25113

PWR, direct heating containment vessel interaction code DHCVIC 7-62043

PWR, flow distrib. calcs. in heated parallel channels (German) 7-25107

PWR, fuel element vibration effects on neutron flux fluctuations 7-25019

PWR, heat transfer during LOCA 7-25151

PWR, high conversion, core performance parameters, sensitivity anal. 7-49524

PWR, LOCA, simulation using TREAT source term expt. 7-42169

PWR, local coolant boiling monitoring by neutron noise anal. (German) 7-15259

PWR, n- γ shielding designs in France 7-25133

PWR, primary loop modelling, appl. of cascaded state feedback control 7-56776

PWR, probabilistic analysis of allowed outage times relaxation 7-42125

PWR, reactivity temperature coeff. meas. by noise method, theory 7-25117

PWR, reactor analysis package for set-point methodology 7-25028

PWR, steam generator tube bundle flow, turbulence force correlation 7-62003

PWR, thermal hydraulic behaviour during loss of offsite power transient without scram (Japanese) 7-56712

PWR, water chemistry guidelines 7-25029

PWR core monitoring, backfit appl. of advanced technology 7-36204

PWR fuel rod, pellet-cladding interaction study (Japanese) 7-5330

PWR fuel rods, power ramp data, FROST and THERMOST codes, cladding deform. rod elongation 7-62034

PWR leak detection studies, dew point, dry bulb temp. and flow rate monitoring 7-42157

PWR load following operation control 7-5353

PWR LOCA, best estimate anal. with thermal hydraulic codes 7-49502

PWR plant-specific availability modelling 7-10198

PWR power plant design for optimum load following capability 7-5317

PWR pressure vessels, fast neutron fluxes using Monte Carlo methods 7-36097

PWR pressurizer, accident and transient anal., nonequilibrium three-region model 7-36195

PWR prestressed containments, response to earthquakes, gas cloud explosions and aircraft impact 7-10264

PWR refuelling using revolving cylinder manipulator crane 7-56739

PWR safety anal. using BIK ID neutron kinetics program 7-5319

PWR turbulence modeling during high pressure coolant injection, COM-MIX-1B code 7-10255

PWRs, neutronic aspects of different moderator-to-fuel volume ratios (German) 7-36185

PYTHIA code for global burnup and flux calcs. in WWER-type reactors (German) 7-56714

RAHAB calc. for lattice parameters of CANDU type reactors 7-36100

RBMK reactors, neutron physics considerations for fuel use efficiency improvements 7-30513

RBMK-1000, energy liberation field calcs. 7-49498

RBMK-1500, fuel pin assemblies, critical power determ. 7-36076

RCC-M code for design and development of PWR components 7-49507

reactor burnup and heavy nuclide nuclear data 7-30510

reactor components, dynamic reliability model for damage accumulation processes 7-30535

reactor neutronic and thermal-hydraulic problems, solns. using engineering workstation 7-36084

reactor refuelling, conf., Newcastle-upon-Tyne, England (May 1985) 7-55891

reinforced concrete shear walls in nuclear power plants, probab.-based design criteria 7-36078

RELAPS/MOD2 code for PWR transient anal. 7-10201

relaxed core stress in ratcheting evaluation for elevated temp. design 7-49521

reliability and risk allocation in nuclear power plants, decision theoretic anal. 7-36081

ROCS/MC code system for coarse mesh reactor anal. 7-10204

RP-10 reactor trip module, availability anal. 7-10238

safe reactor designs 7-15276

safety system design and anal. 7-15288

safety system reliability, design stage quantitative anal. 7-62020

SAFR, 350 MWe inherently safe fast reactor, design and development in USA 7-30472

seed/blanket core, power-sharing formula 7-30603

sensitivity anal. using computer calculus 7-30477

separated flow effect modelling in horizontal heated channel refill 7-10202

shell-and-tube heat exchangers, velocity distrib. comparison for expt. and predictions 7-15275

simplified GPT calculational procedure 7-5315

simulated consolidated BWR fuel, thermal performance predictions using COBRA-SFS code 7-10229

simulation, parallel-processing modular system 7-10197

single group approx. for n transport, perturbation theory method 7-30468

fission reactor theory and design continued

sizewell B PWR, degraded core anal., accident risks 7-62033

Sizewell B PWR, steam generator design for nondestructive exam. requirements 7-56793

SLOWPOKE III, comparison of thermalhydraulic computer codes 7-10260

small HTR in underground silo, concept for urban siting 7-15233

SNR 2 fast breeder reactor development project (German) 7-15303

SNR-300 LMFBFR, design, erection and testing of steel containment 7-25024

SOPHT verification for parallel channel flow stability 7-10206

spallation breeding facilities, neutronics calcs. using Monte Carlo methods 7-10180

spherical head pressure vessels, large deflection anal. 7-5321

SSYST-3 fuel rod behaviour analysis program (Hungarian) 7-56724

stability tests, limit cycles and bifurcations in nuclear systems 7-30618

stability-enhancing two-step method for Transient Reactor Analysis Code 7-10200

steady state operation of nuclear reactor, contributions to control design (German) 7-25105

steam supply system, microcomputer data base 7-36093

steel, low alloy ferritic, strain induced corrosion cracking prevention for BWR piping 7-13641

strain estimation for external event loads 7-10189

structural dynamic models for nuclear plant design, CAE appl. 7-25023

subchannel anal., numerical technique using finite difference method 7-10209

subchannel void fraction predictions using drift-flux anal. 7-30605

supercritical heat transfer in an annular channel with bilateral heating 7-36179

synthetic acceleration of transport calcs. 7-36074

synthetic coarse mesh few group diffusion calcs., finite difference formulation 7-61947

system reliability analysis via generalized perturbation theory methods 7-30498

system state monitoring method using state space trajectory patterns 7-49570

thermal hydraulic anal. on mini- and microcomputers 7-30500

thermal hydraulics calcs., anomalies in 1D 7-10203

thermal power section, parameter sampling (Russian) 7-49527

thermal reactors in perspective 7-61944

thermal stratification predictions due to high-pressure injection in circulating reactor loop 7-30602

thermalhydraulic aspects of natural circulation loop 7-10195

third order Taylor series expansion, nonuniform cell thermal utilization 7-61949

THTR-300 power operation (German) 7-5318

time independent 2D neutron transport problems with voids, discrete cones method 7-15227

time-dependent Nodal Integral Methods in linear and nonlinear heat conduction 7-30491

tornado missile hazard to nuclear plants, numerical methods for risk assessment 7-15293

TRAC analysis of upper plenum thermal-hydraulic phenomena in the Slab Core Test Facility 7-42152

TRAC-PFI/MOD1 code assessment for annular, annular-mist, stratified flow 7-15234

TRANS7 algorithm for transient anal. in reactor loops 7-30589

transient analysis, safety aspects of improved plant behaviour 7-49581

TRANSLOOP code for PWR transients 7-49501

turbulent diffusion in rod arrays with sodium coolant 7-36178

two-dimensional space-time kinetics benchmarks, ADEP code 7-15239

uncertainty propag. in fault trees, quantile arithmetic methodology 7-36095

very high temperature gas cooled reactor, control system design and dynamics 7-768

vessel meth through by molten core materials, time calcs. (Czech) 7-62025

VVER, in-reactor monitoring systems 7-5343

VVER 440 and VVER 1000 nuclear power plants, coolant compensation processes (Czech) 7-766

VVER reactors, neutron physics considerations for fuel use efficiency improvements 7-30513

VVR-M5, thin-walled fuel elements 7-25031

VVRS reactor, neutron flux spectra in channels 7-56718

water level and pressure perturbations using Oyster Creek RETRAN model 7-62037

water moderated reactor, oscillating control element, damping and added mass (German) 7-56779

Westinghouse fifteen years of reactor refuelling experience 7-56749

WWER, fuel assembly outlet temperatures (German) 7-15257

WWER 440, bubbling depressurisation containment, reliability anal. (Czech) 7-62026

WWER-1000 fuel element performance, model computations (German) 7-19355

WWER-40, primary coolant circuit pressure oscillations (German) 7-19392

WWER-70, axial dependence of coolant temp. noise (German) 7-15258

WWER-70, measurement of spectral neutron flux density at boiling conditions (German) 7-15260

WWER-70, unsteady boiling with expt. fuel assemblies, computer anal. (German) 7-15256

Zion Probabilistic Safety Study, methodology for PRA reviews 7-15295

Zircaloy-4, α -phase, burst data, CANSWEL-2 code anal. 7-36159

Zircaloy-4 fuel sheaths, failure model, circumferential temp. effect 7-728

²⁴²Cm(n,f), 0.1 eV-100 keV, fission cross section meas. for reactor apps. 7-42083

⁵⁶Fe(n, γ), capture in 1.15 keV resonance using Moxon-Rae detectors, reactor appl. 7-36004

^AKr(n, γ), 4-250 keV, capture cross sections for A=78-86, reactor appl. 7-36005

Na, rate limited molten fuel coolant interaction model 7-36102

^APu, A=23, 241, reactor parameters, uncertainties in scientific measurements 7-42085

^ARb, A=94, 95, P_n values by β - γ spectroscopic method 7-30507

^ARb, A=94,95, P_n values measured by β - γ spectroscopic method 7-5194

^AU, A=233, 235, reactor parameters, uncertainties in scientific measurements 7-42085

²³⁵U, aqueous critical assemblies, Monte Carlo anal. with ENDF/B-V data 7-30476

fission reactor theory and design continued

- ²³⁵U(n,f), delayed neutron activity, few-group anal. 7-42084
²³⁵U(n,f), international fission foil mass intercomparison, α -decay rates 7-42086

fission reactors

- see also *fission reactor decommissioning; fission reactor materials; fission reactor operation; fission reactor theory and design; fission research reactors; hybrid reactors; nuclear engineering; nuclear physics; nuclear power stations*
 breeder reactors, Na removal from components, test program 7-42174
 CANDU reactors, economic threats from reduced cost enrichment processes 7-10306
 Chernobyl reactor surface temp. analysis using Landsat TM images 7-49585
 conference, ANS winter meeting, Washington, DC, USA, (Nov. 1986) 7-29591
 geological natural nuclear reactor at Oklo, Gabon, Africa (French) 7-28954
 PWR reactor simulation for operator training, use of computer graphics 7-55940
 soft X-ray diode array diagnostic for JET 7-1787

fission research reactors

- see also *fission reactor core control and monitoring; fission reactor instrumentation; fission reactor theory and design*
 computer codes for operational control 7-15232
 conf., Toronto, Ont., Canada (1986) 7-9587
 coolant boiling in research reactors, expts. in WWR-SM facility (German) 7-56781
 development research of nuclear reactors in France (French, English) 7-19398
 DIORIT research reactor, activation product distrib. in shielding materials (German) 7-49536
 EBR II, superheater SU-712, duplex-tube performance, statistical anal. of data 7-19395
 EBR-II, delineations of power and power-to-flow feedback components 7-42132
 EBR-II, ramped power transients, feedback simulation using transfer functions in EROS code 7-42188
 Experimental Steam Generating Facility, PWR secondary water chemistry study (German) 7-25116
 FFTF, fuel rotation or reorientation for extended burnup 7-30546
 FFTF, GEM shutdown device appl., use in unprotected LOF events 7-36227
 FFTF, reactivity worth of gas expansion modules 7-42131
 FFTF as an irradiation test bed for fusion materials and components 7-49662
 FR2 research reactors, chemical and radiochemical meas. 7-25040
 FRJ-2 reactor, design developments (German) 7-61945
 fuel in-storage criticality safety during manufacturing 7-730
 Hanford N Reactor, core simulation, development and appls., DELPHI code 7-42112
 Hanford N Reactor, flux flattening programme, core physics calcs. 7-42133
 HENDEL, gas bearing circulator, bearing characteristics 7-10249
 HFIR irradiation facility, HIFI Project 7-49615
 HFR, nuclear exptl. program. (Dutch) 7-19175
 in-core management calculations for the EWA research reactor 7-49523
 instrumental elementary anal., fission research reactor equipment complex 7-39932
 JOYO radiation streaming, energy-space dependent error propagation in Monte Carlo coupling calculations 7-19335
 LEU fuel conversion of test and research reactors, related problems 7-36106
 LOFT facility, rewet, NCC, stratified flow and plant recovery procedure studies 7-49564
 Maple Research Reactor, beam tube performance assessment 7-5365
 Maple Research Reactor, core and fuel selection 7-5335
 MORSE-CG code for pulsed fast reactor problems, Monte Carlo anal. 7-15229
 NRU, early innovation during operation 7-10253
 NRX, early innovation during operation 7-10253
 nuclear reactor control information, provision in presence of instrument failures 7-5367
 Petten HFR, reactor vessel replacement, dismantling, segmentation, waste disposal, doses 7-5488
 PGN-200M loop steam generators, noise level measurements 7-61982
 PROTEUS, high converter LWR test lattices, fuel enrichment effects on characteristics 7-19396
 pulsed source experiments, use of ex-core epithermal detectors, kinetic distortion 7-56771
 RKFB, reactor kinetic code with feedback for materials testing reactors 7-36099
 ROSA-III, break location effects on thermal-hydraulics during intermediate break LOCA expts. 7-49589
 Rossendorf Research Reactor, computer-based γ -ray area monitoring system (German) 7-19552
 Rossendorf research reactor, coolant boiling expts. (German) 7-56786
 RP-10 reactor trip module, availability anal. 7-10238
 SEFOR test reactor, gamma anal. of soil following decommissioning 7-30726
 SLOWPOKE III, comparison of thermalhydraulic computer codes 7-10260
 TRIGA reactors, LiF thermoluminescent dosimeter appl. in n- γ mixed field dosimetry 7-49733
 UPTF PWR LOCA expt. program 7-49583
 VVR-M5, thin-walled fuel elements 7-25031
 ZPPR fast reactor, nodal diffusion and transport methods for critical expt. anal. 7-19325
 Cd plates, reactivity worth in MTR-fuel-type reactor 7-56772

fissures see *cracks***flame sprayed coatings**

- powdered materials, gas-thermal coating, substrate porosity effect 7-53999
 sintered materials, coating deposition process character. 7-54002
 TiCN-Ni-Mo composite powders and coatings, prep. and characteris. 7-3255

flame spraying

- ceramic engine component fabrication techniques 7-3243
 powdered materials, gas-thermal coating, substrate porosity effect 7-53999

flame spraying continued

- sintered materials, coating deposition process character. 7-54002
 thermographic look at plasma spraying 7-24648
 SiC whisker reinforced Al, flame spraying fabrication and forging, whisker distrib. and strengths 7-59483
 TiCN-Ni-Mo composite powders and coatings, prep. and characteris. 7-3255

flames

- see also *chemically reactive flow; combustion; fires*
 acetylene-O₂, flame, temp. and OH-conc. profile, IR spectroscopic determ. (French) 7-25513
 annular premixed propane flame, mass transfer, residence time in recirculation zone 7-17790
 atomised liquid fuel, turbulent diffusion flame, fine struct., using pneumatic nozzle 7-17791
 behaviour during cylindrical vessel explosions 7-59760
 chemically reacting transverse turbulent jet, flame struct. and vorticity 7-20809
 coal dust flame acceleration, feedback control model for unsteady flow 7-65326
 counter-flow premixed flames, flame interference effects on flammability limits 7-23020
 cross-beam polarisation spectroscopy with pulsed dye laser 7-13771
 curved, nonlinear thermal diffusive theory 7-57941
 diagnosis by laser Raman spectroscopy, 3D distrib. of temp. and conc. (Chinese) 7-59804
 diagnostics by pulsed photothermal and photoacoustic deflection spectroscopy 7-23016
 diffusion, bluff-body stabilised, near-wake region, CARS meas. 7-8282
 dissipative systems, stationary soliton soln. investig. 7-51034
 ethylene premixed flame, soot particle inception, O₂ profiles 7-23019
 fluctuating temp. meas. by thermocouple 7-56264
 front propag. convective vertex form. 7-13777
 fuel drop-air mixtures, flame propag. 7-23018
 gaseous mixture wrinkled flames, reactive-diffusive model 7-46849
 hydrodynamic instability, nonlinear theory, weak thermal-expansion approx. calcs. 7-59764
 jet diffusion flame in co-flowing air stream, turbulence struct. 7-43996
 jet diffusion flames, flow visualisation using Mie scatt. method 7-11566
 jet diffusion flames, swirl effect on stability 7-23017
 laser Doppler anemometer for vel. meas. in enclosed flames (German) 7-18765
 laser induced fluoresc. imaging calibration 7-59759
 Linan's premixed flame regime, stability 7-17797
 magnetic field effects on biological and chem. processes 7-47135
 methane and propane in diluted air, diffusion flames, extinction limits 7-3590
 methane-air laminar counterflow diffusion flames, struct., CARS meas. 7-57939
 methane-air laminar diffusion flames, struct. 7-65327
 methane-air turbulent diffusion flames laminar-flamelet modelling 7-57938
 multiphoton excitation techniques for combustion diagnostics 7-17789
 one dimensional unsteady flame propagation, nonlinear partial diff. eqn. system (French) 7-65320
 one-dimensional premixed, wave characts. 7-8279
 plane premixed flame, nonlinear differential system modelling (French) 7-28313
 premixed flame, struct. and extinction limit, Lewis no. effects (Chinese) 7-11559
 premixed laminar flames in stagnation point flow, calculation of extinction limits 7-59762
 propagation, unsteady and ID, mathematical anal. 7-57944
 propagation emission tomography 7-61368
 propane jet flames, near-nozzle region, flow struct. 7-8280
 propane-air flames, explosion venting, 2D Navier-Stokes eqns. 7-51340
 reacting flows, combustion and chem. reactors, book 7-4644
 rotational CARS generation through multiple four-colour interaction 7-50632
 suspensions, reactive, flames, radiative transfer as propag. mechanism 7-17796
 turbulence generation and suppression 7-8281
 turbulent, struct. calc. 7-65321
 turbulent reactive flow, num. computation (French) 7-57943
 CO in combustion flows, two-photon digital imaging using planar laser-induced fluorescence 7-46896
 H₂ flames, two-step saturated fluoresc. detect. 7-19759
 H swirling turbulent diffusion flames, turbulence intensity study 7-26287
 H₂, turbulent jet diffusion flame, conserved scale probability density functions 7-26260
 H₂-O₂, flame, temp. and OH-conc. profile, IR spectroscopic determ. (French) 7-25513
 H₂-O₂-N₂ flames, one-dimensional simulation, mathematical and numerical aspects 7-39893
 KCl, solute trapped from air-acetylene flame, morphological investig. 7-28362
 Na atoms in flame, laser-probed resonant Voigt effect, analytical detection sensitivity 7-19764
 O atom, flame diagnostics by two-photon fluoresc., UV laser appl. 7-23015
 OH in flames, excited state rot. population study using laser induced fluoresc. 7-3592
 OH radicals in spray flames, planar laser-induced-fluorescence monitoring 7-59766

flare stars

- YZ CMi, dwarf M flare star, simultaneous IUE and VLA obs. 7-47931
 YZ CMi, photoelectric monitoring and flare characts. (1980 to 1984) 7-4493
 YZ CMi, simultaneous X-ray and optical monitoring 7-24151
 YY Gem, components atm. activity, IUE and H β spectra anal. 7-55677
 HEAO A-1 all-sky survey of fast X-ray transients 7-60836
 L726-8A, narrow-band radio flares, mechanisms anal. and UHF obs. 7-60679
 EV Lac, Bulgarian flare obs. (1986 Aug.) 7-55658
 EV Lac, eclipsing UV Cet star, photometric obs. of flares 7-66614
 EV Lac, photoelectric monitoring and flare characts. (1980 to 1984) 7-4493
 EV Lac, UV Cet star, mass expulsion episode, obs. characts. 7-55672
 EV Lac, UV Cet star, UV radiation rot. modulation 7-47933
 AD Leo, dwarf M flare star, simultaneous IUE and VLA obs. 7-47931

flare stars continued

- AD Leo, narrow-band radio flares, mechanisms anal. and UHF obs. 7-60679
 AD Leo, periodic var. 7-14582
 AD Leo, photoelectric monitoring and flare characts. (1980 to 1984) 7-4493
 AD Leo, UV Cet star, flare activity anal. 7-29487
 AD Leo, UV Cet star, giant flare UV and visible obs. 7-55676
 AU Mic, BY Dra star, IUE spectra of fluxes 7-47939
 AT Mic, dMe star, UV and visible obs. 7-47934
 AT Mic, flare far-UV spectra compared with solar flares 7-47937
 AT Mic, UV Cet star, quiescent emission at 843 MHz 7-34998
 TZ Ori, flaring Orion variable, photometric characts. 7-40818
 Orion Nebula region flare stars, survey 7-14591
 southern objects, search for 843 MHz radio emission from active stars 7-55671
 Taurus T-associations, photometric study of flare stars 7-24136

flares, solar *see solar flares***flash lamp annealing** *see incoherent light annealing***flash lamps**

- low-pressure, background radiation from ablation phenomena 7-43282
 microsecond discharges in flash lamps, elec. cct. matching 7-10978
 Xe, photoelectronic source for swarm expts. in high-density gases 7-9925

flash photolysis *see photolysis***flashover**

- bipolar electric field flashover of vacuum interfaces in accelerator cavities 7-30750
 epoxy spacers exposed to sparks and SF₆ arcing byproducts, surface characterisation 7-39692
 iced insulator string flashover mechanism; role of water film 7-51556
 insulators, electrical damage, fluorescence probes 7-51525
 interelectrode flashover in the presence of a weakly ionised plasma channel created by laser irradiation 7-44281
 polymer flashover potential, surface anal. using ESCA 7-33990
 surface flashover in insulator with reduced E-field 7-64569
 N₂, flashover at dielectric interfaces: the interaction of surface and volume processes 7-51549
 SF₆, discharge characts. and insulating props., review of Japanese research 7-44279

flaw detection*see also crack detection*

- analytical signal convertor for US flaw detection 7-31621
 ball bearing defect detection using non-periodic analysis 7-13707
 boiler tube NDT inspection systems 7-20549
 broadband ultrasonic flaw detector system 7-65276
 ceramic tubes, acoustic anal., nondestructive examination method 7-13705
 ceramic-metal interfaces, grain boundaries, bonding and interfacial structure 7-26765
 ceramics, brittle, non-oxide, flaw charactn., computer-aided US testing 7-54064
 cylindrical ferromag. specimen, surface slit, open circuit remagnetisation, cavity mag. field meas. 7-54051
 cylindrical object, simulated corrosion wastages detection, US waveguide technique 7-59729
 defect detection using ultrasonic B-scan, transducer beam divergence effects 7-31617
 defects, US scatt., surface roughness effects 7-54062
 eddy current flaw detectors, impedance components for probe coils, standardisation prediction 7-33891
 eddy current flaw inversion algorithm, experimental verification 7-54059
 electrically conducting half-space, analytic Green's dyads 7-10821
 electronic materials and their microstructure, thermal wave imaging studies 7-8237
 electroradiography inspection method for castings 7-65262
 fatigue damage detection by position-sensitive detector, X-ray diff. profile singularity change (*Japanese*) 7-8236
 flat layer insulators, RF flaw detection, diff. 7-54053
 fluorescent dye penetrant inspection, UV radiation safety and visual enhancement 7-40311
 fluoroscope, portable, with image intensifier, optimal screen characts. 7-61407
 glass fibre reinforced plastic cylinders, burst pressure, stress wave factor correl., US meas. 7-13709
 glass fibre reinforced polyester laminate, hydrothermal ageing, degradation, US obs. 7-13708
 graphite fibre reinforced epoxy laminates, holographic investigation of stressing techniques for detecting flaws 7-59732
 high temp. crystallisation, flaw form., AE detection, automatic system 7-3557
 high-resolution holographic techniques for visualization of surface acoustic waves 7-28251
 hot steel slabs, eddy current method (*Japanese*) 7-53771
 internal imperfections, NDE, thermal flux method (*German*) 7-13718
 joints, adhesive, defect detection, NDT techniques 7-28248
 Lamb wave flaw inspection appls. 7-20540
 laminate, holographic investigation of stressing techniques for detecting flaws 7-59732
 laminate flaws, pulsed photothermoelastic quantitative eval. 7-54048
 laminated materials, flaw detection, signal recognition automation using linear prediction model 7-3561
 LWR piping, flaw detection by US systems, digital techniques 7-46782
 magnetic, of pipelines, eddy currents as interfering factor 7-39822
 magnetic inspection of internal defects in components using combined magnetization 7-28242
 magnetic particle inspection, visibility and magnetisation (*German*) 7-8239
 magnetostatic leakage fields of surface defects, math. model and defect size determ. applic. 7-39819
 metals, surface-breaking defect characterization using laser-generated ultrasound 7-46774
 metals, void detection, thermography appl. 7-28256
 microfocus X-ray-units, focal spot size, stability, defect visibility (*German*) 7-13712
 nuclear NDT development at Harwell, review 7-65270
 online acoustic emission monitoring of cracks in nuclear systems, review 7-54066
 optical fibre strength, break detect. in mandrel static fatigue process 7-50769
 optical methods in composites, conf., Keystone, USA (Nov. 86) 7-55894

flaw detection continued

- Peach Bottom 3 BWR, creviced safe ends, US inspection for cracks 7-46781
 plane parallel components, US inspection, shear wave beam multiple reflection 7-54055
 polymeric materials, computed tomography appl. 7-28254
 polypropylene film, fibrillation, sonic pulse propag., stress-strain meas. 7-26669
 portable flaw detector with built-in LCD thickness meter 7-13704
 production line NDT appls., holographic and visual inspection methods 7-39837
 pulsed photoacoustic materials characterization 7-46755
 reconstruction of flaws, using model-based elastic wave inverse scattering 7-54069
 rectangular slot, mag. field intensity concentrator calc. 7-3560
 refractory products, US flaw detection 7-22960
 sapphire, sub-surface, defect obs., by Rayleigh wave reflection in scanning acoustic microscope 7-13710
 scanning acoustic microscopy, NDT appl. 7-3564
 sizing of defects in steel constructions by ultrasound 7-33907
 steel, austenitic stainless, US response from artificial defects 7-46762
 steel, C, LWR piping, flaw evaluation 7-46652
 steel, rail, US inspection signal rel. to microstruct. and surface condition 7-3556
 steel, stainless, crack growth in BWR piping, meas. techniques 7-39839
 steel rolled sheet, distorted form effect on inspection results by shadow method 7-39815
 steel tubes, eddy current testing using electromagnet technique 7-39826
 steel wire rope, defect detection., Hall effect mag probe 7-33885
 structural ceramics, flaw detection, holographic interferometry techniques 7-46760
 subsurface defect acoustic imaging in composites and roughened samples 7-3568
 thermal wave imaging with thermoacoustic detection 7-43586
 ultrasonic models for nondestructive evaluation techniques, design and validation 7-46775
 US defect location and sizing, technique developments 7-65269
 US flaw detection, liquid contacting layer, inclined incidence beam, pulsed radiation 7-54056
 US flaw detector, measuring errors of pulse parameters with different specimens 7-28246
 US flaw detectors, generator schemata comparison, electroacoustic criteria 7-54057
 US NDT, dynamic scanning systems 7-13715
 US shadow method of inspection of rolled sheets, distorted form effect 7-39815
 US signal processing for near surface defect detect. and thickness meas. 7-39830
 welds, NDE calibration, prod. and sizing of uniform 2D flows 7-17757
 X-ray, adaptive multichannel systems 7-39817
 X-ray real-time imaging for weld inspection, methods and equipment 7-54045
 Bi₁₂SiO₂₀, photorefractive, hologram recording, real-time defect enhancement using inversion props. 7-25771
- flexoelectricity**
 chiral smectic-C liq. cryst., light diff. props. in external elec. field 7-64604
 crystalline dielectrics, piezoelec. and flexoelec. responses, surface contribs., unified approach 7-22193
 MBBA hybrid nematic liq. cryst. cell, flexo-electric effect study 7-11904
 nematic liq. cryst., flexoelectric instability 7-63460
 nematic liq. crystal, symmetrically realigned, refl. of a plane TM wave 7-44367
 nematic liq. crystals, surface anchoring energy, validity of Rapini-Papoular form 7-26625
 nematic liquid crystal, light scattering in elec. field 7-1843
 nematic liquid crystals, flexoelectric effect, statistical theory 7-21083
 smectic C chiral liquid crystals, elastic free energy 7-11900
- flexural strength** *see bending strength*
- flexural waves** *see elastic waves*
- flicker noise** *see random noise*
- flight control** *see aerospace control*
- flight simulation** *see aerospace simulation*
- flip-chip devices**
see also thin film circuits
 No entries
- flip-flops**
 digital optical computers, threshold device tolerance requirements 7-57410
 interferometric devices, two-beam, with in-phase outputs, optical bistability 7-62764
 optical parallel logic gate using Pockels effect modulators, fundamental components for optical digital computing 7-43347
- floating zone method** (*crystal growth*) *see zone melting*
- floating zone refining** (*see zone refining*)
- flocculation**
see also colloids; sedimentation
 clay kaolin aqueous suspensions, particle association, floc formation, shear, time-dependent properties 7-8308
 in-undecane, emulsion in sodium oleate stabilised water, conc. effect on aggregation 7-39926
- flow**
see also boundary layers; chemically reactive flow; compressible flow; Couette flow; electrohydrodynamics; external flows; flow instability; flow measurement; flow simulation; flow through porous media; Knudsen flow; laminar flow; multiphase flow; non-Newtonian flow; nonequilibrium flow; pipe flow; plasma flow; Poiseuille flow; pulsatile flow; rotational flow; shear flow; stagnation flow; stratified flow; supersonic flow; swirling flow; transonic flow; turbulence
 hyperbolic systems of 3D fluid flow, numerical methods 7-51022
 incompressible fluid flow, viscous, fractal dimension of attractors 7-9677
- flow birefringence**
 anisotropic fluids, viscous behaviour, transport phenomena 7-32272
 aromatic copolyamide, conformational and optical characts., flow birefringence data (*Russian*) 7-44420
 aromatic polyester, hydrodynamic and dynamooptical props. (*Russian*) 7-39077
 carboxymethylcellulose, monosubstituted, cadoxene solns., diffusion, sedimentation and flow birefringence (*Russian*) 7-63859

flow birefringence continued
comb-like polymers, with mesogenic side fragments, conform. and optical anisotropy (*Russian*) 7-63516
polyamidobenzimidazole solns., hydrodynamic and optical props. (*Russian*) 7-26619
solution of rodlike molecules, flow, phase separation, orientation distrib. 7-43989
surfactant systems, drag reduction, physico-chem. props., rheology 7-43992

flow charts see *flowcharting*

flow control

capillary viscometer for evaluating low-viscosity solutions at elevated temperatures 7-11570
desalination ion exchange installations, meas. and control 7-28339
fluid control and meas., conf., Tokyo, Japan (Sept. 1985) 7-29593
gas flow regulation and meas., based on pressure drop determ. 7-48711
plasma spray deposition process parameters control, math. model 7-3477
radial attaching jet flow control, flow before reattachment point 7-20769
reverse osmosis desalination meas. and controls 7-28338
Solar Process Heat System supplanting induction-heated boilers 7-8366
turbomolecular pump, automatic ventilation system 7-18797

flow diagrams see *flowcharting*

flow instability

ablation front instability in presence of layer acceleration 7-1536
active suppression of flow-excited cavity oscillations (*French, English*) 7-31774
air boundary layer, active transition fixing and control 7-31740
air cross flow over heated cylinder, heat transfer coeff. investig. 7-43892
air-water countercurrent flow in horizontal tubes, flooding study 7-57902
alloys, binary, freezing, convective and morphological instabilities 7-32615
annular jet, wake and wake-induced shear layer excitation 7-37508
atmosphere, manifestations of Charney baroclinic-instability with Rossby wavetrains 7-18287
atmosphere barotropic motion, effects of orography (*Russian*) 7-29130
baroclinic chaos numerical anal. 7-57893
baroclinic instability of basic current in 2-layer ocean model 7-29068
baroclinic instability over topography, nonlinear evolution 7-57804
Benard convection, 2D and 3D, num. simulation 7-37465
Benard-Marangoni's instability, nonuniform temp. gradient and Coriolis force effect 7-43886
binary liquid mixture, late-stage phase separation and hydrodynamic flow, light scatt. meas. 7-58486
blood oscillatory flow in viscoelastic tube, wave motions near instability limit 7-51316
boiling liquid, first crisis, elementary hydrodynamic model, additive generalisation 7-31746
boundary-layer transition, roughness trips with rows of spherical elements 7-51050
buoyancy-driven convection in horizontal fluid layer extending over porous substrate 7-51136
buoyancy-driven instabilities of low-viscosity zones, appl. to magma rich zones 7-8930
CANDU heat transport system, stability criterion for flow oscillations 7-10205
CANDU-600 heat transport system flow stability 7-30607
cavity flows, 2D laminar and chaotic mixing 7-16263
cellular automata for 2D hydrodynamic flow simulation (*French*) 7-16158
channel flow, instabilities and bifurcations 7-26352
coal dust flame acceleration, feedback control model for unsteady flow 7-65326
colloidal crystals, shear melting and Taylor instabilities 7-43858
completely confined porous medium, onset of hydromagnetic thermal convection, stability 7-6205
compressible isentropic spiral flow between two coaxial circular cylinders, instability 7-6216
confined Bernard problem, nonlinear phenomena, numerical parametric anal. 7-30482
convection, finite-amplitude axisymmetric, between rigid rotating planes 7-26272
convection, rectangular box, oscillatory instability, 3D Boussinesq eqns. 7-51129
convection, rot. cylindrical annulus, instabilities of columns 7-51128
convective equation, weak nonlinear instability of Euler explicit scheme 7-57832
convective instability in packed or porous beds with throughflow 7-11383
Couette-Taylor instability, hydrodynamic and phase-transition descriptions, expt. study of connection 7-20691
counter-rotating vortex pair induced flow at wall 7-31810
cryogenic flow instability during adiabatic boiling 7-11385
cryogenics, geometry and rot. effects on convection onset 7-57833
detonation shock waves, transonic flow behind wave front, stationarity conditions 7-63174
dielectric liquid, stationary instabilities, unipolar injection and thermal gradient effects 7-26357
dissipative systems, stationary soliton soln. investig. 7-51034
distributed roughness effect on transition enhancement 7-37433
dusty gas, conducting, channel flow, graphical anal. 7-63214
dynamic thermocapillary liquid layers instability mechanism 7-38303
electrolyte solution surfaces, hydrodynamic instabilities caused by elec. forces. 7-51322
elliptical flow, 3D instability 7-20690
film condensation instability at surface of a cylinder 7-37526
film flow on a rotating disk 7-31749
finite amplitude convection in a rotating porous medium 7-57842
finite element methods in flow problems, conference, Antibes, France (June 1986) 7-41009
flame propagation, unsteady and ID, mathematical anal. 7-57944
flames, curved, nonlinear thermal diffusive theory 7-57941
flames, hydrodynamic instability, nonlinear theory, weak thermal-expansion approx. calcs. 7-59764
flames, Linan's premixed flame regime, stability 7-17797
flexible cylinder array, fluidelastic in stability in cross-flow 7-16089
flow-induced surface instabilities, Kramer-type compliant surfaces, irreversible processes effects 7-16159
fluidelastic instability of rectangular plates under shearing load in subsonic flow 7-51057
free mixing layer, weakly nonlinear stability theory, Landau constant 7-63118

flow instability continued

free surface flows, triangular elements development 7-51051
free-convection, unsteady boundary-layer flow, semisimilar solns. 7-57834
front motion, metastability and subcritical bifurcations 7-51056
fuel drops combustion, stability loss mechanism in stream of oxidising gas 7-31892
gas-liquid dispersions in bubble columns, flow instability 7-11498
gravitating rotating gaseous disk, nonlinear convective instability development calcs. 7-66766
gravity waves, N-layer stratified shear flow, Kelvin-Helmholtz instability 7-43951
gravity-capillary waves, nonlinear 2D, 3D instabilities 7-51194
hairpin vortices, generation in laminar boundary layers, obs. 7-57797
heavy fluid, gravity-elastic wave excitation, unsteady problems 7-31747
Hele-Shaw cells, imperfect, flow properties 7-6184
Hele-Shaw flow stability, wetting-layer effect 7-12404
heterogeneous shear flows, generalisation of stability theory (*Chinese*) 7-26248
homocentric rotating torus, dynamical instability and growth rate upper limit 7-47693
homogeneous uniformly rot. McLaurin spheroid in mag. field, equilb. and stability, stellar appl. 7-47686
Hopf bifurcation in the Lorenz model by the 2-timing method 7-31802
hydromagnetic stability of stratified compressible fluid between two rotating cylinders 7-57936
ideal fluid, shear flow stability, effect of stratification 7-26249
ideal incompressible fluid, rot. motion, stability study 7-51164
ideal isothermal gas, 2D unsteady viscous compressible flows, global solns. 7-26304
immiscible displacement in porous medium, viscous fingering instability 7-11491
immiscible viscous fluids, fingering in Hele-Shaw cells 7-43854
incompressible fluid eqns., oscillations and concentrations in weak solns. 7-57802
inert gas, shock wave instability, anomalous relaxation mechanism 7-31834
interfacial wave generation, investigation through flow visualisation and LDA 7-37438
interfacial waves, finite amplitude stability, effect of basic current shear 7-43946
interstellar gas clouds in galactic bulges, Rayleigh-Taylor instability rel. to clouds dynamics 7-66707
inverse energy cascade, 2D turbulence, vortices meas. in a square box 7-16190
inviscid barotropic flow over topography, nonlin. stability and statistical mechanics 7-57806
inviscid counter-rotating vortices, nonlinear evolution 7-26293
inviscid fluid, universal short-wave instability of 2D eddies 7-20689
jet diffusion flames, swirl effect on stability 7-23017
jet impingement on wedge, edge-tone flowfield 7-11483
jets, initially circular, flow development and control, shear layer growth 7-11482
jets, wave struct., Rayleigh linear inviscid instability anal., 7-51054
Kelvin ship-wave pattern, cusp lines, unsteady and nonlinear effects 7-57845
Kelvin-Helmholtz instability, nonlinear theory 7-11387
laminar flow stability criteria and lower critical Reynolds number 7-1530
laminar flow through axisymmetric sudden expansions, shear layer instabilities obs. 7-11376
laminar natural convective flow along isothermal vertical surface, stability 7-31744
large elliptical warm-core rings 7-8995
laser-Doppler anemometer, pipe flow, laminar to turbulent flow transition, sinusoidal flow modulation 7-16262
laser-induced convection, instability, laminar to turbulent transition 7-37464
line plume, laminar, falling in fluid, stability investig. 7-57807
linear stability of hydromagnetic flow for nonaxisymmetric disturbances 7-63230
liquefied hydrocarbon gases, unsteady-state discharge, num. anal. 7-6185
liquid drop, instability development in elec. field 7-31850
liquid droplet deformation in gas flow, anal. 7-51278
liquid film, disintegration by gas press. difference 7-52195
liquid film downflow, Orr-Sommerfeld eqn. soln., optimal approach 7-51119
liquid N₂ heat exchanger, two-phase flow instability, LUSH-EX code 7-6294
liquid solution, diffusion coeff., hydrodynamic stability 7-63115
liquid thread breakup in linear flow 7-57805
liquid-gas interface, linear stability of liq. film with counter-current gas flow (*French*) 7-1533
magnetic fluids, Taylor instability, mag. field effects 7-31738
magnetic liquid, film flow stability 7-51329
magneto-gravitational instability of a rotating and finitely-conducting fluid 7-11555
MHD channel flow through porous medium 7-57932
MHD convection, overstability study 7-51333
MHD laminar flow, vortex behaviour 7-63228
micropolar fluid, unsteady flow past flat plate 7-63113
miscible displacement stability in porous media, rectilinear flow 7-31750
modal amplitudes in interacting triads, probability distrib. with arbitrary random forcing 7-9097
modulated Taylor-Couette flow as a dynamical system, linear stability 7-11431
natural convection flow on inclined flat plates with uniform surface heat flux, wave instability 7-20725
natural convection in narrow-gap spherical annuli, stability to axisymmetric disturbances 7-31789
nematic flows, unit-sphere description 7-20688
nematic liquid layers, convective flow, multiple spatial periodicities, EHD instability 7-43909
nonlinear convection with variable coefficient of thermal expansion 7-6207
nonlinear gravity-capillary waves, stability 7-16161
nonlinear stability analysis of stratified fluid equilibria 7-6186
nonlinear viscous fluid, stability of flow (*Russian*) 7-57803
ocean stratified bottom current, nature of structural instability 7-14310
4-n-octyl-4'-cyano-biphenyl nematic liq. cryst., torsional shear flow, tumbling instability obs. 7-11386
Oldroyd fluid through circular pipe, unsteady flow 7-63112
one-dimensional unsteady gas motions, stability 7-20687
onset, parametric modulation effects 7-43857

flow instability continued

- oscillating cascades, unsteady flow, asymptotic solns. 7-37437
 oscillating free-connection flow past infinite porous vertical limiting surface, effects of mass transfer 7-14479
 oscillation excitation is supersonic boundary layer by external acoustic field 7-51046
 oscillatory turbulent flow in a cylindrical channel 7-57820
 parallel free flow, nonlinear stability theory, Landau equation and mean flow distortion 7-1534
 particle image displacement velocimetry for 2D flow visualisation 7-31893
 penetrative double-diffusive convection, stability anal. 7-57838
 pipe flow, unsteady, attenuation prediction, num. method appl. 7-31732
 pipe laminar thermal energy region, transient unsteady convective heat transfer 7-31775
 plane pipe, nonsteady heat convection study 7-63135
 plasma jet stagnation region, blunt body heat transfer coeff. investig. 7-43892
 Poiseuille flow stability, suspended particle effect 7-1613
 potential flows, linear and nonlinear acoustic wave eqns. 7-16015
 power plant combustion chamber, combustion stability 7-31890
 quantum liq.-quantum cryst. phase interface, hydrodynamic eqns., sound transmission calcs. 7-32746
 Rayleigh's inflexion-point theorem and its extensions 7-11384
 Rayleigh-Benard convection patterns, wavenumber distrib. and time dependence 7-43914
 Rayleigh-Benard instability, external noise influence 7-43853
 Rayleigh-Benard instability, stochastic perturbations, random rot. effect 7-31751
 Rayleigh-Taylor instabilities in geology, relation between initial conditions and late stages 7-66108
 Rayleigh-Taylor instability, steady solns. in 3D bounded domain, bifurcation theory 7-16228
 Rayleigh-Taylor instability in laser accelerated foils, track detector study 7-37435
 Rayleigh-Taylor problem in vertical slot, moving contact lines, stability 7-43855
 reacting shock waves, theoretical and num. structure 7-20759
 rippled interface between liqs. of different densities, shock wave effects 7-58572
 Rivlin-Ericksen fluid, viscoelastic, unsteady flow through rectilinear tube 7-57884
 Rossby waves, triad reson. interactions in ocean 7-29067
 rotary-wing aeroelasticity, time-domain unsteady aerodynamics appls. 7-20686
 rotating Benard convection, transition to turbulent flow, instability heat transfer meas. 7-26253
 rotating differentially heated annulus with unstable stratification, convection characts. (Russian) 7-29129
 rotating fluid, baroclinic vortex pairs 7-51168
 rotating ideal fluid, equilib. conditions in parameterised post-Newtonian formalism 7-1651
 rotating porous medium, unsteady free convective flow 7-51139
 rotating vortex patch stability, spectral anal. and variational methods 7-16184
 Saffman-Taylor experiment, dendritic growth 7-1531
 Saffman-Taylor instability, narrow fingers 7-37436
 Saffman-Taylor meniscus during flow between plates, gravity effect 7-63915
 salinity-temperature front, double-diffusive horizontal intrusions, linear stability theory 7-26250
 secondary flow patterns, flow visualization and centrifugal instability in curved tubes 7-37550
 shear flow, spatial instability, Orr-Sommerfeld eqn. 7-51052
 shear-flow instability waves, wave action density analysis 7-16169
 shear-induced order-disorder transition, possible instability 7-35287
 sheared disturbances, instability solns. 7-57808
 shock waves, stability in media with arbitrary eqn. of state, quasi 1D anal. and numerical modelling 7-63180
 shock waves propagation in gas with cosmic rays, instability (Russian) 7-40652
 simple Benard problem with permeable boundaries 7-57809
 solidification, stirred, Taylor vortices influence on morphology 7-22657
 solitary rotational water waves, Lyapunov stability, oceanic appl. 7-63164
 SOPHT verification for parallel channel flow stability 7-10206
 sparsely packed porous layer, double diffusive convection 7-11531
 spatial oscillations in confined rotating fluid, temporal development 7-16186
 spatially periodic parallel flows, nonlinear stability theory 7-31748
 spatially-forced thermal convection, resonance and phase solitons 7-51138
 spherical fluid inclusion, convective instability 7-43856
 stationary planar Euler flows in an unbounded strip, nonlinear stability 7-31883
 stationary states or flows in regions extended in one direction, stability conditions 7-1535
 steady and unsteady non-parallel boundary layers, 3D instabilities, cross flow 7-63117
 steam-water violent condensation shock mechanism 7-57901
 stirred reactor, flow characts., flow visualisation and torque meas. 7-57963
 stratified fluids, Squire's theorem 7-11490
 stratified laminar shear layer, stability 7-43849
 stratified shear flow, explosive processes, multidimensional and self-similar props. 7-37434
 stratified shear flow, stability, Richardson's criterion 7-37511
 streaklines in unsteady vortices, flow reversal 7-37472
 subsonic shear flow, ordered structure development, acoustic oscills. influence 7-20742
 supersonic flow, past 2D plate cascade, vorticity inhomogeneities 7-57875
 supersonic vortex rings, differential interferometry study 7-51220
 surface gravity waves in deep water, class I and II instabilities, modified Zakharov eqn. 7-51195
 surface rippling during laser material processing, thermohydraulics anal. 7-58574
 swirl flows with free surfaces, stability criteria 7-1579
 Taylor instability in streamer and bubble amplitude 7-11389
 Taylor-Couette flow, stability limits, flow visualisation and numerical study 7-43844
 Taylor-Couette systems, phase instabilities and end effects 7-11432
 tearing instability in MHD flows 7-51053
 thermal stability of a fluid layer under variable body forces 7-63116

flow instability continued

- thin films, thermocapillary convection and stability 7-12409
 Tollmien-Schlichting waves and flows governed by interactive boundary-layer eqns., Taylor-Görtler instabilities 7-26300
 tomographic visualisation, improved method 7-37568
 transient dispersed-film flows in channels containing fuel rod bundles 7-10236
 transition to chaotic convection 7-11422
 transonic speeds on an aerofoil, shock wave interference, shock/boundary-layer interactions 7-6241
 transonic/supersonic diffuser, shock wave stability to pressure disturbances (Japanese) 7-11462
 turbulence theory, closure, stabilization principle 7-16165
 turbulent periodic unidirectional 3D flow, negative-viscosity phenomena 7-57810
 turbulent transfer processes, flow swirl effect 7-43927
 two-component fluid-fluid system, convective instability 7-31776
 two-layer immiscible fluids with thermally insulated boundaries, convective instability 7-51122
 two-phase flow, fluid-heated, dynamic instabilities, meas. and anal. 7-51276
 unstable fronts in a porous medium, stochastic numerical scheme 7-57919
 unsteady compressible viscous flow over airfoils, integro-differential and finite-difference methods 7-31821
 unsteady flow around spherical bodies, use of spherical shaped current meter 7-6227
 unsteady flow force measurement in inline and staggered heat exchanger tubes 7-6187
 unsteady free-convection flow past accelerated plate, skin friction 7-4321
 unsteady heat transfer in gas-swept bed of spherical granules 7-31803
 unsteady incompressible turbulent boundary layer flow over a longitudinal cylinder 7-6195
 unsteady incompressible two-dimensional and axisymmetric turbulent boundary layer flows 7-1540
 unsteady incompressible viscous flow over circular cylinder, body-fitted coordinates 7-43851
 unsteady jets, 3D surface shape estimation by image processing 7-37573
 unsteady laminar forced convection from impulsively started sphere, temp. field 7-43852
 unsteady MHD flow past vertical porous plate, mass transfer and free convection effects with constant suction 7-54332
 unsteady MHD flow past vertical porous plate, mass transfer and free convection effects with variable suction 7-54333
 upper convected Maxwell fluid, plane Couette flow, linear stability 7-16160
 variable viscosity revolving fluid between rotating cylinders, flow instability 7-57854
 vertical wind tunnel for water drop studies 7-6293
 vertically stratified thin accretion disks, baroclinic waves 7-14477
 viscoelastic fingering, time effects 7-57800
 viscoelastic fluid, unsteady flow through ducts, impulsive pressure gradient 7-57885
 viscoelastic liquids, tricritical codimension-2 point near convection onset 7-51055
 viscous flow Saffman-Taylor model, random walk techniques, review 7-57811
 viscous flows in two dimensions, complex analytic methods, book contrib. 7-51059
 viscous flows in two dimensions 7-11388
 viscous fluid convective thermal motion instability in tube 7-31804
 viscous fluid flow in porous medium, num. anal. 7-63207
 viscous fluid in porous medium, stability criteria for convection, eigenvalue problems 7-44033
 viscous incompressible flow in 2D flat torus, stability props. 7-57801
 viscous incompressible flow in a narrow channel with one free wall and fluid supply through a porous insert 7-1636
 viscous incompressible nonhomogeneous fluid, hydromagnetic stability 7-63114
 viscous liq. drop breakup, capillary wave instabilities, transient effect 7-43954
 viscous stratified fluid, unsteady flow, variable mag. induction 7-63193
 vortex breakdown model, axisymmetric flow stability 7-26282
 vortex instability in natural convection flow on an inclined uniform-heat-flux surface (Chinese) 7-11430
 vortex structure in plane mixing layers, meas. and models 7-16191
 vortices, rot. config., nonlinear evolution 7-43932
 wakes behind stationary cylinders, vortex street formation, wake instability model 7-16182
 water, arbitrary depth, 3D Stokes waves, stability anal., fourth order evolution eqns. 7-16162
 water, pure and saline, thermal buoyancy induced flow stability 7-1532
 wavenumber selection and Eckhaus instability in Couette-Taylor flow 7-43843
 waves, instability problems, finite-difference soln. methods 7-11437
 weld pool steady fluid flow, 2D model, surface skin effects 7-20730
 wetting films on fibres, peristaltic instability (French) 7-32751
 Ar, metastable population meas. and flow instability due to shock wave, comparison with models 7-16207
 Ga, liquid, electrohydrodynamics, ion source appls. 7-31887
 He, liq., flow stability at supercrit. press., nonuniform heat flux distrib. in channel 7-51058
⁴He superfluid, critical vel. regime at low temps. 7-27042
 Hg layer, rotating, heated from below, subject to mag. field, oscillatory instability 7-16193

flow measurement

- see also *anemometry; flow visualisation; flowmeters; laser velocimetry*
 acceleration measurements using laser Doppler anemometry 7-31904
 acoustic Doppler current profiler, vessel-mounted, for use in rivers and estuaries 7-9262
 air flow vel. gradient meas. using nematic liq. cryst. orientation 7-32283
 arterial blood-flow waveform meas. in intact animals: digital radiographic technique 7-54837
 axial flow in square lattice rectangular rod bundle, wall shear stress meas. 7-16282
 behaviour during cylindrical vessel explosions 7-59760
 block-implicit multigrid calculation of two-dimensional recirculating flows 7-26242
 blood, instantaneous flow, estimation from indicator-dilution curve after bolus injection of indicator 7-65867

flow measurement continued

blood, regional flow meas., theoretical anal. of transient clearance method 7-28736
 blood, using scanning X-ray imaging system 7-40266
 blood, vol. flow in human common femoral artery. meas. using a duplex US system 7-28630
 blood rate detector, one chip VLSI implementation using PPL 7-65881
 Borda connector, wall thickness coeff. (*French*) 7-6331
 boundary layer transition detector, using differential interferometer 7-20822
 brain, regional cerebral blood flow, meas. method for freely moving, unstressed rats 7-28790
 bubble-driven flow, fluid and bubble meas., numerical soln. 7-16237
 capillary holes diameter meas., in 0.2 to 2 mm range 7-4807
 cavitation in large scale shear flows 7-51244
 cavitation nuclei meas. using optical system 7-51243
 cavitation tunnel, flow meas. using laser Doppler velocimeter 7-37607
 cavity-mounted press. transducer, input press. effects on freq. characts. 7-37595
 cerebral blood-flow meas. in ventilated premature babies, ^{133}Xe , inhalation system 7-23434
 cerebrospinal fluid shunt flow meas., reproducible radionuclide procedure 7-65836
 circular jet with initially laminar boundary layers, turbulent interaction region 7-11486
 circulating fluidised beds, flow structs., meas. technique development (*German*) 7-16243
 combustion diagnostics by pulsed photothermal and photoacoustic deflection spectroscopy 7-23016
 complex flow measurement, two component LDV system (*Chinese*) 7-26366
 compressible turbulent free shear layer interaction 7-51078
 conference, Prague, Czechoslovakia (April 1985) 7-48169
 confined air-water jets flow-field measurements and physical processes 7-37527
 contaminant monitor for fluid power applications 7-37613
 convergent tube, oscillatory incompressible fluid laminar flow 7-20794
 coronary blood flow, absolute, online computer meas. using a H_2 dilution catheter 7-28742
 Couette-Taylor flow, quasiperiodic to turbulent transition, strange attractors 7-63120
 Couette-Taylor instability, hydrodynamic and phase-transition descriptions, expt. study of connection 7-20691
 cyclone dust collectors, spherical, cone and semi-spherical forms, turbulent rot. air flows 7-16183
 cylindrical surface modifications effect, H_2 bubble wire flow visualisation and anemometry meas. 7-6196
 debris flows, noncontact speed sensors 7-40615
 Doppler flowmetry, perturbation meas. using power spectrum analysis 7-50852
 Doppler US 7-8672
 drag anemometry for measuring velocities in electromagnetically driven flows 7-44076
 droplet entrainment in vertical annular flow and its contrib. to momentum transfer 7-11492
 eddy viscosity in a turbulent boundary layer on a cylinder 7-51091
 EM flow-rate meter electrically-conducting fluid, flow rate meas. using (*Russian*) 7-11571
 experimental verification of numerical simulation of flows in cyclones and hydrocyclones 7-26296
 fibre laser Doppler anemometer and boundary-layer meas. appl. 7-37609
 fibre optic petal flowmeter for low gas pipe flows 7-44081
 fibre optic sensors, development, configs., and appls., review 7-31485
 fibre optics in laser Doppler velocimetry 7-50771
 fibre-optic liquid film sensor for 2-phase annular and stratified flow 7-37611
 flames, diffusion, bluff-body stabilised, near-wake region, CARS meas. 7-8282
 float-area type flowmeters, float instabilities in conduits, coupled vibration 7-20818
 flow parameters in presence of shock waves, interferometry 7-43982
 fluid control and meas., conf., Tokyo, Japan (Sept. 1985) 7-29593
 fluid-particle motion in isotropic turbulent field, Lagrangian meas. 7-57962
 fluidic transducers for flow meas. 7-37561
 fluidic volumetric-flow, mass-flow density and viscosity meter 7-26367
 fluidised beds, freeboard, vel. meas. using laser Doppler anemometer 7-11527
 forced Rayleigh scattering appl. to hydrodynamic meas. 7-11572
 free liquid film flow measurement by laser Doppler velocimeter 7-37606
 gas dispersion in aerated turbine agitated vessels, flooding phenomenon 7-44011
 gas flow distribution meas. system using nonlinear US sounding 7-37586
 gas flow regulation and meas., based on pressure drop determ. 7-48711
 gas flow velocity distribution meas. based on nonlinear effect of ultrasonics (*Japanese*) 7-31905
 gas flow velocity meas. by photothermal deflection spectroscopy 7-11563
 gas-flow rate through conducting pipe, three-point-pressure meas. technique 7-51350
 gas-liquid flows, capillary waves, spectral behaviour 7-11521
 gas-liquid slug flow in horizontal pipelines, press. meas. 7-57921
 gas-solid fluidised bed, freeboard region, two-phase flow behaviour 7-63209
 gasdynamic system for flow meas. using microcomputer data-acquisition system 7-51349
 grid mixing tank, turbulence meas. using laser-Doppler anemometer 7-1656
 high specific centrifugal compressors, flow measurement 7-26371
 horizontal annular flow measurements using pulsedphoton activation and film thickness distributionmodelling 7-5357
 hot wire anemometry, book 7-51357
 hot-film anemometer meas., correction for ambient temperature changes 7-57946
 hot-film anemometers, const. temp., calibration in water 7-11567
 hot-wire anemometry, turbulent flow meas., evaluation of analytical systems 7-16274
 hot-wire data corrections for high intensity turbulence 7-37448
 hot-wire probes calibration, using self-contained motorised cart 7-31899
 hot-wire procedures and appraisal through simulation 7-44078
 hot-wire techniques for Reynolds stress tensor determ. for 3D flows 7-57945

flow measurement continued

hydraulic pipeline, single capsule motion 7-26339
 IC microtransducer for air flow and differential pressure sensing 7-61329
 imaging of temp. fields in air using laser-induced fluoresc. of O_2 7-41384
 incompressible viscous fluid, MHD flow in infinite channel 7-6326
 instantaneous flowrate measurement of transient air flow 7-31906
 interfacial wave generation, investigation through flow visualisation and LDA 7-37438
 interfacial wave measurement method involving light polarisation and optical activity 7-4201
 internal gravity waves, stratified shear flow, wave-action model study 7-43948
 inverse energy cascade, 2D turbulence, vortices meas. in a square box 7-16190
 inviscid axial flow in compressor rotor, leading-edge effects, flowfield meas. 7-11562
 laminarisation and reversion to turbulence of low Reynolds no. flow 7-51039
 large range flow calibrated by changeable water level system with computer simulation 7-37592
 laser Doppler anemometer arrangement measurements (*Polish*) 7-57965
 laser Doppler anemometry, counter based in wet steam flow 7-57969
 laser Doppler interferometry methods for highly accurate flow meas. 7-44073
 laser Doppler velocimetry, multi-pt. system using phase diffraction grating 7-37605
 laser double-pulsed velocimetry, image shifting technique to resolve directional ambiguity 7-37559
 laser interferometer skin-friction meter, numerical and expt. study 7-16276
 laser-Doppler anemometer, pipe flow, laminar to turbulent flow transition, sinusoidal flow modulation 7-16262
 leak rate units and flow rates 7-18735
 LOFT pressurizer, on-line instrument failure detection, Kalman gain approach 7-5354
 low-velocity flow measurement by bubble/dye tracing technique 7-16283
 membranes with locatable single pores generation, obs. and testing 7-298
 metal, liq., flow rate measurement using EM flowmeter, error in corr. method 7-57954
 metering system with direct flanged differential pressure transducer design (*German*) 7-44070
 methane, turbulent jet discharge, planar imaging 7-20767
 meteorological support to means of measuring flow rate for liquid cryogenic media 7-44074
 monolithic gas flow sensor with polyimide athermal insulator 7-6332
 multichannel time counter and data acquisition system 7-37571
 NMR imaging technique for flow measurements 7-1653
 nonperturbing boundary-layer transition detector for hypersonic wind tunnel, based on laser interferometry 7-20821
 ocean, surface current meas., CODAR intercomparison, Delaware Bay (1984) 7-9254
 ocean current meas. from motional electric fields and currents 7-9257
 ocean current sensing, space-time analysis of acoustic scintillations 7-9258
 ocean meas. under sea ice, medium-resolution turbulence cluster 7-9271
 oceanographic, surface mooring in shallow water, VMCM S4 current meter intercomparison 7-9249
 oceanographic acoustic Doppler current profiler, intercomparison with conventional instruments and tidal flow model 7-9266
 oceanographic acoustic Doppler current profiling, form volunteer commercial ship 7-9261
 oceanographic acoustic Doppler profile current meter, field evaluations 7-9264
 oceanographic acoustic Doppler profiler intercomparison expt., Delaware Bay (1984) 7-9263
 oceanographic current meas., Conf., Airlie, VA, USA (Jan. 1986) 7-4633
 oceanographic current meas. by vane vector averaging meter and dual orthogonal propeller meter 7-9250
 oceanographic current meters intercomparison, laboratory and field meas. 7-9256
 oil-water core-annular flow in pipe loop, turbulent lubricating film model 7-57922
 optical measurement of velocity and acceleration with colour coding 7-11568
 optical measurements of porosity and fluid motion in packed beds 7-6304
 optical particle sizing and concentration meas. system 7-48694
 orifice flowmeter, flow coeff. meas. for large diameter pipe 7-37590
 particle motion study in concentrated dispersions, tracer diffusion method 7-51351
 particles in flows, simultaneous velocity and size meas. using laser technique 7-9814
 photoacoustic effect in flowing liquid 7-44695
 pipeline flow meas. in flow straightener/flowmeter package 7-57948
 plethysmograph for meas. of digital blood flow 7-40324
 plunging breaking waves, velocity and force measurements in the splash zone, laser anemometry 7-63237
 poststenotic flow disturbance in dog aorta as measured with Doppler US 7-8668
 proximity sensors, flow meas. with beam-scanning LDV 7-37604
 pulse blood flow of limbs, quantitative eval. using rheography 7-40352
 pulsed supersonic He free-jet expansions, time-of-flight characterisation 7-11457
 quasi-steady state isochoric plane flow meas., noisy data anal. 7-63727
 radial attaching jet flow control, flow before reattachment point 7-20769
 rate meas. by speed-area method using convergent nozzles 7-57959
 reacting and non-reacting turbulent liquid mixing layer, entrainment and mixing, composition meas. 7-16174
 refractive index fields, spatially extended, speckle photography 7-41431
 retinal blood flow visualisation and meas. by laser speckle photography 7-47212
 rhodamine 6G, hydrodynamically focused flow, laser induced fluoresc. detection 7-59811
 ribbed wall channel, turbulent flow study using 2-component laser Doppler anemometry 7-37547
 rotating concentric cylinders, same or opposite directions, turbulence and vortices 7-16255
 semielliptical afterbody near-wake, turbulence intensities 7-51150
 sensor, swirling jet type, and flow field 7-37562
 sensors with hydrodynamic smoothing for conductometry of turbulent flows 7-57961

flow measurement continued

- separated Poiseuille flow downstream of step, generation and development of perturbations 7-44045
- ships, flow around aft section, static pressure meas. 7-37594
- silicone rubber and silicone oil, convergent flow into rectangular slit, rel. distrib. meas. 7-6339
- small flow rates of liquids and gases 7-6335
- smart acoustic current meters, experiences in Lake St. Clair, Canada/USA 7-9255
- solid particle acceleration by gaseous detonation products 7-20778
- solid-liquid two-phase flow, laser Doppler velocimeter meas. and turbulence props. 7-37533
- spectral method of flow-velocity measurement 7-36182
- Stirling engine regenerators, flow inhomogeneity 7-65559
- stratified fluids, gravity currents, turbulence effect 7-43949
- supersonic expansion, density meas. using beam-deflection optical tomography 7-44080
- synthetical radiographs, numerical image computation, high velocity flow anal. appl. 7-44082
- thermal plume, turbulent struct., vel. field (French) 7-31762
- thermography and thermal engineering conf., Budapest, Hungary (April 1987) (Hungarian) 7-56258
- three-phase flow meas., tomographic imaging 7-51355
- time-of-flight NMR flow imaging: selective saturation recovery with gradient refocusing 7-14095
- transient liquid/gas interfaces, US system for detection, by pulse-echo technique 7-1657
- transient velocity profiles, real-time estimation using Kalman filtering techniques 7-37582
- transit time method using radioactive tracers (Finnish) 7-57970
- transonic speeds on an aerofoil, shock wave interference, shock/boundary-layer interactions 7-6241
- turbopiston method development, based on hydrodynamic suspension of rotor 7-44075
- turbulence, laser homodyne technique meas. 7-26254
- turbulence, measurements, pot.-difference method 7-57816
- turbulence measurement using a laser-2-focus velocimeter 7-57967
- turbulence measurement with inclined hot wire probe, 3D angle calibration method (Japanese) 7-6338
- turbulent boundary layer, heated, hot-wire meas. of velocity and temp. fluctuations 7-63236
- turbulent boundary layers external factors effect with directional injection and suction 7-6199
- turbulent boundary layers subject to strong press. gradients wall shear stress meas. 7-26265
- turbulent boundary-layer skin-friction drag reduction meas. 7-51081
- turbulent developing flow in U-bend of circular cross section 7-16267
- turbulent flow and mass transfer of unstabilised stream in channel with obstacle 7-11391
- turbulent flow characts. in wake of circular cylinder (Russian) 7-1574
- turbulent flow meas. in ribbed-wall flow channel and comparison with model 7-57947
- turbulent plane wake, heat transport meas. 7-31760
- turbulent slugs in pulsatile pipe flow, behaviour 7-37551
- two-phase boundary layer, frictional stress meas. 7-44018
- two-phase bubbly flow, simultaneous bubble and liquid vel. meas. using LDV 7-20777
- two-phase flow measurement method, by digital tomography 7-16281
- ultrasonic flow cytometer, tests using small particle suspensions 7-20529
- underwater optical probe for laser Doppler anemometry 7-16279
- unsteady 3D flow, meas. using 5-hole pressure probe, design procedure 7-37593
- unsteady flow around spherical bodies 7-6227
- unsymmetrical 2-D diffuser characts. in steady and unsteady flows (Japanese) 7-6203
- US, freq. modulated, errors in flow meas. 7-57951
- US meas. of liquids in closed pipe-lines, compensation method (German) 7-26373
- vapor bubbles in liquid filled pipe, US imaging system 7-6333
- variable area flowmeter for mass flow meas. (German) 7-26369
- velocimeter, fibre optic, low cost 7-20444
- velocity meas. in stirred tanks, hot-film const. temp anemometer probes 7-16273
- velocity profile meas. by US Doppler shift method 7-51346
- vibrating-rod densimeter theory 7-31894
- void fraction meas. 7-43430
- void fraction meas. by capacitance transducers, parametric effects 7-1652
- vortex flow meters for computerised vapour-heat flow measurement (German) 7-11564
- vorticity measuring apparatus using reciprocal ultrasonic transmission method 7-20819
- wall attachment device, turbulent flow field, control flow effects 7-20697
- water velocity meas. in porous medium by fast neutron transmission 7-37584
- wind towers, air flow rate estimation and pressure coefficients eval. 7-39956
- YEWFLOW vortex flowmeter, small size and cryogenic versions (Japanese) 7-51356
- Ar-H₂O, two-phase mixture, voids fraction meas. 7-44072
- O₂ swirling flow combustor, gas densities, laser scatt. meas. 7-6218

flow process charts see flowcharting**flow reattachment** see flow separation**flow resistance** see viscosity**flow separation**

- arbitrary obstacle, 3-D boundary layer calc. (French) 7-11382
- bluff bodies, vortex wake interaction 7-51165
- by-passing flow in a supersonic nozzle with optical windows (Japanese) 7-51263
- circular cylinder in cross flow, tripping wire effect on boundary layer transition 7-43847
- coherent struct. in reattaching laminar and turbulent shear layers 7-51079
- complex shear flows, turbulence modelling 7-51077
- compressible separated turbulent shear flow, mixing, flow meas. 7-51080
- compressible turbulent free shear layer interaction 7-51078
- conference, Cambridge, England (March 1986) 7-40987
- cylinders subject to transverse streamline flow, turbulent boundary layer separation (Russian) 7-11400
- droplets of lower channels, separation, channel profile geometry effect 7-44017

flow separation continued

- dynamic compartmental models for separation processes 7-44066
- ellipsoid of revolution, incompressible turbulent boundary layers, inverse mode calc. 7-31768
- energy separation in fluid streams 7-31896
- flow around a cylinder near a plane screen, num. modeling 7-63123
- fluid separation in rotating tube, cavitation investig. by Runge-Kutta method (German) 7-51245
- free cavern separation zone pulsation at supersonic stream vel. 7-11458
- heat transfer, simulation for separated and reattached flow on flat plate 7-51107
- heated plate, acoustically perturbed 2D separated flow 7-16195
- immiscible fluid mixture in shear flow, phase separation, spinodal decomposition under shear 7-21464
- incompressible 2D jet reattachment, augmented thrust and mass flow 7-51248
- laminar boundary layer eqns. fast approx. soln. 7-16155
- laminar boundary-layer flows, separation point determ. 7-31741
- laminar flow past sudden expansions, Navier-Stokes solns. 7-43846
- laminar incompressible separated flows, iterative boundary-layer-type solver 7-11380
- laminar natural convection above horizontal isothermal square cylinder, separation 7-31783
- laminar small Reynolds-number flow over wavy walls 7-43840
- liquid-gas, nonuniform stratified flow through horizontal tubes 7-31862
- liquid-gas flow through coarse particle beds, 1D model 7-57904
- local separation zones in viscous jets, existence and nonuniqueness 7-1595
- magnetic fluid, thin layer coating, hydrodynamic drag, num. investig. 7-51061
- nonlinear viscous flow, 3D separation patterns, Navier-Stokes eqn. soln. 7-43837
- orbital flow past cylinder, vorticity-transport and stream function eqns. 7-43929
- perturbed flows in a longitudinal gravity field 7-1594
- polymer flooding of oil formations with bottom water, quasi-1D model 7-51359
- potential flow, 2D with separation in unsymmetrical bends 7-11538
- roughness trips, effect on boundary layer transition 7-16167
- semielliptical afterbody near-wake, turbulence intensities 7-51150
- separated Poiseuille flow downstream of step, generation and development of perturbations 7-44045
- separation structures on cylindrical wings (French) 7-11451
- single-step wedge with sideplates at yaw angles, supersonic flow, expt. study 7-51219
- supersonic laminar flow with strong viscous-inviscid interaction 7-51212
- supersonic Laval nozzle separated regions, heat transfer investig. 7-31831
- transonic flow, Navier-Stokes computations with two-eqn. turbulence model 7-31829
- tube, periodically constricted, transition to inertial and nonsteady flows 7-11541
- turbulence modelling of separation bubble 7-31756
- turbulent boundary layer 2D separation mean flow similarity 7-31767
- turbulent boundary layers, barriers, flow and heat transfer 7-51100
- turbulent flow behind disk, press.-strain correl model 7-31758
- turbulent flow field in wall attachment device, characts. 7-26255
- turbulent flow over nonrotating cylinder, press. distrib. and fluctuations meas. 7-43868
- turbulent incompressible flow around aerofoils, separation bubbles 7-31761
- two-dimensional magnetogasodynamical boundary layer flow in aligned mag. field, similarity solns. 7-57937
- unheated end shape influence on heat transfer of cylinder in longitudinal flow 7-43893
- unsteady compressible viscous flow over airfoils, integro-differential and finite-difference methods 7-31821
- volcanic eruption, two-phase magma flow in pipe from magma chamber 7-40451
- wake analysis, physical and schematic viscosity influence 7-26281
- wave loading on offshore structs. 7-51172
- wing profile, flow separation, aerodynamic hysteresis 7-57870
- wings, thin, perturbing supersonic flow of perfect gas, optimal lifting surface 7-20754

flow simulation

- 4-cylinder internal combustion engine, 2D intake manifold flow digital simulation 7-63170
- advection, positive definite schemes, comparison and eval. 7-16151
- advection eqn., 1D, 3-pt. 2-level finite difference methods 7-16149
- advection eqn., 1D, improved 5 pt. implicit finite difference methods 7-16150
- advection-diffusion eqn., accurate finite difference methods and Pascal listing 7-16148
- atmospheric convection, comparison of GR FEM models 7-18298
- AZTEC software for 1D gas dynamics 7-26237
- Benard convection, 2D and 3D, num. simulation 7-37465
- block-implicit multigrid calculation of two-dimensional recirculating flows 7-26242
- bubble-driven flow, fluid and bubble meas., numerical soln. 7-16237
- buoyancy-driven convection in horizontal fluid layer extending over porous substrate 7-51136
- buoyant vapour bubbles modelling growth and collapse, rigid boundary, stagnation flow 7-16220
- CANDU-600 heat transport system flow stability, modelling using computer codes 7-30607
- cellular automata for 2D hydrodynamic flow simulation (French) 7-16158
- channel flow, molecular dynamics simulation 7-37418
- circular orifice, 3-D hydrodynamic interaction of a finite sphere, num. soln. 7-51303
- coocurrent two-phase upward flow through packed bed, liq. hydrodynamics simulation 7-57897
- combustion, flow simulation in vortex struct., variational entropy method (French) 7-44064
- compressible flow, accuracy of nonuniform-mesh schemes 7-51202
- compressible flow, moving finite-element modelling 7-51222
- computer graphics techniques for flow pattern visualisation in fluid mechanics education 7-55939
- contour dynamic, rotational flow simulation appl. 7-16194
- convective boundary layer simulation, efficiency of different higher order turbulence models atm. appl. 7-57819

flow simulation continued

Czochralski method simulation using tetradecane, Flow transitions visualisation 7-22463
 degenerate equilibria, determinacy 7-57782
 dense systems of spherical particles under shear dynamics 7-6258
 detached flow problems, soln. using finite element method 7-18599
 dielectric liquids, stressed, transient EHD motion, computer simulation 7-1643
 electrically boosted glass melting tank, 3D model for flow simulation and heat transfer 7-20805
 experimental verification of numerical simulation of flows in cyclones and hydrocyclones 7-26296
 fluid jet models, one-dimensional, numerical comparisons, appl. to drop-on-demand ink-jet printing 7-31851
 fractured rock masses, fluid flow simulation, hybrid boundary element-finite element analysis procedure 7-34478
 fully developed turbulent flow in rot. channel, large-eddy simulation 7-37450
 gases, premixed turbulent combustion, second-order closure prediction 7-57942
 heated plate, acoustically perturbed 2D separated flow 7-16195
 Hele-Shaw fingering, num. simulation 7-51030
 implicit solution methods in computational fluid dynamics 7-51020
 incompressible fluid, flow eqn. soln. 7-6179
 incompressible fluid in closed cavity, free convection, numerical simulation 7-63134
 inf-sup conditions, equivalent forms and applications 7-1431
 inviscid flow, supersonic to subsonic transition, quasi-conservative lambda formulation 7-11454
 laminar boundary layers, active stabilisation, turbulence transition, drag reduction 7-20683
 laminar duct flow, heat cond., numerical soln. 7-57790
 laminar end-wall vortex and boundary layer, numerical simulation 7-51181
 lifting bodies, 2D and 3D Euler computations, finite element method 7-43961
 LMFBR, accelerated two-phase flow through perforated plates during core-disruptive accident 7-30609
 marine weather prediction, 3D models 7-55245
 meandering channels, flow and pollutant dispersion, 3D modelling 7-44052
 molten metal flow pattern calc. in induction furnace (*German*) 7-31729
 Monte Carlo turbulence simulation using rotational approx. to von Karman spectra 7-31759
 moving interface problems in slow viscous flows, FEM 7-16157
 N waves, evolution and decay, Burgers eqn. anal. 7-43980
 nonviscous flow simulation, upwind scheme (*French*) 7-57878
 null-collision technique in the direct-simulation Monte Carlo method, rarefied gas dynamics 7-31841
 numerical expt., computational methods 7-43836
 numerical simulation of viscous flows in hydraulic turbomachinery by the finite element method 7-26256
 oil-bearing stratum, incompressible two-phase flow simulation (*French*) 7-44032
 open-channel network flow model (*Japanese*) 7-35285
 orbital flow past cylinder, vorticity-transport and stream function eqns. 7-43929
 pipe flow., unsteady, attenuation prediction, num. method appl. 7-31732
 plane jet at low Reynolds number confined in rectangular channel, numerical analysis 7-37507
 random choice method for reactive gas with many chemical species 7-20812
 rarefaction or shock wave/duct area change interaction, numerical soln. 7-11461
 reliability considerations in the numerical solution of elastoplastic, viscoplastic and flow problems 7-1452
 reservoir simulation, displacement in two phase flow in porous media, finite element simulation 7-51295
 separated and reattached flow on flat plate, simulation of heat transfer 7-51107
 separation flow around a cylinder near a plane screen, num. modeling 7-63123
 shallow water equations, complex flow, boundary fitted grids 7-6231
 shear dispersion in parallel flow, computational method 7-16152
 shear-flow instability waves, wave action density analysis 7-16169
 SIMPLE hydrodynamics benchmark, restructuring for CHiP architecture 7-16145
 sink-flow boundary layers, num. simulations 7-43882
 Spencer Gulf, tidal computer model 7-18207
 steady Euler eqns., multiple-grid and Osher's scheme 7-51021
 stiff ODE solver software, selection 7-26239
 Stokes equations, soln. for incompressible fluid in multiconnected domain 7-20797
 surface-mounted obstacles, wakes, trailing vortices, channel-flow expts. and num. simulation 7-57844
 swirling flow in diffusers, turbulent pipe flow, Navier-Stokes eqns. 7-6222
 thin liquid films, vortex couples, von Karman wakes, turbulence 7-43935
 tides, 2D eqns., num. soln. by method of characts. 7-18187
 tides, 2D eqns., soln. by method of characts., adaptation to wind-induced currents and storm surges 7-18188
 topographic Rossby waves, 1D models, elongated basins, various lake cross sectional distributions 7-18220
 transonic flows, least squares FEM for simulation 7-26309
 transonic full potential eqn., intermediate boundary condition in Holst AF2 scheme 7-26308
 turbulence near a wall, limiting behaviour, Navier-Stokes computational models 7-16170
 turbulent channel flow 7-57926
 turbulent flow meas., hot-wire anemometry, evaluation of analytical systems 7-16274
 turbulent flow struct. in rot. channel, large-eddy simulation 7-37442
 turbulent flows, helical nature, num. simulation 7-31763
 turbulent flows-elastic shell interaction, finite element anal. 7-43874
 turbulent mass transfer at mobile interface, computer simulation 7-43865
 turbulent reacting flow simulation, based on spectral characts. eqns. 7-26361
 turbulent thermally buoyant flow, statistical modelling 7-31731
 two-dimensional gasdynamic currents on variable struct. grid, numerical simulation (*Russian*) 7-20680
 two-fluid flow through porous media, Monte Carlo simulation 7-31734

flow simulation continued

unsteady incompressible viscous flow over circular cylinder, body-fitted coordinates 7-43851
 viscoelastic flow problems, integral constitutive models 7-16213
 viscous flow, stress ensemble calcs. 7-43838
 vortex breakdown, num. study 7-26283
 vortex breakdown model, axisymmetric flow stability 7-26282
 vortex breakdown simulation, multigrid method 7-26284
 vortex dynamics and singularities, Biot-Savart eqn. soln. 7-51183
 vorticity distrib. simulation, Monte Carlo techniques 7-37471
 wakes behind stationary cylinders, vortex street formation, wake instability model 7-16182
 H₂-air turbulent mixing in coaxial jets 7-37505
 H₂-O₂-Ar mixture, reflected-shock flowfield calcs., random choice method appl. 7-20812
 H₂-O₂-N₂ flames, one-dimensional simulation, mathematical and numerical aspects 7-39893

flow stress see plastic flow**flow through porous media**

absorbed polyelectrolytes, effect on convective flow and diffusion in porous membranes 7-11536
 adaptive methods to solve free boundary problems 7-66182
 annular packed-sphere bed with wall effects, fully-developed forced convective flow 7-51110
 areal micellar polymer flooding calc. 7-6307
 asymptotic laminar boundary layer, mass transfer effects on transient behaviour 7-4323
 boundary collocation method, boundary integral elements method 7-6311
 brinkman equation, fractal model for porous media, and viscosity renormalization 7-44042
 buoyancy-driven convection in horizontal fluid layer extending over porous substrate 7-51136
 capillary condensation in cylindrical pore, stability 7-1623
 capillary-porous bodies, heat and mass transfer, mathematical models 7-62957
 capillary-porous structures, heat transfer during vapour formation, regimes and laws 7-31865
 chemical dissolution by reactive fluid 7-44062
 circular orifice, 3-D hydrodynamic interaction of a finite sphere, num. soln. 7-51303
 circulating fluidised beds, flow structs., meas. technique development (*German*) 7-16243
 clay soil, filtration prop. form., adsorbed H₂O struct. role 7-51297
 compact heat exchangers, with permeable wall, friction and heat transfer 7-51143
 completely confined porous medium, onset of hydromagnetic thermal convection, stability 7-6205
 composites, transport props., pore-size parameter studies 7-38657
 conducting viscous incompressible flow near an oscillating porous flat plate 7-6322
 convective flow structure in porous media (*French*) 7-16246
 convective instability in packed or porous beds with throughflow 7-11383
 Couette flow with porous walls of a dilute suspension 7-51037
 crack in porous medium, elastic-hydrodynamic problem of fluid inflow 7-11534
 deep bed filtration, stochastic compartmental model 7-6301
 diffusion, interfacial surface statistics 7-16236
 diffusion-limited-aggregation in porous medium, effect of morphological disorder on viscous fingers 7-56173
 dilute adsorbable gases, heat of transport through pores, pore struct. form. 7-54175
 dispersion and convection in periodic porous media 7-51140
 dispersion in one-phase flow 7-6302
 dispersion in two-phase flow 7-6303
 dispersive transport in porous media, modelling, second order approach, appl. 7-63212
 dispersive transport modelling in porous media, solute motion in pipes and capillary tubes 7-23753
 dispersive transport modelling in porous media, theoretical development of second-order approach 7-23752
 displacement in two phase flow in porous media, finite element simulation 7-51295
 drying, filtration process, hydrodynamics 7-57918
 dual-gamma attenuation for the determination of porous medium saturation with respect to three fluids 7-51307
 dynamic analysis of saturated porous media, higher order, mixed, and Hermitean finite element procedures 7-14263
 dynamic response of saturated porous media, evaluation of u-w and u- π finite element methods 7-14262
 dynamical growth systems, fractal patterns, flow in porous media appl. 7-37540
 elastically deformable porous medium, gas filtration during dynamic expansion of cavity 7-16248
 fibrous medium, thermally induced hygroscopic mass transfer 7-44037
 filler evaporation from porous body with plane surface 7-51230
 film condensation and natural convection along interface between porous and open space 7-43903
 filtration through gas-liquid foam, fluid flow model 7-51301
 finite amplitude convection in a rotating porous medium 7-57842
 finite element methods in flow problems, conference, Antibes, France (June 1986) 7-41009
 fixed bed catalytic reactors, 1D heat transfer coefficient 7-6298
 flat surface, porous, movement in parallel free stream, boundary layer behaviour 7-43919
 flow properties w.r.t. cryogenic appls. 7-52171
 flowing packed particle beds in circular tubes, const. wall heat flux, local Nusselt numbers 7-1626
 fluid displacement in porous medium, fluctuations, viscous fingering and diffusion-limited aggregation 7-37539
 fluid displacement in porous medium, interphase mass transfer and phase transform. 7-51300
 fluid in porous medium, stability criteria for convection, eigenvalue problems 7-44033
 fluid inertia and fibre proximity of airflow through fibrous filter 7-11535
 fluidised bed stability, influence of gravity, chemical reactors appl. 7-16242
 fluidised beds, gas-solid-liquid, fluid dynamics, correls. 7-16250
 fluidized beds, electric behaviour, capacitor model 7-6305
 fractal patterns from chemical dissolution 7-44061
 fractured porous rock, contaminant transport 7-55027

flow through porous media continued

fractured rock masses, fluid flow simulation, hybrid boundary element-finite element analysis procedure 7-34478
gas mixture nonequib. flow through narrow channels, phonon drag effects 7-16253
gels, drying induced shrinkage, liquid flow and chem. reactions 7-23069
Green-Ampt analysis for falling water table in stratified profile 7-23764
groundwater, porous flow model for steady state Ra transport 7-23725
groundwater flow in permeable geologic media for nuclear waste evaluation using 3D-SEEP code 7-60103
groundwater pollution, solute dispersion in multidimensional periodic saturated porous media 7-23731
heat exchange between tube and surrounding water-saturated soil 7-63153
heat-conducting fluid flow through porous media, appl. in Martian regolith 7-16249
homogeneous fluid flow rate in porous media 7-51298
homogeneous soil matrix containing population of macropores, infiltration 7-23743
horizontal flow past partially heat infinite vertical cylinder embedded in porous medium 7-6309
hot water storage in aquifer, underground heat and fluid flow models 7-65600
hydromagnetic free convection flow along porous plate with mass transfer, Hall effects 7-63141
ice, melting in porous media, solid-liq. interface motion, temp. distrib. 7-50926
ice-air composite materials, melting process study 7-26335
ideal gas diffusion through porous plug, finite-time thermodynamics 7-31914
idealised spiral wound membrane module, fluid flow 7-6312
immiscible displacement in porous medium, viscous fingering instability 7-11491
immiscible viscous fluids, fingering in Hele-Shaw cells 7-43854
inclined porous channel, viscous MHD flow in the presence of a mag. field 7-6320
incompressible three-phase flow in porous media, conservation laws 7-51286
kidney, artificial, press. losses in apparatus with capillary channels made of semipermeable film 7-28772
linearised unsteady multidimensional infiltration in soil 7-55108
liquid phase sintering, pore filling, critical grain size for liq. flow 7-46364
liquid-gas flow through coarse particle beds, 1D model 7-57904
lumped model for multicomponent adsorptions in fixed beds 7-6300
magma ascent by porous flow, role of magmons 7-8928
magneto-gravitational instability of a rotating and finitely-conducting fluid 7-11555
mass transport, generalised Darcy's and Fick's laws 7-57915
mass transport, macroscopic balance laws 7-57914
mass transport in discrete fracture networks, prediction by geometric field data use 7-66192
material transfer and absorpt., boundary regime optimisation 7-26341
membrane spargers, elastic and flow mechanics 7-31877
membranes transport process meas. techniques 7-28337
membranes with locatable single pores generation, obs. and testing 7-298
MHD channel flow through porous medium 7-57932
miscible displacement stability in porous media, rectilinear flow 7-31750
mixed convection flow over horizontal cylinder or sphere in saturated porous medium 7-1562
Monte Carlo simulation of two-fluid flow through porous media 7-31734
multicomponent multiphase fluid flow in porous media, probability approach 7-44028
multilayer porous materials, data correl. for internal hydraulic resistances 7-51302
natural convection, book 7-60909
natural convection experiments in a stratified liquid-saturated Porous Medium 7-63150
natural convection from cylindrical heat source in water saturated porous medium, radwaste appl. 7-806
natural convection in porous media, non-Darcian effects 7-31785
natural gas separation using supported liquid membranes 7-11526
network models of porous media, hydrodynamic dispersion 7-1625
non-Newtonian fluid flow past infinite porous plate, existence theorem 7-4695
nonDarcy free convection boundary layer on axisymmetric and 2D bodies of arbitrary shape 7-43904
nonequilibrium gas-solid system, transport processes, kinetic theory calcs. 7-16254
oil displacement from porous rock by micellar solns., analytic and expt. study 7-6278
oil reservoir flow models, book 7-48219
oil-bearing stratum, incompressible two-phase flow simulation (French) 7-44032
oil-water gravitational separation in beds of limited thickness 7-51299
one dimensional porous media, turbulent filtration eqn. 7-31879
optical measurements of porosity and fluid motion in packed beds 7-6304
oscillating flow past infinite vertical plate, suction and free convection effects 7-1555
oscillating free-convection flow past infinite porous vertical limiting surface, effects of mass transfer 7-14479
packed bed catalytic reactor, local thermal equilibrium 7-6276
packed bed heat exchanger, evaluation for residential appliances use 7-31779
packed beds, flow, drag force, wall effect 7-51292
percolation model of an inhomogeneous anisotropic medium 7-1624
percolation of a compressible fluid in a nondeformable porous medium 7-44035
perturbation propagation in porous granulated media, lin. theory 7-6306
pipe, vertical, internally cooled, embedded in porous medium, condensation 7-32624
pipe flow, gas, permeable walls, turbulent flow, heat transfer, phys. props. temp. depend effect 7-63217
plate, nonisothermal flat, free convection flow influenced by blowing or suction 7-11529
PMMA, swelling caused by CS₂ imbibition, light scatt. investig. 7-62628
polymer films, multicomponent gas permeation, meas. method 7-51304
polystyrene diffusion in porous silica 7-12351
porous media, degenerate parabolic eqns., difference schemes 7-51306
porous media, nonlinear conservation law, FEM (French) 7-44031
porous-bed solar air heater, functional aspects 7-28412

flow through porous media continued

porous-walled duct flow with gas injection, acoustic boundary layer 7-20793
pressure drop, shear force, Kozeny-Darcy relationship 7-51305
pressure wave propagation in fluid flowing through porous medium 7-6310
radionuclide migration through sandy soil layer 7-8458
rock, porous, permeability, percolation concept anal. 7-47436
rotating porous medium, unsteady free convective flow 7-51139
second-order fluid flow between two porous coaxial circular cylinders, finite element method 7-11530
second-order fluid flow through channel with porous walls under mag. field 7-20762
shallow water wave propagation, effects of permeable breakwater 7-66165
shield-vacuum heat insulation, gas permeability 7-44038
singular soln. of porous media eqn. with absorption 7-29763
sloped porous layers, 3 D convective cells (French) 7-16247
slow viscous flow past a random array of spheres, macroscopic descript. 7-11537
soil, infiltration from cavities, num. soln. 7-18254
soil column with central hole, infiltration 7-18253
soil water, analytical-numerical approach to one-dimensional infiltration in homogeneous soils 7-29082
solid-fluid mixtures, boundary conditions 7-6854
solute transport in infinite medium with mobile and immobile zones, 3D solns. 7-23248
sparsely packed porous layer, double diffusive convection 7-11531
sparsely packed porous medium, double diffusive convection, rot. effect 7-1553
spheres in beds in lengthwise flow, fluid friction and convective exchange 7-57917
steady gas flow past blunt bodies screened by permeable surface 7-51216
streamline routing through fracture junctions 7-55028
thermal osmosis near a buried heat source 7-51296
thermoconsolidating media, acceleration wave prop. and decay 7-1622
thermoelastic response of fluid-saturated porous rock 7-14267
three-phase flow meas., tomographic imaging 7-51355
tracer dispersion in a binary mixture of spheres (French) 7-63211
tracer dispersion in sintered glass beads (French) 7-63210
transient 3D 3-phase 3-component nonequib. flow in porous bodies by 3-velocity fields. 7-56782
transient heat transfer in porous media—a two-temperature model 7-16181
transverse thermal dispersion in forced convective flow through packed bed 7-51105
trickle packed towers, fluid dynamics, mass transfer at high press (German) 7-16244
tubes and channels, porous-walled, injection-induced flows 7-31876
turbulent boundary layer in channel, injection through porous wall, accel. and turbulence influence, investig. 7-26263
turbulent flow in cylindrical tube with internal perforated baffles, drag crisis 7-43867
two-dimensional flow past bluff flexible low porosity membranes 7-16241
two-sphere hydrodynamic interactions and mobilities in a porous medium 7-26340
ultrafiltration, modelisation and structure modulus (French) 7-16245
unsaturated flow of liquids in porous media, free boundary problem 7-37538
unstable fronts in a porous medium, stochastic numerical scheme 7-57919
unsteady free-convection flow past accelerated plate, skin friction 7-4321
unsteady heat transfer in gas-swept bed of spherical granules 7-31803
unsteady interface between two fluids in a porous medium 7-14319
unsteady MHD flow past vertical porous plate, mass transfer and free convection effects with constant suction 7-54332
unsteady MHD flow past vertical porous plate, mass transfer and free convection effects with variable suction 7-54333
vapor condensation on an inclined plate within aporous medium 7-1572
vapour dryness degree distrib., thermal action on oil seams 7-20791
velocity effects on dispersion in porous media with a single heterogeneity 7-20792
viscoelastic boundary layer flow past stretching plate with suction and heat transfer 7-6313
viscoelastic porous media, fluid eqn. soln. and applic. (Chinese) 7-18222
viscoplastic liquid impregnation of heated filler, axisymm. problem 7-44040
viscous fingers and diffusion limited aggregates near percolation 7-16252
viscous fluid, time depend. rotational flow over infinite porous disk with magnetic field 7-26290
viscous fluid flow, Brinkman's eqns., Foldy's approx., porous media with large number of scales 7-16251
viscous fluid flow in porous medium, num. anal. 7-63207
viscous incompressible flow in a narrow channel with one free wall and fluid supply through a porous insert 7-1636
viscous incompressible fluid flow through porous medium and mass transfer 7-11532
viscous stratified fluid, unsteady flow, variable mag. induction 7-63193
water free and forced convective flow through porous medium 7-11533
water velocity meas. in porous medium by fast neutron transmission 7-37584
weak disturbance velocity measurement, bulk density in porous media 7-31826
wet porous beds, natural convection determ. 7-31786
Al₂O₃ porous ceramics, elec. cond. and fluid flow permeability correls. 7-38566
He-H₂O, gas/vapour mixtures in porous medium, natural convection 7-1554
³He, superfluidity suppression in small cylindrical pores 7-63898
Hg injection into porous media, elec. resist. devil's staircase, fluid displacement kinetics and thermodynamics 7-44041
N₂-H₂O, gas/vapour mixtures in porous medium, natural convection 7-1554

flow visualisation

3-D vector-values data visualization method (Japanese) 7-51031
3D flow obs. by interferometry and image processing 7-37576
air flow visualisation in clean rooms using laser light sheet method (Japanese) 7-57966
air jet, development and breakaway, coanda effect, interferometric, Schlieren and shadowgraph investigs. 7-51358

flow visualisation continued

annular cascade oscill. in transonic flow, unsteady aerodynamic characts. 7-37490
 arch-type vortex, form. behind normal plate in laminar boundary layer 7-26288
 axisymmetric free jets having parabolic profiles at nozzle exit, hot-wire turbulence meas. 7-51260
 behaviour during cylindrical vessel explosions 7-59760
 by-passing flow in a supersonic nozzle with optical windows (*Japanese*) 7-51263
 cavitating flow in duct, high speed cine photographic obs. 7-51240
 cavity flow, buoyancy effect (*Chinese*) 7-11429
 channel flow, rectangular turbulent promoters, computer generation 7-37549
 chronographic technique based on split-timer cct. 7-51353
 circular cylinder rotating in rectangular tank, induced flow 7-37475
 coherent struct. in reattaching laminar and turbulent shear layers 7-51079
 cold, transient and steady-state vertical natural convection flow, meas. and visualisations 7-43902
 composite channel flow, periodical large surface eddies generation 7-20803
 compressible separated turbulent shear flow, mixing, flow meas. 7-51080
 computer graphics techniques for flow pattern visualisation in fluid mechanics education 7-55939
 convective flow patterns in cylindrical layer, wave-vector field 7-51352
 creeping flow around spherical gas-bubble in liquid, Oseen's eqn. soln. 7-37513
 crystal growth, image processing of Czochralski bulk flow 7-53544
 curved pipes, dilute polymer soln. flow, drag reduction, pressure loss in 360° bends 7-16211
 cylinder, circular, sectional aerodynamic calcs., free-stream turbulence scale effects (*Japanese*) 7-51206
 cylindrical surface modifications effect, H₂ bubble wire flow visualisation and anemometry meas. 7-6196
 Czochralski method simulation using tetradecane, Flow transitions visualisation 7-22463
 distributed roughness effect on transition enhancement 7-37433
 droplet field visualization and characterization via digital image analysis 7-37577
 falling water films on vertical cylinder with downward step 7-6334
 fibre optic sensors and their appls., conf., Cannes, France (Nov. 1985) 7-40999
 fibre suspensions in Newtonian fluids and polymer solns., capillary flow 7-6318
 fluid control and meas., conf., Tokyo, Japan (Sept. 1985) 7-29593
 fluids possessing yield stress, cavern sizes and mixing performance, X-ray-heavy metal tracer method 7-11565
 gas concentration and gradient meas. in photoacoustically perturbed jet 7-37560
 gas jet impacting a cavity, temp. and velocity meas., flow anal. 7-43999
 gas velocity imaging using photothermal deflection effect 7-20817
 gravity current on sloping bottom, rot. flow interaction, shelf wave generation, flow visualisation expts. 7-43947
 hairpin vortices, generation in laminar boundary layer, obs. 7-57796
 hairpin vortices, generation in laminar boundary layers, obs. 7-57797
 historical and recent developments 7-35189
 horizontal annular pipes, two-phase flow regimes during heat transfer crisis 7-63200
 horizontal eccentric annular cavity, natural convective heat transfer reduction by baffles 7-20701
 horizontal gas-liq. two-phase flow, flow pattern identification using differential pressure fluctuations 7-37534
 inlet through circular orifice, effect of viscosity on flow characts. 7-6330
 instabilities, tomographic visualisation, improved method 7-37568
 interfacial wave generation, investigation through flow visualisation and LDA 7-37438
 interfacial wave measurement method involving light polarisation and optical activity 7-4201
 internal flow visualisation by 3D dynamic laser sheets (*French*) 7-31900
 jet diffusion flames, flow visualisation using Mie scatt. method 7-11566
 jet flow visualisation, image processing using streamline coordinates 7-37572
 jet impingement on wedge, edge-tone flowfield 7-11483
 jets, initially circular, flow development and control, shear layer growth 7-11482
 Karman vortex flowmeter, fluid flow around bluff body 7-37601
 laminar heat transfer and flow in curved square channels, elliptic nature, numerical visualisation 7-37432
 laminar juncture flow, unsteady characteristics, visualisation 7-57799
 laminar natural convective flow along isothermal vertical surface, stability 7-31744
 laser light sheet method for building environmental engineering 7-37570
 light slicing technique 7-44067
 liquid crystal thermography for wall heat transfer and flow visualisation 7-35520
 liquid surfaces, slightly deformed, visualisation using K.-Moire method 7-37483
 longitudinal flow past plates with blunt trailing edges, wake investig. (*German*) 7-20824
 longitudinal vortices in straight open channel, flow visualisation 7-37476
 low vel. field in plenum, meas. using flow visualisation 7-37567
 low-velocity flow measurement by bubble/dye tracing technique 7-16283
 MOCVD reactor, vertical vs. horizontal design, optical study of gas phase 7-22534
 MOCVD reactor cell, visualisation of flow and temp. profiles, appl. of holographic interferometry 7-22532
 modern developments, review 7-11561
 MOVPE growth, flow patterns in vertical reactors 7-22535
 multi-spark visualization of typical combustor flowfields 7-26372
 multiphase flow visualisation study, holography appl. 7-51287
 natural convection, partially filled rectangular enclosure, heat transfer study 7-31625
 natural convection, partitioned enclosures, heat transfer study 7-31626
 natural convection in partially divided enclosures 7-63146
 natural convection in rapidly spinning systems, heat transfer and flow visualisation 7-63161
 noise generation in transonic flow, investig. (*German*) 7-31833
 oscillating air foil-vortex interaction, flow visualisation study 7-20816
 parallel rotating heat pipe, heat transfer characts. (*Japanese*) 7-57841

flow visualisation continued

particle image displacement velocimetry for 2D flow visualisation 7-31893
 particle motion study in concentrated dispersions, tracer diffusion method 7-51351
 pattern anal. using observed data and numerical anal., appl. to air deflecting device 7-37420
 photographic recording, computer-aided data processing 7-6329
 photographs from third annual fluid-mechanics photo contest 7-11569
 pipe flow, visualization in steel pipes using real-time neutron radiography 7-37583
 plane detonation wave at convex corner, diffr. 7-57880
 plate with jet impingement, holographic visualisation of pressure distrib. 7-37569
 pollutant dispersion, wind tunnel expts. 7-1573
 propane jet flames, near-nozzle region, flow struct. 7-8280
 radial fingering pattern of immiscible liqs. in circular Hele-Shaw cell 7-63160
 radial reattachment turbulent jet flow, press. distrib. 7-26324
 real-time neutron radiography applications in dynamic fluid flow studies 7-33903
 real-time neutron radiography of lubricant dynamics 7-33902
 retinal blood flow visualisation and meas. by laser speckle photography 7-47212
 ring vortices, smoke visualisation 7-37566
 rotating concentric cylinders, same or opposite directions, turbulence and vortices 7-16255
 rotating cylinder in quiescent fluid, turbulent shear flow, flow visualisation, eddies 7-16168
 rotating cylindrical annulus, imposed temp. gradient, flow regimes study 7-43933
 salinity distrib. meas. in salt-stratified, double-diffusive systems, by optical deflectometry 7-23092
 secondary flow patterns, flow visualization and centrifugal instability in curved tubes 7-37550
 soap-mineral oil lubricating grease, 12 Li-hydroxystearate greases, thick film, ambient pressure, shear flow transient tests (*French*) 7-6169
 steady and unsteady flow visualisation using spark velocimetry 7-57968
 stirred reactor, flow characts., flow visualisation and torque meas. 7-57963
 stratified flow, entrainment, sheared density interface study 7-51266
 streamlines and pathlines, plotting on microcomputer 7-16272
 subsonic shear flow, ordered structure development, acoustic oscills. influence 7-20742
 supersonic air ejector, primary flow oscill. 7-37492
 swirling flow, axisymmetric vortex breakdown in circular pipe 7-26286
 swirling flow in narrow annuli with tangential air inlets 7-43926
 Taylor-Couette flow, stability limits, flow visualisation and numerical study 7-43844
 thermal plume in thermally stratified medium holographic visualisation 7-11489
 thermohaline system with mixed layer circulation, gradient layer entrainment 7-65601
 time-dependent convective flow pattern rotation, comment and reply 7-1560
 transition sensitivity, in flow around a circular cylinder, oil-flow photographs anal. 7-43848
 transonic flows, unsteady phenomena, visualization and registration 7-37491
 trapped internal waves from body moving in ocean thermocline, phase config, visualisation 7-31854
 tunnel test sections for optical measurements 7-57964
 turbine cascade in wind tunnels, transonic flow meas. 7-26313
 turbulent, fully developed 2D channel flow, visualisation and image processing 7-37574
 turbulent boundary layers, wall-pressure peaks generation, flow struct. obs. 7-57821
 turbulent boundary-layer, surface drag reduction by riblet modification, visualisation study 7-11394
 turbulent channel flow, 3D coherent structures in near-wall region 7-37548
 turbulent channel flow, ejections and bursts, struct. and timescales 7-51088
 turbulent flow field in wall attachment device, characts. 7-26255
 turbulent flowfield visualisation, computer generated, for flow around cubic model 7-37447
 turbulent open-channel flow, struct., flow visualisation study 7-51071
 turbulent plane jet, organised struct., role in momentum and heat transport 7-44000
 two layer flow, chemically reacting mixing layer, vortical struct., flow visualisation anal. 7-44007
 unsteady jets, 3D surface shape estimation by image processing 7-37573
 velocity field visualisation by single exposure holospeckle interferometry 7-50518
 velocity vector, automatic determ. from pathline photograph 7-37575
 velocity-field measurement by pixel-based temporal mutual-correlation analysis of dynamic image 7-20823
 vertical wind tunnel for water drop studies 7-6293
 vessel filling, flow visualisation, inlet orifice position effects 7-11560
 viscous Newtonian and nonNewtonian fluids, power and Taylor nos., Taylor vortices 7-51158
 volume cycling in tapered pipe, dye streak meas., Eulerian and Lagrangian velocity profiles 7-44051
 vortex filament interactions, expt. study 7-37474
 vortex form. processes in wakes behind bluff bodies 7-51174
 vortex structure in plane mixing layers, meas. and models 7-16191
 vortex-pairing mechanism, interaction of free-stream turbulence with shear layer vortices 7-43931
 vortices, far-wake structures behind bluff bodies 7-51175
 VPE, organometallic, reactor design optimisation, flow visualisation studies 7-22533
 wakes, turbulent, pseudo 2D, development 7-57846
 wall attachment device, turbulent flow field, control flow effects 7-20697
 water pollution, Seto Inland Sea hydraulic model, dye conc. pattern anal. 7-40058
 Ar, inductively coupled plasma torch, gas flow dynamics, light scatt. technique 7-11795
 DF chemical lasers, mixing enhancement using supersonic nozzle. design 7-5878
 GaAs, MOCVD, uniform growth on multi-wafers 7-22536
 H flame-out in air flow, gas dynamic struct., interaction effect 7-26315

flow visualisation continued

- I_2 , supersonic flow study by 3D visualization and laser-induced fluorescence 7-20751
- N_2 7-26268
- UF₆, laser induced breakdown and appl. to flow diagnostics 7-20832

flowcharting

- see also *programming; systems analysis*
- solar still performance synthesis and predictions 7-23217

flowmeters

- see also *anemometers; flow measurement; laser velocimeters*
- acoustic continuity transducer for flowmeters with two-phase media 7-57960
- Borda connector, wall thickness coeff. (French) 7-6331
- calibration, computer-aided test system 7-37591
- complex flow measurement, two component LDV system (Chinese) 7-26366
- differential pressure transducer, directly flanged, design (German) 7-44070
- domestic gas meter using coherently modulated US carrier 7-1659
- Doppler flowmeters, differential, with single-mode fibre waveguides 7-44079
- Doppler ultrasonic flowmetry, signal analysis using PLL 7-50851
- electromagnetic flowmeter sensitivity with two-phase flow 7-37522
- electromagnetic flowmeter without settling section 7-51348
- EM, for liq. metal flow rate meas., error in correl. method 7-57954
- EM flow-rate meter electrically-conducting fluid, flow rate meas. using (Russian) 7-11571
- EM flowmeters, noise reduction 7-37599
- error components determination 7-57955
- fibre optic petal flowmeter for low gas pipe flows 7-44081
- flexible orifice flowmeter 7-37589
- float-area type flowmeters, float instabilities in conduits, coupled vibration 7-20818
- fluidic flowmeters with wide measuring range 7-37564
- fluidic volumetric-flow, mass-flow density and viscosity meter 7-26367
- hot wire air flow meter for automobile engine intake mass air flow rate meas. 7-37587
- hot-wire anemometer compensated for ambient temperature variations 7-16275
- jet generator based, medical instrumentation appl. (Bulgarian) 7-28740
- Karman vortex flowmeter, fluid flow around bluff body 7-37601
- liquid meter checking system, automatic 7-57957
- mass flowmeter using heat transfer for dense phase solid-gas two-phase flow 7-37579
- mass hydrometry, Oval micromotion mass flowmeter (Japanese) 7-56225
- medical pulsed US air flowmeter, design and construction 7-3845
- medical US Doppler flowmeter for use in theatre 7-47188
- metrological support to means of measuring flow rate for liquid cryogenic media 7-44074
- microcomputerised system, accuracy estimation 7-57956
- micronozzles for flow rate meas., calibration system 7-51347
- milliwatt power consumption type electromagnetic flowmeter 7-37600
- new hydrodynamic oscillator type flowmeter 7-37565
- NMR, front sampling parameters effect on systematic error 7-57952
- NMR, relax. error elimination method 7-57953
- nuclear fuel reprocessing, fluid flow meas., microcomputer-based multi-channel polarity cross-correlator 7-42121
- obstructionless flowmeters survey 7-63235
- orifice flowmeter, flow coeff. meas. for large diameter pipe 7-37590
- oscillating LPA for measuring flow and pressure 7-37563
- PAT loop for AGR fuel testing, flow meters for coolant 7-26370
- PC-I type of mini-flowmeter, development (Chinese) 7-1654
- Peltier probe flowmeter, performance analysis 7-44083
- pipeline flow meas. in flow straightener/flowmeter package 7-57948
- propeller type, vibration effects 7-37597
- pulsation effects in vortex and orifice types 7-37596
- pulverised coal/air two-phase flowmeter 7-37580
- solid-gas two-phase flowmeter for blast furnace pulverized coal injection 7-37578
- tagging type, error structure 7-57950
- temperature compensated Doppler flowmeter for small diameter pipe 7-20820
- temperature-independent design using modified sing-around method 7-37612
- transient velocity profiles, real-time estimation using Kalman filtering techniques 7-37582
- turbine type, calibration curve prediction 7-37598
- turbine-type working with cryogenic products, conversion factor 7-57958
- US, freq. modulated, errors in flow meas. 7-57951
- US blood flowmeter, pulsed Doppler system, serial data processing (Korean) 7-3846
- variable area and pressure difference flowmeters, review 7-44077
- variable area flowmeter for mass flow meas. (German) 7-26369
- velocity profile measurement by ultrasound Doppler shift method 7-37585
- vortex flow meters for computerised vapour-heat flow measurement (German) 7-11564
- vortex flowmeters, bluff body design 7-37603
- vortex shedding flowmeter with piezoelectric sensor 7-37602
- water meter, weighted mean error components analysis and standardisation 7-57949
- YEWFO vortex flowmeter, small size and cryogenic versions (Japanese) 7-51356
- He, liquid, flow rate meas., IMGC calibration facilities 7-63234

fluctuations

- see also *Brownian motion; critical fluctuations; current fluctuations; noise; random processes*
- $\phi^2 + \phi^4$ field, quantum fluctuations around soliton at finite temp. 7-41593
- adiabatic thermal explosion in small systems, stochastic theory, numerical results 7-9764
- augmented Langevin description of multiplicative noise and nonlinear dissipation in Hamiltonian systems 7-29898
- background fluctuations and Wegner corrections 7-281
- biological motion, coordinated, nonequilibrium phase transitions, critical fluctuations 7-28564
- Bose fluid, interacting, nonlinear quantum and classical renormalization-group trajectories 7-35396
- Bose superfluid, fluctuation dispersion of transport coeffs. 7-38284
- bubble growth and collapse, transient boiling heat transfer in narrow channel 7-26346

fluctuations continued

- cellular automata, Langevin equations, and unstable states 7-18703
- cooperative phenomena, statistical mechanical theory, fluctuations, coherent anomalies and scaling exponents 7-48658
- correlations and fluctuations in charged fluids 7-56149
- critical behaviour finite cutoff and higher transient effects 7-282
- curvature and torsion from matter, Lorentz gauge symm. 7-41208
- cylinder, circular, sectional aerodynamic calcs., free-stream turbulence scale effects (Japanese) 7-51206
- damped quantum mechanical oscillators with thermal fluctuations 7-48410
- diffusion-reaction systems, fluctuations, adiabatic elimination of transport modes 7-39855
- directed polymers in random medium, fluctuations 7-33199
- discs with fluctuating radii, simulation of elastic response 7-56040
- dissipative linear quantum systems, repeated meas. 7-48394
- distinguishability or indistinguishability in classical and quantum statistics 7-41244
- drift-wave fluctuations in sheared magnetic field, 3D particle simulation 7-44237
- dynamical structure factor of a fluid in nonequilibrium steady states 7-31752
- dynamical systems and statistical physics conf., Koszeg, Hungary, Aug.-Sept. 1984 7-48194
- effective classical potential for fluctuating field systems of finite size 7-14866
- electron whistlers in plasmas, EM modulation 7-58000
- energy-density fluctuations in de Sitter space 7-18668
- extended irreversible thermodynamics, linear Burnett coeffs. and thermodynamic fluctuations 7-285
- fermi system, correlation functions of order-parameter fluctuations 7-56145
- ferromagnets, dilute, lines and domain walls 7-33199
- field correls. in a fluctuating homogeneous medium, spectral coherence, dynamical struct. factor determ. 7-4119
- fluid surfaces, effective bending rigidity calcs., integration meas. 7-58571
- free cavern separation zone pulsation at supersonic stream vel. 7-11458
- gamma-rays emitted by solid, effects of vac. fluctuation 7-7626
- generalized wave-particle fluctuations, Einstein's separation 7-4712
- heavy particle tunnelling in condensed media, fluctuation and vibration effects 7-21981
- Heisenberg ferromagnet, thermal boson expansion at finite temp. 7-2885
- imaging method diagnostics for plasma density fluctuations 7-1738
- interacting Brownian particles in hydrodynamical limit, bulk diffusion and equilibrium fluctuations 7-48585
- interacting diffusions, fluctuation phenomena, tightness problem, stochastic evolution 7-211
- intermediate-valence system, fluctuations and photoemission props. calc. in tetrahedral-cluster model 7-39354
- intermittent chaos, global spectral structs. for periodic laminar motions with turbulence 7-41271
- irreversible processes formulated in a superspace, quantum theory, variation principle 7-14869
- Ising model disordered ferromag. binary system, phase diagram 7-59041
- isenthalpic-isobaric ensemble, fluctuation formulae 7-279
- Josephson junction, macroscopic current states decay rate determ. 7-52912
- Kaluza-Klein model in 5D, quantum fluctuations and residual length 7-48507
- kinetic theory of liquids, maximum entropy ensembles and equilib. soln. 7-26605
- laser-assisted collisions, random telegraph noise 7-50044
- light quantum particle motion in metallic environment, path-integral formalism calcs. 7-52459
- light wave interference, quantum fluctuation effects, laser gravitational obs. sensitivity implications 7-43039
- Lorenz attractor, effective noise, stochastic differential eqn. 7-223
- macroscopic system, variables, theory of meas. 7-48442
- macroscopic systems, fluctuation phenomena in localisation kinetics 7-64177
- membrane, stack structures, fluctuation pressure 7-47014
- membranes, fluctuation pressure between walls 7-3604
- mesoscopic systems, transport props., book contrib. 7-52553
- metallic wires, small, conductance fluctuation 7-64201
- microstructures, noise effects, device sensitivity 7-52713
- monomolecular reactions, diffusion-induced, fluctuations and rotation 7-39864
- multicomponent systems, thermodynamics props., pairwise fluctuations 7-14900
- multiplicative random walk, self-similarity of fluctuations 7-231
- nonlinear bound on unstable fluctuation level in low-density non-neutral plasma 7-57998
- nonlinear gyrokinetic theory, direct interaction and anomalous thermal transport in tokamaks 7-37638
- nonpolar liquid mixtures, fluctuon self-localised state of electrons 7-16993
- nonpremixed gases, turbulent diffusion combustion 7-1648
- open reactive systems, centre manifold onset, far-from-equilib. fluctuations scaling, virtual size parameter calcs. 7-35484
- optical wave phase fluctuations through atm. turbulence, probability density function 7-57246
- order parameter fluctuations, role in finite size effects determ. in system undergoing phase transformation 7-2143
- p^n junctions, impact ionisation rates, field fluctuation effects, Monte Carlo simulation 7-64323
- paramagnetic medium, completely disordered, magnetisation fluctuations, CPA approx. 7-2808
- particle in fixed dispersed layer, fluctuation hydrodynamics of Brownian motion 7-24560
- phase transitions, fluctuation effects in exactly solvable model 7-41318
- photon correlation spectroscopy, laser fluctuation compensation 7-41487
- plasma, ion acoustic turbulence evolution 7-51451
- plasma heavy ion beam probe, temperature and fluctuation correlation meas. 7-1755
- polymer solutions, spinodal separation kinetics (Russian) 7-16392
- quartz, crystal growth, pragmatic model for simulation of self-induced striations 7-11973
- random surfaces, triangulated, intrinsic geometry, mean size fluctuations, model anal. 7-61226
- random surfaces, triangulated, intrinsic geometry, mean size fluctuations, Monte Carlo simulation of critical props. 7-61227

fluctuations continued

- randomly diluted resistor network, resistance fluctuations calcs. 7-64193
 rare-earth magnets, spin reorientation phase transitions, fluctuation effects, critical behaviour (*Russian*) 7-52990
 reacting particles, stochastic clustering and loss kinetics, fluctuations spectrum anal. 7-39851
 regression, self-similarity 7-48550
 semiconductors, zero-gap, carrier temp. and density, nonequib. fluctuations 7-38576
 serrated yielding, computer simulation using negative resist. characts. 7-2089
 small particles, quasi-melting 7-32608
 spectra fluctuations in random media, Lenz shift phenomena 7-48577
 squeezed quantum fluctuations, dissipation effect 7-24476
 stationary state, noise-induced, stability and dynamics 7-227
 statistically nonuniform emitters, noise and emission props., Markov model 7-48582
 stochastic particle systems, equilibrium fluctuations 7-48586
 structural phase transitions in highly anisotropic systems, dynamics 7-32605
 SU(2) gauge theory, topological mass induced by radiative corrections 7-420
 SU(2) nonAbelian gauge theory, quantum fluctuations of Copenhagen vacuum 7-61436
 TCA Tokamak, density fluctuations, long wavelength turbulence 7-1727
 thermal fluctuations in a Knudsen flow system 7-63183
 thermal ion-acoustic fluctuations in collisionally dominated plasmas, laser scatt. meas. 7-11711
 tokamak, toroidally symmetric, thermal instability MARFE phenomena review 7-63290
 transient optical bistability fluctuations 7-62756
 transition metal dichalcogenides, CDW transition effects of lattice fluctuations 7-21831
 transition-strength fluctuations and the onset of chaotic motion 7-35335
 transverse fluctuations in multidimens. tunnelling, asymptotic behaviour 7-123
 two-dimensional rotor system, relaxation processes 7-9807
 two-step chemical reaction, nonequib. conc., steady state fluctuations and struct. factor 7-13726
 Ag₂O-Al₂O₃ ceramics and single crysts., cond. fluctuations and contact noise meas. 7-58840
 Al films and wires, fluctuation and localisation effects 7-64176
 CdIn_{0.3}Cr_{1.7}S₄ spin glass, equilibrium mag. fluctuations 7-64452
 CoO, heat capacity in vicinity of strong fluctuations, nonpower-law behaviour 7-2865
 CsNiFeF₆ spin glass, equilibrium mag. fluctuations 7-64452
 Cu, crystal surface and interface, heterophase fluctuations (*Russian*) 7-8650
 Fe₈₁B₁₉ amorphous alloy, thermally activated time fluctuations of nucl. spin orientation 7-7622
 (Fe₇Ni₉₃)₇Si₁₀B₁₃ amorphous spin glass, dynamic mag. susceptibility and critical phenomena (*Russian*) 7-7511
 GaAs devices, 1/f fluctuation, surface states effects (*Japanese*) 7-21955
 H transfer in double minimum potential, kinetic props. and quantum dynamics 7-54104
³He in superfluid ⁴He, correcting dil. solns., superfluid turbulence 7-44946
 Kr ion laser, perturbations obs. in 0-10 kHz range 7-5871
 Sm, four-wave light mixing, collision-and stochastic-fluctuation induced Hanle reson. 7-15559

fluctuations in superconductors

- used only for thermal (thermodynamic) fluctuations around the order parameter near the critical point
 dirty superconductors, conductivity and diamag. susceptibility fluctuations near Anderson localisation 7-45563
 dirty superconductors, weak localisation and supercond. fluctuations 7-64403
 disordered granular superconductor near percolation, phase transitions 7-17140
 Josephson contacts, critical current quantum renormalisation 7-12921
 Josephson junctions, phase fluctuations, thermal excitation and zero-point motion effects calcs. 7-7450
 Josephson-junction array in mag. field, resistance oscillations 7-2789
 magnetic superconductor, coexistent states of ferro- and antiferromagnetism 7-58950
 metallic glasses, weak localisation, magnetoresistance meas. 7-52574
 one-dimensional interacting electron systems, charge density and superconducting fluctuations 7-22061
 phonon pumping of superconductors 7-33125
 random fields, weakly first-order phase transition 7-22068
 short superconducting point contacts, equilb. fluctuations, nonzero energy relax. time (*Russian*) 7-52897
 superconducting-normal metal networks, noise exponent 7-38652
 triplet bipolaron systems, superconducting A and B phases (*Chinese*) 7-58949
 two-dimensional and three-dimensional superconductivity, interplay with electron localisation 7-64392
 Ba-La-Cu-O system, possible high T_c superconductivity 7-2770
 Nb thin films, resistive transition smearing in parallel magnetic field (*Russian*) 7-52918
 Nb-Si films, superconducting fluctuations weak localisation and electron interactions 7-2783
 Sn-GeO granular films, struct., resistivity and superconducting props. study 7-45082
 V thin films, resistive transition smearing in parallel magnetic field (*Russian*) 7-52918

fluctuations of cross sections *see statistical theory of nuclear reactions and scattering***flue gas desulphurisation** *see air pollution detection and control***fluidics** *see fluidics***fluid composition control** *see chemical variables control***fluid composition measurement** *see chemical variables measurement***fluid dynamics**

- see also aerodynamics; astrophysical fluid dynamics; biological fluid dynamics; drag; flow; geophysical fluid dynamics; hydrodynamics; liquid oscillations; Navier-Stokes equations; rarefied fluid dynamics; relativistic fluid dynamics; surface waves (fluid); turbulence; wakes*
 3D compressible Euler eqns., conservation laws 7-56046
 acceleration-dependent fluid forces 7-31907
 aeronautics, conf., Aix-en-Provence, France, (April 1986) 7-48191

fluid dynamics continued

- applications of the power-fluidics oscillator in the process of mass transfer 7-26245
 approximate random choice method for scalar conservation laws 7-20679
 astrophysical, equilibria and instabilities of polytropic configurations within homogeneous background matter 7-4316
 astrophysical, numerical calcs. on viscous jets 7-4565
 astrophysical, strong shock wave propag. in medium with exponentially varying density 7-14481
 Babuska-Brezzi conditions for two kinds of rectangular elements (*Chinese*) 7-51029
 boundary conditions at outflow for a problem with transport and diffusion 7-61109
 Burgers equation, low order analogue, truncation effects 7-14782
 compressible gas dynamical eqns., rapidly oscill. solns. (*Russian*) 7-55181
 conference, Japanese Physical Soc. Nishinomiya-shi, Nyogo-ken, Japan (Sept. 1986) (*Japanese*) 7-48186
 cylinder translation between 2 parallel walls, viscous flow in Stokes regimes (*French*) 7-31885
 cylindrical cavities, sound generation due to flow excitation 7-43500
 dissipative flows, local dimens.-2 bifurcations, nonequib. pot. 7-61302
 Euler eqn. calcs., zonal-boundary scheme 7-20676
 FEA, discontinuity-capturing operator for multidimensional advection-diffusion systems 7-26241
 finite amplitude waves, gas dynamic approx. 7-51188
 finite element formulation, generalized streamline operator for multidimensional advective diffusion systems 7-26240
 flow through packed beds, surface roughness effect 7-51239
 flow with free surface past bodies, hydraulic modelling of drag and friction resistance 7-31822
 fluid control and meas., conf., Tokyo, Japan (Sept. 1985) 7-29593
 fluid movement by a profile carrying a source (*French*) 7-63100
 fluidised beds, fluid dynamic charactn. (*German*) 7-51294
 free surface flow anal., 3D, FEM 7-43839
 free surface flow due to reservoir sink, investig. 7-57787
 galactic disks, solitary vortices theory 7-14657
 galaxies, disk wave pattern generation by satellite with retrograde motion 7-4553
 gas flow, nonequib. processes on free boundary 7-57940
 Ginzburg-Landau eqn., instabilities, secondary bifurcation 7-37419
 Glimm's method, introduction and FORTRAN listing (*Spanish*) 7-20678
 heavy fluid pot. flow under gate 7-37614
 hemicellulose suspensions, gelation, flow (*German*) 7-13830
 hydrostatic fields of multicomponent fluids in liquid and gaseous layers (*Spanish*) 7-48368
 hyperbolic problems, soln. with spectral methods, shock-fitting techniques (*French*) 7-61110
 incompressible couple stress flows (*German*) 7-31735
 incompressible flow problems, finite element stability anal. 7-31730
 incompressible fluid, flow eqn. soln. 7-6179
 incompressible viscous fluid with density, initial boundary value problem, weak soln. 7-61112
 incremental multigrid strategy for fluid dynamic eqn. soln. 7-51019
 internal waves, nonstationary theory, existence theorems (*Russian*) 7-61130
 isoperimetric inequalities for capacity, polarisation and virtual mass 7-31208
 liquid trickle flow through packed beds, residence time distrib. 7-44034
 LNG vapour plume, interaction with storage tanks, simulation 7-1593
 low Mach number flow, spectral method 7-9676
 lubricated squeezing flow anal. 7-31728
 Maxwell fluid flow, extra-stress eigenvalues sign (*French*) 7-31844
 mechanics of deformable media, book 7-35135
 modal amplitudes in interacting triads, probability distrib. with arbitrary random forcing 7-9097
 monotonic scheme of through calculation using implicit algorithm (*Russian*) 7-20681
 multiatomic gases, relaxation processes 7-31916
 numerical expt., computational methods 7-43836
 oil reservoir water flooding, anal. of hyperbolic conservation laws 7-18602
 oscillating free-connection flow past infinite porous vertical limiting surface, effects of mass transfer 7-14479
 panel method based on special interpolation functions for flow anal. 7-14780
 perfect fluid flow past body with conical singularity 7-56044
 plane flows of smooth nearly elastic circular disks, boundary conditions 7-26374
 planetary atmosphere and stellar convection, zero-gravity expts. 7-29393
 ponderomotive drift, single-particle and fluid theories 7-56043
 radiative gas dynamics (book) 7-55910
 Saturn ring system, nonlinear study of Mimas 5:3 density wave 7-24057
 shock layers in perturbed systems related to steady conservation laws 7-61113
 spatial differencing scheme for 3D full potential eqn. 7-6176
 sphere, vibr. in spherical vol. of viscous fluid 7-50971
 steady flow past a sluice gate 7-51360
 steady flow problems, press.-vel. components, algorithm comparison 7-37417
 steady self-superposable flows 7-1524
 steam injection expts., low flow rate, Grassberger Procaccia dimension determ. 7-11573
 stellar atmospheres, effect of rot. and mag. field on thermosolutal-convective instability 7-14557
 Stoke's flow in plane multiply connected domains, computation method 7-57783
 Stokes problems in multiple connected domains, press. pot. formulation 7-63105
 super long waves, dispersive generalisations of wave eqns. 7-24434
 symmetric total variation diminishing schemes, explicit and implicit construction 7-48370
 time dependent boundary conditions for hyperbolic systems 7-48369
 tubular flow chemical reactors, stochastic axial dispersion model 7-14864
 two dimensional flow, boundary fitted grids 7-6178
 two-dimensional gasdynamic calculations, modified boundary conditions 7-1373
 two-dimensional slow viscous flows past obstacles in a half-plane 7-57788
 ultraviolet problem and analytical properties of classical field theories 7-61134
 van der Waals fluid with entropy rate admissibility criterion, Riemann problem for nonisothermal system 7-18600

fluid dynamics continued

- vapour axial deposited preform stretching, numerical model for internal distortion 7-11133
 viscous creeping motion equations, soln, using cartesian-tensors 7-14778
 viscous flow boundary element analysis by penalty function formulation 7-37415
 water flow in capillary, surface and kinetic energy, laboratory exercise 7-18528
⁴He, superfluid, props. and appls. 7-48751
 U, isotope separation using nozzle effects, fluid dynamic analysis 7-61975

fluid flow *see flow***fluid instability** *see flow instability***fluid mechanics**

- see also capillarity; cavitation; compressibility of gases; compressibility of liquids; fluid dynamics; hydrostatics; Mach number*
 brachistochrone problem with gravit. pot., Bernoulli's method with ray eqn. approach 7-61111
 Galerkin finite element analysis of complex viscoelastic flows 7-16143
 mechanics of deformable media, book 7-35135
 mixtures, diffusion induced by nonhomogeneous shearing deform. field 7-14765
 nonlinear partial differential equations, hybrid boundary integral-Taylor series approach 7-61108
 numerical expt., computational methods 7-43836
 numerical methods, innovative, in engineering, conf., Atlanta, GA, USA (March 1986) 7-12
 stream function and stream-function-coordinate (SFC) formulation for inviscid flow field calculations 7-26289
 TK!Silver for students in Fluid Mechanics Laboratory 7-16260

fluid rheology *see rheology***fluid theory, dense** *see liquid theory***fluid valves** *see valves***fluidic amplifiers**

- see also hydraulic amplifiers*
 flow/pressure meas. using oscillating fluidic LPA 7-37563

fluidic devices

- flow measurement utilizing fluidic technology 7-37561
 flowmeter, hydrodynamic oscillator type 7-37565
 flowmeters with wide measuring range 7-37564

fluidic logic *see fluidics***fluidics**

- attachment process of switching of a jet in a wall-attachment device 7-26327
 numerical study of swirling flow field in a vortex device 7-20682

fluidised beds

- ash-agglomerating gasifier, fluidised-bed, high pressure operation 7-65394
 blow close-packed bed of fruit and vegetables, heat transfer, num. anal. 7-63139
 coal, fluidised-bed combustion, mathematical model 7-6308
 coal char combustion in fluidised bed 7-37537
 coal combustion, in fluidised bed furnace, mechanism investig., balance eqn. formulation 7-65322
 correlation for heat transfer between immersed surfaces and large-particle gas-fluidised beds 7-26127
 electrodes, mass transport 7-20789
 fluid dynamic charactn. (German) 7-51294
 freeboard, vel. meas. using laser Doppler anemometer 7-11527
 gas distributor plate of fluidised and bubbled beds, aerodynamical modelling 7-57916
 gas-fluidised beds, two-phase models, axial conc. profiles 7-6299
 gas-liquid-solid fluidised bed, correl. for solids holdup 7-51291
 gas-solid fluidised bed, freeboard region, two-phase flow behaviour 7-63209
 gas-solid transport, clustering under electrostatic force influence 7-20790
 gas-solid-liquid, fluid dynamics, correls. 7-16250
 granular solids, fluidised-bed drying, mathematical model 7-50917
 heat exchange with submerged heated surface, mechanism 7-51099
 heat transfer in retarded fluidised bed, oscill. model 7-26269
 heat-sensitive substances, drying using vibration- and air-fluidised beds, fluid dynamics 7-44036
 horizontal boiler tubes, dryout criteria for nonuniform heat flux 7-20713
 liquid-solid fluidised bed containing binary mixture of particles, solids layer inversion prediction 7-51290
 minimum fluidization velocity at elevated temperatures and pressures 7-37536
 sludge treatment, advanced anaerobic process 7-65595
 solids circulation pattern and particle mixing in large jetting fluidised bed 7-63208
 turbulent, mass transfer, burning rate 7-59761
 two- and three-phase, heat transfer characts. 7-31878
 unsteady heat transfer in gas-swept bed of spherical granules 7-31803
 zeolites, synthetic, thermal regeneration in thermofluidised bed, heat and mass transfer, mathematical model 7-51120

fluidised powders *see powders***fluidity** *see viscosity***fluids**

- see also bubbles; classical theories of fluid structure; disperse systems; fluid mechanics; fluidised beds; gases; gravity waves; liquids; non-Newtonian fluids; quantum fluids; quantum theories of fluid structure*
 No entries

fluorescence

- see also atomic fluorescence; fluorescent lamps; fluorescent screens; molecular fluorescence; nonradiative transitions; X-ray fluorescence analysis*

- alkylcyanobiphenyl-phenylcyclohexanecarboxylate mesomorphic mixtures, binary phase diagrams, fluoresc. spectral determ. 7-27765
 alumina, UV laser sputter etching effects, laser-induced fluoresc. and interferometry studies 7-26798
 anthracene in benzene, fluorescence spectral shifts, laser-driven shock compression 7-27781
 anthracene-pyromellitic N,N'-dimethylidiimide, triplet exciton contact pairs 7-64093
 azacoumarin dyes, fluorinated, laser dye stability, lifetimes, fluoresc. 7-59237
 benzoic acid:thioindigo(selenoindigo) impurity-induced double proton transfer, fluorescence decays 7-33420

fluorescence continued

- biological systems, fluorescent microscopy enhancement using imaging 7-28795
 1,4-bis(β -pyridyl-2-vinyl)benzene-2,5-distyryl pyrazine mixed crystals, photopolymerisation kinetics, fluoresc. spectra studies 7-33928
 1,4-bis(β -pyridyl-2-vinyl)benzene and hydrochloride derivative, photopolymerisation kinetics, fluoresc. spectra studies 7-33928
 cellulose acetate hollow-fibre membranes, ZnTPP modified, photosensitivity and photosynthesis 7-13811
 chemical sensors based on oxygen detection by optical methods 7-43426
 conifers exposed to environmental pollutants, time-resolved fluoresc. rel. to photosynthetic system 7-47156
 cyclohexane, liq., geminate electron-hole pairs, props. 7-64679
 detector for fluorescent X-ray adsorption spectroscopy 7-24751
 β -9,10-dichloroanthracene, triplet excitons, zero field DF ODMR 7-27631
 Dicke model and the theory of driven and spontaneous emission, review 7-5864
 dimyristoylphosphatidic acid: cholesterol spiral liq. cryst., fluoresc. microscopic obs. 7-58129
 9,10-diphenylanthracene, energy transfer from mesitylene and benzene 7-22316
 DNA luminescence, dependence on excitation energy (Russian) 7-28470
 droplet field visualization and characterization via digital image analysis 7-37577
 droplet shape and size variations from morphology-depend. reson. in fluoresc. spectra 7-29970
 dye solutions, quantum efficiency of fluoresc., determ. by diffraction at laser induced phase grating 7-3081
 epoxy resins, cure monitoring, fluoresc. method using organic dyes 7-22339
 flames laser induced fluoresc. imaging calibration 7-59759
 flavin derivatives, adsorbed on oxide layers, photophysics study 7-7738
 fluorescein dye in ionic gel near phase transition, fluorescence obs. 7-13190
 fluorometer, fibre-optic, freq.-scanned, for subnanosec. lifetime determ. 7-48851
 four-wave mixing, use in intracollision dynamics anal. 7-10509
 gas-solid fluidised bed, freeboard region, two-phase flow behaviour 7-63209
 glass:Nd, transition metal doped, fluorescence and absorption spectra 7-13229
 glass:Nd absorption thermometer with fluorescent referencing, fibre optic temp. sensor 7-25996
 glass:Yb³⁺, time resolved fluorescence line narrowing 7-13230
 glass, transition metal doped, optical absorpt. and luminesc. spectra 7-13186
 glycerol, fluorescence spectral shifts, laser-driven shock compression 7-27781
 HeLa cells, changes in UV-fluoresc. intensity in irradiated cells (Russian) 7-14056
 hematoporphyrin.2HCl, dye, energy transfer excitation (Japanese) 7-22342
 indolecarboxylic acids, proton transfer reactions in excited singlet state, fluoresc. spectra study 7-22318
 inorganic materials, activator ion doped luminescence (French) 7-27774
 insulators, electrical damage, fluorescence probes 7-51525
 kidney tissues, normal and cancerous, fluoresc. polarisation spectroscopy and time-resolved fluoresc. kinetics, rat obs. 7-8646
 Lake Sevan, determ. of organic matter and chlorophyll using laser fluorescence 7-23713
 Langmuir monolayers, phase transitions, fluoresc. microscopy 7-32867
 laser fluorescence velocimeter 7-44068
 laser-induced fluorescence spectroscopy, excitation anisotropy 7-28367
 leaves, clover, fluorescence lifetime meas., single-photon counting technique 7-22311
 liquids, mixing, conc. meas. by fluoresc. technique 7-65366
 long-range energy transfer for inhomogeneous spatial distrib. and indirect donor-donor interaction 7-33419
 lymphocyte, free energy of accumulation of a fluoresc. cation probe within the mitochondria 7-40118
 medical fluorescence imaging, digital background subtraction 7-40247
 metal trimer clusters photodissoc., bound-free transitions fluoresc. study 7-23045
 methane, liquid, fluorescence spectra near needle electrode under divergent fields 7-7737
 syn-(methyl,methyl)bimane aq. soln., lasing action obs., absorpt. and fluoresc. spectra meas. 7-43083
 micelles, cylindrical, intramolecular fluoresc. quenching rate const. 7-54189
 microscopy, astron. hypersensitisation techniques applied to photomicrography, Kodak 2415 film 7-56363
 molecular structures, impure, noncoherent excitation migration and fluorescence quenching 7-59247
 naphthalene:pyrene, triplet excitons, prompt and delayed fluoresc. 7-22298
 4-octyloxy-4'-heptyl- α -cyanostilbene, excimer fluorescence (Russian) 7-3093
 octyloxycyanobiphenyl and octylcyanobiphenyl, smectic Ad phases, time-resolved fluorescence studies 7-2194
 orcein dye treatment, fluoresc. reactions and appls. 7-60140
 pearls, fluorescence spectra, mother oyster distinction 7-28793
 pentacene in naphthalene, two-level impurity fluorescence in strong resonant field 7-13222
 photofading and drift-induced errors, minimisation by spectrum scanning strategy 7-48852
 photomultiplier anode current variation obs., for continuous and pulsed gamma radiation 7-30888
 poly(N-vinylcarbazole) films and solns., localised exciton hopping, fluoresc. studies 7-52435
 poly(N-vinylcarbazole; solns., nonexponential picosec trapping, electronic energy transport 7-13198
 polyethylene terephthalate glycol, films, uniaxially stretched, amorphous orientation and induced crystallisation 7-16448
 polyethylene terephthalate glycol, uniaxially stretched, amorphous orientation and induced crystallisation 7-11956
 polymers, isolated flexible chains, tagged with chromophores, electronic excitation transport 7-15751
 polypropylene oxide, undiluted state diffusion coeff., temp. depend. 7-38255
 polystyrene, photodegradation, spectral differences, solvent effects 7-6675
 polystyrene solns., excimer fluoresc., conc. depend. 7-7743

fluorescence continued

- polyvinyl alcohol film with natural dyes, optical props., effect of dye conc. 7-22324
- polyvinyl alcohol films, fluorescence lifetime meas., single-photon counting technique 7-22311
- polyvinyl carbazole donor-acceptor complexes, luminesc. and photoemission spectra 7-46115
- PVC, thermal degradation, fluoresc. study 7-33422
- pyrene substituted polyacrylic acid solns., interpolymer interactions, photo-physical obs. 7-46109
- radiation absorpt., high-power, generalised nonlinear master eqns. with finite correlation time. 7-25863
- Raman spectroscopy using gated intensified diode array detector, fluorescence rejection 7-15009
- redistribution functions, in plasma, model (*French*) 7-11604
- reflection nebulae, fluoresc. model for I-band excess emission 7-55773
- relativistic ions-laser photons collisions, spectrum and polarisation of γ -rays produced 7-50002
- rhodamine dye intercalated smectite, fluorescence props. 7-22325
- rigid probe mobility in bulk elastomer, stationary fluorescence depolarisation obs. 7-7744
- ruby, Cr weakly coupled ions, cooperative photon emission 7-59256
- ruby, fluorescence, radiative trapping effects, 77 to 300K 7-53395
- ruby, R, fluoresc. line lifetime meas., high press. conditions, modulation fluorometry technique 7-22307
- semiconductor face-pumped laser, bimolecular recombination, bistability theory 7-57336
- semiconductors, fluorescence line shape anal. for free-to-bound transitions 7-46097
- Seyfert galaxy nuclei, near-UV spectroscopy rel. to reddening and Bowen fluoresc. 7-55801
- sodium silicate as combined fluoresc./refl. coating for broad band detector (*German*) 7-4891
- spectrometer, frequency-domain, for picosecond rotational-correlation times determ. 7-56347
- spectrometer for single electrostatically levitated microparticle 7-9905
- sputtering, laser-induced fluorescence studies 7-59333
- squeezing in collective resonance fluorescence 7-25788
- surface layer struct., study using depth controlled EXAFS, near edge spectroscopy 7-59297
- surface-enhanced spectroscopy appl. to change of optical props. of microenvironment of small scattering object 7-18852
- switch plasma diagnostics using laser induced fluorescence, H thyratron plasma 7-32099
- synchronous excitation spectrofluorometry, scatt. background elimination 7-54203
- 7,7',8,8'-TCNQ, semicond., fluorescence spectra and electronic energy levels 7-27769
- temperature sensor, fluoresc. decay, with optimised signal processing 7-41386
- tetracene in ethanol glass, appl. of hole-burning spectroscopy as a tool to eliminate inhomogeneous broadening 7-46104
- vibronic systems, resonance fluorescence stationary spectrum 7-49994
- X-ray diff. in the grazing incidence Bragg-Laue geometry, fluorescence radiation yield 7-53403
- AlNbO₄:Cr³⁺ tunable IR laser crystals, fluorescent spectra 7-43110
- Al₂O₃, laser ablation, laser-induced fluorescence study 7-46249
- Al₂O₃:Cr,Ga, ruby, Cr-Ga complexes, luminesc. study 7-22320
- AlTaO₄:Cr³⁺ tunable IR laser crystals, fluorescent spectra 7-43110
- Al₂(WO₄)₃:Cr³⁺, tunable IR laser crystals, fluorescent spectra 7-43110
- BaF₂:ThF₄-YbF₄ glass, electron irradiation effects, Yb³⁺ optical transitions 7-27764
- BeAl₂O₄:Ni²⁺, chrysoberyl, laser induced fluoresc. and decay lifetime 7-46135
- Be₃Al₂(SiO₃)₆:Cr³⁺, emerald, spectral energy transfer, fluorescence line narrowing 7-33441
- CO, selection rule in two-photon absorption spectra 7-10693
- CaF₂:Er³⁺, H⁻(D⁻), IR excitation and absorpt. spectra anal. of sites 7-53306
- CaF₂:Sm²⁺, electronic Raman transitions study 7-46017
- CaO-TiO₂:SiO₂:Eu³⁺ sphere ceramic, impurity laser-excited site-selective fluorescence line-narrowing spectra 7-13200
- Ca(PO₃)₂:Duo³⁺ glass, highly doped, fluorescence spectral width of ³D₀-F₀ transition 7-13189
- CeF₃:Ho³⁺, fluorescence decay characts. of Green emission 7-7747
- Cr compounds, sputtering of Cr atoms, laser-induced fluorescence spectra studies 7-59334
- CsI, two-photon induced luminesc. 7-64696
- Cu monolayer on Au (111), fluoresc. detected surface EXAFS 7-46235
- DyP₂O₁₄, absorpt. spectra intensity parameters, fluoresc. radiative transition probabilities (*Chinese*) 7-39141
- Eu(II)- β -alumina, luminescence, order-disorder effects, optical, structural and ion transport props. 7-46114
- Fe-graphite structures, ion induced mixing, sputtering yield, fluoresc., RBS depth profile meas. 7-64844
- GaAs laser induced etching in carbon tetrachloride atm., fluoresc. 7-59700
- GaAs:Te, struct. environment of dopant, study by EXAFS in fluorescence mode. 7-59300
- H₂O, shocked water, temp. meas. using fluorescence probe thermometer 7-24653
- KAl(MoO₄)₂:Cr³⁺ tunable IR laser crystals, fluorescent spectra 7-43110
- KNd₂Gd_{1-x}P₄O₁₂, isolated ion pair interaction, fluoresc. quenching study 7-46117
- La, X-ray M_{4,5} fluorescent emission spectrum, hole-induced shakedown processes. 7-53450
- LaF₃:Pr³⁺, ³P₀ fluorescence quenching processes 7-22314
- LaF₃:Pr³⁺ Nd³⁺, energy up-conversion, UV fluoresc. obs. 7-53401
- LaF₃:Pr³⁺ Gd³⁺, two-photon excitation and interconfigurational energy transfer 7-3083
- LiF, F₃⁺ and F₂ colour centres optical study (*Chinese*) 7-37984
- LiNbO₃ waveguide, parametric fluoresc. amplification and oscill. 7-25894
- LiYF₄:Ho³⁺, Er³⁺, Tm³⁺, excited-state absorpt., energy transfer, fluoresc. study 7-22322
- NaBr:CN⁻, IR vibrational fluoresc. obs. 7-27775
- NaCl:Co, doped and undoped, thermoluminescence and X-ray fluorescence spectra 7-22356
- NaCl:Eu single cryst., EuCl₂ phase precipitation, fluoresc. and X-ray diff. studies 7-46108

fluorescence continued

- Na₂O-Al₂O₃:SiO₂:Eu³⁺ glass, impurity laser-excited site-selective fluorescence line-narrowing spectra 7-13200
- Na₂O-CaO-Al₂O₃-TiO₂:SiO₂:Eu³⁺ glass ceramic, impurity laser-excited site-selective fluorescence line-narrowing spectra 7-13200
- Nd₂O₃:P₂O₅-GeO₂, phase equilibria, X-ray diff., thermal anal., fluoresc. spectra 7-6758
- Nd₂Y_{1-x}PO₄, excitation energy transfer and ion-ion interaction 7-33421
- Ne discharge, high-current, low-pressure, radial distrib. of neutral gas density 7-20952
- O₂+B(BO), gas-phase oxidation, rate consts., fluoresc. and chemiluminesc. study 7-22985
- PbHPO₄, photostimulated luminescence near ferroelec. Curie temp. 7-64697
- PbMoO₄ crystals, point defects, absorpt. and fluoresc. props. 7-64674
- PbWO₄:Nd³⁺(Pr³⁺), optical spectra 7-39146
- Pd polycrystalline surface, internal energy distrib. of recombinatively desorbing D₂ 7-2350
- PrCl₃ organic complexes, spectral energies and oscillator strengths 7-3067
- SiO₂, porous silicas, direct energy transfer in restricted geometries as probe of pore morphology 7-59251
- SiO₂:Yb³⁺ glass, energy transfer among impurity ions, time resolved fluoresc. line narrowing meas. 7-46124
- SiO₂-Al₂O₃-MgO-TiO₂-Cr₂O₃ based glass ceramics, Cr³⁺ laser emission and excitation spectra 7-22299
- SiO₂-B₂O₃-Na₂O-Al₂O₃ glasses, corroded, grazing incidence fluorescence EXAFS, near edge spectroscopy 7-59296
- SrB₄O₇:Sm²⁺, fluorescence shift, pressure depend. (*French*) 7-4805
- ThCl₄:U⁴⁺ incommensurate struct., absorption and emission spectra studies 7-33439
- β -ThCl₄:Pr³⁺, site selective laser fluorescence spectroscopy 7-64687
- ThO₂:Np⁴⁺, absorption and emission spectra of Np⁴⁺ 7-27763
- ThSiO₄:Np⁴⁺, absorption and emission spectra of Np⁴⁺ 7-27763
- UO₂²⁺ ion fluorometry in nitric acid soln. 7-61974
- YAG:Mn⁴⁺, luminesc. and fluoresc. line narrowing studies 7-46105
- YAG:Nd, Ce, energy transfer mechanisms between Ce³⁺ and Nd³⁺ at low temp. 7-64691
- YAG:Pr³⁺, up-conversion, stepwise photon absorpt. process 7-13193
- YAG:Tb, electron-phonon relax. in ³D₄ of Tb³⁺ 7-2130
- YAG:Tb, crystal. field anal. of Tb³⁺, site selective polarisation spectroscopy 7-2546
- ZnS:Ho³⁺, radiative transitions and nonradiative processes (*Chinese*) 7-59235
- fluorescence of atoms** see atomic fluorescence
- fluorescence of molecules** see molecular fluorescence
- fluorescent lamps**
- eye fatigue caused by reflected glare under intense illumination from fluorescent lamps (*Japanese*) 7-34130
- plasma computer modelling 7-20929
- fluorescent screens**
- see also electroluminescence
- image perception, fluctuation theory 7-34146
- X-ray fluorescent, for use in portable fluoroscope 7-61407
- Gd₂O₃:SiTb X-ray fluorescent screen for use in portable fluoroscope 7-61407
- fluorimetry** see spectrochemical analysis
- fluorine**
- see also nuclei with
- adsorbed ions on W surface, photo- and electron-stimulated desorption 7-12465
- adsorption on Si (100) and (111) exposed to XeF₂, XPS studies 7-2379
- atom, 2nd Rydberg series correl., HF-term energy separation 7-30939
- atom, electron impact ionisation cross sections meas., TOF spectra 7-42770
- atom, spin and charge densities, HF and UHF calcs. 7-19684
- atom and ion, MBPT and coupled cluster calc., comparison with CI 7-49899
- atomic and mol. reactions with Si surface, XPS studies 7-28350
- chemisorption on (111) and (100) surfaces of Si 7-6979
- desorption from LiF surface, Ar⁺ and Ar²⁺ bombarded, secondary ion mass spectra study 7-21661
- detector based on chemiluminescence, excimer laser monitor appl. 7-20216
- diffusion in SiO₂, consts. and profiles meas. 7-58540
- films, transparent conducting oxides, H₂ plasma treatment 7-3528
- gas laser using fast plasma mixing excitation 7-15899
- low current arc, spectroscopic study 7-26581
- molecule, electron impact ionis. cross section calc. 7-50380
- molecule, electronic struct., X-ray emission spectra 7-50174
- molecule, f ²F₂ state, electron impact, laser photon emission 7-5778
- molecule, photoionisation cross section, ground state inversion pot. method/diff. theory 7-944
- molecule, pot. energy surfaces, multireference coupled cluster theory calc. 7-49970
- molecule, stretching force consts. inner-shell polarisation effect, HF calcs. 7-15588
- multiphoton ionisation spectroscopy 7-10534
- radioisotope production, anal. and appl., conf., Banff, Canada, Sept. 1985 7-24254
- tektites, F and Cl contents 7-34501
- F I, excited levels, photoionisation cross-sections, Thomas-Fermi calcs. 7-10423
- F IX, excitation by laser flame recharging in plasma 7-20851
- F⁺, electron affinity calc. with fourth order many-body perturbation theory 7-42471
- F²⁺, quintet transitions, beam-foil spectra anal. 7-31004
- F-He, van der Waals mol., interaction pot., MBPT calcs. 7-42721
- F+Au, X-ray emission from multiply ionized atoms (*Rumanian*) 7-15699
- F+Be⁺, K-shell X-ray prod. cross section meas. 7-15680
- F+H₂, bond angle-bond distance coordinate system, energy conserving trajectories 7-28287
- F+H₂, reactive scattering, hybrid solution to coupled equations 7-57164
- F+H₂(HD)(D₂), quantum reaction probabilities, hyperspherical coordinates 7-13754
- F+H₂→HF+H, collinear transition state, CI calcs. 7-54105
- F+I₂, reaction dynamics, quasiclassical trajectory studies 7-22998
- F+I₂, reactive collision, IF laser induced fluoresc. (*French*) 7-13727

fluorine continued

$F^{8+} + Ne$, k-k charge transfer, excitation patterns, Auger spectra 7-15682
 $F^{9+} + Ne$, k-k charge transfer, excitation patterns, Auger spectra 7-15682
 F_2 laser at 157.6 nm excited by electric discharge 7-25803
 F_2 solid, high-pressure behaviour at low temps. 7-37923
 F_2^+ , excited state spin-orbit interaction 7-49962
 F_2 -He discharge pumped laser, 157.6 nm, efficiency 7-43077
 $F_2 + CS_2$, reaction, mol. electronic emission spectrum 7-3577
 $F_2 + I_2$, room-temp. reaction, obs. of I, IF chemiluminesc. 7-28289
 $F^{18}F$, radioisotope production for biomedical applications 7-60087
 $F^{18}F$, radioisotope prod. for medical appl., review 7-28693
 $F^{18}F$, single-passage extraction in rabbit bone 7-40249
 $F^{18}F$, aqueous, radioisotope production for biomedical applications 7-60087
 ^{19}F NMR appls. in medicine 7-23427
 ^{19}F nuclei in single-electron ions, Coulomb excited, γ -angular correls. 7-49292
 $a-GaAs:H:F$, electronic struct., dangling bonds, cluster-Bethe lattice method calcs. 7-12592
 $a-Ge:Si:H:F$, multijunction solar cells, performance data 7-40011
 $GeO_2:F-GeO_2$, doped cladding-pure core single-mode fibre, dispersion study 7-43382
 $a-Ge:Si:D,F$, D NMR lineshapes and spin-lattice relax. studies 7-45836
 $a-Ge:Si:H:F$ double Schottky barrier structures, surface photovoltage meas. and calc. 7-17093
 H -like, plasma, spectral series (*French*) 7-11794
 H_2-F_2 laser, atmospheric pressure, feasibility of short radiation pulse generation 7-25807
 H_2-F_2 -HF gaseous mixture, light initiated chain reaction, stimulated light scatt. study 7-62778
 $KCl:F^{2+}:Eu^{3+}$, optical absorpt., excitation and luminesc. spectra 7-59250
 $PbTiO_3:Fe^{3+}$, F^- charge compensating cluster form., EPR spectra studies 7-64518
 Si , HF passivated, surface chemistry, XPS and ion scatt. spectra 7-33857
 $Si:B$, F implanted amorphous layers, struct. and elec. props., ESR and Hall effect meas. 7-26634
 $a-Si:D,F$, D NMR lineshapes and spin-lattice relax. studies 7-45836
 $a-Si:D,F$, plasma deposited, deuteron magnetic resonance 7-27626
 $Si:F$, implanted, dry oxidation kinetics, impurity effects 7-13667
 $a-Si:F$, mobility edge, density of states and carrier activation energy calcs., random Bethe lattice approach 7-16937
 $Si:F,H$, amorphous, high efficiency solar cells fabrication and props. 7-17901
 $a-Si:F,H$ films, glow discharge deposition, B doping efficiency 7-17436
 $a-Si:H,F$ by thermal CVD, photosensitivity, spin density, conductivity and p-n type 7-17454
 $a-Si:H,F$ films, dark discharge mechanism of surface potential (*Japanese*) 7-17034
 $a-Si:H,F$ films, glow discharge decomposition from Si_2F_6 7-64924
 $a-Si:H,F$ films, H-radical-assisted CVD, hole transport 7-64264
 $a-Si:H,F$ films, initial carrier trapping states observed by femtosecond spectroscopy 7-27301
 $a-Si:H,F$ films, prep. using H radical assisted CVD (*Japanese*) 7-17430
 $a-Si:H,F$ multijunction solar cells, performance data 7-40011
 $a-Si:H,F$ solar cells, radiation hardness to 1 MeV protons 7-23180
 $a-Si:H,F/a-Si:Ge:H,F$ superlattices, elec. transport studies 7-38716
 $a-Si:H,F/a-Si:H,F,Ge$ multiple junction solar cells on stainless steel substrates 7-13902
 $a-Si:H,F/a-Si:Ge:H,F$ multiple layered films for enhancement in photore-sponse in near IR spectrum 7-52668
 $a-Si:H,F-Si_0.4Ge_{0.6}:H,F$ superlattices, carrier scatt., optical absorpt. study 7-38711
 $Si:H(F)-Si:Ge:H(F)$ amorphous multilayer struct., fabrication and near IR photoconductivity characts. 7-52797
 $Si:C,F$, amorphous, electronic and structural props. 7-17054
 $Si:C,H,F$ amorphous films, struct., elec. and optical props. 7-22360
 $a-Si:Ge:D,F$, vibr. modes, Fourier transform IR spectra studies 7-46053
 $a-Si:Ge:D,F$, plasma deposited, deuteron magnetic resonance 7-27626
 $Si:Ge:F,H$, amorphous, high efficiency solar cells fabrication and props. 7-17901
 $a-Si:Ge:F$ solar cells, chemical basis for high efficiency 7-17884
 $a-Si:Ge:H,F$ glow discharge films, elec. and optical props. 7-46169
 $a-Si:Ge:H,F$ alloy films, F incorporation and annealing props. 7-54588
 $a-Si:Ge:H,F$ alloys for solar cells, prep. by DC and RF discharge deposi-tion 7-17900
 $a-Si:Ge:H,F$ films, glow discharge deposition and elec. props. 7-64917
 $a-Si:Ge:H,F$ glow discharge films, microcrystallinity studies 7-45088
 $a-Si:Ge:H,F$ glow discharge films, electronic transport and density of states 7-45114
 $a-Si:Ge:H,F$ solar cells, radiation hardness to 1 MeV protons 7-23180
 $a-Si:Ge:H,F/Pd(Au)(Ni)$, Schottky barrier height, internal photoemission meas. 7-45501
 $a-Si_{1-x}Ge_x:H,F$, light-induced degradation meas. 7-45397
 $a-Si_{1-x}Ge_x:H,F$ alloy films, RF glow discharge deposition in ultrahigh vacuum reactor 7-53619
 $Si_0.9Ge_{0.1}:H,F$ amorphous films, struct., elec. and optical props. 7-22360
 $SiO_2:F$, P fibres, dopant materials behaviour in MCVD process 7-20462
 $SiO_2:F$, quartz glass, struct. study using ^{19}F -NMR (*Japanese*) 7-21122
 $SiO_2:F$, vitreous, substitutional impurity, semiempirical calcs. 7-32464
 $SiO_2:F$ cladding for pure SiO_2 monomode fibres, prep. by MCVD process 7-1289
 $SiO_2:F$ layers, modified CVD 7-53608
 $SnO_2:F$ CVD films, UV absorpt. props. study 7-22370
 $SnO_2:F$ coatings, evacuated window glazings for energy efficient buildings 7-54352
 $SnO_2:F$ electrodes, surface modification by underpotential deposition of noble metals 7-44998
 $SnO_2:F$ films, CVD growth using hydrofluoric acid as doping material 7-7871
 $SnO_2:F$ thin film, uses for $a-Si:H/a-Si_{1-x}C_x:H$ solar cells 7-46952
 $SnO_2:F$ thin films, CVD deposition, elec. and optical props. 7-7425
 $SnO_2:F-n-Si(poly)$ solar cells fabricated by CVD, characterisation 7-59859
 $SnO_2:F-CuInS_2$ sprayed solar cells, photovoltaic props. 7-54322

fluorine compounds

atmospheric of India, fluoride in precipitation; natural background levels 7-14329

fluorine compounds continued

fluoride glasses doped with YbF_3 and ErF_3 , efficient optical freq. up-conversion via energy transfer 7-50634
 FA ($A=Li, Be, B, C, N, O, F$), chem. bonding, kinetic energy anisotropy investig. 7-10396
 FBS^{2+} , electron impact prod., $\bar{A}^2\Sigma^+$ to $X^2\Pi$, emission spectrum 7-50158
FCP and higher-lying isomer, struct., stabilities, ab initio study 7-864
FDF $^-$, IR spectrum, ab initio calcs. 7-25506
FHF $^-$, IR spectrum, ab initio calcs. 7-25506
FNC isomerisation to FCN, MINDO calcs. 7-56979
 FNO_2 , semi-empirical MO-LCAO method validity eval. 7-15482
 F_2SeO , geometry optimisation using energy exponent 7-25344
 F_2SeO complexes ($X=F, Cl, Br$) H bonding ab initio calcs. 7-56960
 MF_2 type fluorides, stability under high pressure (*French*) 7-63568
 MMF_4 type fluorides, stability under high pressure (*French*) 7-63568
fluoroscopy *see radiography*
flux (magnetic) *see magnetic flux*
flux (neutron) *see neutron flux*
flux creep
see also flux pinning
No entries
flux crystal growth *see crystal growth from solution*
flux flow
see also flux pinning
Josephson junction, DC driven, inhomogeneous damped, many-fluxon kinetics 7-45571
planar superconductor, vortex pair dissociation kinetics calcs. (*Russian*) 7-58560
superconducting thin plate, magnetic flux dynamics eqns. 7-33132
superconductors, type II, magnetic instability, thermodynamic anal. 7-52921
thin film superconductors, Kosterlitz-Thouless transition analytic soln. of renormalisation equations 7-27480
Nb-Ti, superconducting composites, critical current distributions 7-38833
Nb $_3$ Sn, superconducting composites, critical current distributions 7-38833
flux-line lattice
anisotropic type II superconductors, mag. props. 7-38814
ferromagnetic superconductors, intermediate state and easy-axis mag. ani-sotropy 7-38831
ferromagnetic superconductors, intermediate state and easy-plane magnetic anisotropy 7-38832
type II superconductor, critical state, surface barrier struct. 7-52916
type II superconductors, flux-line lattice, elastic and plastic props. 7-27481
type II superconductors, pinning strength and range, collective flux-line lattice interaction calcs. 7-2795
Al thin supercond. film, nonlinear RF props., vortex pair creation, critical effects 7-17137
flux line motion *see flux flow*
flux pinning
see also flux-creep; flux flow
ferromagnetic-nonferromagnetic supercond. superlattices, vortex pinning 7-45591
Josephson cross-strip junction, elementary pinning force for a supercon-ducting vortex 7-45592
type II superconductor, critical state, surface barrier struct. 7-52916
type II superconductors, flux-line lattice, elastic and plastic props. 7-27481
type II superconductors, pinning strength and range, collective flux-line lattice interaction calcs. 7-2795
Cu-Nb composite superconductors, critical parameters and surface flux pinning studies 7-38830
 $Cu_{33}Zr_{67}$, glassy metals, peak effect, flux pinning (*Chinese*) 7-12929
 $Cu_{33}Zr_{67}$ metallic glasses, flux pinning and critical current peak effect studies 7-22079
Nb foil, He bubbles, magnetic flux pinning, temp. and field depend. stu-dies 7-2794
Nb superconducting bicrystals, flux pinning by symmetrical grain bounda-ries 7-64419
Nb, superconducting bicrystal, flux pinning by special grain boundary 7-64420
Nb-Al-Ge superconductors, pinning force, mech. meas. 7-64417
Nb-Ti, superconducting composites, critical current distributions 7-38833
NbN microbridges, current-voltage characts., magnetic field effects (*Rus-sian*) 7-7460
Nb $_3$ Sn multifilamentary composite superconductor, bronze processed, glo-bal pinning force, critical mag. field, grain size 7-22078
Nb $_3$ Sn, superconducting composites, critical current distributions 7-38833
 $Ni_{33}Zr_{67}$, glassy metals, peak effect, flux pinning (*Chinese*) 7-12929
 $Ni_{33}Zr_{67}$ metallic glasses, flux pinning and critical current peak effect studies 7-22079
Pb-Bi superconducting alloys with Bi precipitates, critical current density 7-17146
Pt-Bi (22 wt.%), supercond. films, pinning in appl. mag. field (*Russian*) 7-64418
 V_3Ga superconducting tapes, grain boundaries, elementary pinning force 7-22080
Zr-Ni(V) amorphous superconductors, struct. and supercond. props. 7-27482
 $Zr_{70}Cu_{30}$ melt spun ribbons, collective flux pinning dimensional crossover obs. 7-17143
flux vortex flow *see flux flow*
flux vortex lattice *see flux-line lattice*
fluxmeters
see also magnetic field measurement; magnetic flux
No entries
fluxoid array *see flux-line lattice*
FMR *see ferromagnetic resonance*
foams
see also bubbles
cellular foams, fn. between aeration ratio and electric cond. ratio. 7-39922
dry, rheology, 2D model 7-16238
filtration through gas-liquid foam, fluid flow model 7-51301
high-multiplicity, optical density as a fn. of interface structure 7-39923
liquids in downcomers, foam behaviour, expts. (*German*) 7-54192
nuclear waste vitrification, melt foaming, foam stability and redox studies 7-5452

foams continued

- polymers, gas-filled, action as cutoff optical filters in the IR region 7-57529
- polyurethane foam, form., exotherm data acquisition using microcomputer 7-54118
- polyurethane foams, shock wave attenuation capabilities 7-33972
- porous layered media, Biot waves propagation 7-6028
- seawater, wind-wave breaking crests and foam patches in Pacific (*Russian*) 7-23670
- soap-film networks, 2D, mean-field theory 7-28361
- two-dimensional soap froth, shear elastic const. 7-3610

focal planes *see image sensors; infrared imaging***focused collision sequences** *see sputtering***focusing***see also self-focusing*

- 3D imaging, spatial frequency cut-off 7-15823
- accelerating and focusing systems, structural and parametric optimisation, design 7-25280
- acetone, induced absorption and stimulated scattering of focused radiation 7-62780
- acoustic microscope, elastic wave propag. focusing props. of small-aperture lenses 7-43473
- acoustic microscope planar focusing lens design and operation 7-1341
- acoustic microscope spherical focusing transducers, ray-optical analysis 7-1371
- Applied-B ion diode expts. on Particle Beam Fusion Accelerator-I 7-10310
- aspherical focusing lenses for high-power multi-wavelength laser systems 7-62808
- aspherical lenses, wide-aperture objectives for radiation concentration 7-43302
- atomic beam, deflection and focusing by reson. light field 7-42786
- autocollimation focusing devices for optical systems, photoresistors used as image analyzer 7-37110
- automatic focus control for head alignment 7-5968
- BESSY multipole magnet, electron opt. props. and electron trajectories 7-42254
- cameras, automatic focusing systems, IC testing 7-41517
- cathode lenses, design, Pontryagin's max. principle 7-42885
- centrifugal electrostatic focusing system, bunching mechanism and kinetic anal. of relativistic electron beam 7-36871
- ceramics NDT by acoustic microscopy with single zoom lens 7-3570
- combined electric-magnetic focusing-deflection system, relativistic fifth order geom. aberration eqn. 7-10838
- combined electrostatic focusing-deflection systems, asymptotic aberrations 7-10835
- conic mirror, on-axis focusing formula 7-43289
- cryogenic pulsed ion source focusing, beam characteristic 7-30655
- deflecting focusing kinoform for lasers 7-25736
- diffractive Raman scattering in focused geometry, coupled pump and Stokes differential eqns. 7-20339
- electron beam in combined electromagnetic focusing-deflection system with spherical cathode, relativistic aberration theory 7-62613
- electron beams, aberrations in combined electromagnetic focusing spherical cathode lens, theory (*Chinese*) 7-36868
- electron beams, relativistic aberrations in combined electromagnetic focusing-deflection system, theory (*Chinese*) 7-36869
- electron microscopes astigmatism detection using radon transform (*Japanese*) 7-18931
- electrons, radial focusing in biperiodic slow-wave struct. with high accel. rate 7-41550
- flux concentrator, nonimaging, axially symmetric, concentration ratio calc. 7-57506
- gasdynamic focusing in supersonic jets, chemical anal. appl. 7-20752
- gaseous media, THG, compensation for inhomogeneous nonlinear phase mismatch 7-31394
- Gaussian beam diffracted through finite lens, focus 7-42893
- Gaussian beam focusing through hemispherical microlens 7-11090
- Gaussian beams, oscillations and discontinuity in focal shift 7-31374
- grating element for the entry and focusing of radiation in a planar waveguide 7-37126
- high intensity neutrino beam prod. at meson factories, focusing device, magnets 7-5517
- holographic sharp-focusing technique, sensitivity 7-36920
- ion beam generation and focusing from conical pinched electron beam diode 7-11806
- ions, multiply charged energetic, focusing using solenoidal B and radial E lenses 7-56899
- large-F-number systems, aperture-lens separation effect on focal shift 7-57231
- laser beam in medium containing droplets, nonlinear refraction phase compensation 7-4183
- laser beams, multimode with variable beam parameters 7-11021
- laser focusing element development for materials processing 7-11023
- laser focusing system, dimensioning (*German*) 7-31378
- lens, focus of high-numerical-aperture objectives, light distribution 7-43290
- lens, graded-index, light distribution near foci 7-43287
- lens design, automatic, use of multi-image plane merit function 7-43310
- magnetic focusing and deflection systems of camera tubes (*Chinese*) 7-10837
- micro-Fresnel lens arrays, rectangular-apertured, fabrication by electron beam lithography 7-57505
- microscope for microsurgery, self focusing 7-54705
- mirrors, focusing, thermooptic aberrations, heat transfer study 7-57509
- multilayer films, focusing, X-ray reflectance calc. 7-1247
- multilayer focusing films, computing X-ray reflectance 7-30143
- multilayered X-ray optics on cylindrical reflector and ellipsoidal focusing ring, monochromatisation 7-1246
- neutron beam spatial condensation by asymmetric diff. in thermal neutron monochromatisation 7-16363
- nonlinear distortion compensation of light beams with restricted deform. of control mirror 7-50622
- oblique scanning acoustic microscope confocal beam formation 7-1340
- optical systems of finite fresnel number, imaging 7-5847
- proton beam focusing by z-discharged plasma channel, expt. and theoretical results 7-11804
- quadratic media, longit. homogeneous, with absorpt. or amplification, correlated coherent states 7-50621
- quadrupole free electron laser spontaneous radiation 7-31334

focusing continued

- relativistic electron beams, periodic permanent magnet field-transport 7-57226
- relativistic fifth order geometrical aberration eqn. of combined focusing-deflection system (*Chinese*) 7-36867
- RF ion source, focusing system, expt. and theoretical investigs. 7-10840
- scanning ion beam systems, in-lens deflection 7-42889
- scanning microscope with confined EM waves 7-41461
- seismic waves, effects of focusing on amplitudes at antipode 7-28864
- seismic waves, subsurface focusing, rel. to strong ground motion prediction in Puget Sound region 7-3980
- semiconductor lasers, beam location and focusing using computer-controlled spot-centring technique 7-5934
- shaped multilayer X-ray interference mirrors focusing props. 7-61417
- SHG, autocorrelation functions, deformation and reconstruction 7-15819
- soft X-ray focusing for longitudinally pumping short wavelength lasers 7-18955
- stimulated Raman scattering conversion efficiency, effects of focusing parameters (*Chinese*) 7-5951
- synchrotron radiation mirror, lacquer-coated, irradi. with undulator light, surface heating 7-43307
- TEM image quality criteria; appl. on thin phase objects (*German*) 7-56379
- thermal-wave lens, ray diagrams, focusing 7-54046
- three-element electrostatic lens, focusing property investig. 7-36870
- US transient diffraction and focusing in absorbent media, modal analysis 7-1305
- variable focus, single lens, 3 CRT dichroic color graphics projector 7-25933
- window heating by pulsed laser, focal lengths and rise times 7-43179
- X-ray Fourier images, formation 7-18953
- zoom converter with focusing and thermal compensation functions 7-31516
- Au liquid metal ion source, focused droplet beam 7-30801
- NH₃ superradiant Raman FIR laser with nonlinear reson. four-wave mixing generation of medium IR emission 7-50657
- Na atomic neutral beam, laser technique for collimating and focusing 7-62610
- SiCl₄, liquid, phase conjugation of microsecond pulses in stimulated Brillouin scatt. of focused beams 7-57467

focusing, particle *see focusing; particle optics***fog**

- England and Wales, fog cover at night AVHRR observations 7-4216
- extinction profile meas. by lidar using Klett's inversion method 7-9184
- FOG-82, cooperative field study of radiation fog, exptl. design and results 7-9068
- ice, microscopic filament form. in elec. field 7-14362
- Indianapolis, USA, fog chemistry at urban Midwest site 7-55187
- light scattering, 10.6- μ m extinction coeff., forward-scatter meter 7-57238
- optical attenuation coeffs. 7-34672
- pesticides at high concentration in fog droplets in USA 7-60365
- radiation fog, 1D numerical model rel. to obs. 7-66255
- radiative transfer theory, small-angle approx. and numerical soln. 7-36878
- remote sensing of patchy nighttime fog using satellite IR radiometry (AVHRR) 7-4216
- sound attenuation in water fog 7-37239
- supercooled fogs artificial dispersal, anal. by lidar 7-34733

foils

- brass L80, grain struct. form. after isothermal annealing 7-53761
- Cliff-Lorimer k_{AB} factors at zero foil thickness, extrapolation method 7-39935
- composition modulated layered structs., elastic strain, X-ray diff. studies 7-27086
- electron beam excitation using glass foils 7-35627
- manganin foil stress gauges, piezoresist. response meas. 7-29998
- membranes with locatable single pores generation, obs. and testing 7-298
- metal, Hall effect and magnetoresistance 7-52575
- metal foil prep. by melt overflow rapid solidification 7-22609
- metal foils, surface loss intensity of incident electrons, angular distribution 7-64836
- metal superlattices, elastic and plastic props. 7-27085
- metallic, comp. modulated, mech. props., book contrib. 7-27222
- metallic glass reinforced Al composite fabrication by multi-lamina explosive compaction 7-59482
- polyvinylidene fluoride, modifications under high energy heavy ion, X-ray and electron irradi., XPS study 7-38076
- positron-annihilation apparatus for layerwise analysis of defects in solids 7-39219
- steel, austenitic stainless, foil, air oxidation, Cr depletion, Mossbauer spectra 7-39702
- steel, eutectoid, 1.3 wt.% Cr, specimen prep. technique influence on analytical TEM obs. of partitioning 7-22950
- steel, foils, H charged, internal friction, quasi-molecular state (*Russian*) 7-59561
- tensile testing of foils and films, specimen-deformation machine for X-ray diffractometers 7-33874
- ultra-thin foil thickness determination from large-angle convergent beam electron diffraction patterns 7-63406
- Al, alumina form. by O₂⁺ implantation, sheet resistance and XPS meas. 7-26780
- Al electron absorpt. and scatt. energy spectra, Monte Carlo calcs. 7-22399
- Al-Cu-Mg, 2024, TEM specimen prep. parallel and perpendicular to machined surfaces 7-39808
- Al-Zn-Mg, TEM specimen prep. parallel and perpendicular to machined surfaces 7-39808
- Au thin foil, Rutherford backscatt., low energy background studies 7-3132
- C, beam-foil convoy electron double differential distrib. for proton irradi. 7-22408
- C, convoy electron yield, target thickness depend. from C^{q+} collisions 7-27839
- C, electron absorpt. and scatt. energy spectra, Monte Carlo calcs. 7-22399
- C stripper foils, long lived, development 7-15436
- Co foil surface, preadsorbed K, CO adsorption, XPS and AES studies 7-8296
- Co single crystal foils, α - and β -phase, ion transmission and sputtering 7-59322

foils continued

- Cu, electron absorpt. and scatt. energy spectra, Monte Carlo calcs. 7-22399
- Cu, excimer laser assisted gas phase etching 7-54015
- Fe foils, H charged, internal friction, quasi-molecular state (*Russian*) 7-59561
- Fe₅₀Ni₅₀ alloy foils, N₂⁺ implantation, oxidation behaviour, conversion electron Mossbauer spectra study 7-22877
- In foils, ion bombarded, desorbed neutral energy distrib. studies 7-22406
- Ni foils, H charged, internal friction, quasi-molecular state (*Russian*) 7-59561
- Ni, N ion energy loss meas. and calcs. 7-63694
- Pb, electron absorpt. and scatt. energy spectra, Monte Carlo calcs. 7-22399
- Pd-Rh, high temp. air oxidation, surface comp., AES 7-22891
- PdFe ordered alloy, discontinuous domain coalescence (*Russian*) 7-2025
- δ-Pu-Ga (1.5 wt.%) foils, cold rolling, annealing, microstruct., TEM obs. 7-59544
- Rh foils, ion bombarded, desorbed neutral energy distrib. studies 7-22406
- Si, amorphous foil, time-resolved X-ray absorption during pulsed laser irradiation 7-12128
- a-Si foils, pulsed laser irradi., clusters and plasmas, time resolved X-ray absorpt. meas. 7-64755
- Si, ingot and foil casting 7-53711
- TaD₄ foils, D desorpt., Auger electron and thermal desorpt. spectra studies 7-32800
- W, chemical etching, ion bombardment effects, AES study 7-28212
- Yb foils, piezoresistance response studies 7-32985

Fokker-Planck equation

- ID system, master eqn. and Fokker-Planck eqn. in thermodynamic limit 7-276
- anharmonic oscillator, nonlinear system under combined periodic and random excitation 7-9699
- averaged Kolmogorov-Fokker-Planck eqns. in random vibr. theory, integrability condition 7-88
- axisymmetric MHD stable sloshing ion distributions 7-57985
- bistable system, equistability criterion 7-35418
- Brownian particle, diffusion in bistable potential, general inverse friction expansion 7-29950
- charged particle transport calcs., finite element method, ICF appl. 7-36244
- charged particle transport in fully ionized plasma, flux-limited diffusion model 7-36246
- conservative finite difference schemes 7-61278
- diffusion coefficient, coloured noise, projection approach calcs. 7-35412
- dislocations, fluctuation unpinning from point defects, one-dimensional diffusion eqn. 7-26752
- electron cyclotron heating in tokamaks, Fokker-Planck studies 7-51405
- electron-electron scatt., energy loss to phonons, integral eqn. 7-52478
- energy relaxation, during tail-anisotropy instability in lower-hybrid current rise 7-6385
- gas laser, positive *P* representation and the laser equations 7-10909
- heated particle in rarefied gas, Brownian movement, kinetic description 7-51231
- lattice stochastic algorithms, generalised Fokker-Planck eqn., lattice gauge theory appl. 7-24770
- isothermal desorpt., Fokker-Planck eqn. for physisorption kinetics 7-52257
- K-distributed noise, Fokker-Planck description, stochastic diff. eqns. 7-61236
- kinetic gas theory formulation for Boltzmann-Fokker-Planck eqn. 7-63239
- laser fusion, direct drive, thermal electron transport, review 7-26391
- laser-abeted plasma, collisional Weibel instability, nonlocal anal. 7-58013
- lattice gauge theory, stochastic quantization using Langevin and Fokker-Planck eqns. 7-24792
- linear transport eqns. in a random medium, projection operator methods 7-61287
- lower hybrid current drive, simulation model 7-11597
- multimode self-pulsing in optical systems, quantum statistical treatment 7-10898
- non-autonomous mechanical systems, Fokker-Planck-Kolmogorov eqns., random oscils. 7-85
- nondissipative quantum diffusion eqns., comment and reply 7-41309
- nonlocal electron heat transport by not quite Maxwell-Boltzmann distributions 7-16300
- plasma transport coefficients for nonsymmetric toroidal confinement systems 7-11678
- plasmas, laser-produced, nonlocal heat flow, model 7-20912
- polynomial expansion and integral eqn. methods 7-61291
- potential energy barrier crossing rates, 2D Fokker-Planck eqn. 7-270
- quantum-beat laser theory, Fokker-Planck approach 7-57292
- random vibrations of nonlinear systems, non-Gaussian moment method (*Chinese*) 7-24542
- runaway electrons, velocity-space struct. 7-11586
- solidification, shear flow influence on phase transition 7-32620
- stochastic particle acceleration and statistical closures 7-9763
- storage rings, transverse mode coupling instability, Fokker-Planck theory 7-814
- subsystem interaction with boson field, kinetics 7-32591
- time-dependent systems, density functional theory 7-41254
- transport theory conf., Montecatini Terme, Italy, June 1985 7-60874
- turbulence theory, generalised Kolmogorov-Fokker-Planck equations 7-51062
- two-level atoms, excited, microscopic maser theory 7-15837
- two-step chemical reaction, nonequilib. conc., steady state fluctuations and struct. factor 7-13726
- velocity distribution functions, magnetised Fokker-Planck eqn. with quasi-lin. diffusion 7-11590
- weakly coloured noise, effective Fokker-Planck eqn. uniform convergence 7-24557
- AlGaAs laser, mode hopping suppression by saturable absorber 7-62696
- He, positron thermalisation and annihilation 7-63245
- Ne positron thermalisation and annihilation 7-63245

food processing industry

- milk pasteurization using solar pipe collectors 7-23218
- poultry processing plant refrigeration heat recovery system 7-8428

forbidden gap see energy gap

Forbush decreases see cosmic ray variations

force

- see also atomic forces; coercive force; Coriolis force; force measurement; molecular force constants
- plate bending element, bilinear, force evaluation 7-57707
- force constants see lattice dynamics; molecular force constants
- force measurement
 - see also dynamometers
 - attraction force meas., using torsion balance and capacitive position transducer 7-41407
 - fibre optic evanescent-wave coupling force transducer, using He-Ne laser 7-41367
 - impact analysis and obs., effect of mass on transducer sensitivity 7-16137
 - microbend fibre optic sensors, principle and appls. (*Slovak*) 7-11123
 - paper web tension profile meas. by contactless acoustic instrument 7-1336
 - photoelastic fibre optic sensor, force, pressure, acceleration and sound meas. (*German*) 7-11159
 - photoelastic pressure sensor, using low-birefringence fibre 7-43429
 - quartz tuning fork resonator transducers 7-35512
 - split point drills, TiN and ZrN coatings performance charact. meas. 7-65244
 - vibration characterisation by force and acceleration meas. 7-9812

force meters see force measurement

forecasting, technological see technological forecasting

forecasting theory

- long-range prediction, GMDH approach, weather forecasting appl. 7-18270
- meteorological/climatological prediction models, group method of data handling method 7-29125
- URFOR, urban-scale computer model for short-term prediction of air pollution (*Polish*) 7-66205

forestry see natural resources

forging

- compressible materials, complex math. model of plastic flow 7-64959
- slow, frictionless ring forming: further exact solutions for a wide class of ductile materials 7-6111
- steel, high-speed, cast and wrought, impact-fatigue strength 7-39656
- steel, low C, cold forgeability, notches, geometry, friction conditions, microstruct. 7-33697
- steel, low-C, wrought, thermal strengthening methods effectiveness 7-46524
- steel, tool, heat treatment cycles, original struct. and deform. influence on mech. props. 7-39560
- steel surface at moderate heating temps., relationship between emissivity and exoemissive props. 7-43641
- Fe, cast, diffusion interaction with steel in forging, explosive treatment and thermal cycling 7-28070
- Fe powder, ultrafine, and hot forged specimens, reduction temp. effect on struct. form. and props. 7-53670
- Mo alloys, forging, crystallographic texture, X-ray diffr. (*Russian*) 7-39538
- SiC whisker reinforced Al, flame spraying fabrication and forging, whisker distrib. and strengths 7-59483
- Ti-Al-V (6.4 wt.%), α morphology rel. to thermomech. treatment 7-46520

form factors, atomic see atomic structure

form factors (elementary particles)

- see also form factors (nuclear)
- π NN form factor in the Skyrme model 7-15159
- π -form factor model, construction using conformal mapping, ρ -meson contributions 7-30270
- baryonium, influence of relativistic effects on level widths 7-10064
- electromagnetic struct. of nuclei and nucleons, review 7-30315
- electromagnetic transitions and deformations in nucleons and deltas 7-41812
- electroweak form factors of the Skyrminion 7-415
- electroweak interactions with the nucleon and tests of the standard model 7-61513
- EM form factors and $\pi\pi$ scattering, consistency in $\rho(1600)$ region, dispersion relation anal. 7-567
- fermion-scalar system, potential model anal. of magnetic moment and form factors 7-61691
- form factors and static props. in relativistic potential model 7-15157
- gluon-exchange quark model and baryon-nucleon spin-orbit forces 7-61544
- low energy cross sections and quark confinement radius 7-35899
- neutrinos, polarization loss and induced electric charge in plasmas 7-41685
- neutron electric form factor from $\bar{e}d \rightarrow e'n p$ 7-35880
- nucleon axial vector form factor in perturbative QCD 7-522
- nucleons, core motion effects on static props. 7-15158
- pseudoscalar meson charge radii from QCD sum rules, SU(3) breaking 7-10033
- pseudoscalar meson electric form factor calcs. lattice QCD anal. 7-35801
- scalar lattice QCD, hadron static props., form factors, charge radii, lepton widths 7-49080
- singlet form factors and local observables in the Glashow-Weinberg-Salam model 7-5014
- Skyrme model, expressions for various currents using gauge transformations 7-30162
- two-pion exchange three-nucleon potential, modifications, inclusion of form factors 7-49251
- VPP-interaction, chiral anomalies, low-energy theorems and form factors 7-41813
- weak form factors and supersymmetry 7-61490
- d charge form factor in perturbative QCD 7-41719
- $e(\mu,\gamma)$ N elastic scattering, nucleon form factors from polarized lepton scatt. 7-56556
- $ed \rightarrow e'n p$, dynamics in light cone, nucleon form factors (*Russian*) 7-15165
- e^+e^- heavy baryons, perturbative QCD anal. 7-35887
- $eN \rightarrow e\Delta$, high Q^2 , N- Δ form factors, perturbative QCD anal. 7-19119
- $e\pi$ scattering, $E_\pi=300$ GeV, space-like pion EM form factor meas. 7-10062
- $\gamma n \rightarrow W^+ p$, high-energy photoproduction of W bosons 7-35881
- $\gamma p \rightarrow W^+ n$, high-energy photoproduction of W bosons 7-35881
- K, charge radius meas. by direct scatt. 7-10063

form factors (elementary particles) continued

- $K^- \rightarrow \pi^0 e^- \bar{\nu}_e$, decay probability, form factor meas. 7-56538
 $IN \rightarrow X$, deep inelastic scatt., two-photon collisions 7-19115
 N form factor, QCD anal. 7-61686
 N form factor, QCD and perturbation theory calcs. 7-61685
 N form factor zeros, quark model anal. 7-61690
 NN interaction model with π -exchange, overlapping nucleon form factors 7-35952
 Ωp elastic scatt., Chou-Yang model for differential cross section 7-41833
 pp charge exchange reactions, low energy cross sections and quark confinement radius 7-35899
 $pp \rightarrow n\Delta^{++}$, one-pion exchange model anal. of $^1H(^3He, t\Delta^{++})$ 7-24988
 $pp \rightarrow pn\pi^+$ at 800 MeV, one-pion exchange model and Faddeev eqn. 7-41846
 π form factor, QCD anal. 7-61686
 $\pi^0 \rightarrow e^+ e^-$, branching ratio two-photon processes, form factor 7-35855
 $\pi^0 \rightarrow e^+ e^- \gamma$, form factor information 7-15145
 $\pi^+ \rightarrow e^+ \nu_e \gamma$, axial vector to vector weak π^+ form factor meas. 7-10055
 $\pi^+ \rightarrow e^+ \nu_e \gamma$, pion axial-vector to vector form factor ratio meas. 7-41802
 $\pi\pi$ scattering, three channel N/D model anal., π form factors and vertex fns. 7-61739
 $\Sigma\pi$ elastic scatt., Chou-Yang model for differential cross section 7-41833
 $W \rightarrow l\nu$ ($\bar{u}d$)($\bar{c}s$), electroweak one-loop corrections, form factor, calc. scheme 7-5091
 Ξp elastic scatt., Chou-Yang model for differential cross section 7-41833
 $H(e, e'n)$, d disintegration by pol e^- , neutron electric form factor 7-61862

form factors (nuclear)

- $^A O(e, e')$, $A=16, 18$, form factors and transition charge densities 7-35942
 $A=5-8$, breathing cluster model for two s-wave clusters, charge form factors 7-24942
 charge distribution, central depression 7-19160
 cluster transfer reaction, microscopic form factor 7-30319
 E2 form factor, continuity-equation constraint and the non-uniqueness of the vector potential decompositions 7-49296
 elastic transfer between similar nuclei, parity dependent contribution to optical potential 7-10131
 electromagnetic struct. of nuclei and nucleons, review 7-30315
 EMC effect, QCD and Fermi gas model interpretations 7-15188
 future prospects for struct. studies with high energy projectiles and probes 7-56611
 gluon condensate modification in nuclei 7-49279
 IBM, electromagnetic and hadronic form factors and operators 7-5154
 isovector transition densities and isobar spin potential deformation, semimicroscopic approach 7-30389
 multi-quark correlations in nuclei quark cluster model anal. of nuclear structure functions 7-56633
 $N=82$ isotones, Coulomb form factors, core polarization effects on transition densities 7-61847
 NNN system, properties and electromagnetic observables, form factors 7-61803
 nucleus-nucleus collisions, deformed nuclei, form-factor calcs. using proximity-plus-Coulomb potential 7-19285
 quark percolation in finite size nuclei 7-591
 quark-gluon plasma and EMC effect studies at CERN 7-49273
 random phase approx. spin-isospin nuclear response in deep inelastic region 7-5157
 three-nucleon bound state, struct. function calcs. using Faddeev wave function 7-5151
 trinucleon charge densities and three-nucleon forces, form factor calcs. 7-19161
 Tucson-Melbourne force, role in binding energies and charge form factors 7-61805
 Δ isobar Landau-Migdal parameters and high momentum props. of spin-isospin response functions 7-5180
 (e, e) , model independent densities from scatt. data, form factors 7-657
 (e, X) deep inelastic scatt., vector meson dominance and EMC effect 7-30317
 (γ, π^0) , Pauli exclusion effects on form factors and s-wave repulsion 7-24968
 $(I, \phi X)$, nuclear enhancement effect, colour oscillation mechanism 7-41987
 (I, X) , deep inelastic scatt., two-photon collisions 7-19115
 NNN form factors, isospin structure 7-61793
 (π^+, π^-) , $A=12-56$, nonanalogue double charge exchange, cross sections, form factors, transitions, shell model 7-30456
 7-41892
 $^{27}Al(p, p)^{27}Al$, spin-spin potential determ. in optical model from depolarisation 7-660
 ^{10}B , electromagnetic struct., Cohen-Kurath wave functions (Korean) 7-24935
 ^{11}B , electromagnetic struct., Cohen-Kurath wave functions (Korean) 7-24935
 ^{12}B , aligned nucleus, beta-ray angular distribution anal. 7-5195
 ^{12}C , dynamic and static longitudinal structure factors, RPA anal. 7-41884
 $^{12}C(e, e)$, dispersive effects in form factor meas. 7-5227
 $^{13}C(\alpha, p)$, differential cross section meas. and DWBA calcs. 7-30343
 $^{14}C(e, e')$, form factors and stretched M4 configurations, shell model comparisons 7-41981
 ^{40}Ca , dynamic and static longitudinal structure factors, RPA anal. 7-41884
 $^{19}F(e, e)$, form factor calcs. using projected Hartree-Fock function 7-30413
 ^{56}Fe , dynamic and static longitudinal structure factors, RPA anal. 7-41884
 ^{56}Fe , proton form factor, valon model (Chinese) 7-10100
 ^{147}Gd ($A=156, 158, 160$), (e, e') form factor and BM1 probability calcs. 7-56591
 2H charge form factor in perturbative QCD 7-41719
 2H , EM form factors in quark based model 7-41888
 2H , electromagnetic structure of the deuteron in the Skyrme model 7-49235
 2H , magnetic form factor, topological exchange current contrib. 7-35941
 2H , magnetic form factor meas. at high Q^2 7-35938
 2H , NN pot. and phase shifts with quark degrees of freedom 7-41886
 2H , quadrupole moment, rms radius and form factors from local NN potential 7-5165

form factors (nuclear) continued

- $^2H(e, e'N)$, nucleon momentum distrib. using y-scaling 7-5226
 $^2H(e, e')$, nucleon momentum distrib. using y-scaling 7-5226
 $^2H(\pi, X)$, absorption form factor and off-shell behaviour, perturbative approach 7-5295
 3H , charge form factors, hybrid quark hadron model anal. 7-24933
 3H , EM form factors, hybrid-quark-hadron model anal. 7-56673
 3H , electromagnetic struct., nonnucleonic degrees of freedom and relativity effects 7-35937
 $^3H(\pi, \pi)$, 142, 180, 217 MeV, matter form factors, comparisons with $^3He(\pi, \pi)$ 7-56600
 $^3H(\pi, \pi)^3H$, elastic scatt., form factor determ. 7-61926
 3He , charge form factors, hybrid quark hadron model anal. 7-24933
 3He , EM form factors, hybrid-quark-hadron model anal. 7-56673
 3He , electromagnetic struct., nonnucleonic degrees of freedom and relativity effects 7-35937
 $^3He(e, e'N)$, nucleon momentum distrib. using y-scaling 7-5226
 $^3He(e, e')$, longitudinal spectra in the low-energy scheme 7-41986
 $^3He(e, e')$, nucleon momentum distrib. using y-scaling 7-5226
 $^3He(\pi, \pi)$, 142, 180, 217 MeV, matter form factors, comparisons with $^3H(\pi, \pi)$ 7-56600
 $^3He(\pi, \pi)^3He$, elastic scatt., form factor determ. 7-61926
 (N, X) , low energy interactions in semimicroscopic approach 7-10142
 ^{12}N , aligned nucleus, beta-ray angular distribution anal. 7-5195
 $^{14}N(e, e')$, 2.313 MeV state, transverse scatt. form factors and phenomenological wave fn. 7-41982
 $^{14}N(e, e')$, form factors and stretched M4 configurations, shell model comparisons 7-41981
 $^{14}N(e, e)$, ground state, transverse scatt. form factors and phenomenological wave fn. 7-41982
 ^{16}N , multiparticle-multi-hole strength, DWBA calcs. and spin-parity assignments 7-30343
 $^{16}O(^{16}O, X)$, elastic transfer effects in subbarrier fusion, barrier penetration model 7-42061
 $^{16}O(e, e')$, $A=17, 18, 15-23$ MeV, excitation of M4 transitions, form factor meas. 7-19238
 $^{208}Pb(e, e')$, high spin state form factor calcs. 7-49218
 ^{110}Pd , Coulomb form factors, core polarization effects on transition densities 7-61847
 $^{28}Si(e, e'P)$, coincidence studies in the giant resonance region 7-49384
 $^{28}Si(e, e')$, coincidence studies in the giant resonance region 7-49384
 $^{154}Sm(^{12}C, ^{14}C)$, pair transfer, macroscopic description, form factor 7-25000
 ^{116}Sn , Coulomb form factors, core polarization effects on transition densities 7-61847
 $^{238}U(e, e')$, 5-23 MeV, coincidence cross section meas. 7-19240
 ^{90}Zr , second 0^+ state excitation, form factors and transitions, CC anal. of (n, n') , (p, p') and (α, α') 7-30369

formal logic

- see also computability
 logical cover spaces 7-29779
 quantum logics, Gudder conjecture and joint distrib. 7-18625
 symbolic substitution logic, optical implementation using polarisation for coding 7-10860

formation, heat of see heat of formation**forming processes**

- see also casting; electroforming
 brass, pressed component, strain distrib. 7-13530
 metal sheet, forming limit diagram in negative minor strain region 7-65090
 metal sheet, superplastic bulging, technological anal. 7-65093
 metals, ductile, new workability criterion 7-13533
 metals, plastic forming operations, Bauschinger effect 7-46557
 metals, sheet, history depend. forming limits, hardening models 7-59542
 metals, sheet, press formability and anisotropic yield, Bassani-type criteria 7-28068
 sheet metal forming limits under complex strain paths using void growth and coalescence model 7-13532
 simulation using arbitrary Eulerian-Lagrangian formulation 7-6105
 steel, duplex stainless, ferrite-austenite flow localisation during plane strain punch stretching 7-17593
 steel, ferritic-martensitic stainless, warm forming (Polish) 7-13507

FORTRAN

- see also FORTRAN listings
 RPHIN—a FORTRAN 77 program for acquiring axial ratios, long axis orientations and centroid positions of elliptical strain markers 7-17581
 spatial trend analysis of streamline glacial features 7-18216

FORTRAN listings

- beams/columns subjected to non-uniform axial loads, vibration and buckling 7-6140
 chemical analysis of igneous rocks and CIPW norm calculations 7-29263
 clay constituents, apportionment into structural formula 7-65999
 contouring algorithm in FORTRAN 7-66312
 displacement in two phase flow in porous media, finite element simulation 7-51295
 drainage network simulation 7-55088
 electrostatic lens for positron studies, transfer-matrix subroutines 7-62616
 extraterrestrial solar radiation on inclined surfaces, FORTRAN program 7-55138
 FIRECRACKER 3, computer program for X-ray powder diffractometers calibration 7-14931
 fluid dynamics, Glimm's method, introduction and FORTRAN listing (Spanish) 7-20678
 mineral melt evolution simulation, Rayleigh fractionation 7-65998
 petroleum resource appraisal program, FORTRAN listing 7-40576
 polar coordinate transformation to new pole 7-54846
 radiative cooling in valleys and hollows 7-55134
 rock microstructure, image analysis of particles, FORTRAN V program 7-66311
 running averages, an efficient algorithm 7-8465
 sea bed contour map construction from random data, iterative method 7-34725
 seismology, algorithm for synthetic seismograms for oil and gas prospecting 7-60395
 stratigraphically constrained cluster analysis, FORTRAN 77 program 7-66114
 stream gauge data adjustment for urbanization effects 7-34567
 thermophysical properties, calcs., microcomputer interactive FORTRAN programs 7-11260

FORTRAN listings continued

- water level computation between high and low tides, FORTRAN program 7-55077
- well-log evaluation for carbonate reservoir in Kansas, microcomputer based program, WSULOG 7-40580
- WSU-MAP: a microcomputer-based reconnaissance mapping system for Kansas subsurface data 7-40584
- WSUTREND, trend-surface analysis in oil fields 7-40583

Foucault currents see *eddy currents*

fountain effect see *superfluid helium-4*

Fourier analysis

- see also *Fourier transforms; harmonic analysis; waveform analysis*
- 2D digitised images, object boundaries anal. 7-36906
- cardiac nuclear medicine images, length-based Fourier anal. in pre-excitation syndrome 7-65879
- Cepheids, light curves, Fourier decomp. parameters 7-40826
- crystal structure determ. using automatic Fourier, Patterson and superposition methods 7-32219
- earthquakes, Fourier analysis for computation of focal mechanisms 7-18131
- elliptic partial differential eqns., iterative soln. by local discrete Fourier anal. 7-18572
- EMG, short time Fourier anal.: fast movements and constant contraction 7-54537
- FTIR photoacoustic spectra, resolution enhancement by Fourier self-deconvolution 7-48881
- geomagnetic PC 1 micropulsations, Fourier analysis of wave packets, freq-spectra 7-14416
- heat conduction, 2D, isoparametric line and transition finite elements 7-43628
- image anal., similarity measures between images 7-42999
- leap-frog finite difference schemes, nonlinear instabilities 7-29694
- RR Lyr stars, light curves, Fourier decomp. parameters 7-40826
- magnetic oxide recording media, static hysteresis loops, Fourier anal. 7-33213
- microfunctions, sheaf flabbiness 7-48320
- microfunctions with values in a Clifford algebra 7-48321
- mismatched overlayers, dislocation depinning, mol. dynamics investig. 7-7011
- nuclear ventriculography, ejection fraction determ. by combined inverse Fourier anal. and second-derivative technique 7-40254
- optical image deblurring by spectrum analysis (*Korean*) 7-57256
- optical pulses, time-dependent spectral analysis, resolution limits 7-42955
- overlapped bands resolution by Fourier method 7-48885
- protein structure by FTIR self-deconvolution 7-54476
- pulse power radial transmission line, matching problems 7-32075
- STEM focused electron probes, Fourier analysis 7-18934
- transient heat transfer in porous media—a two-temperature model 7-16181
- two-window Fourier transform technique, $Pb_{1-x}Sn_xTe$ quantum oscils. spectrum anal. 7-52404
- CdSe:Cu, transient photocond. anal. 7-64288
- $K_2H(IO_3)_2Cl$, cryst. struct., neutron diffr. studies (*Chinese*) 7-12005
- Si, X-ray structure factor, Pendellosung method meas. 7-32362

Fourier series see *series (mathematics)*

Fourier transform optics

- see also *Fourier transform spectroscopy*
- astronomical telescopes, imaging props. of large reflecting telescopes 7-66461
- Cauchy/Schwarz inequality, constraint in power spectrum/autocorrelation anal. and image reconstruction 7-42996
- coded aperture imaging, Fourier space anal. 7-57250
- computer-generated holography, 3D image display using 1D transforms 7-31274
- correlation, compact minicorrelator for pattern recognition 7-57523
- dense particle fields, laser diffraction meas. correction for multiple scatt. 7-1212
- discrete Fourier transforms by single-mode star networks 7-42989
- electro-optical pre-detector signal processing 7-5852
- filter with limited rotation invariance for target recognition 7-10872
- focus of high-numerical-aperture objectives, light distribution 7-43290
- forced Rayleigh scattering appl. to hydrodynamic meas. 7-11572
- Fresnel holograms, in-line, phase retrieval and twin-image elimination 7-43008
- FTIR microanalysis principle and appls. 7-24699
- GRIN lens with revolution symmetry, paraxial Fourier transforming and imaging props. 7-31420
- Hartley transform intensity for image reconstruction 7-31260
- high-dimensionality pattern recognition feature space production 7-25725
- holography, Fourier phases, signal processing 7-57275
- hybrid pattern recognition by features extracted from object and Fraunhofer diffr. patterns 7-42942
- image processing of Fourier magnitudes, continuous object distributions reconstruction 7-42959
- image processing of Fourier transform, complex-valued objects reconstruction 7-42960
- image reconstruction from Fourier transform, phase retrieval from two intensity measurements 7-42964
- image reconstruction from Fourier-transform phase using moments 7-42985
- image restoration, automatic multidimensional deconvolution 7-42967
- image restoration from Fourier-transform magnitudes by generalized projections 7-42974
- interferogram Fourier transform., optical data processed FT spectrometer 7-24707
- inverse source problem comparison for quasihomogeneous, partially coherent sources in two and three dimens. 7-62597
- medical images, pseudocolour encoding with white light 7-3861
- metal surface roughness parameter measurement, diamond turned, light scattering technique 7-61318
- modulation transfer function for the display engineer 7-25730
- multiple matched filter design for character recognition 7-50718
- optical/digital hybrid system for calculating geometric moments 7-25724
- particle velocity and displacement distribs. from double-exposure holograms using opt. and digital processing 7-31277
- phase front reconstruction of light wave by Fourier optics method 7-36893
- phase retrieval, improvement in logarithmic Hilbert transform evaluation 7-31262
- phase retrieval algorithm using sampling theorem 7-62632

Fourier transform optics continued

- phase retrieval based on theoretical models for multi-dimens. band-limited signals 7-62636
- phase retrieval with complex image 7-62634
- phase-only image reconstruction from offset Fourier data 7-50509
- phase-retrieval stagnation problems and solutions 7-31257
- plane diffr. grating, resolution and wavefront evaluation by FFT 7-31266
- randomisation techniques for moire fringe suppression 7-42980
- range images, segmentation using sine wave coding and Fourier transformations 7-42951
- reconstruction of complex-valued propagating wave fields by Hilbert-Hankel transforms 7-42975
- speckle modulation methods, transverse rel. to longitudinal displacement (*Korean*) 7-29965
- speckle statistical theory, Fourier optics 7-42927
- split-step fast Fourier transform method, optical coherence calcs. 7-1022
- Strehl ratio phase-space representation, ambiguity function 7-57257
- telescope for subarcsecond imaging of solar flare x-rays and γ -rays 7-40706
- theta decoder, lensless using Lau effect 7-25719
- wavefront estimation from difference meas. using discrete Fourier transform 7-31255
- Wigner distribution function from single object transparency, optical system for efficient display 7-31259

Fourier transform spectrometers see *Fourier transform spectroscopy; interference spectrometers*

Fourier transform spectroscopy

- acetylene vibr. excited, chaos and dynamics on 0.5 to 300 ps time scale, Fourier transform spectra 7-42634
- 2-adamantanone, order-disorder transition obs. by FRIR spectroscopy 7-53342
- ADC errors in quantitative FTIR spectroscopy 7-48877
- albumin solution, struct. determ. by FTIR 7-54471
- n-alcohols, IR intensities in liq. phase, OH vibrs., assoc. model 7-53336
- alkali metal chlorate ion pairs, coord. structs., FT IR matrix isolation spectra 7-62367
- alkaline earth, cpds. laser and Fourier transform spectroscopy 7-19872
- n-alkanes, liq., energy difference between specific and localised conform. isomers, FTIR spectra 7-42615
- allene-d, (-1,1-d₂), pure rot. spectra, microwave FT spectrosc. 7-5669
- analytical spectroscopy methods review 7-54226
- anvil cell, high press., development for microscopy/IR spectroscopy 7-54224
- apodization effects in Fourier transform IR difference spectra 7-48896
- aromatic aldehydes in cyclohexane solvent, internal mobility study, far-IR and microwave Fourier transform spectra anal. 7-64631
- asbestos, fibres, Fourier transform photoacoustic spectroscopy 7-51952
- atmospheric Fourier transform spectral analysis of far IR emission 7-14379
- atmospheric microwave plasma emission characteristics in near IR 7-55318
- atmospheric trace gas measurements using matrix isolation-FTIR spectroscopy 7-55316
- ATP-transition and nontransition metal complexes, struct., PMR and IR spectra 7-8493
- bacteria, pathogenic, ultrarapid differentiation and identification using FTIR techniques 7-54835
- benzene-d, 1₀₁-0₀₀ rot. transition, Stark shift, microwave FT spectrosc. 7-57110
- benzonitrile, liq., FTIR and Raman obs. on dynamic and interaction processes 7-53344
- biological membranes, lipid/protein interaction, Fourier transform IR studies 7-54498
- bisphenol-A polycarbonate, stressed, reversible mol. orientation, IR studies 7-50428
- blood component platelet activating factor, IR spectroscopic characterisation 7-54499
- cells, live, Fourier transform IR spectroscopy 7-54507
- cellulose, particle size and order changes, ¹³C NMR and NIR diffuse reflectance spectroscopy responses 7-27610
- chalcocarbonyl(5,10,15,20-tetraphenylporphinato) iron II complexes, IR and NMR spectra 7-33394
- chlorophyll carbonyls, IR band resolution enhancement, computer techniques 7-39096
- cyanooacetylene, ν_5 and ν_6 fundamental bands, FT IR obs. 7-923
- 4-cyanopyridine, rot. spectrum, nucl. quadrupole coupling effects 7-57055
- cyclopropane, ν_{10} and ν_{11} fundamentals in IR Fourier transform spectra 7-50052
- data manipulation, UNIX based computer workstation 7-48859
- DEFT with 2D pulse sequence, solvent reson. suppression or differentiation 7-48798
- diatomic molecules, high resolution Fourier spectroscopy 7-50138
- diatomic mols. laser and Fourier transform spectroscopy 7-19872
- diazirine, ν_3 fundamental, rovibr. anal., IR spectra 7-10583
- 1,2-trans-dichloroethylene, vibr. distribs., time-resolved FTIR photofragment emission spectroscopy 7-25508
- difluoromethane pumped by ¹²C¹⁸O₂, ¹²C¹⁸O₂ lasers, submillimetre emission assignment 7-36944
- dual beam FTIR, dynamic range considerations in ultimate sensitivity 7-48890
- electrical contact surface, two-dimens. FTIR mapping 7-48882
- electroactive species, Fourier transform IR reflectron absorpt. spectra 7-23093
- electronic materials characterisation, recent trends (*Japanese*) 7-13163
- ethylene-acrylic acid copolymers, struct. analysis using Fourier self-convolution of IR spectra 7-53337
- ethyne adsorbed on zeolite, time resolved FTIR obs. 7-54182
- far IR spectroscopy with 4 m path difference interferometer 7-48887
- ferrofluid, near mm wavelength studies of refr. indices by dispersive Fourier transform spectra 7-53289
- ferrofluid-Al particle composite, microwave absorption studies 7-59306
- FIR spectroscopy, review 7-35608
- fluid under high pressure, FTIR spectra interpret. 7-50402
- fluorenone ketyl radical cation, single channel quadrature FT ESR spectra 7-25570
- formic acid, ν_3 band, sub-Doppler laser-stack and Fourier transform spectroscopy 7-62430
- Fourier transform ion cyclotron reson. spectra, residual spatial mag. field gradient effects 7-42550

Fourier transform spectroscopy continued

- FT IR spectroscopic system, high press., with cell for catalytic reactions obs. 7-35606
- FT photoelectron spectroscopy, correl. fn. and harmonic oscillator approx. 7-10665
- gallstone and bezoar, FTIR spectra, protein bands and secondary struct. 7-54473
- gas chromatograms, reconstruction from GC/IR spectrometry data 7-17832
- gas chromatograph/FTIR system, optimal design 7-48891
- gas phase reaction kinetics, rapid scanning FTIR time-resolved spectrometry technique 7-48886
- E-glass fibre composite interfaces, surface studies using diffuse reflectance and photoacoustic FTIR spectra 7-46044
- graphite fibre reinforced epoxy composite, characterisation by diffuse reflectance Fourier transform IR 7-53332
- hazardous gas monitoring system in chem. manufacturing facility, open path FTIR air monitor 7-54416
- heavy atom spectra sources for use with high resolution Fourier transform spectrometer 7-50403
- heterocyclic aromatic polymers, laser desorption FT mass spectrosc. anal. 7-23085
- hormonal steroids, physiological levels detection by Fourier transform IR spectroscopy 7-54833
- hydrocarbon systems, gas and liq. phase, in situ modelling using FTIR at high press. 7-54221
- IBM AT-based FTIR spectrometer 7-24713
- ice, cubic, proton transport, FTIR obs. 7-53340
- ICP Fourier transform spectrometer, signal to noise ratio characts. 7-35600
- ICR cell excitation, axial and radial motion coupling 7-48855
- ICR mass spectrometry, dynamic range extension 7-48901
- IR difference spectroscopy for elucidating biomolecular mechanisms 7-54832
- IR emission accessory for surface analysis, ellipsoidal mirror 7-54225
- IR Fourier transform spectroscopy for investigating elementary processes in gas-solid interaction 7-33986
- IR photoluminescence by Fourier transform spectroscopy 7-46134
- IR photothermal beam deflection spectroscopy of complex gas/solid systems 7-41497
- IR quantitative analysis, Fourier domain, processing vector representations 7-35599
- IR spectral emittance meas., 2 to 20 μm 7-30104
- IR spectroscopy, biological and biomedical appl. 7-54831
- IR spectroscopy, math. representation, resolution and role of model in anal. 7-48875
- IR spectroscopy, Ottawa, Ont., Canada (June 1985) 7-48160
- IR spectroscopy, quantitative intensity meas. 7-48869
- IR spectroscopy, spectral searching 7-48874
- IR spectroscopy, theoretical limits 7-48873
- IR spectroscopy, today and tomorrow 7-48876
- IR spectroscopy for industrial materials characterisation 7-48868
- IR spectroscopy from space, ATMOS expt. on Spacelab-3 7-55314
- IR techniques, in-situ spectroelectrochemistry 7-54144
- cis-1,4-isoprene, mol. orientation, FT IR dichroism 7-17322
- Kevlar 49 fibres, N-H groups, photoacoustic Fourier transform IR spectra 7-39118
- Kevlar fibre surface, diffuse reflectance FTIR spectroscopy, fibre accessibility and water absorption 7-46040
- lanthanide thenoyltrifluoroacetate pyridine, Raman and FTIR spectra 7-57061
- laser wavelength comparison, using Fourier transform spectrometer 7-20311
- lipid A, free, multilayer, phase transition behaviour, FTIR, endotoxic principle of gram-negative bacteria outer barrier 7-54500
- liquid crystalline polymer, electric field FT-IR reflectance spectra 7-25688
- long-chain amphiphile on solid substrate, thermally induced disorder, Fourier transform IR spectra 7-12467
- magnetic modulation for detection of paramagnetic species 7-48856
- mass spectrometry in microelectronics processing, book contrib. 7-41529
- mathematics of spectral treatment in the Fourier domain 7-48870
- matrix-isolated molecules, FTIR vibr. circular dichroism 7-50104
- metal oxide catalysts, IR emission spectrosc. 7-39098
- methacrylic acid copolymers, struct. analysis using Fourier self-convolution of IR spectra 7-53337
- methane, absolute strengths and self-broadened widths in IR spectra 7-36622
- methane, gaseous, low temp. collision-induced IR absorpt. 7-10562
- methane- d_4 , pentad rovibr. levels, line parameters study, Fourier transform IR spectra anal. 7-50115
- methanol, adsorpt. on Al_2O_3 , Fourier transform IR spectra 7-38345
- methyl cyanide-acetylene dimer, pulsed nozzle FT microwave spectrosc. 7-36593
- 2-methyl oxetan, vibr. circular dichroism spectra, expt. and theoretical results 7-50208
- methyl silane, rot.-vibr. anal., Fourier transform IR spectra 7-19846
- s-cis methyl vinyl ether, coupled torsional and bending motions, microwave Fourier transform spectra 7-62355
- Michelson interferometer, hand-held, design and sensitivity for Space Shuttle glow obs. 7-55421
- Michelson interferometer, slightly-cooled high-resolution, for limb emission meas. from space 7-55317
- micro-emission FTIR accessories, performance 7-48845
- microsample analysis using IR dual-mode microscope 7-48844
- millimeter wave dielectric meas. of birefringent and ceramic materials 7-14978
- modulation spectroscopy 7-48872
- molecular cluster selective formation in cryogenic matrices, FTIR spectroscopy obs. 7-48895
- molecular diffusion, FT pulsed gradient spin echo investig. 7-22161
- nitrile ylides, matrix photolysis of phenyl and azidostyrenes, isotopic shift, mol. struct. FT IR spectra anal. 7-31035
- NMR, pulse sequence for acoustic ringing suppression 7-35553
- NMR spectroscopy oversampling technique improvement of dynamic range 7-24667
- nonadecane, liq., energy difference between specific and localised conform. isomers, FTIR spectra 7-42615
- nonlinear detectors for distortion free interferograms 7-41476
- nyquist frequency extension by interleaved data acquisition, Fourier transform NMR spectroscopy 7-24680

Fourier transform spectroscopy continued

- one-sided interferograms in Fourier spectrometers, recovery of linear phase errors 7-35581
- optical data processed Fourier transform spectrometer 7-24707
- organic films, on inorganic substrates, FT IR reflection spectrosc. 7-39097
- organic molecules at surfaces, Fourier transform IR studies 7-54220
- organometallic free radicals, laser and Fourier transform spectroscopy 7-18872
- overlapped bands resolution by Fourier method 7-48885
- PEEK, melting behaviour, molecular anal. using Fourier transform spectroscopy, thermal anal. 7-12244
- PET, films, depth-profiling, FTIR photoacoustic spectroscopy 7-25686
- photoacoustic, FTIR, use in depth profiling expts. 7-48880
- photoacoustic near-, mid- and far-IR, noise sources and reduction strategies 7-48888
- photoacoustic spectra, FTIR, phase analysis 7-48878
- photoacoustic spectra, FTIR, resolution enhancement by Fourier self-deconvolution 7-48881
- photoacoustic spectroscopy of solids 7-41496
- photoluminescence analysis, of trace impurities and defects in Si 7-53412
- poly(vinyl acetate) film on Cu, FTIR surface EM wave spectroscopy, Otto config. 7-46162
- poly-L-lysine, deuterated, Fourier transform vibr. circular dichroism in amide I bands 7-54475
- poly-vinylacetate-Cu, thin polymer films, Fourier transform IR ellipsometry 7-53334
- polyacetylene, cond., fast FTIR and IR intensity spectra, struct. and electronic props. 7-53335
- polybutylene terephthalate fibres, phase transitions, surface characterisation, spectrosc. methods 7-63505
- polydimethylsiloxane oligomers, FT-IR spectra, Fourier self-deconvolution appl. 7-25687
- polyethylene oxide-disubstituted benzene intercalates, Fourier transform IR spectra 7-13153
- cis-1,4-polyisoprene, mol. orientation, FT IR dichroism 7-13159
- polymer blend, intensity spectroscopy and FTIR as tool for struct. and inter mol. interactions determ. 7-53338
- polymer blend films, Fourier transform IR/ATR spectroscopy studies 7-53333
- polymer film on metal substrate, FTIR surface EM wave spectroscopy, Otto config. 7-46162
- polymers, conducting, laser desorption/Fourier transform mass spectral analysis 7-1920
- polymers permittivity, loss tangent and refractive index meas., dispersive Fourier transform technique 7-18820
- polypropylene, isotactic, polymorphic forms, FTIR far-IR obs. 7-53339
- polyurethane insulation, thermal and elec. aging, prebreakdown phenomena, FTIR spectra study 7-39568
- polyvinylidene fluoride, films, depth-profiling, FTIR photoacoustic spectroscopy 7-25686
- porous and fibrous materials, radiative transfer, IR spectra study of oxide crystals 7-53305
- propyne, $2\nu_3$ band study, Fourier transform IR spectra anal. 7-50119
- protein in aqueous solution, FTIR spectra, automatic water subtraction procedure 7-54836
- protein structure by FTIR self-deconvolution 7-54476
- protein structure determination by FTIR 7-54471
- protein structure-spectra correlations, nonaqueous solvent effects using FTIR and ATR flow cell 7-54472
- proteins and lipids, FTIR spectra, water subtraction procedure 7-54834
- pulsed MM wave Fourier transform microwave spectrometer, rot. transition detect. in mols. 7-350
- PVC, pure and plasticized, orientation, Fourier transform IR study 7-44661
- pyridine- d_5 (d_1), HFS, quadrupole coupling, Fourier transform microwave spectra 7-19827
- quartz, FTIR spectrum of crystals, press. effects, phonon band splitting 7-46039
- Raman, appls. 7-56346
- rare earth naphthalene complexes, extract phase, FTIR and subtraction spectra 7-50142
- reactive intermediates determination by matrix isolation FTIR spectroscopy 7-54417
- reflection-absorbance FT IR spectra of chromatograph effluent, continuous recording 7-15016
- resonant classical motion, EBK quantisation, Fourier transform approach, semiclassical eigenvalues 7-42587
- ribonuclease, FTIR obs. of folding 7-54470
- rubber, natural, mol. orientation, FT IR dichroism 7-13159
- rubber, natural, mol. orientation, FT IR dichroism 7-17322
- sample cell, Invar, low temp., for FTIR spectroscopy, thermal calibration 7-41507
- sample handling methods for FTIR analysis 7-46899
- sample transfer accessory for thin-layer chromatography/Fourier transform infrared spectrometry 7-30101
- sampling techniques for FTIR studies of liquefied and crystallised gas mixtures 7-48894
- SCRIBE interferometer atmospheric emission spectra 7-55319
- short-chain molecules, liquid-phase, motion, ^{13}C and ^1H NMR investig. 7-15624
- silica gel surface, variable temp. diffuse reflectance FT IR spectrosc. obs. 7-53294
- skin, living human, thermo spectral anal. by Fourier transform IR spectroscopy 7-54707
- slice selection in the presence of chemically shifted species 7-48821
- Solar Max samples, erosion studies 7-46743
- solid-liq. interface, Fourier-transform IR spectroscopy with photothermal beam deflection appl. 7-52234
- solvent suppression pulse sequence for biomolecule ^1H NMR spectroscopy 7-28788
- spectrometer, high resolution IR, for atomic, mol. and cryst. spectroscopy 7-41505
- spectrometer, Los Alamos design with microprocessor control 7-48860
- spectrometer, microcomputer-controlled, path difference control 7-48861
- spectrometer, near-IR, with IR vidicon 7-48889
- spectrometer, phase correction, computational algorithm 7-41504
- spectrometer, research grade, Digilab FTS to, design and performance 7-48892
- spectrophotometer, rotary scanning, props. and performance 7-48893

Fourier transform spectroscopy continued

stratosphere, far-IR spectrum, high resolution meas. with Fourier transform spectrometer 7-55262
stratospheric far-IR emission analysis, synthetic spectra and FTIR meas. comparison 7-55315
stratum corneum, lipophilic pathway, Fourier transform IR spectroscopy studies 7-54510
structural analysis using interferometric data 7-54222
surface analysis in far IR, triple modulation FTIR spectrometry 7-54223
surface EM wave FTIR spectroscopy of very thin films 7-41506
surface FTIR reflectance spectroscopy characterisation 7-46043
surface FTIR-ATR spectroscopy, lower limit of thickness of measurable surface layer 7-41508
surfaces and adsorption complexes, FTIR characteris. 7-46042
tetrachlorodibenzodioxins, isomers, identification, micro-diffuse reflectance and matrix isolation FT-IR techniques 7-25502
tetraglycidyl methylene dianiline, ¹H spectrum, FT 2D NMR obs. 7-19899
thin film dielectrics, characterisation 7-53435
time resolved spectroscopy, rapid scan, for gas phase systems, IR source development 7-48879
trifluoromethane, interacting states, high resolution FTIR absorpt. spectra 7-57065
two dimensional Fourier transform ESR spectra 7-19904
two-dimensional FTIR mapping of curved surfaces 7-48882
two-window Fourier transform technique, Pb_{1-x}Sn_xTe quantum oscills. spectrum anal. 7-52404
urea, rot. transition, N quadrupole coupling, HFS, microwave spectra 7-10559
N-urethanyl- α -amino acids, Fourier transform vibr. circular dichroism of carbonyl stretching modes 7-50207
vinyl chloride, vibr. distrib., time-resolved FTIR photofragment emission spectroscopy 7-25508
violacein, thin layer chromatography and FTIR analysis 7-54469
VUV spectrometer, design and performance 7-41490
water, liq., FTIR spectra, fine struct., molar absorptivities of vibr. modes 7-53343
Al₂Si₂O₅(OH)₄, kaolinite, FTIR photoacoustic spectra 7-48881
As-S (Se) chalcogenide glasses, far-IR absorption spectra and spatial charge fluctuation 7-7696
BaCl₂, B² Σ^+ -X² Σ^- transition, rot. anal., FTS and diode laser spectra 7-10581
BrF₃, FT IR spectra, rot. struct. 7-922
C cluster ions, trapped FT ICR mass spectrometry 7-1000
a-C:H plasma grown films, struct., physical props. 7-58713
C₂⁺, excited state, prod., ion-mol. reactions, FT mass spectra investig. 7-54087
C_n⁺-D₂(O₂) cluster ions, ion+mol. reactions 7-50432
C₂N₂-Ar gaseous mixture, collision-induced absorpt., quadrupole moments, IR and microwave spectra 7-50098
CO solid films, Fourier transform IR spectra 7-59214
CO₂ FTIR spectra, band intensities 7-50264
CO₂-Ar gaseous mixture, collision-induced absorpt., quadrupole moments, IR and microwave spectra 7-50098
CaO-SiO₂ polycryst. silicates, FTIR and Raman spectra, isotopic shifts and force consts. 7-53341
Cd(ClO₄)₂.6H₂O, low-temperature phase transitions characterisation by Fourier transform IR spectroscopy 7-52046
Cd_{1-x}Mn_xTe mixed cryst., far IR Fourier transform spectra, acoustic local mode and TA band mode 7-53378
CIF, FT IR spectra, rot. struct. 7-922
CuH, vibr.-rot. spectra obs. using FTIR 7-50139
DOCl, FTIR spectrum, band origins 7-50140
Fe-Cr alloy, oxide film form., FTIR reflectance spectroscopy characterisation 7-46043
GaAs, electronic intrasite transitions and local vibr. modes 7-53377
GaAs, substrates, multi-technique approach to defect microstructure characterisation 7-52215
GaP-electrolyte interfaces, Fourier transform IR spectroscopy 7-27124
H-bonds in molecular biology, FTIR spectra, strongly anharmonically coupled vibr. 7-47009
(HCN)_n microcluster selective formation in cryogenic matrices, FTIR spectroscopy obs. 7-48895
HCl, IR spectra, Ar- and N₂-broadened linewidths, rot. spectrum 7-50113
H₃GeD, Fourier transform IR spectra, rovibr. anal. 7-25516
H₃N-HCl, H-bonded dimer charactn., rot. FT microwave spectrum 7-25490
HNC, 2100 cm⁻¹ bands, IR Fourier transform spectra anal. 7-50117
H₂¹⁸O, energy levels, line intensities, Fourier transform IR spectra 7-5674
HOCl, FTIR spectra, vibr. rot. consts. and harmonic force field 7-50140
H₂S adsorbed on SiO₂/Na, FTIR and Raman spectra obs., Na promotion of Claus process 7-46869
H₂S, in O₂ matrix, FT IR spectra 7-36606
(H₂S)₂, in O₂ matrix, FT IR spectra 7-36606
H₂SiD, Fourier transform IR spectra, rovibr. anal. 7-25516
H₂SiF, Coriolis coupling, FT IR spectrum, rovibr. anal. 7-5679
H₂SnBr, rovibr. anal., harmonic force field calc., Fourier transform IR spectra study 7-50122
H₃¹¹⁶Sn⁷⁹Br, FT IR spectra, rovibr. investig. 7-921
H₃SnCl, rovibr. anal., harmonic force field calc., Fourier transform IR spectra study 7-50122
H₃¹¹⁶Sn³⁵Cl, FT IR spectra, rovibr. investig. 7-921
H₃SnI, rovibr. anal., harmonic force field calc., Fourier transform IR spectra study 7-50122
H₃¹¹⁶SnI, FT IR spectra, rovibr. investig. 7-921
HgCdTe and HgTe-CdTe superlattices, IR photolum. by Fourier transform spectroscopy 7-46134
KCl_{1-x}Br_x mixed powder crystals, long wavelength optical phonons; 7-12220
K_{1-x}Rb_xI mixed crystals, FIR props., optical phonons 7-46011
KTaO₃, Fourier transformed EXAFS spectra, comparison with NaTaO₃ 7-64749
Kr, Fourier transform EXAFS spectra; nonstructural low-R peak 7-64744
⁶Li, 2 Σ_g^+ state, isotope effect, Fourier transform spectroscopy 7-5660
 γ -methacryloxypropyltrimethoxysilane, chem. reaction on PbO surface, Fourier transform IR spectra 7-53308
N₂, chemisorpt. on (110) surface, FT IR refl-absorpt. spectrosc. obs. 7-27100

Fourier transform spectroscopy continued

N₂ glow discharge, pulsed, time-resolved Fourier transform spectra of IR emission 7-51538
N₂ solid films, Fourier transform IR spectra 7-59214
N₂-methane gaseous mixture, collision-induced absorpt., IR and microwave Fourier transform spectra anal. 7-50097
NF, b'² Σ^+ -X² Σ^- system, line assignments, transition moments, visible Fourier-transform spectra anal. (French) 7-50153
NH, A³ Π -X³ Σ^- transition, Fourier transform spectroscopy, vibr. levels, fine struct., rot. consts. 7-50080
NH, Fourier transform spectroscopy of c¹ Π -a¹ Δ transition 7-5786
NH radical, rot.-vibr. anal. for X² Σ^- state, IR Fourier transform spectra 7-19847
(NH₄)₂NaFeF₆, low-temperature phase transitions characterisation by Fourier transform IR spectroscopy 7-52046
NaTaO₃, Fourier transformed EXAFS spectra, comparison with KTaO₃ 7-64749
NeH⁺, vibr.-rot. spectra obs. using FTIR 7-50139
O₂ solid films, Fourier transform IR spectra 7-59214
OF₂, ν_2 fundamental, rovibr. study, Fourier transform IR spectra anal. 7-50123
OH, adsorbed on SiO₂, FTIR characteris. 7-46042
OH radical study of Sun at National Solar Observatory 7-55482
S₂, b'² Σ^+ -X² Σ_g^- system consts., IR and microwave spectra anal. 7-19848
SF₆ clusters, supersonic jet, Fourier transform IR spectra 7-15598
SO₂ adsorbed on SiO₂/Na, FTIR and Raman spectra obs., Na promotion of Claus process 7-46869
SO₂-HCN (SO₂-DCN) dimers., anti-H-bonded, rot. spectrum, mol. geometry 7-36592
Si:C,O wafers, C and O contents., Fourier transform IR spectra studies, book contrib. 7-44596
Si:H, impurity effects on IR absorpt. bands of Si-H centres, irradi. and unirrad. crysts. 7-53379
Si:H, polycrystalline, chemistry of grain boundary passivation 7-12375
a-Si:H films, light-induced bond breaking 7-12517
Si-electrolyte interface, Fourier transform IR spectroscopy 7-27124
Si₂, IR emission band spectrum 7-57062
a-SiGe:D, F, vibr. modes, Fourier transform IR spectra studies 7-46053
SiO₂, with adsorbed OH, FTIR characteris. 7-46042
SiO₂/Na with adsorbed SO₂ and H₂S, FTIR and Raman spectra obs., Na promotion of Claus process 7-46869
TiN compound layer prepared by ion implantation, XPS and FTIR obs., depth profile analysis of ion etched samples 7-59373
Va, singly ionised, lifetimes and oscillator strengths meas., fluoresc. and Fourier-transform spectra anal. 7-30986
WF₆+Si_n (n=2 to 6), Fourier transform ion cyclotron reson. mass spectrometry 7-31200
Zr, Fourier transform EXAFS spectra, nonstructural low-R peak 7-64744

Fourier transforms

see also fast Fourier transforms; Fourier analysis; Fourier transform optics
acoustic complex wave fields propagation, reconstruction using Hilbert-Hankel transform 7-43514
acoustical reflection coefficients determ. for dispersive systems, cepstral methods 7-43543
Axiom A dynamical systems, resonance location, simple model 7-29893
band structure occupancy determ. using Fourier-transformed Compton profile 7-21801
Boltzmann equation, transport coeffs. (Korean) 7-24605
convective equation, weak nonlinear instability of Euler explicit scheme 7-57832
cross sectional images, ultrasonic 7-43609
detecting system response function determ. 7-62240
diffraction tomography and maximum entropy Fourier synthesis 7-65884
diffraction tomography reconstruction, max. entropy method 7-47256
finite function spatial spectrum in 2D case, relation of components 7-50503
granular films, kinematic diffraction, numerical simulation 7-64025
Landsat data, Fourier filtering for information extraction in surveying and mapping 7-47582
Lau interferometry and diffraction correlation (Chinese) 7-57247
medical Fourier transform NMR imaging, 2D, respiratory effects 7-14098
MFFT package for 2D and 3D vectorised discrete Fourier transforms 7-41060
musical transitions between notes, discrete short-time Fourier analysis 7-62927
noisy inverse scattering problem, Fourier transform and Born approx. 7-35306
Pascal-Sierpinski gaskets, spatial Fourier transforms 7-14756
polystyrene films, craze microstruct., low angle electron diff., Fourier transforms of TEM images 7-13560
polystyrene solutions, slit-length-smeared SAXS curves evaluation using indirect Fourier transformation routines 7-51571
positron lifetime spectra anal., Fourier transform method 7-39282
propagators for quantum systems with electromagnetic fields, constructive representations 7-48420
radiative transfer in plane-parallel medium with space-depend. albedo, Fourier transform soln. 7-34850
series-termination and break-off waves anal. 7-61031
solar insulation data analysis by means of Allan variance and Fourier transform 7-60371
solar irradiation simulation using Markov processes and Fourier analysis 7-8433
telluric anomalies analysis in lower half-space, Fourier transforms method 7-28826
textural feature extraction procedure for remote sensing 7-9207
thermoelasticity, spectral theorems via eigenfunction expansions 7-26149
time-variable signals, computer averaging by autocorrelation 7-18768
waveform complexity, Fourier transform formulated, theory and expt. 7-37266
X-ray photoelectron spectra, Ka₂ satellite subtraction, Fourier transform formalism 7-27869
Al cylindrical tank, water-filled, damping characteristic determ. from vibration meas. 7-16200
Cu-Ni-Fe, alloy decomposition and periodic struct. coarsening 7-53735
H₂, ortho-para conversion, non-dissociative, on mag. surfaces, theory review 7-17781

Fourier transforms continued

- MgO, directional Compton profiles and autocorrelation function 7-3103
- Ni (001), adsorbed Na, photoelectron diffraction spectrum calc. and Fourier transform anal. (*Chinese*) 7-13326
- Ni (011), adsorbed S, struct., angle-resolved-photoemission extended fine struct. studies 7-63950

fractals

- 1/f spectra in nonlinear dynamics, noise-induced trapping at attractor boundaries 7-48557
- aerosol particles with fractal structure, effect of coagulation on diffusive spread 7-18728
- Aerosol-OT, stabilised microemulsion, X-ray scatt. data, fractal anal. 7-54190
- aggregates, fractal props., statistical methods conf., Oaxtepec, Mexico, Jan. 1986 7-24268
- aggregates, imaging, in-line holograms, digital decoding 7-10884
- aggregation phenomena and fractal aggregates (*French*) 7-9757
- alloys, icosahedral and amorphous structures, fractal coefficients 7-26646
- angiographic images, anal. and interpolation by use of fractals 7-34271
- anisotropic and isotropic fluids, single-particle trajectories and isojets, fractal behaviour 7-26608
- anomalous diffusion on fractal, first passage time problem 7-277
- area-preserving maps, fat-fractal scaling exponent 7-56160
- atoms, adsorbed on fractal surface, crit. temps., van der Waals eqn. calcs. 7-2352
- Aubry model, 1D, for any irrational number, fractal splitting props. 7-38429
- basin boundary constructed by superposition of Weierstrass function 7-4658
- batteries, discharge capacity dependence on electrode fractality 7-3631
- bounds for the fractal dimension of space 7-35257
- bovine serum albumin-lithium dodecyl sulphate complexes, struct. and fractal dimension 7-40093
- branched polymers, asymptotic props. on a fractal lattice 7-48595
- brinkman equation, fractal model for porous media, and viscosity renormalization 7-44042
- catalyst surface, fractal clustering of reactants 7-3605
- Cayley trees, randomly closed, and fractal dimensionality 7-4784
- chaos, ergodic theory 7-62657
- chaotic dynamic system, temporal intermittency as multifractality in history space 7-24549
- chaotic repellers as eigenvalues, charact. exponents 7-41250
- chemical dissolution, assoc. fractal patterns 7-44061
- chiral fermion propagation on 2D fractal structs. 7-48981
- circle mappings, renormalisation group methods 7-56168
- classical fluids, particle trajectories, fractal anal. 7-37828
- cluster form. by aq. nanodroplets in apolar media, dielec. 7-39921
- cluster-cluster aggregation, intrinsic anisotropy of clusters 7-18694
- coherent tunnelling, squeezing, chaotic behaviour and fractal dimension in a bistable potential 7-35410
- coherent tunnelling propagator and chaotic bistability 7-35315
- complex Sierpinski carpets, phase transform. 7-61303
- computer-generated uniform disk close packing round rhomboidal seeds, orientational order 7-61271
- conservative dynamical systems, apparent fractal dimensions 7-24555
- cosmic strings, fractal geometry and galaxy and cluster correlation functions 7-56115
- crystals, fractal nature of slip 7-16561
- deterministic fractal defect structs., hard disk close packings round rhomboidal seeds 7-2033
- Devil's staircase 7-48574
- 4,4'-dibromobenzophenone-1,4-dibromonaphthalene in polymer films, phosphoresc. study 7-59244
- diffusion, combinatorial algebra 7-269
- diffusion noise of fractal networks and percolation clusters 7-35415
- diffusion on loopless fractals, mapping to hopping on hierarchical structures 7-24574
- diffusion-limited aggregation, anomalous diffusion for regular and random models 7-239
- diffusion-limited aggregation, generalization and fractal dimensions 7-247
- diffusion-limited aggregation with tunable lattice anisotropy 7-245
- dimensional reduction via dimensional shadowing 7-35752
- disordered chains, fractal behaviour, 2D stochastic maps 7-41268
- distribution and entropy of clusters in growth models 7-29915
- dynamical growth systems, fractal patterns, flow in porous media appl. 7-37540
- dynamical system, fractal dimension universality at period-doubling chaos onset 7-48570
- dynamical system, time ordering and thermodynamics of fractal invariant measure 7-4790
- Eden trees on square lattice, deterministic fractal model 7-14885
- Eden trees on the Sierpinski gasket 7-14886
- electrodeposition, dendritic and fractal structures, diffusion and current fields 7-45102
- electron spin-lattice relaxation in fractal structures 7-45802
- fat fractals in quantum chaos 7-4713
- Feigenbaum attractor, fractal dimension, calc., comments 7-35413
- Feigenbaum attractors for a class of 1D maps, fractal dimension 7-217
- gelation, 3D kinetic model, critical behaviour 7-14904
- generalised random walks in 1D, fractal props. 7-9785
- generalized diffusion limited aggregation model, Monte Carlo simulations 7-244
- generating function and its formal derivatives for dynamical systems 7-18705
- growth oscillations; deterministic models 7-48571
- growth probability and harmonic measure, fractal struct., scaling props. 7-61268
- Hausdorff dimension as intrinsic metric prop. of fractals 7-24566
- ID random field Ising model, characteristic fractal dimension calc. 7-45719
- immiscible viscous fluids, fingering in Hele-Shaw cells 7-43854
- incommensurate systems, fractal spectra, Aubry model energy spectrum 7-12581
- incompressible fluid flow, viscous, fractal dimension of attractors 7-9677
- infinite cluster at percolation threshold, Monte Carlo renormalisation approach to fractal dimensions 7-35439
- ion beam damage in solids, fractal concepts 7-58380
- ion-implanted polymers, fractal elec. cond., current transients, percolative transition calcs. 7-2645
- Ising model, critical exponents in non-integer dimensions 7-56172

fractals continued

- Ising model, fractal clusters, scaling, distrib. fn. 7-35462
- Ising model, random-field, formation of domains 7-45602
- Ising model Glauber spin dynamics on fractal lattices, numerical simulation 7-64472
- Ising spin dynamics on 2 D fractal lattice, Monte Carlo study 7-2874
- iterated mappings, one-dimensional, chaos and fractal dimension of strange repellers 7-9775
- Josephson junction in microwave field, devil's staircase fractal dimension and decay constants 7-38821
- kinetic gelation clusters in 3D anomalous diffusion, random walks 7-61279
- lattice gas of diffusing interacting particles in concentration gradient, Monte Carlo simulation 7-48596
- light quasilastic-scattering linewidths and relaxation times for surface and mass fractals 7-1030
- linear polymers, collapse transition on fractal lattices, interacting self-avoiding walk model 7-48603
- low field Hall effect, self-dual fractal models near percolation threshold 7-12699
- metal-electrolyte rough interface, AC response, inverse-Cantor-bar model anal. 7-22012
- metal-insulator transition, 2D continuum percolation clusters, fractal prop. 7-18716
- metric space-time as renormalisation group eqn. fixed point on fractal structs. 7-48505
- microstructure, systematic description 7-22633
- model particle packings having multiple generations of agglomerates, fractal dimensions 7-39451
- multi-dimensional intertwined basin boundaries and kicked double rotor 7-29902
- multifractality in diffusion-limited aggregation model, exptl. evidence 7-41264
- multiparticle diffusion, fractal kinetics 7-24604
- needle crystal formation in two dimensions 7-38421
- nematic liquid crystals, transitions of viscous fingering patterns 7-12273
- NGC 5506, Seyfert galaxy, fractal anal. of X-ray time variability and spectral invariance 7-66764
- nonlinear dynamical systems, fat fractals and scaling exponents 7-24559
- nonlinear resistor networks, resistance noise 7-56162
- one-dimensional random field Ising model, characteristic fractal dimension calc. 7-18724
- Pacific Ocean, chaotic behaviour in large and mesoscale motions of Kuroshio current 7-55073
- particle shape and size determination, concurrent spatial harmonic and fractal analysis 7-31263
- Pascal-Sierpinski gaskets, spatial Fourier transforms 7-14756
- Penrose chain, 1d, vibr. spectrum and spectral dimension. 7-32582
- percolation at surface, fractal dimension 7-14867
- percolation clusters, two-dimensional, fractal dimension of hull, Monte Carlo calcs. 7-241
- periodic nonlinear media, nonperturbative bistability 7-20320
- phase separation on regular and fractal lattices in two dimensions 7-14887
- phase transitions on fractal lattices with long-range interactions 7-29928
- polypyrrole, diffusion-controlled polymerisation, growth instability 7-28311
- porous medium, chemical dissolution by reactive fluid 7-44062
- porous medium, fractal networks, anomalous diffusion, NMR field gradient expt., spin-echo amplitude 7-27627
- porous medium with fractal struct., nucl. mag. relax. 7-27625
- position space renormalisation group approach to fractal dimens. at percolation threshold 7-48605
- Potts model, antiferromagnetic, critical phases on fractals 7-24583
- Potts model on Sierpinski carpets, Migdal-Kadanoff bond-moving renormalisation anal. 7-24588
- proteins, fractons and fractal dimension self-avoiding walk model 7-48590
- pyrrole polymerisation, diffusion-controlled statics and dynamics, fractal and dendritic growth in electrochem. cell 7-59758
- quantum fluctuations and the Lorenz equations 7-9696
- quasicrystalline chain, vibr. and electronic spectral props., perturbative approach 7-45116
- quasicrystals, 1D tight-binding model, critical wave functions and Cantor-set spectrum 7-64189
- quasiperiodic Schrodinger equation, global scaling props. of spectrum 7-283
- random fractals, Debye-Huckel theory 7-212
- random fractals, measure theory 7-9766
- random fractals 7-9767
- random resistor fractal networks, infinite set of exponents 7-236
- random systems, d-dimensional, fracton scatt. and Ioffe-Regel criterion 7-44727
- random walker on fractal lattice, superuniversality of acceleration corrs. 7-61258
- reaction-limited cluster aggregation kinetics, Smoluchowski eqns. modeling 7-41261
- regular-random fractal model for cluster numbers and structure in percolation 7-35427
- repellers, chaotic, smooth stationary distrib. 7-225
- Riemann hypothesis, fractal random walk approach 7-14896
- San Andreas fault, California, United States, fractal geometry and seismicity 7-66030
- San Andreas fault, United States, fault geometry, appl. of fractal anal. 7-66348
- scaling indices and routes to chaos 7-48624
- scaling properties for the surfaces of fractal and nonfractal objects: an infinite hierarchy of critical exponents 7-18715
- self-affine clusters and generalised Cantor bars generation, spatial convolution techniques 7-9796
- self-avoiding walks on a crumpled fractal 7-41260
- shape analysis, fractal dimensions of topographic surfaces, 7-54845
- Sierpinski carpet, random walk problem, spectral dimensionality and hyperscaling 7-18720
- Sierpinski gasket, duality construction 7-48606
- Sierpinski gasket, hierarchy of current cumulants 7-52551
- Sierpinski gasket, self-similarity and Hilbert curve self affinity 7-24570
- Sierpinski gasket, two-dimensional with anisotropic interactions, density of states calcs. 7-242
- Sierpinski gasket fractals, hierarchical model relaxation, diffusion generalisation 7-9784

fractals continued

- silica, colloidal, gelation 7-46877
- silica aerogels, photon-fracton crossover, Brillouin scatt. meas. 7-46878
- silica gel, fractal vibr. modes; low freq. Raman scatt. 7-26890
- sine map and driven damped pendulum cross-over 7-18593
- singularities on a measure, singularity meas. on a fractal 7-35467
- solar granulation, fractal dimension anal. rel to granules critical scale 7-66550
- solid fractal surfaces, diffusion, relation to observable diffusion 7-61280
- solid state electrolyte, δ -transfer and diffusion (French) 7-17801
- solids, optical spectra dimensionality, fractional calculus anal. 7-45958
- solids, prebreakdown and dielec. breakdown, fractal model anal. 7-2973
- solute transport in aquifers, dispersion in fractal fracture networks 7-23772
- spin glasses, critical fractal cluster model, relax. behaviour 7-45692
- spreading phenomena in which growth sites have a distribution of lifetimes 7-35438
- square lattice, truly kinetic random walks, multifractal nature 7-56161
- statistical physics and field theory conf., Groningen, Netherlands, Aug. 1985 7-55899
- steady-state chemical kinetics on fractals, segregation of reactants 7-41295
- strong resonances of periodic patterns 7-61230
- surface, periodic, scalar scattering, effect of modeling errors 7-41162
- turbulence, fractals 7-51070
- universality in phase transitions on inhomogeneous structs. 7-41279
- viscous fingers and diffusion limited aggregates near percolation 7-16252
- Vycor leached porous glass, fractal struct., SANS, SAXS, and energy transfer meas., comment and reply 7-44398
- Yang-Lee edge singularity on fractals 7-18722
- AgI-Ag₂O-B₂O₃ glasses, superionic, crossover freq. between phonon and fracton regimes, scaling behaviour 7-44728
- Ag₂S, fractal dimensionalities of ionic trails and isojets in superionic conductors 7-6869
- Ag₂S, superionic conductor, single-particle trajectories and isojets, fractal behaviour 7-26608
- Al(OH)₃, aggregate fractal structs., X-ray scatt. functions 7-32381
- Au film, optical props. 7-17296
- Au, small metallic particles, surface fractal dimension 7-38308
- Cu metal leaves, electrodeposited, Hausdorff dimension or fractal nature 7-12523
- Fe aggregated particles fractal dimension meas. by electron microscopy 7-26598
- n-GaAs, oscillations and chaotic current fluctuations 7-64253
- ⁴He, superfluid, fractal surface, third sound, capillary condensation 7-27041
- In-Ge thin films, anomalous structures 7-21733
- NH₄Cl, irregular fractal-like crystal growth, diffusion-limited aggregation model 7-2445
- Na-colloid in NaCl, low freq. surface enhanced Raman scatt. from NaCl-Na interface localized fractal vibrational modes 7-59195
- Pd, small metallic particles, surface fractal dimension 7-38308
- Pt, small metallic particles, surface fractal dimension 7-38308
- SiO₂ aggregates, fractal props., light scatt. studies 7-28358
- SiO₂ colloidal fractal aggregates, hydrodynamic behaviour 7-59797
- SiO₂, porous silicas, direct energy transfer in restricted geometries as probe of pore morphology 7-59251
- YIG, charact. of chaotic states of parallel-pumped magnons 7-52961

fractional programming see nonlinear programming

fractionation see distillation

fractography

- fatigue crack length and closure/opening stress, automated estimation 7-43811
- PEEK, fracture toughness, temp. and strain-rate effects 7-39660
- PEEK glass fibre reinforced plastics, fracture toughness, temp. and strain-rate effects 7-39660
- SEM crack distributions on plane sections, correction of window size distortion 7-59711
- steel, fatigue fracture surface at elevated temps., X-ray fractographic study (Japanese) 7-8098
- steel, low alloy, fatigue fracture in air and 3.5% NaCl soln., X-ray fractography (Japanese) 7-8099
- steel fibre reinforced Cu composites, extruded, struct. and fractography 7-13595
- C fibre reinforced epoxy resin composites, fractography 7-8080
- Fe, cast, pearlitic, nodular, fractographic anal. 7-53882
- Mo fibre reinforced Cu or Fe composites, extruded, struct. and fractography 7-13595
- Ni, intergranular cavitation in high temp. creep, fractographic techniques appl. 7-53804
- SiC particle reinforced Al-Cu-Mg composite, failure mechanism, SEM obs. 7-65132
- Ti-Al-V (6.4 wt.%), annealed fatigue crack growth in water, SEM fractography (Chinese) 7-8076

fracture

- see also brittle fracture; crack-edge stress field analysis; cracks; creep fracture; ductile-brittle transition; ductile fracture; embrittlement; fatigue; fracture mechanics; fracture toughness; stress corrosion cracking alloys, superplastic, necking, fracture, strain rate sensitivity, cavity growth 7-28087
- alumina polycrystalline ceramics, shock fracture and recompaction, double impact technique study 7-33880
- barium oxalate dihydrate single crystals, Vickers microhardness meas. 7-63736
- bone, fracture healing, assessment by spectral anal. 7-8730
- brittle materials, containing spherical voids, tensile fracture loci 7-12200
- BWR piping research in Italy, IGSCC tests, fracture and cracks 7-53890
- cast Fe, flake and nodular graphite, breaking behaviour of perforated notched specimens 7-17606
- cavitation and residual creep life 7-50962
- cellulose fibre reinforced polyester, prep., and props. 7-3265
- cement-based composite, strain rate effects on fracture, conf., Boston, USA (Dec. 1985) 7-14712
- ceramics, microfracture prediction via microcontact model 7-16678
- ceramics and coated carbides for matching stainless steels, failure mechanisms 7-3432
- coatings, friction and adhesion meas. using microtribometer 7-46742
- compact tension specimen, J-integral functions for fracture and fatigue anal. 7-63055

fracture continued

- composite, failure criteria, tensor-polynomial type, exptl. verification of efficiency 7-22812
- composite shell, conical, stability calc. with allowance for cracking of binder in layers 7-16084
- composites, response in adverse environment, reliable modelling, implication of 7-65169
- concrete, microplane model for progressive fracture, microcracking 7-15248
- conference on the safety and reliability of reactor pressure components, Stuttgart, Germany, (Oct. 1985) 7-9583
- crack initiation sites, determ. using digital NDE workstation 7-65277
- crystalline minerals, fracture characteristics using ²²²Rn and ²²⁰Rn as probes 7-23893
- crystalline solid bodies, conditions of elastic equilb. of submicrocracks (Russian) 7-58407
- curved water pipe, freezing pipe 7-26347
- damage cumulation, self-similarity for different loading conditions 7-20658
- dimethacrylate paste with silanated silicate particles, photopolymerised, filler influence on fracture 7-3426
- dynamic fracture studies by stress intensity factor tracer method 7-63081
- dynamically loaded pipes with circumferential flaws, behaviour under internal pressure and external loads 7-13577
- elastoplastic solids, dynamic deform. processes, computation with allowance for continual failure 7-43696
- fibre composites, orthogonally reinforced, fracture criteria 7-1494
- fibres, natural, fracture behaviour, empirical evaluation of struct.-prop. relationships 7-39633
- fractal structure in architectural features of fracture fields in rocks (French) 7-66100
- fractographic features caused by impact load and microstruct. effect of impact vel. (Japanese) 7-51929
- friction and wear, crit. transition points 7-26853
- fused quartz particulate composite, fracture behaviour (Chinese) 7-8079
- glass, crack propagation, effect of inhomogeneities (Japanese) 7-22823
- glass, helicopter windshield, chemically tempered impact fracture 7-28108
- glass, number of cracks at fracture rel. to ultimate stress 7-22809
- glass and C fibre reinforced epoxy laminates, cross-ply cracking 7-39617
- glass ceramic, failure kinetics using composite glass-crystal system model 7-59631
- glass fibre reinforced epoxide resin, tensile props. under superposed hydrostatic press., failure mechanisms 7-28078
- glass fibre reinforced epoxy and polyester composites, flexural failure mechanisms, global stress plane 7-8082
- glass fibre reinforced polyester, aligned, AE stress corrosion cracks 7-59722
- grain boundary segregation, free energy considerations and fracture 7-38110
- graphite, fracture criterion, acoustic emission studies (Japanese) 7-8088
- graphite, polygranular, failure models assessment 7-46596
- graphite fibre reinforced Al-Mg-Fe, unidirectional and angle-ply, strength and fracture anal. 7-59605
- graphite fibre reinforced epoxy laminates, dynamic response at high shear strain rates 7-3371
- graphite isotropic, fine grained, oxidation effect on crack extension rate (Japanese) 7-56754
- inclined crack under biaxial load, fracture stress 7-57747
- internal damage in struct. solid, stochastic approach 7-37965
- ivory, tensile props. and fracture rel. to comp. and struct. 7-14032
- joints of dissimilar metals, adhesively bonded strength evaluation 7-46791
- Li₂ ordered alloys, grain boundary strength and fracture, electronic and struct. studies 7-33756
- life fraction rule, modified, determ. of times-to-rupture under changing loading conditions 7-26847
- lignocellulosic fibres, phys. and mech. props. 7-53883
- line spring model, equivalent relation 7-57746
- liquid, impulsive failure, energy threshold 7-32539
- long-spindle insulator damage by shotgun (Japanese) 7-22787
- marble, development of conjugate-shear fracture (Chinese) 7-34474
- material fracture energy, eval. from heat content 7-52019
- mechanoluminescence studies of crystal structure 7-59268
- metal superlattices, elastic and plastic props. 7-27085
- metal-H system, internal grain-boundary crack opening by H (Russian) 7-33764
- metallic superlattices, mech. props. and diffusion 7-52377
- metals, deuteron irradiation, multiple fracture planes, bubble growth 7-58372
- metals, polycryst., expt. simulation of intercryst. sliding and fracture 7-2095
- metals, strength, durability and fracture, time depend. in microsecond range 7-46597
- metals and alloys, environmentally assisted cracking at high vel. 7-65213
- Mo-Ni, activated sintered, sintering behaviour and mech. props. 7-7929
- monolithic fuel cell tapes, three-layer ceramic composite, stress and fracture analysis 7-3407
- mother-of-pearl, fracture surfaces, analytical techniques appl. 7-8781
- mullite, Al₂O₃ and ZrO₂ particle reinforced, prep. by reaction sintering, fractographic study 7-22800
- necking development under uniaxial tensile deform., strain hardening, geometric defects, elongation to failure 7-33742
- nonequilibrium statistical theory of fatigue fracture, fatigue crack growth 7-39665
- optical fibres, strength meas. by bending 7-43384
- optical silicate glass melt, fracture in laser beam 7-43278
- orthotropic materials, fracture propag., finite element modelling 7-57751
- path-independent integrals in fracture dynamics using auxiliary fields 7-1495
- petrographic parameters quantification, appl. of digital image processing (Spanish) 7-34740
- plastics, yield condition under biaxial stress fields, prediction (Japanese) 7-46563
- plates, deformation and fracture under thermal shock 7-43763
- plates and cylinders, surface-cracked, J-integral and HRR dominance under large-scale yielding 7-63080
- PMMA, environmental fatigue, initiation of wavy striation (Japanese) 7-33814
- PMMA, environmental stress cracking in methanol, mol. props. effects 7-65153

fracture continued

- PMMA, failure at high loading rates, correlation of relaxation and energy characteristics 7-46598
 PMMA based materials, craze resist., struct., water absorpt. 7-59602
 poly(p-phenylene terephthalamide) fibres mech. props., stochastic model 7-39661
 poly(p-phenylene benzobisthiazole-epoxy composite, adhesive behaviour 7-65278
 1,2-polybutadiene-natural rubber blends, tear failure, blend ratio, cross-linking, HAF black content 7-65126
 polycarbonate, failure at high loading rates, correlation of relaxation and energy characteristics 7-46598
 polycarbonate, fracture, effect of rolling orientation on ductile-brittle transition 7-46644
 polycarbonate-polyarylatarylene sulfonoxide block copolymer blends, crit. stress determ., nick self-dulling model (*Russian*) 7-44681
 polychloroprene, tear strength, crosslinking, viscoelastic loss mechanisms 7-39632
 polyester, clay-filled, tensile behaviour 7-3382
 polyethylene, charged particle exoemission rel. to deform. and fracture 7-7827
 polyethylene, extended under press., hydrostatic press. effect on damage accumulation, struct. reorganisation 7-8065
 polyethylene-polyacrylic acid copolymer, radiation grafted, struct.-morphology, obs. (*Russian*) 7-16452
 polymeric dielectric, in partial discharge, depression rel. to elec. ageing (*Russian*) 7-26577
 polyphosphazene, tear strength, crosslinking, viscoelastic loss mechanisms 7-39632
 polypropylene, mica-reinforced, fracture behaviour, effect of coupling agent, flake orientation and degradation 7-13593
 polystyrene, monodisperse, fracture, chain scission, mol. wt., temp. depend. 7-33776
 porous-brittle solids, micromechanical model 7-26849
 post-yield fracture, 3D finite element simulation 7-26216
 PVC, impact fracture regularities, matrix morphological struct. effects (*Russian*) 7-16677
 radioactive waste repository, heat induced fracturing of rock in an existing uniaxial stress field 7-5484
 revolving bodies, dynamic contact with rigid wall, deform. and fracture investig. 7-31663
 rock mass, 2D continuity, stochastic evaluation 7-55019
 rock salt form Gulf Coast domes, uniaxial and triaxial mechanical expts. 7-47428
 rocks, EM emission and light radiation (*Chinese*) 7-29000
 rocks, fracture anal. 7-66106
 rocks, single fracture characts. and gas flow 7-23641
 SCARE postprocessor program to MSC/NASTRAN, ceramic components reliability anal. 7-17750
 shock wave fracture, interferometric investig. 7-44683
 shock waves in condensed matter, conference, Spokane, WA, USA (July 1985) 7-18501
 shock-induced solid-solid phase transformations, nonequilib. mol. dynamics calcs. 7-17646
 silk fibre filled thermoplastic elastomer, tensile rupture 7-39635
 solid materials, bonding, external electrostatic field effects 7-26693
 steel, alloy, H-induced delayed fracture under mode II loading (*Chinese*) 7-65119
 steel, austenitic, Mn-Cr, fatigue crack growth behaviour 7-59593
 steel, austenitic stainless, grain boundary microstruct., He embrittlement resistance 7-56829
 steel, austenitic stainless, single cryst., SCC and pot. depend. in $MgCl_2$ soln. (*Japanese*) 7-33831
 steel, austenitic stainless, tensile and impact props., effect of grain boundary carbides 7-33785
 steel, carbon, thin walled square pipes subjected to compressive load, local buckling strength 7-17578
 steel, carbon and stainless, pipe fracture safety analysis using limit load and J-integral techniques 7-13585
 steel, cast, nonmetallic inclusions influence on fracture character 7-3421
 steel, Cr-Mo, mech. stability of retained austenite, absence of H influence 7-28125
 steel, ferrite-pearlite, viscous-brittle transition model (*Russian*) 7-3401
 steel, ferrite-pearlite and pearlite-free, microfracture resistance (*Russian*) 7-33765
 steel, ferritic, fracture behaviour after warm prestressing, effects of subcrit. crack growth 7-46601
 steel, ferritic, yielding and fracture in transition region of quasistatic to dynamic loading 7-13581
 steel, high strength, defect enhanced diffusion process and hydrogen delayed fracture 7-39673
 steel, low alloy, damaged surface, comp., displacement dislocations, Auger spectra (*Russian*) 7-59620
 steel, low alloy, oxides on fracture surfaces, failure anal. examination 7-13586
 steel, low alloy, pearlite free, fracture energy, effect of microstruct. parameters (*Russian*) 7-33787
 steel, martensitic, intergranular crack nucleation, fractographic and acoustic emission meas. (*Russian*) 7-33766
 steel, mech. props. and failure character after repeated thermomech. strengthening of surface layer 7-53994
 steel, mild, crit. stress intensity factor, influences of grain size and precracking load 7-59607
 steel, Mn, influence of S on failure mechanism in dual α/γ phase (*French*) 7-33760
 steel, Mn-Mo-V, reactor piping material, strength, deformation and fracture behaviour 7-13578
 steel, Ni-Co-Mo, managing, ultrahigh strength, delayed fracture in H environment 7-28135
 steel, Ni-Co-Mo, maraging, lath martensite boundary cracking near threshold stress intensity factor (*Japanese*) 7-53846
 steel, Ni-Cr, deform. dislocation struct., fracture 7-33740
 steel, Ni-Cr-Mo, H embrittlement in artificial seawater, effect of H content (*Japanese*) 7-53868
 steel, Ni-Mo, LWR pressure vessel cladding, irradiation effects and flaw structs. 7-53888
 steel, stainless, clad fuel rod, failure behaviour 7-61965
 steel, stainless, duplex, austenitic-ferritic, cavitation erosion 7-65149
 steel, stainless, heavy section, fracture studies, welds, neutron irradiation, crack arrest 7-13587

fracture continued

- steel, stainless, pipe, subjected to bending deform., fracture instability, effect of multiple circumferential through-wall cracks 7-65122
 steel fibre reinforced Cu composites 7-13595
 steel sheet, disc-shaped lamination development under tension and hydrogen impregnation 7-17695
 stress-rupture strength, temp-time prediction 7-28133
 styrene-butadiene rubber, tear strength, crosslinking, viscoelastic loss mechanisms 7-39632
 surface fracture during He^+ ion bombardment 7-21294
 surfaces, semi-automated topographic mapping through stereophotogrammetry 7-13691
 symmetric and asymmetric fully plastic crack growth, macromech. anal. 7-51931
 TEM observation of in-situ fracture, influence of several parameters 7-6713
 tensile fractures, radiation patterns in glass plates and ice 7-60182
 thermal shock loadings in PTS accidents, J-integral concept appl. 7-13696
 tibial bone, bovine, fracture props. 7-34177
 tribochemistry, chemical reaction increase by friction 7-46868
 viscoplastic finite element analysis of rapid fracture 7-63061
 wollastonite reinforced polyamide 6, strength props., depend. on humidity and temp. 7-39636
 Zircaloy, claddings, creep deform., bulge growth, time to failure 7-59589
 Zircaloy-4, α -phase, burst data, CANSWEL-2 code anal. 7-36159
 Zircaloy-4 fuel sheaths, failure model, circumferential temp. effect 7-728
 Al based composite, rheocasting, microstruct., fracture, worn surface (*Chinese*) 7-13407
 Al, cracking behaviour during liquid Hg embrittlement 7-22816
 Al, fracture, size effect tests 7-59595
 Al, heterogeneous shock wave response, holographic interferometry studies 7-32571
 Al, plastic deformation under impact loading, metallography, SEM and TEM studies (*Russian*) 7-3361
 Al-base alloy, IN-9021, fatigue morphology 7-39653
 Al-base alloys, IN-9021, SCC fracture behaviour 7-39744
 Al-Cu-Li-Mn-Cd alloy, 2020, micromechanisms governing elevated temp. fracture resist. 7-22803
 Al-Cu-Mg, fracture behaviour, influence of fine transition-metal particles and grain struct. 7-3406
 Al-Li-Cu-(Mg), fracture, effect of subgrain struct. and ageing practice 7-13563
 Al-Mg-Zn system, fracture viscosity rel. to surplus phase morphology 7-46610
 Al-Zn-Mg-Cu, 7475, environment sensitive fracture using shadow optical method of caustics 7-39647
 Al-Zn-Mg-Cu, notched and unnotched bars, macroscopic shear localisation and fracture 7-46633
 Al_2O_3 fibre reinforced Al composites, compressive failure modes, dead weight or machine loading 7-39663
 Al_2O_3 , strengthening, mech. props. and microstruct. (*Japanese*) 7-22820
 β - Al_2O_3 - Na_2O , ZrO_2 toughened solid electrolyte, failure initiation, critical current density, AE obs. 7-38252
 $Al_2(TiO_3)_3$ ceramics, sintering, microstruct., bending strength, additives effect (*Japanese*) 7-17601
 B fibre reinforced Al, strength characts. 7-33768
 B fibre reinforced Al matrix composites, transverse mech. props., isothermal exposure effect 7-39688
 BN, graphite-like powder particles, shock compression effects 7-39453
 C fibre reinforced Al-Cu(Mg) composites, tensile strength, fracture, interfacial bond strength 7-33744
 C fibre reinforced C, multidirectional composites, macroporosity and interfacial cracks 7-46513
 C fibre reinforced epoxy, unidirectional, fracture strength, role of matrix resin 7-53845
 C fibre reinforced epoxy laminates, matrix splitting, K_I - K_{II} interaction (*German*) 7-22829
 C fibre reinforced epoxy resin composites, fractography 7-8080
 C fibre reinforced polymer cracks, lightweight construction appl. (*German*) 7-22825
 C fibres, B modified, effect on mech. props. 7-17570
 C fibres, Celion, mechanical and fracture behaviour 7-22786
 C, fractographic studies 7-17645
 C-sunhemp fibre reinforced polyester hybrid composite, tensile strength and fracture 7-13522
 Cu, dynamic elongation determ. expanding ring test, 2D hydro-plasto-dynamic code anal. 7-33755
 Cu-Co, dynamic fracture characts., void nucleation at incoherent precipitates 7-17628
 Cu-Zr (0.5 wt.%), high strength, high cond., prod. by rapid solidification technology 7-28029
 D+D reaction, detection of occurrence during shock fracture of D_2O ice 7-39874
 (Fe,Ni)₃V, LRO alloys, mech. props., effects of strain rate and long-term ageing 7-53796
 Fe, (001) oriented single crystals, hydrogen induced cracking and hydrogen embrittlement (*Japanese*) 7-33782
 Fe, BCC, effective fracture energy assoc. with cleavage crack growth 7-44678
 Fe, cast, pearlitic, nodular, fractographic anal. 7-53882
 Fe-Ni, creep in vacuum and air, relationships governing deform. and failure 7-28097
 Fe-P-C system, ferritic, grain boundary segregation of P and C 7-39530
 Fe₈₄B₁₆ amorphous alloy, interstitial element segregation during fracture (*Russian*) 7-53875
 FeCrNiW amorphous alloys SCC behaviour 7-39727
 Fe₄₀Ni₄₀B₂₀ metallic glass ribbon, failure mechanics and atom probe study correlations 7-28139
 FeNiCr, grain boundary solute segregation 7-56833
 LiF, fracture, mag. field effects 7-16675
 LiF plastic crystals, formation of cracks at cleavage fracture front 7-44674
 LiF, pore-grain boundary configs., fracture surface, SEM obs. 7-32458
 LiNbO₃, heterogeneous shock wave response, holographic interferometry studies 7-32571
 MgAl₂O₄He spinel, implanted, high temp. electron irradi., structural damage 7-51829
 Mo fibre reinforced Cu or Fe composites, extruded, struct. and fractography 7-13595

fracture continued

- Ni-Al-Cr, melt spun ribbons, microstruct., mech. props., Cr conc. effect 7-28031
 Ni-Cr, bonding to dental glass 7-39844
 Ni-Mo (20 at.%), ageing, yield strength rel. to prior α grain size 7-39507
 NiAl single crystal, surface oxide softening 7-39751
 Ni₃Al, polycrystalline, grain boundary fracture model 7-53896
 Ni₇₅Si₁₀B₁₂, metallic glass, shear crack propag. 7-65113
 Pb-Al-Mg-Sn-Li, strength and microstruct. 7-8047
 Pb-Li, strength and microstruct. 7-8047
 SiC fibre reinforced Al alloys, whisker or particulate hybrids, mech. props. 7-13537
 SiC particle reinforced Al-Cu-Mg composite, failure mechanism, SEM obs. 7-65132
 α -SiC, sintered, non-equilib. surface conditions and microstruct. changes following pulsed laser irradi. and ion beam mixing of Ni overlayers 7-65170
 SiC whisker reinforced Al, flame spraying fabrication and forging, whisker distrib. and strengths 7-59483
 SiC whiskers, tensile fracture rel. to defects 7-58722
 Si₃N₄, sintering, under rotary bending, mirrorlike region of fractured surface (Japanese) 7-3436
 Si₃N₄-Y₂O₃-Al₂O₃, pressureless sintering 7-17503
 Ta, dynamic elongation determ. expanding ring test, 2D hydro-plasto-dynamic code anal. 7-33755
 Ta-T system, distortion by He form. 7-51717
 Ti alloy, two-phase, microstruct. and failure nature correl. 7-8110
 Ti alloys, microstruct. and slip characters. 7-8050
 Ti, fracture, deform., porosity effect 7-22750
 Ti-Al-V, spall strength and fracture mechanism 7-46627
 Ti-Al-V (6.4 wt.%), fracture, deform., porosity effect 7-22750
 Ti-Al-Zr-Mo-Si, creep resistance, silicides obs., effect on mechanical props. and fracture 7-8051
 Ti-coated Be substrate, bond failure, thin film fracture 7-59600
 W base heavy metal alloys, mech.-props., porosity, impurity effects 7-17495
 W-Re alloys, mech. props., conc. depend. in different struct. conditions (Russian) 7-53876
 WC-Co, TiN-coated, residual stress and strength, X-ray diffr. study (Japanese) 7-8101
 W-Cu bond, mechanical properties, fusion reactor divertor plate appl. 7-26848
 Zn-Al-Cu, superplastic, cavitation damage 7-65080
 ZrO₂, MgO partially stabilised, SrO sintering aid addition, microstruct. and chem. aspects 7-64983
 ZrO₂, MgO partially stabilised ceramics, thermal treatment, mech. props., microstruct. 7-65067
 ZrO₂, Y₂O₃ stabilised, CeO₂ doped on surface, thermal stability improvement 7-13619
 (ZrO₂)_{0.9}(Y₂O₃)_{0.1} flintite crystals, bending and compressive strength temp. depend. meas. 7-44653

fracture mechanics

- 3D crack terminating at interface, stress intensity factors 7-11351
 adhesive debonding equation in fracture mechanics, derivation 7-20656
 bar, elliptical, with asymm. internal crack under anti-plane shear deform. 7-26208
 bars, tensile, void coalescence, plastic localisation, failure modes 7-6108
 biaxial loading effects in stress intensity factor calcs. 7-63074
 BIBLS-B reactor pressure vessel, fracture mech. anal. for thermal shock transients 7-10220
 brittle material, crack stability and toughness characts., book contrib. 7-26224
 brittle materials, contact flaws, strength, lateral crack growth effects 7-8091
 brittle-matrix, fibre-reinforced composites, matrix cracking mechanisms 7-65129
 BWR piping, fracture mech. research in Japan 7-53891
 ceramic-metal interfaces, grain boundaries, bonding and interfacial structure 7-26765
 ceramics, engineering performance prediction, fracture mechanics 7-3416
 cholesteric liquid crystals, freeze fracture 7-11906
 components under complex loading, stress anal. incorporating fracture mech. and materials aspects 7-13584
 composite, failure in compression, surface delamination along macrocrack 7-6155
 concrete, inelastic behaviour, damage mechanics constitutive theory, FEM model 7-53833
 concrete, structures, micro- and macroscale damage 7-43766
 concrete micromechanical damage model 7-53837
 conference on water reactor safety, Gaithersburg, MD, USA, (Oct. 1985) 7-48152
 CR-39 track detector, treeing during electrochemical etching, fracture mech. study 7-30877
 crack tip fields asymptotic small scale yielding solns. and double limits 7-26215
 crack under mode I loading, coherent-light-shadow spot, theory and expt. 7-63089
 cracked-lap shear specimen thickness for interlaminar fracture toughness determ., delamination vs. adherend failure 7-1510
 creep, damage localisation theory 7-50990
 creep crack growth parameters, finite element and exptl. investigs. comparison 7-39674
 critical element model, modelling philosophy 7-43767
 cumulative fatigue damage analysis re-examination 7-53836
 cylinder weakened by system of reduced strength layers under dynamic loading, behaviour 7-11345
 damage and fatigue, conf., Haifa, Israel (Jul. 1985) 7-48139
 damage cumulation, self-similarity for different loading conditions 7-20658
 defect and fracture mechanics, conf., Bad Honnef, Germany (Jan. 1985) 7-24260
 dynamic fragmentation, particle size distrib., random Poisson process calcs. 7-31708
 dynamic materials testing using fibre optic sensors 7-46778
 elastomers, sliding friction mechanics, asperities adhesion fracture 7-53922
 elastoplastic problem of antiplanar deform. of crack-containing body, discontinuous solns. 7-11343

fracture mechanics continued

- end-notch flexure specimen, mode II interlaminar fracture toughness, finite element anal. 7-1509
 engineering materials, general yield criterion depend. on void growth 7-1444
 epoxide resin composites, particulate filled, static fatigue, time to failure predictions 7-13562
 fatigue crack initiation under cyclic torsion 7-43799
 fibre optic sensors appl. in materials testing (German) 7-11162
 fibre reinforced composites, fracture, micromechanical and macromech. criterion 7-17609
 fibre reinforced polymeric composite, cracked orthotropic, long-time strength under constant tensile load 7-6156
 films, decohesion from ceramic or semiconductor substrates 7-21711
 glass, number of cracks at fracture rel. to ultimate stress 7-22809
 glassy polymers, fracture mechanisms, scaling analysis 7-46618
 granite, stick slip and shear fracture energy at elevated press. 7-47427
 graphite, polygranular, failure models assessment 7-46596
 HTGR, fracture criteria of reactor graphite under multi-axial stress (Japanese) 7-61946
 hydraulic fracturing mechanics, explicit approx. solns. 7-6158
 ice, freshwater, crack resist. determ. 7-12195
 inhomogeneous elastic body with circular crack, equil. problem 7-16127
 interface in uniform stress field, crack problem soln. 7-16125
 joints, adhesive, engineering failure envelope 7-33763
 laminates, centrally notched, residual strength determ. (Chinese) 7-13557
 laminates, strain energy release rate of edge delamination, residual thermal and moisture influences 7-1508
 linear elastic fracture mechanics, computerised R-functions method 7-63066
 linear elastic fracture mechanics, singular nine-noded distorted isoparametric elements 7-63054
 local approach of fracture, continuum damage mechanics 7-50988
 macrocrack growth kinetics in aging viscoelastic bodies under variable loads 7-63071
 material, creep rupture mechanics 7-53835
 material, mechanical behavior representation rel. to internal damage 7-53838
 metals, creep crack growth prediction by a local approach 7-53841
 micro-cracking induced by Rayleigh wave 7-43794
 mode III crack kinking with delay time, analytical approx. 7-26217
 moving defect with irreversible deformation zone and criterion of non-linear dynamic fracture of solids 7-26204
 nonlinear, path-independent integral, finite element approach 7-63068
 nonlinear 3D fracture dynamics, path-independent integrals 7-63069
 nonlinear coupled thermomechanical system crack propagation 7-63067
 notch tips, plane, stress singularity 7-26220
 NRC Degraded Piping Programme, LWR piping fracture research, Phase II progress 7-53889
 panels, tensile, elastic-plastic models of surface cracks 7-63077
 plastic asymmetric crack growth near single shear band 7-20654
 plastic rupture during compression along near-surface fractures 7-43795
 plate, infinite, of crack-weakened hereditary material, limiting equil. 7-31705
 plate, multilayer reinforced, with through crack, stress state and limiting equil. 7-11344
 plates, centre-cracked biaxially loaded, plastic plane stress solns. 7-43800
 PMMA layers, metal-polymer struct., degrad. during mech. fracture (Russian) 7-20660
 polycarbonate, J-integral as fracture criterion 7-39631
 polyimide adhered films, solvent induced crack-like defects 7-46653
 polymers, ductile fracture, essential work 7-53842
 polystyrene, slow crack propag., crazing and fracture, acoustic emission study 7-32555
 pre-rupture state, free vibration model 7-44668
 PWR coolant pump flywheel radial crack testing, caustic curve method 7-15266
 reactor piping systems, cycle-dependent material props. 7-10222
 reactor pressure vessels, fracture mechanics of cracks under cyclic thermal shock 7-10218
 rock cracking due to thermal stress, for granite, diabase, limestone 7-40466
 rocks, hydraulic fracturing, dynamics using finite difference theory 7-55041
 rubber toughened plastic, surface embrittlement, fracture mechanics 7-28161
 sapphire, crack propagation threshold, surface energy determ. 7-58401
 solids, brittle, in nonuniform strain field, fracture 7-43784
 square specimen, compressed, with longit. or diagonal crack, stress intensity factors calc. 7-16118
 steel, heavy section, Ni-Mo, elastodynamic fracture analysis of large crack-arrest experiments 7-53887
 steel, low C, small fatigue crack growth, effects of microstruct. and limitations of linear elastic fracture mechanics 7-39625
 steel, Ni-Cr-Mo-V for turbine disc, fracture mechanics anal. 7-13589
 steel, pressure vessel with surface fatigue cracks, leak-before-break failures analysis 7-65141
 steel, stainless, LWR piping systems, LBB feasibility eval., fracture criteria 7-61968
 steel LWR piping fracture mechanics database 7-53892
 steel sheet, disc-shaped lamination development under tension and hydrogen impregnation 7-17695
 strength size effects and fracture mechanics, phys. evidence 7-57756
 stress intensity factor field extent during crack growth under dynamic loading conditions 7-11350
 strip, infinite, with cracks and holes, singular integral eqn. soln. 7-26219
 structural elements, crit. stresses, theoretical-expt. determ. 7-31707
 surface crack, normal-separation, profile opening, comparison of calc. and expt. 7-20659
 surface crack, stress intensity factor variation and back surface displacement 7-57762
 surface crack growth in lubricated rolling/sliding spherical contact 7-11354
 surface crack profile measurement method and results 7-22939
 surface flaw, stress intensity distrib. and fatigue crack growth predictions 7-63075
 ultrasonic models for nondestructive evaluation techniques, design and validation 7-46775
 universal optimum quarter point element 7-16117
 wedge test for adhesive joints, mechanics 7-33872
 Weibull parameters estimation using weight function 7-22934

fracture mechanics continued

Weibull plots, modulus of rupture, probability estimators 7-39639
 Al_2O_3 fibres, strength distrib., multi-model Weibull distrib. 7-28081
 As_2Se_{100-x} , chalcogenide glass, Vickers microhardness indentation and fracture mechanics 7-21342
 SIC fibres, strength distrib., multi-model Weibull distrib. 7-28081

fracture strength *see fracture toughness***fracture strength testing** *see fracture toughness testing***fracture toughness**

see also notch brittleness; notch ductility; notch strength
 advanced instrumented impact testing facility for characterization of dynamic fracture behavior 7-13692
 $Al-Zn-Mg-Cu$, impact toughness improvement by intermediate thermomech. treatment 7-53907
 aramid fiber reinforced epoxy, delamination fracture toughness 7-53900
 B_2C , thermal stress fracture, grain size and porosity effects (Japanese) 7-8087
 biaxial loading effects in stress intensity factor calcs. 7-63074
 brittle material, crack stability and toughness characts., book contrib. 7-26224
 brittle materials, contact flaws, strength, lateral crack growth effects 7-8091
 brittle materials, fracture toughness, crack front irregularity effect 7-57740
 bronze BR4Zn, elec. discharge sintering of powder from swarf, electrophys. and mech. props., microstruct. 7-27974
 cement paste, low-porosity, subcrit. crack growth in alcohol media 7-59650
 cement-based composite, strain rate effects on fracture, conf., Boston, USA (Dec. 1985) 7-14712
 ceramic part, heat resistance under two-dimens. strain conditions 7-59630
 ceramics, fracture toughness evaluation using chevron-notched specimens (Japanese) 7-59613
 ceramics, structural, flaw size distrib. 7-22818
 ceramics, toughening by strong reinforcements, fracture toughness, microstruct. 7-22783
 ceramics, transformation toughening, shear, shape and orientation effects 7-39626
 clays, fracture permeability study for radioactive waste repositories 7-10293
 conference on the safety and reliability of reactor pressure components, Stuttgart, Germany, (Oct. 1985) 7-9583
 corundum-graphite refractories, thermomech. props. 7-22806
 crack arrest with externally bonded ligaments 7-26221
 cracked-lap shear specimen thickness for interlaminar fracture toughness determ., delamination vs. adhering failure 7-1510
 cutting tool materials, mech. props., wear-resist. relations 7-3443
 ductile fracture, plane stress, essential work of fracture vs. energy dissipation rate 7-20649
 duplex fibre reinforced materials, fracture toughness development 7-22804
 end-notch flexure specimen, mode II interlaminar fracture toughness, finite element anal. 7-1509
 epoxide resins, particulate filled, parameters determining strength and toughness 7-65071
 epoxy resin, aminimide-cured, mica reinforced, improved mech. props. 7-59489
 fatigue crack growth rate and fracture life under mixed mode loading (Japanese) 7-58406
 ferritic spent fuel casks, predrop test anal., stresses and fracture toughness 7-46651
 fibre reinforced composite, planar, in tension, optimum crack-resistant design 7-16126
 gilsonite, microstructure and mechanical props. 7-44838
 glass, number of cracks at fracture rel. to ultimate stress 7-22809
 glass fibre reinforced epoxy, cross-reinforced wound, deform. and failure in tensile loading 7-17633
 glass fibre reinforced plastic, cross-layered reinforcement strength criteria 7-17631
 glass fibre reinforced polyester resin composite, fracture toughness and microfractures, AE obs. (Japanese) 7-33779
 graphite, bend strength and fracture strain under press. 7-46595
 graphite, nucl. grade, fracture processes and oxidation effects 7-28157
 graphite, nucl. grade, pitchcoke, irradi., mech. props., radiolytic oxidation effect 7-25032
 graphite fiber reinforced epoxy, delamination fracture toughness 7-53900
 graphite fibre reinforced epoxy, interlaminar fracture toughness, effects of rad. 7-33773
 hard alloy, cyclic cracking resist. determ. method 7-13682
 ice, columnar grained, fracture toughness using large specimens (Japanese) 7-59612
 ice, single crystal, fracture toughness and macrofractography (Japanese) 7-16676
 ivory, tensile props. and fracture rel. to comp. and struct. 7-14032
 J-integral fracture toughness, under modes I, II and III, effect of notch root radius 7-63060
 Kevlar 29 fibre reinforced bone and dental cements, mech. props. 7-28080
 laminates, strain energy release rate of edge delamination, residual thermal and moisture influences 7-1508
 lower-shelf, probabilistic model, theory and appl. 7-43770
 metal tubes, ductile, no. of cracks in axial splitting 7-59597
 metal-ceramic composite, dynamic fracture toughness (Japanese) 7-13559
 metallic materials, cracking resistance, effect of strain rate and test temp. 7-13548
 metals and alloys, high-melting, fracture toughness (Polish) 7-44679
 mullite-alumina composites, sintering and charactn. 7-3252
 notched and precracked ISO-V specimens, loading rate effects on fracture resistance 7-13580
 nylon 6 composites, formed by in situ polymerisation of caprolactam, mech. performance 7-39575
 one-dimensional crystals, effect of quantum statistics on low temp. strength 7-38105
 oriented polymers, time-depend, fracture strength, microscopic mol. kinetics, statistical calcs. 7-32556
 PEEK, fracture toughness, temp. and strain-rate effects 7-39660
 PEEK glass fibre reinforced plastics, fracture toughness, temp. and strain-rate effects 7-39660

fracture toughness continued

plate, multilayer reinforced, with through crack, stress state and limiting equil. 7-11344
 PMMA, stress cracking in air, mol. wt. distrib. effect 7-50992
 polycarbonate, fatigue crack propag. and fracture toughness, specimen thickness and geometry influence (German) 7-3438
 polycarbonate, J-integral as fracture criterion 7-39631
 polycomponent composite materials, fracture toughness estimation (Chinese) 7-8075
 polyethylene, fracture toughness, high press. tension testing 7-28111
 polymer composites, particle filled, mechanical strength/filler content relationship 7-13594
 polymer fibre, discontinuous strength spectrum 7-17610
 polymer honeycomb filter, strength and stiffness in shearing determ. 7-17634
 polypropylene, glass-flake reinforced, impact fracture 7-39659
 PVC, rubber modified or filled, damage kinetics, AE analysis 7-54063
 rubber toughened epoxy polymers, toughness rel. to dispersed rubber phase vol. fraction 7-65125
 rubber-epoxy materials exhibiting increased crack resistance 7-17509
 sapphire, ion implantation, mechanical surface property modifications 7-32473
 β -sialon composite ceramics, microstruct., hardness, tool appls. 7-65144
 size effect, Irwin β_{lc} adjustment 7-43780
 square specimens, compressed, with longit. or diagonal crack, stress intensity factors calc. 7-16118
 statistical analysis of cleavage fracture ahead of sharp cracks and rounded notches 7-13540
 steel, alloy type, low-C, tempering temp. effect on mech. props. and crack resist. 7-39654
 steel, austenitic stainless, BWR pipe welds, toughness and tensile props. 7-46650
 steel, austenitic stainless, creep rupture properties of heavy section Type 304 forgings for LMFBRs 7-13582
 steel, austenitic stainless, pipe weldments, toughness at LWR operating temps. 7-13599
 steel, austenitic stainless, strength and toughness at 4K, fusion energy magnets appl. 7-53793
 steel, C-Mn, arc welds, as-deposited strength, toughness, microstruct. 7-13555
 steel, cast, nonmetallic inclusions influence on fracture character 7-3421
 steel, constructional carbon type, original charge purity influence on microstruct. hardenability and mech. props. 7-46521
 steel, Cr-Mo, elevated temp. strength, H attack resistivity and stress relief cracking suscept. improvements 7-13583
 steel, Cr-Mo, normalised heavy section plate, weld cold cracking susceptibility (Japanese) 7-3425
 steel, Cr-Mo, plate, directional solidification, rolling, strength, toughness, microstruct., weldability 7-59622
 steel, Cr-Mo, toughness, impurity element effects 7-53856
 steel, Cr-Mo ferritic-martensitic, fracture toughness precip. of Laves phases 7-53849
 steel, Cr-Mo type, ageing effect on heat resist. props. after cold deform. and tempering 7-22813
 steel, Cr-Mo type, deformed, struct. and mech. props. after long ageing 7-8106
 steel, Cr-Mo type, temp. and deform. rate conditions influence on mech. props. 7-33752
 steel, Cr-Mo-Fe-C, crack resist., temp. and comp. depend. study (Russian) 7-13553
 steel, Cr-Mo-Ni, temper embrittlement, effect of V additions 7-13575
 steel, Cr-Mo-V type, service props. in different struct. conditions 7-8107
 steel, Cr-Ni, microsegregation phenomena in long-term holding at 400°C 7-13458
 steel, Cr-Ni high-temp. type, N and heat treatment effect on struct. and mech. props. 7-33688
 steel, Cr-Ni type, temper hardened, strain rate effect on plastic deform. resist. and energy characts. 7-39601
 steel, Cr-Ni-Co VKS6, struct. and mech. characts., effects of Ni, Co and heat treatment 7-8108
 steel, Cr-Ni-Mo, fracture toughness rel. to austenitising temp. (Japanese) 7-33778
 steel, Cr-Ni-Mo, maraging, mech.-props. rel. to heat treatment (Japanese) 7-53792
 steel, Cr-Ni-Mo type, austenitisation conditions effect on austenite decomp. kinetics and mech. characts. 7-39557
 steel, cracking resistance, effect of strain rate and test temp. 7-13548
 steel, cryogenic, Al alloying effect on mech. and mag. props. 7-39679
 steel, cyclic fracture toughness, evaluated by use of concept of specific fracture work 7-28129
 steel, die, heat-resistant, optimum hardening temps., struct. and mech. props. 7-8022
 steel, dislocation struct. rel. to cyclic bending strain 7-22760
 steel, ferritic, HT-9, mech. props. as function of heat treatment 7-53858
 steel, ferritic and austenitic welded joints, thermally loaded, struct. and mech. props. 7-8102
 steel, forged powder, prod. from water-sprayed Astalloy powders, fracture toughness 7-13572
 steel, fracture toughness assessment using elec. pot. method in comparison with standardized multiple specimen method 7-22932
 steel, fracture toughness of specimens with mixed microstruct., prediction using conc. model 7-13570
 steel, fracture toughness prediction from Charpy impact test results (Japanese) 7-59611
 steel, hardened and tempered, struct. aspects of cyclic crack resist. 7-17613
 steel, heat treatment method effect on struct. and mech. props. 7-39561
 steel, heat-resistant, N and V influence on mech. and service props. 7-8105
 steel, high Mn, impact toughness depend. on Mn/C ratio 7-39657
 steel, high speed, powders, transform., struct. and props., prior annealing effect 7-13452
 steel, high strength, fracture toughness, US meas. 7-28238
 steel, high-alloy, specimen dims. effect on cracking resist. determ. accuracy 7-13549
 steel, high-speed p/m tungstenless, Mo and V effect on microstruct. and operating props. 7-33788
 steel, high-strength low-C weldable, C content effect on struct. and mech. props. 7-46583
 steel, HSLA, Nb, ductile fracture, plastic deform. mechanisms 7-28115
 steel, HSLA, TM-rolling, role of reverse temper embrittlement 7-8112

acture toughness continued

- steel, HY series, laser weldments, S and Ni effects on mech. props. 7-13602
- steel, low alloy, oxides on fracture surfaces, failure anal. examination 7-13586
- steel, low-alloy, H-beams, controlled rolling effect on mech. props. 7-39562
- steel, low-alloy construction, nonmetallic inclusions influence on impact strength and fracture type 7-8085
- steel, low-C, Ni influence on struct., fracture resist. and fractographic features 7-3420
- steel, low-C, wrought, thermal strengthening methods effectiveness 7-46524
- steel, low-pearlite, subjected to controlled rolling, complex microalloying effect 7-46523
- steel, managing, precip. and notch toughness, effect of Cr (*Japanese*) 7-22798
- steel, martensitic stainless, precipitation hardened, impact toughness rel. to Mo content, AES obs. 7-39666
- steel, mild, fast fracture, crack arrest behaviour (*Japanese*) 7-59610
- steel, Mn, fatigue resist., effect of Mo and V alloying, carbide precip. 7-8109
- steel, Mn-V, low-pearlitic, normalized, struct. and mech. props., sheet thickness depend. 7-8006
- steel, Ni-Co-Mo, maraging, fracture toughness rel. to heat treatment, precip., Auger spectra 7-65124
- steel, Ni-Cr-Mo, weldments, dynamic fracture toughness, split Hopkinson bar technique 7-13685
- steel, Ni-Cr-Mo-V, for turbine disc, fracture mechanics anal. 7-13589
- steel, Ni-Mo, upper shelf fracture toughness rel. to prestrain 7-17622
- steel, nuclear pressure vessel, dynamic fracture toughness, crack tip strain behaviour, EM force appl. 7-28126
- steel, pressure vessel with surface fatigue cracks, leak-before-break failures analysis 7-65141
- steel, roll type, crack resist. as criterion of effectiveness, alloying and heat treatment parameters influence 7-53884
- steel, Si-Mn-Mo, austenitising, bainite transform., lump-like composite struct., mech. props. (*Chinese*) 7-13477
- steel, stainless, austenitic, valve type, heat treatment schedule effect on failure nature 7-3423
- steel, stainless, austenitic-pearlitic, N effect on phase comp. and props. 7-53754
- steel, stainless, cryogenic structural material, low-temp. strength under action of elec. current pulses 7-22814
- steel, stainless, LWR piping systems, LBB feasibility eval., fracture criteria 7-61968
- steel, stainless, superalloy, fracture toughness, tensile props., T and ^3He effect 7-46616
- steel, structural, cleavage fracture toughness predictions 7-13544
- steel, structural, fracture toughness, rapid austenitisation, effect of conditions (*Russian*) 7-39651
- steel, tool, Cr-Mo-V, hot working, ductility, C content, toughness, eutectic carbide segregation 7-59592
- steel, tool, fracture toughness, effect of nonmetallic inclusions 7-59635
- steel, tool, fracture toughness rel. with grain size 7-59634
- steel structure, biaxially-loaded connections, fracture condition (*Japanese*) 7-58403
- steel weld joint, austenitic surfacing-pearlitic transition zone, cyclic crack resist. 7-17691
- steel-VC composites, cold sintered, mech. props., bonding integrity 7-39471
- steels, tool, M2 and H13, fracture toughness, influence of microstruct. 7-46632
- stress intensity factor and energy release rate for three-point bend specimen 7-26205
- stress singularity and generalised fracture toughness at vertex of re-entrant corners 7-57749
- structural member, endurance in creep conditions, accuracy of prediction 7-32561
- structurally stress concentrated regions, brittle fracture strength eval. method 7-3424
- sunhemp fibre reinforced polyester composites, tensile and impact props. 7-39592
- superalloys, stress rupture notch sensitivity, grain boundary precip. (*Chinese*) 7-13541
- surface crack, normal-separation, profile opening, comparison of calc. and expt. 7-20659
- surface crack, stress intensity factor variation and back surface displacement 7-57762
- surface flaw, stress intensity distrib. and fatigue crack growth predictions 7-63075
- thickness effect in fracture toughness, probabilistic anal. 7-65123
- three-point bend ductile fracture specimen, dynamically loaded, anal. 7-26206
- unidirectional fibre composites, two in-plane fracture toughnesses relationship 7-53844
- Weibull plots, modulus of rupture, probability estimators 7-39639
- Al alloy, cracking resistance, effect of strain rate and test temp. 7-13548
- Al alloys, fracture toughness, all modes 7-65121
- Al-Cu-Li, cryogenic toughness, orientation effects 7-39669
- Al-Cu-Li-Mn-Cd alloy, 2020, micromechanisms governing elevated temp. fracture resist. 7-22803
- Al-Fe-V rapidly solidified sheets, mech. props., hot rolling effects 7-22838
- Al-Li alloys, grain boundary fracture 7-39644
- Al-Li base alloys, deform. and fracture 7-39594
- Al-Li-Cu-Mg-Zr die forgings, mech. props., microstruct. 7-46636
- Al-Li-Cu-Zr, fracture, ageing and comp. depend. 7-22784
- Al-Li-Cu-(Mg), stress corrosion resist. and mech. props. 7-33833
- Al-Mg, rapidly solidified powders, effect of extrusion parameters on props. 7-39595
- Al-Mg and Al-Zn-Mg alloys, plasma-coated, heat treatment effect on fine struct. and failure mechanism 7-3496
- AlNiFe_{0.5}, reactor fuel cladding, corrosion resistance, rupture strength, neutron irradiation effects testing 7-59670
- Al₂O₃ ceramics, microstruct.-mech. prop. relationship 7-65147
- Al₂O₃ discs, thermal shock reliability, Weibull parameters, bending and fracture testing 7-3408
- Al₂O₃, joining by inducing localised reducing conditions 7-46787
- Al₂O₃, polycrystalline, fracture toughness, R-curve behaviour rel. to grain size 7-46615

fracture toughness continued

- B'-Al₂O₃-Na₂O-ZrO₂ ceramics, transform toughened, fabrication, mech. props. ionic resist. 7-65143
- Al₂O₃-SiC composites, microstruct. and mech. props. (*Japanese*) 7-22821
- Al₂O₃-TiC-TiN composite ceramics, microstruct., hardness, tool appls. 7-65144
- Al₂O₃-ZrO₂ composite ceramics, microstruct., hardness, tool appls. 7-65144
- Al₂O₃-ZrO₂ composites, high temp. behaviour and microstruct. study with HVEM (*Japanese*) 7-22819
- AlSi₃Ni, reactor fuel cladding, corrosion resistance, rupture strength, neutron irradiation effects testing 7-59670
- As₂Se_{100-x}, chalcogenide glass, Vickers microhardness indentation and fracture mechanics 7-21342
- B fibre reinforced Al alloy, corrosive media influence on crack resist. 7-17668
- BN polycrystals, heat treatment conditions effect on mech. and service props. 7-53894
- Bi alloy impregnated Ti, composite pseudoalloy, mech. props., Bi alloy content depend. 7-28095
- C fibre reinforced C composites, tensile props. and fracture toughness at high temps. up to 2400°C (*Japanese*) 7-53864
- C fibre reinforced epoxy, failure in static and fatigue loading 7-17632
- C fibre reinforced plastic laminate; impeding edge-delamination development effect on tension-tension loading (*German*) 7-22827
- C fibre reinforced plastic, cemented lap joint, stress-strain state and strength 7-33794
- C fibre/glass fibre reinforced polyester hybrid laminates, impact and perforation props. (*Japanese*) 7-13569
- Ca₂Na₂K₂Si₂O₃₀F₄, chain-silicate canasite glass-ceramic, thermal shock behaviour, effect of crystn. 7-46613
- Ca₂Nd₄(SiO₄)₆O₂Cm ceramic simulated nuclear waste forms, radiation effects on microstruct. and fracture props. 7-58373
- CaPuTi₂O₇, substituted zirconolite, high level waste, self-irrad. effects, mech. props. 7-805
- CaZrO₃, sintering, porosity, mech. props., corrosion resist. 7-39664
- Co-Mo-Cr-Si, wear resist. alloy development 7-3440
- Cu-Ni-P alloy, P addition effect on struct. and strength 7-53669
- Fe powders, hot pressing, fracture toughness, intergranular failure rel. to porosity 7-13596
- Fe-Cr-C-B hard surfacing weld deposits, abrasive wear resist. and microstruct. 7-22847
- Fe-Cr-Ni-Mn-N (18, 20, 5, 0.16 wt.%), weld metal, fully austenitic, tensile and fracture props. at 4K 7-53901
- Fe-graphite compacts, sintering, alloying, mech. props. 7-39455
- Fe-VC composites, cold sintered, mech. props., bonding integrity 7-39471
- Fe₃₀Cr₁₀Ni₄₀B₂₀ metallic glass, fracture toughness rel. to prep. and struct. 7-53870
- Fe₄₀Ni₄₀B₂₀ metallic glass, fracture toughness rel. to prep. and struct. 7-53870
- GaAs solar cells, fracture strength as function of manufacturing process steps 7-3696
- LaCrO₃-Cr cermets, mech. props., interparticle welding 7-39630
- MgO-Al₂O₃-SiO₂ glass-ceramics, nucleation crystallisation, modulus of rupture, acousto-US obs. 7-59723
- MgO-ZrO₂, dispersed, phase transform., toughening 7-65034
- Mo-W (30 wt.%) alloy, temp. depend. of crack resist. 7-22808
- Mo-ZrO₂, sintered composites, mech. props. microstruct. (*Japanese*) 7-13558
- Na₂O-CaO-Al₂O₃-SiO₂ glass ceramic system, spherulitic growth, mech. props. 7-46405
- Na₂O-CaO-SiO₂ glass, indentation strength comparisons 7-3410
- Ni-Cr alloy, wrought, Hf effect on struct. and mech. props. 7-33689
- Ni-Fe-Cr, Inconel 600 and Incoloy 800, fracture toughness 7-59596
- Ni₆₀Si₁₀B₁₀ metallic glass, fracture toughness rel. to prep. and struct. 7-53870
- Ni₆₀Si₁₀B₁₀ metallic glass, fracture toughness rel. to prep. and struct. 7-53870
- Si-Al-O-N Syalon, bonding investig., active Ti additive role, fracture strength and microstruct. 7-39846
- SiC fibre reinforced SiC, high heat flux, low activation struct. materials 7-49635
- SiC, high-pressure, self-combustion sintering from fine mixed powders of Si and C (*Japanese*) 7-3249
- α -SiC polycryst., pulsed laser annealing and ion beam mixing surface modification studies 7-16657
- SiC, sintered, fracture after Li exposure 7-28103
- α -SiC, sintered, hot corrosion by molten salts, strength degradation mechanism 7-33813
- SiC whisker or particle reinforced Al composites, deform. thermal expansion, strengthening mechanisms 7-3373
- SiC whisker reinforced Si₃N₄, microstruct. and props. 7-22824
- SiC whisker reinforced Si₃N₄ ceramics, fracture toughness (*Japanese*) 7-28138
- SiC:Si, reaction bonded composite, mech. props. and microstruct. anisotropy 7-65146
- SiC-Si₃N₄ fibres, prep. by polycarbosilazane precursors pyrolysis 7-27988
- Si₃N₄ based powder materials with SiC component, comp. effect on mech. props. 7-27998
- Si₃N₄ ceramics, hot pressed, fatigue test with Knoop indentation, residual stress effects (*Japanese*) 7-17640
- Si₃N₄, fracture toughness measured with short-bar chevron-notched specimens 7-59599
- Si₃N₄, gas press. sintering, fracture toughness, fibre like struct., additions effect 7-13414
- Si₃N₄, hot-pressed, friction and wear 7-59642
- Si₃N₄ powders, high press. not pressing, mech. props., thermal cond. temp. depend. 7-3231
- Si₃N₄, surface flaws effect on strength 7-59638
- Si₃N₄, with MgO addition, phys. and tribological props., effect of hot-pressing temp. (*Japanese*) 7-65150
- Si₃N₄-SiC film, hybrid material prepared by plasma CVD, microhardness and internal stress 7-13616
- Si₃N₄-SiC reaction sintered ceramics, oxidation effect on strength 7-65163
- Si₃N₄-TiC composites, densification, matrix-dispersoid reaction, mech. props. microstruct., impurities effect 7-64994
- Si₃N₄-TiC composites, mech. props., wear resist., dispersoid-matrix interaction 7-65145

fracture toughness continued

- Si₃N₄-Y₂O₃, hot pressed, fracture, flexural strength, temp. degradation 7-13546
- Ti alloy, cracking resistance, effect of strain rate and test temp. 7-13548
- Ti alloy, two-phase, microstruct. and failure nature correl. 7-8110
- Ti-Al-Cr-Mo alloy VT3-1 mech. props. depend. on decomp. product morphology for metastable phases 7-39655
- Ti-Al-Mo-Cr alloy, VT3-1, cooling regimes in heat treatment effect on mech. props. 7-8026
- Ti-Al-Mo-Cr alloy, VT3-1, vac. annealing of blanks after isothermal deform., hydrogen plasticising effect 7-8027
- Ti-Al-Sn, weld metal, cryogenic toughness (*Japanese*) 7-46620
- Ti-Al-V (6, 4 wt.%) plates, rolling, heat treatment, microstruct., mech. props., turbine blade appl. 7-17644
- Ti-Al-V alloys, VT20 and VT6, annealing temp. effect on mech. props. of semifinished products 7-39558
- Ti₃Al-Nb alloys, ductility and fracture toughness, dispersoid modification effects 7-22779
- TiB₂ ceramics, pure and liq. phase sintered, processing and microstruct. development 7-3251
- TiC/TiN double layer coated cemented carbide milling tools, wear mechanisms 7-53932
- TiC-Fe-Cr alloyed with Si, high-Cr, sinterability and mech. props. improvement 7-64986
- TiC-Mo₂C-Ni hardmetals, high temp. strength 7-3404
- TiC(N) coated cemented carbide milling tools, wear mechanisms 7-53932
- TiN protective coatings on cemented carbides, adhesion and toughness 7-65159
- W, strength of defect-free crystals, temp. depend. 7-38104
- WC-Co composites, fracture toughness rel. to hardness, microstruct. model 7-17637
- WC-TaC-Co, N contained cemented carbides, sinterability, mech. props. rel. to prep. 7-17507
- ZrO₂ advanced ceramics, props. and appl. 7-13416
- ZrO₂, CeO₃ containing tetragonal polycrystals, thermal stability, mech. props. 7-28101
- ZrO₂ ceramics, strength, effect of freeze-drying of Zr(OH)₂ 7-13415
- ZrO₂ transform. toughened ceramics, fracture toughness rel. to transform. temp. 7-46614
- ZrO₂, Y₂O₃ partially stabilised, crack config. (*Japanese*) 7-65138
- ZrO₂, Y₂O₃ stabilised, fracture toughness and transformability, grain size depend. 7-13566
- ZrO₂, Y₂O₃ stabilised powder, spray pyrolysis, sintering, microstruct., fracture toughness 7-27983
- ZrO₂, Y₂O₃ stabilised, amorphous second phase, sintering, grain morphology, fracture roughness, surface degradation 7-46612
- ZrO₂, Y₂O₃ stabilised, phase transform., mech. props., surface struct. rel. to polishing (*Japanese*) 7-53791
- ZrO₂, Y₂O₃-doped, powders, sinterable, chemically coprecipitated in non-aq. medium 7-64982
- ZrO₂:Ti, ion implantation, mech. props. 7-28102
- ZrO₂-CaO-P₂O₅-SiO₂ glass ceramics, prep. and mech. props. (*Japanese*) 7-7942
- ZrO₂-Y₂O₃ ceramics, toughened, prep., microstruct., mech. props. 7-3409
- ZrO₂-Y₂O₃ partially stabilized, Al₂O₃ effect on retaining tetragonal particles, matrix toughening 7-59485

fracture toughness testing

- see also notch testing*
- acrylic resin, fracture toughness, effect of notch sharpness and plate thickness (*Japanese*) 7-51007
- brittle material, through cracked-starter notched beam specimen, crack stability 7-65252
- ceramics, fracture toughness evaluation using chevron-notched specimens (*Japanese*) 7-59613
- comparison of fracture toughness testing methods 7-37402
- crack arrest stage, specimen-testing machine system compliance effect on crack resist. 7-22940
- dynamic materials testing using fibre optic sensors 7-46778
- dynamic stress intensity factors, meas. using FFT analyser, appl. to drop weight impact three-point bend testing (*Japanese*) 7-59712
- fibre optic sensors appl. in materials testing (*German*) 7-11162
- fibre reinforced ceramics, test techniques for mech. props. 7-13698
- fibre reinforced composites, compact shear test specimens 7-39793
- flexure specimen, end-notched, for mode II testing, design and anal. 7-51005
- glassy epoxy polymer V notched specimens, quasi brittle fracture (*Polish*) 7-46744
- hard alloy, cyclic cracking resist. determ. method 7-13682
- instrumented Charpy test, dynamic elastic-plastic fracture toughness parameters, accuracy of meas. 7-59705
- material inhomogeneity, stress distrib., loading equipment imperfections, fracture origin freq., distrib. (*German*) 7-33873
- metal-ceramic composite, dynamic fracture toughness (*Japanese*) 7-13559
- metallic glasses, specimens with central sharp crack 7-53870
- optical methods in composites, conf., Keystone, USA (Nov. 86) 7-55894
- PMMA, surface crack profile measurement method and results 7-22939
- polyethylene, fracture toughness, high press. tension testing 7-28111
- R-curve, effect of initial fatigue crack applic. conditions and crack length meas. method 7-22945
- SCARE postprocessor program to MSC/NASTRAN, ceramic components reliability anal. 7-17750
- small specimens, fracture toughness estimation 7-39795
- split Hopkinson pressure bar method use in dynamic testing, review 7-22944
- steel, alloy, crack arrest toughness, moment modified compact tension specimen, PTS conditions 7-13695
- steel, ductile, static crack resist. determ., specimen geom. and loading type selection 7-22947
- steel, fracture toughness testing methods, comparison 7-37402
- steel, high strength, fracture toughness, US meas. 7-28238
- steel, high-alloy, specimen dimens. effect on cracking resist. determ. accuracy 7-13549
- steel, Ni-Cr-Mo, weldments, dynamic fracture toughness, split Hopkinson bar technique 7-13685
- steel, structural, welds, dynamic fracture toughness by instrumented impact testing (*Korean*) 7-28235
- steels, alloy, crack arrest toughness, proposed ASTM test method, European experience 7-13694
- Stripa granite drill cores meas. 7-55017

fracture toughness testing continued

- surface crack profile measurement method and results 7-22939
- tension-torsion creep-fracture testing device 7-46739
- thin side-grooved specimens, fracture toughness determ. 7-59706
- Weibull parameters estimation using weight function 7-22934
- Al alloy, pulsed laser weldability 7-13702
- Al-Cu-Mg r-curve behaviour of double edge notched tensionspecimens in plane stress 7-13701
- Al₂O₃ discs, thermal shock reliability, Weibull parameters, bending and fracture testing 7-3408
- Cu tubes, creep-fracture tests 7-46739
- SiC, instrumented impact testing, absorbed energy 7-28237
- SiC, stress intensity factor meas. using notched and surface flaw specimens 7-65251
- WC-Co cemented carbides, compression fatigue crack growth 7-28119
- ZrO₂, partially stabilised, instrumented impact testing, absorbed energy 7-28237

francium

see also nuclei with

- atom, isotope shifts, relativistic DF contrib., reson. doublet, UV laser spectroscopy 7-10475
- atom, second resonance doublet, wavelength meas. fine-, hyperfine structure, isotope shifts 7-57020
- ²²¹Fr, radioactive isotope detection, laser resonant photoionisation method 7-42572
- ²²⁶Fr, ground state hyperfine struct. determ. by RF mag. reson. and laser optical pumping 7-25681

francium compounds

No entries

Franc-Condon factors

- azulene, S₀-S₁ absorpt. spectra and Raman excitation profiles, vibr. intensity distrib., quantum-chem. anal. 7-42619
- cobaltocene, gaseous, self-exchange electron-transfer kinetics, Franck-Condon barriers 7-36745
- dibucaine, H bonding nature and vibr. structure, birefringence emission spectra anal. 7-19935
- 5,6-dihydrobenzo(c)xanthylum salts, synthesis, struct. and spectral props 7-57050
- ferrocene, gaseous, self-exchange electron-transfer kinetics, Franck-Condon barriers 7-36745
- four-wave mixing, use in intracollision dynamics anal. 7-10509
- FT photoelectron spectroscopy, correl. fn. and harmonic oscillator approx 7-10665
- insulin, UV reson. Raman spectra anal. 7-41481
- jets, Raman scatt., Franck-Condon and double reson. study 7-31082
- manganocene, gaseous, self-exchange electron-transfer kinetics, Franck-Condon barriers 7-36745
- methane ion, photoelectron spectrum, Jahn-Teller effect, ab initio SCI and CI calcs. 7-42683
- NH vibr. transition probabilities and r-centroids 7-50262
- phenylalanine, UV reson. Raman spectra anal. 7-41481
- polyatomic molecules, Franck-Condon factors, calc. for undergraduate quantum chem. 7-60919
- pyrene, vibronic coupling and intramol. dynamics, fluoresc. excitation spectra 7-57118
- ruthenocene, gaseous, self-exchange electron-transfer kinetics, Franck-Condon barriers 7-36745
- species-state transition probabilities, calc. for rearranged systems (*German*, 7-36694
- two-centre harmonic oscillator matrix elements and recursion relations 7-36691
- tyrosine, UV reson. Raman spectra anal. 7-41481
- A/O (B²⁺-X²⁺) system, Franck-Condon factors, isotope effect 7-10671
- AlO, B=X system in sunspot spectra 7-60525
- Ar⁺+N₂, charge transfer collision, Franck-Condon principle at low collision energies study 7-62511
- CO, b²Σ⁺-a¹Π, system, Kaplan bands, UV obs. 7-62395
- CO₂, autoionisation and isotope effect in threshold UPS 7-19948
- Cl⁺, charge transfer reactions with organic mols., cross section anal. 7-15701
- GaAs:O LEC crystals, deep photoluminesc. band, fine struct. 7-46110
- GaO, lower electronic states, SCF-X_α SW calcs. 7-30948
- GeH⁺(GeD⁺) in He afterglow, a¹Π₀₊₁-X¹Σ⁺ visible band system 7-50152
- H⁺+H₂ double capture, collisions, H⁺ ion excitation energy meas. Franck-Condon calcs. 7-36751
- H₂, photoionisation and photodissociation, six photon ionisation, vibrational levels 7-10682
- Hg-Ar complex, electronic states struct., pot. energy curves, visible fluoresc. spectra anal. 7-36631
- Hg+NH₃, photosensitised reaction, complex form., luminesc. spectra 7-8256
- Hg₂, GO₂⁺ state vibr. anal., visible and UV fluoresc. spectra study 7-19933
- I₂, F(0_g⁺) ion-pair state anal., OODR and fluoresc. excitation spectrum 7-19931
- InCl molecule, C¹Π-X¹Σ⁺ system, emission spectrum and dissociation energy 7-5694
- InO, lower electronic states, SCF-X_α SW calcs. 7-30948
- KCl:Ti³⁺-type phosphors, Jahn-Teller-induced A-absorption and A-emission bands 7-53398
- LiNbO₃, F⁺ centre wave function calc. 7-44540
- ¹Li₂, A²Σ_u⁺-X¹Σ_g⁺ and B¹Π_u-X¹Σ_g⁺ 7-36691
- N₂, electron impact on N₂, A²Π_u state excitation rate meas. 7-19934
- NH₃, jets, Raman scatt., Franck-Condon and double reson. study 7-31082
- NO, autoionisation of ν=3 Rydberg states, branching ratios, multiphoton spectra anal. 7-36718
- NO, photoexcitation and ionisation cross sections, Stieltjes-orbital representations, HF calcs. 7-19677
- N₂O, photoionis. dynamics and vibr. branching ratios, fluoresc. spectra 7-15653
- O₂, C³Π_g Rydberg state, excited-state photoelectron spectra 7-50250
- O₂+H⁺, charge transfer collisions, vibr. state resolved meas. 7-5762
- O₃, photodetachment cross sections Franck-Condon anal. 7-57139
- PbO, D¹-X¹Σ⁺ system, band intensities distrib. 7-50082
- SF₆ jets, Raman scatt., Franck-Condon and double reson. study 7-31082
- Si, optical props. of isolated dangling bond 7-38507
- a-Si:H films, deep levels in the mobility gap 7-12670

Frank-Condon factors continued

SiF₄ core-excited Rydberg state, SCF calcs. 7-851
ZnD, B²Σ⁺ state, spectrosc., rot. anal. 7-5665

Frank-Read sources

crystal with dislocations, first-order phase transitions 7-38178

Fraunhofer lines *see solar spectra*

Free-electron approximation

metals, EM generation of acoustic waves, theory 7-51945
scanning tunneling microscopy model, appl. to semicond. surface 7-11864
Sugiyama phase sum rule, inapplicability to very thin films 7-17117
Ag particles in Ag-O-Cs photoemitters and Ag aerosols 7-33518
K_α direct EM, ultrasound generation, polarisation dependence expt. 7-2110

Free electron lasers

AC, using relativistic electron beams 7-10973
active guiding in small signal regime 7-1167
almost concentric resonators for low gain FEL, alignment and performance 7-43155
amplification, freq. spectrum oscillating phenomenon 7-43122
amplification and phase shift meas. 7-36973
amplifier, kinetic energy injection 7-15878
annular reflectors for an FEL resonator 7-1146
antiferromagnetic crystal wiggler synchrotron radiation and free electron lasers 7-57223
autoresonant electron laser nonlinear theory 7-10976
beam brightness from a relativistic, field-emission diode with a velvet covered cathode 7-1121
betatron-synchrotron resonances and misalignment in free electron laser oscillators with quadrupole focusing 7-1172
bunched beam laser, transient anal. 7-1175
Cherenkov 100 μm laser expt., operating principles 7-1147
circular free electron lasers, theoretical and expt. aspects (*Japanese*) 7-20242
coherent short wave radiation from a solid state free electron laser 7-1151
cold electron beam sources for Raman FEL 7-1118
collective (Raman) free electron laser gain measurements 7-1156
Compton and Raman regimes, Hamiltonian model 7-57348
Compton scattering free electron laser system, electron beam trapping expt. 7-1136
conf., Rochester, NY, USA 7-9595
conference, Tahoe City, CA, USA (Sept. 1985) 7-6
DC EM wigglers, performance limitations for FEL 7-1125
dielectric mirror damage due to high K undulator radiation 7-1142
distributed feedback, dynamics 7-50588
electromagnetically pumped, with EM wiggler and axial-guide mag. field, linear gain 7-1176
electron beams, high-power, modulation in corrugated waveguide 7-10839
electron trapping and phase-area displacement in electron beam interaction with two counterpropagating laser beams 7-42875
ELF microwave free electron laser expt., comparisons with 2D FRED code simulations 7-1190
EM wave propag. through free-electron laser amplifier, phase change meas. 7-62715
ENEA FEL, above threshold operation, recent exptl. results 7-1137
ENEA-FEL experiment, variable gap permanent magnet linear undulator 7-1191
energy model (*Chinese*) 7-5896
EUV, three-dimens. simulation 7-43131
even-harmonic generation mechanism 7-43127
FIR, review 7-36974
gain, radiation force effects 7-57347
gain degradation and electron beam quality 7-43128
gain maximization modes in low gain-small signal regime 7-1166
gain props., gradient magnetic field effect calcs. 7-20238
gas loaded FEL, benefits and costs 7-1148
gyrotron powered electromagnetic wigglers 7-57346
Hamiltonian model 7-50572
helical wiggler mag. field, sideband instability, kinetic anal. 7-15879
high brightness electron injector for FEL driven by RF linacs 7-1117
High Brightness Test Stand 7-1114
high current electron guns, brightness enhancement 7-1119
high gain 35 GHz FEL amplifier with guide mag. field, parametric behaviour 7-1158
high gain free electron laser oscillators, spatial and temporal evolution of multiple modes 7-1129
high-gain and large-diffraction regimes of the FEL 7-1161
high-gain free electron lasers as generators of short wavelength coherent radiation 7-20232
Hughes low-voltage Free Electron Laser Program 7-1139
hybrid undulator design considerations for FEL 7-1123
induced magnetobremstrahlung of electrons in an undulator field and an axial guide field 7-50574
induced resonance electron cyclotron (IREC) quasi-optical maser 7-1157
induced resonance electron cyclotron quasi-optical maser in an open resonator 7-20176
induction linacs and free electron laser amplifiers, fusion program appl. 7-10287
injector designs for high electron beam qualities, numerical anal. 7-1120
insertion device beam line optics, review 7-43305
insertion devices for synchrotron sources, conf., Stanford, CA, USA (Oct. 1985) 7-29584
intense low emittance beams prod. in electron linacs 7-1116
inverse noncollinear Compton laser for electron acceleration 7-49744
laser electron acceleration in stimulated Compton scatt. 7-50645
LELA experiment, cavity alignment tests and status 7-1135
linac preparatory study for free electron laser project at JAERI 7-20244
line broadening due to classical and quantum noise 7-50573
longitudinal wiggler free electron laser, experimental demonstration 7-43121
Los Alamos FEL, electron micropulse diagnostics 7-1108
Los Alamos FEL, linear accelerator noise control 7-62115
Los Alamos FEL, oscillator expt. 7-1107
Los Alamos FEL, status 7-1106
low voltage FEL design, Hughes program 7-10982
micro-undulator free electron lasers 7-1188
Microtron accelerator for a free electron laser 7-1113
microtron FEL Cherenkov 7-10970
millimeter wave radiation from rotating electron ring 7-1155
millimetre wave operation, gain and extraction efficiency 7-1189

free electron lasers continued
mirror degradation and performance requirements 7-43152
MM-wave, sideband control 7-62716
mode competition in Raman free electron lasers 7-1160
modulated axial mag. field system 7-10974
multimode dynamics in a free electron laser with energy shift 7-1169
multimode oscillator, electron energy drift effect, instability 7-15880
NBS CW microtron, FEL expts. 7-1140
noncollinear, off-axis schemes 7-15877
nonlinear traveling waves in a free electron laser 7-1159
off-axis gain enhancement in long undulator regime 7-25833
operational conditions using a standing wave wiggler 7-43123
optical cavities, alignment, tuning 7-1143
optical coating damage, performance requirements 7-1141
optical guiding in an FEL 7-1165
optical guiding simulations for high gain-shortwavelength FELs 7-1162
optical klystron, theory 7-360
optical klystron, XXUV laser harmonic generation, effects of wiggler errors 7-1127
optical mode gain and evolution 7-43126
optimisation criteria 7-36972
Orsay optical klystron, goals 7-31231
Orsay storage ring FEL, operating point modifications 7-1110
parametric FEL theory 7-43125
particle dynamics and beam energy with planar undulator 7-10975
particle simulations vs. small signal FEL theory 7-10971
permanent magnet field source for circularly polarised radiation production via helical FEL 7-31349
permanent magnet helical wiggler model for FEL off-axis orbit anal. 7-1124
picosecond beam propagation for gas-loaded free electron lasers 7-1152
planar metal-grating free-electron lasers 7-10969
planar wiggler free electron laser, kinetic small signal gain anal. in strong wiggler regime 7-1133
plasma, HF amplification by laser wiggler beat waves 7-20117
pulse amplification, transient and asymptotic small signal gain 7-43048
quadrupole free electron laser spontaneous radiation 7-31334
quantized field formulation of the free electron laser in the Heisenberg picture 7-1174
quantum description with uniform mag. field and corrugated slow-wave struct. 7-10972
quantum theory, intrinsic linewidth and photon statistics 7-43130
quantum-mechanical equations transition probabilities 7-1105
radiation force corrections to planar wiggler FEL gain 7-1170
Raman FEL at 2 mm wavelength 7-1153
Raman regime, frequency resolved radiations, temporal evolutions 7-57344
relativistic electron beam, quantum-kinetic theory 7-43124
research using 35 MeV linac at NERL (*Japanese*) 7-20243
review (*Japanese*) 7-1177
ring resonators, mode rotation, intracavity beam divergence, alignment sensitivity 7-1144
self amplified spontaneous emission 7-1163
self-amplified spontaneous emission and coherent amplification 7-15881
single particle FEL equations with overtones for linear polarized wiggler 7-1168
small signal FEL performance with two waveguide modes 7-1131
soft X-ray overtone production 7-20234
solid FEL, possibility of obtaining coherent short wave radiation 7-20237
spiking mode operation for a uniform-period wiggler 7-1109
spontaneous radiation of an electron beam in a free-electron laser with a quadrupole wiggler 7-5898
Stanford Mark III infrared free electron laser 7-1112
steady state FEL, particle dynamics in two beam accelerator 7-1173
stimulated head-on scatt., self-modulation study 7-43132
stimulated Raman scatt. based FEL action, radiation output and meas. (*Chinese*) 7-57345
stimulated-Cerenkov free electron laser, multiple scatt. effect 7-25832
storage ring for high power XUV FEL 7-31351
superradiant harmonic radiation, 3D model 7-20233
tapered, beam density, deceleration and spatial exponentiation rate limits calc. 7-43129
tapered wiggler for FEL, desirable excitation patterns 7-1122
tapered-wiggler, high-efficiency microwave radiation extraction 7-20241
three-dimensional free electron laser gain and evolution of optical modes 7-1164
three-dimensional simulations of free electron laser physics 7-1171
transverse correlations in start-up from noise 7-20236
trapped particle instability in FEL oscillators and amplifiers 7-1130
two-stage, quasioptical cavity, cold testing 7-1145
two-stage FEL, design issues 7-1149
Ubitron/FEL amplifier with axial guide field, three-dimens. simulation 7-1154
UCSB FEL 400 μm expt., spectral characteristics 7-1111
UCSB free electron laser, linearly polarized undulator, laser gain depression 7-1126
UCSB two-stage FEL experiment 7-1150
UK free electron laser project, status 7-1134
undulator, linear, variable gap permanent magnet, for ENEA free electron laser expt. 7-43151
undulator, long, evolution of radiation beam system 7-42880
undulator technology and synchrotron radiation source requirements 7-31350
visible wavelength FEL oscillator 7-1192
VUV harmonic generation on storage ring of optical klystron for pulsed and free electron lasers 7-1229
VUV/soft X-ray, options for development 7-31333
wiggler and alternating-gradient quadrupole field for free electron laser, electron beam envelopes and matching conditions 7-1128
wiggler for IR FEL and coherent harmonic generation 7-31352
working state anal. (*Chinese*) 7-5897
X-ray amplifier pumped by kinetic energy of clusters 7-20239
X-ray free electron laser and laser electron acceleration based on megagauss mag. fields 7-20240
X-ray free electron lasers, high gain, feasibility study 7-1132
XUV, RF-linac-driven, gain physics 7-20235
XUV FEL, high-gain, storage-ring design 7-1115
XUV FEL oscillator at Stanford X-ray Centre Storage Ring 7-1138
XUV free electron laser oscillators, options and issues 7-20231

free energy

- 2D nucleation in elec. field, form. free energy 7-58434
 ϵ -expansion of the surface tension in an external field 7-2305
 n -vector model and polymers, parametric eqn. of state 7-51986
 A_2BX_4 -type crystals, incommensurate phase, zig-zag domain wall structure 7-33342
acceleration wave propagation and evolution in thermoelastic solids (*Italian*) 7-20616
alkali halide mixtures, binary, common-anion, correl. of thermochem. and phase-diagram data 7-3286
alkali halide solid solns., thermodynamic props. calc. model 7-52086
alkali metal atomic fluids, thermodynamic and electronic props. 7-45157
alkali metal ions, free energy, additivity rules (*German*) 7-2233
alkyl nitriles, conformational kinetics calcs., gas and liquid phases, MR spectra 7-19896
alkyl nitriles gas and liquid phases, syn-anti conformer equilb., MR chem. shift study 7-19895
alkyne isomer groups, chemical thermodynamic props. data 7-60901
alloy thin films, co-deposited, phase form. 7-59492
alloys, binary, phase diagrams and short range order, Monte Carlo simulations 7-53704
alloys, liquid, binary, high order perturbative effects 7-52085
alloys, solvent and solute diffusion enhancement, effect of non-random solute distrib. around vacancies 7-63868
analytical Gibbs fields, regularity props. in the high-temp. region 7-48672
antiferromagnetic, X-Y model, triangular lattice in mag. field, phase diagram, spin wave free energy calcs. 7-17178
aqueous soln., free energies of hydration, ionisation pots., electron affinities 7-65292
asymptotic growth shapes developed from 2D nuclei 7-58180
atom, interacting with blackbody radiation, thermodynamic perturbation theory 7-910
Baxter model, free-energy amplitude in finite-size scaling 7-48604
binary alloys, crystal-amorphous transformation, thermodynamics and kinetics 7-21108
binary alloys, Monte Carlo calc. of configurational entropy and combinatoric factor 7-63846
binary fluid mixtures, comparative anal. by extended irreversible thermodynamics and kinetic theory 7-16290
block copolymer-homopolymer system, phase separation, statistical theory 7-38213
butylamine binary liq. mixtures, viscosity meas., free energy and intermol. interactions studies 7-63862
charged solid-liq., interfaces, dipolar hard spheres, density functional theory study 7-63414
chiral smectic C liq. crystals, mol. theory 7-1867
commensurate-incommensurate transition, phase and amplitude modulation 7-32600
complex dynamical systems, phase transform. 7-29954
Coulombic systems, interacting, thermodynamic functions and self-energy 7-16963
crystal shape, equilibrium, numerical evaluation 7-63530
cubic systems, superconducting p -wave pair states, collective excitations, spin-orbit interaction and cryst. field effect 7-7440
CVD, adsorption on Si (111) of Si-H system species, rel. to temp., super-saturation, bond strength and press. 7-33583
deformed paramagnetic tetragonal system, field-induced symmetry change in the free energy 7-12324
1,2-dichloroethane- n -alkane or -2,2,4-trimethylpentane liq. mixtures, excess enthalpy meas. and calcs. 7-6827
difluorodichloromethane, mol. consts., force field study, thermodynamics props. 7-19814
diglycine nitrate, spontaneous polarisation and electrocaloric effect near the ferroelectric transition 7-17273
dimethylether-Xe, vap. press. and density, excess molar enthalpy and entropy 7-12319
dipolar fluid, effective pair pot. for orientational correls. in elec. field 7-37826
dipolar fluids, density functional theory, orientational correls. in linear chains 7-37827
discommensuration patterns, dynamics 7-44749
discotic liq. cryst. strands, freely suspended, cross sectional shape 7-37845
dispersion forces, free energy via response functions 7-57144
effective classical partition functions for anharmonic oscillators and double-well pot. 7-35334
electrocrystallisation, kinetics, computer simulation studies 7-58173
electron gas, diamagnetic susceptibility at low temps., surface effects 7-21841
element, single, ionisation equilb. theory, approximate soln. 7-19787
epoxide networks, crosslinked, sorption and diffusion of chloroform vapours (*Russian*) 7-27021
equations of state and constitutive equations 7-21389
ethane, orthopositronium annihilation rates 7-62543
exactly solvable IRF model, Gordon-generalisation hierarchy, free energy parameterisation 7-24592
excess Gibbs free energy of binary liquid mixture, numerical differentiation appl. 7-14899
ferroelectric liquid crystals, distortion free energy density, electrostatic screening 7-37844
ferromagnet, free energy, anisotropy and rotational invariance 7-59007
ferromagnetic Heisenberg model, one- and two-dimensional, free energy and susceptibility 7-45722
ferromagnetic semicond., donor state, thermally induced abrupt shrinking 7-52510
ferromagnetic superconductor, phase diagrams and order parameters 7-17127
ferromagnetic systems, critical point phenomenology and neglect of irrelevant variables, renormalisation group results anal. 7-64468
ferromagnetic-nonferromagnetic supercond. superlattices, vortex pinning 7-45591
finite compression of solids, second order thermoelastic anal. 7-43708
finite systems, hyperuniversality and renormalisation group, finite-size scaling 7-56203
finite-size scaling in strips, log. corrections, Potts model appl. 7-35429
flexible polymers, in limited volumes, behavior (*Russian*) 7-25694
fluid hierarchical reference theory, smooth cut-off formulation 7-6491
fluid-solid interface, one order parameter theory 7-27098
four-sublattice Jahn-Teller crystals., phase transitions, free energy and symm. props. calcs. 7-2544

free energy continued

- free-electron gas diamagnetic props. in external helical magnetic fields 7-45610
Gibbs field uniqueness in ν -dimensional lattice systems 7-48671
Gibbs free energy calc., symmetric minimum-norm updates 7-39912
glasses, surface singularities, topological origin 7-12444
grain boundary segregation, free energy considerations and fracture 7-38110
group IIB-VA liquid metal systems, Gibbs energy, composition depend. 7-52080
haemoglobin, human, cooperative free energies for nested allosteric models 7-23272
hard parallel spherocylinder fluid, smectic order and nematic-smectic transition 7-11905
HCL, condensation on charged CO_2 walls, Stockmayer model calcs. 7-63784
Heisenberg classical magnetoelastic chains, lattice distortions and short range mag. order 7-17195
Heisenberg ferromagnet, 3D, susceptibility, correl. length, free energy, twelfth order series study 7-27488
hexafluorobenzene-benzene- n -hexadecane ternary mixtures, vapour press. and excess vol. meas. at 298.15K 7-12315
icosahedral quasi-crystalline struct., mechanism for stabilisation 7-6753
II-VI and III-V semicond., solid solns., short range order and free energy of mixing, EXAFS meas. 7-63573
III-V semiconductor-metal interface, thermodynamic stability considerations 7-21490
III-V semiconductors, MBE, thermodynamic anal. 7-46328
inert gases, hydrophobic hydration, free energy, mol. dynamics study 7-46821
inhomogeneous one-dimens. models, construction of exact solns. 7-35453
interaction round a face model, free energy expression 7-196
ion-molecule association and clustering form., thermochemical data 7-18514
Ising model, 2D with layered quenched bond randomness, free energy and specific heat calcs. 7-7531
Ising model, 3D thermodynamic functions at $T > T_c$ (*Ukrainian*) 7-9781
Ising model, 1D, in a variety of random fields 7-33188
Ising model, random-field, with trimodal distrib., phase diagram 7-56182
Ising model, spin-glass transition, domain wall scaling, energy and free energy distrib. calcs. 7-38891
Ising spin glass, three-dimensional, entropy and free energy, Monte Carlo simulation 7-17184
Ising triangular lattice, 2×1 and 2×2 structures, phase transitions 7-63765
lattice animals, collapse transition and asymptotic scaling behaviour, low temp. expansion 7-29921
lattice spin models, infinite range soln. and free energy calcs. 7-24593
Lennard-Jones crystals, free energies, mol. dynamics calc. 7-12318
Lennard-Jones fluid mixtures, infinite-dilution activity coeffs., computer simulation 7-16383
liquid flat aggregates embedded in crystal matrix, interfacial free energies per unit area 7-6973
low angle symmetric tilt boundary, thermal fluctuations 7-21220
lymphocyte, free energy of accumulation of a fluoresc. cation probe within the mitochondria 7-40118
macroscopic quantum systems, weakly coupled, limiting Gibbs state calcs., appl. to Josephson oscillator 7-45582
magnet properties, thermodynamic pot. technique 7-41327
magnetic fluids, internal rot., constitutive eqn. 7-43922
magnetic hard-square lattice gas, scaling form for free energy 7-48607
magnetically ordered regions in crystals with dislocations, static susceptibility 7-38851
MBBA hybrid nematic liq. cryst. cell, flexo-electric effect study 7-11904
Meldrum's acid, ionisation rot. barriers 7-62307
metallic fine particles, surface free energy anisotropy determ. 7-32783
metals, thermodynamic functions of relative temps. 7-38225
metals, thermodynamics during high-pressure shock 7-21352
2-methoxy-2-oxo-1,3,2-oxazaphosphorinane, conformer struct. and populations, IR, NMR and X-ray spectra anal. 7-25509
micelles, spherical and nonspherical, asymmetrisation, free energy, conc. depend. 7-8321
Migdal-Kadanoff renormalisation, appl. to Potts model 7-24600
mixtures with supercritical gases, vapour-liq. equilb. calcs., excess Gibbs energy method 7-6768
molten surfaces, roughening 7-52194
muonium+benzoic acid derivatives, addition reaction in aq. solns., Hammett free energy 7-15744
muonium radicals in allyl benzene and styrene, resulting from insertion, role of substituents 7-42788
nematic liq. cryst., line defect dynamics, viscous damping effects study 7-44365
noninteracting electrons, nonequilibrium thermodynamic pot. functional, \hbar^2 -order terms, gradient expansion 7-48667
organic O O contrary comps. in C_1 to C_4 range, ideal gas thermodynamic props. 7-60904
 p -wave pair states, spin-orbit interaction and crystal field effects 7-38806
 n -pentane-dichloromethane, excess thermodynamic props. 7-52079
phase transitions, equilibrium, with bulk, interfacial and boundary energy 7-41313
polaron theory, time-ordered products method for equilb. thermodynamic props. 7-38470
poly(1,3-propylene phosphate), hypercoiled to extended coil state transition study 7-31194
polyelectrolyte, weakly charged, in poor solvent, struct. phase transitions 7-51600
polyethylene, dielec. and mechanical relaxations, rate theory eqn. calcs. 7-26983
polymer nets, high elasticity, mol. theory with allowance for topological constraints 7-37839
polymer solutions, thermodynamic props. 7-16386
polymer solutions, thermodynamic props. prediction by group contrib. method 7-32683
polymer surface and interface dynamics study 7-63917
polymers, excluded-volume interaction, Flory-Huggins theory 7-2151
Potts model, cluster-size distrib. and mag. props. 7-33136
propylammonium tetrachloromanganate, incommensurate γ phase, elastic neutron and X-ray scatt. 7-16538
pyrene solubility in binary solvent systems, meas. and NIBS model calcs. 7-63829
random field Ising model, higher-order cumulants 7-53016

free energy continued

- Sb₂O₃, thermodynamic stability, EMF obs. 7-46828
 second order phase transition, wave vector depend. susceptibility, elastic coupling effects, mean field theory 7-32599
 sine-Gordon thermodynamics using Bethe ansatz, classical limit 7-41319
 single ions, transfer between two solvent, free energy 7-17785
 smectic C chiral liquid crystals, elastic free energy 7-11900
 solid cyanoadamantane, phenomenological approach to phase transitions 7-32636
 soliton systems, statistical mechanics, collective coordinate approach, non-canonical method 7-18690
 solution of rodlike molecules, flow, phase separation, orientation distrib. 7-43989
 spin glass phase, generalised random energy model, partition functions, magnetic props. and $q(x)$ function calcs. 7-17177
 spinodal systems, nonlinear theory of mag. ageing 7-3344
 steel, C, thermodynamics of phase boundaries 7-65007
 trans-stilbene-fumaronitrile ion pair, back-electron transfer, solvent effects 7-39873
 superconductor, sinusoidal magnetic order and superconductivity coexistence 7-7442
 superfluid films and interfaces, at $T=0$, local interactions 7-38283
 system with coupled order parameters, ring approx. 7-41315
 tetraethyleneglycol-alcohol-cyclic ether, excess Gibbs free energies at 298.15K 7-44851
 2-thio-1,3,2-oxazaphosphorinane, conformer struct. and populations, IR, NMR and X-ray spectra anal. 7-25509
 transition metal alloys, amorphous, short-range order, approx. to coherent locator (*Russian*) 7-58731
 transition metals, liquid, thermodynamic props. 7-12323
 transverse Ising model in random parallel field, internal energy expansion 7-33189
 triplet bipolaron systems, superconducting A and B phases (*Chinese*) 7-58949
 type II superconductor, mixed state, free energy, interpolation method 7-52920
 vapour phase homogeneous nucleation, interfacial tension rel. to droplet size 7-58435
 XY model, 3D, critical surface free energy, universal finite scaling amplitude, direct Monte Carlo sampling 7-61305
 Zamolodchikov model, 3D, free energy, partition function per site 7-35424
 Ag-Au-Zn ternary system, liq., thermodynamic functions (*German*) 7-44856
 Ag-Mg, commensuration and discommensuration characteristics, modulation periods 7-46463
 AgIn₂Se₈ photoelectrodes, thermodynamic stability in electrolytes 7-54330
 Al, Gibbs free energy at melting nonstructural contribution estimation 7-2156
 Al, thermodynamics during high-pressure shock 7-21352
 Al-Li (9.5 at.%), coarsening of δ' -Al₃Li precipitates, var. of average Li content in Al matrix 7-3313
 Al₂O₃, mixing of metal overlayers, ion beam irradi., rapid thermal annealing, pulsed laser irradi. 7-58330
 Al₂TiO₂ ceramics, form. by solid state reaction of Al₂O₃ and TiO₂ powders 7-46385
 N-aryl-4-t-butyl-thiazoline-2-thiones, rot. barrier, enantiomer separation 7-13759
 Au-Si, liq., thermodynamic analysis of conc. fluctuations and homogeneous nucleation, glass form. 7-44852
 BaO-CeO₂, phase relations, thermodynamic parameters 7-6829
 Bi-Sn, liq., thermodynamic analysis of conc. fluctuations and homogeneous nucleation, glass form. 7-44852
 Ca(OH)₂Zn(OH)₂·2H₂O, chem. comp., solubility in KOH, thermodynamic props., reaction equilib. 7-26962
 Cd-Bi(Sb), thermodynamic functions are modelled by chemical-physical theory, Gibbs energy 7-52051
 CdSe-polysulphide photoelectrochem. system. corrosion reactions, thermodynamic stability calcs. 7-28320
 CoCr films, texture formation, appl. for perpendicular mag. recording 7-39539
 CoO-MnO system, thermodynamic props., phase diagram, miscibility gap 7-53706
 CsCuCl₃, Jahn-Teller induced helical deformations 7-7178
 Cu-Si alloys, thermodynamic props. determ. by Knudsen cell mass spectrometry 7-26976
 CuInS₃ photoelectrodes, thermodynamic stability in electrolytes 7-54330
 F₂ solid, high-pressure behaviour at low temps. 7-37923
 Fe epitaxial monolayers on the Au (100), surface magneto-optic Kerr effect 7-59080
 Fe, passive, adsorption and absorpt. of Cl⁻ ions 7-28340
 Fe, polymorphism interpretation 7-51700
 Fe thermodynamic props., data tables and reviews 7-18512
 Fe-Al disordered alloys, mag. props., site-diluted Ising model calcs. 7-2873
 Fe-Co, liq., thermodynamic mixing functions, Knudsen cell mass spectrometry (*German*) 7-21470
 Fe-Mn(S), surface comp. and surface tension, effect of S and Mn (*Chinese*) 7-6916
 Fe-N system, phase diagram, thermodynamic calc. 7-7973
 Fe-Ni FCC alloys, low temp. phase equilib., mag. effects 7-26914
 Fe-Ni system, liq., phase equilib., above 1200K, mag. contrib., thermodynamic analysis 7-7966
 Fe-Ni system, phase equilibria, mag. contrib. to thermodynamic functions, below 1200K 7-7965
 Fe-Ni-W system, phase equilib., expt. and theoretical study 7-28013
 Fe-Si (3 wt.%), secondary recrystallisation, seed grain formation, influence of elastic anisotropy energy 7-13470
 GaSb, crystal growth and synthesis, thermodynamics, optimisation algorithm appl. 7-16461
 Ge₂₀Te₈₀ glasses, heat capacity, relax. and thermodynamic kinetics during annealing 7-44843
³He, superfluid, free energy symmetry and stationary points 7-2293
³He, superfluid A and B phases, order parameter dynamics, spin and orbital dynamics 7-44943
 Hg₃-AsF₆, chain compound, paraconductivity, Sugiyama-Gutfreund-Weger model 7-52584
 I, arc in air, plasma comp., Gibbs free energy calcs. 7-37795
 In crystallites, surface free energy anisotropy 7-27091
 In-Bi-Pb system, liq., thermodynamic props. (*Japanese*) 7-53699

free energy continued

- In-Pb, liq., activities, temp. depend., EMF obs. (*Japanese*) 7-12320
 In-Tl, liq., activities, temp. depend., EMF obs. (*Japanese*) 7-12320
 Li, arc in air, plasma comp., Gibbs free energy calcs. 7-37795
 LiBr-LiCl binary mixed crystal system, critical nucleus, melt comp. 7-58445
 Mg-Cu alloys, vap. press. meas. by boiling temp. method, thermodynamic props. 7-44778
 Mg(I), vap. press. meas. by boiling temp. method, thermodynamic props. 7-44778
 MgO-Ca²⁺ (100), entropy of segregation calcs. 7-2323
 Mn-P melts, free energy of mixing and Mn₃P form. 7-65042
 Mo porous electrodes for alkali metal thermoelec. convertor, voltammetric studies 7-28405
 Mo-Ni-Co-Sn, liq. phase sintering, grain boundary migration, coherency strain effect 7-22604
 Nb, BCC, thermodynamic props. 7-6828
 Nb-Al₂O₃, high temp. interactions, X-ray diffr., DTA studies 7-8259
 Nb-Cr₂O₃, high temp. interactions, X-ray diffr., DTA studies 7-8259
 Nb-Y₂O₃, high temp. interactions, X-ray diffr., DTA studies 7-8259
 NbC_{1-x}, thermodynamic props., 1200-2500 K 7-44849
 Ni alloys, thermodynamic anal. of gas phase in thermal diffusion aluminosiliconising 7-1660
 Ni-Al alloy phase transforms. during ion beam mixing, electron diffr. and microscopy studies 7-16655
 Ni-Si system, phase diagram, thermodynamics 7-46424
 NpO_{2-x}, hypostoichiometric, O dissociation press., partial thermodynamic functions 7-17520
 Pb₂GeO₁₁, sound velocity discontinuities at the phase transition 7-17274
 Pd-B alloys, thermodynamic props. (*German*) 7-21486
 Pt anode in fuel cell, performance in presence of CO and CO₂, CO poisoning adsorption parameters calc. 7-13855
 Pu-O system, phase equilib., thermodynamics, 1400-1610 K 7-59496
 Sb-Ge-Zn system, thermodynamic investig. (*German*) 7-53703
 Sb-Sn system, phase diagram, thermodynamics 7-3283
 Sb_{1-x}Bi_xSi crystals, elec. props. at ferroelec. Curie point 7-2991
 Si, thermodynamic props., data tables and reviews 7-18512
 Si-Cu(Au), deep level position in forbidden gap, charactn. using ionisation Gibbs free energy (*Chinese*) 7-58760
 Si-binary alloy interfacial interactions, Rutherford backscattering spectrometry, TEM 7-12505
 SiC ceramics, reactivity with various additives, uses as effective sintering aids 7-46383
 SiC, mixing of metal overlayers, ion beam irradi., rapid thermal annealing, pulsed laser irradi. 7-58330
 SiC:P(N)(B)(Al) thin films, impurity 7-27192
 Si₃N₄, mixing of metal overlayers, ion beam irradi., rapid thermal annealing, pulsed laser irradi. 7-58330
 SiO₂, mixing of metal overlayers, ion beam irradi., rapid thermal annealing, pulsed laser irradi. 7-58330
 SiO₂-Al₂O₃, glassy system, thermal capacity, thermodynamic props. 7-12307
 SiO₂-TiO₂, glassy system, thermal capacity, thermodynamic props. 7-12307
 TaC_{1-x}, thermodynamic props., 1200-2500 K 7-44849
 U_{1-x}Ce_xO_{2+x}, nonstoichiometry, chemical thermodynamics 7-52083
 U_{1-x}Ln_xO_{2+x} (Ln=Y, La, Nd, Gd), nonstoichiometry, chemical thermodynamics 7-52083
 U_{1-x}Pu_xC, mixed carbide fuel, thermodynamic props., effect of O and N impurities 7-58507
 V-N system, phase equilib., crystallography, thermodynamic props. 7-28011
 VC_{1-x}, thermodynamic props., 1200-2500 K 7-44849
 W, BCC, thermodynamic props. 7-6828
 Xe plasma, equilib. comp., numerical methods study 7-31935
 Y_{1-x}Ln_x (x=1,2) equilib. reaction, thermodynamic parameters evaluation, Knudsen effusion mass spectrometry 7-23054
 Zn-Ho alloy, two-phase, partial thermodynamic props., 690 to 1020K 7-7963
 Zn-Sb, thermodynamic functions are modelled by chemical-physical theory, Gibbs energy 7-52051
 ZnSO₄-Na₂SO₄ reactions in CoCrAlY hot corrosion 7-28188
 Zr-Sn, diffusion, chem. activity, modified evaporation method 7-38243
 Zr-Ti, diffusion, chem. activity, modified evaporation method 7-38243
 ZrO₂, Y₂O₃ partially stabilised, phase diagram, microstruct. (*Japanese*) 7-53707
 ZrS₂, thermodynamic props., 298 to 1600K 7-28022
- free field rooms** see *anechoic chambers*
free induction decay (optical) see *optical coherent transients*
free radical reactions
 acrylamide, UV irradi., free radical reactions with gases, ESR obs. 7-10633
 butane radical, absorpt. cross section and reaction rate consts. meas. using molecular modulation spectrometry 7-22997
 dichlorofluoromethylperoxy radical + NO₂ forming peroxyxynitrate, rate const. at stratosphere conditions 7-23802
 difluoromethyl diradical, form. obs., dimerisation rate const. determ. 7-28291
 ethyl radical, absorpt. cross section and reaction rate consts. meas. using molecular modulation spectrometry 7-22997
 formaldehyde radical + formaldehyde radical, absorpt. cross section and rate const. determ. 7-28269
 methacrylamide, UV irradi., free radical reactions with gases, ESR obs. 7-10633
 methanol + OH, rate coeff. determ., flow tube temp. effect 7-59740
 methyl + H(D), rate const. determ., laser photolysis and reson. fluoresc. 7-8250
 methyl thiol radical + NO(NO₂)(O₂), reaction rate consts., mol. fluoresc. anal. 7-19917
 methyldioxy radical self-reaction, rate constant, flash photolysis and UV spectral study 7-54075
 OH radical dynamics in pulse radiolysis of Ar sensitised water vapour 7-8292
 polyethylene, radiation effects at high press. 7-21260
 polypropylene, macroradical termination, segmented mobility and low-mol. radicals (*Russian*) 7-65312
 polystyrene, incorporation of stilbene (p-fluorostilbene) during radical polymerisation, NMR investig. 7-39890
 propionamide, UV irradi., free radical reactions with gases, ESR obs. 7-10633

free radical reactions continued

- stellar atmosphere di- and tri-atomic molecules, dissociation functions 7-24002
 styrene-butadiene-styrene block copolymer, thermoxidative degradation kinetics, fission track study 7-39877
 tetrachloroethene discharges, radical reactions, spectrosc. investig. 7-20990
 tetrachloroethene-O₂ discharges, radical reactions, spectrosc. investig. 7-20990
 tetrafluoromethane plasma, etching of Si, chemistry, model 7-3544
 tetrafluoromethane-O₂ discharge, plasma etching, chem. processes 7-3475
 trifluoromethyl+O₂, rate const. meas., laser photolysis and time-resolved mass spectrometry 7-8249
 vinylbenzyl ester-maleic anhydride donor-acceptor complex, alternating copolymerisation (*Russian*) 7-65319
 C₂, a π_n radical, form. and decay in methane pulse discharge 7-23003
 CH+H₂, rate const. meas., fluoresc. detect. 7-17763
 HO₂+HO₂, rate constant, flash photolysis and UV spectral study 7-54075
 HO₂+methylidoxo radical, rate constant, flash photolysis and UV spectral study 7-54075
 HO₂+O₃, reaction rate const. meas. by photofragment fluoresc. detect. 7-22990
 Mn₂(CO)₁₀, gas-phase, photodissoc. pathways and recomb. kinetics 7-59771
 NH+NO(NO₂), reaction rate const. 7-3578
 NO₃+dimethyl sulphide, reaction rate coeff. meas. 7-22987
 O+CH₃, exothermic reactions, rate const., classical trajectory study 7-17783
 O+formaldehyde, rate const. meas., laser-induced fluoresc., time-resolved detect. 7-46815
 O+NO₂ (ClO) stratospheric reactions, rate const. meas. 7-8265
 OH, photodissociation processes in astrophysical environment 7-23042
 OH+CO, reaction kinetics at atmospheric conditions 7-40529
 Si, etching in CF₄ plasma, chemistry, model 7-3544

free radicals

- see also *free radical reactions; paramagnetic resonance of free radicals*
 acetone, positive muon irradi., radiolysis, radical form. 7-17813
 acridine, radical anion in stretched polyethylene films, polarised absorpt. spectra 7-50083
 alanine system sensitivity, fast neutron irradiation effects 7-34188
 alkene nitrite isomers, radicals, EPR investig. 7-36653
 alkoxy radicals, electronic struct., rot. resolved spectra 7-62352
 α -aminoalkyl radicals, electrochemical detection, bond dissoc. energies determ. using oxidation pots. 7-28286
 anthracene, radical anion in stretched polyethylene films, polarised absorpt. spectra 7-50083
 anthraquinone anion radicals, frozen soln., ENDOR spectra, temp. depend. 7-7610
 ascorbic acid radical, strong perchloric acid soln., free radical protonation equilib., ESR study 7-33918
 ascorbic acid radical anion, Ca²⁺ exchange, ESR line broadening meas. of rate const. 7-28270
 ascorbic acid radicals, stability, semiempirical MNDO calcs. 7-36480
 bicyclooctene, mol. plastic cryst., muonium adduct radicals, temp. depend. 7-53207
 bipyridine, dications and cation radicals, conformational struct. ab initio calc. 7-15497
 2,2'-bipyridine radical ions, absorpt. spectra, counter ion effects 7-49934
 bis(chlorophyll)cyclophane, radical cations, ENDOR and TRIPLE reson. 7-42655
 camphorquinone radical anion, photogenerated, time-resolved CIDEP spectra 7-57102
 CH mol., photodissoc., ab initio SCF with CI calcs. 7-42499
 chlorophyll a, radical cations, ENDOR and TRIPLE reson. 7-42655
 colour centre laser spectroscopy 7-18890
 crown ether-anion radical salt complexation, electrical cond. investig. 7-58842
 cyanomethanes, He(I) photoelectron spectrum; vertical ionisation energies, LBCO-MO model 7-50249
 cycloheptatriene, muonium addition, ring inversion kinetics of radicals 7-42792
 diarylphosphonyl radical, kinetic and spectrosc. characterisation 7-62419
 dibenzotetraphene, radical cations, electronic and photoelectron spectra 7-57079
 dichlorofluoromethylperoxy radical + NO₂ forming peroxyxynitrate, rate const. at stratosphere conditions 7-23802
 dichloromethylene radical, fluoresc. decay meas., lifetime determ. 7-25594
 difluoromethyl diradical, form. obs., dimerisation rate const. determ. 7-28291
 dimethylamine radical cation, hyperfine coupling tensors, ab initio UHF calcs. 7-25373
 3,4-diphenyl-2,5-dimethyl-2,4-hexadiene, free radicals, γ -irradiation generated, visible absorpt. and EPR spectra 7-57100
 1,2-diphenyl-3,3,4,4-tetramethylcyclobutene, free radicals, γ -irradiation generated, visible absorpt. and EPR spectra 7-57100
 DNA, oriented, neutron-induced free radicals 7-23391
 ethyl, ethenyl and ethynyl anions, structs. and rearrangement processes, ab initio MO calcs. 7-59757
 ethyl radical, muonated, first detection in gas phase 7-42790
 ethynyl radicals, vibr. excited, colour centre laser spectra 7-62362
 fluorenone ketyl radical cation, single channel quadrature FT ESR spectra 7-25570
 fluoroethylene radical anions, dissoc. electron attachment 7-50349
 formic acid radical cation and its isomers, pot. energy surface, ab initio quantum chemical methods appl. 7-42521
 formyl ion, dissociative recombination of interstellar ion, electronic struct. calc. 7-20064
 formyl pair, anharmonic vibr. effects, ab initio SCF-CI calcs. 7-10444
 formyl radical-d₀(d₁), third-order anharmonic pot. const. equilib. structure parameters, calc. procedure 7-10544
 hydrazyl radicals, muonium substituted hyperfine coupling constants 7-42793
 hydrocarbon peroxy radicals, ab initio MO and electron correl. calcs. 7-49951
 hydroxymethylperoxy radical, thermal stability, ESR spectra 7-62415
 iso-propyl radicals, radiolysis rate const. determ., UV absorpt. spectra 7-46860

free radicals continued

- iso-propylperoxy radicals, radiolysis rate const. determ., UV absorpt. spectra 7-46860
 isocyanic acid, heat of form., photodissoc. study, time-of-flight and laser-induced fluoresc. spectra anal. 7-31105
 lithium phthalocyanine radical, optical and mag. props. 7-62417
 methoxy-(d₃) radicals, gas-phase detection by reson.-enhanced multiphoton ionisation spectroscopy 7-31134
 methyl+H(D), rate const. determ., laser photolysis and reson. fluoresc. 7-8250
 methyl methacrylate radicals, ESR spectra, temp. depend., 77 to 300 K 7-62420
 methyl radical, pyrolytic precursors, electronic spectrum, EELS anal. 7-42760
 methyl radicals, etching of metal films in discharges 7-3507
 methyl thiol radical+NO(NO₂)(O₂), reaction rate const., mol. fluoresc. anal. 7-19917
 methylamine radical cation, hyperfine coupling tensors, ab initio UHF calcs. 7-25373
 methylbenzyl radicals, photoelectron spectrosc., thermochem. 7-10664
 methylene, ¹A₁-³B₁ separation, full CI calcs. 7-36486
 methylene, pot. energy surface and singlet-triplet splitting, calcs. 7-10397
 methylene, triplet, ν_2 fundamental band, IR spectra 7-10568
 methylene, vibr. band broadening, Raman spectra 7-10597
 methylene, X³B₁, IR rot. transitions, diode laser absorpt. obs. 7-10567
 methylene radical, ¹A₁ state and ¹A₁-³B₃ coupling, visible absorpt. and mag.-rot. spectra 7-49903
 methylene radical, ³B₁ state, visible absorpt. and mag.-rot. spectra 7-50155
 methylnitrene, matrix-isolated, IR and UV absorpt. spectra 7-42637
 3-methylpentane, radical cation, struct., ESR 7-42653
 methylviologen, radical cation dimers, adsorbed on colloidal CdS surface, relax. 7-27095
 mm wave spectra of interstellar molecules 7-24196
 muon spin rotation spectroscopy, compliment to ESR spectroscopy 7-42787
 muonium adducts of carbonyl bond, hyperfine coupling const. 7-50409
 muonium radicals in allyl benzene and styrene, resulting from insertion, role of substituents 7-42788
 muonium-organic radical systems, struct., muon spin rot. studies 7-50410
 naphthalene radical ions, absorpt. spectra, counter ion effects 7-49934
 nitrobenzenes para-substituted, solvated anion radicals reaction kinetics in liq. NH₃, ESR spectra anal. 7-19907
 nitroxy radicals, anisotropically rotating, 2 mm EPR spectra calcs. 7-15630
 nitroxyl radicals, in aq. glycerol soln., superslow rotation investig. 7-62422
 norbornene, mol. plastic cryst., muonium adduct radicals, temp. depend. 7-53207
 olefin radical cations from hydrocarbon radiolysis, time-resolved fluoresc.-detected mag. reson. 7-57099
 organic free radicals, avoided level crossing muon spin rotation 7-42789
 organic liquids, detection of short-lived muonium via spin trapping 7-42791
 organic radical cations, electronic visible-UV spectra, LNDO/s PERTCI calcs. 7-50169
 organic radicals, muonium-containing, H⁺-Mu isotope effects 7-15745
 organometallic free radicals, laser and Fourier transform spectroscopy 7-19872
 2,2,5,7,8-pentamethylchroman-b-oxyl-¹³C, radical, ESR spectra and hyperfine coupling const. 7-36652
 pentaphenes, radical cations, electronic and photoelectron spectra 7-57079
 pentynylidene radical (C₅H), in interstellar space, hyperfine struct. obs. 7-60749
 perchlorotriphenylmethyl, spatially resolved EPR tomography 7-5708
 phenazine, radical anion in stretched polyethylene films, polarised absorpt. spectra 7-50083
 phenazine derivatives, partly hydrogenated radicals, hyperfine const., EPR (*French*) 7-31079
 polyacetylene, muon spin resonance studies 7-53202
 cis-polyacetylene, muonium substituted radical, hyperfine coupling constant 7-50407
 polyacrylate radicals trapped in polymeric network, struct. and stability, EPR obs. 7-5801
 production in aqueous solns. due to diagnostic US 7-50900
 propylene oxide cation radical, unimol. dissoc. reaction, nonergodic behaviour 7-39857
 radical anions, single cryst., dissoc., struct. investig. 7-33275
 squaric acid radical, HYSCORE 2D ESR investig. 7-25565
 stellar atmosphere di- and tri-atomic molecules, dissociation functions 7-24002
 4,4'-1-terphenylenebisgalvinoxyl biradical, nematic liquid crystal, ENDOR and EPR spectra anal. 7-19908
 tetraaryldiphosphine radical cations, ESR linewidths rel. to struct. 7-50201
 tetrafluoromethane-O₂ discharge, plasma etching, chem. processes 7-3475
 tetrafluoromethane/O₂ plasma etching reactor, CF and CF₂ radicals, laser induced fluorescence detection 7-58068
 transient species in supersonic, free jet expansion, laser induced fluoresc. 7-31099
 tribromomethyl radical, geometry and electronic struct., SWX α calcs., ab initio UHF calcs. 7-19703
 trichloromethyl radical, struct. and electronic states, ab initio UHF SWX α calcs. 7-30949
 trifluoromethyl+O₂, rate const. meas., laser photolysis and time-resolved mass spectrometry 7-8249
 trimethylamine radical cation, hyperfine coupling tensors, ab initio UHF calcs. 7-25373
 vitamin E(¹³C) radical, ESR spectra and hyperfine coupling const. 7-36652
 AlF₄⁺, matrix ESR and CI investig. 7-15629
 BS₂, photolysis products, UV electronic absorpt. spectra 7-23041
 C-centres radicals, merostabilisation energy calcs. 7-30924
 C₂, a π_n radical, form. and decay in methane pulse discharge 7-23003
 CCH, X² Σ^+ state, rot.-vibr. energies, ab initio calc. using nonrigid bender Hamiltonian 7-25422
 CF radical, far IR laser mag. reson. spectrum 7-50202
 CF⁺, near-equilib. pot. and electric dipole moment calc. by SCEP-CEPA method 7-25368

free radicals continued

- CF₃ chemisorption on GaAs (001), electronic struct., RHEED, photoelectron spectra, HF SCF calcs. 7-53497
 CH+H₂, rate const. meas., fluoresc. detect. 7-17763
 CN, generation by photolysis of NCNO, removal by H₂, HCl and HBr, fluoresc. 7-46812
 CN radical, anal. of perturbation between B²Σ⁺ ν=5 and A² Π₁ ν=17 levels 7-50067
 CNH₂⁺, laboratory generation, mass spectra 7-46811
 Cl₃, electronic struct., ab initio SCF and CI study 7-5605
 DO₂, third-order anharmonic pot. consts. equilb. structure parameters, calc. procedure 7-10544
 HO₂ radical, third-order anharmonic pot. consts. equilb. structure parameters, calc. procedure 7-10544
 HOO radical, orbital energies, UHF calcs. phys. interpretation 7-56931
 HPO₃ radical, strong perchloric acid soln., free radical protonation equilb., ESR study 7-33918
 K + methyl iodide (ethyl iodide) (n-propyl iodide), reactive collision, medical group effect, mol. beam study, cross section meas. 7-39900
 N₂, plasma jet, post-discharge, radical spatial distrib. 7-20969
 NCO, MODOR and intermodulated fluoresc., hyperfine coupling consts. 7-50206
 NCl, radicals, electronic struct., radiative lifetime eval., MRD CI calcs. 7-42492
 NF, metastable radical, microwave spectrum 7-42603
 NF, radicals, electronic struct., radiative lifetime eval., MRD CI calcs. 7-42492
 NH radical, form. by electron impact 7-36800
 NH radical, rot.-vibr. anal. for X²Σ⁻ state, IR Fourier transform spectra 7-18487
 NH radicals, in plasma jet, spatial distrib. 7-20969
 NH+NO(NO₂), reaction rate consts. 7-3578
 NH₂, excited radical, fluoresc., Einstein coeff. and oscillator strength calc. 7-42668
 NH₃⁺ radical cation, hyperfine coupling tensors, ab initio UHF calcs. 7-25373
 NO₃, visible and UV absorpt. spectra, temp. depend. 7-10608
 OH, A²Σ_{1/2}⁺, first excited electronic state ρ-doublet transition obs., UV-microwave double reson. 7-10636
 OH, A²Σ⁺→X²Π fluoresc. excitation function 7-42669
 OH, desorpt. on TiO₂(NaCl)(SrF₂) surfaces, kinetic and internal energy, determ., fluoresc. detect. 7-8298
 OH in atmosphere, concentrations in AD 1860 to 2035 period 7-29153
 OH in tropical clouds, cloud chemistry model 7-18290
 OH, photodissociation processes in astrophysical environment 7-23042
 OH radical, orbital energies, UHF calcs. phys. interpretation 7-56931
 OH radicals in spray flames, planar laser-induced-fluorescence monitoring 7-59766
 OH + H₂, rot. excitation cross sections, close-coupling calcs. 7-25639
 OH+CO, reaction kinetics at atmospheric conditions 7-40529
 OH+N, state specific collision dynamics 7-20014
 SF₃ radicals, electronic struct., ab initio SCF CI calcs. 7-19716
 SH₃ radicals, electronic struct., ab initio SCF CI calcs. 7-19716
 SO radical, A³Π₁-X³Σ⁻ transition, 0-0 band spectrum, rot.-vibr. levels, rot. consts. 7-10542
 SO₂ radical, strong perchloric acid soln., free radical protonation equilb., ESR study 7-33918
 SPCl₂F⁻ radical, ESR and ab initio quantum chem. study 7-42654
 SiCl₂ radical, laser-induced fluoresc. investig. 7-31090
 SiCl₂, UV emission spectrum, vibr. anal. 7-31024
 SiH₂, intracavity laser absorpt. spectra. 7-15616
 SiH₂ radicals, singlet-triplet energy separation, SCF CI calcs. 7-19718
 SiH_n, (n=1 to 3), photoion yield and thresholds, photoionisation mass spectra study 7-50242

freezing

- see also refrigeration*
 alloys, binary, freezing, convective and morphological instabilities 7-32615
 binary alloy, freezing, morphological instability evolution, model cryst. growth system 7-1925
 biological specimen visualisation by cryoHVEM 7-40380
 biological tissue, fresh, propane-jet freezing without ice form. 7-40379
 cylindro-inner cones, freezing point, radiant emission characts. 7-56254
 density functional theories, appl. in 2D and 3D 7-32621
 density functional theory with reference liq., appl. to hard sphere system 7-16718
 density wave theory, thermodynamic consistency and entropy change calcs. 7-63845
 drop freezing data anal. using mathematical technique 7-58444
 energy transfer in soils with nonequilibrium phase transition 7-66104
 freezing problem, moisture migration allowance study 7-55094
 hard discs and hyperspheres, freezing 7-44768
 hard sphere liquid, freezing into FCC against HCP structures, density functional theory 7-44765
 heat transfer, 2-dimens., with melting and freezing, finite element soln. algorithm 7-1381
 ice, formation of cubic phase from water aerosol droplets 7-60364
 ice, nucleation activity of AgI particles 7-26918
 icosahedral and decagonal quasicrystals, twins of 820-atom cubic cryst. 7-58189
 liquid metals approximate struct. theory, hot cryst. vacancy form. energy calcs. 7-63421
 liquids in porous glass, geometrical supercooling 7-16720
 magnetic fluids, liquid and frozen, magnetisation processes 7-59060
 non-Newtonian freezing liquid, buried pipeline wall icing investig. 7-63189
 one component plasma, triple correlations in freezing transition 7-63773
 polydisperse colloidal crystals, stability anal. 7-8315
 porous media, liq. sat., freezing 7-62966
 sandy rock, pore moisture thawing and freezing, aq.-phase press. influence 7-52004
 skeletal muscle fibres, frog, quick-freezing following electrical stimulation 7-28798
 steady-state freezing of liquids in laminar flow between two parallel plates 7-51036
 Stefan problems, multidimensional, efficient finite difference scheme 7-6069
 supercooled liquid, freezing dynamics 7-12239
 thermoplastic, freezing, developing flows with very low heat generation 7-6084

freezing continued

- thermoplastics, injection moulding, fully-developed flows 7-11264
 tissue culture cells, imaging intracellular elemental distrib. and ion fluxes using ion microscopy, freeze-fracture 7-60139
 1,3,5-trimethylbenzene, melting point meas., liq. self-diffusion study, hard-spheres method 7-52003
 underground pipe, freezing liquid transport, cooling effect 7-57923
 water, alkanolic acids and their mixtures, freezing temp. determ. using kinetic technique 7-44762
 water, freezing, surfaces influence 7-6763
 water, initially superheated, solidification in horizontal cylinder study 7-58443
 water flow in curved pipe, freezing fracture 7-26347
 Al, thermodynamic temp. meas. between 683K and 933K using IR pyrometer 7-18788
 Al-Si LM 13 alloy with graphite particles, gravity die cast, dispersed graphite effect on freezing rate 7-59506
 FEMs for solidification problems, comparison 7-14759
 He liquefier, condensing and freezing purification system 7-56280
 He, liq., in Vycor glass, thermodynamics of freezing and melting 7-52169
 MnBi/Bi eutectic, freezing rates, convection effect on microstruct. 7-22652

Frenkel defects

- metal displacement cascade damage computer simulation using binary collision approx. code (*Japanese*) 7-32535
 metals with close-packed structure, solid-liq. phase transitions, atomic processes 7-52012
 recombination zone, influence of uniaxial tension (*Russian*) 7-37970
 solid solutions, precipitate growth under irradiation, theory 7-12296
 Ag, Frenkel pair production cross sections, calc. fission-fusion neutron spectrum sensitivity 7-51849
 Al, Frenkel pair formation energy, pseudopot. theory anal. (*Russian*) 7-6617
 Al-H, H-point defect interactions, extended Huckel mol. orbital calcs. 7-44533
 Cu, Frenkel pair production cross sections, calc. fission-fusion neutron spectrum sensitivity 7-51849
 Ge, ionisation-stimulated annealing of Frenkel pairs under electron or gamma irradiation 7-38061
 Ge, mixed group III and group V ion implantation 7-21243
 KCl, Frenkel defect recomb., thermally stimulated electron emission obs. 7-64869
 KCl, vibronic mechanisms of excitation decay, defect formation 7-39158
 MgAl₂O₄, spinel single cryst., low dose neutron irradi., swelling, defect interaction 7-51842
 MgO, proton-irradiated, cross-stabilisation of Frenkel defects 7-44627
 Mo, Frenkel pair production cross sections, calc. fission-fusion neutron spectrum sensitivity 7-51849
 NaCl:Ag Frenkel defect recomb., thermally stimulated electron emission obs. 7-64869
 Ni, ⁵⁷Ni labelled, ⁵⁷Fe Mossbauer emission spectroscopy of internal radiation damage 7-13061
 Ni, defects created by low-energy ion bombardment, investig. by slow electron diffr. (*Russian*) 7-58374
 Si, electron beam irradiated at different temps., formation of complexes 7-12153
 Si, ionisation-stimulated annealing of Frenkel pairs under electron or gamma irradiation 7-38061
 Si, mixed group III and group V ion implantation 7-21243
 UO₂, Frenkel disorder, estimate of enthalpy contributions 7-6618
 W, Frenkel pair production cross sections, calc. fission-fusion neutron spectrum sensitivity 7-51849

Frenkel-Poole effect *see* Poole-Frenkel effect

frequency allocation

- HF skywave remote sensing, frequency management 7-40646
 ionospheric forecasting, short-term, problems 7-40645
 TV VHF signal propagation, far beyond primary service zone 7-34768

frequency changers *see* frequency convertors

frequency control

- see also automatic frequency control*
 800 MHz bandwidth with acousto-optical spectrometer at Helsinki Observatory 7-60561
 conference, Philadelphia, PA, USA (May 1986) 7-55893
 He-Ne laser at 0.633 μm, frequency stabilisation, using polarisation modulation 7-20295

frequency convertors

- see also mixers (circuits); optical frequency conversion*
 n-GaAs/Al_xGa_{1-x}As multilayer heterostructs., nonlinear high-freq. effects during vertical transport 7-2694
 TaS₃, quasi-1-dimens. conductor, dynamic behaviour, possible electronic appls. 7-38548

frequency convertors, optical *see* optical frequency conversion

frequency division multiplexing

- coupled lightguides, filter operation, parameters choice 7-37111
 coupler, WDM active, bidirectional transmission on single fibre 7-15994
 dielectric guides in integrated optics, wavelength multiplexer/demultiplexer (*German*) 7-62848
 fibre optic couplers, connectors and splices, conf., San Diego, CA, USA (Aug. 1985) 7-24277
 fibre optic fused biconical monomode directional couplers, power transfer wavelength selectivity control 7-37159
 fibre optical sensors, FDM using FM laser source 7-15986
 fibre optics, single-mode WDM systems using Fabry-Perot interferometers, wavelength-selective filters appl. 7-57557
 flat passband birefringent wavelength-division multiplexers 7-57604
 grating coupler/demultiplexer for fibre optic LANs using WDM 7-37152
 heterodyne/coherent optical fibre communications, ultimate performance 7-31490
 holographic optical element wavelength multi-demultiplexer in near IR 7-25756
 holographic wavelength demultiplexer for optical fiber communications 7-25774
 narrowband tunable optical filter for channel selection in densely packed WDM systems 7-11174
 optical parallel array logic system, architecture without memory elements 7-20144

frequency division multiplexing continued

- optical waveguide horn-grating demultiplexer circuit, single-mode operation 7-62846
- semiconductor laser amplifier, optical freq., selective amplification 7-57311
- single-mode fibres, chromatic dispersion meas. technique using WDM 7-11140
- wavelength-tunable single-mode fibre grating reflector 7-31442

frequency-domain analysis

- see also frequency-domain synthesis*
- groundwater quality, freq. domain anal. 7-23789
- phase-change material storage design for passive solar heating 7-8447
- quasi interferometric set up, pseudocolour encoding, spatial frequency domain 7-62640
- speech, nonstationary analysis model 7-47127

frequency-domain synthesis

- see also frequency-domain analysis*
- nonlinear articulatory speech synthesizer using both time- and frequency-domain elements 7-43558

frequency hop communications *see* radiocommunication**frequency measurement**

- see also atomic clocks*
- absolute, of CH₄ stabilised laser, NRLM work relating to precision meas. 7-14915
- acoustic signal freq. meas. techniques (*Japanese*) 7-31592
- atomic frequency standards (*French*) 7-9822
- carbonyl fluoride, laser lines, optically pumped, heterodyne freq. meas. 7-36943
- difluoromethane, CO₂ laser pumped, freq. meas. on FIR laser emissions 7-1084
- ethyl iodide, laser lines, optically pumped, heterodyne freq. meas. 7-36943
- FIR lasers, using point-contact-type Josephson harmonic mixer 7-20310
- frequency control, conf., Philadelphia, PA, USA (May 1986) 7-55893
- fundamentals of time and frequency measurements (*French*) 7-9820
- intense single-pulse microwave sources diagnostics 7-9845
- interferometric laser frequency division and stabilization 7-20314
- Laboratoire Primaire du Temps et des Frequences, metrological activities in 1986 (*French*) 7-9821
- laser frequencies measurement (*French*) 7-29983
- laser frequency standard accuracy improvement, based on saturation absorption method 7-18761
- methane hyperfine line, stabilised He-Ne laser expt. 7-20190
- methyl chloride, CO₂ laser pumped, freq. meas. on FIR laser emissions 7-1084
- methyl fluoride-d₃, and isotopic, laser lines, optically pumped, heterodyne freq. meas. 7-36943
- NBS calibration service based on GPS common view data 7-14926
- nuclear quadrupole resonance thermometers, freq.-temp. conversion (*Russian*) 7-41385
- optical frequency standard based on Ramsey excitation in Ca atomic beam 7-14925
- proton gyromagnetic ratio in H₂O determ., by low field method 7-14916
- reproduction standards, automatic 7-41352
- ring dye laser for probing trapped ions, optical frequency standard appl. 7-20285
- servo-controlled lasers progress and appls. 7-20307
- standard, metrological certification of radiooptical freq. bridge 7-56210
- standard based on Ramsey resonance of alkali hyperfine doublet 7-19733
- standard of frequency deviation unit for FM oscillations 7-48772
- standard units automatic comparison, software 7-41353
- standards, statistical analysis based on classical variance 7-18736
- standards based on stored ions 7-14924
- time and frequency standards comparison along radiometric channel, instruments design 7-56209
- to-and-fro zone plate method for 3D frequency characts. obs. 7-20393
- YIG single-crystal ferrites, relation between biasing magnetic field and linewidth 7-4868
- Ag atomic beam frequency standard, optically pumped 7-18763
- Cs alkali gas cell atomic freq. standards 7-41357
- Cs atomic beam freq. standards, distributed phase shift minimization 7-41356
- Cs atomic beam frequency reference, metrological analysis 7-41351
- Cs atomic clock, PTB design, preliminary results 7-18756
- Cs atomic clock, velocity distrib. determ. 7-18755
- Cs beam freq. standards, atom transit time effect on stability 7-41355
- Cs beam frequency standard with narrow atomic velocity distrib. ranges, Ramsey patterns 7-18758
- Cs beam frequency standard, optically pumped, progress 7-41354
- Cs beam primary frequency standard, C-field setting, transitions and disturbances 7-18757
- Cs clocks charactn. in perturbed environment (*French*) 7-29984
- Cs₂ reference for freq. stabilisation of 1.06 μ m Nd:YAG laser 7-57403
- H maser atomic standard, built at Johns Hopkins University, long term performance 7-18759
- H maser miniature passive clock, NBS design, characts. and performance 7-18760
- He/Ne/methane laser, absolute frequency meas. at 88 THz 7-18762
- Pb salt diode laser calibration, wavemeter 7-5930
- Rb alkali gas cell atomic freq. standards 7-41357
- RuO₄ transitions in ν_3 band, freq. meas. 7-36624

frequency modulation

- see also frequency shift keying*
- deformation meas. using spatial frequency modulation of holographic interferometry, moire method (*Japanese*) 7-56218
- DFB lasers, phase tunable type, 1.5 μ m operation, FM and spectral characts. study 7-43171
- fibre optic interferometer using FM laser diodes 7-31470
- fibre optical sensors, FDM-using FM laser source 7-15986
- laser FM measurement technique, suppression of residual AM 7-15919
- laser heterodyne bias frequency-locking for coherent optical communication (*Chinese*) 7-57382
- methane/He-Ne ring lasers stabilised using FM resonances, frequency reproducibility 7-1206
- optical fibres, multisolution pulse interaction, FM influence 7-43390
- phase-switched optical pulses, compression in resonant absorber 7-1238
- semiconductor junction DFB laser direct FM characts. meas. using delayed self-homodyne technique 7-11014
- semiconductor lasers field spectra computing asymmetry due to noise obs. (*Japanese*) 7-15862

frequency modulation continued

- standard of frequency deviation unit for FM oscillations 7-48772
- unified standard for RF signal shape and spectrum parameter meas., design 7-48773
- US flowmeter, freq. modulated, errors in flow meas. 7-57951
- UV generation using FM dye laser 7-50644
- CO₂ laser radar, coherent FM CW, signal amplitude distrib. meas. 7-40570
- H₂O, vap., pressure-broadening, amplitude modulation servo control in FM spectroscopy 7-18888
- InGaAsP 1.3 μ m diode laser, ultra-high-speed modulation 7-5924
- InGaAsP-InP DFB laser monolithically integrated with tunable external cavity, linewidth and FM characts. 7-57316
- InGaAsP-InP laser, single-mode, 1.3 μ m, analog FM 7-37002
- LiNbO₃ waveguide electro-optic freq. translators, appl. to coherent optical fibre systems 7-20468

frequency modulation, optical *see* frequency modulation; optical modulation**frequency regulation *see* frequency control****frequency response**

- active anti-vibration platform, multivariable control 7-29991
- hearing aid frequency response damping, effects on speech clarity and preferred listening level 7-8763
- hot wire, oscillating, response 7-37588
- measurement equipment for subscriber optical lines 7-62856
- polyvinylidene fluoride sheet evaluation for large sonar arrays 7-2986
- strain gauge calibration procedure for modal analysis, correction 7-56251
- tall thin piezoelectric bar, two-dimensional equivalent circuit 7-1366
- variable-pressure sensors, four-mass method of examining vibrational frequency characts. 7-48708
- wind turbine test data correl. optimisation using frequency response matching 7-8357
- GaAlAs laser diodes, stripe geometry, directly modulated in microwave range, freq. response study 7-11017
- InGaAsP-InP DFB laser with modified double-channel planar BH struct., 1.3 μ m high-speed operation 7-15896
- Pt thin-film thermometers, frequency response investig. 7-48741

frequency selective surfaces *see* antenna theory**frequency shift keying**

- fast frequency-tunable external-cavity laser, FSK modulation, 100 Mbits/s 7-57383

frequency stability

- see also frequency control; laser frequency stability*
- 800 MHz bandwidth acousto-optical spectrometer at Helsinki Observatory 7-60561
- Casagrain antennas, phase and frequency stability, appls. 7-60547
- high-quality quartz crystals, production developmental results 7-59823
- quartz crystal resonators, growth and sweeping of high quality quartz 7-39369
- quartz crystal resonators radiation sensitivity with different Al impurity content 7-58335
- H active masers for VLBI appls. 7-43042
- H maser at temp. below 1K 7-43043
- H masers, single-state selection system 7-43045
- H microwave-pumped cryogenic maser 7-43044
- He-Ne Zeeman lasers for coherent optical fibre system 7-50786

fretting *see* wear**friction**

- see also internal friction; lubrication*
- 3D contact problems with friction, mathematical programming approach 7-16131
- 3D contact problems with friction, static and dynamic analysis 7-43804
- 3D elastic bodies, contact problems, mathematical models of friction 7-51002
- abrasive wear mechanism clarification, contact surface deform. effect on wear and friction 7-8134
- adverse press. gradient boundary layers, k- ϵ turbulence model 7-16172
- AE technique for friction and wear obs. and seizure prediction (*Japanese*) 7-59721
- aerial multiple pipe system, pulling force estimation and design of optical cord (*Japanese*) 7-6016
- alloys, amorphous, friction and wear behaviour rel. to microstruct. and surface chem. 7-8127
- anisotropic solid friction model (*French*) 7-6160
- anisotropic surface friction coefficient tensor 7-26851
- asbopolymer material, friction and wear characts. vs. metal friction pairs 7-28153
- asperity pair elastic joints, friction resistance 7-11363
- axial flow in square lattice rectangular rod bundle, wall shear stress meas. 7-16282
- ball rolling on rotating plane, inclusion of viscosity and friction, diff. eqn. soln. 7-41097
- Blasius flow, skin friction, heat transfer, variational soln. 7-20699
- bodies moving with slip, contact temp. 7-11252
- boundary layer flow and frictional resistance of uniformly accelerating or decelerating flat plate 7-1544
- bowed string, vibrations, flexural rigidity and internal friction effects 7-20617
- bowed string vibration, friction-vel. characts. 7-50943
- bronze-steel pair, friction surface, local X-ray spectra study 7-3449
- bundles of twisted tubes, heat transfer and fluid friction 7-57827
- buoyant and combusting flow, turbulence model 7-51083
- C thin films, RF discharge deposition, mech., elec. and optical props. 7-22509
- cantilever in dry friction, additional and differential harmonic oscillations 7-22843
- ceramic materials, wear mechanism in dry rolling friction 7-59643
- ceramic matrix composite frictional stress evaluation along fibre-matrix interface 7-28143
- ceramics, friction and wear measured by a pin-on-disk method (*Japanese*) 7-22850
- circular plate, self-excited vibration and frictional forces calcs. 7-26187
- circular plate, self-excited vibration and frictional forces, internal resons. effects calcs. 7-26188
- coatings, friction and adhesion meas. using microtribometer 7-46742
- compact heat exchangers, with permeable wall, friction and heat transfer 7-51143
- conference, tribology and lubrication, Tokyo, Japan (July 1985) 7-4631
- contact noise, conf., Delft, Netherlands (June 1985) 7-48168

friction continued

contact problems with nonlinear friction laws, existence of local uniqueness of solns. 7-37397
cotton fibre reinforced polyester composites, friction and wear 7-13610
Coulomb friction law use in contact problems soln. by finite element method 7-31711
CVD and PVD coatings, structural, mechanical and tribological props. and applications 7-53935
cylinder, unsteady boundary layer eqns., frictional forces 7-1392
cylinders with parallel axial displacement, overlap coeff. in end friction 7-16135
discs, inelastic frictional, shearing assemblies, viscosity, granular temp., stress calcs. 7-37398
discs and rings, subjected to rolling contact, stress intensity factors for small cracks in rim 7-57761
duct, cross shaped cross section, parametric study of friction and heat transfer 7-26276
duct, scalene triangular, rib-roughened, turbulent friction factors study 7-57812
ducts, finned, triangular, fully developed flow, friction factors 7-63224
dynamic friction characteristics during interaction with elastic system, pattern form. anal. 7-1519
dynamic three-point bending test, finite element anal. considering contact and frictional effects (*Japanese*) 7-57776
elastic film on rigid substrate, contact stress and strain with friction, finite element anal. 7-57769
elastomers, sliding friction mechanics, asperities adhesion fracture 7-53922
end-notch flexure specimen, mode II interlaminar fracture toughness, finite element anal. 7-1509
fibre reinforced composites, damping by dry friction of dynamic loads 7-32563
flow properties of coal-oil slurries at low Reynolds number 7-20801
fluid flow with free surface past bodies, hydraulic modelling of drag and friction resistance 7-31822
flycasting mechanics, flyline investig. 7-50
fuel-rod bundles model, hydraulic drag 7-10237
general contact boundary conditions and friction system anal. 7-43807
hard materials, frictional behavior of diamond and cubic BN abrasives 7-3461
hard materials, fundamentals of wear 7-3456
heated gas flow in circular tube, friction factor studies (*Japanese*) 7-57924
Hertzian contact, stress hypotheses and material stresses 7-1521
high viscosity fluid in heated or cooled pipe, flow with viscosity gradient and frictional resistance 7-26350
incompressible fluid at technically rough surface, boundary layer parameter calc. 7-63125
incompressible laminar boundary layer flow, MHD with heat and mass transfer 7-20806
Inconel 625 matrix-carbide particle composite surface layers, wear resistance improvement 7-53912
inertial moment, slip method determ. using functional force and impulse 7-41038
inhomogeneous fluid, tracer diffusion, kinetic theory 7-58111
laminar incompressible 2D boundary layer eqns. similarity solns. 7-51042
laminar incompressible oscillating flow, mean-parameter modeling 7-63109
laser interferometer skin-friction meter, numerical and expt. study 7-16276
magnetic tapes, friction reduction by acoustic excitation 7-65148
material compatibility, subsurface processes 7-16679
material compatibility, surface processes 7-26850
materials, wear, conf., Vancouver, BC, Canada (April 1985) 7-14701
metal surfaces, ion implanted, durability 7-53918
metal-carbide composites, implantation modified, friction, surface chemistry 7-46660
metal-polymer composites, wear resist., damping device appl. 7-17657
metallic glasses, amorphous material behaviour in friction 7-28151
metallic materials, surface refinement by ion implantation, friction, abrasive and corrosion resist. (*German*) 7-53949
metallic sliding friction, fatigue wear mechanism 7-8135
metallic surfaces, friction mechanisms 7-53921
microbubble skin friction reduction on an axisymmetric body in turbulent boundary layer 7-31772
micropolar fluid, unsteady flow past flat plate 7-63113
moving load on viscoelastic half-plane, anal. 7-57764
multidimensional mechanical systems with freq.-independ. friction, identification problems 7-87
nonstationary interaction 3D contact problems for elastic solids with friction, variational method 7-43806
nylon, friction and wear props., temp. effects 7-8132
PET, friction and wear under water lubrication, degree of crystallinity effect 7-3454
phenolic resin composites, optimisation for friction materials 7-39475
pipe friction experiment, appl. of TKI/Silver for students in Fluid Mechanics Laboratory 7-16260
plane anisotropic contact problems, Green's function soln. 7-6163
plate, circular, subjected to frictional forces, self-excited vibration, internal reson. effect 7-37364
plate, nonisothermal flat, free convection flow influenced by blowing or suction 7-11529
polyatomic ions in soln., rot., Hubbard-Onsager-Felderhof's dielectric friction theory 7-17281
polycarbonate, friction and wear, molecular orientation, uniaxial prestraining effect 7-13609
polydiphenylborosiloxane/aminimide-cured epoxy resin composites, friction and abrasion props. 7-39677
polyimide thin films, friction and wear rel. to struct. 7-8130
polyions, charged spherical, time depend. electrolyte friction calc. 7-21067
polymers, friction, electrophysical phenomena 7-17654
precision function components, improvements made by ion implantation (*Chinese*) 7-53919
pressure sensitive adhesives, ball rolling motion, friction coefficient, viscoelastic props. 7-28234
projection equipment, wearout in Geneva mechanisms (*Russian*) 7-11096
PTFE antifriction coatings, thickness and uniformity, X-ray fluoresc. method 7-17661
PVC, friction and wear, molecular orientation, uniaxial prestraining effect 7-13609

friction continued

rectangle, elastic, compressible object, contact interaction of two stressed half-planes 7-1518
rocks, fracture anal. 7-66106
rocks, friction and faulting 7-60251
rolling bearings, friction, wear and corrosion control 7-46658
rough disks, shear flow, constitutive relations 7-35267
rough surfaces, elastoplastic deform. in real contact zones, friction coeffs. calc. 7-16136
rough tubes, in staggered bundles, local features of flow 7-1628
rubber modified epoxy resin, tribological props. 7-17664
rubber vulcanizates, natural and styrene butadiene, environment effect on friction and wear 7-8131
sea-bed-structure interaction in the presence of frictional effects for submarine pipelines 7-20664
skin friction and wall shear stress meas. instrument 7-37406
solid struct. calcs. 7-51932
sphere, twisting, induced stress field 7-11314
spheres in beds in lengthwise flow, fluid friction and convective exchange 7-57917
stearic acid-Langmuir-Blodgett films, boundary lubricant efficiency (*Japanese*) 7-8118
steel, austenitic stainless, crack tip cyclic plastic work, load ratio, frictional work 7-53897
steel, austenitic stainless, high temp. sliding wear in CO₂ atm., effect of low conc. additions of O₂ 7-33806
steel, austenitic stainless, N-bearing, Nitronic 60, fretting wear at temps. up to 600°C 7-17653
steel, austenitic stainless, unlubricated reciprocating sliding wear in CO₂ at 20 to 600°C 7-17662
steel, Cr-Mo, friction pair, contact zone surface struct. and mech. props. (*Russian*) 7-59640
steel, Cr-Mo, friction pair, surface layer structural modifications (*Russian*) 7-39678
steel, low C, cold forgeability, notches, geometry, friction conditions, microstruct. 7-33697
steel, martensitic stainless, bearing appls., Ti and C ion implantation, enhanced lubricated sliding wear resistance 7-53916
steel, medium C, wear, influences of materials and operating parameters 7-8133
steel, Mn, austenitic, friction induced martensitic transform., wear resist., work hardened surface layer 7-17531
steel, stainless, O-alloyed friction structures, under conditions of thermal action, stability (*Russian*) 7-59673
steel, stainless, unlubricated 316, friction and sliding wear in air at room temp., 0.5 to 90 N load range 7-3451
steel, stainless SUS304, fretting props. in vac. environment, oxidative and adhesive wear 7-8122
stick-slip friction, acoustic output 7-50905
surface film formation in friction, physicochem. processes 7-21347
surface friction layers, study by AES method (*Russian*) 7-59674
surface modification and coatings, conf., Toronto, Ont., Canada (Oct. 1985) 7-41004
thermally affected layer caused by friction, temp. field, calc., experimental study 7-45095
thin hard coatings, adhesion test methods, review 7-46741
tribochemistry, chemical reaction increase by friction 7-46868
tubes fitted with helical heat transfer enhancers, fluid friction 7-57828
turbulent boundary layer, integral characts. 7-11395
turbulent boundary layers, mean flow, drag reduction, review 7-16171
turbulent boundary-layer skin-friction drag reduction meas. 7-51081
twisted circular-sector ducts, fluid flow and heat transfer anal. 7-11374
twisted oval tube, heat transfer and hydraulic drag coeffs. 7-1631
two-phase boundary layer, frictional stress meas. 7-44018
unsteady free-convection flow past accelerated plate, skin friction 7-4321
viscoelastic rarefied gas, MHD natural convection flows, buoyancy effects 7-6321
viscous incompressible fluid flow through porous medium and mass transfer 7-11532
water free and forced convective flow through porous medium 7-11533
wear and friction, crit. transition points 7-26853
Ag-brass, mixing layer, friction props., ion beam mixing (*Chinese*) 7-51888
Al-Si, graphitic, hot extruded powders, sintering, antifriction props. 7-13409
Al-Sn, bearing alloys, run-in kinetics, friction, contact resist., AE signals 7-17655
Al₂O₃ ceramics, friction and wear measured by a pin-on-disk method (*Japanese*) 7-22850
Al₂O₃-ZrO₂ toughened ceramics, dry friction and wear against steel 7-8125
a-C:H polymeric plasma-activated CVD films, tribological and mechanical props. studies 7-16920
Co-Cr perpendicular recording media with oxidised surface layer, wear resistance 7-28185
CrC_x coatings, tribological props., comp. depend. studies 7-53914
Cr₃C₂-based tribological coating for use to 900°C, appl. to Stirling engine 7-46696
Cu alloy base powder materials with MoS₂(Se₂), self-lubricating, tribotech. characts. 7-28146
Cu, dislocation-diffusion mechanism of wear reduction in selective transfer 7-17658
Cu powder, porosity influence on mech. and tribotech. characts. in high-speed friction 7-8119
Cu-composite material contact, sliding characts. and contact resistance (*Japanese*) 7-8120
Cu-Cu contact, sliding characts. and contact resistance (*Japanese*) 7-8120
Fe based eutectic alloy powder, plasma coatings with interstitial phases, tribotechnical props. 7-17731
Fe/Ti multilayered struct., wear and friction, ion beam mixing effects 7-28141
Fe-Cr-Mn-C alloy, laser clad, microstruct. and wear props. 7-13652
Fe-Ti/AISI 304 stainless steel system, ion beam mixed, wear and friction studies 7-46657
⁴He, superfluid, quantised vortex lines, turbulent motion 7-52168
HfN, sputtered coatings, wear and friction 7-33800
KCl crystals, rolling friction, elastoplastic deform. 7-16681
MoN_x sputtered coatings, tribological props. in contact with Cu 7-53911
MoS₂-based double layer solid lubricant, friction-reducing coatings 7-46669

friction continued

- $\text{Ni}_{52.5}\text{Mo}_{38}\text{Cr}_{10}\text{B}_{1.5}$ metallic glass, shock consolidated, wear props. 7-28154
 SiC ceramics, friction and wear measured by a pin-on-disk method (Japanese) 7-22850
 Si_3N_4 ceramics, friction and wear measured by a pin-on-disk method (Japanese) 7-22850
 Si_3N_4 , hot-pressed, friction and wear at 150 to 800°C 7-28142
 Si_3N_4 , hot-pressed, friction and wear 7-59642
 Si_3N_4 , with MgO addition, phys. and tribological props., effect of hot-pressing time (Japanese) 7-65150
 TiB₂-MoB base electrode materials for elec. spark alloying 7-28205
 TiC₂ coatings, tribological props., comp. depend. studies 7-53914
 TiN coatings, ion implanted, wear resistant props. (Japanese) 7-46698
 TiN, sputtered coatings, wear and friction 7-33800
 TiN thin films, activated reactive evaporation deposited, vacuum annealing, struct., mech. props. 7-8010
 W-C coatings on stainless steel, sputter deposited, mechanical props., effect of interlayers 7-53983
 WC₂ coatings, tribological props., comp. depend. studies 7-53914
 ZrN, sputtered coatings, wear and friction 7-33800
 ZrO₂ ceramic, partially stabilised, friction and wear meas. by a pin-on-disk method (Japanese) 7-22850
 ZrO₂-Y₂O₃, ZrO₂-MgO toughened ceramics, dry friction and wear against steel 7-8125

friction, internal see internal friction

frictional electricity see triboelectricity

FSK see frequency shift keying

fuel

see also coal; fission reactor fuel

- Chinese energy consumption growth forecast and implications for atmospheric CO₂ increase 7-28418
 coke dust, polydisperse, combustion kinetics 7-13776
 diesel fuel conversion using 2-stage hydrodesulfurization, suitable for H₃PO₄ fuel cells 7-65458
 drops combustion, stability loss mechanism in stream of oxidising gas 7-31892
 ethanol fuel production from wheat, technico-economic aspect (French) 7-28385
 gaseous, and solid fuel combustion, energy efficiency calc. (German) 7-8354
 hog fuel predrying by flue gas heat recovery 7-8356
 landfill gas recovery, natural and induced gas migration through cover materials 7-65396
 natural gas hydrate deposits prospecting, acoustic and resistivity meas. on rock samples containing tetrahydrofuran hydrates 7-55026
 natural gas pyrolysis in Ar arc plasmatron 7-39886
 Raman spectroscopy, role in study of energy sources, literature review since 1977 7-59827
 renewable resources, microbiological conversion into liquid fuels 7-65512
 waste fuels in the cement industry 7-28386
 CO₂ emission reduction from fossil fuels in future energy planning (French) 7-40053

fuel batteries see fuel cells

fuel cells

- alkaline fuel cells, low cost, development and hydrogen economy appls. 7-39950
 automotive long range highway vehicle propulsion system using fuel cells, R&D needs 7-65456
 battery technology trends (1981-6) and prospects (Japanese) 7-65429
 ceramic oxides, cond., for use as molten carbonate fuel cell electrodes 7-13854
 glycol/air fuel cells, electrode catalyst and fuel electrolyte soln. 7-39987
 Matsushita molten carbonate fuel cell development (Japanese) 7-65455
 molten carbonate fuel cell, performance model, oxidant depend. (Japanese) 7-65453
 molten carbonate fuel cell develop. and system anal. 7-65459
 molten carbonate fuel cell electrolyte structures, fabrication techniques 7-46934
 molten carbonate fuel cell program by US Department of Energy 7-65461
 molten carbonate fuel cells, corrosion, anal. using Cr-Li-K-C-O system phase relationships 7-28020
 molten carbonate fuel cells, fabrication of bubble press. barriers 7-13856
 molten carbonate fuel cells, performance model (Japanese) 7-59836
 molten carbonate fuel cells with low press. electrolyte, effect of carbonate content on cell performance (Japanese) 7-17858
 monolithic fuel cell tapes, three-layer ceramic composite, stress and fracture analysis 7-3407
 protonic solid electrolyte fuel cells, polarisation model 7-65454
 spacecraft batteries, testing facilities at the European Space Battery Test Centre 7-55412
 technology breakout in energy conversion, conf., San Diego, CA, USA (Aug. 1986) 7-60875
 trifluoromethanesulphonic acid electrolyte in fuel cells, O solubility, diffusion coeff., reduction rate, adsorption on Pt surface 7-28395
 ZrO₂ thin-film fuel cells, vacuum evaporation prep. (Japanese) 7-23132
 H₃PO₄ 500 W prototype fuel cell develop. 7-65457
 H₃PO₄ electrolyte in fuel cells, O solubility, diffusion coeff., reduction rate, adsorption on Pt surface 7-28395
 H₃PO₄ fuel cell, 11 MW International Fuel Cells-Bechtel demonstration project 7-28397
 H₃PO₄ fuel cell, mixing of reactant gases to simulate gas crossover 7-65460
 H₃PO₄ fuel cell develop. and system anal. 7-65459
 H₃PO₄ fuel cells using converted diesel fuel, 2-stage hydrodesulfurization 7-65458
 La_{1-x}Sr_xMO₃ (M=Cr, Mn, Fe, Co), electrodes for high temp. oxide fuel cells 7-54291
 Ni anodes for molten carbonate fuel cells, stabilisation 7-39988
 NiO porous cathode model for molten carbonate fuel cell 7-3640
 Pt anode in fuel cell, performance in presence of CO and CO₂, CO poisoning adsorption parameters calc. 7-13855
 Pt anode in phosphoric acid fuel cell electrolyte, H₂S poisoning 7-46933
 SrCeO₃ proton-conductive solid electrolyte fuel cell performance with ethane, CO and ethanol fuels 7-3641
 ZrO₂-Y₂O₃ solid oxide fuel cell development to 5 kW 7-28396

fugacity

see also kinetic theory of gases

- Malankhand Cu sulphide deposit, India, f(O₂), f(S₂) and pH conditions during ore deposition 7-29025
 H-CO₂ binary mixtures, H fugacity coeff. meas., physical equilib. technique 7-16296
 H-propane and H-methane binary mixtures, H fugacity coeff. meas., physical equilib. technique 7-16295
 H₂-CO₂ binary mixtures, H component fugacities, press. depend. 7-51367

full wave rectification see rectification

full wave rectifiers see rectifiers

function approximation

see also Chebyshev approximation; interpolation

- coupled dynamic thermoelasticity, approx. solns. 7-16062
 elasticity, unilateral BVPs, num. methods 7-24427
 ferromagnetic substance magnetisation curve descriptive function 7-64490
 linear second order differential eqn., prolate spheroidal functions with large parameters, uniform asymptotic expansions 7-35243
 multidimensional wave eqn., absorbing boundary conditions for difference approxs. 7-48384
 porous media, degenerate parabolic eqns., difference schemes 7-51306
 regression design on unit sphere in Hilbert space with limited resources 7-29736
 well-posedness of one-way wave equations and absorbing boundary conditions 7-48383

function evaluation

Bessel functions of complex argument, computation 7-41083

Fredholm determinant associated with path integrals, exact evaluation 7-61035

function generators

see also pulse generators; signal generators; time bases

programmable, multifunction dual-channel waveform generator for visual psychophysics 7-60006

functional analysis

see also harmonic analysis

- δ -function method for infinite series 7-48310
 algebraic function fields of genus one over real closed fields, isomorphism theorem 7-60994
 amplified climbing-sine map, non-diffusive aspects 7-72
 analytic continuation of local representations of symmetric spaces 7-55981
 analytic martingale convergence 7-29705
 Axiom A dynamical systems, resonance location, simple model 7-29893
 Banach algebras produced by 2D integral operators 7-60938
 Banach lattices, additive mean ergodic theorem (French) 7-55974
 basin boundary constructed by superposition of Weierstrass function 7-4658
 Bazilevic functions, determ. of geometric subclass 7-18561
 Bogolyubov generating functional method, transformation analog to collective variables 7-29870
 Bogolyubov generating functional method and analogue of transform. to collective variable in grand canonical ensemble 7-41230
 boundary circles for area-preserving maps 7-4660
 bounded holomorphic functions, explicit extension formula 7-55980
 circle maps, composition operator, existence of fixed points 7-24375
 concrete universally topological categories and subcategories, classification 7-60992
 constrained Lagrangian submanifolds over singular constraining varieties and discriminant varieties 7-60979
 convergence of images of probabilistic measures 7-48330
 correlation inequalities of FK_g type for monotone functions 7-14870
 cosine families in Banach spaces, perturbation 7-18563
 counterflow heat exchanger analysis, appl. of some special functions 7-62955
 cubic subcomplexes in regular lattices (Russian) 7-48594
 decreasing rearrangement of functions 7-61026
 degenerate system, Lagrangian and Hamiltonian constraints 7-61032
 density theorems for almost periodic functions 7-61028
 differential equation approach to functional equations, exact soln. 7-73
 Dirac formalism, mathematical introduction, book 7-60896
 Dirichlet discontinuity factor analogue for non-self-adjoint extensions of a Laplace operator (Russian) 7-60991
 Dirichlet forms and the density of real random variables on Wiener spaces (French) 7-29704
 discrete time bilinear models, minimality and invertibility (French) 7-60989
 dual mapping with a scale function 7-29693
 eigenvalues, sensitivity under elementary matrix perturbations 7-60955
 elliptic equations, local behaviour of solutions 7-55970
 elliptic equations, semilin., positive solns., symmetry-breaking 7-35210
 elliptic motion of arbitrary eccentricity and semi-major axis, expansion theory, general periodic function 7-60510
 elliptic systems, analytic singular perturbations 7-61021
 ergodic properties of linear dynamical systems 7-61044
 Euler-MacLaurin sum rules, zeta-function derivation for infinite series 7-61034
 explicit solution of the inverse periodic problem for Hill's equation 7-61046
 first integrals for π -systems, DISSYS program 7-48299
 fitting function determination method based on maximal errors 7-60981
 fractional calculus operators, appls. to classes of analytic and multivalent functions 7-61016
 functional integration, measure and support 7-9655
 generalized Fejer and Lanczos kernels 7-61055
 global blow-up of a nonlinear heat equation 7-62968
 global maximum, of function of several variables, numerical method determ. (Russian) 7-61060
 ground states and Dirichlet problems for $-\Delta u - f(u)$ in \mathbb{R}^2 7-41058
 growth, motion and 1-parameter families of symmetry sets 7-55960
 growth of harmonic functions in hyperspheres 7-61023
 Hadamard factorization of Selberg zeta function on compact Riemann surface 7-24392
 heat kernels for root systems and symmetric spaces of type B₂ (French) 7-55972
 heat transfer with viscous dissipation between infinite parallel plates, functional analysis 7-37459
 heat transfer with viscous dissipation in semi-infinite tube, functional analysis 7-37458

functional analysis continued

- Henon map unstable manifold, functional equation for segment 7-4661
 holomorphic functions on unbounded domains of C^n , boundary values (French) 7-60985
 Hopf bifurcation and symmetry, travelling and standing waves on circle, reaction-diffusion eqns. 7-56192
 hyperbolic-parabolic systems of conservation eqns., solns. large-time behaviour 7-55998
 invariant circles for the piecewise linear standard map 7-24376
 invariant density distrib. evolution under a discrete time quadratic map 7-35230
 Laplace transform of G function 7-18580
 Laquerre theorem extension to entire functions of exponential type 7-61024
 Legendre functions, closed analytical expressions and integrals 7-61005
 linear operators on matrices, invariance of decomposable numerical range 7-48274
 linear system with contractive propagator, Naimark's theorem on dilation, scatt. operators 7-35346
 Liouville-type results for fourth order elliptic equations 7-24393
 Ljapunov equation, appl. to 1D diffusion eqn. stabilisation 7-61283
 mathematical models in mechanics, book 7-55906
 matrix convex functions, connection with monotonicity 7-48283
 Meixner multinomials, use in the approximate calculation of integrals 7-61001
 minimisers, near singular points, behaviour of derivatives 7-41057
 mixed Schur functions, inequalities 7-29714
 monoenergetic neutron transport, solution to a parametric equation in transport theory 7-10179
 multi-valued functional construction, general method 7-61033
 multicomponent linear conjugation problem, asymptotic props. of solns. 7-29722
 multivalued differential systems, integral equivalence 7-18564
 Navier-Stokes equation, boundary conditions on pressure 7-9674
 Neveu Schwarz model, scattering amplitude calcs. using supersheet functional integration 7-442
 operator identities related to the SO_3 group 7-61142
 operator theory, symposium, Athens, Greece (Aug. 1985) 7-55878
 operators with closed ranges in spaces of analytic vector-valued functions 7-29702
 parabolic and elliptic equations, comparison soln. results 7-60982
 plane premixed flame, nonlinear differential system modelling (French) 7-28313
 pointwise convergence of densities under iteration of Ulam and von Neumann's map 7-35234
 positive functionals, unique extension 7-35218
 positivity in functional analysis, conf., Tübingen, Germany, (June 1985) 7-4638
 quantum field theory, progress, book 7-9602
 quantum logics, Gudder conjecture and joint distrib. 7-18625
 quantum oscillator in radiation field, interaction energy 7-29806
 quasi-invariant measures of infinite dimens. Grassmann manifolds 7-55949
 quasilinear elliptic equation, numerical solution of first boundary value problem (Russian) 7-55975
 (e) function calculation, maximal error method appl., plastic anisotropy coeff. 7-61101
 real singularities of singular Sturm-Liouville expansions 7-61052
 recovery in noisy network data by local splines (Russian) 7-61059
 regression design on unit sphere in Hilbert space with limited resources 7-29736
 representation projections for polygonal Bazilevic functions 7-18559
 Riemann hypothesis, fractal random walk approach 7-14896
 rim-finite spaces and the property of universality 7-18584
 Runge approximation theorems in complex Clifford anal. 7-55978
 Schauder condition in the critical point theory 7-14752
 second quantization and pseudodifferential operators 7-29815
 semilinear Dirichlet problem, multiple solutions 7-18560
 semilinear equations in large balls, set of positive solns. 7-61039
 space-periodically driven codimension-two bifurcations 7-18581
 spaces L_p with mixed norm in an infinite-dimensional torus 7-60940
 spectral methods using rational basis functions on an infinite interval 7-61076
 stable analytic continuation with a condition of uniform boundedness 7-29711
 stationary planar Euler flows in an unbounded strip, nonlinear stability 7-31883
 Stokes equations, collocation method, variational problem (French) 7-55973
 superlinear elliptic Dirichlet problems in almost spherically symmetric exterior domains 7-41059
 Toeplitz operators and quantum mechanics 7-14812
 Toeplitz operators on Bergman space, spectral theorems 7-60996
 transfer functions and operator theory 7-55983
 transversal heteroclinic points and Cherry's example of a nonintegrable Hamiltonian system 7-29697
 Tsirelson superspaces and l_p 7-29703
 universal functional equation for period doubling in constant jacobian maps 7-30183
 weighted composition semigroups on Hardy spaces 7-55964
 wigner quantized operator and Bogolyubov's generating functional method in nonequilibrium statistical physics 7-41239
 yield surfaces, initial and subsequent, translated deviator stress tensor 7-16061

functional equations

- dynamics and the calculus of variations 7-61085
 electron-phonon interacting systems, thermal Green's function generating functional from functional integrals with one-sided boundary conditions 7-52447
 nonconvex integral functionals, absolutely continuous subgradients 7-55994
 plates and shells, hybrid strain technique for FEA 7-20603
 probability and energy density currents, expression as density functionals 7-117
 retarded functional differential equations, heteroclinic orbits 7-18574

functionals *see functional equations***functions**

- see also Bessel functions; Boolean functions; describing functions; Green's function methods; random functions; recursive functions; transfer functions; vertex functions; Walsh functions*
 Airy functions, use of in integral evaluation 7-70
 algebras of functions similar to Lie functions 7-60941
 alternative algebras of functions 7-35206
 associated Legendre functions, alternate forms for use in geomag. modelling 7-14186
 Bessel function roots, summability 7-35201
 Bessel function zeros, monotonicity properties 7-35200
 bounded analytic functions, Banach algebra, closed and prime ideals 7-24349
 coupled stationary bifurcations in non-flux boundary value problems 7-29717
 divergence free functions, polynomial approx. (French) 7-60987
 empirical orthogonal functions, developments in use for mapping meteorological fields 7-29142
 Euler-MacLaurin sum rules, zeta-function derivation for infinite series 7-61034
 Fitting functors in finite solvable groups, behaviour with respect to direct products 7-29681
 fractional calculus operators, appls. to classes of analytic and multivalent functions 7-61016
 global inverse spectral problems for rational matrix functions 7-60961
 holomorphic functions on unbounded domains of C^n , boundary values (French) 7-60985
 inclination functions in artificial Earth satellites theory, connection with Tisserand's polynomials 7-47664
 infinite series of Bessel and Struve functions, closed expressions 7-61013
 L-pseudosolutions, generalised discrepancy principle (Russian) 7-61166
 Legendre functions, closed analytical expressions and integrals 7-61005
 multi-valued mappings approximation, marginal function differentiability (Russian) 7-60990
 n-circular domains of bounded holomorphicity and Liouville's theorem 7-35221
 nonlinear functions, minimization using Hessian matrix modified Cholesky factorizations 7-41074
 rational complex planar splines, mapping props. for interpolants from polynomial functions 7-29716
 Riemann derivatives and general integrals 7-24372
 S-function infinite series and non-compact Lie groups 7-35229
 $SO(3, 2)$ representation, special functions 7-35729
 Sobolev resonant function approx. use for the Ambartsumian-Chadrasekhar and Hopf functions determ. 7-40717
 stable analytic continuation with a condition of uniform boundedness 7-29711
 starlike univalent functions, characterisation 7-60993
 triangle functions, non-causal 7-48312
 V-function geometry and Liapunov stability theory 7-55989
 Wiener process, Brownian motion, Mobius' function and models (Russian) 7-24544

fundamental constants *see constants***fundamental law tests**

- electron mag. moment, fine struct. const., QED determ. 7-15109
 gravity probe-B expts., using superconducting thin film gyroscope 7-14855
 periastron precession in general relativity 7-48244
 servo-controlled lasers progress and appls. 7-20307

fundamental particles *see elementary particles***fundamental physics concepts** *see physics fundamentals***fundamentals of physics** *see physics fundamentals***furnaces**

- see also electric furnaces; refractories*
 analysis of the stability of heating processes from the point of view of measurement (Hungarian) 7-59765
 coal combustion, in fluidised bed furnace, mechanism investig., balance eqn. formulation 7-65322
 floating zone imaging furnace, molten zone temp. distrib., calc. method 7-17416
 gas radiation tubes, internal and external heat transfer, combined soln. 7-11415
 heat-pipe oven, superheating addition 7-36553
 mass flowmeter using heat transfer for dense phase solid-gas two-phase flow 7-37579
 massive optically dense body, short-time heating by radiant flux 7-11256
 multiheliostat solar furnace, anal. of subsystems structure 7-46920
 pulverised coal/air two-phase flowmeter 7-37580
 solid-gas two-phase flowmeter for blast furnace pulverised coal injection 7-37578
 tubular heat pipe furnace charact., gas-controlled 7-41375
 Au film, for LPE growth system, IR reflectivity (Korean) 7-33606
 NO_x in-furnace reduction, reburning, bench scale process evaluation 7-17798
 W ribbon furnace for electrothermal at. absorpt. spectrometry. temp. meas. 7-30017

Furry theorem *see quantum electrodynamics***fuses, electric** *see electric fuses***fusion** *see melting***fusion, nuclear** *see nuclear fusion***fusion-fission reactors** *see hybrid reactors***fusion reactor fuel**

- advanced fuels in a field-reversed configuration 7-56855
 ASDEX fusion experiment, particle balance, data anal. 7-49669
 conf., Austin, Texas, USA (Nov. 1985) 7-14703
 cryogenic falling liquid film He separator for T production, design concept 7-800
 cryogenic pulsed ion source focusing, beam characteristic 7-30655
 cryogenic pulsed ion source with stirling cycle refrigerator 7-30654
 fuel density-radius product of inertial confinement fusion targets, determ. using secondary nuclear fusion reactions 7-5405
 ICF, fuel ion temperature meas. using single-hit detector array 7-30646
 tandem mirror reactors, fuelling requirements 7-15317
 Tara tandem mirror, heating, gas press. meas. and control 7-63337
 thermonuclear fuel cycles, analysis 7-49679
 time-dependent net core breeding gain of fusion-fissionsymbiotic systems 7-804

fusion reactor fuel continued

- TRIDEX experiment, effective cross sections and prod. rates for tritium, blanket dev. 7-19428
 tritiated water, enrichment and vol. reduction using an electrolysis cell with a permeable cathode 7-49668
 Tritium Systems Test Assembly, current operations and experiments 7-36257
 DT ion-beam inertial fusion targets, compression and burn results, HIBALL-II reactor appl. 7-10282
³H, chemistry in fission and fusion reactors 7-25234
³H production in fusion blanket, on-line meas. method 7-62078
³H₂ recovery from inert gas by precious metal catalyst 7-62076
 Li flashover ion source development 7-30652
 LiD fusion plate design 7-19438
⁶LiD cylinder irradiated by 14 MeV neutrons, T and ⁴He prod., comparison with TART code 7-36245
 T breeder materials, BeO/Li ceramic, sphere-pac forms, thermal cond. 7-52163
 T breeding performance of self-cooled water-based blanket 7-56840
 T, extraction in and out of pile from LiAlO₂ and LiAl₂O₃ 7-49655
 T, near surface depth profiling in Li₂O and LiAlO₂ ceramics 7-49653
 T, recovery and inventory in fusion solid breeders, surface desorption effect 7-49651
 T, recovery from γ-LiAl₂ breeder blanket 7-49645
 T, release, in-pile from LiAlO₂, Li₂SiO₃ and Li₂O in EXOTIC expts. 7-49648
 T, release from fusion breeder blanket materials 7-49652
 T, release from LiO₂ and LiAlO₂ spheres, diffusion coeffs. 7-49643
 T release from tritiated Y, Y-Th and Y-Nb in Ar gas flow, 973-1173 K 7-56836
 T, retention in fast neutron irradiated Li based oxide ceramics 7-49649
 T retention in solid breeder blankets 7-49650
 T, surface adsorption on LiAlO₂ 7-52246
 T, transport modelling in solid γ-LiAlO₂ breeder blanket 7-49642

fusion reactor ignition

- see also *fusion reactor materials; plasma heating; plasma production*
 100 TW particle beam fusion accelerator for inertial confinement fusion program 7-30664
 ablative macroparticle accelerator using electron beam diodes as impact fusion drivers 7-36266
 AC tokamak reactor, 8 hour discharges 7-30660
 anode plasma production processes of low temperature type pulsed ion source 7-6423
 Applied-B ion diode expts. on Particle Beam Fusion Accelerator-I 7-10310
 ATF neutral beam injection system, description of basic parameters 7-19518
 Aurora Krf laser system, design and performance of large area monolithic electron guns 7-36987
 battery energy storage for fusion programs 7-15321
 boil off Li vapour source for PBFA II ICF expts. 7-25293
 cannonball target, absorpt. of 0.53 μm laser light 7-20923
 cluster ion accelerator using triangle-shaped accelerated waves 7-42246
 Common Long Pulse Accelerator, thermal and struct. anal. for TFTR, Doublet, MFTF 7-19434
 Common Long Pulse Source, mechanical baseline design 7-19433
 compact tokamak ignition expts., ohmic ignition prospects 7-15338
 compact torus, self-consistent modeling of quasi-steady state evolving to ignition 7-56854
 conf., Austin, Texas, USA (Nov. 1985) 7-14703
 cryogenic pulsed ion source focusing, beam characteristic 7-30655
 cryogenic pulsed ion source with stirling cycle refrigerator 7-30654
 cryogenic pulsed on beam research in Japan 7-25235
 DIII-D long pulse neutral beam system 7-19520
 ECRH to provide access to tokamak second stability region 7-26465
 electron beam accelerator, vacuum pulse conditioning and risetime sharpening 7-30659
 electron cyclotron reson. heating of mag. confined plasmas using TE01 to TM11 mode converters 7-37708
 EM mass driver, projectile velocity calc. 7-49671
 gas jet neutralizer for MFTF-B pure beam injectors 7-19436
 GEKKO XII high power Nd:glass laser, harmonic conversion 7-50571
 gyrotron appls. in fusion research 7-49617
 gyrotron development in the framework of the European Fusion Programme 7-49618
 gyrotrons for plasma diagnostics, development 7-1780
 HDCT design for study of tokamak plasma close to ignition 7-16330
 heavy ion ICF, current status and future prospects 7-62081
 high gain fusion target development facility 6-10 MJ driver 7-19490
 ICF, effect of UV irradiation on anode plasma production 7-6424
 ICF, experimental approaches to heavy ion fusion 7-6425
 ICF, numerical analysis for nonuniform implosion of target 7-6387
 ICF, observation of hydrodynamic instability in spherical target implosion with GeKKO XII green laser 7-5440
 ICF, power plant by LIB 7-5442
 ICF, self-similar ion beam fusion plasmas 7-5443
 ICF, vaporising liquid metal first wall 7-5441
 ICF target experiments, preliminary performance with Nova 7-15371
 ICF target implosion, moving finite element method 7-5439
 ICRH 1.5 MW generators for fusion reactor heating 7-15395
 Ignition Spherical Torus, enhanced elongation and paramagnetism 7-15331
 Ignition Studies Project, limiter design 7-25206
 Ignitor and LITE type compact ignition tokamak design spaces 7-19493
 imploding advanced fuel pellet, neutron heating effects, simulation 7-6421
 imploding shell during coasting phase, inner surface perturbations, amplitude variation 7-56844
 induction linac driver for inertial fusion, cost/performance analysis 7-25209
 inertial confinement fusion, Nova laser facility 7-1778
 inertial fusion drivers, Krf laser appl., cost/performance anal. between different systems 7-25210
 ion beam opening switch and plasma opening switch performance 7-26545
 ion diode, beam production and propagation 7-30656
 JET, impact of active phase, remote handling and fuel recycling 7-49678
 JET, neutral beam heating expts. 7-25163
 JET, neutral injection and ICR heating, status 7-30649
 JET, upgraded ICRF heating system, design and technology 7-49674

fusion reactor ignition continued

- JET, wall effects and impurities 7-56845
 JET additional heating expts. using ion cyclotron waves 7-25165
 JET and TFCC, plasma performance with sawtoothing, ignition 7-1685
 JET ICRF system, engineering design and performance 7-19504
 JET neutral injection system, operational test in test bed 7-25169
 JET neutral injection/RF heating power supplies, design 7-15322
 JET plasma heating 7-25166
 JFT-2M, ICRF heating, confinement studies 7-11660
 JFT-2M 60 GHz second harmonic electron cyclotron heating 7-62079
 JFT-2M pneumatic-gun pellet injector 7-56851
 JFT-2M tokamak, design and fabrication of ECRH system 7-19522
 JP JIPPT-IIU tokamak, Ion Bernstein Wave heating 7-6416
 JT-60, computer system for neutral beam injection equipment 7-25237
 JT-60 gas injection valve 7-19500
 JT-60 neutral beam injectors, cryopumps and cryogenic systems 7-19519
 JT-60 neutral beam injectors, performance at test bed facility 7-25168
 large-area liquid-lithium ion source for inertial confinement fusion 7-25296
 laser ablation studies, planar multilayered targets preparation 7-19426
 laser fission progress 7-802
 laser-imploded glass shells, study by multi-frame X-ray shadowgraphy. 7-30645
 laser-pellet fusion, collisionless plasma expansion, plasma wake study 7-31950
 launching system of LHRF and ICRF heating on JT-60 7-19502
 light ion beam fusion target development facility, design 7-25208
 linear stability of counter-streaming two strong ionbeams 7-6422
 LITE-R4, machine parameters, toroidal field coil 7-19474
 Long Pulse Accelerator, thermal and struct. anal. for TFTR, Doublet, MFTF 7-19434
 lower hybrid current drive, circuit anal. on tokamak 7-16328
 MFTF, design of mode-selective directional couplers for ECRH 7-19523
 MFTF, industrially fabricated ion source, test and conditioning 7-19435
 MFTF ICRH system, control and data acquisition 7-15396
 MFTF-B ICRH system—design summary and construction status 7-19501
 microparticle-initiated losses in magnetically insulated transmission lines 7-30658
 MIDAAS, ion diode, extraction performance 7-30657
 neutral beam line power flow 7-19437
 ohmic-heating coils, design optimization using simplex method (Chinese) 7-5421
 particle beam fusion, Nagoya, Japan (Nov. 1985) 7-4636
 particle beam fusion accelerator for inertial confinement fusion program, construction projection 7-30665
 particle beam fusion accelerator I (PBFA I), automated features of control/monitor system 7-30754
 Particle Beam Fusion Accelerator II (PBFA II), computer model of vacuum system design 7-30773
 Particle Beam Fusion Accelerator II (PBFA II), energy storage system 7-30765
 Particle Beam Fusion Accelerator II (PBFA II), energy transport meas. and computer simulation 7-30764
 Particle Beam Fusion Accelerator II (PBFA II), laser triggering optical system 7-30771
 Particle Beam Fusion Accelerator II (PBFA II), laser trigger system design 7-30772
 Particle Beam Fusion Accelerator II (PBFA II), quality assurance of R&D project 7-30763
 particle beam fusion accelerator II (PBFA II), vacuum insulator stack failure mechanisms 7-30749
 particle beam fusion accelerator II (PBFA II) control/monitor system 7-30751
 particle beam fusion accelerator II (PBFA II) data acquisition system with waveform recorders 7-30753
 Particle Beam Fusion Accelerator II (PBFA II) engineering design of pulse forming system 7-30770
 particle beam fusion accelerator II (PBFA II) high speed multi-channel data acquisition system 7-30752
 Particle Beam Fusion Accelerator II (PBFA II) Marx generator engineering and assembly line technology 7-30768
 particle beam fusion accelerator-II (PBFA-II), design of applied-B ion diode 7-36343
 PBFA II accelerator assembly and characterisation 7-30762
 PBFA II Plasma Erosion Opening Switch geometry effect on current transfer 7-26543
 PBFA-II photoactivation, fusion breakeven experiments, radiation protection problems 7-30775
 pellet compression schemes, indirect irradiation by relativistic electron beam 7-11808
 pellet injection into hot plasma, review 7-6437
 pipe gun for H pellet injection 7-19427
 plasma generator for long pulse 10×40 neutral beam 7-32007
 plasma opening switch experiments on PBFA I using flashboards 7-26542
 plasma opening switch performance on Supermite and PBFA II 7-26541
 plasma-filled applied-B diode 7-25297
 PLT, RF heating techniques and equipment, review 7-25176
 PPPL Ignition Studies Project 7-19473
 proton source, high purity, pulsed with cryogenic plasma diode 7-30815
 pulsed power accelerator for fusion research, SF₆ reprocessing system 7-30769
 pulsed power research facilities, successful long-term operation, contributing factors, PBFA-I as example 7-30778
 relativistic electron beam diodes, electrode design and appls. 7-20967
 relativistic electron gun, laser-pulsed 7-30653
 reversed field pinch at HBTX, basic principles 7-30663
 reversed field pinch fusion power reactor, 1000 MWe, plasma parameters (Japanese) 7-16319
 self sustained plasma in tokamak reactor, burn control by H feeding 7-795
 spherical fuel pellet compression using laser beams 7-32027
 steam, high density, initiation of electrical discharge, target ignition appl. 7-15324
 surface discharges as soft X-ray flashlamps 7-25236
 tandem mirror reactors, fuelling requirements 7-15317
 TARA neutral beam injector system, ion source electrical characterisation 7-19439
 TDF reaction chamber, fatigue lifetime analysis 7-25200
 TEXTOR neutral injectors, arc power supply 7-19476

fusion reactor ignition continued

TEXTOR neutral injectors, auxiliary power supplies design 7-19477
 TFTR, D and T pellet injector systems 7-19497
 TFTR, recent results 7-30650
 TFTR, tritium pellet injector design 7-19498
 TFTR deuterium pellet injector gun design 7-19499
 TFTR neutral beam heating system, present status 7-25167
 TFTR status and recent results 7-15310
 thermonuclear plasma, thermal stability for temp. depend. confinement time, Kaye-Goldston scaling 7-30647
 three-temperature plasma model, soln. method, inertial confinement fusion target design studies appl. 7-10278
 TMX-U, ECRH, quality assurance 7-19443
 TMX-U, ECRH control system 7-15397
 TMX-U, gyrotron anode modulation of ECRH 7-19525
 TMX-U, ICRH loop antenna 7-15394
 TNT-A Tokamak, localized electron heating expts. by ion Bernstein waves 7-1713
 Tokamak, compact ignition designs, plasma predictions 7-15315
 tokamak, compact ignition experiments, startup, confinement, α -effect assessments 7-15316
 tokamak devices with ohmic-heating dominated startup 7-15332
 Tokamak ignition devices, physics parameter space anal. using physics systems code 7-25214
 tokamak ignition-burn experimental research with TIBER 7-19472
 tokamak systems code, high-field ignition devices 7-15330
 tokamaks, plasma operating regimes and ignition conditions, contour anal. 7-15329
 two-dimensional modeling of the plasma opening switch 7-26544
 US Common Long Pulse neutral beam source, prototype testing 7-19432
 US ignition devices, experimental plans, machine design alternatives 7-15312
 WT-III, wave heating tokamak, design and manufacture 7-19521
 X-ray drive ICF, radiation transport modelling 7-6420
 CO₂ laser system for plasma heating 7-32031
 D-T direct drive implosions, neutron sources for diagnostics development 7-1776
 DT ion-beam inertial fusion targets, compression and burn results, HIBALL-II reactor appl. 7-10282
 KrF laser produced plasma, stimulated Brillouin scatt. 7-32032
 KrF laser system, Aurora, for inertial confinement fusion studies 7-15894
 KrF lasers, inertial confinement fusion appl. 7-10288
 Li ion source for PBFA II ICF research 7-25292
 Li plasma anode layers for PBFA II ion diode 7-25295
 Li plasma generation for large area ion diode 7-25294

fusion reactor instrumentation

see also fission reactor instrumentation
 actively cooled Langmuir probe for long pulse appls., design and fabrication 7-26517
 Alcator C tokamak, nonthermal electron distrib. functions during LH heating and current drive 7-11740
 Alcator C vertical viewing electron cyclotron emission diagnostic 7-11742
 ASDEX data acquisition system, local area network 7-19464
 coincidence techniques for fusion product meas. 7-11728
 conf., Austin, Texas, USA (Nov. 1985) 7-14703
 DIII-D, plasma diagnostic set, design, installation and operation, eng. and physics problems 7-25217
 DIII-D tokamak, grating spectrometer for electron cyclotron emission meas. 7-11741
 double scatter in time of flight spectrometer for fusion plasma, electronics implementation 7-15368
 fiber sensor neutron streak camera for ICF diagnostics 7-11721
 high temperature plasma diagnostics, conf., Hilton Head Island, SC, USA, (Mar. 1986) 7-9585
 ICF, fuel ion temperature meas. using single-hit detector array 7-30646
 inertial confinement fusion light balance meas., light-integrating cylinder 7-44253
 ion speed distrib. meas. in DD plasma 7-11723
 JAIERI reactor engineering dept 1985-6 annual report 7-56725
 JET diagnostic systems, interfacing aspects 7-15369
 JET neutron spectrometry 7-11713
 JET soft X-ray diode array diagnostic 7-25164
 JET tokamak, single Langmuir probes, spurious values of electron temp. 7-49677
 JT-60 discharge optimization, plasma modelling and simulation study 7-15360
 JT-60 integrated performance test 7-15361
 layered synthetic microstructures, X-ray diagnostic for magnetic fusion device instabilities 7-37748
 MEQALAC low- β in accelerator for plasma diagnostics 7-26528
 MFTF-B, background gas pressure diagnostic, electrical and mech. design 7-25220
 MFTF-B, mag. field alignment diagnostic for magnet system, design 7-25221
 MFTF-B mag. field alignment diagnostic, electron-beam source development 7-25222
 microchannel plate, use as collimators for high-energy charged particles, fusion plasma appl. 7-15124
 Mirror Fusion Facility, local control station development 7-19463
 Multichannel far infrared interferometer, MIRI, signal processing for electron density meas. 7-25232
 multichannel FIR collective scatt. and interferometry systems for fusion diagnostics 7-25215
 neutral beam source conditioning with AI techniques 7-19462
 neutron calorimeter as a fusion diagnostic 7-11726
 neutron diagnostics on TFTR utilizing the Campbell technique 7-11724
 neutron fluctuation measurements on TFTR 7-11729
 neutron streak tube for ICF meas 7-11722
 Nova, ICF, neutron spectroscopy 7-11715
 plasma control on the Tokamak de Varennes 7-15336
 plasma edge diagnostics, charged particle transmission through probe apertures 7-25159
 plasma fluctuations meas., integrated data acquisition and handling system based on digital time series anal. 7-25231
 radiochemistry and secondary reactions for the diagnostics of laser-driven fusion plasmas 7-11716
 soft X-ray average recombination coeff., average charge for metallic impurities 7-11761

fusion reactor instrumentation continued

SPRED VUV spectrograph, synchrotron radiation calibration 7-24711
 streak camera performance characs., with cooled CCD 7-19425
 TARA tandem mirror, heavy ion beam probe design 7-25223
 TEXT, diagnostic neutral beam system for impurities 7-25216
 TEXT, digital spectral anal. diagnostic for transport, turbulence and scatt. 7-25233
 TEXT, ECRH absorption and propagation studies via collective Thomson scattering 7-11749
 TEXT diagnostics, digital complex demodulation applied to interferometry 7-11752
 TEXTOR tokamak, current distrib. meas. by FIR polarimetry 7-11738
 TFTR, 14.7 MeV proton emission meas. 7-11730
 TFTR, detached plasma regime study using MIRI FIR interferometer 7-11760
 TFTR, neutral beam interlock system using infrared pyrometry 7-6469
 TFTR, neutron activation system analysis program 7-11725
 TFTR, nuclear reaction diagnostics of fast confined and escaping alpha particles 7-11732
 TFTR, optically thin electron cyclotron emission meas. using Michelson interferometer 7-11755
 TFTR neutral beam ion source fault detector 7-15401
 time-resolved 14-MeV neutron detector for triton confinement studies 7-11733
 time-resolved X-ray photography of laser imploded fusion targets 7-18960
 time-resolved X-ray spectrographic instrumentation for laser fusion and X-ray laser studies 7-18961
 TMX-U, E||B end-loss-ion analyser 7-25218
 TMX-U, neutral particle time-of-flight analyser for escaping particle vel. distrib. 7-25219
 TMX-U, plasma potential diagnostic, hardware and calibration system 7-25224
 TMX-U E||B end-loss ion spectrometers 7-11735
 TMX-U overview, plasma pot. control system development 7-15358
 tokamak plasma, 2D density distrib. using phase imaging interferometry 7-11739
 tokamaks, α -particle diagnostic approaches 7-11714
 Wolter X-ray microscope calibration 7-24750
 Si surface barrier detector for fusion neutron spectroscopy 7-11727
 ZnS scintillator for TFTR fusion product emission meas. 7-11731

fusion reactor materials

see also fusion reactor fuel; radioactive waste
 Advanced Toroidal Facility, helical field coils, assembly 7-19451
 Advanced Toroidal Facility, vertical field coils, design and manufacture 7-19452
 bonded armour tiles for in-vessel components, residual stresses 7-5416
 breeder blanket fluids, T extraction, Pd catalyzed oxidative diffusion 7-49641
 breeder blanket materials, expts. and test facilities 7-49621
 Canadian fusion breeder blanket program, Chalk River irradiation facilities 7-49664
 ceramic electrical insulators for liquid metal blankets 7-49624
 ceramic materials and technology survey 7-10215
 ceramics, props. meas., conf., Soverato, Italy (Sept. 1986) 7-9582
 coatings, review 7-42193
 conf., Austin, Texas, USA (Nov. 1985) 7-14703
 conference, Chicago, IL, USA (Apr. 1986) 7-48145
 Cr-MoVW ferritic steel, ductile-brittle transition temp., irradiation flux depend. 7-56825
 crack growth behavior, appl. of H embrittlement models 7-53850
 DEMO fusion reactor blanket, time-depend neutron effects, burnup calcs. 7-797
 design study of Fusion Material Irradiation Test Facility in Japan 7-56835
 DIII-D, vacuum protection system, limiter design 7-25230
 DIII-D tokamak, thermal insulation blankets and heater jackets for vacuum vessel and ports 7-25192
 direct conversion electrodes, material effects on energy conversion efficiency, neutral beam injection system appl. (Japanese) 7-10277
 disc bend test, parameterize anal. 7-54039
 divertor materials, heat load expts. with electron beam facility 7-49638
 divertor plate, mechanical properties of W-Cu bond 7-26848
 divertor plate for Next European Torus, testing and theoretical analysis 7-25198
 dual-ion irradiation station at Tokyo Univ. for fusion materials. testing 7-51875
 FCC pure metals, neutron irradiated, thermal stability of cascade defects, annealing expt. 7-51856
 FER first wall and divertor plate materials performance 7-56847
 first granules layer, protection in Cascade reactor 7-15392
 first wall, implantation-driven permeation characs. 7-49640
 first wall, materials selection 7-25155
 first wall, plasma disruption damage calc. 7-791
 first wall, sheath potential and thermionic emission, wall temp. dependence 7-30651
 first wall candidate alloys, HFIR irradiation microstruct. development 7-56824
 first wall candidate ferrite alloys, Ni doped, postirradiation tensile behaviour 7-56827
 first wall material candidates, thermal shock behavior 7-25189
 first wall materials, plasma-wall interactions 7-25156
 first wall materials for high-power-density reactor 7-19515
 first wall/blanket structures, comparison of tokamak and tandem mirror designs 7-25190
 first walls, ion debris and X-ray energy deposition and response 7-49639
 first-wall component testing, ORNL facilities 7-25186
 force flow cooled superconductor bends, mechanical invasions and failure criteria 7-15356
 Frenkel pair production cross sections, calc. fission-fusion neutron spectrum sensitivity 7-51849
 fusion blanket, self-cooled water-based, tritium breeding performance, neutronics anal. 7-56840
 fusion damage simulation, alloy irradiation 7-49660
 Fusion Neutronics Source (FNS) Facility 7-30819
 fusion nuclear technology experiments and facilities 7-19491
 gamma-ray emission rate effects on cross section meas. 7-30672
 gas diffusion and temperature dependence of bubble nucleation during irradiation 7-51874
 graphite, first wall thermal performance in ICF reactor 7-49634

fusion reactor materials continued

graphite, He ion irradiation, thermal desorption 7-52245
 graphite, nuclear material, corrosion and irradiation induced porosity 7-51836
 graphite, plasma interactive component surfaces, H recycling properties 7-63295
 graphite, pyrolytic, sputtering with O ions at various target temperatures 7-49633
 graphite, sublimation and hydrocarbon production under intense energy deposition 7-49629
 graphite, surface erosion by D_2^+ irradiation, structure 7-51869
 graphite, tokamak limiter, thermal properties, effusivity 7-49630
 graphite, tokamak limiter material, high heat load tests using 120 kW electron beam 7-26803
 graphite tokamak limiter, outgassing of impurities 7-49631
 HT-9 martensitic steel, radiation induced segregation 7-56830
 hybrid reactor pebble bed blanket, magnetohydraulic flow in Na-K eutectic mixture 7-15366
 Incoloy 800 H, oxidation, EMPA profiles in depletion zone 7-17727
 Inconel 600, H permeation studies for fusion reaction 7-5435
 Inconel 617, oxidation, EMPA profiles in depletion zone 7-17727
 irradiation, He effects control 7-51845
 irradiation, model for interstitial dislocation loop nucleation and growth kinetics 7-51817
 JET, limiters and first wall, use of graphite tiles 7-19513
 JET nuclear fusion plant, gas-insulated HV cable for neutral injector (German) 7-62064
 laser-imploded glass shells, study by multi-frame X ray shadowgraphy 7-30645
 Light Ion Beam Fusion Target Development Facilities, activation studies 7-49732
 limiter design for Ignition Studies Project 7-25206
 limiter-first wall structure, tritium movement predictions using TMAP safety code 7-36258
 low activation, tempering, toughness, ductile-brittle transition properties 7-53862
 Low-Temperature Neutron Irradiation Facility for fusion materials research 7-49665
 MARS blanket lifetime prediction, dimensional scaling and material property uncertainties, STAIRES code 7-5417
 metals, bubble nucleation and growth under neutron and proton irradiation, nonequilibrium statistics 7-51848
 metals, He production and long-term activation by protons and deuterons, fusion reactor application 7-58371
 metals, irradiation-induced transient creep during pulsed irradiation 7-13528
 near term fusion reactors, key materials issues 7-49620
 NET, first wall protection 7-49622
 neutron irradiation, defect structure 7-51844
 neutron irradiation, dosimetry and damage calculations 7-51847
 neutron irradiation damage on metals (Japanese) 7-32508
 neutron requirements and sources for fusion development 7-19492
 neutron sources for fusion subcomponent testing 7-15442
 nuclear data and integral neutronics experiments for fusion reactors 7-30674
 nuclear data for fusion blanket neutronics 7-30675
 nuclear data status for fusion reactor structural materials 7-30673
 nuclear fusion superconducting magnets development 7-5408
 organic coolant, radiation stability 7-62059
 organic coolants, fusion reactor application 7-56841
 organic coolants for fusion applications 7-25160
 OSIRIS instrumentation for fusion reactor material irradiation tests; 7-49568
 oxide breeders, T recovery and inventory, surface desorption effect 7-49651
 plasma interactive components, neutron damage, sputter erosion 7-49623
 plasma limiter materials, operating performance, plasma-induced degradation 7-26818
 plasma-first wall interactions in tokamaks, effects of vapour shield formation 7-19514
 plasma-wall interaction in fusion devices, conf. Princeton, NJ, USA (May 1986) 7-60861
 plasma-wall interactions, redeposited material behaviour and structural changes 7-51458
 polyethylene film, low density, electrical properties relative to nuclear irradiation, 5K 7-53232
 precipitation modelling under cascade damage 7-52059
 preoxidation procedures for high temp. alloys 7-5436
 RFX, first wall and vacuum vessel design, technological aspects 7-25187
 RTNS-II fusion materials irradiation facility, status 7-49667
 S-1 Spheromak flux core, use of explosive forming to manufacture resistive vacuum torus 7-25204
 selection, safety and environmental challenges 7-49626
 self-cooled heavy water breeding blanket concept 7-15364
 self-cooled heavy water fusion breeding blanket, neutronics analysis in 1D 7-15365
 self-cooled liquid metal blankets, analysis of MHD effects 7-15363
 SIRIUS-M, ICF test facility, materials testing 7-49663
 SIRIUS-M, symmetric illumination, inertially confined direct drive materials test facility 7-49661
 solid breeder blankets, thermomechanical properties, T retention 7-49650
 solid breeder materials, irradiation effects using FFTF 7-49662
 sources for materials testing 7-15388
 sputtering, preferential, collisional aspects using Monte Carlo method 7-53464
 sputtering yields and plasma contamination 7-56843
 stainless steel, electron beam heating, vaporisation and melting measurements, first wall application 7-26929
 steel, austenitic, ^{59}Ni doped, design of single variable He effects experiment for FFTF irradiation experiments 7-49666
 steel, austenitic, Cr-Mn, thermal and mechanical properties, fusion reactor application 7-53795
 steel, austenitic, first wall material, H permeability study 7-62058
 steel, austenitic, fusion reactor first wall material, development and testing 7-53860
 steel, austenitic, in fusion reactor first wall, gas thermal desorption by plasma streams 7-49616
 steel, austenitic, low-activation, constitution, structural and mechanical properties 7-42195
 steel, austenitic, stainless, high temp. ductility, H and He effects 7-5406
 steel, austenitic Cr-Mn, corrosion in thermally convective Li 7-53960

fusion reactor materials continued

steel, austenitic stainless, compatibility with liquid and solid T breeding materials 7-53966
 steel, austenitic stainless, corrosion in flowing PbLi eutectic 7-53958
 steel, austenitic stainless, electron beam welded, void swelling under electron irradiation 7-51830
 steel, austenitic stainless, FT limiters structure and chemical modifications compared with disruption simulation damage 7-51521
 steel, austenitic stainless, fusion reactor blanket material, oxidation and volatilisation rates in air 7-53957
 steel, austenitic stainless, fusion reactor first wall, fast neutron irradiation, microstructure evolution model 7-51846
 steel, austenitic stainless, fusion reactor first wall behaviour after plasma disruption, electron beam experiment 7-62068
 steel, austenitic stainless, grain boundary microstructure, He embrittlement resistance 7-56829
 steel, austenitic stainless, He-induced creep ductility loss, prediction and analysis 7-53854
 steel, austenitic stainless, in-beam creep rupture properties at 873K 7-53851
 steel, austenitic stainless, in-reactor deformation 7-56826
 steel, austenitic stainless, low activation, development, mechanical properties, fusion reactor structural material 7-53799
 steel, austenitic stainless, materials erosion and redeposition studies at PISCES facility, net erosion under redeposition 7-49637
 steel, austenitic stainless, precipitation stability, during heavy ion irradiation 7-58367
 steel, austenitic stainless, strength and toughness at 4K, fusion energy magnets application 7-53793
 steel, austenitic stainless, swelling under dual ion beam irradiation 7-44629
 steel, austenitic stainless, void stability, effect of O 7-58262
 steel, austenitic stainless and Cr-Mo, corrosion in flowing Li environment, temperature and purity depend 7-53961
 steel, austenitic stainless and Cr-Mo, corrosion in molten thermally convective Pb-Li 7-53962
 steel, austenitic stainless and CrMo, corrosion in flowing Pb-Li environment 7-53959
 steel, austenitic stainless radiation damage process observations using high voltage electron microscopy 7-51831
 steel, Cr-Mo, cyclic softening, creep and fatigue, fusion reactor applications 7-53757
 steel, Cr-Mo, ferritic, reduced activation fusion reactor structural material, development 7-53665
 steel, Cr-Mo, normalised, tempered, neutron irradiation, 390-550°C, tensile properties 7-17621
 steel, Cr-Mo, toughness, impurity element effects 7-53856
 steel, Cr-Mo ferritic-martensitic, fracture toughness precipitation of Laves phases 7-53849
 steel, ferrite, low activation, correlation of hot microhardness with elevated temperature tensile properties 7-53797
 steel, ferritic, fusion reactor first wall material, development and testing 7-53860
 steel, ferritic, HT-9, mechanical properties as function of heat treatment 7-53858
 steel, ferritic, unirradiated, low activation, microstructure and mechanical properties 7-53863
 steel, ferritic stainless, 11 MeV proton irradiation behaviour 7-58369
 steel, ferritic stainless, cavity formation, effect of electron/He dual beam irradiation 7-58341
 steel, ferritic stainless, He-doped, microstructure evolution following 14 MeV Ni ion irradiation 7-58363
 steel, ferritic stainless, Mo, welding, heat affected zones, microstructure, thermal history 7-53769
 steel, Mo stainless, microstructure relative to heat treatment 7-53770
 steel, pressure vessel and stainless, low dose neutron irradiation, spectral effects on yield stress 7-51850
 steel, rapid solidification, fusion reactor application 7-49657
 steel, reduced activation alloys, development, fusion material application 7-53664
 steel, stainless, H degradation by disc. press. test 7-53855
 steel, stainless, martensitic, low-activation, for first wall and blanket structures, development prospects 7-42194
 steel, stainless, neutron irradiated, defect clusters, positron annihilation lifetime measurements 7-51853
 steel, stainless, neutron irradiation effects on mechanical properties, damage and yield stress 7-51865
 steel, stainless, radionuclide deposition from Na coolant 7-62060
 steel, stainless, superalloy, fracture toughness; tensile properties, T and ^3He effect 7-46616
 steel, stainless, surface deuterium recombination 7-62063
 steel, stainless, type 316, neutron damage USA-Japan studies 7-56834
 steel martensitic, stainless, low activation, hardening, tempering, mechanical properties 7-53861
 steels, stainless, α -particle irradiated, mechanical properties and microstructure 7-51872
 structural materials, neutron irradiation effects (Japanese) 7-19424
 structural alloys, irradiation, creep fracture by grain boundary cavitation, modelling 7-53859
 structural materials, swelling after neutron and ion irradiation, comparison 7-58357
 supercond. mag. material, fusion reactor conditions simulation 7-52922
 superconducting coil, mechanical behaviour 7-15345
 SUS316, 40 keV Cu^+ , Fe^+ and fission neutron irradiation effects 7-56823
 TCA Tokamak, first wall damage, H recycling models 7-801
 TEXTOR, plasma boundary structure, effects on impurity release, density measurements 7-16325
 TEXTOR liner, radial H flux measurements 7-63352
 TFTR bumper limiter, dynamic analysis 7-56837
 TFTR bumper limiter and final protective plate engineering, fabrication and assembly 7-25195
 Tokamak de Varennes, disruption-induced currents in vacuum vessel and liner 7-15352
 toroidal field coils for compact tokamak ignited experiments, structural evaluation 7-15346
 Al and Al alloys, 800 MeV proton irradiation, gas accumulation at grain boundaries 7-58361
 Al, fusion reactor first wall behaviour after plasma disruption, electron beam experiment 7-62068
 Al-Mg-Bi-Cr, low activation alloy development for reacting plasma experiment 7-15384
 Al-Mg-Cu-Zr, low activation alloy development for reacting plasma experiment 7-15384

fusion reactor materials continued

- Al-Mg-Li, 14 MeV neutron irradi., mech. props. microscopic struct. 7-56820
- Al-Mg-Si, high-purity, nucleation and growth of precipitates and the bubbles, effect of 600 MeV protons 7-58364
- Al₂O₃, electrical props., radiation effects 7-52617
- Al₂O₃, neutron irradi., microstruct., mech. props. 7-51843
- Au, cascade overlap effect on defect struct. after repeated neutron irradiation 7-51859
- Au, defect development from displacement cascade damage in low temp. neutron irradiation 7-51851
- Au, neutron irradiated, recoil energy effects on cascade defect structures 7-51855
- Au, surface deuterium recombination 7-62063
- BE prototype limiter for JET, thermal fatigue tests, microcracking 7-5415
- Be, energy multiplier in fusion reactor blanket, costs and benefits 7-49625
- Be, fusion machine wall material erosion and impurity prod. 7-62074
- Be limiter material, effect of heat and particle fluxes in ISX-B* 7-20866
- Be limiter material for ISX-B tokamak 7-19422
- BeO, neutron multiplication study by shift register coincidence technique 7-30467
- BeO/Li ceramic, sphere-pac forms, T breeder materials, thermal cond. 7-52163
- BeO/LiAlO₂ blanket, neutron activation calcs. in Cascade 7-15380
- C, fusion machine wall material erosion and impurity prod. 7-62074
- C, fusion reactor first walls, ion debris and X-ray energy deposition and response 7-49639
- Cr, He production in HFIR neutron irradiated pure elements 7-51852
- Cr-Mo ferritic steel, 14 MeV neutron irradi., mech. prop. changes 7-56821
- Cr-Mo-Ni ferritic-martensitic steel, irradi. in RTNS-II, TEM study 7-58345
- CrMoV ferritic steels, He containing, fatigue behaviour in fusion reactor 7-56828
- CrMoVNbNi steel, Ni addition effect on void formation following irradi. 7-56822
- CrMoVWNi steel, Ni addition effect on void formation following irradi. 7-56822
- Cu alloys, candidate materials for high heat load appl. in neutron environments 7-49636
- Cu alloys, high-strength, rad.-enhanced recrystn. 7-51871
- Cu alloys, irradi. in FFTF to 16 dpa at 450°C, microstruct. eval. 7-51837
- Cu alloys, neutron irradi., cond. changes, porosity swelling and transmutation contrib. 7-51838
- Cu alloys, neutron irradi., 13 dpa, mech. prop. and elec. cond. changes 7-51839
- Cu alloys, rapid solidification, fusion reactor appl. 7-49657
- Cu alloys, rapidly solidified powder metallurgy, irradi. to 13.5 dpa with neutrons, microstruct. evolution and swelling 7-51840
- Cu and alloys, neutron irradi. effects, elec. cond., fusion reactor appl. 7-51835
- Cu, cascade overlap effect on defect struct. after repeated neutron irradiation 7-51859
- Cu commercial alloys, low neutron dose effects on tensile props., yield stress 7-51863
- Cu, damage correlation of high energy neutron and ion irradiation, sub-cascades 7-51860
- Cu, defect development from displacement cascade damage in low temp. neutron irradiation 7-51851
- Cu, electron beam heating, vaporisation and melting meas., first wall appl. 7-26929
- Cu Foametal, high thermal conductivity material, thermal, mechanical and vacuum props. 7-25191
- Cu, He production in HFIR neutron irradiated pure elements 7-51852
- Cu, ion irradiated, mech. prop. meas. 7-51873
- Cu, low dose neutron irradiation, spectral effects on yield stress 7-51850
- Cu, low neutron dose effects on tensile props., yield stress 7-51863
- Cu, materials erosion and redeposition studies at PISCES facility, net erosion under redeposition 7-49637
- Cu-Li, prep. and props. 7-53663
- Cu-Ni-Fe, irradi., stability of periodic decomp. struct. 7-58366
- Cu-Zn alloys, electron irradiation, interstitial cluster form., diffusion rates, resistivity 7-2013
- Cu-Zr, ion irradiated, mech. prop. meas. 7-51873
- Cu₂Au, irradiation disordering and reordering by fusion neutrons, electrical resistivity meas. 7-51864
- CuPd, disordering by 14 MeV Cu ions between 296 and 823 K 7-51877
- (Fe,Ni)₂V, LRO alloys, mech. props., effects of strain rate and long-term ageing 7-53796
- Fe, He production in HFIR neutron irradiated pure elements 7-51852
- Fe, neutron irradiated, defect clusters, positron annihilation lifetime meas. 7-51853
- Fe, neutron irradiation effects on mech. props., damage and yield stress 7-51865
- Fe, zone refined, radiation hardening by 14 MeV neutrons, temp. depend. 7-51857
- Fe-9Cr ferritic steel, 40 keV Cu⁺, Fe⁺ and fission neutron irradi. effects. 7-56823
- Fe-Cr, neutron irradiated, defect clusters, positron annihilation lifetime meas. 7-51853
- Fe-Cr (12 at.%), ferritic alloy, He⁺ implantation and Fe⁺ irradi., bubble nucleation and growth 7-58362
- Fe-Cr-Ni, austenitic, electron irradi., conversion of stacking fault tetrahedra to voids 7-58342
- Fe-Ni-Cr, high-purity, irradi., void swelling and nucl.-induced phase transformations. 7-58340
- Fe-Ni-Cr (25,15 wt.%), MC stabilized, fatigue life, effects of implanted He 7-53852
- Fe-Ni-Cr austenitic alloys, MC carbide dispersed, void swelling and precip. behaviour following proton irradi., dose depend. 7-58365
- Fe-Ni-Cr-Mo-Ti-C, JPCA, He injected and creep ruptured, microstruct. obs. 7-53853
- Fe-Ni-Cr-P, ion irradi., swelling suppression, effect of P modification 7-58358
- FeCrNiWMo alloys, sputtering effects on props 7-36240
- FeNiCr, grain boundary solute segregation 7-56833
- He cooled, high flux heat removal, assessment study 7-25194

fusion reactor materials continued

- Li based ceramics, fusion breeder blanket, irradi., high burnup, large temp. gradients 7-49644
- Li based oxide ceramics, fusion breeders, chemical compatibility with stainless steels 7-49646
- Li ceramics, thermal stability with fusion reactor structural materials 7-38227
- Li containing ceramic, T breeder material, thermal cond. 7-10280
- Li flow in transverse magnetic fields, heat transfer and temp. fluctuations, fusion reactor cooling appl. 7-6327
- Li, flowing environment, corrosion of steels 7-53961
- Li, liq. fusion reactor blanket, mass transfer in dynamic environment, corrosion damage 7-49659
- Li, thermally convective, corrosion of austenitic Cr-Mn steels 7-53960
- Li-Pb, liq., T breeder material, compatibility with austenitic stainless steel 7-53966
- Li-Pb, liq. fusion reactor blanket, mass transfer in dynamic environment, corrosion damage 7-49659
- γ-LiAlO₂, ceramic, T breeding material, compatibility with austenitic stainless steel 7-53966
- γ-LiAlO₂, breeder blanket, T recovery 7-49645
- LiAlO₂ ceramic breeder material, fabrication for NET programme 7-798
- LiAlO₂ ceramic breeder material, post irradi. T recovery 7-49647
- LiAlO₂, ceramics, fast neutron irradi., T and He retention, high temp. vacuum extraction 7-49649
- LiAlO₂ ceramics, near surface T depth profiling, low energy nuclear reactions 7-49653
- LiAlO₂, fabrication, irradi., in-pile T release, EXOTIC expts. 7-49648
- LiAlO₂, fusion blanket material, effects of sweep gas, extraction vessel material and ceramic props 7-49664
- LiAlO₂, fusion breeder blanket, in-situ T release 7-49652
- γ-LiAlO₂, fusion reactor breeder blanket, T transport modelling 7-49642
- γ-LiAlO₂, neutron irradi. effects 7-51841
- LiAlO₂, surface adsorpt. isotherms, T inventory appl. 7-52246
- LiAlO₂, T ceramic breeder material, Italian fusion technology programme review 7-10279
- LiAlO₂, T extraction in and out of pile 7-49655
- LiAl₂O₃, T extraction in and out of pile 7-49655
- LiNO₃/LiNO₂ as fusion reactor coolant fluid, thermochemical assessment 7-62073
- Li₂O, elastic and creep props., porosity and temp. depend. 7-53780
- Li₂O, ceramic breeder material, post irradi. T recovery 7-49647
- Li₂O, ceramics, fast neutron irradi., T and He retention, high temp. vacuum extraction 7-49649
- Li₂O ceramics, near surface T depth profiling, low energy nuclear reactions 7-49653
- Li₂O, fabrication, irradi., in-pile T release, EXOTIC expts. 7-49648
- Li₂O, fusion blanket material, effects of sweep gas, extraction vessel material and ceramic props. 7-49664
- Li₂O single crystals, compressive creep and plastic deform. at high temp. 7-51920
- Li₂Pb₃, breeding blanket, NET, LOCA, mechanical anal. 7-19444
- Li₂SiO₃, fabrication, irradi., in-pile T release, EXOTIC expts. 7-49648
- Li₂SiO₃, fusion breeder blanket, in-situ T release 7-49652
- Li₂SiO₃, Li₄SiO₄, Li₆SiO₅, breeder materials, prep. in alcoholic media 7-49654
- Li₂SiO₃ pellets, sintering, density, struct., porosity 7-53682
- Li₄SiO₄, fusion breeder blanket, in-situ T release 7-49652
- Li₂ZrO₃, ceramics, fast neutron irradi., T and He retention, high temp. vacuum extraction 7-49649
- ⁶LiD cylinder irradiated by 14 MeV neutrons, T and ⁴He prod., comparison with TART code 7-36245
- MgAl₂O₄, neutron irradi., microstruct., mech. props. 7-51843
- MgAl₂O₄, spinel single cryst., low dose neutron irradi., swelling, defect interaction 7-51842
- MgAl₂O₄:He spinel, implanted, high temp. electron irradi., structural damage 7-51829
- Mo, He pipe diffusion along dislocations 7-58544
- Mo single crystal, cold worked, He pipe diffusion along dislocation, thermal desorption spectra 7-52142
- Mo single crystals, neutron irradiation embrittlement, yield strength 7-51854
- Mo, thermodynamic stability in a fusion reactor environment, H, O and C implantation and diffusion 7-49658
- Mo, TiC coated, H absorption under glow discharge fusion reactor appl. 7-52244
- Mo, TiC coated, low cycle fatigue behaviour 7-53848
- Mo, tokamak limiter material, high heat load tests using 120 kW electron beam 7-26803
- Na cooled reactors, radionuclide behaviour 7-25038
- (Nb,Ti)₃Sn, supercond. mag. material, fusion reactor conditions simulation 7-52922
- Nb, electron beam heating, vaporisation and melting meas., first wall appl. 7-26929
- Nb, He production in HFIR neutron irradiated pure elements 7-51852
- Nb, neutron irradiated, effect of irradiation temp. and O impurity on yield strength 7-58344
- Nb-Sn composite wires, effectiveness of V as diffusion barrier material 7-15353
- Nb-Ti, supercond. mag. material, fusion reactor conditions simulation 7-52922
- NbN composites, fusion reactor magnet appls., sputter deposition, critical props. 7-49627
- Nb₃Sn coil, high field performance 7-15354
- Ni alloys, high temp. ductility, H and He effects 7-5406
- Ni alloys, thin oxide films for H barriers, growth study 7-2434
- Ni, creep, electron bombardment effect, 200 to 500°C 7-8062
- Ni defect development from displacement cascade damage in low temp. neutron irradiation 7-51851
- Ni, He production in HFIR neutron irradiated pure elements 7-51852
- Ni, irradi. with energetic ions, defect prod. and recovery 7-58370
- Ni, Ni ion irradi., 14 MeV, void form., gas effects 7-58360
- Ni, radionuclide deposition from Na coolant 7-62060
- Ni, T-induced He bubbles on grain boundaries migration and coalescence 7-58289
- Ni, void stability, effect of O 7-58262
- Ni-Si, ductility, influence of rad.-induced segregation 7-53798
- Ni-Si alloy, Ni₃Si precipitation during electron and ion irradiation 7-51876
- Pb-Li, flowing environment, corrosion of fusion reactor structural steels 7-53959

fusion reactor materials continued

- Pb-Li, molten, thermally convective, corrosion of austenitic stainless and Cr-Mo steels 7-53962
 PbLi eutectic, flowing, corrosion of stainless steel 7-53958
 Pb(n,X), 14 MeV, neutron multiplication, leakage rate from sphere, fusion reactor appls. 7-62061
 SiC fibre reinforced Al composite wires, neutron irradi., mech. props., fusion reactor appl. 7-49628
 SiC fibre reinforced SiC, high heat flux, low activation struct. materials 7-49635
 SiC fibres, neutron irradi., mech. props., fusion reactor appl. 7-53794
 SiC, fusion reactor first walls, ion debris and X-ray energy deposition and response 7-49639
 SiC-Al composites, heat treatment and neutron irradi. effects on mech. props. 7-65081
 SiC-C alloy coated graphite as armour tiles, post-exposure anal. after high heat loadings 7-49632
 Si₃N₄, hot pressed, elec. cond., microstruct., fusion reactor insulator appl. 7-52619
 T production rate in Li blanket, TLD meas. (German) 7-15309
 Ta-T system, distortion by He form. 7-51717
 Ti, electron beam welded, neutron irradi. effects 7-56832
 Ti, He production in HFIR neutron irradiated pure elements 7-51852
 Ti-6Al-4V, electron beam welded, neutron irradi. effects 7-56832
 Ti_{1-x}B_x films deposited onto Mo by co-sputtering, D retention 7-51870
 TiC and TiB₂ coatings, effect of stoichiometry on D retention, thermal desorption study 7-6997
 V alloys, neutron irradiation effects 7-53750
 V, oxidation in moist He coolant gas 7-53963
 V, radiation hardening by 14 MeV neutrons, athermal effects 7-51858
 V-20Ti pressurized tubes, creep response to neutron irradi. 7-56831
 V-CR-Ti (15, 15 wt.%), mech. props., effect of heat treatment and impurity conc. 7-53857
 V-Cr-Fe, corrosion in pressurized water, 288°C 7-53967
 V-Cr-Ti, corrosion in pressurized water, 288°C 7-53967
 V-Cr-Ti, fusion reactor blanket, surface alloying, oxidation resist. to high temp. He coolant 7-53964
 V-Cr-Ti, fusion reactor first wall, oxidation and volatility 7-53965
 V-Cr-Ti, ion-irradi., swelling and microstruct. evolution, effect of He 7-58359
 V-Cr-Ti, V-Cr, oxidation in moist He coolant gas 7-53963
 V-Ti, corrosion in pressurized water, 288°C 7-53967
 VB, 14 MeV neutron irradi., TEM dislocation obs. 7-56819
 VO solid solution, vaporisation study by mass spectrometric method, fusion reactor material 7-52027
 W, thermodynamic stability in a fusion reactor environment, H, O and C implantation and diffusion 7-49658
 W-Cu duplex struct., brazed test pieces, durability against thermal fatigue (Japanese) 7-56818
 Y, T release in Ar gas flow, 973-1173 K 7-56836
 Y-Nb, T release in Ar gas flow, 973-1173 K 7-56836
 Y-Th, T release in Ar gas flow, 973-1173 K 7-56836
 Zn, fusion reactor first wall behaviour after plasma disruption, electron beam expt. 7-62068
 Zr, neutron irradiated, solute effects on damage production and recovery 7-51861
 Zr-Ti (Sn)(Dy)(Au), neutron irradiated, solute effects on damage production and recovery 7-51861
 Zr-Ti(Sn)(Au), low temp. damage prod. and recovery after fusion neutron irradiation 7-51862
 ZrO₂, partially stabilised, phase stability, elec. cond., fusion reactor elec. insulator appl. 7-52618
 Zr₃Pb₃, fusion blanket neutron multiplier, fabrication and props. 7-49656

fusion reactor safety

- Cat-D fueled reversed-field pinch reactor assessment 7-5419
 conf., Austin, Texas, USA (Nov. 1985) 7-14703
 FFTF as an irradiation test bed for fusion materials and components 7-49662
 fusion damage simulation, alloy irradiation 7-49660
 JET, ⁴He leak detection in the presence of high D₂ partial pressure 7-49675
 maintenance reliability influence on safety and availability 7-19468
 materials selection, safety and environmental challenges 7-49626
 MINIMARS, tandem mirror direct converter design for high-temperature heat recovery 7-25212
 NET, preliminary design considerations, ³H control 7-49670
 neutral beam injection duct concrete shield, differential gamma dose rate 7-36242
 steel, austenitic stainless, fusion reactor blanket material, oxidation and volatilisation rates in air 7-53957
 steel, austenitic stainless, fusion reactor first wall behaviour after plasma disruption, electron beam expt. 7-62068
 superconducting magnet system with internal short, MSCAP code appl. 7-15351
 Al, fusion reactor first wall behaviour after plasma disruption, electron beam expt. 7-62068
 D-T neutrons transmitted through rare earth mixed concretes, neutron spectrum 7-25158
 Zn, fusion reactor first wall behaviour after plasma disruption, electron beam expt. 7-62068

fusion reactor theory and design

- see also fusion reactor ignition; fusion reactor materials; plasma confinement; plasma heating; plasma production
 AC tokamak reactor, 8 hour discharges 7-30660
 advanced concept, axisymmetric tandem mirror and heliac stellarator aspects 7-5407
 advanced fuels in a field-reversed configuration 7-56855
 Advanced Toroidal Facility, design and construction 7-15359
 Advanced Toroidal Facility, helical field coils, assembly 7-19451
 Advanced Toroidal Facility, vacuum vessel, design and fabrication 7-25202
 Advanced Toroidal Facility, vertical field coils, design and manufacture 7-19452
 Alcator C-Mod magnetic systems, conceptual design 7-15373
 anode plasma production processes of low temperature type pulsed ion source 7-6423
 ASDEX data acquisition system, local area network 7-19464
 ASDEX fusion experiment, particle balance, data anal. 7-49669
 ATF, helical field coils, thermal and electrical joint test 7-15339

fusion reactor theory and design continued

- ATF, mechanical testing and development of helical field coil joint 7-15341
 ATF neutral beam injection system, description of basic parameters 7-19518
 ATF torsatron at ORNL, facility design and preparation 7-25226
 ATFSR, moderate aspect ratio torsatron, design and confinement models 7-25177
 AVSYS code for fusion plant availability calc. 7-19440
 axisymmetric tokamak plasma, dynamical modeling of transport and positional control 7-11629
 AYMAN fusion and hybrid blanket design, cylindrical blanket with D-T driver 7-803
 BELTEM code for transient electromagnetic and structure analysis of bellows type vacuum vessels 7-25181
 bifurcation, nonlinear dynamics, chaos 7-30481
 BIG DEE tokamak vacuum fabrication 7-25183
 blanket activation and afterheat for the compact reversed-field pinch reactor 7-15382
 bond graph model of a pool-type nuclear reactor 7-5438
 bonded armour tiles for in-vessel components, residual stresses 7-5416
 CALIF computer code for fusion reactor first wall lifetime anal. 7-25188
 Cascade ICF reactor, recondensation of vaporized material 7-15391
 Cascade inertial confinement fusion reactor, design 7-15327
 Cat-D fueled reversed-field pinch reactor assessment 7-5419
 charged particle transport calcs., finite element method, ICF appl. 7-36244
 charged particle transport in degenerate electron gases, ICF plasma appls. 7-36241
 charged particle transport in fully ionized plasma, flux-limited diffusion model 7-36246
 CODAS large scale multicomputer control system for JET 7-56846
 commercial tokamak fusion reactors, FEDC design options 7-794
 Common Long Pulse Accelerator, thermal and struct. anal. for TFTR, Doublet, MFTF 7-19434
 Common Long Pulse Source, mechanical baseline design 7-19433
 compact ignition device poloidal field system trade-studies using an equilibrium field expansion technique 7-15378
 compact ignition experiment, structural anal. of alternative concepts 7-15344
 compact reversed field pinch reactors, conceptual design issues 7-5418
 compact tokamak device for ignition studies, systems studies at PPPL 7-25173
 compact toroidal ignition machine, facilities and auxiliary systems 7-25170
 compact torus, self-consistent modeling of quasi-steady state evolving to ignition 7-56854
 computational continuum dynamics, parallel algorithms 7-4683
 computer codes for engineering design 7-56849
 conf., Austin, Texas, USA (Nov. 1985) 7-14703
 conf., Rochester, NY, USA 7-9595
 conf., Saskatoon, Canada, May 1986 7-29595
 CTR, development and evaluation of cryosorption and cryotrapping pumps 7-25185
 Culham Conceptual Tokamak Reactor Mk. II, manning requirements and radiological exposure durations 7-56850
 D+T, rate enhancement in nonuniform magnetoplasma 7-42196
 D-T tokamak, use of D-D reactions to aid burning 7-19423
 DEMO fusion reactor blanket, time-depend neutron effects, burnup calcs. 7-797
 digital signal processing for noise removal from plasma diagnostics 7-15400
 DIII-D, vacuum protection system, limiter design 7-25230
 DIII-D, vacuum vessel design and anal. 7-25182
 DIII-D long pulse neutral beam system 7-19520
 DIII-D tokamak, data acquisition and control system 7-36252
 DIII-D tokamak, vacuum control system, design 7-36253
 DIII-D tokamak, vacuum heating system, design 7-25203
 DIII-D tokamak device, mechanical assembly 7-16329
 direct energy converter for open magnetic traps 7-25154
 divertor plate for Next European Torus, testing and theoretical analysis 7-25198
 Doublet DIII-D tokamak, toroidal field coil modifications 7-19458
 Doublet III-D tokamak, computerised operation of neutral beams 7-19466
 drive systems for pulsed synchronous machines 7-19482
 economic requirements for competitive laser fusion power production 7-19429
 eddy current analysis in multiply connected shells using a circuit network model 7-15386
 eddy current models for a tokamak reactor vessel and blanket/shield 7-15385
 ELMO Bumpy Square, design features 7-19455
 elongated tokamak commercial reactor design 7-15390
 energy deposition of fast α -particles in a fully ionized deuterium-tritium plasma 7-10289
 energy experiment controlled by an expert system 7-5437
 energy transport requirements for tokamak reactors in the second ballooning stability regime 7-15333
 engineering aspects of high availability resistive magnet commercial tokamak reactors 7-15389
 ETI, high elongation ignition tokamak, design with sliding joints 7-25174
 fast-fission tokamak breeder reactors 7-62067
 FER divertor plasma, effects of closed geometry 7-56853
 first granules layer, protection in Cascade reactor 7-15392
 FIRST STEP, two-dimensional nucleonics calcs. for ICF conceptual design 7-15381
 first wall, sheath potential and thermionic emission, wall temp. dependence 7-30651
 first wall materials for high-power-density reactor 7-19515
 first wall/blanket structures, comparison of tokamak and tandem mirror designs 7-25190
 flowing packed particle beds in circular tubes, const. wall heat flux, local Nusselt numbers 7-1626
 force flow cooled superconductor bends, mechanical invitations and failure criteria 7-15356
 force-cooled superconductors, protection considerations 7-19507
 FRX-C/T compact toroid translation expt., design and performance 7-25225
 FTU Tokamak, main mechanical, thermal loads and stresses 7-56842
 FTU Tokamak, poloidal field coils, thyristor convertors 7-36263

fusion reactor theory and design continued

FTU tokamak machine, vacuum vessel thermal and mechanical problems 7-25179
fusion blanket, self-cooled water-based, tritium breeding performance, neutronics anal. 7-56840
fusion energy prod., magnetically confined ion beam fusion reactor investigation, 7-63346
fusion engineering database 7-19441
fusion machines, plasma-surface interactions, design studies 7-63298
Fusion Neutronics Source (FNS) Facility 7-30819
fusion nuclear technology experiments and facilities 7-19491
fusion reaction kinetics in plasma focus, gyrating particle model 7-63345
fusion reactor core, one-dimensional transport model (*Chinese*) 7-5420
gas jet neutralizer for MFTF-B pure beam injectors 7-19436
HDCT design for study of tokamak plasma close to ignition 7-16330
heavy ion ICF reactor, critical system issues, linac design 7-25211
Hefei Tokamak Hybrid Reactor, physics conceptual design 7-25238
helical coil alignment in the Advanced Toroidal Facility 7-19454
high current electrical joint design and evaluation 7-19475
high field tokamaks, advantages for fusion reactor development 7-62066
high gain fusion target development facility 6-10 MJ driver 7-19490
high-beta tokamak operation in the second stability regime 7-37722
hot-electron generation and transport in high-intensity laser interaction 7-26431
hybrid reactor pebble bed blanket, magnetohydraulic flow in Na-K eutectic mixture 7-15366
ICF, 2D Lagrangian simulations 7-11676
ICF, effect of UV irradiation on anode plasma production 7-6424
ICF, experimental approaches to heavy ion fusion 7-6425
ICF, numerical analysis for nonuniform implosion of target 7-6387
ICF, observation of hydrodynamic instability in spherical target implosion with Gekko XII green laser 7-5440
ICF, power plant by LIB 7-5442
ICF, self-similar ion beam fusion plasmas 7-5443
ICF, vaporising liquid metal first wall 7-5441
ICF target implosion, moving finite element method 7-5439
ICRF antenna and feedthrough development at ORNL 7-26457
ICRH 1.5 MW generators for fusion reactor heating 7-15395
IFSMTF, large coil test structural analysis 7-19509
IFSMTF, use of Kapton insulated high voltage cable 7-19511
IFSMTF power and switch system 7-19479
Ignition Spherical Torus, enhanced elongation and paramagnetism 7-15331
Ignitor and LITE type compact ignition tokamak design spaces 7-19493
IGNITOR structural evaluations, finite element models 7-15348
impinging advanced fuel pellet, neutron heating effects, simulation 7-6421
implosion shell during coasting phase, inner surface perturbations, amplitude variation 7-56844
improved reactor designs, needs and prospects 7-62071
induction linacs and free electron laser amplifiers, fusion program appl. 7-10287
inherently safe fusion power plant designs 7-792
integrated blanket-coil concept for spherical torus 7-15362
internally cooled cable superconductors, enhanced heat transfer calcs. 7-15355
ion trapping rates in tandem mirror reactors 7-15334
ISP, coil design study 7-19457
ISP compact tokamak, mechanical design, sliding joint for TF coil 7-25172
JAERI tokamak, high field superconducting coil 7-15372
JET, articulated boom, design and operation 7-19430
JET, asymmetric k_{\perp} spectrum excitation by phasing the ICRF antennae 7-49672
JET, impact of active phase, remote handling and fuel recycling 7-49678
JET, MHD equilibrium profile depend. on p and q profiles, ESCO code anal. 7-25161
JET, poloidal field system, β plasma shaping and mag. separatrix formation 7-56848
JET, relevance to the requirements for a fusion power reactor 7-25162
JET, sawtooth oscillation rapid collapse 7-5433
JET, upgraded ICRF heating system, design and technology 7-49674
JET, wall effects and impurities 7-56845
JET and TFCX, plasma performance with sawtoothing, ignition 7-1685
JET ICRF system, engineering design and performance 7-19504
JET joint undertaking, 1985 annual report 7-6474
JET machine, design, mfg. and assembly 7-15306
JET neutral injection beamline system, manufacture and assembly 7-19516
JET nuclear fusion plant, gas-insulated HV cable for neutral injector (*German*) 7-62064
JET nuclear fusion project 7-19421
JET plasma, vertical position stabilization and shape control 7-15314
JFT-2M poloidal field coils, power supply and control system 7-15323
JFT-2M tokamak, data processing system 7-15405
JFT-2M tokamak, design and fabrication of ECRH system 7-19522
JFT-2M tokamak, vertical instability anal. 7-36247
JFT-2M tokamak data acquisition system 7-15404
JT-60, plasma feedback control system 7-36250
JT-60, toroidal field coil power supply, 4 GJ flywheel motor-generator 7-36260
JT-60, toroidal field power supply, tests 7-36261
JT-60 discharge optimization, plasma modelling and simulation study 7-15360
JT-60 divertor plate, 2D inverse heat conduction anal. 7-25193
JT-60 gas injection valve 7-19500
JT-60 integrated performance test 7-15361
JT-60 neutral beam injectors, cryopumps and cryogenic systems 7-19519
JT-60 tokamak, mechanical props. in power tests (*Japanese*) 7-5409
JT-60 toroidal field power supply, rectifier, voltage regulation characteristics 7-36262
large coil program, General Electric coil, engineering problems 7-19456
laser fusion, direct drive, thermal electron transport, review 7-26391
launching structures for FT and FTU 7-19505
launching system of LHRR and ICRF heating on JT-60 7-19502
Light Ion Beam Fusion Target Development Facilities, activation studies 7-49732
limiter design for Ignition Studies Project 7-25206
linear stability of counter-streaming two strong ionbeams 7-6422
liquid metal two-phase mixture with and without mag. field, shock waves 7-5410

fusion reactor theory and design continued

Long Pulse Accelerator, thermal and struct. anal. for TFTR, Doublet, MFTF 7-19434
low activation fusion ignition experiments, design aspects 7-15383
magnetic diffusion effects in TF systems for compact ignition devices 7-15375
magnetic fusion reactors, melting and evaporation during disruptions, approx. analytical soln. 7-56839
maintenance reliability influence on safety and availability 7-19468
MARS, implications of probabilistic risk assessment for fusion decision making 7-793
MARS blanket lifetime prediction, dimensional scaling and material prop. uncertainties, STAIRES code 7-5417
MCFR superconducting magnet system, irradiation and mechanical design features 7-19510
MFTF, design of mode-selective directional couplers for ECRH 7-19523
MFTF, industrially fabricated ion source, test and conditioning 7-19435
MFTF, mag. field strength meas. using NMR 7-15403
MFTF ICRH system, control and data acquisition 7-15396
MFTF-B, mag. shielding for long-pulse, pure-beam source neutralizers 7-19447
MFTF-B, structural mechanics methods for design optimisation 7-5411
MFTF-B data triggered data processing 7-15399
MFTF-B ICRH system—design summary and construction status 7-19501
MHD equation implications for inertial confinement fusion concept 7-44213
MIMIMARS halo model and computer code 7-15335
MINIMARS, design 7-15328
MINIMARS, engineering overview 7-15326
MINIMARS, tandem mirror direct converter design for high-temperature heat recovery 7-25212
Mirror Fusion Facility, local control station development 7-19463
modular tokamak magnetic system, coil designs 7-15376
modular-multiplex or single large fusion power plants, utility advantages and disadvantages 7-25213
MOSFET power switches for diagnostic neutral beam decelerating supply 7-19480
multi-group double-differential cross-sections using PROF-DD code system 7-56852
Multipinch, design and construction of composite vacuum vessel 7-25229
muon production for fusion catalysis 7-62069
muon-catalysed fusion, physics and prospects for power prod. 7-62080
Nagoya University Institute of Plasma Physics, Annual Review (April 1985-March 1986) 7-63249
NET, first wall protection 7-49622
NET, preliminary design considerations, ^3H control 7-49670
NET, superconducting toroidal field coil power supply and protection systems 7-15350
neutral beam injection duct concrete shield, differential gamma dose rate 7-36242
neutral beam injectors, heat absorption panels, design and fabrication 7-19517
neutral beam source conditioning with AI techniques 7-19462
neutronics calculational benchmarks 7-15308
noncircular tokamaks, ideal MHD props., ballooning and kink modes, stable β -values 7-11628
nonresonant thermonuclear reaction rates, analytic representations 7-30463
nuclear data and integral neutronics experiments for fusion reactors 7-30674
nuclear data conference, Tokai, Ibaraki, Japan (Nov. 1985) 7-29600
nuclear data for fusion blanket neutronics 7-30675
nuclear data review 7-10284
nuclear data status for fusion reactor structural materials 7-30673
numerical simulation, book 7-48214
ohmic heating power supply for HL-1 tokamak 7-19483
ohmic-heating coils, design optimization using simplex method (*Chinese*) 7-5421
optical data links, field experience in fusion reactor environment 7-15995
optimal design, thermonuclear fuel cycles, analysis 7-49679
oscillating field current drive for ZT40M, design and construction 7-19506
particle accelerators for heavy ion fusion 7-10285
particle beam fusion, Nagoya, Japan (Nov. 1985) 7-4636
PBFA II facility, status and plans 7-15370
PBX upgrade, coil design 7-15374
plasma channels for light ion beam propag. in target development facility 7-15357
plasma containment, appl. of spectral theory and to ideal MHD eqns. 7-34854
plasma focus drivers, efficiency parameters for reactor conditions 7-63373
plasma generator for long pulse 10×40 neutral beam 7-32007
plasma heating by collisional magnetic pumping 7-16315
plasma-first wall interactions in tokamaks, effects of vapour shield formation 7-19514
PLT rotatable graphite limiter, thermal analysis 7-25207
poloidal field coil design from plasma equilibrium parameters, Green's fn. computer code anal. 7-15318
poloidal field coil system for an elongated tokamak 7-19461
poloidal field coils for DIII-D, fabrication 7-19460
power balance, heating efficiency effect 7-15393
power transmission and shine-through calorimetric meas. during NBI in TFR 7-58056
PPPL Ignition Studies Project 7-19473
Princeton Beta Experiment 7-19496
pulsed high power high tension voltage source with inductive energy storage 7-19481
pump limiter, large area design 7-25197
quality requirements, formulation and implementation 7-19471
radiative Gaunt factors 7-49673
radio-frequency heating apparatus for JT-60, controlling system 7-19503
REPUTE-1, RFP plasma, relaxation processes 7-32050
reversed field pinches, fusion application prospects 7-16327
RFP, current driven instabilities, nonlinear evolution 7-30648
RFX, data acquisition and anal. system design 7-15398
RFX, first wall and vacuum vessel design, technological aspects 7-25187
RFX fusion expt., Italy, AC network transient anal. 7-30666
RFX fusion expt., Italy, design criteria for switching units 7-30667

fusion reactor theory and design continued

- RFX fusion expt., Italy, power supply protection against plasma disruption and fault conditions 7-30668
 RFX machine-supply system anal. 7-19488
 RFX poloidal magnetic field system, fault anal. and protection concepts 7-15349
 RFX stabilising shell, electromechanical design 7-25228
 RFX vacuum vessel, structural and thermal anal. using FEM 7-25178
 rotating magnetic fields, RF driven, plasma confinement appl., self-consistent calc. 7-796
 S-1 Spheromak flux core, use of explosive forming to manufacture resistive vacuum torus 7-25204
 self sustained plasma in tokamak reactor, burn control by H. feeding 7-795
 self-cooled heavy water breeding blanket concept 7-15364
 self-cooled heavy water fusion breeding blanket, neutronics anal. in ID 7-15365
 self-cooled liquid metal blankets, anal. of MHD effects 7-15363
 self-fusion reaction rate expressions, heuristic formulation 7-62062
 sensitivity theory for inertial confinement pellet fusion system 7-30670
 sliding joint concept from toroidal field coils of a tokamak 7-15340
 sliding joint design and testing for toroidal field coil 7-15342
 Spherical Torus Experiment, STX, engineering features of proposed design 7-25227
 spin polarised plasmas in a fusion reactor, performance benefits 7-36243
 SPTR-P tokamak reactor, tube panel first wall, thermohydraulic and mechanical design assessment 7-62070
 STARFIRE, implications of probabilistic risk assessment for fusion decision making 7-793
 stellarator conductor design limitations for modular coils 7-19453
 stellarator reactor, modular coils, field distribution, stresses and strains 7-20968
 STOR-1M tokamak, new developments 7-30661
 SUPERCOIL code for tokamak design NET and ASDEX upgrade appls. 7-5413
 superconducting coil, mechanical behaviour 7-15345
 superconducting coils, compensated current control 7-19508
 superconducting magnet system with internal short, MSCAP code appl. 7-15351
 superconducting magnets in fusion reactor design, review 7-49680
 superconducting pulsed poloidal coil for next tokamak 7-15377
 superconducting tokamak, medium sized, design study 7-15379
 Tandem Mirror Experiment Upgrade, computer aided design 7-15387
 tandem mirror reactors, fuelling requirements 7-15317
 tandem mirrors, macroscopic model of trapped-particle modes (*Chinese*) 7-6430
 TANDEM program for axisymmetric tandem mirror device magnetic configs. 7-42192
 TEXT, capacitor banks for diagnostic neutral beam and ECH expts. 7-19485
 TEXT diagnostic beam source, arc snubber system, HV cabling 7-19486
 TEXT ECH expts., modulator/regulator/crowbar design 7-19487
 TEXT tokamak, 60 MJ pulsed homopolar generator power supply, design 7-15320
 TEXTOR neutral injectors, arc power supply 7-19476
 TEXTOR neutral injectors, auxiliary power supplies design 7-19477
 TEXTOR solid-state accelerator power supplies 7-36265
 TEXTOR tokamak, power supply, upgrading to 3 T operation 7-36264
 TFCX, current density determ. for superconducting toroidal field coils 7-5414
 TFR, 60 GHz gyrotrons, power supply and operating system 7-19489
 TFTR, D and T pellet injector systems 7-19497
 TFTR, maintenance manipulator development 7-19431
 TFTR, plasma-wall interactions heating and diagnostics study 7-63291
 TFTR, poloidal field coil system, thermal anal. 7-19459
 TFTR, power system, electrical characteristics, computer simulation 7-19478
 TFTR, tritium pellet injector design 7-19498
 TFTR adiabatic compression expts., vacuum vessel eddy current modelling 7-799
 TFTR bumper limiter, dynamic analysis 7-56837
 TFTR bumper limiter and final protective plate engineering, fabrication and assembly 7-25195
 TFTR bumper limiter and protective plate graphite tile, computer aided, design/manufacture 7-25196
 TFTR decontamination and decommissioning plan 7-19445
 TFTR deuterium pellet injector gun design 7-19499
 TFTR high accuracy cryogenic temperature measuring system 7-15402
 TFTR lower hybrid current drive launcher, thermal considerations 7-26454
 TFTR lower hybrid current drive launcher design, predictive model 7-26453
 TFTR neutral beam computer control system 7-19465
 TFTR neutral beam ion source fault detector 7-15401
 TFTR poloidal field coil, finite element modeling 7-15343
 TFTR poloidal field coils, MSC/NASTRAN expert techniques 7-15347
 TFTR status and recent results 7-15310
 thermal stabilization of an elongated tokamak by variation of plasma elongation 7-15337
 thermonuclear Alfvén loss-cone instability in mirror reactor, quasilinear theory 7-51435
 thermonuclear fusion research by sheet plasma, vol. prod. H^- and D^- ion source 7-32105
 thermonuclear plasma, thermal stability for temp. depend. confinement time, Kaye-Goldston scaling 7-30647
 thermonuclear plasmas, collective modes and high-energy components 7-51491
 THIDA-2 code for transmutation, activation, decay heat and dose rate calc. 7-15307
 three-temperature plasma model, soln. method, inertial confinement fusion target design studies appl. 7-10278
 TIBER superconducting ignition tokamak, mechanical configuration 7-25171
 time-resolved derivation of heat fluxes from quantitative infrared thermography and its relationship to photoacoustics 7-44210
 TMAP, fusion safety analysis code for tritium movement and inventory predictions 7-36258
 TMX-U, drift pumping, concepts and development 7-26494
 TMX-U, ECRH, quality assurance 7-19443
 TMX-U, ECRH control system 7-15397
 TMX-U, gyrotron anode modulation of ECRH 7-19525

fusion reactor theory and design continued

- TMX-U, halo recycler, design, operation 7-25201
 TMX-U, ICRH loop antenna 7-15394
 TMX-U, mag. drift pumping, electrical configurations 7-19446
 TMX-U, magnet system operation 7-19448
 TMX-U, octupole coil configuration 7-19449
 TMX-U, plasma potential control system 7-36248
 TMX-U, Ti-Ta sublimation getter pumping system and performance, computer control 7-25184
 TMX-U, trim coils for improved mag. field mapping 7-19450
 TMX-U 80 kW SCR VLF power source for drift-pump-coil excitation 7-19484
 TMX-U diagnostic computer system, improvements 7-36255
 TMX-U overview, engineering developments 7-15358
 TMX-U tandem mirror experiments 7-30662
 Tokamak, compact ignition designs, plasma predictions 7-15315
 tokamak, modular design 7-15325
 tokamak, noncircular cross-section, plasma transport/stability anal. 7-16324
 Tokamak de Varennes, disruption-induced currents in vacuum vessel and liner 7-15352
 tokamak devices with ohmic-heating dominated startup 7-15332
 tokamak energy confinement and ignition, fusion alpha heating effects 7-11677
 Tokamak ignition devices, physics parameter space anal. using physics systems code 7-25214
 tokamak ignition-burn experimental research with TIBER 7-19472
 tokamak plasma, quasilinear analysis 7-63325
 tokamak plasmas, feasibility of using positrons for transport studies 7-6450
 tokamak structural components, 3D analysis of eddy currents using boundary element method 7-25199
 tokamak systems code, high-field ignition devices 7-15330
 tokamak-pinch expt., design and operation 7-15367
 tokamaks, anomalous transport theories, conceptual and expt. bases 7-37641
 Tokamaks, controlled nuclear fusion (*German*) 7-62065
 tokamaks, plasma operating regimes and ignition conditions, contour anal. 7-15329
 tokamaks, superconducting poloidal field coils design, CAD program system development 7-5412
 TORE SUPRA tokamak, cryogenic system design 7-1716
 toroidal field coils for compact tokamak ignited experiments, structural evaluation 7-15346
 toroidal resistive MHD instabilities, time stepping code calc., INTOR appl. 7-11621
 torus reactor, magnetic field calc. (*Russian*) 7-25157
 transport scalings in tokamaks, thermodynamic approach 7-44214
 TRIDEX experiment, effective cross sections and prod. rates for tritium, blanket dev. 7-19428
 US Common Long Pulse neutral beam source, prototype testing 7-19432
 US ignition devices, experimental plans, machine design alternatives 7-15312
 vertical position control of INTOR elongated plasma 7-62075
 WT-III, wave heating tokamak, design and manufacture 7-19521
 X-ray drive ICF, radiation transport modelling 7-6420
 X-ray perpendicular bremsstrahlung emission of suprathermalelectrons 7-1784
 ZENKEI, JT-60 central control system, design and testing 7-36249
 Be, energy multiplier in fusion reactor blanket, costs and benefits 7-49625
 Be limiter material for ISX-B tokamak 7-19422
 BeO/LiAlO₂ blanket, neutron activation calcs. in Cascade 7-15380
 D⁺ JET tokamak plasma, ion cyclotron emission spectra meas. 7-58067
 D⁺ neutron energy determination 7-30671
 DT ion-beam inertial fusion targets, compression and burn results, HIBALL-II reactor appl. 7-10282
 H⁺, D⁺ vol. prod. ion source by sheet plasma, proton accelerator and thermonuclear fusion research applications (*Japanese*) 7-5511
 He cooled, high flux heat removal, assessment study 7-25194
 Li liquid flow through thin walled elbow in uniform magnetic field 7-37555
 γ-LiAlO₂, fusion reactor breeder blanket, T transport modelling 7-49642
 LiD fusion plate design 7-19438
 Li₁₇Pb₈₃ breeding blanket, NET, LOCA, mechanical anal. 7-19444
⁶Li(n,X), 15 MeV, a=6, ⁷He prod. cross sections, fusion reactor appl. 7-36006

fusion reactors

- see also fusion reactor ignition; fusion reactor materials; fusion reactor safety; fusion reactor theory and design; hybrid reactors; nuclear engineering; plasma heating
 2T-40M reversed-field pinch, plasma-surface interactions 7-63336
 Alcator C edge plasma, directional asymmetries 7-63300
 ASDEX Tokamak, ohmic and auxiliary heating, impurity prod. 7-63293
 charcoal sorbents for He cryopumping 7-62077
 conference, ANS winter meeting, Washington, DC, USA, (Nov. 1986) 7-29591
 conference, Japanese Physical Soc. Nishinomiya-shi, Nyogo-ken, Japan (Sept. 1986) (*Japanese*) 7-48186
 cryopumping for fusion power applications 7-25205
 cryopumping for fusion reactors 7-56838
 DITE tokamak, detached plasmas, density and temp. profiles 7-63339
 electrical assembly recovery, removal of dielectric insulation systems 7-19512
 fusion nuclear technology experiments and facilities 7-19491
 high power density fusion machines, MFAC report 7-15313
 ICF, use of pulsed power technology 7-10286
 IFSMTF power supply regulator 7-19467
 JAERI Fusion Research Center April 1984-March 1985 report 7-10283
 JET, 1985 progress report 7-5434
 JET, edge phenomena, probe diagnostics 7-63334
 JET, evolution, status and prospects 7-15305
 JET, Ohmic heating 7-5430
 JET, optimization and development plans 7-15311
 JET, scrape-off layer, probe meas. 7-63351
 JET, technical and scientific performance, future plans 7-49676
 JET, vacuum systems 7-5432
 JET project, energy from fusion 7-56817
 JT-60, installation and testing 7-19442
 JT-60, ohmic heating, diagnostics study 7-63335

fusion reactors continued

- JT-60 power tests from mechanical and thermal viewpoints of tokamak machines 7-25175
 JT-60 tokamak, global particle balance in ohmically heated divertor discharge 7-20927
 JT-60 vacuum vessel, leak tests and surface conditioning for commissioning 7-25180
 Langmuir calorimeter probe heads in TFTR, use of graphite 7-1768
 mirror loop system for TFTR 7-1771
 multichannel tangential bolometer on PBX, operation 7-1774
 NET, plasma-wall interaction study 7-63297
 NET, superconducting toroidal field coil power supply and protection systems 7-15350
 nonfuel O&M costs from laser and heavy-ion fusion power plants 7-19494
 nuclear fusion energy, prospects for use (*Korean*) 7-49619
 particle balance meas. using diagnostic system in TMX-U 7-1767
 performance and cost sensitivities associated with superconducting devices 7-19495
 PISCES facility, erosion and redeposition expt. 7-63292
 plasma-wall interaction in fusion devices, conf. Princeton, NJ, USA (May 1986) 7-60861
 poloidal β meas. in JET with diamagnetic loop 7-1772
 probe measurements of the density and temperature profiles in the JET plasma boundary 7-5431
 probes for edge plasma studies in TFTR 7-1779
 PROTO II accelerator power flow modification in insulator stack 7-30669
 pulse neutral beam source, 10×40 cm, 120 kV testing 7-32008
 refrigerators for large superconducting devices, thermodynamic optimisation 7-48753
 reversed field pinch fusion power reactor, 1000 MWe, plasma parameters (*Japanese*) 7-16319
 RF linear accelerators, use in fusion research and strategic defence 7-10317
 soft X-ray diode array diagnostic for JET 7-1787
 T-10 tokamak, plasma-wall interactions 7-63294
 T-15 tokamak, plasma-wall interactions, diagnostics 7-63299
 test facility for the evaluation of microwave transmission components 7-19524
 TEXTOR, plasma-wall interactions, heating, review 7-63289
 TFTR, detached plasma, MARFEs phenomena, diagnostics 7-63341
 TFTR, detached plasmas, impurities study 7-63340
 TFTR, electron cyclotron meas. with fast scanning heterodyne radiometer, temp. meas. 7-11747
 TFTR, parametric study of electron density profile evol. following injection 7-11759
 TFTR, scrape-off layer, probe meas. 7-63351
 TFTR plasmas, Faraday rotation and line electron density meas. using FIR interferometer 7-11754
 TFTR systems availability analysis and growth methodologies 7-19470
 TFTR test cell basement, neutron and photon spectral data 7-19469
 TFTR with D⁰ neutral beam injection, fusion neutron prod., reaction rate meas. 7-62072
 tokamaks, carbonisation, plasmachemical in situ deposition 7-63296
 tokamaks, plasma-wall interactions, impurity behaviour 7-63338
 toroidal variation of power radiated from TFTR 7-1769
 vertical high-resolution Bragg X-ray spectrometer for the tokamak fusion test reactor 7-10281
 X-ray diagnostics for mag. fusion 7-1783
 X-ray imaging system for TFTR, MHD studies 7-1786
 X-ray imaging systems for TFTR 7-1785
 Z-pinches, neutron prod. mechanism 7-63329
 T-cycle process computer modelling 7-62082
²³³U fuel for naval and space reactors produced in a fusion reactor blanket 7-61964

future developments see *technological forecasting***fuzzy set theory**

- λ -additive fuzzy measures, entropy 7-60947
 CT, reconstruction from limited projection data using fuzzy sets 7-28672
 incident control, simulation of man machine interaction 7-15287
 measurement accuracy improvement using a priori information 7-14908
 reinforced concrete members, reliability of crack control, fuzz set anal. (*Chinese*) 7-20655
 skeletal maturity, fuzzy grammars for syntactic recognition from X-rays 7-34317
 solar proton flares forecasting, appl. of fuzzy clustering theory to short-term forecasts (*Chinese*) 7-4389

g-factor

- see also *gyromagnetic ratio; nuclear magnetic moment; Zeeman effect*
 alkali metal atoms, orientation, alignment and HFS 7-50278
 alkali metal tetrafluorotetracyanoquinodimethane (TCNQ₄), charge transfer salts, comparative EPR studies 7-53114
 anomalous Zeeman effect and its influence on the line absorption and dispersion coefficients 7-60513
 ascorbic acid radical, strong perchloric acid soln., free radical protonation equilib., ESR study 7-33918
 ascorbic acid radical anion, Ca²⁺ exchange, ESR line broadening meas. of rate const. 7-28270
 azurin, g-values, EPR spectra, temp. depend. 7-57098
 (BEDT-TTF)₂I₃, α and β phases, CESR 7-2930
 bis(benzene)-vanadium S=1/2 dopant in nickelocene lattice, large impurity anisotropic g-shift obs., mol. field anal. 7-13017
 bis(n-toluene)vanadium, matrix isolated, magnetisation props., MCD meas. 7-57112
 chromium(III)tris(acetylacetonate), matrix isolated, magnetisation props., MCD meas. 7-57112
 copper phthalocyanine iodide, quasi 1D conductor, transition of local moments coupled to itinerant electrons 7-2815
 cyclopentadienyl-cycloheptatrienyl-vanadium S=1/2 dopant in nickelocene lattice, large impurity anisotropic g-shift obs., mol. field anal. 7-13017
 decamethylcobaltocene, electronic struct. and dynamic Jahn-Teller effect EPR 7-59104
 decamethylnickelocenium, electronic struct. and dynamic Jahn-Teller effect EPR 7-59104
 diatomic molecules, Zeeman quantum beats during transient process, after ground electronic state optical depopulation 7-36545
 electromagnetic properties of high-spin isomers 7-35928
 ferredoxins, g strain, EPR study 7-25567

g-factor continued

- fine structure constant, electron self-field interaction and internal resonance 7-41701
 four-lattice rhombic antiferromagnet, reson. props., exchange, and high freq. suscept. calcs. (*Russian*) 7-13037
 graphite, ultrafine, heats of combustion, ESR meas., depend. on exposure to air 7-33266
 ground states, MCD saturation behaviour 7-57111
 hydroxymethylperoxy radical, thermal stability, ESR spectra 7-62415
 IBM, g boson signature from g-factor variations 7-41917
 imidazole, rot. Zeeman effect 7-57109
 iron(III)tris(acetylacetonate), matrix isolated, magnetisation props., MCD meas. 7-57112
 nuclear high spin levels, g-factor determ. using tilted-multifoil hyperfine interaction 7-56604
 nucleon g_q factor, effects of renormalization on anomalous E1 conversion processes (*Russian*) 7-597
 PAA uniaxial nematic liquid crystals, orientational order using ESR of solute molecules 7-1872
 phenazine derivatives, partly hydrogenated radicals, hyperfine const., EPR (*French*) 7-31079
 plastocyanin, g-values, EPR spectra, temp. depend. 7-57098
 polycetylene, alkali metal doped, role of spin-orbit coupling in EPR spectra 7-64527
 polythiophene, radiation-induced doping, elec. and ESR studies 7-38545
 pyrazole, rot. Zeeman effect 7-57109
 rare earth adsorbates on metal surfaces, EPR line shapes 7-53129
 semiconductors with zinc-blende structure, electron spin relax. in a quantising mag. field 7-45822
 semiquinone cation radical, immobilised, EPR spectral simulation calcs. 7-50200
 strong perchloric acid soln., free radical protonation equilib., ESR study 7-33918
 TCNQ salt, N-n-propyl phthalazinium 7,7,8,8 TCNQ₂, struct., elec., mag. props., EPR meas. 7-33005
 three-level atoms, optical free induction decay quantum beat 7-57482
 transient magnetic field acting on swift neutral moving in magnetized solids 7-49243
 transition metal dithiolates and diselenolates, molecular and electronic structs. 7-52397
 ultra-high-resolution echo spectroscopy in a strong magnetic field 7-43264
¹⁶⁴Dy, g-factors and effective boson charges for M1-, E2-, M3-IBA transition operators 7-49299
⁷Be, electromagnetic props., resonating group model description 7-30330
 Ag conduction electrons, gyromag. factor calcs. 7-7099
¹⁰⁸Ag, spin determ. by nucl. orientation and NMR 7-41893
 Au conduction electrons, gyromag. factor calcs. 7-7099
 Ba, fast atomic beam laser fluoresc. 7-10483
 BaTiO₃Mn(Cr), impurity electronic struct., molecular-orbital calcs. 7-45213
¹³⁸Ba, microscopic struct. of semimagic nuclei 7-30304
¹⁴²Ba, 2₁⁺ state g-factor, hydrodynamic model and IBA-2 anal. 7-30332
 Ca₃Ga₂Ge₂O₁₂Cr³⁺ garnet, ESR and ultrasonically modulated ESR studies 7-22139
 CaO, light sensitive centres with tetragonal symmetry, EPR study 7-53133
 Cd_{1-x}Mn_xTe semimag. semicond., ESR line shape meas., comp. and temp. depend. 7-7584
 Ce, odd-mass isotopes, backbending, IBA anal. 7-19149
¹⁴⁰Ce, microscopic struct. of semimagic nuclei 7-30304
 Co complexes, bis(dimethylglyoximate)cobalt(II), frozen soln., EPR and ENDOR investig. 7-57097
 Cr, matrix isolated, magnetisation props., MCD meas. 7-57112
 CsI, excitons, three-photon magnetoabsorpt. meas., g-value determ. 7-2498
 Cu complexes, L-phenylalanine salt, EPR study 7-59106
 Cu(NO₃)₂·2.5 H₂O, EPR and magneto-microwave birefringence powder spectra 7-45810
 Cu₂S, stoichiometry and phase transitions, Cu²⁺ EPR studies 7-17219
 Cu₂Si₂O₈·6H₂O, Diopside crystals, Cu²⁺ EPR and optical absorpt. spectra studies 7-53120
 Dy₂(SO₄)₃·8H₂O, magnetic and hyperfine props., cryst. field effects calcs. 7-27305
 Er₂(SO₄)₃·8H₂O, magnetic and hyperfine props., cryst. field effects calcs. 7-27305
¹⁶⁶Er, gyromagnetic ratios of excited states in ground and gamma bands 7-30335
 Eu₂Y_{3-x}Fe_xGa₃O₁₂ LPE garnet films, ferromagnetic relax. meas. 7-38911
 Fe ultra thin films, Brillouin scatt. 7-27728
 Fe-Pt, dilute alloys, ferromagnetic, internal mag. fields, impurity conc. dependence 7-38858
⁴Fr, A=207-228, g-factors ground state spin and single particle structure 7-49244
 GaAs:Ti³⁺, EPR 7-45811
 GaInAs-InP quantum well, CESR of 2D electrons 7-38941
 GaP:Cu, 1.65 eV luminescence, optically detected mag. resonance studies 7-64547
 Gd-Fe evaporated amorphous alloy films, mag. props. and FMR behaviour studies 7-45825
 Ge, high spin states, B(E2) values, g-factors IBM coupled calcs. 7-35930
 Ge:Ga, impurity g-factor determ. piezo-Zeeman spectra obs. 7-16982
⁶⁸Ge, g-factor meas., evidence for higher multipole forces and states 7-49240
 H₂, b² Σ_u^+ , excited states, mag. effects, ab-initio calcs. 7-10413
 HPO₃ radical, strong perchloric acid soln., free radical protonation equilib., ESR study 7-33918
 He-Ne laser, mode-crossing reson., intracavity distance and mode-locking quality anal. 7-31373
 InSb, conduction electrons g-factor anisotropy, spin-orbit splitting calcs., comment 7-38441
 InSb, electron inversion layers, cyclotron and electron spin resonance 7-38736
 InSb, free-electron g-factor meas. by spin-flip Raman scatt. gain method 7-2470
¹¹⁷In, A=106, 108, spin determ. by nucl. orientation and NMR 7-41893
¹¹⁷In, 589 keV state, lifetime and g-factor 7-49304
 Ir, itinerant electron Zeeman splitting anisotropy meas. 7-52536
 K[(OH)₂PO₃], irradiated single crystal struct. study, ESR and ENDOR anal. 7-38962

g-factor continued

- ⁶Li, A=6.7, electromagnetic props., resonating group model description 7-30330
 (NH₄)₂Pb(Cu(NO₂)₆) struct. phase transform., ESR study 7-13026
 NdIG, mag. props. 7-45662
²⁰Ne, 4⁺ g-factor meas., critical assessment 7-10102
 PbTe:Mn²⁺, superhyperfine struct., EPR spectra 7-27595
¹³⁵Pb, A=204, 206, g-factor from recoil in vacuum expt., reanal. 7-10135
²⁰³Pb, g-factor of 21/2⁺ isomer, meas. using time differential perturbed ang. distrib. technique 7-41896
 Pd conduction electrons, gyromag. factor calcs. 7-7099
 Pd, X-pocket holes, anisotropy of conduction electron Zeeman splitting 7-32963
 Pd-Fe(Ni) dilute alloys, Fermi surface exchange splitting, de Haas-van Alphen effect studies 7-52405
¹⁴³Pm, microscopic struct. of semimagic nuclei 7-30304
 PrIG, mag. props. 7-45662
 Pr₂(SO₄)₃·8H₂O, magnetic and hyperfine props., cryst. field effects calcs. 7-27305
¹⁴¹Pr, microscopic struct. of semimagic nuclei 7-30304
 Pt conduction electrons, gyromag. factor calcs. 7-7099
 PtMn dilute alloy, longitudinal magnetoresist. meas. 7-12700
 Rh complexes, Rh₂(acetate)₄(H₂O)₂⁺, aq. soln., χ_{RhRh} odd electron orbital evidence, ESR spectrum 7-15628
 Si (001) inversion layers in parallel mag. fields, electronic g-factor 7-12783
 Si neutron irradiated float zone crystals, triclinic symm. defect, EPR study 7-53134
 Si, thermal donors, alignment by uniaxial stress, EPR and optical studies 7-59227
 Si²⁺ transversing Fe and Gd foils transient mag. fields 7-10537
 Si:Au, Li, Au-Si pair paramagnetic state, EPR studies 7-45817
 Si:Ge, irradiated, photoluminescence spectra 7-13207
 a-Si:H, broken bond local environment relax., g-factor, cluster calcs. 7-37876
 Si:P, EPR temp. depend. g-shifts obs. 7-27600
 Si:Se(Te), chalcogenide pairs, electronic structs., Green's function calc. (Chinese) 7-58759
 Si-Si₃N₄, SOI structs. formed by N⁺ implantation EPR of defects 7-33273
 Si-SiO₂, SOI structs. formed by O⁺ implantation, EPR of defects 7-33272
 SmB₂Er³⁺, Jahn-Teller phenomena in valency-mixing surroundings 7-45240
¹⁴⁴Sm, microscopic struct. of semimagic nuclei 7-30304
⁴Sn, A=109, 111, microscopic struct. of semimagic nuclei 7-30304
 SrF₂Tm²⁺, g-factor signs, optically detected ESR 7-32948
¹²⁵Te, A=122, 125, 130, energy level g factor meas., transitional-field method anal. 7-30327
 TiO₂:V⁴⁺, anatase and rutile phases, EPR study 7-2923
²³⁵U, spectral line classification, isotope shifts, Lande g factors, pattern-recognition technique 7-62309
 (VO)₂P₂O₇, 1D spin 1/2 Heisenberg antiferromagnet, mag. susceptibility meas. 7-45639
¹⁶⁸W, g-factor above the first backbend, 12⁺ state, stretched neutron config. fig. 7-15191
 Zn_{1-x}Mn_xTe semimag. semicond., ESR line shape meas., comp. and temp. depend. 7-7584
 ZnTe:Cl(Al), crystals, vacancy-impurity complexes, ODMR studies 7-2530
 ZrF₄ based glasses, reduced species, EPR and optical studies 7-64665
 ZrF₄-LaF₃-BaF₂-NaF glasses, EPR of Cu²⁺ ions 7-27593

gadolinium

- see also nuclei with
 adsorption on W (110) 7-27118
 atom, autoionising states, electric field effects, UV spectra anal. 7-42531
 cathode, hot, evaporating, in stationary vacuum arc with diffuse cathode emission, thermal conditions 7-58087
 Curie point thermomagnetic engine, demonstration of Carnot principle 7-48233
 Curie temp. press. depend., Fermi surface struct. effects 7-7509
 equal magnetisation lines, effective field const., paramag. Curie temp. and magnetocaloric effect 7-7546
 ferromagnetic, electronic quasiparticle struct., temp. depend. 7-32908
 foil, transient mag. field effect on Si²⁺ 7-10537
 lanthanum ethylsulphate: Gd³⁺, spin correlated cryst. fields and zero-field splittings, intersite contrib. calcs. 7-16996
 mean square amplitude of vibr. and Debye temp. 7-21368
 monolayer on W, ferromag. order and orit. exponent, ESR study 7-45680
 monolayer on W (110), magnetic resonance 7-59113
 optical radiation generated by electrons (Russian) 7-53415
 point contacts, microcontact spectroscopy, contact temp. determ. 7-12790
 PWR, reactivity control of first cycle using Gd burnable poison system 7-56773
 spin-polarised Auger electron spectroscopy 7-33489
 surface, evidence for ferromag. order above bulk Curie temp. 7-33173
 BaFCl:Gd³⁺, charge transfer excitation and emission spectra 7-64688
 BiVO₄:Gd³⁺, ESR spectra, temp. depend. 7-22137
 CdF₂:Gd crystals, local field-enhanced electronic conduction, activation energy and Poole-Frenkel const. calcs. 7-38570
 CdS:Gd, Cl film solar cells, gamma radiation effects on photoelectric properties 7-34032
 CeO₂:Gd³⁺, grain boundary effect, elec. meas. 7-38248
 CsCaF₂:Gd³⁺, transferred hyperfine interaction of impurity centres, ENDOR, EPR meas. 7-32946
 CsMF₃:Gd³⁺ (M=Cd,Ca), transferred hyperfine interactions, ¹⁹F ENDOR studies 7-53177
 GaSb:Gd, Ho crystal grown by horizontal zone melting, precipitate identification 7-21462
 Gd, μ SR studies, Knight shifts and relax. above Curie temp. 7-45877
 Gd³⁺ compounds, Y-diluted energy migration, luminescence study 7-33443
 Gd:Ce, hyperfine field and relax. rate, intermediate valence model 7-7184
 Gd-Co compositionally modulated mag. film props. study 7-7566
 Gd-Y single crystal superlattices, struct. and mag. props. 7-27160
¹⁵³Gd production for medical scanning appl., nuclear data 7-34274
 KTaO₃:Gd³⁺, ESR, effect of external electric field 7-38933

gadolinium continued

- LaF₃:Pr³⁺Gd³⁺, two-photon excitation and interconfigurational energy transfer 7-3083
 LuPO₄:Gd³⁺, mag. hyperfine interactions, ³¹P and ⁵¹V ENDOR spectra 7-27630
 LuVO₄:Gd³⁺, mag. hyperfine interactions, ³¹P and ⁵¹V ENDOR spectra 7-27630
 Pb₂Ge₂O₁₁:Gd³⁺, impurity ion reorientation kinetics 7-45940
 PbTe:Gd, mag. props. EPR study 7-53126
 Pt-Gd contact, mag. order destruction by cold current 7-52980
 Si:Gd, grown from melt, electrical and optical props., residual impurities 7-63636
 Si:Gd, neutron irradi., Hall effect, elec. cond., IR absorpt. spectra 7-51834
 Si:Gd,C profiled single cryst., electronic parameters and SiC inclusions 7-32944
 SmB₂:Gd³⁺ energy gap temp. depend., impurity ESR study 7-45151
 TbCl₄:Gd³⁺, impurity-vacancy centre EPR probe for incommensurate phase 7-17220
 UBe₁₃-Gd, EPR in superconducting phase 7-33269
 YVO₄:Gd³⁺, mag. hyperfine interactions, ³¹P and ⁵¹V ENDOR spectra 7-27630

gadolinium alloys

- Al-Ti-Gd, rapidly solidified ribbons, aged, ternary phase precipitate identification 7-3311
 Cd(Cu_{1-x}Al_x)₂, mag. and cryst. props. 7-27506
 Cd(Cu_{1-x}Ni_x)₂, mag. and cryst. props. 7-27506
 Co-Gd-Tb-based thin films, properties and stability for magneto-optic recording 7-53075
 Cu-Gd, thermodynamic props. rel. to glass forming ability 7-38204
 Gd-Co, amorphous, influence of hydrogenation or mag. props. 7-2899
 Gd-Co, amorphous and crystalline, hydrogenation, pressure-composition isotherm 7-3606
 Gd-Co, anisotropic ferrimagnets in high mag. fields 7-17200
 Gd-Co films, amorphous, spontaneous spin-reorientation transition (Russian) 7-45763
 Gd-Co-Mo amorphous magnetic thin films, spin wave mode linewidth meas. 7-45826
 Gd-Cr-C system, phase equilib., struct. 7-46423
 Gd-Fe, amorphous Faraday rotation 7-64612
 Gd-Fe evaporated amorphous alloy films, mag. props. and FMR behaviour studies 7-45825
 Gd-Fe sputtered amorphous films, structural relax., positron lifetime meas. 7-37870
 Gd-Fe-Co, amorphous Faraday rotation 7-64612
 Gd-Mg system, phase equilib. study 7-26935
 Gd-Pd, formation enthalpies, calorimetric determ. 7-65341
 Gd-Pt, formation enthalpies, calorimetric determ. 7-65341
 Gd-Sb, phase diagram, peritectic reactions, congruent melting, DTA, microstructural and X-ray anal. 7-39481
 Gd-Tb alloys, temp. depend. of magnetostrictive coeffs. 7-64505
 Gd-Tb-Co-Fe sputtered amorphous films, Kerr magneto-optical effect, anisotropy dispersion effects 7-38913
 Gd(Al_{1-x}Ga_x)₂, cryst. struct., paramag. susceptibility, elec. resist. meas. 7-16492
 GdAuCu₄, cubic alloys, mag. props. 7-52936
 GdCo amorphous, Faraday rotation 7-64612
 GdCo and GdTbFeCo alloys, amorphous thin films, thermomag. recording, magnetisation reversal, coercivity 7-64459
 GdCo-based glasses, double transition behaviour induced by anisotropy 7-22109
 GdCo₂, ¹⁵⁵Gd 105.3 KeV transition, Mossbauer effect study 7-38971
 GdCo₂, magnetocrystalline anisotropy, rare earth contribution 7-45659
 GdCo glasses, electronic struct., photoemission and magnetism 7-64060
 GdCo(Fe) amorphous films with perpendicular anisotropy, Hall loop meas., mag. struct. studies 7-7205
 GdCoSi₃, amorphous film, mag. and magnetoopt. props., thickness depend. 7-33239
 GdCu, optical props. and electronic struct. investigs. (Russian) 7-13174
 Gd(Cu_{1-x}Co_x)₂, mag. and crystallographic props. 7-38903
 GdFe and GdCo amorphous thin films, electrical conductivity, influence of mag. order 7-7409
 Gd₂Fe₁₄B alloys, magnetic anisotropy and spin reorientations 7-38855
 Gd₂Fe_{14-x}Mn_xB system, mag. characts. 7-27523
 Gd₂Fe_{12-x}Mn_xCo₂B, mag. props. 7-27500
 GdIn₃, antiferromagnetic alloys, thermolec. power meas., band gap form. 7-38543
 Gd₂In, mag. transitions under press. 7-59013
 Gd_{2-x}La_xAl, pseudobinary cpd., mag. props., disorder effects 7-7523
 Gd₂La_{65-x}Co₂₅B₁₀ mixed glasses, mag. props., phase transitions, microstruct. effects 7-64465
 GdM₂ (M=Al, Ni), paramag. fluctuations, μ SR study 7-45878
 GdMn₂, magnetic structure, tight binding approx. 7-2819
 GdNi amorphous ferrimag. anisotropic films, Hall voltage polarity voltage and temp. depend. studies 7-7206
 GdNi₃, paramag. suscept. studies 7-52935
 GdPd₃, electronic structure and intrinsically selective absorption 7-38444
 Gd₂Si_{1-x}, x=0.18, 0.59, 0.87, amorphous, thermal, elec. and mag. props. 7-53039
 GdTbFe, corrosion resistance improvement by metal coatings 7-53952
 Mg-Gd supersaturated solid soln., precipitate cryst. struct. (Russian) 7-33665
 Sn-Gd binary system, phase diagram and equilb. 7-7961
 Sn(La-Gd)₃Rh₄Sn₁₂ crystals, structural distortion and chem. bonding, X-ray diff. studies 7-1947
 Tb_{0.05}Gd_{0.95}Al₂, NMR of ¹⁵⁹Tb (Russian) 7-45832
 Tb₂Gd_{1-x}Al₂, intrinsic low field susceptibility studies 7-45633
 Tb₂Gd_{1-x}Al₂, intrinsic coercive field 7-45729
 U₂Gd_{1-x}Ga_x, Curie temp., loss of ferromagnetism, comp. depend. competing exchange interactions 7-12970

gadolinium compounds

- see also gadolinium alloys
 H-D exchange, H desorption 7-28304
 oxychlorides, phase equilib., X-ray diff. and spectro-luminesc. anal. 7-46143
 Ba_{1-x}Gd_xF_{2+x}, defect struct., ionic thermocurrents, dielec. meas., EPR obs. 7-44907
 (BiDySmLuGd)(FeGa)₂O₁₂ bubble garnet films, Bi-substituted, LPE growth rate reduction 7-45049

gadolinium compounds continued

- (BiGdTm)₃(FeGa)₅O₁₂ single cryst. film, reverse-magnetisation domain nucleation studies 7-17208
 (BiGdTm)₃(FeGa)₅O₁₂ epitaxial films, microdomain nucleation near moving domain walls 7-45778
 CaGdAlO₄ crystals, growth by Czochralski method 7-22460
 Cr,Nd:(Gd,Sc)₃Ga₅O₁₂ laser crystals, growth and quality 7-13346
 Cr,Nd:GdScGa₅O₁₂ laser Q switching for optimising use of stored energy 7-25851
 Cr,Nd:GdScGa₅O₁₂ laser rods losses and efficiency meas. 7-43106
 Cr³⁺:Gd₃Sc₂Al₃O₁₂ laser, flash-lamp pumped 7-15902
 CrGd₂S₇ synthesis, physicochemical props. 7-44470
 (Gd,Bi)₃(FeGaAl)₅O₁₂ garnet films, selected area liq. phase epitaxy, local ion implantation effects 7-21726
 (Gd,Sc)₃Ga₅O₁₂ laser materials, high strength, development 7-10961
 Gd₂(Co_{1-x}Mn_x)₁₇, Co contribution to magnetocrystalline anisotropy, point charge model 7-45665
 GdBO₃, luminesc. of Sb³⁺ 7-33442
 GdBO₃:Pr³⁺, Tb³⁺(Sm³⁺)(Dy³⁺), host lattice sensitisation, energy transfer and photolum. 7-46113
 (GdBi)₃(FeAlGa)₅O₁₂ garnet films, LPE growth 7-59463
 Gd_{3-x}Bi_xFe₅O₁₂ crystal growth for 0.8 μm optical isolator 7-57605
 GdCl₃, frozen soln., coordination environment investig., ENDOR 7-25576
 GdFe₄B₄, cryst. struct. and interatomic distances 7-32380
 GdFe_{1-x}Mn_xO₃, orthoferrite, mag. behaviour characts. 7-45657
 GdFeO₃ orthoferrite crystals, RF mag. props. and frozen rare earth sublattice 7-17225
 Gd₃Fe₂O₁₂ ferrogarnets, heat of crystallisation, scanning calorimetry obs. 7-2154
 Gd₃Fe₂O₁₂ garnet, spin-reorientation phase transition, NMR obs. 7-38861
 Gd₃Fe₂O₁₂, initial permeability peak at low temperature 7-33212
 GdGG laser material, characts. of polishing cpds. 7-37212
 GdGG, paramag., mag. lin. birefr. meas. 7-53265
 Gd₃(Ga_{1-x}Fe_x)₅O₁₂ and Gd₃[Al₃(Ga_{1-x}Fe_x)₂]O₁₂, mag. solid soln. systems for regenerator materials 7-59015
 Gd₃Ga₅O₁₂ laser materials, high strength, development 7-10961
 Gd₃Ga₅O₁₂, pure and doped, photoelectret, photoconductivity 7-45919
 Gd₃Ga₅O₁₂, refrigerant characts. for Carnot mag. refrigerator 7-56286
 Gd₃Ga₅O₁₂, sintered, mag. refrigerant, Kapitza conductance to He II 7-58603
 Gd₃Ga₅O₁₂, use in mag. refrigerator for He liquefaction 7-56283
 Gd₃Ga₅O₁₂, use in rot. mag. refrigerator for He liquefaction 7-56282
 Gd₃Ga₅O₁₂-YIG-ZnO, surface magnetostatic wave scatt. by SAW 7-64507
 GdIG, Faraday effect meas. 7-64616
 Gd₂MSb₂Zn₃O₁₂ (M=Sr,Ca), rare-earth activated garnets, cathodolum. 7-7763
 Gd₂(MoO₄)₃, improper ferroelectrics, energy spectrum and vacuum UV spectra 7-33413
 Gd₂(MoO₄)₃:Eu³⁺, nonresonant energy transfer between two different Eu³⁺ ion sites 7-46125
 Gd₂O₃ 7-30014
 Gd₂O₃, reflection spectra, 4d ionisation threshold 7-46234
 Gd₂O₃-P₂O₅ phosphors, Eu³⁺ activated, luminesc. spectra, cryst. symm. 7-3080
 Gd₂O₃-UO₂, nuclear fuel, interdiffusion coeff. study using autoradiographic technique 7-36157
 Gd₂O₃-UO₂, solid solution, lattice parameters, O/U thermal conductivity meas. 7-21180
 Gd₂O₃-UO₂ fuel pellets, thermal expansion meas. at 293-1973 K 7-49538
 Gd₂O₃-ZrO₃-Nb₂O₅ structure investig. 7-46427
 Gd₂O₃:SiTb X-ray fluorescent screen for use in portable fluoroscope 7-61407
 GdS, lattice thermal cond., two-made cond. of phonons 7-27039
 GdScGa₅O₁₂:Cr, Tm crystals, dual freq. lasing study 7-43117
 Gd_{2.957}Sc_{1.905}Ga_{3.138}O₁₂ garnet, congruently melting, cryst. growth 7-59412
 Gd₃Sc₂Ga₅O₁₂, garnets 7-21045
 Gd₃Sc₂Ga_{5-x}O₁₂:Cr³⁺ garnet, laser spectral analyser 7-31362
 GdSi_{2-x}Si_x, silicide thin films, phase composition, conductance, surface morphology 7-7072
 Gd₃SiO₃:Ce(Tb), Czochralski growth 7-53556
 Gd_{1-x}Sc_xCrO₃, coordination number and elec. cond., EXAFS and XANES studies 7-64785
 Gd₃Te₂Li₃O₁₂:R, cathodoluminescence study (German) 7-22354
 Gd₂Ti₂O₇:Ce, radiation effects, appl. for nuclear waste disposal 7-32522
 Gd_{2.813}Tm_{0.17}Hf_{0.017}Sc_{0.005}Ga_{4.95}O₁₂, laser active medium operating in 2 μm range 7-50568
 Gd₂Zr₂O₇, defect behaviour, computer-based atomistic simulation studies 7-16548
 HfO₂-Gd₂O₃, solid soln. single crystals, physicochem. props. 7-2097
 HfO₂-Gd₂O₃, solid solution single crystal growth 7-7838
 KGd(WO₄)₂:Ho³⁺, luminesc. kinetics, visible and UV spectra anal. 7-46144
 KNd₂Gd_{1-x}P_xO₁₂, isolated ion pair interaction, fluoresc. quenching study 7-46117
 K₂O-Al₂O₃-B₂O₃-Fe₂O₃-Gd₂O₃ glasses, mag. props., composition dependences 7-2823
 LiGdP₂O₁₂, flux cryst. growth 7-13345
 Nd,Cr:(Gd,Sc)₃Ga₅O₁₂, spectroscopic, optical and thermo-mechanical props. and laser performance 7-10963
 Pb₉₃Gd₀₅Te, antiferromag. exchange constant between nearest-neighbour Gd³⁺ ions 7-59002
 PbTe-Gd₂Te₃ system, solid solns., synthesis and props. 7-21458
 Pr_{0.1}Gd_{0.9}(SiO₄)₆O₂, sensitisation of Gd³⁺ luminesc. by the Pr³⁺ ion 7-3082
 Rb₂Gd(MoO₄)₄, palmierite-type cpd., cryst. struct. determ. 7-21174
 (SmLuGd)₃(FeGaSc)₅O₁₂ films, with submicron domain structures, mag. inhomogeneity 7-45782
 (U,Gd)₂O₃ solid solns., O/M ratio, gravimetry meas. 7-30560
 U_{1-x}Gd_xO₂ solid soln., microcharacterisation by ESR, XPS and mag. susceptibility meas. 7-12957
 Y_{1.5}Gd_{1.5}Fe₅O₁₂ garnet, γ-irradiated, mag. props. (Russian) 7-27502
 Y₂Pr_{0.03}Gd_{0.97}Al₅O₁₂, sensitisation of Gd³⁺ luminesc. by the Pr³⁺ ion 7-3082
 (YSmLuGd)₃(FeGa)₅O₁₂ garnet film struct. and mag. props., mag. bubble memory apps. (Japanese) 7-7575
 ZrF₄-BaF₂-GdF₃-AlF₃-NaF-FeF₃, optical fibre glasses, trace amounts of Fe, characterisation 7-2956

gain (amplification) *see* amplification

gain measurement

- dye lasers, pulsed, expression for small signal gain 7-15889
 optical, spontaneous emission amplification obs. 7-14989
 KrF laser gain meas. system 7-62717

gait analysis *see* biomechanics

galactic cosmic rays

- acceleration by supernova remnant shock-waves, orbit averaged Darwin quasi-neutral hybrid code 7-14425
 acceleration in collapsing gas clouds 7-55390
 acceleration of protons and electrons in EM field of rot. orthogonal mag. dipole, theory 7-9339
 atmosphere, north-south asymmetry, solar mag. field effects 7-66409
 Compton-Getting effect, frame transformation of spherical-harmonic coefficients of differential particle intensity 7-18337
 cosmions in solar neutrino. problem, particle physics models 7-55457
 Cyg X-3, cosmic glueballinos source, discussion 7-48105
 Cyg X-3, H dihyperon from high energy muon obs. 7-47992
 Cygnus X-3, radiation source, role of antineutrinos and photinos 7-24242
 Cygnus X-3, underground muons, new evidence from Soudan 1 7-40863
 density gradient perpendicular to ecliptic plane pointing southward, correl. with Sun northern activity excess 7-24111
 electrons of superhigh energy, spectrum formation 7-4278
 highest energy cosmic rays, energy spectrum, directional anisotropy and origin 7-55389
 intensity enhancement near interplanetary mag. field annihilation region 7-23960
 intensity profiles, effects of solar wind compound stream 7-47656
 leaky box model for cosmic ray propag., antiprotons production model and p/p ratios estimation 7-40654
 light nuclide production from interstellar matter-cosmic ray interactions 7-47836
 long term variations of galactic cosmic rays, Monte Carlo calcs. 7-34842
 M31, possibilities for detect. at γ-ray wavelengths, implications for cosmic rays 7-60782
 Neogene flux variations, implications of cosmogenic isotope and track records in meteorites 7-29440
 neutron stars, neutrino lumin., implications of collective effects of nucleon medium 7-47967
 positron annihilation in interstellar H₂ environment, laboratory simulation 7-14426
 positron observations from 10 to 20 GeV, balloon-borne meas. using geomag. east-west asymmetry 7-66411
 positrons and γ-rays in diffusion model (Russian) 7-40655
 propagation in solar wind 7-35124
 protons and static cosmic ray-supported galactic corona, model 7-60787
 space-time flux variations, implications of radionuclide depth profiles in Dhajala chondrite 7-29439
 supernovae (book) 7-60914
 ultra-high-energy cosmic rays, accel. and transport in Galactic wind and termination shock 7-66403
³⁹Ar activity, galactic cosmic ray intensity 7-23957
 H and He isotopes in galactic cosmic radiation, meas. rel. to source abundances and interstellar propag. 7-55394
 He nuclei interstellar pathlength, implications of He rigidity spectrum and ³He/⁴He ratio at high energies 7-66410
³He/⁴He ratio rel. to origin of cosmic-ray He nuclei 7-60497
⁴He solar modulation 7-47648
 Mg isotopic characts. 7-60645

galactic nuclei

- 7-9552
 0133+476, 0235+164, 1749+096, 2131-021, variable quasars, multifreq. radio obs. 7-40955
 0754+101, BL Lac object, V-magnitude obs. during new visual outburst (1986 September 30) 7-29540
 1701+610, QSO with tidal tail, CCD imaging and spectroscopic obs. 7-4589
 accretion disks, model of hydromagnetic turbulence in differentially rotating disks 7-18354
 active galactic nuclei, computational methods for emission-line spectrum 7-9534
 active galactic nuclei, distrib. function description of cloud props. 7-29535
 active galactic nuclei, effects of one-generation pair production in synchrotron self-Compton sources 7-55452
 active galactic nuclei, electron pair prod. rel. to bimodal spectral behaviour 7-9510
 active galactic nuclei, emission line profiles from Keplerian cloud ensembles 7-4586
 active galactic nuclei, emission spectrum of high-density photoionisation models and low-ionisation lines 7-9535
 active galactic nuclei, flux-redshift relations in chronometric cosmology rel. to luminosity evolution 7-24237
 active galactic nuclei, magnetodynamic jets form. through accretion of rotating magnetised mass 7-55460
 active galactic nuclei, new accretion disk models rel. to optical and UV spectra 7-60813
 active galactic nuclei, phenomena arising from nonstationary central black hole 7-60795
 active galactic nuclei, spectroscopic obs. and red shifts 7-4566
 active galactic nuclei, two-epoch VLBI obs. of low frequency variable radio sources 7-4579
 active galaxies, IUE meas. rel. to X-ray characts. 7-66770
 active galaxies, matter inflow to nucleus triggered by companion galaxies 7-55788
 active galaxies, radio cores polarisation props. 7-60803
 active galaxies, supercritical winds 7-55437
 active galaxies, supermassive central black holes ejection 7-60797
 active nuclei, narrow emission line region O III 500.7 nm forbidden line 7-40933
 active nuclei and primaevial QSOs 7-60827
 active nuclei characts. (French) 7-66759
 active nuclei variability, gravit. lens hypothesis, microlensing effects 7-55791
 Arp 220, molecular gas, mm interferometry 7-55815
 Arp 220, peculiar galaxy (IR bright), far-IR and optical observations 7-40931
 barred spiral galaxies, radio emission from galactic nuclei 7-24203
 bipolar jets, prod by turbulent Alfvén waves 7-60523

galactic nuclei continued

- 3C 120, Seyfert galaxy, UV and optical obs. in two different states 7-55832
 4C 18.68, quasar, radio core and halo struct. 7-4588
 3C 371, N-galaxy/BL Lac object, EXOSAT obs. 7-55802
 3C 428, neglected 3C radio sources VLA obs. 7-14672
 Cen A (NGC 5128), X-ray intensity and spectrum obs. from Tenma 7-55828
 Cen A (NGC 5128) obs. at MeV gamma-ray energies 7-66754
 Einstein normal galaxy sample, radio and X-ray props. of elliptical and S0 galaxies 7-66753
 ESO 428-G14, new Seyfert 2 galaxy, evidence for nonthermal power-law source 7-9538
 FIRST observational potential 7-48093
 G1200-2038, dwarf galaxy with Seyfert characts., spectroscopy and imaging obs. 7-48069
 Galaxy, 43-GHz continuum obs. of central region 7-24219
 Galaxy, 511 keV annihilation line and positronium monoenergetic beams 7-62547
 Galaxy, ^{12}CO and ^{13}CO obs. of unusual mol. cloud complex (Clump 1) 7-48044
 Galaxy, black hole at galactic centre, observational evidence, review 7-29541
 Galaxy, common origin for gamma-ray lines at 0.51 and 1.81 MeV 7-24238
 Galaxy, mol. obs. with University of Cologne 3 m telescope at Gornergrat Observatory 7-60557
 Galaxy, neutral disk, CO and CS obs. 7-35040
 Galaxy, prominent polarised plumes and their mag. field, linear polarisation obs. 7-14656
 Galaxy, spatial distrib. and vel. field of H_2 line emission from central region 7-9528
 Galaxy, twin-jet model for centre lobe rel. to former Seyfert stage 7-66740
 high-mass stars formation, role of cloud-cloud collisions 7-55610
 IC 5063 (PKS 2048-57), discovery of polarized nonthermal nucleus 7-66762
 intermediate Seyferts, emission line spectra, composite models 7-40913
 interstellar Na I line strength versus reddening relation, influence on stellar population synthesis 7-9526
 IR spectra, 3.28 μm feature and continuum emission obs. 7-9533
 IRAS minisurvey galaxies, near-IR photometry 7-40923
 isotropic stellar systems, linear oscills., non-radial modes 7-35014
 Kerr black holes, optically-thick gas steady spherically-symm. accretion, outgoing radiative flux 7-35044
 BL Lac candidates, X-ray selected, optical spectroscopy of six objects 7-48085
 BL Lac objects, updated list and relation to galaxies and quasistellar objects 7-47732
 M31, near-UV obs. with ESA Photon Counting Detector 7-4562
 M51, M100, obs. of stellar ovals and nuclear rings in galactic interiors 7-4568
 M82, interstellar medium in central 1 kpc 7-55816
 Markarian 231, Seyfert 1 galaxy, morphology and nuclear spectroscopy 7-48067
 Markarian 231, Seyfert galaxy/QSO, CO ($J=1-0$) emission detect. and optical imaging 7-66757
 Markarian 306, double nucleus galaxy, spectroscopic investigation 7-24199
 Markarian 35 (=NGC 3353), spectrophotometric characts. 7-40910
 Markarian 490, high ionisation starburst galaxy, spectroscopic and imaging obs. 7-4574
 Markarian 705, Seyfert ring galaxy, B and V surface photometry 7-66732
 Markarian galaxies, catalogue 7-55496
 narrow-line regions, anal. of interstellar gas clouds dynamics in galactic bulges 7-66707
 NGC 1068, Seyfert 2 galaxy, radio struct. in inner 1 arcsecond 7-48068
 NGC 1068, Seyfert galaxy, detect. of broad UV Fe II lines in spectrum of nucleus 7-14663
 NGC 1097, barred spiral galaxy with ring of star formation at centre 7-60777
 NGC 1275, Seyfert galaxy, submm continuum characts. 7-48099
 NGC 2798, interacting galaxy, evidence from UV spectroscopy from starburst in galactic nucleus 7-55830
 NGC 3079, 3998, and 4258, kpc structure from $\text{H}\alpha$ CCD images of galaxies with compact radio nuclei 7-55810
 NGC 3256, galaxy, evidence from UV spectroscopy from starburst in galactic nucleus 7-55830
 NGC 4051, Seyfert galaxy, EXOSAT obs. of low-freq divergent X-ray variability 7-66763
 NGC 4151, Seyfert 1 galaxy, C IV 155 nm line profile obs. (1978 to 1983) 7-60814
 NGC 4151, Seyfert 1 galaxy, obs. of new outflowing absorpt. component in Mg II line profile 7-55834
 NGC 4151, Seyfert galaxy, detect. of intense Fe line emission at 6.4 keV 7-18452
 NGC 4922, binary galaxy, spectrophotometric investigation 7-24200
 NGC 5506, Seyfert galaxy, EXOSAT obs. of fractal X-ray time variability and spectral invariance 7-66764
 NGC 5548, Seyfert 1 galaxy, double broad-line emitting regions as evidence for supermassive binary system 7-66756
 NGC 5548, Seyfert 1 galaxy, evidence for black hole accretion event, He II obs. 7-35052
 NGC 5548, Seyfert 1 galaxy, optical spectrum vars. rel. to multiple-component broad-line region 7-66750
 NGC 613, barred spiral galaxy with collimated outflow from nucleus 7-60779
 NGC 6240, far IR spectra of luminous interacting galaxy 7-40932
 NGC 7469, Seyfert 1 galaxy, EXOSAT obs. of rapid hard X-ray variability and soft X-ray excess 7-48077
 NGC 7469, type 1 Seyfert galaxy, emission lines mapping rel. to circum-nuclear starburst 7-29536
 OJ 287, BL Lac object, optical variation and outburst obs. (1980 to 1984) (Chinese) 7-4548
 PG 0946+301, broad absorption line QSO, spectrum from 550 to 4250 Å 7-55852
 PKS 0521-36, radiogalaxy, optical jet and nucleus photometric characts. 7-55789
 PKS 2155-304, BL Lac object, IUE obs. (1979 to 1985) 7-55833
 Q0800+608, quasar, VLA obs. of remarkable one-sided jet 7-9555

galactic nuclei continued

- Q1100+772, Q2201+315, intermediate-redshift quasars, line profiles from high signal-to-noise UV spectra 7-55850
 quasars, brightness scale length of outer regions rel. to active nuclei characts. (Russian) 7-55826
 quasars, characts. review 7-48098
 quasars, energy puzzle of broad line region 7-9553
 quasars, low-redshift, archival study of IUE obs. 7-60835
 quasars, perturbed galaxy disk models rel. to tidal triggering 7-9537
 radio galaxies, role of magnetic energy dissipation in force-free jets 7-29391
 radio jets, general relativistic decollimation theory 7-60522
 radio sources, model for rapid flux variations (Chinese) 7-4577
 radiogalaxies, milliarcsecond VLBI nuclei positions 7-14671
 Seyfert 1 galaxies, emission line profiles and profile ratios 7-55818
 Seyfert galaxies, brightness scale length of outer regions rel. to active nuclei characts. (Russian) 7-55826
 Seyfert galaxies, emission-line variability 7-14648
 Seyfert galaxies, IUE obs. and comparison with low-redshift quasars 7-60835
 Seyfert galaxies, luminosity function and space density 7-24202
 Seyfert galaxies, narrow-line, with permitted Fe II emission (Mrk 507, 5C 3.100, I Zw 1), optical, X-ray, and IR props. 7-66751
 Seyfert galaxies, perturbed galaxy disk models rel. to tidal triggering 7-9537
 Seyfert galaxies, radio props. of type 1.8 and 1.9 galaxies rel. to galactic nuclei differences 7-29537
 Seyfert galaxy nuclei, near-UV spectroscopy rel. to reddening and Bowen fluoresc. 7-55801
 Seyfert-1 galaxies, UV spectra rel. to nature of broad-line region 7-55831
 Sgr A West region, ionised gas dynamics and comp. 7-40935
 spectroscopy of galactic nuclei, results for complete sample of galaxies 7-40921
 stability of a hypothetical binary at the galactic center 7-55793
 starburst galaxies, spectroscopic study of nuclear starburst regions 7-24222
 stellar encounters, cross sections for tidal capture binary form. and stellar merger 7-29519
 supercritical winds, Comptonisation, dynamics and obs. diagnostics 7-55438
 supernova frequency, possible implications for binary stars occurrence 7-66601
 support due to energy from mag. monopole catalytic reaction of nucleon decay (Chinese) 7-66439
 thin disk model for UV excess of quasars and Seyfert 1 galaxies 7-40956
 Ursa Major I(S) group galaxies, ^{12}CO and far-IR obs. 7-29548
 violent indicator rel. to central black hole 7-18449
 viscous jets dynamics, numerical calcs. 7-4565
 X-ray emission from galactic nucleus explosion and hot interstellar matter effects 7-40962
 X-ray luminosity-redshift relationship for extragalactic objects, observational data 7-14679
 C IV emission line behaviour in active nuclei, IUE spectra 7-60790
 H_2O masers in nuclei of nearby galaxies, 22-GHz obs. 7-14661
 OH-IR stars near galactic centre, luminosities and progenitor characts. 7-14584

galactic radio waves see radiofrequency cosmic radiation

galaxies

- see also galactic nuclei; Galaxy; Magellanic Clouds; Markarian galaxies; radiogalaxies; Seyfert galaxies
 Abell cluster galaxies, 11.1-cm radio maps and obs. at 6.3 and 2.8 cm 7-18454
 active dwarf galaxies, star formation rates and efficiency 7-55806
 active galaxies, visible photometric obs. 7-66784
 active nuclei, distrib. function description of cloud props. 7-29535
 active nuclei variability, gravit. lens hypothesis, microlensing effects 7-55791
 Anon 0052-07, SN 1986K spectral obs. 7-4495
 Arp 205 system, modelling 7-35041
 Arp 220, molecular gas, mm interferometry 7-55815
 Arp 220, peculiar galaxy (IR bright), far-IR and optical observations 7-40931
 automated surface photometry, calibration and validation of photometric technique 7-60575
 bars, dynamical models, truncated perfect elliptical disk 7-60786
 biased formation model, anal. of spatial correl. of Abell clusters 7-9548
 biased galaxy formation 7-14658
 blue compact galaxies, spectrophotometric anal. 7-40920
 blue irregular galaxies, massive star content determ. from IUE obs. 7-48088
 brightest cluster galaxies, gravit. amplification by foreground clusters 7-24206
 burnt-out galaxies and galaxy clusters, relation to quasar pairs 7-35051
 Byurakan second spectral sky survey in UMa field 7-4352
 3C 275.1, CCD imaging of host galaxy and gas cloud surrounding quasar 7-55848
 Carina dwarf galaxy, photometric obs. of RR Ly stars 7-4570
 Case emission-line galaxies in direction of Bootes void, spectroscopic survey 7-29534
 cD-type galaxies, equilib. of gas in galaxy gravit. field 7-24204
 Centaurus cluster, struct. and distrib. of different galaxy types 7-9547
 central galaxies in southern clusters, optical spectra rel. to evidence for star form. 7-55821
 CfA galaxies clustering, correl. length rel. to cluster-cluster correl. function 7-48092
 in CG 1116+51, He in dwarf irregular rel. to primordial abundance 7-55804
 chemical abundances and evolution of irregular and blue compact galaxies 7-60775
 chemical evolution, He and heavy-element enrichment of interstellar medium 7-40905
 chemical evolution, secondary metallicity in analytical models 7-66743
 chemical evolution models construction techniques 7-40721
 chemical evolution of galaxies 7-48083
 colour-luminosity relations in optical and IR, determ. for complete galaxy redshift sample 7-24213
 Coma cluster galaxies, positions and vels. rel. to cluster mass 7-40945
 Coma/A 1367 Supercluster, radio continuum props. of galaxies in different density environments 7-29547

galaxies continued

- compact blue dwarf galaxies, stellar populations and evol. 7-48078
 conf., Erice, Italy (April 1986) 7-41001
 Conference on nebulae and abundances, Austin, TX, USA (April 1986) 7-35096
 correlation functions, closure of BBGKY hierarchy in phase space 7-29546
 cosmic ray-supported coronae, model 7-60787
 cosmic string induced galaxy formation 7-9543
 cosmic strings, fractal geometry and galaxy and cluster correlation functions 7-56115
 cosmological model, self-similar, galactic scale phenomena and dark matter 7-35076
 dark galactic haloes 7-60530
 dark matter in the Universe 7-60851
 dark matter nature 7-60658
 DDO 155, distance modulus and field star VM No.1 nature 7-66588
 deformed galaxy model with large degree of stochasticity 7-60780
 diffuse microwave background radiation, temps. of galactic and cosmic components at 12 cm wavelength 7-55859
 disk galaxies, gas flow simulation, tilts and corrugation waves evol. 7-60806
 disk galaxies, populations of subclasses of ordinary and barrel spirals in various environments 7-24215
 disk galaxies form. at high red-shift 7-55794
 disk wave pattern generation by satellite with retrograde motion 7-4553
 Draco dwarf galaxy, magnitudes of bright variable stars 7-9483
 Dressler 36, ring galaxy discovery 7-14652
 dwarf galaxies, low surface brightness, in Virgo cluster, H I synthesis obs. and surface photometry 7-4560
 dwarf galaxies, luminosity classification anal. 7-60794
 dwarf galaxies, role in origin of quasars absorpt. lines 7-40952
 dwarf galaxies, spatial struct. determ. 7-29527
 dwarf galaxies of low surface brightness, SHF continuum obs. 7-40916
 dwarf galaxy in Phoenix, H I survey 7-24229
 dwarf irregular galaxies, CNO abundances determ. 7-40939
 dwarf irregular galaxies, search for ^{12}CO emission from twelve objects 7-35033
 dwarf star content of elliptical and lenticular galaxies, near-IR spectra 7-60792
 dynamical models, adaptation to globular cluster systems 7-14613
 dynamics, completely analytical family of anisotropic Plummer models 7-55741
 dynamics, stability of multi-component gravit. systems described by Boltzmann eqn. 7-4525
 E50-390-G 05, abundance determ., spectrophotometric obs. anal. 7-66722
 early-type elliptical galaxies in Virgo cluster, colour distrib. from surface-brightness meas. 7-48070
 early-type galaxies, H I content versus star form. and ionised gas 7-29528
 early-type galaxies, prevalence of cooling flows from interstellar gas density profiles 7-14664
 early-type galaxies, X-ray surface brightness distrib. and spectral props. 7-55799
 early-type galaxies with emission lines, catalogue 7-60578
 edge-on galaxies with box and peanut-shaped bulges, minor axis brightness profiles 7-29526
 Einstein normal galaxy sample, radio and X-ray props. of elliptical and S0 galaxies 7-66753
 elliptical galaxies, circumgalactic shells morphology rel. to dark matter 7-66748
 elliptical galaxies, more precise L- σ distance indicator 7-9541
 elliptical galaxies, orbital characts. of dynamical models 7-35046
 elliptical galaxies, phase space density 7-55795
 elliptical galaxies, radial vels. rel. to non-uniform Hubble flow 7-24225
 elliptical galaxies, self-regulated cooling flows and low-mass star form. 7-66741
 elliptical galaxies, wind model, chem. and photometric props. 7-66733
 elliptical galaxies in groups and clusters, mass determ., X-ray emission anal. 7-4552
 elliptical galaxy near BAL QSO 1E 0104.2+3153, obs. 7-66787
 emission nebulae and abundances in galaxies, review 7-40903
 evolutionary relations between dwarf irregular and elliptical galaxies 7-35053
 explosive galaxy formation, percolation rel. to galaxy-galaxy correl. scale 7-29533
 extragalactic H II regions, collisional effects in He I triplets rel. to primordial He abundance 7-55446
 extragalactic H II regions in SA 94, identifications from objective-prism classification of quasar candidates 7-66779
 faint galaxies as probes for distant Universe 7-4610
 faint galaxies photometry, implications for cosmology and galaxy clustering 7-60915
 faint H α emission-line galaxies, spectral obs. 7-35032
 field galaxies, red shifts and fluxes used to determine Universe mass density 7-40968
 first-ranked galaxies in poor clusters, luminosities determ. 7-55843
 formation, assoc. cosmic rays origin and accel. 7-55390
 formation, equilibria and instabilities of polytropic configurations within homogeneous background matter 7-4316
 formation, evolution and clustering of rich clusters in hierarchical theories 7-9546
 formation, evolution of adiabatic perturbations in baryonic Universe 7-4597
 formation, implications of baryon concentration in string wakes (at $z \geq 200$) 7-14687
 formation, implications of temp. fluctuations of microwave background due to gravit. lensing 7-4595
 formation, Population II stars as 'dirty' primordial Population III 7-29470
 formation, quantum creation theory 7-14487
 formation, recent developments in cosmic string theory 7-14694
 formation, role of cosmic strings 7-48117
 formation, string-induced, compatibility with inflation 7-66765
 formation, triggering by evolution of large-scale density perturbations 7-66794
 formation rel. to material content of Universe, conference, London, England (October 1985) 7-55884
 Fornax dwarf spheroidal galaxy, globular clusters radial vel. 7-14649

galaxies continued

- G0053-076, anonymous galaxy in Cetus, discovery, precise position, and magnitude estimate of SN 1986K 7-9502
 galaxies, redshift-magnitude formula for Universe with cosmological const. and radiation press. 7-40924
 galaxy formation, cosmic string basis 7-14693
 gas flow in spiral galaxies: effects of rotation, thermal processes, and self-gravitation 7-29531
 gas-rich dwarfs and QSO absorption lines origin 7-60828
 gaseous disk spiral wave packets, stability 7-4318
 general textbook contribution 7-60912
 gravitational Bohr orbits in double galaxies 7-14670
 gravitational lens effects, flux conservation rel. to random gravit. lensing of quasars 7-23994
 gravitational micro-lensing by stars in galaxies, astrophysical appls. 7-9364
 H II regions, abundances and spectra 7-66742
 halo dark matter, particle mass limits from beam-dump expts. 7-49186
 halos, rotation, density and string-seeded spirals 7-29562
 high-velocity clouds collisions with galactic disks, 2D hydrodynamic simulations 7-48065
 IC 1194, ring galaxy discovery 7-14652
 IC 4553, megamaser galaxy, 5 cm OH absorption 7-40911
 interacting pairs, rotation curves and mass estimates 7-29530
 interstellar gas clouds orbits in galactic bulges, cloud stability anal. 7-66707
 interstellar giant molecular clouds in galaxies, N-body simulation of random vel. generation and accel. 7-18445
 interstellar molecular clouds form. in galaxies with different Z, opacity-driven fragmentation of diffuse clouds 7-40908
 interstellar Na I line strength versus reddening relation, influence on stellar population synthesis 7-9526
 intervening galaxy effects on quasar counts and colours 7-55847
 intervening galaxy towards QSO B2 1225+317, high-resolution spectroscopy of $z=1.79$ absorpt. line system 7-66782
 IRAS colours of normal galaxies 7-55813
 IRAS galaxies, sub-millimetre obs. 7-9532
 IRAS galaxies of very high lumin., ages and star form. characts 7-66767
 IRAS minisurvey galaxies, near-IR photometry 7-40923
 IRAS sources, two-dimensional covariance function determ. 7-14677
 irrotational and zero angular momentum ellipsoids in the Dirichlet problem 7-4557
 IUE and UV astronomy, conf., London, England (July 1986) 7-41012
 large-scale clustering of galaxies with massive dark halos, general struct., two-point corrs. and binaries 7-29544
 large-scale structure in Corona Borealis region, redshift survey 7-40922
 late-type galaxies, star formation rates determ. (*German*) 7-24207
 lensing galaxy of triple QSO PG 1115+080, photometric obs. rel. to redshift 7-66781
 Local Group Sb and Sbc galaxies, physical and star form. props., H I obs. 7-60809
 Local Supercluster galaxies, rot. axes orientation 7-14662
 luminosity function determination, non-parametric method for magnitude-limited samples 7-24212
 luminosity profile analysis for galaxies by curve matching 7-55825
 luminosity profiles, statistical study using spheroid-disk composite models 7-55817
 luminous axion clusters, photon decay, measurable luminosities 7-47694
 Lyman alpha disk absorbers towards QSOs, surface brightness limits 7-4587
 M101, kinematic detection of supernova remnants in giant H II regions 7-55764
 M31, globular cluster candidates in $3^\circ \times 3^\circ$ square field 7-66478
 M31, halo and disk populations from two-colour photometry 7-4569
 M31, interstellar H I holes and supernova rate 7-35036
 M31, M33, IUE and optical obs. of massive early-type stars 7-47881
 M31, massive stars props. from obs. of OB associations 7-40926
 M31, NE spiral arm mol. complex, CO mapping 7-66734
 M31, possibilities for detect. at γ -ray wavelengths, implications for cosmic rays 7-60782
 M31, red supergiants, lumin. characts., BV obs. 7-60785
 M31 and M33, SNR characts. 7-14621
 M33, 102 MHz obs. (*Russian*) 7-24217
 M33, H I survey Ing Westerbork Synthesis Radio Telescope 7-66739
 M33, OB 112 and OB 110 stellar associations, photometry characts. 7-40927
 M51, M100, obs. of stellar ovals and nuclear rings in galactic interiors 7-4568
 M81, O and N abundance gradients from spectrophotometry of H II regions 7-40941
 M87 close companions, photometric and spectral characts. 7-66735
 magnetic fields, general aspects (book) 7-48216
 merged galaxies remnants, vel. dispersions and evol., spectral obs. 7-55797
 mergers in relation to elliptical galaxies form., implications of globular cluster frequencies 7-4572
 metal-poor galaxies, determ. of primordial He abundance 7-40978
 modal analysis of rotating polytropic cylinders, gravitationally unstable mode and relation to r-mode 7-18453
 molecular content of interacting and isolated galaxies, star formation efficiency 7-55812
 MR 2251-178, quasar, underlying galaxy characts. 7-35060
 multicolour photometry of field galaxies to 24th magnitude 7-60793
 nearby galaxies, giant extragalactic H II regions integrated H α profiles 7-14624
 nearby galaxies, motion characts. 7-55835
 nearby galaxies catalogue, effect of Virgo-centric flow model on observed rels. 7-40723
 Newton's second law at small accelerations, test from disc galaxies grav. radiation 7-48081
 NGC 1023-1023A as interacting galaxies, spectral and photometric characts. 7-35037
 NGC 1097, barred spiral galaxy with ring of star formation at centre 7-60777
 NGC 1381, edge-on S0 galaxy, components, surface photometry anal. 7-55792
 NGC 1559, SN 1986L, UBV and visual magnitude estimates 7-40852
 NGC 1559, spectroscopic obs. and visual magnitude estimates of SN 1986L 7-18428
 NGC 1559, supernovae discovery in Oct. 1986, SN 1986L 7-18425

galaxies continued

- NGC 1559, visual magnitude estimates for SN 1986L (1986 November 1 to December 11) 7-47953
 NGC 1566, barred spiral galaxy, imaging spectroscopy of spiral arm 7-24214
 NGC 1667, spectral type and precise position of SN 1986N 7-47956
 NGC 1667, supernova discovery, of 1986N 7-47954
 NGC 2227, discovery, approximate position, and magnitude estimate of SN 1986O 7-47958
 NGC 2227, spectra of SN 1986O, Type Ia object 7-55692
 NGC 2403, spiral galaxy, chemical comp. gradient and stellar mass limit 7-40940
 NGC 253, photometric examination 7-55819
 NGC 2798, interacting galaxy, evidence from UV spectroscopy from starburst in galactic nucleus 7-55830
 NGC 3256, galaxy, evidence from UV spectroscopy from starburst in galactic nucleus 7-55830
 NGC 3347, spiral galaxy, UBVR photometry rel. to light vars. 7-35034
 NGC 3359, barred spiral galaxy, H I distrib. and kinematics 7-66745
 NGC 3448, amorphous galaxy, photometry and H I dynamics 7-35041
 NGC 3923, shell galaxy, shell system struct. rel. to alternatives to dark matter hypothesis 7-66749
 NGC 3923 and 3051, shell galaxies, shell lumin. characts., spectrophotometric obs. 7-55796
 NGC 4214, 4449, blue irregular, galaxies, kinematics of H II regions 7-40925
 NGC 4486, 4472 and 4406, elliptical galaxies in Virgo Cluster, colour gradients 7-35054
 NGC 4594, mass distrib. 7-40914
 NGC 4618, optical light curve of SN 1985F 7-40851
 NGC 4618, SN 1985F, light curve characts. (Russian) 7-24156
 NGC 4861, He in dwarf irregular rel. to primordial abundance 7-55804
 NGC 4922, binary galaxy, spectrophotometric investigation 7-24200
 NGC 5023, edge-on dwarf galaxy, H I layer thickness 7-24208
 NGC 5236(M83), surface photometry and lumin. characts. 7-29538
 NGC 5383, barred spiral galaxy, CO obs. 7-55827
 NGC 5430, galaxy with Wolf-Rayet knot, stellar population study 7-60778
 NGC 55, magellanic-type galaxy, H I and radio continuum obs. 7-9539
 NGC 5850, discovery in Feb. 1987 of SN 1987B supernova 7-66633
 NGC 5850, SN 1987B, Type II SN, spectral characts. 7-66639
 NGC 5850, supernova 1987B, Feb. 1987 observations 7-66635
 NGC 613, barred spiral galaxy with collimated outflow from nucleus 7-60779
 NGC 6166, g-band photometric decomposition of multiple-nucleus galaxy 7-55803
 NGC 6240, far IR spectra of luminous interacting galaxy 7-40932
 NGC 6946, spiral galaxy, catalogue and characts. of 643 H II regions 7-29414
 NGC 7499, SN 1986M prediscovery and 1986 Dec. magnitudes 7-47952
 NGC 7499, spectroscopic identification of SN 1986M as type Ib supernova 7-47956
 NGC 7499, supernova discovery, of SN 1986G 7-40853
 NGC 891, prediscovery radioobservations of SN 1986J 7-47955
 NGC 891, spectrum and radio detections of SN 1986J 7-9503
 NGC 891, supernova SN 1986J, prediscovery microwave flux densities 7-18426
 NGC 891, upper limits on B-magnitude of radio supernova SN 1986J 7-18429
 NGC 891, VLBI observation of SN 1986J supernova 7-47957
 opposite pairs effect in 'small universe', relation to topological struct. of Universe 7-60844
 orbital motion within galaxy clusters, numerical expts. 7-24231
 origin, constraints from small-scale cosmic background radiation anisotropy and galaxy clustering 7-48082
 origin, evolution and star form. 7-48087
 overlapping pair of galaxies, gravit. pot. energy 7-60784
 Palomar-Westerbork survey of northern spiral galaxies 7-40724
 PHL 1070, Q50, spiral galaxy nature, four-colour obs. 7-14675
 photometry, improved formulae for transformation of CGCG magnitudes to B_r^s system 7-48086
 photometry, proceedings, Toulouse, France (September 1984) 7-24298
 Pisces-Perseus supercluster galaxies, 21-cm survey in declination zone $+21.5^\circ$ to $+27.5^\circ$ 7-4576
 protogalaxies, IR line emission of H I and H₂ 7-4600
 Q0957+561A,B, edge-on galaxy model for gravit. lens 7-60829
 Q1146+111B,C,D,E, photometric identification of possible lens galaxy 7-29554
 Q 1548+114A, B, QSO pair, gravit. lensing by foreground QSO host galaxy 7-9554
 QSOs in fields of nearby galaxies (NGC 55, 253, 300 and 5364) 7-18461
 quadrupole gravitational lens, theory, images multiplicity and positions determ. 7-66453
 quantum double galaxies, possible mass limits 7-18455
 quasars association, surveys of intermediate-redshift quasars fields 7-55495
 quasispherical galaxy, numerical comparison of resonant orbits for 1/1 resonance 7-55740
 R² cosmology, inflation without a phase transition 7-40973
 radial periodic orbits instability for galactic potentials 7-66681
 radial velocities of galaxies near groups of galaxies 7-4550
 red shift quantisation evidence 7-60812
 red shift-number test implications 7-35079
 RI photometry of three distant galaxy cluster, results rel. to BVRI photometry in comparison fields 7-29542
 ring galaxies, classification and statistics 7-18451
 rotating triaxial galaxies, relaxation and dynamical friction in non-integrable stellar systems 7-4524
 rotation curves 7-47692
 satellite orbits decay by dynamical friction, 3D modelling 7-60801
 Schmidt law for the molecular gas profiles of disk galaxies 7-55814
 Sculptor dwarf galaxy, metal abundances and origins of anomalous Cepheids 7-4571
 Sculptor dwarf galaxy, radial vel., vel. dispersion and M/L ratio 7-14654
 Sculptor Group galaxies, radio continuum emission 7-60810
 secular redshift variations, effects of cosmological deceleration and peculiar motion 7-60796
 self-focusing as a mechanism for the formation of dense structures in Newtonian cosmology 7-40964
 Sex A, brighter stars visible photometric obs. 7-60808

galaxies continued

- Shane-Wirtanen counts, observer and time-depend. effects 7-55838
 Shane-Wirtanen counts, plate correction factors and correl. function 7-55837
 Shapley-Ames elliptical galaxies, interstellar dust content from IRAS obs. 7-66758
 shell elliptical galaxies, radio emission search 7-60807
 shells around elliptical galaxies, tests for mass distrib. and 3-D shape 7-9536
 small groups and pairs, H I spectral spectral characts. 7-14669
 solitary vortices in galactic disks, 2D hydrodynamic theory 7-14657
 South Galactic Pole, galaxy and quasar candidates, correl. studies (Chinese) 7-66731
 South Galactic Pole field, IRAS point sources identification 7-35067
 southern spiral galaxies, BV photometry and radial vel. 7-66768
 spatial correlations at high redshift, implications for quasars environment 7-24216
 spectroscopy of galactic nuclei, results for complete sample of galaxies 7-40921
 spherical galaxies, dynamics of head-on collisions 7-48072
 spiral density waves damping, role of interstellar clouds collisions 7-66755
 spiral galaxies, χ^2 minimisation scheme for bulge-to-disk ratios determination 7-48071
 spiral galaxies, central vel. gradients classification 7-60781
 spiral galaxies, flat rot. curves, antigravity as possible cause 7-35377
 spiral galaxies, H I deficient, in Virgo cluster, orbits determ. 7-24230
 spiral galaxies, large scale props. determ. from kinematics 7-35048
 spiral galaxies, mass radial distrib., effects of decaying dark matter 7-29557
 spiral galaxies, star form characts., far-IR lumin. and CO line obs. anal. 7-4563
 spiral galaxies, star-formation triggers and chemical evolution 7-40936
 spiral galaxies, very small dust particles and IR emission characts. 7-24209
 spiral galaxies in Virgo cluster, threshold in star formation processes 7-60776
 spiral galaxy structure, due to percolation phase transition 7-4575
 spiral structure development in gaseous disks, due to nonlinear convective instability 7-66766
 star formation triggered by density waves, limitations 7-60789
 starburst galaxies, spectroscopic study 7-24222
 stochastic stellar orbits in galaxies, Melnikov's method in $n \geq 3$ dimensions 7-9519
 sub-millimetre/far-IR emission from warm and cold dust, observational review 7-48022
 superconducting cosmic strings, form. of moderate redshift galaxies on gravit. unstable shells 7-24518
 supergiant ellipticals, spectroscopic studies, dissertation 7-66769
 supernovae as distance indicators, proceedings, Cambridge, MA, USA (September 1984) 7-24296
 supernovae host galaxies, flocculent and grand design spirals 7-60696
 surface brightness distrib. 7-40909
 tidally stripped galaxies, density profile calculation 7-40930
 timelike worldlines, past extension rel. to general upper limits to age of Universe 7-4603
 triaxiality and pressure anisotropy induced by tidal interactions between galaxies 7-40942
 Tully-Fisher relation, type effect and Malmquist bias 7-14646
 two-point correlations of galaxies and rich clusters, effects of non-Gaussian mass density fluctuations 7-29545
 UGC 8508—a dwarf galaxy associated with the M101 group 7-9550
 undisturbed background disk galaxies, surface brightnesses radial distrib. 7-66736
 Ursa Major I(S) group galaxies, ¹²CO and far-IR obs. 7-29548
 Ursa Minor dwarf galaxy, star proper motions and bright-star photometry 7-14653
 UV photometry, ANS obs. of M31, M33, M81, M101, NGC 2403, and Zwicky galaxies 7-29529
 UV-excess galaxies, Kiso survey 7-4351
 violent indicator rel. to central black hole 7-18449
 Virgo Cluster, struct. and use of lumin. index as distance indicator 7-14668
 Virgo cluster galaxies, possible associations with quasars 7-35063
 Virgo cluster spiral galaxies, 2.8 cm radio continuum emission distrib. 7-9540
 warped disks, haloes and gravity 7-66744
 whole-sky distribution of galaxies, MCG-ESO(B)-UGC comparison 7-9551
 X-ray luminosity-redshift relationship for extragalactic objects, observational data 7-14679
 CNO abundances evol. 7-40934
 H I content of lenticular and early-type galaxies, comparison between field and Virgo cluster samples 7-4559
 H II galaxies, He abundance and dY/dZ meas. 7-40937
 H II regions, He ionisation struct. rel. to He/H abundance ratio 7-40906
 H II regions, photoionisation models rel. to abundances and ionising star temp. determ. 7-40907
 H II regions and star form. in galaxies, depend. on Hubble type 7-48084
 H₂O masers in nearby galaxies, luminosities and line profiles 7-14661
 OH absorption in extragalactic sources, Arcibo survey 7-40895

Galaxy

- 7-47832
 age and chemical evolution, general constraints 7-55809
 arm structure determ. from H II regions obs. 7-60746
 black hole at centre, observational evidence, review 7-29541
 bulge, star counts, colour distrib. and colour lumin. arrays 7-14651
 bulge, stars nature, IRAS data anal. 7-47733
 cataclysmic binary stars, space densities and evol. 7-60672
 cataclysmic binary stars, space distrib. rel. to observational selection in magnitude-limited sample 7-29479
 central region, 43-GHz continuum obs. 7-24219
 central region, ¹²CO and ¹³CO obs. of unusual mol. cloud complex (Clump I) 7-48044
 central region, nonthermal radio emission from continuum arc 7-55844
 centre, common origin for gamma-ray lines at 0.51 and 1.81 MeV 7-24238
 centre, neutral disk, CO and CS obs. 7-35040
 centre, spatial distrib. and vel. field of H₂ line emission 7-9528

Galaxy continued

centre direction, constraints on ionised gas props. from low-freq. radio recomb. lines 7-66719
 centre region, mol. obs. with University of Cologne 3 m telescope at Gornegrat Observatory 7-60557
 centre region, prominent polarised plumes and their mag. field, linear polarisation obs. 7-14656
 chemical evolution, He and heavy-element enrichment of interstellar medium 7-40905
 chemical evolution and light nuclide origin 7-47836
 chemical evolution solar neighbourhood, implications for Type I supernova rate 7-24155
 cosmic ray-supported corona, model 7-60787
 differential rotation and interstellar vel. gradients 7-60755
 diffuse galactic 380 μm emission 7-48090
 diffuse interstellar lines, line strength depend on galactic longit. 7-48021
 diffuse submm emission obs. 7-48091
 disk, evidence for local chemical inhomogeneities from classical Cepheids 7-34997
 disk, obs. from $l=-150^\circ$ to $l=82^\circ$ in sub-millimetre range 7-4558
 disk chemical evolution, implications of red giants metallicity function 7-4451
 disk interstellar medium, IUE evidence for diffuse collisionally ionised C IV and Si IV below $Z=1$ kpc 7-55783
 dwarf spheroidal galaxies orbiting, around galactic centre, numerical expts. 7-24231
 extended nonthermal sources in galactic plane, 57.5 MHz obs. 7-40897
 faint blue stars at high galactic latits., UV and visual spectra 7-47878
 fountain energetics 7-4537
 galactic halo study using γ -rays from WIMP annihilation 7-9542
 galactic nucleus explosion and hot interstellar matter effects on galactic ridge X-ray emission 7-40962
 gamma-ray line emission, constraint on origin of mass 22 nuclei in astrophysical environments 7-35069
 gaseous corona, IUE obs. rel. to kinematics, ionisation, and abundances 7-48054
 gaseous disk spiral wave packets, stability 7-4318
 gaseous halo support, evolution of superbubbles driven by sequential supernova explosions 7-55778
 general textbook contribution 7-60912
 globular cluster orbits around galactic centre, numerical expts. 7-24231
 halo, cold dark matter candidates, limits from deep underground detectors 7-23998
 halo gas properties, form. of C IV and Si IV ions 7-24171
 halo population in solar neighbourhood, luminosity function 7-60657
 high-latitude molecular clouds, distances and extinctions 7-35022
 initial collapse, implications of kinematics of 1125 high-proper-motion stars 7-47843
 inner galactic rot. curve shape 7-35050
 interstellar extinction curve, very broad struct. profile 7-14645
 interstellar H I obs. 7-60768
 interstellar matter, struct. 7-66725
 interstellar Na I line strength versus reddening relation, influence on stellar population synthesis 7-9526
 interstellar [Fe X] 637.5 nm absorpt. in galactic halo and LMC, implications for million degree gas 7-55758
 invisible axion detectors 7-10012
 IR absorption characts. 7-48089
 IR radiation characts., implications for existence of very small dust particles 7-24209
 IR sources and characts. (French) 7-29555
 IRS 16 NW+object A in Sgr A* direction, interpretation 7-40959
 K-type giant stars of galactic disk, metallicity variance 7-60640
 large-amplitude wave in gas disk, stationary periodic wave theory 7-23987
 local interstellar medium, multi-component vel. struct. 7-35018
 luminous axion clusters, photon decay, measurable luminosities 7-47694
 RR Lyr stars in Baade Window, radial vels. for 17 stars 7-55666
 M-type stars in SAO catalogue, galactic latit. and longit. distrib. rel. to luminosity classes 7-4435
 magnetic field characts. 7-40963
 magnetic field small-scale variations, anal. from rot. measure vars. across extragalactic radio sources 7-29524
 mass determ. 7-14654
 missing mass in halo and disk, constraints on objects masses 7-14650
 molecular clouds and stellar kinematics 7-48025
 molecular gas mass in Galaxy, review 7-9530
 motion in Virgo Cluster 7-55835
 nebulous objects in outer Galaxy, catalogue for vel. field in Southern Hemisphere 7-18359
 NGC 2420 field, stellar populations distrib. and RGU three-colour photometry 7-60783
 NGC 3603, giant H II region, speckle masking obs. of central object (HD 97950) 7-29502
 NGP, far-UV diffuse background, Voyager 2 obs. 7-60839
 novae space density in The Galaxy 7-40832
 nucleus, 511 keV line and positronium beams 7-62547
 nucleus Kerr black holes, optically-thick gas steady spherically-symm. accretion, outgoing radiative flux 7-35044
 OH-IR stars at Galactic Centre, showing SiO maser emission 7-60666
 rot. cloud comets injection to inner Solar System by galactic tidal fields 7-47738
 open clusters, age distrib. and total lifetimes 7-14618
 perturbations of long-period cometary orbits, numerical and analytic calcs. 7-34935
 populations of stars, distrib. 7-24169
 positron annihilation in an experimentally simulated low-density galactic environment 7-40944
 positron annihilation radiation from galactic centre 7-40943
 proper-motion stars, UV photometry and radial vels. 7-47844
 pulsar population in 10-100 msec range from two surveys 7-60702
 radio patrol of northern Milky Way, catalogue of sources 7-4356
 radio recombination lines of galactic ridge, origin from H22 α lines survey 7-66718
 radio sources in galactic plane near $l=54^\circ$, WSRT radio continuum obs. 7-35057
 Sgr A West region, ionised gas dynamics and comp. 7-40935
 SHF emission, contrib. to background radiation 7-55463
 size and rotation, scale change repercussions 7-14659
 small-scale interstellar dust distrib. towards NGC 2516 open cluster 7-35043

Galaxy continued

solar neighborhood, past star formation rate and IMF 7-47829
 solar neighbourhood missing mass 7-48079
 solar system tidal radius, boundary set by Galaxy according to King Innanen formula 7-4357
 South Galactic Cap stars, astrometry, trigonometric parallaxes, proper motions and photometry 7-47734
 South Galactic Pole: radial velocities of 157 O-F8 stars 7-60659
 South Galactic Pole, space distrib. of G5-M stars 7-4448
 South Galactic Pole and Magellanic Stream, dust and H I distrib. 7-66721
 South Galactic Pole field, star counts and colour indices 7-4573
 spiral arms vertical structure, energetics of vel. active regions 7-24220
 spiral density waves damping, role of interstellar clouds collisions 7-66755
 spiral structure in Vela 7-24227
 stability of a hypothetical binary at the galactic center 7-55793
 stars distribution in Orion Association 7-55477
 stellar VRI photoelectric sequence towards South Galactic Pole, meas. 7-40880
 sub-millimetre/far-IR emission from warm and cold dust, observational review 7-48022
 surface brightness of northern Milky Way, V photometry 7-4556
 total gamma-ray emission (Russian) 7-40655
 twin-jet model for galactic centre lobe, implications for former Seyfert stage 7-66740
 ultra-high-energy cosmic rays, accel. and transport in Galactic wind and termination shock 7-66403
 UV-excess objects in Galactic plane, KPD survey for white dwarfs and subdwarfs 7-9383
 variable stars in South Galactic Cap, photographic survey 7-14593
 Vela Star Cloud, foreground reddening struct., photometry obs. 7-35015
 vertex deviation of young stars 7-24226
 wind, role in cosmic rays origin and accel. 7-55390
 X-ray emission from a galactic ridge, contrib. from supernova remnants 7-24221
 X-ray sources in galactic bulge and globular clusters, radio obs. 7-29511
²⁶Al production by Wolf-Rayet stars, galactic yield and gamma-ray line emissivity 7-47830
 CNO abundances evol. 7-40934
 D abundance, chem. evol. model (Russian) 7-24218
 H I layer shape in outer Galaxy, volume densities atlas in cuts through composite data cube 7-18358
 H I small-scale structure and soft X-ray background 7-55769
 H I survey of Southern Milky Way, 21-cm obs. 7-40894
 H II regions, galactic electron temp. gradient, dust effects 7-48073
 Li enrichment in disk gas rel. to abundance in M67 cluster 7-55746
 Na enrichment in Galaxy, dwarf stars spectral characts. anal. 7-4446
 OH interstellar clouds vel., use for Sun-galactic centre distance determ. 7-4554
 OH-IR stars near galactic centre, luminosities and progenitor characts. 7-14584

gallium
 see also nuclei with

Al₂O₃:Cr,Ga, Cr-Ga complexes, energy transfer 7-22321
 adsorbed on Si (111), X-ray photoelectron and Auger electron diffraction 7-27116
 atom, 4s²nd²D series, lifetimes and oscillator strengths, MCHF wave fn. calcs. 7-62324
 atom, hyperfine struct., magnetic-dipole- and electric quadrupole coupling consts., atomic fluoresc., MCHF method 7-30985
 atom during trimethylgallium CVD reaction, multiphoton-ionisation/mass spectrometric detection 7-25471
 atom radiative lifetimes, fluoresc., MCHF calcs. 7-30946
 atoms, photofragment from trimethylgallium fluoresc. study 7-23046
 crystalline film amorphisation by pulsed excimer laser irradi., residual resist. and T_g meas. 7-12140
 Czochealski growth, mag., expt. model 7-44428
 determination in gallium and aluminium oxinate mixtures, fluorimetry 7-54231
 electron impact ionisation function meas. 7-50367
 film, vac. condensates, struct. and opt. characts. 7-2404
 fine particle layers, enhanced supercond. 7-7436
 growth into supercooled melt, faceted solid-liq. interface kinetics, kinetic roughening 7-58172
 liquid, elec. resist. meas. 7-38532
 liquid, electrohydrodynamics, ion source appls. 7-31887
 liquid, electron distrib., struct. factors, neutron diffraction. determ. 7-26620
 liquid ion source at low emission currents 7-30798
 liquid metal ion source, influence of substrate geometry on emission props. 7-53508
 liquid surface, In monolayer, sputtering, computer simulation studies 7-17387
 melting and triple points realisation, comparison of sealed cells 7-61333
 reference sample, absolute isotropic abundance ratio and at. weight 7-42779
 resonant atomic state, autoionis., electron spectra 7-900
 small metallic clusters, vol. and surface plasmons, EELS studies 7-27271
 solid and liquid, high press. phase transitions, EMF pulse study (Russian) 7-2166
 sound attenuation oscillatory deviation in weak mag. field, Fermi surface cross section and electron rel. determ. 7-2106
 thin evaporated films, nucleation and growth mechanism 7-46327
 ultra-fine ion probes for SIMS imaging microanalysis 7-4908
 ultrathin amorphous films, superconductivity threshold studies 7-22059
 Al₂O₃:Cr,Ga, ruby, Cr-Ga complexes, luminesc. study 7-22320
 BaTiO₃:Ce,Mg,Ga, double doping study 7-2037
 Bi-Ga two-layer film compositions, refl. and microstruct., temp. depend. 7-53428
 CdCr₂Se₄-Ga, lightly doped, ferromag., photoconductivity, band struct. 7-7278
 CdF₂:Ga crystals, local field-enhanced electronic conduction, activation energy and Poole-Frenkel const. calcs. 7-38570
 DyIG:Ga,Bi, RF sputtered films for magneto-optical memory, mag. props. 7-64613
 Ga I and II, stellar line Stark broadening 7-55690
 Ga II and Ga III lines in HD 25823 and HD 17081, UV spectrum synthesis compared with IEU obs. 7-47943

gallium continued

- Ga to Kr, Coulomb and exchange operators, valence electron only SCF calcs. 7-15507
 Ga VII, optical spectrum, $3d^7-3d^64p$ transitions, Hartree-Fock calcs. 7-57018
 Ga⁺ impurity ion in alkali halide crystals, triplet excited relaxed states, ODMR study 7-2953
 Ga⁺ in alkali halide crystals, polarised luminesc., model of impurity centre 7-27753
 Ga-GaP liquid metal-semiconductor contact, transition from rectifying to ohmic operation 7-52833
 Ga⁺+H⁺, charge transfer and ionis. 7-31162
 Ga₂, electronic states, CASSCF and FOCI calcs. 7-62267
 Ga(In), growth dislocations, in-situ detection using Seebeck effect 7-32451
 p-Ge:Ga, annealing kinetics of radiation defects, influence of impurity binding energy 7-39547
 Ge:Ga, impurity g-factor determ. piezo-Zeeman spectra obs. 7-16982
 p-Ge:Ga, resistivity at low temp. appl. to bolometers 7-41471
 Ge:Ga extrinsic photoconductor material, cryst. growth and characterisation 7-64893
 Ge:Ga single crystals, tracer diffusion coeff. and isotope effect, SIMS meas. 7-27019
 Ge:Sb(Al)(Ga)(In), heavily doped, charge carrier scatt., elec. cond., Hall effect meas. 7-7228
 InAs:Sb(Ga)(Mn), single crystal, elec. inhomogeneity, effects of isovalent impurities 7-7229
 InP:Fe,Ga,Sb, LEC growth, dislocation density, resistivity, SIMS obs. 7-53552
 InP:Ga,As,Sb single crystals, LEC growth, isoelectronic doping, dislocation density, X-ray topography 7-33549
 InP:S,Ga,Sb, LEC growth, appl. mag. field method, dislocation etching 7-53553
 Pb_{0.8}Sn_{0.2}:Te:Ga solid solns., diffusion coeff., temp. depend. study 7-2254
 PbTe:Ga, doping during vapour phase growth, elec. props. 7-26774
 PbTe_{0.92}Se_{0.08}:Ga solid solns., diffusion coeff., temp. depend. study 7-2254
 Si:B(Ga)(As)(Sb) 7-2040
 Si:Ga, electron irradiated and annealed, photoluminescence spectra 7-13206
 Si:Ga, highly cond. shallow junction layer form. by ion implantation 7-38037
 Si:Ga epitaxial layers, growth induced planar defects 7-38414
 Si:Ga MBE layers, ion implantation doping using liq. metal ion source, carrier conc., spreading resist., SIMS profiles 7-12563
 Si:Ga thermal donor props., impurity effects, DLTS, Hall effect, and admittance spectra meas. 7-21851
 Si:Ge, irradiated, photoluminescence spectra 7-13207
 Si_{0.9}Ge_{0.1}:Ga, resistivity and Hall constant, temp. depend. 7-7231
 YIG:Ga, Bi, RF sputtered films for magneto-optical memory, mag. props. 7-64613
 YIG:La-Ga-YIG:La double layered film, different magnetisation and anisotropy, magnetostatic mode spectra 7-64498
 ZnO:Ga thin films, temp. depend. of conductivity, effect of H₂O vapour chemisorbed states 7-7427
 ZnSe:Ga, impurity diffusion coefficients, cathodoluminesc. study 7-27017
 ZnSe:Ga, impurity segregation model calcs., elec. props., precipitate effects 7-16762

gallium alloys

see also *gallium compounds*

- Ag-Ge-Ga-Al FCC alloys, faulted structure, X-ray diffr. studies 7-58292
 Al-Ga, low temp. diffusion and trapping of muons 7-45865
 Al-Ga (1.0 wt.%), atmospheric oxidation in range 150 to 500 °C. 7-28197
 AuGa₂ intermetallic cpds., charge redistrib., L-edge XANES study 7-64816
 AuGa₂-GaAs (001), chemically unreactive interfaces formation 7-7050
 Bi-Ga, liq., elec. resist. meas. 7-38532
 Ca-Al-Ga metallic glasses, electron transport 7-45264
 Co-Ga binary system, β -phase solid soln., positron annihilation studies 7-46185
 CoGa, electronic struct. of vacancies 7-16975
 Co₅₀Ga₅₀ film samples, interband optical conductivity (Ukrainian) 7-13244
 Cr-Ga intermetallic cpds., mag. suscept. meas. 7-12942
 Cu-Ga, random alloys, residual electrical resistivity, first-principles calc. 7-2569
 Cu-Ge-Ga-Al FCC alloys, faulted structure, X-ray diffr. studies 7-58292
 Fe-Si-Ga, atomic ordering and mechanical props. 7-11990
 Fe-Si-Ga, high-Si, alloy elements influence on plasticity and mag. props. 7-8067
 FePGa, amorphous, magnetoelastic props. 7-27591
 Ga-In, liq., surface segregation, ion bombard. photon emission study 7-32265
 Ga-In-Sn liquid alloy, electron field emission studies 7-33535
 Ga-Te system, phase diagram, DTA 7-46425
 GaSb+V₂Ga₃, eutectic alloys, elec. props., anisotropy 7-12717
 Gd(Al_{1-x}Ga_x)₂, cryst. struct., paramag. susceptibility, elec. resist. meas. 7-16492
 In_{0.95}Ag_{0.045}Ga_{0.005}, ¹¹¹Cd quadrupole interaction, temp. dependence, lattice electric field gradients (Chinese) 7-7183
 In_{0.95}Ag_{0.045}Ga_{0.005} alloy, quadrupole interactions, TDPAC study 7-38521
 K₁₀Na₁₀Ga₄₉, synthesis and cryst. struct. 7-6584
 LiGa B32-type Zintl phases, mag. props., exchange enhancement, APW calcs. 7-27504
 Mg-Ga liquid alloys, Hall effect, meas. 7-32991
 Mn-Ga, amorphous film, prep. by ionised cluster beam deposition 7-3205
 Mn₃GaC temp.-induced metamagnets, dipol-octopole interaction calcs. 7-17191
 Na-Ga, liq., phase diagram and electrical resistivity 7-21408
 Nb₂Sn₂Ga, crystal growth and superconductivity 7-27451
 NiCoGa, thermal vacancies 7-51764
 Ni₃Ga, 2D electron-positron momentum density and Fermi surface 7-45127
 Ni₃Ga, alloying addition lattice location, phenomenological description 7-32463
 Ni₃Ga, atomic ordering, strain disruption (Russian) 7-53808
 Ni₃Ga, L1₂ ordered alloys, grain boundary strength and fracture, electronic and struct. studies 7-33756

gallium alloys continued

- Ni₃Ga, momentum density distrib., Compton scatt., positron annihilation, symmetrised APW method 7-64069
 Ni₃MnGa, Heusler alloys, Curie temp., effect of hydrostatic press. 7-64455
 δ -Pu-Ga (1.5 wt.%) foils, cold rolling, annealing, microstruct., TEM obs. 7-59544
 RGA₂Co₂ (R=Ce, Pr, Eu), cryst. struct., mag. props. 7-45614
 RGA₂Fe₂ (R=La, Ce, Pr, Nd, Sm), cryst. struct., mag. props. 7-45614
 Sc-Ga(In)(Sb), alloy form, thermodynamics 7-22637
 ScGa₃, band struct., coupling energy (Russian) 7-58732
 a-Tb_{0.4}Fe_{0.6}Ga₁₆, mag. phase transition behaviour in random anisotropy system 7-2864
 U-Ga dilute alloys, microstructure study 7-16780
 UGaNi(Co)(Ru) ternary alloys, magnetic behaviour, elec. resist. and sp. ht. meas., 5f electron effects 7-12999
 U₂Gd_{1-x}Ga₂ Curie temp., loss of ferromagnetism, comp. depend, competing exchange interactions 7-12970
 U₂Y_{1-x}Ga₂, Curie temp., loss of ferromagnetism, comp. depend, competing exchange interactions 7-12970
 V₃Ga films, supercond. electron-phonon interaction spatial function, electron tunnelling spectra study 7-45578
 V₃Ga, superconducting Al₁₅ cpds., resistivity and magnetoresistance 7-32982
 V₃Ga superconducting tape 7-7456
 V₃Ga superconducting tapes, grain boundaries, elementary pinning force 7-22080

gallium arsenide

- (001)GaAs, rel. between etch pit density and dislocation density 7-51771
 2D electron gas, dynamical cond., IR cyclotron reson. meas., electron interaction effects 7-45195
 (100) films, mol. beam epitaxy system (Czech) 7-7854
 absorbing zinc-blende type material, backward Raman scatt., ang. dispersion calcs. 7-22338
 absorption-induced nodal plane shifts of X-ray stationary waves, angular depend. 7-32196
 acoustic charge transport device using SAWs, signal processing appl., principles and performance 7-57653
 adsorption of O₂ on GaAs, UPS 7-59371
 p-AlGaAs/GaAs modulation-doped heterostruct., liq. phase epitaxy and carrier props. 7-33074
 ambient induced surface effects, O adsorption, photolum., conductivity 7-45429
 amorphous, optical absorpt. and refractive index spectra 7-27735
 amorphous films, dynamics of laser annealing by transient grating method 7-12122
 annealing, high temp., prevention of thermal surface damage 7-39546
 anomalous photovoltage films X-ray irradiation effects studies 7-58834
 antisite defects formation during plastic deformation 7-37988
 atomic layer epitaxy, review 7-13362
 atomic layer epitaxy growth, photolum., Hall meas. 7-22527
 atomic layer epitaxy in low press. MOCVD system 7-53628
 backwall Schottky barrier solar cells, minority carrier current collection, built-in elec. field enhancement limitations 7-54305
 band structure, polarisation-dependent angle-resolved photoemission spectroscopy 7-21814
 band-gap shifts 7-22333
 biased semi-insulating, cross modulation effect 7-50731
 CCD, high resistivity gate struct., radiation effects 7-6683
 characterisation by a microwave photoconductance technique 7-7281
 chemical beam epitaxial growth investig. 7-7878
 chemical etching by Cl, thermodynamically predicted depend. on press. and temp. 7-22919
 chemisorption of O₂ on (110) surface, photoemission evidence for surface growth 7-2356
 clusters, TOF mass spectra 7-20084
 concentrator cells, design options and constraints 7-3698
 conduction band, deformation splitting and intervalley scattering 7-2548
 conference on semiconductors, Jevnaker, Norway (June 1986) 7-14705
 covalent cryst., electronic struct., cluster approx. 7-52403
 crack formation, quenching by dislocation ensembles (Russian) 7-44680
 crystal defects, IR light scattering tomography and IR absorption microscopy 7-46023
 crystal growth, semiconductor industry needs 7-53540
 crystal polarity, convergent beam electron diff. study 7-21162
 crystalline and amorphous, L near-edge structure, X-ray photoabsorpt. spectra 7-64766
 crystals, liquid-phase electroepitaxial growth, dislocation density reduction 7-58681
 crystals, selective etching and photoetching of CrO₃-HF aq. solns. 7-32442
 current limiters, impact ionisation breakdown 7-52639
 CVD, laser selective deposition on GaAs and Si substrates 7-22546
 Czochralski grown, defect. conc., spatially resolved photoluminesc. 7-22341
 Czochralski growth of high quality crystals. 7-53548
 DC conductivity, surface conductivity 7-21919
 decomposition during rapid thermal annealing 7-13657
 deep centres in semiconductors, book 7-18510
 deep level nonradiative carrier capture press. depend. calcs. 7-12735
 deep levels, scanning optical fibre microscope, laser beam induced current images 7-48846
 defect mapping by in-water photocorrosion 7-59692
 defect structure charactn., US meas. 7-21363
 defects, positron lifetime spectra 7-37979
 defects, strain-induced, EPR anal. 7-45821
 detector material, applications 7-45307
 device picosecond electro-optic sampling 7-53278
 device structures, γ -ray effects, surface generation-recombination processes 7-64349
 devices, 1/f fluctuation, surface states effects (Japanese) 7-21955
 devices and materials, conf., Tokyo, Japan (Aug. 1986) 7-48173
 DH laser struct., external injection of spontaneous emission 7-31328
 dielectric protective coatings during heat treatment 7-33852
 dielectric response and electronic states 7-33320
 diffusion of Fe, from sputtered layer, temp. depend. 7-6875
 diffusivity-mobility ratio, modified form of Einstein rel. in presence of electric and mag. field 7-45356
 diode, active layer <1 μ m, low temp. current flow 7-52757

gallium arsenide continued

dislocated and In-doped dislocation free, inhomogeneities obs. by video-enhanced IR topography 7-32446
 dislocation containing, positron annihilation 7-39279
 dislocation core struct. 7-38007
 dislocation density reduction in crystal growth 7-2020
 dislocation loops, TEM image profiles, electron diffr. two-beam dynamical theory 7-12071
 dislocation network density, thermal wave microscopy 7-51778
 dislocation rosette generation round Vickers indentations, mobility and twinning, TEM study 7-63618
 dislocation-complex defect interactions, photoluminescence studies 7-16608
 dislocations, obs. by transmission IR microscopy 7-32447
 dislocations, stereographic obs. by IR light scatt. 7-32235
 DLTS meas. using lock-in amplifier, at freq. up to 2000 Hz 7-327
 dopant profiles modification due to surface and interface modifications 7-58306
 doped, oxidation, in situ TEM obs. 7-28215
 doping superlattices, efficient room temp. electroluminescence, tunability 7-27782
 doping superlattices, pulsed and CW photoluminescence obs. 7-46138
 dry etching, radiation damage 7-54024
 effect on surface depletion potential 7-38678
 EL2 and As antisite defect props., review (*Japanese*) 7-7152
 EL2 centre stability under electron-hole recomb. conditions 7-16978
 EL2 clusters, scattering and absorpt. of IR light 7-53382
 EL2 defect, identification 7-38502
 EL2 defect profiling, DLTS 7-12652
 electron beam irradi., carrier density, anomalous temp. depend. 7-52610
 electron density distrib., X-ray refl. anal. 7-44497
 electron drift vel.-elec. field characts. 7-38569
 electron impact ionisation rate in nonuniform elec. fields, simulation 7-33021
 electron irradiated, defect profiling, DLTS 7-12652
 electron irradiation induced defects, DLTS study 7-58338
 electron scattering in quantum limit 7-38552
 electron-electron interaction, quantum effects, magnetoresist. studies 7-38591
 electron-electron interactions, appl. for hot electron decay 7-32934
 electron-hole plasma diffusion, spatially resolved gain and luminesc. spectra 7-12747
 electron-hole plasma dynamics under subpicosecond optical excitation, optical absorption saturation 7-27356
 electron-irradiated, relative density of levels of radiation defects 7-52500
 electron-LO phonon dynamics, subpicosecond Raman spectroscopy 7-46052
 emission lines, lifetimes and ionisation energies 7-22306
 energy bands, cohesive energy, form. energy, self-consistent calcs. 7-21995
 epilayers, MOCVD on Si for solar cell appls. 7-27928
 epilayers grown on Ge or Ge/Si substrates, defects 7-21778
 epitaxial film on (001) oriented Si and Ge substrates, structural props. 7-58687
 epitaxial film shallow homojunction solar cells fabrication by Zn solid state diffusion method 7-17860
 epitaxial films, domain form., crystallographic analysis 7-58690
 epitaxial films, growth by close-spaced vapour transport, unwanted doping, X-ray diffr., SEM obs. 7-27187
 epitaxial films, MOCVD growth on Si substrates, substrate offset angle effects 7-22567
 epitaxial films, MOCVD growth using tertiarybutylarsine source 7-59439
 epitaxial films, switched laser MOVPE stepwise monolayer growth 7-13372
 epitaxial growth, $\delta(z)$ doping layer, electronic states 7-52729
 epitaxial growth, thermodynamic equil. displacement controlled 7-53616
 epitaxial layer, EL2 midgap electron trap prod. by rapid thermal annealing, DLTS study 7-64154
 epitaxial layers, grown in temp.-gradient field, effects on dislocation density 7-13393
 epitaxial layers, large scale MOVPE growth 7-22552
 epitaxial layers, MOCVD grown, influence of growth parameters on residual impurities 7-7047
 epitaxial layers, MOCVD growth, boundary layer effects, photoluminesc. study 7-64923
 epitaxial layers, native deep level defects 7-12888
 epitaxial layers, OMCVD growth, optimisation using photoluminesc. analysis 7-39396
 epitaxial layers, OMVPE growth on Si (100) 7-3190
 epitaxial layers, selective growth in MOMBE and MOCVD systems 7-22555
 epitaxial layers, vacancy doping 7-6656
 epitaxial layers and heterostructures grown on Si substrates, material props. 7-7046
 epitaxial layers grown directly on Si (100) by low press. MOVPE 7-27924
 epitaxial nucleation and growth kinetics, substrate orientation depend., numerical anal. 7-64020
 epitaxial wafers, highly uniform growth by large capacity MOCVD reactor 7-22551
 etalons, pulsed optical logic 7-57412
 etching in Ar-tetrachloromethane RF discharge 7-32167
 excimer laser projection etching 7-13662
 excimer-laser-stimulated CVD, polycryst. thin film growth and props. 7-64912
 exciton-exciton and exciton-electron collisions, ultrafast phase relaxation 7-12618
 excitons, picosecond phase coherence, orientational relax. 7-16948
 fast-neutron irradiated, electrical behaviour during thermal recovery 7-13029
 faulted dislocation dipoles, electron diffr. and high-resolution TEM studies 7-44551
 femtosecond carrier dynamics 7-58829
 FET arrays, electrical parameter mapping 7-32438
 film, substrate for CaF_2 epitaxial growth 7-39204
 film on NaCl, heteroepitaxial growth and composition 7-7052
 films, initial stages of MBE growth on Si (100) 7-63995
 films, MBE growth and structural characterisation 7-21775
 films, single domain epitaxial growth on Ge (100) 7-22578
 Films, vacuum chemical epitaxy 7-39406

gallium arsenide continued

films on amorphous insulating substrates, laser recrystallisation 7-38397
 films on oxidised Si, zone melting recrystallisation 7-38396
 Fresnel waveguide grating lenses, aberration corrected, simulation 7-26036
 FTIR spectra of acceptors, electronic intrasite transitions and local vibr. modes 7-53377
 fundamental energy gap, temp. depend. 7-7115
 $\text{Ga}_{0.93}\text{In}_{0.07}\text{As}$, transient transport in central-valley-dominated ternary III-V alloys 7-7253
 gas phase epitaxial growth, layer thickness uniformity, flow conditions depend. meas. and model calcs. 7-52348
 Gault process for semiconductor crystals growth 7-46300
 giant-exciton resonance in nonlinear optical activity 7-45167
 gratings, submicrometre, direct maskless fabrication 7-62855
 guided-wave bistable devices, semicond. clad dielectric, periodic coupling 7-57426
 H_2 production by photoelectrolysis of water using GaAs semiconductor electrodes 7-3723
 Hall effect measurement in the diamond anvil high-pressure cell 7-30041
 heavily doped, carrier-carrier and carrier-dopant interactions 7-21903
 heterostructures, noise meas. of two-dimensional electron gas, SQUID flux-transformer-coupled instrument 7-18830
 heterostructures, valence subbands, excitons and luminescence 7-7321
 highly doped, polarised hot electron photoluminescence 7-46121
 highly doped quantum wells, mobility enhancement 7-64325
 homoepitaxial growth, cross hatch defect structure 7-45054
 horizontal Bridgman growth, semi-insulating props. characts. 7-64896
 hot anti-Stokes luminesc., picosecond spectroscopy 7-22336
 hot electron spectroscopy, extreme nonequilibrium electron transport dynamics 7-12726
 hot optically excited carriers in a spin-split-off subband, energy relax. 7-22302
 hot-electron 1/f noise 7-21927
 hydride VPE layers, deep level incorporation and background doping 7-17120
 impact ionisation, soft-threshold lucky drift theory, mean free path calcs. 7-64256
 impact ionisation coeffs., lucky drift model including soft threshold energy 7-64258
 impurity atom site location using channelling enhanced microanalysis 7-38023
 impurity doping by photonuclear reactions 7-16589
 $\text{In}_{0.93}\text{Ga}_{0.07}\text{As}$:Fe metalorganic CVD epitaxial growth and elec. props. 7-63993
 InGaAsP epitaxial films, X-ray diffr. charactn. (*Japanese*) 7-63399
 inhomogeneous characteristics, photoconductivity and optical absorption meas. 7-32439
 injection laser, twin-stripe, lateral behaviour, self-consistent model 7-15861
 integrated waveguides as all-optical logic devices, GaAs Mach-Zehnder interferometer 7-25869
 interatomic force consts. and normal modes, group theoretical method calcs. 7-32588
 internal thermal conversion, material for integrated circuits 7-12767
 intraband relaxation dynamics of photo-excited carriers 7-52691
 inversion layers, hot free electron gas, intraband absorpt. coeff. calc. 7-33083
 ion implant depth profiles, channelling, Monte Carlo simulation 7-51811
 ion implantation, H^+ , He^+ , Ar^+ , elastic vibrations 7-12094
 ion implanted, flash tube annealing 7-39551
 ion implanted, rapid thermal annealing, review 7-58296
 ion implanted, stoichiometry violation, electron microscopy studies 7-12303
 ion implanted and laser irradiated, defect studies 7-32432
 ion irradi. high-resistivity layer, thickness and resistance, free carrier density and cryst. orientation dependence 7-58354
 IR imaging 7-32238
 IR tomography and transmission images, numerical processing 7-32236
 JFET devices, elec. resist., Hall effect, influence of electronic subband mag. depopulation 7-38740
 junction, temp. meas. using capacitance change of space-charge region 7-48742
 large dislocation-free cryst. growth for LSI appls. 7-64895
 laser diode, single-quantum well, carrier temperature and wavelength-switching 7-43097
 laser direct writing and laser-assisted CVD of III-V cpds. on GaAs 7-13373
 laser evaporation, spectroscopic study 7-58324
 laser excited with several electron beams, light pulse formation 7-43098
 laser induced etching in carbon tetrachloride atm., fluoresc. 7-59700
 laser material, intervalence band absorpt. coeff. calc. 7-3015
 laser materials processing developments at GEC Hirst Research Centre (UK) 7-53581
 laser MOVPE growth 7-33580
 laser-assisted MOVPE growth 7-64928
 laser-enhanced oxidation, X-ray photoelectron and Auger electron spectroscopy 7-17739
 laser-induced damage and ion emission at $1.06\text{ }\mu\text{m}$ 7-37008
 laser-induced melting and nonlinear optical studies 7-12432
 lattice dynamics and electron-phonon interactions, quasi-ion approach calcs. 7-58422
 Laue zone effects, nonzerofth order, atom location by channelling enhanced microanal., X-ray fluorescence anal. 7-46905
 layers, MBE, oval defects 7-59433
 layers, MOVPE, Zn acceptor impurities, magnetophotolum. 7-22308
 layers and quantum well struct., MOVPE growth chemistry 7-22550
 LEC, semi-insulating, undoped, C origin and melt comp. depend. 7-17410
 LEC, undoped, stoichiometry 7-53563
 LEC grown, obs. of Ga precipitates 7-32663
 LEC grown, threshold for dislocation form., role of cryst. dia. and impurity hardening 7-53551
 LEC growth, solid-liq. interface, meniscus shape, X-ray image processing appl. 7-17406
 LEC growth configuration, thermal stresses, effect of liq. encapsulation, thermoclastic anal. 7-59414
 LEC growth for IC technology appls. 7-64894
 LEC semi-insulating crystals, pure and In-doped, IR absorpt. WRT resistivity 7-64629
 LEC single cryst. homogeneity, effect of strong mag. field 7-53549

gallium arsenide continued

- LEC substrates, EL2 deep donor kinetics under annealing, IR absorpt., DLTS, Hall effect meas. 7-32955
- LEC wafers, cathodolum. mapping, IR absorpt., X-ray topography obs. 7-33462
- length scale near metal-insulator transition 7-52425
- liquid/semiconductor junction, device performance improvement 7-17098
- longitudinal optical phonons, interaction with nonequilib. plasmons 7-45192
- low frequency 1/f noise, new scale invariance 7-12770
- low-frequency Raman scattering anomaly 7-27710
- LPE from soln. in laminar flow, high growth rates 7-33605
- LPE growth from Ga-As-Bi soln., kinetics, edge growth effects 7-39444
- LPE layers, heavily doped and compensated, hopping cond., density of states at Fermi level, carrier conc. determ. 7-2753
- LPE on channelled (100) GaAs substrates 7-13391
- magneto-optical photoluminescent spectra studies 7-46148
- maskless ion beam assisted etching 7-22923
- MBE films, oval defects and whiskers 7-13364
- MBE growth, acceptor impurity background reduction 7-3173
- MBE growth, defect reduction using superlattice structures 7-13359
- MBE growth, transient behaviour, RHEED oscillations 7-64904
- MBE growth mechanisms, in situ RHEED 7-53603
- MBE growth of high quality P-type GaAs films (*Chinese*) 7-33566
- MBE heteroepitaxial layers, lattice distortions, X-ray diff. and Raman studies (*Japanese*) 7-27219
- MBE initial growth stage on (100) Si substrate, RHEED, AES and TEM 7-52356
- MBE layer growth and surface anal. (*Korean*) 7-2417
- MBE layers, bias-dependent capture-emission processes, DLTS anal. 7-64166
- MBE layers, deep level defects, passivation by H₂ plasma exposure 7-21850
- MBE layers, deep level defects and impurities 7-22051
- MBE layers, oval defects, particulate effects during growth 7-21194
- MBE layers on Si (100), crystalline quality, rapid thermal annealing effects 7-12519
- melt growth, theoretical and expt. fundamentals of decreasing dislocations 7-53547
- MESFET devices, elec. resist., Hall effect, influence of electronic subband mag. depopulation 7-38740
- MESFETs, reactive ion etching, DC characteristics (*Japanese*) 7-59701
- metal contacts, interfacial microstruct., elec. props., phase diagrams 7-45495
- metalorganic MBE 7-53601
- metastable defects, electronic Raman scatt. of nonequilibrium holes 7-26748
- metastable state annealing 7-27297
- microwave absorption transient spectroscopy for investigation of deep levels in semiconductors 7-52520
- midgap levels, quenching and recovery spectra measured by double-beam photoconductivity 7-58769
- MIS struct., light scatt. from inversion layer 7-3033
- MISS, common anion rule, density distrib., photoionisation 7-38765
- mixed electron-hole conductivity 7-58808
- MOCVD, design of safe facility 7-22529
- MOCVD, gas phase depletion and flow dynamics in horizontal reactors 7-17433
- MOCVD, H₂ carrier gas effect 7-17432
- MOCVD, plasma stimulation, growth kinetics, elec. props. 7-22548
- MOCVD, uniform growth on multi-wafers 7-22536
- MOCVD epitaxial layer photolum. spectral shift and Si, Se doping efficiency obs. (*Japanese*) 7-45076
- MOCVD growth, thermal decomp. rates 7-22540
- MOCVD growth on Ge (100) and Si (100) substrates, antiphase and single domains 7-27925
- MOCVD growth on Ge substrates for high efficiency tandem solar cell appl. 7-3671
- MOCVD growth on Si, band gap energy and stress 7-38368
- MOCVD growth on Si with superlattice intermediate layers, material props. 7-27923
- MOCVD growth using CIME₂GaAsEt₃ adduct, chemisorption and thermal heterogeneous decomp. 7-22558
- MOCVD in inverted stagnation point flow, deposition from TMAs and TMGa 7-22531
- MOCVD layers, lateral growth mechanisms 7-64032
- MOCVD layers on Si substrates with superlattice intermediate layers, DLTS studies 7-38501
- modulation-doped heterostructs., quantum transport effects 7-52767
- molecular beam epitaxial layers, defect density reduction by thermal annealing, TEM study 7-45041
- molecular layer epitaxy, UV light effects, photo-assisted reactions and adsorpt. phenomena (*Japanese*) 7-7048
- molten, temp. fluctuation meas., 1125 to 937 K 7-58123
- monolithic integrated optics, performance in space environment 7-26028
- monolithic optoelectronic ICs for high-speed fibre optic transmission 7-37203
- monovacancy electronic struct. and positron states, self-consistent LMTO calcs. 7-2536
- morphological stability in epitaxy, appl. to optoelectronic monolithically integrated structures 7-27172
- MOVPE, conf., Universal City, CA, USA (Apr. 1986) 7-18477
- MOVPE, laser assisted, selective area irradi., carrier conc. 7-22545
- MOVPE growth, flow patterns in vertical reactors 7-22535
- MOVPE growth rate, orientation depend. 7-22556
- multilayer structure, calc. elastic scattering spectra 7-13311
- multiple quantum wells, absorption-induced optical bistability 7-57444
- multiple quantum wells, charge-carrier dynamics, contactless microwave photocond. meas. 7-21998
- n⁺-n⁺ struts., quasi-elastic inter-Landau-level scattering processes 7-17086
- n-i-p-i doping superlattices, selective contacts, MBE growth through shadow mask 7-13356
- n-type, depletion and accumulation layer profiles, self-consistent Hartree approx. calcs. 7-27375
- n-type, electron-irradiated, photoionization cross sections of E levels 7-64152
- n-type, free carrier IR absorpt. spectra, scattering mechanisms, RPA calcs. 7-2604
- n-type, Hall factor calcs. 7-52657
- n-type, impurity bands and band tailing 7-21809

gallium arsenide continued

- n-type, intervalley processes, nonequib. phonon spectroscopy and hydrostatic compression, Monte Carlo study 7-58425
- n-type, ionised-impurity-mediated free-carrier absorption 7-17335
- n-type, oscillations and chaotic current fluctuations 7-64253
- n-type, proton irradiated, effects of annealing on optical properties 7-28155
- n-type cleaved surfaces, elec.-field-induced Raman scatt., reson., temp. and screening effects 7-27717
- n-type compensated samples, MOVPE grown, Hall effect meas. 7-27348
- n-type films, electron-hole plasma stratification and blue luminesc. near static domain 7-52666
- n-type films, magneto-optical studies under high hydrostatic press. 7-13247
- n-type sawtooth gratings, photoelectrochemical fabrication 7-50726
- n-type surface, cleaved clean (110), initial band bending cause, noble metal deposition 7-22017
- n-type surface, photoelectrochemical etching, orientational depend. 7-65224
- narrow n⁺ wires, universal magnetoconductance fluctuations 7-64272
- near-surface structure, analysing He⁺ ion beam effects 7-7808
- negative magnetoresistance and electron localisation in the region of a metal-insulator transition 7-12737
- negative magnetoresistance and nonequib. electron cooling 7-17042
- neutral shallow donor inter-excited-state transitions, far IR photocond. in mag. field study 7-22249
- neutron damaged, photoconducting flat response detectors from UV to X-ray region 7-5563
- neutron transmutation doped, thermal annealing effects, channelling anal. (*Chinese*) 7-12178
- neutron transmutation doped, variable range hopping studies 7-33012
- neutron-irradiated, vacancy annealing, positron-lifetime study 7-64727
- nonlinear Fabry-Perot resonator, GaAs filled, picosec. light pulse changes (*Russian*) 7-50620
- nonlinear refractive index, dispersive nonlinearities meas. 7-43192
- nonradiative states of optically illuminated sample, phonon detection by superconducting tunnel junction 7-3074
- nucleation and growth on Ge, antiphase boundary struct. 7-2420
- ohmic contact, form. using ion beam mixing 7-21299
- ohmic contact resist. limitations 7-52838
- OMVPE, low pressure growth from trimethylgallium+AsH₃ 7-17439
- optical inverted rib, phase modulators grown by VPE, optical and electrooptical anal. 7-31450
- optical logic gate, ultrafast, based on MQW bistable device 7-57415
- all-optical logic gate arrays, fabrication and characterisation 7-57414
- optical nonlinearities, freq. depend. 7-25867
- optical reflection anisotropy due to surface band bending 7-39062
- optical transient current spectroscopy determ. of deep centres 7-52498
- optical waveguide, thermal index changes by optical absorpt., all-optical signal processing 7-31381
- optical waveguides in bulk and multiple-quantum-well structures, optical nonlinearities 7-57553
- optically induced far-IR absorption from residual acceptors 7-22287
- organometallic VPE growth, use of tertiarybutylarsine 7-45047
- overlapping etch pits, density, evaluation technique 7-32443
- p-doped, dielec. functions, band-gap narrowing anal. 7-52482
- p-n homojunction diode, photocurrent meas. of defect distribution 7-32851
- p-n junction, scanning tunneling potentiometry study 7-45439
- p-n junction, space charge region, electrooptic effect investig. 7-52756
- p-type, electron irradi.-induced trap defects, DLTS study 7-12155
- p-type, excitons bound to pairs of shallow impurities 7-45169
- partially excited electron hole plasmas thermodynamics 7-16962
- passivation, by a-P and alkali metal polyporphides 7-39778
- patterning using photoelectrochem. etching and focused ion beams 7-22924
- phonon and plasmon deformation potentials, FIR spectra under uniaxial stress 7-26886
- phonon dispersion, dispersive corrections to continuum elastic theory 7-26887
- phonon hot spot, subTHz acoustic phonon emission 7-2118
- phonon-plasmon coupling in electron transport 7-33041
- photocathode development for TeV e⁺e⁻ linear collider (*Japanese*) 7-19589
- photocathodes, NEA, photoelectron energy spectra 7-13325
- photoconductive device, drive for synchronously operated streak camera 7-18903
- photoconductivity, slow-relaxation phenomena 7-58837
- photoconductivity and Hall voltage kinetics, recombination and scattering centre recharging 7-27364
- photoconductivity oscillations, monochromatic IR illuminations in mag. field 7-12763
- photoelectrochemical etching of holographic gratings 7-26051
- photoemission electron source, operating experience 7-41535
- photoholes in the spin-split band, energy relax. and spin depolarisation 7-22301
- photoluminescence lines, mag. and strain field splitting 7-3079
- photoluminescence rel. to Si substrate orientation 7-53411
- photoreflectance of doping superlattices 7-53368
- photorefractive, enhanced two-beam mixing gain using alternating electric fields 7-43203
- photorefractive beam coupling with picosec. pulses 7-31386
- photorefractive effect, temperature and intensity dependence 7-45951
- photovoltaic concentrator research progress 7-17903
- piezoelectric, SAW slowness surfaces 7-38315
- PIN electro-optic travelling-wave modulator at 1.3 μm 7-1287
- plasma etching damage, Raman scatt. study 7-54023
- plasma etching in H glow discharge 7-32168
- plastically deformed, Hall effect meas. 7-27351
- plastically deformed, spatial distrib. of dominant electron and hole traps 7-7160
- plastically deformed or electron or neutron irradiated, antisite defects 7-37987
- point defects, props. and processes, dislocation form. and characterisation (*Japanese*) 7-7151
- polar semicond., carrier-carrier interaction and picosecond phenomena 7-45309
- polycrystalline solar cell, electron beam generated carriers in presence of grain boundaries 7-64262
- polycrystalline solar cells, influence of grain boundaries on performance 7-17892

gallium arsenide continued

polycrystalline thin films, RF sputter deposition on silica substrates, light transmission props. 7-46320
 positron lifetime, electron beam effects and temp. depend. 7-39280
 proton bombard., optoelectronic effects 7-21295
 proton bombarded, H platelets, TEM obs. 7-12164
 pure and Si, Mn or Cu doped crystals, impurity and defect props., heat treatment, photolum. studies 7-39163
 pure and Te doped (*Chinese*) 7-13254
 quantised inversion layers, hot 2D electron gas, spectral acoustic phonon emission intensity 7-52452
 quantum Hall effect, resistance meas. appl., US legal unit monitoring 7-18808
 quantum well structures, metal-insulator transition due to surface roughness scatt. 7-27400
 quantum wells, 2D hot-electron mobility 7-45470
 quantum wells, band offsets, inelastic light scatt. studies 7-7362
 quantum wells, electron interference effects, obs. of bound and reson. states 7-64334
 quantum wells, optical high-field transport expts. 7-52638
 quantum wells, optical Stark effect on excitons 7-31384
 quantum wells, space-charge induced, inelastic light scattering by electronic excitations in semiconductor heterostructures 7-13171
 quantum-well wire hydrogenic impurity state binding energy and lowest exciton state lum. efficiency calc. 7-2683
 radiation-induced defects, review 7-48201
 Raman phonon piezospectroscopy, IR meas. 7-64647
 Raman scatt. by LO phonons, interference effects 7-59213
 rapid thermal annealing, heating behaviour 7-21258
 reactive ion etching, AES, photoluminescence, SEM obs. 7-65241
 refractive index dispersion, Fabry-Perot cavity oscillations obs. 7-59171
 residual acceptor assessment, Raman and selective pair luminescence studies 7-26771
 resistance standard appl., precise comparisons of quantized Hall resistances 7-18809
 sawtooth doping superlattices, photoluminescence, transport props. 7-52825
 sawtooth doping superlattices, prep., LED and laser appls. 7-7372
 scanning DLTS study of deep level defects 7-21865
 scanning tunnelling microscopy of cleaved semiconductor surfaces 7-21051
 Schottky barrier formation, effect of surface annealing 7-12785
 Schottky barrier lowering by submicron ohmic contacts 7-7332
 Schottky contacts in GaAs microelectronics (*German*) 7-52735
 Schottky-barrier behaviour, Monte Carlo simulation 7-45491
 Schottky-barrier formation and microscopic metal clusters 7-45497
 secondary electron emission, effect of illum. in space charge region 7-17374
 selective growth by reduced press. MOCVD 7-53627
 SEM-EBIC characterisation, semiconducting and semi-insulating LEC materials 7-51777
 semi-insulating, AL metallisation, electromigration failure anal. 7-44927
 semi-insulating, deep levels, nondestructive microwave DLTS measurements 7-45210
 semi-insulating, IR light scattering from defect centres 7-64620
 semi-insulating, LEC grown, midgap native donor concentration 7-33547
 semi-insulating, nonstoichiometry study, lattice parameter meas. 7-38220
 semi-insulating, photoluminescence imaging using laser scanning microscope 7-53384
 semi-insulating, surface photocond., surface topography meas. using scanning tunnelling microscopy 7-45376
 semi-insulating, switching effect, deep level spectroscopy appl. 7-38630
 semi-insulating bulk with thin conducting layer, optical DLTS distortions calcs. 7-58766
 semi-insulating cryst. characts., IC substrate appls. (*Japanese*) 7-6622
 semi-insulating LEC crystals, thermal conversion, DLTS studies 7-7150
 semi-insulating thin wafers, EL2 defect and dislocation mapping, near-IR transmittance meas. 7-63605
 semi-insulating wafer, inhomogeneity characterization by scanning photo-induced current transient spectroscopy 7-7164
 semiconducting/semi-insulating reversibility 7-21939
 semiinsulating, electrophysical props., dislocation effects 7-16557
 semiinsulating LEC substrate, elec. homogeneity evaluation, thermally stimulated drain conductance meas. 7-32954
 semiinsulating LEC substrates, defect etching 7-59694
 semiinsulating LEC wafers, radiative centres, local photoluminescence study 7-33458
 semiinsulating slices, spatial inhomogeneities, near IR transmission imaging techniques 7-33400
 shallow acceptor levels, photoluminesc. study 7-45209
 shallow-homojunction solar cells, junction depth effect on photovoltaic parameters 7-3673
 short n^+nn^+ structs., elec. transport props. in high elec. and mag. fields 7-33084
 short semicond. structs., photoexcited electron-hole plasma instability, numerical simulation 7-45367
 single crystals, high temp. mechanical props., effects of doping and environment 7-21326
 single domain layer growth on Si wafers by MOCVD/MBE, heteroepitaxy 7-52357
 single quantum well, doubly resonant LO-phonon Raman scatt. via deform. pot., polarisation obs. 7-39114
 single quantum wells, free excitons, phase coherence and line broadening 7-45170
 single-junction solar cells, concentrator module with 19% efficiency 7-17906
 single-particle excitations, dynamic correl. corrections, local density theory 7-45115
 solar array design, weight-efficient rigid panel structure 7-13881
 solar cell arrays with point focus concentration for spacecraft 7-3662
 solar cell concentrators, optimised top contact design 7-8385
 solar cell parameters, theoretical temp. depend. 7-23161
 solar cell with 25.5% efficiency AMO 7-3665
 solar cells, circulation meas. and spectral error reduction 7-13903
 solar cells, comparison with InP and Si cells in space 7-65484
 solar cells, crossed-lens photovoltaic concentrator appl. 7-17905
 solar cells, depletion layer recombination effects on radiation damage hardness 7-13888
 solar cells, elec. parameter mapping by numerical image processing of light beam induced current topography 7-33051

gallium arsenide continued

solar cells, fracture strength as function of manufacturing process steps 7-3696
 solar cells, perform. and temp. dependencies of proton irradiated n-p and p-n cells 7-3702
 solar cells, sequential irradiation effects of electrons and protons 7-13877
 solar cells, transient current studies of junction activity 7-8409
 solar cells fabrication on Si substrates by MOCVD 7-23183
 solar cells for space appls., potential efficiency 7-65482
 solar cells for thermophotovoltaic appls. theoretical efficiency 7-59855
 solar cells with corrugated surface, computer code for performance eval. 7-3667
 solar cells with varying junction depths, spectral mismatch correction 7-65475
 solar concentrator cells, perform. under 1 MeV electron irradiation 7-3704
 solar panel performance of LIPS-II satellite 7-13883
 solar panels with LPE and metal organic CVD circuits, satellite power 7-65493
 solid phase epitaxial growth of GaAs layers, effect of impurities 7-16907
 solid-phase-epitaxy, interface structure and impurity effects 7-2407
 space qualified solar cell production by organic metal CVD, performance testing 7-65492
 space-charge layer effective mass in parallel mag. field 7-2469
 sputtered, comp. depth profiles, AES, XPS, inverse Laplace transforms 7-22390
 sputtered films, optical props., effective medium models (*Chinese*) 7-7774
 stepwise monolayer growth by switched laser MO-VPE 7-53626
 stimulated Raman gain spectroscopy, below bandgap studies 7-22231
 stress distribution, EL2 conc., near-IR absorption mapping 7-52522
 stress-induced doubly resonant Raman scattering 7-46029
 sublattices direct resolution and identification by high-resolution TEM 7-37813
 submicron $n^+n^-n^+$ multilayers, single impurity-assisted tunnelling 7-38710
 submicron wires, conductance fluctuations in magnetoresistance 7-38597
 substrate, MBE grown refractory metals growth 7-21755
 substrate, multi-technique approach to defect microstructure characterisation 7-52215
 substrate, plasma deposition of C dielectric films 7-39420
 substrate, ZnSe MBE layers, lattice mismatch effects, TEM, photolum. and X-ray diffr. studies 7-45042
 substrate for GeSi thermally evaporated epitaxial heterolayers, Si distrib. (*Russian*) 7-63988
 substrate for MBE growth, thermal etching 7-7861
 substrate for MBE growth of magnetic Fe films 7-27584
 substrates, (100) oriented, growth of HgTe-CdTe superlattices by MBE 7-12520
 substrates, laser-induced metal and alloy plating, silicide form. 7-39448
 substrates, W films, electrical resistivity after high temp. annealing 7-64366
 substrates and devices, surface anal., SIMS appl. 7-22417
 superheating during picosecond laser melting 7-12246
 superlattice solar cell structure with high efficiency and radiation tolerance 7-8414
 surface, (001), chemisorption of CF_3 radicals, RHEED, photoelectron spectra, HF SCF calcs. 7-53497
 surface, (100), oxidation 7-59703
 surface, (100), UV-ozone cleaning, for device appl. 7-28228
 surface, (110), with ordered Sb overlayers, ARUPS 7-59378
 surface, (110), with Sb overlayers, electronic band bending at interface 7-58895
 surface, (111), alkali metal covered, adsorption of O_2 7-63957
 surface, (111), sorption of O_2 , surface struct., AES anal. 7-53457
 surface, anisotropically etched, p-n junction formation by MOCVD 7-13374
 surface, Fermi level unpinning by flowing water 7-58843
 surface, formation of gratings in laser photoemission wet etching 7-8205
 surface, interaction with H_2 7-58632
 surface (001), etch pits, depend. on Burgers vectors of dislocations 7-39767
 surface (100), chemical etching and oxidation, XPS characterisation 7-21591
 surface (100), Fermi level unpinning in air using photochem. 7-2655
 surface (100), MBE growth parameter influence on surface kinetic processes, RHEED specular beam intensity meas. 7-2424
 surface (100), thermal and ion-assisted reactions with Cl_2 7-3537
 surface (110), adsorption of O_2 , confirmation of two-step uptake model 7-2355
 surface (110), O_2 adsorption, electronic props., contact pot. meas. 7-2353
 surface (110), oxidation, photoemission spectra studies 7-3147
 surface (110), substrate for In growth, RHEED study 7-2425
 surface (110) adsorption of Al, soft X-ray photoemission spectra study 7-53494
 surface (110) $p(1 \times 1)$, adsorbed Sb, domain size, LEED profile anal. 7-7075
 surface (111), (2×2) reconstruction, geometric struct. model 7-6950
 surface (111) orderly faceted struct., LEED pattern anal. 7-21579
 surface (311)(1×1), atomic geometry and electronic struct. 7-2311
 surface and bulk nonradiative recombinations, photoacoustic study 7-33438
 surface H_2S adsorption, orientation and temp. depend. 7-58634
 surface morphology, in HNO_3 -HF- H_2O etching system (*Korean*) 7-28225
 surface morphology of crystals grown by gas-source MBE using trimethylgallium and As_4 7-17424
 surface oxidation, AES, XPS and ellipsometry studies 7-22927
 surface oxidation, effect of anodizing conditions 7-13669
 surface oxide desorption, temp. meas., Auger anal. 7-58608
 surface potential barrier in ion-etched (100) surface, electron-voltaic effect 7-7819
 surface recombination velocity and bulk minority carrier lifetime 7-17037
 surface region, heat-treated, photoluminescence, antisite defect obs. 7-39167
 surface structure with adsorbed Te 7-12460
 surfaces, (111) and $(-1-1-1)$, electronic props., angle resolved photoemission studies 7-7327
 surfaces, picosecond laser interactions, time-resolved optical studies 7-12134
 surfaces, picosecond laser melting and evaporation 7-12120
 surfaces (511) and (711), struct. studies using LEED AES, and EELS 7-2312

gallium arsenide continued

thin film photovoltaic cells, large-scale manufacture, hazard characterisation of AsH_3 gas and GaAs waste 7-39998
 thin films, on glass substrates, transport props. 7-2742
 thin semi-insulating wafers, EL2 distrib., dislocation network correl., near IR absorpt. maps and X-ray topographs 7-21203
 third order elastic constants, US displacement interferometry 7-2087
 transient thermal processing 7-16601
 transport properties, charge collection microscopy 7-52649
 tunnelling through III-V heterostructures, relevance to electronic devices 7-58885
 ultrasound, anharmonic props. under intense excitation 7-20488
 ultrathin layers, liquid phase epitaxial growth on GaAlAs substrate 7-53645
 ultrathin layers, protection for $\text{Al}_x\text{Ga}_{1-x}\text{As}$, AES sputter depth profiles 7-54022
 undoped, thermal activation of plastic deform., 528-813 K 7-6710
 undoped semi-insulating, dislocations, deep trap levels, FET meas. (Chinese) 7-12643
 uniformity imaging 7-32481
 unpinned (100) surface, picosecond transient reflectivity 7-59168
 V_F -T characteristics of p-n junction at low temp. (Chinese) 7-12792
 vapour etching, buried interface, carrier traps 7-28213
 vapour levitation epitaxy, system design and performance 7-59445
 variation of EL2 with As press. during heat treatment 7-58770
 VPE grown, defect formation leading to deep levels, review 7-64151
 VPE growth, reaction mechanisms 7-58693
 VPE growth in hydride system, elec. props. 7-2751
 wafers, LEC-grown, semi-insulating, two-dimens. high-resolution EL2 topography 7-53381
 wafers, subsurface structural defects, photon backscattering studies 7-12059
 X-ray diffr., anomalous dispersion effects, thermal vibrs. and bonding charges 7-44733
 X-ray topographic examination 7-32225
 (Al, Ga)As films, doped, Si migration during MBE growth 7-27171
 (Al,Ga)As/(Ca,Sr) F_2 multilayer structures, MBE grown, broadband high-reflectivity mirrors fabrication 7-11091
 (Al, Ga)As/GaAs undoped quantum wells, Al and Ga interdiffusion, photoluminesc. study 7-2271
 Al honeycomb substrate, flat-plate space solar panels interconnector design 7-13879
 Al-GaAs, pure and Si or Zn doped interfaces, composition depth profile, pulsed laser atom probe study 7-32842
 Al-GaAs (100) interface, Schottky barrier form. 7-2717
 Al-GaAs interfaces, convergent beam electron diffr. patterns 7-27156
 Al-GaAsO-GaAs structures, energy diagram 7-33096
 Al-Si $_3\text{N}_4$ -GaAs strucs., interface state density profile determ., DLTS spectra interpretation 7-38733
 $\text{Al}_{0.3}\text{Ag}_{0.7}\text{As}$, femtosecond carrier dynamics 7-58829
 AlAs/GaAs modulated struct., high resolution double-cryst. X-ray diffr. studies 7-7029
 AlAs/GaAs superlattices, X-point excitons 7-33069
 AlAs/GaAs superlattice/GaAs interface, inversion holes, long term storage 7-45442
 AlAs/GaAs superlattice mixing induced by Si $^+$ implantation 7-58649
 AlAs/GaAs:Si super-doped strucs., short-period superlattice electrical and defect props. (Japanese) 7-7353
 AlAs/GaAs/AlAs quantum wells, eigenvalues calcs. 7-12820
 AlAs-GaAs double-barrier structures, resonant tunnelling, room temp. effects 7-21985
 AlAs-GaAs Fibonacci superlattice, quasiperiodic ordering, X-ray scatt. study 7-2692
 AlAs-GaAs MIS capacitors, dynamic storage of holes 7-33071
 AlAs-GaAs quantum-wells, low temp. growth by modified MBE 7-39386
 AlAs-GaAs superlattices, Si ion implantation, dose-dependent mixing 7-12500
 AlAs-GaAs superlattice waveguides in separate confinement heterostructure laser diodes, threshold current density 7-20267
 AlAs-GaAs superlattice, Si $^+$ implantation, depth dependent mixing 7-27032
 AlAs-GaAs superlattices, disordering by Si and S implantation 7-45024
 AlAs-GaAs superlattice, compositional disordering control by Ar ion implantation 7-51806
 AlAs-GaAs superlattices, lattice vibration, Raman spectra 7-63937
 $\text{Al}_{1-x}\text{Ga}_x\text{As}$ layers, form. by regrowth on surface of GaAs during contact with undersaturated liq. containing Al 7-46311
 $\text{Al}_{0.5}\text{Ga}_{1-x}\text{As}$ -GaAs multiple quantum wells, photoluminescence studies, press. depend. (Chinese) 7-13194
 $\text{Al}_{0.5}\text{Ga}_{1-x}\text{Te}$, low press. OMVPE, Te doping, Hall effect, carrier conc., photolum. 7-21242
 AlGaAs BH laser with flared waveguides, high power operation 7-57352
 AlGaAs, chemical beam epitaxial growth investig. 7-7878
 AlGaAs, DX centres, DLTS signature anal. 7-45204
 AlGaAs epitaxial layers and superlattices, X-ray diffr. analysis 7-21047
 AlGaAs epitaxial layers, large scale MOVPE growth 7-22552
 AlGaAs epitaxial layers, OMVCD, compositionally graded growth technique for device strucs. 7-22553
 AlGaAs epitaxial wafers, highly uniform growth by large capacity MOVPE reactor 7-22551
 AlGaAs heterostructs., low temp. LPE growth 7-64939
 AlGaAs high-power pulsed laser 7-10997
 AlGaAs high-power ridge-waveguide GRIN-SCH laser diode 7-10988
 AlGaAs injection heterolasers and integrated laser-photodetector pairs, prepared by microcleaving 7-31343
 AlGaAs integrated-hybrid Bragg heterostruct. laser thermal stability of distributed-refl. spectral bands 7-57393
 AlGaAs intraband relaxation dynamics of photo-excited carriers 7-52691
 AlGaAs laser, mode hopping suppression by saturable absorber 7-62696
 AlGaAs laser, tunability and mode-transition characteristics 7-20293
 AlGaAs laser, tunability, appl. to Cd^+ ion drift velocity meas. (Japanese) 7-20294
 AlGaAs laser arrays with Si disordered facet windows, high power operation 7-43140
 AlGaAs laser diode, HF stabilisation 7-15864
 AlGaAs laser diode array travelling-wave amplifier, high peak power, gateable picosec. optical pulses 7-20252
 AlGaAs laser diodes, MOVPE grown, struct. fabrication and characts. (Japanese) 7-20272
 AlGaAs laser diodes, MBE grown, fabrication and characts. (Japanese) 7-20273

gallium arsenide continued

AlGaAs laser rib-waveguide, gain- to index-guiding transition 7-31315
 AlGaAs, laser-assisted MOVPE growth 7-64928
 (AlGa)As lasers, separately pumped, continuous control 7-20287
 AlGaAs layer, separating on GaAs surface, growth mechanism, Auger depth profiling 7-44434
 AlGaAs layers MOCVD using dimethyl aluminium hydride, C acceptors, photolum. 7-22517
 AlGaAs low current threshold visible laser diodes, (AlGaAs) $_m$ (GaAs) $_n$ superlattice quantum well 7-10926
 AlGaAs, low press. MOVPE grown, surface morphology and defects 7-64023
 AlGaAs, MOVPE, design of safe facility 7-22529
 AlGaAs, MOVPE growth on Ge substrates for high efficiency tandem solar cell appl. 7-3671
 AlGaAs, MOVPE growth, refractive indices meas. by in situ reflectometry 7-59270
 AlGaAs, MOVPE, laser assisted, selective area irradi., carrier conc. 7-22545
 AlGaAs MQW lasers, index-guided, fabrication by selective disordering using Be focused ion beam implantation 7-20269
 AlGaAs monolithic three-junction solar-cells, computer modelling 7-3672
 AlGaAs superlattice for visible laser diode, energy band structure (Japanese) 7-12823
 AlGaAs superlattices, donor state instability, DLTS and Hall meas. 7-12663
 AlGaAs surface cleaning using ECR radical beam gun 7-54028
 AlGaAs terrestrial solar cells, high-efficiency concepts 7-8390
 AlGaAs, triethylgallium pyrolysis temp. in presence of AsH_3 or trimethylaluminium 7-22541
 AlGaAs:Mg LPE layers, Mg doping and injection laser threshold current 7-12092
 AlGaAs:Mg-GaAs:Se concentrator solar cells, 26 percent efficient 7-3699
 AlGaAs:Sb, MBE growth, Sb doping 7-2038
 AlGaAs:Si-GaAs 2D electron gas structure, scatt. mechanisms 7-38718
 AlGaAs:Si(Zn), MOVPE, impurity induced disordering, quantum well laser fabrication and characts. 7-27934
 AlGaAs/AlAs multiquantum-well strucs., staggered band alignments 7-7361
 AlGaAs/GaAs, abrupt heterojunction structures, large area uniformity, MOVPE reactor design 7-22524
 AlGaAs/GaAs DBR laser with multiquantum well active/passive waveguides 7-57350
 AlGaAs/GaAs DFB laser diodes, MOVPE growth, CW operating characts. 7-25836
 AlGaAs/GaAs heterointerface solid-state far IR emitter utilising 2D plasmon 7-53414
 AlGaAs/GaAs heterojunction bipolar transistor, self-aligned with InGaAs emitter cap 7-45492
 AlGaAs/GaAs heterostruct., quasicrystalline system, electronic struct. studies 7-38699
 AlGaAs/GaAs laser diodes, advanced optoelectronic technology 7-1187
 AlGaAs/GaAs long cavity ridge waveguide DFB lasers, spectral linewidth reduction 7-1179
 AlGaAs/GaAs modulation-doped heterojunctions, 2D electron gas, DX centres 7-38694
 AlGaAs/GaAs ridge waveguide quantum well lasers with high quantum efficiency 7-15905
 AlGaAs/GaAs selectively doped heterointerface under high elec. field appl., 2D plasmon 7-52637
 AlGaAs/GaAs solar cells, proton irradiated, defect production 7-46936
 AlGaAs/GaAs superlattice 7-64324
 AlGaAs/GaAs two-junction monolithic cascade solar cell in lattice-matched system 7-13862
 AlGaAs/GaAs waveguide phase modulators, wavelength depend. 7-43361
 AlGaAs/GaAs:Si heterostruct., MBE growth on polar surfaces 7-7863
 AlGaAs/GaAs/AlGaAs selectively doped double heterojunction FET system, high mobility electron subband struct. studies 7-12838
 AlGaAs/GaAs/AlGaAs selectively doped double heterostructs., electron conc. and mobility 7-12839
 AlGaAs/GaAs/AlGaAs single quantum well, negative differential mobility and drift vel. overshoot 7-52803
 AlGaAs/GaAs/Ge multijunction solar cell, model for calc. of displacement damage by radiation 7-13878
 AlGaAs/GaAs/InGaAs multijunction solar cell, model for calc. of displacement damage by radiation 7-13878
 AlGaAs/GaInAs two-junction monolithic cascade solar cell in lattice-mismatched system 7-13862
 AlGaAs/GaInAs two-terminal multijunction solar cell spectral response meas. 7-13871
 AlGaAs-GaAs, band-gap discontinuity, determ. by quantum oscillations of photolum. intensity 7-13217
 AlGaAs-GaAs, DFB lasers, low threshold, 0.88 μm emission, MOVPE fabricated with ridge waveguide struct. 7-5906
 AlGaAs-GaAs, modulation doped heterostructs., high field transient transport 7-12836
 AlGaAs-GaAs, selectively doped heterojunctions, energy relax. of 2D electrons, deformation potential constant 7-12801
 AlGaAs-GaAs 2D electron gas strucs., scatt. mechanisms 7-52783
 AlGaAs-GaAs cascade solar cells, efficient two-junction monolithic, grown by MOVPE 7-65483
 AlGaAs-GaAs concentrator solar cells with high efficiency, design and fabrication 7-3669
 AlGaAs-GaAs DFB-TJS external-cavity laser with optical phase control loop, spectral linewidth 7-20222
 AlGaAs-GaAs DH injection lasers, MOVPE growth on Si substrates 7-57356
 (AlGa)As-GaAs DQW-SCH lasers grown by MOVPE, design, fabrication and characterisation 7-36990
 AlGaAs-GaAs GRIN-SCH SQW laser, wide-stripe, injection locking 7-20290
 AlGaAs-GaAs graded barrier quantum well heterostructure laser diodes with compositionally graded and superlattice buffer layers 7-57353
 AlGaAs-GaAs heteroepitaxial wafer for solar cell appls., uniform growth by MOVPE 7-64929
 AlGaAs-GaAs heteroface space solar cells with 21 percent conversion efficiency 7-3694
 AlGaAs-GaAs heteroface solar cells, role of window layer 7-3695
 AlGaAs-GaAs heterointerface, ballistic transport of quasi-2D electron gas 7-52788

gallium arsenide continued

- AlGaAs-GaAs heterostructures, organometallic VPE grown, galvanomagnetic effect 7-12800
- AlGaAs-GaAs heterostructures, dissipationless quantum Hall effect, size-depend. quantised breakdown 7-45469
- AlGaAs-GaAs heterostructure travelling-wave amplifier based on injection laser diode 7-62694
- AlGaAs-GaAs index-guided lasers with mode filter, props. study 7-5905
- AlGaAs-GaAs laser diodes, elec. field depend. of photoconductivity spectra 7-20227
- AlGaAs-GaAs MQW CCD spatial light modulators using electroabsorption effects 7-20407
- AlGaAs-GaAs narrow spectral linewidth semiconductor optical-fiber ring laser 7-25817
- AlGaAs-GaAs selectively doped heterostructures, orientation effect on contact resistance 7-38680
- AlGaAs-GaAs self-pulsing lasers, quasiperiodic route to chaos under large signal current modulation 7-62706
- AlGaAs-GaAs single quantum well, MBE growth interruption, well width fluctuations 7-7865
- AlGaAs-GaAs single quantum wells with growth interrupted heterointerfaces, photoluminesc. 7-39168
- AlGaAs-GaAs solar cells, MOCVD on GaAs, Ge and Ge-Si substrates 7-3650
- AlGaAs-GaAs solar cells, high efficiency DH cells fabrication using MOCVD 7-3693
- AlGaAs-GaAs solar cells, fabrication on Si substrates 7-46937
- AlGaAs-GaAs solar cell fabrication, elec. characts. and space appl. 7-54307
- AlGaAs-GaAs space solar cells, LPE production and characterisation 7-3666
- AlGaAs-GaAs split gate heterojunction FET, elec. resist., Hall effect, influence of electronic subband mag. depopulation 7-38740
- AlGaAs-GaAs superlattices, impurity electron states (*Japanese*) 7-12662
- AlGaAs-GaAs superlattices, Si-Be co-doping, compositional disordering suppression, SIMS study 7-16878
- AlGaAs-GaAs superlattices, Se (Si)(Mg)(Be) ion implantation, intermixing, residual damage 7-26782
- AlGaAs-GaAs-AlGaAs single quantum well heterostruct., negative differential mobility and drift velocity overshoot 7-52787
- AlGaAs-GaAs-Si, Be superlattices, correlation between Si diffusion and Si-induced disordering 7-38034
- AlGaAs-GaInAs cascade solar cells, efficient two-junction monolithic, grown by MOCVD 7-65483
- AlGaAs-GeAs n-n heterojunction, thermionic current and capacitance, effect of subband quantisation in 2D electron gas 7-17090
- AlGaAs-Si mechanically stacked multijunction solar cells, optical effects of thin film adhesives 7-3670
- Al_{0.25}Ga_{0.75}As multilayer structures, vertical transport 7-38719
- Al_{0.26}Ga_{0.74}As, instability of electron-nuclear spin system in strong mag. field, luminesc. study 7-7729
- Al_{0.26}Ga_{0.74}As/GaAs heterojunction, high mobility 2-D hole gas 7-2679
- Al_{0.28}Ga_{0.72}As, photoluminescence half-width and intensity, temp. depend. 7-39179
- Al_{0.3}Ga_{0.7}As, thermal and ion-assisted reactions with Cl₂ 7-28349
- Al_{0.3}Ga_{0.7}As/GaAs quantum wells, photocond. of confined donors 7-7282
- Al_{0.3}Ga_{0.7}As-GaAs optically-pumped multiple quantum well laser 7-5922
- Al_{0.3}Ga_{0.7}As-GaAs quantum well structure, electric-field-induced optical modulation, theory using Monte Carlo approach 7-17077
- Al_{0.55}Ga_{0.45}As:Te edge region photocapacitance at constant bias, anal. 7-7287
- Al₁Ga_{1-x}As, hot-electron capture at DX centres 7-45344
- Al₁Ga_{1-x}As, AlAs and GaAs epitaxial multilayers as optical interferometric elements 7-342
- Al₁Ga_{1-x}As bandgap determ. by Schottky barrier spectral response meas. 7-2667
- Al₁Ga_{1-x}As cascade solar cells, OM-VPE growth, in-situ-grown tunnel junction 7-8387
- Al₁Ga_{1-x}As crystals, DX centre props. 7-2534
- Al₁Ga_{1-x}As, DX centre, theory 7-12654
- n-Al₁Ga_{1-x}As epitaxial layers, graded-gap, resistance, press. dependence 7-33113
- Al₁Ga_{1-x}As film formation by laser beam interaction with AlAs/GaAs multilayer structure 7-12570
- Al₁Ga_{1-x}As films and multilayer structures, MOCVD growth and characterisation, review 7-33586
- Al₁Ga_{1-x}As, Ga interstitial identification by ODMR 7-33302
- Al₁Ga_{1-x}As heteroepitaxial layers formed by metalloorganic chem. hydride method, electrophys. props., comp. effect 7-64370
- Al₁Ga_{1-x}As heterojunction, tunnelling current modulation by optical photons 7-27394
- Al₁Ga_{1-x}As homojunctions, minority-carrier diffusion, TOF studies 7-12797
- Al₁Ga_{1-x}As layers and quantum well struct., MOVPE growth chemistry 7-22550
- Al₁Ga_{1-x}As, low press. OMVPE, selective growth embedding in etched grooves on GaAs 7-22554
- Al₁Ga_{1-x}As MBE layers, deep electron traps, flux ratio effects 7-12641
- Al₁Ga_{1-x}As, MOCVD, equilib. gas phase species 7-22542
- Al₁Ga_{1-x}As p-n junction solar cell radiation-induced defects obs. using DLTS 7-13875
- Al₁Ga_{1-x}As solar cells, MOCVD growth and characterisation, review 7-34043
- Al₁Ga_{1-x}As surface, protection by As and GaAs ultrathin layers, AES sputter depth profiles 7-54022
- Al₁Ga_{1-x}As, thin films, Raman spectroscopy, characterisation 7-53354
- Al₁Ga_{1-x}As:Be epitaxial layers, ion implanted, rapid thermal annealing 7-21257
- Al₁Ga_{1-x}As:Mg/GaAs:Se quantum well heterostruct., photopumped laser operation 7-25818
- Al₁Ga_{1-x}As:Si, deep donor centres 7-45217
- Al₁Ga_{1-x}As:Si, LEDs, luminesc. props. (*Korean*) 7-27786
- Al₁Ga_{1-x}As:Si, Si diffusion from sputtered Si film 7-58537
- Al₁Ga_{1-x}As/GaAs, multilayer and superlattice structs., electronic subbands 7-58877
- Al₁Ga_{1-x}As/GaAs multi-quantum-well Zn-diffused mesa BH lasers, sub-milliwatt lasing 7-10991
- Al₁Ga_{1-x}As/GaAs photoexcited heterojunction, charge transfer calcs. 7-12688
- Al₁Ga_{1-x}As/GaAs quantum wells, photolum., periodic variation investig. 7-2688

gallium arsenide continued

- Al₁Ga_{1-x}As-AlAs quantum well, magneto-optical absorpt. study 7-7681
- Al₁Ga_{1-x}As-GaAs BH quantum well edge-injection laser array 7-57355
- Al₁Ga_{1-x}As-GaAs broad area quantum well lasers, single-mode single-lobe operation 7-10930
- Al₁Ga_{1-x}As-GaAs double heterostruct. injection laser, power-current characteristics study 7-62704
- Al₁Ga_{1-x}As-GaAs heterostructures, 2D electron space charge layers, plasmon and magnetoplasmon excitation 7-38696
- Al₁Ga_{1-x}As-GaAs heterointerface, 2D electron gas density 7-45448
- Al₁Ga_{1-x}As-GaAs heterostruct. injection laser with coupled cavity, dynamic stability 7-62705
- Al₁Ga_{1-x}As-GaAs heteroface solar concentrator cells, space and terrestrial appls. 7-65486
- Al₁Ga_{1-x}As-GaAs LOC lasers for high power low threshold current density operation, optimisation 7-10934
- Al₁Ga_{1-x}As-GaAs layered structures, metal organic VPE grown, depth profiles, SIMS anal. 7-21684
- Al₁Ga_{1-x}As-GaAs mesa BH MQW lasers with 880 μ A threshold current at 77 K 7-50595
- Al₁Ga_{1-x}As-GaAs stripe-geometry quantum well heterostructure lasers defined by defect diffusion 7-1181
- Al₁Ga_{1-x}As-GaAs superlattices, ion implanted, defect struct. 7-26783
- Al₁Ga_{1-x}As-AlAs heterojunctions, band discontinuities meas. 7-27407
- AlGaInAs layers on InP, LPE growth 7-33608
- AlInAs-GaInAs superlattices, electronic transport and depletion by tunnelling 7-27395
- AlInAs-GaInAs selectively doped heterostructs., MOCVD growth, HIFET fabrication appl. 7-17429
- AlInAs-GaInAs superlattices, quantum photoconductivity, effective mass filtering 7-12847
- Al_{0.48}In_{0.52}As-Ga_{0.47}In_{0.53}As SQW, electron temp. depend. on well width, photolum. obs. 7-12810
- Al_{1-x}In_xAs-GaAs strained layer superlattices, X-ray diffraction and excitation spectroscopy studies 7-12853
- Au-GaAs, annealed, interface erosion 7-21683
- Au-GaAs, contact, structural and elec. props. 7-27424
- Au-GaAs, interface state meas. at Schottky contacts, admittance characterisation technique 7-2718
- Au-GaAs, Schottky contact, interface states, trap characterisation 7-27421
- Au-GaAs (001), short range potential variations at interface 7-45500
- Au-GaAs (110) interface, photoemission studies, temp. effects 7-33517
- Au-GaAs Schottky-barrier diode hot-electron temperature measurement, method 7-52623
- Au-Ge-GaAs, interfacial reactions, struct. after annealing 7-27154
- Au-Ge-Ni-GaAs, non-alloyed ohmic contact, solid phase epitaxy 7-27423
- Au-Ni-Au-Ge-Ni-GaAs, ohmic contacts, alloying, specific contact resistivity 7-27425
- Au-TiB₂-Au-Ge-Ni-GaAs, ohmic contacts, alloying, specific contact resistivity 7-27425
- AuGe₂-GaAs (001), chemically unreactive interfaces formation 7-7050
- AuGe-GaAs, ion beam induced phenomena 7-12166
- AuGe-Nb-GaAs, ohmic superconducting contacts to GaAs 7-33088
- CaF₂-GaAs (100), surface morphology, elec. props. 7-39392
- nCdS-n-GaAs photoanode, flux anal. of multiple junction solar cells 7-23162
- Cr₂O₃-GaAs, struct. and electrophysical props. 7-17109
- Cu-GaAs (110), electron struct., synchrotron radiation photoelectron spectroscopy 7-27420
- Ga-As-AlGaAs superlattice, laser induced disordering and Si impurity incorporation 7-45018
- Ga-In-As-P system, ternary alloys, E₁ energy gap, CPA calc. 7-58740
- GaAs:Be, MOVPE, diethylberyllium dopant source, elec. characts. 7-22521
- GaAs-GaAlAs MQW waveguides, nonlinear propag. 7-26033
- a-GaAs_{1-x}H_x, plasma deposition in RF capacitively coupled system 7-64927
- GaAlAs channelled-substrate-planar laser, measuring modulus and phase of chirp/modulated power ratio 7-57391
- GaAlAs DH laser amplifier, Fabry-Perot type, gain and frequency bandwidth 7-20228
- GaAlAs diode laser, frequency shift in magnetic field 7-5885
- GaAlAs diode laser, gain compression, picosecond transmission meas. 7-20289
- GaAlAs heterostructures with an insulating layer 7-12866
- GaAlAs injection lasers, single-frequency, linewidth investig. 7-25819
- GaAlAs, LIMA anal., effect of alloy composition on secondary ion yields 7-28376
- GaAlAs laser, collinear nearly degenerate four-wave mixing in amplifying media 7-11071
- GaAlAs laser, LPE grown, effect of crystal defects on reliability 7-36960
- GaAlAs laser amplifier, high sensitivity picosecond optical pulse detection 7-50565
- GaAlAs laser diode, extremely weak feedback, lasing wavelength shift anal. 7-31325
- GaAlAs laser diodes, stripe geometry, directly modulated in microwave range, freq. response study 7-11017
- GaAlAs laser diodes, self-coupling effects and appls. 7-57386
- GaAlAs laser diodes under microwave intensity modulation, linearity charactn. 7-10944
- GaAlAs laser structs., double crystal X-ray rocking curves, interference peaks 7-44303
- GaAlAs laser-diode array, high-speed electronic beam steering 7-43185
- GaAlAs lasers, injection, photodetection props. 7-31379
- GaAlAs lasers, polarisation-resolved low-frequency noise 7-15863
- GaAlAs MOCVD layers, stoichiometry variation determ., pulsed laser atom probe anal. 7-12305
- GaAlAs, MOVPE growth rate, orientation depend. 7-22556
- (GaAl)As monolithic composite-cavity laser, chem. etching technique 7-50579
- GaAlAs morphological stability in epitaxy, appl. to optoelectronic monolithically integrated structures 7-27172
- GaAlAs passive waveguide, intrinsic optical bistability obs. 7-57425
- GaAlAs semiconductor laser coupled with short external cavity, stable single longitudinal mode operation 7-62737
- GaAlAs single freq. heterostruct. injection lasers, LPE and VPE growth 7-62699
- GaAlAs strip waveguides, optical transistor effects, expt. study 7-37026
- GaAlAs substrate, GaAs ultrathin layers, liquid phase epitaxial growth 7-53645

gallium arsenide continued

GaAlAs wideband free-space lasercom transmitter, design 7-31354
 GaAlAs wideband lasercom transmitter, performance 7-31355
 GaAlAs:Si, DX centres, nonexponential thermal emission kinetics 7-12640
 GaAlAs/GaAs, junction isolated LED structures, MOCVD, characts. 7-27935
 GaAlAs/GaAs, semicond. superlattice heterojunction interface, SIMS anal. (Japanese) 7-2396
 GaAlAs/GaAs circular BH surface emitting lasers, fabrication using selective meltback method 7-5911
 GaAlAs/GaAs heterostructure, absorption coeff. and thermal conductivity meas. by photothermal spectroscopy 7-41474
 GaAlAs/GaAs MOCVD growth for surface emitting lasers 7-53630
 GaAlAs/GaAs single quantum well laser, current pumped, second quantised state lasing 7-50559
 GaAlAs/GaAs surface-emitting linear laser arrays with etched mirrors 7-20255
 GaAlAs/GaAs TJS lasers on Si substrates, MOCVD growth 7-62691
 GaAlAs/GaAs:C quantum wells interface struct. and luminesc. efficiency 7-7735
 GaAlAs-GaAs DFB lasers with double channel planar buried heterostructure, low threshold operation 7-20256
 GaAlAs-GaAs DFB laser with double-channel planar BH 7-50594
 GaAlAs-GaAs epitaxial superlattice, X-ray double crystal characterisation, rocking curves calc., computer simulation technique 7-58105
 GaAlAs-GaAs heterostructures grown by MOCVD, transition region, ellipsometric anal. 7-2388
 GaAlAs-GaAs heterostructure solar cells, multijunction with bulk graded bandgap/p-n junction 7-3676
 GaAlAs-GaAs laser diodes, catastrophic optical damage, electrolum., cathodolum., EBIC and TEM obs. 7-57329
 GaAlAs-GaAs laser failure causes and distrib., laboratory service life tests 7-62692
 GaAlAs-GaAs MOCVD solar cells on Ge and Ge/Si substrates 7-23182
 GaAlAs-GaAs MQW structure, compositional fluctuations, STEM/EDX microanal. 7-45077
 GaAlAs-GaAs microcavity surface-emitting laser 7-57361
 GaAlAs-GaAs multi-heterostructures, MOCVD growth for surface emitting lasers 7-59440
 GaAlAs-GaAs quantum well superlattices, applied electric field, quasi-eigenstates and eigenenergies, determ. 7-33072
 GaAlAs-GaAs ridge waveguide DFB lasers, lateral anal. 7-62686
 GaAlAs-GaAs solar cells grown by MBE, material props. and device parameters 7-23164
 GaAlAs-GaAs superlattice, Auger sputter depth profiling 7-21254
 GaAlAs-GaAs superlattice struct., dynamic SIMS profiles 7-22417
 GaAlAs-GaAs surface-emitting laser diodes, lateral pumping struct. 7-57359
 GaAlAs-GaAs surface-emitting laser with $\text{TiO}_2\text{-SiO}_2$ dielec. multilayer reflector 7-59427
 GaAlAs-Mo junctions, Schottky barrier height, electrical props. 7-64346
 ($\text{Ga}_{0.5}\text{Al}_{0.5}\text{As}$), MBE grown, elastic consts., diffuse X-ray scatt. study 7-16918
 $\text{Ga}_{0.60}\text{Al}_{0.40}\text{As}$, electron-hole plasma diffusion, spatially resolved gain and luminesc. spectra 7-12747
 $\text{Ga}_{0.65}\text{Al}_{0.35}\text{As}$ -GaAs quantum wells, elect. field-induced decrease of exciton lifetimes 7-45481
 $\text{Ga}_{0.8}\text{Al}_{0.2}\text{As}$ -GaAs- $\text{Ga}_{0.8}\text{Al}_{0.2}\text{As}$ quantum well structs., electroreflectance spectra, model 7-33365
 $\text{Ga}_{1-x}\text{Al}_x\text{As}$, indirect-gap crystals, hot photolum., polarisation characts. 7-46092
 $\text{Ga}_{1-x}\text{Al}_x\text{As}$, ion-implanted, defect creation 7-21240
 $\text{Ga}_{1-x}\text{Al}_x\text{As}$ -GaAs- $\text{Ga}_{1-x}\text{Al}_x\text{As}$ heterostructures, tunneling through indirect-gap barriers 7-21999
 $\text{Ga}_{1-x}\text{Al}_x\text{As}$, Al concentration profiling using nucl. resonances 7-6811
 $\text{Ga}_{1-x}\text{Al}_x\text{As}$ and GaAs multilayer structures, metalorganic MBE growth 7-7860
 $\text{Ga}_{1-x}\text{Al}_x\text{As}$, DX centres, inner and outer crossing lattice relax. 7-45218
 $\text{Ga}_{1-x}\text{Al}_x\text{As}$, disorder effects of Raman scatt. 7-7704
 $\text{Ga}_{1-x}\text{Al}_x\text{As}$ MIS and SIS structures, prep. by metallorganic chem. hydride method, electrophysical props. 7-22018
 $\text{Ga}_{1-x}\text{Al}_x\text{As}$ quantum-well wires, Wannier excitons, binding energies 7-64092
 $\text{Ga}_{1-x}\text{Al}_x\text{As}$ solid soln. epitaxial layer composition, Raman determ. 7-64628
 $\text{Ga}_{1-x}\text{Al}_x\text{As}$:S(Se), MBE growth, dopant incorporation 7-12533
 $\text{Ga}_{1-x}\text{Al}_x\text{As}$:Si, electrical current induced liq. phase epitaxy 7-27955
 $\text{Ga}_{1-x}\text{Al}_x\text{As}$ /Ga $_{1-x}\text{Al}_x\text{As}$ /GaAs double barrier tunneling struct., negative resist. calcs. 7-45451
 $\text{Ga}_{1-x}\text{Al}_x\text{As}$ -GaAs, thickness and conc. of thin $\text{Ga}_{1-x}\text{Al}_x\text{As}$ epitaxial films, determ. by photoemission jumps method (French) 7-38381
 $\text{Ga}_{1-x}\text{Al}_x\text{As}$ -GaAs quantum wells, diamag. shift of exciton energy levels 7-21824
 $\text{Ga}_{1-x}\text{Al}_x\text{As}$ -GaAs- $\text{Ga}_{1-x}\text{Al}_x\text{As}$ quantum well, donor ion dielec. response 7-45417
 GaAlAsGaAs quantum well heterostructures, grown by MOCVD, props. 7-45479
 GaAlAsSb/GaSb/GaInAsSb injection double heterostructure laser, room temp. operation 7-62697
 $\text{Ga}_{1-x}\text{Al}_x\text{As}$ -GaAs superlattice, exciton CW-photoluminesc., excitation intensity depend. 7-59252
 GaAs - Ag (Au), excimer laser annealed Au(Ag) contacts 7-12857
 GaAs (100)-Ni interface, effect of O on diffusion and compounding 7-21539
 GaAs and GaAs-Ge, extrinsic photoeffect obs., with X-ray diffraction apparatus 7-32221
 GaAs doping superlattices, optically induced absorpt. modulation 7-7713
 GaAs doping superlattices, temp. depend. of tunable lumin. 7-39182
 GaAs epilayers, plasma enhanced metalorganic CVD 7-46336
 n-GaAs metal-dielectric-semiconductor system, field effect, transistor studies 7-52841
 GaAs quantum wells, hot-carrier phonon interactions, steady-state and picosecond meas. 7-12837
 GaAs quantum wells, n-modulation-doped, negative absolute mobility of holes 7-7337
 GaAs, valence charge density, X-ray diffr. study, comparison with calculated results (French) 7-16940
 GaAs: S, Sn, epitaxial layers, photoluminescence spectra 7-46095
 GaAs: Si(Se)(Zn)(Be), ion implanted, rapidly annealed, damage removal process 7-17043

gallium arsenide continued

GaAs:Al, surface layer, degree of disordering, effect of dopant 7-63929
 GaAs:Al⁺(P⁺), ion implantation damage 7-38024
 GaAs:B, as-grown Czochralski crystals, EPR signal 7-38935
 GaAs:B, internal friction temp. depend. studies 7-38112
 GaAs:B, ion implanted, near-intrinsic and extrinsic photocapacitance due to the EL2 level 7-7147
 GaAs:B, ion implanted, struct. and damage distrib., TEM study 7-51893
 GaAs:B buried isolation layer form. by focused ion beam, FIBI-MBE system 7-51804
 GaAs:Be⁺, ion implanted, residual microstruct., TEM studies 7-32675
 GaAs:Bi, epitaxial layers, purification by Bi doping 7-58301
 GaAs:C, impurity content meas., IR absorpt., room temp. meas. 7-22289
 GaAs:C, impurity levels determ. 7-32949
 GaAs:C, LVM absorpt. temp. depend. (Chinese) 7-59225
 GaAs:C, low C conc., crystal growth using pyrolytic BN coated graphite 7-59398
 GaAs:C, O, trace determ. by ³He-activation anal. 7-58308
 n-GaAs:Co, impurity double acceptor state, Hall effect and resistivity meas., temp. and press. depend. 7-12656
 GaAs:Cr, deep levels characterisation using photo-induced transient spectroscopy 7-16973
 p-GaAs:Cr, excited and metastable states of Cr-related double centres 7-7153
 GaAs:Cr, meas. of residual stress by Cr-related luminesc. lines 7-7726
 GaAs:Cr, photorefractive behaviour using two-beam coupling 7-31387
 GaAs:Cr,Se, impurity complex, luminescence study 7-53396
 GaAs:Cr free and metallised surfaces, SAW absorpt. meas., hybrid SAW semicond. device appls. 7-52217
 GaAs:Cr impurity level studies 7-33084
 GaAs:Cr seminsulating LEC wafers, microhardness cartography 7-32886
 GaAs:Cr/ZnSe heterostructure, interface stress 7-38352
 GaAs:Cs, impurity ion beam effects, SIMS depth profiling 7-22419
 GaAs:Cu, neutral state of deep acceptors, photoluminescence spectra, Jahn-Teller effect 7-64149
 GaAs:Er MBE layer, dopant trapping level, photolum. obs. 7-44581
 GaAs:Ge,Se, diffused contact regions, rapid thermal annealing 7-17103
 GaAs:He, ion implanted, damaged layers, IR Raman probing 7-59191
 GaAs:H, vibrational excitations, impurity-host atom complexes, IR absorpt. data interpretation 7-44724
 GaAs:H amorphous sputtered films, AC cond. studies 7-21947
 a-GaAs:H:F, electronic struct., dangling bonds, cluster-Bethe lattice method calcs. 7-12592
 GaAs:Ho, electroluminescence and injection currents 7-13232
 GaAs:In, B, electrical props., role of residual B impurity, liquid encapsulated Czochralski growth 7-45312
 GaAs:In, doped and undoped, EL2 maps from computer based IR image analysis 7-32237
 GaAs:In, LEC growth, annealing, solid soln. hardening, dislocation density, elec. props. 7-17404
 GaAs:In, lattice distortions, NMR study 7-2933
 GaAs:In, low In conc., LEC cryst. growth employing thermal stress anal. 7-46305
 GaAs:In, semi-insulating substrates and ingots, In content, nondestructive meas. 7-58305
 GaAs:In, strain effects, electrorefl. and photocapacitance study 7-22224
 GaAs:In, VPE growth, isoelectronic In doping, etch pit densities 7-46340
 GaAs:In (B)(Si), dislocation free crystals, LEC grown, microscopic defects, eutectic etching 7-16545
 GaAs:In annealed substrates, In distribution in surface region 7-44959
 GaAs:In crystals, dislocations, in situ X-ray topographic studies 7-21207
 GaAs:In crystals, LEC growth, grown-in dislocation elimination 7-22465
 GaAs:In LEC crystals, dislocation etch pits 7-38000
 GaAs:In MBE layers, defect density reduction by isoelectronic In doping 7-3176
 GaAs:In(Cr), doped and undoped, microdefects obs. by IR light scatt. tomography 7-32662
 GaAs:Mg, MOVPE, p-type doping using an organometallic Mg precursor 7-22522
 GaAs:Mg MBE layers, photoluminescence 7-22295
 GaAs:Mg⁺, formation of p-type layers using ion implantation and rapid thermal annealing 7-45311
 GaAs:Mo (W), impurity electronic struct. excitation and ionisation, cluster approach, X_α multiple scatt. calcs. 7-2535
 GaAs:Nb photolum., Zeeman spectra study 7-39175
 GaAs:Ni, acceptor like electron trap, DLTS study 7-7166
 n-GaAs:O, semi-insulating, impurity centres, electron capture 7-52643
 GaAs:O LEC crystals, deep photoluminesc. band, fine struct. 7-46610
 GaAs:P, ion implanted and pulse laser annealed, Raman study 7-6653
 GaAs:Pr(Nd)(Yb), IR photoluminescence of rare earth impurities 7-64692
 GaAs:S,Si epitaxial layers, close space vapour transport growth, photoluminescence and electrical props. 7-21776
 GaAs:S layers obtained by gas-phase epitaxy, electrophysical props. 7-7418
 GaAs:S surface elec. props. modification by plasma exposure 7-27346
 GaAs:Sb, deep level formed by Sb doping 7-52496
 GaAs:Se, ion implanted, annealing mechanism 7-26777
 GaAs:Si, annealing behaviour of impurities in presence of stress 7-65060
 GaAs:Si, dislocations, STEM and CTEM micrographs 7-1825
 GaAs:Si, distorted impurity configuration 7-52501
 GaAs:Si, electrical props. of p-type layer 7-12722
 GaAs:Si, FET structs., rapid optical annealing for improved uniformity 7-16620
 GaAs:Si, flow-rate modulation epitaxy, Si planar doping 7-17443
 GaAs:Si, ion implanted, amorphisation and epitaxial regrowth, defect depth profiles 7-12088
 GaAs:Si, ion implanted, rapid thermal annealing effects 7-21259
 GaAs:Si, ion implanted and rapid thermal annealed, activation efficiency, crystal stoichiometry effects 7-51791
 GaAs:Si, MBE growth, carrier concentration, dislocation effects 7-58682
 GaAs:Si, semi-insulating, ion implanted, LEC growth, elec. activation efficiency, stoichiometry dependence 7-46298
 GaAs:Si, shallow donor neutralisation by atomic H, photoluminescence study 7-22294
 GaAs:Si,Be, MBE, dopant interaction 7-52362
 GaAs:Si,Ge, local modes, isotopic fine struct., IR spectra 7-38145
 GaAs:Si heteroepitaxial growth on sapphire, low press. MOCVD three-step method 7-27927
 GaAs:Si wafer, failure, dislocation distrib., etching 7-12067
 GaAs:Si/Al_{1-x}Ga_xAs quantum wells, photolum. studies 7-39178

gallium arsenide continued

GaAs:Si/AlAs multiquantum well structs., band struct. and photolum. studies 7-12843
GaAs:Si-AlAs:Si superlattices, MBE growth and electrical props. 7-22052
GaAs:Si⁺ wafers, implant at. profiles, planar and residual channelling effects 7-12181
GaAs:Si(B)-Ga_{0.25}Al_{0.75}As:Si(B) quantum wells, ion implanted, TEM and photolum. studies 7-58865
GaAs:Si(Be)(Mg), rapid annealing, temp. depend. of damage removal and carrier activation 7-17032
GaAs:Si(S), LEC grown, struct. defects, influence of Si and S doping 7-53550
GaAs:Sn, epitaxial layers, current carrier distrib. 7-12530
GaAs:Sn, photolum. spectra, line shape anal., conduction band to deep acceptor transition 7-46098
GaAs:Sn epilayers, MOCVD using triethylgallium and tetraethyltin, characterisation 7-22515
GaAs:Sn LPE layers, heavily doped, Mossbauer study 7-38967
GaAs:Sn(Te)(Zn) surface layers, luminesc., electrophys. parameters, effect of annealing 7-64680
GaAs:Te, annealing encapsulation props. of SiO₂, Si₃N₄ and Si_xN_yO_z films 7-8030
GaAs:Te, low press. OMVPE, Te doping, Hall effect, carrier conc., photolum. 7-21242
GaAs:Te, struct. environment of dopant, study by EXAFS in fluorescence mode. 7-59300
GaAs:Te films, flash evaporation, annealing, elec. props. 7-64373
GaAs:Te VPE, vacancy-impurity complex capture, photolum. study 7-58678
GaAs:Ti, optical spectra 7-7720
GaAs:Ti³⁺, EPR 7-45811
GaAs:V, electromodulation spectra, deep level energy positions 7-38496
GaAs:V, photocond. props. and thermally stimulated currents 7-7284
GaAs:V²⁺ (Cr²⁺) single crystals, acoustic relax. phenomena, phonon-impurity coupling, ultrasonic attenuation meas. 7-32581
GaAs:Zn, ion damage and recrystn. annealing, conversion electron EXAFS meas. 7-64821
GaAs:Zn, ion-implanted, acceptor-associated emission, selective self-optical compensation effect 7-22304
GaAs:Zn, Zn diffusion by open-tube technique 7-38260
GaAs:Zn:Si, selective double diffusion using sputtered Si masks 7-51805
GaAs:Zn epilayers, metalorganic CVD, Zn incorporation 7-63996
GaAs:Zn(C) epilayers, low pressure MOCVD growth, impurity incorporation 7-59442
GaAs/(GaAl)As LOC lasers, MOCVD growth and characts. 7-25835
GaAs/Al epitaxial contacts, MBE growth 7-22488
GaAs/Al quantum wells, MBE growth, photoluminescence and absorption linewidth studies 7-7749
GaAs/Al_{0.38}Ga_{0.62}As lattice-matched superlattice photoelectrochem. electrodes, photocurrent spectra 7-45377
GaAs/Al_{1-x}Ga_xAs modulation-doped heterostructs., 2D electron gas mobility meas. and calcs. 7-12840
GaAs/Al_{1-x}Ga_xAs, superlattices, layered electron gas plasmons, Raman scatt., Green's functions calcs. 7-17313
GaAs/Al_{1-x}Ga_xAs 3D ICs, selection rule for epitaxial growth techniques, LPE, MOVPE and MBE 7-46326
GaAs/Al_{1-x}Ga_xAs heterostruct., 2-D density of states in extreme quantum limit 7-2455
GaAs/Al_{1-x}Ga_xAs heterostructs., 2D electron gas, polaron screening effects, optical absorpt. calcs. 7-2511
GaAs/Al_{1-x}Ga_xAs heterostructure interfaces, band discontinuities, electrical meas. 7-52814
GaAs/Al_{1-x}Ga_xAs heterojunction photodiodes, band discontinuities 7-58871
GaAs/Al_{1-x}Ga_xAs heterostruct. localisation and interaction in a strong mag. field 7-64343
n-GaAs/Al_{1-x}Ga_xAs multilayer heterostructs., nonlinear high-freq. effects during vertical transport 7-2694
GaAs/Al_{1-x}Ga_xAs multi-quantum well structs., photoluminescence studies 7-3078
GaAs/Al_{1-x}Ga_xAs modulated structs., MBE growth kinetics, RHEED studies 7-7066
GaAs/Al_{1-x}Ga_xAs modulation doped heterostruct., high temp. annealing effects (Chinese) 7-12805
GaAs/Al_{1-x}Ga_xAs MBE grown superlattices, effect of barrier config. and interface quality on props. 7-52790
GaAs/Al_{1-x}Ga_xAs quantum-well bound states, valence-band offsets 7-7313
GaAs/Al_{1-x}Ga_xAs quantum wells, excitonic transitions, photocurrent spectra studies 7-7816
GaAs/Al_{1-x}Ga_xAs RIE using CCl₂F₂, selectivity 7-22920
GaAs/Al_{1-x}Ga_xAs superlattices, magnetophonon oscills. damping, polar-optical phonon contrib. calcs. 7-27391
GaAs/Al_{1-x}Ga_xAs superstructure, TEM images, composition anal. by thickness fringes, simulation 7-38353
GaAs/Al_{1-x}Ga_xAs superlattices, optical transitions involving unconfined states, barrier width depend., photolum. spectra 7-52773
n-GaAs/Al_{1-x}Ga_xAs/n⁺-GaAs capacitors, accumulation layers magnetotunnelling obs. 7-12880
GaAs/Al_{1-x}Ga_{x-1}As, tunnelling through III-V low-barrier heterostructures 7-52799
GaAs/AlAs, short period superlattices, MOCVD growth, Raman scatt., AES, X-ray diffr. 7-27386
GaAs/AlAs 1-D MBE superlattice, struct. parameters, X-ray double cryst. diffr. studies (Chinese) 7-12503
GaAs/AlAs doped quantum well waveguides, IR intersubband absorpt. 7-59192
GaAs/AlAs double barrier struct., electron transport, scatt. matrix theory 7-12822
GaAs/AlAs heterostruct., transition layer form. during LPE 7-45074
GaAs/AlAs MBE superlattice, interface struct., HREM study 7-17096
GaAs/AlAs MQW structures, life-time-free switching of luminescence by elec. fields 7-52791
GaAs/AlAs MQW structure, exciton-induced dispersion of electroluminescence at room temp. 7-53277
GaAs/AlAs quantum wells, photoexcited transport 7-2674
GaAs/AlAs quantum well structures, electroluminescence spectra and field-induced refractive index modulation 7-13135
GaAs/AlAs single quantum well heterostructures confined by short-period superlattices, photoluminesc. 7-22296

gallium arsenide continued

GaAs/AlAs superlattice, optical phonons and interface thickness, Raman scatt. studies 7-7705
GaAs/AlAs superlattices, electronic band structure, pseudopot. method calc. 7-17084
GaAs/AlAs superlattices, folded acoustical Raman line intensities 7-46050
GaAs/AlAs:Mg/GaAs tunnel structs., current transport mechanisms 7-7357
GaAs/AlAs/GaAs:Se heterojunctions, elec. behaviour, DLTS studies 7-7360
p⁺-GaAs/AlGaAs, double barrier, hot electron energy distrib. study using resonant tunnelling electron spectroscopy 7-45447
GaAs/AlGaAs 2D electron gas MBE structures, carrier mobility and density meas. 7-64321
GaAs/AlGaAs heterostructs. on Si substrate, MOCVD and MBE growth 7-7883
GaAs/AlGaAs modulation doped heterostructs., transport props. studies 7-52752
GaAs/AlGaAs multi-quantum well heterostructures, optical gain, well width depend 7-46130
GaAs/AlGaAs multiple quantum well structures, hot-carrier relaxation, femtosecond optical meas. 7-52750
GaAs/AlGaAs multiple-quantum-well structures, shallow donors, far infrared spectroscopy 7-39121
GaAs/AlGaAs pair-groove-substrate MQW laser with self-aligned stripe geometry 7-20260
GaAs/AlGaAs quantum wells, MBE growth, interface disorder studies 7-7026
GaAs/AlGaAs quantum wells, MBE growth and energy levels, photoluminescence meas. 7-7067
GaAs/AlGaAs quantum wells and double heterostruct. lasers, chemical beam epitaxy, photolum. 7-22523
GaAs/AlGaAs quantum well structures, MOCVD growth, photolum., TEM obs. 7-27929
GaAs/AlGaAs quantum wells, Monte Carlo study of hot electron transport 7-52804
GaAs/AlGaAs separate confinement heterostructure lasers, LPE prep. 7-10940
GaAs/AlGaAs single and coupled double wells, energy depend. light hole mass, photolum. spectra anal. 7-38691
GaAs/AlGaAs single heterojunction quantum well structs., photolum. characts. 7-46085
GaAs/AlGaAs single quantum wells, interrupted MBE growth and temperature-dependent optical spectra 7-46082
GaAs/AlGaAs superlattice, compositional disordering by focused ion beams 7-6695
GaAs/AlGaAs superlattices, Si implanted, compositional disordering, SIMS studies 7-12091
GaAs/AlGaAs superlattices, hydrogenic impurity ground level wave function calcs., variational procedure 7-12664
GaAs/AlGaAs superlattice heterostructures, MBE on nonplanar substrates 7-59425
GaAs/AlGaAs superlattices, valence band electronic struct., pseudopot. calcs. 7-64339
GaAs/Al(Mn)(Ag) interfaces, interactions, XPS and elec. transport studies 7-7384
GaAs/Au contacts, growth modes, AES, UPS, XPS and RHEED studies 7-21753
GaAs/Au contacts, interface morphology 7-45020
GaAs/Au-Ge/Ni ohmic contacts, ion implantation and metallisation prep. 7-22014
n-GaAs/AuGe-Ni, ohmic contact fabrication RBS anal. 7-32840
p-GaAs/AuZnNi/Ti/Au ohmic contacts, low-resistance 7-7385
GaAs/Au(Cr) Schottky barriers, hole diffusion length, photon and electron excitation studies 7-2707
GaAs/Ca,Sr_{1-x}F₂ (100) SOI structures, epitaxial GaAs films, antiphase disorder 7-52315
GaAs/CaF₂ system, MBE growth processes, growth chamber transfers 7-64902
GaAs/CdTe heterojunction, defect and impurity states, photovoltage meas. 7-17065
p-GaAs/electrolyte, photoelectron emission spectra, thermodynamic consts. 7-12856
GaAs/Ga_{1-x}Al_xAs, short period superlattices, MOCVD growth, Raman scatt., AES, X-ray diffr. 7-27386
GaAs/Ga_{1-x}Al_xAs graded interface superlattice band struct. calcs. 7-58879
GaAs/Ga_{1-x}Al_xAs multilayered structures, polariton dispersion relations 7-7125
GaAs/Ga_{1-x}Al_xAs quantum well struct., exciton linewidth calcs., polar optical phonon scatt. 7-2491
GaAs/GaAl_{1-x}As heterojunctions, anomalous quantum Hall effects 7-17085
GaAs/GaAlAs 2D electron gas, cyclotron resonance study 7-2676
GaAs/GaAlAs disordered superlattices, carrier localisation obs. 7-12818
GaAs/GaAlAs double quantum well structures, ambipolar carrier transport, optical TOF study 7-12802
GaAs/GaAlAs double-well superlattice, ultra-fast optical modulator 7-52801
GaAs/GaAlAs graded gap superlattices, high velocity vertical transport 7-52802
GaAs/GaAlAs HJFET and HJBT 7-52811
GaAs/GaAlAs heterostructure, quantized Hall resistance measurement at the National Measurement Laboratory, Australia 7-14965
GaAs/GaAlAs heterostruct. laser with monolayer superlattice, threshold currents 7-62698
GaAs/GaAlAs planar MQW structure, nonlinear coupling of guided waves 7-11106
GaAs/GaAlAs quantum-well structures, optical time-of-flight investigation 7-52800
GaAs/GaAlAs single quantum wells, steady-state photoluminescence studies 7-7750
GaAs/GaAlAs single quantum well laser, threshold current density 7-25816
GaAs/GaAlAs superlattice, optical phonons and interface thickness, Raman scatt. studies 7-7705
GaAs/GaAlAs superlattice structs., metalorganic MBE growth 7-7864
GaAs/GaAlAs TEGFET, resistance laboratory unit determ., using quantum Hall effect 7-18812

gallium arsenide continued

- GaAs/GaAlAs ultrathin layer systems, MOCVD growth and struct. props. 7-7063
- GaAs/GaAlAs/GaAs heterostructure barriers, tunnel current and electron tunnelling times with mag. field 7-52810
- GaAs/GaInAs interface, EELS near a single misfit dislocation 7-33497
- GaAs/GaPAsSb, double heterostruct., LPE, lattice matching, X-ray diffr., luminesc. 7-58884
- GaAs/Ge heterojunction interfaces, cyclic behaviour of band discontinuities 7-7365
- n-GaAs/In_{0.1}Ga_{0.9}As compositionally graded non-alloyed ohmic contacts 7-38695
- GaAs/Langmuir-Blodgett MISS devices, switching characts. 7-38751
- GaAs/LiNbO₃ struct., SAW parametric generation with light pumping 7-63934
- GaAs/metal interface microstruct. and reactions, stability and elec. props., TEM and STEM studies 7-12515
- GaAs/metal Schottky barrier diode, electrical props. 7-27426
- GaAs/n-AlGaAs MBE-grown selectively doped heterostructs., 2D electron gas, transport props. 7-21988
- GaAs/Ni Schottky barrier, current-voltage characts. under electron distrib. disturbance 7-52733
- GaAs/PTCDA rectifying junction, nondestructive semicond. props. eval. method 7-12876
- GaAs/Ta_{0.5}Cu_{0.5} amorphous thin-film diffusion barriers, thermal and structural stabilities 7-52321
- n-GaAs/Ti-Pt system, Schottky barrier height, doping depend. 7-2708
- GaAs/ZnSe interface, MOCVD grown, ZnSe film stoichiometry 7-39415
- GaAs-(Al,Ga)As double heterojunction lasers, dislocation control, electroluminescence 7-7046
- GaAs-(Al,Ga)As heterojunction barrier, tunneling current, probe pressure effect 7-45441
- GaAs-(AlGa)As heterostructure, modulation-doped, valence band mixing, and optical emission 7-7344
- GaAs-(AlGa)As heterojunctions, low temp. elec. transport props. 7-33084
- GaAs-(AlGa)As inelastic light scattering by electronic excitations in semiconductor heterostructures 7-13171
- GaAs-(Ca,Sr)F₂ heterostructure interfaces, twinning, Raman spectra 7-13148
- GaAs-Al junction, interface states, DLTS study 7-58892
- GaAs-Al Schottky barrier contacts, MBE grown, interface reactions, vacuum annealing effects 7-45022
- GaAs-Al_{0.37}Ga_{0.63}As quantum wells, photolum. studies, MBE growth, effect of interruption 7-39150
- GaAs-Al_{0.3}Ga_{0.7}As, thin single quantum well, MBE growth kinetics, normal and inverted interfaces 7-45045
- GaAs-Al_{0.44}Ga_{0.56}As quantum wells, MBE grown, tunnelling assisted photon emission, photoluminescence meas. 7-46120
- GaAs-Al_{0.4}Ga_{0.6}As, intraband recomb., luminesc. spectra anal. 7-53387
- GaAs-Al_{0.65}Ga_{0.35}As, transverse junction stripe laser, lateral heterobarrier by diffusion enhanced alloy disordering 7-10929
- GaAs-Al_{0.7}Ga_{0.3}As single quantum well, photolum., transient response to electric field, carrier lifetime 7-7757
- GaAs-Al_{0.7}Ga_{0.3}As SQW structure, photolum. switching by pulsed elec. field 7-13197
- GaAs-Al₂O₃, interface struct., dielectric film mol. beam epitaxial growth 7-38360
- GaAs-Al_{0.1}Ga_{0.9}As, multiple quantum well struct., expansion of electron-hole plasma, time-resolved Raman studies 7-22258
- GaAs-Al_{0.1}Ga_{0.9}As-AlAs, p-type quantum wells, resonant Raman scatt. 7-22259
- GaAs-Al_{0.1}Ga_{0.9}As, internal photoemission method for determ. of band offsets 7-12832
- GaAs-Al_{0.1}Ga_{0.9}As, heterojunction form. anal. 7-39436
- GaAs-Al_{0.1}Ga_{0.9}As, superlattices, carrier behaviour, mag. field effect 7-45449
- GaAs-Al_{0.1}Ga_{0.9}As, p-n junction waveguide, phase modulation, orientation depend. 7-57536
- GaAs-Al_{0.1}Ga_{0.9}As, modulation-doped quantum wells, photoabsorpt., electronic props. 7-64330
- GaAs-Al_{0.1}Ga_{0.9}As (001) superlattices, periodicity, charge density and zone folding effects 7-2685
- GaAs-Al_{0.1}Ga_{0.9}As heterojunctions, subband Landau-level spectroscopy 7-21996
- GaAs-Al_{0.1}Ga_{0.9}As heterostructures, voltage-controlled dissipation in the quantum Hall effect 7-27393
- GaAs-Al_{0.1}Ga_{0.9}As heterojunction, chemical pot. of electrons, effect of mag. field 7-38682
- GaAs-Al_{0.1}Ga_{0.9}As heterostructures, selectively doped, electron transport in strong electric fields 7-38687
- GaAs-Al_{0.1}Ga_{0.9}As junction, 2D electron gas, plasmons, radiation absorpt. and emission 7-2686
- GaAs-Al_{0.1}Ga_{0.9}As multiple quantum well, electron-phonon interaction 7-2684
- GaAs-Al_{0.1}Ga_{0.9}As multiple quantum well struct., nonequilib. LO phonons 7-12457
- GaAs-Al_{0.1}Ga_{0.9}As modulation-doped structure, parallel cond. in quantum limit 7-12808
- GaAs-Al_{0.1}Ga_{0.9}As multiple-quantum-well struct., electron heating below 1K 7-12817
- GaAs-Al_{0.1}Ga_{0.9}As MBE superlattices, low temp. photoluminesc. spectra 7-22340
- GaAs-Al_{0.1}Ga_{0.9}As MQW and superlattice structures, for IR reflectivity 7-27724
- GaAs-Al_{0.1}Ga_{0.9}As multiple heterostructures, variable angle of incidence spectroscopic ellipsometry 7-39055
- GaAs-Al_{0.1}Ga_{0.9}As MOCVD quantum well structures, time-resolved photolum. 7-53410
- GaAs-Al_{0.1}Ga_{0.9}As quantum well structure, recomb. dynamics, photolum. obs. 7-12809
- GaAs-Al_{0.1}Ga_{0.9}As quantum wells, doubly resonant LO-phonon Raman scatt. obs. 7-27722
- GaAs-Al_{0.1}Ga_{0.9}As quantum wells, homogeneously broadened 2D excitonic transitions, optical dephasing 7-45461
- GaAs-Al_{0.1}Ga_{0.9}As quantum wells, photorefectance spectra, hydrostatic press. 7-52784
- GaAs-Al_{0.1}Ga_{0.9}As quantum wells, doubly reson. LO phonon Raman scatt., photoluminescence spectra 7-53327
- GaAs-Al_{0.1}Ga_{0.9}As quantum wells, parabolic, light scatt. studies. 7-64651

gallium arsenide continued

- GaAs-Al_{0.1}Ga_{0.9}As superlattice, composition anal., electron microscopy studies 7-7028
- GaAs-Al_{0.1}Ga_{0.9}As semicond. superlattice, exciton transitions study 7-52432
- GaAs-Al_{0.1}Ga_{0.9}As superlattice, dimensionality of subbands, plasmon dispersion 7-52765
- GaAs-Al_{0.1}Ga_{0.9}As superlattices, integer quantum Hall effect at microwave frequencies 7-52820
- GaAs-Al_{0.1}Ga_{0.9}As solar cell, operation with band-gap gradient in space charge region 7-54295
- GaAs-Al_{0.1}Ga_{0.9}As superlattice, hole subbands (*Chinese*) 7-58873
- GaAs-Al_{0.1}Ga_{0.9}As superlattices, electronic and optical props., alloying and press. effects 7-64327
- GaAs-Al_{0.1}Ga_{0.9}As type I superlattices, electronic struct., tight binding calcs. 7-45475
- GaAs-Al_{0.1}Ga_{0.9}As-GaAs, multilayer struct., variable angle of incidence spectroscopic ellipsometric study 7-48830
- GaAs-Al_{0.1}Ga_{0.9}As-GaAs, perpendicular transport, tunnelling, thermionic emission studies 7-52781
- GaAs-Al_{0.1}Ga_{0.9}As-GaAs transverse magnetic field effects on tunnelling 7-58874
- GaAs-Al_{0.1}Ga_{0.9}As(In_{0.1}Ga_{0.9}As) lattice-mismatched heterojunctions, misfit strain relaxation, X-ray study 7-21718
- GaAs-AlAs, solid soln., temp.- and current-controlled LPE, theoretical model 7-39447
- GaAs-AlAs superlattices, mixing, ion implantation, rapid thermal annealing, Raman scattering 7-53355
- GaAs-AlAs Al_{0.1}Ga_{0.9}As-AlAs, multi quantum well struct., picosecond spectra. 2D excitons 7-13215
- GaAs-AlAs alternate monolayer compounds structures, MBE growth 7-21716
- GaAs-AlAs device struct., MBE prep. using In-free mounting techniques 7-3183
- GaAs-AlAs heterojunctions, asymmetrically doped, photoresponse under external bias 7-38692
- GaAs-AlAs MBE MQW struct., photoluminesc. spectra (*Chinese*) 7-52940
- GaAs-AlAs MQW structures, Ga⁺ ion implantation defects 7-44585
- GaAs-AlAs multiple quantum wells, photoconductivity, photorefectance and photolum. meas. 7-27368
- GaAs-AlAs short period superlattice, photoexcited carriers, dynamics 7-53402
- GaAs-AlAs superlattice struct., lithographic fabrication of TEM cross-sections 7-370
- GaAs-AlAs superlattices, acoustic and electronic props. 7-6730
- GaAs-AlAs superlattices, 2D excitons, magneto-optical study (*Japanese*) 7-13139
- GaAs-AlAs superlattice, energy bands, cohesive energy, form. energy, self-consistent calcs. 7-21995
- GaAs-AlAs superlattices, Se implantation, effect on compositional disordering 7-26784
- GaAs-AlAs superlattices, folded acoustic branches, leakage-induced and disorder-activated modes 7-33389
- GaAs-AlAs superlattices, confined longitudinal and transverse phonons, phonon spectrum calc. 7-38142
- GaAs-AlAs superlattices, Raman scattering finite size effects 7-39105
- GaAs-AlAs superlattices and GaAs, energy band gap calc., self-interaction correction to local density approx. 7-45144
- GaAs-AlAs superlattices, lattice dynamics 7-52220
- GaAs-AlAs ultra-thin layer semicond. superlattices, energy band and stable struct. study 7-52789
- GaAs-AlAs-GaAs heterostructure, tunnelling transmission probability, many-band pseudopotential model 7-38701
- GaAs-AlAs(GaAlAs) superlattices, Si migration during MBE growth 7-27171
- GaAs-AlAs(InAs) superlattices, lattice distortions 7-12510
- GaAs-AlGaAs, high quality MOVPE quantum wells, optical props. 7-53406
- GaAs-AlGaAs, hot carriers in quasi-2D polar semiconductors 7-12807
- GaAs-AlGaAs, MBE materials for high-speed digital heterostructure devices 7-45480
- GaAs-AlGaAs, multiple quantum well struct., 2s state, excitons, luminesc. study 7-22337
- GaAs-AlGaAs, noise, localised states, quantum Hall effect 7-45413
- GaAs-AlGaAs and GaAs-AlAs quantum well struct., resonant Raman scatt., depend. on electric field 7-7707
- GaAs-AlGaAs as IR sensor material, characts. (*Japanese*) 7-56339
- GaAs-AlGaAs DFB struct. with multiquantum well for surface emitting laser 7-10939
- GaAs-AlGaAs DH injection laser, optical and transport props., emission energy shift, threshold current meas. 7-1101
- GaAs-AlGaAs extended state superlattices, shallow donor state transition energies 7-33082
- GaAs-AlGaAs heterointerface, band offsets, overview 7-12831
- GaAs-AlGaAs heterojunctions, Be⁺, O⁺ ion implantation, impurity profiles, elec. characts. meas., SIMS, annealing 7-12813
- GaAs-AlGaAs heterojunctions, fractional quantum Hall effect of 2D electrons (*Japanese*) 7-12827
- GaAs-AlGaAs heterojunctions, energy band discontinuities, internal photoemission meas. 7-13331
- GaAs-AlGaAs heterojunction, narrow 2D electron gas, mag. depopulation of 1D subband 7-17080
- GaAs-AlGaAs heterojunctions, scanning tunnelling microscopy, potentiometry 7-52780
- GaAs-AlGaAs heterostructures, 2D electron system, collective excitations, light scatt. (*Japanese*) 7-12633
- GaAs-AlGaAs heterostruct., band discontinuity determ., DLTS, interface charge density, trap conc. 7-12833
- GaAs-AlGaAs heterostructures, energy band alignment, thermionic emission of holes 7-13319
- GaAs-AlGaAs heterostructures, equipotential distrib. in quantum Hall effect 7-21994
- GaAs-AlGaAs heterostructures, zero mag. field thermopower meas., temp. var. 7-33075
- GaAs-AlGaAs heterostructures, transport props. of 2D electron and hole gases 7-52812
- GaAs-AlGaAs heterostructures, density of states of Landau levels 7-52822
- GaAs-AlGaAs high-power laser array of phase-locking free struct. 7-62725

gallium arsenide continued

GaAs-AlGaAs large optical cavity semicond. laser arrays 7-10989
GaAs-AlGaAs MQW, intraband relaxation dynamics of photo-excited carriers 7-52691
GaAs-AlGaAs MQW electroabsorpt. modulator for non-resonant optoelectronic logic gate 7-37139
GaAs-AlGaAs MQW optical NOR gate, exciton and carrier dynamics, time resolved obs. 7-50628
GaAs-AlGaAs MQW structures, MBE grown, material parameters meas. 7-38721
GaAs-AlGaAs modulation-doped quantum wells, photolum., giant oscillations, influence of mag. fields 7-7751
GaAs-AlGaAs modulation-doped heterointerface, photoluminescence spectra studies 7-46137
GaAs-AlGaAs multiple quantum well lasers, voltage-controlled optical bistability, 2D exciton 7-5883
GaAs-AlGaAs multiple quantum wells, temp. depend. of photoreflectance 7-7753
GaAs-AlGaAs multiple quantum well structs., photolum. under high laser excitation 7-13213
GaAs-AlGaAs quantum wells, high electric field, interband transitions, photocurrent spectra obs. 7-7289
GaAs-AlGaAs quantum well heterostructures, spectroscopy of excitons and phonons 7-7706
GaAs-AlGaAs quantum wells, Stark shifts for heavy- and light-hole levels, well size depend. 7-12794
GaAs-AlGaAs quantum wells, picosecond photolum. photocurrent spectra 7-13214
GaAs-AlGaAs quantum wells, etched ultrasmall structs., photolum. excitation spectra meas. 7-22293
GaAs-AlGaAs quantum well structs., luminesc. from 2s heavy hole exciton, low temp. 7-22338
GaAs-AlGaAs quantum well heterostruct. devices, atm. press. MOVPE growth 7-22574
GaAs-AlGaAs quantum wells in waveguides, physics and appls. 7-26034
GaAs-AlGaAs quantum well heterostructures, electronic props. 7-27405
GaAs-AlGaAs quantum wells, MBE grown, photolum. study 7-27758
GaAs-AlGaAs quantum wells, hot electrons, Monte Carlo study 7-38708
GaAs-AlGaAs quantum wells, field-induced lifetime enhancements, ionisation of excitons 7-39181
GaAs-AlGaAs quantum wells, electron-phonon scatt. rate reduction by total spatial quantisation 7-45482
GaAs-AlGaAs quantum wells, FIR studies of shallow donors 7-52819
GaAs-AlGaAs SCH lasers, lasing gain and threshold current 7-31327
GaAs-AlGaAs short cavity multiquantum well lasers, dry etching, threshold current and single mode operation 7-20253
GaAs-AlGaAs superlattice, surface and interface optical phonons, EELS studies 7-6955
GaAs-AlGaAs superlattice, lattice images, high contrast TEM obs. 7-7027
GaAs-AlGaAs superlattices, band structure of holes (*Japanese*) 7-12825
GaAs-AlGaAs superlattices and superstructures, growth by metal organic CVD (*Japanese*) 7-13386
GaAs-AlGaAs superlattice defects, DLTS study 7-21854
GaAs-AlGaAs superlattices, electronic props., calc. methods 7-27406
GaAs-AlGaAs superlattice, hot electrons, real space transfer effect, photolum. studies 7-39180
GaAs-AlGaAs superlattices, magnetotransport 7-45471
GaAs-AlGaAs three-terminal cascade solar cells with selective electrodes 7-23184
GaAs-AlGaAs-GaAs heterostructure barriers, quantum tunnelling 7-52816
GaAs-AlGaAs-GaAs large area graded gap diodes, discrete resistance levels obs. at low temps. 7-52749
GaAs-AlGaAs-InGaAs strained-layer quantum well heterostructures, negative differential resistance 7-45443
GaAs-anodic oxide interfaces, annealing, As enrichment, photoluminescence, Rutherford backscattering anal. 7-21687
GaAs-Au, contacts, elec. and struct. props. 7-2711
GaAs-Au contacts, proton bombard., I-V characts. 7-7386
GaAs-Au Schottky diodes, DLTS 7-58896
GaAs-AuGeNi contacts, interface composition and barrier heights 7-58891
GaAs-AuNiGe (TiSi₂)(Au) interfaces, struct. and elec. props. 7-22013
GaAs-AuNiGe ohmic contacts, microstruct. anal. and contact resist. meas. 7-2393
GaAs-Bi, distrib. coeff. of Bi, crystn. from molten solns. 7-46428
GaAs-CaF₂, interface struct., dielectric film mol. beam epitaxial growth 7-38360
GaAs-CdTe heteroepitaxial interface, at. resolution HVEM study 7-2392
GaAs-Fe interface, simultaneous epitaxy and substrate out-diffusion 7-38355
GaAs-Ga_{0.3}Al_{0.7}As quantum wells, uniaxial stress depend. of spatially confined excitons 7-33078
GaAs-Ga_{0.7}Al_{0.3}As heterojunction, donor-acceptor radiative recomb. mechanism, photolum. spectra study 7-17083
GaAs-Ga_{1-x}Al_xAs superlattices and heterojunctions, electronic struct. 7-12821
GaAs-Ga_{1-x}Al_xAs superlattices, shallow impurity state binding energies 7-45416
GaAs-Ga_{1-x}Al_xAs, semiconductor superlattice, effective mass, mag. quantisation influence 7-52754
GaAs-Ga_{1-x}Al_xAs 2D quantum well heterostructures, magneto-impurities, mag. field and press. effects 7-52728
GaAs-Ga_{1-x}Al_xAs heterojunction, 2D electron and hole mobilities 7-7350
GaAs-Ga_{1-x}Al_xAs heterojunctions, electron energy levels 7-17082
GaAs-Ga_{1-x}Al_xAs heterojunctions, impurities, optical props. 7-27396
GaAs-Ga_{1-x}Al_xAs heterostruct., light interf. meas. of thickness and comp. during epitaxial growth 7-64026
GaAs-Ga_{1-x}Al_xAs modulation-doped quantum well, photoluminesc. studies 7-2687
GaAs-Ga_{1-x}Al_xAs multiple quantum wells, intrinsic and extrinsic photolum. 7-39183
GaAs-Ga_{1-x}Al_xAs multiple well heterostructures, far IR absorpt. by shallow donors 7-45458
GaAs-Ga_{1-x}Al_xAs quantum well, electronic states in semiconductor heterostructures 7-7307
GaAs-Ga_{1-x}Al_xAs quantum wells, interband photocond. and excitonic Landau level transitions in mag. field 7-27390

gallium arsenide continued

GaAs-Ga_{1-x}Al_xAs quantum well structures, energy spectra of donors and acceptors, spatially dependent screening effects 7-45459
GaAs-Ga_{1-x}Al_xAs quantum well, hydrogenic donor low-lying excited states, reson. states, positions and widths 7-45460
GaAs-Ga_{1-x}Al_xAs quantum well structures, electronic props. 7-52817
GaAs-Ga_{1-x}Al_xAs quantum wells, with indirect gas semicond. barriers, electron tunnelling 7-64340
GaAs-Ga_{1-x}Al_xAs superlattices, optical props. 7-3007
GaAs-Ga_{1-x}Al_xAs superlattices, Brillouin scatt. 7-3063
GaAs-Ga_{1-x}Al_xAs superlattice, phonons, acoustic and optic modes 7-12455
GaAs-Ga_{1-x}Al_xAs superlattice localised states in barrier 7-17079
GaAs-Ga_{1-x}Al_xAs superlattice, plasmon propagation across layers 7-27276
GaAs-Ga_{1-x}Al_xAs superlattices, in appl. elec. field, interband optical transitions 7-53274
GaAs-Ga_{1-x}Al_xAs undoped quantum wells, excitonic spectrum, valence band coupling and Fano resonance effects calcs. 7-27256
GaAs-Ga₂Se₃, insulating coating, stoichiometric vacancies, carrier mobility 7-52846
GaAs-Ga₂Al_{1-x} heterojunction, nonequilibrium electron-phonon scatt. 7-45457
GaAs-GaAlAs, modulation doped heterostructures, spectroscopy of 2D plasmas 7-2702
GaAs-GaAlAs, multiple quantum well struct., transient photoconductivity characterisation 7-52692
GaAs-GaAlAs, quantum well lasers, characts., comparison with GaInAs-InP 7-5891
GaAs-GaAlAs, quantum well wires and boxes, optically detected carrier confinement, cathodolum 7-39188
GaAs-GaAlAs, structures, 2D localisation and interaction effects 7-52531
GaAs-GaAlAs diode laser array, diffraction-limited emission, aperture graded-index lens external cavity 7-11005
GaAs-GaAlAs fast MQW absorber for mode locking of semicond. lasers. 7-50655
GaAs-GaAlAs heterojunction, 2D system, high order fractional quantisation obs. 7-27397
GaAs-GaAlAs heterojunctions, cyclotron resonance, screening effects 7-38706
GaAs-GaAlAs heterojunction bipolar transistors, ²⁴Mg and ⁶⁴Zn implanted profiles 7-44591
GaAs-GaAlAs heterojunctions, electron-phonon interactions, cyclotron and magnetophonon reson. meas. 7-45463
GaAs-GaAlAs heterojunctions, fractional quantum Hall effect obs. 7-52821
GaAs-GaAlAs heterostructures, dissipationless quantum Hall effect, crit. current density meas. 7-2696
GaAs-GaAlAs heterostructure, LPE grown, interface photoluminescence spectra 7-53390
GaAs-GaAlAs interface dislocations, stereographic obs. by IR light scatt. 7-32235
GaAs-GaAlAs laser, light-activated, negative resistance, characts. (*Chinese*) 7-5901
GaAs-GaAlAs MQW, optical bistability due to induced absorpt., model 7-5943
GaAs-GaAlAs MQW optical waveguides, nonlinear props. 7-37027
GaAs-GaAlAs MQW structures, exciton-exciton interaction 7-52439
GaAs-GaAlAs MQW ultrafast all-optical gate with subpicosecond ON and OFF response time 7-11026
GaAs-GaAlAs modulation doped quantum wells, hot carrier energy relax., time resolved photoluminescence spectra 7-52828
GaAs-GaAlAs monolithic laser amplifier, C³, with bistable characts. 7-25842
GaAs-GaAlAs multilayer structures, Auger depth profiles using a dual ion gun system 7-22429
GaAs-GaAlAs multiple quantum well structs., quasi-2D electron-hole plasma, band-filling effects, band gap renormalisation 7-7754
GaAs-GaAlAs multiple quantum well structs., band-gap renormalisation 7-58888
GaAs-GaAlAs passive MQW waveguide resonators, all-optical switching effects, expt. study 7-15967
GaAs-GaAlAs pnpn laser, carrier transport in heterostructure base region, carrier confinement factor in lasing region 7-43094
GaAs-GaAlAs pnpn laser diode, optical bistability and switching characts. 7-62752
GaAs-GaAlAs quantum wells, exciton binding energy, magneto-optical determ. 7-7752
GaAs-GaAlAs quantum wells, extrinsic photolum. 7-7755
GaAs-GaAlAs quantum well structs., recomb. dynamics of carriers 7-12830
GaAs-GaAlAs quantum well excitons, interface disorder and mobility 7-52808
GaAs-GaAlAs quantum wells, nonlinear optics and electro-optics 7-52809
GaAs-GaAlAs quantum wells, excitonic coupling in elec. field, photolum. spectra 7-64094
GaAs-GaAlAs quantum-box lasers, 3D, gain and threshold current density 7-10937
GaAs-GaAlAs resonant injection quantum well diodes and lasers 7-43104
GaAs-GaAlAs superlattice, electronic struct., envelope function approx., phonon limited mobility, Boltzmann eqn. 7-2698
GaAs-GaAlAs superlattice, mag. levels 7-52476
GaAs-GaAlAs superlattice structs., impact ionisation coeff., lucky drift model 7-52793
GaAs-GaAlAs superlattices, electron states in microstructs. 7-52807
GaAs-GaAlAs superlattices, density of states of Landau levels, sp. ht., magnetisation meas. 7-52823
GaAs-GaAlAs:Si modulation doped quantum wells, electron mobility, temp. depend. 7-45473
GaAs-GaAlAs-GaAs heterojunction barriers, single particle tunnelling, five level k.p theory 7-64341
GaAs-GaAs cascade solar cells, OM-VPE growth, in-situ-grown tunnel junction 7-8387
GaAs-GaAs MOVPE epitaxially-grown interfaces, anomalous C-V carrier conc. profiles, model 7-52648
GaAs-GaAs:Cr(Te), VPE grown, photoluminescence study, effect of substrate doping 7-27771

gallium arsenide continued

- GaAs-GaAs:In epitaxial layers, dislocation reduction, device performance effects 7-7354
 GaAs-GaAs-Al_xGa_{1-x}As heterostructures, photosensitivity spectra 7-64319
 GaAs-Ga_{1-x}H₂, dissolution of GaAs, crystallographic characteristics 7-12415
 GaAs-GaSb high efficiency mechanically stacked two-colour solar batteries 7-59851
 GaAs-Ge, and clean surfaces, atomic, electronic and vibronic props. 7-2307
 GaAs-Ge crystal growth on Ta₂O₅-coated Si substrates, zone melting and MOCVD 7-53579
 GaAs-Ge epitaxial interface, extended defects, geometrical character 7-6640
 GaAs-Ge heteroepitaxy on Si substrates, recrystallised Ge-on-insulator intermediate layers 7-52358
 GaAs-Ge-SiO₂, semiconductor MBE layers on Ge islands on insulator, photolum. study 7-33455
 GaAs-GeMo ohmic contact, fabrication and characts. study 7-45490
 GaAs-In_xGa_{1-x}As strained layer superlattices, photolum. microimaging of dislocations 7-27161
 GaAs-InAs, in situ contacts, MBE grown 7-45444
 GaAs-InAs strain layer modulated structures, MBE grown, cross-sectional TEM 7-7032
 GaAs-InAs superlattice, reflection electron diffraction intensity oscillation 7-7030
 GaAs-LaB₆ interfaces, thermal stability, high energy ion scattering studies 7-21680
 GaAs-Langmuir-Blodgett film MIS devices 7-55918
 GaAs-metal interfaces, Fermi level pinning 7-2714
 GaAs-Mn(V), extrinsic surface states, core level UPS study 7-2713
 GaAs-Mo Schottky diodes, elec. characts. and microstruct. study 7-22015
 GaAs-Nb, oriented Nb films, electron beam evaporation in ultrahigh vacuum 7-3175
 GaAs-Nb(NbN) Schottky barriers, interdiffusion obs. 7-58856
 GaAs-Ni interfacial reactions, contact elec. props. 7-12504
 GaAs-oxide interfaces, defect stabilised electronic properties 7-38748
 GaAs-P reacted ohmic contact charactn., effect of Mg layer 7-7387
 GaAs-Si, nucleation and growth of GaAs 7-45038
 a-GaAs-Si (100), epitaxial regrowth by excimer laser annealing, FET fabrication 7-32875
 GaAs-Si cells, photovoltaic 7-17903
 GaAs-Si heteroepitaxial interface, at. resolution HVEM study 7-2392
 GaAs-Si heteroepitaxial interface, atomic structure 7-52298
 GaAs-Si mechanically stacked multijunction solar cell 7-8402
 GaAs-Si p-n heterojunctions, interface charge polarity 7-38686
 GaAs-Si thin film solar cells, radiation damage 7-65465
 GaAs-Si₃N₄ interface, multipolar plasma deposition, high resolution electron microscopy study 7-12499
 GaAs-SiO₂N_y films, props. of insulation film as selective diffusion barrier 7-2440
 GaAs-SiON interface, plasma enhanced CVD deposited SiON, NH₃ plasma pretreatment effects 7-7874
 GaAs-thermal oxide interfacial chem. reactions, Raman spectra, AES 7-27145
 GaAs-W(W₂Si₅) Schottky contacts, electrical and metallurgical studies 7-27422
 GaAs-ZnSe, MBE growth on GaAs epilayers, nucleation and characterisation 7-45046
 GaAs₂ semicond. cluster anions, photodetachment and photofragmentation 7-36837
 GaAsAl_xAlGa_{1-x}As, 2D electron gas, edge depletion width 7-58866
 GaAs_{1-x}Al_xAs MQW, MOCVD grown, excitons, photoluminescence spectra 7-38702
 (GaAs)₂₈(AlAs)₂₄ superlattices, lattice distortion, X-ray diffr. studies 7-63974
 GaAsP, DX centres, DLTS signature anal. 7-45204
 p-GaAsP, longitudinally polarised electron bombarded, circularly polarised recomb. radiation emission 7-27807
 GaAsP, MOCVD growth, IR laser assisted grading 7-27945
 GaAsP monolithic three-junction solar cells, computer modelling 7-3672
 GaAsP on GaP solar cells in tandem with Si cells, design, fabrication 7-3674
 GaAsP terrestrial solar cells, high-efficiency concepts 7-8390
 GaAsP, V_F-T characteristics of p-n junction at low temp. (Chinese) 7-12792
 GaAsP-GaAs(P) strained-layer superlattices, MOCVD and device prep. 7-7876
 GaAs_{0.12}P_{0.88}N, Te and GaP:N, Si(Te) epitaxial layers, minority carrier lifetimes, surface and interface recombination effects 7-7424
 GaAs_{0.6}P_{0.4} degraded LEDs, origin of nonradiative centres, photocapacitance, electrolum. spectra 7-53413
 GaAs_{0.6}P_{0.4} LEDs, MOCVD growth on Si substrates 7-17438
 GaAs_{0.7}P_{0.3}GaP solar cell, high efficiency mech. stack, performance meas. 7-8401
 GaAs_{0.75}P_{0.25} solar cells, high efficiency, grown by one atmosphere MOCVD 7-3697
 GaAs_{1-x}P_xBe⁺-GaP:Be⁺ strained-layer superlattices, ion implantation doping, structural study 7-38030
 GaAs_{1-x}P_xBe⁺-GaP:Be⁺ strained layer superlattices, ion implantation doping, optical and elec. props., device appls. 7-44583
 GaAs_{1-x}P_x epitaxial structs., radiative characts., deep centres effects 7-45220
 GaAs_{1-x}P_x solid solns., indirect band gap temp. depend., electrolum. spectra studies 7-38448
 GaAs_{1-x}P_x crystals, electron-traps, DLTS study (Japanese) 7-7146
 GaAs_{1-x}P_x, EL2 level 7-21859
 GaAs_{1-x}P_xN, bound excitons, energy spectrum, optical absorpt. cross section, two-band model 7-16945
 GaAs_{1-x}P_xN, cathodoluminesc. efficiency, N-bound excitons influence 7-7768
 GaAs_{1-x}P_xN epitaxial layers, N conc. determ. 7-63989
 GaAsP_{1-x} and GaAs, energy band calculations (Chinese) 7-38446
 GaAsSb terrestrial solar cells, high-efficiency concepts 7-8390
 GaAs_{1-x}Sb_x, alloy disorder broadening of defect energy levels 7-52516
 GaAs_{1-x}Sb_x-Au Schottky barriers, I-V characts., temp. depend. 7-64344
 GaAs_{1-x}Sb_{1-y} relaxed zinc-blende lattice, EXAFS study 7-64759
 n-GaAs_{1-x}Sb_y epitaxial film, impurity distrib., cond. and Hall mobility study 7-51808

gallium arsenide continued

- GaAs(110)-Al, Schottky barrier form., effect of surface and interface kinetics 7-2668
 GaAs(110)-In, interfacial chem. reaction, UPS study 7-2276
 GaInAs, anodic oxides, growth and composition 7-39781
 GaInAs, Czochralski-grown, dislocation effects investig. 7-7261
 GaInAs epitaxial layer on InP, depth profiling and interface detection using anodic oxidation 7-45057
 GaInAs films and structures, gas source MBE, review 7-33572
 GaInAs, pn junction formation by simultaneous implantation and diffusion annealing 7-38028
 GaInAs, ternary solid soln., miscibility gap in phase diagram 7-52057
 GaInAs terrestrial solar cells, high-efficiency concepts 7-8390
 GaInAs/GaAs single quantum well pseudomorphic structs., high electron mobility meas. 7-12841
 GaInAs/InP, nonlinear optical absorpt. at room temp. 7-59169
 GaInAs/InP heterojunction, 2D electron gas nonequilib. cyclotron reson. obs. 7-12845
 GaInAs/InP heterostructures, VPE, homogeneity, mobilities 7-58882
 GaInAs/InP quantum wells, atmospheric organometallic vapour phase epitaxial growth 7-27912
 GaInAs-AlInAs heterostruct., alloyed NiGeAuAgAu ohmic contacts, charact. 7-22016
 GaInAs-AlInAs heterojunctions, parallel conduction, quantum Hall effect, hydrostatic press. 7-52764
 GaInAs-AlInAs(InP) and GaAs-AlGaAs superlattice avalanche photodiodes, impact ionisation theory appl. 7-58886
 GaInAs-GaInAsP(InP) quantum-box lasers, 3D, gain and threshold current density 7-10937
 GaInAs-InP, quantum well lasers, characts., comparison with GaAs-GaAlAs 7-5891
 GaInAs-InP, quantum well structures, adduct MOVPE, photolum., magnetoresist charactn. 7-27388
 GaInAs-InP double-barrier heterostructs., room temp. resonant tunnelling, neg. resist. effects 7-58814
 GaInAs-InP epitaxial superlattice, X-ray double crystal characterisation, rocking curves calc., computer simulation technique 7-58105
 GaInAs-InP quantum well, CESR of 2D electrons 7-38941
 GaInAs-InP quantum-box lasers, 3D, gain and threshold current density 7-10937
 GaInAs-SiO₂ system, annealing behaviour, SIMS and elec. meas. 7-38270
 Ga_{0.28}In_{0.72}As/Al_{0.28}In_{0.72}As photodiode heterostructures, atm. press. MOCVD, 2 μm, sensitivity, structural charactn. 7-27933
 Ga_{0.3}In_{0.7}As-InP strained layer superlattice, inter-band magneto-absorption 7-45998
 Ga_{0.47}In_{0.53}As, laser material, intervalence band absorpt. coeff. calc. 7-3015
 Ga_{0.47}In_{0.53}As:Be epitaxial films, ion implanted, rapid thermal and furnace annealing 7-22729
 Ga_{0.47}In_{0.53}As/Al_{0.7}In_{0.3}As superlattices, electronic struct., strain-induced elec. field effects 7-7358
 Ga_{0.47}In_{0.53}As/Al_{0.48}In_{0.52}As quantum well, interband magnetoabsorpt. meas., effective mass determ. 7-17088
 Ga_{0.47}In_{0.53}As/Al_{0.48}In_{0.52}As superlattices grown by MBE, structural charactn. 7-52792
 Ga_{0.47}In_{0.53}As/InP heterojunction, chem. beam epitaxy grown, 2D electron gas 7-12803
 Ga_{0.47}In_{0.53}As-InP heterojunction, with three electron subbands, hydrostatic press. effect 7-2695
 Ga_{0.47}In_{0.53}As-InP heterojunction, MOCVD grown, 2D hole gas 7-21992
 Ga_{0.47}In_{0.53}As-InP junction lasers, chem. beam epitaxy and performance characts. 7-20254
 Ga_{0.47}In_{0.53}As-InP quantum wells, photocurrent and dark current, multiple steps obs. 7-12796
 Ga_{0.47}In_{0.53}As-InP superlattices, MOCVD grown, room temp. excitons 7-21986
 Ga_{0.47}In_{0.53}As-InP:Fe(S), deep defect levels, photoluminescence, DLTS meas. 7-33457
 Ga_{0.47}In_{0.53}As-Si₃N₄(SiO₂) interface, elec. charact. 7-38752
 Ga_{1-x}In_xAs, high-temperature hardness 7-44675
 Ga_{1-x}In_xAs, solid soln. strengthening, mech. props. 7-32452
 Ga_{1-x}In_xAs/InP heterostructures, MOVPE, electron mobility, exciton peak, magnetotransport 7-58883
 Ga_{1-x}In_xAs-Al_{1-y}In_yAs superlattices, electronic struct., depend. on growth axis 7-64329
 Ga_{0.7}In_{0.3}As, photoluminescence line shape of excitons 7-3087
 Ga₂In_{1-x}As, heterostruct., local composition, CBED anal. 7-16529
 Ga₂In_{1-x}As, low-pressure MOVPE growth 7-7873
 Ga₂In_{1-x}As/Al_{1-x}In_xAs MBE grown superlattices, effect of barrier config. and interface quality on props. 7-52790
 Ga₂In_{1-x}As/GaAs heterostructures, low press. MOVPE, photolum., Auger profiling 7-27389
 Ga₂In_{1-x}As-GaAs strained layer superlattices, low temp. photolum. 7-53407
 GaInAsP DFB lasers, 1.3 μm, single-mode, realisation and characts. (German) 7-57357
 GaInAsP epitaxial layers, double axis X-ray diffractometry at glancing angles 7-37805
 GaInAsP epitaxial layers, X-ray double crystal characterisation, rocking curves calc., computer simulation technique 7-58105
 GaInAsP films and structures, gas source MBE, review 7-33572
 GaInAsP integrated coupled-cavity lasers, design and fabrication 7-25843
 GaInAsP strip-loaded planar waveguide for high-speed electroabsorpt. modulator 7-31449
 GaInAsP:Er semiconductor injection laser, single longitudinal model operation at 1.5 μm 7-50558
 GaInAsP/InP heterostructures, MOVPE, press. control, reactor design 7-39399
 GaInAsP/InP, planar single mode heterostructures, calculated characts. 7-31326
 GaInAsP/InP entirely VPE-grown 1.5 μm DFB lasers with low threshold currents 7-50577
 GaInAsP/InP heterojunctions, atmospheric press. MOVPE growth TEM studies 7-3196
 GaInAsP/InP heterostruct., luminescence polarisation, quantum size effects 7-13210
 GaInAsP/InP laser diodes, amplification piezoeffect 7-5889
 GaInAsP/InP stressed heterostructure lasers, lifetimes meas. 7-5890
 GaInAsP/InP surface emitting laser with flat surface circular buried heterostructure 7-31358

gallium arsenide continued

GaInAsP-InP BH laser fabrication, MOCVD epitaxy, validation by photoluminescence imaging 7-31360
GaInAsP-InP CW phase-locked semiconductor laser array, MOCVD growth 7-57351
GaInAsP-InP double heterostructure lasers, 1.5 μm , chemical beam epitaxial growth 7-57310
GaInAsP-InP etched mirror laser, passivation with angled sputtering 7-57358
GaInAs(P)-InP heterostructures, gas source MBE growth 7-53598
GaInAsP-InP lasers, single-step LPE fabrication 7-10996
GaInAsP-InP laser, anisotropic deform. influence on radiative characts., threshold, polarisation and watt-ampere charact. 7-43100
GaInAsP-InP laser, anisotropic deform. influence on radiative characts., spectral characts. 7-43101
GaInAsP-InP substrate, integrated optoelectronics, micrograting form. by HV electron beam lithography 7-31443
GaInAsP-InP surface-emitting laser with circular BH, low temp. CW operation 7-31337
Ga_{0.29}In_{0.72}As_{0.6}P_{0.4} laser material, intervalence band absorpt. coeff. calc. 7-3015
Ga_{1-x}In_yAs_{1-y}P_{1-x} effective masses and alloy disorder effects, shallow donor photocond. 7-64289
GaInAsSb, MOVPE, band gap rel. to growth temp. 7-39409
GaInAsSb/AlGaAsSb injection lasers, threshold current density reduction 7-5886
Ga_{0.85}In_{0.05}As_{0.13}Sb_{0.87}/Al_{0.4}Ga_{0.6}As_{0.035}Sb_{0.965} DH lasers, MBE grown, 2.07 μm laser oscillation 7-43096
Ga_{1-x}In_yAs_{1-y}Sb_{1-y} system, low temp. phase equil. 7-52001
GaInP-AlGaInP-GaAs heterostructures, MOVPE, Hall effect, photolum. 7-39401
GaInP₂-GaAs, current-matched and lattice-matched tandem cell efficiency 7-8403
Ga_{1-x}In_yP_{1-x}/GaAs heterojunction band discontinuity determ., C-V profiling 7-58880
Ga_{1-x}In_yP_{1-x}/GaAs (Al_{1-x}Ga_xAs) heterostructures, OMVPE, photolum., lattice matching 7-39402
Ga_{1-x}In_yP_{1-x}As_{1-y} solid solns., thermodynamic stability 7-21453
Ga_{1-x}In_yP_{1-x}As_{1-y}-InP heterojunction interfaces, electron energy band structure (*Chinese*) 7-33070
GaP/GaAsP epitaxial layers, MOCVD growth on Si, TEM and SEM 7-38416
GaP-GaAs₂P_{1-x} strained layer superlattices, photolum. microimaging of dislocations 7-27161
Ga_{1-x}P_{1-x}-GaP-Si mechanically stacked multijunction solar cells, p-n junction model 7-3668
GaP_{0.9}As_{0.8} strained-layer superlattice, low-temp. pressure-depend. magneto-optic meas. 7-12793
GaSb-GaAs photodiode, low-temp. growth by plasma process (*Japanese*) 7-7061
GaSb_{1-x}As_x 7-16529
Ge/GaAs multijunction monolithic cascade solar cells with patterned Ge tunnel junctions 7-13863
Ge-GaAs heterostructures, lattice theory, phonon propagation 7-58602
Ge_{1-x}Si_xGaAs-Si, multispectral high efficiency solar cells, semicond. selection criterion 7-8399
InGaAsP lasers, high speed design and performance 7-62700
In/GaAs:Cu/In struct., I-V characts., carrier recomb. and generation, impurity thermionic field ionisation effects (*Russian*) 7-22030
In-Ga-As-P films highly excited, ps band filling 7-43261
In-Ga-P-As, gap width, temp. depend. 7-12602
In-GaAs reactions, interfacial native oxide layer effects 7-12501
In-Pt-GaAs, heterojunction ohmic contacts, interfacial struct. 7-27155
In_{0.53}Ga_{0.47}As-InP, epitaxial single quantum wells, spectroscopy of excited states 7-46126
InAlAs/InGaAs modulation-doped heterostructs., 2D electron gas mobility meas. 7-12842
InAlAs-InGaAs resonant tunnelling barrier struct., MBE grown, NDR characts. 7-52796
In_{0.18}Al_{0.82}As-GaAs strained layer superlattices, Raman studies 7-12854
In_{1-x}Al_xAs/GaAs strained-layer superlattices, effective mass reversal 7-17078
n-InAs/GaAs SNS heterostructure weak link with Nb electrodes 7-52898
InAs/GaAs single quantum well structures grown by atomic layer epitaxy 7-22486
InAs/GaAs strained-layer superlattices, band struct., TEM, X-ray and photolum. spectra 7-38722
InAs-GaAs strained-layer superlattices, pseudo-alloy behaviour 7-7376
InAs-GaAs superlattices grown by beam-separation MBE, surface morphology and elastic strain 7-7031
InAs-GaAs superlattice, electronic props. 7-52817
InGaAlAs, props. for integrated optics/optoelectronics in optical fibre communication systems, review 7-11178
InGaAs and InGaAsP, nonuniform, dynamical X-ray rocking curve simulations 7-2408
InGaAs, CVD growth by VPE, review 7-39417
InGaAs, chemical beam epitaxial growth investig. 7-7878
InGaAs epitaxial films, MO-chloride VPE growth 7-22566
InGaAs epitaxial layers on InP substrates, ion beam crystallography 7-32863
InGaAs films, organometallic CVD growth mechanisms, adduct formation 7-33588
InGaAs, high-field autovariance coeff., diffusion coeff., and noise at 300 K 7-64260
InGaAs, ion beam damage-induced masking for photoelectrochem. etching 7-44628
InGaAs, LPE diffusion-limited growth 7-21277
InGaAs layers on InP, LPE growth 7-33608
InGaAs, MISS, common anion rule, density distrib., photoionisation 7-38765
InGaAs monolithic three-junction solar cells, computer modelling 7-3672
InGaAs, patterning using photoelectrochem. etching and focused ion beams 7-22924
InGaAs, reactive ion etching 7-65241
InGaAs strained-layer superlattices, valence-band nonparabolicity and tailorable hole masses 7-12798
InGaAs, vapour levitation epitaxy, system design and performance 7-59445
InGaAs:Si LED, electrical and luminesc. props., ultrasonically-induced changes 7-22350

gallium arsenide continued

InGaAs/GaAs GRIN SCH SL quantum well laser, MOCVD grown 7-50557
InGaAs/GaAs lattice-strained double heterojunction bipolar struct., comp., recomb. props. and device performance 7-64322
InGaAs/GaAs(InP) quantum well structures, localised states, strain depend. 7-7312
InGaAs/InAlAs MQW pin diodes, room temp. current oscillations 7-45454
InGaAs/InAlAs multiple quantum well struct., nonlinear spectroscopy 7-1236
n⁺-InGaAs/InAlAs/n⁻-InGaAs, conduction band discontinuity determ. by current-voltage meas. 7-7352
InGaAs/InP heteroepitaxial struct., misfit stress, elastic eqns., comment 7-21676
InGaAs/InP heterostructures, chloride VPE, interface form. control 7-58656
InGaAs/InP multiple quantum well waveguides, low loss, MOCVD growth 7-43358
InGaAs/InP photodiodes, MOCVD growth and characts. 7-27932
InGaAs/InP quantum wires and boxes, low temp. photoluminesc. 7-59238
InGaAs/InP single quantum wells, transport and persistent photocond. props. 7-27385
InGaAs/InP superlattices, effective mass filtering obs. 7-12799
InGaAs-GaAs, quantum well struct., p-type modulation doped, Hall effects, influence of built-in strain 7-7339
InGaAs-GaAs and GaAs-GaPAs strained layer superlattices, press. depend. magneto-optic meas. at low temp. 7-27404
InGaAs-GaAs MOVPE epitaxially-grown interfaces, anomalous C-V carrier conc. profiles, model 7-52648
InGaAs-InAlAs MQW structure, anisotropic electroabsorpt. and optical modulation 7-13134
InGaAs-InAlAs multiple quantum wells, long wavelength optical modulation, electro-optical effects 7-7677
InGaAs-InAlAs strained-layer superlattices, MBE grown, optical characterisation 7-13142
InGaAs-InP, direct growth on GaAs substrates using MOVPE 7-22510
InGaAs-InP 1.5 μm photodetectors, optical communication appls. 7-37202
InGaAs-InP heterostruct., rare earth doped, elec. and photoluminescence props. 7-46133
In_{0.2}Ga_{0.8}As-GaAs cascade solar cells, OM-VPE growth, in-situ-grown tunnel junction 7-8387
In_{0.2}Ga_{0.8}As-GaAs strained-layer superlattice, low-temp. pressure-depend. magneto-optic meas. 7-12793
In_{0.5}Ga_{0.5}As quantum wells, quantized energy levels, conduction-band nonparabolicity effects 7-2675
In_{0.52}Ga_{0.48}As/In_{0.52}(Ga_{1-x}Al_x)_{0.48}As heterostructures, conduction band edge discontinuity 7-12815
In_{0.53}Ga_{0.47}As, impact ionisation coeffs., lucky drift model including soft threshold energy 7-64258
In_{0.53}Ga_{0.47}As, LPE growth on semiinsulating InP:Fe, SEM studies 7-22591
In_{0.53}Ga_{0.47}As, surface analysis using organic-on-inorganic contact barriers 7-21991
In_{0.53}Ga_{0.47}As:Be, high dose implants, rapid thermal annealing 7-16602
In_{0.53}Ga_{0.47}As/In_{0.52}Al_{0.48}As quantum wells, lamp annealing interdiffusion and optical props. 7-12502
In_{0.53}Ga_{0.47}As-In_{0.52}Al_{0.48}As modulation-doped heterostructs., interface roughness scatt. 7-2678
In_{0.53}Ga_{0.47}As-InP, double-barrier struct., tunnelling 7-45446
In_{0.53}Ga_{0.47}As-InP, quasi-2D heterostructures, suppression of current filament by mag. field 7-52760
In_{0.53}Ga_{0.47}As-InP heterointerfaces, CV profiling 7-12834
In_{0.53}Ga_{0.47}As-InP layers, photolum. and laser emission 7-7739
In_{0.53}Ga_{0.47}As-W-InP structures, LPE growth on structured substrates 7-46353
In_{0.69}Ga_{0.31}As-InP strained-layer effective-mass superlattices 7-7378
In_{1-x}Ga_xAs, MOCVD, optical and elec. props. rel. to growth temp. 7-53613
In_{1-x}Ga_xAs-InP heterostructure APD for 1.55 μm optical fibre communication system (*Japanese*) 7-62843
InGa_{1-x}As-GaAs single-quantum-well heterostructs., pseudomorphic, optical characterisation 7-22303
InGa_{1-x}As (100)-metal interfaces, Fermi level pinning and chem. interactions 7-2712
InGa_{1-x}As, atomic displacements detection using channelled electron induced X-ray emission 7-21311
InGa_{1-x}As, atomic layer epitaxy growth, photolum., Hall meas. 7-22527
InGa_{1-x}As, gas source MBE growth 7-52361
InGa_{1-x}As, MBE growth rates, temp. dependence 7-17426
InGa_{1-x}As, magnetophonon resonance effect 7-21942
InGa_{1-x}As, photoluminescence determ. of effects due to In alloying 7-46096
InGa_{1-x}As pseudomorphic quantum well lasers, carrier collection and stimulated emission 7-10928
InGa_{1-x}As/In_{0.52}Al_{0.48}As and (InAs)_m(GaAs)_n superlattices, MBE grown, optical studies 7-13221
InGa_{1-x}As/InP heterostructures, OMVPE growth, quality, source comp., press. effect 7-39400
InGa_{1-x}As-InAl_{1-y}As superlattices, lattice-matched and lattice-mismatched, dislocation filtering 7-21671
InGa_{1-x}As-InAl_{1-y}As heterojunction, cyclotron resonance linewidth due to alloy scatt. 7-27399
InGaAsP 1.3 μm diode laser, ultra-high-speed modulation 7-5924
InGaAsP 1.5 μm DFB laser diodes, optical communication appls. 7-37202
InGaAsP 1.55 μm mode-locked laser with single-mode fibre output 7-50600
InGaAsP (001), surface, dislocation etch pits, new etchant props. 7-59699
InGaAsP BH lasers, radiative, Auger and nonradiative currents 7-57312
InGaAsP buried crescent injection lasers, differential quantum efficiency 7-25815
InGaAsP buried crescent injection lasers, low threshold 1.5 μm operation 7-43136
InGaAsP buried heterostructure lasers, polarisation, effect of stress relax. caused by repetitive temp. change 7-62690
InGaAsP constricted mesa laser, 8 Gbit/s return-to-zero modulation by gain switching 7-31366

gallium arsenide continued

- InGaAsP DFB lasers, extremely low-noise facet-reflectivity-controlled 7-31320
 InGaAsP DFB laser, phase noise and linewidth 7-31322
 InGaAsP device fabrication using HBr-H₂O etching soln. 7-46728
 InGaAsP directly modulated semicond. lasers, gain nonlinearity effects calcs. 7-20218
 InGaAsP double heterostructures for laser diodes, LPE growth, influence of P vapour ambient 7-46355
 InGaAsP epitaxial films, strain mapping by an X-ray diffraction technique 7-21786
 InGaAsP film, defect struct. and strain anal., X-ray topography 7-52344
 InGaAsP films, dense electron-hole plasmas, picosecond dynamics, acoustic phonon generation 7-45373
 InGaAsP injection lasers, mode-locked and gain-switched, timing jitter 7-11013
 InGaAsP, ion beam damage-induced masking for photoelectrochem. etching 7-44628
 InGaAsP, LPE growth on GaAs_{0.7}P_{0.3} substrate, crosshatch pattern 7-59472
 InGaAsP laser, LPE grown, effect of crystal defects on reliability 7-36960
 InGaAsP laser amplifiers, recombination, gain and bandwidth characs. 7-57334
 InGaAsP lasers, injection, photodetection props. 7-31379
 InGaAsP layers, LPE on GaAs, immiscibility region, lattice matching 7-59465
 InGaAsP layers, VPE growth, X-ray characterisation 7-21780
 InGaAsP layers on InP (001), origin of grown-in dislocations 7-38415
 InGaAsP, layers on InP, rel. lattice parameter meas., convergent beam electron diffraction 7-52371
 InGaAsP local struct., EXAFS and near-edge struct. studies 7-64006
 InGaAsP, MOVPE system, gas switching mass spectrometry 7-22526
 InGaAsP materials, OMVPE growth for long wavelength detectors and emitters 7-27931
 InGaAsP, optical gain spectra, effects of energy band struct. (Chinese) 7-59239
 InGaAsP, patterning using photoelectrochem. etching and focused ion beams 7-22924
 InGaAsP, props. for integrated optics/optoelectronics in optical fibre communication systems, review 7-11178
 InGaAsP ridge waveguide laser threshold current optimisation, simplified hybrid optical model 7-57321
 InGaAsP, spinodally decomposed, elastic relax. effects on TEM 7-52378
 InGaAsP system, transferred electron effect anal. 7-64259
 InGaAsP TM-wave injected BH laser, ps switching optical bistability 7-50629
 InGaAsP, vapour levitation epitaxy, system design and performance 7-59445
 InGaAsP wideband semicond. lasers, limitations on switching speed 7-10943
 InGaAsP/InP, semicond. superlattice heterojunction interface, SIMS anal. (Japanese) 7-2396
 InGaAsP/InP 1.3 μ m lasers grown on p-InP substrates, low threshold, high T₀ operation 7-1180
 InGaAsP/InP DFB lasers, DFB mode oscillation, temp. range 7-5910
 InGaAsP/InP double heterostructures, microcathodoluminescence studies 7-39189
 InGaAsP/InP heterostructures, carrier lifetimes and quantum efficiencies, photoluminesc. studies 7-64675
 InGaAsP/InP laser wafers, pinhole defects, identification of source 7-46356
 InGaAsP/InP multiquantum well layers, LPE, photolum., X-ray diff. 7-53640
 InGaAsP/InP multiple quantum well waveguide phase modulator 7-57531
 InGaAsP/InP superlattices, gas-source MBE grown, X-ray diff. and TEM studies 7-32839
 InGaAsP/InP:Fe buried crescent lasers with wide-bandwidth and high power 7-50560
 n-InGaAsP/p-GaAs diodes, photocurrent meas. of defect distribution 7-32851
 InGaAsP-GaAs double heterostructures, luminescence efficiency and surface recombination velocity 7-13196
 InGaAsP-InP, 1.5 μ m laser with high external quantum efficiency and controlled emission wavelength 7-57323
 InGaAsP-InP, heterolaser struct., distributed feedback conditions, luminesc. spectra anal. 7-50561
 InGaAsP-InP, integrated external cavity laser 7-36993
 InGaAsP-InP, long-wavelength components by VPE 7-46343
 InGaAsP-InP, quantum well wire, Auger recombination 7-7374
 InGaAsP-InP, solid-phase epitaxial Pd-Ge ohmic contacts 7-2706
 InGaAsP-InP bistable lasers, temp. depend. 7-5887
 InGaAsP-InP buried heterostructure lasers, internal thermal stress distrib. 7-10931
 InGaAsP-InP DFB lasers with monolithic external cavity, spectral characs. for 1.3 μ m 7-20281
 InGaAsP-InP DFB laser monolithically integrated with tunable external cavity, linewidth and FM characs. 7-57316
 InGaAsP-InP DFB laser, waveguiding props. 7-57319
 InGaAsP-InP distributed-feedback injection laser, fabrication by LPE and VPE 7-57337
 InGaAsP-InP double heterostructures, luminescence efficiency and surface recombination velocity 7-13196
 InGaAsP-InP Fabry-Perot and DFB lasers, VPE transport fabrication 7-20277
 InGaAsP-InP heterostruct. laser output characs., quantum size effect active layer thickness variation effects 7-31323
 InGaAsP-InP heterostructures, light emission and degradation characs. 7-45455
 InGaAsP-InP high power long wavelength laser diode 7-10998
 InGaAsP-InP high-performance 1.3 μ m laser structures with both facets etched 7-20259
 InGaAsP-InP laser diodes, low resist. contacts on p-side 7-20276
 InGaAsP-InP laser, ridge waveguide, threshold current anal. 7-31338
 InGaAsP-InP laser, single-mode, 1.3 μ m, analog FM 7-37002
 InGaAsP-InP laser failure causes and distrib., laboratory service life tests 7-62692
 InGaAsP-InP low-threshold separate-confinement heterostruct. laser characs. 7-31324

gallium arsenide continued

- InGaAsP-InP optical switches, carrier induced refractive index change 7-57606
 InGaAsP-InP planar surface BH lasers with hydride VPE-grown Fe-doped current blocking layers 7-20261
 InGaAsP-InP waveguides, optical parameters 7-62831
 InGaAsP-InP-ridge waveguide lasers, LPE fabricated, design and 1.5 μ m low-threshold operation 7-15897
 In_{1-x}Ga_xAs_{1-y}P_y/InP heterojunctions, MOCVD grown, spectroscopic ellipsometry study 7-39195
 In_{1-x}Ga_xAs_{1-y}P_y/InP quarter-wavelength-shifted DFB laser source for 1.55 μ m underwater optical cable system (Japanese) 7-62720
 In_{1-x}Ga_xAs_{1-y}P_y cpd. semicond. alloys, lattice and band struct. props., review (Japanese) 7-7109
 In_{1-x}Ga_xAs_{1-y}P_y/Cd on InP, activation energy of impurity 7-32942
 In_{1-x}Ga_xAs_{1-y}P_y/Te films, Fermi energy, dopant conc. depend. 7-52867
 In_{1-x}Ga_xAs_{1-y}P_y-InP quantum well, 2D electron gas, self-consistent calcs. 7-58890
 InGaAsSb/AlGaSb DH lasers, MBE grown, room-temperature 2.2 μ m operation 7-20219
 In_{1-x}Ga_{1-x}As_{1-y}Sb_{1-y}, mid-IR source and detector material 7-36964
 InP-GaAs, LPE growth on GaAs, immiscibility effects 7-39442
 InGaPAs/GaAs interface stress, Cr-related luminescence study 7-46101
 InP/GaInAs/InP heterostructures, OMVPE, high speed p-n photodiodes, photolum., Hall meas. 7-27387
 InP/InGaAs heterojunction bipolar transistors, open-tube Zn diffusion 7-44914
 InP/InGaAs near-IR detector self-calibration feasibility determ. 7-15002
 InP/InGaAsP antiresonant reflecting optical waveguides, chemical beam epitaxy and propagation losses 7-57537
 InP/InGaAsP device structures, LPE growth 7-33610
 InP-Ga_{0.47}In_{0.53}As superlattice, electron and hole impact ionisation rates 7-17076
 InP-Ga_{1-x}In_xAs_{1-y}P_y double heterostructs., device quality, growth by MOVPE 7-7877
 InP-GaInAs, 2D electron gas, persistent photoconductivity 7-33046
 InP-GaInAs planar BH lasers, OMVPE growth 7-1183
 InP-InGaAs single quantum wells, transport and persistent photoconductivity 7-38709
 Mn/GaAs interface formation on clean and oxidised (110) surfaces 7-45029
 Ni/GaAs film/surface reaction, TEM 7-39920
 Ni-AuGe-GaAs, ion beam induced phenomena 7-12166
 Ni-AuGe-GaAs, ohmic contacts, interface reactions, elec. behaviour 7-27031
 Ni-GaAs, barrier height meas., UV-ozone cleaning of GaAs (100) 7-28228
 Ni-GaAs, interphase contact and interaction 7-16880
 Ni-GaAs, lateral reactions, hot-stage TEM 7-27030
 Ni-GaAs, metallurgical reactions, heavy ion Rutherford backscattering spectrometry 7-53488
 NiTa-GaAs, phase separation, cross-sectional TEM 7-27152
 Pd/GaAs film/surface reaction, TEM 7-39920
 Pd-GaAs, metallurgical reactions, heavy ion Rutherford backscattering spectrometry 7-53488
 Pd-GaAs, phase formation sequence, morphology 7-27153
 Pt-GaAs, metallurgical reactions, heavy ion Rutherford backscattering spectrometry 7-53488
 Pt_{1-x}Si_x/n-GaAs contacts, elec. and metallurgical characs. 7-64345
 Rh/GaAs Schottky contact, correlation between solid-state reaction and electrical props. 7-58655
 Si bicrystals and thin films, grain boundaries, electronic props. 7-7172
 Si-GaAs_{0.7}P_{0.3} multijunction solar cell, solid state photovoltaic research status at SERI 7-8389
 Si-GaAsP-GaP solar cell, high efficiency mech. stack, performance meas. 7-8401
 Si₃N₄/GaAs buried interface, EXAFS studies in total reflection and dispersive modes 7-64765
 TaIr-GaAs Schottky barrier contacts 7-17102
 W-GaAs diode system, Schottky barrier degradation after high temp. annealing 7-33089
 WSi₂-GaAs interface, thermal stability 7-52302
 ZnSe/GaAs, electron beam pumped lasing action obs. 7-43093
 ZnSe-GaAs:Cr, meas. of residual stress by Cr-related luminesc. lines 7-7726

gallium compounds

- see also gallium alloys; gallium arsenide
 InGaAsP epitaxial films, X-ray diff. charactn. (Japanese) 7-63399
 InGaP/InGaAlP double heterostructure and multiquantum-well laser diodes, MBE growth and characterisation 7-62689
 -7-38565
 AgGa_{1-x}In_xS₂, solid solns., conc. depend. of band gap 7-52423
 AgGa_{1-x}In_xSe₂ thin films, evaporated, photosensitivity and optical props. study (Korean) 7-53423
 AgGaS₂, reflectivity spectra, 1.2 to 25 eV, contrib. of electronic transitions 7-46067
 AgGaSe₂, broadly tunable infrared parametric oscillator 7-11052
 AgGaSe₂ crystals, light scatt. and transparency, annealing expts. 7-3338
 AgGaSe₂, reflectivity spectra, 1.2 to 25 eV, contrib. of electronic transitions 7-46067
 AgGaSe(Te)₂, valence band struct., spin-orbit and cryst. field splittings, p-d hybridisation effects calcs. 7-27252
 AgGaX₂ (X=S,Se), low temp. reflectivity spectra 7-53366
 AlGaAs-GaAs, heterostructures, density of states of Landau levels 7-52822
 AlGaAs-GaAs DH injection laser, optical and transport props., emission energy shift, threshold current meas. 7-1101
 AlGaAs-GaAs extended state superlattices, shallow donor state transition energies 7-33082
 AlGaAs-GaAs heterojunctions, Be⁺, O⁺ ion implantation, impurity profiles, elec. characs. meas., SIMS, annealing 7-12813
 AlGaAs-GaAs heterostructures, zero mag. field thermopower meas., temp. var. 7-33075
 AlGaAs-GaAs split gate heterojunction FET, elec. resist., Hall effect, influence of electronic subband mag. depopulation 7-38740
 Al_{0.28}Ga_{0.72}As, photoluminescence half-width and intensity, temp. depend. 7-39179
 Al_{0.44}Ga_{0.56}As-GaAs quantum wells, MBE grown, tunnelling assisted photon emission, photoluminescence meas. 7-46120

gallium compounds continued

Al_{1-x}Ga_x-As-GaAs heterostructures, 2D electron space charge layers, plasmon and magnetoplasmon excitation 7-38696
Al_{1-x}Ga_x-As-GaAs layered structures, metal organic VPE grown, depth profiles, SIMS anal. 7-21684
Al_{1-x}Ga_x-As-GaAs quantum wells, doubly reson. LO phonon Raman scatt., photoluminescence spectra 7-53327
Al_{1-x}Ga_x-As-GaAs superlattices, integer quantum Hall effect at microwave frequencies 7-52820
AlGaInP, MOCVD, photolum., quantum wells, double heterostruct. laser appl. 7-39405
AlGaInP visible semicond. lasers, mesa stripe struct., MOVPE grown, 621 nm CW operation at 0°C 7-20262
AlGaInP visible semiconductor lasers grown by metalorganic vapor phase epitaxy 7-50590
Al_{1-x}Ga_x-N epitaxial layers, MOCVD, growth mechanism, Ga incorporation rate 7-39411
Al_{1-x}Ga_x-N MOVPE growth, struct. and elec. props. 7-21729
Al_{1-x}Ga_x-N, photoluminescence in the edge emission region 7-27778
Al_{0.4}Ga_{0.6}Sb-GaSb-Al_{0.4}Ga_{0.6}Sb MBE strained layer DH, optically pumped laser oscill. 1.6 to 1.8 μ m 7-5888
AlSb-GaSb superlattices, low-temp. growth by plasma process (*Japanese*) 7-7061
AlSb-GaSb superlattices, X-ray diffr. analysis 7-21047
Au/Cd stearate/n-GaP electroluminescent device struct., electron-hole recomb. luminesc., minority carrier injection mechanism 7-59260
BaGeO₃-Ga₂O₃-CaO-CaF glasses, IR transmission spectra, depend. on composition 7-3031
BaMnGaF₇, exchange interactions, mag. susceptibility meas. 7-45654
BiX₂-Ga₂X₃ complex; X=Cl, Br; struct. Raman spectra study 7-46020
Ca₃Ga₂Ge₂O₁₂:Cr³⁺ garnet, ESR and ultrasonically modulated ESR studies 7-22139
Ca₃Ga₂Ge₂-xSi_xO₁₂:Tb, cathodoluminescence, photoluminescence props. 7-53404
Ca₃(NbGa)₂Ga₃O₁₂:Nd³⁺, Nd³⁺ ions, two channels of stimulated emission 7-22285
Ca_{2-x}Nd_xGa_{2+x}Si_{1-x}O₇, Ga gehlenite, cryst. struct. and optical props. 7-16525
CdGa₂S₄, luminesc. associated with defect complexes 7-27757
CdGa₂S₄ single crystals, chemical vapour transport growth, microhardness, crack patterns 7-7833
CdGa₂S₄ single crystals, phase transforms., photoluminesc. studies 7-2171
CdGa₂(Se)₄ defect chalcopyrite struct. crystals., linear optical response, atomic core electron contrib. calcs. 7-39061
CdlGaS₄ in MSM surface-barrier structures., photovoltaic effect and SCL currents 7-52687
CdS-CuGaSe₂ solar cell fabrication 7-22047
CoGaInS₄, cpd. with FeGa₂S₄ struct., prep. and characts (*German*) 7-1984
CoGaInS₄ layer cpds., struct. and mag. props., XPS studies 7-44498
CoGaInS₄ pseudoternary layers cpds., optical props., comp. depend. studies 7-39072
Co_{0.2}Ga_{0.8}S₂ single crystals., optical props. and impurity energy levels meas. 7-13122
CsO-Nb₂O₅-Ga₂O₃ glass structure, Raman spectroscopy 7-1902
CuAl_{1-x}Ga_xSe₂, chem. transport reactions, growth and morphology 7-7830
CuGa_{1-x}In_xS₂, solid solns., conc. depend. of band gap 7-52423
CuGa_{1-x}In_xSe₂ mixed chalcopyrite local struct., K-edge EXAFS meas. 7-63574
CuGaS₂, cathodoluminescence from iodine transport method grown crystals (*Japanese*) 7-3096
CuGaSe₂ thin films, flash evaporated, optical and elec. props. 7-7417
CuGaSe₂ thin films, physical props. and photovoltaic potential 7-22047
CuGaSe₂-CdS solar cells, physical properties and photovoltaic potential of CuGaSe₂ thin films 7-12889
CuGaSe₂-ZnCdS wide bandgap solar cells for thin film tandem structs. 7-23172
CuGaSe(S)₂, valence band struct., spin-orbit and cryst. field splittings, p-d hybridisation effects calcs. 7-27252
CuGaSe₂(1-x)Te₂, solid solns., prep. and characteris. 7-21169
CuGaSbSe₂, valence band struct., spin-orbit and cryst. field splittings, p-d hybridisation effects calcs. 7-27252
CuGaTe₂ thin films, elec. cond., 100-300K 7-22042
CuIn_{1-x}Ga_xSe₂ absorber materials, electroplating prep. 7-17894
CuIn_{1-x}Ga_xSe₂, liquid-encapsulated Bridgman-Stockbarger melt growth and props. 7-59403
ErCl₃-GaCl₃-SOCl₂ system, solution viscosity 7-21500
(Fe_{0.8}Ga_{0.2})₂TiO₅ spin glass, remanent magnetization reduction, Heisenberg and Ising comparison 7-53019
Ga-In-As-P system, ternary alloys, E₁ energy gap, CPA calc. 7-58740
Ga-Se-Te, phase change optical recording, write erase characteristics 7-57491
GaAlAs-GaAs heterojunctions, fractional quantum Hall effect obs. 7-52821
GaAlAs-GaAs heterostructures, dissipationless quantum Hall effect, crit. current density meas. 7-2696
GaAlAs-GaAs modulation doped quantum wells, hot carrier energy relax., time resolved photoluminescence spectra 7-52828
GaAlAs-GaAs superlattice, electronic struct., envelope function approx., phonon limited mobility, Boltzmann eqn. 7-2698
GaAlAs-GaAs superlattice struct., dynamic SIMS profiles 7-22417
GaAlAs-GaAs superlattices, density of states of Landau levels, sp. ht., magnetisation meas. 7-52823
Ga_{1-x}Al_xAs, quantitative anal. by SIMS (*Chinese*) 7-54239
Ga_{1-x}Al_x-GaAs 2D quantum well heterostructures, magneto-impurities, mag. field and press. effects 7-52728
Ga_{1-x}Al_x-GaAs heterojunctions, impurities, optical props. 7-27396
Ga_{1-x}Al_x-GaAs multiple well heterostructures, far IR absorpt. by shallow donors 7-45458
Ga_{1-x}Al_x-GaAs quantum well structures, energy spectra of donors and acceptors, spatially dependent screening effects 7-45459
Ga_{1-x}Al_x-GaAs quantum well, hydrogenic donor low-lying excited states, reson. states, positions and widths 7-45460
Ga_{1-x}Al_x-GaAs superlattices, in appl. elec. field, interband optical transitions 7-53274
GaAlAsSb/GaSb/GaInAsSb injection double heterostructure laser, room temp. operation 7-62697
Ga_{1-x}Al_x-GaAs superlattice, exciton CW-photoluminesc., excitation intensity depend. 7-59252

gallium compounds continued

GaAlSb/GaSb (111) heterostructures, signs of misfit dislocations, X-ray topographic determ. 7-38349
Ga_{0.94}Al_{0.06}Sb/GaSb epitaxial struct., misfit dislocations anomalous visibility, Bragg geometry X-ray topograms 7-2019
Ga_{0.96}Al_{0.04}Sb layers, liq. phase epitaxial growth, elec. and photoelec. characterisation 7-39443
Ga_{1-x}Al_xSb epitaxial layers, MOCVD, morphology rel. to growth conditions 7-39408
GaAs films, changes of optical consts. stimulated by external effects, determ. 7-22362
GaAs/GaPAsSb, double heterostruct., LPE, lattice matching, X-ray diffr., luminesc. 7-58884
GaAs-AlAs double barrier heterostructures, resonant tunnelling through quantum well states 7-58870
GaAs-Ga_{1-x}H₂, dissolution of GaAs, crystallographic characteristics 7-12415
GaAs-GaSb high efficiency mechanically stacked two-colour solar batteries 7-59851
GaAs_{1-x}Al_xAs MQW, MOCVD grown, excitons, photoluminescence spectra 7-38702
GaAsP, CVD, laser selective deposition on GaAs and Si substrates 7-22546
GaAsP, DX centres, DLTS signature anal. 7-45204
p-GaAsP, longitudinally polarised electron bombarded, circularly polarised recomb. radiation emission 7-27807
GaAsP, MOCVD growth, IR laser assisted grading 7-27945
GaAsP monolithic three-junction solar cells, computer modelling 7-3672
GaAsP on GaP solar cells in tandem with Si cells, design, fabrication 7-3674
GaAsP terrestrial solar cells, high-efficiency concepts 7-8390
GaAsP, V_F-T characteristics of p-n junction at low temp. (*Chinese*) 7-12792
GaAsP-GaAs(P) strained-layer superlattices, MOCVD and device prep. 7-7876
GaAs_{0.12}P_{0.88}N, Te and GaP:N, Si(Te) epitaxial layers, minority carrier lifetimes, surface and interface recombination effects 7-7424
GaAs_{0.7}P_{0.3}-GaP solar cell, high efficiency mech. stack, performance meas. 7-8401
GaAs_{0.75}P_{0.25} solar cells, high efficiency, grown by one atmosphere MOCVD 7-3697
GaAs_{1-x}P_x:Be⁺-GaP:Be⁺ strained-layer superlattices, ion implantation doping, structural study 7-38030
GaAs_{1-x}P_x:Be⁺-GaP:Be⁺ strained layer superlattices, ion implantation doping, optical and elec. props., device appls. 7-44583
GaAs_{1-x}P_x, epitaxial structs., radiative characts., deep centres effects 7-45220
GaAs_{1-x}P_x crystals, electron-traps, DLTS study (*Japanese*) 7-7146
GaAs_{1-x}P_x, EL2 level 7-21859
GaAs_{1-x}P_x:N, cathodoluminesc. efficiency, N-bound excitons influence 7-7768
GaAs_{1-x}P_x:N epitaxial layers, N conc. determ. 7-63989
GaAsSb terrestrial solar cells, high-efficiency concepts 7-8390
GaAs_{1-x}Sb_x, alloy disorder broadening of defect energy levels 7-52516
GaAs_{1-x}Sb_x-Au Schottky barriers, I-V characts., temp. depend. 7-64344
GaBr₃, vapour phase, vibr. anal., high temp. IR spectra 7-31050
Ga(CO)₂, form. in hydrocarbon matrices, magnetic parameters, EPR and IR spectra anal. 7-19906
GaCl, isotopic derivatives, Dunham pot. for electronic ground state, microwave spectra anal. 7-31029
GaCl Raman-Stokes spectrum, intensity and band shape calcs. (*French*) 7-15606
Ga_{2-x}Fe_xO₃, precipitation in MgO-Ga₂O₃-Fe₂O₃ (*French*) 7-6798
 α -Ga₂GeO₈, tunnel structures 7-44480
Ga₄Ge₃O₁₂, tunnel structures 7-44480
Ga_{0.47}In_{0.53}As, laser material, intervalence band absorpt. coeff. calc. 7-3015
Ga_{0.47}In_{0.53}As/Al_{0.48}In_{0.52}As modulated struct., high resolution double-cryst. X-ray diffr. studies 7-7029
Ga_{0.47}In_{0.53}As-InP:Fe(S), deep defect levels, photoluminescence, DLTS meas. 7-33457
GaInAsP DFB lasers, 1.3 μ m, single-mode, realisation and characts. (*German*) 7-57357
GaInAsP films and structures, gas source MBE, review 7-33572
GaInAsP integrated coupled-cavity lasers, design and fabrication 7-25843
GaInAsP strip-loaded planar waveguide for high-speed electroabsorpt. modulator 7-31449
GaInAsP-InP heterostructures, MOVPE, press. control, reactor design 7-39399
GaInAsP-InP, planar single mode heterostructures, calculated characts. 7-31326
GaInAsP-InP entirely VPE-grown 1.5 μ m DFB lasers with low threshold currents 7-50577
GaInAsP-InP heterojunctions, atmospheric press. MOVPE growth TEM studies 7-3196
GaInAsP-InP heterostruct., luminescence polarisation, quantum size effects 7-13210
GaInAsP-InP BH laser fabrication, MOCVD epitaxy, validation by photoluminescence imaging 7-31360
GaInAsP-InP double heterostructure lasers, 1.5 μ m, chemical beam epitaxial growth 7-57310
GaInAsP-InP etched mirror laser, passivation with angled sputtering 7-57358
GaInAs(P)-InP heterostructures, gas source MBE growth 7-53598
GaInAsP-InP lasers, single-step LPE fabrication 7-10996
GaInAsP-InP surface-emitting laser with circular BH, low temp. CW operation 7-31337
Ga_{0.28}In_{0.72}As_{0.6}P_{0.4}, laser material, intervalence band absorpt. coeff. calc. 7-3015
Ga_xIn_{1-x}As_yP_{1-y}, effective masses and alloy disorder effects, shallow donor photocond. 7-64289
GaInAsSb, MOVPE, band gap rel. to growth temp. 7-39409
GaInP-AlGaInP-GaAs heterostructures, MOVPE, Hall effect, photolum. 7-39401
GaInP₂-GaAs, current-matched and lattice-matched tandem cell efficiency 7-8403
Ga_{1-x}In_xP/GaAs heterojunction band discontinuity determ., C-V profiling 7-58880
Ga_xIn_{1-x}P epitaxial layers, OMVPE, surface morphology, photolum. 7-22557

gallium compounds continued

- Ga_{1-x}In_xP layers, MOVPE, photolum., comp. and growth temp. depend. 7-39403
- n-Ga_{1-x}In_xP, light scatt. by free carriers 7-17328
- Ga_{1-x}In_xP, OMVPE growth and characterisation 7-3192
- Ga_{1-x}In_{1-x-y}P/GaAs (Al_yGa_{1-y}As) heterostructures, OMVPE, photolum., lattice matching 7-39402
- Ga_{1-x}In_xP,As_{1-y}In_y heterojunction interfaces, electron energy band structure (*Chinese*) 7-33070
- Ga_{1-x}In_xSb epitaxial layers, MOCVD, morphology rel. to growth conditions 7-39408
- n-Ga_{1-x}In_xSb:Se(S), impurity states, press. and comp. depend., Hall coeff. and elec. resist. meas. 7-2533
- GaN, band struct., pseudopotential method anal. 7-52421
- GaN crystals, polarisation props. of band-edge emission, dispersion theory appl. 7-64694
- GaN, electron-hole plasma generation 7-27358
- GaN films, epitaxial growth by reactive ion plating, elec. props. 7-3206
- GaN films, OMVPE, Hall mobilities, impurity band 7-39410
- GaN, undoped and control doped films, luminesc. studies 7-27790
- GaN, X-ray phase anal., elastic props. 7-45050
- GaN:Sb, antisite dopant incorporation, Mossbauer spectra study 7-12086
- GaN:Zn, pure and doped, electrophysical props., nonhomogeneous semiconductor model 7-27292
- GaN:Zn films, MOVPE, electron cyclotron resonance plasma excitation, low temp. growth 7-22549
- GaN:Zn(Cd), time-resolved photoluminesc. study 7-22347
- GaO, lower electronic states, SCF-X_α SW calcs. 7-30948
- Ga₂O, He I photoelectron spectra, relativistic DVM SCC X_α calcs. 7-50252
- Ga₂O₃, chem. transport in Ga₂O₃/H-Cl system 7-17401
- Ga₂O₃, chem. transport in Ga₂O₃/N-H-Cl system 7-53519
- β-Ga₂O₃, chem. transport using Cl₂ as transporting agent 7-17400
- Ga₂O₃, surface O photoactivation, struct. (*Russian*) 7-63552
- β-Ga₂O₃:Fe³⁺(Cr³⁺), zero-field splittings and site distortions 7-59119
- Ga₂O₃-CaO system, comp., structural props., X-ray diff. study 7-37942
- GaP (110), with ordered Sb overlayers, ARUPS 7-59378
- GaP and GaP:N diodes, electroluminescence, high press. effects 7-27787
- GaP anomalous photovoltage films X-ray irradiation effects studies 7-58834
- GaP, Ar⁺ irradiated, damage profile, backscattering spectra, anal. by computer program 7-64840
- GaP, band structure, polarisation-dependent angle-resolved photoemission spectroscopy 7-21814
- GaP bicrystals, potential barriers of grain boundaries 7-21976
- GaP coating for passivation of Si solar cells 7-65479
- GaP, coherent optical phonon generation and decay 7-33040
- GaP crystal, low temp. negative thermal expansion coeff. 7-6837
- GaP, deep centres in semiconductors, book 7-18510
- GaP, deep level centres at excited states, study by transient optical absorpt. spectroscopy 7-13188
- GaP, defects, optical detection of magnetic resonance studies 7-22165
- GaP electrical conductivity meas., high pressure, in diamond anvil cells at cryogenic temp. 7-56299
- GaP emitters, secondary electron energy distrib. rel. to work function 7-46256
- GaP, energy band calculations (*Chinese*) 7-38446
- GaP epitaxial layers, MOCVD growth on Si, TEM and SEM 7-38416
- GaP, epitaxial structs., radiative characs., deep centres effects 7-45220
- GaP films, MBE grown on Si, antiphase domain structures 7-64014
- GaP films, MBE growth on Si(211), defects obs. 7-58695
- GaP Films, vacuum chemical epitaxy 7-39406
- GaP finite cluster, local electronic struct., recursion method calcs. 7-2464
- GaP, floating zone melting prep., elec. props. 7-64238
- GaP, implanted with He ions and protons, microhardness rel. to damage density 7-51883
- GaP, ion-induced Auger electron emission under shadowing conditions 7-64841
- GaP LPE layers, reuse of Ga melt for LED prep., effect on electrical characs. 7-22592
- GaP, LPE macrosteps, shape of atomic steps and interface supersaturation 7-58689
- GaP MBE heteroepitaxial layers, lattice distortions, X-ray diff. and Raman studies (*Japanese*) 7-27219
- GaP, MISS, common anion rule, density distrib., photoionisation 7-38765
- GaP, microcrystals, amorphous-like Raman signals 7-53349
- GaP, neutron irradiated and as-grown, vacancy defects, positron studies 7-2012
- GaP on Si substrate, MOCVD growth and characterisation 7-27926
- GaP, phonon shifts due to temp. and pressure rise induced by a laser beam 7-2125
- GaP, phonons, ps laser induced transient dynamics 7-39113
- GaP, photoexcited plasmon-phonon modes, time-resolved Raman scatt. 7-39106
- p-GaP, powder, metal-loaded, photoinduced electron-hole pair separation 7-59770
- GaP semiconductor crystals growth using Gault process 7-46300
- GaP single crystals, high energy ion implantation, damage profiles 7-16590
- GaP single crystals, anisotropic deep centres, polarised photolum. and thermolum. studies (*Russian*) 7-21867
- GaP, single-particle excitations, dynamic correl. corrections, local density theory 7-45115
- GaP, sublattices direct resolution and identification by high-resolution TEM 7-37813
- GaP, thermo-EMF of high press. phase 7-38604
- GaP thin films, optical props., meas. by surface plasmon excitation 7-46166
- GaP, V_T-T characteristics of p-n junction at low temp. (*Chinese*) 7-12792
- GaP: Te(Zn), doping superlattices, growth and props. 7-64684
- GaP:B, internal friction temp. depend. studies 7-38112
- GaP:Cr, impurity ion-lattice coupling, reson. phonon scatt. spectra 7-58420
- GaP:Cr, optically induced changes in impurity-related absorpt. line struct. 7-17334
- GaP:Cu, 1.65 eV luminescence, optically detected mag. resonance studies 7-64547
- GaP:Fe, deep levels formed by Fe complexes 7-12657
- GaP:He⁺, implanted, swelling, strain and radiation damage 7-6694

gallium compounds continued

- GaP:Ni²⁺, absorpt. spectrum of Ni²⁺ 7-53373
- GaP:O, review 7-48201
- GaP:Pr(Nd)(Yb), IR photoluminescence of rare earth impurities 7-64692
- GaP:Zn, electron irradiation induced defects, DLTS study 7-52513
- GaP/GaAsP epitaxial layers, MOCVD growth on Si, TEM and SEM 7-38416
- GaP-electrolyte interfaces, Fourier transform IR spectroscopy 7-27124
- GaP-Ga semiconductor-liquid metal contact, transition from rectifying to ohmic operation 7-52833
- GaP-GaAs_{1-x}P_x strained layer superlattices, photolum. microimaging of dislocations 7-27161
- GaP-In semiconductor-liquid metal contact, transition from rectifying to ohmic operation 7-52833
- Ga_{1-x}P_x-GaP-Si mechanically stacked multijunction solar cells, p-n junction model 7-3668
- Ga_{0.2}As_{0.8} strained-layer superlattice, low-temp. pressure-depend. magneto-optic meas. 7-12793
- GaP(As)O(S)₄, dielec. const. meas. w.r.t. bond ionicity (*French*) 7-38988
- GaPO₄ orthophosphate crystals, hydrothermal synthesis 7-53531
- GaPSb, ternary solid soln., miscibility gap in phase diagram 7-52057
- GaP(Sb):H, vibrational excitations, impurity-host atom complexes, IR absorpt. data interpretation 7-44724
- GaS, layered, high temp. e-h liq., radiative recomb., luminesc. spectra study 7-17343
- Ga₂S₃-MnS phase diagrams, metastable phases, thermal and structural features 7-38165
- Ga₂Se_{1-x} crystals, phase transitions under press., exciton-phonon interaction 7-44785
- GaSb (110), intrinsic intergap surface state, angle-resolved photoemission 7-45423
- GaSb, band structure, polarisation-dependent angle-resolved photoemission spectroscopy 7-21814
- GaSb, crystal growth and synthesis, thermodynamics, optimisation algorithm appl. 7-16461
- GaSb high press. phase, β-Sn-type struct., pseudopot. perturbation calcs. 7-51938
- n-GaSb impurity Auger hole recomb. via deep acceptor, electron density depend. calcs. 7-38573
- GaSb, impurity doping by photonuclear reactions 7-16589
- GaSb, impurity level calcs., effective mass pseudopotential method 7-7163
- GaSb, LPE growth from Ga and Sn solns. 7-59467
- p-GaSb, low-temp. growth by plasma process (*Japanese*) 7-7061
- GaSb single crystals, intrinsic point defects and microdefects, TEM studies 7-44529
- GaSb:Gd, crystal grown by horizontal zone melting, precipitate identification 7-21462
- GaSb:Se, resist. and thermoelec. power meas. at metal-insulator transition 7-45403
- GaSb:Te(Se)(Si)(Ge) single crystals, Czochralski growth, carrier conc. rel. to dopant conc. 7-22462
- GaSb/Al_{0.5}Ga_{0.5}Sb MBE grown superlattices, effect of barrier config. and interface quality on props. 7-52790
- GaSb/AlSb single quantum wells, electroreflectance and photoluminescence studies 7-46136
- GaSb/AlSb strained-layer heterojunction valence band discontinuity, XPS core level meas. 7-21984
- GaSb/GaSb:Si (111) epitaxial structures, signs of misfit dislocations, X-ray topographic determ. 7-38349
- GaSb/InAs/GaSb quantum wells, carrier densities and mobilities, magnetotransport meas. 7-12846
- GaSb-Al interfacial chem. reactions, surface refl. Raman Scatt. study 7-2275
- GaSb-Al_{0.5}Ga_{0.5}Sb multi quantum wells, excitons, electric field effect, phototransist. spectra obs. 7-7288
- GaSb-AlSb multiple quantum well structs., size-induced direct to indirect gap transition 7-7373
- GaSb-AlSb quantum well lasers, reduction of Auger effect, 1-5 μm wavelength region 7-5893
- GaSb-AlSb quantum wells, optical transitions, obs. 7-46086
- GaSb-AlSb quantum-well structures, 2E_g transitions 7-46128
- GaSb-AlSb strained quantum well, electronic states in semiconductor heterostructures 7-7307
- GaSb-AlSb strained-layer superlattices, electronic props. 7-52817
- GaSb-based wafers, determ. of (110) and (-110) directions by etching 7-59696
- GaSb-GaAs photodiode, low-temp. growth by plasma process (*Japanese*) 7-7061
- GaSb+GaV₃Sb₅, eutectic alloys, elec. props., anisotropy 7-12717
- GaSb+V₃Ga₅, eutectic alloys, elec. props., anisotropy 7-12717
- (GaSb)_{1-x}(Ge₂)_x metastable thin film alloys, struct. phase transitions, ion-channeling studies 7-58462
- GaSb_{0.5}AlSb quantum wells, nonparabolic behaviour under hydrostatic press. 7-64328
- e-GaSe, acoustoelectronic interaction, piezoelectric effect 7-45399
- GaSe amorphous film, high field kinetics of photocurrent 7-2748
- GaSe, evidence of exciton-plasma transition in emission spectra 7-59249
- GaSe, excitons, room temp. self screening 7-45166
- GaSe, gamma irradi., photoluminescence spectra, temp. depend. 7-17336
- GaSe laminar semicond. intercalation cpds., phase equilibria and stability studies (*Russian*) 7-21409
- GaSe layer cpd., Al dopant intercalation, Auger and IR spectra studies (*Russian*) 7-32476
- GaSe, layered cryst., Raman scatt. intensities and atomic bonding 7-22257
- GaSe layered intercalated crystals, formation of electric state 7-38994
- GaSe, photoexcited localised excitons thermalisation, stacking disorder effects, photolum. study 7-27770
- GaSe, screening of excitons by free carriers, transmission, reflection and luminescence spectra 7-38460
- GaSe, single cryst. growth by I₂ vap. transport 7-17399
- GaSe single crystal, surface bending, radius of curvature determ., Berg-Barret method (*Russian*) 7-38305
- GaSe, spontaneous and stimulated photoluminescence studies 7-22315
- GaSe, subpicosecond relax., nonlinear susceptibility 7-43198
- GaSe, surface phonons, inelastic electron tunnelling spectroscopy 7-63935
- GaSe:Mn single crystals, optical props. 7-27777
- GaSe-Li, intercalated layer compounds, conc. depend. of electrode potential 7-7230

gallium compounds continued

- Ga₂Se₃ films on GaAs substrates, insulating coating, stoichiometric vacancies, carrier mobility 7-52846
 Ga₂Ta₂S₇, intercalation reactions, nucl. quadrupole interactions, TDPAC meas. 7-17245
 Ga₂₀Te₉₀, double glass transition and double stage crystn., X-ray diffr. studies 7-58157
 Ga₂Te₂In₂Se₃ solid solns., cryst. struct., X-ray powder diffr. studies 7-16526
 Ga₉Tl₃O₂S₁₃, crystal struct. investig. (*French*) 7-12000
 HgGa₂S₄-HgIn₂S₄ system, new multinary layered compound 7-53516
 HgGa₂Se₄, photocond., photoluminescence spectra, annealing and ion implantation effects 7-39152
 HgS-Ga₂S₃, phase diagram, incongruently melting compounds 7-13436
 In GaAsP lasers, high speed design and performance 7-62700
 In-Ga-As-P films highly excited, ps band filling 7-43261
 InAs/GaSb quantum well, 2D electron gas, cyclotron reson. oscills. meas. 7-38944
 InAs-GaSb superlattice dispersion relations, electronic states in semiconductor heterostructures 7-7307
 InAs-GaSb superlattices, transient photovoltaic effect 7-12764
 InAs-GaSb superlattice, band offset press. depend., magneto-optical studies 7-38698
 InAs-GaSb superlattices, band line-up under hydrostatic press. 7-52782
 InAs-GaSb superlattices, electronic props. 7-52817
 InAs-GaSb thin film heterostr., superlattice, electron transverse effective mass 7-21990
 InAsSb/GaSb n-n heterojunctions, band discontinuities, C-V and I-V meas. 7-7366
 In_{0.5}Ga_{0.5}P layers, LPE, elec. and optical props. 7-17119
 InGaAsP epilayers, MOCVD, laser appl. 7-39404
 InGaAsP transverse mode stabilized visible laser diodes fabricated by MOCVD selective growth 7-50591
 InGaAs-GaAs and GaAs-GaPAs strained layer superlattices, press. depend. magneto-optic meas. at low temp. 7-27404
 InGaAsP 1.5 μm DFB laser diodes, optical communication appls. 7-37202
 InGaAsP (001), surface, dislocation etch pits, new etchant props. 7-59699
 InGaAsP buried heterostructure lasers, polarisation, effect of stress relax. caused by repetitive temp. change 7-62690
 InGaAsP constricted mesa laser, 8 Gbit/s return-to-zero modulation by gain switching 7-31366
 InGaAsP DFB laser, phase noise and linewidth 7-31322
 InGaAsP device fabrication using HBr-H₂O etching soln. 7-46728
 InGaAsP directly modulated semicond. lasers, gain nonlinearity effects calcs. 7-20218
 InGaAsP double heterostructures for laser diodes, LPE growth, influence of P vapour ambient 7-46355
 InGaAsP epitaxial films, strain mapping by an X-ray diffraction technique 7-21786
 InGaAsP film, defect struct. and strain anal., X-ray topography 7-52344
 InGaAsP laser, LPE grown, effect of crystal defects on reliability 7-36960
 InGaAsP laser amplifiers, recombination, gain and bandwidth characts. 7-57334
 InGaAsP lasers, injection, photodetection props. 7-31379
 InGaAsP layers, LPE on GaAs, immiscibility region, lattice matching 7-59465
 InGaAsP layers, VPE growth, X-ray characterisation 7-21780
 InGaAsP layers on InP (001), origin of grown-in dislocations 7-38415
 InGaAsP local struct., EXAFS and near-edge struct. studies 7-64006
 InGaAsP, MOVPE system, gas switching mass spectrometry 7-22526
 InGaAsP materials, OMVPE growth for long wavelength detectors and emitters 7-27931
 InGaAsP, optical gain spectra, effects of energy band struct. (*Chinese*) 7-59239
 InGaAsP, patterning using photoelectrochem. etching and focused ion beams 7-22924
 InGaAsP, props. for integrated optics/optoelectronics in optical fibre communication systems, review 7-11178
 InGaAsP, spinodally decomposed, elastic relax. effects on TEM 7-52378
 InGaAsP system, transferred electron effect anal. 7-64259
 InGaAsP TM-wave injected BH laser, ps switching optical bistability 7-50629
 InGaAsP/InP, semicond. superlattice heterojunction interface, SIMS anal. (*Japanese*) 7-2396
 InGaAsP/InP multiquantum well layers, LPE, photolum., X-ray diffr. 7-53640
 InGaAsP/InP:Fe buried crescent lasers with wide-bandwidth and high power 7-50560
 n-InGaAsP/p-GaAs diodes, photocurrent meas. of defect distribution 7-32851
 InGaAsP-GaAs double heterostructures, luminescence efficiency and surface recombination velocity 7-13196
 InGaAsP-InP, integrated external cavity laser 7-36993
 InGaAsP-InP, quantum well wire, Auger recombination 7-7374
 InGaAsP-InP, solid-phase epitaxial Pd-Ge ohmic contacts 7-2706
 InGaAsP-InP DFB lasers with monolithic external cavity, spectral characts. for 1.3 μm 7-20281
 InGaAsP-InP DFB laser monolithically integrated with tunable external cavity, linewidth and FM characts. 7-57316
 InGaAsP-InP distributed-feedback injection laser, fabrication by LPE and VPE 7-57337
 InGaAsP-InP double heterostructures, luminescence efficiency and surface recombination velocity 7-13196
 InGaAsP-InP Fabry-Perot and DFB lasers, VPE transport fabrication 7-20277
 InGaAsP-InP heterostr. laser output characts., quantum size effect active layer thickness variation effects 7-31323
 InGaAsP-InP heterostructures, light emission and degradation characts. 7-45455
 InGaAsP-InP high power long wavelength laser diode 7-10998
 InGaAsP-InP laser diodes, low resist. contacts on p-side 7-20276
 InGaAsP-InP laser, ridge waveguide, threshold current anal. 7-31338
 InGaAsP-InP laser, single-mode, 1.3 μm, analog FM 7-37002
 InGaAsP-InP low-threshold separate-confinement heterostr. laser characts. 7-31324
 InGaAsP-InP optical switches, carrier induced refractive index change 7-57606

gallium compounds continued

- InGaAsP-InP planar surface BH lasers with hydride VPE-grown Fe-doped current blocking layers 7-20261
 InGaAsP-InP waveguides, optical parameters 7-62831
 InGaAsP-InP-ridge waveguide lasers, LPE fabricated, design and 1.5 μm low-threshold operation 7-15897
 In_{1-x}Ga_xAs_{1-y}P_{1-y} cpd. semicond. alloys, lattice and band struct. props., review (*Japanese*) 7-7109
 In_{1-x}Ga_xAs_{1-y}P_{1-y}:Cd on InP, activation energy of impurity 7-32942
 In_{1-x}Ga_xAs_{1-y}P_{1-y}:Te films, Fermi energy, dopant conc. depend. 7-52867
 In_{0.5}Ga_{0.5}As_{1-y}P_{1-y}InP quantum well, 2D electron gas, self-consistent calcs. 7-58890
 InGaAsSb/AlGaSb DH lasers, MBE grown, room-temperature 2.2 μm operation 7-20219
 In_{0.5}Ga_{0.5}As_{1-y}Sb_{1-y}, mid-IR source and detector material 7-36964
 InGaP-InGaAsP MQW struts., room temp. excitons 7-58745
 In_{1-x}Ga_xP solid solns., indirect band gap temp. depend., electrolum. spectra studies 7-38448
 In_{1-x}Ga_xP, epitaxial films, radiative recomb. 7-59257
 In_{1-x}Ga_xP epitaxial layers, LPE, surface morphology rel. to lattice mismatch 7-33604
 In_{0.5}Ga_{0.5}P LPE layers lattice-matched to GaAs, Hall mobility meas. and MESFET fabrication 7-7905
 InP/InGaAsP device structures, LPE growth 7-33610
 InP-Ga_{1-x}In_xAs_{1-y}P_{1-y} double heterostr., device quality, growth by MOVPE 7-7877
 K₂O-Ga₂O₃-SiO₂ glasses, Raman spectra 7-3035
 K₂O-Ga₂O₃-SiO₂-Al₂O₃-Fe₂O₃-FeO melts, struct. role of Fe³⁺, Ga³⁺, Al³⁺, Fe redox ratio 7-26635
 K₂O-Nb₂O₅-Ga₂O₃ glass structure, Raman spectroscopy 7-1902
 La₃Ga₂SiO₁₄, elastic and piezoelectric consts., temp. depend. 7-53242
 La₂S₃-La₂O₃-Ga₂O₃-Ga₂S₃ glassy and crystalline chalcogenides, EXAFS structural study 7-63481
 Li_{1-x}Ga_{1-x}Mg(Zn)_xO₄ solid solns., ionic cond. comp. depend. meas. 7-12366
 Li₂GaSe intercalation cpd., elec. resist. and Hall effect meas. 7-12719
 Li₂TiGaSe₂, ion intercalated, dark current and photocurrent relax. meas. 7-38622
 Mg₂Ga₂GeO₁₂, spineloid related cpd., cryst. struct., powder X-ray diffr. determ. 7-63564
 MgO-Ga₂O₃-Fe₂O₃ system, precipitation of Ga_{2-x}Fe_xO₃ (*French*) 7-6798
 20(NaK)₂O-xGa₂O₃-(80-x)SiO₂ glasses, elec. conductivity, mixed alkali effect 7-27001
 Na₂O-B₂O₃-Ga₂O₃-Y₂O₃ glass, porous, leaching and sintering 7-7953
 Na₂O-Ga₂O₃-SiO₂ glasses, Raman spectra 7-3035
 Na₂O-K₂O-Ga₂O₃-SiO₂ glasses, glass transform temps., mixed alkali effect 7-6793
 (PBr₄)⁺(GaBr₄)⁻ complex, mol. vibr., Raman and IR spectra anal. 7-46021
 PbF₂-GaF₃ glass films, vacuum deposition 7-64905
 PbF₂-ZnF₂-GaF₃-AlF₃-YF₃-LaF₃:Mn II, Nd III, energy transfer 7-1889
 Sb₂X₂-Ga₂X₄ complex; X=Cl, Br; struct. Raman spectra study 7-46020
 Si-GaAs_{0.9}P_{0.1} multijunction solar cell, solid state photovoltaic research status at SERI 7-8389
 Si-GaAsP-GaP solar cell, high efficiency mech. stack, performance meas. 7-8401
 TiGaS₂ crystals, photolum., magneto-optical characts. study 7-46089
 TiGaS₂, exciton states, absorpt. and refl. spectra 7-46066
 TiGaSe₂ crystals, exciton spectrum, phase transitions 7-7124
 TiGaSe₂, electric field induced photoconductivity 7-52676
 YGG:Nd waveguide laser amplifiers for fibre-optic communication 7-31359
 ZnGa₂S₆ and ZnInGaS₆, thermal stability in air 7-22914

galvanising see surface treatment

galvanoluminescence see luminescence

galvanomagnetic effects

see also Hall effect; magnetoresistance; Suhl effect; thermomagnetic effects

- Aharonov-Bohm effect, influence of electron-phonon interaction 7-21895
 conducting specimens in mag. fields, reverse-field reciprocity 7-58789
 degenerate semicond., diffusivity-mobility ratio, modified form of Einstein rel. in presence of electric and mag. field 7-45356
 electron gas, galvanomag. props., interaction effects, applied electric and mag. fields 7-52477
 graphite fibres, galvanomag. props., weak localisation and carrier interaction effects calcs. (*Russian*) 7-27347
 graphite-AsF₃ intercalation cpd., galvanomag. props. 7-58822
 metal, universal conductance fluctuations, effects of finite temp., interactions and mag. field 7-64196
 metal loop, elastic scattering causing resistive electronic behaviour 7-12690
 metallic cylinders, phase transition of Aharonov-Bohm periodicity 7-52580
 meter, core-magnet type, moving coil, flat, indicating errors caused by external mag. field (*Japanese*) 7-4873
 normal metal, Aharonov-Bohm effect, quantum coherence and transport, review 7-52559
 Onsager reciprocal relations, symmetries of magnetoconductivity tensor 7-7193
 photogalvanomagnetic effect, short-circuit current in relaxational conditions 7-52680
 quantum transport equation for electric and magnetic fields 7-52550
 semiconductor superlattices, type I, memory function and dynamic conductivity in a mag. field 7-52775
 semiconductors, electrical meas. in applied mag. fields, reverse-field reciprocity 7-58789
 semiconductors, magnetoconcentration effect, inhomogeneous mag. field 7-12743
 semiconductors, photoelectrons subjected to parallel elec. and quantising mag. fields 7-64280
 ternary calcopyrite semiconductor, gate capacitance in n-channel inversion layers, quantising mag. field 7-2733
 thermogalvanomagnetic props. of 2D two-component systems 7-64204
 thin metal wire, effect of shape of cross section 7-17015
 transverse conductivity of nondegenerate two-dimensional electrons scattered from longitudinal optical phonons in a strong magnetic field 7-21885
 two dimensional electron gas, nonlinear cond. in quantising mag. field, electron-acoustic phonon scatt. (*Russian*) 7-17004

galvanomagnetic effects continued

- AlGaAs/GaAs/AlGaAs selectively doped double heterojunction FET system, high mobility electron subband struct. studies 7-12838
 Bi band parameter temp. depend. galvanomag. coeffs. and mobility, L-hole effect calcs. 7-2461
 Cd_{0.9}Hg_{0.1}Te, galvanomag. props. after metal-insulator transition 7-52655
 GaAs, electron scattering in quantum limit 7-38552
 n-GaAs, oscillations and chaotic current fluctuations 7-64253
 GaAs short n⁺nn⁺ structs., elec. transport props. in high elec. and mag. fields 7-33084
 GaAs, space-charge layer effective mass in parallel mag. field 7-2469
 GaAs/GaAlAs/GaAs heterostructure barriers, tunnel current and electron tunnelling times with mag. field 7-52810
 GaAs-Al_{0.1}Ga_{0.9}As-GaAs transverse magnetic field effects on tunnelling 7-58874
 GaAs-AlGaAs superlattices, magnetotransport 7-45471
 GaAs-AlGaAs-GaAs heterostructure barriers, quantum tunnelling 7-52816
 Ge, carrier conc., mag. gradient effect (*Russian*) 7-17040
 p-Ge, threshold switching and microwave-induced spontaneous emission in static magnetic field 7-52707
 Hg_{0.8}Cd_{0.2}Te, low temp. hot electron energy relax. time in extreme quantum limit mag. fields 7-33035
 HgCr₂Se₄ spinel magnetic semicond., electronic struct., elec. props., defects and ferromag. anisotropy 7-38857
 InSb, impurity bands and their conductivity in strong mag. fields 7-45152
 NbSe₃, CDW magnetodynamics, complex AC cond. meas. 7-32998
 n-nP, Anderson transition in a mag. field 7-16944
 Pb_{1-x}Sn_xTe_{1-y}Se_y solid soln. single crystals., density, comp., lattice const. and galvanomag. props. (*Russian*) 7-44500
 PbTe:Ga, doping during vapour phase growth, elec. props. 7-26774
 Te (0001), conductivity of size-quantised holes, hydrostatic pressure effects 7-45428

galvanomagnetism *see electromagnetism***galvanometers**

- mirror design with optimal high resolution 7-31427

galvanothermodynamic effects *see thermodynamic effects***game theory**

- see also information theory*
 complexity of games and percolation on trees of winning strategies 7-48601
 estimation problem with unmodelled accel., soln. algorithm 7-55434
 evolutionary game theory 7-54430
 solar collector/heat exchanger system, differential game control 7-65578

gamma fission reaction *see photofission***gamma radiation** *see gamma-rays***gamma-ray absorption**

- solutions, f' problem, Mossbauer effect investig. 7-64548
²⁴Mg, 10.71 MeV bound state, γ resonant absorption 7-30363

gamma-ray angular distribution

- see also gamma-ray spectra*
 oriented nuclei, MQNMR study 7-49286
 superdeformed states in Z=66 and 68 isotopes, γ -ray energy correlations 7-49298
 (n, γ), E1 giant resonance excitation, partial cross sections in optical shell model 7-30421
¹⁰Be(γ , π^+)¹⁰Be*, recoil nuclear polarization study, γ -circular polarization asymmetry meas. 7-24969
¹²C(¹⁴N, γ X), 20, 30, 40 MeV/nucleon, gamma-ray energies, angular distrib. meas. 7-5286
¹²C(α , γ)¹⁶O, 0.94-2.84 MeV, absolute cross sections, γ -ray distrib., excitation fn. meas. 7-42037
¹²C(π , π'), 116-226 MeV, π - γ angular correlation meas., Δ -hole model predictions 7-19307
¹¹⁰Cd, angular correlation meas., gamma-transitions, multipole mixing ratio determ. 7-49314
¹⁵²Dy, quasicontinuum γ -rays from collective high-spin states, internal conversion coeff., multipolarity meas. 7-56639
¹⁶³Dy(³⁵Cl,X), 160 MeV, ¹⁶³Dy ground state band study, γ - γ coincidence, angular distn. meas. 7-56640
¹⁶³Dy(⁵⁸Ni, X), 250 MeV, ¹⁶³Dy ground state band study, γ - γ coincidence, angular distn. meas. 7-56640
¹⁹F nuclei in single-electron ions, Coulomb excited, γ -angular correls. 7-49292
⁴Fe(n,n' γ), A=54, 56, 58, gamma distrib., excited level schemes, B(E2) values 7-30419
⁶⁷Ga ¹⁵/2⁺ 3578 keV level, mag. moment meas. from ⁵⁶Fe(¹⁶O, α p) 7-35946
²³Na(p, γ)²⁴Mg, resonance strength (*Korean*) 7-24978
²⁰⁸Pb(¹⁴N, γ X), 20, 30, 40 MeV/nucleon, gamma-ray energies, angular distrib. meas. 7-5286
⁴⁵Sc(p, γ X), 2-4 MeV, gamma-ray ang. distrib., low-lying levels anal. 7-19168
¹¹⁰Sn, nuclear shape study using γ - α angular correlations 7-41891
⁸⁶Sr, yrast decay schemes, gamma-ray data and shell model calcs. 7-15198
⁴⁸Ti(α , γ), particle-gamma angular correlation meas. 7-30370
²¹³U, E2/M1 multipole mixing ratios, ang. correlations 7-19194
⁴Y, A=87-90, yrast decay schemes, gamma-ray data and shell model calcs. 7-15198
¹⁷⁰Yb, nuclear shape study using γ - α angular correlations 7-41891
⁴Zn(n,n' γ), A=64, 66, 68, 70, gamma distrib., excited level schemes, B(E2) values 7-30419
⁶⁴Zn(¹⁴N, γ X), 20, 30, 40 MeV/nucleon, gamma-ray energies, angular distrib. meas. 7-5286
⁴Zr, A=87-89, yrast decay schemes, gamma-ray data 7-15198
⁹⁶Zr(¹Li,2np)¹⁰⁰Mo, 32.5 MeV, yrast states, γ - γ coincidence meas. 7-24926

gamma-ray applications

- see also radiation therapy*
 dual energy gamma radiation system for soil water content meas., 7-23917
 Inconel welds joining dissimilar metals, radiographic evaluation 7-39828
 radioactive solution level gauging, meas. system resolving power, γ -detection 7-24741
 selective gamma-gamma method inversion probe in geophysics (*Russian*) 7-34708

gamma-ray astronomical observations

- Cas γ -1 (=4U 0115+63), transient gamma-ray source, obs. of 3.6-s. pulses at TeV energies 7-60838
 Cen A (NGC 5128) obs. at MeV gamma-ray energies 7-66754
 2CG 006-00 (=PSR 1802-23), COS B source, pulsed very high energy gamma ray emission obs. 7-66788
 2CG 195+5, γ -ray emission characts. 7-55857
 Crab Nebula, γ -ray spectral obs. 7-55857
 Cyg X-3, evidence for free precession of neutron star from obs. of 12.59 ms γ -ray pulse period 7-66649
 Cyg X-3, obs. of very-high-energy gamma rays 7-60916
 Cyg X-3, Oct. 1985 RF burst and gamma-ray event, cosmic ray shower observations 7-66790
 Geminga, search for very high energy gamma ray pulsed emission 7-55854
 GRB 830801b, burst characts. (*Russian*) 7-24241
 NGC 1275, search for γ -ray emission 7-55857
 NGC 4151, broad-band study (γ -ray to IR) 7-60791
 ρ Oph dark cloud, multi-freq. obs. 7-48024
 PSR 0531+21, search for γ -ray emission 7-55857
 PSR 0531+21 (Crab pulsar), obs. of very-high-energy gamma rays 7-60916
 Signe 2MP9 γ -ray burst expt. results (*Russian*) 7-24240
 Sun, limb flare of 1981 April 4, hard X-ray and γ -ray emissions 7-29457
 Wolf-Rayet stars, new evidence at X-ray and gamma-ray freqs., for non-thermal phenomena 7-55640

gamma-ray astronomy

- 1TeV gamma-ray telescope, design and evaluation 7-34884
 Buckland Park cosmic ray air shower array for UHE γ -ray astronomy 7-60565
 COS-B, telescope in-flight calibration of sensitivity and background behaviour of instrument 7-60539
 cosmic ray acceleration in supernova remnants, large-scale intensity variations 7-18339
 cosmic ray measurement by atmospheric Cherenkov technique 7-66470
 diffuse gamma-ray line emission, constraint on origin of mass 22 nuclei in astrophysical environments 7-35069
 Fourier transform telescope for subarcsecond imaging of solar flare X-rays and γ -rays 7-40706
 galactic halo study using γ -rays from WIMP annihilation 7-9542
 Galaxy, total gamma-ray emission (*Russian*) 7-40655
 high energy gamma-ray telescopes, source location capability 7-9376
 light curves analysis, appl. of kernel density estimators 7-47718
 M31, possibilities for detect. at γ -ray wavelengths, implications for cosmic rays 7-60782
 polarised electron-positron pairs annihilation in strong mag. fields, one-quantum annihilation cross-section 7-47674
 positron annihilation in an experimentally simulated low-density galactic environment 7-40944
 positron annihilation radiation from galactic centre 7-40943
 relativistic plasma, bremsstrahlung electron, positron and gamma-ray spectra 7-40684
 star camera and aspect determ. system for balloon-borne payloads 7-55418
 Sun, flares, X-ray and γ -ray time profiles, particle propag. effects 7-24106
 very-high-energy gamma rays from astronomical objects, obs. of Cyg X-3 and Crab pulsar 7-60916
 VHE and UHE gamma-ray studies, review 7-55856
 White Cliffs Solar Power Station VHE γ -ray instruments 7-60566
 e⁺e⁻ annihilation in interstellar H₂ gas, laboratory simulation 7-14426

gamma-ray detection and measurement

- see also gamma-ray spectrometers; radioactivity measurement*
 $4\pi\beta$ sources for $4\pi\beta$ - γ coincidence counting, thin source preparation 7-36439
 actively shielded 86 cm³ Ge detector for astron. spectra meas. 7-55857
 anticoincidence counting system, absolute activity meas. (*Korean*) 7-25329
 axial neutron distribution inertialess monitoring in reactors using triaxial gamma chambers 7-61979
 backscatter density gauges modelling 7-34716
 BGO γ -detector, interpolation method for functions of the two variables 7-36400
 bioassay procedures for radionuclides for atomic radiation workers 7-8696
 camera, electronically collimated, gas scintillation utilisation 7-65845
 coal fly ash radionuclides chemical anal. using alpha, gamma and X-ray fluorescence spectroscopy 7-23266
 complex Ge detector systems and Compton suppression spectrometers, Monte Carlo simulation 7-5530
 contaminant control in nuclear facility environment by γ -spectrometry (*Rumanian*) 7-10300
 cosmic ray measurement by atmospheric Cherenkov technique 7-66470
 DELPHI forward EM calorimeter, edge effects (*Spanish*) 7-49789
 direct discharge detector, γ -ray calcs. in output lines using Monte Carlo method (*Russian*) 7-5564
 dosimeter energy dependence 7-30713
 DOSKMF2 code for gamma radiation field meas. on high dose rate radiation equipment 7-15417
 Fourier transform telescope for subarcsecond imaging of solar flare x-rays and γ -rays 7-40706
 gamma camera for positron emission tomography, development study 7-47221
 gamma-ray skyshine calcs., effects on nuclear facility design 7-42239
 GEMS environmental monitoring system for γ -ray emissions 7-10298
 high intensity positron beam and ang. correl. expt. techniques and apparatus, Cu single cryst. data 7-42274
 high-energy gamma ray spectrometer for heavy-ioninduced experiments 7-5528
 high-pressure ionisation chamber, appl. to meas. mean neutron energy or γ -ray dose fraction in a mixed neutron- γ field 7-34280
 high-pressure ionisation chamber to meas. mean neutron energy and γ -ray dose fraction 7-34281
 in-core self-powered neutron detectors, burnout determ. of Rh emitters 7-62239
 intelligent multichannel analyzer for themeasurement of gamma spectra 7-5533
 inversion probes, new designs for prospecting (*Russian*) 7-34703

gamma-ray detection and measurement continued

- Karlsruhe 4π BaF_2 γ -detector, time-and-energy resolution of prototype crystals 7-5543
 large tapered BGO crystals, performance for 6-20 MeV photons 7-62235
 molecular fraction method for personnel radiation dose meas. 7-62096
 Mossbauer spectra meas. with high count rate 7-36425
 multichannel scintillation detector for high energy photon radiation 7-25304
 multilayer composite material for X-, γ - and β -ray detector windows 7-5570
 multiple detector CAMAC controlled system, 3 photon annihilation spectroscopy sum energy analyser, SiO_2 fine powder data 7-42435
 neutron gamma logging, rock models, min. dimensions (*Russian*) 7-34477
 peak fitting programme for γ -ray spectra measured in semicond. detectors (*Czech*) 7-62205
 photoconductor X/ γ -ray detectors and X-ray bolometers 7-10361
 plastic track detectors, gamma dose discrimination props. 7-30863
 position sensitive γ -ray detector for nuclear medicine, efficient design 7-14122
 priority switching in measurement of time spectra of gamma-gamma coincidences 7-10369
 quartz piezoelectric resonators, electron and gamma radiation dosimetry appls. 7-15416
 radioactive solution level gauging, meas. system resolving power, γ -detection 7-24741
 radioassay of Pu or Am in biological samples, low-energy photon detector 7-54819
 relative gamma intensities in decay of ^{110m}Ag , ^{133}Br , ^{182}Ta , ^{192}Ir , spectrometer calibration appl. 7-5568
 Rossendorf Research Reactor, computer-based γ -ray area monitoring system (*German*) 7-19552
 sealed radioactive check sources for liq. scintillation counters, American standards 7-36370
 SEFOR test reactor, gamma anal. of soil following decommissioning 7-30726
 single photon detectors with optically shielded wires, operation in transverse mag. fields 7-30847
 spent nuclear fuel assemblies, nondestructive burnup meas. at reprocessing plant (*Japanese*) 7-17753
 superhard photon detector using aligned single crystals 7-823
 tissue equivalent radiochromic waveguide dosimeters for X, γ and fast neutron meas. 7-34279
 TMI-2 reactor vessel, gamma scanning of primary shield cavity, results 7-42238
 WWR-SM type fuel assemblies, γ -spectrometric burn-up study method 7-49552
 γ -ray source radiation field near interface of different density material 7-36361
 n- γ radiation field dosimetry using miniature Si photodiodes 7-25262
 BaF_2 scintillators, positron lifetime meas., Ag thermal vacancy form. data 7-42434
 BeO thermoluminescent phosphor, γ and in dosimetry using electrical conductivity 7-62095
 $\text{CaF}_2\text{:Mn}$ thermoluminescent phosphor, γ and in dosimetry using electrical conductivity 7-62095
 ^{109}Cd , γ -ray emission rate meas. with well-type NaI(Tl) detector 7-25332
 ^{252}Cf radiation, phys. and biological dosimetries 7-28711
 CsF detectors, use in lifetime spectrometers for e^+e^- annihilation studies 7-5554
 ^{137}Cs decays, X- and γ -ray intensity meas. 7-61838
 $^{57}\text{FeF}_3\cdot 3\text{H}_2\text{O}$, resonance scintillators for recoilless 14.4 keV γ -quanta 7-62202
 Ge γ -detectors, correlation between deep-level parameters and energy resolution 7-15454
 Ge-NaI(Tl) anti-Compton spectrometer, on-line neutron response, γ prod. 7-5532
 $\alpha\text{-HgI}_2$ crystals, recent progress in material characterization for X- and γ -ray detectors 7-44577
 HgI_2 detector, electrical characteristics 7-49838
 HgI_2 solution-grown crystals, X-ray and γ -ray irradi. effect on elec. props., radiation detector performance 7-58838
 HgI_2 , timing techniques for γ -ray detector performance 7-49815
 ^{203}Hg decays, X- and γ -ray intensity meas. 7-61838
 $\text{K}_2^{57}\text{Fe(CN)}_6\cdot 3\text{H}_2\text{O}$, resonance scintillators for recoilless 14.4 keV γ -quanta 7-62202
 $\text{Li}_2\text{B}_4\text{O}_7\text{:Mn}$ thermoluminescent phosphor, γ and in dosimetry using electrical conductivity 7-62095
 LiF thermoluminescent dosimeter appl. in n- γ mixed field dosimetry in TRIGA reactors 7-49733
 Mg/Ar ionisation chambers used as γ -ray dosimeters in mixed neutron-photon fields, characts. 7-34282
 NaI(Tl) spectrometer, γ -ray response function, energy resolution 7-62200
 $^{23}\text{Na(p,}\gamma)^{24}\text{Mg}$, gamma-ray angular distrib. (*Korean*) 7-24978
 ^{103}Pd decay, absolute photon intensities determ. by coincidence method 7-5569
 ^{226}Ra mass-unit standard 7-48698
 ^{226}Rn determ. using activated C and high purity Ge detector 7-2827
 Si internal target of 1.3 GeV synchrotron, coherent bremsstrahlung generation and meas. 7-15434
 Si photodiodes, use for dose depth distrib. meas. in oncology 7-60092
 Xe gamma-quantum detector, position sensitive 7-36412

gamma-ray diffraction

- water, structure, quantum effects, gamma-ray diffr. obs. 7-26609
 LiBnO_3 , charactn. by γ -ray diff. 7-54061
 Si, Pendellosung intensity beat meas. with γ -radiation 7-46170
 Si surface, Mossbauer diffraction from rotating single crystal (*Russian*) 7-27071
 SrTiO_3 , 100 K phase transition charact. by high-resolution γ -ray diffraction 7-52040

gamma-ray effects

- see also biological effects of gamma-rays; radiolysis
 air, ionisation currents in cylindrical chambers 7-37778
 $\gamma\text{-Al}_2\text{O}_3\text{:Co}$, spinel phase composite, study of γ -ray irradi. effects on optical absorpt. spectra 7-46071
 calcium tartrate single crystals, dielectric props. rel. to X-ray on γ -ray irradi. 7-59161
 cellulose crystallinity, gamma radiolysis effect 7-32500
 compound semiconductors, radiation induced defects (*Japanese*) 7-21280

gamma-ray effects continued

- cycloaliphatic epoxy resin, ageing, irradiation environmental conditions effect 7-33707
 cyclohexane, α and γ induced solute fluoresc., single photon counting expts. 7-62448
 1,4-dichlorobutane radiolysis, gamma irradiation yield meas. and stable products identification 7-65333
 1,4-dichlorobutane-2 radiolysis, gamma irradiation yield meas. and stable products identification 7-65333
 3,4-diphenyl-2,5-dimethyl-2,4-hexadiene, free radicals, γ -irradiation generated, visible absorpt. and EPR spectra 7-57100
 1,2-diphenyl-3,3,4,4-tetramethylcyclobutene, free radicals, γ -irradiation generated, visible absorpt. and EPR spectra 7-57100
 Dralon fibres, gamma-irradiated, optical props. 7-39068
 elastomers, stress relax rig for use in γ -irrad. environments 7-8224
 epoxy resin, elec. props., γ -irradiation effects 7-39023
 glass, gamma-irradiated, plasma production by laser beams 7-44379
 insulating oils, gamma-ray effects on elec. props. 7-48829
 KCl, single crystal, growth of hole defects (*Russian*) 7-16628
 metal complex systems, ^{7}Be recoil implantation behaviour from $^{14}\text{C}(\gamma,\text{Na})^{7}\text{Be}$ process 7-21281
 methylmethacrylate-dimethacrylate oxymethylanthracene polymer blend, γ -irrad., recomb. luminesc. spectra anal. 7-46145
 MOS capacitors, interface state generation by ionising radiation, oxide thickness depend. 7-58900
 MOS capacitors, radiation-induced interface state generation 7-58899
 MOS structure, gamma irradi. effects, mech. stress depend. 7-58903
 multilayered devices, algorithm for dose profile calc. using personal computer 7-56877
 muscovite mica, effect of high γ -ray doses on thermal props. 7-8270
 optical fibre, single-mode, pure-silica-core, transmission characts. and reliability 7-11145
 optical fibres, radiation resistance characts. 7-11144
 organic fusion reactor coolant, radiation stability 7-62059
 paper filtration props., gamma irradiation effects 7-32499
 particle beam fusion accelerator II (PBFA II), vacuum insulator stack failure mechanisms 7-30749
 photomultiplier anode current variation obs., for continuous and pulsed gamma radiation 7-30888
 PMMA, modified, γ -ray effects, dielec. props. 7-22185
 polyethylene film, low density, elec. props. rel. to nuclear irradi., 5K 7-53232
 polyethylene films, electrical conduction, breakdown characts., effects of gamma radiation 7-27658
 polypropylene-polyethylene blends, γ -irrad., mech. and thermal props. 7-21137
 polythiophene, radiation-induced doping, elec. and ESR studies 7-38545
 polynylidene fluoride, Form I, ferroelectric switching characts., microdomain nucleation and growth model 7-22197
 PTFE, amorphous and cryst., irradiated, thermal characts. (*Russian*) 7-6681
 PTFE-polypropylene copolymer soln., γ -irrad. effects 7-63658
 PVC-thermoplastic copolyester elastomer blends, γ -irrad., mech. props., fractography 7-21317
 quartz:Al, static magnetisation of Al-O^- centres, electric field effects 7-38900
 α -quartz, synthetic, defects 7-63603
 quartz ceramic reflectors, γ -irrad. effects on Nd:YAG laser energy characts. 7-50575
 quartz crystal resonators radiation sensitivity with different Al impurity content 7-58335
 radioactive waste, gamma radiation effects on Climax Stock and Westerly granite 7-19538
 semiconductors, impurity doping by photonuclear reactions 7-16589
 silanopentyl radical formation in γ -irradiated silanopentanes at 77K (*Japanese*) 7-38943
 silica glass optical fibres, γ -irradiated and H_2 treated, 1.52 μm absorption band 7-37145
 soil, photon attenuation, particle size effects 7-21279
 steel, austenitic stainless, corrosion, γ -radiation effect 7-28173
 styrene-butadiene rubber, C-black loaded, elec. props., effect of gamma irradi., dosimetry appls. 7-33006
 TGS crystals, paraelec. phase, gamma irradiated, nonlinear dielec. props. studies 7-53214
 triglycine selenate crystals, dielectric props. at high hydrostatic press. 7-7631
 vinyl pyrrolidone copolymers, highly swollen hydrogels preparation 7-21073
 Al, γ -ray attenuation coeff. obs. incorporating detector resolution 7-63656
 Al_2O_3 , thermoluminescence from F and F^+ centres (*Korean*) 7-27795
 As_2S_3 , vitreous, γ -irradiated, EPR of radiation-stimulated paramag. centres (*Russian*) 7-2929
 Au-Al interfaces, dose profiles for 100 to 1250 keV photons, ONETRAN calcs. 7-56874
 BaF_2 crystals, γ -irrad., optical absorpt. 7-58275
 $\text{BaO-B}_2\text{O}_3$ glass, containing Fe_2O_3 , heat treatment and γ -irrad., IR study 7-16627
 $\text{BaO-B}_2\text{O}_3\text{-Fe}_2\text{O}_3$ glasses, γ -irradiated and heat treated, elec. conductivity and crystn. 7-21510
 $\text{Ba(PO}_3)_2\text{-LiF}$ gamma irradiated activated glasses, optical absorpt. and ESR spectra corrls. 7-13030
 $\text{Bi}_2\text{Ge}_3\text{O}_{12}$ crystals, positron annihilation parameters determ., gamma irradi. effects 7-46223
 $\text{CaF}_2\text{:Mn}$, gamma irradiation-induced defects, absorpt. and excitation spectra studies 7-26801
 $\text{CaF}_2\text{:Nd}$ single crystals, ionic conductivity study 7-21521
 $\text{CaSO}_4\text{:Dy}$, gamma radiation damage on thermolum. 7-38059
 $\text{n-Cd,Hg}_{1-x}\text{Te}$, single crystal, γ -irradiation, electrophysical props. in strong elec. field 7-7251
 CdIn_2S_4 optical props., annealing and γ -ray irradiation effects 7-13211
 $\text{CdAl}_2\text{O}_4\text{-P}_2\text{O}_5$ glasses, EPR spectra, synthesis effects 7-64530
 CdS:Gd , Cl film solar cells, gamma radiation effects on photoelectric properties 7-34032
 $\text{Co}_{33}\text{Fe}_2\text{Si}_{17}\text{Ge}_{15}\text{B}_{25}$, amorphous alloy, struct. changes after γ -irrad. (*Russian*) 7-58336
 CsH_2AsO_4 and $\text{CsH}_{2x}\text{D}_{2(1-x)}\text{AsO}_4$, ferroelectric, optical props., radiation effects 7-33406
 CsI , cryst., γ -irrad., acoustic nucl. reson. (*Russian*) 7-22152
 CsI:Ti , γ -ray radiation damage, recovery 7-63657
 Cu, gamma-irradiated, anomalous effect of small doses 7-12151

gamma-ray effects continued

- Cu- γ -ray attenuation coeff. obs. incorporating detector resolution 7-63656
 $\text{Fe}_2\text{O}_3/\text{Ti}(\text{Sn},\text{Nb})$, γ -ray damage, impurity effects on annealing 7-6679
 GaAs device structures, γ -ray effects, surface generation-recombination processes 7-64349
 GaSe, gamma irradi., photoluminescence spectra, temp. depend. 7-17336
 Ge, ionisation-stimulated annealing of Frenkel pairs under electron or gamma irradiation 7-38061
 GeO₂, γ -irrad., majority carrier mobility meas. 7-27334
 GeO₂ glass, gamma-ray irradi., defect centres, ESR studies 7-6678
 HgI₂ solution-grown crystals, X-ray and γ -ray irradi. effect on elec. props., radiation detector performance 7-58838
 InGaAsP-InP heterostructures, light emission and degradation characts. 7-45455
 p-InP, γ -ray irradiated low temp., nonradiative-recomb.-enhanced defect struct. transformation 7-2062
 KBr microcrystalline powders, interstitial cluster stability 7-32485
 KCl, γ -irradiated, influence of plastic deformation on colour centre conc. 7-44538
 KCl X-ray and γ -irrad., F-centre destruction owing to subsequent laser light excitation, luminesc. spectral characts. 7-27772
 KCl:Ca, γ -irrad., Z₁-centre growth, effect of dislocations, thermolum. study 7-32487
 KCl:Ca, γ -irrad., Z₁ colour centres, mech. bleaching form. 7-6620
 KCl(Br) γ -irrad. single crystals, piezolum. and thermolum. spectral shift meas. 7-27796
 KH₂PO₄ and KH₂D₂(1-x)PO₄, ferroelectric, optical props., radiation effects 7-33406
 KNO₃, dielectric props., effect of X-ray or γ -ray irradiation 7-53215
 LiF crystals with F₂[•] centres, inactive losses, investig. of mechanism 7-3072
 LiF, γ -irrad., positron annihilation, temp. depend. 7-3110
 LiF, γ -irradiated, influence of plastic deformation on colour centre conc. 7-44538
 LiF γ -irradiated crystals, F-centres, positron annihilation and optical absorpt. meas. 7-44542
 LiIO₃, ferroelectric, optical props., radiation effects 7-33406
 LiNbO₃, γ -irradiated, elastic and piezoelectric props. 7-45935
 LiNbO₃:Fe, and undoped crystals, decay of γ -centres 7-7658
 LiNbO₃:Ni(Cu), γ -irradiated, ESR spectra of impurity centres 7-17218
 MgO:Fe, gamma irradi., thermoluminescence and TSC studies 7-33464
 MgO:Fe, gamma-ray and electron radiation-induced conductivity 7-33015
 MoO₃, amorphous films, X- and γ -irradiated, color center form. 7-44541
 NaCl positron annihilation parameters, irradi. effects determ. 7-46224
 NaCl, X-ray and γ -irrad., F-centre destruction owing to subsequent laser light excitation, luminesc. spectral characts. 7-27772
 NaCl:Eu²⁺, gamma irradi., optical absorpt. spectra, TSC meas. 7-58337
 NaCl:Eu²⁺ crystals, γ -irradiated, colourability 7-12062
 NaCl:Eu²⁺ crystals, mechanical strength, dopant distrib. and γ -irrad. effects study 7-26800
 NaCl:OH⁻, Cd²⁺ single cryst., gamma irradi., electronic and IR spectra 7-53320
 NaF:OH⁻, X⁺, X=impurities, vibr., radiation effects, IR spectra 7-53321
 NbTi alloy, neutron and γ -ray irradi. effects near supercond. transition temp. (Russian) 7-33119
 Ni and Ni-Cu, gamma-irradiated, point defect migration 7-6893
 Ni-Cu, heterodiffusion, effect of γ -rad. (Russian) 7-44617
 PLZT ferroelectric ceramics, gamma, electron and neutron irradi. effects study 7-6677
 PLZT, transparent ferroelectric ceramic, irradiation effects 7-59157
 Pb, buildup factors and spectra for point isotropic γ -sources near the K-edge 7-36301
 Pb, γ -ray attenuation coeff. obs. incorporating detector resolution 7-63656
 Pb(Sr_{0.5}Nb_{0.5})O₃ ferroelectric ceramics, gamma, electron and neutron irradi. effects study 7-6677
 Pb(Sr_{0.5}Nb_{0.5})O₃, transparent ferroelectric ceramic, irradiation effects 7-59157
 n-Si, gamma-irrad., intrinsic defects, Hall effect and elec. cond. meas. 7-6615
 p-Si, gamma-ray irradi., recombination centres, p-n junction meas. 7-37985
 Si, ionisation-stimulated annealing of Frenkel pairs under electron or gamma irradiation 7-38061
 Si, isoelectronic structurally bistable defect configs. study 7-16546
 Si p⁺-i-n⁺ diodes, gamma irradi., capacitance detected mag. resonance 7-17243
 Si, radiation defect thermal ionisation, effect of dislocations on activation energy 7-6680
 Si, recombination channels, dislocations interaction with point defects, luminesc. study 7-46094
 Si, ribbons, γ -irradiated, defect form., photoluminesc. investig. 7-46147
 Si single-crystal, gamma-ray effects on micro defects and electrophysical props. 7-16629
 Si, transmutation-doped, carrier recomb. props. at gamma-irrad. defects, transport meas. 7-38575
 a-Si:H, glow discharge deposited, light soaking effects 7-52872
 a-Si:H, light soaked, dangling bond creation 7-12150
 a-Si:H films, electronic props., effects of γ -irradiation 7-38584
 Si:O, γ -irrad., majority carrier mobility meas. 7-27334
 Si/SiO₂/TiSi₂(WSi₂) MOS capacitors, radiation-induced interface traps 7-58897
 Si-SiO₂ interface, study using variable energy positron beam 7-38063
 Si-SiO₂-Si layered struct., dose calcs. for X-ray and X-ray irradi. 7-58333
 SiO₂, amorphous, densified, O diffusion kinetics, annealing, gamma-ray effects 7-52127
 SiO₂, γ -ray induced defect centres, thermal bleaching 7-63659
 SiO₂, laser-induced breakdown, radiation induced defects 7-12147
 SiO₂ quartz glass, γ -irradiated, phase relax. of E' centres, spin echo study 7-38938
 SiO₂ silica glasses, doped, radiation-induced defect centres, EPR and optical studies 7-13033
 SiO₂ sol-gel glass structures, effects of water content of gels, EPR study 7-6526
 SiO₂ sol-gel glasses, structure, paramagnetic defect centres 7-11945
 SiO₂-GeO₂ optical fibre, drawing- and radiation-induced paramagnetic defects 7-11084

gamma-ray effects continued

- SiO₂-GeO₂ sol-gel glasses, paramagnetic states 7-13035
 SiO₂-P₂O₅ optical fibres, γ -irradiated, phosphorus oxygen hole centres 7-11083
 Ti-Mo, electrochemical behaviour in brine, gamma radiolysis effect 7-65185
 W, gamma-irradiated, anomalous effect of small doses 7-12151
 W-Co alloy, gamma-irradiated, anomalous effect of small doses 7-12151
 YAlO₃:Pr³⁺ single crystals, colour centres, optical absorption spectra studies 7-63610
 Y₃Al₅O₁₂, room temp. γ -irrad., colour centre investig 7-6621
 Y_{1.5}Gd_{1.5}Fe₂O₁₂ garnet, γ -irradiated, mag. props. (Russian) 7-27502
 YIG, γ -irradiated, amplification effects and nuclear relax. in domain walls 7-7603
 ZrF₄-BaF₂-LaF₃-AlF₃ optical fibres, gamma irradiation, EPR and IR studies 7-37183
- gamma-ray interactions**
 see also gamma-ray scattering
 No entries
- gamma-ray lasers**
 coherent and incoherent upconversion pumping schemes 7-10947
 conference, laser science advances, Dallas, TX, USA (Nov. 1985) 7-9573
 electronic heat conduction under high pressure 7-10955
 field-enhanced internal conversion, appl. to γ -ray laser 7-10125
 flash X-ray source for γ -ray laser candidate material evaluation 7-10954
 interlevel transfer mechanisms 7-10948
 kinetic behavior 7-25825
 LLNL expts. for gamma-ray laser development 7-10950
 Mossbauer crystals, multi-beam Borrmann modes, γ -ray lasing conditions 7-10953
 Mossbauer effect in long-lived nucl. states, observational techniques 7-10124
 nuclear excitation by laser driven coherent outer shell electron oscillation, gamma-ray laser appl. 7-10121
 nuclear interlevel transfer, resonant electronic states, gamma-ray laser possibilities 7-10119
 nuclear isomeric states for gamma ray laser appl. 7-10951
 nuclear properties for gamma-ray laser based on upconversion 7-10952
 nuclear structure properties for gamma-ray lasers 7-10946
 nuclear superradiance kinetics 7-10949
 proposals, critical review 7-10945
 relativistic e⁻e⁺ γ -ray laser 7-10906
 relativistic electron-positron gamma-ray laser 7-1070
 transfer levels for isomeric deexcitation in γ -ray lasers 7-10908
¹⁹⁹Hg, nuclear isomer separation, for gamma-ray laser 7-10091
²³⁵U, 73 eV first excited state, nuclear excitation, graser possibilities 7-10120
- gamma-ray polarisation**
 high energy γ -quanta, polarisation in strong EM fields 7-62243
 relativistic ions-laser photons collisions, spectrum and polarisation of γ -rays produced 7-50002
¹⁰Be($\gamma,\pi^+)¹⁰Be⁺, recoil nuclear polarization study, γ -circular polarization asymmetry meas. 7-24969
¹²C* 4.43 MeV emission from solar flares, linear polarisation as indicator of particle directions 7-66563
¹⁸F, parity mixing of 0⁺ states, γ -ray polarization meas. 7-5155
¹⁶O* 6.13 MeV emission from solar flares, linear polarisation as indicator of particle directions 7-66563
¹⁵¹Sm(⁴N, γ X), 20, 35 MeV/nucleon, deflection of non-equilibrium light particles by nuclear mean field, γ -polarization meas. 7-5283$
- gamma-ray production**
 antiferromagnetic crystal wiggler synchrotron radiation and free electron lasers 7-57223
 Cas γ -1, transient TEV source, GT 0116+622 and 4U 0115+634 as radio-counterparts 7-18459
 industrial gamma irradiators, design innovations 7-9933
 monochromatic and polarized gamma-ray beams for few body interaction studies 7-62154
 multipurpose prompt gamma facility 7-30804
 radiation from gamma-ray sources, Leontovich boundary condition calcs. 7-31233
 relativistic ions-laser photons collisions, spectrum and polarisation of γ -rays produced 7-50002
 pp- γ X, 300, 460 MeV/c, gamma-spectra meas., baryonium state search 7-49172
- gamma-ray radiography** see radiography
- gamma-ray scattering**
 see also Compton effect; gamma-ray interactions
 backscatter density gauges modelling 7-34716
 concrete shield, heat-resistant, in nuclear reactor, capture γ -ray refl. and transmission 7-49532
 hydrides, amorphous and crystalline, comparative studies via incoherent scatt. 7-21798
 inhomogeneous slabs in a ⁶⁰Co beam scatt. anal.: differential tissue-air ratio method 7-23436
 W, J-shell electrons, gamma ray Compton scatt., intensity distrib. 7-13252
- gamma-ray sources** see gamma-ray production; radioactive sources
- gamma-ray sources (astronomical)**
 1979 March 5 γ -ray transient model 7-24239
 black holes, neutrino and γ -ray emission due nucl. reactions of accreting matter (Russian) 7-24160
 burst sources, one-quantum annihilation of polarised electron-positron pairs in strong mag. fields 7-47674
 burst sources, spectra and thermal synchrotron radiation 7-48103
 burster sources, size-freq.-distrib., study of temporal and spectral selection effects 7-40960
 bursters and possible optical bursts 7-47929
 3C 273, quasar, consequences of gravit. lensing for gamma radiation 7-9552
 Cas γ -1, identification with variable radio source (GT 0116+622) 7-4356
 Cas γ -1 (=4U 0115+63), transient gamma-ray source, obs. of 3.6-s pulses at TeV energies 7-60838
 Cen A (NGC 5128) obs. at MeV gamma-ray energies 7-66754
 2CG 006-00 (=PSR 1802-23), COS B source, pulsed very high energy gamma-ray emission obs. 7-66788
 2CG 195+5, γ -ray emission characts. 7-55857
 Crab Nebula, γ -ray spectral obs. 7-55857

gamma-ray sources (astronomical) continued

- Crab Nebula, EAS obs. rel. to ultrahigh-energy gamma-ray emission 7-14461
- Cyg X-3, cosmic glueballinos source, discussion 7-48105
- Cyg X-3, EAS obs. rel. to ultrahigh-energy gamma-ray emission 7-14461
- Cyg X-3, evidence for free precession of neutron star from obs. of 12.59 ms γ -ray pulse period 7-66649
- Cyg X-3, H dihypon from high energy muon obs. 7-47992
- Cyg X-3, obs. of very-high-energy gamma rays 7-60916
- Cyg X-3, Oct. 1985 RF burst and gamma-ray event, cosmic ray shower observations 7-66790
- Cygnus X-3, cygnet particle flux predictions 7-30303
- Cygnus X-3, radiation source, role of antineutrinos and photinos 7-24242
- Cygnus X-3, underground muons, new evidence from Soudan 1 7-40863
- galactic 511 keV line and positronium beams 7-62547
- galactic centre, common origin for gamma-ray lines at 0.51 and 1.81 MeV 7-24238
- Geminga, hour-mass binary model and 59 s periodicity 7-55855
- Geminga, period rel. to Earth rotation nonuniformities 7-28809
- Geminga, search for very high energy gamma ray pulsed emission 7-55854
- GRB 830801b, burst characts. (*Russian*) 7-24241
- GRBS 1979 March 25b (1810+31), approx. position and magnitudes of possible optical counterpart 7-35068
- hard γ -ray sources, possibilities for polarisation meas. 7-4593
- Her X-1, γ -ray emission mechanism 7-47975
- Her X-1, companion-star beam steering of high-energy particles rel. to gamma-ray emission 7-14611
- light curves analysis, appl. of kernel density estimators 7-47718
- neutron star magnetosphere, pair formation 7-40860
- NGC 1275, search for γ -ray emission 7-55857
- point cosmic gamma-ray sources 7-35865
- positron annihilation, gamma-ray burst events 7-40859
- PSR 0531+21 (Crab pulsar), obs. of very-high-energy gamma rays 7-60916
- rotating black hole, gamma-ray emission from accretion 7-55700
- Signe 2MP9 γ -ray burst expt. results (*Russian*) 7-24240
- superconducting cosmic strings, γ -ray background contrbs. 7-24518
- synchrotron self-Compton sources, one-generation pair production theory 7-55452
- Wolf-Rayet stars, new evidence at X-ray and gamma-ray freqs., for non-thermal phenomena 7-55640
- X-ray binary systems, mechanism for ultra-high-energy gamma-ray emission 7-47971
- ²⁶Al, interstellar, gamma-ray line emissivity from Wolf-Rayet star prod. 7-47830

gamma-ray spectra

- see also gamma-ray angular distribution; gamma-ray spectra of liquids and solids; gamma-ray spectroscopy; nuclear decay theory
- DELPHI, γ -ray spectrum analysis code 7-15201
- graphite shielding slabs, penetration of 2.75 MeV γ -rays 7-30712
- peak fitting programme for γ -ray spectra measured in semicond. detectors (*Czech*) 7-62205
- steel, shielding slabs, penetration of 2.75 MeV γ -rays 7-30712
- terrestrial gamma-ray surveys, altitude depend. model 7-47440
- (n, γ), determ. of absolute intensities, time-of-flight γ - and neutron-spectra meas. 7-56678
- (n, γ), El giant resonance excitation, partial cross sections in optical shell model 7-30421
- pp- γ X, 300, 460 MeV/c, gamma-spectra meas., baryonium state search 7-49172
- pp- γ X, at rest, search for narrow signals in γ -spectrum, branching ratio 7-49190
- ²²⁸Ac in natural background γ -radiation spectrum 7-19550
- Al shielding slabs, penetration of 2.75 MeV γ -rays 7-30712
- C(¹⁴N,X), 20-40 MeV/N, high energy γ -ray prod., intranuclear NN collision model 7-36041
- ¹²C*, 4.43 MeV emission from solar flares, linear polarisation as indicator of particle directions 7-66563
- ¹³C(K, π^-), s¹p²o_{SA}, s¹p²o_{PA} state spectra, baryon decays, neutron spectra, nuclear and hypernuclear γ -spectra 7-56634
- ⁴⁰Ca isospins level-widths, 9.5 to 10.5 MeV, from ³⁹K(p, γ) (*Chinese*) 7-35972
- ⁴⁰Ca(⁴⁰Ca, γ)⁸⁰Zr*, 55-79 MeV, ⁷⁶Rb isomer obs., half-life meas., level structure 7-10109
- ¹³²Ce, effective moment of inertia, γ -ray spectra study and cranking model comparison 7-49209
- Cu₂Hf₄₃ amorphous alloy, local Hf environment, TDPAC spectra study 7-32303
- ¹⁵²Dy, quasicontinuum γ -rays from collective high-spin states, internal conversion coeff., multipolarity meas. 7-56639
- ⁶⁷Ga 15/2⁺ 3578 keV level, mag. moment meas. from ⁵⁶Fe(¹⁶O,ap) 7-35946
- ¹⁵⁸Gd(⁴⁰Ar,X), 44 MeV/N, γ -rays from peripheral and central collisions, fragment stat. decay 7-61917
- Ge(Li) detector system, monoenergetic γ -ray spectrum modeling 7-30898
- ⁴Hg (d,p γ), A=202, 204, γ -ray and conversion electron meas., neutron hole states 7-49432
- ⁴⁰K in Makhmur Plain soil, N Iraq, α -ray spectroscopical analysis 7-34487
- ²⁴Mg(π^+ , N), 200 MeV, single nucleon removal, γ -rays, diff. cross sections, PWIA, intranuclear cascade 7-30455
- (n, γ), gamma-ray spectra, P-violating effects 7-49425
- Nb-Hf-Ta-O dilute alloy system, O-induced nonaxially symmetric elec. field gradient, TDPAC meas. 7-12686
- ¹⁵⁴Nd, effective moment of inertia, γ -ray spectra study and cranking model comparison 7-49209
- ¹⁵⁶Nd, effective moment of inertia, γ -ray spectra study and cranking model comparison 7-49209
- ¹⁴⁴Nd(¹⁶O, γ)¹⁶⁰Er, E_{lab}=76-105 MeV, ¹⁶⁰Er statistical decay, giant dipole resonance effects, statistical model comparisons 7-10173
- Ni multiple scattering profile, gamma-ray Compton study 7-17356
- Ni-Bi amorphous alloys, crystallisation produced by ion implantation, TDPAC study 7-32288
- ¹⁶O*, 6.13 MeV emission from solar flares, linear polarisation as indicator of particle directions 7-66563
- Pb shielding slabs, penetration of 2.75 MeV γ -rays 7-30712
- Pb(¹⁴N,X), 20-40 MeV/N, high energy γ -ray prod., intranuclear NN collision model 7-36041

gamma-ray spectra continued

- ²⁰¹Po, m and g isomers, decay scheme construction from time-sequenced spectra 7-30365
- ²¹⁰Po α -source, use in determining Al, F, N content in samples 7-65360
- ⁸⁵Rb^m, isomer shift, mag. moment, laser induced nuc. orientation 7-10106
- ⁴Rn, A=223, 226, 227, half-life meas. 7-49291
- ⁴⁵Sc(p, γ X), 2-4 MeV, gamma-ray ang. distribns., low-lying levels anal. 7-19168
- ⁸⁶Sm, A=150,152, electromagnetic decay of O₂⁺ and O₃⁺ states 7-15199
- ⁸⁶Sr(n, γ), level struct. and transition strength study 7-41899
- ²³²U, gamma-ray spectroscopy up to spin 20 7-15200
- ¹⁷⁵Yb-¹⁷⁵Lu, gamma-spectra, ¹⁷⁵Lu level anal. 7-49313
- gamma-ray spectra of liquids and solids**
- see also Mossbauer effect
- Ag-¹¹¹In, O agglomeration in presence of radiation defects 7-26791
- graphite surface, adsorbed N₂ mol. zero-point energies, out-of-plane orientation, nucl. reson. photon scatt. study 7-32819
- irradiated metals, isochronal annealing PAC monitored defect reactions anal. 7-44623
- vacuum fluctuation effects on gamma-rays emitted by solid 7-7626
- YIG, ⁵⁷Fe enriched, quantum beats from synchrotron radiation pulses 7-2960
- Ag/In thin film couples, interface AgIn₂ cpd. form. and props., gamma ray spectra 7-21688
- Al-Hf dilute quenched cold-worked alloys, vacancy migration recovery processes, PAC and positron annihilation studies 7-39545
- Au/In thin film couples, interface AuIn₂ cpd. form. and props., gamma-ray spectra 7-21688
- Au-Fe, mag. hyperfine field, temp. and composition depend. 7-45243
- Bi₂Ge₃O₁₂ single cryst. growth, characterisation and appls. 7-33550
- Cd-In alloys, vacancy-induced elec. field gradient temp. depend., PAC meas. 7-52541
- Cu/In thin film couples, interface CuIn₂ cpd. form. and props., gamma ray spectra 7-21688
- Cu-In alloys, vacancy-induced elec. field gradient temp. depend., PAC meas. 7-52541
- Fe-Pt, dilute alloys, ferromagnetic, internal mag. fields, impurity conc. dependence, PAC study 7-38858
- HoVO₄, enhanced nucl. order, nucl. orientation study 7-64550
- In_{0.95}Ag_{0.045}Ga_{0.005}, ¹¹¹Cd quadrupole interaction, temp. dependence, lattice electric field gradients (*Chinese*) 7-7183
- In_{0.95}Ag_{0.045}Ga_{0.005} alloy, quadrupole interactions, TDPAC study 7-38521
- InCl₃ mixed valence cpds., nuclear electron capture aftereffects, quadrupole interactions, γ ray ang. correl. anal. 7-53182
- K₂HfF₆, polymorphism, TDPAC investig. 7-2188
- (NH₄)₂HfF₆, thermally activated α - β transition 7-12258
- Nb₂O₅, H and D trapping, perturbed ang. correl. obs. 7-27641
- ²⁰Ne⁺ and ²²Ne⁺, ion implantation in elemental solids, range profile, gamma-ray spectra 7-2959
- Si single cryst., electron axial and planar channelling, gamma-ray emission studies 7-44636
- Si:¹¹¹Cd, hyperfine interactions, temp. depend., gamma-ray spectra studies 7-64553
- Si:As,In, formation of In-As complexes, perturbed angular correlation technique obs. 7-17254
- Ta₂S₃, electrochem. intercalation reactions with Li, K, H, In, Ga, In_{0.17}Ga_{0.83}, nucl. quadrupole interactions, TDPAC meas. 7-17245
- TiC, effective and Debye temps. of Ti, gamma ray reson. scatt. meas. 7-44731
- TiH₂, effective and Debye temps. of Ti, gamma ray reson. scatt. meas. 7-44731
- TiO₂, effective and Debye temps. of Ti, gamma ray reson. scatt. meas. 7-44731
- Zn-In alloys, vacancy-induced elec. field gradient temp. depend., PAC meas. 7-52541
- Zr₆₈Hf₃₂Cu₃₀ amorphous and cryst. alloy, elec. field gradient, TDPAC meas. 7-2958

gamma-ray spectrometers

- see also gamma-ray spectra; gamma-ray spectroscopy
- actively shielded 86 cm³ Ge detector for astron. spectra meas. 7-55857
- complex Ge detector systems and Compton suppression spectrometers, Monte Carlo simulation 7-5530
- Compton spectrometer, fluorescent sources 7-15449
- controller for electrodynamic drive of Mossbauer spectrometer 7-35508
- counting losses not eliminated by dead time correction circuitry 7-4938
- data acquisition circuitry, long-term stability 7-19624
- high-energy gamma ray spectrometer for heavy-ioninduced experiments 7-5528
- hodoscopic scintillation gamma spectrometers with light-guide spectrum mixers 7-10351
- intelligent multichannel analyzer for the measurement of gamma spectra 7-5533
- Mossbauer spectrometer and data anal. system, IBM PC-based 7-18959
- Mossbauer spectrometers, cryostat design (*Chinese*) 7-61338
- transverse BGO Compton suppression shield for Ge γ -spectrometer, expt. and Monte Carlo study 7-25300
- ultra low level counting with Ge spectrometers, α -induced background from ²¹⁰Pb decay 7-25299
- CsF detectors, use in lifetime spectrometers for e⁺e⁻ annihilation studies 7-5554
- Ge gamma-ray spectrometer, calibration using ¹⁵²Eu decay 7-42275
- Ge-BGO Compton suppression spectrometer system, time pickoff for BGO suppression shield 7-5529
- Ge-NaI(Tl) anti-Compton spectrometer, on-line neutron response, γ prod. 7-5532
- NaI:TI, triple-coincidence spectrometer for ²⁶Al, ²²Na 7-25317
- NaI:TI spectrometer, γ -ray response function, energy resolution 7-62200
- Xe, liquid scintillation spectrometer 7-62199

gamma-ray spectroscopy

- accuracy of half-lives determined by γ -ray spectrometry 7-24958
- activation analysis, high sensitivity, using underground laboratory for gamma spectroscopy 7-24743
- calibration, using relative gamma intensities in decay of ^{110m}Ag, ¹³³Br, ¹⁸²Ta, ¹⁹²Ir 7-5568
- contaminant control in nuclear facility environment by γ -spectrometry (*Rumanian*) 7-10300
- counting losses not eliminated by dead time correction circuitry 7-4938
- data acquisition circuitry, long-term stability 7-19624
- EMG gasmaspectroscopic analyser system (*Hungarian*) 7-49784

gamma-ray spectroscopy continued

- high resolution spectroscopy, semiconductor detector electronics for measurements in heavy overload conditions 7-42439
 ionisation chamber based, with compressed Xe 7-10350
 Mossbauer spectra meas. with high count rate 7-36425
 Mossbauer spectroscopy, hydrostatic pressure effect on the minimum temperature of a helium-3 cryostat 7-18970
 neutron-activation detectors, activity meas. by gamma spectrometry, systematic errors 7-49793
 priority switching in measurement of time spectra of gamma-gamma coincidences 7-10369
 remote sensing neutron dosimetry using prompt γ -ray spectrometry 7-49727
 Pu content of Mururoa Atoll coral samples, gamma spectrometry study 7-54415
 U concentration meas. in soil and rocks by γ -ray spectrometry 7-54373
 ^{238}U , isotopic composition determ., nuclear spectrometric method 7-62198
 ^{133}Xe , activity determination by γ -ray spectrometry, nuclear plant effluent air check 7-25298

gamma-ray transport *see photon transport theory***gamma-rays**

No entries

gamma transition *see glass transition (polymers)***Gamow-Teller transitions** *see beta-decay***garnets**

- includes ferrimagnetic insulators, $\text{M}_3\text{Fe}_2\text{O}_{12}$, for rock-type garnets, $\text{MM}'(\text{SiO}_4)_3$, *see minerals*
see also ferrimagnetic properties of substances
 bubble films, H_2^+ -implanted, thermal stability and aging 7-22124
 bubble films, H_2^+ -implanted, H out-diffusion suppression of overlayers 7-38259
 bubble garnet films, coercive force determ., microwave absorpt. meas. 7-59096
 bubble materials, stripe domain structures, undulation instabilities 7-59097
 chemical bonds, ionicity, covalency (*Russian*) 7-16483
 epitaxial layers, Bloch line behaviour in an in-plane field 7-53101
 ferrimagnetic, vertical Bloch line motion, memory appls. 7-53024
 ferromagnetic garnets, magneto-optical effects and appls. (*French*) 7-59190
 film, strip domain stretching, computer simulation 7-59083
 film, stripe domain stabilisation by grooving 7-59084
 films, Co-containing, domain-wall dynamics, magnetic after-effect 7-64504
 films, $\text{He}^+(\text{H}_2^+)$ implanted, magnetisation and uniaxial anisotropy meas. 7-7576
 films, isolated stripe domain deformation instability study (*Russian*) 7-2916
 films, orthorhombic, optical modes, phase matching 7-11110
 garnet epitaxial thin film, FMR investig. 7-53069
 laser material, spectroscopic props. 7-10957
 LPE films, lattice relax. around cracks 7-7054
 $(\text{LuYBiPb})_3(\text{FeGa})_5\text{O}_{12}$, crystn. from soln. melt, component distrib. 7-21149
 magnetic garnet films, stress induced optical anisotropy 7-53430
 ornamental, general method of formulation and crystal growth 7-53252
 rare earth Ga-Fe garnets, $\text{R}_3\text{Fe}_{5-x}\text{Ga}_x\text{O}_{12}$, dissoln. forms 7-58481
 rare earth iron garnet films, surface-spin orientations, depth-selective Mossbauer spectroscopy 7-2907
 rare earth iron garnets, Bi-doped, growth-induced anisotropy 7-22103
 YAG: rare earth crystals, impurity content, absorpt., spectrophotometric obs. 7-13843
 YIG: Ca films, magneto-optical props., reducing treatment effects 7-64617
 YIG, ^{57}Fe enriched, quantum beats from synchrotron radiation pulses 7-2960
 $(\text{YSmLuCa})_3(\text{FeGe})_5\text{O}_{12}$, bubble lattice, magnetisation curves 7-53094
 $(\text{Bi,Tm})_3(\text{Fe,Ga})_5\text{O}_{12}$ garnet films, magnetisation reversal, pulsed mag. field nonuniformity effect 7-45783
 $\text{Bi}_{1-x}\text{Ca}_x\text{Fe}_{3-x}\text{In}_x\text{V}_x\text{O}_{12}$ single crystal, Mossbauer spectroscopy (*Chinese*) 7-17250
 $\text{Bi}_{1-x}\text{Ca}_x\text{Fe}_{3-x}\text{V}_x\text{O}_{12}$, sublattice magnetisation and Faraday rotation (*Chinese*) 7-17308
 $\text{Bi}_2\text{Dy}_{1-x}\text{Fe}_{3.8}\text{Al}_{0.2}\text{O}_{12}$ garnet films, magneto-optical props. 7-64614
 $(\text{BiDySmLu})_3(\text{FeAl})_5\text{O}_{12}$ bubble garnet films, Bi-substituted, LPE growth rate reduction 7-45049
 $(\text{BiDySmLuGd})_3(\text{FeGa})_5\text{O}_{12}$ bubble garnet films, Bi-substituted, LPE growth rate reduction 7-45049
 $\text{Bi}_3(\text{GaFe})_5\text{O}_{12}$, epitaxial films, mag. and magneto-optical props. 7-53102
 $(\text{BiGdTm})_3(\text{FeGa})_5\text{O}_{12}$ single cryst. film, reverse-magnetisation domain nucleation studies 7-17208
 $(\text{BiGdTm})_3(\text{FeGa})_5\text{O}_{12}$ epitaxial films, microdomain nucleation near moving domain walls 7-45778
 BiIG films, selected-area sputter epitaxy 7-7845
 $(\text{BiLu})_3(\text{FeGa})_5\text{O}_{12}$ epitaxial films, microdomain nucleation near moving domain walls 7-45778
 $(\text{BiLu})_3(\text{FeGa})_5\text{O}_{12}$ film, magnetic bubble motion, Rayleigh surface wave effects 7-33245
 $\text{Bi}_2\text{Lu}_2\text{Y}_{1-x}\text{Fe}_3\text{O}_{12}$, ferrimagnetic garnets characterisation for MSW optical diff. 7-13040
 $(\text{BiR})_3(\text{FeGa})_5\text{O}_{12}$, garnet films, pulsed magnetisation reversal, in-plane mag. field 7-45736
 $(\text{BiTm})_3(\text{FeGa})_5\text{O}_{12}$ epitaxial films, microdomain nucleation near moving domain walls 7-45778
 $(\text{BiTm})_3(\text{FeGa})_5\text{O}_{12}$, garnet films, pulsed magnetisation reversal, influence of temp. on integral characts. 7-45735
 $(\text{BiYLu})_3(\text{FeGa})_5\text{O}_{12}$, garnet films, pulsed magnetisation reversal, influence of temp. on integral characts. 7-45735
 $(\text{BiYLu})_3(\text{FeGa})_5\text{O}_{12}$ epitaxial films, microdomain nucleation near moving domain walls 7-45778
 $(\text{BiYSmTbGdHoCa})_3(\text{FeSiGe})_5\text{O}_{12}$ bubble films, rare earth substitution effects 7-59095
 $\text{Ca}_3\text{Al}_2\text{Ge}_{3-x}\text{Si}_x\text{O}_{12}$:Tb, cathodoluminescence, photoluminescence props. 7-53404
 $\text{Ca}_2\text{Ga}_2\text{Ge}_3\text{O}_{12}$: Cr^{3+} garnet, ESR and ultrasonically modulated ESR studies 7-22139
 $\text{Ca}_2\text{Ga}_2\text{Ge}_{3-x}\text{Si}_x\text{O}_{12}$:Tb, cathodoluminescence, photoluminescence props. 7-53404*

garnets continued

- $\text{Ca}_3\text{Mn}_2\text{Ge}_3\text{O}_{12}$ single domain crystals, birefringence and spontaneous phase transitions 7-17303
 $\text{Ca}_3\text{Sc}_2\text{Ge}_{3-x}\text{Si}_x\text{O}_{12}$:Tb, cathodoluminescence, photoluminescence props. 7-53404
 $\text{Ca}_3\text{Y}_2\text{Ge}_{3-x}\text{Si}_x\text{O}_{12}$:Tb, cathodoluminescence, photoluminescence props. 7-53404
 $(\text{Ca}_2\text{Y})\text{Sn}_2\text{Fe}_3\text{O}_{12}$, ion distrib., Mossbauer spectra anal. 7-33306
 Cr,Nd: $(\text{Gd,Sc})_3\text{Ga}_5\text{O}_{12}$ laser crystals, growth and quality 7-13346
 Cr,Nd:GdScGa $_5\text{O}_{12}$ laser rods losses and efficiency meas. 7-43106
 Cr^{3+} :Gd $_3\text{Sc}_2\text{Al}_2\text{O}_{12}$ laser, flash-lamp pumped 7-15902
 $\text{Dy}_3\text{Al}_5\text{O}_{12}$, refrigerant characts. for Carnot mag. refrigerator 7-56286
 $\text{Dy}_3\text{Al}_5\text{O}_{12}$, exchange metamagnetism 7-2841
 DyIG:Ga,Bi, RF sputtered films for magneto-optical memory, mag. props. 7-64613
 ErIG, mag. prop. calc. 7-52977
 (Eu, Lu, La) $_3\text{Fe}_5\text{O}_{12}$ films, gyromagnetic ratio, damping parameter and mag. anisotropy 7-45777
 Eu $_x\text{Y}_{3-x}\text{Fe}_5\text{Ga}_5\text{O}_{12}$ LPE garnet films, ferromagnetic relax. meas. 7-38911
 Fe garnet epitaxial films, near a nonmagnetic metallic disk, domain struct., mech. stress effects 7-38922
 Fe garnet film, epitaxial growth from weakly dissociated molten soln. 7-64944
 Fe garnet films containing Bi, comp. study, and chemical etching anal. 7-45083
 (Gd,Bi) $_3(\text{FeGaAl})_5\text{O}_{12}$ garnet films, selected area liq. phase epitaxy, local ion implantation effects 7-21726
 (Gd,Sc) $_3\text{Ga}_5\text{O}_{12}$ laser materials, high strength, development 7-10961
 (GdBi) $_3(\text{FeAlGa})_5\text{O}_{12}$ garnet films, LPE growth 7-59463
 Gd $_3\text{-x}\text{Bi}_x\text{Fe}_5\text{O}_{12}$ crystal growth for 0.8 μm optical isolator 7-57605
 Gd $_3\text{Ga}_5\text{O}_{12}$ ferrogarnets, heat of crystallisation, scanning calorimetry obs. 7-2154
 Gd $_3\text{Fe}_5\text{O}_{12}$ garnet, spin-reorientation phase transition, NMR obs. 7-38861
 Gd $_3\text{Fe}_5\text{O}_{12}$, initial permeability peak at low temperature 7-33212
 GdGG laser material, characts. of polishing cpds. 7-37212
 GdGG, paramag., mag. lin. birefr. meas. 7-53265
 Gd $_3(\text{Ga}_{1-x}\text{Fe}_x)_5\text{O}_{12}$ and Gd $_3(\text{Al}_{1-x}\text{Fe}_x)_5\text{O}_{12}$, mag. solid soln. systems for regenerator materials 7-59015
 Gd $_3\text{Ga}_5\text{O}_{12}$ laser materials, high strength, development 7-10961
 Gd $_3\text{Ga}_5\text{O}_{12}$, pure and doped, photoelectret, photoconductivity 7-45919
 Gd $_3\text{Ga}_5\text{O}_{12}$, refrigerant characts. for Carnot mag. refrigerator 7-56286
 Gd $_3\text{Ga}_5\text{O}_{12}$, sintered, mag. refrigerator, Kapitza conductance to He II 7-58603
 Gd $_3\text{Ga}_5\text{O}_{12}$, use in mag. refrigerator for He liquefaction 7-56283
 Gd $_3\text{Ga}_5\text{O}_{12}$, use in rot. mag. refrigerator for He liquefaction 7-56282
 Gd $_3\text{Ga}_5\text{O}_{12}$ -YIG-ZnO, surface magnetostatic wave scatt. by SAW 7-64507
 GdIG, Faraday effect meas. 7-64616
 Gd $_2\text{MSb}_2\text{Zn}_3\text{O}_{12}$ (M=Sr,Ca), rare-earth activated garnets, cathodolum. 7-7763
 GdScGa $_5\text{O}_{12}$:Cr, Tm crystals, dual freq. lasing study 7-43117
 Gd $_{2.95}\text{Sc}_{1.05}\text{Ga}_{3.135}\text{O}_{12}$ garnet, congruently melting, cryst. growth 7-59412
 Gd $_3\text{Sc}_2\text{Ga}_3\text{O}_{12}$ garnets 7-21045
 Gd $_3\text{Sc}_2\text{Ga}_3\text{O}_{12}$: Cr^{3+} garnet, laser spectral analyser 7-31362
 Ho $_3\text{Fe}_5\text{O}_{12}$ ferrogarnets, heat of crystallisation, scanning calorimetry obs. 7-2154
 Mn $_3\text{Cr}_2\text{Ge}_3\text{O}_{12}$ garnets, cryst. growth, chemical vapour transport, struct. 7-53518
 Mn $_3\text{Fe}_2\text{Ge}_3\text{O}_{12}$ garnets, cryst. growth, chemical vapour transport, struct. 7-53518
 Mn $_3\text{Ga}_2\text{Ge}_3\text{O}_{12}$ garnets, cryst. growth, chemical vapour transport, struct. 7-53518
 Na $_4\text{Zr}_2\text{Si}_3\text{O}_{12}$ -Y $_3\text{Fe}_5\text{O}_{12}$ composite ceramics, prep., thermal expansion 7-63853
 Nb:YAG picosec. laser pulse characterisation by self diffraction 7-10965
 Nd,Cr:(Gd,Sc) $_3\text{Ga}_5\text{O}_{12}$, spectroscopic, optical and thermo-mechanical props. and laser performance 7-10963
 Nd:YAG CW mode locked laser, simultaneous amplification and compression 7-10966
 Nd:YAG laser, 1.06 μm Cs $_2$ reference for freq. stabilisation 7-57403
 Nd:YAG miniature oscillator, freq. doubled, laser diode pumped 7-15876
 Nd $^{3+}$:La $_3\text{Lu}_2\text{Ga}_3\text{O}_{12}\text{ZZ}$ 7-10957
 Nd $_3\text{Ga}_5\text{O}_{12}$ garnet, cryst. field studies of excited states 7-33407
 Nd $_3\text{Ga}_5\text{O}_{12}$, photoelectret, photoconductivity 7-45919
 NdIG, mag. props. 7-45662
 Nd, Y $_3\text{-x}\text{Fe}_5\text{O}_{12}$ garnets, growth anisotropy, Mossbauer study 7-38973
 PbFe $_{1-x}\text{Ga}_x\text{O}_{10}$ (x=0, 1, 3, 4), magneto-optical props. 7-53281
 PrIG, mag. props. 7-45662
 Pr $_2\text{Y}_{1-x}\text{Fe}_5\text{O}_{12}$ garnets, growth anisotropy, Mossbauer study 7-38973
 SiAlON-YAG ceramics, Auger electron microscopic quantification of phase comp. 7-22951
 Sm $_3\text{Ga}_5\text{O}_{12}$, photoelectret, photoconductivity 7-45919
 SmIG, low temp. evolution of Faraday rotation 7-64615
 SmLu(FeGa) $_5\text{O}_{12}$ films, with submicron domain structures, mag. inhomogeneity 7-45782
 (SmLuGd) $_3(\text{FeGaSc})_5\text{O}_{12}$ films, with submicron domain structures, mag. inhomogeneity 7-45782
 Tb $_3\text{Fe}_5\text{O}_{12}$ ferrogarnets, heat of crystallisation, scanning calorimetry obs. 7-2154
 Tb $_3\text{Fe}_5\text{O}_{12}$, magnetic struct., X-ray absorpt. spectra magnetic dichroism meas. 7-39315
 (TmBi) $_3(\text{FeGa})_5\text{O}_{12}$ indicator film, visualisation of mag. field profile of thin-film magnetic heads 7-61359
 Tm $_3\text{Fe}_5\text{O}_{12}$, double phase transition, EXAFS studies 7-63799
 Tm $_3\text{Fe}_5\text{O}_{12}$ ferrogarnets, heat of crystallisation, scanning calorimetry obs. 7-2154
 (Y,Gd) $_3\text{Fe}_5\text{O}_{12}$:Mn, thin films, noncubic mag. anisotropy origin 7-53068
 (Y,Sc) $_3\text{Ga}_5\text{O}_{12}$: Cr^{3+} , Er^{3+} , spectral, luminesc. and lasing props., Stark sublevel lifetimes 7-25827
 YAG laser materials, high strength, development 7-10961
 YAG:Mn $^{4+}$, luminesc. and fluoresc. line narrowing studies 7-46105
 YAG:Nd, Ce, energy transfer mechanisms between Ce $^{3+}$ and Nd $^{3+}$ at low temp. 7-64691
 YAG:Nd activated crystals, coherent propag. of small-area pulses 7-43038
 YAG:Nd crystals, high quality, growth by temp. gradient technique 7-22464
 YAG:Nd $^{3+}$, impurity two-photon absorpt. cross section meas. 7-53375
 YAG:Nd $^{3+}$, luminescence decay 7-17342

garnets continued

- YAG:Nd(Nd,Ce) single crystals, luminesc. and laser props. 7-10967
 YAG:Ni(Ni, Zr) (Fe), defect and optical props. 7-59258
 YAG:Pr³⁺, up-conversion, stepwise photon absorpt. process 7-13193
 YAG:Tb, electron-phonon relax. in ⁵D₄ of Tb³⁺ 7-2130
 YAG:Tb cryst. field anal. of Tb³⁺, site selective polarisation spectroscopy 7-2546
 YAlO₃:Pr³⁺ single crystals, colour centres, optical absorption spectra studies 7-63610
 Y₃Al₅O₁₂, room temp. γ -irrad., colour centre investig 7-6621
 (YBi)₃(FeGa)₅O₁₂, epitaxial films, mag. bubble lattices, influence of external stresses 7-64503
 (YBi)₃Fe₅O₁₂, magneto-optic materials and their applications 7-27703
 (YEuLuCa)₃(FeGe)₅O₁₂ films, mag. bubble motion in the presence of a modulated bias field 7-53098
 (YEuTmCa)₃(FeGe)₅O₁₂ films, planar anisotropy and magnetisation, ion irrad. effects study 7-2906
 (YEuTmCa)₃(FeGe)₅O₁₂, epitaxial films, O ion adsorpt. bubble diameter variation effect 7-22125
 (YEuTmCa)₃(FeGe)₅O₁₂/(YLa)₃Fe₅O₁₂, ferrite/garnet layered structs., domain wall and ferromag. reson. props. (Russian) 7-45828
 (YEuTmCa)₃(FeGe)₅O₁₂ films, double layer, mag. bubbles, translational velocity 7-45781
 Y₃Fe_{4.5}Ga_{0.5}O₁₂, single cryst., NMR, ang. depend. 7-53148
 Y₃Fe_{5- γ} Ga _{γ} O₁₂ epitaxial film, high freq. threshold props. studies (Russian) 7-45775
 Y₃Fe_{5- γ} Ga _{γ} O₁₂ garnet films, magnetostatic wave props. 7-52958
 Y₃Fe₅O₁₂:Si, epitaxial film, domain struct. rearrangement, unpolarised light influence 7-45784
 YGG:Nd waveguide laser amplifiers for fibre-optic communication 7-31359
 Y_{1.5}Gd_{1.5}Fe₂O₁₂ garnet, γ -irradiated, mag. props. (Russian) 7-27502
 YIG, charact. of chaotic states of parallel-pumped magnons 7-52961
 YIG, critical mag. relaxation, ESR linewidth 7-22106
 YIG cryst., domain wall dynamics, optical polarisation study 7-45732
 YIG double-layered films, thermal detection of FMR, microwave freq. appls. 7-45766
 YIG, epilayers, SIMS anal. 7-27207
 YIG epitaxial film, magnetic grating, Raman-Nath diffr. of surface magnetostatic waves 7-58999
 YIG, epitaxial layers, Faraday rot. meas., Bi and Pb ion contribs. 7-53071
 YIG, FZ growth for magneto-optic devices in fibre-optic communication systems 7-27892
 YIG, ferrimagnetic garnets characterisation for MSW optical diffr. 7-13040
 YIG, ferromagnet, domain struct., transform. in alternating mag. fields 7-53027
 YIG, ferromagnetic hysteresis loop, grain size distrib. effect 7-27556
 YIG film, nonuniformly magnetised, group delay characts. of magnetostatic forward vol. waves 7-45764
 YIG film tangentially magnetised dielec. layered struct., nonlinear magnetostatic wave mixing (Russian) 7-45649
 YIG films, ferromag. resonance absorpt., influence of exchange interaction, weak surface pinning 7-2931
 YIG films, H₂ annealed, Mossbauer study 7-45847
 YIG films, low dose ion implanted, magnetostatic backward vol. waves 7-45765
 YIG films, symmetrical single-mode magneto-optic waveguides, phase matching by stress appl. 7-45972
 YIG films, tangentially magnetised, magnetoelastic effects 7-22130
 YIG, γ -irradiated, amplification effects and nuclear relax. in domain walls 7-7603
 YIG, irradiation by high energy heavy ions, electronic stopping power effects on damage rate 7-58352
 YIG LPE films, mag. mode fine struct. (Chinese) 7-13007
 YIG, LPE films, microwave magnetostatic waves, magnetic induction probe studies 7-58996
 YIG mixed cryst. films, LPE, segregation 7-53641
 YIG, multicomponent systems, synthesis, microwave characts., mathematical modelling 7-33626
 YIG, optical reflectivity meas. by synchrotron radiation spectroscopy 7-59135
 YIG powder, FMR line shape, test of independent powder particle model 7-64533
 YIG single crystal films, FMR foldover, Subl instability 7-53141
 YIG single crystals, thermodepolarisation studies (Russian) 7-33029
 YIG solubility in PbO-B₂O₃ flux validity of anionic model 7-52062
 YIG, superexchange interactions, inelastic neutron scatt. studies 7-33161
 YIG, toroidal ferrimagnetic polycrystals, domain-wall continuity 7-33197
 YIG:Ga, Bi, RF sputtered films for magneto-optical memory, mag. props. 7-64613
 YIG-H, ion implanted, elastic recoil analysis using 44 MeV Cl ions 7-12107
 YIG-H, sp. ht. and annealing behaviour, conversion-electron Mossbauer spectroscopy study 7-17253
 YIG:Ho³⁺, laser mag. reson. study, quasi-Ising model 7-53147
 YIG:La-Ga-YIG:La double layered film, different magnetisation and anisotropy, magnetostatic mode spectra 7-64498
 YIG:Ne⁺ ferrite films, surface magnetostatic wave damping, ion implantation effects (Russian) 7-33242
 YIG:Si epitaxial films, mag. anisotropy and spin reorientation under unpolarised white light irrad. (Russian) 7-33246
 YIG/ferroelec. struct., surface magnetostatic wave propag. charact. meas. 7-52965
 (YLuBi)₃(FeGa)₅O₁₂, Ne⁺ implanted, CEMS study (Chinese) 7-7620
 (YLuBi)₃(FeGa)₅O₁₂:Ne⁺ films, stripe domain stabilisation by ion implantation 7-53100
 (YLuSmCa)₃(FeGe)₅O₁₂ epitaxial films, transition layer 7-45779
 Y₂MSb₂Zn₃O₁₂ (M=Sr,Ca), rare-earth activated garnets, cathodolum. 7-7763
 Y₂Pr_{0.03}Gd_{0.97}Al₅O₁₂, sensitisation of Gd³⁺ luminesc. by the Pr³⁺ ion 7-3082
 (YSm)₃(FeGa)₅O₁₂ garnet film, demagnetisation, elongation of striped domain struct. 7-45737
 (YSmLuCa)₃(FeGe)₅O₁₂ epitaxial layer, conversion electron Mossbauer spectra 7-48926
 (YSmLuCa)₃(FeGe)₅O₁₂ epitaxial films, Faraday rot., Sm³⁺ conc. effect. 7-53070
 (YSmLuCa)₃(FeGe)₅O₁₂ film, stripe domain stabilisation for Bloch line memory 7-59087

garnets continued

- (YSmLuGd)₃(FeGa)₅O₁₂ garnet film struct. and mag. props., mag. bubble memory appls. (Japanese) 7-7575
 (YTMBi)₃(FeGa)₅O₁₂ films, bubble wall states generation in rotating gradient expt. 7-53097
 Y_{3- γ} Yb _{γ} A₅O₁₂, thermal conductivity, temp. and composition dependences 7-38274
 YbAG, paramag., mag. lin. birefr. meas. 7-53265
 YbGG, paramag., mag. lin. birefr. meas. 7-53265
- gas *see* gases
 gas analysis *see* chemical analysis
 gas blast circuit breakers
 ablation controlled arcs, stagnation press. elec. field strength 7-26332
 arc mantle studies in dual flow plasmas 7-26559
 asymmetric dual-flow interrupter nozzles, flow field study 7-26331
 nozzle arc dynamic behaviour 7-26556
 SF₆ puffer-type circuit breakers, effects of aerodynamic shocks on performance 7-51223
 gas breakdown *see* electric breakdown of gases
 gas bubbles *see* bubbles
 gas-discharge displays
 AC plasma displays, discharge development 7-21012
 AC plasma displays, discharge ignition 7-21017
 gas discharge lamps *see* discharge lamps
 gas-discharge tubes
see also gas-discharge displays; ion sources; thyatrons
 electric field calculations using the ELF codes glow discharge switches and electrode design 7-32134
 heavy atom spectra sources for use with high resolution Fourier transform spectrometer 7-50403
 image convertor, gas discharge, operating in avalanche mode, intrinsic blurring and freq. contrast characts. 7-4937
 metal plasma arc switches, appl. of particle orbit theory 7-37768
 pulsed power supplies, IEEE conf., Arlington, VA, USA (1985) 7-35110
 triggered cascade gas switches for PBFA I 7-30747
 UV sustained radial glow discharge opening switch investigation 7-32133
 uV-sustained glow discharge opening switch experiments 7-32132
 Ar/C₂F₆ mixtures, Penning ionisation for diffuse discharge switching appls. 7-37622
 Ne-Ar mixtures, transient cataphoretic segregation in a discharge tube 7-20988
 Xe gas discharge triodes 7-37789
- gas discharges *see* discharges (electric)
 gas dynamic lasers *see* gasdynamic lasers
 gas dynamics *see* aerodynamics; flow
 gas ionisation *see* ionisation of gases
 gas lasers
see also chemical lasers; excimer lasers; gasdynamic lasers; ion lasers
 air stream parameter effects on glow discharge, CO₂ laser appl. 7-51531
 ALGOS II He-Ne laser alignment equipment (Rumanian) 7-11001
 Asterix IV I laser, design and performance 7-10913
 ATF, FIR interferometer, development of high power FIR lasers 7-11757
 carbonyl fluoride, laser lines, optically pumped, heterodyne freq. meas. 7-36943
 CO₂-N₂ laser containing isotopically substituted molecules, active medium props. 7-43055
 condensed- and compressed-gas lasers, review 7-36952
 conference, laser science advances, Dallas, TX, USA (Nov. 1985) 7-9573
 15-N cyanogen fluoride FIR laser lines, CW optically pumped 7-25799
 dibromomethane, optically pumped laser, FIR laser line meas. 7-57306
 difluoromethane, CO₂ laser pumped, freq. meas. on FIR laser emissions 7-1084
 difluoromethane laser pumped by CO₂ laser source, Stark cell stabilisation 7-43134
 difluoromethane pumped by ¹²C¹⁶O₂, ¹²C¹⁸O₂ lasers, submillimetre emission assignment 7-36944
 diiodomethane, optically pumped laser, FIR laser line meas. 7-57306
 discharge laser, photo-initiated, electrically excited, electron density meas. 7-31335
 double-pass amplifier with phase conjugate mirror, different frequencies counterpropagating waves amplification 7-50598
 ethyl iodide, laser lines, optically pumped, heterodyne freq. meas. 7-36943
 fast plasma mixing excitation method for CW gas lasers 7-15893
 fast plasma mixing excitation method for gas lasers 7-15899
 FIR lasers, high power, review 7-36976
 FIR lasers, optically pumped, appl. in plasma diagnostics 7-5877
 FIR molecular lasers, optically pumped, freq. meas., 0.1 to 8 THz, review 7-43068
 FIR science and technology, conf., Quebec, Canada (June 1986) 7-35095
 fluoromethane, FIR laser, simultaneous tunable Raman and fixed frequency oscillations 7-57302
 fluoromethane, optically pumped laser, FIR laser line meas. 7-57306
 fluoromethane laser, helical feedback, higher modes 7-15844
 fluoromethanes, ¹²CH₃F and ¹³CH₃F, tunable far-infrared lasers 7-36951
 He-Ne lasers, single frequency, anal. (Chinese) 7-5870
 He-Ne lasers stabilized to ¹²⁷I₂ at 605 nm 7-20309
 He-Ne/ZZ 7-18761
 HeNe/methane laser, absolute frequency meas. at 88 THz 7-18762
 high reliability, anal. methods (German) 7-20188
 high-power, twin-frequency FIR lasers for plasmadiagnostic applications 7-11751
 inert gas, hollow cathode discharge, at. energy level excitation, laser lines 7-1804
 laser, compact high-power finite-impulse-response, pumped in CO₂ laser cavity 7-5907
 medical hand-held surgical CO₂ lasers, advanced appls. 7-34219
 metal atoms and ions, lasing mechanism and energy characts., relax. processes of metastable states 7-62673
 metal halides, in double pulse lasers, vapour press. eqn. 7-50542
 metal strip gratings as submillimetre laser output couplers, power transmission theory 7-43339
 methane-d₂ laser, submillimetre molecular, new emission lines 7-1089
 methanol, FIR laser transitions, FIR and IR spectroscopic studies 7-36625
 methanol, FIR lasers, intracavity triple reson. spectroscopy 7-10560
 methanol FIR laser, optical pumping by powerful stable CO₂ laser 7-10993

gas lasers continued

- methanol high power FIR cavity laser system with long-term stability 7-36982
- methanol laser lines from torsionally excited CO stretch states, and from OH-bend, CH₃-rock, and CH₃-deformation states 7-36942
- methanol pumping by CO₂ waveguide laser, FIR lines 7-20263
- methanol pumping sources, differ free stabilisation using absorption cell 7-11756
- methanol-d₁ lasing lines on IR pumping by CW CO₂ laser 7-1082
- methanol-d₄ lasing lines on IR pumping by CW CO₂ laser 7-1082
- methyl chloride, CO₂ laser pumped, freq. meas. on FIR laser emissions 7-1084
- methyl fluoride-d₃, and isotopic, laser lines, optically pumped, heterodyne freq. meas. 7-36943
- methylene chloride, far IR laser, optically pumped by CO₂ laser 7-62670
- molecular lasers, optically pumped, instabilities 7-25804
- multimode, total electric field strength, temporal evolution 7-15848
- photoacoustic spectroscopy of humid and polluted air using CO and CO₂ lasers 7-20569
- plasma diagnostics, CO₂ laser Thomson scatt., detection limits for α -particle meas. 7-1763
- Polish lasers and masers, development (*Polish*) 7-15907
- positive *P* representation and the laser equations 7-10909
- propargyl fluoride FIR laser lines, CW optically pumped 7-25799
- pump injection into FIR laser resonator using Al₂O₃ waveguide 7-43356
- pumping gas lasers, spectral transform. of Sun's radiation by black body 7-43066
- RF cavity for gas laser excitation 7-57378
- ring laser with two-anode element, reactive oscillations 7-50589
- ring lasers, asymmetry in wave interaction 7-36995
- self-sustained volume discharge initiation in lasers by radioisotopes 7-50534
- single-mode operation, inertial props. 7-62660
- small optically pumped CW far-infrared laser tunability and dynamics in high press. regime 7-20197
- soft X-ray laser development at Princeton, progress 7-20251
- statistical characteristics of emission of laser with nonlinearly absorbing cell 7-20215
- thermal processing of materials using CO₂ and solid state lasers (*Rumanian*) 7-16624
- vinyl chloride FIR laser lines, CW optically pumped 7-25799
- volume discharges, high pressure in gas lasers, review 7-36953
- water vapour-He laser, pulsed and CW operation at 28 μ m 7-36939
- waveguide lasers with diffraction grating, frequency selectivity and resonator losses 7-43158
- wavelength comparison, using Fourier transform spectrometer 7-20311
- Ar, automatic calibration system for laser power standard, expt. and performance eval. (*Japanese*) 7-11019
- Ar fibre laser, stimulated Brillouin scattering, single-mode and multimode pumped, spontaneous mode locking 7-1079
- Ar milliwatt laser with modern capillary design (*German*) 7-20274
- Ar⁺ laser, 514 and 458 nm, for use in holography 7-62721
- Ar-N₂, proton beams angle and energy characts. determ. appl. 7-36368
- Ar-N₂ laser pumping by plasma focus generated charged particle beams, num. calcs. 7-63367
- Ar-Xe laser at 1.73 μ m, electron beam and electric field pumped 7-1077
- Ar-Xe pulse-periodic large-volume electron beam-controlled laser, IR transitions in Xe atom 7-43059
- Au vapour laser, design, construction and performance (*Chinese*) 7-5903
- Ba vapour laser, mechanism limiting pulse repetition freq. 7-43071
- CO electroionisation lasers, injection of laser mixture in liquid phase 7-10921
- CO laser amplifier, electroionisation, saturated amplification mode 7-5876
- CO laser discharges, electron-beam-controlled, maximum input energy and field intensity 7-44285
- CO laser four-wave mixing, phase conjugation in carbon tetrachloride 7-31401
- CO lasers, electroionisation radiation, spectral brightness increase 7-5875
- CO visible multiline laser, lifetime improvement 7-50582
- CO₂ amplifier with mirror utilizing degenerate four-wave interaction 7-25837
- CO₂ annular gain laser, multiple pass unstable resonator 7-36991
- CO₂, CW laser, unsaturated gain coeffs., saturation intensity (*Korean*) 7-25797
- CO₂ CW lasers, DC discharge in pin plate electrode configuration with auxiliary electrode 7-51526
- CO₂ compact wide-aperture single-mode TE laser with low chirp rate 7-50580
- CO₂ continuous-flow laser with unstable resonator, acoustic vibrs. 7-25796
- CO₂ gas laser, double coupled waveguide, RF excitation expt. exam. 7-31361
- CO₂ gas laser, preionisation using α particles study 7-62508
- CO₂ high power fast flow laser facility 7-57296
- CO₂ high power laser, pumping by self-sustained volume discharge, electron beam initiated 7-57297
- CO₂ high-power long-pulse laser design for plasma diagnostics 7-1762
- CO₂ high-pressure discharge laser with plasma cathode 7-57298
- CO₂ high-pressure laser, direct optical pumping with pulsed HF pump laser 7-50533
- CO₂ homogeneously broadened ring laser, optical bistability and instabilities due to mode-mode competition 7-62735
- CO₂ hybrid laser, longitudinal mode selection for subthreshold operation 7-25795
- CO₂, in laser surgery, speculum surface finish effect on beam refl. 7-65830
- CO₂, intramode and Fermi relax. influence on multiple-pass short pulse energy extraction 7-57156
- CO₂ laser, 4.3 μ m, longitudinal-discharge output parameters 7-43056
- CO₂ laser, active medium vibr. relax., decay rate, phase absorpt. method 7-43058
- CO₂ laser, chaotic attractors in crisis 7-43178
- CO₂ laser, compact axial flow, multikilowatt operation 7-57295
- CO₂ laser, continuous electroionis., output characts. (*Russian*) 7-20182
- CO₂ laser, electronic current source, power modulation capability (*German*) 7-50601
- CO₂ laser, form. of self-maintained volume discharge using compact electrode system 7-63394
- CO₂ laser, gain-modulated single mode CW laser instabilities and chaos 7-43057

gas lasers continued

- CO₂ laser, gas transport, cylindrical geometry, high power, development 7-43149
- CO₂ laser, high-power industrial, operation 7-43054
- CO₂ laser, hot-cell-free, at 4.3 μ m 7-15891
- CO₂ laser, intracavity optically controlled cryst. modulators 7-10911
- CO₂ laser, line centre stabilised, frequency shift 7-15839
- CO₂ laser, modulated, single-mode, dynamic behaviour and dimens. chaos 7-1074
- CO₂ laser, optical bistability, regular- to sequence-band switching 7-5947
- CO₂ laser, optogalvanic Lamb dip freq. stabilisation 7-31301
- CO₂ laser, piezoelectric Q switching 7-50608
- CO₂ laser, pulse generator supply 7-1195
- CO₂ laser, Raman conversion from far-wave mixing in p-H₂ 7-25877
- CO₂ laser, short pulse cold-cathode glow-discharge electron beam pumped 7-43150
- CO₂ laser, single-mode operation, inertial props. effect 7-62660
- CO₂ laser, synchronisable, injection locked, Q-switched, mode-locked, cavity dumped 10 atmosphere 7-62736
- CO₂ laser, TE CW, influence of electrical discharge homogeneity 7-50537
- CO₂ laser, TEA, tunable multiline and single line operation at 10.6 μ m and 9.4 μ m 7-31300
- CO₂ laser, TEA, with three cavity mirrors, two-line operation 7-5869
- CO₂ laser, TEA, with unstable resonator, influence of external radiation injection 7-36936
- CO₂ laser, transverse flow, elec. discharge parameters 7-20279
- CO₂ laser, ultrashort pulse generation by square-wave mode locking and cavity dumping 7-43177
- CO₂ laser amplifier, multiatmosphere high gain, characts. and gain at 9.294 μ m 7-57366
- CO₂ laser array, 2D effective phase locking studies 7-50607
- CO₂ laser beam, kinetic self-focusing in air 7-20299
- CO₂ laser cathode systems, characts. 7-15900
- CO₂ laser detection, using CdHgTe detector 7-5915
- CO₂ laser discharges, electron-beam-controlled, maximum input energy and field intensity 7-44285
- CO₂ laser emission freq. continuous tuning band, widening using combined resonators 7-25847
- CO₂ laser gas transport system, compact axial flow 7-57367
- CO₂ laser heterodyne bias frequency-locking for coherent optical communication (*Chinese*) 7-57382
- CO₂ laser P(16) transition, temp. variation of linewidth 7-36934
- CO₂ laser pulse duration control by intracavity IR absorbing gas cell 7-43174
- CO₂ laser pulse shaping and passive mode-locking with nonlinear Michelson interferometer 7-15914
- CO₂ laser pumping source for CH₂F₂ laser, Stark cell stabilisation 7-43134
- CO₂ laser radar, coherent FM CW, signal amplitude distrib. meas. 7-40570
- CO₂ laser radar, imaging, Q-switched 7-5937
- CO₂ laser radar performance, target and atmospheric influence 7-40571
- CO₂ laser spectrum monitoring and displaying instrument 7-5935
- CO₂ laser system for plasma heating 7-32031
- CO₂ laser TE, tunable using near grazing incidence grating, performance 7-43052
- CO₂ laser welding, nuclear reactor fuel cladding repair (*Japanese*) 7-15243
- CO₂ lasers, CW, tunable, length reduction using Fabry-Perot resonators 7-11010
- CO₂ lasers, high energy picosecond 10 μ m pulses 7-62665
- CO₂ lasers, SiC ceramic optical waveguide (*Japanese*) 7-6001
- CO₂ lasers, unconventional material processing appl. 7-17759
- CO₂ lasers with high pressure volume discharges, review 7-36953
- CO₂ lasing characts., effect of waveguide statistical surface roughness 7-50536
- CO₂ lidar systems, high speed tuning mechanism 7-36978
- CO₂ longitudinal, with multisegment hollow cathode discharge 7-1075
- CO₂ mini-TEA lasers, He-free emissions 7-50535
- CO₂ powerful stable laser, optical pumping of methanol FIR laser 7-10993
- CO₂ pulse-periodic laser, gas mixture comp. stabilisation by hopcalite 7-25838
- CO₂ pulse-periodic laser radiation for metal processing, physical laws 7-51824
- CO₂ pulsed laser, medium repetition rate, materials processing appls. 7-20184
- CO₂ pulsed laser freq. dynamic tuning, multispike lasing using intracavity cell with IR absorbing gas 7-62663
- CO₂ pump laser cavity for compact high-power NH₃ laser 7-5907
- CO₂ round-trip amplifier with wavefront-reversing mirror, energy characts. 7-43053
- CO₂ scanning therapeutic laser, thermal effect on tissues 7-47162
- CO₂ single and multilongit. mode laser emissions, SHG in CdGeAs₂ 7-43211
- CO₂ TEA laser, characteristics of confocal unstable resonator (*Korean*) 7-25848
- CO₂ TEA laser, high-power modulation by injection-locked mode-beating 7-62738
- CO₂ TEA laser, Q-switching effect 7-15841
- CO₂ TEA laser, self-sustained volume discharge initiation in lasers by radioisotopes 7-50534
- CO₂ TEA laser, single-mode, using self filtering unstable resonator configuration 7-25850
- CO₂ TEA laser, tunable travelling-wave, single mode operation 7-15840
- CO₂ TEA laser emitting in 11 μ m region, gain and output parameters 7-1073
- CO₂ TEA lasers, spectral control by injection-seeding 7-25857
- CO₂ thin film-coated waveguide lasers, output power characteristics 7-62664
- CO₂ thin-film-coated waveguide laser, RF excited 7-5908
- CO₂ transversely excited lasers, use in Compton scattering free electron laser system, beam trapping expt. 7-1136
- CO₂ tunable waveguide laser with expanded tuning range 7-36981
- CO₂ ultrashort laser pulse optical free induction decay, freq. spectrum 7-31405
- CO₂ waveguide laser, anomalous refr. indices of amplifying medium 7-36933
- CO₂ waveguide laser, Cohen model 7-20183
- CO₂ waveguide laser, design and performance 7-15906

gas lasers continued

- CO₂ waveguide laser, tunable, for optical pumping 7-20263
 CO₂ waveguide laser as tunable IR radiation source 7-31298
 CO₂ waveguide lasers, DC and RF-excited, life problems 7-11000
 CO₂ waveguide lasers with RF excitation, emission freq. tuning 7-43147
 CO₂-He-N₂ laser glow discharge, influence of magnetic fields on instability growth 7-5868
¹⁴CO₂-¹²CO₂ isotope laser 7-31299
 CO₂ laser emitting in 4.2 μm range, construction and props. 7-1186
¹²C¹⁸O₂, ¹²C¹⁶O₂ laser pumps for difluoromethane, submillimetre emission assignment 7-36944
 Cd⁺ recombination laser oscillation, obs. 7-43075
 Co₂, Nd:YAG dual wavelength laser system for surgery 7-47198
 Co₂-N₂-He laser mixture, beam-driven discharge, gasdynamic processes 7-50538
 Cu halides, vapour lasers, resonance radiation trapping effects 7-62669
 Cu II laser with spherical and circularly slotted hollow cathodes, output power and operation period 7-50587
 Cu II laser with tulip shaped hollow cathode 7-43145
 Cu vapour laser, four-wave mixing obs. 7-20359
 Cu vapour laser, molecular gas impurities effects 7-36948
 Cu vapour laser, pumping of dye laser, U isotope separation appl. 7-50553
 Cu vapour laser, self-heated, thermal conditions and stimulated emission characts. 7-25802
 Cu vapour laser, structure and characts. (*Chinese*) 7-10994
 Cu vapour laser for U isotope separation 7-50546
 Cu vapour laser using metallic walls for discharge confinement 7-43146
 Cu vapour laser with self-pumped wavefront reversing mirror 7-1185
 Cu vapour laser with unstable resonator, background radiation influence on dye lasing 7-25856
 Cu vapour laser with wavefront-reversing mirror induced in active medium 7-1199
 Cu vapour lasers, resonance radiation trapping effects 7-62669
 CuCl laser radiation at 510 nm, internal attenuation 7-36949
 D₂O, optically pumped laser, FIR laser line meas. 7-57306
 F₂, f ¹¹I_g state, electron impact, laser photon emission 7-5778
 F₂ laser at 157.6 nm excited by electric discharge 7-25803
 F₂-He discharge pumped laser, 157.6 nm, efficiency 7-43077
 H₂, maximum specific deposited energy, role of VV processes 7-31303
 HF pulsed pump laser, direct optical pumping of high-press. CO₂, N₂O lasers 7-50533
 He-Ar(Ne) lasers, pumping by CO₂-laser induced optical break-down 7-62668
 He-Cd hollow cathode laser, green line oscillations, lower levels population 7-43065
 He-Cd positive column discharge 441.6 nm laser level (*French*) 7-11811
 He-Ne, automatic calibration system for laser power standard, expt. and performance eval. (*Japanese*) 7-11019
 He-Ne, fibre optic evanescent-wave coupling force transducer 7-41367
 He-Ne, I₂ saturated absorption lines identification at 543 nm 7-20372
 He-Ne, performance assessment of laser wavemeter (*Korean*) 7-24692
 He-Ne, stabilised by I₂ external absorption cell 7-20308
 He-Ne laser, internal mirror, freq. and power stabilisation using fan (*Korean*) 7-25849
 He-Ne laser, methane stabilised, frequency meas. of methane hyperfine line 7-20190
 He-Ne laser, mode-crossing reson., intracavity distance and mode-locking quality anal. 7-31373
 He-Ne laser, photothermal deflection, trace gas anal. appls. 7-61381
 He-Ne laser, stabilised by saturated absorption of methane, frequency shifts obs. 7-20192
 He-Ne laser, standardisation for metrological purposes 7-5909
 He-Ne laser, three-mode, frequency resonance 7-36937
 He-Ne laser, transportable, methane stabilised 7-20191
 He-Ne laser as light source in schlieren optics methods 7-57503
 He-Ne laser at 0.633 μm, frequency stabilisation, using polarisation modulation 7-20295
 He-Ne laser at 612 nm, stabilised by external absorption cell 7-20270
 He-Ne laser beam meas. using direct looking apparatus for light intensity distribution (*Japanese*) 7-56314
 He-Ne laser for optical fibres fault location 7-31545
 He-Ne laser heterodyne bias frequency-locking for coherent optical communication (*Chinese*) 7-57382
 He-Ne laser stabilised by methane saturable absorption, effects leading to frequency shifts 7-50540
 He-Ne laser stabilised by Lamb dip, emission frequency scatter, causes 7-62667
 He-Ne laser tuned by axial mag. field, mode competition 7-50539
 He-Ne laser wavelength meas. using 0.63 μm transition 7-1208
 He-Ne laser with high specific output power (*German*) 7-20187
 He-Ne lasers as sources of stable subnanosecond pulses 7-43060
 He-Ne Q-switched laser, radiation laser, radiation growth 7-15842
 He-Ne Zeeman laser, nearly degenerate four wave mixing and high order effects 7-1078
 He-Ne Zeeman lasers for coherent optical fibre system 7-50786
 He-Se laser discharge, population density ratios determ. from Kirchhoff's law for excited He I states 7-58072
³He-Ne gas laser, neutron pumping from tokamaks 7-62666
 Hg, laser, optical pumped with UHF excitation 7-36946
 I₂, photodissociation laser with thermal recirculation (*Czech*) 7-57301
 Kr lasing action, output pulse lengths achieved with electron beam pumping 7-15843
 KrF laser produced plasma, stimulated Brillouin scatt. 7-32032
 KrF laser-matter interaction in the long pulse, low intensity regime 7-32030
 La_{0.7}Sr_{0.3}CoO₃ cathodes for CO₂ waveguide lasers, electrical and emission characts. 7-59383
 Mn halides, vapour lasers, resonance radiation trapping effects 7-62669
 Mn vapour laser, emission spectrum and its time evolution 7-1088
 Mn vapour lasers, resonance radiation trapping effects 7-62669
 Mo, optical gain following Mo(CO)₆ multiple photon dissociation 7-31124
 N₂, electron beam induced lasing at atmospheric pressures 7-15845
 N₂ gas laser, peak power and starting voltage 7-15851
 N₂ laser, effect of organic additives 7-5874
 N₂ laser, plasma electrode, discharge characteristics, optimisation 7-43138
 N₂ laser freq. conversion by H₂ stimulated Raman scatt. 7-57452
 N₂ subnanosecond laser, transient photoconductivity meas. of amorphous conductors 7-18806
 N₂ TEA-TE laser, high power, spectrosc. appls. 7-36954

gas lasers continued

- N₂⁺ laser, pulse shortening in active media 7-43196
 N₂-CO₂-CS₂ mixture, calc. of gains for vibrational transitions 7-1087
 NH₃ CW MIR laser, intensity and half-widths, absorpt. meas. 7-36941
 NH₃ laser, compact high-power finite-impulse-response, pumped in CO₂ laser cavity 7-5907
 NH₃ lasers, FIR, instabilities and chaotic emission 7-15849
 NH₃ lasers, line-tunable operating at wavelengths of 11 to 14 μm 7-5872
 NH₃ lasers, optically pumped, CW operation in mid-IR 7-36950
 NH₃ Raman laser, single-mode homogeneously broadened, self-pulsing instabilities 7-10922
 NH₃ superradiant Raman FIR laser with nonlinear reson. four-wave mixing generation of medium IR emission 7-50657
¹⁴NH₃ and ¹⁵NH₃ laser pumped transversely by CO₂ laser 7-1085
¹⁵NH₃ laser with two-photon optical pumping 7-43069
 N₂O high-pressure laser, direct optical pumping with pulsed HF pump laser 7-50533
 Na₂, collisional energy transfer, dimer laser action 7-5757
 Na₂ photoionisation pumping via two-electron shakeup 7-20195
 Na₂ violet bands, electronic assignments 7-15846
 Na₂3 laser emission studied using heat pipe oven device 7-15882
 Nd_{0.7}Sr_{0.3}CoO₃ cathodes for CO₂ waveguide lasers, electrical and emission characts. 7-59383
 Ne 3.39 μm line, diaphragmed laser near field (*French*) 7-43180
 Ne I lines, laser generation in water cooled helical hollow cathode discharge 7-57299
 Ne laser, superradiance under delayed excitation, asymmetry 7-1076
 Ne laser based on 3p-3s transitions with electron beam excitation 7-20185
 Ne lasing action, output pulse lengths achieved with electron beam pumping 7-15843
 Ne pulsed transverse discharge, population inversion, secondary process influence 7-58084
 Pb vapour pulsed laser operating at high excitation pulse repetition freqs. 7-43072
 Se anti-Stokes Raman laser, high-power, radiating at 169 and 146 nm 7-43076
 Se XXV plasma, laser produced, electron impact, laser transitions 7-26508
 Xe gas laser, neutron pumping from tokamaks 7-62666
 Xe lasing action, output pulse lengths achieved with electron beam pumping 7-15843
 Xe-He active medium, HF H-discharge excited, characts. investig. 7-20189
 XeCl laser, with coaxial ceramic pulse-forming line 7-43061
 XeF laser in Ar and Ne diluent, improved performance 7-25800

gas permeability see permeability

gas phase electron diffraction

- acetylacetone, mol. struct. determ. by gas phase electron diffraction 7-50358
 2-azido-1,3-butadiene, vibr. spectra, mol. struct., conform., GPED anal., Raman and IR spectra anal. 7-36608
 bis(dichlorophosphoryl)methane, struct., conformational equilib., GPED, Raman and IR spectra 7-57176
 trans-1-chloro-2-butene, conformation and mol. struct. determ. by gas phase electron diffraction 7-50356
 2,3-diazido-1,3-butadiene, vibr. spectra, mol. struct., conform., GPED anal., Raman and IR spectra anal. 7-36609
 1,2-dichloroethene, isomeric mixtures, determ. of struct. and comp., GPED spectra anal. 7-36763
 diisopropylamine, mol. struct. and conform., GPED, Raman IR spectra, MO calcs. 7-20043
 1,3-dioxolanes, pseudorotation, gas-phase electron diffraction. investig. 7-50354
 dodecafluorooctahydrothiophene, gas phase, geometric struct., GPED spectra anal. 7-36764
 ethane-1,2-dithiol, mol. struct., conform., electron diffraction. obs. 7-50355
 ethylamine, geometrical structural parameters calcs. GPED 7-20042
 monocyclic free mols., conformation trends, electron diffraction data 7-15709
 propanal, struct. determ. by gas phase electron diffraction 7-50359
 1,1,2,2-tetrabromodisilane, gas phase, mol. struct., conform. comp., GPED spectra anal. 7-36762
 tetrachloromethylenediphosphine struct., GPED 7-57175
 s-triazine, gas phase, mol. struct., GPED anal., ab initio force field calcs. 7-36457
 sym-tribromobenzene, struct., vibr., GPED 7-57177
 trifluoromethyl phosphorane, conform. and struct., GPED anal. 7-20044
 trimethylsilylthiocyanate in gas phase, mol. struct. determ. by electron diffraction 7-50357
 vinyl formate, gas phase structure anal., ab initio calcs., molecular mechanics calcs., IR spectra 7-19691
 ClO₂ struct., pot. functions, electron diffraction and spectroscopic data 7-15708
 CsAlF₄ struct., GPED automatic background subtraction 7-15710
 HgBr₂ struct., GPED automatic background subtraction 7-15710
 SbCl₃ struct., GPED automatic background subtraction 7-15710
 SeO₂ struct., pot. functions, electron diffraction and spectroscopic data 7-15708
 WCl₆ struct. parameters, GPED statistical anal. 7-57174
 W₂Cl₆ mol. struct., GPED 7-5770

gas-surface interactions see sorption

gas technology, natural see natural gas technology

gas turbines

- see also turbogenerators
 alloys, heat resistant gas turbine, creep behaviour (*German*) 7-3389
 CAD system with Denton scheme for flow program, comparison with expt. results 7-63177
 coatings and coating processes for steam turbine blades, characterisation 7-46313
 coatings in high performance gas turbines, high temp. behaviour, laboratory tests 7-46694
 computer-aided interactive design system, Denton scheme for flow program 7-63176
 electrodeposits for high temp. oxidation and corrosion resistance, appl. for gas turbines 7-46358
 engineering ceramics, gas turbine engine appls. 7-3241
 superalloys, columnar grained and single-crystal, high-temp. strength with surface recrystallised layer (*Japanese*) 7-53788
 ZrO₂, Y₂O₃, dip process thermal barrier coatings for gas turbines 7-46314

gasdynamic lasers

- alkali metal-mol. gas mixture, cooling in supersonic nozzle, population inversion of electronic states 7-31304
- microwave excited flow lasers, configs. and operation (*German*) 7-36986
- nonequilibrium flows, transient processes, EM radiation field effect, shock wave effects 7-43979
- supersonic jets, chemical anal. appl. of gasdynamic focusing 7-20752
- unstable resonator with dihedral corner reflector in gasdynamic laser, props. 7-62729
- CO₂ laser, high-power transverse-flow, props. 7-36935
- CO₂-N₂-H₂ gasdynamic laser with 2D nozzles, gain optimisation 7-50541
- CO₂-N₂-H₂O gasdynamic lasers, collisional relaxation mechanisms 7-20181
- N₂O downstream mixing gasdynamic laser, numerical simulation 7-36940

gaseous insulation

- alpha-particle corona streamer counter 7-55333
- electrostatic precipitators back-corona initiation, anal. 7-51555
- ignition voltage of spark gaps in technically important gases (*Czech*) 7-32144
- impulse surface discharge in compressed air in nonuniform field, characts. 7-51550
- magnetic switches, formative time lags, extension of Davidson's theory 7-51547
- strongly electronegative gases; figure of merit meas. 7-51553
- N₂ flashover at dielectric interfaces: the interaction of surface and volume processes 7-51549
- SF₆ and air, impulse breakdown voltage for nonuniform field gaps with different wavefronts 7-51546
- SF₆ and SF₆ mixtures, streamer, leader and corona formation under positive impulse 7-37773
- SF₆ and SF₆ mixtures, streamer to leader transition under positive impulse 7-37774
- SF₆ conditioning under repetitive positive HV conditions 7-51552
- SF₆ discharge characts. and insulating props., review of Japanese research 7-44279
- SF₆ gas, Paschen's law, impurity effects 7-37771
- SF₆, high-current discharges, optical diagnostics 7-37775
- SF₆ puffer-type circuit breakers, effects of aerodynamic shocks on performance 7-51223
- SF₆ under DC stress, potential distortion from change on solid insulators 7-51554
- SF₆ + Freon 113 mixtures in nonuniform field gaps, breakdown 7-51551
- SF₆ + O₂, decomp. rate of SF₆, influence of O₂ in corona 7-51548

gases

- see also aerodynamics; compressibility of gases; density of gases; dielectric properties of gases; diffusion in gases; electric breakdown of gases; electrical conductivity of gases; equations of state of gases; ionisation of gases; kinetic theory of gases; liquefaction of gases; luminescence of gases; Scott effect; Senfleben-Beenakker effect; specific heat of gases; thermal conductivity of gases; thermal diffusion in gases; viscosity of gases*
- mixtures, standard, specifications for pure gases as initial components 7-56212

gate arrays *see cellular arrays***gate turn-off devices** *see thyristors***gauge field theory**

- see also Weinberg model; Yang-Mills theory*
- 3D Abelian gauge model, simplicial pseudorandom lattice study, lattice as extremum of action 7-4975
- θ -sectors in OS construction, quantum mech. and gauge theory examples 7-56088
- ϕ^4 theory, stochastic quantization simulation with slave eqns. 7-48960
- abelian (V-A) theories in 4D, fermion number nonconservation and cold neutral matter 7-41595
- abelian gauge field dynamics, acceleration 7-405
- Abelian gauge theories, systematic search in n-dimens. Minkowski space 7-4973
- abelian lattice gauge theories, large Wilson loop averages from the Schwinger-Dyson equation 7-61456
- Abelian lattice gauge theories, mean field methods for strings and monopoles 7-24772
- Abelian quark-gluon plasma, gauge invariant eqns. of motion, QED derivation 7-61823
- Abelian theories, gauge-invariant regularizations 7-61471
- Abelian U(1) lattice gauge theory, mag. monopoles and charged states 7-24760
- action functional for general gauge field theory, local minimality 7-18983
- action principle and quantization of gauge fields 7-48985
- Adler-Bell-Jackiw anomaly in lattice gauge theory (*Chinese*) 7-48978
- Aharonov-Bohm effect, analogue in spin gauge theory 7-30196
- analytic structure in presence of fermions in arbitrary symmetry 7-30170
- anisotropic homogeneous cosmological models, gauge-invariant perturbations 7-48494
- anomalous gauge theories, path integral quantization 7-56427
- antisymmetric string actions for free bosonic string on external flat space 7-35825
- Atiyah-Singer index theorem, boundary conditions and vacuum quantum numbers 7-61447
- axial gauge non-Abelian gauge theory, stochastic quantisation, Langevin eqn. 7-41627
- axial vector current props., γ_5 and dimensional regularisation 7-61504
- axially symmetric higher-dimensional gravity, Belinsky-Zakharov N-soliton transforms. 7-41207
- axially symmetric higher-dimensional gravity, Neugebauer-Kramer transforms. 7-41206
- Batalin-Fradkin-Vilkovisky formalism for higher-order theories 7-56410
- Becchi-Rouet-Stora transform for open algebra theories (*French*) 7-4943
- book, gauge field theory introduction 7-35134
- book, supersymmetry, superfields, supergravity 7-14724
- boson-fermion duality in 4D, photon construction from neutrino pairs 7-41585
- bosonic massless gauge fields with arbitrary spin and permutation symm. 7-4960
- bosonic string, Hamiltonian and Lagrangian constraints and gauge fixing 7-19088
- bosonic string compactification, conformal subalgebras of Kac-Moody algebras 7-35826
- bosonic string field theories, gauge invariant action construction 7-10042

gauge field theory continued

- BRS transformations and anomalies, differential geometric interpretation 7-56457
- BRST hamiltonian quantization of the supersymmetric particle in relativistic gauges 7-30213
- canonical quantization, Lagrangian and Hamiltonian formalisms 7-41586
- Cartan's contortion, relation to Eotvos torsion expt. 7-4326
- charged lepton, mass, gauge field theory 7-61433
- chiral anomalies in gauge and gravitational interactions, ID SUSY path integral approach 7-41661
- chiral gauge theories, anomalies and Weyl modes 7-56447
- chiral gauge theories, gauge-invariant point-splitting procedure 7-56425
- chiral gauge theory, anomalous, quantization and inclusion of anomaly cancelling fermions during regularization 7-56428
- chiral QCD, topological anomalies from Dirac equation 7-49051
- chiral SU(2)×SU(2) lattice theory with spin 3/2 action in 2D; Monte Carlo anal. 7-15067
- chordal gauge symmetry in string theory, local gauge theory of extended object 7-56454
- closed bosonic and Neveu-Schwarz free strings and their gauge invariance 7-24860
- closed string, spacetime gauge invariance origin, quantisation 7-35827
- closed strings in open-string field theory 7-56529
- Coleman-Weinberg transition on a lattice, mean field anal. 7-35705
- compactified superstrings and torsion, light-cone gauge investigation 7-35816
- complex Langevin equation and Monte Carlo simulations of actions with static charges 7-24769
- conference, strong interactions and gauge theories, Les Arcs, Savoie, France (March 1986) 7-60876
- conformal and current algebras on a general Riemann surface 7-56475
- conformally invariant scalar field, anisotropy damping and particle prod. at finite temp. 7-56132
- constraint and functional methods in field theory 7-56452
- continuum regularization of gauge theory with fermions 7-35723
- correspondence formula for gauge theories with and without ghost fields 7-402
- correspondence principle, gauge theories with Weyl fermions 7-56484
- coset space dimens. reduction of antisymm. tensor fields, Becchi-Rouet-Stova supersymmetry 7-41581
- cosmic axion decay to photons in microwave and IR regions 7-14695
- cosmology, gauge-invariant perturbations in generalised inflationary models 7-48112
- Coulomb-gauge QED, one-loop vertex function in parametric integral form 7-19059
- Coulomb-like gauge for massive gauge fields, SU(2) model appl. 7-4957
- covariant and consistent anomalies in even-dimensional chiral gauge theories 7-19019
- covariant factor ordering of gauge systems 7-35696
- covariant heterotic strings, classical gauge and BRST struct. 7-49105
- covariant heterotic strings, supergauge field theory 7-35834
- covariant string field theory, gauge fixing, physical degrees of freedom 7-5072
- covariant string field theory, gauge-fixed action and BRS transformation 7-19087
- covariant superstring with N=1 global supersymmetry, quantum geometry 7-35735
- critical behavior and renormalization of quantum fields 7-49004
- curvature and torsion from matter, Lorentz gauge symm. 7-41208
- dimensional phase transitions, interacting spinors, gauge fields, background gravity, cell complex 7-35697
- dimensional reduction, spontaneous symm. breaking and absence of chiral fermions 7-41594
- dimensional reduction of gauge theories yielding unified models spontaneously broken to SU₃×SU₂×U₁ 7-35773
- Dirac equation symmetry, with external non-Abelian gauge field 7-41589
- Dirac fermion propag. on hypercubic lattice with random hopping parameters 7-4967
- Dirac operator coupled to non-Abelian gauge fields, two-dimensional chiral anomaly calc., validity 7-61463
- Dirac-like equations for gauge fields 7-4978
- discretization effects on classical Klein-Gordon lattice 7-35668
- double cohomology series, family index theorem (*Chinese*) 7-56399
- E₇ unified model based on coset space dimensional reduction scheme, fermion masses 7-61536
- E₈×E₈ superstring theory, gauge hierarchies for intermediate mass scale 7-41686
- E₈×E₈ superstring theory, low-energy gauge interactions, renormalisation group anal. 7-41687
- effective gauge action on a finite-size lattice, SU(2) theory simulations 7-41620
- effective gauge theory for low energy mesons, stable and unstable classical solns. 7-427
- Eguchi-Kawai model, triangle-lattice quenched, Monte Carlo study 7-30156
- Eguchi-Kawai models, stochastic quantisation 7-56450
- Einstein-Maxwell eqns., gauge freedom of plane symmetric line elements 7-18652
- electroweak SU(2)×U(1) lattice gauge theory with variable-length Higgs fields 7-24791
- elementary scalar particle existence, U(1) Higgs model and scalar electrodynamics 7-10017
- Eotvos anomaly, gauge field coupled to fermion number interpretation 7-18682
- Euclidean lattice, unified treatment of Poincare, de Sitter and conformal gravity 7-56131
- Euclidean SU(2) gauge theory, elliptic solns. 7-4974
- EXCALC code applied to general relativity and Poincaré gauge theory 7-61174
- extra gauge field structure uncovered in the Kaluza-Klein framework 7-164
- factorisation condition for bidimensional and pseudo-Euclidean groups 7-48946
- Faddeev-Popov ghosts and BRS symmetry in string theories 7-35830
- fast fermion algorithm 7-61477
- fermion-gauge field interactions, regularized determinants and non-perturbative definition of chiral anomalies 7-30176
- fermionic fields, species doubling and transfer matrices 7-56431
- fermionic string, interacting string formalisms 7-35839
- finite temperature SU(2) gauge theory, correlation length temp. depend., screening, deconfinement 7-41606

gauge field theory continued

free bosonic string, worldsheet reparametrizations and Tomonaga-Schwinger-Dirac formalism 7-35837
 free massive bosonic fields of arbitrary spin, gauge invariant action construction 7-10042
 free strings, gauge invariant field theories 7-30254
 functional determinant of massless fermions in nonAbelian gauge pot., perturbative derivation 7-30169
 gap equation models for chiral symm. breaking in QCD 7-35738
 gauge dynamics in the C-representation 7-18993
 gauge field coupled to axial U(1) charge in gravitational field, CP-effective action anal., spectral asymmetry 7-41601
 gauge potential estimation for given gauge field on M^4 7-9947
 gauge string fields from the light cone 7-48971
 gauge transformation generators in phase space/velocity phase space 7-9971
 gauge transformation group, smoothness of action on connections 7-18976
 gauged SUSY σ -model in 4D, visualisation by Killing pots. 7-4988
 Gelmini-Roncadelli model, one-loop renormalisation group anal., ν mass generation 7-24817
 general relativity, generalised harmonic gauge conditions as field eqns. for lapse and shift 7-47678
 global gauge anomalies and scattering theory 7-35701
 global gauge anomalies in higher dimensions, Z_3 anomalies in $(4k+2)$ dimensions 7-9955
 globally supersymmetric preon models with gauged colour-flavour symm. 7-19079
 glueball (0^{++}) , mass scaling, SU(N) Hamiltonian lattice calcs., Monte Carlo anal. 7-35807
 glueball mass in SU(2), effect of dynamical quarks 7-61501
 glueball mass spectrum calculation by light-cone quantization (*Russian*) 7-61594
 glueballs, tensor and scalar, mass calcs., in lattice gauge theory 7-61587
 gluon mass, gluon propagator calcs. in Landau gauge, SU(3) lattice anal. 7-61588
 gravitation, gauge theory in higher dimensional space-time and dimens. reduction 7-56127
 gravitation, Lorentz gauge theory, canonical formalism (*Chinese*) 7-9721
 gravitation and supergravity, gauge theory formulation 7-9744
 graviton propagator and infrared divergences in de Sitter space 7-48508
 gravitons, matter-induced topological mass term, fermion and gauge field contrib. 7-18669
 gravity, gauge theories and quantum cosmology, book 7-48512
 Gupta-Bleuler quantisation of the free massless spin 2 field 7-48929
 hadron-hadron interactions, orthogonal lattice gauge field configurations, nucleon-nucleon system 7-41842
 hamiltonian analysis of gauge theories with interacting p -forms 7-15055
 Hamiltonian dynamics of gauge systems 7-35695
 Hamiltonian systems with even and odd Poisson brackets, conservation laws duality 7-49015
 heat-kernel regularization of gauge theory, vanishing gluon mass 7-41624
 heavy quark forces and potentials in SU(2) lattice gauge theory (*Chinese*) 7-35657
 Hehl's Poincare gauge theory, diffeomorphisms for conformal and de Sitter groups 7-48941
 helicity amplitude calculations 7-49014
 heterotic string theory in 4D with families of chiral fermions and standard gauge symm. 7-49033
 hidden supersymmetry and spectral asymm., fermion number fractionization and anomalies 7-24800
 hierarchy problem, mass generation by nonperturbative quantum effects 7-19007
 Higgs boson masses, perturbative calcs. 7-61452
 Higgs-boson doublets, model, with no increase in parameters 7-15110
 higher dimensional matter-gravity coupled theory, 2 pots., 1 gauge group 7-61200
 hot QCD, nonAbelian Debye screening, singlet pot. and gauge symm. breaking 7-49075
 hybrid stochastic algorithms, generalised Fokker-Planck eqn., lattice gauge theory appl. 7-24770
 hypothetical long-range interaction weaker than gravity 7-24516
 induced gauge fields in a nongauged quantum system 7-41153
 induced vacuum quantum numbers in $2+1$ dimensions 7-15063
 inflation, oscillation and quantum creation in gauge extended supergravity 7-35380
 instantons and the U(1) anomaly in QCD, review 7-5048
 interacting bosonic gauge fields of any spin and parity 7-15071
 interacting bosonic strings, gauge-invariant action 7-61630
 interacting field theory in 2D, Sugawara-Sommerfield construction 7-48986
 interacting gauge-covariant bosonic string, symm. and transformations 7-35684
 interacting string dynamics, gauge invariance over a group as the first principle 7-5074
 interacting string field theory, operator formulation 7-61609
 invisible axion detectors 7-10012
 Kac-Moody current algebras of 2D massless gauge theories 7-61505
 Kaluza-Klein monopoles, motion at low energy 7-14839
 Kaluza-Klein theory, self-consistent dimensional reduction and effective action 7-41218
 Kaluza-Klein theory, SO(4) \times U(1) vacuum solns. and nonvanishing cosmological constant 7-4753
 Kaluza-Klein theory for SU(2) particle scatt. off Euclidean instanton 7-35750
 Kaluza-Klein theory with elementary gauge fields, symm. breaking mechanism 7-41192
 Kaluza-Klein theory with multiply connected extra space, gauge field coupling constants (*French*) 7-41672
 Lagrangian density of gravit. field, gauge principle and Riemannian geometry 7-61201
 Lagrangian wave equations of arbitrary helicity, gauge invariance 7-18985
 lattice action sum rules, appl. to glueballs and static quark pots. 7-48959
 lattice fermion derivative formulation, locality and chirality without spectrum doubling 7-41632
 lattice fermions in odd dimensions 7-61430
 lattice gauge theories, analytical approach based on dynamical eqns. 7-15066
 lattice gauge theories with matter fields, order parameter 7-61486

gauge field theory continued

lattice gauge theory, baryon mass calc., quark mass renormalization 7-30155
 lattice gauge theory, boundary condition effects on interior plaquettes 7-41582
 lattice gauge theory, continuum limit and renormalized trajectory, weak coupling expansions 7-19009
 lattice gauge theory, disordered fermion couplings and fermion doubling problem 7-9964
 lattice gauge theory, geometric anal. of lattice actions 7-56414
 lattice gauge theory, global symmetry restoration in high temperature Higgs theories 7-61423
 lattice gauge theory, H dibaryon mass using bag model parameters 7-61485
 lattice gauge theory, heat bath method for vectorized processing 7-18974
 lattice gauge theory, high-temperature QCD and quark matter 7-56416
 lattice gauge theory, microcanonical ensemble techniques 7-48934
 lattice gauge theory, Monte Carlo renormalization group methods 7-61476
 lattice gauge theory, Monte Carlo renormalization group transformation, β -fn. anal. 7-9957
 lattice gauge theory, propagator of Susskind fermions 7-35683
 lattice gauge theory, static screening lengths in finite-temperature pure gluon plasma 7-19003
 lattice gauge theory, stochastic quantization using Langevin and Fokker-Planck eqns. 7-24792
 lattice gauge theory, surface representations of Wilson loop expectations, confinement 7-24771
 lattice gauge theory, topology and instanton struct., Monte Carlo simulation 7-61482
 lattice gauge theory simulation using the APE computer 7-61488
 lattice gauge theory simulations, conf., Wuppertal, Germany, Nov. 1985 7-60883
 lattice gauge theory with Wilson fermions, hadron mass calcs. 7-61483
 lattice gauge-Higgs theories with local \times global symmetry groups including exact solutions 7-18992
 lattice Gross-Neveu model, recovery of chiral symm. 7-19010
 lattice Higgs model, analytic and Monte Carlo methods 7-61480
 lattice N=2 Wess-Zumino model, local Hamiltonian Monte Carlo study 7-15052
 lattice QCD, chiral symm. breaking in strong coupling limit 7-56514
 lattice QCD, deconfining phase transition and continuum limit 7-61568
 lattice QCD, deconfining transition 7-56508
 lattice QCD, improved actions, redundant operators and scaling 7-56513
 lattice QCD, large scale computing aspects 7-49068
 lattice QCD, numerical simulation of interacting fields and static interquark pot. 7-61575
 lattice QCD, quenched SU(2) simulation with staggered fermions, chiral limit 7-61602
 lattice QCD, t-expansion method 7-61573
 lattice QCD, with Wilson fermion action, finite temp. behaviour, implication on spectroscopic studies 7-19066
 lattice QCD at finite density 7-56509
 lattice QCD sum rules and spontaneous chiral symm. breaking, Monte Carlo simulation 7-61603
 lattice QCD with quark loops, Lanczos algorithm simulation 7-61571
 lattice QCD with staggered fermions, chiral props. 7-61576
 lattice QCD with Susskind fermions, current algebra relation 7-41730
 lattice QED, parity-violating fermionic vacuum currents, numerical study 7-19058
 lattice Schrodinger operators with exponential disorder, cut discontinuity, large order behaviour 7-9937
 lattice SU(2) chiral model, complex Langevin simulation on non Abelian group 7-61479
 lattice SU(3) gauge theory, deconfined phase, gluon plasma thermodynamic props. 7-41741
 lattice SU(N) QCD study at finite chem. pot. and baryon density 7-474
 lattice theory, Hamiltonian formulation for gauged nonanomalous chiral theories 7-19001
 lattice theory, weak matrix element calcs., chiral behaviour and multipoint Green's fns. 7-61484
 lattice U(1) gauge Higgs model, free charge in confining phase 7-48966
 lattice U(1) gauge Higgs model, Monte Carlo study of confinement 7-468
 lattice U(1) Higgs gauge theory, phase structure 7-4983
 lepton number/flavour nonconservation and gauge theories 7-56468
 lepton number/flavour violation, phenomenological implications of gauge theories 7-35728
 light-like integrability of string superalgebras 7-35841
 lightest glueball mass in SU(2) and SU(3) gauge theories, lattice size depend. 7-41722
 linear perturbations of gauge fields 7-9942
 linearised Toda lattice, gauge field-Toda amplitude duality 7-48621
 local baryon gauge invariance and Eotvos expt. 7-4959
 local implementations of gauge symmetries in local quantum theory 7-24757
 local Lorentz symm. breaking and space-time dimens. in gravit. theory 7-24803
 longitudinally polarised W and Z bosons, relationship to Goldstone partners, gauge invariance 7-41702
 Lorentz, conformal and gauge anomalies in external fields 7-41219
 Lorentz gauge field and spin angular-momentum 7-35715
 low-energy gauge couplings and the mass gap of N=1 supersymmetry 7-61503
 many-electron atoms, relativistic HF and RPA calcs. 7-19675
 massive gauge superfields, N=2 in harmonic superspace 7-4958
 massive spin-1 and -2 fields, gauge-invariant actions from constraint Hamiltonian dynamics 7-41611
 massless higher-spin fields, coupling and gauge algebra, rel. to string theories 7-177
 massless scalar field with gravity, Einstein's field eqns. in 3D space-time 7-41209
 massless SUSY QCD, vacuum stability, instanton-anti-instanton contrib. to vacuum energy 7-41725
 mean fields and self consistent normal ordering of lattice spin and gauge field theories 7-9978
 metric space-time as renormalisation group eqn. fixed point on fractal structs. 7-48505
 minimal N=2 supergravity in superspace 7-56135
 monopole asymptotic scatt., bound-state spectrum and dynamical symm. 7-56424

gauge field theory continued

monopoles, self-dual, scattering of gauge and Higgs fields 7-30177
 multiflavour QCD, nonAbelian bosonization and baryon mass formulae 7-61579
 multilocal model and relativistic string theory 7-35831
 $N=1$ conformal supergravity, 2D and 3D, constraints and actions, spinning strings, SUSY σ -models 7-4756
 $N=1$ supergravity, Newtonian limit, gauge soln. and torsion 7-18677
 $N=1$ supergravity, SL(2,C) gauge theory 7-24529
 $N=1$ supergravity, $SU(3)\times SU(2)\times U(1)$ models, superparticle and t -quark masses 7-41228
 $N=2$ conformal supergravity, linearized theory, $SU(2)$ extended superfield formulation 7-61204
 $N=2$ supersymmetric gauge theory, action in harmonic superspace 7-56422
 neutrino mass, lepton flavour and lepton number nonconservation 7-9989
 Nielsen identities for gauge-fixing vectors and composite effective potentials 7-61449
 non-Abelian gauge theories, Gauss' Law and antiscreening 7-24799
 non-local gauge field theory, non-Abelian field 7-48997
 nonAbelian, Gribov non-single valuedness, harmonic mappings 7-56448
 nonabelian anomaly in the light-cone gauge, superstring theories 7-30187
 nonAbelian chiral anomaly from lattice regularization 7-15072
 nonAbelian family symm., origin of fermion masses and mixing angles 7-19041
 nonabelian gauge theories, exotic string configurations 7-61458
 nonAbelian gauge theories, ghostless Feynman rules 7-48990
 nonabelian gauge theories with Cherry-Simons term, charged vortex of finite energy 7-9962
 nonabelian gauge theory, appl. of double-dimensional regularisation 7-19015
 nonAbelian gauge theory, scalar formalism using Klein-Gordon-type wave eqn. 7-4952
 nonAbelian gauge theory, Wilson loop renormalisation beyond leading order 7-61451
 nonlinear σ -model coupled to metric tensor field, spontaneous compactification 7-165
 nonperturbative effects in phase transitions through the loop corrections of matter fields 7-61429
 nonperturbative inconsistency of stochastic quantization in odd dimensions 7-61442
 nonperturbative method in field theory, gauge technique, infrared region solns. 7-41616
 nonrenormalization Theorems in superstring theory 7-41633
 nonsemisimple gauge groups, new topological terms in gauge invariant actions 7-61459
 numerical simulation using Cray supercomputers 7-61557
 $O(3)$ σ model, possible fractional spin phase transition 7-56436
 $O(3)$ nonlinear σ model, numerical simulation by Parisi-Wu stochastic quantization 7-19008
 octonions in gauge theories, soln. using composition algebras 7-35713
 one loop effective potential with spontaneous compactification, stability 7-61187
 one-loop effective action, covariant derivative expansion, Schwinger-Fock gauge condition 7-4970
 one-plaquette $U(N)$ gauge model with fermions, leading order topological expansion 7-35721
 open bosonic Polyakov string, saddle-point spectrum anal. and chiral anomaly 7-56528
 open bosonic strings, covariant and gauge invariant theories 7-35835
 open interacting string, auxiliary field system, nilpotent BRS operator 7-61616
 open superstring theory, vector field effective action 7-5076
 open superstrings, effective action for vector field 7-500
 orthogonal lattice-gauge field configurations for hadron-hadron interactions 7-41841
 p-form electrodynamics gauge theory generalization 7-30166
 parallel computing in lattice theory 7-61487
 parity invariance, strong and electromagnetic interactions 7-9995
 particles in the early universe, conference, Thessaloniki, Greece (June 1985) 7-9596
 path integral formulation using corner variables 7-48998
 Pauli formalism for Abelian gauge fields 7-30182
 periodic generalization of static, self-dual $SU(2)$ gauge fields 7-41621
 phase structure of finite temperature lattice gauge theories 7-49002
 phase transitions in the early universe, nonabelian gauge theories 7-9570
 Poincare gauge theory, diffeomorphisms, transformation laws and space-time symm. 7-4951
 Poincare gauge theory of gravit. 7-9741
 Poincare gauge theory of gravity (3+1)-space-time structure 7-56124
 Poincare gravitational gauge theory, torsion soln. existing with Schwarzschild metric 7-56107
 Poincare group, group scaling, classical gauge theory and gravit. corrections 7-24762
 Prasad-Sommerfield monopoles at wide separation, dynamics 7-48930
 propagating modes in gauge field gravit. theory 7-24523
 propagation of boundary effects in large systems on vectorprocessors 7-4989
 pseudoscalar lattice mesons, relative charge distrib. for qq pair 7-49072
 QCD, finite temperature Monte Carlo simulations 7-61567
 QCD, gauge configuration props. in 3D 7-35783
 QCD, gauge theories with imaginary chemical potential 7-35781
 QCD, gauge-invariant variables and infrared confinement in finite space-time 7-61564
 QCD, lattice quantum field theory (Czech) 7-5042
 QCD, perturbative, IR asymptotic, behaviour, contour gauges, renormalization group anal. 7-61596
 QCD, quenched lattice approximation, hadron mass calcs. 7-61581
 QCD and CP^N model, collective phenomena, deconfining and chiral transitions 7-15120
 QCD and the lattice, introductory remarks 7-56507
 QCD flux tubes and glueballs, soliton interactions in gauge theories 7-5051
 QCD gluon Wigner operator, quantum transport eqns. derivation 7-5046
 QCD in 2D, chiral symm. breaking and condensate calcs. 7-49073
 QCD lattice gauge theory, updating fermions with Lanczos method 7-49052
 QCD light cone gauge, integral equation for multiplicity distribution 7-15115
 QCD nonperturbative effects modelling, 2D sigma models and 4D gauge theories 7-35664

gauge field theory continued

QCD spin-depend. static pots., SPINSUB vectorised code for Monte Carlo computation 7-41721
 QCD-like theories, stability of chiral symm. breaking solns. 7-49076
 QED, discretized light-cone quantization and lattice gauge calcs. 7-56497
 QED, superfield formalism using loop functionals 7-61539
 QED, threshold effects in spontaneously broken theories, gauge and scheme depend. 7-5041
 QED, topological mass quantization and parity violation 7-41693
 quantisation on a torus 7-18994
 quantum gravity and nonAbelian gauge field, unification 7-35376
 quantum strings interaction, path group anal. 7-30259
 quantum strings with a dynamic geometry 7-501
 quantum symmetries from quantum phases, fermions from bosons, a Z_2 anomaly and Galilean invariance 7-48970
 quark matter, conference, Pacific Grove, CA, USA (April 1986) 7-55881
 quark-gluon plasma, perturbative and nonperturbative theory, review 7-56510
 quasi-Riemannian gravit. with local $SO(3)$ invariance and broken Lorentz symm. 7-18670
 quaternion fields, spontaneous symmetry breaking and the Higgs mechanism 7-56460
 quenched QCD hadron mass calcs. on 16^4 spacetime lattice 7-61604
 radiative corrections to vector boson masses for heavy Higgs bosons 7-30272
 random lattice, doubling problem and chiral symm. breaking 7-394
 random lattice gauge systems and interacting gaussian surfaces, strong coupling expansion 7-48958
 real- and imaginary-time field theory at finite temperature and density 7-48983
 real-space normalisation, Kakutani metric appls. to small Ising systems and gauge-field quantisation 7-41294
 reduction and reparametrization of quantum field theories 7-35711
 regularisation, nonAbelian anomalies 7-61469
 relativistic many-fermion systems, vacuum-induced Friedel-type oscillations 7-29887
 renormalised Coulomb gauge self-energy fn., integral representation 7-56437
 Ricci-flat supersymmetric σ -models, counterterm counterexamples. 7-61446
 Riemann-Hilbert problem, gauge theories, holonomy operator, Yang-Mills fields 7-35672
 Rubakov-Callan effect, nonabelian interactions 7-10013
 Rydberg atoms, QED approach to energy level calcs. 7-62302
 S^2 nonlinear σ -model with Abelian gauge field, string-like solns. 7-61437
 Savvidy model, absence of deconfining phase transition at one-loop order 7-41735
 scalar Casimir energies in $M^4\times S^N$ for even N 7-41678
 scalar field theory and gauge theory, renormalized coupling constants by Monte Carlo methods 7-41618
 scalar glueball mass estimate, pure gauge lattice QCD calcs., four-parameter improved action 7-487
 scalar notivarg, alternative description 7-61419
 scalar sector of gauge theories and the quest for unified theory 7-10007
 scale invariant gauge theories and self-duality in higher dimensions 7-15060
 Schrodinger equation, local equivalent, with relativistic kinematics, WKB approximation 7-56406
 Schwarzschild black holes, nucleation of vacuum phase transitions, Euclidean action 7-56102
 Schwinger model, vacuum structure and the fermion-boson transformation 7-19004
 Schwinger-DeWitt proper-time method in odd-dimensional gauge theory 7-4954
 semi-off-shell string amplitudes, local operator expansion 7-41759
 sine-lattice eqn., nearly integrable soliton props. of kink solns. 7-392
 singlet form factors and local observables in the Glashow-Weinberg-Salam model 7-5014
 singleton dipole in de Sitter space 7-61425
 SL(2,C) gauge theory, $N=1$ supergravity and torsion 7-24761
 SO_3 gauge field interacting with isovector Higgs field, radiative corrections, monopole model 7-15090
 $SO(32)$ superstring theory, infinity cancellation mechanisms 7-35836
 $SO(3)$ Georgi-Glashow model, $(SU(2)$ gauge-Higgs), phase structure 7-30188
 $Sp(2)\wedge T(2)$ Grassmann Euclidean group, extended BRST SUSY, pseudomass, pseudospin 7-61491
 $Sp(2N)$, N fermion generation gauge group, existence of \hat{Z}^0 for $N=4$ 7-9994
 spin and lattice gauge models, topological excitations, mean field methods 7-9973
 spin-1/2 singleton dipole, canonical form. for second order wave eqn. of spin 1/2 field 7-48954
 spin-5/2 gauge field, grav. interaction, gauge symmetry, nonminimal grav. coupling 7-14842
 spinless relativistic particle, BRS Hamiltonian quantisation in rel. gauges 7-14825
 standard model, development to GUTs and supergravity 7-30219
 standard $SU(2)$ Higgs model, Monte Carlo study on lattices 7-9949
 static potentials from an extended gauge symmetry, confinement mech. 7-24838
 static potentials from bosonic string models, lattice Monte Carlo calcs. 7-61612
 statistical QCD, deconfinement and chiral symm. restoration, Monte Carlo anal. 7-61569
 stochastic quantization of gauge fields and constrained systems 7-15051
 strict QCD inequality and mechanisms for chiral symmetry breaking, instantons role 7-30241
 string action on group manifold, Kac-Moody groups and anomaly cancellation 7-24824
 string field algebra for gauge-invariant interaction of bosonic string 7-49109
 string field theories, gauge covariant formulation 7-24859
 string field theories, gauge invariant, covariant quantisation 7-56531
 string theory, lower critical dimens. and curved backgrounds 7-41763
 strong interacting two-doublet and doublet-singlet Higgs models 7-15097
 SU_2 lattice gauge theory, strong-coupling anal. of space-time critical dimensionality 7-56430
 $SU_c(4)$, gauge symmetry and supersymmetry breaking 7-15083
 $SU(2)_3$ noncompact lattice gauge simulations 7-35690

gauge field theory continued

- SU(2)_{global}×U(1)_{local} gauge-Higgs model, phase props., chiral symmetry breaking 7-398
 SU(2)_L×SU(2)_R×U(1) gauge model, electroweak interaction anal. 7-35751
 SU(2)×U(1) gauge theory, Majorana D and CP violation in leptonic sector 7-24790
 SU(2)×U(1) lattice gauge theory, phase transitions, Monte Carlo anal. 7-406
 SU(2) deconfining phase transition, correlation length and susceptibility, Monte Carlo methods 7-56515
 SU(2) gauge theory, Monte Carlo renormalisation study of deconfining transition 7-15073
 SU(2) gauge theory, topological mass induced by radiative corrections 7-420
 SU(2) gauge theory, transverse fluctuations in multidimens. tunnelling 7-123
 SU(2) gauge theory on R×S³ topology 7-61431
 SU(2) gauge-Higgs model with scalar doublet, continuum limit 7-41604
 SU(2) lattice gauge Higgs theory, Monte Carlo anal. at finite temp. 7-24796
 SU(2) lattice gauge theory, evidence against asymptotic freedom 7-41631
 SU(2) lattice gauge theory, finite temperature, Migdal renormalization group anal. 7-9966
 SU(2) lattice gauge theory, instanton density calcs. 7-4985
 SU(2) lattice gauge theory, Monte Carlo renormalization group study 7-19002
 SU(2) lattice gauge theory, phase structure, Schwinger-Dyson eqn. of a Wilson loop, deconfinement 7-24780
 SU(2) lattice gauge theory, quark and gluon string tensions 7-417
 SU(2) lattice gauge theory, renormalisation and continuum limit of composite operators 7-19017
 SU(2) lattice gauge theory, spontaneously broken, chiral symmetry realization 7-9958
 SU(2) lattice gauge theory with dynamical fermions, glueball mass calcs. 7-9959
 SU(2) lattice gauge theory with dynamical fermions, static quark pot. 7-61478
 SU(2) lattice gauge theory with mixed action, Z(2) monopoles and specific heat 7-48962
 SU(2) nonAbelian gauge theory, quantum fluctuations of Copenhagen vacuum 7-61436
 SU(3) gauge theory, finite size results 7-35704
 SU(3) gauge theory for quark-gluon plasma 7-41623
 SU(3) lattice gauge theory, Δβ and asymptotic scaling 7-4955
 SU(3) lattice gauge theory, Hamiltonian connected movements, expectation values 7-41605
 SU(3) lattice gauge theory, Monte Carlo calcs. of gluon propagator 7-61474
 SU(3) lattice gauge theory, Monte Carlo simulation of fermionic fields 7-48964
 SU(3) lattice gauge theory, sweep-sweep correlations of Polyakov loops 7-413
 SU(3) lattice gauge theory, topological susceptibility Monte Carlo calcs. 7-61455
 SU(3) lattice gauge theory, topology for β>5.6 7-56453
 SU(3) lattice gauge theory on 32⁴ lattices, sweep to sweep corrs. of Polyakov loops 7-15075
 SU(5) model, monopole-fermion interactions, Abelian and nonAbelian anomalies 7-9996
 SU(N) gauge theories, effects of self-dual fourth-rank tensor scalar fields on asymptotic freedom 7-390
 SU(N) gauge theories at finite temp. and chem. pots., rel. partition function 7-41623
 SU(N) gauge theory with independent metric and connection fields, quantisation 7-35693
 SU(N) lattice gauge theories, topological charge in Monte Carlo simulation 7-48938
 SU(N) lattice gauge theory, Langevin eqns. and stochastic quantization 7-35691
 SU(N) nonAbelian gauge theory, gauge fixing and stochastic smeared regularization incompatibility 7-41637
 SU(N) SUSY QCD, instanton superfield calcs. in Higgs phase 7-56512
 SU(n/n) graded Lie algebra 7-49008
 superconducting cosmic strings, cosmological effects 7-24518
 supergravity theories based on free differential algebras, factorisation and gauge transforms, in supergravity theories based on free differential algebras 7-187
 supermembrane in 6D SUSY gauge theory, spontaneous breaking of D=4 N=2 global supersymmetry 7-30212
 superpropagators for broken supersymmetric abelian gauge theories 7-19023
 superstring compactifications, large radius expansion 7-41758
 superstring theory, classical symmetries in the low-energy limit 7-24804
 superstrings, energy splitting of gauge field vacua 7-35842
 supersymmetric effective action in 3D, parity violation and renormalisation procedure 7-48992
 supersymmetric GUT scale, no-scale models and gravitino mass 7-18665
 supersymmetric model with E₆ gauge group and matter 27-plet, valley construction 7-41667
 supersymmetric nonAbelian gauge models, exact β-function from one-loop perturbation theory 7-41644
 SUSY extension of gauge anomaly, direct proof of uniqueness 7-5006
 SUSY gauge theories, coupling constant reparameterization and finite fieldtheories 7-9950
 SUSY gauge theories and Wilson operator expansion, anomaly puzzle solution 7-15059
 SUSY SU(N) gauge theory, Higgs field mass parameter variation 7-408
 T, CP, and CPT transformations in the presence of vacuum degeneracy 7-35741
 technicolour theories, chiral hierarchies, perturbation and breaking 7-41728
 temporal-gauge finite-time Feynman rules and Gauss's law 7-19000
 ten dimensional heterotic string, supersymmetric compactification on coset manifolds 7-24823
 ten-dimensional heterotic strings from Niemeier lattices 7-30255
 three gluon vertex in light cone gauge, nonlocal BRS counterterms 7-5060
 three gluon vertex in light cone gauge, renormalisation anal., nonlocal terms 7-5059

gauge field theory continued

- topological charge of lattice gauge fields 7-35663
 topologically massive chromodynamics at finite temperature 7-41726
 topologically massive gauge theories, monopoles and string tension 7-48989
 topology massive gravity in the dreibein light-front gauge 7-41188
 toroidal compactification of heterotic superstrings 7-41679
 triangle anomaly in the light-cone gauge 7-9975
 twisted Eguchi-Kawai model, complete set of twists 7-41648
 twisting toroidally compactified heterotic strings with enlarged symmetry groups 7-35822
 two-dimensional gauge theories, vector boson mass generation 7-426
 type-I superstring, one-loop gauge anomaly 7-35736
 U(1) Abelian gauge theory, phase struct. study, nonlattice nonperturbative calcs. 7-24755
 U(1) and SU(2) average plaquette energies up to third order approx. in cumulant expansion 7-41579
 U(1) lattice gauge theory, 3D, meson mass calcs. in quenched approx. 7-15068
 U(1) lattice gauge theory, analytical results for average plaquette energy 7-61426
 U(1) lattice gauge theory, iterative approach, d=4 β-function and free energy 7-30189
 U(1) lattice gauge theory, mass gap, variational calcs. 7-30157
 U(1) lattice gauge theory, renormalisation group transformations (*Chinese*) 7-35658
 U(1) lattice gauge theory with Higgs fields, 4 dimens., monopoles, matter representations role 7-41603
 U(1) lattice gauge-Higgs model, zero temperature, phase diagram anal. 7-56401
 U(1) varied-modular Higgs model, phase struct. simulation 7-18973
 U(N) gauge theories, topological aspects of loops 7-24756
 U(n) Veneziano model, Wick-rotated light cone gauge, nonperturbative study 7-24854
 unified action for higher spin gauge bosons from covariant string theory 7-49028
 unitary positive energy representations of the gauge group 7-61441
 vacuum decay rate at zero temp. in gauge theories 7-30168
 vacuum transition as tunnelling effect in 1D winding space 7-15053
 vector meson radiative decay in lattice QCD 7-35879
 vortices and electrically charged vortices in non-Abelian gauge theories 7-41607
 wavelike solutions to the Einstein equations coupled to neutrino and gauge fields 7-35349
 Weinberg, chiral model, saddle points and skyrmion solns. 7-15100
 Wess-Zumino gauge, translational invariance consistency, superfield anal. 7-41658
 Wess-Zumino terms and chiral jacobians, boundary conditions 7-9963
 Weyl-Dirac equation for an SU(2) gauge theory with spherical symmetry 7-41622
 Z₂ gauge theory, finite lattice effects 7-389
 Z(2) Higgs model, nonlocal order parameters 7-10006
 Z(2) lattice gauge theory, critical exponents, finite temp. calcs. 7-49054
 Z(2) lattice gauge theory, Polyakov loop effective couplings, Monte Carlo calc. 7-41619
 Z(2) spin-gauge system, mean field study, temporal and unitary gauges 7-4987
 Z(3) lattice gauge model, entropy and free energy, Monte Carlo calcs. 7-9956
 e⁺e⁻→ff, asymmetries and cross section, superstring gauge boson effects 7-499
 e⁺e⁻→ff, f≠e, ν_e, t, forward-backward and polarization asymmetries for SU(2)_L×U(1)_Y×U(1)_V and SU(2)_L×SU(2)_R×U(1)_{B-L} 7-61708
 e⁺e⁻→W⁺W⁻, probing the weak boson sector, anomalous couplings search, helicity amps. 7-56533
 e⁺e⁻→X, effects of Z'-bosons from superstring or nonlinear σ models 7-444
 ep→ep, scattering asymmetries, superstring gauge boson effects 7-499
 η' mass and topology in SU(3) lattice gauge theory 7-24783
 η' effects and instanton physics in low energy axion dynamics 7-30191
 η' mass in SU(3) lattice gauge theory, topology 7-429
 ↳γγγ, constraints due to topological susceptibility and chiral Ward identities 7-5097
 K⁺→π⁺π⁺e⁺ν, gauged nonlinear σ model with Wess-Zumino condition 7-41790
 p→π⁰e⁺, lattice QCD Monte Carlo simulations 7-35763
 π-η mass difference in lattice QCD, U(1) problem, strong coupling expansion 7-41810
 W boson contrib. to γ polarization propagator in external mag. field 7-61438
- Gaussian noise** see random noise
Gaussian orbital calculations see GO calculations
Gaussian-type orbital calculations see GTO calculations
Ge-Si alloys
 amorphous films, photochemical vapour deposition, review 7-46345
 coherently strained bulk alloys on Ge (001) substrate, indirect band gap and band alignment calcs. 7-2481
 epitaxial growth, conf., Toronto, Ont., Canada (May 1985) 7-9588
 epitaxial growth, struct., and elec. props. 7-52354
 Ge_{1-x}Si_xCu, supersaturated solid solution, decomposition 7-32654
 lattice thermal cond. reduction by point defects at intermediate temps. 7-52161
 MBE on Si substrates, stacking fault tetrahedra form. 7-21769
 p-n junctions, photoelectric props., effects of electron bombardment 7-7351
 piezoresistance under uniaxial elastic deform. (*Russian*) 7-58813
 semiconductor alloys, ordering and decomposition 7-6574
 Si-SiGe strained superlattices on Si substrates, MBE growth, characterisation, appl. for HEMT 7-27218
 solar cells, electron radiation effects 7-34031
 strained layer epitaxy, review of developments 7-52343
 surface, interaction with H₂ 7-58632
 surface (100), shape resonances of chemisorbed OH groups 7-6998
 surfaces, (111) vicinal, step-band formation, cross-sectional TEM studies 7-12412
 thermally evaporated epitaxial heterolayers on GaAs substrate, Si distrib. (*Russian*) 7-63988
 thermoelectric devices, fabrication, materials and properties 7-65499
 thermoelectric materials, ZrO₂ commercial paints as coatings 7-65503
 Ge:Si, ion-implanted amorphous surface layers, EXAFS 7-27823

Ge-Si alloys continued

- a-Ge-Si:H,F, multijunction solar cells, performance data 7-40011
 a-GeSi:D,F, D NMR lineshapes and spin-lattice relax. studies 7-45836
 a-GeSi:H, deposition kinetics and structural control 7-45087
 a-GeSi:H,F double Schottky barrier structures, surface photovoltage meas. and calc. 7-17093
 a-GeSi:H,F/a-Si:H superlattices, elec. transport studies 7-38716
 a-GeSi:H alloy tandem-type solar cells, conversion efficiency 7-40014
 GeSi/Si strained layer superlattices, electronic and optical props. 7-7359
 GeSi-Si heterostructures, MBE grown, structural props., quality, electron diff., imaging obs. 7-7036
 GeSi-Si strained layer superlattices, growth using limited reaction processing 7-39430
 GeSi-Si strained superlattices, order-disorder transitions, obs. 7-27166
 GeSi-Si strained-layer superlattices, elastic relax. effects on TEM 7-52378
 GeSi-Si superlattice, strain-induced order-disorder transition 7-21437
 Ge_{0.6}Si_{0.4} rib waveguide avalanche photodetectors for 1.3 μ m optical fibre communication 7-9896
 Ge_{1-x}Si_x/Si superlattice, use to improve quality of Si heteroepitaxy on CaF₂-Si 7-22497
 Ge_{0.9}Si_{0.1-x}Si multilayers, MBE grown, thermally annealed, Ge diffusion, strain relax., ion channelling, backscattering anal. 7-6896
 Ge_{0.9}Si_{0.1-x}Si strained layer heterojunctions, selectively doped, hole mobilities, temp. depend. 7-7383
 Ge_{0.9}Si_{0.1-x}Si strained layer superlattices, bandgap meas. 7-27408
 Ge_{0.9}Si_{0.1-x}Si strained-layer heterostructure, transport, optical props. and appls. 7-7349
 Ge_{0.9}Si_{0.1-x}Si strained-layer superlattice, zone folding induced quasi-direct gap, optical absorpt. probability 7-27409
 Ge_{0.9}Si_{0.1-x}Si structures, epitaxial growth 7-39387
 Ge_{0.9}Si_{0.1-x}Si superlattices, Raman scatt. involving umklapp processes 7-3043
 Si:Ge, Ge⁺ preamorphisation implants, effect on extended defect formation during subsequent solid phase epitaxy 7-16599
 a-Si:H,F-Si_{0.4}Ge_{0.6}H,F superlattices, carrier scatt., optical absorpt. study 7-38711
 Si:H(F)-SiGe:H(F) amorphous multilayer struct., fabrication and near IR photoconductivity characs. 7-52797
 Si:Sb-SiGe modulation doped superlattices, growth and props. 7-7379
 Si/Ge_{1-x}Si_x superlattices, conduction band interactions and splitting, envelope-function approx. calcs. 7-64332
 Si/Ge_{0.9}Si_{0.1-x} convergent beam electron diffraction and imaging of strained-layer superlattices 7-17095
 Si/Si_{0.5}Ge_{0.5} strained layer superlattices, 2D electron systems 7-7380
 Si-Ge:Au, reaction of Au centres to optical pumping 7-12755
 Si-Ge:O, single crystal, thermodynamic rel. to solubility of O 7-12648
 Si-Si_{1-x}Ge_x strained layer superlattices, electronic struct. 7-38707
 Si-SiGe strained-layer superlattices, optical and electronic props. 7-53353
 SiGe superlattice structures, Sb doped, MBE grown, comp., doping profiles, SIMS, Rutherford backscattering spectra 7-7035
 a-SiGe:D, F, vibr. modes, Fourier transform IR spectra studies 7-46053
 SiGe:F,H, amorphous, high efficiency solar cells fabrication and props. 7-17901
 a-SiGe:F solar cells, chemical basis for high efficiency 7-17884
 SiGe:H, amorphous, electronic and structural props. 7-17054
 SiGe:H, amorphous, p-n solar cells, stability behaviour, impurities and doping residues effect 7-17912
 SiGe:H, amorphous, solar cell efficiency improvement using graded band-gap layer at i/n interface 7-54327
 a-SiGe:H, F glow discharge films, elec. and optical props. 7-46169
 a-SiGe:H,F alloy films, F incorporation and annealing props. 7-44588
 a-SiGe:H,F alloys for solar cells, prep. by DC and RF discharge deposition 7-17900
 a-SiGe:H,F films, glow discharge deposition and elec. props. 7-64917
 a-SiGe:H,F glow discharge films, microcrystallinity studies 7-45088
 a-SiGe:H,F glow discharge films, electronic transport and density of states 7-45114
 a-SiGe:H,F solar cells, radiation hardness to 1 MeV protons 7-23180
 a-SiGe:H,F/Pd(Au)(Ni), Schottky barrier height, internal photoemission meas. 7-45501
 a-SiGe:H alloys for solar cells, electronic and optical props. 7-17899
 SiGe:H amorphous films, glow discharge deposited, photoconductivity, microstructure effects 7-58831
 a-SiGe:H films, CVD, electrical and optical props. 7-33596
 a-SiGe:H films, NMR, ESR and IR studies 7-45833
 a-SiGe:H films, photo-assisted CVD and opto-electronic characterisation 7-33595
 a-SiGe:H glow discharge films, field effect density of states determ. 7-21796
 a-SiGe:H solar cells preparation by photo-CVD 7-17885
 a-SiGe:H thin films for solar cells, electrical and structural properties relationship 7-17898
 a-SiGe:H/a-Si:H multilayers, reactive deposition 7-33592
 SiGe-Si strained layer superlattices, electric subbands 7-2700
 SiGe-Si structures, MBE growth mode and interface structure 7-52311
 a-SiGe_xH_{1-x}F/a-Si:H multiple layered films for enhancement in photore-sponse in near IR spectrum 7-52668
 Si_{0.55}Ge_{0.45}-Si modulation doped superlattice, MBE grown, electron mobility enhancement, Hall meas. 7-7382
 a-Si_{1-x}Ge_xH/Al Schottky barrier form. and characs. 7-12787
 a-Si_{1-x}Ge_xH/a-Si:H/Al Schottky barrier form. and characs. 7-12787
 Si_{1-x}Ge_x films, optical band gap, photocond. props. 7-52672
 Si_{1-x}Ge_x MBE crystals, ordering study 7-58709
 a-Si_{1-x}Ge_xH, electron and hole transport 7-7259
 a-Si_{1-x}Ge_xH, F, light-induced degradation meas. 7-45397
 a-Si_{1-x}Ge_xH,F alloy films, RF glow discharge deposition in ultrahigh vacuum reactor 7-53619
 Si_{1-x}Ge_xH amorphous alloys, electronic struct., soft X-ray and photoelectron spectra studies 7-7857
 Si_{1-x}Ge_xH films, amorphous, bond lengths, comp. depend., EXAFS study 7-64757
 Si_{1-x}Ge_xS(Se)(Te) solid solns., deep levels investig. 7-2529
 Si₃₀Ge₇₀, model alloy system, liquid-solid interface dynamics, rapid solidification 7-6761
 Si_xGe_{1-x}Ga, resistivity and Hall constant, temp. depend. 7-7231
 Si_xGe_{1-x}H,F amorphous films, struct., elec. and optical props. 7-22360
 Si_xGe_{1-x}Si strained layer superlattices, folded phonon dispersion 7-44718
 Si_xGe_{1-x}Si superlattices, strain induced confined electron states 7-7311

gegensein see zodiacal light

Geiger counters

- organic-type Geiger-Muller tube with third electrode, design and performance 7-19627
 pulse height distributions 7-36383
 Kr-He-H₂ mixtures, self-quenching streamer or Geiger-Muller region 7-19669

Geiger Muller counters see Geiger counters

gelatin

- see also gels
 dichromated gelatin, powered refl. HOEs 7-25747
 dichromated gelatin achromatic reflection display holograms 7-25750
 dichromated gelatin and light sensitivity for holographic purposes 7-25741
 dichromated gelatin transmission HOEs, reflective and refractive optics 7-25748
 holographic solar concentrators development 7-50517
 water-gelatin system mixed crystal formation and glassy solidification 7-16717
 wetting by water, effect of gelation time 7-39927
 AgBr, desorption of gelatin by means of sodium polystyrene sulphonate 7-15022

gels

- 3D kinetic gelation model, crit. behaviour 7-14904
 agar-agar gel, effect of gelation time on wetting by water 7-39927
 atactic polystyrene solns., gelation, viscous flow meas. 7-32254
 casein gel, effect of gelation time on wetting by water 7-39927
 ceramic synthesis from molecular precursors, conf., Palo Alto, USA (Apr. 1986) 7-35113
 composites, porous and dense, prep. from sol-gel 7-65002
 contact gel as a source of error in X-ray films of the skull (German) 7-65855
 copolymer gels, water swellable, with L-lysine pendant group, optical resolution of DL-lysine 7-64601
 deoxyhaemoglobin S, solns. and gels, quasi-elastic laser light scatt. 7-28464
 drying induced shrinkage, liquid flow and chem. reactions 7-23069
 elastomer gels, swollen cis-trans isomerisation, network density effects 7-8273
 epoxy-amine networks, build-up and etherification, statistical structural model 7-13768
 fibrin gels, proton spin-lattice relax. 7-34112
 film and flat plate, drying behaviour, anal. 7-59794
 fluorescein dye in ionic gel near phase transition, fluorescence obs. 7-13190
 gelatin, effect of gelation time on wetting by water 7-39927
 gelatin gels with coloured component at reduced pH values, turbidity, optical rot., viscoelastic props. 7-8320
 glass-making, review 7-3259
 gradient index glass rods prep. by sol-gel index modifying ion interdiffusion process 7-7952
 hemicellulose suspensions, gelation, flow (German) 7-13830
 human joint fluids, rheological characs. and lubrication props. 7-40178
 hydroxypropyl guar gels in capillary tubes, slip vels. meas. 7-11550
 kinetic gelation, spatial correlations 7-35446
 Liesegang ring form., microcomputer algorithm 7-17827
 membranes, bilayer, double-chain amphiphiles, phase transitions, DSC obs. 7-54496
 membranes, bilayer, single- and triple-chain amphiphiles, phase transitions, DSC obs. 7-54497
 PMMA, syndiotactic, thermoreversible gelation 7-65358
 poly(vinyl acetate), network, mechanical and swelling behaviour investig. 7-12185
 poly(vinyl alcohol), network, mechanical and swelling behaviour investig. 7-12185
 poly(vinyl alcohol) fibres, high modulus, zone drawing 7-59487
 poly(vinyl alcohol) hydrogels, elastodynamics, Brillouin scatt. meas. 7-39136
 polyacrylamide gels, spontaneous birefringence and photoelasticity 7-22217
 polydimethylsiloxane, swollen in benzene, network struct., cryoscopic obs. 7-21135
 polymer gel in pure and mixed solvent media, phase transition 7-63431
 polymer gels, NMR line shape 7-17229
 polymer gels, self-diffusion coeff. calcs. 7-52099
 polymer gels, zinc phthalocyanin containing, fluoresc., photosynthesis model 7-8515
 polymer macromols., dil. solns., spontaneous symmetry breaking, replica method 7-15758
 polymer nets, high elasticity, mol. theory with allowance for topological constraints 7-37839
 polymer solutions, branched polymers, viscoelastic props. near gelation threshold, frequency dependence 7-58390
 polymer solutions, gel form. during elongational flow 7-51237
 polymer solutions, gelling, rheology, mol. network model 7-51016
 polystyrene-cis-decalin gels, isotactic, compression modulus, conc. depend. 7-32536
 polytrimethylamine-p-vinylbenzimidazole, aq. solns., negative thixotropy and thermoreversible gelation 7-51608
 polyvinyl alcohol gel, effect of gelation time on wetting by water 7-39927
 PVC, gels, Brillouin light scatt. 7-42798
 rubber, gel and mol. wt. influence on mech. props. 7-37904
 scleroglucan solns., low temp. sol-gel transition, rheological behaviour, optical rot. 7-51018
 sediment form., Brownian dynamics simulation, colloidal and hydrodynamic interaction effect 7-13825
 silica, colloidal, gelation 7-46877
 silica, sol-gel processing, role of catalysts 7-22630
 silica aerogels, ethyl versus methyl sol-gel comparison, polar nephelometry studies 7-8312
 silica aerogels, photon-fraction crossover, Brillouin scatt. meas. 7-46878
 silica gel, fractal vibr. modes, low freq. Raman scatt. 7-26890
 silica gel surface, variable temp. diffuse reflectance FT IR spectrosc. obs. 7-53294
 silica monolithic gels, autoclave prepared Raman studies 7-8314
 sol-gel thin films used in solar energy appls. 7-37106
 tetramethoxysilicon, light scatt., below sol-gel transition 7-46058
 transition metal oxides, sol-gel process synthesis, electronic and ionic props. 7-33618

gels continued

- vinyl pyrrolidone copolymers, highly swollen hydrogels preparation 7-21073
 Al_2O_3 - SiO_2 gel, IR and ^{27}Al NMR.MAS spectra AlO_6 , AlO_4 vibr. freq. (French) 7-64534
 Al_2O_3 - Li_2O sol-gel technique for LiAlO_2 felt prep., phase transitions in gels 7-22601
 Al_2O_3 - MgO , diphasic xerogels, densification, sintering, isostructural seed, epitaxy 7-27987
 Al_2O_3 - SiO_2 , mullite, prep. by sol-gel method, microstruct. and mech. props. 7-46386
 $\text{Al}(\text{OH})_3$ sols, gelation, pH, temp., ageing time 7-46875
 AlOOH , stacking fault and size effects on X-ray diffr. line profile calc. 7-2032
Au fine powder, synthesis from metallic aerogels 7-3216
 B_2O_3 - SiO_2 glass, borosiloxane bond formation, sol-gel process, spectroscopic study 7-59117
Cu fine powder, synthesis from metallic aerogels 7-3216
 Li_2O - 2SiO_2 sol-gel glass, prep. and devitrification behaviour 7-58158
 Na_2O - CaO - Al_2O_3 - SiO_2 system, synthesis of glasses by sol-gel process 7-64997
 Na_2O - CaO - SiO_2 , high-silica glass, sol-gel prep. method 7-46402
 Na_2O - SiO_2 binder solns., ester curing, equilibria and kinetics, NMR study 7-8311
 Na_2O - $n\text{SiO}_2$ +propylene carbonate, gels form., comp. of phases and rheological props. meas. 7-39875
Pd fine powder, synthesis from metallic aerogels 7-3216
 SiO_2 aerogel, kinetic energy of positronium emitted from surface 7-39310
 SiO_2 gel, adsorpt. of O_2^- photoform., rot. dynamics, ESR obs. 7-25566
 SiO_2 gels, prep. using tetraethoxysilane, elastic moduli 7-46537
 SiO_2 glasses, gel-derived, defect studies 7-11944
 SiO_2 , silica aerogels, SAXS study 7-28355
 SiO_2 , silica sol-gel derived coatings, thickness, prep. by dipping 7-27193
 SiO_2 sol-gel glass structures, effects of water content of gels, EPR study 7-6526
 SiO_2 xerogels, structural changes during low temp. dehydration 7-28366
 SiO_2 - Al_2O_3 , mullite form. from xerogels, X-ray and IR obs. 7-46391
 SiO_2 - GeO_2 system, gels and gel-glasses, struct. study using vibr. spectroscopy 7-44381
 TiO_2 gel, formation by hydrolysis of Ti alkoxides, molecular precursor modification by acetic acid 7-59793
 TiO_2 -Cr, sol-gel process, ESR study 7-59108
 V_2O_5 gel, V site struct., polarised EXAFS and XANES studies 7-65355
 $\text{Y}_4\text{Al}_3\text{O}_9$, $\text{Y}_3\text{Al}_5\text{O}_{12}$, YAlO_3 , synthesis by sol-gel process 7-13420
 Y_2O_3 - Al_2O_3 system, prepared by sol-gel process, IR vibr. spectra study 7-33384
 ZrO_2 gel, transparent, glass-like, thermal evolution 7-28356

general relativity

- see also *gravitation*; *Schwarzschild metric*; *space-time configurations*; *unified field theories*
accretion disks in bimetric gravit. theory as test for general relativity 7-9365
angular momentum flux carried by gravitational radiation 7-29831
anisotropic cosmological model, Boltzmann and Vlasov kinetic eqns. 7-61189
anisotropic fluid distributions in bimetric general relativity 7-34846
arbitrary dispersive media, operational concepts and transformation laws of space-time coordinates 7-61176
astrophysical jets, general relativistic decollimation theory 7-60522
asymptotic approximation applied to simple harmonic oscillator/scalar field problem 7-61173
asymptotically Minkowskian semi-global solutions of Einstein's equations (French) 7-61168
attractor in superstring model, Einstein theory, Friedmann universe, inflation 7-41201
axially symmetric higher-dimensional gravity, Belinsky-Zakharov N-soliton transforms. 7-41207
axially symmetric higher-dimensional gravity, Neugebauer-Kramer transforms. 7-41206
barotropic perfect fluid, cosmological shock waves in general relativity 7-66797
Bianchi type-I homogeneous universe, exact solns. in general relativity 7-41204
Bianchi types of a three-parameter group of curvature collineations 7-24497
Bianchi-type VIII models, chaos in the long-term behaviour 7-60843
Big Crunch, strong black hole thermodynamics, unified geometrical approach 7-4749
binary stars, eqns. of motion for extended bodies 7-4510
Birkhoff's theorem for electromagnetic fields in scalar-tensor theory 7-56105
Born-Infeld electrodynamics, motion of gravitationally interacting particles 7-48479
bounded source in general relativity, radiation field calc. 7-4734
canonical Hamiltonian for vierbein general relativity 7-29823
Cartan's contortion, relation to Eotvos torsion expt. 7-4326
Cauchy problem in general relativity 7-29843
causality conditions, distinguishing props. 7-61179
causality in general relativity, recovery 7-160
charged perfect fluid obeying equation of state, shear free motion 7-24495
charged spinning fluid in Einstein-Cartan theory, consistency eqns. for energy-momentum tensor 7-41184
classical and quantum gravity, spinorial variables, Hamiltonian formulation 7-24527
closed universes, dynamical torsion and the indefinite metric, general relativistic anal. 7-9571
colliding planar shells of matter, gravitational effect, Einstein's eqns. solns. 7-150
compact space-times and the no-return theorem 7-24496
conformal collineations and anisotropic fluids in general relativity 7-18648
conformal invariance and torsion in general relativity 7-56095
conformal motions, charged matter and one-parameter group 7-24488
conformal motions, charged matter and one-parameter group 7-24489
conservation laws in spacetimes with boundary 7-29829
consistent spinor equations, σ -symbols and Levi-Civita connection 7-61175
constraint equation evolution 7-56096

general relativity continued

- cosmic censorship hypothesis in cosmological space-times 7-48470
cosmological constant, non-compact symmetries and Weyl invariance 7-4611
cosmological Einstein-Rosen metrics, generalised soliton solns. 7-41166
cosmological models with variable G, Λ , energy nonconservation reanalysis 7-48121
cosmological paradox resolution using concepts from general relativity 7-35172
cosmology, gauge-invariant perturbations in generalised inflationary models 7-48112
cosmology, general upper limits to age of Universe 7-4603
covariant observer-dependent Hamiltonian formalism for the relativistic particle 7-41179
covariant quantum field theory of gravitation, scaling limit and space-time metric 7-56134
curvature and torsion from matter, Lorentz gauge symm. 7-41208
cylindrical waves in general relativity 7-48482
dipole particle, Papapetrou and Dixon eqns. of motion anal. 7-29837
Dirac matrices, in gravitational field, construction mode 7-56098
Doppler shifting of a distant light source in a Schwarzschild gravitational field 7-4319
double-null coordinates for the Vaidya metric 7-35352
 $E=mc^2$, validity for gravitational energy in general relativity 7-56094
Earth satellite motion, relativistic effects in generalized Fermi frame 7-23985
Einstein's eqns., similarity solns. relevant to the early Universe 7-48481
Einstein's equations, integration using the Bondi metric 7-61172
Einstein's field eqns., existence of n-geodesically complete or future complete solns. 7-48463
Einstein's field eqns., vacuum solns. with flat 3-dimens. hypersurfaces 7-4728
Einstein's field equations, dimensional reduction in a multi-dimensional cosmology 7-29830
Einstein action, 3+1 Regge calculus with conserved momentum and Hamiltonian constraints 7-48465
Einstein eqns., vacuum solns. for conformal Killing field and cosmological constant 7-41172
Einstein equation, higher dimensional, exact solutions in presence of matter 7-162
Einstein equations, black hole solns. in asymptotically flat space-times 7-24486
Einstein equations, self-consistent solutions with one-loop quantum gravity corrections 7-161
Einstein equations, spherically symm. nonstatic separable solns. in comoving frame 7-9716
Einstein equations with fourth-order derivative terms, appl. to Bianchi-type I space times 7-48111
Einstein field eqns. without symmetries, perfect fluid solns. 7-41171
Einstein gravity, extended with Gauss-Bonnet term, cosmological solns. 7-24500
Einstein solutions, spatially inhomogeneous cosmologies with heat flow 7-35075
Einstein-Born-Infeld theory, duality rotations and type-D solns. 7-47683
Einstein-Cartan theory, equation of state of spinning fluids, variational methods 7-56104
Einstein-Cartan theory, matter field torsion and conservation laws 7-41195
Einstein-Hilbert lagrangian, higher dimensional cosmological solns. 7-14835
Einstein-Kalb-Ramond cosmology 7-48122
Einstein-Maxwell eqns., gauge freedom of plane symmetric line elements 7-18652
Einstein-Maxwell equations, type one soln., charged analogue of Schwarzschild's interior soln. 7-35357
Einstein-Maxwell solutions, conformally Ricci flat, null EM field 7-24508
Einstein-Maxwell space-time, asymptopia of quasi-local mass and momentum 7-29841
Einstein-Rosen metrics generated by the inverse scattering transform 7-24494
Einstein-scalar eqns., spherically symmetric, solns. in large data limit. 7-9712
Einstein-Weyl space-times with geodesic and shear free neutrino rays 7-61169
electric and gravitational forces, and the ballistic theory of light 7-29836
electric source problem in Hermite-symmetric Einstein field theory 7-29838
electrically charge solns. in (2+1) dimens. space-time 7-9713
electrostatic self-force in Reissner-Nordstrom spacetime 7-35350
elementary particle stability, catastrophe theory on the space-time manifold 7-24808
energy propag. and mass-energy equivalence derivation from fundamental symmetries (French) 7-29622
energy-momentum vector of the classical electron 7-24498
Eotvos experiment, new force or thermal gradient 7-14854
Eotvos experiment, nonexistence of intermediate range coupling 7-29861
equivalence principle to gravitational wave detection (German) 7-18680
Euclidean Einstein metrics, complex manifold, triaxial vacuum metric 7-48475
Euler's equations in complicated models of continuous media 7-41175
everywhere invariant spaces of metrics and isometries 7-24492
EXCALC code applied to general relativity and Poincaré gauge theory 7-61174
extended form, many-values representation, dimensionalities (Russian) 7-14837
extended manifolds of general relativity, tachyon prod. 7-35348
field equations for lapse and shift, appl. of generalised harmonic gauge conditions 7-47678
fourth dimension, energy conversion eqn. 7-24487
fourth-order theories of gravity and general relativity, equivalence, cosmological singularity 7-41178
Friedmann-Lemaître-Robertson-Walker models in Lyra's manifold 7-40966
gauge theories and quantum cosmology, book 7-48512
generalized covariant field theory of electrodynamics, flat space-time limit 7-41694
geometrical gauge approach for electromagnetism and gravitation 7-29851
gravitation, new relativistic theory rel. to Friedmann universe and gravit. collapse (Russian) 7-60533

general relativity continued

- gravitation, relativistic theory, radio signal delay 7-29860
- gravitation singularities and space-time foliations in general relativity 7-48489
- gravitation theory taking vacuum into account 7-35347
- gravitational bags from spontaneous compactification 7-41177
- gravitational energy-momentum pseudotensor and the de Donder condition 7-4731
- gravitational field energy, covariant definition in state space-time 7-18643
- gravitational radiation coupled to torsional motion, metric elasticity in a collapsing star 7-48484
- gravitational spin-spin interaction, rel. to Curzon masses 7-61177
- gravitational two-body problem with acceleration-depend. spin terms 7-9722
- gravitational wave emission, tensorial linear theory 7-163
- gravitational waves, inverse-scattering method of generation 7-61181
- gravitationally-induced supercurrents in Schwarzschild fields appl. of jellium model 7-45595
- gravitons in general relativity, implications of photon hypothesis in electrodynamics 7-41164
- Green's function in curved space-time, Hadamard construction (*German*) 7-66444
- Higgs field coupled gravitation theory, high-freq. perturbations and gravitational collapse 7-40681
- homogeneous anisotropic cosmological models with viscous fluid and magnetic field 7-24503
- homogeneous cosmos of Weyssenhoff fluid in Einstein-Cartan space 7-48480
- hydrodynamics of a topologically nontrivial metric 7-29835
- inflation and bubbles in general relativity 7-35351
- inflationary Universe, effective grav. Lagrangian and energy-momentum tensor 7-4606
- inflationary universe, phenomenological cosmological model w.r.t. general relativity 7-48130
- inhomogeneous cosmological model, generalized vacuum soliton soln. of Einstein's eqns. 7-9715
- interferometric tests, use of squeezed states 7-4329
- Kaluza-Klein gravitational theory, astrophysical data and cosmological solns. 7-9363
- Kaluza-Klein model, cosmological solns. for homogeneous, spatially isotropic metric 7-9723
- Kaluza-Klein monopoles, motion at low energy 7-14839
- Kaluza-Klein theory, barrier penetration and initial values 7-29842
- Kaluza-Klein theory, scale invariance, Killing vector and size of fifth dimens. 7-24524
- Kasner spacetime, exact solns. for electromagnetic, neutrino and gravit. fields 7-41173
- Kerr black hole, charged, structure of pseudo-Newtonian force 7-4498
- Kerr black hole, null geodesics in stationary Ernst-Wild space-time 7-61170
- Kerr black hole metrics, colinear, superposition, space-time structure (*Chinese*) 7-40861
- Kerr spacetime, polar orbits, geodesic effect 7-14836
- Killing vectors and Maxwell collineations in general relativity 7-48486
- light deflection, corrected Li expression, for astrolabe obs. 7-66431
- linear conformal gravit. in de Sitter space 7-48504
- linear frames field as fundamental self-interacting system 7-41180
- locality hypothesis and extension of relativity to general coord. systems 7-29782
- Lorentz equations of motion and connections in a principal bundle 7-56120
- Lyra's manifold, vacuum Friedmann cosmological models 7-35074
- macroscopic intermediate range forces, influence on stellar struct. 7-56119
- magnetized cosmological model for perfect fluid distribution 7-24505
- many-body Lagrangian 7-9718
- mass and linear momentum concepts in Galilean thermodynamics 7-56198
- massive particles with integer spin in arbitrarily curved space-time, Lagrangian (*German*) 7-48464
- massless scalar field with gravity, Einstein's field eqns. in 3D space-time 7-41209
- Maxwell's eqns., soln. in curved space-time, Green's function adiabatic expansions 7-41183
- Maxwell's equations in curved space-time 7-9725
- McVittie metric, physical props. of nonquadratic solns. 7-48472
- McVittie metrics, noninteracting solns. for perfect fluid spheres 7-24504
- multipole moment formation in vacuum region for nonasymptotically flat systems 7-48478
- $N=1$ supergravity, Newtonian limit, gauge soln. and torsion 7-18677
- naked singularity space-time having strong curvature 7-29819
- neutron stars, core phase transformations, equilib. configurations in general relativity 7-60705
- neutron stars with solid internal shell, limiting mass in general relativity 7-47966
- Newman-Penrose formalism; general transformation laws 7-29822
- non-Euclideanism in general relativity and cosmology, mathematical formalism 7-34851
- nonlinear electrodynamics generated via gravitational nonminimal coupling 7-24512
- nucleus as a source in Kerr-Newman geometry 7-48476
- null surface geometrodynamics, dynamical struct. of Einstein's theory of gravity 7-149
- $O(N)$ symmetric model, effective pot. in static homogeneous spacetimes 7-18673
- orthogonal perfect fluid and vacuum solutions, self-similar spatially homogeneous cosmologies 7-29824
- Penrose's quasi-local mass in Newtonian limit of general relativity 7-151
- perfect fluid, and vacuum metrics with flat 3-dimens. hypersurfaces 7-4727
- perfect fluid in FRW space-time, kinematic and dynamic properties of conformal Killing vectors in anisotropic fluids 7-48466
- perfect fluid space-time, topology 7-56091
- periastron precession in general relativity 7-48244
- perturbed light beam, linearized field eqns. and gravitational solns. 7-4737
- photon propagators and renormalised stress tensors in curved space-time 7-4730
- plane-fronted gravit. waves, isometry groups 7-24501

general relativity continued

- planetary N-body problem, Hamiltonian eqns. in post-Newtonian approximation 7-47672
- Plebanski metric perturbations in general relativity, fermion field perturbations 7-18645
- Plebanski metric perturbations in general relativity, grav. perturbations eqns. 7-18644
- Poincare group, group scaling, classical gauge theory and gravit. corrections 7-24762
- positive energy proof for weakly asymptotically flat space-times 7-29821
- positive-energy theorem, asymptotically flat metrics 7-29820
- power law singularities in the scale covariant theory 7-48467
- pseudo-Newtonian potentials 7-158
- PSR 1913+16, binary pulsar, proper motion determ. from periastron times 7-55696
- quantum mechanics from general relativity, theory of inertia, book 7-48215
- quantum mechanics of free relativistic particle, canonical and path integral formulations 7-18631
- quantum Regge calculus in the Lorentzian domain and its Hamiltonian formulation 7-175
- quantum space-time, classical particle dynamics 7-24525
- quasi-local mass for small surfaces 7-29827
- radiated gravitational energy calc. using second-order Einstein tensor 7-35355
- radiative gravitational fields, asymptotic behaviour at future null infinity 7-61178
- radiative gravitational fields in general relativity, field struct. outside the source 7-41176
- radio interferometry, representation of time delay and interference freq. in coordinate-independent form 7-60571
- radio signal delay in relativity theory of gravitation 7-4732
- rapidly rotating compact stars, equilib. configurations and gravit. effects (*Chinese*) 7-4305
- relativistic and non-relativistic classical field theory on five-dimensional spacetime 7-154
- relativistic astrophysics and gravitation, conference, Potsdam, Germany (October 1985) 7-40980
- relativistic corotating spherical mass shells, singularities and gravimetric effects 7-41182
- relativistic objects, event horizons and intertransitions, systematics (*Russian*) 7-159
- relativistic theory of gravitation 7-56099
- relativistic wave mechanics of spinless particles in a curved space-time 7-18646
- Riemann-Hilbert problem, gauge theories, holonomy operator, Yang-Mills fields 7-35672
- Riemannian curvature spinor in general space-time 7-29825
- right-conformally equivalent hyperheavenly spaces, Einstein eqn. solns. 7-41169
- rigidly rotating dust with magnetic pressure in general relativity 7-155
- rigidly rotating perfect fluids in general relativity, Wahlquist soln. 7-47680
- Robertson-Walker metric, affine collineation 7-4729
- rocket borne clock expt., kinematical and gravitational anal. 7-29833
- rotating axisymmetric expanding universe with an electromagnetic field 7-24245
- rotating body gravitational field, motion of particles and photons 7-55704
- rotating cosmic string surrounded by grav. radiation, Einstein eqns. solns. 7-18464
- rotating Kaluza-Klein monopoles and dyons 7-9730
- rotating perfect fluid, generalised soln. 7-41174
- satellite orbital period calcs. in relativistic gravit. and general relativity 7-40690
- scalar-tensor theory and baryonic interaction 7-18350
- Schwarzschild black hole, Ernst space-time representation, particle trajectory stability 7-55701
- second rank tensors, representation as linear combination of tensors 7-4733
- self-creations cosmologies, Raychaudhuri-type equations 7-24251
- self-similar perfect fluid, singularities in self-similar spacetimes 7-29826
- self-similar perfect fluid space-times in general relativity 7-41168
- sigma-model superstring corrections to the Einstein-Hilbert action 7-4961
- singularity theorems and curvature growth 7-48471
- $SL(2, \mathbb{C})$ gauge theory, $N=1$ supergravity and torsion 7-24761
- $SO(2)$ space, general relativistic stability of Q matter 7-4741
- space-time structure, relation to quantum mechanics 7-47679
- spacetime curvature and rotation effects on pulse arrival times from fast pulsars 7-60700
- spherical charge and mass distrib., general relativistic anal. 7-18651
- spherically symmetric charged bodies, Einstein-Maxwell eqn. soln. 7-4736
- spherically symmetric free fall collapse for perfect fluid 7-29839
- spin-1/2 particle trajectories in a grav. field, classical limit 7-24490
- spin-tensorial concomitants of the spin-tensor field 7-18647
- Stanford Gravity Probe-B expt., using superconducting thin film gyroscope 7-14855
- static space-times, collision-free gases 7-18649
- stationary axisymmetric vacuum, conformal potential 7-47682
- Stephani-Krasinski solution, anal. of viability as model of universe 7-66800
- strictly positive mass theorem for isolated gravit. system 7-56110
- supernovae, Type II, general relativistic and nuclear matter equation of state anal. 7-47960
- supernovae and high density nuclear matter 7-55693
- superstring modifications of Einstein's equations 7-9727
- symmetric-space fields reduced from axially symmetric Einstein and Yang-Mills eqns., integrability 7-4971
- test particles with internal struct., general Lagrangian approach to eqns. of motion 7-41165
- thermo propagators and real time finite temp. Green functions in general relativity 7-153
- time-dependent gravitational fields, influence on superconducting oscillatory cts. 7-41181
- torsion potentials, dual field and first-order actions 7-9714
- transmission line gyroscopes, general relativistic electromagnetic effects 7-29859
- twisting Einstein vacuum metrics with Weyl tensors of Petrov type II or III 7-41170
- unboundedness of the gravitational partition function 7-48468

general relativity continued

- uncertainty principle, role of general relativity 7-152
- vacuum Einstein eqn. solns., cylindrical waves and cosmic strings of Petrov type D 7-48477
- vacuum Einstein eqns., solitonic approach to self-gravitating disks and rings 7-48473
- vacuum Einstein equations in 4+K dims., spherically symmetric dyonic solns., Kaluza-Klein theories 7-35362
- vacuum Friedman-Robertson-Walker universe, generation of gravitational waves 7-29832
- vacuum Kerr-Schild space perturbations, complex relativity and real solns. 7-24510
- vacuum polarization in curved backgrounds deduced from Hadamard kernels 7-48503
- vacuum space-times that admit no maximal slice 7-9717
- Vaidya spacetimes, shell-focusing singularity strengths 7-56097
- vector parallel transport, physical meaning 7-24491
- vector-spinor space and field equations 7-56092
- viscous fluid solns. and conformal transformations 7-4726
- wavelike solutions to the Einstein equations coupled to neutrino and gauge fields 7-35349

generator coordinate method

- boson images of fermion operators 7-5169
- local-scale point transformations within the generator coordinate method 7-56623
- rare-earth nuclei, multipole moments, generator coordinate method anal. 7-41895
- $^{16}\text{O}(\alpha, \gamma)$, forbidden E1 transitions, microscopic calcs. using generator coord. method 7-30373

generators, acoustic *see acoustic generators***generators, electric** *see electric generators***genetics** *see cellular biophysics***geochemistry**

- 6th international conference on geochronology, cosmochronology and isotope geology, Cambridge, England (June-July 1986) 7-8
- acid rain from Masaya volcanic, Nicaragua, comp., distrib. and neutralisation 7-9145
- Ackley Granite, SE Newfoundland, geochemical trends rel. to magmatic-metallogenic processes 7-8941
- actinide isotopes in the marine environment 7-40314
- Aegean arc, recent magmatism, geodynamics and isotope geochemistry 7-23589
- Afro-Arabian dome, volcanic rocks comp. rel. to geological evolution 7-29027
- Aileu Formation, East Timor, Indonesia, interpretation of $^{40}\text{Ar}/^{39}\text{Ar}$ and K/Ar dating 7-28916
- Ain-Franin geothermal water, Algeria, instrumental neutron activation anal. 7-60289
- Alai Range, USSR, mineral exposures and tectonic associations 7-8883
- Albiges, France, relict clinopyroxenes in Paleozoic metabasites, indication of distensive transitional-to-tholeiitic volcanism (French) 7-66003
- continental alkali basalt origin, as mixtures of kimberlite and depleted mantle 7-23605
- Amazon, sediment processes on continental shelf 7-34457
- Amazon River, continental shelf, clay mineral reactions effect on Al distrib. in sediments and waters 7-34551
- Amazon River, continental shelf organic C accumulation, stable isotope characts. 7-34463
- Amazon River, continental shelf sediment accumulation and transport ^{210}Pb anal. 7-34462
- Amazon River continental shelf, suspended sediments effect on geochem. processes 7-34550
- Amazon River continental shelf, Th partitioning between dissolved and particulate phases 7-34549
- Amitsoq gneisses (early Archaean) of Isukasia area, W Greenland, geochronology and isotopic var. 7-34485
- anion adsorption on oxides, clay minerals and soils 7-54379
- Antarctic meteorites, clay-mineraloid weathering products 7-34951
- apatite, decomposition to dense polymorph of $\text{Ca}_3(\text{PO}_4)_2$ for mantle conditions 7-44796
- apatite, fission tracks thermal annealing, chem. comp. effects 7-60252
- N. Apennines, deformation phases dating using K-Ar and $^{40}\text{Ar}/^{39}\text{Ar}$ techniques 7-40459
- Appalachians of Quebec and Nova Scotia; Ti, P, Zr, Nb, Y geochemistry 7-23587
- Archaean continent formation and anomalous sub-continental mantle link, mineralogical anal. 7-47408
- Late Archaean granites of Napier Complex, Enderby Land, Antarctica, Rb-Sr, Sm-Nd and U-Pb systematics 7-14231
- Archaean high-grade metasediments, rare earth element patterns and tectonic significance 7-34486
- central Arctic Ocean, Pleistocene calcite lysocline and palaeocurrents, climatic implications 7-23696
- Arctic Ocean, water masses and chemical constituents in W Nansen Basin 7-29065
- Arctic Ocean crust, seafloor geology and petroleum potential 7-18146
- argillaceous media, geochemical barrier capacity for radwaste disposal 7-5466
- Auger spectroscopy method for mineral grain surface analysis 7-60426
- Aurora U deposit, McDermitt Caldera Complex, Oregon, He soil gas survey 7-40441
- E. Australian marine sediments containing phosphorite, ages, chemistry and deposition 7-23631
- Barberton Mt. Land, S. Africa, U and Th content of Archaean granitoids 7-18153
- basalt, shock implantation of noble gases 7-55581
- basaltic glasses, N isotope geochemistry rel. to mantle degassing and structure 7-60193
- basalts, tectonic settings discrimination using trace element abundances 7-28957
- basalts from S Atlantic hotspots, geochemical correl. with southern African kimberlites 7-34409
- biotite-sillimanite-spinel assemblages in high-grade metamorphic rocks, thermobarometric appl. 7-40434
- Bir Safsaf-Aswan uplift, SW Egypt, petrology, geochemistry, and structural development 7-66118
- Black Hills of S Dakota, USA, Precambrian rock origin, isotope geochemical constraints 7-60205
- borehole water and gas sampling technique using polyamide tube 7-66310
- geochemistry continued**
- British Columbia, Canada, Au and Ag mineralization of Early Cretaceous age 7-65997
- SW British Columbia, Canada, Hozameen fault system and Coquihalla serpentine belt 7-4009
- S. Bulgarian Black Sea coast, abraded cliffs heavy minerals characts. (Russian) 7-34483
- buried metal sulphide deposits, exploration, effects of chem. processes on emitted gases meas. 7-40439
- Cainozoic basalts of E. China, Pb, Sr and Nd isotope systematics and chemical characts. 7-29011
- calc-alkaline volcanic rocks of Namaqua mobile belt, South Africa, evidence for Middle Proterozoic volcanic arc 7-34493
- California, groundwater Rm as earthquake fluid phase precursor 7-40424
- California, San Andreas and Calaveras faults, H_2 due to fault strips and earthquakes 7-40438
- Cape Breton Highlands, Nova Scotia, geology of Cheticamp pluton 7-65989
- Cevennes Medians, France, vaugneritic magma evol. and characts. 7-40472
- China, tectonic activity anal., use of fluid-geochem. methods 7-40421
- Churchill Province, Canada, Nd evidence of extensive Archaean basement 7-65996
- clay constituents, apportionment into structural formula 7-65999
- Colorado Peaks volcanic rocks, USA, isotope and trace element geochemistry 7-60203
- continental crust, comp. and evol. (book) 7-60913
- continental crust, origin and early growth rate 7-14229
- cordierite-diatexites, Aubusson, France, petrography, composition, age (French) 7-66099
- inner core chemical composition density model indicating elements other than Fe 7-54958
- core-mantle chemical reactions, implications of high-pressure metallisation of FeO 7-66101
- core-mantle separation in accreting Earth, effects of atmosphere form. on thermal history 7-54840
- cosmic-ray-produced isotopes in volcanic rocks at summit of Maui, Hawaii 7-54959
- Cretaceous-Tertiary extinction event, palaeoceanography characts., isotopic and geochem. anal. 7-18104
- crystalline minerals, fracture characteristics using ^{222}Rn and ^{220}Rn as probes 7-23893
- Cuba, ophiolite assoc. struct. 7-28926
- Dakongbeng geothermal area, SW China, hot spring activity 7-4064
- deep sea radwaste disposal, radionuclide dispersion by physical, geochemical and biological processes 7-5468
- deep-sea sediments, O isotope stratigraphy, graphic correl., appl. to Late Quaternary 7-23894
- Devonian shales from Appalachian Basin, C and S relations as indicator of deposition environment 7-65988
- Donegal plutons, Ireland, emplacement ages and geochemistry 7-66011
- Earth core chemistry, S and O contents rel. to inner core accretion growth and geomag. dynamo 7-66027
- earthquake precursory changes in chemistry of emitted gases, review 7-34394
- East Pacific Rise and Guaymas Basin, hot springs U-Th-Pb systematics 7-40462
- Efate, Vanuatu, thermal springs hydrology and chem. 7-60282
- Eifel periodotite xenoliths, trace element and isotope geochemistry rel. to subcontinental lithosphere 7-34484
- Elbe valley, lithospheric geochemistry and petrology in fault zone 7-54946
- England, Ar isotope geochemistry of W mineralisation 7-8876
- environmental standard reference materials, determ. of sampling constants 7-34748
- equilibrium distrib. of two-phase system in grav. field 7-34404
- Etna volcanic plume geochemistry and chemical relations 7-34428
- Etna volcano, Sicily, radioactive isotope study of magma chamber processes 7-60230
- European Association for Geochemistry and British Isotope Geology Group, Goldsmith Centennial Meeting, London, England (January 1986) 7-9
- fire areas (of red sediments and vegetation carbonization) in California, USA, due to hot groundwater 7-23654
- tropical forest soils, emission of N_2O , methane, CO_2 to atmosphere 7-40528
- fulgurites, form., extreme reduction and metal silicate liquid immiscibility 7-47439
- garnet-hornblende thermometry, $\text{CaMgSi}_2\text{O}_6$ activity rel. to min. press. limits for garnet amphibolites 7-29005
- gas geochemistry, volcanism, earthquakes, prospecting, etc., conf., Honolulu, USA (Dec. 1984) 7-29576
- glassy submarine basalts dating and He isotope disequilibrium 7-66352
- granites of E. Zambia, initial $^{87}\text{Sr}/^{86}\text{Sr}$ ratios and Rb-Sr ages 7-18147
- Great Artesian Basin, Australia, very old groundwater ^{36}Cl dating and chem. 7-66194
- Grenville Front, Labrador, Canada, Sr, Nd, Pb isotope geochemistry 7-60199
- Grenville Province, Ontario, Canada, O isotope geochem. and source regions 7-65995
- groundwater of E. Siberia, Au and Ag content of mineral waters 7-28922
- gypsiferous-sodic desert soil, leaching simulation 7-29105
- haematite, chemical remanent magnetisation and structural-sensitivity characterisation 7-29004
- Hawaiian lavas, geochemical and geophysical constraints on origin 7-8943
- Higashi-Izu monogenetic volcano group, Japan, petrology and geochemistry 7-8892
- HLW, influence of redox environments on the geochemical behaviour of radionuclides 7-5474
- hornblende, Al content as empirical igneous barometer 7-55029
- hydrothermal alteration of upper oceanic crust (DSDP Hole 504B), chemistry of seawater-basalt interactions 7-28993
- hydrothermal plumes of E. Pacific Rise, Fe, He, Mn obs. showing Fe enrichment 7-9028
- NW Iapetus Ocean, Early Palaeozoic mudstone characts. 7-23694
- Iberian margin, continental tholeiitic magmatism (French) 7-66065
- Island, geothermal activity and gases and volcanism, review 7-34430
- SW Idaho batholith, USA, erosional and chemical denudation rates meas. 7-9038

geochemistry continued

- igneous petrology, effects of convection and mixing in magma chambers 7-4028
- igneous rocks, chemical analysis, CIPW norm calculations, FORTRAN listing 7-29263
- SW India, monsoon fluctuations in 20000 yr BP O isotope/pollen records 7-47532
- Indian Ocean, Quaternary temps. determ. and sediment planktic foraminifera chem. anal. 7-29074
- indochinite tektites, K, Rb and Li concs, rel. to selective volatilisation and imperfect mixing 7-34500
- inert gas abundances in mid-ocean ridge basalts 7-60198
- inert gas isotope geochemistry, for well gases in Harding County, New Mexico, USA 7-60226
- ion microprobe and SIMS methods for chemical analysis of rocks 7-60427
- isotopic data multidimensional treatment method 7-66315
- isotopic records in deep-sea sediments and Holstein interglaciation 7-47529
- Jabal Tifl layered gabbro, SW Saudi Arabia, mineral chemistry rel. to magma origin 7-29015
- Johnson Camp, Arizona, Cu-Zn ore bodies determ. from soil and soil gas comp. anal. 7-40591
- Kamchia River mouth, Bulgaria, Fe in sediments, river and sea water 7-29085
- Kerch' Peninsula, USSR, hydrocarbon exploration using remote sensing data 7-60223
- Kilauea volcano, Hawaii, Rn soil gas emissions rel. to geology activity 7-34424
- Kilauea volcano, Hawaii, volcanic gas exsolution from magma during eruptions 7-34423
- Kilbourne Hole maar, New Mexico, USA, origin of continental alkali basalts 7-23605
- kimberlites from southern Africa, geochemical correlation with S Atlantic hotspots 7-34409
- komatiites alteration, role of spurious correl. in development of alteration model 7-55039
- central Krak Massif, USSR, struct. and petrology 7-28925
- Kraternaya Bay region, Yankicha Island, Kuril Islands, water chem. and isotopic comp. 7-29078
- lake acidification, role of groundwater 7-23247
- Laurel Mountains peat bog, USA, atm. chemicals deposition chronology 7-9075
- Laurentian Trough sediments, Gulf of St. Lawrence, radionuclide profiles, sedimentation rates, and bioturbation 7-28995
- Lena-Tunguska oil and gas province in eastern USSR 7-54942
- W Leone-Liberian shield area, tectonic development and metallogeny 7-60240
- Loihi Seamount, hydrothermal plumes containing methane and ^3H 7-28994
- low-level counting techniques 7-29296
- magma chamber dynamics and chemical fractionation due to Soret effect 7-28950
- magnioferrite from the Cretaceous-Tertiary boundary, Caravaca, Spain 7-40473
- magnetite compositions in Holocene tephra, appl. of discriminant function and for tephra identification 7-8893
- Malanjkhand Cu sulphide deposit, India, physico-chemical conditions of ore deposition 7-29025
- upper mantle, geochemical implications of viscosity of partial melts 7-8934
- mantle chemical heterogeneities origin 7-66315
- mantle chemistry, effects of chemical and phase transitions on intermediate mantle struct. (Russian) 7-66038
- mantle convective mixing, effects of chemical density differences 7-28969
- mantle depletion, implications of partial melting for Archean lithosphere stabilisation and heat loss 7-34398
- mantle diapirs evolution, effects of comp. and thermal buoyancies 7-8890
- mantle differentiation, buoyancy-driven instabilities of low-viscosity zones as models of magma-rich zones 7-8930
- mantle heterogeneities and deep subduction 7-66039
- mantle isotopic heterogeneity with different size scales 7-8889
- Mariana Trough back-arc basin, hydrothermal plumes containing methane, but no ^3H 7-28994
- Mariana Trough basalt glasses, light noble gases comp. anal. 7-40436
- marine sediments of Pacific, trace metal chemistry of metalliferous sediments 7-23633
- Marydale Group, southern Africa, metamorphosed banded Fe formation, Pb-Pb dating and assoc. geochem. 7-60189
- Masaya Caldera Complex, Nicaragua, Sand Halogen gas emissions 7-34426
- McCloud Lake, soft water acidic lake in Florida, ions sources and sinks 7-23763
- Mediterranean Sea, geochemistry of sediments of different ages, book 7-29608
- metal-silicate fractionation in growing Earth, energy source for magma ocean 7-8888
- metallogenesis rel. to tectonic lineaments 7-29256
- methane biological production in soil and sediments, enhanced due to increase atmos. CO_2 levels 7-29152
- MEXAMS metal transport model 7-9043
- mid-ocean ridge basalt glasses, oxidation states 7-8880
- milk River aquifer, Canada, old groundwater ^{36}Cl dating and chem. 7-66195
- mineral melt evolution simulation, Rayleigh fractionation 7-65998
- mineral resource deposits at D. latitude positions with high seismicity 7-65966
- mineralogy of deep-sea sediments, results from drillholes near East Pacific Rise 7-14260
- minerals, $^{40}\text{Ar}/^{39}\text{Ar}$ dating, errors due to ^{39}Ar loss during neutron activation 7-60390
- minerals, radiation damage and trace water relationship 7-32489
- Mississippi River delta area, ^{226}Ra , in sediments and water column 7-66168
- mixed groundwaters dating, appl. of T corrected ^{14}C and atm. noble gas corrected ^4He 7-9044
- Momotombo volcano, Nicaragua, fumarole gas chemistry and prediction of eruptions 7-34425
- Mont Saint Hilaire plutonic complex, Quebec, Canada, Ar isotopes and emplacement history 7-4007

geochemistry continued

- Muong Nong type tektites from moldavite and North American strewn fields, implications of element abundances 7-55050
- Nagano, Japan, $^3\text{He}/^4\text{He}$ ratio anomalies in hot spring gases, assoc. with 1984 September 14 earthquake 7-40422
- Nagano region, Japan, gas anomalies at mineral springs and fumarole before earthquake 7-40423
- natural gas wells in Sacramento basin, California, He isotope and mantle origin 7-60206
- neutron activation analysis method, calc. for case when sample contains strong absorbers 7-23851
- Nevado del Ruiz volcano, Colombia 7-8897
- New Brunswick, Canada, petrochemistry and tectonics of Carboniferous volcanic rocks 7-65992
- New Zealand, geothermal systems exploration and devel., use of applied chem. 7-13848
- natural nuclear reactor at Oklo, Gabon, Africa (French) 7-28954
- Obaku fault, Uji, Japan, gamma-ray survey of active fault 7-18157
- ocean chemistry, high nitrite levels off N Peru as signal of instability in marine denitrification rate 7-29080
- ocean chemistry, Mn geochemistry near high-temp. vents in Mid-Atlantic Ridge rift valley 7-34468
- ocean CO_2 content var. 7-34640
- Ocean Station P, Pacific Ocean, T time series 7-47466
- ocean water, statistical anal. of relative ionic composition data 7-14315
- oceanic basalts, siderophile and chalcophile abundances rel. to Pb isotope evolution and growth of Earth's core 7-34397
- oceanic basalts of Oceanographer transform, Mid-Atlantic Ridge, three-component isotropic heterogeneity 7-54956
- oceanic crust, seawater-rock interactions rel. to O isotopic profile through upper kilometer 7-34467
- oceanic crust vein mineral deposition, Rb/Sr ages and U-Th-Pb geochemistry 7-60204
- oceanic sediment barrier, geological and geochemical props. for HLW disposal 7-5463
- oceans of Archean era, reducing power of ferrous Fe, contrib. of photosynthetic O_2 7-60277
- oil and gas deposits occurrence patterns on continental shelves 7-34411
- Okinawa Trough, sediments chem. comp. and characts. (Chinese) 7-47420
- Onverwacht Group, Archean flow-top alteration zones form. in low-temp. sulphate-rich environment 7-34488
- Outer Hebrides, evidence for enriched lithospheric keel, mantle xenoliths comp. anal. 7-47407
- oxidation state of rocks formed during normal and reversed geomagnetic polarity times 7-55023
- NW Pacific, crust struct. and composition near Emperor fault 7-34412
- SW Pacific islands, Pb, Sr, Nd isotope and element abundances study 7-8874
- Pacific Ocean floor, hydrocarbons identification in sediments and bottom water layer 7-29079
- East Pacific Rise, hydrothermal clay mineral formation from basalt 7-14256
- palaeoceanography and biogeochemical processes affected by tectonic processes 7-23843
- Palaeozoic ocean, O and C isotopic records anal. 7-9029
- Palo Duro Basin, Texas, USA, groundwater inert gas chemistry 7-66179
- partial melting phenomena in Earth and planetary evolution, conference, Eugene, Oregon (September 1984) 7-4625
- peat dating by U-Th disequilibrium, geochem. aspects 7-60392
- peridotite, melting phase relations up to 14 GPa rel. to origin of peridotitic upper mantle 7-8937
- Phanerozoic, natural divisions, mass extinctions and chem. comp. anal. 7-47403
- Phanerozoic, seawater, SR isotopic comp. var. 7-60273
- Phlegrean Fields, Italy, volcanic activity rel. to uplift, thermal activity, geochemistry 7-34429
- plagioclase-muscovite geothermometer 7-34475
- early Precambrian decomposition reactions, implications of Al_2O_3 -rich rocks of Kaapvaal Craton 7-29020
- Precambrian ophiolites and basement in Central Asian foldbelt, Mongolia, structural-metamorphic evolution 7-34495
- Precambrian palaeopedology, conference, Raleigh, North Carolina (June 1985) 7-24275
- Precambrian palaeosols of Dominion and Pongola Groups, Transvaal, chemistry and mineralogy 7-29018
- Precambrian palaeosols on basaltic and granitic parent materials, elemental concs. profiles 7-29019
- Precambrian rocks of Ural Mountains, petrochemistry rel. to geodynamic regimes 7-34494
- primary lavas from Okmok volcano, central Aleutians, geochemistry rel. to arc magmatogenesis 7-28949
- pristine mantle composition analysis, implications for Earth accretionary history 7-40390
- Early Proterozoic bimodal volcanic rocks in central Colorado, petrogenesis and tectonic setting 7-23645
- Proterozoic mafic volcanic rocks of Nagu-Korpo area, SW Finland, stratigraphy and geochemistry 7-14275
- Early Proterozoic supracrustal rocks of SW United States, geochemistry and tectonic setting 7-55037
- proto-mantle differentiation in accreting Earth, effects of atmosphere form. on thermal history 7-54840
- pyrope ($\text{Mg}_3\text{Al}_2\text{Si}_2\text{O}_{12}$), melting up to 10 GPa rel. to press.-induced struct. change in pyrope melt 7-8936
- pyroxene, structural formulae and end member calculation, APL program 7-66313
- radioactive waste disposal, actinide solubility in the near-field 7-5473
- radionuclide migration over recent geological time, meas. in granite pluton 7-28917
- radionuclides in marine sediments, alpha scintillation counting method 7-4199
- Rainy Lake area, Ontario, Canada, geochemical study of mantle heterogeneity and crustal cycling 7-60202
- Roberts Victor eclogites, oceanic crust metamorphism rel. to mantle metasomatism 7-55042
- Rock Creek, USA, alkalisation due to bridge construction 7-23787
- Rockall Plateau, dipping-reflector passive margin struct., Pb isotopic evidence 7-66037
- Sakurajima volcano, Japan, volcanic gas geochemistry rel. to volcanic activity 7-34422
- salt bearing formations during Palaeozoic, book 7-35137

geochemistry continued

- sandstone-mudstone suites, tectonic setting determ. using SiO_2 content and $\text{K}_2\text{O}/\text{Ni}_2\text{O}$ ratio 7-29014
- Saskatchewan, Canada, well water He and methane anomalies origin 7-40440
- Scotland, Caledonian Pb isotope geochemistry and mantle source 7-23590
- sea-bed mineral formation, geochemical modelling, Mn nodules 7-28998
- seafloor geology and crustal generation since 116 Myr BP, foraminifera Li content evidence 7-23632
- seafloor hydrothermal plumes from S Pacific seafloor, Mn tracing of dispersal patterns 7-9027
- seawater K and Ca concentrations, potentiometric determ. over wide salinity range via admixture technique 7-14311
- Seychelles microcontinent, chem., comp. determ. 7-40452
- Sharyzhalgai complex, Baikal region, USSR, ultrabasics geochem. characts. 7-23603
- S Siberia, metallogenic evolution of Phanerozoic folded systems 7-23595
- E Siberian Platform, petroleum formation and accumulation in Mesozoic troughs 7-54944
- silicate systems, natural, crystallisation 7-8938
- simulated borosilicate radwaste glass, granite and water, geochemical interactions, repository appl. 7-807
- soil, chloride content meas. by neutron counting 7-56291
- soil, gas composition analysis use for geochemical exploration for mineral resources 7-40590
- soil, ion transport, effects of heterogeneous adsorption behaviour 7-29104
- soil water extractor for minimising CO_2 degassing and pH errors 7-23916
- Solea graben, Mediterranean Sea, ore deposition and off-axis hydrothermal metamorphism 7-60247
- solid state nuclear track detectors, conference, Rome, Italy (Sept. 1985) 7-40991
- South China Sea, palaeoclimate and palaeoceanography during Holocene, sediment O isotopic anal. (Chinese) 7-55264
- Sredne-Tersa ultrabasic massif, deep structure and rock composition 7-14223
- stable isotopes in high-temp. geological processes, book 7-35126
- Stillwater Complex, Montana, rare-earth element evidence for form. of Ultramafic Series 7-65987
- stream chemistry, appl. to hydrological parameters estimation 7-23771
- stream water, prediction of pH, alkalinity and total acidity during episodic events 7-23777
- sulphate deposition from atm., adsorption by soil, implications for dynamics in hydrological systems 7-29102
- sulphate deposition from atm., conc. in streams 7-28426
- sulphate deposits in fractured till in S Alberta, Canada, origin and distrib. 7-23726
- TAG geothermal field, Mid-Atlantic Ridge, hydrothermal activity dating 7-8915
- Tariat Depression, Mongolia, geochemistry of spinel peridotite xenoliths 7-60200
- Tariat Depression, Mongolia, Nd, Sr isotope study and subcontinental lithosphere evolution 7-60201
- Tawhai State Forest, New Zealand, catchments, runoff characts. 7-29100
- Tawhai State Forest, New Zealand, storm runoff, hillslope and low order stream response 7-29101
- tektites, F and Cl contents 7-34501
- tholeiitic dike swarm of NE Brazil, oxidation effects on rock magnetism and palaeomagnetism 7-34869
- till deposits in drumlins near Caledonia, S Ontario, geochemical characts. of inverse-graded units 7-9033
- Verkhoynay folded zone, eastern USSR, fault dislocations and petroleum prospect 7-28918
- Vestfold Block, Antarctica, age and geochem. of mafic dyke swarm 7-14228
- volatiles distribution in accreting Earth, implications of shock-induced volatile loss from Murchison carbonaceous chondrite 7-34949
- volcanic plumes from Etna and Mt. St. Helens, particle geochemistry 7-34427
- volcanic rocks from Yap-Mariana trenches intersection, petrology, geochemistry, and tectonic implications 7-34469
- Vulcano, Italy, fumarole gas chemical composition observations 7-4202
- Vulcano, Italy, fumarole gas chemical composition study 7-4015
- Vulcano, Italy, volcanic fumarole gas chemistry and water origin 7-4016
- weathering of mafic and ultramafic rocks in Archaean atmosphere, expt. meas. 7-29021
- xenoliths, kinetics of partial melting and dissolution 7-8944
- Yangbajing fault, isotopic depth 7-28973
- Yukon rivers, dissolved O_2 depressions under ice cover 7-55106
- zircon, dating of gabbro-dioritic complex in Ivrea-Verbano zone, Italy (French) 7-18136
- Ag vein deposits, conf., London, Ontario, Canada (May 1984) 7-48136
- As, seasonal var. of methylarsenic compounds in airborne particulate matter 7-34638
- Au placer deposits in upper Yukon River, Alaska 7-66042
- ^{10}Be content of Mono Lake sediments, California, record of Pleistocene geomagnetic variation and atmospheric ^{10}Be 7-23842
- C cycle, atmospheric disturbance and impact upon biosphere 7-40546
- ^{14}C activity of atmosphere, response of hydrological systems 7-23253
- Cu-Ni sulphide deposits, formation conditions 7-23599
- $\text{Fe-H}_2\text{O}$ reaction under high pressure, implications for evolution of Earth 7-8887
- ^3He in volcanic rocks, of cosmogenic origin, in situ production 7-60500
- Hg dispersion patterns around El Sid-Fawakhir Gold Mine, Eastern Desert, Egypt, stream sediments meas. 7-18148
- Ir abundances across Ordovician-Silurian boundary stratotype, relation to erosion of exposed upper mantle rocks 7-4014
- K residing in Fe core of Earth 7-40437
- K-rich lamprophyres of S Scotland, geochemistry rel. to primary magma origin 7-4032
- ^{40}K in Makhmur Plain soil, N. Iraq, α -ray spectroscopical analysis 7-34487
- Mg_2SiO_4 - MgSiO_3 system, melting and phase relations at 20 GPa under hydrous conditions 7-8935
- Mn fluxes from Juan de Fuca Ridge, regional perspective from hydrothermal plume meas. 7-66095
- Mn prospecting method, borehole γ -ray logging—neutron activation technique 7-55284

geochemistry continued

- Ni sulphides, electrochemical transfer characts. in Western Australia localities, nonlinear complex resist. anal. 7-47553
- O_2 transport in dry rocks, exptl. study 7-54954
- Os, isotopic composition in terrestrial samples from accelerator mass spectrometry meas. 7-23611
- Pb in river sediments, Christchurch, New Zealand 7-13934
- Pb isotope evolution rel. to Earth core growth, implications of siderophile and chalcophile abundances in oceanic basalts 7-34397
- Pb-Pb isochron dating method for deeply weathered terrains geochronology 7-60391
- ^{210}Pb in soil, meas. use to determine atm. aerosol scavenging characts. 7-55188
- Ra in groundwater, porous flow model for steady state transport 7-23725
- Rb-Sr geochronological system, isochrons time-temp. relation 7-66008
- Rn concentration variations in active volcanoes and seismic regions 7-54963
- Rn outgassing related to geothermal faults 7-54964
- ^{222}Rn in Gulf Coast geopressed-geothermal reservoirs, United States 7-8881
- ^{222}Rn transport from soil, role of channels 7-40442
- ^{232}Th concentrations in seawater, meas. techniques and results 7-34554
- Tl, determ. by atomic absorption spectrometry for river sediment, coal, coal fly ash 7-59801
- U and Th, concentrations in geological samples, plastic track detector study 7-40596
- U, determ. of isotope ratio, simultaneous anal. with Th, delayed neutron counting method 7-3615
- ^{238}U ($A=238$, ^{234}U) ratios in seawater, meas. techniques and results 7-34554
- V and V cpds. in marls and shaly limestones 7-14219

geochronology

- 7-34495
- 6th international conference on geochronology, cosmochemistry and isotope geology, Cambridge, England (June-July 1986) 7-8
- N Aegea, Greece, Oligocene formations palaeomag. data, tectonic implications 7-47417
- Afro-Arabian dome, geological evolution 7-29027
- Aileu Formation, East Timor, Indonesia, interpretation of $^{40}\text{Ar}/^{39}\text{Ar}$ and K/Ar dating 7-28916
- Altai-Sayan folded region, USSR, arch-block stage magmatism and tectonic magmatic activation, stratigraphy 7-23602
- N Amazon Basin, Holocene fires as climatic indicators, dating 7-47531
- Amazon River, continental shelf, high-resolution seismic stratigraphy, sedimentological interpretation 7-34465
- Amazon River, continental shelf sediment accumulation and transport ^{210}Pb anal. 7-34462
- Amazon River subaqueous delta, sedimentary structures distrib. 7-34464
- Amtsoq gneisses (early Archaean) of Isukasia area, W Greenland, geochronology and isotopic var. 7-34485
- apatite, external detector comparison for fission track dating 7-54962
- apatite fission track plateau age dating, reproducibility of meas. 7-40597
- N Apennines, deformation phases dating using K-Ar and $^{40}\text{Ar}/^{39}\text{Ar}$ techniques 7-40459
- W Arabian continental margin, S Red Sea, ages of faulting and igneous intrusions 7-14276
- Archaean-Proterozoic boundary, implications of basinal and shelf sedimentation 7-34492
- archaeomagnetic dating method, applicability in Hungary 7-8803
- central Arctic Ocean, Pleistocene calcite lysocline and palaeocurrents, climatic implications 7-23696
- SE Arizona, USA, Jurassic palaeomagnetism and age of Patagonia Mts. 7-28835
- Askoy mafic pluton, Norway, events of Caledonian metamorphic remagnetisation, palaeomag. anal. 7-47339
- Atlantic Ocean, mean sea-surface temperature variations (0-20000 BP) 7-18201
- N Atlantic Ocean, residual geoid-age relation and tectonic implications 7-28814
- E Australian marine sediments containing phosphorite, ages, chemistry and deposition 7-23631
- Bajocian-Bathonian boundary calibration, ^{40}K , ^{40}Ar and palaeomag. data from Les Vignes basaltic complex (France) 7-47389
- Baltic Shield, 1.9-1.8 Gyr strike-slip megashears and plate tectonic implications 7-14284
- E Baltic Shield, polar wander path from palaeomagnetism of Archaean and Proterozoic basic intrusives 7-28828
- Bassariide Belt, Guinea-Senegal, evidence for Panafrican tectonics events (French) 7-66060
- biostratigraphic data collection and analysis, computer analysis and methods 7-40435
- Bir Safsaf-Aswan uplift, SW Egypt, petrology, geochemistry, and structural development 7-66118
- Black Hills of S Dakota, USA, Precambrian rock origin, isotope geochemical constraints 7-60205
- Black Sea, temp.-age relation of abyssal waters (Russian) 7-66156
- blueschist metamorphism in S Alaska, Ar isotope dating 7-14220
- Boso and Miura peninsulas, Japan, collision area, convergence changes tectonic record 7-66066
- British Columbia, Canada, Au and Ag mineralization of Early Cretaceous age 7-65997
- N Brittany, France, Lower Carboniferous dolerite dykes, palaeomag. anal. and K-Ar dating 7-18110
- Cape Breton Highlands, Nova Scotia, geology of Cheticamp pluton 7-65989
- Caradocian tuff horizon, Welsh Borders, radiometric dating 7-47384
- Upper Carboniferous time scale, improvement using $^{40}\text{Ar}/^{39}\text{Ar}$ ages of tonstein and tuff sandines 7-47388
- Carmacks Group, Yukon, Canada, andesites dated to Upper Cretaceous 7-65991
- S Carpathians, age of igneous rocks from Banat Hills 7-60227
- E Carpathians Arc Bend, Romania, shallow vs. deep and old vs. recent tectonic movements 7-28987
- SE Caucasus, USSR, north slope chaotic complexes, morphology and stratigraphy 7-29013
- Cenozoic global plate motions, determ. relative to hot spot reference frame 7-40455
- Central African Republic, Proterozoic chronology and granodiorite ages 7-34405
- Chopin ash layer, stratigraphic marker at 8500 y BP (French) 7-66051

geochronology continued

- Colorado Plateau, palaeomag. data anal. rel. to tectonic rotation 7-14251
 Colorado Plateau, palaeomag. evidence for tectonic rotation 7-14250
 Columbia River, Washington, USA, Late Holocene flood freq., fluvial deposits anal. 7-47470
 continental crust, comp. and evol. (book) 7-60913
 continental rifting, crustal thinning time scales of thermomechanical model 7-14247
 corals, ²³⁸U, ²³⁴U, ²³⁰Th dating over past 500 kyears 7-60394
 cordierite-diatexites, Aubusson, France, petrography, composition, age (French) 7-66099
 mid-Cretaceous geology, book 7-48218
 Late Cretaceous time scale, isotopic ages of alkaline igneous rocks from Nemuro Group, Hokkaido 7-47390
 Cretaceous-Tertiary extinction event, palaeoceanography characts., isotopic and geochem. anal. 7-18104
 Cyprus, rot. and translation, palaeomagnetic timing 7-66067
 Dabusan Lake, Tibet, magnetostratigraphy and age of 528 m borehole core 7-8817
 Dead Sea, high level of lake at 6700 yr BP, salt deposit evidence 7-55087
 Deccan flood basalts, relation to Cretaceous-Tertiary boundary 7-34417
 Deccan trap volcanism as a cause of biologic extinctions at the Cretaceous-Tertiary boundary? (French) 7-18137
 deep-sea sediments, O isotope stratigraphy, graphic correl., appl. to Late Quaternary 7-23894
 Devonian rocks of Kvamshesten, W Norway, tectonic implications of Solundian (Upper Devonian) magnetisation 7-34376
 diamonds, cubic, from Zaire, K-Ar isochron dating 7-23612
 Dnieper-Donets Basin, Devonian volcanism rel. to deep crustal struct. along Kiev-Gomel' DSS profile 7-47394
 Donegal plutons, Ireland, emplacement ages and geochemistry 7-66011
 DSDP site 577, Shatsky Rise, Pacific Ocean, evidence for Cretaceous-Tertiary boundary extinctions 7-23706
 Earth accumulation and initial state, chronology 7-34367
 East Pacific Rise, dispersed minerals in sediments rel. to plates motion 7-14260
 Eifel volcanic field, ⁴⁰Ar/³⁹Ar age determs. rel. to age and duration of Middle Pleistocene cold period 7-47392
 Elatina varve record of solar activity, Hilbert transform anal. 7-47811
 Ellesmere Island, Canada, Late Quaternary sea-level changes and glacial history 7-66128
 NE Ellesmere Island, NWT, Canada, glacial geology and marine stratigraphy 7-4062
 England, Carboniferous sandstones origin, determ. from zircons dating 7-47409
 Eocene-Oligocene boundary age, implications of ⁴⁰Ar/³⁹Ar dating of tektite fragments for Barbados 7-47391
 Ercall Granophyre, Shropshire, England, geochronological study 7-66014
 Finland, tectono-exogenic evolution of Precambrian supracrustal rocks 7-34490
 firm closure, lattice models, percolation on interstices of BCC lattice, bubble age 7-14320
 fission track age determination, neutron dosimetry, neutron energy effects 7-47570
 fission track dating, grain allocation in population method 7-47568
 fission track dating of annealed minerals and non-unique populations, clustering technique 7-47572
 Flysch della Laga formation, Italy, fission track dating 7-40598
 geodynamics since Archaean, implications of previous higher mantle temp. 7-54994
 geomagnetic attractor and 3-disc dynamo system, strange attractor, dimensions and K₂ entropies 7-3978
 glacier advance of Nigardsbreen, SW Norway, ¹⁴C dating and palaeoenvironment 7-9037
 glaciolacustrine sediments of Yukon Territory, stratigraphic, isotopic and micrological evidence for early Holocene thaw unconformity 7-9034
 glassy submarine basalts dating and He isotope disequilibrium 7-66352
 glauconite, sedimentary authigenic, annealing temp. and time effects on fission tracks 7-54966
 glauconite from sedimentary formations, extra-peninsular India, fission track dating 7-54965
 Glen Feshie, Cairngorms, Scotland, age of river terraces 7-34497
 Gorringer Bank, N Atlantic, Ar isotope ages of alkaline volcanism 7-8873
 Great Artesian Basin, Australia, very old groundwater ³⁶Cl dating and chem. 7-66194
 W Greenland, 3820 Ma zircons from tonalitic Amitsoq gneiss 7-8878
 W Greenland, age and Pb loss for Isua supracrustal belt 7-23591
 greenschist belts tectonic evolution, conf., Houston, USA (January 1986) 7-41017
 NW Himalaya, rot. overthrusting chronology from palaeomag. data for Riasi thrust sheet 7-34379
 W Hoggar, Algeria, Pan-African crustal decoupling zone in Timagouine area 7-34439
 Central Hoggar, Algeria, struct., geochronology and tectonic evolution 7-54997
 Late Holocene climatic changes in S Sierra Nevada, California, implications of upper timberline vars. 7-55251
 Holocene palaeoclimate of Mount Kenya, significance of sand dunes in Mutonga drainage 7-18186
 Holstein interglaciation, time-stratigraphic position and correl. to deep-sea sediments stable isotope stratigraphy 7-47529
 Holsteinian interglaciation, N Germany, stratigraphy and ESR dating 7-34669
 Huron, USA, lake levels during Holocene, Lake Nipissing transgression 7-66174
 Illinois Basin, tectonic subsidence anal. rel. to Ordovician time-scale 7-54984
 SW India, monsoon fluctuations in 20000 yr BP O isotope/pollen records 7-47532
 Indian Ocean, Quaternary temps. determ. and sediment planktic foraminifera chem. anal. 7-29074
 Indo-Antarctic metamorphic terrain, Late Proterozoic dates from India rel. to sapphirine granulites correl. 7-34414
 last interglacial-glacial transition in Baffin Bay, land-ocean corals. 7-34568
 Josephine ophiolite of Klamath Mountains, N California, timing and kinematics of emplacement 7-14282
 Juan de Fuca plate, kinematic history from diffuse boundary model for Gorda deformation zone 7-28968
 Kamchatka, USSR, tectonics and volcanism 7-28963

geochronology continued

- Karelian granite-greenstone terrain, geological evolution 7-34489
 Karisimbi volcano, Virunga, Rwanda-Zaire, K-Ar ages of Pleistocene lava 7-34419
 Kennett Formation, E Klamath Mountains, California, island arc sedimentation in Middle Devonian 7-29017
 Kentland, Indiana, cryptoexplosion struct., palaeomag. estimate of age and thermal history 7-29030
 Koobi Fora Formation, Lake Turkana, Kenya, magnetostratigraphy study 7-28838
 Lake Karewa, India, palaeoclimate characts. determ. from sediments anal. 7-4175
 Las Vegas Valley, USA, Late Quaternary environmental changes 7-47414
 Laurel Mountains peat bog, USA, atm. chemicals deposition chronology 7-9075
 Laurentian Trough sediments, Gulf of St. Lawrence, radionuclide profiles, sedimentation rates, and bioturbation 7-28995
 lithosphere thinning under conditions of large heat flows, time for steady-state soln. 7-28928
 Los Angeles Basin, two-dimensional model of extension, subsidence and thermal evolution 7-66080
 low-level counting techniques 7-29296
 Ludlovian bentonites from Welsh Borders, Great Britain, K-Ar biotite data 7-47386
 Maghribi Formation, SW Egypt, deposits from mixed estuarine and tidal-flat environment of Cenomanian age 7-18185
 Malan loess age from Luochuan profile TL study 7-60224
 Marydale Group, southern Africa, metamorphosed banded Fe formation, Pb-Pb dating and assoc. geochem. 7-60189
 NW Massif Central, France, chronology of Neogene and Quaternary geologic events (French) 7-60235
 Mediterranean geosynclinal belt, Carpathian and E Alps, segments, pre-Alpine evol. and main tectonic boundaries 7-34437
 Merida Andes, Venezuela, struct. and stratigraphy rel. to Neo-gene transcurrent motion 7-14283
 Mesozoic dike swarm in NE Brazil, K-Ar ages rel. to rock magnetism and palaeomagnetism 7-54869
 meteorites found in Antarctica, terrestrial ages 7-60608
 Miami Pliocene coral reefs, geomorphology and Atlantic coastal ridge in Florida 7-29028
 Mianwali re-entrant and W Salt Range, Pakistan, palaeomag. constraints on form. 7-34380
 mica Ar isotope dating method, the two ⁴⁰Ar/³⁹Ar age spectra shapes 7-23860
 SW Michipicoten Greenstone Belt, Ontario, evidence for complex Archean deform. history 7-55040
 milk River aquifer, Canada, old groundwater ³⁶Cl dating and chem. 7-66195
 Mindoro Island, Philippines, chronology of allochthonous terrane evolution 7-14249
 mineral cooling ages determ. method 7-12167
 mineral isochrons, time-temperature relation, thermodynamic model, Rb-Sr system as example 7-66008
 minerals, ⁴⁰Ar/³⁹Ar dating, errors due to ³⁹Ar loss during neutron activation 7-60390
 Miocene solar cycle, evidence from tree rings for 7-year cycle 7-9456
 mixed groundwaters dating, appl. of T corrected ¹³C and atm. noble gas corrected ⁴He 7-9044
 Mkushi Gneiss Complex, central Zambia, Rb-Sr and K-Ar, geochronology 7-14230
 Mongolia, tectono-magmatic devel., Late Palaeozoic and Early Mesozoic stages 7-28960
 Mongolia, Trans-Altai zone tectonics and history 7-28961
 Mono Craters, E central California, date of most recent eruption 7-40447
 Mont Saint Hilaire plutonic complex, Quebec, Canada, Ar isotopes and emplacement history 7-4007
 Morocco Basin, stratigraphy of sediment accumulation during Late Quaternary 7-14259
 Missi norite, Morocco, K/Ar dating, petrography and palaeomagnetism 7-8882
 Missi norite (S Morocco), 140 Ma K/Ar age 7-60195
 Muria volcano, Java, magmatic series (French) 7-66050
 Napier Complex, Enderby Land, Antarctica, Rb-Sr, Sm-Nd and U-Pb systematics of Late Archaean granites 7-14231
 SE New England, ⁴⁰Ar/³⁹Ar ages rel. to Late Palaeozoic cooling curve and tectonic model 7-4029
 New Zealand, palaeomag. evidence for large tectonic rot. in last 5 Myr 7-34377
 Northern Hemisphere, volcanic activity and climate since 1500 AD (German) 7-9161
 Northern Hemisphere Quaternary glaciations 7-55051
 oceanic lithosphere, heat flow-time relation for young lithosphere 7-18177
 Olary Block, South Australia, stratigraphic and structural constraints on Proterozoic tectonic history 7-55045
 Oman obduction, chronological datum from Companion Radiolarians faunas (French) 7-66001
 NW Ontario, U-Pb ages of Precambrian rocks 7-4008
 Oxford-Kimmeridgian boundary breccia of SW France, new stratigraphic framework (French) 7-14273
 N Pacific Ocean-atm. system, Pliocene-Pleistocene evol., fossil diatoms anal. 7-23695
 palaeosol, 2200 Myr old, near Waterval Onder, South Africa, reappraisal 7-29022
 Palo Duro Basin, Texas, USA, groundwater inert gas chemistry 7-66179
 Paris Basin, France, chronology of Neogene and Quaternary geologic events (French) 7-60235
 peat dating by U-Th disequilibrium, geochem. aspects 7-60392
 Peerless Formation, Colorado, Early and Late Palaeozoic remagnetisation 7-8813
 Perth region, Australia, Holocene sealevel var., crystal effects 7-47462
 Phanerozoic, natural divisions, mass extinctions and chem. comp. anal. 7-47403
 Phanerozoic, seawater, Sr isotopic comp. var. 7-60273
 Phanerozoic time scale calibration, recent advances 7-47383
 Phanerozoic time scale calibration symposium, Strasbourg, France (April 1985) 7-40983
 Pisco Formation, Peru radioisotope dating age estimation (French) 7-54941

geochronology continued

- plate convergence rate during Taconic arc-continent collision, geological evidence 7-28966
- plate movements, appl. of cladistic methods in Palaeozoic continental reconstruction 7-4019
- plates motion and an expanding Earth, fossil data anal. 7-47418
- Middle Pleistocene cold period, age and duration from $^{40}\text{Ar}/^{39}\text{Ar}$ ages from Eifel volcanic field 7-47392
- Late Pleistocene-Recent volcanics from S Italy, appl. of Cassinoli K-Ar dating technique 7-47393
- Plio-Pleistocene marine sequence of North Island, New Zealand, mag. polarity stratigraphy 7-34378
- polar ice air bubbles for pollution monitoring and bubble age 7-4068
- W Portugal, palaeomagnetism, ages and tectonics of Cretaceous igneous rocks 7-47327
- Poyang Lake, China, Quaternary evol., sediment anal. (Chinese) 7-55105
- Precambrian geology, 27th IGG Congress, Moscow (August 1984) 7-29580
- Precambrian-Cambrian boundary age, implications of study of Ercall Granophyre England 7-66014
- Upper Proterozoic carbonates, ^{13}C stratigraphy rel. to palaeoenvironment 7-47544
- Qingdao coast, China, changes of palaeogeographical environment during past 20000 years (Chinese) 7-55011
- Quelccaya Ice Cap, Peru stratigraphic record of Little Ice Age 7-34670
- radiocarbon dating method for sediments, by accelerator mass spectrometry 7-9240
- Reykjanes Ridge rift valley, Upper Quaternary sediments stratigraphy, foraminiferal anal. 7-29073
- river terraces in Scottish upland valleys, soil stratigraphy and terrace dating 7-34497
- Roberts Victor eclogites, Nd/Sm and Pb/Pb ages of ancient oceanic crust 7-55042
- Ruby Mountains-East Humboldt Range, Nevada, K-Ar and $^{40}\text{Ar}/^{39}\text{Ar}$ studies 7-28986
- Ruby Mts.-E Humboldt Range, Nevada, USA, chronology of tectonic denudation 7-54999
- Samos Is., Greece, Miocene deposits containing fossil mammals, magnetostratigraphy 7-23524
- San Juan Is., Washington, USA, geochronology and tectonic development 7-65994
- sand dunes, thermoluminescence dating method used for Sri Lanka red-sand beds 7-23847
- Santa Cruz County, California, magnetostratigraphy of Pliocene Purisima Formation 7-8799
- West Sayan and Gorniy Altai, USSR, age of flyschoid series rocks 7-28919
- NW Sayan region, USSR, Precambrian granitoids isotopic age 7-23601
- SW Scotland, Luga and other sills, age and geology 7-66013
- young sediment palaeomagnetism, conf., Louvain-la-Neuve, Belgium (Jul.-Aug. 1984) 7-4628
- sedimentary basin analysis (book) 7-35129
- sedimentary basin stratigraphy, effects of lithosphere in-plane stress 7-14278
- Seychelles microcontinent, younger igneous rocks isotopic and geochronological anal. 7-40452
- Sharyzhalgai complex, Baikal region, USSR, ultrabasics Rb-Sr isochrone anal. 7-23603
- Shebandowan greenstone belt, Ontario, Canada, magmatism age and regional deformation 7-23585
- Siberia, Jurassic continental and marine palynostratigraphy 7-23594
- Siberia, stratigraphy of Phanerozoic 7-54943
- NE Siberia (Yakutiya), USSR, crust evol. 7-23593
- Sierras Pampeanas of Argentina, chronology of Late Cenozoic foreland deform. 7-66113
- Silurian-Devonian boundary volcanic rocks from Vendee (W France), U-Pb zircon dating 7-47387
- Snake River Plain, United States, contrasting climatic histories resulting from multiple thermal maxima 7-47530
- solid state nuclear track detectors, conference, Rome, Italy (Sept. 1985) 7-40991
- Solomon Islands arc, Neogene displacements rel. to geology and arc configuration 7-66082
- Sopron, Hungary, archaeological baked clay, archaeomagnetic ages (Hungarian) 7-18113
- South China Sea, palaeoclimate and palaeoceanography during Holocene, sediment O isotopic anal. (Chinese) 7-55264
- sphe from Lower Seve Nappe, Sweden, fission track age temp. method 7-40600
- Stanovoi area, USSR, granulites isotopic age and geological implications 7-23600
- stratigraphically constrained cluster analysis, FORTRAN 77 program 7-66114
- subcontinental lithosphere evolution, implications of trace element and isotope geochemistry of Eifel periodotite xenoliths 7-34484
- subducting oceanic lithosphere, effect of age and thermal state on mag. signatures detected by MAGSAT 7-65938
- TAG geothermal field, Mid-Atlantic Ridge hydrothermal Mn oxide deposits dating 7-8915
- tektite fragments for Barbados, $^{40}\text{Ar}/^{39}\text{Ar}$ laser-probe dating rel. to Eocene-Oligocene boundary age 7-47391
- thermoluminescence dating of epidote, effects of radiation damage 7-51818
- thermoluminescence dating of sphe, radiation damage effects 7-51889
- Tibet, Ar dating of Meso- and Cenozoic rocks, and geodynamic significance 7-8875
- S Tien Shan, greenschist metamorphism conditions and geotectonic evol. model 7-34401
- Toba tuffs, stratigraphy, palaeomagnetism and mag. fabric rel. to sources and eruptive styles 7-28958
- Transantarctic Mountains-Ross Embayment region, asymmetric extension and assoc. uplift and subsidence 7-40453
- Triassic megaporphyritic monzogranites of S California, intrusive ages rel. to offset along San Andreas Fault 7-55043
- Troodos microplate, Cyprus, palaeorotation in Meso-Cenozoic plate tectonic framework of E Mediterranean 7-34441
- SW United States, geochronology and tectonic setting of Early Proterozoic volcanic rocks 7-55037
- Ural Mountains, Precambrian geodynamic regimes 7-34494
- Urgonian platform emplacement, Infra-Urgonian hemipelagic facies age (French) 7-66002

geochronology continued

- central USA, basement Precambrian ages and tectonic significance 7-8877
- Vestfold Block, Antarctica, age and geochem. of mafic dyke swarm 7-14228
- volcanic rock eruption age determ. method using ESR 7-66316
- volcaniclastic materials, thermoluminescence ages, meas. apparatus 7-47571
- Washington-Idaho, Mesozoic tectonic evolution rel. to metamorphism of Priest River Complex 7-4033
- Wenlockian pyroclastic biotites of Gotland (Sweden), radiometric K-Ar ages (French) 7-47385
- West Virginia, chronology of mesostructures development in detached folds 7-4030
- Western Australia, relations between Archaean high-grade gneiss and granite-greenstone terrain 7-34491
- Yangtze Platform, Upper Proterozoic carbonates, ^{13}C stratigraphy rel. to palaeoenvironment 7-47544
- Zabargad Island, struct. and Red Sea rifting 7-66034
- Zambia, provisional metamorphic maps and explanatory notes 7-18184
- E Zambia, Rb-Sr studies of metamorphic and igneous events 7-18147
- zircon crystals, isotope age method and crystal morphology for rock history 7-18183
- zircons, dating of gabbro-dioritic complex in Ivrea-Verbano zone, Italy (French) 7-18136
- $^{13}\text{C}/^{12}\text{C}$ ratios, stratigraphic tool in East Mediterranean (French) 7-60190
- ^{14}C , radiocarbon dating using low energy cyclotron 7-55310
- ^3He of cosmic ray origin, use for dating of lava flows 7-60500
- K-rich lamprophyres of S Scotland, Rb-Sr and K-Ar ages 7-4032
- ^{138}La , beta-decay half-life and dating of gneiss rocks from Scotland 7-49312
- Pb-Pb isochron dating method for deeply weathered terrains geochronology 7-60391
- ^{210}Po -coated geological and synthetic samples, ESR dating 7-47569
- U veins in biotite from Bancroft, Canada, fission track dating 7-40599
- U-Pb zircon and titanite ages, N Western Gneiss Region, Norway 7-60194
- geodesic lenses see aspherical lenses; integrated optics; lenses
- geodesics see differential geometry
- geodesy
- ID time series anal. for sphere, appl. in geomag. and gravimetric geodesy 7-9239
- 1979, assoc. vertical crustal deform. and implications for fault behaviour 7-54929
- absolute gravity meter 7-9224
- adjustment model for geodesy and surveying, validity of mathematical model (German) 7-40400
- anomalous geopotential fields, parameters of regularized continuation of 2D fields 7-60149
- antidensity gravity anomaly calc. using quadratic density function 7-23514
- Atalandi fault-zone, Greece, recent vertical movements 7-28977
- N Atlantic Ocean, residual geoid anomalies and tectonic implications 7-28814
- Atlantic Ocean, variability of dynamic topography and surface geostrophic currents in central tropical Atlantic 7-14304
- N Bay of Biscay continental margin, isostasy gravity and tectonic model 7-8902
- bodies of zero external gravit. pot., forgotten results and present state 7-8789
- S California, levelling refr. 7-8791
- Cape Verde Rise, in N Atlantic, heat flow anomaly and geoid indicating mantle plume support 7-47396
- Great Caucasus, USSR, gravity anomalies for earthquake prediction 7-65971
- Charleston region, South Carolina, vertical crust movements, levelling data anal. 7-8911
- combined terrestrial and satellite control networks, hybrid stochastic model 7-34369
- conference, Kensington, NSW, Australia (Nov. 1985) 7-35082
- constant part of Earth tides in Earth figure theory 7-65916
- coordinate transformation (geodetic to grid coords.), the Lambert conical orthomorphic projection 7-65917
- core rotation rel. to C_{21} and S_{21} geodetic gravity coeffs. 7-47399
- crustal movements in Central and South America, symposium, Maracaibo, Venezuela (February 1985) 7-24291
- crustal tilt anomaly patterns assoc. with earthquakes, features and classification (Chinese) 7-34388
- deformation and surface movements data analysis by statistical methods 7-28803
- deformation due to tidal forces, implications for rot. characts. (Russian) 7-40397
- deformation nets, distance and distance ratio meas. sensitivity (German) 7-23520
- deformation of Earth due to surface tractions Green's function theory 7-54850
- departure from hydrostatic equilibrium 7-54848
- digital terrain model for flat areas by least squares techniques on mini-computer 7-40410
- doming caused by postseismic viscoelastic relaxation following 1959 Hebgen Lake earthquake 7-14245
- dynamical flattening, implications for normal density Earth models 7-18154
- Earth gravity models, freq. windows and resonant solns. as test of accuracy 7-3966
- Earth thermal expansion, temp. profile and radial deform. assoc. with heat cond. in elastic Earth 7-23592
- earthquake prediction, using solid Earth tide tilt and strain near to dilatant region 7-3996
- East Germany, gravity var. and temporal heights near gravimetric W-E profile 7-14177
- Europe, combined geophysical-thermal models of crust and upper mantle 7-28933
- Fruioli area, Italy, crustal deform. and 1976 earthquakes 7-54948
- geodynamics spatial problem soln. using repeated geodetic meas. 7-23623
- geoid anomalies, appl. to core-mantle boundary topography determ. 7-66021
- geoid determ. methods 7-55331
- geoid shape in Sudan, by astrogeodetic and satellite observations 7-40394

geodesy continued

- geometrical levelling automation, appl. of digital linear measuring system (*German*) 7-3972
- geopotential field computation method, for 3D density and magnetization distrib. (*Chinese*) 7-3964
- geopotential harmonics of order 15 and 30, determ. from orbital resons. of 25 satellites 7-65923
- global nondynamic orbit improvement for altimetric satellites 7-14392
- global satellite laser ranging use for tectonic deform. anal. 7-55287
- GPS radionavigation, 1 to 2 parts per 10⁷ geodetic accuracy 7-34686
- GPS radionavigation, data processing algorithms 7-34685
- GPS radionavigation satellite, orbit determ. by regional network double difference carrier phase obs. 7-34684
- GPS satellite methods for geodetic networks (*German*) 7-18108
- gravity, anomalous field due to horizontal layer of Poisson random sources 7-34381
- gravity anomalies, direct problem for vertical cylindrical bodies 7-23510
- gravity anomalies of sedimentary basin, basin depth estimation by anomaly inversion 7-3968
- gravity anomaly, nonlinear data inversion using Schmidt-Lichtenstein approach 7-65920
- gravity anomaly decompensation theory 7-14175
- gravity anomaly due to 2-D body with variable density contrast 7-54842
- gravity anomaly global model using error covariance function (*German*) 7-18109
- gravity anomaly inertial surveying 7-4196
- gravity anomaly interpretation, by multiparameter functional minimization algorithm 7-60150
- gravity anomaly interpretation using deterministic approach 7-28811
- gravity anomaly prospecting, stable difference methods for continuation 7-55303
- gravity field mapping, relative motion of geodynamic twin satellite 7-4285
- gravity network design, based on approx. of variance-covariance matrix 7-65918
- gravity nontidal variations continuous meas. 7-8792
- gravity surveying using inertial navigation 7-4194
- ground control network, hybrid analysis with sparse matrix techniques (*German*) 7-40401
- central Gulf of California, geodetic meas. of plate motions 7-66069
- harmonic function derivatives for geophysical anomalies, method for integral relations 7-60148
- Hawaiian swell, compensation depth estimation using linear filters 7-54986
- Hollister, California, dislocation model for aseismic crustal deform. 7-40445
- horizontal pendulums of capacitive type, laboratory test method 7-29250
- Indian Ocean, geopotential hours and core-mantle interface depressions 7-47412
- inertial geodesy, network adjustment theory (*German*) 7-65924
- inertial positioning problem in Hamiltonian mechanics 7-4195
- isomorphic geodetic and electrical networks, airborne survey analysis 7-47309
- Central Japan, gravity and magnetotelluric study of Fossa Magna region 7-23609
- NE Japan Arc, horizontal crustal strain and tectonics 7-18175
- Kerguelen Plateau province, crust struct. from gravity anomaly and seismic refl. obs. 7-28952
- Kyoto, Japan, earthquake occurrence possibility, from geodetic observations 7-65954
- La Grande-2 Reservoir, Quebec, crust vertical movement and gravity var. 7-8793
- laser ranging, extended Kalman filter for automatic target following of lunar reflectors (*German*) 7-23521
- least squares in geodetic surveying computations, soln. method 7-65914
- levelling survey, elimination of bias caused by variable spacing 7-65912
- Long Valley caldera, California, USA, geodetic trilateration and gravity surveys 7-40449
- mantle convection, geoid anomalies and topography 7-28971
- marine geodesy in North America 7-47312
- maximum likelihood estimate of variance components 7-65915
- Mississippi Embayment, gravity field temporal var. due to crust elevation 7-8794
- Mojave Desert, California, USA, geodetic deformation on faults 7-40395
- network adjustment accuracy for hybrid adjustment of terrestrial and satellite data (*German*) 7-65925
- New York and Connecticut, USA, geodetic obs. of horizontal deformation 7-40456
- North American-Pacific relative plate motion in S California, determ. from VLBI meas. 7-28978
- North azimuth determination using suspended gyrocompasses 7-66309
- nutration, rotational variations and solid Earth tides, influence mantle anelasticity 7-23512
- oceanic geoid global point-mass adjustment using satellite altimetry 7-47310
- oceanic geoid least-squares collocation based on satellite altimetry 7-47311
- oceanic geoid rel. to global seafloor depth 7-65919
- outlier detection by distribution theory 7-40391
- W Pacific, trench-trench-trench triple junction off SE Japan 7-34415
- palaeorotation since Silurian period, and Earth shape and gravity field 7-23511
- Phlegrean Fields, Italy, volcanic activity rel. to uplift, thermal activity, geochemistry 7-34429
- portable absolute gravimeter for vertical crustal motions anal. 7-9225
- precise relative geoid heights determ. from gravimetry 7-8295
- precision geodesy and crustal deform. meas. instrument, hydrostatic levels 7-9229
- projective transformation of space imagery into mosaics and photomaps, minimisation of Earth curvature effect 7-65922
- radionavigation, GPS local 3D geodetic network layout using TI4100 receivers (*German*) 7-40614
- radionavigation, optimum Doppler positioning using new data processing method 7-29249
- radionavigation methods, differences between nautical charts and the geodetic datum (*Japanese*) 7-66353
- rangefinding by optical method, precision, for long baseline meas., error of point approx. method for air integral refr. index 7-66342
- road engineering surveying using GPS satellite 7-34687
- Sacramento Valley, California, USA, 3D geodetic network established using GPS and MACROMETER II 7-34371

geodesy continued

- San Andreas fault, central branch, gravity anomalies and earthquake epicentres 7-65972
- San Andreas fault at Parkfield, California, geodetic strain obs. and slip deficit 7-28979
- satellite geodesy, trigonometric series representations of orbital inclination function 7-4299
- satellite laser ranging, chord and relative height estimation from single data passes (*Chinese*) 7-3961
- satellite laser ranging, observations smoothing via correction of orbital parameters and station coordinates 7-54844
- satellite laser ranging to STARLETTE, ground station coords. and baselines 7-65913
- Saugus-Palmdale, California, atm. refr. error in historical levelling surveys 7-8790
- sea-level monitoring, use of geodetic radio interferometric surveying 7-18312
- solid Earth tide recording, digital data acquisition system 7-29245
- solid Earth tides and geodynamics 7-28804
- spherical harmonics of geopotential temporal variations 7-28805
- spherically stratified model, response to body force and surface pots. load (*Chinese*) 7-18105
- Stanford Gravity Probe-B expt., using superconducting thin film gyroscope 7-14855
- strain measurement, prediction of thermoelastic strain in half-space covered by unconsolidated material 7-29001
- strainmeter and tiltmeter techniques and design, review 7-23906
- surveying, GPS navigation radio receiver sets, MINI-MAC system by Litton 7-34370
- Takase Dam, Japan, tiltmeter obs. rel. to microearthquake activity 7-23572
- digital terrain model, on a triangular base 7-28806
- tide in solid Earth, measurement with feedback gravity meter 7-40396
- tiltmeter of water-tube half-filled type, instrumental noise (*Japanese*) 7-4231
- two step static deformation model, proof of resulting identity (*German*) 7-40399
- vertical crust motion meas. by mobile VLBI and GPS, effects of atm. water vapour 7-9226
- VLBI applications 7-55325
- VLBI for vertical crust motion meas., atm. water vapour correction 7-9227
- VLBI geodetic measurement, influence of atmospheric pressure deformation of land 7-4213
- VLBI method, variance and covariance matrix theory 7-40392
- VLBI station location determination in terrestrial reference frame (*French*) 7-66314
- volcanic area displacement and stresses due to centre of dilation 7-23642
- Wairakei Geothermal Field, exploitation induced gravity var. due to groundwater effects 7-28812
- World projections for environment mapping, application 7-14399
- Yamaguchi earthquake, Japan, crustal movements observations 7-65926

geodetics see geodesy

geolectricity see terrestrial electricity

geography

- Barbados, palaeogeography and tectonics of quartzose sandstones 7-28981
- Canada's electronic atlas 7-40407
- database, Minute Man National Historical Park, map input software 7-47319
- generalised cartography, computer aided 7-47322
- Landsat and SPOT high resolution satellite images: a new component for geographic data bases 7-40405
- Palaeozoic continental reconstruction, appl. of cladistic methods 7-4019
- resources management master planning, GIS and remote sensing role 7-4072
- soil survey, use of Landsat and digital elevation data 7-4233
- undersea features name file for personal computer, database description 7-65927
- water resource planning, geographic information systems for encoding soil information 7-47473
- watershed acidification, computer simulation 7-14322

geology

- 17th Congress of Geological Survey of Finland, conf., Helsingfors, Finland (May 1986) 7-48179
- Ackley Granite, SE Newfoundland, geochemical trends rel. to magmatic-metallogenic processes 7-8941
- Adrar des Iforas, Mali, tectonometamorphic evolution of gneissic Kidal assemblage rel. to Pan-African thrust tectonics 7-66117
- Africa, central and E central region, geology and petroleum resources 7-47438
- Pan-African tectonics and geology of Trans-Saharan belt in Mali 7-34453
- Afro-Arabian dome, geological evolution 7-29027
- Agly, France, pressure of metamorphic events in granulite terrains (*French*) 7-34689
- Alai Range, USSR, mineral exposures and tectonic associations 7-8883
- Albigensis, France, relict clinopyroxenes in Palaeozoic metabasites, indication of distensive transitional-to-tholeiitic volcanism (*French*) 7-66003
- Aldanian shield, USSR, phlogopite and apatite deposits and tectonophysical environment 7-60222
- Western Alps, lithospheric sections assuming that the Sezia zone is not of South Alpine origin (*French*) 7-66004
- Altai-Sayan folded region, USSR, arch-block stage magmatism and tectonic magmatic activation, stratigraphy 7-23602
- Alyat Ridge, SE Caucasus, USSR, horizontal compression structures, clay diapirs and mud volcanoes 7-23643
- Annual Review of Earth and Planetary Sciences 7-9606
- Appalachian Basin, USA, C and S relations in Devonian shales as indicator of depositional environment 7-65988
- Appalachians of Quebec and Nova Scotia; Ti, P, Zr, Nb, Y geochemistry 7-23587
- W Arabian continental margin, S Red Sea, tectonic configuration 7-14276
- Arc basin, France, crack-seal mechanism in limestone as deform. factor in strike-slip faulting 7-29010
- Archaean high-grade metasediments, rare earth element patterns and tectonic significance 7-34486
- Archeozoic oceans, reducing power of ferrous Fe, contrib. of photosynthetic O₂ 7-60277

geology continued

- Arctic Ocean crust, seafloor geology and petroleum potential 7-18146
 Arctic shorelines of USSR, shoreline changes and sea levels during Cainozoic 7-4022
 Armenia volcanic highland, USSR, Late Cainozoic volcanic geology, petrology etc. 7-8884
 Asia (West-Central region), Kimmerian movements and structural development 7-60242
 S Atlantic, Miocene and Pliocene stratigraphy and palaeoceanography 7-23634
 S Atlantic, Oligocene palaeocean and palaeoclimate conditions 7-23698
 N Atlantic off W coast of Spain, seafloor geology (*French*) 7-60191
 S Atlantic Ridge, geology in 20 to 30 degrees South area 7-34410
 S Australia, Precambrian periglacial varvites, palaeomagnetism, palaeoaltitude and palaeoclimate 7-8798
 E Australia metagenesis and tectonics, conf., Sydney, Australia (August 1984) 7-55882
 Australia-Antarctica, reconstruction of tectonic break-up process 7-8899
 E Australian marine sediments containing phosphorite, ages, chemistry and deposition 7-23631
 Axial Seamount, Juan de Fuca Ridge, acoustic noise due to hydrothermal vents 7-23558
 Baffin Bay, sediments rel. to land-ocean corals. during last interglacial-glacial transition 7-34568
 Bahia, Brazil, pressure of metamorphic events in granulite terrains (*French*) 7-34689
 Baltic Shield, 1.9-1.8 Gyr strike-slip megashears and plate tectonic implications 7-14284
 banded Fe formations and chemistry of Archeozoic oceans 7-60277
 Barberton Mt. Land, S Africa, U and Th content of Archaean granitoids 7-18153
 basalt formation, peridotite root zone beneath Grand Lagon Nord, New Caledonia (*French*) 7-66087
 Bassaride Belt, Guinea-Senegal, evidence for Panafrican tectonics events (*French*) 7-66060
 Bay of Islands Ophiolite, 2D seismic reflection modelling of fossil oceanic crust-mantle transition 7-40428
 Benue Valley savanna, Nigeria, soil survey performed by LANDSAT satellite 7-23652
 Betic Cordillera, Spain, Fe oxides mineralogy of Triassic sediments from Kubelka-Munk colour theory 7-66098
 Bhatsa area, Maharashtra, India, tectonic struct. rel. to reservoir-induced seismicity 7-23567
 Bir Safsaf-Aswan uplift, SW Egypt, petrology, geochemistry, and structural development 7-66118
 Black Hills of S Dakota, USA, Precambrian rock origin, isotope geochemical constraints 7-60205
 Black Sea trough, crust struct., geology and tectonics 7-60214
 blueschist metamorphism in S Alaska, Ar isotope dating 7-14220
 Bridge River terrane, British Columbia, Canada, geology and tectonics 7-55001
 British Columbia, Canada, Au and Ag mineralization of Early Cretaceous age 7-65997
 SW British Columbia, Canada, Hozomeen fault system and Coquihalla serpentine belt 7-4009
 Bugaboo Glacier, BC, Canada, lateral moraine and glacial history 7-23720
 Bushveld Complex, South Africa, palaeomagnetism and igneous intrusion emplacement 7-8800
 Caledonia, drumlin field, S Ontario, inverse-graded units within till 7-9033
 Caledonian orogen collapse and 'Old Red Sandstone' characts. 7-4013
 California, Quaternary faults props. rel. to seismic hazard 7-40430
 N California, USA, geology of Franciscan Complex and Coast range ophiolite 7-54969
 Cambrian paleogeographic modelization of northwestern Montagne Noire (Sorezois, France) (*French*) 7-55032
 E Canada, continental rifting and diabase from Northumberland Strait 7-4018
 Canadian Appalachians, effects of Devonian batholiths on crustal heat flow 7-66041
 Canadian Cordillera, seismic refl. geometry of Columbia River fault zone and Shuswap metamorphic complex 7-14281
 Cape Breton Highlands, Nova Scotia, geology of Cheticamp pluton 7-65989
 Cape depression, SE Atlantic, bathymetry and dredged rocks 7-40465
 carbonate platform stratigraphy as record of past earthquakes 7-8859
 Carboniferous pre orogenic magmatism in Central Jebilet Morocco (*French*) 7-66007
 Upper Carboniferous tonstein and tuff sandines, $^{40}\text{Ar}/^{39}\text{Ar}$ ages rel. to time scale improvement 7-47388
 Cariboo gold belt, BC, Canada, imbricated terrane geology and tectonics 7-23584
 S Carpathians, age of igneous rocks from Banat Hills 7-60227
 Castle Mountain (Alaska) fault system, Sutton earthquake rel. to activity on Talkeetna segment 7-3984
 SE Caucasus, USSR, north slope chaotic complexes, morphology and stratigraphy 7-29013
 Central African Republic, Proterozoic chronology and granodiorite ages 7-34405
 Cevennes Medianes, France, vaugneritic magma evol. and characts. 7-40472
 Cezallier hydromineral system, Massif Central, France (*French*) 7-66115
 Chalk River, Ontario, groundwater flow system in fractured monzonitic gneiss block 7-29120
 Charlotte belt, N and S Carolina, USA, deformed composite batholith 7-18141
 E China, Pb, Sr and Nd isotope systematics and chemistry of Cainozoic basalts 7-29011
 China, SE coastal region, regional gravity field and geological structures 7-47337
 Chouchou, Massif du Nord, Haiti, uppermost Eocene chaotic complex and North Caribbean left-lateral faulting (*French*) 7-66116
 Churchill Province, Canada, Nd evidence of extensive Archean basement 7-65996
 Circle quadrangle, Alaska, S central region, petrological evidence for terrane boundary 7-47437
 coal deposits of USA, lignite deposits of Texas to Georgia region 7-18139
 Col de la Cine faulting during Mesozoic (*French*) 7-18161

geology continued

- central Colorado, petrogenesis and tectonic setting of Early Proterozoic bimodal volcanic rocks 7-23645
 central Colorado, petrography and stratigraphy of Early Proterozoic bimodal volcanic rocks 7-23644
 Colorado Plateau, palaeomag. evidence for tectonic rotation 7-14250
 conference on geology, Kingsley Dunham volume, Durham, England (April 1985) 7-24303
 continental denudation balanced by accretion of oceanic crust 7-4021
 cosmic-ray-produced isotopes in volcanic rocks at summit of Maui, Hawaii 7-54959
 cratonization and mantle thermal evolution 7-23622
 creep behaviour of ice and importance for rocks 7-55096
 mid-Cretaceous geology, book 7-48218
 Cretaceous-Tertiary boundary in N America, vegetation, climate and floral changes 7-29031
 Cretaceous/Tertiary boundary in E Hokkaido, evidence for flora devastation 7-40476
 Crete, geological linear features seen by satellite 7-47402
 Crimea-Romania, lithosphere struct. along Geotraverse V 7-60207
 Cuba, ophiolite assoc. struct. 7-28926
 Dakota (North and South), USA, Precambrian basement geology 7-23586
 Darazo, Nigeria, elec. resist. survey of Kerri-Kerri Formation rel. to water resources 7-18219
 Deccan flood basalts, relation to Cretaceous-Tertiary boundary 7-34417
 deep-sea sediments, O isotope stratigraphy, graphic correl., appl. to Late Quaternary 7-23894
 Derbyshire Dome, UK, Dinantian sedimentation and basement struct. 7-66012
 Diamond Craters, Oregon, USA, alkali olivine basalt crystallization history 7-66052
 diapiric structures, relation between initial conditions and late stage of Rayleigh-Taylor instabilities 7-66108
 Donegal plutons, Ireland, emplacement ages and geochemistry 7-66011
 Donets Basin, USSR, Carboniferous deposits parting fractures 7-34403
 earthquakes recorded in stratigraphy as record of past earthquakes 7-8859
 East African rift and northeast lineaments, possible continental spreading-transform system 7-66071
 East Timor, Indonesia, $^{40}\text{Ar}/^{39}\text{Ar}$ and K/Ar ages from Aileu Formation 7-28916
 economic and applied geology, book 7-29609
 Eifel volcanic field, $^{40}\text{Ar}/^{39}\text{Ar}$ age determs. rel. to age and duration of Middle Pleistocene cold period 7-47392
 El-Kharga area, SW Egypt, Maghribi Formation as mixed estuarine and tidal flat deposits 7-18185
 Elatina varve record of solar activity, Hilbert transform anal. 7-47811
 NE Ellesmere Island, NWT, Canada, glacial geology and marine stratigraphy 7-4062
 emplacement of compositionally stratified magma and basal reversed intrusions 7-18152
 England, Ar isotope geochemistry of W mineralisation 7-8876
 Eocene-Oligocene boundary age, implications of $^{40}\text{Ar}/^{39}\text{Ar}$ dating of tektite fragments for Barbados 7-47391
 Eromanga Basin, N Australia, seismic study of crust and Carboniferous orogeny 7-65960
 fault geometries in basement-induced wrench faulting under different initial stress states 7-40458
 fault lineament analysis, comparative study of remote sensing imagery in Nigeria 7-55292
 fault trace by α -particle track etch method, Pleistocene gravel bed surface (*Japanese*) 7-34688
 Fergana intermontane basin, USSR, geology from remotely sensed images 7-66029
 SW Finland, stratigraphy and geochemistry of Proterozoic mafic volcanic rocks of Nagu-Korpo area 7-14275
 Finland, tectono-exogenic evolution of Precambrian supracrustal rocks 7-34490
 fire areas (of red sediments and vegetation carbonization) in California, USA, due to hot groundwater 7-23654
 fluid mechanical problems 7-55036
 geotechnics dictionary 7-55908
 geotherms of eroding mountain belts, geotherm extremal bounds from metamorphic data 7-47397
 Gombé subcatchment, Benue Valley, Nigeria, hydrogeology 7-18217
 Gondwana Proterozoic dyke emplacement 7-14228
 Gotland (Sweden), radiometric K-Ar ages of Wenlockian pyroclastic biotites (*French*) 7-47385
 Great Valley, California, 2D seismic vel. struct. along synclinal axis 7-28861
 Great Valley, California, vel. and Q struct. of sedimentary section from seismic refr. data 7-3988
 E Greenland, classification of remotely sensed data using additional variables and hierarchical struct. 7-4222
 greenstone belts tectonic evolution, conf., Houston, USA (January 1986) 7-41017
 Higashi-Izu monogenetic volcano group, Japan, petrology and geochemistry 7-8892
 Himalayan-Andaman Arc, earthquakes rel. to deformational structs. (seismites) in Holocene sediments 7-66120
 W Hoggar, Algeria, Pan-African crustal decoupling zone in Timgaouine area 7-34439
 Hokkaido, Japan, isotopic ages of alkaline igneous rocks rel. to Late Cretaceous time-scale points 7-47390
 Holstein interglaciation, time-stratigraphic position and correl. to deep-sea sediments stable isotope stratigraphy 7-47529
 Holsteinian interglacial sediments, N Germany, stratigraphy and ESR dating 7-34669
 hydraulic fracturing of rock, 3D dynamics using finite difference theory 7-55041
 hydrocarbon deposit exploration and exploitation the stratigraphic approach 7-18311
 hydrothermal plumes of E Pacific Rise, Fe, He, Mn obs. showing Fe enrichment 7-9028
 Hyllingen Series, Norway, basal reversal in layered intrusion 7-18152
 Iceland, Tertiary and Quaternary geology rel. to accretionary volcanic processes and crustal struct. 7-66081
 Iforas Pan-African Belt, Mali, pre-tectonic tholeiitic volcanism and transitional plutonism 7-34407
 igneous cumulates, evidence for magmatic heat pump 7-47406

geology continued

- N Illinois, possible impact spherules from near base of Middle Ordovician 7-34499
 Illinois Basin, tectonic subsidence anal. rel. to Ordovician time-scale 7-54984
 Imperial Valley, California, travel-time, time-term, and basement depth maps 7-28860
 Indo-Antarctic metamorphic terrain, Late Proterozoic dates from India rel. to sapphirine granulites correl. 7-34414
 Inuyama area, central Japan, paleomagnetism rel. to tectonic history of Pacific Northwest 7-54871
 W Ireland, Caledonides Palaeozoic terrane accretion 7-55004
 Isukasia area, W Greenland, geochronology and isotopic var. of Early Archaean Amitsoq gneisses 7-34485
 S Italy, appl. of Cassinoli K-Ar dating technique to Late Pleistocene-Recent volcanics 7-47393
 N Italy, surface geology rel. to crustal struct. from Liguria to Po Valley 7-14240
 Jabal Tifl layered gabbro, SW Saudi Arabia, mineral chemistry rel. to magma origin 7-29015
 Japan Sea, U and Th contents of basalts as indicators of continental-type volcanism 7-14274
 Kaapvaal Craton, early Precambrian Al_2O_3 -rich rocks as indicators of palaeosols 7-29020
 N Kapuskasing uplift, Ontario, deep crustal struct. and tectonic history 7-14277
 Karelian granite-greenstone terrain, geological evolution 7-34489
 karst aquifer at Castle Meadows, Alberta, Canada, structure and function 7-4060
 Kazakhstan and Central Asia, zoning of Devonian orogenic volcanism 7-60215
 Kentland, Indiana, cryptoexplosion struct., palaeomag. estimate of age and thermal history 7-29030
 Kerch Peninsula, USSR, hydrocarbon exploration using remote sensing data 7-60223
 Kerguelen Plateau province, crust struct. from gravity anomaly and seismic refl. obs. 7-28952
 Kerguelen-Heard Plateau, sediments and stratigraphy (French) 7-66092
 Kiev-Gomel DSS profile, struct. of deep crustal layers and sedimentary cover 7-47394
 Kilbourne Hole maar, New Mexico, USA, origin of continental alkali basalts 7-23605
 kimberlite xenolith of rare type, graphite-bearing harzburgite 7-28921
 Kinki district, SW Japan, crustal stress and lineaments 7-66086
 E Klamath Mountain, California, island arc sedimentation in Middle Devonian Kennett Formation 7-29017
 Klamath Mountains, N California, timing and kinematics of emplacement of Josephine ophiolite 7-14282
 Klamath Mts., California, USA, native terrane geology and evolution 7-54968
 Kodiak convergent margin, episodic growth of accretionary prism 7-54992
 Kola deep borehole, petrology and comp. of Precambrian continental crust 7-34413
 Kola Peninsula, upper crustal struct. along Pechenga Bay-Kovdor-Alakurti profile from geophysical data 7-47395
 Koralbikha ore deposits, Rudnyi Altai, USSR, geologic-genetic model 7-14224
 central Krak Massif, USSR, struct. and petrology 7-28925
 Kulyab, Tajikistan, USSR, earthquakes due to active salt doming 7-47372
 Kuznets basin, USSR, coal measure concentric folding 7-14222
 Kvamshesten, W Norway, tectonic implications of Solundian (Upper Devonian) magnetisation of Devonian rocks 7-34376
 Las Vegas Valley, USA, Late Quaternary environmental changes 7-47414
 Lena-Tunguska oil and gas province in eastern USSR 7-54942
 W Leone-Liberian shield area, tectonic development and metallogeny 7-60240
 Les Vignes basaltic complex (France), ^{40}K - ^{40}Ar and palaeomag. data rel. to Bajocian-Bathonian boundary calibration 7-47389
 Port Lianyangang, muddy beach geology and erosion on Yellow Sea coast (Chinese) 7-55013
 lineament analysis of Landsat MSS imagery of N Wales and W England 7-55033
 lineament imaging and identification using remotely sensed data 7-66333
 Lizard front, SW England, Variscan strain pattern in Palaeozoic series 7-14279
 Loess Hills region of Iowa, USA, Quaternary geology and geomorphology 7-47441
 Loihi Seamount, hydrothermal plumes containing methane and ^3H 7-28994
 Long Valley, California, borehole seismograms anal. rel. to caldera struct. 7-40448
 Long Valley caldera, California, deep crustal struct. from extremal inversion of travel-time residuals 7-28862
 magma chamber, inclined plane boundary with cooling and crystallisation 7-8942
 magma chamber beneath volcano., multicomponent crystallisation and convection 7-54972
 magma chamber dynamics and chemical fractionation due to Soret effect 7-28950
 magma chambers, magma convection and mixing 7-4028
 Malankhand Cu sulphide deposit, India, physico-chemical conditions of ore deposition 7-29025
 S Mangyshlak, Kazakhstan, USSR, oil and gas deposits 7-66028
 map production by remote sensing, methodological problems 7-55295
 Mariana Trough back-arc basin, hydrothermal plumes containing methane but no ^3He 7-28994
 marine mineral resources in USA exclusive economic zone, geological distrib. and potential development 7-66096
 marine sediments of Pacific, trace metal chemistry of metalliferous sediments 7-23633
 Marlboro Mts. Outlier, New York, USA, geology of arenite sequence 7-18142
 Maryland Piedmont, USA, flood plain sediment deposition since 1730 AD 7-29081
 NW Massif Central, France, chronology of Neogene and Quaternary geological events (French) 7-60235
 North Massif Central, gravimetry contribution to model of igneous intrusions emplacement (French) 7-18135

geology continued

- Maui, Hawaii, volcanic rocks at summit, isotopes due to cosmic rays 7-54959
 Mecsek Mts., SW Hungary, tectonic rotation, palaeomagnetism and volcanic history 7-14243
 Mediterranean Sea, geochemistry of sediments of different ages, book 7-29608
 megathrust zones, role of strain heating in tectonic evolution 7-40443
 melt evolution simulation, Rayleigh fractionation 7-65998
 melt migration, the role of surface tension 7-40474
 Merida Andes, Venezuela, struct. and stratigraphy rel. to Neo-gene transcurrent motion 7-14283
 mesofractures anal. using space images, appl. to oil and gas exploration 7-66337
 Mesozoic Mogollon Highlands, Arizona, Early Cretaceous rift shoulder model 7-29016
 metallogenesis rel. to tectonic lineaments 7-29256
 metamorphism, continents and subduction zones (Russian) 7-8945
 metamorphism on regional scale, tectonic settings, conf., London, England (Jan. 1986) 7-60867
 Miami Pliocene coral reefs, geomorphology and Atlantic coastal ridge in Florida 7-29028
 Mianwali re-entrant and W Salt Range, Pakistan, palaeomag. constraints on form. 7-34380
 Mica Creek, British Columbia, min. press. limits for garnet amphibolite metamorphism 7-29005
 SW Michipicoten Greenstone Belt, Ontario, evidence for complex Archean deform. history 7-55040
 Milankovitch cycles through geologic time, conf., Princeton, USA (May 1985) 7-55883
 Mindoro Island, Philippines, allochthonous terrane evolution 7-14249
 mineral resource deposits at D latitude positions with high seismicity 7-65966
 Mkushi Gneiss Complex, central Zambia, Rb-Sr and K-Ar, geochronology 7-14230
 Mohr diagram and 3D strain 7-40594
 molten rock viscosities, expts. on diopside-albite rock melts 7-60248
 Inner Mongolia, palaeo-plate tectonics and geology 7-55002
 Mongolia, structural-metamorphic evolution of Precambrian ophiolites and basement in Central Asian foldbelt 7-34495
 Mongolia, Trans-Altai zone tectonics and struct. 7-28961
 Mono Craters, E central California, date of most recent eruption 7-40447
 Mont Saint Hilaire plutonic complex, Quebec, Canada, Ar isotopes and emplacement history 7-4007
 Montagne Noire, France, magnetotectonic study of Devonian limestones 7-23541
 Monte La Queglia (Abruzzo, Central Italy), geophysical investigations of carbonate struct. 7-40477
 Morocco Basin, stratigraphy of sediment accumulation during Late Quaternary 7-14259
 Mssisi norite, Morocco, K/Ar dating, petrography and palaeomagnetism 7-8882
 S Mugodzhar, USSR, Palaeozoic oceanic crust, geological characts. 7-23606
 Muria volcano, Java, magmatic series (French) 7-66050
 Mygdonian graben, Greece, struct., microearthquake data anal. 7-66010
 Namaqua mobile belt, South Africa, calc-alkaline volcanism assoc. with Middle Proterozoic volcanic arc 7-34493
 Napier Complex, Enderby Land, Antarctica, Rb-Sr, Sm-Nd and U-Pb systematics of Late Archaean granites 7-14231
 Near-Caspian basin, USSR, basement structures seen from space 7-60221
 Neogene continental crust structural devel., conf., Moscow, USSR (January 1985) 7-18474
 E Nepal, petro-structural study of ductile Himalayan layers (French) 7-23617
 S Nevada, USA, palaeomagnetism of plastically deformed welded tuff 7-40416
 SE New England, tectonic model for Late Palaeozoic history 7-4029
 E New York State, plate convergence rate during Taconic arc-continent collision 7-28966
 New Zealand, tectonic setting of sandstone-mudstone suites from SiO_2 content and $\text{K}_2\text{O}/\text{Na}_2\text{O}$ ratio 7-29014
 Nile delta sediment deposition history at Rosetta and Damietta, promontories 7-34565
 North Island, New Zealand, mag. polarity stratigraphy of Plio-Pleistocene marine sequence 7-34378
 Northern Hemisphere Quaternary glaciations 7-55051
 Norway, Caledonian thrust front and palaeospastic restorations 7-40475
 S Norway and adjacent offshore areas, lineaments study 7-29026
 Norwegian Sea, volcanism, continental crust rifting, climatic fluctuations (French) 7-66089
 Nubia, Egypt, lithologic units identification and groundwater prospecting 7-34698
 natural nuclear reactor at Oklo, Gabon, Africa (French) 7-28954
 nuclear waste disposal in plutonic rock masses, disposal sites characterisation 7-10296
 Obaku fault, Uji, Japan, gamma-ray survey of active fault 7-18157
 oceanic crust vein mineral deposition, Rb/Sr ages and U-Th-Pb geochemistry 7-60204
 Ocoee Supergroup in eastern USA, origin of Late Precambrian sedimentary sequence 7-28915
 oil and gas deposits occurrence patterns on continental shelves 7-34411
 oil fields, trend surface anal. 7-40583
 oil reservoir flow models, book 7-48219
 S Oklahoma aulacogen, appl. of quasi-ideal spatial filters to gravity anomalies mapping 7-28808
 Olary Block, South Australia, stratigraphic and structural constraints on Proterozoic tectonic history 7-55045
 NW Ontario, U-Pb ages of Precambrian rocks 7-4008
 Onverwacht Group, Archaean flow-top alteration zones form. in low-temp. sulphate-rich environment 7-34488
 ophiolite sheets and slivers, evidence for tectonic stratification of crust and lithosphere (Russian) 7-66076
 Oradea-Inand area, Romania, Pannonian sequence seismic facies interpretation (Rumanian) 7-8946
 Ordovician-Silurian boundary stratotype, Ir abundances meas. 7-4014
 Orfordville Belt, New Hampshire, press., temp. and structural evolution 7-55044
 Oslo Graben, Norway, anatexis cumulates and residues 7-28951

geology continued

- Osmanagar reservoir, Hyderabad, India, geology rel. to microearthquakes 7-23573
- Oxfordian-Kimmeridgian boundary breccia of Quercy, SW France, typology and genetic interpretation (*French*) 7-14273
- NW Pacific, crust struct. and composition near Emperor fault 7-34412
- S Pacific, Eltanin fault system, tectonic and magmatic ridges 7-23610
- SW Pacific, Miocene and Pliocene stratigraphy and palaeoceanography 7-23634
- East Pacific Rise, hydrothermal clay mineral formation from basalt 7-14256
- palaeoceanography and biogeochemical processes affected by tectonic processes 7-23843
- palaeoceanographic events as cause of regional marine sediment horizons 7-18202
- palaeosol, 2200 Myr old, near Waterval Onder, South Africa, reappraisal 7-29022
- Palaeozoic continental reconstruction, appl. of cladistic methods 7-4019
- Palaeozoic terranes of the central Argentine-Chilean Andes 7-28982
- Paris Basin, France, chronology of Neogene and Quaternary geologic events (*French*) 7-60235
- E Pennsylvania, USA, Valley and Ridge Province geology 7-18140
- peridotites, petrology and geodynamics evolution, review 7-54967
- Persian Gulf and Gulf of Oman, geology and tectonics 7-23615
- Pesterevskii and Malo-Salairka limestone geology, W Siberia, USSR 7-14221
- petroleum exploration, computer appl. conf., Wichita, KS, USA (Oct., 1985) 7-35083
- petroleum exploration, geological and computer traps 7-40582
- petroleum geology of USA Gulf Coast, Niger and Beaufort-Mackenzie area 7-18138
- petroleum resource appraisal program, FORTRAN listing 7-40576
- Phanerozoic time scale calibration, recent advances 7-47383
- Phanerozoic time scale calibration symposium, Strasbourg, France (April 1985) 7-40983
- Pharusian Range, Silet area, Hoggar, Algeria, stratigraphy and struct. (*French*) 7-60192
- Piedmontese Tertiary Basin in N Italy, mag. anomalies and geological struct. 7-54858
- Piton de la Fournaise, Reunion Island, discovery of old magmatic chamber, volcanological implications (*French*) 7-66048
- W Portugal, palaeomagnetism, ages and tectonics of Cretaceous igneous rocks 7-47327
- Precambrian atmosphere, transition to O₂-rich state, geological evidence 7-18304
- Precambrian basinal and shelf sedimentation relation to Archaean-Proterozoic boundary 7-34492
- Precambrian geology, 27th IGG Congress, Moscow (August 1984) 7-29580
- Precambrian palaeopedology, conference, Raleigh, North Carolina (June 1985) 7-24275
- Precambrian palaeosols of Dominion and Pongola Groups, Transvaal, chemistry and mineralogy 7-29018
- Precambrian palaeosols on basaltic and granitic parent materials, elemental concs, profiles 7-29019
- Precambrian permafrost horizons, appl. as indicators of palaeoclimate 7-29023
- Precambrian-Cambrian boundary age, implications of study of Ercall Granophyre England 7-66014
- pressure of metamorphic events, granulite terrain geobarometry methods (*French*) 7-34689
- Priest River Complex, Washington-Idaho, mylonite zone metamorphism rel. to tectonic evolution 7-4033
- Proterozoic ophiolite preservation problem and prevailing plate tectonics, and Venus comparison 7-28980
- Pyrenees, geological evolution, symposium, Strasbourg (April 1985) 7-24290
- N Pyrenees, tectonostratigraphic units rel. to apparent western termination of North Pyrenean fault 7-14280
- Pyrenees occidentales, France, cover and tilted fault blocks gliding (*French*) 7-66000
- Rajmahal Hills, E India, gravity field over Palaeo-Mesozoic continental margin 7-28820
- Red Sea rift seafloor, sedimentary cover structure near 18°N 7-34472
- remote sensing of rocky surface mineralogy by optical and IR reflectance spectroscopy 7-29291
- research management and organisation, for geology 7-40480
- Reunion Island, Indian Ocean, noble gas systematics in basalts and dunite nodule 7-29012
- Reykjanes Ridge rift valley, Upper Quaternary sediments stratigraphy, foraminiferal anal. 7-29073
- rheology, for viscous inclusion embedded in matrix, Eshelby's eqns. 7-55046
- Riasi thrust sheet, NW India, palaeomag. evidence for rot. overthrusting of NW Himalaya 7-34379
- Ries crater, fluidisation and hydrothermal alteration of suevite deposit, and implications for Mars 7-55049
- rock strain analysis, theory of deformable inclusions in flowing matrix 7-55046
- Rocky Mountains, SW Alberta, Canada, duplex structures in Lewis thrust sheet 7-54989
- Saint-Clement Subbrianconnais Flysch, French Alps, dynamics of marine nummulitic deposits (*French*) 7-18182
- salt bearing formations during Palaeozoic, book 7-35137
- San Jacinto graben California, gravity anomalies of trapezoidal model with quadratic density function 7-28819
- San Juan Is., Washington, USA, geochronology and tectonic development 7-65994
- Santa Cruz County, California, magnetostratigraphy of Pliocene Purisima Formation 7-8799
- E Sayan, USSR, magmatic geology 7-23598
- West Sayan and Gornyi Altai, USSR, age of flyschoid series rocks 7-28919
- SW Scotland, Lugar and other sills, age and geology 7-66013
- S Scotland, regional zone of Late Caledonian primitive K-rich lamprophyre dykes and vents 7-4032
- seafloor geology and crustal generation since 116 Myr BP, foraminifera Li content evidence 7-23632
- seafloor hydrothermal plumes in S Pacific, Mn tracing of dispersal patterns 7-9027
- second childhood of ancient science, review (*Russian*) 7-60254

geology continued

- young sediment palaeomagnetism, conf., Louvain-la-Neuve, Belgium (Jul.-Aug. 1984) 7-4628
- sedimentary basin analysis (book) 7-35129
- sedimentary basin stratigraphy, effects of lithosphere in-plane stress 7-14278
- sedimentary basins geology, heterogeneous stretching model with simple shear 7-34399
- sediments of seafloor, NMR imaging, method for organic rich layers 7-9198
- Sette-Daban ridge, S Verkhoyany, USSR, Carboniferous basalt geology 7-23596
- Shebandowan greenstone belt, Ontario, Canada, magmatism age and regional deformation 7-23585
- Shelve inlier, Welsh Borders, radiometric dating of Caradocian tuff horizon 7-47384
- Shirshov Ridge, Bering Sea, topography and struct. of seafloor 7-34473
- NW Siberia, aerospace imagery of lineament zones rel. to presence of oil and gas 7-66335
- Siberia, Jurassic continental and marine palynostratigraphy 7-23594
- S Siberia, metallogenic evolution of Phanerozoic folded systems 7-23595
- Siberia, stratigraphy of Phanerozoic 7-54943
- W Siberian Plate, geology of Palaeozoic carbonate facies 7-23597
- E Siberian Platform, petroleum formation and accumulation in Mesozoic troughs 7-54944
- Sierra Leone, diamond-source kimberlite paradox 7-34406
- Sierras Pampeanas of Argentina, modern analogue of Rocky Mountain foreland deformation 7-66113
- Solomon Islands arc, Neogene displacements rel. to geology and arc configuration 7-66082
- Sredne-Tersa ultrabasic massif, deep structure and rock composition 7-14223
- Sriramsagar reservoir, Andhra Pradesh State, India, geology rel. to induced microearthquakes 7-23575
- Stanovoi area, USSR, granulites isotopic age and geological implications 7-23600
- Stillwater Complex, Montana, rare-earth element evidence for form. of Ultramafic Series 7-65987
- stratigraphically constrained cluster analysis, FORTRAN 77 program 7-66114
- strike-slip duplexes 7-40457
- structural geology, appl. of stream function and Gauss's principle of least constraint 7-29009
- subsurface geology from well logs, color images, Kansas 7-40581
- Tethys oceanic crust movement during Austrian phase (cretaceous) 7-8904
- thermal IR multispectral scanner, airborne instrument for mineral deposits detection 7-14393
- thermoluminescence sensitivity-metamorphism relation for ordinary chondrites and terrestrial systems 7-24087
- Tibet, Ar dating of Meso- and Cenozoic rocks, and geodynamic significance 7-8875
- Tibetan Plateau, 1985 Chinese/British expedition results 7-8913
- S Tien Shan, greenschist metamorphism conditions and geotectonic evol. model 7-34401
- Tien-Shan region, geological significance of isostatic gravity anomalies 7-28965
- Toba tuffs, stratigraphy, palaeomagnetism and mag. fabric rel. to sources and eruptive styles 7-28958
- Tomioka, Fukushima, Japan, borehole logging of crust and seismic wave amplification (*Japanese*) 7-18115
- Transantarctic Mountains-Ross Embayment region, asymmetric extension and assoc. uplift and subsidence 7-40453
- Transylvanian Depression, struct. and morphology (*Rumanian*) 7-8891
- Triassic climate, orbital forcing indicated by lake sediment record 7-66300
- Troodos microplate, Cyprus, palaeorotation in Meso-Cenozoic plate tectonic framework of E Mediterranean 7-34441
- Ulu Jelai River basin, Peninsular Malaysia, geological mapping from enhanced satellite imagery 7-17848
- SW United States, geochemistry and tectonic setting of Early Proterozoic supracrustal rocks 7-55037
- Upper Silesian Massif, Poland, pre-Permian tectonic position (*French*) 7-66054
- trans-Ural marginal downwarp, numerical interpretation of regional mag. anomaly 7-29279
- Ural Mountains, Precambrian geodynamic regimes 7-34494
- central Urals region, USSR and geological devel. 7-23549
- USA, lignite deposits of Texas to Georgia region 7-18139
- USSR, ore deposits characters. (*Russian*) 7-40478
- Uttar Pradesh (N India), utility of Landsat imagery in data base for small-scale soil mapping 7-4205
- Vendee (W France), U-Pb zircon dating of Silurian-Devonian boundary volcanic rocks 7-47387
- Venetian region, N Italy, Ir anomaly in Middle-Lower Jurassic marine sequence 7-55038
- Verkhoyany folded zone, eastern USSR, fault dislocations and petroleum prospect 7-28918
- Vermilion granitic complex, NE Minnesota, USA, multiple folding and pluton emplacement 7-65990
- Vestfold Block, Antarctica, age and geochem. of mafic dyke swarm 7-14228
- volcanic rock eruption age determ. method using ESR 7-66316
- Welsh Borders, Great Britain, K-Ar biotite data for Ludlovian bentonites 7-47386
- West Virginia, mesostructures development in detached folds 7-4030
- Western Australia, relations between Archaean high-grade gneiss and granite-greenstone terrain 7-34491
- W.H. Mathews Symposium, Vancouver, British Columbia (October 1984) 7-4620
- Whirlpool Sandstone (Ontario), horizontal laminae formation under upper flow regime plane bed conditions 7-4031
- Wilcox aquifer, Texas, groundwater flow rel. to sand body interconnectedness in multiple-aquifer system 7-23760
- Woodlark basin in SW Pacific, tectonically controlled origin of 3 rock suites 7-54970
- Wopmay Orogen in Canada, geology of metamorphic internal zone 7-54998
- WSU-MAP: a microcomputer-based reconnaissance mapping system for Kansas subsurface data 7-40584

geology continued

- Yamada fault region, Kinki district, Japan, geological, geophys. and hydrological study (*Japanese*) 7-66085
 Yinchuan graben, N China, seismicity rel. to fault scarps produced by AD 1739 earthquake 7-28859
 Yukon Territory, stratigraphic, isotopic and micrological evidence for early Holocene thaw unconformity 7-9034
 Zambia, provisional metamorphic maps and explanatory notes 7-18184
 E Zambia, Rb-Sr studies of metamorphic and igneous events 7-18147
 Zhelin reservoir, E China, active faulting rel. to induced earthquakes 7-23571
 zircon crystals, isotope age method and crystal morphology for rock history 7-18183
 Ag vein deposits, conf., London, Ontario, Canada (May 1984) 7-48136
 Au placer deposits in upper Yukon River, Alaska 7-66042
 Cu-Ni sulphide deposits, formation conditions 7-23599
 Fe, phase transitions at high-pressure and Earth core conditions 7-38179
⁴⁰K in Makhmur Plain soil, N Iraq, α -ray spectroscopic analysis 7-34487
²³⁴U/²³⁸U activity ratios in geological materials, determ. by α spectrometry 7-60255

geomagnetic storms *see magnetic storms***geomagnetic variations**

- 11-year cycle, characteristic parameters anal. rel. to solar 11-year cycle 7-18114
 Absaroka Mountains, WY, USA, Eocene thick lava flows, recorded rapid secular geomag. var. 7-65931
 AE-index, relation to comp and plasma props. of magnetotail plasma sheet 7-34789
 Baikal Rift region, USSR, elec. cond. anomalies identification by magnetovariation methods 7-23525
 Baikal-Amur Main Line, USSR, elec. struct., mag. var. profiling anal. 7-23527
 Late Brunhes epoch geomagnetic excursions from European data 7-8818
 C9-index, longit distrib. rel. to solar background mag. field distrib. 7-18400
 Canadian Geomagnetic Reference field, for 1985 AD 7-47335
 SE China, quiet diurnal vars. rel. to depth of mantle high-cond. layer (*Chinese*) 7-34374
 core westward drift and Earth rotation rel. to secular geomagnetic changes 7-23515
 core-mantle boundary, models for fields of 1715, 1777 and 1842 AD 7-54870
 Czechoslovakia, field variations at Hurbanovo during 1984 AD 7-32
 E₂ enhancements rel. to local geomagnetic k-index in Far East (*Chinese*) 7-18330
 East Germany, tectonomagnetic field var. 7-14183
 European geomagnetic observatories annual means, solar effects 7-14184
 field reversals periodicity, role of mantle plumes 7-65934
 geomagnetic attractor and 3-disc dynamo system, strange attractor, dimensions and K₂ entropies 7-3978
 historical times geomag. field from palaeo- and archaeo-magnetic records 7-23538
 India, effect of source-field geometry on EM induction Earth 7-28821
 S India, magnetotelluric study of geoelectric anomalies 7-8804
 intermediate anomalies, extraction and structure 7-14180
 Jaramillo-Matuyama mag. polarity transition, Tadzhiik Depression palaeomagnetism 7-8811
 Jurassic apparent polar wander for N America, and tectonic plate movements 7-28834
 K_p-index, effect on equatorial ionospheric scintillations 7-34762
 K_p-indices, use to define max. external contributions to mid-latitude Magsat data 7-14191
 Central Karelia, magnetotelluric sounding in 10⁻³ to 10⁴ s period interval 7-28829
 loess deposit palaeomagnetic method for Pleistocene field variations 7-8816
 long-term variations, effects of mantle dregs and convection on core heat flux 7-66022
 lunar geomagnetic tide at night 7-60159
 magnetic indices rel. to interplanetary parameters (1966-75) (*Chinese*) 7-18336
 Matuyama-Brunhes mag. polarity transition, Tadzhiik Depression palaeomagnetism 7-8811
 Murmansk block, Kola Peninsula, magnetotelluric sounding in 10⁻³ to 10⁴ s period interval 7-28829
 north magnetic dip pole, present position and geomag. variations 7-23522
 north polar currents in winter, geomag. activity effects 7-60450
 north-south asymmetry of geomag. activity, effect of By-component of interplanetary mag. field 7-9336
 Pacific Ocean, deep magnetovariation sounding curve determ. using continuum spectrum method 7-40569
 Papua New Guinea, mag. field var. due to solar eclipse (*Chinese*) 7-55346
 Pleistocene geomagnetic excursion, study of Mono Lake ¹⁰Be record 7-23842
 Late Pleistocene secular variations at Lac du Bouchet, France 7-8815
 Pleistocene secular variations from palaeomagnetic record, New Zealand cave sediments 7-54860
 Pliocene-Pleistocene field for NE Greenland 7-8819
 polarity epochs duration during Middle Triassic, determ. from palaeomag. study of Japanese red cherts 7-54872
 reversals of Earth's magnetic field, review 7-23539
 reversals triggered by extraterrestrial object impact on Earth, precise mechanism 7-40413
 S_p worldwide anomalies 7-23944
 secular variation, 1903-82, spine representation of temporal change 7-14185
 secular variation at Earth's surface, appl. to determ. of steady surficial core motions 7-66023
 secular variation models, appl. to steady flows determ. at top of Earth's core 7-40444
 secular variations, effects of linear trend and mean value on maximum entropy spectral analysis 7-29305
 secular variations, implications of mag. fields fluctuations in coupled-disk dynamo models 7-14187
 secular variations, implications of thermal and topographic coupling of core dynamo and mantle 7-65933
 secular variations dynamo model 7-47326
 secular variations in Europe, for AD 1960 to 1978 period 7-60156

geomagnetic variations continued

- secular variations in Europe during Holocene and late Würmian times 7-8805
 secular variations seen in lake sediments at Lac du Bouchet, France 7-8815
 solar influence on Earth liquid core and geomag. variations 7-34382
 Sq day-to-day var. in geomag. conjugate areas, current effects 7-60452
 surface level field perturbation due to ionospheric currents 7-60454
 ULF pulsations, study of ground-level transient magnetic fields 7-34806
 USSR, intermediate anomalies, extraction and structure 7-14180
 World Magnetic Charts for 1985, main field and secular variation 7-54859

geomagnetism

- see also geomagnetic variations; magnetic storms; palaeomagnetism; rock magnetism*
 1D mag. field data vertical gradients, approximation methods comparison 7-23861
 1D time series anal. for sphere, appl. in geomag. and gravimetric geodesy 7-9239
 2D topographic responses in magnetotellurics, finite element modelling 7-47333
 3D transient EM responses for grounded source 7-47332
 aeromagnetic data, topographic effects 7-65932
 aeromagnetic surveying, variable-magnetisation terrain correction method 7-66325
 anomalies due to magnetite, possible correl. with hydrocarbons occurrence 7-60253
 anomalies due to dipping beds, faults and anticlines, theory 7-28841
 anomalies interpretation, numerical optimisation methods 7-29279
 anomalous field due to horizontal layer of Poisson random sources 7-34381
 anomalous geopotential fields, parameters of regularized continuation of 2D fields 7-60149
 anomaly interpretation using generalised inverse matrix theory (*Chinese*) 7-3974
 anomaly over structurally complex bodies, use of subtended solid angle DEC BASIC-PLUS-2 program 7-9192
 Astrid Ridge off Queen Maud Land, Antarctica, fracture zone nature, magnetic obs. 7-66035
 Atlantic Ocean magnetisation modelling using Magsat data 7-40414
 Baijing-Beigehuang profile, magnetotelluric data inversion via continuous resist. var. model (*Chinese*) 7-34375
 Canadian Geomagnetic Reference field, for 1985 AD 7-47335
 Carpathian Mountains, USSR, geomag. anomaly and geoelectric model 7-40411
 cathodically protected pipelines, effects on aeromag. surveys 7-28824
 Chile Ridge-Chile Trench interaction, mag., thermal and bathymetric characts. 7-66074
 SE China, quiet diurnal vars. rel. to depth of mantle high-cond. layer (*Chinese*) 7-34374
 China, SE coastal region, geomag. anomalies from deep crustal sources 7-47337
 controlled source audiofrequency MT soundings in Japan rel. to Schlumberger sounding (*Japanese*) 7-66318
 core dynamo, effects of lateral heterogeneity at core-mantle boundary due to mantle dregs-convection interaction 7-66022
 core dynamo, for Couette-Poiseuille flow 7-65941
 core dynamo coupling with mantle, thermal and topographic coupling models 7-65933
 core of Earth, expulsion of magnetic flux, 2D model 7-23532
 core-mantle boundary, models for fields of 1715, 1777 and 1842 AD 7-54870
 core-mantle boundary magnetic field maps rel. to thermal core-mantle interactions 7-54960
 coupled-disk dynamo models, mag. fields fluctuations and implications for geomag. secular vars. 7-14187
 cyclotron harmonic waves, propagation paths in mag. meridian plane 7-9313
 deep seated anisotropic oblique zones assoc. multiple elec. discontinuities mapping, magnetotelluric freq. sounding use 7-47573
 dipole source and layered Earth (*Japanese*) 7-23528
 dissipative structure, laminar and turbulent flow 7-28842
 dynamo problem and mag. fields turbulent transport 7-60511
 dynamo theory, implications of accretion growth of inner core 7-66027
 dynamo theory, role of fluctuations 7-60512
 earthquakes hazard and prediction, conf., Tokyo, Japan (1985) 7-60859
 EM induction anomalies of two-dimensions, freq. response 7-47334
 EM modelling program for 2D structures 7-34714
 E Europe and Middle East, lithosphere mag. suscept. anomalies 7-23535
 field correlation with gravity field 7-47318
 field models, appl. to determ. of steady surficial core motions 7-66023
 field morphology and geodynamo 7-54874
 field reversals periodicity, role of mantle plumes 7-65934
 Fourier power spectra of geomag. field for circular paths on Earth's surface 7-28833
 general aspects (book) 7-48216
 geopotential field computation method, for 3D density and magnetization distrib. (*Chinese*) 7-3964
 global geomagnetic modelling, appl. of alternate forms of assoc. Legendre functions 7-14186
 Gorda deformation zone, Juan de Fuca diffuse plate boundary model rel. to marine mag. anomalies 7-28968
 groundwater flow generated elec. currents causing magnetic anomalies 7-23533
 harmonic function derivatives for geophysical anomalies, method for integral relations 7-60148
 historical times geomag. field from palaeo- and archaeo-magnetic records 7-23538
 horst structure, EM field from multiple freq. sounding and transient sounding 7-54864
 Ile-Ife, Nigeria, possible fault zone, elec.-geomag. surveys and minerals existence 7-47330
 Indian Ocean, geopotential hours and core-mantle interface depressions 7-47412
 Indian region, geomagnetic anomalies at satellite altitude 7-23534
 Indian region, residual trend in Magsat pass data 7-54857
 ionosphere, mag. field meas. rel. to longit. currents in cusp as function of IMF orientation 7-4261
 ionosphere, relationship between EM drift components at mid and low latitudes 7-9315

geomagnetism continued

- N Italy, geophysical exploration of upper crust from Ligurian coast to N Po Valley 7-14240
- Central Karelia, magnetotelluric sounding in 10^{-3} to 10^4 s period interval 7-28829
- Karelian granite-greenstone terrain, mag. anomalies rel. to geological evolution 7-34489
- Kenya, failed Jurassic rift and triple junction, geomag. and gravity evidence 7-60197
- Kola Peninsula, upper crustal struct. along Pechenga Bay-Kovdor-Alakurti profile from geophysical data 7-47395
- lateral EM field of vertical dipole, props. and appl. 7-23537
- lithosphere mag. field, origin and dynamics of long wavelength anomalies 7-47338
- lower crust magnetic anomalies, conf., Prague, Czechoslovakia (August 1985) 7-40992
- magnetic crust, bottom depth estimation method 7-47575
- proton magnetometer, DPM-1 instrument from USSR for marine surveys 7-40602
- magnetometric mise-a-la-masse method (*Japanese*) 7-23856
- magnetosheath, MHD turbulence obs. 7-34786
- magnetosphere, storm-time reconfiguration as cause of strong precip. of energetic protons 7-9316
- magnetotail, mag. field configuration rel. to charged particle motion 7-9335
- magnetotail, mag. field results from ISEE-3 Geotail Mission 7-29369
- magnetotelluric data inversion using localised cond. constraints 7-28823
- magnetotelluric impedance for 3D cond. structures 7-23536
- magnetotelluric method for 2D structures, resolving power (*Japanese*) 7-66317
- magnetotelluric response of a laterally inhomogeneous anisotropic inclusion 7-14190
- magnetotelluric sounding, telluric anomalies analysis in lower half-space 7-28826
- magnetotelluric sounding at sea, methods of elec. field meas. in medium with extraneous fields 7-47444
- magnetotelluric sounding data in class of quasi-1D models, interpretation 7-54867
- main field anal. at core-mantle boundary, spherical harmonics compared with harmonic splines 7-65935
- main field models, appl. to steady flows determ. at top of Earth's core 7-40444
- marginal seas, small ocean basins and deep sea basins, magnetic anomaly patterns 7-54873
- marine magnetic anomalies, implications of mag. struct. of upper oceanic crust at DSDP Hole 504B 7-29007
- MHD, improved model for Earth's mag. field 7-34383
- MHD model for the Earth's magnetic field with spatially dependent electrical conductivity 7-60165
- MHD theory, system of eqns. on special Riemann manifold 7-65939
- MHD theory, system of eqns. using Riemann theta functions 7-65940
- MINI-MOSES magnetometric resist. method for deep-sea floor polymetallic sulphide exploration 7-23863
- Monte La Queglia (Abruzzo, Central Italy), geophysical investigations of carbonate struct. 7-40477
- Murmansk block, Kola Peninsula, magnetotelluric sounding in 10^{-3} to 10^4 s period interval 7-28829
- Nagano Prefecture earthquake, Japan, geomagnetism in fault area (*Japanese*) 7-65942
- Narmada-Son lineament on W India continental margin, magnetic anomalies and tectonics 7-54991
- north magnetic dip pole, present position and geomag. variations 7-23522
- Northumberland Trough magnetic anomaly in N England, interpretation using 2D current model 7-23530
- S Norway and adjacent offshore areas, aeromagnetic data rel. to lineaments trends 7-29026
- ocean eddy, EM field components calc. 7-55063
- oceanic upper mantle, effective mag. suscept., Magsat data anal. 7-47331
- oil pipeline, induced EM fields due to electrojet current sources 7-8814
- W Pacific, trench-trench-triple junction off SE Japan 7-34415
- palaeofield (quadrupole and octupole) and dynamo model since 200 Myr BP, from palaeomagnetic record 7-28832
- Paris Basin, Variscan overthrusts characts. 7-4012
- Piedmontese Tertiary Basin in N Italy, mag. anomalies and geological struct. 7-54858
- potential field data between irregular surfaces, upward continuation 7-8787
- proto-Earth contraction, implication for mag. field and origin of Earth-Moon system 7-23509
- rectangular harmonic analysis, numerical evaluation (*Chinese*) 7-54854
- reversals of Earth's magnetic field, review 7-23539
- reversals triggered by extraterrestrial object impact on Earth, precise mechanism 7-40413
- Rikitake two-disk dynamo rel. to polarity intervals 7-65936
- scalar audiomagnetotellurics applied to base-metal exploration in Finland 7-29272
- Schlumberger soundings, rel. to controlled source audiofrequency MT soundings in Japan (*Japanese*) 7-66318
- Scotia arc, evol. and continental mag. anomalies 7-60155
- S Senegal basin, geoelectromagnetic meas. 7-47413
- shipboard-three component magnetometer, characts. and meas. of geomag. anomalies 7-29276
- simultaneous correlation analysis of gravity, magnetic and seismic data, appl. to deep crustal investigations 7-47552
- spherical Earth model field, mantle appl. (*German*) 7-8796
- static magnetic dipole, method for location and dipole moment components estimation 7-9203
- stratospheric balloons use for geomag. anomalies meas. 7-47574
- subduction zones, interpretation of mag. signatures detected by MAGSAT 7-65938
- TEM response of 3D body in layered Earth 7-29271
- theoretical TEM response curves over thin dipping dyke in free space for separated inline loop config. 7-9197
- Tornquist-Teisseyre zone (Poland), deep crustal struct. in contact zone of Palaeozoic and Precambrian platforms 7-14235
- toroidal fields, Namikawa-Matsushita antidynamo theorem extension 7-18352
- total magnetic field of two-dimens. body of arbitrary shape, calc. program 7-34718
- transfer functions robust estimation analysis 7-18313
- transformations 7-47329

geomagnetism continued

- transient EM anomalies, inline and broadside, characts. 7-9191
- transient EM anomalies, topography effects 7-8802
- Transylvanian Depression, struct. and morphology (*Rumanian*) 7-8891
- United States, crust struct., Magsat data anal. 7-47411
- trans-Ural marginal downwarp, numerical interpretation of regional mag. anomaly 7-29279
- World Magnetic Charts for 1985, main field and secular variation 7-54859
- Xikang-Yunnan continental palaeorift zone, China, Curie isotherm depths determ. from geomag. obs. (*Chinese*) 7-28914
- Zyoso Terrace, Japan, ELF magnetotelluric surveying (*Japanese*) 7-23604
- Fe ore fields, inhomogeneously magnetised models selection optimisation 7-23526

geometric programming

- chemical equilibria computation using geometric programming technique 7-39850

geometrical optics

- acoustic microscope spherical focusing transducers, ray-optical analysis 7-1371
- airborne scatterers, multi-(bi)-static HF (PO/GO) radar target imaging 7-25706
- astigmatism in laser beam optical systems 7-5829
- axicon, thin linear, diffraction patterns and zone plates 7-37083
- backscattering from triangular cylinder and hexahedron 7-42865
- branching waveguides, distrib.-index, phase space evaluation 7-31453
- caustic method for stress intensity factor determ. (*German*) 7-20672
- classical and quantum optics, unification using statistical ensemble theory 7-10900
- complex optical systems, optical beam wave propag. 7-50492
- complex point sources and Gaussian beam summation method 7-42894
- concentrator design, criteria for quality evaluation 7-50710
- conic mirror, on-axis focusing formula 7-43289
- conjugate lateral shear interferometry and its implementation 7-30067
- conserved vector flux, construction from plane waves 7-25926
- curvilinear cylindrical cavity, harmonic elastic wave propag., geometrical optics methods 7-1479
- cylinder lens design for X-ray laser 7-43317
- Czerny-Turner monochromator: astigmatism in the classical and in the crossed beam dispositions 7-20396
- display holograms and HOEs, image blurring 7-25752
- energy transport with partially coherent light 7-43326
- Fabry-Perot interferometer, mirror random phase inhomogeneity influence, resonator use 7-24689
- Fermat's principle, nonminimum time paths 7-24340
- Fermat's principle used to derive $F=ma$ eqn. in medium of varying refractive index 7-35145
- fibre, graded index, total acceptance angle 7-11155
- fibres and preform rods refractive index profile reconstruction from transverse interferometric data 7-11113
- flux concentrator, nonimaging, axially symmetric, concentration ratio calc. 7-57506
- focusing of multimode laser beams with variable beam parameters 7-11021
- Fresnel diffraction computation, review 7-18521
- Gaussian beams, generally astigmatic, propag. along skew ray paths 7-62623
- geodesic lens family design, theoretical analysis 7-57507
- ghosts's shadows and superluminal occultations 7-35154
- gradient index lenses, ray tracing, computation of ray-surface intersection 7-31418
- GRIN lens with revolution symmetry, paraxial Fourier transforming and imaging props. 7-31420
- GRIN lenses, optical performance assessment 7-31538
- Hermite-Gaussian beam transformation by shifted spherical lens 7-42891
- holographic optical element construction optics, design considerations 7-50715
- image formation by plane mirror, teaching 7-48254
- inhomogeneous media with smooth spatial-temporal inhomogeneities quadratic characts. of waves 7-62625
- lamellar transmission gratings in soft X-ray region, behaviour 7-20402
- laser resonators, ray matrices for tilted interfaces 7-57370
- laser-diode/multimode-fibre coupling analysis using a planoconvex GRIN lens 7-31480
- layered inhomogeneous uniaxial media, light propag., pseudo-Stokes parameters, geometric optics approx. 7-57244
- lens design, automatic, use of multi-image plane merit function 7-43310
- lens design, Brixner optimisation procedure 7-50683
- lenses, planar geodesic, anisotropic aberrations, definition 7-15818
- mirror design for producing specified raster shape 7-43296
- mirrors particulate contaminated, model for scattering 7-42910
- misaligned first-order optics, canonical operator theory 7-5832
- multilayer films, focusing, X-ray reflectance calc. 7-1247
- multilayer X-ray imaging systems, assessment of imaging props. 7-41568
- multilayer X-ray optics design 7-41567
- multimode branching waveguide, distrib.-index, evaluation by phase space 7-31451
- multiple reflector antennas, diffraction losses calc., asymptotic transition region theory 7-50471
- multiple scattering correction in meas. of particle size and density by diffraction method 7-9815
- multivariate aberration series, acceleration of convergence 7-5846
- multivariate Lagrangian aberration functions, singularities 7-5844
- multivariate Lagrangian aberration series, extension of convergence 7-5845
- noncollinear light propag. in rippled waveguide, geometrical optics approach 7-50742
- ophthalmic optics, tracing axial pencils through systems including astigmatic surfaces at random axes 7-23334
- passive resonators, transverse modes, reference light field choice (*Chinese*) 7-5965
- pinhead mirror as imaging device 7-5966
- pixel-selected ray-tracing for image generation (*Japanese*) 7-57264
- plasma, geometric optics at lower hybrid frequencies 7-37693
- plasmas, laser sustained, imaging of continuum emission for diagnostics 7-20930
- polygonal scan wheels, geometrical relationships 7-50707
- pseudo-Brewster angle, analytical soln. 7-31240

geometrical optics continued

- pseudomages formed by 3D holographic elements, intensity anal. 7-36915
- radar cross-sections, higher order diffractions from a circular disk 7-42866
- radar cross-sections calc., equivalent currents, flat plates with surface impedance coatings anal. 7-42867
- radar cross-sections of polygonal cylinders and flat plates, TGD calc. 7-42864
- random medium, edge diffraction of high-frequency coherence functions 7-42922
- ray series method appl. to axisymmetric nonstationary problems of dynamic elasticity 7-41114
- ray tracing for crossed beam photothermal deflection spectroscopy 7-41477
- ray transfer flow graphs, misaligned optical systems appl. 7-9644
- ray-tracing program integrated with solid-modelling CAD system, Traz program for opt. system design 7-50679
- reversible lens, limitations on performance 7-50694
- Riemann-Cartan space-time 7-1010
- schematic eye predictions of relative spectacle magnification in unilateral aphakia 7-34131
- Schwartzschild objective in X-ray optics, image form. in multilayer optics, SHADOW program 7-30144
- SDI driving optics development 7-48824
- seasonally adjusted, geometrical optical performance evaluation 7-46918
- sound reproduction from old wax phonographic cylinders, laser beam reflection method use 7-37014
- spectrometer, high-resolution, using spherically curved quartz crystals, design 7-4895
- spherical aberration, diffraction intensities 7-57259
- spherical aberration, intermediate, geometric and diffractive parameters, comparison 7-42983
- stationary saddle-type points, heuristic criteria 7-10850
- surface fabrication errors of optical systems, wavefront deformations calcs. 7-57262
- systems of finite fresnel number, imaging 7-5847
- Taylor series for point charact. of refracting plane 7-25713
- teaching approach, rel. to wave optics 7-35176
- thermal-wave lens, ray diagrams, focusing 7-54046
- toroidal and spherocylindrical surfaces, ray tracing 7-10842
- toroidal reflectors with multilayered optical coatings, figured X-ray optics, unified geom. design 7-30140
- two-component objective calc. 7-43294
- unstable cavity, aberration sensitivity, second-order theory 7-31256
- unstable resonators with 90° beam rotation 7-5918
- unstable-cavity sensitivity to spatially localized intracavity phase aberrations 7-25717
- vignetted pupil of optical systems, fast method calc. (Chinese) 7-15814
- volume holographic gratings diffraction efficiency calc. 7-1025
- Wood and GRIN rod lenses, third- and fifth-order aberrations 7-31419

geometry

- see also computational geometry; space time configurations*
- alignments in hierarchically clustered populations, implications for QSOs triple alignments 7-60830
- approximation of zonoids by zonotopes 7-61067
- cosmology, appl. of geometrical structures 7-35073
- Friedmann-Lemaître-Robertson-Walker models in Lyr's manifold 7-40966
- icosahedral structures and tiling, geometry and crystallography 7-1930
- interacting open superstrings, noncommutative supergeometry 7-41760
- local geometry of constitutive sets 7-60950
- Lyr's manifold, vacuum Friedmann cosmological models 7-35074
- Neufeld's connectivity, internal geometry 7-61073
- non-Euclideanism in general relativity and cosmology, mathematical formalism 7-34851
- polypase structures fed by complex current systems, global geometry (Italian) 7-31207
- quasiperiodic tilings obtained by projection 7-1931
- rigid cohomology and abelian varieties 7-61068
- transformation laws, algebraic approach 7-48270
- transformation laws, supersymm., no. system of octonions 7-49009
- transformation laws of geometrical objects, algebraic approach 7-29656
- Tsirelson superspaces and \mathbb{P}_0 7-29703
- two polygons, algorithm for computing every angle of movable separability (Japanese) 7-29729

geomorphology

- see also topography (Earth)*
- alluvial river channel, modelling of channel development 7-18234
- Alyat Ridge, SE Caucasus, USSR, horizontal compression structures, clay diapirs and mud volcanoes 7-23643
- Arctic shorelines of USSR, shoreline changes and sea levels during Cainozoic 7-4022
- S Australia, beach-ridge behaviour density during Holocene 7-4025
- barchan sand dune, development by numerical model 7-4036
- black shale, climatic cycle evidence (French) 7-66288
- book 7-48211
- Bugaboo Glacier, BC, Canada, lateral moraine and glacial history 7-23720
- Caledonia, drumlin field, S Ontario, inverse-graded units within till 7-9033
- Cape Shoalwater, Washington, USA, rapid coastal erosion 7-28991
- SE Caucasus, USSR, north slope chaotic complexes, morphology and stratigraphy 7-29013
- cliff erosion at Chesapeake Bay, Maryland, USA, due to groundwater 7-66123
- coastal wetland erosion accompanying coastal submergence 7-29029
- Columbia River, Washington, USA, Late Holocene flooding and channel morphology 7-47470
- conference, Durham, England (Jan. 1984) 7-48138
- Cooper Creek, SW Queensland, Australia, Quaternary drainage patterns and stratigraphy 7-34496
- Deccan upland region, India, late Quaternary alluvial history and climate 7-60287
- Delaware Bay, USA, coastal wetland erosion accompanying sea level rise 7-29029
- desertification, review and definitions of concept 7-9157
- desertification in irrigated regions 7-8450
- desertification indicators 7-8452

geomorphology continued

- desertification process, importance of drought in intensification of desert conditions 7-8453
- desertification processes responsible for land degradation 7-8449
- developments and applications, book 7-55912
- Ellesmere Island, Canada, Late Quaternary sea-level changes and glacial history 7-66128
- NE Ellesmere Island, NWT, Canada, glacial geology and marine stratigraphy 7-4062
- encyclopedia of beaches and coastal environments 7-35127
- erosion by wind, theory of climatic factor 7-8948
- S Europe, desertification processes 7-8451
- Everglades of Florida, USA, geomorphology and Pliocene coral reefs 7-29028
- fault geometries in basement-induced wrench faulting under different initial stress states 7-40458
- geotechnics dictionary 7-55908
- Glen Feshie, Cairngorms, Scotland, age of river terraces 7-34497
- hillslope failure due to groundwater seepage 7-29112
- ice-push caves in platform limestones of Montreal area, Canada 7-66121
- Japan, river flooding and land-slides during July 1985 in Noto area (Japanese) 7-18226
- karst aquifer at Castle Meadows, Alberta, Canada, structure and function 7-4060
- Kavaratti atoll, sandy beach sediment transport processes (in Indian Ocean) 7-14257
- Port Lianyangang, muddy beach geology and erosion on Yellow Sea coast (Chinese) 7-55013
- Loess Hills region of Iowa, USA, Quaternary geology and geomorphology 7-47441
- Louisiana coast, USA, coastal changes accompanying rapid land subsidence 7-4023
- marine terraces along Alpine fault, New Zealand, uplift rates 7-66077
- Maryland Piedmont, USA, flood plain sediment deposition since 1730 AD 7-29081
- meandering stream, secondary flows and the pool-riffle unit 7-34562
- Miami Pliocene coral reefs, geomorphology and Atlantic coastal ridge in Florida 7-29028
- Mississippi delta barrier islands, geomorphic recovery after hurricane erosion 7-4024
- Mongolia, ring structures and fractures, assoc. gravity and topographic characts. 7-28962
- Montreal areas, Quebec, Canada, ice-push caves in platform limestones 7-66121
- Nile Delta, Egypt, Holocene sediment accumulation history 7-23653
- Nile delta sediment deposition history at Rosetta and Damietta, promontories 7-34565
- central North Sea, valley asymmetry as evidence for periglacial activity 7-14285
- Northern Hemisphere Quaternary glaciations 7-55051
- Ohau River (braided), New Zealand, bedload movement and bar development 7-34563
- Pamlico Sound, USA, coastal wetland erosion accompanying sea level rise 7-29029
- permafrost mapping method for forest areas, Landsat Thematic Mapper method 7-29302
- permafrost of Alaska, temp. profile and evidence for climate change 7-66299
- protalus ramparts of lateglacial age in upland Britain 7-34498
- Qingdao coast, China, changes of palaeogeographical environment during past 20000 years (Chinese) 7-55011
- Quebec and Ontario, Canada, glacial striae and ice flow directions 7-66173
- rain splash erosion beneath tropical forest canopy, study of rain throughfall 7-34561
- river, sandy river bed instability due to bed load motion (Japanese) 7-18224
- river sand waves, bed form response to sudden flow decrease (Japanese) 7-18223
- river terraces in Scottish upland valleys, soil stratigraphy and terrace dating 7-34497
- river with sandy bed, bridge pier scouring and dune migration (Japanese) 7-18225
- ivers, conf., Jackson, MS, USA (March to April 1986) 7-41008
- Saharan dust transport by atmosphere, review 7-9073
- sand dune migration and shaping due to wind, for isolated dune 7-4036
- sand dunes, thermoluminescence dating method used for Sri Lanka red-sand beds 7-23847
- sand dunes in Mutonga drainage, Mount Kenya, origin and palaeoclimatic-ecological significance 7-18186
- Shithatha area, Iraq, gravity study of faults 7-34373
- soil degradation in drylands 7-8455
- soil erosion by wind, measurement apparatus, book 7-35136
- soil erosion planning, vectorization of Landsat TM land cover classification data 7-47443
- soil erosion planning in Dane County, Wisconsin 7-47442
- strike-slip duplexes 7-40457
- E USA, agriculture impact on soil erosion in Chesapeake Bay area 7-23707
- valleys morphology on Hawaii, evidence for groundwater sapping and comparison with Martian valleys 7-55095
- Volga River Delta, USSR, hydrographic map from space images 7-66184
- W.H. Mathews Symposium, Vancouver, British Columbia (October 1984) 7-4620
- wind erosion vulnerable areas, detection by satellite remote sensing of dust storms 7-8949
- Yellow River outlet, coastline changes due to sedimentation 7-55089

geons *see* gravitons**geophones *see* seismometers****geophysical aspects of cosmic rays**

- atmospheric showers initiated by cosmic accelerators 7-18342
- Buckland Park cosmic ray air shower array for UHE γ -ray astronomy 7-60565
- cosmic-ray induced ionization intensities near Kaohsiung, Taiwan, ground, sea-level meas. (Chinese) 7-55399
- cosmogenic nuclides in meteorites and terrestrial matter, workshop, Los Alamos, New Mexico (July 1984) 7-29601
- Cygnus X-3, underground muons, new evidence from Soudan 1 7-40863
- D_{81} correlated cosmic ray variations 7-4279

geophysical aspects of cosmic rays continued

- depth-intensity relation in sea water, determ. from primary cosmic ray energy spectra 7-4281
- detector materials in Earth orbit, disintegration products 7-66425
- diurnal anisotropy of cosmic rays, implications for heliospheric transport parameters 7-66408
- EAS, latitudinal devel. 7-14454
- EAS of low energy, characts. 7-34812
- galactic cosmic rays in atmosphere, north-south asymmetry, solar mag. field effects 7-66409
- geomagnetic activity and local modulations of cosmic rays 7-66404
- gravitational wave detection experiments, correl. of geophys. factors 7-47697
- hadron characteristics at Mt. Kambala 7-34813
- ionisation induced by cosmic rays, intensity meas. 7-40308
- magnetosphere, allowed regions for particle motion in superposed dipole and uniform mag. fields 7-14482
- matter-antimatter symmetry, COSMIC radiation study 7-23958
- muon intensities at deep underground facilities, atm. effects 7-34811
- neutrinos, oscillations, effect of transmission through the Earth 7-41677
- neutrinos in atmosphere, energy spectrum calc. 7-40660
- neutrons of cosmic ray origin, altitude and latitude effects on intensity and energy spectra 7-9346
- nuclear particle flux propagation in atmosphere, model (*Russian*) 7-66413
- possibility of reconstructing a hadron cascade of arbitrary form in the atmosphere 7-14458
- solar diurnal anisotropy of cosmic rays, secular changes in upper cut-off rigidity 7-66407
- solar particle fluxes, relation to nitrate flux on Ross Ice Shelf, Antarctica 7-55091
- solar wind two-sector struct. responsible for enhanced diurnal variations 7-55391
- stratospheric level, galactic cosmic ray modulation at mid-latitudes 7-9344
- tachyon search in EAS 7-66414
- temporal fluctuations at rigidities 4 to 180 GV, power spectral density (1976 to 1980) 7-14427
- Trapped Ions in Space expt., linear energy transfer spectra in low Earth orbit 7-60479
- volcanic rocks at Maui, Hawaii, Ne and He isotopes due to cosmic ray bombardment 7-54959
- ¹⁰Be production during Pleistocene geomagnetic excursion 7-23842
- He nuclei, rigidity spectrum rel. to ³He/⁴He ratio at high energies 7-66410
- ³He production in volcanic rocks (in situ), and geophysical applications 7-60500

geophysical equipment

- see also atmospheric measuring apparatus; hydrological equipment; oceanographic equipment; seismometers*
- 4-camera video system, development and use 7-4235
- absolute gravity meter 7-9224
- apatite, external detector comparison for fission track dating 7-54962
- Archaeon rock weathering apparatus, appl. to expt. weathering of mafic and ultramafic rocks 7-29021
- Australian class A pan evaporation network, evaporation reduction due to bird screen 7-4193
- automatic cloud classification 7-9214
- borehole water and gas sampling technique using polyamide tube 7-66310
- cameras for aerial photography, comparison of three modern aerial cameras (*French*) 7-47307
- consolidated rocks thermal conductivity meas. instrumentation 7-40609
- data acquisition system (digital) for solid Earth tide recording 7-29245
- data logger with 8085 microprocessor 7-9179
- debris flows, noncontact speed sensors 7-40615
- digital linear measuring system, appl. to automation of geometrical levelling (*German*) 7-3972
- discharge equipment for rock AF demagnetization 7-55274
- displacement gauge including linear variable differential transformer, rock mechanics appl. 7-34695
- ERASME airborne side-looking C-band radar, data processing and calibration 7-9205
- ERS-1 satellite, Australian involvement 7-4294
- extended marine arrays versus simulated extended arrays 7-47365
- ferroprobe azimuth transducers, instrumental errors (*Russian*) 7-34706
- gamma-method inversion probes, new designs (*Russian*) 7-34703
- gamma-source backscatter density gauges modelling 7-34716
- geodetic horizontal pendulums of capacitive type, laboratory test method 7-29250
- gravimeter, electrostatic feedback method 7-18319
- groundwater direction and velocity meas. system 7-9185
- gyroscope, passive resonant ring laser, progress 7-20440
- India's development activities at Instrumentation Group of National Geophysical Research 7-18308
- induced polarization meas. device, noise resistance maximization (*Russian*) 7-34700
- inverter, half-bridge HF variable voltage-fed, used for geophysical survey transmitter 7-23879
- IR CCD coupling structure for space appls., using CMT detector 7-29309
- JEOS, JANUS Earth Observation Satellite instrumentation 7-34824
- laboratory magnetometer bench, with shield and regulator 7-30049
- low-energy cyclotron for radiocarbon dating 7-55310
- magnetic field strength meas. equipment (*Russian*) 7-34699
- proton magnetometer, DPM-1 instrument from USSR for marine surveys 7-40602
- magnetometer for geophysical exploration, compensation display device (*Russian*) 7-30045
- proton magnetometer for marine surveys, Chinese CTZY-1 instrument (*Chinese*) 7-4188
- microprobes for elec. logging with flat field in medium with cylindrical boundaries (*Russian*) 7-34704
- multidimensional seismic wave recording systems, efficiency anal. 7-47345
- multipurpose space experiment for land studies, concept and dimensions 7-66336
- non-metric cameras, calibration using finite element method 7-3969
- oblique CCD reconnaissance camera operation, atmospheric effects 7-18900

geophysical equipment continued

- optical converter for marine quartz gravimeter 7-29262
- optical remote sensing from space, conf., Cannes, France (Nov. 1985) 7-35094
- opton displacement sensor [geophysical application] appl. 7-4809
- P400 seismic watergun source 7-9196
- PDA-2 pressure transducer for geophysics (*Russian*) 7-34711
- photogrammetry, auxiliary apparatus for parallel orientation of camera base to datum plane 7-3970
- aerial photography, retractable camera rig for light aircraft 7-29304
- portable absolute gravimeter for vertical crustal motions anal. 7-9225
- portable neutron chloride meter for soil anal. 7-56291
- precision geodesy and crustal deform. meas. instrument, hydrostatic levels 7-9229
- proton magnetometer, intra-cycle build-up to increase accuracy (*Russian*) 7-30046
- push-broom linear array scanner, design of all-reflective flat-field objective 7-55320
- Radarsat synthetic aperture radar system for remote sensing satellite 7-47578
- radiometers, absolute cavity (PMO6), and expt. charactn. 7-35562
- remote sensing image sensors, conf., Stuttgart, Germany (Sept. 1986) 7-60886
- remote sensing of Earth resources, imaging spectropolarimeter-photometer for satellite 7-40604
- remote sensing of land surface, use of ultralight aircraft 7-8952
- remote sensing optical sensor technology (*Japanese*) 7-60420
- rock acoustic emission meas. apparatus, co-axial outlet design 7-18322
- rock thermal conductivity meas. equipment (*Rumanian*) 7-8940
- rock thermophysical characts. determ., automatic meas. system 7-9219
- Romania geodynamic observatories, sensors and auxiliary apparatus characts. for Earth tides obs. (*Rumanian*) 7-9243
- seafloor exploration remotely operated vehicle, ARGO/JASON system 7-55328
- seismic exploration, outlook for development of methods and equipment 7-47341
- seismic explosive source for ocean floor seismic work 7-55309
- seismic measuring transducers, possibility of unification 7-28889
- seismic reflection profiling, MIPEX data acquisition system using personal computer (*Japanese*) 7-55265
- seismic shallow layer reflecting survey system for Japan Geographical Survey Office (*Japanese*) 7-23855
- seismic shear wave source, vibrator with vertical dipole (*Chinese*) 7-4191
- seismic telemetry system of large dynamic range, design and performance 7-28870
- seismological application of borehole volume strainmeter 7-66350
- selective gamma-gamma method inversion probe (*Russian*) 7-34708
- shipboard-three component magnetometer, characts. and meas. of geomag. anomalies 7-29276
- SNARE, earthquake detect. and recording system for small seismograph networks 7-28873
- snow fork for density and wetness profiles determ., permittivity meas. 7-9206
- snow penetrometer, appl. to determ. of strength characts. of loose snow 7-9052
- soil erosion by wind, measurement apparatus, book 7-35136
- space camera lenses, design 7-43314
- spaceborne radiometer antenna reflector, MM wave, development 7-23920
- spaceborne remote sensing systems (book) 7-41027
- spaceborne synthetic aperture radar sensor technology 7-4234
- SPOT satellite series, characts. 7-47551
- strainmeter and tiltmeter techniques and design, review 7-23906
- strong-motion seismic arrays, effect of array configuration on source inversion 7-28853
- subseafloor profiling using seismic waves (*Japanese*) 7-47559
- aerial survey camera trials, for Wild RC10A and Zeiss RMK A 15/23 cameras 7-28817
- surveying, GPS navigation radio receiver sets, MINI-MAC system by Litton 7-34370
- terrain data interactive image processing, digital SM-4 Omega system 7-66334
- thermal conductivity meas. apparatus for drill cuttings 7-29270
- thermal IR multispectral scanner, airborne instrument for mineral deposits detection 7-14393
- tiltmeter of water-tube half-filled type, instrumental noise (*Japanese*) 7-4231
- unfocused electrode-type elec. logging devices, dynamic model 7-23864
- VChV-5 humidimetric system 7-55300
- VLF transmitter for geological fracture mapping 7-14386
- volcaniclastic materials, thermoluminescence ages, meas. apparatus 7-47571
- zenith angle transducers in deviation recorders, accuracy (*Russian*) 7-34707
- U and Th, concentrations in geological samples, plastic track detector study 7-40596

geophysical fluid dynamics

- 3D convective motion in spherical shells 7-57823
- N Adriatic Sea, current struct. of M2 tidal component from rotary anal. of Taylor model 7-40486
- anisotropic flow in layered asthenosphere 7-60209
- W Atlantic Ocean, frontal surveys with towed profiling cond./temp./depth meas. package (SeaSoar) 7-14298
- atmosphere, periodic solns. of non-stationary eqn. for vertical rel. 7-18296
- atmosphere barotropic motion, effects of orography (*Russian*) 7-29130
- atmospheric dynamics, linearised barotropic and baroclinic equations, Arnoldi's method 7-61078
- axisymmetric vortices, momentum diffusion effects, appl. in tornado simulation 7-57850
- balance equations in periodic domain, numerical model, balanced turbulence 7-34604
- baroclinic and barotropic instability spectra as functions of *N* in *N*-level models 7-34590
- baroclinic chaos numerical anal. 7-57893
- baroclinic flow transitions in annulus 7-26351
- baroclinic instability of basic current in 2-layer ocean model 7-29068
- baroclinic instability over topography, nonlinear evolution 7-57804
- baroclinic solitary waves with radial symm. 7-57863
- barotropic geostrophic turbulence free evol. 7-29066

geophysical fluid dynamics continued

- barotropic jet with slow streamwise var., instability 7-66230
- barotropic study of free and forced planetary waves 7-60335
- capillary-gravity ripples generation by strongly non-linear waves on deep fluid surface (*Russian*) 7-29040
- upper Chesapeake Bay, anal. of tidal propag. signals from two bay systems 7-66164
- convection in planetary atmospheres and stars, zero-gravity expts. 7-29393
- convection in spherical shell, onset of time-dependence in mantle 7-60212
- core dynamo, for Couette-Poiseuille flow 7-65941
- current on sloping bottom, rot. flow interaction, shelf wave generation, flow visualisation expts. gravity current on sloping bottom, rot. flow interaction, shelf wave generation, flow visualisation expts. 7-43947
- diapiric structures, relation between initial conditions and late stage of Rayleigh-Taylor instabilities 7-66108
- dilatational model for elastic-plastic deformation of anisotropic media 7-55035
- downdraught windstorms, supercritical flow in stratified fluid 7-66234
- dual-gamma attenuation for the determination of porous medium saturation with respect to three fluids, appl. to groundwater 7-51307
- Earth core, steady flows at core-mantle boundary from geomag. field models 7-40444
- Earth core steady surficial motions determ. from geomag. field models, alternate method 7-66023
- finite element methods in flow problems, conference, Antibes, France (June 1986) 7-41009
- fluid mechanical problems 7-55036
- fluid outer core, inertial waves identification 7-60225
- Fofonoff's mode 7-60262
- frontogenesis, variable resolution finite-element model 7-34622
- gravity currents, stratified fluids, turbulence effect 7-43949
- gravity-capillary waves, wind-generated, period-doubling 7-43952
- Hadley circulations on a nonuniformly heated rotating plate 7-63159
- heterogeneous shear flows, generalisation of stability theory (*Chinese*) 7-26248
- lakes, wind-induced free surface flow anal., 3D, FEM 7-43839
- large-scale currents calc. from density data 7-29297
- linear development of quasi-geostrophic baroclinic disturbances with condensational heating 7-60340
- linearised unsteady multidimensional infiltration in soil 7-55108
- magma chamber beneath volcano., multicomponent crystallisation and convection 7-54972
- magma chamber convection with stagnant bottom layer, laboratory expts. 7-23616
- magma flow in pipe from magma chamber, two-phase flow calcs. 7-40451
- magma migration mechanism, of buoyancy-driven crack propagation 7-54973
- mantle fluid dynamics, soln. of Rayleigh-Taylor problem 7-66084
- mantle plumes, contrib. to periodicity of mag. field reversals 7-65934
- mass transport in porous media, macroscopic balance laws 7-57914
- E Mediterranean Sea, water masses and circulation patterns in deep water layer 7-29063
- MHD theory, system of eqns. on special Riemann manifold 7-65939
- MHD theory, system of eqns. using Riemann theta functions 7-65940
- molten rock viscosities, expts. on diopside-albite rock melts 7-60248
- mushroom-like currents (vortex dipoles), obs. in ocean and laboratory tank 7-29033
- mushroom-shaped ocean currents, regularities in development inferred from satellite imagery anal. 7-66143
- nonlinear gravity-capillary waves, free surface accel., oceanic appl. 7-43955
- nonlinear waves on a coupled density front 7-63163
- ocean, direction and vel. determ. for internal tide wave via single-station meas. 7-40483
- ocean currents, Doppler acoustic current meas. in high currents 7-66166
- ocean currents, field performance of NBIS Smart ACMS with EG&G Sea Link VMCMs 7-66366
- ocean currents, separation and forecasting of mass transport components (*Chinese*) 7-55068
- ocean currents monitoring, appl. of elec. field meas. in sea 7-47444
- ocean tides, microcomputer tide prediction utility 7-66163
- oceanography, relation between daily mean sea level and tidal range and dynamical explanation 7-40481
- oil reservoir flow models, book 7-48219
- oil-bearing stratum, incompressible two-phase flow simulation (*French*) 7-44032
- quasigeostrophic vortices, Lyapunov-stable solns. 7-43925
- Red Sea, hydrographic props. and exchanges with Indian Ocean in summer 7-29064
- river flow modelling and forecasting (book) 7-48199
- rocks, single fracture characts. and gas flow 7-23641
- Rossby and gravity wave breaking, definition of concept 7-29213
- Rossby waves, triad reson. interactions in ocean 7-29067
- Rossby-Haurwitz waves weak nonlinear coupling in atm. 7-60318
- rotating cylindrical annulus, imposed temp. gradient, flow regimes study 7-43933
- rotating differentially heated annulus with unstable stratification, convection characts. (*Russian*) 7-29129
- salinity-temperature front, double-diffusive horizontal intrusions, linear stability theory 7-26250
- shallow water equations, complex flow, boundary fitted grids, breaking wave, reflected wave 7-6231
- shallow water flow incident upon slender orography, semi-geostrophic response to elongated ridge 7-29122
- shallow water wave propagation, effects of permeable breakwater 7-66165
- solitary rotational water waves, Lyapunov stability, oceanic appl. 7-63164
- steady infiltration from buried discs and other sources 7-23786
- stratified shear flow in ocean, wind mixing 7-34504
- streamline routing through fracture junctions 7-55028
- supercritical dynamics of baroclinic disturbances in the presence of asymmetric Ekman dissipation 7-34588
- surface gravity waves in deep water, class I and II instabilities, modified Zakharov eqn. 7-51195
- synoptic scale disturbances with circular symmetry 7-34625
- Taiwan Strait, numerical investigation of three-dimensional diurnal wave (*Chinese*) 7-55069
- thermoelasticity of two-phase media with mass exchange between phases 7-55034

geophysical fluid dynamics continued

- three-dimensional flow in bounded domain, stochastic anal. 7-23761
- time-dependent flow problems, vertical structure functions determ. 7-47576
- transient quasi-geostrophic eddies, 3D propagation 7-29139
- transport in porous media, generalised Darcy's and Fick's laws 7-57915
- trapped internal waves from body moving in ocean thermocline, phase config, visualisation 7-31854
- turbulent entrainment and the entrainment assumption 7-55064
- turbulent exchange coeffs., modified Ertel method in oceanography 7-29072
- two-layer model, direction of energy movement in wave number 7-57864
- Typhoon No. 7507, kinematical fields from upper air obs. (1975 August 17 to 23) 7-40510
- viscous flow past right circular cylinder on β -plane 7-57847
- wave boundary layer, numerical model, ocean appl. 7-55053

geophysical prospecting

- 2D structures, resist. modelling by finite element method (*Chinese*) 7-55270
- 3D transient EM responses for grounded source 7-47332
- aerogeophysical prospecting, knowledge-based analysis system 7-29308
- aeromagnetic surveying, variable-magnetisation terrain correction method 7-66325
- Africa, central and E central region, geology and petroleum resources 7-47438
- airborne gamma-ray surveys, altitude depend. model 7-47440
- airborne gravity gradiometer survey data analysis using isomorphic geodetic and electrical networks 7-47309
- APEX, aerogeophysical prospecting expert system (*Chinese*) 7-55268
- apparent resistivity computation using exponential approx. of kernel functions 7-28822
- Aurora U deposit, McDermitt Caldera Complex, Oregon, He soil gas survey 7-40441
- Basin and Range province, USA shallow subsurface temp. surveys 7-60398
- book, economics and applied geology 7-29609
- borehole electroprospecting, influence of surface deposits on const. current field in anisotropic medium 7-28831
- borehole EM induction logging, moving and stationary transmitter methods 7-4226
- borehole NMR logging method, free fluid index for oil reservoir 7-29253
- borehole well logging by EM method, HFILIS method for producing oil wells 7-55279
- buried metal sulphide deposits, exploration, effects of chem. processes on emitted gases meas. 7-40439
- Calgary area, Canada, geothermal energy potential 7-28924
- Canadian petroleum exploration, appl. of remote sensing 7-40585
- chromite ore prospecting in Zimbabwe underground mine, appl. of high-resolution seismic refl. technique 7-65950
- coal seam exploration, seismic reflection profiling method using shear waves 7-14385
- coal seams, tectonic disturbances and quality changes, geoelectric anal. method 7-34712
- cokriging: multivariable analysis in petroleum exploration 7-40578
- conference on geology, Kingsley Dunham volume, Durham, England (April 1985) 7-24303
- continuation of geophysical fields meas. on a curvilinear surfaces, computation scheme 7-55302
- controlled source audiofrequency MT soundings in Japan rel. to Schlumberger sounding (*Japanese*) 7-66318
- cross-borehole electrical surveys, geological noise effects 7-28825
- deep-sea floor polymetallic sulphide exploration, MINI-MOSES expt. 7-23863
- dipole source and layered Earth (*Japanese*) 7-23528
- vertical electric sounding curves, data interpretation improvements 7-14389
- electrical exploration by resistivity method, numerical soln. for two-dimensional problem 7-8810
- electrical potential due to point current source over layered conducting Earth with dipping anisotropy 7-8801
- electrical prospecting, potential field of stationary elec. current, Fredholm's integral eqns. calc. 7-14181
- electrical prospecting, potential soln. for nonuniform thin vein with transverse conductance variability 7-28830
- electrical prospecting direct problem, numerical soln. method 7-29267
- electrical resistivity method for exploration of thin slab struct. 7-29310
- electrical sounding, HF variable-voltage-fed inverter 7-23879
- electrical sounding, relations between elec. parameters of rocks and chemical comp. 7-18181
- electrical sounding, uniqueness of determ. of 3D underground structs. from surface meas. 7-8809
- EM modelling program for 2D structures 7-34714
- EM prospecting method, finite element modelling (*Japanese*) 7-55280
- EM prospecting of quasiplanar conducting layers, approx., boundary conditions 7-55304
- EM prospecting theory, optimized digital filter for the Fourier transform 7-14387
- EM response of buried thin sheets in uniformly conducting half-space 7-66326
- EM sounding of an electrochemically active half-space 7-23853
- EM subsurface radar using transient field radiated by wire antenna 7-23866
- gamma-method inversion probes, new designs (*Russian*) 7-34703
- gas reservoirs seismic response 7-9194
- geochemical exploration for mineral resources using soil gas comp. 7-40590
- geodetic gravity anomaly interpretation using deterministic approach 7-28811
- geomagnetic depth sounding method, use of line current analogues 7-34719
- geostastical analysis of gas potential in Devonian shales of West Virginia 7-40586
- glaciated terrain, conference, Kuopio, Finland (September 1986) 7-18497
- gravity anomalies and vertical gradient over cavities in brittle rock 7-47308
- gravity prospecting, theory of bodies of zero external gravit. pot. 7-8789
- groundwater in Kasserine Basin, Tunisia, multistage exploration 7-4067
- horst structure, EM field from multiple freq. sounding and transient sounding 7-54864

geophysical prospecting continued

hydrocarbon deposit exploration and exploitation the stratigraphic approach 7-18311
hydrocarbons and authigenic magnetite, occurrence correl. 7-60253
Ile-Ife, Nigeria, possible fault zone, elec.-geomag. surveys and minerals existence 7-47330
India's development activities at Instrumentation Group of National Geophysical Research 7-18308
induced polarisation logging in borehole, theory 7-23864
induced polarisation method for exploration of thin slab struct. 7-29310
induced polarisation method for study of buried 3D body in a two-layered Earth 7-55286
induced polarisation surveys, EM coupling removal 7-9190
induced polarisation meas. device, noise resistance maximization (*Russian*) 7-34700
induction method for stratum axial symmetry determ. (*Russian*) 7-34705
inverse gravimetric problem, choice of norm 7-18106
inverse logarithmic potential problem, uniqueness of solns. 7-29280
Johnson Camp, Arizona, Cu-Zn ore bodies determ. from soil and soil gas comp. anal. 7-40591
Kerch' Peninsula, USSR, hydrocarbon exploration using remote sensing data 7-60223
laser spectroscopy, principles and appls. (*Slovak*) 7-24706
magnetic anomaly over structurally complex bodies, use of subtended solid angle, DEC BASIC-PLUS-2 program 7-9192
magnetic field strength meas. equipment (*Russian*) 7-34699
magnetometer for geophysical exploration, compensation display device (*Russian*) 7-30045
magnetotelluric data inversion using localised cond. constraints 7-28823
magnetotelluric impedance for 3D cond. structures 7-23536
magnetotelluric method for 2D structures, resolving power (*Japanese*) 7-66317
magnetotelluric response of a laterally inhomogeneous anisotropic inclusion 7-14190
magnetotelluric sounding in 2-D, stable finite element soln. 7-47328
magnetotelluric sounding method for hilly terrain, E-polarization case 7-29252
magnetotelluric sounding method in hilly terrain, using H-polarization 7-29251
magnetotelluric sounding method using H polarization, physical modeling 7-29255
magnetotelluric sounding of 2-layered 3D structs., approx. soln. 7-29254
magnetotelluric sounding of Earth struct., Rayleigh-fast fourier transform method 7-9181
S Mangyshlak, Kazakhstan, USSR, oil and gas deposits 7-66028
marine electrical prospecting with pulsed signal, synchronous noise (*Russian*) 7-34701
minerals gas emission causing bubbles in overlying ice, use in prospecting 7-23709
mining, conf., Santiago, Chile (November 1986) 7-35111
mise-a-la-masse anomalies near vertical contact, behaviour 7-9189
natural gas hydrate deposits prospecting, acoustic and resistivity meas. on rock samples containing tetrahydrofuran hydrates 7-55026
Near-Caspian Depression, USSR, oil reservoir below salt beds, detection method using remote sensing 7-55294
network theory appls. in Euclidean space (*French*) 7-23647
neutron gamma logging, rock models, min. dimensions (*Russian*) 7-34477
New Zealand, geothermal systems exploration and devel., use of applied chem. 7-13848
Nubia, Egypt, aerial techniques for groundwater prospecting 7-34698
oil and gas exploration, anal. of mesofractures visible in space images 7-66337
oil and gas reserves, discovery patterns 7-23648
oil and gas seismic prospecting, computer algorithm for synthetic seismograms 7-60395
oil exploration, induced polarisation method (*Chinese*) 7-55269
oil fields, trend surface anal. 7-40583
oil/gas presence prediction, appl. of aerospace imagery 7-66335
optoelectronic meas. of mineral content (*Russian*) 7-9241
ore deposit EM prospecting method metallogenesis rel. to tectonic lineaments 7-29256
ore deposits, PCM station for investigating contact and contact-free polarisation curve methods (*Russian*) 7-34702
Pacific Ocean floor, hydrocarbons identification in sediments and bottom water layer 7-29079
petroleum exploration, coconditional simulation appl. 7-40577
petroleum exploration, computer appl. conf., Wichita, KS, USA (Oct., 1985) 7-35083
petroleum exploration, geological and computer traps 7-40582
petroleum resource appraisal program, FORTRAN listing 7-40576
radiation logging curves, recording scale automatic displacement (*Russian*) 7-34710
radioisotope XFA of copper content in Zongtiaoashan copper mine (*Chinese*) 7-8337
resistivity logs, appl. of digital filter technique (*Chinese*) 7-29261
resistivity spectral transformation, dilution factor use (*Chinese*) 7-54855
sampling and minimum phase from continuous and discrete point of view 7-14384
Saskatchewan, Canada, well water He and methane anomalies, use for hydrocarbon prospecting 7-40440
scalar audiomagnetotellurics applied to base-metal exploration in Finland 7-29272
Schlumberger geosounding, lateral effects reduction method 7-9193
Schlumberger soundings, rel. to controlled source audiofrequency MT soundings in Japan (*Japanese*) 7-66318
seismic data interpretation using a priori information 7-14383
seismic data processing and 4. appl. to investigations at site of Krivoi Rog superdeep hole 7-47343
seismic diffraction tomography and multisource holography applied to seismic imaging 7-66321
seismic exploration, anal. of multidimensional seismic wave recording systems 7-47345
seismic exploration, long streamer appls. 7-28910
seismic exploration, new approach to study of crustal and upper mantle struct. 7-47342
seismic exploration, outlook for development of methods and equipment 7-47341
seismic exploration, three-component meas. via polarisation method 7-47344
seismic exploration of coal mines, in seam reflection technique (*Hungarian*) 7-66351

geophysical prospecting continued

seismic holography, computer simulation 7-18124
seismic inverse problem, definition of velocity change in wave eqn. soln. 7-14198
seismic inversion algorithm, 2.5 D Born inversion with arbitrary reference 7-66322
seismic method in search for oil and gas, development trends 7-4225
seismic migration algorithm, for fast plane-wave and single-shot migration 7-34393
seismic profiling, computer model for image ray tracing 7-3994
seismic profiling, fast time-domain computation of 1D synthetic profiles 7-14204
seismic profiling from drifting ship using light-weight streamer 7-34742
vertical seismic profiling method, separation of upgoing and downgoing waves 7-55283
seismic prospecting, common-midpoint stacked data, with automatic phase correction 7-66324
seismic prospecting, medium response parameter optimal estimation 7-65978
seismic prospecting problems, Cauchy problem (*Chinese*) 7-28846
seismic prospecting with multispread 3D logging method (*Rumanian*) 7-9245
seismic refl. profiling, 3D data inversion for velocity and depth depend. reflectivity 7-60174
seismic reflection method for coal prospecting in China (*Japanese*) 7-23854
seismic reflection profiling, 2D velocity inversion and synthetic seismograms 7-66323
seismic reflection profiling, common depth point method for small velocity inhomogeneities 7-23852
seismic reflection profiling, edge effects in cylindrical slant stacks 7-47350
seismic reflection profiling, reflection and transmission and generalized primary wave 7-23553
seismic reflection profiling in deep water, suppression of peg legs and multiples 7-55281
seismic reflection profiling method using reverse-time migration 7-14203
seismic reflection profiling of coal measures, use of discriminant analysis method 7-4211
seismic reflection profiling using multiwave exploration methods in W Siberia 7-54899
seismic reflection tomography method for subsurface velocity struct. 7-23555
seismic refraction profiling, extension of linear regime of waveform inversion problem 7-40417
seismic shallow layer reflecting survey system for Japan Geographical Survey Office (*Japanese*) 7-23855
seismic shear wave source, vibrator with vertical dipole (*Chinese*) 7-4191
seismic sounding, nonuniform waves propag. in space divided by thin fluid-filled fracture 7-28891
seismic study of oceanic crust, seafloor theoretical seismograms for underwater explosions 7-23563
seismic thin bed analysis using 3D scale model expts. 7-28909
seismic tomographic study of crust struct., algorithms and filter selection 7-23872
seismic trace stacking, for estimation of acoustic impedance function (*Hungarian*) 7-18123
seismogram synthesis for use in acoustic well-logging 7-47364
seismology, algorithm for determining pulse response of medium, z-transformation method 7-60396
seismology iterative inversion for seismic velocity using waveform data 7-47346
selective gamma-gamma method inversion probe (*Russian*) 7-34708
shallow prospecting on land by means of a novel electroacoustical P-Wave pulse generator 7-34751
shallow seismic sources, field comparison 7-47374
soil, dielectric profile retrieval, use of iterative optimisation 7-9204
sonic logging, 2D spectrum anal. 7-4203
sonic logging, 2D spectrum anal. 7-55332
static magnetic dipole, method for location and dipole moment components estimation 7-9203
subsurface anomaly free surface response to SH wave with source on surface 7-28905
subsurface geology from well logs, color images, Kansas 7-40581
surface borehole exploration with direct current for oil and gas deposits contouring 7-23849
telluric method, results for faulted structures 7-34713
TEM response of 3D body in layered Earth 7-29271
TeV neutrino beams, physical bases and geophysical appls., review 7-40587
theoretical TEM response curves over thin dipping dyke in free space for separated inline loop config. 7-9197
thermal IR multispectral scanner, airborne instrument for mineral deposits detection 7-14393
transient EM anomalies, inline and broadside, characts. 7-9191
transient EM anomalies, topography effects 7-8802
transient response of a deposit excited by a pulse of current 7-8808
central Urals region, USSR and geological devel. 7-23549
vibroseis observations, amplitude-phase spatial analysis method 7-29266
VLF transmitter for geological fracture mapping 7-14386
well-log evaluation for carbonate reservoir in Kansas, microcomputer based program, WSULOG 7-40580
well-log information correction for computer processing and analysis 7-40579
Well-logs zoning and correl., computer techniques reviews 7-9195
Wiener filter of time-varying type 7-14388
X-ray radiometric logging (*Russian*) 7-34709
Fe ore deposits, magnetic field strength meas. equipment (*Russian*) 7-34699
Fe ore fields, inhomogeneously magnetised models selection optimisation 7-23526
⁴⁰K in Makhmur Plain soil, N. Iraq, α -ray spectroscopical analysis 7-34487
Mn nodules on seafloor, acoustic method for conc. determ. 7-34741
Mn prospecting method, borehole γ -ray logging-neutron activation technique 7-55284
Ni sulphides, electrochemical transfer characts. in Western Australia localities, nonlinear complex resist. anal. 7-47553
U prospecting, soil survey using Rn α -detection 7-55311

geophysical techniques

see also atmospheric techniques; hydrological techniques; oceanographic techniques

1D magnetic field data vertical gradients, approximation methods comparison 7-23861

1D time series anal. for sphere, appl. in geomag. and gravimetric geodesy 7-9239

aerial digital images enhancement, high altitude, histogram specification techniques 7-40608

aerial survey camera trials, for Wild RC10A and Zeiss RMK A 15/23 cameras 7-28817

aerial techniques for groundwater prospecting 7-34698

aerogeophysical prospecting, knowledge-based analysis system 7-29308

aeromagnetic surveying, variable-magnetisation terrain correction method 7-66325

aerospace imagery, appl. to prediction of presence of oil and gas 7-66335

agricultural remote sensing, database design (hardware and software) 7-60410

airborne geophysical data, statistical multivariate anal. 7-34715

airborne gravity gradiometer survey data analysis using isomorphous geodetic and electrical networks 7-47309

airborne reconnaissance, operational cartography appl. 7-23517

airborne remote sensing from remotely piloted aircraft 7-55289

apatite fission track plateau age dating, reproducibility of meas. 7-40597

apparent resistivity computation using exponential approx. of kernel functions 7-28822

automatic interpolation methods for mapping piezometric surfaces, appl. to groundwater reservoirs 7-40574

bathymetric mapping in USA economic zone, sonar digital swath method 7-66360

bathymetric surveying data acquisition and processing system (SDS III) 7-66361

biostratigraphic data collection and analysis, computer analysis and methods 7-40435

book, economics and applied geology 7-29609

borehole electroprospecting, influence of surface deposits on const. current field in anisotropic medium 7-28831

borehole EM induction logging, moving and stationary transmitter methods 7-4226

borehole NMR logging method, free fluid index for oil reservoir 7-29253

borehole water and gas sampling technique using polyamide tube 7-66310

borehole well logging by EM method, HFILIS method for producing oil wells 7-55279

boundary element method for 3D problems transient elastodynamic anal. 7-34694

Canadian petroleum exploration, appl. of remote sensing 7-40585

cartographic digital data utilization, electronic delivery for users of data 7-66306

cartography, quasi-ideal spatial filters for large maps 7-28808

chemical analysis of mineral grain surfaces, Auger spectroscopy method 7-60426

chemical techniques for use in New Zealand geothermal systems exploration and devel. 7-13848

coal mines, in-seam seismic exploration technique (Hungarian) 7-60416

coal seam exploration, seismic reflection profiling method using shear waves 7-14385

coal seams, tectonic disturbances and quality changes, geoelectric anal. method 7-34712

co-kriging: multivariable analysis in petroleum exploration 7-40578

computer mapping, minimal requirements for CAD 7-40402

continuation of geophysical fields meas. on a curvilinear surfaces, computation scheme 7-55302

contouring algorithm in FORTRAN 7-66312

controlled source audiofrequency MT soundings in Japan rel. to Schlumberger sounding (Japanese) 7-66318

crust EM sounding using field generated by ocean currents, feasibility study 7-9222

crust vertical motions, obs. via vertical gravity meas. 7-9225

crustal stress field determ. from earthquakes focal mechanism, appl. to S Great Basin of Nevada 7-54884

crystalline minerals, fracture characteristics using ^{222}Rn and ^{220}Rn as probes 7-23893

data acquisition system (digital) for solid Earth tide recording 7-29245

data analysis for continuous observations, problems of numerical realization 7-60397

dating method based on archaeomagnetism, applicability in Hungary 7-8803

dating of lava flows, by analysis of cosmogenic ^3He contents 7-60500

dating of rocks by La-Ce method, and ^{138}La beta-decay half-life 7-49312

dating of rocks by mica isotope method, the two $^{40}\text{Ar}/^{39}\text{Ar}$ age spectra shapes 7-23860

day length fluctuations error estimation method 7-14176

delayed neutron counting method for U/Th analysis and U isotope ratio determ. 7-3615

diffraction tomography, shallow appl. 7-9202

digital elevation models, performance evaluation of two bivariate processes using transfer functions 7-3971

digital filter technique, appl. to resist. logs (Chinese) 7-29261

dipole induction profiling above sphere buried in homogeneous half-space, anomaly evaluation 7-28827

disjunctive kriging, appl. to elec. cond. distrib. 7-23755

disjunctive kriging, estimation and conditional probability 7-23754

Earth (2,2) gravity coefficient time vars. detect. sensitivity of LAGEOS 7-34825

Earth core steady surficial motions determ. from geomag. field models, alternate method 7-66023

Earth gravitational potential expansion, convergence improvement methods 7-47742

Earth rotation parameters determ., appl. of lunar laser ranging data (Chinese) 7-3959

Earth rotation parameters determ. estimation of accuracy in different freq. bands 7-54843

Earth rotation parameters. determ. from six techniques, comparison (Chinese) 7-29247

Earth rotation parameters determ. methods, comparison (Chinese) 7-29246

Earth rotation parameters determ. optimal conditions (Chinese) 7-3960

Earth rotation parameters determination, atm. limitations on accuracy 7-60412

earthquake depth determination methods, review 7-54933

geophysical techniques continued

earthquake detection and recording by small seismograph networks, results from SNARE system 7-28873

earthquake hypocentre location errors appraisal, complete approach for single-event locations 7-54892

earthquake hypocentre location method, using nonlinear inversion scheme 7-23859

earthquake location and analysis methods, review 7-54932

earthquake precursor detection methods used at Tokai, Japan (Japanese) 7-8834

earthquake prediction, appl. of Bayes theorem to strong earthquakes in Mexico City 7-14210

earthquake prediction, model of EM emission during seismic activity 7-8856

earthquake prediction research in Japan, results (1978 to 1986) 7-4000

earthquake record in lake sediments 7-3993

earthquake rupture process determ., by waveform inversion method 7-65955

earthquake source parameters estimation by waveform data inversion, appl. to global seismicity (1981-3) 7-54882

earthquake sources, dynamic rupture process, numerical methods for simulation (Chinese) 7-54876

earthquakes, Fourier analysis for computation of focal mechanisms 7-18131

eigenvalues, efficient computation 7-18323

elastic waves computation, fourth-order accurate finite-difference scheme 7-3991

electrical exploration by resistivity method, numerical soln. for two-dimensional problem 7-8810

electrical prospecting, potential field of stationary elec. current, Fredholm's integral eqns. calc. 7-14181

electrical prospecting, potential soln. for nonuniform thin vein with transverse conductance variability 7-28830

electrical prospecting direct problem, numerical soln. method 7-29267

electrical resistivity method for exploration of thin slab struct. 7-29310

electrical sounding, air-subsoil coupling effects in field diffusion in three-dimensional conductor (French) 7-28843

electrical sounding, HF variable-voltage-fed inductor 7-23879

electrical sounding, relations between elec. parameters of rocks and chemical comp. 7-18181

electrical sounding, uniqueness of determ. of 3D underground structs. from surface meas. 7-8809

EM modelling program for 2D structures 7-34714

EM prospecting method, finite element modelling (Japanese) 7-55280

EM prospecting of quasipolar conducting layers, approx., boundary conditions 7-55304

EM prospecting theory, optimized digital filter for the Fourier transform 7-14387

EM response of buried thin sheets in uniformly conducting half-space 7-66326

EM sounding of an electrochemically active half-space 7-23853

EM subsurface radar using transient field radiated by wire antenna 7-23866

environmental change, remote detect., data struct. appls. 7-4240

environmental standard reference materials, determ. of sampling constants 7-34748

environmental standard reference materials, instrumental neutron activation anal. results 7-34747

environmental standard reference materials, role of neutron activation anal. in certification 7-34746

ERASME airborne side-looking C-band radar, data processing and calibration 7-9205

erosion by wind, satellite remote sensing of dust storms for erosion vulnerable areas 7-8949

erosion rate measurement for lava flows, by cosmogenic ^3He content analysis 7-60500

extended marine arrays versus simulated extended arrays 7-47365

fault imaging from space for civil engineering purposes 7-60406

fault rupture determ. method, by principal parameter analysis of after-shocks 7-8828

FEM for thermo-mech. evolution of Atlantic-type continental margins 7-54950

finite difference eigenvalues, asymptotic correction 7-18324

finite element methods for 2D structures resist. modelling (Chinese) 7-55270

fission track dating, grain allocation in population method 7-47568

fission track dating of annealed minerals and non-unique populations, clustering technique 7-47572

fluid-geochemical methods, use for seismic and tectonic activity anal. 7-40421

Flysch della Laga formation, Italy, fission track dating 7-40598

focal mechanisms use for stress determination 7-66072

forestry, vegetation biomass determ. by microwave transmission method 7-23876

forestry and range applications of high altitude reconnaissance technology 7-23905

Fourier-based textural feature extraction procedure for remote sensing 7-9207

fractal analysis applied to characteristic segments of the San Andreas fault 7-66348

frequency response functions gain and phase, estimation of confidence intervals 7-23857

gas reservoirs seismic response 7-9194

generalisation, cartographic, data types 7-47323

generalisation from large to medium and small scale Ordnance Survey maps using expert systems techniques 7-47324

geodetic 3D network establishment using GPS and MACROMETER II 7-34371

geodetic 3D network layout using GPS-TI4100 receivers (German) 7-40614

geodetic anomaly inertial surveying method 7-4196

geodetic baseline determination by VLBI, influence of air pressure 7-4213

geodetic deformation and surface movements data analysis by statistical methods 7-28803

geodetic gravity anomaly interpretation using deterministic approach 7-28811

geodetic gravity surveying using inertial navigation 7-4194

geodetic horizontal pendulums of capacitive type, laboratory test method 7-29250

geophysical techniques continued

- geodetic network establishment using GPS satellite system (*German*) 7-18108
- geodetic radio interferometric surveying for sea-level monitoring 7-18312
- geodetic satellite for laser ranging (STARLETTE), ground station coords. and baselines 7-65913
- geodetic VLBI method, variance and covariance matrix theory 7-40392
- geoid determ. methods 7-55331
- geological fault trace by α -particle track etch method, Pleistocene gravel bed surface (*Japanese*) 7-34688
- geological remote sensing, rocky surface mineralogy by optical and IR reflectance spectroscopy 7-29291
- geological remote sensing method using multispectral images 7-66029
- geomagnetic activity prediction, appl. of characteristic parameters of solar 11-year cycle 7-18114
- geomagnetic anomaly interpretation using generalised inverse matrix theory (*Chinese*) 7-3974
- geomagnetic depth sounding method, use of line current analogues 7-34719
- geomagnetic field modelling, appl. of alternate forms of assoc. Legendre functions 7-14186
- geomagnetic main field anal. at core-mantle boundary, spherical harmonics compared with harmonic splines 7-65935
- geomagnetic transfer functions robust estimation analysis 7-18313
- geomagnetic variation in Pleistocene times, loess-palaeomagnetism method 7-8816
- geometrical levelling automation, appl. of digital linear measuring system (*German*) 7-3972
- geopotential field computation method, for 3D density and magnetization distrib. (*Chinese*) 7-3964
- geosound signal detection, appl. of adaptive dig. filtering (*Chinese*) 7-20508
- geothermometer using plagioclase-muscovite Na-K exchange reaction 7-34475
- glacier velocity determ. in Antarctica using satellite images 7-66190
- glassy submarine basalts dating and He isotope disequilibrium 7-66352
- global satellite laser ranging use for tectonic deform. anal. 7-55287
- GLORIA, long-range sidescan sonar for deep ocean mapping 7-47583
- GPS baseline determ., bias fixing and water vapour radiometer corrections 7-9228
- GPS radionavigation, 1 to 2 parts per 10^7 geodetic accuracy 7-34686
- GPS radionavigation, data processing algorithms 7-34685
- GPS radionavigation satellite, orbit determ. by regional network double difference carrier phase obs. 7-34684
- graphic correlation of deep-sea sediments isotope stratigraphy, appl. to Late Quaternary 7-23894
- gravimetric observation processing, one-stage net drift effects 7-40611
- gravity anomalies interpretation, theory for trapezoidal model with quadratic density function 7-28819
- gravity anomaly, nonlinear data inversion using Schmidt-Lichtenstein approach 7-65920
- gravity anomaly prospecting, stable difference methods for continuation 7-55303
- gravity field mapping, relative motion of geodynamic twin satellite 7-4285
- gravity measurement, reduction of free-fall accel. values 7-29278
- gravity models testing, freq. windows and resonant solns. 7-3966
- ground cover thematic classification map, use of multitemporal data 7-8951
- ground stress measurement by borehole deform. meas. using pre-pressed multi-probe unit (*Chinese*) 7-29259
- heat flow determ. for lake sediments, influence of different sediment layer props. 7-65993
- heat flow estimation at lower boundary of Earth's crust, methods for 2D geothermal models 7-18155
- historical levelling surveys, atm. refr. error 7-8790
- Holocene tephras identification using magnetite comp., appl. of discriminant function anal. 7-8893
- hybrid boundary element-finite element analysis procedure for fluid flow simulation in fractured rock masses 7-34478
- hydrocarbon deposit exploration and exploitation the stratigraphic approach 7-18311
- hydrogeological map production using remote sensing, methodological problems 7-55295
- hydrographic survey information processing system 7-47421
- ice remote sensing, model for calc. of thermal emission 7-60264
- igneous geobarometry, appl. of Al content of hornblende 7-55029
- image correction for radiometric effects in remote sensing 7-55290
- imagery from satellite, video technology appls. (*Japanese*) 7-66349
- Indian upper mantle rocks, pressure-temp. studies for Gruneisen coeff. and specific heat 7-55267
- induced polarisation logging in borehole, theory 7-23864
- induced polarisation method for exploration of thin slab struct. 7-29310
- induced polarisation method for study of buried 3D body in a two-layered Earth 7-55286
- induced polarisation surveys, EM coupling removal 7-9190
- induction method for stratum axial symmetry determ. (*Russian*) 7-34705
- inertial navigation for geodetic surveying, Ferranti, Huxwell and Litton systems 7-4197
- inertial positioning problem in Hamiltonian mechanics 7-4195
- inertial surveying missions over short distances, methods for high accuracy 7-4198
- inverse logarithmic potential problem, uniqueness of solns. 7-29280
- inverse problems for Earth structure investigation, new approaches (*Chinese*) 7-4190
- inverse scattering for a variable background, geophysical problems, seismology appl. 7-34721
- inversion methods for elastic media, state-space approach 7-47554
- inversion technique for aeromagnetic anomalies inversion to mag. suscept. 7-23535
- ion microprobe and SIMS methods for chemical analysis of rocks 7-60427
- IR imaging of hillside at range of 300 metres, radiance statistics versus ground resolution 7-4035
- isotopic data multidimensional treatment method 7-66315
- iterative geophysical tomography 7-40612
- komatiites alteration analysis, role of spurious correl. in development of alteration model 7-55039
- LAGEOS satellite Earth rotation parameters meas. anal. 7-40398
- land surface, remote sensing techniques and methodologies 7-8947

geophysical techniques continued

- land surface radar remote sensing; FINRACS file of radar cross-sections 7-23877
- land-cover mapping from synthetic aperture radar obs., importance of radiometric correction 7-4200
- Landsat and digital elevation data use for soil surveys 7-4233
- Landsat data, Fourier filtering for information extraction in surveying and mapping 7-47582
- Landsat data applications, data base approach 7-4223
- Landsat MSS remote sensing, principal component analysis theory 7-47564
- lattice filtering applications to earthquake observation 7-9248
- least-squares smooth fitting for irregularly spaced data: finite-element approach using the cubic B-spline basis 7-47555
- levelling surveys, refr. determ. 7-8791
- lineament analysis, comparative study 7-55292
- linear inversion in potential theory; implications of bodies of zero external gravit. pot. 7-8789
- low-level counting techniques 7-29296
- magnetic anomaly over structurally complex bodies, use of subtended solid angle, DEC BASIC-PLUS-2 program 7-9192
- magnetic crust, bottom depth estimation method 7-47575
- magnetic field meas. from stratospheric balloons 7-47574
- magnetometer based on ring laser sensor, for weak fields (*Chinese*) 7-4189
- magnetometric mise-a-la-masse method (*Japanese*) 7-23856
- magnetotelluric data inversion using localised cond. constraints 7-28823
- magnetotelluric frequency sounding, use for deep seated anisotropic oblique zones assoc. multiple elec. discontinuities mapping 7-47573
- magnetotelluric inverse problem in one-dimension, discrete freq. inequality theory 7-3976
- magnetotelluric method for 2D structures, resolving power (*Japanese*) 7-66317
- magnetotelluric sounding at sea, methods of elec. field meas. in medium with extraneous fields 7-47444
- magnetotelluric sounding for archipelago area, laboratory model expts. 7-60157
- magnetotelluric sounding in 2-D, stable finite element soln. 7-47328
- magnetotelluric sounding method for hilly terrain, E-polarization case 7-29252
- magnetotelluric sounding method in hilly terrain, using H-polarization 7-29251
- magnetotelluric sounding method using H polarization, physical modeling 7-29255
- magnetotelluric sounding of 2-layered 3D structs., approx. soln. 7-29254
- magnetotelluric sounding of Earth struct., Rayleigh-fast fourier transform method 7-9181
- magnetovariation sounding curve determ. using continuum spectrum method 7-40569
- mantle heat flow anomaly determ., inverse problem for spatial struct. 7-28953
- map production using Thematic Mapper 7-28816
- marine electrical prospecting with pulsed signal, synchronous noise (*Russian*) 7-34701
- marine sedimentology, bulk physical props. estimation at depth from seafloor geophysical meas. 7-55009
- marine seismology, location methods for underwater shots in Gulf of Genoa 7-14217
- maximum entropy spectral analysis, effects of linear trend and mean value 7-29305
- median filtering of seismic data, response in high-freq. range 7-66357
- meteorological data, statistical interpolation by means of successive corrections 7-47519
- micropulsations in magnetosphere, magnetogram deconvolution method for Pi 2 pulsations 7-4271
- microwave sensors, satellite borne, Earth Observation appls. (*German*) 7-40616
- mineral cooling ages determ. method 7-12167
- minerals gas emission causing bubbles in overlying ice, use in prospecting 7-23709
- MINI-MOSES magnetometric resist. method for deep-sea floor polymetallic sulphide exploration 7-23863
- mise-a-la-masse anomalies near vertical contact, behaviour 7-9189
- MM-wave radiometer system for remote sensing appls. 3 mm operation, aircraft/helicopter installation 7-23880
- Mohr diagram and 3D strain 7-40594
- moraine ridges dating, appl. of ^{14}C dating to historical glacier advance of Nigardsbreen, SW Norway 7-9037
- multispectral imagery dimension reduction and interpretable, Chebyshev polynomials 7-4236
- W Nansen Basin, Arctic Ocean, water masses and chemical constituents 7-29065
- natural gas hydrate deposits prospecting, acoustic and resistivity meas. on rock samples containing tetrahydrofuran hydrates 7-55026
- nautical charting system II for National Ocean Service 7-47423
- Near-Caspian Depression, USSR, oil reservoir below salt beds, detection method using remote sensing 7-55294
- neutrino beam interaction with stressed medium, acoustic response anal. 7-14397
- neutrino oscillations, geophysical investigations 7-5033
- neutron activation analysis for mineral assay, low neutron flux technique 7-54212
- neutron activation analysis method, calc. for case when sample contains strong absorbers 7-23851
- neutron activation analysis of Hawaiian volcanic samples 7-34745
- nonlinear complex resistivity use for Ni sulphides electrochemical transfer characts. determ. 7-47553
- North azimuth determination using suspended gyrocompasses 7-66309
- nuclear explosions monitoring, seismic discrimination capabilities anal. using regional data from W United States events 7-3989
- numerical approximation methods for vertical mixing determ. in lake and sea sediment cores 7-66183
- numerical optimisation, appl. to interpretation of gravity and mag. anomalies 7-29279
- oil and gas seismic prospecting, computer algorithm for synthetic seismograms 7-60395
- oil exploration, induced polarisation method (*Chinese*) 7-55269
- optical remote sensing from space, conf., Cannes, France (Nov. 1985) 7-35094
- ore deposit EM prospecting method metallogenesis rel. to tectonic lineaments 7-29256

geophysical techniques continued

- palaeomagnetic data analysis, appl. to tectonic rot. of Colorado Plateau 7-14251
 palaeomagnetic direction determination for multicomponent system 7-8806
 palaeomagnetic field statistical estimation 7-54866
 palaeomagnetism, methods for correcting tectonic deformation effects 7-23636
 Palaeozoic continental reconstruction, appl. of cladistic methods 7-4019
 passive microwave remote sensing, scatt. from layered medium connected with rough interfaces 7-20109
 peat dating by U-Th disequilibrium, geochem. aspects 7-60392
 peat water-content meter, IR, physical principles 7-55299
 permafrost mapping method for forest areas, Landsat Thematic Mapper method 7-29302
 petrographic parameters quantification, appl. of digital image processing (Spanish) 7-34740
 petroleum exploration, coconditional simulation appl. 7-40577
 petroleum exploration, computer appl. conf., Wichita, KS, USA (Oct., 1985) 7-35083
 petroleum exploration, geological and computer traps 7-40582
 petroleum resource appraisal program, FORTRAN listing 7-40576
 photogrammetry, close-range, parallel orientation of stereometric camera base to datum plane 7-3970
 photogrammetry, image displacement on film during exposure due to motion of camera platform 7-54847
 photogrammetry, non-metric cameras calibration via finite-element method 7-3969
 polar ice air bubbles for pollution monitoring and bubble age 7-4068
 precise relative geoid heights determ. from gravimetry 7-8795
 pressure of metamorphic events, granulite terrain geobarometry methods (French) 7-34689
 projective transformation of space imagery into mosaics and photomaps, minimisation of Earth curvature effect 7-65922
 prospecting, use of Wiener filter of time-varying type 7-14388
 prospecting by vertical electric sounding curves, data interpretation improvements 7-14389
 prospecting in areas of glaciated terrain, conference, Kuopio, Finland (September 1986) 7-18497
 prospecting theory, sampling and minimum phase from continuous and discrete point of view 7-14384
 radar imaging of Earth's surface, effect of meteorological conditions on satellite imagery 7-66217
 radar remote sensing of Earth surface, optimal Doppler centroid estimation 7-23650
 radar remote sensing of Earth surface by SAR method, compensation for antenna motion 7-23878
 radarclinometry, mathematical theory and algorithm 7-34372
 radiation logging curves, recording scale automatic displacement (Russian) 7-34710
 radioactive waste repository barrier efficiency and stability of host rock, geological anal. 7-49709
 radioisotope XFA of copper content in Zongtiaoashan copper mine (Chinese) 7-8337
 radionavigation, optimum Doppler positioning using new data processing method 7-29249
 radionavigation for surveying for road engineering, using GPS satellite 7-34687
 radionuclides in marine sediments, alpha scintillation determ. method 7-4199
 rangefinding by optical method, precision, for long baseline meas., error of point approx. method for air integral refr. index 7-66342
 raster-formatted geodata, image processing techniques 7-66367
 ray tracing and seismic modeling 7-29313
 reflectance spectra of ore minerals, use of diagnostics 7-29264
 remote sensing, cartographic projection for reference TV mosaic data bank 7-55048
 remote sensing, colour enhancement of multispectral images 7-60424
 remote sensing, correl. of spectral radiance parameters measured from multiband space images 7-66339
 remote sensing, data classification improvement using additional variables and hierarchical struct. 7-4222
 remote sensing, development of MM-wave radiometer antenna reflector 7-23920
 remote sensing, different meanings and definitions of concept 7-29301
 remote sensing, digital processing of side-looking radar imagery from Cosmos-1500 satellite 7-66340
 remote sensing, errors arising due to imprecise knowledge of water permissibility 7-66331
 remote sensing, model taxonomy 7-14396
 remote sensing, multipurpose space experiment for land studies 7-66336
 remote sensing, multispectral scanner surveying, specular-spot and hotspot regions 7-60403
 remote sensing, pattern recognition problem for imaging of land surface 7-66332
 remote sensing, radiometric correction method for MKF-6 camera remote sensing 7-60408
 remote sensing, space imaging by Spot (satellite probe for Earth observation) (French) 7-60505
 remote sensing, spatial diversity index mapping of classes in grid cell maps 7-4221
 remote sensing, surface properties influence on spectral relationships (narrow to broadband) for clear sky conditions 7-60257
 remote sensing, terrain illumination influence on imaging from space 7-60402
 remote sensing, vector soln. for mean EM fields in layer of random particles 7-14365
 remote sensing applications in Pakistan, current status and future programmes 7-4206
 remote sensing by commercial satellites 7-14398
 remote sensing by radar SAR method, stereo viewing of opposite-side image pairs 7-29300
 remote sensing for soil surveys, symposium, Wageningen, Netherlands (March 1985) (French/English) 7-18476
 remote sensing image sensors, conf., Stuttgart, Germany (Sept. 1986) 7-60886
 remote sensing imaging of land surface, effect of shadowing by topography and clouds 7-23883
 remote sensing method for geothermal anomalies and faults, by satellite photography 7-28920
 remote sensing methods for arid and semiarid regions 7-9186

geophysical techniques continued

- IR remote sensing of Earth surface, selection of spectral band optimal pairs 7-66330
 remote sensing of environment, 19th international conf., Ann Arbor, MI, USA (Oct 1985) 7-15
 remote sensing of land surface, automated thematic processing 7-55297
 remote sensing of land surface, cloud removal method and mosaicking 7-23882
 remote sensing of land surface, context classifier for pixel analysis of images 7-23873
 remote sensing of land surface, optical and IR radiometry responsivity normalization 7-60407
 remote sensing of land surface, use of ultralight aircraft 7-8952
 remote sensing of linear features on land surface, using visual model 7-60404
 remote sensing of outlines on land surface, interactive procedures for aerial images 7-60401
 remote sensing training system for digital image processing theory, using microcomputer 7-18542
 remote sensing using polar orbiting platform, conf., Avignon, France (June 1986) 7-48190
 remote sensing with LANDSAT MSS, sensor and data processing methods 7-55323
 remote sensing with SAR radar, data processing using NEDIPS computer 7-47579
 resistivity spectral transformation, dilution factor use (Chinese) 7-54855
 resolution enhancement of processed seismic data using prior weighting functions 7-26084
 rock deformation modelling, straining of cross-bed populations 7-4034
 rock fracture characts. determ. from light emission anal. (Chinese) 7-29000
 rock magnetite particle size measurement, by magnetic remanence method 7-23858
 rock microstructure, image analysis of particles, FORTRAN V program 7-66311
 rock porosity measurement technique 7-23846
 rock type recognition, computer-aided drainage network anal. form Landsat imagery 7-4238
 rocks, elastic wave velocity determ. methods (Japanese) 7-29312
 rocks strain analysis, use of Fry's method 7-40593
 rocks thermal conductivity meas., heat pulse line source method 7-40609
 rough surface autoradiography method, radwaste repository rock radionuclide distrib. appl. 7-54410
 sand dunes, thermoluminescence dating method used for Sri Lanka red-sand beds 7-23847
 sandstone cores, oil and water content meas. using microwave techniques 7-55288
 SAR data, spaceborne, registration to topographic maps 7-4237
 satellite laser ranging, chord and relative height estimation from single data passes (Chinese) 7-3961
 satellite laser ranging, observations smoothing via correction of orbital parameters and station coordinates 7-54844
 satellite remote sensing, Doppler props. of radars in circular orbits 7-4288
 satellite remote sensing, orbit selection to ensure round-the-clock coverage 7-55298
 satellite remote sensing, simultaneous Earth obs. from two satellites 7-4204
 scalar audiomagnetotellurics applied to base-metal exploration in Finland 7-29272
 Schlumberger geosounding, lateral effects reduction method 7-9193
 Schlumberger soundings, rel. to controlled source audiofrequency MT soundings in Japan (Japanese) 7-66318
 seafloor Fe-Mn nodules, acoustic method for conc. determ. 7-34741
 seafloor geoaoustic properties determ., appl. of three related reson. methods 7-66097
 sediment chemical analysis for Cd, Ag, Pd, Tl, atomic absorpt. method 7-40601
 sediment radiocarbon dating method, using accelerator mass spectroscopy 7-9240
 sediments of seafloor, NMR imaging, method for organic rich layers 7-9198
 seismic damage prediction and understanding appl. of OR techniques 7-60169
 seismic data anal., diffraction separation, Karhunen-Loeve, transform appl. 7-57618
 seismic data interpretation using a priori information 7-14383
 seismic data inversion technique 7-65949
 seismic data processing, appl. of homomorphic system concept (Rumanian) 7-9244
 seismic data processing and 4. appl. to investigations at site of Krivoi Rog superdeep hole 7-47343
 seismic data time-spectral analysis in structural formation anal. 7-23850
 seismic diffraction tomography and multisource holography applied to seismic imaging 7-66321
 seismic exploration, anal. of multidimensional seismic wave recording systems 7-47345
 seismic exploration, long streamer appls. 7-28910
 seismic exploration, new approach to study of crustal and upper mantle struct. 7-47342
 seismic exploration, outlook for development of methods and equipment 7-47341
 seismic exploration, post-stack depth migration in freq.-space domain 7-8836
 seismic exploration, three-component meas. via polarisation method 7-47344
 seismic exploration of coal mines, in seam reflection technique (Hungarian) 7-66351
 seismic explosive source for ocean floor seismic work 7-55309
 seismic geophone differencing to attenuate horizontally propagating noise 7-23862
 seismic ground motion measurement, index for effects of topography 7-14201
 seismic hazard calc. method 7-55301
 seismic hazard mapping using 4D Markov model of seismic regime 7-60183
 seismic holography, computer simulation 7-18124
 seismic inverse problem, definition of velocity change in wave eqn. soln. 7-14198

geophysical techniques continued

- seismic inversion algorithm, 2.5 D Born inversion with arbitrary reference 7-66322
- seismic method in search for oil and gas, development trends 7-4225
- seismic migration algorithm, for fast plane-wave and single-shot migration 7-34393
- seismic migration by diffraction stack method 7-14382
- seismic N^{th} root stacking, theory, appl. and examples 7-29273
- seismic nonlinear elastic inversion strategy for refl. data 7-29274
- seismic observation network in Japan, automatic event detection and location system 7-66359
- seismic P-wave modelling with cellular automata 7-66320
- seismic profiling, computer model for image ray tracing 7-3994
- seismic profiling, fast time-domain computation of 1D synthetic profiles 7-14204
- seismic profiling from drifting ship using light-weight streamer 7-34742
- vertical seismic profiling method, separation of upgoing and downgoing waves 7-55283
- seismic prospecting, common-midpoint stacked data, with automatic phase correction 7-66324
- seismic prospecting, medium response parameter optimal estimation 7-65978
- seismic prospecting with multispread 3D logging method (*Rumanian*) 7-9245
- seismic refl. profiling, 3D data inversion for velocity and depth depend. reflectivity 7-60174
- seismic reflection, appl. as high-resolution exploration tool within Zimbabwe underground mine 7-65950
- seismic reflection method for coal prospecting in China (*Japanese*) 7-23854
- seismic reflection profiling, 2D velocity inversion and synthetic seismograms 7-66323
- seismic reflection profiling, common depth point method for small velocity inhomogeneities 7-23852
- seismic reflection profiling, edge effects in cylindrical slant stacks 7-47350
- seismic reflection profiling, MIPEX data acquisition system using personal computer (*Japanese*) 7-55265
- seismic reflection profiling, reflection and transmission and generalized primary wave 7-23553
- seismic reflection profiling in deep water, suppression of peg legs and multiples 7-55281
- seismic reflection profiling method for very shallow struct. 7-23557
- seismic reflection profiling method using reverse-time migration 7-14203
- seismic reflection profiling of coal measures, use of discriminant analysis method 7-4211
- seismic reflection profiling of deep crust, using wide range of incidence angles 7-40418
- seismic reflection profiling using multiwave exploration methods in W Siberia 7-54899
- seismic reflection surveys for deep crust anal. 7-14394
- seismic reflection tomography inversion method 7-28911
- seismic reflection tomography method for subsurface velocity struct. 7-23555
- seismic refraction profiling, extension of linear regime of waveform inversion problem 7-40417
- seismic risk trend analysis, appl. of human-computer interaction method to real example (*Chinese*) 7-34385
- seismic signal analysis for seismometer arrays 7-66319
- seismic signal processing using L_1 deconvolution 7-34717
- seismic single-sweep recording, processing techniques and data improvement 7-23559
- seismic sounding, nonuniform waves propag. in space divided by thin fluid-filled fracture 7-28891
- seismic source inversion, effect of strong-motion array configuration 7-28853
- seismic source time functions determ., appl. of regularisation method to teleseismic body waves 7-8824
- seismic study of oceanic crust, seafloor theoretical seismograms for underwater explosions 7-23563
- seismic tomographic study of crust struct., algorithms and filter selection 7-23872
- seismic tomography appl. to thermal convection in Earth interior (*French*) 7-23618
- seismic tomography for 3D struct. and vel. determ. 7-29268
- seismic trace stacking, for estimation of acoustic impedance function (*Hungarian*) 7-18123
- seismic travel times estimation method 7-23895
- seismic velocity analysis by ray parameter method, for marine survey data (*Chinese*) 7-54931
- seismic velocity determ. in source region 7-8865
- seismic vibroseis records, deconvolution processing (*Rumanian*) 7-8862
- seismic water gun cavity collapse behaviour and far-field pattern 7-55282
- seismic wave-eqn. datuming for vel. replacement before stack, appl. to submarine canyons 7-29269
- seismic wavefield extrapolation by linearly transformed wave eqn. 7-28878
- seismogram synthesis for use in acoustic well-logging 7-47364
- seismograph operations and data availability in Canada, for 1984 AD (*French English*) 7-65959
- seismology, 3D vector-wave field imaging of seismic sources in anisotropic heterogeneous media 7-28872
- seismology, algorithm for determining pulse response of medium, z-transformation method 7-60396
- seismology, appl. of techniques for systematic errors determ. in magnitude estimates using Parkfield data 7-54891
- seismology, body wave amplitude fluctuations modelling via 3D slowness method 7-40426
- seismology, estimation of slowness-dependent source and receiver corrections for P-wave travel times 7-54893
- seismology, extremal inversion of travel-time residuals 7-28862
- seismology, inversion of seismic sections, by generalized linear inversion (*Hungarian*) 7-60186
- seismology, linear inversion of band-limited refl. seismograms 7-23583
- seismology, moving-window analyzer using maximum entropy analysis 7-55285
- seismology, order clustering methods for seismogenic process of strong earthquakes (*Chinese*) 7-34384
- seismology, resolution matrix calc. via tomographic inversion method 7-14212

geophysical techniques continued

- seismology, rupture length and propag. speed determ. from seismic and acoustic data 7-8855
- seismology, simultaneous estimation of hypocentres and velocity parameters for inclined-layer velocity model 7-14207
- seismology, simultaneous smoothing of phase and group vels. from multi-event surface wave data 7-28865
- seismology, singlet stripping and nonlinear parameter estimation rel. to Earth aspherical struct. 7-28892
- seismology, statistical anal. and mathematical models of induced seismicity 7-23576
- seismology, strong ground motion prediction in Puget Sound region rel. to 1965 Seattle earthquake 7-3980
- seismology, synthesis of near-field ground motion 7-54897
- seismology, tomographic source imaging of $M_L \sim 3$ earthquakes near Anza, S California 7-40431
- seismology iterative inversion for seismic velocity using waveform data 7-47346
- SEM and EPMA analysis appl. in experimental geology 7-34481
- shallow subsurface temperature surveys 7-60398
- ship-board echo location system accuracy and system for East-Scheldt storm barrier construction 7-47558
- simultaneous correlation analysis of gravity, magnetic and seismic data, appl. to deep crustal investigations 7-47552
- smoothing error dynamics in mapping problems 7-8788
- smoothing method for Earth tides obs. data (*Chinese*) 7-55271
- soil, dielectric profile retrieval, use of iterative optimisation 7-9204
- soil, gas composition analysis use for geochemical exploration for mineral resources 7-40590
- soil and gas chem. comp. used for Cu-Zn ore bodies prospecting 7-40591
- soil erosion planning, vectorization of Landsat TM land cover classification data 7-47443
- soil erosion planning in Dane County, Wisconsin 7-47442
- soil mapping, utility of Landsat imagery in data base for small-scale mapping 7-4205
- soil mechanics, evaluation of u-w and u- π finite element methods for dynamic response of saturated porous media 7-14262
- soil mechanics, higher order, mixed, and Hermitean finite element procedures for dynamic anal. of saturated porous media 7-14263
- soil motion reconstruction from seismograms 7-23546
- soil surveying, LANDSAT remote sensing method with machine data processing 7-23652
- soil testing, BASIC program 7-34735
- solid Earth tides, measurement with feedback gravity meter 7-40396
- sonic logging, 2D spectrum anal. 7-4203
- sonic logging, 2D spectrum anal. 7-55332
- space images interpretation, mesofractures anal. rel. to oil and gas exploration 7-66337
- spaceborne remote sensing systems (book) 7-41027
- spectrum analysis by narrow-band method 7-66356
- spent fuel repository, Sweden, site characterization techniques 7-49707
- sphene from Lower Seve Nappe, Sweden, fission track age temp. method 7-40600
- SPOT and Landsat imaging and equipment, conf., Innsbruck, Austria (April 1986) 7-55887
- static magnetic dipole, method for location and dipole moment components estimation 7-9203
- statistics for geographers and Earth scientists, book 7-35138
- step-wise remagnetisation method for palaeointensity var. 7-54865
- stereo-radargrammetry, implications of Gestalt formations for Venus Radar Mapper 7-9379
- strain measurement, prediction of thermoelastic strain in half-space covered by unconsolidated material 7-29001
- strainmeter and tiltmeter techniques and design, review 7-23906
- subduction zone mantle struct. by teleseismic imaging first-arrival time method 7-23566
- superposed epoch analysis method 7-34743
- surface albedo vars. meas. method using Meteosat images of Africa 7-55272
- surface borehole exploration with direct current for oil and gas deposits contouring 7-23849
- surveying, GPS navigation radio receiver sets, MINI-MAC system by Litton 7-34370
- tectonic lineament imaging and identification using remotely sensed data 7-66333
- telluric anomalies analysis in lower half-space, Fourier transforms method 7-28826
- telluric method, results for faulted structures 7-34713
- TEM response of 3D body in layered Earth 7-29271
- temperature of land surface, microwave remote sensing method 7-60411
- terrain data interactive image processing, digital SM-4 Omega system 7-66334
- TeV neutrino beams, physical bases and geophysical appls., review 7-40587
- thematic mapper data geodetic correction to cartographic standards 7-60425
- thematic mapping from Landsat and collaterall data, past experience and future potential 7-3967
- theoretical TEM response curves over thin dipping dyke in free space for separated inline loop config. 7-9197
- tiltmeter of water-tube half-filled type, instrumental noise (*Japanese*) 7-4231
- transient EM anomalies, inline and broadside, characts. 7-9191
- tsunami generation and propag. modelling, microcomputer code 7-8830
- tsunami warning, implications of T-wave duration rel. to earthquake magnitudes and seismic moment 7-14208
- two-wavelength IR-thermography, subresolution meas., accuracy 7-4239
- underground explosions-earthquakes discrimination using discriminant functions, examples for Eurasia and North America 7-28849
- underground structure probing using radar system 7-47580
- vertical crust motion meas. by mobile VLBI and GPS, effects of atm. water vapour 7-9226
- vertical seismic profiling 1D inverse problem, soln. 7-34390
- vertical seismic profiling data migration by ray eqn. extrapolation in 2D variable vel. media 7-8846
- vibroseis observations, amplitude-phase spatial analysis method 7-29266
- VLBI for vertical crust motion meas., effects of atm. water vapour 7-9227
- VLBI station location determination in terrestrial reference frame (*French*) 7-66314
- VLBI use for Earth rot. parameters determ. (*Chinese*) 7-29248

geophysical techniques continued

- VLBI use of Earth parameters determ. 7-55325
- VLF transmitter for geological fracture mapping 7-14386
- volcanic fumarole gas chemical analysis methods 7-4202
- volcanic lava flow type discrimination, SIR-B radar method 7-60231
- volcanic rock eruption age determ. method using ESR 7-66316
- well logging, nodal discrete ordinates methods 7-19328
- well logs use for subsurface geology colour images 7-40581
- well-log evaluation for carbonate reservoir in Kansas, microcomputer based program, WSULOG 7-40580
- well-log information correction for computer processing and analysis 7-40579
- Well-logs zoning and correl., computer techniques reviews 7-9195
- World projections for environment mapping, application 7-14399
- WSU-MAP: a microcomputer-based reconnaissance mapping system for Kansas subsurface data 7-40584
- X-ray radiometric logging (*Russian*) 7-34709
- $^{40}\text{Ar}/^{39}\text{Ar}$ dating of minerals, errors due to ^{39}Ar loss during neutron activation 7-60390
- Fe ore fields, inhomogeneously magnetised models selection optimisation 7-23526
- Fe oxides mineralogy determ. in sediments, appl. of Kubelka-Munk colour theory 7-66098
- K-Ar dating, appl. of Cassinog technique. to Late Pleistocene-Recent volcanics form S Italy 7-47393
- Mn prospecting method, borehole γ -ray logging—neutron activation technique 7-55284
- Pb-Pb isochron dating method for deeply weathered terrains geochronology 7-60391
- ^{210}Po -coated geological and synthetic samples, ESR dating 7-47569
- ^{220}Rn radioactivity from volcanic fumaroles, scintillation meas. technique 7-9199
- ^{238}U , ^{232}Th dating of corals over past 500 kyears 7-60394
- U and Th, concentrations in geological samples, plastic track detector study 7-40596
- U concentration meas. in soil and rocks by γ -ray spectrometry 7-54373
- U veins in biotite from Bancroft, Canada, fission track dating 7-40599
- $^{234}\text{U}/^{238}\text{U}$ activity ratios in geological materials, determ. by α spectrometry 7-60255

geophysics

see also *geophysical fluid dynamics*

- 17th Congress of Geological Survey of Finland, conf., Helsingfors, Finland (May 1986) 7-48179
- Annual Review of Earth and Planetary Sciences 7-9606
- Earth as a planet, conf., Orlando, FL, USA (October 1985) 7-41015
- low-level counting, conference, Bratislava, Czechoslovakia (Oct. 1985) 7-24272
- magma ascent by porous flow, role of magmons 7-8928
- magma ascent in deformable vent, vent response to magma reservoir press. 7-8929
- partial melting phenomena in Earth and planetary evolution, conference, Eugene, Oregon (September 1984) 7-4625
- partially molten systems, permeabilities and interfacial areas and curvatures 7-8926
- shock waves in condensed matter, conference, Spokane, WA, USA (July 1985) 7-18501
- static high pressure research, review 7-21350
- tidal energy dissipation, comparison between astronomical and geophysical estimates 7-14301
- W.H. Mathews Symposium, Vancouver, British Columbia (October 1984) 7-4620

geophysics computing

see also *computerised instrumentation*

- acid rain modelling, turbulent spiral boundary layer and thermal wind simulator 7-14370
- aerogeophysical prospecting, knowledge-based analysis system 7-29308
- aerometric database for field experiment, real-time display and development 7-54407
- AFMS-2, microcomputer-based automatic remote transmitting meteorological station (*German*) 7-4228
- agricultural remote sensing, database design (hardware and software) 7-60410
- air pollution, CPU-time reduction for IFDM computer model 7-54399
- air pollution, Monte Carlo simulation of plume dispersion in turbulence 7-54396
- air pollution, plume rise and dispersion, Salford software model 7-54398
- air pollution chemistry, computer simulation 7-54393
- air pollution in Kuwait, modelling of Shuaiba Industrial Area 7-54400
- air pollution modelling, num. method and computer simulation 7-54394
- air pollution monitoring using Commodore 64 home computers 7-54418
- air pollution screening model, development of MICROGAUSS-I 7-54401
- air quality simulation models, computerized system for evaluation 7-54409
- air quality simulations, nonGaussian climatological model 7-55243
- airborne microwave rain scatterometer/radiometer, DP software system (*Japanese*) 7-23908
- airborne microwave rain scatterometer/radiometer, hardware system development (*Japanese*) 7-23907
- airborne microwave rain scatterometer/radiometer system, microwave backscatter expt. of ocean surface (*Japanese*) 7-23910
- airborne microwave rain scatterometer/radiometer system, rain meas. and data anal. (*Japanese*) 7-23909
- APEX, aerogeophysical prospecting expert system (*Chinese*) 7-55268
- atmosphere sulphur deposition, spreadsheet-based model 7-54397
- atmospheric boundary layer parameterization, FORTRAN programs 7-55246
- atmospheric turbulence classification, computer program 7-55247
- automatic cloud classification 7-9214
- bathymetric surveying data acquisition and processing system (SDS III) 7-66361
- Beaufort wind scale—measured speed conversion, BASIC program 7-55235
- biostratigraphic data collection and analysis 7-40435
- Canadian petroleum exploration, appl. of remote sensing 7-40585
- cartographic digital data utilization, electronic delivery for users of data 7-66306
- cartography and photogrammetry, digital computerised line-matching problem 7-47315
- chemical speciation in water, computer program for equilib. calcs. 7-66178

geophysics computing continued

- CHEMSIMUL code appl. to groundwater radiolysis in HLW repository 7-49693
- clay constituents, apportionment into structural formula 7-65999
- climatological data banks, design and use for monthly data records 7-9178
- coastal flow, numerical modelling 7-55078
- coastal wave climate categorization, software packages 7-55254
- cokriging: multivariable analysis in petroleum exploration 7-40578
- computer graphics for water-quality investigations 7-9030
- computer mapping, minimal requirements for CAD 7-40402
- computer vision system for automatic seismic wave-field movement anal. 7-23902
- continuous Rn monitor for groundwater research, automated operation and characts. 7-40424
- contouring algorithm in FORTRAN 7-66312
- CRACUK model description, UK version CRAC2 weather model 7-29228
- data analysis for continuous observations, problems of numerical realization 7-60397
- digital elevation models 7-40403
- drainage network simulation 7-55088
- earthquake catalogue (worldwide), software for data bank 7-65975
- EM modelling program for 2D structures 7-34714
- environmental science appls., conf., Los Angeles, CA, USA (Nov. 1986) 7-48175
- ERS-1 satellite, Australian involvement 7-4294
- extraterrestrial solar radiation on inclined surfaces, FORTRAN program 7-55138
- flood control, drainage master plan 7-66188
- flood control, drainage master plan 7-66189
- flooding due to urbanization 7-54384
- Fourier-based textural feature extraction procedure for remote sensing 7-9207
- fractal dimensions of topographic surfaces, computation using C program 7-54845
- geographic database, Minute Man National Historical Park, map input software 7-47319
- geostatistical analysis of gas potential in Devonian shales of West Virginia 7-40586
- GLORIA, long-range sidescan sonar for deep ocean mapping 7-47583
- GPS radionavigation, data processing algorithms 7-34685
- groundwater contaminant transport, variable BEM soln. 7-55115
- groundwater flow, transport velocity representation, environmental appls. 7-55114
- groundwater systems management, coupling of finite element and optimisation methods 7-60278
- HS1 digital ocean bottom seismograph (*Chinese*) 7-29260
- hydrographic data, digital, requirements 7-47422
- hydrographic survey information processing system 7-47421
- ice floes, interacting around an obstacle, simulation methodology 7-55081
- igneous rocks, chemical analysis, CIPW norm calculations, FORTRAN listing 7-29263
- IR satellite image processing, kinetic temp. image modelling 7-23899
- lake pollution, computer assessment of eutrophication countermeasures 7-55112
- lakes and oceans, 1D models of thermal stratification 7-55076
- land surface radar remote sensing; FINRACS file of radar cross-sections 7-23877
- low-cost satellite image reception and analysis facility 7-66305
- magnetic anomaly over structurally complex bodies, use of subtended solid angle, DEC BASIC-PLUS-2 program 7-9192
- meteorological computer graphics, stereo display terminals for McIDAS system 7-60389
- meteorological station with automatic data transmission, software and test results (*German*) 7-55266
- meteorology, algorithms for checking weather data (*German*) 7-55330
- meteorology teaching with microcomputers, software packages review 7-60
- meteosat IR meas., surface and cloud-top temp. determ. atmospheric correction scheme 7-18310
- MEXAMS metal transport model 7-9043
- microcomputer-based solar and meteorological data acquisition and control system 7-4186
- mineral melt evolution simulation, Rayleigh fractionation 7-65998
- minicomputer appl. for radiocarbon anal. control and meas. 7-34682
- multispectral imagery dimension reduction and interpretable, Chebyshev polynomials 7-4236
- nautical charting system II for National Ocean Service 7-47423
- NOAA data processing system (*Japanese*) 7-4287
- NODC archives cataloguing on NASA Ocean Data System, results from drifting buoy data loading 7-66307
- ocean imagery, dual-freq. SAR, calibration 7-4244
- ocean tides, microcomputer tide prediction utility 7-66163
- ocean wave models 7-34503
- ocean wave modeling 7-34502
- oceanographic image anal. expert system, knowledge-based, features 7-23901
- oil fields, trend surface anal. 7-40583
- ore minerals, preliminary diagnostics, use of refl. spectra as part of automated system 7-29264
- P-T-X phase diagrams calc. using FORTRAN 77 programs PT-SYSTEM, TX-SYSTEM and PX-SYSTEM 7-38161
- petroleum exploration, coconditional simulation appl. 7-40577
- petroleum exploration, computer appl. conf., Wichita, KS, USA (Oct., 1985) 7-35083
- petroleum exploration, geological and computer traps 7-40582
- petroleum resource appraisal program, FORTRAN listing 7-40576
- photogrammetry, block adjustment with COBLO program for microcomputers 7-28818
- plane layered media, global matrix formulation of wave phenomena 7-61125
- polar coordinate transformation to new pole 7-54846
- Profs weather prediction network 7-47476
- pyroxene, structural formulae and end member calculation, APL program 7-66313
- radiative cooling in valleys and hollows 7-55134
- radionuclide spills and discharge plumes, Lake Ontario, microcomputer-based model 7-13942
- rainfall-runoff-percolation model using programmable spreadsheet 7-55116

geophysics computing continued

- raster-formatted geodata, image processing techniques 7-66367
- regional acid deposition calculations with the IBM PC Lotus 1-2-3 system 7-54408
- remote sensing archiving systems, ERS-1 Data Centre 7-40567
- remote sensing digital imaging processing theory, microcomputer training system 7-18542
- remote sensing of environment, 19th international conf., Ann Arbor, MI, USA (Oct 1985) 7-15
- remote sensing of land surface, context classifier for pixel analysis of images 7-23873
- remote sensing of power station thermal discharges 7-40503
- remote sensing with SAR radar, data processing using NEDIPS computer 7-47579
- research management and organisation, for geology 7-40480
- rock failure during uniaxial loading, 2D computer model 7-8922
- rock microstructure, image analysis of particles, FORTRAN V program 7-66311
- rock type recognition, computer-aided drainage network anal. form Landsat imagery 7-4238
- RPHIN—a FORTRAN 77 program for acquiring axial ratios, long axis orientations and centroid positions of elliptical strain markers 7-17581
- SACUDIDA program for seismic hazard calc. 7-55301
- SAR data, spaceborne, registration to topographic maps 7-4237
- SAR sea ice imagery, geophys. anal., computer-assisted techniques 7-4243
- satellite laser ranging, observations smoothing via correction of orbital parameters and station coordinates 7-54844
- satellite passive microwave ice map, near real-time data system 7-4242
- sea bed contour map construction from random data, iterative method 7-34725
- sea bed contour map construction from random data, spline method 7-34726
- sea bed contour map construction from random data, spline method 7-34728
- sea bed contour map construction from random data by interpolation 7-34727
- seismic data processing at University of Durham 7-65985
- seismic holography, computer simulation 7-18124
- seismic migration by diffraction stack method 7-14382
- seismic P-wave modelling with cellular automata 7-66320
- seismic profiling, computer model for image ray tracing 7-3994
- seismic reflection profiling, MIPEX data acquisition system using personal computer (*Japanese*) 7-55265
- seismic shallow layer reflecting survey system for Japan Geographical Survey Office (*Japanese*) 7-23855
- seismic signal image interpretation system, rule-based, features 7-23903
- seismic tomography for 3D struct. and vel. determ. 7-29268
- seismology, algorithm for determining pulse response of medium, z-transformation method 7-60396
- seismology, algorithm for synthetic seismograms for oil and gas prospecting 7-60395
- SEISOBS, modified version of SEIS83 for ocean bottom seismograms (*Japanese*) 7-65979
- sensitivity anal. using computer calculus, nucl. waste isolation appl. 7-30477
- shallow water eqns., two-stage FEM Fortran program, FEUDX 7-55080
- shipboard-three component magnetometer control 7-29276
- shore wave field, numerical modelling by boundary element method 7-55079
- side scan sonar records, use of image processing 7-66368
- simulation studies of tidal analysis using meteor echo returns 7-40623
- soil erosion planning, vectorization of Landsat TM land cover classification data 7-47443
- soil erosion planning in Dane County, Wisconsin 7-47442
- soil survey, use of Landsat and digital elevation data 7-4233
- soil surveying, LANDSAT remote sensing method with machine data processing 7-23652
- solid Earth tide recording, digital data acquisition system 7-29245
- spatial trend analysis of streamline glacial features 7-18216
- static magnetic dipole, method for location and dipole moment components estimation 7-9203
- stratigraphically constrained cluster analysis, FORTRAN 77 program 7-66114
- stream gauge data adjustment for urbanization effects 7-34567
- subsurface geology from well logs, color images, Kansas 7-40581
- terrain data interactive image processing, digital SM-4 Omega system 7-66334
- tidal model of Spencer Gulf 7-18207
- Topographic Air Pollution Analysis System 7-54395
- total magnetic field of two-dimensions, body of arbitrary shape, calc. program 7-34718
- tsunami generation and propag. modelling, microcomputer code 7-8830
- two expert systems used in weather forecasting 7-66284
- undersea features name file for personal computer, database description 7-65927
- VIDARS anal. station, photogrammetric tools for panoramic sector scan imagery 7-18901
- water level computation between high and low tides, FORTRAN program 7-55077
- water level measurement stations prototype network, test and evaluation software 7-66364
- water level measurement system, management information systems 7-66162
- water pollution, Seto Inland Sea hydraulic model, dye conc. pattern anal. 7-40058
- water quality model, parameter estimation using prototype expert system 7-55111
- water resource planning, geographic information systems for encoding soil information 7-47473
- water resources engineering, research projects, computer support 7-18215
- watershed acidification, computer simulation 7-14322
- well flow with CO₂ and NaCl present, numerical study 7-3624
- well-log evaluation for carbonate reservoir in Kansas, microcomputer based program, WSULOG 7-40580
- well-log information correction for computer processing and analysis 7-40579
- Well-logs zoning and correl., computer techniques reviews 7-9195
- WSU-MAP: a microcomputer-based reconnaissance mapping system for Kansas subsurface data 7-40584

geophysics computing continued

- CO, personal exposure monitor with automatic data-logging 7-3943
- SO₂ pollution forecasting around thermal power stations 7-55244
- geopotential see *geodesy*
- geothermal power
 - Beijing area, China, geothermal resource of hot water aquifer 7-3622
 - Calgary area, Canada, geothermal energy potential 7-28924
 - Dakongbeng geothermal area, SW China, hot spring activity 7-4064
 - demand-side planning, role of Earth-Coupled Heat Pump 7-8359
 - depletion of geothermal reservoir (vapour dominated reservoirs) 7-3623
 - geothermal energy resource utilization, hydraulic investigations 7-28387
 - hybrid staging of energy conversion processes 7-65405
 - hydrocarbon mixed working fluids for geothermal power plants, vaporisation and condensation 7-65408
 - New Zealand, geothermal systems exploration and devel., use of applied chem. 7-13848
 - Regina, Saskatchewan, Canada, geothermal reservoir numerical model 7-18156
 - subterranean thermal water resources (*Rumanian*) 7-9054
 - technology breakout in energy conversion, conf., San Diego, CA, USA (Aug. 1986) 7-60875
 - vertical ground coupled heat pump system design and performance 7-8431
 - well flow with CO₂ and NaCl present, numerical study 7-3624
 - B sources and distrib. in geothermal fluids 7-23121
- geothermal power stations
 - Brawley geothermal pilot plant programme 7-65406
 - Heber binary cycle plant in Southern California 7-8358
 - Mammoth geothermal power plant, operational characts. 7-65407
 - physics of geothermal boilers, installed power and development work (*Polish*) 7-23120
 - well flow with CO₂ and NaCl present, numerical study 7-3624
- germanate glasses
 - gamma-ray irradi., defect centres, ESR studies 7-6678
 - heavy metal oxide germanate glasses, absolute Raman intensities, global criteria. 7-59201
 - B₂O₃-GeO₂ glass, vibrational spectra of structural units 7-3034
 - BaGeO₃-Ga₂O₃-CaO-CaF glasses, IR transmission spectra, depend. on composition 7-3031
 - CdO-B₂O₃-GeO₂ network struct., coordination and bonding, comp. depend., NMR study 7-6535
 - (CdO)_x(B₂O₃)_{1-x}(GeO₂)₂ glasses, struct. and vibrational props.; IR spectra study 7-7694
 - GeO₂ glass, high resolution EXAFS and XANES studies 7-27817
 - GeO₂:F-GeO₂, doped cladding-pure core single-mode fibre, dispersion study 7-43382
 - GeO₂-Bi₂O₃-ZnO, coloration mechanism due to Bi₂O₃ and effects of ZnO addition 7-22291
 - GeO₂-PrCl₃ glasses, elec. props., effect of PrCl₃ content 7-21907
 - GeO₂-PrCl₃ glasses, optical props. rel. to comp. 7-13150
 - GeO₂-TeO₂-V₂O₅ system, phase diagram and equil., quasi-binary section investig. 7-21405
 - GeO₂-ZnO-Bi₂O₃ IR transmitting glasses 7-43276
 - Li₂O-TiO₂-GeO₂ glass form., phase equilibria (*Russian*) 7-21118
 - (Na,Rb)₂O-GeO₂ glasses, mixed alkali effect 7-12367
 - NaGe₂P₂O₁₂ glass-ceramic, synthesis, thermal expansion meas. 7-46406
 - Na₂O-Al₂O₃-GeO₂ glasses, ionic transport meas., packing density depend. 7-32710
 - Na₂O-GeO₂ glasses, ionic transport studies 7-6864
 - Na₂O-TiO₂-GeO₂ glasses, refractive index, density 7-59170
 - SiO₂-GeO₂ integrated optical waveguides, laser heating effect on opt. props. 7-50792
 - SiO₂-GeO₂, influence of impurities on loss increase, expt. study 7-43380
 - SiO₂-GeO₂ core optical fibres, fabrication by the sol-gel method 7-46404
 - SiO₂-GeO₂ optical fibre, drawing- and radiation-induced paramagnetic defects 7-11084
 - SiO₂-GeO₂ sol-gel glasses, paramagnetic states 7-13035
 - SiO₂-GeO₂:Ho very high-rejection optical fibre filters, design and characts. 7-15974
 - SiO₂-GeO₂-P₂O₅, doped silica glass, dopant effect on OH absorpt. 7-27715
 - TiO₂-GeO₂ glasses, crystallisation, ion coordination, X-ray diff., IR spectra 7-6523
- germanium
 - see also *nuclei with*
 - (111) surface structure, lattice gas model anal., DAS structure 7-2309
 - adsorbed on Si (111), X-ray standing wave studies 7-58629
 - adsorption on Si (111), $\sqrt{3} \times \sqrt{3}$ adatom models 7-7008
 - amorphous, molecular dynamics simulation, struct. of solid phases 7-32293
 - amorphous and partially crystallised, X-ray absorpt. investig. of struct. (*German*) 7-46241
 - amorphous films, dynamics of laser annealing by transient grating method 7-12122
 - amorphous films, laser induced image storage 7-11078
 - amorphous films, laser-induced phase transitions, time resolved TEM study 7-38056
 - amorphous films, struct. and crystn., EXAFS study 7-64005
 - amorphous layers on GaAs, solid phase epitaxial Growth during annealing 7-21777
 - anomalous muonium, vacancy-associated model 7-51758
 - anomalous photovoltage films X-ray irradiation effects studies 7-58834
 - atom, odd parity energy levels, precise spectroscopic assignments 7-846
 - atomic-scale surface modifications by scanning tunnelling microscope 7-58583
 - avalanche photomultiplication in the far infrared 7-45375
 - band gap determ. method 7-35155
 - bicrystal, grain boundary dislocations, struct., steps, HREM study 7-16488
 - bicrystal boundaries, transient spectra of dislocation levels 7-52497
 - carrier concentration, mag. gradient effect (*Russian*) 7-17040
 - carrier mobility meas., Haynes-Shockley expt. use for student laboratory 7-55933
 - cathode sputtering process statistical modelling, optical layer deposition 7-39375
 - channeling effects in radiative emission of electrons 7-2074
 - cleaved (111) surface, optical props. and atomic struct. 7-58595
 - cleaved surface in liquid He, photo-EMF production, quasi-2D carrier diffusion in surface cond. gradient 7-38636
 - clusters, TOF mass spectra 7-20084

germanium continued

coated circular metallic hollow waveguides for IR radiation, electrodeposition prep. (*Japanese*) 7-31463
 coincidence spectrometer with scintillation and planar detectors, time characts. 7-36438
 crystal, disordered surface layer, standing X-ray wave excited photoelectron emission, energy dispersion meas. 7-366
 crystal, exciton gas-electron-hole liq. interactions, phase diagram, nuclei drift effects 7-2488
 crystals, band structure, LMT0 calcs. 7-2477
 crystals, high temp. deform., fine slip band struct. (*Russian*) 7-44561
 crystals, surface phonon modes and reconstructions, Green's function method calcs. 7-2339
 crystals with equidistantly-curved reflecting surfaces, scatt. of plane X-ray with three wave diff. (*Russian*) 7-51560
 cubic crystals, electron struct., cluster approx., Xalpha calcs. 7-38445
 curved cryst X-ray optics, inelastic scatt. expts., X-ray spectrometer design parameters 7-16354
 Czochralski growth, cryst. wt. rel to melt temp. variation 7-7841
 defects produced by electron and X-ray irradiation, surface effects 7-6687
 deformed single cryst., AC conductivity at 4.2K 7-7245
 detector, solder natural radioactivity effects in low background expts. 7-62220
 dielectric response and electronic states 7-33320
 diode geometry effect on solar cell reverse recovery expts. 7-34038
 dislocation transmission through $\Sigma=9$ symm. tilt boundaries, synchrotron X-ray topography, HVEM obs. 7-63646
 dislocation transmission through $\Sigma=9$ symm. tilt boundaries, dynamic and crystallographic anal. 7-63647
 dissolution, in Bi-Te liquid, diffusion controlled 7-44820
 dopant profiles modification due to surface and interface modifications 7-58306
 drag thermolec. power, anisotropy parameter, carrier density depend. 7-38603
 droplets, undercooled, microstruct. 7-65013
 dynamical recovery of (III) oriented single crystals 7-13475
 electric avalanche breakdown, chaotic and hyperchaotic states 7-52630
 electron channelling 7-21305
 electron correlation, band gaps and quasiparticle energies 7-27278
 electron escape fns., determ. by methods of calibrated amorphous layers and total external reflection 7-39362
 electron irradi., annealing kinetics, impurity effects 7-16630
 electron irradi., hole effective mass parameters, cyclotron reson. 7-58730
 electron mean free path needed for excitation of volume and surface plasmons 7-21838
 electron-hole liq., ultrasonic attenuation calcs., intraband collision effects 7-12214
 electron-hole plasma transport 7-7272
 electronic struct. of incoherent grain boundary, recursion approach 7-64161
 energy gap, indirect meas. 7-7107
 epitaxial films, CVD growth on Ge substrates, surface morphology 7-53618
 epitaxial films, remote plasma-enhanced CVD 7-39395
 epitaxial growth on CaF_2/Si (111), film quality improvement by Ge predeposition 7-7070
 extrinsic, freq. locking, quasiperiodicity and chaos 7-2618
 extrinsic photoconductors, nonlinear dynamics and chaos 7-52685
 fast neutron scattering in Ge crystals (*Russian*) 7-1820
 film, polycryst., preferred orientation control by two-step growth method 7-21728
 film growth on (HgCd)Te substrates, surface preparation effects 7-45037
 films on amorphous substrates, prep. by surface-energy-driven grain growth 7-38385
 floating zone growth, lateral solute segregation rel. to gravity conditions 7-53576
 fourth-order thermal expansion coeff. fn. 7-44868
 free exciton diffusion and decay, lumin. 7-32918
 gamma-ray spectrometer, calibration using ^{152}Eu decay 7-42275
 Ge^{2+} impurity ion in alkali halide crystals, triplet excited relaxed states, ODMR study 7-2953
 grain boundary energies, computer calcs. 7-6639
 growth surface optical characts. oscills. during MBE, automatic reflection ellipsometry meas. 7-64715
 heavy holes, Landau level spectrum, optical gap form. 7-45191
 heteroepitaxy on CaF_2/Si (111) 7-22497
 heteroepitaxy on CaF_2/Si structures, planarised growth by electron beam exposure to predeposited layers 7-52855
 highly ionised atoms injected into PLT and TFTR discharges, spectra 7-19748
 holes optical effective mass, determ. by interf. method 7-17290
 hot hole FIR laser action investig. 7-57341
 hot-hole cyclotron resonance maser with negative effective hole masses 7-15838
 impurity doping by photonuclear reactions 7-16589
 ion beam deposition on (100) single cryst. substrate, interface, thin film and damage form. 7-17423
 ion cluster beam deposition substrates for MOCVD GaAs solar cells 7-23182
 ionisation-stimulated annealing of Frenkel pairs under electron or gamma irradiation 7-38061
 IR absorpt. coeff. meas. with compensating calorimeter 7-56270
 IR objective, use of proustite crystal in performance meas. 7-57511
 Kikuchi lines, contrast reversal near reflex points with same indices in crystals, with defects (*Russian*) 7-51582
 large crystal growth by Stepanov method 7-33543
 laser heated, time-dependent X-ray reflectivity 7-26796
 laser irradiated, electron-hole plasma dynamics investigated by time-resolved spectroscopy 7-13276
 laser irradiated, thermal excitation 7-38137
 lattice dynamics, real-space force consts., adiabatic bond-charge model 7-32589
 lattice dynamics and electron-phonon interactions, quasi-ion approach calcs. 7-58422
 Lege-type detector, time props. 7-62216
 lenses, diamond-machine for IR, quality and performance 7-25932
 light hole Landau level inversion, light amplification in crossed elec. and mag. fields 7-31293
 liquid, structural phase transitions, photoemission studies 7-1836

germanium continued

MBE growth on CaF_2/Si (111), structural and electrical characteristics 7-45051
 MBE on Si, role of surface reconstruction, LEED, Rutherford backscattering, channelling meas. 7-7034
 metastable phases, vibr. props. 7-2126
 microcrystals, amorphous-like Raman signals 7-53349
 microcrystals, gas-evaporated, thermal annealing, Raman and electron microscopic study 7-64635
 mixed group III and group V ion implantation 7-21243
 multibeam streaming of heavy holes 7-12728
 multipoint field photocathodes, fabrication and emission characteristics 7-13323
 muon channelling, evidence for ponium formation 7-51897
 n-type, many-valley semicond., surface photogalvanic effect calcs. 7-52679
 n-type, Nernst-Ettingshausen coeff. in the case of scatt. by impurities in quantising mag. fields 7-12745
 n-type, room temp. anomalous Hall effect 7-38595
 n-type and ultrapure samples, electron transport and press. coeffs. 7-2615
 nonequilibrium carrier recomb., electron-hole drops in strongly excited Ge 7-38461
 nonlinear I-V characts. and spontaneous current oscillations 7-52631
 nonlinear transport, morphogenetic reaction-diffusion model 7-27337
 nuclear radiation detector, spherical coaxial structure, elec. field distrib. 7-5562
 overlayers on Si (111) surfaces, angle-resolved photoelectron spectra 7-3150
 p-n junction solar cell radiation-induced defects obs. using DLTS 7-13875
 p-type, cubic crystals, magnetic field-induced circular photocurrent drag effect calcs. 7-58833
 p-type, Hall effect, mag. field and temp. depend., transport eqn. soln. 7-52651
 p-type, hot electron transport, perturbed acoustic phonon distrib. effects, Monte Carlo anal. 7-64254
 p-type, hot hole intersubband transitions, stimulated emission and gain, quantum oscills. 7-1052
 p-type, nonlinear light absorpt. coeff., IR intensity study 7-53258
 p-type, solid-state radiation source for submillimeter and far IR waves 7-37079
 p-type, spatial correlations of chaotic oscillations in post-breakdown regime 7-64255
 p-type, stimulated submillimetre emission props. 7-46074
 p-type, threshold switching and microwave-induced spontaneous emission in static magnetic field 7-52707
 p-type, undoped, electron irradiation, defect level annealing and DLTS 7-12660
 p-type far IR multiphoton absorption 7-27723
 partially excited electron hole plasmas thermodynamics 7-16962
 periodic surface microrelief, determ. optical constants of laser-irradiated material 7-63926
 photodiode, pyrometer for 60 to 1400°C range (*Rumanian*) 7-4856
 photodiodes, temperature and uniformity effects 7-61378
 photon drag effect in p-type Ge (*Chinese*) 7-33042
 point contacts, nonlinear elec. cond. effects due to electron-phonon interactions (*Russian*) 7-52628
 polycrystalline films, photoassisted CVD prep. 7-3200
 polycrystalline planar channelling radiation energy levels, variational calcs. 7-63696
 profiled crystals, growth by Stepanov's method, appl. for optical components 7-31409
 pulsed laser melting, time-resolved reflectivity meas. 7-2158
 pure and heavily doped, dielec. function, impurity conc. depend., spectroellipsometric meas. 7-2525
 quartz:Ge, luminescence 7-46152
 quenched, SA_2 acceptor, uniaxial stress effects, far IR optical study 7-64673
 rain erosion resistance improvement of a-C:H diamond-like coating on Ge 7-31435
 reflectivity meas. during pulsed laser irradiation 7-12132
 scattering inhomogeneities, two-wavelength probe meas. 7-46063
 semiconductor plasma, laser produced, ultrafast switching simulation 7-11020
 semiconductor surfaces, atomic, electronic and vibronic props. 7-2307
 shallow donor levels, valley-orbit splitting in mag. field, zero-radius central cell model calcs. 7-58763
 SHG, cryst. orientation depend. 7-50640
 single cryst., native oxide and nitride insulator layers, microstruct. and props. 7-12574
 single crystal, microstruct. of fragments (*Russian*) 7-38107
 single crystal, optical constants, surface polishing effects 7-59175
 single crystals, plasticity meas. near yield peak (*Russian*) 7-44664
 single-particle excitations, dynamic correl. corrections, local density theory 7-45115
 six-beam X-ray spherical wave diff., intensity distrib. 7-32198
 solar cell parameters, theoretical temp. depend. 7-23161
 solar cells for thermophotovoltaic appls. theoretical efficiency 7-59855
 spin-orbit splitting, determ. from ab initio pseudopotential 7-2547
 sputtered (100) textured film, TEM grain growth obs. 7-45040
 structural props., ab initio pseudopotential calcs. 7-44797
 substrate, (001) oriented, with GaAs epitaxial film, structural props. 7-58687
 substrate, resonance Raman scattering of Si film 7-64017
 substrate for MOCVD growth of AlGaAs and GaAs, tandem solar cell appl. 7-3671
 substrate for single-domain epitaxial growth of GaAs 7-22578
 superconductivity and electron-phonon interactions 7-12899
 surface, (100), substrate for ZnSe layers, MBE growth and photoluminesc. 7-7858
 surface, (111), pure and As doped, surface electronic struct., photoemission studies 7-2658
 surface, evanescent X-ray diffraction during total external reflection, struct. studies 7-26590
 surface, GeO stabilisation on laser irradi., X-ray photoelectron spectra anal. 7-46723
 surface, H_2S adsorption, orientation and temp. depend. 7-58634
 surface, NO scattering, energy distributions, state-resolved measurements 7-53477

germanium continued

- surface (001) (2×1), electronic struct., first principles self-consistent calc. 7-12778
- surface (011), field emission flicker noise and electron states 7-33533
- surface (100), H adsorption, high resolution energy loss spectra study 7-38331
- surface (110), electron states calc., tight-binding muffin-tin orbital Green's function method 7-52721
- surface (111), adsorbed Pb, atomic geometry, surface X-ray diffr. 7-52277
- surface (111), adsorbed Pb monolayers, photoelectron scatt., temp. depend. 7-13328
- surface (111), chemisorption of atomic H, nonempirical cluster-model study 7-38332
- surface (111), Sn adsorbate geometry determ., X-ray photoelectron diffr. study (*Japanese*) 7-11852
- surface (111), stability and struct. of 7×7 reconstruction 7-2310
- surface laser irradiation, ionic cluster desorption, time-of-flight meas. 7-12138
- surface phonon generation and picosecond light pulse detection 7-12456
- surface plasmons, electron energy loss peaks 7-7305
- surface potential, photomemory effects 7-12775
- surface state characts., surface struct. and low temp. annealing effects 7-45426
- surface structure, optical transitions 7-12439
- swirl defects formation 7-51753
- thermal donor states 7-7155
- thermal expansion of solids, three-terminal capacitance cell construction and calibration 7-29966
- thermally scattered X-rays, anomalous transmission obs. 7-51573
- thermodynamic interrelation between amorphous, diamond cubic and liquid states 7-12245
- thin film bolometer with fast response 7-56261
- third order elastic constants, US displacement interferometry 7-2087
- tilt boundary struct., computer modelling 7-16579
- tubular hole distrib. under streaming conditions, scatt. anisotropy effects calcs. 7-58802
- ultra-thin films, self-implantation, grain growth enhancement, TEM study 7-12173
- ultrafine particles, Raman and X-ray scatt. study 7-64627
- ultrasound, anharmonic props. under intense excitation 7-20488
- uniaxially stressed, internal strain parameters, surface effects 7-44980
- valence electron subsystem, local and exchange pot. approxs. calcs. 7-38477
- vibrational correlation functions 7-51966
- volume capture effect for relativistic electrons, computer simulation 7-12156
- X-ray interferometry image of deform. field around dislocation cluster (*Russian*) 7-51575
- X-ray phase determination using multiple-beam effects 7-32210
- X-ray resonators tuned to the spectral interval wavelength CoK_{α1} 7-24736
- Al-Ge-Si, heterojunction ohmic contacts 7-27432
- AlGaAs/GaAs/Ge multijunction solar cell, model for calc. of displacement damage by radiation 7-13878
- Au-Ge-GaAs, interfacial reactions, struct. after annealing 7-27154
- Au-Ge-Ni-GaAs, non-alloyed ohmic contact, solid phase epitaxy 7-27423
- Au-Ni-Au-Ge-Ni-GaAs, ohmic contacts, alloying, specific contact resistivity 7-27425
- Au-TiB₂-Au-Ge-Ni-GaAs, ohmic contacts, alloying, specific contact resistivity 7-27425
- Cr-Ge thin film interface, interdiffusion, reaction and intermixing, soft X-ray photoemission study 7-27028
- Fe-Ge (110) interface, electronic struct. calc., mag. effects 7-45496
- GaAs:Ge,Se, diffused contact regions, rapid thermal annealing 7-17103
- GaAs:Ge,Si, local modes, isotopic fine struct., IR spectra 7-38145
- GaAs-Ge crystal growth on Ta₂O₅-coated Si substrates, zone melting and MOCVD 7-53579
- GaAs-Ge-SiO₂, semiconductor MBE layers on Ge islands on insulator, photolum. study 7-33455
- GaSb:Ge single crystals, Czochralski growth, carrier conc. rel. to dopant conc. 7-22462
- Ge + He⁺, L shell X-ray prod. cross sections meas. first Born approx. and ECPSR theory anal. 7-36526
- Ge (111) and Ge (220), EXAFS surface structure studies at Daresbury SRS, in 60 to 11100 eV range 7-33486
- p-Ge, correlation between deep-level parameters and energy resolution in γ-detectors, trapped hole re-emission effects 7-15454
- Ge I, line profiles, Stark widths meas. 7-10489
- Ge I, mpnd and mspm³ configs., J=3⁰ energy level calcs. 7-36451
- p-Ge, spatio-temporal coherence and chaos, conf. Los Alamos, USA, Jan. 1986 7-48158
- Ge, vapour phase growth on Ge substrates, influence of p and n doping 7-3198
- Ge²⁺ in alkali halide crystals, polarised luminesc., model of impurity centre 7-27753
- Ge²⁺ microcluster, pulsed conc. spectra, bonding and growth kinetics 7-19740
- p-Ge:As, Hall effect and electrical conductivity, temp. corrections 7-38592
- Ge:As(Sb)(Te)(Bi), implanted, heavy ion damage, TEM, annealing studies 7-63676
- n-Ge:Au, electron heating, photocond., photo-Hall effect 7-12765
- p-Ge:B(Al)(Ga)(In), annealing kinetics of radiation defects, influence of impurity binding energy 7-39547
- Ge:CuH(D)₂, acceptor electronic state symm., isotope effects study 7-21863
- a-Ge:D,H, plasma deposited, deuteron magnetic resonance 7-27626
- Ge:Ga, impurity g-factor determ. piezo-Zeeman spectra obs. 7-16982
- p-Ge:Ga, resistivity at low temp. appl. to bolometers 7-41471
- Ge:Ga single crystals, tracer diffusion coeff. and isotope effect, SIMS meas. 7-27019
- Ge:Ga(Be)(Zn) extrinsic photoconductor material, cryst. growth and characterisation 7-64893
- a-Ge:H, B, P, As, dopant incorporation and doping efficiency 7-44587
- a-Ge:H, elec. props., effect of H plasma press. (*Korean*) 7-27332
- Ge:H, H composition at surfaces and interfaces 7-27083
- Ge:H(Be,Zn), shallow acceptor complexes 7-45219
- Ge:H films, post-deposition hydrogenated, electrical props. 7-32296
- a-Ge:H glow discharge deposited thin films, H content determ., spectroscopic ellipsometry study 7-38365
- germanium** continued
- a-Ge:H/Si:H superlattice struct., light absorption and photocond. studies 7-38715
- a-Ge:H/a-Si:H multilayer films, photoconductivity enhancement 7-27443
- Ge:H-Si:H amorphous superlattices, electrical transport 7-7336
- Ge:Na(K), impurity addition by electrolysis 7-44578
- Ge:Ni, inhomogeneously photoexcited, cond. random spontaneous oscills. 7-52675
- n-Ge:Ni, photocond., spontaneous oscills. in an electric field 7-52670
- Ge:O, γ-irrad., majority carrier mobility meas. 7-27334
- Ge:O, Li, IR absorption spectra and bands, Li-O complexes 7-33375
- Ge:O, thermal donor binding energies 7-16989
- Ge:P crystals, seeded growth in soft lined crucible, dopant distrib. 7-53559
- Ge:Sb, Cu, impurity photoconductivity, field and spectrum dependences, exclusion effect 7-38635
- n-Ge:Sb, electron heating, photocond., photo-Hall effect 7-12765
- Ge:Sb, mobility anisotropy coeff. determ. 7-12715
- Ge:Sb single cryst., extended defects, X-ray topography meas. 7-38020
- Ge:Sb(Al)(Ga)(In), heavily doped, charge carrier scatt., elec. cond., Hall effect meas. 7-7228
- Ge:Si, ion-implanted amorphous surface layers, EXAFS 7-27823
- Ge:Zn, electron-hole droplet transport, suppression by deep impurities 7-58746
- Ge:Zn, large electron-hole drop, Alfven wave dimensional reson., impurity scatt. effects 7-16950
- Ge:Zn, photolum. spectrum, effect of (001) uniaxial stress 7-33450
- Ge:Zn deep impurity, shallow positive acceptor, far IR photocond. meas. 7-7157
- a-Ge/au interfaces, atomic intermixing, asymmetries 7-21682
- Ge/GaAs heterojunction interfaces, cyclic behaviour of band discontinuities 7-7365
- Ge/GaAs multijunction monolithic cascade solar cells with patterned Ge tunnel junctions 7-13863
- a-Ge/Pb/a-Ge trilayers, melting transition of Pb 7-32884
- Ge/Si amorphous layered system, implanted ion depth distrib. 7-21250
- Ge/Si ion cluster beam deposition substrates for MOVCD GaAs solar cells 7-23182
- Ge-Al₂O₃:Cr, layer-substrate structs., ESR, line-shape, nondestructive contactless meas. of layer conductivity 7-38924
- Ge-AlPO₄ MIS structures, inversion layers obs. 7-45502
- Ge-CaF₂-Si, MBE of CaF₂ on Si and overgrowth with Ge, characts. 7-22495
- Ge-CaF₂-Si epitaxial structures, growth, structural and electrical props. 7-38356
- Ge-CaF₂-Si heteroepitaxial structures, MBE grown, twinning, topography, channelling, TEM, SEM 7-12566
- Ge-GaAs, epitaxial film on GaAs, extrinsic photoeffect obs. with X-ray diffraction apparatus 7-32221
- Ge-GaAs epitaxial interface, extended defects, geometrical character 7-6640
- Ge-GaAs heteroepitaxy on Si substrates, recrystallised Ge-on-insulator intermediate layers 7-52358
- Ge-GaAs heterostructures, lattice theory, phonon propagation 7-58602
- Ge-GeO₂, defect formation, during thermal oxidation 7-65237
- Ge-GeO₂, symmetry forbidden Raman scatt. from (100) oxidised surfaces 7-46002
- Ge-metal interfacial atomic struct. and cpd. form., FIM studies 7-32846
- Ge-Si interface, solid phase epitaxy, intermixing, EXAFS, AES, LEED obs. 7-63973
- Ge-Si multilayered structures, Bi ion implanted, projected range distrib., glancing angle RBS anal. 7-63689
- Ge-Si superlattices, structurally induced optical transitions, electroreflectance spectra 7-59184
- Ge-Sn heterostructure, MBE growth in ultra-high vac. system 7-2423
- Ge-Sn interface form., growth mode, AES, RBS studies 7-58666
- Ge+Ge⁴⁺, L-shell ionisation, X-ray yield, threshold behaviour 7-10734
- Ge_n⁻ semicond. cluster anions, photodetachment and photofragmentation 7-36837
- Ge_n³⁺ clusters, produced by liq. metal ion source, stability and struct. 7-31205
- Ge(Li) detector system, monoenergetic γ-ray spectrum modeling 7-30898
- InP:Ge, Fermi level, determ. from phase diagram data of InP-Ge system 7-21808
- InP:Ge,S, LEC-growth, dislocation-free 7-17409
- InSb:Ge, heterogeneity study 7-21476
- Pb-Ge multilayers, cumulative disorder and X-ray line broadening 7-32847
- Pb_{0.75}Sn_{0.25}Te:In, Ge(S)(Se), elec. resist., photocond., Hall effect meas. 7-17050
- Pd-Ge ohmic contacts to InGaAsP-InP, solid-phase epitaxial growth 7-2706
- Si surfaces, (7×7)-Ge and (5×5)-Ge superstructures, angle-resolved EELS studies 7-21583
- Si:Ge, Ge⁺ preamorphisation implants, effect on extended defect formation during subsequent solid phase epitaxy 7-16599
- Si:Ge,P(B), IR absorpt. band broadening 7-64669
- Si:Ge/Pt system, impurity migration during silicidic form. 7-6895
- Si:Ge⁺, ion implanted and annealed, crystalline to amorphous transformation, TEM study 7-32643
- a-Si:H,F/a-Si:H,F,Ge multiple junction solar cells on stainless steel substrates 7-13902
- Si:H,Ge alloy thin films, optical constants determ., device modelling appl. 7-7666
- a-Si:H,Ge single junction and tandem solar cells, thin film properties and corollary plasma diagnostics 7-13893
- Si/Ge amorphous multilayer films, interdiffusion, neutron scatt. meas. 7-32722
- Si-B⁺, Ge⁺, preamorphised shallow junctions, end-of-range and mask edge lateral damage 7-38071
- Si-Ge, epitaxial growth of Ge, study using an MBE system with automatic ellipsometer, nondestructive anal. 7-7058
- Si-Ge heterojunction, structural and electronic props. 7-21997
- a-Si-Ge multilayer films, interdiffusion, modulation wavelength depend. 7-27033
- a-Si-Ge multilayer interfaces, Raman scatt., X-ray diffr. characterisation 7-27167
- Si-Ge-Si epitaxial layer structs., particle channelling study, statistical equilib. 7-58386
- SiO₂:Ge, impurity charge trapping props., EPR spectra 7-27290
- SiO₂:Ge integrated optical waveguides, plasma CVD 7-27941

germanium continued

- SiO₂-GeO₂ core Al-coated fibre, high-temp. effects 7-11146
 TeO₂-Ge₂Sn films, optical props., thermal stability 7-39207
 V-Ge(111) interface, temp. depend. intermixing, core level photoemission study 7-21542

germanium alloys

see also Ge-Si alloys

- crystalline alloys with immiscible metallic particles, superconducting props. 7-2791
 ternary germanides, M-M'-Ge, (M=Ca,Sr,Sc,Y,La-Lu; M'=Co,Rh,Ir), structural and superconducting props. (French) 7-44491
 Ag-Ge, liq., activity coeffs. of O 7-3284
 Ag-Ge granulated films, Coulomb gap and hopping conduction 7-38774
 Ag-Ge liq. eutectic alloys, elec. resist. and struct., 600 to 900 K (German) 7-45334
 Ag-Ge liquid alloy, structural phase transitions, photoemission studies 7-1836
 Ag-Ge-Ga-Al FCC alloys, faulted structure, X-ray diffr. studies 7-58292
 Al-Ge, dilute alloys, quenched, formation and growth of vacancy type clusters, positron annihilation study 7-39294
 Al-Ge, low temp. diffusion and trapping of muons 7-45865
 Al-Ge, TEM anal. of Ge precip. morphology 7-46489
 Al-Ge (12 at.%), alloy ribbons, prep. by centrifuge melt spinning, effect of process variables on characts. 7-46366
 Al-Ge alloys, obs. of Ge pentagonally twinned precipitate needles 7-12297
 Al-Ge dilute alloys, divacancy effect, annihilation radiation Doppler broadening meas. 7-37982
 Al-Ge eutectic alloy interaction with SiC whisker reinforced Al matrix composites 7-46689
 Al-Ge mixture, H implanted, evidence for metal-insulator transition in Al 7-2483
 Al-Ge-X, amorphous ductile, with two separate phases, form. range and props. for X=Mn, Fe, Co or Ni 7-59493
 Al-Li-Ge, corrosion rel. to Ge content 7-39715
 Au-Ge/Ni/GaAs ohmic contacts, ion implantation and metallisation prep. 7-22014
 AuGe-GaAs and Ni-AuGe-GaAs interfaces, ion beam induced phenomena 7-12166
 AuGe-Nb-GaAs, ohmic superconducting contacts to GaAs 7-33088
 AuGe-Ni/n-GaAs, ohmic contact fabrication RBS anal. 7-32840
 AuGeNi-GaAs contacts, interface composition and barrier heights 7-58891
 AuNiGe-GaAs interfaces, struct. and elec. props. 7-22013
 AuNiGe-GaAs ohmic contacts, microstruct. anal. and contact resist. meas. 7-2393
 CO-Ge, disordered ϵ' martensite struct. (Russian) 7-58207
 Co-Ge, 1D disordered structural states, form., quenching, X-ray diffr. study 7-44784
 Co_{33.5}Fe₃Si_{7.5}Ge_{1.5}B_{2.5}, amorphous alloy, struct. changes after γ -irrad. (Russian) 7-58336
 Cr-Ge dilute alloys, elec. resist. temp. and press. depend. studies 7-32980
 Cr_{1-x}Mn_xGe, cryst. and amorphous, mag. characts., substitution effects 7-59009
 Cu-Ge, random alloys, residual electrical resistivity, first-principles calc. 7-2569
 Cu-Ge (15.0 wt.%), Fermi surface, 2D angular correlation of positron annihilation radiation 7-39243
 α -Cu-Ge alloys, determ. of quantum mechanical density matrix from angular correlation of positron annihilation data 7-39245
 Cu-Ge-Ga-Al FCC alloys, faulted structure, X-ray diffr. studies 7-58292
 Cu-Mn-Ge system, phase equilib. in Cu-rich alloys 7-3277
 CuGe random alloys, positron state, rel. to 2D ang. correlation 7-45230
 EuCu₂Si_{2-x}Cu_x, Eu valency 7-58787
 Fe-Ge amorphous and cryst. layers, short range order and valence bands 7-13266
 FeGe₂ single cryst., magnetisation, temp. depend. (Russian) 7-2891
 Fe₂Ge_{1-x} amorphous magnetic alloys, d-band occupancy, EELS study 7-64059
 Ge-Au, temp. and conc. depend. diamag. susceptibility 7-2811
 Ge-Ba, liq. alloys, enthalpy of form. 7-23050
 Ge-Pd, temp. and conc. depend. diamag. susceptibility 7-2811
 Ge-Sr, liq. alloys, enthalpy of form. 7-23050
 Ge-transition metal eutectic alloys, cryst. growth by directional crystallisation 7-64887
 GeMo-GaAs ohmic contact, fabrication and characts. study 7-45490
 In-Ge thin films, anomalous structures 7-21733
 La(Cr₂Mn_{1-x})₂Ge₂, layer struct. intermetallic cpd., mag. props. comp. depend. studies 7-7489
 La₁₁Ni₄Ge₆, cryst. struct., trigonal-prismatic coordination of atoms 7-21159
 Mn₁₁Ge₈, intermetallic compound, mag. props. 7-52985
 δ -Mn₂Ge₂, high temp. phase structs., electron microscopy obs. 7-26697
 δ -Mn_{5.11}Ge₂, cryst. struct. 7-58202
 Mo₂Ge, neutron irrad., NMR and mag. suscept. studies (Russian) 7-13051
 Nb-Al-Ge superconductors, pinning force, mech. meas. 7-64417
 Nb-Ge alloys, processed in inert gas in 100 m drop tube 7-7986
 Nb_{3+x}Ge_{1-x} and Nb₃Ge₂, superconducting alloys, thermoreflection spectra, electron struct. 7-33370
 Nb₃(Al-Ge), high T_c supercond., Raman spectra studies 7-7699
 Nb₃(Ge,Si), Al₅ phase, Si stabilisation, supercond. transition temp., sp. ht. meas. 7-45532
 Nb₃Ge Al₅ material, displacement correl. functions temp. depend. calcs. 7-51962
 Nb₃Ge films, obtained by joint evaporation technique, microstruct. (Russian) 7-59435
 Nb₃Ge, high supercond. transition temp., struct. instabilities and electronic props. 7-58943
 Nb₃Ge tape conductors, CVD deposited, compositional distrib. and superconducting props. 7-58936
 Nb₃Ge/Pb magnetron sputtered Josephson tunnel junction props., film deposition conditions dependence 7-58955
 Nd₂Co₂Ge₂, cryst. struct., X-ray diffr. studies 7-44450
 NdGe₃ Czochochalski single cryst. growth using tri-arc furnace 7-7836
 Ni-AuGe-GaAs, ohmic contacts, interface reactions, elec. behaviour 7-27031
 Ni-Ge amorphous and cryst. layers, short range order and valence bands 7-13266

germanium alloys continued

- Ni₃Ge, alloying addition lattice location, phenomenological description 7-32463
 NiGeAuAgAu alloyed ohmic contacts to AlInAs-GaInAs heterostruct., charact. 7-22016
 PbGeTe, thermal cond. minimum, thermoelectric appl. 7-38276
 Sb-Ge-Zn system, thermodynamic investig. (German) 7-53703
 a-(Si-Ge):H, prep. in rotary plasma isolated reactor and props. 7-7891
 Sn-Ge granulated films, Coulomb gap and hopping conduction 7-38774
 Tb₂Co₂Ge₄, crystal struct. determ. 7-16495
 TbGe₂Si₂, first-order mag. phase transition, neutron diffr., mag. struct. study 7-45673
 Te-Ge thin films, laser irrad. effects, refl. meas., optical data storage appl. 7-12144
 TiNi-Ge, premartensitic effects (Russian) 7-53692
 Ti₇₅Ni₂₀Ge₅ metallic glasses, corrosion rates in the H₂SO₄ and HCl solns. 7-28199
 Ti₂GeSe₃-Ti₂SnSe₃ systems, phase equilibria 7-6760
 Ti₂GeSe₄-Ti₂SnSe₄ systems, phase equilibria 7-6760
 V₃Ge solid solns. of Fe, Cr and Co, elec. resist. (Russian) 7-45273

germanium compounds

see also germanate glasses; germanium alloys

- chalcogenide-metal contacts, interdiffusion, struct., comp., electron irrad. effects 7-21686
 [Ag₂GeP₂]₂(Ge(Si))₆, bonding relationships and electronic struct. calcs. 7-16941
 As-Ge-Se-Te chalcogenide glass fibres for thermal IR transmission 7-37193
 AsGeSe, IR transmitting fibre optics, spectral props. 7-37179
 As₁₀Ge₂₂Se_{67.5} glass grating couplers, fabrication using electron beam induced Ag doping (Japanese) 7-62817
 As₂Ge₃₀-Se₅₀, amorphous struct. study, positron lifetime spectra meas. 7-37886
 As₄₀Ge₁₀Se₂₅S₂₅ glass grating couplers, fabrication using electron beam induced Ag doping (Japanese) 7-62817
 Bi-Ge-S chalcogenide glasses doping mechanism and structural effects, EXAFS study 7-1909
 CdGeAs₂, glassy, optoelectronic props., photoelectrochemical investigation 7-45382
 CdGeAs₂, n-channel inversion layers, oscillatory diffusivity-mobility ratio, quantising mag. field 7-45419
 CdGeAs₂, SHG of single and multilongit. mode CO₂ laser emissions 7-43211
 p-CdGeAs₂ semicond., hole mobility and scatt., temp. depend. study 7-52609
 CdGeAs₂, ternary chalcopyrite semiconductor, gate capacitance in n-channel inversion layers, quantising mag. field 7-2733
 CdGeAs₂/Ni amorphous films, elec. cond., low temp. impurity breakdown, high field effects 7-52625
 CdGeF₂, glassy, optoelectronic props., photoelectrochemical investigation 7-45382
 CeGe_{1-x}Si_x nearly ferromag. props., temp. and comp. depend. study 7-7493
 Cu-GeO₂, dispersion hardened polycryst., intermediate temp. embrittlement 7-53903
 Fe-Ge-Te, compound formation, microstructure, X-ray diffraction, dilatometry studies 7-7980
 (GaSb)_{1-x}(Ge₂)_x, metastable thin film alloys, struct. phase transitions, ion-channelling studies 7-58462
 Ge-As-S, glasses, elastic properties 7-21323
 Ge-As-Se chalcogenide glasses, structural models, medium range order and interference functions, first sharp diffr. peak calcs. 7-6540
 Ge-As-Se chalcogenide optical glass fibres, prep. and characterisation 7-37194
 Ge-As-Se-Te chalcogenide glass fibres for transmission in the 8 to 12 μ m range 7-37192
 Ge-GeO₂, defect formation, during thermal oxidation 7-65237
 Ge-S+bi chalcogenide glasses, struct., DTA and X-ray diffr. studies 7-6543
 Ge-Sb-S glasses, bulk and thin film samples, optical and photo-acoustic props. study 7-22211
 Ge-Sb-Se glasses, crystallisation ability, high energy electron irrad. effects (Russian) 7-32306
 Ge-Sb-Se IR chalcogenide tube waveguides 7-37195
 Ge-Sb-Te system, diffusion of Fe, Cr and Ni impurities 7-21527
 Ge-Se-Ag amorphous films, Ag doping profiles, ellipsometric studies 7-7779
 Ge-Se-As glasses, elastic constants, rigidity percolation 7-44648
 Ge-Te liq. eutectic alloys, elec. resist. and struct., 600 to 900 K (German) 7-45334
 Ge₃₀As₂₀Se₅₀, glassy semiconductor, structural models 7-44393
 Ge₁₀As₄₀Se₂₅S₂₅ and Ge_{22.5}As₁₀Se_{67.5} glass films, photodarkening effect, exposure characts. (Japanese) 7-64706
 GeBr₂, ground and triplet state, bond angle, density functional calc. 7-854
 GeCl₂, ground and triplet state, bond angle, density functional calc. 7-854
 GeCl₄ + X⁺(X=He,Ne,Ar,H), optical emission spectra rel. to PCVD 7-26531
 GeCl₄, effects on thermal oxidation of Si 7-65238
 GeCl₄, liq., stimulated Brillouin and thermal scatt. of Nd μ s pulses 7-62777
 GeCl₄, liq. struct., X-ray diffr. obs. (German) 7-58118
 GeCl₄, liq. struct., X-ray diffr. investig. (German) 7-58119
 GeCl₄, neutron diffr. intermol. scatt. functions and RISM partial scatt. functions 7-31145
 GeF₄ + X⁺(X=He,Ne,Ar,H), optical emission spectra rel. to PCVD 7-26531
 GeFe₂O₄, ⁵⁷Fe²⁺ Mossbauer quadrupole splitting and orbit-lattice interaction 7-12684
 α -GeH, electronic and transport props., coherent potential approx. 7-27241
 GeH₄, CO₂ laser irradiation, IT multiphoton absorpt. spectra 7-62474
 GeH₄, Rydberg transitions, fluoresc. and VUV absorpt. spectra 7-19880
 GeH₄, Jahn-Teller, struct. and energy distortions ab initio CI calcs., HF calcs. 7-15523
 GeH₄D(GeD₃H), bending mode triad, anal. model, IR spectra 7-19822
 GeH⁺(GeD⁺) in He afterglow, a- Π_{0+1} -X²⁺ visible band system 7-50152
 GeH₄(GeD₄), intermol. force const. and normal mode calcs. 7-56937

germanium compounds continued

- GeN₃:H, amorphous, reactively sputtered, optical and electronic props. 7-58830
- Ge₃N₄ native insulator layer on Ge single cryst., microstruct. and props. studies 7-12574
- GeO films, phase comp. and struct., substrate temp. effects 7-2219
- GeO-BaO thin films between metallic electrodes, elec. props. 7-22054
- GeO₂, dipole polarisabilities, cohesive energies and press. derivatives of bulk moduli 7-2967
- GeO₂ native insulator layer on Ge single cryst., microstruct. and props. studies 7-12574
- GeO₂ rutile crystals, electronic struct., scalar-relativistic muffin-tin-orbital calcs. 7-64077
- GeO₂:Cu thin films, optical absorpt. edge 7-53431
- GeO₂:F-GeO₂, doped cladding-pure core single-mode fibre, dispersion study 7-43382
- GeO₂-core/SiO₂-cladding optical fibres, modified CVD deposition and stimulated Raman appl. 7-43378
- GeO₂-P₂O₅-Nd₂O₃, phase equilibria, X-ray diff., thermal anal., fluoresc. spectra 7-6758
- GeO₂-SiO₂:N optical fibres, N-related absorpt. bands 7-59226
- Ge₂₈Sb₇₂ glasses, surface pot. relax., TSC meas. 7-64261
- GeS and GeSe, chalcogenide glasses for IR fibres, plasma deposition 7-37191
- GeS single cryst., absorpt. coeff. meas., optical energy gap determ., 2D and 3D model anal. 7-17289
- GeS₂ amorphous films, persistent photocurrent 7-45389
- GeS₂ glass, photostructural effects, EXAFS study 7-64758
- GeS₂, vaporisation, torsion and Knudsen effusion technique 7-2163
- GeS₂ amorphous system, struct. anal. by X-ray spectroscopy 7-26653
- Ge₂₀Sb₈₀Bi chalcogenide glasses, doping, coordination number and cond. transition, EXAFS study 7-64764
- a-Ge₃₀S₇₀ films, irreversible photobleaching 7-17353
- Ge₃₀S₇₀:Ag chalcogenide films, Ag photodoping, optical transmission spectra 7-59231
- Ge₃S₆₅ films, evaporated, structural changes on illumination and heat treatment (*Japanese*) 7-22489
- Ge₄₀S₆₀, amorphous film, photoinduced bleaching 7-13618
- Ge₃S_{1-x}, glass, dielectric meas. 7-13077
- GeS₂AgAu films prep. by simultaneous vacuum evaporation, Au effect on metal-photosurface deposition (*Japanese*) 7-3177
- Ge₂₀Sb₈₀Bi_x, amorphous, electronic cond. props. under high press. 7-45328
- Ge₂₅S₇₅(Se₇₅)(Te₇₅), amorphous, anomalous photoinduced transformations study 7-45070
- GeSe amorphous films, persistent photocurrent 7-45389
- GeSe, cryst. growth in Xe atmosphere, expts. performed on Spacelab D1 mission 7-21145
- GeSe₂ amorphous films, persistent photocurrent 7-45389
- GeSe₂ glass, photostructural effects, EXAFS study 7-64758
- GeSe₂ glasses, short and medium range order, Mossbauer studies 7-13069
- GeSe₂, vitreous and crystalline states, energy difference, bond energy, calorimetry study 7-59775
- a-Ge₂₀Se₈₀Bi films, n-type, electron transport props. studies 7-7422
- Ge₂₅Se₇₅ glass films, photodarkening effect, exposure characts. (*Japanese*) 7-64706
- Ge₃Se_{1-x}, glass, dielectric meas. 7-13077
- a-Ge₂₀Se₈₀Bi₁₀ thin film, photoconductivity 7-17052
- (GeSe₂)₇₀(GeTe)₁₅(Sb₂Te₃)₁₅, glass transition, thermodynamic and thermokinetic characts. 7-26953
- GeSeSb, IR transmitting fibre optics, spectral props. 7-37179
- Ge₄Se_{6-x}Te_x amorphous chalcogenide, elec. cond., prep. technique effects 7-7237
- Ge₄Se_{6-x}Te_x amorphous chalcogenide, elec. cond., bulk and thin film effects 7-7238
- Ge_{1-x}Si_xGaAs-Si, multispectral high efficiency solar cells, semicond. selection criterion 7-8399
- Ge_{1-x}Sn_x amorphous films, structural changes on annealing 7-16422
- Ge_{1-x}Sn_xSe₂ glasses, elec. cond. rel. to Mossbauer and Raman spectra 7-64250
- (Ge_{1-x}Sn_x)_{1-x}Se₂(S_x) glasses, percolation transition and strain accumulation 7-11939
- Ge_{0.08}Sn_{0.92}Te, acoustic mode vibr. anharmonicity 7-63751
- GeTe, α - γ phase transformation kinetics, effect of heat treatment 7-63795
- GeTe, dipole-dipole interactions and ferroelectric props. 7-39046
- GeTe, energy bands, relativistic empirical tight binding theory 7-45149
- GeTe, ferroelec. phase transition, electron-phonon interaction 7-13106
- GeTe, slight nonstoichiometry and high free carrier density, phase diagram study (*Russian*) 7-2191
- GeTe, solid and liquid states, electrophysical props. 7-52654
- GeTe, valence and energy spectrum, supercond. state 7-45534
- GeTe:Cd(In)(Sb), solution mechanism of impurities, effect of heat treatment 7-21455
- GeTe-GeSe₂, polythermal section of Ge-Te-Se, effects of deviations from stoichiometry 7-7977
- GeTe-PbSe, phase transformations, cation-anion substitution, electrophysical props. 7-7978
- a-GeTe amorphous films, struct. changes by annealing 7-63467
- a-Ge₂₀Te₈₀ films, crystallisation behaviour and local order 7-44386
- Ge₂₀Te₈₀ glasses, heat capacity, relax. and thermodynamic kinetics during annealing 7-44843
- Ge₅₀Te₅₀, Auger elemental depth profiling, preferential sputtering 7-54247
- GeX, X=S,Se,Te, thin film, electron irradi. effect 7-16636
- Ge_xX_{1-x} (X=S,Se), chalcogenide glasses, stochastic random network model 7-63493
- Li₂O-TiO₂-GeO₂, glass form., phase equilibria (*Russian*) 7-21118
- MgO-Al₂O₃-SiO₂-GeO₂ cordierite ceramics, sintering, microstruct., thermal props. 7-52088
- Ni-GeCl₄, binding energy rel. to Ni chem. state, XPS 7-17820
- Ni_{1-x}Ge_xFe₂O₄ spinel ferrite, AC susceptibility and Mossbauer studies 7-64441
- PbGeS₃, vibr. props., spectral study 7-3032
- Pb_{0.93}Ge_{0.07}Te, glassy and cryst., defect struct., positron annihilation studies 7-46221
- Sb-Ge-Se-Mn, effect of Mn impurity on comp. and physicochemical props. 7-11922
- Se_{100-x}Ge_x amorphous alloy, photodarkening, structure model anal. 7-3003

germanium compounds continued

- Si-Te-As-Ge chalcogenide glass film, electronic processes in strong elec. field 7-45524
- α -SiGeH, electronic and transport props., coherent potential approx. 7-27241
- SiO₂:GeO₂ integrated optical waveguides, laser heating effect on opt. props. 7-50792
- SiO₂:GeO₂ optical fibres reaction of diffused H₂ with defect centres 7-57591
- SiO₂-GeO₂ film, oxide flow during H₂ treatment, planarization technique 7-2426
- SiO₂-GeO₂ optical fibre surfaces, formation mechanism of H-associated defect centre 7-65158
- SiO₂-GeO₂ system, gels and gel-glasses, struct. study using vibr. spectroscopy 7-44381
- Sn-GeO₂ granular films, struct., resistivity and superconducting props. study 7-45082
- Te-Ge alloy glass, isothermal surface crystallisation 7-58576
- (Te₉₀Ge₅In₅)_{100-x}O, Auger elemental depth profiling, preferential sputtering 7-54247
- Tl-Ge-Se, bulk glass formation region, elec. and struct. characts. 7-58159
- Tl₂S(Se)-GeS(Se), polythermal sections, physicochemical anal. 7-7975
- Zn_{1-x}Ge_xFe₂O₄, ferrites, atomic, mag. and electronic disorder (*French*) 7-44477
- ZnGeP₂, single crystals, prep. and characterisation 7-2612
- ZrO₂-GeO₂-NaOH-H₂O system, hydrothermal crystn. investig. 7-2152

getters

see also vacuum techniques

- GaAs wafers, LEC-grown, semi-insulating, two-dimens. high-resolution EL2 topography 7-53381
- GaAs:B, ion implanted, struct. and damage distrib., TEM study 7-51893
- H₂ isotope sorption and recovery by nonevaporable getter with chem. compressor material 7-48760
- Si, CVD thin film backside gettering effectiveness 7-38217
- Si, Czochralski grown, interdependence of contamination and defect formation 7-32467
- Si gettering, review of phenomenology 7-38215
- Si, impurity gettering, defect-defect interaction mechanisms 7-16585
- Si, interstitial-based intrinsic gettering process appl. to multilevel defects struct. 7-38048
- Si, intrinsic gettering by butterfly-type defects 7-38047
- Si materials science and technology, conf., Boston, MA, USA (May 1986) 7-29598
- Si:Fe, intrinsic gettering, EPR and TEM study 7-38216
- Si:Fe:O, Fe intrinsic gettering, EPR studies 7-16553
- Si:O, O precipitation, numerical models 7-16775
- n⁺-Si:O, O precipitation and minority carrier generation lifetimes 7-16774
- Si:O, P, Sb wafers, O precipitation during simulated CMOS cycles 7-38218
- Si:O Czochralski crystals and melts, internal gettering, review 7-32341
- Si:O substrate materials, heavily doped, control of O and precipitation behaviour 7-32665
- Si:O(N), impurity-dislocation interactions, review 7-16610
- Si:transition metals, anomalous diffusion and gettering 7-2264
- Ti-Ta sublimation getter pumping system and performance, computer control at TMX-U 7-25184

GFRP see glass fibre reinforced plastics

giant pulsations (Earth) see micropulsations

giant resonances see nuclear collective states and giant resonances

giant stars

see also OH-IR stars; symbiotic stars

- AC 211, X-ray binary system in globular cluster M15, red giant or HB star model 7-14596
- AGB and post-AGB stars, heavy element synthesis 7-47856
- AGB and post-AGB stars of low mass, neutron synthesis 7-47855
- AGB stars in LMC globular clusters, luminosity function determ. 7-4561
- λ And, two-component coronal model for EXOSAT obs. 7-40800
- δ And (K3 III), IRAS source with unusual UV spectrum, IUE obs. 7-55623
- γ Aql, hybrid chromosphere star, wind characts. and line form. region characts. 7-55630
- FF Aqr, RS CVn star, G-type giant star surface and atm. struct., IUE obs. 7-55730
- α Ari, K-type giant star, spectral lines identifications and heliocentric radial vel. 7-14574
- UX Ari, RS CVn star, autumn 1981 photoelectric obs. of starspot activity 7-9513
- θ As, chromospheric variability of semi-regular M7 giant star 7-66616
- asymptotic giant branch (1.0-3.0 M_⊙), evol. depend. on mass on comp. 7-60650
- asymptotic giant branch stars, intermediate-mass, effects of connective overshooting on He and N abundances 7-40797
- asymptotic giant branch stars, mass loss determ. 7-24127
- binary systems with evolved primary components, relation to props. of main-sequence binaries 7-29505
- Bok globules, characts. determ. from background giants IR obs. 7-35027
- α Boo, ang. diameter and effective temp. meas. 7-14563
- α Boo, IUE high-dispersion echelle spectrograms of K1-giant 7-60656
- τ Cas, K-type giant, non-variability in light and vel. 7-9468
- α Cas, K-type giant star, spectral lines identifications and heliocentric radial vel. 7-14574
- 2 Cen M-type giant star, IUE spectral characts. 7-55674
- 5 Cen, ellipsoidal variable star, rot. vel. and mass ratio determ. 7-40878
- \circ Cet, Te abundance in Mira 7-47899
- \circ Cet stars, circumstellar shell vel. fields, two-fluid model (*Chinese*) 7-66591
- chromospheric Mg II emission lines, influence of interstellar Mg II absorpt. 7-47840
- circumstellar dust shells around late type stars, models for IRAS obs. 7-9461
- circumstellar shells, diagnostic IR signatures of refractory grain processing in circumstellar shells 7-55611
- circumstellar shells, FIRST obs. possibilities 7-47891
- circumstellar shells, molecular abundances and processes, submm astronomy 7-47892
- circumstellar shells, SO₂ and SO emission obs. 7-4429
- close binary, evol. of giant component 7-60633
- FK Com stars, outer atm. characts., UV spectral obs. 7-47936

giant stars continued

- cool giant and supergiant stars, atm. characts., EUV emission anal. 7-47871
 T CrB, recurrent nova, UBV photometry rel. to short-term light vars. 7-55660
 ?20 CVn, δ Sct star, radial vel. vars. obs. 7-9496
 RS CVn stars, H α and Li I obs. of σ Gem, α Aur, HR 6469, and 93 Leo 7-18437
 χ Cyg, Te abundance in Mira variable 7-47899
 δ Del stars, Li abundance, reson. doublet obs. 7-60669
 evolving low-mass stars, activity-related characts. of convective envelopes 7-4440
 TZ For, eclipsing Capella-like system observed with IEU, UV emission-line fluxes meas. 7-47996
 G5 to M-type stars at South Galactic Pole, density distrib. from spectroscopic and photometric surveys 7-4448
 G-type stars, general characts. 7-24135
 globular cluster giants, radial velocity meas. technique 7-40718
 globular star clusters, giant star radial velocity obs. 7-40886
 β Gru, late type giant star, outer atm. struct. and UV spectra 7-34974
 HD 199178, FK Com star, rot. and radial vel., spectral characts. 7-14583
 HD 55510, double-lined spectroscopic binary, orbital elements from photoelectric radial vels. 7-4518
 g Her, SRb star, outer atm., IUE spectral characts. 7-55674
 high-luminosity non-coronal stars, Fe II emission line profiles 7-47867
 HR 6902, composite-spectrum star, spectral types, orbital elements and mass ratio determ. 7-66674
 IR spectra, detection of 12 μ m Mg I and OH absorption lines 7-24132
 IRAS 00193-4033, 22231-4529, O-rich unidentified IRAS sources, optical and IR obs. 7-55853
 IRC+10216, $^{28}\text{SiC}_2$ and $^{30}\text{SiC}_2$ detect. in millimetre-wave spectrum 7-29474
 IRC+10216, brightness distrib. at various wavelengths, radiative transfer in shell 7-60520
 IRC+10420, post AGB star, mass-loss region, circumstellar environment and atm. characts. 7-66583
 K and early M-type giants, evidence for subclass with abnormally high wind expansion vels. 7-47873
 K-type giant stars of galactic disk, metallicity variance 7-60640
 K-type stars, orange giants and dwarfs, review 7-4457
 HK Lac, RS CVn star, long-term light vars. obs. rel. to starspots distrib. 7-60724
 late M-type stars, dust condensation process 7-14565
 late-type giant stars, abundance anal. rel. to departures from LTE in Na and Al 7-60662
 late-type giant stars, outer atmospheres struct. from IUE spectra 7-47872
 long-period and semiregular variables, AAVSO 1986 predictions 7-24144
 long-period variable stars, linear pulsation survey 7-60682
 LSI +65°010 (=2S 0114+650), visible and UV spectra of X-ray binary indicating mass ejection 7-29516
 luminous red giant stars, circumstellar dust and gas props. from IRAS and mol. obs. 7-55609
 R Lyr, no Te lines detected in Mira variable 7-47899
 M-type giants and supergiants, shell and mass loss characts., CO obs. 7-60649
 M-type stars in SAO catalogue, luminosity classes 7-4435
 mass loss rates in Shapley-Ames elliptical galaxies, determ. from IRAS obs. 7-66758
 in metal-rich globular clusters, Washington system photometry and metallicities 7-9523
 mild Ba stars, precursors mass determ. 7-60680
 Mira stars, SiO emission 7-47951
 Mira variable stars, Mg II emission flux meas. from shock waves 7-47938
 Mira variables of short period, search for OH and SiO maser lines 7-14580
 MS-type stars, search for white dwarf companions, UV spectral obs. 7-47935
 neutron stars-giant stars collisions in globular clusters, contrib. to ultra-short period binaries form. 7-66667
 NGC 4833, globular cluster, red giants IR photometry 7-60740
 NGC 6401, globular cluster, variable stars light curves 7-14615
 NGC 6752, globular cluster, photographic photometry of giant, asymptotic, and horizontal branches 7-29520
 NSV 917, red variable star in Fornax, period determ. from photometric obs. 7-24149
 old long-period variable stars in LMC, vel. dispersion determ. 7-55605
 open clusters, subgiants and lower giant branch Ca II emission 7-60741
 RZ Oph, long-period eclipsing binary, photometric and radial vel. study 7-29504
 RS Oph, recurrent nova, optical spectrum and photometry in quiescence 7-24139
 RS Oph, recurrent nova, radio obs. rel. to conditions in nova remnant 7-60695
 4=0¹ Ori, MS star, white dwarf companion detect. and characts., UV spectra anal. 7-55681
 oscillation of stellar atmospheres, response of isothermal atmosphere with nonlinear waves 7-4439
 57 Peg, semiregular variable, photometric and spectral characts. 7-55664
 AG Peg, symbiotic star, spectrophotometric obs. rel. to red giant component heating by hot star (Russian) 7-55669
 pentynylidyne radical (C₅H), detect. of $^{21}\text{N}_{3/2}$ state (in IRC+102.16) 7-23988
 ρ Per, SRb star, outer atm., IUE spectral characts. 7-55674
 Population II, empirical colour-metallicity relations 7-55616
 Population II giant stars, C isotopic ratios determ. 7-60654
 Population II giants, Washington photometry, abundance calibrations 7-9471
 proper-motion stars, parallaxes from photographic astrometry 7-4296
 TX Psc, C star, UV spectral characts. 7-55675
 TX Psc, UV emission var. in cool C star, IUE obs. 7-60684
 R136a, group of 8 massive stars within Tarantula Nebula 7-55749
 R-type stars, model atm. and struct. 7-60674
 rapidly-rotating single late-type giants, evolutionary status and emission fluxes 7-47864
 red giants, $^{18}\text{O}(\text{He},\text{d})^{19}\text{F}$, sub threshold resonance 7-698
 red giants, mass loss characts. and subsequent planetary nebula nature 7-60651
 red giants, metallicity function 7-4451

giant stars continued

- red giants in globular clusters NGC 6171 and NGC 6723, DDO photometry and metallicities 7-9522
 red giants in open cluster M67, chromospheric UV emission obs. 7-47876
 red giants undergoing mass loss, expanding shells IR continuum radiation modelling 7-66582
 rotation and macroturbulence in bright giants 7-47847
 S and MS stars, chem. comp. determ. 7-60681
 m Sculptor dwarf galaxy, radial vel. anal. 7-14654
 semi-regular variables of short period, search for OH and SiO maser lines 7-14580
 semiregular variables, TA obs. (1985 August-1986 January) 7-14586
 16 Ser, binary Ba star, heavy element abundances 7-60680
 LR Sgr, Mira variable, photometric obs. rel. to identity with reported possible nova 7-4479
 stellar coronae in late-type stars, low-g model for dividing line in H-R diagram 7-66569
 Y Tau, C star, effective temp. from occultation and spectroscopic obs. 7-47927
 α Tau, late type giant star, outer atm. struct. and UV spectra 7-34974
 α Tri, hybrid chromosphere star, wind characts. and line form. region characts. 7-55630
 RR UMi, semiregular variable in binary system, revised spectroscopic orbit 7-4520
 variable stars in globular cluster NGC 6637, spectroscopic identification as Mira variable 7-47906
 SS Vir, annual proper motion of Mird variable 7-40845
 g Vir, Ba star, heavy element abundance 7-60680
 $^{27}\text{Al}(\text{He},\text{d})^{28}\text{Si}$, proton threshold states in $^{28}\text{Si}^*$, astrophysical significance 7-19267
 $^{27}\text{Al}(\alpha,\text{t})^{28}\text{Si}$, proton threshold states in $^{28}\text{Si}^*$, astrophysical significance 7-19267
 Ba stars, VLA radio continuum survey 7-47894
 C stars, colour temps. determ., spectrophotometric obs. 7-4461
 C stars, line blanketing in model atm. 7-24141
 C stars, mol. absorpt. bands spectrophotometry 7-40819
 C stars, self-consistent models for dust-driven stellar winds 7-55641
 C stars as symbiotic stars cool components 7-40820
 C stars in Fornax dwarf spheroidal galaxy globular clusters, use for vel. dispersion anal. 7-14649
 C stars with circumstellar silicate dust, spectral characts. 7-40834
 CH stars, synthetic spectra for 255 to 320 nm 7-55673
 CN-strong stars, origin due to binary coalescence 7-66601
 γ Dra, K-type giant, atmospheric props. and Fe/H ratio from spectroscopic anal. 7-14573
 He I 1083 nm chromospheric line, obs. in bright late-type stars 7-55612
 OH-IR stars, IRAS obs. rel. to asymptotic giant branch luminosity function 7-29475
- Gibbs free energy** *see free energy*
Gibbs function *see free energy*
Ginzburg-Landau theory
 antiferromagnetic superconductor, spin wave spectrum 7-38852
 CDW systems, Ginzburg-Landau theory for hysteresis 7-7136
 chaotic soln. integrability and structural stability 7-37480
 critical regimes, periodic perturbation entrainment 7-3575
 cubic systems, superconducting p-wave pair states, collective excitations, spin-orbit interaction and cryst. field effect 7-7440
 disordered granular superconductor near percolation, phase transitions 7-17140
 ferromagnetic superconductors, intermediate state and easy-axis mag. anisotropy 7-38831
 ferromagnetic superconductors, intermediate state and easy-plane magnetic anisotropy 7-38832
 ferromagnetic superconductors, mixed state, surface tension 7-52919
 Josephson tunnel junction, ordered magnetic impurities in barrier region near critical temp. 7-58961
 magnetic superconductor, coexistent states of ferro- and antiferromagnetism 7-58950
 one-dimens. flow system, spatial develop., use of strange attractors 7-51076
 open-flow systems, rel.-depend. Lyapunov exponents as measure of chaos 7-61240
 order-disorder transition, 7-44748
 organic superconductors, S-based, superconductivity, volume property 7-2779
 quasi-one-dimensional electron systems, phase transitions, theory 7-52408
 spin-orbit interaction and crystal field effects 7-38806
 SQUID without Josephson junctions, nonlinear Ginzburg-Landau eqns. 7-45577
 superconducting microbridge, Ginzburg-Landau equations, soln. stability (Chinese) 7-12907
 superconductor-ferromagnet-superconductor contacts, steady state Josephson effect (Russian) 7-7446
 superconductors, random fields, weakly first-order phase transition 7-22068
 superconductors in strong mag. field, Fermi liquid interaction influence 7-52896
 (TMTSF)₂X quasi-1D conductors, SDW transition temperature, superconductivity 7-45705
 triplet local-electron-pair systems 7-45547
 type II superconductors, flux-line lattice, elastic and plastic props. 7-27481
 CePb₃ heavy fermion system, theory of mag. field induced supercond. state 7-45546
 ^3He , superfluid, dynamics in flow channels with restricted geometries 7-38287
 Hg₃-AsF₆ chain compound, paraconductivity, Sugiyama-Gutfreund-Weger model 7-52584
 In-Pb whiskers, critical currents and Ginzburg-Landau parameters 7-17144
 In-Pb whiskers, quasi 1D supercond., weak to strong coupling transition, I-V characts. study 7-38835
 Nb superconducting bicrystals, flux pinning by symmetrical grain boundaries 7-64419
 Pd/Ni interface, strongly paramagnetic layer, magnetisation distrib. 7-7475
- glaciology**
 air bubble trapping in polar ice and importance for air pollution monitoring 7-4068

glaciology continued

- Alaska's galloping glacier, what happens within a glacier in motion 7-18228
 alpine snowfields, influence of longwave radiation on energy balance 7-23727
 Antarctic ice core, record of aerosol concs. in atmosphere 7-55208
 E Antarctic ice sheet, basal melting and climate warming 7-66181
 Antarctica, glacier velocities from satellite images 7-66190
 Baffin Bay, land-ocean correls. during last interglacial-glacial transition 7-34568
 Banff National Park, Alberta, Canada, lake sediments and Holocene glaciation 7-23721
 Bugaroo Glacier, BC, Canada, lateral moraine and glacial history 7-23720
 creep behaviour of ice, dynamic recrystallization and fabric development during shear deformation 7-55096
 Dome C firn layer, debris from Tunguska explosion 7-60605
 Ellesmere Island, Canada, Late Quaternary sea-level changes and glacial history 7-66128
 NE Ellesmere Island, NWT, Canada, glacial geology and marine stratigraphy 7-4062
 extraterrestrial object impacts and triggering of geomagnetic reversals, mechanism involving polar cap growth 7-40413
 Fennoscandinavian ice sheet, thickness determ. using postglacial uplift data 7-34440
 Filchner-Ronne Ice Shelf, Antarctica, numerical flow model and ice thickness 7-18221
 glaciolacustrine sediments of Yukon Territory, stratigraphic, isotopic and micrological evidence for early Holocene thaw unconformity 7-9034
 Greenland, ice sheet folding 7-66186
 Greenland ice cap, cosmic dust placers in blue ice lakes 7-14548
 Hans Glacier, Spitsbergen, upper layer stresses and icequakes 7-14316
 Himalaya mountains, glaciation upper limit and assoc. characts. 7-55090
 Hubbard glacier, 1986's spectacular movement (*French*) 7-60288
 ice age northern hemisphere ice sheet and climate cycles 7-23708
 ice ages and cometary breakup hypothesis re-examination 7-60605
 ice remote sensing, model for calc. of thermal emission 7-60264
 ice-push caves in platform limestones of Montreal area, Canada 7-66121
 Laurentide ice sheet, thickness determ. using postglacial uplift data 7-34440
 Mt Logan, Yukon, Canada, nitrate in ice cores, due to nuclear weapons testing 7-46982
 Melville Island, Canada, ground ice conditions 7-66175
 Montreal areas, Quebec, Canada, ice-push caves in platform limestones 7-66121
 Nevado del Ruiz volcano, Columbia, ice cap melting rel. to lahars during 1985 November 13 eruption 7-8896
 Nigardsbreen, SW Norway, ¹⁴C dating and palaeoenvironment of 'Little Ice Age' glacier advance 7-9037
 Northern Hemisphere Quaternary glaciations 7-55051
 Norwegian and Greenland seas during Pleistocene, ice shelf existence and climate 7-23699
 Norwegian Channel, in Skagerrak-Kattegat region, seismic evidence for glacial erosion model 7-14233
 Ossau Valley, France, sedimentology and morphology (*French*) 7-66177
 periglacial activity in central North Sea, evidence from valley asymmetry 7-14285
 Pleistocene glaciations, relation to lake retreat in Qinghai-Xizang (Tibet) Plateau (*Chinese*) 7-55104
 Quelccaya Ice Cap, Peru stratigraphic record of Little Ice Age 7-34670
 spatial trend analysis of streamline glacial features 7-18216
 Tianmushan glacial table, palaeoclimatological significance 7-55098
 till deposits in drumlins near Caledonia, S Ontario, inverse-graded units 7-9033
 two dimensional line element for glacier flow problems 7-4063
 Vavilov glacier, Arctic USSR, sulphate content over last 90 years from glacier ice 7-23252
 VLF radiosignal diffraction round Antarctic ice cap 7-47491
 W.H. Mathews Symposium, Vancouver, British Columbia (October 1984) 7-4620
 Wisconsinan ice sheet, flow directions from striae in Abitibi-Timiskaming region 7-66173
 Yala Glacier, Nepal, tritium vertical profile in glacier ice 7-40082

glass

- for semiconductor glasses see amorphous semiconductors and chalcogenide glasses
 see also aluminosilicate glasses; amorphous semiconductors; borate glasses; chalcogenide glasses; germanate glasses; glass fibres; glass industry; glass-metal seals; glass structure; metallic glasses; optical glass; phosphate glasses; phosphosilicate glasses; vitreous state; vitrification
 absolute Raman intensities, determ. 7-59200
 absorbed thickness optimisation for Mossbauer study 7-33305
 acoustic emission source characteristics from thermal crack 7-21341
 actinides in glasses, leaching (*French*) 7-19353
 activation enthalpy for diffusion 7-38236
 alkali silicate glasses, internal friction, amplitude depend., cooperative movement parameter near the glass transition temp. 7-2099
 bonding and struct., conf., Reston, VA, USA (May 1983) 7-60879
 brittle fracture threshold under effect of pulsed electron beam, effect of geometrical dimensions 7-3399
 ceramic, advanced, developments and research on cracking tendency 7-27989
 ceramic, failure kinetics using composite glass-crystal system model 7-59631
 ceramic materials, liq. phase separation, nucleation and crystn., book 7-24327
 characterisation by electron bombardment 7-32506
 colour, origins 7-13114
 conference, Alfred, NY, USA (July 1985) 7-3
 contoured substrate, post magnetron sputter and reactive sputter coating 7-53588
 crack propagation, effect of inhomogeneities (*Japanese*) 7-22823
 critical behaviour of double-well potentials, two-level systems model 7-32305
 crystallisation and liquid-phase separation 7-26649
 defects in glasses, conf., Boston, MA, USA (Dec. 1985) 7-9594
 dielectric losses in MM and subMM regions 7-39000
 dielectric relaxation studies, high-resolution laser techniques 7-39006

glass continued

- dispersion eqn. for complex dielectric constant and dispersion analysis of reflection spectra 7-2962
 dynamic fatigue limit, determ. method 7-8221
 elastic properties, theory 7-12189
 electric glass furnace, 3D model for glass flow and Joule heat release calc. 7-20707
 electromigration and charging effects during Auger and XPS analysis of insulators 7-17393
 equations of state and constitutive equations 7-21389
 fiberglass, solar collector cover-plate transmissivities determ. from solar simulator 7-65584
 float glass, solar collector cover-plate transmissivities determ. from solar simulator 7-65584
 fluoride and oxide glasses, reflection spectra in extreme UV region 7-22278
 fluoride glass:Er³⁺, impurity luminesc. and absorpt. spectra studies 7-53386
 fluorozirconate, chem. durability, reaction with water 7-39682
 foils for electron beam excitation 7-35627
 Fourier Transform Infrared spectra, Si-O chem. bond 7-53435
 fracture, number of crack rel. to ultimate stress 7-22809
 fulgurites, form., extreme reduction and metal silicate liquid immiscibility 7-47439
 Furko glasses, quenched, isothermal relaxation of density and stresses 7-1893
 gas bubbles, calibration of dynamic small-sample analysis systems 7-65370
 glass:Ce(Eu), stable and metastable impurity valence states, spectral props. (*Russian*) 7-27747
 glass:CuCl₂Br_{1-x}, x=0-1, colloid exciton spectrum (*Chinese*) 7-38459
 glass:Hg systems, luminescence under strong pulsed laser irradi. 7-33427
 glass:Nd, transition metal doped, fluorescence and absorption spectra 7-13229
 glass:Yb³⁺, time resolved fluorescence line narrowing 7-13230
 glass ceramics, development in China, review 7-6527
 glass ceramics, struct., phase relations 7-7982
 glass-phenol formaldehyde resin hollow microspheres, inverse sedimentation in rubber solutions 7-38325
 glass-plastic melt, thermal cond., effect of type and content of binder 7-58553
 halide glasses, phase equilibria, thermodynamic model 7-2150
 helicopter windshield, chemically tempered, impact fracture 7-28108
 high fluence D implantation, trapping and desorption, saturation conc. studies 7-26781
 HLLW solidification, review of alternative wasteforms and processes 7-36296
 HLW conditioning and glass specification at Sellafield 7-56860
 ideal homopolar, delocalised charge carrier mobility, temp. depend. 7-52613
 immiscibility of glass forming systems, immiscibility 7-2214
 insulators, radiation effects, conf., Guildford, England (July 1985) 7-29590
 interfacial bonding and adhesion, conf., Aspen, CO; USA (Aug. 1985) 7-24269
 ion exchange, surface investig. by XPS and X-ray spectra studies 7-13614
 ion implantation, effect on mechanical and optical props. (*Chinese*) 7-51796
 ionic conductivity mechanism 7-44902
 laser exposure, repeated, absence of below-threshold ionisation and cumulation effect 7-63653
 laser irradiated with picosecond high-power pulses, long-range structural changes 7-12123
 leached, analytical electron microscopy studies using ultramicrotomic thin sections 7-6544
 low temperature properties, below transition temp., relaxation 7-1910
 Mariana Trough basalt glasses, light noble gases comp. anal. 7-40436
 melts, gas bubble dissolution and growth 7-2302
 melts, nonisothermal, meas. of standard Seebeck coeffs. by means of ZrO₂ electrodes 7-3597
 3-methylpentane-tetrachloromethane glass, radiolysis, optical absorpt. band assignment 7-46861
 mixed transfer processes in glass technology 7-7948
 molten, jet formation during absorpt. wave propag. 7-46251
 molten glass layer, temp. convection, anal. 7-57822
 nonlinear relaxational acoustic attenuation, perturbation theory calcs. 7-32578
 nuclear waste glass, comparison of leaching in natural and synthesized groundwaters 7-19530
 nuclear waste glass, devitrification, role of melt insolubles 7-6525
 nuclear waste glass suitability study, systems approach 7-5447
 nuclear waste vitrification, melt foaming, foam stability and redox studies 7-5452
 nuclear waste/natural glasses, aqueous corrosion, comparative hydration rates in liquid/vapour environments 7-8141
 optical basicity and refractivity 7-7660
 optical impurities dephasing 7-53376
 oxide, bond strength and characteristic temp., three-band theory 7-63500
 oxide, low temp. US relax., correl. with phys. props. 7-51961
 oxide, low-temp. acoustic relax. analysis methods 7-12216
 oxide, low-temp. internal friction, longit. and transverse two-well systems rel. contrib. 7-12202
 oxide, relax. time and loss peak correl. with DC cond. 7-22181
 oxide glasses, phase equilibria, thermodynamic model 7-2150
 oxynitride glass development, book contrib. 7-28003
 phonon localisation and thermal cond. 7-21379
 photoelastic constants, evaluation method 7-39080
 plexiglass, solar collector cover-plate transmissivities determ. from solar simulator 7-65584
 polymers, glassy, time depend. nonlinear deform. 7-63733
 porous, sintered, pore size distrib. meas., dynamic water expulsion method improvement 7-13678
 preparation, review 7-3259
 quartz, glass, thermal expansion coeff., two-level system contrib. (*Russian*) 7-21495
 quartz glass, radiation-induced centres, ESR studies 7-12149
 radiation optical props., manifestation of electrification effects 7-64592
 radiation-induced defects and ESR spectra 7-2050
 Rayleigh and Brillouin scattering spectra, Bayesian deconvolution 7-13173

glass continued

- relaxation, mechanical, electrical and structural 7-26650
 relaxation from Levy stable distrib. 7-32299
 relaxational processes, eqn. of state 7-21386
 resorufin, in ethanol, glass, photon echo and hole burning meas. 7-15955
 resorufin, in ethanol glass, photon echo, temp. depend. 7-43256
 rubber-glass interfaces, form. and rupture (*French*) 7-54072
 Savannah River Plant waste glass, interaction with canister and overpack metals 7-8142
 shock loaded target, stress meas. using transverse piezoresist. gauge 7-29999
 shock wave propagation phenomena 7-51941
 silicate, Na desorption during X-ray microanalysis 7-23114
 silicate, radiation-induced centres, ESR studies 7-12149
 silicate, structure and bonding, NMR studies 7-63503
 silicate glass, dissolution in closed glass/water system 7-63828
 silicate glasses, cation environments, EXAFS and NEXAFS studies 7-63482
 silicate glasses, magic-angle spinning NMR, review 7-64536
 silicate glasses containing alkali and alkaline earth metals, alkali ion mobility (*Japanese*) 7-27007
 silicate minerals and glasses, Fe K-edge EXAFS studies, Fe coordination 7-59287
 soda lime glass detectors, chemical etching characts. 7-30868
 softening point determ., numerical method, calculator program (*Czech*) 7-6796
 spacecraft HV solar cell array glass encapsulation for protection against plasma 7-65490
 specific heat calcs. at low temp. 7-44846
 sphenc glass ceramics, radioactive waste immobilisation, sintering, porosity 7-27984
 stabilised, low temp. relax., pot. barrier model. 7-43714
 strip, cracked, thermal shock, temp. depend. material props. 7-16114
 structural relaxation, US absorption, IR divergence response (*Chinese*) 7-6520
 substrate, periodic microrelief, laser irradiation, of nitrocellulose film 7-63927
 surface, graphite thin absorber layer influence on thermal-wave appls. 7-48723
 surface, He atom scatt. 7-64863
 surface, polished, thermal Cs atom reflection 7-22411
 surface recomb. of electrons and ions, kinetic theory 7-46263
 surface singularities, topological origin 7-12444
 surface structure minimal disturbance under ion bombardment 7-12419
 suspensions, beads and fibre, flow through flat orifices, elastic props. influence (*German*) 7-6296
 synthetic silica glass, X-ray induced absorpt. and luminesc., heat treatment effects study 7-7733
 tektites formation and Cretaceous-Tertiary extinctions 7-8953
 tensile fractures, radiation patterns in glass plates and ice 7-60182
 thermal conductivity and heat capacity, hydrostatic pressure dependence obs. 7-306
 tiling model, relax. behaviour, Monte Carlo simulation 7-44816
 transition metal doped, optical absorpt. and luminesc. spectra 7-13186
 transparent ferroelectric ceramics, cryst. chem. and struct. props. and modifications 7-6590
 tubing, thermally induced crack propagation (*German*) 7-22805
 tunnel modes and kinetic props. at low and high temps. 7-21115
 turbid glasses, for calibration and checking of nephelometers and turbidimeters 7-20141
 two-dimensional quenched Lennard-Jones systems, glassy order, Monte Carlo study 7-63494
 two-level systems, density of states and distrib. functions derivation 7-12583
 vitreous silica, two-level tunnelling system-strain coupling const., double well asymm. energy contrib. 7-6538
 Vycor, adsorbed ^4He superfluid transition, constrained randomness, Harris criterion 7-44935
 Vycor, thermodynamics of freezing and melting of liq. ^4He in small pores 7-52169
 Vycor leached porous glass, fractal struct., SANS, SAXS, and energy transfer meas., comment and reply 7-44398
 X-ray diffraction analysis of amorphous materials, features and rel. between methods (*Japanese*) 7-21119
 AgI-Ag₂MoO₄ glasses, ionic conductors, mechanical and electrical relax. 7-44687
 AgI-Ag₃AsO₄ superionic conducting glass, cond. and glass form. studies 7-32711
 AgI-AgPO₃ glasses, thermoelec. power 7-6867
 AgPO₃-based glasses, struct. and elec. props., Raman spectra and ionic cond. meas. 7-6550
 AlF₃-CaF₂-BaF₂ glasses, Raman spectroscopic study 7-7692
 Al₂O₃ glass, gel produced, optical transmission rel. to heat treatment 7-27733
 BaF₂-ThF₄-YbF₄ glass, electron irradiation effects, Yb³⁺ optical transitions 7-27764
 BeF₂-based glasses, thermal conductivity meas. 7-12382
 CaF₂-BaF₂-AlF₃ glasses, struct., transition metal ion EPR studies 7-6545
 Ca₃Na₄K₂Si₂O₁₀F₄, chain-silicate canasite glass-ceramic, thermal shock behaviour, effect of crystn. 7-46613
 CaO-SiO₂-CaF₂, structural analysis for fluorosilicate glasses by X-ray photoelectron spectroscopy (*Japanese*) 7-33510
 CdO-Bi₂Ru₂O₇ thick film resistors with high TCR for temperature sensing 7-48735
 Cr₂O₃ in mullite transparent glass-ceramics, X-ray absorpt., emission and EPR spectra 7-7728
 Cr₂O₃ in transparent glass-ceramic, crystn. and spectroscopic props., melting conditions and heat treatment influence 7-7588
 Cs₂O-SiO₂ glasses, intrinsic and recomb. luminesc. and fundamental absorpt. spectra 7-13195
 Cs₂O-SiO₂-based glasses, Cs⁺ ion distrib., energy dispersive X-ray diff. studies 7-21113
 Cu halides, photochromic glasses, elastic props., 20-500 °C (*Russian*) 7-21365
 Fe₂O₃-SrO system, glass ribbon prep. by melt spinning, charactn. 7-53690
 In-glass, glow discharge induced changes 7-12577
 In-glass composite 7-38656
 K-Ca-NO₃-H₂O glasses, low temp. dielectric study 7-38999
 K₂O-CaO-SiO₂ system, cryst. growth kinetics, morphology, melt comp. depend. 7-46303

glass continued

- K₂O-Ga₂O₃-SiO₂ glasses, Raman spectra 7-3035
 K₂O-PbO-SiO₂, props. rel. to phase diagram 7-13117
 K₂O-PbO-SiO₂ glasses 7-3036
 K₂O-SiO₂ glass melts, structure 7-1831
 K₂O-SiO₂ glasses, intrinsic and recomb. luminesc. and fundamental absorpt. spectra 7-13195
 K₂O-SiO₂ glasses, struct., X-ray diff., molecular dynamics calc. 7-6551
 Li-P-O-N glass, prep. and characterisation 7-26654
 Li₂O-MgO-SiO₂, multicomponent glasses, sequence of cryst. phases 7-26648
 Li₂O-SiO₂ glass, critical cooling rates for nucleating agents 7-6795
 Li₂O-SiO₂ glass, phase nucleation, melting temp. depend. 7-6549
 Li₂O-SiO₂ glass, Pt catalysed crystallisation 7-6524
 Li₂O-SiO₂ glasses, intrinsic and recomb. luminesc. and fundamental absorpt. spectra 7-13195
 Li₂O-SiO₂ glasses, struct., X-ray diff., molecular dynamics calc. 7-6551
 Li₂O-2SiO₂ sol-gel glass, prep. and devitrification behaviour 7-58158
 Mo group glasses, anomalously high bulk cond. meas. in metal-glass structs. 7-17029
 20(NaK)₂O-xGa₂O₃-(80-x)SiO₂ glasses, elec. conductivity, mixed alkali effect 7-27001
 Na₂O-3SiO₂ glass, Tb³⁺ activated, temp. depend. of tunnel lumin. 7-59265
 Na₂O-CaO-SiO₂, high-silica glass, sol-gel prep. method 7-46402
 Na₂O-CaO-SiO₂ glass, indentation strength comparisons 7-3410
 Na₂O-CaO-SiO₂ glass, grinding, crack branching, crushing mechanism 7-3472
 Na₂O-CaO-SiO₂ glass, melting using natural fine-powdered quartz 7-7950
 Na₂O-CaO-SiO₂ glass, hydration, fluid flow effects 7-13758
 Na₂O-CaO-SiO₂ glass, cracktip blunting kinetics, annealing, corrugated surface 7-46611
 Na₂O-CaO-SiO₂ glass, dynamic fatigue, indentation flaws, surface treatment 7-46629
 Na₂O-CaO-SiO₂ glass with subthreshold flaws, dynamic fatigue 7-8111
 Na₂O-CaO-SiO₂ glasses, IR spectra 7-3036
 Na₂O-Ga₂O₃-SiO₂ glasses, Raman spectra 7-3035
 Na₂O-K₂O-CaO-SiO₂ glass, mixed alkali effect on chemical durability 7-8145
 Na₂O-SiO₂ glass, longitudinal electrostriction tensor component 7-2982
 Na₂O-SiO₂ glass, relative defect-production efficiency for fission fragments, alpha decay and electron irradiation 7-12167
 Na₂O-SiO₂ glass melts, structure 7-1831
 Na₂O-SiO₂ glasses, intrinsic and recomb. luminesc. and fundamental absorpt. spectra 7-13195
 Na₂O-SiO₂:Eu³⁺, laser-induced refractive-index gratings, four-wave-mixing techniques 7-11102
 Na₂O-SiO₂-NaF, structural analysis for fluorosilicate glasses by X-ray photoelectron spectroscopy (*Japanese*) 7-33510
 Na₂O-TeO₂-Cr₂O₃ glasses, IR absorpt., visible and UV spectra studies 7-27720
 Na₂O-Y₂O₃-MO-SiO₂ glass, (M=Mg, Sr, Ca), Na⁺ conductivity 7-5134
 Na₂O-Y₂O₃-SnO₂-SiO₂ glass, Na⁺ conductivity 7-52134
 Na₂O.3SiO₂:Eu³⁺, UV-irradiated formation of colour centres 7-12063
 Na₂O.3SiO₂ glass, Na leaching rates in H₂O and D₂O, comparison 7-63885
 Nd, in glass, energy transfer rate, luminesc. 7-13192
 PbO-SiO₂ glass, elastic props. and short- and medium-range structs. (*Japanese*) 7-65077
 PbO-SiO₂ glass sputtered antireflection coatings on semiconductor laser facets 7-15964
 PbO-SiO₂ glasses, IR spectra 7-3036
 PbO-SiO₂ glasses, struct. anal., X-ray diff. studies 7-6532
 PbO-SiO₂-K₂O coloured and colourless glasses, near IR absorpt. temp. depend. study 7-13146
 Pt group glasses, anomalously high bulk cond. meas. in metal-glass structs. 7-17029
 Rb₂O-SiO₂ glasses, intrinsic and recomb. luminesc. and fundamental absorpt. spectra 7-13195
 Si-pyrex, irreversibility of anodic bonding 7-33910
 SiO₂-K₂O-CaO-MgO-CdO glass melts, evaporation 7-2160
 SiO₂-K₂O-PbO glass melts, evaporation 7-2160
 SiO₂, amorphous, intrinsic defects, theory 7-11936
 SiO₂ amorphous, photoinduced paramagnetic defects 7-13031
 SiO₂ amorphous, point defects, review 7-11942
 SiO₂, amorphous, thermal, UV irradiation induced compaction and photoetching 7-12146
 SiO₂, dry silica, UV induced defect creation, ESR study 7-13032
 SiO₂ glass, surface analysis by laser ionisation 7-13275
 SiO₂ glass and cryst., luminescence props. 7-33428
 SiO₂ glasses, gel-derived, defect studies 7-11944
 SiO₂ glasses, prep. by sol-gel technique, dielec. props. 7-45918
 SiO₂, laser-induced breakdown, radiation induced defects 7-12147
 SiO₂ liq., stretched and compressed, glass transition, ion dynamics simulation 7-16747
 SiO₂ thin films, intrinsic bonding defects and impurities, EPR studies 7-13034
 SiO₂, vitreous, aluminium-oxygen hole centre, chemical annealing 7-51646
 SiO₂:OH, X-irrad. induced defect centres, EPR obs. 7-45221
 SiO₂ transition metals, fused quartz, impurity sites, X-ray absorption spectroscopy 7-13263
 SiO₂:Yb³⁺ glass, energy transfer among impurity ions, time resolved fluorescence line narrowing meas. 7-46124
 SiO₂-Al₂O₃ glass, roller-quenched, NMR evidence for 4-, 5- and 6-fold Al sites 7-44384
 SiO₂-CaO-MgO-Na₂O glass, frequency dependent equation of state 7-51987
 SiO₂-TiO₂ vitreous systems, low temp. sp. ht. and thermodynamic props. study 7-63842
 SiO_x thin films, obliquely evaporated, cross sectional TEM studies 7-12571
 SiS₂-Li₂S-LiI glass, ionic cond. meas. 7-38251
 SnO₂ glass, thick film, elec. resistance, effect of struct. 7-7300
 TeO₂-based halide glasses, prep., thermal, mechanical, elec. and optical props. characterisation (*French*) 7-37884
 TeO₂-ZnCl₂ system, glass prep. and composition 7-46403
 ThO₂ based, localisation of 5f states, XANES study 7-64794
 U glasses, unoccupied 5f states, XANES study 7-39318

glass continued

- UO₂ based, localisation of 5f states, XANES study 7-64794
 Y-Si-Al-O-N glasses, Si coordination, NMR studies 7-1906
 Yb, in glass, energy transfer rate, luminesc. 7-13192
 ZnCl₂ pure glass, elastic consts. and struct. 7-63716
 ZnO-AlN-glass, SAW characts. study 7-12448
 ZnO-SiO₂ amorphous system, structure, mol. dynamics computer simulation studies 7-21114
 ZrF₄ based glasses, reduced species, EPR and optical studies 7-64665
 ZrF₄-BaF₂-AlF₃ glass, viscous flow vs. phase separation, DSC study 7-44383
 ZrF₄-BaF₂-LaF₃-AlF₃-NaF glass, crystal growth and microstruct. 7-1896
 ZrF₄-BaF₂-LaF₃-AlF₃-LiF glass, X-ray radiation damage, EPR studies 7-21278
 ZrF₄-BaF₂-LaF₃-AlF₃ fluoride glasses, lanthanide J-levels high yield luminesc. study 7-22309
 ZrF₄-BaF₂-LaF₃-AlF₃, heavy metal fluoride glass system, viscosity and crystallisation 7-37883
 ZrF₄-BaF₂-NaF glasses, crystallisation study 7-11933
 ZrF₄-BaF₂-NaF-AlF₃ glass, crystn. (Japanese) 7-26659
 ZrF₄-BaF₂-NaF-AlF₃-LaF₃ glasses, crystallisation study 7-63491
 ZrF₄-BaF₂-ThF₄-LiF quaternary glasses, ionic cond. and NMR studies 7-6865
 ZrF₄-based fluoride glasses, Fe ions anal. 7-64672
 ZrF₄-LaF₃-BaF₂-NaF glasses, EPR of Cu²⁺ ions 7-27593
 ZrF₄-PbF₂-AlF₃-LiF-KF glasses, mixed alkali effect, DC cond. 7-63873
 ZrF₄-PbF₂-AlF₃-NaF-KF glasses, mixed alkali effect, DC cond. 7-63873

glass fibre reinforced composites

- see also glass fibre reinforced plastics*
 digital image correlation methodology use for deform. quantification 7-59718
 E-glass fibre composite interfaces, surface studies using diffuse reflectance and photoacoustic FTIR spectra 7-46044
 metallic glass reinforced Al composite fabrication by multi-lamina explosive compaction 7-59482
 polypropylene, molten, glass fibre reinforced, rheological props. (French) 7-11369
 relaxation property anisotropy 7-46534

glass fibre reinforced plastics

- binder content in impregnated reinforcement, contactless US inspection use 7-3565
 cross-layered reinforcement strength criteria 7-17631
 cross-reinforced wound, deform. and failure in tensile loading 7-17633
 cylinders, burst pressure, stress wave factor correl., US meas. 7-13709
 cylindrical shells, buckling under external press. 7-37358
 designing with plastics and advanced plastic composites, book 7-4642
 digital image correlation methodology use for deform. quantification 7-59718
 epoxide matrix 7-28078
 epoxy and polyester matrices, flexural failure mechanisms, global stress plane 7-8082
 epoxy laminates, cross-ply cracking 7-39617
 epoxy matrix, average stress-strain curves 7-33733
 epoxy matrix, cross-ply plates, micromech. initial failure anal. 7-62975
 epoxy matrix, fatigue life and static strength, statistical study 7-39618
 epoxy matrix, unidirectional glass fibre, impact behaviour, temp. influence 7-3427
 epoxy matrix panel, whole-field strain determ. using coherent opt. processing 7-57779
 epoxy-amine matrices, improvement of phys. and mech. props. 7-39574
 fibreglass-filled rubber-modified phenolic resin, sp. ht. and thermomech. expansion meas., thermal decomp. 7-6822
 flexible, nonlinear elastic behaviour 7-39570
 glass fibre reinforced epoxy resin insulator, interface treeing phenomena study 7-39012
 honeycomb filler, strength and stiffness in shearing determ. 7-17634
 hydrothermal behaviour, mech. props. rel. to water absorpt. 7-46665
 laminates, yield and ultimate strengths 7-22785
 nylon 6 composites, formed by in situ polymerisation of caprolactam, mech. performance 7-39575
 PEEK glass fibre reinforced plastics, fracture toughness, temp. and strain-rate effects 7-39660
 polyester laminates, fatigue tests 7-3428
 polyester matrix, aligned fibres, AE stress corrosion cracks 7-59722
 polyester matrix, random short fibre SMC, interlaminar fatigue crack growth interlaminar fatigue crack growth 7-33772
 polyester matrix hybrid laminates, impact and perforation props. (Japanese) 7-13569
 polyester resin, glass sphere filled aligned fibre reinforced, Young's and flexural moduli 7-3350
 polyester resin, glass-reinforced, stress corrosion cracks, acoustic emission monitoring 7-53926
 polyester resin matrix, fracture toughness and microfractures, AE obs. (Japanese) 7-33779
 polyester resin matrix laminate, hydrothermal ageing, degradation, US obs. 7-13708
 polypropylene matrix, damping characts. 7-59565
 polypropylene matrix, fibre and matrix orientations 7-39478
 polypropylene matrix, short-fibre, struct. and mech. props., effects of moulding geometry 7-3348
 polypropylene matrix, subjected to pure bending, dynamic tensile props. 7-46545
 production line NDT appls., holographic and visual inspection methods 7-39837
 PTFE matrix, sliding and abrasive wear rel. to fibre content 7-28144
 PVC matrix, short glass fibre reinforced, acoustic emission during irreversible deform. 7-3380
 short fibre reinforced polymer composites, fibre orientation developments in moulding 7-3264
 surface deformation modelling 7-2236
 thermoplastic polymers, molten state, with glass fibres, rheological props. (French) 7-63097
 tubes, radial impact strength 7-59709
 C/glass fibre reinforced hybrid composites, aligned short fibres, SCC prop. 7-13615
 C/glass hybrid fibre reinforced epoxy, tensile, compressive, flexural and shear props., review 7-39532

glass fibres

- see also fibre optics; glass fibre reinforced composites; glass fibre reinforced plastics; optical fibres*
 acoustic and optical waveguides, similarities and differences 7-1298
 diameter meas., diff. pattern analysis, holography appl. 7-25762
 E-glass batch melting redox and its effect on specific glass properties 7-7947
 fibre optic sensors appl. in materials testing (German) 7-11162
 heavy-metal fluoride glass fibres, impurity anal. using selectively excited photolum. 7-31473
 lasers and optical fibres, technology, theory, propagation and nonlinear optical phenomena, review 7-43437
 lecture on glass, light and the information revolution 7-24253
 mid-IR fibre ultralow-loss communications 7-11175
 (Na₂O)₂₅(Li₂O)₂₅(P₂O₅)₅₀ glass fibres, struct., birefringence, density and thermal shrinkage, drawing parameters depend. 7-6536
 optical, strength meas. by bending 7-43384
 softening point determ., numerical method, calculator program (Czech) 7-6796
 spinning process in liq. state 7-3258
 ultralow-loss glasses, book contrib. 7-25917
 Al coated, extinction props., thermal cond. meas. 7-52162
 CaO-BaO-P₂O₅ glass fibres, stress optical studies 7-7673
 (CaO)₂₅(BaO)₂₅(P₂O₅)₅₀ glass fibres, struct., birefringence, density and thermal shrinkage, drawing parameters depend. 7-6536
 Na₂O-Li₂O-P₂O₅ glass fibres, stress optical studies 7-7673
 Na₂O-SiO₂-Ag₂O, Na⁺=Ag⁺ ion-exchanged, elec. conduction 7-27002
 SiO₂-GeO₂ optical fibre surfaces, formation mechanism of H-associated defect centre 7-65158
 SiO₂-GeO₂-P₂O₅, doped silica glass, dopant effect on OH absorpt. 7-27715
 ZrO₂-containing glass fibres, alkali corrosion process, XPS study (Japanese) 7-3480

glass formation *see vitrification***glass industry**

- container industry in European Community, research and development 7-28001
 container industry in US, review 7-28000

glass-metal seals

- In-glass, adhesion strength, meas. method 7-59715

glass structure

- alkali metal nitrate dil. solns., IR spectra anal. 7-19857
 alkali metal perchlorate dil. solns., IR spectra anal. 7-19857
 alkaline earth metasilicate glasses, P₂O₅ added, struct., ³¹P and ²⁹Si NMR 7-32302
 alloys, amorphous, friction and wear behaviour rel. to microstruct. and surface chem. 7-8127
 aluminosilicate glasses, magic-angle spinning NMR, review 7-64536
 binary amorphous alloys, structural models (Chinese) 7-37873
 bond equilibrium theory anal. 7-63499
 borate glasses, basicity and geometry studies, MNDO calcs. 7-6529
 borate glasses, structural groupings, NMR studies 7-11940
 borate glasses, structure and bonding, NMR studies 7-63503
 borosilicate glass leaching behaviour, mol. struct. effects 7-21530
 ceramic materials, intergranular glass phases, equilib. film thickness 7-46433
 chalcogenide glasses, photodarkening process and defects 7-13112
 conference, Alfred, NY, USA (July 1985) 7-3
 E-glass, coord. of iron, ESR and mag. meas. 7-13021
 gamma-irradiated, plasma production by laser beams 7-44379
 glass, tunnel modes and kinetic props. at low and high temps. 7-21115
 glass ceramics, struct., phase relations 7-7982
 glasses, leached, analytical electron microscopy studies using ultramicrotomic thin sections 7-6544
 low alkali borosilicate glasses, electrical resistivity, depend. on composition 7-58806
 low temperature properties, below transition temp., relaxation 7-1910
 luminescence centre struct., rare earth elements in activated glasses 7-27754
 metallic, defects, SANS studies 7-51659
 metallic, short-range order, correlation functions 7-51660
 metallic glasses, atomic radial distrib. functions, ultradispersed eutectic structural model 7-11923
 metallic glasses, laser annealed struct. and magnetoelastic props., effects of surface characts. 7-45785
 metallic glasses, magnetic relaxation and struct. transformations 7-27557
 metallic glasses, surface melting, by plasma, laser or electron beams 7-63495
 metallic glasses-H₂, prep., struct. and props. 7-26663
 microdefect accumulation kinetics during optical irradiation 7-38050
 (Na₂O)₂₅(Li₂O)₂₅(P₂O₅)₅₀ glass fibres, struct., birefringence, density and thermal shrinkage, drawing parameters depend. 7-6536
 oxide, bond strength and characteristic temp., three-band theory 7-63500
 proteins, glass model 7-13953
 quartz glass, microdefect accumulation kinetics during optical irradiation 7-38050
 radiation effects in glasses 7-32518
 radiation-induced defects and ESR spectra 7-2050
 rare earth phosphate glasses, structural investigation 7-6522
 relaxation from Levy stable distrib. 7-32299
 silica glasses, surface structure, mol. dynamics simulations 7-12443
 silica optical fibres, defect struct. and drawing-induced absorption, drawing depend. 7-3071
 silicate, structure and bonding, NMR studies 7-63503
 silicate glass, structural inhomogeneities 7-11941
 silicate glasses, cation environments, EXAFS and NEXAFS studies 7-63482
 silicate glasses, magic-angle spinning NMR, review 7-64536
 silicate porous glass, wear resistance and grinding hardness, struct. effect, grinding method meas. 7-57614
 strength, structure and relaxation of glasses 7-1897
 transition metal-metalloid metallic glasses, struct. relax. and segregation (Russian) 7-32300
 vibrational spectra of structural units 7-3034
 vibrational spectra studies, localised interactions 7-63502
 Vycor leached porous glass, fractal struct., SANS, SAXS, and energy transfer meas., comment and reply 7-44398
 X-ray diffraction analysis of amorphous materials, features and rel. between methods (Japanese) 7-21119

glass structure continued

- Ag_{0.15}As_{0.425}Se_{0.425-x}Te_x chalcogenide glasses, ionic and electronic cond., comp. depend. study 7-12768
- AgI-Ag₂MoO₄ glasses, ionic conductivity, effect of structural relax. 7-44903
- AgI-Ag₂MoO₄ system, conductivity in the liquid and glassy states 7-44881
- AgI-Ag₂O-B₂O₃ fast ion conducting glasses, struct., XANES studies 7-63483
- (As₂Se₃)_{0.1}(B₂O₃)_{0.9} glass network struct., mol. dynamics study 7-6539
- (As₂O)_x(B₂O₃)_{100-x} glasses, microstruct. and electronic cond. studies 7-6534
- AgPO₃-based glasses, struct. and elec. props., Raman spectra and ionic cond. meas. 7-6550
- Ag₂P₂O₇ glassy and cryst. states, thermal props., IR spectra 7-44845
- Al-R (R=Er,Nd,Gd) rapidly solidified alloys, microstruct. and thermal props. 7-22667
- Al₂O₃ ceramics, microstruct.-mech. prop. relationship 7-65147
- Al₂O₃-SiO₂-CaO glasses containing rare alkali oxides, struct. and elec. props 7-6528
- As-Se, amorphous, short range structures, EXAFS studies (Chinese) 7-37871
- As₂S₃, amorphous, bulk glass and thin films, photostructural changes, EXAFS meas. 7-39314
- As₂S₃, amorphous, charact. control using acoustic domain 7-20576
- As₂S₃ glass, photostructural effects, EXAFS study 7-64758
- (As₂Se₃)_x(As₂Te₃)_{1-x} glasses, molecular struct., chemical equivalence of ¹²⁵Te absorpt. and ¹²⁵I emission Mossbauer spectroscopy 7-59129
- As₂O₃Se_{0.5}Te_{0.5} chalcogenide glass, struct. models, X-ray diff. and Monte Carlo calcs. 7-6548
- As_{0.45}Se_{0.10}Te_{0.45} glassy alloy, struct. model and switching props. 7-1904
- (As₂Se₃)_{1-x}(Te₂Se₃)_x elec. and thermal transport props., effect of TI addition 7-38200
- B₂O₃-GeO₂ glass, vibrational spectra of structural units 7-3034
- B₂O₃-PbO-Al₂O₃ glasses, phase separation, dynamical scaling 7-1908
- BaF₂-ZrF₄ glass, Zr local environment, EXAFS studies 7-63485
- BaF₂-ZrF₄-FeF₂ glasses, Raman scatt. study 7-27713
- BaO-Al₂O₃-B₂O₃ glass, constitution 7-21120
- BaO-Fe₂O₃-B₂O₃-based glasses, crystallisation behaviour, nucleating agent effects 7-16560
- Ba(PO₃)₂-LiBa(Mg)AlF₆ glasses, Raman spectra and network struct. studies 7-7695
- Bi-Zn-Fe-O amorphous films, struct. and mag. props. 7-51645
- CaF₂-BaF₂-AlF₃ glasses, struct., transition metal ion EPR studies 7-6545
- CaO-Al₂O₃-B₂O₃ glass, constitution 7-21120
- CaO-SiO₂-CaF₂, structural analysis for fluorosilicate glasses by X-ray photoelectron spectroscopy (Japanese) 7-33510
- (CaO)₂₅(BaO)₂₅(P₂O₅)₅₀ glass fibres, struct., birefringence, density and thermal shrinkage, drawing parameters depend. 7-6536
- CdO-B₂O₃-Si(Ge)O₂ network struct., coordination and bonding, comp. depend., NMR study 7-6535
- CdO-SiO₂-M₂O (M=Na,K,Li), glasses, thermal expansion, free volume 7-58152
- (CdO)_x(B₂O₃)_y(GeO₂)_z glasses, struct. and vibrational props., IR spectra study 7-7694
- Co-B alloy, amorphous, thermodynamic, thermomag. and struct. studies (French) 7-16438
- Co_{83.5}Fe₅Si_{7.5}Ge_{1.5}B_{2.5}, amorphous alloy, struct. changes after γ -irrad. (Russian) 7-58336
- Co₈₈Ni₁₀Fe₂B₁₆Si₁₁, metallic glass, reversible struct. transformation 7-1907
- Co₈₈Ni₁₀Fe₂B₁₆Si₁₁ amorphous ferromagnet, prep. and struct. 7-22605
- Cs₂O-Nb₂O₅-Ga₂O₃ glass structure, Raman spectroscopy 7-1902
- Cs₂O-SiO₂-based glasses, Cs⁺ ion distrib., energy dispersive X-ray diff. studies 7-21113
- Cu-based alloys, rapid solidified and ion implanted, struct. studies 7-21130
- Cu_{1.5}As₂₄Se₅₁, glassy semiconductor, tetrahedral bonding 7-32304
- Cu₉₀Ti₁₀ metallic glass, atomic neighbouring struct., EXAFS study (Chinese) 7-6519
- Cu₂Ti_{100-x}, x=50,66, metallic glasses, crystn., DTA, X-ray diff., hardness meas. 7-63489
- Cu₃₃Y₆₇ metallic glasses, partial struct. factors, chem. short range order 7-63486
- Er-Cu (Ni) metallic glass form. by near-isothermal cold rolling 7-22610
- Fe-B, amorphous, structural characterisation by laboratory EXAFS spectrometer 7-1911
- Fe-B metallic glasses, imperfection struct., positron annihilation studies 7-37885
- Fe-B metallic glasses, struct. relax., Curie temp. meas. 7-21124
- Fe-Cr-B metallic glasses, imperfection struct., positron annihilation studies 7-37885
- Fe-Cr-Si-B metallic glass wires, corrosion rel. to crystallinity and comp. 7-46701
- Fe-Ni based metallic glasses, quenched-in excess vol. and structural relax. 7-6531
- Fe-Ni-B, amorphous, shock loading, inclusions dissolving, domain struct. (Russian) 7-63487
- Fe-Ni-B metallic glasses, crystallisation, microhardness (Russian) 7-59617
- Fe-Ni-Si-B metallic glasses, imperfection struct., positron annihilation studies 7-37885
- Fe-P, amorphous alloys, electrodeposition and melt spinning prep., struct. anal. 7-11934
- Fe-R-B (R=rare earth) metallic glass permanent magnets, TEM studies 7-26661
- Fe-R-B (R=rare earth) metallic glass permanent magnets, struct. and mag. props. 7-27565
- Fe-W-B metallic glasses, imperfection struct., positron annihilation studies 7-37885
- Fe₈₀B₂₀, amorphous, partial pair distribution function determ. 7-51640
- Fe₈₃B₁₇, metallic glass, struct. relax. X-ray and neutron diff. study 7-6521
- Fe₈₉B₁₁Si₁₀, amorphous, very small angle neutron scatt. 7-44392
- Fe₇₉B₁₃Si₉ amorphous and partially crystalline alloy, high resolution TEM studies 7-21127
- (Fe_{1-x}Co_x)₇₇Si₁₀ amorphous alloys, Mossbauer study 7-7623
- (Fe_{1-x}Mn_x)₇₈B₂₂, amorphous alloys, lattice parameters, annealing, X-ray diff., elec. resist. 7-37878
- Fe₄₀Ni₄₀B₂₀, amorphous metallic films, SAX investig. (Russian) 7-51576
- Fe₄₀Ni₄₀B₂₀ metallic glass, neutron diff. struct. factors determ. 7-51654

glass structure continued

- Fe_{45.5}Ni_{44.5}B_{10.3}, amorphous, internal friction, thermo-EMF struct., annealing effect (Russian) 7-59560
- Fe₄₀Ni₄₀P₁₄B₆ amorphous alloy, relax. struct. transforms., 80 to 300K 7-1890
- Fe₄₀Ni₄₀P₁₄B₆ metallic glass, heterogeneous struct., EXAFS study 7-27816
- (Fe_{1-x}Ni_x)₇₇Si₁₀B₁₃, amorphous, structural anal. (Korean) 7-26655
- Fe₄₀Ni₄₀Si₁₆B₄ metallic glass, positron trap depth distrib. determ., lifetime and Doppler effect meas. 7-39304
- FeO-PbO-P₂O₅ glasses, atomic environments, EXAFS studies 7-64787
- Fe₂O₃-BaO-B₂O₃-V₂O₅ glasses, Fe³⁺ site occupancy, Mossbauer studies 7-6541
- Fe₂O₃-P₂O₅-K₂O glasses, mixed valence, EXAFS studies 7-64786
- Fe₂O₃-SrO system, glass ribbon prep. by melt spinning, charactn. 7-53690
- Fe₈₀P₂₀, amorphous ribbons, structural relax., crystallisation, Mossbauer spectra (Chinese) 7-11918
- Fe_{90-x}Si₁₀B₁₀ amorphous alloys, multistep-micro-crystallisation studies 7-21129
- Fe₈₀Si_{20-x} amorphous alloys, struct., mag. and elec. props. (Korean) 7-2893
- Ga₂₀Te₈₀, double glass transition and double stage crystn., X-ray diff. studies 7-58157
- Ge-As-Se chalcogenide glasses, structural models, medium range order and interference functions, first sharp diff. peak calcs. 7-6540
- Ge-As-Se-Te chalcogenide glass fibres for transmission in the 8 to 12 μ m range 7-37192
- Ge-S-bi chalcogenide glasses, struct., DTA and X-ray diff. studies 7-6543
- Ge₃₀As₂₀Se₅₀, glassy semiconductor, structural models 7-44393
- GeO₂ glass, gamma-ray irradi., defect centres, ESR studies 7-6678
- GeO₂ glass, high resolution EXAFS and XANES studies 7-27817
- GeO₂-ZnO-Bi₂O₃ IR transmitting glasses 7-43276
- GeSe₂ glass, photostructural effects, EXAFS study 7-64758
- GeSe₄ amorphous system, struct. anal. by X-ray spectroscopy 7-26653
- Ge₃₅Se₆₅ films, evaporated, structural changes on illumination and heat treatment (Japanese) 7-22489
- Ge₂₀Se_{80-x}Bi_x, n-type amorphous semiconductors, morphological struct. 7-51652
- GeSe₂ glass, photostructural effects, EXAFS study 7-64758
- GeSe₂ glasses, short and medium range order, Mossbauer studies 7-13069
- Ge_{1-x}Sn_xSe₂ glasses, elec. cond. rel. to Mossbauer and Raman spectra 7-64250
- (Ge_{1-x}Sn_x)_{1-x}Se_x(S_x) glasses, percolation transition and strain accumulation 7-11939
- a-Ge_{1-x}Te_x films, crystallisation behaviour and local order 7-44386
- Ge₂X_{1-x} (X=S,Se), chalcogenide glasses, stochastic random network model 7-63493
- Hf_{1-x}Cu_x metallic glass, thermal stability and phase transformations 7-21125
- K₂O-Ga₂O₃-SiO₂ glasses, Raman spectra 7-3035
- K₂O-Nb₂O₅-Ga₂O₃ glass structure, Raman spectroscopy 7-1902
- K₂O-P₂O₅-TiO₂ glass, IR spectra 7-46025
- K₂O-P₂O₅-WO_{3-x} mixed valence glasses, local order, EXAFS and X-ray diff. studies 7-1903
- K₂O-PbO-SiO₂ glasses, chemically nonuniform struct., Rayleigh and Mandelstam-Brillouin scatt. 7-1891
- K₂O-PbO-SiO₂ glasses 7-3036
- K₂O-SiO₂, melt, degree of polymerisation, SiO₄ tetrahedra 7-11921
- K₂O-SiO₂ glasses, molecular dynamics simulation 7-1901
- K₂O-SiO₂ glasses, struct., X-ray diff., molecular dynamics calc. 7-6551
- La-Al, short-range struct., pulsed neutron and X-ray diffraction 7-1912
- La-Si, short-range struct., pulsed neutron and X-ray diffraction 7-1912
- Li borate glasses, density w.r.t. atomic arrangements, comp. depend. 7-6533
- Li₂O-Al₂O₃-SiO₂ glass, cryst. phase nucleation, DTA, X-ray diff. 7-58156
- Li₂O-B₂O₃, ion conducting glass, effect of CaO substitutions on transport and physical props. 7-58535
- Li₂O-B₂O₃ glasses, rapidly quenched, struct. investig. by Raman spectra 7-1913
- Li₂O-SiO₂ glasses, molecular dynamics simulation 7-1901
- Li₂O-SiO₂ glasses, struct., X-ray diff., molecular dynamics calc. 7-6551
- Li₂O-SiO₂ glasses prepared under microgravity and 1-g melting conditions, homogeneity 7-21117
- xLi₂OyLi₂Si₄B₂O₃, IR and Raman spectra, vibr. study and struct. 7-37879
- Li₄TeO₄ glassy electrolyte, vibrational, thermal and elec. charact. study 7-6866
- Mg-Zn metallic glasses, room temp. stability, crystallisation and precipitation 7-11931
- Na₂O-Al₂O₃-SiO₂ glasses, elastic props., annealing and Al substitution effects 7-8035
- Na₂O-Al₂O₃-SiO₂ glass system, strength and struct. features 7-58150
- Na₂O-B₂O₃ glass struct., comparison with pyroborax 7-44391
- Na₂O-B₂O₃ glasses, effect of Na₂O addition, thermal expansion, sp. ht. meas. 7-44862
- Na₂O-B₂O₃-Al₂O₃ glass struct., NMR and computer simulation 7-1898
- Na₂O-B₂O₃-CuO glasses, B ions coordination state studied by X-ray and Raman spectroscopy 7-1892
- Na₂O-B₂O₃-SiO₂, interaction with HNO₃, effect of volumes, radii of channels 7-13613
- Na₂O-B₂O₃-SiO₂ glass ceramic, prep., SiO₂ replacement, phase separation, struct. 7-13428
- Na₂O-B₂O₃-SiO₂ glass, Na⁺ self-diffusion and elec. cond. studies 7-21515
- Na₂O-CaO-Al₂O₃-SiO₂ glass ceramic system, spherulitic growth, mech. props. 7-46405
- Na₂O-CaO-SiO₂ glasses, IR spectra 7-3036
- Na₂O-Fe₂O₃-SiO₂ systems, glass formation and props. 7-2203
- Na₂O-FeO-SiO₂ systems, glass formation and props. 7-2203
- Na₂O-Ga₂O₃-SiO₂ glasses, Raman spectra 7-3035
- Na₂O-SiO₂, melt, degree of polymerisation, SiO₄ tetrahedra 7-11921
- Na₂O-SiO₂ glasses, molecular dynamics simulation 7-1901
- Na₂O-SiO₂:Tb³⁺ glasses, colour centre formation during UV irradiation 7-2049
- Na₂O-SiO₂:Yb³⁺ glass struct. model, Monte Carlo method 7-51644
- Na₂O-SiO₂-FeCO₃-Fe₂O₃ glass system, prep., props and struct. 7-1900

glass structure continued

- Na₂O-SiO₂-NaF, structural analysis for fluorosilicate glasses by X-ray photoelectron spectroscopy (*Japanese*) 7-33510
- Na₂O-SiO₂-TiO₂ system, struct. of glasses and melts (*Japanese*) 7-21121
- Na₂O-SnO₂-SiO₂ glass, diffusion of cations, 500-800°C 7-12371
- Na₂O-TiO₂-GeO₂ glasses, refractive index, density 7-59170
- Na₂O-ZrO₂-Al₂O₃-SiO₂ glasses, ionic cond., glass transition temp. meas. 7-26998
- (Na₂O.2SiO₂)_{1-x}(Fe₂O₃)_x glasses, Fe ions, ionic state and coordination geometry 7-63492
- Na₃Ti₂S₂P₂O₁₂, NASICON-based glass and glass ceramics, synthesis and characterisation 7-44908
- Nb₂O₅-Al₂O₃-B₂O₃-Na₂O-SiO₂ phase separable glass, heat treatment leaching, X-ray diffraction anal. 7-51658
- Ni-B alloy, electroless, heat induced struct. changes 7-13639
- Ni-based metallic glasses, quenched-in excess vol. and structural relax. 7-6531
- Ni-P coating, electrolytic, electron microscope obs. of struct., P content depend., amorphous layer form. 7-8157
- Ni-P glasses, local atomic struct., NMR and EXAFS studies 7-63504
- (Ni-Pd)₈₀Si₁₈ amorphous alloys, corrosion behaviour, struct. relax. effects. 7-8166
- Ni₆₄B₃₆ amorphous alloy, struct., boundary effects, computer simulation study (*Chinese*) 7-11920
- Ni₆₄B₃₆ metallic glass, struct. relax. X-ray and neutron diffr. study 7-6521
- Ni₆₀Nb_{40-x}Al_x metallic glasses, form. and stability, X-ray diffr., DSC obs. 7-58155
- Ni₇₇P₂₃ amorphous alloy, struct. relax. and crystn., elec. resist. and X-ray diffr. obs. 7-1894
- Ni₃₃Y₆₇ metallic glasses, partial struct. factors, chem. short range order 7-63486
- Ni₆₄Zr₃₆ amorphous, short range order, EXAFS 7-44388
- P₂O₅-Dy₂O₃(Pr₂O₃) glasses, struct., mag. and thermal props. 7-26658
- Pb glaze glass system, local coordination EXAFS studies 7-63484
- PbCl₂-Sb₂O₃ glass system, structural aspects 7-44389
- PbF₂-ZnF₂-GaF₃-AlF₃-YF₃-LaF₃:Mn II, Nd III, energy transfer 7-1889
- PbO-B₂O₃-Fe₂O₃ glass, ESCA study 7-26651
- PbO-Fe₂O₃-P₂O₅ glasses, liquid chromatography and Raman scattering studies 7-11946
- PbO-K₂O-Sb₂O₃-As₂O₃ flint type glasses, viscosity near annealing temp., depend. on PbO conc. 7-58151
- PbO-SiO₂ glass, elastic props. and short- and medium-range structs. (*Japanese*) 7-65077
- PbO-SiO₂ glasses, IR spectra 7-3036
- PbO-SiO₂ glasses, struct. anal., X-ray diffr. studies 7-6532
- Pb(PO₃)₂-Fe₂O₃ glass, struct. props., chromatography and Raman spectra studies 7-21112
- Pd-Si base metallic glasses, viscous flow, comp., thermal stability (*Chinese*) 7-12341
- Pd-U-Si glassy state, quasicrystalline phase form., X-ray and electron diffr. studies 7-26645
- PdCuSi, amorphous, reversible and irreversible changes in the thermal conductivity 7-45267
- Pd_{78.5}Cu₆Si_{15.5} metallic glasses, structural relax., vitrification, sp. ht., DSC obs. (*Russian*) 7-37880
- PdO-CdO-B₂O₃ glasses, elec. cond. and density meas. 7-1895
- Pb_{1-x}(ND₄)_xD₂PO₄ structural glass phase, X-ray scatt. meas. 7-26660
- Se, glassy state, phys. props., chem. bonds and defects 7-6530
- Se_{100-x}Ge_x amorphous alloy, photodarkening, structure model anal. 7-3003
- SiO₂, cluster approx. of electron struct. 7-12591
- SiO₂ glass, radiation damage 7-32520
- SiO₂ glass, structural EXAFS study 7-64762
- SiO₂, radial distrib. functions, glassy struct. and bond angles, Monte Carlo method 7-11924
- SiO₂ sol-gel glass structures, effects of water content of gels, EPR study 7-6526
- SiO₂ sol-gel glasses, structure, paramagnetic defect centres 7-11945
- SiO₂, vitreous, Raman structural correlations 7-63501
- SiO₂, vitreous, surface struct., mol. dynamics simulation studies 7-63497
- SiO₂:F, quartz glass, struct. study using ¹⁹F-NMR (*Japanese*) 7-21122
- SiO₂:OH, X-irrad. induced defect centres, EPR obs. 7-45221
- SiO₂-Al₂O₃, thermal capacity, thermodynamic props. 7-12307
- SiO₂-Al₂O₃ glass, roller-quenched, NMR evidence for 4-, 5- and 6-fold Al sites 7-44384
- SiO₂-Al₂O₃-Li₂O-ZnO-TiO₂-ZrO₂-As₂O₃-Cr₂O₃:Cr, glass ceramic, time resolved spectra 7-63478
- SiO₂-GeO₂ system, gels and gel-glasses, struct. study using vibr. spectroscopy 7-44381
- SiO₂-Na₂O-Al₂O₃-ZnO-Fe₂O₃-Si glass system, Fe behaviour at various compositions and reducing conditions 7-1899
- SiO₂-P₂O₅ glass, reflow characts, rapid thermal annealing 7-59553
- SiO₂-P₂O₅ glass films, deposited by different CVD methods, phys. props. 7-27220
- SiO₂-TiO₂, thermal capacity, thermodynamic props. 7-12307
- SiP₂O₇ glass, vibrational spectra of structural units 7-3034
- Si₃Se_{1-x} glass system, diffr. isobestic points and structural systematics 7-44390
- Si₃Se_{1-x} glasses, intermediate range order 7-11938
- Si₃Se_{1-x} low dimensional inorganic polymer glasses, cross-linked chain cluster model 7-11937
- Si₃X_{1-x}(X=S,Se), chalcogenide glasses, stochastic random network model 7-63493
- Te-Cl and Te-Cl-S, chalcogen halogen glasses, IR transmitting materials (*French*) 7-1905
- Te-Ge alloy glass, isothermal surface crystallisation 7-58576
- Ti-Ni-Cu system metallic glasses, superplastic props. in vitrification temp. range 7-3356
- TiO₂-GeO₂ glasses, crystallisation, ion coordination, X-ray diffr., IR spectra 7-6523
- Ti₈₄Si₁₆ metallic glass, total struct. factors, neutron and X-ray diffr. studies 7-6546
- Tl-Ge-Se, bulk glass formation region, elec. and struct. characts. 7-58159
- Y-Si-Al-O-N glasses, Si coordination, NMR studies 7-1906
- Y₂O₃-Al₂O₃-B₂O₃ system, glass formation, props. and struct. 7-2205
- ZnO-SiO₂ amorphous system, structure, mol. dynamics computer simulation studies 7-21114
- ZnO-SiO₂-M₂O (M=Li,K,Na), glasses, thermal expansion, free volume 7-58152

glass structure continued

- Zr-Ni(V) amorphous superconductors, struct. and supercond. props. 7-27482
- Zr₇₀Au₃₀, spontaneous oxidation in air, effect of humidity, pulverisation 7-3510
- ZrF₄-BaF₂-CsF glasses, ionic conductivity 7-52129
- ZrF₄-BaF₂-ThF₄-LiF quaternary glasses, ionic cond. and NMR studies 7-6865
- glass transition (glasses)
- see also vitrification
- alkali silicate glasses, internal friction, amplitude depend., cooperative movement parameter near the glass transition temp. 7-2099
- alloys, local atomic struct., computer simulation 7-58160
- 2-chlorobutane, solns., glass transition, conformational equilib., IR spectra 7-31044
- chlorocyclohexane, solns., glass transition, conformational equilib., IR spectra 7-31044
- cholesteryl acetylferulate, liq. cryst. transitions, glass transition and cold crystn., DSC study 7-63814
- cholesteryl hydrogen phthalate, glass transition study, positron lifetimes meas. 7-38201
- condensed nucleation systems, size effects on glass temp., percolation theory 7-58473
- crystal melting and liquid quenching in two-dimensions 7-16748
- trans-1,2-dichlorocyclohexane, solns., glass transition, conformational equilib., IR spectra 7-31044
- dynamical theory 7-58476
- fluctuating nonlinear hydrodynamics 7-2206
- freezing as kinetics time scale singularity 7-26954
- gelatin-water system mixed crystal formation and glassy solidification 7-16717
- glass temp. derivation, condensed nucleation, percolation theory appl. 7-6794
- glucose, water mixtures, liq. and glassy states, dielectric relaxation study 7-33325
- glycerol, specific heat near glass transition 7-2207
- heat capacity at the glass transition 7-63817
- internal energy effects 7-16744
- Kirkpatrick's theory, nonlinear integral equation 7-44814
- Lennard-Jones system, close to glass transition, dynamics 7-38198
- master-equation approach to the glass transition 7-63818
- material analysis, computer-based, conf., Boston, MA, USA (Dec. 1985) 7-14709
- memory effects 7-2204
- metallic glasses, struct. relax., theory (*Russian*) 7-44397
- mixed alkali borate glasses, transform. range viscosity, thermal expansion 7-52103
- multicomponent glass forming systems, devitrification under diffusion control, theory 7-12279
- neutron spin-echo study of dynamic correlations near liq-glass transition 7-44817
- polyethylene oxide-water system, high molecular, calorimetric obs. (*Russian*) 7-12325
- propylene glycol, specific heat near glass transition 7-2207
- relaxational processes, eqn. of state 7-21386
- silicate glasses containing alkali and alkaline earth metals, alkali ion mobility (*Japanese*) 7-27007
- simple molten salt, relaxation near liquid-glass transition 7-6492
- softening point determ., numerical method, calculator program (*Czech*) 7-6796
- supercooled liquids interacting with repulsive Yukawa pot., glass transition 7-63856
- triphenylchloromethane-o-terphenyl, sp. ht. capacity and glass transition temp. meas., thermodynamic config. anal. 7-21446
- viscous flow in supercooled liquids, transport theory anal. 7-63863
- water, quenched to low temp., glassy state, Monte Carlo simulation 7-26633
- AgI-Ag₂MoO₄ glasses, ionic conductivity, effect of structural relax. 7-44903
- AgI-Ag₂MoO₄ system, conductivity in the liquid and glassy states 7-44881
- AgI-Ag₂AsO₄ superionic conducting glass, cond. and glass form. studies 7-32711
- Al₂O₃ glass, gel produced, optical transmission rel. to heat treatment 7-27733
- As-Sb-Se glasses, calorimetric meas. 7-26652
- (As₂Se₃)_{1-x}Tl_x, elec. and thermal transport props., effect of Tl addition 7-38200
- CaMgSi₂O₆, diopside, thermal expansion and glass transition, quenched defects effects 7-12333
- Co₂O₄-P₂O₅ system, thermal analysis from room temp. to softening pt., vibr. anharmonicity, US vel. 7-12221
- CsBSi₂O₆, glassy and crystalline, IR spectra 7-59199
- Cu_{0.96}Fe_{0.04}SiF₆.6H₂O Jahn-Teller cryst., glass transition, calorimetry and Mossbauer studies (*Russian*) 7-26952
- Fe-M-B metallic glasses (M=Ti,V,Cr,Mn,Co,Ni,Cu,Pd,C,Si,Ge,Sn), formation kinetics, thermal stability 7-58474
- Fe-Ni based metallic glasses, quenched-in excess vol. and structural relax. 7-6531
- Ga₂₀Te₈₀, double glass transition and double stage crystn., X-ray diffr. studies 7-58157
- Ge-S+bi chalcogenide glasses, struct., DTA and X-ray diffr. studies 7-6543
- GeS and GeSe, chalcogenide glasses for IR fibres, plasma deposition 7-37191
- (GeSe₂)₇₀(GeTe)₁₅(Sb₂Te₃)₁₅, glass transition, thermodynamic and thermokinetic characts. 7-26953
- Ge₂₀Te₈₀ glasses, heat capacity, relax. and thermodynamic kinetics during annealing 7-44843
- KBSi₂O₆, glassy and crystalline, IR spectra 7-59199
- K₂O.2B₂O₃ glasses, pulse irradiated, optical absorpt. spectra, temp. effects on the decay process (*Japanese*) 7-22281
- Li₂O-B₂O₃, ion conducting glass, effect of CaO substitutions on transport and physical props. 7-58535
- Li₂O-P₂O₅-PON, nitrogen phosphate glasses, preparation from PON (*French*) 7-26657
- Li₂O-SiO₂ glass, critical cooling rates for nucleating agents 7-6795
- Li₂O.2SiO₂ sol-gel glass, prep. and devitrification behaviour 7-58158
- MoO₃-P₂O₅ glasses, thermal anal. between room temp. and softening point 7-12329

glass transition (glasses) continued

- Na₂O-B₂O₃-SiO₂ glass, porous, sintering temp, glass transition temp. (Japanese) 7-7954
- Na₂O-Fe₂O₃-SiO₂ systems, glass formation and props. 7-2203
- Na₂O-FeO-SiO₂ systems, glass formation and props. 7-2203
- Na₂O-K₂O-Ga₂O₃-SiO₂ glasses, glass transform temps., mixed alkali effect 7-6793
- Na₂O-P₂O₅-PON, nitrogen phosphate glasses, preparation from PON (French) 7-26657
- Na₂O-Y₂O₃-MO-SiO₂ glass, (M=Mg, Sr, Ca), Na⁺ conductivity 7-52134
- Na₂O-Y₂O₃-SnO₂-SiO₂ glass, Na⁺ conductivity 7-52134
- Na₂O-ZrO₂-Al₂O₃-SiO₂ glasses, ionic cond., glass transition temp. meas. 7-26998
- Na₂O.2B₂O₃ glasses, pulse irradiated, optical absorpt. spectra, temp. effects on the decay process (Japanese) 7-22281
- NaPO_{2-x}N_y glass prep. and props., comp. calcs. 7-7951
- Ni-based metallic glasses, quenched-in excess vol. and structural relax. 7-6531
- Ni₄₀Pd₄₀P₂₀ alloy glass, solid-liq. interfacial energy 7-2208
- Ni₄₀Pd₄₀P₂₀ glass transition, internal friction by Collette torsion pendulum 7-38199
- Ni₄₅Pd₃₅P₂₀ metallic glass, decomposition, crystallisation and embrittlement, atom-probe FIM study 7-33639
- P₂O₅ glass transition and viscosity meas. 7-58475
- Pd-Si base metallic glasses, viscous flow, comp., thermal stability (Chinese) 7-12341
- Rb, supercooled liquid, structural relax. 7-37840
- RbBSi₂O₆, glassy and crystalline, IR spectra 7-59199
- RbCN, cryst., phase transition and glass transition 7-12260
- Rb_{1-x}(ND₄)_xD₂PO₄, NMR in random fields, cluster formation and local dynamics of D glass 7-38959
- Rb_{1-x}(NH₄)_xH₂PO₄, press. depend. of proton glass freezing, dielec. props. 7-2209
- SiC fibre reinforced Li₂O-Al₂O₃-SiO₂ glass ceramic composite, thermomech. mismatch 7-46538
- SiO₂ liq., stretched and compressed, glass transition, ion dynamics simulation 7-16747
- Si₃Te_{100-x} glasses, crystallisation, DSC studies 7-6542
- TeO₂-based halide glasses, prep., thermal, mechanical, elec. and optical props. characterisation (French) 7-37884
- Tl-Ge-Se, bulk glass formation region, elec. and struct. characts. 7-58159
- Tl₂Se_{100-x} glasses, glass transition, melting, recrystallisation, elec. transport 7-64246
- Y₂O₃-Al₂O₃-B₂O₃ system, glass formation, props. and struct. 7-2205
- ZrF₄-BaF₂-AlF₃ glass, viscous flow vs. phase separation, DSC study 7-44383
- ZrF₄-BaF₂-LaF₃-AlF₃, heavy metal fluoride glass system, viscosity and crystallisation 7-37883
- ZrF₄-BaF₂-NaF glasses, crystallisation study 7-11933

glass transition (polymers)

- amorphous polymers, secondary relax. processes, thermal history effect 7-63819
- amorphous polymers, yield stress rel. to ageing, nonequilib. glassy state 7-46562
- bisphenol-A-based epoxy resins, physical props. rel. to curing 7-46539
- epoxy aniline phenolformaldehyde binder, mol. mobility and relax. processes, C filler conc. influence (Russian) 7-21447
- epoxy polymers, amine cured, struct., positronium annihilation spectroscopy 7-46176
- equations of state, multiple hole energy model 7-21388
- excluded-volume interaction, Flory-Huggins theory 7-2151
- films, stress development during thermal cycling, bending beam technique 7-28063
- fluoroelastomer copolymers and tercopolymers, glass transition temps. 7-12280
- fluoroelastomer copolymers and terpolymers, glass transition temps. calcs. 7-16745
- glass temp. derivation, condensed nucleation, percolation theory appl. 7-6794
- hydrocarbons and fluorocarbons, plasma polymerised, cross-linking and average coordination 7-8276
- oligocaprolactone glycol-PVC, amorphous matrix, crystallisation (Russian) 7-11969
- partially crystalline, viscoelastic and acoustic props. on hydrostatic compression 7-33719
- PEEK, cryst., mech. relax., electron beam irradiation effects 7-16686
- PET, biaxially oriented, effects of thermal treatment 7-12193
- PET, high-temp. viscoelasticity and heat-setting, strain recovery meas. 7-63721
- PMMA, brittle-viscous transition, mechanism (Russian) 7-21448
- PMMA, glass transition, Gibbs-DiMarzio theory 7-12281
- PMMA, glass transition, high press. (Russian) 7-63821
- PMMA, glass transition temp. and stress relax. 7-52049
- PMMA, photon correl. spectra above T_g evidence of two relax. processes 7-32650
- PMMA, relax. transforms. from relax. spectrometry (Russian) 7-63822
- PMMA, T_g and T_m tacticity depend., DSC investig. 7-12277
- poly(acrylic acid)-ceramic filler composite, filler chem. influence on T_g behaviour, dynamic mech. spectroscopy 7-59559
- poly(ether sulphone)-poly(dimethylsiloxane)-poly(ether sulphone), elastic modulus in glass transition range 7-63722
- poly-α-methylstyrene, glass transition, Gibbs-DiMarzio theory 7-12281
- polyaryl ether ketone blends, isomeric behaviour, miscibility, glass transition and melting temps. 7-44416
- polyaryl-ether-ether-ketone, semicryst., mech. relax., electron beam irradiation effects 7-12204
- polyarylate, mol. motions in glass transition region, thermally stimulated depolarisation current 7-38586
- polyarylate, relaxation time, viscosity, above glass transition 7-12344
- 1,2-polybutadiene, mol. motion, glass transition, loss curve, NMR, ¹³C spin-lattice relax. 7-17234
- polybutadienes, high-temp, struct. transition obs. (Russian) 7-63820
- polybutyl methacrylate, tensile flow, stress-strain behaviour, temp. depend., mol. wt. 7-6847
- polydimethylsiloxane, refr. index and thermal expansion coeff. variations with temp. 7-39060
- polyetheretherketone, phys. ageing characts. 7-65110
- polyethylene, branched, phase transforms. obs., positron lifetime meas. 7-46231

glass transition (polymers) continued

- polyethylene, spherulitic low density, dielec. relax. of dipolar aromatics, glass transition 7-45924
- polyethylene glycol, phosphate ester crosslinked complexes, ionic cond., temp. depend., glass transition 7-52128
- polyethylene terephthalate, glass transition and crystallisation studies, positron annihilation meas. 7-46230
- polyimide thin films, friction and wear rel. to struct. 7-8130
- polyisobutylene, glass transition, mol. wt., Gibbs-DiMarzio statistical mech. theory 7-44815
- cis-polyisoprene, relax. time discontinuous spectra, relax. transitions (Russian) 7-44642
- polymeric glasses, enthalpy relax. determ. (Japanese) 7-38197
- polymers, internal friction, amplitude depend., cooperative movement parameter near the glass transition temp. 7-2099
- polymers, semicrystalline, EPR, elastic modulus data, mol. mobility phenomena 7-37900
- polypropylene, microindentation hardness and dynamic mech. moduli near glass transition 7-13564
- polypropylene, quenched, isotactic, glass transition, effect of drawing 7-12278
- polypropylene oxide 4000, liq. and glassy states, dielec. props. 7-17266
- polypropylene oxide 4000, liq. and glassy states, dielec. relax. and permittivity 7-13083
- polypropylene-ethylene-propylene copolymer blends, isotactic, mechanical props. and morphology 7-63539
- polystyrene, atactic, uniaxially drawn, CO₂ sorption 7-32812
- polystyrene, glass transition, enthalpy relax. kinetics (Russian) 7-6797
- polystyrene, glass transition, Gibbs-DiMarzio theory 7-12281
- polystyrene, solid, liq., p-substituted, and crosslinked, heat capacity 7-44844
- polystyrene/styrene-methyl methacrylate random copolymer blend, DSC obs. of miscibility 7-12291
- polysulfone, relaxation time, viscosity, above glass transition 7-12344
- polytrimellitimide films, dynamic mech. props., glass transition, molecular aggregation effect 7-53782
- polyurethane-CaCO₃ composites, segmented, dielec. relax., glass transition 7-45926
- polyvinyl methyl ether, ageing, enthalpy relax. meas. 7-8029
- polyvinyltrimethyl silane, plasticised, low-mol. cpd. translational and rot. mobility (Russian) 7-44818
- PVC, brittle-viscous transition, mechanism (Russian) 7-21448
- PVC, glass transition, Gibbs-DiMarzio theory 7-12281
- PVC-chlorinated PVC, miscible blends, rheological and mech. props. 7-8040
- PVDF/PMMA blends, electret props., effects of structure, open-circuit thermally stimulated current anal. 7-13087
- styrene copolymers, glass transition, enthalpy relax. kinetics (Russian) 7-6797
- tetrafluoroethylene-perfluoroethylene copolymers, composition-props. correls. (Russian) 7-16746
- N-vinyl carbazole-alkyl methacrylate random copolymers, thermodynamic props. (Russian) 7-26982
- vinyl pyrrolidone copolymers, highly swollen hydrogels preparation 7-21073
- C fibre reinforced plastics, strength, thermomech. props. thermal spiking and moisture absorpt. effect 7-28085

glasses see glass

glassy state see vitreous state

glide, dislocation see slip

Global Positioning System see radionavigation; satellite relay systems

globular star clusters

- ages, colloquium, Rome (April 1986) 7-55879
- ω Cen, rot., vel. dispersion, and mass determ. 7-9520
- ω Cen, RR Lyr stars spectroscopy 7-34979
- ω Cen, search for double-mode RR Lyr stars 7-4469
- ω Cen, soft X-ray obs. with EXOSAT 7-29506
- characteristics and member stars 7-24169
- colour-magnitude diagrams, bibliography 7-60917
- core collapse, effects of two-body tidal capture of main sequence stars and white dwarfs 7-4500
- dark matter nature 7-60658
- dynamical modelling 7-14613
- dynamics, completely analytical family of anisotropic Plummer models 7-55741
- dynamics, stability of multi-component gravit. systems described by Boltzmann eqn. 7-4525
- E2, E3, deep CCD photometry and colour-magnitude diagrams 7-66685
- E2, intermediate-age LMC cluster, colour-magnitude diagram rel. to age and metallicity 7-40883
- in elliptical galaxies, implications for galaxy mergers 7-4572
- formation, Population II stars as 'dirty' primordial Population III 7-29470
- formation redshift, implications for zero-value cosmological const. 7-24250
- Fornax dwarf spheroidal galaxy, globular clusters radial vel. 7-14649
- giant star radial velocity observations 7-40886
- giant stars, Washington photometry, abundance calibrations 7-9471
- head-on binary collisions in globular clusters, collision probabilities 7-60739
- horizontal-branch stars, cosmon effects on HB lifetime rel. to solar neutrino problem 7-55436
- IC 4499, double-mode RR Lyr stars, pulsation characts. and masses, photometric obs. 7-14616
- interstellar Na I line strength versus reddening relation, influence on stellar population synthesis 7-9526
- isotropic stellar systems, linear oscills., non-radial modes 7-35014
- LMC clusters, age determ., metallicity-age relation and AGB stars luminosity function 7-4561
- RR Lyr star light curves, Fourier analysis 7-66599
- M14, Nova Oph 1938 optical candidate 7-60678
- M15, discovery of emission-line object in cluster core 7-14596
- M15, EXOSAT obs. of X-ray source 7-60732
- M15, Fourier analysis of RR Lyr light curves 7-66599
- M15, X-ray binary AC 211, photometric and spectroscopic periods 7-29514
- M15, X-ray modulation period for 4U 2129+12 (=AC 211) 7-29515
- M15 (=NGC 7078), globular cluster, stellar evolution and pulsation theory 7-60736
- M22, stellar proper motions, membership, and photometry 7-4530

globular star clusters continued

- in M31, cluster candidates in $3^\circ \times 3^\circ$ field 7-66478
M4 (=NGC 6121), globular cluster, stellar evolution and pulsation theory 7-60736
M62, colour-magnitude diagram characts. 7-60737
in M87, spectroscopy of cluster system 7-48001
M92, main sequence colour-magnitude diagram 7-66689
Magellanic Clouds clusters, effects of AGB mass loss on AGB luminosity-age relation 7-24127
main sequence mass functions, determ. from CCD photometry and stellar models 7-66586
main-sequence luminosity functions, effects of mass segregation 7-40884
mean field fluctuations and the evolution of self-gravitating systems 7-14619
metal rich globular clusters, spectral characts. 7-14614
metal-poor field subdwarfs, age and temp. characts. 7-47865
metal-rich clusters, metal abundance, metallicity scale 7-40881
metal-rich globular clusters, Washington system photometry and metallicities of giant stars 7-9523
NGC 1904 (M79), radial velocities of giant stars 7-40886
NGC 288, radial velocities of giant stars 7-40886
NGC 330 in SMC, supergiant A7 composition anal. 7-34970
NGC 4147, radial velocities of giant stars 7-40886
NGC 4833, red giants IR photometry 7-60740
NGC 5272 (M3), radial velocities of giant stars 7-40886
NGC 5466, radial velocities of giant stars 7-40886
NGC 5904 (M5), radial velocities of giant stars 7-40886
NGC 6121 (M4), radial velocities of giant stars 7-40886
NGC 6171, NGC 6723, DDO photometry and metallicities of giant stars 7-9522
NGC 6171 and 6723, Fourier analysis of RR Lyr light curves 7-66599
NGC 6388, RR Lyr stars photometry 7-35016
NGC 6397, metal-poor globular cluster, spectroscopy of hot horizontal-branch stars 7-47859
NGC 6397, NLTE-analysis of ROB 162, sdO star 7-40805
NGC 6401, variable stars light curves 7-14615
NGC 6624, 4U 1820-30 period anal. 7-9512
NGC 6624, discovery of 685-s orbital period for X-ray binary star (4U 1820-30) 7-66666
NGC 6624, SAS-3 obs. of X-ray binary 4U 1820-30 rel. to 685-s period 7-9511
NGC 6624, study of neutron star in 4U 1820-30 X-ray burster 7-60703
NGC 6637, spectroscopic identification of new variable as Mira-type star 7-47906
NGC 6752, photographic photometry of giant, asymptotic, and horizontal branches 7-29520
NGC 7078 (M15), radial velocities of giant stars 7-40886
NGC 7492, CCD photometric obs. 7-60738
orbital motion, around galactic centre, numerical expts. 7-24231
post-collapse evolution, N-body statistical stellar dynamics model 7-40885
quasars absorption lines form., role of globular clusters 7-40952
radial motion of giant stars, spectroscopic measurement technique 7-40718
red giants, empirical colour-metallicity relations 7-55616
relativistic collapse of cluster to black hole 7-66682
SMC globular clusters, spectral classification of bright stars 7-4354
SMC globular clusters, spectral classification of bright stars 7-29412
SMC star clusters, observed radii and structural parameters 7-4564
stellar encounters, cross sections for tidal capture binary form. and stellar merger 7-29519
47 Tuc, rot., vel. dispersion, and mass determ. 7-9520
ultrashort period binary stars in globular clusters, form. mechanism 7-66667
Universe age, constraints from globular clusters and cosmic expansion rate 7-55869
X-ray sources in galactic bulge and globular clusters, radio obs. 7-29511
CN-strong stars, origin due to binary coalescence 7-66601

glossaries

No entries

glow curves see *thermoluminescence*

glow discharge deposition see *plasma deposition*

glow discharge lamps see *discharge lamps*

glow discharge microphones see *microphones*

glow discharges

- air stream parameter effects on glow discharge, CO₂ laser appl. 7-51531
atomic beam production by hollow-cathode discharge, characterization by fluorescence spectroscopy 7-365
carbon tetrachloride glow discharges, spectral and probe diagnostics 7-32153
cathode region, electron energy, spectrosc. investig. 7-21007
cathode spot, entry into capillary hole 7-32160
cathode spot in normal glow discharge, distinctive feature 7-20989
DC, two dims. model 7-21004
DC discharge in pin plate electrode configuration with auxiliary electrode, CW CO₂ laser appl. 7-51526
dispersive plasma-satellites of dipole-forbidden transition 7-63391
electric field calculations using the ELF codes for glow discharge switches and electrode design 7-32134
electron beam production, high-power production and appl. (Czech) 7-56373
electron beams, abnormal glow discharge creation, energy spectrum 7-26564
electron distribution fn. in anode sheath of glow discharge, kinetic problem soln. 7-37627
FTIR/time resolved spectrometry, rapid scan, for gas phase systems, IR source development 7-48879
helical hollow cathode discharge, water cooled, laser generation of Cu II, Kr II, Ar II and Ne I lines 7-57299
high voltage discharge, electron beam meas, using photographic technique 7-63376
high voltage discharge, electron density, temp. meas. using Langmuir probe 7-63375
hollow anode glow, characteristics 7-44282
hollow cathode discharge, optogalvanic effects 7-20992
hollow cathode discharge at direct and HF current, temp. meas., spectroscopic study 7-20994
inert gas, hollow cathode discharge, at. energy level excitation, laser lines 7-1804

glow discharges continued

- ion gun, applic. to sputtering yield meas. 7-13303
ion source, ion energy distributions 7-4914
ion source performance improvement in glow discharge mass spectrometry 7-9916
ionised gases, atomic and mol. physics, conf. Greifswald, Germany (Aug. 1986) 7-18499
metals, emission spectrochemical anal. using glow discharge, appl. to in-depth anal. (Japanese) 7-63886
methane, glow discharge, stimulation of methanol formation 7-32178
modeling, theoretical and computational problems 7-37796
multiple-cavity hollow cathode, arc discharge, gas containing alkali metal atom additions 7-32179
nonlinear structures, algebra of attractors 7-37788
nonself maintained discharge with nonuniform external ionisation, current-cond. channel form. 7-58090
optical detection voltage for glow discharge in DC mag. field 7-15000
optical spectrometry, glow discharge, for quantitative surface anal. 7-28373
plasma deposition using directional evaporator with hollow cathode, flow cross section, ion current density 7-3202
plasma electron emitter, grid-stabilised, expt. 7-44297
poloidal magnetic field effects 7-21023
polyethylenes, supermol. struct., glow-discharge induced transformations (Russian) 7-63523
positive corona, math. anal. of glow and dark space regions 7-20982
pulsed electron beam generation by cold cathode plasma guns, appl. to laser excitation 7-26534
RF plasma sheath, ion transport, Monte Carlo modeling 7-37797
shock wave acceleration 7-6478
spectroscopic source for anal. of powders, at. transport phenomena 7-30097
stability, Schottky theory calcs. 7-21018
steel, stainless, surface corrosion products after exposure to liq. alkali metals, glow discharge optical spectroscopy, SIMS anal. 7-22896
steel spectra layer-by-layer anal., using glow discharge 7-54241
super-dense hollow cathode discharge, plasma light amplification (Japanese) 7-6476
surface analysis, glow discharge optical spectroscopy (French) 7-20998
tokamaks, carbonisation, plasmachemical in situ deposition 7-63296
torus, H₂/CH₄ and H₂ glow discharge cleaning (Chinese) 7-6431
UV sustained radial glow discharge opening switch investigation 7-32133
uV-sustained glow discharge opening switch experiments 7-32132
UV-sustained glow discharge opening switches 7-26538
Ar high press. discharge, X-ray initiated, laser appls., anal. 7-63385
Ar, hollow cathode glow discharge, Fe, I-line excitation processes, investig. 7-19775
Ar, hollow cathode glow discharge, UV radiation and positive ions, investig. 7-21000
Ar, RF glow discharges, low-pressure, large-signal time domain modeling 7-58076
Ar, spectral line press. broadening and shift 7-42553
Ar-hexamethyldisiloxane glow discharge, charge carrier prod. 7-32172
Ar-tetrafluoromethane glow discharge etching of Si 7-32170
CO₂-He-N₂, vibr. nonequib. flow in axisymmetric channel with glow discharge 7-20741
CO₂-N₂-He mixtures, self-sustained and nonself-sustained glow discharges 7-44290
Cd⁺, ion drift velocity in He glow discharge, meas. using AlGaAs laser (Japanese) 7-20294
Cl₂, plasma etching reactor, atomic Cl conc. and gas temp., laser spectroscopic meas. 7-58069
Cu₂, glow discharge sputtering, laser-excited fluoresc. 7-10647
H discharge, atmospheric pressure, transition region, static V-I characteristics 7-51536
H glow discharge, plasma etching of Si and GaAs 7-32168
H₂ discharge, electron beam energy relax. mechanism in electrode sheath 7-51464
H₂, glow discharge, C cathode chem. sputtering 7-32171
He DC glow discharge positive column, gas temp. 7-32151
He diaphragmed discharge, multiple contraction 7-20972
He discharge, atomic and molecular metastables, population transient behaviour 7-37783
He glow discharge, cathode fall, spectroscopic diagnostics 7-37763
He glow discharge, wall effects on electron component in ion sound regime 7-21029
He, glow discharge positive column, radial behaviour, self-consistent soln. 7-21034
He positive column, population difference and pulse-mode optogalvanic effect 7-26570
He-Kr⁺ laser operation, DC He and He-Kr discharges in Al hollow cathode tubes 7-10912
He-SF₆, low pressure glow discharge, magnetic control 7-32161
He-SF₆ glow discharge, mag. control, electron energy distrib. 7-26555
He+He, associative ionisation in glow discharges 7-62506
In-glass, glow discharge induced changes 7-12577
N₂, glow discharge, I⁺ absorpt. system, gas heating dynamics 7-37790
N₂, glow discharge, electron kinetics, Boltzmann and vibr. rate balance eqns., self-consistent solns. 7-21035
N₂ laser, atmospheric pressure, asynchronous progress of excitation across glow 7-44286
N₂, pulsed, time-resolved Fourier transform spectra of IR emission 7-51538
N₂ quasisteady glow discharges, current contraction study 7-32152
N₂, subnormal glow discharge, instability study 7-32181
NH₃D⁺, ν_4 fundamental band, IR difference-freq. laser spectra 7-50096
Ne, high-frequency discharge, dissoci. recomb. of excited atoms in after-glow 7-10456
Ne, optogalvanic spectra using tunable laser radiation 7-61389
Ne₂⁺ glow discharge, time depend. of spectral line intensities from after-glow plasma 7-32142
O₂, glow discharge, C cathode chem. sputtering 7-32171
O₂ glow discharge, IR band sequence at 0.1 Torr, obs. 7-37784
O₂, glow discharge, metastable at. and mol. processes 7-16342
Pb₂, glow discharge sputtering, laser-excited fluoresc. 7-10647
SF₆, corona and glow discharges, electrode-F reaction influence 7-26565
SiH₄ glow discharge, ion-molecule reactions and amorphous Si deposition 7-65325
SiH₄, Si₂H₆ and SiH₂Cl₂ plasmas, optical emission spectroscopy, mass spectrometry and laser-induced fluorescence 7-37764

glow discharges continued

- SiH₄+Si₂H₆+Ar+H₂, plasma enhanced CVD of a-Si:H, integrated model 7-39423
 TiCl₄+NH₃; RF glow discharge, plasma enhanced CVD of TiN 7-39427

glueballs see colour model; meson resonances; quark confinement**gluon plasma** see nuclear matter**gluonia** see colour model; meson resonances; quark confinement**GO calculations**

see also GTO calculations

- atoms and ions, H to Ne, relativistic Gaussian basis sets 7-36468
 Cartesian Gaussian orbitals, pseudopotential matrix elements (*Russian*) 7-15489
 pseudopotential in Cartesian Gaussian orbitals, matrix elements, recurrence formulae (*Russian*) 7-25377
 Be₂, bonding, appl. of local spin density approx., comparison with other studies 7-25371
 Cr₂, bonding, appl. of local spin density approx., comparison with other studies 7-25371

gold

see also nuclei with

- acoustic-jet plating of 7.5 MHz 7-59462
 adsorbate layer struct. on Mo (110), Auger electron peak shape study 7-46254
 adsorbed monomolecular layer, giant Raman scatt. effect 7-52255
 adsorbed on Si (111), SEM, LEED and scanning Auger microscopy obs. 7-21056
 adsorbed on W (110), thermal desorption spectroscopy 7-27119
 adsorption on W (110), calcs. based on nonadditive effective binding pot. 7-12483
 Alai Range, USSR, mineral exposures and tectonic associations 7-8883
 aqueous colloids, diffusion- and reaction-limited kinetic aggregation, cluster-mass distrib. meas., dynamic scaling 7-21467
 archaeological artifacts, light element determ. by nuclear reactions 7-59814
 atom, photon cross section meas. 7-57016
 atom, valence energy and polarisability, semiempirical pseudopot. calcs. 7-56926
 atoms, diffusion through oxide layers on Al 7-8200
 binding energies and elastic constants, one-parameter model pseudopotential calc. 7-44650
 British Columbia, Canada, Au and Ag mineralization of Early Cretaceous age 7-65997
 calorimetric study of laser-irradiated thin foil targets 7-32026
 cascade damage under heavy ion irradiation at high temp., in situ obs. 7-58368
 cascade overlap effect on defect struct. after repeated neutron irradiation 7-51859
 cathode photoelectric detectors, absolute photon sensitivity characterisation 7-24704
 clusters, electron microscopy of small particles 7-1824
 clusters and bulk samples, Debye temps., EXAFS studies 7-2136
 clusters on highly oriented pyrolytic graphite, scanning tunnelling microscopy study 7-12413
 coated Ag spheres, single crystals, superheating 7-44767
 coated Fe-Ni Reed blades, AES/SEM study 7-44972
 coating on abrasive paper, highly reflecting diffusers, middle-IR region, develop. status study 7-57615
 colloidal particles, optical nonlinearities, surface resonances and quantum size effects 7-50648
 conduction electrons, gyromag. factor calcs. 7-7099
 core holes, final-state screening, total energy calcs. 7-2526
 crystal, H⁺ ion channelling, catastrophe theory 7-21312
 crystallites, annealing, grain boundary untwisting and untwisting, dislocation climb and glide 7-12076
 crystallites, diffusion process on (100) cleavage planes of KBr, KCl, NaCl 7-21590
 crystals, small, surface twin form., high resolution electron microscopy 7-44566
 CVD by laser induction 7-22564
 defect development from displacement cascade damage in low temp. neutron irradiation 7-51851
 defect struct. evolution following DT neutron irradiation 7-58346
 defects in multiply-twinned particles 7-16558
 deposited on NaCl, elastic surface wave anomalies near cluster to layer transition 7-21606
 deposition onto sputtered and cleaved Hg_{1-x}Cd_xTe surfaces, UPS study 7-33514
 deuteron irradiation, multiple fracture planes, bubble growth 7-58372
 discontinuous films, charge carrier mobility, temp. depend. 7-22035
 discontinuous films, percolation metal-insulator transition, nonlinear behaviour 7-45156
 discontinuous metallic thin films, on amorphous and crystalline substrates, electron irradiation stimulated coalescence 7-2437
 displacement cascade damage computer simulation using binary collision approx. code (*Japanese*) 7-32535
 electrical resistivity, temp. depend. 7-58792
 electrodeposition from acidic plating baths, minute amounts of metal ions effect (*Japanese*) 7-3503
 electron localisation and size effect in single-crystal films 7-17118
 electron mean-free-path calculations using a model dielectric function 7-52583
 energy loss straggling of protons and He ions, 0.1 to 1.0 MeV/u 7-12182
 epitaxial growth on W (100), adsorbate props. 7-38329
 epitaxial ultra-thin films, X-ray diffraction studies 7-27204
 etching by photochem. machining 7-22909
 Fermi surface curvature, de Haas-van Alphen effect meas. 7-2467
 film, adhesion on sapphire, ion beam induced enhancement 7-21292
 film, early stages of reaction with amorphous Ni-Nb films 7-21703
 film, furnace for LPE growth system, IR reflectivity (*Korean*) 7-33606
 film, optical props. 7-17296
 film growth on semicond. surfaces, scanning tunnelling microscopy studies 7-21053
 film on Al and its alloys, surface superconducting appl. in electronic devices (*Spanish*) 7-27483
 film on sapphire substrate, adhesion, mechanical resonance spectra 7-21712
 films, (H₂O)_nH⁺ energetic cluster impact, transmission electron microscopy 7-13304
 films, characterisation by SIMS, Auger spectroscopy and TEM 7-12550

gold continued

- films, CVD from Au complexes 7-64915
 films, focused ion beam induced deposition 7-46334
 films, rapid crystn. kinetics under laser irradiation, picosec. transient reflectance meas. 7-11915
 films, surface plasmon modes 7-7316
 films, with surface adsorbed ethylene, adsorbate-substrate bonding 7-52292
 films on amorphous substrates, prep. by surface-energy-driven grain growth 7-38385
 fine powder, synthesis from metallic aerogels 7-3216
 foil, H⁺ induced ridge electrons emission 7-46270
 geological placer deposits in upper Yukon River, Alaska 7-66042
 groundwater of E Siberia, Au and Ag content of mineral waters 7-28922
 initial stages of epitaxy on Si(111), UHV electron microscopy study 7-27210
 interfacial surface energy atomistic estimation and adhesion meas. (*Japanese*) 7-58657
 internal friction background, low-frequency 7-38113
 ion beam, residual ranges in various media, time of flight spectra and adsorption meas. 7-25333
 ions, energy levels, radiation effects and corrections 7-49960
 ions, laser produced spectra and QED effects 7-37747
 laser deposition from triphenylphosphine complexes 7-46341
 layer on GaP, emission spectrochemical anal. using glow discharge, appl. to in-depth anal. (*Japanese*) 7-63886
 liquid, thermoelectric power calc. 7-12704
 liquid metal ion source, focused droplet beam 7-30801
 locally discontinuous thin films, gas-sensitive electrical conduction 7-12882
 mesh IR diffractive filters fabricated by electron beam lithography, spectral and polarising characts. 7-62816
 metal and clusters, dynamical props., EXAFS studies 7-64805
 metal films, mech. props., relation between different quantities 7-8041
 metal-metal and metal-dielectric systems, adhesion calc. 7-7023
 mirror, absorbance meas. at glancing incidence, photoacoustic calorimetry 7-20380
 monolayer on Ni, partial sputtering cross sections 7-59331
 muon arrhenius jump rates, neutrino emission 7-27643
 narrow rings and lines, low-temp. magnetoresist., aperiodic struct. 7-64206
 neutron irradiated, recoil energy effects on cascade defect structures 7-51855
 neutron irradiated, thermal stability of cascade defects, annealing expt. 7-51856
 ordered overlayer on Si (111), surface states, inverse photoemission studies 7-2660
 overlayer an amorphous W-Si thin films, interfacial reactions 7-21763
 overlayer on Ni films, Ni out-diffusion 7-12511
 overlayer on Si(111), room temp. oxidation behaviour, XPS study 7-13676
 overlayer on Si (111), inverse photoemission spectroscopy 7-59280
 particle faces, restructuring TEM study 7-12418
 particles impregnated in NaY zeolite, positron lifetime spectra 7-17358
 particles on NaCl substrate, crystal structure 7-27209
 permeability of H in Ag-Pd, Pt, Ag, Au alloys and metals at 2 kbar and high temp. 7-27011
 phonon spectra, dynamical pseudopot. shell model calcs. 7-51965
 plasma, atomic processes, collisional-radiative and average-ion hybrid models 7-51387
 plasma, heating by Raman-compressed KrF laser, electron temp. meas., radiation loss and radiative energy transport 7-37713
 plasma, X-ray spectroscopic diagnostics (*French*) 7-6445
 plasma laser produced, X-ray line absorpt. 7-20878
 point contacts, electronic thermal cond. temp. depend. study (*Russian*) 7-12789
 polycrystalline tips, grain rotation and grain boundary annihilation, in situ SEM study 7-32460
 positron lifetime in vacancy clusters 7-39259
 positronium work function, temp. depend. 7-58859
 quartz crystal, Sn or Au coated, surface polariton propag. 7-27259
 quenched, vacancy clustering, positron annihilation 7-44534
 shank overlayer effects on Si field ion imaging, photoillumination and field-induced image-size effects 7-33534
 single-layer metallic structures obs. in EUV and VUV 7-22215
 small metallic particles, surface fractal dimension 7-38308
 small particles on amorphous substrates, dynamic atomic-level rearrangements 7-12542
 smooth surface with adsorbed crystal-violet molecules, resonant Raman scatt., charge-transfer excitation 7-17320
 specular refl. of protons, excited state form. dist., reson. charge exchange, multichannel theory 7-46266
 sputtered films, optical and elec. props., influence of surface scatt. of electrons 7-52858
 static compression, basis for ruby pressure scale calibration 7-18802
 steel, stainless, laser alloying with Au(Mo), Rutherford backscattering and channelling studies 7-28206
 structural rearrangements in small metal particles at atomic resolution 7-16576
 structural stability of reconstructed (110) surfaces 7-7326
 submonolayers on Si laser annealed surfaces, Kapitza anomaly reentry obs. 7-38318
 substrate, Ag monolayer electronic struct. and binding energy, photoemission studies 7-39359
 substrate, ferromag. resonance of thin Co films 7-2932
 surface, (100), FCC, hexagonal reconstruction 7-58591
 surface, (100), reconstruction, embedded-atom simulation 7-52199
 surface, (100), reconstruction, glue model 7-32777
 surface, (100), with epitaxial Fe monolayers, surface magneto-optic Kerr effect 7-59080
 surface, (110)2x1, surface structure, X-ray diffraction studies 7-12438
 surface, (110), clean and oxidised, adsorption and oxidation of CO and CO₂, surface reactions 7-59782
 surface, (110), clean and oxidised, adsorption of formic acid and formaldehyde, acid-base and nucleophilic reactions 7-59783
 surface, (110), struct., low energy ion backscattering determ. 7-52205
 surface, (110) (1x2), sp. ht. anomaly for order-disorder transition, LEED study 7-12310
 surface, (111), electronic struct., angle-resolved XPS studies 7-17060
 surface, (111), with adsorbed layers of inert gases, He atom-surface scatt. 7-27851

gold continued

- surface, adsorbed halide and pseudohalide, SERs, metal-adsorbate vibr. freqs., surface bonding 7-12468
- surface, H^+ Auger neutralisation, transition rate calcs. 7-3140
- surface, large angle scattering of H, D and He atoms 7-64854
- surface, laser stimulated desorption during Cl_2 reactions 7-53453
- surface, low energy K^+ small angle scatt. 7-53484
- surface (110), 180° enhancement of ion backscatt. surface peak yield 7-3131
- surface (110), adsorbed benzene and azabenzene, electron affinity levels studied by inverse photoemission 7-44991
- surface (110), adsorbed Xe layers, final state screening in inverse photoemission spectra 7-3104
- surface (110), electron emission, interaction of multiply charged ions with surface 7-53473
- surface (110), struct. and surface energy, Monte Carlo study 7-6945
- surface (111), Cu monolayer, fluoresc. detected surface EXAFS 7-46235
- surface (111), electron state spectroscopy with scanning tunnelling microscope 7-7306
- surface deuterium recombination 7-62063
- surface layer comp., Auger spectra (Russian) 7-58703
- surface reconstruction phase transformations 7-2326
- surface struct., RHEED and reflection electron microscopy studies 7-32232
- surfaces, (111) and (100)-(5 \times 20), surface-atom valence-band photoemission 7-22447
- target, He^{+} electron capture and stripping cross sections 7-10753
- texture of leaf fabricated by hammering 7-39541
- thermal equilibrium vacancies, positron lifetime studies 7-44535
- thermodynamic props., universal eqn. of state of solids 7-44736
- thin film based transparent IR reflectors, prep. and optical props. 7-39201
- thin film form. on Mo (110) chemically modified surface 7-12489
- thin films, on Au (111), surface-diffusion-induced ageing processes 7-45080
- thin films, phase transition temp., thickness depend., thermodynamic theory 7-26922
- thin films, quantum size effect in optical transmission and refl. spectra 7-59275
- thin films, X-ray telescope mirrors, surface scatt. meas. by triple axis spectrometer 7-37104
- thin foil, Rutherford backscatt., low energy background studies 7-3132
- tip crystals, morphological evolution and surface self-diffusion, in situ scanning electron microscopy study 7-32239
- twin boundary struct. determ. of twinned bicrystals, convergent-beam electron diffraction study 7-51786
- two-photon bremsstrahlung in the Coulomb field 7-42766
- ultra-high pressure shock generation using UV high power lasers 7-30028
- underpotential deposit on SnO_2/F electrode 7-44998
- vapour laser, design, construction and performance (Chinese) 7-5903
- wires, very thin, fatigue 7-39671
- X-ray photoabsorption cross sections 7-46240
- XPS, background removal 7-39355
- Ag-Au, thin interface regions, EXAFS studies 7-59285
- Ag-Au bilayers, EXAFS and X-ray reflectivity meas. 7-27821
- Al/ Al_2O_3 /Au thin film struct., dielec. props. meas. and equivalent circuit anal. 7-17115
- Al/ Al_2O_3 /Au tunnel junction, electromagnetic modes anal. 7-27439
- Al- Al_2O_3 -Au MIM structs. biased near breakdown voltage, optical emission 7-52853
- Al- Al_2O_3 -Au sandwich struct., forming process in high elec. field (Japanese) 7-22028
- Al_2O_3 /Au, wettability of single crystals, between metal melting point and 1673 K (French) 7-63902
- Au - GaAs, excimer laser annealed Au(Ag) contacts 7-12857
- Au + $N_2^+(Ne^+)$, impact ionisation, L_3 subshell alignment, coupled states anal. 7-25643
- Au I vapor laser, room temperature operation 7-10919
- Au thin films, optical characterisation using surface plasmon-polaritons 7-53425
- Au^{51+} , Ni-like, population inversion, ionisation model 7-25462
- Au/Ne^+ , ion implantation in elemental solids, range profile, gamma-ray spectra 7-2959
- Au^4He system, Kapitza resistance between Au and superfluid, singularity 7-58559
- Au/a-SiGe:H,F, Schottky barrier height, internal photoemission meas. 7-45501
- Au/Cd stearate/n-GaP electroluminescent device struct., electron-hole recomb. luminesc., minority carrier injection mechanism 7-59260
- Au/CeO₂ thin films on Ni-Cr Inconel superalloy substrates, diffusional processes 7-45098
- Au/GaAs contacts, growth modes, AES, UPS, XPS and RHEED studies 7-21753
- Au/GaAs Schottky barriers, hole diffusion length, photon and electron excitation studies 7-2707
- Au/i-ZnS/n-ZnS electroluminescent device struct., electron-hole recomb. luminesc., minority carrier injection mechanism 7-59260
- Au/In thin film couples, interface $AuIn_2$ cpd. form. and props., gamma-ray spectra 7-21688
- Au/Ni thin film diffusion couples (French) 7-12576
- Au-Ag sandwiches, grain boundary electron scatt. (Russian) 7-12883
- Au-Al interfaces, dose profiles for 100 to 1250 keV photons, ONETRAN calcs. 7-56874
- Au-Bi₂GeO₂₀-Au MSMS, short-wave light illuminated, photocurrent kinetics 7-22029
- Au-CdIn₂S₂Se₂-In Schottky diodes, I-V charact. 7-33010
- Au-Co compositionally modulated multilayered films, magneto-optical Kerr rot., wavelength depend. 7-3100
- Au-Cr superlattices, elastic props., effect of strain 7-52376
- Au-Cr superlattices, electrical resistivity 7-27384
- au-ethylene-vinylacetate copolymer metal-polymer contact, pot. barrier electronic props., photocurrent spectra meas. 7-27419
- Au-Fe compositionally modulated multilayered films, magneto-optical Kerr rot., wavelength depend. 7-3100
- Au-GaAs, annealed, interface erosion 7-21683
- Au-GaAs, contact, structural and elec. props. 7-27424
- Au-GaAs, interface state meas. at Schottky contacts, admittance characterisation technique 7-2718
- Au-GaAs, Schottky contact, interface states, trap characterisation 7-27421
- Au-GaAs (001), short range potential variations at interface 7-45500

gold continued

- Au-GaAs (110) interface, photoemission studies, temp. effects 7-33517
- Au-GaAs contacts, elec. and struct. props. 7-2711
- Au-GaAs contacts, proton bombard., I-V characts. 7-7386
- Au-GaAs interfaces, struct. and elec. props. 7-22013
- Au-GaAs Schottky-barrier diode hot-electron temperature measurement, method 7-52623
- Au-GaAs_{1-x}Sb_x Schottky barriers, I-V characts., temp. depend. 7-64344
- Au-Ge-GaAs, interfacial reactions, struct. after annealing 7-27154
- Au-Ge-Ni-GaAs, non-alloyed ohmic contact, solid phase epitaxy 7-27423
- Au-HCl₄.5H₂O electrode-electrolyte interface, double layer capacity, temp. and freq. depend. 7-59769
- Au-III-V semiconductor system, heat treatment, gaseous species evolution, mass spectra studies 7-39881
- Au-InP, solid-state reactions, Au₂P₃ formation 7-58550
- Au-InP high-speed internal photoemission detectors enhanced by grating coupling to surface plasma waves 7-52688
- Au-InP interface, Fermi level pinning, growth characts., photoemission spectra 7-22009
- Au-InP Schottky barriers, defects introduced by mech. polishing 7-39768
- Au-Ni-Au-Ge-Ni-GaAs, ohmic contacts, alloying, specific contact resistivity 7-27425
- Au-Ni-Cu, diffusion of Au and Cu through Ni layer, depend. on ambient 7-38266
- Au-PbTe electrical contacts, photothermal deflection meas. 7-38784
- Au-polychlorotrifluoroethylene composite films, optical response in visible region, effective medium approach 7-53433
- Au-polyethylene, adhesion of metal films, effects of Ar⁺ bombardment 7-28267
- Au-polymer composite thin films, plasma deposition, optical props. 7-27947
- Au-polymer composite thin films, elec. behaviour 7-52856
- Au-Si, high energy density pulsed ion beam irradiation, study of reacted layers 7-52151
- Au-SiO₂-Bi, low temp. hot electron energy relaxation and inelastic collision times in thin metal films 7-27441
- Au-SiO₂-Si MIS structures, Au-SiO₂ boundary anal. 7-12867
- Au-TiB₂-Au-Ge-Ni-GaAs, ohmic contacts, alloying, specific contact resistivity 7-27425
- Au-TiO₂-Nb diodes, trapping states, admittance spectra study 7-45494
- Au-vacuum-Au tunnelling, room temp. expts. 7-45438
- Au-vacuum-W junctions, quasi-self-consistent barrier calc. 7-33065
- Au-WO₃-LiF-Au, solid state electrochromic struct. study 7-53275
- Au + F, X-ray emission from multiply ionized atoms (Rumanian) 7-15699
- Au + H⁺, L subshell ionisation probabilities vacancy sharing 7-15697
- Au + S, X-ray emission from multiply ionized atoms (Rumanian) 7-15699
- (Au)_n⁺, mass distrib., mass spectra 7-50431
- AuBe-Cr-Au-InP, improved ohmic contact 7-64310
- C-Au films, ion implanted, projected ranges and range stragglings, RBS anal. 7-63690
- a-C-Au thin multilayer struct., vacuum condensation, interface development, sheet cond., thickness 7-21681
- Cu/Au thin film systems, interdiffusive kinetics, EXAFS studies 7-16819
- Fe-Au-Fe double layers, exchange coupling 7-27510
- Fe-Ni-Au trilayer film, structural depth profiling by glancing angle X-ray diffraction 7-26593
- GaAs/Au contacts, interface morphology 7-45020
- p-GaAs/AuZnNi/Ti/Au ohmic contacts, low-resistance 7-7385
- GaAs-Au Schottky diodes, DLTS 7-58896
- n-Ge:Au, electron heating, photocond., photo-Hall effect 7-12765
- a-Ge/Au interfaces, atomic intermixing, asymmetries 7-21682
- In₂Al₃-Au Schottky barrier heights, composition dependence 7-45431
- InAs-superthin insulator-Au struct., inelastic electron tunnelling spectra 7-27436
- n-InP/Au Schottky contacts, surface treatment by plasma-induced O radicals 7-38674
- InP-Au, metallic contact layers, thermal dissociation, P loss 7-23005
- InP-Cu(Au)(Ag), interphase contact interaction 7-33087
- In₂-Sn₂O₃-y-WO₃-MgF₂-Au, electrochromic coatings for solar windows 7-53621
- Ni-Ag(001), Au doped, thin films, interphase boundaries, struct. and composition 7-27158
- NiFe-Co-Au trilayer film, structural depth profiling by glancing angle X-ray diffraction 7-26593
- Si (111)/Au interfaces, structural and electronic props., annealing effects 7-21679
- Si:Au, deep level carrier capture and emission press. depend. meas., lattice relax. determ. 7-21862
- Si:Au, deep level position in forbidden gap, charactn. using ionisation Gibbs free energy (Chinese) 7-58760
- Si:Au, deep levels, multiexponential anal. of deep level transient spectroscopy 7-52524
- Si:Au, electron irradi. stimulated impurity diffusion 7-63878
- Si:Au, laser radiation effects on impurity levels 7-12645
- Si:Au, Li, Au-Si pair paramagnetic state, EPR studies 7-45817
- Si:Au, self-consistent one-electron states of 5d transition-atom impurities 7-32950
- Si:Au, supersaturated low-temp. substitutional impurities, annealing 7-6665
- Si:Au,Fe-SiO₂, MOS struct., trap centres 7-7388
- Si:Au n-n⁺ isotype junction, enhanced magnetosensitivity 7-7370
- Si:Au U- and W-shaped impurity diffusion profiles investigation 7-16805
- Si:C:Au, intrinsic point defects and impurity interactions 7-16611
- Si/Au buried interface struct. determ., optical second harmonic generation studies 7-63982
- a-Si/Au thin film bilayers, Si crystallisation study 7-21699
- Si-Au interface, atomic bonding 7-58663
- Si-Au-Pt interfaces, PtSi formation, RBS studies 7-58547
- Si-Co₅₀Mo₅₀-Au, amorphous Co₅₀Ta₅₀ alloys as diffusion barriers 7-44923
- Si-Cu-Au layered struct. reflectivity and EXAFS study 7-59292
- Si-Ge:Au, reaction of Au centres to optical pumping 7-12755
- Si-SiO₂-Ag(Cu)(Au)(Pd)(Ti) MOS structures, diffusion coeff. meas. in elec. fields, solid solubilities 7-2279
- SiO₂:Au, ion implanted, projected ranges and range stragglings, RBS anal. 7-63690

gold continued

- ZnSe:Au, cationic substitutional impurities and metal vacancy, microscopic models 7-27296
ZrO₂:Au, powders, result of oxidation of Zr₇₀Au₃₀ in humid air 7-3510

gold alloys

see also gold compounds

- dilute, EFG, asymmetry parameter calcs. 7-2545
dilute alloys, electron irradiation, positron lifetime meas. 7-39250
Ag-Au, external surface adsorption isotherm 7-6978
Ag-Au, valence level splitting 7-45139
Ag-Au-Zn ternary system, liq., thermodynamic functions (German) 7-44856
Ag₂Au_{1-x}, Al-K_α XPS intensities 7-27870
AgMnAu spin glasses, crit. behaviour, Dzyaloshinsky-Moriya interactions 7-7525
An-In liq. alloys, magnetic and thermodynamic props. 7-2812
Au-Ag-Cu-Pd, cast microstructure, segregation, TEM obs. 7-39495
Au-Al alloy, superconductor film structs., fabrication and appls. (Spanish) 7-27483
Au-Cd (47.5 at.%), stress induced martensitic transform., pseudoelasticity 7-39610
Au-Cu alloys, polycryst., room temp. interdiffusion 7-2274
Au-Cu alloys, surface composition, sequential ion scatt. spectroscopy-Auger electron spectroscopy meas. 7-22394
Au-Cu alloys, vapour deposition on NaCl single crystals, nucleation and growth 7-39391
Au-Cu sputtered alloys, segregation, surface compositional changes 7-58585
Au-Cu-Pd, corrosion resist. 7-39739
Au-Er dilute alloys, Er³⁺ crystalline electric fields, screening effects 7-27307
Au-Fe, dil., Kondo system, mag. scatt. time of conduction electrons meas. 7-21902
Au-Fe, mag. hyperfine field, temp. and composition depend. 7-45243
Au-Fe (10 to 35 at.%), early stage clustering struct. 7-59536
Au-Ge/Ni/GaAs ohmic contacts, ion implantation and metallisation prep. 7-22014
Au-Mn (15 at.%), disordered phase, high resolution electron microscopy study 7-63834
Au-Pd, preferential sputtering and surface segregation 7-59339
Au-Pd films, electron scatt. times, weak localisation studies 7-64367
Au-Pd thin films and wires, localisation and electron-electron interaction effects, magnetoresist. meas. 7-52863
Au-Sd transition metal alloys, heat of form. and cryst. struct., linear augmented STO calcs. 7-51705
Au-Si, liq., thermodynamic analysis of conc. fluctuations and homogeneous nucleation, glass form. 7-44852
Au-Si codeposited films, oxidation, SiO₂ form., alloy comp. depend. 7-13654
Au-Si eutectic alloy liquid metallic ion source (Chinese) 7-33600
Au₂Ag intermetallic cpds., charge redistrib., L-edge XANES study 7-64816
AuAl alloys, Al diffusion, NMR study 7-33287
AuAl₃ intermetallic cpds., charge redistrib., L-edge XANES study 7-64816
AuCr, competing antiferromagnet, mag. phase diagram 7-59023
AuCr spin glass, remanent magnetization reduction, Heisenberg and Ising comparison 7-53019
Au₄Cr, atomic ordering, X-ray struct. anal. (Russian) 7-1933
AuCu₃, ordered alloy, antiphase boundary form. energy, atomic config., Morse pot. approx. (Russian) 7-46419
Au₃Cu short range order, EXAFS study 7-63555
Au₇₅Cu₂₅ and Au₇₀Cu₃₀, local order, X-ray diffuse scatt. meas. 7-26972
AuFe re-entrant spin glass, magnetoresist. and AC susceptibility studies 7-7518
AuGa₂ intermetallic cpds., charge redistrib., L-edge XANES study 7-64816
AuGa₂-GaAs (001), chemically unreactive interfaces formation 7-7050
AuGe-GaAs, ion beam induced phenomena 7-12166
AuGe-Nb-GaAs, ohmic superconducting contacts to GaAs 7-33088
AuGe-Ni-n-GaAs, ohmic contact fabrication RBS anal. 7-32840
AuGeNi-GaAs contacts, interface composition and barrier heights 7-58891
AuIn₂₊₃ thin films, resistivity 7-7410
Au₇₇Mg₂₃, atom sublattices, selective high resolution electron microscopy 7-6486
Au₄Mn, atom sublattices, selective high resolution electron microscopy 7-6486
Au₈₀Mn₂₀ disordered alloy, free and frozen magnetisations 7-53037
Au₂Na, NA vapour sensor based on conductivity variation 7-18774
Au₂Ni_{1-x}, Al-K_α XPS intensities 7-27870
AuNiGe-GaAs interfaces, struct. and elec. props. 7-22013
AuNiGe-GaAs ohmic contacts, microstruct. anal. and contact resist. meas. 7-2393
Au₆₀Pd₄₀ narrow rings and lines, low-temp. magnetoresist., aperiodic struct. 7-64206
Au₆₀Pd₄₀ thin films, warm electron energy loss meas. 7-2739
Au₂Pt_{1-x}, Al-K_α XPS intensities 7-27870
Au₂Pt_{1-x}, mag. susceptibility, 77 to 450K 7-17164
AuSi liquid ion sources, alloy composition 7-35623
AuZn layer on GaP, emission spectrochemical anal. using glow discharge, appl. to in-depth anal. (Japanese) 7-63886
Au₃Zn, non-periodic antiphase boundaries, obs. by HREM 7-63550
CdTe-AuCu, AC contact impedance, influence on high freq., low temp. on fast transient junction meas. 7-64311
Co-Au-Fe, dil., local structural and mag. environments of Fe 7-26965
Cu-Au, disordered, short-range ordering, X-ray split diffuse intensity maxima separation 7-2222
Cu-Au, phase diagrams and short range order, Monte Carlo simulations 7-53704
Cu-Au quenched alloys, diffuse X-ray scatt., microdomain model anal. 7-6814
CuAu I and II, initial ordering stages, twinning, periodic antiphase boundaries, electron microscopy 7-28032
CuAu, ordering and recrystallisation, TEM studies (Russian) 7-16479
(CuAu)-Co single crystals, under- and over-aged, additivity of precip. and solid soln. hardening 7-65051
Cu₃Au alloy, displacement cascade collapse at low temp. 7-51892
Cu₃Au, electron irradiation, long range ordering, recovery, vacancy migration and clustering, positron lifetime study 7-39543

gold alloys continued

- Cu₃Au, irradiation disordering and reordering by fusion neutrons, electrical resistivity meas. 7-51864
Cu₃Au, L1₂ ordered intermetallic cpds., symm. tilt boundaries, geometrical models 7-32454
Cu₃Au, quenched, vacancies, ordering and annealing, positron lifetime and elec. resist. meas. 7-39544
Cu_{70-x}Au₃₀Fe_x, ferromagnetic interactions, EXAFS and XANES anal. of Fe atom environment and clustering 7-64808
CuMnAu alloys, homogeneous and inhomogeneous spin freezing, μ SR studies 7-45687
CuMnAu spin glasses, crit. behaviour, Dzyaloshinsky-Moriya interactions 7-7525
Fe-Au, dilute alloys, electron irradiated, vacancy-solute interaction, positron lifetime, muon spin rotation studies 7-39288
Fe-Au, solute segregation, grain boundary structural transform. 7-22687
Fe-Au system, low Au conc., low temp. nucl. orientation and NMR-ON studies 7-2936
Fe(Pd_{1-x}Au_x)₂ disordered alloys, atomic and mag. structs., Mossbauer studies (Russian) 7-17247
p-GaAs/AuZnNi/Ti/Au ohmic contacts, low-resistance 7-7385
Ge-Au, temp. and conc. depend. diagraph, susceptibility 7-2811
Hg-Au, core holes, final-state screening, total energy calcs. 7-2526
LaAu nonmagnetic metallic glasses, negative TCR and electronic struct. studies 7-52562
MnHg_{1-x}Au_x, cubic to orthorhombic transition and mag. suscept. meas. 7-52037
Nb-NbO_x-PbInAu, Josephson tunnelling current depend. on normal state tunnelling resist. 7-22073
Nb-NbO_x-PbInAu Josephson junction fabrication by ion beam oxidation 7-22074
Nb₇₆Au₂₄, with Cr and Fe impurities, supercond. transition temp., impurity conc. depend. 7-2768
Ni-Au (110), Au-enriched by surface segregation, LEED 7-27080
Ni-AuGe-GaAs, ion beam induced phenomena 7-12166
Ni-AuGe-GaAs, ohmic contacts, interface reactions, elec. behaviour 7-27031
Ni₇₇Au₂₃, amorphous, mag. scatt. influence on transport props. 7-33001
NiGeAuAgAu alloyed ohmic contacts to AlInAs-GaInAs heterostruct., charact. 7-22016
Pb-In-Au alloy films, hillock growth during heat treatment 7-16893
Pb-In-Au fine-grained codeposited alloy films, RF plasma oxidation 7-53970
Pb-In-Au thin films, hillock growth kinetics, grain boundary diffusion, SEM study 7-27221
RAuCu₄ (R=Gd, Tb, Dy, Ho, Er), cubic alloys, mag. props. 7-52936
Se-Te-Au(Ag) liq. mixtures, electronic props. 7-64247
Th-Au system, phase diagram, DTA, micrograph, X-ray anal. 7-17512
Ti-Ni-Au, martensite cryst. lattice distortions, comp. depend. 7-22679
TiNi-TiAu alloys, martensitic transformations and shape memory effects (Russian) 7-17529
Ti₅₀Ni₄₀Au₁₀, martensitic transform., TEM study 7-59522
Ti₅₀Ni₄₅Au₅, martensite, interstitial H-induced extra reflection, TEM and electron diff. study 7-59521
UAu₃, band struct., theoretical XPS intensities 7-39353
UAuCu₄ magnetic props., X-ray diff., NMR and mag. suscept. meas. 7-52948
V₃Au, superconducting A15 cpds., resistivity and magnetoresistance 7-32982
YbAuCu₄, strong electronic correlations 7-45194
Zn-Au dilute alloy single crystals, thermally activated and quantum creep, impurity effects (Russian) 7-26755
Zr-Ti (Sn)(Dy)(Au), neutron irradiated, solute effects on damage production and recovery 7-51861
Zr-Ti(Sn)(Au), low temp. damage prod. and recovery after fusion neutron irradiation 7-51862
Zr₇₀Au₃₀, spontaneous oxidation in air, effect of humidity, pulverisation 7-3510
- gold compounds**
see also gold alloys
Au₂(TeO₂)_{1-x} thin films, nanosecond laser annealing, Au cluster redistrib., growth and coalescence 7-12145
Au complex, Au₅₅(PPh₃)₁₂Cl₆, high-nuclearity cpd., DC conductivity 7-33016
AuH bonding, ab initio fully relativistic calcs. 7-15531
(AuO₂)_x complexes, (x=1,2), bonding and configuration, matrix isolation ESR spectra anal. 7-19905
Cs₂Ag^{III}Au^{III}X₆ (X=Cl,Br), valence study by X-ray absorption spectra at Au L₃ edge 7-7791
Cs₂Au^{III}Au^{III}Cl₆, valence study by X-ray absorption spectra at Au L₃ edge 7-7791
Eu(Cu_{1-x}Au_x)₂Si₂, substitution effects on mixed valence behaviour, Mossbauer and XANES studies 7-64183
EuPd_{2-x}Au_xSi₂, valence determ., Mossbauer and X-ray absorpt. studies 7-64800
(S₂N₂)(AuCl₄), crystal struct. studies (German) 7-12004
- goniometers**
3-axis type, for trunk range of motion meas. of worker in worksite 7-28567
adjustable goniometer mount for the spark-planing of metal single crystals 7-32220
channelling contrast microscopy, He⁺ microbeam, semiconductor impurity profiles 7-51587
cooling device for operation at 10K, mounting without rot. seals on four-circle diffractometer 7-14954
electrogoniometer, flexible, applying electroconductive rubber, clinical use (Japanese) 7-14139
electrogoniometer for thoracolumbar rot. meas. 7-28786
ESR crystallography, two/three circle ESR goniometers (Japanese) 7-44328
interference, operating reliability, effect of lateral beam displacement 7-41452
layered synthetic microstructure spectrogoniometer, performance for X-ray spectroscopy 7-41559
layered synthetic microstructure spectrogoniometer for soft X-ray spectroscopy 7-35647
null detector, interference-type, for ang. position of object meas. 7-56327
quartz crystal resonator blanks, X-ray machine 7-37806
sample manipulator for Auger angular dependence studies 7-35626

goniometers continued
Siemens texture goniometer, modified with microcomputer controlled stepping motors 7-44306
texture attachment for quantitative X-ray texture analysis 7-8214

government data processing
see also town and country planning
acid rain deposition modelling for policy anal. 7-13944

GP zones see Guinier-Preston zones

GPS see radionavigation; satellite relay systems

graded index optics see gradient index optics

gradient index optics
antireflection coatings, achromatic, graded-index, for broad spectral region 7-43323
binocular objective design, gradient-index 7-31414
branching waveguides, distrib.-index, phase space evaluation 7-31453
cable, losses resulting from excess fibre length (*Japanese*) 7-50782
cylindrical microlenses with graduated refractive index, appls. (*Italian*) 7-15961
diffuser with controlled divergence 7-5969
Fermat's principle used to derive $F=ma$ eqn. in medium of varying refractive index 7-35145
fibre, graded index, total acceptance angle 7-11155
fibre connector and splices, low-loss, theoretical and exptl. study 7-43438
fibre optic reflective sensing technique employing GRIN rod lens 7-43387
fibres, graded index, longit. strain meas. techniques 7-43418
fibres, GRIN, nonlinear inhomogeneous, solitons transmission 7-20463
fibres and preform rods refractive index profile reconstruction from transverse interferometric data 7-11113
fusion-spliced fibres, Zeiss-Linnik interferometric exam. 7-31531
glass rods prep. by sol-gel index modifying ion interdiffusion process 7-7952
GRIN, speckle and modal noise techniques for coupling 7-20427
GRIN lenses, optical performance assessment 7-31538
GRIN-rod lenses used in single-mode optical devices, aberration anal. 7-31421
group delays meas. of guided modes, in optical fibre waveguides (*Czech*) 7-57596
heterostructure laser, graded-index separate-confinement, carrier capture time 7-1100
high-bandwidth fibre optic system using laser diode transmitters 7-25978
holographic endoscopy with gradient-index optical imaging systems and optical fibres 7-31271
imaging systems, gradient index, conf., Palermo, Sicily, Italy (Sept. 1985) 7-29570
integrated optical lens design using GRIN lens techniques 7-43449
integrated-optic coupling elements based on 2D refractive-index gradient 7-20411
laser diodes, index guided, 1.3 μm , far-field fine struct. study 7-57389
laser-diode/multimode-fibre coupling analysis using a planoconvex GRIN lens 7-31480
lens, graded-index, light distribution near foci 7-43287
lens, gradient index, for low-loss coupling of laser diode to single-mode fibre 7-31465
lens, GRIN, with revolution symmetry, paraxial Fourier transforming and imaging props. 7-31420
lens system design, gradient index, for disc format cameras 7-30105
lenses, gradient index, ray tracing, computation of ray-surface intersection 7-31418
lenses for fibre optic thin film temperature sensor 7-25992
matrix of gradient microlenses fabricated by electrostimulated diffusion, optical connectors development 7-25967
multimode branching waveguide, distrib.-index, evaluation by phase space 7-31451
multimode cabled coated optical fibres, graded-index, losses at low temp. 7-50749
planar graded waveguides, parameters meas. in near IR, refractometric method 7-37150
planar microlens, distrib.-index, and stacked planar optics, review of progress 7-31416
planar microlens fabrication by ion exchange/diffusion, distrib. index profile 7-31417
planar waveguides with nonlinear cover medium, guided waves 7-37141
planoconvex graded-index rod lens for coupling laser diode to single-mode fibre 7-15973
rod, degrees of freedom and quality of image formed 7-42982
rod lens array, testing method based on boiling phenomenon of laser speckle 7-43319
rods, tapered GRIN, imaging and transforming transmission 7-25961
short multimode graded-index optical fibre, intensity fluctuations (*French*) 7-62840
single-mode graded-index fibres; trial field for non-Gaussian field distrib. 7-11120
slab lens, gradient-index, with high numerical aperture 7-31415
spherical gradient-index sphere lens, modified suspension polymerisation fabrication 7-31527
splice attenuation in gradient fibres (*German*) 7-1277
taper coupler for integrated optics formed by ion-exchange under nonuniform electric field 7-50740
tapered quadratic index media, metal waveguide modelling 7-50747
transmission line circuit models for inhomogeneous optical fiber 7-62833
waveguides, finite-cladding, core-mode cutoff 7-31452
Wood and GRIN rod lenses, third- and fifth-order aberrations 7-31419
AlGaAs high-power ridge-waveguide GRIN-SCH laser diode 7-10988
AlGaAs/GaAs ridge waveguide quantum well lasers with high quantum efficiency 7-15905
AlGaAs-GaAs GRIN-SCH SQW laser, wide-stripe, injection locking 7-20290
Al₂O₃-SiO₂ GRIN glass, delta- n control by additives in AgCl diffusion baths 7-31528
As₂S₃ chalcogenide glass, photoinduced gradient waveguide form. (*Russian*) 7-43374
GaAs-GaAlAs diode laser array, diffraction-limited emission, aperture graded-index lens external cavity 7-11005
Hg_{1-x}Cd_xTe optical waveguides, high band gap, for 10.6 μm 7-37157
InGaAs/GaAs GRIN SCH SL quantum well laser, MOCVD grown 7-50557
Li₂O-P₂O₅-Eu³⁺, laser-induced refractive-index gratings, four-wave-mixing techniques 7-11102

gradient index optics continued
Na₂O-SiO₂-Eu³⁺, laser-induced refractive-index gratings, four-wave-mixing techniques 7-11102
P₂O₅-Eu³⁺, laser-induced refractive-index gratings, four-wave-mixing techniques 7-11102
TiO₂-SiO₂ r-GRIN glass rods prep. by sol-gel method 7-13427
ZnS₂Se_{1-x} gradient IR optical material prepared by CVD 7-31408

graft polymers see polymer blends

grain boundaries
see also bicrystals; grain boundary diffusion; grain boundary segregation; subboundary structure; tilt boundaries; twin boundaries; twist boundaries
7-33321
alloys, ordered, L2₀ and L1₂, grain boundary structs., twist boundaries, geometrical models 7-63628
alumina, grain boundary glassy phase, ion milling of TEM specimens 7-44327
alumina, neutron irradi., permittivity and dielec. loss studies 7-33321
atomic structure models, electron microscope images, computer simulation 7-16380
austenitic steels, small precip., moire imaging in TEM 7-46490
bicrystal, grain boundary dislocations, struct., steps, HREM study 7-16488
bicrystal model, grain-boundary melting transitions, mol. dynamics simulations 7-21419
bicrystals, shear incompatible, approx. evaluation method for elastic stresses by virtual array of dislocations (*Japanese*) 7-32841
binary alloys, crystal-amorphous transformation, thermodynamics and kinetics 7-21108
 α -brass, SCC initiation after exposure to NaNO₂ soln. 7-65173
 β -brass bicrystals, Bauschinger effect, grain boundary contrib. 7-46574
cavity-growth kinetics determ. from cavity-size distrib. during creep and continuous nucleation 7-26767
ceramic materials, intergranular glass phases, equilib. film thickness 7-46433
ceramic-metal interfaces, grain boundaries, bonding and interfacial structure 7-26765
ceramics, ion milling of TEM specimens, grain boundary glassy phase 7-44327
coincidence site lattice misorientation, specialness and deviation criteria 7-21221
crack initiation at grain-boundary triple points in high-temp. deform., continuum mech. model 7-28104
creep crack growth by grain boundary cavitation 7-21340
crystallography, practical approach to determ. 7-21224
dislocations, extrinsic and intrinsic boundary types 7-63616
dislocations, grain boundary sources, analytical treatment 7-44568
disordering transitions, nucleation mechanism, review 7-44743
double Schottky barrier, grain boundaries, elec. props. in presence of deep bulk traps, appl. to ZnO varistors 7-7334
elastic properties of grain boundary dislocations 7-21205
electron microscope analysis 7-37818
epitaxial metal bicrystals containing grain boundaries, UHV deposition apparatus 7-39390
fatigue crack growth at elevated temps., grain boundary oxidation 7-6714
films, coercive force establishment, magnetoelastic interaction effects (*Russian*) 7-7558
films, grain structures and grain growth 7-16903
fluid inclusion in grain boundary, unstable spreading under normal stress 7-26761
fusion reactor structural alloys, irradi., creep fracture by grain boundary cavitation, modelling 7-53859
grain growth, local texture development, STEM selected area channelling 7-16575
grain growth, secondary and normal, relative rates 7-65003
graphite surface pulsed laser irradiation, SEM, TEM and STEM microstructural studies 7-12139
high resolution electron microscopy in materials science (*German, English*) 7-39806
IN738LC, Ni base superalloy, low cycle and thermal fatigue, small crack initiation and growth (*Japanese*) 7-13567
Inconel X-750, air environment/creep interactions, prior exposure times effect 7-13499
interfaces, internal, diff. effects, general considerations and grain boundary effects 7-12495
interfacial bonding and adhesion, conf., Aspen, CO, USA (Aug. 1985) 7-24269
interfacial melting, 2D model, computer simulation 7-58448
intergranular phase, continuous, morphological stability 7-63772
ionic crystals, grain boundaries, review 7-6632
L1₂ intermetallics, localised grain-boundary electronic states and intergranular fracture calcs. 7-45215
L1₂ ordered alloys, grain boundary strength and fracture, electronic and struct. studies 7-33756
L1₂ ordered intermetallic cpds., symm. tilt boundaries, geometrical models 7-32454
material analysis, computer-based, conf., Boston, MA, USA (Dec. 1985) 7-14709
materials design using a hierarchy of structural models 7-16350
melting at grain boundaries and surfaces 7-32619
metal tritides, disorder induced by aging 7-21199
metal-H system, internal grain-boundary crack opening by H (*Russian*) 7-33764
metals, BCC and FCC cryst. struct., H trapping, thermal anal. obs. 7-22830
metals, bulk and thin film samples, polycrystalline, DC conductivity 7-52566
metals, grain boundary energies from local-electron-density distributions 7-6634
metals, grain boundary interactions with dislocations (*Russian*) 7-63645
metals, grain boundary structure (*German*) 7-44571
metals, internal interfaces, grain boundary struct., intergranular fracture 7-26766
metals, polycryst., expt. simulation of intercryst. sliding and fracture 7-2095
microcrack behaviour near low angle grain boundary 7-2096
movement analogous to dislocation movement, anal. 7-6637
Nimonic 80, coupled plastic and creep damage at finite deform. (*Japanese*) 7-33736

grain boundaries continued

- Nimonic 80A, coupled effect of plastic damage and creep damage at finite deform. 7-46599
oxide scales, chem. mapping using electron energy loss imaging microscope 7-37812
petrographic parameters quantification, appl. of digital image processing (Spanish) 7-34740
polysilicon for solar cell appls., DLTS study 7-38512
polysilicon thin films for VLSI, elec. props. 7-38789
positron annihilation at the grain boundaries of polycrystals 7-46196
positron trapping at grain boundaries 7-39264
power-law matrix, containing aligned penny-shaped cracks constitutive models 7-37386
Schottky p-type polycryst. junction 7-7331
semiconductor bicrystal, diffusion length and grain boundary recomb. vel. determ. by laser excitation 7-41402
semiconductor grain boundary photovoltaic effect, scanning laser beam obs. anal. 7-12766
semiconductors, electrical breakdown at grain boundaries 7-45339
semiconductors, grain boundaries, at. struct. 7-6638
semiconductors, polycrystalline, beam induced current characterisation, appl. to Si solar cells 7-7267
semiconductors, polycrystalline, conf., Erice, Italy (July 1984) 7-4632
semiconductors, polycrystalline, extended interfacial defects, geometrical character 7-6640
semiconductors, polycrystalline, grain-boundary barrier heights, grain curvature effects 7-2607
semiconductors, polycrystalline, localised defects, EBIC studies 7-21933
Si solar cells, SILSO, grain boundary charact., meas./test techniques 7-13858
sialon ceramics, processing, Al ion redistrib., crystallisation EDX analysis 7-3237
SOI films, thermal stresses during zone melting recrystallisation, sub-boundaries, in-plane orientation 7-33554
SOI technology by zone-melting recrystn. on quartz substrates 7-21736
solar cell, polycrystalline, grain boundary parameters determ. using EBIC signal derivative 7-3882
steel, alloy, impact behaviour, influence of grain boundary carbide density 7-13574
steel, alloy, trace element precipitation and segregation, hot brittleness effects (French) 7-17608
steel, austenitic stainless, biaxial loading, high temp. intergranular crack growth 7-53902
steel, austenitic stainless, extrinsic grain boundary dislocations, spreading kinetics 7-44569
steel, austenitic stainless, grain boundary microstruct., He embrittlement resistance 7-56829
steel, austenitic stainless, He-induced creep ductility loss, prediction and anal. 7-53854
steel, austenitic stainless, in-beam creep rupture props. at 873K 7-53851
steel, austenitic stainless, low cycle fatigue damage, crack initiation (Japanese) 7-33780
steel, C, brittle fracture micromechanism in specimens containing intergranular cementite (Russian) 7-59621
steel, cast, nonmetallic inclusions influence on fracture character 7-3421
steel, Cr-Mo-Fe-C, crack resist., temp. and comp. depend. study (Russian) 7-13553
steel, Cr-Mo-V, rotor, high temp. creep, prior austenite grain size effect 7-53828
steel, Cr-Ni-Mo, fracture toughness rel. to austenitising temp. (Japanese) 7-33778
steel, high strength, near threshold fatigue crack growth behaviour, effect of prior austenitic grain size 7-53906
steel, high-speed, produced from machining waste, liq. phase forming during sintering 7-3226
steel, Nb-V microalloyed, matrix and grain boundary precipitation, effect of heat treatment 7-46493
steel, Ni-Co-Mo, maraging, lath martensite boundary cracking near threshold stress intensity factor (Japanese) 7-53846
steel, Ni-Cr, anelastic props. of grain boundaries and transition temp., effect of temper embrittlement 7-22815
steel, stainless, FCC structure, multiple grain-boundary contacts (Russian) 7-12079
steel, stainless, surface segregation and grain boundary precipitation during heating, atom probe study 7-33672
steel, stainless and alloy, electron radiation damage in fusion reactor materials, voids 7-2064
steel, structural, temper embrittlement, preferential segregation, Auger spectra 7-53737
steels, stainless, α -particle irradiated, mech. props. and microstruct. 7-51872
structure and properties under external influences, review 7-12080
superalloys and ceramics, electron microscopy studies, symposium, Nantes France (July 1986) 7-18479
superplastic deformation, boundary migration, grain growth 7-17600
superplastic deformation, grain-boundary slip velocity and microstruct. (Russian) 7-3362
superplastic to non-superplastic deform., transition at high strain rates 7-46586
surface diffusivity variation on surface morphology and electromigration 7-63920
surface features, thermal wave imaging studies in a SEM 7-44874
symmetrical grain boundary classification, geometrical criteria 7-2029
tensile test, creep failure by microstruct. degradation and grain boundary cavitation 7-65117
theory based on dipolar array of dislocations 7-6635
transparent ferroelectric ceramics, comp., struct. and props. characts. anal. 7-7647
trap occupancy and recomb. models anal. 7-64266
tribochemistry, chemical reaction increase by friction 7-46868
Zircaloy-2, cold worked, irradi. growth, point defect trapping, computer simulation 7-16613
zircaloy-4, polycryst., high temp. internal friction 7-17571
ZnO:Bi (Sb) (transition metal), Schottky-like barriers, ion implantation, annealing 7-58860
YZ-LiNbO₃, domain structure and lattice defects, effects of piezoelectricity, TEM anal. 7-2999
Ag ultrathin films, elec. cond., size effects (Russian) 7-45520
Al and Al alloys, 800 MeV proton irradi., gas accumulation at grain boundaries 7-58361
Al bicrystals, grain boundary rumpling during sliding 7-2030

grain boundaries continued

- Al, creep rate, role of grain boundary movements 7-44666
Al disks, He ion implanted, He re-emission ratios and surface obs. (Japanese) 7-12089
Al, grain boundaries, Na and H impurities, small cluster quantum chemical calcs. 7-38017
Al, grain boundary energies, from local-electron-density distributions 7-6634
Al quenched, tensile flow stress, effect of grain size and strain 7-22756
Al recrystallisation, cryst. boundary stresses, synchrotron X-ray topography study 7-26684
Al, relaxation process studied by positron annihilation 7-6698
Al single cryst. and bicrystal, polygonisation substruct., grain boundary effects (Russian) 7-58287
Al thin films, stress relax. mechanisms 7-21784
Al thin films, vacancy redistrib. kinetics, machine modelling study (Russian) 7-6860
Al-Cu, creep rupture under tri-axial tension 7-53839
Al-Cu (2.5 wt.%), creep deform., effect of θ precipitates 7-65088
Al-Cu-Li alloys, cyclic fracture, mechanisms 7-46634
Al-Cu-MG, annealed, creep, 623-723 K 7-53802
Al-Cu-Mg, fracture behaviour, influence of fine transition-metal particles and grain struct. 7-3406
Al-Li-Cu-Mg quaternary alloy, initiation of voiding at second-phase particles 7-39645
Al-Mg (5 wt.%) polycrystals, high temp. deform., microstruct. 7-13501
Al-Mg alloys, steady-state creep, microstruct. development 7-53817
Al-Mg and Al-Zn-Mg alloys, plasma-coated, heat treatment effect on fine struct. and failure mechanism 7-3496
Al-Mg-Si, high-purity, nucleation and growth of precipitates and the bubbles, effect of 600 MeV protons 7-58364
Al-Si-Pb-Bi, duplex alloys, melt quenching, microstruct. supercond. props. 7-45593
Al-Ti, rapid solidification processed/mechanically alloyed, high temp. deform. 7-65100
Al-Zn-Mg-Cu, notched and unnotched bars, macroscopic shear localisation and fracture 7-46633
Al-Zr-Mg (Cu), grain boundary struct. and superplasticity, electron microscopy studies (Russian) 7-6630
Al-(Mg), AE during deform., effect of struct. state (Russian) 7-38127
Al₄Mn alloy, decagonal and icosahedral phase coexistence, electron diff. studies 7-11991
Al₂O₃ ceramic, grain boundaries, microanal. 7-16577
Al₂O₃ ceramics, microstruct.-mech. prop. relationship 7-65147
Al₂O₃, cryst. growth from melt, phase boundary displacement mechanism, defect distrib. 7-32328
Al₂O₃, neutron irradi., microstruct., mech. props. 7-51843
Al₂O₃ profiled crystals, prod. from gas-saturated liq., struct., effects of growth conditions 7-32327
Al₂O₃, sintered, erosion and strength degradation 7-17663
Al₂O₃, spinel growth, interface struct. investig. 7-16566
Al₂O₃, vitreous bonded, crack nucleation and growth at elevated temps. 7-33770
Al₂(TiO₃)₃ ceramics, sintering, microstruct., bending strength, additives effect (Japanese) 7-17601
Au polycrystalline tips, grain rotation and grain boundary annihilation, in situ SEM study 7-32460
Au-Ag sandwiches, grain boundary electron scatt. (Russian) 7-12883
(Ba_{1-x}La_x)TiO₃ semiconducting ceramic props., grain boundary and dopant effects (Japanese) 7-6631
BaTiO₃ ceramics, Maxwell-Wagner relax. and degradation 7-2970
BaTiO₃, grain boundary inhomogeneity phenomena, microcontact meas. (German) 7-58893
Be, superplastic flow, electron microscopy studies (Russian) 7-3360
 α -brass, hot rolled, recrystallized microstruct., deform. processes 7-13500
CaCO₃, calcite, grain growth, effect of second-phase particles 7-39476
Cd, polycrystalline, work-hardening and recovery during steady-state creep 7-63734
Cd, positron lifetimes, prevacancy effect 7-37973
CdS films, spray deposited, laser annealing, struct., carrier mobility 7-58318
CdTe, polycrystalline, grain boundaries elec. and optical characts. 7-38012
CeO₂, doped with trivalent cations, grain boundary effect, microstruct. and microanal. 7-38249
CeO₂:Y³⁺(Gd³⁺)(La³⁺), grain boundary effect, elec. meas. 7-38248
CoCr films, texture formation, appl. for perpendicular mag. recording 7-39539
CoNiCr-Cr sputtered thin films, film struct., mag. props. 7-33227
Cr thin films, intrinsic stress, elasticity modulus, thermal expansion and struct. 7-16889
Cu alloys, rapidly solidified powder metallurgy, irradi. to 13.5 dpa with neutrons, microstruct. evolution and swelling 7-51840
Cu, creep rupture under tri-axial tension 7-53839
Cu, crystal surface and interface, heterophase fluctuations (Russian) 7-58650
Cu electrodeposits, decorated grain boundary dislocations, electron microscopy obs. 7-27185
Cu, FCC structure, multiple grain-boundary contacts (Russian) 7-12079
Cu, hot rolled, recrystallized microstruct., deform. processes 7-13500
Cu, isoaxial bicrystals, with (001) tilt boundaries, dynamic recrystn., effect of grain boundaries 7-17549
Cu, polycrystalline, multiaxial low cycle fatigue, crack initiation, slip bands, damage mechanics 7-53840
Cu-Al, dynamic recrystallisation, grain boundary bulging 7-39540
Cu-Al bilayers, EXAFS and X-ray reflectivity meas. 7-27821
Cu-Al₂O₃, dispersion strengthened powder alloys struct. and mech. props. 7-53667
Cu-Al-Ni, shape memory alloys, polycrystalline, cyclic deform., fatigue above transform temp. 7-3434
Cu-Co, dynamic fracture characts., void nucleation at incoherent precipitates 7-17628
Cu-GeO₂, dispersion hardened polycrystals, intermediate temp. embrittlement 7-53903
Cu-Ni, dynamic recrystallisation, grain boundary bulging 7-39540
Cu-Si (6 at.%), secondary grain boundary dislocation nodes at junction of three grains 7-63648
Cu-Sn, low cycle fatigue damage, crack initiation (Japanese) 7-33780
Cu-Sn-B(Mg)(P), ductility at high temp., alloying additions effect (Japanese) 7-13515

grain boundaries continued

- CuInSe₂ thin films, polycrystalline, elec. props., effect of excess Cu 7-52871
- α -Fe, grain boundaries of island crystals, lattice mismatch, graphical description method 7-38016
- Fe powders, hot pressing, fracture toughness, intergranular failure rel. to porosity 7-13596
- Fe-base alloys, grain boundary internal adsorption of C and P, segregation study (*Russian*) 7-6961
- Fe-C, ferrite nucleation at austenite grain edges, kinetics 7-7991
- Fe-C-Mn(Ni)(Co)(Si), ferrite nucleation at austenite grain edges, kinetics 7-7991
- Fe-C-Mn(Ni)(Co)(Si)(Mo), nucleation of proeutectoid ferrite at austenite grain boundaries 7-8003
- Fe-Cr-C, martensite nucleation, dislocations, grain boundaries, plastic accommodation 7-28040
- Fe-Cr-Co-Mo permanent magnet ribbons, mag. props., influence of modulated structure 7-53043
- Fe-Cu, sintering, form. of Cu pockets in Fe grains 7-7922
- Fe-Ni-Cr (25,15 wt.%), MC stabilized, fatigue life, effects of implanted He 7-53852
- Fe-Ni(-C), martensite nucleation, dislocations, grain boundaries, plastic accommodation 7-28040
- Fe-Si sheets, grain oriented, orientation of individual grains by means of Kossel patterns (*Japanese*) 7-22716
- Fe-Si-Al, carbide precip. kinetics, core loss 7-8001
- (FeMg)₂SiO₄, spinel growth, interface struct. investig. 7-16566
- Fe₇₁Nd₁₅B₈, sintered permanent magnets, domain wall obs. 7-27544
- FeNiCr, grain boundary solute segregation 7-56833
- FeNiCrSbP, grain boundary segregation, Auger and energy dispersive X-ray mapping 7-16571
- GaAs, crack form., quenching by dislocation ensembles (*Russian*) 7-44680
- GaAs epilayers grown on Ge or Ge/Si substrates, defects 7-21778
- GaAs polycrystalline solar cells, influence of grain boundaries on performance 7-17892
- GaAs polycrystalline solar cell, electron beam generated carriers in presence of grain boundaries 7-64262
- GaAs thin films, grain boundaries, electronic props. 7-7172
- GaAs, transport props., charge collection microscopy 7-52649
- GaAs-Ge epitaxial interface, extended defects, geometrical character 7-6640
- GaP bicrystals, potential barriers of grain boundaries 7-21976
- Ge, electronic struct. of incoherent grain boundary, recursion approach 7-64161
- Ge:H, H composition at surfaces and interfaces 7-27083
- HoMo₈S₈ ferromagnetic films, supercond. props., temp. and mag. field depend. 7-45538
- In, positron lifetimes, prevacancy effect 7-37973
- InP, undoped and Zn(Cd) doped thin films, prep. and characts., appl. for solar cells 7-17895
- KBr, US vibration, 20-300°C block boundaries effect 7-32457
- KCl, US vibration, 20-300°C block boundaries effect 7-32457
- LiBnO₃, charactn. by γ -ray diff. 7-54061
- LiF, US vibration, 20-300°C block boundaries effect 7-32457
- YZ-LiNbO₃, dislocation electric fields and small-angle grain boundaries, ferroelectric domains 7-3000
- Mg, transformation matrices for hexagonal and trigonal crystals 7-63541
- MgAl₂O₄, neutron irradi., microstruct., mech. props. 7-51843
- MgO bicrystals, (110) tilt boundaries and (100) twist boundaries (*Japanese*) 7-21232
- Mo permalloy films, mag. domain walls stability, external mag. field, Lorentz microscopy 7-45780
- Mo, single cryst., recrystallised after hydraulic extrusion, wide-angle boundaries of anomalous grain 7-44563
- MoS₂ films, RF magnetron sputtered, elec. and optical props. 7-2747
- Mo_{0.9}W_{0.1}O_{3-x}, electrical conductivity, mag. susceptibility and IR spectra 7-38546
- NaCl, US vibration, 20-300°C block boundaries effect 7-32457
- Nb, superconducting bicrystal, flux pinning by special grain boundary 7-64420
- Nb-Al₂O₃ interface, grain boundary struct., elemental comp. determ., TEM obs. 7-21225
- Nb-based alloys, grain boundary internal friction investig. (*Russian*) 7-13490
- Nb-Zr (1 wt.%) alloy, hydroextruded, optimum degree of deform., microstruct. 7-3325
- Nd-Dy-Fe-B-based sintered magnet, microstruct., heat treatment effects 7-53767
- Nd-Fe-B permanent magnet, microstructure and coercivity 7-27559
- Nd-Fe-B permanent magnets, BCC phase mag. props. at grain boundaries 7-53044
- Nd-Fe-B rapidly solidified permanent magnet materials, magnetisation processes and domain wall motion 7-38902
- Nd-Fe-B rapidly solidified ribbons, magnetisation, quench rate depend. 7-53034
- Ni base superalloys, techniques for required props. prod. (*Turkish*) 7-59657
- Ni films, vacancy migration, impurity quenching, complex bonding energy (*Russian*) 7-44531
- Ni, H trapping phenomena, meas. by desorption thermal anal. technique 7-6673
- Ni-base wrought superalloy, thermal fatigue resist. improvement by laser-glaze 7-22840
- Ni₃Al, computer simulation of grain boundaries, effect of comp. 7-21228
- Ni₃Al, L₁2 struct., grain boundary ordering configs. 7-32456
- Ni₃Al, polycrystalline, grain boundary fracture model 7-53896
- Ni₃Al-B, grain boundary adhesion 7-16350
- Ni₃B/Ni eutectic, SEM and HREM struct. and chem. anal. 7-17515
- Ni₄Mo-Cr, isothermal annealing, structural changes 7-46462
- NiO ceramics, grain boundary struct., TEM obs. 7-21225
- NiO, spinel growth, interface struct. investig. 7-16566
- NiSi₂-Si epitaxial interface, extended defects, geometrical character 7-6640
- Pb-Sn solder, deform. props. 7-46590
- PbTe films grown by hot-wall epitaxy on KCl and BaF₂, TEM anal. 7-59432
- Pd, single crystals, high temp. elastic props. 7-63710
- PdFe ordered alloy, discontinuous domain coalescence (*Russian*) 7-2025
- SOI films, halogen lamp recrystallised, minority carrier lifetime studies 7-33101

grain boundaries continued

- Si, as-grown and annealed bicrystals, conductance of grain boundaries 7-64245
- Si bicrystals, grain boundaries, electronic states, transient capacitance spectroscopy meas. 7-7173
- Si bicrystals, grain boundary carrier recombination, chemical origin 7-17039
- Si bicrystals and thin films, grain boundaries, electronic props. 7-7172
- Si, charged defect states at grain boundaries 7-44564
- Si films on insulator, lamp zone melting, defect entrainment 7-53642
- Si, grain boundary pot. barrier and role of distorted bonds 7-46080
- Si, low-angle silicon sheet (LASS) material, microstructure exam. 7-21231
- Si, neutron-transmutation doped, spatially resolved carrier lifetime meas. 7-7257
- Si, polycrystalline, for solar cell appls., photovoltaic props., effect of impurities and defects 7-38639
- Si, polycrystalline, grain boundary recomb. vel. eval. from spectral response of solar cells 7-41403
- Si, polycrystalline films, laser-recrystallized, grain boundary location using antireflection cap 7-46312
- Si, polycrystalline layers, growth shape and struct. investig. 7-2405
- Si polycrystalline layers, elec. props. and grain boundary carrier dynamics under solar illumination 7-38625
- Si polycrystalline solar cell p-n junction, carrier lifetime, effective recomb. vel. and diffusion length, EBIC meas. 7-23138
- Si, reconstructed structures of symmetrical (011) tilt grain boundaries 7-51785
- Si solar cells, eval. of density of grain boundary states 7-34028
- Si solar cells, polycrystalline, interface state characterization by electric noise meas. 7-13920
- Si thin films, polycrystalline, elec. props. 7-33117
- Si:Ar⁺, ion implanted thin film, defect form., dose depend. study 7-51793
- Si:As(B)(P), impurities at dislocations and grain boundaries, high-resolution TEM imaging 7-37815
- Si:H, H composition at surfaces and interfaces 7-27083
- Si:H, polycrystalline, chemistry of grain boundary passivation 7-12375
- Si:H, polycrystalline, grain boundary interactions 7-12117
- Si:P, polycrystal, thin film, carrier transport, temp. depend. study 7-22043
- Si:P polycrystalline films, segregation at grain boundaries, NMR study 7-38953
- Si:P thin films, surface energy-driven grain growth during rapid thermal annealing 7-63994
- Si:Ti(V)(Cr)(Fe)(Zr) polycrystalline solar cells, structural, elec., photovoltaic props., impurity effects 7-39990
- α -SiC, sintered, occurrence and distrib. of B-containing phases 7-39466
- α -SiC, static fatigue limit at elevated temps., thermodynamics 7-17629
- SiC:Si reaction bonded composite ceramics, interface struct., grain boundaries 7-64995
- SiC-based ceramics, sintered and hot isostatically pressed, microanalytical investigation 7-27991
- Si₃N₄, grain boundary phases, EM anal. 7-16569
- Si₃N₄, surface flaws effect on strength 7-59638
- Si₃N₄, yield at elevated temps. (*Japanese*) 7-3388
- Si₃N₄:AlN, grain boundary phases, EM anal. 7-16569
- Si₃N₄:Y₂Al₂O₇, grain boundary phases, EM anal. 7-16569
- Si₃N₄-Al₂O₃-Y₂O₃(CeO₂)(La₂O₃) ceramics, sintered, IR and Raman spectra 7-46000
- Si₃N₄-Y₂O₃-Al₂O₃, pressureless sintering 7-17503
- SiO₂-Al₂O₃ powders, prep. by spray pyrolysis, sinterability, effect of chem. comp. (*Japanese*) 7-3246
- Sn alloys, surface and interphase phenomena, grain boundaries and growth 7-13431
- β -Sn, positron lifetimes, prevacancy effect 7-37973
- SrTiO₃ ceramics, Maxwell-Wagner relax. and degradation 7-2970
- Ta grain boundary studies, field ion microscopy, optimal conditions 7-32461
- Ti alloy sheet, vac. annealing temp. influence on surface relief 7-17688
- Ti binary alloys, reduced technological plasticity and struct. (*Russian*) 7-17583
- Ti, impact produced adiabatic shear bands, deform. twins, dislocation density, HVTEM obs. 7-22753
- Ti polycrystals, <1123>{1011} slip 7-38011
- Ti-SiO₂-TiSi₂, high temp. reaction between Ti and SiO₂, XPS, sputtering (*Japanese*) 7-7022
- TiB₂-TiC composite, hot pressed, degradation in liq Al 7-28156
- TiN coatings on steel substrates, growth, struct., props. 7-33799
- U_{0.86}Gd_{0.14}O_{2+x} pellets, reaction with Cs fission product, annealing, diametral expansion 7-56756
- UO_{2+x} pellets, reaction with Cs fission product, annealing, diametral expansion 7-56756
- V₃Ga superconducting tapes, grain boundaries, elementary pinning force 7-22080
- W grain boundary studies, field ion microscopy, optimal conditions 7-32461
- W wire, grain boundary struct. annealing above 1800K 7-6636
- W-Cu duplex struct., brazed test pieces, durability against thermal fatigue (*Japanese*) 7-56818
- WC-Co composite, grain boundary films, mean inner pot. determ. by Fresnel technique 7-16431
- Zn-Al-Mg alloy, defect and grain boundary diffusion-controlled positron trapping study 7-39301
- ZnO, grain boundary inhomogeneity phenomena, microcontact meas. (*German*) 7-58893
- ZnO varistor, grain boundary pot. barrier, effects of annealing 7-16568
- ZnO varistor, grain junction barrier height, majority carrier effects (*French*) 7-17033
- ZnO varistor, single grain junction barrier height, minority carrier effects (*French*) 7-21929
- ZnO varistors, bulk electron traps 7-45348
- ZnO varistors, electroluminescence temp. depend. and conduction mechanisms 7-17349
- ZnO:In films, microstruct., elec. and optical props., film thickness depend. study 7-16895
- Zr, internal friction due to grain boundary relax. 7-65076
- ZrO₂ ceramic, grain boundaries, microanal. 7-16577
- ZrO₂/mullite composite ceramic, grain boundary HREM study 7-16427
- ZrO₂-Y₂O₃-Co₃O₄ materials, Co₃O₄ effect on struct. and phase comp. 7-27990

grain boundary diffusion

- bicrystal structurally inhomogeneous boundaries, grain boundary atom diffusion (*Russian*) 7-16796
 cohesive energy, noncoherent intergranular boundaries (*Russian*) 7-58291
 diffusion induced grain boundary migration, misorientation depend. 7-21229
 diffusion-induced grain boundary migration, effect of thermomech. treatment 7-26764
 diffusional creep, grain boundary dislocation geometry 7-38013
 disordered systems, impurity diffusion (*Russian*) 7-52145
 films, oriented crystalline, on amorphous substrates, prep. by zone melting recrystallisation and surface-energy-driven grain growth 7-38385
 Inconel 600, recovery kinetics, X-ray determ. 7-22722
 kinetics of press. assisted final stage densification, pore size distrib., computer simulation 7-59477
 ledges, cavity nucleation 7-21217
 metals, fine grained structure, grain boundary diffusion theory (*Russian*) 7-6853
 metals, grain boundary diffusion mechanisms, review 7-52143
 multilayer ferromag. thin films, NMR freq. anisotropy (*Russian*) 7-45830
 polycrystals, high temp. internal friction, rel. to grain boundary diffusion 7-63743
 powder densification by interface-reaction controlled grain boundary diffusion 7-64950
 semiconductors, polycrystalline, grain boundary segregation and diffusion 7-6641
 sintering, intermediate and final-stage, microstruct. development 7-64952
 sintering, solid-state, neck shape and limiting grain boundary diffusion/surface diffusion 7-64951
 sliding of grain boundaries by diffusion 7-44560
 slip grain boundary interaction, role in cavity nucleation 7-21219
 steel, die, heat-resistant, optimum hardening temps., struct. and mech. props. 7-8022
 steel, dual-phase, Mn-partitioning, austenite form. 7-39552
 steel, Mo-Ni-Mn, creep fracture mechanisms and rupture life 7-65137
 theory of migration of grain boundaries (*Russian*) 7-58290
 Ag-Ag, thin film system, phase growth, electron microscope obs. 7-58488
 Al-Cu compact, struct. form. during sintering 7-53675
 Al-Li, grain boundary precipitate free zone growth kinetics 7-33662
 Al-Mo, rapid solidification processed, diffusion-induced dislocation migration 7-65047
 Al₂O₃-MgO-TiO₂-Na₂O system, sintering and creep, Na₂O influence, Cable and Reijnen-Readley models (*German, English*) 7-7933
 Au crystallites, annealing, grain boundary untwisting and untilting, dislocation climb and glide 7-12076
 Au/CeO₂ thin films on Ni-Cr Inconel superalloy substrates, diffusional processes 7-45098
 Bi₂-Sb₂Te₃ polycryst. semicond. films, laser annealing effects 7-58317
 CdTe, polycrystalline, grain boundaries elec. and optical characts. 7-38012
 CeO₂-ZrO₂ solid solutions, O self-diffusion, effect of grain boundary movement 7-21522
 Cr₂O₃, pure and MgO doped, sintering kinetics 7-13418
 Cu bicrystals, fatigued at high temp., microstruct. obs. in vicinity of cavity grain boundaries 7-38019
 Cu, vacancy diffusion along (100) twist boundaries (*Russian*) 7-2265
 Cu-Ag, surface segregation 7-44829
 Cu-In (15 wt.%), lamellar precipitates, cellular dissolution kinetics, grain boundary diffusion 7-28047
 Cu-Zn system, diffusion induced grain boundary migration 7-21227
 Cu₃S films, field assisted chemiplating for CdS/Cu₃S heterostruct., growth mechanism 7-59470
 Fe, cast, nodular, ferritising action of increased Mg content on struct. 7-3292
 Fe/Zn diffusion couple, anomalously fast diffusion 7-16818
 Fe-Si, H-induced grain boundary migration 7-21230
 LiF, pore-grain boundary configs., fracture surface, SEM obs. 7-32458
 Mo-Ni-Co-Sn, liq. phase sintering, grain boundary migration, coherency strain effect 7-22604
 Nb₃Sn film, grain size, grain boundaries and diffusion, TEM study 7-21222
 Ni alloy, heat-resisting, hot strain rate effect on microstruct. and mech. props. 7-39559
 Ni, grain boundaries in very clean tips, SEM, FEM obs. 7-52148
 Ni, intergranular H embrittlement kinetics 7-65134
 Ni powder, ultradisperse, recrystallisation inhibition at high press. (*Russian*) 7-59481
 Ni, T-induced He bubbles on grain boundaries migration and coalescence 7-58289
 Ni-Cu diffusion contact, mass transfer at grain boundaries in fields of diffusion-concentration stresses 7-2272
 NiO, coincidence boundary migration, calc. of activation energy for defect movement using computer simulation techniques 7-21218
 NiO, diffusion processes down coincident tilt boundaries 7-38253
 PLZT ceramics, hot pressed, chemically induced grain boundary migration and recrystallisation 7-27027
 Pb-In-Au thin films, hillock growth kinetics, grain boundary diffusion, SEM study 7-27221
 Pb-Sn, cellular transform., directional invariance of grain boundary migration 7-22695
 Pb-Sn (2 wt.%), high temp. fatigue, dynamic recrystallisation 7-39667
 PbS polycryst. semicond. films, laser annealing effects 7-58317
 Pd, H diffusion and segregation in grain boundaries 7-63632
 Si, polycrystalline p-type, Al and Cu diffusion effects on electronic properties 7-17038
 Si:As films, preannealed and As ion implanted, structural changes during transient pot-annealing 7-16904
 Si:P(As)(P,B)(As,B) films, surface energy driven secondary grain growth 7-22740
 Sn grain boundary diffusion in Ni, temp. depend. 7-63877
 Ta, grain boundaries in very clean tips, SEM, FEM obs. 7-52148
 ThO₂-UO₂, polycryst., lattice and grain boundary diffusion 7-58519
 TiSi₂:B(P)(As) films on Si, impurity diffusion 7-7077
 V-Ge(111) interface, temp. depend. intermixing, core level photoemission study 7-21542
 W, grain boundaries in very clean tips, SEM, FEM obs. 7-52148
 Zn-Al, bicrystals, and polycrystals, creep grain boundary strengthening 7-22747
 Zn-Al-Cu, superplastic, cavitation damage 7-65080

grain boundary migration *see* grain boundary diffusion

grain boundary segregation

- Astrolurgy, LC, Nirbase superalloy, hot isostatic pressing, powder metallurgy, second phase particle anal. 7-17497
 free energy considerations and fracture 7-38110
 interaction of doping atoms with grain boundaries (*Russian*) 7-51781
 L1₂ intermetallics, localised grain-boundary electronic states and intergranular fracture calcs. 7-45215
 Monel K-500, precip. of intermetallic γ' phase and carbide phases 7-33678
 Nimonic 105, Ni-base superalloys, precip. and tensile deform. behaviour 7-65078
 nonequilibrium grain-boundary segregation kinetics 7-59525
 semiconductors, polycrystalline, grain boundary segregation and diffusion 7-6641
 solute atom segregation to grain boundaries statistical and struct. effects 7-32651
 stainless steel, ion irradiated, X-ray microanalysis, of equilibrium and nonequilibrium segregation 7-46488
 stainless steel-Sb, X-ray microanalysis, of equilibrium and nonequilibrium segregation 7-46488
 steel, austenitic stainless, corrosion and grain boundary Cr depletion, comparison in modified strauss test 7-39728
 steel, austenitic stainless, creep cavitation rel. to S and P impurity segregation 7-39587
 steel, austenitic stainless, intercrystalline corrosion causes and countermeasures (*German*) 7-17729
 steel, austenitic stainless, N segregation to grain boundaries 7-59537
 steel, austenitic stainless, precipitation and B grain boundary segregation studies 7-33673
 steel, austenitic stainless, tensile and impact props., effect of grain boundary carbides 7-33785
 steel, B-containing, H-embrittled grain boundaries, Auger anal. 7-59633
 steel, C-Mn and Nb treated, high temp. ductility loss, grain boundary segregation 7-46573
 steel, Cr-Mo, crack initiation under sustained load, effect of impurity segregation 7-65111
 steel, Cr-Mo, ion nitriding, transform. of (Cr,M)₇C₃-type carbides 7-17701
 steel, dual-phase, Mn-partitioning, austenite form. 7-39552
 steel, high temp. ductility, effects of B 7-46588
 steel, low C, Al killed sheet, overaging, continuous annealing, carbide precip., hardness (*Korean*) 7-46474
 steel, martensitic stainless, precipitation hardened, impact toughness rel. to Mo content, AES obs. 7-39666
 steel, medium and high C, coalescence recrystallisation, cementite particles effect 7-46515
 steel, microalloyed, hot ductility rel. to grain size and precip. 7-28088
 steel, Mn, lath martensite, embrittlement in specimens containing 6 to 10% Mn (*Japanese*) 7-33774
 steel, Ni-Co-Mo, maraging, fracture toughness rel. to heat treatment, precip., Auger spectra 7-65124
 steel, Ni-Cr, ductile-to-brittle transition temp. shift due to temper embrittlement and neutron irradiation evaluation by small-punch test 7-28114
 steel, stainless, ferritic, irradiation, grain boundary segregation, STEM microanalysis 7-22701
 steel, stainless, superalloy, fracture toughness, tensile props., T and ³He effect 7-46616
 steel, structural, STEM-EDS X-ray microanalysis of grain boundary segregation 7-22702
 structural steels, coercivity and Barkhausen noise power spectrum, stress depend. meas. 7-7548
 superalloys, hot corrosion processes, diffusion and overlayer coating struct. effects 7-53985
 superalloys, stress rupture notch sensitivity, grain boundary precip. (*Chinese*) 7-13541
 thick-film resistors, conduction threshold, segregation effects, percolation model 7-27372
 X-ray microanalysis, of equilibrium and nonequilibrium segregation 7-46488
 Ag-O solid solutions, annealing, grain boundary segregation of O 7-33679
 Al-Al₂O₃-MgO, cast particulate composites, microstruct. and mech. props. 7-65086
 Al-Li, grain boundary precipitate free zone growth kinetics 7-33662
 Al-Li alloys, grain boundary fracture 7-39644
 Al-Li base alloys, deform. and fracture 7-39594
 Al-Li-Cu-Zr, fracture, ageing and comp. depend. 7-22784
 Al-Mg (6.5 wt.%), grain boundary segregation, STEM-EDX analysis 7-39518
 Al-Mo, rapid solidification processed, diffusion-induced dislocation migration 7-65047
 Al-V films, precip. from metastable solid solns. 7-65048
 Al-Zn, fatigue particle coarsening, vacancy creation 7-53895
 Al-Zn-Mg, 7075, grain boundary precip., crystallographic orientation depend. 7-22686
 Au-Ag-Cu-Pd, cast microstruct., segregation, TEM obs. 7-39495
 Co-Cu, Y ion-implant, growing Cr₂O₃ film, obs. of coherent perovskite particles 7-39738
 Cu-Al-Ni, β -phase alloys, fracture rel. to grain boundary precip. and Ni content 7-59604
 Cu-Al-Ni-Ti-Zr, shape memory alloy, grain refinement, fracture mode, Ti and Zr additions effect 7-3301
 Cu-Ni-Al, two-step ageing, microstruct., mech. props. 7-39565
 Cu-Zr (0.5 wt.%), high strength, high cond., prod. by rapid solidification technology 7-28029
 Fe, cast, pearlitic, nodular, fractographic anal. 7-53882
 Fe high temp. ductility, effects of B 7-46588
 Fe, porous, segregation of impurity elements, alloying elements selection and activated sintering 7-53742
 Fe-Au, solute segregation, grain boundary structural transform. 7-22687
 Fe-C-Mn(Ni)(Co)(Si)(Mo), nucleation of proeutectoid ferrite at austenite grain boundaries 7-8003
 Fe-Cr-Al-Ce, microstruct., high temp. corrosion rel. to Ce additions 7-13648
 Fe-Ni-C and Fe-C, bainite reaction kinetics, austenitising temp. effect 7-13453
 Fe-Ni-Sb, grain boundary segregation of Ni and Sb 7-22689
 Fe-P-C system, ferritic, grain boundary segregation of P and C 7-39530

grain boundary segregation continued

Mo alloys, grain boundary enrichment by O and C, nonmonotonic temp. depend. (*Russian*) 7-59534
 Nb, pure, tensile deform., brittle fracture, H effect, SEM obs. (*Chinese*) 7-8078
 Ni base superalloys, pressure vessel performance, strength, ductility, comp., struct. 7-3365
 Ni(B)s, grain-boundary cohesion, impurity segregation effects, density-functional cluster model calcs. 7-44835
 Ni-B, precipitation and B grain boundary segregation studies 7-33673
 Ni-Cr superalloy IN738LC creep induced damage identification using electron backscatt. patterns 7-46748
 Ni-Sn, ageing, discontinuous coarsening of cellular precipitate at grain boundary 7-39528
 Ni₃Al, rapidly solidified, B segregation to grain boundaries, atom probe FIM 7-22688
 Ni₃Al, rapidly solidified, C segregation to grain boundaries 7-46483
 Ni₃Al-B rapidly solidified alloy, B distrib. at grain and antiphase boundaries, atom probe FIM and TEM studies 7-33637
 Ni₃Al-B-Hf alloys, B and Hf grain boundary segregation, ductility, atom probe FIM study 7-33675
 Ni₃Al-Be, ductility, strength, grain boundary segregation, solid soln. strengthening, Be addition effect 7-39608
 Pb-Al-Mg-Sn-Li, strength and microstruct. 7-8047
 Pb-Li, strength and microstruct. 7-8047
 Pd, H diffusion and segregation in grain boundaries 7-63632
 SiC:Si reaction bonded composite ceramics, interface struct., grain boundaries 7-64995
 SiC-based ceramics, sintered and hot isostatically pressed, microanalytical investigation 7-27991
 Sn grain boundary diffusion in Ni, temp. depend. 7-63877
 Ti-Co (3.2 at.%), grain boundary allotriomorphs, nucleation, growth and transform. kinetics 7-28035
 Ti-Cr (6.6 at.%), grain boundary allotriomorphs, nucleation, growth and transform. kinetics 7-28035
 TiO₂-SnO₂ system outside coherent spinodal, phase transform. kinetics, role of aliovalent dopants 7-46432
 W-Cu pseudoalloy, Si alloying effect on solute redistrib. and ductility characts. 7-53741
 WC-TiC-Co hard alloy T15K6, heat treatment effect on failure mechanism 7-13550
 Y₂O₃, elec. cond. as function of O₂ partial press. in wet and dry atm. 7-45405

grain boundary sliding *see slip*

grain growth

electrical steels, physical metallurgy, conf., New York, USA (Feb. 1985) 7-4626
 films, grain growth phenomena and microstructural evolution during deposition, Monte Carlo simulation 7-52336
 films, grain structures and grain growth 7-16903
 films, oriented crystalline, on amorphous substrates, prep. by zone melting recrystallisation and surface-energy-driven grain growth 7-38385
 Inconel X-750, air environment/creep interactions, prior exposure times effect 7-13499
 material analysis, computer-based, conf., Boston, MA, USA (Dec. 1985) 7-14709
 metal films, characterisation by SIMS, Auger spectroscopy and TEM 7-12550
 metals, dual-phase, simulation of growth process of minor phase grains 7-65050
 Monte Carlo simulation 7-17561
 PVC, suspensions, grain formation 7-22694
 secondary and normal grain growth, relative rates 7-65003
 sintering, intermediate and final-stage, microstruct. development 7-64952
 steel, constructional carbon type, original charge purity influence on microstruct. hardenability and mech. props. 7-46521
 steel, Cr-Mo-V, rail, fatigue crack growth 7-8114
 steel, Cr-Mo-V, thermal fatigue resist., effect of initial struct. 7-28132
 steel, die, heat-resistant, optimum hardening temps., struct. and mech. props. 7-8022
 steel, fine-grained, Zr effect on struct. and phase comp. 7-39525
 steel, high-speed p/m tungstenless, Mo and V effect on microstruct. and operating props. 7-33788
 steel, low C, capped, grain growth during subcritical annealing 7-46519
 steel, low-alloy, Te-containing, nonmetallic inclusions and austenite grains 7-39522
 steel, microalloyed, abnormal grain growth in austenite range (*German*) 7-7958
 steel, Mn-V, low-pearlitic, normalized, struct. and mech. props., sheet thickness depend. 7-8006
 steel, Si, recrystallised grain growth, 650 to 850°C 7-46509
 steel, structural heredity in heat cycling 7-33703
 steels, microalloyed, high strength, phys. metallurgy and appls. 7-65066
 superplastic alloys, plastic instabilities and uniaxial tensile ductilities, effect of grain growth 7-53820
 superplastic deformation, boundary migration, grain growth 7-17600
 superplastic flow, void growth mechanism 7-28086
 Al-Cu compact, struct. form. during sintering 7-53675
 Al-Mg (0.2 wt.%), subgrain growth rel. to prior cold work and annealing temp. 7-17551
 Al₂O₃ ceramics, sintering, effect of TiO₂ (*Japanese*) 7-3248
 Al₂O₃-MgO, diphasic xerogels, densification, sintering, isostructural seed, epitaxy 7-27987
 B⁺-Al₂O₃-Na₂O-ZrO₂ ceramics, transform toughened, fabrication, mech. props. ionic resist. 7-65143
 Al₂O₃-TiO₂, mech. props. and microstruct., influence of TiO₂ additions. (*Japanese*) 7-22706
 Au/CeO₂ thin films on Ni-Cr Inconel superalloy substrates, diffusional processes 7-45098
 BaTiO₃ ceramics, sintering, liq. phase enhanced discontinuous grain growth control 7-46384
 CaCO₃, calcite, grain growth, effect of second-phase particles 7-39476
 Cu coating, ion plating on steel, deposition conditions effect on coating struct. 7-39748
 Cu powders, sintering, densification, grain growth (*Japanese*) 7-53662
 Cu-Al-Ni-Ti-Zr, shape memory alloy, grain refinement, fracture mode, Ti and Zr additions effect 7-33301
 Cu-Sn-Pb system, struct. form. during sintering 7-64967
 Cu-Zn-Al shape memory alloys, grain refinement 7-53774
 Fe powders, sintering, densification, grain growth (*Japanese*) 7-53662

grain growth continued

Fe-Cr coating, ion plating on steel, deposition conditions effect on coating struct. 7-39748
 Fe-Cu, sintering, form. of Cu pockets in Fe grains 7-7922
 Fe-Si, rapidly quenched ribbons, grain growth, mag. props. 7-8017
 Fe-Si (3 wt.%), continuously cast slabs, high temp. grain growth during reheating 7-8019
 Fe-Si (3 wt.%), grain oriented, texture development for regular and high permeability 7-8008
 Fe-Si (3 wt.%), microstructure, change in stereological characteristics on secondary recrystallisation 7-13468
 Fe-Si powders, grain size, influence of α - γ transform. 7-7992
 Fe-Si-Ni (6.5, 2 wt.%), development of Goss texture, lowering of core loss 7-33693
 Ge sputtered (100) textured film, TEM grain growth obs. 7-45040
 Ge ultra-thin films, self-implantation, grain growth enhancement, TEM study 7-12173
 Li ferrites, microstruct. effects on mag. props. (*German*) 7-59052
 MgO, sinterability, microstruct. changes during sintering 7-22624
 Mo, single cryst., recrystallised after hydraulic extrusion, wide-angle boundaries of anomalous grain 7-44563
 (Na_{0.5}K_{0.5})NbO₃, sintering, densification and elec. props., effect of Ba additions 7-46387
 Ni alloy, heat-resisting, hot strain rate effect on microstruct. and mech. props. 7-39559
 Ni-base superalloys and intermetallics, rapidly solidified, mech. props. 7-22839
 Ni-based consolidated rapidly solidified alloys, strengthening mechanisms 7-22712
 Ni-Cr alloy, wrought, Hf effect on struct. and mech. props. 7-33689
 Ni-Cr superalloy, high-temp. material, microstruct. and mech. props. with high-temp. heating 7-3341
 PLZT ceramics, grain growth during hot pressing 7-3232
 Rn, electrodeposition from sulphate solns., grain growth, additive effect (*Japanese*) 7-17481
 Si films on glass substrates, laser recrystallisation 7-38395
 Si:P thin films, surface energy-driven grain growth during rapid thermal annealing 7-63994
 Si:P/Ti, enhanced grain growth by silicide form. 7-27142
 Si:P(As)(P)(B)(As,B) films, surface energy driven secondary grain growth 7-22740
 Si:P(B) LPCVD films, amorphous and polycrystalline, struct., elec. resist. meas. 7-52870
 β -SiC powder, sintering, phase transform. rel. to additives (*Japanese*) 7-17527
 Si₃N₄ powder, physico chem. characts. before sintering (*Japanese*) 7-64980
 Si₃N₄, with MgO addition, phys. and tribological props., effect of hot-pressing time (*Japanese*) 7-65150
 Sn alloys, surface and interphase phenomena, grain boundaries and growth 7-13431
 (Ti,Cr)B₂ sintered electrode exposed to liq. Al, degradation, effect of segregated Cr 7-28045
 Ti-Al-Mo-V-Cr alloy VT22, metallographic study of β -solid soln. decomp. 7-39523
 TiB₂ ceramics, pure and liq. phase sintered, processing and microstruct. development 7-3251
 TiC-Ni-Mo sintered carbides, struct. and physicochem. props. 7-3256
 W films on GaAs substrates, electrical resistivity after high temp. annealing 7-64366
 W, grain growth, impurity effects 7-28044
 W wire, K-doped, non-sag struct. form., model 7-7957
 WC-Co compact, stereological analysis of struct. form. during consolidation of carbide powder 7-53688
 Zn-Al-Cu, superplastic, cavitation damage 7-65080
 Zn-Al-Cu (ZZ.0.5%), superplastic behaviour 7-28093
 Zn-based alloys, mechanical props., alloying addition effects (*Japanese*) 7-8090
 ZnO ceramic, grain growth kinetics during synthesis, optimum elec. props. 7-46398
 ZrCo₉₈, sintered polycryst., primary recrystn. process 7-28056
 ZrO₂-Y₂O₃-TiO₂ ceramics, transport, sintering behaviour 7-13421

grain refinement

brass, two-phase, Al-B Masteralloy addition, B redistrib. during solidification, grain refining effect 7-22664
 CVD coating morphology, trace impurity effects 7-3191
 steel, Cr-Mo-V, porosity assoc. with insoluble carbides, probable effect on rolling contact fatigue 7-17639
 steel, high-speed, cast and wrought, impact-fatigue strength 7-39656
 steel, superhardenability treated, transform kinetics 7-39535
 Al-Cu, superplasticity rel. to grain refining addition elements 7-46561
 Al-Si, grain refinement, effect of solute content 7-59503
 Al-Zn-Mg, superplasticity rel. to grain refining addition elements 7-46561
 Al-Zn-Mg-Cu alloy, microalloying effect on struct. and mech. props. 7-53755
 Au-Cu-Pd, corrosion resist. 7-39739
 Cu-Al-Ni-Ti-Zr, shape memory alloy, grain refinement, fracture mode, Ti and Zr additions effect 7-33301
 Cu-Zn-Al shape memory alloys, grain refinement 7-53774
 Ge droplets, undercooled, microstruct. 7-65013
 Ni-Cr alloy, wrought, Hf effect on struct. and mech. props. 7-33689
 Ni-P coating, electrolytic, electron microscope obs. of struct., P content depend., amorphous layer form. 7-8157
 Pb-Sb, grain refinement, effect of solute content 7-59503
 Ti-Al-Mo-V-Cr alloy VT22, metallographic study of β -solid soln. decomp. 7-39523

grain size

see also grain growth; grain refinement
 α -Al₂O₃ powders, high press. compaction, density, pore size, grain size 7-13413
 Al-Zn-Mg-Cu, impact toughness improvement by intermediate thermomech. treatment 7-53907
 alkaline earth sulphide phosphors, prep. and thermolum., review 7-17488
 Alloy 718, Ni-base superalloy, fatigue crack propag. under hold-time cycling, effect of grain size 7-28106
 alloys, rapid solidification technology, review 7-39493
 B₂C, thermal stress fracture, grain size and porosity effects (*Japanese*) 7-8087

grain size continued

- Bauschinger effect, influence of alloying elements and grain size (*German*) 7-17605
- biphase polycrystalline materials, max. plasticity, struct. conditions (*Russian*) 7-51921
- brass, pressed component, strain distrib. 7-13530
- brass, Sn alloyed, disordered areas in three component solid solns. 7-21157
- brass L80 foil, grain struct. form. after isothermal annealing 7-53761
- brass sheet formability, grain struct. and stress raisers influence 7-3376
- ceramics, microstruct. charactn. by image anal. 7-3547
- ceramics, structural, flaw size distrib. 7-22818
- ceramics NDT by acoustic microscopy with single zoom lens 7-3570
- cordierite glass and glass-ceramic, comparative single-point diamond scratching behaviour 7-46654
- deformation curve, relationship between σ_0 and Hall-Petch parameters (*Russian*) 7-38092
- dielectric coatings, mol. struct. and phys. props. Raman studies 7-45063
- liquid phase sintering, pore filling, critical grain size for liq. flow 7-46364
- magnetic multidomain material, screening of domain moments and remanence stability 7-47430
- MIS solar cells, polycryst., barrier height anal. 7-46941
- misch metal-Fe-B melt-spun magnets, mag. and structural props. 7-53032
- Mo-Ni, activated sintered, sintering behaviour and mech. props. 7-7929
- natural polycrystalline quartz aggregates, grain size sensitive plastic flow 7-53824
- phase separation, cluster kinetics and self-similar structure functions 7-44836
- sialon ceramics, processing, Al ion redistrib., crystallisation EDX analysis 7-3237
- snow, IR meas. of grain size and melting degree 7-23719
- stage II fatigue crack growth behaviour of granular bainitic microstructures 7-28134
- steel, alloyed structural, struct. rel. to cold deformability, softening heat treatment methods development 7-39556
- steel, austenitic stainless, Mo and/or N alloyed, recrystn. after hot working 7-3326
- steel, austenitic stainless, strength and toughness at 4K, fusion energy magnets appl. 7-53793
- steel, C-Mn, hot ductility, influence of grain size 7-3374
- steel, constructional carbon type, original charge purity influence on microstruct. hardenability and mech. props. 7-46521
- steel, Cr, austenitisation, recrystallisation, pearlite transform. rel. to hot deform. 7-28033
- steel, Cr-Mo-V, porosity assoc. with insoluble carbides, probable effect on rolling contact fatigue 7-17639
- steel, Cr-Mo-V, rotor, high temp. creep, prior austenite grain size effect 7-53828
- steel, die, heat-resistant, optimum hardening temps., struct. and mech. props. 7-8022
- steel, die, preliminary heat treatment schedule 7-8023
- steel, dual phase, effective grain size, cleavage crack propag. 7-28118
- steel, eutectoid, fully pearlitic, cleavage fracture stress, microstruct. effects 7-28123
- steel, eutectoid, phase rot., effect of recrystn. processes during heat deform. (*Russian*) 7-53760
- steel, ferrite-pearlite, viscous-brittle transition model (*Russian*) 7-3401
- steel, high strength, near threshold fatigue crack growth behaviour, effect of prior austenitic grain size 7-53906
- steel, high-speed p/m tungstenless, Mo and V effect on microstruct. and operating props. 7-33788
- steel, high-strength low-C weldable, C content effect on struct. and mech. props. 7-46583
- steel, hot rolled microalloyed, proeutectoid ferrite transform. kinetics, microstruct. modelling 7-17526
- steel, hot working of austenite, transition from multiple- to single-peak recrystn. 7-65057
- steel, HSLA, mech. props. rel. to ferrite substruct. and grain size. 7-13531
- steel, HSLA, Nb, ductile fracture, plastic deform. mechanisms 7-28115
- steel, low alloy, arc weld deposits, austenite grain struct. 7-39494
- steel, low alloy, pearlite free, fracture energy, effect of microstruct. parameters (*Russian*) 7-33787
- steel, low C, Al-killed, H diffusion 7-6886
- steel, low C, capped, grain growth during subcritical annealing 7-46519
- steel, low C, cold rolled lamination, mag. props., Mn and S contents effect 7-7550
- steel, low C, dynamic recrystn., transition of flow behaviour 7-53756
- steel, low C, magnetoacoustic emission, magnetisation, Barkhausen effect in decarburised steel 7-33207
- steel, low C, structurally free cementite form. rel. to Cr and Mn addition 7-22675
- steel, low C lamination, decarburization, grain size, carbide morphology 7-8016
- steel, low C pearlitic, microstruct.-flow stress relationship 7-33739
- steel, medium and high C, coalescence recrystallisation, cementite particles effect 7-46515
- steel, microalloyed, hot ductility rel. to grain size and precip. 7-28088
- steel, microstructural monitoring by laser-ultrasonic attenuation and forward scattering 7-33889
- steel, Mo stainless, microstructure rel. to heat treatment 7-53770
- steel, N alloyed, mech. prop.-struct. relationship 7-3316
- steel, Ni, bainite transform. kinetics, influence of grain size 7-65030
- steel, Ni maraging, austenite form. characts. (*Russian*) 7-46466
- steel, Ni-Cr-Mn, ferromag., mag. hysteresis loops, effects of grain size, hardness and stress 7-64482
- steel, Ni-Cr-Mo, hydrogen embrittlement susceptibility, austenitising heat treatment prior-austenite grain size effect 7-3415
- steel, rapid solidification, fusion reactor appl. 7-49657
- steel, stainless, ferromag., mag. hysteresis loops, effects of grain size, hardness and stress 7-64482
- steel, stainless, films, sputter deposited, vacuum annealing-induced solute depletion 7-64012
- steel, structural heredity in heat cycling 7-33703
- steel, tool, fracture toughness rel. with grain size 7-59634
- steel, tool, heat treatment cycles, original struct. and deform. influence on mech. props. 7-39560
- steels, microalloyed, high strength, phys. metallurgy and appls. 7-65066

grain size continued

- steels, tool, M2 and H13, fracture toughness, influence of microstruct. 7-46632
- structural steels, coercivity and Barkhausen noise power spectrum, stress depend. meas. 7-7548
- superplastic deformation, boundary migration, grain growth 7-17600
- superplastic to non-superplastic deform., transition at high strain rates 7-46586
- thin films, stress meas. during deposition, review 7-52380
- US attenuation spectral analysis of grain size and dislocation content 7-65271
- AgCl_{0.95}Br_{0.05}, IR transmitting fibres, optical props. 7-37185
- Al alloys, IN9021 and 7090, powder metallurgy, fatigue crack growth, influence of load ratio 7-28124
- Al evaporated films, O contaminated, recrystn., after annealing 7-38412
- Al film deposition on amorphous substrates 7-21770
- Al quenched, tensile flow stress, effect of grain size and strain 7-22756
- Al single cryst. and bicrystal, polygonisation substruct., grain boundary effects (*Russian*) 7-52887
- Al/Al₂O₃ films, ion plated in Ar-O₂ gas mixture, structure anal. 7-7899
- Al-Cu compact, struct. form. during sintering 7-53675
- Al-Cu-Mg, deformed, dislocation struct., AE obs., electron microscopy (*Russian*) 7-39832
- Al-Cu-Mg-Al₂O₃-Al₄C₃, IN 9021, mechanically alloyed precip. hardened, tensile behaviour 7-13525
- Al-Mg, deformed, dislocation struct., AE obs., electron microscopy (*Russian*) 7-39832
- Al-Mn-Si, quasicryst., X-ray diffr., TEM and SEM study 7-12299
- Al-Si, grain refinement, effect of solute content 7-59503
- Al-Ti, rapid solidification processed/mechanically alloyed, high temp. deform. 7-65100
- Al-Ti-based homogeneous alloy films, elec. resist., microstruct., electromigration, comp. effects 7-21765
- Al-Zn-Mg-Cu, 7475, superplasticity, constitutive eqn., evaluation of parameters 7-65085
- Al-Zn-Mg-Cu-Ni-Zr, modified 7075, prod. by liq. dynamic compaction, struct. and props. 7-46437
- Al-Zn-Mg-Mn-Si, rapid solidification, superplasticity 7-53826
- Al₂O₃ ceramics, grindability, effect of microstruct. 7-22862
- Al₂O₃, engineering ceramics, texture 7-28057
- Al₂O₃, polycrystalline, fracture toughness, R-curve behaviour rel. to grain size 7-46615
- B⁺-Al₂O₃-Na₂O solid electrolytes, degradation in Na-S batteries 7-3466
- Al₂O₃-SiC composites, microstruct. and mech. props. (*Japanese*) 7-22821
- Al₂O₃-TiO₂, mech. props. and microstruct., influence of TiO₂ additions. (*Japanese*) 7-22706
- Al₂O₃-ZrO₂ ceramics, hot forging characts., grain size 7-3370
- Al₂(TiO₃)₃ ceramics, sintering, microstruct., bending strength, additives effect (*Japanese*) 7-17601
- BN, cubic, polycryst., influence of sintering conditions on phys. props. 7-22618
- BaCuFe₁₀O₂₇ W-type hexagonal ferrite, intermediate valency, oxidation annealing, magnetisation and neutron diffr. studies 7-7187
- BaFe₁₂O₁₉, microcrystalline powders, prep. by glass synthesis method (*French*) 7-46394
- Ba_{0.9}Sr_{0.1}TiO₃Sb, positive temp. coeff. of resist., synthesis method depend. 7-45324
- BaTiO₃ ceramics, sintering, liq. phase enhanced discontinuous grain growth control 7-46384
- BaTiO₃ ceramics, zone sintering, dielec. props. rel. to microstruct. 7-13078
- BaTiO₃ composites, dielec. and elec. props., rel. to prep. and microstruct. 7-64559
- BaTiO₃, form. from metallo-organic precursors, kinetics 7-39465
- Al₂O₃-Nd, ceramics, diffuse phase transform 7-16731
- Be, AE as function of grain size during plastic deform. (*Russian*) 7-59582
- α -brass, hot rolled, recrystallized microstruct., deform. processes 7-13500
- CaCO₃, calcite, grain growth, effect of second-phase particles 7-39476
- Cd-Zn electroplated steel, extrusion, deform. force rel. to comp. and struct. 7-3367
- CdS films, spray deposited, laser annealing, struct., carrier mobility 7-58318
- CdS/CdTe sintered solar cell photovoltaic props. rel. to CdS film sintering conditions (*Korean*) 7-65476
- CdSe thin film liquid-junction photovoltaic cell, photoelectrochem. charactn. 7-54331
- Co-Al-Fe(Ni), B2, slow plastic flow props. between 1100 and 1400 K 7-46565
- Co-Pt thin films, sputtered, TEM study 7-21757
- CoCr films, texture formation, appl. for perpendicular mag. recording 7-39539
- CoCr sputtered films, struct. and mag. props., role of atomic mobility during film growth 7-33224
- CoCrTa sputtered films, microstruct. and mag. props. studies 7-12575
- Co₈₄Nb₁₆B₆ fully crystallised metallic glass, fracture processes 7-22841
- Cr-Si system, thin film silicide phases, formation and microstructure 7-2435
- Cr₂O₃ film, growing on Y ion-implanted Co-Cu alloy, obs. of coherent perovskite particles 7-39738
- Cu alloys, high-strength, rad.-enhanced recrystn. 7-51871
- Cu alloys, rapid solidification, fusion reactor appl. 7-49657
- Cu coating, ion plating on steel, deposition conditions effect on coating struct. 7-39748
- Cu, dislocation-mechanics-based constitutive relations for material dynamics calcs. 7-63706
- Cu filled polypropylene films, struct. and elec. cond. 7-64301
- Cu, hot rolled, recrystallized microstruct., deform. processes 7-13500
- Cu, polycrystalline, cyclic stress-strain curve, grain size effect 7-53803
- Cu, polycrystalline, high cycle fatigue behaviour, effect of grain size 7-46626
- Cu powders, sintering, densification, grain growth (*Japanese*) 7-53662
- Cu-Co (2 at.%), underaged, fatigue props., comparison of single crystals and polycrystals. (*German*) 7-46648
- Cu-Sn, ductility at elevated temps., effect of small amounts of B, P or Mg 7-53904
- Cu-Za-Al ribbons, rapidly, quenched, martensitic transform., stabilisation 7-22678
- Cu-Zn-Al-Zr, shape memory alloys, grain-refined, effect of grain size on transform. temp. 7-39512

grain size continued

Cu-Zr (0.5 wt.%), high strength, high cond., prod. by rapid solidification technology 7-28029
 Fe, electrodeposited, grain struct. and size, positron lifetime study 7-46209
 Fe powder, ultrafine, and hot forged specimens, reduction temp. effect on struct. form. and props. 7-53670
 Fe powders, sintering, densification, grain growth (*Japanese*) 7-53662
 Fe-base ferrite alloys, deform. behaviour, influence of mech. twinning (*German*) 7-17603
 Fe-Cr coating, ion plating on steel, deposition conditions effect on coating struct. 7-39748
 Fe-Cr-C, martensite nucleation, dislocations, grain boundaries, plastic accommodation 7-28040
 Fe-Nd-B permanent magnets, prep. by liquid dynamic compaction 7-53661
 Fe-Ni austenitic alloys, martensitic transformations, grain size effects (*Russian*) 7-46465
 Fe-Ni-C and Fe-C, bainite reaction kinetics, austenitising temp. effect 7-13453
 Fe-Ni(C), martensite nucleation, dislocations, grain boundaries, plastic accommodation 7-28040
 Fe-Si (3 wt.%), dynamic remagnetisation, structural depend. of losses 7-12994
 Fe-Si (3 wt.%), microstructure, change in stereological characteristics on secondary recrystallisation 7-13468
 Fe-Si (3 wt.%), recrystallisation texture regulation using small deformations 7-13472
 Fe-Si alloy wires, rapidly solidified by in-rotating-water-spinning method, prod. and props. (*Japanese*) 7-22654
 Fe-Si powders, grain size, influence of α - γ transform. 7-7992
 Fe₂O₃ reactivity, decomposition mechanism depend., reaction vol. and densification meas. 7-28308
 GaAs excimer-laser-stimulated CVD, polycryst. thin film growth and props. 7-64912
 GaAs films on amorphous insulating substrates, laser recrystallisation 7-38397
 GaAs films on oxidised Si, zone melting recrystallisation 7-38396
 Ge droplets, undercooled, microstruct. 7-65013
 InP films on oxidised Si substrate, laser recrystallisation 7-38398
 KCl:Ti, X-ray luminescence, grain size effects (*Russian*) 7-27767
 LaB₆ dispersed powders and compact specimens, struct. and morphology 7-64976
 LiAlO₂, Li₂SiO₃ and Li₂O, breeder ceramics, fabrication, irr., T release, EXOTIC expts. 7-49648
 Mg-Mn, MA8, superplastic behaviour, effect of grain struct. (*Russian*) 7-59584
 Mg₂SiO₄, fosterite-based ceramic with BaO addition, synthesis, sintering, struct. and props. 7-46397
 Mo CVD coating on graphite, struct., thermal resist. props. 7-52375
 Mo, recrystallised, microstruct. and creep charact. (*Russian*) 7-39600
 Nb, supercond., nondestructive inspection by scanning laser acoustic microscope 7-3566
 Nb-Zr (1 wt.%) alloy, hydroextruded, optimum degree of deform., microstruct. 7-3325
 Nb₃Al₂Si₄B_{0.5}, A-15 superconducting tapes for high mag. fields, fabrication 7-33133
 Nb₃Ge films, obtained by joint evaporation technique, microstruct. (*Russian*) 7-59435
 Nb₃Sn multifilamentary composite superconductor, bronze processed, global pinning force, critical mag. field, grain size 7-22078
 Nd-Fe-B, microstructure, scanning tunnelling microscopic studies 7-58494
 Ni alloy, heat-resisting, hot strain rate effect on microstruct. and mech. props. 7-39559
 Ni base superalloys, pressure vessel performance, strength, ductility, comp., struct. 7-3365
 Ni, faceted fatigue fractures, occurrence 7-53879
 Ni powder, ultradisperse, recrystallisation inhibition at high press. (*Russian*) 7-59481
 Ni ultradisperse powders, recrystallisation induced dilatation effect 7-39537
 Ni-base superalloy, IN-100, rheocast, processing-struct. charactn. 7-46449
 Ni-base superalloys and intermetallics, rapidly solidified, mech. props. 7-22839
 Ni-based consolidated rapidly solidified alloys, strengthening mechanisms 7-22712
 Ni-Cr superalloy, high-temp. material, microstruct. and mech. props. with high-temp. heating 7-3341
 Ni-Cr-W superalloy, experimental, tensile props., effect of carburisation and aging 7-59576
 Ni-Mo (20 at.%), ageing, yield strength rel. to prior α grain size 7-39507
 Ni-Mo-Cu-Fe-Mg, coarse-grained PC permalloys, annealing-twin density (*Japanese*) 7-3330
 Ni-Si interface, struct., RHEED, Rutherford backscattering spectrometry 7-27143
 NiAl, slow plastic creep props. between 1200 and 1400 K, effect of comp. and grain size 7-65084
 Ni₃Al produced by shock compaction, TEM 7-39480
 Ni₃Al-B rapidly solidified alloy, B distrib. at grain and antiphase boundaries, atom probe FIM and TEM studies 7-33637
 Ni₃Al(B,Ti), rapidly solidified powders, struct. of consolidated products 7-3222
 Ni₇₃B₁₇Si₁₀, ultrafine fine-grained, prep. from amorphous ribbon, creep deform. 7-22748
 Ni₂Si growth kinetics from Ni and Ni-V films on Si surfaces, TEM, AES, X-ray diffr. and backscatt. studies 7-45032
 PLZT ceramics, grain growth during hot pressing 7-3232
 Pb alloy base electrode Josephson junction, self-positioned, fabrication 7-52906
 Pb-Bi-Sn(In), alloy filaments, prod. by glass-coated melt spinning, enhancement of supercond. 7-58937
 Pb-In-Au fine-grained codeposited alloy films, RF plasma oxidation 7-53970
 Pb-Sb, grain refinement, effect of solute content 7-59503
 Pb_{0.9}Sn_{0.1}Te thin films, structural and elec. props., pulsed laser-irr. effects study 7-21270
 PbTiO₃, form. from metallo-organic precursors, kinetics 7-39465
 PdFe ordered alloy, discontinuous domain coalescence (*Russian*) 7-2025

grain size continued

Rh polycrystalline films, electrical size effects 7-7412
 Sc thin films, vacuum-deposited, struct. and optical props. 7-58698
 Si films, grain size and texture enhancement by seed selection through ion channelling 7-38401
 Si polycrystalline CVD film, etch rate free carrier depend., doping level and grain size depend. meas. 7-28219
 Si, polycrystalline film SOI structures, recrystn. by laser irradiation 7-32856
 Si polycrystalline films, sheet resistance, rapid thermal annealing prior to and post As ion implantation 7-12886
 Si, polycrystalline layers, TEM meas. of grain size 7-32672
 Si polycrystalline layers, elec. props. and grain boundary carrier dynamics under solar illumination 7-38625
 Si:As films, preannealed and As ion implanted, structural changes during transient pot-annealing 7-16904
 Si:As(B) polycrystalline films, rapid thermal processing before and after ion implantation, effect on cond. 7-22046
 Si:B (As) diffusion source, diffusion into single crystal Si 7-32727
 Si:H, microcrystalline, photo-CVD growth 7-13382
 Si:P films, CVD and electrical props. 7-64913
 SiC whisker reinforced Al matrix composites, interaction, with eutectic brazing alloys 7-46689
 SiC:Si, reaction bonded composite, mech. props. and microstruct. anisotropy 7-65146
 SiC-AlN ceramics, elevated temp. creep, role of grain size 7-39584
 a-SiGe:H:F glow discharge films, microcrystallinity studies 7-45088
 SiO₂:P films, pure and doped, low press. CVD growth, structural, optical, elec. props. 7-27186
 SrCl₂-Al₂O₃ system, enhancement of ionic conductivity 7-2256
 Ta grain boundary studies, field ion microscopy, optimal conditions 7-32461
 Ti alloy, heat cycling regimes and effects 7-8028
 Ti polycrystalline films, electron beam bombardment, recrystallisation, oxidation and phase transforms. 7-21746
 Ti-Al-Nb, rapidly solidified, microstructural studies 7-22668
 Ti₃Al-Zr, rapidly solidified, microstructural studies 7-22668
 TiC coated cemented carbide cutting tool inserts, performance and material props. 7-46712
 TiCN, TiC and TiN CVD coatings, high-temperature microhardness profiles 7-28181
 U, texture anisotropy, as-cast and heat treated 7-46518
 UO₂, oxidative sintering, microstruct. 7-3239
 W doped wire, effect of dopants on microstruct. (*Korean*) 7-17547
 W films prep. by various deposition methods, effects on elec. resist. 7-52860
 W grain boundary studies, field ion microscopy, optimal conditions 7-32461
 W LPCVD film struct., IC appls. 7-58692
 W reactively sputtered films, elec. resist., microstructure, effects of N or O partial press. 7-52861
 W-Re alloys, annealed and sintered, elevated temp. softening, appl. for thermionic energy conversion 7-28077
 WC-Co, erosion rate 7-3464
 WC-Co cemented carbides, tensile creep, 800-900°C, grain boundary sliding 7-17585
 WC-Co hard metals, thermal conductivity and thermal diffusivity (*German*) 7-27036
 YIG, ferromagnetic hysteresis loop, grain size distrib. effect 7-27556
 (Yb_{0.95}Eu_{0.05})₂O₃, luminophor, granulometric composition 7-22715
 ZnO ceramic, grain growth kinetics during synthesis, optimum elec. props. 7-46398
 ZnO:In films, microstruct., elec. and optical props., film thickness depend. study 7-16895
 Zn₃P₂, vacuum deposited films, struct., transmission electron microscopy and X-ray diffr. 7-52316
 ZrC_{0.98}, sintered polycryst., primary recrystn. process 7-28056
 ZrO₂ ceramics, hot forging characts., grain size 7-3370
 ZrO₂, MgO partially stabilised, SrO sintering aid addition, microstruct. and chem. aspects 7-64983
 ZrO₂, partially stabilised, phase stability, elec. cond., fusion reactor elec. insulator appl. 7-52618
 ZrO₂, Y₂O₃ partially stabilised, microstruct. after ageing at high temp. 7-65061
 ZrO₂, Y₂O₃ stabilised, fracture toughness and transformability, grain size depend. 7-13566
 ZrO₂, Y₂O₃-doped, powders, sinterable, chemically coprecipitated in non-aq. medium 7-64982
 ZrO₂-Y₂O₃, Y-TZP, superplastic, compressive deform. props. and microstruct. (*Japanese*) 7-22774
 ZrO₂-Y₂O₃-Co₃O₄ materials, Co₃O₄ effect on struct. and phase comp. 7-27990
 Zr₃Pb₃, fusion blanket neutron multiplier, fabrication and props. 7-49656
grain structure *see crystal microstructure*
grain subboundaries *see subboundary structure*
grammars
 epileptic electroencephalogram, syntactic analysis 7-34126
 skeletal maturity, fuzzy grammars for syntactic recognition from X-rays 7-34317
gramophones
 No entries
Granato-Lucke theory *see dislocation damping*
grand unified theory *see unified field theories*
granular materials
see also granular structure
 cation-exchange resin, granulated, ionic composition, pulsed elec. field effects 7-54134
 composites, failure anal. in conditions of adverse medium 7-33686
 DC cond. and percolation threshold calcs., metal-insulator composite mean-field theories 7-45253
 deflagration-to-detonation transition, two-phase mixture theory 7-37518
 discs, inelastic frictional, shearing assemblies, viscosity, granular temp., stress calcs. 7-37398
 fabrication by EM pulveriser (*French*) 7-3218
 flow, conf., Blacksburg, VA, USA (Feb. 1985) 7-35086
 fluidised-bed drying, mathematical model 7-50917
 granular superconductors, phase-locking transition, phase-number representation 7-38803
 jet flow perpendicular to flat plate, shear stress meas. by erosion technique 7-31898

granular materials continued

- loose, effective thermal conductivity calc. 7-1385
- metals, granular, hopping conduction 7-17007
- mullite-corundum refractories, creep behaviour rel. to struct. features 7-22770
- propellants, combustion, two-phase transient flow, modelling 7-37520
- shear band analysis by Cosserat theory (*German*) 7-20598
- superconductors, 3D, short-range order and phase diagrams 7-22062
- Ag-Ge granulated films, Coulomb gap and hopping conduction 7-38774
- Al₂O₃-Cu, effective thermal cond. determ. 7-27037
- Sn-Ge granulated films, Coulomb gap and hopping conduction 7-38774

granular metallic thin films *see discontinuous metallic thin films***granular structure**

- see also granular materials*
- ceramic semiconductors, granular struct. and elec. props. (*German*) 7-58495
- granular metals with potential disorder, conduction 7-52554
- mullite-corundum refractories, creep behaviour rel. to struct. features 7-22770
- Fe-SiO₂ granular films, mag. relax., DC SQUID magnetometry, Mossbauer spectra 7-45761

graph theory

- see also directed graphs; trees (mathematics)*
- benzenoid hydrocarbons, combinatorial Clar sextet theory 7-15510
- bond graph model of a pool-type nuclear reactor 7-5438
- chemical graph theory 7-30916
- electroacoustic transducers for sound-powered telephone, bond graph modelling 7-57660
- EM topology, alternative labeling schemes 7-10810
- Hamiltonian circuit in a graph, heuristic determ. method 7-60943
- ice floes, interacting around an obstacle, simulation methodology 7-55081
- infinite graphs with the least limiting eigenvalue greater than -2 7-24357
- irreducible endospectral graphs and endospectral trees 7-29661
- NP-complete problem without local minima 7-29673
- optical relational-graph rule-based processor for structural-attribute knowledge bases 7-10861
- polycyclic aromatic hydrocarbons, periodic table, characteristic polynomial, struct. invariants 7-56924
- polymer representation, matching polynomial of a polygraph 7-5796
- quasi-invariant measures of infinite dimens. Grassmann manifolds 7-55949
- radiotherapy, fractionated, graphical method to simplify the appl. of the linear-quadratic dose-effect eqn. 7-28660
- random graphs, Poisson convergence and semi-induced properties 7-48289
- random walks on graphs and stochastic infinite particle processes, approach to equilibrium 7-18693
- ray transfer flow graphs, misaligned optical systems appl. 7-9644
- sign patterns of matrices and their inverses 7-60957
- structure factor of characteristic polynomial and proof of Hosoya-Randic conjectures 7-14748

graphic equipment, computer *see computer graphic equipment***graphics, computer** *see computer graphics***graphite**

- 1.43 MeV γ -ray penetration of shields, benchmark data 7-5487
- adsorbed layers on Pt (110), nucleation and orientation 7-21664
- adsorbed SF₆ monolayer, X-ray diffraction studies 7-6965
- adsorbed Xe-Kr mixtures, X-ray diffraction studies 7-6966
- adsorption, of Ar, fluid-solid monolayer transition, simulation 7-32796
- adsorption, of ethane, phase transitions, thermodynamics and struct. anal., LEED obs. 7-32797
- adsorption of methane, multilayer growth mode 7-32795
- adsorption of methane, multilayers, adsorp. isotherms and heat of adsorp. 7-32794
- adsorption of N₂, second surface virial coefficient 7-6970
- adsorption of N₂, surface layer motion investig. 7-32792
- AGR fuel sleeves, irradi., bending, AE obs. 7-723
- amorphous struct., X-ray diff. studies 7-58143
- atomic structure, ultrasmall scanning tunnelling microscope for use in a liquid-helium storage Dewar 7-20075
- basal plane, adsorbed methane, bilayer and trilayer 7-2363
- basal plane, adsorbed N₂, computer simulation 7-52297
- beam-solid interactions and phase transformations, conference, Boston, MA, USA (Dec. 1985) 7-9590
- bend strength and fracture strain under press. 7-46595
- cast Fe, flake and nodular graphite, breaking behaviour of perforated notched specimens 7-17606
- chemical reactor design for SO₂ removal by injected limestone sorbents 7-22978
- contamination-mediated deformation, scanning tunnelling microscope study 7-44967
- corundum-graphite refractories, thermomech. props. 7-22806
- crystal interplanar binding, Englert-Schwinger eqn. calcs. 7-21846
- degeneracy lifting, perturbational approach 7-52399
- dispersed powder, C atom vibr. dynamics in IR absorpt. spectrum 7-53322
- divertor materials, heat load expts. with electron beam facility 7-49638
- dynamic simulation of interstitial atom, self-energy and migration energy calcs. 7-2014
- electron microscopy, past, present, future 7-16379
- electron momenta, Hartree-Fock-Roothaan calc. 7-42466
- electronic band struct., unoccupied, angle-resolved inverse photoemission study 7-64725
- electronic struct. of alkali metal overlayers on graphite, initial stages of intercalation 7-53503
- exfoliated surface, O monolayer study by positron annihilation 7-38346
- failure models for polygranular graphites 7-46596
- fiber, benzene-derived, exfoliation and characters. 7-46663
- fiber reinforced epoxy laminate, dynamic moire interferometry of stress wave propag. 7-59717
- fiber reinforced epoxy laminates, holographic interferometry analysis of bending rigidity loss 7-59733
- fiber reinforced epoxy laminates, holographic investigation of stressing techniques for detecting flaws 7-59732
- fiber reinforced glass sandwich reflectors for far-IR astronomy, thermal stability 7-37093
- fiber reinforced PEEK, quasi-isotropic laminate, shear strain meas. by moire interferometry 7-65253

graphite continued

- fibres, galvanomag. props., weak localisation and carrier interaction effects calcs. (*Russian*) 7-27347
- films, plasma fluorination, surface structure determ. 7-27196
- films, pyrolysed from polyoxadiazole condensation polymer, elec. and thermal props. 7-2736
- first wall thermal performance in ICF reactor 7-49634
- fracture criterion, acoustic emission studies (*Japanese*) 7-8088
- fusion reactor, surface erosion by D₂⁺ irradi., struct. 7-51869
- fusion reactor first wall, thermal shock behavior 7-25189
- fusion reactor wall, sublimation and hydrocarbon production under intense energy deposition 7-49629
- graphite-Br intercalation cpds., 2D stripe-domain system, melting transition 7-58449
- graphite-Fe structures, ion induced mixing, sputtering yield, fluoresc., RBS depth profile meas. 7-64844
- highly oriented, low temp. anomalies in thermoelec. power 7-17044
- highly oriented pyrolytic graphite, surface with deposited Ag(Au) clusters, scanning tunnelling microscopy study 7-12413
- HTGR, fines behaviour and recycling during fluidised bed operation 7-19363
- HTGR severe air ingress accident, graphite/O₂ reaction kinetics for various graphites 7-19415
- incommensurate overlayer on Pt (111), LEED 7-63930
- intercalated fibre elec. conductors, passivating coatings 7-8140
- intercalated with alkali metals, electron struct., soft X-ray emission spectroscopy 7-45117
- intercalated with Br, electromech. effect on heating 7-45414
- intercalated with Br, struct. and phase transitions, review 7-52041
- intercalated with ClF₃, electrical conductivity 7-7295
- intercalated with Cs, C₂₄Cs(H₂)_x, domain mobility and rot. tunnelling spectrum 7-63525
- intercalated with FeCl₃, mag. suscept. and low temp. transition meas. 7-58993
- intercalated with FeCl₃, spin-lattice relax. time meas., AC suscept. bridge techniques 7-13054
- intercalated with HNO₃, absolute Pauli spin suscept. meas., Fermi level density of states determ., ESR/NMR method 7-12940
- intercalated with HNO₃, C₂₀HNO₃, low-temp. struct. 7-51721
- intercalated with HSO₄·2H₂SO₄, C₂₄H₂SO₄·2H₂SO₄, quasi-2D, cond. electron state transform. in microwave field, ESR meas. 7-64508
- intercalated with K, C₈K, anisotropic binding of K, nuclear resonance photon scatt. of bremsstrahlung 7-51695
- intercalated with K, C₈K, electronic band struct., angle resolved UPS study 7-27232
- intercalated with K, C₈K, positron annihilation spectra, effect of H absorption 7-39270
- intercalated with K, high-stage struct., temp. depend., X-ray diff. study 7-63592
- intercalated with K, KC₂₄, kinetically-hindered low-temp. staging transition, P-T phase diagram, resist. anomaly meas. 7-6786
- intercalated with K, positron localisation 7-39271
- intercalated with K and Rb, KC₂₄ and RbC₂₄, 2D layer melting dynamics, neutron scatt. meas. 7-21420
- intercalated with KHg, KHgC₄ and KHgC₈, valence bands, XPS studies 7-16932
- intercalated with Li, Li_xC₆, elastic effects, comp. depend. staging studies 7-63707
- intercalated with Na, B doped, Fermi level displacement, diamag. anisotropy and Hall effect meas. 7-16933
- intercalated with SbCl₅, stage 2, based plane resistivity and phase diagram 7-45258
- intercalation compound, 2D Rb liquid, modulation potential, X-ray study 7-44639
- intercalation compound, C_{1-x}F_x, resistivity and ESR study 7-64197
- intercalation compound, C₈K, density of states, interlayer band occurrence 7-2454
- intercalation compound with H₂SO₄, optical study of K-point π -band dispersion 7-17317
- intercalation compound with HNO₃, diffusion, charge transfer and strain fields, ESR study 7-53117
- intercalation compounds, first stage, with heavy alkali metals, electronic props. 7-2463
- intercalation compounds with MnCl₂ and CoCl₂, mag. susceptibility meas. 7-45638
- intercalation compounds with SbC₁₀F_{5-m}, struct., X-ray 7-12008
- intercalation cpd., stage transformation, stochastic model 7-21433
- intercalation cpd. with AlCl₃, phases and phase transform., X-ray crystallography (*French*) 7-44783
- intercalation cpd. with AsF₅, stage 1, nonresonant intercalant modes, Raman scatt. studies 7-38136
- intercalation cpd. with AsF₆, Raman scatt., coupled electron-phonon excitation 7-46045
- intercalation cpd. with CuCl₂, ideal resistivity studies 7-32976
- intercalation cpd. with Fe, atomic structure, EXAFS studies 7-12011
- intercalation cpd. with KH₂, struct. and electronic props. 7-27234
- intercalation cpd. with KHg, supercond. props., density of states model 7-27457
- intercalation cpds., 2D magnetism, review 7-59033
- intercalation cpds., staging, struct., dynamical and magnetic props., review 7-1966
- intercalation cpds., staging dislocation electronic struct., electron scatt. rates, residual resist. 7-52558
- intercalation cpds., staging walls charge profile, Thomas-Fermi description 7-12687
- interstellar grains, effect of cavities and mantles on UV extinction peak 7-4546
- island formation on Pt surface, FEM, SEM and AES studies 7-32805
- isotropic, fine grained, oxidation effect on crack extension rate (*Japanese*) 7-56754
- JET, limiters and first wall, use of graphite tiles 7-19513
- laser ablation, small-scale expts. 7-65157
- laser excitation effects, time resolved picosecond reflectivity study 7-12136
- laser heated, optical characts. 7-32686
- laser-induced vaporization mass spectrometry of refractories 7-23079
- layers on diamond surfaces, optical anisotropy, effect of crystallographic orientation 7-53267
- limiter, porous, effective thermal props., photoacoustic meas. 7-44239
- moderator, Light Ion Beam Fusion Target Development Facilities, activation studies 7-49732

graphite continued

- molecular dynamics simulation and Raman spectrum, atom configs. and interactions, honeycomb struct. 7-58200
monolayer, on Re surface, struct. and props., AES, TDS and thermionic emission anal. 7-45017
monolayer on Ir (111), adsorbed Cs atoms, photo- and electron-stimulated deformation of monolayer 7-58627
multilayer melting transition of adsorbed methane 7-6992
NET, first wall protection 7-49622
neutron irradiation, macrostruct. and porosity studies 7-2069
nonmagnetic samples, ferromag. behaviour 7-53040
nuclear grade, fracture processes and oxidation effects 7-28157
nuclear grade, pitchcoke, irradi., mech. props., radiolytic oxidation effect 7-25032
nuclear grade, polycryst., deform. under press., elastic moduli, rel. to struct., neutron irradi. effect 7-28069
nuclear grade, polycryst. beam, finite contact area effect on impact stresses 7-28050
nuclear grade, thermally and radiolytically corroded, microstruct. rel. to elastic modulus 7-25033
nuclear material, corrosion and irradi. induced porosity 7-51836
overlayer dissolution into the substrate 7-26966
particle dispersed Al-Si LM 13 alloy, gravity die cast, dispersed graphite effect on freezing rate 7-59506
particulate composites, opt. and scanning electron microscope obs. of graphite struct. 7-22933
phase diagram and transitions of adsorbed tetrafluoromethane layers 7-38338
phonon dispersion, two-body pot. 7-44715
physisorbed monolayer methane, thermodynamic study 7-16863
physisorbed submonolayer mixtures of CO, N₂, Ar, LEED study 7-2364
physisorbed surfaces, positron lifetime studies 7-39269
plasma interactive component surfaces, H recycling props. 7-63295
PNP-500 pebble bed reactor, massive water ingress accidents, computer anal., graphite corrosion (*German*) 7-5371
polarization effects in galvanic corrosion 7-39706
powder, elec. resistivity, rel. to degree of comminution 7-45257
pulsed laser melting, impurity redistrib., RBS channelling, Raman scatt. and TEM meas. 7-12135
pyrographite, highly irradi., property change on thermal annealing 7-63665
pyrolytic, sputtering with O ions at various target temps. 7-49633
pyrolytic, highly oriented, intercalation reaction with K vapour, neutron diff. study 7-1999
pyrolytic, neutron irradi., ESR studies, exchange coupling model 7-7590
pyrolytic, surface, sticking probabilities of evaporated C₁, C₂ and C₃ species 7-52273
reactor, thermal expansion, effect of rad. 7-26804
relax. time, parametrisation 7-2513
resistivity at high temp. calc., anisotropy, temp. depend. 7-52556
scattering of He atoms from rare-gas-plated graphite 7-3136
secondary-electron emission and electron-energy loss spectra 7-33491
shielding effect on 14 MeV neutrons, meas. and calcs. 7-42104
shielding slabs, penetration of 2.75 MeV γ -rays 7-30712
siliconized, property variations during neutron irradi. 7-36105
sound velocity determ. by time of flight neutron diff. 7-32575
stopping cross section of ¹²C projectiles 7-51899
strength and structure in carbons and graphite, conf., Liverpool, England (Sept. 1985) 7-24257
structure, determ. by radial distrib. function 7-16485
substrate, adsorbed carbon tetrafluoride, nonwetting growth and cluster formation 7-2359
substrate, adsorbed Xe, thermodynamic's of first-order and continuous melting 7-2358
substrate, Ar physisorbed monolayers, melting transition, high resolution synchrotron X-ray diff. study 7-63780
substrate, Kr submonolayer film, phase diagram, relax. mechanisms, density functional theory calcs. 7-63953
substrate, methane adsorbed layer, heat capacity calcs., quantum cell model 7-52076
substrate, Xe monolayers, low temp. struct. and incommensurate-commensurate transition, electron diff. study 7-38335
substrate with Cu clusters, Auger spectra, effect of cluster size on line-widths 7-53455
substrate with Kr monolayers, domain wall modes 7-38333
surface, (0001), adsorption of Cs, induced work function changes, LEED obs. 7-33064
surface, (001), phonon dispersion, inelastic atom scatt. study 7-52227
surface, adsorbed benzene, rot. dynamics and orientation, NMR spectra 7-53161
surface, adsorbed ethylene, layering and layer-critical-point transitions 7-12471
surface, adsorbed Kr, 2-D system with competing interactions, phase transitions 7-6791
surface, adsorbed Kr incommensurate phase, computer simulation studies 7-7009
surface, adsorbed Kr monolayer, dislocation interactions 7-2357
surface, adsorbed N₂ and CO, pinwheel and herringbone structs. 7-7015
surface, adsorbed N₂ mols., zero-point energies, out-of-plane orientation, nucl. reson. photon scatt. study 7-32819
surface, adsorbed O films, triple point wetting and surface melting 7-45007
surface, adsorbed Xe monolayer, dislocation interactions 7-2357
surface, adsorption isotherm meas. near commensurate-incommensurate transition of adsorbed Kr 7-38337
surface, adsorption of Xe, incommensurate-commensurate phase transition, X-ray diff. obs. 7-32793
surface, Br₂ inelastic scatt., Monte Carlo classical trajectory calcs. 7-27837
surface, giant corrugations, scanning tunnelling microscopy 7-44320
surface, isosteric heats of adsorption of ethylene, phase diagram 7-6972
surface, layering and mixing in coadsorbed Xe-ethylene films 7-58624
surface, methane adsorption, incomplete wetting at low temps. 7-32798
surface, NO molecule scatt. 7-13316
surface, O₂ monolayer, struct. and mag. order, thermodynamic behaviour 7-52242
surface, order-disorder transition of adsorbed ⁴He 7-58563
surface, ordering and phase separation of adsorbed binary mixtures 7-21651
surface, physisorbed o-D₂ monolayers, specific heat studies 7-52271
surface, with physisorbed Ar, N₂ or O₂, positronium formation 7-33483

graphite continued

- surface (0001), SF₆ covered, Kr physisorption studies (*French*) 7-32799
surface (0001)-(2 × 2)K intercalated structure, LEED calcs. 7-6952
surface chemisorption of N on basal plane, ab initio calcs., finite cluster models 7-16869
surface in air and water, scanning tunneling microscopy study 7-21585
surface laser irradiation, ionic cluster desorption, time-of-flight meas. 7-12138
surface pulsed laser irradiation, SEM, TEM and STEM microstructural studies 7-12139
surface pulsed laser melting, cluster form. and evaporative loss, nanosecond time resolved reflectivity meas. 7-12137
surface structure, scanning tunnelling microscopy studies 7-18921
surface with adsorbed ³He-⁴He or H₂-D₂ mixtures, phase diagrams 7-52180
surface with adsorbed H₂, rotational states of physisorbed molecules 7-52278
surface with adsorbed methane, LEED 7-27129
surface with Xe monolayer, H atom scatt. resonances 7-64864
synchrotron-radiation-excited angle-resolved photoemission from single-crystal graphite 7-17391
thin absorber layer on Cu and glass, thermal wave appls. 7-48723
Tokamak limiter, outgassing of impurities 7-49631
Tokamak limiter, thermal props., effusivity 7-49630
tokamak limiter material, high heat load tests using 120 kW electron beam 7-26803
ultrafine, heats of combustion, ESR meas., depend. on exposure to air 7-33266
velocity of sound meas. by pulsed neutron diffraction 7-38125
- (*Japanese*) 7-13384
Al-Si, graphitic, hot extruded powders, sintering, antifriction props. 7-13409
AsF₅-graphite, intercalation compounds, staging phenomenon studied using Ising model 7-58464
BaTiO₃-graphite-rubber composites, varistors fabrication 7-58841
C-graphite heat-shielding coating, destruction and heat transfer in N₂ plasma flow 7-63263
C₂₈Br₂ intercalation cpd., 2-D system with competing interactions, phase transitions 7-6791
C₈Cs, first stage intercalation cpd., self-consistent band struct. calc. 7-52395
C₁₀CuCl₂ intercalation cpd., Shubnikov-de Hass effect, amplitude behaviour (*Russian*) 7-52571
C₂F₆ six-spin system, mol. diffusion of acetone, NMR 7-7598
C₆I₂Cl intercalation cpd., Shubnikov-de Hass effect, amplitude behaviour (*Russian*) 7-52571
C₆K and C₄K layered cpds., superconductivity 7-12904
C₈K and C₂₄K intercalation cpds., angle-depend. X-ray emission bands 7-46248
C₈K first stage intercalation cpd., self-consistent band struct. calc. 7-52395
C₈K type graphite intercalation cpds., mol. dynamics study of model system 7-63430
C₈Rb, first stage intercalation cpd., self-consistent band struct. calc. 7-52395
CoCl₂-graphite intercalation compound, obs. of magnetic state, high magnetic field 7-59008
Cr-graphite powder mixture, coatings form. in shock wave treatment 7-8183
CsBi₃-graphite intercalation cpds., stage 1, α and β phases, X-ray diff. study 7-58226
CsC_x (x=8,24), intercalation cpds., XANES studies, polarisation effects 7-59294
Cu-graphite contacts prep. using atomised Cu powder 7-27976
Fe-graphite compacts, sintering, alloying, mech. props. 7-39455
Fe-graphite diffusion chromised materials, high-temp. interaction in hydrogen 7-17671
FeCl₃-graphite intercalates, high resolution electron microscopy 7-16433
He ion irradi., thermal desorpt. 7-52245
KC₂₄ intercalation cpd., low temp. structural transition 7-21431
KC₈ intercalation cpd., polarisation depend. XANES study 7-59298
KC_x (x=8, 24), intercalation cpds., XANES studies, polarisation effects 7-59294
KH₀₈C_x, polarisation depend. XANES study 7-59298
K(NH₃)₂C₂₄ intercalation cpd., 2D diffusion-limited kinetics 7-58552
RbC₈, 2D graphite intercalation cpds., bond angle determ. EXAFS study, Debye-Waller anisotropy. 7-59293
RbC_x (x=8, 24), intercalation cpds., XANES studies, polarisation effects 7-59294
Si-C-W hot shells for thermionic energy converters, CVD deposition 7-27914
SiC-C alloy coated graphite as armour tiles, post-exposure anal. after high heat loadings 7-49632
graphite fibre reinforced composites *see carbon fibre reinforced composites*
graphite fibre reinforced plastics *see carbon fibre reinforced plastics*
graphite fibres *see carbon fibres; graphite*
graphitic steel *see carbon steel*
graphitisation
diamond, surface graphitisation (*Russian*) 7-17667
multiple activation processes, graphical anal. 7-3574
graphitising
Fe, cast, graphite, directionally solidified, struct. transitions 7-13443
graphs
see also Bode diagrams; nomograms
black-body radiation densities estimation, in IR range 7-4890
eyepiece, two-component, design and correction, calc. process 7-25921
gratings (diffraction) *see diffraction gratings*
gratings (optical) *see diffraction gratings*
gratings (spectra) *see diffraction gratings*
gravimeters
absolute gravity meter 7-9224
electrostatic feedback method for gravimeters 7-18319
JILA absolute gravimeters 7-18327
optical convertor for marine quartz gravimeter 7-29262
portable absolute gravimeter for vertical crust motions study 7-9225
quartz gravity meters, behaviour under high freq. vertical motion 7-40610

gravimeters continued

Stanford Gravity Probe-B expt., using superconducting thin film gyroscope 7-14855

superconducting gravity gradiometer for space and terrestrial applications 7-55305

gravimetric instruments *see gravimeters*gravimetry *see density measurement; weighing*

gravitation

see also general relativity; gravitational collapse; gravitational lenses; gravitational waves; quantum field theory of gravitation; Schwarzschild metric; unified field theories

5D space-time-mass gravity in a vacuum, cosmological soln. 7-60842

accretion disks in bimetric gravit. theory as test for general relativity 7-9365

anisotropic cosmological model, Boltzmann and Vlasov kinetic eqns. 7-61189

astrophysical jets, spacetime curvature defocusing rel. to jet decollimation 7-60522

Barker's theory of gravit., homogeneous and isotropic cosmological models 7-48495

Bianchi type-I homogeneous universe, exact solns. in general relativity 7-41204

Bianchi types of a three-parameter group of curvature collineations 7-24497

Bianchi-type VIII models, chaos in the long-term behaviour 7-60843

bimetric gravitational theory, harmonic maps, field eqn. solns. and spherical gravitational waves 7-35361

Birkhoff's theorem for electromagnetic fields in scalar-tensor theory 7-56105

Birkhoff's theorem in Einstein-Cartan theory for dust sphere 7-4740

Born-Infeld electrodynamics, motion of gravitationally interacting particles 7-48479

Born-Infeld theory, Einstein generalised, canonical approach 7-18663

Born-Infeld theory, Einstein-generalised, multisymplectic description 7-18662

Brans-Dicke-Jordan gravitation theory, stationary axially symmetric exterior solns. in 5D 7-35368

Cartan's contortion, massless spin-2 fields interpretation 7-56117

Cartan's contortion, relation to Eotvos torsion expt. 7-4326

Cauchy problem in general relativity 7-29843

causality in general relativity, recovery 7-160

charged perfect fluid obeying equation of state, shear free motion 7-24495

charged spinning fluid in Einstein-Cartan theory, consistency eqns. for energy-momentum tensor 7-41184

classical and quantum gravity, spinorial variables, Hamiltonian formulation 7-24527

compact space-times and the no-return theorem 7-24496

conservation laws in spacetimes with boundary 7-29829

cosmic censorship hypothesis in cosmological space-times 7-48470

cosmic strings, gravit. effects and temp. discontinuity 7-14841

cosmological constant, non-compact symmetries and Weyl invariance 7-4611

coupling constants, evidence for variation 7-41670

curved spaces, dynamics 7-35359

cylindrical waves in general relativity 7-48482

deflationary universe as de Sitter universe instability 7-35078

diffeomorphisms, anomaly struct. in theories with external gravity 7-4738

dimensionless const. in gravitation theory 7-29624

Einstein's field equations, dimensional reduction in a multi-dimensional cosmology 7-29830

Einstein action, 3+1 Regge calculus with conserved momentum and Hamiltonian constraints 7-48465

Einstein equation, higher dimensional, exact solutions in presence of matter 7-162

Einstein equations, self-consistent solutions with one-loop quantum gravity corrections 7-161

Einstein solutions, spatially inhomogeneous cosmologies with heat flow 7-35075

Einstein-Cartan theory, equation of state of spinning fluids, variational methods 7-56104

Einstein-Cartan theory, matter field torsion and conservation laws 7-41195

Einstein-Maxwell solutions, conformally Ricci flat, null EM field 7-24508

Einstein-Maxwell space-time, asymptopia of quasi-local mass and momentum 7-29841

Einstein-Rosen metrics generated by the inverse scattering transform 7-24494

Einstein-Weyl space-times with geodesic and shear free neutrino rays 7-61169

electric and gravitational forces, and the ballistic theory of light 7-29836

electromagnetism and gravitation, contributions to theories 7-36845

elementary particle stability, catastrophe theory on the space-time manifold 7-24808

Eotvos expt., null results, reanalysis 7-4748

Ernst coordinates 7-4747

Euclidean gravity, appl. of Schwinger-Dyson formulation of coordinate-invariant regularization 7-61464

everywhere invariant spaces of metrics and isometries 7-24492

Finsler space fields, structural features 7-48490

fourth-order gravitation, Newtonian limit 7-47684

fourth-order theories of gravity and general relativity, equivalence, cosmological singularity 7-41178

Friedmann universe and compact internal spaces in 4+N gravity theories 7-9733

galaxies, overlapping pair gravit. pot. energy 7-60784

gauge field coupled to axial U(1) charge in gravitational field, CP-effective action anal., spectral asymmetry 7-41601

general relativistic self-similar perfect fluid; singularities in self-similar spacetimes 7-29826

general relativity, angular momentum flux carried by gravitational radiation 7-29831

geometrical gauge approach for electromagnetism and gravitation 7-29851

geometrical gravitational theory based on a metric-affine manifold 7-18664

gravitational analogies, rel. between electromagnetism and gravitation 7-41187

gravitation continued

gravitational equilibria of self-interacting scalar fields, boson stars maximum mass calcs. 7-24519

gravitomagnetic pole and mass quantisation, comment 7-182

gravitometric pole and mass quantisation, comment 7-181

Green's function in curved space-time, Hadamard construction (*German*) 7-66444

higher dimensional Einstein-Cartan gravity, dimensional reduction 7-61188

induced causality in astrophysics, alternatives to general relativity 7-47676

isotropic universe, longitudinal plasma oscillations generated by gravit. perturbations 7-61185

Jordan-Brans-Dicke theory, isotropic flat space cosmology 7-4601

Kasner spacetime, exact solns. for electromagnetic, neutrino and gravit. fields 7-41173

Kerr black hole, null geodesics in stationary Ernst-Wild space-time 7-61170

light deflection corrected Li expression for astrolabe obs. 7-66431

local Lorentz symm. breaking and space-time dimens. in gravit. theory 7-24803

Lorentz gauge theory, canonical formalism (*Chinese*) 7-9721

Maxwell's equations in curved space-time 7-9725

McVittie metric, physical props. of nonquadratic solns. 7-48472

McVittie metrics, noninteracting solns. for perfect fluid spheres 7-24504

modified gravitation theories, alternatives to dark matter models 7-47692

modified Newtonian dynamics (MOND), appl. to shell system of elliptical galaxy (NGC 3923) 7-66749

momentum current picture of gravitational field of Earth-Moon system 7-55934

multipole moment formation in vacuum region for nonasymptotically flat systems 7-48478

naked singularity space-time having strong curvature 7-29819

Newman-Penrose formalism; general transformation laws 7-29822

Newton's second law at small accelerations, test from disc galaxies grav. radiation 7-48081

Newtonian cosmology based on Yukawa-type pot. 7-41189

non-conservative gravitation and Kaluza-Klein cosmology 7-14689

nonlinear eqns., boundary-value problem solns. 7-24507

null surface geometrodynamics, dynamical struct. of Einstein's theory of gravity 7-149

open bosonic strings in gravitational, tensor and Yang-Mills fields, renormalization props. 7-24826

orthogonal perfect fluid and vacuum solutions, self-similar spatially homogeneous cosmologies 7-29824

passive gravitational mass and inertial mass inequality of extended body 7-9372

perfect fluid, self-gravitating, Einstein-Maxwell and scalar field eqns. solns. 7-51344

perfect fluid in FRW space-time, kinematic and dynamic properties of conformal Killing vectors in anisotropic fluids 7-48466

perfect fluid space-time, topology 7-56091

perfect fluid spheres admitting flat 3-dimensional slices 7-61184

Poincaré gauge theory of gravity (3+1)-space-time structure 7-56124

Poincaré group, group scaling, classical gauge theory and gravit. corrections 7-24762

positive energy proof for weakly asymptotically flat space-times 7-29821

positive-energy theorem, asymptotically flat metrics 7-29820

potential determ. for arbitrary mass distrib. Poisson integral expansion method 7-66447

power law singularities in the scale covariant theory 7-48467

primordial inflation with broken symm. gravit. theory 7-14840

PSR 1913+16, binary pulsar, proper motion determ. from periastron times 7-55696

quantum double galaxies, possible mass limits 7-18455

quasi-local mass for small surfaces 7-29827

$R+R^2$ gravitation in Riemann-Cartan space, general relativistic limit and dynamical torsion 7-4744

$R+R^2$ gravity, first order formalism treatment conformally metric theory 7-41200

radiative gravitational fields in general relativity, field struct. outside the source 7-41176

radio signal delay in relativity theory of gravitation 7-4732

relativistic corotating spherical mass shells, singularities and gravimetric effects 7-41182

relativistic gravitation theory, implications for Friedmann universe and gravit. collapse (*Russian*) 7-60533

relativistic particles in curved space-time and electromagnetic fields in Kaluza-Klein space 7-35356

relativistic theory, radio signal delay 7-29860

relativistic theory of gravit., gravit. restraint 7-29846

relativistic theory of gravitation 7-56099

Riemannian curvature spinor in general space-time 7-29825

rocket borne clock expt., kinematical and gravitational anal. 7-29833

Rosen's bimetric gravitation theory conformally related fields 7-18657

rotating body gravitational field, motion of particles and photons 7-55704

satellite orbital period calcs. in relativistic gravit. and general relativity 7-40690

scalar-tensor theory and baryonic interaction 7-18350

scalar-tensor theory of fourth-order gravity, Universe scale factor 7-61190

self-creations cosmologies, Raychaudhuri-type equations 7-24251

self-focusing as a mechanism for the formation of dense structures in Newtonian cosmology 7-40964

singularities and space-time foliations in general relativity 7-48489

space-time structure, relation to quantum mechanics 7-47679

spherically symmetric free fall collapse for perfect fluid 7-29839

spinor particles in gravit. field, relativistic quantum theory 7-35717

stationary axisymmetric vacuum gravit. field, conformal potential 7-47682

strictly positive mass theorem for isolated gravit. system 7-56110

string-induced gravity and ghost-freedom 7-4743

superconducting; gravitationally induced, in Schwarzschild field of Earth, appl. of jellium model 7-45595

supernovae and high density nuclear matter 7-55693

superstring theory, elementary introduction (*Japanese*) 7-41205

theory taking vacuum into account 7-35347

time-dependent gravitational fields, influence on superconducting oscillatory ccts. 7-41181

gravitation continued

- Tolman-Bondi model, Hawking mass test in expanding dustlike universe 7-18650
- topology massive gravity in the dreibein light-front gauge 7-41188
- transmission line gyroscopes, general relativistic electromagnetic effects 7-29859
- traveling round without feeling it and uncurving curves 7-35159
- two-body problem with acceleration-depend. spin terms 7-9722
- ultralocal limit of the gravitational field coupled to a scalar field 7-41214
- unboundedness of the gravitational partition function 7-48468
- universal gravitation law (*Italian*) 7-18654
- universal master equation for the gravitational violation of quantum mechanics 7-4723
- vacuum Friedman-Robertson-Walker universe, generation of gravitational waves 7-29832
- vector parallel transport, physical meaning 7-24491
- vector-spinor space and field equations 7-56092

gravitational collapse

- classical horizons and quantum corrections, Hawking radiation 7-48506
- closed-universe recollapse conjecture 7-48119
- collisionless gravitating systems, spherical collapse stability 7-40678
- globular clusters, effects of two-body tidal capture of main sequence stars and white dwarfs 7-4500
- Higgs field coupled gravitation theory, high-freq. perturbations and gravitational collapse 7-40681
- interstellar cold clouds, CO radio-line profiles interpretation 7-4544
- interstellar collapsing gas clouds, cosmic ray accel. 7-55390
- interstellar isothermal spherical gas clouds, condensations, similarity solns. 7-35028
- interstellar matter, Jeans collapse in a turbulent medium 7-60752
- interstellar small spherical non-gravitationally bound cool clouds, condensation 7-60751
- metric elasticity in a collapsing star, gravit. radiation coupled to torsional motion 7-48484
- polytropic configurations within homogeneous background matter, equilibria and instabilities 7-4316
- relativistic gravitation theory, implications for Friedmann universe and gravit. collapse (*Russian*) 7-60533
- relativistic theory of gravit., gravit. restraint 7-29846
- spherically symmetric free fall collapse for perfect fluid 7-29839
- stellar cores, entropy generation and deleptonization during collapse 7-55691

gravitational constant

- cosmological variations, effect on cosmic nucleosynthesis 7-40979
- JILA absolute gravimeters 7-18327
- Kaluza-Klein gravitational theory, astrophysical data and cosmological solns. 7-9363
- spaceborne meas. using artificial binary 7-9746
- superstring theory, time variation of Newton's gravit. constant 7-18661
- time dependence, implications of characteristic actions $\hbar^{(4)}$ in struct. of Universe 7-4602

gravitational experiments

- artificial binary for spaceborne meas. of gravitational constant 7-9746
- British long-baseline gravit. wave observatory, feasibility study 7-29408
- correlated spontaneous emission lasers for gravitational radiation detection 7-35387
- cryogenic gravitational wave antenna with resonant capacitive transducer and d.c. SQUID amplifier 7-34881
- dynamic null experiment to test the law of gravitation 7-48517
- Eotvos anomaly, gauge field and symm. breakdown interpretation 7-18682
- Eotvos experiment, new force or thermal gradient 7-14854
- Eotvos experiment, nonexistence of intermediate range coupling 7-29861
- Eotvos experiment, theoretical models for possible nonzero effect 7-9745
- Eotvos experiment, thermal gradient model explanation 7-18681
- Eotvos experiments, anal. for fifth force evidence 7-35385
- Eotvos expt., search for intermediate-range modification 7-48516
- Eotvos-type expts. for medium-range force detection 7-14853
- equivalence principle to gravitational wave detection (*German*) 7-18680
- gravitational waves detection, antenna patterns of interferometric detectors for linearly polarised waves 7-55453
- Hubble constant determ. method involving observation of gravitational waves 7-9559
- laser gravitational obs. sensitivity, light wave interference, quantum fluctuations effects 7-43039
- mechanically modulated microwave cavity for detection of low-frequency gravitational radiation 7-35388
- quantum gravity, experimental test 7-48500
- quantum gravity, \bar{p} gravitational acceleration meas., proposed expt. 7-48501
- radiation detector, impedance matching element 7-61212
- Stanford Gravity Probe-B expt., using superconducting thin film gyroscope 7-14855
- superconducting gravity gradiometer for space and terrestrial applications 7-55305
- three-mode 1200 kg gravitational radiation detector instrumented with a DC SQUID, sensitivity 7-41229
- transmission line gyroscopes, general relativistic electromagnetic effects 7-29859

gravitational lenses

- amplification distribution function by random gravit. lensing, flux conservation theory 7-23994
- background radiation perturbation by moving gravit. lens 7-35070
- 3C 273, quasar, consequences of gravit. lensing for gamma radiation 7-9552
- cosmic microwave background, temp. fluctuations induced by gravitational lensing 7-4595
- dark galactic haloes as lensing objects 7-60530
- diffraction effects in gravitational lensing by low mass objects (stars and planets) 7-40682
- distant radiogalaxies overluminosity, gravit. amplification as possible cause 7-35035
- Doppler shifting of a distant light source in a Schwarzschild gravitational field 7-4319
- double clusters of galaxies 7-9549
- 40 Eri A, gravit. lens effect during appulse to background star 7-47861
- galaxies, effects of gravit. amplification of brightest cluster galaxies by foreground clusters 7-24206
- images classification, role of Fermat's principle and caustics 7-55439

gravitational lenses continued

- inhomogeneous universes, lens effect probabilities 7-40965
- * marginal gravitational lenses of large separation: probing superclusters 7-55456
- micro-lensing, astrophysical appls. 7-9364
- microlensing, implications for gravit. lens hypothesis for origin of active galactic nuclei variability 7-55791
- multiple quasars for multiple images, alternative hypothesis 7-9556
- PG 1115+080, triple quasar, detect. of lensing galaxy 7-66781
- Q0957+561A,B, edge-on galaxy model for gravit. lens 7-60829
- Q1146+111B,C, double QSO, colours of field objects rel. to gravit. lens/string model 7-29554
- Q 1146+111 B, C constraints on gravit. lens models from isotropy of nearby microwave background 7-40961
- Q 1548+114A, B, implications of possible gravit. lens effects by foreground quasar 7-9554
- quadrupole gravitational lens, theory, images multiplicity and positions determ. 7-66453
- quasar micro-lensing causing parallax effect 7-29392
- quasar pairs, role of lensing by burnt-out galaxies and galaxy clusters 7-35051
- wave effects in gravitational lensing of electromagnetic radiation 7-9371

gravitational radiation *see gravitational waves***gravitational red shift**

- DA white dwarfs, Si III Stark shift, modified semiempirical formula 7-55638
- electric and gravitational forces, and the ballistic theory of light 7-29836
- rapidly rotating compact stars (*Chinese*) 7-4305

gravitational waves*see also gravitons*

- absorption by mass triangle, response to polarisation states, cross sections 7-18683
- angular momentum flux carried by gravitational radiation 7-29831
- bimetric gravitational theory, harmonic maps, field eqn. solns. and spherical gravitational waves 7-35361
- bosonic nonlinear σ -models, graviton coupling to massive fields 7-4977
- bounded source in general relativity, radiation field calc. 7-4734
- box to hold grav. radiation in thermal equilb., impossibility 7-61180
- British long-baseline gravit. wave observatory, feasibility study 7-29408
- close binary stars, orbital ang. momentum losses by gravit. waves rel. to evolution 7-24121
- colliding waves, new type of singularity 7-48485
- cosmic and geophysical noise in measurements of small displacements 7-4757
- cosmic strings, gravit. radiation and microwave background 7-14838
- cryogenic gravitational wave antenna with resonant capacitive transducer and d.c. SQUID amplifier 7-34881
- cylindrical waves in general relativity 7-48482
- detection, influence of time-depend. gravit. fields on superconducting oscillatory ccts. 7-41181
- detection by correl. spontaneous emission lasers 7-35387
- detection experiments, correl. of geophys. factors 7-47697
- detection of linearly polarised waves, antenna patterns of interferometric detectors 7-55453
- detector, impedance matching element 7-61212
- disordered radiation, confinement by action of a Higgs vacuum 7-48483
- Earth rotation, intradiurnal nonuniformity, cosmic radiation effects 7-28809
- Einstein's field eqns., vacuum solns. with flat 3-dimens. hypersurfaces 7-4728
- Einstein-Maxwell eqns., gauge freedom of plane symmetric line elements 7-18652
- enhanced emission from perturbed wide binary stars, effects of black hole recoil 7-60730
- Eotvos experiment, thermal gradient model explanation 7-18681
- equivalence principle to gravitational wave detection (*German*) 7-18680
- general relativity interferometric tests, use of squeezed states 7-4329
- gravitational-gyroscopic wave equations, ang. pot. appls. (*Russian*) 7-61183
- Hubble constant determ. method involving observation of gravitational waves 7-9559
- interferometric gravitational-wave detectors, radiation-pressure induced fluctuations reduction 7-35386
- inverse-scattering method of generation 7-61181
- light transversing a gravitational wave background, red-shift, rel. scatt. coherence 7-4735
- low-mass X-ray binaries, gravit. radiation losses rel. to soft X-ray transients 7-55707
- * mechanically modulated microwave cavity for detection of low-frequency gravitational radiation 7-35388
- Newton's second law at small accelerations, test from disc galaxies grav. radiation 7-48081
- perturbed light beam, linearized field eqns. and gravitational solns. 7-4737
- plane-fronted gravit. waves, isometry groups 7-24501
- quantum limit for successive position measurements, grav. waves detection 7-35338
- quantum Regge calculus in the Lorentzian domain and its Hamiltonian formulation 7-175
- radiated gravitational energy calc. using second-order Einstein tensor 7-35355
- radiating system of two coupled strings, normal modes, stars 7-18656
- relativistic stars, nonradially pulsating, g-modes damping time due to gravit. radiation 7-9463
- relativistic string in Peres space-time, gravitational wave propagation 7-35354
- Robinson-Trautman pure radiation solns., asymptotic behaviour 7-9719
- rotating cosmic string surrounded by grav. radiation, Einstein eqns. solns. 7-18464
- superconducting cosmic strings, cosmological effects 7-24518
- three-mode 1200 kg gravitational radiation detector instrumented with a DC SQUID, sensitivity 7-41229
- torsional motion coupling, metric elasticity in a collapsing star 7-48484
- vacuum Einstein eqn. solns., cylindrical waves and cosmic strings of Petrov type D 7-48477
- vacuum Friedman-Robertson-Walker universe, generation of gravitational waves 7-29832
- wave emission, tensorial linear theory 7-163
- Weber-type gravit. wave antenna coupled to reson. transducer, quantum nondemolition observables 7-61182

gravitons

- bosonic nonlinear σ -models, graviton coupling to massive fields 7-4977
- closed strings in background fields, β -functions and vertex operators 7-49118
- closed strings in open-string field theory 7-56529
- D=11 supergravity theory, cosmological constant contribs. from quantized gravitino sector 7-18678
- de Sitter space, graviton propagator and infrared divergences 7-48508
- Einstein-Maxwell- σ theory, 6D, spontaneous breaking of global and local symmetries 7-35369
- Euclidean lattice, unified treatment of Poincare, de Sitter and conformal gravity 7-56131
- general relativistic gravitons, implications of photon hypothesis in electrodynamics 7-41164
- gravity as the limit of the type-II superstring theory, graviton-graviton scatt. 7-4751
- Kaluza-Klein ansatz for chiral $N=2$ D=10 supergravity on round 5-sphere, truncations 7-183
- kasner-type cosmological solutions in $N=1$ supergravity, gravitino ghost field 7-41221
- linear conformal gravit. in de Sitter space 7-48504
- matter-induced topological mass term 7-18669
- minimal $N=2$ supergravity in superspace 7-56135
- $N=2$ supergravity model with a light graviphoton 7-41227
- quantum cosmological perturbations in pure gravity, graviton field theory 7-180
- semi-off-shell string amplitudes, local operator expansion 7-41759
- supersymmetric GUT scale, no-scale models and gravitino mass 7-18665

gravity

see also gravitation

- 1D time series anal. for sphere, appl. in geomag. and gravimetric geodesy 7-9239
- acceleration due to gravity, meas. using bouncing rubber ball 7-48237
- airborne gravity gradiometer survey data analysis using isomorphic geodetic and electrical networks 7-47309
- anomalies and vertical gradient over cavities in brittle rock 7-47308
- anomalies interpretation, numerical optimisation methods 7-29279
- anticline gravity anomaly calc. using quadratic density function 7-23514
- 31 Aql, possible pole-on binary system, spectroscopic gravity determ. method 7-4434
- Bali Basin, tectonic origin, anal. of gravity, bathymetry and earthquake data 7-66073
- N Bay of Biscay continental margin, isostasy gravity and tectonic model 7-8902
- bidispersion, dil., sedimentation and diffusion, Onsager symmetry, kinetic coeffs. 7-26322
- binary stars, pole-on, spectroscopic gravity determ. method and appl. to 31 Aql 7-4434
- bodies of zero external gravit. pot., forgotten results and present state 7-8789
- bubble, rising, free streamline model 7-11520
- California, absolute gravity meas. 7-9224
- Great Caucasus, USSR, gravity anomalies for earthquake prediction 7-65971
- China, SE coastal region, regional gravity field and geological structures 7-47337
- core rotation rel. to C_{21} and S_{21} geodetic gravity coeffs. 7-47399
- crust calculations, use of continental crust density-seismic vel. relationship 7-18144
- crustal movements in Central and South America, symposium, Maracaibo, Venezuela (February 1985) 7-24291
- density distribution, choice of norm 7-18106
- Earth, external gravit. field and dynamical flattening rel. to normal density Earth models 7-18154
- Earth, gravit. potential rel. to trigonometric series representations of satellite orbital inclination function 7-4299
- Earth, sensitivity of LAGEOS to time vars. in (2,2) gravity coeffs. 7-34825
- Earth gravity field, spherical harmonics of geopotential temporal variations 7-28805
- Earth gravity field mapping, relative motion of geodynamic twin satellite 7-4285
- Earth gravity models, freq. windows and resonant solns. as test of accuracy 7-3966
- Earth model, spherically stratified, response to body force and surface pots. load (*Chinese*) 7-18105
- Earth shape and gravity quadrupole moment since Silurian period, from palaeorotation data 7-23511
- Earth tide gravity vars., indirect effects of ocean tides on KAPG stations 7-28813
- East Germany, gravity var. and temporal heights near gravimetric W-E profile 7-14177
- electric and gravitational forces, and the ballistic theory of light 7-29836
- Europe, combined geophysical-thermal models of crust and upper mantle 7-28933
- external potentials expansions of ellipsoidal bodies, analytical continuation 7-47719
- field correlation with mag. field 7-47318
- film, gravitational flow, initial velocity field 7-57784
- free-fall acceleration values, reduction 7-29278
- Galapagos spreading centre, 3D gravity study of 95-5°W propagating rift 7-60196
- geodesy, anomalous field due to horizontal layer of Poisson random sources 7-34381
- geodesy, constant part of Earth tides in Earth figure theory 7-65916
- geodesy, gravity network design, based on approx. of variance-covariance matrix 7-65918
- geodetic anomaly inertial surveying method 7-4196
- geodetic gravity anomalies, direct problem for vertical cylindrical bodies 7-23510
- geodetic gravity anomaly, nonlinear data inversion using Schmidt-Lichtenstein approach 7-65920
- geodetic gravity anomaly decompensation theory 7-14175
- geodetic gravity anomaly due to 2-D body with variable density contrast 7-54842
- geodetic gravity anomaly global model using error covariance function* (*German*) 7-18109
- geodetic gravity anomaly interpretation, by multiparameter functional minimization algorithm 7-60150

gravity continued

- geodetic gravity anomaly interpretation using deterministic approach 7-28811
- geodetic gravity anomaly prospecting, stable difference methods for continuation 7-55303
- geodetic gravity surveying using inertial navigation 7-4194
- geoid anomalies, appl. to core-mantle boundary topography determ. 7-66021
- geopotential 14th-order resonance, Intercosmos 13 rocket (1975-22B) inclination var. analysis 7-55419
- geopotential 15th-order harmonics from Tournesol rocket orbit analysis 7-55420
- geopotential anomalous fields, parameters of regularized continuation of 2D fields 7-60149
- geopotential field, Newtonian potential term alteration rel. to satellite relativistic eqns. of motion 7-34826
- geopotential field anomalies, harmonic function derivatives 7-60148
- geopotential harmonics of order 15 and 30, determ. from orbital reons. of 25 satellites 7-65923
- geopotential harmonics of order 15 and 30 from Cosmos 58 orbit 7-54852
- gravimetric observations affected by one-stage net drift, processing 7-40611
- heat pipes, rotating, in gravity field, with separate vapour and liq. ducts, performance 7-1550
- Indian Ocean, geopotential hours and core-mantle interface depressions 7-47412
- inverse logarithmic potential problem, uniqueness of solns. 7-29280
- N Italy, geophysical exploration of upper crust from Ligurian coast to N Po Valley 7-14240
- Central Japan, gravity, and magnetotelluric study of Fossa Magna region 7-23609
- Kerguelen Plateau province, crust struct. from gravity anomaly and seismic refl. obs. 7-28952
- Kola Peninsula, upper crustal struct. along Pechenga Bay-Kovdor-Alakurti profile from geophysical data 7-47395
- La Grande-2 Reservoir, Quebec, crust vertical movement and gravity var. 7-8793
- Long Valley caldera, California, USA, geodetic trilateration and gravity surveys 7-40449
- North Massif Central, gravimetry contribution to model of igneous intrusions emplacement (*French*) 7-18135
- Mississippi Embayment, gravity field temporal var. due to crust elevation 7-8794
- modified Karhunen-Loeve model of the gravity disturbance vector 7-65921
- Mongolia, ring structures and fractures, assoc. gravity and topographic characts. 7-28962
- Newton's law of gravity modified, celestial mechanical consequences 7-9661
- nontidal variations continuous meas. 7-8792
- N Norway and adjacent offshore areas, gravity data rel. to lineaments trends 7-29026
- ocean, mantle component calc. from crust seismic vel. profiles anal. 7-54849
- S Oklahoma aulacogen, appl. of quasi-ideal spatial filters to gravity anomalies mapping 7-28808
- Olympus Mons, isostatic gravity and elastic bending models 7-29419
- W Pacific, trench-trench-trench triple junction off SE Japan 7-34415
- Paris Basin, Variscan overthrusts characts. 7-4012
- planetary potential expansion, convergence improvement methods 7-47742
- portable absolute gravimeter for vertical crustal motions anal. 7-9225
- potential determ. for axisymmetric mass distrib., hydrodynamic test results 7-66446
- potential field data between irregular surfaces, upward continuation 7-8787
- potential in spherical coordinates, Poisson integral radial recursive integration 7-9367
- precise relative geoid heights determ. from gravimetry 7-8795
- Rajmahal Hills, E India, gravity field over Palaeo-Mesozoic continental margin 7-28820
- San Andreas fault, central branch, gravity anomalies and earthquake epicentres 7-65972
- San Jacinto Graben, California, USA, gravity anomalies 7-54842
- San Jacinto graben California, gravity anomalies of trapezoidal model with quadratic density function 7-28819
- second zonal harmonic, effects of time vars. on lunisolar precession-nutation 7-28810
- sedimentary basin gravity anomalies, basin depth estimation by anomaly inversion 7-3968
- seismic waves propagation, effect of couple stress and gravity on Lamb's plane problem in thermoelastic solid 7-6128
- Shithatha area, Iraq, gravity study of faults 7-34373
- simultaneous correlation analysis of gravity, magnetic and seismic data, appl. to deep crustal investigations 7-47552
- Stanford Gravity Probe-B expt., using superconducting thin film gyroscope 7-14855
- Sun, polar flattening and influence on planetary orbits 7-29452
- Tien-Shan region, isostatic gravity anomaly from isostatic compensation models 7-28965
- Tornquist-Teisseyre zone (Poland), deep crustal struct. in contact zone of Palaeozoic and Precambrian platforms 7-14235
- Transylvanian Depression, struct. and morphology (*Rumanian*) 7-8891
- universal gravitation law (*Italian*) 7-18654
- Venus, gravity studies of Aphrodite Terra 7-34899
- Wairakei Geothermal Field, exploitation induced gravity var. due to groundwater effects 7-28812

gravity meters *see gravimeters***gravity waves**

- accelerations in steep gravity waves, subsurface accelerations 7-9009
- Alfven-gravity spectrum of an incompressible slab, astrophysical appl. 7-57991
- atmosphere, effects of Doppler shifts on wave spectra observed by MST radar 7-47490
- atmosphere, scidar/lidar ground-based study 7-9166
- atmospheric Rossby-gravity wave model, slow manifold of primitive eqn. system 7-9100
- atmospheric turbulent flow over progressive water wave, eddy viscosity model 7-51193

gravity waves continued

- capillary-gravity wave at free surface of viscous incompressible liq., dispersion eqn. 7-43943
- capillary-gravity waves, symmetry and bifurcation 7-43941
- deep water gravity waves, subharmonic instability (*French*) 7-31817
- deep-water gravity-capillary waves fourth-order evolution eqn. 7-37482
- finite-amplitude gravity waves in fluid, nonlinear 3D Schrodinger eqn. 7-16199
- free surface gravity waves, surface impedance formulation 7-57869
- gas-liquid flows, capillary waves, spectral behaviour 7-11521
- gravity-capillary waves, wind-generated, period-doubling 7-43952
- hydrostatic atmospheric gravity waves, influence of Coriolis force due to Earth's rot. (*French*) 7-18271
- inertio-gravity waves effects on a decaying two-dimensional turbulence in rotation (*French*) 7-16197
- internal gravity waves, stratified shear flow, wave-action model study 7-43948
- ionosphere, radiointerferometric obs. of gravity waves 7-4253
- liquid surface gravity wave propag., interfacial props. influence 7-37479
- magnets-acoustic-gravity waves propag., solar appl. (*Chinese*) 7-4306
- middle atmosphere, gravity wave effects under solstice conditions with 3-D circulation model 7-47597
- middle atmosphere, gravity wave motions 7-47587
- N-layer stratified fluid, variational formulation 7-43950
- N-layer stratified shear flow, Kelvin-Holmholz instability 7-43951
- nonlinear 2D gravity-capillary waves, 3D instabilities 7-51194
- nonlinear balance and gravity-inertial wave saturation in a simple atmospheric model 7-1582
- nonlinear gravity waves and capillary waves on surface of infinitely cond. liq., MHD effects 7-44058
- nonlinear gravity-capillary waves, free surface accel. 7-43955
- ocean, capillary-gravity ripples generation by strongly non-linear waves on deep fluid surface (*Russian*) 7-29040
- ocean, surface gravity waves, average values evol. (*Russian*) 7-29042
- oscillation instability while radiating surface and internal waves 7-20775
- planetary scale flow interactions, GFDL SKYHI general circulation model simulation 7-34592
- stability of nonlinear gravity-capillary waves 7-16161
- steep gravity waves: Havelock's method revisited 7-11441
- stellar internal gravity waves produced by convection 7-60631
- stratified fluids, gravity currents, turbulence effect 7-43949
- surface gravity waves in deep water, class I and II instabilities, modified Zakharov eqn. 7-51195
- surface regular gravity wave diffraction by circular cylinders in incompressible fluid 7-6228
- surface wave excitation by disk pitching oscills., variational approx. 7-57865
- surface waves, Eulerian and Lagrangian aspects 7-51191
- viscous terms in subsonic flows, consistent approximation methods 7-34845
- water capillary-gravity waves, fundamental singularities 7-63165
- water waves, shore singularity 7-40501
- wave asymmetry over slopes with variable-depth water 7-6229

greasing see lubrication

Green's function methods

- see also CPA calculations; KKR calculations
- 1D disordered system, random chains and complex transfer matrix attractors 7-61250
- 2D blunt body sampling, mathematical theory, flow calcs. 7-31867
- 2D magnetic field problems, boundary and finite element methods combined 7-62584
- $\phi^3 + \phi^4$ field, quantum fluctuations around soliton at finite temp. 7-41593
- ϕ^4 theory, stochastic quantization simulation with connected Green's fns. 7-48960
- acoustic microscope, elastic wave propag., accurate field anal. 7-43472
- alkali halides, XANES spectra, single site approx. via ideal crystal Green's functions 7-64747
- angle-resolved photoemission spectra, low-energy modelling 7-46275
- anisotropic crystals with chain structure, elastic Green tensor 7-6700
- anisotropic Heisenberg ferromagnet, low temp. props., spectral density method 7-2803
- antiferromagnets with two nuclear spin systems, NMR enhancement effects 7-38947
- arbitrary continuous superlattices, general anal. 7-7322
- Ashkin-Teller model, 2D conformal symmetry and critical 4-spin correl. fns. 7-48999
- atom, Thomas-Fermi kinetic energy functional, Weizsacker-type gradient corrections 7-36475
- atomic clusters, multiple-scatt. theory, appl. of a non-muffin-tin pot. general pot. develop. 7-36839
- atoms, four-level, multiphoton processes, fluoresc. spectra calcs. 7-62318
- atoms, photoionisation, ang. depend. electronic Green's fn., finite basis-sets 7-42570
- atoms in a low field, review 7-898
- band theory, convergence props. 7-27235
- bare pomeron trajectory calcs., vacuum Regge singularity Green's function in QCD 7-41773
- beams, elastoplastic, biaxial dynamic bending 7-62999
- o-benzene, valence ions. energy and mol. geometry, green fn. method, CI and GVB calcs. 7-62290
- Bethe lattice, localisation transition 7-29940
- Bethe-Salpeter equation, renormalized forms for connected N-point Green fns. 7-15048
- biphonon line broadening caused by acoustic phonon interactions 7-44721
- bis(π -allyl) nickel, photoelectron spectrum, semi-empirical and ab initio Green's Function methods 7-30950
- bond-diluted Heisenberg ferromagnets, spin wave damping near percolation threshold, Green's function calcs. 7-17193
- carrier transport theory, picosecond processes 7-45342
- Casimir effect with uniformly moving mirrors 7-41699
- charge-monopole scattering, Green fn. calc. 7-56584
- chemisorption, substrate impurity effects 7-63964
- chloromethane, UV angle resolved photoelectron spectra using synchrotron radiation 7-30246
- collision cascades, linear, variance calc. 7-63686
- composite dielectric materials, interface response theory of electromagnetism 7-62564
- conformal invariant field theory, Green's functions and Feynman rules on $S^3 \times S^1$ hypertorus 7-41597

Green's function methods continued

- conformally-flat Riemannian metrics, Schrodinger operators and semiclassical approx. 7-56074
- continuous composite materials, interface response theory 7-64039
- Coulomb Green's functions, in an n -dimensional Euclidean space 7-41133
- Coulomb-like pot., bound and resonant state calcs. 7-48428
- critical phenomena, field theory applications 7-41578
- crystal with sinusoidal potential, 1D, paramagnetic susceptibility 7-17153
- cylinder, circular, sliding over dissimilar thermally conducting half-plane 7-20666
- cylinders, finite and semi-infinite, vibration characteristic eqn. 7-26197
- degenerate Bose system, many-time Green's functions kinetic asymptotics, variational determ. (*Russian*) 7-41245
- diamond crystals, surface phonon modes and reconstructions, Green's function method calcs. 7-2339
- dielectric materials, linear isotropic, lattice defects 7-26749
- dipole EM radiation in chiral media 7-1005
- disordered monatomic solid, dynamics, force constants distribution 7-12222
- disordered multilayered systems, local density of states determ., recursion method 7-52528
- disordered oxide-semiconductor interface, inversion layer electronic density of states 7-58852
- disordered solid, phonon-like excitations, Green's fn. soln. 7-44729
- disordered solids, 3rd order elastic constants, Green's function approach 7-38088
- eddy currents, EM half-space problems, anal. using Green's functions 7-62579
- Edwards Hamiltonian of polymer physics, stochastic quantisation study 7-48945
- electric fields, dyadic Green's function expansions in spherical coordinates 7-62570
- electrically conducting half-space, analytic Green's dyads 7-10821
- electron correlation, band gaps and quasiparticle energies calcs. for semiconductors and insulators 7-27278
- electron gas, 2D, density of states for high Landau levels and random potential 7-58753
- electron scatt. in a laser field, modified perturbation theory 7-36572
- electron-phonon interacting systems, thermal Green's function generating functional from functional integrals with one-sided boundary conditions 7-52447
- elliptic boundary value problems 7-35240
- EXAFS, inelastic processes, semiclassical treatment 7-64741
- Fermi liquid systems, mag. props. 7-12387
- ferromagnetic multilayers, propagating spin waves 7-52959
- ferromagnetic semiconductors, spin-depend. phonon Raman scatt., theory 7-46013
- ferromagnetic thin films, density of energy for localised retarded modes 7-7569
- ferromagnets, insulating, surface and interface magnetisation changes with temp., Green's function calcs. (*Chinese*) 7-38869
- ferromagnets, non-Heisenberg systems, random phase approx. and Green's function anal. (*Russian*) 7-45597
- fluid, wave-diffraction, submerged cylinder of arbitrary shape, second-order num. soln. 7-51192
- fluoromethane, UV angle resolved photoelectron spectra using synchrotron radiation 7-30246
- fourth order elliptic boundary value problem, symmetries Green's theorem appl. 7-35239
- general relativity, Hadamard construction of Green's function in curved space-time (*German*) 7-66444
- groundwater flow, stochastic anal. of three-dimensional flow in bounded domain 7-23761
- growth probability distribution in kinetic aggregation processes 7-2145
- Hadamard and minimal renormalisations of scalar field in curved space-time 7-48511
- half-space, prestressed elastic, general spatial static contact problem 7-1516
- harmonic oscillator, time-depend. mass, with driving force, exact soln. 7-35331
- heavy fermion metals, supercond. upper crit. field, temp. depend. 7-45587
- heavy quarkonium pot. models, Green's function Schrodinger eqn. calcs. 7-15121
- Heisenberg ferromagnet, diagram technique for Green functions 7-17150
- Hulthen pot., s states, path-integral treatment, use of time transform. trick. 7-35333
- ideal MHD equations, Galerkin method for differential equations with regular singular points 7-11624
- incomplete crystals, surfaces, defects, interfaces and layered structures, theory 7-16926
- incompressible viscous flow, Green's function method for nonlinear problems (*Chinese*) 7-26342
- induction equation in spherical region with boundary, Green's function determ. 7-66445
- induction equation on regions with a boundary 7-1640
- inhomogeneous elastic media, Green's tensor and its potentials 7-62997
- integral quantum Hall effect and localisation 7-64274
- interfaces and superlattices, phonons, Green's function method 7-2340
- intermediate states, Pauli principle and Green function technique 7-5578
- ionisation spectra calc., Green's function method 7-36684
- isolated polyatomic mol., intramolecular vibrational relax. rate, threshold energy depend. calcs. 7-31023
- jets, wave struct., Rayleigh linear inviscid instability anal., 7-51054
- Landau diamagnetism, perimeter corrections for free electron gas 7-38843
- laser diode arrays with heat sinks, temperature profile model 7-20221
- lattice field theories with fermion degrees of freedom, near algorithm for numerical simulation 7-41602
- lattice QCD with Susskind fermions, current algebra relation 7-41730
- lattice theory, weak matrix element calcs., chiral behaviour and multipoint Green's fns. 7-61484
- linear transport eqns. in a random medium, projection operator methods 7-61287
- Lippmann-Schwinger equation solution for short-range potentials 7-19034
- liquid metals, capillary wave dispersion relation modifications due to electric charge, surface Green fn. matching method 7-21575
- Lloyd model, localisation and phase coherence length 7-45106
- many-electron systems, stopping power calculation due to Green's function method 7-4758

Green's function methods continued

- massive scalar field in the static space-time of a cosmic string 7-41217
 matrix construction for stratified elastic half-space (*Russian*) 7-61106
 Maxwell's eqns., soln. in curved space-time, Green's function adiabatic expansions 7-41183
 Maxwell's equations, advanced solns. 7-42834
 metal particles, randomly distributed in a dielectric medium, Anderson localisation of EM waves 7-31218
 metallic thin films, surface electron light absorpt. Green's function method study (*Russian*) 7-21970
 metals, surface lattice dynamics of ordered overlayers 7-2342
 mixed valent compounds, electronic properties, theory 7-21880
 molecular absorption and fluoresc. line shapes, eigenstate-free Green function calcs. 7-25596
 multiple core holes, electronic system response and spectra prod., many-body theory 7-42477
 narrow energy band systems, insulator-metal transition 7-38455
 nematic liq. crystals, light scatt. and. propag. characts. 7-39078
 neutron flux wave excitation in reactor core transients, Green's fn. anal. 7-30601
 nonequilibrium dissipative system, spontaneous symm. breaking and Nambu-Goldstone mode 7-35739
 nonequilibrium open systems, statistical theory 7-198
 nonideal plasma, elec. cond., multiple scatt. contrib. in H 7-16299
 nonlocal metal optics, screened electromagnetic propagators, Green's function calcs. 7-27260
 nonperturbative canonical formulation and Ward-Takahashi relations at finite temp. 7-48932
 nonrelativistic interaction models with infinities, renormalisation, Green's function 7-30171
 nonrelativistic multichannel scatt., strong limit of operator values sequence 7-29818
 nonrelativistic two-particle Coulomb Green's function at positive energy with explicitly separated singularities (*Ukrainian*) 7-9659
 nuclear excitation energy-temperature relation, correlation effects, RPA anal. 7-19214
 nuclear microscopic model with 1p1h and 2p2h configurations, Green's function methods 7-41919
 nuclear time independent mean field theory of collisions, on- and off-shell convergence 7-41951
 numerical analytical continuation method 7-41065
 one-dimensional mol. chain, electron transfer kinetic coeff., donors and acceptors perturbative influence, Davydov solitons 7-27266
 one-dimensional periodic holographic lattices, point spectrum 7-43006
 organic molecules, effective π -electron Hamiltonians, Green's function Monte Carlo calcs. 7-25412
 orthorhombic paramagnet, $J=1$, external field induced Jahn-Teller effect (*Polish*) 7-7179
 parallel thin dielec. cylinders of finite length, scattering study 7-31217
 paramagnets, tetragonal, magnetoelastic excitations and struct. phase transitions 7-27489
 Pauli quenching effects in a simple string model of quark/nuclear matter 7-35828
 periodic metal-semicond. array, depletion layer profile calc. 7-22010
 phonon-assisted quantum diffusion, self-consistent mode mixing. 7-45436
 photon dispersion in strong mag. field with positronium formation 7-41690
 photon propagators and renormalised stress tensors in curved space-time 7-4730
 plane anisotropic contact problems, Green's function soln. 7-6163
 plasma electrical transport, Zubarev-McLennan states, appl. of linear response theory 7-44110
 plasma free boundary calculations in 3D using spectral Green's function method 7-51414
 poloidal field coil design from plasma equilibrium parameters, Green's fn. computer code anal. 7-15318
 polyacetylene, order parameter and optical absorption, quantum fluctuations 7-63750
 trans-polyacetylene, photoinduced IR vibrational modes, lattice dynamical calcs. 7-26891
 polyatomic mol., intramolecular vibr. relax., threshold energy depend. 7-911
 positron annihilation, crystal lattice effects 7-39222
 potential scattering R matrix, Wigner infinite product representation 7-131
 proximity systems, low-dimensional, Josephson current, field effect, appl. to Nb-InAs-Nb system 7-45573
 QED, photon splitting in a strong electromagnetic field 7-35779
 quantum decay into a continuum at weak bias 7-35330
 quantum Hall effect, one-particle wave functions, local density of states and spatial structuring 7-2631
 quantum systems, disordered, interacting, dynamics 7-56147
 quantum theory on surface of a regular tetrahedron 7-48417
 quantum transport eqns., generalised Kadanoff-Baym ansatz 7-38529
 quantum-mechanical Green's function and nonlinear superposition law 7-14817
 quasi-one-dimensional wire, cond., thermopower, effect of lifetime broadening 7-45252
 quasiparticles, polarisation operator in condensed media (*Russian*) 7-16923
 random walk, correlated, on a BCC lattice with next-nearest-neighbour hops, self-consistent decoupling approx. 7-41259
 rare earth semiconductors, valence changes, many-impurity Anderson model 7-7186
 rare earth systems, weak correl. regime, localised 4f states, quasi-particle energy calcs. 7-52492
 reactive scattering by large systems, space-time correl. fn. representation 7-28281
 real O^3+O^4 field in (1+1) dimens. at finite temp., soliton solns. 7-9944
 relativistic Schrodinger equation, Green function calc. (*Chinese*) 7-48437
 s-f model with antiferromag. s-f exchange 7-45653
 scalar Casimir energies in $M^4 \times S^N$ for even N 7-41678
 Schrodinger equation, generalized Green's functions and spectral densities in the complex energy plane 7-29797
 Schrodinger-Coulomb-Green's function, derivation from scatt. expansion, wave functions 7-61159
 semiconductor 2D struct., time-depend. soln. 7-2755
 semiconductor superlattices, layered electron gas plasmons, Raman scatt., Green's functions calcs. 7-17313
 semiconductors, cubic, phonon scatt. at electronically degenerate defect states 7-21827

Green's function methods continued

- semiconductors, electron-phonon weak scatt. in high elec. fields, Boltzmann eqn. 7-2625
 semiconductors, ferromagnetic, dielectric function and reflectivity above T_c 7-7661
 semiconductors, highly excited, nonequilibrium Green's functions and kinetic equations 7-32889
 semiconductors, highly excited nonlinear optical and transport props. of many-exciton system 7-32920
 sheet, orthotropic, adhesively bonded to a stringer, crack tip stress intensity factors 7-1497
 spectra fluctuations in random media, Lenz shift phenomena 7-48577
 stars, photospheric plasmas, time-dependent radiative transfer, analytical methods 7-55451
 strongly anisotropic layer crystals, elastic Green tensor, calc. 7-44645
 surface and interface electronic states calc., tight-binding muffin-tin orbital Green's function method 7-52721
 surfaces and interfaces, electronic states, multiple-scatt. treatment 7-45420
 T matrix, Schwinger variational functionals 7-48949
 thermo field dynamics, development and generalization 7-9984
 thermo propagators and real time finite temp. Green functions in general relativity 7-153
 Thirring model, derivative coupling model equivalence and fermionic Green's fns. 7-48993
 tight-binding itinerant ferromagnet, spin wave anal. 7-2833
 (TMTSF) $_2ClO_4$, transverse spin susceptibility and nuclear spin-lattice relax. rate of field-induced spin-density waves 7-45611
 transition metal dichalcogenides, CDW transition effects of lattice fluctuations 7-21831
 transition metal fluorides, mixed, Raman scatt. by localised and magnon modes 7-46027
 transition metal perovskite type oxides, electronic struct. of point defects 7-16979
 transition metals, Knight shift spin and orbital contribs., real-space formulation, Green's function method 7-2940
 tunnel junctions, prism coupled light emission 7-38770
 tunnelling spectroscopy of a macroscopic variable 7-45435
 uniform asymptotic solution for the Green's function for the two-dimensional acoustic equation 7-62868
 unitary or asymptotic completeness equations, analytic struct. 7-49007
 US pulse diffraction in lossless media, Fourier domain calc. 7-1306
 Ward identities on the lattice for Wilson fermions 7-56419
 wave phenomena in plane layered media, global matrix formulation 7-61125
 X-ray absorption innershell spectra, multiple scatt. theory 7-64736
 XANES, one-electron Green's function, analytical props. 7-64746
 Yang-Mills theory in the light cone gauge, BRS formalism and renormalisation 7-48987
 $Z^{\gamma\gamma}$ and Z^0Z^0 Green's functions, Ward identity derivation 7-41817
 AgCl:I, impurity centre local electron states 7-45207
 AgCrS₂, two dimens. superionic conductor, DC cond. theory 7-16804
 AlH₃, isolated H impurity vibr. spectrum, isotope depend. (*Russian*) 7-16703
 BaTiO₃, ferroelectric solid, microwave absorpt., Curie temp. and ultrasonic attenuation 7-39049
 Be, electronic energy, Green's fn. calc. 7-10445
 Be⁺, metastable ion, shape resons. scaled local density calcs. 7-42464
 CdS platelet, nonlinear optical and transport props. of many exciton system 7-32920
 Ce compounds, heavy-fermion state in the Anderson lattice 7-7476
 Ce, photoelectron and bremsstrahlung isochromat spectra 7-7817
 CoAl, electronic struct. of antistructure Co atoms and Co-vacancies 7-7165
 EuS, mag. ordered and paramag. phases, Raman scatt. 7-22246
 GaAs, electron-electron interactions, appl. for hot electron decay 7-32934
 GaAs, monovacancy, electronic struct. and positron states, self-consistent LMTO calcs. 7-2536
 n-GaAs slabs, ionised-impurity-mediated free-carrier absorption 7-17335
 Ge crystals, surface phonon modes and reconstructions, Green's function method calcs. 7-2339
 H electric field effects, Feynman path-integral formalism 7-42547
 H, external electric field, first-order perturbed wave fn. 7-36465
 H, impurity in metals, electronic struct., higher order approx. 7-52518
 H, multiphoton ionisation by intense laser field, integral eqn. approach 7-62339
 H non-ideal plasma, effect of electron scatt. on conductivity 7-44109
 H₂, electron impact, in laser field, one-photon free-free transitions 7-980
³He, superfluid, dissipative flow through thin channels 7-38288
³He, superfluid, dynamics in flow channels with restricted geometries 7-38287
⁴He, superfluid, critical temp. and nonzero momentum condensation 7-21557
 HfB, electronic struct., chem. bonding, Green's function methods 7-58741
 K, two- and three-photon ionis. 7-30993
 KD₂PO₄-type ferroelectrics, central peak, deuteration effects 7-64586
 Li isoelectronic sequence, quantum defect determ. from negative-energy reaction matrix 7-42480
 LiF, electron beam irrads., desorbed ground state Li atoms, signal time depend. 7-52260
 LiH, electronic energy, Green's fn. calc. 7-10445
 Mg⁺, metastable ion, shape resons. scaled local density calcs. 7-42464
 Mo, electronic struct. of mag. 3d impurities, local density approx. 7-64432
 NaCl, cation self-diffusion by single vacancy mechanism, reaction coordinate approach calcs. 7-32706
 NaCl-type crystal, Green's fn. calc. in Montrose-Potts model 7-58419
 Nb, electronic struct. of mag. 3d impurities, local density approx. 7-64432
 NbC, vacancy electronic struct., muffin tin Green's function method calcs. 7-2531
 Ni (100), adsorption of CO, poisoning in heterogeneous catalysis, role of electronegativity 7-13818
 Ni (111) surface, electronic structure, S effects on heterogeneous catalysis 7-54185
²⁰⁸Pb, isobaric analogue state width determ. using TDA Green function 7-61848
 Rh (111) surface, electronic structure, S effects on heterogeneous catalysis 7-54185

Green's function methods continued

- S₂N₂, photoelectron spectrum, valence ionic state calc. by many-body Green's function method 7-10667
- Si crystals, surface phonon modes and reconstructions, Green's function method calcs. 7-2339
- Si, monovacancy electronic struct. and positron states, self-consistent LMTO calcs. 7-2536
- Si:S(Se)(Te), chalcogenide pairs, electronic structs., Green's function calc. (Chinese) 7-58759
- Si_{1-x}Ge_x:S(Se)(Te) solid solns., deep levels investig. 7-2529
- α-Sn crystals, surface phonon modes and reconstructions, Green's function method calcs. 7-2339
- SrTiO₃:Fe³⁺(V³⁺), impurity energy levels, tight binding model, Green's function method calcs. 7-21856
- TiB, electronic struct., chem. bonding, Green's function methods 7-58741
- U compounds, heavy-fermion state in the Anderson lattice 7-7476
- ZnS:Cu²⁺, multimode Jahn-Teller effect in the luminescence spectrum 7-12675
- ZrB, electronic struct., chem. bonding, Green's function methods 7-58741

GRIN lenses see gradient index optics; lenses

GRIN optics see gradient index optics

grinding

- ceramics, grinding, crack branching, crushing mechanism 7-3472
- crack parameter, finite element modelling of grinding residual stress effects 7-16113
- large aspheric optics, rapid fabrication using computer-controlled opt. surfacing unit 7-37224
- large optics generation, optimum parameters 7-37221
- optical components, large aspherical, fabrication 7-26046
- optical glasses, relative grinding hardness eval. 7-43279
- orientation device for grinding of semiconductor crystals 7-41363
- quartz particles, α-β inversion, structural damage effects, micro DTA study 7-2185
- sialon, abrasive polishing problems 7-53939
- silicate porous glass, wear resistance and grinding hardness, struct. effect, grinding method meas. 7-57614
- ultrasonic optical component processing 7-20478
- ultrasound technical processes, automatic output parameter regulation 7-11232
- Al₂O₃ ceramics, grindability, effect of microstruct. 7-22862
- Cd_{1-x}Mn_xSe, powder, stress effects, amorphisation (Korean) 7-27960
- Ni electroless plated mirrors, diamond-turned, surface finish meas. 7-37218
- Si, thin crystals, grinding, surface defect struct., X-ray diffr. (Russian) 7-38304
- SiC ceramics, hot pressed, grinding, surface damage, bending strength (Japanese) 7-17602
- TiC based hard metals, abrasive polishing problems 7-53939

grinding mills see grinding

groove guides see waveguides

grounding see earthing

groundwater

- 3D flow and solute transport in multilayer systems, finite element algorithms for simulation 7-23742
- Ain-Franin geothermal water, Algeria, instrumental neutron activation anal. 7-60289
- S Alberta, Canada, role of groundwater in origin of sulphates in fractured till 7-23726
- Alberta Basin, Canada, terrestrial heat flow, temp. gradients and groundwater flow 7-28944
- Anambra Basin, Nigeria, water supply of Njikoka and Awka areas 7-18218
- unconfined aquifer, unsaturated flow during gravity drainage, theory 7-18241
- aquifer contaminant transport, orthogonal-upstream finite element modelling 7-23780
- aquifer dewatering, boundary element and optimisation techniques 7-60303
- aquifer optimal management, for large-scale aquifers 7-23746
- aquifer parameters estimation under transient and steady state conditions, max. likelihood method 7-23734
- aquifer parameters estimation under transient and steady state conditions, uniqueness, stability, and soln. algorithms 7-23735
- aquifer parameters estimation under transient and steady state conditions, appl. to synthetic and field data 7-23736
- aquifers, contaminants transport 7-28427
- Argentina, site preselection for radwaste repository (Spanish) 7-42225
- artificially weathered fly ash, trace elements mobilisation and attenuation 7-28437
- automatic interpolation methods for mapping piezometric surfaces, appl. to groundwater reservoirs 7-40574
- Beijing area, China, geothermal resource of hot water aquifer 7-3622
- Bhatsa area, Maharashtra, India, water percolation rel. to reservoir-induced seismicity 7-23567
- W Black Sea, electrical anomaly rel. to filtration anomaly 7-54856
- Bohemian Cretaceous Basin of Czechoslovakia, heat flow and groundwater 7-28945
- book, economics and applied geology 7-29609
- borehole water and gas sampling technique using polyamide tube 7-66310
- boundary element approach for modelling groundwater movement 7-4059
- bounded two-aquifer system with aquitard, crossflow problem soln. 7-29099
- Calgary area, Canada, aquifers and geothermal energy 7-28924
- California, groundwater Rm as earthquake fluid phase precursor 7-40424
- Canadian approach to site characterization for a nuclear fuel waste disposal vault 7-42224
- Chalk River, Ontario, groundwater flow system in fractured monzonitic gneiss block 7-29120
- CHEMSIMUL code appl. to groundwater radiolysis in HLW repository 7-49693
- China, tectonic activity anal., use of fluid-geochem. methods 7-40421
- coastal aquifer, determ. of salt-freshwater interface using borehole, theory 7-29107
- coastal aquifer, unsteady interface between fluids 7-14319
- conference on radwaste underground repositories, Hannover, Germany (Mar. 1986) 7-41010
- contaminant plume in groundwater, migration using Galerkin models 7-60298

groundwater continued

- contaminant transport, variable BEM soln. 7-55115
- contaminant transport model for aquifer 7-23751
- contaminated groundwater in fractured porous rock 7-55027
- contamination of shallow unconfined aquifers through infiltration beds 7-23242
- continental crust, seismic reflectors, elec. cond., water and stress 7-4011
- coupled groundwater flow and heat transfer in granite rock locality 7-55110
- crystalline minerals, fracture characteristics using ²²²Rn and ²²⁰Rn as probes 7-23893
- crystalline rocks, nonsorbing species porosity and diffusivity 7-23639
- Dakongbeng geothermal area, SW China, hot spring activity 7-4064
- Darazo, Nigeria, elec. resist. survey of Kerri-Kerri Formation rel. to water resources 7-18219
- dating of mixed groundwaters, appl. of T corrected ¹⁴C and atm. noble gas corrected ⁴He 7-9044
- deep geological radwaste disposal, basic geological studies for storage environment (French) 7-42226
- deep groundwater flow, governing principles, effects on geological radwaste disposal 7-5462
- diffusion-advection eqn. integral soln. for contaminants transport 7-28424
- direction and velocity meas. system 7-9185
- dispersion of solute in unbounded stratified porous media, theory 7-29115
- dispersive transport in porous media, modelling, second order approach, appl. 7-63212
- dispersive transport modelling in porous media, solute motion in pipes and capillary tubes 7-23753
- dispersive transport modelling in porous media, theoretical development of second-order approach 7-23752
- Donets Basin, USSR, Carboniferous deposits parting fractures, role of pore fluids 7-34403
- drainage from uniform soil layer on hillslope simple hydrological model 7-23756
- Efate, Vanuatu, thermal springs hydrology and chem. 7-60282
- electric currents due to water flow causing magnetic anomalies 7-23533
- environment monitoring system for multiphase and porous media, modelling 7-59904
- falling-rising water table sequence in sand, theory 7-60296
- fire areas (of red sediments and vegetation carbonization) in California, USA, due to hot groundwater 7-23654
- fissured rock areas, groundwater circulation influence on geothermal gradients 7-28941
- flow, transport velocity representation, environmental appls. 7-55114
- flow in low-permeability environments 7-29097
- flow in permeable geologic media for nuclear waste evaluation using 3D-SEEP code 7-60103
- flow in thick multiple-aquifer system, role of sand body interconnectedness 7-23760
- flow modelling, inverse problem soln. for two-dimensional steady state flow 7-23762
- flow simulation, adaptation of Carter-Tracy water influx calc. 7-23745
- fluid flow and energy transport assoc. with high-level radioactive waste disposal in unsaturated alluvium 7-23767
- fractured rock masses, fluid flow simulation, hybrid boundary element-finite element analysis procedure 7-34478
- geothermal energy resource utilization, hydraulic investigations 7-28387
- Gombe subcatchment, Benue Valley, Nigeria, hydrogeology 7-18217
- gravel pits in Rhine Valley north of Strasbourg, hydrological balance with groundwater (French) 7-47468
- Great Artesian Basin, Australia, very old groundwater ³⁶Cl dating and chem. 7-66194
- Great Plains of USA, surface heat flow altered by groundwater circulation 7-28943
- Green-Ampt analysis for falling water table in stratified profile 7-23764
- gypsiferous-sodic desert soil, leaching simulation 7-29105
- Hawaii, large valleys morphology rel. to groundwater sapping and comparison with Martian valleys 7-55095
- heat flow anomalies due to groundwater flow 7-28940
- heat flow near to surface, influence of water table configuration 7-28939
- heterogeneous adsorption behaviour in soil, effect on ion transport 7-29104
- HLW disposal in salt formations, field expts., groundwater, corrosion 7-5465
- hydrocarbons, microbial biodegradation in groundwater, numerical simulation 7-46977
- hydromagmatic eruptions, implications for volcanic hazard in Italy 7-66053
- Iceland, geothermal system prospecting using borehole temperature observations 7-28948
- ILW deep disposal in UK, geological environments 7-42227
- immiscible organic solvent transport at Hyde Park Landfill, New York State, numerical modelling 7-23724
- infiltration from cavities, num. soln. 7-18254
- intermittent flux studies in unsaturated soils, numerical hysteresis model 7-29096
- karst aquifer at Castle Meadows, Alberta, Canada, structure and function 7-4060
- karstic, rock areas, groundwater circulation influence on geothermal gradients 7-28941
- Kasserine Basin, Tunisia, multistage groundwater exploration 7-4067
- Kraternaya Bay region, Yankicha Island, Kuril Islands, water chem. and isotopic comp. 7-29078
- La Grande-2 Reservoir, Quebec, gravity var. due to water transport 7-8793
- lake acidification, role of groundwater 7-23247
- Lalitpur District, Uttar Pradesh, India, groundwater and water supply in granitic terrain 7-4065
- land disposal of radwaste, optimum groundwater transport model for health effects 7-808
- large multiaquifer system, flow, conjugate gradient finite element model 7-23783
- Laurel Mountains peat bog, USA, atm. chemicals deposition chronology 7-9075
- leached radwaste radionuclides, migration by groundwater, math. modelling 7-5461
- low-level counting techniques 7-29296
- MacCormack method for free surface water problems 7-55119
- Madison aquifer, N Great Plains, USA, regional aquifer flow model 7-60292

- groundwater continued**
 magnetic anomalies arising from electric currents due to water flow 7-23533
 mass transport in discrete fracture networks, prediction by geometric field data use 7-66192
 McClood Lake, soft water acidic lake in Florida, groundwater chemistry rel. to ion sources and sinks 7-23763
 measurement, scale, and scaling, relations rel. to subsurface hydrology 7-23914
 mechanics and fluid flow of jointed rock masses, coupled model 7-60297
 milk River aquifer, Canada, old groundwater ³⁶Cl dating and chem. 7-66195
 minerals, radiation damage and trace water relationship 7-32489
 Mobile, USA, two-well tracer test, performance, anal. and simulation 7-23785
 Momotombo hydrothermal area, Nicaragua, thermal evolution modelling 7-23937
 Nagano, Japan, ³He/⁴He ratio anomalies in hot spring gases, assoc. with 1984 September 14 earthquake 7-40422
 Nagano region, Japan, gas anomalies at mineral springs and fumarole before earthquake 7-40423
 natural convection from cylindrical heat source in water saturated porous medium, radwaste appl. 7-806
 near-field solubility constraints on radionuclide mobilisation, influence on radwaste package design 7-5460
 New Mexico, USA, Pleistocene climate indicated by groundwater isotopes 7-23838
 New Mexico, USA semiarid sand site, soil water movement and recharge 7-23774
 Nubia, Egypt, aerial techniques for groundwater prospecting 7-34698
 nuclear waste disposal in plutonic rock masses, disposal sites characterisation 7-10296
 nuclear waste glass, comparison of leaching in natural and synthesized groundwaters 7-19530
 one-dimensional infiltration in homogeneous soils, combined analytical-numerical approach 7-29082
 S Ontario, Canada, hydrochemical interpretation of shallow aquifer 7-4061
 organic solvent movement after release to groundwater system 7-17926
 Palo Duro Basin, Texas, USA, groundwater inert gas chemistry 7-66179
 parameter identification procedures in groundwater hydrology, inverse problem 7-23730
 particulate contaminant migration through porous media 7-60301
 phreatic aquifer, water table region, specific discharge profiles anal. 7-29098
 pollutant organic compounds, transport with saturated groundwater flow, theory 7-23240
 pollutant organic compounds transport with saturated groundwater flow, expt. results 7-23241
 pollutant transport in aquifers, finite element calc. 7-28428
 pollution, convection-dispersion eqn. for transfer function model of solute transport through soil 7-23739
 pollution, fundamental concepts of transfer function model for solute transport through soil 7-23737
 pollution, illustrative appls. of transfer function model for solute transport through soil 7-23738
 pollution in developing countries, aquifer-oriented protection policy 7-3731
 ponds of shallow depth, water infiltration to underlying rocks 7-18251
 pore water effect on freq. depend. seismic wave propag. in rocks 7-28883
 porous media with viscoelastic props., fluid eqn. soln. and applic. (Chinese) 7-18222
 Pripyat River, groundwater regime and balance in forest and marsh landscapes of right bank 7-9050
 quality, freq. domain anal. 7-23789
 radial dispersion problem (recharge of aquifer), analytical soln. 7-29117
 radiocarbon accelerator mass spectrometry for hydrological investigations 7-29295
 radiocolloids near Australian U ore bodies 7-28430
 radioisotope distribution in precipitation, surface and groundwaters in NW Yugoslavia 7-23254
 radionuclide migration in fissured crystalline rock, from nucl. waste repository 7-23246
 radionuclide transport from borehole to porous formation with fracture 7-23244
 radionuclide transport in fast channels in crystalline rock 7-28425
 radwaste disposal in shallow tunnels in glacial till or clayey soil, geotechnical considerations 7-42217
 Regina, Saskatchewan, Canada, geothermal reservoir numerical model 7-18156
 rock porosity changes associated with mechanical stress relief 7-23640
 sand aquifer, hydraulic cond. spatial var., role in dispersion process 7-66200
 sand aquifer, natural gradient expt. on solute transport, nonreactive tracers motion 7-66197
 sand aquifer, natural gradient expt. on solute transport, organic solutes, long-term behaviour during transport 7-66198
 sand aquifer, natural gradient expt. on solute transport, organic solutes sorption, effect on mobility 7-66199
 sand aquifer, natural gradient expt. on solute transport, plume movement 7-66196
 Saskatchewan, Canada, well water He and methane anomalies origin 7-40440
 saturated soil, freezing 7-60279
 seepage direction detector, development and appl. (Chinese) 7-9236
 seepage flow through porous dam, free boundary problem soln. 7-66182
 sensitivity anal. using computer calculus, nucl. waste isolation appl. 7-30477
 separate phase organic contaminants transport 7-51307
 soil, water movement and solute movement 7-23778
 soil column with central hole, infiltration 7-18253
 solute dispersion in multidimensional periodic saturated porous media, asymptotic Gaussian approximations 7-23731
 solute transport in aquifers, dispersion in fractal fracture networks 7-23772
 solute transport in aquifers and field soils, stochastic convection-dispersion model 7-23729
 solute transport in infinite medium with mobile and immobile zones, 3D solns. 7-23248
 solute transport in vadose zone 7-60290
- groundwater continued**
 solute transport parallel to interface separating dissimilar porous media 7-60293
 solute transport simulation, time advancement problem 7-23249
 statistical inference of spatial random functions 7-23779
 statistical theory for flow and transport, at laboratory, formation and regional scales 7-18237
 stochastic theory for heterogeneous aquifer flow 7-18238
 stratified aquifers at Chalk River and Mobile, N America, simulation of two-well tracer tests 7-23784
 streamline routing through fracture junctions 7-55028
 structured soils, equilib. and first order kinetic transport models, validity constraints 7-23243
 subterranean thermal water resources (Rumanian) 7-9054
 subterranean waters, motion into bore in inhomogeneous stratified seam during pumping from two layers 7-23714
 surface saturation zones prediction in natural catchments, appl. of topographic anal. 7-23770
 Switzerland, deep groundwater circulation and heat flow maps 7-28942
 systems management, coupling of finite element and optimisation methods 7-60278
 Tawhai State Forest, New Zealand, catchments, runoff characts. 7-29100
 Tawhai State Forest, New Zealand, storm runoff, hillslope and low order stream response 7-29101
 Tengchong geothermal field region, China, tectonics, thermal springs and active structures 7-60219
 Tengchong geothermal systems, China, evolution (since 1639) 7-60218
 thermal dynamics of a block-filled underground hot water store 7-46972
 three-dimensional flow in bounded domain, stochastic anal. 7-23761
 transient flow response of 3D sparsely fractured rock masses, model 7-60295
 transport simulation in stratified aquifers, curvilinear finite element model 7-23759
 two-dimensional variably saturated flow, finite-element collocation method 7-29111
 unconfined groundwater flow expt. 7-23744
 United States and Canada, 1986 July, water conditions 7-29094
 United States and Canada, 1986 June, water conditions 7-9053
 United States and Canada, 1986 September, water conditions 7-55100
 unsaturated zone water flow and solute transport, review 7-18236
 variably saturated porous media, water flow by 3D finite-element model 7-60294
 variations, correl. with ground self pot. var. 7-29275
 Vulcano, Italy, volcanic fumarole gas chemistry and water origin 7-4016
 Wairakei Geothermal Field, exploitation induced gravity var. due to groundwater effects 7-28812
 water and air intake of surface-exposed rock fractures 7-18250
 water movement in unsaturated zone under irrigated area, investigation using environmental T content 7-23757
 water permeation from artificial reservoirs, relation to seismicity changes in Japan 7-23569
 water pollution by fertilisers and pesticides, book 7-24314
 well water level fluctuations due to Earth tide and atmos. press. 7-9045
 wetland surface water dynamics 7-66193
 Yangbajing fault, isotopic depth 7-28973
 Zhelin reservoir, E China, contrib. of water pore press. to induced earthquakes 7-23571
 Au and Ag content of mineral waters of E Siberia 7-28922
¹⁴C activity of atmosphere, response of hydrological systems 7-23253
¹⁴C concentration in groundwater using liquid scintillation counting 7-23892
 He isotopes in sedimentary basins, relation to form. mechanism 7-47405
⁸¹Kr, analysis in groundwater using laser resonance ionisation spectroscopy 7-29095
 Ra in groundwater, porous flow model for steady state transport 7-23725
²²⁶Ra, meas. method and results in fresh water 7-23262
²²⁸Ra, prediction of occurrence in groundwater, rel. to public drinking water supplies 7-54380
²²²Rn conc. dynamics close to ground surface (Japanese) 7-59884
²²²Rn, meas. method and results in fresh water 7-23262
⁹⁰Sr radioactive pollution at U-plant in Rhode Island, USA 7-23245
 U mill tailings pile causing groundwater pollution, model of plume 7-59885
 UO₂, parametric studies in groundwater 7-25253
²³⁴U/²³⁸U ratio as redox indicator in briny aquifers 7-5470
- group method of data handling** see forecasting theory; identification
- group theoretical schemes**
 see also O groups; SO groups
 E(1+6, 7, 8) SUSY nonlinear σ -models, global anomalies 7-9969
 SO(10) → SU(2)_L × SU(2)_R × SU(4)_C
 SU(2)_L × SU(2)_R × SU(3)_C × U(1)_{B-L} × D unified models, Higgs potential calcs. 7-454
 U(3) × U(3) symmetric effective chiral Lagrangian for baryons 7-49084
- group theory**
 see also Clebsch-Gordan coefficients; crystal symmetry; elementary particle theory; group theoretical schemes; Lie groups; renormalisation; SU_N theory
 abelian and central extensions of aspherical groups 7-29675
 Abelian group, locally compact, quasi-translation invariance and absolute continuity, equivalence 7-48298
 Abelian groups, locally compact topologies 7-48297
 Abelian groups without twisting with periodic groups of automorphisms 7-60973
 adamantane, T_d skeleton, point groups 7-29634
 algebraic groups as products to two subgroups, one of which is solvable 7-18555
 amenable semigroups, solns. to problems 7-55965
 analytic continuation of local representations of symmetric spaces 7-55981
 anisotropic superconductivity, lattice distortion, group theoretical anal. 7-58264
 atomic orbitals, group theoretical treatment 7-836
 automorphic forms and number theory, conference, Sendai, Japan (Nov. 1983) 7-48196
 Bose field, symmetric group characters and Young diagrams 7-401
 bosonic string, classification of subgroup truncations 7-30227
 bosonic string, interacting, 26-dimensional, torus compactification for non-simply laced groups 7-30226
 central-limit theorems on groups 7-41233

group theory continued

- character values, conjugacy classes and a problem of Feit 7-18553
 commutative semigroups, normal extensions 7-35204
 commutative semigroups without idempotents, structural isomorphisms 7-60976
 complex fuzzy events in classical and quantum information systems, algebraic props. 7-61152
 conference, group and semigroup rings, Johannesburg, South Africa (July 1985) 7-4637
 conformal invariant field theory, current algebra, group theoretic anal. 7-35710
 crystal phase transitions, appl. of group theory 7-55926
 crystallographic and metacrytallographic groups, book 7-18517
 cubic crystalline field eigenstates and energies, group-theoretical computational approach 7-21877
 cubic lattices, regular and optimal subdivisions into sublattices 7-16456
 density matrices geometry, superoperators and unitary invariance 7-201
 diffeomorphisms, anomaly struct. in theories with external gravity 7-4738
 differential equations, nonlinear, symmetries and linearization 7-55963
 differential equations, solution by group theoretical methods 7-61065
 Ellis groups and group extensions 7-18554
 Eulerian parametrization of Wigner's little groups, rotations and Lorentz boosts 7-4656
 finite soluble groups, large centralizers 7-24366
 Fitting functors in finite solvable groups, behaviour with respect to direct products 7-29681
 free modules over algebras of finite groups, characterisation 7-60971
 free pro-p-products, subgroups 7-48296
 free semigroups, elementary theories 7-60974
 functions, alternative algebras 7-35206
 gauge fields, factorisation condition for bidimensional and pseudo-Euclidean groups 7-48946
 gauge transformation group, smoothness of action on connections 7-18976
 graded calculus of variations, algebraic model 7-29672
 gradient property of group representations, weaker condition 7-60978
 heavy electron superconductors, p-wave pairing consequences 7-2772
 Hehl's Poincare gauge theory, diffeomorphisms for conformal and de Sitter groups 7-48941
 homogeneous Kaluza Klein cosmologies, group theoretical classification 7-48491
 homomorphisms of general and special linear groups 7-24371
 imaginary Abelian number fields, ideal class group exponents 7-24365
 infinite symplectic group, Riesz ring approach 7-55962
 integral transforms for square group representations 7-29683
 inverse semigroups, recurrence and nonrecurrence of random walk 7-61233
 irreducible representation calcs. of a finite group 7-18557
 Kac-Moody and gauge groups, nonrepresentability of cohomology classes 7-65
 Kadomtsev-Petviashvili eqn., infinite-dimensional symm. group and Backlund transforms. 7-24370
 Klein-Gordon equation, nonlinear, maximal symmetry group 7-391
 Lorentz-group representation products, abstract group-theoretical reduction 7-66
 Maeda's theorem, generalization 7-35303
 methane, T_d skeleton, point groups 7-29634
 molecular vibrational spectroscopy, group theoretical method of constructing symm. coords. 7-36582
 N-atom polar deltahedra, tensor surface harmonic theory, pairing principle 7-50439
 nonlinear evolution equations, semigroups 7-55982
 open bosonic string, dilaton tadpole 7-49114
 operator theory, symposium, Athens, Greece (Aug. 1985) 7-55878
 orthosymplectic groups $OSP(2|2p)$, generalised atypical supertableaux 7-41055
 p-group, $p=2$, derived group analysis 7-48295
 parameterization of the linear zeros of $6j$ coefficients 7-41052
 partially ordered set, generalized upper bound 7-35208
 point groups, rel. to mol. symm. teaching approach 7-29634
 quantum system, group-related coherent states 7-4706
 reduced three-wave resonant system with nonconstant coeffs., group props. 7-41067
 reducing matrices, generating relations and corepresentations 7-4652
 Schrodinger non-relativistic conformal symmetries and invariant tensor fields 7-35674
 semigroup algebras of commutative and cancellative semigroups, radicals 7-24364
 semigroup rings, n-generator property 7-60970
 semigroups and lattices, independence of groups of automorphisms and retracts 7-60975
 semiprimary algebra-group cross product with identity 7-35205
 $Sp(2)/\Lambda T(2)$ Grassmann Euclidean group, extended BRST SUSY, pseudomass, pseudospin 7-61491
 $sp(4, \mathbb{R})$ symplectic algebra generators, matrix representation 7-60948
 spinors and diffeomorphisms 7-9646
 stable and unstable groups, algebraic structure 7-14750
 structural phase transitions, total condensate of normal vibrs., group theory anal. (Russian) 7-44740
 superconformal algebras in two dimensions 7-4982
 symmetries of disorder ensembles with superconducting order 7-64388
 time-continuous random walks on finite groups, transition probability calcs. 7-48337
 transformation laws of geometrical objects, algebraic approach 7-29656
 $U(n_1) \times U(n_2)$ reduced matrix elements and reduced Wigner coeffs. 7-4654
 $U(N)$ gauge theories, topological aspects of loops 7-24756
 $U(n)$ matrix element evaluation in composite basis 7-5604
 unitary representations induced from maximal parabolic subgroups 7-24369
 vector coherent state theory in a group with non-commuting raising generators 7-60977
 weighted composition semigroups on Hardy spaces 7-55964
 Weyl group rotation subgroups, projective representations using $O(l)$ and $SO(l)$ 7-29680
 $e^+e^- \rightarrow X$, asymmetries from E_8 GUTs 7-448
 ^3He , superfluid, free energy symmetry and stationary points 7-2293
 PrO_x , fluorite prototype struct., interfaces and domain form. study 7-58498
 TbO_x , fluorite prototype struct., interfaces and domain form. study 7-58498

Gruneisen coefficient

- 2-adamantanone, order-disorder phase transition, high press. effect, Raman study 7-38183
 alkaline earth fluorite crystals, US attenuation 7-51944
 binary cubic cpds., mode Gruneisen parameter~phonon freqs. ratio correl. formula 7-26894
 cryocrystal: O_2 , thermodynamic props., impurity mol. exchange interaction effects calcs. (Russian) 7-12308
 cubic solids, fourth order theoretical model (French) 7-63761
 disordered systems, two-level system ensemble, low-temp. thermal expansion anomalies 7-2234
 fluorite struct. crystals, phys. props., effective pot. calcs. 7-26692
 heavy fermion systems, Gruneisen parameter electron-phonon coupling 7-2138
 II-VI tetrahedral cpds, mode Gruneisen parameters 7-44732
 III-V covalent crystals, thermal expansion coeffs. calc. 7-44869
 Indian upper mantle rocks, pressure-temp. studies for Gruneisen coeff. and specific heat 7-55267
 ionic solids, overlap interactions and bonding 7-1940
 mean stress dependence of the thermoelastic constant 7-65248
 measurement from shock attenuation in a strongly decaying shock wave 7-21384
 polydiacetylene cryst., Raman spectra, press. depend. 7-27726
 styrene-butadiene rubber, thermoelastic coeff. Gruneisen parameter, thermal effects 7-39576
 $(\text{Ag}_6\text{Sn}_2\text{P}_{12})\text{Ge}_6$ cluster cpd., elastic behaviour and vibr. anharmonicity 7-12223
 Al, fourth-order thermal expansion coeff. fn. 7-44868
 $\text{AlP}(\text{As})(\text{Sb})$, elastic coefficients, pressure effects 7-63720
 BaF_2 , linear thermal expansion meas. 7-44863
 CaF_2 , linear thermal expansion meas. 7-44863
 CeRu_2Si_2 , heavy-fermion system, magnetoacoustic effects in high mag. fields 7-64506
 Cr, magnetovolume, thermal expansion and Gruneisen parameters 7-33260
 Cr-V alloy, magnetovolume, thermal expansion and Gruneisen parameters 7-33260
 CsI, Hugoniot overtake sound-rel. meas. 7-44705
 Cu, fourth-order thermal expansion coeff. fn. 7-44868
 GaP crystal, low temp. negative thermal expansion coeff. 7-6837
 Ge, fourth-order thermal expansion coeff. fn. 7-44868
 $\text{Ge}_{0.98}\text{Sn}_{0.02}\text{Te}$, acoustic mode vibr. anharmonicity 7-63751
 He, Gruneisen parameter at critical points (Chinese) 7-24609
 NaCl, Anderson-Gruneisen parameters, temp. variation 7-2137
 $\text{Pb}_{47}\text{Ba}_{93}\text{Ge}_3\text{O}_{11}$, rhombohedral, acoustic symmetry and vibr. anharmonicity 7-16695
 PbF_2 , linear thermal expansion meas. 7-44863
 $\text{Pb}_5\text{Ge}_3\text{O}_{11}$, high pressure Raman scatt., phonon modes and Gruneisen parameters 7-33391
 $\text{Pb}_5\text{Ge}_3\text{O}_{11}$, rhombohedral, acoustic symmetry and vibr. anharmonicity 7-16695
 PbS , acoustic mode vibr. anharmonicity 7-63751
 PbSe and other IV-VI cpds, acoustic mode vibr. anharmonicity 7-63751
 PbTe , acoustic mode vibr. anharmonicity 7-63751
 S, thermal expansion coeffs., Gruneisen parameter, X-ray powder diffr. determ. 7-2235
 Si, fourth-order thermal expansion coeff. fn. 7-44868
 SiC, cubic, ab initio calc. of ground state props. 7-6751
 $\text{SrF}(\text{Cl})_2$, linear thermal expansion meas. 7-44863
 UPt_3 , heavy-fermion system, magnetoacoustic effects in high mag. fields 7-64506

GTO calculations

- see also GO calculations
 energy-optimised GTO basis sets for LCAO calcs., gradient approach 7-10376
 LCGTO $X\alpha$ method, appl. to photodissociation and conform. energy problems 7-25393
 methane, force field, HF SCF and GAS SCF calcs. 7-62268
 molecular orbital wave functions; interaction parameters, GTO calcs. 7-15506
 H, Griffin-Hill-Wheeler eqn., discretisation, Gaussian type orbitals calcs. 7-30945
 H-like atoms, relativistic corrections to ground state energies, Dirac eqn. variation perturbation method 7-24766
 N_3^- , spectroscopic props. ab initio GTO CEPA study 7-15525

GTO devices see thyristors

Gudden-Pohl effect see electroluminescence

guided electromagnetic wave propagation

- see also guided light propagation; waveguides
 Earth-ionosphere waveguide, ELF mode constants calc., noniterative procedure 7-40636
 HF refraction insertion into ionospheric waveguide 7-14406
 radiowave propagation along highly conducting surface in uniform motion 7-10825

guided light propagation

- see also optical waveguides
 acoustooptical Bragg diffraction, devices and appls. 7-45983
 active guided wave devices, coupled mode anal. 7-62829
 electro-optic materials for guided-wave optical devices 7-37134
 FEL active guiding in small signal regime 7-1167
 fibres, pulse propag., theoretical study (Spanish) 7-37168
 fibres, transmission principles and manufacture (French) 7-15991
 fibres single-mode, nonlinear propag. at zero dispersion wavelength 7-15987
 film-guided waves, nonlinear propag., numerical anal. 7-5998
 garnet films, orthorhombic, optical modes, phase matching 7-11110
 GRIN planar waveguides with nonlinear cover medium, guided waves 7-37141
 interference diagnostics of planar optical waveguides 7-25960
 liquid crystals, nonlinear guided waves, optical hysteresis 7-57551
 nonlinear, TE_0 mode excitation by Gaussian beams 7-1258
 nonlinear guided waves in low-index self-focusing thin films 7-25907
 nonlinear p-polarised optical waves, exact calcs. 7-62802
 nonlinear TE polarised surface plasmon polaritons guided by metal films 7-5946
 nonlinear TM-polarised nonlinear waves guided by thin dielectric films, calc. 7-5993
 optical guiding in an FEL 7-1165
 rods, tapered GRIN, imaging and transforming transmission 7-25961

guided light propagation continued

- single-mode single-polarisation fibre using resonant absorbing effect, theoretical study 7-43381
- spinor formalism and guided waves 7-5996
- super-Gaussian optical pulses, frequency-chirped, propag. along fibre 7-6013
- 22-tricosenoic acid Langmuir-Blodgett films, guided optical waves in ATR geometry 7-31462
- GaAs/GaAlAs planar MQW structure, nonlinear coupling of guided waves 7-11106

Guinier-Preston zones

- Al-Ag, steady-state creep, effect of isochronal ageing 7-17598
- Al-Ag (5.9 at.%), precip., positron study 7-46485
- Al-Ag alloys, isothermal ageing, hardness and creep behaviour 7-8068
- Al-Zn, fatigue particle coarsening, vacancy creation 7-53895
- Al-Zn, Guinier-Preston zones, size distrib., small angle X-ray scatt. studies 7-28043
- Al-Zn (12 at.%) alloy, size-shape relation of Guinier-Preston zones, SAXS study 7-13455
- Al-Zn (15 at.%), precip. during ageing, interaction of continuous and cellular mechanism 7-13454
- Al-Zn alloys, quenching effect on growth of Guinier-Preston zones, resistivity 7-22733
- Al-Zn-Ag, phase diagram tielines, anomalous SAXS studies 7-53705
- Al-Zn-Mg (4.5, 1.75 at.%), ageing, specific surface energy of Guinier-Preston zones 7-28046
- Ti-Cu alloys, Guinier-Preston zones, multi-layer struct., atom probe FIM study 7-33674

Gulyaev-Bluestein waves *see surface acoustic waves***Gunn devices**

- see also Gunn diodes*
- No entries

Gunn diodes

- No entries

Gunn effect

- see also limited space charge accumulation; negative resistance effects*
- Korteweg-de Vries equations for Gunn's effect 7-12725
- n-GaAs films, electron-hole plasma stratification and blue luminesc. near static domain 7-52666
- InGaAsP system, transferred electron effect anal. 7-64259
- PbTe whisker crystals, Gunn-type oscills. 7-52626

Gunn effect devices *see Gunn devices***Gunn oscillators**

- analytical microwave spectrometer employing a Gunn oscillator locked to the rotational absorption line 7-15008

guns, plasma *see plasma guns***gyration** *see rotation***gyromagnetic effect**

- see also gyromagnetic ratio; magnetic resonance*
- electron beam trapping into gyromagnetic autoresonance, Coulomb field effects 7-42887

gyromagnetic ratio

- see also g-factor; magnetic resonance*
- ampere reproduction from proton gyromag. ratio and quantum magnetoresonance phenomena 7-61309
- magnetised plasma, neutron excitation of Landau and collective modes 7-7134
- protons in spherical water sample, gyromagnetic ratio meas. in terms of quantum magnetic flux 7-61687
- Ag conduction electrons, gyromag. factor calcs. 7-7099
- Al conduction electrons, gyromag. factor calcs. 7-7099
- Co-Cr films, mag. parameters, Brillouin light scattering study 7-53357
- ¹⁶⁶Er, gyromagnetic ratios of excited states in ground and gamma bands 7-30335
- (Eu, Lu, La)₂Fe₂O₁₂ films, gyromagnetic ratio, damping parameter and mag. anisotropy 7-45777
- Pd conduction electrons, gyromag. factor calcs. 7-7099
- Pt conduction electrons, gyromag. factor calcs. 7-7099
- ¹¹⁷Sn, gyromagnetic ratio of 3/2⁺ state 7-30334

gyromonotrons *see microwave tubes***gyroscopes**

- see also navigation*
- Coastal Ocean Dynamics Experiment, shipboard Doppler current profiling 7-9260
- complete separation of motion in some gyroscopicsystems 7-11267
- correctable gyrocompass under progressive base oscillations (Russian) 7-30003
- directional coupler, polarisation-preserving, appls. 7-1279
- fiber-optic gyro for space applications 7-30005
- fiber optic, noise problems 7-20439
- fiber optic, phase modulated, coherent backscatter analysis 7-43427
- fiber optic closed loop, performance 7-20438
- fiber optic directional coupler, polarisation preserving for gyroscope 7-25999
- fiber optic gyroscope, noise due to birefringence modulation 7-31479
- fiber optic gyroscope, passive ring cavity-type, 1.5-μm DFB InGaAsP laser appl. 7-57562
- fiber optic gyroscope, self-pumped phase-conjugate 7-31509
- fiber optic sensors for rotation rate meas. (German) 7-11161
- fiber polarisation components, birefringent, for sensor appls. 7-20450
- fiber-optic gyroscope technology, state-of-the-art, review 7-20441
- gyrocompass, integration of eqns. of motion 7-43652
- gyromagnetic compass bearings anal., appl. of current flow junction (Polish) 7-30051
- gyroscopic motion with friction, two time scale anal. 7-48353
- gyrostabiliser under base oscillations, dynamics and errors (Russian) 7-30002
- laser, correlated emission type 7-41368
- laser gyroscope reliability for inertial navigation platforms (Italian) 7-25860
- motion of a gyroscope with small self-excitation, rotation evolution 7-43654
- noncontact gyroscope in resistive medium, run-up system 7-43653
- North azimuth determination using suspended gyrocompasses 7-66309
- optical passive ring resonator gyro, reson. characs. of backscatt. 7-50753
- optical passive ring resonator gyroscope, semiconductor laser and integrated optics use 7-25998
- passive laser gyros, servo-controlled lasers progress and appls. 7-20307
- passive resonant ring laser, progress 7-20440

gyroscopes continued

- pendulum, gyroscopic, with ideal unilateral constraint, motion with respect to angle of nutation 7-43655
- ring laser, doubly dithered, harmonic mixing signal 7-42872
- ring laser gyroscope, skewed probability densities, coloured noise effect 7-41369
- ring-laser gyroscope, random dither modulation 7-57376
- solid state, optical, review 7-20437
- superconducting thin film gyroscope readout for gravity probe-B 7-14855
- torque measurement using high performance gyroscopes 7-48720
- transmission line gyroscopes, general relativistic electromagnetic effects 7-29859
- two-wavelength fibre gyroscope with wide dynamic range 7-1270
- LiNbO₃ integrated optical components for fibre gyroscopes 7-20472

gyrotrons *see microwave tubes***gyrotropy (optical)** *see optical rotation***H-centres**

- KCl, vibronic mechanisms of excitation decay, defect formation 7-39158
- KX (X=Cl, Br), H-interstitials, struct. and crowding mechanism 7-38939
- RbX (X=Cl, Br), H-interstitials, struct. and crowding mechanism 7-38939

H I regions

- 21-cm line observations, appl. of acousto-optical spectrometer for RATAN-600 radio telescope 7-66463
- in active galaxies, H I 21-cm emission obs. 7-48066
- chemistry of interstellar clouds, dynamical perspective 7-24194
- in dwarf galaxies, 21-cm line widths rel. to luminosity classification extension 7-60794
- in dwarf galaxies, low surface brightness, in Virgo cluster, H I synthesis obs. 7-4560
- in early-type galaxies, H I content versus star form. and ionised gas 7-29528
- expanding H I supershells around OB associations, nature 7-4527
- G24.6+0.0 (Scutum ring), obs. of ring of H II regions assoc. with CO and H I shells 7-18447
- in galactic spiral arms, vertical vel. struct. rel. to energetics of vel. active regions 7-24220
- in galaxies, H I content of lenticular and early-type galaxies in field and in Virgo cluster 7-4559
- outer Galaxy H I layer, volume densities atlas in cuts through composite data cube 7-18358
- HD 88500, H I bubble related to WC star 7-40808
- high velocity H I clouds, relation to twin jet in galactic nucleus and former Seyfert galaxy stage 7-66740
- high-velocity clouds, search for dust, IR emission search 7-40893
- large-scale structures, effects of high-velocity clouds collisions with galactic disks 7-48065
- LkHα 101, VLA obs. of H II region and small-scale struct. in nearby H I 7-48038
- Lyman alpha absorption, correction for effects on observed stellar Lyman alpha profiles 7-60637
- Lyman alpha disk absorbers towards QSOs, surface brightness limits 7-4587
- M16, star-forming complex, obs. of giant stellar wind shell assoc. with H II region 7-18446
- in M33, 21-cm survey by Westerbork Synthesis Radio Telescope 7-66739
- neutral gas shell surrounding H II region, dynamical evolution 7-66692
- in NGC 5023, edge-on dwarf galaxy, H I layer thickness 7-24208
- NGC 55, magellanic-type galaxy, H I and radio continuum obs. 7-9539
- in quasars, H I 21-cm emission obs. 7-48066
- in radio galaxies with OH absorptions H I absorpt. obs. 7-40895
- Southern Milky Way, fully-sampled HI survey 7-40894
- submm spectral characts. 7-48058
- supernova remnants, colliding, oblique shock refls. rel. to anomalous H I vel. features 7-24175
- supernova remnants, H I 21-cm emission during radiative expansion stage 7-60744
- H I bubble around O7 star (HD 91824) in Carina region, prod. by stellar wind of O-type star 7-60760

H II regions

- in CG 1116+51, He in dwarf irregular rel. to primordial abundance 7-55804
- chemistry of interstellar clouds, dynamical perspective 7-24194
- compact galactic H II regions, extinction and reddening anal. 7-60747
- compact H II regions, IRAS meas. 7-66695
- Conference on nebulae and abundances, Austin, TX, USA (April 1986) 7-35096
- cosmological H II regions, dynamics rel. to photoionisation of intergalactic medium 7-40938
- 30 Dor, area spectroscopy of northern part of core 7-66698
- 30 Dor nebula region, LMC, average interstellar UV extinction curve 7-35042
- dust effects 7-40901
- in dwarf irregular galaxies, CNO abundances determ. 7-40939
- in early-type galaxies, H I content versus star form. and ionised gas 7-29528
- element abundances determ., implications of new atomic data for astrophysics 7-40689
- in external galaxies, ANS UV obs. in M31, M33, M81, M101, NGC 2403, and Zwicky galaxies 7-29529
- extragalactic H II regions, abundances and spectra 7-66742
- extragalactic H II regions, collisional effects in He I triplets rel. to primordial He abundance 7-55446
- extragalactic H II regions, modelling rel. to abundances determ. 7-40903
- extragalactic H II regions in SA 94, identifications from objective-prism classification of quasar candidates 7-66779
- extragalactic H II regions, He abundance and dY/dZ meas. 7-40937
- G24.6+0.0 (Scutum ring), obs. of ring of H II regions assoc. with CO and H I shells 7-18447
- G333.3-0.4, low density ionized gas, H166α radio recombination line obs. 7-24190
- G34.3+0.2, compact H II region, NH₃ obs. of warm molecular core 7-24173
- G53.9+0.3, H II ring, WSRT radio continuum map 7-35057
- galactic electron temp. gradient, dust effects 7-48073
- galactic nuclei, 3.28 μm feature and continuum emission obs. 7-9533
- in galactic nuclei, spectroscopic obs. 7-4566
- in galactic nuclei, spectroscopic obs. for complete sample of galaxies 7-40921

H II regions continued

galactic ridge H II regions, low-density envelopes as source of radio recombination lines 7-66718
 in galaxies, H II regions and star form. rel. to Hubble type 7-48084
 giant extragalactic H II regions in nearby galaxies, integrated H α profiles 7-14624
 giant H II regions in Markarian 35 (=NGC 3353) 7-40910
 giant H II regions in primordial galaxies, IR line emission 7-4600
 grains and photoelectric heating 7-18442
 Gum Nebula, globules, dark clouds and T Tau stars 7-55750
 internal motions in H II regions, ordered and random components 7-40902
 LkH α 101, VLA obs. of H II region and small-scale struct. in nearby H I 7-48038
 LMC H II regions, H $_2$ O masers obs. 7-14661
 Lyman alpha disk absorbers towards QSOs, surface brightness limits 7-4587
 Lynds 792, fossil H II region, relation to cometary struct. of nearby dark globule (Lynds 810) 7-24178
 in M101, kinematic detection of supernova remnants in giant H II regions 7-55764
 M16, star-forming complex, obs. of giant stellar wind shell assoc. with H II region 7-18446
 M17, expanding shock-mol. cloud interaction 7-60745
 M17, low density ionized gas, H16 α radio recombination line obs. 7-24190
 M17 (Omega Nebula), H α vel. field 7-66704
 in M81, giant H II regions, radio obs., 7-55798
 M8 E, IR spectrum obs. rel. to evidence for circumstellar CO 7-48040
 in M81, spectrophotometry rel. to O and N abundance gradients 7-40941
 Markarian 306, double nucleus galaxy, spectroscopic obs. of H II regions 7-24199
 in Markarian 490, high ionisation starburst galaxy, spectroscopic and imaging obs. 7-4574
 methyldene (CH), rotationally excited interstellar molecule in direction of W51 H II region 7-24193
 Mon R2 star form. region, IR sources and polarisation obs. 7-60753
 N44C1, LMC H II region, exciting start characts. 7-40892
 nebulous objects in outer Galaxy, catalogue for vel. field in Southern Hemisphere 7-18359
 neutral gas shell surrounding H II region, dynamical evolution 7-66692
 in NGC 1068, high-excitation extranuclear gas, spectrophotometry of Seyfert galaxy 7-24211
 in NGC 1566, barred spiral galaxy, imaging spectroscopy of H II regions 7-24214
 NGC 2024, VLA maps of formaldehyde absorpt. 7-48041
 in NGC 2403, spiral galaxy, chemical comp. gradient and stellar mass limit 7-40940
 NGC 3603, giant H II region, speckle masking obs. of central object (HD 97950) 7-29502
 in NGC 4214, 4449, blue irregular, galaxies, kinematics of H II regions 7-40925
 in NGC 4861, He in dwarf irregular rel. to primordial abundance 7-55804
 NGC 5430, galaxy with Wolf-Rayet knot, stellar population study 7-60778
 NGC 55, magellanic-type galaxy, radio continuum obs. rel. to star form. 7-9539
 NGC 6357, IR obs. rel. to star form. 7-48009
 in NGC 6946, spiral galaxy, catalogue and characts. of 643 H II regions 7-29414
 NGC 7469, type 1 Seyfert galaxy, emission lines mapping rel. to circum-nuclear starburst 7-29536
 optical H II regions, possible connection with mol. clouds, CO obs. 7-40887
 Orion A, He abundance, spectral obs. (Russian) 7-40951
 Orion Nebula, element abundance determ. from IUE lines 7-55784
 Orion Nebula intense 6.7-keV Fe X-ray emission line detect. from high-temp. plasma 7-55780
 photoionisation models, appl. to abundances and ionising star temp. determ. 7-40907
 physical properties and spectral obs. 7-35032
 PK 97+3 $^{\circ}$ 1 (A 77), misclassified planetary nebulae, identification as compact H II region 7-4541
 projection on supernova remnants, new selection effect in statistical investigations 7-24170
 radio recombination line emission 7-60746
 radiosources, VLA survey in outer Galaxy 7-14655
 RCW 74, low density ionized gas, H16 α radio recombination line obs. 7-24190
 Rosette Nebula, assoc. dark globules radial systems 7-4536
 Sh2-235, mol. cloud-ionised emission nebula interface modelling, C recomb. lines obs. anal. 7-48012
 Sharpless 252, assoc. dust and gas, UBVRI polarimetry and molecular line obs. 7-48023
 Sharpless H II regions at 1 \sim 190 $^{\circ}$, eight-colour photometry of assoc. stars 7-55604
 submm spectral characts. 7-48058
 Tarantula Nebula, massive star system of R136a 7-55749
 Trifid reflection nebulae, dust grain characts. 7-35024
 Ursa Major I(S) group galaxies, far-IR obs. rel. to dust and H II regions heating 7-29548
 very low excitation compact nebulae in LMC, UV and optical spectra of exciting stars 7-47883
 W3, assoc. interstellar dust distrib. from stellar colour excesses 7-48004
 W3(OH), hot NH $_3$ obs. towards H $_2$ O masers near W3(OH) 7-9525
 W3 core region, millimetre-wave continuum obs. at 6.5 and 4 mm 7-55781
 W49, exptl. 'zoned relay' obs. at RATAN-600 radio telescope 7-60822
 W51, methyldene detection in direction of W51 H II region 7-24193
 W51, NH $_3$ maser and thermal emission obs. toward star-forming region (IRS 2) 7-66702
 H $_2$ O masers search 7-4539
 He and heavy-element enrichment of interstellar medium, results from H II regions 7-40905
 He ionisation structure in H II region complexes, implications for He/H abundance ratio 7-40906
 O II forbidden lines, improved radiative transition probabilities 7-66442
 OH, obs. of highly excited states towards galactic H II regions 7-24177

Hadfield steel see alloy steel**hadron classification schemes**

nonassociativity as the generating source of the mass levels of hadrons and leptons 7-61637

hadron current

see also *current algebra*
 Skyrme model, expressions for various currents using gauge transformations 7-30162
 $^{12}\text{C}(\bar{p}, \bar{p})$, cross sections, anal. of (0+0 \rightarrow 1+0) isoscalar transition, hadron current structure 7-5228
 $^{14}\text{N}(\bar{p}, \bar{p})$, cross sections, anal. of (1+0 \rightarrow 2+0) isoscalar transition, hadron current structure 7-5228

hadron decay

see also *baryon decay*; *meson decay*
 h \rightarrow lWH, higgs-boson production via bremsstrahlung from heavy quarks 7-41683
 $\pi^+p \rightarrow$ charm hadrons, 360 GeV/c, hadron decay props. 7-562

hadron-deuteron interactions

see also *hadron-deuteron scattering*; *hyperon-deuteron interactions*; *meson-deuteron interactions*; *proton-deuteron interactions*
 hd \rightarrow pX, π rescattering contrib. to p cumulative prod. 7-41861

hadron-deuteron scattering

see also *hadron-deuteron interactions*; *hyperon-deuteron scattering*; *meson-deuteron scattering*; *proton-deuteron scattering*
 Nd \rightarrow Nd, elastic scatt., vector analysing power data 7-61721

hadron electroproduction

$e^+e^- \rightarrow$ hadrons, asymmetries, electroweak radiative corrections, Z_0 resonance 7-15166
 $e^+e^- \rightarrow$ 2 mesons+ γ , high energies, QCD perturbation theory anal., cross sections, wave functions 7-19123
 $e^+e^- \rightarrow$ 3 jets, average hadron multiplicities, total multiplicity formula 7-5105
 e^+e^- annihilation, 29 GeV, p-A corrs., local baryon number conservation 7-49163
 $e^+e^- \rightarrow D^+ (D^0) X$, 29 GeV, lifetime meas. 7-19098
 $e^+e^- \rightarrow e^+e^- +$ hadrons, 7-70 (GeV/c) 2 , photon structure fn. meas. QCD, parton model comparisons 7-540
 $\bar{e}^+e^- \rightarrow f\bar{f}\gamma$, bremsstrahlung amplitude calcs. 7-61712
 $e^+e^- \rightarrow$ hadrons, 35 GeV, α_s determ., corrections to corrected data, second-order QCD anal. 7-30275
 $e^+e^- \rightarrow$ hadrons, total hadronic cross sections, α_s , $\text{Sin}^2\theta_W$ 7-61703
 $e^+e^- \rightarrow$ hadrons, washing out final state interactions for longit. pol. asymmetry 7-24896
 e^+e^- high energy annihilation, quark and gluon fragmentation, Feynman diagrams 7-24901
 $e^+e^- \rightarrow$ jets, geometric struct. anal. review, QED tests, review 7-541
 $e^+e^- \rightarrow \pi^+\pi^-$, $2\pi^+2\pi^-$, $\pi^+\pi^- \pi^0\pi^0$, observation of $\rho'(1600)$ 7-61711
 $e^+e^- \rightarrow \pi\pi\pi\pi$, cross sections, N/D model anal. 7-61739
 eN \rightarrow eA, high Q 2 , N-d form factors, perturbative QCD anal. 7-19119
 $e^+e^- \rightarrow$ hyperons, 10 GeV, obs. of octet and decuplet hyperons 7-61704

hadron-hadron interactions

see also *baryon-baryon interactions*; *hadron-hadron scattering*; *meson-baryon interactions*; *meson-meson interactions*
 backwards evolved initial state parton showers, Monte Carlo model 7-15128
 charm hadroproduction in H and Be, nuclear depend. 7-61719
 European Hadron Facility, conference, Maine, Germany (March 1986) 7-48154
 hadronic systems eqn. of state, S-matrix statistical mechanics formulation, many-particle process effects (Russian) 7-41772
 high energy hadron-nucleus interactions, grey particle energy and angular spectra 7-5246
 high mass dilepton production in hadron collisions, review 7-56574
 hyperon polarization in hadronic collisions 7-35908
 inclusive reactions, numerical results from quasi-nuclear quark model 7-24922
 low transverse momentum transfer reactions, colour superconducting treatment 7-41738
 Monte Carlo simulation of hard hadronic processes, review 7-56563
 nondiffractive hadron-hadron collisions, rapidity dependence of multiplicity distributions 7-61741
 orthogonal lattice gauge field configurations, nucleon-nucleon system 7-41842
 orthogonal lattice-gauge field configurations 7-41841
 P matrix parameters, model calcs. 7-61720
 quark-gluon degrees of freedom, inclusion in hadron-hadron interactions, dispersion approach 7-5008
 short-distance hadronic cross sections, soft-gluon corrections 7-24907
 short-distance hadronic cross-sections, soft gluon corrections 7-41840
 spectroscopy, European Hadron Facility 7-49185
 spin effects in hadronic reactions 7-49184
 ultra-heavy quarks, prod. and decay props., quarkonia prod. in hh and e^+e^- 7-30242
 ultra-relativistic hadronic collisions, pion interferometry in inside-outside cascade model 7-24908
 hh \rightarrow W(Z)+jet, QCD parton shower Monte Carlo model 7-41852
 hh \rightarrow X, approach to chaos in high energy collisions 7-49187
 hh \rightarrow X, central fireball, momentum and mass distrib. 7-41851
 h $_1$ h $_2 \rightarrow$ V(t)X, V(t) $\rightarrow\gamma$, Z 0 , Z $^0 \rightarrow$ ll, weak neutral currents, expt. possibilities, lepton longitudinal polarization 7-5098
 hN $\rightarrow\gamma\gamma_{\text{opp}} + X$, qq $\rightarrow\gamma\gamma$, gg $\rightarrow\gamma\gamma$, qg \rightarrow q $\gamma\gamma$ mechanisms, perturbative QCD anal. 7-61592
 hN \rightarrow h'X, 100 GeV, longitudinal hadron momentum distrib. calcs. and reg-geon, pomeron exchange, quark-parton model anal. 7-61749
 hh \rightarrow X, secondary hadron transverse momentum distrib. 7-41828

hadron-hadron scattering

see also *baryon-baryon scattering*; *hadron-hadron interactions*; *meson-baryon scattering*; *meson-meson scattering*
 elastic scattering, effects on spin asymmetries at 90 $^{\circ}$ 7-30291
 elastic scattering amplitude calcs., model anal. for $\sigma_{\text{el}}/\sigma_{\text{tot}} \rightarrow 1$ 7-61746
 hadron scattering, importance in particle/nuclear physics intersections 7-35892
 high energy hadron scattering, elastic amplitude phase, momentum transfer dependence 7-61745
 large angle scatt., spin effects 7-24912
 scaling and s-channel helicity conservation via optimal state description of hadron-hadron scattering 7-61718

hadron-hadron scattering continued

- spin asymmetries in hadron elastic scatt. at 90° , exchange contribs. 7-30298
 hh-hh, inelastic scatt., flux tube or bremsstrahlung 7-35893

hadron interactions *see hadron-deuteron interactions; hadron-hadron interactions***hadron leptoproduction**

- see also baryon production; hadron electroproduction; meson production*
 No entries

hadron mass

- see also baryon mass; meson mass*
 Friedberg-Lee soliton bag model with iterative one-gluon exchange, hadron static props. 7-49090
 lattice gauge theory, hadron mass calcs., conf., Wuppertal, Germany, Nov. 1985 7-60883
 lattice gauge theory with Wilson fermions, hadron mass calcs. 7-61483
 nonassociativity as the generating source of the mass levels of hadrons and leptons 7-61637
 QCD, quenched lattice approximation, hadron mass calcs. 7-61581
 quenched ACD, chiral props. and hadron spectrum in alternate directions implicit method 7-61577
 quenched QCD hadron mass calcs. on 16^4 spacetime lattice 7-61604
 squared mass spectrum, stochastic approach 7-30261
 stochastic approach, link with quarkonium model 7-49121
 stochastically quantized field theories, hadron mass, energy gap derivation 7-35706

hadron-nucleus reactions

- see also hadron-hadron interactions; hyperon-nucleus reactions; meson-nucleus reactions; nucleon-nucleus reactions*
 charm hadroproduction in H and Be, nuclear depend. 7-61719
 Drell-Yan process, anal. of nuclear A dependence of q,q nuclear density distances 7-49423
 EMC effect, breaking of additivity of nucleons 7-24984
 high energy hadron-nucleus interactions, grey particle energy and angular spectra 7-5246
 multistring models, test of hadron-nucleus and nucleus-nucleus interactions 7-41771
 quasideikonal approximation, cross section calcs. 7-5206
 quasideikonal approximation 7-5206
 superhigh energy cross sections in critical and supercritical Pomeron models 7-19090
 ^{21}Al (hadron, X), 45 MeV, hadron yield meas. for $^{69}\text{Cu}(\text{A,X})$, $\text{A}=\text{He}, ^{12}\text{C}$ (Russian) 7-24987
 ^{12}C (hadron, X), 20 MeV, hadron yield meas. for $^{69}\text{Cu}(\text{A,X})$, $\text{A}=\text{He}, ^{12}\text{C}$ (Russian) 7-24987
 $^2\text{H}(\text{h,pX})$, π rescattering contrib. to p cumulative prod. 7-41861

hadron-nucleus scattering

- see also hadron-hadron scattering; hyperon-nucleus scattering; meson-nucleus scattering; nucleon-nucleus scattering*
 Coulomb phase shift in hadron-light-nucleus scattering 7-24977

hadron photoproduction

- see also baryon photoproduction; meson photoproduction*
 baryon resonance photoproduction, helicity amplitudes in Skyrme model 7-19118
 deep inelastic QED Compton scatt., topological isolation, inclusive cross sections 7-49157
 quark model with charm and colour 7-41737
 $\gamma\gamma$ → hadrons, data compilation, struct. functions, resonance widths, cross sections 7-14722
 $\gamma\gamma$ reactions, inclusive and exclusive final states, jets and total cross sections 7-61783
 $\gamma\gamma^*$ collisions, P_T and Q^2 depend. of multijet prod., 2, 3, and 4 jets 7-5137

hadron production

- see also baryon production; hadron leptoproduction; hadron photoproduction; meson production*
 anomalous correl. between hadrons and electromagnetic particles, Chacaltaya emulsion chamber obs. 7-34816
 cosmological quark-hadron transition, effects on primaeval nucleosynthesis 7-47677
 nucleus-nucleus collisions, ultrarelativistic, hydrodynamical evolution of matter, transverse momentum distribts. 7-19188
 penetrative high energy showers, Chacaltaya emulsion chamber obs. 7-34815
 e^+e^- → hadrons, sub-Poissonian hadronic multiplicity distribts. 7-19121
 e^+e^- → hadrons, superclusters and hadronic multiplicity distribution 7-19132
 e^+e^- → q $\bar{q}g$, parity violating structure function calcs. 7-10067
 $\bar{\nu}\nu$ → hadrons, sub-Poissonian hadronic multiplicity distribts. 7-19121
(p,X), X = hadrons, inclusive process, multi-quark configurations in nuclei 7-61882
pp → hadrons, superclusters and hadronic multiplicity distribution 7-19132
pp → X, impact parameter representation of multiplicity distribts. 7-10080
 π p → hadron jets, 40 GeV/c, jet props., quark, diquark fragmentation 7-61753

hadron scattering *see hadron-deuteron scattering; hadron-hadron scattering***hadron spin and parity**

- see also baryon spin and parity; meson spin and parity*
 spin asymmetries in hadron elastic scatt. at 90° , exchange contribs. 7-30298
 hh large angle scatt., spin effects 7-24912

hadronic atoms

- see also mesic atoms*
 antiprotonic atoms, vacuum polarization effects on l-dependent level shifts 7-5793
 protonium, pp interaction, p parameter/optical model comparisons 7-10069
p atoms, X-ray meas., strong interaction shift, width determ. 7-50404
p-nucleus annihilation, two-nucleon mechanism, cross section, p atoms 7-61880
 ^{14}N , antiprotonic atom, 4f strong interaction level width 7-31191
 ^{23}Na , antiprotonic atom, 4f strong interaction level width 7-31191
O, antiprotonic atom, 4f strong interaction level width 7-31191
 $^{\text{A}}\text{O}$, A = 16,17,18, antiprotonic, strong interaction isotope effects, 3d level shifts and widths 7-5791
T, spin-polarized hypernuclear-atom systems, Efimov effect 7-31189

hadrons

- see also baryon resonances; baryons; hadron classification schemes; hadron current; hadron decay; meson resonances; mesons*
 collective excitations of a superfluid coloured quark liquid 7-5044
 early Universe, bubble growth and droplet decay in quark-hadron phase transition 7-9562
 flux tube model in nucl. matter, EMC effect 7-49272
 hadron fields from anisotropic space, interactions 7-35670
 lattice QCD, light hadron and quark masses, large lattice results 7-15139
 mass spectrum, stochastic approach 7-30262
 nonlocal light-cone hadron operators, one-loop approx. 7-41649
 phase transition between hadron matter and quark-gluon plasma, bag model study 7-41752
 Skyrme model and future directions in hadron spectroscopy 7-35659
 spectroscopy, European Hadron Facility 7-49185
 spectroscopy, gluonic containing hadrons 7-49078
 spectroscopy, particle and nucl. physics intersections conf., Lake Louise, Canada, May 1986 7-29569
 spectroscopy, QCD aspects 7-30245
 static properties, quark bag model 7-41716

haemodynamics

- see also blood*
 aorta, human foetus, interdependence of pulse wave variables, US obs. 7-40198
 aorta, time domain resolution of forward and refl. waves 7-3900
 aortic porcine valves, orifice area flow dependency obs. 7-34185
 arterial bifurcation, numerical simulation of pulsatile blood flow 7-65794
 arterial blood press, and ECG, rhythm anal. 7-54653
 arterial blood pressure and heart rate variability signals, normal and pathological subjects evaluation appl. 7-34312
 arterial blood-flow waveform meas. in intact animals: digital radiographic technique 7-54837
 arterial flow at a 90° bifurcation, effects of nonNewtonian viscoelasticity and wall elasticity 7-3812
 arterial flow in the presence of a stenosis, model 7-34176
 arterial mean pressure, simple device for meas. and for calibration of arterial press. monitors. 7-8731
 arterial occlusive disease, US, diagnosis, some failings of pulsatility index and damping factor 7-47187
 arterial pressure, mean, computer control with Na nitroprusside: adaptive model-based system 7-40359
 arterial pressure pulses, simulations using a transmission line model 7-23388
 arterial pulse as a soliton, nonlinear differential eqn. 7-60023
 arterial system, HF characts., dog obs. 7-28554
 arterial system, human, under periodic body accel., finite element anal. of blood flow through model 7-34178
 arterial vessels, bio-medico-mech. behaviour under constant and variable internal pulsatile press. flow test in vitro 7-65799
 atrial and venous press. waves spectral anal.: methods and results 7-65795
 biochemical and haemodynamic, factors interactions, rel. to transient ischaemic attacks and strokes 7-65786
 blood flow meas. using NMR imaging technique, cardiovascular disease detection appl. 7-54694
 blood gases, effect of ventilation and blood flow in lung 7-34173
 blood oscillatory flow in viscoelastic tube, wave motions near instability limit 7-51316
 blood pressure regulation during surgery using self tuning controller 7-54805
 blood pressure variations playing video games (French) 7-34171
 blood rate detector, one chip VLSI implementation using PPL 7-65881
 blood-rate detector, one-chip VLSI implementation using PPL 7-28756
 brachial artery, Doppler US vel. waveforms, vector based approach to age-related changes 7-65822
 brain, regional cerebral blood flow, meas. method for freely moving, unstressed rats 7-28790
 brain, regional cerebral blood flow meas. by ^{133}Xe , Alzheimer's disease diagnosis appl. 7-28676
 brain tumors, regional cerebral blood flow meas. obs. 7-23390
 cardiac arrhythmia haemodynamics, simulation with a real-time computer model 7-3826
 cardiac indices meas. from freq. transformed TAV Doppler US signals 7-28626
 cardiac left-to-right shunts, quantitation using digital subtraction angiography 7-40285
 cardiac output determination, first-pass radionuclide, effect of region of interest selection 7-40256
 cardiac output monitoring by impedance cardiography during treadmill exercise 7-28733
 cardiovascular models for real time applications 7-34094
 carotid artery blood flow: single factor classification of Doppler waveforms 7-3844
 carotid siphon model, pulsatile blood flow anal. 7-40197
 Casson's fluid, pulsatile flow through stenosed arteries with appls. to blood flow 7-40186
 cerebral blood flow meas. using ^{133}Xe inhalation and dual detectors (Chinese) 7-8629
 cerebral blood flow measurement, indicator elution curves analysis by microcomputer 7-40389
 cerebral blood flow measurement, multicompartment analysis of trace clearance 7-18010
 cerebral blood-flow meas. in ventilated premature babies, ^{133}Xe , inhalation system 7-23434
 cerebral circulation in man, global math. model 7-40193
 colour display of quantitative blood flow and cardiac anatomy in a single NMR cine loop 7-60065
 common carotid artery, vol. flow meas. with duplex scanning 7-18036
 computerized autoradiographic technique for the simultaneous high-resolution mapping of myocardial blood flow and metabolism 7-60113
 conference on biomechanics, Mons, Belgium (Sept. 1986) (French) 7-9578
 control systems, closed loop identification 7-60027
 coronary arteries microembolisation, computer simulation of hyperemic flow 7-18007
 coronary blood flow, absolute, online computer meas. using a H_2 dilution catheter 7-28742
 coronary blood vel., phasic, clinical assessment using digital subtraction angiography 7-3873

haemodynamics continued

coronary sinus haemodynamics in transient ischaemia 7-40205
 critical and emerging issues in artificial organs 7-65807
 CW Doppler US spectra, comparison with spectra derived from a flow visualisation model 7-14071
 diastolic arterial press. in human fingers, meas. method using vol. oscillometry 7-3915
 Doppler US blood flow meas., error bounds 7-8672
 exercise test protocols for haemodynamically compromised subjects, digital filtering and data processing 7-8727
 femoral artery branch model, phasic and spatial press. meas. for pulsatile flow 7-8634
 flow imaging by cine mag. resonance 7-14083
 flow parameters estimation using pulse Doppler US with corrections for spectral broadening 7-8671
 flow phase detection on digital subtraction angiography 7-47257
 flow velocity meas. in intraarterial digital subtraction angiography, pulsed-injection method 7-14128
 flow/haematocrit relationship in larger blood vessels, changes, rabbit obs. 7-3814
 flush-mounted hot film anemometer accuracy in pulsatile flow 7-8735
 forearm, blood flow response to local temp., effect of nerve block 7-8532
 heart, artificial, adaptive control technique, rel. to blood press. and flow 7-3933
 heart rate and arterial blood press. variability signals, auto-spectral and cross-spectral anal. 7-47270
 heart rate and blood press., closed-loop identification of beat-to-beat interactions 7-8640
 Hofkessel: an artificial afterload for cardiovascular research 7-18096
 instantaneous flow, estimation from indicator-dilution curve after bolus injection of indicator 7-65867
 intravascular signal in NMR imaging: differentiation of blood-flow signal from intraluminal disease 7-28652
 IR fibre optic device for cardiac cycle timing and photoplethysmography 7-3856
 kidney, artificial, press. losses in apparatus with capillary channels made of semipermeable film 7-28772
 left ventricle and aorta of chronically instrumented dogs, beat-to-beat anal. of high-fidelity signals 7-18008
 left ventricular assist device, pulsed US Doppler rel. obs. 7-8667
 left ventricular ejection fraction, continuous monitoring using a miniature NaI detector and microcomputer 7-34305
 left ventricular ejection fraction calc. through anal. of model, effect of scintigram background correction 7-54728
 mass transfer in fluids flowing through rot. nonaligned straight tubes, medical device appl. 7-65803
 measurement using scanning X-ray imaging system 7-40266
 median eminence microvascular, 3D reconstruction 7-34356
 MHD oscillatory flow through channels of variable cross section 7-28551
 microcirculation pressure meas., math. model of transducer (*Chinese*) 7-28784
 microcomputer-assisted haemodynamic and respiratory monitoring 7-40329
 myocardial infarction, acute, computer-aided decision in haemodynamic-based treatment 7-40360
 neonatal haemodynamics assessment, use of Doppler US 7-28629
 neuroradiology, transcranial Doppler sonography rel. to angiography 7-18035
 NMR angiography, methods that create projection images based on flowing blood 7-14080
 NMR tomography, phase encoding method using a slice selection gradient for high speed flow vel. meas. 7-23426
 non-invasive ultrasonic method for blood flow and pressure measurements to evaluate the haemodynamic properties of the cerebro-vascular system 7-54646
 ophthalmic diagnosis use of blood circulation meas. 7-8746
 oscillometric determination of diastolic, mean and systolic blood press., numerical model 7-65805
 photoacoustic effect in flowing blood stream 7-44695
 plasmapheresis, increase of filtration by pulsatile blood flow (*French*) 7-3930
 plethysmograph for meas. of digital blood flow 7-40324
 poststenotic coronary flow, assessment of changes by computer anal. of digitised coronary angiograms 7-28687
 poststenotic flow disturbance in dog aorta as measured with Doppler US 7-8668
 pressure measurement in postoperative hypertensive patients, comparison of intra-arterial and automated oscillometric methods 7-34297
 pressure sensor for fibrillation detect. method, implantable defibrillator output circuit evaluation (*Japanese*) 7-14160
 pressure signals, continuous long-term, decomposition into root components 7-34311
 prosthetic heart valve, Ionescu-Shiley aortic, in vitro vel. obs. downstream 7-3936
 prosthetic heart valve test apparatus, microcomputer-based data acquisition system 7-40364
 pulmonary blood flow, estimation by single-breath method, anal. 7-8622
 pulsatile flow through a transverse clip stenosis, rat obs. 7-14038
 pulse blood flow of limbs, quantitative eval. using rheography 7-40352
 regional flow meas., theoretical anal. of transient clearance method 7-28736
 regulation modelling 7-54667
 regurgitant flow through heart valves: hydraulic model applicable to US Doppler meas. 7-28563
 retinal blood flow visualisation and meas. by laser speckle photography 7-47212
 review, flow in tubes and arteries: a comparison 7-3815
 skin and RIF-1 tumour of mice, heat-induced changes, quantification by laser Doppler flowmetry 7-65711
 spleen haemodynamics, quantitative evaluation from radiocolloidal dynamic scintigraphy 7-3865
 steady-state macromolecular transport across a multilayered arterial wall, math. model 7-65793
 stenosis and bulb induced spectral changes in CW Doppler US, in vitro obs. 7-65821
 superior vena caval blood flow vels. in adults, Doppler echocardiographic study 7-8623
 synchronous HF jet ventilation during acute hypovolemia, haemodynamic effects, dog obs. 7-8616
 thermal pulse decay method for simultaneous meas. of local thermal cond. and blood perfusion 7-8734

haemodynamics continued

thin-walled collapsible tubes, self-excited oscills., blood appl. 7-3827
 thrombi, haemodynamic and embolising forces, effect of pulsatile blood flow 7-28555
 time-of-flight NMR flow imaging: selective saturation recovery with gradient refocusing 7-14095
 toroidal rotary seal of IBM 2997 continuous flow cell separator, vels. and stress levels of axisymmetric azimuthal flow 7-3907
 transcranial Doppler sonography, exam. technique and normal reference values 7-14070
 ultrasound diagnosis advances, human blood flow meas., conf., Dubrovnik, Yugoslavia (Sept. 1985) 7-25
 umbilical artery, Doppler US indices derived from max. vel. waveforms 7-47185
 umbilical artery, Doppler US indices derived from mean vel. and first moment waveforms 7-47186
 US Doppler flowmeter for use in theatre 7-47188
 US Doppler signals of blood vel. and adaptive filtering 7-8670
 vascular and urethral parameters meas., microprocessor-based signal processing system 7-54686
 velocity profile measurement by ultrasound Doppler shift method 7-37585
 velocity waveforms of superior mesenteric artery, pulsatility index, Doppler US obs. 7-28565
 venous pressure in microgravity 7-8721
 ventricle, method for computing flow fields around moving bodies 7-65789
 ventricular pressure-volume relationships, automated anal. by digital ventriculography 7-28692
 volume flow in human common femoral artery. meas. using a duplex US system 7-28630
 whole-body γ -irrad., changes in ECG and haemodynamics (*Russian*) 7-8659

haemoglobin see proteins**haemorheology see biorheology; blood****hafnium**

see also nuclei with

Aegean arc, recent magmatism, geodynamics and isotope geochemistry 7-23589
 etching by photochem. machining 7-22909
 film, sputtered in oscillatory electron discharge, structural features 7-12548
 high-temperature corrosion film characterization using Raman microscopy 7-46772
 surface nitridation by powerful CW CO₂ laser irradiation in air 7-2051
 valve metal, corrosion under influence of Pu, oxide layer formation 7-17699
 Cu-Hf multilayers, interface EXAFS study 7-64811
 Hf:Ne⁺, ion implantation in elemental solids, range profile, gamma-ray spectra 7-2959
 Hf/Si amorphous multilayer X-ray reflectors, layer imperfections effects 7-25936
 Hf-Si multilayers, X-ray optical props. rel. to layer imperfections 7-37097

hafnium alloys

see also hafnium compounds

V-Hf-Zr-Ta C-15 phase superconducting alloys, phonon props., inelastic neutron scatt. spectra 7-51969
 Al-Hf dilute quenched cold-worked alloys, vacancy migration recovery processes, PAC and positron annihilation studies 7-39545
 Al-Zn-Mg-Cu-Hf, microalloying effect on struct. and mech. props. 7-53755
 AuHf, heat of form. and cryst. struct., linear augmented STO calcs. 7-51705
 Co-Cr-Al-Hf, high temp. oxidation rel. to alloying additions, ion implantation, Rutherford backscatt. 7-53987
 Cu₅₇Hf₄₃ amorphous alloy, local Hf environment, TDPAC spectra study 7-32303
 Hf-Os, electronic, mag., supercond. and glass forming ability rel. to stability 7-38846
 HfCo₂₊₅ C15 Laves phase system, ferromag. props., comp. depend. study 7-7490
 Hf₂Co, surface oxidation, XPS 7-8184
 HfCo(Ni)Sn, Pauli paramagnet, mag. suscept. and cryst. struct. determ. (*Russian*) 7-1952
 Hf_{1-x}Cu_x metallic glass, thermal stability and phase transformations 7-21125
 HfFe₂, electronic struct. and mag. props., tight-binding approx. calcs. 7-2475
 HfNi, amorphous phase form. by solid-state reaction, dominant moving species 7-21706
 Hf_{1-x}Pd_x(Rh)₂H₂, crystal-amorphous transformation, thermodynamics and kinetics 7-21108
 HfPt, electronic struct. calcs. 7-45200
 Nb-Hf-B system, phase equilib. in Nb corner 7-46415
 Nb-Hf-Ta-O dilute alloy system, O-induced nonaxially symmetric elec. field gradient, TDPAC meas. 7-12686
 Ni-Cr, wrought, Hf effect on struct. and mech. props. 7-33689
 Ni₃Al-B-Hf alloys, B and Hf grain boundary segregation, ductility, atom probe HF study 7-33675
 Ni₃AlHfB/Ni couples, up-hill Hf interdiffusion studies 7-12378
 Zr₆₈Hf₃₂Cu₃₀ amorphous and cryst. alloy, elec. field gradient, TDPAC meas. 7-2958

hafnium compounds

see also hafnium alloys

HfRuSi, equiatomic ternary silicides, superconductivity, rel. to cryst. struct. 7-6607
 HfTe₂, electronic props. 7-2610
 Hf-Mo-N, phase equilibria between high melting nitrides and refractory binder metals 7-28018
 Hf-N coatings on high-speed steel substrates, characterisation by Auger electron spectroscopy and X-ray photoelectron spectroscopy 7-53982
 HfB, electronic struct., chem. bonding, Green's function methods 7-58741
 HfC, HfN, refractories, basic props., survey 7-64883
 HfC tool coatings, wear resistance, mechanistic model calcs. 7-53915
 HfC₂N_{0.93}-xO_{0.07}, thermodynamic props. in temp. range 298 to 1500 K 7-44854
 HfGeO₄, cryst. struct. determ. 7-26718
 HfN films, colour, aging and tempering effects 7-46159

hafnium compounds continued

- HfN, sputtered coatings, wear and friction 7-33800
 HfN, vibrational entropy 7-6745
 HfN(C) reactively sputtered wear resistant coatings, struct., hardness and adhesion props. study 7-52330
 HfO₂, laser evaporation, luminescence of generated plasma 7-63354
 HfO₂-Ln₂O₃, (Ln=Y,Gd,Tb,Er,Yb), solid soln. single crystals, physicochem. props. 7-2097
 HfO₂-MgO system massive vacuum condensates, structure (Ukrainian) 7-12527
 HfO₂-R₂O₃, R=Sc, Y, Nd, Gd, Tb, Er, Yb, solid solution single crystal growth 7-7838
 HfOsSi, equiatomic ternary silicides, superconductivity, rel. to cryst. struct. 7-6607
 HfRhSi, equiatomic ternary silicides, superconductivity, rel. to cryst. struct. 7-6607
 HfTe₅, Fermi surface, effective masses, energy bands, determ. from Schubnikov-de Haas effect 7-64051
 HfTe₅, unit cell dimensions and positional parameters, powder X-ray and neutron diffr. studies 7-16527
 HfU₂S₅, mag. props. 7-22120
 K₂HfF₆, polymorphism, TDPAC investig. 7-2188
 Li₂HfF₆, hyperfine interactions, temp. depend. 7-12679
 (NH₄)₂HfF₆, thermally activated α - β transition 7-12258
 Na₂Hf₂Ge₂O₁₂, ionic conductor, hydrothermal crystallisation and cryst. struct. 7-37935
 Sr_{0.2}Hf_{0.8}O_{1.8} solid soln., enthalpy of form. 7-3600
 TiHfC tool coatings, wear resistance, mechanistic model calcs. 7-53915

half adders *see adders***half-lives (radioactive)** *see radioactive decay periods***half wave rectification** *see rectification***half wave rectifiers** *see rectifiers***halides**

- see also compounds of individual elements, e.g. "tungsten compounds" and "organic compounds"*
see also alkali metal halides; halogens
 chloride-inert gas excimers, interaction with simple cryogenic liquids 7-42776
 fluoride-inert gas excimers, interaction with simple cryogenic liquids 7-42776
 ions, adsorbed on Cu electrode, electoreflectance obs. 7-13132
 lamellar, incipient triple point in physisorbed inert gas films 7-16722
 metal halides, in double pulse lasers, vapour press. eqn. 7-50542
 organic-inorganic double halides, SHG meas. 7-43227
 solar insolation simulation by compact-source iodide lamps 7-23122
 solid, excitonic processes, book chapters 7-29610
 He-X⁺ (X=halide), gas, interaction pot. 7-19739
 TlBr:I indirect exciton transition, effects of disorder 7-2489

Hall constant *see Hall effect***Hall effect**

- see also quantum Hall effect*
 actinides bulk magnetic and transport props. 7-12953
 Anderson model, transport props. at low temps. 7-27311
 anisotropic composites, kinetic Hall and seebeck coeffs., critical behaviour calcs. 7-45411
 Couette flow with heat transfer, Hall effects 7-37554
 disordered metal-nonmetal mixtures, percolation, anisotropic conductivity, Hall effect, thermopower 7-52555
 double layer thin films, Hall coeff. 7-12740
 drift velocity, direct demonstration using the Hall effect 7-48229
 electron gas, two-dimensional, correlation functions and Laughlin quasiparticle operators 7-16965
 graphite:B-Na intercalation cpd., Fermi level displacement, diamag. anisotropy and Hall effect meas. 7-16933
 graphite films, pyrolysed from polyoxadiazole condensation polymer, elec. and thermal props. 7-2736
 graphite-AsF₅ intercalation cpd., galvanomag. props. 7-58822
 HfTe₂, electronic props. 7-2610
 hydromagnetic channel flow in inclined magnetic field, Hall effects 7-51334
 hydromagnetic free convection flow along porous plate with mass transfer, Hall effects 7-63141
 II-V semiconds., cryst. growth, characterisation and appls., review 7-26685
 III-V semiconductors, carrier concentration and mobility profiling 7-45315
 III-V semiconductors, Hall effect in semiconductor assessment 7-17041
 InP:Si, ion implanted, rapid thermal annealing and solid phase epitaxy 7-21296
 low field Hall effect, self-dual fractal models near percolation threshold 7-12699
 measurement in diamond anvil high-pressure cell 7-30041
 mesoscopic systems, transport props., book contrib. 7-52553
 metal foils and films, Hall effect and magnetoresistance 7-52575
 metal-Hall insulator transition 7-52708
 plasma, mag. relax. Hall effect 7-57988
 quasi 2D quantum wells, linear and nonlinear electrical conduction 7-64331
 semiconductors, acoustical Hall effect 7-58823
 semiconductors, Hall effect, finite element simulation 7-21940
 SOI films, inhomogeneous carrier transport props., influence of temp. 7-33094
 SOS, ion beam improved, elec. characts. 7-17114
 stellar atmospheres, Hall current effects 7-18401
 (TMTSF)₂PF₆ field induced quantum oscillations, Hall effect studies 7-45280
 (TMTSF)₂ClO₄, mag. field induced phases, phase diagram studies 7-45752
 (TMTSF)₂PF₆, Hall effect study of field-induced stabilities at 10.5 kbar 7-7214
 (TMTSF)₂ReO₄, Shubnikov de Haas oscils. and (0.1/2 1/2) anion ordering 7-45281
 (TMTSF)₂X Bechgaard salts, field-induced phase transitions 7-45409
 (TMTSF)₂X salts, quasi-1D, cascade of field-induced SDW phases 7-45701
 transition metal disilicide films, electrical transport props. 7-58908
 transition metals, resistivity and superconducting transition temp. 7-17013
 two-dimensional carrier systems, parallel transport 7-52827
- Hall effect continued**
 two-electrode semiconductor systems, electric field, resistance and current distrib. calc. 7-38600
 weakly disordered polycrystalline systems, nonlinear conductivity, Hall effect 7-38594
 Ag₂S(Se)-Ag₂Te(Se) liq. and glassy semicond., activation energy of carrier thermal generation, elec. meas. 7-17035
 Ag₂S(Se)(Te)-Cu₂S(Se)(Te) liq. and glassy semicond., activation energy of carrier thermal generation, elec. meas. 7-17035
 Ag_{1/3}TiS₂ intercalation cpd., transport and mag. props. 7-52572
 Al-base icosahedral alloys, elec. resist. and Hall coeff. studies 7-27316
 AlGaAs superlattices, donor state instability, DLTS and Hall meas. 7-12663
 AlGaAs-GaAs heterostructures, organometallic VPE grown, galvanomagnetic effect 7-12800
 Al_{1-x}Ga_xAs:Be epitaxial layers, ion implanted, rapid thermal annealing 7-21257
 Al_{1-x}Ga_{1-x}As:Te, low press. OMVPE, Te doping, Hall effect, carrier conc., photolum. 7-21242
 AlGaInAs layers on InP, LPE growth 7-33608
 Al_{1-x}Ga_{1-x}N MOVPE growth, struct. and elec. props. 7-21729
 AlN films, OMVPE, Hall mobilities, impurity band 7-39410
 Ba(Bi,Pb)O₃, semiconducting props., X-ray powder diffr. and transport meas. (Japanese) 7-64237
 Bi-Sb:Te(Sn) thin films, elec. props 7-64376
 Bi₂GeO₂₀ piezoelec. semicond., photovoltaic displacement current, Hall component meas. 7-64286
 Bi₂Te₃ doped crystals, energy formation of antisite defects 7-21204
 (CdHg)Te, LPE growth, use of in-situ wash melts 7-59466
 Cd_{0.1}Hg_{0.9}Te, galvanomagnetic props., effect of US treatment 7-38593
 Cd_{1-x}Hg_xTe, abrupt interfaces using thermal and photo-MOVPE, Hall meas. 7-27917
 Cd_{1-x}Hg_{1-x}Te, LPE and MOVPE grown, elec. props. and annealing 7-53512
 Cd_{1-x}Hg_{1-x}Te MOVPE layers, elec. props. and Hall effect behaviour 7-27444
 CdIn₂O₄ RF sputtered films, transparent heat mirror characts., elec. and optical meas. 7-39199
 CdIn₂O₄ thin films, DC reactive sputtered, elec. and optical props. 7-38788
 n-Cd_{1-x}Mn_xSe, magnetoresist. and Hall effect meas. near metal-insulator transition 7-12741
 CdSe crystals, laser beam defocusing, rel. to Hall mobility and carrier density 7-52652
 CdSe, optimally annealed in molten Cd, DC galvanomagnetic props. 7-27352
 CdSe,Te_{1-x} inhomogeneous solid soln., semicond. films; Hall effect temp. depend. meas. 7-58915
 Cd₂SnO₄ transparent thin film electrodes prepared by DC reactive sputtering from Cd-Sn alloy targets 7-22477
 p-CdTe, complex-formation processes at high concentrations of intrinsic defects 7-37963
 CdTe grown on Si by LPMOCVD, physical props., Hall meas. 7-27181
 CdTe-HgTe superlattices, IR material characterisation, transport phenomena anal. 7-64338
 Ce intermetallic cpds., Hall effect meas. 7-12702
 CeAl₃ Kondo lattice, coherent regime, Hall effect temp. depend. study 7-52581
 CeAl₃ nonmagnetic Kondo lattices, coherent regime, Hall effect temp. depend. meas. 7-52582
 CeCu₆, heavy fermion system, temp. and mag. field depend. of Hall effect 7-2579
 CeCu₆, heavy-fermion material, coherent and incoherent behaviour, Hall effect and magnetoresist. 7-32992
 CeCu₂Si₂ nonmagnetic Kondo lattices, coherent regime, Hall effect temp. depend. meas. 7-52582
 Ce_{0.8}La_{0.2}Al₃ nonmagnetic Kondo lattices, coherent regime, Hall effect temp. depend. meas. 7-52582
 CeSi₃, galvanomag. and thermoelec. props. 7-38537
 Co-transition metal amorphous films, mag. and galvanomag. props. 7-53079
 CoFeSiB inhomogeneous magnetic alloys, anomalous Hall effect-magnetic polarisation corrls. 7-7208
 CoSi₂, thin film, electrical transport props. 7-27442
 Cu-Mg amorphous alloys, 2D weak localisation effects 7-21871
 CuBe, scatt. anisotropy of conduction electrons 7-38536
 CuFe alloys, anomalous Hall effect 7-52577
 CuInSe₂, flash evaporation, elec. and optical props. 7-7892
 CuInSe₂ thin films, polycrystalline, elec. props., effect of excess Cu 7-52871
 DgTb amorphous ferrimag. anisotropic films, Hall voltage polarity voltage and temp. depend. studies 7-7206
 Fe, Hall effect, anomalous, and energy band struct. (Russian) 7-52414
 Fe_{5.85}Co_{7.15}Mo₂B₁₅Si₅ amorphous ribbons traversed by DC electric currents excess resistance, collective motion of ferromag. domain walls 7-32989
 Fe_{1-x}Si_x amorphous films, Hall effect and mag. anisotropy 7-2911
 GaAs:Be, MOVPE, diethylberyllium dopant source, elec. characts. 7-22521
 GaAs, atomic layer epitaxy growth, photolum., Hall meas. 7-22527
 n-GaAs compensated samples, MOVPE grown, Hall effect meas. 7-27348
 GaAs, electron beam irr., carrier density, anomalous temp. depend. 7-52610
 GaAs epitaxial films, MOCVD growth using tertiarybutylarsine source 7-59439
 GaAs epitaxial layers, MOCVD grown, influence of growth parameters on residual impurities 7-7047
 GaAs films on oxidised Si, zone melting recrystallisation 7-38396
 n-GaAs, Hall factor calcs. 7-52657
 GaAs, horizontal Bridgman growth, semi-insulating props. characts. 7-64896
 GaAs, hydride VPE layers, deep level incorporation and background doping 7-17120
 GaAs LEC substrates, EL2 deep donor kinetics under annealing, IR absorpt., DLTS, Hall effect meas. 7-32955
 GaAs, MBE growth, acceptor impurity background reduction 7-3173
 GaAs MESFET and JFET devices, elec. resist., Hall effect, influence of electronic subband mag. depopulation 7-38740
 GaAs, mixed electron-hole conductivity 7-58808

Hall effect continued

GaAs, neutron transmutation doped, thermal annealing effects, channelling anal. (*Chinese*) 7-12178
 GaAs, photoconductivity and Hall voltage kinetics, recombination and scattering centre recharging 7-27364
 GaAs, plastically deformed, Hall effect meas. 7-27351
 GaAs, semiconducting/semi-insulating reversibility 7-21939
 GaAs thin films, on glass substrates, transport props. 7-2742
 GaAs, undoped semi-insulating, dislocations, deep trap levels, FET meas. (*Chinese*) 7-12643
 GaAs, uniformity imaging 7-32481
 GaAs, VPE growth in hydride system, elec. props. 7-2751
 GaAs: Si(Si₂(Zn)(Be), ion implanted, rapidly annealed, damage removal process 7-17043
 n-GaAs:Co, impurity double acceptor state, Hall effect and resistivity meas., temp. and press. depend. 7-12656
 GaAs:Cr, deep levels characterisation using photo-induced transient spectroscopy 7-16973
 GaAs:Er MBE layer, dopant trapping level, photolum. obs. 7-44581
 GaAs:Mg²⁺, formation of p-type layers using ion implantation and rapid thermal annealing 7-45311
 GaAs:S layers obtained by gas-phase epitaxy, electrophysical props. 7-7418
 GaAs:S surface elec. props. modification by plasma exposure 7-27346
 GaAs:Si,Be, MBE, dopant interaction 7-52362
 GaAs:Si(Be)(Mg), rapid annealing, temp. depend. of damage removal and carrier activation 7-17032
 GaAs:Sn epilayers, MOCVD using triethylgallium and tetraethyltin, characterisation 7-22515
 GaAs:Sn LPE layers, heavily doped, Mossbauer study 7-38967
 GaAs:Te, low press. OMVPE, Te doping, Hall effect, carrier conc., photolum. 7-21242
 GaAs:Zn epilayers, metalorganic CVD, Zn incorporation 7-63996
 GaAs:Zn(Cd) epilayers, low pressure MOCVD growth, impurity incorporation 7-59442
 GaAs/Al_{1-x}Ga_xAs modulation doped heterostruc., high temp. annealing effects (*Chinese*) 7-12805
 n-GaAs_{1-x}Sb_xP_y epitaxial film, impurity distrib., cond. and Hall mobility study 7-51808
 Ga_{0.47}In_{0.53}As-InP heterojunction, with three electron subbands, hydrostatic press. effect 7-2695
 Ga_{1-x}In_xAs/InP heterostructures, MOVPE, electron mobility, exciton peak, magnetotransport 7-58883
 GaInP-AlGaInP-GaAs heterostructures, MOVPE, Hall effect, photolum. 7-39401
 n-Ga_{1-x}In_xSb:Se(S), impurity states, press. and comp. depend., Hall coeff. and elec. resist. meas. 7-2533
 GaN films, epitaxial growth by reactive ion plating, elec. props. 7-3206
 GaN films, OMVPE, Hall mobilities, impurity band 7-39410
 GaP LPE layers, reuse of Ga melt for LED prep., effect on electrical characts. 7-22592
 GaSb+GaV₃Sb₅, eutectic alloys, elec. props., anisotropy 7-12717
 GaSb+V₂Ga₃, eutectic alloys, elec. props., anisotropy 7-12717
 GdCo(Fe) amorphous films with perpendicular anisotropy, Hall loop meas., mag. struct. studies 7-7205
 GdNi amorphous ferrimag. anisotropic films, Hall voltage polarity voltage and temp. depend. studies 7-7206
 Ge, drag thermoelec. power, anisotropy parameter, carrier density depend. 7-38603
 p-Ge, Hall effect, mag. field and temp. depend., transport eqn. soln. 7-52651
 Ge, MBE growth on CaF₂/Si (111), structural and electrical characteristics 7-45051
 Ge, n-type and ultrapure samples, electron transport and press. coeffs. 7-2615
 n-Ge, room temp. anomalous Hall effect 7-38595
 p-Ge:As, Hall effect and electrical conductivity, temp. corrections 7-38592
 n-Ge:Au, electron heating, photocond., photo-Hall effect 7-12765
 Ge:Ga(Be)(Zn) extrinsic photoconductor material, cryst. growth and characterisation 7-64893
 Ge:P crystals, seeded growth in soft lined crucible, dopant distrib. 7-53559
 n-Ge:Sb, electron heating, photocond., photo-Hall effect 7-12765
 Ge:Sb(Al)(Ga)(In), heavily doped, charge carrier scatt., elec. cond., Hall effect meas. 7-7228
 GeTe, solid and liquid states, electrophysical props. 7-52654
 n-HgCdTe, acceptor densities, photo-Hall determ. 7-58836
 HgCdTe epitaxial layers and structures, characterisation of intentional dopants 7-12552
 HgCdTe epitaxial layers, Hall effect and elec. resist. characterisation 7-64375
 p-HgCdTe, minority carrier characterisation using light-modulated Hall effect 7-21934
 p-Hg_{0.78}Cd_{0.22}Te:Sb LPE films, elec. props. 7-7426
 Hg_{0.79}Cd_{0.21}Te, metal-insulator transition, mag. field induced, low temps. 7-45158
 Hg_{0.8}Cd_{0.2}Te:Cu, activation energy of Cu shallow acceptors 7-64153
 Hg_{1-x}Cd_xTe with metallic donor clusters, anomalous Hall effect below mag. field induced metal insulator transition 7-2485
 Hg_{1-x}Cd_xTe, zero gap, acceptor levels 7-27287
 Hg_{1-x}Mn_xTe, Hall coeff., magnetoresist. meas., exchange interaction, field, temp. effects 7-64270
 Hg_{1-x}Mn_xTe, magnetoresist. meas., effect of valence band spectrum quantisation at low temps. 7-52653
 Hg_{1-x}Mn_xTe, spontaneous Hall effect studies 7-45360
 p-HgTe-CdTe superlattices, magnetotransport props. 7-33076
 HgTe-HgCdTe superlattices grown on lattice-mismatched GaAs substrates 7-52341
 HoNi amorphous ferrimag. anisotropic films, Hall voltage polarity voltage and temp. depend. studies 7-7206
 In single crystal, Hall coeff. anisotropy, Fermi surface effects 7-12701
 InAs, In_{0.9}Ga_{0.1}As, atomic layer epitaxy growth, photolum., Hall meas. 7-22527
 n-InAs, metal-Hall insulator transition 7-52708
 n-InAs:Sn,Te, LPE growth, elec. characts. 7-33603
 In_{0.5}Ga_{0.5}P layers, LPE, elec. and optical props. 7-17119
 InGaAs/InP single quantum wells, transport and persistent photocond. props. 7-27385
 InGaAs-GaAs, quantum well structs., p-type modulation doped, Hall effects, influence of built-in strain 7-7339

Hall effect continued

In_{0.9}Ga_{0.1}P LPE layers lattice-matched to GaAs, Hall mobility meas. and MESFET fabrication 7-7905
 In₂O₃:Sn evaporated films, optical props. and applications to energy-efficient windows 7-46157
 In₂O₃:Sn vapour deposited films, growth, struct., electronic props. 7-12535
 In₂O₃:Sn(In)(Cd) films, optical and elec. props. 7-22365
 In₂O₃·x, Hall coeff., noncritical behaviour at mobility edge 7-32993
 n-InP compensated samples, MOVPE grown, Hall effect meas. 7-27348
 InP epitaxial films, MOCVD grown, identification of acceptors and donors 7-58688
 InP epitaxial layers, MOVPE, elec. characts., photolum. 7-22519
 InP films, hydride VPE, impurity incorporation, defect charactn. 7-53614
 InP films on oxidised Si substrate, laser recrystallisation 7-38398
 n-InP, Hall factor calcs. 7-52657
 InP, Hall scatt. factor 7-45361
 InP synthesis by modified horizontal Bridgman method, elec. props. 7-58821
 InP:Fe wafer, semi-insulating, elec. characteristics 7-45323
 InP:Ge, Fermi level, determ. from phase diagram data of InP-Ge system 7-21808
 InP:Ti, Hg, semi-insulating, impurity electron state compensation mechanism, SRS, SSMS, EPR and Hall effect meas. 7-64164
 InP:Yb LPE layers, luminesc. and elec. props. 7-59464
 n-InP:Zn, Zn diffusion 7-63882
 InP/GaInAs/InP heterostructures, OMVPE, high speed p-i-n photodiodes, photolum., Hall meas. 7-27387
 n-InSb low-temp. growth by plasma process (*Japanese*) 7-7061
 InSb, coherent spontaneous oscills. under transverse breakdown conditions, high frequencies 7-17046
 InSb, metal-insulator transition, mag. field induced, low temps. 7-45158
 InSb with metallic donor cluster, anomalous Hall effect below mag. field induced metal insulator transition 7-2485
 InSb:Te, resonance absorpt. of electromag. wave due to impurity band 7-52499
 InSb:Te(Se)(S)(Cd)(Zn) thin films, doping, Hall effect meas. 7-21743
 InSe₂S₃(Li), electrical transport props. 7-21917
 K_{0.9}MoO₃, Peierls semiconductor, nonlinear Hall effect, sliding of CDW 7-45357
 Li₂GaSe intercalation cpd., elec. resist. and Hall effect meas. 7-12719
 Mg-Ga liquid alloys, Hall effect, meas. 7-32991
 Mg₂Si(Ge)(Sn)(Pb), Hall effect in solid and liq. states 7-38647
 MoS₂ films, RF magnetron sputtered, elec. and optical props. 7-2747
 NbSe₂, CDW and magnetotransport, mag. field effects to 230 kG 7-64215
 NdZn, antiferromag. skew scatt. Hall effect 7-52578
 Ni, Hall effect, anomalous, and energy band struct. (*Russian*) 7-52414
 Ni₂MnIn(Sb) Heusler alloys, galvanomag. props. and magnetisation meas., fermi level shift effects 7-7207
 NiSi₃, thin film, electrical transport props. 7-27442
 NpAs₂, single crystals, Hall resistivity 7-12739
 PbS, epitaxial film, weak-field magnetoresistance, multi-valley model (*Korean*) 7-33114
 PbSe films, photosensitivity mechanism 7-58923
 PbSe₂Te_{1-x} thin films, localised defect states and Hall effect 7-2752
 Pb_{0.75}Sn_{0.25}Te:In, Ge(S)(Se), elec. resist., photocond., Hall effect meas. 7-17050
 Pb_{1-x}Sn_xTe solid solns., intrinsic defect donor states characts. Hall effect temp. depend. meas. 7-58762
 Pb_{1-x}Sn_xTe:Bi, free carrier density 7-38572
 PbTe, epitaxial film, weak-field magnetoresistance, multi-valley model (*Korean*) 7-33114
 PbTe, solid and liquid states, electrophysical props. 7-52654
 PbTe:Ti(Tl,Na) films, superconducting transition 7-38797
 Pb_{1-x}Te:Ti, quasilocal level and transport props. 7-38492
 PdSiCo inhomogeneous magnetic alloys, anomalous Hall effect—magnetic polarisation corrls. 7-7208
 ReS₂, single cryst. growth by chem. vapour transport, elec. resist., Hall mobility meas. 7-64251
 ReSe₂, single cryst. growth by chem. vapour transport, elec. resist., Hall mobility meas. 7-64251
 Sb₂Te₃ crystal, semimetallic, semicond. behaviour at low temps. 7-12716
 Sb₂Te₃ doped crystals, energy formation of antisite defects 7-21204
 ScN compensated semimetal single crystals, electronic struct., reflectivity and elec. props. meas. 7-27253
 Si (111) in MIS struct., Hall resistivity of 2D electron gas in strong mag. fields 7-7391
 p-Si conductivity and Hall mobility calcs., impurity scatt., anisotropic-nonparabolic effects 7-12720
 Si doping superlattices, anomalous mobility enhancement 7-7381
 Si, epitaxial growth using photochem. vapour deposition at 200°C 7-39431
 Si films, solid phase epitaxial regrowth on epitaxially grown MgO.Al₂O₃ 7-38399
 n-Si, gamma-irrad., intrinsic defects, Hall effect and elec. cond. meas. 7-6615
 Si, MBE growth on CaF₂/Si (111), structural and electrical characteristics 7-45051
 Si, neutron-irradiated, photoluminescence study of annealing process 7-51833
 Si polycrystalline film, mobility temp. depend. (*Chinese*) 7-2744
 a-Si, prep. by low press. CVD, characts. 7-7884
 Si, radiation defect thermal ionisation, effect of dislocations on activation energy 7-6680
 Si, transmutation doped, carrier lifetime and hall effect, high temp processing effects 7-33027
 Si, transmutation-doped, carrier recomb. props. at gamma-irrad. defects, transport meas. 7-38575
 Si:As, ion implanted, electronic transport props. 7-7233
 Si:As films, heavily doped, grown by partially ionised MBE, phys. and elec. characts. 7-12561
 Si:As ion implanted films, defects charactn. by AC Hall effect meas. 7-38601
 Si:As on sapphire, ion beam recrystallised and laser annealed, elec. props. 7-16649
 Si:Au, supersaturated low-temp. substitutional impurities, annealing 7-6665
 Si:B, F implanted amorphous layers, struct. and elec. props., ESR and Hall effect meas. 7-26634

Hall effect continued

- Si:B(Al)(Ga)(P)(Sb) thermal donor props., impurity effects, DLTS, Hall effect, and admittance spectra meas. 7-21851
 Si:Co, impurity energy levels, Hall and DLTS meas. 7-52509
 Si:Er(Dy)(Yb)(Ho)(Gd), neutron irradi., Hall effect, elec. cond., IR absorpt. spectra 7-51834
 Si:H films, ion implant redistribution 7-16921
 Si:O, C, thermal donor form., $T < 800\text{K}$ 7-27294
 P-Si:O, new donor state, optical, elec. and TEM studies 7-32956
 Si:O,B⁺, ion implanted, reverse annealing 7-16617
 Si:P, quenching thermodefect prod. Hall effect, EPR meas. 7-27293
 Si:Sb, pot. enhanced doping during MBE growth, elec., optical props., cryst. quality 7-12112
 Si/Si_{0.5}Ge_{0.5} strained layer superlattices, 2D electron systems 7-7380
 Si-Si_{0.55}Ge_{0.45} modulation doped superlattice, MBE grown, electron mobility enhancement, Hall meas. 7-7382
 β -SiC crystals, free carrier conc., Raman scattering 7-59197
 SiC, cubic, electrically active centres 7-12736
 SiC, cubic, epitaxial films, compensation 7-7268
 Si_xGe_{1-x}Ga, resistivity and Hall constant, temp. depend. 7-7231
 SnO₂F films, CVD growth using hydrofluoric acid as doping material 7-7871
 SnO₂F thin films, CVD deposition, elec. and optical props. 7-7425
 SnTe, conc. depend. props. in region of homogeneity 7-45366
 SnTe, solid and liquid states, electrophysical props. 7-52654
 SnTe:Bi epitaxial layers, vacuum deposition, optical and electrical props. 7-59430
 SrTi_{0.97}Zr_{0.03}O₃ ceramics, superconducting transitions from states with low normal conductivity 7-27452
 SrTi_{0.97}Zr_{0.03}O₃, superconductivity at low carrier conc. and indications of charged Bose gas 7-27453
 Ta-H system, T migration in Hall field, effect of temp. 7-6890
 TaH_{0.015}, ³H migration in Hall field, temp. effect 7-32729
 TbNi amorphous ferrimagn. anisotropic films, Hall voltage polarity voltage and temp. depend. studies 7-7206
 TiN_x epitaxial layers, atomic and electronic struct., growth, physical props. 7-32854
 TiPrSe₂ (Se₂)(Te₂), elec. cond., Hall effect and thermoelec. studies 7-2606
 UBe₁₃, heavy fermion system, unusual low temp. Hall voltage behaviour obs. 7-38540
 V-Si films, electrical transport props. 7-33108
 W single crystals, galvanomagnetic props., low temp. Fermi surface local features effects (*Russian*) 7-27320
 Y₂Co₉, resistivity and Hall effect temp. depend. meas. 7-52568
 Y₂Ni₉, sputtered amorphous film, Hall effect (*Chinese*) 7-64202
 Y₂Ni₉H₂, amorphous thin films, mag. and elec. transport props., H content effect, 1.5 to 400K (*Chinese*) 7-38909
 Yb intermediate valent intermetallic cpds., Hall effect studies 7-12703
 Yb_{1-x}Tm_xSe, anomalous Tm valence, lattice parameters, diamag. suscept. and Hall effect meas. 7-16998
 ZnGeP₂, Hall effect and conductivity in zinc vapours, high temp. meas. 7-27350
 Zn_xHg_{1-x}Se, electrophysical props. and carrier scatt. mechanisms 7-17024
 n-ZnSe, heavily doped strongly compensated crystals, electron mobility 7-7247
 ZnSiP₂ and ZnGeP₂, single crystals, prep. and characterisation 7-2612
 Zr-H system, T migration in Hall field, effect of temp. 7-6890
 ZrH_{0.015}, ³H migration in Hall field, temp. effect 7-32729

Hall effect devices

- digital sweeper and Hall-generator magnetic field stabilizer as combined set for magnetic resonance spectrometers (*Polish*) 7-9862
 steel wire rope, defect detection., Hall effect mag probe 7-33885

Hall effect transducers

- magnetic measuring apparatus for cryogenic electrical engineering installations 7-56308
 manometric thermometers with liquid and Hall transducers, manufacturing possibilities (*Rumanian*) 7-48734

Hall generators *see* Hall effect devices**halogen lamp annealing** *see* incoherent light annealing**halogens**

- see also* astatine; bromine; chlorine; fluorine; halides; iodine
 alkali metal cation-halogen anion microclusters, structs. and energetics 7-8266
 halogen thiocyanates (isothiocyanates), ionis. pots., photoelectron spectrosc. and ab initio calcs. 7-25601

halting problem *see* computability**Hamidashi effect** *see* ferroelectricity**handicapped aids**

- audiobiofeedback system for sensory aid to handicapped persons 7-34344
 critical and emerging issues in rehabilitation engineering 7-65894
 DC motors in wheelchairs and prostheses, switching converters for efficient control 7-34355
 EGG, articulatory function assessment 7-40136
 electronic cochlear neuroprosthesis development, Czechoslovak project 7-8766
 electrooculographic control system, discrete, for severely handicapped persons 7-8736
 eye position controlled communication aid for the disabled 7-47290
 eye word processor and peripheral controller using eye movement (*Japanese*) 7-8764
 functional elec. stimulation hand grasp orthoses, tracking performance 7-28777
 human prosthesis systems, control properties 7-18095
 integrated communication aids for the blind 7-40367
 joint angle sensors for closed-loop control of movements in paraplegics 7-28766
 manipulation aids for handicapped with upper extremity impairment 7-34351
 personal computers for disabled people, UK survey (*Japanese*) 7-40363
 physically disabled assistive devices, speech control 7-37282
 rehabilitation of handicapped, technology, conf., Minneapolis, MN, USA (June 1986) 7-29599
 Rehabilitation R&D Progress Reports 7-28774
 speech communication technology for the disabled and its commercial apps. 7-8598
 speech training devices for profoundly deaf children 7-37278

handicapped aids continued

- speech training systems for handicapped children using vocal tract lateral shapes 7-37279
 three channel cochlear neuroprosthesis for the deaf, implantable receiver/portable transmitter config. 7-8765
 Tri-sensor ultrasonic aid for blind people 7-14157
 vocal synthesis and voice recognition, developments (*Italian*) 7-60123

handling, materials *see* materials handling**Hanle effect**

- collision-assisted zeeman, Hanle reson., transverse optical pumping, relationship 7-10514
 diatomic molecules, Lande g factor and relax. rate of ground state, simultaneous determ. using Hanle effect 7-31120
 resonance scattering spectra appl. to very weak mag. fields diagnostics in diffuse media 7-23991
 Ca, atomic beam, two-photon Hanle effect in Ramsey interrogation 7-15560
 O VI 103.2 nm line polarisation use for coronal mag. field determ. on Sun 7-34958
 P, II levels, hollow cathode discharge, self-alignment and radiative lifetime meas. 7-10678
 Sm, $F_1 \rightarrow F_0^0$ transition, Hanle effect, obs. of incoherent population effect and ground-state incoherence components 7-10515
 Sm, four-wave light mixing, collision-and stochastic-fluctuation induced Hanle reson. 7-15559

hard metals *see* cermets**hard soldering** *see* brazing**hard-sphere fluids** *see* classical theories of fluid structure; liquid theory; quantum theories of fluid structure; statistical mechanics**hardening**

- see also* dispersion hardening; quench hardening; radiation hardening; softening (metallurgical); solid solution hardening; surface hardening; work hardening
 alkali metal halides, hardening, effect of dislocation elec. charge 7-51816
 bearing type, austenite transform. kinetics and internal stresses in bainitic hardening 7-39563
 composite, winding, stress form. in frontal hardening 7-17491
 constitutive equations of hardening, analytical integration, elastic-plastic finite element analysis 7-63016
 creep-plasticity constitutive models suitable for thermal loading 7-51925
 elastic-plastic shrink fit with supercritical interference 7-43662
 epoxy resins, effects of epoxy number and hardener on properties (*German*) 7-22973
 finitely deforming rigid-plastic materials, Lagrangian strain space formulation 7-6109
 gypsum, initial hardening with cement, pulse rheometry investig. 7-37411
 kinematic hardening and large plastic deformations 7-6110
 kinematic hardening in finite deform. plasticity, corotational rates 7-1433
 laser surface treatment, recent developments 7-21274
 materials, transform. toughened, transformed zone size during steady state cracking 7-39641
 metal, cyclic hardening, hardening law and fatigue damage 7-58400
 peroxide urea-formaldehyde oligomers, structurisation, IR spectra 7-39126
 plasticity, cyclic, time-independent constitutive theories 7-1439
 porous ductile material, yield surface curvature and void nucleation effect on plastic flow 7-51919
 rotating elastic-plastic shrink fit with hardening 7-43663
 steel, austenitic, Mn-Cr, hardening characts. and hydroextrusion parameters (*Russian*) 7-59540
 steel, austenitic stainless, dislocation structure and secondary cyclic hardening at 600°C 7-33783
 steel, austenitic stainless, mechanical properties, H effects (*Russian*) 7-46603
 steel, constructional carbon type, original charge purity influence on microstruct. hardenability and mech. props. 7-46521
 steel, Cr-Mo, cyclic stress-strain response at elevated temps. 7-39624
 steel, Cr-Mo-V, porosity assoc. with insoluble carbides, probable effect on rolling contact fatigue 7-17639
 steel, Cr-Si type parts, mag. characts. after isothermal hardening, heat treatment quality inspection method 7-65261
 steel, die, heat-resistant, optimum hardening temps., struct. and mech. props. 7-8022
 steel, die, preliminary heat treatment schedule 7-8023
 steel, low C pearlitic, microstruct.-flow stress relationship 7-33739
 steel, low-C, wrought, thermal strengthening methods effectiveness 7-46524
 steel, low-pearlite, rules of austenite decomp. in continuous cooling 7-3339
 steel, martensitic stainless, low activation, hardening, tempering, mechanical props. 7-53861
 steel, micro-alloyed, low C, B containing, heat-affected zone props. 7-17543
 steel, Mn-V, continuously cooled, hardness rel. to martensite vol. fraction 7-28121
 steel, strengthening of parts and semifinished products in the last stage of heat treatment 7-8024
 steel, superhardenable treated, transform kinetics 7-39535
 steel, tool, 65Nb, tough strengthening heat treatment (*Chinese*) 7-3318
 steel, tool, heat treatment cycles, original struct. and deform. influence on mech. props. 7-39560
 steel structural, powder, hardenability and hardness penetration; effect of comp. and porosity 7-22807
 strengthening diagram, relationship with dislocation kinetics (*Russian*) 7-53753
 time depend. plasticity theory, stress relax., creep, plastic flow 7-43703
 viscoelastic solid growth under frontal hardening conditions, stressed state form. 7-43712
 AgBr-AgI crystals, strain-ageing 7-6627
 AgCl, strain ageing, temp. depend. 7-65065
 Al quenched, tensile flow stress, effect of grain size and strain 7-22756
 Al single crystals, cyclic deform. at low const. plastic strain amplitude 7-65114
 Al-Ag, decay and short-range ordering (*Russian*) 7-44795
 Al-Li-Se, cast, decomp., mech. props., struct. (*Russian*) 7-59532
 Al-Zn, disintegration kinetics, hardening temp. effects 7-52055
 Al₂O₃-H₂O-based heterogeneous monotype systems, hardening and binding props. 7-65052
 Cu-Nb, supercond. composites, low temp. plasticity, annealing hardening, strength (*Russian*) 7-59579

hardening continued

Fe, Armo and Vacofer, yielding behaviour, H influence 7-33753
 Fe-Cr-Ni, hardening at low temp. (*Russian*) 7-39554
 Fe-Ni-Nb alloys, shape memory effect, effect of phase hardening (*Russian*) 7-53809
 Fe₉₃B₂, amorphous alloy, elec. resist. and crystn. on hardening from different temps. 7-44380
 Nb single crystals, cyclic deform., dislocation behaviour 7-63729
 Ni-based consolidated rapidly solidified alloys, strengthening mechanisms 7-22712
 Ni-P alloy electroless deposits, hardening by baking treatments (*Japanese*) 7-33759
 PbO₂-H₂O-based heterogeneous monotype systems, hardening and binding props. 7-65052
 TaC, high temp. hardness, stacking faults, hardening rel. to C diffusion 7-3369
 Ti, hardened from β -region, fine struct. study (*Russian*) 7-32450
 Ti-Al-V (6, 4 wt.%), hardness and alpha/beta ratio, effect of O 7-3430
 WC-Co sintered carbides, X-ray diff. obs. of microstruct. after hardening, optimum heat treatment cycle 7-65063
 Zn, dislocation motion across two-component forest dislocations and point obstacles (*Russian*) 7-58277
 Zn-Al, bicrystals and polycrystals, creep grain boundary strengthening 7-22747
 ZrO₂, tetragonal, ferroelastic domain switching as toughening mechanism 7-33712

hardness

see also abrasion; hardness testing
 alkali metal halide microcrystalline powders, correl. between coloration stability and microhardness 7-32486
 alloys, two-phase, models of tensile behaviour from components 7-46570
 barium oxalate dihydrate single crystals, Vickers microhardness meas. 7-63736
 bronze BrAZh, elec. discharge sintering of powder from swarf, electro-phys. and mech. props., microstruct. 7-27974
 C thin films, RF discharge deposition, mech., elec. and optical props. 7-22509
 ceramic coatings, plasma sprayed on stainless steel, hot isostatic pressing, hardness, bond strength 7-13624
 ceramic eutectic composites, microstruct. and mech. props. 7-64991
 ceramics, engineering, rel. between Rockwell hardness and Vickers hardness (*Japanese*) 7-65140
 charge-induced effect on creep and hardness 7-21598
 cracks, small, ΔK_{th} , effect of hardness and crack geometry (*Japanese*) 7-58405
 crystalline materials, dislocation glide, tension, hardness effects (*Spanish*) 7-51779
 CVD and PVD coatings, structural, mechanical and tribological props. and applications 7-53935
 dimethacrylate paste with silanated silicate particles, photopolymerised, filler influence on fracture 7-3426
 dynamically overloaded cold profiled cylindrical compression springs calc. using Spectrum 48 k (*Croatian*) 7-22705
 Elinvar alloys, dispersion hardening and softening, elastic limit studies (*Russian*) 7-59539
 friction and wear, crit. transition points 7-26853
 haematite, Fe₂O₃, microhardness meas. up to 900°C 7-21343
 hard materials, fundamentals of wear 7-3456
 Inconel 625 matrix-carbide particle composite surface layers, wear resistance improvement 7-53912
 materials selection for hard coatings, multicomponent refractory material systems 7-46668
 metal superlattices, elastic and plastic props. 7-27085
 metal wear resistance, ion implantation and ion assisted coatings 7-3513
 metal/ceramic, diffusion welded layered composites, transition zone metallography, struct., hardness (*German, English*) 7-8226
 metallic superlattices, mech. props. and diffusion 7-52377
 metals, low-melting, microhardness 7-22797
 metals and alloys, plastic deform. in conditions of quasihydrostatics (*Russian*) 7-59586
 mullite-alumina composites, sintering and charactn. 7-3252
 Nimonic 105, Ni-base superalloys, precip. and tensile deform. behaviour 7-65078
 nitride and carbide thin films, high-rate reactive sputtering processes and props. study (*Polish*) 7-33559
 optical coating, improvements from deposition using cryopumps 7-3185
 optical glasses, relative grinding hardness eval. 7-43279
 paraffins, lamellar crystals, microhardness and temp. variation 7-12197
 pineapple leaf fibre reinforced rubber, phys. and mech. props. 7-3378
 polymer surfaces, erosive wear by steel ball blasting 7-3446
 polymer surfaces, IR laser irradiation, physico-chem. and chem. transforms 7-65350
 polypropylene, microindentation hardness and dynamic mech. moduli near glass transition 7-13564
 polysulphide rubber-butadiene-acrylonitrile copolymer/PVC blend, mech. props., ageing and solvent resist. 7-39593
 refractory metal nitride, sputtered coatings, wear and friction 7-33800
 Rene 80, Ni-base superalloy, creep rupture props., influence of coating treatment and directional solidification 7-28116
 sapphire, ion implantation, mechanical surface property modifications 7-32473
 β -sialon composite ceramics, microstruct., hardness, tool appls. 7-65144
 silicate porous glass, wear resistance and grinding hardness, struct. effect, grinding method meas. 7-57614
 steel, austenitic, bombarded with Ar ions, ageing temp. effects on structure, microhardness and sputtering 7-65120
 steel, C, microhardness load depend., influence of surface roughness (*Japanese*) 7-46622
 steel, C-Mn, creep crack growth at 360°C, effect of microstruct. 7-28113
 steel, C-Mn, Nb-modified, creep crack charactn. at 360°C 7-46631
 steel, Cr-Mo, sintered, ageing and steam oxidation, effect of P 7-7930
 steel, CR-Mo-Ni, temper embrittlement, effect of V additions 7-13575
 steel, Cr-Mo-V, ion nitriding charactn. (*Korean*) 7-8162
 steel, die, heat-resistant, optimum hardening temps., struct. and mech. props. 7-8022
 steel, duplex stainless, manual metal arc weld metals, microstruct. and phase transform. 7-59526
 steel, duplex stainless, sintered, mech. props., corrosion resist. and high temp. oxidation resist. 7-7928

hardness continued

steel, ferrite, low activation, correl. of hot microhardness with elevated temp. tensile props. 7-53797
 steel, ferrite-pearlite and pearlite-free, microfracture resistance (*Russian*) 7-33765
 steel, ferritic, HT-9, mech. props. as function of heat treatment 7-53858
 steel, ferritic stainless, 11 MeV proton irradi. behaviour 7-58369
 steel, forged powder, prod. from water-sprayed Astalloy powders, fracture toughness 7-13572
 steel, high speed, powders, transform., struct. and props., prior annealing effect 7-13452
 steel, high speed, service performance rel. to Ca and Zr microalloying 7-3366
 steel, high speed, wear, role of primary carbides 7-33807
 steel, high strength line pipe, H induced cracking susceptibility, comp. and treatment effect 7-39619
 steel, high-speed, ion beam metallurgy processing, influence on surface props. (*Chinese*) 7-53764
 steel, high-speed p/m tungstenless, Mo and V effect on microstruct. and operating props. 7-33788
 steel, HSLA, Ti and Nb additions effect on coarse grained heat affected zone 7-17665
 steel, linepipe weldments, ductility rel. to cathodic protection 7-39578
 steel, low alloy, structural transformations during continuous cooling and isotherms 7-22636
 steel, low C, Al killed sheet, overaging, continuous annealing, carbide precip., hardness (*Korean*) 7-46474
 steel, low C, alloying using high-intensity sources 7-28179
 steel, low C, microhardness, temp. depend in coarse-plastic transition region (*Russian*) 7-46638
 steel, low-pearlite, rules of austenite decomp. in continuous cooling 7-3339
 steel, managing, 18 Ni, erosion, effect of microstruct. and mech. props. 7-22849
 steel, medium C, wear, influences of materials and operating parameters 7-8133
 steel, mild, cold-form-rolled, rotary bending fatigue behaviour (*Japanese*) 7-53866
 steel, Mn-V, continuously cooled, hardness rel. to martensite vol. fraction 7-28121
 steel, Ni-Co-W, managing, martensite isothermal aging, hardness, struct. and elec. resist. kinetic behaviour study 7-17553
 steel, Ni-Cr-based, high temp. strength, modified ausforming effects (*Japanese*) 7-8089
 steel, Ni-Cr-Mn, ferromag., mag. hysteresis loops, effects of grain size, hardness and stress 7-64482
 steel, nitrided layer, hardness distrib. prediction model 7-39746
 steel, nitrided layers, surface strength and hardness prediction 7-3495
 steel, roll type, crack resist. as criterion of effectiveness, alloying and heat treatment parameters influence 7-53884
 steel, secondary hardening, alloy carbide precipitation, FIM atom probe studies 7-33671
 steel, stainless, (Cr,Fe)₂₃C₆ compact specimens, corrosion-electrochem. and phys. props. w.r.t. comp. 7-54000
 steel, stainless, ferromag., mag. hysteresis loops, effects of grain size, hardness and stress 7-64482
 steel, stainless, microstruct., aging effects, atom probe FIM, optical and analytic electron microscopy studies 7-33700
 steel, structural, diffusion chromised, elevated temp. effect on comp., struct. and mech. props. 7-8178
 steel, tool, fracture toughness, effect of nonmetallic inclusions 7-59635
 steel, tool, fracture toughness rel. with grain size 7-59634
 steel, tool, H-13 hot-work, partial substitution of Nb for V 7-13463
 steel, tool, heat treatment cycles, original struct. and deform. influence on mech. props. 7-39560
 steel, tool, high speed, splat quenched, microstruct. variations 7-46439
 steel, wear resist. under wet-abrasive erosion conditions 7-22848
 steel structural, powder, hardenability and hardness penetration, effect of comp. and porosity 7-22807
 steels, C and austenite welded joint, microhardness, effect of C redistrib. 7-13571
 steels, stainless, ion-nitrided, struct. and props. 7-22884
 steels, tool, M2 and H13, fracture toughness, influence of microstruct. 7-46632
 transition metal amorphous alloy coatings, microindentation response, microstruct. and composition effects 7-46625
 Vickers microhardness number derivation from penetration depth calcs. 7-63739
 Ag₂O-Ti₂O₃-B₂O₃ glasses, physical props. and tandem monovalent ions effect 7-3013
 AgX (X=Cl,Br), extruded fibres, optical and material props. 7-37184
 Al, anodising by chromic acid, surface struct., abrasion resist., hardness, adhesion props. 7-13646
 Al, charge-induced effect on creep and hardness 7-21598
 Al, hardness, effect of thermomech. history 7-53873
 Al, repeated cold rolling effect on recrystn. Vickers hardness obs. 7-59543
 Al, shocked, polycryst. positron annihilation ang. correlation studies 7-46197
 Al thin films on Si substrates, plastic props., meas. by submicron indentation hardness, substrate curvature techniques 7-58720
 Al-Ag alloys, isothermal ageing, hardness and creep behaviour 7-8068
 Al-Al₂O₃-MgO, cast particulate composites, microstruct. and mech. props. 7-65086
 Al-based sputtered hard compound films, struct. and props. 7-46318
 Al-Cu (1.87 wt.%), stability of metastable defects at elevated temps. 7-38207
 Al-Cu (3.76 wt.%), rheocast, partially homogenised; ageing response, microhardness 7-46499
 Al-Cu-Mg-Al₂O₃-Al₄C₃, IN 9021, mechanically alloyed precip. hardened, tensile behaviour 7-13525
 Al-Fe-R, R=Ce, Er, Nd or Gd, rapidly solidified microstruct. 7-59502
 Al-Li-B alloys, rapidly solidified, microstruct. eval. 7-22656
 Al-Li-Cu-Mg-Zr powder alloy, superplastic, high modulus and hardness 7-53816
 Al-Mg-Si, Al-Mg, cast, mica particle dispersed composites, struct., strength, hardness 7-59574
 Al-R (R=Er,Nd,Gd) rapidly solidified alloys, microstruct. and thermal props. 7-22667
 Al-Si, talc particle reinforced composites, prep., wear and mech. props. 7-13408

hardness continued

- Al-Si-SiO₂ sand composites, prep. and mech. props. 7-17500
 Al-Si-Zn-Mg-Ti-(Sr) system alloys, mech. props., Sr microalloying effect 7-3377
 Al-Ti, powder metallurgy alloys, mech. and thermal stability 7-64973
 Al-V films, precip. from metastable solid solns. 7-65048
 Al-Zn, disintegration kinetics, hardening temp. effects 7-52055
 Al-Zr-V, rapid solidification, age hardening, solid soln. form. (Korean) 7-46475
 Al₂O₃ CVD coatings, high-temperature microhardness profiles 7-28181
 Al₂O₃ refractory ceramic, wettability and contact angle with Al melt, nitride additive effects (Russian) 7-12402
 Al₂O₃ strengthening, mech. props. and microstruct. (Japanese) 7-22820
 Al₂O₃-SiC composites, microstruct. and mech. props. (Japanese) 7-22821
 Al₂O₃-SiO₂, mullite, prep. by sol-gel method, microstruct. and mech. props. 7-46386
 Al₂O₃-TiC-TiN composite ceramics, microstruct., hardness, tool appls. 7-65144
 Al₂O₃-ZrO₂ composite ceramics, microstruct., hardness, tool appls. 7-65144
 Al₂O₃-ZrO₂ composites, microstruct. charactn. by Raman spectroscopy (Japanese) 7-22684
 As₂Se_{100-x}, chalcogenide glass, Vickers microhardness indentation and fracture mechanics 7-21342
 B fibre reinforced Al matrix composites, transverse mech. props., isothermal exposure effect 7-39688
 BN, cubic, polycryst., influence of sintering conditions on phys. props. 7-22618
 BN, film, optical energy gap, density, hardness 7-39204
 c-BN, high press. sintering 7-22615
 BN polycrystals, heat treatment conditions effect on mech. and service props. 7-53894
 BN, wurtzite compacts, sintered, particle size distrib., hardness, phase comp. 7-59603
 Ba ferrite filled styrene-isoprene-styrene composite, dynamic mech., elec. and mag. props. 7-13001
 Bi alloy impregnated Ti, composite pseudoalloy, mech. props., Bi alloy content depend. 7-28095
 C diamondlike films, deposition with C⁺ and hydrocarbon ion beams, mechanical props., comparison 7-59417
 C fibre reinforced plastics, hardness anisotropy 7-8081
 C films, diamond like, prep. and props. 7-22472
 C, hard type, B-doped, prep., phys. and mech. props. 7-39571
 C layers, arc plasma deposition, struct., mech. props. (Russian) 7-22581
 C layers, deposition, by RF plasma decomp., physical props. 7-22508
 C sputtered films, ion enhancement, struct. prop. relationships studies 7-52332
 a-C:H, film, optical energy gap, density, hardness 7-39204
 a-C:H diamond-like coating on Ge, rain erosion resistance improvement obs. 7-31435
 a-C:H films, plasma deposited, optical props. 7-27799
 C-Sn composite sputtered films, ion enhancement, struct. prop. relationships studies 7-52332
 C-Ti composite sputtered films, ion enhancement, struct. prop. relationships studies 7-52332
 C-ZnX (X=S, Se), adherence of diamondlike C films, use of intermediate layers 7-46624
 CaMoO₄, microhardness anisotropy meas., quenching and annealing temp. effect 7-63738
 CaPuTi₂O₇, substituted zirconolite, high level waste, self-irrad. effects, mech. props. 7-805
 Ca₂Sr_{1-x}F₂, mixed crystals., microhardness study 7-51928
 CaZrO₃, sintering, porosity, mech. props., corrosion resist. 7-39664
 CdGa₂S₄, single crystals, chemical vapour transport growth, microhardness, crack patterns 7-7833
 CdIn₂S₄, single cryst., chem. vapour transport growth and Vickers microhardness 7-21345
 Co-Al, precipitation product dissolution (Russian) 7-58479
 Co-Cr-Re system, phase equilib., struct., microstructural, X-ray phase and durometric analyses 7-17513
 CoSi layers, prep. by Co silicisation using Si₂Cl₆ source by diffusion and CVD processes, microhardness meas. 7-17700
 Co₂Si layers, prep. by Co silicisation using Si₂Cl₆ source by diffusion and CVD processes, microhardness meas. 7-17700
 Cr, electrodeposits from Cr₂(SO₄)₃-potassium formate baths, hardness (Japanese) 7-59471
 Cr, electroplated deposits, hardness rel. to C content, heat treatment, bath comp. (Japanese) 7-17480
 Cr evaporated and ion assisted deposited coatings, microstruct., electron microscope obs. 7-52335
 Cr, vacuum-deposited, hardness and struct. studies 7-33761
 Cr-Mo ferritic steel, 14 MeV neutron irrad., mech. prop. changes 7-56821
 CrC coatings on high speed steel, deposition process and mechanical props. 7-64011
 Cu, ion irradiated, mech. prop. meas. 7-51873
 Cu, polycrystalline, US and neutron irrad., struct. and mech. props. (Russian) 7-3402
 Cu powder, porosity influence on mech. and tribotech. characts. in high-speed friction 7-8119
 Cu-Al bronze, hot deform. and annealing, mechanical props. and softening kinetics 7-17552
 Cu-Al-Ag (5.4, 5.2 wt.%), ageing, hardness, precip. energy 7-65127
 Cu-Mn-Ge system, phase equilib. in Cu-rich alloys 7-3277
 Cu-Ni-Al, two-step ageing, microstruct., mech. props. 7-39565
 Cu-Ni-Al (7.5, 2.5 at.%), thermomech. treatment (Japanese) 7-8013
 Cu-Ni-Cr, spinodal decomp., X-ray diff. and TEM study 7-22732
 Cu-Ni-P alloy, P addition effect on struct. and strength 7-53669
 Cu-Sn, dual phase, struct.-prop. correl., hardness obs. 7-8094
 Cu-Sn-Pb system, struct. form. during sintering 7-64967
 Cu-Su, amorphous system, high press. melt quenching, microhardness, X-ray obs. (Russian) 7-44396
 Cu-Ti (5.7 at.%), diffusion of products of cellular dissoln. (Russian) 7-58485
 Cu-Zr, ion irradiated, mech. prop. meas. 7-51873
 Cu-Zr (0.5 wt.%), high strength, high cond., prod. by rapid solidification technology 7-28029
 Cu₂Ti_{100-x}, x=50,66, metallic glasses, crystn., DTA, X-ray diff., hardness meas. 7-63489
 Dy-Re-Fe(CO)(Ni), intermetallide-based solid solns., phase equilib. and mag. props. 7-22639

hardness continued

- Fe based eutectic alloy powder, plasma coatings with interstitial phases, tribotechnical props. 7-17731
 Fe, cast, high-strength, form. of wear resistant structs. corresponding to Charpy principle 7-28180
 Fe, cast, laser surface hardening, optimisation of process variables 7-13645
 Fe, cast, surface melting, composition and impurity effects 7-21423
 Fe, cast, white, Cr-Mo, unidirectionally solidified, sclerometric study 7-3455
 Fe, cementation layer struct., Mossbauer spectra, radioisotope method, microhardness obs. (Russian) 7-39741
 Fe, ductile and grey cast, laser surface hardened, sliding wear 7-17650
 Fe powder, ultrafine, and hot forged specimens, reduction temp. effect on struct. form. and props. 7-53670
 Fe, pure, diffusion of H, dislocation trapping, interstitial impurities effect (Japanese) 7-52140
 Fe surface layers under toluene, laser irradiated, supersaturation with C 7-51820
 Fe/Ni Reed blades, Au coated, AES/SEM study 7-44972
 Fe-C-based alloys, high C, rapidly solidified, mech. props. 7-22673
 Fe-Cr-Mo-Mn-C-P, sintered, ageing and steam oxidation, effect of P 7-7930
 Fe-Cr-Ni, hardening at low temp. (Russian) 7-39554
 Fe-Cr-Re system, interaction of intermediate phases, phase equilibria 7-17514
 Fe-Cu-P, sintered, ageing and steam oxidation, effect of P 7-7930
 Fe-Ni-B metallic glasses, crystallisation, microhardness (Russian) 7-59617
 Fe-Si-B (10, 15 at.%), metallic glass, plastic deform. resist. 7-13521
 Fe-Si-B metallic glasses, wear resist. 7-13604
 Fe-TiB₂ eutectic system, microhardness, modulus of elasticity (Russian) 7-39648
 Fe₄₀Ni₄₀B₂₀ amorphous alloy, effect of plastic deform. on mech. and mag. props. (Russian) 7-53810
 Fe₈₀P₁₃C₇ alloy, metallic glass surface layers by rapid quenching, microhardness 7-3512
 GaAs, crack form., quenching by dislocation ensembles (Russian) 7-44680
 GaAs, dislocation rosette generation round Vickers indentations, mobility and twinning, TEM study 7-63618
 GaAs:Cr semiinsulating LEC wafers, microhardness cartography 7-32886
 Ga_{1-x}In_xAs, high-temperature hardness 7-44675
 Ga_{1-x}In_xAs, solid soln. strengthening, mech. props. 7-32452
 GaP, implanted with He ions and protons, microhardness rel. to damage density 7-51883
 Gd-Sb, phase diagram, peritectic reactions, congruent melting, DTA, microstructural and X-ray anal. 7-39481
 GeO₂-ZnO-Bi₂O₃ IR transmitting glasses 7-43276
 HfN(C) reactively sputtered wear resistant coatings, struct., hardness and adhesion props. study 7-52330
 HfO₂-Ln₂O₃ (Ln=Y,Gd,Tb,Er,Yb), solid soln. single crystals, physico-chem. props. 7-2097
 HgZnTe bulk crystals, travelling heater method growth, and charactn. 7-59387
 KCl microcrystalline powders, correl. between microhardness, dislocation mobility and coloration stability 7-32436
 LaNi₅, anisotropic H migration, deposition potentials, hardness, brittleness meas. 7-6873
 Li-P-O-N glass, prep. and characterisation 7-26654
 LiF, N ion implanted and X-irrad., microhardness response 7-21344
 Li₂O-P₂O₅-PON, nitrogen phosphate glasses, preparation from PON (French) 7-26657
 Mn-Sn, homogenised, mag. props., thermal expansion 7-2900
 Mo, boriding by immersion process in fused salts (Japanese) 7-59663
 Mo CVD coating on graphite, struct., thermal resist. props. 7-52375
 Mo, microhardness, temp. depend in coarse-plastic transition region (Russian) 7-46638
 Mo single cryst., rolling, dynamic recovery rel. to deform. temp. (Russian) 7-65095
 Mo-Re (27 wt.%), rolling, reorientation, annealing effect (Russian) 7-39598
 Mo-V(Nb)(Ti)(Zr), solid soln. hardening, alloying element effects, Vickers hardness meas. (Korean) 7-3319
 Na₂O-P₂O₅-PON, nitrogen phosphate glasses, preparation from PON (French) 7-26657
 NaPO₂+N₂ glass prep. and props., comp. calcs. 7-7951
 Nb, shock-synthesised superconductor, characterisation 7-38116
 Nb-Ti-W (30, 20 wt.%), nitriding, hardness, wear and corrosion resist. 7-46713
 Nb_{100-x}B_x alloy films, sputtered, elec. cond., hardness, amorphous and crystal struct. 7-13354
 Ni-base self-fluxing alloys, wear resist. of detonation coatings 7-28152
 Ni-based consolidated rapidly solidified alloys, strengthening mechanisms 7-22712
 Ni-Co-Cr-Al-Y coatings, electron beam deposition, oxidation rel. to pretreatment 7-46702
 Ni-Fe-Cu, mag. props., hardness, elec. resist., V, Nb and Ta additions effect (Japanese) 7-12998
 Ni-Mo (20 at.%), ageing, yield strength rel. to prior α grain size 7-39507
 Ni-Mo₂C eutectic, directional solidification oriented struct., strength, hardening mechanism (Russian) 7-59507
 Ni-Mo-Cr-B powders, amorphous and microcrystalline, shock consolidated, wear props. 7-46655
 Ni-P alloy electroless deposits, hardening by baking treatments (Japanese) 7-33759
 Ni-P electroless deposited amorphous coatings, wear resistance, crystallisation effects 7-53913
 Ni-P-B electroless coatings, prep. and deposit characts. 7-59671
 Ni₃Al produced by shock compaction, TEM 7-39480
 Ni₃₀B₅₄C₁₆, B-rich amorphous alloy prep. by rapid quenching, crystn., hardness and elec. resist. 7-13441
 Ni₂Cr, order-disorder transform. kinetics, P content effect 7-13446
 Ni₂Cr, recrystn. kinetics and mech. props., influence of P 7-22718
 Ni₈₉Cr₇Fe₃Si₄B₃, amorphous alloy, crystallisation (Chinese) 7-6518
 Ni₅₂Mo₃₈Cr₈B_{1.5} metallic glass, shock consolidated, wear props. 7-28154
 NiSn-SiC composite coatings, electrodeposition, wear resist., hardness, porosity 7-33613
 PLZT, elastic-plastic contact damage 7-39627

hardness continued

PbTe-Gd₂Te₃ system, solid solns., synthesis and props. 7-21458
PbTe-Tb₂Te₃, solid solns., physicochemical anal. 7-21456
Pt-Zr internally oxidised alloys, morphology, struct. and stability (*Russian*) 7-33687
SbSI, crystals grown from melt, microhardness study 7-12196
SbSeI, crystals grown from melt, microhardness study 7-12196
Si, indentation dislocation rosettes length, influence of Vickers indenter edge orientation rel. to slip directions 7-58284
SiC, high-press. self-combustion sintering from fine mixed powders of Si and C (*Japanese*) 7-3249
SiC powder compacts, formed by cold isostatic pressing, influence of shape and size on homogeneity (*Japanese*) 7-64981
Si₃N₄ powders, high press. not pressing, mech. props., thermal cond. temp. depend. 7-3231
Si₃N₄, with MgO addition, phys. and tribological props., effect of hot-pressing time (*Japanese*) 7-65150
Si₃N₄-SiC composite, sintering, Vickers hardness (*Japanese*) 7-8116
Si₃N₄-SiC film, hybrid material prepared by plasma CVD, microhardness and internal stress 7-13616
Si₃N₄-TiC composites, densification, matrix-dispersoid reaction, mech. props. microstruct., impurities effect 7-64994
SiO₂ evaporated and ion assisted deposited coatings, microstruct., electron microscope obs. 7-52335
Sm₂(CoCu)₁₇ magnets, cast, coercivity and microhardness 7-53880
SnTe, conc. depend. props. in region of homogeneity 7-45366
SnTe, Mossbauer spectra and microhardness, stoichiometry deviation effects, vacancy conc. and distrib. 7-26973
Ta₅₅-It₄₅ amorphous alloy, crystallisation study 7-58145
TaC, high temp. hardness, stacking faults, hardening rel. to C diffusion 7-3369
Ta₂O₅ evaporated and ion assisted deposited coatings, microstruct., electron microscope obs. 7-52335
Ta₂Si electrodeposited coatings, composition, morphology and hardness meas. 7-27191
TeO₂-based halide glasses, prep., thermal, mechanical, elec. and optical props. characterisation (*French*) 7-37884
(Ti,Al)N layers on high speed steel, morphology and props., deposition temp. and sputtering atmosphere depend. 7-53975
Ti alloy metastable phases, plasticity (*Russian*) 7-33729
Ti, nitriding in rarefied activated nitrogen 7-8181
Ti-Al-Cr-Mo alloy VT3-1 mech. props. depend. on decomp. product morphology for metastable phases 7-39655
Ti-Al-Mo-Cr, VT3-1, struct. changes during US case hardening (*Russian*) 7-53991
Ti-Al-Nb (6,2 wt.%), fusion weld, defect regions, cracking, porosity, interstitials analysis 7-28109
Ti-Al-V (6,4 wt.%), hardness and alpha/beta ratio, effect of O. 7-3430
Ti-based sputtered hard compound films, struct. and props. 7-46318
B-Ti-Mo, single crystals., age and quench hardening, effects of cryst. orientation and surface condition (*Japanese*) 7-22709
Ti-N ion deposited film, struct., phase comp. and mechanical props., comp. depend., X-ray diffr. study 7-12573
Ti-Ni-Al rapidly quenched amorphous alloys, thermal stability studies 7-21123
TiAlN coatings, sputter ion plating, struct. and protective props. 7-53976
TiC coated cemented carbide cutting tool inserts, performance and material props. 7-46712
TiC coatings on high speed steel, deposition process and mechanical props. 7-64011
TiC sputtered films, influence of ion bombardment 7-3171
TiC-Ni-Mo sintered carbides, struct. and physicochem. props. 7-3256
TiC-steel hard alloys, wear resist. in abrasive jet, methods of improvement 7-3448
TiC-WC-TaC-Co hard metals, Ta conc. effect on comp. and physicochem. of carbide and Co phases 7-53708
TiCN, TiC and TiN CVD coatings, high-temperature microhardness profiles 7-28181
TiCN-Ni-Mo composite powders and coatings, prep. and characteris. 7-3255
TiN coating, on steel, ion-plasma appl., laser alloying, dynamic surface strength 7-17730
TiN coatings, ion implanted, wear resistant props. (*Japanese*) 7-46698
TiN coatings on steel substrates, growth, struct., props. 7-33799
TiN film deposition by reactive sputtering, hardness and optical props. 7-22481
TiN thin films, activated reactive evaporation deposited, vacuum annealing, struct., mech. props. 7-8010
TiN-C(BN), hard composite coatings, deposition and props. 7-46623
TiN-coated gear cutting hobs, wear characteristics, mechanical and structural props. 7-53980
TiN-coated high-speed steel cutting tools, coating quality and surface finish., tool metallurgy and design 7-53979
TiN_x epitaxial layers, atomic and electronic struct., growth, physical props. 7-32854
TiN(C) 7-52330
TiNi shape memory alloys, wear resist. and hardness, influence of heat treatment (*Korean*) 7-17647
TiO₂ evaporated and ion assisted deposited coatings, microstruct., electron microscope obs. 7-52335
Ti₂GeSe₃-Ti₂SnSe₃ systems, phase equilibria 7-6760
Ti₄GeSe₄-Ti₄SnSe₄ systems, phase equilibria 7-6760
(U_{0.3}Pu_{0.7})C, hyperstoichiometric, hot hardness, 293-1573K 7-59608
V and alloys, dispersion hardened, strength changes and recrystn. 7-17545
W thin films on Si substrates, plastic props., meas. by submicron indentation hardness, substrate curvature techniques 7-58720
WC coatings on stainless steel, sputter deposited, mechanical props., effect of interlayers 7-53983
W-Re alloys, annealed and sintered, elevated temp. softening, appl. for thermionic energy conversion 7-28077
WC coatings on high speed steel, deposition process and mechanical props. 7-64011
WC thin films, RF reactive magnetron sputtering and hardness meas. 7-7844
WC-Co, erosion, effect of hardness 7-17648
WC-Co, TiN-coated, residual stress and strength, X-ray diffr. study (*Japanese*) 7-8101
WC-Co composites, fracture toughness rel. to hardness, microstruct. model 7-17637

hardness continued

WC-TaC-Co, N contained cemented carbides, sinterability, mech. props. rel. to prep. 7-17507
Y₂O₃-ZnO-Al₂O₃-SiO₂, glass form. and crystn., effect of ZnO additions 7-44382
Zn, microhardness, temp. depend in coarse-plastic transition region (*Russian*) 7-46638
Zn-based alloys, mechanical props., alloying addition effects (*Japanese*) 7-8090
ZnS_{1-x}Se_x, gradient IR optical material prepared by CVD 7-31408
Zr-Co, amorphous alloys, microhardness and struct. relax. (*Chinese*) 7-65069
Zr-Ir, hardening by dispersed ω-phase particles, annealing effect (*Russian*) 7-65053
Zr-Nb (1 wt.%), laser irradi., hardness, struct., corrosion resist. 7-3400
Zr-Nb (20 wt.%), ageing behaviour, effect of H 7-46527
Zr-Ni, amorphous alloys, microhardness and struct. relax. (*Chinese*) 7-65069
Zr-Os, hardening by dispersed ω-phase particles, annealing effect (*Russian*) 7-65053
e-ZrH₂, shape memory effect (*Russian*) 7-59577
ZrN(C) reactively sputtered wear resistant coatings, struct., hardness and adhesion props. study 7-52330
ZrO₂ advanced ceramics, props. and appl. 7-13416
ZrO₂, CeO₂ containing tetragonal polycrystals, thermal stability, mech. props. 7-28101
ZrO₂ single crystals, stabilised, growth by skull melting technique, char-actn. 7-53560
ZrO₂:Ti, ion implantation, mech. props. 7-28102
ZrO₂-CaO-P₂O₅-SiO₂ glass ceramics, prep. and mech. props. (*Japanese*) 7-7942
ZrO₂-Y₂O₃ partially stabilized, Al₂O₃ effect on retaining tetragonal particles, matrix toughening 7-59485

hardness testing
coatings, microindentation hardness testing, techniques and data interpretation 7-33868
coatings, ultralow load hardness testing in a scanning electron microscope 7-46740
holographic evaluation of laser hardening of instrument parts 7-5857
metals, low-melting, microhardness 7-22797
microhardness correction procedures evaluation 7-3550
microhardness for film material testing (*Russian*) 7-61395
optimum device, new scale appl. (*German*) 7-13690
PVC, rigid, stabilised, crystallinity detection by hardness testing 7-8223
thin films, mechanical properties meas., depth-sensing indentation instruments 7-8211
thin films, quality testing using hardness meas. in SEM 7-8210
US nondestructive testing, microcomputer appls. in thickness meters and hardness testing (*French*) 7-54068
C fibre reinforced plastics, hardness anisotropy 7-8081

harmonic analysis
see also waveform analysis
Earth core-mantle boundary topography, harmonic expansion from travel-time residuals 7-66036
Earth tides, harmonic anal. of strain tidal data in Shanghai City (*Chinese*) 7-34368
elastic waves in a periodic band (*French*) 7-11336
geomagnetic field modelling, appl. of alternate forms of assoc. Legendre functions 7-14186
geomagnetic main field anal. at core-mantle boundary, spherical harmonics compared with harmonic splines 7-65935
geopotential harmonics of order 15 and 30, determ. from orbital resons. of 25 satellites 7-65923
gravitational potential determ. for arbitrary mass distrib. Poisson integral expansion method 7-66447
particle shape and size determination, concurrent spatial harmonic and fractal analysis 7-31263
radiative-transfer problems with reflective boundary conditions, modified spherical-harmonic method 7-34853

harmonic generation
see also optical harmonic generation
free electron laser soft X-ray overtone production 7-20234
Josephson tunnel junctions, microwave-driven, one-third harmonic generation 7-52899
weakly nonlinear dispersive media, three-wave interaction including frequency doubling effects 7-43215
Al alloy US nonlinearity dependence on second phase precipitates, obs. 7-2111

harmonic oscillators
3D harmonic oscillator function calcs. 7-2537
active rotator model with phase transitions 7-35270
active rotator systems subject to noise, two-dimensional, cooperative phenomena and phase transitions 7-4673
algebraic time-ordering techniques, time depend. freq. 7-14828
anharmonic asymmetric oscillator, classical and quantum treatment 7-18619
anharmonic oscillator, $\kappa X^2 + \beta X^4$, nonperturbative method study 7-61164
anharmonic oscillator, activated and tunnelling transitions between forced oscillation regimes 7-35343
anharmonic oscillator, convergence props., 1/D expansion 7-14830
anharmonic oscillator, equations of motion of interacting particles in external field, elliptic solns. 7-41140
anharmonic oscillator, limitations of Birkhoff-Gustavson normal form anal. 7-56081
anharmonic oscillator, nonlinear system under combined periodic and random excitation 7-9699
anharmonic oscillator, one-dimensional, Birkhoff-Gustavson transformation, quantum corrections 7-9706
anharmonic oscillator, perturbation and Pade summability method 7-146
anharmonic oscillator, Rayleigh-Schrodinger perturbation theory 7-56084
anharmonic oscillator, short-lived quasi-stationary states (*Russian*) 7-24462
anharmonic oscillator, squeezed light interaction, SU (1,1) coherent states appl. 7-62655
anharmonic oscillator, Yukawa pot., interdimensional degeneracies 7-14808
anharmonic oscillator with two external periodic forces, chaotic behaviour 7-18624
anharmonic oscillators, classical path treatment 7-30918
anharmonic oscillators, dynamical behaviour 7-9707

harmonic oscillators continued

anharmonic oscillators, energies from divergent perturbation series 7-24477
 anharmonic oscillators, expansion parameter, spatial dimension 7-14829
 anharmonic oscillators, quartic and sextic, Schrodinger eqn., eigenvalues, lower bounds calc. 7-41126
 asymptotic approximation applied to simple harmonic oscillator/scalar field problem 7-61173
 benzonitriles, substituted, thermodynamic functions 7-52082
 binary random harmonic chains, special freqs. and Lifshitz singularities 7-35404
 carbon tetrafluoride, Morse oscillators, Miller's classical path approx. appl. 7-25624
 chain of anharmonically coupled oscillators, broken ergodicity 7-61087
 charged oscillator, U-matrix theory anal. 7-61157
 charmonium and bottomonium spectra, introductory physics course 7-18534
 circle maps with bistable dynamics, basin-struct. invariance 7-9708
 coupled anharmonic oscillators, algebraic reson. quantisation 7-24450
 coupled axial-torsional oscillator with neo-Hookean spring 7-35265
 damped, nonisolated system, QED formulation (*Russian*) 7-19062
 damped, propagator evaluation, path integral method (*Korean*) 7-24464
 damped, quantisation 7-41035
 damped, wave function, energy expectation value (*Korean*) 7-24465
 damped nonlinear oscillator, Markovian master eqn. 7-35329
 damped quantum oscillator, functional integration method anal. 7-24479
 dispersive optical bistability model, limit cycle quantisation for dissipative driven anharmonic osc. 7-11045
 dissipative linear quantum systems, repeated meas. 7-48394
 dynamical supersymmetries of the harmonic oscillator 7-24801
 effective classical partition functions for anharmonic oscillators and double-well pot. 7-35334
 exact propagator, eval. in time-varying mag. field 7-133
 exciton-biexciton two-oscillator model, chaos 7-31390
 Feynman-Hellman theorem, central force problems, radial expectation values 7-35156
 Frenkel-Kontorova Aubry Model, driven dynamics 7-9662
 fundamental commutator and quantum relax. 7-41139
 Gaussian wave-packet dynamics 7-48409
 general damped anharmonic oscillator, intensity distrib., spectral behaviour 7-143
 Green matrix construction for stratified elastic half-space (*Russian*) 7-61106
 gyrodendulum, Rydberg states in crossed fields 7-25437
 Hamiltonian, resonance perturbation by mode coupling (*Chinese*) 7-35264
 Hamiltonian system, 2D, stability-instability transitions, analytic soln. 7-18628
 Henon-Heiles and two coupled quartic anharmonic oscillator systems, invariance and integrability 7-24412
 inert gas atoms, physisorbed, induced dipole moment 7-52243
 instability of the harmonic oscillator with small noise 7-4770
 interacting self-oscillators, discrete-time population dynamics 7-4675
 Kratzer oscillators, perturbed, rovibr. energy levels and expectation values 7-5656
 Lagrangian and Hamiltonian formulation 7-18524
 Langevin equation, generalised, for oscillator 7-29746
 linear systems with strong relax., transition to aperiodic motion 7-29937
 methane ion, photoelectron spectrum, Jahn-Teller effect, ab initio SCF and CI calcs. 7-42683
 Morse pot., matrix elements, appl. of 2D harmonic oscillator 7-56071
 multiboson Holstein-Primakoff squeezed states for SU(2) and SU(1,1) 7-18632
 multidimensional wavepacket propag. theory 7-9685
 nonlinear, Lyapunov stability and attractors 7-147
 nonlinear anharmonic motion eqn., series solns. 7-24383
 nonlinear driven oscillator, periodic orbit systematics, prototype model 7-18629
 nonlinear driven oscillators, periodic orbit systematics, analytic treatment 7-9658
 nonlinear oscillator, parametrically excited bifurcations 7-56070
 nonlinear oscillator coupled to FM wave, stochastic behaviour 7-61225
 nonlinear oscillators, weakly coupled systems, chaos and order 7-56164
 nonlinear quantum oscillator, linear damping of arbitrary magnitude; exact Hamiltonian 7-48403
 nonlinear Schrodinger equation with an external field, soliton studies 7-41121
 nonlinear stochastic oscillator, linear response 7-9704
 nonrelativistic bound-state problems in momentum space 7-116
 nonseparable systems, higher order resons., eigenvalues, semiclassical calc. 7-4705
 nonstationary quantum singular oscillator, correlation fns., density matrix element calcs. 7-24455
 one-dimensional, two-step coherent state approx., modified operator method 7-35326
 oscillator shell model, spin cutoff parameter calc., exciton model, state density angular momentum dependence 7-35960
 particle dynamics in Coulomb pot. anisotropic harmonic oscillator pots. 7-61163
 particle in a box, thermodynamics 7-41238
 phonon damped, scattering response 7-2114
 pumped, energy absorption calcs. 7-11271
 quantum kinematics of Newtonian symmetry group 7-41131
 quantum Markov chains, translation-invariant distrib. 7-61265
 quantum mechanics, supersymmetry 7-35158
 quantum oscillator basis, matrix elements, centre-of-mass coordinates elimination 7-24483
 quantum-mechanical Green's function and nonlinear superposition law 7-14817
 quartic harmonic oscillators, Schrodinger equation with polynomial potential, soln. using numerical method 7-41125
 quasi-integrable Hamiltonian systems, stability of motions near resonances 7-29800
 random, Lyapunov exponent and rot. number, asymptotic anal. 7-4720
 random chain of coupled oscillators, special frequencies and asymptotics 7-56061
 recurrence relations for two-center harmonic oscillator integrals 7-48416
 relativistic linear oscillator, generalized coherent states and semiclassical quantization 7-35341
 rotating harmonic, 3D, and doubly anharmonic oscillators, Schrodinger eqns., confinement pots. 7-35313

harmonic oscillators continued

Schrodinger equation and canonical perturbation theory 7-48401
 second-quantized molecular time scale generalized Langevin equation theory: coupled oscillator model 7-24452
 semiclassical mechanics, time independ. methods 7-9691
 simple pendulum as an anharmonic oscillator 7-9657
 simplex structure of harmonic oscillator classical states 7-48400
 spatially extended EM system in zero-point radiation, thermal effects of radiation, class. oscillators 7-41185
 squeezed quantum fluctuations, dissipation effect 7-24476
 strangulation on damping, Kanai-Caldirola Hamiltonian energy dissipation anal. 7-24474
 system coupled to harmonic bath, quantum mech., basis set methods 7-56072
 thermal averages and Bloch's second theorem 7-48657
 time-depend. mass, with driving force, exact soln. 7-35331
 time-dependent invariant associated to nonlinear Schrodinger-Langevin equations 7-41134
 time-dependent oscillator, constants of motion 7-24408
 two dimensional isotropic oscillator, coherent angular momentum states 7-56077
 two-centre harmonic oscillator matrix elements and recursion relations 7-36691
 Van der Pol-Duffing oscillator chaos 7-11272
 vibrationally excited molecules, steady-state flux distrib. of populations over levels 7-15583
 visual theorem, applications 7-35174
 Weber-type gravit. wave antenna coupled to reson. transducer, quantum nondemolition observables 7-61182
 NH₃, vibr., inversion doubling, variational calcs., use of intramol. pair pots. 7-31014
 SiF₄, stretching vibr. overtone and combination states, multiphoton processes 7-25488

harmonics

see also harmonic analysis
 finite element analysis of steady nonlinear harmonic oscillations of axisymmetric shells 7-6133
 liver, pulsed finite-amplitude US passing through, harmonic distortion development 7-34190
 optical fibres, single-mode, mode field radius meas., harmonics detection appl. 7-37163
 pyrodetector responsivity for harmonic and pulse modulation of IR radiation (*Slovak*) 7-9897
 string vibrating against rigid fixed obstacle, motion 7-61090
 LiNbO₃ SAW bifurcation and chaotic state obs. 7-2333

Hartmann lines see *Luders bands***Hartree calculations** see *SCF calculations***Hartree-Fock approximation** see *HF calculations***Hartree-Fock calculations** see *HF calculations***hashing functions** see *file organisation***Hasiguti relaxation** see *anelastic relaxation; dislocation damping***Hastelloy** see *iron alloys; molybdenum alloys; nickel alloys***HCMOS** see *CMOS integrated circuits***He** see *helium***He-3-A** see *superfluid helium-3***He-3-B** see *superfluid helium-3***headphones**

see also earphones
 personal Hi-Fi, hearing impairment effects (*Japanese*) 7-47110
 responses on real ears and a head and torso simulator 7-40368

health care

used for systems approach only
 see also patient care
 American health care technology evolution, economic and ethical implications 7-4648

health effects of radiation see *biological effects of radiation***health hazards**

see also biological effects of radiation
 actinide isotopes in the marine environment 7-40314
 air ions, biological significance 7-28496
 airborne radioactive gases inside a nuclear reactor containment building, Monte Carlo program to calc. exposure rate 7-54766
 asbestos workers autopsied lung tissue, Mossbauer effect study 7-65849
 biomedical electronic instruments safety and testing Electrotechnical Testing Institute practices (*Czech*) 7-18090
 broadcast transmitting station radiation hazards 7-14045
 building materials used in the Netherlands, proposed standard for radioactivity 7-34287
 coal fly ash, element bioaccumulation in rats 7-34366
 coastal water, routine discharges from CEBG nuclear power stations; crit. group radiation exposure 7-40306
 CT, use of effective dose equivalent, H_g, as risk parameter 7-40294
 cyclotron, residual radioactivity in components and surroundings 7-8701
 dental photopolymerisation sources, curing efficiency and ocular hazards 7-60064
 electric shock effects on the human body 7-24337
 electrical shock, heart muscles effect (*German*) 7-3776
 electricity production, mutagenicity (*French*) 7-28802
 environmental movement, dynamic model for prediction 7-54372
 epidemiological investigation of mutational diseases in the high background radiation area of Yangjiang, China 7-18019
 fluorescent dye penetrant inspection, UV radiation safety and visual enhancement 7-40311
 gamma radiation in Swedish dwellings 7-3884
 generic probabilistic risk analysis for a high-level waste repository 7-28225
 human head internal heating by pulsed microwave irradiation, thermal stress calc. (*Japanese*) 7-47166
 Japanese Tritium Programme, biomedical research at NIRS, Chiba 7-54772
 laser hazard analysis, nominal hazard zone 7-60094
 laser hazards, controls 7-65812
 logistic estimate of the final incidence of lateration effects 7-8653
 long lived radionuclides, transfer through marine food chains, data review 7-28728
 medical irradiation, effect of utilising age and sex dependent factors for detriment calc. 7-54734

health hazards continued

- natural radiation exposure, correl. with cancer mortality in Japan 7-18022
- neutron leakage through an Fe shield at an accelerator, rel. to concrete augmentation of shielding 7-54764
- nuclear facilities, prod. of air pollutants leeward (*German*) 7-65664
- nuclear issues in New Zealand, health physics aspects 7-8697
- nuclear medicine workshop. Chalk River, Ont., Canada (Aug. 1985) 7-24308
- patient doses and risks from diagnostic radiology in north-east Italy 7-60089
- personnel exposure in interventional radiology, shielding method 7-47261
- portable gas chromatograph evaluation for transformer site polychlorinated biphenyl meas. 7-46994
- prenatal obstetric X-ray exam., unborn child cancer risk, Oxford survey analysis 7-8694
- radar workers at civilian airports, exposure survey of microwave radiation, Australia 7-47161
- radiation, biological basis of radiological protection and its appl. to risk assessment, conf., Bristol, England (April 1986) 7-48134
- radiation carcinogenesis, cumulative empirical distrib. functions, risk projection models 7-28705
- radiation epidemiology, individual and collective dose estimation method for subthreshold detection 7-28704
- radiation risks and radiation protection at Chalk River Nuclear Lab. 7-25268
- radiation risks in perspective 7-54681
- radioactive cloud, dose reduction factors for large buildings, computer codes 7-54759
- radioactive contamination of manufactured products 7-28721
- radiotherapy shielding block fabrication, pot. exposure to metal fumes, particulates, and organic vapours 7-40277
- satellite transmit earth station, RF radiation hazards, menace or myth 7-18018
- scattered radiation reaching doors and windows of diagnostic X-ray rooms 7-60076
- thin film solar cells manufacture, elec. and EM hazards 7-59849
- thin-film photovoltaic cell production, gas, health and safety hazard controls 7-17876
- ²⁴¹Am electrodeposition geometry in the assay of environmental samples 7-28718
- CO, personal exposure monitor with automatic data-logging 7-3943
- ¹³⁷Cs, A=134,137, comparative pathway analysis in Hudson River estuary, dose assessment 7-8699
- GaAs thin film photovoltaic cells, large-scale manufacture, hazard characterisation of AsH₃ gas and GaAs waste 7-39998
- HTO, accidental intake: report of 2 cases 7-40316
- HTO and H₂O, differences in behaviour in soil after condensation from atm. 7-54378
- ³H, accidental releases from fusion reactors 7-54777
- ³H atmospheric release rel. to precipitation contamination 7-54382
- ³H content in tissue free water of Japanese bodies 7-60102
- ³H control in NET, preliminary design considerations 7-49670
- ³H, elementary, uptake by the soil 7-54377
- ³H, environmental and human risks, conf., Karlsruhe, Germany (Feb. 1986) 7-48163
- ³H gas, fixation by rats 7-60099
- ³H in drinking water, background information for development of a standard 7-60101
- ³H in plants, review 7-54779
- ³H in the aquatic environment, current literature review 7-54381
- ³H metabolism in animals, review 7-60097
- ³H metabolism in newborn mice and estimation of accumulated dose 7-60100
- ³H, modelling 7-54371
- ³H, normal releases from fusion processes and environmental radiation doses 7-54775
- ³H, organically bound, given during pregnancy and lactation, retention in young pigs 7-60098
- ³H releases from nuclear power plants and nuclear fuel reprocessing plants 7-54776
- ³H, survey methods in Paks nuclear power plant, development and appl. 7-56881
- ²³⁷Np, amount in environment (*French*) 7-40315
- ²³⁷Np and ⁹⁹Tc, plant uptake under field conditions 7-28729
- ²³⁷Np determination in sediments from Sellafield, UK, by neutron activation anal. 7-28731
- ²³⁷Np from global fallout after atm. testing, human tissue sample obs. 7-34291
- ²³⁷Np inhalation in rats 7-54768
- ²¹⁰Pb concs. and states of equilib. with ²³⁸U, ²³⁴U and ²³⁰Th in U miners' lungs 7-28724
- Pu fallout, food ingestion in Japan 7-28723
- ²³⁹Pu, A=239,240, conc. in Japanese human tissues 7-18081
- ²³⁹Pu and ²⁴⁴Cm, lung clearance and translocation following inhalation, rat obs. 7-34290
- ²⁴¹Pu in low-level radioactive wastes from reactors, determ. 7-30516
- ²²⁶Ra, A=226,228, intake by early Ra dial workers in Illinois, health risks 7-8700
- ²²⁶Ra, prediction of occurrence in groundwater, rel. to public drinking water supplies 7-54380
- Rn daughter exposure and cigarette smoking, lung cancer in Navajo men, U mining relationship 7-8703
- Rn daughters in indoor air, Swedish limitation schemes 7-34286
- Rn, indoor, seasonal variation in houses, southwestern USA 7-28722
- Rn, indoor and soil meas. in Albuquerque, NM, USA 7-28726
- ²²²Rn, A-220, 222, progeny inhalation, lung cancer risk at low doses of α particles 7-28608
- ²²⁶Rn, concs. determ. by scintillation counting method, appl. to Japanese fumaroles and hot springs 7-9199
- ²²⁶Rn determ. using activated C and high purity Ge detector 7-28727
- ²²²Rn in exhaled breath of Th plant workers, obs. 7-54767
- ²²²Rn concentration meas. in Greek radon spas 7-23465
- ²²²Rn concentrations in USA homes, contrib. to lung cancer risk 7-65666
- ²²²Rn, surface deposition of short lived decay products, fan induced air motion effect 7-8698
- ²²²Rn transport through a cool season grass growing on uranium mill wastes 7-28730
- U acute accidental inhalation by 3 men: 38 yr. follow-up 7-34289
- U content in tobacco, SSNTD anal. 7-49829
- U mills, final product dust median aerodynamic diameters 7-8702

health hazards continued

- U mine tailings disposal, radiation exposure estimation 7-5445
- U refinery in Canada, U dust distrib. and radiation dose to public 7-59887
- UO₂, in vitro dissolution characts. 7-14137
- ²³⁵UO₂(NO₃)₂, A=232, 233, inhaled by rats, deposition and early disposition 7-54769
- ¹³³Xe packaging contamination 7-3888
- health physics** see dosimetry; health hazards; radiation monitoring; radiation protection
- hearing**
 - see also bioacoustics; ear; hearing aids; speech
 - adaptation, rapid, of auditory-nerve fibres: fine struct. at high stimulus intensities in gerbils 7-40171
 - adaptive array with binaural processor 7-31579
 - adult listeners, auditory tests, differences between individuals 7-65768
 - aliasing components, psychoacoustic tests on audibility (*German*) 7-1332
 - AM/FM detection at low modulation freqs. 7-47079
 - amplitude comparator for RF signals analogous to cricket's auditory system 7-14024
 - analytical studies (*Japanese*) 7-65741
 - audiological investigations using microcomputer system 7-65882
 - audiological test data analysis by microcomputer 7-40176
 - auditory brain stem responses from human adults and infants: wave V tuning curves 7-65766
 - auditory nerve level, speech analysis/synthesis 7-43557
 - auditory representation of symmetrical CVC syllables 7-37270
 - auditory thresholds and cochlear mechanisms 7-47081
 - binaural cross-correlation model, lateralization of pure tones 7-47096
 - binaural cross-correlation model, law of the first wave front 7-47097
 - binaural integration of acoustical cues 7-14019
 - binaural sensitivity in Tri-sensor ultrasonic aid for blind people 7-14157
 - binaural versus monaural loudness: supersummation of tone partially masked by noise 7-54601
 - brain, mouse, left hemisphere advantage for recognising US communication calls 7-54607
 - brainstem auditory evoked pots. in rhesus monkey, neural generators 7-8581
 - brainstem auditory evoked responses in the hamster 7-54595
 - brainstem evoked pots., finite impulse response digital filters appl. 7-23491
 - brainstem response using excitatory and inhibitory neuron elements (*Japanese*) 7-8597
 - brainstem responses, effects of presbycusis and other types of hearing loss 7-54609
 - brainstem responses from human adults and infants: restriction of freq. contrib. by notched-noise masking 7-34159
 - categorical perception of syllable boundaries 7-47083
 - cats, effect on hearing of intense low freq. acoustic impulses 7-34160
 - cerebral cortical contribs. to sensory evoked pots., hydranencephaly obs. 7-23342
 - children, differential effects of various causes of deafness on eyes, refr. errors, and vision 7-8555
 - chinchilla auditory filter shapes 7-8590
 - cochlea computational model, expts. 7-47117
 - cochlea representation in primary auditory cortex of ferret 7-8585
 - cochlear frequency selectivity, effects of section of medial efferent tracts in guinea pigs 7-40170
 - cochlear frequency selectivity and efferent tracts in guinea pigs 7-40169
 - cochlear mechanics and physiology, interrelationships (*French*) 7-47082
 - cochlear vibrations, model of effect of outer hair cell motility 7-8586
 - comodulation masking release: effects of varying the level, duration, and time delay of the cue band 7-47101
 - comparative learning of pitch and loudness identification 7-54602
 - complex pitch, central adaptation 7-47104
 - computer model of peripheral auditory processing incorporating phase-locking, suppression and adaptation effects 7-37269
 - consonance judgements of musical chords by musicians and untrained listeners 7-37296
 - consonant recognition by young and elderly subjects with normal hearing 7-47095
 - consonant recognition in quiet and in noise with aging among normal hearing listeners 7-47094
 - continuous evoked pots., visual and auditory, MTF obs. 7-8556
 - critical masking interval meas. for click in wideband noise 7-57634
 - cross-modality matching of auditory and lingual vibrotactile sensations, magnitude estimation instrumentation 7-14028
 - deafness due to exposure to music, Japanese study (*Japanese*) 7-47113
 - decision rules in detection of simple and complex tones 7-47100
 - detection and intensity discrimination of a sinusoid 7-47087
 - dichotic stimulation for central auditory testing, audio tape production, computer programs 7-47084
 - discrimination and response bias for CV syllables differing in voice onset time among children and adults 7-28540
 - discrimination of sound signals simulating sound source movement, role of dog's auditory cortex 7-40166
 - discrimination of spectral-peak amplitude by normal and hearing-impaired subjects 7-65770
 - diving helmet noise, instrumentation methods for meas., diver hearing appl. 7-60146
 - ear canal meas. of eardrum sound pressure level in simulators 7-8592
 - electrical stimulation of auditory system in vivo using multichannel photolithographic electrode arrays, cat obs. 7-3799
 - envelope-induced pitch shifting 7-65769
 - event-related potentials to speech sounds and tones, habituation 7-34155
 - evoked dipole source potentials of the human auditory cortex 7-8580
 - evoked electric responses, individual differences, absolute latencies of brainstem vertex-positive peaks 7-28544
 - evoked potential components, mid and long latency, law of 3.5 c/sec 7-3771
 - evoked potential maps in learning disabled children 7-8558
 - evoked response, auditory nerve-brainstem, depression in hypoxaemia: mechanism and site of effect 7-54584
 - evoked responses, apparent response incompatibility effects rel. to task 7-65764
 - evoked responses, midlatency: differential recovery cycle charact. 7-65763
 - evoked responses during NREM sleep stage 2 in man, late component variants 7-23370
 - FIR digital filter, hearing impaired subjects, speech discrimination assessment 7-37274

hearing continued

flight simulation, vestibular and visual perception cues, coordination 7-14011
 frequency coding in the inferior colliculus, gerbil obs. 7-54596
 frequency difference limens as a function of interstimulus interval 7-54582
 frequency discrimination in the mammalian cochlea: theory versus experiment 7-54599
 frequency discrimination of tones presented in filtered noise 7-47102
 frequency specificity of auditory brainstem responses 7-28543
 headphone responses on real ears and a head and torso simulator 7-40368
 helmet noise and divers' hearing 7-60019
 high-frequency audiometric assessment of a young adult population 7-65775
 human freq.-following response for low pitched complex tones 7-47103
 impaired speech perception of Japanese monosyllables 7-14023
 impairment caused by loud music (*Japanese*) 7-47109
 impedance audiometry of children 7-28628
 industrial audiometric procedures 7-28542
 inferior colliculus, guinea pig, spontaneous activity of single units, salicylate-induced changes 7-47120
 inferior colliculus, rat, dynamic props. of responses of single neurons 7-40163
 infrasound, human perception levels 7-50841
 intensity just-noticeable-differences, 1st order calcs. 7-47088
 interaural magnification theory 7-54598
 Japanese music, effect on performers' hearing (*Japanese*) 7-47111
 layered neural network model applied to the auditory system 7-54581
 LF auditory fibre responses in 2 anuran amphibians, freq. and time domain comparison 7-54594
 loud music, effect on hearing (*Japanese*) 7-47112
 loudness estimation for pure tones (*French*) 7-47080
 low freq., narrow-band signals, detection of temporal gaps 7-47090
 masked speech reception threshold of sentences, amplitude-freq. response 7-65773
 masker-bandwidth dependence in homophasic and antiphasic tone detection 7-65772
 masking, temporal effects and psychophysical tuning curves 7-47099
 masking additivity in the hearing-impaired 7-54585
 mechanical point impedance of the human head, with and without skin penetration 7-34296
 medial geniculate body, cat, functional props. and interactions of neuron pairs simultaneously recorded 7-54592
 memory-intensive recognition for word articulation training 7-37281
 middle-ear input admittance, changes during postnatal auditory development in chicks 7-40165
 midlatency auditory evoked responses: differential effects of sleep in the cat 7-8582
 midlatency auditory evoked responses: differential effects of sleep in the human 7-8583
 military service and hearing damage noise-induced HF losses, study on 38, 294 conscripts 7-54613
 minimum spectral contrast for vowel identification by normal-hearing and hearing-impaired listeners 7-54604
 modulation detection by patients with 8th-nerve tumours 7-8596
 muff-type hearing protectors, effects on speech intelligibility in noise 7-40172
 multi-modality evoked potentials in hypoxaemia, cat obs. 7-54583
 multi-modality evoked responses vs. temp. and thermal dose with whole-body hyperthermia in water bath 7-8500
 musical interval tuning expts. 7-14020
 neural temporal coding of low pitch, human freq.-following responses to complex tones 7-54589
 nonlinear response in evaluating the subjectivediffusiveness of sound fields 7-6050
 occupational noise, hearing loss development during long-term exposure 7-54615
 offset tuning curves rel. to simultaneous and forward masking in mouse and gerbil 7-8587
 otosclerosis, normative multifreq. tympanometric data 7-54610
 P300 potential complex to auditory stimuli, subcortical correlates in man 7-23369
 partition-stereophony to reproduce spatial hearing events (*Japanese*) 7-20571
 pathological high impedance tympanograms, simulation 7-47115
 perceived height of octave-related complexes 7-47089
 perception of front vowels: the role of harmonics in the first formant region 7-65776
 perceptual space for repetitive impulses and environmental noises (*Japanese*) 7-47114
 peripheral auditory system, computational model, speech recognition research appl. 7-43555
 peripheral auditory transduction model using phase vocoder with modified channel signals 7-47116
 personal Hi-Fi, hearing impairment effects (*Japanese*) 7-47110
 phase effects in masking related to dispersion in the inner ear 7-47098
 pictorial information transmission using point sound image, study for visually handicapped sensory aids appl. (*Japanese*) 7-34341
 pipistrelle bat, detection of normal and reversed replicas of its sonar pulses 7-3804
 pitch ambiguity, tone affinity and identification of successive intervals (*German*) 7-3795
 pitch identification of simultaneous dichotic two-tone complexes 7-34158
 pitch perception model 7-40174
 pitch shifts of pure tones due to partially masking sounds (*German*) 7-65761
 populations with special auditory problems in large areas (*Chinese*) 7-60016
 protector test procedures 7-37244
 pure tone detection thresholds in ferrets 7-40168
 pure-tone AM, detect. rel. to sensation level from 8 to 14 kHz 7-8588
 relative loudness of third-octave bands of speech 7-54606
 release from masking by continuous, random, notched noise 7-65767
 reverberation time difference limens for artificial reverberation signals under monophonic listening condition (*Japanese*) 7-31569
 rooms, localization of sound, onset and duration effects 7-47106
 sensory information processing mechanisms (*Japanese*) 7-14003
 short-latency auditory evoked pots. in the monkey, intracranial generators 7-3798

hearing continued

short-latency auditory evoked pots. in the monkey, wave shape and surface topography 7-3797
 signal duration effects on 500 Hz masking-level difference 7-54612
 sinusoid detection, influence of place synchrony 7-65771
 sound localization of frequency-modulated sinusoids by Old World monkeys 7-8591
 speaker-independent isolated word recognition based on emphasized spectral dynamics 7-43556
 speaking clearly for the hard of hearing, acoustic characts. of clear and conversational speech 7-47122
 speech anal. devices for speech and hearing people diagnosis and education 7-37280
 speech identification under simulated hearing and freq. response characts. 7-34157
 speech intelligibility, masking source direction effects (*French*) 7-3796
 speech intelligibility improvement with disturbed temporal resolution rel. to hearing aid design (*German, English*) 7-60120
 speech perception, spectral transition studies 7-34156
 speech production rel. to reduced auditory information 7-47125
 speech recognition by hearing-impaired and normal-hearing listeners, appl. of articulation index and speech transmission index 7-47123
 speech recognition using a cochlear model 7-43554
 speech training devices for profoundly deaf children 7-37278
 state of the art of audiology 7-8593
 stereo reproduction, relationship between cross-correlation function and sound image width (*Japanese*) 7-47108
 stereocilia micromechanics, changes following overstimulation in metabolically blocked hair cells 7-40164
 synchronised responses of primary auditory fibre-populations in caimans to single tones and clicks 7-8584
 temporal characteristics of sound, sensitivity of neurons in auditory mid-brain of grassfrog 7-40167
 temporal discrimination for single components of nonspeech auditory patterns 7-47105
 temporal gap resolution in listeners with high-frequency sensorineural hearing loss 7-54603
 temporal resolution, expedient meas. method for speech intelligibility (*German, English*) 7-60017
 temporal resolution capacity of hearing for various hearing loss types, clinical investigation (*German, English*) 7-60018
 threshold characteristics of the human auditory brain stem response 7-54600
 thresholds as predictors of speech prod. performance 7-54614
 thresholds of perception of irregular signal/frequency changes 7-14022
 thresholds of perception of jump frequency changes for a decaying signal 7-14021
 tinnitus, magnitude estimation and 'paradoxical' loudness 7-8595
 tinnitus, treatment by external elec. therapy 7-28762
 tinnitus as a source of internal noise 7-8594
 tuning curves, whole nerve action pot. and auditory brainstem response, comparison in guinea pigs 7-54591
 vertebrate hearing, evolution rel. to noise 7-54588
 vowel errors in noise and in reverberation by hearing-impaired listeners 7-8589
 vowel identification, inherent spectral change role modelling 7-47086
 vowel intelligibility in the absence of the acoustic reflex: performance-intensity characteristics 7-65777

hearing aids

active free-field equalizer for TDH-39 earphones 7-28768
 bandwidth-compression-limited amplification in profoundly deaf persons' hearing aid 7-34161
 bone conduction microphone for noisy conditions (*Japanese*) 7-43612
 electronic aids for hearing impaired, visible voice or speech transmission, assessment 7-40173
 electronic cochlear neuroprosthesis development, Czechoslovak project 7-8766
 extracochlear electrode, temporary, use in preoperative testing of permanent implant candidates 7-54611
 frequency response damping, effects on speech clarity and preferred listening level 7-8763
 headphone responses on real ears and a head and torso simulator 7-40368
 implantable electronic devices reliability, case studies 7-60122
 medical electronics developments, review (*Italian*) 7-18094
 noise cancellation 7-40175
 prescription technique comparison using computerised filter adjustment for aid simulation 7-34163
 REDMASK noise reduction filtering for the hearing-impaired 7-34162
 Rehabilitation R&D Progress Reports 7-28774
 Siemens' hearing aids of various sizes (*Dutch*) 7-23485
 Siemens in ear technology (*Dutch*) 7-54608
 speech intelligibility improvement with disturbed temporal resolution (*German, English*) 7-60120
 speech processor with lateral inhibition, 8 channel cochlear implant, subject testing evaluation 7-37275
 three channel cochlear neuroprosthesis for the deaf, implantable receiver/portable transmitter config. 7-8765
 wearable pocket-sized processor for digital hearing aid and hearing prostheses 7-37277
 Zn-air button type battery appls. (*Japanese*) 7-65890

heart see cardiology

heart valves see cardiology; prosthetics

heat

see also heat transfer; heating; latent heat; specific heat; temperature; terrestrial heat; thermal variables control; thermal variables measurement; thermodynamic properties; thermodynamics
 CR-39, response to α -particles, heat and humidity effects 7-30861
 thermal power plants, chemical regeneration of heat for improved efficiency 7-37319

heat capacity see specific heat

heat conduction

see also thermal conductivity
 anisotropic solid, heat conducting second sound and internal energy 7-57669
 axisymmetric, FEM analysis with temperature and temperature gradients as primary variables 7-6071
 bistable thermal equilibrium systems, initial temp. profile, asymptotic evolution 7-31632

heat conduction continued
boundary temperature discontinuities and infinite short-circuit diffusion phenomena 7-1377
boundary value problems, eigenvalues eval. 7-62949
buoyancy-driven flows of gases above liquids with nonuniform heating 7-31790
cassette radioelectronic apparatus, forced ventilation cooling, optimisation algorithm 7-63138
circular tube, heat transfer problems with axial cond., soln. using linear operator method 7-20726
circular tubes in semiinfinite medium, heat transfer, numerical model 7-63152
combined mode heat transfer analysis utilizing radiation scaling 7-63225
composite slab, transient heat conduction, convective and radiative cooling 7-11246
conjugated convection-conduction anal. for vertical plate fin, microstruct. effects 7-63149
continued fraction expansions, thermodynamic aspects 7-11249
continuous versus on-off heating 7-37310
convection/diffusion phase change, enthalpy formulation anal. 7-51118
coupled conduction and radiation in participating slab geometry, short time soln. 7-1378
crystal growth, Czochralski furnace, numerical calc. of heat transfer 7-53543
Dirichlet problem in crescent-shaped domain, solution 7-57670
disequilibrium and self-organisation, book 7-24328
drift rippling mode stabilisation, parallel electron heat conduction 7-16304
in elastic Earth, temp. profile and radial deform. 7-23592
clastomers, impurity containing, exposed to laser pulses, thermooptic lenses, form. kinetics 7-51671
electron beam annealing, pseudo-line, thermal anal., 2D finite element method (*Japanese*) 7-32507
equivalent transformations of grid models 7-11250
fluid flow in channel, nonsteady heat transfer calc. method 7-63223
focusing mirrors, thermooptic aberrations, heat transfer study 7-57509
function analysis of heat transfer with viscous dissipation in semi-infinite tube 7-37458
functional analysis of heat transfer with viscous dissipation between infinite parallel plates 7-37459
gas flows, slow, viscous, heat conducting, calc. 7-51025
gas trunk-line transportation, math. model including turbulence and heat conduction 7-63220
glass-copper laminate, one-dimens. unsteady heat cond., appl. to thermal diffusivity meas. 7-31624
heat flux and temp. gradient relation 7-18540
heat flux distrib. determ. on PF anode surface 7-63258
heat theory principles, historically and critically elucidated, book 7-48265
heat transfer, 1D problem solns. polynomial approx. 7-50907
heat-flux distrib. in semiinfinite bodies, heat-conduction boundary problem soln. 7-62951
heat-sensitive half space heat cond., generalised problem 7-62952
hyperbolic heat conduction, dissipation inequality 7-26123
ice, melting in porous media, solid-liq. interface motion, temp. distrib. 7-50926
inclined square enclosure, natural convection, wall conduction influence 7-26122
insulating materials, surface destruction, self-similar heating regime study 7-62950
interference filters, laser-induced heat flow 7-43333
inverse problem, Duhamel's integral transform. 7-43626
inverse problem, surface temp. and heat flux study 7-43627
inverse problem for the heat equation 7-37309
irreversible processes, Lagrange formalism 7-24617
isoparametric line and transition finite elements of 2D heat conduction 7-43628
JT-60 divertor plate, 2D inverse heat conduction anal. 7-25193
laminar duct flow, heat cond., numerical soln. 7-57790
laser absorption wave structure in thermal dissociation presence 7-26119
laser melting of solids, theory 7-21267
liquid inclusions movement in soluble solids, inverse Stokes' law 7-11263
low temperature measurement by Pt resistance thermometer, errors 7-9833
metals, heating at free surface by laser irradiation, electron kinetic theory 7-6073
meteoroids ablation, radiative heat exchange determ. using radiant heat conduction approximation 7-34948
micropolar thermoelasticity, heat flux dependent 7-6092
monatomic Bose gas, heat conduction, thermo field dynamics methods 7-11251
moving boundary region problems, orthogonal Watson operator, expansion calcs. 7-43629
multidimensional heat cond. in solids, thermal histories, Z-transfer method 7-57668
multilayer composite wall with effects of internal thermal radiation and cond., transient temp. distrib. 7-11262
natural convective heat transfer on vertical plate, heat conduction effect 7-26124
nonlinear heat conduction, moving boundary problems, appl. of Backlund transformation 7-6074
nonlinear inverse ID problem 7-50911
nonlinear unsteady heat conduction problem, verification of experimental B_{ik} and S_k numbers 7-50910
optical storage, digital media, transient thermal conduction 7-57490
orthotropic plate with inclusion, heated, heat cond. 7-11247
oxide, laser reduction to metal, effect of heat conduction 7-17674
paraboloidal systems, steady heat conduction, temp. distrib. 7-50912
phase change problems, curved interface straightening, isoparametric finite elements 7-62963
phase-change material during melting, heat cond. and natural convection, moving boundary problem 7-43900
plate, translucent, radiative-cond. heat transfer 7-43643
porous media, liq. sat., freezing 7-62966
problems with discontinuous boundary condition of second kind, inverse Laplace transformation 7-43631
quasi-analogies and problems of heat conduction (*Russian*) 7-6072
sapphire, single cryst., heat pulse propag. 7-27034
semiconductor and electrical engineering devices, cooling device design 7-37314
semiconductor multilayer systems, non-Fourierian heat conduction 7-43632

heat conduction continued
semiinfinite body, surface temp. distrib., annular heat source effects 7-43630
semitransparent material temp. profile, thermal radiation contrib. calc. technique 7-6080
slabs, planar, short-circuit diffusion phenomena 7-26121
solid, moving, semiinfinite, subjected to pulsed laser irradi. 7-62964
solid cylinder, nonlinear 1D thermal conduction with exponential heat generation 7-6076
space-time behaviour, thermo field dynamics methods 7-11251
surface temp. meas. of poor heat conducting materials radiation technique accuracy 7-26133
synchronous interaction of nonlinear acoustic waves with heat pulses 7-43493
thermal engine connected to finite heat sources, performance 7-16054
thermal problems, time integration, least-squares schemes 7-50908
thermoelastic shells, 2D nonlinear eqns. 7-57685
thermophysical characteristics determination 7-26120
time optimal control in two-dimensional problems of heatconduction 7-11248
transient conduction in a plate cooled by free convection 7-51108
transient problem, Rayleigh-Ritz soln. Lanczos method 7-50909
transport processes approximate soln., nonintegral technique 7-9804
vacuum shield insulation, heat exchange calc. allowing for end effects 7-31629
vapour bubble growth in superheated liquid vol., heat flux calc. 7-63204
variable explicit finite element methods for unsteady heat conduction equations 7-26118
variational techniques for nonlinear heat conduction problems 7-62953
viscoelastic material, Kelvin-type, thermal effect anal. 7-57667
viscous fluid, heat-conducting, relax., variational principle 7-51027
viscous heat-conductive gas, asymptotic behaviour of initial value problem solns. 7-50913
water, initially superheated, solidification in horizontal cylinder study 7-58443
He, free convective heat transfer from horizontal cylinder with large temp. head 7-63142
Sn, crystal growth and Stefan problem, stochastic theory comparison 7-21415

heat content *see* **enthalpy**
heat convection *see* **convection**
heat dissipation *see* **cooling**
heat engines
adiabatic diesel engine, combustion characts. of powdered coal fuel 7-65596
Brayton cycle engines with reciprocating work components, thermodynamics realities 7-65518
Brayton cycle with positive displacement compression and expansion, piston-speed-related inefficiency effect on performance 7-65519
ceramics, reciprocating engine requirements 7-3242
coal conversion and heat-engine ceramic technology, US instrumentation 7-1344
combined solar-fuel power plant with Stirling engine, heat exchange in radiation pipe 7-46922
conversion efficiency limits 7-65521
diesel engine, partial adiabatic cycle heat loss 7-65522
DOE/NASA Automotive Stirling Engine Project overview 86 7-65533
EcoEnergy Power Cycle, alternative to the organic Rankine cycle 7-65517
electric solar power plant for small community 7-65413
endoreversible engines, maximum power calc. 7-65514
fluidyne pumping engine with minimal tuning line, liquid-feedback design 7-65562
free-piston linear alternator solar Stirling engine concept 7-65539
intrinsically irreversible or natural engines, thermoacoustic aspects 7-13927
liquid metal thermoacoustic engine, MHD generator 7-65495
low-grade heat sources, Rankine vs. trilateral cycle engine comparison 7-3714
multivane expander simulation, design and operation optimisation 7-3713
optimization rules in thermal cycle models 7-65520
organic Rankine cycle electric generator with nuclear reactor heat source 7-65569
organic Rankine system for energy recovery, optimisation and economic evaluation strategy 7-40024
pV cycle area rel. to work done 7-35170
Rankine cycles optimisation for low temp. heat recovery 7-65523
Ringbom Stirling engines, displacer spring effects, math. model 7-65558
Ringbom-Stirling engine design, solar operated 7-65544
Ringbom-Stirling engines, parameter effects expt. study 7-65536
Ross linkage for Stirling engines 7-65563
shape memory heat engine performance and optimum stress calc. 7-23207
shuttle heat transfer losses in split-cycle Stirling refrigerator 7-56287
solar water lifting unit with external heat supply engines and solar concentrator 7-33995
Space Station solar dynamic power system, simulation 7-65494
space vehicle appls. of solar dynamic systems using heat engines, overview 7-34070
Stirling cryocoolers, trends and development 7-65535
Stirling cycle simulation, globally-implicit finite-difference method 7-65553
Stirling engine, appendix gap heat transfer losses eval. 7-65555
Stirling engine, flat-plate, recent development 7-65545
Stirling engine, free-piston, RE-1000 hydraulic output system description 7-65542
Stirling engine, gas-fired, 3 kW, perform. anal. and improvement 7-65541
Stirling engine, inverted yoke drive, improvements 7-65546
Stirling engine, pressure drops anal. under reversing flow conditions 7-65548
Stirling engine, regenerator effect on performance 7-65547
Stirling engine, two-phase, two-component, anal. techniques comparison 7-65552
Stirling engine, variable-stroke, testing 7-65537
Stirling engine 3 kW class and heat pump system progress 7-65538
Stirling engine analysis method based upon moving gas nodes 7-65556
Stirling engine components, meas. with reversing flow test facility 7-65551
Stirling engine development in Japan, overview 7-65534

heat engines continued

- Stirling engine for model aircraft propulsion, design and test 7-65543
- Stirling engine heat exchangers, oscillating flow 7-65550
- Stirling engine heater tubes, single and double-row, heat transfer 7-65549
- Stirling engine performance optimization with different working fluids, H₂, He, air and methane 7-65557
- Stirling engine powered torpedo 7-65564
- Stirling engine regenerators, flow inhomogeneity 7-65559
- Stirling engines, moderate temp., mechanical losses in rolling seals 7-65561
- Stirling engines, shaft power producing combustor for thermal efficiency improvement 7-65560
- Stirling engines advantages and appl. 7-65531
- Stirling five-cylinder double-acting engine development for heat pump system 7-65540
- Stirling free-piston space-power module at NASA Lewis Research Center 7-65532
- sun-tracking concentration dish/Stirling engine solar electric system 7-65566
- technology breakout in energy conversion, conf., San Diego, CA, USA (Aug. 1986) 7-60875
- thermal energy storage, phase change materials testing, space appls. 7-65627
- thermal energy storage for space solar power system, phase change materials compatibility 7-65628
- thermal engine connected to finite heat sources, performance 7-16054
- V4-275R Stirling engine, submarine appls. 7-65565
- CO₂ liq. finite sink for atmospheric heat engine 7-40022
- Cr₃C₂-based tribological coating for use to 900°C, appl. to Stirling engine 7-46696
- H⁺ ion heat engine for direct conversion to electricity 7-28409
- NH₄Cl aq. soln. finite sink for atmospheric heat engine 7-40022
- NH₄NO₃ aq. soln. finite sink for atmospheric heat engine 7-40022
- Ni-Ti, nitinol, shape memory alloy, phase transitions, thermal energy conversion appl. 7-39514

heat exchange see heat transfer**heat exchangers**

- see also cooling towers*
- boiling curves, calcs. from unsteady-state quenching tests 7-54257
- bundles of twisted tubes, heat transfer and fluid friction 7-57827
- capillary porous heat exchangers, heat transfer improvement 7-11417
- cavity type solar receiver with thermodynamic transducer, heat loss investigation 7-54341
- combined solar-fuel power plant with Stirling engine, heat exchange in radiation pipe 7-46922
- compact heat exchangers, with permeable wall, friction and heat transfer 7-51143
- contact-type exchangers, heat transfer efficiency 7-11410
- counterflow heat exchanger analysis, appl. of some special functions 7-62955
- crawl space assisted heat pump performance 7-65515
- crossflow heat transfer in tube bundles at low Reynolds numbers 7-63151
- cyclic temperature transient influence on creep behaviour 7-10186
- design, thermoeconomic perspective 7-65516
- design for optical components manufacture 7-31541
- diffusion, in shear flows, Taylor limit investig. 7-57925
- exchangers with oval-shaped tubes, heat transfer and press. drop on shell-side 7-51112
- exergetic efficiency of heat exchangers 7-6079
- fin assemblies, optimum dimensions calcs. 7-1380
- flow and heat-transfer at the intake of a radially symmetrical longitudinal flow heat exchanger (*German*) 7-30619
- fluidized bed heat exchange with a submerged heated surface, mechanism 7-51099
- Incoloy 800 H, permeability of ³H and H in heat exchanger tubes (*German*) 7-56759
- jet cooling and finned walls for improved heat transfer in power installations 7-63140
- large-scale heat accumulation at low temp. for domestic, industrial and farm heating (*Portuguese*) 7-13931
- liquid N₂ heat exchanger, two-phase flow instability, LUSH-EX code 7-6294
- liquid solar collector using mixed dye solution 7-65579
- low-cost solar-energy stimulated absorption refrigerator for vaccine storage 7-65576
- matrix recuperator-heat exchanger calc. procedure 7-26130
- mixing process in heat exchanger, heat and mass transfer 7-37452
- modular HTGR plant, steam generator design considerations 7-62014
- organic Rankine system for energy recovery, optimisation and economic evaluation strategy 7-40024
- packed bed heat exchanger, evaluation for residential appliances use 7-31779
- parallel-horizontal cylinder rows under corona discharge, heat transfer 7-43634
- perforated plate, for small capacity He refrigerators 7-56279
- phase flow regimes, heat exchange with vapour condensation in horizontal tubes 7-31858
- plate-fin and tube heat exchanger, fluid flow and heat transfer 7-20703
- pressure losses in finned air coolers during frost formation 7-57829
- Rankine cycles optimisation for low temp. heat recovery 7-65523
- satellite refrigerator efficiency, influence of heat exchanger longit. heat cond. 7-56274
- shell and tube heat exchanger, heat transfer and press. drop, interbaffle spacing 7-43896
- shell-and-tube heat exchange, thermal performance 7-30006
- shell-and-tube heat exchangers, velocity distribs. comparison for expt. and predictions 7-15275
- solar collector/heat exchanger system, differential game control 7-65578
- solar heating units for wine materials heat-processing 7-34067
- Stirling engine, inverted yoke drive, improvements 7-65546
- Stirling engine analysis method based upon moving gas nodes 7-65556
- Stirling engine heat exchangers, oscillating flow 7-65550
- Superphenix reactor heat exchanger and pump development (*French*) 7-769
- thermochemical energy transfer systems, direct work output 7-54334
- transfer surfaces (*Spanish*) 7-56255
- tubes fitted with helical heat transfer enhancers, fluid friction 7-57828
- tubes with internal turbulence promoters, heat transfer coeffs. 7-43889

heat exchangers continued

- tubular, control with tube-side chemical reaction fouling, simulation 7-16055
- unsteady flow force measurement in inline and staggered heat exchanger tubes 7-6187
- unsteady heat and mass transfer in a heat exchanger with twisted tubes 7-31794
- void fraction meas. in two-phase flow, using fibre optic sensor 7-43430
- Al alloys as heat exchanger materials for OTEC 7-65571
- He Joule-Thomson satellite refrigerator, advantages 7-48755

heat flow see heat transfer**heat insulation see thermal insulation****heat losses**

- see also thermal insulation*
- cavity type solar receiver with thermodynamic transducer, heat loss investigation 7-54341
- central, room and package terminal heat pump installation performance 7-23214
- diesel engine, partial adiabatic cycle heat loss 7-65522
- greenhouse insulation using double glazing and thermal curtains 7-46925
- shape memory heat engine performance and optimum stress calc. 7-23207
- shuttle heat transfer losses in split-cycle Stirling refrigerator 7-56287
- solar collectors, engineering method for heat-transfer coeff. and heat loss calc. 7-54342
- solar water heater, investig. of thermal-energy characts. by dynamic method 7-46966
- Stirling engine, appendix gap heat transfer losses eval. 7-65555
- thermal energy transportation from solar collector field to energy conversion facility 7-65590
- thin plate two-dimensional diffusivity tensor meas. by thermal pattern analysis 7-2285
- transient thermal processes anal. in oil and low-temp. gas pipelines 7-11418

heat measurement see thermal variables measurement**heat of adsorption**

- bond-order conservation, bond making and breaking on transition metal surfaces 7-21653
- coadsorption, promotion and poisoning effects, analytic modelling based on band-order conservation 7-27121
- CVD, adsorption on Si (111) of Si-H system species, rel. to temp., super-saturation, bond strength and press. 7-33583
- graphite surface, isosteric heats of adsorption of ethylene, phase diagram 7-6972
- graphite surface, methane adsorption, incomplete wetting at low temps. 7-32798
- methane, adsorp. on graphite, multilayers, adsorp. isotherms and heat of adsorp. 7-32794
- Ag (110), adsorption of ethylene oxide, surface interactions, XPS, TDS, AES, EELS studies 7-33963
- C, activated, adsorption of Ag, mathematical model 7-44999
- CO adsorption on Cu (111)-Fe cryst. 7-21616
- Mo (100), clean and with S or C overlayers, adsorption and reactions of hydrocarbons 7-28345
- Mo-H system, neutron irradi., H-void interactions 7-44604
- Ni (111), isothermal adsorption/desorption parameters of CO, EELS meas. 7-6971
- NO, adsorption of NO, IR transmission spectra, calorimetry studies 7-58640
- Pd monolayer on Ta (110), heat of adsorp. estimates from core-level shifts 7-52258
- Pt (111), adsorption and desorption of NO, CO or H₂ 7-21643
- Pt (111), adsorption of ethylene oxide, surface interactions, XPS, TDS, AES, EELS studies 7-33963
- Pt (111), Xe adsorption, thermodynamic meas. 7-6982
- Pt monolayer on Ta (110), heat of adsorp. estimates from core-level shifts 7-52258
- Ru (001), clean and O covered, adsorption of NO₂, EELS, thermal desorption mass spectrometry 7-52267
- Si surfaces, (111) and (100), chemisorption of halogen atoms 7-6979
- W (100), Nd thermal desorption, anomalous kinetics 7-45010

heat of combustion

- graphite, ultrafine, heats of combustion, ESR meas., depend. on exposure to air 7-33266
- heterogeneous materials, multikilogram capacity calorimeter, design and construction 7-41390
- solar thermochemical conversion by steam reforming of methane 7-8426

heat of crystallisation

- Gd₃Fe₅O₁₂ ferrogarnets, heat of crystallisation, scanning calorimetry obs. 7-2154
- Ho₃Fe₅O₁₂ ferrogarnets, heat of crystallisation, scanning calorimetry obs. 7-2154
- Tb₃Fe₅O₁₂ ferrogarnets, heat of crystallisation, scanning calorimetry obs. 7-2154
- Tm₃Fe₅O₁₂ ferrogarnets, heat of crystallisation, scanning calorimetry obs. 7-2154

heat of dissociation

- atomisation enthalpies for organic compounds from band increments (*German*) 7-25388
- ethanediazonium ions, unimol. dissoc., ab initio and semiempirical MNDOC calcs. 7-15513
- metal hydrides, thermodynamics of hysteresis at high pressures 7-39911
- methanediazonium ions, unimol. dissoc., ab initio and semiempirical MNDOC calcs. 7-15513
- propanediazonium ions, unimol. dissoc., ab initio and semiempirical MNDOC calcs. 7-15513
- Kr clathrate hydrates, sp. heat, compositions and heat of dissoc. in range 85 to 270K, calorimetric determ. 7-26974
- Nb₂O₄, gaseous, atomisation energy determ., mass spectrometric study 7-28331
- Nb₂O₅, gaseous, atomisation energy determ., mass spectrometric study 7-28331
- Nb₄O₁₀, gaseous, atomisation energy determ., mass spectrometric study 7-28331
- Nb₄O₉, gaseous, atomisation energy determ., mass spectrometric study 7-28331

heat of dissociation continued

Xe clathrate hydrates, sp. heat, compositions and heat of dissoc. in range 85 to 270K, calorimetric determ. 7-26974
YrC_x (x=1,2) equil. reaction, thermodynamic parameters evaluation, Knudsen effusion mass spectrometry 7-23054

heat of formation

alkali borate glasses, M₂O-B₂O₃, (M=Li, Na, K, Rb, Cs), thermodynamic props. 7-2211
alkali metal hydroxide vapour, ion clustering struct., chem. equil., mass spectra 7-17814
alkali metal monohydroxides, high temp. photoelectron spectroscopy, ab initio MO calcs. 7-50251
alkyne isomer groups, chemical thermodynamic props. data 7-60901
benzenes, substituted, ionisation pots., electron affinity, HAM/3 study 7-19710
chloranil-mesitylene(benzene), charge transfer complexes, thermodynamic and spectrophotometric study 7-33950
chloranil-pyrene charge transfer complex, solvent effects, visible spectra study 7-42636
ethylene-HCl van der Waals mol., dissociation energies and heats of formation, photoionisation study 7-19966
growing crystal, correl. between chemoeptaxial temp. and thermodynamic characts. (Russian) 7-58704
hydrocarbons, heats of form., off-diagonal matrix elements, IOC- ω technique calcs. 7-39910
hydrophobic effects in soln. chem., integral eqn., Monte Carlo study 7-59751
intercalation cpd. struct., enthalpy of reaction 7-46841
ion-molecule association and clustering form., thermochemical data 7-18514
isocyanic acid, heat of form., photodissoc. study, time-of-flight and laser-induced fluoresc. spectra anal. 7-31105
metal hydrides, thermodynamics of hysteresis at high pressures 7-39911
methanol, associates, H bonding, struct. CNDO/BW calcs. 7-56985
methanol-trimethylamine, associates, H bonding, struct. CNDO/BW calcs. 7-56985
1-methylallyl cation, photoionisation mass spectrometry, heat of form., ionisation energies, ab initio MO calcs. 7-13798
methylcyclobutane-do(d₃), conformational stability, low freq. Raman spectra anal. 7-50146
polymers elastic moduli, semiempirical method calc. 7-51908
silicides, d-metal, heat of form. evaluation from X-ray emission spectra (Russian) 7-59776
sputtering, slow collisional, surface binding energy 7-59329
transition metal alloys, heat of formation, X-ray emission centres (Russian) 7-37919
transition metal borides, AlB₂ type, electronic struct. study, heats of formation anal., HMO calcs. 7-25409
transition metal crystal, BCC, metal-H bond investig. 7-32360
urethane form. reaction, H bonding, CNDO/BW calcs. 7-56985
Ag, thermal equilibrium vacancies, positron lifetime studies 7-44535
AlOH, enthalpy of form., mass spectrometric determ., equil. const., ionisation pot. 7-59777
Au, thermal equilibrium vacancies, positron lifetime studies 7-44535
Au-Sd transition metal alloys, heat of form. and cryst. struct., linear augmented STO calcs. 7-51705
BaTe, vapourisation thermodynamics and formation enthalpies (German) 7-26930
C₆, cyclic ground state, struct., ab initio calcs. 7-42819
Ca(OH)₂Zn(OH)₂2H₂O, chem. comp., solubility in KOH, thermodynamic props., reaction equil. const. 7-26962
CaTe, vapourisation thermodynamics and formation enthalpies (German) 7-26930
CdSe-polysulphide photoelectrochem. system. corrosion reactions, thermodynamic stability calcs. 7-28320
Co, thermal equilibrium vacancies, muon spin resonance studies 7-51757
Co-B alloy, amorphous, thermodynamic, thermomag. and struct. studies (French) 7-16438
CoH system, ferromag., heat of formation, total energy calcs. 7-45198
Cr vacancy formation enthalpy, positron annihilation studies 7-44536
Cu, thermal equilibrium vacancies, positron lifetime studies 7-44535
Cu, vacancy formation enthalpy, positron annihilation studies 7-7787
Cu-Dy, thermodynamic props. rel. to glass forming ability 7-38204
Cu-Er, thermodynamic props. rel. to glass forming ability 7-38204
Cu-Gd, thermodynamic props. rel. to glass forming ability 7-38204
Cu-La, thermodynamic props. rel. to glass forming ability 7-38204
CuSb(In), vacancy formation enthalpy, positron annihilation studies 7-7787
ErSi₂, behaviour under ion bombard. and O exposure, AES, EELS 7-33506
 α -Fe, H-H binding energy, lattice location and heat of formation 7-32361
Fe, thermal equilibrium vacancies, muon spin resonance studies 7-51757
Fe-Co, thermal equilibrium vacancies, muon spin resonance studies 7-51757
FeF₂ - FeF₃, ion-molecule equilibria, mass spectra, heat of form., electron affinity 7-46862
Gd-Pd, formation enthalpies, calorimetric determ. 7-65341
Gd-Pt, formation enthalpies, calorimetric determ. 7-65341
Ge-Ba, liq. alloys, enthalpy of form. 7-23050
Ge-Sr, liq. alloys, enthalpy of form. 7-23050
GeSe₂, vapourisation, torsion and Knudsen effusion technique 7-2163
GeSe₂, vitreous and crystalline states, energy difference, bond energy, calorimetry study 7-59775
Hg_{0.8}Cd_{0.2}Te, Hg vacancies, heat of form. determ. 7-37969
In, monovacancy formation enthalpy, positron annihilation Doppler broadening studies 7-37976
In, positron annihilation parameters, prevacancy effect 7-39251
Li cpds., energy stability, struct., vibr. spectra, MO LCAO SCF calcs. 7-15512
MoO₃, oxidation and heat of formation 7-65156
(NH₄)_{0.32}F_{0.16}WO₃, intercalation cpd. struct., enthalpy of reaction 7-46841
(NH₄)_{1.84}V₃O₈, intercalation cpd. struct., enthalpy of reaction 7-46841
NaPO₂, form. enthalpy from NaPO₃ mass spectra 7-33952
Nb (110), vacancy formation, positron studies 7-44537
NbC_{1-x}, thermodynamic props., 1200-2500 K 7-44849
NbH, β - and γ -phases, electronic struct. and phonon anharmonicity 7-45199
Ni, single and multiple defect props., mol. dynamics simulations 7-12060

heat of formation continued

Ni/Zr thin film diffusion couples, amorphisation, DSC studies 7-26639
PO_{2-x}, form. enthalpy from NaPO₃ mass spectra 7-33952
PO_{2-x}, form. enthalpy from NaPO₃ mass spectra 7-33952
POBr, gaseous, form., mass spectrometric and matrix IR investig. 7-39908
Pa vapour press. meas., form. enthalpy and bond dissociation energy calcs. 7-10765
PaO₂ and PaO vapour press. meas., form. enthalpy and bond dissociation energy calcs. 7-10765
PbBi₄Te₇, synthesis and physicochemical props. 7-13349
Pd-Ni alloys, formation enthalpies and lattice parameters, embedded atom calc. 7-44455
PdH_x films, H absorption, press.-composition isotherm studies 7-52248
Re₆Te₁₅, cluster type struct., X-ray diffr. study, thermodynamical form. consts. determ. 7-44494
SiH_n, (n=1 to 4), photon yield and thresholds, photoionisation mass spectra study 7-50242
Si₂H₄, struct. and stability, ab initio calcs., heat of form. 7-10441
Sr_{0.2}Hf_{0.8}O_{1.8} solid soln., enthalpy of form. 7-3600
SrTe, vapourisation thermodynamics and formation enthalpies (German) 7-26930
TaC_{1-x}, thermodynamic props., 1200-2500 K 7-44849
TiCl₂, crystn. heat of form. and entropies data base 7-18511
TiCl₃, crystn. heat of form. and entropies data base 7-18511
TiCl₄, heat of form. and entropies data base 7-18511
Ti, positron lifetimes, temp. depend. 7-39253
Ti₂GeSe₂, phase equil. in Ti₂S(Se)-GeS(Se) polythermal sections 7-7975
V-N system, phase equil., crystallography, thermodynamic props. 7-28011
VC_{1-x}, thermodynamic props., 1200-2500 K 7-44849
W, vacancy formation enthalpy, positron annihilation studies 7-37974
YBa₂, enthalpy of form., high temp. calorimetric meas. 7-39909
YrC_x (x=1,2) equil. reaction, thermodynamic parameters evaluation, Knudsen effusion mass spectrometry 7-23054
Zr-Sn, diffusion, chem. activity, modified evaporation method 7-38243
Zr-Ti, diffusion, chem. activity, modified evaporation method 7-38243

heat of fusion
4,4'-di-n-alkoxy-2-hydroxybenzalazines, liq. cryst. props., effect of mol. central core geometry changes 7-1866
4,4'-di-n-alkoxybenzalazines, liq. cryst. props., effect of mol. central core geometry changes 7-1866
eutectic systems, simple, latent heat of fusion, temp. and conc. relationships (Russian) 7-38170
glassy materials, fusion, boundary-value problem soln. 7-21416
growing crystal, correl. between chemoeptaxial temp. and thermodynamic characts. (Russian) 7-58704
lattice spin system, microscopic anisotropy influence on phase boundary macroscopic behaviour 7-18730
metal alloys, amorphisation from melt, determ. 7-6516
poly 4-methyl pentene-1, heat of fusion calc., PVT meas., X-ray diffr. 7-52007
polybutene-1, heat of fusion, X-ray diffr. obs. 7-52008
PVC-chlorinated PVC, miscible blends, rheological and mech. props. 7-8040
steel, austenitic stainless, quenching from liq. state, cooling rate calc. 7-22726
whisker-type monocrystal, elastic limit rel. to phys. characts. 7-2443
Bi, solidification of undercooled liquid, nucleation, pressure effects 7-38169
Fe, polymorphic forms stability, elastic consts. in 20 to 1470°C range, enthalpy of fusion rel. to self-diffusion activation energy 7-6781
Li₂MoO₄, high-press. polymorphs, calorimetric study 7-32638
Li₂WO₄, high-press. polymorphs, calorimetric study 7-32638
Pb-Bi system, heat of fusion (Russian) 7-44766
Sn-Bi system, heat of fusion (Russian) 7-44766

heat of mixing
alkali halide mixtures, binary, common-anion, correl. of thermochem. and phase-diagram data 7-3286
n-alkyl formate-n-alkanol mixtures, excess molar enthalpies at 298.15K 7-44823
alloys, liquid, binary, high order perturbative effects 7-52085
calorimetric measurement, high temp. (Japanese) 7-14949
cyclohexane-methanol, liq.-liq. critical point, eqn. of state 7-12230
derivation using Flory-Huggins lattice theory 7-14735
3,3-dimethylbutan-1-ol-n-hexane mixtures, excess molar enthalpy, heat capacity and molar vol. 7-44850
ethanol-water, excess enthalpies at 323.15, 333.15, 348.15 and 373.15K and from 0.4 to 15 MPa 7-26958
group IIB-VA liquid metal systems, Gibbs energy, composition depend. 7-52080
hexanol-hexane (cyclohexane)(benzene), excess molar enthalpies at 298.15K 7-26956
III-V ternary alloy semiconductors, short-range order 7-44821
lost work and the entropy of mixing 7-29628
4-methoxybenzylidene-4'-propylaniline-n-hexane (benzene) mixtures, enthalpy (Russian) 7-63833
methyl methacrylate-n-heptane, excess enthalpies and vols. at 298.15K 7-44824
methyl methacrylate-n-hexane, excess enthalpies and vols. at 298.15K 7-44824
polymer mixtures, H bonding, enthalpy-IR freq. shift correl., acid-base interaction 7-51667
polystyrene-poly 2-chlorostyrene blend system, miscibility, vol. changes 7-44830
propan-1-ol-benzene-tetrachloromethane, excess molar enthalpies at 298.15K 7-26957
propan-1-ol-tetrachloromethane, excess molar enthalpies at 298.15K 7-26957
propan-2-ol-benzene-tetrachloromethane, excess molar enthalpies at 298.15K 7-26957
propan-2-ol-tetrachloromethane, excess molar enthalpies at 298.15K 7-26957
solid solutions, surface composition, multilayer adsorption 7-6938
tetrachloromethane-alcohol-cyclic ether, excess Gibbs free energies at 298.15K 7-44851
toluene-n-decane (n-dodecane), isothermal compressibility at various temp., excess functions calc. 7-26822
Al-Mg, liq., excess entropy of mixing, resist. calcs. 7-2571

heat of mixing continued

- CO₂-pentane, excess enthalpies at 348.15, 373.15, 413.15, 470.15 and 573.15K 7-44826
 Cd-Bi(Sb), thermodynamic functions are modelled by chemical-physical theory, Gibbs energy 7-52051
 Cu-Dy, thermodynamic props. rel. to glass forming ability 7-38204
 Cu-Er, thermodynamic props. rel. to glass forming ability 7-38204
 Cu-Gd, thermodynamic props. rel. to glass forming ability 7-38204
 Cu-La, thermodynamic props. rel. to glass forming ability 7-38204
 Cu-Zr, compositionally modulated amorphous films, sputter deposition prep. 7-22482
 Fe-Co, liq., thermodynamic mixing functions, Knudsen cell mass spectrometry (*German*) 7-21470
 Fe-Cr system, thermodynamic characts., mass spectrometry 7-53736
 Fe-Ti compositionally modulated amorphous films, sputter deposition prep. 7-22482
 HF-H₂O, vap.-liq. equilib. and partial press. formulae 7-21427
 Hg_{1-x}Cd_xTe, pseudobinary melts, heat capacity, enthalpy of melting, thermal cond. 7-21477
 In-Bi, liq., heat of mixing, calorimetric study 7-12283
 In-Pb, liq., activities, temp. depend., EMF obs. (*Japanese*) 7-12320
 In-Tl, liq., activities, temp. depend., EMF obs. (*Japanese*) 7-12320
 Li-Mg, liq., excess entropy of mixing, resist. calcs. 7-2571
 Li-Sn, liq. alloy, mixing enthalpies, high temp. calorimetry, EMF obs. 7-65044
 Mo film ion beam mixing of marker atoms, heat of mixing effect 7-21304
 NH₃-N₂(methane), excess molar enthalpy and heat capacity 7-44825
 (Ni,Pd,Pt)-(Al,In) liq. alloys, enthalpies of mixing 7-46487
 Ru film, ion beam mixing of marker atoms, heat of mixing effect 7-21304
 Si:As, highly doped, spinodal decomposition and clustering 7-52063
 SiO₂-MgO(SrO)(La₂O₃)(Y₂O₃) systems, liq. immiscibility 7-6807
 Ti-Co, liq.-alloys, thermodynamic props., mass spectrometry (*Japanese*) 7-52084
 UC-UN solid soln., vapour press. meas., chem. activity and heat of mixing eval. 7-12290
 Zn-Sb, thermodynamic functions are modelled by chemical-physical theory, Gibbs energy 7-52051

heat of reaction

- see also *heat of combustion; heat of dissociation; heat of formation*
 alkali metal hydroxide vapour, ion clustering struct., chem. equilib., mass spectra 7-17814
 bromodifluoriodoethane, photodissoc. translational spectroscopy 7-62463
 cytosine and thio derivatives, tautomerism, ab initio study 7-837
 dual temperature thermal storage with complex compounds 7-65620
 fibreglass-filled rubber-modified phenolic resin, sp. ht. and thermomech. expansion meas., thermal decomp. 7-6822
 isocytosine, and thio derivatives, tautomerism, ab initio study 7-837
 methanol, vapour, homogeneous nucleation rates, heat of assoc. effects 7-26926
 methyl halides, nucleophilic substitution reactions, quantum-mechanical model, HMO calcs. 7-36482
 pivalic acid in dil. solution, dimerisation, IR spectroscopy 7-65313
 uracil and thio derivatives, tautomerism, ab initio study 7-837
 BaO-CeO₂, phase relations, thermodynamic parameters 7-6829
 Ca²⁺+D-ribose (D-arabinose), enthalpies, sp. heat and molal vols. at 25°C 7-8253
 Li/SOCl₂ cell, corrosion, calorimetric study 7-46929
 MoO₃, oxidation and heat of formation 7-65156
 Nb-Al₂O₃, high temp. interactions, X-ray diff., DTA studies 7-8259
 Nb-Cr₂O₃, high temp. interactions, X-ray diff., DTA studies 7-8259
 Nb-Y₂O₃, high temp. interactions, X-ray diff., DTA studies 7-8259
 U₃Si, U₃Si₂ powders dispersed in Al matrix, heat of reaction, DTA 7-719

heat of solution

- alkali borate glasses, M₂O-B₂O₃, (M=Li, Na, K, Rb, Cs), thermodynamic props. 7-2211
 alkali metal binary alloys, low temp. phase diagram, compression effects 7-33641
 nonelectrolytes in water, heat of soln., enthalpic pair interaction coeffs. 7-28328
 oxidic actinide cpds., systematic props., oxidation states, fluorite lattice and thermodynamic props., review 7-12013
 polymer gel in pure and mixed solvent media, phase transition 7-63431
 transition metal-H system, heats of soln. and vacancy trapping 7-6804
 urea in water-alkanol mixtures, heat of soln., enthalpic pair interaction coeffs. 7-28328
 water, partial molar enthalpies of solution in n-alkan-1-ols, esters 7-52056
 water in benzene and some n-alkanes, heat of soln. at 298.15, 308.07 and 313.14K 7-26959
 Hg-Au, core holes, final-state screening, total energy calcs. 7-2526
 Mo-H system, neutron irradi., H-void interactions 7-44604
 Nb-C alloy, thermotransport of C 7-46479
 V-C alloy, thermotransport of C 7-46479

heat of sublimation

- nucleic acids, energy minimisation and dynamics, empirical energy functions 7-34097
 Cu, vapour press. and heat of sublimation 7-58454
 Zr-Sn, diffusion, chem. activity, modified evaporation method 7-38243
 Zr-Ti, diffusion, chem. activity, modified evaporation method 7-38243

heat of transformation

- see also *heat of crystallisation; heat of fusion; heat of sublimation; heat of vapourisation*
 alkali metals, condensed phase, thermodynamic props. study 7-32684
 convection/diffusion phase change, enthalpy formulation anal. 7-51118
 cyclosilanes, plastic and condit. crystals, thermal anal. 7-37910
 lead (II) carboxylates, thermotropic phase transitions, DSC meas. 7-21441
 melting lines of simple substances, thermodynamic similarity and thermal props. calcs. 7-6762
 mercury carboxylates, thermotropic phase transition temps. and heats of phase changes 7-2155
 octyloxybenzoyloxybenzylidene, reentrant transition enthalpies, frustrated spin-glass model 7-63816
 4-(4-n-pentyloxybenzylideneamino)azobenzene, liq. cryst. transitions 7-63812
 polymer, thermotropic, structure and structure formation, transition enthalpy/entropy 7-11962

heat of transformation continued

- polymethylenes, melting characts., continuum model (*Russian*) 7-63782
 polystyrene, glass transition, enthalpy relax. kinetics (*Russian*) 7-6797
 smectic A₁ binary mixture, nematic phase creation, phase diagram, transition enthalpy comp. depend. study 7-12269
 styrene copolymers, glass transition, enthalpy relax. kinetics (*Russian*) 7-6797
 Al-Mn quasicrystalline and metastable phases, phase form. and thermal stability 7-26644
 Fe, polymorphism interpretation 7-51700
 Fe thermodynamic props., data tables and reviews 7-18512
 Li₂MoO₄, high-press. polymorphs, calorimetric study 7-32638
 LiNaSO₄, BCC, rotator phase, solid electrolyte behaviour, thermodynamic props. 7-21139
 Li₂WO₄, high-press. polymorphs, calorimetric study 7-32638
 (NH₄)₂SO₄, partially deuterated, phase transition, heat of transition 7-53246
 Ni-Ti, Nitinol, thermodynamics 7-58506
 Rb₂KMF₆, (M=Al, Cr, Fe, Y, Br), structural phase transitions 7-52044
 Si, thermodynamic props., data tables and reviews 7-18512

heat of vapourisation

- 1-alkanols, vapour press. and thermal data simultaneous correls. 7-6767
 material fracture energy, eval. from heat content 7-52019
 DCl, molar vol., vapour press. meas. 7-44779
 Fe thermodynamic props., data tables and reviews 7-18512
 GeS₂, vapourisation, torsion and Knudsen effusion technique 7-2163
 HCl, molar vol., vapour press. meas. 7-44779
 Pb overlayer of Cu (100), growth, phase transitions and struct., thermal energy He atom scatt. study 7-63943
 Si, thermodynamic props., data tables and reviews 7-18512

heat of wetting see wetting**heat pipes**

- antigravity, wick pore dimensions, optimisation 7-1549
 'antigravity', operation, adverse accels. effects 7-44050
 black-body reflectometer for room temp. emissivity meas. 7-14990
 capillary porous materials for heat pipes, struct. and hydraulic props. 7-44039
 corrugated wicks, heat output and max. heat transfer 7-11414
 high-temperature parameters, conjugate problem calc. 7-51104
 horizontal annular pipes, two-phase flow regimes during heat transfer crisis 7-63200
 integrated heat pipe-thermal storage design for a solar receiver, design anal. 7-65626
 liquid flow in coaxial pipes, heat transfer study 7-63137
 oven devices for broadband excitation laser studies 7-15882
 parallel rotating heat pipe, heat transfer characts. (*Japanese*) 7-57841
 plane pipe, nonsteady heat convection study 7-63135
 rotating, in gravity field, with separate vapour and liq. ducts, performance 7-1550
 semiconductor and electrical engineering devices, cooling device design 7-37314
 sintered capillary structures, wetting, macroscopic boundary angles 7-12397
 solar cookers using heat-pipe principle 7-13928
 superheating in heat-pipe oven, appl. to spectroscopy 7-6070
 superheating in heat-pipe oven 7-36553
 tubular heat pipe furnace characts., gas-controlled 7-41375
 vapour flow characts. of slender cylindrical heat pipes 7-11375
 vapour flow in low temp. heat pipes, effect of evaporation and condensation zones 7-63136
 S-I working fluid, max. heat flux transferable in thermosiphon 7-50930

heat pumps

- absorption heat pump systems, H₂O-LiBr based, operating temps. and concs. 7-59866
 air conditioner/heat pump, new concept 7-65526
 assisted distillation system operating characteristics with R11 external working fluid 7-65513
 central, room and package terminal heat pump installation performance 7-23214
 compressor life anal. 7-23211
 crawl space assisted heat pump performance 7-65515
 demand-side planning, role of Earth-Coupled Heat Pump 7-8359
 design, economic viability and performance estimates 7-8430
 dyeing, appl. of waste heat-recovery heat pumps (*Japanese*) 7-59867
 fluidyne pumping engine with minimal tuning line, liquid-feedback design 7-65562
 gas fired heat pump concept using complex compounds as working fluid 7-65524
 hybrid heat pump appl. study 7-23213
 hydride chemical heat pump thermodynamics, alloy selection 7-40023
 industrial heat pumps, comparative economic evaluation 7-65529
 industrial heat pumps, novel approach to placement, sizing and selection 7-65527
 industrial waste heat and flat-plate collector solar heat upgrading by reversed absorption heat pump 7-65419
 integration vs. heat pumping, new challenge 7-65528
 Nevada desert test site heat pump strategy 7-8429
 poultry processing plant refrigeration heat recovery system 7-8428
 radiative heat pumps using narrow-bandgap semiconductors 7-40019
 refrigeration and heat pump cycles, maximum capabilities 7-37457
 service life and compressor survival in northern climate 7-23212
 solar assisted heat pump, control strategy, bilinear model 7-59868
 solar collector with heat pump for food and agricultural products drying 7-54344
 solar-powered solid-adsorption ice maker design 7-65585
 solid gas adsorption cooling system, refrigerator and heat pump using natural zeolite 7-65567
 Stirling engine, gas-fired, 3-kW, perform. anal. and improvement 7-65541
 Stirling engine 3 kW class and heat pump system progress 7-65538
 Stirling engine development in Japan, overview 7-65534
 Stirling five-cylinder double-acting engine development for heat pump system 7-65540
 Stirling heat-actuated heat pumps using liq. pistons, isothermalization 7-65525
 thermal energy storage by thermochemical energy conversion and heat pumps 7-65568
 thermal energy storage in solar house, heat pump coupled to solar collector 7-65619
 thermoeconomic optimisation of heat pump system 7-23210

heat pumps continued

- TRNSYS/GROCS simulation of horizontal coil ground coupled heat pump 7-8427
 utilisation in process industry evaporators 7-65420
 vacuum freezing process in heat pump for subzero climates 7-65530
 vertical ground coupled heat pump system design and performance 7-8431
 Vuilleumier cycle heat pump for domestic appl., computer simulation 7-65554
 water-LiBr absorption cooling system thermodynamic design data 7-23208
 water-to-water heat pump system, performance anal. 7-54336
 H₂O-LiBr absorption heat pumps, thermodynamic design data, heating 7-23209
 LaNi_{4.77}Al_{0.22}-LaNi₅, hydride chem. heat pump, thermodynamics 7-13926

heat radiation

- 3D and 2D radiative transfer in the diffusion approx. 7-10853
 absorbing liquid, radiant heating, numerical modeling 7-11258
 angular coefficients, generalised, with selective absorpt. 7-11257
 black-body radiation, photon radiant and radiant exitance, analytic expression (*Chinese*) 7-50922
 blackbody radiant source, low temp. large area, with heat pipe (*Chinese*) 7-50923
 combined mode heat transfer analysis utilizing radiation scaling 7-63225
 combined solar-fuel power plant with Stirling engine, heat exchange in radiation pipe 7-46922
 composite slab, transient heat conduction, convective and radiative cooling 7-11246
 convective and radiative heat transfer during blowing into layer of two-phase prods. from ablation 7-20755
 coupled conduction and radiation in participating slab geometry, short time soln. 7-1378
 crystal growth, Czochralski furnace, numerical calc. of heat transfer 7-53543
 emission integrals eval. 7-50921
 emissivity of diffuse cylindro-inner-cone with specular lid 7-43637
 ERM thermal anal., heat radiation case study using finite element method 7-20588
 finite element solution of coupled natural convection and radiation in an axisymmetric cavity 7-37311
 floating zone imaging furnace, molten zone temp. distrib., calc. method 7-17416
 fluid frame, radiation transfer 7-20587
 fly ash and coal, radiative characts. 7-43640
 gas-particle mixture, heat transfer under direct radiant heating 7-31780
 glass fibre processing, spinning process in liq. state 7-3258
 heat theory principles, historically and critically elucidated, book 7-48265
 IR heating, physical considerations (*Spanish*) 7-16057
 IR methods of temp. and process control 7-6082
 irradiance calc. in D* determ., precision improvement (*Chinese*) 7-48825
 laser-generated intense Planck radiation 7-16056
 low resolution IR gas transmissivities, line-by-line approach 7-51386
 massive optically dense body, short-time heating by radiant flux 7-11256
 Monte Carlo method, computing time reduction 7-43638
 multilayer composite wall with effects of internal thermal radiation and cond., transient temp. distrib. 7-11262
 optical glasses, radiation heating, radiation source selective props. and temp. effects 7-11255
 optically thick medium exposed to laser beam, anisotropic back scatt. 7-62629
 phase transition temp. determ. in optical ovens for refractory materials 7-30014
 plane-parallel media, radiation transfer, natural eigenfunctions anal. 7-6081
 plasma-molecular systems, spatially nonuniform, thermal radiation power spectral distrib. calcs. (*Russian*) 7-44122
 plate, translucent, radiative-cond. heat transfer 7-43643
 radiant heat fluxes, distrib. over bodies in supersonic ideal-gas flow 7-1589
 radiative heat fluxes in supersonic flow of inviscid gas over 3D bodies 7-43972
 radiative ignition in a planar medium 7-50925
 selectively emitting and absorbing medium, radiative and combined heat transfer in spherical volume 7-1551
 semitransparent material temp. profile, thermal radiation contrib. calc. technique 7-6080
 shells, linear thermoelastic, mech. contact, uniqueness theorem 7-37340
 steel surface at moderate heating temps., relationship between emissivity and exoemissive props. 7-43641
 surface temp. meas. of poor heat conducting materials radiation technique accuracy 7-26133
 temperature fields, finite elements nonlinear anal. 7-50924
 thermal energy storage by thermochemical energy conversion and heat pumps 7-65568
 thermal radiation in turbulent flows—temperature and concentration fluctuations 7-26258
 thermal radiation transfer, diff. theory appl., mathematical aspects 7-43639
 thermal radio emission at sea surface 7-60268
 thin films, radiative heat transfer models validity 7-26132
 transfer eqns., implicit difference eqns. (*Russian*) 7-43642
 tubular thermal solar absorbers, numerical study and THEK appl. (*French*) 7-54353
 vacuum shield insulation, heat exchange calc. allowing for end effects 7-31629
 water vapour, radiation absorpt., generalised ang., coeffs. 7-11257
 CO₂ gas, radiation absorpt., generalised ang., coeffs. 7-11257
 H₂-He mixture, radiant heat transfer body shape influence 7-20715
 Si:P slotted surface, IR emission showing organ pipe resonant modes 7-44873

heat sinks

- laser diode arrays with heat sinks, temperature profile model 7-20221
 CO₂ liq. finite sink for atmospheric heat engine 7-40022
 NH₄Cl aq. soln. finite sink for atmospheric heat engine 7-40022
 NH₄NO₃ aq. soln. finite sink for atmospheric heat engine 7-40022

heat systems

- see also boilers; heating
 No entries

heat transfer

- see also condensation; convection; cooling; evaporation; heat conduction; heat radiation; radiative transfer; thermal diffusivity
 7-46438
 adiabatic curvilinear surface, turbulent wall jets, integral relations 7-11488
 advection equation, linearised, 2D, finite element approximations, stability and phase speed 7-37455
 aerosol spherical particles at arbitrary Knudsen no., thermophoresis, gas-kinetic eqn. 7-44030
 air, laminar flow and heat transfer in tube bank, finite element calcs. 7-51313
 air cross flow over heated cylinder, heat transfer coeff. investig. 7-43892
 air crossflow operation of tube bundles, heat transfer enhancement 7-26128
 air flow, rot. and vibr. spheres heat transfer 7-43928
 air flow in pipes, local heat transfer coeffs. meas. 7-11412
 air flow with fine droplets, evaporative cooling heat transfer 7-11508
 air-water (hexadecane), natural convection in complex enclosed space, heat transfer 7-11421
 air-water-sand flow in horizontal pipe, heat transfer and pressure drop 7-37515
 annular duct, convective heat transfer, turbulent to laminar reverse transition (*Japanese*) 7-11543
 annular thermal entry problem, num. solns. 7-16180
 axial flow in square lattice rectangular rod bundle, wall shear stress meas. 7-16282
 binary gas mixtures, thermodiffusion ratio determ. 7-57972
 binary liquid mixtures, heat and mass transport 7-1559
 binary semiconductor alloys, directional solidification, convection, segregation, ampoule and furnace design 7-59501
 Blasius flow, skin friction, heat transfer, variational soln. 7-20699
 blow close-packed bed of fruit and vegetables, heat transfer, num. anal. 7-63139
 blunt cone lateral surface heat exchange in boundary layer flow 7-1529
 boiling, capillary porous coating thickness effect 7-51101
 boiling, coefficient, plasma-deposited coating particle size effect 7-50916
 boiling, flow, critical heat flux prediction 7-43898
 boiling heat transfer, anal. using hot ball quenching method (*Chinese*) 7-49596
 boilup heat transfer obs., using fibre optic probe 7-50778
 boundary layer, heat and mass transfer, external turbulence effects 7-1541
 boundary layers, three-dimensional unsteady flow due to stretching surface 7-51044
 bubble and transition-boiling regimes, heat transfer coeff. 7-11416
 bubble growth and collapse, transient boiling heat transfer in narrow channel 7-26346
 bundles of twisted tubes, heat transfer and fluid friction 7-57827
 buoyancy-driven turbulent flow in rectangular cavity 7-51068
 buoyant and combustng flow, turbulence model 7-51083
 capillary porous heat exchangers, heat transfer improvement 7-11417
 capillary-porous bodies, heat and mass transfer, mathematical models 7-62957
 capillary-porous structures, heat transfer during vapour formation, regimes and laws 7-31865
 CARS, applications in chemical reactors, combustion and heat transfer 7-17788
 channel, vertical, partially blocked, laminar mixed convection 7-43842
 Chebyshev collocation methods for parabolic eqns., heat eqn., advection-diffusion eqn. 7-48649
 chemical boiling, heat and mass transfer, gas liberation and free convection 7-43907
 chemical reactions, exothermic, in coupled nonisothermal continuous stirred tank reactors, dynamics 7-13732
 chemical reactions, homogeneous, wall to gas heat transfer coeffs. 7-8258
 3D chemically nonequilibrium viscous shock layer on catalytic surface 7-20810
 circular tube, heat transfer problems with axial cond., soln. using linear operator method 7-20726
 circular tubes, average heat transfer coeff., empirical correl. 7-1565
 circular tubes in semiinfinite medium, heat transfer, numerical model 7-63152
 coherent structures in the far field of a turbulent wake 7-31773
 combined solar unit, heat flow balance in working chamber 7-54345
 combined solar-fuel power plant with Stirling engine, heat exchange in radiation pipe 7-46922
 compact heat exchangers, with permeable wall, friction and heat transfer 7-51143
 compensated heat flow meter, thermal flux meas. at elevated radiation influence 7-4838
 complexity of PDEs 7-48385
 composite material, diffusion and heat transfer, practical eqns. 7-6855
 composite thermal energy storage systems, high temp., for industrial appls. 7-65636
 compressible flow, boundary layer excitation by surface heating or cooling, numerical simulation 7-6181
 compressible laminar boundary layer flow with heat transfer, quasi-linearization technique 7-26247
 compressible Navier-Stokes eqns., pseudo-time algorithm for integration to steady state 7-26302
 condensation, solid-state, heat transfer and cryodeposit props. 7-63789
 condensation of flowing vapour on horizontal elliptic cylinder 7-58452
 confined Bernard problem, nonlinear phenomena, numerical parametric anal. 7-30482
 conjugate film condensation on one side of vertical wall and natural convection on other side 7-63147
 contact melting, latent heat thermal energy storage 7-43646
 contact temp. in bodies moving with slip 7-11252
 contact-type exchangers, heat transfer efficiency 7-11410
 continuous longitudinal-transverse motion of liq. in annular heat generating layer (*Russian*) 7-49578
 corner flow, incompressible fluid with suction, heat transfer eval. 7-26277
 correlation for heat transfer between immersed surfaces and large-particle gas-fluidised beds 7-26127
 corrosion testing, heat transfer effect, dimensionless groups appl. 7-39792
 counterflow heat exchanger analysis, appl. of some special functions 7-62955
 coupled groundwater flow and heat transfer in granite rock locality 7-55110

heat transfer continued

critical heat flux of boiling Freon, correls. at high subcrit. press. 7-1389
critical heat flux prediction via Katto's correls. and Whalley's model 7-51339
crossflow boiling heat transfer in tube bundles 7-11511
crossflow heat transfer in tube bundles at low Reynolds numbers 7-63151
crossflow rough tube bundles, heat transfer efficiency 7-26129
cryogenic engineering conf., Berlin, Germany (April 1986) 7-48183
crystal growth, Czochralski furnace, numerical calc. of heat transfer 7-53543
crystal growth, heat and mass transfer in microgravity and on Earth 7-53510
crystal surface, temp. distrib., induced by local heat pulse 7-57671
customised shear layers on smooth and rough surfaces, development 7-51082
cylinder in cross flow of water with injection into boundary layer, heat transfer and drag 7-43888
cylinders, elliptic, in tandem arrangement, heat transfer 7-63145
cylinders subject to transverse streamline flow, turbulent boundary layer separation (*Russian*) 7-11400
cylindrical electrical conductor, heat transfer eqn. soln. using optimal linearization method 7-57672
Czochralski growth, global finite element calc. 7-39370
deflector type effect, blades with cooling gas crossflow 7-43635
deformation, linear reversible, thermodynamics 7-32551
diesel engine, partial adiabatic cycle heat loss 7-65522
direct surface heat flow measurement and the optimisation of thermal insulations (*Hungarian*) 7-58500
disperse systems, nonstationary heat transfer, internal heat source influence 7-63202
drainage discs effect on condensing heat transfer of vertical fluted tubes 7-20711
droplets, accelerated, in nonisothermal flow, heat transfer (*Russian*) 7-16179
drops, evaporation anal. taking account of variability of gas props. 7-44029
dropwise condensation heat transfer on a horizontal tube 7-20704
duct, cross shaped cross section, parametric study of friction and heat transfer 7-26276
duct, rectangular, turbulence promoters, geometric shapes effect 7-37443
duct blocking effect on crossflow and heat transfer in cylinder 7-1629
dust-gas mixture, slow burning conditions 7-13778
dynamics of heat exchange in natural heat flowmeter (*Russian*) 7-6212
earth, oil-bearing, heat and mass transfer 7-56189
Earth's temp. field, stationary heat eqn., temp. optimisation 7-8871
Earth mantle, heat transfer, 2D model 7-54940
electric arc, deflected wall-stabilised relax. process, thermodynamics soln. 7-44273
electric glass furnace, 3D model for glass flow and Joule heat release calc. 7-20707
electrically boosted glass melting tank, 3D model for flow simulation and heat transfer 7-20805
electrothermal processes, one-dimensional, boundary-value problems (*German*) 7-31623
entropy layer absorption effect on supersonic flow heat transfer of submerged circular cone 7-43975
equation, smoothness of soln. in singular domain of R^{n+1} 7-62967
exchangers with oval-shaped tubes, heat transfer and press. drop on shell-side 7-51112
exergetic efficiency of heat exchangers 7-6079
explosive flashing, effective heat of vapourisation 7-1547
falling films, surface temp. meas., rel. to gas and vapour sorption 7-56263
falling liq. film, vapour generation nucleate boiling, acoustic diagnostic technique 7-11502
film condensation instability at surface of a cylinder 7-37526
fin, rectangular, heat transfer rate, power-law temp. depend. 7-1561
fin assemblies, optimum dimensions calcs. 7-1380
finned tube, transverse flow of viscous fluid, local heat transfer (*Russian*) 7-31881
finned tubes, transverse flow of viscous fluid, heat transfer (*Russian*) 7-31882
fission reactors, uncovered-bundle heat transfer under high-pressure boil-off conditions 7-5359
fixed bed catalytic reactors, 1D heat transfer coefficient 7-6298
flat plate thermometer, heat transfer characteristics, effect of variable fluid property 7-43910
flat surface, porous, movement in parallel free stream, boundary layer behaviour 7-43919
flow and heat-transfer at the intake of a radially symmetrical longitudinal flow heat exchanger (*German*) 7-30619
fluid flow in channel, nonsteady heat transfer calc. method 7-63223
fluid flow through porous media, heat cond. 7-16249
fluidised beds, two- and three-phase, heat transfer characts. 7-31878
fluidized bed heat exchange with a submerged heated surface, mechanism 7-51099
fluids, enhanced heat diffusion by oscillation 7-51116
forced oscillatory compressible flow past yawed cylinder, heat transfer 7-1585
free-convection boundary layer at heated vertical plate, heat transfer and temp. profiles 7-31795
fuel drop, liq., moving, combustion, thin-flame theory, variable density effect 7-26364
fuel element bundles, 3D heat-carrier flow, numerical modelling 7-61981
furnace gas radiation tubes, internal and external heat transfer, combined soln. 7-11415
gas flow in cylindrical channel, interactions of electric arc 7-44056
gas-liq. descending annular flow, phase boundary turbulence and heat exchange 7-63201
gas-liquid two-phase flow of drag reducing fluids, heat transfer 7-16175
gas-particle mixture, heat transfer under direct radiant heating 7-31780
gasdynamic model, heat exchange, press. distrib. in high enthalpy air stream 7-1587
global blow-up of a nonlinear heat equation 7-62968
granular propellants, combustion, two-phase transient flow, modelling 7-37520
graser electronic heat conduction under high pressure 7-10955
heat absorption demonstration using incorrectly installed bulb 7-48257
heat carriers in vertical pipes of low-head natural circulation systems, limiting thermal loads 7-43917

heat transfer continued

heat equation, ill-posed Cauchy problem, error estimates for numerical method 7-50932
heat equation with absorption, singular soln. 7-37318
heat flux and temp. gradient relation 7-18540
heat pipe, high-temperature parameters, conjugate problem calc. 7-51104
heat pipe with corrugated wicks, heat output and max. heat transfer 7-11414
heat source movement over heat conducting medium surface 7-1379
Hele-Shaw flows, free boundary problem solns., periodicity and almost periodicity 7-57840
hexadecane-water, natural convection in complex enclosed space, heat transfer 7-11421
n-hexane, flashing liq., steady-state ejection, expt. unit 7-6209
high temperature gases in annular channel with cold walls, heat transfer in turbulent flow (*Russian*) 7-1557
high-enthalpy gas flow, heat and mass transfer on catalytic wall 7-11510
high-temperature oxidizer heaters for a 500-MW MHD power station 7-63232
Hopf bifurcation in the Lorenz model by the 2-timing method 7-31802
horizontal annular pipes, two-phase flow regimes during heat transfer crisis 7-63200
horizontal boiler tubes, dryout criteria for nonuniform heat flux 7-20713
human exercise and heat exchange in thermal environments 7-63154
hydrocarbon, pyrolysis, wall to gas heat transfer coeffs. 7-8258
hypersonic viscous shock layer investig., on rotating bodies 7-20756
ice-air composite materials, melting process study 7-26335
incompressible laminar boundary layer, MHD flow past non-isothermal cone 7-11554
incompressible laminar boundary layer flow, MHD with heat and mass transfer 7-20806
ingot solidification, temp. field, ZD simulation 7-33650
internally cooled cable superconductors, enhanced heat transfer calcs. 7-15355
irregularly shaped bodies, heat and mass transfer, numerical simulation 7-48639
isovectors of class of nonlinear diffusion equations 7-24603
jet cooling and finned walls for improved heat transfer in power installations 7-63140
laminar boundary layers on continuous moving surface, momentum and heat transfer 7-63111
laminar falling liquid film, heat transfer from horizontal smooth tube 7-63131
laminar fully developed flow in plate fin passages, heat transfer, fin shape effect 7-63110
laminar heat transfer and flow in curved square channels, elliptic nature, numerical visualisation 7-37432
laminar incompressible 2D boundary layer eqns. similarity solns. 7-51042
laminar incompressible flow with large negative long. press. gradient, friction and heat transfer 7-51047
laminar incompressible oscillating flow, mean-parameter modeling 7-63109
latent heat storage unit with finned tube, heat transfer characts. 7-43647
latent heat storage unit with finned tube, solidification, heat transfer characts. 7-43648
lighting generators for commercial vehicles, oil cooled, heat transfer coefficients comparison (*German*) 7-37312
linear polymers, struct., thermophys., props. (*Russian*) 7-12334
liquid boiling, heat and mass transfer 7-31627
liquid boiling heat transfer in porous struct. 7-51102
liquid crystal thermography for wall heat transfer and flow visualisation 7-35520
liquid film, laminar downflow over cylindrical surface, thermal entry region, heat transfer 7-51096
liquid films, heat transfer coeff., surface nonisothermicity 7-11411
liquid flow in coaxial pipes, heat transfer study 7-63137
liquid with vapour bubbles, finite duration pulses and shock wave evol. 7-6250
liquid-gas flow through coarse particle beds, 1D model 7-57904
liquid-liquid spray column, heat transfer model 7-1567
liquid/liquid two-phase annular flow, flow behavior and heat transfer to flowing liquids (*German*) 7-16176
liquids, radiation heat transfer influence on effective thermal conductivity 7-6898
local coefficients from staggered bundles of rough tubes in crossflow, expt. 7-43894
longitudinal flow operation of fins, heat transfer, num. anal. 7-51103
low temperature thermal storage using latent heat and direct contact heat transfer 7-65618
LWR safety anal., steam direct contact condensation on slowly moving water 7-5358
macroscopically inhomogeneous anisotropic media, kinetic phenomena, review (*Russian*) 7-56195
magnetic refrigerator, Ericsson, regenerator and working material heat transfer process 7-56284
material destruction rate, heating type effects 7-46848
matrix recuperator-heat exchanger calc. procedure 7-26130
melting around horizontal tube, axial fins effects 7-51106
melting in tube in presence of circumferentially nonuniform heating 7-43897
meridional sections of 3D boundary layer, heat transfer calcs. 7-51125
metal equipment struck by lightning, temp. distrib. anal. and heat fluxes (*Russian*) 7-43649
metallic mould/casting thermal response characts., transient temp. field anal. 7-65019
MHD boundary layers, heat transfer, Joule heating and transpiration effects 7-37556
MHD Couette flow with heat transfer, Hall effects 7-37554
MHD heat transfer in cylinder, temp. distrib., implicit calcs. 7-51324
magnetopolar fluid in magnetic field, laminar free convective heat transfer, suction/injection effects 7-57824
mirror, honeycomb sandwich, thermal design 7-37089
mixed-convective heat transfer to liquids at supercrit. press. in vertical pipes 7-57830
mixing process in heat exchanger, heat and mass transfer 7-37452
molten reactor core/concrete interactions in HCDA, mass and heat transfer simulation 7-25138
molten salts, chemical resistance of valve packing and sealing materials 7-65586
motionless medium, heat transfer, heat flux relaxation 7-57666

heat transfer continued
 multilayer fusing heat insulating coating, weight minimisation algorithm 7-65154
 natural convection enclosure flow, temp. and heat flux distrib. 7-1563
 natural convection in partially divided enclosures 7-63146
 natural convection in rapidly spinning systems, heat transfer and flow visualisation 7-63161
 nonisothermal continuous stirred tank reactor, multivariable, global control using moving model 7-13729
 nonlinear eqn. soln., singularities development 7-37341
 nonlinear heat eqn. with absorption, regularity of solns. and interfaces 7-62959
 nonNewtonian flow, transient mass and heat transfer from drops or bubbles 7-11473
 nonNewtonian laminar falling liquid film, thermal entrance region, heating and evaporation 7-51235
 nonNewtonian media, highly viscous, hydrodynamics and heat transfer 7-43985
 nonsteady heat transfer calcs. in bed using special functions 7-43918
 nucleate pool boiling, surface roughness and polymeric additive effect 7-11512
 oceanographic heat transport in Pacific and Indian oceans, annual var. 7-55066
 oceans contrib. of Ekman flows to annual heat flux variations across Tropic circles 7-8992
 open-type vortex cooler for power semicond. instruments, thermal resist. study 7-11405
 optical crystals, growth, Bridgman-Stockbarger method, thermal modelling 7-22461
 oscillating flow past infinite vertical plate, suction and free convection effects 7-1555
 oscillating flow subjected to axial temp. gradient, temp. and spatial distrib. of heat flux 7-51114
 OTEC, open cycle heat and mass transfer expts. 7-65575
 OTEC, plate type condenser, performance tests (*Japanese*) 7-54337
 OTEC shell and plate type evaporator, performance tests (*Japanese*) 7-54338
 oval twisted tubes, transverse streamline gas flow, characts. (*Russian*) 7-11548
 packed bed catalytic reactor, local thermal equilibrium 7-6276
 packed bed heat exchanger, evaluation for residential appliances use 7-31779
 parallel plates at arbitrary Knudsen numbers heat transfer study 7-57883
 parallel rotating heat pipe, heat transfer characts. (*Japanese*) 7-57841
 parallel-horizontal cylinder rows under corona discharge, heat transfer 7-43634
 particles diffusion and heat flux in the initial stage of the transport process 7-20589
 pellets, cylindrical, heat transfer 7-43651
 phase change process in cylindrical annulus with axial fins on inner tube 7-51273
 phase flow regimes, heat exchange with vapour condensation in horizontal tubes 7-31858
 pipe, vertical, internally cooled, embedded in porous medium, condensation 7-32624
 pipe flow, gas, permeable walls, turbulent flow, heat transfer, phys. props. temp. depend effect 7-63217
 plane two-layer medium of different optical props., radiative and complex heat transfer (*Russian*) 7-1383
 plane-linear induction magnetohydrodynamic pump, thermophysical study (*Russian*) 7-11254
 plasma jet stagnation region, blunt body heat transfer coeff. investig. 7-43892
 plasma-electrolyte metal heating mechanism 7-46857
 plate, flat, with vectored surface mass transfer, heat transfer characts. (*Chinese*) 7-11398
 plate array aligned in rectangular duct flow, heat transfer, press. drop 7-31788
 plate-fin and tube heat exchanger, fluid flow and heat transfer 7-20703
 point sink on plane with magnetic field, heat and mass transfer 7-1618
 polyethylene, form-stable high density, latent thermal storage unit performance 7-65602
 polyethylene, high density, latent thermal storage unit, heat transfer, numerical anal. 7-65603
 polymer melts, elongational flow, thermodynamics nonlinear theory 7-43991
 pool boiling, role of macrolayer evaporation at high heat flux 7-50927
 pool boiling, thermodynamic state of bulk-sat. liq. prediction 7-50928
 porous material, diffusion and heat transfer, practical eqns. 7-6855
 porous slab, phase change, heat and mass transfer 7-31863
 power plant condensers, 2D flow and heat transfer computation 7-51148
 profiled crystals, Stepanov growth, conf., Leningrad, USSR (March 1985) 7-29573
 propagation problem, Laplace-Hankel transformation 7-6075
 rarefied plasma flow, heat transfer to metallic or nonmetallic particle 7-20868
 Rayleigh-Benard instability, stochastic perturbations, random rot. effect 7-31751
 RBMK-1000 reactors, heat transfer during accidental emissions, numerical anal. (*Russian*) 7-5402
 reactive shear bands, dimensional anal., numerical integration 7-33931
 reactor nucleate pool boiling using heated multirod, pressure effects 7-56715
 reattachment of flow downstream of sudden pipe expansion, turbulent heat transfer 7-51134
 refrigerant R-142, boiling, heat flux in low press. natural circulation coding system 7-11505
 refrigeration and heat pump cycles, maximum capabilities 7-37457
 retarded fluidised bed, heat transfer, oscill. model 7-26269
 review of 1985 literature 7-48221
 rough annuli, heat transfer anal. 7-1548
 round jets, turbulent and heated, similarity solns. 7-1598
 salt-stratified layer, double-diffusive convection induced by discrete heat source 7-43901
 sapphire, growing crystals, hot zone heat transfer simulation 7-32321
 SCALE, nuclear waste cask analysis software, heat transfer analysis capabilities 7-15412
 SCALE, spent fuel cask analysis software, conf., Saclay, France, (June 1986) 7-14700
 selectively emitting and absorbing medium, radiative and combined heat transfer in spherical volume 7-1551

heat transfer continued
 self similar cylindrical shock wave in radiating magnetogasdynamics, astrophysical appl. 7-34847
 separated and reattached flow on flat plate, simulation of heat transfer 7-51107
 shell and tube heat exchanger, heat transfer and press. drop, interbaffle spacing 7-43896
 shock wave structure, liq. with bubbles, transient heat and mass transfer effect 7-6249
 shock waves from point-sources in a heat-conducting gas 7-34849
 shuttle heat transfer losses in split-cycle Stirling refrigerator 7-56287
 simple Benard problem with permeable boundaries 7-57809
 solar collector, flat-plate type electronic, heat transfer coeff. digital meter 7-23220
 solar collectors, engineering method for heat-transfer coeff. and heat loss calc. 7-54342
 solar convective loop air thermocirculation (*Italian*) 7-20729
 solar cooling by direct evaporation from sprays 7-37532
 solar flat-plate collector, dynamic behaviour (*French*) 7-28414
 solid adsorbent grain, spherical, submitted to adsorbable vapor press. step temp., conc. and press. distrib. (*French*) 7-1386
 solid particle acceleration by gaseous detonation products 7-20778
 solid state laser systems heat transfer and thermoelasticity effects, alternating direction implicit method 7-50567
 spatial components of energy release functions in two-dimens. heat cond. problems (*Russian*) 7-51147
 sphere in cylindrical tube, fluid flow and heat transfer 7-20706
 spherical particle surface, heat transfer investigated using mol. kinetic methods 7-63184
 spiral tube bundles, heat and mass transfer 7-43905
 stationary vapour on corrugated surface of horizontal tube, heat transfer, condensation 7-50919
 steady heat flow, BGK kinetic model 7-43636
 steady heat source moving through stratified flow, resulting flow patterns, atm. appl. 7-4127
 steady-state flow in channels, heat transfer calcs., three-parameter model 7-51123
 steady-state freezing of liquids in laminar flow between two parallel plates 7-51036
 steam, dropwise condensation, heat transfer study, falling drops effect 7-43890
 steel, Al killed, tensile testing, deform. heating 7-65105
 steel, quenching, effect of martempering on thermal stress and strain 7-46532
 Stefan problem, two-phase, with interfacial energy and entropy 7-43633
 Stefan problem with one spatial var., simulation of permafrost zone, soil thawing and freezing 7-47469
 Stefan problems, multidimensional, efficient finite difference scheme 7-6069
 Stefan systems, stochastic two-phase, state and free boundary estimations 7-62956
 Stirling cycle simulation, globally-implicit finite-difference method 7-65553
 Stirling engine, appendix gap heat transfer losses eval. 7-65555
 Stirling engine, two-phase, two-component, anal. techniques comparison 7-65552
 Stirling engine components, meas. with reversing flow test facility 7-65551
 Stirling engine heat exchangers, oscillating flow 7-65550
 Stirling engine heater tubes, single and double-row, heat transfer 7-65549
 storage of hot water in aquifer, underground heat and fluid flow models 7-65600
 subcooled boiling flow in vertical eccentric annular channel, heat transfer study 7-51310
 subcooled liquid, film boiling in channels, heat transfer and hydraulic resistance 7-51145
 superheated liq., flashing in glass capillaries 7-13797
 superheating in heat-pipe oven, appl. to spectroscopy 7-6070
 supersonic Laval nozzle separated regions, heat transfer investig. 7-31831
 surface exposed to vapour with noncondensable gas, simultaneous melting and condensation 7-51274
 surface rippling during laser material processing, thermohydraulics anal. 7-58574
 surface roughness effects on adiabatic wall temp. 7-20700
 surface thermophysical properties effect on heat transfer in turbulent flow 7-26271
 suspensions, reactive, flames, radiative transfer as propag. mechanism 7-17796
 swirled plumes, shear stresses, turbulent heat flux 7-6220
 symmetry planes of differently shaped bodies, heat and mass transfer characts. 7-11447
 synchrotron beam line critical elements, heat transfer studies 7-42255
 tensile tests, nonisothermal, anal. using measured temp. distrib. 7-65245
 thermal loading, transient heat transfer thermo-elastic anal. 7-50951
 thermal osmosis near a buried heat source 7-51296
 thermal regime identification of complex structure 7-26131
 thermal stability of a fluid layer under variable body forces 7-63116
 thermal transport problem modelling using boundary element methods 7-51149
 thermochemical energy transfer systems, direct work output 7-54334
 thermogrammetry and thermal engineering conf., Budapest, Hungary (April 1987) (*Hungarian*) 7-56258
 thermophysical research automation at BSSR Institute of Heat and Mass Transfer 7-4823
 thermosiphon, transients, heat transfer calcs. 7-11506
 thermosiphon, two-phase, inclination angle influence on limiting heat flux 7-51097
 thermosyphonic solar water systems, pipe thermal insulation effects 7-40040
 thin liquid layers, thermal conductance, meas. 7-16827
 toluene, laminar flow, heat transfer in thermal inlet region 7-43895
 transient boiling, heat transfer mechanism 7-11253
 transient thermal processes anal. in oil and low-temp. gas pipelines 7-11418
 truncated-cone chamber, radiative heat transfer, zonal method soln. 7-50915
 tube, vertical, with crossflow of condensing steam, heat transfer to surface 7-51144
 tube and surrounding water-saturated soil, heat exchange 7-63153

heat transfer continued

- tube banks, staggered, heat transfer characts. in crossflow of air with varying temp. differences (*Russian*) 7-1556
- tube bundle with spacers, flow of water, convective heat transfer 7-51146
- tubes, liquid filled, heat transport 7-37542
- tubes fitted with helical heat transfer enhancers, fluid friction 7-57828
- tubes with internal turbulence promoters, heat transfer coeffs. 7-43889
- tubular heat exchanger, control with tube-side chemical reaction fouling, simulation 7-16055
- tubular specimen under HF induction heating, temp. distrib. anal. 7-43650
- turbulent boundary layers, barriers, flow and heat transfer 7-51100
- turbulent boundary layers, finite element anal. 7-31771
- turbulent channel flow, heat and mass transfer modelling 7-26257
- turbulent flow characts. in wake of circular cylinder (*Russian*) 7-1574
- turbulent heat transfer from shrouded longitudinal fin array, tip to shroud clearance effect 7-63121
- turbulent liquid film, freely-falling, momentum and heat transfer 7-20712
- turbulent nonpremixed series parallel reaction, mixing effect 7-31889
- turbulent pipe flow, heat transfer 7-43860
- turbulent plane jet, organised struct., role in momentum and heat transport 7-44000
- turbulent plane wake, heat transport meas. 7-31760
- twisted circular-sector ducts, fluid flow and heat transfer anal. 7-11374
- twisted oval tube, heat transfer and hydraulic drag coeffs. 7-1631
- two-dimensional, with melting and freezing, finite element soln. algorithm 7-1381
- two-dimensional linear advection equation, high resolution schemes 7-37456
- two-phase disperse boundary layer, condensate pulsation characts., effects on heat transfer and friction 7-51281
- two-phase flow, fluid-heated, dynamic instabilities, meas. and anal. 7-51276
- two-phase thermosiphons, heat and mass transfer 7-11409
- underheated liquid, surface boiling, forced motion, Reynolds analogy appl. 7-31806
- unheated end shape influence on heat transfer of cylinder in longitudinal flow 7-43893
- unsteady heat and mass transfer in a heat exchanger with twisted tubes 7-31794
- unsteady heat transfer in gas-swept bed of spherical granules 7-31803
- vapor condensation on an inclined plate within aporous medium 7-1572
- vapour bubbling of moving underheated liquid, condensation and heat exchange 7-37525
- vapour condensation in cylindrical borehole, heat transfer 7-11408
- vapour flow in low temp. heat pipes, effect of evaporation and condensation zones 7-63136
- Venus ionosphere, two-dimensional model of thermal struct. 7-24039
- vibrating tubes in air crossflow, heat transfer behaviour, temp. and velocity fluctuations 7-51094
- vibrating tubes in crossflow, local and average heat transfer coeffs. 7-51095
- viscoelastic boundary layer flow past stretching plate with suction and heat transfer 7-6313
- viscous gas flow, intense heat release in channels 7-31797
- viscous incompressible fluid in half-plane, Chorin-Marsden product formula convergence 7-11372
- viscous incompressible liquid flow and heat exchange, grid method calc. 7-26270
- viscous Newtonian and non-Newtonian heat transfer for helical ribbon mixers 7-6208
- Volterra equation, homogenization 7-35480
- vortex flow meters for computerised vapour-heat flow measurement (*German*) 7-11564
- vortex flows, ballistics of objects in system 7-11427
- VVER-1000 reactor, heat transfer during accidental emissions, numerical anal. (*Russian*) 7-5402
- wall jet diffusion combustion, heat exchange process, num. investig. 7-26266
- wall temperature nonuniformity effect on natural convection in heated enclosure 7-51109
- water, cold, horizontal buoyant flows, multiple steady-state solns. 7-43899
- water, cold, natural convection near its density maximum in rectangular enclosure 7-57836
- water, supercritical, heat transfer and turbulent flow in vertical tube 7-51142
- water flow in tubes, heat transfer crisis, control expt. errors 7-63130
- water heater, 2-phase solar, operation and comparison with thermosiphon heater 7-65580
- water waves, impact on ice surface, heat transfer 7-51098
- wedges with leading edge sweep, heat transfer, premature transition 7-6211
- weld pool steady fluid flow, 2D model, surface skin effects 7-20730
- wide-band absorption coefficient integration kernel 7-51338
- yawed finned tube, heat transfer, temp. distrib., orientation effects 7-1564
- York, England (Jul. 1986) 7-48142
- zeolites, synthetic, thermal regeneration in thermofluidised bed, heat and mass transfer, mathematical model 7-51120
- Al single cryst. spheres, superheating 7-44767
- Al-Si, chill-cast, heat flow and dendritic arm spacing during solidification 7-53714
- C-graphite heat-shielding coating, destruction and heat transfer in N₂ plasma flow 7-63263
- CO₂, vibr. relax. during injection into ionosphere 7-34087
- CdS, absorpt. optical bistability, lattice heating study 7-43205
- FEMs for solidification problems, comparison 7-14759
- He, channelled cryogenic liquids, heat transfer and hydrodynamics 7-16261
- He, film boiling, heat transfer, centrifugal forces effects 7-50920
- He, liq., flow stability at supercrit. press., nonuniform heat flux distrib. in channel 7-51058
- He liquefaction, condensation heat transfer enhancement for mag. refrigerator performance improvement 7-56283
- He, liquid, heat transfer with nucleate boiling in channels 7-11524
- He transfer tubes, construction (*Japanese*) 7-320
- ⁴He, superfluid, props. and appls. 7-48751
- Hg arc discharge, high-pressure, heat transport obs. 7-21009

heat transfer continued

- Hg layer, rotating, heated from below, subject to mag. field, oscillatory instability 7-16193
- K self-broadened reson. line, heat-pipe oven, superheating effect study 7-36553
- Li flow in transverse magnetic fields, heat transfer and temp. fluctuations, fusion reactor cooling appl. 7-6327
- Li-SOCl₂ primary cells, heat dissipation study 7-34009
- N₂, channelled cryogenic liquids, heat transfer and hydrodynamics 7-16261
- N₂ liq., electrical breakdown in presence of thermally induced bubbles 7-63377
- N₂ liq., forced flow in horizontal pipe, film boiling 7-51277
- N₂O₄ condensation in equilibrium maintaining chemical reaction, heat and mass transfer (*Russian*) 7-51341
- NaNO₃-KNO₃ molten salts for solar central receiver appls. 7-65587
- Nb-Ti composite superconductors, influence of heat transfer on current carrying capability 7-64422
- Ni-Ag overlayers, pulsed electron beam irradiation, heat flow model 7-38062
- Ni-H₂ secondary cells heat generation and transfer rates 7-65452
- P₂O₅-SiO₂ glass in multilayer struct., laser-induced flow modelling 7-38057
- Pb, use in Ericsson mag. refrigerator, regenerator and working material heat transfer process 7-56284
- Pt, wire, heat transfer characteristics 7-12693
- Si, thin sheets, EFG, thermal capillary mechanism for growth limit 7-17407
- Sn superconducting films, resistive state visualisation using laser beam scanning 7-17142

heat treatment

- see also annealing; normalising; quenching (*thermal*); spheroidizing; tempering; thermomagnetic treatment; thermomechanical treatment
- bearing type, austenite transform. kinetics and internal stresses in bainitic hardening 7-39563
- bimetal cylinder, temp. fields and residual stresses in cooling 7-33705
- ceramics, multiphase, sintering 7-64963
- chemicothermal treatment conditions of metals, form. kinetics of irreversible deform. 7-17692
- electrical steels, physical metallurgy, conf., New York, USA (Feb. 1985) 7-4626
- electrodeposits for high temp. oxidation and corrosion resistance, appl. for gas turbines 7-46358
- graphite fibre, benzene-derived, exfoliation and characters. 7-46663
- heterogeneous ceramics, processing for dielectric appls. 7-64984
- Khrovangal alloy, phonon thermal cond., heat treatment effects 7-12696
- laminated composite with unique microstruct., development by C diffusion control 7-17501
- LR-115 films, background heat treatment studies 7-30865
- metal-Al₂O₃-InP structs., improved elec. props. with heat resist. interface 7-38753
- PEEK, fracture toughness, temp. and strain-rate effects 7-39660
- PEEK glass fibre reinforced plastics, fracture toughness, temp. and strain-rate effects 7-39660
- PET, high-temp. viscoelasticity and heat-setting, strain recovery meas. 7-63721
- PET fibres, heat treatment kinetics 7-44407
- poly(p-phenylene) films, elec. cond. enhancement by heat treatment 7-64361
- poly(p-phenylene) films, heat treated, electrical conductivity, thermoelectric power 7-52557
- poly(p-phenylene vinylene) films, highly graphitisable, elec. conductivity, thermoelectric power 7-32916
- polyamides, aliphatic, nonhomogeneous thermooxidative degradation during heat ageing (*Russian*) 7-28060
- polybutylene terephthalate fibres, heat treatment kinetics 7-44408
- polycarbonate, impact props. and residual stress state, thermal treatment effects 7-32557
- polymers, oriented, thermally stimulated shrinkage forces, induction time 7-13484
- polymers, oriented, thermally stimulated shrinkage forces, induction time 7-17560
- polynaphthylene films, elec. cond. enhancement by heat treatment 7-64361
- polyphenylacetylene:1, conformational defects, ESR studies 7-64531
- polyvinyl alcohol films, heat treatment, light irr., polyene mixtures, absorpt. spectra 7-53432
- powder sinterability characteristics linked with manuf. method, mech. processing and heat treatment effects 7-53652
- powder sintering, temp. jump behaviour, manufacture method and impurities effect 7-13402
- α -quartz, synthetic, defects 7-63603
- rapid thermal processing, bibliography 7-14727
- refractory metal nitride, sputtered coatings, wear and friction 7-33800
- silicone rubber, vulcanised, elec. props. 7-7302
- stainless steel, 304, strain effects on sensitisation developments, STEM/EDS and electrochemical potentiokinetic reactivation methods 7-54014
- steel, abrasion resistance after heat treatment 7-17697
- steel, alloyed structural, struct. rel. to cold deformability, softening heat treatment methods development 7-39556
- steel, austenitic stainless, intercrystalline corrosion causes and counter-measures (*German*) 7-17729
- steel, austenitic stainless, sensitisation resistance improvement, application of analytical electron microscopy 7-39762
- steel, cast duplex stainless, spinodal reaction and G-phase precipitation, FIM atom probe anal. 7-33670
- steel, composition-treatment-structure property correlation, computer software development 7-3329
- steel, constructional carbon type, original charge purity influence on microstruct. hardenability and mech. props. 7-46521
- steel, Cr, austenitisation, recrystallisation, pearlite transform. rel. to hot deform. 7-28033
- steel, Cr-Mn(V), bainite transform. kinetics, austenitising and working conditions effect 7-22674
- steel, Cr-Mo-Fe-C, crack resist., temp. and comp. depend. study (*Russian*) 7-13553
- steel, Cr-Ni high-temp. type, N and heat treatment effect on struct. and mech. props. 7-33688

heat treatment continued

- steel, Cr-Ni-Mo, fracture toughness rel. to austenitising temp. (*Japanese*) 7-33778
- steel, Cr-Ni-Mo, Ge and melting method influence on mech. props. at high temp. 7-8025
- steel, Cr-Ni-Mo type, austenitisation conditions effect on austenite decomp. kinetics and mech. characts. 7-39557
- steel, Cr-Si type parts, mag. characts. after isothermal hardening, heat treatment quality inspection method 7-65261
- steel, die, heat-resistant, optimum hardening temps., struct. and mech. props. 7-8022
- steel, die, preliminary heat treatment schedule 7-8023
- steel, dispersoid, mech. props. rel. to presence of H 7-8113
- steel, dual-phase, micro alloyed, mech. props. and struct., effect of process variables 7-65108
- steel, duplex stainless, manual metal arc weld metals, microstruct. and phase transform. 7-59526
- steel, ferritic, fracture behaviour after warm prestressing, effects of subcrit. crack growth 7-46601
- steel, ferritic stainless, Mo, welding, heat affected zones, microstruct., thermal history 7-53769
- steel, forged powder, prod. from water-sprayed Astalloy powders, fracture toughness 7-13572
- steel, heat treatment method effect on struct. and mech. props. 7-39561
- steel, heat-resistant, N and V influence on mech. and service props. 7-8105
- steel, high strength line pipe, H induced cracking susceptibility, comp. and treatment effect 7-39619
- steel, high-speed W-Mo, nitrogen effect of stabilisation of austenite 7-8021
- steel, HSLA, mech. props. rel. to ferrite substruct. and grain size. 7-13531
- steel, low alloy, structural transformations during continuous cooling and isotherms 7-22636
- steel, low C pearlitic, microstruct.-flow stress relationship 7-33739
- steel, low-C, cost, failure micromechanism in fatigue crack propag. after different heat treatments 7-46641
- steel, low-C, wrought, thermal strengthening methods effectiveness 7-46524
- steel, low-pearlite, rules of austenite decomp. in continuous cooling 7-3339
- steel, martensitic stainless, brittle failure rel. to overheating, fractography 7-22796
- steel, martensitic transformation, residual stresses establishment 7-33657
- steel, medium and high C, coalescence recrystallisation, cementite particles effect 7-46515
- steel, Mn, influence of S on failure mechanism in dual α/γ phase (*French*) 7-33760
- steel, Mn-V, continuously cooled, hardness rel. to martensite vol. fraction 7-28121
- steel, Ni-Co-Mo, maraging, fracture toughness rel. to heat treatment, precip., Auger spectra 7-65124
- steel, Ni-Co-Mo, maraging, ultrahigh strength, H embrittlement rel. to coatings 7-28136
- steel, Ni-Co-Mo, maraging, ultrahigh strength, H embrittlement rel. to Ni or Cu coating 7-28137
- steel, Ni-Co-W, maraging, martensite-austenite reversible transforms. during tensile deform. and thermal cycling 7-17528
- steel, Ni-Cr-Mo, H embrittlement in artificial seawater, effect of H content (*Japanese*) 7-53868
- steel, Ni-Cr-Mo, hydrogen embrittlement susceptibility, austenitising heat treatment prior-austenite grain size effect 7-3415
- steel, pearlite-austenite transformation during heating, kinetics problems 7-33633
- steel, roll type, crack resist. as criterion of effectiveness, alloying and heat treatment parameters influence 7-53884
- steel, secondary hardening, alloy carbide precipitation, FIM atom probe studies 7-33671
- steel, Si-Mn-Mo, austenitising, bainite transform., lump-like composite struct., mech. props. (*Chinese*) 7-13477
- steel, stainless, austenitic, valve type, heat treatment schedule effect on failure nature 7-3423
- steel, stainless, cold rolled sheet, struct. form. during recrystn., optimum heat treatment schedule 7-3340
- steel, stainless, laser surface melted, residual stresses 7-3506
- steel, stainless, martensitic, cooling rate and heat treatment effect on chem. microinhomogeneity 7-3294
- steel, stainless, surface segregation and grain boundary precipitation during heating, atom probe study 7-33672
- steel, strengthening of parts and semifinished products in the last stage of heat treatment 7-8024
- steel, structural, fracture toughness, rapid austenitisation, effect of conditions (*Russian*) 7-39651
- steel, structural heredity in heat cycling 7-33703
- steel, tool and struct., nitrided, prior heat treatment effect on mech. props. 7-46707
- steel surface at moderate heating temps., relationship between emissivity and exoemissive props. 7-43641
- steel surfaces, lubricated flat, oil supply effect on fretting wear 7-8123
- steels, tool, M2 and H13, fracture toughness, influence of microstruct. 7-46632
- substrate degassing effects on sputter deposition of Co-Cr films 7-27904
- superalloy single crystals, directional solidification, mech. anisotropy, fatigue, creep 7-3293
- synthetic silica glass, X-ray induced absorpt. and luminesc., heat treatment effects study 7-7733
- XLPE insulation, water treeing 7-39026
- Al alloys, heat treatment, prediction of start of exposure phase 7-33698
- Al and alloys, dynamic restoration during hot rolling 7-22724
- Al single crystals, helical dislocations with low dislocation density 7-51774
- Al-Cu (2 wt.%) single crystals, rolled, shear band form., θ precip. 7-28099
- Al-Cu (3.76 wt.%), rheocast, partially homogenised, ageing response, microhardness 7-46499
- Al-Hg-Si, dil., solidification, intermetallic cpd. form. 7-13442
- Al-Mg and Al-Zn-Mg alloys, plasma-coated, heat treatment effect on fine struct. and failure mechanism 7-3496
- Al-Mg surface layers, electronic and atomic structs., heat treatment effects (*Russian*) 7-58575
- Al-Nb amorphous films, elec. props. and charactn. (*Japanese*) 7-32977

heat treatment continued

- Al-R (R=Er,Nd,Gd) rapidly solidified alloys, microstruct. and thermal props. 7-22667
- Al-Si, brittle failure rel. to overheating, fractography 7-22796
- Al-Si, cold worked, damping characts. 7-28064
- Al-Si, talc particle reinforced composites, prep., wear and mech. props. 7-13408
- Al-Si-Zn-Mg-Ti-(Sr) system alloys, mech. props., Sr microalloying effect 7-3377
- Al₂O₃ glass, gel produced, optical transmission rel. to heat treatment 7-27733
- Al₂O₃-ZrO₂ composites, high temp. behaviour and microstruct. study with HVEM (*Japanese*) 7-22819
- Al₂O₃-ZrO₂-Y₂O₃ system, synthesis and props. 7-22614
- AlPO₄, heat treated, IR meas., temp. coeff. of delay and insertion loss 7-13486
- B fibre reinforced Al, strength characts. 7-33768
- BN polycrystals, heat treatment conditions effect on mech. and service props. 7-53894
- BN pyrolytic crucibles for MBE, AES, XPS, SIMS, and bulk anal. after vac. baking 7-53596
- BaFe₁₂O₁₉, synthesis by hydrolysis of barium acetate and tris (acetylacetonate) iron (*Japanese*) 7-46392
- BaO-B₂O₃ glass, containing Fe₂O₃, heat treatment and γ -irrad., IR study 7-16627
- BaO-B₂O₃-Fe₂O₃ glasses, γ -irradiated and heat treated, elec. conductivity and crystn. 7-21510
- BaO-Fe₂O₃-B₂O₃-based glasses, crystallisation behaviour, nucleating agent effects 7-51650
- Be, technical grade, size instability during low temp. thermal cycling (*Russian*) 7-33699
- Bi₂SiO₂₀, photogalvanically active centres 7-45380
- C fibre reinforced C, multidirectional composites, macroporosity and interface cracks 7-46513
- CaO-Fe₂O₃ system, solid state reactions, ferrite growth and morphology 7-3236
- CdS epitaxial films, initial oxidation stages, diffusion mass transport between CdO islands 7-8206
- CdTe LPE layers, matrix atom diffusion, SIMS studies 7-21513
- CdTe, polycrystalline, grain boundaries elec. and optical characts. 7-38012
- CdTe:Sn, impurity compensation effect on elec. resist. and mobility 7-52614
- Ce(Co,Cu,Fe)₆, magnetically hard, heat treatment effects on struct. and mag. characts. 7-27564
- Co₂, reduction by thermal treatment in vacuum or H₂ atmosphere, IR, PMR and ESR spectra 7-59756
- CoCrAlY electron beam physical vapour deposition coating microstruct., TEM characterisation 7-52334
- CoFeCr sputtered films, struct. and mag. props. 7-27175
- CoO-Al₂O₃ dispersed oxides, positron annihilation 7-39275
- Cr, residual macrostress distrib. after cyclic heat treatment, US and X-ray study (*Russian*) 7-53772
- Cr₂O₃, in transparent glass-ceramic, crystn. and spectroscopic props., melting conditions and heat treatment influence 7-7588
- Cu based alloys, internal friction, Young's modulus, amplitude relationship (*Russian*) 7-65075
- Cu-Al-Ni-Fe-Mn bronze, cast, laser surfacing, improved corrosion resist., microstruct. characteris. 7-13651
- Cu-Ni-Fe-Mn, physical props. rel. to precip. and thermal treatment (*German*) 7-12698
- Cu-Zn-Al shape memory alloys, rapidly solidified, microstruct. and props. (*Chinese*) 7-8043
- CuIn(Ga)Se₂ thin film solar cells, ESCA anal. 7-23197
- Cu₂MnAl, Heusler alloy, heat and press. processed, changes in phys. props. during heating (*Russian*) 7-59645
- CuO-Al₂O₃ dispersed oxides, positron annihilation 7-39275
- Fe, cast, bainitic ductile, microstruct. rel. to comp. and heat treatment 7-39579
- Fe cast, Cr-type, duplex nature of eutectic carbides 7-13440
- Fe, cast, diffusion interaction with steel in forging, explosive treatment and thermal cycling 7-28070
- Fe, cast, ductile, austempering techniques 7-59552
- Fe, cast, high-Cr, wear-resistance, laser and heat treatment effect on struct. and props. 7-8174
- Fe, cast, metastable austenite form. rel. to initial treatment and struct. 7-46455
- Fe, cast, Sn plating, heat diffusion method, corrosion resist in H₂SO₄ (*Japanese*) 7-53956
- Fe, solubility of Nd, positron annihilation study 7-46208
- Fe/Cu microlaminate condensates, creep and struct. investig. (*Russian*) 7-33749
- Fe-Al-Si system, electronic struct. interatomic bonding, X-ray emission spectra analysis (*Russian*) 7-39320
- Fe-Co-Cr-Mo alloys, electronic struct. and mag. props., X-ray spectra studies (*Russian*) 7-32902
- Fe-Ni, austenite form. during continuous heating (*Russian*) 7-17557
- Fe-Ni-C and Fe-C, bainite reaction kinetics, austenitising temp. effect 7-13453
- Fe-Ni-based amorphous alloys, relax. spectra, effect of pulse treatment 7-46536
- Fe-Si, structure, texture and mag. props. 7-12995
- Fe-Zr alloy formation at Fe/Zr thin film interfaces, Mossbauer study 7-63975
- Fe₇Co₃B₁₀S metallic glass, magnetic aftereffect, thermal treatment, positron lifetime study 7-38907
- FeH₃(PO₄)₂·2.5H₂O, pyrite-phosphate mixtures, X-ray phase and electron microscopic studies 7-33652
- Fe₇Nd₁₃B₃-based melt spun ribbons, crystallisation and mag. props. 7-26662
- Fe₂SiO₄, spinels, cryst. struct. as function of temp. and heating duration 7-16522
- GaAs, dielectric protective coatings during heat treatment 7-33852
- GaAs, electron beam irrad., carrier density, anomalous temp. depend. 7-52610
- GaAs, transient thermal processing 7-16601
- GaAs, variation of EL2 with As press. during heat treatment 7-58770
- Gd-Co films, amorphous, spontaneous spin-reorientation transition (*Russian*) 7-45763
- Ge₂S₆ films, evaporated, structural changes on illumination and heat treatment (*Japanese*) 7-22489

heat treatment continued

- GeTe: Cd(In/Sb), solution mechanism of impurities, effect of heat treatment 7-21455
 $H_{(3-9)}$ (PV, Mo₍₁₂₋₉₎O₁₀).XH₂O, stability to dehydration in air and vacuum, ESR study 7-38929
 HgCdTe, homogenization, wetting elimination 7-38221
 Hg_{1-x}Cd_xTe crystals, anodic oxide capped, thermal stability 7-65225
 α -HgI₂ crystals, recent progress in material characterization for X- and γ -ray detectors 7-44577
 InAs:Sb(Ga)(Mn), single crystal, elec. inhomogeneity, effects of isovalent impurities 7-7229
 InGaAsP buried heterostructure lasers, polarisation, effect of stress relax. caused by repetitive temp. change 7-62690
 InP MIS structures, thermal treatment in P overpressure 7-7394
 InP-Au, metallic contact layers, thermal dissociation, P loss 7-23005
 InSb MOS structures, heat treatment effects 7-8031
 In_{2-x}Sn_xO_{3-y} thin films, RF reactive sputtering prep., elec. and optical props. 7-39378
 In_{2-x}Sn_xO_{3-y}/Ag/In_{2-x}Sn_xO_{3-y} magnetron sputtered transparent heat-reflective films, thermal stability study 7-53426
 KCl, heat treated, alpha particle dechannelling, range meas. by F-coloration depth determ. 7-32512
 LiKSO₄ single crystals, optical activity, ferroelec. and ferroelastic props. 7-27687
 Li₂O-Al₂O₃-SiO₂ glass, cryst. phase nucleation, DTA, X-ray diff. 7-58156
 Mg thin films, initial oxidation stages, emission phenomena 7-13629
 MgO (001), initial stages of Cu deposition, EELS 7-63959
 MgO sputtered coatings on metal substrates, adhesion and structural props. 7-52337
 MgO:Al crystals, cathodolum., effect of heat treatment 7-7767
 MgO-SiO₂ high-temperature composites, calcination temp. and mech. strength 7-33651
 Mn-Sn, homogenised, mag. props., thermal expansion 7-2900
 Mn_{1-x}Zn_xFe₂O₄ substrates, Auger microprobe temperature profiles of contamination residue 7-59822
 Mo-Ag, pseudoalloys, Ni and Co effect on interphase interaction 7-27975
 Mo-H system, neutron irradiat., H-void interactions 7-44604
 NaCl, pure and Mg doped, electron range vel. to heat treatment 7-21283
 Na₂O-B₂O₃-SiO₂ glass ceramic, prep., SiO₂ replacement, phase separation, struct. 7-13428
 Na₂O-CaO-Al₂O₃-SiO₂ glass ceramic system, spherulitic growth, mech. props. 7-46405
 Na₂O-V₂O₅-P₂O₅, crystallised glass, containing V bronze crystals, elec. cond. 7-21922
 Nb film, elec. props., temp. cycling effects 7-38804
 Nb film supercond. props., α particle bombardment and thermal cycling effects 7-33704
 Nb surface, enhanced field emission sites during heat treatment 7-33531
 Nb₃Al superconducting tape prepared by CO₂ laser beam irradiation 7-17145
 Nb₂O₅-Al₂O₃-B₂O₃-Na₂O-SiO₂, phase separable glass, heat treatment leaching, X-ray diffraction anal. 7-51658
 Nb₃Sn-Ti(In) multifilamentary superconducting composites, growth dynamics, struct. and props., additive and heat treatment effects 7-22056
 Nd-Dy-Fe-B-based sintered magnet, microstruct., heat treatment effects 7-53767
 Nd-Fe-B permanent magnets, BCC phase mag. props. at grain boundaries 7-53044
 Nd-Fe-B system, permanent magnet, mag. props. (Korean) 7-7554
 Ni-B alloy, electroless, heat induced struct. changes 7-13639
 Ni-base superalloy, carbide precip., influence of alloy chem. 7-46481
 Ni-base superalloy, IN 939, high Cr, effects of heat treatment on mech. props. 7-13526
 Ni-base superalloy, single cyst., SRR99, creep behaviour 7-17587
 Ni-base wrought superalloy, thermal fatigue resist. improvement by laser-glaze 7-22840
 Ni-Cr superalloy, heat-resistant, heat treatment effect on ductile props. in cold deform. 7-46584
 Ni-P, electroless coatings, wear rel. to counterface materials and heat treatment 7-33802
 Ni-Zn ferrite and Ni ferrite films, prep., mag. props. 7-13378
 Ni₂SiO₄, spinels, cryst. struct. as function of temp. and heating duration 7-16522
 NiTa-GaAs, phase separation, cross-sectional TEM 7-27152
 Pb-In-Au alloy films, hillock growth during heat treatment 7-16893
 Pb-In-Au thin films, hillock growth kinetics, grain boundary diffusion, SEM study 7-27221
 PbO-B₂O₃ optical glass, props. and structure, effect of heat treatment 7-20377
 PbO-Fe₂O₃-B₂O₃ glass ceramics, mag. props. and EPR spectra of precipitated mag. phases 7-45748
 Pb_{1-x}Sn_xTe surfaces, AES, LEED and Kikuchi pattern obs. 7-52200
 Pb(Zn_{1/3}Nb_{2/3})O₃-PbTiO₃, perovskite ceramic powder, prep. dielec. and piezoelec. props. 7-46380
 Pd monolayers on Ta(110), morphology and struct. phase transitions 7-38374
 Si, Czochralski grown, interdependence of contamination and defect formation 7-32467
 Si, rapid thermal oxidation and nitridation 7-33861
 Si:As, high dose implanted, defect density reduction by low temp. oxidation 7-58297
 Si:B,O, thermal donor formation, bending stress effects 7-17563
 Si:B,O epitaxial wafers, internal gettering heat treatments and O precipitation 7-45059
 Si:C,O, heat-treated, photoconductivity relax., α traps 7-52677
 Si:C,O, solubility, segregation, diffusion and precipitation 7-16777
 a-Si:H stable heterojunction solar cells develop., thermal degradation phenomenon 7-65477
 Si:O, Czochralski grown, electron irradiated, thermal donor formation 7-44619
 Si:O, diffusion of O during thermal donor form. 7-38262
 n-Si:O, donor states of O rel. to heat treatment 7-12647
 Si:O, influence of growth microdefects on microdefect formation during heat treatment 7-17559
 Si:O, optical transition at thermal donors 7-17346
 Si:O, structure and props. of the thermal donor 7-16766

heat treatment continued

- Si:O epitaxial wafers, preanneal heat treatment effect on precipitation 7-38219
 Si:O, thermal donor formation and structure, review 7-17562
 Si:(O,C), impurity aggregation, SIMS 7-16778
 Si:(O,H), heat treated, DLTS 7-16991
 a-Si/Au thin film bilayers, Si crystallisation study 7-21699
 SiC whisker reinforced Al alloy, powder metallurgy, corrosion susceptibility, influence of metallurgical variables 7-65152
 SiC-Al composites, heat treatment and neutron irradiat. effects on mech. props. 7-65081
 SiO₂ films thermally grown on Si, decomposition acceleration factors 7-63999
 SiO₂, gate dielectric films, growth by rapid thermal processing, material and electrical props. 7-16906
 SiO₂, spherical particles synthesis, thermal behaviour (Japanese) 7-7943
 SiO₂-Al₂O₃-MgO-Cr₂O₃ glass, magnetism of spinel microcrystals, ESR study 7-27594
 SiO₂-GeO₂ film, oxide flow during H₂ treatment, planarization technique 7-2426
 Sm₂(Co, Fe, Cu, Zr)₁₇ sintered compact permanent magnet, mag. props., comp. and heat treatment effects (Korean) 7-2894
 SnO₂ glass, thick film, elec. resistance, effect of struct. 7-7300
 SnO₂:Sb spray deposited coatings, comp., elec. props. thermal treatments, AES study 7-22393
 SnTe: Cd(In/Sb), solution mechanism of impurities, effect of heat treatment 7-21455
 Sr ferrite fine particles, prep., mag. props. (Japanese) 7-53065
 TaH_{0.07}, lattice location of H by channelling method 7-1975
 Ti alloy, heat cycling regimes and effects 7-8028
 Ti film on Si, heat treatment in O₂, N₂ or O₂/N₂, Ti silicides, TiO and TiN formation 7-65191
 Ti, films on Si, heat treatment, TiSi₂ form. 7-46530
 α -Ti, mutual interactions of O and H during heat treatment, diffusion coeffs. meas. 7-39549
 Ti, rolling, texture form., metastable high press. phase transform (Russian) 7-65029
 Ti/Si:B,As,Sb interface, dopant redistrib. during silicide form. by rapid thermal processing 7-63641
 Ti-Al, brittle failure rel. to overheating, fractography 7-22796
 Ti-Al-Mo-Cr alloy, VT3-1, cooling regimes in heat treatment effect on mech. props. 7-8026
 Ti-Al-Mo-V-Cr alloy VT22, metallographic study of β -solid soln. decomp. 7-39523
 Ti-Al-V, spall strength and fracture mechanism 7-46627
 Ti-Al-V (6, 4 wt.%), powder metallurgy, fatigue props. rel. to microstruct. 7-8096
 Ti-Al-V (6, 4 wt.%) plates, rolling, heat treatment, microstruct., mech. props., turbine blade appl. 7-17644
 Ti-Al-V-Mo-Cr alloy, VT23, gas impregnation influence in heat treatment, rapid heating effect 7-17696
 Ti₃Al, struct., phase comp. rel. to crystallisation rate and heat treatment 7-46442
 Ti₂Mo₂C₂TiO₂-C black mixture, complex carbide interactions on heat treatment, homogenisation 7-53684
 TiNi shape memory alloys, wear resist. and hardness, influence of heat treatment (Korean) 7-17647
 TiNi-X, X=Fe, Ge, Re or Ni, struct. transitions in premartensitic range (Russian) 7-39504
 TiO₂-GeO₂ glasses, crystallisation, ion coordination, X-ray diff., IR spectra 7-6523
 U, texture anisotropy, as-cast and heat treated 7-46518
 U-Ti dilute alloys, phase transformations 7-16730
 URu₂Si₂ single crystal, Czochralski growth, charact. 7-53557
 W-Ag pseudoalloys, Ni and Co effect on interphase interaction 7-27975
 W-Ni-Fe, sintered, ductility and precip. 7-17589
 WC-Co, plasma sprayed coatings, wear, adherence, heat treatment effect 7-33555
 WC-Co sintered carbides, X-ray diff. obs. of microstruct. after hardening, optimum heat treatment cycle 7-65063
 WC-TiC-Co hard alloy Ti15K6, heat treatment effect on failure mechanism 7-13550
 YAG powders, hydrothermal growth, controlled nucleation, CRT phosphor prep. 7-13412
 Y₂O₃-ZrO₂-Fe, high dose ion implanted, profile shapes and electronic cond. 7-32472
 ZnO (1010), initial stages of Cu deposition, EELS 7-63959
 ZnO ceramic, grain growth kinetics during synthesis, optimum elec. props. 7-46398
 ZnO with tri-valent donor impurities, elec. props., heat treatment effects 7-2611
 ZnO/Ag/ZnO magnetron sputtered transparent heat-reflective films, thermal stability study 7-53426
 ZnTe, cathodoluminescence, Zn-vapour and Te-vapour heat treatment effects 7-46151
 ZrO₂ gel, transparent, glass-like, thermal evolution 7-28356
 ZrO₂, tetragonal, cryst. growth 7-17417
 ZrO₂-CaO-P₂O₅-SiO₂ glass ceramics, prep. and mech. props. (Japanese) 7-7942

heated cathodes see thermionic cathodes

heating

- see also electric heating; induction heating; ovens; plasma heating; refractories; space heating
 absorption heat pump systems, H₂O-LiBr-based; operating temps. and concs. 7-59866
 adsorbed atoms on coated transparent crystal, laser heating 7-63654
 aquifer thermal energy storage for Canada Centre 12-storey office building 7-65607
 built-in type solar water heater performance analysis 7-3719
 commercial and industrial water heating by low-cost shallow solar pond system 7-8443
 continuous versus on-off heating 7-37310
 corrugated water-trickle collector, expt. and theoretical study of thermal performance 7-65581
 cryoturbogenerator rotors, heating and convection of boiling fluid 7-31796
 crystal surface, temp. distrib., induced by local heat pulse 7-57671
 heat source movement over heat conducting medium surface 7-1379
 IR heating, physical considerations (Spanish) 7-16057
 massive optically dense body, short-time heating by radiant flux 7-11256

heating continued

metal bulk sample, laser heating and combustion by obliquely incident radiation 7-26795
molten semiconductors, structural changes caused by heating, acoustic investigations 7-51942
molten semimetals, structural changes caused by heating, acoustic investigations 7-51942
orthotropic plate with inclusion, heated, heat cond. 7-11247
oven type solar cooker using spiral solar energy concentrator 7-65410
polymer thermal destruction in nonsteady heating in hot gas stream 7-26126
radiative heat pumps using narrow-bandgap semiconductors 7-40019
solar air heater design for cost-effectiveness 7-3626
solar air heating systems, analytic model for performance prediction 7-59875
solar heating of fluid in semi-transparent plate, transient anal. 7-40039
solar heating units, paint coat thickness effects on radiation characts. 7-46968
solar heating units for wine materials heat-processing 7-34067
Solar Process Heat System supplanting induction-heated boilers 7-8366
solar water heater, investig. of thermal-energy characts. by dynamic method 7-46966
solar water heaters with variable volume storage, energy balance eqns. 7-59873
solar water heating system design criteria for schools 7-8442
solar water heating system with n-tanks in series, anal. 7-40036
steel, stainless, type 302, ignition of bulk by laser heating 7-3516
suspended flat-plate solar air heater, transient anal. 7-40027
thermophysical characteristics meas., error due to heat capacity of heater 7-56256
thermosiphonic solar water heater, modelling 7-40034
thin film pulsed heating, thermal and plasma models 7-26946
tubular specimen under HF induction heating, temp. distrib. anal. 7-43650
water heater, 2-phase solar, operation and comparison with thermosiphon heater 7-65580
Al, deformed, acoustic emission on heating 7-51958
Al₂O₃ powder, metallised, heater appl. (*Japanese*) 7-23204
GaAs, rapid thermal annealing, heating behaviour 7-21258
InP, rapid thermal annealing, heating behaviour 7-21258

heating, buildings *see space heating*

heavily doped semiconductor materials *see heavily doped semiconductors*

heavily doped semiconductors

see also degenerate semiconductors; superconducting semiconductors
Si:O, heavily doped, SIMS meas. of O conc. 7-17388
chalcogenide glass films, metal ion doped, impurity effects 7-11943
elemental, electron-phonon mobility variation with carrier density 7-64249
ferromagnets with low carrier densities, indirect exchange 7-33162
films, optical absorption band shift 7-7776
multilayer isotopic n⁺-n heterostructures, S-type current-voltage characts. 7-52758
p-type, band-gap shifts 7-22333
polyacetylene:Br(I), polarised EXAFS and near edge spectra studies 7-64778
SOI wafers, O implantation prep., background doping effects 7-32478
superlattices, optical properties, plasma wave effects 7-64599
- 7-38565
AlAs:Si films and AlAs:Si-GaAs:Si superlattices, MBE growth and electrical props. 7-22052
AlGaAs/GaAs modulation-doped heterojunctions, 2D electron gas, DX centres 7-38694
GaAs, band-gap shifts 7-22333
GaAs, heavily doped, carrier-carrier and carrier-dopant interactions 7-21903
GaAs, highly doped, polarised hot electron photoluminescence 7-46121
GaAs highly doped quantum wells, mobility enhancement 7-64325
GaAs LPE layers, heavily doped and compensated, hopping cond., density of states at Fermi level, carrier conc. determ. 7-2753
GaAs:Sn LPE layers, heavily doped, Mossbauer study 7-38967
n-Ga_{1-x}In_xSb:Se(S), impurity states, press. and comp. depend., Hall coeff. and elec. resist. meas. 7-2533
GaN:Zn, pure and doped, electrophysical props., nonhomogeneous semiconductor model 7-27292
Ge, pure and heavily doped, dielec. function, impurity conc. depend., spectroellipsometric meas. 7-2525
p-Ge:As, Hall effect and electrical conductivity, temp. corrections 7-38592
Ge:Sb(Al)(Ga)(In), heavily doped, charge carrier scatt., elec. cond., Hall effect meas. 7-7228
Hg_{1-x}Mn_xTe, Hall coeff., magnetoresist. meas., exchange interaction, field, temp. effects 7-64270
p-Hg_{1-x}Mn_xTe, highly doped, ground state of shallow acceptor 7-7167
Hg_{1-x}Mn_xTe, magnetoresist. meas., effect of valence band spectrum quantisation at low temps. 7-52653
InAs-GaAs, in situ contacts, MBE grown 7-45444
In₂O₃:Sn films, theoretical model for optical props. in 0.3 to 50 μ m range 7-39200
n-Si, heavily doped, carrier conc. and activation energy, Lee-McGill model calcs. 7-58819
Si, heavily doped, thermoreflectance, study 7-45999
Si, heavily doped crystals, behaviour of O and dopants 7-32483
Si junctions very shallow, elec. field anal. 7-21989
Si, laser deposition for interconnections 7-53632
Si, n- and p-type, band-gap narrowing 7-7108
Si solar cells, alloyed inversion layer, with n-type substrates and TiO₂ antireflection coatings 7-17864
Si solar cells, heavy doping effects 7-3653
n-Si, ultraheavily doped, Rayleigh surface waves, Brillouin scatt. study 7-21605
Si:As, highly doped, spinodal decomposition and clustering 7-52063
Si:As,Sb(P,Sb), Sb diffusion 7-44915
Si:As films, heavily doped, grown by partially ionised MBE, phys. and elec. characts. 7-12561
Si:As substrate, dopant effects on formation kinetics of Pt silicides 7-21697
Si:As surface, TiSi₂ formation 7-12551
Si:As⁺, heavily doped, ion implant deactivation 7-17567
Si:As(Sb)(In), heavily doped, laser induced oxidation 7-13672

heavily doped semiconductors continued

Si:B, critical supercond. current induced by proximity effect, mag. field depend. 7-22069
Si:B, O, heavily doped, O precipitation, diffuse X-ray scatt. studies 7-32669
Si:B,O(Sb,O), heavily doped Czochralski wafers, O precipitation, 450°C thermal annealing 7-58477
Si:B,P highly doped epitaxial layers, growth by low press. VPE 7-39432
Si:B film deposition in Si₂H₆-B₂H₆-He gas system, doping effect 7-27184
a-Si:H film, photoenhanced deposition and characts. 7-53635
Si:O substrate materials, heavily doped, control of O and precipitation behaviour 7-32665
Si:P, heavily doped, plasma etching with trifluorochloromethane-Ar discharges, modelling of ion bombard. energy distrib. 7-28222
Si:P, heavily doped, plasma etching with trifluorochloromethane-Ar discharges, modelling of etching rate and directionality 7-28223
Si:P, heavily implanted, influence of precipitation on P diffusivity 7-6879
Si:P, meas. of heavy doping parameters 7-12855
Si:P heavily doped, plasma etching with trifluorochloromethane-Ar discharges, parametric modelling and impedance anal. 7-28221
Si:P slotted surface, IR emission showing organ pipe resonant modes 7-44873
ZnS:Mn heavily doped phosphors, mechano and electroluminesc. 7-13240

heavy fermion superconductors *see heavy fermion systems; type II superconductors*

heavy fermion systems

d-wave superconductivity in the large-degeneracy limit of the Anderson lattice 7-45551
actinide systems, photoelectron spectroscopy, review of present status 7-39348
anisotropic supercond. under uniaxial stress, possibility of additional phases 7-64382
anisotropic superconductors, Meissner effect 7-45557
characteristic props., muon spin rotation studies 7-45883
conf., Neuchatel, Switzerland, April 1986 7-40984
d-wave superconductors, sp. ht., thermal cond., US absorpt. 7-64400
degenerate Kondo lattice, magnetic instability and sp. ht. calcs. 7-58977
dense Kondo heavy fermion systems, Cooper pairs attractive interactions freq. depend. 7-58951
disorder and coherence 7-21888
effective magnetic moments and Wilson ratio for Kondo lattices 7-22091
f-electron and conduction electron superconductivity, periodic Anderson model, self-consistent calcs. 7-12908
Fermi liquid aspects 7-27275
Gruneisen parameter electron-phonon coupling 7-2138
Gutzwiller method for heavy electrons 7-27228
heavy electron systems, Fermi liquid theory anal. of specific heat and magnetic susceptibility 7-38484
heavy Fermi liquids and narrow band metals, characteristic temps. 7-45689
hydrodynamic fluctuations 7-44708
intermediate valence and heavy fermion model systems, review 7-33122
itinerant f-electron model 7-38808
Kondo exponent, conc. depend., in heavy fermion alloys 7-27495
Kondo exponent, conc. depend. 7-27497
low temp. lattice Anderson model, large-orbital-degeneracy expansion in the Kondo limit 7-64037
metal-insulator transition, modified Gutzwiller theory, appl. to heavy-fermion systems 7-32915
metals, strongly correlated, containing heavy fermions, thermodynamic and transport parameters 7-38458
metals, supercond. upper crit. field, temp. depend. 7-45587
muon spin resonance, conference, Uppsala, Sweden (June 1986) 7-48141
nearly antiferromagnetic itinerant fermion systems, possible superconductivity 7-38802
p-wave superconductors, ultrasound attenuation 7-27468
singlet superconductivity, mean field theories in extended Hubbard models 7-27461
superconducting materials, advances and developments (*French*) 7-27476
superconducting p-wave pair states, spin-orbit interaction and crystal field effects 7-38806
superconducting state, temp. depend. of nucl. spin-lattice relax. 7-17136
superconductivity, conduction band and virtual bound states, Kondo-like interaction, periodic Anderson Hamiltonian calcs. 7-27460
superconductivity in itinerant ferromagnets (*Chinese*) 7-38805
superconductors, Cooper pairing 7-33123
superconductors, FIR spectroscopy 7-38816
superconductors, normal impurity effects, excitation spectrum 7-27462
superconductors, observability of order parameter collective modes 7-38807
superconductors, spin-fluctuation-mediated even-parity pairing 7-38812
superconductors, transport and thermal props. 7-38809
superconductors in strong mag. field, Fermi liquid interaction influence 7-52896
superconductors with heavy fermions, Josephson effect 7-33131
thermodynamic props., lattice-gas anal. using heavy fermion-boson mixture 7-58505
transport properties of heavy fermion systems 7-45553
triplet bipolaron systems, superconducting A and B phases (*Chinese*) 7-58949
Ce compounds, heavy-fermion state in the Anderson lattice 7-7476
Ce metallic systems, valence band photoemission spectra anal. 7-13332
CeAl₃, heavy fermion system, fluctuating bands 7-58736
CeB₃, heavy fermion system, muon Knight shift study 7-45886
CeCu₆, heavy fermion substance, magnetoresistance under press. 7-52579
CeCu₆, heavy fermion system, temp. and mag. field depend. of Hall effect 7-2579
CeCu₆, heavy-fermion material, coherent and incoherent behaviour, Hall effect and magnetoresist. 7-32992
CeCu_{2-x}Ni_xSi₂, Kondo-lattice system, resist. anomalies 7-58799
CeCu₂Si₂, heavy fermion superconductor, magnetic field penetration, muon spin relax. studies 7-45886
CeCu₂Si₂, heavy-fermion superconductors, induced moment mag. form factors 7-12909
CeH_{2.7}, heavy electron system, muon spin rot., Knight shift and relax. studies 7-45885
CeO₂, electronic struct. determ. 7-52417
CePb₃, heavy fermion material, magnetism and superconductivity 7-52880
CePb₃, heavy fermion system, theory of mag. field induced supercond. state 7-45546

heavy fermion systems continued

- CePb₃, possible superconductivity in nearly antiferromagnetic itinerant fermion systems 7-38802
 CePb(Al)₃ heavy fermion system, muon Knight shift study 7-45886
 CePd₂Bo₆ heavy fermion cpd., thermal and mag. anomalous cryst. field effects 7-45239
 CePd₂Si, heavy fermion cpd., thermal and mag. anomalous cryst. field effects 7-45239
 CeRu₂Si₂, heavy fermion, magnetism and spin fluctuation effects induced by partial substitution 7-38850
 CeRu₂Si₂, heavy-fermion system, magnetoacoustic effects in high mag. fields 7-64506
 U alloys, heavy-electron ground state, chemical comp. effects, low temp. sp. ht. and superconductivity 7-63841
 U alloys, high press. magnetic and superconducting props., review 7-12952
 U compounds, heavy-fermion state in the Anderson lattice 7-7476
 U-based heavy Fermion systems, final-state effects in inverse photoemission 7-53437
 UAu₃, band struct., theoretical XPS intensities 7-39353
 UBe₁₃, elec. resist., Press. and mag. field effects 7-45562
 UBe₁₃, electron-phonon coupling calcs., unconventional superconductivity mechanism 7-38811
 UBe₁₃, heavy fermion cpd., lattice dynamics, EXAFS study 7-64792
 UBe₁₃, heavy fermion system, unusual low temp. Hall voltage behaviour obs. 7-38540
 UBe₁₃, heavy-fermion superconductors, induced moment mag. form factors 7-12909
 UBe₁₃, heavy-fermion superconductors, Landau-Khalatnikov US damping 7-12912
 UBe₁₃, obs. of antiferromag. correlations 7-22093
 UBe₁₃ single crystals., normal and supercond. states, thermal cond. temp. depend. meas. 7-52166
 UBe₁₃, superconductivity, simple transition metal-type and heavy fermion behaviour 7-12897
 UBe₁₃-Gd, EPR in superconducting phase 7-33269
 UCd₁₁ heavy electron system, antiferromag. phase transition, muon spin rot. and relax. meas. 7-45668
 U₆Co, heavy fermion superconductor, penetration depth rel. to saturation spin moment 7-52893
 UCu₅ magnetic heavy electron materials, muon spin rotation studies 7-45884
 U₆Fe, heavy fermion superconductor, penetration depth rel. to saturation spin moment 7-52893
 UIr₃, band struct., theoretical XPS intensities 7-39353
 U₆Mn, heavy fermion superconductor, penetration depth rel. to saturation spin moment 7-52893
 UPd₂Sn, heavy electron behaviour, elec. resist., mag. susceptibility, sp. ht. meas. 7-32679
 UPt₃, band struct., theoretical XPS intensities 7-39353
 UPt₃, heavy fermion supercond., Cooper pair states, atomic representation 7-45550
 UPt₃ heavy fermion supercond., muon spin relax. and Knight shift meas. 7-45888
 UPt₃, heavy fermion superconductivity and normal state props. 7-52412
 UPt₃ heavy fermion system, muon Knight shift study 7-45886
 UPt₃ heavy-fermion superconductors, induced moment mag. form factors 7-12909
 UPt₃, heavy-fermion superconductors, Landau-Khalatnikov US damping 7-12912
 UPt₃, heavy-fermion system, development of antiferromag. correlations 7-64435
 UPt₃, heavy-fermion system, magnetoacoustic effects in high mag. fields 7-64506
 UPt₃, possible superconductivity in nearly antiferromagnetic itinerant fermion systems 7-38802
 UPt₃, superconductivity, simple transition metal-type and heavy fermion behaviour 7-12897
 UPt₃, superconductivity, one-component Fermi liquid theory 7-22066
 URu₂Si₂, heavy electron system, competing electronic correlations, press. effect 7-45539
 URu₂Si₂, heavy fermion system, core levels and band struct., electron spectra studies 7-52418
 U_{1-x}Th_xBe₁₃ heavy fermion superconds., muon Knight shift and zero-field relax. meas. 7-45887
 U₂Zn₁₇ magnetic heavy electron materials, muon spin rotation studies 7-45884
 U₂Zn₁₇, point contact spectroscopy meas. 7-52748
 YbPd₂Si₂, moderate heavy fermion system, sp. ht. 7-58504

heavy ion excited X-ray emission *see ion microprobe analysis***heavy ion-nucleus reactions**

- for inelastic heavy ion-nucleus scattering, see "heavy ion-nucleus scattering"*
⁶⁰Ni(¹⁴N,pn), lowest three yrast transitions in ⁷²Se, lifetime meas. 7-10099
^{Asn}(^{38,64}Ni,X), A=112-124 fusion fission, excitation functions 7-49450
 adiabatic model for heavy-ion fusion, geometric interpretation 7-5265
 angular and mass distribution of fission fragments 7-35993
 anisotropic hydrodynamics analysis, cross sections 7-25005
 anisotropic hydrodynamics and isotropization of momentum 7-42053
 anomalous search in heavy ion reactions using SSNTDs 7-19276
 anomalous positron peaks and Dirac eqn., comment and reply 7-56697
 atomic nuclei, high energy collisions, expt. results 7-42048
 backward flow of mesonic fluid at ultra-high energy 7-19295
 baryon recoil and the fragmentation regions in ultrarelativistic nuclear collisions 7-5294
 baryon rich quark-gluon plasma produced in rel. heavy ion collisions, decay 7-5175
 bremsstrahlung in the incoherent limit, simplified fireball model 7-61907
 collective flow of nuclear matter 7-5217
 collective flow of pions produced in nucleus-nucleus collisions 7-5218
 collision term in heavy ion collisions 7-5207
 compound heavy ion reactions, stat. ang. distrib., applicability of classical descript. 7-19296
 compound nuclear reactions, total number of stages and Fermi energy 7-15217
 compound nuclei, limiting excitation energy 7-61909
 compound nucleus fission, tilting mode dynamics 7-5274
 compound nucleus formation, dynamical hindrance 7-19272
 compound nucleus reactions, time reversal symmetry breaking 7-30404

heavy ion-nucleus reactions continued

- compound nucleus temperature, validity of determ. using fragment excitation data, statistical mechanics anal. 7-5255
 conf., Copper Mountain, Colorado, USA (Feb. 1986) 7-4634
 conf., Leningrad, USSR, April 1985 7-29574
 conference heavy ion reaction, nuclear chemistry, with tandem accelerators, Tokai, Japan (Jan. 1986) 7-35116
 deep inelastic heavy ion collisions, relative nucl. motion 7-30441
 deep inelastic scattering, ambiguities in the description of nucleon transfer 7-5279
 dilepton emission and the QCD phase transition in ultrarelativistic nuclear collisions 7-5219
 dinotor model for anomalous nuclei 7-24940
 direct heavy-ion reactions, quasiclassical DWBA anal. 7-56699
 dissipation in fission and heavy-ion reactions 7-5221
 dissipation-fluctuation dynamics of the formation of fission-fragment mass distributions 7-42090
 dissipative diabatic dynamics in heavy-ion collisions 7-49466
 dissipative nuclear collisions, Ericson fluctuations 7-49352
 double differential cross-section, momentum and energy distrib. 7-36029
 E=54-70 MeV, isospin nonconservation 7-5272
 energetic photons at intermediate energies 7-49412
 entropy in high energy heavy ion collisions 7-5215
 entropy production, information and measurement theory 7-61901
 equation of state from subthreshold kaon prod. 7-5293
 evaporation reactions, pn to d and α pn to α d emission ratio meas. 7-5263
 evaporation residues, limiting angular momenta in heavy ion fusion reactions 7-36050
 event generator model, collective flow in central Ca+Ca and Nb+Nb collisions 7-5214
 fission fragment mass distribution for nuclei lighter than Th 7-42089
 fission in a narrow J-window and J-dependent fission barriers 7-19231
 fusion in terms of Rutherford trajectories in elastic model 7-25014
 fusion-fission systematics, effect of compound nucleus spin distribution 7-704
 fusion-like processes in hot nuclei, Hartree-Fock and Thomas-Fermi approx. 7-61826
 Gamow states in realistic two-centre pot. 7-10168
 Hartree-Fock approach for thermal nuclei 7-36044
 heavy ion fragmentation, abrasion model differences, optical/geometric model anal. 7-19289
 heavy ion physics and nuclear/quark matter 7-35968
 high energy, flattening of distrib. of large transverse energy prod. 7-42068
 high energy collisions, average transverse momentum and energy density meas. in emulsion chamber 7-42063
 high energy gamma rays emitted from highly excited states in the continuum 7-36043
 high energy nucleus-nucleus collisions, Boltzmann eqn. anal. 7-19282
 high energy particle emission from heavy ion collisions at energies up to 10 MeV/N 7-10165
 IBM, quadrupole sum rule violation and E2 matrix elements 7-61819
 inclusive breakup reactions, coupled channels Born approximation formalism 7-49351
 incomplete fusion in light heavy-ion induced reactions 7-19301
 incomplete fusion reactions, fragment emission, influence of projectile cluster props. 7-19315
 incomplete-fusion reactions, projectile cluster property effects on fragment spectra, direct-transfer model anal. 7-49436
 information-theoretical analysis of heavy ion collisions, constraint on \sqrt{E} and exciton number 7-5271
 intermediate energies, results from CERN synchrocyclotron 7-49459
 intermediate energy reaction mechanism, linear momentum transfer 7-5288
 intermediate energy reactions, fusion process in Landau-Vlasov dynamics 7-25002
 ion projectile break-up, Serber model 7-42069
 isospin correlated nucleon exchange, mass, charge distrib. 7-10172
 isotopically resolved intermediate-mass fragment emission, thermodynamic quantities 7-30444
 Landau-Vlasov transport theory anal. of heavy ion collisions, medium effects 7-56696
 leading particle explanation for linear momentum transfer systematics 7-49463
 lepton and dilepton production, low p_T and low pair mass anal. 7-35896
 light pseudoscalar particle production in heavy-ion collisions 7-19292
 local-scale point transformations within the generator coordinate method 7-56623
 low mass dilepton production in heavy ion collisions, background from quark-gluon plasma 7-35795
 microcanonical simulation of nuclear disassembly 7-5292
 model description of neutron emission 7-42071
 multifragmentation in intermediate energy heavy ion collisions 7-5291
 multifragmentation of hot and compressed nuclei within a time dependent Thomas Fermi and percolation model 7-30450
 multistructure models, test of hadron-nucleus and nucleus-nucleus interactions 7-41771
 N=82 region, fusion-evaporation reactions (French) 7-19192
 neutron emission in large amplitude collective motions 7-42072
 non-interacting quarks and gluons in a slab, thermodynamics, plasma in HI collisions 7-49444
 nonfusion yield in heavy residue spectra 7-5289
 nonspectator nucleons, increase due to energy and baryon stopping 7-42067
 nuclear fragmentation, cluster distributions, lattice model anal. 7-24950
 nuclear matter droplet formation dynamics in heavy ion collisions 7-30359
 nuclear polarization potential due to single-particle transfer 7-5276
 nuclear shapes studied by Coulomb excitation, review 7-56598
 nuclear transfer in heavy ion-reactions, correspondence of random walk and Markovian master eqns. 7-41969
 nucleus-nucleus collisions, deformed nuclei, form-factor calcs. using proximity-plus-Coulomb potential 7-19285
 orbiting and fusion processes, statistical model anal. 7-5278
 particle and nucl. physics intersections conf., Lake Louise, Canada, May 1986 7-29569
 particle emission from static nucleus, energy depend. of source sizes in nuclear interferometry 7-36039
 peripheral relativistic HI collisions, multistep fragmentation and high-lying state EM excitation 7-36034

heavy ion-nucleus reactions continued

- photon interferometry for heavy ion collisions 7-49446
photon production mechanisms 7-49455
pion production in heavy-ion collisions, microscopic anal. 7-49467
positron production in heavy ion collisions 7-36020
positron spectra, interference effects between atomic and nuclear processes 7-61902
positrons from heavy ion collisions 7-56702
precompound reactions, statistical theory of multistep compound process 7-19225
projectile fragmentation, Monte Carlo simulations of anomalous expts. 7-614
projectile fragments in relativistic heavy ion reactions, nuclear chemistry anal. 7-19299
QED plasma, relativistic, screening effect appl. to heavy ion collisions 7-10018
quantal model for heavy ion-collisions 7-49464
quantal permeation currents in nuclear heavy ion reactions 7-49465
quark matter, conference, Pacific Grove, CA, USA (April 1986) 7-55881
quark-gluon plasma undergoing a phase transition, rel. hydrodynamic eqns. 7-19184
Rayleigh criterion for neck stability 7-5268
reaction duration meas. using e^+ and e^- spectra and product distribns., review 7-42044
relativistic, anomalously short mean free paths, parameter-free theoretical anal. 7-25004
relativistic collisions, baryon-quark phase transition effects on nuclear matter flow, oblique shock wave production 7-24949
relativistic collisions, impact parameter dependence of specific entropy and fragment yield 7-19280
relativistic heavy ion collisions, EM processes, giant resonances, π and e^+e^- prod. 7-19270
relativistic heavy ion collisions, metastable strange-quark droplet production 7-36019
relativistic heavy ion collisions, nuclear matter compression and expansion 7-19297
relativistic heavy ion collisions, subthreshold antikaon production 7-36018
relativistic heavy ion collisions relationship to nuclear matter equation of state 7-35969
relativistic heavy ion reactions, Lund model 7-49458
relativistic heavy-ion collisions, heavy lepton production, cross section calcs. using equivalent photon method 7-56695
relativistic heavy-ion collisions, subthreshold kaon production and compression effects 7-49448
relativistic hydrodynamics, entropy, π prod., quark-gluon plasma, review 7-615
resonant e^+e^- prod. in heavy ion collisions, QED external field problem 7-5038
reviews of particle and nuclear physics, book 7-55907
semimicroscopic nuclear fragmentation model 7-56689
short-range rapidity fluctuations in high energy collisions 7-61781
spectator residues, fragment apparent temp. in breakup 7-49454
storage rings for heavy-ion atomic and nuclear physics 7-36346
strangeness evolution in central region with transverse flow effects 7-15220
strangeness in relativistic heavy ion collisions, review 7-5260
sub-barrier fusion reactions, review 7-56703
sub-barrier fusion-fission reactions, anomalously broad spin distrib., comment with reply 7-10178
superheavy elements, nuclear properties and laboratory synthesis, review 7-61904
ultra-relativistic heavy ion collisions, strangeness in the central region 7-56691
ultra-relativistic nucleus collisions, dilepton production 7-56690
ultra-relativistic heavy-ion collisions, one-dimensional hydrodynamics 7-19291
ultra-relativistic nuclear collisions, initial temp. 7-61918
ultra-relativistic nuclear collisions, stopping power in dual parton model 7-61780
ultra-relativistic nucleus-nucleus collisions, ϕ mass shift predictions by lepton-pair production 7-19077
ultra-relativistic nucleus-nucleus collisions, dilepton emission and the QCD phase transition 7-19290
ultra-relativistic nucleus-nucleus collisions, hydrodynamical evolution of matter, transverse momentum distribns. 7-19188
unequal nuclei collisions at high energy, rapidity distribns. and hydrodynamic model 7-9350
UNILAC heavy-ion reaction searches for superheavy elements 7-19298
very-heavy-ion collisions, critical distance for fusion, fusion barriers 7-19316
vibrational modes of solids, nuclear reaction spectroscopy 7-21371
(e^+e^-) resonance as possible source for anomalous e^+ peak in HI collisions 7-49445
 Λ production in nucleus-nucleus reactions, polarization study 7-5253
 ϕ production in heavy ion collisions (light pseudoscalar boson), QED calcs. 7-36022
Ag(Ar,X), 1.5 GeV/N, central collisions, kinematics and hydrodynamic effects 7-49447
Ag(^{56}Fe ,X), 1.7 GeV/N, anomalous search using plastic SSNTDs 7-19275
Ag(^{14}N ,X), effect of ^8Be decay on nucl. temp. meas. 7-5261
Ag(^{32}S ,X), nuclear temperature measurements and feeding from particle unbound states 7-19305
Ag(^{132}Xe ,X), 14 MeV/N, multipronged events, fission and quasi-fission contribs., SSNTD use 7-19273
 ^{107}Ag (^{12}C ,X), 4.5 GeV/c/nucleon, proton emission multiplicity distribution, Koba-Neilsen-Olesen scaling 7-49438
 ^{107}Ag (^{132}Xe ,X) 7-49437
 ^{107}Ag (^{132}Xe ,X), in AgBr, 0.5-1.2 GeV/nucleon, collective flow in nuclear matter, transverse-momentum anal. 7-19277
 ^{107}Ag (^{197}Au ,X) in AgBr, 0.5-1.2 GeV/nucleon, collective flow in nuclear matter, transverse-momentum anal. 7-19277
 ^{107}Ag (^{238}U ,X) in AgBr, 0.85 A GeV, projectile-target fragment angular correlations 7-19283
 ^{107}Ag (^{32}S ,X), 715 MeV, inclusive fragment cross sections, γ -ray transition cross sections from fragment decays 7-42047
 ^{27}Al (^{16}O ,X), coincidence meas. of light particles and evaporation residues 7-61906
 ^{27}Al (^{16}O ,X), light particle inclusive cross section meas. 7-5262
 ^{27}Al (^{16}O , α), 62, 84.5 MeV, α energy spectra and ang. distribns., direct emission mech. 7-30440

heavy ion-nucleus reactions continued

- ^{27}Al (^{19}F ,X), deep inelastic transfer reactions at 64-88 MeV (Rumanian) 7-15221
 ^{27}Al (^{40}Ar ,X), 600 MeV, composite system formation and decay, multifragmentation and light particle emission 7-36036
 ^{27}Al (^{40}Ar ,X), cross-sections and angular distribns. 7-36024
 ^{27}Al (^{40}Ar ,X), energy spectra and ang. distrib. meas., statistical model comparison 7-42062
 ^{27}Al (^{84}Kr ,X), prod. and decay of highly excited systems, sequential decay model comparison 7-42057
 ^{27}Al (A,X), A= ^4He , ^{12}C , 3.65 GeV/nucleon, cross-section meas. (Russian) 7-24987
 ^{27}Al (A,X), ^{18}F , A= ^4He , ^{12}C , 3.65 GeV/nucleon, cross-section meas. (Russian) 7-24987
(Ar,X), far from stable nuclei, props. and prod. 7-49220
(Au,X), 1 GeV/N in emulsion, multifragmentation, reaction mech., exclusive expt. results 7-36033
Au(Kr,X), 35.44 MeV/u, correlated sources of heavy fragments 7-36040
Au(^{132}Xe ,X), 14 MeV/N, multipronged events, fission and quasi-fission contribs., SSNTD use 7-19273
 ^{197}Au (^{12}C ,f), ang. distribns. and excitation functions (Chinese) 7-25013
 ^{197}Au (^{14}N ,X), 35 MeV/nucleon, source radii and emission temperature meas. 7-5285
 ^{197}Au (^{14}N ,X), linear momentum transfer depend. on source radii and emission temp. 7-19300
 ^{197}Au (^{16}O ,X), light particle inclusive cross section meas. 7-5262
 ^{197}Au (^{20}Ne , ^{20}Ne), quasi-elastic reactions, partition of excitation energy 7-25001
 ^{197}Au (^{20}Ne ,X), 11 MeV/nucleon, 3-body final states, nuclear clustering and projectile excitation 7-5281
 ^{197}Au (^{40}Ar ,X), 27 MeV/nucleon, nuclei deexcitation near nuclear matter instability temp. 7-19279
 ^{197}Au (^{40}Ar ,X), 60 MeV/N, multiplicity depend. light particle corrls., participant-spectator anal. 7-30446
 ^{11}B (^7Li , ^7Li), state excitations, DWBA and coupled channels calcs. 7-42051
 ^{134}Ba (^{24}Mg ,nf), 180 MeV, neutron emission prior to fission 7-5273
 ^9Be (^4B ,O)H, bound and unbound levels in ^4H , ^3H , ^2H 7-36027
 ^9Be (^6Li , ^3B)/He, 72 MeV, excited state search in ^8He , ^7He 7-30338
 ^9Be (^6Li ,5), 32 MeV, ^{12}C levels, spectroscopic strength, ^3He cluster struct., Hauser-Feshbach anal. 7-35965
 ^9Be (^8B , ^8He), 82 MeV, excited state search in ^8He , ^7He 7-30338
 ^{209}Bi (^{18}O , X), 1550 MeV, reaction products study using SSNTD 7-36023
 ^{209}Bi (^{12}C ,f), ang. distribns. and excitation functions (Chinese) 7-25013
 ^{209}Bi (^{50}Ti ,X), $z=102$ to 105 isotope synthesis from fusion reactions 7-24996
 ^{79}Br (^{12}C ,X), 4.5 GeV/c/nucleon, proton emission multiplicity distribution, Koba-Neilsen-Olesen scaling 7-49438
 ^{79}Br (^{12}C ,X), in AgBr, 4.5A GeV/c, central collisions, comparative pseudorapidity spectra study, quark matter formation 7-42045
 ^{79}Br (^{12}C ,X) 7-49437
 ^{79}Br (^{132}Xe ,X), in AgBr, 0.5-1.2 GeV/nucleon, collective flow in nuclear matter, transverse-momentum anal. 7-19277
 ^{79}Br (^{197}Au ,X) in AgBr, 0.5-1.2 GeV/nucleon, collective flow in nuclear matter, transverse-momentum anal. 7-19277
 ^{79}Br (^{238}U ,X) in AgBr, 0.85 A GeV, projectile-target fragment angular correlations 7-19283
 ^{107}Br (^{12}C ,X), in AgBr, 4.5A GeV/c, central collisions, comparative pseudorapidity spectra study, quark matter formation 7-42045
 ^{12}C (^{14}N ,X), 20-40 MeV/N, high energy γ -ray prod., intranuclear NN collision model 7-36041
 ^{12}C (X), 4.5 GeV/c/N, comparison with p-Em 7-49439
 ^{12}C (X), heavy fragment production in intermediate energy heavy ion reactions 7-19303
 ^{12}C (X), spectra of p, d and t, comparison with coalescence model 7-42070
 ^{12}C (^{12}C ,X), low energy fusion, coupled channel formalism 7-707
 ^{12}C (^{12}C , ^{12}B), Δ excitations and shell-model information 7-49457
 ^{12}C (^{12}C ,X), 40 MeV/nucleon, large angle p-p correlations 7-5287
 ^{12}C (^{12}C , α), ^{20}Ne , g-factor meas., critical assessment 7-10102
 ^{12}C (^{12}C , α), ^{16}O , ^{20}Ne , excited states, low-lying bands 7-61911
 ^{12}C (^{12}C , π^-), 4.2, 4.5 A GeV/c, reaction analysis 7-708
 ^{12}C (^{14}N , ^{10}B), ^{16}O , E=54-70 MeV, isospin nonconservation 7-5272
 ^{12}C (^{14}N ,X), correlations between α particles and evaporation residues in complete and incomplete fusion 7-42052
 ^{12}C (^{14}N , γ X), 20, 30, 40 MeV/nucleon, gamma-ray energies, angular distrib. meas. 7-5286
 ^{12}C (^{16}O , ^{16}O), 608 MeV, elastic, inelastic scatt., angular dist. meas. 7-19288
 ^{12}C (^{16}O ,X), fusion channels, intermediate resonances 7-36049
 ^{12}C (^{16}O ,X), light particle inclusive cross section meas. 7-5262
 ^{12}C (^{16}O ,X), doorway states and cross-section fluctuations 7-19287
 ^{12}C (^{16}O , α), ^{24}Mg , 40-67 MeV, obs. of high spin γ -decaying state at 16.9 MeV 7-5139
 ^{12}C (^{19}F , α), ^{27}Al , intermediate structure excitation functions and ang. distribns. 7-49453
 ^{12}C (^{20}Ne ,X), ^{28}Si highly excited spin states 7-705
 ^{12}C (^{24}Mg ,X), 15 MeV/nucleon, 3-body final states, nuclear clustering and projectile excitation 7-5281
 ^{12}C (^6Li ,p), ^{17}O , energy level study and Hauser-Feshbach calcs. 7-15218
 ^{12}C (^{84}Kr ,X), prod. and decay of highly excited systems, sequential decay model comparison 7-42057
 ^{12}C (A,X), ^{11}C , A= ^4He , ^{12}C , 3.65 GeV/nucleon, cross-section meas. (Russian) 7-24987
 ^{13}C (^7Li , ^7Li), state excitations, DWBA and coupled channels calcs. 7-42051
 ^{14}C (^6Li , ^6He), ^{14}N , angular distributions of elastic, inelastic and charge exchange reactions 7-61910
 ^{14}C (^6Li , ^6He), ^{14}N charge exchange reaction, differential cross section meas., refraction effects study 7-49462
(Ca,X), far from stable nuclei, props. and prod. 7-49220
 ^{40}Ca (^{16}O ,X), 69.3-87.3 MeV, A=40, 44 fission-like yields, fusion-fission reaction mech. 7-36038
 ^{40}Ca (^{16}O ,X), A=40,44, nuclear clustering effects in colliding N=Z and N \neq Z nuclei 7-49468
 ^{40}Ca (^{20}Ne , ^{20}Ne), ^{40}Ca , at 92, 149 and 213 MeV, projectile breakup processes 7-30442
 ^{40}Ca (^{23}Na ,X), 260, 287 MeV, complete and incomplete fusion-evap. residue cross-sections, limiting ang. momenta effects 7-30462

heavy ion-nucleus reactions continued

- ⁴⁰Ca(²⁸Si,X), 298, 327 MeV, complete and uncomplete fusion-evap. residue cross-sections, limiting ang. momenta effects 7-30462
⁴⁰Ca(³⁶Ar,2pα), 115 MeV, ⁷⁰Se lifetime meas. 7-10099
⁴⁰Ca(³⁶Ar,4p), lowest three yrast transitions in ⁷²Se, lifetime meas. 7-10099
⁴⁰Ca(⁴⁰Ca,X), dissipative diabatic dynamics 7-49466
⁴⁰Ca(⁴⁰Ca,γ)⁸⁰Zr*, 55-79 MeV, ⁷⁰Rb isomer obs., half-life meas., level structure 7-10109
⁴⁸Ca(³³Al), 198 MeV, ³³Al mass excess 7-49227
¹⁰⁶Cd(³²S,X), A=137-144 exotic neutron-deficient nuclei, shape and γ-decay 7-19201
¹⁰⁶Cd(³⁵Cl,X), A=137-144 exotic neutron-deficient nuclei, shape and γ-decay 7-19201
¹¹⁰Cd(¹³C,3n), ¹²⁰Xe yrast band and backbending using in-beam γ-ray spectroscopy 7-36028
¹¹⁷Cd(²C,3n), ¹²⁰Xe yrast band and backbending using in-beam γ-ray spectroscopy 7-36028
Cl(Ar,X), 1.5 GeV/N, three pion correlations in relativistic collisions 7-36035
³⁵Cl(⁴⁰Ar,X), 1.2, 1.89 A GeV, in KCl, collective flow and stiffness in compressed nuclear matter 7-36021
Cm(Th,X), anomalous e⁺ prod. 7-30439
Cm(Th,X), narrow positron peak observation 7-49470
Cm(U,X), anomalous e⁺ prod. 7-30439
²⁴⁸Cm(⁴Ca,X), A=40,48 actinide yields 7-24994
²⁴⁸Cm(⁴⁸Ca,X), superheavy element production 7-24993
²⁴⁸Cm(¹⁸O,X), below target yields 7-19304
²⁴⁸Cm(⁴⁰Ca,X), below target yields 7-19304
²⁴⁸Cm(Xe,X), actinide prod. cross section dependence on projectile mass number 7-42058
¹³³Cs(²²Ne,X), complete fusion, excitation functions and high-spin isomeric species 7-5266
⁶⁹Cu(¹²C,X), 3.65 GeV/nucleon, hadron yields, angular distrib. meas. (Russian) 7-24987
¹⁶³Dy(³⁵Cl,X), 160 MeV, ¹⁶³Dy ground state band study, γ-γ coincidence, angular distrib. meas. 7-56640
¹⁶³Dy(⁵⁸Ni,X), 250 MeV, ¹⁶³Dy ground state band study, γ-γ coincidence, angular distrib. meas. 7-56640
²⁵⁴Es, transactinide production by multinucleon transfer reactions 7-24992
⁵⁴Fe(²⁰Ne,X), reaction mechanism 7-701
⁵⁴Fe(²⁸Si,X), angular-momentum limitations in the high-spin gamma-decay of medium-mass evaporation residues 7-10170
¹⁵⁶Gd(¹⁶O,αp), ⁶⁷Ga 15/2⁺ 3578 keV level, mag. moment meas. 7-35946
¹⁵⁶Gd(⁴⁰Ar,X), 44 MeV/N, γ-rays from peripheral and central collisions, fragment stat. decay 7-61917
¹⁶⁰Gd, nucleon transfer reactions to rot. states induced by ²⁰⁶Pb, ²⁰⁸Pb 7-49210
¹⁶⁰Gd(¹⁸O,X), A=74,76, yrast decay in fusion-evaporation reaction products 7-15198
²H(⁶Li,α)⁴He, off-resonance analyzing power meas. 7-5204
¹⁸¹Hf(¹⁸O,X), 1550 MeV, reaction products study using SSNTD 7-36023
¹⁶⁵Ho(¹⁴N,X), neutron emission from high temp. region 7-36045
¹⁶⁵Ho(¹⁴N,X), 35 MeV/N, neutron-fragment coincidence meas. 7-36037
¹⁶⁵Ho(¹⁴N,X), excitation of discrete particle-unbound states in heavy-ion collisions 7-61914
¹⁶⁵Ho(¹⁶O,4n), 78-84.5 MeV, ¹⁷⁷Re single quasi-proton states, deformation depend., level scheme, cranking model, anal. 7-41877
¹⁶⁵Ho(⁴⁰Ar,X), 27 MeV/nucleon, nuclei deexcitation near nuclear matter instability temp. 7-19279
¹⁶⁵Ho(⁵⁶Fe,X), SOS MeV, fragment analysis 7-5275
¹⁶⁵Ho(⁵⁸Ni,X), 5.9, 6.5 MeV/N, mass asymmetry degree-of-freedom relaxation, fragment correl. 7-30448
¹⁶⁵Ho(⁵⁸Ni,αX), 8.2 MeV/nucleon, signatures for fast α-emission, velocity distrib., angular correlations 7-5282
¹¹¹In(¹²C,X), residual nuclei recoil study 7-19302
K(Ar,X), 1.5 GeV/N, three pion correlations in relativistic collisions 7-36035
³⁹K(⁴⁰Ar,X), 1.2, 1.89 A GeV, in KCl, collective flow and stiffness in compressed nuclear matter 7-36021
(Kr,X), heavy fragment production in intermediate energy heavy ion reactions 7-19303
¹³⁹La(¹³⁹La,X), 40 MeV/u, fragmentation anal. 7-5284
¹³⁹La(¹³⁹La,X), π⁻ multiplicity and nucl. matter response 7-42066
⁶Li(⁶He), on A=7-90, 210 MeV, spin-transfer strength probe, Gamow-Teller transitions 7-25003
⁶Li(αd), coupled channel study 7-36048
⁷Li(αt), coupled channel study 7-36048
⁷Li(⁷Be)⁷He, 70 MeV, excited state search in ⁸He, ⁷He 7-30338
¹⁷³Lu(¹²C,f) (Chinese) 7-25013
²⁴Mg(¹⁹F,X), deep inelastic transfer reactions at 64-88 MeV (Rumanian) 7-15221
²⁴Mg(¹²C,X), excitation fns., intermediate structures, comparisons with orbiting-cluster model 7-56692
²⁴Mg(¹⁶O,X), deep inelastic transfer reactions at 64-88 MeV (Rumanian) 7-15221
Mo(¹⁶O, xnp), ¹⁰⁵⁻¹⁰⁸In beta⁺-decay energies determ., Q_{BC} values 7-19209
⁹⁴Mo(⁶⁰Ni,pn)¹⁵²Tm, E=240-250 MeV, yrast level anal. 7-10098
⁹⁴Mo(⁶Li,p2n), 20-34 MeV, ⁹⁷Ru excited states, level schemes, spins and transitions 7-35921
¹⁴N(²⁸Si,X), forward-angle yield, equilibration in orbiting reactions 7-5270
¹⁴N(⁷Li,t)¹⁸F*, α clustering, DWBA anal. 7-700
⁹²Nb(²⁷Al,X), 8-40 MeV/u, intermediate mass fragment emission 7-5290
⁹²Nb(¹²C,X), 8-40 MeV/u, intermediate mass fragment emission 7-5290
⁹²Nb(²⁰Ne,X), complete and incomplete fusion, inclusive fragment spectra meas. 7-42055
⁹²Nb(⁶⁰Ni,2pn)¹⁵⁰Ho, E=240-250 MeV, yrast level anal. 7-10098
⁹²Nb(⁶Be,X), 8-40 MeV/u, intermediate mass fragment emission 7-5290
¹⁴²Nd(¹⁶O,γ)¹⁵⁸Er, 207 MeV, enhancement of pre-fission neutron multiplicities w.r.t. statistical model predictions 7-10174
¹⁴²Nd(¹⁶O,nf), 207 MeV, neutron emission prior to fission 7-5273
¹⁴²Nd(¹⁶O,nf), 207 MeV, neutron emission prior to fission 7-5300
¹⁴²Nd(¹⁶O,γ)¹⁶⁰Er, E_{lab}=76-105 MeV, ¹⁶⁰Er statistical decay, giant dipole resonance effects, statistical model comparisons 7-10173
²⁰Ne(¹²C,X), excitation fns., intermediate structures, comparisons with orbiting-cluster model 7-56692

heavy ion-nucleus reactions continued

- (²²Ne,X), fragmentation on photoemulsion nuclei, topological characts. 7-10163
⁴⁰Ne(B,π⁻Δ), B=¹⁶O, ¹²C, 4.5 A GeV/c, reaction analysis 7-708
(Ni,X), far from stable nuclei, props. and prod. 7-49220
Ni(¹⁴N,X), 35 MeV/N, neutron-fragment coincidence meas. 7-36037
Ni(¹⁴N,X), neutron emission from high temp. region 7-36045
⁶¹Ni(²⁸Si,X), A=58,62, transfer cross sections near Coulomb barrier 7-36052
⁵⁴Ni(¹⁴N,γX), 35 MeV/n, bremsstrahlung angular distrib. 7-5254
⁵⁸Ni(³²N,pn), 39 MeV, ⁷²Se lifetime meas. 7-10099
⁵⁸Ni(³²S,X), selective γ-decay of fission-like fragments 7-42059
⁵⁸Ni(³⁶S,X), 94-112 MeV, quasi-elastic transfer cross section meas., effects on sub-barrier fusion 7-61915
⁵⁸Ni(⁴⁰Ar,X), 600 MeV, composite system formation and decay, multifragmentation and light particle emission 7-36036
⁵⁸Ni(⁵⁴Fe,X)¹¹²Xe*, groundstate proton radioactivity meas. 7-49350
⁵⁸Ni(⁵⁸Ni,X)¹¹⁶Ba*, groundstate proton radioactivity meas. 7-49350
⁵⁸Ni(⁷Li,⁸He), 76.5 MeV, ⁵⁷Cu ground state Q-value and mass excess, cross section 7-35935
⁶¹Ni(¹²C,X), light particle energy spectrum anal. (Chinese) 7-24999
⁶⁴Ni(³²S,X), 94-112 MeV, quasi-elastic transfer cross section meas., effects on sub-barrier fusion 7-61915
⁶⁴Ni(Li,d), DWBA anal., exptl. comparisons 7-56699
⁶⁴Np, A=243,244, separation and identification by centrifuge system 7-24995
(¹⁶O,X), in emulsion, anomalous behaviour of singly charged relativistic secondary particles 7-5264
(¹⁶O,X), heavy fragment production in intermediate energy heavy ion reactions 7-19303
¹⁶O(¹⁶O,¹²C)²⁰Ne, ang. distrib. at energies near Coulomb barrier 7-36026
¹⁶O(¹⁶O,X), fusion cross-sections in classical microscopic equations of motion approach 7-56698
¹⁶O(¹⁶O,α)²⁴Mg, small angle cross-sections, resonances and compound fluctuations 7-49449
¹⁶O(¹⁶O,α)²⁸Si, small angle cross-sections, resonances and compound fluctuations 7-49449
¹⁶O(¹⁶O,πX), 40-80 MeV/nucleon, microscopic anal. 7-49467
¹⁶O(¹⁶O,πX), π-production cross section calcs., TDHF anal. 7-24998
¹⁶O(Li,⁸Be)¹⁶Ba*, direct and sequential processes 7-10167
¹⁶O(Li,xy), 4-10 MeV, complete fusion in Coulomb threshold region, total cross section 7-19314
Pb(Ar,X), 1.8 GeV/N, three pion correlations in relativistic collisions 7-36035
Pb(¹²C,f), ang. distrib. and excitation functions (Chinese) 7-25013
Pb(¹⁴N,X), 20-40 MeV/N, high energy γ-ray prod., intranuclear NN collision model 7-36041
Pb(Pb,X), 5.7 MeV/n, e⁻ and e⁺ spectra, sudden rearrangements of electronic shells 7-49441
²⁰⁸Pb(⁴⁸Ca,X), A=206,208, Z=102 to 105 isotope synthesis from fusion reactions 7-24996
²⁰⁸Pb(⁶⁰Ti,X), A=207,208, Z=102 to 105 isotope synthesis from fusion reactions 7-24996
²⁰⁶Pb(²³N,X), subbarrier fusion cross sections and tensor analyzing powers 7-19293
²⁰⁸Pb(⁵⁸Ni,⁵⁹Ni), quasielastic transfer meas. and DWBA anal. 7-42065
²⁰⁸Pb(⁵⁸Ni,⁵⁹Ni), quasielastic transfer meas. and DWBA anal. 7-42065
²⁰⁸Pb(¹²C,X), spallation residues, velocity and ang. distrib. 7-61913
²⁰⁸Pb(¹⁴N,γX), 20, 30, 40 MeV/nucleon, gamma-ray energies, angular distrib. meas. 7-5286
²⁰⁸Pb(¹⁶O,¹⁵N), transfer to discrete levels, semiclassical selection rules and DWBA formalism 7-36032
²⁰⁸Pb(¹⁶O,¹⁵O), transfer to discrete levels, semiclassical selection rules and DWBA formalism 7-36032
²⁰⁸Pb(¹⁶O,f), 76.8, 77.3, 80.2 MeV, fragment angular distrib. 7-19286
²⁰⁸Pb(²⁰Ne,nX), 390 MeV/nucleon, low-energy neutron angular distrib. meas. 7-19284
²⁰⁸Pb(⁴⁸Ti,X), 300 MeV, transition between quasi-elastic and deep-inelastic reactions 7-5277
²⁰⁸Pb(⁸⁶Kr,X), 10, 13, 18.2 MeV/u, quasielastic reactions, role of inelastic excitation and nucleon transfer 7-5280
¹⁰⁸Pd(⁵⁰Ti,nf), 216 MeV, neutron emission prior to fission 7-5273
Pb(¹²C,f), ang. distrib. and excitation functions (Chinese) 7-25013
²⁴⁰Pu, compound nucleus, enhanced neutron emission, fission calcs., diffusion model anal. 7-61903
²⁴²Pu(¹²C,X), actinide prod. cross section meas. 7-5267
Re(¹²C,f), ang. distrib. and excitation functions (Chinese) 7-25013
³²Si(¹²C,X), excitation fns., intermediate structures, comparisons with orbiting-cluster model 7-56692
⁴⁵Sc(⁴⁰Ar,X), 600 MeV, composite system formation and decay, multifragmentation and light particle emission 7-36036
²⁸Si(¹²C,X), excitation fns., intermediate structures, comparisons with orbiting-cluster model 7-56692
²⁸Si(¹²C,X), 43-70.5 MeV, complete fusion excitation function (Chinese) 7-49443
²⁸Si(¹⁸O,¹⁸F), 19.6 MeV/N, one-step direct contrib., cross-sections, double folding DW anal. 7-30401
²⁸Si(²⁸Si,N), E_{lab}=151.25 MeV, cross section meas. 7-19281
²⁸Si(²⁸Si,xnp), E_{lab}=151.25 MeV, cross section meas. 7-19281
²⁸Si(³²Ar)³⁶Ar, Mg, ang. distrib. meas., energy dependence 7-10166
²⁸Si(³⁸Ni,³⁹Ni), transfer cross section meas., isotopic dependence, DWBA anal. 7-5256
²⁸Si(⁶²Ni,⁶³Ni), transfer cross section meas., isotopic dependence, DWBA anal. 7-5256
¹⁴⁴Sm(¹²C,X), ¹⁵⁶Er production, evaporation residue cross sections and average neutron multiplicities, stat. anal. 7-30445
¹⁴⁴Sm(¹⁶O,γ), E_{lab}=63-72 MeV, fusion cross section meas. at sub-barrier energies 7-5257
¹⁵²Sm, nucleon transfer reactions to rot. states induced by ²⁰⁶Pb, ²⁰⁸Pb 7-49210
¹⁵⁴Sm(¹²C,¹⁴C), pair transfer, macroscopic description, form factor 7-25000
¹⁵⁴Sm(¹²C,X), incomplete and complete fusion in intermediate energy heavy ion reactions 7-49461
¹⁵⁴Sm(¹⁴N,γX), 20, 35 MeV/nucleon, deflection of non-equilibrium light particles by nuclear mean field, γ-polarization meas. 7-5283
¹⁵⁴Sm(¹⁶O,X), incomplete and complete fusion in intermediate energy heavy ion reactions 7-49461
¹⁵⁴Sm(¹⁶O,X), linear and angular momentum transfer in incomplete fusion reactions 7-42054

heavy ion-nucleus reactions continued

- $\text{Sn}^{(38}\text{Ni},\text{X})$, subbarrier nucleon transfer and doorway fusion states 7-42064
 $\text{Sn}^{(40}\text{O},\text{X})$, A-16,18, subbarrier nucleon transfer and doorway fusion states 7-42064
 $^{117}\text{Sn}^{(32}\text{S},\text{X})$, A=137-144 exotic neutron-deficient nuclei, shape and γ -decay 7-19201
 $^{117}\text{Sn}^{(35}\text{Cl},\text{X})$, A=137-144 exotic neutron-deficient nuclei, shape and γ -decay 7-19201
 $^{118}\text{Sn}^{(12}\text{C},\text{X})$, preequilibrium reactions, coincidence spectra 7-49460
 $^{118}\text{Sn}^{(64}\text{Ni},\text{X})$, compound nucleus angular distrib. and fission cross sections, elastic fusion model comparisons 7-56694
 $^{127}\text{Sn}^{(208}\text{Pb},\text{X})$, quasi-elastic recoil and elastoplasticity in central collisions 7-5258
 $^{128}\text{Sn}^{(38}\text{Ni},\text{f})$, cross sections and compound nucleus angular distrib., elastic fusion model comparisons 7-56694
 $^{181}\text{Ta}^{(12}\text{C},\text{X})$, 4.2 GeV/c, central collisions, anal. using data and cascade-evaporation model 7-56701
 $^{181}\text{Ta}^{(12}\text{C},\text{f})$, ang. distrib. and excitation functions (*Chinese*) 7-25013
 $^{181}\text{Ta}^{(20}\text{Ne},\alpha)$, DWBA anal., exptl. comparisons 7-56699
 $^{181}\text{Ta}^{(40}\text{Ar},\text{X})$, 44 MeV/A, $X=^{14}\text{N},^{16}\text{O},^{19}\text{F}$, mass meas. of fragmentation products 7-5148
 $^{181}\text{Ta}^{(40}\text{Ar},\text{X})$, observation of ^{22}C exotic nucleus 7-10164
 $^{187}\text{Th}^{(19}\text{F},\text{X})$, 181 MeV, particle-bound excited state yields 7-5269
 $^{128}\text{Te}^{(32}\text{S},\text{nf})$, 180 MeV, neutron emission prior to fission 7-5273
 $^{130}\text{Te}^{(28}\text{Si},\text{X})$, transfer reactions, optimum Q-values (*Korean*) 7-24997
 $^{130}\text{Te}^{(40}\text{Ar},\text{X})$, 180 MeV, ^{166}Yb high spin states, lifetimes meas., B(E2) values 7-35924
 $\text{Th}^{(Th},\text{X})$, anomalous e^+ prod. 7-30439
 $\text{Th}^{(Th},\text{X})$, narrow positron peak observation 7-49470
 $\text{Th}^{(U},\text{X})$, anomalous e^+ prod. 7-30439
 $^{235}\text{Th}^{(40}\text{Ar},\text{X})$, 240 MeV, cross section for evaporative α -particles, α -yield 7-36042
 $^{235}\text{Th}^{(40}\text{Ar},\text{X})$, fragmentation, shell effects in mass asymmetry evolution 7-30449
 ^{235}Th , nucleon transfer reactions to rot. states induced by ^{206}Pb , ^{208}Pb 7-49210
 $^{232}\text{Th}^{(16}\text{O},\text{f})$, 77-86 MeV, ^{248}Cf compound nucleus spin determ. from fragment angular distrib. 7-19286
 $^{235}\text{Th}^{(238}\text{U}, \gamma\gamma\text{X})$, 6 MeV/nucleon, two-photon spectrum, correlated narrow-peak structure 7-19294
 $\text{Ti}^{(40}\text{Ar},\text{X})$, cross-sections and angular distrib. 7-36024
 $\text{Ti}^{(Zr},\text{X})$, subbarrier fusion, adiabatic representation 7-702
 $^{46}\text{Ti}^{(35}\text{Cl},\text{X})$, damped reaction products, coincidence study 7-36051
 $^{48}\text{Ti}^{(23}\text{Na},\text{X})$, subbarrier fusion cross sections and tensor analyzing powers 7-19293
 $^{48}\text{Ti}^{(31}\text{Cl},\text{X})$, damped reaction products, coincidence study 7-36051
 $^{167}\text{Tm}^{(12}\text{C},\text{f})$, ang. distrib. and excitation functions (*Chinese*) 7-25013
 $\text{U}^{(Li},\text{p})$, backward angle proton emission in central collisions 7-5305
 $\text{U}^{(Th},\text{X})$, anomalous e^+ prod. 7-30439
 $\text{U}^{(Th},\text{X})$, narrow positron peak observation 7-49470
 $\text{U}^{(U},\text{X})$, anomalous e^+ prod. 7-30439
 $^{236}\text{U}^{(12}\text{C},\text{f})$, 60-68 MeV, ^{248}Cf compound nucleus spin determ. from fragment angular distrib. 7-19286
 $^{238}\text{U}^{(12}\text{C},\text{f})$, 81, 90 MeV, fragment angular distrib. 7-5303
 $^{238}\text{U}^{(16}\text{O},\text{X})$, actinide prod. cross section meas. 7-5267
 $^{238}\text{U}^{(22}\text{Ne},\text{f})$, 125, 143, 175 MeV, fragment angular distrib. 7-5303
 $^{238}\text{U}^{(238}\text{U}, ^{239}\text{U})$, sub-Coulomb transfer, excitation functions and ang. distrib. 7-5259
 $^{238}\text{U}^{(238}\text{U},\text{X})$, 50 GeV/nucleon, one-dimensional hydrodynamics anal. 7-19291
 $^{238}\text{U}^{(32}\text{S},\text{X})$, fragmentation, shell effects in mass asymmetry evolution 7-30449
 $^{238}\text{U}^{(4}\text{He},\text{f})$, 25, 35 MeV, fragment angular distrib. 7-5303
 $\text{W}^{(12}\text{C},\text{f})$, ang. distrib. and excitation functions (*Chinese*) 7-25013
 $^{184}\text{W}^{(16}\text{O}, \text{xn})$, $^{194-196}\text{Pb}$ energy level conversion coeff. meas. 7-19206
 $^{64}\text{Zn}^{(14}\text{N},\gamma\text{X})$, 20, 30, 40 MeV/nucleon, gamma-ray energies, angular distrib. meas. 7-5286
 ^{65}Zn compound system, preequilibrium α -emission, angular momentum effects 7-56693
 $^{68}\text{Zn}^{(40}\text{Ar},\text{X})$, inclusive variables, random walk model calcs. 7-42050
 $^{90}\text{Zr}^{(40}\text{Ar},\text{X})$, 600 MeV, composite system formation and decay, multifragmentation and light particle emission 7-36036
 $^{90}\text{Zr}^{(90}\text{Zr},\text{X})$, dissipative diabatic dynamics 7-49466
 $^{90}\text{Zr}^{(90}\text{Zr},\gamma)$, ^{180}Hg nuclear shape coexistence, γ -decay, energy levels 7-19163
 $^{92}\text{Zr}^{(60}\text{Ni},\text{pn})$, ^{150}Ho , E=240-250 MeV, yrast level anal. 7-10098
 $^{92}\text{Zr}^{(64}\text{Ni},\text{X})$, ^{156}Er production, evaporation residue cross sections and average neutron multiplicities, stat. anal. 7-30445
 $^{96}\text{Zr}^{(7}\text{Li},2\text{np})$, ^{100}Mo , 32.5 MeV, yrast states, $\gamma\gamma$ coincidence meas. 7-24926

heavy ion-nucleus scattering

- $^{24}\text{Mg}^{(24}\text{Mg},^{24}\text{Mg})$, R-matrix formalism with physical boundary conditions 7-36025
 absorptive potential, closure approximation 7-703
 conference on nuclear scatt. data eval. methods, Berlin, Germany (June 1985) 7-21
 elastic collisions, nuclear masses, energy density formalism 7-25006
 elastic scatt., parity depend., two-centre harmonic oscillator model 7-42046
 elastic scattering and energy storing in compressed nuclear matter 7-706
 factorized density-dependent interaction in the folding model 7-30393
 high energy, flattening of distrib. of large transverse energy prod. 7-42068
 inelastic scatt., optical potential deformation 7-49442
 interaction radii of stable and unstable nuclei 7-49452
 nuclear polarization potential, role in heavy-ion collisions 7-5276
 optical potential analyses, stat. regularisation method appl. 7-620
 quantised adiabatic time-dependent Hartree-Fock theory 7-61900
 $\text{SO}(2,3)$ S-matrix, strong factor, heavy ion appls., phase shifts 7-30391
 tidal symmetry in scatt. of polarised projectiles. 7-15208
 vibrational modes of solids, nuclear reaction spectroscopy 7-21371
 $^{28}\text{Si}^{(16}\text{O},^{16}\text{O})$, stochastic regularisation appl. to phase shift anal. 7-709
 $\text{Al}^{(6}\text{Li},^6\text{Li})$, scatt. study using LR-115 SSNTD 7-19274
 $^{12}\text{C}^{(12}\text{C},^{12}\text{C})$, 1016 MeV, optical pot. using inverse scatt. method 7-49440
 $^{12}\text{C}^{(12}\text{C},^{12}\text{C})$, ^{24}Mg symmetric fission following inelastic scatt. 7-36031
 $^{12}\text{C}^{(12}\text{C},^{12}\text{C})$, ^{24}Mg decay, excitation energies 7-36030
 $^{12}\text{C}^{(12}\text{C},^{12}\text{C})$, 1449 and 2400 MeV, phase shift anal. 7-30447

heavy ion-nucleus scattering continued

- $^{12}\text{C}^{(12}\text{C},^{12}\text{C})$, elastic scattering angular distrib., total reaction cross-section 7-49451
 $^{12}\text{C}^{(12}\text{C},^{12}\text{C})$, effects of vacuum polarisation on sub-Coulomb scatt. 7-49469
 $^{12}\text{C}^{(12}\text{C},^{12}\text{C})$, elastic scatt., surface transparency 7-61912
 $^{13}\text{C}^{(12}\text{C},^{12}\text{C})$, Landau-Zener transition due to molecular orbitals, coupled channels model 7-42060
 $^{14}\text{C}^{(6}\text{Li},^6\text{Li})$ elastic scatt. differential cross section meas., refraction effects study 7-49462
 $^{14}\text{C}^{(6}\text{Li},^6\text{Li})$, angular distributions of elastic, inelastic and charge exchange reactions 7-61910
 $^{40}\text{Ca}^{(12}\text{C},^{12}\text{C})$, elastic scattering angular distrib., total reaction cross-section 7-49451
 $^{248}\text{Cm}^{(136}\text{Xe},^{136}\text{Xe})$, E2 properties of ground state band 7-10093
 $^{248}\text{Cm}^{(58}\text{Ni},^{58}\text{Ni})$, E2 properties of ground state band 7-10093
 $^{19}\text{F}^{(12}\text{C},^{12}\text{C})$, back-angle anomalous scatt. 7-10171
 $^{19}\text{F}^{(16}\text{O},^{16}\text{O})$, phase anomaly for elastic and inelastic scatt. 7-36046
 $^{160}\text{Gd}^{(Pb},\text{Pb})$, rotational state population close to Coulomb barrier 7-49210
 $^A\text{Mg}^{(28}\text{Si},^{28}\text{Si})$, A=24, 26, backward-angle excitation functions and ang. distrib. 7-30443
 $^{60}\text{Ni}^{(16}\text{O},^{16}\text{O})$, ^{60}Ni , polarisation potential in optical model 7-19271
 $^{16}\text{O}^{(12}\text{C},^{12}\text{C})$, optical pot. determ. using quasi-classical inversion 7-61905
 $^{16}\text{O}^{(12}\text{C},^{12}\text{C})$, ^{16}O , intermediate width structures, angular momenta 7-49456
 $^{16}\text{O}^{(16}\text{O},^{16}\text{O})$, ang. distrib. at energies near Coulomb barrier 7-36026
 $^{18}\text{O}^{(58}\text{Ni},^{58}\text{Ni})$, 60 MeV, optical-potential phase-shifts, phase-integral calcs. 7-19278
 $^A\text{Os}^{(32}\text{S},^{32}\text{S})$, A=190, 192, 100 MeV, nuclear deorientation during recoil in vacuum, γ -ray ang. correls. 7-10135
 $^{208}\text{Pb}^{(100}\text{Mo},^{100}\text{Mo})$, 350 MeV, Coulomb excitation, $8^+ \rightarrow 6^+$ transition, B(E2) meas. 7-24926
 $^{208}\text{Pb}^{(12}\text{C},^{12}\text{C})$, 1449 and 2400 MeV, phase shift anal. 7-30447
 $^{208}\text{Pb}^{(12}\text{C},^{12}\text{C})$, ^{208}Pb , elastic scattering angular distrib., total reaction cross-section 7-49451
 $^{208}\text{Pb}^{(16}\text{O},^{16}\text{O})$, ^{208}Pb , polarisation potential in optical model 7-19271
 $^{208}\text{Pb}^{(16}\text{O},^{16}\text{O})$, DWBA anal., exptl. comparisons 7-56699
 $^{208}\text{Pb}^{(16}\text{O},^{16}\text{O})$, ^{208}Pb , Coulomb nuclear interference in excitation 7-10169
 $^{208}\text{Pb}^{(17}\text{O},^{17}\text{O})$, high energy continuum excitation 7-42049
 $^{208}\text{Pb}^{(32}\text{S},^{32}\text{S})$, high energy continuum excitation 7-42049
 $^A\text{Pt}^{(12}\text{C},^{12}\text{C})$, A=194,196,198 electric quadrupole moments of first excited states 7-10103
 $^A\text{Pt}^{(16}\text{O},^{16}\text{O})$, A=194,196,198 electric quadrupole moments of first excited states 7-10103
 $^A\text{Pt}^{(32}\text{S},^{32}\text{S})$, A=194, 196, 100 MeV, nuclear deorientation during recoil in vacuum, γ -ray ang. correls. 7-10135
 $^{195}\text{Pt}^{(32}\text{S},^{32}\text{S})$, 125 MeV, levels and transitions, B(E2) values, SUSY classification in IBFM 7-30310
 $^{28}\text{Si}^{(14}\text{N},^{14}\text{N})$, spin-orbit term in optical pot. 7-36047
 $^{28}\text{Si}^{(16}\text{O},^{16}\text{O})$, 29-35 MeV, optical model, coupled-channel method anal., role of collective excitations 7-56700
 $^{28}\text{Si}^{(16}\text{O},^{16}\text{O})$, 21.1, 34.8 MeV, optical model pots. from pot. inversion at fixed energy 7-5208
 $^{28}\text{Si}^{(16}\text{O},^{16}\text{O})$, $E_{\text{lab}}=94$ MeV/nucleon, angular distrib., double-folded potential comparisons 7-61916
 $^{152}\text{Sm}^{(Pb},\text{Pb})$, rotational state population close to Coulomb barrier 7-49210
 $^{154}\text{Sm}^{(24}\text{Mg},^{24}\text{Mg})$, 150 MeV, DWBA anal. using proximity-plus-Coulomb potential calculated form factors 7-19285
 $^{120}\text{Sn}^{(7}\text{Li},^7\text{Li})$, differential cross section and analysing power meas., coupled channels calcs. 7-15219
 $^{120}\text{Sn}^{(7}\text{Li},^7\text{Li})$, analyzing power and spin-orbit interaction, coupled channels formalism 7-61908
 $^{232}\text{Th}^{(Pb},\text{Pb})$, rotational state population close to Coulomb barrier 7-49210
 $^{235}\text{U}^{(84}\text{Kr},^{84}\text{Kr})$, 370, 450 MeV, band strucls., moments of inertia, multipole moments, transition probabs. 7-35922
 $^{238}\text{U}^{(40}\text{Ar},^{40}\text{Ar})$, multiple Coulomb nucl. excitation to high spin states, iteration method of soln. 7-42056
 $^{238}\text{U}^{(84}\text{Kr},^{84}\text{Kr})$, multiple Coulomb nucl. excitation to high spin states, iteration method of soln. 7-42056
 $^A\text{W}^{(32}\text{S},^{32}\text{S})$, A=182, 184, 186, 100 MeV, nuclear deorientation during recoil in vacuum, γ -ray ang. correls. 7-10135
 $^{90}\text{Zr}^{(12}\text{C},^{12}\text{C})$, ^{90}Zr , elastic scattering angular distrib., total reaction cross-section 7-49451

heavy leptons

- branching fraction meas. 7-41805
 fermion production and decay via W bosons, helicity projection techniques 7-61762
 heavy-ion collisions, relativistic, heavy lepton production, cross section calcs. using equivalent photon method 7-56695
 lepton spectrum derivation using the TLVP EM model 7-61638
 leptonium, radiative corrections to one-photon annihilation leptonic decays 7-35871
 standard model, heavy neutral lepton search techniques 7-30221
 α decay modes, standard electroweak model predictions 7-41804
 $\text{E}-\bar{\text{e}}$ mixing in E_μ , effects on $\text{e}^+\text{e}^- \rightarrow \text{Z}^0\gamma$ 7-61645
 $\text{e}^+\text{e}^- \rightarrow \tau^+\tau^-$, cross section determ. from 14 to 465.8 GeV 7-15142
 $\text{L} \rightarrow \bar{\nu}\nu(\bar{\nu}\nu)$ (L=heavy lepton), event search at CERN collider 7-61680
 $\nu \rightarrow \gamma\text{X}$, lifetime constraints from primordial light-element photodestruction anal. 7-10059
 $\nu_\mu, \nu_e \rightarrow \nu_\tau$, oscillations limits, $\nu_\mu, \nu_e \rightarrow \tau^+\tau^-$ direct coupling 7-35768
 $\text{pp} \rightarrow$ heavy leptons, 10-40 TeV, cross section calcs. in E_μ 7-19138
 $\text{pp} \rightarrow$ heavy leptons, missing-pr-plus-jets signal anal. 7-61761
 $\text{pp} \rightarrow \text{L}^+\text{L}^- + \text{jets}$, N=heavy neutrino, event signature anal. 7-19137
 $\text{pp} \rightarrow \text{W}^\pm \nu_\tau (\text{Z}^0 (\text{W}^\pm \gamma) \rightarrow \text{L}^+\text{L}^-)$, heavy lepton production through vector boson fusion processes 7-10078
 $\tau \rightarrow 3\pi\nu_\tau$, 3π spectral function, implications for A_1 mass 7-49141
 $\tau \rightarrow \bar{\nu}_\mu \nu_\tau$, ν_τ mass limits 7-24884
 τ mass, gauge field theory 7-61433
 $\tau \rightarrow \mu \bar{\nu}_\mu$, branching ratio determ. 7-15142
 τ neutrinoless decay, lepton-number and lepton-flavour violation search 7-61675
 $\tau \rightarrow \nu_\mu \pi$, branching fraction meas. 7-49144
 $\tau \rightarrow \nu \gamma \tau(p)$, radiative 3-body decays 7-15152
 $\tau \rightarrow \nu \mu \nu$, $\text{K}^0 \nu_\tau$, branching ratios, effects of asymptotic flavour symmetry, QCD anal. 7-49143

heavy leptons continued

- τ^- branching ratio meas. 7-61677
- $\tau^- \rightarrow \nu_\tau e^- \bar{\nu}_e$, branching fraction meas. 7-61676
- $\tau^- \rightarrow \nu_\tau \pi^-$, $\nu_\tau \pi^- \pi^0$, $\nu_\tau \pi^- (\pi^0, n > 1)$, branching fraction meas. 7-61676
- $\tau^- \rightarrow \nu_\tau \pi^- \pi^0 +$ neutral meson(s), inclusive branching fraction meas. 7-15154
- $\tau^- \rightarrow \nu_\tau \pi^- \pi^+ \pi^-$, $\nu_\tau \pi^- \pi^+ \pi^- (\pi^0, n > 0)$, branching fraction meas. 7-61676
- $\tau^- \rightarrow \omega \pi^-$, branching ratio meas., $e^+ e^- \rightarrow \tau^+ \tau^-$ expt. 7-61674
- $\tau^- \rightarrow \omega \pi^- \pi^-$, branching ratio 7-35874
- $\tau^\pm \rightarrow \nu_\tau \pi^\pm$, branching fraction meas. 7-41805
- $\tau^\pm \rightarrow \nu_\tau \pi^\pm \pi^\pm$, branching fraction meas. 7-41805
- $\tau^\pm \rightarrow \nu_\tau \pi^\pm$, branching fraction meas. 7-41805

heavy water

- decylammonium-D₂O, surfactant aggregates, correl. time determ., relax. meas. 7-25540
- deuterium ion source for plasma chromatograph and mass spectrometer 7-4909
- deutero-isobutyric acid (coax)-D₂O, critical mixtures, isotope effects 7-12253
- distillation process, steady and unsteady state models 7-6340
- equation of state, international standard 7-51988
- fusion reactor self-cooled heavy water breeding blanket concept 7-15364
- molecule, H- and D-bonded dimers, relative stabilities, IR spectra 7-62364
- molecule, quantum state selective detection by (2+1) REMPI 7-36706
- molecule, rot. levels, isotope effects, three-parameter model 7-31018
- neutron scatt. by molecules, inelasticity corrections using a synthetic scatt. function 7-20069
- optically pumped laser, FIR laser line meas. 7-57306
- phenol-d₆-D₂O, critical mixtures, isotope effects 7-12253
- salt/water/aprotic solvent mixtures, alkali cation influence, IR spectra anal. 7-19856
- water-caesium pentadecafluorooctanoate discoid micelle solns., order-disorder transitions, X-ray scatt., elec. cond., NMR meas. 7-26949
- D₂O⁺, B²B₂ state predissoc., intramol. dynamics, photoelectron spectroscopy 7-42699
- D₂O⁺, mol. beam photoelectron spectrosc., femtosec. intramol. dynamics 7-36688
- HDO, vibr. modes, rot. decoupling 7-57042
- H₂O-D₂O liq. mixture, thermal transport props. 7-16826
- HTO, mol. vibr.-rot., IR spectra anal. 7-50116

HEED see high energy electron diffraction**height measurement**

- optical position sensing using Si photodetectors 7-48691
- satellite altimetry for oceanic eddy transport estimation 7-40595
- satellite laser ranging, chord and relative height estimation from single data passes (Chinese) 7-3961
- sea surface, global nondynamic orbit improvement for altimetric satellites 7-14392

Heisenberg model

- anisotropic ferromagnet, low temp. props., spectral density method 7-2803
- anisotropic Heisenberg chain, high temp. dynamics, moment methods study 7-12989
- anisotropic Heisenberg chain, Monte Carlo study of crossover behaviour and solitons 7-7532
- anisotropic Heisenberg ferromagnet with biquadratic exchange 7-12987
- antiferromagnet, corrections to power-law behaviour 7-33137
- antiferromagnetic, 1-D, ground state struct. 7-45721
- antiferromagnetic chain, S=1/2 random-exchange, correlation effects 7-52928
- antiferromagnetic ground state, possible description without introducing anomalous means 7-45604
- antiferromagnetic quantum spin chains, random exchange effects, Monte Carlo study 7-64475
- antiferromagnetic rings, finite lattice extrapolations for ground state energies 7-38896
- antiferromagnets, multicritical points 7-27541
- bond-diluted Heisenberg antiferromagnet, spin damping near percolation threshold 7-17194
- bond-diluted Heisenberg ferromagnets, spin wave damping near percolation threshold, Green's function calcs. 7-17193
- charge transfer compounds, thermodynamic and dynamic props. 7-59048
- classical anisotropic ferromagnet, dynamical props., stereographic representation 7-2882
- classical compressible Heisenberg chain, soliton canonical transform. calcs. 7-17192
- classical easy-plane models, 2D, Monte Carlo studies 7-27542
- classical magnetoelastic chains, lattice distortions and short-range mag. order 7-17195
- classical spin chains, dil., effects of mag. field on thermodynamics 7-38840
- compressible anisotropic classical Heisenberg chain, spin dynamic eqns., soliton solns. 7-2804
- cyclohexyl ammonium copper tribromide-d₁₄, S=1/2 ferromag. chain system, short and long range correlations 7-17159
- dilute ferromagnetic alloys, magnetisation and Curie temp. calcs., approximated Heisenberg model 7-7549
- easy-plane ferromagnets, different-ion anisotropy, arbitrary site spin, low temp. props. 7-33193
- ferrimagnetic sphere spin waves, derivation 7-52956
- ferromagnet, 3D, susceptibility, correl. length, free energy, twelfth order series study 7-27488
- ferromagnet, anharmonic spin-one, order of phase transitions, effect of press. 7-53018
- ferromagnet, anisotropic, thermodynamic props., Monte Carlo Method calcs. 7-38894
- ferromagnet, diagram technique for Green functions 7-17150
- ferromagnet, easy-axis, phase transitions, mech. model 7-41034
- ferromagnet, interaction anisotropy influence on surface magnetism 7-52970
- ferromagnet, S=1/2, thermal boson expansion at finite temp. 7-2885
- ferromagnet, semi-infinite, Curie temp. calcs. 7-45603
- ferromagnetic chain, bound states, correl. functions 7-64474
- ferromagnetic chains, classical and quantum, momentum and cryst. momentum 7-12932
- ferromagnetic Heisenberg model, one- and two-dimensional, free energy and susceptibility 7-45722
- ferromagnetic Heisenberg spin chain, compressible, static π -kink 7-53020
- ferromagnets, paramagnetic neutron scatt. temp. depend. anal. 7-38848

Heisenberg model continued

- ferromagnets, paramagnetic zero-field susceptibility, modified power law study 7-45612
- finite-size scaling calcs. 7-56179
- ground state of Heisenberg linear chains, influence of third-nearest-neighbour interactions 7-38841
- Heisenberg ferromagnet, dynamic structure factors, real space renormalization group calcs. 7-2878
- Heisenberg spin glasses, rotational symmetry breaking 7-53022
- integrable S=1 isotropic quantum spin chain, mag. field props. calcs. 7-22087
- Ising-like Heisenberg antiferromagnets on a triangular lattice, mag. props. 7-27540
- large-N Heisenberg model, improved block-spin transformations and redundant operators 7-4777
- magnetic chains, anisotropic, of arbitrary spin, Bethe ansatz for two-magnon bound states 7-53015
- multicomponent generalizations of integrable nonlinear partial differential eqns. 7-74
- nonlinear σ -model classical version, spin waves and soliton solns. 7-2886
- one-dimensional classical anisotropic Heisenberg ferromagnet, numerical study 7-12933
- one-dimensional Heisenberg antiferromagnet, soft modes 7-2832
- one-dimensional spin-1 bilinear-biquadratic exchange Hamiltonian, crossover effects 7-7464
- paramagnet, spin autocorrel. function, high freq. asymptotics calcs. 7-52927
- paramagnets, thermodynamics, influence of crystal field anisotropy 7-12988
- quantum fluctuations and phase diagram of Heisenberg models with competing interactions 7-38895
- quantum spectral transform 7-48630
- quasi-one-dimensional systems, spin-Peierls transition 7-59047
- simple magnets and spin glasses, zero field muon spin relax. 7-53193
- spin 1/2 triangular antiferromagnet, thermodynamic props. 7-59046
- spin glass, 3D short-range, computer simulation 7-33190
- spin glass, sp. ht., strong spin dynamics effects 7-64476
- spin glasses, anisotropy-induced Heisenberg-Ising crossover 7-38890
- spin-1/2 Heisenberg antiferromagnet, triangular lattice, Ising-like exchange anisotropy, magnetisation process 7-53021
- spin-1/2 Heisenberg chains, critical region, finite-size corrections and numerical calcs. 7-59045
- superlattices, Heisenberg magnetism study (Chinese) 7-27485
- surface and interface magnetism, dilution effects and influence of nature of interaction 7-59032
- transition metal dimers, antiferromagnetic coupling, ligand spin polarisation, broken symmetry UHF calcs. 7-22084
- two dimensional, easy-plane exchange anisotropy, Monte Carlo study 7-17196
- two-dimensional antiferromag. Heisenberg model, correl. fns. 7-2880
- XXZ Heisenberg chain, ground state finite-size corrections 7-27539
- AgMnAu spin glasses, crit. behaviour, Dzyaloshinsky-Moriya interactions 7-7525
- AgMo₂, (M=Cr, Fe, Co), delafossite-type cpds., mag. props. 7-2879
- AuCr spin glass, remanent magnetization reduction, Heisenberg and Ising comparison 7-53019
- B clusters, magnetic properties, Heisenberg Hamiltonian 7-57199
- Ba₂CaCu₂Fe₂F₁₄, exchange interactions, mag. susceptibility meas. 7-45654
- BaMnAlF₄, exchange interactions, mag. susceptibility meas. 7-45654
- BaMnF₄, 2D Heisenberg magnet, spin dynamics and EPR linewidth 7-38932
- BaMnGaF₇, exchange interactions, mag. susceptibility meas. 7-45654
- CsMnCl₃·2H₂O, 1D Heisenberg magnet, spin dynamics and EPR linewidth 7-38932
- CsNiF₃, dynamical critical slowing down, spin fluctuation relax. time, mag. suscept. meas. 7-38897
- CsVCl₃, one-dimens. Heisenberg antiferromag., mag. excitations, neutron scatt. study 7-7482
- CuMo₂, (M=Cr, Fe, Al, Co), delafossite-type cpds., mag. props. 7-2879
- CuMn spin glass, remanent magnetization reduction, Heisenberg and Ising comparison 7-53019
- CuMnAu spin glasses, crit. behaviour, Dzyaloshinsky-Moriya interactions 7-7525
- a-DyNi, critical props. and universality class of disordered systems 7-2884
- EuS Heisenberg ferromagnet, diverging and finite suscept. below T_c 7-7444
- Eu₂Sr_{1-x}S mag. sp. ht., field and temp. depend., numerical simulation 7-2883
- (Fe_{0.8}Ga_{0.2})₂TiO₅ spin glass, remanent magnetization reduction, Heisenberg and Ising comparison 7-53019
- β -O₂ solid, rhombohedral Heisenberg antiferromag., neutron scatt. 7-7480
- Pd₃Fe disordered alloy, low-energy spin-wave excitations, Heisenberg model calcs. 7-2829
- Pd₃MnSn, cubic ferromagnet, high temp. spin dynamics 7-2881
- PdMo₂, (M=Cr, Fe), delafossite-type cpds., mag. props. 7-2879
- (VO)₂P₂O₇, 1D spin 1/2 Heisenberg antiferromagnet, mag. susceptibility meas. 7-45639

Heising modulation see amplitude modulation**helical dislocations** see screw dislocations**helicity (elementary particles)**

- ^t Hooft-Polyakov monopole, charge-exchange and helicity-flip scattering 7-19043
- axial vector coupling constant and quark confinement 7-24835
- baryon resonance photoproduction, helicity amplitudes in Skyrme model 7-19118
- basis states for relativistic three-body calculations of particles with spin 7-19032
- boson resonance decay width calcs., Reggeon anal. 7-5009
- Feynman diagrams representing partial helicity amplitudes, substitution rules 7-49023
- four-quark two-gluon amplitude, extension to equal flavour quarks 7-482
- heavy fermion production and decay via W bosons, helicity projection techniques 7-61762
- helicity amplitude calculations 7-49014
- Lagrangian wave equations, arbitrary-helicity, systematics 7-56412
- N=1 supergravity, torsion term in Einstein-Cartan action 7-14850
- B- γ X, helicity suppression and colour thaw problem 7-61590

helicity (elementary particles) continued

- $\delta^+e^- \rightarrow e^+e^- \gamma$, bremsstrahlung amplitude calcs. 7-61712
- $\delta^+e^- \rightarrow H\gamma(\mu^+ \mu^-)$, helicity amplitudes, cross section calcs. 7-61641
- $e^+e^- \rightarrow W^+W^-$, probing the weak boson sector, anomalous couplings search, helicity amps. 7-56533
- $e^+e^- \rightarrow W^+W^- WZ, W\gamma ZZ$, tri-boson gauge coupling effects, standard model calcs. 7-24868
- ν properties, review 7-30218
- pp, 3 GeV/c, pure helicity states, total cross section meas. 7-30278
- $\pi \rightarrow \nu$, lepto-quark effects in E_6 superstring models, helicity unsuppressed amplitude anal. 7-61651
- $\pi^+p \rightarrow (\eta^0, \omega^0)\Delta^{++}$, 16 GeV/c, helicity amplitude anal. 7-15173

helicons

- see also solid-state plasma
- alkali metals, low temp. nonlocal electromagnetic ultrasound generation calcs. (Russian) 7-7294
- contactless measurement of carrier mobility and concentration in semiconductors 7-30036
- metals, EM generation of acoustic waves, theory 7-51945
- oblique incidence of helicons on a plane boundary between magnetoactive plasma and anisotropic medium (Slovak) 7-57987
- semiconductor superlattices, helicon wave propag., collision-induced instabilities study 7-2633
- semiconductor superlattices, helicon wave quantised undamping 7-45466
- semiconductors, surface magnetoplasmons, dispersion characteristics 7-12636
- surface, electron beam interactions, energy exchange and magnetic damping calcs. (Russian) 7-21949
- Ge:Zn, large electron-hole drop, Alfvén wave dimensional reson., impurity scatt. effects 7-16950
- In single-crystal plate, acoustohelicon resons. 7-52695
- InSb, solid-state electron plasma magnetised, circular antenna directivity diagram 7-45372

helicopters

- impulsive noise, theory and expt. 7-11214

heliotron see plasma devices

helium

- see also nuclei with
- see also helium atoms; helium films; liquid helium; solid helium
- abundance in NGC 7492 globular cluster 7-60738
- ALGOCS II He-Ne laser alignment equipment (Rumanian) 7-11001
- atom, diffraction from NaCl (001) surface, interaction potentials for diffraction 7-22425
- atom, with turbulent flow, two electron group model for RF ionisation 7-31921
- atomic beam source, metastable, for time-of-flight appls. 7-41533
- atoms, scatt. with adsorbed CO, potentials and scatt. cross-sections 7-59363
- atoms, scattering from rare-gas-plated graphite 7-3136
- Aurora U deposit, McDermitt Caldera Complex, Oregon, He soil gas survey 7-40441
- basalts of mid-ocean ridges, inert gas abundances 7-60198
- Bianchi cosmologies, He production, time scale arguments 7-40972
- binding energies on simple metal surfaces, van der Waals energy 7-38663
- breakdown in discharges, emission study 7-26574
- bubbles in Nb foil, magnetic flux pinning, temp. and field depend. studies 7-2794
- bubbles in Ni, He densities, SANS and TEM studies 7-58266
- bubbles migration and coalescence during creep in T charged Ni 7-65102
- cooler, closed cycle, simplified cold head design 7-56277
- cooling systems for apparatus, cooldown mass flow requirements calc. 7-56281
- cosmic nucleosynthesis, relation between ^4He , ^2H and ^3He prod. 7-40979
- cosmic ray $^3\text{He}/^4\text{He}$ ratio at high energies, implications of rigidity spectrum of He nuclei 7-66410
- cosmology, primordial ^3He abundances 7-60840
- DC glow discharge positive column, gas temp. 7-32151
- diaphragmed discharge, multiple contraction 7-20972
- diffusion and embrittlement of irradiated fusion reactor materials 7-51845
- dimer, dispersion energy, partial wave expansion and damping phenomenon 7-50283
- dimer, interat. interactions in van der Waals region, Epstein Nesbet calc. 7-36491
- discharge, atomic and molecular metastables, population, transient behaviour 7-37783
- discharge, positive column, electron energy distrib. function calcs. 7-21031
- doped Cr-Ni-Mo-Nb steel, precipitates formation, effect of He 7-13460
- extragalactic H II regions, He abundance and dY/dZ meas. 7-40937
- field adsorbed on metal surfaces, atom-probe spectroscopy studies 7-32803
- field absorption and evaporation on W 7-32802
- field adsorption and diffusion on W, atom-probe field ion microscopy studies 7-32808
- field adsorption on W 7-32816
- free convective heat transfer from horizontal cylinder with large temp. head 7-63142
- fusion materials, gas diffusion and temperature dependence of bubble nucleation during irradiation 7-51874
- gas, formation of monoenergetic positronium 7-36784
- gas, low temperature bath for $\text{Cu-}^{57}\text{Co}$ Mossbauer source, oscillations after heating by an RF pulse 7-59128
- gas pressure effect on arc cathode erosion and cathodic plasma expansion 7-32164
- gas recovery system, automatic control of gas purity 7-318
- geochemistry, cosmic ray induced ^3He production in volcanic rocks 7-60500
- glassy submarine basalts dating and He isotope disequilibrium 7-66352
- glow discharge, cathode fall, spectroscopic diagnostics 7-37763
- glow discharge, electron conc. meas. in anode region 7-11788
- glow discharge, shock wave acceleration 7-6478
- glow discharge, wall effects on electron component in ion sound regime 7-21029
- glow discharge positive column, radial behaviour, self-consistent soln. 7-21034
- Grüneisen parameter at critical points (Chinese) 7-24609
- He-Ne lasers, single frequency, anal. (Chinese) 7-5870
- He-Ne lasers stabilized to $^{127}\text{I}_2$ at 605 nm 7-20309

helium continued

- He-Ne/ZZ 7-18761
- HeNe/methane laser, absolute frequency meas. at 88 THz 7-18762
- high flux heat removal, fusion reactor cooling appl. 7-25194
- HTGR, adsorpt. removal of CO_2 from He coolant 7-30514
- hybridisation interaction between He and metal surface 7-38664
- ion, ionisation by electron and position collisions, cross. section calc. 7-15726
- ion capture effects on Zr (0001) HCP to BCC phase transition, AES, TDS and SIMS studies 7-58590
- ion implanted Al disks, He re-emission ratio and surface obs. (Japanese) 7-12089
- ion scattering, from Ni, energy distrib. surface peak of scattered He ions and atoms 7-64855
- ionisation by positron impact 7-36785
- ionisation structure in H II region complexes, implications for He/H abundance ratio 7-40906
- ions, multiple scatt. at TaC (001) surfaces 7-22426
- IRAS 1912+172P09, new binary planetary nebula, He/H ratio 7-48046
- isotopic abundances in sedimentary basins, relation to form. mechanism 7-47405
- liquefaction, condensation heat transfer enhancement for mag. refrigerator performance improvement 7-56283
- liquefaction, refrigerant characts. of $\text{Dy}_2\text{Al}_2\text{O}_{12}$ and $\text{Gd}_3\text{Ga}_5\text{O}_{12}$ 7-56286
- liquefaction, rot. mag. refrigerator design 7-56282
- liquefier, condensing and freezing purification system 7-56280
- liquefier with turbo-expanders, prediction method for cool-down characts. 7-56276
- metals, He bubble nucleation and growth under neutron and proton irradiation, nonequilibrium statistics 7-51848
- microwave-induced plasma in laminar flow torch, spectrosc. temp. determ. 7-37738
- molecule, metastable state, reactivity, rate coeff. determ., fluoresc. 7-19760
- Moon, solar cosmic ray inert gases in regolith minerals 7-14507
- multielectron multiphoton ionisation 7-19795
- Nagano, Japan, $^3\text{He}/^4\text{He}$ ratio anomalies in hot spring gases, assoc. with 1984 September 14 earthquake 7-40422
- natural gas wells in Sacramento basin, California, He isotope and mantle origin 7-60206
- NGC 5548, Seyfert 1 galaxy, evidence for black hole accretion event, He II obs. 7-35052
- Nova Vul 1984 No.1 (PW Vul) slow nova, abundances, visible and IR obs. 7-40850
- Orion A, He abundance, spectral obs. (Russian) 7-40951
- pipe diffusion along dislocations in cold worked Mo single crystals, thermal desorption spectra 7-52142
- plasma, forbidden lines intensities, diagnostics 7-51516
- plasma, heating with H^+ beam, spectrosc. appls. 7-48864
- plasma, hot-electron instability in mirror geometry 7-31960
- plasma, spatial resolved line-intensity meas., electron density determ. 7-36641
- plasma, spectral line Stark broadening for theta-pinch turbulent plasma parameter meas. 7-44255
- plasma, Stark parameters meas. of 447.15 nm line electron density determ. 7-36540
- plasma, Stark parameters meas. of 492.2 nm line, electron density determ. 7-36541
- plasma in multiple mag. mirror electron cyclotron instability 7-44227
- plasmosphere, H^+ and He^+ flow along mag. field lines 7-9299
- platelets, nucleation and growth in Ni, computer simulation 7-58269
- positron annihilation and elastic scatt. cross sections 7-42763
- positron impact ionisation of He atom 7-36786
- positron thermalisation and annihilation 7-63245
- primordial He abundance, implications of collisional effects in He I triplets 7-55446
- primordial He abundance determ. from metal-poor galaxies 7-40978
- proportional counter for low temps. and appl. to cryogenic resonance-electron Mossbauer spectroscopy 7-62234
- pulsed supersonic He free-jet expansions, time-of-flight characterisation 7-11457
- Raman scattering of laser radiation to far UV by excited states of He and Ne 7-25886
- retention in fast neutron irradiation. Li based oxide ceramics 7-49649
- S and MS stars, He burning and s-process 7-60681
- Saskatchewan, Canada, well water He and methane anomalies origin 7-40440
- scattered ion yields from neutral or ion bombard. of solids 7-13313
- scattering apparatus for gas-surface interaction studies 7-33503
- seafloor hydrothermal plumes of E Pacific Rise, Fe, He, Mn obs. showing Fe enrichment 7-9028
- selective adsorpt. on Ag (110), bound-state reson. meas., interaction pot. electron density depend. 7-21631
- solar wind, energetic H^+ and He fluxes associated with interplanetary shocks 7-23967
- solid, pair potential, effective medium approach 7-45201
- sorption by Ti hydride, interatomic bond study (Russian) 7-38022
- stereotactic radiosurgery of central nervous system disorders, He ion beam 7-40270
- Sun, small-scale energy release observed on limb. He I D3 lines characts. 7-24113
- supply and importance to cryoengineering 7-48748
- temperature and density meas. in decaying plasma 7-31934
- thermal desorpt. from ion irradiated graphite 7-52245
- thyatron with linear geometry, excited state densities 7-20963
- total ionisation cross sections for positrons 7-36787
- total positronium formation cross sections 7-42796
- transition metal surfaces, He atom scattering potential energy surfaces, vibr. substrate relax. effects 7-53478
- turbulent convection at supercritical press. under nonisothermal conditions 7-31805
- Venus atmosphere, radiative transfer theory rel. to He I 58.4 nm emission meas. 7-9396
- Wolf-Rayet stars, He ionisation state rel. to mass loss rates 7-9475
- Z-pinch plasma, visible emission in afterglow 7-32092
- CO_2 -He dilute mixtures, liq.-vapour curve, ^3He partial contrib. 7-32625
- CO_2 -He- N_2 vibr. nonequilibrium flow in axisymmetric channel with glow discharge 7-20741
- CO_2 - N_2 -He mixtures, self-sustained and nonself-sustained glow discharges 7-44290

helium continued

- $\text{CO}_2\text{-N}_2\text{-He}$ laser mixture, beam-driven discharge, gasdynamic processes 7-50538
 Cu:He vacancy cluster stability calcs., void form., O and the impurity effects 7-51763
 Cu:B:He , neutron irradiated, annealing behaviour of defects, positron annihilation study 7-39291
 $\text{F}_2\text{-He}$ discharge pumped laser, 157.6 nm, efficiency 7-43077
 Fe:He , distribution and migration of interstitial impurities in the field of a screw dislocation core 7-6669
 GaP:He^+ , implanted, swelling, strain and radiation damage 7-6694
 HCl/Xe/He gas mixture, kinetic model of discharge (*Russian*) 7-11577
 HCl-Xe-He self-sustained discharge, population dynamics of electronic states of atoms and ions 7-37781
 $^3\text{H-}^3\text{He}$ atomic mass difference, effects of $^3\text{He}^+$ metastable $2^2\text{S}_{1/2}$ state, mass spectrometric anal. 7-5782
 He I 1083 nm chromospheric line, obs. in bright late-type stars 7-55612
 He I laser action in stellar envelopes, theory 7-4438
 He^+ tandem multipole ion source, Langmuir probe meas. 7-10336
 He^+ + tetrafluoromethane, absolute excitation cross sections 7-20010
 He^+ , channelling contrast microscopy, semiconductor impurity profiles 7-51587
 He^+ photoionisation pumping via two-electron shakeup 7-20195
 He^+ , Rutherford backscatt. from Ni (100) and (110), continuum approx. parameter effects 7-46271
 He^+ , Rutherford backscattering-particle induced X-ray emission analysis 7-54251
 He^+ , vibr. excitation by charge exchange with mols., TOF anal. (*German*) 7-57170
 He^{2+} , electron capture cross section calc. by distorted-wave perturbation theory 7-50336
 He^{2+} recombination lasers in VUV excited by intense proton beams 7-25798
 He:H , isotope composition, spectrosc. determ. 7-50395
 He/H , ratio in globular cluster NGC 6752, determ. from photographic photometry 7-29520
 He/H ratio in Hyades, implications of H-R diagram position of eclipsing binary star (HD 27130) 7-66665
 He/H ratios in B-type stars, determ. for members of open clusters and associations (*Russian*) 7-55626
 He-Ar mixture, density meas. up to 8000 bar, Lennard-Jones comparison 7-1669
 He-Ar(He) lasers, pumping by CO_2 -laser induced optical break-down 7-62668
 He-Cd discharge in concentric hollow-cathode struct., spectrosc. obs. 7-20953
 He-Cd hollow cathode laser, green line oscillations, lower levels population 7-43065
 He-Cd laser, noise reduction by discharge current modulation 7-31348
 He-Cd laser transitions, level width determ., double-mode lasing state 7-43080
 He-Cd positive column discharge 441.6 nm laser level (*French*) 7-11811
 He-Cd^+ white light laser, hollow cathode, power stabilisation 7-57385
 He-H_2 , rot. inelastic scatt., forward and inverse functional var. 7-5753
 He-H_2 system, density inversions between fluid and solid phases at high pressures 7-58451
 $\text{He-H}_2\text{O}$, gas/vapour mixtures in porous medium, natural convection 7-1554
 He -hydrogenic trace mixtures, temp. depend. of thermal diffusion factor, role of column calibration factor 7-63240
 He-Kr^+ laser operation, DC He and He-Kr discharges in Al hollow cathode tubes 7-10912
 He-metal impact, density functional approach, dynamic response at metal surfaces, van der Waals interaction, excitation of electron-hole pairs 7-3129
 He-N_2 laser, pulsed electric-discharge, laser props. investig. 7-62675
 He-N_2 mixture, calc. of classical cross sections related to the Senftleben-Beenakker effect 7-16287
 He-N_2 mixtures, metastable the electron impact excitation coeffs. 7-20059
 He-N_2 green laser, I_2 saturated absorption lines identification at 543 nm 7-20372
 He-Ne laser, automatic calibration system for laser power standard, expt. and performance eval. (*Japanese*) 7-11019
 He-Ne laser, damage to $\text{LiNbO}_3\text{:Fe}$, linear electro-optic effect (*Korean*) 7-27698
 He-Ne laser, fibre optic evanescent-wave coupling force transducer 7-41367
 He-Ne laser, internal mirror, freq. and power stabilisation using fan (*Korean*) 7-25849
 He-Ne laser, methane stabilized, frequency meas. of methane hyperfine line 7-20190
 He-Ne laser, mode-crossing reson., intracavity distance and mode-locking quality anal. 7-31373
 He-Ne laser, performance assessment of laser wavemeter (*Korean*) 7-24692
 He-Ne laser, photothermal deflection, trace gas anal. appls. 7-61381
 He-Ne laser, stabilised by saturated absorption of methane, frequency shifts obs. 7-20192
 He-Ne laser, stabilised by external absorption cell 7-20270
 He-Ne laser, stabilised by I_2 external absorption cell 7-20308
 He-Ne laser, standardisation for metrological purposes 7-5909
 He-Ne laser, three-mode, frequency resonance 7-36937
 He-Ne laser, transportable, methane stabilized 7-20191
 He-Ne laser as light source in schlieren optics methods 7-57503
 He-Ne laser at 0.633 μm , frequency stabilisation, using polarisation modulation 7-20295
 He-Ne laser beam 'divergence' meas. using LiNbO_3 SAW interaction 7-1211
 He-Ne laser beam meas. using direct looking apparatus for light intensity distribution (*Japanese*) 7-56314
 He-Ne laser for optical fibres fault location 7-31545
 He-Ne laser stabilised by methane saturable absorption, effects leading to frequency shifts 7-50540
 He-Ne laser stabilised by Lamb dip, emission frequency scatter, causes 7-62667
 He-Ne laser tuned by axial mag. field, mode competition 7-50539
 He-Ne laser wavelength meas. using 0.63 μm transition 7-1208
 He-Ne laser with high specific output power (*German*) 7-20187
 He-Ne lasers as sources of stable subnanosecond pulses 7-43060
 He-Ne mixtures collision induced far IR translational absorpt. 7-10563

helium continued

- He-Ne Q-switched laser, radiation laser, radiation growth 7-15842
 He-Ne Zeeman laser, nearly degenerate four wave mixing and high order effects 7-1078
 He-Ne Zeeman lasers for coherent optical fibre system 7-50786
 He-Ne/methane ring lasers stabilised using FM resonances, frequency reproducibility 7-1206
 He-SF_6 glow discharge, mag. control, electron energy distrib. 7-26555
 He-Ne laser discharge, population density ratios determ. from Kirchhoff's law for excited He I states 7-58072
 He-water vapour laser, pulsed and CW operation at 28 μm 7-36939
 He-Xe pulsed discharge, $\text{Xe}(\text{P}_2)$ radial distrib. 7-26573
 He-Xe-HCl excimer laser discharge growth dynamics 7-1086
 He-Zn laser with transverse HF excitation 7-1090
 He-Zn metal vapor mixture, laser excitation by electron guns 7-26534
 $\text{He}^+\text{Ca}^+(\text{Mg}^+)$, pot. curves reson. line broadening and shift parameters 7-53032
 He^+I_2^* , collision, rotational energy transfer 7-36734
 He^+Na , scatt. precession induced fluore. modulation 7-19928
 $\text{He}^+ + \text{H}_2$, nondissociative and single ionis., cross section meas. 7-31147
 $\text{He}^+ + \text{H}_2(\text{D}_2)$, rate const. determ. 7-17774
 $\text{He}^+ + \text{H}^+$, ionis., beam-pulsing expt. 7-31160
 $\text{He}^+ + \text{He}$, ejected electron distrib. shape, series expansion and fitting anal. 7-15675
 $\text{He}^+ + \text{He}$, single and double ionis., cross section meas. 7-31148
 $\text{He}^+ + \text{tetrafluoromethane}$, excitation cross sections 7-62501
 $\text{He}^+ + \text{Ti}$, inner-shell ionis. polarisation effect, variational wave fn. calc. 7-62491
 $\text{He}^{2+} + \text{He}$, ejected electron distrib. shape, series expansion and fitting anal. 7-15675
 $\text{He}^{2+} + \text{Li}$, electron capture, Coulomb integral eval. 7-15679
 He_2 , intermolecular interaction energies, SCF calcs., variation-perturbation procedure 7-15505
 He_2^+ , mobility, temp. and field depend. 7-51380
 $\text{He}_2^+ + \text{Ne}_2$, reaction kinetics at atm. press., three-body processes 7-22984
 $\text{He}_2^+ + \text{Ne}(\text{N}_2)(\text{CO}_2)$, charge transfer reaction rate consts. 7-22983
 HeN^{7+} quasi-molecule, autoionisation 7-62459
 ^3He polarised target 7-10328
 ^3He , use in gas scintillation counters 7-30897
 ^3He -He mixtures adsorbed on graphite, phase diagrams 7-52180
 $^3\text{He-Ne}$ gas laser, neutron pumping from tokamaks 7-62666
 ^4He anomalous cosmic ray component solar modulation 7-47648
 ^4He , atm. inert gases corrected, use for mixed groundwaters dating 7-9044
 ^4He , dynamic temp. and second virial coeff. meas. using constant-volume gas thermometer 7-48738
 ^4He , superfluid, props. and appls. 7-48751
 Kr-He-H_2 mixtures, self-quenching streamer or Geiger-Muller region 7-19669
 $\text{LiNbO}_3\text{:He}^+$ implanted waveguide stability 7-43364
 $\text{LiNbO}_3\text{:He}^+$ optical waveguides, thermal annealing 7-15983
 $\text{LiNbO}_3\text{:He}^+$ optical waveguides, ion implanted, Li outdiffusion modelling 7-62832
 $\text{MgAl}_2\text{O}_4\text{:He}$ spinel, implanted, high temp. electron irradi., structural damage 7-51829
 $\text{N}_2\text{-He}$ mixture, depolarized Rayleigh light scattering, temp. dependence 7-31053
 $\text{N}_2\text{-He-SF}_6$ laser, high power, UV preionised, characts. 7-25805
 Na+Rg optical collisions, (RG = He, Ne, Ar, Kr, Xe), fine struct. branching ratio determ. 7-10704
 Nb:He^+ films, radiation defects produced by ion implantation 7-7059
 Ni , He implanted, defects study by monoenergetic positron beam 7-39293
 Ni-He , electronic state or interstitial He atoms, MO calcs. of model clusters 7-16969
 Pt (111), adsorbed CO, He thermal beam scattering 7-53475
 Xe-He active medium, HF H-discharge excited, characts. investig. 7-20189

helium, liquid see liquid helium

helium, solid see solid helium

helium-3 interactions see helium 3-nucleus reactions

helium 3-nucleus reactions

for inelastic helium 3-nucleus scattering, see "helium 3-nucleus scattering"

multistring models, test of hadron-nucleus and nucleus-nucleus interactions 7-41771

180 W (^4He , fission), mass distributions of fission fragments from heated nuclei and the drop model 7-42041 $^{27}\text{Al}(\text{He,d})^{28}\text{Si}$, proton threshold states in $^{28}\text{Si}^*$, astrophysical significance 7-19267 $^{27}\text{Al}(\text{He},\pi^+)$, 263 MeV, angular distribs., total cross sections 7-24989 $^{34}\text{Ar}(\text{He,n})^{36}\text{K}$, structure studies using time-of-flight spectrometer 7-696 $^{10}\text{B}(\text{He},\alpha)^9\text{B}$, excitation energy and width of state 7-15216 $^{11}\text{B}(\text{He},^4\text{Li})^8\text{Be}$, transitions to ground and excited states 7-19153 $^9\text{Be}(\text{He},\alpha\alpha)^4\text{He}$, 3-12 MeV, anal. of quasi-free process using virtual $^3\text{He}(\text{He},\alpha)^4\text{He}$ 7-19266 $^{12}\text{C}(\text{He},^4\text{Be})$, 41 MeV, ang. distribs. and α spectroscopic factors, DWBA anal. 7-15190 $^{12}\text{C}(\text{He,X})$, diffraction dissociation at 90 MeV by nuclei with a diffuse edge 7-42043 $^{12}\text{C}(\text{He,pp})$, differential cross sections and analysing powers 7-42032 $^{12}\text{C}(\text{He},\pi^+)^{15}\text{N}$, 181.4 MeV, obs. using recoil detection technique 7-19269 $^{12}\text{C}(\text{He},\pi^+)$, 263 MeV, angular distribs., total cross sections 7-24989 $^{13}\text{C}(\text{He},p)^{14}\text{N}$, 13.7 MeV, polarization comparisons with $^{15}\text{N}(p,^3\text{He})^{13}\text{C}$ analyzing power meas. 7-5251 $^{38}\text{Ca}(\text{He,n})^{40}\text{Sc}$, structure studies using time-of-flight spectrometer 7-696 ^{162}Dy (^4He , fission), mass distributions of fission fragments from heated nuclei and the drop model 7-42041 $\text{Fe}(\text{He,X})$, 27 MeV, ^{54}Fe and ^{55}Co medium spin structure, shapes and transitions, HF and shell anal. 7-41873 $^{54}\text{Fe}(p,^3\text{He})$, 65 MeV, reaction mech. investigation, optical pots. 7-627 $^1\text{H}(\text{He,X})^2\text{H}$, high resolution search for narrow dibaryons 7-5209 $^1\text{H}(\text{He,t}\alpha)^{4+}$, one-pion exchange model anal. 7-24988 $^3\text{H}(\text{He,d})^4\text{He}$, 18-33 MeV, analyzing power meas., charge symmetry violation anal. 7-5252 $(^3\text{He,f})$, $E=270$ MeV, target nuclei Nb, Ag, La, Ce, Pr, Nd, Dy, fission mass distrib. 7-5304

helium 3-nucleus reactions continued

- ³He(³He, α)⁴He, virtual reaction, use in anal. of ⁹Be(³He, α)⁴He, excitation fn. meas. 7-19266
- ¹⁷F(³He, fission), mass distributions of fission fragments from heated nuclei and the drop model 7-42041
- ⁷Li(³He, α)²H, low energies, ⁷Li(p,d)⁴He contributions 7-10156
- ²²Mg(³He,n)²⁴Al, structure studies using time-of-flight spectrometer 7-696
- ²⁴Mg(³He, ⁷Be), 41 MeV, ang. distrib. and α spectroscopic factors, DWBA anal. 7-15190
- ²⁶Mg(³He,n)²⁸Si, 23, 45 MeV, neutron angular distrib., DWBA, coupled channel comparisons, ²⁸Si level anal. 7-42036
- ⁵⁸Ni(³He), 65 MeV, reaction mech. investigation, optical pots. 7-627
- ¹⁶O(³He, d), 12 MeV, angular distributions, optical, DWBA and CC anals. 7-24990
- ¹⁷O(³He,p), 18 MeV, ¹⁹F positive parity levels, ang. distrib., DWBA and shell anals. 7-15181
- ¹⁸O(³He,d)¹⁹F, sub threshold resonance in red giants 7-698
- ²⁰⁶Pb(³He,3n), 27 MeV, ²⁰⁶Po yrast structure, transitions, T_{1/2} and isomer 7-41878
- ²⁰⁸Pb(³He, π^+), 263 MeV, angular distrib., total cross sections 7-24989
- ²⁶Si(³He,n)²⁸P, structure studies using time-of-flight spectrometer 7-696
- ²⁸Si(³He, d), 12 MeV, angular distributions, optical, DWBA and CC anals. 7-24990
- ³⁰Si(³He, α), CCBA, DWBA anal. 7-42034
- Sn(³He,X), 20.9-27.5 MeV, ¹¹⁴⁻¹¹⁷Te vibrational and quasiparticle structs. coexistence, states and spectra, shell model anal. 7-41874
- ¹⁸¹Ta (³He, fission), mass distributions of fission fragments from heated nuclei and the drop model 7-42041
- ²³²Th(³He,X), 270 MeV, intermediate mass fragment emission 7-5249
- ¹⁶⁹Tm (³He, fission), mass distributions of fission fragments from heated nuclei and the drop model 7-42041
- U(³He,pf), 21.3 to 90 MeV, backward angle proton emission in central collisions 7-5305
- ⁵¹V(³He,X), diffraction dissociation at 90 MeV by nuclei with a diffuse edge 7-42043
- ⁸⁹Y(³He, π^+), 263 MeV, angular distrib., total cross sections 7-24989
- ⁹⁰Zr(³He, t), 200 MeV/nucleon, collective mode excitations, DWIA anal. 7-56687
- ⁹⁰Zr(³He,X), diffraction dissociation at 90 MeV by nuclei with a diffuse edge 7-42043
- ⁹¹Zr(³He, α), matrix element determ. allowing for I_n mixing 7-61897

helium 3-nucleus scattering

- ¹²C(³He, ³He), 12 MeV, angular distributions, optical, DWBA and CC anals. 7-24990
- (³He, ³He), 10-220 MeV, optical model anal. 7-42035
- ¹⁶O(³He, ³He), 12 MeV, angular distributions, optical, DWBA and CC anals. 7-24990
- ²⁸Si(³He, ³He), 12 MeV, angular distributions, optical, DWBA and CC anals. 7-24990
- ⁹⁰Zr(³He,t), 600 MeV, Gamow-Teller strength, Δ -isobar quenching effects 7-49422

helium-3 scattering see helium 3-nucleus scattering

helium atoms

- 1 s4d config. fine struct., Zeeman sublevels crossing fields 7-50015
- 3 ¹D state electron impact excitation, electron-polarised photon coincidence study 7-36774
- 3 ³P state, electron polarised photon coincidence expts. 7-5772
- 3 ³P state lifetime, electron-photon delayed coincidence technique meas. 7-62533
- ¹p⁻ symmetry, Wannier two-electron ionis. ladder, wave fn. calc. 7-62274
- 7-31104
- alignment and orientation, electron impact excitation 7-50373
- antikaonic, evidence for narrow nucl. \bar{K} bound state 7-5788
- atom, electron impact excitation, orientation parameter anal., exam. of Steph-Golden model 7-20053
- atom scattering, from Ni, energy distrib. surface peak of scattered He ions and atoms 7-64855
- atomic scattering, from Cu, Au and Ni, energy spectrum, scattering trajectories 7-64854
- autoionising states, laser-induced transition 7-42566
- autoionising states, use of virial theorem in wavefunction calcs. 7-25465
- beam hyperfine struct. evolution and tensor polarisability determ. in elec. field. 7-57028
- broadening of Ca⁺ IR triplet 7-62323
- collisional depopulation rate by Rb thermal collisions (German) 7-15694
- collisions with fast highly charged ions, electron capture to continuum 7-20026
- correlated wavefunctions, dynamical anal. 7-49941
- correlation energy, Fulde's local approach studies 7-30957
- dipole-quadrupole dispersion coefficients, ab initio coupled HF calcs. 7-11986
- doubly excited states, correl. wavefunction calcs. (French) 7-10454
- doubly excited autoionising resonance states, Hylleraas-type wave fn. calcs. 7-30940
- doubly excited states, electron impact excitation. generalised oscillator strengths 7-873
- electron impact autoionisation, triple differential cross sections, first-order model calcs. 7-25466
- electron impact excitation, electron-photon polarisation correl. 7-10761
- electron impact excitation, excited state polarisation and ang. correl. 7-36772
- electron impact excitation, fine-struct. effect, electron spin polarisation fn. 7-50374
- electron impact excitation, metastable state, laser induced fluoresc. 7-50372
- electron impact excitation, Stokes' parameters, electron-photon coincidence spectra anal. 7-50377
- electron impact ionisation, cross sections, fast-neutral beam method, TOF spectra 7-42769
- electron impact ionisation, distorted-wave impulse approx. 7-31175
- electron impact ionisation, intermediate energy 7-25664
- electron impact ionisation cross section, modified-Glauber-approx. study, higher-order effects 7-42771
- electron impact triple differential ionisation cross-section calcs. 7-36773
- electron scatt. below excitation threshold, phase shift anal. 7-15715
- electron thermalisation processes obs. by pulse-radiolysis microwave cond. method 7-20051
- energy levels, relativistic correction, variational calcs. 7-869
- exchange correlation energies, E_h method calcs. 7-56993

helium atoms continued

- fast electron impact ionisation, triple differential cross section calcs. 7-25657
- ground state, correl. energy eval., correl. fn. influence 7-36447
- ground state, gas discharge, longit. nucl. relax. time, temp. depend. 7-20997
- ground state, one-electron loss cross section in H₂ gas 7-50338
- ground state energies, Dirac-Coulomb eqn., relativistic perturbation soln. 7-24767
- ground state energy calcs. using hyperspherical coords. 7-49880
- HF eqns., Griffin-Hill-Wheeler version 7-42459
- interactions, second-order exchange-dispersion energy, nonadditivity 7-49901
- ion implantation effects on Al polycryst. near-surface struct. 7-58302
- ionisation by positron impact, partial cross-section meas. 7-36777
- ionisation energies, g-Hartree ab initio calcs. 7-15488
- ionised gas-laser interaction, dynamic Stark effect (French) 7-6395
- isoelectronic sequence, relativistic second-order many-body corrections 7-870
- isoelectronic series, application of a variational fn. to ground-state energies 7-15485
- isoelectronic series, binding energies and radiative lifetimes, Dirac Hamiltonian, relativistic variational soln. 7-25456
- isoelectronic series, correl. effects, local level, CI partitions 7-49940
- kaonic, coupled channels problem soln. 7-5789
- Kohn-Sham time-depend. orbital density functional theory, hydrodynamic formulation 7-25678
- low energy triply differential electron impact ionisation cross sections 7-15722
- metastable state, positive column, ionis. process investig. 7-20057
- metastable state, reactivity, rate coeff. determ., fluoresc. 7-19760
- modified HF SCF equation 7-56970
- multiple ionisation by intense laser pulse 7-62332
- multiply charged ions collisions, semiclassical model, double electron transitions 7-10733
- muonic, Lamb shift at low temps. 7-57192
- n ²D₂ levels, alignment and orientation in elec. field 7-865
- N-electron atom, electronic energy in a space of constant curvature (French) 7-36500
- optically orientated He plasma density, kinetic model calcs. 7-51391
- photoelectron satellite branching ratios, asymmetry parameters, UV PES anal. 7-62333
- photoelectron satellites at threshold, photoelectron spectra anal. 7-36564
- photoionisation, partial cross-sections and Rydberg series resons. 7-903
- plasma, collision induced transitions between singlet and triplet levels, laser fluoresc. 7-20846
- plasma, excited state lifetimes determ. 7-20947
- plasma, ion collisions, low-energy charge exchange, XUV spectra 7-20032
- plasma diagnostics using injected neutral He beam 7-1757
- plasma ion temperature diagnostic based on He neutral beam scatt. 7-1742
- population difference and pulse-mode optogalvanic effect 7-26570
- positron collisions, positronium form. cross sections 7-15724
- positron elastic scatt., 2-pot. calcs. 7-36766
- positron elastic scattering, empirical correl. pot. calcs. 7-36770
- positron impact excitation of ²S and ²P states, distorted wave approximation. calcs. 7-36795
- positron impact triplet-triplet excitation 7-36789
- positron mobility edge, Monte Carlo simulation 7-44086
- positron scattering, cross-section meas. 7-20054
- positron scattering, inelastic and superelastic, calcs. 7-36790
- positronium form. by positron scatt., cross-section calcs. 7-36796
- Rydberg atoms, QED approach to energy level calcs. 7-62302
- Rydberg state, absolute photoionisation cross section 7-62331
- scattering from O chemisorbed layer on Ni (001), cluster model calcs. 7-53471
- small angle differential cross sections for electron elastic scatt. 7-15713
- spin and charge densities, HF and UHF calcs. 7-19684
- stilbene-He(Ne), coherent photodissoc., picosec. polaris. obs. 7-36715
- threshold double photoionisation 7-19804
- transition probabilities and oscillator strengths for singly excited states 7-48207
- two-electron doubly excited states, quantum number classification 7-49886
- Ar+Na, optical collisions, fine struct. branching cross-sections, nonadiabatic theory 7-959
- Ca+He, saturated two-photon absorpt. in perturber bath 7-888
- Ca+He, spin-changing collision cross section 7-25641
- F-He, van der Waals mol. interaction pot., MBPT calcs. 7-42721
- H₂-He, photodissociation processes, CARS (French) 7-5726
- H₂-He collision complexes, roto-vibr. spectra. SCF CEPA calcs. 7-42478
- H₂-He mixture, radiant heat transfer body shape influence 7-20715
- HF-He, mol. interactions, nonexpanded dispersion and induction energies, damping functions 7-42474
- He⁺ + Ne(Ar), charge exchange into excited states in collisions 7-31155
- He + Br₂(I₂)(ICl)(IBr), bound and continuum states, excitation transfer, optical and electron spectroscopy investig. 7-36689
- He + CO⁺ + CO, association reactions, third-order kinetics, temp. depend. 7-46817
- He + Ca⁺ (Eu⁺), collisional lasers, high specific output energy 7-43078
- He + H₂, V - T rate const., numerical and anal. calcs. 7-20022
- He + H₂ in interstellar and gaseous planetary matter 7-10720
- He + H⁺ in solar wind, elastic collision cross sections 7-47654
- He + H⁺(H⁺), single and double ionisation by fast antiproton and proton impact 7-20027
- He + Li, electric field effect, fluoresc. and radiative decay rate determ. 7-20009
- He + Ti, Ti excited state total ang. momentum charge, radiation quenching 7-42735
- He + Ti, triplet state quenching and excitation transfer processes 7-19761
- He + vinylidene radical, collisional quenching, rate const., time resolved spectra 7-31104
- He, fast electron impact ionisation, triple differential cross sections, Coulomb wave fns. calcs. 7-50365
- He, ground states, Rayleigh-Schrodinger perturbation expansions 7-844
- He I, transition wavelengths among doubly excited states 7-49980
- He I triplets, collisional excitation cross sections and implications for primordial He abundance 7-55446

helium atoms continued

- He II, recombination line intensities Case B calcs. 7-57023
 He para-difluorobenzene, vibr. energy transfer 7-50318
 He, positron scatt., superelastic and inelastic processes 7-15711
 He⁺, ³S resonant state, projection-operator formalism, CI calcs. 7-36498
 He⁺ + light target atoms (28 ≤ Z ≤ 46), L shell X-ray prod. cross sections meas., first Born approx. and ECPSR theory anal. 7-36526
 He⁺ bombard. of target atoms, shadow cone form. calc. 7-36731
 He⁺ low energy ion-surface scatt., reionisation process theory 7-22413
 He⁺, photoionisation production and fluorescence angular distrib. 7-25451
 He²⁺, charge exchange collisions, multiply charged closed K shell targets, exponential model study 7-25426
³He, hyperfine struct., relativistic contribs. contribs. 7-42509
 He-alkali metal atom, Rydberg energy levels, Coulomb and Coulomb-Stark-Green fn. 7-42476
 He-H mixtures, positron annihilation, simulation 7-36792
 He-like systems, energies and widths of singlet and triplet S resonances 7-36508
 He-Ne van der Waals mol. pot., ab initio HF SCF calcs. 7-36459
 He-X⁺ (X=halide), gas, interaction pot. 7-19739
 He-¹⁷⁴Yb, collisional velocity thermalisation, echo techniques 7-36732
 He⁺(He²⁺)(C⁶⁺)(O⁸⁺), electron capture cross section calc. by distorted-wave perturbation theory 7-50336
 He+Ar, 2¹P₁ state quenching 7-62319
 He+Ar⁺(Ne⁺), charge exchange into excited states in collisions 7-31155
 He+Ar⁴⁺ (I⁹⁺), total one-electron capture cross sections 7-10754
 He+Ar(N₂)(O₂), bimolecular and termolecular, deexcitation reactions (French) 7-10724
 He+B³⁺(O⁴⁺)(Si⁴⁺), double- and single-electron capture and loss cross section meas., OBK scaling calcs. 7-42756
 He+Be⁴⁺, charge exchange cross sections, quasimolecule Feshbach method calcs. 7-36754
 He+C³⁺, transfer excitation, electron emission, forward-backward asymmetries 7-973
 He+C⁴⁺, double charge transfer process, differential cross sections, quantum study 7-62512
 He+C⁴⁺, two-electron capture cross sections, comparison of calc. methods 7-15703
 He+C⁶⁺(Ne¹⁰⁺) electron capture, bound and continuum states, impulse approx. 7-50329
 He+C⁶⁺(O⁸⁺), intermediate energy collisions, electron capture cross sections, AO expansion method calcs. 7-25381
 He+CO(CO₂), vibr. relax., coupled states calcs. 7-50317
 He+Cs⁺, low-energy collisions, absolute total cross section meas., curve-crossing model anal. 7-36749
 He+Cs(Rb), He²P₁ and 2¹S₀ state quenching 7-57153
 He+Fe(Ti), thick target bombardment, X-ray production cross sections 7-20025
 He+ferrocene (Fe(CO)₅), dissociation, excitations, mol. orbital correls. 7-10735
 He+H, differential scatt. cross-sections for neutral particle precipitation 7-5739
 He+H, electron capture cross sections 7-10747
 He+H₂, collision-induced rototranslational spectra 7-15677
 He+H₂, collisional excitation, translational-vibr. transition probability computation 7-42732
 He+H₂, vibr. transition probabilities, semiclassical algebraic description 7-25636
 He+H₂ autoionising systems, Born-Oppenheimer approx., diatomic-molecules calcs. 7-5742
 He+H₂⁺, elastic and inelastic scatt. mechanisms, energy loss spectra 7-15671
 He+H₂⁺, reaction, quantum infinite order sudden approx. 7-54097
 He+H₂⁺ collisions, dissociation and electron capture cross section meas. 7-31156
 He+H₂⁺ reaction, expt. and quantum mech. results 7-3584
 He+H₂⁺ → HeH⁺+H, endothermic reaction on ab initio pot. energy surface, dynamics 7-54103
 He+H₂(O₂), vibr.-translation energy transfer determ. 7-57160
 He+H₂ → HeH+H, quasiclassical trajectory calcs. 7-39876
 He+H⁺, collisional detachment neutralization at high energy 7-15685
 He+H⁺, electron detachment, energy and ang. distrib. 7-20013
 He+H⁺, single-electron detachment, time correlated electron spectrum study 7-36741
 He+H⁺, 2l-electron capture, first-Born-type approximation, cross sections 7-10743
 He+H⁺, charge transfer, second-order Born and Faddeev-Watson approx. 7-62516
 He+H⁺, electron ejection, double differential cross section meas. 7-20024
 He+H⁺, simultaneous single-electron capture, H²⁺ production, existence of critical scatt. angle 7-10750
 He+H⁺, united atom rot. coupling collisions 7-958
 He+H⁺ collisions, secondary electron spectra, Wannier ridge obs. 7-10736
 He+H⁺(H⁺), double ionisation, ab initio calcs. 7-42737
 He+H₂, angular momentum collisional alignment Born approx. calcs. 7-964
 He+He, associative ionisation in glow discharges 7-62506
 He+He, ionis. cross section meas. 7-62494
 He+He⁺, excitation fns., transition moment and pot. energy curves (Japanese) 7-50307
 He+He⁺, single and double ionis., cross section meas. 7-31148
 He+He⁺(H₂⁺), electron loss to the continuum, absolute cross sections 7-50304
 He+He⁺(He²⁺), ejected electron distrib. shape, series expansion and fitting anal. 7-15675
 He+He²⁺, time-depend. HF wave functions, variationally improved transition amplitude 7-36739
 He+K, fine-struct. transitions, differential cross section meas. 7-62493
 He+Kr⁴⁺, state-selective electron capture, translational energy spectra 7-50337
 He+Li₂, rot. energy transfer cross sections, studied using polarisation ratio vel. depend. 7-42740
 He+Li₂, total integral scatt. cross-sections 7-36728
 He+Li²⁺, n=Z levels, alignment and orientation (French) 7-10723
 He+Li³⁺(C⁶⁺)(O⁸⁺), electron capture, Coulomb integral eval. 7-15679
 He+Li(Na)(k)(Rb)(Cs), Penning ionisation, pot. well depth calcs., electron energy spectra anal. 7-62510

helium atoms continued

- He+N₂, potential energy surface, multiproperty obs. 7-25633
 He+N₂, reaction kinetics at atm. press., three-body processes 7-22984
 He+N₂⁺, rot. transfer coeff. determ. (French) 7-10708
 He+NH₃, Rydberg atom ionis., rot. deexcitation 7-36737
 He+NO, rot. inelastic cross section determ. sudden approx. 7-25637
 He+Na, fine-struct. branching ratios, meas. 7-15676
 He+Na, Na D line broadening and shift (French) 7-10501
 He+Na₂, state selected rot. transitions, scatt. induced ang. momentum alignment 7-20005
 He+Na₂, collisional depolarisation, fluoresc. spectra anal. 7-19924
 He+Na(K)(Pb)(Cs), inelastic collisions at thermal energies 7-983
 He+Ne, electronically excited atoms, beam sources 7-20008
 He+Ne excitation transfer processes, quasimolecule form. 7-5758
 He+Ne²⁺, collisional transition probabilities, avoided crossing, nonadiabatic effects (French) 7-10727
 He+Ne²⁺, transfer excitation in low-energy collisions, spectroscopic meas. 7-15696
 He+Ne⁴⁺, collisions, nonadiabatic transitions 7-62487
 He+Ne⁴⁺, polarization effects in collision-induced intramultiplet mixing 7-5749
 He+O, van der Waals interaction, mol. beam study 7-20001
 He+O₂, rot. inelastic collision, polaris.-preserving propensities 7-36736
 He+O₂(N₂)(NO), scatt., total differential cross-sections 7-39865
 He+O₂⁺, reson. transfer and excitation to specific LS-coupled states, 0⁺ AES 7-36744
 He+O⁵⁺, resonant transfer excitation, Auger spectra obs. 7-50309
 He+O⁶⁺(C⁴⁺), one-step double electron capture 7-50344
 He+O⁶⁺(C⁶⁺), (quasi)-two-electron collision systems 7-5764
 He+positronium, annihilation spectrum 7-62547
 He+Rb, afterglow, inelastic collisions quenching cross sections 7-42746
 He+Rb oscillator strength, pot. curves (French) 7-10728
 He+Sr⁺(Ca⁺)(Mg⁺), reson. line broadening and shift rates, pot. calc. 7-15683
 He⁺+Ca(Cr)(Cu), target K-shell ionis., cross-sections and probabilities 7-50343
 He⁺+Cd(2n), exothermic charge exchange with excitation cross sections 7-42755
 He⁺+H₂, elastic and inelastic scatt. mechanisms, energy loss spectra 7-15671
 He⁺+H₂, ion-molecule reaction rate at low-temp. conditions of interstellar space 7-23007
 He⁺+H₂(N₂)(O₂)(CO)(NO), metastable state, collisional quenching cross section 7-62315
 He⁺+H⁺, Fine-struct. excitation, plasma screening effects, ion-sphere and Debye-Huckel models 7-62509
 He⁺+He collisions, projectile ionization, doubly differential cross section study 7-971
 He⁺+He⁺, electron capture cross sections, SCF-CI calcs. 7-15526
 He⁺+He(Ne)(Ar)(H₂), electron loss to the continuum, absolute cross sections 7-50304
 He⁺+Ne(Kr)(Xe), analytic repulsive pot. calc. 7-50308
 He⁺+Ne(Na)(Mg), multiple ionisation, charge transfer cross sections 7-15706
 He⁺+Pt, L subshell ionisation probabilities vacancy sharing 7-15697
 He⁺+Zn, Penning and charge transfer reactions, Zn²⁺ levels excitation 7-5746
 He²⁺+Ar, electron emission, impact parameter depend., TOF, coincidence spectra anal. 7-42747
 He²⁺+He, symmetric resonant charge transfer collisions in ultralow collision energy range 7-31164
 He²⁺+K, ionisation and charge transfer collisions, cross section meas. 7-20031
 He²⁺+Na, charge transfer, excitation processes coupled state impact parameter model 7-62518
³He+³He(He), elastic scatt. cross section ratio, nucl. spin lattice relax. time anal. 7-42652
 He₂²⁺, ground-state pot. curve, Moller-Plesset perturbation calcs., bond lengths 7-42455
 He²⁺CO₂, CO₂ gas laser preionisation study 7-62508
³He²⁺ electron capture and stripping cross section in Al, Ni, Ag and Au targets 7-10753
⁴He, three atoms interacting through intermol. pot., Efimov state 7-5738
 He⁺, odd-parity coherence in beam-foil excitation 7-909
 He⁺+Ne, collisions, nonadiabatic transitions 7-62487
 He⁺+Zn, Penning and charge transfer reactions, Zn²⁺ levels excitation 7-5746
 He⁺(2S), muonic, binding in He gas, quenching mechanism study 7-36812
 He=Na, optical collisions, fine struct. branching cross-sections, nonadiabatic theory 7-959
 N₂⁺+He, electron beam excitation at 391.4 and 427.8 nm 7-10917
 Ne+Na, optical collisions, fine struct. branching cross-sections, nonadiabatic theory 7-959
 Si:He, ground state one-electron energies, SCF MS X_α calcs. 7-44582

helium compounds

- BaZrF₆, ionic conductivity 7-52129
 He-H₂ van der Waals mol., diagrammatic perturbation theory 7-5607
 He-I₂, complex scaling method appl. 7-42565
 HeBCH, ground state, MP4 (SDTQ)/6-311G**//MP2/6-31G**+ZPE level calcs. 7-25480
 HeBeO, ground state, MP4 (SDTQ)/6-311G**//MP2/6-31G**+ZPE level calcs. 7-25480
 HeH⁺, dissociative charge exchange in HeH⁺+Cs collisions 7-5766
 HeH⁺, orbital energies, multipole moments and electric field gradients, HF calcs. 7-62270
 HeH⁺, vibr.-rot., IR photodissociation spectra 7-31009
 HeH⁺+C, fast mol. ion dissoc., charged fragment wake effects (French) 7-50345
 HeH⁺+Cs, HeH bound excited state form., predissoc. and radiative dissoc. 7-20033
 HeH(D) visible emission spectra obs. and rovibrational energy-level calcs. 7-42633
 He₂H⁺(He₂D⁺), rot.-vibr. states calcs. 7-36576
 HeLi₂, van der Waals system, pot. energy surface 7-62261
 (HeNe)²⁺, pot. energy curves, semi-diabatic model (French) 7-10464
 HeRh²⁺, adsorbed compound ion, field dissociation by atomic tunneling 7-33919
 HeRh²⁺, cpd. ion, dissoc. in high elec. field, at. tunnelling, orientational and isotope effects 7-42777

helium films

- boiling, heat transfer, centrifugal forces effects 7-50920
 liquid, thinning effect at λ point, 3D XY model, direct Monte Carlo sampling 7-61305
 superfluid, one-dimensional electron system, localisation, ripples, scatt. and Coulomb interaction effects (*Russian*) 7-27050
³He, adsorbed on Grafoil, nuclear ferromagnetism and surface ferromagnetic effect 7-2296
³He, adsorbed on solid surface, magnetism (*Japanese*) 7-21564
³He films, gapless superfluidity, diffuse boundary scatt. effects 7-44939
³He spins on exfoliated graphite surface, detection of ferromag. domains 7-38291
³He, superfluid A-phase, normal current in thin film 7-21560
³He, superfluid films, modified XY model 7-4774
³He-⁴He films, superfluid phase transitions 7-21565
³He-A, superfluid, anomalous currents and fractional charge associated with domain walls 7-2297
⁴He, adsorbed on graphite order-disorder transition, sp. ht. anal. 7-58563
⁴He, liq. films, first and second sound 7-32734
⁴He saturated superfluid, spin polarised H thermal accommodation meas. 7-38299
⁴He, superfluid, fractal surface, third sound, capillary condensation 7-27041
⁴He-³He mixture films, surface superfluidity, vortex pair pot. energy (*Chinese*) 7-12391

helium I see *liquid helium-4*

helium II see *superfluid helium-4*

helium nuclei see *nuclei with mass number 1 to 5; nuclei with mass number 6 to 19*

Hellman-Feynman theorem see *quantum theory*

Helmholtz free energy see *free energy*

hemoglobin see *proteins*

hemorheology see *bioreology; blood*

HEMT see *high electron mobility transistors*

hereditary systems see *distributed parameter systems*

Hertzsprung-Russell diagram see *stellar evolution*

heterodyne detection see *demodulation*

heterodyne wavemeters see *wavemeters*

HEXFET see *insulated gate field effect transistors*

HF calculations

see also *Xalpha calculations*

- A=4-90, single particle energies as functions of binding energies, HF sum rules 7-56588
 Abelian quark-gluon plasma, gauge invariant eqns. of motion, QED derivation 7-61823
 acetylidimethyl phosphine, geometries and rotation barriers, structures, ab initio calcs. 7-15501
 acetylene, binding energies, ab initio HF calcs. 7-49894
 actinide-transition metal alloys, AM₂, A=U-Np, M=Fe-Ni, magnetism and electronic props. 7-27505
 alkali halides, colour centres, Hartree-Fock cluster computations 7-16985
 alkali metal hydrides, X²⁺ state, HF quality Slater basis sets 7-19719
 alkali-metal atoms, photoionisation cross sections, ab initio RPPA calcs. 7-36462
 alkaline earth oxides, colour centres, Hartree-Fock cluster computations 7-16985
 annulene and annulene ions, aromaticity, HF instabilities 7-15521
 ATDHF theory, non-uniqueness of the collective submanifold 7-15195
 atom, electron elastic scatt., electron spin polarisation, HF calcs. 7-25369
 atom, transition and ionisation energies, g-Hartree ab initio calcs. 7-15488
 atomic and mol. electronic struct., calcs., relativistic effects 7-36504
 atomic exchange energy functionals, rational fn. representation, HF calcs. 7-49905
 atomic ionisation energy and electron affinity, correl. energy estimation by local approx. 7-56991
 atomic kinetic energy density, approx. functionals study, HF calcs. 7-36476
 atoms, closed-shells, s-state and total electron density, convolution relation, HF calcs. 7-42475
 atoms, microscopic stress tensors 7-42481
 atoms, semiclassical self-consistent field 7-42484
 atoms and ions, H to Ne, relativistic Gaussian basis sets 7-36468
 atoms and mols., spin and charge densities, HF and UHF calcs. 7-19684
 Auger electron spectra of the metallic elements ₄₇Ag to ₅₁Sb, main and satellite structures 7-7795
 bacteriochlorophyll a, config. for photosynthesis, SCF HF INDO calcs. 7-858
 basis extension in the Roothaan method 7-30943
 benzene, vibronic perturbations, pseudopotential propensity rules 7-25397
 p-benzoquinone, struct. and vibr. anal., ab initio HF calcs. 7-25372
 p-benzoquinone radical anion, struct. and vibr. anal. ab initio HF calcs. 7-25372
 chiral mols., vibr. mag. dipole transition moments, rot. strengths, SCF HF calcs. 7-49885
 closed shell ions, electric field gradient Sternheimer function 7-12681
 collective motions and collisions, TDHF and other theories 7-49270
 collective vibrations, phase space description using Vlasov eqn. plus quantum corrections 7-30306
 compound metal clusters, struct. and electronic structs. calcs. 7-15783
 core polarization effects in odd nuclei, HF and RPA schemes 7-61821
 core polarization effects of giant resonances on transition densities of open-shell nuclei 7-61847
 cyclopolyenes, orbital mag. moment, paratropicity, HF eqns. 7-56968
 deep inelastic heavy ion collisions, relative nucl. motion 7-30441
 di-*t*-butyl silylene, triplet ground-state, electronic and stearic effects, ab initio calcs. 7-25419
 diamond, interstitial H or muonium, Hartree-Fock analysis 7-32947
 diamond, muonium, anomalous, model as body-centered interstitial muonium, HF calc. 7-45899
 diamond, muonium-related paramagnetic centres, UHF calcs. 7-38980
 diamond anomalous muonium, vacancy-associated model 7-51758
 diatomic systems orbital energies, multipole moments and electric field gradients, HF calcs. 7-62270
 1,2-difluoroethane, gauche and trans conformers, stability, ab initio calcs. 7-15500
 trans-difluoroethylene ozonide, struct. dipole moment, ab initio HF calcs., microwave spectra 7-10557

HF calculations continued

- dimers, antiferromagnetic coupling, ligand spin polarisation, broken symmetry UHF calcs. 7-22084
 dimethyl silylene, triplet ground-state, electronic and stearic effects, ab initio calcs. 7-25419
 dimethylamine radical cation, hyperfine coupling tensors, ab initio UHF calcs. 7-25373
 dimethylphosphinic acid cation, geometry optimisation, approximate Hessian 7-25345
 Dirac-Hartree-Fock calcs. for relativistic description of nucl. ground state props. 7-5174
 dirty superconductors, strong-coupling eqns., disorder effects 7-64393
 dithioformic acid, conform. struct. and stability, rot. barrier, SCF and HF calcs. 7-25427
 electron momentum density, near HF limit analytic wave fns., atoms and mols. 7-49884
 electron plasma, pure, strong mag. field states 7-45185
 electronic struct. and dynamics, conf., Snowbird, UT, USA (April 1986) 7-55877
 electronic struct. of impurities in metals, valence-electron-only molecular orbital calcs. 7-2528
 equation soln. using algorithms 7-15495
 ethene, multicentre integrals, Slater fn. translation transform. calcs. 7-10417
 ethylene, C-C bond description, HF and VB LCAO calcs. 7-25415
 ethylene, nuclear spin-spin coupling constants evaluated using manybody methods 7-5705
 evaporation residues, limiting angular momenta in heavy ion fusion reactions 7-36050
 fast ion dechannelling, electronic diffusion coeff. calc. 7-44635
 first-row atoms, exchange correlation energies, E_x method calcs. 7-56993
 formaldehyde, protonated, rot. const., ab initio MO calcs. 7-25349
 formaldehyde, vibr.-rot. interaction const., RHF closed-shell wave function 7-19818
 formylphosphine, geometries and rotation barriers, structures, ab initio calcs. 7-15501
 fractional quantum Hall states, size depend. in small system calcs. 7-2517
 Gamow-Teller β -decay of even nuclei near ¹⁰⁰Sn, struct. model calcs. 7-49330
 giant Resonances in Hot and rotating nuclei 7-35933
 graphite, electron momenta, Hartree-Fock-Roothaan calc. 7-42466
 Hartree-Fock approach for thermal nuclei 7-36044
 heavy-ion scattering, quantised adiabatic time-dependent Hartree-Fock theory 7-61900
 hexahalo complexes, vibronic coupling and state Jahn-Teller effect 7-19725
 1,3,5- hexatriene, conform. struct, vibr. anal., ²H substitution effects, RHF calcs. 7-25386
 highly ionized atoms, hyperfine splitting, Hartree-Fock-Dirac calcs. 7-30974
 hot nuclei, semiclassical calcs. using Hartree-Fock and Thomas-Fermi approx. 7-61826
 hydrides, H⁺ states, HF theory 7-19679
 hypernuclei, pionic decay rate calcs. using DDHF single-particle wave functions 7-5183
 inert-gas atoms, elastic scatt. of electrons, phaseshifts and differential cross sections, local-density approx. 7-19695
 interaction radii of stable and unstable nuclei 7-35943
 ions, in cryst., dipole-quadrupole dispersion coefficients, ab initio coupled HF calcs. 7-11986
 M X-ray energy shifts, relativistic Dirac-Fock wave fns. calc. 7-19727
 many-body problems of proton-neutron interaction, HF theory 7-30350
 many-electron atoms, relativistic HF and RPA calcs. 7-19675
 many-electron Schrödinger eqn. for molecular systems, computational considerations 7-4700
 many-fermion system, TDHF extension with Grassmann variables, formulation using Dirac's canonical theory of constraints 7-56629
 many-fermion system, TDHF extension with Grassmann variables, canonical invariance and coordinate system specification 7-56630
 many-fermion systems, microscopic theory of one-body dissipation, TDHF calcs. 7-61822
 mean field approx. for fermion or pseudo-spin boson interaction 7-32590
 medium-Z elements, K α' satellite, transition assignment, nonrelativistic single configuration HF calcs. 7-30941
 metalloporphyrin dianions, electronic struct., RHF calcs. 7-56946
 methane, binding energies, ab initio HF calcs. 7-49894
 methane, electron momenta, Hartree-Fock-Roothaan calc. 7-42466
 methane, force field, HF SCF and GAS SCF calcs. 7-62268
 methane, multicentre integrals, Slater fn. translation transform. calcs. 7-10417
 methanimine, fluorination effect on double bonds, SCF HF and MP2 ab initio calcs. 7-10384
 methylamine radical cation, hyperfine coupling tensors, ab initio UHF calcs. 7-25373
 1-methyluracil, isotopic derivatives vibr. spectra, ab initio Hartree-Fock SCF calcs. 7-15589
 molecular crystals, electron density distrib. calcs., X-ray diffr. 7-26587
 molecular electron affinities evaluation 7-5591
 molecular nucl. mag. shielding consts. ab initio wave function calcs. 7-5594
 molecular polarisability, Cauchy moments, nonempirical HF perturbation theory calcs. 7-49918
 molecular systems, semiempirical MND0C calcs., size consistency corrections 7-62292
 monohalomethane, harmonic force fields and vibr. spectra, ab initio HF calc. 7-50064
 multiple core holes, electronic system response and spectra prod., many-body theory 7-42477
 muonium energy profiles, unrestricted Hartree-Fock cluster calcs., comment and reply 7-45907
 neutral atoms, energy investg. using statistical formulas 7-57004
 nitromethane, isomers, struct., quantum mech. harmonic force field calcs. 7-56952
 nuclear matter, saturation density and Skyrme functional, Hartree-Fock calcs. 7-49276
 nuclear matter, thermodynamic properties, anal using saturating chiral field theory, relativistic Hartree approximation calcs. 7-24948
 nuclear matter effective interaction, Dirac-Brueckner HF/Brueckner HF calcs. 7-24938
 nuclei, hot, thermal response 7-24945

HF calculations continued

octatetraene, vibronic perturbations, pseudoparity propensity rules 7-25397
 open-shell SCF wavefunctions, anal. energy third derivatives 7-25341
 orbital optimisation scheme, spin projected HF method 7-838
 organic compounds., electronic density, transferability of atomic descriptions, mol. pot. calcs., HF STO calcs. 7-25355
 periodic polypeptides, band struct. ab initio HF cryst. orbital calcs. 7-23298
 periodic TDHF solutions, physical interpretation and quantisation 7-30358
 perturbation-theory method of calculating the energies and excitation energies of atomic, molecular, and solid-state systems 7-5596
 phonon-assisted quantum diffusion, self-consistent mode mixing. 7-45436
 phosphamethane, fluorination effect on double bonds, SCF HF and MP2 ab initio calcs. 7-10384
 planar four-coordinated metal complexes, symm. effects, RHF MO SCF calcs. 7-56963
 polyacetylene, electron momenta, Hartree-Fock-Roothaan calc. 7-42466
 polyacetylene, N-containing analogues, electronic structures, conduction props., ab initio study 7-32911
 polyacetylene, solitons, electronic props., local space approx. 7-52506
 polyatomic mols., stretching force consts., inner-shell polarisation effect, HFD calcs. 7-15588
 polyene chains, electronic struct., long-range electrostatic effects and terminal group influence 7-56987
 polyenes, cyclic, stability props., spin restricted and spin-projected HF methods 7-10435
 polyenes, long, low-lying electronic excitations, PPP-MRD-CI calcs. 7-36488
 polyisothianaphthene, electronic struct. and conduction properties 7-45119
 polymer, band struct., direct space exchange lattice sums, convergence props. 7-21797
 polymethynes, restricted HF MINDO/3 calcs. 7-10432
 prop-1-en-2-ol, geometry optimisation, approximate Hessian 7-25345
 purines, tautomeric equilib., gas phase and aq. soln., HF calcs., MNDO calcs. 7-25403
 pyrimidines, tautomeric equilib., gas phase and aq. soln., HF calcs., MNDO calcs. 7-25403
 QCD-based relativistic Hartree-Fock calculations for identical quarks 7-15112
 quantum systems, microscopic stress tensors 7-41147
 quasi-1D infinite linear atomic chain, Hartree-Fock eqns., numerical soln. 7-21793
 quasi-relativistic methods in Hartree-Fock theory, one-electron integrals 7-10381
 superconducting nuclei, nucleon-number conservation in self-consistent collective-coord. method 7-19180
 TDHF approximation for soluble models with large degeneracies 7-24944
 TDHF theory, dynamical collective submanifold for large-amplitude collective motion 7-19181
 TDHF theory, quantum theory of dynamical collective subspace for large-amplitude motion 7-19182
 thermal linear response theory for dissipative high spin quantum states 7-19223
 tribromomethyl radical, geometry and electronic struct., SWX α calcs., ab initio UHF calcs. 7-19703
 trichloromethyl radical, struct. and electronic states, ab initio UHF SWX α calcs. 7-30949
 trimethylamine radical cation, hyperfine coupling tensors, ab initio UHF calcs. 7-25373
 two dimensional electron gas, thermodynamic props., interaction and disorder effects, HF approx. calcs. 7-2516
 vibration potential function in effective nuclear charge model, energetic consideration 7-25364
 wave equations consistency of use in basis set variational solns. with Dirac hole theory 7-19692
 Z=56 to 66 neutron-deficient nuclei, nucleon stability, Hartree-Fock method calcs. (Russian) 7-30384
 H₂S, normal and deuterated, K-shell X-ray absorption spectra, double excitation 7-62404
 Al, hyperfine struct., magnetic-dipole- and electric quadrupole coupling consts., atomic fluoresc., MCHF method 7-30985
 Al_n clusters, (n=5,9,13), electronic struct. and bonding 7-15775
 Ar, 3s-subshell excitation, photoabsorption spectra anal., HF calcs., config. interaction calcs. 7-30947
 Ar, dipole (e,2e) cross sections, plane-wave Born calcs. 7-30935
 Ar, fast electron bremsstrahlung cross sections 7-36780
 Ar, H-like and doubly excited He-like, dielectronic satellite spectra, transition rates and energies 7-51512
 Ar, kinetic energy density, nonlocal correl. fn., CI wave fns. and HF calcs. 7-42496
 Ar⁺, 3p⁴ configuration, multielectron photoionisation, relativistic HF calcs. 7-36567
 Ar²⁺, energy level radiation lifetime calcs. 7-25455
 Au, valence energy and polarisability, semiempirical pseudopot. calcs. 7-56926
 BF₃, electric-field gradients, NMR shielding tensors, NQR coupling consts., ab initio HF calcs. 7-19693
 B₂H₂, polyboranes, nucl. coupling const. HF calcs. 7-19688
 Ba, energy struct., HF-Dirac method 7-30938
 Ba, valence energy and polarisability, semiempirical pseudopot. calcs. 7-56926
 Be, excitation energies, oscillator strengths, polarisabilities, HF calcs. 7-56929
 Be, HF eqns., Griffin-Hill-Wheeler version 7-42459
 Be isoelectronic series, fine struct. multiconfigurational DF calcs. 7-62266
 Be, kinetic energy density, nonlocal correl. fn., CI wave fns. and HF calcs. 7-42496
 Be, modified HF SCF equation 7-56970
 Be, multi-config. HF and many-body perturbation theory calcs. 7-19699
 Be⁺, shape reson., complex-rotated HF method 7-842
 Be²⁺-H₂O, geometry and vibr. freqs., ab initio HF calcs. 7-49881
 C-centres radicals, merostabilisation energy calcs. 7-30924
 C-containing mols., X-ray emission spectra, ab initio MO HF calcs. 7-36642
 Cs, geometric isomers, ab initio calc. of equil. struct. 7-62291
 CF₃ chemisorption on GaAs (001), electronic struct., RHEED, photoelectron spectra, HF SCF calcs. 7-53497

HF calculations continued

CO, 5 σ photoions, reson. effects calcs. 7-36705
 CaSiO₃, perovskite type, cryst. struct., lattice dynamics and eqn. of state 7-58248
⁴⁰Ca, deformed excited 0⁺ states, HF and α -cluster calcs. 7-41879
⁴⁰Ca(p,p), optical pot., dispersion relation approach to extrapolation to negative energy 7-41958
 Cd, oscillator strengths and excitation energies, relativistic CI and MCRHF calcs. 7-50260
 Cl isoelectronic sequence, allowed 3-3 transitions, Slater parameter optimisation, HF CI calcs. 7-48205
⁵⁴Co medium spin structure, shapes and transitions, HF and shell anal. of ⁵⁴Fe(He,X) 7-41873
 Cr²³⁺, dielectronic satellite spectra CI HFS calcs. 7-42506
^ACr, A=48, 50, single particle spectra and shape from deformed HF calcs. (Chinese) 7-5186
 Cs, isotope shifts, relativistic DF contrib., reson. doublet, UV laser spectroscopy 7-10475
 Cu surface, Raman intensity of adsorbate vibr., cluster-model calc. 7-27089
 Cu₂, STF HF wave function 7-25365
 CuCl, low-lying excited states, HF approx. 7-62254
 D, spin-polarized, ground state props., GFHF calcs. 7-27055
 Er, low-lying states electronic density, ab initio multiconfiguration DF calcs. 7-15486
¹⁷⁰Er, deformations, pair gaps and giant resonances, temp. depend., finite temp. HFB calcs. 7-30320
 F VI, 2nd Rydberg series correl., HF-term energy separation 7-30939
¹⁹F(e,e), form factor calcs. using projected Hartree-Fock function 7-30413
 Fe XV, allowed transitions, Hartree-Fock and Dirac-Fock calcs. 7-15494
 Fe₂, diatomic molecules, electronic configuration, ⁵⁷Fe Mossbauer data 7-10640
 Fe(H₂O)₂²⁺ clusters, intermol. pot. fn. and pot. energy surface, ab initio UHF calcs. 7-25354
⁵⁴Fe medium spin structure, shapes and transitions, HF and shell anal. of ⁵⁴Fe(He,X) 7-41873
 Fr, isotope shifts, relativistic DF contrib., reson. doublet, UV laser spectroscopy 7-10475
 Ga, 4snd 2D series, lifetimes and oscillator strengths, MCHF wave fn. calcs. 7-62324
 Ga, hyperfine struct., magnetic-dipole- and electric quadrupole coupling consts., atomic fluoresc., MCHF method 7-30985
 Ga, radiative lifetimes, fluoresc., MCHF calcs. 7-30946
 Ga VII, optical spectrum, 3d⁷-3d⁶4p transitions, Hartree-Fock calcs. 7-57018
 Ge (111), chemisorption of atomic H, nonempirical cluster-model study 7-38332
 Ge, anomalous muonium, vacancy-associated model 7-51758
 GeH₄⁺, Jahn-Teller, struct. and energy distortions ab initio CI calcs., HF calcs. 7-15523
^AGe, A=68,70,72,74, high spin yrast levels, microscopic study 7-5143
 H atom in molecule, polarisability change calcs. (Russian) 7-62279
 H-bonded systems, polarisation function SCF calcs. 7-19685
 H₂ formulation of ab initio optical potential for electron elastic scatt. 7-15714
 H₂, interat. interactions in van der Waals region, Epstein Nesbet calc. 7-36491
 H₂⁺, interat. interactions in van der Waals region, Epstein Nesbet calc. 7-36491
 H₂+NH₃, ab initio potential-energy surface, HF, SCF calcs. 7-10716
 HCN, vibr.-rot. interaction const., RHF closed-shell wave function 7-19818
 HD, nuclear spin-spin coupling constants evaluated using manybody methods 7-5705
 HF, nuclear spin-spin coupling constants evaluated using manybody methods 7-5705
 HF, vibr. transition, H bonding derivative HF theory 7-19680
 HF-He, mol. interactions, nonexpanded dispersion and induction energies, damping functions 7-42474
 H₃GeX (X=F, Cl, Br, I), harmonic force fields and vibr. spectra, ab initio HF calc. 7-50064
 H₂O, vibr.-rot. interaction const., RHF closed-shell wave function 7-19818
 HOO radical, orbital energies, UHF calcs. phys. interpretation 7-56931
 HSOH, CI analytic energy second derivatives, IR intensities and vibr. freqs. prediction 7-5608
 H₃SiX (X=F, Cl, Br, I), harmonic force fields and vibr. spectra, ab initio HF calc. 7-50064
 H₃SnX (X=F, Cl, Br, I), harmonic force fields and vibr. spectra, ab initio HF calc. 7-50064
 He, exchange correlation energies, \bar{E}_x method calcs. 7-56993
 He, HF eqns., Griffin-Hill-Wheeler version 7-42459
 He, modified HF SCF equation 7-56970
 He, photoionisation, partial cross-sections and Rydberg series resons. 7-903
 He⁺ low energy ion-surface scatt., reionisation process theory 7-22413
 He-like ions, electron excitation, distorted-wave polarised orbital approach 7-62531
 He-like ions, multiconfiguration DF study 7-62298
 He-like ions, radiative corrections, multiconfigurational DF study 7-62299
 He+He²⁺, time-depend. HF wave functions, variationally improved transition amplitude 7-36739
 He₂, interat. interactions in van der Waals region, Epstein Nesbet calc. 7-36491
 HeLi₂ van der Waals system, pot. energy surface 7-62261
⁴He, finite temperature Hartree Fock calcs. with quasiparticle (nucleon, Δ (1232) isobar) basis 7-35966
 Hg, oscillator strengths and excitation energies, relativistic CI and MCRHF calcs. 7-50260
 Hg, valence energy and polarisability, semiempirical pseudopot. calcs. 7-56926
 In, hyperfine struct., magnetic-dipole- and electric quadrupole coupling consts., atomic fluoresc., MCHF method 7-30985
 K⁺-CO₂ system, pot. energy surfaces calc. 7-57015
 Kr, kinetic energy density, nonlocal correl. fn., CI wave fns. and HF calcs. 7-42496
 Kr, two-electron-one-photon excitations, X-ray photoabsorpt. studies 7-36527
 Kr²⁺ energy level radiation lifetime calcs. 7-25455

HF calculations continued

La, fast electron bremsstrahlung cross sections 7-36780
Li, crystal and electronic struct., ab initio HF cluster method 7-44443
Li I, oscillator strengths, transition matrix elements, Dirac-Fock approx. 7-843
Li, ultrafine structure, nonrelativistic approx. 7-5612
Li-CO₂ complex, pot. energy surface, covalent ionic nature 7-30967
Li₂, photoionisation and Auger electron emission, HF calcs. 7-36703
LiCN(LiNC), struct., electron correl. calcs. 7-30956
LiH, electronic struct., mol. cluster calcs. 7-7110
LiH⁺, ground and first excited state electron affinities, extended-Koopman's-theorem, ab initio calcs. 7-25352
Li₂S, triplet ground-state, electronic and stearic effects, ab initio calcs. 7-25419
methanol, protonated, rot. const., ab initio MO calcs. 7-25349
Mg, 3snl excited series, CI HF calcs. 7-36496
Mg, exchange correlation energies, \bar{Z}_4 method calcs. 7-56993
Mg II, core-excited states, energy levels and lifetimes, HF calcs. 7-867
MgO (001), ab initio Hartree-Fock calcs. 7-27378
MgO, directional Compton profiles and autocorrelation function 7-3103
MgSiO₃, perovskite type, cryst. struct., lattice dynamics and eqn. of state 7-58248
²⁴Mg, approximate angular momentum states, thermal response in finite temp. HF approximation 7-19155
Mo V, HF calcs. and spectra 7-10477
N at. and mol. chemisorption on graphite finite cluster models, HF calcs. 7-16869
N₂, photoionis. cross section, HF calcs. 7-42693
NH₃⁺ radical cation, hyperfine coupling tensors, ab initio UHF calcs. 7-25373
(NH₃)₂, dimer struct., electron spectra anal., HF calcs. 7-36686
NH₄⁺, methyl-substituted, H-bond and hydration energies relationship, HF MO calcs. 7-15490
NH₂NO, struct. and vibr. freqs. calc. using basis sets ranging from STO-3G to 6-311G** 7-10385
NO, photoexcitation and ionisation cross sections, Stieltjes-orbital representations, HF calcs. 7-19677
NS, spin-orbit coupling consts. calc. using restricted HF wavefunctions 7-56949
Na-like ions, Rydberg states, dynamic polarisability, HF calcs. 7-62273
Na⁺-CO₂ system, pot. energy surfaces calc. 7-57015
NaCN, ab initio coupled HF calcs. of multipole moments and dipole polarisability of CN⁻ 7-5587
Na₂Cl, microclusters, ionisation induced structural transitions, pseudo-potential, HF calcs. 7-25379
NaI core-excited states, energy levels and lifetimes, HF calcs. 7-867
Ne, atom, dielectric satellite lines of X resonance line, calcs. 7-5621
Ne, dipole (e,2e) cross sections, plane-wave Born calcs. 7-30935
Ne, kinetic energy density, nonlocal correl. fn., CI wave fns. and HF calcs. 7-42496
Ne-He van der Waals mol. pot., ab initio HF SCF calcs. 7-36459
Ni (100), (111) and (110), N₂ chemisorption, molecular cluster calcs. 7-52280
Ni, quasi-particle and band-calc. spectra, w.r.t. valence band photoemission meas. 7-2474
Ni₄H clusters, charge distrib., Hartree-Fock SCF INDO calcs. 7-52411
NiO₂Cl₂ microclusters, ionisation induced structural transitions, pseudo-potential, HF calcs. 7-25379
O, orbital energies, UHF calcs. phys. interpretation 7-56931
O₂, photoionis. cross section, HF calcs. 7-42693
OH radical, orbital energies, UHF calcs. phys. interpretation 7-56931
OH₃⁺, methyl-substituted, H-bond and hydration energies relationship, HF MO calcs. 7-15490
OI, dipole transition probabilities, HF wave functions calcs. 7-5634
¹⁶O, deformed excited 0⁺ states, HF and α -cluster calcs. 7-41879
¹⁶O(¹⁶O, π X), π -production cross section calcs., TDHF anal. 7-24998
^AO_s, A=186, 188, deformations, pair gaps and giant resonances, temp. depend., finite temp. HFB calcs. 7-30320
P VI-XIII, in plasmas, spectra, 22-92 Å 7-15537
²⁰⁸Pb, thermal props., constrained Hartree-Fock calcs. 7-19183
Pb, electron momentum spectra, multiconfiguration DF wavefunction 7-50351
Pb, valence energy and polarisability, semiempirical pseudopot. calcs. 7-56926
²⁰⁸Pb charge density shape, influence of ground state correlations 7-30318
²⁰⁸Pb(N,N), optical pot., dispersion relation approach to extrapolation to negative energy 7-41958
Pd V, fifth spectrum anal. 7-42532
PdGe, bonding, electronic states, ab initio HF-CI calcs. 7-42497
S isoelectronic series, transition probabilities and wavelengths 7-15550
SF₃ radicals, electronic struct., ab initio SCF CI calcs. 7-19716
SF₆, electron affinity, HF SCF calcs. 7-49907
SH₃ radicals, electronic struct., ab initio SCF CI calcs. 7-19716
Si₄N₄²⁺ dication, HF instabilities 7-15508
Se, trigonal, optical props., local field effects 7-22204
^ASe, A=70,72,74,76, high spin yrast levels, microscopic study 7-5143
^ASe(e,e), A=78,80, differential cross section meas. and phase shift anal. 7-41985
Si (111), Br chemisorption, SCF HF cluster calculation 7-52251
Si (111), chemisorption of atomic H, nonempirical cluster-model study 7-38332
Si, anomalous muonium, vacancy-associated model 7-51758
Si clusters, in presence of O, Si-Si bond breaking, total energy calcs. 7-50438
Si, energy calcs. using four-centre integrals 7-27227
Si isoelectronic sequence, allowed 3-3 transitions, Slater parameter optimisation, HF CI calcs. 7-48206
Si, lattice images, screening effect 7-51592
Si, muonium, anomalous, model as body-centered interstitial muonium, HF calc. 7-45899
Si, normal muonium, location and hyperfine props., Hartree-Fock cluster calcs. 7-52539
Si, self-consistent Hartree-Fock and screened exchange calcs. 7-12585
Si:N(O), pseudo Jahn-Teller effect and chemical rebonding 7-16992
SiC₂, protonated isomers, struct. and proton affinity, ab initio HF MO calcs. 7-25384
SiF, spin-orbit coupling consts. calc. using restricted HF wavefunctions 7-56949
SiF₄, electric-field gradients, NMR shielding tensors, NQR coupling consts. ab initio HF calcs. 7-19693

HF calculations continued

SiH₄, electron impact cross sections, spherical-complex-optical pot., ab initio HF calcs. 7-49904
SiH₄⁺, Jahn-Teller, struct. and energy distortions ab initio CI calcs., HF calcs. 7-15523
SiH₄+e⁺, optical pot. approach 7-30933
SiH₄F₆ (a+b=4), NMR shielding consts., ab initio coupled HF calcs. 7-42646
¹⁴⁸Sm, deformations, pair gaps and giant resonances, temp. depend., finite temp. HFB calcs. 7-30320
SnH₄⁺, Jahn-Teller, struct. and energy distortions ab initio CI calcs., HF calcs. 7-15523
Sr+Ar, ¹P fluoresc. line broadening, ab initio close-coupled scatt. calcs. 7-36494
TeF₆, electron affinity calcs. 7-36453
Th, plasma, XUV spectra, isotope line identification, HF and DF calcs. 7-15487
^ATi, A=44, 46, 48, 50, single particle spectra and shape from deformed HF calcs. (Chinese) 7-5186
Ti, valence energy and polarisability, semiempirical pseudopot. calcs. 7-56926
Ti⁺, shielding of external elec. field, Hartree-Fock calcs. 7-15532
W (110), hyperthermal K⁺ scattering, HFS-LCAO pair potential 7-22412
W, fifth spectrum, 2300-450 Å 7-885
Xe, fast electron bremsstrahlung cross sections 7-36780
Xe, two-photon one-electron ionisation cross sections, RPA, LDA HF calcs. 7-49912
⁹⁰Zr, thermal props., constrained Hartree-Fock calcs. 7-19183
HGMS see magnetic separation
hierarchical systems
phyllotaxis, universal model considering entropy and hierarchical primordia 7-65676
upper arm prosthesis, intelligent control system (Chinese) 7-60127
Higgs particles see intermediate bosons
high electron mobility transistors
III-V semiconductor, strained layer superlattice research developments 7-52766
K-band receiver, cryogenically cooled HEMT for radio astronomical obs. 7-60548
microstructures and microdevices, conf., Goteborg, Sweden (Aug. 1986) 7-35097
picosecond electro-optic sampling 7-53278
quantum heterostructure materials and devices 7-52786
Si-SiGe strained superlattices on Si substrates, MBE growth, characterisation, appl. for HEMT 7-27218
AlGaAs/GaAs/AlGaAs selectively doped double heterojunction FET system, high mobility electron subband struct. studies 7-12838
AlGaAs-GaAs, modulation doped heterostruc., high field transient transport 7-12836
AlInAs-GaInAs heterointerface FET, MOCVD growth fabricated, characts. 7-17429
GaAs-Al_{1-x}Ga_{1-x}As MODFETs, hot-electron capture at DX centres 7-45344
GaAs-AlAs device structs., MBE prep. using In-free mounting techniques 7-3183
Ge-Si alloys, strained layer epitaxy, review of developments 7-52343
SiGe-Si structures, MBE growth mode and interface structure 7-52311
high-energy cosmic ray interactions
antiprotons production at ultrahigh energies rel. to p/p ratios, appl. of leaky box prop. model 7-40654
Centauro phenomenon, search in pp, 900 GeV 7-30297
charmed particle prod. and long-range avalanches in cosmic ray showers 7-14446
Cygnus X-3, radiation source, role of antineutrinos and photinos 7-24242
gamma-families formed at ultrahigh energies, spatial characts., Monte Carlo calcs. 7-14431
hadron families, energy spectra and spatial distrib. at ultrahigh energy 7-14432
hadron interaction range for E>20 TeV in Pb chambers 7-14470
hadron-nucleus reactions, superhigh energy cross sections in critical and supercritical Pomeron models 7-19090
jet phenomena in a giant superfamily 7-14468
multidimensional characts. of e⁻-photon showers, analytic solns. 7-14450
multijet family event at super-high energy (Chinese) 7-14443
neutrino-induced EAS, detection possibilities 7-9349
neutrino production in atmosphere, energy spectrum calc. 7-40660
nucleus-nucleus collisions, average transverse momentum and energy density meas. in emulsion chamber 7-42063
nucleus-nucleus interactions, cosmic ray results from the JACEE experiments 7-60499
Pamir expt. data, comparison with strong interaction model 7-10038
secondary particles with large transverse momentum, X-ray emulsion chamber study 7-14429
ultra-high energy cosmic-ray spectrum, implications of Fly's Eye detector results 7-4280
unequal nuclei collisions at high energy, rapidity distrib. and hydrodynamic model 7-9350
nn→X, high energy cosmic rays, particle production, multiplicity 7-47652
high energy electron diffraction
see also reflection high energy electron diffraction
binary cubic solid solns., structure factor determ. 7-16374
Ag-CdTe (100) interface, photoemission studies, surface struct., growth behaviour, Schottky barrier and surface photovoltage 7-39352
CdTe (100), photoemission studies, surface struct., growth behaviour, Schottky barrier and surface photovoltage 7-39352
Fe-N, implantation at 77 K, surface comp., microstructure, AES, HVEM, transmission HEED studies 7-38033
 β -NiAl, electron charge distrib., HEED meas. 7-16502
SiO₂, amorphous film, ionic character, HEED study 7-63468
SiO₂, natural oxide on a-Si, structure, HEED study 7-63469
high-energy nuclear reactions and scattering see nuclear reactions and scattering
high field effects
see also Gunn effect; hot carriers; impact ionisation; limited space charge accumulation; Poole-Frenkel effect; Schottky effect; Zener effect
2D systems, proceedings of Winter School, Mauterndorf, Austria (Feb. 1986) 7-48131

high field effects continued

- Bloch electrons, quantum transport in homogeneous time depend. elec. fields 7-52633
 carrier transport theory, picosecond processes 7-45342
 current discharge, n-filamentous Z-pinch, radial movement anal., high electric field effect 7-63261
 dielectrics with deep traps, currents in strong elec. fields 7-33023
 disordered polycrystalline semiconductor, nonlinear percolation conductivity, alternating electric field 7-58816
 electron-electron scatt. in nondegenerate semiconductors, anisotropic electron distrib., displaced Maxwellian 7-2624
 ethylene copolymers, electric breakdown and high-field conduction meas. 7-39011
 ferromagnetic semiconductors, hot magnons 7-22099
 ferromagnetic superconductors, superlattices formed by coherent light beams 7-2622
 inhomogeneous semiconductor, polarisation by strong HF elec. field 7-52664
 insulating polymers, elec. cond. and breakdown phenomena 7-45306
 metal-vacuum interface, tunneling from a self-energy approach 7-52745
 multilayer isotypic n^+-n heterostructures, S-type current-voltage characts. 7-52758
 narrow band gap semicond., with symm. electron and hole spectra, pinch effect 7-17047
 p-n junction, nonlinear transport problems, use of electron temp. concept 7-7371
 polyethylene, electron beam charged, space charge decay currents 7-27338
 polyethylene, low density, electric breakdown and high-field conduction meas. 7-39011
 polyethylene naphthalate, electrolum. and electronic conduction in high DC fields 7-27788
 polystyrene film, electron thermalisation and trapping 7-27343
 quantum transport eqns., generalised Kadanoff-Baym ansatz 7-38529
 quantum transport theory for small-geometry structures 7-52640
 quantum well heterostructures, intraband photocond. 7-64318
 quasi 2D quantum wells, linear and nonlinear electrical conduction 7-64331
 SCL current with nonlinear velocity-field relationship, I-V characts. 7-33020
 semiconductor, carrier transport in built-in and external fields 7-52634
 semiconductor, nondegenerate, diffusion noise and hot-electron noise at arbitrary drift vels. 7-64299
 semiconductor thin film, band population inversion under strong alternating elec. field 7-64371
 semiconductors, disordered, with dispersive transport, elec. transient process 7-17074
 semiconductors, electron-phonon weak scatt. in high elec. fields, Boltzmann eqn. 7-2625
 semiconductors, photoelectrons subjected to parallel elec. and quantising mag. fields 7-64280
 semiconductors, slow current relax. and assoc. effects 7-52671
 semiconductors, tunnel delocalisation of electrons 7-33022
 semiconductors, unipolar injection in presence of deep centres with negative Hubbard energy 7-38568
 Si_3N_4 MONOS structures, negative hopping magnetoresist. meas. 7-64357
 two-dimensional carrier systems, parallel transport 7-52827
 Al- Al_2O_3 -Au sandwich struct., forming process in high elec. field (Japanese) 7-22028
 AlGaAs-GaAs, modulation doped heterostructs., high field transient transport 7-12836
 AlGaAs-GaAs heterointerface, ballistic transport of quasi-2D electron gas 7-52788
 $\text{Al}_{0.3}\text{In}_{0.7}\text{As}$, transient transport in central-valley-dominated ternary III-V alloys 7-7253
 As_2Se_3 single crystals, geminate pair recomb., photocond., photoluminescence meas. 7-38581
 $\text{Ba}_2\text{NaNb}_2\text{O}_{15}$ single crystals, spatio-temporal electrical instabilities 7-52632
 $\text{Bi}_{1-x}\text{Sb}_x$ narrow-gap semicond., intraband breakdown, current-voltage characts., size effect conditions 7-52624
 $\text{Bi}_2\text{Si}(\text{Ge})\text{O}_{20}$, light-induced field redistrib., photocond. studies 7-38623
 CdGeAs_2 , Ni amorphous films, elec. cond., low temp. impurity breakdown, high field effects 7-52625
 n- $\text{Cd}_x\text{Hg}_{1-x}\text{Te}$, single crystal, γ -irradiation, electrophysical props. in strong elec. field 7-7251
 CdTiO_3 , nonlinear props. in high electric fields 7-7668
 GaAs diode, active layer $<1 \mu\text{m}$, low temp. current flow 7-52757
 GaAs, electron drift vel.-elec. field characts. 7-38569
 GaAs LPE layers, heavily doped and compensated, hopping cond., density of states at Fermi level, carrier conc. determ. 7-2753
 GaAs quantum wells, optical high-field transport expts. 7-52638
 GaAs-Al $_x$ Ga $_{1-x}$ As heterostructures, selectively doped, electron transport in strong electric fields 7-38687
 GaAs-AlGaAs quantum wells, high electric field, interband transitions, photocurrent spectra obs. 7-7289
 $\text{Ga}_{0.9}\text{In}_{0.1}\text{As}$, transient transport in central-valley-dominated ternary III-V alloys 7-7253
 GaSe amorphous film, high field kinetics of photocurrent 7-2748
 p-Ge, electric avalanche breakdown, chaotic and hyperchaotic states 7-52630
 Ge:Ni, inhomogeneously photoexcited, cond. random spontaneous oscills. 7-52675
 $\text{Hg}_{0.8}\text{Cd}_{0.2}\text{Te}$, low temp. hot electron energy relax. time in extreme quantum limit mag. fields 7-33035
 InGaAs, high-field autovariance coeff., diffusion coeff., and noise at 300 K 7-64260
 $\text{Na}_2\text{B}_4\text{O}_7$ - PbO_4 -CuO glasses, elec. props., effect of added CuO 7-2605
 Si, charge carrier-lattice interaction, X-ray diff. study 7-51975
 n-Si, electron heating and intervalley redistribution in strong electric fields 7-27336
 Si MOS structures, high field stressing, ESR study 7-33091
 Si metal tunnel-thin insulator-semiconductor structures, effects of high field corners 7-64348
 Si-Al struct., cond., transverse elec. field depend. 7-27417
 Si-SiO $_2$ interface, positive charge generation; rel. to high field electron transport in SiO $_2$ 7-38571
 Si-Te-As-Ge chalcogenide glass film, electronic processes in strong elec. field 7-45524
 Si_3N_4 , amorphous hopping cond. in high elec. and mag. fields 7-64257

high field effects continued

- Si_3N_4 thin films in MNOS structs., charge transport in elec. fields 7-12730
 SiO $_2$, behaviour under high elec. field/current stress conditions 7-7254
 SiO $_2$ films, ballistic electron transport 7-45531
 SiO $_2$, high field electron transport, rel. to positive charge generation at Si-SiO $_2$ interface 7-38571
high-frequency discharges
 electric field strength, detect. by dynamic Stark effect 7-21001
 electric fields, ions and chemistry in RF discharges 7-26579
 electronegative gas microwave discharge, layerless kinetic instability 7-37792
 glow discharges, modeling, theoretical and computational problems 7-37796
 high-current microwave discharge plasma, time varying ion acceleration 7-11815
 hollow cathode discharge at direct and HF current, temp. meas., spectroscopic study 7-20994
 microwave discharge, nonself-sustained, energy deposition into high-pressure gas 7-21014
 microwave discharge, plasma corona, large amplitude plasma waves and particle acceleration 7-63380
 microwave discharge, plasma parameters in contracted region, ionis. wave propag. 7-21013
 microwave discharge, spatial profiles and time evolution of gas parameters 7-21015
 microwave discharge in TE wave beam intersection, ionisation instability 7-37793
 microwave generated plasma characteristics 7-26578
 plasma jet prod., thermophysical and gasdynamic parameters 7-11812
 powder production in low press. nonequil. HF discharge 7-53650
 RF discharge, coupled CO $_2$ waveguide laser form. 7-31361
 RF discharge, diode type, plasma and electrode potentials 7-26571
 RF discharge, electron acceleration by self-generated stochasticity 7-32166
 RF discharge, optogalvanic detected IR spectra 7-20970
 RF discharge, sheath props. 7-21021
 RF discharge as low press. contactless sonic wave sensor 7-43585
 RF discharges, characterisation by electrode self-bias voltage 7-21020
 RF planar discharges, model 7-44283
 RF plasma reactors, plasma sheaths, modelling 7-31991
 RF plasma sheath, ion transport, Monte Carlo modeling 7-37797
 solutions, emission spectroscopic analysis, matrix composition effects 7-54240
 thioformaldehyde, RF discharge, optogalvanic detected IR spectra 7-20970
 tokamaks, carbonisation, plasmachemical in situ deposition 7-63296
 trifluorochloromethane-Ar discharges, for plasma etching of Si:P, parametric modelling and impedance anal. 7-28221
 trifluorochloromethane-Ar discharges, for plasma etching of Si:P, modelling of ion bombard. energy distrib. 7-28222
 Ar gas, surface-wave produced microwave discharges 7-63389
 Ar RF discharge plasma, electron and ion transport meas. 7-20874
 Ar, RF glow discharges, low-pressure, large-signal time domain modeling 7-58076
 CO, RF molecular plasma, electron energy distrib. functions 7-37636
 Cl $_2$ discharge, 13.56-MHz, optogalvanic effect 7-32148
 He, atom, with turbulent flow, two electron group model for RF ionisation 7-31921
 He-Zn laser with transverse HF excitation 7-1090
 N $_2$ gas breakdown by 13.56 MHz electric field 7-1806
 N $_2$ in RF discharge, low press., pulsed laser optogalvanic spectroscopy 7-37769
 N $_2$ microwave nonself-sustained discharge, instability 7-37791
 Ne, high-frequency discharge, dissociation recomb. of excited atoms in afterglow 7-10456
 O $_2$ RF discharge, electron energy distrib. function determ. 7-21032
 P, II levels, hollow cathode discharge, self-alignment and radiative lifetime meas. 7-10678
 SF $_6$, RF breakdown and discharges, continuum modelling 7-37798
 SF $_6$, RF molecular plasma, electron energy distrib. functions 7-37636
 SF $_6$ -O $_2$ discharges, LF and RF, etching and surface modification of polyimide films 7-22858
 SiH $_4$ (Si $_2$ H $_6$) RF discharges, radical fluxes, plasma enhanced CVD 7-26580
 SiH $_4$ -Ar plasma, particle number densities, masses and size distrib. meas. 7-37761

high-frequency effects

- see also helicons; hot carriers; skin effect; solid-state plasma
 chalcogenide glasses, AC conduction, theoretical models and expt. data, review 7-64252
 graphite-HSO $_4$ ·2H $_2$ SO $_4$ intercalation cpd., $\text{C}_{24}\text{H}_{12}\text{SO}_4$ ·2H $_2$ SO $_4$, quasi-2D, cond. electron state transform. in microwave field, ESR meas. 7-64508
 HF measurements on chip components (German) 7-45368
 high freq. phonon generation in antiferromagnets, nonresonant parallel pumping (Russian) 7-33157
 inhomogeneous semiconductor, polarisation by strong HF elec. field 7-52664
 metal, quasi-2D conductivity, high freq. effects (Russian) 7-33038
 metallic crystals, magneto-optical Kerr effect, charge carrier plasma reson. enhancement calcs. 7-45997
 photoconductivity, time-resolved microwave cond., semiconductor material characterisation 7-52692
 propylene carbonate-1,2-dimethoxyethane mixtures in electrolyte solns., dielectric props. 7-33322
 semiclassical processes in a high-frequency field 7-52743
 semiconductor superlattices, surface EM waves, amplification 7-17075
 semiconductors, intrinsic, solid-state plasma, local impact ionisation regions form. 7-52663
 semiconductors, narrow gap, spontaneous oscills. under plasma resonance conditions 7-38605
 TCNQ salt, conducting Langmuir-Blodgett film, electronic transport props. 7-38782
 n-WSe $_2$ -electrolyte interface, microwave photoelectrochemistry studies 7-27413
 AgI, submillimeter cond., permitt. spectra meas. 7-44901
 Al, induction-heated conductor, relax. temp.-electric self-oscillations (Russian) 7-52665

high-frequency effects continued

- n-Cd,Hg_{1-x}Te, single crystal, γ -irradiation, electrophysical props. in strong elec. field 7-7251
 CdS, single crystal, US wave absorption, impurity distrib. effect., electron-probe X-ray anal. 7-53241
 CdSe, single crystal, US wave absorption, impurity distrib. effect., electron-probe X-ray anal. 7-53241
 CoFeMoB amorphous thin films, prep. and high-freq. impedance studies 7-53585
 CuInS₂, heterogeneous, VLS growth, electronic defects, photocurrent spectra, photolum., EBIC analysis 7-27288
 FeS₂ polycryst. photoactive MOCVD films, photocond. and time-resolved microwave cond. meas. 7-45386
 GaAs, characterisation by a microwave photoconductance technique 7-7281
 GaAs multiple quantum wells, charge-carrier dynamics, contactless microwave photocond. meas. 7-21998
 GaAs:Si(Be)(Mg), rapid annealing, temp. depend. of damage removal and carrier activation 7-17032
 n-GaAs/Al_{0.3}Ga_{0.7}As multilayer heterostructs., nonlinear high-freq. effects during vertical transport 7-2694
 GaAs-Al_{0.3}Ga_{0.7}As superlattices, integer quantum Hall effect at microwave frequencies 7-52820
 GaAs-GaAlAs modulation doped quantum wells, hot carrier energy relax., time resolved photoluminescence spectra 7-52828
 Ge deformed single cryst., AC conductivity at 4.2K 7-7245
 p-Ge, threshold switching and microwave-induced spontaneous emission in static magnetic field 7-52707
 H, stretched, microwave-driven, level mixing 7-42524
 In_{0.53}Ga_{0.47}As-InP, quasi-2D heterostructures, suppression of current filament by mag. field 7-52760
 InSb, coherent spontaneous oscills. under transverse breakdown conditions, high frequencies 7-17046
 K_{0.3}MoO₃, blue bronze, microwave conductivity 7-45370
 K₂Pt(CN₄)Br_{0.3}·3.2H₂O, quasi 1D conductor, near IR conductivity, pseudogap model 7-45298
 MoSe₂, melt grown layered crystals., optoelectronic props. 7-21946
 Pb_{1-x}Sn_xTe narrow-gap semicond., electron-electron interaction, effect on permitt., two-band model 7-52420
 RbNO₃ cryst., AC cond. near first-order phase transition points 7-21948
 p-Si (100), chemical etching with aq. K₂Cr₂O₇, XPS, UPS, LEED and TRMC meas. 7-46719
 Si, characterisation by a microwave photoconductance technique 7-7281
 Si epitaxial film, with current filament radiation temp. coordinate distrib. 7-38650
 Si single cryst. wafer, charge carrier kinetics, excess microwave cond. meas. 7-38580
 a-Si:H films, charge carrier dynamics, influence of preparation conditions 7-33053
 SiO-SnO₂, vac. evaporated films, AC elec. props. 7-45528
 TaS₂, 1T, submillimetre conductivity, dielectric function 7-12749
 Te, cyclotron reson. characts. of nonequilibrium carriers at low temps. 7-64532
 WSe₂, melt grown layered crystals., optoelectronic props. 7-21946
- high-frequency electronic transport** *see high-frequency effects*
high-frequency heating *see radiofrequency heating*
high level languages
see also FORTRAN; Modula; Pascal; PROLOG
 position sensitive detector data treatment, possible use of OCCAM and transputers 7-10355
- high-pass filters**
 ECG baseline wander reduction using linear phase filters 7-18086
 Landsat data, Fourier filtering for information extraction in surveying and mapping 7-47582
- high power amplifiers** *see power amplifiers*
- high-pressure effects in solids**
see also high-pressure solid-state phase transformations; piezo-optical effects
 acetylene, solid, high-pressure. props., polymerisation paths 7-58412
 alkali halides, powdered, electrophysical investigation during molding 7-7232
 (BEDT-TTF)₂X, (X=SbF₆, AsF₆), metal-insulator transition, EPR study under hydrostatic press. 7-53115
 B-(BEDT-TTF)₂I₃, shear-induced superconductivity 7-45583
 β -(BEDT-TTF)₂I₃, superconductivity, proton irradi. effects 7-45544
 β -(BEDT-TTF)₂I₃ high T_c state, upper critical field meas. 7-45589
 (BEDT-TTF)₂ReO₄, band electronic struct. 7-7094
 B-(BEDT-TTF)₂X organic metal, high T_c supercond. state 7-45542
 B-(BEDT-TTF)₂X organic superconds., Meissner effect under press. 7-45559
 (BEDT-TTF) BrO₄, band electronic struct. 7-7094
 bisethylammonium copper tetrachloride rhombic antiferromagnet, magnetic phase diagram, press. effects study (Russian) 7-52981
 (BMDT-TTF)TCNQ, molecular conductor, dimensionality, struct. and electrical props. 7-52595
 dl-borneole, mol. reorientation dynamics, proton NMR study under hydrostatic press. 7-50175
 dl-camphene, methyl reorientation, high press. NMR study 7-27609
 corundum (α -Al₂O₃), elasticity and high pressure instabilities 7-66103
 diamond, optical phonons and elasticity at megabar stresses 7-21375
 diamond, radiation damage prod. of 5RL centres, phonons, absorpt. spectra, cathodoluminescence studies 7-33461
 Earth lower mantle minerals, press. depend. of thermal cond. rel. to interpretation of D" zone 7-66020
 electronic structure change, high press. appl., review (Czech) 7-58411
 electronic structure change in solids, high press. effect 7-44788
 ethylsulphate:Nd³⁺, high press. spin-lattice relax. and ground state 7-38934
 glass, thermal cond. and heat capacity obs., hydrostatic pressure dependence 7-306
 glass fibre reinforced epoxide resin, tensile props. under superposed hydrostatic press., failure mechanisms 7-28078
 graphite, bend strength and fracture strain under press. 7-46595
 graphite, nucl. grade, polycryst., deform. under press., elastic moduli rel. to struct., neutron irradi. effect 7-28069
 Group VII hydrides, high-pressure. cryst. struct. 7-21183
 inorganic crystals, atomic coordination numbers and defects, geometric estimate 7-63571
 manganese formate, Mn(HCOO)₂·2H₂O, magnetic transitions, compression and mag. dilution effects 7-52986

high-pressure effects in solids continued

- materials modification and synthesis under high pressure shock compression, book contrib. 7-27957
 metal hydrides, thermodynamics of hysteresis at high pressures 7-39911
 metals, bulk modulus and its press. derivative 7-21322
 metals, compression pulses, nanosecond, attenuation 7-58413
 metals, ion implantation of inert gases, high press. precip. phases 7-38031
 metals and alloys, plastic deform. in conditions of quasihydrostatics (Russian) 7-59586
 Ni, electron core states overlap at very high compressions 7-21849
 α -perylene, crystals., excitons, hydrostatic press. effects 7-52430
 poly(propylene oxide) elec. relax. time, high press. effects study 7-32703
 poly(propylene oxide)-Li salt complexes, ionic cond., high press. effects study 7-32703
 poly 2,6-dimethyl-1,4-phenylene oxide and poly styrene-co-p-fluorostyrene blends, miscibility, press. depend. 7-17533
 polyacetylene:I, metallic, effective mass, magnetoreflexion studies 7-64056
 polycarbonate doped with pyrazolines, photoconductivity and carrier mobility, press. effects 7-27363
 polydiacetylene cryst., Raman spectra, press. depend. 7-27726
 polyethylene, extended under press., hydrostatic press. effect on damage accumulation, struct. reorganisation 7-8065
 polyethylene, fracture toughness, high press. tension testing 7-28111
 polyethylene, monoclinic form, hydrostatic compression effect 7-44690
 polystyrene plasma deposited thin films, ionic cond., free vol. model calcs. and meas., press. depend. 7-27009
 polyvinylidene fluoride sheet evaluation for large sonar arrays 7-2986
 precious metals, H₂ permeability at 2 kb press. and elevated temp. 7-27011
 quartz, FTIR spectrum of crystals, press. effects, phonon band splitting 7-46039
 quartz, H₂ diffusional uptake and hydrolytic weakening 7-40469
 rare earth metals, high-performance phases, crystal structure models 7-16489
 rarefaction wave velocities determ. at high pressures, use of Manganin stress gauges 7-48713
 rock deformation, viscosity of partial melts in upper mantle 7-8934
 rocks, crystalline, pore vol. and transport prop. changes during press. cycling 7-40471
 rocks, effect of press. on elastic and strain-strength props. 7-47424
 static high pressure research, review 7-21350
 steel, austenitic stainless, high press. deform., twinned struct., TEM obs. (Russian) 7-46578
 steel, Cr type, dislocation struct. after hydraulic pressing followed by austempering 7-3334
 stishovite (SiO₂), elasticity and high pressure instabilities 7-66103
 styrene-butadiene rubber, thermoelastic coeff. Gruneisen parameter, thermal effects 7-39576
 tetrathiofulvalene bis(bis-(4,5 dimercapto-1,3-dithiole-2-thione) Ni(II)), 3D mol. supercond. 7-45594
 tetrathiofulvalene-p-chloranil, mixed-stack charge-transfer cryst., elec. cond. and phase diagram 7-52586
 (TMTSF)₂BF₄, anion ordering, press. effects 7-2596
 (TMTSF)₂PF₆, cryst. struct., neutron low temp. and X-ray high press. diff. studies 7-44502
 (TMTSF)₂PF₆, Hall effect study of field-induced stabilities at 10.5 kbar 7-7214
 (TMTSF)₂PF₆, unified phase diagram, magnetotransport data anal. 7-45410
 (TMTSF)₂PF₆(ClO₄)(ReO₄) organic metals, mag. suscept. press. depend. meas. 7-12943
 (TMTSF)₂ReO₄, quantum oscillations and field-induced transitions 7-45300
 triglycine selenate crystals., dielectric props. at high hydrostatic press. 7-7631
 AgN₃, elec. cond. under high press., decomp. by dielec. breakdown 7-27010
 Ag₄P₂O₇, high-pressure. polymorph, characterisation 7-1991
 Al, polycrystalline, high temp. creep, strain hardening rates during primary stage 7-65104
 Al, reflectivity meas. on shock-unloading solids 7-27693
 Al, superconducting transition temperature, press. depend. 7-22058
 Al_{0.3}Ga_{0.7}As-GaAs multiple quantum wells, photoluminescence studies, press. depend. (Chinese) 7-13194
 n-Al_{0.3}Ga_{0.7}As epitaxial layers, graded-gap, resistance, press. dependence 7-33113
 Al₂O₃, minerals, shock induced radiation 7-27694
 AlP(As)(Sb), elastic coefficients, pressure effects 7-63720
 Ar, high press. eqn. of state, interatomic pots. 7-58431
 Ar, solid, high press. eqn. of state 7-21396
 As, Fermi surface characts., hydrostatic press. depends. (Russian) 7-32896
 β -(BEDT-TTF)₂I₃, organic supercond., cryst. and mol. struct., X-ray diff. study at 9.5 kbar 7-44504
 c-BN, high press. sintering 7-22615
 BN, polymorphism studies, temp. and press. effects 7-1934
 Ba, thermoelectric power meas. up to 8 GPa 7-64208
 Ba₃Ge₂O₃(OH)₄, high press. phase, cryst. struct., X-ray diff. study 7-32412
 BaPb_{1-x}Bi_xO₃, supercond. props., press. effects 7-45533
 BaPb_{1-x}Bi_xO₃, supercond. characts., press. effect versus composition effect 7-58941
 BaSe, pressure-induced metallisation 7-52698
 Bi, solidification of undercooled liquid, nucleation, pressure effects 7-38169
 Br₂ solid, high press. X-ray absorpt. study, energy dispersive mode 7-59299
 CS₂, spectroscopic studies at high press. 7-27742
 CaF₂:Eu³⁺, O₂⁻, quadrupole coupling and crystal-field shielding under hydrostatic press. 7-2551
 Cd, high pressure magnetoresist. near electronic topological transition (Russian) 7-7204
 Cd, polycrystalline rolled sheets, flow stress, hydrostatic press. effect, 600 MPa (Japanese) 7-33735
 Cd-Hg, ω -phase lattice parameters, influence of temp. and press. (Russian) 7-51704
 CdInGaSe₄, optical absorption spectra, hydrostatic pressure dependence 7-59222

high-pressure effects in solids continued

- CdSe, Te_{1-x} , bowing parameter of direct band gap, press. depend. 7-38453
- CeCu₆, heavy fermion substance, magnetoresistance under press. 7-52579
- CeS, continuous valence transition under high press. 7-32965
- CeSb, mag. ordering and critical fluctuations, uniaxial pressure effects 7-33174
- CoH system, ferromag., heat of formation, total energy calcs. 7-45198
- Cr, Neel temp. and thermal expansion press. depend., strain gauge meas. 7-6724
- Cs, positron annihilation and pressure-induced electronic s-d transition 7-22378
- CsCl(Br)(I), luminescence quenching in *F* centers under pressure 7-22334
- CsI, high press. metallisation, relativistic self-consistent APW calcs. 7-21812
- CsSbF₆, high press. cryst. struct., Raman spectra studies 7-26860
- Cs[Pd(S₂C₂(CN)₂)₂].0.5 H₂O, low-dimensional metal at low-temp. and high-press. 7-45290
- CuCl, off-centre model, vibr. and struct. props. 7-17316
- Cu₂MnAl, Heusler alloy, heat and press. processed, changes in phys. props. during heating (*Russian*) 7-59645
- Cu₈₀Sn₁₅, amorphous melt-quenched alloys, crystn. (*Russian*) 7-37881
- Eu-Yb, high press. mag. and elec. props. studies 7-7541
- EuS, mag. props. under high press., competing magnetic interactions 7-7542
- F₂ solid, high-press. behaviour at low temps. 7-37923
- Fe and alloys, alloying with N under high press. 7-3266
- Fe, electrical resistivity, high temp. and press. 7-38534
- Fe, Fermi surface change near the mag. transition 7-16935
- Fe-Mg-Si-O system, phase equilibria at high press. and temp., thermochemical data base 7-21407
- Fe_{100-x}B_x metallic glass system, elec. resist. under press. 7-7200
- FeH₂, prep. under high press., Mossbauer obs. 7-33313
- Fe₃₀Ni₃₅Cr₁₂Mo₂Si₃B₁₅, amorphous alloy, Curie temp., press. effect 7-52976
- Fe_{0.94}O, metallisation at elevated press. and temp., shock wave elec. resist. meas. 7-7297
- Fe₃O₄, magnetite, cryst. struct. under press. 7-16524
- Fe₃O₄, magnetite, high press. cryst. chemistry 7-16521
- Fe₂P, mag. props. under high press., competing magnetic interactions 7-7542
- GaAlAs:Si, DX centres, nonexponential thermal emission kinetics 7-12640
- Ga_{1-x}Al_xAs, DX centres, inner and outer crossing lattice relax. 7-45218
- GaAs, deep level nonradiative carrier capture press. depend. calcs. 7-12735
- n-GaAs films, magneto-optical studies under high hydrostatic press. 7-13247
- GaAs, phonon and plasmon deformation potentials, FIR spectra under uniaxial stress 7-26886
- n-GaAs:Co, impurity double acceptor state, Hall effect and resistivity meas., temp. and press. depend. 7-12656
- GaAs/Al_xGa_{1-x}As quantum-well bound states, valence-band offsets 7-7313
- GaAs-Al_xGa_{1-x}As quantum wells, photorefectance spectra, hydrostatic press. 7-52784
- GaAs-Al_xGa_{1-x}As superlattices, electronic and optical props., alloying and press. effects 7-64327
- GaAs-AlGaAs-GaAs heterostructure barriers, quantum tunnelling 7-52816
- GaInAs-AlInAs heterojunctions, parallel conduction, quantum Hall effect, hydrostatic press. 7-52764
- Ga_{0.47}In_{0.53}As-InP heterojunction, with three electron subbands, hydrostatic press. effect 7-2695
- n-Ga_{1-x}In_xSb:Se(S), impurity states, press. and comp. depend., Hall coeff. and elec. resist. meas. 7-2533
- GaP and GaP:N diodes, electroluminescence, high press. effects 7-27787
- GaPO₄ orthophosphate crystals, hydrothermal synthesis 7-53531
- GaSb:Se, resist. and thermoelec. power meas. at metal-insulator transition 7-45403
- GaSb_{0.4}AlSb_{0.6} quantum wells, nonparabolic behaviour under hydrostatic press. 7-64328
- Gd-Co, amorphous, influence of hydrogenation or mag. props. 7-2899
- Gd₂In, mag. transitions under press. 7-59013
- Ge, n-type and ultrapure samples, electron transport and press. coeffs. 7-2615
- Ge, uniaxially stressed, internal strain parameters, surface effects 7-44980
- Ge₂₀Sn₈₀Bi_x, amorphous, electronic cond. props. under high press. 7-45328
- H₂, dynamic isentropic loading, high press. eqn. of state, computational simulations 7-32747
- HF solid, elastic and photoelastic anisotropy at high press. 7-2083
- Hf-Mo-N, phase equilibria between high melting nitrides and refractory binder metals 7-28018
- HgCdTe, 0⁻ giant oscillation near semimetal-semiconductor transition 7-64053
- HgCdTe:B, bulk and thin film, resonant impurity levels, magneto-transport studies 7-64162
- InAs-GaSb superlattice, band offset press. depend., magneto-optical studies 7-38698
- InAs-GaSb superlattices, band line-up under hydrostatic press. 7-52782
- InSb bicrystals, n-inversion layers, pressure dependence electron states 7-45468
- InSb, carrier lifetime, pressure depend. 7-52644
- K, compression and polymorphism, up to 400 kbar 7-32632
- KCl, minerals, shock induced radiation 7-27694
- KCl(Br)(I), luminescence quenching in *F* centers under pressure 7-22334
- KH₂PO₄, hydrostatic pressure effect on ferroelectric relaxational mode, light scatt. study 7-2971
- K₂OsCl₆, mode softening and phase transition, press. depend., NQR study 7-26896
- K₂SO₄-Cr(SO₄)₃.24H₂O, alum, optical spectra, press. shifts 7-64666
- La-Ba-Cu-O system, superconducting transition above 4 K, high press. 7-58946
- LaMgAl₁₁O₁₉, elastic and anharmonic props., acoustic meas. 7-44706
- LiF, minerals, shock induced radiation 7-27694
- Lu₂Ir₂Si₁₀, superconducting, electronic phase transition and partially gapped Fermi surface 7-12902
- MF₂ type fluorides, stability under high pressure (*French*) 7-63568

high-pressure effects in solids continued

- MMF₄ type fluorides, stability under high pressure (*French*) 7-63568
- Mg-based amorphous alloys, elec. resist., press. depend. 7-7199
- MgAl₂O₄ spinel, high press. cryst. chemistry 7-16521
- MgO, minerals, shock induced radiation 7-27694
- MgO, thermal cond. and heat capacity obs., hydrostatic pressure dependence 7-306
- X-Mn, Neel temp. and thermal expansion press. depend., strain gauge meas. 7-6724
- Mn_{0.615}Cr_{0.385}As, press.-induced helimagnetic-ferromagnetic transition 7-52984
- Mn_{1-x}Ni_xAs, structural and magnetic phase diagrams 7-6784
- Mo, creep, stress factors (*Russian*) 7-33750
- Mo, polygonisation under high press. (*Russian*) 7-51939
- NaCl, minerals, shock induced radiation 7-27694
- Nb films, superconducting, synthesis under Mbar dynamic pressures 7-2757
- NbSe₃-I-Pb, tunnel junctions under press. 7-52594
- Ni, electrical resistivity, high temp. and press. 7-38534
- Ni, Fermi surface change near the mag. transition 7-16935
- Ni powder, ultradisperse, recrystallisation inhibition at high press. (*Russian*) 7-59481
- Ni-based alloys, magnetic props. under high press., effects on s and d band electrons 7-7542
- Ni₂MnM (M=Al,Ga,In,Sb), Heusler alloys, Curie temp., effect of hydrostatic press. 7-64455
- NpAl₂, high press. studies 7-16689
- O₂ transport in dry rocks, exptl. study 7-54954
- P, high-pressure superconductivity studies 7-38799
- Pb, self-consistent relativistic band struct., normal and high press. 7-52413
- Pb₄₇Ba_{0.3}Ge₃O₁₁, rhombohedral, acoustic symmetry and vibr. anharmonicity 7-16695
- PbBi₄Te₇, synthesis and physicochemical props. 7-13349
- Pb₂Ge₂O₁₁, high pressure Raman scatt., phonon modes and Gruneisen parameters 7-33391
- Pb₂Ge₂O₁₁, rhombohedral, acoustic symmetry, and vibr. anharmonicity 7-16695
- PbSe and other IV-VI cpds., acoustic mode vibr. anharmonicity 7-63751
- PbTiO₃, spontaneous strain, anomalous press. depend. 7-26833
- PtMnGa, Curie temp., hydrostatic press. effect 7-27527
- RbCl:Ag⁺, hydrostatic press. depend. of tunnelling splitting 7-64590
- Rb_{1-x}(NH₄)_xH₂PO₄, press. depend. of proton glass freezing, dielec. props. 7-2209
- ReO₃, bridging angle, high press. EXAFS studies 7-64781
- Ru, electronic, structural and cohesive props., theoretical study 7-37922
- α -S orthorhombic, elastic behaviour under pressure, lattice dynamics anal. 7-16667
- Sb, muon Knight shift press. depend. meas. and mol. cluster calcs. 7-45890
- SbCl₂, intercalated graphite, stage 2, basal plane resistivity and phase diagram 7-45258
- Se, amorphous, elec. resist. and Hugoniot shock wave vel. meas. 7-32567
- Si, crystal data for high-press. phases 7-16486
- Si, superconducting transition temp., press. depend. 7-33121
- Si, total energy and superconductivity, pseudopotential method 7-32358
- Si, uniaxially stressed, internal strain parameters, surface effects 7-44980
- Si:B, implant redistribution during high pressure oxidation, SIMS and C-V meas. 7-27020
- Si-P, dopant redistribution during high pressure oxidation, four-point probe meas. 7-27020
- SiC, high-press. self-combustion sintering from fine mixed powders of Si and C (*Japanese*) 7-3249
- Si₃N₄ powders, high press. not pressing, mech. props., thermal cond. temp. depend. 7-3231
- SiO₂, fused, frequency dependent equation of state 7-51987
- SiO₂, minerals, shock induced radiation 7-27694
- SiO₂-CaO-MgO-Na₂O glass, frequency dependent equation of state 7-51987
- Sm, phase transitions at high pressures 7-64457
- SmSe, high press. EXAFS studies at 77 K 7-64799
- SmSe, thermoelec. power, elec. resist., meas. near semiconductor-metal transition, press. up to 12 GPa 7-45404
- TaSe₃, orthorhombic, press. and field depend. of DC resistance 7-52592
- TaSe₃, transport props., uniaxial stress effect 7-38801
- Te (0001), conductivity of size-quantised holes, hydrostatic pressure effects 7-45428
- Te superconducting films at high press. 7-33120
- ThC powders, structural stability, eqn. of state, press. up to 36 GPa 7-16688
- Ti-Mo(W)-N, phase equilibria between high melting nitrides and refractory binder metals 7-28018
- TiNi alloy, amorphisation by high press. shear deform. (*Russian*) 7-8053
- U alloys, high press. magnetic and superconducting props., review 7-12952
- U-Nb-Zr (7.5, 2.5 wt.%), SCC in gaseous O₂ and H₂ (*French*) 7-17619
- UBe₁₃, elec. resist., Press. and mag. field effects 7-45562
- UPt₃ Kondo lattice, low-temp. sp. ht., suscept. and resist. meas., press. depend. anal. 7-7220
- UPt₃, superconductivity, one-component Fermi liquid theory 7-22066
- URu₂Si₂, heavy electron system, competing electronic correlations, press. effect 7-45539
- (U_{1-x}Th_x)Be₁₃, superconductivity under pressure 7-12903
- WC, high press. sintering, microstruct. 7-39470
- WC-Co, high press, sintering, microstruct. 7-39470
- Xe, solid, luminescence of trapped excitons, press. effects 7-64690
- Y electronic struct., electron-phonon matrix and superconductivity, high press. effects, KKR calcs. 7-21805
- Y, pressure-induced superconductivity, band struct. and sp. ht. press. depend. calcs. 7-7431
- ZN single crystals, creep, dislocation struct., high press. effect (*Russian*) 7-59578
- Zn, amplitude-dependent internal friction, press. depend. (*Russian*) 7-58409
- ZnTiF₆.6H₂O:Mn²⁺, ESR spectrum, axial press. effects 7-22136
- Zr-Mo-N, phase equilibria between high melting nitrides and refractory binder metals 7-28018
- ZrO₂, high press. phase, cryst. struct. 7-16523

high-pressure phenomena and effects

- see also *high-pressure effects in solids*
 alcohol-water mixture, volumetric behaviour, high press. study 7-51904
 alkali metal binary alloys, low temp. phase diagram, compression effects 7-33641
 anthracene in benzene, fluorescence spectral shifts, laser-driven shock compression 7-27781
 binary fluid mixtures, eqn. of state, high temp. and high press. 7-21385
 brine-saturated fractured rock, elec. cond. for various confirming press. 7-29002
 bromotrifluoromethane, liq. and gaseous phases, compression factor, vapour press. meas. 7-51905
 caesium perfluoro-octanoate, lyotropic liq. cryst., press. depend. of nematic-isotropic transition 7-32647
 chlorocyclohexane, conformational enthalpy and vol. changes, Raman spectroscopy determ. 7-62383
 diethyl fumarate, polymerisation rates at high pressures 7-39889
 dimethyl sulphoxide, dendritic solidification and surface-press.-induced wetting transition in narrow gaps 7-27223
 DPPC bilayers, aqueous assemblies, high press. IR studies 7-54501
 ethanol, aq. solns., viscosity, high press. effect 7-52102
 trans-ethyl cinnamate, polymerisation rates at high pressures 7-39889
 fluid under high pressure, FTIR spectra interpret. 7-50402
 fused silica, laser-driven shock wave dynamics study 7-44691
 gases, supercontinuum generation with femtosecond pulses 7-25908
 glycerol, fluorescence spectral shifts, laser-driven shock compression 7-27781
 granite, stick slip and shear fracture energy at elevated press. 7-47427
 hydrocarbon systems, gas and liq. phase, in situ modelling using FTIR at high press. 7-54221
 liquids, thermal expansion and heat capacity at high pressure 7-6818
 lyotropic liq. crystals, high press. phase diagrams, re-entrant phenomenon obs. 7-12270
 methanol, aq. solns., viscosity, high press. effect 7-52102
 methanol, compressed gas and liq. PVT props. meas., pseudoisochores determ. 7-16713
 methyl alcohol, ^{13}C NMR chem. shifts, intermol. interactions effects 7-50193
 2-methyl-2-propanol, aq. solns., viscosity, high press. effect 7-52102
 microscopic system, high press. effects, P,T thermodynamic description 7-48655
 microscopic system, high press. effects, P,T thermodynamic description, appls. 7-48656
 nematic liquid crystals, Frank constants, effects of compression 7-63702
 nematic liquid crystals, rotational viscosity under high press. 7-32695
 n-pentane, vol. ratios, compressibilities, 278-338K, pressures up to 280 MPa 7-51906
 peridotite, melting phase relations up to 14 GPa rel. to origin of peridotitic upper mantle 7-8937
 polyethylene, dilation by sorption of CO_2 7-12469
 polyethylene, radiation effects at high press. 7-21260
 polymers, macromolecular dynamics, hydrostatic press. effects (*Russian*) 7-16690
 2-propanol, aq. solns., viscosity, high press. effect 7-52102
 pyrope ($\text{Mg}_3\text{Al}_2\text{Si}_3\text{O}_{12}$), melting up to 10 GPa rel. to press.-induced struct. change in pyrope melt 7-8936
 rock salt form Gulf Coast domes, uniaxial and triaxial mechanical expts. 7-47428
 rocks, elastic props. at high temp. and press., laboratory anal., lithosphere appl. 7-55015
 rocks, stress-strain state at high press., appl. of nonlinear heredity models 7-55021
 ruby, R. fluoresc. line lifetime meas., high press. conditions, modulation fluorometry technique 7-22307
 supercritical water, vel. of sound meas. at high temp. and press. 7-16691
 AgNO_3 , electrical resistance effects accompanying high pressure and temperature melting and decomposition 7-16719
 Al alloy, binary, alloying capacity for solid soln. obtained by casting under press. 7-53716
 Ar gas, surface-wave discharges, wave propagation and diagnostics 7-63390
 CS_2 liquid, time-resolved IR spectral photography of shock-induced chemistry 7-27727
 CS_2 , shocked liquid, absorpt. spectra 7-27743
 CaF_2 , powder compacts, shock wave effects 7-51936
 $\text{Co}(\text{NO}_3)_2 \cdot 6\text{H}_2\text{O}$, electrical resistance effects accompanying high pressure and temperature melting and decomposition 7-16719
 Csl, Hugoniot overtake sound-rel. meas. 7-44705
 Cu-Su, amorphous system, high press. melt quenching, microhardness, X-ray obs. (*Russian*) 7-44396
 Fe, high-press. melting curve, implications for temps. in Earth's outer core 7-23614
 Fe- H_2O reaction under high pressure, implications for evolution of Earth 7-8887
 Ga, solid and liquid, high press. phase transitions, EMF pulse study (*Russian*) 7-2166
 H_2O , shocked water, temp. meas. using fluorescence probe thermometer 7-24653
 $^4\text{H}_2$, liq. and solid, elastic props., and density up to 20 GPa 7-32733
 He- H_2 system, density inversions between fluid and solid phases at high pressures 7-58451
 Hg arc discharge, high-pressure, heat transport obs. 7-21009
 Hg, solid and liquid, high press. phase transitions, EMF pulse study (*Russian*) 7-2166
 K, vapour, density meas. 1500-2100K, 1.4-4.0 MPa 7-51371
 KTiOPO_4 , solubility in KF aq. soln., high temp. and press., hygrothermal growth 7-58482
 LiCsSO_4 , dielec. props., press. effect 7-64555
 MoS_2 , high press. synthesis, characterisation 7-26716
 N_2 fluid, high temp. and press. vibrational spectra, CARS study 7-53326
 PLZT hot pressed ceramic, polarisation reversal studies under hydrostatic press. 7-59160
 Rb vapour, density meas. 1450-2000K, 1.7-5.2 MPa 7-51371
 Se-Te liquid mixtures, mass density at high temp. and press. 7-63701

high-pressure solid-state phase transformations

- AB_2N compounds, press.-induced phase transitions 7-52039
 2-adamantanone, order-disorder phase transition, high press. effect, Raman study 7-38183
 apatite, decomposition to dense polymorph of $\text{Ca}_3(\text{PO}_4)_2$ under high press. and temp. conditions 7-44796

high-pressure solid-state phase transformations continued

- β -(BEDT-TTF) $_2\text{I}_3$, conductor, thermal expansion and structural phase transitions 7-44870
 binary crystals, structural stability, chem. trends 7-21153
 crystalline materials, press.-induced first-order phase transition, nearest-neighbour distance changes calcs. 7-7623
 diamond, high pressure phase transitions total energy methods 7-63802
 Earth mantle, effects of chemical and phase transitions on intermediate mantle struct. (*Russian*) 7-66038
 Group IA hydrides, high-press. phase transitions 7-21438
 Group IIIA hydrides, high-press. phase transitions 7-21438
 Group IVA hydrides, high-press. phase transitions 7-21438
 ice clathrate containing tetrahydrofuran molecules, transformation on compression at 77 K 7-37862
 PMMA, glass transition, high press. (*Russian*) 7-63821
 polyphenyls, phase transitions and IR spectra under press. 7-6725
 squaric acid, press. depend. of cryst. struct. 7-32417
 static high pressure research, review 7-21350
 thermotropic polyester, press.-induced enantiotropic transition at room temp. 7-1916
 (TMTSF) $_2\text{ClO}_4$, conductor, thermal expansion and structural phase transitions 7-44870
 (TMTSF) $_2\text{ReO}_4$, organic supercond., anion-ordering phase diagram studies 7-21434
 transition metal cpds., high press. metal-insulator insulator transition, extended Hubbard model calcs. (*Russian*) 7-32917
 vinylidene-trifluoroethylene copolymer, ferroelec. phase transition, X-ray diffr. investig. 7-53249
 zinc-blende semiconductors, high pressure phase transitions total energy methods 7-63802
 Ag-rare earth alloys, press.-induced structural transitions and mag. props. 7-7542
 Al-Mn, pressure induced quasi-crystal to crystal transition for melt span alloys 7-16726
 AlAs-GaAs superlattices, phase transitions under high press. 7-64016
 BN, wurtzite, sintered polycryst., texture form. during hot compacting at high press., sphalerite transition 7-53685
 BN, wurtzite-like, deformation and high-press. phase transitions 7-44804
 BN, wurtzite-type and zincblende-type, struct. changes by shock treatments 7-22676
 BaF_2 , phase transitions, influence of shear deformation 7-21429
 Bi, high press. phase transitions, EMF pulse study (*Russian*) 7-2166
 Bi, phase diagrams, appl. for online press. and temp. calibration 7-4853
 CaTiO_3 (perovskite), high press. phase transformations and isothermal compressibility 7-14269
 $\text{Cd}_{1-x}\text{Mn}_x\text{Te}$, semimagnetic semiconductor, optical absorpt. edge, press. dependence (*Chinese*) 7-39139
 $\text{Cd}_2\text{Nb}_2\text{O}_7$ ceramic, high press. phase transition and dielec. props. 7-2177
 Ce-Sc (B at.%), γ to α transition, EMF generation, press. depend. near crit. point (*Russian*) 7-53723
 CeSc alloys, gamma to alpha transform., press. and alloying effects (*Russian*) 7-12257
 Cr-Ge dilute alloys, elec. resist. temp. and press. depend. studies 7-32980
 Cs high press. phase, β -Sn-type struct., pseudopot. perturbation calcs. 7-51938
 Csl, press. induced structural instability, ab initio pseudopotential techniques 7-52042
 Cu-Pt (48.1 at.%), elec. resist. var. during ordering under press. (*Russian*) 7-33810
 Cu-Zr, amorphisation under action of high press. and shear deform. (*Russian*) 7-58163
 CuBr, X-ray absorption study at higher press. 7-17362
 Cu_2HgI_4 , order-disorder transition, differential scanning calorimetry, high-press. phase diagrams 7-58463
 Cu_2MnAl , high press. phase transition, elec. resist., saturation magnetisation, lattice parameters (*Russian*) 7-46457
 Fe, phase diagram and Earth interior conditions 7-38179
 Fe, phase diagrams, appl. for online press. and temp. calibration 7-4853
 Fe, positron annihilation, high press. Doppler broadening expts. in diamond anvil 7-46189
 Fe-Ni-P-C, amorphisation under action of high press. and shear deform. (*Russian*) 7-58163
 FeO, high-press, metallisation obs. and implications for Earth's core 7-66101
 $\alpha\text{-Fe}_2\text{O}_3$ powder compacts, shock-modified, Morin transition, Mossbauer and magnetisation studies 7-2852
 Ga, solid and liquid, high press. phase transitions, EMF pulse study (*Russian*) 7-2166
 GaP, thermo-EMF of high press. phase 7-38604
 $\text{GaS}_2\text{Se}_{1-x}$ crystals, phase transitions under press., exciton-phonon interaction 7-44785
 GaSb high press. phase, β -Sn-type struct., pseudopot. perturbation calcs. 7-51938
 Ge, structural props., ab initio pseudopotential calcs. 7-44797
 He, high density props., exponential-six pot. 7-32742
 Hg phase diagrams, appl. for online press. and temp. calibration 7-4853
 Hg, solid and liquid, high press. phase transitions, EMF pulse study (*Russian*) 7-2166
 I, metallisation and struct. transform. under press. 7-44800
 I, monatomic metallic, press. induced FCC phase 7-63805
 In-Tl (23 at.%) alloy, FCC, thermodynamics of ferroelastic phase transition 7-2189
 K, compression and polymorphism, up to 400 kbar 7-32632
 KBr, martensitic character of press. induced B1-B2 phase transition 7-6789
 KSF_6 , high press. cryst. struct., Raman spectra studies 7-26860
 LiKSO_4 phase diagram, critical points determ., press. depend., differential thermal anal. 7-6780
 Li_2MoO_4 , high-press. polymorphs, calorimetric study 7-32638
 Li_2WO_4 , high-press. polymorphs, calorimetric study 7-32638
 Mg phase diagram determ., HCP to BCC transition, fusion curve calc. 7-52043
 MgGa_2O_4 - Mg_2GeO_4 system, spinelloid phases charact. 7-37946
 Mg_2SiO_4 - Fe_2SiO_4 system rel. to seismic discontinuity at 400 km and olivine in upper mantle 7-47404
 Mg_2SiO_4 - MgSiO_3 system, melting and phase relations at 20 GPa under hydrous conditions 7-8935
 MnAs, phase transitions, effect of external press. and chemical substitutions 7-63798
 MnAs, press. induced transitions 7-26941
 $\text{MnAs}_{0.8}\text{Sb}_{0.2}$, press. induced transitions 7-26941

high-pressure solid-state phase transformations continued

- N₂ crystals, molecular-to-nonmolecular transformation at high press., theory 7-21432
 NpO₂, high press. studies 7-16689
 PZT, paraelectric phase transition broadening due to coexistence of ferroelectric and antiferroelectric phases 7-45942
 Pb phase diagrams, appl. for online press. and temp. calibration 7-4853
 PbHAsO₄, ferroelec. phase transitions, proton tunnelling effect, NQR study 7-53172
 PbMg_{1/3}Nb_{2/3}O₃ ceramic, elastic moduli and diffuse ferroelec. phase transition, press. depend. 7-63717
 Pd-H system, struct. changes, phase rels. 7-22643
 PrRuO₃, perovskite phase, effects of high press. 7-2103
 Rb high press. phase, β -Sn-type struct., pseudopot. perturbation calcs. 7-51938
 RbI single cryst. high press. Brillouin scatt. meas. 7-3061
 Si 7-51938
 Si₂ HCP-FCC transition, at 78 GPa and studies to 100 GPa 7-63804
 Si, superconducting high-press. phases, occurrence and props. 7-2646
 Sm, phase transitions at high pressures 7-64457
 Sn, high press. phase transitions and compressions, in situ X-ray diffr. study 7-6722
 Sn phase diagrams, appl. for online press. and temp. calibration 7-4853
 β -Sn, superconducting high-press. phases, occurrence and props. 7-2646
 Sn-Sb system, high press. phase transitions, X-ray diffr. study 7-6779
 SrF₂, phase transitions, influence of shear deformation 7-21429
 TaSe₃, transport props., uniaxial stress effect 7-38801
 ThAl₂, press. induced AlB₂ to MgCu₂-type struct. transition 7-12263
 Ti-S system, synthesis of sulphides under high press., phase diagram 7-44791
 Ti₅₀Ni₄₇Fe₃, intermetallic cpd., martensitic transform. at high press. (*Russian*) 7-59520
 TI phase diagrams, appl. for online press. and temp. calibration 7-4853
 UC, high press. struct. study, X-ray diffr., synchrotron radiation 7-16729
 UP(Sb), bulk moduli and phase transforms., high press. X-ray diffr. study 7-12206
 Zr-Nb, high press. β - ω transformation (*Russian*) 7-16727
 ZrO₂, high press. phase, cryst. struct. 7-16523
 ZrO₂, nondestructive phase transform. of single cryst. at high press. 7-59511

high-pressure techniques

- anvil cell development for microscopy/IR spectroscopy 7-54224
 anvil-type high-pressure apparatus using prolate tetragonal anvil 7-323
 balanced puff valve for impinging gas-puff experiments 7-324
 beveled diamond anvil cells design, finite element analyses 7-41398
 chemical reaction rates meas. 7-33913
 creep rupture, high press. testing in 20 MPa H₂ atmosphere at high temp. 7-3548
 crystal growth, high temp., and phase diagram studies, high purity auto-claves 7-53511
 diamond anvil cell, Mbar pressures generation and measurement (*Japanese*) 7-18800
 diamond anvil cell for IR spectroscopy of gas and liquid 7-56300
 diamond anvils, sintered, ultrahigh pressure generation, X-ray diffraction calibration 7-18799
 diamond nucleation and growth at high press., colloidal theory 7-46301
 diamond polycrystals, synthesis using refractory metal catalysts, press. up to 13 GPa 7-53646
 diamond-anvil cell and closed-cycle refrigerator system 7-41400
 electrical conductivity meas., high pressure, in diamond anvil cells at cryogenic temp. 7-56299
 FT IR spectroscopic system, high press., with cell for catalytic reactions obs. 7-35606
 galvanomagnetic studies of organic metals, at high pressures and low temp. 7-30035
 Hall effect measurement in the diamond anvil high-pressure cell 7-30041
 hydrostatic pressure electric resistance cell, for 30 kbars (*Korean*) 7-24656
 laser-driven flyers backed by high impedance windows, vel. meas. 7-30029
 light gas gun for shock initiation studies, 63mm diameter 7-30031
 machine for tensile and compressive testing of materials with application of pressure 7-33876
 magnetic properties measurement, hydrostatic pressure, low temp. technique in mag. field (*Japanese*) 7-48790
 magnetic susceptometer, SQUID-based high pressure 7-41410
 magnetic valve for high-pressure gas injection, plasma fusion confinement 7-11683
 mechanical tests of tubular specimens, high-press. chamber 7-59716
 metallic samples, shock loaded, mass ejection meas. techniques 7-30032
 Microshell-tipped optical fibres, high-press. shock detectors 7-30030
 MuSR, high pressure, low temp. system 7-49843
 NMR in diamond anvil cell 7-56301
 peridotite melting under ultrahigh pressure 7-34481
 polymer solutions cloud points meas., using pressurised apparatus 7-9871
 rolling-ball viscometer up to 1 GPa 7-1655
 ruby, luminescent R-line emission, pressure calibration to shock wave eqn. of state of Au and Cu 7-18802
 sample transfer system for surface studies over pressure range 10⁻⁷ to 10⁶ Pa 7-61323
 sapphire anvil cell for high pressure research 7-9841
 shock wave compression, review 7-21351
 shock waves in condensed matter, conference, Spokane, WA, USA (July 1985) 7-18501
 thermal properties measurement, hydrostatic pressure, low temp. technique in mag. field (*Japanese*) 7-48790
 ultra-high pressure shock generation using UV high power lasers 7-30028
 US level sensor for liquids under high pressure 7-11235
 US measurements, high-pressure apparatus up to 8 GPa 7-14960
 X-ray diffr. data collection and processing, high press. study 7-3944
 X-ray diffraction apparatus, energy-dispersive with synchrotron source 7-18801
 Ar, refractive index meas. in diamond anvil cell 7-35534
 H, liq. and solid, cryogenic, high press. eqn. of state, laser interferometric meas. method 7-30027
 Hg, high pressure decaying arc., spectroscopic temp. meas. 7-11809
 NH₃, cryogenic, high press. shock temp. meas. 7-32566

high speed steel see tool steel**high spin states (nuclear) see nuclear collective states and giant resonances****high-temperature phenomena and effects**

- see also *refractories*
 Alloy 718, Ni-base superalloy, fatigue crack propag. under hold-time cycling, effect of grain size 7-28106
 Alloy 800 H, high temp. fatigue, damage mechanism (*German*) 7-17604
 alloys, high temp. corrosion in sulphidising/oxidising environments, review 7-39737
 alloys, solvent and solute diffusion enhancement, effect of non-random solute distrib. around vacancies 7-63868
 aluminate layers on Ti, high temp. cyclic oxidation 7-17719
 anisotropic Heisenberg chain, high temp. dynamics, moment methods study 7-12989
 apatite, decomposition to dense polymorph of Ca₃(PO₄)₂ for mantle conditions 7-44796
 binary fluid mixtures, eqn. of state, high temp. and high press. 7-21385
 ceramics, engineering, tensile strength (*Japanese*) 7-53800
 electrical and thermal conductivity investigation in solids at high temp. 7-32730
 electrodeposits for high temp. oxidation and corrosion resistance, appl. for gas turbines 7-46358
 fatigue crack growth at elevated temps., grain boundary oxidation 7-6714
 fatigue life prediction, new method, high temp. low cycle conditions 7-39797
 graphite, reactor, thermal expansion, effect of rad. 7-26804
 high temp. behaviour, coatings in high performance gas turbines 7-46694
 impurity in W, morphology and behaviour of K bubbles at varied temps. 7-2223
 Incoloy 800H, multilayer oxide scales in gas atmosphere, Ti distribution 7-53972
 Inconel X-750, Ni-base superalloy, SCC susceptibility in high-temp. water, effect of chloride 7-39729
 intermetallic phases, appl. as high temp. materials, review 7-22775
 journal bearings, numerical modelling of thermal effects 7-51004
 latt. dynamics, phonon line shapes at high temp. 7-2122
 metals, high temp. oxidation under time-dependent gas press. 7-33837
 methanol, compressed gas and liq. PVT props. meas., pseudoisochores determ. 7-16713
 Nimonic 80A, crack growth under sulphidising conditions, metallography 7-59680
 nonmetallic crystals, radiation-induced struct. changes, mechanisms and criteria 7-63651
 nontronite, effects of shock and thermal alteration on physical props., and implications for Martian surface 7-55024
 polycrystals, high temp. internal friction, rel. to grain boundary diffusion 7-63743
 polyethersulphone, temp.-dependent mech. behaviour, use as matrices for short fibre reinforced laminates 7-17620
 polyimide, temp.-dependent mech. behaviour, use as matrices for short fibre reinforced laminates 7-17620
 polymers, conducting, high temperature, synthesis reactions 7-2594
 polyvinylidene fluoride sheet evaluation for large sonar arrays 7-2986
 pressure testing at elevated temps., portable equipment 7-13689
 quasi 2D quantum wells, linear and nonlinear electrical conduction 7-64331
 rocks, elastic props. at high temp. and press., laboratory anal., lithosphere appl. 7-55015
 sialon, commercial, static fatigue and creep resist. 7-59601
 spent fuel rods, accelerated high-temperature tests under dry storage conditions 7-36153
 steel, austenitic stainless, biaxial loading, high temp. intergranular crack growth 7-53902
 steel, austenitic stainless, corrosion product release in lithiated high temp. water, mechanism and kinetics 7-65172
 steel, austenitic stainless, creep strain, resulting changes in subboundary mesh size 7-46575
 steel, austenitic stainless, high temp. sliding wear in CO₂ atm., effect of low conc. additions of O₂ 7-33806
 steel, austenitic stainless, plastic creep, laws of high temp. behaviour (*French*) 7-13523
 steel, austenitic stainless, tensile, creep and low-cycle fatigue props., effect of prestrain (*Japanese*) 7-46621
 steel, Cr-Mo, cyclic stress-strain response at elevated temps. 7-39624
 steel, Cr-Mo, elevated temp. erosion-corrosion 7-3518
 steel, Cr-Mo, erosion-corrosion, effect of temp. 7-3519
 steel, Cr-Mo, tube, fatigue crack growth at high temp. 7-59632
 steel, Cr-Mo-V, cyclic creep accel. and retardation at room and elevated temp. 7-39581
 steel, Cr-Mo-V, multistep cycling and cycling with compression hold at elevated temps. 7-13576
 steel, duplex stainless, sintered, mech. props., corrosion resist. and high temp. oxidation resist. 7-7928
 steel, ferrite, low activation, correl. of hot microhardness with elevated temp. tensile props. 7-53797
 steel, stainless, high temp. corrosion by oxidising gases (*Korean*) 7-8161
 steels, creep-fatigue cracks, high temp., strain range partitioning anal. (*Japanese*) 7-33781
 superalloys, columnar grained and single-crystal, high-temp. strength with surface recrystallised layer (*Japanese*) 7-53788
 supercritical water, vel. of sound meas. at high temp. and press. 7-16691
 transition metal cluster oxides, high-temp. multiphoton ionis. and fragmentation 7-36835
 zircaloy-4, polycryst., high temp. internal friction 7-17571
 Ag₃P₂O₇, high-press. polymorph, characterisation 7-1991
 Al alloy, high temp. creep, role of surface layer in power law breakdown 7-65089
 Al alloys, hot workability, determ. of high temp. flow stress (*Korean*) 7-28076
 Al-Ti, rapid solidification processed/mechanically alloyed, high temp. deform. 7-65100
 Al₂O₃ CVD coatings, high-temperature microhardness profiles 7-28181
 Al₂O₃:Fe,Y, high temp. DC elec. cond. rel. to superalloy oxide scale adherence 7-52615
 Al₂O₃-Cr₂O₃-ZrO₂ system, subsolidus, high temp. phase relation 7-17519
 Al₂O₃-ZrO₂ composites, high temp. behaviour and microstruct. study with HVEM (*Japanese*) 7-22819
 Au, cascade damage under heavy ion irradi. at high temp., in situ obs. 7-58368

high-temperature phenomena and effects continued

B₄C, fast neutron irradiated, thermal cond. meas. 7-6900
BaTiO₃, perovskite, TEM study of dislocations 7-38003
C fibre reinforced C composites, tensile props. and fracture toughness at high temps. up to 2400°C (*Japanese*) 7-53864
Co-Al-Fe(Ni), B2, slow plastic flow props. between 1100 and 1400 K 7-46565
Co+Cr₂O₃, wear protective dispersion coating for use at high temp. 7-46667
Cu bicrystals, fatigued at high temp., microstruct. obs. in vicinity of caviated grain boundaries 7-38019
Cu, dynamic softening during deform. at high temps. and strain rates 7-33690
Cu, single crystals, mech. instability during tension at high temps. 7-13505
Cu, single crystals, with different orientations, strain localisation during high temp. deform. 7-13506
Cu-Al₂O₃, dispersion strengthened powder alloys struct. and mech. props. 7-53667
EuXO₃, (X=Group, IV, V or IVA element), gaseous, stability 7-38224
Fe alloys, high-temp. creep, rel. between dislocation density and internal stress 7-13524
Fe, electrical resistivity, high temp. and press. 7-38534
Fe, ferromagnetic sp. ht. meas. by pulse-heating technique 7-7513
Fe/Cu microlaminate condensates, creep and struct. investig. (*Russian*) 7-33749
Fe-Al, al alloying for oxidation resist. improvement, comparison between ion implantation and laser irradiation 7-22883
Fe-Cr, high temp. oxidation, effect of various amounts of Ce and CeO₂ 7-53945
Fe-Cr, high-temp. air corrosion products, distrib. and charactn. by Raman microscopy 7-65205
Fe-Cr-Al, C solubility, influence of Ti and Nb, high-temp. oxidation resist. 7-22876
Fe-Cr-Ni-Al-Si-Mn, oxidation from 700 to 1000°C 7-65207
Fe-Mg-Si-O system, phase equilibria at high press. and temp., thermochemical data base 7-21407
Fe-CrAlY coatings, ion-implanted, oxidation behaviour 7-53974
Fe₂Mn_{1-x}S, high temp. metal-nonmetal transition 7-7117
FeO, high-press, metallisation obs. and implications for Earth's core 7-66101
Fe_{0.95}O, wustite, defect arrangement at high temps. 7-21196
Fe_{0.94}O, metallisation at elevated press. and temp., shock wave elec. resist. meas. 7-7297
Fe₂Si, near-stoichiometric high temp. creep and struct. investig. 7-22762
Fe₂SiO₄, spinels, cryst. struct. as function of temp. and heating duration 7-16522
Ge crystals, high temp. deform., fine slip band struct. (*Russian*) 7-44561
HoI₃, mass spectra, vapour press. and thermodynamic props. 7-26927
K, vapour, density meas. 1500-2100K, 1.4-4.0 MPa 7-51371
KBr films, high temp., phonon anharmonicity, IR spectra study 7-33469
K₂TiOPO₄, solubility in KF aq. soln., high temp. and press., hygrothermal growth 7-58482
KZnF₃, high temp. mean square ionic displacements 7-2259
(Mg,Fe)₂SiO₄, olivine, electrical conductivity changes due to creep at Earth mantle conditions 7-18180
MgGa₂O₄-Mg₂GeO₄ system, spineloid phases charact. 7-37946
MgO single crystals, high temp. creep and dislocation struct. at low stresses 7-21336
MgO-Cr₂O₃-ZrO₂ system, subsolidus, high temp. phase relation 7-17519
MgO-M₂O₃-ZrO₂ 7-17519
MgO-SiO₂ high-temperature composites, calcination temp. and mech. strength 7-33651
Mo, oxidation-preventing coating, high temperature, low-pressure plasma spraying 7-28182
Mo single crystals, high temp. deep following ion thermal treatment (*Russian*) 7-53813
Mo/Inconel 601 bimetallic strips, explosively welded, thermal effects (*German*) 7-27144
Mo-TiC eutectic composites, yield strength in temp. range 285 to 2270 K 7-53831
Mo₂Si₃-Mo, lowest silicide phase coating, phase changes at high temps. 7-3497
N₂ fluid, high temp. and press. vibrational spectra, CARS study 7-53326
N₂, fuse jets, high-temp., rot. relax. 7-62500
N₂, liquid, molecular dissociation and shock-induced cooling at high densities and temperatures 7-28307
NF₃, high temperature absorpt. of laser radiation 7-51385
NH₃, high temperature absorpt. of laser radiation 7-51385
Nb, BCC, thermodynamic props. 7-6828
Ni base high temp. alloys, corrosion in simulated HTGR He environments 7-17703
Ni, electrical resistivity, high temp. and press. 7-38534
Ni-base superalloy, IN 939, high Cr, effects of heat treatment on mech. props. 7-13526
Ni-base superalloy, oxidation in steam at 800°C, role of Al and Ti 7-65203
Ni-base superalloys, fatigue endurance at high temps., influence of struct. and surface oxidation 7-59626
Ni-base ternary alloys and superalloys, hot corrosion in SO₂/O₂ atm. 7-65175
Ni-base ternary alloys and superalloys, hot corrosion mechanism in SO₂/O₂ atm. 7-65176
Ni-Cr-Al (20, 12.5 wt.%), coatings containing dispersed oxides, high temp. oxidation 7-33842
NiAl, slow plastic creep props. between 1200 and 1400 K, effect of comp. and grain size 7-65084
Ni₃Al-B, elevated temp. ductility, effect of testing environment 7-39614
Ni₃Al-B, with and without Hf additions, dynamic embrittlement at 600°C 7-65112
NiMn₂O₄, elec. cond. and cation distrib. 7-33009
Ni₂SiO₄, spinels, cryst. struct. as function of temp. and heating duration 7-16522
O₂ transport in dry rocks, exptl. study 7-54954
Pb-Sn (9 wt.%), solid soln. alloy 7-8066
Pd, single crystals, high temp. elastic props. 7-63710
PdTi, enthalpy of form. by high temp. calorimetry 7-21410
Pt-Al-Cr coatings, structure and 700°C hot corrosion behaviour 7-53973
Rb vapour, density meas. 1450-2000K, 1.7-5.2 MPa 7-51371
SF₆, high temperature absorpt. of laser radiation 7-51385
Se-Te liquid mixtures, mass density at high temp. and press. 7-63701

high-temperature phenomena and effects continued

Si ribbons, dendritic web grown, high temp. mech. behaviour, strain rate and temp. depend. of yield stress 7-65099
Si-based structural ceramics, high-temp oxidation 7-39681
SiC fibres, prep. from polycarbosilane, heat treatment, Raman study 7-65062
α-SiC, static fatigue limit at elevated temps., thermodynamics 7-17629
SiC-AlN ceramics, elevated temp. creep, role of grain size 7-39584
SnSe, high temp. oxidation mechanism 7-3536
Ta-ir alloy, amorphous, rapidly solidified, high temp. oxidation 7-33841
(Ti,Mo)C, solid solution hardening of TiC by Mo 7-46498
β-Ti alloys, superplastic deform. props. 7-65092
Ti-Si, oxidation between 550 and 700°C 7-65202
TiC-Mo₂C-Ni hardmetals, high temp. strength 7-3404
TiCN, TiC and TiN CVD coatings, high-temperature microhardness profiles 7-28181
UO₂, electron emission studies using laser and conventional heating techniques 7-7810
UO₂, Frenkel disorder, estimate of enthalpy contributions 7-6618
UO₂, solid and liq., exptl. derivations of sp.ht. 7-6817
W, BCC, thermodynamic props. 7-6828
W, electron emission studies using laser and conventional heating techniques 7-7810
W grain growth, impurity effects 7-28044
W-Re alloys, annealed and sintered, elevated temp. softening, appl. for thermionic energy conversion 7-28077
ZnO films, with high elec. resistance, conductivity-controlled preparation 7-17122
ZrO₂, Y₂O₃ partially stabilised, microstruct. after ageing at high temp. 7-65061
ZrO₂-MgO-P₂O₅ system, phase equilib. at 1573K 7-28023
ZrO₂-Sc₂O₃, cubic to β martensitic transform. 7-22681

high-temperature techniques
see also pyrometers; refractories
amorphous thin films, elec. resist. meas. at high temps. (*German*) 7-33118
bolometric measurements on high temp. plasma 7-1734
compensating leads for carbide thermocouples 7-48737
compression creep equipment for low stresses 7-17751
conversion electron Mossbauer spectroscopy using high temp. proportional detector 7-48926
creep rupture, high press. testing in 20 MPa H₂ atmosphere at high temp. 7-3548
crystal growth, high temp., and phase diagram studies, high purity auto-claves 7-53511
emissivity measuring apparatus, vac. high-temp. system 7-56272
fibre optic pyrometric sensor 7-41393
heat of mixing, high temp. calorimetric meas. (*Japanese*) 7-14949
laser-heated materials, temp. distrib. meas. method 7-9837
melt, high temp., density meas. method (*Chinese*) 7-4817
oxide melts, thermal conductivity and diffusivity measurements at high temps. 7-61335
photoelectron spectrometer for vapour-phase species studies >2000K 7-35522
plastic strain-limit control in cyclic deformation testing using servohydraulic testing machine 7-28233
self-flushing optical window to prevent collection of condensates 7-1254
shock wave compression, review 7-21351
supersonic jet spectrometry with pulsed nozzle, gas chromatographic appls. 7-15005
transparent materials, spectral emissivity exam., using fast automatic system 7-4855
US cavitation, sonochemical reaction and local temp. determ. 7-3594
US high-temperature thermometer 7-313
vibrating magnetometer for magnetic moments of magnetic materials meas., temp. dependences 7-30050
MoS₂, amorphous thin films, elec. resist. meas. at high temps. (*German*) 7-33118
YB₄, enthalpy of form., high temp. calorimetric meas. 7-39909

high vacuum gauges *see vacuum gauges*

high-voltage engineering
see also high-voltage techniques
ions from high-voltage equipment 7-29234

high-voltage techniques
airgap breakdown characts. obs., under ambient conditions of reduced air density 7-20978
capacitance meas. bridge, frequency dependent errors 7-18813
compressed gas capacitors, precise capacitance meas. appl. 7-18814
DC electric field meter with fiber-optic readout 7-30040
double impulse tests of long airgaps, engineering problems 7-20974
double impulse tests of long airgaps, leader decay and reactivation 7-20975
double impulse tests of long airgaps, voltage front perturbation effects 7-20976
kilovoltmeter with optical feedback 7-30038
pulse neutral beam source, 10×40 cm, 120 kV testing 7-32008
regulator for field emission 7-30039

hip joint replacements *see prosthetics*

history
1066, September, sea state in English Channel, chroniclers' records anal. 7-29650
ancient comets and meteor showers, temporal correlations and genetic associations 7-55543
archaeoastronomy and roots of science, conference San Francisco (January 1980) 7-41019
Bauschinger effect, hundred years (*German*) 7-41046
biological electron probe X-ray microanal., current status, history 7-8782
cluster beams, history 7-15766
α Cma (Sirius), historical colour records as evidence for white-dwarf thermonuclear runaway 7-34977
colour vision standards within the transport industry, origins 7-23350
comets, history of research, book 7-24330
cosmic ray research, the early history, 1900 to 1927 7-48263
cryogenics, speculations and reminiscences 7-48266
Einstein-Podolsky-Rosen problem, consistent history anal. 7-48227
electrodynamic potential propagation, Carl Neumann vs. Rudolf Clausius 7-63
electron microscope development and electron optics 7-41049
electron microscopists, successive generations 7-41045
electron microscopy, AEI contribution in UK 7-4926

history continued

- electron microscopy, Australian historical background 7-4928
 electron microscopy, UK involvement in development 7-4925
 entropy, theory, Rudolf Clausius's contribution 7-35190
 error and its effects in scientific progress, historical discussion (*German*) 7-29652
 film role in UK TV over 50 years from 1936 7-41524
 flood frequency analysis, appl. of historical and palaeoflood information 7-23769
 flow visualisation, historical and recent developments 7-35189
 founding fathers of physics, Christian beliefs 7-60931
 U Gem, dwarf nova, evidence for prolonged quiescence and large-amplitude flickering from early obs. 7-66621
 glacier advance of Nigardsbreen, SW Norway, ^{14}C dating and palaeoenvironment 7-9037
 Harwell van de Graaff accelerator, 1950s fundamental research 7-29654
 health care technology evolution in USA, economic and ethical implications 7-4648
 heat theory principles, historically and critically elucidated, book 7-48265
 Henry Rowland and astronomical spectroscopy, conference, Baltimore, Maryland (June 1984) 7-18493
 J. Tebbutt (1834-1916) and his obs. of Halley's Comet 7-55943
 lasers, Romanian, history and state of the art 7-14747
 lasers and masers development in Poland (*Polish*) 7-15907
 liquid-mirror telescope, history of concept 7-9374
 LWRs, thermal hydraulics research, history and present status 7-29653
 Magnus effect, early investigations and question of priority, review 7-41048
 metallurgical appl. of electron microscope in Cambridge 7-4927
 Moon, acceleration (book) and motion 7-41050
 Mount Wilson Observatory 7-48264
 Pluto, planet discovery and announcement, historical account by discoverer 7-18546
 remote physiological sensing: historical perspective, theories and preliminary developments 7-34298
 Roentgen's X-ray absorpt. obs. in 1895, implications 7-24346
 SN 1408, probably spurious supernova, anal. of Chinese and Japanese obs. 7-47962
 Stephen Gray, discoverer of electrical conduction 7-41047
 telecommunication, 1650 to 1985 7-55944
 turbulence, statistical theory, history 7-9643
 underwater sound, historical perspective on sea surface loss in surface ducts and shallow water 7-66160
 Uranus satellites discovery, historical anal. for Ariel and Umbriel 7-66501
 Venus atmosphere, research history (*Russian*) 7-24042
 vibrating string controversy of mid-1700s, classical wave eqn. 7-48262
 weak interactions, evolution and history 7-18548
 zodiacal stars, Chinese names (in 4th-6th centuries) (*Chinese*) 7-24347
 ^{252}Cf , historical review of discovery and development, radiotherapy appl. 7-24348
 O_2 , discovery by Scheele, involvement in biological reactions 7-60927

HIXE see ion microprobe analysis; X-ray chemical analysis

HMO calculations

- acyclic azines, substituted, fluorescence props. 7-62444
 bis arene sandwiches, $\text{C}_6\text{R}_5\text{FeC}_6\text{R}_6$ where $\text{R}=\text{H}$ or CH_3 , and $(\text{C}_6(\text{CH}_3)_6)_2\text{Fe}^+$, hyperfine and mag. props. 7-12680
 conjugated molecules, topological spectra, HMO calcs. 7-49933
 metal-metal multiple bonding, cluster electron count and geometries, HMO calcs. 7-25410
 methyl halides, nucleophilic substitution reactions, quantum-mechanical model, HMO calcs. 7-36482
 molecular vibrational theory, comparison with Huckel MO theory 7-29636
 one-dimensional polymer, vibronic interactions, HMO calcs. 7-26878
 polycyclic aromatic hydrocarbons, periodic table, characteristic polynomial, struct. invariants 7-56924
 polydicyanoacetylene, bond alternation, Huckel model anal. 7-5602
 polydihalogenoacetylene, band alternation and soliton excitations, Huckel model anal. 7-5601
 transition metal borides, AlB_2 type, electronic struct. study, heats of formation anal., HMO calcs. 7-25409
 C_{60} , cage-like struct., HMO calcs. 7-15520
 Fe complex $[(\text{ethyl})_4\text{N}]_6[\text{Ti}_6\text{Fe}_{10}(\text{CO})_{36}]$, struct. and bonding study, HMO calcs. 7-25411
 $\text{Mo}_4\text{Cl}_8(\text{PET}_3)_4$, metal-metal multiple bonding, cluster electron count and geometries, HMO calcs. 7-25410
 $\text{Sc}_2\text{Cl}_6\text{B}(\text{N})$ infinite chain phases, single cryst. struct. studies 7-32385
 $\text{Sc}_2\text{Cl}_{12}\text{B}(\text{N})$ metal-metal bonded cluster phases, single cryst. struct. studies 7-32385
 $\text{Te}_6\text{Br}_{12}$, metal-metal multiple bonding, cluster electron count and geometries, HMO calcs. 7-25410

HMOS integrated circuits see field effect integrated circuits

H_3O^+ see hydroxonium ion

hodoscopes see cosmic ray apparatus

HOE see holographic optical elements

hole burning (optical) see optical hole burning

hole capture see hole traps

hole mobility see carrier mobility

hole theory of liquids see liquid theory

hole traps

- see also electron traps
 alumina, polycrystalline, X-ray and proton irradi., elec. cond. studies 7-33014
 amorphous semiconductors, multiple trapping, effect of defect level 7-27237
 anthracene: acridine crystals, conduction mechanism and trap levels, TSC meas. 7-27342
 anthracene single crystals, structural imperfections as triplet exciton traps, defect recovery 7-64160
 disordered solids, dispersive hopping and trapping transport, mean field theory 7-38554
 dispersive trap-controlled carrier transport, surface pot. decay, space charge effects, finite difference calcs. 7-38588
 grain boundary trap occupancy and recomb. models anal. 7-64266
 ion-implanted polymers, fractal elec. cond., current transients, percolative transition calcs. 7-2645
 metal-insulator-semicond. structs., interface state density profile determ., DLTS spectra interpretation 7-38733

hole traps continued

- MIS structure, small-signal DLTS response from insulator semiconductor interfacial traps, model anal. 7-64147
 MOS structure, gamma irradi. effects, mech. stress depend. 7-58903
 MOS structure, X-ray irradi., interface trap annealing, two-reaction model 7-58901
 MOS structure, X-ray irradi., trapped hole spatial depend., tunnelling anal. and annealing meas. 7-58902
 MOSFET, substrate hole current, oxide breakdown 7-12863
 naphthalene crystals, indole admixture trap form., thermolum. study (*Russian*) 7-22357
 nondegenerate semiconds., charged dislocation hole capture, hole thermal ionisation and free density calcs. 7-38574
 polysilicon for solar cell appls., DLTS study 7-38512
 quartz, luminescence of pure and Ge-activated samples 7-46152
 semiconductor thin films, bulk trap spectroscopy by temp.-modulated space-charge-limited current meas. 7-45338
 semiconductors, compensated, impurity photoconductivity, field and spectrum dependences, exclusion effect 7-38635
 semiconductors, cubic, photoionisation of deep acceptors, drag of holes by light 7-12754
 semiconductors, deep level carrier capture and emission press. depend. meas., lattice relax. determ. 7-21862
 semiconductors, disordered, with dispersive transport, elec. transient process 7-17074
 AgCl:I , impurity centre local electron states 7-45207
 $\text{As}_2\text{Se}_{100-x}$, vitreous chalcogenide semicond. layers, deep trapping levels, photostimulated effects (*Russian*) 7-2754
 $\alpha\text{-As}_2\text{Te}_3$ films, hole transport investigation by transient field-effect and time-of-flight methods 7-22040
 Au-TiO_2 :Nb diodes, trapping states, admittance spectra study 7-45494
 $\text{Ba}(\text{PO}_3)_2\text{-LiF}$ gamma irradiated activated glasses, optical absorpt. and ESR spectra corrls. 7-13030
 $\text{Bi}_2\text{SO}_{20}$, trapping levels, obs. using photorefractive effect 7-12639
 CdSe:Cu , deep levels investigated by photoconductivity and space-charge region capacitance techniques 7-7148
 p-CuInS_3 , strongly sublinear photocond. 7-52667
 GaAs, deep level nonradiative carrier capture press. depend. calcs. 7-12735
 p-GaAs, electron irradi.-induced trap defects, DLTS study 7-12155
 GaAs, plastically deformed, spatial distrib. of dominant electron and hole traps 7-7160
 GaAs, scanning DLTS study of deep level defects 7-21865
 GaAs, semi-insulating bulk with thin conducting layer, optical DLTS distortions calcs. 7-58766
 GaAs, vapour etching, buried interface, carrier traps 7-28213
 GaAs, variation of EL2 with As press. during heat treatment 7-58770
 GaAs-Mo Schottky diodes, elec. characts. and microstruct. study 7-22015
 GaP single crystals, anisotropic deep centres, polarised photolum. and thermolum. studies (*Russian*) 7-21867
 p-Ge, undoped, deep level defects produced by electron irradiation, annealing 7-12660
 HgCr_2Se_4 spinel magnetic semicond., electronic struct., elec. props., defects and ferromag. anisotropy 7-38857
 InGaAs/InP superlattices, effective mass filtering obs. 7-12799
 p-InP, electron irradi., atomic displacement threshold energy 7-2066
 InP, electron irradi. damage, impurity effects 7-12154
 p-InP, γ -ray irradiated low temp., nonradiative-recomb.-enhanced defect struct. transformation 7-2062
 InP:Fe, transient photoconductive response 7-52681
 InP:Mn, deep acceptor level, props. 7-21853
 $\text{K}_2\text{Cd}_2(\text{SO}_4)_3\text{Sm}$, doped and undoped, thermoluminescence 7-39191
 LiNbO_3 , pure and Mg, Fe doped crystals, photoconductivity props. studies 7-38624
 $\text{Mg}_2\text{Cd}_3\text{Se}$ single cryst. solid solns., local centres parameters determ. (*Russian*) 7-32953
 Se vitreous chalcogenide semicond. layers, deep trapping levels, photostimulated effects (*Russian*) 7-2754
 Si bicrystals and thin films, grain boundaries, electronic props. 7-7172
 Si, charged defect states at grain boundaries 7-44564
 a-Si, generation-recombination rate 7-33032
 Si, neutron-irradiated, relax. space-charge-limited current spectroscopy 7-38493
 Si, oxidation, trap generation by avalanche electron injection, HCl effects 7-3531
 Si p-amorphous/n-cryst. anisotype heterojunction characts., acceptor doping level depend. 7-7355
 Si polycrystalline layers, elec. props. and grain boundary carrier dynamics under solar illumination 7-38625
 Si, pyrogenic oxides, carrier trapping and breakdown, rel. to H_2O partial press. 7-64267
 Si, rapidly annealed with incoherent light, defect state generation 7-52504
 Si, recombination activity of dislocations 7-12733
 Si thin films, polycrystalline, elec. props. 7-33117
 Si wafers, doped by neutron transmutation, minority carrier lifetime, photocond., annealing 7-38785
 Si:B, carrier lifetime meas., capture and recombination 7-38585
 Si:C, electron irradiated, photolum. defect spectra, obs. of interstitial C 7-59253
 Si:C,O, heat-treated, photoconductivity relax., α traps 7-52677
 a-Si:H, carrier trapping and recombination, IR enhancement spectra of photoconductivity 7-33052
 a-Si:H, photoconductivity exponent for recombination at dangling bonds 7-33054
 a-Si:H, surface deep hole trap, photocurrent studies 7-45424
 a-Si:H,F films, initial carrier trapping stages observed by femtosecond spectroscopy 7-27301
 a-Si:H,P, electron lifetime, excitation energy depend. 7-45349
 a-Si:H solar cells, hydrogenated microvoids and light-induced degradation 7-54294
 Si:O, energy levels and capture cross-sections of thermal donors 7-16988
 Si:O, new donors, bound exciton recomb., photolum. study 7-22300
 Si:O, optical transition at thermal donors 7-17346
 Si:Ti, deep level transient spectroscopy, transient capacitance data anal. 7-52526
 Si:Ti, ion implanted, deep level charactn. 7-38513
 Si/SiO $_2$, ion implantation-induced interface states generation and charge trapping study 7-12874

hole traps continued

Si/SiO₂, two-step oxidation of thin gate oxides, trapping characts., hot electron effect study 7-64351
Si/SiO₂ interface, oxide trap capture cross section and tunnelling emission, DLTS study 7-12875
Si-SiO₂ interface, electrically active defects 7-33102
Si-SiO₂ MOS capacitors, defect struct. and interface state generation 7-7399
SiO₂:N ultrathin films, carrier conduction, nitriding effects obs. 7-38790
SiO₂ hot carrier trapping characts., effect of post-oxidation annealing 7-64268
SiO₂ thermal oxide films on Si substrate, ramp-voltage-stressed I-V characts. 7-17112
SiO₂:Ge, impurity charge trapping props., EPR spectra 7-27290
TiGaSe₂, electric field induced photoconductivity 7-52676
Zn_{0.25}Cd_{0.75}Se mixed crystals, electron and hole deep level traps 7-16980
ZnO:In films, microstruct., elec. and optical props., film thickness depend. study 7-16895
ZnS:Al, Cr, Fe crystals, recomb. luminesc., EPR and photocond. meas. 7-3076
ZnTeO, red cathodolum. kinetics, two-step electron capture model calcs. 7-59262

hollow cathodes see cathodes

holmium

see also nuclei with
antiferromagnetic phase transition, second order, μ SR study 7-45880
atom, ionic bombardment, continuous spectrum form. 7-42528
surface, ion sputtering, emission spectra studies 7-64853
BaFCl:Ho³⁺, charge transfer excitation and emission spectra 7-64688
CeF₃:Ho³⁺, fluorescence decay characts. of Green emission 7-7747
GaAs:Ho, electroluminescence and injection currents 7-13232
GaSb:Gd, Ho crystal grown by horizontal zone melting, precipitate identification 7-21462
Ho,Cr,Tm:YAG laser spectroscopic pumping scheme for 2 μ m band 7-36968
Ho:YAG laser, 2.1 μ m, GaAlAs laser diode array pumped 7-1182
KA(WO₄):Ho³⁺, A=Y, Gd, Lu, luminesc. kinetics, visible and UV spectra anal. 7-46144
LaF₃:Dy³⁺(Ho³⁺), surface temp. meas., fluoresc. appl. 7-19947
LiLuF₆:Ho³⁺, stimulated emission spectroscopy 7-13179
LiYF₄:Ho³⁺,Er³⁺,Tm³⁺, excited-state absorpt., energy transfer, fluoresc. study 7-22322
Lu₃Al₅O₁₂:Cr³⁺,Fm³⁺,Ho³⁺, 2 μ m stimulated emission of Ho³⁺ ions, spectral composition and kinetics 7-46073
Pt-Ho contact, mag. order destruction by cold current 7-52980
Si:Ho, neutron irradi., Hall effect, elec. cond., IR absorpt. spectra 7-51834
SiO₂-GeO₂:Ho very high-rejection optical fibre filters, design and characts. 7-15974
SrF₂:2YF₃:Ho³⁺, interionic interaction, occupation kinetics, stimulated emission 7-46072
Y₃Al₅O₁₂:Tm³⁺,Cr³⁺,Ho³⁺, 2 μ m stimulated emission of Ho³⁺ ions, spectral composition and kinetics 7-46073
YBO₃:He³⁺, nonradiative energy transfer, activator ion interactions, laser-excited luminesc. study (Russian) 7-22345
YIG:Ho³⁺, laser mag. reson. study, quasi-Ising model 7-53147
ZnS:Ho³⁺, radiative transitions and nonradiative processes (Chinese) 7-59235

holmium alloys

HoAuCu₄, cubic alloys, mag. props. 7-52936
HoCo₃, magnetocrystalline anisotropy, rare earth contribution 7-45659
Ho₂Co₁₇, intersubattice mol. field calc. 7-27511
HoCo₃Cu₂, ferrimag. cpds., mag. anisotropy, temp. depend. 7-64450
Ho₂(CoFe)₁₇ intermetallics, high field magnetisation studies 7-53038
Ho₂CoSn₂₃ cryst. struct. and mag. suscept. studies (Russian) 7-21161
Ho₂Fe₄, amorphous ribbons, mag. props. 7-33177
Ho₂Fe₁₄B alloys, magnetic anisotropy and spin reorientations 7-38855
Ho₂Fe₁₄B single crystals, mag. anisotropy and magnetisation 7-27547
Ho₂Fe₁₄B spin reorientation, NQR meas. 7-52960
HoNi amorphous ferrimag. anisotropic films, Hall voltage polarity voltage and temp. depend. studies 7-7206
Ho_{1-x}Y_xCo₃, orientational phase transitions and elec. resist. (Russian) 7-7506
NdHoDyFeB permanent magnets with zero temp. coeff. of induction 7-53047
Zn-Ho, two-phase, partial thermodynamic props., 690 to 1020K 7-7963

holmium compounds

see also holmium alloys
concentrated crystals, interionic interaction, stimulated emission 7-27744
formate dihydrate, circular dichroism meas. 7-17301
intracentre transition probabilities and luminesc. self-quenching 7-22332
CrHo₂S₇, synthesis, physicochemical props. 7-44470
Dy₂O₃-Er₂O₃-Ho₂O₃, mixtures, IR reflectance spectrum, wavelength standard 7-41330
Er_{0.187}Ho_{0.813}Rh₄B₄ re-entrant superconductor US attenuation obs. 7-2782
Er_{0.705}Ho_{0.295}Rh₄B₄ re-entrant superconductor US attenuation obs. 7-2782
Gd_{2.815}Tm_{0.17}Ho_{0.017}Sc₂Cr_{0.05}Ga_{4.95}O₁₂, laser active medium operating in 2 μ m range 7-50568
HoCl₃·3H₂O, cryst. field levels, assignment 7-27766
HoFeO₃ crystals, flux growth, secondary phase and microdiscs form. 7-13344
Ho₃Fe₂O₁₂ ferrogarnets, heat of crystallisation, scanning calorimetry obs. 7-2154
HoH₂ films, H annealing, elec. resist 7-64000
Hol₃, mass spectra, vapour press. and thermodynamic props. 7-26927
Ho(Ir_{0.7}Rh_{0.3})₄, antiferromag. superconductors, upper crit. mag. field (Russian) 7-58963
Ho₃Ir₄Si₁₃, existence and electrical props. (French) 7-17008
HoMo₆S₈ ferromagnetic supercond., coexistence phase, spin-orbit scatt. effects 7-22077
HoMo₆S₈ ferromagnetic films, supercond. props., temp. and mag. field depend. 7-45538
HoMo₆S₈, quenched superconductivity by rapid cooling to low temps. below T_{c2} 7-45545
Ho₂O₃, solids and liqs., photoacoustic spectroscopy, optical absorpt. coeffs. 7-51951
Ho₃Os₄Si₁₃, existence and electrical props. (French) 7-17008

holmium compounds continued

Ho₂S₃ films, optical parameters 7-33466
HoSi_{2-x}Si, silicide thin films, phase composition, conductance, surface morphology 7-7072
Ho₂Si₂H₂, H-D exchange, H desorption 7-28304
HoVO₄, enhanced nucl. order, nucl. orientation study 7-64550
KHo(MoO₄)₂, Ho³⁺ ground state, low temp. sp. ht., Stark components 7-44840
LiHoP₄O₁₂, Li(Ho,Y)P₄O₁₂ and Li(Ho,Er,Tm)P₄O₁₂, flux cryst. growth 7-13345
LiMo₆Li_{1-x}F₄, dilute dipolar-coupled magnet, ferromagnetism, glassiness, metastability 7-22098

holograms see holography

holographic gratings

aberration-corrected, design for use with Seya-Namioka monochromators 7-25947
associative memory using optical resonator 7-20157
asymmetric profile synthesis from double grating interferometer 7-9885
bacteriorhodopsin appl. in detection of small US vibrations by dynamic holographic method 7-57279
book, laser-induced dynamic gratings 7-9605
computer generated holograms, distortion-free, for optical element testing (Japanese) 7-10892
concave gratings, appl. in prime-focus spectrographs for Canada-France-Hawaii Telescope 7-4341
concave gratings for use with off-plane constant-deviation monochromator 7-43336
dichromated gelatin hologram recording process 7-43003
direct production and appls. 7-43346
display holograms and HOEs, image blurring 7-25752
dynamic holography of ultrashort light pulses 7-62648
dynamic resonance holography using scanning techniques 7-43019
excitation by ultrashort light pulses in nonlinear cubic media 7-10888
fabrication by tunable pulsed dye laser 7-5983
fibre optic interferometric sensor system, optically multiplexed 7-25986
glass:Eu³⁺, erasable holographic grating obs. at room temp. 7-31276
holographic grating storage, photorefractive piezoelectric cryst. boundary influence on induced field struct. 7-43344
image correlation using pulsed dynamic holography, expt. study 7-20147
interactions between gratings in holograms recorded with two object waves 7-10880
laser differentiating interferometer with hologram grating, use in mechanical vibr. meas. 7-56330
light diffraction by holographic gratings in media with photoinduced scattering 7-57277
light model recording and readout in 3D hologram 7-43010
LiNbO₃:Cu(Er)(Mg)(H), laser-induced grating characteristics 7-62746
multilayer holographic functional element in an analog-digital converter 7-62647
one-dimensional periodic holographic lattices, point spectrum 7-43006
optical erasure of sinusoidal holographic gratings in photorefractive materials, kinetics 7-10886
phase conjugation by holographic gratings in electrooptic crystals 7-37046
phase diffraction gratings, 3-dimens., effective thickness 100 μ m 7-10893
phase-modulated holography, hologram form. mechanism and appls. 7-62645
phase-shifted diffraction-grating fabrication using holographic wavefront reconstruction 7-50512
photochemical reactions, irreversible, study using grating expts. 7-10891
photochemistry, solid-state, phase-modulated holographic investig. 7-62645
photopolymer for matched spatial filtering, hologram grating recording 7-57527
photorefractive anisotropic media, holographic beam coupling 7-57273
photorefractive crystals, dynamic holographic recording process, microphotometric study 7-43005
photorefractive cubic crystals, hologram diffraction efficiency and diffracted light polaris., optical activity effect 7-43020
photorefractive materials, grating interactions 7-25948
photorefractive polymer for optical recording of waveguide gratings 7-5963
photoresist gratings on reflecting substrates interference pattern 7-1042
plane gratings for analytical instruments 7-5984
Polaform process, holographic embossing at Polaroid 7-25751
polarization grating holograms with a high diffraction efficiency 7-57278
polymer recording media, diffusion processes studied by holographic relaxometry 7-36914
polymethine dye grazing-incidence laser using holographic grating (Russian) 7-50583
production on plastic substrates, diffraction efficiency 7-43004
progress in holographic appls., conf., Cannes, France (Dec. 1985) 7-24280
reconstruction accuracy and uniformity, moire anal. 7-5859
recording techniques and appls. 7-57276
recording using laser interferometer 7-18867
reflection grating real-time holography, multistability 7-5856
reflective properties, recorded on threshold materials, num. investig. 7-43343
Schottky detectors, frequency and polarisation-selective 7-41470
semiconductor laser with transmission grating feedback, tunable narrow-band emission 7-1099
semiconductors, photoelectrochemical etching of holographic gratings 7-26051
solid-state photochemistry investig. by holographic methods 7-10890
spectrograph, small-size wide-aperture, using holographic grating 7-41483
two-dimensional optical beam switching techniques using dynamic holography 7-25755
ultrasonic wave generation with picosecond holographic grating 7-10889
unsalted diffr. gratings in phase hologram recording material DMP-128 7-25949
volume holographic gratings diffraction efficiency calc. 7-1025
volume reflection holograms with multiple gratings 7-43000
Ag halide emulsion multiple holographic transmission gratings 7-57267
BaTiO₃ photorefractive devices, effect of temp. variation 7-20368
Bi₁₂SiO₂₀ monocrystals, holographic grating recording, improvement 7-10885
Bi₁₂SiO₂₀ photorefractive crystals, hologram fixing at room temp. 7-20160

holographic gratings continued

- LiNbO₃:Fe photorefractive crystals, light-induced scattering 7-10887
- LiNbO₃, doped, holographic recording of gratings, microphotometric investig. 7-25735
- LiNbO₃, picosecond photography and four-wave mixing 7-20161
- LiNbO₃ piezoelectric photorefractive crystal, hologram writing and reconstruction 7-57268
- LiNbO₃:Fe crystals, refractive index gratings, microphotometric study 7-62649
- LiTaO₃:Cr crystal, photoinduced light scatt., noise holographic grating mechanism 7-62775
- NaCl crystals, electron-coloured, transmission and holographic props. 7-43001
- PLZT transparent ferroelec. ceramic, hologram recording energy transfer, light scatt. effects study 7-5855
- α -SiC, wedgelike sample, self-diffraction, 2D character 7-5858

holographic instruments

- see also holography*
- 3D holographic miniprojector, integrated circuits assembly and quality control appl. 7-25763
- automatic holographic particulate meas., fundamental study (*Japanese*) 7-18745
- deflection matrices, optical switching appl. 7-37206
- lensless holographic line scanner 7-25784
- point of sale hologram scanner, optical design 7-25783
- projection type holographic microscope for microcircuits assembly and QC 7-62650
- scanning system, design and commercial appl. 7-25770
- X-ray holographic microscopy using synchrotron radiation 7-41554

holographic interferometry

- 3D displacement and strain meas., automated evaluation by quasi-heterodyne holographic interferometry 7-31287
- 3D flow obs. by interferometry and image processing 7-37576
- 3D object motion meas., compensation method 7-25768
- asymmetric profile synthesis from double grating interferometer 7-9885
- automatic fringe analysis in double exposure and live fringe holographic interferometry 7-31286
- beams, vibrating, holographic and finite element studies 7-31718
- camera using photothermoplastic film 7-43016
- ceramics, parameter meas. by laser interferometry 7-9888
- combustion processes of coal particles 7-25734
- computer-aided holography, new developments 7-31285
- computer-based fringe interpretation 7-31264
- crack stress intensity factor determ. 7-43816
- crack tip propagation measurement by pulsed holographic microscopy (*Japanese*) 7-46780
- crystal growth from soln., holographic interferometry appl. to conc. distrib. and hydrodynamics 7-53526
- deformation and shape meas. 7-43817
- deformation meas. using spatial frequency modulation of holographic interferometry, moiré method (*Japanese*) 7-56218
- deformation measurement using holographic interferometry and moiré fringes 7-48685
- diffusely scatt. objects, dynamic deform. meas. by holographic moiré and speckle interferometry 7-46764
- disk, rotating bladed, vibrating anal. using holographic interferometry and laser vibrometry 7-31719
- dye laser with diffraction grating in resonator for holographic interferometry 7-43159
- elastomer, viscoelasticity meas. by electronic speckle pattern interferometry 7-33877
- electron holographic interferometry, quantitative phase anal. and magnetic field meas. appl. 7-41538
- electronic speckle pattern and holographic interferometry compared (*German*) 7-9890
- electronic speckle pattern interferometry, technique and advantages (*German*) 7-61371
- endoscopy, holographic, with gradient-index optical imaging systems and optical fibres 7-31271
- engineering meas., conf., Cannes, France (Dec. 1985) 7-29586
- engineering measurements, optical methods, review 7-30072
- fibre optic interferometer, appl. to integrated optic grating device manufacture 7-25757
- fibre optics combinations 7-25773
- film deposit assessment with hologram interferometry 7-1291
- flaw detection, high-resolution holographic techniques for visualization of surface acoustic waves 7-28251
- free-vortex nozzle, supersonic jet struct. study using pulse holographic interferometry 7-51256
- fringe pattern analysis, holographic-moiré technique 7-20164
- fringe pattern analysis using holographic interferometry 7-15817
- glasses, optical, holographic interferometry of instantaneous deform. (*Chinese*) 7-57611
- graphite fibre reinforced epoxy laminates, holographic interferometry analysis of bending rigidity loss 7-59733
- graphite fibre reinforced epoxy laminates, holographic investigation of stressing techniques for detecting flaws 7-59732
- grating spacing error testing using holographic interferometry 7-37216
- heterodyne, write/readout system 7-20163
- holospecklegram orthogonal polarisation props. 7-24695
- image differentiation using an optical filter (*Japanese*) 7-5843
- in-plane strain anal. by reflection holography (*Polish*) 7-43818
- IR holographic interferometry, displacement meas. appl. 7-10882
- IR interferometers at 10 μ m 7-35582
- laminate, holographic investigation of stressing techniques for detecting flaws 7-59732
- laser hardening of instrument parts, holographic evaluation 7-5857
- local deformations, reflection-hologram interferometry 7-41457
- macromolecular diffusion coeffs. meas. using holographic interferometry, digital image processing 7-31272
- market trends, embossed holograms, opt. elements and NDT systems 7-25742
- materials testing by holographic contouring 7-31283
- medical device industry, holographic testing appls. 7-40366
- minute spatial displacement field determ. from multiple interferometric holograms, fast algorithm (*Chinese*) 7-56215
- MOCVD reactor cell, visualisation of flow and temp. profiles, appl. of holographic interferometry 7-22532
- NDT, conf., Los Angeles, CA, USA (Jan. 1986) 7-35090
- NDT by real-time holographic interferometry 7-28239

holographic interferometry continued

- nondestructive evaluation methods, holography and shearography comparison 7-39836
- optical methods in composites, conf., Keystone, USA (Nov. 86) 7-55894
- optical NDT in China 7-30075
- optical nondestructive evaluation at the National Bureau of Standards 7-39835
- particle velocity and displacement distrib. from double-exposure holograms using opt. and digital processing 7-31277
- phase measurement system for optical element testing 7-57270
- phase shifting holographic interferometry 7-31288
- phase-shifting, stroboscopic, appl. to vibration meas. 7-41449
- photorefractive crystals., uses in holographic vibrometry 7-43819
- plasma, holographic interferometric determ. of electron density distrib. in race track plasma 7-11707
- plasma diagnostics, holographic interferometry appls. 7-58066
- plate with jet impingement, holographic visualisation of pressure distrib. 7-37569
- plates, flat, clamped, expt. eigenvalues and mode shapes 7-63035
- plates, flat clamped, vibration, eigenvalues and mode shapes 7-31670
- production line NDT appls., holographic and visual inspection methods 7-39837
- pulsed holographic interferometry, NDT appls. 7-39838
- real-time moiré holography 7-24696
- residual stress determination through combined use of holographic interferometry and blind-hole drilling 7-63087
- sandwich holography appl. to stress anal. of paintings on canvas 7-31284
- sandwich holospeckle interferometry for 3D displacement determination 7-50519
- shearing interferometry, high angular resolution 7-47717
- shock waves initiated by gigawatt CO₂ laser pulse in transparent target 7-38052
- skull, dry, initial tooth and bone displacements, optical laser techniques meas. 7-65796
- small components, load-deflection characts., hologram interferometry 7-35587
- specimen magnetic structure and thickness distrib., holographic interference electron microscopy appl. 7-5860
- structural ceramics, flaw detection, holographic interferometry techniques 7-46760
- surface contouring by electronic speckle pattern interferometry 7-29971
- systems with HOE and optical fibres 7-25772
- tomography and interferometry, regularisation, expt. errors and accuracy 7-35583
- triple-exposure heterodyne, optical path difference meas. sensitivity and nonlinearity 7-9882
- velocity field visualisation by single exposure holospeckle interferometry 7-50518
- vibration measurement using phase-shifting speckle-pattern interferometry 7-35576
- vibration measurement using phase-shifting time-average holographic interferometry 7-35575
- wind tunnels research appl., alignment and photographic problems 7-18872
- Al alloy plates, crack opening after discontinuous growth, laser interferometry studies (*Russian*) 7-46604
- Al, heterogeneous shock wave response, holographic interferometry studies 7-32571
- Co₂-N₂-He laser mixture, beam-driven discharge, gasdynamic processes 7-50538
- LiNbO₃, heterogeneous shock wave response, holographic interferometry studies 7-32571
- Nd-glass laser, double-pulse, use in holographic interferometry 7-15829
- Se X-ray laser targets, hydrodynamic aspects, four-frame holographic interferometry 7-20208
- Si pressure sensor diaphragm, displacement and slope analysis, holospeckle-shearing interferometry 7-29972

holographic lenses *see* holographic optical elements; lenses**holographic optical elements**

- see also holographic gratings*
- 3D holographic miniprojector, integrated circuits assembly and quality control appl. 7-25763
- aberration coefficients of curved holographic optical elements 7-36887
- achromatic combinations of holographic and refractive optical elements 7-50716
- achromatic single-component kinoform objective, with circular aberration coeff. 7-25737
- chronophotography, light beam superfast scanning 7-48898
- construction optics, design considerations 7-50715
- correlator, signal parameters, medium nonlinearity and filter spatial limitations effect 7-50514
- correlator for pattern recognition using Fresnel holographic filter and extended source 7-62633
- cylindrical kinoform lenses for monochromatic light, effect of fabrication errors 7-25923
- deflecting focusing kinoform for lasers 7-25736
- design innovations 7-50674
- dichromated gelatin achromatic reflection display holograms 7-25750
- dichromated gelatin and light sensitivity for holographic purposes 7-25741
- dichromated gelatin transmission HOEs, reflective and refractive optics 7-25748
- display holograms and HOEs, image blurring 7-25752
- head-up displays, holographic diffractive optics progress 7-25749
- Holocoupler-Selfoc fibre system, coherent transfer matrix description 7-26016
- holographic lenses, on-axis, coupled-wave anal. 7-5839
- holographic solar concentrators development 7-50517
- image lens, optimal design 7-43007
- industrial appls. in display systems 7-25753
- kinoform lens fabrication errors, effect on pupil function 7-25739
- kinoforms phase structure synthesis 7-25738
- lens design, conf., Cherry Hill, USA (June 1985) 7-48161
- lens for laser beam expansion, design 7-62812
- lensless holographic line scanner 7-25784
- long focus objective, holographic method of testing, optimum conditions calc. 7-57512
- market trends, embossed holograms, opt. elements and NDT systems 7-25742

holographic optical elements continued

- multimode fibre, 1D image transmission, holographic optical elements 7-62836
- off-axis HOE based on phase conjugation 7-50515
- optimised, design 7-43007
- Polaform process, holographic embossing at Polaroid 7-25751
- polyvinyl carbazole material for HOEs 7-25745
- powered reflection HOE, analysis and construction 7-25747
- progress in holographic appls., conf., Cannes, France (Dec. 1985) 7-24280
- projection type holographic microscope for microcircuits assembly and QC 7-62650
- pseudocolors formed by 3D elements, intensity anal. 7-36915
- recording techniques and appls. 7-57276
- satellite datalink using hologram laser beam corrector-collimator 7-25754
- solar concentrator, feasibility and basic principles 7-46919
- systems with optical fibres 7-25772
- transform performance using holographic lenses, theory 7-10868
- wavelength multi-demultiplexer in near IR 7-25756
- wavelengths demultiplexer for optical fibre communications 7-25774
- wide angle distortion free holographic head-up display 7-25766

holographic storage

- associative memory using phase-conjugate resonator 7-25733
- electro-optic materials for data storage and processing 7-43021
- imaging props. of static and Doppler 3D holograms 7-50510
- multilayer holographic functional element in an analog-digital converter 7-62647
- neural networks and optical resonators 7-54512
- nonlinear optical associative memories using thresholding devices and volume hologram 7-57408
- storage capacity of holographic associative memories 7-42986
- Bi₂GeO₂₀ Czochralski-grown crystals., comp. anal., holographic storage props., stoichiometry depend. 7-63837

holography

- see also acoustic holography; computer-generated holography; holographic gratings; holographic instruments; holographic interferometry; holographic optical elements; holographic storage; microwave holography
- 3D representation of characters, graphics and pictures (*German*) 7-5861
- acoustic signals, holographic matched filtering, membrane modulator appl. 7-43541
- acousto-optical devices, holographic filtering use 7-20409
- aperture-limited in-line far-field hologram, nonlinearities 7-36911
- associative memories based on photorefractive oscillations 7-20154
- automated holographic mass production 7-25778
- automatic holographic particulate meas., fundamental study (*Japanese*) 7-18745
- bacteriorhodopsin-biochrome films, reversible media for optical recording 7-57495
- bovine serum albumin, photoinduced ionisation by holographic relax. method 7-14046
- bubble chamber, neutrino detection, holographic recording techniques 7-25321
- bubble chamber recording, Q-switched ruby laser pulse stretching 7-43169
- calibration of cloud physics instrumentation 7-23897
- camphorquinone, mass diffusion in polystyrene studied by holographic relax. studies 7-21529
- cinematography, single and double exposure recording 7-25767
- colour hologram recording 7-36912
- colour reflection hologram recording and reconstruction 7-25781
- computing appls. (*French*) 7-57274
- copying lenses, requirements for use in devices for information entry by holography 7-20383
- copying using incoherent light 7-25759
- CW pulse transfer for high security holograms 7-25761
- degenerate holographic four-wave mixing as Sturm-Liouville problem 7-43251
- demonstration in high school science classroom 7-24342
- device for recording rectilinear discharge propag. on a surface, lighting simulation 7-26575
- dichromated gelatin achromatic reflection display holograms 7-25750
- dichromated gelatin and light sensitivity for holographic purposes 7-25741
- diffusely scattering objects image contrast, prod. by thick-layer transmission phase holograms 7-36921
- digital image recovery from shifted phase holograms 7-57254
- display holograms and HOEs, image blurring 7-25752
- dynamic hologram writing, nonsymmetric beam interactions, nonstationary energy exchange obs. (*Russian*) 7-31289
- dynamic resonance holography using scanning techniques 7-43019
- echo holograms, with 3-pulse excitation of resonant media, form. 7-57281
- education, single beam projects 7-24345
- electric-optic crystals with bipolar conductivity, holographic gains 7-20162
- electron holography approaching atomic resolution 7-43018
- endoscope for optical fibre holography 7-25769
- engineering measurements, optical methods, review 7-30072
- far-field in-line holography, nonblocked zero-freq. filtering 7-36917
- fibre optic sensors, extrinsic, for remote meas., impact on meas. techniques 7-11154
- fibre optic sensors for remote measurement 7-43394
- fibre optics combinations 7-25773
- fibres, multimode, polaris.-modulated signals transmission and holographic multiplexing 7-37199
- Fourier phases, signal processing 7-57275
- fractal aggregates, imaging, in-line holograms, digital decoding 7-10884
- Fresnel holograms, in-line, phase retrieval and twin-image elimination 7-43008
- high luminosity system for recording long distance objects 7-25760
- high spatial resolution track chambers, holographic data systems 7-36382
- high-speed photography, videography and photonics, conf., San Diego, CA, USA (Aug. 1985) 7-18486
- hologrammetry for automatic inspection in hostile environments 7-31280
- image correlation using pulsed dynamic holography, expt. study 7-20147
- image recording using computer control 7-25758
- image-plane holography of astigmatic system (*Chinese*) 7-5854
- IR objective testing, holographic method using graphitised photographic emulsions 7-57513

holography continued

- iridescent holograms of false-colour images, recording and copying 7-50516
- light model recording and readout in 3D hologram 7-43010
- long focus objective, holographic method of testing, optimum conditions calc. 7-57512
- market trends, embossed holograms, opt. elements and NDT systems 7-25742
- materials testing, optical techniques 7-33897
- measurement, influence of holography 7-43009
- multichannel optoelectronic processor with correlation-function processing 7-25740
- multiphase flow visualisation study, holography appl. 7-51287
- NDT, conf., Los Angeles, CA, USA (Jan. 1986) 7-35090
- nonlinear optics, conf., Los Angeles, CA, USA (1986) 7-18488
- one-step rainbow holography, limitations 7-10883
- one-step white light in-line holography of 2-D transparencies 7-31270
- Orsay optical klystron, goals 7-31231
- partially coherent holography, props. and appls. 7-62646
- particle sizing and spray analysis, conf., San Diego, USA (Aug. 1985) 7-29583
- particulate analysis, filtering effects in far-field in-line holography and diff. pattern analysis 7-31279
- particulates in three-dimensional sample, coherent imaging, meas. accuracy 7-31278
- phase holograms, 1D nonlinear representation, space transform. 7-43011
- phase inhomogeneity visualisation in holographic method (*Russian*) 7-16375
- phase measurements with image holography 7-25782
- phase media with absorption holographic analysis 7-50513
- photorefractive anisotropic media, holographic beam coupling 7-57273
- photorefractive cubic crystals, hologram diffraction efficiency and diffracted light polaris., optical activity effect 7-43020
- point of sale hologram scanner, optical design 7-25783
- Polaform process, holographic embossing at Polaroid 7-25751
- poly-N-vinylcarbazole as holographic recording material 7-25746
- polyvinyl carbazole material for HOEs 7-25745
- practical appls., conf., Los Angeles, CA, USA (Jan. 1986) 7-24281
- progress in holographic appls., conf., Cannes, France (Dec. 1985) 7-24280
- pulsed holographic art practice 7-25777
- rainbow hologram prod., 2D transparency (*Chinese*) 7-57271
- rainbow holography, one-step using spherical mirror 7-10881
- rainbow holography with a multimode laser source 7-25764
- real-time optical image subtraction based on wave polarization 7-57260
- recording features on two-layer photographic material 7-43015
- recording materials used in holography, general review 7-25744
- recording techniques and appls. 7-57276
- recording with filter, glass fibre dia. meas. 7-25762
- reflection holography, sheet film processing problems 7-25765
- rotating objects through distorting medium, holographic image form. 7-43012
- scanning system, design and commercial appl. 7-25770
- sharp-focusing technique, sensitivity 7-36920
- signal correlation with phase-conjugate holographic reconstruction using a BaTiO₃ crystal 7-20155
- skull, computer-aided tomogram, multiplex hologram 7-65883
- soft X-ray interferometry and holography 7-18950
- solar concentrator, feasibility and basic principles 7-46919
- solar concentrators, critical review 7-54272
- solar control tunable Lippmann hollowindows 7-36919
- space-time holograms, recording and reproduction in selective photochromic media 7-57280
- special effects techniques for integral holograms 7-25775
- spectroscopy for refraction indicators determ., layer thickness meas. appl. 7-9877
- spherical droplets, semi-transparent, hologram structure 7-31281
- table design with rubberised coil as vibration absorber 7-31275
- testing of stretchable concave imaging mirrors by holography 7-31282
- time diagnostics with picosecond resolution 7-43014
- transmission, display with white light source 7-36913
- volume reflection holograms with multiple gratings 7-43000
- waveguide holograms of 2D objects 7-57269
- white light cylindrical holograms 7-25776
- white light reflection holograms, processing techniques 7-25779
- wide angle distortion free holographic head-up display 7-25766
- wooden plates, vibration mode meas. using TV-holographic and electroacoustical methods 7-31716
- X-ray and electron holography using local reference beam 7-20159
- X-ray applications, prospects 7-24739
- X-ray partially coherent radiation, props. and appls. 7-24738
- Ag halide emulsion multiple holographic transmission gratings 7-57267
- Ag halide materials for hologram mass production 7-25780
- Ag halides photographic plates, relief-phase holograms, copying 7-43013
- Ag ultradisperse particles in holographic emulsion, photolum. 7-33446
- As₂S₃ thin films, photodarkened, reversible recording and erasure of holograms 7-50511
- Bi₂GeO₂₀, real time holographic image recording, diffraction efficiency (*Korean*) 7-25743
- Bi₁₂SiO₂₀, photorefractive, hologram recording, real-time defect enhancement using inversion props. 7-25771
- LiNbO₃, picosecond holography and four-wave mixing 7-20161
- LiNbO₃:Fe, Czochralski growth and holography appl. 7-59404
- LiNbO₃:Fe planar optical waveguide, hologram recording, dopant conc. depend. 7-15828
- Si_{0.75}Ba_{0.25}Nb₂O₆:Ce self-starting passive phase conjugate mirror 7-43243

homogenising see heat treatment

homopolymers see polymers

hopping conduction

- amorphous films, transverse hopping cond. temp. depend. mesoscopic behaviour anal. 7-17028
- amorphous solid, e⁻ scavenging, generalized master eqn. theory 7-21884
- anisotropic 2D square lattice, random hopping model, percolation, diffusion and conductivity 7-61282
- aromatic hydrocarbons, semicond., nondispersive transport, model of diff. jumps 7-58812
- chalcogenide glasses, AC conduction, theoretical models and expt. data, review 7-64252
- diamond:B, hopping photoconductivity 7-38617

hopping conduction continued

- disordered 2D system, AC cond., anomalous permitt. 7-45406
 disordered solids, dispersive hopping and trapping transport, mean field theory 7-38554
 DNA, aperiodic, electronic structure and cond. props. 7-23297
 DNA electronic structure and cond. props., calcs. 7-23296
 fluorinated ethylene-propylene copolymer, hole schubweg models 7-21936
 granular metals, conc. depend. of hopping conductivity 7-32969
 ion-implanted polymers, fractal elec. cond., current transients, percolative transition calcs. 7-2645
 metals, granular, hopping conduction 7-17007
 organic layers, carrier drift mobility, anomalous field depend. 7-58928
 organic layers, electric field dependent hopping mobility 7-21920
 trans-polyacetylene, random soliton distrib., localisation and density of states calcs., renormalised virtual cryst. method 7-52453
 polyethylene films with Si incorporation, localized gap states, space-charge-limited current 7-52530
 polymer, molecularly doped, charge carriers, pseudo-percolation, Monte Carlo study 7-2613
 polymers, conducting, electronic cond., conjugation length depend. 7-64228
 polyperinaphthalene, pristine and doped, elec. conductivity 7-2589
 proteins, aperiodic, electronic struct., ab initio calcs. 7-23273
 proteins, electronic structure and cond. props., calcs. 7-23296
 quasi one-dimensional inversion layers, hopping magnetoconductance fluctuations 7-12868
 quasi-1D mol. systems, polaron struct., interchain electron hopping effects calcs. 7-16959
 ruby:Cr, alternating-sign resonant photocond., impurity ion excitation 7-2643
 semiconductors, acoustic props. under hopping conduction conditions 7-16692
 semiconductors, hopping thermoelectric power near the mobility edge, critical behaviour 7-52661
 Si₃N₄ MONOS structures, negative hopping magnetoresist. meas. 7-64357
 SIPOS-Si heterojunction current flow props. 7-38713
 site-disordered d-dimensional lattices, hopping transport 7-45291
 small polaron hopping regime, thermoelec. power, temp. and coupling strength effects 7-7196
 superionic conducting materials, ionic thermoelec. power, heuristic treatment 7-45345
 TCNQ salt, conducting Langmuir-Blodgett film, electronic transport props. 7-38782
 TCNQ salts, semiconducting, dielec. response in submillimetre range 7-45916
 theory of hopping conduction by the path-probability method 7-45308
 transient small polaron hopping motion 7-38563
 Ag-Ge granulated films, Coulomb gap and hopping conduction 7-38774
 AlN_x nonstoichiometric sputtered films, electron localisation, transport props. 7-58929
 As₂Se₃:Ni films, electronic struct. and transport props. 7-12595
 α-As₂Te₃ films, hole transport investigation by transient field-effect and time-of-flight methods 7-22040
 Bi₂O₃-V₂O₅-CaO system, vitreous oxide semiconductor, polarisation processes 7-59139
 Bi₁₂SiO₂₀, photorefractive effect, simplified band transport model 7-27700
 CuGaTe₂ thin films, elec. cond., 100-300K 7-22042
 CuInTe₂ film, amorphous, flash evap., DC cond. mechanisms, density of states 7-22041
 CuInTe₂ thin films, flash evaporated, elec. conductivity, optical absorption 7-7428
 CuO-P₂O₅ glasses containing NiO or CoO, elec. cond. 7-17025
 FeO, wustite, defect agglomeration at high temps., elec. conduction model 7-21197
 Fe₃O₄ single cryst., dielec. and conducting props. study below Verwey point 7-53230
 Fe₃O₄, small polaron conduction and short-range order 7-7239
 Fe₂Sb_{100-x}, amorphous, metal-insulator transition and effects of localisation and correlation 7-45407
 Fe₂Se₃ and As₂Se₃-Fe₂Se₃ films, electronic props. 7-58922
 Fe₂ZrSe₂, intercalated layered cpd., thermopower and low DC field magnetisation study 7-17199
 Ga_{1-x}Al_xAs MIS and SIS structures, prep. by metallorganic chem. hydride method, electrophysical props. 7-22018
 GaAs LPE layers, heavily doped and compensated, hopping cond., density of states at Fermi level, carrier conc. determ. 7-2753
 GaAs, neutron transmutation doped, variable range hopping studies 7-33012
 a-Ge:H, elec. props., effect of H plasma press. (Korean) 7-27332
 a-Ge₂₀Se₈₀:Bi films, n-type, electron transport props. studies 7-7422
 Ge₄Se₆-Te_x amorphous chalcogenide, elec. cond., prep. technique effects 7-7237
 In, granular films, metal-insulator transition, conducting props. study (Russian) 7-7116
 InP:Mn, deep acceptor level, props. 7-21853
 KH₂(IO₃)₃, proton cond. and cryst. struct., X-ray and neutron diffr. studies 7-12026
 NH₄H₂(IO₃)₃, proton cond. and cryst. struct., X-ray and neutron diffr. studies 7-12026
 Ni_{1-x}Fe_xO₄, elec. cond., thermoelec. power meas., 10-300K 7-38648
 a-P, sputtered, response to intense ion bombardment 7-27447
 PbTe oxidised disordered films, magnetoresist. quantum oscils. obs. 7-64271
 Si, accumulation layers, quasi-1D transport, strong localisation 7-64359
 a-Si, low temp. electron transport near mobility edge 7-38562
 Si:As, ion implanted, electronic transport props. 7-7233
 Si:B, electron-irradiated, AC hopping conductivity and DLTS 7-44624
 a-Si:H/SiO₂-N:H heterostruct., transport props 7-38768
 Si:Na MOSFET struct., hopping cond. in 2D impurity band 7-45512
 a-SiC:H film prepared by magnetron sputtering, elec. and optical props. (Japanese) 7-12887
 Si₃N₄, amorphous hopping cond. in high elec. and mag. fields 7-64257
 Si₃N₄ thin films, reactively sputtered, hopping cond., defect states 7-52620
 a-Si_{1-x}Te_x amorphous alloys, electronic and optical props. 7-7234
 Sn-Ge granulated films, Coulomb gap and hopping conduction 7-38774
 V₂O₅ and Li_{1-x}V₂O₅, amorphous thin films, electrical conductivity 7-58921
 V₂O₅-P₂O₅-Bi₂O₃(Sb₂O₃) glasses, DC conductivity 7-45316
 V₂O₅-TeO₂-PbO, glass, elec. and optical props. (Korean) 7-27330

hopping conduction continued

- WO₃ amorphous evaporated film, complex cond., temp. and freq. depend studies 7-2756
 WS_{2+x} elec. cond. and permittivity, temp. and freq. depend. studies 7-7235
 YFe₂O₄, elec. resist. and Seebeck coeff. studies 7-21914
 ZnO-V₂O₅ glasses, DC conductivity 7-27327
horn antennas see *directive antennas; waveguide antennas*
horology see *time measurement*
hospital administration see *medical administrative data processing*
hospital engineering see *biomedical engineering*
hospital information systems see *medical administrative data processing*
hot carrier conduction see *hot carriers*
hot carriers
 degenerate semiconds., anisotropic hot carrier distrib., transport eqn. solns anal. 7-58815
 direct-gap semiconductor, reversible picosecond brightening during inter-band absorpt. of intense light pulses 7-12761
 hexatriacontane, hot electron cond. and relax., internal photoemission for transport anal. method 7-45340
 hot electron dynamics in tunnel junctions, surface plasmon emission as probe 7-2735
 III-V semicond. alloys, vel.-field characs., band struct. effects, CPA calcs. 7-64243
 III-V semiconductors, hot-electron photoluminescence, polarisation 7-46118
 layer inhomogeneous semiconds., hot electron effects, N-type current-voltage characs. calcs. 7-38689
 mobility overshoot of hot electrons 7-52636
 multilayer isotypic n⁺-n heterostructures, S-type current-voltage characs. 7-52758
 narrow band gap semicond., with symm. electron and hole spectra, pinch effect 7-17047
 p-n junction, nonlinear transport problems, use of electron temp. concept 7-7371
 pentane isomers, ionis. and electron thermalisation distances, mol. shape and density effects 7-50347
 polar semiconductors, quasi-2D, hot carriers 7-12807
 polyethylene dielec. thin films, hot-electron-induced damage and charge storage, electron spectra studies 7-27662
 quantum well ground state, 2D gas, electron temp. and energy losses 7-17092
 resonant tunnelling electron spectroscopy, technique for hot electron energy distrib. determ. in semiconductors 7-45447
 semiconducting quantum well wires, hot electron transport 7-7356
 semiconductor, carrier transport in built-in and external fields 7-52634
 semiconductor, nondegenerate, diffusion noise and hot-electron noise at arbitrary drift vels. 7-64299
 semiconductor heterojunctions, 2D hot electron time-depend. energy relax. nonequilib. optical phonon effects 7-64102
 semiconductor heterojunctions, nonequilibrium electron-phonon scatt. 7-45457
 semiconductor heterostructures, ultrafast switching mechanism 7-38693
 semiconductor n⁺-n-n⁺ submicron struct., ballistic electron transport 7-22004
 semiconductor structures, hot electron transient behaviour, numerical model 7-12729
 semiconductor thin films and wires, hot electrons under quantum size effect conditions 7-38780
 semiconductors, compensated, impurity photoconductivity, field and spectrum dependences, exclusion effect 7-38635
 semiconductors, electrical breakdown at grain boundaries 7-45339
 semiconductors, extrinsic n-type, stochastic self-oscillations under intense illumination 7-2639
 semiconductors, hot-carrier transport, Monte Carlo and Davydov calcs. 7-45341
 semiconductors, intraband luminesc., anal. 7-27759
 semiconductors, magnetic two-phonon resonance involving acoustic phonons 7-45355
 semiconductors, Raman scatt. in the presence of photoexcited nonequilibrium carriers 7-27719
 solid dielectrics, breakdown and prebreakdown phenomena, charge transport and dielectric aging 7-39014
 steady-state hot electron transport, quantum theory of thermal noises 7-33024
 superlattice APDs, impact ionisation, theory 7-12850
 superlattices, hot electron diffusion study by Monte Carlo technique 7-45483
 superlattices, microstructures and microdevices, conf., Goteborg, Sweden (Aug. 1986) 7-35097
 two-dimensional carrier systems, parallel transport 7-52827
 vertical transport in multilayer semiconductor structures 7-38705
 AG, hot electron luminescence 7-17337
 AlGaAs/GaAs selectively doped heterointerface under high elec. field appl., 2D plasmon 7-52637
 AlGaAs-GaAs, selectively doped heterojunctions, energy relax. of 2D electrons, deformation potential constant 7-12801
 AlGaAs-GaAs-AlGaAs single quantum well heterostruct., negative differential mobility and drift velocity overshoot 7-52787
 Al_{1-x}Ga_xAs, hot-electron capture at DX centres 7-45344
 Al_{0.48}In_{0.52}As-Ga_{0.47}In_{0.53}As SQW, electron temp. depend. on well width, photolum. obs. 7-12810
 AlSb, hot electron luminesc. 7-46119
 Au-InP high-speed internal photoemission detectors enhanced by grating coupling to surface plasma waves 7-52688
 Au-SiO₂-Bi, low temp. hot electron energy relaxation and inelastic collision times in thin metal films 7-27441
 Au₆₀Pd₄₀ thin films, warm electron energy loss meas. 7-2739
 n-Cd₂Hg_{1-x}Te, single crystal, γ-irradiation, electrophysical props. in strong elec. field 7-7251
 CdSe, strongly excited, electron-phonon interaction screening, luminesc. meas. 7-38606
 Ga_{1-x}Al_xAs, indirect-gap crystals, hot photolum., polarisation characs. 7-46092
 GaAs, electron-electron interactions, appl. for hot electron decay 7-32934
 GaAs, highly doped, polarised hot electron photoluminescence 7-46121
 GaAs, hot anti-Stokes luminesc., picosecond spectroscopy 7-22336
 GaAs, hot electron spectroscopy, extreme nonequilibrium electron transport dynamics 7-12726

hot carriers continued

- GaAs, hot optically excited carriers in a spin-split-off subband, energy relax. 7-22302
 GaAs, hot-electron 1/f noise 7-21927
 GaAs hot-electron temperature measurement, method 7-52623
 GaAs, inversion layers, hot free electron gas, intraband absorpt. coeff. calc. 7-33083
 GaAs quantised inversion layers, hot 2D electron gas, spectral acoustic phonon emission intensity 7-52452
 GaAs quantum wells, 2D hot-electron mobility 7-45470
 GaAs quantum wells, hot-carrier phonon interactions, steady-state and picosecond meas. 7-12837
 n-GaAs:O, semi-insulating, impurity centres, electron capture 7-52643
 p⁺-GaAs/AlGaAs, double barrier, hot electron energy distrib. study using resonant tunnelling electron spectroscopy 7-45447
 GaAs/AlGaAs multiple quantum well structures, hot-carrier relaxation, femtosecond optical meas. 7-52750
 GaAs-Al_xGa_{1-x}As multiple-quantum-well struct., electron heating below 1K 7-12817
 GaAs-AlGaAs, hot carriers in quasi-2-D polar semiconductors 7-12807
 GaAs-AlGaAs quantum wells, hot electrons, Monte Carlo study 7-38708
 GaAs-AlGaAs superlattice, hot electrons, real space transfer effect, photolum. studies 7-39180
 GaAs-Ga_xAl_{1-x} heterojunction, nonequilibrium electron-phonon scatt. 7-45457
 GaAs-GaAlAs modulation doped quantum wells, hot carrier energy relax., time resolved photoluminescence spectra 7-52828
 GaInAs/InP heterojunction, 2D electron gas nonequilib. cyclotron reson. obs. 7-12845
 GaInAs-InP, quantum well lasers, characts., comparison with GaAs-GaAlAs 7-5891
 p-Ge, hot electron transport, perturbed acoustic phonon distrib. effects, Monte Carlo anal. 7-64254
 Ge, hot hole FIR laser action investig. 7-57341
 p-Ge, hot hole intersubband transitions, stimulated emission and gain, quantum oscills. 7-1052
 Ge hot-hole cyclotron resonance maser with negative effective hole masses 7-15838
 Ge, multibeam streaming of heavy holes 7-12728
 p-Ge, spatial correlations of chaotic oscillations in post-breakdown regime 7-64255
 n-Hg_{0.8}Cd_{0.2}Te, condensed electron system, heat capacity, comment 7-58503
 Hg_{0.8}Cd_{0.2}Te, low temp. hot electron energy relax. time in extreme quantum limit mag. fields 7-33035
 Hg_{1-x}Mn_xTe LPE crystals, magnetophonon reson. recomb. with phonon emission 7-63755
 n-InSb, magnetic two-phonon resonance involving acoustic phonons 7-45355
 n-Si, electron heating and intervalley redistribution in strong electric fields 7-27336
 Si, hot hole dispersion laws 7-52629
 Si, hot-electron 1/f noise 7-21927
 Si light-enhanced oxidation, hot electron injection, electron population depend. study 7-46720
 Si quantised inversion layers, hot 2D electron gas, spectral acoustic phonon emission intensity 7-52452
 a-Si:H/a-Si_{0.2}C_{0.8}:H superstructures, hot electron conduction 7-45453
 Si:H-Si_{1-x}C_x:H amorphous super struct., hot electron generation 7-52794
 Si/CoSi₂/Si struts., parallel and perpendicular transport, supercond. props. 7-45518
 Si/SiO₂, two-step oxidation of thin gate oxides, trapping characts., hot electron effect study 7-64351
 Si₃N₄ MIS struct., electron transport and heating, vacuum emission studies 7-2723
 SiO₂, high field electron transport, rel. to positive charge generation at Si-SiO₂ interface 7-38571
 SiO₂, hot carrier trapping characts., effect of post-oxidation annealing 7-64268
 SiO₂N_x MIS struct., electron transport and heating, vacuum emission studies 7-2723

hot cathode tubes *see thermionic tubes***hot cathodes** *see thermionic cathodes***hot electrons** *see hot carriers***hot pressing**

- Astrology, LC, Nirbase superalloy, hot isostatic pressing, powder metallurgy, second phase particle anal. 7-17497
 ceramic coatings, plasma sprayed on stainless steel, hot isostatic pressing, hardness, bond strength 7-13624
 ceramic composites, liq. phase sintered, hot isostatic pressing 7-64989
 ceramic engine component fabrication techniques 7-3243
 epitaxial metal bicrystals containing grain boundaries, UHV deposition apparatus 7-39390
 metal powders, hot isostatic pressing, empirical model 7-46365
 Mo-Ni, activated sintered, sintering behaviour and mech. props. 7-7929
 parts production by hot isostatic pressing, applic. of rheological model for porous materials (*French*) 7-13400
 piezoceramic narrow-strip element resonance freq. dispersion diagrams, texture and ionic substitution effects 7-1363
 polypropylene, hot isostatic pressing, mech. strength improvement 7-7955
 powder densification by interface-reaction controlled grain boundary diffusion 7-64950
 steel structural, powder, hardenability and hardness penetration, effect of comp. and porosity 7-22807
 steel surface at moderate heating temps., relationship between emissivity and exoemissive props. 7-43641
 superalloys, oxide dispersion strengthened, manufacturing process developments 7-27979
 Al-Mg and Al-Zn-Mg alloys, plasma-coated, heat treatment effect on fine struct. and failure mechanism 7-3496
 AlN, hot pressed, elec. cond. rel. to CaO addition 7-38559
 Al₂O₃, joining by inducing localised reducing conditions 7-46787
 Al₂O₃-TiN composite, interfacial reaction and mass transport of components during sintering 7-3254
 Al₂O₃-ZrO₂ ceramics, densification kinetics 7-27992
 BN polycrystals, heat treatment conditions effect on mech. and service props. 7-53894
 BN, wurtzite, sintered polycryst., texture form. during hot compacting at high press., sphalerite transition 7-53685

hot pressing continued

- Ba(Ca_{1/3}Nb_{2/3})O₃-PbZrO₃-PbTiO₃ ceramics, hot-pressed, ferroelectric phase transitions 7-7652
 BaTiO₃, fine-grained superplastic creep in reducing environment 7-28075
 Be mirror for large optics, fabrication by hot isostatic pressing 7-37228
 CaLa₂S₄ optical ceramic, powder synthesis 7-37067
 Co₇₅Si₁₀B₁₅, amorphous powder, static consolidation, mechanical and mag. props. 7-3217
 Fe powders, hot pressing, fracture toughness, intergranular failure rel. to porosity 7-13596
 Fe/Fe-FeO/Al₂O₃ systems, diffusion bonded, interface chemistry, bonding strength 7-28079
 Fe-C-based alloys, high C, rapidly solidified, mech. props. 7-22673
 LaB₆ dispersed powders and compact specimens, struct. and morphology 7-64976
 LaCrO₃-Cr cermets, mech. props., interparticle welding 7-39630
 La₂O₃, thermal expansion coeff. below room temp. 7-12332
 MgAl₂O₄ spinel, preparation and IR optical applications 7-37066
 Ni-Co-Cr-Mo-Al-Ti prealloyed powder, parts prod. by hot pressing (*French*) 7-13400
 Ni-W-Co-Cr superalloys, creep rupture and tensile props. rel. to hot pressing or aluminising 7-3363
 PLZT ceramics, grain growth during hot pressing 7-3232
 PLZT ceramics, hot pressed, chemically induced grain boundary migration and recrystallisation 7-27027
 Pb(Sr_{0.5}Nb_{0.5})O₃ transparent ferroelec. ceramic production by hot pressing and props. 7-7934
 Pb(Sr_{1/2}Ta_{1/2})O₃, single crystals and hot pressed ceramics, ordering, domain struct., TEM obs. 7-26936
 SiC ceramics, hot pressed, grinding, surface damage, bending strength (*Japanese*) 7-17602
 SiC, sintered, microstruct. and props., influence of fabrication method (*Japanese*) 7-22622
 SiC whisker reinforced Si₃N₄, microstruct. and props. 7-22824
 SiC-AlN ceramics, elevated temp. creep, role of grain size 7-39584
 SiC-based ceramics, sintered and hot isostatically pressed, microanalytical investigation 7-27991
 Si₃N₄ ceramics, hot pressed, fatigue test with Knoop indentation, residual stress effects (*Japanese*) 7-17640
 Si₃N₄, hot isostatic pressing with BeAl₂O₄ addition (*Japanese*) 7-27994
 Si₃N₄, hot pressed, elec. cond., microstruct., fusion reactor insulator appl. 7-52619
 Si₃N₄, hot-pressed, friction and wear 7-59642
 Si₃N₄, hot-pressed, tensile strength at room and elevated temp. (*Japanese*) 7-65139
 Si₃N₄ powders, high press. not pressing, mech. props., thermal cond. temp. depend. 7-3231
 Si₃N₄, with MgO addition, phys. and tribological props., effect of hot-pressing time (*Japanese*) 7-65150
 Si₃N₄/ferritic stainless steel, joining with soft metal interlayers, tensile strength 7-28266
 Si₃N₄-Y₂O₃, hot pressed, fracture, flexural strength, temp. degradation 7-13546
 Sr(La_{1/2}Nb_{1/2})O₃-PbZrO₃-PbTiO₃, hot-pressed ceramics, dielectric, piezoelectric and optical props. 7-64583
 Ta₆W₁₈O₉₄-Super Invar composite, thermal expansion coeff. 7-12331
 TaVO₅, thermal expansion coeff. below room temp. 7-12332
 Ta₆W₁₈O₉₄, thermal expansion coeff. below room temp. 7-12332
 Ti parts prod. from TiH₂ powder by hot pressing 7-27973
 Ti-Al-Mo-Cr alloy, VT3-1, vac. annealing of blanks after isothermal deform., hydrogen plasticising effect 7-8027
 TiB₂-TiC composite, hot pressed, degradation in liq Al 7-28156
 TiO₂, amorphous reactive ion beam deposition, crystallisation 7-45091
 ZnO ceramic, grain growth kinetics during synthesis, optimum elec. props. 7-46398
 ZrO₂, Y₂O₃ partially stabilised, hot isostatic pressing, high temp. mech. props. 7-28082
 ZrO₂-Y₂O₃, Y-TZP, toughened, microstruct., TEM and electron diffr. study (*Japanese*) 7-22634
 ZrO₂-Y₂O₃ ceramics, toughened, prep., microstruct., mech. props. 7-3409
 Zr₅Pb₃, fusion blanket neutron multiplier, fabrication and props. 7-49656

hot rolling

- α-brass, hot rolled, recrystallized microstruct., deform. processes 7-13500
 steel, C, dislocation structure, rolling temp. effects (*Russian*) 7-44552
 steel, Cr-Mo-V, porosity assoc. with insoluble carbides, probable effect on rolling contact fatigue 7-17639
 steel, Cr-Ni-Mo, Ge and melting method influence on mech. props. at high temp. 7-8025
 steel, high-strength low-C weldable, C content effect on struct. and mech. props. 7-46583
 steel, hot rolled microalloyed, protoeutectoid ferrite transform. kinetics, microstruct. modelling 7-17526
 steel, low C lamination, decarburization, grain size, carbide morphology 7-8016
 steel, low-alloy, H-beams, controlled rolling effect on mech. props. 7-39562
 steel, low-C, wrought, thermal strengthening methods effectiveness 7-46524
 steel, low-pearlite, rules of austenite decomp. in continuous cooling 7-3339
 steel, low-pearlite, subjected to controlled rolling, complex microalloying effect 7-46523
 steel, Ni-Cr-based, high temp. strength, modified ausforming effects (*Japanese*) 7-8089
 steel, p/m, heat treatment effect on strength and yield parameters 7-53775
 steel, stainless, cold rolled sheet, struct. form. during recrystn., optimum heat treatment schedule 7-3340
 steel, stainless, ferritic, annealed hot-rolled plates, texture heterogeneous, correl. with plastic deform. struct. (*French*) 7-13483
 surface flaw detection for hot steel slabs, eddy current method (*Japanese*) 7-53771
 Al alloys, liquid dynamic compaction, microstruct. and precipitation, TEM study 7-59529
 Al and alloys, dynamic restoration during hot rolling 7-22724
 Al-Al₂Cu eutectic alloys, chill cast, directionally solidified, hot rolling microstruct. 7-46447
 Al-Al₂Ni eutectic alloys, chill cast, directionally solidified, hot rolling microstruct. 7-46447

hot rolling continued

- Al-Fe-V rapidly solidified sheets, mech. props., hot rolling effects 7-22838
 Al-Mg alloys 5056 and 5083, recrystn. kinetics after hot deform. 7-3328
 Cu, recrystallisation texture, deformation temp. effects (*Russian*) 7-8007
 Cu-Zn-Al shape memory alloys, grain refinement 7-53774
 Fe-Si, grain oriented, hot rolling texture, thickness variations 7-8009
 Fe-Si, plasticity, influence of thermomechanical parameters 7-13512
 Fe-Si (2 wt.%), microstruct., mag. props., thermomech. history effect 7-7551
 Fe-Si (3 wt.%), Goss orientation rel. to hot rolling conditions 7-8018
 Fe-Si (3 wt.%), grain oriented, texture development for regular and high permeability 7-8008
 Fe-Si (3 wt.%), hot rolling, austenite formation 7-13481
 Fe-Si-B, normalising, decarburisation, secondary recrystallisation, mag. induction obs. 7-8020
 Fe-Si-Ni (6.5, 2 wt.%), development of Goss texture, lowering of core loss 7-33693
 Mo single cryst., rolling, dynamic recovery rel. to deform. temp. (*Russian*) 7-65095
 Ti-Al-V (6, 4 wt.%) texture stability during rolling in two-phase field 7-46508

hot shortness *see* **brittleness****hot strength** *see* **tensile strength****hot working**

- see also* **hot rolling**
 simulated hot deformation, determ. of CCT diagrams by thermal anal. 7-59557
 steel, austenitic stainless, Mo and/or N alloyed, recrystn. after hot working 7-3326
 steel, austenitic stainless, Mo-N alloyed, static recrystn. and hot ductility 7-3327
 steel, austenitic stainless, softening mechanism in hot working 7-3333
 steel, C, n (*Japanese*) 7-17558
 steel, constructional, struct. and props. after high-temp thermomech. isothermal working 7-46522
 steel, Cr, austenitisation, recrystallisation, pearlite transform. rel. to hot deform. 7-28033
 steel, Cr-Mn(V), bainite transform. kinetics, austenitising and working conditions effect 7-22674
 steel, ferritic-martensitic stainless, warm forming (*Polish*) 7-13507
 steel, high strength line pipe, H induced cracking susceptibility, comp. and treatment effect 7-39619
 steel, hot working of austenite, transition from multiple- to single-peak recrystn. 7-65057
 steel, low alloy, hot forming, transform. behaviour, struct. (*German*) 7-59518
 steel, martensitic stainless, brittle failure rel. to overheating, fractography 7-22796
 steel, P/M, produced by hot forming, strength characts., influence of porosity, C content and compacting method 7-53823
 steel, tool, Cr-Mo-V, hot working, ductility, C content, toughness, eutectic carbide segregation 7-59592
 steel, tool, heat treatment cycles, original struct. and deform. influence on mech. props. 7-39560
 Al alloys, hot workability, determ. of high temp. flow stress (*Korean*) 7-28076
 Al-Cu-Mg, hot workability, recrystallisation during torsional deform. (*Korean*) 7-46559
 Al-Si, brittle failure rel. to overheating, fractography 7-22796
 Al₂O₃-ZrO₂ ceramics, hot forging characts., grain size 7-3370
 Co-Si-B, change of elongation, rel. to conditions for hot working 7-3384
 Cu-Al bronze, hot deform. and annealing, mechanical props. and softening kinetics 7-17552
 Fe, hot deformed, metadynamic recrystn. 7-3335
 Fe-Mn-Al, processing and props., effect of Si and C additions 7-17707
 Ni alloy, heat-resisting, hot strain rate effect on microstruct. and mech. props. 7-39559
 Ni-Cr superalloy, high-temp. material, microstruct. and mech. props. with high-temp. heating 7-3341
 Ti-Al, brittle failure rel. to overheating, fractography 7-22796
 TiAl, deform. at high temp., flow and brittle fracture stress (*Japanese*) 7-13516
 ZrO₂ ceramics, hot forging characts., grain size 7-3370

household appliances *see* **domestic appliances****housings** *see* **packaging****HSLA steel** *see* **alloy steel****Hubbard model**

- 1D, ground state energy, variational calc. 7-38425
 Anderson-Hubbard model, real-space renormalisation group method 7-38842
 degeneracy and quantum effects in the Hubbard model 7-7469
 disordered interacting electron system, extreme-short-range-force, Hubbard interaction calcs. 7-22089
 elements, monovalent, electron correlations and chemical bonds, Hubbard model 7-58755
 Fermi gas, 1D, Bethe-ansatz soln., simple approx. 7-61221
 functional-integral approaches and diagrammatic many-body theory of the Hubbard model 7-64428
 Gutzwiller-Hubbard-Kanamori model, crystallization props. 7-58974
 heavy electron Fermi liquids, Hubbard model anal., similarities to ³He 7-2522
 itinerant electron model with crystalline or mag. long-range order 7-17152
 magnetic semiconductors, anisotropic, narrow-band, elementary excitations 7-59001
 magnetic thin films, surface spin waves, tight-binding and Coulomb parameter effects 7-27572
 metal-insulator transition, modified Gutzwiller theory, appl. to heavy-fermion systems 7-32915
 metal-insulator transition, nonlocal correlation in Hubbard model 7-38456
 mixed-stack cpds., electronic states, soliton structs. 7-52451
 monovalent systems, low-lying excited states, metal-insulator transition, modified Hubbard model, Gutzwiller variational calcs. 7-7119
 narrow energy band systems, insulator-metal transition 7-38455
 one-dimensional degenerate Hubbard model, Monte Carlo simulations 7-45609
 one-dimensional disordered Hubbard chain, high-field dynamical theory far from equil. 7-2447

Hubbard model continued

- one-dimensional Hubbard model, one- and two-hole excitation spectra 7-22088
 one-dimensional systems with weak coupling, Peierls instability 7-32938
 orbitally degenerate model, phase transitions 7-64041
 organic crystals, neutral-ionic transition, Monte Carlo simulation of modified Hubbard model 7-2554
 Peierls-Hubbard model, exact and approximate solns. 7-52383
 phonon coupling, finite Hubbard model 7-12582
 polarons, small radius, effective mass studies 7-38465
 trans-polyacetylene, photogenerated exciton-breather state 7-21823
 quasi-1D conductors, Coulomb correlation effects 7-52485
 random Hubbard alloys, localisation-affected conductivity, numerical studies 7-45223
 segregated-stack organic charge transfer solids, mag. props. 7-17151
 semiconductors, unipolar injection in presence of deep centres with negative Hubbard energy 7-38568
 singlet superconductivity, mean field theories in extended Hubbard models 7-27461
 statistical physics and field theory conf., Groningen, Netherlands, Aug. 1985 7-55899
 strongly correlated Fermi systems, Gutzwiller saddle-point approx., functional integral approach 7-207
 superconducting electron pairing, exchange and correl. contributions 7-45574
 surface ferromagnetism in transition metals, Hubbard model 7-33139
 TCNQ salts, quarter-filled band, optical absorption studies 7-46033
 TCNQ salts, quasi 1D molecular crystals, optical props., Hubbard model generalization, cond. calc. 7-45952
 temperature-induced metal insulator transitions (*Russian*) 7-45153
 three dimensional, d-wave pairing near a spin-density-wave instability 7-45608
 three-dimensional half-filled band sector, magnetic props., Monte Carlo simulation 7-58971
 transition metal cpds., high press. metal-insulator insulator transition, extended Hubbard model calcs. (*Russian*) 7-32917
 two-dimensional, mag. props., mean-field phase diagram and spin-spin correl. 7-64429
 world-line and determinantal functional-integral formulations 7-4781
 InSb, impurity bands and their conductivity in strong mag. fields 7-45152
 Ni, magnetic props., Hubbard model 7-2806
 Ni, quasi-particle and band-calc. spectra, w.r.t. valence band photoemission meas. 7-2474
 USi₃(Ir₃) intermetallics, correlation effects, XPS and bremsstrahlung isochromat spectra 7-21844

Hubble model *see* **cosmology****Huckel molecular orbital calculations** *see* **HMO calculations****hue** *see* **colour****Hugoniot diagrams** *see* **equations of state****human engineering** *see* **ergonomics****human factors**

- see also* **behavioural sciences**; **biocybernetics**; **ergonomics**; **man-machine systems**; **speech intelligibility**; **user interfaces**
 7-28682
 colour, direction and speed of motion, perceived relations 7-47078
 colour perception, display technology implications 7-14005
 conf., Dayton, OH, USA (Sept.-Oct. 1986) 7-35114
 criticality safety, replacing aged professionals 7-759
 display image quality, human detection of undersampled gratings 7-14004
 electric power industry Inter-RAM conference, Syracuse, NY, USA (June 1986) 7-9592
 incident control, simulation of man machine interaction 7-15287
 IPI semiautomated inspection devices for inspectors 7-54546
 joint motion clusters in servomanipulator operations 7-36177
 lens design software, human dimension 7-50675
 nuclear power, human factors reliability (*Czech*) 7-61990
 nuclear power plants, human factors in risk assessment 7-30637
 nuclear power stations, human approach to process control and predictive information 7-30612
 nuclear power stations, systematic human action reliability procedure, benchmark process 7-30634
 nuclear safety, system design and anal. 7-15288
 peripheral information display 7-40162
 peripheral information extraction: cognitive load effects 7-40161
 peripheral vision advances 7-40159
 peripheral visual sensitivity, foveal load 7-40160
 retinal adaptation to non-uniform fields: average luminance or symbol luminance? 7-54562
 task difficulty effects on steady state visual evoked response 7-54544
 VDU perceived flicker prediction method 7-54572
 VDU visibility aspects, contrast and luminance 7-54570
 VDUs, practical guide to flicker measurement: using the flicker-matching technique 7-54573
 vision research and image technology, human functions of information processing (*Japanese*) 7-28499

human-machine systems *see* **man-machine systems****human relations** *see* **behavioural sciences**; **social sciences****humidity**

- see also* **atmospheric humidity**; **hygrometers**
 corona and breakdown mechanisms obs. in rod-plane gap 7-20979
 CR-39, response to α -particles, heat and humidity effects 7-30861
 fibrous medium, thermally induced hygroscopic mass transfer 7-44037
 powders and porous media, thermal diffusivity, photoacoustic technique meas., effect of humidity 7-4837
 XLPE, dielectric properties modification due to corona discharges, humidity effects 7-39022
 Zr₇₀Au₃₀, spontaneous oxidation in air, effect of humidity, pulverisation 7-3510

humidity control

- measuring devices and controllers (*Japanese*) 7-56296

humidity measurement*see also* **hygrometers**

- calibration of neutron probe for soil humidity measurement (*French*) 7-47581
 gas hygrometer, ionisation type, charge carrier mobility meas. 7-56295
 hygrometry standard, design principles 7-56293
 intelligent ventilated psychrometer with autocalibration 7-4860

humidity measurement continued

- laser photoacoustic spectroscopy of humid and polluted air 7-20569
- measuring devices and controllers (*Japanese*) 7-56296
- NBS developments of humidity standards 7-4859
- PTFE, chem. modified, humidity sensor appls. 7-9839
- relative humidity measurement using alpha-particle corona streamer counter 7-55333
- sensor, burnt zircon with alkali hardener, sensitivity 7-18793
- UK standards development at NPL 7-4858
- $\text{Cu}_2\text{O}-\text{Al}_2\text{O}_3$ -Al moisture transducer, design and development 7-41395
- LiNbO_3 SAW oscillator for humidity and temp. meas. 7-4232
- $\text{Mg}_{0.98}\text{Na}_{0.02}\text{Fe}_2\text{O}_4$, spinel struct., EXAFS and XANES studies, humidity sensor appls. 7-64784
- $\text{Zn}_{0.98}\text{Na}_{0.02}\text{Fe}_2\text{O}_4$, spinel struct., EXAFS and XANES studies, humidity sensor appls. 7-64784
- ZrSiO_4 , burned, humidity sensor with H_3PO_4 , sensitivity rel. to acidic groups 7-9838

HV engineering *see high-voltage engineering***HVDC** *see high-voltage engineering***HVEM** *see electron microscopy***hybrid computer methods** *see hybrid simulation***hybrid integrated circuits***see also flip-chip devices*

fibre-optic hybrid receiver uses thick film technology 7-26021

hybrid reactors

- AYMAN fusion and hybrid blanket design, cylindrical blanket with D-T driver 7-803
- Hefei Tokamak Hybrid Reactor, physics conceptual design 7-25238
- pebble bed blanket, magnetohydraulic flow in Na-K eutectic mixture 7-15366
- time-dependent net core breeding gain of fusion-fissionsymbiotic systems 7-804
- ^{233}U -Pu hybrid cycle power system, growth, anal. calcs. 7-49681
- ^{233}U -Pu hybrid fuel cycle systems, reactor strategy (*Japanese*) 7-49682

hybrid simulation

thermohydraulic aspects of natural circulation loop 7-10195

hybrid turbine cycle power stations *see combined cycle power stations***hydrated electrons** *see solvated electrons***hydration** *see solvation***hydraulic amplifiers**

No entries

hydraulic control equipment*see also hydraulic amplifiers*

- fluid control and meas., conf., Tokyo, Japan (Sept. 1985) 7-29593
- material listing equipment, Instron 1340 Series 7-8209

hydraulic systems

- contaminant monitor for fluid power applications 7-37613
- network, large-scale, nonlinear conservation laws 7-10196
- optical to hydraulic interface 7-5975
- pump driven by low-level temp. difference 7-54335
- Stirling engine, free-piston, RE-1000 hydraulic output system description 7-65542

hydraulic turbines

- draft tube, 3D turbulent flow anal. 7-51026
- tidal power barrage sites in UK, environmental problems caused by schemes 7-33994

hydroacoustics *see underwater sound***hydrodynamics***see also electrohydrodynamics; jets; liquid waves; magnetohydrodynamics; viscosity of liquids*

- adiabatic multiphase fluids, hydrodynamics and EHD 7-1611
- alkali metal-alkali halide mixtures, liq., longitudinal collective modes 7-6744
- Antilles-Guiana countercurrent, struct. in vicinity of Demerara Rise 7-14305
- aromatic polyester, hydrodynamic and dynamooptical props. (*Russian*) 7-39077
- axisymmetric body, force in linearised time-depend. motion 7-26303
- Black Sea, vel. distrib. of surface current in vicinity of N Caucasus coast 7-14306
- boiling liquid, first crisis, elementary hydrodynamic model, additive generalisation 7-31746
- Bose superfluid, fluctuation dispersion of transport coeffs. 7-38284
- carboxymethylcellulose, monosubstituted, cadoxene solns., diffusion, sedimentation and flow birefringence (*Russian*) 7-63859
- cellular automata for 2D hydrodynamic flow simulation (*French*) 7-16158
- cellular automation fluid models, continuum eqns. for large-scale behaviour 7-35286
- coocurrent two-phase upward flow through packed bed, liq. hydrodynamics simulation 7-57897
- collapse of MRL 38 mm shaped charge, database for computer modelling 7-63192
- columns in liq. circulation regime, hydrodynamics 7-11499
- constrained gas-liquid jet in isothermal coocurrent flow, hydrodynamics 7-44015
- convection-diffusion equations, bracket formulation 7-6214
- dense gases, transport processes, kinetic theory 7-6342
- detached flow around profiles with ang. points, computer modelling 7-43924
- diffusion hydrodynamic model for drainage system evaluations 7-4058
- diffusive transport in spatially periodic hydrodynamic flows 7-31801
- dilute dimple gas, equilibrium eigenmodes 7-16291
- disperse streams, dynamics in presence of boundaries 7-43845
- dynamical structure factor of a fluid in nonequilibrium steady states 7-31752
- elastohydrodynamic lubrication of soft, highly deformed contacts under conditions of nonuniform motion 7-57770
- electrophoresis, continuous flow, hydrodynamics (*French*) 7-39901
- eutrophication process in coastal bay, 3D eco-hydrodynamic model 7-55082
- finite difference method and spurious reflection of waves in layer of fluid 7-51185
- fluid flow, sound radiation 7-50891
- foils, laser-irrad., radiation hydrodynamics 7-1649
- forced Rayleigh scattering appl. to hydrodynamic meas. 7-11572
- gas interaction with light, transport phenomena 7-16288

hydrodynamics continued

- gas-liquid contact in Karr columns, press. drop, gas holdup and interfacial area 7-6284
- gel-like sediment form., Brownian dynamics simulation, colloidal and hydrodynamic interaction effect 7-13825
- Hookean dumbbell suspensions in steady state shear flow, hydrodynamic interaction, num. investig. 7-31868
- incompressible fluid with gas bubbles hydrodynamics eqns. soln. 7-11501
- Lake Balkhash, USSR, macrocirculation movements arising from seiche action 7-9051
- Liapunov exponents from time series, calcs., algorithm 7-41077
- linear causal system, Kramers-Kronig relations, asymptotic consequences 7-51190
- liquid-gas interface, linear stability of liq. film with counter-current gas flow (*French*) 7-1533
- liquid-glass transition, fluctuating nonlinear hydrodynamics 7-2206
- macromolecules, transport props. by Brownian dynamics 7-10789
- magnetic fluid, thin layer coating, hydrodynamic drag, num. investig. 7-51061
- many-body hydrodynamic interactions between spherical drops in an emulsion 7-16147
- nematic flows, unit-sphere description 7-20688
- non-stationary gas flows, hydrodynamic fields, dynamics of space-time correlations 7-26243
- nonequilibrium fluid with constant shear flow, Rayleigh line calcs. 7-26252
- nonlinear hydrodynamic eqns., integrability, gradient algorithm and Lax representation 7-61114
- nonNewtonian media, highly viscous, hydrodynamics and heat transfer 7-43985
- nonpropagating hydrodynamic soliton, expt. discovery 7-11445
- nonstationary Stokes equation, boundary element spectral method 7-37421
- ocean circulation, characts. of synoptic motions on sphere 7-14303
- ocean near-bottom density currents, vertical struct. 7-14308
- ocean Vaisala-Brunt frequency, calc. from hydrologic obs. using rational interpolation splines 7-14312
- oil displacement by active soln., nonmonotonic effect on flow distrib. fn. 7-1615
- packed tubes, hydrodynamics, functional relationships 7-44084
- particle in fixed dispersed layer, fluctuation hydrodynamics of Brownian motion 7-24560
- penetration of compressible liquid by axially symmetric solid 7-11370
- poly-m-phenylenisophthalamide, in dimethyl acetamide, hydrodynamic props., conform. characts. (*Russian*) 7-11894
- poly-p-decylstyrene solns., optical and hydrodynamic investig. (*Russian*) 7-13167
- polyamidobenzimidazole solns., hydrodynamic and optical props. (*Russian*) 7-26619
- polymer solutions, hydrodynamic interaction, dumbbell kinetic theory, structural approach, vector model (*French*) 7-6259
- polymer solutions, weak-flow effects, renormalisation-group anal. 7-20764
- porous medium with crack, elastic-hydrodynamic problem of fluid inflow 7-11534
- potential flow hydrodynamic coeffs., energy derived, algorithm 7-6177
- preplanetary nebula, gas flow rel. to solid material form. and chondrites comp. 7-24024
- propagation of molecular chaos theorem, hierarchies 7-56047
- quantum liq.-quantum cryst. phase interface, hydrodynamic eqns., sound transmission calcs. 7-32746
- quasigeostrophic vortices, Lyapunov-stable solns. 7-43925
- rhodamine 6G, hydrodynamically focused flow, laser induced fluoresc. detection 7-59811
- rod penetration models, extension of hydrodynamic theory 7-20665
- sensors with hydrodynamic smoothing for conductometry of turbulent flows 7-57961
- SIMPLE hydrodynamics benchmark, restructuring for CHiP architecture 7-16145
- smectic A liquid crystals, screw dislocation dynamics 7-21090
- smectic liq. cryst., A phase, hydrodynamics, US meas. 7-1876
- smoothed particle hydrodynamics, hypersonic flow appl. 7-16206
- solid body hinge-suspended in a fluid flow, vibrations 7-1394
- solid particulates and aerosol droplets at entrance of pore, hydrodynamic and mol. wall interaction effects 7-51270
- soliton turbulence, transport by negative eddy viscosity 7-14790
- spheres moving in viscous fluid, transport props. and hydrodynamic interactions 7-11522
- superheated water flow, vaporisation, heterogeneous mechanism 7-6265
- surface waves in cylinder of fluid oscillated vertically, low-dimensional chaos 7-11442
- two-sphere hydrodynamic interactions and mobilities in a porous medium 7-26340
- viscous flows in two dimensions, complex analytic methods, book contrib. 7-51059
- water waves and floating bodies, workshop, MIT, Cambridge, MA, USA (Feb. 1986) 7-48143
- ^3He , superfluid, hydrodynamic boundary conditions and cooling 7-63897
- ^4He , superfluid, dissipative flow in absolute zero limit 7-12386
- Se X-ray laser targets, hydrodynamic aspects 7-20208
- SiO_2 colloidal fractal aggregates, hydrodynamic behaviour 7-59797

hydroelasticity *see elasticity***hydroelectric power stations**

- see also dams; hydraulic turbines; pumped-storage power stations; tidal power stations; water supply; wave power generation*
- downstream fish migration protection technologies 7-34075
- Gabcikovo-Nagymaros hydroelectric power scheme 7-29087
- hydro resources identification using enhanced satellite imagery, example from Peninsular Malaysia 7-17848
- instream flow need determ. methods and their test procedures 7-39963
- Sanmen Gorge project, China, environmental impact of sedimentation in reservoir 7-29086
- variable head multireservoir power system, optimisation for long term regulation 7-23119

hydrogen*see also nuclei with*

- see also deuterium; hydrogen ions; hydrogen neutral atoms; hydrogen neutral molecules; protons; solid hydrogen; tritium*
- absorption, amorphous Gd-Co alloys, pressure-composition isotherm 7-3606
- absorption, by $\text{TiCr}_{2-x}\text{Fe}_x$ alloys, investig. 7-32832

hydrogen continued

- absorption, Gd-Co amorphous alloys, influence on mag. props. 7-2899
 absorption, in disordered solids, model 7-26970
 absorption in amorphous and crystalline Cu-Ti alloys 7-2369
 absorption in graphite-K intercalation cpd., effect on positron annihilation spectra 7-39270
 absorption kinetics on Pd (110) with impurity S coverage 7-6995
 absorption on TiC coated Mo under glow discharge, fusion reactor appl. 7-52244
 absorption on TiFe(Ti₄Fe₂O), Mossbauer obs. 7-27642
 active maser, VLB1 appls. 7-43042
 adsorbed layer on Ni (110), struct. determ., LEED studies 7-45004
 adsorbed layers on Si, phonon scatt. at crystal surface 7-21609
 adsorbed on Ni(Pd) surfaces, order-disorder transitions, theory 7-12492
 adsorbed on Ni (110), competing surface reconstruction mechanisms 7-7004
 adsorbed on Ni (111), phase diagrams based on model interactions 7-21650
 adsorbed on Pd (100) and (111), surface resonances in vibr. spectroscopy 7-52229
 adsorbed on Pd (110), row pairing model 7-2370
 adsorbed on Pt (111), reaction with coadsorbed C₂N₂ 7-54186
 adsorbed on Si(100)2x1, surface structure, high resolution, IR spectroscopy 7-13169
 adsorbed on Si (001), RHEED intensities 7-27123
 adsorbed on Si (110), atomic configuration, LEED studies 7-2314
 adsorbed on W, Mo, Re, high-field corrosion, field-ion microscopy studies 7-33830
 adsorbed on W (001), displace surface reconstructions, incommensurate sandwiches 7-52223
 adsorbed on W (100), long and short range fluctuations, lattice dynamical model 7-7002
 adsorbed on Zn (0001), thermal desorption spectra 7-21646
 adsorption, on metals, kinetics model of chemisorption layer (Korean) 7-32813
 adsorption, on Nb, kinetic model (Korean) 7-32814
 adsorption and desorpt. on Fe_{1-x}Nd(Y)(Ce)₂B fine particles prep., mag. props., recording appls. 7-53660
 adsorption and desorption on Pt (111) 7-21643
 adsorption and overlayer ordering on Ni and Pd (110) surfaces, embedded-cluster model anal. 7-52256
 adsorption of H(D) on Rh(110), form. of high density chemisorbed phase, LEED investigations 7-27094
 adsorption on Ce (001), initial stages of hydride form., UPS, LEED and EELS studies 7-21629
 adsorption on Cu (110), adsorbate movement-induced subsurface reconstruction, LEED and atom diff. meas. 7-27114
 adsorption on Fe, pulsed laser atom probe studies 7-32811
 adsorption on Ge (100), high resolution energy loss spectra study 7-38331
 adsorption on LaNi₅ oxide surface layers, kinetics 7-32833
 adsorption on Ni (100), X-ray induced secondary electron emission 7-27866
 adsorption on Pd (001), coverage depend. props., ab initio calcs. 7-38340
 adsorption on Si (111), electronic struct. calcs. 7-27377
 adsorption on Si (111), generalised Bethe lattices, chemisorpt. theory 7-7318
 adsorption on SiO₂ supported Fe microcrystals, positron annihilation studies 7-39311
 adsorption on W (001), commensurate-incommensurate phase transitions 7-7010
 adsorption on W (100) and (110) surfaces, very low electron energy refl. study 7-12488
 adsorption sites on Ru (001) at saturation coverage, LEED 7-58645
 air-H₂ turbulent mixing in coaxial jets 7-37505
 alkali halides:H, trapped atomic H and muonium 7-45900
 amorphous and disordered solids, H impurities, conference, Rhodes, Greece (Sept. 1985) 7-24302
 amplifiers, efficient high-gain, beam cleanup and low-distortion amplification 7-20341
 upper atmosphere, D and H concentrations in daytime thermosphere 7-60437
 upper atmosphere, exosphere H concs. influenced by solar cycle 7-55338
 atom, 2D, reciprocal expansions of polar and parabolic bases of continuous spectrum 7-29813
 atom, Dirac equation, separation and eigenvalue anal., hyperfine splitting in IS state, 2S state shift 7-36807
 Be stars, H α profiles atlas and shell struct. 7-14577
 bulk, surface state densities, Bethe lattice method, CPA calcs. 7-32898
 California, San Andreas and Calaveras faults, H₂ due to fault strips and earthquakes 7-40438
 carbonaceous chondrites, O and H isotopic relations in water and acid residues 7-9443
 chemisorbed monolayer on Cu-Ni alloy, induced surface segregation calcs. 7-21465
 chemisorbed on metal clusters ionisation threshold, photoionisation TOF mass spectra 7-20085
 chemisorbed on Ni (100), vibr. motion, high resolution EELS 7-12458
 chemisorbed on Ni (110), induced (1x2) reconstruction 7-58851
 chemisorbed on Si (100), transition from the dihydride to the monohydride phase 7-58631
 chemisorption, dissoci., on Ni and Cu surfaces, morphology and surface temp. effects 7-13808
 chemisorption at Nb(100) surface, EELS, LEED and work function meas. 7-32815
 chemisorption on ferromag. transition metal surface, self-consistent model 7-16862
 chemisorption on Ge (111), nonempirical cluster-model study 7-38332
 chemisorption on Ni and Pd, tight-binding approach, s-orbital hopping parameters calc. 7-21625
 chemisorption on Si (111), dihydride phases, TDS studies (Chinese) 7-38321
 chemisorption on Si (111), nonempirical cluster-model study 7-38332
 chemisorption on TiO₂(110) stoichiometric and defective surfaces 7-6983
 chemisorption on transition metal surfaces, binding energy, sum rules 7-16868
 chemisorption on W (110) 7-21663
 chemisorption phases on Pd (110), selective population of H subsurfaces sites, He diff., thermal desorption spectra study 7-6958
 coadsorption with CO on Ni (100) 7-27117
 coadsorption with ethylene as (001) surface 7-32789

hydrogen continued

- P/Comet Halley (1982i), H α and 630 nm meas. 7-18378
 compact torus form. by rot. relativistic electron beam 7-37729
 composition between 500 and 20000K 7-39944
 compressed, stimulated Raman scatt., excitation by XeCl low divergence laser 7-57468
 CRL 618, proto-planetary nebula, H₂ S(1) line profile 7-35031
 RS CVn stars, H α emission and X-ray characs. (Chinese) 7-29501
 DA stars, effective temps., Ly α profiles 7-55633
 degradation reduction in optical cables, materials selection 7-11172
 dense plasma, H α line Stark-broadened profile meas. 7-20935
 depth profile meas. by reson. nucl. reactions 7-3617
 desorption from Si (100) surface, reactivity enhancement by electronic excitation 7-2366
 diamond, interstitial H or muonium, Hartree-Fock analysis 7-32947
 diffusion and trapping in Fe-Cr alloys: 7-27018
 diffusion and trapping in Nb, NMR obs. 7-27616
 diffusion coefficient in Pd, influence of subsurface layer on meas. 7-6892
 diffusion in α - and β - phases of LaNi₅ 7-6874
 diffusion in long-range ordered alloys 7-21508
 diffusion in PbO₂, electrochem. meas. 7-16807
 diffusion in Pd membranes, transport coeffs. and energetics 7-21533
 diffusion in pure Fe, dislocation trapping, interstitial impurities effect (Japanese) 7-52140
 diffusion in Si-SiO₂ system 7-21531
 diffusion in solid solution alloys, FCC and BCC lattice structs. 7-21532
 diffusion in Ta, internal friction, 100-400K (Chinese) 7-6872
 diffusion on low C steel, trapping by TiC precipitates (Chinese) 7-7998
 diffusivity and solubility in Pd-polymer membranes, meas. by nonequilib. stripping potentiostatic method 7-6809
 Dirac operators, consistency of use in basis set variational solns. with Dirac hole theory 7-19692
 discharge, at. and mol. meas. using reson. multiphoton ionisation 7-20955
 discharge, atmospheric pressure, transition region, static V-I characteristics 7-51536
 discharge, electron beam energy relax. mechanism in electrode sheath 7-51464
 dissociative adsorption and reduction of Fe oxide surface layers 7-8297
 duoplasmatron arc, plasma emission mechanism 7-26532
 electrochemical evolution from In surface, in US field 7-11231
 electron swarm development in nonuniform electric field crossed with mag. field 7-51390
 faint H α emission-line galaxies, spectral obs. 7-35032
 field adsorption and desorption on W (110), atom probe FIM 7-21647
 galaxy pairs and small groups, H I spectral characs. 7-14669
 garnet bubble films, H₂⁺-implanted, H out-diffusion suppression of over-layers 7-38259
 gas, low pressure, in light guide, as high-power forward Raman amplifier 7-20344
 gas, Raman beam combination of two-line XeF laser sources 7-20336
 gas, stimulated Raman scatt., Ar₂ excimer laser tunable intense radiation generation 7-20328
 gas, supercontinuum generation with femtosecond pulses 7-25908
 gas diffusion into Pd alloy tubes 7-20828
 generation from optical fibre cable materials 7-11170
 generation from optical fibre coatings UV curable acrylated resins 7-11171
 glow discharge, shock wave acceleration 7-6478
 ideal gas, modified Gibbs state 7-44087
 implantation and diffusion in fusion reactor structural materials, Mo and W 7-49658
 impurity in Nb₉₀V₁₀ alloys trapping, precipitation and nucleation, localised vibr. mode meas. 7-2133
 impurity in Pd, molecular dynamics simulation model for mobility and thermotransport props. 7-58554
 interaction at metal surfaces and interfaces 7-21670
 interaction with LaB₆ (001), effect on field evaporation 7-21652
 interaction with semiconductor surfaces 7-58632
 internal friction in amorphous Ni₃Si₂ 7-39577
 interstellar H₂, assoc. e⁻e⁺ annihilation laboratory simulation 7-14426
 interstellar H I in halo and LMC 7-60768
 interstellar local material ionisation characs. 7-14628
 ion implants in metals, trapping coefficients 7-6884
 ion microanalysis of solid surface layers during H admission 7-18929
 isotope separation by selective multiphoton dissociation 7-42780
 isotope sorption and recovery by nonevaporable getter with chem. compressor material 7-48760
 jets, ignition behind reflected shock waves 7-37504
 kaonic, Klein-Gordon eqn. with phenomenological pots. 7-42794
 laser radiation frequency conversion by stimulated Raman scattering in H₂ 7-43226
 LDN 1641, second mol. cloud core discovery, HCN and H₂ mapping 7-14622
 lines in arc plasma, shift meas. 7-11709
 liquid, cryogenic, high press. eqn. of state, laser interferometric meas. method 7-30027
 liquid, with immersed Ne impurity, polarisation effects on core levels 7-64158
 M31, interstellar H I holes and supernova rate 7-35036
 Magellanic H I bridge, 160 pc shell feature characs., stellar wind or SNR origin 7-35049
 maser, operation below 1K 7-1069
 maser at temps. below 1K 7-43043
 maser atomic standard, built at Johns Hopkins University, long term performance 7-18759
 maser miniature passive clock, NBS design, characs. and performance 7-18760
 masers, single-state selection system 7-43045
 metal-H systems, anelastic props. 7-26856
 metal-H system, surface props. investig. 7-33487
 metal-H systems, bonding, statistical thermodynamic aspects 7-21472
 metallic glasses-H₂, prep., struct. and props. 7-26663
 methane-H₂ mixture, isochoric meas. at temp. from 140 to 273.15K, eqn. of state, density 7-26377
 methane-H₂ plasma, epitaxial growth mechanism of diamond crystal 7-12532
 microwave-pumped cryogenic maser 7-43044
 molecular beam impact with Cu (100), resonant sticking coeff. 7-13308
 molecular chemisorpt. on Ni (100) stepped surface 7-21632
 molecular cryst., IR absorpt. spectra in first overtone region 7-59209

hydrogen continued

molecular diffusion in pure crystals, continuous-time correlated walk with unrestricted jumps model appl. 7-27015
 molecules, adsorbed by metals, kinetics, oxide layer effects at room temp. 7-33965
 monolayer on Pt surface, He atom diff. intensity calcs. 7-3139
 NGC 3448, amorphous galaxy, photometry and H I dynamics 7-35041
 nonlinear susceptibility, third-order, electronic hyperpolarisability dispersion 7-20316
 overpotentials on Pd(Pd alloy) electrode surfaces 7-23031
 Palomar-Westerbork survey of northern spiral galaxies 7-40724
 para-H₂ cell, Raman conversion from far-wave mixing of CO₂ laser 7-25877
 para-H₂ concentration meas. using thermal conductivity cell 7-54229
 parametric Raman gain suppression 7-43232
 passivation, of polycrystalline Si, grain boundaries 7-26769
 passivation of dislocations in Si at high H₂ press. 7-39763
 pellet fuelling system for plasma fusion confinement magnetic valve design 7-11683
 permeability at high-temp. and -press., in Ag-Pd, Au, Ag, Pt metals 7-27011
 permeation, S surface segregation on V effect, AES anal. 7-32660
 permeation in Fe, plastic deform., dislocation traps 7-65082
 permeation through metal membranes (*German*) 7-57971
 photoinjected in MoO₃, effect on adsorptivity 7-63942
 photoinjected in V₂O₅, effect on adsorptivity 7-63942
 photoinjected in WO₃, effect on adsorptivity 7-63942
 physisorption interaction with simple metals 7-12480
 plasma, α line shift and profile 7-44243
 plasma, β spectral line peak asymmetry 7-51518
 plasma, Balmer- α line Stark broadening, simulation 7-11697
 plasma, computer simulated binary collision hypotheses, Stark broadening 7-10492
 plasma, electrical conductivity 7-1677
 plasma, electron scattering, momentum transfer 7-51389
 plasma, low n Balmer line intensities, T-tube glass-to-plasma boundary layer study 7-37701
 plasma, low-density, H Lyman- α line, Stark broadening 7-32086
 plasma, nonideal elec. cond., multiple scatt. contrib. is H 7-16299
 plasma, phase transitions study 7-37633
 plasma, strongly degenerate two-component, thermodynamics 7-16962
 plasma, T-tube boundary layer effects on spectral intensities ratios, temp. determ. 7-37635
 plasma, thermodynamic functions and self-energy 7-16963
 plasma diagnostics using ion impact Stark broadening 7-51517
 plasma parameters, electronic device for taking probe current second derivative (*Czech*) 7-32080
 plasma passivation of Si, subsurface H barrier layer obs. 7-17745
 plasma-broadened H α line, theory of two-photon polarisation spectroscopy 7-20936
 plasmas, ionised Fe atom miscibility under solar interior conditions 7-14555
 polyimide surface, in situ anal. of H,C,N and O using direct recoil time-of-flight technique 7-54242
 production of low energy atoms, energy and particle reflection coeff. meas. 7-26448
 pulsed plasma, stability measures Balmer- β line spectrum 7-11615
 quartz, H₂ diffusional uptake and hydrolytic weakening 7-40469
 Raman amplifier, Stokes phase preservation 7-20342
 Raman conversion, high efficiency and brightness via capillary waveguide amplifier 7-15944
 Raman generator, stimulated Stokes emission spatial mode structure 7-15937
 Raman generators, spatial mode struct. of stimulated Stokes emission 7-20345
 Raman oscillator, synchronously pumped, picosecond Stokes pulse generation 7-15933
 Saturn H₂ number density in upper atmosphere, calc. using temperature models 7-14517
 self-diffusion on Cu(100) surface, isotope and substrate motion effects 7-38237
 sensors using MOS structures with Pd-Ag gates 7-65364
 a-Si:H, structural characterisation, hyperfine interaction, ESR, ENDOR 7-53135
 a-Si:H solar cells stability, role of Si-H bonds studied by Fourier transform infrared spectroscopy 7-13896
 solar wind, energetic H⁺ and He fluxes associated with interplanetary shocks 7-23967
 solubility diffusion in amorphous Pd₈₀Si₂₀ 7-26969
 solubility in Li-LiH-Na systems, press. and temp. depend. 7-21471
 sorption on Ni_{4.15}Fe_{0.85}R-Al matrix (R = Mischmetal), nonequilibrium parameter 7-32836
 steel, H anomalous diffusion, nonlinear partial differential eqns., C² solns. 7-58525
 storage systems using thermochemical compression for transportation appl. 7-34072
 Sun, coronal loops, Lyman α emission, filtergram anal. 7-24092
 Sun, filaments, oscillations in H α and C IV lines 7-60614
 Sun, flare non-LTE calcs. (*Chinese*) 7-29442
 Sun, flares in chromosphere, H non-thermal excitation and ionisation 7-34843
 Sun, H β line form. in chromosphere magnetic field (*Chinese*) 7-29441
 Sun, H spectra, visible and IR lines in photospheric models 7-29454
 Sun, quiescent filament, H α and C IV vel., centre-limb anal. 7-14551
 swirling turbulent diffusion flames, turbulence intensity study 7-26287
 thermal absorption or desorption studies, microcomputer controlled apparatus 7-21668
 trace anal. in thin films using extremely high vacuum SIMS 7-54243
 transfer in double minimum potential, kinetic props. and quantum dynamics 7-54104
 transition metals:H, local impurity environment in cubic lattices 7-21236
 transition metals-H₂, disordered, NMR studies 7-27618
 trapping in Fe during cathodic charging 7-21256
 trapping in Nb:O, perturbed ang. coring. obs. 7-27641
 trapping phenomena in metals, with BCC and FCC struct., meas. by desorption thermal anal. technique 7-6673
 turbulent jet diffusion flame, conserved scale probability density functions 7-26260
 United States E and Gulf coasts, atm. H₂ conc. and sources 7-55197
 Uranus, H Lyman α emission characts. 7-9414

hydrogen continued

Venus atmosphere, H velocity distrib. influenced by charge exchange 7-55509
 VUV anti-Stokes Raman line generation using excimer lasers 7-57450
 Z-discharge plasma, H atom density from H α and H β spectral line intensities 7-26512
 Al-killed 1006 steel, H diffusion effect on enamelling 7-33816
 Al-Si:Ar:H, ion implanted ultrahigh Schottky barriers, interfacial traps, DLTS study 7-45489
 Ar-H₂ mixture, plasma jet, 941.04 Å emission 7-11704
 Ar-H₂ mixtures, transport and relax. cross-sections, close-coupling calcs. 7-51363
 a-C:H, diamondlike, dielectric film, props. rel. to deposition parameters 7-39419
 a-C:H, film, optical and compositional props. 7-39206
 a-C:H, film, optical and electronic props. rel. to deposition parameters 7-38406
 a-C:H, film, optical energy gap, density, hardness 7-39204
 a-C:H, film, plasma emission spectroscopy, chem. anal. 7-38407
 a-C:H, films, plasma deposition characterisation of hydrocarbons used 7-39422
 C:H, homogeneous and heterogeneous chemistry of methane deposition plasma 7-39424
 a-C:H, props., review 7-51630
 a-C:H films, glow discharge deposited, valence electron props., electron energy loss spectra study 7-13288
 a-C:H films, plasma deposited, optical props. 7-27799
 a-C:H plasma grown films, struct., physical props. 7-58713
 a-C:H polymeric layers, plasma-activated CVD produced, spectroscopic investigations 7-22572
 a-C:H polymeric plasma-activated CVD films, tribological and mechanical props. studies 7-16920
 CO-H system, magnetisation study 7-38901
 CO-N₂-H₂ gasdynamic laser with 2D nozzles, gain optimisation 7-50541
 CaF₂:Er³⁺, H⁺, IR excitation and absorpt. spectra anal. of sites 7-53306
 Cl₂-H₂ cells containing PbCl₂ solid electrolyte, cathodic characts; effect of vac. deposited FeCl₃ (*Japanese*) 7-13850
 Co-Cr-H₂ films, sputter deposited, effects of additive gases on mag. props. 7-27575
 α -Fe:H, H induced softening, yield stress reduction 7-39607
 Fe:H(D), lattice strains, meas. 7-2268
 Fe-H system, dislocated single crystals, positron trapping reduction on H charging 7-39262
 Fe-H system, H-defect interactions study by positron annihilation 7-38046
 γ -Fe₂O₃:H, H content, DTA, mag. anal. and Mossbauer studies (*Chinese*) 7-12104
 γ -Fe₂O₃:H, hydrogen probe using thermal neutron transmission gauge (*Chinese*) 7-6666
 Fe₇₃Ti₂₇-H₂ amorphous alloys, Mossbauer spectra 7-33308
 GaAs:H, ion implanted, damaged layers, IR Raman probing 7-59191
 GaAs:H, proton bombarded, H platelets, TEM obs. 7-12164
 GaAs:H amorphous sputtered films, AC cond. studies 7-21947
 a-GaAs:H:F, electronic struct., dangling bonds, cluster-Bethe lattice method calcs. 7-12592
 GaAs-Ga_{1-x}H₂, dissolution of GaAs, crystallographic characteristics 7-12415
 GaAs(P)(Sb):H, vibrational excitations, impurity-host atom complexes, IR absorpt. data interpretation 7-44724
 Gd₃Si₂H₇, H-D exchange, H desorption 7-28304
 a-Ge:D,H, plasma deposited, deuteron magnetic resonance 7-27626
 a-Ge:H, B, P, As, dopant incorporation and doping efficiency 7-44587
 a-Ge:H, elec. props., effect of H plasma press. (*Korean*) 7-27332
 Ge:H,Be(Zn), shallow acceptor complexes 7-45219
 a-Ge:H glow discharge deposited thin films, H content determ., spectroscopic ellipsometry study 7-38365
 a-Ge:H/Si:H superlattice struct., light absorption and photocond. studies 7-38715
 Ge:H:Si:H amorphous superlattices, electrical transport 7-7336
 a-Ge:Si:H,F, multijunction solar cells, performance data 7-40011
 a-Ge:Si:H, deposition kinetics and structural control 7-45087
 a-Ge:Si:H:F double Schottky barrier structures, surface photovoltage meas. and calc. 7-17093
 a-Ge:Si:H,F/a-Si:H,F superlattices, elec. transport studies 7-38716
 a-Ge:Si:H alloy tandem-type solar cells, conversion efficiency 7-40014
 H I IR line emission from protogalaxies and protocluster pancakes 7-4600
 H I obs. of Per A and Vir A 7-60774
 H II regions, H radical recombination line emission 7-60746
 H neutrals in bounded plasma slab, kinetic theory, analytical solns. 7-57981
 H plasma, collisions, Stark broadening calcs. 7-10493
 H, T-tube plasma, β -line central dip, ion dynamic effects anal. 7-36542
 H/hydrocarbon ion beam passivation of Si, surface layer characterisation 7-17746
 H-C-C relay investig. of unprotonated C atoms 7-35558
 H-CO₂ binary mixtures, H fugacity coeff. meas., physical equilib. technique 7-16296
 H-D exchange, fast atom bombardment mass spectrometric obs. 7-50392
 H-metal disordered systems, neutron vibr. spectroscopy, review 7-21381
 H-propane and H-methane binary mixtures, H fugacity coeff. meas., physical equilib. technique 7-16295
 H₂, chemisorption on W (100), free carrier surface scatt., IR obs. of adsorbate induced changes 7-22268
 H₂ effect on CO-induced struct. changes in supported Rh 7-23063
 H₂ evolving electrode with superimposed electrolyte flow, mass transfer 7-46852
 H₂ IR line emission from protocluster pancakes and protogalaxies 7-4600
 H₂, reaction with different Cu surfaces with adsorbed O 7-59784
 H₂-Ar, externally sustained discharge, instability mechanism 7-63381
 H₂-Ar mixture, frequency conversion by stimulated Raman scattering 7-43233
 H₂-D₂ mixtures adsorbed on graphite, phase diagrams 7-52180
 H₂-D₂ system, CO₂ laser induced breakdown 7-6352
 H₂-F₂ laser, atmospheric pressure, feasibility of short radiation pulse generation 7-25807
 H₂-hydrocarbon vapour-liquid equilibria and saturated densities at high press. and temp. 7-16707
 H₂-metal impact, density functional approach, dynamic response at metal surfaces, van der Waals interaction, excitation of electron-hole pairs 7-3129

hydrogen continued

- H₂-O₂-N₂ flames, one-dimensional simulation, mathematical and numerical aspects 7-39893
 H₂ profiles at high electron densities from optical discharges 7-6447
 HCl/H₂ gas etchant for Si surfaces 7-65220
 HCl/H₂ gas etchant for Si, gas composition analysis 7-65221
³H labeled compounds, gasoline as primary solvents in liquid scintillation counting 7-36417
 He-H, isotope composition, spectrosc. determ. 7-50395
 He-H₂, rot. inelastic scatt., forward and inverse functional var. 7-5753
 He-H₂ system, density inversions between fluid and solid phases at high pressures 7-58451
 He-hydrogenic trace mixtures, temp. depend. of thermal diffusion factor, role of column calibration factor 7-63240
 Ho₂Si₂H₂, H-D exchange, H desorption 7-28304
 KCl:H, F-centre accumulation during proton irradiation 7-46076
 Kr-He-H₂ mixtures, self-quenching streamer or Geiger-Muller region 7-19669
 LaNi₅:H films, resist. rel. to hydrogenation 7-58910
 α-LaNi₅-H, multiply cycled, inelastic neutron scatt. 7-32835
 LaNi₄Al_{0.5}H₂-n-undecane suspension, H₂ absorpt. kinetics 7-33966
 LaNi₅H₂O, dissociation press., O content depend. 7-63825
 LaNi₅H₂-n-octane suspension, H₂ absorpt. kinetics 7-33966
 Li-H systems, localised nature of chemisorption bond, calc. of chemisorption energies 7-2361
 Li₃N:H, doped and undoped fast ionic conductor, positron annihilation 7-39276
 LiNbO₃:H, laser-induced grating characteristics 7-62746
 LiNbO₃:H channel waveguides, anal. 7-26023
 LiNbO₃:H optical waveguides, devices, charactn. and future prospects 7-26022
 LiNbO₃:H ring resonators, operation at 0.79 μm and 1.3 μm 7-26029
 LiNbO₃:Ti(H) waveguides, photorefractive susceptibility, charactn. methods 7-26024
 Mg-SiO-H₂, nucleation, physical spinodal theory 7-21428
 MgO:H, C single crystals, ion implanted, C and H diffusion behaviour, SIMS studies 7-32714
 Nb-H⁺ films, radiation defects produced by ion implantation 7-7059
 Nb-H systems, muon diffusion, μSR study 7-45868
 Nb-H-O(N) system, supercond., tunnelling of H trapped by O(N) anelastic relax. meas. 7-39572
 Nb-Ti-H(D), anomalous anelastic relax., statistical model 7-28065
 Nb-Ti-H(D), substitutional alloys, intermediate temp. relax., Fermi-Dirac model 7-26858
 NbH₂, Compton profiles 7-59281
 NbH_x, interstitial H total cross-section determ., localised modes and diffusion, neutron transmission meas. 7-12061
 Ni-H, diffusivity, diffusion-elastic effect and Gorsky effect 7-27023
 Ni-H system, band structure calcs. 7-45140
 Ni-H₂ aerospace batteries, low Earth orbit test program 7-34025
 Ni-H₂ aerospace cells for low Earth orbit appls., research technology advances 7-34022
 Ni-H₂ batteries, 40 Ah, bipolar, for space appls., parametric testing 7-34027
 Ni-H₂ batteries for space appls., proceeding of NASA/Goddard workshop, Greenbelt, MD, USA (Nov. 1985) 7-29578
 Ni-H₂ cell for space appls., 4.5 inch IPV development program 7-34026
 Ni-H₂ cells, lightweight, direct radiating, for space appls. 7-34023
 Ni-H₂ cells technology for RADARSAT spacecraft appls., test program 7-34024
 Ni-H₂ secondary cells for low-Earth-orbit satellites, reliability and life testing 7-65451
 Ni-H₂ secondary cells heat generation and transfer rates 7-65452
 NiZr-H₂, metallic glass, pressure-concentration isotherms 7-26665
 Ni₄Zr₃₆, amorphous, electrical resistance meas. in gaseous H₂ 7-32978
 Pd-B-H alloys, internal friction, elastic consts. 7-26857
 Pd-B-H dilute solutions, statistical mechanics 7-21669
 Pd-Ce-H, electrical resistance meas. 7-32984
 Pd-H system, H conc. determ. in absorbing metallic thin films 7-23117
 Pd-H₂, Pd-based ternary system, hydrogen absorption, model 7-26970
 Pd₈₀Si₂₀H₃, metallic glass, H diffusion, quasielastic neutron scatt. study 7-21534
 Pd₃CeH₂, H solubility in ordered/disordered Pd alloys 7-21473
 Pd_{1-x}Fe_xH₂ system, isomeric shift, fluctuations of hyperfine interaction, Mossbauer study 7-45843
 PdH, thin film thickness depend. resistivity changes meas. 7-33109
 PdH_x, dilute alloys, Pd substituted, interaction of H with impurities, EXAFS study 7-64806
 β-PdH_x, spin polarisation torsional spectroscopy 7-33280
 Pd₃MH₂ (M=Fe, Mn), H solubility in ordered/disordered Pd alloys 7-21473
 Pd_{82-y}Ni₁₈, amorphous, electrical resistance meas. in gaseous H₂ 7-32978
 Pd_{100-y}Si_y, amorphous, electrical resistance meas. in gaseous H₂ 7-32978
 S-B-H Schottky and n⁺-p junction diodes, electrical transport of acceptor-compensating defect 7-16823
 ScH₂, H diffusion 7-52117
 Si surface, 100, in situ anal. of H,C,N and O using direct recoil time-of-flight technique 7-54242
 Si-B, H, hydrogenation of B acceptor during electron injection by Fowler-Nordheim tunnelling 7-45504
 a-Si:D,H, deuteron mag. resonance, annealing effects 7-33292
 a-Si:F,H, amorphous, high efficiency solar cells fabrication and props. 7-17901
 a-Si:H, ²⁹Si and ¹H NMR spectra, peak position and line shape 7-2934
 Si-H, acceptor neutralizing species, low temp. injection mechanisms 7-32482
 a-Si:H, ambipolar drift length meas. using steady-state photocarrier grating technique 7-45390
 α-Si:H, amorphous, coherent potential approx., potential well analogy 7-27240
 Si:H, amorphous, dendritic web, Czochralski flat plate modules and concentrator module, price comparison 7-17904
 Si:H, amorphous, p-i-n solar cells, stability behaviour, impurities and doping residues effect 7-17912
 Si:H, amorphous, solar cells, current-induced and light-induced degradation, non-equivalence 7-17908
 Si:H, amorphous, transient photoconductivity characterisation 7-52692
 Si:H, amorphous film, optical absorption and bandgap rel. to temp. (Korean) 7-59228

hydrogen continued

- a-Si:H, amorphous to microcrystalline structure transformation, phase stabilisation 7-63475
 a-Si:H, B, P, As, dopant incorporation and doping efficiency 7-44587
 a-Si:H, B, P-type, increased elec. cond. studies 7-45337
 a-Si:H, B₂H₆(PH₃), localised density of states, electrophotography study 7-32957
 a-Si:H, broken bond local environment relax., g-factor, cluster calcs. 7-37876
 a-Si:H, C superlattice struct., solar cell performance 7-46945
 a-Si:H, carrier trapping and recombination, IR enhancement spectra of photoconductivity 7-33052
 a-Si:H, conductivity, fundamental pre-exponential factor, Meyer-Neldel rule 7-7249
 Si:H, conf., Boston, MA, USA (Dec. 1985) 7-14711
 a-Si:H, configurational models and adiabatic potentials of H 7-51632
 a-Si:H, contact resist. meas. technique 7-24658
 a-Si:H, deep trapping, transient photocurrent saturation 7-21952
 a-Si:H, defect structure, ab initio theory 7-32298
 Si:H, dendritic web cryst., solar cells and modules fabrication status 7-8391
 a-Si:H, density of states, SCLC meas., effect of injection electrodes 7-64265
 a-Si:H, distrib. of states study by capacitance-voltage method 7-7089
 a-Si:H, divacancy electron struct., semiempirical CNDO/2 cluster calcs. 7-38495
 a-Si:H, doped, electronic transport 7-21916
 a-Si:H, EXAFS, spherical wave anal. and multiple scatt. effects 7-64740
 a-Si:H, elastic properties 7-21323
 a-Si:H, electronic density of states, DLTS and capacitance transient spectra anal. 7-45134
 a-Si:H, electronic struct., inadequacy of the conventional view 7-32961
 a-Si:H, electronic struct. modelling with small clusters 7-64057
 a-Si:H, electronic transport 7-33004
 a-Si:H, evaporated samples, post-hydrogenation, characts. 7-59103
 a-Si:H, extended state mobility and tail-state distrib. 7-2617
 a-Si:H, fluctuation induced gap states 7-27242
 a-Si:H, form. by ion flux control under toroidal mag. field (Japanese) 7-17446
 a-Si:H, gas-phase and ion-implantation doped, doping efficiencies 7-51790
 a-Si:H, glow discharge deposited, light soaking effects 7-52872
 a-Si:H, glow discharge deposition, surface roughness evolution 7-64933
 a-Si:H, glow discharge prepared, steady-state photoconductivity 7-38632
 a-Si:H, glow discharge thin films, deposition rate, optical props., influence of substrate temp. 7-59460
 a-Si:H, H clustering, multiple quantum NMR 7-32671
 Si:H, impurity clustering, hydride form. on dislocations, TEM study 7-26964
 a-Si:H, influence of H on defects and instabilities 7-26647
 a-Si:H, intrinsic glow-discharge, elec. noise meas. 7-64297
 Si:H, ion implanted and annealed, H depth distrib. 7-26785
 a-Si:H, light induced degradation at high illum., inverse Staebler-Wronski effect 7-23195
 a-Si:H, light-induced electron spin resonance 7-33274
 a-Si:H, localised electronic state, light soaking and current injection 7-16994
 a-Si:H, metastable defect states, capacitance studies 7-45225
 a-Si:H, mobility edge, density of states and carrier activation energy calcs., random Bethe lattice approach 7-16937
 a-Si:H, NMR props. of ortho-H₂ centres 7-2935
 a-Si:H, neutral dangling bond defect, photocarrier processes 7-32962
 a-Si:H, non-exponential photocurrent decay, anal. 7-38633
 a-Si:H, optical dispersion relations, determ. 7-33353
 a-Si:H, photo-CVD deposition, initial processes (Japanese) 7-7053
 a-Si:H, photocond. response, light soaking effects 7-45396
 a-Si:H, photoconductivity and light-induced changes 7-2640
 a-Si:H, photoconductivity exponent for recombination at dangling bonds 7-33054
 a-Si:H, photoinduced absorpt., ps decay 7-27684
 a-Si:H, photolum. and photoconductivity studies 7-33456
 a-Si:H, photoluminescence, thermal quenching 7-53389
 a-Si:H, picosecond photoinduced absorption and transmission 7-3006
 a-Si:H, picosecond photoinduced absorption decays, interference effects 7-3012
 a-Si:H, plasma deposited NMR, Pake doublet 7-27617
 a-Si:H, plasma enhanced CVD, integrated model 7-39423
 Si:H, polycrystalline, chemistry of grain boundary passivation 7-12375
 Si:H, polycrystalline, grain boundary interactions 7-12117
 Si:H, polycrystalline, plasma hydrogenation, ESR study 7-45819
 a-Si:H, prep. in rotary plasma isolated reactor and props. 7-7891
 a-Si:H, RF glow discharge prod., high deposition rate study 7-7889
 a-Si:H, recomb. at dangling bonds and steady-state photocond. Fermi level depend. calcs. 7-12734
 Si:H, Si-H IR stretching bands, models, CNDO calc. 7-53314
 a-Si:H, Si-H-Si three centre bonds IR spectra, LCAO-MO-SCF-STO-3G calcs. 7-6741
 a-Si:H, Staebler-Wronski effect and metastable light-induced defect creation kinetics model 7-64284
 a-Si:H, structural props., EXAFS study 7-64760
 Si:H, summary of present state of research 7-16584
 a-Si:H, surface deep hole trap, photocurrent studies 7-45424
 a-Si:H, thermal-equilib. processes, electronic transport 7-64167
 a-Si:H, triplet exciton recomb., ODMR studies 7-2490
 a-Si:H,B, effective p⁺ doping by plasma-assisted B diffusion 7-38036
 a-Si:H,B, RF sputtered films, optical and electrical props. 7-33470
 a-Si:H,B, thin films, thermoelectric power 7-58826
 a-Si:H,B films, hole transport, time-of-flight meas. 7-45320
 a-Si:H,B p-i-n and n-i-p solar cells, doping profile effects 7-46947
 a-Si:H,B/a-Si:H,P doping modulated superlattice, photo-induced excess conductivity 7-17051
 a-Si:H,B(As) RF sputtered coatings, gas-phase doping efficiency 7-63471
 a-Si:H,B(P) films, dopant conc. meas. and depth profiling by means of (p,γ) resonant reactions 7-12555
 a-Si:H,Cl glow discharge films, Raman scatt. 7-39116
 a-Si:H,D, H abstraction from surface, HD formation 7-39914
 a-Si:H,F by thermal CVD, photosensitivity, spin density, conductivity and p-n type 7-17454
 a-Si:H,F films, dark discharge mechanism of surface potential (Japanese) 7-17034

hydrogen continued

- a-Si:H,F films, initial carrier trapping stages observed by femtosecond spectroscopy 7-27301
- a-Si:H,F films, prep. using H radical assisted CVD (*Japanese*) 7-17430
- a-Si:H,F multijunction solar cells, performance data 7-40011
- a-Si:H,F solar cells, radiation hardness to 1 MeV protons 7-23180
- a-Si:H,F/a-Si:Ge,H,F superlattices, elec. transport studies 7-38716
- a-Si:H,F/a-Si:H,F,Ge multiple junction solar cells on stainless steel substrates 7-13902
- a-Si:H,F/a-Si:Ge,H,F multiple layered films for enhancement in photoreponse in near IR spectrum 7-52668
- a-Si:H,F-Si_{0.4}Ge_{0.6}H,F superlattices, carrier scatt., optical absorpt. study 7-38711
- a-Si:H,Ge single junction and tandem solar cells, thin film properties and corollary plasma diagnostics 7-13893
- a-Si:H,N thin films, activated reactive evaporation 7-13355
- a-Si:H,P multilayer films, plasma CVD and elec. cond. studies 7-39428
- a-Si:H,P(B) films, ion implanted, photoelectric and optical props. 7-38615
- a-Si:H,P(B) p-i-n solar cells, open-circuit volt., wavelength depend. 7-46948
- a-Si:H (C,H) (O,H) (N,H), annealing of metastable defects 7-3343
- Si:H (100) proton bombarded surface, complex refractive index profile, ellipsometry study 7-22216
- a-Si:H and a-Si films, electrical conductivity and struct. 7-52866
- a-Si:H and a-Si:H, B films, photoinduced changes in elec. props. 7-38634
- a-Si:H and a-Si:H,P, electron nuclear double resonance expts. 7-2950
- Si:H and near-surface damage of Si caused by H ions, review 7-16813
- Si:H based alloy thin films, optical constants determ., device modelling appl. 7-7666
- a-Si:H based alloys for solar cells, elec. props. and degradation behaviour 7-52642
- a-Si:H biased activated reactive layer evaporation and charactn. 7-59428
- Si:H binary alloys, crystallisation of polysilane 7-21105
- a-Si:H CVD coating, high temp. elec. cond. meas. 7-45336
- a-Si:H CVD films, density of states distrib., I-V characts. meas. 7-45113
- a-Si:H doping modulated films, photocond., carrier separation effects 7-38641
- a-Si:H doping modulated multilayers, light-induced excess conductivity 7-38643
- a-Si:H doping modulated superlattices, light-induced excess cond., deposition effects 7-27410
- a-Si:H doping superlattice interface struct. charactn. 7-58652
- a-Si:H evaporated layer production from RF discharge, growth mechanism and props. 7-64898
- a-Si:H film, photo-assisted plasma CVD 7-33593
- a-Si:H film, photoenhanced deposition and characts. 7-53635
- a-Si:H film prep. by compressed mag. field magnetron sputtering (*Japanese*) 7-46323
- a-Si:H films, annealing, compressive stress, H evolution 7-28059
- a-Si:H films, CVD, electrical and optical props. 7-33596
- a-Si:H films, CVD, optical and electronic props. 7-33597
- a-Si:H films, carrier transport 7-17023
- a-Si:H films, charge carrier dynamics, influence of preparation conditions 7-33053
- a-Si:H films, columnar morphology, evolution of vibr. spectra 7-64646
- a-Si:H films, contact potential difference, surface photovoltage and conductivity 7-58855
- a-Si:H films, deep levels in the mobility gap 7-12670
- a-Si:H films, defects and microvoids, positron annihilation study 7-45086
- a-Si:H films, density of states and photoconductivity 7-45392
- a-Si:H films, depth profiling of constituents and impurities, elastic proton scatt. 7-45044
- a-Si:H films, discharge and CVD deposition, surface reactions 7-33601
- a-Si:H films, electron irradi., photocond., absorpt. coeff. spectral depend. 7-64279
- a-Si:H films, electronic props., effects of γ -irradiation 7-38584
- a-Si:H films, glow discharge deposition 7-65325
- a-Si:H films, glow-discharge-deposition, initial nucleation and growth 7-63997
- a-Si:H films, growth and photovoltaic appls. 7-64236
- a-Si:H films, growth habit, influence of substrate struct., ellipsometry study 7-45055
- Si:H films, H content meas. 7-12553
- a-Si:H films, high rate deposition and impurity doping effects (*Japanese*) 7-13385
- a-Si:H films, high rate deposition by RF planar magnetron sputtering (*Japanese*) 7-39373
- a-Si:H films, illumination effects on conductivity 7-7291
- Si:H films, ion implant redistribution 7-16921
- a-Si:H films, light-induced bond breaking 7-12517
- a-Si:H films, metal-semiconductor contacts, characterisation 7-38724
- a-Si:H films, metastable optically induced ESR, time depend. 7-45800
- a-Si:H films, photo-enhanced CVD 7-33594
- a-Si:H films, photocond. characts. stabilisation (*Japanese*) 7-45393
- a-Si:H films, photoconductivity, thermal quenching obs. 7-52686
- a-Si:H films, plasma CVD, deposition kinetics (*Japanese*) 7-17450
- a-Si:H films, RF glow discharge deposition, optical and electrical props. 7-33598
- a-Si:H films, reactive deposition 7-33592
- a-Si:H films, sputter deposition, optical and ESR props. 7-33565
- a-Si:H films, thermal-equilibrium defect processes 7-26640
- a-Si:H films and p-i-n solar cells, photo-assisted CVD and opto-electronic characterisation 7-33595
- a-Si:H films and solar cells, light induced effects 7-46954
- a-Si:H films deposited by dual ion beam sputtering, characterisation 7-32882
- a-Si:H films high-rate deposition by RF planar magnetron sputtering (*Japanese*) 7-17419
- a-Si:H films photo-CVD, photoelectric and structural props. 7-7869
- Si:H floating zone single crystals, neutron irradi., isochronal annealing behaviour, positron annihilation studies 7-21288
- a-Si:H heterojunction solar cell modules, fabrication by laser scribing 7-13900
- a-Si:H high efficiency p-i-n solar cells using superlattice p-layers 7-23177
- a-Si:H junction position sensitive photodetector 7-56343
- a-Si:H large area integrated solar cells, fabrication 7-40013
- a-Si:H material and p-i-n cell, light-induced charge 7-17055
- a-Si:H material and solar cells, light induced effects 7-23139

hydrogen continued

- Si:H microcrystalline films, glow discharge prep., elec. and optical props. 7-7415
- a-Si:H modulation doped multilayers, persistent photocond. studies 7-38642
- a-Si:H modulation doped multilayers, planar and perpendicular cond. meas. 7-38717
- aSi:H multijunctions, charge carrier transport, theoretical anal. 7-38690
- a-Si:H multilayer films, charge transfer doping, cond., photocond. meas. 7-38735
- a-Si:H n^+-i-n^+ struct., freq.-depend. noise studies 7-45484
- a-Si:H p^+-n-i structs., memory switching, transient current instability study 7-52762
- a-Si:H p-i-n solar cells, behaviour after light soaks through p-layer and n-layer 7-8398
- a-Si:H p-i-n solar cells, light induced degradation, effects of impurities and temp. 7-17886
- a-Si:H pin solar cells, open-circuit volt., temp. and light intensity depend. 7-46949
- a-Si:H pin solar cells, photocurrent, transient behaviour 7-46950
- a-Si:H semiconductor-metal system, field effect problems, I-V meas. 7-38728
- a-Si:H short range order, impurity distrib. effects, EXAFS study 7-64761
- aSi:H solar cell characts. change due to long term temp. stresses 7-8393
- a-Si:H solar cell on polymer substrate, roll-to-roll prep. 7-59861
- a-Si:H solar cell prep. by laser-induced CVD of SiH₄ 7-7890
- a-Si:H solar cell technology in Japan, recent advances 7-40009
- a-Si:H solar cells, density of states asymmetry effects 7-46946
- a-Si:H solar cells, dynamic equilibrium dangling bond density 7-17878
- a-Si:H solar cells, effect of texturing 7-13857
- Si:H solar cells, H passivation by ion beams 7-17867
- a-Si:H solar cells, hydrogenated microvoids and light-induced degradation 7-54294
- a-Si:H solar cells, i-layer stability thickness dependency 7-17880
- a-Si:H solar cells, impurities and metastable centres 7-40010
- a-Si:H solar cells, integrated series connection 7-40015
- a-Si:H solar cells, kinetics of light-induced degradation and thermal annealing 7-17909
- a-Si:H solar cells, leakage currents, electrochem. treatment effects 7-65467
- a-Si:H solar cells, optically induced degradation 7-59848
- a-Si:H solar cells, p-layer doping by plasma assisted B diffusion 7-13898
- a-Si:H solar cells, photo-CVD prep. 7-17885
- a-Si:H solar cells, photoconductivity-open cct. voltage relation 7-8396
- a-Si:H solar cells, radiation damage by 12 MeV protons and annealing 7-13895
- a-Si:H solar cells, turn-off character, wavelength depend. 7-46951
- a-Si:H solar cells, uses of transparent conducting oxides 7-46953
- a-Si:H solar cells deposited from disilane, blue response and efficiency improvement 7-17877
- a-Si:H solar cells on textured glass substrate with SiO₂ film 7-13899
- a-Si:H solar cells prod. by positive-column glow-discharge method 7-8397
- a-Si:H sputtered film, low-temp. optical props. 7-3101
- a-Si:H sputtered films, intrinsic stress, H effects 7-7078
- a-Si:H stable heterojunction solar cells develop., thermal degradation phenomenon 7-65477
- a-Si:H surfaces and interfaces, microstruct., ellipsometry studies 7-38362
- a-Si:H thin film photovoltaic production, safety and industrial engineering 7-13894
- Si:H thin film solar cell technology, design and appls. 7-17872
- a-Si:H thin film solar cells, device properties 7-13897
- Si:H thin film solar cells, transparent module development 7-13911
- a-Si:H thin film solar cells, repeatable meas. system for accelerated stress testing 7-23174
- a-Si:H thin film solar cells, light soaking condition effects 7-46956
- a-Si:H thin films, bulk and interface struct., in situ ellipsometry study 7-27200
- a-Si:H thin films, elec. and optical props., thickness depend. 7-46168
- a-Si:H thin films, ohmic and quasi-ohmic contacts 7-38729
- a-Si:H two-junction, two-terminal tandem solar cells, stability and efficiency 7-46957
- a-Si:H ultrathin layers, CW photoluminescence, layer thickness depend. 7-13202
- a-Si:H ultrathin layers, photoluminescence characts., layer thickness depend. in variety of sample configurations 7-46123
- a-Si:H/CuInS₂ heterojunctions, photovoltaic behaviour, c-v meas. 7-7340
- a-Si:H/Ge:H superlattice struct., light absorption and photocond. studies 7-38715
- a-Si:H/Pd system, silicide form., struct. and electronic props. 7-38363
- a-Si:H/SiC tandem solar cell, thermal and light-induced degradation 7-46955
- a-Si:H/SiN_x interface, slow states, transient photoconductivity studies 7-38670
- a-Si:H/SiN_x:H (a-SiC:H) double-barrier structs., resonant tunnelling coeffs. 7-45467
- a-Si:H/SiO₂/N,H heterostruct., transport props 7-38768
- a-Si:H/SiO₂/metallic gate struct., capacitance-volt. characts. 7-45515
- a-Si:H/Ti/Al system, solid state reactions, TEM and SAD studies 7-3602
- a-Si:H/a-Ge:H multilayer films, photoconductivity enhancement 7-27443
- n^+-i-n^+ a-Si:H/a-Si:H/a-SiC:H heterostructures, electrophotographic props. 7-45485
- a-Si:H/a-Si_{0.5}C_{0.5}H solar cells, light trapping on SnO₂:F 7-46952
- a-Si:H/a-Si_{0.5}N_{0.5}H superlattices, plasma deposition methods 7-39439
- a-Si:H/a-SiGe:H multilayers, reactive deposition 7-33592
- a-Si:H/a-SiN_x:H, amorphous multilayer structures, optical props. 7-3014
- a-Si:H/a-SiN_x:H interface system, struct. and electronic props. 7-38361
- a-Si:H/a-SiN_x:H interface, deep states and photoluminescence spectra, transistor characts. 7-39186
- a-Si:H/a-SiN_x:H multilayer films, coplanar conductance, voltage-induced anomalies study 7-2729
- a-Si:H/a-SiN_x:H superlattices, interface struct., optical reflectance determ. 7-12497
- a-Si:H/a-SiN_x:H superlattices, interface defects and disorder 7-52306
- a-Si:H/a-SiN_x:H superlattice interface struct. charactn. 7-58652
- a-Si:H/a-SiN_x:H superlattice films, prep., struct., and optical props. (*Chinese*) 7-58676
- a-Si:H/a-SiO₂:H superlattice micropores, pyrene molecules adsorption and confinement 7-27112

hydrogen continued

- a-Si:H/a-SiO(N)_xH multilayer films, interface electroabsorpt. meas. 7-2689
- a-Si:H/crystalline Si heterojunction, photosensitivity studies 7-38714
- a-Si:H/metal junction, pot. profile determ. 7-2715
- Si:H-CuInSe₂ tandem modules, thin film design and fabrication 7-13913
- a-Si:H-CuInSe₂ thin film tandem solar cells, energy based perform. and eval. 7-13890
- a-Si:H-Pt Schottky barrier contact, photocurrent excitation nonadditivity effects 7-17099
- Si:H-Si_{1-x}C_xH amorphous super struct., hot electron generation 7-52794
- a-Si:H-Si₃N₄H double barrier structs., resonant tunnelling 7-52848
- Si:H-SiC:H heterojunction, amorphous solar cell anal. (Chinese) 7-34029
- a-Si:H-SiN_xH interface, compositional profile, Rutherford backscatt. study 7-13292
- a-Si:H-SiN_xH layered structures, effect of a-SiN_xH composition on band bending near interface 7-45510
- a-Si:H-based films, photochemical vapour deposition, review 7-46345
- a-Si:H-based heterojunction stacked solar cells, design and fabrication 7-40012
- Si:H(F)/SiGe:H(F) amorphous multilayer struct., fabrication and near IR photoconductivity characts. 7-52797
- Si:H(Sn,H)(C,H), amorphous alloy fabrication and characterisation 7-8389
- Si:O:H, heat treated, DLTS 7-16991
- a-Si:Se(Te) thermally evaporated films, photoelectronic props. 7-38640
- a-Si_{1-x}C_xH films prepared by plasma CVD method, props. (Japanese) 7-12543
- a-(Si-Ge)-H, prep. in rotary plasma isolated reactor and props. 7-7891
- a-SiC:H films, photo-assisted CVD and opto-electronic characterisation 7-33595
- SiC:H, amorphous, electronic and structural props. 7-17054
- SiC:H, amorphous CVD film, electron optical characterisation 7-52372
- a-SiC:H, elec., optical and local structure props. 7-45089
- a-SiC:H, B, effective p⁺ doping by plasma-assisted B diffusion 7-38036
- a-SiC:H,B, thin films, thermoelectric power 7-58826
- SiC:H,F amorphous films, struct., elec. and optical props. 7-22360
- SiC:H amorphous films, glow discharge deposited, photoconductivity, microstructure effects 7-58831
- a-SiC:H film prepared by magnetron sputtering, elec. and optical props. (Japanese) 7-12887
- a-SiC:H films, CVD, electrical and optical props. 7-33596
- a-SiC:H glow discharge films, IR vibr. spectra 7-53434
- a-SiC:H glow-discharge plasma deposition, photosensitivity, prep. conditions depend. 7-46338
- a-SiC:H thin films, glow discharge deposition, energy gap and activation energy 7-46352
- a-SiC:H/a-Si:H double-barrier structs., resonant tunnelling coeffs. 7-45467
- a-SiC:H(B), thin film, solar cells fabricated by plasma deposition (Korean) 7-33585
- a-SiC-a-Si:H stable heterojunction solar cell 7-23178
- a-Si_{1-x}C_xH, B(P) films, valence band localised holes, light-induced ESR spectra studies 7-53110
- a-Si_{1-x}C_xH, Si-K β spectra, soft X-ray emission spectra (Japanese) 7-13268
- a-Si_{1-x}C_xH,B(P) thin films, H bonding and H content, IR spectra studies (Chinese) 7-12524
- Si_{1-x}C_xH films, amorphous, bond lengths, comp. depend., EXAFS study 7-64757
- a-Si_{1-x}C_xH thin films, struct. investig., electron diff. studies 7-2430
- Si₂C_{1-x}H, amorphous, local atomic arrangement, EELS and electron diffraction 7-44378
- a-Si₂C_{1-x}H films, adsorbates influence on conductance, surface state 7-33115
- SiGe:F,H, amorphous, high efficiency solar cells fabrication and props. 7-17901
- SiGe:H, amorphous, electronic and structural props. 7-17054
- SiGe:H, amorphous, p-i-n solar cells, stability behaviour, impurities and doping residues effect 7-17912
- SiGe:H, amorphous, solar cell efficiency improvement using graded band-gap layer at i/n interface 7-54327
- a-SiGe:H, F glow discharge films, elec. and optical props. 7-46169
- a-SiGe:H,F alloy films, F incorporation and annealing props. 7-44588
- a-SiGe:H,F alloys for solar cells, prep. by DC and RF discharge deposition 7-17900
- a-SiGe:H,F glow discharge films, microcrystallinity studies 7-45088
- a-SiGe:H,F glow discharge films, electronic transport and density of states 7-45114
- a-SiGe:H,F solar cells, radiation hardness to 1 MeV protons 7-23180
- a-SiGe:H,F/Pd(Au)(Ni), Schottky barrier height, internal photoemission meas. 7-45501
- a-SiGe:H alloys for solar cells, electronic and optical props. 7-17899
- SiGe:H amorphous films, glow discharge deposited, photoconductivity, microstructure effects 7-58831
- a-SiGe:H films, CVD, electrical and optical props. 7-33596
- a-SiGe:H films, NMR, ESR and IR studies 7-45833
- a-SiGe:H films, photo-assisted CVD and opto-electronic characterisation 7-33595
- a-SiGe:H glow discharge films, field effect density of states determ. 7-21796
- a-SiGe:H solar cells preparation by photo-CVD 7-17885
- a-SiGe:H thin films for solar cells, electrical and structural properties relationship 7-17898
- a-SiGe:H/a-Si:H multilayers, reactive deposition 7-33592
- a-Si_{1-x}Ge_xH/Al Schottky barrier form. and characts. 7-12787
- a-Si_{1-x}Ge_xH/a-Si:H/Al Schottky barrier form. and characts. 7-12787
- a-Si_{1-x}Ge_xH, F, light-induced degradation meas. 7-45397
- Si_{1-x}Ge_xH amorphous alloys, electronic struct., soft X-ray and photoelectron spectra studies 7-27857
- Si_{1-x}Ge_xH films, amorphous, bond lengths, comp. depend., EXAFS study 7-64757
- Si₂Ge_{1-x}H,F amorphous films, struct., elec. and optical props. 7-22360
- SiH₄+Si₂H₆+Ar+H₂, plasma enhanced CVD of a-Si:H, integrated model 7-39423
- a-SiN_xH CVD film, IR and ²⁹Si NMR studies 7-38952
- a-SiN_xH dielectric films with low defect density 7-39036
- SiN_xH films, amorphous, glow discharge deposited, IR absorpt. and Raman scatt. spectra 7-46003
- SiN_xH films, amorphous, bond lengths, comp. depend., EXAFS study 7-64757

hydrogen continued

- a-SiN_xH plasma-enhanced CVD film props. rel. to SiH₄-N₂ gas vol. ratio, RF power and substrate temp. (Korean) 7-3201
- a-SiN_xH/a-Si:H double-barrier structs., resonant tunnelling coeffs. 7-45467
- a-SiN_xH/a-Si:H interface system, struct. and electronic props. 7-38361
- a-SiN_xH/a-Si:H interface, deep states and photoluminescence spectra 7-39186
- a-Si_{1-x}N_xH,B films, ESR and IR spectra studies 7-7780
- a-Si_{1-x}N_xH films, H₂ evolution 7-17445
- a-Si₃N₄H films, plasma enhanced CVD, chemical and mech. props. 7-38420
- a-Si₃N₄H films deposited by plasma enhanced CVD, optical and elec. props. 7-39205
- a-Si₃N₄H/a-Si:H superlattices, plasma deposition methods 7-39439
- SiO₂H₂, nucleation, physical spinodal theory 7-21428
- SiO₂ glass:H₂ fibres, IR optical loss 7-11143
- SiO₂:GeO₂ optical fibres reaction of diffused H₂ with defect centres 7-57591
- a-SiO₂H films, local struct. EXAFS study 7-59291
- SiO₂N₂H/a-Si:H heterostruct. transport props. 7-38768
- a-SiSn:Cl,H glow discharge films, elec. and optical props. (Chinese) 7-58805
- a-Si_{1-x}Sn_xH films, electronic structure of divalent defects 7-32960
- STiO₂H, O-H stretching vibr. under applied electric field and uniaxial stress 7-44723
- Ta:H(D)(T), heat of transport, isotope and temp. depend. 7-27024
- Ta-H system, elec. resist., phase transition (Russian) 7-46458
- TaH_{0.015}, ³H migration in Hall field, temp. effect 7-32729
- Ta₂O₅H films, NPL standard, distrib. of H, AES and SIMS 7-26789
- Ta₂S₅H polypolytype form. and stability, impurity effects 7-44440
- TaSe₂H, polypolytype formation, impurity conc. depend. 7-63801
- TiCu-H₂, thermal stability of hydrides 7-26664
- U-Co system, mag. props., influence of hydriding 7-45750
- U-V (0.2 wt.%), hydriding reaction kinetics (French) 7-23062
- V-Ti-H(D), substitutional alloys, intermediate temp. relax., Fermi-Dirac model 7-26858
- V-Ti-Fe-H₂ system, V-rich, dihydride form., lattice parameters, thermodynamics 7-32369
- VB₂, Compton profiles 7-59281
- VB₂, (0.60 < x < 0.67), optical reflectivity meas. 7-33398
- V₂Zr:H solns., phase transitions rel. to H conc. (Russian) 7-59513
- Xe-Ar:H, plasma, comp. eval. 7-17133
- YIG:H, ion implanted, elastic recoil analysis using 44 MeV Cl ions 7-12107
- YIG:H, sp. ht. and annealing behaviour, conversion-electron Mossbauer spectroscopy study 7-17253
- ZnO:H, quantised accumulation layers on ZnO surfaces, photoenhancement 7-7304
- ZnS:Cu, Mn (H), electroluminesc., simultaneous action of AC and DC fields 7-64699
- ZnSe:H, proton implanted, localised vibr. mode, IR transmission spectra 7-51981
- Zr-H₂ system, phase equilib. 7-21412
- Zr-Mn-H system, equilibrium props. 7-16756
- ZrH_{0.015}, ³H migration in Hall field, temp. effect 7-32729
- Zr₂Pd-H₂, thermal stability of hydrides 7-26664
- Zr₂Rh-H₂, amorphous alloy formation, solid state reactions 7-27982
- Zr₃Rh-H₂, thermal stability of hydrides 7-26664

hydrogen bonds

- 4-trifluoromethyl-6-phenyl-3-cyano-2-pyridone X-ray struct. study 7-21192
- N-acetyl-1-aminocyclohexanecarboxylic acid N'-methylamide, conformations, PMR and NOE studies 7-62424
- alcohols in glassy media, dielectric and IR spectral study 7-2968
- 1-azabicyclo[2.2.2]octane, binary solvent system, solute-solvent interactions, ¹³C and ¹⁵N spin-lattice relax. study 7-31069
- barbiturates, cryst. struct. anal., H bond geometry and types 7-23300
- beef liver catalase, refined struct. 7-17938
- benzenes monosubstituted, H-bonded complexes with fluoroalkanol and fluoroalkyl ethers, ¹H NMR study 7-42651
- substituted benzoylaminopropionic acid esters, conformational equilib., IR spectra, steric effects 7-57066
- biologically active peptides in soln., NMR and IR studies 7-28471
- bromide salt hydrates, H-bonded (H₂O.Br)₂, 7-51738
- butylamine, adsorbed on SiO₂, Al₂O₃ and CaO, thermal desorption and IR study 7-39110
- carbazole, complexes with alkyl cyanides, bonding, fluoresc. excitation spectra anal. 7-31093
- carbazole+4-cyanopyridine (benzonitrile), H bonding interaction 7-17784
- cellulose substrate, room-temp. phosphoresc., H-bonding props. 7-31102
- chloronitroacetic acid, amide, ammonium salt, molecular and defect cryst. struct. 7-21188
- α -cyanoacetohydrazide, crystal struct., neutron diff. anal., ab initio MO calcs. 7-36458
- cyclobutenediyl dyes, electron transfer rate consts. and fluoresc. lifetime determ. 7-25587
- cyclohexanediol:benzene cyclamer, 6:1, solid-state struct. characterisation 7-12040
- 1,3-cyclohexanedione, solid-state struct. characterisation 7-12040
- diacetylene-HF complexes in solid Ar, IR spectra, H-bonding 7-10574
- p-substituted N,N-dialkylanilines, TICT states, fluoresc., H-bonds 7-15644
- 4,4'-diaminophenyl sulphone, intramol. charge transfer state, H-bonded cluster information, fluoresc. and IR spectra 7-50213
- 1,3-diaza-6,9-dioxo-2-cycloundecanthione, cryst. and molecular struct. 7-21189
- 1,2-dibromethane-alcohol mixtures, excess vol., comp. depend. meas. 7-63704
- dibucaine, H bonding nature and vibr. structure, birefringence emission spectra anal. 7-19935
- dichloroacetic acid complex with substituted pyridines, solvent effects, IR and ¹H NMR spectra anal. 7-62365
- 2-N,N'-diethylamino-N-oxymethyl-4,6-dichlorophenol, OHO H-bond, X-ray diff., IR and UV spectra 7-26731
- N,N'-dihydroxyethylthiooxamide-do(d₄), vibr. anal., X-ray diff., NMR, Raman, IR, visible and UV spectra 7-51741
- dimers, H bonded, intermol. interactions, quantitative model 7-36721
- dimethyl ether-HCl (DCI), H bonded complexes, IR spectra 7-19840

hydrogen bonds continued

12,2-dimethyl-1,3-dioxolane-4-methanol, OH stretching band, free and H bonded species equilib., dichroism and IR spectra 7-10641
 2,4-dimethylaniline, freq. assignments, IR and Raman spectra 7-22261
 disulphide bond, S-S dihedral angle, ab initio SCF MO calcs. 7-15504
 ethane-1,2-dithiol, mol. struct., conform., electron diff. obs. 7-50355
 N-ethyl carbazole, complexes with alkyl cyanides, bonding, fluoresc. excitation spectra anal. 7-31093
 ethylene-acrylic acid copolymers, struct. analysis using Fourier self-convolution of IR spectra 7-53337
 ethylenediammonium hexachlorometallates, struct., H bonds and phase transitions 7-16535
 fatty alcohol monolayers at air-H₂O interface, spin model 7-27104
 ferroelectrics, H-bonded, one-dimensional Schrodinger eqn. with double-well pot. 7-29807
 fluoroacetones, protonated, intramol. H bonding, STO-3G MO calcs. 7-49878
 FTIR spectra of H-bonds in molecular biology, strongly coupled anharmonic vibr. 7-47009
 guanidinium aluminium pentafluoride dihydrate single crystals, struct. and symm. determ., X-ray diff. study (French) 7-37960
 hydrates, solid, mol. stretching freq. versus H bond distance correlation anal. 7-21370
 hydrophobic effects in soln. chem., integral eqn., Monte Carlo study 7-59751
 hydroxides, solid, OH stretching freq., interionic influences 7-50129
 4'-hydroxy-1-methylstilbazolium, solvatochromism, spectra study, solvatochromic comparison method anal. 7-25519
 8-hydroxy-2-piperidinoquinoline, cryst. and molecular struct. 7-21191
 9-hydroxyphenalenone-de(di) Shpolskii matrix isolated, H bonding, phosphoresc. 7-19926
 8-hydroxyquinoline, intramol. H bonding, UV photoelectron spectra and MO calcs. 7-25367
 8-hydroxyquinoline-N-oxide, intramol. H bonding, UV photoelectron spectra and MO calcs. 7-25367
 ice stretching vibr., red shift 7-22236
 incoherent neutron scatt. cross-sections 7-990
 indoloquinoline, excited state, radiative rates, fluoresc. spectra 7-62433
 macromolecular structure refinement programs, PROTON and PROLSQ, addition of symmetry-related contact restraints 7-51572
 medium effect on H bond, model pot. 7-15533
 mercaptopyrimidines, substituted, vibr. IR, Raman and UV spectra 7-31043
 methacrylic acid copolymers, struct. analysis using Fourier self-convolution of IR spectra 7-53337
 methanol, associates, H bonding, struct. CNDO/BW calcs. 7-56985
 methanol+fulminic acid (acetonitrile oxide), reaction pathway, MNDO SCF calcs. 7-3582
 methanol, liq., cross-correl. fn., diffusional dynamics study 7-37822
 methanol-trimethylamine, associates, H bonding, struct. CNDO/BW calcs. 7-56985
 2-methoxyethylamine, H bonded config. mol. rot., rot. isomerism barrier, quadrupole coupling consts., microwave spectra 7-50093
 methyl cyanide-HF(DF), hyperfine struct., rot. spectra 7-31012
 methyl fluoride, pot. surface studied using ab initio MO theory with electron correl. energy 7-42494
 methyl fluoride, proton bound dimer, hydrogen bond energy determ. gas-phase mass spectra anal. 7-28365
 methyl-substituted amine-HF complexes, methylation effect, IR spectra anal. 7-19855
 N-methylacetamide, liq., low-freq. Raman spectra 7-50144
 N-methylacetamide-formamide, varying H bond geometry, N-H bond vibr. properties, ab initio calcs. 7-10407
 methylenefluoronium ylide, pot. surface studied using ab initio MO theory with electron correl. energy 7-42494
 molecular crystals, van der Waals at. radii 7-62301
 molecular H-bonded systems, interaction energies, polarisation counterpoise corrections 7-62262
 monomer orientation in H bonded and weakly bonded complexes, elec. influence 7-954
 2-morpholine-8-hydroxyquinoline, cryst. and molecular struct. 7-21191
 nitromethane dimer, non-bonded and H-bonded interactions, SCF calcs. 7-25357
 nitrophenol-trialkylamine ionic complexes, spectral characts. 7-15596
 1S,4R-norcamphor, circular dichroism, solvent effects and vibronic coupling perturbations calc. 7-42658
 nylon films, thermally stimulated and pyroelectric currents, H-bond struct. effects 7-27664
 olefin-H₂O complexes, matrix isolation study, IR spectra, H-bonds 7-31032
 organic sulphur cpds., liq., Monte Carlo simulations, develop. of suitable intermol. pot. fns. 7-31140
 oxalic acid, isomerisation and unimol. dissoc. channels, MO calcs. 7-28295
 pentachlorophenol-hexachlorobenzene, solid soln., H-bonding and phase transitions 7-17310
 phenol-benzene H bonded complex, supersonic jet spectroscopy study 7-57129
 pivalic acid in dil. solution, dimerisation, IR spectroscopy 7-65313
 PMMA based materials, craze resist., struct., water absorpt. 7-59602
 polar compound in alcoholic solvents, time depend. fluoresc. shift, solute-solvent interaction 7-62436
 polarisation function SCF calcs. 7-19685
 polymer mixtures, H bonding, enthalpy-IR freq. shift correl., acid-base interaction 7-51667
 polyurethanes, molecular struct., morphology, phase mixing, mech. props. 7-51664
 potassium dihydrogen triacetate, cryst. struct. study 7-44503
 proton conductivity of hydrogen-bonded chain, light and ultrasonic effects 7-44891
 purines, cryst. struct. anal., H bond geometry and types 7-23300
 pyrazine-d₄, spectral anal., Lennard-Jones-H-bonding pot. energy calcs. 7-5734
 pyrazine-d₄-pyrimidine, spectral anal., Lennard-Jones-H-bonding pot. energy calcs. 7-5734
 pyrazine-h₄-pyrazine-d₄, spectral anal., Lennard-Jones-H-bonding pot. energy calcs. 7-5734
 pyridine-water complexes, intermolecular pot. functions 7-62480
 pyrimidines, cryst. struct. anal., H bond geometry and types 7-23300
 sodium nitrophenolates-crown ethers, proton transfer complexes, spectral characts. 7-15596

hydrogen bonds continued

soliton dynamics of finite 1D H-bonded system 7-2112
 1'-sucrose derivatives, intramol. H bonding, SIMPLE ¹H NMR spectrosc. 7-10620
 terephthalic acid, linear chain struct., order-disorder phenomena, Raman scatt. study 7-21150
 tetramethylsilane, ¹³C NMR chemical shifts, solvent effects 7-50198
 tetraphenylloxalamidine, double H transfer, conforms., tautomerism, NMR and IR obs. 7-57083
 TGS group crystals, thermal anomalies, evaporation products mass spectra study (Russian) 7-44781
 thiamin thiazolone, cryst. struct., transition state analogue 7-51736
 thiosemicarbazide, bonding and struct., effect of protonation, ¹⁴N quadrupole reson. spectra anal. 7-33295
 thiosemicarbazide hydrochloride, bonding and struct., effect of protonation, ¹⁴N quadrupole reson. spectra anal. 7-33295
 thiourea, paraelectric phase, mol. dynamics simulation 7-37920
 tracer diffusion in dense ethanol, correl. for nonpolar and H-bonded solvents 7-32688
 trifluoroacetic acid, H-bonded complex with esters, lifetimes, IR absorpt. spectra 7-50133
 trifluoroacetic acid-isoquinoline complexes, H bond, H⁺ transfer, medium effects 7-46833
 tris-sarcosine calcium chloride, deuterated, ferroelectric props. 7-39050
 urethane form. reaction, H bonding, CNDO/BW calcs. 7-56985
 water, liquid, H-bonds, spatial correls., Raman spectra 7-13156
 water, thin liquid layers, thermal cond. and diffusivity 7-16828
 water molecular chains, orientation defects motion, kink soliton solution mechanism (Russian) 7-32260
 water-methanol mixed clusters, H-bonded networks, stability, thermochemistry 7-62559
 weakly bound dimers complexes, bending force consts., internal dynamics 7-31011
 AlCl₃·6H₂O single cryst., polarised IR reflection spectra 7-3054
 BaBr₂·H₂O, cryst. struct., comparative study with isotopic halides, bifurcated H bonds 7-63543
 BaCl₂·H₂O, cryst. struct., comparative study with isotopic halides, bifurcated H bonds 7-63543
 BaI₂·H₂O, cryst. struct., comparative study with isotopic halides, bifurcated H bonds 7-63543
 Ba(NO₃)₂·D₂O, lattice vibr., mol. contrib., Raman spectra 7-46007
 ((CO)₂W-H-W(CO)₂)₂⁻, struct., H atom dynamics, spectrosc. investig. 7-15613
 Ca(UO₂)₂(SiO₃OH)₂·5H₂O, β-uranophane, refined cryst. struct., thermal anal., IR spectra 7-55031
 caesium 4-trifluoromethyl-6-phenyl-3-cyano-2-pyridone, X-ray struct. study 7-21192
 Cd(BrO₃)₂ · 2H₂O(D₂O), H bonding, crystal struct., ¹H and ²D NMR anal., IR spectra 7-22156
 CsH₂PO₄(d₂), polarised IR and Raman spectra, internal vibr. 7-50125
 CsH₂PO₄(d₄), polarised IR and Raman spectra, transition dipole moments, orientation calcs. 7-50124
 CsHSO₄, cryst. struct. IR spectra study 7-63588
 Cs₂[Fe(CN)₅NO]·H₂O, thermal behaviour and vibr. spectra 7-64632
 D+D reaction, detection of occurrence during shock fracture of D₂O ice 7-39874
 D₂O, H- and D-bonded dimers, relative stabilities, IR spectra 7-62364
 H₂-HF complex, struct., bonding, vibr. freq. shift 7-19817
 HCN free jet spectroscopy by coherent Raman methods 7-15003
 HCN-HF, Coriolis coupling const., eval. for ν₃ estimation 7-5583
 HCN-HF H bonded complexes, hot bands Doppler limited laser spectroscopy 7-19835
 HDO, H- and D-bonded dimers, relative stabilities, IR spectra 7-62364
 HF complexes, H-bonded, vibr. transition freqs., red shifts 7-10546
 HF, vibr. transition, H bonding derivative HF theory 7-19680
 HF weakly bound dimers complexes, bending force consts., internal dynamics 7-31011
 HF-H₂N, H-bonded complex, force consts. calc. for vib. modes, correl. effects 7-19823
 (HF)₂, vibr. predissoc. IR spectra 7-19971
 H₂N-HCl, H-bonded dimer charactn., rot. FT microwave spectrum 7-25490
 H₂N-HF-HF, H bond cooperativity, structural and energetic props., ab initio calcs. 7-19697
 (H₂O)_n, H-bond strengths, MNDO calcs. 7-15519
 H₂O, associated species, stretching force consts., mol. interaction effects, CNDO calcs. 7-25396
 H₂O clusters, Raman spectra 7-42826
 H₂O, H- and D-bonded dimers, relative stabilities, IR spectra 7-62364
 H₂O, liq., network defect density, determ. from Raman spectra 7-15603
 H₂O-H₂O₂ mixtures, defects, network construction, Raman spectrum 7-64630
 H₂P-HF-HF, H bond cooperativity, structural and energetic props., ab initio calcs. 7-19697
 H_nPO₄, n=1-3, tetrahedra distortion depend. on H bond length 7-63542
 H₂S, liq., Monte Carlo simulations, develop. of suitable intermol. pot. fns. 7-31140
 HX-HCP complexes (X=F, Cl, Br) H bonding ab initio calcs. 7-56960
 HX-HNC complexes (X=F, Cl, Br) H bonding ab initio calcs. 7-56960
 HX-HCN complexes (X=F, Cl, Br) H bonding ab initio calcs. 7-56960
 K_xH(F) (x=2.5, 3), homologous anions, crystal struct. anal. 7-26711
 KF·(HO)₂Cl, cryst. struct., neutron diff. studies (Chinese) 7-12005
 KHSeO₄ single crystal, polarised IR spectra anal., rel. to cryst. struct. 7-46047
 MnNa(H₂PO₃)₃·H₂O orthorhombic struct., bond lengths and angles, X-ray diff. study 7-32372
 ND₄SCN, phase transitions, spin lattice relax. study 7-33286
 NH₃+HX where X=Cl, Br, I, gas phase charge transfer complexes, pot. curves 7-13733
 NH₄⁺, methyl-substituted, H-bond and hydration energies relationship, HF MO calcs. 7-15490
 NH₄H₂PO₄, antiferroelectricity, role of H bonds 7-64582
 (NH₄)₂SO₄, partially deuterated, phase transition, heat of transition 7-53246
 NaF, thermal hopping of μ⁺ between FμF centres 7-45903
 NaF·OH⁻, X⁺, X=impurities, vibr., radiation effects, IR spectra 7-53321
 NaH(D)SeO₃, neutron diff., DMR investigation 7-21178
 Na₂(H₂W₂O₄), cryst. and mol. struct. studies 7-6596
 OCN⁻-H₂O interaction, pot. surface, SCF MO calcs. 7-56967
 OH+cytosine, ab initio SCF MO calcs. 7-8478

hydrogen bonds continued

- OH₃⁺, methyl-substituted, H-bond and hydration energies relationship, HF MO calcs. 7-15490
 Pd complexes, with dithiooxamides, vibr., IR spectra 7-3053
 Rb_{1-x}(ND₄)_xD₂PO₄ structural glass phase, X-ray scatt. meas. 7-26660
 RbHSeO₄ single cryst. ferroelec., H bond vibr., polarised IR spectra studies 7-27707
 Rb_{1-x}(NH₄)_xH₂(P,As)O₄, mixed system, proton localisation, obs. by incoherent neutron scatt. 7-12224
 Rb_{1-x}(NH₄)_xH₂PO₄, press. depend. of proton glass freezing, dielec. props. 7-2209
 a-Si:H,B, RF sputtered films, optical and electrical props. 7-33470
 a-Si_{1-x}C_xH,B(P) thin films, H bonding and H content, IR spectra studies (Chinese) 7-12524
 a-SiGe:H alloys for solar cells, electronic and optical props. 7-17899
 SrBr₂H₂O, cryst. struct., comparative study with isotopic halides, bifurcated H bonds 7-63543
 Sr(BrO₃)₂·H₂O(D₂O), EFG parameters, H bonding, PMR, deuteron mag. reson. 7-27612
 SrCl₂·H₂O, cryst. struct., comparative study with isotopic halides, bifurcated H bonds 7-63543
 Srl₂H₂O, cryst. struct., comparative study with isotopic halides, bifurcated H bonds 7-63543
 Zn(BrO₃)₂·6H₂O, H bonding, PMR study 7-33277

hydrogen compounds

- see also deuterium compounds; hydroxonium ion; ice; steam; tritium compounds; water
 ethylene-HCl van der Waals mol., dissociation energies and heats of formation, photoionisation study 7-19966
 fluorosilanes, protonated, structs., energetics, ab initio MO calcs. 7-56956
 formyl ion, dissociative recombination of interstellar ion, electronic struct. calc. 7-20064
 Group IA hydrides, high-pressure phase transitions 7-21438
 Group IIIA hydrides, high-pressure phase transitions 7-21438
 Group IVA hydrides, high-pressure phase transitions 7-21438
 HBF₄⁺, Γ_8 struct., bond lengths, microwave spectra 7-62357
 HCL, condensation on charged CO₂ walls, Stockmayer model calcs. 7-63784
 HSO₄·2H₂SO₄ intercalation cpd. with graphite, C₂₄H₂SO₄⁻·2H₂SO₄, quasi-2D, cond. electron state transform. in microwave field, ESR meas. 7-64508
 hydrides, first and second row, NMR chem. shift bond length derivatives 7-42644
 methyl-substituted amine-HF complexes, methylation effect, IR spectra anal. 7-19855
 pot. energy surfaces 7-10468
 potassium hydrogen phthalate, cryst. growth, influence of impurities, in situ obs. of [010] face 7-46289
 repeat 1st entry 7-36724
 H₂S, normal and deuterated, K-shell X-ray absorption spectra, double excitation 7-62404
 Ar-HCl, energy levels, ab initio close coupling calcs. 7-50292
 Ar-HCl van der Waals complexes, IR spectra, secular eqn. calc. 7-31031
 Ar-HF binary complex, long-lived metastable systems 7-36515
 BaCl₂·HCl, cond. meas. at 298.15 K, anal. using Lee and Wheaton eqn. 7-16792
 CsH₃AsO₄ ferroelec. cryst., EPR studies of AsO₄⁴⁻ centres 7-45816
 CsH_{0.1}D_{0.9}AsO₄, melting pt., phase diagram 7-21417
 H₂-Ar pairs collision-induced rototranslational spectra, ab initio dipole-moment surface 7-15493
 H₂-F₂-HF gaseous mixture, light initiated chain reaction, stimulated light scatt. study 7-62778
 H₂-HF complex, struct., bonding, vibr. freq. shift 7-19817
 HAlOH, struct. and vibr. freqs., SCF calcs. 7-10386
 H₃AsO₃+IO₃⁻, stirring effects and bistability, coalescence-dispersion model 7-46801
 HBF₄⁺, rot. anal., microwave spectra 7-19832
 HDO detection by discharge modulated IR diode laser spectroscopy 7-25505
 H₃BO₃:fluorescein glass, nonlinear optical interactions 7-1239
 HBOH, struct. and vibr. freqs., SCF calcs. 7-10386
 HBeOH, struct. and vibr. freqs., SCF calcs. 7-10386
 HBr + CN, time-resolved laser induced fluoresc. 7-46812
 HBr, d shell photoionisation, shape resonances study 7-19964
 HBr, electron impact, Auger and Coster-Kronig spectra 7-15719
 HBr, pot. energy curve construction method 7-36512
 HBr, VUV photoabsorpt. and fluoresc. spectra 7-19927
 HBr+H₂, vibr. transition probabilities, semiclassical algebraic description 7-25636
 HCF, mag. interactions obs. by intermodulated fluoresc. technique, hyperfine struct. 7-25593
 HCN cluster form. in carbon tetrachloride matrix, IR spectra 7-19841
 HCN detection in Periodic Comet Halley (1982i) 7-60598
 HCN, dipole moment geometric derivatives from nucl. electric screening 7-25428
 HCN, elec. polarisabilities, ab initio calcs. 7-5585
 HCN, formation on Pd (111) and (100) by hydrogenation of adsorbed CN 7-6985
 HCN free jet spectroscopy by coherent Raman methods 7-15003
 HCN, in atmosphere of Titan (Saturn VI), 88 GHz emission detect. 7-9410
 HCN in circumstellar shell of IRC+10420 peculiar O-rich evolved supergiant 7-9464
 HCN, in discharged He flow, CN(B²Σ⁺) form. 7-25476
 HCN isotopes, quartic approx. of pot. function, mech. spectroscopic problem 7-50288
 HCN, isotopic species, electronic states, pot. surface, dissoci. vibr. anal., CI calcs. 7-62297
 HCN J=1-0 rotational transition in P/Comet Halley (1982i) 7-24072
 HCN mapping in LDN 1641, EHF obs. 7-14622
 HCN, optimised geometries and harmonic freqs., MP2 calcs. 7-62255
 HCN, overtone transitions, self-broadening and intensity, photoacoustic spectra rot. relax. 7-20016
 HCN, vibr. energy levels calc. using ab initio pot. energy function, CI calcs. 7-25484
 HCN, vibr.-rot. interaction const., RHF closed-shell wave function 7-19818
 HCN, X-ray emission spectra, ab initio MO HF calcs. 7-36642
 HCN/HNC abundance ratio vars. in Orion molecular cloud 7-48033

hydrogen compounds continued

- HCN-HF, Coriolis coupling const., eval. for ν_2 estimation 7-5583
 HCN-HF, excited vibr. states, gas-phase IR spectrum 7-50108
 HCN-HF H bonded complexes, hot bands Doppler limited laser spectroscopy 7-19835
 (HCN)_n microcluster selective formation in cryogenic matrices, FTIR spectroscopy obs. 7-48895
 HCN-H³⁵Cl, gas phase rovibr. anal. 7-25477
 HCP and higher-lying isomer, struct., stabilities, ab initio study 7-864
 HCa₂Nb₂O₇, intercalation of n-alkylamines, structural studies 7-65306
 HCl + CN, time-resolved laser induced fluoresc. 7-46812
 HCl + OH (OD), reaction rates, vibr. excitation and isotopic substitution effect 7-22996
 HCl and NaOH interdiffusion meas. at 25°C in aqs. soln. 7-6841
 HCl BF₃, struct. determ. mol. beam electric reson. spectroscopy 7-15591
 HCl, boiling concentrated solution, corrosion behaviour of amorphous Ni-base alloys 7-3511
 HCl condensation in winter polar stratospheres, contrib. to Antarctic O₃ hole 7-55162
 HCl, Cooper minimum, photoelectron dynamics 7-942
 HCl, countercurrent diffusion with AgNO₃ in cellulose and Nafion films 7-12377
 HCl desorpt. from Ar (111) surface, internal state depend. 7-6963
 HCl detection in atm. by laser-induced fluorescence of CO₂ 7-46993
 HCl, IR spectra, Ar- and N₂-broadened linewidths, rot. spectrum 7-50113
 HCl, IR transitions, vibr.-rot. matrix elements 7-50131
 HCl, in Ar and Kr matrices far IR spectra, press. effects 7-22240
 HCl in atm., ground-based IR solar spectra anal. 7-40538
 HCl in middle stratosphere, obs. and modelling 7-14363
 HCl in stratosphere, near-IR satellite remote sensing and interference from OH airglow 7-23926
 HCl, interaction with Si (111) single crystal, 190-720K 7-13817
 HCl, low-energy electron collisions, inelastic processes, R matrix theory anal. 7-31180
 HCl, molar vol., vapour press. meas. 7-44779
 HCl, nucl. mag. shielding consts. ab initio wave function calcs. 7-5594
 HCl, photodissoc. branching ratios pot. energy curves 7-31128
 HCl, photodissociation processes in astrophysical environment 7-23042
 HCl, photoionisation cross section, ground state inversion pot. method/diff. theory 7-944
 HCl photoionisation cross section by Stieltjes technique, channel coupling effect 7-31123
 HCl, soln., elec. surface pot. change with conc. and surface age (Russian) 7-27063
 HCl, vibr. transition probabilities, reactive field effect 7-36584
 HCl⁺, bound electronic states, ab initio Born-Oppenheimer calcs. 7-42469
 HCl/H₂ gas etchant for Si surfaces 7-65220
 HCl/H₂ gas etchant for Si, gas composition analysis 7-65221
 HCl/Xe/He gas mixture, kinetic model of discharge (Russian) 7-11577
 HCl-Ar gas mixtures, electron irradi., negative differential conductivity 7-63243
 HCl-Kr, mixture, vibr. relax., rate const. meas. 7-15687
 HCl-SrCl₂ mixed electrolyte, thermodynamic study, appl. of Pitzer's eqns. 7-33940
 HCl-Xe, mixture, vibr. relax., rate const. meas. 7-15687
 HCl-Xe-He self-sustained discharge, population dynamics of electronic states of atoms and ions 7-37781
 HCl+1,3-butadiene, addition, internal excitation effect, rate const. meas. 7-17761
 HCl+Cl, prod. rot. distrib., centrifugal sudden distorted wave study 7-46808
 HCl+ClONO₂, homogeneous and heterogeneous components, kinetics, implications for stratosphere chem. 7-54091
 HCl+ClONO₂, kinetics, implications for stratospheric O₃ 7-54089
 HCl+Li, laser catalysed reaction, pot. surfaces and transition dipoles 7-39861
 HCl+O, steric requirements, reagent rot. effect 7-57150
 HCl₅·5H₂O-Au electrolyte-electrode interface, double layer capacity, temp. and freq. depend. 7-59769
 HCo(CO)₃, hydroformylation, quantum chem. calcs. 7-54115
 HCo(CO)₄, hydroformylation, quantum chem. calcs. 7-54115
 HDNCC, rot.-inversion spectrum in region from 100 to 400 GHz 7-25494
 HDO and D₂O, IR spectra, vibro-rot. transitions, line intensity meas. 7-50109
 (HF)₂, IR and Raman spectra, vibr. calcs., secondary basis set superposition error 7-25478
 HF, 1s core orbital, inadequate representation, basis set superposition error 7-25346
 HF, chem. laser, modeling based on standing detonation wave 7-62681
 HF dimer, dissoci., excitation energy transfer meas. (German) 7-57163
 HF dimer, vibr. predissoc. lifetime 7-5729
 HF, gaseous and solid, electronic structure, X-ray spectra studies 7-10614
 HF, intermol. pot. model including polarisability 7-25623
 HF, MBPT and coupled cluster calc., comparison with CI 7-49899
 HF, macroscopic solvation, electron distrib. ab initio INDO SCF calcs. 7-54099
 HF, nuclear spin-spin coupling constants evaluated using manybody methods 7-5705
 HF pulsed pump laser, direct optical pumping of high-pressure CO₂, N₂O lasers 7-50533
 HF solid, elastic and photoelastic anisotropy at high press. 7-2083
 HF, stretching force consts., inner-shell polarisation, HF calcs. 7-15588
 HF, two photon bound-bound electronic transition calcs. 7-31136
 HF, vibr. transition, H bonding derivative HF theory 7-19680
 HF, vibr. transition probabilities, reactive field effect 7-36584
 HF weakly bound dimers complexes, bending force consts., internal dynamics 7-31011
 H¹⁸F, radioisotope production for biomedical applications 7-60087
 HF-Ar, trimers, mol. rot., hyperfine struct., spectra anal. and calcs. 7-50060
 HF-DF chemical laser, electrically initiated (Chinese) 7-5879
 HF-diacylene complexes in solid Ar, IR spectra, H-bonding 7-10574
 HF-H₂O, vap.-liq. equilib. and partial press. formulae 7-21427
 HF-H₃N, H-bonded complex, force consts. calc. for vib. modes, correl. effects 7-19823
 HF-He, mol. interactions, nonexpanded dispersion and induction energies, damping functions 7-42474

hydrogen compounds continued

- HF-methyl cyanide, hyperfine struct., rot. spectra 7-31012
 HF+DF dimer, collisional vibr. relax., rate consts. meas. 7-50320
 HF+H₂(N₂), total differential scatt. cross sections 7-13743
 HF+H⁺, charge transfer processes, ab initio calcs. 7-5744
 HF+H⁺, rot. energy transfer, pot. energy surface 7-967
 HF+Li, 3D reaction, differential cross section calc. 7-59739
 (HF)₂, degenerate rearrangement, tunneling splitting, reaction-path anal. 7-22979
 (HF)₃, vibr. predissoc. IR spectra 7-19971
 H₂GeD, Fourier transform IR spectra, rovibr. anal. 7-25516
 H₂GeX (X=F, Cl, Br, I), harmonic force fields and vibr. spectra, ab initio HF calc. 7-50064
 H⁺(H₂O)_n, ion mobility in water vapour, TOF mass spectra 7-11582
 H(H₂O)₂BiO₃, prep. from KBiO₃ by ion exchange, high proton cond. 7-2260
 HI, Ar matrix, conc. effects, binary complexes with impurities, IR spectra anal. 7-31034
 HI, d shell photoionisation, shape resonances study 7-19964
 HI in solid N₂, IR spectra in temp. range 9 to 30 K 7-50127
 HI, vibr. transition probabilities, reactive field effect 7-36584
 HI-HF complexes, struct. and microwave spectra 7-50087
 HI+I, 3D trajectory study 7-42729
 HMgBH₄, relative energy characts., electronic correl. in ab initio calcs. 7-15528
 HMgOH, struct. and vibr. freqs., SCF calcs. 7-10386
 HN₃, rot. anal. for ground, v₅ and v₆ states, IR spectra 7-19850
 H₂N-HCl, H-bonded dimer charactn., rot. FT microwave spectrum 7-25490
 H₂N-HF-HF, H bond cooperativity, structural and energetic props., ab initio calcs. 7-19697
 HNC, 2100 cm⁻¹ bands, IR Fourier transform spectra anal. 7-50117
 H₂NC⁺, interstellar mol., pot. energy surfaces, ab initio MO theory 7-19687
 HNO₃, ag. soln., Raman spectra 7-39125
 HNO₃, air pollution due to nuclear explosions in atmos., glacier ice core record 7-46982
 HNO₃ and N cpds., troposphere conc. observations in Colorado, USA 7-18288
 HNO₃ and nitrates in Antarctic snow, tropospheric and stratospheric sources 7-55227
 HNO₃, boiling concentrated solution, corrosion behaviour of amorphous Ni-base alloys 7-3511
 HNO₃, collision-free photodissociation at 266 nm, OH prod. 7-8293
 HNO₃ condensation in winter polar stratospheres, contrib. to Antarctic O₃ hole 7-55162
 HNO₃ in cold Antarctic stratosphere, role in form. of springtime O₃ hole 7-47508
 HNO₃, intercalated in graphite, diffusion, charge transfer and strain fields, ESR study 7-53117
 HNO₃ intercalation cpd. with graphite, C₂₀HNO₃, low-temp. struct. 7-51721
 HNO₃, treatment of Na₂O-B₂O₃-SiO₂, effect of volumes, radii of channels 7-13613
 HNO₃-graphite intercalation cpds., absolute Pauli spin suscept. meas., Fermi level density of states determ., ESR/NMR method 7-12940
 HNO₃-HF-H₂O, etching of GaAs, surface morphology (Korean) 7-28225
 HN₃O⁺, millimetre-wave spectrum and mol. consts. 7-29387
 HNSF⁺, struct. and bonding investigated at SCF level, electron correl. effects 7-10439
 HnBO₃, electrical conductivity meas. 7-16802
 HO₂ radical, third-order anharmonic pot. consts. equilib. structure parameters, calc. procedure 7-10544
 HO₂⁺, electronic struct., MRD-CI calcs. 7-10450
 HO₂+H, abstraction reaction, saddle point geometries and barrier heights, ab initio SDCI calcs. 7-46806
 HO₂+HO₂, rate constant, flash photolysis and UV spectral study 7-54075
 HO₂+methyldioxy radical, rate constant, flash photolysis and UV spectral study 7-54075
 HO₂+O₃, reaction rate const. meas. by photofragment fluoresc. detect. 7-22990
 H₂O, shocked water, temp. meas. using fluorescence probe thermometer 7-24653
 H₂O-H₂O₂, mixtures, long-range intermol. interaction energies using RPA/moment function methods 7-10698
 H₂O-H₂O₂ mixtures, defects, network construction, Raman spectrum 7-64630
 H₂O₂ and CH₃OOH, photochemical formation in boundary layer of atmosphere 7-29155
 H₂O₂ behaviour in RBMK-1000 BWR safety control system coolant circuit 7-30631
 H₂O₂, collision-free photodissociation at 266 nm, OH prod. 7-8293
 H₂O₂ in polar ice cores, long-term record 7-55229
 H₂O₂, long-range intermol. interaction energies using RPA/moment function methods 7-10698
 H₂O₂, overtone excited states, torsion-vibr. interactions 7-50072
 H₂O₂, photodissoc., fluoresc., VUV spectra 7-57140
 H₂O₂, photodissoc., OH product state and spectroscopy 7-13795
 H₂O₂, photofragmentation dynamics at 193 nm, laser-induced fluoresc., rot. and vibr. distrib. 7-42700
 H₂O₂+S(IV), reaction kinetics in rainwater samples 7-29170
 H₃O⁺, electron impact dissoc. fragment cross sections 7-5777
 H₃O⁺, IR diode laser spectroscopy, rot. lines, inverse pot. function 7-10564
 H₃O⁺ in cometary comae, origin 7-66517
 H₃O⁺, v₃ fundamental band meas. with colour centre laser 7-57064
 HOCl, FTIR spectra, vibr. rot. consts. and harmonic force field 7-50140
 HOCl, gaseous, UV absorpt. spectrum, rel. to atm. modelling 7-25534
 HOCl, IR spectra, v₂ and v₃ bands, a-type and b-type transitions 7-50112
 HO₂H and HO₂D, intramol. energy flow and overtone-induced dissoc., classical trajectory study 7-28303
 HONO, laser induced chem. processes anisotropies, OH ejection 7-19973
 HO₂NO₂, IR spectra of stratosphere at 802 cm⁻¹ and conc. profile 7-9168
 HOO radical, orbital energies, UHF calcs. phys. interpretation 7-56931
 (H₂O)₂O₂⁻ clusters, charge transfer interaction investigated using ab initio MO theory, binding energy calc. 7-5809
 H₂P₂ isomers, electronic states, ab initio mol. electronic struct. theory 7-36934

hydrogen compounds continued

- H₂P₂, unimol. rearrangement, ab initio investig. 7-25342
 H₂P₂⁺, unimol. rearrangement, ab initio investig. 7-25342
 H₂P-HF-HF, H bond cooperativity, structural and energetic props., ab initio calcs. 7-19697
 H₃PMo₁₂O₄₀·nH₂O, polycryst., NMR and H⁺ conductivity investig. 7-17230
 HPNH, photoionisation cross-sections, MS X α calcs. (French) 7-5599
 HPO₃ radical, strong perchloric acid soln., free radical protonation equilib., ESR study 7-33918
 H₃PO₄ 500 W prototype fuel cell develop. 7-65457
 H₃PO₄ electrolyte in fuel cells, O solubility, diffusion coeff., reduction rate, adsorption on Pt surface 7-28395
 H₃PO₄ fuel cell, 11 MW International Fuel Cells-Bechtel demonstration project 7-28397
 H₃PO₄ fuel cell, mixing of reactant gases to simulate gas crossover 7-65460
 H₃PO₄ fuel cell develop. and system anal. 7-65459
 H₃PO₄ fuel cells using converted diesel fuel, 2-stage hydrodesulfurization 7-65458
 H₂PO₄, n=1-3, tetrahedra distortion depend. on H bond length 7-63542
 H₂POOH, bonding, ab initio calcs., proton exchange reactions 7-5589
 H₂POSH, bonding, ab initio calcs., proton exchange reactions 7-5589
 H₂PSSH, bonding, ab initio calcs., proton exchange reactions 7-5589
 H₂(3+n)(PV_nMo_{12-n}O₄₀)·XH₂O, stability to dehydration in air and vacuum, ESR study 7-38929
 H₂S adsorbed on SiO₂/Na, FTIR and Raman spectra obs., Na promotion of Claus process 7-46869
 H₂S adsorption on Ge and GaAs, substrate orientation and temp. depend. 7-58634
 H₂S, air pollution, release from natural gas well blowout in Alberta, Canada 7-40072
 H₂S atmospheric pollution from geothermal power plants (Polish) 7-23120
 H₂S electrolysis in aqueous alkaline solutions 7-65649
 H₂S, electron scatt., low energy, absolute total cross-sections meas. 7-25650
 H₂S, gas, electron swarm characteristic energies 7-63388
 H₂S, in O₂ matrix, FT IR spectra 7-36606
 H₂S, inner valence shell, photoionisation, ang. distrib. in 40 to 70 eV photon energy range 7-57131
 H₂S, K X-ray yield, chem. environment effect 7-3618
 H₂S, liq., Monte Carlo simulations, develop. of suitable intermol. pot. fns. 7-31140
 H₂S photoelectrolysis using n-CdSe photoanode, photoelectrochemical cell for H₂ production 7-54328
 H₂S poisoning of Pt anode in phosphoric acid fuel cell electrolyte 7-46933
 H₂S, pot. energy surfaces 7-10468
 H₂S, pot. energy surfaces, spectroscopic props., ab initio CEPA calcs. 7-19686
 H₂S⁺, pot. energy surfaces, spectroscopic props., ab initio CEPA calcs. 7-19686
 (H₂S)₂ in O₂ matrix, FT IR spectra 7-36606
 HSCN (HNCS), ionis. pots., photoelectron spectrosc. and ab initio calcs. 7-25601
 HSO₃⁻, formation in atmospheric clouds, model 7-18290
 H₂SO₄, 1-1 electrolyte theory 7-9631
 H₂SO₄ and H₂ production from electrolysis of aqueous S slurry 7-3724
 H₂SO₄ and NH₃ reactions for chemical storage of solar energy, kinetics 7-40048
 H₂SO₄ decomposition and synthesis for chemical energy storage and transportation system 7-65639
 H₂SO₄ intercalated with graphite, optical study of K-point π-band dispersion 7-17317
 H₂SO₄, kinetics of heterogeneous reactions for chemical storage of energy 7-23229
 HSOH, CI analytic energy second derivatives, IR intensities and vibr. freqs. prediction 7-5608
 H₂Se, E, band, rot. contour analysis and predissoc. mechanisms, VUV spectra anal. 7-25537
 H₂Se, geometry optimisation using energy exponent 7-25344
 H₂Se, photoionisation, ionisation pot. and bond energies 7-19979
 H₂Se, photoionisation and autoionisation, UV spectra 7-10524
 H₂Se, Rydberg series identification, VUV spectra anal. 7-25538
 H₂SeO, geometry and energy, role of optimum supplementary d-orbitals 7-25344
 H₂Si₂⁺, electronic struct., MC SCF CI and CEPA calcs. 7-56992
 H₂Si-B₂H₆, form., geometry, ab initio calcs. 7-25376
 HSiCl+SiH₄(SiH₂Cl₂), insertion reaction rate const. meas., laser-excited fluoresc. detect. 7-46813
 H₂SiD, Fourier transform IR spectra, rovibr. anal. 7-25516
 HSiF, mag. interactions obs. by intermodulated fluoresc. technique, hyperfine struct. 7-25593
 H₂SiF, Coriolis coupling, FT IR spectrum, rovibr. anal. 7-5679
 H₂SiO₄, force fields, ab initio MO calcs. 7-25375
 HSiOH, struct. and vibr. freqs., SCF calcs. 7-10386
 H₂SiX (X=F, Cl, Br, I), harmonic force fields and vibr. spectra, ab initio HF calc. 7-50064
 H₂SnBr, rovibr. anal., harmonic force field calc., Fourier transform IR spectra study 7-50122
 H₂¹¹⁶Sn⁷⁹Br, FT IR spectra, rovibr. investig. 7-921
 H₂SnCl, rovibr. anal., harmonic force field calc., Fourier transform IR spectra study 7-50122
 H₂¹¹⁶Sn³⁵Cl, FT IR spectra, rovibr. investig. 7-921
 H₂SnI, rovibr. anal., harmonic force field calc., Fourier transform IR spectra study 7-50122
 H₂SnI, FT IR spectra, rovibr. investig. 7-921
 H₂SnX (X=F, Cl, Br, I), harmonic force fields and vibr. spectra, ab initio HF calc. 7-50064
 H_{0.33}TaS₂, host lattice-intercalant strong interaction, proton mobility hysteresis, PMR study 7-53159
 H₃Ta₂, intercalation reactions, nucl. quadrupole interactions, TDPAC meas. 7-17245
 H₂Te, E, band, rot. contour analysis and predissoc. mechanisms, VUV spectra anal. 7-25537
 H₂Te, Rydberg states, high resol. VUV spectra 7-50173
 HUO₂PO₄·4H₂O intercalation with piperidine, hydrazine, pyridine, pyrazine or (dimethylaminomethyl) ferrocene 7-65304
 HX-HCP complexes (X=F, Cl, Br) H bonding ab initio calcs. 7-56960
 HX-HNC complexes (X=F, Cl, Br) H bonding ab initio calcs. 7-56960

hydrogen compounds continued

- HX-XCN complexes (X=F, Cl, Br) H bonding ab initio calcs. 7-56960
 He-H₂ van der Waals mol., diagrammatic perturbation theory 7-5607
 He-Xe-HCl excimer laser discharge growth dynamics 7-1086
 H₂O-H₂O₂ system vapour pressure determ. using static phase equilib. apparatus 7-23049
 K-Ca-NO₃-H₂O glasses, low temp. dielectric study 7-38999
 KH₂PO₄ crystal, bifurcation response near ferroelectric transition 7-39051
 Li + XF (where X = Mu, ¹H, ³H, ¹⁰H), quasiclassical trajectory calcs., isotopic and orientational study 7-33923
 Li+HBr, complex optical pots., large angle elastic scatt. calcs. using WKB theories 7-42728
 Li_{1-x}H_xNbO₃, struct. and props. 7-12017
 Li_{3-x}H_xTaO₄, prep. by means of hydrothermal synthesis and protolysis 7-39449
 N₂-HF, IR spectrum and vibr. predissoc. 7-50106
 NH₃+HX where X=Cl, Br, I, gas phase charge transfer complexes, pot. curves 7-13733
 PbHAsO₄, ferroelec. phase transitions, proton tunnelling effect, NQR study 7-53172
 Pt/H₂(PMo₁₂Mo₄₀).22H₂O-polyethylene oxide interface, audiofrequency behaviour 7-52693
 SO₂-HF(DF), mol. geometry, ¹⁹F spin-spin and D-nucl. quadrupole coupling consts., rot. spectrum 7-5666
 Xe:HCl, cooperative photoabsorpt. induced charge transfer reaction dynamics 7-28297

hydrogen distribution *see* **hydrogen economy****hydrogen economy**

- 500 kW solar energy generating facility for H₂ production by electrolysis (German) 7-28417
 alkaline fuel cells, low cost, development and hydrogen economy appls. 7-39950
 Chinese literature bibliography 7-35141
 electrochemical H₂ production, electrocatalytic materials comparison and eval. 7-65645
 electrolysis of water, H₂ evolution kinetics at Ni-Mo-Cd electrocoated cathodes 7-3728
 graphite, plasma interactive component surfaces, H recycling props. 7-63295
 hydride chemical heat pump thermodynamics, alloy selection 7-40023
 ion exchange membrane water electrolysis, alkaline type, for H₂ energy storage 7-3727
 metal hydride hydrogen storage beds, temp.-comp. relations, computer calcs. 7-8448
 mobile solar energy H₂ generating system 7-65652
 natural gas processing using solar energy 7-54346
 paired metal hydrides, operational characts. and dynamic behaviour 7-32609
 photoelectrochemical cell for H₂ production, photoelectrolysis of H₂S using n-CdSe photoanode 7-54328
 photoelectrolysis of water using semiconductor electrodes 7-3723
 photoevolution by Rhodospseudomonas palustris in light-dark cycles 7-3722
 photovoltaic solar energy electrolysis for H₂ production, review 7-3726
 production from coal and petroleum coke, technical and economical perspectives 7-40050
 production processes, thermodynamic perform. anal. and comparison 7-65650
 solar H₂ production, S-I₂ cycle versus water vapour electrolysis 7-65651
 solar H₂ technology, water electrolysis (German) 7-65642
 solar photovoltaic converter and electrolyser for H₂ production 7-3721
 solar-hydrogen project, dimensions, costs and timing (German) 7-46938
 steam raising from H₂ for power generation (German) 7-23233
 storage systems using thermochemical compression for transportation appl. 7-34072
 technology breakout in energy conversion, conf., San Diego, CA, USA (Aug. 1986) 7-60875
 thermochemical production of the H₂ at Joint Research Centre, Ispra, Italy 7-40049
 two-step water photo-decomposition reactions for H₂ production 7-54365
 vehicle fuel appls. in USSR (French) 7-54368
 water electrolyser for H₂ production, membrane electrolysis 7-23230
 water electrolyses and the use in electrolytic H₂ and NH₃ production 7-23231
 CeNi₅ based hydride systems, hydriding characts. and stability 7-40051
 H₂ adsorpt. on La-Mg alloy, H storage investig. 7-52241
 H₂ as energy carrier, H₂ production using alkaline water electrolysis cell (German) 7-65641
 H₂ energy and technology in USSR, bibliography 7-65648
 H₂ energy R and D in India, overview 7-65643
 H₂ generation using solar battery and electrolyser unit, optimisation 7-54361
 H₂ production by impingement of steam jet on high temp. ZrO₂ surface 7-54362
 H₂ production efficiency from light energy conversion by photosynthetic bacterium Rhodospirillum rubrum 8703 7-65644
 H₂ production from hydrocarbons using steam reforming 7-23232
 H₂ production from water electrolysis (French) 7-59879
 H₂ sorption, kinetic models and appls. to H₂-M systems 7-65646
 H₂ storage by Mg₂Ni, dehydriding kinetic rates 7-54363
 H₂ technology for energy needs of human settlements 7-54367
 H₂-air mixtures, 1-D tube combustion processes, numerical calc. 7-65647
 H₂O electrolysis for H₂ production using photovoltaic power unit 7-46973
 H₂S electrolysis in aqueous alkaline solutions 7-65649
 H₂SO₄ and H₂ production from electrolysis of aqueous S slurry 7-3724
 La_{2-x}Ca_xMg₁₇, H₂ storage appl. 7-40052
 La_{0.3}Nd_{0.2}Ni_{2.5}Co_{2.4}Si_{0.1} electrode, storage capacity investig. 7-33946
 LaNi₅, anisotropic H migration, deposition potentials, hardness, brittleness meas. 7-6873
 α-LaNi₅-H, multiply cycled, inelastic neutron scatt. 7-32835
 LaNi₄AlH₂ and LaNi_{4.5}Al_{0.5}H₂, dynamical disorder of H, quasi-elastic neutron scatt. study 7-21535
 LaNi₄MH₂ (M=Mn, Cu), dynamical disorder of H, quasi-elastic neutron scatt. study 7-21535
 Mg solvated in organic matrices, H absorption studies 7-34073
 Mg surface, air exposed, XPS after hydrogenation-dehydrogenation cycles 7-17923
 Mg-Cu solvated in organic matrices, H absorption studies 7-34073

hydrogen economy continued

- NaH, thermodynamic characterisation using phase diagrams and electrochemical meas. for H₂ storage 7-54366
 Ni_{100-x}Zr_x metallic glasses, H storage, press.-conc. isotherms, site occupation, binding energies 7-58153
 PrNi₅ based hydride systems, hydriding characts. and stability 7-40051
 SrCeO₃ based proton conductive solid electrolyte in high temp steam electrolysis for H₂ production 7-54364
 T₂O water decomposition using ZrO₂-Pt cell for H₂ production 7-3581
 Ti-Cu, H storage, theory 7-34074
 Ti-Fe H storage, theory 7-34074
 Ti-Ni, H storage, theory 7-34074
 TiCr_{2-x}Fe_x alloys, H absorpt. and storage investig. 7-32832
 TiFe, H absorpt., Mossbauer obs. 7-27642
 Ti₄Fe₂O₇, H absorpt., Mossbauer obs. 7-27642
 TiO₂ thin film electrodes of photoelectrolysis solar cells for H₂ production 7-3725
 WC cathodes in acid electrolytes for H₂ production 7-3729
 ZrMnFe₂ system, H storage material, effect of hyperstoichiometric Fe 7-45000

hydrogen embrittlement

- fusion reactor materials, crack growth behavior, appl. of H embrittlement models 7-53850
 high tensile steel electroplating, H₂ embrittlement fracture prevention (German) 7-33767
 metal electrodes, H atom diffusion and trapping, meas. by potentiostatic double-step method 7-21524
 metal electrodes, H atom diffusion and trapping, meas. by potentiostatic double-step method 7-21525
 metallic glasses-H₂, prep., struct. and props. 7-26663
 metals, BCC, H-dislocation interaction mechanism, embrittlement and dislocation motion 7-44600
 metals, BCC and FCC cryst. struct., H trapping, thermal anal. obs. 7-22830
 metals, internal interfaces, grain boundary struct., intergranular fracture 7-26766
 metals and alloys, environmentally assisted cracking at high vel. 7-65213
 SCC mechanism based on surface mobility mechanism 7-53943
 steel, 4340, positron annihilation parameter and H behaviour, effects of tempering temps. 7-46205
 steel, alloy, H-induced delayed fracture under mode II loading (Chinese) 7-65119
 steel, austenitic, martensite transform. start temp. increase in electrolytic H impregnation, internal microstresses role 7-17690
 steel, austenitic stainless, cold-worked, SCC and hydrogen embrittlement 7-13637
 steel, austenitic stainless, creep, effect of hydrogen charging (Chinese) 7-8042
 steel, austenitic stainless, mechanical properties, H effects (Russian) 7-46603
 steel, austenitic stainless, microstructure rel. to cathodic H charging 7-28039
 steel, austenitic stainless, SCC, delayed fractures under mode III loading
 H induced cracking 7-53898
 steel, austenitic stainless, surface phase transform. rel. to H charging and ageing 7-17530
 steel, B-containing, H-embrittled grain boundaries, Auger anal. 7-59633
 steel, C, interaction with H₂ investig. (Russian) 7-13552
 steel, C type, corrosion acceleration in boiling annular crevices, 100°C chloride solns. 7-65219
 steel, corrosion inhibitor development 7-17684
 steel, Cr-Mo, elevated temp. strength, H attack resistivity and stress relief cracking suscept. improvements 7-13583
 steel, Cr-Mo, mech. stability of retained austenite, absence of H influence 7-28125
 steel, dispersoid, H embrittlement, mechanical props. 7-33795
 steel, dispersoid, mech. props. rel. to presence of H 7-8113
 steel, ferrite-pearlite, H occlusivity and embrittlement, effect of C content 7-3417
 steel, H diffusivity from electropermeation transients under galvanostatic charging 7-6887
 steel, high strength, defect enhanced diffusion process and hydrogen delayed fracture 7-39673
 steel, high strength, H assisted cracking in aq. environment 7-3393
 steel, high strength, H induced SCC rel. to galvanisation (German) 7-3521
 steel, high strength line pipe, H induced cracking susceptibility, comp. and treatment effect 7-39619
 steel, high-strength wire, prod. parameters influence on corrosion cracking tendency in H₂S media 7-17693
 steel, HSLA, H-induced crack propag., method to evaluate crit. H conc. 7-65116
 steel, HSLA, partially coated, SCC, non-uniform H charging effect 7-3483
 steel, linepipe, H-induced cracking 7-22881
 steel, linepipe weldments, ductility rel. to cathodic protection 7-39578
 steel, low alloy, sulphide cracking, role of H 7-39726
 steel, low alloy Ni-Cr-Mo-V, with 850 N/mm² yield strength, hydrogen-induced crack form. 7-3437
 steel, low C, Al-killed, H diffusion 7-6886
 steel, low C, spheroidised, H degradation 7-8104
 steel, medium C, H degradation by disc. press. test 7-53855
 steel, mild, H diffusivity meas. using electropermeation transients 7-22903
 steel, Ni-Co-Mo, managing, ultrahigh strength, delayed fracture in H environment 7-28135
 steel, Ni-Co-Mo, managing, ultrahigh strength, H embrittlement rel. to coatings 7-28136
 steel, Ni-Co-Mo, managing, ultrahigh strength, H embrittlement rel. to Ni or Cu coating 7-28137
 steel, Ni-Cr, tensile flake form., H damage, dislocation transportation (Chinese) 7-8077
 steel, Ni-Cr-Mo, crack branching in H embrittlement (Japanese) 7-53847
 steel, Ni-Cr-Mo, H embrittlement in artificial seawater, effect of H content (Japanese) 7-53868
 steel, Ni-Cr-Mo, hydrogen embrittlement susceptibility, austenitising heat treatment prior-austenite grain size effect 7-3415
 steel, pressure vessel, fatigue crack growth rates under various conditions of loading and environment 7-28203

hydrogen embrittlement continued

- steel, stainless, H degradation by disc. press. test 7-53855
 steel, stainless, superalloy, fracture toughness, tensile props., T and ^3H effect 7-46616
 steel sheet, disc-shaped lamination development under tension and hydrogen impregnation 7-17695
 Al-H, H-point defect interactions, extended Huckel mol. orbital calcs. 7-44533
 Fe, (001) oriented single crystals, hydrogen induced cracking and hydrogen embrittlement (*Japanese*) 7-33782
 Fe, Armco, mag. internal friction, cathodic charging effect 7-17212
 Fe, cathodic charging, H trapping 7-21256
 Fe electrodes, H atom diffusion and trapping, meas. by potentiostatic double-step method 7-21525
 Fe-Al-Mn, austenitic, SCC in NaCl soln. 7-8195
 Fe-graphite diffusion chromised materials, high-temp. interaction in hydrogen 7-17671
 Fe-Ni-Co alloy, H damage, lattice distortion, defect and crack generation, positron lifetime study 7-39675
 Nb, H embrittlement, crack propag., 120-300K, hydride form. 7-33757
 Nb, pure, tensile deform., brittle fracture, H effect, SEM obs. (*Chinese*) 7-8078
 Ni 201 discs, H-induced rupture 7-3418
 Ni, intergranular H embrittlement kinetics 7-65134
 Ni₃Al-Be, ductility, strength, grain boundary segregation, solid soln. strengthening, Be addition effect 7-39608
 Ni₄₀Nb₆₀ glass ribbons, H embrittlement susceptibility, effects of cold working 7-46503
 Ti-Al-Cr-FeSi, AT3 alloy, corrosion resist. and hydrogenation susceptibility in dil. H₂SO₄ soln. 7-17685
 Ti-Al-V (6.4 wt.%), annealed fatigue crack growth in water, SEM fractography (*Chinese*) 7-8076
 Ti-Mo (15 wt.%), Young's modulus, cohesive energy, H effect (*Chinese*) 7-8033

hydrogen energy see hydrogen economy

hydrogen ion activity see pH

hydrogen ion concentration see pH

hydrogen ions

- atomic data relevant to edge plasmas 7-20063
 Auger and resonant neutralisation on Al surface, charge capture probability, parameter-free perturbation theory calcs. 7-3141
 Auger neutralisation at Al and Au surfaces, transition rate calcs. 7-3140
 channelling in Au cryst., catastrophe theory 7-21312
 charge exchange with optically pumped Na target 7-50342
 diffusion coefficient in plasma, gyro-radius effect 7-31936
 extraction from large magnetic multipole source 7-58037
 H₂⁺, higher vibr.-rot. levels calcs., relativistic connections 7-42588
 implantation effects on Al polycryst. near-surface struct. 7-58302
 isotopes, relative abundance, mass spectrometric meas., computer-assisted null point method 7-25489
 low energy implantation for passivation of polycryst. Si solar cells 7-23157
 molecule, interat. interactions in van der Waals region, Epstein Nesbet calc. 7-36491
 molecule, ground and excited states binding energies, variational calcs. 7-25684
 neutral carriers, for solvent polymeric membrane electrodes 7-17834
 plasma, beat wave saturation by collisional damping meas. 7-58058
 plasmasphere, H⁺ and He⁺ flow along mag. field lines 7-9299
 pulsed ion beam, inductive post-acceleration obs., beam energy meas. 7-11805
 transverse field focusing matching/pumping system for beam injection 7-15440
 H⁺ ion prod., dependence on plasma and wall parameters 7-25288
 H⁺ multicusp ion source, wall effect on volume prod. 7-25289
 H ions, Stark-broadening effect, simulation technique applied to models for Lyman α line 7-15721
 H⁺, $^3\text{P}_0$ symmetry, Wannier two-electron ionis. ladder, wave fn. calc. 7-62274
 H⁺, 30 kV accelerator for negative ion beams 7-18916
 H⁺ beam from pulsed magnetically insulated diodes 7-10343
 H⁺ beamline, pressure in transverse field focusing matching/pumping system 7-15441
 H⁺ charge-exchange injection into synchrotron, stripping C foil 7-62159
 H⁺, D⁺ vol. prod. ion source by sheet plasma, proton accelerator and thermonuclear fusion research applications (*Japanese*) 7-5511
 H⁺ density in large mag. multipole source 7-10329
 H⁺ discharge, atomic processes investig. 7-51527
 H⁺ extraction, effect of weak mag. field in front of plasma electrode 7-10341
 H⁺ extraction and electron control in multipole ion source 7-18915
 H⁺ extraction from volume sources 7-15447
 H⁺ formation by H⁺ bombardment of cesiated W surface 7-17390
 H⁺ formation in H⁺-surface collisions 7-17389
 H⁺, free-free absorpt. coeff., R-matrix method 7-62524
 H⁺ generation and cathode plasma formation in magnetically insulated diode 7-10342
 H⁺, ground state energy calcs. using hyperspherical coords. 7-49880
 H⁺, ground states, Rayleigh-Schrodinger perturbation expansions 7-844
 H⁺, ground-state energy, comparison of a variational fn. with previous calcs. 7-15485
 H⁺ hybrid and tandem sources, high resolution VUV light emission meas. 7-10346
 H⁺ hybrid volume source, ion and electron density profiles 7-10340
 H⁺ ion beam, steady-state, production from plasma source 7-36365
 H⁺ ion extraction from mirror ECR source 7-10334
 H⁺ ion form. on low work function surfaces 7-15444
 H⁺ ion high current density accelerator, design and diagnostics 7-15429
 H⁺ ion source, effect of magnetic filter on volume production typenegative ion source 7-526
 H⁺ ion sources, conf., Palaiseau, France, March 1986 7-9601
 H⁺ ion volume prod., effect of chamber volume and gas pressure 7-10347
 H⁺ ion volume prod. in hybrid multicusp sources 7-10331
 H⁺, laser spectroscopy with relativistic beams 7-19778
 H⁺ loss, PIG ion source 7-36704
 H⁺ magnetic multicusp discharges, e⁻ energy distrib. function modelling 7-10337
 H⁺ multipole plasma source, neutral H level populations, spectroscopic meas. 7-817

hydrogen ions continued

- H⁺ plasma ion source, wall material effects 7-62155
 H⁺, positron impact electron detachment, with excitation, threshold law calcs. 7-25668
 H⁺ production in multicusp source, effect of gas mixing 7-10332
 H⁺ source, H₂ rovibrational population, CARS time-resolved meas. 7-10605
 H⁺ source development at BNL 7-10333
 H⁺, stability, form. from NH₄⁺, pot. energy surfaces, ab initio CI calcs. 7-30955
 H⁺ surface conversion source with hot walls 7-15443
 H⁺ tandem multipole ion source, Langmuir probe meas. 7-10336
 H⁺ tandem multipole ion source, plasma parameter meas. by Langmuir probe anal. 7-10339
 H⁺ tandem multipole source, plasma parameter meas. using Langmuir probe technique 7-10338
 H⁺, two-electron doubly excited states, quantum number classification 7-49886
 H⁺ volume ion sources, modelling of vibrational population distrib. 7-10344
 H⁺ volume prod. ion source, model 7-10335
 H⁺ + H in solar wind, elastic collision cross sections 7-47654
 H⁺ + He, single and double ionisation by fast antiproton and proton impact 7-20027
 H⁺ + He in solar wind, elastic collision cross sections 7-47654
 H⁺ beam, heating of the plasma, spectrosc. appls. 7-48864
 H⁺ bombardment of cesiated W surface, H⁺ form. 7-17390
 H⁺ collisions with atoms, inner-shell ionisation 7-42750
 H⁺, exchangeable, NMR using uniform excitation solvent suppression pulse sequences 7-50192
 H⁺ induced ridge electrons emission in Au, Al and C foils 7-46270
 H⁺ ion heat engine for direct conversion to electricity 7-28409
 H⁺ motion in asymm. double-well pot. interacting with heat bath 7-24533
 H⁺, photoionisation and photodissociation, six photon ionisation, vibrational levels 7-10682
 H⁺, vibr. excitation by charge exchange with mols., TOF anal. (*German*) 7-57170
 H⁺/D⁺ fractionation, NMR investig. with various probe nuclei 7-56312
 H-like ions in laser plasma, freq. redistrib., Stark broadening of lines 7-44203
 H⁺ + H, charge transfer processes, H₂⁺ autodetaching states 7-15705
 H⁺ + He, collisional detachment neutralization at high energy 7-15685
 H⁺ + He, electron detachment, energy and ang. distrib. 7-20013
 H⁺ + He, single-electron detachment, time correlated electron spectrum study. 7-36741
 H⁺ + Xe, collisional excitation and decay of ¹P shape resonance 7-5616
 H⁺ + Al³⁺(Ga³⁺)(In³⁺)(Ti⁴⁺), charge transfer and ionis. 7-31162
 H⁺ + Ar, electron emission, impact parameter depend., TOF, coincidence spectra anal. 7-42747
 H⁺ + Ar, p state ionisation, density matrix parameters meas., DWBA calcs. 7-36743
 H⁺ + Ar, two-electron charge exchange mol. states, nonorthogonal CI calcs. 7-50339
 H⁺ + Ar(Kr) recoil ion prod. from zero-impact-parameter 7-50310
 H⁺ + Au, L subshell ionisation probabilities vacancy sharing 7-15697
 H⁺ + BH(X⁺ Σ ⁺) charge transfer dynamics 7-50331
 H⁺ + Ba, elastic backscatt., K-shell ionis. probability, reson. effect 7-42748
 H⁺ + C(CH₃)(CH₂)(CH₃), methane form. kinetics model 7-5745
 H⁺ + Cs charge transfer collisions, laser radiation influence 7-25646
 H⁺ + D₂, trajectory surface hopping calcs. 7-59747
 H⁺ + Dy(Yb), L-subshell ionisation cross section, X-ray emission 7-50327
 H⁺ + H, electron capture, strong pot. Born approx calcs. 7-972
 H⁺ + H, electron capture at intermediate energies from 1 to 200 keV 7-62515
 H⁺ + H, reson. electron capture from excited 2 s states, cross section calcs. 7-36747
 H⁺ + H, symmetric resonant charge transfer collisions in ultralow collision energy range 7-31164
 H⁺ + H collisions, H₂⁺ system emission and absorpt. processes (*French*) 7-10552
 H⁺ + H₂, nondissociative and single ionis., cross section meas. 7-31147
 H⁺ + H₂, total ang. momentum barriers 7-50294
 H⁺ + H₂, double capture, collisions, H⁺ ion excitation energy meas., Franck-Condon calcs. 7-36751
 H⁺ + H₂(D₂), charge transfer into 2S state, differential cross sections meas. 7-36750
 H⁺ + HF, charge transfer processes, ab initio calcs. 7-5744
 H⁺ + HF(CO₂), rot. energy transfer, pot. energy surface 7-967
 H⁺ + H(Ar), capture theory, first-order Born approx. Coulomb boundary conditions 7-10745
 H⁺ + H(Ar), electron capture, K-shell cross sections 7-10752
 H⁺ + H(He), 2l-electron capture, first-Born-type approximation, cross sections 7-10743
 H⁺ + He, charge transfer, second-order Born and Faddeev-Watson approx. 7-62516
 H⁺ + He, double ionisation, ab initio calcs. 7-42737
 H⁺ + He, electron capture cross section calc. by distorted-wave perturbation theory 7-50336
 H⁺ + He, electron ejection, double differential cross section meas. 7-20024
 H⁺ + He, united atom rot. coupling collisions 7-958
 H⁺ + He collisions, secondary electron spectra, Wannier ridge obs. 7-10736
 H⁺ + He⁺ ionis., beam-pulsing expt. 7-31160
 H⁺ + He⁺(Ne⁹⁺)(Ar¹⁷⁺)(Fe²⁵⁺), Fine-struct. excitation, plasma screening effects, ion-sphere and Debye-Huckel models 7-62509
 H⁺ + inert gas, electron transfer and ionis., δ -electron spectrosc. 7-42685
 H⁺ + K, ionisation and charge transfer collisions, cross section meas. 7-20031
 H⁺ + K charge transfer collisions, laser radiation influence 7-25646
 H⁺ + N₂O, collision excitation, photon emission spectra 7-15678
 H⁺ + Na, excitation cross sections, travelling at. orbital calcs. 7-62505
 H⁺ + Na charge transfer collisions, laser radiation influence 7-25646
 H⁺ + Nd(Sm)(Tm), K-shell ionisation cross sections 7-50326
 H⁺ + Ne, electron capture probabilities at large scatt. angles 7-62517
 H⁺ + Ne(Na)(Mg), multiple ionisation, charge transfer cross sections 7-15706
 H⁺ + O₂, charge transfer collisions, vibr. state resolved meas. 7-5762

hydrogen ions continued

- H^+ + Ru charge transfer collisions, laser radiation influence 7-25646
 H^+ + Sm, 4 MeV collisions, L-subshell ionisation probabilities, impact parameter depend. 7-42749
 H^+ + Sm(Tm)(Ta)(Ho)(Au)(Pb)(W)(Lu), $K\alpha_2$ to $K\alpha_1$ intensity ratio meas. 7-963
 H^+ + Ti, inner-shell ionis. polarisation effect, variational wave fn. calc. 7-62491
 H_2^+ , autodetaching states, Feshbach-type formalism 7-15705
 H_2^+ + Cs, dissociative charge exchange, H_2 predissociation, fragment spectra anal. 7-36753
 H_2^+ and HD^+ , complex scaling method appl. 7-42565
 H_2^+ , Born-Oppenheimer electronic polarisability, perturbational-variational Rayleigh-Ritz formalism appl. 7-10387
 H_2^+ , charge-overlap damping fn.s., Born-Oppenheimer curves calcs. 7-62269
 H_2^+ , damping coeffs. and multipole anal., exact second-order induction energy calcs. 7-62271
 H_2^+ electric dipole polarisability and hyperpolarisability, vibr. effects introduction to calcs. 7-10547
 H_2^+ , electric polarizabilities, perturbation study 7-36664
 H_2^+ , electron impact, autoionising states, avoided crossings 7-950
 H_2^+ , emission and absorpt. processes (French) 7-10552
 H_2^+ , excited states, non-Born-Oppenheimer electric polarisabilities 7-42662
 H_2^+ , molecular description of two-electron atoms 7-845
 H_2^+ , nonadiabatic lower and upper bound calcs. 7-36469
 H_2^+ , OS orbital calcs. 7-56938
 H_2^+ , scattering from Al (110), charge exchange 7-3133
 H_2^+ , scattering from Al (110), resonant transition rates for charge transfer 7-3134
 H_2^+ slow electron impact dissoci. recomb. 7-50382
 H_2^+ + Ar, chemical reaction and charge-transfer processes, RIOSA quantum-mechanical study. 7-31159
 H_2^+ + Ar collisions, dissociation and electron capture cross section meas. 7-31156
 H_2^+ + H_2 , H_3^+ form., quasiclassical trajectory surface hopping method 7-59750
 H_2^+ + He, elastic and inelastic scatt. mechanisms, energy loss spectra 7-15671
 H_2^+ + He, reaction, quantum infinite order sudden approx. 7-54097
 H_2^+ + He collisions, dissociation and electron capture cross section meas. 7-31156
 H_2^+ + He reaction, expt. and quantum mech. results 7-3584
 H_2^+ + He(Ne)(Ar)(H_2) electron loss to the continuum, absolute cross sections 7-50304
 H_2^+ + He \rightarrow H^+ + H + He, degenerate product electronic state distrib. determ. 7-50299
 H_2^+ + He \rightarrow He H^+ + H, endothermic reaction on ab initio pot. energy surface, dynamics 7-54103
 H_2^+ + inert gas, high Rydberg fragments, kinetic energy spectra 7-42745
 H_2^+ + Ne collisions, dissociation and electron capture cross section meas. 7-31156
 H_2^+ + tetrafluoromethane, excitation cross sections 7-62501
 H_2^+ and isotopomers, IR spectra, ab initio calcs. 7-30929
 H_2^+ , dissociative recombination at interstellar cloud conditions 7-23009
 H_2^+ , semiclassical vibr. eigenvalues, adiabatic switching method 7-57043
 H_2^+ , total ang. momentum barriers 7-50294
 H_2^+ , vibr.-rot., IR photodissociation spectra 7-31009
 H_2^+ + tetrafluoromethane, excitation cross sections 7-62501
 H_2^+ cluster ions, ($n=5,7,9,11,13,15$), vibrational predissociation spectroscopy 7-10588
 H_2^+ , even cluster ions, form., reactivity collision-induced dissoci., isotope effects, mass spectra anal. 7-50434
 H_2^+ , $n=5-23$, cluster, dissociation in Ar gas target 7-36844
 H^+ CO_2 , charge transfer reaction cross section and pot. energy curve meas. 7-54086
 HD^+ , $1s\sigma^+$ electronic ground state, vibr.-rot. levels calcs. 7-50078
 HD^+ , electrical props. adiabatic calcs. 7-56927
 HD^+ , electrostatic pot., nonadiabatic effects 7-42457
 HD^+ , higher vibr.-rot. levels calcs., relativistic connections 7-42588
 HD^+ , pot. curves, vibr. and rot. states, adiabatic STO calcs. 7-25380
 HD^+ , vibr.-rot., IR photodissociation spectra 7-31009
 H^+ L(Cr,Fe,Co,Zn), k-shell ionization cross sections and theoretical models 7-5627
 H_2^+ Mg, direct dissociative charge exchange investig. 7-50332
 H^+ (NH_3) cluster, struct., stability, ab initio MO calcs. 7-56965
 H^+ (NH_3) cluster, struct., stability, ab initio MO calcs. 7-56965
 H^+ polarised source ETH, cooling intense atomic beam 7-5521
 $He + H^+$, simultaneous single-electron capture, H_2^+ production, existence of critical scatt. angle 7-10750
 H^+ formation on W surfaces, detection low-energy H atoms from tokamak plasma 7-44248

hydrogen neutral atoms

- see also spin polarised atomic hydrogen
 adsorbed on Ru (0001), adsorbate bonding and vibr. 7-52291
 adsorpt. on La-Mg alloy, H storage investig. 7-52241
 atomic data relevant to edge plasmas 7-20063
 atomic scattering, from Cu, Au and Ni, energy spectrum, scattering trajectories 7-64854
 Br α and γ line studies of NGC 2024 - IRS 2 wind 7-40799
 chemisorption on RU (001), effect of coadsorbed O_2 7-33959
 column density at SGP and in Magellanic Stream 7-66721
 complex scaling method appl. 7-42565
 compressed, energy shift calcs. 7-35175
 degenerate Rydberg states spectrum in crossed fields 7-25437
 diamagnetic Rydberg states, meas. and calcs. 7-5615
 elastic electron scatt., forward-angle dispersion relation 7-15712
 elastic electron scatt., reson. struct. study 7-20045
 electric field effects, Feynman path-integral formalism 7-42547
 electron and positron scatt., exact eikonal approx. 7-50360
 electron capture by bare ions, coupled-state calcs., convergence 7-31166
 electron elastic scatt., second-order eikonal exchange amplitudes, Glauber approx. 7-25655
 electron impact, in laser field, one-photon free-free transitions 7-980
 electron impact excitation, excited state polarisation and ang. correls. 7-36772
 electron impact excited, polarisation and ang. correl. relations 7-31170
 electron impact ionis., second Born triple-differential cross section meas. 7-57179

hydrogen neutral atoms continued

- electron impact ionisation, triple differential cross sections, coupled pseudostate calcs. 7-50376
 electron impact ionisation triple differential cross section at intermediate energies 7-62528
 electron scatt., effect on conductivity in non-ideal plasma 7-44109
 electronic states in uniform mag. field, cylindrical adiabatic approx. calcs. 7-42479
 EM energy density distrib., van der Waals forces 7-50048
 energy levels in mag. field, quantum chaos and statistical props. 7-19765
 excited state, laser spectroscopy in mag. field 7-10460
 excited state, translational energy distrib. in DC discharge, spectroscopic meas. 7-20946
 excited states, 1D atom construction using external electric fields 7-19730
 excited states, photoionisation in strong elec. fields 7-10526
 external electric field, first-order perturbed wave fn. 7-36465
 fast electron impact ionisation, higher-order effects 7-50371
 finite chains, intermediate one-particle states 7-7145
 flames, two-step saturated fluoresc. detect. 7-19759
 flux from wall into plasma, spectroscopic meas. 7-20901
 glow discharge, plasma etching of Si and GaAs 7-32168
 Griffin-Hill-Wheeler eqn., discretisation, Gaussian type orbitals calcs. 7-30945
 ground state, 2 $^{\circ}$ -pole Cauchy moment computation 7-5629
 ground state energies, relativistic corrections, Dirac eqn. variation perturbation method 7-24766
 Hamiltonian system, regularity and irregularity transition 7-56083
 highly excited, quasi-Landau struct. 7-36510
 impurity in metals, electronic struct., higher order approx. 7-52518
 inelastic electron scatt., eikonal Born series study (Spanish) 7-15727
 interstellar, charge transfer reactions rel. to 220 nm extinction feature 7-55787
 interstitial site occupancy in Laves phases and struct. rel. cpds. 7-16549
 ion recomb. and level pops., role of charge exchange 7-31925
 ionisation by electron and positron collisions, cross. section calc. 7-15726
 ionised gas-laser interaction, dynamic Stark effect (French) 7-6395
 kaonic, coupled channels problem soln. 7-5789
 Kepler-Coulomb problem, coherent states and propagators time variables 7-62277
 Lamb shift, proton mass corrections 7-42510
 laser spectroscopy with relativistic beams 7-19778
 laser-assisted electron elastic scatt., differential cross sections, exchange and dressing study 7-20046
 lepton (antilepton) scattering, field theoretic calcs. 7-36769
 line number to line intensity, logarithmic relationship 7-49977
 Local Group Sb and Sbc galaxies, physical and star form. props., H I obs. 7-60809
 Lyman- α line Stark struct. using VUV laser system 7-62321
 mesic 2 s state, elastic and inelastic slow electron scatt. 7-10781
 metastable 2s state, electron impact ionis., triple differential cross-sections 7-25665
 microwave ionisation below classical chaos border 7-57142
 microwave ionisation of highly excited states, stochastic effects 7-15562
 multiphoton absorption above ionisation threshold, Sturmiann expansion appl. 7-36565
 multiphoton excitation techniques for combustion diagnostics 7-17789
 multiphoton ionisation, time-depend. theory 7-42568
 multiphoton ionisation by intense laser field, integral eqn. approach 7-62339
 multiple sum rules, closed-form results 7-62249
 multipole transitions, positions of minima in multipole matrix elements 7-36550
 NGC 3359, barred spiral galaxy, H I distrib. and kinematics 7-66745
 one-dimensional, ionis. by reson. elec. field 7-5780
 periodic orbits, quantisation in mag. field 7-30932
 photoionisation, ang. depend. electronic Green's fn., finite basis-sets 7-42570
 plasma, ion collisions, low-energy charge exchange, XUV spectra 7-20032
 positron annihilation, computer expt. 7-36791
 positron elastic scatt., continued-fraction approach to optical pot. calcs. 7-20048
 positron elastic scattering, empirical correl. pot. calcs. 7-36770
 positron impact ionis. cross section 7-36793
 positron impact ionisation, Faddeev formalism calcs. 7-36794
 positron scattering, inelastic and superelastic, calcs. 7-36790
 propylene reaction with Si surface, effect of addition of H 7-54187
 proton collisions, higher-order electron capture processes 7-25647
 quadrupole moment, relativistic two-body eqn. 7-49959
 radio recombination line broadening in plasma 7-29390
 recombination line intensities, Case B calcs. 7-57023
 Rydberg atom, Lamb shift in waveguides 7-10458
 Rydberg atoms, low-velocity charge transfer, classical scaling failure 7-15707
 Rydberg atoms in uniform magnetic field, quantum stochasticity, eigenvalue spectra calcs. 7-42526
 Rydberg const. meas. via Balmer- α wavelength single-photon determ. 7-36516
 Rydberg states, Doppler-free two-photon spectra 7-10533
 Rydberg states, Rydberg constant determ. by two-photon spectroscopy 7-25433
 Schrödinger equation with polynomial potential, soln. using numerical method 7-41125
 Stark effect and field ionis. 7-5628
 Stark effect in strong field 7-50008
 Stark ionisation, multichannel reson. quantisation 7-50005
 stretched, microwave-driven, level mixing 7-42524
 thermosphere, H dissipation flux density rel. to temp. 7-23922
 two-photon 1s-2s transition, high resol. laser spectroscopy 7-19806
 two-photon spectra of 1s-2s transition 7-10532
 Zeeman resons. at zero-field ionization threshold, semiclassical model 7-15547
 H + H_2 , deactivation rate const., low and high temp. 7-20020
 H + H^+ in solar wind, elastic collision cross sections 7-47654
 H, electron scatt. in chaotic laser field 7-10703
 H, Schrödinger eqn., many dimensional analogue, quantum mechanical many-body problem 7-42460
 H-like atoms, stability, particle in a spherical box theory 7-9629
 H + muonic H, low energy collisions, isotopic derivatives, cross sections, electron screening effect 7-31143

hydrogen neutral atoms continued

- H+Al³⁺, charge-transfer reaction, mol. representation, CI calcs. 7-36485
 H+Ar (N₂)(CO₂)(SF₆), Rydberg atom depopulation, scattering cross section, 7-10732
 H+C³⁺, pot. energy curves, spin-coupled VB theory 7-957
 H+CO, rot. distrib. from reson. and direct scatt., coupled channel scatt. calcs. 7-46826
 H+CO, scatt., rot. distrib. and collision lifetimes calcs. 7-25638
 H+CO vibr. excitation, pot. function, classical trajectory study 7-17783
 H+CO₂, rot. resolved hot atom collisional excitation by time-resolved diode laser spectra 7-10731
 H+C(CH₃)(CH₂)(CH₃), methane form. kinetics model 7-5745
 H+D₂-HD+D, product rot.-state distrib., information-theoretic anal. using perturbation method 7-62495
 H+F₂(Cl₂), kinetic isotope effects, dynamics calcs. 7-54098
 H+fully stripped ion collision, electron capture, travelling MO expansion study 7-50341
 H+H, ion-pair form. reaction, mol. treatment 7-50340
 H+H (H-like ions), 1s-2s excitation, cross sections, Born approx. 7-10730
 H+H₂, collision theory thermal rate consts., on SLTH pot. surface 7-54085
 H+H₂, collision-induced dissociation at interstellar densities 7-55448
 H+H₂, deactivation of vibrationally excited H₂ by collisional transfer 7-10722
 H+H₂, hemiquantal reaction dynamics with ingoing half-trajectory matching 7-28271
 H+H₂, reactive scatt., infinite order sudden approx., discrete variable representation 7-65297
 H+H₂, reactive scattering, hybrid solution to coupled equations 7-57164
 H+H₂, resonant scatt., rot. distrib. 7-39858
 H+H₂ collinear exchange reaction, time depend. arrangement channel quantum mechs. eqns. 7-17780
 H+H₂ reactive scatt., quantum mech. 3-D calcs. 7-50293
 H+H₂ reactive scattering in hyperspherical coordinates 7-57151
 H+H₂ charge transfer processes, H₂⁻ autodetaching states 7-15705
 H+H⁺, 2l-electron capture, first-Born-type approximation, cross sections 7-10743
 H+H⁺, capture theory, first-order Born approx. Coulomb boundary conditions 7-10745
 H+H⁺, electron capture, K-shell cross sections 7-10752
 H+H⁺, electron capture, strong pot. Born approx calcs. 7-972
 H+H⁺, reson. electron capture from excited 2 s states, cross section calcs. 7-36747
 H+H⁺ collisions, H₂⁺ system emission and absorpt. processes (*French*) 7-10552
 H+HO₂, abstraction reaction, saddle point geometries and barrier heights, ab initio SDCl calcs. 7-46806
 H+He(Ar)(Ne)(Kr)(Ne)(H₂), electron capture cross sections 7-10747
 H+He(H₂)(N₂)(O₂), differential scatt. cross-sections for neutral particle precipitation 7-5739
 H+methyl radical, rate const. determ., laser photolysis and reson. fluoresc. 7-8250
 H+methyl-methane, ab initio pot. energy surfaces, channel model calcs. 7-28276
 H+N₂O, hot atom reaction, chem. laser, nonequib. processes 7-1092
 H⁺+H, symmetric resonant charge transfer collisions in ultralow collision energy range 7-31164
 H₂-F₂-HF gaseous mixture, light initiated chain reaction, stimulated light scatt. study 7-62778
 H₂+He(C₂), vibr.-translation energy transfer determ. 7-57160
 H^{*}, excited fragment from mol. dissoc., effect on electron impact excitation cross-sections 7-25671
 He, positron scatt., superelastic and inelastic processes 7-15711
 He-H mixtures, positron annihilation, simulation 7-36792
 M+H⁺, electron capture at intermediate energies from 1 to 200 keV 7-62515
 N+OH, state specific collision dynamics 7-20014

hydrogen neutral molecules

- a ²Σ_g⁺-b³Σ_g⁺ system, dipole moments and transition probabilities 7-917
 absorption in metal hydride systems, kinetics 7-33966
 adsorbed on graphite, rotational states 7-52278
 adsorption on Ni (111), isotope effects, kinetic investig. 7-21624
 adsorption on Ni (115), surface corrugation effects, He diff. study 7-2381
 adsorption rate at H₂-LaNi₅ interphase, diffusion coeff. eval. 7-32696
 atom in molecule, polarisability change calcs. (*Russian*) 7-62279
 atomic data relevant to edge plasmas 7-20063
 autoionising ²Σ_g⁺ and ¹Π_g states, theory 7-5646
 B¹Σ_g⁺ and D¹Π_g states, REMPI, photoelectron spectra 7-62469
 beam diffraction from metal surfaces, multidimensional potential energy surface 7-53490
 bond rupture surfaces, MC SCF calcs. 7-30922
 c³Π_g state, total excitation cross-sections 7-5779
 chemisorption, H-permeation and recycling, molecular chemisorption model 7-8302
 coadsorption with CO, and Rh (100) surface, adsorbate-adsorbate interactions effects 7-44997
 coherent anti-Stokes Raman spectra calcs. 7-50145
 collisional effect on broadening and shift coeff. in vibr.-rot. spectra 7-15584
 desorption, thermal from Ni (111), ang. distrib., rel. to coverage 7-27103
 desorption from Pd surface, rovibr. state distrib., VUV laser induced fluoresc. 7-17826
 diffraction and rot. excitation by collision with solid surfaces, multiple Gaussian wave packet theory 7-10767
 dissociation dynamics, quantum mechanical study on Ni (100) 7-54168
 dissociative adsorption on transition metal surfaces, effect of impurities 7-16876
 dissociative chemisorption dynamics on Si (111) 7-54169
 dissociative single and double photoionisation, photon spectra anal. 7-19984
 double photoionisation cross sections and electron energies, ab initio calcs. 7-15654
 doubly excited states, photodissoc. cross section 7-19980
 E,F¹Σ_g⁺ state, REMPI, ab initio calcs. 7-62470
 E,F state, photodissoc. cross-sections calcs. 7-36714
 electron+H₂, scatt., polarisation pot. calcs. 7-15716

hydrogen neutral molecules continued

- electron beam ionisation luminesc. in high-current discharge, vacuum-UV radiation props. 7-57183
 electron impact, b¹Σ_g⁺ excitation differential cross section meas. 7-31178
 electron impact excitation cross-sections, correction for excited fragment escape 7-25671
 electron impact vibr. excitation, low energy, in He-H₂ mixtures 7-25675
 electron scatt., elastic and vibr. excitation differential cross section calcs. 7-25652
 excited state, multiphoton spectroscopy 7-10695
 excited states, rot. and vibr. branching ratios, UPS 7-5725
 fixed nuclei, elastic electron scatt., cross sections calcs. 7-15717
 gas, thermalised free positron annihilation rate studies 7-50390
 glow discharge, C cathode chem. sputtering 7-32171
 high energy electron scatt. cross sections calcs., revised Bethe theory 7-42507
 hyperpolarisabilities, vibr. contris., CARS 7-57074
 interatomic interactions in van der Waals region, Epstein Nesbet cal. 7-36491
 interstellar, line polarisation obs. in OMC-1 rel. to H₂ refl. nebula 7-14633
 interstellar H₂, form. on amorphous silicate grains 7-24184
 interstellar H₂ 2 μm emission in star-forming clouds, S(1) line mapping rel. to shock waves and jets 7-55760
 isotopes, nonadiabatic eigenvalues and adiabatic matrix elements 7-62381
 isotopomers, rot. transition, Raman line position 7-62380
 low energy elastic positron collisions, R-matrix method 7-50361
 low-energy electron scatt., static exchange calcs. 7-988
 low-energy positron scatt., Z_{eff} calcs. 7-50384
 maximum specific deposited energy, role of VV processes 7-31303
 metastable, discharge rotational temp. and density determ., resonant multiphoton ionisation method 7-44105
 methane-H₂, gaseous mixture, far-IR absorpt. spectrum 7-10577
 Morse oscillator, struct., diagonal matrix elements 7-25629
 MRD-CI pot. surfaces calcs. using balanced basis sets 7-42498
 near-threshold rovibrational excitation cross-sections, first-order non-degenerate adiabatic theory 7-15729
 negative ion generation, atomic processes investig. 7-51527
 nuclear spin relax. times and line shapes 7-42648
 one-electron loss cross section of He in H₂ gas 7-50338
 orbital energies, multipole moments and electric field gradients, HF calcs. 7-62270
 ortho to para transition, decay rate, quantum electrodynamic method 7-10674
 ortho-para conversion, new channel 7-36502
 ortho-para conversion, non-dissociative, on mag. surfaces, theory review 7-17781
 photodissociation of doubly excited states, Lyman-α fluoresc. spectra anal. 7-19945
 photodissociation of metastable states, photofragment spectra anal. 7-36716
 photodissociation processes, CARS (*French*) 7-5726
 photoionisation and photodissociation, six photon ionisation, vibrational levels 7-10682
 physisorbed on Cu (100), quadrupolar mol. rot. damping due to electron-hole pair excitation 7-23064
 plasma, electrode sheath, calcs. 7-37703
 plasma, hot-electron instability in mirror geometry 7-31960
 plasma production, LaB₆ pulsed hot cathode discharge 7-32006
 positron collisions, positronium form. cross sections 7-15724
 positron impact, positronium form. cross-sections 7-36801
 positron impact vibr. excitation 7-36802
 primordial intergalactic gas, heating by background radiation in presence of H₂ 7-24205
 reactant in RF plasma CVD reactor, flow, temp., conc. fields, num. simulation 7-26501
 resonantly enhanced multiphoton dissociative ionis. meas. 7-19968
 resonantly enhanced multiphoton dissociative ionisation, photoelectron spectroscopy 7-15645
 rotational Raman linewidths and line shifts, temp. and density depend. 7-924
 rovibrational population, in H⁺ source, CARS time-resolved meas. 7-10605
 Rydberg states, nonpenetrating, autoionis., energy-level struct. calcs. 7-15492
 short range interactions 7-19999
 single- and multi-photon ionisation process dynamics 7-36701
 solubility in Fe under high press. 7-8887
 sorption on Pd, rate investig. 7-32834
 stepwise two-photon ion-pair production, mol. spectroscopy 7-10683
 stimulated Raman scatt., N₂ laser frequency conversion 7-57452
 stimulated Raman scattering around 126 nm 7-20326
 thermodynamic properties, semiclassical limit 7-51373
 two-photon excitation and stimulated emission in VUV 7-10690
 vibrational energy accommodation coeffs., photoelectron spectrosc. obs. 7-15691
 vibrational excitation by electrons, electron spectra 7-57181
 vibrational population distrib. modelling in volume H⁺ ion source 7-10344
 viscosity, thermal cond., zero density limit data 7-60899
 Ar-H₂, low-press. plasma, form. and vanishing charact. times 7-32097
 Ar⁺+H₂(N₂) collisions, ion energy-loss spectroscopy 7-50324
 CN + H₂, time-resolved laser induced fluoresc. 7-46812
 H+CH, rate const meas., fluoresc. detect. 7-17763
 H+H₂, and isotropic analogs, reactive scatt. 7-17776
 H+H₂, resonant scatt., rot. distrib. 7-39858
 H₂ + H, deactivation rate consts., low and high temp. 7-20020
 H₂ + H₂, rotational-translational energy transfer 7-10720
 H₂ + He rotational-translational energy transfer 7-10720
 H₂ + OH, rot. excitation cross sections, close-coupling calcs. 7-25639
 H₂ + Ti, triplet state quenching and excitation transfer processes 7-19761
 H₂ + vinylidene radical, collisional quenching, rate consts., time resolved spectra 7-31104
 H₂, b³Σ_g⁺, excited states, mag. effects, ab initio calcs. 7-10413
 H₂ cluster detection at 4.2K 7-36843
 H₂ discharge, diagnostics by resonant multiphoton ionization 7-15657
 H₂ formulation of ab initio optical potential for electron elastic scatt. 7-15714
 H₂, high resolution microwave spectroscopy of Rydberg transition 7-15595

hydrogen neutral molecules continued

- H₂, vibrationally excited, rot. excitation and dissociation meas. using resonant multiphoton ionization 7-15658
H₂, vibronic constants, semiempirical determ. 7-42513
H₂-Ar, rot. line broadening calc., projection operator algebra and linked cluster theorem 7-42687
H₂-CO₂ binary mixtures, H component fugacities, press. depend. 7-51367
H₂-H₂, energy levels, ab initio close coupling calcs. 7-50292
H₂-HF complex, struct., bonding, vibr. freq. shift 7-19817
H₂-He, photodissociation processes, CARS (French) 7-5726
H₂-He collision complexes, rovibr. spectra. SCF CEPA calcs. 7-42478
H₂-He mixture, radiant heat transfer body shape influence 7-20715
H₂-methane pairs, roto-translational far IR absorpt. spectra 7-15601
H₂-O₂ flame, temp. and OH-conc. profile, IR spectroscopic determ. (French) 7-25513
H₂-O₂-Ar mixture, reflected-shock flowfield calcs., random choice method appl. 7-20812
H₂-OH, intra- and intermol. energy transfer 7-15689
H₂-octaethylporphyrin in polystyrene, photochemical hole, transmission spectrum, temp. broadening (Russian) 7-15617
H₂+Ar⁺, chemical reaction and charge-transfer processes, RIOSA quantum-mechanical study. 7-31159
H₂+Ar^{q+} (I^{q+}), total one-electron capture cross sections 7-10754
H₂+Ar(Kr)(Xe), pot. energy surfaces calcs. 7-50301
H₂+B⁺, pot. energy surfaces, diatomics-in-molecules calcs. 7-5748
H₂+C⁺(He⁺)(Ne⁺), rate const. determ. 7-17774
H₂+Ca, collisional quenching, time-resolved emission spectra anal. 7-36528
H₂+Cl⁺, reactive collisions, trajectory surface-hopping study 7-3576
H₂+Cr⁺, kinetic and electronic energy effect, mass spectra 7-65293
H₂+Cs, CsH form. kinetics, rot. distrib. (French) 7-13728
H₂+D, mol. beam scatt. study, differential cross sections meas. 7-39860
H₂+D₂-HD+H, quantum mech. reactive scatt. problem, L² soln. 7-62485
H₂+F, bond angle-bond distance coordinate system, energy conserving trajectories 7-28287
H₂+F, quantum reaction probabilities, hyperspherical coordinates 7-13754
H₂+F, reactive scattering, hybrid solution to coupled equations 7-57164
H₂+F-HF+H, collinear transition state, CI calcs. 7-54105
H₂+fully stripped ion collision, electron capture, travelling MO expansion study 7-50341
H₂+H, and isotropic analogs, reactive scatt. 7-17776
H₂+H, collision theory thermal rate consts., on SLTH pot. surface 7-54085
H₂+H, collision-induced dissociation at interstellar densities 7-55448
H₂+H, differential scatt. cross-sections for neutral particle precipitation 7-5739
H₂+H, electron capture cross sections 7-10747
H₂+H, hemiquantal reaction dynamics with ingoing half-trajectory matching 7-28271
H₂+H, reactive scattering, hybrid solution to coupled equations 7-57164
H₂+H, reactive scattering in hyperspherical coordinates 7-57151
H₂+H collinear exchange reaction, time depend. arrangement channel quantum mechs. eqns. 7-17780
H₂+H reactive scatt., quantum mech. 3-D calcs. 7-50293
H₂+H₂, deactivation of vibrationally excited H₂ by collisional transfer 7-10722
H₂+H₂, vibr. excitation, operator algebra study 7-20018
H₂+H₂⁺, H₃⁺ form., quasiclassical trajectory surface hopping method 7-59750
H₂+H⁺, charge transfer into 2S state, differential cross sections meas. 7-36750
H₂+H⁺ double capture collisions, H⁺ ion excitation energy meas., Franck-Condon calcs. 7-36751
H₂+H⁺ total ang. momentum barriers 7-50294
H₂+H⁺(He⁺), nondissociative and single ionis., cross section meas. 7-31147
H₂+HF, total differential scatt. cross sections 7-13743
H₂+He, autoionising systems, Born-Oppenheimer approx., diatomics-in-molecules calcs. 7-5742
H₂+He, collision-induced roto-translational spectra 7-15677
H₂+He, collisional excitation, translational-vibr. transition probability computation 7-42732
H₂+He⁺, elastic and inelastic scatt. mechanisms, energy loss spectra 7-15671
H₂+He⁺, metastable state, collisional quenching cross section 7-62315
H₂+He⁺(H₂⁺), electron loss to the continuum, absolute cross sections 7-50304
H₂+He(HBr), vibr. transition probabilities, semiclassical algebraic description 7-25636
H₂+He-He+H, quasiclassical trajectory calcs. 7-39876
H₂+Kr⁺, spin-orbit state and isotope effects, pot. energy curve, cross sections meas. 7-39859
H₂+Li₂, ab initio study 7-8257
H₂+methyl cation, radiative assoc. rate 7-3585
H₂+methyl ion → CH₃⁺=hv, rate coeffs. rel. to role of electronic transitions in radiative assoc. processes 7-66714
H₂+Mg, reactive collision complex form., far wing laser light scatt. 7-22982
H₂+Mg, reactive collision dynamics by far using laser scatt. 7-28296
H₂+Mu reaction, rate consts., 480 to 675K 7-50412
H₂+MuH, low energy scatt. 7-15674
H₂+N³⁺, electron transfer rate const. calc. 7-33917
H₂+NH₃, ab initio potential-energy surface, HF, SCF calcs. 7-10716
H₂+NH₃⁺(N₂H⁺)(H), ion-molecule reaction rate at low-temp. conditions of interstellar space 7-23007
H₂+Na, energy transfer expts., CARS 7-10719
H₂+Ne⁺ collisions, Ne⁶⁺ excited states, VUV spectra anal. 7-20030
H₂+O, cross section estimation 7-20004
H₂+O, crossed mol. beam expts. involving long-lived collision complexes 7-22999
H₂+O, trajectory isotope effects, pot. energy surfaces 7-65296
H₂+O⁶⁺(C⁴⁺), one-step double electron capture 7-50344
H₂+OH, collisional quenching of OH, rate const. meas. 7-10654
H₂+O-OH+H, reagent translational energy effect, pot. energy surface calc. 7-42739
H₂+Rb, fine-structure transition cross-sections, quantum-mechanical calcs., importance of perturber rotational levels 7-57161
H₂+Sc⁺ endothermic reaction ab initio pot. energy surfaces 7-13746

hydrogen neutral molecules continued

- H₂+vinyl-d₂ cation, reaction cross-section, vibr. state depend., TESICO obs. 7-54102
(H₂)₂ dimer, MP4 interaction energies and basis set superposition errors 7-62479
(H₂)₂, intermolecular interaction energies, SCF calcs., variation-perturbation procedure 7-15505
H₃, MRD-CI pot. surfaces calcs. using balanced basis sets 7-42498
H₃ in ground and first two excited singlet states, pot. energy hypersurfaces 7-57002
H₃+He, V-T rate consts., numerical and anal. calcs. 7-20022
HD Cr⁺, kinetic and electronic energy effect, mass spectra 7-65293
HD, doubly excited states, photodissoc. cross section 7-19980
HD, nuclear spin-spin coupling constants evaluated using manybody methods 7-5705
HD, photoionisation, multichannel quantum defect calcs., rovibr. frame transformation theory 7-25614
HD, rot. transition, Raman line position 7-62380
HD, submm transitions for astronomy 7-47698
HD Tokamak plasma, fast Alfvén wave propag., expt. meas. 7-58014
HD-H₂O, solenolysis, H₂ and D₂ form., H/D isotope exchange 7-13755
HD+F, quantum reaction probabilities, hyperspherical coordinates 7-13754
HD+Kr⁺, spin-orbit state and isotope effects, pot. energy curve, cross sections meas. 7-39859
HD+O, reaction probabilities and rate consts. ab initio pot. energy surface 7-65295
HD+O, reaction rates, variational transition state theory 7-59749
HD+O, trajectory isotope effects, pot. energy surfaces 7-65296
HT, rot. transition, Raman line position 7-62380
HT, rot. vibr., line position meas. in optoacoustic spectra 7-62456
N₂-H₂, gaseous mixture, far IR absorpt. spectrum 7-19858
N₂O-CO-H₂-Ar, superequilibrium pumping, Ar dilution effects 7-25611
- hydrogen power** see *hydrogen economy*
hydrogen production see *hydrogen economy*
hydrogen storage see *hydrogen economy*
hydrogen transmission see *hydrogen economy*
hydrological equipment
acoustic Doppler current profiler, vessel-mounted, for use in rivers and estuaries 7-9262
aquifer well water level fluctuation meas. device 7-9045
borehole water and gas sampling technique using polyamide tube 7-66310
calibration of neutron probe for soil humidity measurement (French) 7-47581
continuous Rn monitor for groundwater research, automated operation and characts. 7-40424
debris flows, noncontact speed sensors 7-40615
dual energy gamma radiation system for soil water constant meas., calibration 7-23917
portable neutron water content meter for soil anal. 7-56291
seepage direction detector, development and appl. (Chinese) 7-9236
smart acoustic current meters, experiences in Lake St. Clair Canada/USA 7-9255
soil water extractor for minimising CO₂ degassing and pH errors 7-23916
Hg monitoring instrument for continuous operation 7-65672
- hydrological techniques**
airborne microwave observations use for differential bare field drainage props. determ. 7-23915
alpha-card measurement technique, appl. to searches for underground water in bedrock (Chinese) 7-9235
coastal aquifer, determ. of salt-freshwater interface using borehole, theory 7-29107
aquifer parameters estimation under transient and steady state conditions, max. likelihood method 7-23734
aquifer parameters estimation under transient and steady state conditions, uniqueness, stability, and soln. algorithms 7-23735
aquifer parameters estimation under transient and steady state conditions, appl. to synthetic and field data 7-23736
atmosphere chemical deposition, stochastic modelling of space-time struct. 7-23239
borehole EM induction logging, moving and stationary transmitter methods 7-4226
borehole water and gas sampling technique using polyamide tube 7-66310
depth determination for shallow waters, photogrammetric method 7-40573
disjunctive kriging, appl. to elec. cond. distrib. 7-23755
disjunctive kriging, estimation and conditional probability 7-23754
dispersive transport modelling in porous media, solute motion in pipes and capillary tubes 7-23753
dispersive transport modelling in porous media, theoretical development of second-order approach 7-23752
distributional parameters estimation for censored trace level water quality data, estimation techniques 7-23237
distributional parameters estimation for censored trace level water quality data, verification and appls. 7-23238
dual-gamma attenuation for the determination of porous medium saturation with respect to three fluids, appl. to groundwater 7-51307
evaporation measurement, by use of pans of water 7-29090
flood frequency analysis, appl. of historical and palaeoflood information 7-23769
flash flood warning systems for real-time operation 7-60388
glacier velocity determ. in Antarctica using satellite images 7-66190
groundwater flow modelling, inverse problem soln. for two-dimensional steady state flow 7-23762
groundwater flow prediction in multiple-aquifer system, app. of sand body interconnectedness data 7-23760
groundwater hydrology, parameter identification procedures for inverse problem 7-23730
groundwater pollution risk assessment in developing countries, aquifer-oriented policy 7-3731
groundwater systems management, coupling of finite element and optimisation methods 7-60278
Hodder catchment evaporation model 7-40589
homogeneity test applied to precipitation data 7-47565
ice cover of lakes, remote sensing method based on nonthermal radiowave emission 7-66141
ice remote sensing, model for calc. of thermal emission 7-60264

hydrological techniques continued

- immiscible organic solvent transport anal., numerical modelling at Hyde Park Landfill, New York State 7-23724
- IR meas. of grain size and melting degree of snow 7-23719
- lake acidification meas., integrated palaeoecological approach 7-65658
- loose snow strength characteristics determ. appl. of conical indenter instrument 7-9052
- low-velocity flow measurement by bubble/dye tracing technique 7-16283
- measurement, scale, and scaling, relations rel. to subsurface hydrology 7-23914
- mixed groundwaters dating 7-9044
- modelling techniques, developments 7-55113
- moraine ridges dating, appl. of ^{14}C dating to historical glacier advance of Nigardsbreen, SW Norway 7-9037
- multiyear drought durations, freq. anal. technique 7-23758
- overland flow velocity determ. by dye tracer method 7-34693
- passive microwave data use for soil hydraulic characts. determ. 7-23868
- permafrost mapping method for forest areas, Landsat Thematic Mapper method 7-29302
- polar ice air bubbles for pollution monitoring and bubble age 7-4068
- porous flow model for groundwater, appl. to steady state Ra transport 7-23725
- precipitation measurement networks characts. (German) 7-4229
- precipitation measuring systems comparison (German) 7-4230
- precipitation network design anal. 7-9048
- remote sensing, generalisation of Landsat MSS interpretations of aquatic areas in SW Finland 7-9035
- remote sensing, subsatellite expts. on water bodies in USSR and Hungary 7-66185
- remote sensing for hydrogeological map production, methodological problems 7-55295
- remote sensing for soil surveys, symposium, Wageningen, Netherlands (March 1985) (French English) 7-18476
- remote sensing of estuaries, overview 7-66158
- remote sensing of land surface, use of ultralight aircraft 7-8952
- river basin parameters estimation, appl. of stream chemistry meas. 7-23771
- river flood modelling and forecasting, empirical relationship 7-40504
- river forecasting, centralised basinwide system for Lower Mekong Basin 7-18227
- river loads estimation by rating curves, underestimation factor 7-23728
- river water mixing coeff. estimation methods (Russian) 7-23666
- rivers missing flow data generation, time series model 7-66172
- rock porosity measurement technique 7-23846
- satellite microwave radiometry use for snow cover water equivalent determ. 7-23711
- scalar dynamic precipitation model, state estimation from time-aggregate obs. 7-23830
- sediment chemical analysis for Cd, Ag, Pd, Tl, atomic absorpt. method 7-40601
- sediment suspended load in lakes, Landsat remote sensing technique 7-29303
- self potential measurements; appl. in hydrogeology 7-29275
- snow cover remote sensing, effect of shadowing by topography and clouds 7-23883
- snow cover remote sensing by microwave radiometry method using classification algorithm 7-23874
- snow cover satellite remote sensing, NOAA-7 imaging method 7-23712
- snowmelt runoff determination, Landsat MSS remote sensing method 7-23875
- soil, minimal moisture capacity determination methods 7-23891
- soil mechanics, evaluation of u-w and u- π finite element methods for dynamic response of saturated porous media 7-14262
- soil mechanics, higher order, mixed, and Hermitean finite element procedures for dynamic anal. of saturated porous media 7-14263
- soil moisture estimation and forecasting for irrigated fields, stochastic method 7-23732
- soil moisture meas., remote sensing in 100 MHz-1 GHz range 7-55273
- soil moisture sensing method, by 19.1 GHz microwave radiometry 7-34564
- soil testing, BASIC program 7-34735
- solute dispersion in multidimensional periodic saturated porous media, asymptotic Gaussian approximations 7-23731
- stochastic convection-dispersion model of solute transport in aquifers and field soils, fundamental problems 7-23729
- surface saturation zones prediction in natural catchments, appl. of topographic anal. 7-23770
- Thematic Mapper data use for water quality modelling 7-34697
- thermal IR remote sensing appl. for water management in humid and arid areas 7-34696
- time series, nonstationarity detection 7-23888
- topographic partitioning of watersheds, appl. of digital elevation models 7-23723
- two-well tracer tests simulation in stratified aquifers, curvilinear finite element model 7-23759
- unsteady flow around spherical bodies, use of spherical shaped current meter 7-6227
- water level measurement stations prototype network, test and evaluation software 7-66364
- water level measurement system, management information systems 7-66162
- water resource planning, geographic information systems for encoding soil information 7-47473
- ^{226}Ra , meas. method and results in fresh water 7-23262
- ^{222}Rn , meas. method and results in fresh water 7-23262

hydrology

- Amazon River, water discharge and suspended sediment concs. (1982 to 1984) 7-23766
- Anambra Basin, Nigeria, water supply of Njikoka and Awka areas 7-18218
- aquifer parameters estimation under transient and steady state conditions, max. likelihood method 7-23734
- aquifer parameters estimation under transient and steady state conditions, uniqueness, stability, and soln. algorithms 7-23735
- aquifer parameters estimation under transient and steady state conditions, appl. to synthetic and field data 7-23736
- atmosphere chemical deposition, stochastic modelling of space-time struct. 7-23239
- Baikal-Amur Mainline area of USSR, surface heat balance study 7-23816

hydrology continued

- Bangladesh, evaporation rates, water pan observations 7-29092
- Charvak reservoir, USSR, statistical anal. and mathematical models of induced seismicity 7-23576
- chemical speciation in water, computer program for equilib. calcs. 7-66178
- cokriging and disjunction kriging in hydrological theory 7-18243
- computer applications, conf., Los Angeles, CA, USA (Nov. 1986) 7-48175
- computer graphics for water-quality investigations, Tickell diagram plotting, BASIC listing 7-9030
- cotton crops, irrigation, evapotranspiration, soil moisture etc. 7-29032
- Darazo, Nigeria, elec. resist. survey of Kerri-Kerri Formation rel. to water resources 7-18219
- diffusion hydrodynamic model for drainage system evaluations 7-4058
- dispersive transport modelling in porous media, solute motion in pipes and capillary tubes 7-23753
- dispersive transport modelling in porous media, theoretical development of second-order approach 7-23752
- drainage from uniform soil layer on hillslope simple hydrological model 7-23756
- drainage pipes under field, finite-element drainage problem with boundary conditions 7-29119
- dynamic analysis of saturated porous media, higher order, mixed, and Hermitean finite element procedures 7-14263
- dynamic response of saturated porous media, evaluation of u-w and u- π finite element methods 7-14262
- estuarine water properties, remote sensing methods 7-66158
- Ethiopia, 1983-4 drought, AVHRR images analysis 7-40505
- evaporation at catchment-scale, parameterization method involving atmos. boundary layer 7-18231
- evaporation from water surface in humid tropical area of India 7-29090
- SW Finland, generalisation of Landsat MSS interpretations of aquatic areas 7-9035
- flood and flash-flood forecasting, generalised stochastic hydrometeorological model, case study 7-66202
- flood and flash-floods forecasting, generalised stochastic hydrometeorological model formulation 7-66201
- flood control, drainage master plan 7-66188
- flood control, drainage master plan 7-66189
- flood estimation research and hydrologic design practice 7-18240
- flood frequency analysis, appl. of historical and palaeoflood information 7-23769
- flood frequency analysis theory 7-23750
- flood frequency analysis using the Cox regression model 7-23775
- flood frequency curves, similarity among river basins 7-29113
- flood hydrology predictive models 7-18232
- flood peak frequency estimation 7-18239
- flooding due to urbanization 7-54384
- flooding studies, use of point rainfall probabilistic model 7-23747
- flow modelling and forecasting (book) 7-48199
- fluid flow and energy transport assoc. with high-level radioactive waste disposal in unsaturated alluvium 7-23767
- free surface unsteady flows having shocks or bores, explicit numerical schemes 7-60302
- global-scale hydrology, dynamic modelling of ocean-atmos.-land system 7-18229
- Gombe subcatchment, Benue Valley, Nigeria, hydrogeology 7-18217
- Green-Ampt analysis for falling water table in stratified profile 7-23764
- groundwater flow in thick multiple-aquifer system, role of sand body interconnectedness 7-23760
- groundwater flow modelling, inverse problem soln. for two-dimensional steady state flow 7-23762
- groundwater hydrology, parameter identification procedures for inverse problem 7-23730
- Housatonic basin, Connecticut, appl. of stream chemistry to hydrological parameters estimation 7-23771
- hydromagmatic eruptions, implications for volcanic hazard in Italy 7-66053
- hydromass behaviour, time-depend., boundary element method appl. 7-55118
- SW Idaho batholith, USA, erosional and chemical denudation rates meas. 7-9038
- immiscible organic solvent transport at Hyde Park Landfill, New York State, numerical modelling 7-23724
- India, droughts and floods in summer monsoon season, AD 1871 to 1984 period 7-66294
- India, droughts in Maharashtra State 7-29093
- India, droughts incidence, seasonal aridity index anal. 7-9049
- induced seismicity, IASPEI symposium, Hyderabad, India (1984) 7-18484
- industrial water use, implications of structural changes 7-29109
- infiltration from cavities, num. soln. 7-18254
- intermittent flux studies in unsaturated soils, numerical hysteresis model 7-29096
- International Association for Great Lakes Research, 29th conference, Scarborough, Ontario (May 1986) 7-18507
- Japan, river flooding and land-slides during July 1985 in Noto area (Japanese) 7-18226
- Kotmale Reservoir, Sri Lanka, relation to seismic activity 7-23570
- lahars from Nevado del Ruiz volcano, Columbia, 1985 November 13, contrib. of ice cap melting 7-8896
- Lake Balaton, Hungary, subsatellite remote sensing expts. 7-66185
- Lake Balkhash, USSR, macrocirculation movements arising from seiche action 7-9051
- Lake Bhatsa, Maharashtra, India, reservoir-induced seismicity 7-23567
- Las Vegas Valley, USA, Late Quaternary environmental changes 7-47414
- laws, relationships and predictive models in hydrology 7-18232
- Leningrad, USSR, flooding in AD 1955, modelling study (Russian) 7-8964
- McCloud Lake, soft water acidic lake in Florida, ions sources and sinks 7-23763
- measurement, scale, and scaling, relations rel. to subsurface hydrology 7-23914
- Lower Mekong Basin, centralised basinwide river forecasting system 7-18227
- Melville Island, Canada, ground ice conditions 7-66175
- model choice for watersheds and floods 7-55117
- multiyear drought durations, freq. anal. technique 7-23758
- Nevado del Ruiz volcano, Colombia 7-8897

hydrology continued

- one-dimensional water infiltration in homogeneous soils, combined analytical-numerical approach 7-29082
- overland flow velocity determ. by dye tracer method 7-34693
- palaeoflood hydrology, theory 7-23750
- porous media with viscoelastic props., fluid eqn. soln. and applic. (*Chinese*) 7-18222
- Precambrian permafrost horizons, appl. as indicators of palaeoclimate 7-29023
- precipitation occurrence, continuous-time renewal and Markov chain models 7-18249
- precipitation surplus or deficit analysis using index method 7-23715
- prediction models of complex processes from noisy expt. data, construction 7-29084
- Pripyat River, groundwater regime and balance in forest and marsh landscapes of right bank 7-9050
- Qinghai-Xizang (Tibet) Plateau, Quaternary lakes retreat and climatic significance (*Chinese*) 7-55104
- raindrop splash, physically-based model of splash droplets dispersion 7-9036
- point rainfall generator probabilistic model for flood studies 7-23747
- rainfall models, role of scale of fluctuations 7-18230
- rainfall-runoff models, importance of convergence criteria in automatic calibration 7-18242
- rainfall-runoff-percolation model using programmable spreadsheet 7-55116
- Rajasthan, India, localized flooding due to heavy rains, meteorological study 7-18283
- regional hydrologic analysis, model error estimators for least squares regression 7-18252
- Rhein-Felsberg basin, Switzerland, snowmelt and runoff remote sensing 7-23875
- Ries crater, fluidisation and hydrothermal alteration of suevite deposit, and implications for Mars 7-55049
- River Don, USSR, subsatellite remote sensing expts. 7-66185
- river flood modelling and forecasting, empirical relationship 7-40504
- Rouge River, Quebec, migration patterns of asymmetric meandering river 7-23765
- surface runoff model, discrete conceptualization of Volterra series model 7-18248
- Sagehen Creek, California, size distrib. of surficial bed material during extreme snowmelt flood 7-23733
- salt marsh creek, River Esk, Cumbria, seasonal changes in surface level 7-8914
- sand-bed streams of American Midwest, flow variability and bankfull depth 7-9040
- scalar dynamic precipitation model, state estimation from time-aggregate obs. 7-23830
- sediment transporting capacity of overland flow, determ. on plane and irregular beds 7-14317
- E Shropshire, England, rainfall, runoff and erosion on bare arable soils 7-9039
- Sichuan flood catastrophe, China, mesoscale analysis of July 1981 event 7-60344
- soil, minimal moisture capacity determination methods 7-23891
- soil, solute dispersion in unsteady flow, velocity-depend. dispersion 7-60300
- soil, water downward percolation rate for intermittent flood irrigation conditions 7-29110
- soil, water infiltration during rainstorm, surface sealing phenomena due to rain 7-9031
- soil, water infiltration from spheroidal cavities 7-60299
- soil moisture, stochastic estimation and forecasting for irrigated fields 7-23732
- soil moisture content remote sensing by 19.1 GHz microwave radiometry 7-34564
- soil water and groundwater flow in unsaturated zone 7-18236
- soil water flow in two-dimensions, calc. of variably saturated flow 7-29111
- soil water physics 7-18235
- solute dispersion in multidimensional periodic saturated porous media, asymptotic Gaussian approximations 7-23731
- solute transport in aquifers, dispersion in fractal fracture networks 7-23772
- solute transport in aquifers and field soils, stochastic convection-dispersion model 7-23729
- solute transport in vadose zone 7-60290
- solute transport parallel to interface separating dissimilar porous media 7-60293
- solute transport through soil, convection-dispersion eqn. for transfer function model 7-23739
- solute transport through soil, fundamental concepts of transfer function model 7-23737
- solute transport through soil, illustrative appls. of transfer function model 7-23738
- spatial functions estimation using Bayesian analysis 7-23748
- spatial-temporal processes, model 7-66203
- statistical inference of spatial random functions 7-23779
- stochastic models for hydrological processes 7-23717
- stream gauge data adjustment for urbanization effects 7-34567
- Sudan, Savanna Zone, NOAA AVHRR monitoring of rainfall and vegetation 7-40506
- sulphate deposits in fractured till in S Alberta, Canada, origin and distrib. 7-23726
- surface saturation zones prediction in natural catchments, appl. of topographic anal. 7-23770
- Takase Dam, Japan, microearthquake activity before and after water impounding 7-23572
- Tengchong volcanic-geothermal region, China, microseismicity and hydrothermal activity (*Chinese*) 7-54875
- E Texas, storm flow and sediment losses from site-prepared forestland 7-23768
- thermal dynamics of a block-filled underground hot water store 7-46972
- three-dimensional flow in bounded domain, stochastic anal. 7-23761
- Tibet Plateau, floods, droughts and snowstorms in historical times (*Chinese*) 7-18255
- topographic partitioning of watersheds, appl. of digital elevation models 7-23723
- trace level water quality, distributional parameters estimation for censored data 7-23237

hydrology continued

- trace level water quality, verification and appls. of distributional parameters estimation for censored data 7-23238
- two-well tracer tests simulation in stratified aquifers, curvilinear finite element model 7-23759
- United States and Canada, 1986 July, water conditions 7-29094
- United States and Canada, 1986 June, water conditions 7-9053
- United States and Canada, 1986 September, water conditions 7-55100
- unsteady interface between two fluids in a porous medium 7-14319
- urban hydrometeorology review 7-9032
- urban water balance, model for daily totals 7-18246
- USA, August 1986 hydrological conditions 7-23718
- USA, October 1986 hydrological conditions 7-55101
- Vancouver, BC, Canada, urban water balance model 7-18247
- variably saturated porous media, water flow by 3D finite-element model 7-60294
- water in planetary bodies, occurrence and physical state 7-34895
- water movement in unsaturated zone under irrigated area, investigation using environmental T content 7-23757
- water permeation from artificial reservoirs, relation to seismicity changes in Japan 7-23569
- water pollution by fertilisers and pesticides, book 7-24314
- water resource valuing, existence values and normative economics 7-29108
- water resources engineering, research projects, computer support 7-18215
- Western Ghats, India, water supply and hydroclimatology 7-29091
- W.H. Mathews Symposium, Vancouver, British Columbia (October 1984) 7-4620
- Yamada fault region, Kinki district, Japan, geological, geophys. and hydrological study (*Japanese*) 7-66085
- Zhelin reservoir, E China, contrib. of water pore press. to induced earthquakes 7-23571
- N pollution in hydrosphere and atmosphere, appls. of isotopic studies 7-48222
- Ra in groundwater, porous flow model for steady state transport 7-23725
- ²²⁶Ra, meas. method and results in fresh water 7-23262
- ²²²Rn, meas. method and results in fresh water 7-23262
- hydromagnetic waves** see magnetohydrodynamic waves
- hydromagnetics** see magnetohydrodynamics
- hydrometers**
see also density measurement
mass hydrometry, Oval micromotion mass flowmeter (*Japanese*) 7-56225
- hydrophones**
see also sonar
air-backed transducer for deep sea work 7-50886
calibration of hydrophones for use in medical US fields 7-60063
composite piezoelectric sensors, elec. characts. hydrophone appl. 7-62943
cylindrical shell transducer with syntactic foam, directivity pattern calcs. 7-20561
fibre optic hydrophone with dual in-line resonant cavity 7-43600
fibre optic sensors and their appls., conf., Cannes, France (Nov. 1985) 7-40999
interference-type optical fibre hydrophone, effect of fibre length 7-43611
polyvinylidene fluoride sheet evaluation for large sonar arrays 7-2986
reflectometric fibre optic hydrophones improvement 7-43601
slow-disc waveguide radiators (*Japanese*) 7-20555
time-delay spectrometry for ultrasonic transducer characterisation 7-16041
ultrasonic field meas. using laser interferometry, use of pulse-excited hydrophones 7-62942
underwater acoustics, finite element analysis appl. (*French*) 7-11209
US attenuation in suspensions meas., coherent scattering contribution 7-16040
US wave field meas. using light beam CT system (*Japanese*) 7-57652
- hydrophotometers** see photometers
- hydrostatics**
atmospheric gravity waves, influence of Coriolis force due to Earth's rot. (*French*) 7-18271
densitometer, absolute meas. of temp. dependences of density and related variables 7-35496
metals and alloys, plastic deform. in conditions of quasihydrostatics (*Russian*) 7-59586
photoviscoplastic polymers, hydrostatic pressure effect meas. 7-11365
testing of nuclear fuel waste disposal containers 7-15406
- hydrothermal crystal growth** see crystal growth from solution
- hydroxonium ion**
electron impact dissoc. fragment cross sections 7-5777
interstellar, search for P(2,1) line emission 7-9524
K_a values 7-9626
H₃O⁺-H₂O molecule, intermolecular energy anal. SCF calcs. 7-15479
- hydroxyl group** see oxygen compounds
- hygiene**
see also medicine
No entries
- hygrometers**
see also humidity measurement
apatite concentrates, water-content measurement system 7-55300
dielometric water-content meter, methodological error in checking by use of water content simulators 7-48757
dielometric water-content meters, metrological characts. 7-48756
electronic hygrometer, cct. (*Spanish*) 7-34744
gas hygrometer, ionisation type, charge carrier mobility meas. 7-56295
gravimetric, UK standards development at NPL 7-4858
humidity measuring devices and controllers (*Japanese*) 7-56296
intelligent ventilated psychrometer with autocalibration 7-4860
linen material, raw, water-content meter 7-56292
liquids, water content meas., IR spectrochemical anal., standard-signal method and microprocessor technique 7-59809
microwave, principle of operation and characts. 7-56294
NBS developments of humidity standards 7-4859
peat water-content meter, IR, physical principles 7-55299
quartz sensor for automatic dew-point hygrometer 7-61344
refractometric water-content meas., systematic error reduction by structural method and microcomputer 7-48832
soil, water and chloride content meas. using neutron counting 7-56291
standard, design principles 7-56293
UHF water-content meters for cotton materials 7-48758
Volna-5 low-inertia hygrometer (*Russian*) 7-41396
Cu₂O-Al₂O₃-Al moisture transducer, design and development 7-41395

hyperfine field interactions (condensed matter)

see also crystal hyperfine field interactions; nuclear screening
aminoxyl(nitroxide) radicals, orientation in nematic liq. cryst., ESR obs.
7-36654
borate glasses, structure and bonding, NMR studies 7-63503
DMSO-water mixture, spin relax. ^{17}O and ^2H NMR study 7-38961
metallic glasses, laser annealed struct. and magnetoclastic props., effects
of surface characts. 7-45785
Mossbauer spectra hyperfine struct. relaxational transformation processes
anal. 7-2954
muonium, anisotropic, random hyperfine distortions, static relaxation
theory 7-13071
PAA uniaxial nematic liquid crystals, orientational order using ESR of
solute molecules 7-1872
poly-p-phenylene sulphide, conducting polymer solution, chemical struc-
ture, EPR and ^{19}F NMR studies 7-2938
polyacetylene, prepared by Durham route, EPR meas. 7-64529
polyphenylacetylene:1, conformational defects, ESR studies 7-64531
randomly disordered compounds, electric field gradients 7-45237
a-Si:H, structural characterisation, hyperfine interaction, ESR, ENDOR
7-53135
silica glass optical fibres, γ -irradiated and H_2 treated, 1.52 μm absorption
band 7-37145
silicate glasses, structure and bonding, NMR studies 7-63503
 BaTiO_3 : ^{57}Fe , multiphonon transitions from modulated hyperfine electric
field gradients 7-27633
Co-B amorphous alloys, ^{59}Co hyperfine field distrib., NMR spin echo
studies 7-53174
Fe-Ni-Zr metallic glasses, Ni contrib. to magnetism 7-53183
Fe-P amorphous alloys, electrodeposition and melt spinning prep., struct.
anal. 7-11934
 $\text{Fe}_{81}\text{B}_{19}$ amorphous ribbon, averaged spin orientation under uniaxial com-
pression, Mossbauer spectra study 7-45792
 $\text{Fe}_{81}\text{B}_{14}\text{Si}_4$ amorphous, mag. hyperfine fields under stress, Mossbauer
study 7-22166
($\text{Fe}_{1-x}\text{Co}_x$) $_{77}\text{B}_{13}\text{Si}_{10}$ amorphous alloys, Mossbauer study 7-7623
 $\text{Fe}_{85}\text{Cr}_5\text{B}_{15}(\text{Ni}_{10}\text{B}_{15})$ metallic glasses, mag. and elec. props. 7-13002
($\text{Fe}_{1-x}\text{Ni}_x$) $_{80}\text{B}_{20}$ amorphous, contribution of Ni to hyperfine fields
(*Korean*) 7-27636
 $\alpha\text{-Fe}_2\text{O}_3$, hyperfine field changes obs., selective Mossbauer refl. spectrum
detection 7-64554
 $\text{Fe}_2\text{O}_3\text{-Na}_2\text{O-B}_2\text{O}_3$ glasses, Mossbauer study 7-7619
 $\text{Fe}_{52}\text{P}_{11}\text{B}_7$ metallic glass, mag. anisotropy and correlated hyperfine interac-
tions 7-7505
 ^{57}Fe , Mossbauer effect, inhomogeneous magnetic hyperfine line broaden-
ing, nonlinear RF spectra 7-45858
Li adatoms on W (110) nuclear quadrupole interactions, NMR study
7-2937
 $\text{N}_2\text{-Ar}$ solid mixtures, orientational ordering, collective versus noncollective
behaviour 7-21103
Na adatoms on W (110), nuclear quadrupole interactions, NMR study
7-2937
 $\text{Na}_2\text{O-B}_2\text{O}_3\text{-Fe}_2\text{O}_3$ glass, hyperfine parameter distrib., ^{57}Fe Mossbauer
study 7-22170
Np cpds., Mossbauer spectroscopy, appl. to solid state chemistry 7-17248
 $\text{Ru}_2\text{Fe}_{80-x}\text{B}_{20}$ amorphous alloys, magnetic phase diagram, magnetisation
and Mossbauer studies 7-53042
 $\text{SiO}_2\text{-GeO}_2$ optical fibre, drawing- and radiation-induced paramagnetic
defects 7-11084
 VPO_3 glass, NMR quadrupole interactions study 7-45838
 $\text{Y}_{100-x}\text{Fe}_x\text{H}_2$ metallic glasses, mag. props., H content effects 7-33155
 $\text{ZrF}_4\text{-LaF}_3\text{-BaF}_2\text{-NaF}$ glasses, EPR of Cu^{2+} ions 7-27593
 $\text{Zr}_{68}\text{Hf}_{32}\text{Cu}_{30}$ amorphous and cryst. alloy, elec. field gradient, TDPAC
meas. 7-2958

hyperfine field interactions in crystals see crystal hyperfine field interactions

hyperfine structure, atomic see atomic hyperfine structure

hyperfine structure, molecular see molecular hyperfine structure

hyperfragments see hypernuclei

hypernuclei

A=12-40, strangeness exchange reactions with the recoil corrected conti-
nuum shell model 7-19190
binding energy, semi-empirical formulae 7-30362
clusterized 3n-quark systems, Pauli blocking effect, quark-cluster model
anal. 7-24833
electromagnetic transitions in hypernuclei and hyperon-nucleon forces
7-49285
exotic hadronic states in nuclei, confinement mechanism 7-49281
heavy hypernuclear production from $^{238}\text{U}(\text{p},\text{X})$ 7-49284
hypernuclear physics, conference summary 7-35970
hypernuclei identification in nuclear emulsions, review (*Polish*) 7-30887
lepton and radiation decompositions, final-state interaction and polarisa-
tion effects (*Russian*) 7-19191
particle and nucl. physics intersections conf., Lake Louise, Canada, May
1986 7-29569
pionic decay rate calcs. using DDHF single-particle wave functions
7-5183
weak decays of hypernuclei 7-49283
(γ, K^+), anal. with Coulomb, optical distortions, hypernuclear excitations
7-41973
(γ, K^+), relativistic bound state wave functions, hypernuclear shell model
studies 7-42073
(K, π), stopped-K hypernuclear expt. at KEK 7-41930
(K, π^-) reaction, hypernuclei and spin-orbit interaction 7-49473
($\text{K}, \pi^+\gamma$), hypernuclear formation, pole graph method anal. 7-42074
 ΔN and NN wave functions in nuclear matter, comparisons 7-41931
 ΔN -interaction, correlations between free and intranuclear interaction,
Brueckner G-matrix anal. 7-41931
 Δ low energy scattering and p-shell hypernuclei pots., binding energies
7-49280
(π^+, K^+), hypernuclear experiment at KEK 7-41930
 $^{10}\text{B}_\Lambda$, spin-dependent interaction parameters 7-30361
 $^{11}\text{B}_\Lambda$, hypernuclear lifetimes, neutron stimulated fraction meas., weak
decay 7-41932
 $^{11}\text{B}_\Lambda$ ground state, nonmesonic lifetimes and branches 7-30361
 $^{12}\text{C}_\Lambda$, exchange force effects on binding energy, microscopic α -cluster
model 7-41935
 $^{12}\text{C}_\Lambda$, glue-like role of Λ , microscopic three-cluster model 7-41934
 $^{12}\text{C}_\Lambda$, spin-dependent interaction parameters 7-30361
 $^{16}\text{O}_\Lambda$, exchange force effects on binding energy, microscopic α -cluster
model 7-41935

hypernuclei continued

$^{12}\text{Be}_\Lambda$, yield from $^{12}\text{C}(\text{K}^-, \pi^+)$, DWIA calcs. 7-5184
 ^{12}C prod. in $^{12}\text{C}(\pi^+, \text{K}^+)$, DWIA calcs. 7-711
 $^{12}\text{C}_\Lambda$, hypernuclear lifetimes, neutron stimulated fraction meas., weak
decay 7-41932
 $^{12}\text{C}_\Lambda$, lifetime for nonmesonic Λ decays 7-41798
 $^{12}\text{C}_\Lambda$, weak decay, AGS data 7-49282
 $^{12}\text{C}_\Lambda$, yield from $^{12}\text{C}(\text{K}^-, \pi^-)$, DWIA calcs. 7-5184
 $^{12}\text{C}_\Lambda$ ground state, nonmesonic lifetimes and branches 7-30361
 $^{12}\text{C}_\Lambda$ interaction parameters and continuum state prod. 7-30361
 $^{12}\text{C}(\text{K}^-, \pi)$, hypernuclear yield calcs. using DWIA 7-5184
 $^{13}\text{C}(\text{K}^-, \pi^-)$, $s^2 p^8 \otimes s_\Lambda$, $s^2 p^8 \otimes p_\Lambda$ state spectra, baryon decays, neutron spec-
tra, nuclear and hypernuclear γ -spectra 7-56634
 $^4\text{He}_\Lambda$, Λ -separate energies, spectra, s-wave phase shifts 7-30348
 $^4\text{He}_\Lambda \rightarrow ^3\text{H} + \pi^-$, energy spectra, angular correlation calcs. 7-56635
 $^4\text{He}_\Lambda \rightarrow ^3\text{He} + n\pi^-$, energy spectra, angular correlation calcs. 7-56635
 $^4\text{He}_\Lambda$, Λ -separate energies, spectra, s-wave phase shifts 7-30348
 $^4\text{He}(\text{K}^-, \pi^-)$, hypernucleus production cross section calcs., PWIA anal.
7-10118
 $^4\text{He}(\text{p}, \text{K}^+)$, hypernucleus production cross section calcs., PWIA anal.
7-10118
 $^4\text{He}(\pi^+, \text{K}^+)$, hypernucleus production cross section calcs., PWIA anal.
7-10118
 $^5\text{He}_\Lambda$, exchange force effects on binding energy, microscopic α -cluster
model 7-41935
 $^6\text{He}_\Lambda$, exchange force effects on binding energy, microscopic α -cluster
model 7-41935
 $^A\text{He}_\Lambda$, A=4,5, hypernuclear lifetimes, neutron stimulated fraction meas.,
weak decay 7-41932
 $^7\text{Li}_\Lambda$, spin-dependent interaction parameters 7-30361
 $\Delta\text{N} \rightarrow \text{NN}$, nonmesonic hypernuclei decay, meson exchange anal. 7-41933
 $^{16}\text{O}_\Lambda$, spin-dependent interaction parameters 7-30361
 $^{238}\text{U}(\text{p}, \text{f})$, delayed fission observation, non-mesonic hypernuclear decay
interpretation 7-42082

hyperon absorption

No entries

hyperon capture

see also hypernuclei

No entries

hyperon decay

beta-decay, Kobayashi-Maskawa angles and SU(3) breaking 7-41788
constituent quark model picture for non-leptonic hyperon decays 7-49139
CP-odd observables in hyperon decay 7-49138
hyperon physics and strange matter props. 7-30265
S-wave nonleptonic hyperon decays in quantum chromodynamics 7-15149
semileptonic decay, bremsstrahlung, integration of photon quadrupole
moment (*Spanish*) 7-61672
semileptonic hyperon decays 7-56545
 Λ nonmesonic decay in hypernuclei, hybrid quark hadron model anal.
7-41798
 $\Lambda^0(\Lambda^0)$ decays, production of polarized p,p beams 7-30796
 $\Lambda_c^+ \rightarrow \text{K}^0 \pi^+ \pi^-$, Λ_c^+ polarization meas. from $^{12}\text{C}(\text{n}, \Lambda_c^+)$, 40-70 GeV/c
7-5088
 $\Lambda_c^+ \rightarrow \Lambda^0 \pi^+ \pi^-$, Λ_c^+ polarization meas. from $^{12}\text{C}(\text{n}, \Lambda_c^+)$, 40-70 GeV/c
7-5088
 $\Lambda_c^+ \rightarrow \Sigma^+ \pi^- \pi^+$, charmed baryon decay, nuclear emulsion obs. 7-15150
 $\Sigma_c^- \rightarrow \text{ne } \bar{\nu}$, mag. moment meas. using spin-precession techniques 7-5093
 $\Sigma^- \rightarrow \text{ne } \bar{\nu}$, electron energy spectrum calcs. with radiative corrections
7-61670
 $\Sigma^- \rightarrow \pi \pi^-$, mag. moment meas. using spin-precession techniques 7-5093
 $\Sigma^0 \rightarrow \Delta\gamma$, transition magnetic moment meas. 7-524
 $\Sigma^+ \rightarrow \pi \gamma$ asymmetry, W-exchange dominance in SU(6) broken quark-
diquark model 7-49153
 $\Sigma^+ \rightarrow \pi^+ \pi^0$, charmed baryon decay, nuclear emulsion obs. 7-15150
 $\Sigma_c^0 \rightarrow \Lambda_c^+ \pi^-$, charmed baryon decay, nuclear emulsion obs. 7-15150
 $\Delta\text{N} \rightarrow \text{NN}$, nonmesonic hypernuclei decay, meson exchange anal. 7-41933

hyperon detection and measurement

No entries

hyperon-deuteron interactions

see also hyperon-deuteron scattering

No entries

hyperon-deuteron scattering

see also hyperon-deuteron interactions

No entries

hyperon effects

No entries

hyperon electric moment

No entries

hyperon interactions see hyperon-nucleon interactions; hyperon-nucleus reactions

hyperon magnetic moment

$\Sigma^- \rightarrow \text{ne } \bar{\nu}$, mag. moment meas. using spin-precession techniques 7-5093
 $\Sigma^- \rightarrow \pi \pi^-$, mag. moment meas. using spin-precession techniques 7-5093
 $\Sigma^0 \rightarrow \Delta\gamma$, transition magnetic moment meas. 7-524

hyperon mass

dihyperon physics and strange matter props. 7-30265

hyperon-nucleon interactions

see also hyperon-nucleon scattering

$\Delta\text{N} \rightarrow \Sigma\text{N}$, low-energy interaction, P-matrix anal. 7-41834
 $\Delta\text{N} \rightarrow \text{NN}$, isospin structure, hypernuclear weak decay 7-41932
 $\Delta\text{N} \rightarrow \text{NN}$, nonmesonic hypernuclei decay, meson exchange anal. 7-41933

hyperon-nucleon scattering

see also hyperon-nucleon interactions

ΔN elastic scattering in $^4\text{He}_\Lambda$, $^4\text{H}_\Lambda$ 7-30348
 $\Delta\text{N} \rightarrow \Delta\text{N}$, quark cluster model 7-49180
 Δ low energy scattering and p-shell hypernuclei pots., binding energies
7-49280
 $\Delta\text{p} \rightarrow \Delta\text{p}$, slope parameter and scaling of differential cross-section 7-56571
 Ωp elastic scatt., Chou-Yang model for differential cross section 7-41833
 $\Sigma \pm \text{p}$ elastic scatt., Chou-Yang model for differential cross section
7-41833
 $\Sigma^- \text{p} \rightarrow \Sigma^+ \text{p}$, elastic scatt., Donnachie-Landshoff model 7-24911
 Σp elastic scatt., Chou-Yang model for differential cross section 7-41833

hyperon-nucleus reactions

for inelastic hyperon-nucleus scattering, see "hyperon-nucleus scattering"
see also hyperon capture; hyperon-nucleon interactions
(Λ , Σ^0), Primakoff production, corrected analysis 7-520

hyperon-nucleus scattering

see also hyperon-nucleon scattering
No entries

hyperon production

- hyperon polarization in hadronic collisions 7-35908
 $e^+e^- \rightarrow \Sigma^- X$, inclusive prod. at 29 GeV 7-56562
 $\gamma p \rightarrow \Lambda p X$, diffractive production meas., cross-sections and distrib. 7-41823
 $\gamma p \rightarrow \Sigma^- p X$, diffractive production meas., cross-sections and distrib. 7-41823
 $K^- d \rightarrow \Lambda n \pi$, three-body multichannel, two body interaction anal. 7-36057
 $K^- d \rightarrow \Lambda n \pi$, three-body multichannel, two body interaction anal. 7-36057
 $K^- p \rightarrow K^0 \Lambda$, source of ss states with even spin 7-41857
 $K^- p \rightarrow \Lambda^0 X$, 150-350 MeV/c, analysis of two-body channels 7-24905
 $K^- p \rightarrow \Sigma^+ \pi^-$, pole plus cut model anal. 7-15174
 $K^+ p \rightarrow \Lambda p X$, hyperon inclusive production 7-41855
 (Λ, Σ^-) , Primakoff production, corrected analysis 7-520
 Λ_c^- inclusive production, quark-gluon-string model 7-41750
 $\Lambda_c^- \rightarrow \Lambda^0 \pi^+ \pi^-$, Λ_c^+ polarization meas. from $^{12}C(n, \Lambda_c^+)$, 40-70 GeV/c 7-5088
 $\nu_\mu N$ -strange particles, inclusive production rates 7-528
 $\bar{p} p \rightarrow \mu^+ \Lambda$, quasielastic production, comparison with Cabibbo scheme 7-41781
 $\bar{p} d \rightarrow \Lambda X$, low-energy annihilation, cross section meas. 7-15169
 $\bar{p} N \rightarrow \Lambda X$, 13, 18 GeV/c, polarization transfer meas. 7-30294
 $\bar{p} p$, 32 GeV/c, inclusive baryonic reson. prod., constitutive model 7-5127
 $\bar{p} p \rightarrow \Lambda X$, one-particle and semi-inclusive hyperon spectra 7-41856
 $\bar{p} p \rightarrow \Lambda^0 X$, $\sqrt{s}=31-62$ GeV, Λ^0 polarization meas. 7-61760
 $\bar{p} p \rightarrow \Lambda \Lambda$, antiproton spin physics expt. at LEAR 7-49170
 $\bar{p} p \rightarrow \Lambda \Lambda$, exchange $K+K^*$ coupled channels analysis 7-5107
 $\bar{p} p \rightarrow \Lambda \Lambda$, K exchange, cross section and ang. distrib. calcs. 7-19126
 $\bar{p} p \rightarrow \Lambda \Lambda$, LEAR data anal., CP invariance in $\Lambda \Lambda$ system 7-49167
 $\bar{p} p \rightarrow \Lambda \Lambda(\Sigma \Sigma)$, low energy, CP violation, asymmetry meas. 7-15082
 $\bar{p} p \rightarrow \Lambda X$, analyzing power and spin transfer meas. 7-41853
 $\pi^- p \rightarrow K^+ \Sigma^+$, pole plus cut model anal. 7-15174
 $^{12}C(p, \pi^- \Lambda)$, 4.2, 4.5 A GeV/c, reaction analysis 7-708
 e^+e^- -hyperons, 10 GeV, obs. of octet and decuplet hyperons 7-61704
 $^7Li(\alpha, \pi^-)$, 3.7 GeV/A, Λ polarization study 7-5253
 $^7Li(\alpha, \pi^- \Lambda)$, 4.5 A GeV/c, reaction analysis 7-708
 $^{20}Ne(p, \Lambda K^0)$, strange particle production expt. 7-49392
 $^{40}Ne(B, \pi^- \Lambda)$, $B=^{16}O$, ^{12}C , 4.5 A GeV/c, reaction analysis 7-708
 $pN \rightarrow \Lambda^0 X$, polarisation in inclusive production, A dependence 7-15177
 $\bar{p} p$, baryon production, quark-quark and quark-diquark reaction mech. 7-5133

hyperon resonances

- dihyperon physics and strange matter props. 7-30265
H, dihyperon, high energy muon obs. in Cyt X-3 7-47992
 $K^- p \rightarrow K^0 \Lambda^0 \pi^+$, source of ss states with even spin 7-41857
 (Λ, Σ^-) , Primakoff production, corrected analysis 7-520
 Λ production in nucleus-nucleus reactions, polarization study 7-5253
 $\bar{p} p \rightarrow \Lambda \Lambda$, exchange $K+K^*$ coupled channels analysis 7-5107
 $\xi(2232)$, a $\Lambda \Lambda$ bond state in quark pair creation model 7-41709

hyperon scattering see hyperon-nucleon scattering; hyperon-nucleus scattering**hyperon spin and parity**

- Λ^0 polarization meas. $\bar{p} p \rightarrow \Lambda^0 X$, $\sqrt{s}=31-62$ GeV 7-61760

hyperons

see also hyperon resonances

- bag radius increase, strangeness-induced size effects 7-19067
CP-odd observables in hyperon decay 7-49138
electromagnetic decays, Skyrme model predictions 7-61696
ground state hyperons, bound kaon-skyrmion anal., baryon number distn. calcs., nonsphericity of baryonic density 7-41599
semileptonic hyperon decays 7-56545
stars of strange matter, energy and chemical potential 7-61829
 $\Lambda(1405)$, KN bound state and 3-quark state model interpretations 7-492
 $\Lambda_c^- \rightarrow K^0 \pi^+ \pi^-$, Λ_c^+ polarization meas. from $^{12}C(n, \Lambda_c^+)$, 40-70 GeV/c 7-5088
 $\Lambda_c^+ \rightarrow \Lambda^0 \pi^+ \pi^-$, Λ_c^+ polarization meas. from $^{12}C(n, \Lambda_c^+)$, 40-70 GeV/c 7-5088
 $\Sigma^- \rightarrow nev$, electron energy spectrum calcs. with radiative corrections 7-61670
 $\Sigma^0 \rightarrow \Lambda \gamma$, transition magnetic moment meas. 7-524
 $K^- p \rightarrow \Lambda X$, Λ polarization, energy dependence and p_t variance, QCD comparisons 7-61754
 $pN \rightarrow \Lambda^0 X$, polarisation in inclusive production, A dependence 7-15177

hypersonic flow

- 3D hypersonic rarefied gas flow around rotating bodies 7-20761
hemisphere and cones in wind tunnels 7-51218
hypersonic viscous shock layer investig., on rotating bodies 7-20756
local interaction theory, aerodynamic calc. 7-43971
nonperturbing boundary-layer transition detector for hypersonic wind tunnel, based on laser interferometry 7-20821
nonviscous flow simulation, upwind scheme (French) 7-57878
prototype physicochemical processes in shock layer during flow past hypersonic wind tunnels 7-63175
radiative and convective heat transfer during blowing into layer of two-phase prods. from ablation 7-20755
shock waves, structure, statistical modelling, weighting schemes (Russian) 7-56019
smoothed particle hydrodynamics, hypersonic flow appl. 7-16206
surface roughness effects on adiabatic wall temp. 7-20700
Taylor-Maccoll soln., const. density approx. 7-20749
wedges and plane ogives, oscillating, unified supersonic/hypersonic similitude 7-6246
wind-tunnel diffuser operating at Mach no.4.4 to 8.5, press. recovery 7-43973

hypersorption see sorption**hypersound** see ultrasonics**hyperthermia** see biothermics**hypertritons** see hypernuclei; tritons**hyperviral theorem** see quantum theory**hypochromism** see light absorption**hypothetical particles**

see also charm particles; heavy leptons; intermediate bosons; magnetic monopoles; quarks; sparticles; tachyons
anyon statistics with single-valued wave functions 7-29879
axions, short-lived, evidence in ^{10}B isoscalar M1 transitions 7-56641

hypothetical particles continued

- bosonic states, $J=1$, from σ -model simulation of strongly interacting Higgs sector 7-48975
cold dark matter, ultralow background solar search 7-55393
cold dark matter candidates, limits from deep underground detectors 7-23998
cosmic axion decay to photons in microwave and IR regions 7-14695
cosmons, effects in Sun and in globular cluster stars 7-55436
cosmons in solar neutrino. problem, particle physics models 7-55457
Cyt X-3, cosmic glueballinos source, discussion 7-48105
cygnet particles associated with Cygnus X-3, flux predictions 7-30303
dark matter in Universe 7-9560
 E_c exotic, mirror and fourth generation lepton production in e^+e^- collisions 7-19093
gaugino masses from radiative corrections in superstring models 7-24864
gluinos, quasi stable, evidence against existence 7-5004
Goldstone-Higgs particle mass, internal subgroup prediction 7-35756
inos in $N=2$ massive gauge superfield formalism 7-4958
invisible axion detectors 7-10012
leptoquark bosons, decay in lepton+quark 7-10019
light neutral particle search in ^{13}C 3.68 MeV state decay 7-30366
paraton existence in U(1) gauge symmetry 7-9992
photinos and primordial nucleosynthesis 7-66793
shadow matter mass/charge constraints, from beam-dump expts. 7-49186
stellar axion emission rates in nonrelativistic degenerate regime 7-55458
supermassive relic particle search, flux upper limits 7-61516
SUSY down-quark mixing in superstring models 7-5022
weakly interacting massive particles and cosmological missing matter problem 7-24246
 E^+ (heavy lepton) $\rightarrow N \mu^+ \nu_e \rightarrow e^+ \mu^+ W^- \nu_e$, preon model anal. 7-56524
 ϕ production in heavy ion collisions (light pseudoscalar boson), QED calcs. 7-36022
 $S(V_1 V_1) \rightarrow \gamma \gamma (\gamma Z^0)$, $V_L = W^\pm$, Z^0 , branching ratios, nonrelativistic bound-state calcs. 7-49154
 Sff , $S\gamma\gamma$, $S\gamma Z^0$ couplings, $S=V_L V_L$, $V_L = W^\pm$, Z^0 , nonrelativistic bound state calcs. 7-49154
 W mass, astrophysical bound 7-5005
 W decay, generalized vector-boson dominance anal. 7-61681
 $^1H(n, \text{axion})^0H$, search for short lived axions 7-56685

hysteresis

see also coercive force; dielectric hysteresis; elastic hysteresis; magnetic hysteresis; remanence

- CDW systems, Ginzburg-Landau theory for hysteresis 7-7136
dynamical system with delayed feedback (Chinese) 7-35263
ferromagnetic superconductor, phase diagrams and order parameters 7-17127
Josephson junction with time-independent driving current, chaotic behaviour 7-52904
liquid cryst. display, SBE type, fundamental characteristics (Japanese) 7-7670
liquid cryst. display, SBE type, supertwisted nematic, display characts., effects of various parameters (Japanese) 7-7669
metal hydrides, thermodynamics of hysteresis at high pressures 7-39911
nematic liquid crystals, supertwisted, hysteresis effect 7-16408
nonlinear optics, latent symmetry of system of equations, hysteresis 7-43194
phase transformations in solids, plastic deformation and thermodynamic hysteresis 7-16714
poly(n-alkyl methacrylates), surface mobility and struct. transitions, dynamic contact angle meas. 7-32758
polyethylene, medium-density, noncontact monitoring of cyclic loading and stress relax. by US backscatter 7-59724
smectic C phases, bistability and domain wall motion induced by strong elec. fields 7-63450
Stirling engines, moderate temp., mechanical losses in rolling seals 7-65561
visual motion direction perception, hysteresis as evidence for neural cooperativity 7-34152
AgCd, martensite transformation and shape memory effect, resistivity and thermoelectric power meas. 7-53729
Ag₂HgI₄, thermochromic phase transition, Raman and optical absorption studies 7-7680
Al, hysteresis behaviour of medium temp. peaks (French) 7-63742
CdS, temperature-electric instability, spontaneous oscillation states 7-38616
GaAs:Si,Se MOCVD epitaxial layer photolum. spectral shift and doping efficiency obs. (Japanese) 7-45076
He, liquid, heat transfer with nucleate boiling in channels 7-11524
InP MIS structures, prep. by RF plasma oxidation, interface elec. props. 7-2731
K_{0.3}MoO₃, electric field hysteresis and relax. 7-52462
(NbSe₄)₃I, phase transition props. 7-44803
Ni-Ti, Nitinol, thermodynamics 7-58506
TaS₃, disequilibrium of pinned CDW state 7-32927

hysteresis motors

- turbomolecular pump with hysteresis motor for particle accelerators (French) 7-30025

I-centres see colour centres**I-II-VI₂ semiconductors** see ternary semiconductors**I-III-VI₂ semiconductors** see ternary semiconductors**IBA** see interacting boson approximation**IBM** see interacting boson approximation**IC** see integrated circuits**IC engines** see internal combustion engines**ice**

- see also sea ice; snow
acoustic emission due to deformation and breaking 7-16053
air bubble trapping in polar ice and importance for air pollution monitoring 7-4068
aircraft, static charging by collisions with ice crystals 7-55212
amorphous, high-density struct. by neutron diff. 7-37865
amorphous films, low temp. elastic props. 7-45099
Antarctic Dome C ice core samples, TEM study of dust microparticles 7-55228
Antarctica, ice core record of $^{13}C/^{12}C$ ratio of atmospheric CO₂ for past two centuries 7-34637
Antarctica, Pb conc. changes in ice core from Dome C 7-40074
atmospheric icing of exposed surfaces, density of accreted ice 7-34648
biological charge transfer processes, IR and microwave spectra 7-3749

ice continued
bridges, over rivers, 7-55092
California Valley, hydrometeor evol. in rainbands 7-4126
cirriform cloud at -83°C, ice particles characts. implications for polar stratospheric clouds 7-4123
clouds, ice splinter production, importance of rimer surface temperature 7-34657
columnar grained, fracture toughness using large specimens (*Japanese*) 7-59612
comet dirty ice grains, albedos evol. 7-24067
cometary comae, micron-size ice grains cloud rel. to exptl. modelling of cometary phenomena 7-66506
comets, dirty ice grain characts. 7-18387
creep behaviour, dynamic recrystallization and fabric development during shear deformation 7-55096
crystal growth in stratiform cirrus clouds rel. to radiative props. 7-66222
cubic, proton transport, FTIR obs. 7-53340
cubic ice (Ic), formation from aerosols in laboratory 7-60364
Denver hailstorm, 1984 June 13, meteorological obs. 7-29127
drop freezing data anal. using mathematical technique 7-58444
films, Kr⁺ bombardment, ion cluster desorption, TOF mass spectra study, astrophysical implications 7-26815
Finland, lake ice freeze-up and break-up dates rel. to air temp. climate 7-14342
firm closure, lattice models, percolation on interstices of BCC lattice, bubble age 7-14320
formation on substrates, crystallographic config., cooling rate and direction (*Japanese*) 7-6569
freezing problem, moisture migration allowance study 7-55094
freshwater, crack resist. determ. 7-12195
front risk and min. temp. surveys 7-4133
frost penetration into water saturated porous medium (*Russian*) 7-47471
graupel growth in supercooled clouds, supersaturation field 7-34591
Greenland ice cap, cosmic dust placers in blue ice lakes 7-14548
growth in anvil of severe thunderstorm during CCOPE 7-66231
hail, remote sensing with S-band dual linear polarization radar 7-66344
hail embryo definition, morphology and growth in clouds (*Chinese*) 7-18260
hail growth in 3D storm cloud model (*Chinese*) 7-4081
hail suppression by cloud seeding, Grossversuch IV expt. in Switzerland 7-14344
Himalaya mountains, glaciation upper limit and assoc. characts. 7-55090
hurricanes, ice distribution and convection 7-4121
ice:RbOH, phase transition, dielec. studies 7-53220
ice clathrate containing tetrahydrofuran molecules, transformation on compression at 77 K 7-37862
ice-air composite materials, melting process study 7-26335
icing of exposed surfaces, accretion onto fixed cylinders 7-34649
Ih phase, X-ray powder spectrum, temp. depend. simulation, Metropolis Monte Carlo sampling 7-16510
insulator string flashover mechanism; role of water film 7-51556
ion bombardment, classical dynamics model 7-23996
Lake Arakhs, USSR, ice gas inclusions and ice sheet radioluminescent temp. 7-23709
low temperature thermal energy storage using ice slurry 7-65622
low-level counting techniques 7-29296
Mars, quantity and condition of underground water 7-24043
Marsian atmosphere, evidence for water ice haze layers from scattered light profiles 7-55513
materials modification with ion beams, review 7-16647
melting around horizontal cylinder, numerical simulation 7-1604
melting in porous media, solid-liq. interface motion, temp. distrib. 7-50926
Melville Island, Canada, ground ice conditions 7-66175
microscopic filament form. in elec. field 7-14362
microwave absorption measurements of melting spherical and nonspherical hydrometeors 7-9106
noctilucent clouds, observational props. rel. to behaviour of upper atmosphere 7-23925
nucleation activity of AgI particles 7-26918
nucleation by AgI-AgBr-CuI system, UV irradiation effect 7-66247
nucleation mechanism under elec. effect 7-52005
nucleation on AgI-AgCl solid solns. 7-58179
periglacial activity in central North Sea, evidence from valley asymmetry 7-14285
permafrost mapping method for forest areas, Landsat Thematic Mapper method 7-29302
permafrost of Alaska, temp. profile and evidence for climate change 7-66299
permafrost zone, soil thawing and freezing, Stefan problem with one spatial var. 7-47469
phase I, pre-melting second-order transform., isothermal compressibility and expansivity meas. 7-32631
planetary satellites, cratering in icy targets 7-34863
polar ice cores, long-term record of atmospheric H₂O₂ 7-55229
positronium formation at low positron energy in cryst. and amorphous ice 7-27815
Precambrian permafrost horizons, appl. as indicators of palaeoclimate 7-29023
pure and doped, US absorpt., dislocation damping 7-26756
Quechaya Ice Cap, Peru stratigraphic record of Little Ice Age 7-34670
remote sensing of lake and sea ice, method using radiowave emissions 7-66141
riming of snowflakes, wind tunnel study of aggregates 7-66229
riming of snowflakes, wind tunnel study of disks and stellars 7-66228
Saturn rings, IUE spectral obs. 7-47759
segregated ice in freezing soil under negligible overburden press., stable growth 7-60279
single crystal, fracture toughness and macrofractography (*Japanese*) 7-16676
single crystal crucible-free growth, weightlessness simulation 7-64888
solar powered solid-adsorption ice maker design 7-65585
sound vel. meas. 7-32576
stretching vibr., red shift 7-22236
tensile fractures, radiation patterns in glass plates and ice 7-60182
tetramethyl urea+water system, solid-liq. phase equil., freezing pts. 7-32616
thin films, ion irradiation erosion effects meas., astrophysical discussion 7-26814
tropical squall line, diagnostic modelling study of stratiform cloud region 7-29136

ice continued
underground pipe, freezing liquid transport, cooling effect 7-57923
uniaxial nonlinear viscoelastic constitutive relation for ice 7-4069
water, quenched to low temp., glassy state, Monte Carlo simulation 7-26633
Yukon rivers, dissolved O₂ depressions under ice cover 7-55106
H₂O-NH₃ ice mixtures, optical consts. determ. 7-23993

iconoscopes *see television camera tubes*

identification
see also correlation methods; frequency response; modelling; parameter estimation; simulation; state estimation
bond graph model of a pool-type nuclear reactor 7-5438
complex natural process prediction model, construction, hydrological appl. 7-29084
dynamic behaviour of sheathed thermocouples under field conditions obs., using online identification 7-4848
haemodynamic control systems, closed loop identification 7-60027
heart rate and blood press., closed-loop identification of beat-to-beat interactions 7-8640
posture control system, max. likelihood identification 7-60022
posture-control system, selection of perturbation parameters for identification 7-28561
sound insulation system, dynamical identification method, conditioned obs. based 7-43526
system theory, conf., Knoxville, TN, USA (Apr. 1986) 7-14714

IETS *see tunnelling spectra; tunnelling spectroscopy*

IEXE *see ion microprobe analysis; X-ray chemical analysis*

IGFET *see insulated gate field effect transistors*

ignition
see also electric ignition
AC plasma displays, discharge ignition 7-21017
flameless peat fires, low temp., kinetic characts. 7-13774
free-resistant material, Sb₂O₃ influence on effectiveness, chem. anal. (*Russian*) 7-65378
fuel spray ignition by hot surface 7-51337
infinite slab, critical local disturbance of temp. field necessary for ignition, reactant consumption effects 7-33932
magnetic linear accelerator (MAGLAC), switching studies 7-36342
nitromethane, shocked, condensed, ignition, rate determining step 7-54124
radiative ignition in a planar medium 7-50925
radiative ignition in propagation of large explosions 7-54127
reactive shear bands, dimensional anal., numerical integration 7-33931
self-ignition conditions for frontal phase transition in cylindrical volume 7-17795
steel, stainless, type 302, ignition of bulk by laser heating 7-3516
thermal explosion and times to ignition in systems with distributed temps., behaviour at criticality and transition 7-54128
transient ignition on a flat plate 7-17794
Al particles, ignition, behind detonation and shock waves 7-8287
H₂, jets, ignition behind reflected shock waves 7-37504
O atom, flame diagnostics by two-photon fluoresc., UV laser appl. 7-23015

II-III₂-VI₄ semiconductors *see ternary semiconductors*

II-IV-V₂ semiconductors *see ternary semiconductors*

II-VI semiconductors
CdS-CuInSe₂ solar cells fabricated by DC magnetron sputtering of Cu₂Se and In₂Se₃ 7-23170
CdTe films, MBE growth, photoluminescence and TEM characterisation 7-22376
deep centres in semiconductors, book 7-18510
electronic struct. of bulk and defect sites, tight-binding recursion method 7-45222
films, prep., electronic props., solar cell appl. (*Japanese*) 7-54299
glass: CdSse gratings, darkening effect, optical phase conjugation 7-57476
Hg_{1-x}Mn_xTe-HgTe dilute mag. semicond. superlattices, MBE growth and props. 7-13357
II-VI-III-V systems, thermodynamics and reactivity 7-16790
IR coating materials, physical effects 7-37065
Jahn-Teller interaction, influence of mag. field 7-16995
laser stimulated desorption, dimerisation enhanced phase transition 7-58619
lattice matched heterojunctions, common anion rule failure 7-7367
low-temperature epitaxial growth, MBE and MOCVD 7-64906
MOCVD, organometallic precursors monitoring by laser mass spectroscopy 7-22547
MOCVD, prep. and props. of metal alkyls 7-22520
moving dislocations in II-VI semiconductors, dislocations, effect on physical props. 7-7224
MOVPE, conf., Universal City, CA, USA (Apr. 1986) 7-18477
shallow donor problem, pseudopot. approach 7-45216
solid solns., short range order and free energy of mixing, EXAFS meas. 7-63573
solid solutions, luminescence, exciton localisation 7-33429
solid solutions with wurtzite structure 7-32348
surface preparation effects 7-45037
tetrahedral cpds, mode Gruneisen parameters 7-44732
transient spectroscopy, deep level characterisation 7-58776
wide-gap II-VI superlattices 7-7346
ZnO:Bi (Sb) (transition metal), Schottky-like barriers, ion implantation, annealing 7-58860
Au/i-ZnS/n-ZnS electroluminescent device struct., electron-hole recomb. luminesc., minority carrier injection mechanism 7-59260
Bi chalcogenides, binding energies, chem. shifts XPS and diffuse refl. spectra (*German*) 7-1943
C-ZnX (X=S, Se), adherence of diamondlike C films, use of intermediate layers 7-46624
(Cd,Mn)Te quantum well structure, wide-gap II-VI superlattices 7-7346
Cd chalcogenides, cryst. growth by SSSR-zone melting method 7-64897
Cd-Hg-Te phase diagram, numerical descriptions, review 7-26913
CdHgTe detector, CO₂ laser detection appl. 7-5915
CdHgTe focal plane arrays, sampling effects reduction 7-30090
(CdHg)Te, LPE growth, use of in-situ wash melts 7-59466
CdHgTe, optical nonlinearities and bistability 7-57435
CdHgTe photodetectors for infrared measuring techniques (*Russian*) 7-4889
Cd_{0.2}Hg_{0.8}Te, galvanomagnetic props., effect of US treatment 7-38593
Cd_{0.2}Hg_{0.8}Te surface, electron-stimulated processes 7-13279

II-VI semiconductors continued

- Cd_{0.23}Hg_{0.77}Te, time-resolved self-defocusing 7-43267
 Cd_{0.23}Hg_{0.77}Te:B⁺, ion implanted, photoreflection spectra in the edge absorption region 7-39099
 Cd_{1-x}Hg_xTe crystals, impurity band elec. conduction, Fermi glass model anal. 7-27328
 Cd_{1-x}Hg_xTe IR heterodyne detectors, intermediate temp. operation 7-35594
 n-Cd_{1-x}Hg_xTe, doped and undoped, minority-carrier lifetime 7-21932
 Cd_{1-x}Hg_xTe, abrupt interfaces using thermal and photo-MOVPE, Hall meas. 7-27917
 Cd_{1-x}Hg_xTe, band gap collapse, effects of Hg 5d electrons 7-64075
 Cd_{1-x}Hg_xTe, Bridgman growth using Accelerated Crucible Rotation Technique 7-46307
 p-Cd_{1-x}Hg_xTe, doped and undoped, minority carrier lifetime 7-45353
 Cd_{1-x}Hg_xTe, galvanomag. props. after metal-insulator transition 7-52655
 Cd_{1-x}Hg_xTe heterostructures, MOVPE, computer controlled reactor, charactn. 7-59446
 Cd_{1-x}Hg_xTe IR photodiodes for 3 to 14 μ m, comparison 7-41466
 Cd_{1-x}Hg_xTe, LPE and MOVPE grown, elec. props. and annealing 7-53512
 Cd_{1-x}Hg_xTe layers, MOVPE, CdTe substrate orientation effect, RHEED, SEM obs. 7-59447
 Cd_{1-x}Hg_xTe MOVPE growth on CdTe/sapphire substrate 7-27918
 Cd_{1-x}Hg_xTe MOVPE layers, elec. props. and Hall effect behaviour 7-27444
 Cd_{1-x}Hg_xTe, p-type, minority carrier exclusion 7-64242
 Cd_{1-x}Hg_xTe, photo-epitaxy, free radical mechanism 7-53612
 n-Cd_{1-x}Hg_xTe, single crystal, γ -irradiation, electrophysical props. in strong elec. field 7-7251
 Cd_{0.6}Mn_{0.4}Te, spin-freezing process, time-depend. of thermoremanent magnetization 7-2863
 Cd_{1-x}Mn_xTe mixed cryst., far IR Fourier transform spectra, acoustic local mode and TA band mode 7-53378
 Cd_{1-x}Mn_xTe, refractive index dispersion and two-mode refl. spectra behaviour calc. model (Russian) 7-45971
 CdS, A-exciton, normal-incidence exciton transmission and refl. spectra 7-39058
 CdS, absorpt. optical bistability, lattice heating study 7-43205
 CdS, absorption-induced optical bistability 7-57444
 CdS, acoustoelectronic system, solitons obs. 7-45401
 CdS, adsorbed methylviologen radical cation dimers, relax. 7-27095
 CdS and Zn_{1-x}Cd_xS, electron-pumped, high-efficiency semiconductor laser 7-5884
 CdS anodic film growth, initial stages, voltammetry and computer simulation studies 7-28216
 CdS based ceramics, radiative recomb. at high excitation levels (Russian) 7-3090
 CdS, bound-exciton states, resonant Brillouin scatt. 7-46062
 CdS, Brillouin spectra of acoustoelectronic interaction 7-7292
 CdS, carrier transport, defect effects, photoacoustic and photocurrent spectra 7-38626
 CdS composite logic gate element and multiplexer for optical computing and optical communications 7-57421
 CdS crystal growth and charact. (Japanese) 7-7829
 CdS crystals, surface polaritons, luminescence 7-64098
 CdS, electron beam irradiated, red flash-like luminescent centres, annealing 7-7740
 CdS, electron-hole exchange interaction for donor-acceptor pairs as a function of separation distance 7-52537
 CdS epitaxial films, initial oxidation stages, diffusion mass transport between CdO islands 7-8206
 CdS evaporated films, cathodolum., effect of thermal annealing 7-22353
 CdS excited state dynamics studied by transient grating techniques 7-12616
 CdS, excitonic polaritons, transmission and damping 7-58748
 CdS, exoelectron emission, phonon drag, inhomogeneous energy distrib. 7-39366
 CdS, film, charge transport, rel. to electrophysical props. 7-17121
 CdS films, formation by spray pyrolysis, characterisation of intermediate complexes 7-39372
 CdS films, superlinearity of light-current characts. 7-64282
 CdS, fine activated, prep. and props. for electrophotographic appl. 7-41514
 CdS induced homojunction formation in p-CuInSe₂ 7-58867
 CdS, integral exciton absorpt. coeff., temp. depend. characts. 7-45959
 CdS inversion layers, carrier effective mass calcs. 7-64055
 CdS laser excited with several electron beams, light pulse formation 7-43098
 CdS, light emission under voltage pulses 7-7764
 CdS, luminesc. associated with defect complexes 7-27757
 CdS, nonradiative recombination, elec. transport, combined photoacoustic and photocurrent spectra 7-38582
 CdS, nonradiative recomb., elec. transport, combined photoacoustic and photoconductive spectra, theory 7-38583
 CdS, optical bistability 7-57432
 CdS, oxidised, SIMS/XPS characterisation 7-39934
 CdS particles deposited on porous vycor glass electron transfer and photoluminesc. dynamics 7-64678
 CdS photoconductive thin films, optimum spray pyrolysis preparation conditions 7-17418
 CdS, photoconductivity spectrum, surface excitons, localised hole in quantum inversion layer 7-12762
 CdS, photolum., exciton scatt. from defects and impurities, depend. on exciting light intensity 7-39156
 CdS photosensitive cryst., 3D light diffr. from acoustic instability 7-33362
 CdS plastically deformed cryst., reorientable defects, polarised luminesc. study 7-51749
 CdS platelet, nonlinear optical and transport props. of many exciton system 7-32920
 CdS platelets, fast all-optical switching 7-57430
 CdS polycryst. layers, photoelec. props. α -Cr₂O₃ regulator 7-45378
 CdS polycrystalline films, temp. variation in thermoelectric power 7-22048
 CdS, powder, metal-loaded, photoinduced electron-hole pair separation 7-59770
 CdS reaction with aq. CuCl, TEM 7-39920
 CdS, refractive index nonlinearity due to excitonic molecule resonance state 7-11044

II-VI semiconductors continued

- CdS resonant self-diffraction from dynamic laser-induced gratings 7-11036
 CdS, semicond. crystallite, quantum size effects, energy spectrum calc. 7-12613
 CdS, shallow donor problem, pseudopot. approach 7-45216
 CdS, single crystal, US wave absorption, impurity distrib. effect., electron-probe X-ray anal. 7-53241
 CdS single crystals, cathodoluminescence, memory effect 7-22352
 CdS single crystals, subsurface region comp., laser radiation effects, AES study (Russian) 7-58329
 CdS single crystals, acoustoelectronic interaction, ultrasonic attenuation and amplification, dislocation motion effects (Russian) 7-21953
 CdS single crystals, nonequib. high-temp. vacuum annealing effects, intrinsic defect transform. 7-58764
 CdS skeletal and hollow crystals grown under time-increasing supersaturation 7-21144
 CdS small crystallites, zero-dimensional excitons 7-12615
 CdS surface rhodamine B mol. adsorpt. kinetics, binding energy determ. (Russian) 7-21667
 CdS surfaces, electron-beam-stimulated processes, real-time atomic-resolution electron microscopy 7-7798
 CdS, temperature-electric instability, spontaneous oscillation states 7-38616
 CdS thermally induced optical bistability study 7-11047
 CdS thin film MIS structs., band bending and interface state density 7-7402
 CdS thin films, deep trap depth, TSC meas. 7-58774
 CdS thin films, deposition by dip technique 7-3210
 CdS thin films, electrochem. bath deposition, photovoltaic cell props. 7-7900
 CdS, three types of electronic optical bistabilities 7-43262
 CdS, transient spectroscopy, deep level characterisation 7-58776
 CdS, transmission and damping of excitonic polaritons 7-58747
 CdS, wide-gap semiconductors, room-temperature optical nonlinearity 7-57440
 CdS, with compensated i-layer, photosimulated deep level transient spectroscopy 7-7765
 CdS, X-ray graphic elastic constants and lattice spectrum 7-32546
 CdS/Cu, Cl photoconducting films, photolum. spectra studies (Russian) 7-46140
 CdS/Gd, Cl film solar cells, gamma radiation effects on photoelectric properties 7-34032
 CdS:In-SnO₂ (glass), spray pyrolysed, photoelectrochemical studies 7-52830
 CdS:Ri³⁺(Kr⁺)(Ar⁺)(Ne⁺), ion implantation damage 7-26812
 CdS/CdTe screen-printed thin-film solar cell for indoor consumer electronics (Japanese) 7-65472
 CdS/CdTe sintered solar cell photovoltaic props. rel. to CdS film sintering conditions (Korean) 7-65476
 CdS/CdTe solar cells, circulation meas. and spectral error reduction 7-13903
 CdS/CdTe solar cells, effects of CdS film thickness on photovoltaic props. 7-65468
 CdS/CuInSe₂ solar cells, modelling and anal. 7-17893
 CdS/CuInSe₂ thin film chalcopyrite solar cells, electroplating prep. 7-17894
 a-CdS/n-Si heterojunctions, elec. props. 7-64342
 CdS/polymer composites, degenerate four-wave mixing 7-62795
 CdS/ZnS, multilayer structures, MOCVD, wide band gap, interdiffusion characts. 7-53610
 CdS-Ag, size quantisation in CdS layer, surface plasma spectroscopy 7-32936
 CdS-CdSe-sulphide-polysulphide multiple junction photoelectrochemical cells 7-59863
 CdS-CdTe heterostructure, closed-tube CVD and charactn. 7-59444
 CdS-CdTe screen printed solar cell modules, long term reliability tests 7-23158
 CdS-Cu₂S solar cells, SEM and Auger microanalysis 7-23189
 CdS-Cu₂S heterojunction, form. by photoelectrochemical process, phys. props. under light irradi. 7-45456
 CdS-Cu₂S solar cells, comp. of differing junction types, AES, SIMS determ. 7-23167
 CdS-CuGaSe₂ solar cells, physical properties and photovoltaic potential of CuGaSe₂ thin films 7-12889
 CdS-CuGaSe₂ solar cell fabrication 7-22047
 CdS-CuInSe₂ Boeing solar cells, I-V characteristics meas. 7-8408
 CdS-CuInSe₂ solar cells, charge transport studies 7-12890
 CdS-CuInSe₂ solar cells, capacitance determ. of interfacial states 7-13916
 CdS-CuInSe₂ thin film solar cell, solid state photovoltaic research status at SERI 7-8389
 CdS-CuInSe₂ thin-film solar cells, junction formation and O role, EBIC studies 7-17915
 CdS-CuInSe₂ backwall solar cells, intrinsic loss mechanisms calc. 7-23187
 CdS-InP solar cells, high efficiency, with thermally evaporated window layers 7-3701
 nCdS-n-GaAs photoanode, flux anal. of multiple junction solar cells 7-23162
 CdS-Si and CdS-CuInSe₂ heterojunctions, struct., elec. and photoelectric props. 7-22001
 CdS+propanol-2 radical, photochemistry and radiation chemistry, nonlinear optical effects 7-46858
 CdS,Se_{1-x} crystal waveguide Bragg light modulators 7-12888
 CdS,Se_{1-x} doped, glass substrates for thin film waveguides 7-5941
 CdS,Se_{1-x} doped filters, femtosecond nonlinearities using opt. Kerr effect 7-50660
 CdS,Se_{1-x} doped glasses, optical nonlinearities 7-57431
 CdS,Se_{1-x} mixed crystal, laser-induced probe-beam defocusing at band edge 7-7657
 CdS(Se)(Te):Mn, impurity EPR spin Hamiltonian parameter correl. calcs. 7-27597
 CdS,Te_{1-x} single crystals, growth form CdCl₂-CdS-CdTe ternary system, liquidus surface anal. 7-33644
 CdSb crystals, band struct., LCAO calcs. 7-58737
 CdSe, Cd vapour pressure determ. by atomic absorption method 7-63790
 CdSe crystals, laser beam defocusing, rel. to Hall mobility and carrier density 7-52652
 CdSe, dielectric fn. and interband crit. points. 7-2480

II-VI semiconductors continued

- CdSe electrodes, photoanodic dissolution in NaCl soln. (*Japanese*) 7-23026
 CdSe, exciton luminesc., polarisation depend. 7-59248
 CdSe, highly excited, exciton dynamics, picosec. time-resolved gain-absorpt. spectra study 7-2494
 CdSe laser with microminiature cryogenic refrigerator 7-43153
 CdSe lattice defects, digital struct. anal. by ion beam thinning for high resolution electron microscopy 7-6616
 CdSe, optimally annealed in molten Cd, DC galvanomagnetic props. 7-27352
 CdSe, ordered structures, field ion microscopy studies 7-32768
 n-CdSe photoanode for H₂S photoelectrolysis, photoelectrochemical cell for H₂ production 7-54328
 CdSe, photogenerated high density electron-hole plasma, energy relax., rapid expansion 7-33039
 CdSe, single crystal, US wave absorption, impurity distrib. effect., electron-probe X-ray anal. 7-53241
 CdSe, stimulated photolum. 7-27776
 CdSe, strongly excited, electron-phonon interaction screening, luminesc. meas. 7-38606
 CdSe thin film liquid-junction photovoltaic cell, photoelectrochem. charactn. 7-54331
 CdSe thin films, electrodeposited from SeSO₃²⁻ soln., comp. performance, polarography, RBS, cyclic voltammetry, power meas. 7-2411
 n-CdSe thin films grown from low purity materials for solar cell appls. 7-65480
 CdSe thin films made by tarnishing 7-22587
 CdSe, transient spectroscopy, deep level characterisation 7-58776
 CdSe, wide-gap semiconductors, room-temperature optical nonlinearity 7-57440
 CdSe, X-ray graphic elastic constants and lattice spectrum 7-32546
 CdSe:Cu, deep levels investigated by photoconductivity and space-charge region capacitance techniques 7-7148
 CdSe:Cu, transient photocond. anal. 7-64288
 CdSe:Cu films, radiative recomb. centres form., photolum. spectra studies (*Russian*) 7-33453
 CdSe/ZnSe, multilayer structures, MOCVD, wide band gap, interdiffusion characts. 7-53610
 CdSe-CdTe-selenide-polyselenide multiple junction photoelectrochemical cells 7-59863
 CdSe-Cu₂Se heterojunction solar cell, dry formation, electron microscope study 7-17916
 CdSe-polysulfide solar cells, nitrite reduction to ammonia 7-39999
 CdSe-polysulfide photoelectrochem. system. corrosion reactions, thermodynamic stability calcs. 7-28320
 CdSe(S) thin films, electrophys. props., electron irradiation effects study, solar cell appl. 7-16894
 CdSeTe-polysulfide solar cells, nitrite reduction to ammonia 7-39999
 CdSe_{0.65}Te_{0.35}/aqueous polysulfide interface, photoelectrochemical props. 7-52829
 CdSe_{0.7}Te_{0.3} and CdSe_{0.8}Te_{0.2}-Cu films, deep local states, photosensitivity, spectral study 7-22371
 CdSe_{0.7}Te_{0.3}, bound excitons, thermal dissoc., photoluminescence, reflectivity meas. 7-46122
 CdSe_{0.7}Te_{0.3}, bowing parameter of direct band gap, press. depend. 7-38453
 CdSe_{0.7}Te_{0.3}, inhomogeneous solid soln., semicond. films, Hall effect temp. depend. meas. 7-58915
 CdSe_{0.7}Te_{0.3}, polycrystalline solid solutions in electrochemical solar cells, photosensitivity 7-54296
 CdTe : B⁺(Cu⁺) ion implantation damage, rapid thermal annealing, photolum. anal. 7-39162
 CdTe (001), Cd and Te desorpt., surface stoichiometry and reaction kinetics, RHEED studies 7-21613
 CdTe (001) films, MBE grown on InSb substrates, low temp. photolum. studies 7-22317
 CdTe (100), photoemission studies, surface struct., growth behaviour, Schottky barrier and surface photovoltage 7-39352
 CdTe (100)-oriented single crystals, lattice dynamics temp. depend., X-ray studies 7-26880
 CdTe, acceptor higher excited states calcs. 7-52511
 CdTe amorphous thin films, electrical and optical props. 7-22045
 CdTe and CdZnTe, single-crystal substrates, struct. characterisation 7-32769
 CdTe, annealing in Cd or Hg vapour, defect concentrations 7-65064
 CdTe anomalous photovoltage films X-ray irradiation effects studies 7-58834
 CdTe, atomic layer epitaxy on CdTe (111) substrates, growth mech. 7-12525
 CdTe, atomic layer epitaxy, review 7-13362
 CdTe, cathode sputtering process statistical modelling, optical layer deposition 7-39375
 CdTe, cathodic electrochemical surface modifications, Cd layer form. 7-65239
 CdTe, closed tube CVD growth using NH₄Cl transport agent 7-27913
 p-CdTe, complex-formation processes at high concentrations of intrinsic defects 7-37963
 CdTe, crystallographic polarity, determ. from Auger electron spectra 7-64830
 CdTe crystals, resistive element defect electromigration, flicker noise enhancement. 7-63889
 CdTe, D plasma etching, surface comp. 7-46730
 CdTe, d-core transitions, reflectivity spectra 7-53364
 CdTe, detector material, applications 7-45307
 CdTe, electrodeposition from acidic aq. solns., voltammetry 7-27188
 CdTe, electron irradi., a (100) dislocation loops 7-6686
 CdTe, epitaxial growth on GaAs (100) 7-21779
 CdTe epitaxial layers, MBE growth on GaAs substrates, photoluminesc. 7-46083
 CdTe epitaxial layers on GaAs substrates, X-ray diffr. 7-27201
 CdTe film, polycryst., grown by UV-enhanced OMCVD, picosecond photocond. 7-52873
 CdTe film in a photovoltaic cell, electrodeposition and props. 7-64938
 CdTe films, detachable oriented, VPE 7-33567
 CdTe films, electrochemically deposited, resistivity, carrier conc. and carrier mobility 7-7419
 CdTe films, electrochemically deposited, comp., struct., AES, electron probe anal., X-ray diffr. spectroscopy 7-58694
 CdTe films, illum. with monochromatic light, anomalous photovoltaic effect 7-52684

II-VI semiconductors continued

- CdTe films, organometallic VPE growth mechanism 7-64914
 CdTe films on InSb, interface struct. and band offsets 7-58664
 CdTe grown on Si by LPMOCVD, physical props. 7-27181
 CdTe, heteroepitaxial growth on GaAs (100) substrates 7-45034
 CdTe high-resistivity undoped crystals, defects, EBIC studies 7-21211
 CdTe homoepitaxy on CdTe (111) by laser MBE, nucleation kinetics 7-22499
 CdTe, IR optical materials, production 7-37075
 CdTe, ion milling, TEM 7-39344
 CdTe LPE layers, matrix atom diffusion, SIMS studies 7-21513
 CdTe layers, electrochemical deposition, struct. and elec. props. 7-12526
 CdTe, low-temperature epitaxial growth, MBE and MOCVD 7-64906
 CdTe, MBE growth, crystallographic orientations and condensation coeffs. 7-3180
 CdTe, MBE growth on GaAs substrates, struct. and optical props. 7-64907
 CdTe, MBE growth on Si using (Ca, Ba)F₂ buffer layer 7-46325
 CdTe MOVPE growth on InSb substrate, characts. 7-27920
 CdTe, MOVPE on {111}CdTe, twin nucleation 7-33579
 CdTe, metal, contacts, interfacial microstruct., elec. props., phase diagrams 7-45495
 CdTe, OMVPE growth on InSb substrates 7-33577
 CdTe, optical anisotropy due to spatial dispersion 7-53266
 CdTe, optical nonlinearities and bistability 7-57435
 CdTe photoelectrochemical solar cells, effects of Ru surface modification 7-40017
 CdTe, polycrystalline, grain boundaries elec. and optical characts. 7-38012
 CdTe polycrystalline thin film solar cells 7-17888
 CdTe, positron annihilation in defects at crystal surface, defect anal. 7-39306
 p-CdTe RF sputtered thin films, resistivity, forbidden gap, optical and X-ray diffr. spectra studies 7-21747
 CdTe, Ru surface modified for solar cells XPS obs. 7-23202
 CdTe, Schottky-barrier height determ. including electron-hole recomb. and electron trapping effects 7-2720
 CdTe, segregation coeffs. of Ag, Co, I and In, recoil implanted radioactive tracer technique 7-21461
 CdTe, single cryst., transmission region optical props., impurities effects 7-39128
 CdTe, single crystal, structural perfection, X-ray topography 7-12070
 p-CdTe, single crystal and thin film, chemical etching study 7-46724
 CdTe single crystals, anisotropy of positron annihilation 7-39214
 CdTe strong-absorbing single crystals, Laue X-ray diffr. thickness depend. anal. and interpretation (*Russian*) 7-44310
 CdTe tetrahedral cpds, mode Gruneisen parameters 7-44732
 CdTe thin film heterojunction solar cells 7-17914
 CdTe thin film solar cells, efficiency improvement 7-17883
 CdTe thin film solar cells fabricated by evaporation (*Japanese*) 7-34044
 CdTe, threshold conditions for oscillation which the aid ofshifted and unshifted dynamic gratings 7-1228
 CdTe, transient spectroscopy, deep level characterisation 7-58776
 CdTe, very high conductivity films, formation and props. 7-45522
 CdTe:Co, Jahn-Teller interaction, influence of mag. field 7-16995
 CdTe:Fe²⁺, impurity vibronic coupling and near IR spectra characts. 7-26889
 n-CdTe:In, high mobility, growth by photoassisted MBE 7-22485
 CdTe:In, photocorrosion, vacancies, photoluminescence spectra 7-27948
 CdTe:P-CdS solar cells, control of open circuit voltage by carrier density variation 7-17887
 pCdTe:Sb epilayers, photoassisted MBE growth 7-53607
 CdTe:Sn, impurity compensation effect on elec. resist. and mobility 7-52614
 CdTe/(Cd,Mn)Te superlattice, optical props. heterointerface effects 7-7736
 CdTe/a-Si:H heterojunction, X-ray image sensor fabrication 7-41557
 CdTe/CdS-CuInSe₂/CdS tandem solar cells 7-17891
 CdTe/GaAs heterojunction, defect and impurity states, photovoltage meas. 7-17065
 CdTe/In₂O₃ solar cells, high efficiency 7-59838
 CdTe/InSb interface, quasi-2D electron gas obs. 7-21987
 CdTe/ZnTe superlattice, quasi-2D excitons in strongly localised regime 7-12617
 CdTe-(Ba,Ca)F₂ layers, MBE growth on non-lattice-matched Si substrates 7-27216
 CdTe-(Cd,Mn)Te MQW, optical and magnetooptical props. 7-13137
 CdTe-Ag interface, photoemission studies, surface struct., growth behaviour, Schottky barrier and surface photovoltage 7-39352
 CdTe-AuCu, AC contact impedance, influence on high freq., low temp. on fast transient junction meas. 7-64311
 CdTe-Cd_{0.6}Mn_{0.4}Te superlattices, high resolution electron microscope study 7-27162
 CdTe-CdMnTe, quantum wells, excitons and kinetics 7-12622
 CdTe-CdMnTe superlattices, photoluminesc. props. 7-13218
 CdTe-Cu interface form., effect of different cation-anion bond strengths 7-27149
 CdTe-Cu_{1.8} thin film polycrystalline solar transducers, photosensitivity spectra 7-34036
 CdTe-GaAs heteroepitaxial interface, at. resolution HVEM study 7-2392
 CdTe-HgTe superlattices, magnetotransport props. 7-33076
 CdTe-HgTe superlattices, IR material characterisation, transport phenomena anal. 7-64338
 CdTe-In₂-Sn₂O_{3-y} solar cells, spray deposited, elec. and photoelec. props. 7-54321
 CdTe(Se) heteroepitaxial layers, deposition on InAs 7-7045
 CdTe-x_{1-y}Se_yS_y, mixed system, optical phonon frequencies 7-2123
 CdZnS/CuInSe₂ solar cells, spray pyrolysis prep. and characts. 7-8374
 CdZnS/CuInSe₂ solar cells, transient current studies of junction activity 7-8409
 n-CdZnS/p-CuInSe₂ polycrystalline solar cells, open circuit voltage 7-17889
 CdZnS-CuInSe₂ solar cell development for space appls. 7-13917
 CdZnS-InP heterojunction solar cell, numerical anal. 7-23155
 Cd_{0.8}Zn_{0.2}S films, solution-sprayed, photocurrent decay times 7-45525
 Cd_{1-x}Zn_xS-CuInSe₂ thin-film solar cells, voltage and light bias-dependent spectral response 7-8375
 CdZnTe, epitaxial growth via low press. CVD, IR detector appls. 7-64926
 CdZnTe, MBE growth on GaAs substrates, struct. and optical props. 7-64907

II-VI semiconductors continued

- Cd_{1-x}Zn_xTe mixed cpd. semicond., lattice const. comp. depend., X-ray diffr. study 7-58246
 Cd_{1-x}Zn_xTe, MBE growth 7-13358
 Cd_{1-x}Zn_xTe:Mn, hyperfine coupling constant, EPR study 7-22138
 Cd_{1-x}Zn_xTe, second-order optical process, transient behavior, luminesc., Raman scatt. 7-64689
 Cu_{2-x}Cd_xTe_{1-x}Se_{0.5}Te_{0.5}Te₁, heterojunction solar cells, fabrication and characterisation (*Korean*) 7-28402
 CuGaSe₂-ZnCdS wide bandgap solar cells for thin film tandem structs. 7-23172
 CuInSe₂-CdS heterojunctions deposition, in-line sputtering system 7-64900
 p-CuInSe₂-CdZnS-ZnO solar cells, device anal. 7-23171
 CuInSe₂-ZnCdS thin film polycryst. solar cell efficiency improvement using antireflection coatings 7-23186
 CuO-ZnO p-n contact, sensor appls. 7-64996
 Cu₂S/CdS large-area solar cells, reactive sputtering 7-46943
 Cu₂S-CdS polycrystalline solar cell, freq. dispersion in admittance 7-65464
 Cu₂S-CdS solar cells, all-evaporation processed, characts. 7-8383
 Cu₂S films, field assisted chemiplating for CdS/Cu₂S heterostruct., growth mechanism 7-59470
 Cu₂S-Cd_{1-x}Zn_xS thin film solar cells perform., depend. on annealing temp. 7-17861
 GaAs, laser-enhanced oxidation, X-ray photoelectron and Auger electron spectroscopy 7-17739
 GaAs-ZnSe, MBE growth on GaAs epilayers, nucleation and characterisation 7-45046
 Hg_{1-x}Cd_x(Mn)_{1-x}Te, refractive index dispersion and two-mode refl. spectra behaviour calc. model (*Russian*) 7-45971
 Hg_{1-x}Cd_x(Mn)_{1-x}Te/CdTe superlattices, twin faults, X-ray obs. 7-45036
 Hg_{1-x}Cd_xSe, reson. Raman Scatt. meas. 7-7701
 HgCdTe, 0⁺ giant oscillation near semimetal-semiconductor transition 7-64053
 HgCdTe 32×32 CCD array for IR camera, for astronomy 7-60560
 n-HgCdTe, acceptor densities, photo-Hall determ. 7-58836
 HgCdTe, ambipolar diffusion and free carrier recombination studied by transient grating technique 7-12731
 HgCdTe and HgTe-CdTe superlattices, IR photolum. by Fourier transform spectroscopy 7-46134
 HgCdTe anodic oxide surface analysis by laser ionisation 7-13275
 HgCdTe as IR sensor material, characts. (*Japanese*) 7-56339
 HgCdTe, bulk melt growth and LPE, defect control 7-64940
 HgCdTe, cryst. growth by travelling heater method 7-64892
 HgCdTe, electrochemical and electrolyte electroreflectance studies 7-64607
 HgCdTe, electronic struct., alloying effects, ETBM calc. method 7-64080
 HgCdTe, epitaxial film, interdiffusion profiling, microreflection spectroscopy 7-53369
 HgCdTe epitaxial layers and structures, characterisation of intentional dopants 7-12552
 HgCdTe epitaxial layers, Hall effect and elec. resist. characterisation 7-64375
 HgCdTe Fabry-Perot IR bistable devices, parameter optimisation 7-57396
 HgCdTe focal plane array photodetectors, growth, performance and array fabrication 7-15001
 HgCdTe, Hg-rich LPE growth using dipping furnace 7-64943
 HgCdTe, high quality LPE on CdZnTe, IR detector anal. 7-64941
 HgCdTe, homogenization, wetting elimination 7-38221
 HgCdTe IR CCD coupling structure for space appls. 7-29309
 HgCdTe IR detectors, epitaxial growth of CdZnTe substrate 7-64926
 HgCdTe, IR nonlinear absorpt., dynamic Burstein-Moss effect (*Chinese*) 7-50615
 HgCdTe IR photodetectors, magnetoresist. and cyclotron resonance characterisation 7-64054
 HgCdTe in MIS struct., electroreflectance at 77K 7-13128
 HgCdTe, LPE growth in multi-slice apparatus 7-64942
 HgCdTe materials for infrared detectors, prep. techniques 7-64019
 p-HgCdTe, minority carrier characterisation using light-modulated Hall effect 7-21934
 HgCdTe, p-type, acceptor conc., IR reflectance studies 7-64600
 HgCdTe photoconducting detector design for IR imaging 7-9900
 HgCdTe, single cryst. growth by travelling heater method 7-64891
 HgCdTe: In, ion implanted, damage and rapid thermal annealing 7-63637
 HgCdTe:B, bulk and thin film, resonant impurity levels, magnetoresistance studies 7-64162
 HgCdTe:B⁺, ion implanted n⁺p junction, lifetime and carrier conc. profile 7-45450
 HgCdTe-CdZnTe heterojunctions, lattice matching 7-21717
 Hg_{0.75}Cd_{0.25}Te-Cu interface form., effect of different cation-anion bond strengths 7-27149
 Hg_{0.78}Cd_{0.22}Te, stoichiometry of anodic oxides, quantitative meas. 7-39782
 p-Hg_{0.78}Cd_{0.22}Te:Sb LPE films, elec. props. 7-7426
 Hg_{0.75}Cd_{0.25}Te, metal-insulator transition, mag. field induced, low temps. 7-45158
 n-Hg_{0.8}Cd_{0.2}Te accumulation layer electrons, tilted field cyclotron resonance 7-7591
 n-Hg_{0.8}Cd_{0.2}Te, condensed electron system, heat capacity, comment 7-58503
 Hg_{0.8}Cd_{0.2}Te, Hg vacancies, heat of form. determ. 7-37969
 Hg_{0.8}Cd_{0.2}Te, low temp. hot electron energy relax. time in extreme quantum limit mag. fields 7-33035
 n-Hg_{0.8}Cd_{0.2}Te, magnetic field-induced metal-insulator transition, threshold field electron density depend. 7-52427
 Hg_{0.8}Cd_{0.2}Te:Cu, activation energy of Cu shallow acceptors 7-64153
 Hg_{1-x}Cd_xTe and related materials, far IR spectroscopy 7-39120
 Hg_{1-x}Cd_xTe crystals, anodic oxide capped, thermal stability 7-65225
 Hg_{1-x}Cd_xTe crystals, lattice defect imaging, high resolution electron microscopy obs. 7-51769
 Hg_{1-x}Cd_xTe, electron-irradiated, positron annihilation 7-38060
 Hg_{1-x}Cd_xTe, epitaxial growth by low temp. metalorganic CVD 7-27911
 Hg_{1-x}Cd_xTe films, LPE using a semiclosed rotational boat 7-64937
 Hg_{1-x}Cd_xTe films, organometallic epitaxial growth on CdTe and characterisation 7-22579
 Hg_{1-x}Cd_xTe heterojunctions, supersymmetry, band-inverting contact 7-52717

II-VI semiconductors continued

- Hg_{1-x}Cd_xTe, low frequency absorption bands (*Chinese*) 7-39095
 Hg_{1-x}Cd_xTe, MBE growth, crystallographic orientations and condensation coeffs. 7-3180
 Hg_{1-x}Cd_xTe MBE layers, plasma oxidation, oxide growth, comp. and surface struct. 7-54018
 Hg_{1-x}Cd_xTe optical waveguides, high band gap, for 10.6 μm 7-37157
 Hg_{1-x}Cd_xTe, photochemical organometallic vapour phase epitaxy 7-27946
 Hg_{1-x}Cd_xTe resistors, Umklapp 1/f noise, Hooge parameter, relativistic correction 7-2649
 Hg_{1-x}Cd_xTe, sputtered and cleaved surfaces, deposition of In and Al reactive metals, UPS study 7-33513
 Hg_{1-x}Cd_xTe surfaces, sputtered and cleaved, deposition of unreactive Au, UPS study 7-33514
 Hg_{1-x}Cd_xTe with metallic donor clusters, anomalous Hall effect below mag. field induced metal insulator transition 7-2485
 Hg_{1-x}Cd_xTe, zero gap, acceptor levels 7-27287
 Hg_{1-x}Cd_xTe:B, ion implanted, annealing, nature oxide encapsulation 7-2036
 Hg_{1-x}Cd_xTe/Ag(Cu)(Al) interfaces, morphology, Hg bonding effects 7-7021
 Hg_{1-x}Cd_xTe/CdTe superlattices, MBE growth and props. 7-53602
 Hg_{1-x}Cd_xTe/Pt interface, overlayer-cation reaction, XPS, UPS and LEED studies 7-65349
 Hg_{1-x}Cd_xTe-CdTe superlattice, MBE growth and props. 7-7345
 Hg_{1-x}Cd_xTe_{1-x}Se_x, existence region of wurzite struct. 7-53709
 HgCdTe thin film solar cells fabrication 7-23188
 α-HgS:Ti single cryst., elec. relax. current 7-64241
 α-HgSe films, elec. conductivity, thermoelectric power, optical absorpt. 7-22050
 HgSe, plastic deformation 7-21331
 HgTe, d-core transitions, reflectivity spectra 7-53364
 HgTe, electron-irradiated, positron annihilation 7-38060
 HgTe films, deposition by photolysis of (t-butyl)HgTe(t-butyl) 7-3197
 HgTe/ZnTe, isothermal interdiffusion expts. 7-52152
 HgTe-based solid solns., low temp. electron mobility, resonance scatt. 7-38558
 HgTe-CdTe as IR sensor material, characts. (*Japanese*) 7-56339
 HgTe-CdTe superlattices, cut-off wavelengths meas. 7-3030
 HgTe-CdTe superlattice, MBE growth and props. 7-7345
 HgTe-CdTe superlattices, growth of GaAs (100) substrates by MBE 7-12520
 HgTe-CdTe superlattices, present status, props. and applications (*Japanese*) 7-12829
 HgTe-CdTe superlattice, semimetallic, band structure calc. 7-12851
 HgTe-CdTe superlattice, IR magneto-optics and band struct. 7-13138
 HgTe-CdTe superlattice, alloying, far IR study 7-13143
 HgTe-CdTe superlattices, IR optical props. 7-13166
 HgTe-CdTe superlattices, IR photoluminesc. spectra 7-13219
 HgTe-CdTe superlattices, struct. characterisation 7-27164
 HgTe-CdTe superlattices, electronic props., calc. methods 7-27406
 p-HgTe-CdTe superlattices, magnetotransport props. 7-33076
 HgTe-CdTe superlattices grown on lattice-mismatched GaAs substrates 7-52341
 HgTe-CdTe superlattices, band struct., optical and magneto-optical studies 7-64337
 HgTe-EuTe system, interactivity 7-6801
 HgTe-Hg_{1-x}Cd_xTe double barrier, single quantum well heterostructures, resonant tunnelling 7-33068
 HgTe-Hg_{1-x}Cd_xTe heterojunctions, hole Hall mobility enhancement 7-33077
 HgTe-ZnTe superlattice, MBE growth and props. 7-7345
 HgZnTe as IR sensor material characts. (*Japanese*) 7-56339
 HgZnTe bulk crystals, travelling heater method growth and charactn. 7-59387
 HgZnTe, electrochemical and electrolyte electroreflectance studies 7-64607
 Hg_{1-x}Zn_xTe solid solns. band gap, temp. and comp. depend. 7-58738
 In₂O₃:Sn-ZnS:Cu,Cl,Mn-Al, surface electrical conductivity in ZnS:Cu,Cl,Mn thin films 7-38672
 LiNbO₃/CdSe multilayer structs. with ohmic contacts, electroacoustic conversion, SAW excitation 7-58839
 Mg₂Cd_{1-x}Se single cryst. solid solns., local centres parameters determ. (*Russian*) 7-32953
 Mg₂Cd_{1-x}Se single crystals, impurity photocurrent temp. activation meas. and calcs. (*Russian*) 7-45394
 Mn₂Cd(Hg)_{1-x}Te, refractive index dispersion and two-mode refl. spectra behaviour calc. model (*Russian*) 7-45971
 MnS thin films, luminesc. and excitation spectroscopy studies 7-7741
 Mn₂Zn_{1-x}Se, energy gap comp. depend., photocond. and absorpt. edge meas. 7-38454
 Ni-ZnSe-SiO₂-Si struct., energy barriers for photocharging of trapping sights in ZnSe layer 7-52844
 PbTe films grown by hot-wall epitaxy on KCl and BaF₂, TEM anal. 7-59432
 (Zn,Mn)Se quantum well structures, wide-gap II-VI superlattices 7-7346
 Zn₂Cd_{1-x}S and ZnS_{1-x}Se_x, electron-pumped, high-efficiency semiconductor laser 7-5884
 Zn₂Cd_{1-x}S thin films, struct. and electrical props. 7-64372
 ZnCdSe, electron beam pumped, cathodolum., gain and stimulated emission 7-64701
 Zn_{0.25}Cd_{0.75}Se mixed crystals, electron and hole deep level traps 7-16980
 Zn₂Cd_{1-x}Te thin film heterojunction solar cells 7-17914
 Zn₂Cd_{1-x}Te, crystals, grown from non-stoichiometric melts, Zn distrib. calc. 7-51678
 Zn₂Hg_{1-x}Se, electrophysical props. and carrier scatt. mechanisms 7-17024
 Zn₂Hg_{1-x}Se, far IR spectra study 7-22262
 ZnO based varistors, sintering, multiparametric anal. 7-64978
 ZnO ceramic, grain growth kinetics during synthesis, optimum elec. props. 7-46398
 ZnO crystals, real struct. during growth process, effect of plastic deform. 7-11974
 ZnO films, DC sputtered, structure changes during growth 7-7848
 ZnO films, elec. props., decomp., chemisorption of O², photocond. meas. 7-27445
 ZnO films, with high elec. resistance, conductivity-controlled preparation 7-17122
 ZnO films on Si substrates, layer acoustic mode propagation, electroelastic effect 7-44978

II-VI semiconductors continued

- ZnO films with high resistance, electrical conductivity, press. and temp. depend. 7-22044
- ZnO, glass-doped, prep., elec. props. and degradation phenomena 7-13425
- ZnO, grain boundary inhomogeneity phenomena, microcontact meas. (*German*) 7-58893
- ZnO multilayers for solar collector coatings 7-3717
- ZnO, on $\text{LiNbO}_3(\text{Bi}_{12}\text{SiO}_{20})$, growth, acoustoelectric props. 7-38645
- ZnO, ordered structures, field ion microscopy studies 7-32768
- ZnO, particulate, surface states (*Japanese*) 7-12774
- ZnO piezoelectric thin films, layer struct., RHEED and X-ray diffr. studies 7-16888
- ZnO powder-polyvinyl butyral films, dark discharge props. 7-58919
- ZnO resonant self-diffraction from dynamic laser-induced gratings 7-11036
- ZnO, solubility product const. determ. 7-13790
- ZnO, surface, interaction with vibr. excited O_2 mols. 7-15692
- ZnO thin film preparation by spray pyrolysis for photoelectrochemical solar cells 7-23166
- ZnO varistor, grain boundary pot. barrier, effects of annealing 7-16568
- ZnO varistor, grain junction barrier height, majority carrier effects (*French*) 7-17033
- ZnO varistor, single grain junction barrier height, minority carrier effects (*French*) 7-21929
- ZnO varistor props., grain boundary characts. (*Japanese*) 7-6631
- ZnO varistors, bulk electron traps 7-45348
- ZnO varistors, electroluminescence temp. depend. and conduction mechanisms 7-17349
- ZnO varistors, grain boundaries, elec. props. in presence of deep bulk traps 7-7334
- ZnO with tri-valent donor impurities, elec. props., heat treatment effects 7-2611
- ZnO, X-ray graphic elastic constants and lattice spectrum 7-32546
- ZnO:Al films, RF reactive sputter deposition, struct., elec. and optical props. (*Japanese*) 7-27900
- ZnO:Co(Ni)(Cu), impurity electron states, optical spectroscopy 7-46127
- ZnO:Ga thin films, temp. depend. of conductivity, effect of H_2O vapour chemisorbed states 7-7427
- ZnO:H, quantised accumulation layers on ZnO surfaces, photoenhancement 7-7304
- ZnO:In films, microstruct., elec. and optical props., film thickness depend. study 7-16895
- ZnO:In films, transparent conducting oxides, H_2 plasma treatment 7-3528
- ZnO:Si thin films, RF magnetron sputtered, conductive and transparent props. 7-22476
- ZnO/Ag/ZnO magnetron sputtered transparent heat-reflective films, thermal stability study 7-53426
- ZnO/ $\text{Y}_{2.9}\text{La}_{0.2}\text{Al}_{0.12}\text{O}_{12}$ SAW resonator struct., amplitude-freq. and phase-freq. characts. 7-16051
- ZnO:AlN-glass, SAW characts. study 7-12448
- ZnO-Cu-SiO₂-Si composite membrane, interdigital transducer generated US Lamb waves 7-11241
- ZnO-electrolyte interface, electrolum. under cathodic and anodic pulsed polarisation 7-13235
- ZnO-electrolyte interface, photoconductivity and photocurrent spectra, influence of exciton absorption 7-45486
- ZnO-Si structures, transverse acoustoelectric effect 7-45398
- ZnO-supported Cu particles, vibr. spectra of adsorbed species, operation of metal surface selection rule 7-53350
- Zn₃P₂ pellets, elec. cond., compacting press. depend. 7-58809
- ZnS, CVD films on sapphire substrates, epitaxial nature 7-3199
- ZnS, clusters, electronic struct., variational cellular method 7-45120
- ZnS, covalent cryst., electronic struct., cluster approx. 7-52403
- ZnS, cryst., p-type cond., luminesc. 7-13226
- ZnS, crystal growth by chem. transport using NH_4Cl transport agent 7-59385
- ZnS cubic cryst., spatially oscillating piezophotovoltaic effect meas. 7-52669
- ZnS, cubic piezoelectric crystals, influence of uniaxial mechanical stresses on linear photovoltaic effect 7-7276
- ZnS, epitaxial film, TEM and photoelectron study 7-53408
- ZnS, film deposition, surface morphology and preferential orientation 7-27906
- ZnS films, MBE growth on Si (100), substrate temp. effects 7-39384
- ZnS, fused polycryst. layers, photocond. and photolum. spectra, defect form. influence 7-46142
- ZnS, hexagonal, four-photon spectroscopy 7-5948
- ZnS, interband two-photon absorpt., freq. depend. 7-33451
- ZnS interference filters, simultaneous optical bistable switching on adjacent pixels, pattern recognition 7-57420
- ZnS, MBE growth on Si (100), photoluminesc. props. 7-3174
- ZnS nonlinear planar waveguides, bistability and self-pulsing using prism couplers 7-57427
- ZnS, polycrystalline, AC driven thin film electrolum. displays 7-7762
- ZnS, rare earth impurities, electrolum. of Schottky barriers, photolum., charge compensation, and impurity electron states 7-64700
- ZnS, single crystal, annealed in O, intrinsic defects rel. to elec. and luminesc. props. 7-12649
- ZnS thin films, radiation enhanced adhesion to SiO_2 substrates 7-32504
- ZnS, transient spectroscopy, deep level characterisation 7-58776
- ZnS wavelength prism coupling, nonlinear coupler example 7-31385
- ZnS:Ag scintillator in detector for fluorescent X-ray adsorption spectroscopy 7-24751
- ZnS:Al, Cr, Fe crystals, recomb. luminesc., EPR and photocond. meas. 7-3076
- ZnS:Al, electron capture processes, role of donors, transient ESR meas. 7-45347
- ZnS:Al, low resistivity, grown by MOVPE 7-27921
- ZnS:Al, temp. depend. of visible photolum., ESR studies 7-46099
- ZnS:Cr³⁺, Fe³⁺ single crystals, impurity centre charge exchange, plastic deform. effects, ESR spectra studies 7-16984
- ZnS:Cr²⁺, Cr excitation spectrum interpretation 7-58775
- ZnS:Cu, electrophosphors, aging phenomena 7-27791
- ZnS:Cu, pure and doped, defects in solids, mol. cluster calc. with modification 7-21857
- ZnS:Cu,Mn films, vacuum deposition and DC electroluminescence 7-7868
- ZnS:Cu,Yb phosphor, AC electrolum. study 7-13233

II-VI semiconductors continued

- ZnS:Cu²⁺, multimode Jahn-Teller effect in the luminescence spectrum 7-12675
- ZnS:Er, impact cross section of Er^{3+} in luminesc. spectra 7-46150
- ZnS:Fe,Cu, three-centre Auger recombination, EPR study 7-45806
- ZnS:Fe electronic struct., K-edge EXAFS study 7-64079
- ZnS:Fe²⁺, impurity vibronic coupling and near IR spectra characts. 7-26889
- ZnS:Ho³⁺, radiative transitions and nonradiative processes (*Chinese*) 7-59235
- ZnS:In, photoluminescence, D-A pair emission 7-22312
- ZnS:In epitaxial films, photoluminescence. decay props. 7-39166
- ZnS:Mn, electrolum. study 7-13234
- ZnS:Mn, impact excitation and Auger quenching 7-27827
- ZnS:Mn electrolum. thin film-based structs., native memory formation, supersonic effects study (*Russian*) 7-3020
- ZnS:Mn electrolum. thin film displays, growth by at. layer epitaxy 7-13362
- ZnS:Mn electroluminescent thin films, photothermal deflection spectroscopy 7-27804
- ZnS:Mn films, struct. and electroluminescence props. (*Japanese*) 7-27783
- ZnS:Mn heavily doped phosphors, mechano and electroluminesc. 7-13240
- ZnS:Mn thin films, DC electrolum. and local destructive dielec. breakdown model calcs. 7-59147
- ZnS:Mn thin films, electrolum., review 7-27784
- ZnS:Mn thin films, local destructive breakdown and DC electrolum., film prep. and test conditions depend. 7-59146
- ZnS:O, Er(Tm)(Dy), activator centres, spectrosc. investig. 7-13184
- ZnS:TbF₃, sputtered thin films, electrolum. and photolum. 7-7727
- ZnS/ZnSe, multilayer structures, MOCVD, wide band gap, interdiffusion characts. 7-53610
- ZnS-CdS:Ag,Ni,Co phosphors, photolum., energy level model 7-59245
- ZnS-ZnSe mixed powders, site selective EXAFS via optical de-excitation 7-53443
- ZnS(Se), IR transmitting windows, protective coatings 7-46731
- ZnS(Se), ion milling, TEM 7-39344
- ZnS(Se), plastic deform., thermal activation anal. 7-2091
- ZnS_{0.9}Se_{0.1} coating for passivation of Si solar cells 7-65479
- ZnS_{0.9}Se_{0.1} gradient IR optical material prepared by CVD 7-31408
- Zn(S_{1-x}Se_x), crystal growth by chem. transport using NH_4Cl transport agent 7-59385
- ZnS_{1-x}Se_x, scatt. of light by polaritons 7-39100
- ZnS_{1-x}Se_x, semicond., optical bowing 7-33352
- ZnS_{1-x}Se_x, single crystals, growth, exciton luminesc. 7-22453
- ZnS_{1-x}Se_x:Mn²⁺, Mn energy levels, photoconductivity bands 7-7156
- ZnS(Se)(Te) tetrahedral cpds, mode Gruneisen parameters 7-44732
- ZnS(Se)(Te):Mn, impurity EPR spin Hamiltonian parameter correl. calcs. 7-27597
- ZnS_{1-x}Te_x, semicond., optical bowing 7-33352
- ZnSe (110) surface atomic geometry and energy states, self-consistent pseudopot. calcs. 7-21582
- ZnSe, bistable interference filters, nanosecond switching at room temp. 7-11028
- ZnSe bistable interference filters, switching processes, steady-state model 7-50617
- ZnSe cryst., low press. melt growth technique, photolum., laser appl. 7-33548
- ZnSe, cryst., spectral broadening about second harmonic generated by laser pulse 7-43236
- ZnSe, crystal growth by chem. transport using NH_4Cl transport agent 7-59385
- ZnSe, dispersive bistability and absorptive switching 7-57434
- ZnSe, donor-acceptor pairs, time-resolved recombination luminescence 7-39165
- ZnSe epitaxial films, twin boundaries, high resolution TEM obs. and computer simulation studies 7-51784
- ZnSe epitaxial layers, MOVPE grown, elec. and photolum. props. 7-7420
- ZnSe epitaxial layers on GaAs(100) substrates, anomalous twin boundaries, TEM obs. 7-27198
- ZnSe films, electrochemical co-deposition, photoelec. conversion characts. 7-46959
- ZnSe films; CVD 7-64909
- n-ZnSe, heavily doped strongly compensated crystals, electron mobility 7-7247
- ZnSe, heteroepitaxial growth on GaAs, energy band gap, elastic strain effects 7-59242
- ZnSe hydrothermal growth, cathodolum. props. 7-63531
- ZnSe IR optical fibres, development, appls. 7-37190
- ZnSe interference filters, thermally deposited and molecular-beam-grown, CW laser pumped bistability 7-25861
- ZnSe interference filter triple bistable-element loop circuit for digital parallel all-optical computer 7-57409
- ZnSe interference filters, simultaneous optical bistable switching on adjacent pixels, pattern recognition 7-57420
- ZnSe laser-induced epitaxial growth on GaAs using organic compounds 7-52366
- ZnSe layer growth by plasma-assisted epitaxy 7-52365
- ZnSe layers on Ge (100), MBE growth and photoluminesc. 7-7858
- ZnSe MBE layers on GaAs, lattice mismatch effects, TEM, photolum. and X-ray diffr. studies 7-45042
- ZnSe, MOCVD, chemical reactions monitoring 7-53611
- ZnSe, MOVPE growth kinetics on GaAs 7-22544
- ZnSe nonlinear interf. filter white light switching, spatial light modulator design 7-57416
- ZnSe nonlinear planar waveguides, bistability and self-pulsing using prism couplers 7-57427
- ZnSe nonlinear visible interf. filter, critical slowing down 7-57419
- ZnSe, optical anisotropy due to spatial dispersion 7-53266
- ZnSe, phonons, ps laser induced transient dynamics 7-39113
- ZnSe photoelastic modulator for IR 7-43348
- ZnSe, shallow donor problem, pseudopot. approach 7-45216
- ZnSe, single crystals, growth, exciton luminesc. 7-22453
- ZnSe, thin films, surface electron states (*Russian*) 7-21971
- ZnSe:Al, MOCVD growth, deep level characterisation 7-52519
- ZnSe:Al(Ca)(In), impurity diffusion coefficients, cathodoluminesc. study 7-27017
- ZnSe:As, MOCVD growth, exciton and deep emission bands 7-52367
- ZnSe:Cl layers grown by MBE, blue photoluminesc. 7-52364
- ZnSe:Cu,Al,Fe crystals, melt-grown, absorpt. coeff., impurity effects 7-3070

II-VI semiconductors continued

- ZnSe:Cu(Ag)(Au), cationic substitutional impurities and metal vacancy, microscopic models 7-27296
 ZnSe:Er³⁺, ion implanted, identification of cathodolum. centres 7-53417
 ZnSe:Fe, impurity ion photoionisation, EPR, photoconductivity spectra 7-52495
 ZnSe:Ga, impurity segregation model calcs., elec. props., precipitate effects 7-16762
 ZnSe:Mn, ⁴E states, spin-orbit interactions and dynamical Jahn-Teller effect 7-21875
 ZnSe:N, MBE growth and doping, photoluminescence studies 7-27749
 ZnSe:Si, single crystal growth, chem. transport method (*Korean*) 7-27880
 ZnSe/(Zn,Mn)Se superlattice, optical props. heterointerface effects 7-7736
 ZnSe/GaAs, electron beam pumped lasing action obs. 7-43093
 ZnSe/GaAs interface, MOCVD grown, ZnSe film stoichiometry 7-39415
 ZnSe/GaAs:Cr heterostructure, interface stress 7-38352
 ZnSe/Zn_{1-x}Mn_xSe strained layer superlattices, electronic energy states and relax. 7-45425
 ZnSe-GaAs:Cr, meas. of residual stress by Cr-related luminesc. lines 7-7726
 ZnSe-In₂₋₃Sn₂₋₃O_{3-y} junctions, microstruct. optical props., influence of deposition method 7-21689
 ZnSe-ZnMnSe, quantum wells, excitons and kinetics 7-12622
 ZnSe-ZnMnSe strained layer superlattices, quantum confinement effects 7-27403
 ZnSe-ZnMnSe superlattices, photoluminesc. props. 7-13218
 ZnSe-ZnS electroluminescent MIS structures, MOCVD growth and charactn. 7-59443
 ZnSe-ZnS strained-layer superlattice, low pressure MOVPE growth 7-53604
 ZnSe-ZnTe strained layer superlattices, MBE growth on InP substrates 7-13366
 ZnSe-ZnTe strained layer superlattice on InP, TEM obs. 7-52778
 ZnSe-ZnTe strained-layer superlattices, lattice strain and lattice dynamics 7-58654
 (ZnSe)_x(CdTe)_{1-x} films, CVD fabricated, phys. props. 7-7055
 ZnSeTe wide bandgap solar cells for thin film tandem structs. 7-23172
 ZnTe, acceptor higher excited states calcs. 7-52511
 ZnTe, cathodoluminescence, Zn-vapour and Te-vapour heat treatment effects 7-46151
 ZnTe, chemical vapour transport and homoepitaxial growth in closed-tube system, thermodynamic analysis 7-33582
 ZnTe, d-core transitions, reflectivity spectra 7-53364
 ZnTe epilayers, chemical transport growth, photoluminesc. props. 7-39413
 ZnTe films, vacuum deposition, elec. resist. and photocond. meas. 7-3179
 ZnTe, nonequilibrium carrier recomb. processes, plasmon effects, luminesc. spectra calcs. 7-58818
 ZnTe, obs. of time evolution from reson. Raman scatt. to excitonic-polariton luminesc. 7-33390
 ZnTe:Cl(Al), crystals, vacancy-impurity complexes, ODMR studies 7-2530
 ZnTe:Cu, impurity related neutral complex with bound exciton, photoluminescence, absorpt., Zeeman meas. 7-45165
 ZnTe:O, hot luminesc., reson. Raman scatt. studies 7-64695
 ZnTe:O, light scattering 7-17333
 ZnTe:O, red cathodolum. kinetics, two-step electron capture model calcs. 7-59262
 ZnTe-ZnCdS wide bandgap solar cells for thin film tandem structs. 7-23172
 ZnTe-ZnSe heterostructures, liq. phase epitaxially grown, luminesc. preps. 7-45477
 ZnTe-ZnSe superlattices, photoluminesc. 7-17339
 ZnTe-ZnSe(S) superlattices, hot wall epitaxial growth and photoluminesc. props. 7-13220
 ZnTe-ZnSe(S) superlattices, MBE and atomic layer epitaxy growth 7-13365
 ZnTeSeS, superlattices, prep. by hot wall epitaxy, props. (*Japanese*) 7-12546

III-V semiconductors

- (*Chinese*) 7-38446
 p-AlGaAs/GaAs modulation-doped heterostruct., liq. phase epitaxy and carrier props. 7-33074
 alloys, val.-field characts., band struct. effects, CPA calcs. 7-64243
 Auger recombination via deep double-charged centres (*Ukrainian*) 7-12732
 BAs, structural and electronic props., pseudopotential method, local density approx. 7-32353
 carrier concentration and mobility profiling 7-45315
 chemical beam epitaxy 7-52360
 conduction electrons, spin relaxation, strain effects 7-38942
 conduction-band-edge charge density, empirical pseudopot. calcs. 7-64046
 covalent crystals, thermal expansion coeffs. calc. 7-44869
 crystal growth using Gault process 7-46300
 deep centres in semiconductors, book 7-18510
 defect mapping by in-water photocorrosion 7-59692
 defect recognition and image processing, conf., Montpellier, France (July 1985) 7-29596
 depolarisation of photolum. emitted by III-V semiconductors, determ. 7-53392
 devices and materials, review 7-58801
 dielectric films, on compound semiconductors, conf., Las Vegas, USA (Oct. 1985) 7-35108
 diffusion in III-V semiconductors, modelling techniques 7-58522
 electrical parameter mapping by numerical image processing of light beam induced current topography 7-33051
 electronic struct. calcs. 7-12608
 electronic struct. of bulk and defect sites, tight-binding recursion method 7-45222
 electrooptic waveguide modulator, microwave performance prediction 7-43349
 epitaxial growth by rapid thermal MOCVD 7-53605
 epitaxial layers, OMCVD, compositionally graded growth technique for device structs. 7-22553
 films, metalorganic MBE 7-53601
 Ga_{0.4}In_{0.6}As, transient transport in central-valley-dominated ternary III-V alloys 7-7253
 Hall effect in semiconductor assessment 7-17041
 hot-electron photoluminescence, polarisation 7-46118

III-V semiconductors continued

- II-VI-III-V systems, thermodynamics and reactivity 7-16790
 In_{0.53}Ga_{0.47}As:Fe metalorganic CVD epitaxial growth and elec. props. 7-63993
 InGaAsP epitaxial films, X-ray diffr. charactn. (*Japanese*) 7-63399
 InGaP/InGaAlP double heterostructure and multiquantum-well laser diodes, MBE growth and characterisation 7-62689
 InP:Cu, band-edge photolum. quenching, impurity recomb. centre effects study 7-39177
 InP:Si, ion implanted, rapid thermal annealing and solid phase epitaxy 7-21296
 InP, electron-electron interaction, quantum effects, magnetoresist. studies 7-38591
 integrated optoelectronics, micrograting form. by HV electron beam lithography 7-31443
 integrated waveguides as all-optical logic devices 7-25869
 interface chemistry of III-V semiconductor-metal interface, thermodynamic stability considerations 7-21490
 interface chemistry of III-V semiconductor-metal interfaces, review 7-21544
 ionic reactive etching (*French*) 7-46735
 laser, effect of LPE grown crystal defects on reliability 7-36960
 laser direct writing and laser-assisted CVD of III-V cpds, on GaAs 7-13373
 laser stimulated desorption, dimerisation enhanced phase transition 7-58619
 lattice defects detection using IR tomography 7-32234
 lattice matched heterojunctions, common anion rule failure 7-7367
 line defects, TEM obs. 7-51751
 localised electron states of substantial transition metal impurities, review 7-27295
 MBE, surface effects and growth dynamics 7-58711
 MBE, thermodynamic anal. 7-46328
 MBE growth, kinetic processes 7-2418
 metal organic MBE and VPE growth, kinetic and thermodynamic aspects 7-7064
 MIS interface elec. charactn. by C-V anal. 7-22021
 MOCVD, organometallic precursors monitoring by laser mass spectroscopy 7-22547
 monolithic optoelectronic ICs for high-speed fibre optic transmission 7-37203
 MOVPE, conf., Universal City, CA, USA (Apr. 1986) 7-18477
 multijunction concentrator solar cells, review 7-3651
 negative magnetoresistance and nonequilib. electron cooling 7-17042
 nonlinear excitation, picosecond laser induced 7-11024
 ohmic contact semiconductors, funds. of theory and methods of technology (*Polish*) 7-64347
 organometallic CVD using metalorganic halides 7-33587
 oxidation, conference, Paris, France (May 1986) 7-60866
 quantum well structures, destruction mechanism due to impurity diffusion 7-63971
 quantum well structures, linear optical props. elec. field depend. waveguide electroabsorb. and sum rules 7-13133
 quantum-well wire hydrogenic impurity state binding energy and lowest exciton state lum. efficiency calc. 7-2683
 quaternary III-V alloy semiconductors, MOVPE, thermodynamic anal. 7-16884
 rare gas ion-enhanced etching 7-22918
 reactive ion etching, AES, photoluminescence, SEM obs. 7-65241
 resonant photovoltaic effect during NMR 7-53158
 selective photoetching studies of defects 7-32426
 semiconductor industry, appl. of SIMS, SAES, XPS 7-16847
 semiconductor-Au system, heat treatment, gaseous species evolution, mass spectra studies 7-39881
 single crystal growth, formation of microinclusions 7-21141
 solid solns., short range order and free energy of mixing, EXAFS meas. 7-63573
 sputtered films, optical props., effective medium models (*Chinese*) 7-7774
 strained layer superlattice research developments 7-52766
 strained-layer effective-mass superlattices 7-7378
 substrate, optical study of a-C:H, BN, CaF₂ insulating films 7-39204
 superlattice band structures of group IV and III-V materials, axial strain effects 7-2697
 superlattices, pseudopotential approach to thermodynamic props. 7-7377
 superlattices and quantum well structures, electronic props. 7-52817
 superlattices dynamical screening, quasi-2D electron gas, electron-phonon interactions 7-45464
 surface (111), EXAFS surface structure studies, at Daresbury SRS, in 60 to 11100 eV range 7-33486
 surfaces, virtual gap states and Fermi level pinning by adsorbates 7-2654
 surfaces (110), Sb p(1 × 1) overlayers, atomic and electronic struct. 7-7007
 ternary alloys, short-range order 7-44821
 ternary solid soln., miscibility gap in phase diagram 7-52057
 transition metal impurities, review 7-48201
 tunnelling through III-V heterostructures, relevance to electronic devices 7-58885
 vapour levitation epitaxy, system design and performance 7-59445
 vertical transport in multilayer semiconductor structures 7-38705
 VPE, interplay between kinetics and diffusion in hot wall reactors 7-46330
 X-ray topography and diffr. imaging 7-32224
 (Al, Ga)As films, doped, Si migration during MBE growth 7-27171
 (Al,Ga)As/(Ca,Sr)F₂ multilayer structures, MBE grown, broadband high-reflectivity mirrors fabrication 7-11091
 (Al, Ga)As/GaAs undoped quantum wells, Al and Ga interdiffusion, photoluminesc. study 7-2271
 Al/III-V semiconductor interfaces, laser-induced chem. reactions 7-7017
 Al-GaAs, pure and Si or Zn doped interfaces, composition depth profile, pulsed laser atom probe study 7-32842
 Al-GaAs (100) interface, Schottky barrier form. 7-2717
 Al-GaAs interfaces, convergent beam electron diffr. patterns 7-27156
 Al-GaAsO-GaAs structures, energy diagram 7-33096
 Al-Si₃N₄-GaAs struts., interface state density profile determ., DLTS spectra interpretation 7-38733
 Al_{0.3}Ag_{0.7}As, femtosecond carrier dynamics 7-58829
 AlAs, atomic layer epitaxy, review 7-13362
 AlAs, energy bands, cohesive energy, form. energy, self-consistent calcs. 7-21995
 AlAs optical props., pseudodielec. function, spectroscopic ellipsometry meas. 7-52487

III-V semiconductors continued

- AlAs, VPE growth by chloride transport method 7-64930
 AlAs:Si films and AlAs:Si-GaAs:Si superlattices, MBE growth and electrical props. 7-22052
 AlAs:Si MBE layers, photoluminesc. 7-39160
 AlAs/GaAs modulated struct., high resolution double-cryst. X-ray diffr. studies 7-7029
 AlAs/GaAs superlattices, X-point excitons 7-33069
 AlAs/GaAs superlattice/GaAs interface, inversion holes, long term storage 7-45442
 AlAs/GaAs superlattice mixing induced by Si⁺ implantation 7-58649
 AlAs/GaAs:Si super-doped structs., short-period superlattice electrical and defect props. (*Japanese*) 7-7353
 AlAs/GaAs/AlAs quantum wells, eigenvalues calcs. 7-12820
 AlAs-GaAs double-barrier structures, resonant tunnelling, room temp. effects 7-21985
 AlAs-GaAs MIS capacitors, dynamic storage of holes 7-33071
 AlAs-GaAs quantum-wells, low temp. growth by modified MBE 7-39386
 AlAs-GaAs superlattices, Si ion implantation, dose-dependent mixing 7-12500
 AlAs-GaAs superlattice waveguides in separate confinement heterostructure laser diodes, threshold current density 7-20267
 AlAs-GaAs superlattice, Si⁺ implantation, depth dependent mixing 7-27032
 AlAs-GaAs superlattices, Si migration during MBE growth 7-27171
 AlAs-GaAs superlattices, disordering by Si and S implantation 7-45024
 AlAs-GaAs superlattice, compositional disordering control by Ar ion implantation 7-51806
 AlAs-GaAs superlattices, lattice vibration, Raman spectra 7-63937
 AlAs-GaAs superlattices, phase transitions under high press. 7-64016
 Al_{1-x}Ga_{1-x}As layers, form. by regrowth on surface of GaAs during contact with undersaturated liq. containing Al 7-46311
 Al_{1-x}Ga_{1-x}As-GaAs multiple quantum wells, photoluminescence studies, press. depend. (*Chinese*) 7-13194
 AlGaAs BH laser with flared waveguides, high power operation 7-57352
 AlGaAs, chemical beam epitaxial growth investig. 7-7878
 AlGaAs, DX centres, DLTS signature anal. 7-45204
 AlGaAs epitaxial layers and superlattices, X-ray diffr. analysis 7-21047
 AlGaAs epitaxial layers, large scale MOVPE growth 7-22552
 AlGaAs, epitaxial wafers, highly uniform growth by large capacity MOCVD reactor 7-22551
 AlGaAs heterostructs., low temp. LPE growth 7-64939
 AlGaAs high-power pulsed laser 7-10997
 AlGaAs high-power ridge-waveguide GRIN-SCH laser diode 7-10988
 AlGaAs injection heterolasers and integrated laser-photodetector pairs, prepared by microcleaving 7-31343
 AlGaAs integrated-hybrid Bragg heterostruct. laser thermal stability of distributed-refl. spectral bands 7-57393
 AlGaAs laser, mode hopping suppression by saturable absorber 7-62696
 AlGaAs laser, tunability and mode-transition characteristics 7-20293
 AlGaAs laser, tunability, appl. to Cd⁺ ion drift velocity meas. (*Japanese*) 7-20294
 AlGaAs laser arrays with Si disordered facet windows, high power operation 7-43140
 AlGaAs laser diode, HF stabilisation 7-15864
 AlGaAs laser diode array travelling-wave amplifier, high peak power, gateable picosec. optical pulses 7-20252
 AlGaAs laser diodes, MOCVD grown, struct. fabrication and characts. (*Japanese*) 7-20272
 AlGaAs laser diodes, MBE grown, fabrication and characts. (*Japanese*) 7-20273
 AlGaAs laser rib-waveguide, gain- to index-guiding transition 7-31315
 AlGaAs, laser-assisted MOVPE growth 7-64928
 (AlGa)As lasers, separately pumped, continuous control 7-20287
 AlGaAs layer, separating on GaAs surface, growth mechanism, Auger depth profiling 7-44434
 AlGaAs layers MOCVD using dimethyl aluminium hydride, C acceptors, photolum. 7-22517
 AlGaAs low current threshold visible laser diodes, (AlGaAs)_m(GaAs)_n superlattice quantum well 7-10926
 AlGaAs, low press. MOCVD grown, surface morphology and defects 7-64023
 AlGaAs, MOCVD growth on Ge substrates for high efficiency tandem solar cell appl. 7-3671
 AlGaAs, MOCVD growth, refractive indices meas. by in situ reflectometry 7-59270
 AlGaAs, MOVPE, laser assisted, selective area irr., carrier conc. 7-22545
 AlGaAs MQW lasers, index-guided, fabrication by selective disordering using Be focused ion beam implantation 7-20269
 AlGaAs monolithic three-junction solar-cells, computer modelling 7-3672
 AlGaAs multiquantum well-buried optical guide lasers, fabrication by Si-induced disordering 7-10995
 AlGaAs superlattice for visible laser diode, energy band structure (*Japanese*) 7-12823
 AlGaAs superlattices, donor state instability, DLTS and Hall meas. 7-12663
 AlGaAs surface cleaning using ECR radical beam gun 7-54028
 AlGaAs terrestrial solar cells, high-efficiency concepts 7-8390
 AlGaAs, triethylgallium pyrolysis temp. in presence of AsH₃ or trimethylaluminium 7-22541
 AlGaAs:Mg LPE layers, Mg doping and injection laser threshold current 7-12092
 AlGaAs:Mg-GaAs:Se concentrator solar cells, 26 percent efficient 7-3699
 AlGaAs:Sb, MBE growth, Sb doping 7-2038
 AlGaAs:Si-GaAs 2D electron gas structure, scatt. mechanisms 7-38718
 AlGaAs:Si(Zn), MOCVD, impurity induced disordering, quantum well laser fabrication and characts. 7-27934
 AlGaAs/AlAs multiquantum-well structs., staggered band alignments 7-7361
 AlGaAs/GaAs, abrupt heterojunction structures, large area uniformity, MOVPE reactor design 7-22524
 AlGaAs/GaAs DBR laser with multiquantum well active/passive waveguides 7-57350
 AlGaAs/GaAs DFB laser diodes, MOCVD growth, CW operating characts. 7-25836
 AlGaAs/GaAs heterointerface solid-state far IR emitter utilising 2D plasmon 7-53414
 AlGaAs/GaAs heterojunction bipolar transistor, self-aligned with InGaAs emitter cap 7-45492

III-V semiconductors continued

- AlGaAs/GaAs heterostruct., quasiatomic system, electronic struct. studies 7-38699
 AlGaAs/GaAs laser diodes, advanced optoelectronic technology 7-1187
 AlGaAs/GaAs long cavity ridge waveguide DFB lasers, spectral linewidth reduction 7-1179
 AlGaAs/GaAs modulation-doped heterojunctions, 2D electron gas, DX centres 7-38694
 AlGaAs/GaAs ridge waveguide quantum well lasers with high quantum efficiency 7-15905
 AlGaAs/GaAs selectively doped heterointerface under high elec. field appl. 2D plasmon 7-52637
 AlGaAs/GaAs solar cells, proton irradiated, defect production 7-46936
 AlGaAs/GaAs superlattice 7-64324
 AlGaAs/GaAs two-junction monolithic cascade solar cell in lattice-matched system 7-13862
 AlGaAs/GaAs waveguide phase modulators, wavelength depend. 7-43361
 AlGaAs/GaAs:Si heterostruct., MBE growth on polar surfaces 7-7863
 AlGaAs/GaAs/AlGaAs selectively doped double heterojunction FET system, high mobility electron subband struct. studies 7-12838
 AlGaAs/GaAs/AlGaAs selectively doped double heterostructs., electron conc. and mobility 7-12839
 AlGaAs/GaAs/AlGaAs single quantum well, negative differential mobility and drift vel. overshoot 7-52803
 AlGaAs/GaAs/Ge multijunction solar cell, model for calc. of displacement damage by radiation 7-13878
 AlGaAs/GaAs/InGaAs multijunction solar cell, model for calc. of displacement damage by radiation 7-13878
 AlGaAs/GaInAs two-junction monolithic cascade solar cell in lattice-mismatched system 7-13862
 AlGaAs/GaInAs two-terminal multijunction solar cell spectral response meas. 7-13871
 AlGaAs-GaAs, band-gap discontinuity, determ. by quantum oscillations of photolum. intensity 7-13217
 AlGaAs-GaAs, DFB lasers, low threshold, 0.88 μ m emission, MOCVD fabricated with ridge waveguide struct. 7-5906
 AlGaAs-GaAs, modulation doped heterostructs., high field transient transport 7-12836
 AlGaAs-GaAs, selectively doped heterojunctions, energy relax. of 2D electrons, deformation potential constant 7-12801
 AlGaAs-GaAs 2D electron gas structs., scatt. mechanisms 7-52783
 AlGaAs-GaAs cascade solar cells, efficient two-junction monolithic, grown by MOCVD 7-65483
 AlGaAs-GaAs concentrator solar cells with high efficiency, design and fabrication 7-3669
 AlGaAs-GaAs DFB-TJS external-cavity laser with optical phase control loop, spectral linewidth 7-20222
 AlGaAs-GaAs DH injection lasers, MOCVD growth on Si substrates 7-57356
 (AlGa)As-GaAs DQW-SCH lasers grown by MOCVD, design, fabrication and characterisation 7-36990
 AlGaAs-GaAs GRIN-SCH SQW laser, wide-stripe, injection locking 7-20290
 AlGaAs-GaAs graded barrier quantum well heterostructure laser diodes with compositionally graded and superlattice buffer layers 7-57353
 AlGaAs-GaAs heteroepitaxial wafer for solar cell appls., uniform growth by MOCVD 7-64929
 AlGaAs-GaAs heteroface space solar cells with 21 percent conversion efficiency 7-3694
 AlGaAs-GaAs heteroface solar cells, role of window layer 7-3695
 AlGaAs-GaAs heterointerface, ballistic transport of quasi-2D electron gas 7-52788
 AlGaAs-GaAs heterostructures, organometallic VPE grown, galvanomagnetic effect 7-12800
 AlGaAs-GaAs heterostructures, dissipationless quantum Hall effect, size-depend. quantised breakdown 7-45469
 AlGaAs-GaAs heterostructure travelling-wave amplifier based on injection laser diode 7-62694
 AlGaAs-GaAs index-guided lasers with mode filter, props. study 7-5905
 AlGaAs-GaAs laser diodes, elec. field depend. of photoconductivity spectra 7-20227
 AlGaAs-GaAs MQW CCD spatial light modulators using electroabsorption effects 7-20407
 AlGaAs-GaAs narrow spectral linewidth semiconductor optical-fiber ring laser 7-25817
 AlGaAs-GaAs selectively doped heterostructures, orientation effect on contact resistance 7-38680
 AlGaAs-GaAs self-pulsing lasers, quasiperiodic route to chaos under large signal current modulation 7-62706
 AlGaAs-GaAs single quantum well, MBE growth interruption, well width fluctuations 7-7865
 AlGaAs-GaAs single quantum wells with growth interrupted heterointerfaces, photoluminesc. 7-39168
 AlGaAs-GaAs solar cells, MOCVD on GaAs, Ge and Ge-Si substrates 7-3650
 AlGaAs-GaAs solar cells, high efficiency DH cells fabrication using MOCVD 7-3693
 AlGaAs-GaAs solar cells, fabrication on Si substrates 7-46937
 AlGaAs-GaAs solar cell fabrication, elec. characts. and space appl. 7-54307
 AlGaAs-GaAs space solar cells, LPE production and characterisation 7-3666
 AlGaAs-GaAs superlattices, impurity electron states (*Japanese*) 7-12662
 AlGaAs-GaAs superlattices, Si-Be co-doping, compositional disordering suppression, SIMS study 7-16878
 AlGaAs-GaAs superlattices, Se (Si)(Mg)(Be) ion implantation, intermixing, residual damage 7-26782
 AlGaAs-GaAs-AlGaAs single quantum well heterostruct., negative differential mobility and drift velocity overshoot 7-52787
 AlGaAs-GaAs-Si, Be superlattices, correlation between Si diffusion and Si-induced disordering 7-38034
 AlGaAs-GaInAs cascade solar cells, efficient two-junction monolithic, grown by MOCVD 7-65483
 AlGaAs-GeAs n-n heterojunction, thermionic current and capacitance, effect of subband quantisation in 2D electron gas 7-17090
 AlGaAs-Si mechanically stacked multijunction solar cells, optical effects of thin film adhesives 7-3670
 Al_{0.25}Ga_{0.75}As multilayer structures, vertical transport 7-38719
 Al_{0.26}Ga_{0.74}As, instability of electron-nuclear spin system in strong mag. field, luminesc. study 7-7729
 Al_{0.26}Ga_{0.74}As/GaAs heterojunction, high mobility 2-D hole gas 7-2679

III-V semiconductors continued

- Al_{0.28}Ga_{0.72}As, photoluminescence half-width and intensity, temp. depend. 7-39179
- Al_{0.3}Ga_{0.7}As, thermal and ion-assisted reactions with Cl₂ 7-28349
- Al_{0.3}Ga_{0.7}As/GaAs quantum wells, photocond. of confined donors 7-7282
- Al_{0.3}Ga_{0.7}As-GaAs optically-pumped multiple quantum well laser 7-5922
- Al_{0.3}Ga_{0.7}As-GaAs quantum well structure, electric-field-induced optical modulation, theory using Monte Carlo approach 7-17077
- Al_{0.35}Ga_{0.45}As:Te edge region photocapacitance at constant bias, anal. 7-7287
- Al_{0.4}Ga_{1-x}As, hot-electron capture at DX centres 7-45344
- Al_{0.4}Ga_{1-x}As, AlAs and GaAs epitaxial multilayers as optical interferometric elements 7-342
- Al_{0.4}Ga_{1-x}As bandgap determ. by Schottky barrier spectral response meas. 7-2667
- Al_{0.4}Ga_{1-x}As cascade solar cells, OM-VPE growth, in-situ-grown tunnel junction 7-8387
- Al_{0.4}Ga_{1-x}As crysts., DX centre props. 7-2534
- Al_{0.4}Ga_{1-x}As, DX centre, theory 7-12654
- n-Al_{0.4}Ga_{1-x}As epitaxial layers, graded-gap, resistance, press. dependence 7-33113
- Al_{0.4}Ga_{1-x}As film formation by laser beam interaction with AlAs/GaAs multilayer structure 7-12570
- Al_{0.4}Ga_{1-x}As films and multilayer structures, MOCVD growth and characterisation, review 7-33586
- Al_{0.4}Ga_{1-x}As, Ga interstitial identification by ODMR 7-33302
- Al_{0.4}Ga_{1-x}As heteroepitaxial layers formed by metalloorganic chem. hydride method, electrophys. props., comp. effect 7-64370
- Al_{0.4}Ga_{1-x}As heterojunction, tunnelling current modulation by optical photons 7-27394
- Al_{0.4}Ga_{1-x}As homojunctions, minority-carrier diffusion, TOF studies 7-12797
- Al_{0.4}Ga_{1-x}As layers and quantum well struct., MOVPE growth chemistry 7-22550
- Al_{0.4}Ga_{1-x}As, low press. OMVPE, selective growth embedding in etched grooves on GaAs 7-22554
- Al_{0.4}Ga_{1-x}As MBE layers, deep electron traps, flux ratio effects 7-12641
- Al_{0.4}Ga_{1-x}As solar cells, MOCVD growth and characterisation, review 7-34043
- Al_{0.4}Ga_{1-x}As surface, protection by As and GaAs ultrathin layers, AES sputter depth profiles 7-54022
- Al_{0.4}Ga_{1-x}As, thin films, Raman spectroscopy, characterisation 7-53354
- Al_{0.4}Ga_{1-x}As:Be epitaxial layers, ion implanted, rapid thermal annealing 7-21257
- Al_{0.4}Ga_{1-x}As:Si, deep donor centres 7-45217
- Al_{0.4}Ga_{1-x}As:Si, LEDs, luminesc. props. (Korean) 7-27786
- Al_{0.4}Ga_{1-x}As:Si, Si diffusion from sputtered Si film 7-58537
- Al_{0.4}Ga_{1-x}As:Te, low press. OMVPE, Te doping, Hall effect, carrier conc., photolum. 7-21242
- Al_{0.4}Ga_{1-x}As/GaAs, multilayer and superlattice structures, electronic subbands 7-58877
- Al_{0.4}Ga_{1-x}As/GaAs multi-quantum-well Zn-diffused mesa BH lasers, sub-milliwatt power lasing 7-10991
- Al_{0.4}Ga_{1-x}As/GaAs photoexcited heterojunction, charge transfer calcs. 7-12688
- Al_{0.4}Ga_{1-x}As/GaAs quantum wells, photolum., periodic variation investig. 7-2688
- Al_{0.4}Ga_{1-x}As-AlAs quantum well, magneto-optical absorpt. study 7-7681
- Al_{0.4}Ga_{1-x}As-GaAs BH quantum well edge-injection laser array 7-57355
- Al_{0.4}Ga_{1-x}As-GaAs broad area quantum well lasers, single-mode single-lobe operation 7-10930
- Al_{0.4}Ga_{1-x}As-GaAs double heterostruct. injection laser, power-current characteristics study 7-62704
- Al_{0.4}Ga_{1-x}As-GaAs heterostructures, 2D electron space charge layers, plasmon and magnetoplasmon excitation 7-38696
- Al_{0.4}Ga_{1-x}As-GaAs heterointerface, 2D electron gas density 7-45448
- Al_{0.4}Ga_{1-x}As-GaAs heterostruct. injection laser with coupled cavity, dynamic stability 7-62705
- Al_{0.4}Ga_{1-x}As-GaAs heteroface solar concentrator cells, space and terrestrial appls. 7-65486
- Al_{0.4}Ga_{1-x}As-GaAs LOC lasers for high power low threshold current density operation, optimisation 7-10934
- Al_{0.4}Ga_{1-x}As-GaAs layered structures, metal organic VPE grown, depth profiles, SIMS anal. 7-21684
- Al_{0.4}Ga_{1-x}As-GaAs mesa BH MQW lasers with 880 μ A threshold current at 77 K 7-50595
- Al_{0.4}Ga_{1-x}As-GaAs stripe-geometry quantum well heterostructure lasers defined by defect diffusion 7-1181
- Al_{0.4}Ga_{1-x}As-GaAs superlattices, ion implanted, defect struct. 7-26783
- Al_{0.4}Ga_{1-x}As-AlAs heterojunctions, band discontinuities meas. 7-27407
- AlGaInAs layers on InP, LPE growth 7-33608
- AlGaInP, MOCVD, photolum., quantum wells, double heterostruct. laser appl. 7-39405
- AlGaInP visible semicond. lasers, mesa stripe struct., MOVPE grown, 621 nm CW operation at 0°C 7-20262
- AlGaInP visible semiconductor lasers grown by metalloorganic vapor phase epitaxy 7-50590
- Al_{0.4}Ga_{1-x}N epitaxial layers, MOCVD, growth mechanism, Ga incorporation rate 7-39411
- Al_{0.4}Ga_{1-x}N MOVPE growth, struct. and elec. props. 7-21729
- Al_{0.4}Ga_{1-x}N, photoluminescence in the edge emission region 7-27778
- Al_{0.4}Ga_{0.6}Sb-GaSb-Al_{0.4}Ga_{0.6}Sb MBE strained layer DH, optically pumped laser oscill. 1.6 to 1.8 μ m 7-5888
- AlInAs-GaInAs superlattices, electronic transport and depletion by tunnelling 7-27395
- AlInAs-GaInAs heterostruct., alloyed NiGeAuAgAu ohmic contacts, charact. 7-22016
- AlInAs-GaInAs selectively doped heterostructs., MOCVD growth, HIFET fabrication appl. 7-17429
- AlInAs-GaInAs superlattices, quantum photoconductivity, effective mass filtering 7-12847
- Al_{0.25}In_{0.75}As, transient transport in central-valley-dominated ternary III-V alloys 7-7253
- Al_{0.48}In_{0.52}As:Si, MBE grown, crystalline and optical props. 7-52322
- Al_{0.48}In_{0.52}As-Ga_{0.47}In_{0.53}As SQW, electron temp. depend. on well width, photolum. obs. 7-12810
- Al_{1-x}In_xAs-GaAs strained layer superlattices, X-ray diffraction and excitation spectroscopy studies 7-12853
- AlN amorphous film, plasma CVD from metal organic Al source 7-52368
- AlN crystal, phonon energy calcs. 7-2119

III-V semiconductors continued

- AlN, electronic struct., first principles LCAO calc. 7-21813
- AlN films, OMVPE, Hall mobilities, impurity band 7-39410
- AlN formed by N ion implantation of Al, electronic struct. 7-58926
- AlN thin crystalline stoichiometric film, electronic struct., electron spectroscopy studies 7-58916
- AlN, undoped and control doped films, luminesc. studies 7-27790
- AlN-sapphire, low temp. epitaxial film growth 7-13387
- AlP(As)(Sb), elastic coefficients, pressure effects 7-63720
- AlSb, hot electron luminesc. 7-46119
- AlSb:Se, donor studies, incoherent laser saturation method 7-27298
- AlSb-GaSb superlattices, low-temp. growth by plasma process (Japanese) 7-7061
- AlSb-GaSb superlattices, X-ray diff. analysis 7-21047
- Au/Cd stearate/n-GaP electroluminescent device struct., electron-hole recomb. luminesc., minority carrier injection mechanism 7-59260
- Au-GaAs, annealed, interface erosion 7-21683
- Au-GaAs, contact, structural and elec. props. 7-27424
- Au-GaAs, interface state meas. at Schottky contacts, admittance characterisation technique 7-2718
- Au-GaAs, Schottky contact, interface states, trap characterisation 7-27421
- Au-GaAs (001), short range potential variations at interface 7-45500
- Au-GaAs (110) interface, photoemission studies, temp. effects 7-33517
- Au-Ge-GaAs, interfacial reactions, struct. after annealing 7-27154
- Au-Ge-Ni-GaAs, non-alloyed ohmic contact, solid phase epitaxy 7-27423
- Au-InP, solid-state reactions, Au₂P₃ formation 7-58550
- Au-InP high-speed internal photoemission detectors enhanced by grating coupling to surface plasma waves 7-52688
- Au-Ni-Au-Ge-Ni-GaAs, ohmic contacts, alloying, specific contact resistivity 7-27425
- AuBe-Cr-Au-InP, improved ohmic contact 7-64310
- AuGe-Nb-GaAs, ohmic superconducting contacts to GaAs 7-33088
- BN MIS structures, form. by reactive pulse plasma method, on Si or SiO₂ substrates, phys. props., annealing effects 7-22023
- BN, polymorphism studies, temp. and press. effects 7-1934
- CaF₂-GaAs (100), surface morphology, elec. props. 7-39392
- nCdS-n-GaAs photoanode, flux anal. of multiple junction solar cells 7-23162
- CdTe-InSb interface struct. and band offsets 7-58664
- CdZnS-InP heterojunction solar cell, numerical anal. 7-23155
- Cr₂O₃-GaAs, struct. and electrophysical props. 7-17109
- Ga-As-AlGaAs superlattice, laser induced disordering and Si impurity incorporation 7-45018
- Ga-In-As-P system, ternary alloys, E₁ energy gap, CPA calc. 7-58740
- GaAs (110), oxidation, photoemission spectra studies 7-3147
- GaAs:Be, MOVPE, diethylberyllium dopant source, elec. characts. 7-22521
- GaAs-GaAlAs MQW waveguides, nonlinear propag. 7-26033
- a-Ga_{0.5}As_{1-x}I_x, plasma deposition in RF capacitively coupled system 7-64927
- GaAlAs channelled-substrate-planar laser, measuring modulus and phase of chirp/modulated power ratio 7-57391
- GaAlAs diode laser, frequency shift in magnetic field 7-5885
- GaAlAs diode laser, gain compression, picosecond transmission meas. 7-20289
- GaAlAs heterostructures with an insulating layer 7-12866
- GaAlAs injection lasers, single-frequency, linewidth investig. 7-25819
- GaAlAs, LIMA anal., effect of alloy composition on secondary ion yields 7-28376
- GaAlAs laser, collinear nearly degenerate four-wave mixing in amplifying media 7-11071
- GaAlAs laser, LPE grown, effect of crystal defects on reliability 7-36960
- GaAlAs laser amplifier, high sensitivity picosecond optical pulse detection 7-50565
- GaAlAs laser diode, extremely weak feedback, lasing wavelength shift anal. 7-31325
- GaAlAs laser diodes, stripe geometry, directly modulated in microwave range, freq. response study 7-11017
- GaAlAs laser diodes, self-coupling effects and appls. 7-57386
- GaAlAs laser diodes under microwave intensity modulation, linearity charactn. 7-10944
- GaAlAs laser structs., double crystal X-ray rocking curves, interference peaks 7-44303
- GaAlAs laser-diode array, high-speed electronic beam steering 7-43185
- GaAlAs lasers, injection, photodetection props. 7-31379
- GaAlAs lasers, polarisation-resolved low-frequency noise 7-15863
- GaAlAs MOCVD layers, stoichiometry variation determ., pulsed laser atom probe anal. 7-12305
- GaAlAs, MOVPE growth rate, orientation depend. 7-22556
- (GaAl)As monolithic composite-cavity laser, chem. etching technique 7-50579
- GaAlAs morphological stability in epitaxy, appl. to optoelectronic monolithically integrated structures 7-27172
- GaAlAs passive waveguide, intrinsic optical bistability obs. 7-57425
- GaAlAs, semiconductor laser coupled with short external cavity, stable single longitudinal mode operation 7-62737
- GaAlAs single freq. heterostruct. injection lasers, LPE and VPE growth 7-62699
- GaAlAs strip waveguides, optical transistor effects, expt. study 7-37026
- GaAlAs wideband free-space lasercom transmitter, design 7-31354
- GaAlAs wideband lasercom transmitter, performance 7-31355
- GaAlAs:Si, DX centres, nonexponential thermal emission kinetics 7-12640
- GaAlAs/GaAs, junction isolated LED structures, MOCVD, characts. 7-27935
- GaAlAs/GaAs, semicond. superlattice heterojunction interface, SIMS anal. (Japanese) 7-2396
- GaAlAs/GaAs circular BH surface emitting lasers, fabrication using selective meltback method 7-5911
- GaAlAs/GaAs heterostructure, absorption coeff. and thermal conductivity meas. by photothermal spectroscopy 7-41474
- GaAlAs/GaAs MOCVD growth for surface emitting lasers 7-53630
- GaAlAs/GaAs single quantum well laser, current pumped, second quantised state lasing 7-50559
- GaAlAs/GaAs surface-emitting linear laser arrays with etched mirrors 7-20255
- GaAlAs/GaAs TJS lasers on Si substrates, MOCVD growth 7-62691
- GaAlAs/GaAs:C quantum wells interface struct. and luminesc. efficiency 7-7735

III-V semiconductors continued

- GaAlAs-GaAs DFB lasers with double channel planar buried heterostructure, low threshold operation 7-20256
- GaAlAs-GaAs DFB laser with double-channel planar BH 7-50594
- GaAlAs-GaAs epitaxial superlattice, X-ray double crystal characterisation, rocking curves calc., computer simulation technique 7-58105
- GaAlAs-GaAs heterostructures grown by MOCVD, transition region, ellipsometric anal. 7-2388
- GaAlAs-GaAs heterostructure solar cells, multijunction with bulk graded bandgap/p-n junction 7-3676
- GaAlAs-GaAs laser diodes, catastrophic optical damage, electrolum., cathodolum., EBIC and TEM obs. 7-57329
- GaAlAs-GaAs laser failure causes and distrib., laboratory service life tests 7-62692
- GaAlAs-GaAs MOCVD solar cells on Ge and Ge/Si substrates 7-23182
- GaAlAs-GaAs MQW structure, compositional fluctuations, STEM/EDX microanal. 7-45077
- GaAlAs-GaAs microcavity surface-emitting laser 7-57361
- GaAlAs-GaAs multi-heterostructures, MOCVD growth for surface emitting lasers 7-59440
- GaAlAs-GaAs quantum well superlattices, applied electric field, quasi-eigenstates and eigenenergies, determ. 7-33072
- GaAlAs-GaAs ridge waveguide DFB lasers, lateral anal. 7-62686
- GaAlAs-GaAs solar cells grown by MBE, material props. and device parameters 7-23164
- GaAlAs-GaAs superlattice, Auger sputter depth profiling 7-21254
- GaAlAs-GaAs superlattice struct., dynamic SIMS profiles 7-22417
- GaAlAs-GaAs surface-emitting laser diodes, lateral pumping struct. 7-57359
- GaAlAs-GaAs surface-emitting laser with $\text{TiO}_2\text{-SiO}_2$ dielec. multilayer reflector 7-59427
- GaAlAs-Mo junctions, Schottky barrier height, electronic props. 7-64346
- $(\text{Ga}_{0.5}\text{Al}_{0.5})\text{As}$, MBE grown, elastic consts., diffuse X-ray scatt. study 7-16918
- $\text{Ga}_{0.60}\text{Al}_{0.40}\text{As}$, electron-hole plasma diffusion, spatially resolved gain and luminescence spectra 7-12747
- $\text{Ga}_{0.65}\text{Al}_{0.35}\text{As}$ -GaAs quantum wells, elect. field-induced decrease of exciton lifetimes 7-45481
- $\text{Ga}_{0.8}\text{Al}_{0.2}\text{As}$ -GaAs- $\text{Ga}_{0.8}\text{Al}_{0.2}\text{As}$ quantum well structs., electroreflectance spectra, model 7-33365
- $\text{Ga}_{1-x}\text{Al}_x\text{As}$, indirect-gap crystals, hot photolum., polarisation characters. 7-46092
- $\text{Ga}_{1-x}\text{Al}_x\text{As}$, ion-implanted, defect creation 7-21240
- $\text{Ga}_{1-x}\text{Al}_x\text{As}$ -GaAs- $\text{Ga}_{1-x}\text{Al}_x\text{As}$ heterostructures, tunneling through indirect-gap barriers 7-21999
- $\text{Ga}_{1-x}\text{Al}_x\text{As}$, Al concentration profiling using nucl. resonances 7-6811
- $\text{Ga}_{1-x}\text{Al}_x\text{As}$ and GaAs multilayer structures, metalorganic MBE growth 7-7860
- $\text{Ga}_{1-x}\text{Al}_x\text{As}$, DX centres, inner and outer crossing lattice relax. 7-45218
- $\text{Ga}_{1-x}\text{Al}_x\text{As}$, disorder effects of Raman scatt. 7-7704
- $\text{Ga}_{1-x}\text{Al}_x\text{As}$ MIS and SIS structures, prep. by metallorganic chem. hydride method, electrophysical props. 7-22018
- $\text{Ga}_{1-x}\text{Al}_x\text{As}$, quantitative anal. by SIMS (*Chinese*) 7-54239
- $\text{Ga}_{1-x}\text{Al}_x\text{As}$ quantum-well wires, Wannier excitons, binding energies 7-64092
- $\text{Ga}_{1-x}\text{Al}_x\text{As}$ solid soln. epitaxial layer composition, Raman determ. 7-64628
- $\text{Ga}_{1-x}\text{Al}_x\text{As:S(Se)}$, MBE growth, dopant incorporation 7-12533
- $\text{Ga}_{1-x}\text{Al}_x\text{As:Si}$, electrical current induced liq. phase epitaxy 7-27955
- $\text{Ga}_{1-x}\text{Al}_x\text{As/Ga}_{1-y}\text{Al}_y\text{As}$ double barrier tunnelling struct., negative resist. calcs. 7-45451
- $\text{Ga}_{1-x}\text{Al}_x\text{As-GaAs}$, thickness and conc. of thin $\text{Ga}_{1-x}\text{Al}_x\text{As}$ epitaxial films, determ. by photoemission jumps method (*French*) 7-38381
- $\text{Ga}_{1-x}\text{Al}_x\text{As-GaAs}$ quantum wells, diamag. shift of exciton energy levels 7-21824
- $\text{Ga}_{1-x}\text{Al}_x\text{As-GaAs-Ga}_{1-y}\text{Al}_y\text{As}$ quantum well, donor ion dielec. response 7-45417
- GaAlAsGaAs quantum well heterostructures, grown by MOCVD, props. 7-45479
- GaAlAsSb/GaSb/GaInAsSb injection double heterostructure laser, room temp. operation 7-62697
- $\text{Ga}_{1-x}\text{Al}_x\text{As-GaAs}$ superlattice, exciton CW-photoluminesc., excitation intensity depend. 7-59252
- GaAlSb/GaSb (111) heterostructures, signs of misfit dislocations, X-ray topographic determ. 7-38349
- $\text{Ga}_{0.94}\text{Al}_{0.06}\text{Sb/GaSb}$ epitaxial struct., misfit dislocations anomalous visibility, Bragg geometry X-ray topograms 7-2019
- $\text{Ga}_{0.96}\text{Al}_{0.04}\text{Sb}$ layers, liq. phase epitaxial growth, elec. and photoelec. characterisation 7-39443
- $\text{Ga}_{1-x}\text{Al}_x\text{Sb}$ epitaxial layers, MOCVD, morphology rel. to growth conditions 7-39408
- GaAs, laser-assisted MOVPE growth 7-64928
- GaAs - Ag (Au), excimer laser annealed Au(492) contacts 7-12857
- GaAs 2D electron gas, dynamical cond., IR cyclotron reson. meas., electron interaction effects 7-45195
- GaAs (001), chemisorption of CF_3 radicals, RHEED, photoelectron spectra, HF SCF calcs. 7-53497
- GaAs (001), rel. between etch pit density and dislocation density 7-51771
- GaAs (001) surface, etch pits, depend. on Burgers vectors of dislocations 7-39767
- GaAs (001)-AuGa₂, chemically unreactive interfaces formation 7-7050
- GaAs (100), ambient induced surface effects, O adsorption, photolum., conductivity 7-45429
- GaAs (100), chemical etching and oxidation, XPS characterisation 7-21591
- GaAs (100), oxidation 7-59703
- GaAs (100), surface Fermi level unpinning in air using photochem. 7-2655
- GaAs (100), UV-ozone clearing, for device appl. 7-28228
- GaAs (100) films, mol. beam epitaxy system (*Czech*) 7-7854
- GaAs, (100) substrates, growth of HgTe-CdTe superlattices by MBE 7-12520
- GaAs (100) unpinned surface, picosecond transient reflectivity 7-59168
- GaAs (100)-Ni interface, effect of O on diffusion and compounding 7-21539
- GaAs (110), adsorption of O_2 , confirmation of two-step uptake model 7-2355
- GaAs (110), adsorption of Al, soft X-ray photoemission spectra study 7-53494

III-V semiconductors continued

- GaAs (110), chemisorption of O_2 , photoemission evidence for surface growth 7-2356
- GaAs (110), O_2 adsorption, electronic props., contact pot. meas. 7-2353
- GaAs (110), substrate for In growth, RHEED study 7-2425
- GaAs (110) Cu, electron struct., synchrotron radiation photoelectron spectroscopy 7-27420
- GaAs (110) p(1 × 1), adsorbed Sb, domain size, LEED profile anal. 7-7075
- GaAs (110) with ordered Sb overlayers, ARUPS 7-59378
- GaAs (110) with Sb overlayers, electronic band bending at interface 7-58895
- GaAs (111), (2 × 2) reconstruction, geometric struct. model 7-6950
- GaAs (111), alkali metal covered, adsorption of O_2 7-63957
- GaAs (111), sorption of O, surface struct., AES anal. 7-53457
- GaAs (111) and (-1-1-1), electronic props., angle resolved photoemission studies 7-7327
- GaAs (111) orderly faceted struct., LEED pattern anal. 7-21579
- GaAs (311)(1 × 1) surface, atomic geometry and electronic struct. 7-2311
- GaAs (511) and (711) surfaces, struct. studies using LEED AES, and EELS 7-2312
- GaAs absorbing zinc-blende type material, backward Raman scatt., ang. dispersion calcs. 7-22238
- GaAs, absorption-induced nodal plane shifts of X-ray stationary waves, angular depend. 7-32196
- GaAs acoustic charge transport device using SAWs, signal processing appl., principles and performance 7-57653
- GaAs, AlGaAs, MOCVD, design of safe facility 7-22529
- GaAs all-optical logic gate arrays, fabrication and characterisation 7-57414
- GaAs and GaAs:Te, defect study by positron annihilation (*Chinese*) 7-13254
- GaAs and GaAs:Ge extrinsic photoeffect obs. with X-ray diffraction apparatus 7-32221
- GaAs, anharmonic props. of ultrasound under intense excitation 7-20488
- GaAs anomalous photovoltage films X-ray irradiation effects studies 7-58834
- GaAs, antisite defects formation during plastic deformation 7-37988
- GaAs, atomic layer epitaxy, review 7-13362
- GaAs, atomic layer epitaxy growth, photolum., Hall meas. 7-22527
- GaAs, atomic layer epitaxy in low press. MOCVD system 7-53628
- GaAs backwall Schottky barrier solar cells, minority carrier current collection, built-in elec. field enhancement limitations 7-54305
- GaAs, band-gap shifts 7-22333
- GaAs biased semi-insulating, cross modulation effect 7-50731
- GaAs bulk and MQW structures, nonlinear channel waveguides 7-57553
- GaAs CCD, high resistivity gate struct., radiation effects 7-6683
- GaAs, CVD, laser selective deposition on GaAs and Si substrates 7-22546
- GaAs cells, crossed-lens photovoltaic concentrator appl. 7-17905
- GaAs cells, photovoltaic concentrator research progress 7-17903
- GaAs, characterisation by a microwave photoconductance technique 7-7281
- GaAs, chemical beam epitaxial growth investig. 7-7878
- GaAs chemical etching by Cl₂, thermodynamically predicted depend. on press. and temp. 7-22919
- n-GaAs, cleaved clean (110) surface initial band bending cause, noble metal deposition 7-22017
- GaAs cleaved semiconductor surfaces, scanning tunnelling microscopy 7-21051
- n-GaAs cleaved surfaces, elec.-field-induced Raman scatt., reson., temp. and screening effects 7-27717
- GaAs cluster, TOF mass spectra 7-20084
- n-GaAs compensated samples, MOVPE grown, Hall effect meas. 7-27348
- GaAs concentrator cells, design options and constraints 7-3698
- GaAs, conduction band, deformation splitting and intervalley scattering 7-2548
- GaAs, covalent cryst., electronic struct., cluster approx. 7-52403
- GaAs, crack form., quenching by dislocation ensembles (*Russian*) 7-44680
- GaAs, crystal defects, IR light scattering tomography and IR absorption microscopy 7-46023
- GaAs, crystal growth, semiconductor industry needs 7-53540
- GaAs, crystal polarity, convergent beam electron diff. study 7-21162
- GaAs crystalline and amorphous, L near-edge structure, X-ray photoabsorpt. spectra 7-64766
- GaAs crystals, liquid-phase electroepitaxial growth, dislocation density reduction 7-58681
- GaAs crystals, selective etching and photoetching of $\text{CrO}_3\text{-HF}$ aq. solns. 7-32442
- GaAs current limiters, impact ionisation breakdown 7-52639
- GaAs, Czochralski grown, defect. conc., spatially resolved photoluminesc. 7-22341
- GaAs, Czochralski growth of high quality crystals. 7-53548
- GaAs, DC conductivity, surface conductivity 7-21919
- GaAs DH laser struct., external injection of spontaneous emission 7-31328
- GaAs, DLTS meas. using lock-in amplifier 7-327
- GaAs, decomposition during rapid thermal annealing 7-13657
- GaAs, deep level nonradiative carrier capture press. depend. calcs. 7-12735
- GaAs, deep levels, scanning optical fibre microscope, laser beam induced current images 7-48846
- GaAs, defect structure charactn., US meas. 7-21363
- GaAs, defects, positron lifetime spectra 7-37979
- n-GaAs, depletion and accumulation layer profiles, self-consistent Hartree approx. calcs. 7-27375
- GaAs, detector material, applications 7-45307
- GaAs device structures, γ -ray effects, surface generation-recombination processes 7-64349
- GaAs devices, 1/f fluctuation, surface states effects (*Japanese*) 7-21955
- p-GaAs, dielec. functions, band-gap narrowing anal. 7-52482
- GaAs, dielectric overlayers, effect on surface depletion potential 7-38678
- GaAs, dielectric protective coatings during heat treatment 7-33852
- GaAs, dielectric response and electronic states 7-33320
- GaAs, diffusion coeff. of Fe, temp. depend. 7-6875
- GaAs diode, active layer <1 μm , low temp. current flow 7-52757
- GaAs, direct maskless fabrication of submicrometre gratings 7-62855

III-V semiconductors continued

- GaAs dislocated and In-doped dislocation free, inhomogeneities obs. by video-enhanced IR topography 7-32446
 GaAs, dislocation containing, positron annihilation 7-39279
 GaAs, dislocation core struct. 7-38007
 GaAs, dislocation density reduction in crystal growth 7-2020
 GaAs, dislocation loops, TEM image profiles, electron diffr. two-beam dynamical theory 7-12071
 GaAs, dislocation network density determ., thermal wave microscopy 7-51778
 GaAs, dislocation rosette generation round Vickers indentations, mobility and twinning, TEM study 7-63618
 GaAs, dislocation-complex defect interactions, photoluminescence studies 7-16608
 GaAs, dislocations, obs. by transmission IR microscopy 7-32447
 GaAs, dislocations, stereographic obs. by IR light scatt. 7-32235
 GaAs, dopant profiles modification due to surface and interface modifications 7-58306
 GaAs, doped, oxidation, in situ TEM obs. 7-28215
 GaAs doping superlattices, optically induced absorpt. modulation 7-7713
 GaAs doping superlattices, efficient room temp. electroluminescence, tunability 7-27782
 GaAs doping superlattices, temp. depend. of tunable lumin. 7-39182
 GaAs doping superlattices, pulsed and CW photoluminescence obs. 7-46138
 GaAs doping superlattices, photoreflectance 7-53368
 GaAs, dry etching, radiation damage 7-54024
 GaAs, EL2 and As antisite defect props., review (*Japanese*) 7-7152
 GaAs, EL2 centre stability under electron-hole recomb. conditions 7-16978
 GaAs, EL2 clusters, scattering and absorpt. of IR light 7-53382
 GaAs, EL2 defect profiling, DLTS 7-12652
 GaAs, electron beam irradi., carrier density, anomalous temp. depend. 7-52610
 GaAs, electron density distrib., X-ray refl. anal. 7-44497
 GaAs, electron drift vel.-elec. field characts. 7-38569
 GaAs, electron impact ionisation rate in nonuniform elec. fields, simulation 7-33021
 p-GaAs, electron irradi.-induced trap defects, DLTS study 7-12155
 GaAs, electron irradiated, defect profiling, DLTS 7-12652
 GaAs, electron irradiation induced defects, DLTS study 7-58338
 GaAs, electron scattering in quantum limit 7-38552
 GaAs, electron-LO phonon dynamics, subpicosecond Raman spectroscopy 7-46052
 GaAs, electron-electron interactions, appl. for hot electron decay 7-32934
 GaAs, electron-electron interaction, quantum effects, magnetoresist. studies 7-38591
 GaAs, electron-hole plasma diffusion, spatially resolved gain and luminesc. spectra 7-12747
 GaAs, electron-hole plasma dynamics under subpicosecond optical excitation, optical absorption saturation 7-27356
 GaAs, electron-irradiated, relative density of levels of radiation defects 7-52500
 GaAs, emission lines, lifetimes and ionisation energies 7-22306
 GaAs, energy bands, cohesive energy, form. energy, self-consistent calcs. 7-21995
 GaAs epilayers, MOCVD on Si for solar cell appls. 7-27928
 GaAs epilayers, plasma enhanced metalorganic CVD 7-46336
 GaAs epilayers grown on Ge or Ge/Si substrates, defects 7-21778
 GaAs, epitaxial film on (001) oriented Si and Ge substrates, structural props. 7-58687
 GaAs epitaxial film shallow homojunction solar cells fabrication by Zn solid state diffusion method 7-17860
 GaAs epitaxial films, domain form., crystallographic analysis 7-58690
 GaAs epitaxial films, growth by close-spaced vapour transport, unwanted doping, X-ray diffr., SEM obs. 7-27187
 GaAs epitaxial films, MOCVD growth using tertiarybutylarsine source 7-59439
 GaAs epitaxial films, switched laser MOVPE stepwise monolayer growth 7-13372
 GaAs, epitaxial growth, $\delta(z)$ doping layer, electronic states 7-52729
 GaAs, epitaxial growth, thermodynamic equilb. displacement controlled 7-53616
 GaAs epitaxial layer, EL2 midgap electron trap prod. by rapid thermal annealing, DLTS study 7-64154
 GaAs epitaxial layers, OMVPE growth on Si (100) 7-3190
 GaAs epitaxial layers, vacancy doping 7-6656
 GaAs epitaxial layers, MOCVD grown, influence of growth parameters on residual impurities 7-7047
 GaAs epitaxial layers, native deep level defects 7-12888
 GaAs, epitaxial layers, grown in temp.-gradient field, effects on dislocation density 7-13393
 GaAs epitaxial layers, large scale MOVPE growth 7-22552
 GaAs, epitaxial layers, selective growth in MOMBE and MOCVD systems 7-22555
 GaAs epitaxial layers, OMCVD growth, optimisation using photoluminesc. analysis 7-39396
 GaAs epitaxial layers, MOCVD growth, boundary layer effects, photoluminesc. study 7-64923
 GaAs epitaxial layers and heterostructures grown on Si substrates, material props. 7-7046
 GaAs epitaxial layers grown directly on Si (100) by low press. MOVPE 7-27924
 GaAs epitaxial nucleation and growth kinetics, substrate orientation depend., numerical anal. 7-64020
 GaAs epitaxial wafers, highly uniform growth by large capacity MOCVD reactor 7-22551
 GaAs etalons, pulsed optical logic 7-57412
 GaAs, etching in Ar-tetrachloromethane RF discharge 7-32167
 GaAs, excimer laser projection etching 7-13662
 GaAs excimer-laser-stimulated CVD, polycryst. thin film growth and props. 7-64912
 GaAs, exciton-exciton and exciton-electron collisions, ultrafast phase relaxation 7-12618
 p-GaAs, excitons bound to pairs of shallow impurities 7-45169
 GaAs FET arrays, electrical parameter mapping 7-32438
 GaAs, FTIR spectra of acceptors, electronic intrasite transitions and local vibr. modes 7-53377
 GaAs, fast-neutron irradiated, electrical behaviour during thermal recovery 7-13029

III-V semiconductors continued

- GaAs faulted dislocation dipoles, electron diffr. and high-resolution TEM studies 7-44551
 GaAs, femtosecond carrier dynamics 7-58829
 GaAs filled nonlinear Fabry-Perot resonator, picosec. light pulse changes (*Russian*) 7-50620
 GaAs, film, substrate for CaF_2 epitaxial growth 7-39204
 GaAs film on NaCl, heteroepitaxial growth and composition 7-7052
 GaAs films, dense electron-hole plasmas, picosecond dynamics, acoustic phonon generation 7-45373
 a-GaAs films, dynamics of laser annealing by transient grating method 7-12122
 n-GaAs films, electron-hole plasma stratification and blue luminesc. near static domain 7-52666
 GaAs films, initial stages of MBE growth on Si (100) 7-63995
 GaAs films, MBE growth and structural characterisation 7-21775
 n-GaAs films, magneto-optical studies under high hydrostatic press. 7-13247
 GaAs Films, vacuum chemical epitaxy 7-39406
 GaAs films on amorphous insulating substrates, laser recrystallisation 7-38397
 GaAs films on oxidised Si, zone melting recrystallisation 7-38396
 n-GaAs, free carrier IR absorpt. spectra, scattering mechanisms, RPA calcs. 7-2604
 GaAs Fresnel waveguide grating lenses, aberration corrected, simulation 7-26036
 GaAs, fundamental energy gap, temp. depend. 7-7115
 GaAs gas phase epitaxial growth, layer thickness uniformity, flow conditions depend. meas. and model calcs. 7-52348
 GaAs, giant exciton resonance in nonlinear optical activity 7-45167
 GaAs growth mechanisms, in situ RHEED 7-53603
 GaAs, Hall effect measurement in the diamond anvil high-pressure cell 7-30041
 n-GaAs, Hall factor calcs. 7-52657
 GaAs, heavily doped, carrier-carrier and carrier-dopant interactions 7-21903
 GaAs heterostructures, valence subbands, excitons and luminescence 7-7321
 GaAs heterostructures, noise meas. using SQUID flux-transformer-coupled instrument 7-18830
 GaAs high quality layers grown on Si by MOCVD 7-27922
 GaAs, high temp. annealing, prevention of thermal surface damage 7-39546
 GaAs, high-resistivity semiconductor, deep centres, determ. by optical transient current spectroscopy 7-52498
 GaAs, highly doped, polarised hot electron photoluminescence 7-46121
 GaAs highly doped quantum wells, mobility enhancement 7-64325
 GaAs, homoepitaxial growth, cross hatch defect structure 7-45054
 GaAs, horizontal Bridgman growth, semi-insulating props. characts. 7-64896
 GaAs, hot anti-Stokes luminesc., picosecond spectroscopy 7-22336
 GaAs, hot electron spectroscopy, extreme nonequib. electron transport dynamics 7-12726
 GaAs, hot optically excited carriers in a spin-split-off subband, energy relax. 7-22302
 GaAs, hot-electron 1/f noise 7-21927
 GaAs hot-electron temperature measurement, method 7-52623
 GaAs, hydride VPE layers, deep level incorporation and background doping 7-17120
 GaAs, IR imaging 7-32238
 GaAs, IR tomography and transmission images, numerical processing 7-32236
 GaAs, identification of EL2 defect 7-38502
 GaAs, impact ionisation, soft-threshold lucky drift theory, mean free path calcs. 7-64256
 GaAs, impact ionisation coeffs., lucky drift model including soft threshold energy 7-64258
 GaAs, impurity atom site location using channelling enhanced microanalysis 7-38023
 n-GaAs impurity bands and band tailing 7-21809
 GaAs, impurity doping by photonuclear reactions 7-16589
 GaAs in MIS struct., light scatt. from inversion layer 7-3033
 GaAs, inhomogeneous characteristics, photoconductivity and optical absorption meas. 7-32439
 GaAs injection laser, twin-stripe, lateral behaviour, self-consistent model 7-15861
 GaAs interatomic force consts. and normal modes, group theoretical method calcs. 7-32588
 GaAs, internal thermal conversion, material for integrated circuits 7-12767
 n-GaAs, intervalley processes, nonequib. phonon spectroscopy and hydrostatic compression, Monte Carlo study 7-58425
 GaAs, inversion layers, hot free electron gas, intraband absorpt. coeff. calc. 7-33083
 GaAs inverted rib, phase modulators grown by VPE, optical and electro-optical anal. 7-31450
 GaAs, ion implant depth profiles, channelling, Monte Carlo simulation 7-51811
 GaAs, ion implanted, flash tube annealing 7-39551
 GaAs, ion implanted, rapid thermal annealing, review 7-58296
 GaAs, ion implanted, stoichiometry violation, electron microscopy studies 7-12303
 GaAs, ion implanted and laser irradiated, defect studies 7-32432
 GaAs, ion irradi. high-resistivity layer, thickness and resistance, free carrier density and cryst. orientation dependence 7-58354
 GaAs junction, temp. meas. using capacitance change of space-charge region 7-48742
 GaAs, LEC, semi-insulating, undoped, C origin and melt comp. depend. 7-17410
 GaAs, LEC, undoped, stoichiometry 7-53563
 GaAs, LEC grown, obs. of Ga precipitates 7-32663
 GaAs, LEC grown, threshold for dislocation form., role of cryst. dia. and impurity hardening 7-53551
 GaAs, LEC growth, solid-liq. interface, meniscus shape, X-ray image processing appl. 7-17406
 GaAs, LEC growth configuration, thermal stresses, effect of liq. encapsulation, thermoelastic anal. 7-59414
 GaAs, LEC growth for IC technology appls. 7-64894
 GaAs LEC semi-insulating crystals, pure and In-doped, IR absorpt. WRT resistivity 7-64629

III-V semiconductors continued

- GaAs, LEC single cryst. homogeneity, effect of strong mag. field 7-53549
- GaAs LEC substrates, EL2 deep donor kinetics under annealing, IR absorpt., DLTS, Hall effect meas. 7-32955
- GaAs LEC wafers, cathodolum. mapping, IR absorpt., X-ray topography obs. 7-33462
- GaAs, LEC-grown wafer, EL2 conc., stress distrib., near-IR absorption mapping 7-52522
- GaAs, LPE from soln. in laminar flow, high growth rates 7-33605
- GaAs LPE layers, heavily doped and compensated, hopping cond., density of states at Fermi level, carrier conc. determ. 7-2753
- GaAs LPE on channelled (100) GaAs substrates 7-13391
- GaAs, large dislocation-free cryst. growth for LSI appls. 7-64895
- GaAs laser diode, single-quantum well, carrier temperature and wavelength-switching 7-43097
- GaAs, laser evaporation, spectroscopic study 7-58324
- GaAs laser excited with several electron beams, light pulse formation 7-43098
- GaAs laser induced etching in carbon tetrachloride atm., fluoresc. 7-59700
- GaAs, laser MOVPE growth 7-33580
- GaAs, laser material, intervalence band absorpt. coeff. calc. 7-3015
- GaAs, laser-induced damage and ion emission at $1.06\ \mu\text{m}$ 7-37008
- GaAs, laser-induced melting and nonlinear optical studies 7-12432
- GaAs, lattice dynamics and electron-phonon interactions, quasi-ion approach calcs. 7-58422
- GaAs, Laue zone effects, nonzerth order, atom location by channelling enhanced microanal., X-ray fluorescence anal. 7-46905
- GaAs layers, effect of impurities on solid phase epitaxial growth 7-16907
- GaAs layers, LPE growth from Ga-As-Bi soln., kinetics, edge growth effects 7-39444
- GaAs layers, MBE, oval defects 7-59433
- GaAs layers, MOVPE, Zn acceptor impurities, magnetophotolum. 7-22308
- GaAs layers and quantum well struct., MOVPE growth chemistry 7-22550
- GaAs, length scale near metal-insulator transition 7-52425
- GaAs, longitudinal optical phonons, interaction with nonequilib. plasmons 7-45192
- GaAs, low frequency $1/f$ noise, new scale invariance 7-12770
- GaAs, low-frequency Raman scattering anomaly 7-27710
- GaAs MBE films, oval defects and whiskers 7-13364
- GaAs, MBE growth, acceptor impurity background reduction 7-3173
- GaAs, MBE growth, defect reduction using superlattice structures 7-13359
- GaAs, MBE growth, transient behaviour, RHEED oscillations 7-64904
- p-GaAs, MBE growth of high quality films (*Chinese*) 7-33566
- GaAs MBE heteroepitaxial layers, lattice distortions, X-ray diffr. and Raman studies (*Japanese*) 7-27219
- GaAs, MBE initial growth stage on (100) Si substrate, RHEED, AES and TEM 7-52356
- GaAs MBE layer growth and surface anal. (*Korean*) 7-2417
- GaAs MBE layers, bias-dependent capture-emission processes, DLTS anal. 7-64166
- GaAs, MBE layers, deep level defects, passivation by H_2 plasma exposure 7-21850
- GaAs MBE layers, deep level defects and impurities 7-22051
- GaAs MBE layers, oval defects, particulate effects during growth 7-21194
- GaAs MBE layers on Si (100), crystalline quality, rapid thermal annealing effects 7-12519
- GaAs MBE substrate refractory metals growth 7-21755
- GaAs MESFET and JFET devices, elec. resist., Hall effect, influence of electronic subband mag.; depopulation 7-38740
- GaAs MESFETs, reactive ion etching, DC characteristics (*Japanese*) 7-59701
- GaAs, MISS, common anion rule, density distrib., photoionisation 7-38765
- GaAs, MOCVD, gas phase depletion and flow dynamics in horizontal reactors 7-17433
- GaAs, MOCVD, H_2 carrier gas effect 7-17432
- GaAs, MOCVD, plasma stimulation, growth kinetics, elec. props. 7-22548
- GaAs, MOCVD, uniform growth on multi-wafers 7-22536
- GaAs, MOCVD growth, thermal decomp. rates 7-22540
- GaAs, MOCVD growth on Ge substrates for high efficiency tandem solar cell appl. 7-3671
- GaAs MOCVD growth on Ge (100) and Si (100) substrates, antiphase and single domains 7-27925
- GaAs, MOCVD growth on Si, band gap energy and stress 7-38368
- GaAs MOCVD growth using $\text{CIME}_2\text{GaAsEt}_3$ adduct, chemisorption and thermal heterogeneous decomp. 7-22558
- GaAs, MOCVD in inverted stagnation point flow, deposition from TMAs and TMGa 7-22531
- GaAs MOCVD layers, lateral growth mechanisms 7-64032
- GaAs, MOCVD layers on Si substrates with superlattice intermediate layers, DLTS studies 7-38501
- GaAs, MOVPE, laser assisted, selective area irr., carrier conc. 7-22545
- GaAs, MOVPE growth, flow patterns in vertical reactors 7-22535
- GaAs, MOVPE growth rate, orientation depend. 7-22556
- GaAs Mach-Zehnder interferometer, integrated waveguides as all-optical logic devices 7-25869
- GaAs, magneto-optical photoluminescent spectra studies 7-46148
- GaAs, maskless ion beam assisted etching 7-22923
- GaAs, melt grown, theoretical and expt. fundamentals of decreasing dislocations 7-53547
- GaAs, metal contacts, interfacial microstruct., elec. props., phase diagrams 7-45495
- n-GaAs metal-dielectric-semiconductor system, field effect, transistor studies 7-52841
- GaAs metalorganic MBE 7-53601
- GaAs, metastable defects, electronic Raman scatt. of nonequilibrium holes 7-26748
- GaAs, metastable state annealing 7-27297
- GaAs microelectronics, role of Schottky contacts (*German*) 7-52735
- GaAs microwave absorption transient spectroscopy for investigation of deep levels in semiconductors 7-52520
- GaAs, midgap levels, quenching and recovery spectra measured by double-beam photoconductivity 7-58769

III-V semiconductors continued

- GaAs, mixed electron-hole conductivity 7-58808
- GaAs modulation-doped heterostruc., quantum transport effects 7-52767
- GaAs molecular beam epitaxial layers, defect density reduction by thermal annealing, TEM study 7-45041
- GaAs molecular layer epitaxy, UV light effects, photo-assisted reactions and adsorpt. phenomena (*Japanese*) 7-7048
- GaAs, molten, temp. fluctuation meas., 1125 to 937 K 7-58123
- GaAs monolithic integrated optics, performance in space environment 7-26028
- GaAs, monovacancy electronic struct. and positron states, self-consistent LMTO calcs. 7-2536
- GaAs morphological stability in epitaxy, appl. to optoelectronic monolithically integrated structures 7-27172
- GaAs, multilayer struct., calc. elastic scattering spectra 7-13311
- GaAs multiple quantum wells, charge-carrier dynamics, contactless microwave photocond. meas. 7-21998
- GaAs, multiple quantum wells, absorption-induced optical bistability 7-57444
- GaAs n^+-n^+ strucs., quasi-elastic inter-Landau-level scattering processes 7-17086
- GaAs n-i-p-i doping superlattices, selective contacts, MBE growth through shadow mask 7-13356
- GaAs, n-type, electron-irradiated, photoionization cross sections of E levels 7-64152
- GaAs, n-type, proton irradiated, effects of annealing on optical properties 7-28155
- GaAs narrow n^+ wires, universal magnetoconductance fluctuations 7-64272
- GaAs, near-surface structure, analysing He^+ ion beam effects 7-7808
- GaAs, negative magnetoresistance and electron localisation in the region of a metal-insulator transition 7-12737
- GaAs, neutral shallow donor inter-excited-state transitions, far IR photocond. in mag. field study 7-22249
- GaAs, neutron transmutation doped, thermal annealing effects, channelling anal. (*Chinese*) 7-12178
- GaAs, neutron transmutation doped, variable range hopping studies 7-33012
- GaAs, neutron-irradiated, vacancy annealing, positron-lifetime study 7-64727
- GaAs, nonlinear refractive index, dispersive nonlinearities meas. 7-43192
- GaAs nonradiative states of optically illuminated sample, phonon detection by superconducting tunnel junction 7-3074
- GaAs, nucleation and growth on Ge, antiphase boundary struct. 7-2420
- GaAs, OMVPE, low pressure growth from trimethylgallium+AsH₃ 7-17439
- GaAs, ohmic contact, form. using ion beam mixing 7-21299
- GaAs, ohmic contact resist. limitations 7-52838
- a-GaAs, optical absorpt. and refractive index spectra 7-27735
- GaAs, optical nonlinearities, freq. depend. 7-25867
- GaAs, optical reflection anisotropy due to surface band bending 7-39062
- GaAs, optically induced far-IR absorption from residual acceptors 7-22287
- GaAs, organometallic VPE growth, use of tertiarybutylarsine 7-45047
- n-GaAs, oscillations and chaotic current fluctuations 7-64253
- GaAs, overlapping etch pits, density, evaluation technique 7-32443
- GaAs p-n homojunction diode, photocurrent meas. of defect distribution 7-32851
- GaAs, p-n junction, scanning tunneling potentiometry study 7-45439
- GaAs p-n junction, space charge region, electrooptic effect investig. 7-52756
- GaAs PIN electro-optic travelling-wave modulator at $1.3\ \mu\text{m}$ 7-1287
- GaAs, passivation, by a-P and alkali metal polyphosphides 7-39778
- GaAs, patterning using photoelectrochem. etching and focused ion beams 7-22924
- GaAs, phonon and plasmon deformation potentials, FIR spectra under uniaxial stress 7-26886
- GaAs, phonon dispersion, dispersive corrections to continuum elastic theory 7-26887
- GaAs, phonon hot spot, subTHz acoustic phonon emission 7-2118
- GaAs, phonon-plasmon coupling in electron transport 7-33041
- GaAs photocathodes, NEA, photoelectron energy spectra 7-13325
- GaAs photoconductive device, drive for synchronously operated streak camera 7-18903
- GaAs, photoconductivity, slow-relaxation phenomena 7-58837
- GaAs, photoconductivity oscillations, monochromatic IR illumination in mag. field 7-12763
- GaAs, photoconductivity and Hall voltage kinetics, recombination and scattering centre recharging 7-27364
- GaAs, photoelectrochemical etching of holographic gratings 7-26051
- n-GaAs, photoelectrochemical etching, orientational depend. 7-65224
- GaAs photoemission electron source, operating experience 7-41535
- GaAs, photoholes in the spin-split band, energy relax. and spin depolarisation 7-22301
- GaAs, photoluminescence lines, mag. and strain field splitting 7-3079
- GaAs photoluminescence rel. to Si substrate orientation 7-53411
- GaAs photorefractive, enhanced two-beam mixing gain using alternating electric fields 7-43203
- GaAs, photorefractive beam coupling with picosec. pulses 7-31386
- GaAs, photorefractive effect, temperature and intensity dependence 7-45951
- GaAs picosecond electro-optic sampling 7-53278
- GaAs, picosecond phase coherence, orientational relax. of excitons 7-16948
- GaAs, piezoelectric, SAW slowness surfaces 7-38315
- GaAs, plasma etching damage, Raman scatt. study 7-54023
- GaAs, plasma etching in H glow discharge 7-32168
- GaAs, plastically deformed, spatial distrib. of dominant electron and hole traps 7-7160
- GaAs, plastically deformed, Hall effect meas. 7-27351
- GaAs, plastically deformed or electron or neutron irradiated, antisite defects 7-37987
- GaAs, point defects, props. and processes, dislocation form. and characterisation (*Japanese*) 7-7151
- GaAs point focus concentrating solar cell arrays for spacecraft 7-3662
- GaAs, polar semicond., carrier-carrier interaction and picosecond phenomena 7-45309
- GaAs polycrystalline solar cells, influence of grain boundaries on performance 7-17892

III-V semiconductors continued

- GaAs polycrystalline solar cell, electron beam generated carriers in presence of grain boundaries 7-64262
- GaAs, polycrystalline thin films, RF sputter deposition on silica substrates, light transmission props. 7-46320
- GaAs, positron lifetime, electron beam effects and temp. depend. 7-39280
- GaAs, proton bombard., optoelectronic effects 7-21295
- GaAs, proton bombarded, H platelets, TEM obs. 7-12164
- GaAs pure and Si, Mn or Cu doped crystals, impurity and defect props., heat treatment, photolum. studies 7-39163
- GaAs quantised inversion layers, hot 2D electron gas, spectral acoustic phonon emission intensity 7-52452
- GaAs quantum Hall effect, resistance meas. appl., US legal unit monitoring 7-18808
- GaAs quantum well structures, metal-insulator transition due to surface roughness scatt. 7-27400
- GaAs quantum wells, 2D hot-electron mobility 7-45470
- GaAs quantum wells, band offsets, inelastic light scatt. studies 7-7362
- GaAs quantum wells, electron interference effects, obs. of bound and reson. states 7-64334
- GaAs quantum wells, hot-carrier phonon interactions, steady-state and picosecond meas. 7-12837
- GaAs quantum wells, n-modulation-doped, negative absolute mobility of holes 7-7337
- GaAs quantum wells, optical Stark effect on excitons 7-31384
- GaAs quantum wells, optical high-field transport expts. 7-52638
- GaAs quantum wells, space-charge induced, inelastic light scattering by electronic excitations in semiconductor heterostructures 7-13171
- GaAs, radiation-induced defects, review 7-48201
- GaAs, Raman phonon piezospectroscopy, IR meas. 7-64647
- GaAs, Raman scatt. by LO phonons, interference effects 7-59213
- GaAs, rapid thermal annealing, heating behaviour 7-21258
- GaAs, Rayleigh wave propag., 7-2334
- GaAs, refractive index dispersion, Fabry-Perot cavity oscillations obs. 7-59171
- GaAs, residual acceptor assessment, Raman and selective pair luminescence studies 7-26771
- GaAs, resistance standard appl., precise comparisons of quantized Hall resistances 7-18809
- GaAs sawtooth doping superlattices, prep., LED and laser appl. 7-7372
- GaAs sawtooth doping superlattices, photoluminescence, transport props. 7-52825
- n-GaAs, sawtooth gratings, photoelectrochemical fabrication 7-50726
- GaAs, scanning DLTS study of deep level defects 7-21865
- GaAs, Schottky barrier formation, effect of surface annealing 7-12785
- GaAs, Schottky barrier lowering by submicron ohmic contacts 7-7332
- GaAs Schottky-barrier behaviour, Monte Carlo simulation 7-45491
- GaAs Schottky-barrier formation and microscopic metal clusters 7-45497
- GaAs, secondary electron emission, effect of illum. in space charge region 7-17374
- GaAs, selective growth by reduced press. MOCVD 7-53627
- GaAs, semi-insulating, AL metallisation, electromigration failure anal. 7-44927
- GaAs, semi-insulating, deep levels, nondestructive microwave DLTS measurements 7-45210
- GaAs, semi-insulating, IR light scattering from defect centres 7-64620
- GaAs, semi-insulating, LEC grown, midgap native donor concentration 7-73547
- GaAs, semi-insulating, nonstoichiometry study, lattice parameter meas. 7-38220
- GaAs, semi-insulating, photoluminescence imaging using laser scanning microscope 7-53384
- GaAs, semi-insulating, switching effect, deep level spectroscopy appl. 7-38630
- GaAs, semi-insulating, surface photocond., surface topography meas. using scanning tunnelling microscopy 7-45376
- GaAs, semi-insulating bulk with thin conducting layer, optical DLTS distortions calcs. 7-58766
- GaAs semi-insulating cryst. charact., IC substrate appls. (Japanese) 7-6622
- GaAs, semi-insulating LEC crystals, thermal conversion, DLTS studies 7-7150
- GaAs semi-insulating thin wafers, EL2 defect and dislocation mapping, near-IR transmittance meas. 7-63605
- GaAs, semi-insulating wafer, inhomogeneity characterization by scanning photo-induced current transient spectroscopy 7-7164
- GaAs, semiconducting and semi-insulating LEC crystals, SEM-EBIC characterisation 7-51777
- GaAs, semiconducting/semi-insulating reversibility 7-21939
- GaAs semiconductor electrodes for H_2 production by photoelectrolysis of water 7-3723
- GaAs semiconductor/liquid junction device performance improvement 7-17098
- GaAs, semiinsulating, electrophysical props., dislocation effects 7-16557
- GaAs semiinsulating LEC substrate, elec. homogeneity evaluation, thermally stimulated drain conductance meas. 7-32954
- GaAs semiinsulating LEC wafers, radiative centres, local photoluminescence study 7-33458
- GaAs, semiinsulating LEC substrates, defect etching 7-59694
- GaAs semiinsulating slices, spatial inhomogeneities, near IR transmission imaging techniques 7-33400
- GaAs, shallow acceptor levels, photoluminesc. study 7-45209
- GaAs shallow-homojunction solar cells, junction depth effect on photovoltaic parameters 7-3673
- GaAs short $n^{++}nn^{++}$ structs., elec. transport props. in high elec. and mag. fields 7-33084
- GaAs short semicond. structs., photoexcited electron-hole plasma instability, numerical simulation photoexcited electron-hole plasma instability, numerical simulation 7-45367
- GaAs, single domain epitaxial growth on Ge (100) 7-22578
- GaAs single domain layer growth on Si wafers by MOCVD/MBE, heteroepitaxy 7-52357
- GaAs single quantum well, doubly resonant LO-phonon Raman scatt. via deform. pot., polarisation obs. 7-39114
- GaAs single quantum wells, free excitons, phase coherence and line broadening 7-45170
- GaAs single-junction solar cells, concentrator module with 19% efficiency 7-17906
- GaAs, single-particle excitations, dynamic correl. corrections, local density theory 7-45115

III-V semiconductors continued

- n-GaAs slabs, ionised-impurity-mediated free-carrier absorption 7-17335
- GaAs solar array design, weight-efficient rigid panel structure 7-13881
- GaAs solar cell concentrators, optimised top contact design 7-8385
- GaAs solar cell parameters, theoretical temp. depend. 7-23161
- GaAs solar cell with 25.5% efficiency AMO 7-3665
- GaAs solar cells, circulation meas. and spectral error reduction 7-13903
- GaAs solar cells, comparison with InP and Si cells in space 7-65484
- GaAs solar cells, depletion layer recombination effects on radiation damage hardness 7-13888
- GaAs solar cells, elec. parameter mapping by numerical image processing of light beam induced current topography 7-33051
- GaAs solar cells, fracture strength as function of manufacturing process steps 7-3696
- GaAs solar cells, perform. and temp. dependencies of proton irradiated n-p and p-n cells 7-3702
- GaAs solar cells, sequential irradiation effects of electrons and protons 7-13877
- GaAs solar cells, transient current studies of junction activity 7-8409
- GaAs, solar cells fabrication on Si substrates by MOCVD 7-23183
- GaAs solar cells for space appls., potential efficiency 7-65482
- GaAs solar cells for thermophotovoltaic appls. theoretical efficiency 7-59855
- GaAs solar cells with corrugated surface, computer code for performance eval. 7-3667
- GaAs solar cells with varying junction depths, spectral mismatch correction 7-65475
- GaAs solar concentrator cells, perform. under 1 MeV electron irradiation 7-3704
- GaAs solar panel performance of LIPS-II satellite 7-13883
- GaAs solar panels with LPE and metal organic CVD circuits, satellite power 7-65493
- GaAs, solid-phase-epitaxy, interface structure and impurity effects 7-2407
- GaAs space qualified solar cell production by organic metal CVD, performance testing 7-65492
- GaAs, space-charge layer effective mass in parallel mag. field 7-2469
- GaAs, sputtered, comp. depth profiles, AES, XPS, inverse Laplace transforms 7-22390
- GaAs, stepwise monolayer growth by switched laser MO-VPE 7-53626
- GaAs, stimulated Raman gain spectroscopy, below bandgap studies 7-22231
- GaAs, strain-induced defects, ERP anal. 7-45821
- GaAs, stress-induced doubly resonant Raman scattering 7-46029
- GaAs, sublattices direct resolution and identification by high-resolution TEM 7-37813
- GaAs submicron $n^{++}n^{++}$ multilayers, single impurity-assisted tunnelling 7-38710
- GaAs submicron wires, conductance fluctuations in magnetoresistance 7-38597
- GaAs, substrate, plasma deposition of C dielectric films 7-39420
- GaAs substrate, ZnSe MBE layers, lattice mismatch effects, TEM, photolum. and X-ray diffr. studies 7-45042
- GaAs substrate for GeSi thermally evaporated epitaxial heterolayers, Si distrib. (Russian) 7-63988
- GaAs substrate for MBE growth, thermal etching 7-7861
- GaAs substrate for MBE growth of magnetic Fe films 7-27584
- GaAs substrates, laser-induced metal and alloy plating, silicide form. 7-39448
- GaAs, substrates, multi-technique approach to defect microstructure characterisation 7-52215
- GaAs substrates, W films, electrical resistivity after high temp. annealing 7-64366
- GaAs substrates and devices, surface anal., SIMS appl. 7-22417
- GaAs, superheating during picosecond laser melting 7-12246
- GaAs superlattice solar cell structure with high efficiency and radiation tolerance 7-8414
- GaAs surface, anisotropically etched, p-n junction formation by MOCVD 7-13374
- GaAs surface, Fermi level unpinning by flowing water 7-58843
- GaAs surface, formation of gratings in laser photoemission wet etching 7-8205
- GaAs surface, H_2S adsorption, orientation and temp. depend. 7-58634
- GaAs surface, interaction with H_2 7-58632
- GaAs, surface and bulk nonradiative recombinations, photoacoustic study 7-33438
- GaAs surface cleaning using ECR radical beam gun 7-54028
- GaAs, surface morphology of crystals grown by gas-source MBE using trimethylgallium and As_4 7-17424
- GaAs, surface morphology, in HNO_3 -HF- H_2O etching system (Korean) 7-28225
- GaAs, surface oxidation, effect of anodizing conditions 7-13669
- GaAs surface oxidation, AES, XPS and ellipsometry studies 7-22927
- GaAs, surface oxide desorption, temp. meas., Auger anal. 7-58608
- GaAs, surface potential barrier in ion-etched (100) surface, electron-voltaic effect 7-7819
- GaAs, surface recombination velocity and bulk minority carrier lifetime 7-17037
- GaAs, surface region, heat-treated, photoluminescence, antisite defect obs. 7-39167
- GaAs, surface structure with adsorbed Te 7-12460
- GaAs surfaces, picosecond laser melting and evaporation 7-12120
- GaAs surfaces, picosecond laser interactions, time-resolved optical studies 7-12134
- GaAs thin film photovoltaic cells, large-scale manufacture, hazard characterisation of AsH_3 gas and $GaAs$ waste 7-39998
- GaAs thin films, grain boundaries, electronic props. 7-7172
- GaAs thin films, on glass substrates, transport props. 7-2742
- GaAs thin semi-insulating wafers, EL2 distrib., dislocation network correl., near IR absorpt. maps and X-ray topographs 7-21203
- GaAs third order elastic constants, US displacement interferometry 7-2087
- GaAs, transient thermal processing 7-16601
- GaAs, transport props., charge collection microscopy 7-52649
- GaAs ultrafast all-optical logic gate based on MQW bistable device 7-57415
- GaAs, ultrathin layers, liquid phase epitaxial growth on GaAlAs substrate 7-53645
- GaAs, undoped, thermal activation of plastic deform., 528-813K 7-6710
- GaAs, undoped semi-insulating, dislocations, deep trap levels, FET meas. (Chinese) 7-12643

III-V semiconductors continued

- GaAs, uniformity imaging 7-32481
 GaAs, V_F-T characteristics of p-n junction at low temp. (*Chinese*) 7-12792
 GaAs, VPE grown, defect formation leading to deep levels, review 7-64151
 GaAs, VPE growth, reaction mechanisms 7-58693
 GaAs, VPE growth in hydride system, elec. props. 7-2751
 GaAs, valence charge density, X-ray diffr. study, comparison with calculated results (*French*) 7-16940
 GaAs, vapour etching, buried interface, carrier traps 7-28213
 GaAs, variation of EL2 with As press. during heat treatment 7-58770
 GaAs wafers, LEC-grown, semi-insulating, two-dimens. high-resolution EL2 topography 7-53381
 GaAs waveguide, thermal index changes by optical absorpt., all-optical signal processing 7-31381
 GaAs with Al honeycomb substrate, flat-plate space solar panels interconnector design 7-13879
 GaAs, X-ray diffr., anomalous dispersion effects, thermal vibr. and bonding charges 7-44733
 GaAs, X-ray topographic examination 7-32225
 GaAs: S, Sn, epitaxial layers, photoluminescence spectra 7-46095
 GaAs: Si(Se)(Zn)(Be), ion implanted, rapidly annealed, damage removal process 7-17043
 GaAs: Al, surface layer, degree of disordering, effect of dopant 7-63929
 GaAs: Al⁺(P⁺), ion implantation damage 7-38024
 GaAs: B, as-grown Czochralski crystals, EPR signal 7-38935
 GaAs: B, internal friction temp. depend. studies 7-38112
 GaAs: B, ion implanted, near-intrinsic and extrinsic photocapacitance due to the EL2 level 7-7147
 GaAs: B, ion implanted, struct. and damage distrib., TEM study 7-51893
 GaAs: B buried isolation layer form. by focused ion beam, FIBI-MBE system 7-51804
 GaAs: Be⁺, ion implanted, residual microstruct., TEM studies 7-32675
 GaAs: Bi, epitaxial layers, purification by Bi doping 7-58301
 GaAs: C, impurity content meas., IR absorpt., room temp. meas. 7-22289
 GaAs: C, impurity levels determ. 7-32949
 GaAs: C, LVM absorpt. temp. depend. (*Chinese*) 7-59225
 GaAs: C, low C conc., crystal growth using pyrolytic BN coated graphite 7-59398
 GaAs: C, O, trace determ. by ³He-activation anal. 7-58308
 n-GaAs: Co, impurity double acceptor state, Hall effect and resistivity meas., temp. and press. depend. 7-12656
 GaAs: Cr, deep levels characterisation using photo-induced transient spectroscopy 7-16973
 p-GaAs: Cr, excited and metastable states of Cr-related double centres 7-7153
 GaAs: Cr, meas. of residual stress by Cr-related luminesc. lines 7-7726
 GaAs: Cr, photorefractive behaviour using two-beam coupling 7-31387
 GaAs: Cr, Se, impurity complex, luminescence study 7-53396
 GaAs: Cr free and metallised surfaces, SAW absorpt. meas., hybrid SAW semicond. device appls. 7-52217
 GaAs: Cr impurity level studies 7-33084
 GaAs: Cr semiinsulating LEC wafers, microhardness cartography 7-32886
 GaAs: Cr/ZnSe heterostructure, interface stress 7-38352
 GaAs: Cs, impurity ion beam effects, SIMS depth profiling 7-22419
 GaAs: Cu, neutral state of deep acceptors, photoluminescence spectra, Jahn-Teller effect 7-64149
 GaAs: Er MBE layer, dopant trapping level, photolum. obs. 7-44581
 GaAs: Ge, Se, diffused contact regions, rapid thermal annealing 7-17103
 GaAs: H, ion implanted, damaged layers, IR Raman probing 7-59191
 GaAs: H amorphous sputtered films, AC cond. studies 7-21947
 a-GaAs: H, F, electronic struct., dangling bonds, cluster-Bethe lattice method calcs. 7-12592
 GaAs: Ho, electroluminescence and injection currents 7-13232
 GaAs: In, B, electrical props., role of residual B impurity, liquid encapsulated Czochralski growth 7-45312
 GaAs: In, doped and undoped, EL2 maps from computer based IR image analysis 7-32237
 GaAs: In, LEC growth, annealing, solid soln. hardening, dislocation density, elec. props. 7-17404
 GaAs: In, lattice distortions, NMR study 7-2933
 GaAs: In, low In conc., LEC cryst. growth employing thermal stress anal. 7-46305
 GaAs: In, semi-insulating substrates and ingots, In content, nondestructive meas. 7-58305
 GaAs: In, strain effects, electrorefl. and photocapacitance study 7-22224
 GaAs: In, VPE growth, isoelectronic In doping, etch pit densities 7-46340
 GaAs: In (B)(Si), dislocation free crystals, LEC grown, microscopic defects, eutectic etching 7-16545
 GaAs: In annealed substrates, In distribution in surface region 7-44959
 GaAs: In crystals, dislocations, in situ X-ray topographic studies 7-21207
 GaAs: In crystals, LEC growth, grown-in dislocation elimination 7-22465
 GaAs: In LEC crystals, dislocation etch pits 7-38000
 GaAs: In MBE layers, defect density reduction by isoelectronic In doping 7-3176
 GaAs: In(Cr), doped and undoped, microdefects obs. by IR light scatt. tomography 7-32662
 GaAs: Mg, MOVPE, p-type doping using an organometallic Mg precursor 7-22522
 GaAs: Mg MBE layers, photoluminescence 7-22295
 GaAs: Mg⁺, formation of p-type layers using ion implantation and rapid thermal annealing 7-45311
 GaAs: Mo (W), impurity electronic struct. excitation and ionisation, cluster approach, X_α multiple scatt. calcs. 7-2535
 GaAs: Nb photolum., Zeeman spectra study 7-39175
 GaAs: Ni, acceptor like electron trap, DLTS study 7-7166
 n-GaAs: O, semi-insulating, impurity centres, electron capture 7-52643
 GaAs: O LEC crystals, deep photoluminesc. band, fine struct. 7-46110
 GaAs: P, ion implanted and pulse laser annealed, Raman study 7-6653
 GaAs: Pr(Nd)(Yb), IR photoluminescence of rare earth impurities 7-46922
 GaAs: S, Si epitaxial layers, close space vapour transport growth, photoluminescence and electrical props. 7-21776
 GaAs: S layers obtained by gas-phase epitaxy, electrophysical props. 7-7418
 GaAs: S surface elec. props. modification by plasma exposure 7-27346
 GaAs: Sb, deep level formed by Sb doping 7-52496
 GaAs: Se, ion implanted, annealing mechanism 7-26777
 GaAs: Si, annealing behaviour of impurities in presence of stress 7-65060
 GaAs: Si, dislocations, STEM and CTEM micrographs 7-1825

III-V semiconductors continued

- GaAs: Si, distorted impurity configuration 7-52501
 GaAs: Si, electrical props. of p-type layer 7-12722
 GaAs: Si, FET structs., rapid optical annealing for improved uniformity 7-16620
 GaAs: Si, flow-rate modulation epitaxy, Si planar doping 7-17443
 GaAs: Si, ion implanted, amorphisation and epitaxial regrowth, defect depth profiles 7-12088
 GaAs: Si, ion implanted, rapid thermal annealing effects 7-21259
 GaAs: Si, ion implanted and rapid thermal annealed, activation efficiency, crystal stoichiometry effects 7-51791
 GaAs: Si, MBE growth, carrier concentration, dislocation effects 7-58682
 GaAs: Si, semi-insulating, ion implanted, LEC growth, elec. activation efficiency, stoichiometry dependence 7-46298
 GaAs: Si, shallow donor neutralisation by atomic H, photoluminescence study 7-22294
 GaAs: Si, Be, MBE, dopant interaction 7-52362
 GaAs: Si, Ge, local modes, isotopic fine struct., IR spectra 7-38145
 GaAs: Si, Se MOCVD epitaxial layer photolum. spectral shift and doping efficiency obs. (*Japanese*) 7-45076
 GaAs: Si heteroepitaxial growth on sapphire, low press. MOCVD three-step method 7-27927
 GaAs: Si wafer, failure, dislocation distrib., etching 7-12067
 GaAs: Si/Al_{0.25}Ga_{0.75}As quantum wells, photolum. studies 7-39178
 GaAs: Si/AlAs multiquantum well structs., band struct. and photolum. studies 7-12843
 GaAs: Si: AlAs: Si superlattices, MBE growth and electrical props. 7-22052
 GaAs: Si⁺ wafers, implant at. profiles, planar and residual channelling effects 7-12181
 GaAs: Si(B)-Ga_{0.25}Al_{0.75}As: Si(B) quantum wells, ion implanted, TEM and photolum. studies 7-58865
 GaAs: Si(Be)(Mg), rapid annealing, temp. depend. of damage removal and carrier activation 7-17032
 GaAs: Si(S), LEC grown, struct. defects, influence of Si and S doping 7-53550
 GaAs: Sn, epitaxial layers, current carrier distrib. 7-12530
 GaAs: Sn, photolum. spectra, line shape anal., conduction band to deep acceptor transition 7-46098
 GaAs: Sn epilayers, MOCVD using triethylgallium and tetraethyltin, characterisation 7-22515
 GaAs: Sn LPE layers, heavily doped, Mossbauer study 7-38967
 GaAs: Sn(Te)(Zn) surface layers, luminesc., electrophys. parameters, effect of annealing 7-64680
 GaAs: Te, annealing encapsulation props. of SiO₂, Si₃N₄ and Si_xN_yO₂ films 7-8030
 GaAs: Te, low press. OMVPE, Te doping, Hall effect, carrier conc., photolum. 7-21242
 GaAs: Te, struct. environment of dopant, study by EXAFS in fluorescence mode. 7-59300
 GaAs: Te films, flash evaporation, annealing, elec. props. 7-64373
 GaAs: Te VPE, vacancy-impurity complex capture, photolum. study 7-58678
 GaAs: Ti, optical spectra 7-7720
 GaAs: Ti³⁺, EPR 7-45811
 GaAs: V, electromodulation spectra, deep level energy positions 7-38496
 GaAs: V, photocond. props. and thermally stimulated currents 7-7284
 GaAs: V²⁺ (Cr²⁺) single crystals, acoustic relax. phenomena, phonon-impurity coupling, ultrasonic attenuation meas. 7-32581
 GaAs: Zn, ion damage and recryst. annealing, conversion electron EXAFS meas. 7-64821
 GaAs: Zn, ion-implanted, acceptor-associated emission, selective self-optical compensation effect 7-22304
 GaAs: Zn, Zn diffusion by open-tube technique 7-38260
 GaAs: Zn, Si, selective double diffusion using sputtered Si masks 7-51805
 GaAs: Zn epilayers, metalorganic CVD, Zn incorporation 7-63996
 GaAs: Zn(C) epilayers, low pressure MOCVD growth, impurity incorporation 7-59442
 GaAs/ (GaAl)As LOC lasers, MOCVD growth and characts. 7-25835
 GaAs/ Al epitaxial contacts, MBE growth 7-22488
 GaAs/ Al quantum wells, MBE growth, photoluminescence and absorption linewidth studies 7-7749
 GaAs/ Al_{0.38}Ga_{0.62}As lattice-matched superlattice photoelectrochem. electrodes, photocurrent spectra 7-45377
 GaAs/ Al_{1-x}Ga_xAs modulation-doped heterostructs., 2D electron gas mobility meas. and calcs. 7-12840
 GaAs/ Al_xGa_{1-x}As, superlattices, layered electron gas plasmons, Raman scatt., Green's functions calcs. 7-17313
 GaAs/ Al_xGa_{1-x}As 3D ICs, selection rule for epitaxial growth techniques, LPE, MOVPE and MBE 7-46326
 GaAs/ Al_xGa_{1-x}As heterostruct., 2-D density of states in extreme quantum limit 7-2455
 GaAs/ Al_xGa_{1-x}As heterostructs., 2D electron gas, polaron screening effects, optical absorpt. calcs. 7-2511
 GaAs/ Al_xGa_{1-x}As heterostructure interfaces, band discontinuities, electrical meas. 7-52814
 GaAs/ Al_xGa_{1-x}As heterojunction photodiodes, band discontinuities 7-58871
 GaAs/ Al_xGa_{1-x}As heterostruct. localisation and interaction in a strong mag. field 7-64343
 n-GaAs/ Al_xGa_{1-x}As multilayer heterostructs., nonlinear high-freq. effects during vertical transport 7-2694
 GaAs/ Al_xGa_{1-x}As multi-quantum well structs., photoluminescence studies 7-3078
 GaAs/ Al_xGa_{1-x}As modulated structs., MBE growth kinetics, RHEED studies 7-7066
 GaAs/ Al_xGa_{1-x}As modulation doped heterostruct., high temp. annealing effects (*Chinese*) 7-12805
 GaAs/ Al_xGa_{1-x}As MBE grown superlattices, effect of barrier config. and interface quality on props. 7-52790
 GaAs/ Al_xGa_{1-x}As quantum-well bound states, valence-band offsets 7-7313
 GaAs/ Al_xGa_{1-x}As quantum wells, excitonic transitions, photocurrent spectra studies 7-7816
 GaAs/ Al_xGa_{1-x}As RIE using CCl₂F₂, selectivity 7-22920
 GaAs/ Al_xGa_{1-x}As superlattices, magnetophonon oscills. damping, polar-optical phonon contrib. calcs. 7-27391
 GaAs/ Al_xGa_{1-x}As superstructure, TEM images, composition anal. by thickness fringes, simulation 7-38353
 GaAs/ Al_xGa_{1-x}As superlattices, optical transitions involving unconfined states, barrier width depend., photolum. spectra 7-52773

III-V semiconductors continued

- n^- -GaAs/ $\text{Al}_x\text{Ga}_{1-x}\text{As}/n^+$ -GaAs capacitors, accumulation layers magnetotunnelling obs. 7-12880
 GaAs/ $\text{Al}_x\text{Ga}_{1-x}\text{As}$, tunnelling through III-V low-barrier heterostructures 7-52799
 GaAs/AlAs 1-D MBE superlattice, struct. parameters, X-ray double cryst. diff. studies (*Chinese*) 7-12503
 GaAs/AlAs doped quantum well waveguides, IR intersubband absorpt. 7-59192
 GaAs/AlAs double barrier struct., electron transport, scatt. matrix theory 7-12822
 GaAs/AlAs heterostruct., transition layer form. during LPE 7-45074
 GaAs/AlAs MBE superlattice, interface struct., HREM study 7-17096
 GaAs/AlAs MQW structures, life-time-free switching of luminescence by elec. fields 7-52791
 GaAs/AlAs MQW structure, exciton-induced dispersion of electroreflectance at room temp. 7-53277
 GaAs/AlAs quantum wells, photoexcited transport 7-2674
 GaAs/AlAs quantum well structures, electroreflectance spectra and field-induced refractive index modulation 7-13135
 GaAs/AlAs single quantum well heterostructures confined by short-period superlattices, photoluminesc. 7-22296
 GaAs/AlAs superlattice, optical phonons and interface thickness, Raman scatt. studies 7-7705
 GaAs/AlAs superlattices, electronic band structure, pseudopot. method calc. 7-17084
 GaAs/AlAs superlattices, folded acoustical Raman line intensities 7-46050
 GaAs/AlAs/Mg/GaAs tunnel structs., current transport mechanisms 7-7357
 GaAs/AlAs/GaAs:Se heterojunctions, elec. behaviour, DLTS studies 7-7360
 p^+ -GaAs/AlGaAs, double barrier, hot electron energy distrib. study using resonant tunnelling electron spectroscopy 7-45447
 GaAs/AlGaAs 2D electron gas MBE structures, carrier mobility and density meas. 7-64321
 GaAs/AlGaAs heterostructs. on Si substrate, MOCVD and MBE growth 7-7883
 GaAs/AlGaAs modulation doped heterostructs., transport props. studies 7-52752
 GaAs/AlGaAs multi-quantum well heterostructures, optical gain, well width depend 7-46130
 GaAs/AlGaAs multiple quantum well structures, hot-carrier relaxation, femtosecond optical meas. 7-52750
 GaAs/AlGaAs multiple-quantum-well structures, shallow donors, far infrared spectroscopy 7-39121
 GaAs/AlGaAs pair-groove-substrate MQW laser with self-aligned stripe geometry 7-20260
 GaAs/AlGaAs quantum wells, MBE growth, interface disorder studies 7-7026
 GaAs/AlGaAs quantum wells, MBE growth and energy levels, photoluminescence meas. 7-7067
 GaAs/AlGaAs quantum wells and double heterostruct. lasers, chemical beam epitaxy, photolum. 7-22523
 GaAs/AlGaAs quantum well structures, MOCVD growth, photolum., TEM obs. 7-27929
 GaAs/AlGaAs quantum wells, Monte Carlo study of hot electron transport 7-52804
 GaAs/AlGaAs separate confinement heterostructure lasers, LPE prep. 7-10940
 GaAs/AlGaAs single and coupled double wells, energy depend. light hole mass, photolum. spectra anal. 7-38691
 GaAs/AlGaAs single heterojunction quantum well structs., photolum. characts. 7-46085
 GaAs/AlGaAs single quantum wells, interrupted MBE growth and temperature-dependent optical spectra 7-46082
 GaAs/AlGaAs superlattice, compositional disordering by focused ion beams 7-6695
 GaAs/AlGaAs superlattices, Si implanted, compositional disordering, SIMS studies 7-12091
 GaAs/AlGaAs superlattices, hydrogenic impurity ground level wave function calcs., variational procedure 7-12664
 GaAs/AlGaAs superlattice heterostructures, MBE on nonplanar substrates 7-59425
 GaAs/AlGaAs superlattices, valence band electronic struct., pseudopot. calcs. 7-64339
 GaAs/Al(Mn)(Ag) interfaces, interactions, XPS and elec. transport studies 7-7384
 GaAs/Au contacts, growth modes, AES, UPS, XPS and RHEED studies 7-21753
 GaAs/Au contacts, interface morphology 7-45020
 GaAs/Au-Ge/Ni ohmic contacts, ion implantation and metallisation prep. 7-22014
 n -GaAs/AuGe-Ni, ohmic contact fabrication RBS anal. 7-32840
 p -GaAs/AuZnNi/Ti/Au ohmic contacts, low-resistance 7-7385
 GaAs/Au(Cr) Schottky barriers, hole diffusion length, photon and electron excitation studies 7-2707
 GaAs/ $\text{Ca}_x\text{Sr}_{1-x}\text{F}_2$ (100) SOI structures, epitaxial GaAs films, antiphase disorder 7-52315
 GaAs/ CaF_2 system, MBE growth processes, growth chamber transfers 7-64902
 GaAs/CdTe heterojunction, defect and impurity states, photovoltage meas. 7-17065
 GaAs/dielectric guided-wave bistable devices, periodic coupling 7-57426
 p -GaAs/electrolyte, photoelectron emission spectra, thermodynamic consts. 7-12856
 GaAs/ $\text{Ga}_{1-x}\text{Al}_x\text{As}$ graded interface superlattice band struct. calcs. 7-58879
 GaAs/ $\text{Ga}_{1-x}\text{Al}_x\text{As}$ multilayered structures, polariton dispersion relations 7-7125
 GaAs/ $\text{Ga}_{1-x}\text{Al}_x\text{As}$ quantum well struct., exciton linewidth calcs., polar optical phonon scatt. 7-2491
 GaAs/ $\text{Ga}_{1-x}\text{Al}_x\text{As}$ (AlAs), short period superlattices, MOCVD growth, Raman scatt., AES, X-ray diff. 7-27386
 GaAs/ $\text{Ga}_{1-x}\text{Al}_x\text{As}$ heterojunctions, anomalous quantum Hall effects 7-17085
 GaAs/GaAlAs 2D electron gas, cyclotron resonance study 7-2676
 GaAs/GaAlAs disordered superlattices, carrier localisation obs. 7-12818
 GaAs/GaAlAs double quantum well structures, ambipolar carrier transport, optical TOF study 7-12802

III-V semiconductors continued

- GaAs/GaAlAs double-well superlattice, ultra-fast optical modulator 7-52801
 GaAs/GaAlAs graded gap superlattices, high velocity vertical transport 7-52802
 GaAs/GaAlAs HJFET and HJBT 7-52811
 GaAs/GaAlAs heterostructure, quantized Hall resistance measurement at the National Measurement Laboratory, Australia 7-14965
 GaAs/GaAlAs heterostruct. laser with monolayer superlattice, threshold currents 7-62698
 GaAs/GaAlAs planar MQW structure, nonlinear coupling of guided waves 7-11106
 GaAs/GaAlAs quantum-well structures, optical time-of-flight investigation 7-52800
 GaAs/GaAlAs single quantum wells, steady-state photoluminescence studies 7-7750
 GaAs/GaAlAs single quantum well laser, threshold current density 7-25816
 GaAs/GaAlAs superlattice, optical phonons and interface thickness, Raman scatt. studies 7-7705
 GaAs/GaAlAs superlattice structs., metalorganic MBE growth 7-7864
 GaAs/GaAlAs TEGFET, resistance laboratory unit determ., using quantum Hall effect 7-18812
 GaAs/GaAlAs ultrathin layer systems, MOCVD growth and struct. props. 7-7063
 GaAs/GaAlAs/GaAs heterostructure barriers, tunnel current and electron tunnelling times with mag. field 7-52810
 GaAs/GaInAs interface, EELS near a single misfit dislocation 7-33497
 GaAs/GaPAsSb, double heterostruct., LPE, lattice matching, X-ray diff., luminesc. 7-58884
 GaAs/Ge heterojunction interfaces, cyclic behaviour of band discontinuities 7-7365
 n -GaAs/ $\text{In}_x\text{Ga}_{1-x}\text{As}$ compositionally graded non-alloyed ohmic contacts 7-38695
 GaAs/Langmuir-Blodgett MISS devices, switching characts. 7-38751
 GaAs/ LiNbO_3 struct., SAW parametric generation with light pumping 7-63934
 GaAs/metal interface microstruct. and reactions, stability and elec. props., TEM and STEM studies 7-12515
 GaAs/metal Schottky barrier diode, electrical props. 7-27426
 GaAs/ n -AlGaAs MBE-grown selectively doped heterostructs., 2D electron gas, transport props. 7-21988
 GaAs/Ni Schottky barrier, current-voltage characts. under electron distrib. disturbance 7-52733
 GaAs/PTCDA rectifying junction, nondestructive semicond. props. eval. method 7-12876
 GaAs/ $\text{Ta}_{1-x}\text{Cu}_x$ amorphous thin-film diffusion barriers, thermal and structural stabilities 7-52321
 n -GaAs/Pi-Pt system, Schottky barrier height, doping depend. 7-2708
 GaAs/ZnSe interface, MOCVD grown, ZnSe film stoichiometry 7-39415
 GaAs-(Al,Ga)As double heterojunction lasers, dislocation control, electroluminescence 7-7046
 GaAs-(Al,Ga)As-GaAs heterojunction barrier, tunneling current, probe pressure effect 7-45441
 GaAs-(AlGa)As heterostructure, modulation-doped, valence band mixing, and optical emission 7-7344
 GaAs-(AlGa)As heterojunctions, low temp. elec. transport props. 7-33084
 GaAs-(AlGa)As inelastic light scattering by electronic excitations in semiconductor heterostructures 7-13171
 GaAs-(Ca,Sr) F_2 heterostructure interfaces, twinning, Raman spectra 7-13148
 GaAs-Al junction, interface states, DLTS study 7-58892
 GaAs-Al Schottky barrier contacts, MBE grown, interface reactions, vacuum annealing effects 7-45022
 GaAs- $\text{Al}_{0.37}\text{Ga}_{0.63}\text{As}$ quantum wells, photolum. studies, MBE growth, effect of interruption 7-39150
 GaAs- $\text{Al}_{0.3}\text{Ga}_{0.7}\text{As}$, thin single quantum well, MBE growth kinetics, normal and inverted interfaces 7-45045
 GaAs- $\text{Al}_{0.44}\text{Ga}_{0.56}\text{As}$ quantum wells, MBE growth, tunnelling assisted photon emission, photoluminescence meas. 7-46120
 GaAs- $\text{Al}_{0.4}\text{Ga}_{0.6}\text{As}$, intraband recomb., luminesc. spectra anal. 7-53387
 GaAs- $\text{Al}_{0.65}\text{Ga}_{0.35}\text{As}$, transverse junction stripe laser, lateral heterobarrier by diffusion enhanced alloy disordering 7-10929
 GaAs- $\text{Al}_{0.7}\text{Ga}_{0.3}\text{As}$ single quantum well, photolum., transient response to electric field, carrier lifetime 7-7757
 GaAs- $\text{Al}_{0.7}\text{Ga}_{0.3}\text{As}$ SQW structure, photolum. switching by pulsed elec. field 7-13197
 GaAs- Al_2O_3 , interface struct., dielectric film mol. beam epitaxial growth 7-38360
 GaAs- $\text{Al}_x\text{Ga}_{1-x}\text{As}$, multiple quantum well structs., expansion of electron-hole plasma, time-resolved Raman studies 7-22258
 GaAs- $\text{Al}_x\text{Ga}_{1-x}\text{As}$ -AlAs, p -type quantum wells, resonant Raman scatt. 7-22259
 GaAs- $\text{Al}_x\text{Ga}_{1-x}\text{As}$, internal photoemission method for determ. of band offsets 7-12832
 GaAs- $\text{Al}_x\text{Ga}_{1-x}\text{As}$, heterojunction form. anal. 7-39436
 GaAs- $\text{Al}_x\text{Ga}_{1-x}\text{As}$, superlattices, carrier behaviour, mag. field effect 7-45449
 GaAs- $\text{Al}_x\text{Ga}_{1-x}\text{As}$, p - n junction waveguide, phase modulation, orientation depend. 7-57536
 GaAs- $\text{Al}_x\text{Ga}_{1-x}\text{As}$, modulation-doped quantum wells, photoabsorpt., electronic props. 7-64330
 GaAs- $\text{Al}_x\text{Ga}_{1-x}\text{As}$ (001) superlattices, periodicity, charge density and zone folding effects 7-2685
 GaAs- $\text{Al}_x\text{Ga}_{1-x}\text{As}$ heterojunctions, subband Landau-level spectroscopy 7-21996
 GaAs- $\text{Al}_x\text{Ga}_{1-x}\text{As}$ heterostructures, voltage-controlled dissipation in the quantum Hall effect 7-27393
 GaAs- $\text{Al}_x\text{Ga}_{1-x}\text{As}$ heterojunction, chemical pot. of electrons, effect of mag. field 7-38682
 GaAs- $\text{Al}_x\text{Ga}_{1-x}\text{As}$ heterostructures, selectively doped, electron transport in strong electric fields 7-38687
 GaAs- $\text{Al}_x\text{Ga}_{1-x}\text{As}$ junction, 2D electron gas, plasmons, radiation absorpt. and emission 7-2686
 GaAs- $\text{Al}_x\text{Ga}_{1-x}\text{As}$ multiple quantum well, electron-phonon interaction 7-2684
 GaAs- $\text{Al}_x\text{Ga}_{1-x}\text{As}$ multiple quantum well structs., nonequilibrium LO phonons 7-12457
 GaAs- $\text{Al}_x\text{Ga}_{1-x}\text{As}$ modulation-doped structure, parallel cond. in quantum limit 7-12808

III-V semiconductors continued

- GaAs-Al_{1-x}Ga_xAs multiple-quantum-well struct., electron heating below 1K 7-12817
- GaAs-Al_{1-x}Ga_xAs MBE superlattices, low temp. photoluminesc. spectra 7-22340
- GaAs-Al_{1-x}Ga_xAs MQW and superlattice structures, for IR reflectivity 7-27724
- GaAs-Al_{1-x}Ga_xAs multiple heterostructures, variable angle of incidence spectroscopic ellipsometry 7-39055
- GaAs-Al_{1-x}Ga_xAs MOCVD quantum well structures, time-resolved photolum. 7-53410
- GaAs-Al_{1-x}Ga_xAs quantum well structure, recomb. dynamics, photolum. obs. 7-12809
- GaAs-Al_{1-x}Ga_xAs quantum wells, doubly resonant LO-phonon Raman scatt. obs. 7-27722
- GaAs-Al_{1-x}Ga_xAs quantum wells, homogeneously broadened 2D excitonic transitions, optical dephasing 7-45461
- GaAs-Al_{1-x}Ga_xAs quantum wells, photoreflectance spectra, hydrostatic press. 7-52784
- GaAs-Al_{1-x}Ga_xAs quantum wells, doubly reson. LO phonon Raman scatt., photoluminescence spectra 7-53327
- GaAs-Al_{1-x}Ga_xAs quantum wells, parabolic, light scatt. studies 7-64651
- GaAs-Al_{1-x}Ga_xAs superlattice, composition anal., electron microscopy studies 7-7028
- GaAs-Al_{1-x}Ga_xAs semicond. superlattice, exciton transitions study 7-52432
- GaAs-Al_{1-x}Ga_xAs superlattice, dimensionality of subbands, plasmon dispersion 7-52765
- GaAs-Al_{1-x}Ga_xAs superlattices, integer quantum Hall effect at microwave frequencies 7-52820
- GaAs-Al_{1-x}Ga_xAs solar cell, operation with band-gap gradient in space charge region 7-54295
- GaAs-Al_{1-x}Ga_xAs superlattice, hole subbands (*Chinese*) 7-58873
- GaAs-Al_{1-x}Ga_xAs superlattices, electronic and optical props., alloying and press. effects 7-64327
- GaAs-Al_{1-x}Ga_xAs type I superlattices, electronic struct., tight binding calcs. 7-45475
- GaAs-Al_{1-x}Ga_xAs-GaAs, multilayer struct., variable angle of incidence spectroscopic ellipsometric study 7-48830
- GaAs-Al_{1-x}Ga_xAs-GaAs, perpendicular transport, tunnelling, thermionic emission studies 7-52781
- GaAs-Al_{1-x}Ga_xAs-GaAs transverse magnetic field effects on tunnelling 7-58874
- GaAs-Al_{1-x}Ga_xAs(In_xGa_{1-x}As) lattice-mismatched heterojunctions, misfit strain relaxation, X-ray study 7-21718
- GaAs-AlAs, solid soln., temp.- and current-controlled LPE, theoretical model 7-39447
- GaAs-AlAs, superlattices, mixing, ion implantation, rapid thermal annealing, Raman scattering 7-53355
- GaAs-AlAs Al_{1-x}Ga_xAs-AlAs, multi quantum well structs., picosecond spectra. 2D excitons 7-13215
- GaAs-AlAs alternate monolayer compounds structures, MBE growth 7-21716
- GaAs-AlAs device structs., MBE prep. using In-free mounting techniques 7-3183
- GaAs-AlAs double barrier heterostructures, resonant tunnelling through quantum well states 7-58870
- GaAs-AlAs Fibonacci superlattice, quasiperiodic ordering, X-ray scatt. study 7-2692
- GaAs-AlAs heterojunctions, asymmetrically doped, photoresponse under external bias 7-38692
- GaAs-AlAs MBE MQW struct., photoluminesc. spectra (*Chinese*) 7-59240
- GaAs-AlAs MQW structures, Ga⁺ ion implantation defects 7-44585
- GaAs-AlAs multiple quantum wells, photoconductivity, photoreflectance and photolum. meas. 7-27368
- GaAs-AlAs short period superlattice, photoexcited carriers, dynamics 7-53402
- GaAs-AlAs superlattice struct., lithographic fabrication of TEM cross-sections 7-370
- GaAs-AlAs superlattices, acoustic and electronic props. 7-6730
- GaAs-AlAs superlattices, 2D excitons, magneto-optical study (*Japanese*) 7-13139
- GaAs-AlAs superlattice, energy bands, cohesive energy, form. energy, self-consistent calcs. 7-21995
- GaAs-AlAs superlattices, Se implantation, effect on compositional disordering 7-26784
- GaAs-AlAs superlattices, folded acoustic branches, leakage-induced and disorder-activated modes 7-33389
- GaAs-AlAs superlattices, confined longitudinal and transverse phonons, phonon spectrum calc. 7-38142
- GaAs-AlAs superlattices, Raman scattering finite size effects 7-39105
- GaAs-AlAs superlattices, GaAs and AlAs, energy band gap calc., self-interaction correction to local density approx. 7-45144
- GaAs-AlAs superlattices, lattice dynamics 7-52220
- GaAs-AlAs ultra-thin layer semicond. superlattices, energy band and stable structs. study 7-52789
- GaAs-AlAs-GaAs heterostructure, tunnelling transmission probability, many-band pseudopotential model 7-38701
- GaAs-AlAs(InAs) superlattices, lattice distortions 7-12510
- GaAs-AlGaAs, high quality MOVPE quantum wells, optical props. 7-53406
- GaAs-AlGaAs, hot carriers in quasi-2-D polar semiconductors 7-12807
- GaAs-AlGaAs, MBE materials for high-speed digital heterostructure devices 7-45480
- GaAs-AlGaAs, multiple quantum well structs., 2s state, excitons, luminesc. study 7-22337
- GaAs-AlGaAs, noise, localised states, quantum Hall effect 7-45413
- GaAs-AlGaAs and GaAs-AlAs quantum well structs., resonant Raman scatt., depend. on electric field 7-7707
- GaAs-AlGaAs as IR sensor material, characts. (*Japanese*) 7-56339
- GaAs-AlGaAs DFB struct. with multiquantum well for surface emitting laser 7-10939
- GaAs-AlGaAs DH injection laser, optical and transport props., emission energy shift, threshold current meas. 7-1101
- GaAs-AlGaAs extended state superlattices, shallow donor state transition energies 7-33082
- GaAs-AlGaAs heterointerface, band offsets, overview 7-12831
- GaAs-AlGaAs heterojunctions, Be⁺, O⁺ ion implantation, impurity profiles, elec. characts. meas., SIMS, annealing 7-12813

III-V semiconductors continued

- GaAs-AlGaAs heterojunctions, fractional quantum Hall effect of 2D electrons (*Japanese*) 7-12827
- GaAs-AlGaAs heterojunctions, energy band discontinuities, internal photoemission meas. 7-13331
- GaAs-AlGaAs heterojunction, narrow 2D electron gas, mag. depopulation of 1D subband 7-17080
- GaAs-AlGaAs heterojunctions, scanning tunnelling microscopy, potentiometry 7-52780
- GaAs-AlGaAs heterostructures, 2D electron system, collective excitations, light scatt. (*Japanese*) 7-12633
- GaAs-AlGaAs heterostruct., band discontinuity determ., DLTS, interface charge density, trap conc. 7-12833
- GaAs-AlGaAs heterostructures, energy band alignment, thermionic emission of holes 7-13319
- GaAs-AlGaAs heterostructures, equipotential distrib. in quantum Hall effect 7-21994
- GaAs-AlGaAs heterostructures, zero mag. field thermopower meas., temp. var. 7-33075
- GaAs-AlGaAs heterostructures, transport props. of 2D electron and hole gases 7-52812
- GaAs-AlGaAs heterostructures, density of states of Landau levels 7-52822
- GaAs-AlGaAs high-power laser array of phase-locking free struct. 7-62725
- GaAs-AlGaAs large optical cavity semicond. laser arrays 7-10989
- GaAs-AlGaAs MQW electroabsorpt. modulator for non-resonant optoelectronic logic gate 7-37139
- GaAs-AlGaAs MQW optical NOR gate, exciton and carrier dynamics, time resolved obs. 7-50628
- GaAs-AlGaAs MQW structures, MBE grown, material parameters meas. 7-38721
- GaAs-AlGaAs modulation-doped quantum wells, photolum., giant oscillations, influence of mag. fields 7-7751
- GaAs-AlGaAs modulation-doped heterointerface, photoluminescence spectra studies 7-46137
- GaAs-AlGaAs multiple quantum well lasers, voltage-controlled optical bistability, 2D exciton 7-5883
- GaAs-AlGaAs multiple quantum wells, temp. depend. of photoreflectance 7-7753
- GaAs-AlGaAs multiple quantum well structs., photolum. under high laser excitation 7-13213
- GaAs-AlGaAs quantum wells, high electric field, interband transitions, photocurrent spectra obs. 7-7289
- GaAs-AlGaAs quantum well heterostructures, spectroscopy of excitons and phonons 7-7706
- GaAs-AlGaAs quantum wells, Stark shifts for heavy- and light-hole levels, well size depend. 7-12794
- GaAs-AlGaAs quantum wells, picosecond photolum. photocurrent spectra 7-13214
- GaAs-AlGaAs quantum wells, etched ultrasmall structs., photolum. excitation spectra meas. 7-22293
- GaAs-AlGaAs quantum well structs., luminesc. from 2s heavy hole exciton, low temp. 7-22338
- GaAs-AlGaAs quantum well heterostruct. devices, atm. press. MOVPE growth 7-22574
- GaAs-AlGaAs quantum wells in waveguides, physics and appls. 7-26034
- GaAs-AlGaAs quantum well heterostructures, electronic props. 7-27405
- GaAs-AlGaAs quantum wells, MBE grown, photolum. study 7-27758
- GaAs-AlGaAs quantum wells, hot electrons, Monte Carlo study 7-38708
- GaAs-AlGaAs quantum wells, field-induced lifetime enhancements, ionisation of excitons 7-39181
- GaAs-AlGaAs quantum wells, electron-phonon scatt. rate reduction by total spatial quantisation 7-45482
- GaAs-AlGaAs quantum wells, FIR studies of shallow donors 7-52819
- GaAs-AlGaAs SCH lasers, lasing gain and threshold current 7-31327
- GaAs-AlGaAs short cavity multiquantum well lasers, dry etching, threshold current and single mode operation 7-20253
- GaAs-AlGaAs superlattice, surface and interface optical phonons, EELS studies 7-6955
- GaAs-AlGaAs superlattice, lattice images, high contrast TEM obs. 7-7027
- GaAs-AlGaAs superlattices, band structure of holes (*Japanese*) 7-12825
- GaAs-AlGaAs superlattices and superstructures, growth by metal organic CVD (*Japanese*) 7-13386
- GaAs-AlGaAs superlattice defects, DLTS study 7-21854
- GaAs-AlGaAs superlattices, electronic props., calc. methods 7-27406
- GaAs-AlGaAs superlattice, hot electrons, real space transfer effect, photolum. studies 7-39180
- GaAs-AlGaAs superlattices, magnetotransport 7-45471
- GaAs-AlGaAs three-terminal cascade solar cells with selective electrodes 7-23184
- GaAs-AlGaAs-GaAs heterostructure barriers, quantum tunnelling 7-52816
- GaAs-AlGaAs-GaAs large area graded gap diodes, discrete resistance levels obs. at low temps. 7-52749
- GaAs-AlGaAs-InGaAs strained-layer quantum well heterostructures, negative differential resistance 7-45443
- GaAs-anodic oxide interfaces, annealing, As enrichment, photoluminescence, Rutherford backscattering anal. 7-21687
- GaAs-Au, contacts, elec. and struct. props. 7-2711
- GaAs-Au contacts, proton bombard., I-V characts. 7-7386
- GaAs-Au Schottky diodes, DLTS 7-58896
- GaAs-AuGeNi contacts, interface composition and barrier heights 7-58891
- GaAs-AuNiGe (TiSi₂)(Au) interfaces, struct. and elec. props. 7-22013
- GaAs-AuNiGe ohmic contacts, microstruct. anal. and contact resist. meas. 7-2393
- GaAs-Bi, distrib. coeff. of Bi, crystn. from molten solns. 7-46428
- GaAs-CaF₂, interface struct., dielectric film mol. beam epitaxial growth 7-38360
- GaAs-CdTe heteroepitaxial interface, at. resolution HVEM study 7-2392
- GaAs-Fe interface, simultaneous epitaxy and substrate out-diffusion 7-38355
- GaAs-Ga_{0.3}Al_{0.7}As quantum wells, uniaxial stress depend. of spatially confined excitons 7-33078
- GaAs-Ga_{0.7}Al_{0.3}As heterojunction, donor-acceptor radiative recomb. mechanism, photolum. spectra study 7-17083
- GaAs-Ga_{1-x}Al_xAs superlattices and heterojunctions, electronic struct. 7-12821

III-V semiconductors continued

- GaAs-Ga_{1-x}Al_xAs superlattices, shallow impurity state binding energies 7-45416
- GaAs-Ga_{1-x}Al_xAs, semiconductor superlattice, effective mass, mag. quantisation influence 7-52754
- GaAs-Ga_{1-x}Al_xAs 2D quantum well heterostructures, magneto-impurities, mag. field and press. effects 7-52728
- GaAs-Ga_{1-x}Al_xAs heterojunction, 2D electron and hole mobilities 7-7350
- GaAs-Ga_{1-x}Al_xAs heterojunctions, electron energy levels 7-17082
- GaAs-Ga_{1-x}Al_xAs heterojunctions, impurities, optical props. 7-27396
- GaAs-Ga_{1-x}Al_xAs heterostruct., light interf. meas. of thickness and comp. during epitaxial growth 7-64026
- GaAs-Ga_{1-x}Al_xAs modulation-doped quantum well, photoluminesc. studies 7-2687
- GaAs-Ga_{1-x}Al_xAs multiple quantum wells, intrinsic and extrinsic photolum. 7-39183
- GaAs-Ga_{1-x}Al_xAs multiple well heterostructures, far IR absorpt. by shallow donors 7-45458
- GaAs-Ga_{1-x}Al_xAs quantum well, electronic states in semiconductor heterostructures 7-7307
- GaAs-Ga_{1-x}Al_xAs quantum wells, interband photocond. and excitonic Landau level transitions in mag. field 7-27390
- GaAs-Ga_{1-x}Al_xAs quantum well structures, energy spectra of donors and acceptors, spatially dependent screening effects 7-45459
- GaAs-Ga_{1-x}Al_xAs quantum well, hydrogenic donor low-lying excited states, reson. states, positions and widths 7-45460
- GaAs-Ga_{1-x}Al_xAs quantum wells, with indirect gap semicond. barriers, electron tunnelling 7-64340
- GaAs-Ga_{1-x}Al_xAs superlattices, optical props. 7-3007
- GaAs-Ga_{1-x}Al_xAs superlattices, Brillouin scatt. 7-3063
- GaAs-Ga_{1-x}Al_xAs superlattice, phonons, acoustic and optic modes 7-12455
- GaAs-Ga_{1-x}Al_xAs superlattice localised states in barrier 7-17079
- GaAs-Ga_{1-x}Al_xAs superlattice, plasmon propagation across layers 7-27276
- GaAs-Ga_{1-x}Al_xAs superlattices, in appl. elec. field, interband optical transitions 7-53274
- GaAs-Ga_{1-x}Al_xAs undoped quantum wells, excitonic spectrum, valence band coupling and Fano resonance effects calcs. 7-27256
- GaAs-Ga₂Se₃, insulating coating, stoichiometric vacancies, carrier mobility 7-52846
- GaAs-Ga₂Al_{1-x} heterojunction, nonequilibrium electron-phonon scatt. 7-45457
- GaAs-GaAlAs, modulation doped heterostructures, spectroscopy of 2D plasmas 7-2702
- GaAs-GaAlAs, multiple quantum well struct., transient photoconductivity characterisation 7-52692
- GaAs-GaAlAs, quantum well lasers, characts., comparison with GaInAs-InP 7-5891
- GaAs-GaAlAs, quantum well wires and boxes, optically detected carrier confinement, cathodolum 7-39188
- GaAs-GaAlAs, structures, 2D localisation and interaction effects 7-52531
- GaAs-GaAlAs diode laser array, diffraction-limited emission, aperture graded-index lens external cavity 7-11005
- GaAs-GaAlAs fast MQW absorber for mode locking of semicond. lasers. 7-50655
- GaAs-GaAlAs heterojunction, 2D system, high order fractional quantisation obs. 7-27397
- GaAs-GaAlAs heterojunctions, cyclotron resonance, screening effects 7-38706
- GaAs-GaAlAs heterojunction bipolar transistors, ²⁴Mg and ⁶⁴Zn implanted profiles 7-44591
- GaAs-GaAlAs heterojunctions, electron-phonon interactions, cyclotron and magnetophonon reson. meas. 7-45463
- GaAs-GaAlAs heterojunctions, fractional quantum Hall effect obs. 7-52821
- GaAs-GaAlAs heterostructures, dissipationless quantum Hall effect, crit. current density meas. 7-2696
- GaAs-GaAlAs heterostructure, LPE grown, interface photoluminescence spectra 7-53390
- GaAs-GaAlAs interface dislocations, stereographic obs. by IR light scatt. 7-32235
- GaAs-GaAlAs laser, light-activated, negative resistance, characts. (Chinese) 7-5901
- GaAs-GaAlAs MQW, optical bistability due to induced absorpt., model 7-5943
- GaAs-GaAlAs MQW optical waveguides, nonlinear props. 7-37027
- GaAs-GaAlAs MQW structures, exciton-exciton interaction 7-52439
- GaAs-GaAlAs MQW ultrafast all-optical gate with subpicosecond ON and OFF response time 7-11026
- GaAs-GaAlAs modulation doped quantum wells, hot carrier energy relax., time resolved photoluminescence spectra 7-52828
- GaAs-GaAlAs monolithic laser amplifier, C³, with bistable characts. 7-25842
- GaAs-GaAlAs multilayer structures, Auger depth profiles using a dual ion gun system 7-22429
- GaAs-GaAlAs multiple quantum well structs., quasi-2D electron-hole plasma, band-filling effects, band gap renormalisation 7-7754
- GaAs-GaAlAs multiple quantum well structs., band-gap renormalisation 7-58888
- GaAs-GaAlAs passive MQW waveguide resonators, all-optical switching effects, expt. study 7-15967
- GaAs-GaAlAs npn laser, carrier transport in heterostructure base region, carrier confinement factor in lasing region 7-43094
- GaAs-GaAlAs npn laser diode, optical bistability and switching characts. 7-62752
- GaAs-GaAlAs quantum wells, exciton binding energy, magneto-optical determ. 7-7752
- GaAs-GaAlAs quantum wells, extrinsic photolum. 7-7755
- GaAs-GaAlAs quantum well structs., recomb. dynamics of carriers 7-12830
- GaAs-GaAlAs quantum well excitons, interface disorder and mobility 7-52808
- GaAs-GaAlAs quantum wells, nonlinear optics and electro-optics 7-52809
- GaAs-GaAlAs quantum wells, excitonic coupling in elec. field, photolum. spectra 7-64094
- GaAs-GaAlAs quantum-box lasers, 3D, gain and threshold current density 7-10937

III-V semiconductors continued

- GaAs-GaAlAs resonant injection quantum well diodes and laser 7-43104
- GaAs-GaAlAs superlattice, electronic struct., envelope function approx. phonon limited mobility, Boltzmann eqn. 7-2698
- GaAs-GaAlAs superlattice, mag. levels 7-52476
- GaAs-GaAlAs superlattice structs., impact ionisation coeff., lucky drift model 7-52793
- GaAs-GaAlAs superlattices, electron states in microstructs. 7-52807
- GaAs-GaAlAs superlattices, density of states of Landau levels, sp. h. magnetisation meas. 7-52823
- GaAs-GaAlAs:Si modulation doped quantum wells, electron mobility temp. depend. 7-45473
- GaAs-GaAlAs-GaAs heterojunction barriers, single particle tunnelling, five level k.p theory 7-64341
- GaAs-GaAs cascade solar cells, OM-VPE growth, in-situ-grown tunnel junction 7-8387
- GaAs-GaAs MOVPE epitaxially-grown interfaces, anomalous C-V carrier conc. profiles, model 7-52648
- GaAs-GaAs:Cr(Te), VPE grown, photoluminescence study, effect of substrate doping 7-27771
- GaAs-GaAs:In epitaxial layers, dislocation reduction, device performance effects 7-7354
- GaAs-GaAs-Al_xGa_{1-x}As heterostructures, photosensitivity spectra 7-64319
- GaAs-Ga_{1-x}H₂, dissolution of GaAs, crystallographic characteristics 7-12415
- GaAs-GaSb high efficiency mechanically stacked two-colour solar batteries 7-59851
- GaAs-Ge, and clean surfaces, atomic, electronic and vibronic properties 7-2307
- GaAs-Ge crystal growth on Ta₂O₅-coated Si substrates, zone melting and MOCVD 7-53579
- GaAs-Ge epitaxial interface, extended defects, geometrical characteristics 7-6640
- GaAs-Ge heteroepitaxy on Si substrates, recrystallised Ge-on-insulator intermediate layers 7-52358
- GaAs-Ge-SiO₂, semiconductor MBE layers on Ge islands on insulator photolum. study 7-33455
- GaAs-GeMo ohmic contact, fabrication and characts. study 7-45490
- GaAs-In_xGa_{1-x}As strained layer superlattices, photolum. microimaging of dislocations 7-27161
- GaAs-InAs, in situ contacts, MBE grown 7-45444
- GaAs-InAs strain layer modulated structures, MBE grown, cross-sectional TEM 7-7032
- GaAs-InAs superlattice, reflection electron diffraction intensity oscillations 7-7030
- GaAs-LaB₆ interfaces, thermal stability, high energy ion scattering studies 7-21680
- GaAs-Langmuir-Blodgett film MIS devices 7-55918
- GaAs-metal interfaces, Fermi level pinning 7-2714
- GaAs-Mn(V), extrinsic surface states, core level UPS study 7-2713
- GaAs-Mo Schottky diodes, elec. characts. and microstruct. studies 7-22015
- GaAs-Nb, oriented Nb films, electron beam evaporation in ultrahigh vacuum 7-3175
- GaAs-Nb(NbN) Schottky barriers, interdiffusion obs. 7-58856
- GaAs-Ni interfacial reactions, contact elec. props. 7-12504
- GaAs-oxide interfaces, defect stabilised electronic properties 7-38748
- GaAs-Pt reacted ohmic contact charactn., effect of Mg layer 7-7387
- GaAs-Si, nucleation and growth of GaAs 7-45038
- a-GaAs-Si (100), epitaxial regrowth by excimer laser annealing, FE-TEM fabrication 7-32875
- GaAs-Si cells, photovoltaic 7-17903
- GaAs-Si heteroepitaxial interface, at. resolution HVEM study 7-2392
- GaAs-Si heteroepitaxial interface, atomic structure 7-52298
- GaAs-Si mechanically stacked multijunction solar cell 7-8402
- GaAs-Si p-n heterojunctions, interface charge polarity 7-38686
- GaAs-Si thin film solar cells, radiation damage 7-65465
- GaAs-Si₃N₄ interface, multipolar plasma deposition, high resolution electron microscopy study 7-12499
- GaAs-SiON interface, plasma enhanced CVD deposited SiON, NH₃ plasma pretreatment effects 7-7874
- GaAs-thermal oxide interfacial chem. reactions, Raman spectra, AES 7-27145
- GaAs-W(W₂Si₃) Schottky contacts, electrical and metallurgical studies 7-27422
- GaAs-ZnSe, MBE growth on GaAs epilayers, nucleation and characterisation 7-45046
- GaAs₂ semicond. cluster anions, photodetachment and photofragmentation 7-36837
- GaAsAl_xAlGa_{1-x}As, 2D electron gas, edge depletion width 7-58866
- GaAs_{1-x}Al_xAs MQW, MOCVD grown, excitons, photoluminescence spectra 7-38702
- (GaAs)₂₈(AlAs)₂₄ superlattices, lattice distortion, X-ray diffraction studies 7-63974
- GaAsP, CVD, laser selective deposition on GaAs and Si substrates 7-22546
- GaAsP, DX centres, DLTS signature anal. 7-45204
- p-GaAsP, longitudinally polarised electron bombarded, circularly polarised recomb. radiation emission 7-27807
- GaAsP, MOCVD growth, IR laser assisted grading 7-27945
- GaAsP monolithic three-junction solar cells, computer modelling 7-3672
- GaAsP on GaP solar cells in tandem with Si cells, design, fabrication 7-3674
- GaAsP terrestrial solar cells, high-efficiency concepts 7-8390
- GaAsP, V_F-T characteristics of p-n junction at low temp. (Chinese) 7-12792
- GaAsP-GaAs(P) strained-layer superlattices, MOCVD and device preparation 7-7876
- GaAs_{0.12}P_{0.88}:N, Te and GaP:N, Si(Te) epitaxial layers, minority carrier lifetimes, surface and interface recombination effects 7-7424
- GaAs_{0.6}P_{0.4} degraded LEDs, origin of nonradiative centres, photocapacitance, electrolum. spectra 7-53413
- GaAs_{0.6}P_{0.4} LEDs, MOCVD growth on Si substrates 7-17438
- GaAs_{0.7}P_{0.3}-GaP solar cell, high efficiency mech. stack, performance measures 7-8401
- GaAs_{0.75}P_{0.25} solar cells, high efficiency, grown by one atmosphere MOCVD 7-3697
- GaAs_{1-x}Be_x:GaP:Be⁺ strained-layer superlattices, ion implantation doping, structural study 7-38030

III-V semiconductors continued

- GaAs_{1-x}P_xBe⁺-GaP:Be⁺ strained layer superlattices, ion implantation doping, optical and elec. props., device appls. 7-44583
- GaAs_{1-x}P_x epitaxial structs., radiative characts., deep centres effects 7-45220
- GaAs_{1-x}P_x solid solns., indirect band gap temp. depend., electrolum. spectra studies 7-38448
- GaAs_{1-x}P_x crystals, electron-traps, DLTS study (*Japanese*) 7-7146
- GaAs_{1-x}P_x, EL2 level 7-21859
- GaAs_{1-x}P_x:N, bound excitons, energy spectrum, optical absorpt. cross section, two-band model 7-16945
- GaAs_{1-x}P_x:N, cathodoluminesc. efficiency, N-bound excitons influence 7-7768
- GaAs_{1-x}P_x:N epitaxial layers, N conc. determ. 7-63989
- GaAs(P)(Sb):H, vibrational excitations, impurity-host atom complexes, IR absorpt. data interpretation 7-44724
- GaAsSb terrestrial solar cells, high-efficiency concepts 7-8390
- GaAs_{1-x}Sb_x, alloy disorder broadening of defect energy levels 7-52516
- GaAs_{1-x}Sb_x-Au Schottky barriers, I-V characts., temp. depend. 7-64344
- GaAsSb_{1-y} relaxed zinc-blende lattice, EXAFS study 7-64759
- n-GaAs_{1-x}Sb_xP, epitaxial film, impurity distrib., cond. and Hall mobility study 7-51808
- GaAs(100), MBE growth parameter influence on surface kinetic processes, RHEED specular beam intensity meas. 7-2424
- GaAs(100), thermal and ion-assisted reactions with Cl₂ 7-3537
- GaAs(110)-Al, Schottky barrier form., effect of surface and interface kinetics 7-2668
- GaAs(110)-In, interfacial chem. reaction, UPS study 7-2276
- GaInAs, anodic oxides, growth and composition 7-39781
- GaInAs, Czochralski-grown, dislocation effects investig. 7-7261
- GaInAs epitaxial layer on InP, depth profiling and interface detection using anodic oxidation 7-45057
- GaInAs films and structures, gas source MBE, review 7-33572
- GaInAs, pn junction formation by simultaneous implantation and diffusion annealing 7-38028
- GaInAs, ternary solid soln., miscibility gap in phase diagram 7-52057
- GaInAs terrestrial solar cells, high-efficiency concepts 7-8390
- GaInAs/GaAs single quantum well pseudomorphic structs., high electron mobility meas. 7-12841
- GaInAs/InP, nonlinear optical absorpt. at room temp. 7-59169
- GaInAs/InP heterojunction, 2D electron gas nonequilibrium cyclotron reson. obs. 7-12845
- GaInAs/InP heterostructures, VPE, homogeneity, mobilities 7-58882
- GaInAs/InP quantum wells, atmospheric organometallic vapour phase epitaxial growth 7-27912
- GaInAs-AlInAs heterostruct., alloyed NiGeAuGaAu ohmic contacts, charact. 7-22016
- GaInAs-AlInAs heterojunctions, parallel conduction, quantum Hall effect, hydrostatic press. 7-52764
- GaInAs-AlInAs(InP) and GaAs-AlGaAs superlattice avalanche photodiodes, impact ionisation theory appl. 7-58886
- GaInAs-GaInAsP(InP) quantum-box lasers, 3D, gain and threshold current density 7-10937
- GaInAs-InP, quantum well lasers, characts., comparison with GaAlAs 7-5891
- GaInAs-InP, quantum well structures, adduct MOVPE, photolum., magnetoresist charactn. 7-27388
- GaInAs-InP double-barrier heterostructs., room temp. resonant tunnelling, neg. resist. effects 7-58814
- GaInAs-InP epitaxial superlattice, X-ray double crystal characterisation, rocking curves calc., computer simulation technique 7-58105
- GaInAs-InP quantum well, CESR of 2D electrons 7-38941
- GaInAs-InP quantum-box lasers, 3D, gain and threshold current density 7-10937
- GaInAs-SiO₂ system, annealing behaviour, SIMS and elec. meas. 7-38270
- Ga_{0.28}In_{0.72}As/Al_{0.28}In_{0.72}As photodiode heterostructures, atm. press. MOCVD, 2 μ m, sensitivity, structural charactn. 7-27933
- Ga_{0.3}In_{0.7}As-InP strained layer superlattice, inter-band magneto-absorption 7-45998
- Ga_{0.47}In_{0.53}As, laser material, intervalence band absorpt. coeff. calc. 7-3015
- Ga_{0.47}In_{0.53}As:Be epitaxial films, ion implanted, rapid thermal and furnace annealing 7-22729
- Ga_{0.47}In_{0.53}As/Al_{0.48}In_{0.52}As modulated struct., high resolution double-cryst. X-ray diff. studies 7-7029
- Ga_{0.47}In_{0.53}As/Al_{0.7}In_{0.3}As superlattices, electronic struct., strain-induced elec. field effects 7-7358
- Ga_{0.47}In_{0.53}As/Al_{0.48}In_{0.52}As quantum well, interband magnetoabsorpt. meas., effective mass determ. 7-17088
- Ga_{0.47}In_{0.53}As/Al_{0.48}In_{0.52}As superlattices grown by MBE, structural charactn. 7-52792
- Ga_{0.47}In_{0.53}As/InP heterojunction, chem. beam epitaxy grown, 2D electron gas 7-12803
- Ga_{0.47}In_{0.53}As-InP heterojunction, with three electron subbands, hydrostatic press. effect 7-2695
- Ga_{0.47}In_{0.53}As-InP heterojunction, MOCVD grown, 2D hole gas 7-21992
- Ga_{0.47}In_{0.53}As-InP junction lasers, chem. beam epitaxy and performance characts. 7-20254
- Ga_{0.47}In_{0.53}As-InP quantum wells, photocurrent and dark current, multiple steps obs. 7-12796
- Ga_{0.47}In_{0.53}As-InP superlattices, MOCVD grown, room temp. excitons 7-21986
- Ga_{0.47}In_{0.53}As-Si₃N₄(SiO₂) interface, elec. charact. 7-38752
- Ga_{1-x}In_xAs, high-temperature hardness 7-44675
- Ga_{1-x}In_xAs, solid soln. strengthening, mech. props. 7-32452
- Ga_{1-x}In_xAs/InP heterostructures, MOVPE, electron mobility, exciton peak, magnetotransport 7-58883
- Ga_{1-x}In_xAs-Al_{1-y}In_yAs superlattices, electronic struct., depend. on growth axis 7-64329
- Ga_{0.7}In_{0.3}As, photoluminescence line shape of excitons 7-3087
- Ga_{0.7}In_{0.3}As, heterostruct., local composition, CBED anal. 7-16529
- Ga_{0.7}In_{0.3}As, low-pressure MOVPE growth 7-7873
- Ga_{0.7}In_{0.3}As/Al_{0.7}In_{0.3}As MBE grown superlattices, effect of barrier config. and interface quality on props. 7-52790
- Ga_{0.7}In_{0.3}As/GaAs heterostructures, low press. MOVPE, photolum., Auger profiling 7-27389
- Ga_{0.7}In_{0.3}As-GaAs strained layer superlattices; low temp. photolum. 7-53407
- GaInAsP DFB lasers, 1.3 μ m, single-mode, realisation and characts. (*German*) 7-57357

III-V semiconductors continued

- GaInAsP epitaxial layers, double axis X-ray diffractometry at glancing angles 7-37805
- GaInAsP epitaxial layers, X-ray double crystal characterisation, rocking curves calc., computer simulation technique 7-58105
- GaInAsP films and structures, gas source MBE, review 7-33572
- GaInAsP integrated coupled-cavity lasers, design and fabrication 7-25843
- GaInAsP strip-loaded planar waveguide for high-speed electroabsorpt. modulator 7-31449
- GaInAsP:Er semiconductor injection laser, single longitudinal model operation at 1.5 μ m 7-50558
- GaInAsP:InP heterostructures, MOVPE, press. control, reactor design 7-39399
- GaInAsP/InP, planar single mode heterostructures, calculated characts. 7-31326
- GaInAsP/InP entirely VPE-grown 1.5 μ m DFB lasers with low threshold currents 7-50577
- GaInAsP/InP heterojunctions, atmospheric press. MOVPE growth TEM studies 7-3196
- GaInAsP/InP laser diodes, amplification piezoeffect 7-5889
- GaInAsP/InP stressed heterostructure lasers, lifetimes meas. 7-5890
- GaInAsP/InP surface emitting laser with flat surface circular buried heterostructure 7-31358
- GaInAsP-InP BH laser fabrication, MOCVD epitaxy, validation by photoluminescence imaging 7-31360
- GaInAsP-InP CW phase-locked semiconductor laser array, MOCVD growth 7-57351
- GaInAsP-InP double heterostructure lasers, 1.5 μ m, chemical beam epitaxial growth 7-57310
- GaInAsP-InP etched mirror laser, passivation with angled sputtering 7-57358
- GaInAs(P)-InP heterostructures, gas source MBE growth 7-53598
- GaInAsP-InP lasers, single-step LPE fabrication 7-10996
- GaInAsP-InP laser, anisotropic deform. influence on radiative characts., threshold, polarisation and watt-ampere charact. 7-43100
- GaInAsP-InP laser, anisotropic deform. influence on radiative characts., spectral characts. 7-43101
- GaInAsP-InP substrate, integrated optoelectronics, micrograting form. by HV electron beam lithography 7-31443
- GaInAsP-InP surface-emitting laser with circular BH, low temp. CW operation 7-31337
- Ga_{0.28}In_{0.72}As_{0.6}P_{0.4} laser material, intervalence band absorpt. coeff. calc. 7-3015
- Ga_{1-x}As_xP_{1-y}, effective masses and alloy disorder effects, shallow donor photocond. 7-64289
- GaInAsSb, MOVPE, band gap rel. to growth temp. 7-39409
- GaInAsSb/AlGaAsSb injection lasers, threshold current density reduction 7-5886
- Ga_{0.85}In_{0.015}As_{0.13}Sb_{0.87}/Al_{0.4}Ga_{0.6}As_{0.035}Sb_{0.965} DH lasers, MBE grown, 2.07 μ m laser oscillation 7-43096
- Ga_{1-y}In_xAs_{1-y}Sb_y system, low temp. phase equilib. 7-52001
- GaInP-AlGaInP-GaAs heterostructures, MOVPE, Hall effect, photolum. 7-39401
- GaInP₂-GaAs, current-matched and lattice-matched tandem cell efficiency 7-8403
- Ga_{1-x}In_xP/GaAs heterojunction band discontinuity determ., C-V profiling 7-58880
- Ga_xIn_{1-x}P epitaxial layers, OMVPE, surface morphology, photolum. 7-22557
- Ga_xIn_{1-x}P layers, MOVPE, photolum., comp. and growth temp. depend. 7-39403
- n-Ga_{1-x}In_xP, light scatt. by free carriers 7-17328
- Ga_xIn_{1-x}P, OMVPE growth and characterisation 7-3192
- Ga_xIn_{1-x}P/GaAs (Al_{1-y}Ga_{1-y}As) heterostructures, OMVPE, photolum., lattice matching 7-39402
- Ga_xIn_{1-x}PAs_{1-y} solid solns., thermodynamic stability 7-21453
- Ga_xIn_{1-x}PAs_{1-y}InP heterojunction interfaces, electron energy band structure (*Chinese*) 7-33070
- Ga_{1-y}In_xSb epitaxial layers, MOCVD, morphology rel. to growth conditions 7-39408
- n-Ga_xIn_{1-x}Sb:Se(S), impurity states, press. and comp. depend., Hall coeff. and elec. resist. meas. 7-2533
- GaN, band struct., pseudopotential method anal. 7-52421
- GaN crystals, polarisation props. of band-edge emission, dispersion theory appl. 7-64694
- GaN, electron-hole plasma generation 7-27358
- GaN films, epitaxial growth by reactive ion plating, elec. props. 7-3206
- GaN films, OMVPE, Hall mobilities, impurity band 7-39410
- GaN, undoped and control doped films, luminesc. studies 7-27790
- GaN, X-ray phase anal., elastic props. 7-45050
- GaN:Sb, antisite dopant incorporation, Mossbauer spectra study 7-12086
- GaN:Zn, pure and doped, electrophysical props., nonhomogeneous semiconductor model 7-27292
- GaN:Zn films, MOVPE, electron cyclotron resonance plasma excitation, low temp. growth 7-22549
- GaN:Zn n-i structures, electrical conductivity 7-38565
- GaN:Zn(Cd), time-resolved photoluminesc. study 7-22347
- GaP (110), with ordered Sb overlayers, ARUPS 7-59378
- GaP and GaP:N diodes, electroluminescence, high press. effects 7-27787
- GaP anomalous photovoltage films X-ray irradiation effects studies 7-58834
- GaP, Ar⁺ irradiated, damage profile, backscattering spectra, anal. by computer program 7-64840
- GaP bicrystals, potential barriers of grain boundaries 7-21976
- GaP coating for passivation of Si solar cells 7-65479
- GaP, coherent optical phonon generation and decay 7-33040
- GaP crystal, low temp. negative thermal expansion coeff. 7-6837
- GaP, deep level centres at excited states, study by transient optical absorpt. spectroscopy 7-13188
- GaP, defects, optical detection of magnetic resonance studies 7-22165
- GaP electrical conductivity meas., high pressure, in diamond anvil cells at cryogenic temp. 7-56299
- GaP emitters, secondary electron energy distrib. rel. to work function 7-46256
- GaP, energy band calculations (*Chinese*) 7-38446
- GaP epitaxial layers, MOCVD growth on Si, TEM and SEM 7-38416
- GaP, epitaxial structs., radiative characts., deep centres effects 7-45220
- GaP films, MBE grown on Si, antiphase domain structures 7-64014
- GaP films, MBE growth on Si(211), defects obs. 7-58695
- GaP Films, vacuum chemical epitaxy 7-39406
- GaP finite cluster, local electronic struct., recursion method calcs. 7-2464

III-V semiconductors continued

- GaP, floating zone melting prep., elec. props. 7-64238
 GaP, implanted with He ions and protons, microhardness rel. to damage density 7-51883
 GaP, ion-induced Auger electron emission under shadowing conditions 7-64841
 GaP LPE layers, reuse of Ga melt for LED prep., effect on electrical characts. 7-22592
 GaP, LPE macrosteps, shape of atomic steps and interface supersaturation 7-58689
 GaP MBE heteroepitaxial layers, lattice distortions, X-ray diffr. and Raman studies (*Japanese*) 7-27219
 GaP, MISS, common anion rule, density distrib., photoionisation 7-38765
 GaP, microcrystals, amorphous-like Raman signals 7-53349
 GaP, neutron irradiated and as-grown, vacancy defects, positron studies 7-2012
 GaP on Si substrate, MOCVD growth and characterisation 7-27926
 GaP, phonon shifts due to temp. and pressure rise induced by a laser beam 7-2125
 GaP, phonons, ps laser induced transient dynamics 7-39113
 GaP, photoexcited plasmon-phonon modes, time-resolved Raman scatt. 7-39106
 p-GaP, powder, metal-loaded, photoinduced electron-hole pair separation 7-59770
 GaP single crystals, high energy ion implantation, damage profiles 7-16590
 GaP single crystals, anisotropic deep centres, polarised photolum. and thermolum. studies (*Russian*) 7-21867
 GaP, single-particle excitations, dynamic correl. corrections, local density theory 7-45115
 GaP, sublattices direct resolution and identification by high-resolution TEM 7-37813
 GaP, thermo-EMF of high press. phase 7-38604
 GaP thin films, optical props., meas. by surface plasmon excitation 7-46166
 GaP, V_F -T characteristics of p-n junction at low temp. (*Chinese*) 7-12792
 GaP:Te(Zn), doping superlattices, growth and props. 7-64684
 GaP:B, internal friction temp. depend. studies 7-38112
 GaP:Cr, impurity ion-lattice coupling, reson. phonon scatt. spectra 7-58420
 GaP:Cr, optically induced changes in impurity-related absorpt. line struct. 7-17334
 GaP:Cu, 1.65 eV luminescence, optically detected mag. resonance studies 7-64547
 GaP:Fe, deep levels formed by Fe complexes 7-12657
 GaP:He⁺ implanted, swelling, strain and radiation damage 7-6694
 GaP:Ni²⁺, absorpt. spectrum of Ni²⁺ 7-53373
 GaP:O, review 7-48201
 GaP:Pr(Nd)(Yb), IR photoluminescence of rare earth impurities 7-64692
 GaP:Zn, electron irradiation induced defects, DLTS study 7-52513
 GaP/GaAsP epitaxial layers, MOCVD growth on Si, TEM and SEM 7-38416
 GaP-electrolyte interfaces, Fourier transform IR spectroscopy 7-27124
 GaP-Ga semiconductor-liquid metal contact, transition from rectifying to ohmic operation 7-52833
 GaP-GaAs_{1-x}P_x strained layer superlattices, photolum. microimaging of dislocations 7-27161
 GaP-In semiconductor-liquid metal contact, transition from rectifying to ohmic operation 7-52833
 Ga_{1-x}P_x-GaP-Si mechanically stacked multijunction solar cells, p-n junction model 7-3668
 GaP_{0.2}As_{0.8} strained-layer superlattice, low-temp. pressure-depend. magneto-optic meas. 7-12793
 GaP(As)(Sb), band structure, polarisation-dependent angle-resolved photoemission spectroscopy 7-21814
 GaPSb, ternary solid soln., miscibility gap in phase diagram 7-52057
 GaSb (110), intrinsic intergap surface state, angle-resolved photoemission 7-45423
 GaSb, crystal growth and synthesis, thermodynamics, optimisation algorithm appl. 7-16461
 GaSb high press. phase, β -Sn-type struct., pseudopot. perturbation calcs. 7-51938
 n-GaSb impurity Auger hole recomb. via deep acceptor, electron density depend. calcs. 7-38573
 GaSb, impurity doping by photonuclear reactions 7-16589
 GaSb, impurity level calcs., effective mass pseudopotential method 7-7163
 GaSb, LPE growth from Ga and Sn solns. 7-59467
 p-GaSb, low-temp. growth by plasma process (*Japanese*) 7-7061
 GaSb single crystals, intrinsic point defects and microdefects, TEM studies 7-44529
 GaSb:Gd,Ho crystal grown by horizontal zone melting, precipitate identification 7-21462
 GaSb:Se, resist. and thermoelec. power meas. at metal-insulator transition 7-45403
 GaSb:Te(Se)(Si)(Ge) single crystals, Czochralski growth, carrier conc. rel. to dopant conc. 7-22462
 GaSb/Al_xGa_{1-x}Sb MBE grown superlattices, effect of barrier config. and interface quality on props. 7-52790
 GaSb/AlSb single quantum wells, electroluminescence and photoluminescence studies 7-46136
 GaSb/AlSb strained-layer heterojunction valence band discontinuity, XPS core level meas. 7-21984
 GaSb/GaSb:Si (111) autoepitaxial structures, signs of misfit dislocations, X-ray topographic determ. 7-38349
 GaSb/InAs/GaSb quantum wells, carrier densities and mobilities, magnetotransport meas. 7-12846
 GaSb-Al interfacial chem. reactions, surface refl. Raman Scatt. study 7-2275
 GaSb-Al_xGa_{1-x}Sb multi quantum wells, excitons, electric field effect, phototurrent spectra obs. 7-7288
 GaSb-AlSb multiple quantum well structs., size-induced direct to indirect gap transition 7-7373
 GaSb-AlSb quantum well lasers, reduction of Auger effect, 1-5 μ m wavelength region 7-5893
 GaSb-AlSb quantum wells, optical transitions, obs. 7-46086
 GaSb-AlSb quantum-well structures, 2E_g transitions 7-46128

III-V semiconductors continued

- GaSb-AlSb strained quantum well, electronic states in semiconductor heterostructures 7-7307
 GaSb-based wafers, determ. of (110) and (-110) directions by etching 7-59696
 GaSb-GaAs photodiode, low-temp. growth by plasma process (*Japanese*) 7-7061
 GaSb_{1-x}As_x 7-16529
 GaSb_{0.1}AlSb quantum wells, nonparabolic behaviour under hydrostatic press. 7-64328
 GaSe amorphous film, high field kinetics of photocurrent 7-2748
 Ge/GaAs multijunction monolithic cascade solar cells with patterned Ge tunnel junctions 7-13863
 Ge-GaAs heterostructures, lattice theory, phonon propagation 7-58602
 Ge_{1-x}Si_x-GaAs-Si, multispectral high efficiency solar cells, semiconductor selection criterion 7-8399
 In As_{1-x}Sb_x epitaxial layers, MOCVD, strained-layer superlattices 7-39407
 In GaAsP lasers, high speed design and performance 7-62700
 In/GaAs:Cu/In struct., I-V characts., carrier recomb. and generation, impurity thermionic field ionisation effects (*Russian*) 7-22030
 In-GaAs-P films highly excited, ps band filling 7-43261
 In-Ga-P-As, gap width, temp. depend. 7-12602
 In-GaAs reactions, interfacial native oxide layer effects 7-12501
 In-Pt-GaAs, heterojunction ohmic contacts, interfacial struct. 7-27155
 In_{0.53}Ga_{0.47}As-InP, epitaxial single quantum wells, spectroscopy of excited states 7-46126
 InAlAs, growth by MBE, alloy clustering, surface quality, role of kinetics and thermodynamics 7-32866
 InAlAs/InGaAs modulation-doped heterostructs., 2D electron gas mobility meas. 7-12842
 InAlAs-InGaAs resonant tunnelling barrier struct., MBE grown, NDR characts. 7-52796
 In_{0.18}Al_{0.82}As-GaAs strained layer superlattices, Raman studies 7-12854
 In_{0.52}Al_{0.48}As optical waveguides, MBE growth on InP 7-11107
 In_xAl_{1-x}As/Au Schottky barrier heights, composition dependence 7-45431
 In_xAl_{1-x}As/GaAs strained-layer superlattices, effective mass reversal 7-17078
 InAs (110), oxidation, correlated changes of electronic surface props. 7-2354
 InAs (110), surface electron states, effect of Al submonolayer coverage, soft XPS study 7-2653
 InAs, atomic layer epitaxy growth, photolum., Hall meas. 7-22527
 InAs, electron-electron interaction, quantum effects, magnetoresist. studies 7-75891
 InAs, impurity doping by photonuclear reactions 7-16589
 n-InAs, Kane-type semiconductors, Einstein relation, mag. quantisation effect 7-52603
 InAs MIS structures, space charge accumulation 7-33097
 n-InAs, metal-Hall insulator transition 7-52708
 InAs, nuclear transmutation doping 7-38025
 InAs quantum well structures, metal-insulator transition due to surface roughness scatt. 7-27400
 InAs substrates and devices, surface anal., SIMS appl. 7-22417
 InAs surface on InP, epitaxial regrowth 7-2431
 InAs:B, internal friction temp. depend. studies 7-38112
 InAs:Sb(Ga)(Mn), single crystal, elec. inhomogeneity, effects of isovalent impurities 7-7229
 n-InAs:Sn,Te, LPE growth, elec. characts. 7-33603
 n-InAs/GaAs SNS heterostructure weak link with Nb electrodes 7-52898
 InAs/GaAs single quantum well structures grown by atomic layer epitaxy 7-22486
 InAs/GaAs strained-layer superlattices, band struct., TEM, X-ray and photolum. spectra 7-38722
 InAs/GaSb quantum well, 2D electron gas, cyclotron reson. oscills. meas. 7-38944
 InAs-GaAs strained-layer superlattices, pseudo-alloy behaviour 7-7376
 InAs-GaAs superlattices grown by beam-separation MBE, surface morphology and elastic strain 7-7031
 InAs-GaSb superlattice dispersion relations, electronic states in semiconductor heterostructures 7-7307
 InAs-GaSb superlattices, transient photovoltaic effect 7-12764
 InAs-GaSb superlattice, band offset press. depend., magneto-optical studies 7-38698
 InAs-GaSb superlattices, band line-up under hydrostatic press. 7-52782
 InAs-GaSb thin film heterostruct., superlattice, electron transverse effective mass 7-21990
 InAs-superthin insulator-Au struct., inelastic electron tunnelling spectra 7-27436
 InAs₂P₃, LEC-grown single crystals, growth defects and lattice strains 7-38001
 InAs_{0.3}Sb_{0.7} IR detector, photoresponsivity meas. 7-7274
 InAs_{1-x}Sb_x IR photodiodes for 3 to 14 μ m, comparison 7-41466
 InAsSbP/InAs bent heterostructures, dislocation distribution 7-21673
 InAsSbP/InAs p-n structures, nonclassical thermal injection current 7-12806
 In_{0.5}G_{0.5}P layers, LPE, elec. and optical props. 7-17119
 InGaAlAs, props. for integrated optics/optoelectronics in optical fibre communication systems, review 7-11178
 In_xGa_{1-x}(Al_{1-x})_xAs, MBE growth rates, temp. dependence 7-17426
 InGaAlP epilayers, MOCVD, laser appl. 7-39404
 InGaAs and InGaAsP, nonuniform, dynamical X-ray rocking curve simulations 7-2408
 InGaAs, CVD, laser selective deposition on GaAs and Si substrates 7-22546
 InGaAs, CVD growth by VPE, review 7-39417
 InGaAs, chemical beam epitaxial growth investig. 7-7878
 InGaAs epitaxial films, MO-chloride VPE growth 7-22566
 InGaAs epitaxial layers on InP substrates, ion beam crystallography 7-32863
 InGaAs films, organometallic CVD growth mechanisms, adduct formation 7-33588
 InGaAs, high-field autovariance coeff., diffusion coeff., and noise at 300 K 7-64260
 InGaAs, ion beam damage-induced masking for photoelectrochem. etching 7-44628
 InGaAs, LPE diffusion-limited growth 7-21727
 InGaAs layers on InP, LPE growth 7-33608

III-V semiconductors continued

- InGaAs, MISS, common anion rule, density distrib., photoionisation 7-38765
- InGaAs monolithic three-junction solar cells, computer modelling 7-3672
- InGaAs, patterning using photoelectrochem. etching and focused ion beams 7-22924
- InGaAs, reactive ion etching 7-65241
- InGaAs strained-layer superlattices, valence-band nonparabolicity and tailorable hole masses 7-12798
- InGaAs:Si LED, electrical and luminesc. props., ultrasonically-induced changes 7-22350
- InGaAs/GaAs GRIN SCH SL quantum well laser, MOCVD grown 7-50557
- InGaAs/GaAs lattice-strained double heterojunction bipolar structs., comp., recomb. props. and device performance 7-64322
- InGaAs/GaAs(InP) quantum well structures, localised states, strain depend. 7-7312
- InGaAs/InAlAs MQW pin diodes, room temp. current oscillations 7-45454
- InGaAs/InAlAs multiple quantum well structs., nonlinear spectroscopy 7-1236
- n^- -InGaAs/InAlAs/ n^- -InGaAs, conduction band discontinuity determ. by current-voltage meas. 7-7352
- InGaAs/InP heteroepitaxial structs., misfit stress, elastic eqns., comment 7-21676
- InGaAs/InP heterostructures, chloride VPE, interface form. control 7-58656
- InGaAs/InP multiple quantum well waveguides, low loss, MOCVD growth 7-43358
- InGaAs/InP photodiodes, MOCVD growth and characts. 7-27932
- InGaAs/InP quantum wires and boxes, low temp. photoluminesc. 7-59238
- InGaAs/InP single quantum wells, transport and persistent photocond. props. 7-27385
- InGaAs/InP superlattices, effective mass filtering obs. 7-12799
- InGaAs-GaAs, quantum well structs., p-type modulation doped, Hall effects, influence of built-in strain 7-7339
- InGaAs-GaAs and GaAs-GaPAs strained layer superlattices, press. depend. magneto-optic meas. at low temp. 7-27404
- InGaAs-GaAs MOVPE epitaxially-grown interfaces, anomalous C-V carrier conc. profiles, model 7-52648
- InGaAs-InAlAs MQW structure, anisotropic electroabsorpt. and optical modulation 7-13134
- InGaAs-InAlAs multiple quantum wells, long wavelength optical modulation, electro-optical effects 7-7677
- InGaAs-InAlAs strained-layer superlattices, MBE grown, optical characterisation 7-13142
- InGaAs-InP, direct growth on GaAs substrates using MOVPE 7-22510
- InGaAs-InP 1.5 μ m photodetectors, optical communication appls. 7-37202
- InGaAs-InP heterostruct., rare earth doped, elec. and photoluminescence props. 7-46133
- $\text{In}_{0.7}\text{Ga}_{0.3}\text{As}$ -GaAs cascade solar cells, OM-VPE growth, in-situ-grown tunnel junction 7-8387
- $\text{In}_{0.2}\text{Ga}_{0.8}\text{As}$ -GaAs strained-layer superlattice, low-temp. pressure-depend. magneto-optic meas. 7-12793
- $\text{In}_{0.5}\text{Ga}_{0.5}\text{As}$ quantum wells, quantized energy levels, conduction-band nonparabolicity effects 7-2675
- $\text{In}_{0.52}\text{Ga}_{0.48}\text{As}/\text{In}_{0.52}(\text{Ga}_{1-x}\text{Al}_x)_{0.48}\text{As}$ heterostructures, conduction band edge discontinuity 7-12815
- $\text{In}_{0.53}\text{Ga}_{0.47}\text{As}$, impact ionisation coeffs., lucky drift model including soft threshold energy 7-64258
- $\text{In}_{0.53}\text{Ga}_{0.47}\text{As}$, LPE growth on semiinsulating InP:Fe, SEM studies 7-22591
- $\text{In}_{0.53}\text{Ga}_{0.47}\text{As}$, surface analysis using organic-on-inorganic contact barriers 7-21991
- $\text{In}_{0.53}\text{Ga}_{0.47}\text{As}$:Be, high dose implants, rapid thermal annealing 7-16602
- $\text{In}_{0.53}\text{Ga}_{0.47}\text{As}/\text{In}_{0.52}\text{Al}_{0.48}\text{As}$ quantum wells, lamp annealing interdiffusion and optical props. 7-12502
- $\text{In}_{0.53}\text{Ga}_{0.47}\text{As}-\text{In}_{0.52}\text{Al}_{0.48}\text{As}$ modulation-doped heterostructs., interface roughness scatt. 7-2678
- $\text{In}_{0.53}\text{Ga}_{0.47}\text{As}-\text{InP}$, double-barrier structs., tunnelling 7-45446
- $\text{In}_{0.53}\text{Ga}_{0.47}\text{As}-\text{InP}$, quasi-2D heterostructures, suppression of current filament by mag. field 7-52760
- $\text{In}_{0.53}\text{Ga}_{0.47}\text{As}-\text{InP}$ heterointerfaces, CV profiling 7-12834
- $\text{In}_{0.53}\text{Ga}_{0.47}\text{As}-\text{InP}$ layers, photolum. and laser emission 7-7739
- $\text{In}_{0.53}\text{Ga}_{0.47}\text{As}-\text{W-InP}$ structures, LPE growth on structured substrates 7-46353
- $\text{In}_{0.69}\text{Ga}_{0.31}\text{As}-\text{InP}$ strained-layer effective-mass superlattices 7-7378
- $\text{In}_{1-x}\text{Ga}_x\text{As}$, MOCVD, optical and elec. props. rel. to growth temp. 7-53613
- $\text{In}_{1-x}\text{Ga}_x\text{As}-\text{InP}$ heterostructure APD for 1.55 μ m optical fibre communication system (Japanese) 7-62843
- $\text{In}_x\text{Ga}_{1-x}\text{As}-\text{GaAs}$ single-quantum-well heterostructs., pseudomorphic, optical characterisation 7-22303
- $\text{In}_x\text{Ga}_{1-x}\text{As}$ (100)-metal interfaces, Fermi level pinning and chem. interactions 7-2712
- $\text{In}_x\text{Ga}_{1-x}\text{As}$, atomic displacements detection using channelled electron induced X-ray emission 7-21311
- $\text{In}_x\text{Ga}_{1-x}\text{As}$, atomic layer epitaxy growth, photolum., Hall meas. 7-22527
- $\text{In}_x\text{Ga}_{1-x}\text{As}$, gas source MBE growth 7-52361
- $\text{In}_x\text{Ga}_{1-x}\text{As}$, magnetophonon resonance effect 7-21942
- $\text{In}_x\text{Ga}_{1-x}\text{As}$, photoluminescence determ. of effects due to In alloying 7-46096
- $\text{In}_x\text{Ga}_{1-x}\text{As}$ pseudomorphic quantum well lasers, carrier collection and stimulated emission 7-10928
- $\text{In}_x\text{Ga}_{1-x}\text{As}/\text{InP}$ heterostructures, OMVPE growth, quality, source comp., press. effect 7-39400
- $\text{In}_{1-x}\text{Ga}_x\text{As}-\text{In}_y\text{Al}_{1-y}\text{As}$ superlattices, lattice-matched and lattice-mismatched, dislocation filtering 7-21671
- $\text{In}_{1-x}\text{Ga}_x\text{As}-\text{In}_y\text{Al}_{1-y}\text{As}$ heterojunction, cyclotron resonance linewidth due to alloy scatt. 7-27399
- InGaAsP 1.3 μ m diode laser, ultra-high-speed modulation 7-5924
- InGaAsP 1.5 μ m DFB laser diodes, optical communication appls. 7-37202
- InGaAsP 1.55 μ m mode-locked laser with single-mode fibre output 7-50600
- InGaAsP (001), surface, dislocation etch pits, new etchant props. 7-59699
- InGaAsP BH lasers, radiative, Auger and nonradiative currents 7-57312

III-V semiconductors continued

- InGaAsP buried crescent injection lasers, differential quantum efficiency 7-25815
- InGaAsP buried crescent injection lasers, low threshold 1.5 μ m operation 7-43136
- InGaAsP buried heterostructure lasers, polarisation, effect of stress relax. caused by repetitive temp. change 7-62690
- InGaAsP constricted mesa laser, 8 Gbit/s return-to-zero modulation by gain switching 7-31366
- InGaAsP DFB lasers, extremely low-noise facet-reflectivity-controlled 7-31320
- InGaAsP device fabrication using HBr-H₂O etching soln. 7-46728
- InGaAsP directly modulated semicond. lasers, gain nonlinearity effects calcs. 7-20218
- InGaAsP double heterostructures for laser diodes, LPE growth, influence of P vapour ambient 7-46355
- InGaAsP epitaxial films, strain mapping by an X-ray diffraction technique 7-21786
- InGaAsP film, defect struct. and strain anal., X-ray topography 7-52344
- InGaAsP films, dense electron-hole plasmas, picosecond dynamics, acoustic phonon generation 7-45373
- InGaAsP injection lasers, mode-locked and gain-switched, timing jitter 7-11013
- InGaAsP, ion beam damage-induced masking for photoelectrochem. etching 7-44628
- InGaAsP, LPE growth on $\text{GaAs}_{0.7}\text{P}_{0.3}$ substrate, crosshatch pattern 7-59472
- InGaAsP laser, LPE grown, effect of crystal defects on reliability 7-36960
- InGaAsP laser amplifiers, recombination, gain and bandwidth characts. 7-57334
- InGaAsP lasers, injection, photodetection props. 7-31379
- InGaAsP layers, LPE on GaAs, immiscibility region, lattice matching 7-59465
- InGaAsP layers on InP (001), origin of grown-in dislocations 7-38415
- InGaAsP, layers on InP, rel. lattice parameter meas., convergent beam electron diffraction 7-52371
- InGaAsP local struct., EXAFS and near-edge struct. studies 7-64006
- InGaAsP, MOVPE system, gas switching mass spectrometry 7-22526
- InGaAsP materials, OMVPE growth for long wavelength detectors and emitters 7-27931
- InGaAsP, optical gain spectra, effects of energy band struct. (Chinese) 7-59239
- InGaAsP, "patterning using photoelectrochem. etching and focused ion beams 7-22924
- InGaAsP, props. for integrated optics/optoelectronics in optical fibre communication systems, review 7-11178
- InGaAsP ridge waveguide laser threshold current optimisation, simplified hybrid optical model 7-57321
- InGaAsP, spinodally decomposed, elastic relax. effects on TEM 7-52378
- InGaAsP system, transferred electron effect anal. 7-64259
- InGaAsP TM-wave injected BH laser, ps switching optical bistability 7-50629
- InGaAsP wideband semicond. lasers, limitations on switching speed 7-10943
- InGaAsP/InP, semicond. superlattice heterojunction interface, SIMS anal. (Japanese) 7-2396
- InGaAsP/InP 1.3 μ m lasers grown on p-InP substrates, low threshold, high T_0 operation 7-1180
- InGaAsP/InP DFB lasers, DFB mode oscillation, temp. range 7-5910
- InGaAsP/InP double heterostructures, microcathodoluminescence studies 7-39189
- InGaAsP/InP heterostructures, carrier lifetimes and quantum efficiencies, photoluminesc. studies 7-64675
- InGaAsP/InP laser wafers, pinhole defects, identification of source 7-46356
- InGaAsP/InP multiquantum well layers, LPE, photolum., X-ray diffr. 7-53640
- InGaAsP/InP multiple quantum well waveguide phase modulator 7-57531
- InGaAsP/InP superlattices, gas-source MBE grown, X-ray diffr. and TEM studies 7-32839
- InGaAsP/InP:Fe buried crescent lasers with wide-bandwidth and high power 7-50560
- n-InGaAsP/p-GaAs diodes, photocurrent meas. of defect distribution 7-32851
- InGaAsP-GaAs double heterostructures, luminescence efficiency and surface recombination velocity 7-13196
- InGaAsP-InP, 1.5 μ m laser with high external quantum efficiency and controlled emission wavelength 7-57323
- InGaAsP-InP, heterolaser struct., distributed feedback conditions, luminesc. spectra anal. 7-50561
- InGaAsP-InP, integrated external cavity laser 7-36993
- InGaAsP-InP, long-wavelength components by VPE 7-46343
- InGaAsP-InP, quantum well wire, Auger recombination 7-7374
- InGaAsP-InP, solid-phase epitaxial Pd-Ge ohmic contacts 7-2706
- InGaAsP-InP bistable lasers, temp. depend. 7-5887
- InGaAsP-InP buried heterostructure lasers, internal thermal stress distrib. 7-10931
- InGaAsP-InP DFB laser with modified double-channel planar BH struct., 1.3 μ m high-speed operation 7-15896
- InGaAsP-InP DFB lasers with monolithic external cavity, spectral characts. for 1.3 μ m 7-20281
- InGaAsP-InP DFB laser monolithically integrated with tunable external cavity, linewidth and FM characts. 7-57316
- InGaAsP-InP DFB laser, waveguiding props. 7-57319
- InGaAsP-InP distributed-feedback injection laser, fabrication by LPE and VPE 7-57337
- InGaAsP-InP double heterostructures, luminescence efficiency and surface recombination velocity 7-13196
- InGaAsP-InP Fabry-Perot and DFB lasers, VPE transport fabrication 7-20277
- InGaAsP-InP heterostruct. laser output characts., quantum size effect active layer thickness variation effects 7-31323
- InGaAsP-InP high power long wavelength laser diode 7-10998
- InGaAsP-InP high-performance 1.3 μ m laser structures with both facets etched 7-20259
- InGaAsP-InP laser diodes, low resist. contacts on p-side 7-20276
- InGaAsP-InP laser, single-mode, 1.3 μ m, analog FM 7-37002
- InGaAsP-InP laser failure causes and distrib., laboratory service life tests 7-62692

III-V semiconductors continued

- InGaAsP-InP low-threshold separate-confinement heterostruct. laser characts. 7-31324
 InGaAsP-InP optical switches, carrier induced refractive index change 7-57606
 InGaAsP-InP planar surface BH lasers with hydride VPE-grown Fe-doped current blocking layers 7-20261
 InGaAsP-InP waveguides, optical parameters 7-62831
 InGaAsP-InP ridge waveguide lasers, LPE fabricated, design and 1.5 μm low-threshold operation 7-15897
 $\text{In}_{1-x}\text{Ga}_x\text{As}_y\text{P}_{1-y}$ /InP heterojunctions, MOCVD grown, spectroscopic ellipsometry study 7-39195
 $\text{In}_{1-x}\text{Ga}_x\text{As}_y\text{P}_{1-y}$ /InP quarter-wavelength-shifted DFB laser source for 1.55 μm underwater optical cable system (Japanese) 7-62720
 $\text{In}_{1-x}\text{Ga}_x\text{As}_y\text{P}_{1-y}$ cpd. semicond. alloys, lattice and band struct. props., review (Japanese) 7-7109
 $\text{In}_{1-x}\text{Ga}_x\text{As}_y\text{P}_{1-y}$ /Cd on InP, activation energy of impurity 7-32942
 $\text{In}_{1-x}\text{Ga}_x\text{As}_y\text{P}_{1-y}$ /Te films, Fermi energy, dopant conc. depend. 7-52867
 $\text{In}_{1-x}\text{Ga}_x\text{As}_y\text{P}_{1-y}$ /InP quantum well, 2D electron gas, self-consistent calcs. 7-58890
 InGaAsSb/AlGaSb DH lasers, MBE grown, room-temperature 2.2 μm operation 7-20219
 $\text{In}_{1-x}\text{Ga}_x\text{As}_y\text{Sb}_{1-y}$, mid-IR source and detector material 7-36964
 InGaP-InGaAlP MQW structs., room temp. excitons 7-58745
 $\text{In}_{1-x}\text{Ga}_x\text{P}$ solid solns., indirect band gap temp. depend., electrolum. spectra studies 7-38448
 $\text{In}_{1-x}\text{Ga}_x\text{P}$, epitaxial films, radiative recomb. 7-59257
 $\text{In}_{1-x}\text{Ga}_x\text{P}$ epitaxial layers, LPE, surface morphology rel. to lattice mismatch 7-33604
 $\text{In}_{1-x}\text{Ga}_x\text{P}$ LPE layers lattice-matched to GaAs, Hall mobility meas. and MESFET fabrication 7-7905
 InGaPAs, LPE growth on GaAs, immiscibility effects 7-39442
 InGaPAs/GaAs interface stress, Cr-related luminescence study 7-46101
 InN, band struct., pseudopotential method anal. 7-52421
 InN films, IR absorption 7-7778
 InP (100), ambient induced surface effects, O adsorption, photolum., conductivity 7-45429
 InP (100), empty surface states, two-photon photoemission 7-53498
 InP (100), prep. by P deposition and annealing, surface reconstruction, LEED, EELS studies 7-38311
 InP (110), oxidation, photoemission spectra studies 7-3147
 InP (110) cleaved surface and Schottky diodes 7-58850
 InP (110) photoexcited surface, time-resolved VUV photoemission spectroscopy 7-18919
 InP (110) surface, picosecond time-resolved photoemission study 7-46280
 InP (111), chemically polished and etched, characterisation of native oxide layer, ion scatt. spectra, AES, ESCA 7-22925
 InP (111) orderly faceted struct., LEED pattern anal. 7-21579
 InP {001} surfaces, chem. etch cleaning procedure 7-13668
 InP, acceptor higher excited states calcs. 7-52511
 InP and InP based materials, epitaxial growth, review 7-33574
 InP, chemical beam epitaxial growth investig. 7-7878
 InP chemical etching by Cl, thermodynamically predicted depend. on press. and temp. 7-22919
 n-InP compensated samples, MOVPE grown, Hall effect meas. 7-27348
 InP crystals and solar cells, radiation-induced defects, room-temperature annealing 7-39993
 InP device fabrication using HBr-H₂O etching soln. 7-46728
 InP, direct synthesis, growth, liquid encapsulated Czochralski method 7-59397
 InP, dislocation density reduction in crystal growth 7-2020
 InP, dislocation-complex defect interactions, photoluminescence studies 7-16608
 InP doping superlattices, nonlinear optical absorption 7-39069
 InP dry etching at room temp. 7-28227
 InP dual-wavelength channelled-substrate BH laser light source 7-62726
 InP, electrochemical C-V profiling 7-27325
 InP electrodes, surface modified, time resolved photoelectrochemical meas. 7-27415
 p-InP, electron irradi., atomic displacement threshold energy 7-2066
 InP, electron irradi. damage, impurity effects 7-12154
 InP epitaxial films, MO-chloride VPE growth 7-22566
 InP epitaxial films, MOCVD grown, identification of acceptors and donors 7-58688
 InP, epitaxial films, radiative recomb. 7-59257
 InP epitaxial layers, MOVPE, elec. characts., photolum. 7-22519
 InP, field assisted plasma grown oxide 7-39772
 InP films, hydride VPE, impurity incorporation, defect charactn. 7-53614
 InP films, MOCVD growth using plasma pre-cracking 7-7880
 InP films and structures, gas source MBE, review 7-33572
 InP films on oxidised Si substrate, laser recrystallisation 7-38398
 InP, floating zone melting prep., elec. props. 7-64238
 InP, grown-in defects, slow positron beam and positron labelling studies 7-44527
 p-InP, γ -ray irradiated low temp., nonradiative-recomb.-enhanced defect struct. transformation 7-2062
 n-InP, Hall factor calcs. 7-52657
 InP, Hall scatt. factor 7-45361
 InP, high resistivity layer form. by ion implantation, ohmic contact characterisation 7-38035
 InP, impact ionisation coeffs., lucky drift model including soft threshold energy 7-64258
 InP, impurity atom site location using channelling enhanced microanalysis 7-38023
 InP, ion beam damage-induced masking for photoelectrochem. etching 7-44628
 InP, ion enhanced chem. etching in Cl₂, thermal pulse model 7-54029
 InP, laser enhanced low temp. oxidation, dissociation of N₂O 7-39780
 n-InP, light scatt. by free carriers 7-17328
 InP, luminesc. associated with defect complexes 7-27757
 InP MIS structs. with amorphous C films, interfacial electronic props. 7-7400
 InP MIS structures, prep. by RF plasma oxidation, interface elec. props. 7-2731
 InP MIS structures, thermal treatment in P overpressure 7-7394
 InP, MISS, common anion rule, density distrib., photoionisation 7-38765
 InP, MOCVD on structured substrates, mass transport 7-39397
 InP, MOVPE on SiO₂ masked substrates at reduced press., vapour etching 7-39398
 InP, MOVPE; morphology, photolum., carrier conc. and mobility 7-22518

III-V semiconductors continued

- InP, maskless ion beam assisted etching 7-22923
 InP, melt grown, theoretical and expt. fundamentals of decreasing dislocations 7-53547
 InP, metal contacts, interfacial microstruct., elec. props., phase diagrams 7-45495
 InP microwave absorption transient spectroscopy for investigation of deep levels in semiconductors 7-52520
 n-InP, minority carrier diffusion length meas. using a photoelectrochemical technique 7-33030
 InP, multiphonon absorption (Chinese) 7-7682
 $\text{InP } n^+n^+$ struct., space-charge limited magnetoconductivity 7-45472
 InP, negative magnetoresistance and electron localisation in the region of a metal-insulator transition 7-12737
 InP, neutral shallow donor inter-excited-state transitions, far IR photcond. in mag. field study 7-22249
 InP, optical generation and phase-sensitive detection of SAWs 7-58598
 InP, passivation, by a-P and alkali metal polyphosphides 7-39778
 InP, passivation by plasma deposited P film 7-3540
 InP, patterning using photoelectrochem. etching and focused ion beams 7-22924
 InP pure and Er doped liquid phase epitaxial films, elec. props. in strong elec. fields 7-38779
 InP, quantitative trace anal. of impurities by SIMS 7-53480
 InP, radiation-damaged photocond., Hertzian dipole meas. of picosecond photoresponses 7-52690
 InP, rapid thermal annealing, heating behaviour 7-21258
 InP, reactive ion etching, AES, photoluminescence, SEM obs. 7-65241
 InP room temp. band edge photolum. intensity interpretation 7-27762
 InP rotating ring-disk electrodes, appl. of redox contacts 7-39982
 InP single crystal (100) surface, atomic scatt., electron-hole pair creation 7-27841
 InP solar cells, potential for use in space radiation environment 7-23181
 InP solar cells, radiation resistant characts. 7-8413
 InP solar cells in space radiation environment, comparison with GaAs, and Si cells 7-65484
 InP stress meas., photoelasticity determ. with aid of computer 7-31725
 InP, sublatitics direct resolution and identification by high-resolution TEM 7-37813
 InP, submicron gratings, reactive ion beam etching and deformation-free LPE overgrowth 7-13659
 InP substrate, integrated optoelectronics, micrograting form, by HV electron beam lithography 7-31443
 InP, substrate, plasma deposition of C dielectric films 7-39420
 p-InP substrate mass transport BH laser, narrow active stripe 7-31357
 InP substrate vapour phase etching, surface morphology, temp. depend. study 7-28220
 InP substrate with GaInAs epitaxial layer, depth profiling and interface detection using anodic oxidation 7-45057
 InP substrates, influence of inhomogeneities on quality of quaternary layers 7-32770
 InP substrates and devices, surface anal., SIMS appl. 7-22417
 InP, surface, for MIS device, As-stabilisation, effect on elec. and physicochemical props. 7-38767
 InP surface, interaction with H₂ 7-58632
 InP, surface analysis using organic-on-inorganic contact barriers 7-21991
 InP surface annealed under As pressure, epitaxial growth of InAs 7-2431
 InP surface metal-p⁺-n enhanced Schottky barriers formed by open tube diffusion technique 7-2710
 InP, surface recombination velocity and bulk minority carrier lifetime 7-17037
 InP surfaces, sputter etched, optoelectronic and structural props. 7-13661
 InP synthesis by modified horizontal Bridgman method, elec. props. 7-58821
 InP thin film solar cells on Si substrate, high efficiency and high radiation resistance 7-59852
 InP, ultrapure, atmospheric pressure OMVPE growth 7-13375
 InP, undoped and Zn(Cd) doped thin films, prep. and characts., appl. for solar cells 7-17895
 InP, VPE using flow modulation 7-7039
 InP waveguide, thermal index changes by optical absorpt., all-optical signal processing 7-31381
 InP:B, internal friction temp. depend. studies 7-38112
 InP:B, multiphonon absorpt. 7-59211
 InP:Be(Si), isothermal anneal techniques, comparison 7-16603
 InP:Bi thin film, epitaxy, impurity distrib., photoluminesc. spectra anal. 7-53388
 InP:Cr, impurity ion-lattice coupling, reson. phonon scatt. spectra 7-58420
 InP:Fe, Czochralski-grown, stoichiometric-related faulted loops, struct. and lumini. props. 7-51772
 InP:Fe, deep levels formed by Fe complexes 7-12657
 InP:Fe, epitaxial layers, MOCVD, doping profiles, SIMS, resist., temp. depend. 7-21248
 InP:Fe, LPE growth, SIMS 7-52363
 InP:Fe, midgap impurity levels, isomer shift and charge state calcs. 7-2538
 InP:Fe, OMVPE grown, electronic and optical props. 7-52868
 InP:Fe, optical spectra 7-53372
 InP:Fe, programmed magnetic field applied LEC crystal growth 7-59399
 InP:Fe, Si-implanted and rapid thermal annealed, photoluminesc. study 7-59243
 InP:Fe, transient photoconductive response 7-52681
 InP:Fe,Ga,Sb, LEC growth, dislocation density, resistivity, SIMS obs. 7-53552
 InP:Fe photoconductive detectors for VUV and soft X-ray regions 7-30084
 InP:Fe semi-insulating layers, MOVPE growth and elec. characts. 7-22511
 InP:Fe wafer, semi-insulating, elec. characteristics 7-45323
 InP:Ga,As,Sb single crystals, LEC growth, isoelectronic doping, dislocation density, X-ray topography 7-33549
 InP:Ge, Fermi level, determ. from phase diagram data of InP-Ge system 7-21808
 InP:Ge,S, LEC-growth, dislocation-free 7-17409
 InP:Hg ion implanted at 200°C, rapid thermal annealing, carrier conc. and mobility 7-32469
 InP:Mg p-n junction waveguide fabricated by Mg ion implantation 7-64326
 InP:Mn, deep acceptor level, props. 7-21853

III-V semiconductors continued

InP:Mn, LPE growth, carrier conc. control and appl. to buried heterostructure laser diodes 7-21774
InP:Mn³⁺, Jahn-Teller effect, mag. suscept. and ESR spectra anal. 7-52534
InP:S, LEC grown, influence of growth conditions on defects 7-32427
InP:S, shallow n⁺ diffusion of S, open-tube diffusion technique, n⁺-p junction formation 7-44912
InP:S,Ga,Sb, LEC growth, appl. mag. field method, dislocation etching 7-53553
InP:S substrate wafers for LPE growth of laser diode heterostructures, polarised IR and X-ray topographic evaluation 7-32453
InP:Si, substrate, encapsulated annealing, using SiN encapsulant 7-39779
InP:Sn substrate/epilayer interface, Sn depth profiling, AES and SIMS studies 7-27146
InP:Ti, Hg, semi-insulating, impurity electron state compensation mechanism, SIMS, SSMS, EPR and Hall effect meas. 7-64164
InP:Ti(Cr)(Ni), LEC growth, precipitate phase identification 7-16754
InP:Yb LPE layers, luminesc. and elec. props. 7-59464
InP:Zn, ion implantation and annealing, Raman studies 7-6652
n-InP:Zn, Zn diffusion 7-63882
InP:Zn(Cd), interstitial-substitutional diffusion, doping effects 7-6878
InP/Al UHV-cleaved and laser annealed interface, acceptor-like electron traps 7-7310
InP/Al(Mn)(Ag) interfaces, interactions, XPS and elec. transport studies 7-7384
n-InP/Au Schottky contacts, surface treatment by plasma-induced O radicals 7-38674
p-InP/Co(Pt) photocathodes for photoelectrochemical solar cells, H₂ evolution from alkaline solns. 7-13922
p-InP/electrolyte, photoelectron emission spectra, thermodynamic consts. 7-12856
InP/GaInAs/InP heterostructures, OMVPE, high speed p-i-n photodiodes, photolum., Hall meas. 7-27387
InP/InGaAs heterojunction bipolar transistors, open-tube Zn diffusion 7-44914
InP/InGaAs near-IR detector self-calibration feasibility determ. 7-15002
InP/InGaAsP antiresonant reflecting optical waveguides, chemical beam epitaxy and propagation losses 7-57537
InP/InGaAsP device structures, LPE growth 7-33610
InP/metal Schottky barrier diode, electrical props. 7-27426
InP/native oxide MIS structures, interface elec. props. 7-33851
InP/Pd (110) interface, chem. reactions, overlayer morphology and Fermi level pinning 7-7020
InP/SrF₂ lattice mismatch, temp. depend. 7-63849
InP-Al, wet anodisation, compositional profiles 7-65216
InP-Al₂O₃-metal struct., improved elec. props. with heat resist. interface 7-38753
InP-aqueous electrolyte interfaces, laser induced photoelectrochemistry 7-27412
InP-Au, metallic contact layers, thermal dissociation, P loss 7-23005
InP-Au interface, Fermi level pinning, growth characts., photoemission spectra 7-22009
InP-Au(Al) Schottky barriers, defects introduced by mech. polishing 7-39768
InP-C based MIS struct., interfacial characts. 7-2732
InP-CdS solar cells, high efficiency, with thermally evaporated window layers 7-3701
InP-Cu(Au)(Ag), interphase contact interaction 7-33087
InP-Ca_{0.47}In_{0.53}As superlattice, electron and hole impact ionisation rates 7-17076
InP-Ga_{1-x}In_xAs_{1-y}P_y double heterostr., device quality, growth by MOVPE 7-7877
InP-Ga_{1-x}In_x-xP_xAs_{1-y} heterojunction interfaces, electronic band struct. (Chinese) 7-33070
InP-GaInAs, 2D electron gas, persistent photoconductivity 7-33046
InP-GaInAs planar BH lasers, OMVPE growth 7-1183
InP-In_{2-x}Sn_xO_{3-y}, solar cells for space appl. 7-3700
InP-InGaAs single quantum wells, transport and persistent photoconductivity 7-38709
InP-InP:As epitaxial layers, dislocation reduction, device performance effects 7-7354
InP-metal interfaces, Fermi level pinning 7-2714
InP-n⁺-i-In_{2-x}Sn_xO_{3-y}, Schottky diode, solar cell props. 7-65474
InP-SiO₂ interface, electron localisation 7-45514
InP-SiO₂ MISFET, electron tunnelling into oxide traps 7-38764
InP:As_{1-y}, solid solutions, temp. depend. of lattice constants and thermal expansion coeffs. 7-21165
InP(As)(Sb), band structure, polarisation-dependent angle-resolved photoemission spectroscopy 7-21814
InP(As)(Sb) surfaces, oxidation processes studied by high-resolution electron microscopy 7-39766
InP(Sb), ion milling, TEM 7-39344
InP(110), P- and In-rich, electronic states, semi-empirical tight binding calcs. (Chinese) 7-12773
InP=Si(Sn)(Be), doping using thermal atomic beams in chemical beam epitaxy 7-44584
InSb, 1/f noise, temp. depend. 7-52710
InSb (-1-1-1) (3 × 3) reconstructed, X-ray diffr. studies 7-6951
InSb (110), LEED surface crystallography and R-Factors 7-26596
InSb (110), surface electron states, effect of Al submonolayer coverage, soft XPS study 7-2653
InSb amorphous films, metal-semicond. transitions, superconductivity 7-64085
InSb, anodic native oxide, interface width, AES profiles 7-22911
InSb array IR imaging camera, for astronomical appls. 7-34865
InSb, a dislocations, motion, small shear stresses 7-44553
InSb bicrystals, n-inversion layers, pressure dependence electron states 7-45468
InSb bistable etalon, regenerative pulsations 7-20318
InSb bistable optical arrays, diffusion effects 7-57447
InSb, carrier lifetime, pressure depend. 7-52644
InSb charge injection device arrays, IR camera for astronomical imaging 7-34872
InSb, coherent spontaneous oscills. under transverse breakdown conditions, high frequencies 7-17046
InSb, conduction band, deformation potential constant 7-7112
InSb, conduction electrons g-factor anisotropy, spin-orbit splitting calcs., comment 7-38441
InSb, cyclotron resonance harmonics in conduction band, obs. 7-53136

III-V semiconductors continued

InSb, Czochralski growth rate and spreading resist. relations (Japanese) 7-26679
InSb, Dember EMF contrib. to capacitor photo-EMF 7-38621
InSb, density of excited electron-hole plasma 7-38608
InSb, density of states and effective mass determ. 7-38433
n-InSb, electron absorption of sound, hopping mechanism 7-17056
InSb, electron inversion layers, cyclotron and electron spin resonance 7-38736
InSb Fabry-Perot IR bistable devices, parameter optimisation 7-57396
InSb films, preparation of highly sensitive magnetoresistance elements 7-7859
InSb, four-wave mixing, degenerate and nondegenerate 7-11069
InSb, free-electron g-factor meas. by spin-flip Raman scatt. gain method 7-2470
InSb, galvanomagnetic luminescence 7-3095
InSb, galvanomagnetic luminesc., radiative heat pump appls. 7-40019
InSb heterostructures, MBE growth 7-27910
n-InSb, impact ionisation electron-hole pair generation, high power optical wave elec. field effect, luminesc. obs. 7-30225
InSb, impurity bands and their conductivity in strong mag. fields 7-45152
InSb, impurity doping by photonuclear reactions 7-16589
InSb, impurity level calcs., effective mass pseudopotential method 7-7163
InSb, large-k acoustic phonon imaging, freq. selectivity and isotopic defect scatt. effects 7-26885
InSb, length scale near metal-insulator transition 7-52425
n-InSb, low-temp. growth by plasma process (Japanese) 7-7061
InSb MIS structures, (BN)_n and Si₃N₄ film formation using plasmachemical methods 7-33584
InSb MOS interfaces, annealing, O diffusion and reaction 7-58665
InSb MOS structures, heat treatment effects 7-8031
n-InSb MOS structures, heterogeneity of generation processes, expt. 7-17106
InSb MOS structures, electric field effects on characteristics 7-38738
n-InSb, magnetic two-phonon resonance involving acoustic phonons 7-45355
InSb, metal-insulator transition, mag. field induced, low temps. 7-45158
InSb metalorganic magnetron sputtered films, structural and compositional characts. 7-21725
InSb, n-type, 60° dislocation motion, etching studies 7-63619
InSb, narrow gap, spontaneous oscills. under plasma resonance conditions 7-38605
InSb, narrow-gap semiconductor, bound excitons, magneto-absorption studies 7-45168
InSb, nondislocating crystals, damaged surface struct., X-ray scatt. (Russian) 7-58581
InSb optical bistable elements as optical computer components 7-37025
InSb, optical reflection anisotropy due to surface band bending 7-39062
InSb optical switching elements, transverse coupling 7-57446
InSb optically bistable etalon, critical slowing-down phenomena 7-5942
InSb passivation, SiO₂, anodic native oxide interfaces studies 7-22917
InSb, pulsed laser evaporation, neutral and charged particle emission 7-3120
InSb, resonant states, strong mag. field, Coulombic impurity pot. 7-32925
InSb, room temp., cascaded bistable optical devices based on two-photon absorpt. 7-57413
InSb shallow magnetodons photo-ionisation spectra studies 7-64165
InSb single cryst., neutron acoustic effect, neutron diff. study 7-26875
InSb, solid-state electron plasma magnetised, circular antenna directivity diagram 7-45372
n-InSb, solid-state plasma, stimulated Raman scatt. of extraordinary mode 7-31398
InSb strong-absorbing single crystals, Laue X-ray diffr. thickness depend. anal. and interpretation (Russian) 7-44310
InSb surface, oxidation at room temp. 7-46734
InSb surface damage layer refl. spectra and thickness meas. 7-22209
InSb, time-resolved self-defocusing 7-43267
InSb, transient grating formation under two-photon excitation 7-11037
InSb transphaser, gain-bandwidth product 7-57417
InSb with metallic donor cluster, anomalous Hall effect below mag. field induced metal insulator transition 7-2485
InSb:Te, Cd, Zn single crystals, Czochralski growth, solute distrib., mag. field effect on melt 7-3158
InSb:Te, resonance absorpt. of electromag. wave due to impurity band 7-52499
InSb:Te crystals, Czochralski growth, layered heterogeneity, melt temp. fluctuations, mag. field effect 7-27888
InSb:Te(Ge)(Cd)(Si), heterogeneity study 7-21476
InSb:Te(Se)(Si)(Cd)(Zn) thin films, doping, Hall effect meas. 7-21743
InSb:Ti, physicochemical behaviour of Ti 7-21452
InSb/CdTe interface, quasi-2D electron gas obs. 7-21987
InSb/LiNbO₃ layered struct. with transverse drift, SAW detection 7-12447
InSb/Teflon SIS structs., EM magnetoplasma Gaussian beams, propag. and size resonances study 7-58905
InSb-NiSb eutectic composite, rel. between metal fibre morphology and elec. props. 7-59644
InSb-SiO₂ MIS structures, photo-CVD fabrication 7-38739
Mn/GaAs interface formation on clean and oxidised (110) surfaces 7-45029
Nb-InAs-Nb proximity system, Josephson current, field effect 7-45573
Ni/GaAs film/surface reaction, TEM 7-39920
Ni-AuGe-GaAs, ohmic contacts, interface reactions, elec. behaviour 7-27031
Ni-GaAs, interphase contact and interaction 7-16880
Ni-GaAs, lateral reactions, hot-stage TEM 7-27030
Ni-GaAs, metallurgical reactions, heavy ion Rutherford backscattering spectrometry 7-53488
NiTa-GaAs, phase separation, cross-sectional TEM 7-27152
n-nP, Anderson transition in a mag. field 7-16944
Pd/GaAs film/surface reaction, TEM 7-39920
Pd-GaAs, metallurgical reactions, heavy ion Rutherford backscattering spectrometry 7-53488
Pd-GaAs, phase formation sequence, morphology 7-27153
Pt-GaAs, metallurgical reactions, heavy ion Rutherford backscattering spectrometry 7-53488
Pt₂Si_{1-x}/n-GaAs contacts, elec. and metallurgical characts. 7-64345
Rh/GaAs Schottky contact, correlation between solid-state reaction and electrical props. 7-58655

III-V semiconductors continued

- Si-GaAs_{0.7}P_{0.3} multijunction solar cell, solid state photovoltaic research status at SERI 7-8389
- Si-GaAsP-GaP solar cell, high efficiency mech. stack, performance meas. 7-8401
- Si-InP (110) heterojunction, characterisation 7-33079
- Si-InSb heterojunction, spectral characts. and detection props. 7-38712
- Si-SiO₂-InSb hybrid struct. spectral characts. and detection props. 7-38712
- Si₃N₄/GaAs buried interface, EXAFS studies in total reflection and dispersive modes 7-64765
- TaIr-GaAs Schottky barrier contacts 7-17102
- W-GaAs diode system, Schottky barrier degradation after high temp. annealing 7-33089
- WSi₂-GaAs interface, thermal stability 7-52302
- ZnSe/GaAs, electron beam pumped lasing action obs. 7-43093
- ZnSe-GaAs:Cr, meas. of residual stress by Cr-related luminesc. lines 7-7726

III-VI semiconductors

- GaAs films, changes of optical const. stimulated by external effects, determ. 7-22362
- GaS, layered, high temp. e-h liq., radiative recomb., luminesc. spectra study 7-17343
- Ga₂Se_{1-x} crystals, phase transitions under press., exciton-phonon interaction 7-44785
- α -GaSe, acoustoelectronic interaction, piezoelectric effect 7-45399
- GaSe, evidence of exciton-plasma transition in emission spectra 7-59249
- GaSe, excitons, room temp. self screening 7-45166
- GaSe, gamma irr., photoluminescence spectra, temp. depend. 7-17336
- GaSe laminar semicond. intercalation cpds., phase equilibria and stability studies (Russian) 7-21409
- GaSe layer cpd., Al dopant intercalation, Auger and IR spectra studies (Russian) 7-32476
- GaSe, layered cryst., Raman scatt. intensities and atomic bonding 7-22257
- GaSe layered intercalated crystals, formation of electretic state 7-38994
- GaSe, photoexcited localised excitons thermalisation, stacking disorder effects, photolum. study 7-27770
- GaSe, screening of excitons by free carriers, transmission, reflection and luminescence spectra 7-38460
- GaSe, spontaneous and stimulated photoluminescence studies 7-22315
- GaSe, surface phonons, inelastic electron tunnelling spectroscopy 7-63935
- GaSe:Mn single crystals, optical props. 7-27777
- InSe crystals, melt-grown, electron diff. study 7-1994
- InSe, excitonic luminescence, influence of macroscopic inclusions 7-13204
- InSe films, formation by double source evaporation 7-59436
- InSe intercalation cpd., with Ag, prep. 7-54146
- InSe laminar semicond. intercalation cpds., phase equilibria and stability studies (Russian) 7-21409
- InSe layer cpd., Al dopant intercalation, Auger and IR spectra studies (Russian) 7-32476
- n-InSe layered crystals, 2D electron gas regions, magnetoresist. meas. 7-45359
- InSe, photoluminescence, defects effects 7-39161
- InSe single crystals, growth by travelling heater method, carrier conc., photoelectrochemical props. 7-59410
- TlSe, thermal expansion coeff. temp. depend. and absorpt. spectra meas. 7-58508
- ZnS, single cryst. growth by gas source MBE 7-17397
- Zn₂Se_{1-x} polariton dispersion with Fermi reson., Raman scatt. cross-section (Ukrainian) 7-12623
- ZnSe:H, proton implanted, localised vibr. mode, IR transmission spectra 7-51981

IIR filters *see* digital filtersIKBS *see* expert systemsillumination *see* lightingimage amplifiers *see* image intensifiers**image converters**

- see also* fluorescent screens; image intensifiers
- gas discharge, operating in avalanche mode, intrinsic blurring and freq. contrast characts. 7-4937
- high-speed photography, videography and photonics, conf., San Diego, CA, USA (Aug. 1985) 7-18486
- liquid crystal spatial light modulators for visible to IR dynamic image converters 7-37133
- liquid-crystal spatial light modulator, coupled to image converter, expt. investig. 7-43440
- optical convertor for marine quartz gravimeter 7-29262
- picosecond electronic framing camera 7-20465
- streak camera performance characts., with cooled CCD 7-19425
- streak recording of picosecond pulses 7-15026
- zoom convertor with focusing and thermal compensation functions 7-31516

image iconoscopes *see* television camera tubes**image intensifiers**

- airglow (OH) imaging system, using image intensifier and solid state sensor 7-29288
- aurora CCD-image intensifier camera, for all-sky observation 7-40603
- binoculars, passive, with ocular disparity, design 7-62813
- biomedical image intensifier digital imaging systems, struct. mottle obs. 7-54721
- biomedical image intensifier TV digital systems, accurate meas. of charact. curves by Al stepwedge technique 7-54726
- digital subtraction radiography technology, equipment and techniques 7-40267
- electro-optical meteor observation, techniques and results 7-47716
- electron analyser with position sensitive detector, scattered electrons influence 7-36377
- electron-optical image luminance amplifiers, resolution capability 7-50784
- energy analyser with MCP calibrated using cellulose nitrate film 7-48914
- fast framing camera with independent frame adjustments 7-18894
- fluoroscope, portable, with image intensifier, optimal screen characts. 7-61407
- ion signal calibration in imaging atom-probe with time-gated intensifier 7-48911
- MCP detection quantum efficiency meas. 7-41542

image intensifiers continued

- microchannel spatial light modulator, high-gamma, for nonlinear optical processing 7-25959
- microchannel spatial light modulator with improved resolution and contrast ratio 7-25954
- multichannel X-ray detector design 7-41555
- nanosecond optical shutters 7-20467
- photometry with image intensifiers and integrating readout devices effect of phosphor persistence 7-9870
- photon counting imaging microchannel plate detectors calibration, for EUV astronomy 7-29404
- picosecond semiconductor lasers for characterizing high-speed image shutters 7-20466
- proximity image intensifier persistence improvements with Y₂O₃S:Tb phosphor 7-57598
- scanning electron microscope, using hemispherical retarding field energy analyser with microchannel plate detector 7-15035
- scanning X-ray imaging system for quantitative arteriography and blood flow meas. 7-40266
- soft X-ray imaging with high-gain MCP detector systems 7-41564
- stripline microchannel plates, subnanosecond spectroscopy appl. 7-24708
- UV imaging photon detector, large format for astronomical spectroscopy 7-56342
- X-ray, with large input aperture and high resolution (Czech) 7-35650
- X-ray spectrometer, 2D imaging, using microchannel plate collimator 7-48927
- In seal and appl. to proximity focussed image intensifier (Chinese) 7-48763

image orthicons *see* television camera tubesimage processing *see* picture processing**image sensors**

- see also* CCD image sensors; television camera tubes
 - amorphous semiconductors, conference, Palo Alto, CA, USA (April 1986) 7-29602
 - amorphous semiconductors for microelectronics appls., conf., Los Angeles, CA, USA (Jan. 1986) 7-24282
 - astronomical observing techniques and instrumentation, book 7-60910
 - coherence image detection theory 7-48849
 - digital image input devices, resolution, curve-fitting method 7-57600
 - far-focus thermal imager system, deep-focus attachment 7-30061
 - fast framing camera with independent frame adjustments 7-18894
 - IR streak camera for use in 1.0 to 1.6 μ m region 7-18896
 - IR technology and appls., conf., San Diego, CA, USA (Aug. 1985) 7-18487
 - IR zoom telescope development 7-31425
 - laser scanner, image capture capabilities and PCB inspection applic. 7-57601
 - linear pyroelectric array IR sensor 7-30089
 - liquid-crystal spatial light modulator, coupled to image converter, expt. investig. 7-43440
 - luminescence imaging document analyser 7-57599
 - meteorological satellite, radiometers, IR detectors and their calibration 7-23898
 - meteorological satellite GOES-I, J, K instruments developed by Kodak 7-23971
 - MM-wave radiometer system for remote sensing appls. 3 mm operation, aircraft/helicopter installation 7-23880
 - MTF measurement methods, anal. (German) 7-20150
 - optical scanning systems, Sawyer motors use 7-57602
 - photon counting detectors for space astronomy, wedge and strip image readout systems 7-47713
 - photon counting image acquisition system, performance analysis 7-30088
 - position/dimension meas., laser-based system with triangulation format 7-24625
 - push-broom linear array scanner, design of all-reflective flat-field objective 7-55320
 - pyroelectric array imager, theoretical and expt. performance 7-18877
 - pyroelectric detector and imaging developments 7-24702
 - real-time imaging of analyzed areas in surface analysis 7-12427
 - scanning optical microscope using sequential imaging 7-48842
 - solid-state imaging arrays, conf., San Diego, CA, USA (Aug. 1985) 7-29582
 - spectrally selective shutter in proximity to focal plane 7-20397
 - thermal imager performance meas., objective meas. of minimum resolvable temp. difference 7-30092
 - thermal imaging system performance assessment 7-30091
 - thermal neutron imaging using position sensitive photomultiplier 7-49819
 - thermoplastic optical recording devices 7-37201
 - UV imaging photon detector, large format for astronomical spectroscopy 7-56342
 - BaTiO₃ imaging threshold detector using phase-conjugate resonator 7-6019
 - CdHgTe focal plane arrays, sampling effects reduction 7-30090
 - CdTe/a-Si:H heterojunction, X-ray image sensor fabrication 7-41557
 - Fe₂O₃/o-toluidine photoelectrochemical imaging system (Japanese) 7-35590
 - HgCdTe focal plane array photodetectors, growth, performance and array fabrication 7-15001
 - Si colour image sensor, based on wavelength dependence of radiation adsorption 7-4892
- image storage tubes**
- data acquisition suites, multichannel, with time-scale conversion and storage CRT, design 7-61321
- imagers** *see* image sensors
- images, optical** *see* optical images
- imaging, acoustic** *see* acoustic imaging
- imaging, infrared** *see* infrared imaging
- imaging, NMR** *see* nuclear magnetic resonance spectroscopy
- IMMA** *see* ion microprobe analysis
- immiscibility** *see* solubility
- impittance, electric** *see* electric impittance
- impact (mechanical)**
- see also* ballistics; impact strength
 - AGR helically wound heat exchanger, impacting phenomena anal. for Heysham 7-56790
 - barrier puncture with brittle fracture by rigid cone 7-43786
 - bars, collision with bar or disk, longit. impact, mech. similarity study 7-37394
 - bars, initially curved, dynamic elastoplastic buckling 7-63024

impact (mechanical) continued

bars, plastic impact, contact duration 7-37393
beams, viscoelastic, strength evaluation under impact load 7-57712
body collision between elastic half-planes, mixed problem soln. 7-43738
body suspended on string with impact interactions, stability of permanent rotations 7-41090
cantilever beam, transversely isotropic, smooth indentation 7-26227
charged microspheres, interaction with extended surfaces 7-59308
colliding bodies, penetration model accounting for ductile props. 7-58398
cylinder, composite with penny-shaped crack, impact response 7-37384
dynamic isochromatic method in expt. contact mechanics (*German*) 7-20667
elastomers, impact wear 7-22844
EM radiation on collision of solids 7-42890
erosion rate, time dependence, probabilistic approach 7-37399
erosion rate 7-3464
flexible multi-body systems, impact response 7-57724
fractographic features caused by impact load and microstruct. effect of impact vel. (*Japanese*) 7-51929
geological targets, penetration expts. 7-14271
glassy polymers, time depend. nonlinear deform. 7-63733
graphite, nucl. grade, polycryst. beam, finite contact area effect on impact stresses 7-28050
hot gas spraying, particle impact interaction with substrate 7-27894
human spinal cord effects of impact loads, full-scale and computational expts. 7-34294
icy targets, cratering, laboratory expts. 7-34863
inner cylindrical surface, erosion by force particle impact 7-26852
laminates, two-layered, subjected to impact load, dynamic response (*Japanese*) 7-50946
nylon-6-rubber-modified rubber blends, mixing effect on morphology, mech. and impact props. 7-37903
plates, composite, impact tensile loading, crack bifurcation modes 7-50993
polymers, deform. under impact, transient high temp. meas. 7-22802
rod, long, plastic wave propag., strain and temp. distrib. (*Japanese*) 7-31678
rod penetration, flow field model 7-11360
rod penetration models, extension of hydrodynamic theory 7-20665
rods, nonlinear propagation of elasto-plastic waves 7-26200
rubber half-space, rigid sphere impact, coeff. of energy absorpt. 7-1520
seated human, response to vibr. and impact 7-3831
semi-infinite target penetration by long rods 7-51001
slightly slanting impact on an elastic cantilever column—an experimental study 7-51008
steel, Cr containing, elevated temp. combined erosion-corrosion, particle impacts 7-3517
steel, Cr-Mo, elevated temp. erosion-corrosion 7-3518
steel, Cr-Mo, erosion-corrosion, effect of temp. 7-3519
steel, stainless, high velocity shock impact, numerical simulation of sample recovery fixture 7-38120
steel, stainless 304, erosion by sharp alumina particles 7-3453
steel tubes, energy dissipation characts. 7-63034
steels, surface degradation in elevated temp. gas-particle streams 7-3520
stepped circular tubes, collapse under impact axial load (*Japanese*) 7-11310
stress strain relationships, elastic deformation, specimen connected with long bar (*Japanese*) 7-11290
strip, infinite orthotropic, finite crack, impact response 7-63082
thermoplastic materials, erosion resistance, angular particle impingement at normal incidence 7-3442
thoraco-abdominal biomechs. research, use of quadruped models 7-40189
vibration-impact systems with moving limiters, nonsmooth transforms. 7-11269
vibroimpact system analysis 7-63041
viscoplastic threads, transverse impact of cone (*Russian*) 7-63083
Al, plastic deformation under impact loading, metallography, SEM and TEM studies (*Russian*) 7-3361
Al₂O₃, shock loaded, release behaviour, plate impact expts. 7-2101
PLTZ, elastic-plastic contact damage 7-39627
WC-Co, erosion rate 7-3464
Zn-based alloys, mechanical props., alloying addition effects (*Japanese*) 7-8090
ZrO₂ base ceramic thermal barrier coatings, erosion rel. to processing and microstruct. 7-3450

impact avalanche transit-time diodes *see* IMPATT diodes

impact ionisation

hexatriacontane, hot electron cond. and relax., internal photoemission for transport anal. method 7-45340
MIS structure, carriers in insulator and at semiconductor-insulator interface, EEPROM appl. 7-2730
MOS systems, interface state generation upon carrier injection 7-38759
multivalent traps, capture to emission ratios 7-7260
p⁺n junctions, impact ionisation rates, field fluctuation effects, Monte Carlo simulation 7-64323
semiconductor, soft energy thresholds and lucky drift model 7-52635
semiconductors, electrical breakdown at grain boundaries 7-45339
semiconductors, intrinsic, solid-state plasma, local impact ionisation regions form. 7-52663
semiconductors, narrow gap, spontaneous oscills. under plasma resonance conditions 7-38605
solid dielectrics, breakdown and prebreakdown phenomena, charge transport and dielectric aging 7-39014
superlattice APDs, impact ionisation, theory 7-12850
superlattice avalanche photodiodes, impact ionisation theory appl. 7-58886
superlattice tunnelling-assisted impact ionisation rate calcs., analytical approx. 7-64324
CaF₂-Si, MBE of CaF₂ on Si and overgrowth with Si or Ge characts. 7-22495
CdS thin films, deep trap depth, TSC meas. 7-58774
GaAs current limiters, impact ionisation breakdown 7-52639
GaAs, electron impact ionisation rate in nonuniform elec. fields, simulation 7-33021
GaAs, impact ionisation, soft-threshold lucky drift theory, mean free path calcs. 7-64256
GaAs, impact ionisation coeffs., lucky drift model including soft threshold energy 7-64258
GaAs, semi-insulating, switching effect, deep level spectroscopy appl. 7-38630

impact ionisation continued

GaAs-GaAlAs superlattice structs., impact ionisation coeff., lucky drift model 7-52793
Ge, extrinsic photoconductors, nonlinear dynamics and chaos 7-52685
Ge, nonlinear transport, morphogenetic reaction-diffusion model 7-27337
p-Ge, spatial correlations of chaotic oscillations in post-breakdown regime 7-64255
In_{0.53}Ga_{0.47}As, impact ionisation coeffs., lucky drift model including soft threshold energy 7-64258
InP, impact ionisation coeffs., lucky drift model including soft threshold energy 7-64258
InP-Ga_{0.47}In_{0.53}As superlattice, electron and hole impact ionisation rates 7-17076
InSb, coherent spontaneous oscills. under transverse breakdown conditions, high frequencies 7-17046
n-InSb, impact ionisation electron-hole pair generation, high power optical wave elec. field effect, luminesc. obs. 7-33025
PbTe, low-voltage electroabsorpt., exciton states, magnetoabsorpt. spectra 7-2501
Si diffused-junction solar cells, shunt resist. and soft reverse characts. 7-17863
Si, fast ionisation waves due to absorpt. and reemission of luminesc. 7-52627
Si, impact ionisation coeffs., lucky drift model including soft threshold energy 7-64258
Si, oxidation, trap generation by avalanche electron injection, HCl effects 7-3531
Si-SiO₂ in MOS structs., charge phenomena in thermal films with avalanche injection 7-2727
SiO₂ thermal oxide films on Si substrate, ramp-voltage-stressed I-V characts. 7-17112
ZnO varistors, electroluminescence temp. depend. and conduction mechanisms 7-17349
ZnO-electrolyte interface, electrolum. under cathodic and anodic pulsed polarisation 7-13235

impact phenomena *see* collision processes

impact strength

see also fracture toughness; notch strength
Al-Zn-Mg-Cu, impact toughness improvement by intermediate thermomech. treatment 7-53907
alumina, polycrystalline ceramics, spall strength, plate impact meas., spall zone model calcs. 7-33797
alumina polycrystalline ceramics, shock fracture and recompaction, double impact technique study 7-33880
bronze BrAZh, elec. discharge sintering of powder from swarf, electrophys. and mech. props., microstruct. 7-29794
cement-based composite, strain rate effects on fracture, conf., Boston, USA (Dec. 1985) 7-14712
Cr-MoVW ferritic steel, ductile-brittle transition temp., irradi. flux depend. 7-56825
fibre reinforced composite tubes, radial impact strength 7-59709
glass, helicopter windshield, chemically tempered impact fracture 7-28108
glass fibre reinforced epoxy, unidirectional, impact behaviour, temp. influence 7-3427
glass fibre reinforced polypropylene, short-fibre, struct. and mech. props., effects of moulding geometry 7-3348
low activation, tempering, toughness, ductile-brittle transition props. 7-53862
nylon 6 and 66, impact strength in dry and moist states 7-3414
polyamide 6-polyethylene blends, miscibility, mech. props. 7-59535
polycarbonate, impact props. and residual stress state, thermal treatment effects 7-32557
polyether sulphone, flexed plate impact testing, moulded notch effect 7-59713
polyethersulphone, flexed plate impact testing of notched specimens 7-22799
polypropylene, glass-flake reinforced, impact fracture 7-39659
polypropylene, hot isostatic pressing, mech. strength improvement 7-7955
polypropylene mica filled composites, struct.-mech. props. relations 7-1919
PVC, impact fracture regularities, matrix morphological struct. effects (*Russian*) 7-16677
PVC, impact strength, morphology influence (*Russian*) 7-44682
PVC, mech. props. in β -transition region (*Russian*) 7-63724
steel, alloy, impact behaviour, influence of grain boundary carbide density 7-13574
steel, alloy type, low-C, tempering temp. effect on mech. props. and crack resist. 7-39654
steel, austenitic, Al-Mn, mech. props., oxidation and corrosion behaviour 7-65218
steel, austenitic, fusion reactor first wall material, development and testing 7-53860
steel, austenitic stainless, tensile and impact props., effect of grain boundary carbides 7-33785
steel, C, Vasco X-2M, precipitation during tempering, rel. to impact toughness 7-46494
steel, cast, nonmetallic inclusions influence on fracture character 7-3421
steel, constructional carbon type, original charge purity influence on microstruct. hardenability and mech. props. 7-46521
steel, Cr-Mo, normalised heavy section plate, weld cold cracking susceptibility (*Japanese*) 7-3425
steel, Cr-Mo, toughness, impurity element effects 7-53856
steel, Cr-Mo type, deformed, struct. and mech. props. after long ageing 7-8106
steel, Cr-Ni-Co VKS6, struct. and mech. characts., effects of Ni, Co and heat treatment 7-8108
steel, Cr-Ni-Mo, Ge and melting method influence on mech. props. at high temp. 7-8025
steel, Cr-Ni-Mo type, austenitisation conditions effect on austenite decomp. kinetics and mech. characts. 7-39557
steel, CrMoV, cold rolled, effects of ageing on mechanical properties (*Russian*) 7-13478
steel, cryogenic, Al alloying effect on mech. and mag. props. 7-39679
steel, die, heat-resistant, optimum hardening temps., struct. and mech. props. 7-8022
steel, dislocation struct. rel. to cyclic bending strain 7-22760
steel, ferritic, fusion reactor first wall material, development and testing 7-53860

impact strength continued

- steel, ferritic, unirradiated, low activation, microstructure and mechanical props. 7-53863
- steel, fracture toughness prediction from Charpy impact test results (*Japanese*) 7-59611
- steel, growth under impact tension 7-28105
- steel, heat treatment method effect on struct. and mech. props. 7-39561
- steel, high Mn, impact toughness depend. on Mn/C ratio 7-39657
- steel, high speed, TiN coated, ductility, impact testing 7-46569
- steel, high-speed, cast and wrought, impact-fatigue strength 7-39656
- steel, high-speed p/m tungstenless, Mo and V effect on microstruct. and operating props. 7-33788
- steel, high-strength low-C weldable, C content effect on struct. and mech. props. 7-46583
- steel, low-alloy, H-beams, controlled rolling effect on mech. props. 7-39562
- steel, low-alloy construction, nonmetallic inclusions influence on impact strength and fracture type 7-8085
- steel, low-C, wrought, thermal strengthening methods effectiveness 7-46524
- steel, low-pearlite, rules of austenite decomp. in continuous cooling 7-3339
- steel, martensitic stainless, low activation, hardening, tempering, mechanical props. 7-53861
- steel, martensitic stainless, precipitation hardened, impact toughness rel. to Mo content, AES obs. 7-39666
- steel, medium C, impact toughness and fracture, prolonged high tempering effects (*Russian*) 7-8083
- steel, Mn-Cr, case carburising, mech. props., influence of inclusion characts. 7-65135
- steel, Mn-Mo-V, reactor piping material, strength, deformation and fracture behaviour 7-13578
- steel, roll type, crack resist. as criterion of effectiveness, alloying and heat treatment parameters influence 7-53884
- steel, secondary-hardening, bainitic embrittlement 7-3405
- steel, stainless, austenitic, valve type, heat treatment schedule effect on failure nature 7-3423
- steel, stainless, austenitic-pearlitic, N effect on phase comp. and props. 7-53754
- steel, tool and struct., nitrided, prior heat treatment effect on mech. props. 7-46707
- sunhemp fibre reinforced polyester composites, tensile and impact props. 7-39592
- wollastonite reinforced polyamide 6, strength props., depend. on humidity and temp. 7-39636
- Al-Cu-Li, cryogenic toughness, orientation effects 7-39669
- Al-Li-Cu-(Mg), stress corrosion resist. and mech. props. 7-33833
- Al-Mg alloys, spall strength, impact stress and strain-rate depend. studies 7-33796
- Al-Mg-Si, squarely extruded, texture and mech. props. (*Japanese*) 7-33694
- B₂O₃-SiO₂ glass, Pyrex, shock loading meas., impact failure modes determ. 7-33798
- Ba ferrite filled styrene-isoprene-styrene composite, dynamic mech., elec. and mag. props. 7-13001
- BeO, beryllia, polycrystalline ceramics, spall strength, plate impact meas., spall zone model calcs. 7-33797
- Bi alloy impregnated Ti, composite pseudoalloy, mech. props., Bi alloy content depend. 7-28095
- C fibre reinforced epoxy, electrodeposition of polymer interphase 7-13592
- C fibre/glass fibre reinforced polyester hybrid laminates, impact and perforation props. (*Japanese*) 7-13569
- Cu powder, porosity influence on mech. and tribotech. characts. in high-speed friction 7-8119
- Fe-Cu, pore form. during sintering, effect on mech. props. 7-64970
- Ni-Cr superalloy, high-temp. material, microstruct. and mech. props. with high-temp. heating 7-3341
- Ti alloy, two-phase, microstruct. and failure nature correl. 7-8110
- Ti-Al-Mo-Cr alloy, VT3-1, vac. annealing of blanks after isothermal deform., hydrogen plasticising effect 7-8027
- Ti-Al-V alloys, VT20 and VT6, annealing temp. effect on mech. props. of semifinished products 7-39558
- TiC-Fe-Cr alloyed with Si, high-Cr, sinterability and mech. props. improvement 7-64986

impact testing

- advanced instrumented impact testing facility for characterization of dynamic fracture behavior 7-13692
- alumina, polycrystalline ceramics, spall strength, plate impact meas., spall zone model calcs. 7-33797
- alumina polycrystalline ceramics, shock fracture and recompaction, double impact technique study 7-33880
- computer-assisted impact testing 7-59707
- concrete, insulating cellular, compressive strength, in situ evaluation using impact device 7-39800
- conference on the safety and reliability of reactor pressure components, Stuttgart, Germany, (Oct. 1985) 7-9583
- fibre reinforced composite tubes, radial impact strength 7-59709
- hammer performance analysis and obs., effect of mass on transducer sensitivity 7-16137
- instrumented, resonance and signal conditioning 7-8225
- material inhomogeneity, stress distrib., loading equipment imperfections, fracture origin freq., distrib. (*German*) 7-33873
- metal-ceramic composite, dynamic fracture toughness (*Japanese*) 7-13559
- noise emission analysis for determining crackinitiation during instrumental notched bar impact testing (*German*) 7-8216
- polycarbonate, shock-loaded, tension-recompression response method study 7-33879
- polyether sulphone, flexed plate impact testing, moulded notch effect 7-59713
- polyethersulphone, flexed plate impact testing of notched specimens 7-22799
- steel, structural, welds, dynamic fracture toughness by instrumented impact testing (*Korean*) 7-28235
- steels, dynamic yield strength determ., embedded manganin gauges, flyer plate impact technique 7-33871
- stress strain relationships, elastic deformation, specimen connected with long bar (*Japanese*) 7-11290
- Al-Mg alloys, spall strength, impact stress and strain-rate depend. studies 7-33796

impact testing continued

- Al-Mg-Si, compression test, high speed, microcomputer system, split Hopkinson bar technique 7-13686
- B₂O₃-SiO₂ glass, Pyrex, shock loading meas., impact failure modes determ. 7-33798
- BeO, beryllia, polycrystalline ceramics, spall strength, plate impact meas., spall zone model calcs. 7-33797
- Cu, dislocation-mechanics-based constitutive relations for material dynamics calcs. 7-63706
- Fe, dislocation-mechanics-based constitutive relations for material dynamics calcs. 7-63706
- H, liq. and solid, cryogenic, high press. eqn. of state, laser interferometric meas. method 7-30027
- Se, amorphous, elec. resist. and Hugoniot shock wave vel. meas. 7-32567
- SiC, instrumented impact testing, absorbed energy 7-28237
- ZrO₂, partially stabilised, instrumented impact testing, absorbed energy 7-28237

IMPATT diodes

- UKIRT mm and submm receivers 7-34880

impedance, acoustic *see acoustic impedance***impedance, electric** *see electric impedance***impedance, electric, measurement** *see electric impedance measurement***impedance, measurement, electric** *see electric impedance measurement***impedance matching**

- thin disc transducers, normalised time-response family model 7-1368
- US transducer construction with screen-printed matching layers 7-1370

imperfections, crystal *see crystal defects***impermeability** *see permeability***implosions** *see explosions***impulse generators** *see pulse generators***impulse testing**

- air, impulse breakdown voltage of slightly nonuniform field gaps, wave-front effect 7-32145
- double impulse tests of long airgaps, engineering problems 7-20974
- double impulse tests of long airgaps, leader decay and reactivation 7-20975
- double impulse tests of long airgaps, pre-existing space charge effects 7-20977
- double impulse tests of long airgaps, voltage front perturbation effects 7-20976
- silane XLPE, electrical breakdown study 7-27659
- N₂, impulse breakdown voltage of slightly nonuniform field gaps, wave-front effect 7-32145
- SF₆, impulse breakdown voltage of slightly nonuniform field gaps, wave-front effect 7-32145

impulse voltages *see transients***impulse welding** *see resistance welding***impurities**

- for impurity vibrations *see "lattice localised modes" or "molecular vibrations in solids"*
- see also chemical analysis; crystal inclusions; crystal purification; diffusion in solids; impurity-defect interactions; impurity distribution; impurity electron states; interstitials; magnetic impurity interactions; phonon-impurity interactions; plasma impurities; segregation; semiconductor doping*
- Si:O, heavily doped, SIMS meas. of O conc. 7-17388
- adsorbed monolayer, Ising model, 2D random field, correlations 7-6754
- alkali halides, F-centre production, impurity aggregate effects 7-21202
- alkali metal halide crystals, impurities, local and gap mode freq. calcs. 7-26888
- aluminum polyfluorophthalocyanine, IF₃ chemical doping 7-52600
- amorphous and disordered solids, H impurities, conference, Rhodes, Greece (Sept. 1985) 7-24302
- Anderson model, Bethe ansatz soln., cryst. field and spin-orbit coupling effects 7-2449
- anthracene molecules in liquid crystal matrix, orientational order, tensor parameter, spectroscopic study 7-37851
- atomic liquids with mol. impurities, similarity law for kinetic coefficients of hot electrons 7-16999
- atomic micro-clusters, electronic struct., ab initio studies 7-31203
- ceramic oxides, cond., for use as molten carbonate fuel cell electrodes 7-13854
- charged impurities in a semiconductor, anal. of diffusion 7-52137
- close-packed crystals, imperfect, self-diffusion of impurities, thermally-activated change in mechanism (*Russian*) 7-58523
- collisional mixing, magnitude and mechanism 7-63677
- conjugated polymers, impurities, nonlinear dynamics 7-64115
- cubic lattices, long-range impurity diffusion, mono- and divacancy mechanisms 7-58526
- deformable sliding CDW, mode locking and interference phenomena 7-21836
- diamond, thermal cond., C-defect effects 7-27035
- diamond, voidites, electron microscopy study 7-32425
- diglycine nitrate, alanine-doped, dielectric props. 7-45908
- dilute mag. alloy system, external mag. field, thermodynamic props. anomalies 7-45666
- diphenyl crystal, interaction of anthracene impurities with surface layers, struct. model of quasiliquid layer 7-58191
- electron gas, 2D, density of states for high Landau levels and random potential 7-58753
- electron irradiation-induced trap defects, DLTS study 7-12155
- energy-dispersive X-ray detector performance, contamination influence 7-23106
- ferroelectrics, incommensurate phase, impurity-order parameter and -soft modes interactions 7-64584
- films grown from a partly ionised molecular beam, computer simulation of structure 7-7060
- fluoride glass optical fibre, Pr³⁺ impurities, photoluminesc. anal. 7-37144
- fractional quantum Hall states, hierarchy termination and impurity effect scaling 7-21978
- garnets, ornamental, general method of formulation and crystal growth 7-53252
- glass:Er³⁺, lasing props. 7-43109
- graphite, pulsed laser melting, impurity redistrib., RBS channelling, Raman scatt. and TEM meas. 7-12135
- graphite dispersed powder, C atom vibr. dynamics in IR absorpt. spectrum 7-53322
- growing crystal surface, impurity atoms and vacancies, nonlinear kinetic effects 7-44575

impurities continued

- heavy electron superconductors, p-wave pairing consequences 7-2772
 heavy fermions and valence fluctuations, conf., Shima Kanko, Japan (April 1985) 7-23
 ice, pure and doped, US absorpt., dislocation damping 7-26756
 II-V semiconds., cryst. growth, characterisation and appls., review 7-26685
 III-V semiconductors, transition metal impurities, review 7-48201
 interface wandering in pure and impure and bulk phases 7-32791
 L₁2 intermetallics, localised grain-boundary electronic states and inter-granular fracture calcs. 7-45215
 lead phthalocyanine, electrical props., influence of I impurity 7-58927
 MBBA liq. cryst., mol. orientational relax. times, luminescence meas. 7-44368
 metal films, characterisation by SIMS, Auger spectroscopy and TEM 7-12550
 metal-H systems, interatomic forces near H impurity 7-58293
 metallic films, growth by laser photolysis of carbonyls, C and O incorporation mechanisms 7-58685
 metallic glasses, atomic transport, diffusivity meas. 7-52144
 metallic glasses, one-component, amorphisation and crystallisation (*Russian*) 7-32301
 metals, irradiated, deformation, impurity atmosphere effects (*Russian*) 7-59569
 metals, proton tunneling, neutron scattering studies 7-6646
 molecule in glassy matrix, inhomogeneous distrib. function and homogeneous spectra 7-50084
 naphthalene with α -bromonaphthalene or α -chloronaphthalene impurities, intercombination conversion during exciton capture 7-46091
 nematic liq. crystal, impurity-molecule luminescence, rotational depolarisation kinetics 7-51629
 nuclear fuels, diffusion processes, review 7-19350
 nuclear spin diffusion induced by paramag. impurities in magic angle conditions 7-27619
 one-dimensional interacting electron systems, charge density and superconducting fluctuations 7-22061
 optical surface defect characts. using pulsed laser damage methods 7-37010
 phthalocyanine metallomacrocyclic assemblies, [Si(Pc)O]_n, molecular metals, conduction props. 7-2585
 phthalocyanine thin films, gas-surface reactions, elec. cond. meas., ESCA 7-52262
 poly-p-phenylene and poly-p-phenylenevinylene, conducting polymers, NH₃ doping effects 7-2583
 polyacetylene:AsF₆, identification of dopant species, X-ray absorpt. and Mossbauer spectra 7-65377
 polyacetylene:I, photoexcitation spectra 7-64657
 trans-polyacetylene:Na, undoped and doped, momentum depend. dielec. functions, EELS study 7-64144
 polyacetylene:SbF₆, identification of dopant species, X-ray absorpt. and Mossbauer spectra 7-65377
 polyacetylene, alkali metal doped, role of spin-orbit coupling in EPR spectra 7-64527
 polyacetylene, alkali metal doped, semiconductor-metal transition, EPR study 7-64528
 polyacetylene, Durham, isomerisation and doping, ESR study 7-64510
 polyazulene, in situ optical and ESR studies during electrochemical doping 7-26670
 polydiacetylene, conductivity enhancement by chemical doping and ion implantation 7-21957
 polyethylene, single cryst. growth mode and lateral habit, impurity effects 7-26668
 polyethylene oxide, single cryst. growth mode and lateral habit, impurity effects 7-26668
 polymer films, I-doped, prep. by glow discharge polymerisation, elec. conductivity 7-22584
 polymers, elec. cond. and breakdown phenomena 7-45306
 powder sintering, temp. jump behaviour, manufacture method and impurities effect 7-13402
 quantum Hall effect, quasiparticles and impurities 7-33036
 quantum paraelectric material with two types of impurity, structural phase transition, CPA calc. 7-44786
 quartz, crystal growth, pragmatic model for simulation of self-induced striations 7-11973
 quartz, positronium-impurity interactions 7-39215
 α -quartz, synthetic, defects 7-63603
 quasi-1D superconductors, effect of impurities 7-45548
 semiconductor crystals, point defect behaviour, influence of isovalent impurities as sources of elastic stresses 7-51756
 semiconductor wafer, ion implanted dopant profile evolution during annealing, diffusion eqn., anal. 7-58536
 semiconductors, charged defects, reaction rates 7-38497
 semiconductors, impurity doping by photonuclear reactions 7-16589
 semiconductors, singular perturbation anal. (*French*) 7-21905
 semiconductors with parabolic density of states, activity coeffs. of electrons and holes 7-27324
 solar cell substrate charactn. techniques 7-40004
 solids in contact, interfacial bonding 7-27148
 steel, Cr-Mo-Ni-Mn, stress relief cracking, impurity effects 7-46635
 steel, Cr-Mo-V, creep ductility, impurity and microstruct. effects 7-46587
 steel, low alloy, rare earth-containing, temper embrittlement susceptibility, effect of S 7-65131
 steel, Ni-Cr, ductile-to-brittle transition temp. shift due to temper embrittlement and neutron irradiation evaluation by small-punch test 7-28114
 steel, stainless, surface corrosion products after exposure to liq. alkali metals, glow discharge optical spectroscopy, SIMS anal. 7-22896
 strong coupling electron systems, CDW, supercond., effect of randomness 7-27459
 substitutional impurity atoms uprise diffusion in cryst. near-surface layers (*Russian*) 7-44920
 surfaces and interfaces, electronic states, multiple-scatt. treatment 7-45420
 surfactant-water-nonaqueous liq. systems, elec. cond. study 7-13789
 three dimensional systems, phase transition of order 2 1/2, possibility of obs. by varying impurity conc. 7-44741
 transition metal crystal, BCC, metal-H bond investig. 7-32360
 transition metal impurities, interstitial, enhanced mobilities and reactivities 7-17769
 transition metal surfaces, dissociative adsorption of H₂, effect of impurities 7-16876

impurities continued

- transition metals:H, local impurity environment in cubic lattices 7-21236
 triglycine sulphate:Ti³⁺, X-ray effects, changes in physical props. 7-22198
 triglycine sulphate, Cr doped, amplitude depend. of dielectric losses 7-64587
 turbulent vortex ring, passive impurity loss 7-11426
 Vycor, thermodynamics of freezing and melting of liq. ⁴He in small pores 7-52169
 AgSn(Sb), impurity-vacancy and impurity-impurity interactions calc. from diffusion enhancement 7-6672
 Al atomic cluster, trapping regions around impurity atoms, charge density 7-53195
 Al evaporated films, O contaminated, recrystn., after annealing 7-38412
 Al foils, U contamination study using CR-39 track detectors 7-54218
 Al, grain boundaries, Na and H impurities, small cluster quantum chemical calcs. 7-38017
 Al-Xe, implanted, form. of solid precipitates and fluid bubbles, TEM obs. 7-38032
 Al_{0.48}In_{0.52}As:Si, MBE grown, crystalline and optical props. 7-52322
 α -Al₂O₃, CVD coating morphology, trace impurity effects 7-3191
 Al₂O₃, cryst. growth from melt, phase boundary displacement mechanism, defect distrib. 7-32328
 Al₂O₃:Cr³⁺, ruby, optically excited crystals, critical Cr conc. depend. of electrical instability 7-7280
 Al₂O₃:Mo, W, Cr, leucosapphire, growth by horizontal directional crystallisation, mass transport of Mo, W 7-22459
 (As₂Se₃)_{1-x}Tl_x, elec. and thermal transport props., effect of Tl addition 7-38200
 B and U impurity concentration in semiconductors, microanalytical estimation 7-38040
 BN:Cs(Br₂)_x intercalation cpd. formation 7-44574
 Bi₁₂MO₂₀V, (M=Si,Ge,Ti), sillenite struct., local vibrs. of impurities, spectral study 7-7718
 Bi₂Te₃-based solid solns., CdCl₂ doped, thermal conductivity studies 7-45363
 a-C:H, film, optical and compositional props. 7-39206
 a-C:H, film, optical energy gap, density, hardness 7-39204
 a-C:H, film, plasma emission spectroscopy, chem. anal. 7-38407
 a-C:H, films, plasma deposition characterisation of hydrocarbons used 7-39422
 a-C:H films, glow discharge deposited, valence electron props., electron energy loss spectra study 7-13288
 a-C:H films, plasma deposited, optical props. 7-27799
 a-C:H plasma grown films, struct., physical props. 7-58713
 C₆₀ and similar substances, inert gas trapping, possible occurrence in meteorites 7-50436
 CdCr₂Se₄-Ga, lightly doped, ferromag., photoconductivity, band struct. 7-7278
 CdTe, single cryst., transmission region optical props., impurities effects 7-39128
 CdTe:Co, Jahn-Teller interaction, influence of mag. field 7-16995
 Co-Cr films, sputter deposited, effects of additive gases on mag. props. 7-27575
 Co-Cr perpendicular recording media, props., effect of impurity gases 7-59069
 Cr-Si, lateral growth of CrSi₂, role of Si transport 7-38272
 Cs₂NaAlF₁₂:Cr³⁺(Fe³⁺), impurity ion spin Hamiltonian parameters, EPR determ. 7-64523
 Cu²⁺ impurity ion in octahedral environment, EPR spectrum, MM field freq. and temp. depend. 7-27596
 CuB:He, neutron irradiated, annealing behaviour of defects, positron annihilation study 7-39291
 Fe, cathodic charging, H trapping 7-21256
 Fe, porous, segregation of impurity elements, alloying elements selection and activated sintering 7-53742
 α -Fe single crystals, activation energy of S diffusion, surface segregation, AES obs. 7-39529
 Fe:H(D), lattice strains, meas. 7-2268
 Fe-Ni (36 at.%), Invar, oxidation, effect of annealing conditions 7-28167
 Fe₈₀B₂₀ ribbons, amorphous and crystallised, surface comp., electronic props., topography, AES, XPS, ion scatt. studies 7-27065
 γ -Fe₂O₃ particles, pure and Co-modified, microstructural defects 7-58497
 FeS containing Cr and Mn, cation vacancy conc. 7-16551
 Fe₃Si, transition metal impurities, electronic struct. and site preference 7-12653
 Ga:In, growth dislocations, in-situ detection using Seebeck effect 7-32451
 GaAs crystals, selective etching and photoetching of CrO₃-HF aq. solns. 7-32442
 GaAs device structures, γ -ray effects, surface generation-recombination processes 7-64349
 GaAs diode, active layer <1 μ m, low temp. current flow 7-52757
 GaAs epitaxial films, growth by close-spaced vapour transport, unwanted doping, X-ray diffr., SEM obs. 7-27187
 GaAs epitaxial layers, MOCVD grown, influence of growth parameters on residual impurities 7-7047
 GaAs epitaxial layers, MOCVD growth, boundary layer effects, photoluminesc. study 7-64923
 GaAs films on amorphous insulating substrates, laser recrystallisation 7-38397
 GaAs, impurity atom site location using channelling enhanced microanalysis 7-38023
 GaAs, ion implanted, rapid thermal annealing, review 7-58296
 GaAs, LEC grown, threshold for dislocation form., role of cryst. dia. and impurity hardening 7-53551
 GaAs layers, effect of impurities on solid phase epitaxial growth 7-16907
 GaAs, MBE growth, acceptor impurity background reduction 7-3173
 GaAs, melt grown, theoretical and expt. fundamentals of decreasing dislocations 7-53547
 GaAs, proton bombarded, H platelets, TEM obs. 7-12164
 GaAs, residual acceptor assessment, Raman and selective pair luminescence studies 7-26771
 GaAs: Si(Se)(Zn)(Be), ion implanted, rapidly annealed, damage removal process 7-17043
 GaAs:C, low C conc., crystal growth using pyrolytic BN coated graphite 7-59398
 GaAs:Cr semiinsulating LEC wafers, microhardness cartography 7-32886
 GaAs:Cs, impurity ion beam effects, SIMS depth profiling 7-22419
 GaAs:In, LEC growth, annealing, solid soln. hardening, dislocation density, elec. props. 7-17404
 GaAs:In, lattice distortions, NMR study 7-2933

impurities continued

- GaAs:In, semi-insulating substrates and ingots, In content, nondestructive meas. 7-58305
 GaAs:S:Si epitaxial layers, close space vapour transport growth, photoluminescence and electrical props. 7-21776
 GaAs:Si, annealing behaviour of impurities in presence of stress 7-65060
 GaAs:Si, FET structs., rapid optical annealing for improved uniformity 7-16620
 GaAs:Si(Be)(Mg), rapid annealing, temp. depend. of damage removal and carrier activation 7-17032
 GaAs:Te, defect study by positron annihilation (*Chinese*) 7-13254
 GaAs:Zn(C) epilayers, low pressure MOCVD growth, impurity incorporation 7-59442
 GaAs-GaAs:Cr(Te), VPE grown, photoluminescence study, effect of substrate doping 7-27771
 GaAs-GaAs-Al_xGa_{1-x}As heterostructures, photosensitivity spectra 7-64319
 GaAs_{1-x}P_x:N, bound excitons, energy spectrum, optical absorpt. cross section, two-band model 7-16945
 GaAs_{1-x}P_x:N epitaxial layers, N conc. determ. 7-63989
 GaP, floating zone melting prep., elec. props. 7-64238
 Ga₂Se₃ films on GaAs substrates, insulating coating, stoichiometric vacancies, carrier mobility 7-52846
 Gd₂O₃-P₂O₅ phosphors, Eu³⁺ activated, luminesc. spectra, cryst. symm. 7-3080
 Ge, electron irradi., annealing kinetics, impurity effects 7-16630
 Ge:Ga(Be)(Zn) extrinsic photoconductor material, cryst. growth and characterisation 7-64893
 Ge:Na(K), impurity addition by electrolysis 7-44578
 Ge:Ni, inhomogeneously photoexcited, cond. random spontaneous oscils. 7-52675
 Ge:Sb(Al)(Ga)(In), heavily doped, charge carrier scatt., elec. cond., Hall effect meas. 7-7228
 Ge-Sb-Te system, diffusion of Fe, Cr and Ni impurities 7-21527
 GeO₂:Cu thin films, optical absorpt. edge 7-53431
 Ge₂₀Se₈₀-Bi_x, amorphous, electronic cond. props. under high press. 7-45328
 GeTe:Cd(In)(Sb), solution mechanism of impurities, effect of heat treatment 7-21455
 H₂-octaethylporphyrin in polystyrene, photochemical hole, transmission spectrum, temp. broadening (*Russian*) 7-15617
 He liquefier, condensing and freezing purification system 7-56280
⁴He, liquid, impurities, variational theory 7-27045
 n-HgCdTe, acceptor densities, photo-Hall determ. 7-58836
 HgCdTe, p-type, acceptor conc., IR reflectance studies 7-64600
 α-HgI₂ crystals, recent progress in material characterization for X- and γ-ray detectors 7-44577
 HoFeO₃ crystals, flux growth, secondary phase and microdiscs form. 7-13344
 InGaAs:Si LED, electrical and luminesc. props., ultrasonically-induced changes 7-22350
 In₂O₃:Sn vapour deposited films, growth, struct., electronic props. 7-12535
 In₂O₃:Sn-ZnS:Cu₂Cl₂Mn-Al, surface electrical conductivity in ZnS:Cu₂Cl₂Mn thin films 7-38672
 In₂O₃:Sn(Te), thin films, etching, comparison of solns. dilute HCl and H₃PO₄ 7-8208
 In₂O₃Sn thin films, prep. by pyrolysis, props. 7-2749
 InP, electron irradi. damage, impurity effects 7-12154
 InP epitaxial films, MOCVD grown, identification of acceptors and donors 7-58688
 InP, floating zone melting prep., elec. props. 7-64238
 InP, impurity atom site location using channelling enhanced microanalysis 7-38023
 InP, melt grown, theoretical and expt. fundamentals of decreasing dislocations 7-53547
 InP, quantitative trace anal. of impurities by SIMS 7-53480
 InP:Ge, Fermi level, determ. from phase diagram data of InP-Ge system 7-21808
 InP:S, shallow n⁺ diffusion of S, open-tube diffusion technique, n⁺-p junction formation 7-44912
 InSb, 1/f noise, temp. depend. 7-52710
 InSb:Te(Ge)(Cd)(Si), heterogeneity study 7-21476
 InSb:Te(Se)(S)(Cd)(Zn) thin films, doping, Hall effect meas. 7-21743
 In₂Se₃:S(Li), electrical transport props. 7-21917
 KAl(SO₄)₂ solutions, effect of impurities on props. 7-6495
 K₂Cd₂(SO₄)₃:Sm, doped and undoped, thermoluminescence 7-39191
 KCl doped crystals, impurity centres, form. processes and thermoactivation solution 7-44576
 KCl, positron lifetime meas. rel. to impurity conc. 7-53438
 KCl:Ca²⁺, Z₂⁺-centres, axial config., pseudopotential perturbation calc. 7-32952
 KCl:Li, F_A-centre crystals, diffraction efficiency of photoinduced gratings 7-62818
 KCl:En solid soln. crystals., thermal and radiation induced decay, impurity aggregation study (*Russian*) 7-2216
 KCl:Mn_{1-x}:Ca(Mn), doped crystals, elastic constants, meas. using US pulse superposition method 7-26827
 K₂HPO₄, cryst. growth from boiling solns. in presence of impurities 7-53529
 K₂SO₄, cryst. growth, nucleation kinetics, habit, Cr(III) effect, soln. pH 7-53539
 KTaO₃:Li, quadrupole ferroelastic phase 7-6778
 KTaO₃:Li, time depend. phase transform., neutron diffr. meas. 7-44799
 KX:O₂⁻ (X=Cl, Br), tunable CW laser operation in 1.45 to 2.16 μm range 7-62707
 KX:Sr,Eu (X=Br,Cl), Sr precipitation, study using Eu³⁺ ions 7-53127
 KZnF₃:Mn²⁺, thermal expansion of the Mn²⁺-F⁻ bond 7-6836
 K₂ZnF₄:Cu²⁺ crystal, possible ligand spin-orbit coupling in CuF₄ clusters 7-38520
 LaNi₅, anisotropic H migration, deposition potentials, hardness, brittleness meas. 7-6873
 LaNi₅, diffusion of H and D, temp. depend. 7-6874
 LaNi₅H_{0.8}:O, dissociation press., O content depend. 7-63825
 LiF:Mg,Ti phosphor layer on borosilicate glass substrate, laser stimulated thermolum. 7-64703
 LiIO₃ crystals, iron-group doped, impurity centres, circular dichroism studies 7-45976
 α-LiIO₃:Co²⁺, ESR and optical absorpt. studies of impurity ions 7-45803
 LiNbO₃:Co²⁺, ESR and optical absorpt. studies of impurity ions 7-45803

impurities continued

- LiNbO₃:Fe, and undoped crystals, decay of γ-centres 7-7658
 LiNbO₃:T surface, acousto-optic interaction, photoelastic and electro-optic contrbs. 7-45982
 LiNbO₃:Ti, acousto-optical diffr. elastic strain and electric field effects 7-45985
 Li₂O-MO-B₂O₃:VO²⁺ (M=Ba,Ca,Mg) borate glasses, ESR of VO²⁺ ion 7-59110
 MgO, positron lifetime spectra, impurity effects 7-39278
 MgO:C, single crystals, solute C and C segregation, SIMS study 7-16759
 MgO:C, single crystals, solute C and C segregation, SIMS study 7-16761
 MgO:C single crystals, solute C and C segregation, SIMS study 7-16760
 Mg₇₀Zn₃₀ and (Mg₇₀Zn₃₀)₉₅Pb₅, metallic glasses, impurity vibr. states, influence on thermodynamic and superconducting props. 7-38148
 Mo, arc melting, impurity content, mech. props. 7-27980
 Mo high purity single crystal, impurity-induced lattice distortions, diffuse X-ray scatt. studies (*Russian*) 7-6644
 Mo, high purity single crystals, distortion charact., effect of point defects, diffuse X-ray scatt. meas. 7-51752
 Mo-N polycrystalline films, implanted, single defects, X-ray diffr. data anal. 7-38372
 MoO_x-WO_x, H insertion, struct. and thermodynamics 7-16506
 MoS₂ single crystals, grown in presence of Co, photoelectrochemical props. 7-8294
 NH₄Cl:Ni, TSC, polarisation meas., 150-500K 7-52645
 NH₄H₂PO₄:SeO₄³⁻, partially deuterated, D concentrations in H₂PO₄⁻ and NH₄⁺ radicals, ESR spectra 7-27671
 (NH₄)₂SO₄, crystal growth, contact nucleation rel. to Cr ion conc. 7-16462
 NaCl:Ca, impurity dipoles, aggregation with dislocations under alternating elec. field 7-44598
 NaCl:Co, doped and undoped, thermoluminescence and X-ray fluorescence spectra 7-22356
 NaCl:K, microcryst. powders, spontaneous colloid form. in electrodeless discharge 7-12065
 NaCl:O₂, tunable CW laser operation in 1.45 to 2.16 μm range 7-62707
 NaF:OH⁻, X⁺, X=impurities, vibr., radiation effects, IR spectra 7-53321
 Na₂O-SiO₂:Tb³⁺ glasses, colour centre formation during UV irradiation 7-2049
 Na₃Ti₃O₂(OH)₂[SiO₄]₄, polymorphous modification of natasite, cryst. struct., X-ray diffr. 7-26709
 Nb, interstitial N, O, H, D, Zwischenreflex scattering 7-51766
 Nb, tunnelling of H and D trapped by O(N), anelastic relax. meas. 7-39572
 Nb:O, H and D trapping, perturbed ang. correl. obs. 7-27641
 Nb-N polycrystalline films, implanted, single defects, X-ray diffr. data anal. 7-38372
 Nb₇₆Au₂₄, with Cr and Fe impurities, supercond. transition temp., impurity conc. depend. 7-2768
 NbH_x, H transfer integral renormalisation 7-12085
 NbO_x, ω phase, point defect induced nucleation 7-1923
 Ne:Ar(Kr)(Xe), solid, local phase transition near impurity center 7-26945
 Ni (100), adsorption of CO, poisoning in heterogeneous catalysis, role of electronegativity 7-13818
 Ni (111), adsorption of Te, adsorbate induced C segregation and dissolution 7-12477
 Ni, D permeation rel. to surface impurities and Ar sputtering 7-52141
 Ni-Ag(001), Au doped, thin films, interphase boundaries, struct. and composition 7-27158
 Ni-Cr based alloys, low impurity content, microanalytical charactn. of microscopic defects 7-58261
 Ni-Mo (6 at.%), oxidation, ESCA study 7-22897
 Ni₂Cr, order-disorder transform. kinetics, P content effect 7-13446
 NiSi₂:Si(BF₂), epitaxial growth of NiSi₂, influence of dopant atoms 7-45039
 Ni₃Ti₆₅, amorphous, internal friction of H 7-39577
 NiZr₂ metallic glasses, crystallisation, influence of O and other trace impurities 7-51633
 PZT:Bi piezoelectric ceramics, vacancies, positron lifetimes 7-37980
 Pb(Mg_{1/3}Nb_{2/3})O₃ ceramics, dielec. props. 7-46382
 PbMg_{1/3}Nb_{2/3}O₃-PbTiO₃, MnO doped, relaxor ferroelec. ceramics, dielec. ageing effects 7-22195
 PbSe:Ag, electron irradi. stimulated impurity diffusion 7-63878
 Pb_{0.75}Sn_{0.25}Te:In, Ge(S)(Se), elec. resist., photocond., Hall effect meas. 7-17050
 Pb_{0.8}Sn_{0.2}Te:In, impurity diffusion, thermoelec. probe meas. 7-63879
 PbTiO₃:La piezoelectric ceramics, vacancies, positron lifetimes 7-37980
 Pd, pulsed current electrodeposition, pulse parameters effect on deposit morphology, H content 7-59473
 Pd-H, single particle dynamics, simulation model 7-27016
 PdH_x, dilute alloys, Pd substituted, interaction of H with impurities, EXAFS study 7-64806
 Pt anode in fuel cell, performance in presence of CO and CO₂, CO poisoning adsorption parameters calc. 7-13855
 Pt surfaces, impurity segregation, high resolution AES studies 7-33668
 Sc₂S₃, solid, elec. cond. (*Japanese*) 7-33002
 Si, amorphisation and crystallisation 7-11914
 Si, axial magnetic Czochralski growth 7-32343
 Si, charged defect states at grain boundaries 7-44564
 Si, crystal growth, impurity effect on formation of microdefects 7-32340
 Si, Czochralski grown, interdependence of contamination and defect formation 7-32467
 Si, diffusing metallic impurities, H implantation effects 7-12370
 Si epitaxial layers, impurity anal. by photoluminescence spectroscopy 7-7057
 Si, impurity gettering, defect-defect interaction mechanisms 7-16585
 Si, in ceramic specimens, for TEM, ion milling, grain boundary glassy phase 7-44327
 Si, lattice distortions and vibr. modes of substitutional impurities 7-51979
 Si, MBE cryst. growth, dopant incorporation 7-12559
 Si MBE films, deep level defects 7-12668
 Si MBE homoepitaxial growth, expt. considerations 7-13369
 Si MBE layers, defect characterisation, luminesc., TEM studies 7-13227
 Si MBE layers, spreading resist., etching, bevelling, staining characterisation techniques 7-12891

impurities continued

Si MOS capacitor elec. parameters, effects of process chemical purity 7-33103
Si materials and process charact. for VLSI, SIMS studies 7-33988
Si, oxidation, growth mechanism of thin oxide films 7-65235
Si, oxidation of damaged surfaces, precipitation at stacking faults 7-38313
Si, surface, laser beam melting and recrystallisation 7-12431
Si, thermal oxidation, effects of GeCl₄ 7-65238
Si, thermal oxidation, growth of very thin films, effect of hydrogenated impurities 7-33850
Si wafers, surface contaminants, identification, depth distrib., SIMS 7-22418
Si, with transition metal impurities, detect. using rapid thermal annealing 7-2044
Si:As, implanted, supersaturated soln., defect struct., TEM obs. 7-58483
Si:As, ion implanted polycrystalline films, electrical activation by rapid thermal annealing 7-58914
Si:As films, heavily doped, grown by partially ionised MBE, phys. and elec. characts. 7-12561
Si:As⁺(As₂⁺), ion implanted, phys. props., spreading resist., TEM, Rutherford backscattering, SIMS 7-26775
Si:As(B)(P), impurities at dislocations and grain boundaries, high-resolution TEM imaging 7-37815
Si:Au, supersaturated low-temp. substitutional impurities, annealing 7-6665
Si:B, H, hydrogenation of B acceptor during electron injection by Fowler-Nordheim tunnelling 7-45504
Si:B, impurity diffusion from BN sources, non-Fickian model 7-27012
Si:B, MBE grown, coevaporation doping 7-12562
Si:B,C,O, O clustering and thermal donor formation kinetics 7-17566
Si:B film deposition in Si₃H₈-B₂H₆-He gas system, doping effect 7-27184
Si:B MBE layers, shallow states, photoluminescence spectra, doping level depend. 7-13228
Si:Bi polycrystal-single cryst. interface, impurity diffusion across boundary 7-27013
Si:BF₃⁺(PF₃⁺), ion implantation damage, backscattering channelling meas. 7-63675
Si:B(As)-Ti(Co), silicide formation using rapid thermal processing, defect behaviour 7-32726
Si:B(Au), electron irradi. stimulated impurity diffusion 7-63878
Si:B(P), lateral diffusion, modeling LOCOS effects 7-33865
Si:C, impurity concentration determ. by photoluminesc. method 7-46084
Si:C, photolum. detection of impurities introduced by dry etching processes 7-27748
Si:C,O grown by gas-assisted solidification, impurities determination 7-16586
Si:F, implanted, dry oxidation kinetics, impurity effects 7-13667
Si:Ga MBE layers, ion implantation doping using liq. metal ion source, carrier conc., spreading resist., SIMS profiles 7-12563
Si:Gd, grown from melt, electrical and optical props., residual impurities 7-63636
a-Si:H, evaporated samples, post-hydrogenation, characts. 7-59103
Si:H, Si-H IR stretching bands, models, CNDO calc. 7-53314
Si:H, summary of present state of research 7-16584
a-Si:H,B, RF sputtered films, optical and electrical props. 7-33470
a-Si:H,B(As) RF sputtered coatings, gas-phase doping efficiency 7-63471
a-Si:H,Cl glow discharge films, Raman scatt. 7-39116
a-Si:H,D, H abstraction from surface, HD formation 7-39914
a-Si:H (C,H) (O,H) (N,H), annealing of metastable defects 7-3343
a-Si:H and a-Si:H,P, electron nuclear double resonance expts. 7-2950
a-Si:H films, columnar morphology, evolution of vibr. spectra 7-64646
a-Si:H films, depth profiling of constituents and impurities, elastic proton scatt. 7-45044
a-Si:H films, electron irradi., photocond., absorpt. coeff. spectral depend. 7-64279
a-Si:H films, high rate deposition and impurity doping effects (*Japanese*) 7-13385
a-Si:H films, light-induced bond breaking 7-12517
a-Si:H modulation doped multilayers, planar and perpendicular cond. meas. 7-38717
a-Si:H/a-SiN_x:H, amorphous multilayer structures, optical props. 7-3014
a-Si:H/a-SiN_x:H superlattices, interface struct., optical reflectance determ. 7-12497
a-Si:H-Pt Schottky barrier contact, photocurrent excitation nonadditivity effects 7-17099
Si:H(He)(Ar), ground state one-electron energies, SCF MS X_α calcs. 7-44582
Si:In⁺, ion implanted, damage prod., incidence angle depend. 7-65242
Si:Na(K), impurity addition by electrolysis 7-44578
Si:O, C, thermal donor form., T<800K 7-27294
Si:O, Czochralski cryst. growth, impurity segregation, high axial mag. field effect 7-26960
Si:O, Czochralski-grown wafers, growth striations, X-ray topography study 7-59400
Si:O, enhanced diffusion at thermal donor formation temp. 7-44911
Si:O, Fourier transform IR spectroscopy and SIMS calibrations for O conc. meas. 7-16606
Si:O, low thermal donor conc. layer formation during annealing 7-17564
Si:O, off-centre, impurities, theory 7-21251
Si:O, positron annihilation study 7-3105
Si:O, review 7-16583
Si:O, thermal donor formation, kinetics 7-6664
Si:O, thermal donor formation and structure, review 7-17562
Si:O(H)(C)(N), conf., Boston, MA, USA (Dec. 1985) 7-14711
Si:P, LPCVD doped, deform. pot. shear const. determ. 7-38086
Si:P(B) LPECVD films, amorphous and polycrystalline, struct., elec. resist. meas. 7-52870
Si:Sb, pot. enhanced doping during MBE growth, elec., optical props., cryst. quality 7-12112
Si:Sb MBE film, doped by electron impact ion source, improved doping characts. 7-12101
Si:Sb MBE layers, doping by secondary implantation 7-12102
Si:Sb(As)(P)(B) epitaxial films, low temp. deposited by low press. CVD, autoping 7-27182
Si:Ti(V)(Cr)(Fe)(Zr) polycrystalline solar cells, structural, elec., photovoltaic props., impurity effects 7-39990
Si:transition metals, anomalous diffusion and gettering 7-2264
Si-Al structures, ion mixing, effect of interfacial oxide 7-21537
Si-Si homoepitaxial interfaces, MBE grown, oxygen trapping 7-32855

impurities continued

SiC short fibred filamentary crystals., phase comp. and morphology 7-65010
SiC:Si reaction bonded composite ceramics, interface struct., grain boundaries 7-64995
Si_{1-x}C_x:H films, amorphous, bond lengths, comp. depend., EXAFS study 7-64757
SiGe superlattice structures, Sb doped, MBE grown, comp., doping profiles, SIMS, Rutherford backscattering spectra 7-7035
Si_{1-x}Ge_x:H films, amorphous, bond lengths, comp. depend., EXAFS study 7-64757
a-SiN_x:H dielectric films with low defect density 7-39036
SiN_x:H films, amorphous, glow discharge deposited, IR absorpt. and Raman scatt. spectra 7-46003
SiN_x:H films, amorphous, bond lengths, comp. depend., EXAFS study 7-64757
Si₃N₄-TiC composites, densification, matrix-dispersoid reaction, mech. props. microstruct., impurities effect 7-64994
SiO₂ thin films, intrinsic bonding defects and impurities, EPR studies 7-13034
SiO₂:Cl films prod. by Si oxidation in Cl containing ambients, impurity distrib. 7-26787
SiO₂:Cs-Si MOS, semicond. flatband voltage depend. on impurity distrib. 7-27433
SiO₂:Ge, impurity charge trapping props., EPR spectra 7-27290
SiO₂:transition metals, fused quartz, impurity sites, X-ray absorption spectroscopy 7-13263
a-SiO_x:H films, local struct. EXAFS study 7-59291
SiO_x:F films, pure and doped, low press. CVD growth, structural, optical, elec. props. 7-27186
SiSe⁺, photothermal release of carriers, deep levels, capacitance spectroscopy 7-16968
SnO₂:Cl coatings, electrical and optical props. 7-58925
SnO₂:Sb thin films, doped and undoped, prep. by photolysis, phys. props. 7-22368
SnTe:Cd(In)(Sb), solution mechanism of impurities, effect of heat treatment 7-21455
SrO.56Fe₂O₃, doped with kaolin and BaB₂O₄, sintering temp., effect on structural and mag. parameters 7-7543
TaH_x, H transfer integral renormalisation 7-12085
TaSe₂:H, polytype formation, impurity conc. depend. 7-63801
TaT_x, lattice deformation due to ³He production 7-21237
TeO₂:Ge,Sn films, optical props., thermal stability 7-39207
Ti thin films, dissolution and diffusion of O, resist., X-ray diffr., particle backscatt. and AES studies 7-58913
Ti-Si, native contamination layer effect on interface props. 7-17104
TiO₂:Cr, sol-gel process, ESR study 7-59108
Ti₇₅Sb₂₅, with Cr and Fe impurities, supercond. transition temp., impurity conc. depend. 7-2768
TiInS₂, crystals, vibr. spectra in vicinity of phase transitions 7-17321
U_{1-x}Pu_x:C, mixed carbide fuel, thermodynamic props., effect of O and N impurities 7-58507
U_{1-x}Th_xRe₂, polymorphic transform., supercond. crit. temp., low temp. sp. ht. meas. 7-17125
VD_x, H distrib. and diffusion near impurities, Mossbauer and PAC obs 7-33314
VH_x, H distrib. and diffusion near impurities, Mossbauer and PAC obs 7-33314
W base heavy metal alloys, mech.-props., porosity, impurity effects 7-17495
W films prep. by various deposition methods, effects on elec. resist. 7-52860
W, grain growth, impurity effects 7-28044
W monocrystals, with P impurities, removal during chem. and metallurgical treatments 7-6645
W selective low press. CVD growth on Ti, TiSi₂ and PtNiSi, surface reactions, struct. 7-27183
W sputter deposited films, impurity effects on elec. props. 7-52862
W wire doped with K, morphology and behaviour of K bubbles at varied temps. 7-2223
WSi_x films, CVD, resistivity and composition changes by annealing 7-2738
YAG:Nd, Ce, energy transfer mechanisms between Ce³⁺ and Nd³⁺ at low temp. 7-64691
YIG:La,Ga-YIG:La double layered film, different magnetisation and anisotropy, magnetostatic mode spectra 7-64498
Y₂O₃, DC cond. as function of water vap. press. 7-45317
Y₂O₃, elec. cond. as function of O₂ partial press. in wet and dry atm. 7-45405
Y₂O₃-P₂O₅ phosphors, Eu³⁺ activated, luminesc. spectra, cryst. symm. 7-3080
Zn, electrodeposition, macromorphology, impurity effects, pot. sweep analysis 7-22595
ZnO films, elec. props., decomp., chemisorption of O⁻, photocond. meas. 7-27445
ZnO with tri-valent donor impurities, elec. props., heat treatment effects 7-2611
ZnS:Mn electrolum. thin film displays, growth by at. layer epitaxy 7-13362
ZnSO₄-Na₂SO₄ reactions in CoCrAlY hot corrosion 7-28188
ZnSe:H, proton implanted, localised vibr. mode, IR transmission spectra 7-51981
ZrF₄-BaF₂-GdF₃-AlF₃-NaF-FeF₃, optical fibre glasses, trace amounts of Fe, characterisation 7-2956
Zr₇₅Rh₂₅ and (Zr₇₅Rh₂₅)₃Be₂, metallic glasses, impurity vibr. states, influence on thermodynamic and superconducting props. 7-38148

impurity and defect absorption spectra of inorganic solids
actinides in hosts, optical absorption spectra 7-27730
γ-Al₂O₃:Co, spinel phase composite, study of γ-ray irradi. effects on optical absorpt. spectra 7-46071
alkali halide crystals, F-centre formation threshold by two-photon absorpt. 7-32437
alkali oxides with antifluorite structure, F⁺-centre absorption energy calcs. 7-12658
cultured quartz Al defects, IR and laser spectroscopic charactn. 7-59234
diamond, radiation damage prod. of 5RL centres, phonons, absorpt. spectra, cathodoluminescence studies 7-33461
diamond, type Ia, IR absorption spectra, platelets 7-7723
emerald, Cr³⁺ absorption spectrum, spin-orbit interaction effects 7-13182

impurity and defect absorption spectra of inorganic solids continued

- fluorapatite, relative defect-production efficiency for fission fragments, alpha decay and electron irradiation 7-12167
 fluoride glass:Er³⁺, impurity luminesc. and absorpt. spectra studies 7-53386
 fluorophosphate glass:Er³⁺, impurity luminesc. and absorpt. spectra studies 7-53386
 glass:Ce(Eu), stable and metastable impurity valence states, spectral props. (Russian) 7-27747
 glass:Nd, transition metal doped, fluorescence and absorption spectra 7-13229
 glass, transition metal doped, optical absorpt. and luminesc. spectra 7-13186
 glasses, optical impurities dephasing 7-53376
 graphite dispersed powder, C atom vibr. dynamics in IR absorpt. spectrum 7-53322
 III-V semiconductors, defect recognition and image processing, conf., Montpellier, France (July 1985) 7-29596
 lanthanide complexes, two-photon absorpt. 7-908
 lanthanide oxysulphides (oxyhalides), Eu³⁺-doped, vibronic spectra 7-51968
 optical glass fibre waveguides, colour centres 7-11081
 optical glass fibres, UV-radiation induced colour centres 7-11082
 phosphate laser glasses, IR absorption of water 7-33416
 polyethylene:Si films, trapping states, TSC, optical absorpt. spectra, photocond. meas. 7-27345
 radiation effects in materials for optical interferometric devices 7-44618
 rare earth trifluorides:Nd³⁺, absorption and luminescence spectra, Stark sublevels 7-3077
 ruby, Cr³⁺ absorption spectrum, spin-orbit interaction effects 7-13182
 ruby, impurities optical dephasing temp. and freq. depend. 7-22286
 sapphire:Ti³⁺ laser material, scattering centre formation mechanism 7-10960
 silica glass optical fibres, γ -irradiated and H₂ treated, 1.52 μ m absorption band 7-37145
 silica optical fibres, defect struct. and drawing-induced absorption, drawing depend. 7-3071
 spectral holes, persistent, in external fields, review 7-5959
 synthetic silica glass, X-ray induced absorpt. and luminesc., heat treatment effects study 7-7733
 transition metal impurities, interstitial, enhanced mobilities and reactivities 7-17769
 YAG: rare earth crystals, impurity content, absorpt., spectrophotometric obs. 7-13843
 YIG:Ca films, magneto-optical props., reducing treatment effects 7-64617
 AlN films, OMVPE, Hall mobilities, impurity band 7-39410
 α -Al₂O₃ foreign phase influence on RE-activated aluminate phosphors UV stability (German) 7-27779
 Al₂O₃, leucosapphire single crystals, transformation of colour centres 7-37986
 Al₂O₃:Cr³⁺, radiation colour centres, excitation energy transfer 7-21200
 AlSb:Se, donor studies, incoherent laser saturation method 7-27298
 As₂S₃:Ag, amorphous, charge fluctuation, Ag doping effects 7-7700
 B₂O₃-SiO₂:U, doped glasses, optical spectroscopy study 7-39145
 BaF₂:ThF₄-YbF₄ glass, electron irradiation effects, Yb³⁺ optical transitions 7-27764
 BaFCl:Sm³⁺(Eu³⁺)(Gd³⁺)(Ho³⁺)(Er³⁺)(Yb³⁺), charge transfer excitation and emission spectra 7-64688
 Ba₃LaNb₃Nd³⁺(Eu³⁺) single crystals, spectral-luminesc. props. 7-39169
 Ba(PO₃)₂:LiF gamma irradiated activated glasses, optical absorpt. and ESR spectra corrls. 7-13030
 BaTiO₃:Mn, Mn oxidation state change near phase transitions 7-16974
 BeAl₂O₄:Cr³⁺, alexandrite, excited, absorpt. spectra, 220-900 nm 7-46075
 BeO, optical props. of F⁺ centres 7-7717
 Bi₂GeO₂₀, pure and doped crystals phys. props. 7-7283
 BiI, intrinsic semiconductor, reverse H-like series, light absorpt. study 7-53370
 Bi₂MO₂₀:V, (M=Si,Ge,Ti), sillenite struct., local vibrs. of impurities, spectral study 7-7718
 Bi₅PO₁₁:Nd³⁺, cryst. growth, spectroscopic props. of Nd³⁺ ions 7-46131
 Bi₂SiO₂₀, pure and doped crystals phys. props. 7-7283
 CaF₂:Ce, Mn crystals, energy transfer, optical absorpt. and luminesc. studies, X-ray irradi. effects 7-27773
 CaF₂:Ce,Mn, optically active sites, optical spectra 7-22305
 CaF₂:Ce³⁺, two-photon absorpt. cross section, anal. of lowest 4f-5d transition 7-46081
 CaF₂:Mn, gamma irradiation-induced defects, absorpt. and excitation spectra studies 7-26801
 CaF₂:O crystals, O-vacancy centres, optical props. 7-7722
 CaF₂:Sm³⁺, electronic Raman transitions study 7-46017
 CaF₂:Sm³⁺:Nd³⁺ energy transfer efficiency 7-7734
 CaF₂:Tm³⁺, absorption spectra of optically excited Tm³⁺ 7-33418
 Ca₃Ga₂O₉:Nd³⁺, luminescence and absorption spectra and stimulated emission 7-7732
 CdCr₂Se₄ thin films, ferromagnetic semicond., multielectron energy struct., absorpt. spectrum, temp. and doping depend. 7-38488
 Cd_{1-x}Mn_xTe mixed cryst., far IR Fourier transform spectra, acoustic local mode and TA band mode 7-53378
 CdSe,Te_{1-x}, bound excitons, thermal dissoc., photoluminescence, reflectivity meas. 7-46122
 CdTe, single cryst., transmission region optical props., impurities effects 7-39128
 CdTe:Fe²⁺, impurity vibronic coupling and near IR spectra characts. 7-26889
 Ce doped fluoride elpasolites, 5d-4f spectra, impact of ion-host interactions 7-39143
 Ce³⁺ in dielectric crystal, 5d-4f spectra, phenomenological cryst. field model 7-39148
 Co_{0.2}Ga_{0.8}S₂ single crystals, optical props. and impurity energy levels meas. 7-13122
 Co_{0.9}In_{0.1}S_{3+x} thin films, spray pyrolysis deposited, structural and optical props. 7-22468
 CsBr:Hg²⁺, Hg²⁺ centres, electronic absorpt. spectrum 7-59229
 CsCl:CN⁻, F_H(CN⁻)-centre absorption bands, pseudopotential method calcs. 7-22292
 CsCl(Br)(I), luminescence quenching in F centers under pressure 7-22334
 CsI:Hg²⁺, Hg²⁺ centres, electronic absorpt. spectrum 7-59229

impurity and defect absorption spectra of inorganic solids continued

- Cs₂O-SiO₂ glasses, intrinsic and recomb. luminesc. and fundamental absorpt. spectra 7-13195
 CuCl₂Br_{1-x} colloids in glasses, x=0-1, exciton spectrum (Chinese) 7-38459
 Eu²⁺ impurity in garnets, compositional shift of spectral lines 7-53252
 Fe₂(SiO₄), defects, Fe³⁺ conc., microscope-spectrometric method 7-17330
 GaAs, crystal defects, IR light scattering tomography and IR absorption microscopy 7-46023
 GaAs, EL2 clusters, scattering and absorpt. of IR light 7-53382
 GaAs, electron-irradiated, relative density of levels of radiation defects 7-52500
 GaAs, FTIR spectra of acceptors, electronic intrasite transitions and local vibr. modes 7-53377
 GaAs, IR imaging 7-32238
 GaAs, inhomogeneous characteristics, photoconductivity and optical absorption meas. 7-32439
 GaAs LEC substrates, EL2 deep donor kinetics under annealing, IR absorpt., DLTS, Hall effect meas. 7-32955
 GaAs, LEC-grown wafer, EL2 conc., stress distrib., near-IR absorption mapping 7-52522
 GaAs, metastable state annealing 7-27297
 GaAs, microwave absorption transient spectroscopy for investigation of deep levels in semiconductors 7-52520
 GaAs, n-type, electron-irradiated, photoionization cross sections of E levels 7-64152
 GaAs, optically induced far-IR absorption from residual acceptors 7-22287
 GaAs, plastically deformed or electron or neutron irradiated, antisite defects 7-37987
 GaAs seminsulating slices, spatial inhomogeneities, near IR transmission imaging techniques 7-33400
 n-GaAs slabs, ionised-impurity-mediated free-carrier absorption 7-17335
 GaAs, uniformity imaging 7-32481
 GaAs wafers, LEC-grown, semi-insulating, two-dimens. high-resolution EL2 topography 7-53381
 GaAs:C, impurity content meas., IR absorpt., room temp. meas. 7-22289
 GaAs:C, LVM absorpt. temp. depend. (Chinese) 7-59225
 p-GaAs:Cr, excited and metastable states of Cr-related double centres 7-7153
 GaAs:Ge,Si, local modes, isotopic fine struct., IR spectra 7-38145
 GaAs:In, doped and undoped, EL2 maps from computer based IR image analysis 7-32237
 GaAs:In, strain effects, electrorefl. and photocapacitance study 7-22224
 GaAs:Ti, optical spectra 7-7720
 GaAs:V, electromodulation spectra, deep level energy positions 7-38496
 GaAs/AlGaAs multiple-quantum-well structures, shallow donors, far infrared spectroscopy 7-39121
 GaAs_{1-x}P_xN epitaxial layers, N conc. determ. 7-63989
 GaAs(P)(Sb):H, vibrational excitations, impurity-host atom complexes, IR absorpt. data interpretation 7-44724
 GaN films, OMVPE, Hall mobilities, impurity band 7-39410
 GaP:Ni²⁺, absorpt. spectrum of Ni²⁺ 7-53373
 Ge, quenched, SA₂ acceptor, uniaxial stress effects, far IR optical study 7-64673
 GeO, Li, IR absorption spectra and bands, Li-O complexes 7-33375
 GeO₂-Bi₂O₃-ZnO glass, coloration mechanism due to Bi₂O₃ and effects of ZnO addition 7-22291
 GeO₂-SiO₂:N optical fibres, N-related absorpt. bands 7-59226
 Ge₃₀S₇₀-Ag chalcogenide films, Ag photodoping, optical transmission spectra 7-59231
 InP, microwave absorption transient spectroscopy for investigation of deep levels in semiconductors 7-52520
 InP:B, multiphonon absorpt. 7-59211
 InP:Fe, optical spectra 7-53372
 InSb shallow magnetodonor photo-ionisation spectra studies 7-64165
 IrBr₂⁻, in A₂MX₆-type host crystals, near-IR absorpt. spectra 7-22232
 IrCl₆⁻, in A₂MX₆-type host crystals, near-IR absorpt. spectra 7-22232
 KAl(SO₄)₂.12H₂O:Cr³⁺, optical absorpt. spectrum study, cryst. field and site symm. determ. 7-59232
 K_{1.5}Bi_{1.5}Nd_{0.5}O₁₅, cryst. growth, spectral props. of Nd³⁺ ions 7-53405
 KBr crystal, radiation defects destruction by electron beam generated pulsed stresses 7-63663
 KBr single crystals, F-band absorpt., X-irrad., thermolum., mag. and elec. field effects 7-59230
 KBr:CN⁻, persistent IR hole burning in vibr. spectrum 7-37057
 KBr:Cu, visible absorpt. spectra 7-3073
 KBr:Se⁻, electronic spectroscopy 7-22319
 KBr:Se⁻, mag. circular dichroism, electric conductivity, mobility of anion vacancies 7-3024
 KBr:Sn²⁺, impurity localised excitons, form. energy calcs., UV spectra anal. 7-64095
 KCl, γ -irradiated, influence of plastic deformation on colour centre conc. 7-44538
 KCl, single crystal, γ -irradiated, growth of hole defects (Russian) 7-16628
 KCl:Cu visible absorpt. spectra 7-3073
 KCl:F⁻:Eu²⁺, optical absorpt., excitation and luminesc. spectra 7-59250
 KCl:H, F-centre accumulation during proton irradiation 7-46076
 KCl:Sn²⁺, impurity localised excitons, form. energy calcs., UV spectra anal. 7-64095
 KCl:Ti³⁺-type phosphors, Jahn-Teller-induced A-absorption and A-emission bands 7-53398
 KCl_{1-x}Bi_xLi mixed crystals, F_A centre absorpt. and emission spectra studies 7-12064
 KCl(Br)(I), luminescence quenching in F centers under pressure 7-22334
 K₂CuX₃ (X=Cl, Br), energy band struct., fundamental optical absorption 7-7093
 KH₂PO₄(D₂PO₄), impurities, UV spectroscopic study 7-33417
 K₂NaScF₆:Cr³⁺ laser material, tunable, crystal growth and spectroscopy 7-13347
 K₂O-SiO₂ glasses, intrinsic and recomb. luminesc. and fundamental absorpt. spectra 7-13195
 K₂SO₄-ZnSO₄:Pr³⁺, impurity ion spectroscopic parameter determ. 7-7719
 KTa_{1-x}Nb_xO₃:CO₃²⁻, impurity detection, IR transmission and Raman scatt. studies 7-13164
 La₃Ga₅Ta_{0.5}O₁₄:Nd³⁺, luminescence and absorption spectra and low-threshold stimulated emission 7-7731

impurity and defect absorption spectra of inorganic solids continued
LaMgAl₁₁O₁₉:Nd(Eu), single cryst., phys. chem. and spectrosc. props. 7-13185
Li-Al₂O₃-P₂O₅:Ag glasses, Ag⁰ centre thermal and photochemical conversion, spectroscopic consequences 7-39906
LiCl: Pb²⁺, absorpt. and luminesc. spectra studies (*Russian*) 7-46141
LiF crystals with F₂⁻ centres, inactive losses, investig. of mechanism 7-3072
LiF, F₂⁻-F₂ mixed centres, laser oscillations at room temp. 7-7714
LiF, F⁻ and F₂⁻ centres induced by ion implantation 7-26747
LiF, γ -irradiated, influence of plastic deformation on colour centre conc. 7-44538
LiF γ -irradiated crystals, F-centres, positron annihilation and optical absorpt. meas. 7-44542
LiF:Ne⁺(Ar⁺), defect and colloid production by ion implantation 7-26746
LiF:U, Ti(U), X-irradiated crystals, absorpt. bands of U⁴⁺ and U³⁺ ions 7-13183
LiH, ¹¹C and ¹³N implantation, chemical effects, radiochromatography study 7-28324
 α -Li₂O:Co²⁺, ESR and optical absorpt. studies of impurity ions 7-45803
LiLuF₄ = Pr³⁺ (Nd³⁺) (Ho³⁺) (Er³⁺), stimulated emission spectroscopy 7-13179
LiNbO₃:Co²⁺, ESR and optical absorpt. studies of impurity ions 7-45803
LiNbO₃:Mg, incorporation of H⁺, IR spectra of OH⁻ ions 7-7724
Li₂O, F⁻ centre absorption energy calcs. 7-12658
Li₂O, neutron and ion irradi. damage, ESR and optical absorption studies 7-32509
Li₂O-B₂O₃-WO₃:Co(Cr) glasses, optical props. 7-46079
Li₂O-SiO₂ glasses, intrinsic and recomb. luminesc. and fundamental absorpt. spectra 7-13195
LiRbSO₄:VO²⁺, optical absorpt. and EPR spectrum, crystal field parameters 7-59109
LiYF₄:Tm³⁺ crystal, Tm optical spectrum, press. induced linear dichroism, electron-phonon interaction 7-3069
MgAl₂O₄:Ni²⁺, Czochralski growth and optical props. 7-59406
MgO, electron irradi., stored energy, differential thermal anal. studies 7-32503
MgO:Cr, Cr³⁺ absorption spectrum, spin-orbit interaction effects 7-13182
Mo, N-vacancy interactions, obs. with thermal He desorption spectrometry 7-58311
NH₄Al(SO₄)₂.12H₂O:Cr³⁺, X-ray radiation damage, EPR and optical absorption studies 7-26799
NH(D)₂Cl:Cu²⁺ crystals, impurity optical absorpt. spectrum temp. depend. study 7-53374
NH₄H₂PO₄:Co²⁺, optical absorption spectrum 7-46077
(NH₄)₂SO₄:Ti, cryst. fields calc., Madelung energies and cryst. pots., optical absorption spectra anal. 7-64180
(NH₄)₂SO₄:Ti, mol. orbitals, EHT calc., rel. to absorption spectra 7-64181
(NH₄)₂SO₄:Ti crystal, temp. depend. of optical absorption bands 7-64671
NO₂⁻ effect on IR absorpt. spectra in Ti halide crystals. 7-39124
NaCl crystals, electron-coloured, transmission and holographic props. 7-43001
NaCl:Cu, visible absorpt. spectra 7-3073
NaCl:Eu²⁺, gamma irradi., optical absorpt. spectra, TSC meas. 7-58337
NaCl:Eu²⁺ crystals, γ -irradiated, colourability 7-12062
NaCl:Mg, X-ray irradi., exciton interactions with impurity-vacancy dipoles, absorpt. and luminesc. spectra 7-45162
NaCl:OH⁻, Cd²⁺ single cryst., gamma irradi., electronic and IR spectra 7-53320
NaCl:Sn²⁺, impurity localised excitons, form. energy calcs., UV spectra anal. 7-64095
NaF:OH⁻, X⁺, X=impurities, vibr., radiation effects, IR spectra 7-53321
Na₂O-B₂O₃ glass, UV absorption spectra of Ag⁺ ion 7-7721
Na₂O-SiO₂ glass, relative defect-production efficiency for fission fragments, alpha decay and electron irradiation 7-12167
Na₂O-SiO₂ glasses, intrinsic and recomb. luminesc. and fundamental absorpt. spectra 7-13195
Na₂O-SiO₂:Tb³⁺ glasses, colour centre formation during UV irradiation 7-2049
Na₂O.3SiO₂:Eu³⁺, UV-irradiated glass, formation of colour centres 7-12063
PbMoO₄ crystals, point defects, absorpt. and fluoresc. props. 7-64674
PbO-SiO₂-K₂O coloured and colourless glasses, near IR absorpt. temp. depend. study 7-13146
PbTe, mag. susceptibility, optical absorpt. spectra, effect of intrinsic defects 7-64670
PbWO₄:Nd³⁺(Pr³⁺), optical spectra 7-39146
Pd₂Th, impurity internal oxidation, EXAFS 7-17360
Pb₃AgI₃, energy band struct., fundamental optical absorption 7-7093
RbBr:Ba²⁺(Ca²⁺)(Eu²⁺)(Sr²⁺), Z₂ colour centres, picosecond relax., non-stationary spectra 7-59233
Rb₂CuX₃ (X=Cl, Br, I), energy band struct., fundamental optical absorption 7-7093
Rb₂Mg(SO₄)₂.6H₂O:CO²⁺ optical absorption spectrum 7-13180
Rb₂Mg(SO₄)₂.6H₂O:Cu²⁺, electronic and EPR spectra 7-13019
Rb₂O-SiO₂ glasses, intrinsic and recomb. luminesc. and fundamental absorpt. spectra 7-13195
Si, grain boundary pot. barrier and role of distorted bonds 7-46080
Si, heavily doped crystals, behaviour of O and dopants 7-32483
Si, optical props. of isolated dangling bond 7-38507
Si porous films, IR absorpt. study 7-39149
Si, thermal donors, alignment by uniaxial stress, EPR and optical studies 7-59227
Si:Er(Dy)(Yb)(Ho)(Gd), neutron irradi., Hall effect, elec. cond., IR absorpt. spectra 7-51834
Si:Ge,P(B), IR absorpt. band broadening 7-64669
Si:H, amorphous film, optical absorption and bandgap rel. to temp. (*Korean*) 7-59228
Si:H, impurity effects on IR absorpt. bands of Si-H centres, irradi. and unirrad. crystals. 7-53379
a-Si:H,F/a-SiGe₂:H,F multiple layered films for enhancement in photore-sponse in near IR spectrum 7-52668
a-Si:H films, thermal-equilibrium defect processes 7-26640
a-Si:H sputtered film, low-temp. optical props. 7-3101

impurity and defect absorption spectra of inorganic solids continued
Si₃N₄, O, impurity complexes as shallow donors, optical absorpt. study 7-39147
SiO₂, Czochralski grown, O-related defects after annealing, IR TEM and resistivity meas. 7-32466
SiO₂, IR absorption meas. of interstitial O conc., calibration 7-33401
a-Si_{1-x}N_x:H films, H₂ evolution 7-17445
V-SiO₂ intrinsic defect electronic struct., optical transitions, cluster-Bethe lattice calcs. 7-2541
SiO₂ silica glasses, doped, radiation-induced defect centres, EPR and optical studies 7-13033
SiO₂-Al₂O₃-Li₂O-ZnO-TiO₂-ZrO₂-As₂O₃-Cr₂O₃:Cr, glass ceramic, time resolved spectra 7-63478
SiO₂-Al₂O₃-MgO-TiO₂-Cr₂O₃ based glass ceramics, Cr³⁺ laser emission and excitation spectra 7-22299
SiO₂-Al₂O₃-ZnO-Li₂O:Cr³⁺ gahnite type glass ceramics, laser excited emission spectra 7-22288
SiO₂-B₂O₃-ThO₂ based glasses, local struct. around actinide, EXAFS and optical spectral studies, appl. for nuclear waste glasses 7-59290
SiO₂-B₂O₃-UO₂ based glasses, local struct. around actinide, EXAFS and optical spectral studies, appl. for nuclear waste glasses 7-59290
SiO₂-GeO₂-P₂O₅, doped silica glass, dopant effect on OH absorpt. 7-27715
SiO₂-P₂O₅ optical fibres, γ -irradiated, phosphorus oxygen hole centres 7-11083
SnO₂, pure and F doped CVD films, UV absorpt. props. study 7-22370
SrCl₂:Eu, defect equilibria, site selective laser spectrosc. 7-46078
SrTiO₃:Mn, Mn oxidation state change near phase transitions 7-16974
TeO₂, paratellurite, circular dichroism and weak absorption bands 7-45977
 β -ThCl₄:Pr³⁺, site selective laser fluorescence spectroscopy 7-64687
ThCl₄:U, optical spectra of U⁴⁺ 7-27732
ThO₂:Np⁴⁺, absorption and emission spectra of Np⁴⁺ 7-27763
ThSiO₄:Np⁴⁺, absorption and emission spectra of Np⁴⁺ 7-27763
ThSiO₄:U, optical spectra of U⁴⁺ 7-27732
TiO₂, absorption and photolysis spectra 7-22290
TiO₂:Al, absorption and photolysis spectra 7-22290
TiO₂:Cd thin films, extension of optical absorpt. range by doping 7-39144
TiO₂:Cr, absorption and photolysis spectra 7-22290
TiO₂:V, absorption and photolysis spectra 7-22290
TiBr₃ indirect exciton transition, effects of disorder 7-2489
(Y,Sc)₃Ga₅O₁₂:Cr³⁺,Er³⁺, spectral, luminesc. and lasing props., Stark sublevel lifetimes 7-25827
YAG:Nd³⁺, impurity two-photon absorpt. cross section meas. 7-53375
YAlO₃:Pr³⁺ single crystals, colour centres, optical absorption spectra studies 7-63610
Y₂Al₂O₇, room temp. γ -irrad., colour centre investig. 7-6621
YLiF₄:Nd³⁺, impurity two-photon absorpt. cross section meas. 7-53375
Y₂O₃:Eu³⁺, impurities optical dephasing temp. and freq. depend. 7-22286
YVO₄:Eu,Ga(Sc)(La), optical props. and electronic struct. 7-33423
Yb²⁺ impurity in garnets, compositional shift of spectral lines 7-53252
ZnAl₂O₄:Cr³⁺ laser excited emission spectra 7-22288
ZnS:Fe²⁺, impurity vibronic coupling and near IR spectra characts. 7-26889
ZnS:Mn electroluminescent thin films, photothermal deflection spectroscopy 7-27804
ZnS:O, Er(Tm)(Dy), activator centres, spectrosc. investig. 7-13184
ZnSe:Cu,Al,Fe crystals, melt-grown, absorpt. coeff., impurity effects 7-3070
ZnSiP₂ cryst., exciton absorpt. spectrum, energy gap and exciton binding energy determ. 7-2500
ZnTe:Cu, impurity related neutral complex with bound exciton, photoluminescence, absorpt., Zeeman meas. 7-45165
ZnTe:O, light scattering 7-17333
ZnWO₄, Czochralski grown, quality, colour rel. to scintillation output 7-59407
ZnWO₄:Fe single crystals, spectroscopic props. 7-7725
Zr³⁺ impurity in garnets, compositional shift of spectral lines 7-53252
ZrF₄-based fluoride glasses, Fe ions anal. 7-64672

impurity and defect absorption spectra of solids
see also impurity and defect absorption spectra of inorganic solids
amorphous solids, optical dephasing of impurity transitions, distrib. functions 7-27746
benzoic acid:thioindigo(selenoindigo) impurity-induced double proton transfer, fluorescence decays 7-33420
homogeneous optical band shape of impurity centres, amorphous and crystalline media 7-38510
indole:naphthalene(anthracene)(tetracene) crystals, impurity complexes, photolum., thermolum. and absorpt. spectra studies (*Russian*) 7-46139
organic mixed crystals, impurities optical dephasing temp. and freq. depend. 7-22286
phonon mechanism of phase relax. of electron excitation 7-38464
phthalocyanine polymer films, I₂ implantation, RBS studies 7-26776
polyacetylene:I₂, semicond. soliton lattice-metal phase transition, photo-modulation spectra studies 7-21819
polyacetylene, I₂-doped, quantitative optical study 7-53380
polyacetylene films, oxygen-exposed, IR transmission spectra 7-13181
polyazulene, in situ optical and ESR studies during electrochemical doping 7-26670
polyethylene films with Si incorporation, localized gap states, space-charge-limited current 7-52530
random organic solids, non-exponential relax. processes. 7-37058
semiconductors, light absorption by dislocations, exciton effects 7-53371

impurity clustering *see segregation*
impurity-defect interactions
see also impurity-dislocation interactions; impurity-vacancy interactions
2D diffusion kinetics, influence of point defects 7-38263
semiconductors, implanted ions diffusion redistribution, effect of radiation defects 7-51810
solid solutions, precipitate growth under irradiation, theory 7-12296
Co_{1-x}O, dopant cations interaction with 4:1 defect clusters, theoretical study 7-63644
Fe-H system, electron and neutron irradi., positron lifetime meas. 7-44603
Fe-H system, H-defect interactions study by positron annihilation 7-38046
Fe_{1-x}O, dopant cations interaction with 4:1 defect clusters, theoretical study 7-63644

impurity-defect interactions continued

- GaAs pure and Si, Mn or Cu doped crystals, impurity and defect props., heat treatment, photolum. studies 7-39163
 InAs:Sb(Ga)(Mn), single crystal, elec. inhomogeneity, effects of isovalent impurities 7-7229
 InP crystals and solar cells, radiation-induced defects, room-temperature annealing 7-39993
 InP, electron irradi. damage, impurity effects 7-12154
 $Mn_{1-x}O$, dopant cations interaction with 4:1 defect clusters, theoretical study 7-63644
 Mo-H proton irradiated system, defect annealing, positron lifetime studies 7-38043
 Mo-H system, neutron irradi., H-void interactions 7-44604
 Mo-N system, neutron irradi., isochronal annealing, positron annihilation studies 7-46531
 NaCl crystal, surface optical breakdown, exoelectronic emission with laser irradiation, impurity effects 7-59384
 Ni, H trapping phenomena, meas. by desorption thermal anal. technique 7-6673
 Ni-H proton irradiated system, defect annealing, positron lifetime studies 7-38043
 $Ni_{1-x}O$, dopant cations interaction with 4:1 defect clusters, theoretical study 7-63644
 Si, defect reactions and atomic diffusion 7-38264
 Si, interstitial-based intrinsic gettering process appl. to multilevel defects structures 7-38048
 Si, intrinsic gettering by butterfly-type defects 7-38047
 Si, polycrystalline, for solar cell apps., photovoltaic props., effect of impurities and defects 7-38639
 Si, ramp assisted foil casting and photovoltaic apps. 7-16609
 Si:As ion implanted films, defects charactn. by AC Hall effect meas. 7-38601
 Si:H floating zone single crystals, neutron irradi., isochronal annealing behaviour, positron annihilation studies 7-21288
 Si:N, N incorporation and behaviour 7-16598
 Si:O, diffusivity and solubility of O review 7-16809
 Si:O, vacancy-enhanced O diffusion 7-16811
 Si:O,C, intrinsic point defects and impurity interactions 7-16611
 $SiO_2:GeO_2$ optical fibres reaction of diffused H_2 with defect centres 7-57591

impurity-dislocation interactions

- see also dislocation locking; dislocation pinning*
 alkali metal halides, hardening, effect of dislocation elec. charge 7-51816
 ice, pure and doped, US absorpt., dislocation damping 7-26756
 metals, BCC, H-dislocation interaction mechanism, embrittlement and dislocation motion 7-44600
 metals, irradiated, deformation rate, radiation swelling and creep (*Russian*) 7-44597
 smectic A liq. crystals., point-like impurity-dislocation interactions, Peach-Koehler formula calcs. 7-11903
 steel, Ni-Cr, tensile flake form., H damage, dislocation transportation (*Chinese*) 7-8077
 Al, hysteresis behaviour of medium temp. peaks (*French*) 7-63742
 Cu-based binary alloys, Young's modulus, microalloying effects (*Russian*) 7-33711
 Fe, Armco, H. charging, Rayleigh wave attenuation, mag. field effect 7-53107
 Fe, Armco and Vacofer, yielding behaviour, H influence 7-33753
 α -Fe, dislocation pair jog, energy characts., mol. dynamics method anal. (*Russian*) 7-32440
 Fe, plastic deform., H permeation, dislocation traps 7-65082
 Fe, pure, diffusion of H, dislocation trapping, interstitial impurities effect (*Japanese*) 7-52140
 Fe, pure, plastic softening by H plasma charging 7-59590
 Fe:He(C), distribution and migration of interstitial impurities in the field of a screw dislocation core 7-6669
 Fe-base alloys, interstitial impurity-dislocation binding energy (*Russian*) 7-58310
 Fe-H system, dislocated single crystals, positron trapping reduction on H charging 7-39262
 Fe-H system, H-defect interactions study by positron annihilation 7-38046
 GaAs, dislocations, obs. by transmission IR microscopy 7-32447
 $MgO:Fe$, small angle [001] twist boundaries, Fe solute effect 7-32459
 Mo, He pipe diffusion along dislocations 7-58544
 Mo single crystal, cold worked, He pipe diffusion along dislocation, thermal desorption spectra 7-52142
 Mo-Fe dilute alloy, Fe solute atom-screw dislocation interaction force, modified tight-binding recursion method calcs. 7-51814
 NaCl:Ca, impurity dipoles, aggregation with dislocations under alternating elec. field 7-44598
 Ni, creep, T charging, He bubble migration and coalescence 7-65102
 Ni, dislocation-impurity C interstitial interaction, computer simulation studies 7-2046
 Ni, electron irradi., H-defect interactions, positron annihilation study 7-6674
 Ni, H trapping phenomena, meas. by desorption thermal anal. technique 7-6673
 Ni, intergranular H embrittlement kinetics 7-65134
 Ni:H, diffusivity, diffusion-elastic effect and Gorsky effect 7-27023
 Ni₂Cr, recrystn. kinetics and mech. props., influence of P 7-22718
 Pd-H system, plastically deformed, H-dislocation interactions 7-6671
 Si, surface layers, local mechanical stresses relaxation 7-21604
 Si:H, impurity clustering, hydride form. on dislocations, TEM study 7-26964
 Si:O, dendritic web growth, plastic flow, O effects 7-16471
 Si₂O(N), impurity-dislocation interactions, review 7-16610
 Ta wire, cold worked, internal friction, hydride precip. (*Chinese*) 7-8034
 Ti, pure, plate, yield strength, H content depend. (*Chinese*) 7-8044
 W-H system, H-defect interactions, positron annihilation studies 7-38045
 Zn-Ag dilute alloy single crystals., thermally activated and quantum creep, impurity effects (*Russian*) 7-26755
 Zn-Au dilute alloy single crystals., thermally activated and quantum creep, impurity effects (*Russian*) 7-26755
 Zr, polycrystalline, low temp. creep, dislocation interactions (*Russian*) 7-3359
 $(Zr_{0.2}O_{0.9}(Y_{2}O_{3})_{0.1})$ fliantite crystals., bending and compressive strength temp. depend. meas. 7-44653

impurity distribution

- see also doping profiles; segregation*
 C fibre reinforced Al, segregation of doping elements, Si, Bi 7-65046
 conversion layers on Al, struct., TEM, LAMMA, AES, XPS, SIMS, ion scatt. spectra 7-23094
 crystals, impurity distribns. due to growth-rate fluctuations 7-44589
 diffusion, with form. of segregation phases at dislocations (*Russian*) 7-52146
 disordered systems, impurity diffusion (*Russian*) 7-52145
 electron gas, galvanomag. props., interaction effects, applied electric and mag. fields 7-52477
 Fe-D formed by D ion implantation, multiple D occupancy of vacancies 7-63643
 inhomogeneous materials, implanted ion depth distribns. 7-21250
 ions implanted into single crystals, depth distributions 7-6667
 p⁺n junctions, impact ionisation rates, field fluctuation effects, Monte Carlo simulation 7-64323
 Peierls-CDW state, ID, impurity distrib., 2k_F distortion 7-44593
 piezoelectric materials, acoustic resonance techniques for temp., stress and impurity characterization 7-45938
 polypyrrole:BF₄⁻O, dopant distrib., atom probe anal. 7-32480
 potassium hydrogen phthalate, cryst. growth, influence of impurities, in situ obs. of {010} face 7-46289
 quartz: Cu⁺ (Fe³⁺)(Nb⁵⁺), ion implanted, coloration and transparency (*Japanese*) 7-7656
 quartz, cultured, grown from +X seeds, Al and OH⁻ distrib. 7-58307
 radiation-stimulated diffusion during ion etching 7-38261
 semiconductor materials characterisation, electron, ion, X-ray and optical probe methods 7-27203
 semiconductor metallisation, Auger depth profiling, interface resolution 7-54246
 semiconductors, depth resolution of SIMS 7-54253
 semiconductors, impurity profile and concentration-dependent diffusion 7-51809
 solid state laser materials, active ion distributions 7-57342
 solids, ion-implanted impurities, steady-state concs., ultimate retained doses, determ. 7-6658
 steel, Cr-Mo, crack initiation under sustained load, effect of impurity segregation 7-65111
 steel, Cr-Mo, toughness, impurity element effects 7-53856
 steel, stainless, nuclear fuel pin cladding, C distrib., SIMS study 7-19360
 ZnO:Bi (Sb) (transition metal), Schottky-like barriers, ion implantation, annealing 7-58860
 Ag-brass, mixing layer, friction props., ion beam mixing (*Chinese*) 7-51888
 Al, disordered films, density of states, electron-electron interactions tunnel conductance meas. 7-52393
 β -Al₂O₃, diffusion of implanted ions (*Chinese*) 7-51798
 α -Al₂O₃:Br, ion implanted, RBS and annealing studies 7-32515
 Al₂O₃:C,S CVD layers, C and S distrib., SIMS anal. 7-6668
 Al₂O₃:Ti³⁺, solid laser material, active ion distributions 7-57342
 BeAl₂O₄:Cr³⁺, solid laser material, active ion distributions 7-57342
 a-C:H, diamondlike, dielectric film, props. rel. to deposition parameters 7-39419
 a-C:H, film, optical and electronic props. rel. to deposition parameters 7-38406
 C:H, homogeneous and heterogeneous chemistry of methane deposition plasma 7-39424
 CdS, single crystal, US wave absorption, impurity distrib. effect., electron-probe X-ray anal. 7-53241
 CdSe, single crystal, US wave absorption, impurity distrib. effect., electron-probe X-ray anal. 7-53241
 CdTe, segregation coeffs. of Ag, Co, I and In, recoil implanted radioactive tracer technique 7-21461
 Fe surface layers under toluene, laser irradiated, supersaturation with C 7-51820
 Fe:He(C), distribution and migration of interstitial impurities in the field of a screw dislocation core 7-6669
 Fe-based metallic glasses, retardation of annealing embrittlement by C microadditions 7-65118
 Fe-N, implantation at 77 K, surface comp., microstructure, AES, HVEM, transmission HEED studies 7-38033
 Fe-P-C system, ferritic, grain boundary segregation of P and C 7-39530
 Fe-Pt-N austenites, thermodynamics 7-63844
 GaAs, epitaxial layers, grown in temp.-gradient field, effects on dislocation density 7-13393
 GaAs, LEC, semi-insulating, undoped, C origin and melt comp. depend. 7-17410
 GaAs LEC wafers, cathodolum. mapping, IR absorpt., X-ray topography obs. 7-33462
 GaAs, uniformity imaging 7-32481
 GaAs:C, O, trace determ. by ³He-activation anal. 7-58308
 GaAs:In annealed substrates, In distribution in surface region 7-44959
 GaAs:Mg²⁺, formation of p-type layers using ion implantation and rapid thermal annealing 7-45311
 GaAs:Si⁺ wafers, implant at. profiles., planar and residual channelling effects 7-12181
 GaAs/GaAlAs single quantum wells, steady-state photoluminescence studies 7-7750
 GaAs-Bi, distrib. coeff. of Bi, crystn. from molten solns. 7-46428
 n-GaAs,_{x-y}Sb,P, epitaxial film, impurity distrib., cond. and Hall mobility study 7-51808
 GaP: Te(Zn), doping superlattices, growth and props. 7-64684
 GaSb:Te(Se)(Si)(Ge) single crystals., Czochralski growth, carrier conc. rel. to dopant conc. 7-22462
 GdTbFe, corrosion resistance improvement by metal coatings 7-53952
 Ge, floating zone growth, lateral solute segregation rel. to gravity conditions 7-53576
 Ge:H films, post-deposition hydrogenated, electrical props. 7-32296
 In-glass, glow discharge induced changes 7-12577
 InAs:Sb(Ga)(Mn), single crystal, elec. inhomogeneity, effects of isovalent impurities 7-7229
 InP:Bi thin film, epitaxy, impurity distrib., photoluminesc. spectra anal. 7-53388
 InP:Fe, programmed magnetic field applied LEC crystal growth 7-59399
 InP-Si(Sn)(Be), doping using thermal atomic beams in chemical beam epitaxy 7-44584
 InSb:Te crystals, Czochralski growth, layered heterogeneity, melt temp. fluctuations, mag. field effect 7-27888
 KCl:Sr, quenched and as-grown crystals., ionic cond., impurity dispersion state effects study 7-26786

impurity distribution continued

K₂Pt(CN₄)Br_{0.3}·3.2H₂O, quasi 1D conductor, near IR conductivity, pseudogap model 7-45298
Mo alloys, grain boundary enrichment by O and C, nonmonotonic temp. depend. (Russian) 7-59534
Mo and alloys, containing pores, segregation effects (Russian) 7-59533
MoSi₂:As-poly Si struct., redistribution of As by silicidation tempering 7-51812
NaCl:Eu²⁺ crystals, mechanical strength, dopant distrib. and γ -irrad. effects study 7-26800
Nb-Li alloys, interstitial impurity distrib., thermodynamic anal. (Russian) 7-32430
NbH₃, coherent phase transition, neutron radiography study 7-32629
Nb₇₅Si₂₅, N⁺ implantations, effect on A15 phase formation 7-63480
Ni, He implanted, defects study by monoenergetic positron beam 7-39293
Ni, ion irradiation-induced implant diffusion and segregation, synergistic effects, kinetic model calcs. 7-16658
Ni(B)s, grain-boundary cohesion, impurity segregation effects, density-functional cluster model calcs. 7-44835
p-Si:As oxidation in HCl ambient, impurity pile-up, bubble pattern form. and local oxide bowing 7-13675
PbSe: Cd, crystal growth and impurity distrib., electron probe X-ray microanal. studies 7-63639
PbTe:In₁, Soret effect, impurity cond. distrib., thermolec. power meas. 7-44930
PbTiO₃:Cr³⁺, ceramic, EPR, ENDOR, ESE investigations. 7-13020
Pd-H, single particle dynamics, simulation model 7-27016
Sb-Ge-Se:Mn, effect of Mn impurity on comp. and physicochemical props. 7-11922
Sb₂Te₃:Sn, Ti, single crystals, X-ray spectral microanalysis 7-44590
Si, Auger electron spectroscopy, sensitivity, contamination levels 7-54245
Si, CVD thin film backside gettering effectiveness 7-38217
Si epitaxial layers, ultrahigh-purity, photoluminesc. studies 7-45033
Si epitaxial layers, VPE growth, charactn. (Japanese) 7-63986
Si, Fourier transform photoluminescence analysis 7-53412
Si gettering, review of phenomenology 7-38215
Si, impurity and carrier conc. profiles, electrochem. C-V method (Chinese) 7-12105
Si, impurity profiles, depth resolution of SIMS 7-54253
Si, interstitial-based intrinsic gettering process appl. to multilevel defects struct. 7-38048
Si, intrinsic gettering by butterfly-type defects 7-38047
a-Si, ion implanted, 2D model of nucleation and regrowth 7-38408
Si MBE, impurity sticking coeffs., substrate orientation depend. 7-52355
Si, polycrystalline, H₂ passivation, grain boundaries, EBIC technique 7-26769
Si, recoil implantation of O₂, characterisation by double-crystal X-ray diffraction, TEM, Monte Carlo simulation 7-51807
Si:Ag, implantation damage regrowth studied via Ag depth profiling 7-22730
Si:Al, depth profiles, redistrib. of annealed Al implants 7-63640
Si:Al surfaces, SIMS anal. of contaminants 7-33989
Si:Al(In), recrystallisation by pulsed electron beam, impurity profiles 7-16605
Si:As films, heavily doped, grown by partially ionised MBE, phys. and elec. characts. 7-12561
Si:As(P)(B)-SiO₂ interface, segregation, transport coeffs. of impurities 7-63880
Si:Au. U- and W-shaped impurity diffusion profiles investigation 7-16805
Si:B, impurity transport in mag. Czochralski growth, computer simulation 7-58182
Si:B, laser microprobe mass analysis, quantitative 7-54250
Si:B,Fe, EBIC and DLTS meas., comparisons 7-7265
Si:B(BF₂) wafers, activated carrier density profile and scatt. rate meas., nondestructive IR attenuated total refl. technique 7-22207
a-Si:B(P)(As), implanted ion distrib., lateral spreading, theoretical predictions and computer simulation 7-16604
Si:Bi, solute trapping by lateral motion of {111} ledges 7-44592
Si:C, polycrystalline, electrical and structural properties 7-12106
Si:Co, supersaturated solid solution, annealing 7-63642
Si:F, implanted, dry oxidation kinetics, impurity effects 7-13667
Si:Fe, intrinsic gettering, EPR and TEM study 7-38216
Si:H, ion implanted and annealed, H depth distrib. 7-26785
Si:H, polycrystalline, grain boundary interactions 7-12117
Si:H, thin film, Raman spectroscopy, characterisation 7-53354
a-Si:H short range order, impurity distrib. effects, EXAFS study 7-64761
Si:Li, ion implanted, impurity redistribution under pulsed laser radiation 7-12098
Si:O, Czochralski cryst. growth, impurity segregation, high axial mag. field effect 7-26960
Si:O, influence of growth microdefects on microdefect formation during heat treatment 7-17559
Si:O, low thermal donor conc. layer formation during annealing 7-17565
Si:O, P, Sb wafers, O precipitation during simulated CMOS cycles 7-38218
Si:Pt, deep levels and diffusion profiles 7-58767
Si:W⁺ layers, implanted and annealed, struct., TEM, electron diffr. studies 7-32858
a-SiN₂:H CVD film, IR and ²⁹Si NMR studies 7-38952
Si₃N₄ LPCVD films, bombardment induced H redistrib. 7-38404
SiO₂:Cl, ion implanted, Cl ion redistrib., SIMS studies 7-21249
SiO₂:Cl films prod. by Si oxidation in Cl containing ambients, impurity distrib. 7-26787
SiO₂:Cs-Si MOS, semicond. flatband voltage depend. on impurity distrib. 7-27433
SiO₂-Si, quantitative distrib. eval. of P, SIMS 7-54254
SnO₂:Sb spray deposited coatings, comp., elec. props. thermal treatments, AES study 7-22393
 α -Ti:Si, ion implanted, diffusion profiles, annealing behaviour 7-12369
Ti/Si:B,As,Sb interface, dopant redistrib. during silicide form. by rapid thermal processing 7-63641
Ti-Al-Nb (6.2 wt.%), fusion weld, defect regions, cracking, porosity, interstitials analysis 7-28109
TiSi₂:As(Sb) layers, dopant redistribution during silicidation by rapid thermal annealing, ion scatt. spectra study 7-21253
TiSi₂:B(P)(As) films on Si, impurity diffusion 7-7077
W (011), pulsed field evaporation, impurity distrib. 7-63956

impurity distribution continued

YIG:H, ion implanted, elastic recoil analysis using 44 MeV Cl ions 7-12107
Y₂O₃:ZrO₂:Fe, high dose ion implanted, profile shapes and electronic cond. 7-32472
Zr, oxidation effect of Ar ion beam mixing (Chinese) 7-53997
ZrO₂, cubic, crystal growth, stabiliser distrib. coeff. 7-53561

impurity electron states
see also A-centres; Anderson model; charge compensation; deep levels; electron traps; heavily doped semiconductors; impurity scattering; OH⁻-centres; U-centres; Z-centres
1D CDW systems, collective modes and impurity effects 7-21832

Al₂O₃:Cr,Ga, Cr-Ga complexes, energy transfer 7-22321
alkali halide crystals, polarised luminesc., model of Ga⁺, Ge²⁺, In⁺, Sn²⁺, Ti⁺, Pb²⁺ centres 7-27753
alkali metals, impurities and defects, electronic structure 7-27299
amorphous semicond. III-V and II-VI cpds., electronic struct. of bulk and defect sites, tight-binding recursion method 7-45222
Anderson impurity model, single particle excitation spectra, scatt. eqns., S-matrix approach 7-52385
Anderson model, Coulomb repulsion between localised and extended states 7-17157
anthracene: acridine crystals, conduction mechanism and trap levels, TSC meas. 7-27342
carrier concentration, temperature dependent data, donor and acceptor behaviour 7-64263
CDW, impurity pinning and depinning, quantum effects 7-52464
chalcogenide glass films, metal ion doped, impurity effects 7-11943
chemisorption, substrate impurity effects 7-63964
crystal impurity centres, interaction with coherent EM field 7-32951
deep levels study, capacitance methods 7-45205
diamond, interstitial H or muonium, Hartree-Fock analysis 7-32947
1,4-dibromonaphthalene:acenaphthenequinone crystals, phosphorescence spectra and decay kinetics temp. depend. (Russian) 7-27751
electron excitations, energy transport, luminesc. of impurity pairs, modelling 7-2508
electronic struct. of impurities in metals, valence-electron-only molecular orbital calcs. 7-2528
emerald, Cr³⁺ absorption spectrum, spin-orbit interaction effects 7-13182
energy transfer and lattice phonons, mutual influence 7-16977
ferromagnetic semicond., donor state, thermally induced abrupt shrinking 7-52510
gapless semiconductor, low temp. density of states near Fermi surface 7-64042
Ge_{1-x}Si_x:Cu, supersaturated solid solution, decomposition 7-32654
Ge²⁺ impurity ion in alkali halide crystals, triplet excited relaxed states, ODMR study 7-2953
heavy electron superconductors, normal impurity effects, excitation spectrum 7-27462
homogeneous optical band shape of impurity centres, amorphous and crystalline media 7-38510
II-VI semiconductors, shallow donor problem, pseudopot. approach 7-45216
III-V semiconductors, hot-electron photoluminescence, polarisation 7-46118
III-V semiconductors, localised electron states of substantial transition metal impurities, review 7-27295
impurity electron transfer selection rules (Russian) 7-16983
impurity ion off-centre dipoles 7-64163
impurity liq. cryst. spectra, complex vibron struct., polarisation absorpt. band splitting studies 7-17332
In_{0.53}Ga_{0.47}As:Fe metalorganic CVD epitaxial growth and elec. props. 7-63993
inert gases implanted in solids, model of diffusion and release behaviour (Chinese) 7-38257
InP:Cu, band-edge photolum. quenching, impurity recomb. centre effects study 7-39177
integer quantum Hall effect, theory 7-52824
intermediate valence and kondo impurities, noncrossing approx. 7-7162
interstitial diffusion in crystals, quantum theory 7-44916
local electron centre config. instability, quasiloocal modes interaction model calcs. 7-58772
local Fermi liquid theory of Anderson impurity model 7-52507
luminescence centre struct., rare earth elements in activated glasses 7-27754
metals, electron impurity states, dynamic spin suscept. calcs. (Russian) 7-12646
metals, strongly correlated, containing heavy fermions, thermodynamic and transport parameters 7-38458
MIM electroluminescent device struct., impurity centre electron impact-induced luminesc. mechanism 7-59260
multivalley semiconductors, excited states of shallow donors 7-52514
nondegenerate semiconductor, resistivity, impurity depend. 7-7240
one-dimensional cryst. with impurity, coherent exciton motion propagator and capture prob. calcs. 7-52436
one-dimensional tight-binding system, localisation by elec. field 7-16967
polyacetylene, ground, excited, polaronic, solitonic and impurity states calcs., doping effects 7-45131
polyacetylene, solitons, electronic props., local space approx. 7-52506
polyethylene:Si films, trapping states, TSC, optical absorpt. spectra, photod. meas. 7-27345
polythiophene, doped, polaron and bipolaron excitations, Huckel approx. calcs. 7-52448
quantized Hall effect, impurity bound state ionisation 7-12742
 α -quartz: AlO₄, hyperfine and quadrupole interactions, ENDOR study 7-2951
quasi-one-dimensional electron gas, screened hydrogenic impurity, binding energy 7-52508
quenching and energy transfer, description, rate eqns. 7-45211
rare earth semiconductors, valence changes, many-impurity Anderson model 7-7186
ruby, Cr³⁺ absorption spectrum, spin-orbit interaction effects 7-13182
ruby, C₃³⁺ ground state, superposition-model analyses of EPR data 7-7158
s-dimensional semiconds., Fermi energy, relativistic corrections, free-Fermi-gas model calcs. 7-2465
semi-infinite type I semicond. superlattice, surface electronic collective excitation modes, ionised donor oscill. current effects 7-21837
semiconducting materials, cryst., and device apps., book 7-60894

impurity electron states continued

- semiconductor doping superlattices, physics and applications 7-52826
 semiconductor heterostructures, inelastic light scatt. by electronic excitations 7-13171
 semiconductors, charged defects, reaction rates 7-38497
 semiconductors, deep centres, book 7-18510
 semiconductors, dispersive transport under conditions of maximum population of localized states 7-52605
 semiconductors, doped, H-like eigenstates, variational alternant MO method 7-25356
 semiconductors, extrinsic n-type, stochastic self-oscillations under intense illumination 7-2639
 semiconductors, fluorescence line shape anal. for free-to-bound transitions 7-46097
 semiconductors, ionised resonant donor and acceptor superlattice form., screened Coulomb interaction, carrier scatt. effects 7-16981
 semiconductors, quasi-1D, bipolaron-impurity complexes 7-45180
 semiconductors, space charge stratification, transient processes 7-64313
 TGS:Cr³⁺ single crystals, valence bands and impurity levels, absorpt, edge meas. 7-33350
 transition metal fluorides, mixed, Raman scatt. by localised and magnon modes 7-46027
 transition metal oxides, impurity and defect electron struct., self-consistent local density theory 7-45208
 transition metal perovskite type oxides, electronic struct. of point defects 7-16979
 transition metals:H, local impurity environment in cubic lattices 7-21236
 transition metals, impurity and defect electron struct., self-consistent local density theory 7-45208
 TTF-chloranil, neutral-ionic transition, phenomenological theory 7-26939
 tunnelling states of off-centre impurities and Jahn-Teller systems, 3D harmonic oscillator function calcs. 7-2537
 two-dimensional electron systems, magnetoelectronic, density and mag. field dependences 7-33033
 weakly bound impurity states, ionisation width in mag. field 7-45206
 Ag alloys, dil., EFG, asymmetry parameter calcs. 7-2545
 Ag₃AsS₂ undoped proustite crystals, photolum. obs., exciton-impurity complexes 7-33445
 AgBr:Rh³⁺, IR radiative recomb. 7-7748
 AgCl:I, impurity centre local electron states 7-45207
 AlAs/GaAs:Si super-doped struts., short-period superlattice electrical and defect props. (Japanese) 7-7353
 Al_{0.5}Ga_{0.5}As-GaAs multiple quantum wells, photoluminescence studies, press. depend. (Chinese) 7-13194
 AlGaAs layers MOCVD using dimethyl aluminium hydride, C acceptors, photolum. 7-22517
 AlGaAs superlattices, donor state instability, DLTS and Hall meas. 7-12663
 AlGaAs-GaAs superlattices, impurity electron states (Japanese) 7-12662
 Al_{0.3}Ga_{0.7}As/GaAs quantum wells, photocond. of confined donors 7-7282
 Al_{0.55}Ga_{0.45}As:Te edge region photocapacitance at constant bias, anal. 7-7287
 Al_{0.5}Ga_{0.5}As crystals, DX centre props. 7-2534
 Al_{0.5}Ga_{0.5}As heteroepitaxial layers formed by metalloorganic chem. hydride method, electrophys. props., comp. effect 7-64370
 Al_{0.5}Ga_{0.5}As/GaAs photoexcited heterojunction, charge transfer calcs. 7-12688
 AlN films, OMVPE, Hall mobilities, impurity band 7-39410
 AlN, undoped and control doped films, luminesc. studies 7-27790
 AlNbO₄:Cr³⁺ tunable IR laser crystals, fluorescent spectra 7-43110
 Al₂O₃:Cr³⁺, V³⁺, electron-phonon interaction and impurity energy levels, APR and EPR studies (Russian) 7-45814
 Al₂O₃:Cr,Ga, ruby, Cr-Ga complexes, luminesc. study 7-22320
 AlSb:Se, donor studies, incoherent laser saturation method 7-27298
 AlTiO₄:Cr³⁺ tunable IR laser crystals, fluorescent spectra 7-43110
 Al₂(WO₄)₃:Cr³⁺, tunable IR laser crystals, fluorescent spectra 7-43110
 As₂S₃:Ni films, electronic struct. and transport props. 7-12595
 Au alloys, dil., EFG, asymmetry parameter calcs. 7-2545
 Au-TiO₂:Nb diodes, trapping states, admittance spectra study 7-45494
 BaF₂:ThF₄:YbF₄ glass, electron irradiation effects, Yb³⁺ optical transitions 7-27764
 BaFCl:Dy(Cu), thermolum., X-irradiated at room temp. 7-53419
 BaO:Al₂O₃:Eu²⁺ Mn²⁺ phosphor, luminesc. props. 7-46112
 BaO:Al₂O₃:Eu²⁺ phosphor, luminesc. props. 7-46112
 BaS:Sm²⁺, photolum. of Sm²⁺ ions 7-59246
 BaTiO₃, acceptor state behaviour, influence of impurities and lattice defects 7-2539
 BaTiO₃:Mn, Mn oxidation state change near phase transitions 7-16974
 BaTiO₃:Mn(Cr), impurity electronic struct., molecular-orbital calcs. 7-45213
 BaY₂F₈:Pr³⁺, stimulated emission spectra, laser action excitation 7-27745
 BeAl₂O₄:Cr³⁺, alexandrite, excited, absorpt. spectra, 220-900 nm 7-46075
 Be₃Al₂(SiO₃)₆:Cr³⁺, emerald, spectral energy transfer, fluorescence line narrowing 7-33441
 BiI₃ extrinsic semiconductor, reverse H-like series, light absorpt. study 7-53370
 Bi₂O₃ thin films, traps, TSC meas. (Japanese) 7-7423
 Bi₃PO_{11.2}:Nd³⁺, cryst. growth, spectroscopic props. of Nd³⁺ ions 7-46131
 Ca₃Al₂Ge_{3-x}Si_xO₁₂:Tb, cathodoluminescence, photoluminescence props. 7-53404
 CaF₂:Ce³⁺, impurity ion-ligand nuclei interactions, ENDOR meas. and operator method calcs. 7-52538
 CaF₂:Ce³⁺, two-photon absorpt. cross section, anal. of lowest 4f-5d transition 7-46081
 CaF₂:Eu³⁺, hyperfine coupling in ⁷F₀ and ⁵D₀ states, ODMR meas., optical hole burning 7-45842
 CaF₂:Eu³⁺, O₂, quadrupole coupling and crystal-field shielding under hydrostatic press. 7-2551
 CaF₂:Sm²⁺, electronic Raman transitions study 7-46017
 CaF₂:Tm²⁺ crystal, dynamic nuclear polarisation, strong hyperfine interaction, ENDOR study 7-45840
 CaF₂-Si interface, with MBE grown insulator, trap states, I-V, C-V meas. 7-7407
 Ca₃Ga₂Ge_{3-x}Si_xO₁₂:Tb, cathodoluminescence, photoluminescence props. 7-53404
 Ca₃(NbGa₂)Ga₃O₁₂:Nd³⁺, Nd³⁺ ions, two channels of stimulated emission 7-22285
 CaS:Sm³⁺, photolum. of Sm³⁺ ions 7-59246

impurity electron states continued

- Ca₃Sc₂Ge_{3-x}Si_xO₁₂:Tb, cathodoluminescence, photoluminescence props. 7-53404
 Ca₃Y₂Ge_{3-x}Si_xO₁₂:Tb, cathodoluminescence, photoluminescence props. 7-53404
 CdCl₂:Mn²⁺, cryst. struct. of CdCl₂, temp. var., determ. from EPR data 7-32382
 CdCr₂Se₄ thin films, ferromagnetic semicond., multielectron energy struct., absorpt. spectrum, temp. and doping depend. 7-38488
 CdF₂:Eu³⁺, electrolum. studies 7-27785
 CdF₂:Eu³⁺, hyperfine coupling in ⁷F₀ and ⁵D₀ states, ODMR meas., optical hole burning 7-45842
 CdGeAs₂:Ni amorphous films, elec. cond., low temp. impurity breakdown, high field effects 7-52625
 CdI₂:Br, indirect excitons, isoelectronic impurity effects, luminesc. spectra 7-27255
 CdS, electron-hole exchange interaction for donor-acceptor pairs as a function of separation distance 7-52537
 CdS, photolum., exciton scatt. from defects and impurities, depend. on exciting light intensity 7-39156
 CdS:Cu,Cl photoconducting films, photolum. spectra studies (Russian) 7-46140
 CdSe:Cu films, radiative recomb. centres form., photolum. spectra studies (Russian) 7-33453
 CdSe:Te_{1-x}, bound excitons, thermal dissoc., photoluminescence, reflectivity meas. 7-46122
 CdSe:Te_{1-x} inhomogeneous solid soln., semicond. films, Hall effect temp. depend. meas. 7-58915
 CdSe:Te_{1-x}:Cu films, deep local levels, photosensitivity, spectral study 7-22371
 CdTe, acceptor higher excited states calcs. 7-52511
 CdTe:Co, Jahn-Teller interaction, influence of mag. field 7-16995
 CdTe/GaAs heterojunction, defect and impurity states, photovoltage meas. 7-17065
 CeN, narrow band material, high resolution photoemission 7-33512
 Co_{0.2}Ga_{0.8}Si_{0.2} single crystals, optical props. and impurity energy levels meas. 7-13122
 Cr impurity ions, d-p electronic energy, coord. sphere radius depend. 7-16971
 CsCaF₃:Gd³⁺, transferred hyperfine interaction of impurity centres, ENDOR, EPR meas. 7-32946
 CsMF₃:Gd³⁺ (M=Cd,Ca), transferred hyperfine interactions, ¹⁹F ENDOR studies 7-53177
 Cu alloy, dil., with 3d impurities, X-ray absorpt. edges (German) 7-46241
 Cu²⁺ impurity ion in octahedral environment, EPR spectrum, MM field freq. and temp. depend. 7-27596
 Cu:Mn(Cr) matrix, electronic struct. calcs. 7-16976
 Cu-based binary dilute alloys, electron struct., X-ray La emission spectra studies 7-12598
 Cu-Fe alloys, electronic structure and impurity states, optical investigations (Russian) 7-32943
 Cu-Mn dil. alloys, electronic struct. of mag. impurities 7-58771
 CuInSe thin films, flash evaporation prep. and characterisation 7-7893
 CuInSe₂ photovoltaic devices, analysis using admittance spectroscopy 7-7171
 Fe alloy, dil., with 3d impurities, X-ray absorpt. edges (German) 7-46241
 Fe(NH₄)₂(SO₄)₂·6H₂O, EPR of Mn²⁺, Mn²⁺-Fe²⁺ exchange interaction 7-2924
 Fe₂Si, transition metal impurities, electronic struct. and site preference 7-12653
 FeSnSb dilute alloys, local lattice relax. around impurity, K-edge EXAFS study 7-64159
 Ga⁺ impurity ion in alkali halide crystals, triplet excited relaxed states, ODMR study 7-2953
 GaAlAs:Si, DX centres, nonexponential thermal emission kinetics 7-12640
 GaAlAs/GaAs:C quantum wells interface struct. and luminesc. efficiency 7-7735
 Ga_{1-x}Al_xAs-GaAs-Ga_{1-x}Al_xAs quantum well, donor ion dielec. response 7-45417
 n-GaAs compensated samples, MOVPE grown, Hall effect meas. 7-27348
 GaAs, defect structure charactn., US meas. 7-21363
 GaAs epitaxial films, growth by close-spaced vapour transport, unwanted doping, X-ray diff., SEM obs. 7-27187
 GaAs, epitaxial growth, δ(z) doping layer, electronic states 7-52729
 p-GaAs, excitons bound to pairs of shallow impurities 7-45169
 GaAs, FTIR spectra of acceptors, electronic intrasite transitions and local vibr. modes 7-53377
 n-GaAs films, magneto-optical studies under high hydrostatic press. 7-13247
 n-GaAs impurity bands and band tailing 7-21809
 GaAs LEC substrates, EL2 deep donor kinetics under annealing, IR absorpt., DLTS, Hall effect meas. 7-32955
 GaAs LEC wafers, cathodolum. mapping, IR absorpt., X-ray topography obs. 7-33462
 GaAs layers, MOVPE, Zn acceptor impurities, magnetophotolum. 7-22308
 GaAs MBE layers, deep level defects and impurities 7-22051
 GaAs, neutral shallow donor inter-excited-state transitions, far IR photocond. in mag. field study 7-22249
 GaAs pure and Si, Mn or Cu doped crystals, impurity and defect props., heat treatment, photolum. studies 7-39163
 GaAs quantum-well wire hydrogenic impurity state binding energy and lowest exciton state lum. efficiency calc. 7-2683
 GaAs sawtooth doping superlattices, photoluminescence, transport props. 7-52825
 GaAs, semi-insulating bulk with thin conducting layer, optical DLTS distortions calcs. 7-58766
 GaAs seminsulating LEC wafers, radiative centres, local photoluminescence study 7-33458
 GaAs, shallow acceptor levels, photoluminesc. study 7-45209
 GaAs submicron n⁺n⁺n⁺ multilayers, single impurity-assisted tunnelling 7-38710
 GaAs:B, as-grown Czochralski crystals, EPR signal 7-38935
 GaAs:C, impurity levels determ. 7-32949
 n-GaAs:Co, impurity double acceptor state, Hall effect and resistivity meas., temp. and press. depend. 7-12656
 GaAs:Cr, meas. of residual stress by Cr-related luminesc. lines 7-7726
 GaAs:Cr,Se, impurity complex, luminescence study 7-53396

impurity electron states continued

GaAs:Cr impurity level studies 7-33084
 GaAs:Er MBE layer, dopant trapping level, photolum. obs. 7-44581
 GaAs:In, B, electrical props., role of residual B impurity, liquid encapsulated Czochralski growth 7-45312
 GaAs:Mo (W), impurity electronic struct. excitation and ionisation, cluster approach, X α multiple scatt. calcs. 7-2535
 GaAs:Ni, acceptor like electron trap, DLTS study 7-7166
 n-GaAs:O, semi-insulating, impurity centres, electron capture 7-52643
 GaAs:Sb, deep level formed by Sb doping 7-52496
 GaAs:Si, distorted impurity configuration 7-52501
 GaAs:Si, shallow donor neutralisation by atomic H, photoluminescence study 7-22294
 GaAs:Sn, photolum. spectra, line shape anal., conduction band to deep acceptor transition 7-46098
 GaAs/AlGaAs multiple-quantum-well structures, shallow donors, far infrared spectroscopy 7-39121
 GaAs/AlGaAs superlattices, hydrogenic impurity ground level wave function calcs., variational procedure 7-12664
 GaAs-Al_{1-x}Ga_xAs quantum well structure, recomb. dynamics, photolum. obs. 7-12809
 GaAs-AlGaAs extended state superlattices, shallow donor state transition energies 7-33082
 GaAs-AlGaAs quantum wells, FIR studies of shallow donors 7-52819
 GaAs-Ga_{0.7}Al_{0.3}As heterojunction, donor-acceptor radiative recomb. mechanism, photolum. spectra study 7-17083
 GaAs-Ga_{1-x}Al_xAs superlattices, shallow impurity state binding energies 7-45416
 GaAs-Ga_{1-x}Al_xAs 2D quantum well heterostructures, magneto-impurities, mag. field and press. effects 7-52728
 GaAs-Ga_{1-x}Al_xAs heterojunctions, electron energy levels 7-17082
 GaAs-Ga_{1-x}Al_xAs heterojunctions, impurities, optical props. 7-27396
 GaAs-Ga_{1-x}Al_xAs multiple well heterostructures, far IR absorpt. by shallow donors 7-45458
 GaAs-Ga_{1-x}Al_xAs quantum well structures, energy spectra of donors and acceptors, spatially dependent screening effects 7-45459
 GaAs-Ga_{1-x}Al_xAs quantum well, hydrogenic donor low-lying excited states, reson. states, positions and widths 7-45460
 GaAs-Ga_{1-x}Al_xAs superlattice localised states in barrier 7-17079
 GaAs-GaAs:Cr(Te), VPE grown, photoluminescence study, effect of substrate doping 7-27771
 GaAs_{1-x}Al_xAs MQW, MOCVD grown, excitons, photoluminescence spectra 7-38702
 GaAs_{1-x}P_x:Be⁺-GaP:Be⁺ strained layer superlattices, ion implantation doping, optical and elec. props., device appls. 7-44583
 GaAs_{1-x}P_x:N, bound excitons, energy spectrum, optical absorpt. cross section, two-band model 7-16945
 Ga_{0.49}In_{0.51}As-InP:Fe(S), deep defect levels, photoluminescence, DLTS meas. 7-33457
 n-Ga_{1-x}In_xSb:Se(S), impurity states, press. and comp. depend., Hall coeff. and elec. resist. meas. 7-2533
 GaN films, OMVPE, Hall mobilities, impurity band 7-39410
 GaN, undoped and control doped films, luminesc. studies 7-27790
 GaN:Zn, pure and doped, electrophysical props., nonhomogeneous semicond. model 7-27292
 GaP:Cr, impurity ion-lattice coupling, reson. phonon scatt. spectra 7-58420
 GaP:Cr, optically induced changes in impurity-related absorpt. line struct. 7-17334
 GaP:Cu, 1.65 eV luminescence, optically detected mag. resonance studies 7-64547
 GaP:Ni²⁺, absorpt. spectrum of Ni²⁺ 7-53373
 GaP:Zn, electron irradiation induced defects, DLTS study 7-52513
 n-GaSb impurity Auger hole recomb. via deep acceptor, electron density depend. calcs. 7-38573
 GaSb, impurity level calcs., effective mass pseudopotential method 7-7163
 GaSe, gamma irradi., photoluminescence spectra, temp. depend. 7-17336
 GaSe:Mn single crystals, optical props. 7-27777
 GdBO₃:Pr³⁺, Tb³⁺(Sm³⁺)(Dy³⁺), host lattice sensitisation, energy transfer and photolum. 7-46113
 Gd₂(MoO₄)₃:Eu³⁺, nonresonant energy transfer between two different Eu³⁺ ion sites 7-46125
 Gd₂O₃-P₂O₅ phosphors, Eu³⁺ activated, luminesc. spectra, cryst. symm. 7-3080
 Ge, electron irradi., annealing kinetics, impurity effects 7-16630
 Ge shallow donor levels, valley-orbit splitting in mag. field, zero-radius central cell model calcs. 7-58763
 Ge, thermal donor states 7-7155
 p-Ge, undoped, deep level defects produced by electron irradiation, annealing 7-12660
 Ge:CuH(D)₂, acceptor electronic state symm., isotope effects study 7-21863
 Ge:Ga, impurity g-factor determ. piezo-Zeeman spectra obs. 7-16982
 Ge:H,Be(Zn), shallow acceptor complexes 7-45219
 Ge:H-Si:H amorphous superlattices, electrical transport 7-7336
 Ge:O, thermal donor binding energies 7-16989
 Ge:Zn, photolum. spectrum, effect of (001) uniaxial stress 7-33450
 H, impurity in metals, electronic struct., higher order approx. 7-52518
 HgCdTe, 0⁻ giant oscillation near semimetal-semiconductor transition 7-64053
 HgCdTe:B, bulk and thin film, resonant impurity levels, magneto-transport studies 7-64162
 p-Hg_{0.78}Cd_{0.22}Te:Sb LPE films, elec. props. 7-7426
 Hg_{0.8}Cd_{0.2}Te:Cu, activation energy of Cu shallow acceptors 7-64153
 Hg_{1-x}Cd_xTe with metallic donor clusters, anomalous Hall effect below mag. field induced metal insulator transition 7-2485
 Hg_{1-x}Cd_xTe, zero gap, acceptor levels 7-27287
 HgCr₂Se₄ spinel magnetic semicond., electronic struct., elec. props., defects and ferromag. anisotropy 7-38857
 p-Hg_{1-x}Mn_xTe, highly doped, ground state of shallow acceptor 7-7167
 Hg_{1-x}Mn_xTe LPE crystals, magnetophonon reson. recomb. with phonon emission 7-63755
 In_{1-x}Ga_xAs,P_{1-y}-Cd on InP, activation energy of impurity 7-32942
 InP, acceptor higher excited states calcs. 7-52511
 n-InP compensated samples, MOVPE grown, Hall effect meas. 7-27348
 InP electrodes, surface modified, time resolved photoelectrochemical meas. 7-27415
 InP, neutral shallow donor inter-excited-state transitions, far IR photocond. in mag. field study 7-22249

impurity electron states continued

InP:Cr, impurity ion-lattice coupling, reson. phonon scatt. spectra 7-58420
 InP:Fe, midgap impurity levels, isomer shift and charge state calcs. 7-2538
 InP:Fe, optical spectra 7-53372
 InP:Fe, Si-implanted and rapid thermal annealed, photoluminesc. study 7-59243
 InP:Mn, deep acceptor level, props. 7-21853
 InP:Mn³⁺, Jahn-Teller effect, mag. suscept. and ESR spectra anal. 7-52534
 InP:Ti, Hg, semi-insulating, impurity electron state compensation mechanism, SIMS, SSMS, EPR and Hall effect meas. 7-64164
 InP-aqueous electrolyte interfaces, laser induced photoelectrochemistry 7-27412
 In₂S₃:Co, photoconductivity, Co impurity energy levels (Korean) 7-33049
 InSb, impurity bands and their conductivity in strong mag. fields 7-45152
 InSb, impurity level calcs., effective mass pseudopotential method 7-7163
 InSb shallow magnetodons photo-ionisation spectra studies 7-64165
 InSb with metallic donor cluster, anomalous Hall effect below mag. field induced metal insulator transition 7-2485
 InSb:Te, resonance absorpt. of electromag. wave due to impurity band 7-52499
 In₂Te₂:Fe, Fe²⁺ elec. inactivity study, mag. suscept., Mossbauer spectra and XPS anal. 7-52494
 KAl(MoO₄)₂:Cr³⁺ tunable IR laser crystals, fluorescent spectra 7-43110
 KAl(SO₄)₂·12H₂O:Cr³⁺, optical absorpt. spectrum study, cryst. field and site symm. determ. 7-59232
 KAlSi₃O₈:Fe³⁺, orthoclase, absorpt. and luminesc. spectra 7-53383
 KBr:CN⁻, persistent IR hole burning in vibr. spectrum 7-37057
 KBr:Eu²⁺, impurity precipitates, Raman spectra meas. during annealing 7-64634
 KBr:Se²⁻, electronic spectroscopy 7-22319
 KBr:Se²⁻, mag. circular dichroism, electric conductivity, mobility of anion vacancies 7-3024
 KBr:Sn²⁺, impurity localised excitons, form. energy calcs., UV spectra anal. 7-64095
 KCl:Ca, γ -irrad., Z₁-centre growth, effect of dislocations, thermolum. study 7-32487
 KCl:Ca²⁺, Z₂⁺-centres, axial config., pseudopotential perturbation calc. 7-32952
 KCl:Eu²⁺, impurity precipitates, Raman spectra meas. during annealing 7-64634
 KCl:Sn²⁺, impurity localised excitons, form. energy calcs., UV spectra anal. 7-64095
 KH₂PO₄:Ti²⁺, impurity centres, ESR line width studies 7-38498
 KI:Eu²⁺, impurity precipitates, Raman spectra meas. during annealing 7-64634
 KI:Ti³⁺ crystals, luminescence polarisation of dimer centres 7-22335
 KI/Ti³⁺, stability of V-type defects 7-26745
 K_{0.3}MoO₃:Fe, CDW state, Mossbauer studies 7-53112
 KTaO₃:Fe³⁺, EPR of Fe³⁺ centres, electric field effect 7-38926
 LaF₃:Nd³⁺, energy value calc. of Stark sublevels (Chinese) 7-38519
 LaF₃:Pr³⁺, spin Hamiltonian spectroscopy, spin-spin cross relax. by optical pumping 7-22228
 LaF₃:Pr³⁺,Nd³⁺, energy up-conversion, UV fluoresc. obs. 7-53401
 Li₂B₄O₇:CuCl₂ crystallised glasses, pure and doped, thermally stimulated exoelectron emission, thermolum. 7-27874
 LiCl:Pr³⁺, absorpt. and luminesc. spectra studies (Russian) 7-46141
 Li₂Cr(Mn)(Fe)(Co)(Ni)O₂ electrode materials, electronic and electrochemical props., ion intercalation, electronic model 7-33945
 LiF:U⁴⁺, Ti(U), X-irradiated crystals, absorpt. bands of U⁴⁺ and U³⁺ ions 7-13183
 LiF:U⁴⁺, cryst. luminesc. excitation of impurity centres 7-13225
 LiLaPO₄:Nd³⁺,Yb³⁺, metaphosphate glasses, Nd³⁺ to Yb³⁺ energy transfer, luminesc. study 7-22323
 LiLuF₄ = Pr³⁺(Nd³⁺)(Ho³⁺)(Er³⁺), stimulated emission spectroscopy 7-13179
 LiNdP₄O₁₂:Yb³⁺, metaphosphate glasses, Nd³⁺ to Yb³⁺ energy transfer, luminesc. study 7-22323
 LiYF₄:Ho³⁺,Er³⁺,Tm³⁺, excited-state absorpt., energy transfer, fluoresc. study 7-22322
 LiYF₄:Tm³⁺ crystal, Tm optical spectrum, press. induced linear dichroism, electron-phonon interaction 7-3069
 LiYbP₄O₁₂:Nd³⁺, metaphosphate glasses, Nd³⁺ to Yb³⁺ energy transfer, luminesc. study 7-22323
 Lu₃Al₂O₁₂:Cr³⁺,Fm³⁺, 2 μ m stimulated emission of Ho³⁺ ions, spectral composition and kinetics 7-46073
 LuPO₄:Gd³⁺, mag. hyperfine interactions, ³¹P and ⁵¹V ENDOR spectra 7-27630
 LuVO₄:Gd³⁺, mag. hyperfine interactions, ³¹P and ⁵¹V ENDOR spectra 7-27630
 Mg,Cd_{1-x}Se single crystals, impurity photocurrent temp. activation meas. and calcs. (Russian) 7-45394
 Mg(NH₄)₂(SO₄)₆·6H₂O, EPR of Mn²⁺, Mn²⁺-Fe²⁺ exchange interaction 7-2924
 MgO:Cr, Cr³⁺ absorption spectrum, spin-orbit interaction effects 7-13182
 MgS:Sm³⁺, photolum. of Sm³⁺ ions 7-59246
 Mn,Si_{1-x}Mo_xS₈, Mn dopant props., supercond. transition temp., EXAFS, XANES, photoemission studies 7-46236
 Mo, electronic struct. of mag. 3d impurities, local density approx. 7-64432
 NaCl:Eu²⁺, gamma irradi., optical absorpt. spectra, TSC meas. 7-58337
 NaCl:Mg, X-ray irradi., exciton interactions with impurity-vacancy dipoles, absorpt. and luminesc. spectra 7-45162
 NaCl:Sn²⁺, impurity localised excitons, form. energy calcs., UV spectra anal. 7-64095
 Na₂Cr(Mn)(Fe)(Co)(Ni)O₂ electrode materials, electronic and electrochemical props., ion intercalation, electronic model 7-33945
 Na₂O-3SiO₂ glass, Tb³⁺ activated, temp. depend. of tunnel lumin. 7-59265
 Nb, electronic struct. of mag. 3d impurities, local density approx. 7-64432
 Ne impurity immersed in liq. metallic H, polarisation effects on core levels 7-64158
 Ni alloy, dil., with 3d impurities, X-ray absorpt. edges (German) 7-46241
 Ni-He, electronic state or interstitial He atoms, MO calcs. of model clusters 7-16969

impurity electron states continued

- NiSbInSb dilute alloys, local lattice relax. around impurity, K-edge EXAFS study 7-64159
 Pb_{0.75}Ge_{0.25}Gd³⁺ impurity ion reorientation kinetics 7-45940
 PbO chemically deposited layers, electrical props. 7-64377
 Pb₃O₄ thin film, electronic props., electrochem. technique characterisation 7-7416
 Pb_{0.75}Sn_{0.25}Te:In, Ge(S)(Se), elec. resist., photocond., Hall effect meas. 7-17050
 Pb_{1-x}Sn_xTe:Bi, free carrier density 7-38572
 Pb_{1-x}Sn_xTe:In, impurity levels, covalent defect theory 7-52515
 PbTe, impurity levels, covalent defect theory 7-52515
 PbTe:In, MIS struct., tunneling spectra of quasilocated impurity states 7-12869
 PbTe:Mn²⁺, superhyperfine struct., EPR spectra 7-27595
 PbTe:Ti(Li,Na) films, superconducting transition 7-38797
 Pb_{1-x}Te:Ti, quasiloal level and transport props. 7-38492
 PbWO₃:Nd³⁺(Pr³⁺), optical spectra 7-39146
 PdCe, Ce impurity, ground state studies, multiplet effects, near-edge XAS 7-64803
 RbCl(Br)(I):Ag⁺(OH⁻) crystals, paraelec. centres, elec. dipole moment temp. depend., dielec. meas. 7-38508
 RbH₂PO₄:Ti²⁺, impurity centres, ESR line width studies 7-38498
 SbSI, elec. cond., ferroelec., phase transition temp. 7-45326
 SbSn dilute alloys, muon Knight shift and trapping, comp. and temp. depend. 7-45889
 ScCe, Ce impurity, ground state studies, multiplet effects, near-edge XAS 7-64803
 Si : BF₂ preamorphised implanted samples, defects and leakage currents abs. 7-38514
 Si crystalline solar cells, conditions for high efficiency 7-23145
 Si, Czochralski grown, electron irradi., thermal donor form. 7-21868
 Si, electron irradi., obs. of IR bands during annealing, kinetic study 7-45214
 n-Si, excitons bound to pairs of shallow impurities 7-45169
 Si, group III acceptors, neutral and ionised states, deep dopant description 7-64155
 Si, heavily doped, band-gap narrowing 7-7108
 n-Si, heavily doped, carrier conc. and activation energy, Lee-McGill model calcs. 7-58819
 Si, impurity and defect props., processes and characterisation (*Japanese*) 7-7151
 Si, impurity ionisation, doping conc. and temp. depend. 7-38509
 p-Si, impurity photocond. type inversion by fundamental absorpt. band illumination 7-64287
 Si, off-centre impurities and defects, local electronic struct. valence-bond theory calcs. 7-2532
 Si p-amorphous/n-cryst. anisotype heterojunction characts., acceptor doping level depend. 7-7355
 Si p-n structures, induced current pot., temp. depend., impurity levels, SEM 7-17073
 n-Si, piezoresistance associated with bending of the energy relief at the bottom of the conduction band 7-13095
 Si, shallow thermal donor series, electronic struct. 7-7154
 Si, thermal donor states 7-7155
 Si, thermal donor-related isoelectronic centres, exciton binding, photoluminescence studies 7-21861
 Si, transition metal dopant complexes photolum., review 7-45203
 Si: transition metals, solubilities, diffusivities and deep levels 7-32465
 Si:As, deep level spectra, ion implanted defects, laser annealing 7-21869
 Si:As,In, formation of In-As complexes, perturbed angular correlation technique obs. 7-17254
 Si:As, deep level carrier capture and emission press. depend. meas., lattice relax. determ. 7-21862
 Si:As, deep levels, multiplexponential anal. of deep level transient spectroscopy 7-52524
 Si:As, laser radiation effects on impurity levels 7-12645
 Si:As, Li, Au-Si pair paramagnetic state, EPR studies 7-45817
 Si:As,Fe-SiO₂, MOS struct., trap centres 7-7388
 Si:B, B-vacancy complex, electronic and atomic struct., ENDOR studies 7-63649
 Si:B, mag. props. of the acceptor system 7-27496
 Si:B,Fe, EBIC and DLTS meas., comparisons 7-7265
 Si:B MBE layers, shallow states, photoluminescence spectra, doping level depend. 7-13228
 Si:B(Al), hydrogenation and annealing kinetics 7-2527
 Si:B(Al)(Ga)(P)(Sb) thermal donor props., impurity effects, DLTS, Hall effect, and admittance spectra meas. 7-21851
 Si:Co, impurity energy levels, Hall and DLTS meas. 7-52509
 Si:Cr,B, optically-induced spin orientation, EPR study 7-2927
 Si:Er(Dy)(Yb)(Ho)(Gd), neutron irradi., Hall effect, elec. cond., IR absorpt. spectra 7-51834
 Si:Ge,P(B), IR absorpt. band broadening 7-64669
 a-Si:H, B₂H₆(PH₃), localised density of states, electrophotography study 7-32957
 Si:H, B(Al)(Ga)(In), polishing, acceptor compensation by atomic H 7-33860
 a-Si:H, non-exponential photocurrent decay, anal. 7-38633
 a-Si:H,B, thin films, thermoelectric power 7-58826
 a-Si:H,B(As) RF sputtered coatings, gas-phase doping efficiency 7-63471
 a-Si:H,F-Si_{0.4}Ge_{0.6}H₂F superlattices, carrier scatt., optical absorpt. study 7-38711
 Si:H and near-surface damage of Si caused by H ions, review 7-16813
 a-Si:H multilayer films, charge transfer doping, cond., photocond. meas. 7-38735
 a-Si:H solar cells, impurities and metastable centres 7-40010
 a-Si:H ultrathin layers, photoluminescence characts., layer thickness depend. in variety of sample configurations 7-46123
 Si:Hg(Au)(Pt)(Ir)(Os)(Re)(W), self-consistent one-electron states of 5d transition-atom impurities 7-32950
 Si:Mg, photothermal ionisation spectroscopy 7-45374
 Si:Mg(Be) metastable impurity levels, self-consistent local-density total-energy calcs. 7-38503
 Si:N, host-impurity interactions, transferability of tight-binding parameters 7-58773
 Si:N, O, impurity complexes as shallow donors, optical absorpt. study 7-39147
 Si:N,O, impurity interactions in optical defects 7-17348
 Si:Na MOSFET struct., hopping cond. in 2D impurity band 7-45512
 Si:Ni reverse-biased p⁺nn⁺ junctions, electron thermal emission rates 7-7169

impurity electron states continued

- Si:O, C, thermal donor form. T<800K 7-27294
 Si:O, diffusion of O during thermal donor form. 7-38262
 n-Si:O, donor states of O rel. to heat treatment 7-12647
 Si:O, electronic struct. and atomic symmetry of the thermal donor 7-16986
 Si:O, energy levels and capture cross-sections of thermal donors 7-16988
 Si:O, IR absorption spectra of thermal donors 7-17326
 P-Si:O, new donor state, optical, elec. and TEM studies 7-32956
 Si:O, new donors, bound exciton recomb., photolum. study 7-22300
 Si:O, oxide precipitate nucleation, thermal donor-formation kinetics 7-32667
 Si:O, structure and props. of the thermal donor 7-16766
 Si:O, thermal donor binding energies 7-16989
 Si:O, thermal donor impurity density of states, formalism and appl. 7-12655
 Si:O, thermal donors, photothermal ionisation spectroscopy and IR transmission meas. 7-16987
 Si:O, thermal donor formation and structure, review 7-17562
 Si:O(O,H), heat treated, DLTS 7-16991
 Si:P, EPR temp. depend. g-shifts obs. 7-27600
 Si:P, many-valley semicond., electron intervalley scatt., optical pumping study 7-52608
 Si:P, quenching thermodefect prod. Hall effect, EPR meas. 7-27293
 Si:P, self-consistent multi-ion screening formalism 7-38505
 Si:Se(Te), chalcogenide pairs, electronic structs., Green's function calcs. (*Chinese*) 7-58759
 Si:Sb, local lattice relax. around impurity, K-edge EXAFS study 7-64159
 Si:Sb,As, cryst. aid amorphous, impurity band form., X-ray spectra studies 7-12650
 Si:Ti, deep level transient spectroscopy, transient capacitance data anal. 7-52526
 Si:Ti, electron and hole energy levels, DLTS and DDLTS meas. 7-32941
 Si:V, impurity self-ENDOR spectrum 7-64545
 Si:Ge:O, single crystal, thermodynamic rel. to solubility of O 7-12648
 Si-SiO₂, buried oxide formation by O⁺ implantation, donor creation, enhanced conductivity 7-32529
 Si-SiO₂ interface, MOS capacitance derivative freq. depend., surface state densities and capture cross section 7-45507
 3C-SiC, n- and p-type epitaxial CVD layers, elec. props. temp. depend. studies 7-58917
 a-SiC:H,B, thin films, thermoelectric power 7-58826
 21R-SiC:N, shallow donor bound electronic transitions, light scatt. study 7-38494
 6H-SiC:P, impurity paramagnetic and elec. props. study 7-53130
 Si:C,Te, N, 6H polypoly, ESR of (TiN)⁰ impurity pairs 7-2926
 a-Si_{1-x}C_xH, B(P) films, valence band localised holes, light-induced ESR spectra studies 7-53110
 Si_{1-x}Ge_xH amorphous alloys, electronic struct., soft X-ray and photoelectron spectra studies 7-27857
 SiO₂-Cs-Si MOS, semicond. flatband voltage depend. on impurity distrib. 7-27433
 SiO₂:OH, X-irrad. induced defect centres, EPR obs. 7-45221
 SiO₂:Yb³⁺ glass, energy transfer among impurity ions, time resolved fluorescence line narrowing meas. 7-46124
 SiO₄-Li, crystalline quartz with Li-associated electron trap, electronic struct. 7-21860
 SnTe:In, superconducting transition 7-38798
 SrF₂:Tm²⁺, g-factor signs, optically detected ESR 7-32948
 SrS:Sm³⁺, photolum. of Sm³⁺ ions 7-59246
 SrTiO₃, acceptor state behaviour, influence of impurities and lattice defects 7-2539
 SrTiO₃:Fe³⁺(V³⁺), impurity energy levels, tight binding model, Green's function method calcs. 7-21856
 SrTiO₃:Mn, Mn oxidation state change near phase transitions 7-16974
 TiO₂, absorption and photolysis spectra 7-22290
 TiO₂:Al, absorption and photolysis spectra 7-22290
 TiO₂:Cr, absorption and photolysis spectra 7-22290
 TiO₂:Cr(Cd) thin films, extension of optical absorpt. range by doping 7-39144
 TiO₂:V, absorption and photolysis spectra 7-22290
 TiO₂:V³⁺, anatase and rutile phases, EPR study 7-2923
 TiX:B (X=C, N, O) electronic struct., chem. bonding, Green's function methods 7-58741
 UO₂, pure and cation doped, elec. conductivity, O potentials, defect structures 7-12718
 YAG:Nd³⁺, impurity two-photon absorpt. cross section meas. 7-53375
 YAlO₃:Eu³⁺, Van Vleck paramagnet, low field Raman heterodyne study 7-53179
 YAlO₃:Nd³⁺, sub-levels R₁ and R₂, thermal shifts 7-32940
 Y₃Al₅O₁₂:Tm³⁺,Cr³⁺,Ho³⁺, 2 μm stimulated emission of Ho³⁺ ions, spectral composition and kinetics 7-46073
 YIG:Ho³⁺, laser mag. reson. study, quasi-Ising model 7-53147
 YLiF₄:Nd³⁺, impurity two-photon absorpt. cross section meas. 7-53375
 Y₂O₃-P₂O₅ phosphors, Eu³⁺ activated, luminesc. spectra, cryst. symm. 7-3080
 YVO₄:Eu,Ga(Se)(La), optical props. and electronic struct. 7-33423
 YVO₄:Gd³⁺, mag. hyperfine interactions, ³¹P and ⁵¹V ENDOR spectra 7-27630
 Zn(NH₄)₂(SO₄)₂·6H₂O, EPR of Mn²⁺, Mn²⁺-Fe²⁺ exchange interaction 7-2924
 ZnO:Co(Ni)(Cu), impurity electron states, optical spectroscopy 7-46127
 ZnO:Ga thin films, temp. depend. of conductivity, effect of H₂O vapour chemisorbed states 7-7427
 ZnO:H, quantised accumulation layers on ZnO surfaces, photoenhancement 7-7304
 ZnO-electrolyte interface, electrolum. under cathodic and anodic pulsed polarisation 7-13235
 ZnS, rare earth impurities, electrolum. of Schottky barriers, photolum., charge compensation, and impurity electron states 7-64700
 ZnS:Al, Cr, Fe crystals, recomb. luminesc., EPR and photocond. meas. 7-3076
 ZnS:Al, electron capture processes, role of donors, transient ESR meas. 7-45347
 ZnS:Al, temp. depend. of visible photolum., ESR studies 7-46099
 ZnS:Cr³⁺, Fe³⁺ single crystals, impurity centre charge exchange, plastic deform. effects, ESR spectra studies 7-16984
 ZnS:Cr²⁺, Cr excitation spectrum interpretation 7-58775
 ZnS:Cu, electrophosphors, aging phenomena 7-27791

impurity electron states continued

- ZnS:Cu, pure and doped, defects in solids, mol. cluster calc. with modification 7-21857
 ZnS:Cu²⁺, multimode Jahn-Teller effect in the luminescence spectrum 7-12675
 ZnS:Fe,Cu, three-centre Auger recombination, EPR study 7-45806
 ZnS:Mn, impact excitation and Auger quenching 7-27827
 ZnS:Mn thin films, electrolum., review 7-27784
 ZnS:TbF₃, sputtered thin films, electrolum. and photolum. 7-7727
 ZnS-CdS:Ag,Ni,Co phosphors, photolum., energy level model 7-59245
 ZnS,Se_{1-x}Mn²⁺, Mn energy levels, photoconductivity bands 7-7156
 ZnSe:Cu(Ag)(Au), cationic substitutional impurities and metal vacancy, microscopic models 7-27296
 ZnSe:Ga, impurity segregation model calcs., elec. props., precipitate effects 7-16762
 ZnSe:N, MBE growth and doping, photoluminescence studies 7-27749
 ZnSe-GaAs:Cr, meas. of residual stress by Cr-related luminesc. lines 7-7726
 ZnTe, acceptor higher excited states calcs. 7-52511
 ZnTe:Cu, impurity related neutral complex with bound exciton, photoluminescence, absorpt., Zeeman meas. 7-45165
 ZnTe:O, hot luminesc. reson. Raman scatt. studies 7-64695
 ZnTe:O, red cathodolum. kinetics, two-step electron capture model calcs. 7-59262

impurity-phonon interactions *see phonon-impurity interactions***impurity scattering**

- used for carrier scattering by impurities*
see also Kondo effect
 1D weak localisation, effects of forward scatt. and incommensurate lattice 7-45202
 Aharonov-Bohm effect with integer and half-integer flux quanta, cond. oscils. 7-52552
 alloys, dilute, electron scatt., many-impurity effects (*Russian*) 7-45305
 Bloch electrons, quantum transport in homogeneous time depend. elec. fields 7-52633
 Boltzmann-Lorentz model for particles with spin, exact calcs. 7-32970
 Boltzmann-Lorentz model for particles with spin, projection-operator technique 7-32971
 charge density waves, microscopic theory in path integral formulation 7-27273
 dense Kondo systems, coherent state and Z⁻¹ expansion 7-2603
 disordered conductors, low temp. current spatial fluctuations, size depend. and coherent length 7-17003
 double quantum well structs., parallel electron transport studies 7-45474
 electron gas, disordered, interacting, quasi-2D, plasmon dispersion relations calcs. 7-38485
 electron gas, galvanomag. props., interaction effects, applied electric and mag. fields 7-52477
 electron-electron interaction effects on Aharonov-Bohm effect 7-12689
 fluctuating valence heavy fermion systems, impurity resistivity temp. depend. calcs. 7-2565
 heavy fermion superconductors, observability of order parameter collective modes 7-38807
 heavy fermion superconductors, transport and thermal props. 7-38809
 heavy fermion systems, disorder and coherence 7-21888
 III-V semiconductors, negative magnetoresistance and nonequilib. electron cooling 7-17042
 magnetic alloys, dilute, negative magnetoresistance; coupling pair model 7-32987
 metals, electroconductivity in const. mag. field, electron relax. time and interactions (*Russian*) 7-32994
 metals, Kondo effect amplification by mag. field 7-52602
 metals and superconductors, electron-phonon interaction 7-38143
 p-type semiconductors, heavily doped, band-gap shifts 7-22333
 quantum sine-Gordon system with single impurity, dielectric constant 7-38530
 quasi-one-dimensional semiconductor, electron mobility investig. 7-2616
 quasi-one-dimensional wire, cond., thermopower, effect of lifetime broadening 7-45252
 semiconductor film, electron scattering by charged impurities 7-21886
 semiconductor quantum well structs., 2-D thermopower studies 7-33081
 semiconductor superlattices, type I, memory function and dynamic conductivity in a mag. field 7-52775
 semiconductors, carrier reson. scatt., effect on transport coeffs. 7-38602
 semiconductors with degenerate electron distribution, runaway effect 7-52607
 ternary semicond. alloy ultrathin wires, alloy scatt. limited mobility calcs. 7-12724
 transport equation for weakly localised electrons 7-7195
 weakly bound impurity states, ionisation width in mag. field 7-45206
 Ag-based dilute alloys, low temp. elec. resist. 7-52565
 Al thin films, elec. cond. quantum size effect, Kubo formalism study 7-22034
 AlGaAs:Si-GaAs 2D electron gas structure, scatt. mechanisms 7-38718
 Au-Pd thin films and wires, localisation and electron-electron interaction effects, magnetoresist. meas. 7-52863
 p-CdGeAs₂ semicond., hole mobility and scatt., temp. depend. study 7-52609
 Cu elec. resist., strain-induced changes in temp. depend. component, magnetic impurity effects 7-52567
 Cu thin films, elec. cond. quantum size effect, Kubo formalism study 7-22034
 Cu-based dilute alloys, low temp. elec. resist. 7-52565
 CuBe, scatt. anisotropy of conduction electrons 7-38536
 CuInS₂ films, RF sputtering, struct. and elec. props. 7-3169
 GaAs, electron scattering in quantum limit 7-38552
 GaAs, heavily doped, carrier-carrier and carrier-dopant interactions 7-21903
 GaAs, inversion layers, hot free electron gas, intraband absorpt. coeff. calc. 7-33083
 GaAs/Al_{1-x}Ga_xAs modulation-doped heterostructs., 2D electron gas mobility meas. and calcs. 7-12840
 GaAs-GaAlAs superlattices, density of states of Landau levels, sp. ht., magnetisation meas. 7-52823
 GaAs-GaAlAs:Si modulation doped quantum wells, electron mobility, temp. depend. 7-45473
 p-Ge, Hall effect, mag. field and temp. depend., transport eqn. soln. 7-2651
 n-Ge, Nernst-Ettingshausen coeff. in the case of scatt. by impurities in quantising mag. fields 7-12745

impurity scattering continued

- Ge:O, γ -irrad., majority carrier mobility meas. 7-27334
 Ge:Zn, large electron-hole drop, Alfvén wave dimensional reson., impurity scatt. effects 7-16950
 InGaAs/InP single quantum wells, transport and persistent photocond. props. 7-27385
 InP:Fe wafer, semi-insulating, elec. characteristics 7-45323
 PbTe:Ti, Na, carrier reson. scatt., effect on transport coeffs. 7-38602
 PbTe_{1-x}S_x, free carrier scatt. near a phase transition 7-38557
 p-Si conductivity and Hall mobility calcs., impurity scatt., anisotropic-nonparabolic effects 7-12720
 Si quantum well struct., 2D electron gas, transport props. 7-52774
 Si:O, γ -irrad., majority carrier mobility meas. 7-27334
 Si:P, many-valley semicond., electron intervalley scatt., optical pumping study 7-52608
 Si-Si_{0.35}Ge_{0.45} modulation doped superlattice, MBE grown, electron mobility enhancement, Hall meas. 7-7382
 3C-SiC, n- and p-type epitaxial CVD layers, elec. props. temp. depend. studies 7-58917
 β -SiC(N) single crystals, CVD grown, elec. props., temp. dependence 7-2740
 W plates with adsorbed layers, transverse magnetoresist. under static skin effect conditions (*Russian*) 7-45369
 n-ZnSe, heavily doped strongly compensated crystals, electron mobility 7-7247

impurity-vacancy interactions

- Ag-¹¹¹In, O agglomeration in presence of radiation defects 7-26791
 alloys, α -FeC, positron annihilation and vacancy-impurity binding 7-39289
 alloys, solvent and solute diffusion enhancement, effect of non-random solute distrib. around vacancies 7-63868
 binding energy, solidus condition 7-44602
 Fe-D formed by D ion implantation, multiple D occupancy of vacancies 7-63643
 metals, radiation swelling, vacancy-interstitial and interstitial-impurity complex form. (*Russian*) 7-58309
 mobile interstitial atom-substitutional impurity complex form. (*Russian*) 7-12372
 semiconductors, vacancy conc. change due to doping with isovalent impurities 7-51813
 solid solutions, precipitate growth under irradiation, theory 7-12296
 steel, stainless, ion irradi., positron annihilation studies 7-46219
 transition metal-H system, heats of soln. and vacancy trapping 7-6804
 AgSn(Sb), impurity-vacancy and impurity-impurity interactions calc. from diffusion enhancement 7-6672
 Al-H, H-point defect interactions, extended Huckel mol. orbital calcs. 7-44533
 Al-H(He) systems, vacancy-impurity centres, positron lifetime meas. 7-39254
 Au dilute alloys, electron irradi., positron lifetime meas. 7-39250
 Cu, H trapping, positron annihilation spectra 7-33482
 Cu, ion mixing and thermochemical props. of markers 7-26805
 Cu:O(He) vacancy cluster stability calcs., void form., O and the impurity effects 7-51763
 Fe, dilute alloys, electron irradi., positron lifetime meas. 7-39250
 Fe single crystals, Bi ion implantation, high substitutional fractions 7-58299
 GaAs:Se, ion implanted, annealing mechanism 7-26777
 GaAs:Te VPE, vacancy-impurity complex capture, photolum. study 7-58678
 In, impurity-induced vacancy clustering, positron studies 7-38044
 KCl:Ca²⁺, Z₂⁺-centres, axial config., pseudopotential perturbation calc. 7-32952
 KCl:Eu²⁺, f to f transitions, two-photon spectra studies 7-3068
 KCl:F⁻:Eu²⁺, optical absorpt., excitation and luminesc. spectra 7-59250
 KCl:Zn, elec. cond., dielec. loss meas., before and after X-irrad. 7-33324
 LiF:C⁶⁺ ion implanted, impurity defects outside implantation zone 7-7773
 MgO, deformed and annealed, red cathodoluminescence spectrum 7-27792
 Mo, N-vacancy interactions, obs. with thermal He desorption spectrometry 7-58311
 Mo:D, ion implanted, impurity trapping 7-38029
 NaCl:Mg, X-ray irradi., exciton interactions with impurity-vacancy dipoles, absorpt. and luminesc. spectra 7-45162
 Nb:He⁺(H⁺) films, radiation defects produced by ion implantation 7-7059
 Nb-H system, alpha-particle irradi., defect annealing behaviour 7-44605
 Ni, electron irradi., H-defect interactions, positron annihilation study 7-6674
 Ni films, vacancy migration, impurity quenching, complex bonding energy (*Russian*) 7-44531
 Ni-C, C-vacancy binding 7-44601
 Ni-H system, H-defect interactions, positron annihilation studies 7-39256
 RbCl, divalently doped, ionic thermocurrent studies 7-7262
 Si, Czochralski, electron-irradiated, DLTS and photoluminesc. studies 7-7149
 Si, Czochralski grown, electron irradi., thermal donor form. 7-21868
 Si, diffusion modelling, point defect interactions 7-32715
 Si, electron irradi., obs. of IR bands during annealing, kinetic study 7-45214
 Si:B, B-vacancy complex, electronic and atomic struct., ENDOR studies 7-63649
 Si:B, electron-irradiated, AC hopping conductivity and DLTS 7-44624
 Si:B, O, heavily doped, O precipitation, diffuse X-ray scatt. studies 7-32669
 Si:B(P)(As)(Sb), retarded and enhanced dopant diffusion related to implantation-induced excess vacancies and interstitials 7-63881
 Si:N, deep level generation and annihilation 7-16612
 Si:O, Czochralski grown, electron irradiated, thermal donor formation 7-44619
 Si:O, defects created by electron irradiation and subsequent thermal treatments, review 7-16642
 Si:O, magnetic resonance of O-related defects 7-17223
 Si:O, review 7-16583
 Si:O, vacancy-enhanced O diffusion 7-16811
 Si:O CZ gram, O precipitation enhanced with vacancies 7-32664
 n-Si:P,C, electron-irradiated and injection-annealed, vacancies, dislocations and C interstitials 7-51815

impurity-vacancy interactions continued

- ThCl₂:Gd³⁺, impurity-vacancy centre EPR probe for incommensurate phase 7-17220
 W-H system, H-defect interactions, positron annihilation studies 7-38045
incandescent lamps *see filament lamps*
inclusions in crystalline material *see crystal inclusions*
inclusive reactions, elementary particle *see elementary particle inclusive interactions*
incoherent light annealing
 InP:Si, ion implanted, rapid thermal annealing and solid phase epitaxy 7-21296
 metal-Si (SiO₂), silicidation reactions, rapid thermal annealing/TEM technique 7-52156
 MOS structure, X-ray irradi., interface trap annealing, two-reaction model 7-58901
 rare earth silicide epitaxial formation by rapid annealing 7-21768
 SOI films, halogen lamp recrystallisation 7-38394
 SOI formation, high dose O⁺ ion implantation, lamp annealing 7-32527
 solar cell high throughput automated fabrication line 7-8417
 Al_{0.5}Ga_{0.5}As:Be epitaxial layers, ion implanted, rapid thermal annealing 7-21257
 CaF₂ epitaxial films on Si, structural and electrical props. improvement by rapid thermal annealing 7-38400
 CoSi₂, self-aligned silicide technology using rapid thermal processing 7-52154
 GaAs (100)-Ni interface, effect of O on diffusion and compounding 7-21539
 GaAs epitaxial layer, EL2 midgap electron trap prod. by rapid thermal annealing, DLTS study 7-64154
 GaAs, ion implanted, flash tube annealing 7-39551
 GaAs, rapid thermal annealing, heating behaviour 7-21258
 GaAs:Si, FET structs., rapid optical annealing for improved uniformity 7-16620
 GaAs:Si, ion implanted, rapid thermal annealing effects 7-21259
 In_{0.53}Ga_{0.47}As/In_{0.52}Al_{0.48}As quantum wells, lamp annealing interdiffusion and optical props. 7-12502
 InP, rapid thermal annealing, heating behaviour 7-21258
 InP:Fe, Si-implanted and rapid thermal annealed, photoluminesc. study 7-59243
 NbSi₂, sputtered films, rapid thermal annealing 7-21739
 Ni-Si interface reactions induced by pulsed incoherent light, silicide formation 7-32725
 Pt on Si, struct. and comp. of silicides formed in photon annealing, Auger obs. 7-2402
 SOI films, halogen lamp recrystallised, minority carrier lifetime studies 7-33101
 Si films, structural changes due to annealing 7-52346
 Si, implanted layers, short time annealing, light source comparisons 7-21263
 Si, ion implanted, amorphous phase transformation during rapid thermal annealing 7-16435
 Si, oxide growth, rapid thermal processing 7-22929
 Si, oxide growth by rapid thermal oxidation 7-22922
 Si polycrystalline films on (100) Si substrate, epitaxial alignment using rapid thermal processing 7-38413
 Si, rapid thermal and furnace oxide growth, meas. and modelling studies 7-13677
 Si, rapidly annealed with incoherent light, defect state generation 7-52504
 Si substrate, insulator growth by rapid thermal processing 7-22921
 Si:As, ion implanted, rapid thermal annealing 7-16615
 Si:As, ion implanted, rapid thermal annealing, metastable activation 7-16616
 Si:As porous layer, impurity diffusion under incoherent light exposure 7-38258
 Si:As(B) polycrystalline films, rapid thermal processing before and after ion implantation, effect on cond. 7-22046
 Si:B, ion implanted, dopant redistrib. during rapid thermal annealing 7-38042
 n-Si:B⁺(BF₂⁺), ion implanted, rapid thermal annealing, DLTS 7-16619
 Si:BF₂⁺ p⁺-n diodes, BF₂⁺-implanted and rapid thermal annealed, junction leakage currents meas. 7-12814
 Si:Ga, highly cond. shallow junction layer form. by ion implantation 7-38037
 Si:O, ion implanted, structure before and after heat-pulse annealing 7-16600
 Si:O:B⁺, ion implanted, reverse annealing 7-16617
 Si:PF₆⁺, ion implanted, recrystallisation kinetics during fast thermal annealing 7-16618
 Si:P(Al), random and channelled implantation profiles and range parameters of dopants 7-21246
 SiO₂, thin film growth, on Si, annealing by lamp heating 7-22930
 TiSi₂ formation by As⁺ ion beam mixing and rapid thermal annealing 7-52153
 W-Si, sputter deposition on Si (100), rapid thermal annealing 7-21548

Incoloy *see chromium alloys; iron alloys; nickel alloys***incommensurate-commensurate transformations** *see commensurate-incommensurate transformations***Inconel** *see chromium alloys; nickel alloys***independent particle model** *see nuclear optical model; nuclear shell model***indeterminacy**

- Bohr's discussion of the fourth uncertainty relation revisited 7-18614
 cosmological constant, uncertainty principle limits 7-14685
 damped harmonic oscillator, wave function, energy expectation value (Korean) 7-24465
 general relativity role in uncertainty principle 7-152
 Lorentz boost generators proportional operators, role as position operators 7-61136
 teaching approach 7-9640
 transactional interpretation of quantum mechanics 7-4719
 uncertainty in particle motion, velocity and higher derivatives anal. 7-14820

indexing

- office, information retrieval system using concepts of the AIR/PHYS physics data bank (German) 7-14721

indium

- see also nuclei with*
 adatom on Si (100), bonding coordination number, synchrotron photoemission studies 7-45071

indium continued

- adhesion to glass, adhesion strength, meas. method for vac. seals 7-59715
 adsorption of n-butane on (110) surface, activation with translational energy 7-39336
 atom, hyperfine struct., magnetic-dipole- and electric quadrupole coupling consts., atomic fluoresc., MCHF method 7-30985
 atom, L X-ray spectra study 7-42536
 Auger electron spectra, main and satellite structures 7-7795
 Auger energy, Slater transition state calcs., metallic and atomic states, jellium model 7-38475
 BCT, force constant models, elastic inconsistency 7-38140
 channelling contrast microscopy, He⁺ microbeam, semiconductor impurity profiles 7-51587
 cold-deposited thin films, H₂ temp. and film thickness depend. study (Russian) 7-27477
 compression feedthroughs, low-temp., for superconducting or Cu wire 7-35527
 cooldown mass flow requirements for He or N cooling systems 7-56281
 crystallites, surface free energy anisotropy 7-27091
 crystallographic equivalence between BCT and FCT structs. 7-37924
 deposition onto sputtered and cleaved Hg_{1-x}Cd_xTe surfaces 7-33513
 discontinuous metallic thin films, on amorphous and crystalline substrates, electron irradiation stimulated coalescence 7-2437
 electron impact ionisation function meas. 7-50367
 equal magnetisation lines, effective field const., paramag. Curie temp. and magnetocaloric effect 7-7546
 equilibrium shapes, critical behaviour of curved regions 7-63529
 film, etching by methyl radicals in discharges 7-3507
 film, irreversible resistivities during annealing process 7-64365
 foils, ion bombarded, desorbed neutral energy distrib. studies 7-22406
 granular films, electron localisation, transition from weak to strong 7-64083
 granular films, metal-insulator transition, conducting props. study (Russian) 7-7116
 growth on GaAs (110), RHEED study 7-2425
 impurity-induced vacancy clustering, positron studies 7-38044
 liquid monolayer on Ga, sputtering, computer simulation studies 7-17387
 metal-metal and metal-dielectric systems, adhesion calc. 7-7023
 monolayer and multilayer surface diffusion, growth mode and thermal stability on W (100) 7-2386
 monovacancy formation enthalpy, positron annihilation Doppler broadening studies 7-37976
 muon trapping and diffusion after electron irradiation, μ SR study 7-45864
 nonequilibrium superconductor, Bernoulli effect meas. (Russian) 7-7455
 positron annihilation parameters, prevacancy effect 7-39251
 positron lifetimes, prevacancy effect 7-37973
 resonant atomic state, autoionis., electron spectra 7-900
 seal and appl. to proximity focussed image intensifier (Chinese) 7-48763
 single crystal, Hall coeff. anisotropy, Fermi surface effects 7-12701
 single-crystal plate, acoustohelicon resons. 7-52695
 sputtered excited neutral atoms vel. distrib. meas. and deexcitation model calcs. 7-875
 superconducting cylinders, mag. flux diffusion, exptl. study 7-38813
 superconducting film, nonequilibrium phenomena under quasiparticle injection (Chinese) 7-27465
 superconducting film, temp. dependent order parameter relax. time determ., critical DC current meas. 7-17147
 superconducting granule, type I, metastable state destruction by external irradiation 7-27475
 surface, electrochem. H evolution in US field 7-11231
 surface, oxidised, in acidic solns., zero charge points 7-13783
 surface oxidation, ion-induced secondary emission target current meas. 7-59684
 ultrathin films on Si, electromigration, scanning AES study 7-63891
 vacancy formation study by positron lifetime spectroscopy with β^+ - γ - and γ - γ coincidences 7-39261
 wire, extrusion for vacuum seals 7-48761
 Ag/In thin film couples, interface AgIn₂ cpd. form. and props., gamma ray spectra 7-21688
 Au/In thin film couples, interface AuIn₂ cpd. form. and props., gamma-ray spectra 7-21688
 CdS:In films for solar cells, control of open circuit voltage by carrier density variation 7-17887
 CdS:In-SnO₂ (glass), spray pyrolysed, photoelectrochemical studies 7-52830
 CdSb-In crystal, In atom electrodiffusion study 7-63890
 n-CdTe:In, high mobility, growth by photoassisted MBE 7-22485
 CdTe:In, photocorrosion, vacancies, photoluminescence spectra 7-27948
 CdTe:In, segregation coeff., recoil implanted tracer technique 7-21461
 Cu/In thin film couples, interface CuIn₂ cpd. form. and props., gamma ray spectra 7-21688
 Ga:In, growth dislocations, in-situ detection using Seebeck effect 7-32451
 GaAs:In, B, electrical props., role of residual B impurity, liquid encapsulated Czochralski growth 7-45312
 GaAs:In, dislocation free crystals, microscopic defects, eutectic etching 7-16545
 GaAs:In, dislocation free, inhomogeneities obs. by video-enhanced IR topography 7-32446
 GaAs:In, EL2 maps from computer based IR image analysis 7-32237
 GaAs:In, LEC growth, annealing, solid soln. hardening, dislocation density, elec. props. 7-17404
 GaAs:In, lattice distortions, NMR study 7-2933
 GaAs:In, low In conc., LEC cryst. growth employing thermal stress anal. 7-46305
 GaAs:In, microdefects obs. by IR light scatt. tomography 7-32662
 GaAs:In, semi-insulating substrates and ingots, In content, nondestructive meas. 7-58305
 GaAs:In, strain effects, electrorefl. and photocapacitance study 7-22224
 GaAs:In, VPE growth, isoelectronic In doping, etch pit densities 7-46340
 GaAs:In annealed substrates, In distribution in surface region 7-44959
 GaAs:In crystals, dislocations, in situ X-ray topographic studies 7-21207
 GaAs:In crystals, LEC growth, grown-in dislocation elimination 7-22465
 GaAs:In LEC crystals, dislocation etch pits 7-38000
 GaAs:In LEC semi-insulating crystals, IR absorpt. WRT resistivity 7-64629
 GaAs:In MBE layers, defect density reduction by isoelectronic In doping 7-3176
 GaAs-GaAs:In epitaxial layers, dislocation reduction, device performance effects 7-7354
 Gd₃Ga₅O₁₂:In, photoelectret, photoconductivity 7-45919

indium continued

- p-Ge:In, annealing kinetics of radiation defects, influence of impurity binding energy 7-39547
 Ge:Sb(Al)(Ga)(In), heavily doped, charge carrier scatt., elec. cond., Hall effect meas. 7-7228
 GeTe:In, solution mechanism of impurities, effect of heat treatment 7-21455
 HgCdTe: In, ion implanted, damage and rapid thermal annealing 7-63637
 In II and III, cascade corrected lifetime meas. 7-50016
 In plasma, laser ablated inner-shell photoionisation-pumped, optical gain at 185 nm 7-20193
 In⁺ in alkali halide crystals, polarised luminesc., model of impurity center 7-27753
 In³⁺, reduction, rel. to coumarin adsorpt. on dropping Hg electrode 7-58609
 In/GaAs:Cu/In struct., I-V characs., carrier recomb. and generation, impurity thermionic field ionisation effects (*Russian*) 7-22030
 In-CdIn₂Se₂-Au Schottky diodes, I-V charact. 7-33010
 In-GaAs reactions, interfacial native oxide layer effects 7-12501
 In-GaAs(110), interfacial chem. reaction, UPS study 7-2276
 In-GaP liquid metal-semiconductor contact, transition from rectifying to ohmic operation 7-52833
 In-glass, glow discharge induced changes 7-12577
 In-glass composite 7-38656
 In-InP Schottky diodes formed on cleaved surfaces 7-58850
 In-Nb point contact, observation of chaotic noise 7-7445
 In-Pt-GaAs, heterojunction ohmic contacts, interfacial struct. 7-27155
 In+He⁺, L-subshell ionisation, X-ray prod. 7-50303
 In+In⁴⁺, L-shell ionisation, X-ray yield, threshold behaviour 7-10734
 In₂O₃:In films, optical and elec. props. 7-22365
^{113m}In-indifor use, patient irradi. doses (*Russian*) 7-3881
 KBr:Ti(In), defect creation by excitons, room temp. (*Russian*) 7-16946
 Mg₂Zn_{1-x}Te-In Schottky barriers, C-V and photoelec. studies 7-64307
 NbN/Pb(In) Josephson junction, Ar⁺ irradi., characs. (*Japanese*) 7-22071
 NbSe₂-I-Pb, tunnel junctions under press. 7-52594
 Pb_{0.75}Sn_{0.25}Te:In, Ge(Si)(Se), elec. resist., photocond., Hall effect meas. 7-17050
 Pb_{0.8}Sn_{0.2}Te:In, impurity diffusion, thermoelec. probe meas. 7-63879
 Pb_{1-x}Sn_xTe:In, impurity levels, covalent defect theory 7-52515
 PbTe:In, MIS struct., tunneling spectra of quasilocal impurity states 7-12869
 PbTe:In, I, Soret effect, impurity cond. distrib., thermoelec. power meas. 7-44930
 Pt-CdInGaS₄-In surface-barrier structs., photovoltaic effect and SCL currents 7-52687
 Si:Al(In), recrystallisation by pulsed electron beam, impurity profiles 7-16605
 Si:As,In, formation of In-As complexes, perturbed angular correlation technique obs. 7-17254
 Si:In, amorphous, low temp. annealing, impurity diffusion, phase separation and crystn. studies 7-16808
 Si:In, heavily doped, laser induced oxidation 7-13672
 Si:In, nucleation of internal melt during pulsed laser irradiation 7-12129
 Si:In, substitutional ion implanted dopants, electron and positron channelling studies 7-26778
 Si:In⁺, ion implanted, damage prod., incidence angle depend. 7-65242
 Si-In, metal implantation using pulsed electron beam 7-6882
 SnTe:In, solution mechanism of impurities, effect of heat treatment 7-21455
 SnTe:In, superconducting transition 7-38798
 ZnO:In films, microstruct., elec. and optical props., film thickness depend. study 7-16895
 ZnO:In films, transparent conducting oxides, H₂ plasma treatment 7-3528
 ZnS:In, photoluminescence, D-A pair emission 7-22312
 ZnS:In epitaxial films, photoluminescence. decay props. 7-39166
 ZnSe:In, impurity diffusion coefficients, cathodoluminesc. study 7-27017

indium alloys

- see also indium compounds
 Ag-¹¹¹In, O agglomeration in presence of radiation defects 7-26791
 Ag-In, atomic radial distrib. function, close order sorting parameter (*Russian*) 7-58206
 Ag-In, liq., activity coeffs. of O 7-3284
 Al-Cu-In alloy, deformed, θ'-phase precipitation 7-22691
 Al-In, monotectic alloy, section prep., micromilling, polishing (*German, English*) 7-22937
 An-In₂ liq. alloys, magnetic and thermodynamic props. 7-2812
 AuIn₂₊₃ thin films, resistivity 7-7410
 Bi-In-Sn alloys system, phase relationships 7-13433
 CaIr₂B₂, structural relationship to BaAl₄ 7-16496
 Cd-In alloys, vacancy-induced elec. field gradient temp. depend., PAC meas. 7-52541
 CeAg_{1-x}In_x, magnetisation process, strain effects 7-64488
 CeIn₃ antiferromagnetic alloys, thermoelec. power meas., band gap form. 7-38543
 (Ce_{1-x}La_x)In₃ antiferromagnetic alloys, thermoelec. power meas., band gap form. 7-38543
 Cu-In (15 wt.%), lamellar precipitates, cellular dissolution kinetics, grain boundary diffusion 7-28047
 Cu-In alloys, vacancy-induced elec. field gradient temp. depend., PAC meas. 7-52541
 CuIn vacancy formation enthalpy, positron annihilation studies 7-7787
 Ga-In, liq., surface segregation, ion bombard. photon emission study 7-32265
 Ga-In-Sn liquid alloy, electron field emission studies 7-33535
 GdIn₃ antiferromagnetic alloys, thermoelec. power meas., band gap form. 7-38543
 Gd₂In, mag. transitions under press. 7-59013
 Hg-In, liq., mag. susceptibility, conc. and temp. depend. 7-27492
 Hg-In liquid alloys, vol. and thermal expansion coeffs., higher-order correlation effects 7-12328
 Hg-In liquid alloys, volume, thermal expansion coeff. 7-56227
 In-Bi, liq., heat of mixing, calorimetric study 7-12283
 In-Bi-Pb system, liq., thermodynamic props. (*Japanese*) 7-53699
 In-Ge thin films, anomalous structures 7-21733
 In-Pb whiskers, critical currents and Ginzburg-Landau parameters 7-17144

indium alloys continued

- In-Pb whiskers, quasi 1D supercond., weak to strong coupling transition, I-V characs. study 7-38835
 In-Sn, diffusion coeffs. of In and Sn determ. by AES using Xe ion bombardment 7-22405
 In-Sn alloys, solid and liquid, surface composition, Auger electron spectra study 7-12421
 In-Sn solid solns., strain ageing kinetics investig. (*Russian*) 7-13467
 In-Tl, liq., activities, temp. depend., EMF obs. (*Japanese*) 7-12320
 In-Tl (23 at.%) alloy, FCC, thermodynamics of ferroelastic phase transition 7-2189
 In-Tl (3 wt.%), adhesion to glass, adhesion strength, meas. method for vac. seals 7-59715
 In-Tl system, absolute thermo-EMF (*Russian*) 7-32996
 In_{0.95}Ag_{0.05}Ga_{0.05}, ¹¹¹Cd quadrupole interaction, temp. dependence, lattice electric field gradients (*Chinese*) 7-7183
 In_{0.95}Ag_{0.05}Ga_{0.05} alloy, quadrupole interactions, TDPAC study 7-38521
 In_{1-x}Sn_x alloys, electronic structure dependence on crystal lattice parameters 7-45141
 Li-In-Sb, ternary phase diagram, electrochem. investig. 7-58441
 LiIn B32-type Zintl phases, mag. props., exchange enhancement, APW calcs. 7-27504
 Lu₂Ir₂Si₁₀, superconducting, electronic phase transition and partially gapped Fermi surface 7-12902
 NaIn B32-type Zintl phases, mag. props., exchange enhancement, APW calcs. 7-27504
 Nb-NbO_x-PbInAu, Josephson tunnelling current depend. on normal state tunnelling resist. 7-22073
 Nb-NbO_x-PbInAu Josephson junction fabrication by ion beam oxidation 7-22074
 NbIr molecules, magnetic moment formation and mag. susceptibility 7-58995
 Nb₂Ir, Al₁₅ cpds., 2D angular correlation of positron annihilation radiation 7-39238
 NbN/Pb-In Josephson junctions, fabrication by Ar⁺ ion bombardment 7-2787
 Nb₃Sn-In multifilamentary superconducting composites, growth dynamics, struct. and props., additive and heat treatment effects 7-22056
 NdIn₃ antiferromagnetic alloys, thermoelec. power meas., band gap form. 7-38543
 Ni-Fe-In ternary Permalloy electroplated films, mag. props. and thermal stability 7-33236
 Ni-In liq. alloys, enthalpies of mixing 7-46487
 Ni₂MnIn Heusler alloys, galvanomag. props. and magnetisation meas., fermi level shift effects 7-7207
 Ni₂MnIn, Heusler alloys, Curie temp., effect of hydrostatic press. 7-64455
 NiSnInSb dilute alloys, local lattice relax. around impurity, K-edge EXAFS study 7-64159
 Pb In type II cylindrical superconductor, AC losses, circular magnetic field effects 7-52895
 Pb-Bi-In, alloy filaments, prod. by glass-coated melt spinning, enhancement of supercond. 7-58937
 Pb-In films, Josephson junction, thermal stress cycles, hillock form. (*Japanese*) 7-12536
 Pb-In-Au alloy films, hillock growth during heat treatment 7-16893
 Pb-In-Au fine-grained codeposited alloy films, RF plasma oxidation 7-53970
 Pb-In-Au thin films, hillock growth kinetics, grain boundary diffusion, SEM study 7-27221
 Pd-In alloys, constitutional and thermal defects, positron lifetime study 7-39299
 Pd-In liq. alloys, enthalpies of mixing 7-46487
 Pt-In liq. alloys, enthalpies of mixing 7-46487
 Pu-Rh-B system, phase equilibria and cryst. struct. 7-16781
 Sc-Ga(In)(Sb), alloy form, thermodynamics 7-22637
 SmIn₃ antiferromagnetic alloys, thermoelec. power meas., band gap form. 7-38543
 UIr₃, band struct., theoretical XPS intensities 7-39353
 UIr₃, hybridisation, electronic struct. and props. 7-45136
 UIr₃ intermetallics, correlation effects, XPS and bremsstrahlung isochromat spectra 7-21844
 Yb-In-Te system, phase equilibria 7-44761
 Yb₂In_{1-x}Cu_x, Yb valence transition 7-45245
 Zn-In alloys, vacancy-induced elec. field gradient temp. depend., PAC meas. 7-52541

indium antimonide

- 1/f noise, temp. depend. 7-52710
 690 GHz bolometer, 2L-He hybrid cryostat 7-30024
 amorphous films, metal-semicond. transitions, superconductivity 7-64085
 anodic native oxide, interface width, AES profiles 7-22911
 anomalous Hall effect below mag. field induced metal insulator transition, InSb with metallic donor cluster 7-2485
 band structure, polarisation-dependent angle-resolved photoemission spectroscopy 7-21814
 bicrystals, n-inversion layers, pressure dependence electron states 7-45468
 bistable etalon, regenerative pulsations 7-20318
 bistable optical arrays, diffusion effects 7-57447
 cascaded bistable optical devices based on two-photon absorption in room temperature InSb 7-57413
 coherent spontaneous oscils. under transverse breakdown conditions, high frequencies 7-17046
 conduction band, deformation potential constant 7-7112
 conduction band spin splitting, spin reson. interaction obs., LMTO and k.p. perturbation calcs. 7-12676
 conduction electrons g-factor anisotropy, spin-orbit splitting calcs., comment 7-38441
 cyclotron resonance harmonics in conduction band, obs. 7-53136
 Czochralski growth rate and spreading resist. relations (*Japanese*) 7-26679
 Dember EMF contrib. to capacitor photo-EMF 7-38621
 density of states and effective mass determ. 7-38433
 dislocation motion under small shear stresses 7-44553
 Fabry-Perot IR bistable devices, parameter optimisation 7-57396
 films, preparation of highly sensitive magnetoresistance elements 7-7859
 four-wave mixing, degenerate and nondegenerate 7-11069
 free-electron g-factor meas. by spin-flip Raman scatt. gain method 7-2470
 galvanomagnetic luminescence, radiative heat pump appls. 7-40019
 galvanomagnetic luminescence 7-3095

indium antimonide continued

- heterostructures, MBE growth 7-27910
 impurity bands and their conductivity in strong mag. fields 7-45152
 impurity doping by photonuclear reactions 7-16589
 impurity level calcs., effective mass pseudopotential method 7-7163
 ion milling, TEM 7-39344
 large-k acoustic phonon imaging, freq. selectivity and isotopic defect scatt. effects 7-26885
 length scale near metal-insulator transition 7-52425
 low-temp. growth by plasma process (*Japanese*) 7-7061
 metal-insulator transition, mag. field induced, low temps. 7-45158
 metalorganic magnetron sputtered films, structural and compositional characts. 7-21725
 MIS structures, (BN)_n and Si₃N₄ film formation using plasmachemical methods 7-33584
 MOS interfaces, annealing, O diffusion and reaction 7-58665
 MOS structures, electric field effects on characteristics 7-38738
 MOS structures, heat treatment effects 7-8031
 MOS structures, heterogeneity of generation processes, expt. 7-17106
 n-type, 60° dislocation motion, etching studies 7-63619
 n-type, electron absorption of sound, hopping mechanism 7-17056
 n-type, impact ionisation electron-hole pair generation, high power optical wave elec. field effect. luminesc. obs. 7-33025
 n-type, magnetic two-phonon resonance involving acoustic phonons 7-45355
 n-type, solid-state plasma, stimulated Raman scatt. of extraordinary mode 7-31398
 narrow gap, spontaneous oscills. under plasma resonance conditions 7-38605
 narrow-gap semiconductor, bound excitons, magneto-absorption studies 7-45168
 negative magnetoresistance and nonequilib. electron cooling 7-17042
 nondislocating crystals, damaged surface struct., X-ray scatt. (*Russian*) 7-58581
 optical bistable elements as optical computer components 7-37025
 optical reflection anisotropy due to surface band bending 7-39062
 optical switching elements, transverse coupling 7-57446
 optically bistable etalon, critical slowing-down phenomena 7-5942
 passivation, SiO_x anodic native oxide interfaces studies 7-22917
 pulsed laser evaporation, neutral and charged particle emission 7-3120
 resonant states, strong mag. field, Coulombic impurity pot. 7-32925
 self-defocusing, time-resolved 7-43267
 shallow magnetodons photo-ionisation spectra studies 7-64165
 single cryst., neutron acoustic effect, neutron diff. study 7-26875
 solid-state electron plasma magnetised, circular antenna directivity diagram 7-45372
 strong-absorbing single crystals, Laue X-ray diff. thickness depend. anal. and interpretation (*Russian*) 7-44310
 surface, (110), LEED surface crystallography and R-Factors 7-26596
 surface, (-1-1-1) (3 × 3) reconstructed, X-ray diff. studies 7-6951
 surface, oxidation at room temp. 7-46734
 surface, oxidation processes studied by high-resolution electron microscopy 7-39766
 surface (110) electron states, effect of Al submonolayer coverage, soft XPS study 7-2653
 surface (111), EXAFS surface structure studies, at Daresbury SRS, in 60 to 11100 eV range 7-33486
 surface damage layer ref. spectra and thickness meas. 7-22209
 transient grating formation under two-photon excitation 7-11037
 transphaser, gain-bandwidth product 7-57417
 CdTe-InSb interface struct. and band offsets 7-58664
 GaInAsSb, MOVPE, band gap rel. to growth temp. 7-39409
 GaInAsSb/AlGaAsSb injection lasers, threshold current density reduction 7-5886
 Ga_{0.85}In_{0.05}As_{0.15}Sb_{0.87}/Al_{0.4}Ga_{0.6}As_{0.035}Sb_{0.965} DH lasers, MBE grown, 2.07 μm laser oscillation 7-43096
 Ga_{1-x}In_xSb epitaxial layers, MOCVD, morphology rel. to growth conditions 7-39408
 n-Ga_{1-x}In_xSb:Se(S), impurity states, press. and comp. depend., Hall coeff. and elec. resist. meas. 7-2533
 In As_{1-x}Sb_x epitaxial layers, MOCVD, strained-layer superlattices 7-39407
 InAs, electron-electron interaction, quantum effects, magnetoresist. studies 7-38591
 InAsSb/GaSb n-n heterojunctions, band discontinuities, C-V and I-V meas. 7-7366
 InAs_{0.3}Sb_{0.7} IR detector, photoresponsivity meas. 7-7274
 InAs_{1-x}Sb_x IR photodiodes for 3 to 14 μm, comparison 7-41466
 InAsSbP/InAs bent heterostructures, dislocation distribution 7-21673
 InAsSbP/InAs p-n structures, nonclassical thermal injection current 7-12806
 InGaAsSb/AlGaSb DH lasers, MBE grown, room-temperature 2.2 μm operation 7-20219
 In_{0.9}Ga_{0.1}As_{1-x}Sb_x, mid-IR source and detector material 7-36964
 InSb, density of excited electron-hole plasma 7-38608
 InSb, electron inversion layers, cyclotron and electron spin resonance 7-38736
 InSb:Te, Cd, Zn single crystals, Czochralski growth, solute distrib., mag. field effect on melt 7-3158
 InSb:Te, resonance absorpt. of electromag. wave due to impurity band 7-52499
 InSb:Te crystals, Czochralski growth, layered heterogeneity, melt temp. fluctuations, mag. field effect 7-27888
 InSb:Te(Ge)(Cd)(Si), heterogeneity study 7-21476
 InSb:Te(Se)(S)(Cd)(Zn) thin films, doping, Hall effect meas. 7-21743
 InSb:Ti, physicochemical behaviour of Ti 7-21452
 InSb/CdTe interface, quasi-2D electron gas obs. 7-21987
 InSb/LiNbO₃ layered struct. with transverse drift, SAW detection 7-12447
 InSb/Teflon SIS structs., EM magnetoplasma Gaussian beams, propag. and size resonances study 7-58905
 InSb-NiSb eutectic composite, rel. between metal fibre morphology and elec. props. 7-59644
 InSb-SiO₂ MIS structures, photo-CVD fabrication 7-38739
 Si-InSb heterojunction, spectral characts. and detection props. 7-38712
 Si-SiO₂-InSb hybrid struct. spectral characts. and detection props. 7-38712

indium compounds

see also indium alloys; indium antimonide
 7-39072

indium compounds continued

- CdS-CuInSe₂ solar cells fabricated by DC magnetron sputtering of Cu₂Se and In₂Se₃ 7-23170
 Ga_{0.4}In_{0.6}As, transient transport in central-valley-dominated ternary III-V alloys 7-7253
 In_{0.53}Ga_{0.47}As:Fe metalorganic CVD epitaxial growth and elec. props. 7-63993
 InGaAsP epitaxial films, X-ray diff. charactn. (*Japanese*) 7-63399
 InGaP/InGaAlP double heterostructure and multiquantum-well laser diodes, MBE growth and characterisation 7-62689
 InP:Cu, band-edge photolum. quenching, impurity recomb. centre effects study 7-39177
 InP:Si, ion implanted, rapid thermal annealing and solid phase epitaxy 7-21296
 InP, electron-electron interaction, quantum effects, magnetoresist. studies 7-38591
 polyacetylene:InI₃, DC elec. cond. studies 7-33018
 AgGa_{1-x}In_xS₂ solid solns., conc. depend. of band gap 7-52423
 AgGa_{1-x}In_xSe₂ thin films, evaporated, photosensitivity and optical props. study (*Korean*) 7-53423
 Ag_{1/2}In_{1/2}PS₃ lamellar cpd., cryst. struct. refinement studies 7-58235
 AgIn₂Se₆ photoelectrodes, thermodynamic stability in electrolytes 7-54330
 AgInTe₂ polycrystalline thin films, elec. and optical props. study 7-58924
 AlGaAs/GaAs/InGaAs multijunction solar cell, model for calc. of displacement damage by radiation 7-13878
 AlGaAs/GaInAs two-junction monolithic cascade solar cell in lattice-mismatched system 7-13862
 AlGaAs/GaInAs two-terminal multijunction solar cell spectral response meas. 7-13871
 AlGaAs-GaInAs cascade solar cells, efficient two-junction monolithic, grown by MOCVD 7-65483
 AlGaInAs layers on InP, LPE growth 7-33608
 AlGaInP, MOCVD, photolum., quantum wells, double heterostruct. laser appl. 7-39405
 AlGaInP visible semicond. lasers, mesa stripe struct., MOVPE grown, 621 nm CW operation at 0°C 7-20262
 AlGaInP visible semiconductor lasers grown by metalorganic vapor phase epitaxy 7-50590
 AlInAs-GaInAs superlattices, electronic transport and depletion by tunnelling 7-27395
 AlInAs-GaInAs heterostruct., alloyed NiGeAuAgAu ohmic contacts, charact. 7-22016
 AlInAs-GaInAs selectively doped heterostructs., MOCVD growth, HIFET fabrication appl. 7-17429
 AlInAs-GaInAs superlattices, quantum photoconductivity, effective mass filtering 7-12847
 Al_{0.25}In_{0.75}As, transient transport in central-valley-dominated ternary III-V alloys 7-7253
 Al_{0.48}In_{0.52}As:Si, MBE grown, crystalline and optical props. 7-52322
 Al_{0.48}In_{0.52}As-Ga_{0.47}In_{0.53}As SQW, electron temp. depend. on well width, photolum. obs. 7-12810
 Al_{1-x}In_xAs-GaAs strained layer superlattices, X-ray diffraction and excitation spectroscopy studies 7-12853
 (Al_{0.02}In_{0.98})₂Se₃, metastable complex defects, ESR studies 7-33270
 As_{2-x}Te_{3-x}In_x and As_{20-x}Te_{80-x}In_x systems, chalcogenides, thin films, optical and electrical props. 7-27446
 Au-CdIn₂S₂Se₂-In Schottky diodes, I-V charact. 7-33010
 Au-InP, solid-state reactions, Au₂P₃ formation 7-58550
 Au-InP high-speed internal photoemission detectors enhanced by grating coupling to surface plasma waves 7-52688
 AuBe-Cr-Au-InP, improved ohmic contact 7-64310
 Bi_{2-x}In_xTe₃, carrier density, depend. of anisotropy parameter 7-7226
 Bi_{2-x}In_xTe₃, doped crystals, energy formation of antisite defects 7-21204
 CdInGaS₄ in MSM surface-barrier structs., photovoltaic effect and SCL currents 7-52687
 CdIn₂O₄ thin films, DC reactive sputtered, elec. and optical props. 7-38788
 CdIn₂S₄, electron trap characts., TSC meas. 7-27340
 CdIn₂S₄ single cryst., chem. vapour transport growth and Vickers microhardness 7-21345
 CdIn₂S₄ single crystals, phase transforms., photoluminesc. studies 7-2171
 CdIn₂S₄Se₂, semicond., optical and elec. props. 7-33010
 CdS-CuInSe₂ Boeing solar cells, I-V characteristics meas. 7-8408
 CdS-CuInSe₂ heterojunctions, struct., elec. and photoelectric props. 7-22001
 CdS-CuInSe₂ thin film solar cell, solid state photovoltaic research status at SERI 7-8389
 CdS-CuInSe₂ thin-film solar cells, junction formation and O role, EBIC studies 7-17915
 CdS-CuInSe₂ backwall solar cells, intrinsic loss mechanisms calc. 7-23187
 CdZnS/CuInSe₂ solar cells, transient current studies of junction activity 7-8409
 CdZnS-InP heterojunction solar cell, numerical anal. 7-23155
 CoGaInS₄ cpd. with FeGa₂S₄ struct., prep. and characts (*German*) 7-1984
 Co₂In₂S_{3+x} thin films, spray pyrolysis deposited, structural and optical props. 7-22468
 Cu₂Ag_{1-x}In_xSe₂, liquid-encapsulated Bridgman-Stockbarger melt growth and props. 7-59403
 CuGa_{1-x}In_xS₂ solid solns., conc. depend. of band gap 7-52423
 CuGa_{1-x}In_xSe₂ mixed chalcopyrite local struct., K-edge EXAFS meas. 7-63574
 CuIn_{1-x}Ga_xSe₂ absorber materials, electroplating prep. 7-17894
 CuInGa_{1-x}Se₂, liquid-encapsulated Bridgman-Stockbarger melt growth and props. 7-59403
 CuInS₂, chemical transport, thermodynamics 7-7832
 CuInS₂, heterogeneous, VLS growth, electronic defects, photocurrent spectra, photolum., EBIC analysis 7-27288
 p-CuInS₂, strongly sublinear photocond. 7-52667
 CuInS₂:P, ion implanted, pulsed electron beam annealing 7-16644
 CuInS₂-SnO₂:F sprayed solar cells, photovoltaic props. 7-54322
 CuInS₂ photoelectrodes, thermodynamic stability in electrolytes 7-54330
 CuInSe₂ coatings, sputter deposition 7-39377
 CuInSe₂ epitaxial films deposited on GaAs and CdS, RHEED studies 7-12549
 CuInSe₂ large grain (112) oriented thin films grown by RF sputtering, solar cell applications 7-17422
 CuInSe₂, p-type, CdS induced homojunction formation 7-58867
 CuInSe₂, pH effects on surface properties 7-23201

indium compounds continued

- n-CuInSe₂ photoelectrochemical cells 7-23199
 CuInSe₂ photovoltaic devices, analysis using admittance spectroscopy 7-7171
 CuInSe₂ polycrystalline thin film solar cells 7-17888
 CuInSe₂ polycrystalline thin film solar cells, donor-acceptor pair luminescence 7-17890
 CuInSe₂, thin film, electron beam evaporation optical props. (Korean) 7-27801
 CuInSe₂ thin film growth 7-13368
 CuInSe₂ thin film photoelectrochemical cells 7-23200
 CuInSe₂, thin films, flash evaporated, electrical cond. and optical absorpt. spectrum 7-33112
 CuInSe₂ thin films, polycrystalline, elec. props., effect of excess Cu 7-52871
 CuInSe₂/CdS, thin film chalcopyrite solar cells, electroplating prep. 7-17894
 CuInSe₂/CdS solar cells, modelling and anal. 7-17893
 CuInSe₂/CdS-CdTe/CdS tandem solar cells 7-17891
 p-CuInSe₂/n-(Cd,Zn)S polycrystalline solar cells, open circuit voltage 7-17889
 CuInSe₂-based photoelectrochem. solar cells, optical and electronic props. studies 7-46958
 CuInSe₂-CdS heterojunctions deposition, in-line sputtering system 7-64900
 CuInSe₂-CdS solar cells and CuInSe₂ thin films, charge transport studies 7-12890
 CuInSe₂-CdS solar cells, capacitance determ. of interfacial states 7-13916
 CuInSe₂-CdZnS solar cell development for space appls. 7-13917
 p-CuInSe₂-CdZnS-ZnO solar cells, device anal. 7-23171
 CuInSe₂-Si:H, tandem modules, thin film design and fabrication 7-13913
 CuInSe₂-Si:H thin film tandem solar cells, energy based perform. and eval. 7-13890
 CuInSe₂-ZnCdS thin film polycryst. solar cell efficiency improvement using antireflection coatings 7-23186
 CuInTe₂ film, amorphous, flash evap., DC cond. mechanisms, density of states 7-22041
 CuInTe₂ thin films, flash evaporated, elec. conductivity, optical absorption 7-7428
 Eu-In-Te systems, phase equilib. investigations 7-2173
 Ga-In-As-P system, ternary alloys, E_i energy gap, CPA calc. 7-58740
 GaAlAsSb/GaSb/GaInAsSb injection double heterostructure laser, room temp. operation 7-62697
 GaAs/GaInAs interface, EELS near a single misfit dislocation 7-33497
 n-GaAs/InGa_{1-x}As compositionally graded non-alloyed ohmic contacts 7-38695
 GaAs-AlAs(InAs) superlattices, lattice distortions 7-12510
 GaAs-AlGaAs-InGaAs strained-layer quantum well heterostructures, negative differential resistance 7-45443
 GaAs-InGa_{1-x}As strained layer superlattices, photolum. microimaging of dislocations 7-27161
 GaAs-InGa_{1-x}As, lattice-mismatched heterojunctions, misfit strain relaxation, X-ray study 7-21718
 GaAs-InAs strain layer modulated structures, MBE grown, cross-sectional TEM 7-7032
 GaAs-InAs superlattice, reflection electron diffraction intensity oscillation 7-7030
 GaInAs, anodic oxides, growth and composition 7-39781
 GaInAs, Czochralski-grown, dislocation effects investig. 7-7261
 GaInAs epitaxial layer on InP, depth profiling and interface detection using anodic oxidation 7-45057
 GaInAs films and structures, gas source MBE, review 7-33572
 GaInAs, pn junction formation by simultaneous implantation and diffusion annealing 7-38028
 GaInAs, ternary solid soln., miscibility gap in phase diagram 7-52057
 GaInAs terrestrial solar cells, high-efficiency concepts 7-8390
 GaInAs/GaAs single quantum well pseudomorphic structs., high electron mobility meas. 7-12841
 GaInAs/InP, nonlinear optical absorpt. at room temp. 7-59169
 GaInAs/InP heterojunction, 2D electron gas nonequilib. cyclotron reson. obs. 7-12845
 GaInAs/InP heterostructures, VPE, homogeneity, mobilities 7-58882
 GaInAs/InP quantum wells, atmospheric organometallic vapour phase epitaxial growth 7-27912
 GaInAs-AlInAs heterostruct., alloyed NiGeAuAgAu ohmic contacts, charact. 7-22016
 GaInAs-AlInAs heterojunctions, parallel conduction, quantum Hall effect, hydrostatic press. 7-52764
 GaInAs-AlInAs(InP) and GaAs-AlGaAs superlattice avalanche photodiodes, impact ionisation theory appl. 7-58886
 GaInAs-GaInAsP(InP) quantum-box lasers, 3D, gain and threshold current density 7-10937
 GaInAs-InP, quantum well lasers, characts., comparison with GaAs-GaAlAs 7-5891
 GaInAs-InP, quantum well structures, adduct MOVPE, photolum., magnetoresist charactn. 7-27388
 GaInAs-InP double-barrier heterostructs., room temp. resonant tunnelling, neg. resist. effects 7-58814
 GaInAs-InP epitaxial superlattice, X-ray double crystal characterisation, rocking curves calc., computer simulation technique 7-58105
 GaInAs-InP quantum well, CESR of 2D electrons 7-38941
 GaInAs-InP quantum-box lasers, 3D, gain and threshold current density 7-10937
 GaInAs-SiO₂ system, annealing behaviour, SIMS and elec. meas. 7-38270
 Ga_{0.28}In_{0.72}As/Al_{0.28}In_{0.72}As photodiode heterostructures, atm. press. MOCVD, 2 μm, sensitivity, structural charactn. 7-27933
 Ga_{0.3}In_{0.7}As-InP strained layer superlattice, inter-band magneto-absorption 7-45998
 Ga_{0.47}In_{0.53}As, laser material, intervalence band absorpt. coeff. calc. 7-3015
 Ga_{0.47}In_{0.53}As:Be epitaxial films, ion implanted, rapid thermal and furnace annealing 7-22729
 Ga_{0.47}In_{0.53}As/Al_{0.48}In_{0.52}As modulated struct., high resolution double-cryst. X-ray diff. studies 7-7029
 Ga_{0.47}In_{0.53}As/Al_{0.7}In_{0.3}As superlattices, electronic struct., strain-induced elec. field effects 7-7358
 Ga_{0.47}In_{0.53}As/Al_{0.48}In_{0.52}As quantum well, interband magnetoabsorpt. meas., effective mass determ. 7-17088

indium compounds continued

- Ga_{0.47}In_{0.53}As/Al_{0.48}In_{0.52}As superlattices grown by MBE, structural charactn. 7-52792
 Ga_{0.47}In_{0.53}As/InP heterojunction, chem. beam epitaxy grown, 2D electron gas 7-12803
 Ga_{0.47}In_{0.53}As-InP heterojunction, with three electron subbands, hydrostatic press. effect 7-2695
 Ga_{0.47}In_{0.53}As-InP heterojunction, MOCVD grown, 2D hole gas 7-21992
 Ga_{0.47}In_{0.53}As-InP junction lasers, chem. beam epitaxy and performance characts. 7-20254
 Ga_{0.47}In_{0.53}As-InP quantum wells, photocurrent and dark current, multiple steps obs. 7-12796
 Ga_{0.47}In_{0.53}As-InP superlattices, MOCVD grown, room temp. excitons 7-21986
 Ga_{0.47}In_{0.53}As-InP:Fe(S), deep defect levels, photoluminescence, DLTS meas. 7-33457
 Ga_{0.47}In_{0.53}As-Si₃N₄(SiO₂) interface, elec. charact. 7-38752
 Ga_{1-x}In_xAs, high-temperature hardness 7-44675
 Ga_{1-x}In_xAs, solid soln. strengthening, mech. props. 7-32452
 Ga_{1-x}In_x/InP heterostructures, MOVPE, electron mobility, exciton peak, magnetotransport 7-58883
 Ga_{1-x}In_x-Al_{1-y}In_yAs superlattices, electronic struct., depend. on growth axis 7-64329
 Ga_{0.47}In_{0.53}As, photoluminescence line shape of excitons 7-3087
 Ga₂In_{1-x}As, heterostruct., local composition, CBED anal. 7-16529
 Ga₂In_{1-x}As, low-pressure MOVPE growth 7-7873
 Ga₂In_{1-x}As/Al₂In_{1-x}As MBE grown superlattices, effect of barrier config. and interface quality on props. 7-52790
 Ga₂In_{1-x}As/GaAs heterostructures, low press. MOVPE, photolum., Auger profiling 7-27389
 Ga₂In_{1-x}As-GaAs strained layer superlattices, low temp. photolum. 7-53407
 GaInAsP DFB lasers, 1.3 μm, single-mode, realisation and characts. (German) 7-57357
 GaInAsP epitaxial layers, double axis X-ray diffractometry at glancing angles 7-37805
 GaInAsP epitaxial layers, X-ray double crystal characterisation, rocking curves calc., computer simulation technique 7-58105
 GaInAsP films and structures, gas source MBE, review 7-33572
 GaInAsP integrated coupled-cavity lasers, design and fabrication 7-25843
 GaInAsP strip-loaded planar waveguide for high-speed electroabsorpt. modulator 7-31449
 GaInAsP:Er semiconductor injection laser, single longitudinal model operation at 1.5 μm 7-50558
 GaInAsP:InP heterostructures, MOVPE, press. control, reactor design 7-39399
 GaInAsP/InP, planar single mode heterostructures, calculated characts. 7-31326
 GaInAsP/InP entirely VPE-grown 1.5 μm DFB lasers with low threshold currents 7-50577
 GaInAsP/InP heterojunctions, atmospheric press. MOVPE growth TEM studies 7-3196
 GaInAsP/InP heterostruct., luminescence polarisation, quantum size effects 7-13210
 GaInAsP/InP laser diodes, amplification piezoeffect 7-5889
 GaInAsP/InP stressed heterostructure lasers, lifetimes meas. 7-5890
 GaInAsP/InP surface emitting laser with flat surface circular buried heterostructure 7-31358
 GaInAsP-InP BH laser fabrication, MOCVD epitaxy, validation by photoluminescence imaging 7-31360
 GaInAsP-InP CW phase-locked semiconductor laser array, MOCVD growth 7-57351
 GaInAsP-InP double heterostructure lasers, 1.5 μm, chemical beam epitaxial growth 7-57310
 GaInAsP-InP etched mirror laser, passivation with angled sputtering 7-57358
 GaInAs(P)-InP heterostructures, gas source MBE growth 7-53598
 GaInAsP-InP lasers, single-step LPE fabrication 7-10996
 GaInAsP-InP laser, anisotropic deform. influence on radiative characts., threshold, polarisation and watt-ampere charact. 7-43100
 GaInAsP-InP laser, anisotropic deform. influence on radiative characts., spectral characts. 7-43101
 GaInAsP-InP substrate, integrated optoelectronics, micrograting form. by HV electron beam lithography 7-31443
 GaInAsP-InP surface-emitting laser with circular BH, low temp. CW operation 7-31337
 Ga_{0.28}In_{0.72}As_{0.6}P_{0.4}, laser material, intervalence band absorpt. coeff. calc. 7-3015
 Ga₂In_{1-x}As₂P_{1-y}, effective masses and alloy disorder effects, shallow donor photocond. 7-64289
 GaInAsSb, MOVPE, band gap rel. to growth temp. 7-39409
 Ga_{1-x}In_xAs₂Sb_{1-y} system, low temp. phase equilib. 7-52001
 GaInP-AlGaInP-GaAs heterostructures, MOVPE, Hall effect, photolum. 7-39401
 GaInP₂-GaAs, current-matched and lattice-matched tandem cell efficiency 7-8403
 Ga_{1-x}In_xP/GaAs heterojunction band discontinuity determ., C-V profiling 7-58880
 Ga₂In_{1-x}P epitaxial layers, OMVPE, surface morphology, photolum. 7-22557
 Ga₂In_{1-x}P layers, MOVPE, photolum., comp. and growth temp. depend. 7-39403
 n-Ga₂In_{1-x}P, light scatt. by free carriers 7-17328
 Ga₂In_{1-x}P, OMVPE growth and characterisation 7-3192
 Ga₂In_{1-x}P/GaAs (Al₂Ga_{1-y}As) heterostructures, OMVPE, photolum., lattice matching 7-39402
 Ga₂In_{1-x}P_yAs_{1-y}, solid solns., thermodynamic stability 7-21453
 Ga₂In_{1-x}P_yAs_{1-y}InP heterojunction interfaces, electron energy band structure (Chinese) 7-33070
 GaSb/InAs/GaSb quantum wells, carrier densities and mobilities, magnetotransport solids 7-12846
 Ga₂Te₃-InSe₃ solid solns., cryst. struct., X-ray powder diff. studies 7-16526
 Ge_{20-x}Se_{80-x}In_{2x} system, chalcogenides, thin films, optical and electrical props. 7-27446
 HgGa₂S₄-HgIn₂S₄ system, new multinary layered compound 7-53516
 InI, spectra and struct., AO⁺ state, rot. and vibr. consts. 7-50081
 ITO antireflection coating for a-Si solar cells with transparent Ag contacts 7-65478
 In As_{1-x}Sb_x epitaxial layers, MOCVD, strained-layer superlattices 7-39407

indium compounds continued

- In GaAsP lasers, high speed design and performance 7-62700
 In-Ga-As-P films highly excited, ps band filling 7-43261
 In-Ga-P-As, gap width, temp. depend. 7-12602
 $\text{In}_{0.53}\text{Ga}_{0.47}\text{As}$ InP, epitaxial single quantum wells, spectroscopy of excited states 7-46126
 InAlAs, growth by MBE, alloy clustering, surface quality, role of kinetics and thermodynamics 7-32866
 InAlAs/InGaAs modulation-doped heterostructs., 2D electron gas mobility meas. 7-12842
 InAlAs-InGaAs resonant tunnelling barrier struct., MBE grown, NDR characts. 7-52796
 $\text{In}_{0.18}\text{Al}_{0.82}\text{As}$ -GaAs strained layer superlattices, Raman studies 7-12854
 $\text{In}_{0.52}\text{Al}_{0.48}\text{As}$ optical waveguides, MBE growth on InP 7-11107
 $\text{In}_x\text{Al}_{1-x}\text{As}/\text{Au}$ Schottky barrier heights, composition dependence 7-45431
 $\text{In}_x\text{Al}_{1-x}\text{As}/\text{GaAs}$ strained-layer superlattices, effective mass reversal 7-17078
 InAs (110), oxidation, correlated changes of electronic surface props. 7-2354
 InAs (110), surface electron states, effect of Al submonolayer coverage, soft XPS study 7-2653
 InAs, atomic layer epitaxy growth, photolum., Hall meas. 7-22527
 InAs, band structure, polarisation-dependent angle-resolved photoemission spectroscopy 7-21814
 InAs, impurity doping by photonuclear reactions 7-16589
 n-InAs, Kane-type semiconductors, Einstein relation, mag. quantisation effect 7-52603
 InAs MIS structures, space charge accumulation 7-33097
 n-InAs, metal-Hall insulator transition 7-52708
 InAs, nuclear transmutation doping 7-38025
 InAs quantum well structures, metal-insulator transition due to surface roughness scatt. 7-27400
 InAs substrates and devices, surface anal., SIMS appl. 7-22417
 InAs surface, oxidation processes studied by high-resolution electron microscopy 7-39766
 InAs surface on InP, epitaxial regrowth 7-2431
 InAs, wavefront reversal system using four-wave interaction with passive optical isolator, reflection efficiency 7-62783
 InAs:B, internal friction temp. depend. studies 7-38112
 InAs:Sb(Ga)(Mn), single crystal, elec. inhomogeneity, effects of isovalent impurities 7-7229
 n-InAs:Sn,Te, LPE growth, elec. characts. 7-33603
 n-InAs/GaAs SNS heterostructure weak link with Nb electrodes 7-52898
 InAs/GaAs single quantum well structures grown by atomic layer epitaxy 7-22486
 InAs/GaAs strained-layer superlattices, band struct., TEM, X-ray and photolum. spectra 7-38722
 InAs/GaSb quantum well, 2D electron gas, cyclotron reson. oscills. meas. 7-38944
 InAs-GaAs, in situ contacts, MBE grown 7-45444
 InAs-GaAs strained-layer superlattices, pseudo-alloy behaviour 7-7376
 InAs-GaAs superlattices grown by beam-separation MBE, surface morphology and elastic strain 7-7031
 InAs-GaAs superlattice, electronic props. 7-52817
 InAs-GaSb superlattice dispersion relations, electronic states in semiconductor heterostructures 7-7307
 InAs-GaSb superlattices, transient photovoltaic effect 7-12764
 InAs-GaSb superlattice, band offset press. depend., magneto-optical studies 7-38698
 InAs-GaSb superlattices, band line-up under hydrostatic press. 7-52782
 InAs-GaSb superlattices, electronic props. 7-52817
 InAs-GaSb thin film heterostruct., superlattice, electron transverse effective mass 7-21990
 InAs-superthin insulator-Au struct., inelastic electron tunnelling spectra 7-27436
 $\text{InAs}_2\text{P}_{1-x}$, LEC-grown single crystals, growth defects and lattice strains 7-38001
 InAsSb/GaSb n-n heterojunctions, band discontinuities, C-V and I-V meas. 7-7366
 $\text{InAs}_{0.3}\text{Sb}_{0.7}$ IR detector, photoresponsivity meas. 7-7274
 $\text{InAs}_{1-x}\text{Sb}_x$ IR photodiodes for 3 to 14 μm , comparison 7-41466
 InAsSbP/InAs bent heterostructures, dislocation distribution 7-21673
 InAsSbP/InAs p-n structures, nonclassical thermal injection current 7-12806
 InBr, A-X system, rot. struct., dissoc. energy 7-50071
 InBr, isotope shift, rot. anal., UV spectra 7-19876
 InBr, rot. anal., use of isotopic effects 7-15587
 $^{113}\text{InBr}$, $\text{A}^*\pi_0\text{-X}^1\Sigma^+$ and $\text{B}^*\pi_1\text{-X}^1\Sigma^+$ subsystems, rot. anal. 7-42592
 $^{115}\text{InBr}$, $\text{A}^*\pi_0\text{-X}^1\Sigma^+$ and $\text{B}^*\pi_1\text{-X}^1\Sigma^+$ subsystems, rot. anal. 7-42592
 InCl molecule, $\text{C}^1\Pi\text{-X}^1\Sigma^+$ system, emission spectrum and dissociation energy 7-5694
 $^{111}\text{InCl}$ and ^{113}InI , ion-molecule collisions in gaseous forms, cross sections 7-20006
 InCl_2 mixed valence cpds., nuclear electron capture aftereffects, quadrupole interactions, γ ray ang. correl. anal. 7-53182
 $\text{InF}_2\text{-PbF}_2\text{-BaF}_2\text{-SrF}_2\text{-YF}_3\text{-AlF}_3\text{-UO}_2\text{F}_2$, luminesc., lifetime meas. 7-27750
 $\text{In}_{0.5}\text{Ga}_{0.5}\text{P}$ layers, LPE, elec. and optical props. 7-17119
 InGaAlAs, props. for integrated optics/optoelectronics in optical fibre communication systems, review 7-11178
 $\text{In}_x\text{Ga}_{1-x}(\text{Al}_{1-x})\text{As}$, MBE growth rates, temp. dependence 7-17426
 InGaAlP epilayers, MOCVD, laser appl. 7-39404
 InGaAlP transverse mode stabilized visible laser diodes fabricated by MOCVD selective growth 7-50591
 InGaAs and InGaAsP, nonuniform, dynamical X-ray rocking curve simulations 7-2408
 InGaAs, CVD, laser selective deposition on GaAs and Si substrates 7-22546
 InGaAs, CVD growth by VPE, review 7-39417
 InGaAs, chemical beam epitaxial growth investig. 7-7878
 InGaAs emitter cap layer for AlGaAs/GaAs heterojunction bipolar transistor 7-45492
 InGaAs epitaxial films, MO-chloride VPE growth 7-22566
 InGaAs epitaxial layers on InP substrates, ion beam crystallography 7-32863
 InGaAs films, organometallic CVD growth mechanisms, adduct formation 7-33588
 InGaAs, high-field autovariance coeff., diffusion coeff., and noise at 300 K 7-64260

indium compounds continued

- InGaAs, ion beam damage-induced masking for photoelectrochem. etching 7-44628
 InGaAs, LPE diffusion-limited growth 7-21727
 InGaAs layers on InP, LPE growth 7-33608
 InGaAs, MISS, common anion rule, density distrib., photoionisation 7-38765
 InGaAs monolithic three-junction solar cells, computer modelling 7-3672
 InGaAs, patterning using photoelectrochem. etching and focused ion beams 7-22924
 InGaAs, reactive ion etching 7-65241
 InGaAs strained-layer superlattices, valence-band nonparabolicity and tailorable hole masses 7-12798
 InGaAs, vapour levitation epitaxy, system design and performance 7-59445
 InGaAs:Si LED, electrical and luminesc. props., ultrasonically-induced changes 7-22350
 InGaAs/GaAs GRIN SCH SL quantum well laser, MOCVD grown 7-50557
 InGaAs/GaAs lattice-strained double heterojunction bipolar struct., comp., recomb. props. and device performance 7-64322
 InGaAs/GaAs(InP) quantum well structures, localised states, strain depend. 7-7312
 InGaAs/InAlAs MQW pin diodes, room temp. current oscillations 7-45454
 InGaAs/InAlAs multiple quantum well struct., nonlinear spectroscopy 7-1236
 $n^+\text{-InGaAs}/\text{InAlAs}/n^-\text{-InGaAs}$, conduction band discontinuity determ. by current-voltage meas. 7-7352
 InGaAs/InP heteroepitaxial struct., misfit stress, elastic eqns., comment 7-21676
 InGaAs/InP heterostructures, chloride VPE, interface form. control 7-58656
 InGaAs/InP multiple quantum well waveguides, low loss, MOCVD growth 7-43358
 InGaAs/InP photodiodes, MOCVD growth and characts. 7-27932
 InGaAs/InP quantum wires and boxes, low temp. photoluminesc. 7-59238
 InGaAs/InP single quantum wells, transport and persistent photocond. props. 7-27385
 InGaAs/InP superlattices, effective mass filtering obs. 7-12799
 InGaAs-GaAs, quantum well struct., p-type modulation doped, Hall effects, influence of built-in strain 7-7339
 InGaAs-GaAs MOVPE epitaxially-grown interfaces, anomalous C-V carrier conc. profiles, model 7-52648
 InGaAs-GaAs strained layer superlattices, press. depend. magneto-optic meas. at low temp. 7-27404
 InGaAs-InAlAs MQW structure, anisotropic electroabsorpt. and optical modulation 7-13134
 InGaAs-InAlAs multiple quantum wells, long wavelength optical modulation, electro-optical effects 7-7677
 InGaAs-InAlAs strained-layer superlattices, MBE grown, optical characterisation 7-13142
 InGaAs-InP, direct growth on GaAs substrates using MOVPE 7-22510
 InGaAs-InP 1.5 μm photodetectors, optical communication appls. 7-37202
 InGaAs-InP heterostruct., rare earth doped, elec. and photoluminescence props. 7-46133
 $\text{In}_{0.2}\text{Ga}_{0.8}\text{As}$ -GaAs cascade solar cells, OM-VPE growth, in-situ-grown tunnel junction 7-8387
 $\text{In}_{0.3}\text{Ga}_{0.8}\text{As}$ -GaAs strained-layer superlattice, low-temp. pressure-depend. magneto-optic meas. 7-12793
 $\text{In}_{0.5}\text{Ga}_{0.5}\text{As}$ quantum wells, quantized energy levels, conduction-band nonparabolicity effects 7-2675
 $\text{In}_{0.52}\text{Ga}_{0.48}\text{As}/\text{In}_{0.52}(\text{Ga}_{1-x}\text{Al}_x)_{0.48}\text{As}$ heterostructures, conduction band edge discontinuity 7-12815
 $\text{In}_{0.53}\text{Ga}_{0.47}\text{As}$, impact ionisation coeffs., lucky drift model including soft threshold energy 7-64258
 $\text{In}_{0.53}\text{Ga}_{0.47}\text{As}$, LPE growth on semiinsulating InP:Fe, SEM studies 7-22591
 $\text{In}_{0.53}\text{Ga}_{0.47}\text{As}$, surface analysis using organic-on-inorganic contact barriers 7-21991
 $\text{In}_{0.53}\text{Ga}_{0.47}\text{As}:\text{Be}$, high dose implants, rapid thermal annealing 7-16602
 $\text{In}_{0.53}\text{Ga}_{0.47}\text{As}/\text{In}_{0.52}\text{Al}_{0.48}\text{As}$ quantum wells, lamp annealing interdiffusion and optical props. 7-12502
 $\text{In}_{0.53}\text{Ga}_{0.47}\text{As}-\text{In}_{0.52}\text{Al}_{0.48}\text{As}$ modulation-doped heterostructs., interface roughness scatt. 7-2678
 $\text{In}_{0.53}\text{Ga}_{0.47}\text{As}-\text{InP}$, double-barrier struct., tunnelling 7-45446
 $\text{In}_{0.53}\text{Ga}_{0.47}\text{As}-\text{InP}$, quasi-2D heterostructures, suppression of current filament by mag. field 7-52760
 $\text{In}_{0.53}\text{Ga}_{0.47}\text{As}-\text{InP}$ heterointerfaces, CV profiling 7-12834
 $\text{In}_{0.53}\text{Ga}_{0.47}\text{As}-\text{InP}$ layers, photolum. and laser emission 7-7739
 $\text{In}_{0.53}\text{Ga}_{0.47}\text{As}-\text{W-InP}$ structures, LPE growth on structured substrates 7-46353
 $\text{In}_{0.69}\text{Ga}_{0.31}\text{As}-\text{InP}$ strained-layer effective-mass superlattices 7-7378
 $\text{In}_{1-x}\text{Ga}_x\text{As}$, MOCVD, optical and elec. props. rel. to growth temp. 7-53613
 $\text{In}_{1-x}\text{Ga}_x\text{As}-\text{InP}$ heterostructure APD for 1.55 μ optical fibre communication system (Japanese) 7-62843
 $\text{In}_x\text{Ga}_{1-x}\text{As}-\text{GaAs}$ single-quantum-well heterostructs., pseudomorphic, optical characterisation 7-22303
 $\text{In}_x\text{Ga}_{1-x}\text{As}$ (100)-metal interfaces, Fermi level pinning and chem. interactions 7-2712
 $\text{In}_x\text{Ga}_{1-x}\text{As}$, atomic displacements detection using channelled electron induced X-ray emission 7-21311
 $\text{In}_x\text{Ga}_{1-x}\text{As}$, atomic layer epitaxy growth, photolum., Hall meas. 7-22527
 $\text{In}_x\text{Ga}_{1-x}\text{As}$, gas source MBE growth 7-52361
 $\text{In}_x\text{Ga}_{1-x}\text{As}$, magnetophonon resonance effect 7-21942
 $\text{In}_x\text{Ga}_{1-x}\text{As}$, photoluminescence determ. of effects due to In alloying 7-46096
 $\text{In}_x\text{Ga}_{1-x}\text{As}/\text{In}_y\text{Ga}_{1-y}\text{As}$ and $(\text{InAs})_m(\text{GaAs})_n$ superlattices, MBE grown, optical studies 7-13221
 $\text{In}_x\text{Ga}_{1-x}\text{As}/\text{InP}$ heterostructures, OMVPE growth, quality, source comp., press. effect 7-39400
 $\text{In}_x\text{Ga}_{1-x}\text{As}-\text{In}_y\text{Al}_{1-y}\text{As}$ superlattices, lattice-matched and lattice-mismatched, dislocation filtering 7-21671
 $\text{In}_x\text{Ga}_{1-x}\text{As}-\text{In}_y\text{Al}_{1-y}\text{As}$ heterojunction, cyclotron resonance linewidth due to alloy scatt. 7-27399
 InGaAsP 1.3 μm diode laser, ultra-high-speed modulation 7-5924
 InGaAsP 1.5 μm DFB laser diodes, optical communication appls. 7-37202

indium compounds continued

- InGaAsP 1.55 μm mode-locked laser with single-mode fibre output 7-50600
 InGaAsP (001), surface, dislocation etch pits, new etchant props. 7-59699
 InGaAsP BH lasers, radiative, Auger and nonradiative currents 7-57312
 InGaAsP buried crescent injection lasers, differential quantum efficiency 7-25815
 InGaAsP buried crescent injection lasers, low threshold 1.5 μm operation 7-43136
 InGaAsP buried heterostructure lasers, polarisation, effect of stress relax. caused by repetitive temp. change 7-62690
 InGaAsP constricted mesa laser, 8 Gbit/s return-to-zero modulation by gain switching 7-31366
 InGaAsP DFB lasers, extremely low-noise facet-reflectivity-controlled 7-31320
 InGaAsP DFB laser, phase noise and linewidth 7-31322
 InGaAsP device fabrication using HBr-H₂O etching soln. 7-46728
 InGaAsP directly modulated semicond. lasers, gain nonlinear effects calcs. 7-20218
 InGaAsP double heterostructures for laser diodes, LPE growth, influence of P vapour ambient 7-46355
 InGaAsP epitaxial films, strain mapping by an X-ray diffraction technique 7-21786
 InGaAsP film, defect struct. and strain anal., X-ray topography 7-52344
 InGaAsP films, dense electron-hole plasmas, picosecond dynamics, acoustic phonon generation 7-45373
 InGaAsP injection lasers, mode-locked and gain-switched, timing jitter 7-11013
 InGaAsP, ion beam damage-induced masking for photoelectrochem. etching 7-44628
 InGaAsP, LPE growth on GaAs_{0.7}P_{0.3} substrate, crosshatch pattern 7-59472
 InGaAsP laser, LPE grown, effect of crystal defects on reliability 7-36960
 InGaAsP laser amplifiers, recombination, gain and bandwidth characts. 7-57334
 InGaAsP lasers, injection, photodetection props. 7-31379
 InGaAsP layers, LPE on GaAs, immiscibility region, lattice matching 7-59465
 InGaAsP layers, VPE growth, X-ray characterisation 7-21780
 InGaAsP layers on InP (001), origin of grown-in dislocations 7-38415
 InGaAsP, layers on InP, rel. lattice parameter meas., convergent beam electron diffraction 7-52371
 InGaAsP local struct., EXAFS and near-edge struct. studies 7-64006
 InGaAsP, MOVPE system, gas switching mass spectrometry 7-22526
 InGaAsP materials, OMVPE growth for long wavelength detectors and emitters 7-27931
 InGaAsP, optical gain spectra, effects of energy band struct. (Chinese) 7-59239
 InGaAsP, patterning using photoelectrochem. etching and focused ion beams 7-22924
 InGaAsP, props. for integrated optics/optoelectronics in optical fibre communication systems, review 7-11178
 InGaAsP ridge waveguide laser threshold current optimisation, simplified hybrid optical model 7-57321
 InGaAsP, spinodally decomposed, elastic relax. effects on TEM 7-52378
 InGaAsP system, transferred electron effect anal. 7-64259
 InGaAsP TM-wave injected BH laser, ps switching optical bistability 7-50629
 InGaAsP, vapour levitation epitaxy, system design and performance 7-59445
 InGaAsP wideband semicond. lasers, limitations on switching speed 7-10943
 InGaAsP/InP, semicond. superlattice heterojunction interface, SIMS anal. (Japanese) 7-2396
 InGaAsP/InP 1.3 μm lasers grown on p-InP substrates, low threshold, high T₀ operation 7-1180
 InGaAsP/InP DFB lasers, DFB mode oscillation, temp. range 7-5910
 InGaAsP/InP double heterostructures, microcathodoluminescence studies 7-39189
 InGaAsP/InP heterostructures, carrier lifetimes and quantum efficiencies, photoluminesc. studies 7-64675
 InGaAsP/InP laser wafers, pinhole defects, identification of source 7-46356
 InGaAsP/InP multiquantum well layers, LPE, photolum., X-ray diffr. 7-53640
 InGaAsP/InP multiple quantum well waveguide phase modulator 7-57531
 InGaAsP/InP superlattices, gas-source MBE grown, X-ray diffr. and TEM studies 7-32839
 InGaAsP/InP:Fe buried crescent lasers with wide-bandwidth and high power 7-50560
 n-InGaAsP/p-GaAs diodes, photocurrent meas. of defect distribution 7-32851
 InGaAsP-GaAs double heterostructures, luminescence efficiency and surface recombination velocity 7-13196
 InGaAsP-InP, 1.5 μm laser with high external quantum efficiency and controlled emission wavelength 7-57323
 InGaAsP-InP, heterolaser struct., distributed feedback conditions, luminesc. spectra anal. 7-50561
 InGaAsP-InP, integrated external cavity laser 7-36993
 InGaAsP-InP, long-wavelength components by VPE 7-46343
 InGaAsP-InP, quantum well wire, Auger recombination 7-7374
 InGaAsP-InP, solid-phase epitaxial Pd-Ge ohmic contacts 7-2706
 InGaAsP-InP bistable lasers, temp. depend. 7-5887
 InGaAsP-InP buried heterostructure lasers, internal thermal stress distrib. 7-10931
 InGaAsP-InP DFB lasers with monolithic external cavity, spectral characts. for 1.3 μm 7-20281
 InGaAsP-InP DFB laser monolithically integrated with tunable external cavity, linewidth and FM characts. 7-57316
 InGaAsP-InP DFB laser, waveguiding props. 7-57319
 InGaAsP-InP distributed-feedback injection laser, fabrication by LPE and VPE 7-57337
 InGaAsP-InP double heterostructures, luminescence efficiency and surface recombination velocity 7-13196
 InGaAsP-InP Fabry-Perot and DFB lasers, VPE transport fabrication 7-20277
 InGaAsP-InP heterostruct. laser output characts., quantum size effect active layer thickness variation effects 7-31323

indium compounds continued

- InGaAsP-InP heterostructures, light emission and degradation characts. 7-45455
 InGaAsP-InP high power long wavelength laser diode 7-10998
 InGaAsP-InP high-performance 1.3 μm laser structures with both facets etched 7-20259
 InGaAsP-InP laser diodes, low resist. contacts on p-side 7-20276
 InGaAsP-InP laser, ridge waveguide, threshold current anal. 7-31338
 InGaAsP-InP laser, single-mode, 1.3 μm , analog FM 7-37002
 InGaAsP-InP laser failure causes and distrib., laboratory service life tests 7-62692
 InGaAsP-InP low-threshold separate-confinement heterostruct. laser characts. 7-31324
 InGaAsP-InP optical switches, carrier induced refractive index change 7-57606
 InGaAsP-InP planar surface BH lasers with hydride VPE-grown Fe-doped current blocking layers 7-20261
 InGaAsP-InP waveguides, optical parameters 7-62831
 InGaAsP-InP-ridge waveguide lasers, LPE fabricated, design and 1.5 μm low-threshold operation 7-15897
 In_{1-x}Ga_xAs_{1-y}P_y/InP heterojunctions, MOCVD grown, spectroscopic ellipsometry study 7-39195
 In_{1-x}Ga_xAs_{1-y}P_y-InP quarter-wavelength-shifted DFB laser source for 1.55 μm underwater optical cable system (Japanese) 7-62720
 In_{1-x}Ga_xP_{1-y} cpd. semicond. alloys, lattice and band struct. props., review (Japanese) 7-7109
 In_{1-x}Ga_xAs_{1-y}P_y-Cd on InP, activation energy of impurity 7-32942
 In_{1-x}Ga_xAs_{1-y}P_y-Te films, Fermi energy, dopant conc. depend. 7-52867
 In₂Ga_{1-x}As_{1-y}P_y-InP quantum well, 2D electron gas, self-consistent calcs. 7-58890
 In₂Ga_{1-x}Sb_{1-y}, mid-IR source and detector material 7-36964
 InGaP, vapour levitation epitaxy, system design and performance 7-59445
 InGaP-InGaAlP MQW structs., room temp. excitons 7-58745
 In_{1-x}Ga_xP solid solns., indirect band gap temp. depend., electrolum. spectra studies 7-38448
 In_{1-x}Ga_xP, epitaxial films, radiative recomb. 7-59257
 In_{1-x}Ga_xP epitaxial layers, LPE, surface morphology rel. to lattice mismatch 7-33604
 In₂Ga_{1-x}P LPE layers lattice-matched to GaAs, Hall mobility meas. and MESFET fabrication 7-7905
 InGaPAs, LPE growth on GaAs, immiscibility effects 7-39442
 InGaPAs/GaAs interface stress, Cr-related luminescence study 7-46101
 In_{0.17}Ga_{0.83}TaS₂, intercalation reactions, nucl. quadrupole interactions, TDPAC meas. 7-17245
 In₂Hg arc, high-pressure, spectroscopic studies 7-44278
 In_{1-x}Li_{3x}VO₄ solid solutions, characterisation, ionic conductivity (French) 7-44833
 InMgGaO₄, luminescence props. 7-17341
 In₂MoSe₈, insertion cpd., synthesis and props. 7-32407
 InN, band struct., pseudopotential method anal. 7-52421
 InN films, IR absorption 7-7778
 InO, lower electronic states, SCF-X_α SW calcs. 7-30948
 InO₂, He I photoelectron spectra, relativistic DVM SCC X_α calcs. 7-50252
 In₂O₃ 3-D disordered samples, Anderson transition, finite temperature aspects 7-7118
 In₂O₃ mixed conductor films in WO₃ based electrochromic windows, recent R&D 7-37122
 In₂O₃:Sn, sputtered films prep. and optical props. 7-53587
 In₂O₃:Sn evaporated films, optical props. and applications to energy-efficient windows 7-46157
 In₂O₃:Sn films, electron effective mass determ., refractive index carrier density depend. meas. 7-38440
 In₂O₃:Sn films, prep. by thermal decomposition of organometallic cpds., optical and electrical props. 7-17483
 In₂O₃:Sn films, theoretical model for optical props. in 0.3 to 50 μm range 7-39200
 In₂O₃:Sn transparent conducting films, electr., optical props., appls. (Korean) 7-59842
 In₂O₃:Sn vapour deposited films, growth, struct., electronic props. 7-12535
 In₂O₃:Sn-ZnS:Cu,Cl,Mn-Al, surface electrical conductivity in ZnS:Cu,Cl,Mn thin films 7-38672
 In₂O₃:Sn(In)(Cd) films, optical and elec. props. 7-22365
 In₂O₃:Sn(Te), thin films, etching, comparison of solns. dilute HCl and H₃PO₄ 7-8208
 In₂O₃/CdTe solar cells, high efficiency 7-59838
 In₂O₃:P, Hall coeff., noncritical behaviour at mobility edge 7-32993
 In₂O₃Sn thin films, prep. by pyrolysis, props. 7-2749
 InP (100), ambient induced surface effects, O adsorption, photolum., conductivity 7-45429
 InP (100), empty surface states, two-photon photoemission 7-53498
 InP (100), prep. by P deposition and annealing, surface reconstruction, LEED, EELS studies 7-38311
 InP (110), oxidation, photoemission spectra studies 7-3147
 InP (110) cleaved surface and Schottky diodes 7-58850
 InP (110) photoexcited surface, time-resolved VUV photoemission spectroscopy 7-18919
 InP (110) surface, picosecond time-resolved photoemission study 7-46280
 InP (111), chemically polished and etched, characterisation of native oxide layer, ion scatt. spectra, AES, ESCA 7-22925
 InP (111) orderly faceted struct., LEED pattern anal. 7-21579
 InP {001} surfaces, chem. etch cleaning procedure 7-13668
 InP, acceptor higher excited states calcs. 7-52511
 InP and InP based materials, epitaxial growth, review 7-33574
 InP, band structure, polarisation-dependent angle-resolved photoemission spectroscopy 7-21814
 InP, chemical beam epitaxial growth investig. 7-7878
 InP chemical etching by Cl₂, thermodynamically predicted depend. on press. and temp. 7-22919
 n-InP compensated samples, MOVPE grown, Hall effect meas. 7-27348
 InP crystals and solar cells, radiation-induced defects, room-temperature annealing 7-39993
 InP device fabrication using HBr-H₂O etching soln. 7-46728
 InP, direct synthesis, growth, liquid encapsulated Czochralski method 7-59397
 InP, dislocation density reduction in crystal growth 7-2020
 InP, dislocation-complex defect interactions, photoluminescence studies 7-16608
 InP doping superlattices, nonlinear optical absorption 7-39069

indium compounds continued

- InP dry etching at room temp. 7-28227
 InP dual-wavelength channelled-substrate BH laser light source 7-62726
 InP, electrochemical C-V profiling 7-27325
 InP electrodes, surface modified, time resolved photoelectrochemical meas. 7-27415
 p-InP, electron irradi., atomic displacement threshold energy 7-2066
 InP, electron irradi. damage, impurity effects 7-12154
 InP epitaxial films, MO-chloride VPE growth 7-22566
 InP epitaxial films, MOCVD grown, identification of acceptors and donors 7-58688
 InP, epitaxial films, radiative recomb. 7-59257
 InP epitaxial layers, MOVPE, elec. characts., photolum. 7-22519
 InP etching by Cl_2 , rare gas ion-enhanced etching 7-22918
 InP, field assisted plasma grown oxide 7-39772
 InP films, hydride VPE, impurity incorporation, defect charactn. 7-53614
 InP films, MOCVD growth using plasma pre-cracking 7-7880
 InP films and structures, gas source MBE, review 7-33572
 InP films on oxidised Si substrate, laser recrystallisation 7-38398
 InP, floating zone melting prep., elec. props. 7-64238
 InP, grown-in defects, slow positron beam and positron labelling studies 7-44527
 p-InP, γ -ray irradiated low temp., nonradiative-recomb.-enhanced defect struct. transformation 7-2062
 n-InP, Hall factor calcs. 7-52657
 InP, Hall scatt. factor 7-45361
 InP, high resistivity layer form. by ion implantation, ohmic contact characterisation 7-38035
 InP, impact ionisation coeffs., lucky drift model including soft threshold energy 7-64258
 InP, impurity atom site location using channelling enhanced microanalysis 7-38023
 InP, ion beam damage-induced masking for photoelectrochem. etching 7-44628
 InP, ion enhanced chem. etching in Cl_2 , thermal pulse model 7-54029
 InP, ion milling, TEM 7-39344
 InP, laser enhanced low temp. oxidation, dissociation of N_2O 7-39780
 n-InP, light scatt. by free carriers 7-17328
 InP, luminesc. associated with defect complexes 7-27757
 InP MIS structs. with amorphous C films, interfacial electronic props. 7-7400
 InP MIS structures, prep. by RF plasma oxidation, interface elec. props. 7-2731
 InP MIS structures, thermal treatment in P overpressure 7-7394
 InP, MISS, common anion rule, density distrib., photoionisation 7-38765
 InP, MOCVD on structured substrates, mass transport 7-39397
 InP, MOVPE, press. control, reactor design 7-39399
 InP, MOVPE on SiO_2 masked substrates at reduced press., vapour etching 7-39398
 InP, MOVPE; morphology, photolum., carrier conc. and mobility 7-22518
 InP, maskless ion beam assisted etching 7-22923
 InP, melt grown, theoretical and expt. fundamentals of decreasing dislocations 7-53547
 InP, metal contacts, interfacial microstruct., elec. props., phase diagrams 7-45495
 InP microwave absorption transient spectroscopy for investigation of deep levels in semiconductors 7-52520
 n-InP, minority carrier diffusion length meas. using a photoelectrochemical technique 7-33030
 InP, multiphonon absorption (*Chinese*) 7-7682
 InP n^+n^+ struct., space-charge limited magnetoconductivity 7-45472
 InP, negative magnetoresistance and electron localisation in the region of a metal-insulator transition 7-12737
 n-InP, negative magnetoresistance and nonequilib. electron cooling 7-17042
 InP, neutral shallow donor inter-excited-state transitions, far IR photocond. in mag. field study 7-22249
 InP, optical generation and phase-sensitive detection of SAWs 7-58598
 InP, passivation, by a-P and alkali metal polyphosphides 7-39778
 InP, passivation by plasma deposited P film 7-3540
 InP, patterning using photoelectrochem. etching and focused ion beams 7-22924
 InP pure and Er doped liquid phase epitaxial films, elec. props. in strong elec. fields 7-38779
 InP, quantitative trace anal. of impurities by SIMS 7-53480
 InP, radiation-damaged photocond., Hertzian dipole meas. of picosecond photoresponses 7-52690
 InP, rapid thermal annealing, heating behaviour 7-21258
 InP, reactive ion etching, AES, photoluminescence, SEM obs. 7-65241
 InP refractive index and its temp. coeff. at 0.96 to 13 μm 7-39070
 InP room temp. band edge photolum. intensity interpretation 7-27762
 InP rotating ring-disk electrodes, appl. of redox contacts 7-39982
 InP semiconductor crystals growth using Gault process 7-46300
 InP single crystal (100) surface, atomic scatt., electron-hole pair creation 7-27841
 InP single crystals, thermal activation of glide 7-21213
 InP solar cells, potential for use in space radiation environment 7-23181
 InP solar cells, radiation resistant characts. 7-8413
 InP solar cells in space radiation environment, comparison with GaAs and Si cells 7-65484
 InP stress meas., photoelasticity determ. with aid of computer 7-31725
 InP, sublattices direct resolution and identification by high-resolution TEM 7-37813
 InP, submicron gratings, reactive ion beam etching and deformation-free LPE overgrowth 7-13659
 InP substrate, integrated optoelectronics, micrograting form. by HV electron beam lithography 7-31443
 InP, substrate, plasma deposition of C dielectric films 7-39420
 p-InP substrate mass transport BH laser, narrow active stripe 7-31357
 InP substrate vapour phase etching, surface morphology, temp. depend. study 7-28220
 InP substrate with GaInAs epitaxial layer, depth profiling and interface detection using anodic oxidation 7-45057
 InP substrates, influence of inhomogeneities on quality of quaternary layers 7-32770
 InP substrates and devices, surface anal., SIMS appl. 7-22417
 InP, surface, for MIS device, As-stabilisation, effect on elec. and physicochemical props. 7-38767
 InP surface, interaction with H_2 7-58632

indium compounds continued

- InP surface, oxidation processes studied by high-resolution electron microscopy 7-39766
 InP, surface analysis using organic-on-inorganic contact barriers 7-21991
 InP surface annealed under As pressure, epitaxial growth of InAs 7-2431
 InP surface metal-p⁺-n enhanced Schottky barriers formed by open tube diffusion technique 7-2710
 InP, surface recombination velocity and bulk minority carrier lifetime 7-17037
 InP surfaces, sputter etched, optoelectronic and structural props. 7-13661
 InP synthesis by modified horizontal Bridgman method, elec. props. 7-58821
 InP thin film solar cells on Si substrate, high efficiency and high radiation resistance 7-59852
 InP, ultrapure, atmospheric pressure OMVPE growth 7-13375
 InP, undoped and Zn(Cd) doped thin films, prep. and characts., appl. for solar cells 7-17895
 InP, VPE using flow modulation 7-7039
 InP, vapour levitation epitaxy, system design and performance 7-59445
 InP waveguide, thermal index changes by optical absorpt., all-optical signal processing 7-31381
 InP:B, internal friction temp. depend. studies 7-38112
 InP:B, multiphonon absorpt. 7-59211
 InP:Be(Si), isothermal anneal techniques, comparison 7-16603
 InP:Bi thin film, epitaxy, impurity distrib., photoluminesc. spectra anal. 7-53388
 InP:Cr, impurity ion-lattice coupling, reson. phonon scatt. spectra 7-58420
 InP:Fe, Czochralski-grown, stoichiometric-related faulted loops, struct. and luminesc. props. 7-51772
 InP:Fe, deep levels formed by Fe complexes 7-12657
 InP:Fe, epitaxial layers, MOCVD, doping profiles, SIMS, resist., temp. depend. 7-21248
 InP:Fe, LPE growth, SIMS 7-52363
 InP:Fe, midgap impurity levels, isomer shift and charge state calcs. 7-2538
 InP:Fe, OMVPE grown, electronic and optical props. 7-52868
 InP:Fe, optical spectra 7-53372
 InP:Fe, photoconducting flat response detectors from UV to X-ray region 7-5563
 InP:Fe, programmed magnetic field applied LEC crystal growth 7-59399
 InP:Fe, Si-implanted and rapid thermal annealed, photoluminesc. study 7-59243
 InP:Fe, transient photoconductive response 7-52681
 InP:Fe,Ga,Sb, LEC growth, dislocation density, resistivity, SIMS obs. 7-53552
 InP:Fe photoconductive detectors for VUV and soft X-ray regions 7-30084
 InP:Fe semi-insulating layers, MOVPE growth and elec. characts. 7-22511
 InP:Fe wafer, semi-insulating, elec. characteristics 7-45323
 InP:Ga,As,Sb single crystals, LEC growth, isoelectronic doping, dislocation density, X-ray topography 7-33549
 InP:Ge, Fermi level, determ. from phase diagram data of InP-Ge system 7-21808
 InP:Ge,Sb, LEC-growth, dislocation-free 7-17409
 InP:Hg ion implanted at 200°C, rapid thermal annealing, carrier conc. and mobility 7-32469
 InP:Mg p-n junction waveguide fabricated by Mg ion implantation 7-64326
 InP:Mn, deep acceptor level, props. 7-21853
 InP:Mn, LPE growth, carrier conc. control and appl. to buried heterostructure laser diodes 7-21774
 InP:Mn³⁺, Jahn-Teller effect, mag. suscept. and ESR spectra anal. 7-52534
 InP:S, LEC grown, influence of growth conditions on defects 7-32427
 InP:S, shallow n⁺ diffusion of S, open-tube diffusion technique, n⁺-p junction formation 7-44912
 InP:S,Ga,Sb, LEC growth, appl. mag. field method, dislocation etching 7-53553
 InP:S substrate wafers for LPE growth of laser diode heterostructures, polarised IR and X-ray topographic evaluation 7-32453
 InP:Si, substrate, encapsulated annealing, using SiN encapsulant 7-39779
 InP:Sn substrate/epilayer interface, Sn depth profiling, AES and SIMS studies 7-27146
 InP:Ti, Hg, semi-insulating, impurity electron state compensation mechanism, SIMS, SSMS, EPR and Hall effect meas. 7-64164
 InP:Ti(Cr)(Ni), LEC growth, precipitate phase identification 7-16754
 InP:Yb LPE layers, luminesc. and elec. props. 7-59464
 InP:Zn, ion implantation and annealing, Raman studies 7-6652
 n-InP:Zn, Zn diffusion 7-63882
 InP:Zn(Cd), interstitial-substitutional diffusion, doping effects 7-6878
 InP/Al UHV-cleaved and laser annealed interface, acceptor-like electron traps 7-7310
 InP/Al(Mn)(Ag) interfaces, interactions, XPS and elec. transport studies 7-7384
 n-InP/Au Schottky contacts, surface treatment by plasma-induced O radicals 7-38674
 p-InP/Co(Pt) photocathodes for photoelectrochemical solar cells, H_2 evolution from alkaline solns. 7-13922
 p-InP/electrolyte, photoelectron emission spectra, thermodynamic const. 7-12856
 InP/GaInAs/InP heterostructures, OMVPE, high speed p-i-n photodiodes, photolum., Hall meas. 7-27387
 InP/InGaAs heterojunction bipolar transistors, open-tube Zn diffusion 7-44914
 InP/InGaAs near-IR detector self-calibration feasibility determ. 7-15002
 InP/InGaAsP antiresonant reflecting optical waveguides, chemical beam epitaxy and propagation losses 7-57537
 InP/InGaAsP device structures, LPE growth 7-33610
 InP/metal Schottky barrier diode, electrical props. 7-27426
 InP/native oxide MIS structures, interface elec. props. 7-33851
 InP/Pd (110) interface, chem. reactions, overlayer morphology and Fermi level pinning 7-7020
 InP/SrF₂ lattice mismatch, temp. depend. 7-63849
 InP-Al, wet anodisation, compositional profiles 7-65216
 InP-Al₂O₃-metal structs., improved elec. props. with heat resist. interface 7-38753
 InP-aqueous electrolyte interfaces, laser induced photoelectrochemistry 7-27412
 InP-Au, metallic contact layers, thermal dissociation, P loss 7-23005

indium compounds continued

- InP-Au interface, Fermi level pinning, growth charact., photoemission spectra 7-22009
 InP-Au(Al) Schottky barriers, defects introduced by mech. polishing 7-39768
 InP-C based MIS struct., interfacial charact. 7-2732
 InP-CdS solar cells, high efficiency, with thermally evaporated window layers 7-3701
 InP-Cu(Au)(Ag), interphase contact interaction 7-33087
 InP-Ga_{0.47}In_{0.53}As superlattice, electron and hole impact ionisation rates 7-17076
 InP-Ga_{1-x}In_xAs_{1-y}P_y double heterostructs., device quality, growth by MOVPE 7-7877
 InP-Ga_{1-x}In_x-P_yAs_{1-y} heterojunction interfaces, electronic band struct. (Chinese) 7-33070
 InP-GaInAs, 2D electron gas, persistent photoconductivity 7-33046
 InP-GaInAs planar BH lasers, OMVPE growth 7-1183
 InP-InGaAs single quantum wells, transport and persistent photoconductivity 7-38709
 InP-InP:As epitaxial layers, dislocation reduction, device performance effects 7-7354
 InP-metal interfaces, Fermi level pinning 7-2714
 InP-n⁺-i-In_{2-x}Sn_xO_{3-y} Schottky diode, solar cell props. 7-65474
 InP-SiO₂ interface, electron localisation 7-45514
 InP-SiO₂ MISFET, electron tunnelling into oxide traps 7-38764
 InP_xAs_{1-x} solid solutions, temp. depend. of lattice constants and thermal expansion coeffs. 7-21165
 InP(As)(S)₄, dielec. const. meas. w.r.t. bond ionicity (French) 7-38988
 InP(110), P- and In-rich, electronic states, semi-empirical tight binding calcs. (Chinese) 7-12773
 InP=Si(Sn)(Be), doping using thermal atomic beams in chemical beam epitaxy 7-44584
 β-In₂S₃ thin films, spray pyrolysis grown, optical energy gaps 7-33467
 In₂S₃:Co, photoconductivity, Co impurity energy levels (Korean) 7-33049
 InSb array IR imaging camera, for astronomical appls. 7-34865
 InSb, carrier lifetime, pressure depend. 7-52644
 InSb charge injection device arrays, IR camera for astronomical imaging 7-34872
 InSe and γ-In₂Se₃ films, formation by double source evaporation 7-59436
 InSe crystals, melt-grown, electron diff. study 7-1994
 InSe, excitonic luminescence, influence of macroscopic inclusions 7-13204
 InSe intercalation cpd., with Ag, prep. 7-54146
 InSe laminar semicond. intercalation cpds., phase equilibria and stability studies (Russian) 7-21409
 InSe layer cpd., Al dopant intercalation, Auger and IR spectra studies (Russian) 7-32476
 n-InSe layered crystals, 2D electron gas regions, magnetoresist. meas. 7-45359
 InSe, photoluminescence, defects effects 7-39161
 InSe single crystals, growth by travelling heater method, carrier conc., photoelectrochemical props. 7-59410
 InSe-Li, intercalated layer compounds, conc. depend. of electrode potential 7-7230
 γ-In₂Se₃ bound layer, elec. props. and surface states (Japanese) 7-22038
 In₂Se₃ films, laser synthesized, optical props. 7-59276
 In₂Se₃ films, synthesis with pulsed ruby laser 7-58707
 In₂Se₃ intercalation cpd. with Ag, prep. 7-54146
 In₂Se₃, layered semicond., photolum. studies 7-7746
 In₂Se₃(S(Li)), electrical transport props. 7-21917
 In_{2-x}Sn_xO_{3-y} films, reactive RF magnetron sputtering prep., elec. and optical props. 7-46324
 In_{2-x}Sn_xO_{3-y} coatings, evacuated window glazings for energy efficient buildings 7-54352
 In_{2-x}Sn_xO_{3-y} films, transparent conducting oxides, H₂ plasma treatment 7-3528
 In_{2-x}Sn_xO_{3-y} protective coatings for Galileo spacecraft, radiation testing 7-59647
 In_{2-x}Sn_xO_{3-y} solar cells, state-of-the-art review 7-40007
 In_{2-x}Sn_xO_{3-y} sputter deposited, elec. cond., oxidation resistant coatings for spacecraft applic. 7-22866
 In_{2-x}Sn_xO_{3-y} thin films, struct. 7-21722
 In_{2-x}Sn_xO_{3-y} thin films, RF reactive sputtering prep., elec. and optical props. 7-39378
 In_{2-x}Sn_xO_{3-y}/Ag/In_{2-x}Sn_xO_{3-y} magnetron sputtered transparent heat-reflective films, thermal stability study 7-53426
 In_{2-x}Sn_xO_{3-y}-CdTe solar cells, spray deposited, elec. and photoelec. props. 7-54321
 In_{2-x}Sn_xO_{3-y}-i-n⁺-InP Schottky diode, solar cell props. 7-65474
 In_{2-x}Sn_xO_{3-y}-InP, solar cells for space appl. 7-3700
 In_{2-x}Sn_xO_{3-y}-WO₃-MgF₂-Au, electrochromic coatings for solar windows 7-53621
 In_{2-x}Sn_xO_{3-y}-SnO₂-Pt-Si:H solar cells 7-8395
 In₁₈Sn₇S₃₄, cryst. struct. determ. (French) 7-58214
 In_xTa_{1-x}S₂, intercalation reactions, nucl. quadrupole interactions, TDPAC meas. 7-17245
 In₂Te₃, vaporisation, torsion-effusion obs., morphology 7-58455
 In₂Te₃:Fe, Fe²⁺ elec. inactivity study, mag. suscept., Mossbauer spectra and XPS anal. 7-52494
 InVO₄-CrVO₄ system, study for solid solns. (French) 7-44833
 InZnGaO₄, luminescence props. 7-17341
 LiInP₂O₇, synthesis and cryst. struct. (French) 7-58223
 LiInSe₂ epitaxial films on GaAs and GaP, RHEED 7-52318
 Na_{1+x}Zr_{2-x}In_x(PO₄)₃ solid soln., Na⁺ ion motion, NMR study 7-44904
 Na₃Zr_{2-x}In_xS_{2-x}P_{1+x}O₁₂ system, chem. composition, cryst. struct. and ionic cond. (Chinese) 7-12006
 Nb-InAs-Nb proximity system, Josephson current, field effect 7-45573
 n-nP, Anderson transition in a mag. field 7-16944
 (PBr₄)⁻(InBr₄)⁺ complex, mol. vibr., Raman and IR spectra anal. 7-46021
 Pb₁₂In₂Bi₂S₁₃, cryst. struct. determ. 7-1962
 PbLiInSe, intercalation-layer compound, dielectric-metal cond. transition 7-7230
 Sb_{2-x}In_xTe₃, doped crystals, energy formation of antisite defects 7-21204
 Si-InP (110) heterojunction, characterisation 7-33079
 SnTe-InSe, quasibinary section of Sn-In-Te-Se, physicochemical props. 7-7979
 (Te₉₀Ge₁₀In_{90-x}O_x), Auger elemental depth profiling, preferential sputtering 7-54247
 β-TiInSn₂, Urbach rule and phase transitions 7-46009

indium compounds continued

- Tl₃In(SO₄)₃, columnar cpds., vibr. spectra and phase transitions 7-17314
 TlInSe₂, electronic struct., synchrotron radiation photoelectron spectra 7-52422
 Yb-In-Te system, phase equilibria 7-44761
 Zn₃In₂S₆ and Zn₃GaInS₆, thermal stability in air 7-22914
 ZnIn₂Se₄, crystal struct. 7-2002
 ZnSe-In_{2-x}Sn_xO_{3-y} junctions, microstruct. optical props., influence of deposition method 7-21689
- INDO calculations**
 acetophenone derivatives, NMR, spin-spin coupling interactions, INDO MO FPT calcs. 7-25395
 acetylenes, substituted, spin-spin coupling consts., 7-31074
 aluminosilicates, at. charges, SCF and semiempirical calcs. 7-2942
 ammonium hydrogen-DL-malate monohydrate, dielec. and pyroelec. props. 7-59138
 bacteriochlorophyll a, config. for photosynthesis, SCF HF INDO calcs. 7-858
 benzaldehyde derivatives, NMR, spin-spin coupling interactions, INDO MO FPT calcs. 7-25395
 benzene, vibronic activity, CNDO/S and INDO/S calcs. 7-49926
 benzophenone derivatives, NMR, spin-spin coupling interactions, INDO MO FPT calcs. 7-25395
 benzyl cyanide, spin-spin coupling consts. and internal rot. pots., determ. 7-50178
 bis(π-allyl) nickel, photoelectron spectrum, semi-empirical and ab initio Green's Function methods 7-30950
 demethyl porphyrins, monosubstituted free-base series, MCD study, INDO and CI calcs. 7-25401
 2,6-dichlorobenzyl cyanide, spin-spin coupling consts. and internal rot. pots., determ. 7-50178
 2,6-difluorobenzyl cyanide, spin-spin coupling consts. and internal rot. pots., determ. 7-50178
 diphenyl group-containing mols., conform. and internal rot. dynamics, CINDO calcs. 7-62285
 diphenylamine, geometry optimisation, semiempirical quantum chem. methods 7-10433
 harmaline, conformation effect, MINDO calcs. 7-56980
 harmine, conformation effect, MINDO calcs. 7-56980
 molecules, macroscopic solvation, electron distrib. ab initio INDO SCF calcs. 7-54099
 organic cpds. excited state H⁺ transfer, state orbital corrs. 7-13760
 oxadiazole derivatives, absorpt. spectra, expt. and quantum-chem. study 7-42488
 oxazole derivatives, absorpt. spectra, expt. and quantum-chem. study 7-42488
 perfluorovinyl radical in Ar matrix, ESR INDO MO calcs., hyperfine struct. 7-31078
 polyacetylene, solitons, electronic props., local space approx. 7-52506
 spin-spin coupling const., polarisation propagator anal., RPA CI INDO calcs. 7-49942
 triatomics, closed shell configs. SINDO method calcs. 7-19705
 triphenylmethane dyes, induced optical activity, INDO/S calcs. 7-19708
 vinylene carbonate, struct. and vibr. spectra, ab initio CNDO/2 and INDO calcs. 7-49930
 C-centres radicals, merostabilisation energy calcs. 7-30924
 Fe complex, nucleophilic attack, activation mechanism, EHT and INDO calcs. 7-39847
 Fe complex (Fe(PH₃)₃(C₆H₁₃)₃)⁺, localised INDO calcs. 7-49927
 HF, macroscopic solvation, electron distrib. ab initio INDO SCF calcs. 7-54099
 Li₂Si₇, chemical bonding, validity of formal electron counting rules 7-63544
 Li₂Si₅, chemical bonding, validity of formal electron counting rules 7-63544
 Li₂Si₅, electronic struct., INDO calcs. 7-38437
 Ni_n (n=3 and 5) clusters, spin states and magnetism quenching, MO INDO calcs. 7-62557
 Ni₃(CO)_m (M=2,4,6) clusters, spin states and magnetism quenching, MO INDO calcs. 7-62557
 Ni₅(CO)_m (m=9 and 12) clusters, spin states and magnetism quenching, MO INDO calcs. 7-62557
 Ni₄H clusters, charge distrib., Hartree-Fock SCF INDO calcs. 7-52411
 TiCl₃ crystal, electronic struct. 7-38449
- INDOR**
 see also nuclear Overhauser effect
 No entries
- induced anisotropy (magnetic)**
 amorphous films, ferromag., induced mag. anisotropy (Russian) 7-52974
 amorphous films, magnetic anisotropy field, elastic deform. effect (Russian) 7-38914
 films, amorphous, mag. anisotropy, influence of plastic deform. (Russian) 7-45660
 permalloy evaporated films, induced mag. anisotropy, thickness depend. study 7-7562
 Permalloy films, field induced uniaxial anisotropy, thickness depend. 7-53086
 (BiLu)₃(FeGa)₅O₁₂ film, magnetic bubble motion, Rayleigh surface wave effects 7-33245
 (BiYSmTbGdHoCa)₃(FeSiGe)₅O₁₂ bubble films, rare earth substitution effects 7-59095
 Co-based metallic glasses, flash annealing under stress 7-52971
 Co-Zr(Ti) amorphous films, induced anisotropy, relax. process 7-53080
 CoTi soft ferromagnetic thin films, structure-related induced anisotropy 7-45663
 Fe₃₀Co₃₀Si₁₀B₁₂, magnetic induced anisotropy, crossover effect 7-17169
 Fe_{80-x}Cr_x(SiB)₂₀ amorphous alloy, induced anisotropy, melt spinning effects (Russian) 7-59004
 γ-Fe₂O₃ sputtered thin films, CoCr-doped, stress-induced perpendicular mag. anisotropy 7-33232
 NdFeB, anisotropic permanent magnet, prep. and investig. 7-52969
 Ni, magnetic biaxial anisotropy induced by plastic deformation 7-59006
 NiCoFe ferrite, permivar, wall displacements, induced anisotropy effect 7-52968
 SmCo₅, anisotropic permanent magnet, prep. and investig. 7-52969
 (YLuBi)₃(FeGa)₅O₁₂, Ne⁺ implanted, CEMS study, stress induced magnetic planar anisotropy (Chinese) 7-7620
- inductance**
 electrostatic discs with parallel and intersecting axes, mean potentials and potential coeffs. (Russian) 7-42835

inductance continued

transducer inductance effects during seismograph calibration 7-40613
 SrTi_{0.97}Zr_{0.03}O₃ ceramics, superconducting transitions from states with low normal conductivity 7-27452

inductance measurement

multipackage induction sensing units, multifrequency, choice of package number and ang. displacement (*Russian*) 7-14962
 polyetherimide, RF elec. props., 10 kHz to 1 MHz 7-48779
 polyethylene, terephthalate, RF elec. props., 10 kHz to 1 MHz 7-48779
 polyimides, RF elec. props., 10 kHz to 1 MHz 7-48779
 standard calibration using ratio transformer unbalanced bridge 7-18833
 standards, LF models comparison 7-18834

induction, electromagnetic *see electromagnetism induction***induction heating**

see also electric furnaces; ovens
 clinical hyperthermia, VLF induced heating 7-54806
 magnetic vortex field, 2D, with boundary conditions of 3rd kind, numerical determ. for tube drawing, inductive heating (*German*) 7-33811
 metallic specimen heating in split-Hopkinson bar expts. using induction coil heaters 7-33870
 molten metal flow pattern calc. in induction furnace (*German*) 7-31729
 slab-heating square inductor vibration and acoustic analysis (*Russian*) 7-62905

induction motors

acoustic noise reduction using optimum PWM waveforms of inverter 7-20499
 photovoltaic pump powered by asynchronous machine, optimal control (*French*) 7-59839
 PWM inverter with 20 kHz switching freq. using Bi-MOS power transistors, acoustic noise 7-62934

inductor microphones *see microphones***inductors**

see also coils; power inductors; transformers
 MEATGRINDER circuit for enhanced energy transfer of inductive energy to imploding plasma loads 7-32131
 PBFA II vacuum magnetically insulated transmission line redesign to inductive energy store 7-30755
 plasma focus drivers, efficiency parameters for reactor conditions 7-63373

industrial atmospheres *see air pollution***industrial economics** *see economics***industrial plants**

heat pump utilisation in process industry evaporators 7-65420
 hot water production, roof collector model 7-3718
 hybrid heat pump appl. study 7-23213
 large-scale heat accumulation at low temp. for domestic, industrial and farm heating (*Portuguese*) 7-13931
 ultrasound technical processes, automatic output parameter regulation 7-11232
 waste heat and flat-plate collector solar heat upgrading by reversed absorption heat pump 7-65419
 water heating by low-cost shallow solar pond system 7-8443

industrial research management *see research and development management***industrial robots**

flexible US scanner for NDT 7-22970
 inspection of irradiated components from decommissioned nuclear plant 7-19420
 Manipulator Comparative Testing Program for nuclear fuel reprocessing appls. 7-49556
 photogrammetric checking 7-56369
 Savannah River DWPF, stainless steel decontamination manipulators for radwaste canisters 7-42203
 stiffness calculations for superlight industrial robots 7-22743
 ultrasonic imaging systems for robot object recognition 7-26097

industrial standards *see standards***industries**

this heading is restricted to those industries which are not covered by other specific headings
see also automobile industry; cement industry; ceramic industry; chemical industry; electricity supply industry; food processing industry; glass industry; metallurgical industries; paper industry; petroleum industry; plastics industry; textile industry
 light beam detectors for industry (*German*) 7-299

inelastic electron tunnelling spectra *see tunnelling spectra***inelastic electron tunnelling spectroscopy** *see tunnelling spectroscopy***inert anodes** *see anodes***inert gas compounds**

see also argon compounds; helium compounds; krypton compounds; neon compounds; radon compounds; xenon compounds
 alkali doped inert gas solids, matrix-bound systems, dipolar excitonic insulator transitions, mean field theory 7-45163
 diatomic dications, dissoci., detect. and charact. 7-46804
 halide cryogenic solns., UV excitation and stimulated emission 7-10645

inert gases

see also argon; helium; krypton; neon; radon; xenon
 adsorbed on metals, interadatom interactions, LEED studies 7-7014
 afterglow, step by step excitation electron distrib. 7-26572
 afterglows, electron distribution function, metastable atom+atom collision effects 7-21030
 alkali, atom-inert gas atom complexes, optical pumping, polaris. effects 7-15536
 alkali-inert gas pair diffusion cross sections, light-induced drift 7-51366
 atom+K, ⁵2P_{1/2}-⁵2P_{3/2} fine struct. mixing 7-50306
 atom+Ti, 6P_{1/2}-7P_{1/2, 3/2} two-photon line broadening and shift 7-49983
 atoms, anisotropic collisions with atoms and ions, intermultiplet mixing 7-57154
 atoms, hyperpolarizabilities, local-density approx. method 7-25630
 atoms, ionisation by CO₂ laser, nonlinearity 7-62335
 atoms, multiphoton ionisation study 7-19798
 atoms, multiple ionisation by intense laser pulse 7-62332
 atoms, physisorbed, induced dipole moment 7-52243
 basalts from Reunion and Grand Comore Islands, Indian Ocean, noble gas systematics 7-29012
 basalts of mid-ocean ridges, inert gas abundances 7-60198
 bubble precipitate solid in Al, defects, high resolution electron microscopy studies 7-32424
 clusters, mol. spectrosc. 7-42824
 cold quasistationary beam plasma, state evaluation 7-31996

inert gases continued

condensation in free jets, scaling laws, similarity relations 7-42825
 contracted discharge, ionisation waves, 2D theory 7-16343
 crystalline solids, electrostatic Madelung and cohesive energies 7-44442
 crystals, surface or bulk location of self-trapped excitons, luminesc. 7-46129
 dense plasmas, temp. and density profiles, Stark linewidth and shift 7-37752
 dimer clusters, ionis. energies, lin. correl. plot 7-25697
 dunite nodule from Reunion Island, Indian Ocean, noble gas systematics 7-29012
 field adsorption on metal surfaces 7-21648
 films, physisorbed on lamellar halides, incipient triple points 7-16722
 geochemistry of well gases in Harding County, New Mexico, USA 7-60226
 hollow cathode discharge, at. energy level excitation, laser lines 7-1804
 hydrophobic hydration, free energy, mol. dynamics study 7-46821
 implanted in solids, model of diffusion and release behaviour (*Chinese*) 7-38257
 inert gas+H⁺, electron transfer and ionis., δ -electron spectrosc. 7-42685
 inert gas atoms+H₂⁺ (D₂⁺) (N₂⁺) (C₂⁺), high Rydberg fragments, kinetic energy spectra 7-42745
 inert gas-NH₃ ion form. by electron ionisation, mass anal. ion kinetic energy spectra 7-13736
 inert gas-O₂-(SF₆) discharges, charged particle induced, O₃ synthesis 7-3587
 isotopic compositions in planetary atmospheres, effects of mass fractionation during transonic escape 7-55508
 liquefied, inherent structure, thermal disruption, mol. dynamics computer simulation 7-26612
 liquefied, viscosity and structural props. 7-6501
 long range interaction between rare gas atoms/molecules and surfaces, calc. 7-3135
 lunar highland breccias, 60018, 67435 and 67455, comp. anal. 7-55501
 Mariana Trough basalt glasses, light noble gases comp. anal. 7-40436
 metal vapour-inert gas mixture, low current steady state and periodic pulse discharge, props. 7-63379
 mixed groundwater dating, appl. of atm. inert gases corrected ⁴He 7-79044
 mixtures adsorbed on graphite and Ag, ordering and phase separation 7-21651
 moderator, transient electron longitudinal and transverse diffusion coeffs., elec. field depend. 7-6347
 multiphoton ionization in intense ultraviolet laser fields 7-19797
 noble gas metastable atoms, interaction with transition metal surface 7-64852
 pair pot., energy density functionals, Thomas-Fermi theory 7-42485
 Palo Duro Basin, Texas, USA, groundwater inert gas chemistry 7-66179
 plasma, phase transitions study 7-37633
 Ragland meteorite, LL 3.4 chondrite find from New Mexico, evidence for noble gas loss 7-9450
 shock wave instability, anomalous relaxation mechanism 7-31834
 solid, excitonic processes, book chapter 7-29610
 solid, phonons, close to melting 7-63757
 terrestrial rare gas systematics 7-60386
 trapping in C₆₀ and similar substances, possible occurrence in meteorites 7-50436
 Wethersfield (1982) chondrite, abundances of cosmogenic radionuclides and noble gases 7-34952
 D₂CO + inert gas, Coriolis enhanced vibr. energy transfer theory and its appls. 7-31153
 SR + inert gases, collisional energy transfer, time resolved fluoresc. meas., quenching cross sections 7-62497
 VO⁺+inert gases, collision-induced dissoci. studied by ion beam tandem mass spectrometer 7-23001

inertial navigation

geodetic gravity surveying using inertial navigation 7-4194
 geodetic surveying, Ferranti, Honeywell and Litton systems 7-4197
 Hamiltonian mechanics theory for inertial positioning 7-4195
 laser gyroscope reliability for inertial navigation platforms (*Italian*) 7-25860
 modified Karhunen-Loeve model of the gravity disturbance vector 7-65921
 North azimuth determination using suspended gyrocompasses 7-66309
 space vehicles, inertial navigation algorithms, for high life-to-drag vehicle during atmospheric entry 7-4289
 surveying missions over short distances, methods for high accuracy 7-4198

inertial systems

clock based on computer controlled servo-driven corotation system 7-14927

inference processes *see artificial intelligence***infinite impulse response filters** *see digital filters***infinite series** *see series (mathematics)***inflammability** *see combustion***information analysis**

see also cataloguing; classification; indexing
 climatological data banks, design and use for monthly data records 7-9178
 quantum Hall effect, publications and citations, anal. 7-48220

information analysis centres *see information centres***information centres**

remote sensing archiving systems, ERS-1 Data Centre 7-40567

information retrieval

see also information storage
 cartographic digital data utilization, electronic delivery for users of data 7-66306
 Fourier transform IR spectroscopy, spectral searching 7-48874
 thermochemical data base 7-18511

information retrieval system evaluation

material properties databases, nonbibliographic, cluster anal. 7-41026

information retrieval systems

see also bibliographic systems; information retrieval system evaluation
 molecular structure information retrieval system, microcomputer based 7-10774
 NASA Ocean Data System, computer-based online data information system 7-66307
 OEKFAK factual database on nuclear technology (*Russian*) 7-35133

information retrieval systems continued

- office information retrieval system using concepts of the AIR/PHYS physics data bank (*German*) 7-14721
- resources management master planning, GIS and remote sensing role 7-4072
- sensor database maintained by Warren Spring Laboratories 7-14933
- spectral line parameters database 7-50017
- thermophysical laboratory database formation, using pulse heat method 7-4828
- USA Water Supply Computerised Information Directory 7-66204

information services

- climatological data banks, design and use for monthly data records 7-9178
- quantum Hall effect, publications and citations, anal. 7-48220
- remote sensing, data base approach to Landsat data appls. 7-4223
- shock compression database 7-18465

information storage

- see also *information retrieval*
- archiving of X-rays: digital or analogue methods? (*German*) 7-62313
- thermochemical data base 7-18511

information storage systems see *information retrieval systems***information systems, management** see *management information systems***information technology** see *office automation***information theory**

- see also *codes; correlation theory; estimation theory; filtering and prediction theory; modulation; signal detection; signal processing; speech intelligibility; switching theory*
- canonical density matrix, derived using principle of least information 7-55929
- chaotic strange attractors for information processing 7-48578
- composite matched filtering with error correction 7-42990
- diffraction tomography reconstruction, max. entropy method 7-47256
- information and thermodynamics 7-29955
- optical quantum communication processes, mathematical model 7-10873
- C₂N₂-Ar, gaseous mixture, collision-induced absorpt., quadrupole moments, IR and microwave spectra 7-50098
- CO₂-Ar gaseous mixture, collision-induced absorpt., quadrupole moments, IR and microwave spectra 7-50098
- N₂-methane gaseous mixture, collision-induced absorpt., IR and microwave Fourier transform spectra anal. 7-50097
- N₂+O—NO+N, reaction rate const., vibr. excitation effect, information theory approx. 7-46832

information use

- climatological data banks, design and use for monthly data records 7-9178

infrared astronomical observations

- A-type stars, CNO abundances from IR lines 7-9472
- AFGL 2591, unipolar bubble in star-forming region 7-55770
- Fo Aqr (H2215-086), intermediate polar, visual and IR polarimetry rel. to origin of pulsations 7-47985
- X Ari, RR Lyr star, distance determ. via Baade-Wesselink method, photometric and spectral obs. 7-66604
- Arp 220, peculiar galaxy (IR bright), far-IR and optical observations 7-40931
- Barnard 62, Bok globule, optical and IR evidence for star form. 7-9527
- Bok globules, characts. determ. from background giants IR obs. 7-35027
- α Boo, ang. diameter and effective temp. meas. 7-14563
- 3C 273, new IR spectral component 7-4590
- 3C 446, quasar, visible and IR photometric obs. 7-35059
- η Car, dust shell internal struct. from six-channel 8 to 13 micron mapping 7-55650
- γ Cas, Be star, IRAS spectra comparison with models 7-4488
- Cas A, fast moving knot, IR spectral and photometric meas. 7-66708
- Cas A, search for stellar remnant, improved brightness limits 7-66705
- Cas A, supernova remnant, surface brightness map at 1.2 mm wavelength 7-24176
- Cepheids in Magellanic Clouds, IR photometry rel. to Cepheids intrinsic props. and Clouds spatial struct. 7-14592
- 1 Ceres, asteroid thermal emission model based on IR and diameter observations 7-40741
- Chamaeleon dark cloud, extinction and distance from JHK photometry 7-60763
- Chamaeleon T-association, extinction, distance and membership from JHK photometry 7-60763
- chemically peculiar stars, IR photometric props. 7-60670
- circumstellar dust shells around late type stars, models for IRAS obs. 7-9461
- classical novae detected in the IRAS survey 7-40829
- P/Comet Halley, (1982i), bacterial grain model for 2 to 4 μ m spectrum 7-34937
- P/Comet Halley (1982i), 3 μ m spectroscopy and photometry 7-24070
- P/Comet Halley (1982i), far-IR photometry obs. 7-18386
- P/Comet Halley (1982i), ground-based obs. of 3.2-3.6 μ m emission features 7-24071
- P/Comet Halley (1982i), JHK IR magnitudes (1986 November 16) 7-24080
- P/Comet Halley (1982i), JHK photometry and visual magnitude estimates (1987 January 28 to February 12) 7-66512
- P/Comet Halley (1982i), near IR obs. from Vega-2 spacecraft 7-14520
- P/Comet Halley (1982i), post-perihelion obs. of H₂O from KAO 7-47786
- P/Comet Halley (1982i), preperihelion IRTF monitoring program obs. 7-34931
- P/Comet Halley (1982i), spectroscopy of 3.4 μ m emission feature 7-55537
- P/Comet Halley (1982i), Vega 1 IKS IR obs. of nucleus 7-40774
- P/Comet Halley (1982i), Vega IKS IR spectrum 7-40775
- P/Comet Halley (1982i), Vega IR spectral obs. (*Russian*) 7-4376
- P/Comet Halley (1982i), Vega-2 TKS expt. obs. (*Russian*) 7-4377
- Comet Wilson (1986i), IR and visual magnitudes (1986 September) 7-9436
- comets, optical and near-IR obs. rel. to wavelength depend. of grain scatt. 7-55535
- compact H II regions, IRAS meas. 7-66695
- Crab Nebula, surface brightness map at 1.2 mm wavelength 7-24176
- R CrB, IRAS detect. and study of fossil circumstellar shell 7-55649
- R CrB stars, IRAS obs. of cool circumstellar dust 7-9495
- R CrB stars and planetary nebulae, IRAS obs. 7-66600

infrared astronomical observations continued

- CRL 618, proto-planetary nebula, H₂ S(1) line profile, wind and dust effects 7-35031
- CH Cyg, symbiotic star, broad-band multicolour photometry 7-47926
- V1016 Cyg, symbiotic star, photometric obs. rel. to dust shell form. (summer 1983) 7-47897
- V1329 Cyg, UBVRJHK photometry (1980-3) 7-29492
- dense molecular cloud cores, formyl radical and formyl ion obs. 7-48064
- diffuse galactic 380 μ m emission 7-48090
- dust clouds, activity centres, spectral study (0.3-1300 μ m) 7-48029
- dwarf novae, IR photometry rel. to ellipsoidal vars. in CW Mon, X Leo, IP Peg, and AF Cam 7-4471
- dwarf star content of elliptical and lenticular galaxies, near-IR spectra 7-60792
- E/S0 galaxies with compact radio cores, far IR excesses 7-24210
- ESO 428-G14, new Seyfert 2 galaxy, photometric and spectroscopic study 7-9538
- field horizontal-branch stars, CNO abundances from IR lines 7-9472
- G-type stars with IR excesses, IRAS survey 7-66575
- galactic and extragalactic diffuse emission study using IR photometer 7-14493
- galactic diffuse submm emission obs. 7-48091
- galactic disk, obs. from $l=-150^\circ$ to $l=82^\circ$ in sub-millimetre range 7-4558
- galactic nuclei, 3.28 μ m feature and continuum emission obs. 7-9533
- galaxies, IRAS colours 7-55813
- galaxies, narrow emission line active objects, UV to IR continuum 7-40912
- galaxies, optical and IR colour-luminosity relations for complete galaxy redshift sample 7-24213
- galaxies of IRAS minisurvey, near-IR photometry 7-40923
- P/Giacobini-Zinner (1984e), thermal IR and visual imaging 7-24073
- giants, IR spectra, detection of 12 μ m Mg I and OH absorption lines 7-24132
- Gum Nebula region T Tau stars, visible and IR characts. 7-55750
- Heiles Cloud 2, magnetic field structure from K-band polarimetry 7-60762
- AM Her, IR photometry of dwarf nova outburst 7-9485
- AH Her stars, IR photometry of secondary star in two systems 7-9514
- HH 1-23 exciting star, nature of IR emission from JHKL photometry 7-60661
- interstellar C I, 809 GHz fine-structure line obs. in dense mol. clouds 7-66717
- interstellar H₂ 2 μ m emission in star-forming clouds, S(1) line mapping rel. to shock waves and jets 7-55760
- interstellar H₂ line emission from centre of Galaxy, spatial distrib. and vel. field 7-9528
- interstellar molecules, IR spectroscopy 7-14638
- IRAS 00193-4033, 22231-4529, O-rich unidentified IRAS sources, optical and IR obs. 7-55853
- IRAS 1912+172P09, new binary planetary nebula, spectroscopy and JHKL photometry 7-48046
- IRAS Circular No.9 sources, OH/IR star candidates, IR photometry 7-66786
- IRAS galaxies, sub-millimetre obs. 7-9532
- IRAS sources, two-dimensional covariance function determ. 7-14677
- IRAS sources assoc. with mol. outflows, far-IR luminosities 7-55766
- IRC +10420, post AGB star, mass-loss region, circumstellar environment and atm. characts. 7-66583
- Jupiter, water vapour abundance and distrib. in atmosphere, IR obs. 7-60594
- L1551 IRS 5, IR polarimetry of nearby refl. nebula 7-24186
- L1551 IRS 5, obs. of extended far-IR emission assoc. with mass outflow from young star 7-66715
- late-type stars, obs. of He I 1083 nm chromospheric line in bright stars 7-55612
- LDN 1642, high-latitude cloud, IRAS mapping, visible surface brightness and extinction 7-48062
- LMC X-3, UV obs. and V, JHK photometry 7-55715
- luminous red giant stars, circumstellar dust and gas props. from IRAS and mol. obs. 7-55609
- RU Lup, RW Aur star, multifrequency obs. 7-47866
- M175SW, molecular cloud, CO submm mapping 7-60748
- M82, interstellar medium in central 1 kpc of active galaxy 7-55816
- M83, near-IR photometry characts. 7-60802
- M8 E, IR spectrum obs. rel. to evidence for circumstellar CO 7-48040
- M-type dwarf stars, photometry and spectra rel. to chromospheric activity, kinematics, and metallicities 7-9466
- main sequence A and B-type stars, IR photometry 7-34976
- molecular clouds in outer Galaxy, far-IR characts. and star form. 7-66709
- Mon R2 star form. region, IR sources and polarisation obs. 7-60753
- MWC 349, velocity-resolved IR spectroscopy 7-60683
- Neptune, occultation determ. of oblateness and chromospheric methane mixing ratio 7-34927
- Neptune, submillimetre and millimetre observations 7-24063
- NGC 1333 (HH12), star-forming cloud, obs. of shocked H₂ and interstellar jets 7-55760
- NGC 2024 - IRS 2, H I Br α and γ line studies of wind 7-40799
- NGC 2071 star-forming cloud, obs. of shocked H₂ and supersonic jets 7-55760
- NGC 2798, interacting galaxy, IR and UV obs. rel. to starburst in galactic nucleus 7-55830
- NGC 3256, merging galaxy, IR and UV obs. rel. to starburst in galactic nucleus 7-55830
- NGC 4151, broad-band study (γ -ray to IR) 7-60791
- NGC 4833, globular cluster, red giants IR photometry 7-60740
- NGC 6240, far IR spectra of luminous interacting galaxy 7-40932
- NGC 6357, H II region, IR obs. rel. to star form. 7-48009
- NGC 7293 (Helix Nebulae), IRAS flux densities 7-66699
- Nova Cen 1986, discovery, position, magnitudes, photometry, prenova identifications 7-24146
- Nova Cen 1986, IR photometry rel. to dust shell form. (1986 December 30 to 1987 January 5) 7-47913
- Nova Cyg 1986, IR and visible obs. (1986 August to September) 7-9481
- Nova Cyg 1986, spectra and magnitude estimates 7-18409
- Nova Vul 1984 No.1 (PW Vul) slow nova, abundances, visible and IR obs. 7-40850
- NRAO 140, quasar, visible and IR photometric obs. 7-35059
- OB supergiant stars, visible and IR continuum spectropolarimetric obs. 7-47845

infrared astronomical observations continued

- OJ 287, BL Lac-type object, IR variability since 1983 outburst 7-48080
 V2051 Oph, IR and optical photometry of eclipsing dwarf nova 7-55670
 V2051 Oph, structure and variability of cataclysmic binary 7-18423
 ρ Oph dark cloud, multi-freq. obs. 7-48024
 α Ori, outer atm. and circumstellar material characts., far-IR spectral obs. 7-60690
 FU Ori stars, evidence for disk accretion IR spectral obs. 7-66581
 Orion Molecular Cloud 1, IR polarisation obs. and discovery of H₂ refl. nebula 7-14633
 Orion Molecular Cloud 2, IR refl. nebulae obs. 7-55765
 Orion Nebula, ionization structure, IR line obs. and models 7-60757
 OX 169, quasar, visible and IR photometric obs. 7-35059
 2 Pallas, asteroid thermal emission model based on IR and diameter observations 7-40741
 IP Peg, near-IR spectroscopy and photometry 7-66619
 II Peg, RS CVn star, 1986 JK photometry and light curves 7-4515
 GK Per (=Nova Per 1901), IR magnitudes of outbursts 7-40844
 PKS 0537-441, multifreq. obs. of blazar in moderately active state 7-55811
 planetary nebulae, identification of misclassified objects from red and near-IR photometry 7-4542
 Pleiades, interstellar dust grains IRAS obs. 7-48003
 pre-main sequence, CO band heads emission 7-66584
 pre-main-sequence stars in Bok globule Barnard 62, optical and IR obs. 7-9527
 reflection nebula near molecular outflow sources, 1 μ m CCD study 7-66696
 Shapley-Ames elliptical galaxies, interstellar dust content from IRAS obs. 7-66758
 Sharpless 140, unipolar bubble in star-forming region 7-55770
 SN 1987A in LMC, optical spectra, radiobrightness and double nature of progenitor 7-66634
 SN 1987A in LMC, photometric and spectral obs. (1987 February 24-26) 7-66632
 SN 1987A in LMC, photometry and spectral characts. (1987 February) 7-66640
 SN 1987A in LMC, progenitor position, photometry, and polarization 7-66631
 SN 1987A in LMC, spectral evolution (1987 Feb. 25-Mar. 1) 7-66641
 solar submillimetre limb brightness profile, appl. to chromospheric modelling 7-55590
 solar-type protostars in nearby mol. cloud cores, IRAS candidates 7-47853
 spectroscopy of point sources and extended objects at high dispersion using echelle/CCD spectrograph 7-66474
 star formation regions, far IR, submm and mm dust emission spectra 7-24180
 sub-millimetre/far-IR emission from warm and cold dust clouds, observational review 7-48022
 Sun, CO vibr.-rot. bands obs. rel. to ¹²C/¹³C and ¹⁶O/¹⁸O ratios in photosphere 7-55598
 Sun, magnetic flux diagnostics using Fe I 1564.854 nm line 7-66531
 symbiotic stars, IRAS observations and energy fluxes 7-34984
 Y Tau, C star, effective temp. from occultation and spectroscopic obs. 7-47927
 Uranus, methane-d, detect. at 1.6 μ m wavelength 7-55529
 Uranus, submillimetre and millimetre observations 7-24063
 Ursa Major I(S) group galaxies, ¹²CO and far-IR obs. 7-29548
 Van Biesbroeck 8, IR speckle interferometry rel. to binary nature 7-66587
 Vega-like stars from IRAS point-source catalogue, IR photometry 7-4456
 Virgo Cluster, dwarf irregular and elliptical galaxies, comparative photometric parameters 7-35053
 young supernova remnants, shock-heated dust obs. rel. to remnant struct. and dynamics 7-55754
 OH-IR stars, IRAS obs. rel. to determ. of absolute luminosities and mass loss rates 7-29475
 OH-IR stars near galactic centre, luminosities and progenitor characts. 7-14584

infrared astronomy

- see also *infrared sources (astronomical)*
 2D detector array, microcomputer-based data acquisition 7-9382
 adaptive flexible mirror, IR background speckle noise 7-55467
 atomic data for astrophysics, collisional data for IR fine-struct. transitions 7-40689
 blackbody source of variable temperature, for use in IR astronomical radiometry 7-40713
 Cagliari Astronomical Observatory, Sardinia, atmospheric water vapour contents rel. to IR astronomy 7-40547
 calibrator for low background infrared bolometers 7-9899
 1 Ceres, asteroid thermal emission model based on IR and diameter observations 7-40741
 P/Comet Halley (1982), dust IR characts. 7-18385
 P/Comet Halley (1982), IR heating of cometary atmosphere 7-34933
 cometary dust studies using ground-based near-IR obs. (Chinese) 7-18357
 common-user submm receiver for UKIRT and UK-NL telescopes 7-34883
 cryogenic optical systems and instruments, conference, Los Angeles, California, (January 1986) 7-24283
 deconvolution method for photometric and spectroscopic obs., theory and appl. 7-4348
 Fabry-Perot multichannel spectrometer 7-55474
 Far Infrared Space Telescope (FIRST), high precision composite sandwich antennas anal. 7-24012
 Far Infrared Submillimetre Space Telescope mission 7-34866
 FIR photometer, improved design 7-14492
 FIRST mission, general outline 7-60508
 FIRST telescope, active optics and spectral range extension in IR 7-60553
 five-band differential IR photometer for balloon-borne observations of diffuse sky radiation 7-14493
 galactic IR absorption var. with latitude 7-48089
 Galaxy, IR radiation characts., implications for existence of very small dust particles 7-24209
 giant planets, atm. study in submm range with FIRST 7-47743
 high-velocity clouds, search for dust, IR emission search 7-40893

infrared astronomy continued

- instrumentation and techniques, conf., Tucson, AZ, USA (March 1986) 7-48162
 instruments and observational possibilities (Japanese) 7-60546
 interplanetary dust, IR and visible obs. anal. 7-47762
 interstellar chemistry and submm astron. 7-48060
 interstellar grains emission, radiative transfer rel. to grain models 7-48013
 interstellar IR silicate bands, exptl. investigations rel. to silicate dusts identification 7-48017
 interstellar submm mol. transitions 7-47698
 Io, ground-based IR obs. anal. 7-34916
 IRAS data, availability and use at Leiden and results 7-47733
 Jupiter, NH₃ abundance and cloud opacities determ. from Voyager IRIS data 7-24051
 Jupiter, upper troposphere, zonal mean characts., Voyager IR obs. anal. 7-24052
 Large Deployable Reflector, characts. 7-60555
 Large Deployable Reflector System concept 7-29399
 Mars atmosphere remote sensing using IR pressure modulation and filter radiometry 7-47747
 molecular astrophysics, NATO conf., Bad Windsheim, Germany (1984 July) 7-9589
 molecular ions, ultrasensitive IR laser studies 7-14490
 Mount Graham Submillimetre Telescope project 7-60554
 2 Pallas, asteroid thermal emission model based on IR and diameter observations 7-40741
 planetary spectra, Gaussian anal. of temp. effects on 1- μ m refl. spectra of mafic minerals 7-29006
 planetary systems, search methods, role of IR astronomy 7-55722
 Saturn, Cassini mission near-IR objectives 7-40755
 SETI, laser signals search from nearby stars 7-34889
 SIRTf, a cryogenically cooled IR telescope 7-34873
 SIRTf, dynamic optical deformations of chopping secondary mirror 7-24008
 solar submillimetre limb brightness profile, appl. to chromospheric modelling 7-55590
 solid-state imaging arrays, conf., San Diego, CA, USA (Aug. 1985) 7-29582
 spacelab-2 experiments 7-23973
 speckle interferometry, 1D system 7-55488
 spectral signatures of refractory grain processing in circumstellar shells, theory 7-55611
 sub-millimetre/far-IR emission from warm and cold dust clouds, observational review 7-48022
 submm astronomy (in 1990s) 7-47736
 submm laser system for local oscillator use in heterodyne receiver 7-34869
 subMM transparency of atm. at Antarctic station Vostok (Russian) 7-23822
 UC Berkeley submm heterodyne receiver for spectroscopy 7-34879
 UKIRT mm and submm receivers 7-34880
 C fibre reinforced sandwich panels for far-IR telescope mirrors, thermal stability tests 7-40705
 CO 2.3 μ m band synthesis in supergiant stars, appl. to band strengths interpretation in Magellanic Cloud stars 7-66577
 InSb array IR imaging camera, for astronomical appls. 7-34865
 InSb charge injection device arrays, IR camera for astronomical imaging 7-34872
 Mg IV forbidden lines, electron impact excitation rate coeffs. for Mg³⁺ 7-55455
 Mg V forbidden lines, electron impact excitation rate coeffs. for Mg⁴⁺ 7-55455
 OH, laboratory meas. of rot. spectrum with tunable far-IR radiation 7-47691
 Si:Bi hybrid array for photometric near-IR spectrometer 7-30103

infrared communication see optical communication**infrared detectors**

- see also *bolometers; photodetectors*
 2I-He hybrid cryostat for 690 GHz InSb bolometer 7-30024
 black-body radiation densities estimation 7-4890
 calibrated thermal imagers, laboratory characterisation 7-24703
 calibrator for low background infrared bolometers 7-9899
 camera with hybrid 32x32 HgCdTe CCD array for astronomy 7-60560
 chalcogenide fibres development and appls. 7-20456
 cold radiation shield design for linear detector array 7-35592
 common-user submm receiver for UKIRT and UK-NL telescopes 7-34883
 computerised IR spectroradiometer, capabilities and appls. 7-30063
 conference, Cannes, France (Nov. 1985) 7-35093
 conference on IR technology and appls., Cannes, France (Nov. 1986) 7-29589
 directions-of-arrival estimation in IR detector arrays, eigenstructure approach 7-56334
 dual waveband imaging radiometer 7-6020
 EM fields, infrared measurements of scattering and electromagnetic penetration through apertures 7-56336
 emissivity distrib. of nonuniform materials meas., NPL thermal imaging facility 7-4849
 far-IR detectors cooling technology (Japanese) 7-56340
 far-IR photoconductive detectors, optical efficiency 7-35513
 FIR heterodyne detectors, review 7-35596
 FIR photometer, improved design 7-14492
 FIR science and technology, conf., Quebec, Canada (June 1986) 7-35095
 five-band differential IR photometer for balloon-borne observations of diffuse sky radiation 7-14493
 heteroepitaxial IV-VI infrared sensors on Si substrates with fluoride buffer layers 7-41468
 ideal bolometer, background power effect on performance 7-56344
 III-V semiconductor, strained layer superlattice research developments 7-52766
 imaging system design, image anomalies avoidance issues 7-11173
 infrared detection and imaging, review 7-56260
 linear pyroelectric array IR sensor 7-30089
 long-wavelength components by VPE 7-46343
 measurement and appls. of IR radiation (Japanese) 7-347
 meteorological satellite, radiometers, IR detectors and their calibration 7-23898
 modulation doped extrinsic semiconductor IR detector, charge distrib., response time 7-61376

infrared detectors continued

- MOVPE, atm. press. growth, operating characts. 7-27930
 NDT of materials, subsurface control by photothermal radiometry 7-33898
 p-i-n diode structures, low gap, Auger suppression and negative resist. 7-12812
 passive radiator for cooling IR detectors in geostationary orbit 7-18878
 photodiodes for 3 to 14 μm , comparison 7-41466
 photothermal radiometer for concentrated sunlight intensity measurements 7-23919
 polymer films, pyroelectric behaviour for IR detection 7-7644
 pyrodetector responsivity for harmonic and pulse modulation of IR radiation (*Slovak*) 7-9897
 pyroelectric detection of laser radiation 7-56341
 pyroelectric detector and imaging developments 7-24702
 pyrometer, thermodynamic temp. meas. between 683K and 933K 7-18788
 quantum well photodetectors, fast response 7-30085
 quartz miniature resonator thermal detector 7-349
 radiothermometer, S/N ratio and sensitivity equations 7-18782
 sampled data systems, MRTD estimation 7-5853
 semiconductor infrared detectors, conf., Innsbruck, Austria (April 1986) 7-60871
 semiconductor IR detectors, non-equilibrium modes of operation 7-9898
 semiconductor radiation detectors and diode lasers appl. 7-15865
 semiconductor radiative lifetime for IR detect. 7-35591
 sensor material, characts. (*Japanese*) 7-56339
 Shuttle Orbiter leeside surface IR imagery, during atmospheric entry, comprehensive analysis 7-29378
 SIRTf, a cryogenically cooled IR telescope 7-34873
 sodium salicylate as combined fluoresc./refl. coating for broad band detector (*German*) 7-4891
 solid state image sensors and their appls., conf., Cannes, France (Nov. 1985) 7-24288
 solid-state imaging arrays, conf., San Diego, CA, USA (Aug. 1985) 7-29582
 SPRITE based thermal imagers, anamorphic detector optics 7-35595
 streak camera for use in 1.0 to 1.6 μm region 7-18896
 submm heterodyne detection system for atm. phys. and astronomy 7-60562
 technology and appls., conf., San Diego, CA, USA (Aug. 1985) 7-18487
 temperature meas. using infrared detectors (*Russian*) 7-4889
 temperatures near ambient, measurement using infrared fibre-optic cable system 7-14945
 thermal IR multispectral scanner, airborne instrument for mineral deposits detection 7-14393
 UC Berkeley submm heterodyne receiver for spectroscopy 7-34879
 UKIRT mm and submm receivers 7-34880
 voltage controlled tunable IR detectors using MIM structures 7-61377
 zoom telescope development 7-31425
 AlGaAs injection heterolasers and integrated laser-photodetector pairs, prepared by microcleaving 7-31343
 Au-InP high-speed internal photoemission detectors enhanced by grating coupling to surface plasma waves 7-52688
 CdHgTe, CO_2 laser detection appl. 7-5915
 CdHgTe focal plane arrays, sampling effects reduction 7-30090
 Cd_{1-x}Hg_xTe IR heterodyne detectors, intermediate temp. operation 7-35594
 Ga_{0.2}In_{0.72}As/Al_{0.25}In_{0.72}As photodiode heterostructures, atm. press. MOCVD, 2 μm , sensitivity, structural charact. 7-27933
 Ge, avalanche photomultiplication in the far infrared 7-45375
 Ge_{1-x}Si_x-Si strained-layer heterostructure, transport, optical props. and appls. 7-7349
 HgCdTe focal plane array photodetectors, growth, performance and array fabrication 7-15001
 HgCdTe, high quality LPE on CdZnTe, IR detector anal. 7-64941
 HgCdTe IR CCD coupling structure for space appls. 7-29309
 HgCdTe IR detectors, epitaxial growth of CdZnTe substrate 7-64926
 HgCdTe IR photodetectors, magnetoresist. and cyclotron resonance characterisation 7-64054
 HgCdTe photoconducting detector design for IR imaging 7-9900
 HgZnTe bulk crystals, travelling heater method growth and charactn., 10 μm detect. wavelength 7-59387
 InAs_{0.3}Sb_{0.7} IR detector, photoresponsivity meas. 7-7274
 InGaAs/InP photodiodes, MOCVD growth and characts. 7-27932
 InGa_{1-x}As_xSb_{1-y}, mid-IR source and detector material 7-36964
 InP, radiation-damaged photocond., Hertzian dipole meas. of picosecond photoresponses 7-52690
 InP/GaInAs/InP heterostructures, OMVPE, high speed p-i-n photodiodes, photolum., Hall meas. 7-27387
 InP/InGaAs near-IR detector self-calibration feasibility determ. 7-15002
 InP/InGaAs:Zn, PIN detectors, OMVPE growth 7-27931
 InSb array IR imaging camera, for astronomical appls. 7-34865
 InSb charge injection device arrays, IR camera for astronomical imaging 7-34872
 (Pb,Sn)Se IR detector arrays, heteroepitaxial growth on fluoride-covered Si substrates 7-39429
 Pb_{1-x}La_xTi_{1-x/4}O₃ thin film pyroelectric infrared sensors 7-56338
 PbTe IR detector arrays, heteroepitaxial growth on fluoride-covered Si substrates 7-39429
 Si p⁺-n junction, superlinear response in IR spectral region (*Chinese*) 7-52751
 Si p-i-n diode, spectral information coding by IR photoreceptors, colour vision analogue 7-35593
 Si:Bi hybrid array for photometric near-IR spectrometer 7-30103
 W-Ni MIM diode as difference frequency IR detector, long-term stability 7-24700

infrared imaging

- aspherical components fabrication, diamond turning with MOORE machine 7-31539
 boiler tube NDT inspection systems 7-20549
 calibrated thermal imagers, laboratory characterisation 7-24703
 cellulose acetate, corona charged, electrothermographic characteristics 7-61391
 chalcogenide fibres development and appls. 7-20456
 coatings development, appl. and testing, with diamond-like props. 7-31434
 composites, thermography makes progress in NDT (*French*) 7-39831
 computerised axial tomography, appl. of IR scanners and inverse heat conduction methods 7-48731

infrared imaging continued

- conference on IR technology and appls., Cannes, France (Nov. 1986) 7-29589
 design of IR imaging systems, critical issues 7-50673
 dual waveband imaging radiometer 7-6020
 electronic materials and their microstructure, thermal wave imaging studies 7-8237
 emissivity distrib. of nonuniform materials meas., NPL thermal imaging facility 7-4849
 far-focus thermal imager system, deep-focus attachment 7-30061
 FIRST telescope, active optics and spectral range extension in IR 7-60553
 focal plane arrays, sampling effects reduction 7-30090
 geophysical prospecting optoelectronic meas. of mineral content (*Russian*) 7-9241
 hillside far IR imaging at 300 metres range, radiance statistics versus ground resolution 7-4035
 image anomalies avoidance issues 7-11173
 imaging optics for the dual-field IR scanner 7-50706
 infrared detection and imaging, review 7-56260
 internal imperfections, NDE, thermal flux method (*German*) 7-13718
 laboratory assessment of camouflage materials effectiveness in the thermal IR 7-4850
 laser beam profile meas., by thermographic technique 7-31377
 lightweight composite mirrors for IR astronomy 7-57519
 linear pyroelectric array IR sensor 7-30089
 material stress inspection by digital thermographic image processing 7-33896
 measurement and appls. of IR radiation (*Japanese*) 7-347
 medical thermogram processing system using a microcomputer (*Chinese*) 7-28643
 medical thermography, review 7-60070
 metals, void detection, thermography appl. 7-28256
 meteorological IR satellite, optical design of imaging system 7-55321
 meteorol. IR meas., surface and cloud-top temp. determ. atmospheric correction scheme 7-18310
 monochromator with concave diffraction grating, spread function determ. 7-50725
 mylar, ultrasonically excited thin sheet, depth-depend. 2D thermal-wave source profiling 7-48725
 NDT of materials, subsurface control by photothermal radiometry 7-33898
 nondestructive evaluation, thermal-wave imaging 7-46754
 passive radiator for cooling IR detectors in geostationary orbit 7-18878
 performance assessment, improved minimum resolvable temp. difference system 7-34154
 performance assessment of thermal imaging system 7-30091
 performance meas. of thermal imager, objective meas. of minimum resolvable temp. difference 7-30092
 plasma spraying obs. 7-24648
 plates and rings, SPATE stress studies under in-plane loading 7-63086
 polygonal scan wheels, geometrical relationships 7-50707
 pulse video thermography appl. to subsurface structures obs. 7-33899
 push-broom linear array scanner, design of all-reflective flat-field objective 7-55320
 pyroelectric detector and imaging developments 7-24702
 sampled data systems, MRTD estimation 7-5853
 satellite image processing, kinetic temp. image modelling 7-23899
 scanned local thermal-wave probing for nondestructive testing 7-46766
 scanner lens design considerations 7-50704
 semiconductor infrared detectors, conf., Innsbruck, Austria (April 1986) 7-60871
 Shuttle Orbiter leeside surface IR imagery, during atmospheric entry, comprehensive analysis 7-29378
 SIRTf, a cryogenically cooled IR telescope 7-34873
 snow, IR meas. of grain size and melting degree 7-23719
 solid-state imaging arrays, conf., San Diego, CA, USA (Aug. 1985) 7-29582
 spectral emittance meas. 2 to 20 μm 7-30104
 SPRITE based thermal imagers, anamorphic detector optics 7-35595
 stress analysis appl. 7-31723
 stress analysis of randomly loaded structures 7-31724
 stress meas. in semiconductor materials and components, photoelasticity determ. 7-31725
 surface features, thermal wave imaging studies in a SEM 7-44874
 technology and appls., conf., San Diego, CA, USA (Aug. 1985) 7-18487
 temperature meas. using infrared detectors (*Russian*) 7-4889
 temperature of atmosphere, estimation from remotely sensed IR data, physical models (*Japanese*) 7-18316
 testing and evaluation of thermal optical systems, two-level process 7-31431
 thermal camera without liquid N₂ coolant (*Swedish*) 7-35514
 thermal IR multispectral scanner, airborne instrument for mineral deposits detection 7-14393
 thermogrammetry and thermal engineering conf., Budapest, Hungary (April 1987) (*Hungarian*) 7-56258
 thermographic methods applied to industrial materials 7-46750
 thermography, video images, digital enhancement techniques 7-65272
 thin plate two-dimensional diffusivity tensor meas. by thermal pattern analysis 7-2285
 time-resolved derivation of heat fluxes from quantitative infrared thermography and its relationship to photoacoustics 7-44210
 tomographic analysis of the evolution of plasma crosssections 7-1741
 tracing the thermic symptom of radiation injuries by infrared image forming (*Hungarian*) 7-60030
 two-wavelength IR-thermography, subresolution meas., accuracy 7-4239
 vision systems for biomedical use, calibration from thermal emissivity standards 7-60117
 welding seams, photothermal nondestructive radiometric eval. 7-46752
 zoom converter with focusing and thermal compensation functions 7-31516
 zoom lens for thermal cameras and video equipment (*Japanese*) 7-57515
 zoom lens tolerances and design concepts 7-31426
 zoom telescope development 7-31425
 GaAs semiinsulating slices, spatial inhomogeneities, near IR transmission imaging techniques 7-33400
 Ge lenses, diamond-machine for IR, quality and performance 7-25932
 HgCdTe photoconducting detector design for IR imaging 7-9900
 InSb array IR imaging camera, for astronomical appls. 7-34865

infrared imaging continued

- InSb charge injection device arrays, IR camera for astronomical imaging 7-34872
 SF₆ gas, infrared radiation wavefront inversion, thermomagnetic image recording 7-43245

infrared-infrared double resonance *see optical double resonance***infrared laser effects** *see laser beam effects***infrared-microwave double resonance** *see microwave-optical double resonance***infrared-radiofrequency double resonance** *see magnetic double resonance; optical double resonance***infrared radiometers** *see radiometers***infrared sources**

- ATF, FIR interferometer, development of high power FIR lasers 7-11757
 blackbody radiant source, low temp. large area, with heat pipe (*Chinese*) 7-50923
 blackbody source, of variable temperature, for use in far-IR astronomy 7-40713
 calibration of IR emitters, using K-100 IR comparator 7-35564
 FIR spectroscopy by synchrotron radiation at UVSOR facility 7-41498
 FTIR/time resolved spectrometry, rapid scan, for gas phase systems, IR source development 7-48879
 heating physical considerations (*Spanish*) 7-16057
 high-power, twin-frequency FIR lasers for plasmadiagnostic applications 7-11751
 irradiance calc. in D* determ., precision improvement (*Chinese*) 7-48825
 methanol pumping sources, differ free stabilisation using absorption cell 7-11756
 multiwavelength linearized diode laser spectra by overlapping frequency scans 7-41492
 particle beams use in radiation generation from IR to γ -rays 7-42877
 photometer calibration, stable source of IR radiation 7-56317
 AlGaAs/GaAs heterointerface solid-state far IR emitter utilising 2D plasmon 7-53414
 AlGaAs/GaAs selectively doped heterointerface under high elec. field appl., 2D plasmon 7-52637
 CO₂ waveguide laser as tunable IR radiation source 7-31298
 p-Ge, solid-state radiation source for submillimeter and far IR waves 7-37079

infrared sources (astronomical)*see also BL Lac-type objects; OH-IR stars*

- active dwarf galaxies, star formation rates and efficiency 7-55806
 AFGL 2591, unipolar bubble in star-forming region 7-55770
 δ And (K3 III), IRAS source with unusual UV spectrum, IUE obs. 7-55623
 V1302 Aql. (IRC+10420), supergiant OH-IR star, new emission features obs. 7-48101
 Arp 220, peculiar galaxy (IR bright), far-IR and optical observations 7-40931
 B335, Bok globule, obs. of cyanoacetylene emission assoc. with far-IR source 7-18448
 Barnard 335, dense mol. cloud, internal sources characts. 7-14625
 Barnard 62, Bok globule, optical and IR evidence for star form. 7-9527
 Becklin-Neugebauer objects, circumstellar dust shells around very young and massive stars 7-48026
 Becklin-Neugebauer objects, evolution and structure 7-48028
 brown dwarf stars, astrophysics, symposium, Fairfax, Virginia (October 1985) 7-18
 brown dwarf stars, evolution and IR spectra 7-29472
 3C 273, new IR spectral component 7-4590
 3C 273, quasar, particle accel. in jet hotspot rel. to radio to IR spectrum 7-14676
 3C 273, quasar, submm continuum characts. 7-48099
 3C 273 jet, swinging relativistic plasma beam model 7-66783
 η Car, dust shell internal struct. from six-channel 8 to 13 micron mapping 7-55650
 η Car, grain size and geometrical effects in dust shell rel. to 8-13 μ m feature 7-9494
 η Car, UV spectrum obs. 7-47942
 η Car, visual features and IR emission characts. 7-60769
 γ Cas, Be star, IRAS spectra comparison with models 7-4488
 Cas A, fast moving knot, IR spectral and photometric meas. 7-66708
 Cas A, supernova remnant, 1.2-mm map rel. to synchrotron and IR spectra 7-24176
 circumstellar dust shells around late type stars, models for IRAS obs. 7-9461
 circumstellar shells, diagnostic IR signatures of refractory grain processing in circumstellar shells 7-55611
 circumstellar shells, SO₂ and SO emission obs. 7-4429
 classical novae detected in the IRAS survey 7-40829
 Cn1-1, planetary nebula, dust and central star characts. 7-35019
 compact H II regions, IRAS meas. 7-66695
 Crab Nebula, 1.2 mm map rel. to synchrotron and IR spectra 7-24176
 R CrB, IRAS detect. and study of fossil circumstellar shell 7-55649
 R CrB stars, IRAS obs. of cool circumstellar dust 7-9495
 CRL 618, proto-planetary nebula, H₂ S(1) line profile, wind and dust effects 7-35031
 V1057 Cyg, circumstellar dust nature and existence, photometric anal. 7-4463
 V1016 Cyg, symbiotic star, photometric obs. rel. to dust shell form. (summer 1983) 7-47897
 V645 Cyg-Duck Nebula complex, characts. and obs. 7-60655
 dwarf stars, radii determ. from IRAS 12 μ m fluxes 7-60644
 E/SO galaxies with compact radio cores, far IR excesses 7-24210
 Egg Nebula (CRL 2688), IR source characts. 7-4540
 emission nebulae, implications of atomic data for astrophysics for element abundances 7-40689
 evolved stars, circumstellar shells, FIRST obs. possibilities 7-47891
 evolved stars, circumstellar shells, molecular abundances and processes, submm astronomy 7-47892
 FIRST observational potential 7-48093
 G-type stars with IR excesses, IRAS survey 7-66575
 galactic bulge, IRAS point sources characts. 7-47733
 galactic disk, obs. from $l=-150^\circ$ to $l=82^\circ$ in sub-millimetre range 7-4558
 galactic nuclei, 3.28 μ m feature and continuum emission obs. 7-9533
 galactic nuclei, high-mass stars formation due to cloud-cloud collisions 7-55610
 galaxies, IRAS colours 7-55813
 galaxies of IRAS minisurvey, near-IR photometry 7-40923
infrared sources (astronomical) continued
 general characts. (*French*) 7-29555
 H₂O masers search 7-4539
 He 2-104, He 2-106, symbiotic stars, spectrophotometric obs. of emission lines 7-9477
 Herbig Ae/Be stars, envelopes dust IR excess and H₂O absorpt. 7-4473
 HH 1-23 exciting star, nature of IR emission from JHKL photometry 7-60661
 high-mass loss rate stars, projected FIRST obs. 7-47842
 IC 443, supernova remnant, multiwavelength investigation 7-40896
 interstellar cirrus, distances 7-35022
 interstellar dust clouds, sub-millimetre/far-IR emission from warm and cold clouds 7-48022
 interstellar grains emission, radiative transfer rel. to grain models 7-48013
 interstellar H₂ 2 μ m emission in star-forming clouds, S(1) line mapping rel. to shock waves and jets 7-55760
 interstellar H₂ line emission from centre of Galaxy, spatial distrib. and vel. field 7-9528
 interstellar molecular clouds, C I fine-structure line obs. at 809 GHz 7-66717
 interstellar sources, submm obs. 7-48058
 IR 1017+08, galaxy, OH maser emission obs. 7-29539
 IRA 03134+5958, optical identification as possible Herbig-Haro object 7-66720
 IRAS 00193-4033, 22231-4529, O-rich unidentified IRAS sources, optical and IR obs. 7-55853
 IRAS 00275-2859, identification as quasar, spectral characts. 7-18462
 IRAS 16293-2422, NRAO 245 GHz obs. of protostellar cloud 7-14561
 IRAS 1629-2422, protostellar source, structure resolved in EHF 7-55621
 IRAS 1912+172P09, new binary planetary nebula, spectroscopy and JHKL photometry 7-48046
 IRAS Circular No.9 sources, OH/IR star candidates, IR photometry 7-66786
 IRAS deep field sources, radio counterparts 7-48102
 IRAS galaxies, sub-millimetre obs. 7-9532
 IRAS galaxies of very high lumin., ages and star form. characts 7-66767
 IRAS low resolution spectra atlas 7-24021
 IRAS low-temp. unidentified print sources, ¹³CO and ¹²CO obs. 7-48006
 IRAS sources, Nancy obs. of assoc. OH circumstellar masers 7-34978
 IRAS sources, two-dimensional covariance function determ. 7-14677
 IRAS sources assoc. with mol. outflows, far-IR luminosities 7-55766
 IRAS sources in mol. clouds, search for H₂O masers 7-35066
 IRC+10216, ²⁹SiC₂ and ³⁰SiC₂ detect. in millimetre-wave spectrum 7-29474
 IRC+10216, brightness distrib. at various wavelengths, radiative transfer in shell 7-60520
 IRC 1 in M17, bipolar outflow source and nebosity, spectral characts. 7-60748
 IRC+10420, post AGB star, mass-loss region, circumstellar environment and atm. characts. 7-66583
 IRS 16 NW+object A in Sgr A* direction, interpretation 7-40959
 L1551 IRS 5, IR polarimetry of nearby refl. nebula 7-24186
 L1551 IRS 5, obs. of extended far-IR emission assoc. with mass outflow from young star 7-66715
 L1551 IRS 5, VLA obs. of assoc. 4.8 GHz H₂CO transition 7-60765
 L 1551 bipolar flow, extended IR radiation 7-40890
 LDN 1551, bipolar nebula IR emission characts. 7-48061
 LDN 1551-IRS 5, circumstellar CO abundance characts. 7-47893
 LDN 1642, high-latitude cloud, IRAS mapping, visible surface brightness and extinction 7-48062
 LDN 723, dense mol. cloud, internal sources characts. 7-14625
 luminous red giant stars, circumstellar dust and gas props. from IRAS and mol. obs. 7-55609
 RU Lup, RW Aur star, multifrequency obs. 7-47866
 Lynds 1457, nearest mol. cloud, discovery of assoc. hard X-ray source (H0253+193) 7-66789
 M83, near-IR photometry characts. 7-60802
 M8 E, IR spectrum obs. rel. to evidence for circumstellar CO 7-48040
 M-type giants and supergiants, shell and mass loss characts., CO obs. 7-60649
 Markarian 231, Seyfert 1 galaxy, morphology and nuclear spectroscopy 7-48067
 Markarian 231, Seyfert galaxy/QSO, CO (J=1-0) emission detect. and optical imaging 7-66757
 Markarian galaxies, catalogue 7-55496
 massive protostars, temp. struct. in accretion flows rel. to emergent IR radiation field 7-29471
 molecular clouds in outer Galaxy, far-IR characts. and star form. 7-66709
 Mon R2 star form. region, IR sources and polarisation obs. 7-60753
 MWC 349, velocity-resolved IR spectroscopy 7-60683
 nearby stars with IR excesses, catalogue rel. to search for planetary systems 7-66480
 nebulae, O and N abundances determ. from far-IR emission-lines 7-40722
 NGC 1275, Seyfert galaxy, submm continuum characts. 7-48099
 NGC 1333 (HH12), star-forming cloud, obs. of shocked H₂ and interstellar jets 7-55760
 NGC 2024, H II region, VLA maps of formaldehyde absorpt. 7-48041
 NGC 2024 - IRS 2, H I Bra and γ line studies of wind 7-40799
 NGC 2071, refl. nebula, nearby bipolar flow source NH₃ obs. 7-24181
 NGC 2071 star-forming cloud, obs. of shocked H₂ and supersonic jets 7-55760
 NGC 2798, interacting galaxy, evidence from UV spectroscopy from starburst in galactic nucleus 7-55830
 NGC 3256, galaxy, evidence from UV spectroscopy from starburst in galactic nucleus 7-55830
 NGC 6240, far IR spectra of luminous interacting galaxy 7-40932
 NGC 6357, H II region, IR obs. rel. to star form. 7-48009
 NGC 7469, type 1 Seyfert galaxy, emission lines mapping rel. to circumnuclear starburst 7-29536
 Nova Cen 1986, IR photometry rel. to dust shell form. (1986 December 30 to 1987 January 5) 7-47913
 NS3, NS12, possible bipolar nebulae, optical polarisation study 7-48047
 α Ori, outer atm. and circumstellar material characts., far-IR spectral obs. 7-60690
 Ori IRC 2, SiO maser emission from expanding shell 7-60646
 FU Ori stars, evidence for disk accretion, IR spectral obs. 7-66581
 Orion IRC 2, vibr. excited cyanoacetylene obs. 7-48063

infrared sources (astronomical) continued

- Orion KL, NH₂D detect. and abundance 7-60754
 Orion Molecular Cloud 1, IR polarisation obs. and discovery of H₂ refl. nebula 7-14633
 Orion Molecular Cloud 2, IR refl. nebulae obs. 7-55765
 Orion-KL region, maps of high-vel. CO outflow 7-29522
 pentynylidyne radical (C₅H), detect. of $\Pi_{3/2}$ state (in IRC+102.16) 7-23988
 planetary nebulae, astrophysical significance (*German*) 7-55776
 pre-main sequence, CO band heads emission 7-66584
 pre-main-sequence stars in Bok globule Barnard 62, optical and IR obs. 7-9527
 protogalaxies and protocluster pancakes, IR line emission 7-4600
 protostar formation regions, submm astronomy with FIRST 7-47890
 quasars, IR characteristics and IRAS meas. 7-60834
 radio galaxies with OH absorption, IR luminosities 7-40895
 red giants undergoing mass loss, expanding shells IR continuum radiation modelling 7-66582
 Red Rectangle (HD 44179), role of visible luminesc. from polycyclic aromatic hydrocarbons 7-48008
 reflection nebulae near molecular outflow sources 7-66696
 RNO 43, young stellar object, CCD obs. of jet assoc. with far-IR source 7-55617
 S140 IRS 1, CO obs. of assoc. bipolar outflow 7-66710
 Serpens Nebula, IR emission characts. 7-48061
 Seyfert galaxies, IR/radio luminosity ratio sequence rel. to radio props. of Seyfert 1.8 and 1.9 galaxies 7-29537
 Seyfert galaxies, narrow-line, with permitted Fe II emission (Mrk 507, 5C 3.100, I Zw 1), optical, X-ray, and IR props. 7-66751
 V4046 Sgr, T Tau star, UV and visible obs. 7-47869
 VX Sgr, VLB1 obs. of SiO masers rel. to physical conditions in circumstellar envelope 7-55619
 Sh2-155, emission region, blue refl. nebula detect., assoc. dust emission, IRAS data anal. 7-66723
 Shapley-Ames elliptical galaxies, interstellar dust content from IRAS obs. 7-66758
 solar-type protostars in nearby mol. cloud cores, IRAS candidates 7-47853
 South Galactic Pole field, IRAS point sources identification 7-35067
 spiral galaxies, star form characts., far-IR lumin. and CO line obs. anal. 7-4563
 spiral galaxies, very small dust particles and IR emission characts. 7-24209
 star formation regions, far IR, submm and mm dust emission spectra 7-24180
 star formation regions in southern hemisphere, CO J=2-1 obs. 7-18441
 submillimetre astronomy, conf., Segovia, Spain (June 1986) 7-41013
 submm sources, characts. 7-48059
 supernovae, IR emission from heated interstellar grains 7-48007
 symbiotic stars, IRAS observations and energy fluxes 7-34984
 Trifid reflection nebulae, dust grain characts. 7-35024
 Vega-like stars from IRAS point-source catalogue, IR photometry 7-4456
 W51 IRS 2, star-forming region, NH₃ maser and thermal emission obs. 7-66702
 Wolf-Rayet stars, new evidence at X-ray and gamma-ray freqs., for non-thermal phenomena 7-55640
 young supernova remnants, constraints on struct. and dynamics from shock-heated dust obs. 7-55754
 C stars with circumstellar silicate dust, spectral characts. 7-40834
 H II regions, highly-excited Oh transitions obs. 7-24177

infrared spectra of diatomic inorganic molecules

- diatomic molecules, high resolution Fourier spectroscopy 7-50138
 diatomic molecules, IR transitions, vibr.-rot. matrix elements 7-50131
 ethylene dimer spectrum, photodissoc. spectrum, hindered rot. bands 7-42607
 Fourier and computerised IR spectroscopy, Ottawa, Ont., Canada (June 1985) 7-48160
 laser photoacoustic spectroscopy of humid and polluted air 7-20569
 peak-separation algorithm for personal computer, appl. to visible emission and IR absorpt. spectra (*Japanese*) 7-31015
 SeS, rot. anal., isotropic shifts, mol. moments, IR Fourier transform spectra 7-62370
 simple molecules, superfine, hyperfine struct., from IR spectra 7-10586
 two-configuration SCF wave functions, IR intensities and polarisabilities evaluation 7-10582
 BaCl, B² Σ -X² Σ transition, rot. anal., FTS and diode laser spectra 7-10581
 BrF, FT IR spectra, rot. struct. 7-922
 CN⁻, oxidation at Pt electrode, polarisation modulation IRRAS 7-17836
 CO, adsorbed on highly dispersed Pd and Pt, vibr. spectra 7-12475
 CO adsorbed on Pt, vibr. spectrum, electrochemical pot., stark tuning rate 7-10570
 CO adsorbed on Pt 111, vibr., site conversion, IR spectra 7-58613
 CO, and mixtures, line interaction effects in IR absorpt. spectra 7-31038
 CO, band intensities, IR absorpt. 7-36619
 CO, ground state, vibr.-rot. matrix elements 7-912
 CO IR atmospheric transmittance, band model 7-40563
 CO molecules, jet cooled IR laser spectroscopy 7-41495
 CO, rovibr. lines, IR spectral linewidth collisional broadening 7-36621
 CO, submm spectroscopy 7-31041
 CO, vibr. energy exchange rates, IR and UV emission 7-966
¹²C¹⁸O, E'^{II}-A'^{II} and B'² $\Sigma^+-A'^{II} transitions, emission spectra 7-50095
 CO+N₂, nonequilibrium vibr. kinetics, IR spectra 7-57158
 CO₂, ν_2 band, diode laser absorpt. 7-10580
 ClF, FT IR spectra, rot. struct. 7-922
 CuH, vibr.-rot. spectra obs. using FTIR 7-50139
 DBr⁺, X'^{II} $\Sigma_{3/2}$ ground state, mol. rot.-vibr., isotope shifts, double modulation Faraday LMR IR spectra 7-62369
 DI, Ar matrix, conc. effects, binary complexes with impurities, IR spectra anal. 7-31034
 H₂-methane pairs, rototranslational far IR absorpt. spectra 7-15601
 HCl, IR spectra, Ar- and N₂-broadened linewidths, rot. spectrum 7-50113
 HCl in atm., ground-based IR solar spectra anal. 7-40538
 HD⁺, vibr.-rot., IR photodissociation spectra 7-31009
 HI, Ar matrix, conc. effects, binary complexes with impurities, IR spectra anal. 7-31034$

infrared spectra of diatomic inorganic molecules continued

- H₂O, liq. state, FTIR spectra, fine struct., molar absorptivities of vibr. modes 7-53343
 H₃O⁺, IR diode laser spectroscopy, rot. lines, inverse pot. function 7-10564
 He-Ne mixtures collision induced far IR translational absorpt. 7-10563
 HeH⁺, vibr.-rot., IR photodissociation spectra 7-31009
 Li salts, ion-molecule interactions in DMF, IR spectrosc. obs. 7-10584
 MgHe, collisional redistrib. profiles meas. 7-42525
 N₂, chemisorpt. on (110) surface, FT IR refl-absorpt. spectrosc. obs. 7-27100
 N₂, gaseous, induced vibr.-rot. and vibr.-translational spectra 7-31037
 N₂ glow discharge, pulsed, time-resolved Fourier transform spectra of IR emission 7-51538
 N₂+N₂, collision induced rototranslational absorpt. spectra 7-60521
 NH radical, rot.-vibr. anal. for X² Σ^- state, IR Fourier transform spectra 7-19847
 NH⁻, IR rot.-vibr. spectrum, high-resolution meas. 7-62373
¹⁵NH⁺, X'^{II} state, IR rot.-vibr. spectrum, isotopic shifts and equilib. consts. 7-50107
 NO, linewidth broadening and strengths, tunable diode laser IR spectroscopy 7-5676
 NO, Zeeman modulated radiometer for remote detection 7-55313
 N₂O spectra in 1100 to 1440 cm⁻¹ region 7-19854
 NS⁺, electronic states study, CI calcs. 7-19714
 Na dimer, lowest triplet transition, laser-induced fluoresc., IR spectra anal. 7-36627
 NeH⁺, vibr.-rot. spectra obs. using FTIR 7-50139
 NpH₆, IR-active fundamentals and combination bands, vibr. force consts. 7-25511
 O₂, A band, line profiles study, IR spectra anal., dye laser excitation 7-50114
 OH, adsorbed on SiO₂, FTIR characteris. 7-46042
 OH, ground state, conc.-profile in premixed oxy-fuel flames, IR spectroscopic determ. (*French*) 7-25513
 OH, laboratory meas. of rot. spectrum with tunable far-IR radiation 7-47691
 PuF₆, IR-active fundamentals and combination bands, vibr. force consts. 7-25511
 Rh, Al₂O₃ supported, CO-induced struct. changes, H₂ effect, IR study 7-23063
 RuO₄ transitions in ν_3 band, freq. meas. 7-36624
 S₂, b'² Σ^+ -X'² Σ_g^- system consts., IR and microwave spectra anal. 7-19848
 SD⁺, X² Σ^- ground state, mol. rot.-vibr., Zeeman consts., mid-IR LMR spectra anal. 7-62368
 SH⁺, IR spectra, laser modulation 7-62363
 SH⁺, electronic transitions, IR laser spectra 7-50100
 Si₂, IR emission band spectrum 7-57062
 SiH, geometric structs., force consts. and vibr. spectra, SCF CI calcs. 7-19713
 VCl₃, Fourier for IR and laser Raman spectra meas., normal coordinate anal., molecular constant calcs. 7-50137

infrared spectra of inorganic liquids and solutions *see spectra of inorganic liquids and solutions***infrared spectra of inorganic solids**

- alcohols in glassy media, dielectric and IR spectral study 7-2968
 alkali cyanides, multipole interaction effects on cohesive and anharmonic props. 7-1942
 alkali halide mixed crystals, phys. props., review 7-37943
 amorphous semiconductor films, photo-assisted CVD and opto-electronic characterisation 7-33595
 apatite ceramics, with microstruct. controlled by Y³⁺ substitution, elec. props. 7-21523
 asbestos-brucite-polyphenylene sulphide composites 7-53925
 β -BoB₂O₄, crystal vibr. assignment, Raman and IR spectra anal. 7-53346
 cobaltites, fine-particles, low temp. prep. by solid solution precursor method 7-59486
 cultured quartz Al defects, IR and laser spectroscopic charactn. 7-59234
 diamond, type Ia, IR absorption spectra, platelets 7-7723
 diamond CVD, Raman and IR spectroscopy study 7-17428
 exciton motion, influence on shape of optical absorption lines, appl. to surface vibrations 7-7317
 FTIR spectrometer, high resolution, for atomic, mol. and cryst. spectroscopy 7-41505
 glass, characterisation by Fourier Transform Infrared spectra 7-53435
 glass, vibrational spectra of structural units 7-3034
 glass structure, vibrational spectra studies, localised interactions 7-63502
 graphite dispersed powder, C atom vibr. dynamics in IR absorpt. spectrum 7-53322
 graphite intercalation compound with H₂SO₄, optical study of K-point π -band dispersion 7-17317
 halide eutectic composites, growth, struct., mech., elec. and optical props. 7-33648
 heavy fermion superconductors, FIR spectroscopy 7-38816
 heavy metal phosphates, IR spectrosc. investig. (*German*) 7-53299
 ice, cubic, proton transport, FTIR obs. 7-53340
 ice biological charge transfer processes, IR and microwave spectra 7-3749
 ice stretching vibr., red shift 7-22236
 III-V semiconductors, defect recognition and image processing, conf., Montpellier, France (July 1985) 7-29596
 intercalation cpd. struct., enthalpy of reaction 7-46841
 layered structures, Raman and IR spectroscopy 7-3059
 mafic minerals, Gaussian anal. of temp. effects on reflectance spectra in 1- μ m region 7-29006
 metal clusters, dispersed in polymeric matrices, synthesis and props. 7-17370
 metal complexes, IR vibrational spectra, coordination bond length correlation 7-13161
 metal films, enhanced IR absorption of adsorbed molecules, electromagnetic effect 7-27805
 metal particles, quantum size effects 7-7597
 metal ribbon lattices, spectral characts., loss effects 7-13162
 (NH₄)₂PCrO₄, polycrystn., internal vibr., IR and Raman spectra 7-22263
 octahaloaluminumtrimethylacetorhenium, press. tuning IR spectral shifts 7-22242
 orthophosphates, vibr., Raman and IR spectra 7-3048

infrared spectra of inorganic solids continued

- peak-separation algorithm for personal computer, appl. to visible emission and IR absorpt. spectra (*Japanese*) 7-31015
 phosphate laser glasses, IR absorption of water 7-33416
 porous and fibrous materials, radiative transfer, IR spectra study of oxide crystals 7-53305
 quartz, cultured, grown from +X seeds, Al and OH⁻ distrib. 7-58307
 quartz, FTIR spectrum of crystals, press. effects, phonon band splitting 7-46039
 quartz, particle size effect on Fourier transform IR photoacoustic spectra 7-9909
 rare earth borides, RB₆, elec., optical and thermal cond. props. 7-21910
 rare earth cpds., RSc₃(BO₃)₄ (R=Ce,Pr,Nd,Sm), preparation, struct. and props. 7-1968
 rare earth phosphate glasses, structural investigation 7-6522
 reststrahlen spectra in IR crystals, review 7-39119
 semiconductor thin films, weakly absorbing, thickness, optical consts. and relax. time determ. 7-39194
 semiconductors, FIR absorption and near-IR photoluminescence spectroscopy of bound excitons 7-39122
 Si:B polycrystalline solar cell substrates, B conc. meas. using IR spectroscopy 7-23176
 silica gel surface, variable temp. diffuse reflectance FT IR spectrosc. obs. 7-53294
 tetra-n-butylammoniumoctahydrohenium, press. tuning IR spectral shifts 7-22242
 thin film dielectrics, characterisation by Fourier Transform Infrared spectra 7-53435
 vibrational spectra, fully automated microcomputer calc. 7-56238
 YIG:Ca films, magneto-optical props., reducing treatment effects 7-64617
 zirconia transparent gel-monolith from Zr alkoxide, controlled hydrolysis prep. 7-8313
 Ag, small particles in amorphous materials, far-IR absorpt. spectra 7-64623
 AgCl_{0.95}Br_{0.05}, IR transmitting fibres, optical props. 7-37185
 Ag₂P₂O₇, glassy and cryst. states, thermal props., IR spectra 7-44845
 Al, IR spectrum, intraband and interband processes 7-22256
 Al, small particles in amorphous materials, far-IR absorpt. spectra 7-64623
 AlCl₃, layer struct., IR vibr. spectra 7-13151
 AlCl₃.6H₂O single cryst., polarised IR reflection spectra 7-3054
 Al₁Ga_{1-x}As film formation by laser beam interaction with AlAs/GaAs multilayer structure 7-12570
 Al₁Ga_{1-x}As-GaAs heterostructures, 2D electron space charge layers, plasmon and magnetoplasmon excitation 7-38696
 Al₂O₃ anodic porous film on Al, microstruct. 7-22882
 Al₂O₃, corundum, single crystals, IR absorpt. and transmission spectra study 7-53305
 Al₂O₃ glass, gel produced, optical transmission rel. to heat treatment 7-27733
 Al₂O₃, leucosapphire single crystals, transformation of colour centres 7-37986
 Al₂O₃ SiO₂ gel, IR and ²⁷Al NMR.MAS spectra AlO₆, AlO₄ vibr. freq. (*French*) 7-64534
 Al₂O₃, uniaxial, transverse bulk polaritons, IR refl. 7-17319
 (Al₂O₃)_{1-x}(AlN)_x film, optical and elec. props., comp. depend. 7-38766
 AlPO₄, berlinite, synthesis and charactn. of new polymorphic modification 7-53534
 AlPO₄, heat treated, IR meas., temp. coeff. of delay and insertion loss 7-13486
 As-S (Se) chalcogenide glasses, far-IR absorption spectra and spatial charge fluctuation 7-7696
 As-S-I semicond. glass system, IR and Raman spectra studies 7-3058
 As₂S₃:Ag, amorphous, charge fluctuation, Ag doping effects 7-7700
 Au, film, furnace for LPE growth system (*Korean*) 7-33606
 Au film, optical props. 7-17296
 Au thin film based transparent IR reflectors, prep. and optical props. 7-39201
 Au thin films, quantum size effect in optical transmission and refl. spectra 7-59275
 B, amorphous, elec., optical and thermal cond. props. 7-21910
 BN, film, optical and compositional props. 7-39206
 B₂O₃-GeO₂ glass, vibrational spectra of structural units 7-3034
 B₂O₃-SiO₂ glass, borosiloxane bond formation, sol-gel process, spectroscopic study 7-59117
 B₂O₃-SiO₂ glass coating films, prep. by sol-gel method 7-46310
 Ba(ClO₃)₂.H₂O single crystal, Fourier transform IR spectroscopy, quantitative intensity meas. 7-48869
 BaFCl, IR lattice vibr., dielectric dispersion and lattice dynamics 7-3044
 BaGeO₃-Ga₂O₃-CaO-CaF glasses, IR transmission spectra, depend. on composition 7-3031
 BaO-B₂O₃ glass, containing Fe₂O₃, heat treatment and γ-irrad., IR study 7-16627
 BaPb_{1-x}Bi_xO₃, semicond. phase, CDW gap, optical meas. 7-53328
 BaSO₄, barite, IR and far IR optical props. 7-13116
 BaTiO₃:Ni ceramic, H defect diffusion 7-58545
 Bi chalcogenides, binding energies, chem. shifts XPS and diffuse refl. spectra (*German*) 7-1943
 Bi complex, MBi(PO₄)₃, M=Cd, Pb, Co, Sr, Bi, structural and spectroscopic data correl., Raman and IR spectra anal. 7-53348
 Bi films, IR and visible spectra, refractive index, extinction coeff. and dielectric const. 7-46156
 Bi films, size quantised, IR spectrum, optical cond., two-band model 7-27803
 Bi₂FeO₆, reflectivity spectra structure, thermorefectance 7-59207
 Bi_{1/2}GeO₂₀(SiO₂₀)(TiO₂₀) and Bi₄Zr₃O₁₂, sillenites, IR transmission spectra 7-59194
 Bi₂Mo₂₀:V, (M=Si,Ge,Ti), sillenite struct., local vibrs. of impurities, spectral study 7-7718
 (Bi_{1-x}Sb_x)₂Te₃ single crystal, optical constants, IR spectra study 7-46030
 Bi_{1/2}Si_{1/2}Ge_{1/2}O₂₀ solid solutions, IR spectra 7-7691
 Bi_{1/2}Si_{1/2}(Ge)(Ti)O₂₀, reflectivity spectra structure, thermorefectance 7-59207
 Bi_{1/2}SiO₂₀ crystals, local vibrs. of Si isotopes, Raman spectra 7-7689
 C, amorphous submicron grains, far-IR extinction meas. and props., astro-physical appl. 7-47699
 C layers, deposition, by RF plasma decomp., physical props. 7-22508
 a-C:H, film, optical and compositional props. 7-39206
 a-C:H, props., review 7-51630

infrared spectra of inorganic solids continued

- a-C:H plasma grown films, struct., physical props. 7-58713
 a-C:H polymeric layers, plasma-activated CVD produced, spectroscopic investigations 7-22572
 C-ZnX (X=S, Se), adherence of diamondlike C films, use of intermediate layers 7-46624
 CO, adsorpt. on KCl film, IR investig. 7-63945
 CO complexes, struct. ang. distortions, stretching modes. IR spectra 7-3052
 CO solid films, Fourier transform IR spectra 7-59214
 CO, terminally bonded on Ru (001), vibr. dephasing 7-17318
 CO₂, amorphous solid, mol. vibr., IR spectra anal. 7-53307
 CO₂ ice, absorpt. coeff. and refr. index, laboratory meas. UV to microwave, review 7-3008
 CS₂, spectroscopic studies at high press. 7-27742
 CaF₂:Er³⁺, H⁻(D⁻), IR excitation and absorpt. spectra anal. of sites 7-53306
 Ca(HSeO₃)₂.H₂O, cryst. struct., IR spectra, thermal behaviour 7-44479
 Ca₂(HSeO₃)₂(Se₂O₃), cryst. struct., IR spectra, thermal behaviour 7-44479
 CaO-SiO₂ polycryst. silicates, FTIR and Raman spectra, isotopic shifts and force consts. 7-53341
 Ca₁₀(PO₄)₆(OH)₂, thermal lattice expansion, 20-600 °C 7-58510
 Ca(UO₂)₂(Si₃O₇)₂.5H₂O, β-uranophane, refined cryst. struct., thermal anal., IR spectra 7-55031
 Ca₈Y₂(PO₄)₆(OH)₂-xO_x, synthesis, struct., dielec. props., AC elec. cond., IR spectra 7-3235
 Cd(ClO₄)₂.6H₂O, low-temperature phase transitions characterisation by Fourier transform IR spectroscopy 7-52046
 Cd_{0.27}Hg_{0.73}Te:B⁺, ion implanted, photorefection spectra in the edge absorption region 7-39099
 Cd_{1-x}Hg_xTe heterostructures, MOVPE, computer controlled reactor, charactn. 7-59446
 CdIn₂O₄ RF sputtered films, transparent heat mirror characts., elec. and optical meas. 7-39199
 CdIn₂O₄ thin films, DC reactive sputtered, elec. and optical props. 7-38788
 Cd_{1-x}Mn_xTe mixed cryst., far IR Fourier transform spectra, acoustic local mode and TA band mode 7-53378
 (CdO)_x(B₂O₃)_{1-x}(GeO₂)₂ glasses, struct. and vibrational props., IR spectra study 7-7694
 3CdSO₄.8H₂O, site symm. of SO₄²⁻ ion, IR absorpt. spectra 7-33374
 CdTe, single cryst., transmission region optical props., impurities effects 7-39128
 CdTe:Fe²⁺, impurity vibronic coupling and near IR spectra characts. 7-26889
 CeB₆, optical props. and band struct., spectroscopic ellipsometry meas. 7-13157
 CeO₂, reduction by thermal treatment in vacuum or H₂ atmosphere, IR, PMR and ESR spectra 7-59756
 Ce₂(SeO₄)₃.5H₂O, vibr., IR and Raman spectra 7-3046
 Co²⁺, complexes, IR spectra, coordination bond length correlation 7-13160
 Co₅₀Ga₅₀ film samples, interband optical conductivity (*Ukrainian*) 7-13244
 CoGaInS₄, cpd. with FeGa₂S₄ struct., prep. and characts (*German*) 7-1984
 Co_{1-x}In_{2x+3} thin films, spray pyrolysis deposited, structural and optical props. 7-22468
 Co_{1-x}Fe_xO₃ selective coatings, spray pyrolysis for high temp. appls. 7-5974
 Co₈₀P₂₀, amorphous films, electrodeposited, optical and NMR spectra, annealing effect (*Russian*) 7-45831
 CrCl₃, layer struct., IR vibr. spectra 7-13151
 Cr₂O₃, in transparent glass-ceramic, crystn. and spectroscopic props., melting conditions and heat treatment influence 7-7588
 CsBSi₃O₆, glassy and crystalline, IR spectra 7-59199
 CsCaF₃, fluoroperovskites, IR refl. spectra, temp. depend. 7-22248
 Cs₂HPO₄Te(OH)₆, vibr. anal., IR and Raman spectra 7-39104
 CsHSO₄, cryst. struct. IR spectra study 7-63588
 CsNO₃, polycryst., IR absorpt. spectra 7-33396
 Cs₃ReBr₆(Cl₆), solid, IR and Raman spectra, vibr. anal. 7-53292
 Cs₃TcBr₆(Cl₆), solid, IR and Raman spectra, vibr. anal. 7-53292
 Cs₃[Fe(CN)₆].[NO].H₂O, thermal behaviour and vibr. spectra 7-64632
 Cu, electronic props., spectrosc. investig. 7-59216
 Cu II complexes, charactn., electronic and ESR parameters 7-2925
 Cu particles, ZnO-supported, vibr. spectra of adsorbed species, operation of metal surface selection rule 7-53350
 Cu²⁺ complexes, IR spectra, coordination bond length correlation 7-13160
 CuCl, off-centre model, vibr. and struct. props. 7-17316
 Cu(ClO₄)₂.2H₂O, electronic absorption spectra, energy splittings 7-64625
 CuInSe₂, thin films, flash evaporated, electrical cond. and optical absorpt. spectrum 7-33112
 CuInTe, thin films, flash evaporated, elec. conductivity, optical absorption 7-7428
 CuO-P₂O₅ glass, containing Pr₆O₁₁, optical props. 7-17292
 Cu₂Si₆O₁₈.6H₂O, Diopside crystals, Cu²⁺ EPR and optical absorpt. spectra studies 7-53120
 Dy₂O₃-Er₂O₃-Ho₂O₃, mixtures, IR reflectance spectrum, wavelength standard 7-41330
 DyP₃O₁₄, absorpt. spectra intensity parameters, fluoresc. radiative transition probabilities (*Chinese*) 7-39141
 Eu chalcogenides, IR optical parameters, rel. to chemical bonds 7-53291
 EuAsO₄ crystal, vibr. spectra and optical absorption studies 7-13145
 Fe-Cr alloy, oxide film form., FTIR reflectance spectroscopy characterisation 7-46043
 FeCl₃, layer struct., IR vibr. spectra 7-13151
 (Fe³⁺_{2-2x}Fe²⁺_{1+x}Ti⁴⁺_x)O₄, submicron synthetic titanomagnetites, oxidation products, IR spectra 7-27716
 α-Fe₂O₃ microcrystals, IR spectra calc. 7-53315
 FePS₃, absorpt. spectra of transition metal ion 7-33411
 FePS₃, optical absorption in near IR, visible and near UV regions 7-46070
 Ga film, vac. condensates, struct. and opt. characts. 7-2404
 GaAs, (100) substrates, growth of HgTe-CdTe superlattices by MBE 7-12520
 GaAs, crystal defects, IR light scattering tomography and IR absorption microscopy 7-46023
 GaAs, EL2 clusters, scattering and absorpt. of IR light 7-53382
 GaAs FET arrays, electrical parameter mapping 7-32438

infrared spectra of inorganic solids continued

- GaAs, FTIR spectra of acceptors, electronic intrasite transitions and local vibr. modes 7-53377
 n-GaAs, free carrier IR absorpt. spectra, scattering mechanisms, RPA calcs. 7-2604
 GaAs, IR imaging 7-32238
 GaAs, IR tomography and transmission images, numerical processing 7-32236
 GaAs LEC semi-insulating crystals, pure and In-doped, IR absorpt. WRT resistivity 7-64629
 GaAs LEC substrates, EL2 deep donor kinetics under annealing, IR absorpt., DLTS, Hall effect meas. 7-32955
 GaAs, LEC-grown wafer, EL2 conc., stress distrib., near-IR absorption mapping 7-52522
 GaAs, neutral shallow donor inter-excited-state transitions, far IR photocond. in mag. field study 7-22249
 GaAs, optically induced far-IR absorption from residual acceptors 7-22287
 GaAs, phonon and plasmon deformation potentials, FIR spectra under uniaxial stress 7-26886
 GaAs, polycrystalline thin films, RF sputter deposition on silica substrates, light transmission props. 7-46320
 GaAs, semi-insulating, IR light scattering from defect centres 7-64620
 GaAs semi-insulating thin wafers, EL2 defect and dislocation mapping, near-IR transmittance meas. 7-63605
 GaAs semiinsulating slices, spatial inhomogeneities, near IR transmission imaging techniques 7-33400
 GaAs thin semi-insulating wafers, EL2 distrib., dislocation network correl., near IR absorpt. maps and X-ray topographs 7-21203
 GaAs, uniformity imaging 7-32481
 GaAs wafers, LEC-grown, semi-insulating, two-dimens. high-resolution EL2 topography 7-53381
 GaAs:C, impurity content meas., IR absorpt., room temp. meas. 7-22289
 GaAs:C, LVM absorpt. temp. depend. (Chinese) 7-59225
 GaAs:Ge,Si, local modes, isotopic fine struct., IR spectra 7-38145
 GaAs:In, doped and undoped, EL2 maps from computer based IR image analysis 7-32237
 GaAs:Sn epilayers, MOCVD using triethylgallium and tetraethyltin, characterisation 7-22515
 GaAs:V, electromodulation spectra, deep level energy positions 7-38496
 GaAs/AlAs doped quantum well waveguides, IR intersubband absorpt. 7-59192
 GaAs/AlGaAs multiple-quantum-well structures, shallow donors, far infrared spectroscopy 7-39121
 GaAs-Al_{1-x}Ga_xAs MQW and superlattice structures, for IR reflectivity 7-27724
 GaAs-Al_{1-x}Ga_xAs superlattices, electronic and optical props., alloying and press. effects 7-64327
 GaAs-AlGaAs quantum wells, FIR studies of shallow donors 7-52819
 GaAs(P)(Sb):H, vibrational excitations, impurity-host atom complexes, IR absorpt. data interpretation 7-44724
 GaInAs, Czochralski-grown, dislocation effects investig. 7-7261
 Ga_{0.28}In_{0.72}As/Al_{0.28}In_{0.72}As photodiode heterostructures, atm. press. MOCVD, 2 μ m, sensitivity, structural charactn. 7-27933
 GaP:Cr, optically induced changes in impurity-related absorpt. line struct. 7-17334
 GaP-electrolyte interfaces, Fourier transform IR spectroscopy 7-27124
 GaSe layer cpd., Al dopant intercalation, Auger and IR spectra studies (Russian) 7-32476
 GdCu, optical props. and electronic struct. investigs. (Russian) 7-13174
 Ge, carrier conc., mag. gradient effect (Russian) 7-17040
 p-Ge, far IR multiphoton absorption 7-27723
 Ge, laser irradiated, electron-hole plasma dynamics investigated by time-resolved spectroscopy 7-13276
 Ge, pure and heavily doped, dielec. function, impurity conc. depend., spectroellipsometric meas. 7-2525
 Ge, quenched, SA₂ acceptor, uniaxial stress effects, far IR optical study 7-64673
 Ge:Ga(Be)(Zn) extrinsic photoconductor material, cryst. growth and characterisation 7-64893
 GeO, Li, IR absorption spectra and bands, Li-O complexes 7-33375
 Ge-Sb-S glasses, bulk and thin film samples, optical and photo-acoustic props. study 7-22211
 Ge-Si superlattices, structurally induced optical transitions, electrorreflectance spectra 7-59184
 GeO₂-PrCl₃ glasses, optical props. rel. to comp. 7-13150
 GeO₂-SiO₂:N optical fibres, N-related absorpt. bands 7-59226
 GeO₂-TeO₂-V₂O₅ system, phase diagram and equil., quasi-binary section investig. 7-21405
 GeO₂-ZnO-Bi₂O₃ IR transmitting glasses 7-43276
 GeS and GeSe, chalcogenide glasses for IR fibres, plasma deposition 7-37191
 a-Ge₂₀S₈₀ films, irreversible photobleaching 7-17353
 Ge₄₀S₆₀, amorphous film, photoinduced bleaching 7-13618
 H, cryst., IR absorpt. spectra in first overtone region 7-59209
 HCl, in Ar and Kr matrices far IR spectra, press. effects 7-22240
 HgCdTe and HgTe-CdTe superlattices, IR photolum. by Fourier transform spectroscopy 7-46134
 HgCdTe, IR nonlinear absorpt., dynamic Burstein-Moss effect (Chinese) 7-50615
 Hg_{1-x}Cd_xTe and related materials, far IR spectroscopy 7-39120
 Hg_{1-x}Cd_xTe, low frequency absorption bands (Chinese) 7-39095
 Hg_{1-x}Cd_xTe/CdTe superlattices, MBE growth and props. 7-53602
 HgTe-CdTe superlattices, cut-off wavelengths meas. 7-3030
 HgTe-CdTe superlattice, alloying, far IR study 7-13143
 HgTe-CdTe superlattices, IR optical props. 7-13166
 HgTe-CdTe superlattices grown on lattice-mismatched GaAs substrates 7-52341
 InGaAs-InAlAs strained-layer superlattices, MBE grown, optical characterisation 7-13142
 In_{0.5}Ga_{0.5}As/In_{0.5}Ga_{0.5}As and (InAs)_m(GaAs)_n superlattices, MBE grown, optical studies 7-13221
 InN films, IR absorption 7-7778
 In₂O₃:Sn films, theoretical model for optical props. in 0.3 to 50 μ m range 7-39200
 In₂O₃:Sn(In)(Cd) films, optical and elec. props. 7-22365
 InP, multiphonon absorption (Chinese) 7-7682
 InP, neutral shallow donor inter-excited-state transitions, far IR photocond. in mag. field study 7-22249
 InSb-SiO₂ MIS structures, photo-CVD fabrication 7-38739

infrared spectra of inorganic solids continued

- InSe layer cpd., Al dopant intercalation, Auger and IR spectra studies (Russian) 7-32476
 Ir complex, (Ir(CO)₂4,4',5,5'-tetracyano-2,2'-biimidazole)⁻, anisotropic conductor, phys. props. 7-7242
 IrBr₆²⁻, in A₂MX₆-type host crystals, near-IR absorpt. spectra 7-22232
 IrCl₆³⁻, in A₂MX₆-type host crystals, near-IR absorpt. spectra 7-22232
 KBrSi₂O₆, glassy and crystalline, IR spectra 7-59199
 K₂Bi(MoO₄)₄, palmierite-type cpd., cryst. struct. determ. 7-21174
 KBi₂(PO₄)₆, structural and spectroscopic data correl., Raman and IR spectra anal. 7-53348
 KBr films, high temp. phonon anharmonicity, IR spectra study 7-33469
 KBr:CN⁻, persistent IR hole burning in vibr. spectrum 7-37057
 KClO₄ single crystals, vibr. anal., optical modes, IR spectra studies 7-22245
 KCl_{1-x}Bi_xLi mixed crystals, F_A centre absorpt. and emission spectra studies 7-12064
 KCl_{1-x}Br_x mixed powder crystals, long wavelength optical phonons; 7-12220
 KD₂(WO₄)₂, vibr. characts. of O bonds, IR and Raman spectra 7-32587
 K₂Fe(CN)₆·1.25 H₂O, DTA-TGA, cryst. and mol. struct. and vibr. props. 7-6597
 K₂HfPCrO₁₀, polycrystn., internal vibr., IR and Raman spectra 7-22263
 KHSeO₄ single crystal, polarised IR spectra anal., rel. to cryst. struct. 7-46047
 KMBi₂(PO₄)₃, M=Cd, Pb, Co, Sr, Bo, structural and spectroscopic data correl., Raman and IR spectra anal. 7-53348
 K₄Mo₂Cl₈, press. tuning IR spectral shifts 7-22242
 K_{0.3}MoO₃, IR reflectivity and Raman scatt. from midgap-state exciton-polaritons 7-33386
 KNO₃-I, orientational mobility of NO₂⁻ ions, IR spectral study 7-7690
 K₂Nd(MoO₄)₄, palmierite-type cpd., cryst. struct. determ. 7-21174
 K₂O-P₂O₅-TiO₂ glass, IR spectra 7-46025
 K₂O-PbO-SiO₂ glass, props. rel. to phase diagram 7-13117
 K₂O-PbO-SiO₂ glasses 7-3036
 K₂PCr₄O₁₆, polycrystn., internal vibr., IR and Raman spectra 7-22263
 K₂Rb_{0.5}I mixed crystals, phonon combination bands, far-IR spectra anal. 7-64650
 K_{1-x}Rb_xI mixed crystals, FIR props., optical phonons 7-46011
 K₂ReBr₆(Cl₆), solid, IR and Raman spectra, vibr. anal. 7-53292
 K₂SO₄-ZnSO₄:Pr³⁺, impurity ion spectroscopic parameter determ. 7-7719
 KSnCl₃·H₂O, near IR spectra, polarised overtone-combination bands 7-7684
 K₂SnCl₄·H₂O, near IR spectra, polarised overtone-combination bands 7-7684
 KTa_{1-x}Nb_xO₃:CO₂²⁻, impurity detection, IR transmission and Raman scatt. studies 7-13164
 K₂TcBr₆(Cl₆), solid, IR and Raman spectra, vibr. anal. 7-53292
 KTiOPO₄ crystals, electrochromic effects obs. (Russian) 7-33367
 KTiOPO₄, IR spectra 7-46025
 KZnF₃, fluoroperovskites, IR refl. spectra, temp. depend. 7-22248
 KBr:ClO₄, X irradiation, paramag. defect prod., EPR, Raman and IR spectra 7-22142
 LaB₆, optical props. and band struct., spectroscopic ellipsometry meas. 7-13157
 LaCO₃OH polymorphs, prep., cryst. data, X-ray powder diff., IR spectra, TGA curves 7-32392
 La₂NiO₄, struct. characterisation of orthorhombic form 7-1990
 LaTiO₃-based perovskites, IR vibr. spectra studies 7-39102
 Li-P-O-N glass, prep. and characterisation 7-26654
 LiBeH₃ and Li₂BeH₄, cryst. struct. and IR absorption 7-51720
 LiH, ⁷Li and ⁶Li implantation, chemical effects, radiochromatography study 7-28324
 α -LiIO₃:Co²⁺, ESR and optical absorpt. studies of impurity ions 7-45803
 LiInS₂, lattice vibr. and interatomic forces, IR reflectivity spectra anal. 7-26882
 LiKSO₄, high temp. phase transitions, IR spectra study 7-7698
 LiMO₂, M=Sc, Ti, V, Cr, Mn, Fe, Co, Ni, Cu props., review 7-64437
 Li_{1-x}MnRu_{1-x}Ti₂O₄ system, characterisation of different phases (German) 7-26971
 LiNbO₃, ilmenite modifications, vibr. spectra 7-22243
 LiNbO₃ planar-optical waveguides, proton-exchanged, chem. and optical props. 7-57544
 LiNbO₃:Co²⁺, ESR and optical absorpt. studies of impurity ions 7-45803
 LiNbO₃:Mg, incorporation of H⁺, IR spectra of OH⁻ ions 7-7724
 Li₂O-B₂O₃ glasses, vibr. spectra and struct. 7-59196
 xLi₂O.yLi₂SO₄.zB₂O₃, IR and Raman spectra, vibr. study and struct. 7-37879
 Li₂SO₄·H₂O, supercooled melts, cryst. and mol. struct., thermal stability 7-21170
 Li₂TeO₄ glassy electrolyte, vibrational, thermal and elec. characts. study 7-6866
 LiVO₃, phase transition near 200°C, elec. resist., mag. susceptibility, X-ray diff., IR spectra, EPR, thermal anal. 7-32914
 MgAl₂O₄:Ni²⁺, Czochralski growth and optical props. 7-59406
 MgO, single crystals, IR absorpt. and transmission spectra study 7-53305
 MgO-Na₂O-B₂O₃ glasses, FIR spectra 7-39123
 Mn(IO₃)₂, electronic absorption spectra, energy splittings 7-64625
 MnPS₃, absorpt. spectra of transition metal ion 7-33411
 Mo₂, preparation, elec. and optical props. 7-64946
 MoW₂O₁₀²⁻, valence force field calcs., influence of metal atoms oxidation state 7-17323
 Mo_{n-1}W₁O_{3n-1}, electrical conductivity, mag. susceptibility and IR spectra 7-38546
 N₂ solid films, Fourier transform IR spectra 7-59214
 NH₄H₂PO₄, temp. depend. IR active lattice modes in para- and antiferro-electric phase 7-46012
 (NH₄)_{0.32}H_{0.16}WO₃, intercalation cpd. struct., enthalpy of reaction 7-46841
 NH₄MnX₃ (X=Cl, F), absorpt. spectra 7-33410
 (NH₄)₂MoBr₆, press. tuning IR spectral shifts 7-22242
 (NH₄)₂NaFeF₆, low-temperature phase transitions characterisation by Fourier transform IR spectroscopy 7-52046
 (NH₄)_{1.84}V₃O₈, intercalation cpd. struct., enthalpy of reaction 7-46841
 N₂O, mol. solid, lattice vibr., IR active modes (Japanese) 7-6731
 Na₂CO₃, incommensurate crystal, Raman and IR spectra 7-17315
 NaCl:CO₂²⁻, cryst. surface, localised intramol. vibrations, IR transmission spectra study 7-2132

infrared spectra of inorganic solids continued

- NaCl:OH⁻, Cd²⁺, single cryst., gamma irradi., electronic and IR spectra 7-53320
- NaF:OH⁻, X⁺, X=impurities, vibr., radiation effects, IR spectra 7-53321
- NaLa(MoO₄)₂, Nd³⁺, Raman and IR spectra study 7-46046
- NaNO₃, solid ferroelectric and paraelectric phases, lattice vibr., Raman and IR spectra anal., mol. dynamics calcs. 7-21373
- NaNbO₃, ilmenite modifications, vibr. spectra 7-22243
- Na₂O-CaO-SiO₂ glasses, IR spectra 7-3036
- Na₂O-K₂O-CaO-SiO₂ glass, mixed alkali effect on chemical durability, IR spectrometry 7-8145
- Na₂O-TeO₂-Cr₂O₃ glasses, IR absorpt., visible and UV spectra studies 7-27720
- (Na₂O.2SiO₂)_{1-x}(Fe₂O₃)_x glasses, Fe ions, ionic state and coordination geometry 7-63492
- Na₃PCr₃O₁₃.3H₂O, polycrystn., internal vibr., IR and Raman spectra 7-22263
- Na₂P₂Se₆, isomeric forms, P₂Se₆⁴⁻ vibr. spectra, normal coordinate anal. (German) 7-22270
- Na_{1+x}Zr₂Si₂P_{3-x}O₁₂, NASICON, superionic cond. and glass-crystal transition 7-6870
- NbW₉O₁₉³⁻, valence force field calcs., influence of metal atoms oxidation state 7-17323
- Nd complex, tetra dimethyl sulphoxide neodymium nitrate, vibr., Raman. IR and luminesc. study 7-33392
- Nd₂Cr(Ce)_{1-x}P₂O₁₄ cryst. growth and characterisation, X-ray diffr., Raman scatt., visible and IR absorpt. meas. 7-44423
- Nd₂Ga₂O₁₂ garnet, cryst. field studies of excited states 7-33407
- Ni (IO₃)₂.2H₂O, electronic absorption spectra, energy splittings 7-64625
- Ni (111), coadsorbed CO and K, adsorbates electrostatic interaction, IR reflection-absorption spectra, TPD, LEED obs. 7-32824
- Ni²⁺ complexes, IR spectra, coordination bond length correlation 7-13160
- Ni-ZnO/ZnS, selective Ni black coating, struct. and optical response 7-58697
- Ni_xM_{1-x}PS₃ where M = Cd, Zn, Mg, IR, visible and UV spectra, dilution and intercalation effects 7-13175
- NiO, adsorption of NO, IR transmission spectra, calorimetry studies 7-58640
- NiPS₂, absorpt. spectra of transition metal ion 7-33411
- NiPS₃, near IR, visible, and near UV optical absorpt. spectra studies 7-46068
- NiS thin films, deposition by soln. growth techniques, X-ray diffr., optical, elec. meas. 7-32870
- NiSe thin films, deposition by soln. growth techniques, X-ray diffr., optical, elec. meas. 7-32870
- NbBi₃(PO₄)₆ structural and spectroscopic data correl., Raman and IR spectra anal. 7-53348
- NoMBi₃(PO₄)₃, M=Cd, Pb, Co, Sr, Bi, structural and spectroscopic data correl., Raman and IR spectra anal. 7-53348
- O₂ solid films, Fourier transform IR spectra 7-59214
- Os single cryst., energy band struct. and optical absorpt. studies 7-16938
- (PBr₄)⁻(MBr₄)⁺ complex, M=B, Al, Ga, In, mol. vibr., Raman and IR spectra anal. 7-46021
- PLZT ferroelec. ceramics, IR optical and electrooptical props. studies 7-7675
- P₂O₅-Dy₂O₃(Pr₂O₃) glasses, struct., mag. and thermal props. 7-26658
- Pb₂(GeO₄)_{1-x}(SiO₄)_x(VO₄)₂, vibr. and impurity mode behaviour, IR spectra studies 7-64649
- PbGeS₃, vibr. props., spectral study 7-3032
- PbO-SiO₂ glasses, IR spectra 7-3036
- PbO-SiO₂-K₂O coloured and colourless glasses, near IR absorpt. temp. depend. study 7-13146
- Pb(S_{1-x}Nb_x)O₃ ferroelec. ceramics, IR optical and electrooptical props. studies 7-7675
- PbTe, mag. susceptibility, optical absorpt. spectra, effect of intrinsic defects 7-64670
- PbTiO₃ based glass ceramics piezoelectricity, pyroelectricity and ferroelectricity 7-7654
- PbWO₄, struct., X-ray, IR absorpt. and Raman spectra 7-37954
- Pd complexes, with dithiooxamides, vibr., IR spectra 7-3053
- Pd/Al₂O₃ surfaces, ethynylene covered, CO adsorpt., IR spectra studies 7-2371
- PdO-CdO-B₂O₃ glasses, elec. cond. and density meas. 7-1895
- PrCl₃ organic complexes, spectral energies and oscillator strengths 7-3067
- PrP₂O₁₄ cryst. growth and characterisation, X-ray diffr., Raman scatt., visible and IR absorpt. meas. 7-44423
- Pt complexes, triphenylphosphine complexes, vibr., IR and Raman spectra 7-33397
- Pt, small particles in amorphous materials, far-IR absorpt. spectra 7-64623
- Pt stepped surfaces with adsorbed CO, coupled harmonic oscillator models 7-52230
- RbBSi₂O₆, glassy and crystalline, IR spectra 7-59199
- RbCaF₃, fluoroperovskites, IR refl. spectra, temp. depend. 7-22248
- Rb₂Gd(MoO₄)₄, palmierite-type cpd., cryst. struct. determ. 7-21174
- RbHSeO₄ single cryst. ferroelec., H bond vibr., polarised IR spectra studies 7-27707
- Rb₂Mg(SO₄)₂.6H₂O.CO²⁺ optical absorption spectrum 7-13180
- RbMnF₃, absorption bands in paramag. state, temp. depend. 7-46069
- Rb₂MoO₃, IR reflectivity and Raman scatt. from midgap-state exciton-polaritons 7-33386
- RbNO₃, polycryst., IR absorpt. spectra 7-33396
- Rb₂ReCl₆, solid, IR and Raman spectra, vibr. anal. 7-53292
- Rb₂TcCl₆, solid, IR and Raman spectra, vibr. anal. 7-53292
- Rh, Al₂O₃ supported, CO-induced struct. changes, H₂ effect, IR study 7-23063
- Ru complex, Creutz-Taube complex with H₂O₂PO₄, synthesis, struct. and oxidation, IR and X-ray spectra anal. 7-46840
- Sb-S, amorphous and thermally annealed, optical props. (Russian) 7-17352
- Sb-Se, amorphous and thermally annealed, optical props. (Russian) 7-17352
- (Sb_{1-x}Bi_x)NbO₄ solid solns. and constituent cpds., vibr. spectroscopic study 7-39115
- Si (100)2×1, adsorbed H, surface structure, high resolution, IR spectroscopy 7-13169
- Si, bulk free-carrier lifetime, IR absorpt., contactless spatially resolved meas. 7-52650

infrared spectra of inorganic solids continued

- Si diffusion layers with high charge carrier densities, IR radiation refl. 7-13123
- Si, doped layers, IR transmission spectra 7-59208
- Si, heavily doped crystals, behaviour of O and dopants 7-32483
- Si, high dose implantation, with Co, Ni, Fe ions struct. and phase modifications 7-12095
- a-Si, IR spectra calcs., static charge effects 7-3040
- Si, laser irradiated, electron-hole plasma dynamics investigated by time-resolved spectroscopy 7-13276
- Si, neutron irradi. induced IR absorpt. bands 7-46004
- Si, polycrystalline cast ingots, bulk free-carrier lifetime, contactless meas. 7-7258
- Si porous amorphous sputtered films, oxidation, IR spectra studies 7-3532
- Si porous films, IR absorpt. study 7-39149
- a-Si, prep. by low press. CVD, characts. 7-7884
- Si surfaces, passivated by H₂/hydrogen mixtures, surface dielectric layers characterisation 7-17746
- Si:B,C,O, O clustering and thermal donor formation kinetics 7-17566
- Si:B⁺(BF₃)⁻, ion implanted, characterisation by IR attenuated total reflection spectroscopy 7-17327
- Si:C, impurity content determ. IR absorpt.-charged particle activation anal. conversion factor 7-26788
- Si:C, polycrystalline, electrical and structural properties 7-12106
- Si:C,O wafers, C and O contents, Fourier transform IR spectra studies, book contrib. 7-44596
- Si:Cu, ion implantation-amorphised, direct imaging of pulsed laser-induced buried molten layers 7-12130
- Si:Er(Dy)(Yb)(Ho)(Gd), neutron irradi., Hall effect, elec. cond., IR absorpt. spectra 7-51834
- Si:Gd, grown from melt, electrical and optical props., residual impurities 7-63636
- Si:Ge,P(B), IR absorpt. band broadening 7-64669
- Si:H, impurity effects on IR absorpt. bands of Si-H centres, irradi. and unirrad. crystals. 7-53379
- Si:H, polycrystalline, chemistry of grain boundary passivation 7-12375
- Si:H, Si-H IR stretching bands, models, CNDO calc. 7-53314
- a-Si:H, Si-H-Si three centre bonds IR spectra, LCAO-MO-SCF-STO-3G calcs. 7-6741
- a-Si:H,B, RF sputtered films, optical and electrical props. 7-33470
- a-Si:H,N thin films, activated reactive evaporation 7-13355
- Si:H and near-surface damage of Si caused by H ions, review 7-16813
- a-Si:H evaporated layer production from RF discharge, growth mechanism and props. 7-64898
- a-Si:H films, CVD, optical and electronic props. 7-33597
- a-Si:H films, columnar morphology, evolution of vibr. spectra 7-64646
- Si:H films, H content meas. 7-12553
- a-Si:H films, light-induced bond breaking 7-12517
- a-Si:H films deposited by dual ion beam sputtering, characterisation 7-32882
- Si:H solar cells stability, role of Si-H bonds studied by Fourier transform infrared spectroscopy 7-13896
- a-Si:H sputtered films, intrinsic stress, H effects 7-7078
- a-Si:H thin films, elec. and optical props., thickness depend. 7-46168
- a-Si:H/a-SiN_x:H superlattices, interface defects and disorder 7-52306
- Si:N, deep level generation and annihilation 7-16612
- Si:O, C, low temp. precipitation, IR and SANS meas. 7-32666
- Si:O, Czochralski grown, O-related defects after annealing, IR TEM and resistivity meas. 7-32466
- Si:O, diffusivity and solubility of O review 7-16809
- Si:O, electronic struct. and atomic symmetry of the thermal donor 7-16986
- Si:O, energy levels and capture cross-sections of thermal donors 7-16988
- Si:O, Fourier transform IR spectroscopy and SIMS calibrations for O conc. meas. 7-16606
- Si:O, IR absorption meas. of interstitial O conc., calibration 7-33401
- Si:O, IR absorption spectra of thermal donors 7-17326
- Si:O, IR spectra of interstitial O 7-17325
- Si:O, influence of glow microdefects on microdefect formation during heat treatment 7-17559
- Si:O, magnetic resonance of O-related defects 7-17223
- P-Si:O, new donor state, optical, elec. and TEM studies 7-32956
- Si:O, optical transition at thermal donors 7-17346
- Si:O, precipitation kinetics, interstitial diffusion 7-44837
- Si:O, thermal donors, photothermal ionisation spectroscopy and IR transmission meas. 7-16987
- Si:O(O,C), impurity aggregation, SIMS 7-16778
- Si/a-SiO₂/ZrO₂-Y₂O₃, SOI system fabrication, charact. 7-22025
- Si-electrolyte interface, Fourier transform IR spectroscopy 7-27124
- Si-N-H glow-discharge films, elec. and optical props., comp. depend. 7-58933
- Si-O amorphous films, structure and defects 7-58700
- Si-SiO₂, new donors effect, interface effect due to internal oxidation 7-33093
- a-Si_{1-x}C_x:H films prepared by plasma CVD method, props. (Japanese) 7-12543
- SiC, hot pressed, IR optical absorpt. and refl. 7-59167
- SiC, polycryst., oxidation 7-28159
- SiC, submicron grains, far-IR extinction meas. and props., astrophysical appl. 7-47699
- a-SiC:H, elec., optical and local structure props. 7-45089
- SiC:H amorphous films, struct., elec. and optical props. 7-22360
- a-SiC:H glow discharge films, IR vibr. spectra 7-53434
- a-Si_{1-x}C_x films, RF sputtered, IR absorpt., X-ray diffr., RHEED (Japanese) 7-53584
- Si_{1-x}C_x thin films, glow discharge deposition and struct. props. 7-64932
- a-Si_{1-x}C_x:H,B(P) thin films, H bonding and H content, IR spectra studies (Chinese) 7-12524
- a-SiGe:D, F, vibr. modes, Fourier transform IR spectra studies 7-46053
- a-SiGe:H, F glow discharge films, elec. and optical props. 7-46169
- a-SiGe:H,F alloy films, F incorporation and annealing props. 7-44588
- a-SiGe:H alloys for solar cells, electronic and optical props. 7-17899
- a-SiGe:H films, NMR, ESR and IR studies 7-45833
- Si₃Ge_{1-x}:H,F amorphous films, struct., elec. and optical props. 7-22360
- a-SiN_x:H CVD film, IR and ²⁹Si NMR studies 7-38952
- SiN_x:H films, amorphous, glow discharge deposited, IR absorpt. and Raman scatt. spectra 7-46003
- a-Si_{1-x}N_x:H,B films, ESR and IR spectra studies 7-7780
- a-Si_{1-x}N_x:H films, H₂ evolution 7-17445
- Si₃N₄ films, plasma deposited, bonds and defects 7-17437

infrared spectra of inorganic solids continued

- a-Si₃N₄:H films deposited by plasma enhanced CVD, optical and elec. props. 7-39205
- Si₃N₄-Al₂O₃-Y₂O₃(CeO₂)(La₂O₃) ceramics, sintered, IR and Raman spectra 7-46000
- Si₃N₄-x amorphous thin films grown by ion beam assisted deposition, IR and ion beam anal. 7-39209
- Si₃N₄ film form. and charact., ion and vapour deposition method 7-13370
- SiO₂ amorphous optical fibers, material dispersion study over IR region 7-7663
- SiO₂ films, IR spectra, plasma treatment effects 7-7693
- SiO₂ films on Si, low-temperature annealing, interfacial props. of MOS structures 7-46526
- SiO₂ RF sputtered thin films, atomic defects and stresses, optical and elec. props. 7-16898
- SiO₂ spherical particles synthesis, thermal behaviour (*Japanese*) 7-7943
- SiO₂ ultrathin films, structure, IR study 7-58674
- SiO₂, water-free fused silica, IR-transparency, laser windows, prep. by reactive atmosphere process 7-59202
- SiO₂, with adsorbed OH, FTIR characteris. 7-46042
- SiO₂:Na with adsorbed SO₂ and H₂S, FTIR and Raman spectra obs., Na promotion of Claus process 7-46869
- SiO₂-Al₂O₃, mullite form. from xerogels, X-ray and IR obs. 7-46391
- SiO₂-GeO₂ system, gels and gel-glasses, struct. study using vibr. spectroscopy 7-44381
- SiO₂-GeO₂-P₂O₅, doped silica glass, dopant effect on OH absorpt. 7-27715
- SiO₂-P₂O₅ glass films, deposited by different CVD methods, phys. props. 7-27220
- SiO₂-Si interface, insulator props. after exposure to H₂+N₂ and NH₃, 7-59693
- SiO₂ films, vibrational spectra and structure (*Russian*) 7-64709
- SiO_x thin films, plasma enhanced CVD deposited, Si chem. states, IR spectra, XPS, AES 7-21721
- SiO_xN_y films, deposited by plasma-enhanced CVD, charact. by FTIR meas. 7-2413
- SiO_xN_y films, IR optical props. 7-7777
- SiO_xN_y films, plasma-enhanced CVD growth 7-22514
- SiO_xN_y films, plasma-enhanced CVD deposited, annealing 7-32861
- SiO_xN_y, plasma-enhanced deposited oxynitride films, IR and UV transmission 7-33474
- Si₃O₈, plasma enhanced CVD, characterisation 7-39426
- SiO₂-TiO₂ solid solutions, phase relationships and spectroscopic features 7-63826
- SiP₂O₇ glass, vibrational spectra of structural units 7-3034
- Si_{1-x}Sn_xO_{1+x} amorphous thin films, optical and structural studies 7-64714
- Si_{1-x}(ZnS)_x:H amorphous films, synthesis and characterisation 7-17420
- SmAsO₄, vibrational spectra, IR and Raman obs., X-ray and thermal analysis 7-59198
- Sm₂O₃, aging in air 7-65160
- SnS, photoacoustic response and transmission spectra, thermoacoustic meas. 7-46014
- SnSe, IR absorpt. edge, transition temp. coeffs. 7-27721
- SrTiO₃ single cryst., H defect diffusion 7-58545
- SrTiO₃:H(D), O-H and O-D stretching vibrs. under applied electric field and uniaxial stress 7-44723
- Te crystalline thin films, laser-induced transform., transient conductance and optical meas. 7-12142
- TeO₂-based halide glasses, prep., thermal, mechanical, elec. and optical props. characterisation (*French*) 7-37884
- Te(OH)₆(NH₄)₂HPO₄, Te(OH)₆(Na₂HPO₄)₂·H₂O, IR and Raman spectra, vibr. anal. 7-13147
- α-ThBr₄:U, Stark energy level determ. of ³H₄ ground state of U⁴⁺ 7-27696
- ThCl₄:U⁴⁺ incommensurate struct., absorption and emission spectra studies 7-33439
- ThO₂:Np⁴⁺, absorption and emission spectra of Np⁴⁺ 7-27763
- ThSiO₄ single crystal, low temp. Raman and room temp. IR spectra 7-13158
- ThSiO₄:Np⁴⁺, absorption and emission spectra of Np⁴⁺ 7-27763
- TiCl₃, α and β forms, vibr. anal., IR spectra study 7-46049
- TiN compound layer prepared by ion implantation, XPS and FTIR obs., depth profile analysis of ion etched samples 7-59373
- TiO₂ single crystals, IR absorpt. and transmission spectra study 7-53305
- TiO₂-GeO₂ glasses, crystallisation, ion coordination, X-ray diff., IR spectra 7-6523
- Tl halide crystals, NO₃⁻ effect on IR absorpt. spectra 7-39124
- TlGaSe₂ crystals, exciton spectrum, phase transitions 7-7124
- TlIn_{0.95}Ga_{0.05}S₂, crystals, vibr. spectra in vicinity of phase transitions 7-17321
- TlInS₂, crystals, vibr. spectra in vicinity of phase transitions 7-17321
- β-TlInS₂, Urbach rule and phase transitions 7-46009
- TlIn(S_{0.8}Se_{0.2})₂, crystals, vibr. spectra in vicinity of phase transitions 7-17321
- Tl₄P₂Se₆, isomeric forms, P₂Se₆⁴⁻ vibr. spectra, normal coordinate anal. (*German*) 7-22270
- VH_x (0.60 < x < 0.67), optical reflectivity meas. 7-33398
- W (100), chemisorption of N₂, O₂, CO, H₂, D₂, free carrier surface scatt., IR obs. of adsorbate induced changes 7-22268
- (Y,Sc)₃Ga₅O₁₂:Cr³⁺,Er³⁺, spectral, luminesc. and lasing props., Stark sublevel lifetimes 7-25827
- YAlO₃:Nd³⁺, sub-levels R₁ and R₂, thermal shifts 7-32940
- YAsO₄, internal and external vibrs., IR and Raman spectra studies 7-64648
- Y₂O₃ film, electron beam evap., struct. characteris. using TEM, opt. props. 7-21732
- Y₂O₃-Al₂O₃ system, prepared by sol-gel process, IR vibr. spectra study 7-33384
- Y₂O₃-Al₂O₃-B₂O₃ system, glass formation, props. and struct. 7-2205
- Y₂Hg_{1-x}Se, far IR spectra study 7-22262
- ZnO multilayers for solar collector coatings 7-3717
- ZnO:Co(Ni)(Cu), impurity electron states, optical spectroscopy 7-46127
- Zn₃P₂ amorphous films, preparation and optical props. 7-13360
- Zn(PO₃)₂-CdCl₂-KCl glasses, electrical conductivity and IR spectra 7-2253
- ZnS:Fe²⁺, impurity vibronic coupling and near-IR spectra characts. 7-26889
- ZnSe:Cu,Al,Fe crystals, melt-grown, absorpt. coeff., impurity effects 7-3070

infrared spectra of inorganic solids continued

- ZnSe:H, proton implanted, localised vibr. mode, IR transmission spectra 7-51981
- ZnSiP₂ and ZnGeP₂, single crystals, prep. and characterisation 7-2612
- ZnWO₄:Fe single crystals, spectroscopic props. 7-7725
- ZrF₄:BaF₂-GdF₃-AlF₃-NaF-FeF₃, optical fibre glasses, trace amounts of Fe, characterisation 7-2956
- ZrF₄:BaF₂-LaF₃-AlF₃ optical fibres, gamma irradiation, EPR and IR studies 7-37183
- ZrO₂, single crystals, IR absorpt. and transmission spectra study 7-53305

infrared spectra of organic molecules and substances

- acetone-d₀(d₃)(d₆), mol. torsion, semirigid rotor model, far-IR spectra anal. 7-50105
- acetonitrile, anharmonic force consts., Fermi coupling, IR and Raman spectra 7-920
- N-acetyl-L-amino acid methylamides solid and soln., conformers, IR and Raman spectra 7-33395
- acetylcholinesterase, immobilised, structure-activity relations, IR-ATR modulation spectroscopy obs. 7-54474
- acetylene, protonated, d₀(d₃), struct., vibr. freqs., IR intensities 7-5677
- acetylene isotopes, IR spectra, vibr.-rot. IR spectra 7-31036
- acetylenedicarboxylic acids and alkali metal salts, Raman and IR spectra (*French*) 7-15609
- acyclic alcohols, hydroxyl stretching freqs., rotamer pop., CNDO calcs., IR spectra anal. 7-36611
- 2-adamantanone, order-disorder transition obs. by FRIR spectroscopy 7-53342
- adsorption of H₂O and pyridine on (VO)₂P₂O₇, IR spectra 7-17818
- albumin solution, struct. determ. by FTIR 7-54471
- n-alcohols, IR intensities in liq. phase, OH vibrs., assoc. model 7-53336
- n-alkanes, conformations, solvent effects, IR spectrosc. obs. 7-5673
- n-alkanes, liq., energy difference between specific and localised conform. isomers, FTIR spectra 7-42615
- alkoxyazoxybenzenes, mol. reorientation, far IR study 7-33383
- allyl phenyl ether, photoisomerisation reaction mechanisms, IR multiphoton excitation study 7-62372
- aluminium polyfluorophthalocyanine, IF₃ chemical doping 7-52600
- ammonium hydrogen bis(trichloroacetate) single cryst., internal modes, IR and Raman spectra studies 7-26877
- aniline, substituted, polymerisation and characterisation 7-33929
- arachidic acid, adsorbed layer on Ag, form. and struct., IR spectra, optical ellipsometry 7-44992
- arachidic acid spontaneously adsorbed monolayer on Ag, surface organisation, IR spectra obs. 7-46164
- aromatic adsorbed on SiO₂ and Al₂O₃-SiO₂, IR spectra 7-10573
- aromatic aldehydes in cyclohexane solvent, internal mobility study, far-IR and microwave Fourier transform spectra anal. 7-64631
- astrophysical molecules, theoretical predictions of the infrared and microwave spectra of small molecules 7-10561
- ATP-transition and nontransition metal complexes, struct., PMR and IR spectra 7-8493
- azide, cyanate and thiocyanate adsorbed on Ag electrodes, pot. difference IR spectra, coverage depend. orientation 7-22252
- 2-azido-1,3-butadiene, vibr. spectra, mol. struct., conform., GPED anal., Raman and IR spectra anal. 7-36608
- azomethine derivatives, kinetic data eval. from freq. shifts of IR absorpt. bands 7-33911
- azulene, S₀-S₁ absorpt. spectra and Raman excitation profiles, vibr. intensity distrib., quantum-chem. anal. 7-42619
- bacteria, pathogenic, ultrarapid differentiation and identification using FTIR techniques 7-54835
- α-(BEDT-TTF)₂(NO₃)₂, electronic excitations, optical study 7-53367
- BEDT-TTF polyhalides, reflectance spectra, temp. depend. 7-46031
- benzaldehyde, IR and Raman spectra, normal coordinate system 7-5671
- benzaldehydes, monosubstituted, vibr., IR spectra 7-31049
- benzene, Fourier transform IR spectroscopy, quantitative intensity meas. 7-48869
- benzene, liq., IR and Raman spectra, interaction between intra- and inter-molecular modes (*Ukrainian*) 7-13144
- benzene, liq., IR spectrum of second and third orders (*Russian*) 7-3057
- benzene clusters, struct., IR photodissoc. and mass spectra study 7-62371
- benzene liquid, intermolecular resonance vibrations, IR absorpt. spectra, isotropic dilution (*Russian*) 7-59215
- benzene-d₆, IR spectra, rot. reson. 7-25514
- benzonitrile, liq., FTIR and Raman obs. on dynamic and interaction processes 7-53344
- substituted benzoylaminopropionic acid esters, conformational equilb., IR spectra, steric effects 7-57066
- bicyclic compounds, valence force field and vibr. wavenumber calcs., IR and Raman data comparison 7-50079
- bicyclohexyl, conformers, phase transform. vib., IR and Raman spectra 7-33393
- biferrocene, intervalence transfer electronic absorpt. band energy, press.-induced freezing effect 7-25507
- biferrocenium hexafluorophosphate, intervalence transfer electronic absorpt. band energy, press.-induced freezing effect 7-25507
- biferrocenium triiodide, intervalence transfer electronic absorpt. band energy, press.-induced freezing effect 7-25507
- binaphthyls, near-IR triplet-triplet spectroscopy and circular dichroism as probes for electron delocalisation 7-31086
- biohelical poly A-poly U complex, hydration, IR spectra, piezogravimetry 7-8491
- biologically active peptides in soln., NMR and IR studies 7-28471
- bis(dichlorophosphoryl)methane, struct., conformational equilb., GPED, Raman and IR spectra 7-57176
- 3,3-bis(nitratomethyl)oxetane, solid and soln., IR lineshape 7-3047
- bis-dithiobiuret copper(II) chloride, Raman and IR spectra 7-62374
- bisphenol-A polycarbonate, stressed, reversible mol. orientation, IR studies 7-50428
- ((bpy)₂ClRu)₂pyz(PF₆)₂, intervalence transfer electronic absorpt. band energy, press.-induced freezing effect 7-25507
- 1-bromo-2-methylpropane, gaseous phase, conformational stability, for IR and LF Raman spectra 7-10602
- bromomethane, submm spectroscopy 7-31041
- bromotrifluoromethane mol., intermolecular and intramolecular vibrational energy distrib. study, IR multiphoton excitation, Raman spectra 7-42594
- butadiene elastomers, soot-filled, struct., IR spectra 7-39127
- n-butane-d₈, C-H bonds, vibr. anal. gas phase IR spectra simulation 7-19825

infrared spectra of organic molecules and substances continued

- butylamine, adsorbed on SiO_2 , Al_2O_3 and CaO , thermal desorption and IR study 7-39110
- 1-butyne, vibr. anal., IR and Raman spectra 7-19852
- cadmium arachidate, Langmuir-Blodgett films, struct. disorder and polymerisation competition at elevated temp., IR spectra obs. 7-46163
- cadmium dithiocarbamate dichloride, intermediate cpd. in formation of CdS films by spray pyrolysis, characterisation 7-39372
- carbenes, intramol. H shifts, spectrosc. obs. 7-62390
- carbons, IR exam. with photothermal beam deflection spectroscopy 7-46010
- carbonyl oxide, IR spectra, harmonic freq. and ^{18}O isotopic shifts 7-62361
- P-carborane, plastic cryst. phases, mol. notions 7-63528
- cellulose, particle size and order changes, ^{13}C NMR and NIR diffuse reflectance spectroscopy responses 7-27610
- chalcocarbonyl(5,10,15,20-tetraphenylporphinate) iron II complexes, IR and NMR spectra 7-33394
- 6-chloro-2,4-dimethoxyppyrimidine, liq. and vapour, electronic and vibr. spectra, UV and IR obs. 7-19859
- 5-chloro-2-hydroxypyridine, tautomerism, IR and UV spectra 7-31047
- 1-chloro-2-methylpropane, gaseous phase, conformational stability, for IR and LF Raman spectra 7-10602
- 2-chloro-4-methylquinoline, vibr., IR and UV-visible spectra 7-19838
- 2-chlorobutane, solns., glass transition, conformational equilib., IR spectra 7-31044
- chlorocyclohexane, solns., glass transition, conformational equilib., IR spectra 7-31044
- chlorodifluoromethane, IR multiphoton dissociation for ^{13}C laser isotope separation using waveguide reactor 7-991
- chlorodifluoromethane, IR spectra, resonant vibr. energy exchange kinetics 7-36617
- chlorodifluoromethane, IR spectra, rot. and vibr. relax. 7-36616
- chloroethane, IR multiphoton excitation probed by CARs, vibr. population distrib. 7-10591
- (chloromethyl) phosphonothioic difluoride, microwave, IR and Raman spectra, conformational stability 7-36599
- 2-(chloromethyl)-2-methyl-1,3-dichloropropane, conformational equilib., Raman and IR spectra study 7-46018
- p-chlorophenyltin, Raman and IR vibr. spectra 7-57058
- chlorophyll *a*, intact and metal-substituted, metal-sensitive bands in Raman and IR spectra 7-25520
- chlorophyll carbonyls, IR band resolution enhancement, computer techniques 7-39096
- chlorotrifluoromethane, ν_1 - ν_3 band, diode laser spectrosc. 7-5680
- chlorotrifluoromethane, IR multiphoton dissociation induced by CO_2 laser pulses 7-992
- chlorotrifluoromethane, overtone spectra, vibr. anal. 7-36613
- crown ether-NaSCN complex, tetrahydrofuran solvent, IR and microwave dielectric spectro anal. 7-31027
- cycanoacetylene, ν_5 and ν_6 fundamental bands, FT IR obs. 7-923
- cyanobicyclohexyls, crystn. and liq. cryst. phase, IR, Raman and dichroic spectra 7-3051
- cyanomethane anion, photodetachment spectroscopy 7-10670
- cyclobutene, IR spectra, vibr. struct. and C-H local mode dynamics 7-25510
- cyclohexanols, hydroxyl stretching freqs., MM2/CNDO model calcs., IR spectra anal. 7-36610
- cyclopentanone, IR spectral band fit optimisation 7-62360
- cyclophane-fluoranyl charge transfer complexes, struct. and stability, IR spectra anal. 7-50143
- cyclophosphazenes, linked to spermine, synthesis, struct. NMR, IR and mass spectro, antitumoural activity anal. 7-23291
- cyclopropane, ν_{10} and ν_{11} fundamentals in IR Fourier transform spectra 7-50052
- cyclopropane, IR spectra, combination bands, vibr.-rot. coupling parameters 7-25515
- decafluorobutane, rot. isomerism and vibro spectra calc. 7-5682
- di-2-pyridyl ketone benzoylhydrazone, electronic UV absorpt. and IR spectra 7-25504
- di-2-pyridyl ketone salicyloylhydrazone, electronic UV absorpt. and IR spectra 7-25504
- diacetylene, IR band intensities prediction using bond polar parameter method 7-50110
- diacetylene-HF complexes in solid Ar, IR spectra, H-bonding 7-10574
- diacyl peroxides, low temp. photolysis, vib. anal. for CO_2 dimer, IR spectra 7-15597
- 4,4'-diaminophenyl sulphone, intramol. charge transfer state, H-bonded cluster importance, fluoresc. and IR spectra 7-50213
- 2,3-diazido-1,3-butadiene, vibr. spectra, mol. struct., conform., GPED anal., Raman and IR spectra anal. 7-36609
- diazirine, ν_3 fundamental, rovibr. anal., IR spectra 7-10583
- 3-diazo-2-butanone - do(d6), vibr. anal., IR and Raman spectra 7-19853
- 1,2-dibromocyclopropane, rot. isomers, mol. vibr., IR and Raman spectra anal. 7-42609
- 1,2-dibromoethane, IR overtone spectra, vibr. anal. 7-10565
- dibromomethane, optically pumped laser, FIR laser line meas. 7-57306
- 1,3-dicarbonyl compounds, enol group, characteristic IR absorpt. freqs. 7-25503
- dichloroacetic acid complex with substituted pyridines, solvent effects, IR and ^1H NMR spectra anal. 7-62365
- 2,6-dichloroaniline, solid, vibr., IR spectra, CNDO/2 calcs. 7-3050
- trans-1,2-dichlorocyclohexane, solns., glass transition, conformational equilib., IR spectra 7-31044
- 1,2-dichloroethane, IR overtone spectra, vibr. anal. 7-10565
- 1,2-trans-dichloroethylene, vibr. distrib., time-resolved FTIR photofragment emission spectroscopy 7-25508
- dichlorofluoromethane, relax. to photophysical steady state during IR absorpt. 7-36618
- 2,2-dichloropropane- $\text{d}_0(\text{d}_6)$, vibr. anal. IR and Raman obs. 7-919
- 2-dicyanomethylene-1,3-indandione-methylated[2.2]paracyclophanes charge transfer complexes, IR and mass spectroscopy 7-25523
- didymium tartrate crystals, gel grown, charactn., thermal behaviour 7-39367
- 2-N,N'-diethylamino-N-oxymethyl-4,6-dichlorophenol, OHO H-bond, X-ray diff., IR and UV spectra 7-26731
- diffusive reflectance IR spectra, absorbing matrices effects 7-17831
- trans-1,2-difluoroethane, Ar_{364} matrix isolated, substitutional defects, consistent force field 7-57059
- difluoromethylene radical photofragment, time-resolved IR spectra 7-19836

infrared spectra of organic molecules and substances continued

- dihalogenomethylene sulphoxides, photochemistry, IR spectra (German) 7-31046
- N,N'-dihydroxyethylthiooxamide- $\text{d}_0(\text{d}_4)$, vibr. anal., X-ray diff., NMR, Raman, IR, visible and UV spectra 7-51741
- diiodomethane, optically pumped laser, FIR laser line meas. 7-57306
- diisopropylamine, mol. struct. and conform., GPED, Raman IR spectra, MO calcs. 7-20043
- dimedone Schiff bases, stretching vibr., IR spectra, solvent effects 7-57057
- 3,5-dimethoxy phenol, vibr., IR absorpt. spectra 7-19839
- 2,5-dimethoxybenzaldehydes, IR and Raman vibr. spectral anal. 7-57070
- dimethyl ether-HCl (DCI), H bonded complexes, IR spectra 7-19840
- 12,2-dimethyl-1,3-dioxolane-4-methanol, OH stretching band, free and H bonded species equilib., dichroism and IR spectra 7-10641
- 2,4-dimethylaniline, freq. assignments, IR and Raman spectra 7-22261
- dimethylbenzonitriles, IR and Raman spectra 7-25501
- 4,4-dimethylheptane, conform. anal., IR and Raman spectra 7-19863
- 3,3-dimethylhexane, conformational anal., IR and Raman spectra obs. 7-15602
- dioxirane, IR spectra, harmonic freq. and ^{18}O isotopic shifts 7-62361
- disodium cromoglycate in water, nematic lyotropic liq. crystal, struct. and order parameter, FTIR spectra 7-11899
- 2,4-dithiobiuret, Raman and IR spectra 7-62374
- dithiolates, cyclic vibr., IR and Raman spectra (German) 7-31045
- DMTCF salts, electronic and vibr. absorption spectra, electronic correlations 7-46034
- DPPE bilayers, aqueous assemblies, high press. IR studies 7-54501
- dye molecules, Raman and IR meas., quantum beat data interpretation 7-42591
- electrooptic parameters, valence optical theory 7-31088
- enzymes, structure-activity relations, IR-ATR modulation spectroscopy obs. 7-54474
- epihalohydrins, IR spectra, vibr. assignments 7-36603
- epoxydiane oligomers, struct., X-ray diff. and IR spectra (Russian) 7-11968
- epoxydiane polymers, struct., X-ray diff. and IR spectra (Russian) 7-11968
- ethane, Q branches of ν_2 fundamental band, laboratory spectra 7-5672
- ethane, vibr. anal. IR and Raman spectra, MNDO calcs. 7-10543
- ethane-Ar, vibr. predissoc. IR spectra 7-19971
- ethene, gas, CO_2 laser irradiation, end-point anal., IR spectroscopy detect. 7-65335
- ethene, laser-induced vibr. predesorption from NaCl 7-58615
- ethene adsorbed on partially exchanged $\text{ZnO-Na}_2\text{O-Al}_2\text{O}_3\text{-SiO}_2$, zeolite, IR and neutron scatt. studies 7-7001
- 3-ethoxy-4-hydroxybenzaldehydes, IR and Raman vibr. spectral anal. 7-57070
- ethyl 2-bromopropionate, mol. orbital study, Raman and IR spectra anal., CNDO calcs. 7-49931
- ethyl 2-chloropropionate, mol. orbital study, Raman and IR spectra anal., CNDO calcs. 7-49931
- 3-ethyl-5-[2-(3-ethyl-2-benzothiazolynylidene)-ethylidene]-rhodanine, polymorphism and electronic props. 7-37959
- ethylene, hydroformylation, in situ IR and EXAFS 7-59755
- ethylene dimer, mol. beam IR laser photodissoc. 7-10576
- ethylene-acrylic acid copolymers, struct. analysis using Fourier self-convolution of IR spectra 7-53337
- ethylene-Li-N $_2$ complexes in solid Ar, IR spectra 7-31033
- ethyne adsorbed on zeolite, time resolved FTIR obs. 7-54182
- ethynyl radicals, vibr. excited, colour centre laser spectra 7-62362
- etioporphyrin metal complexes, isomers, vibr. spectra interpretation 7-42617
- fluorenone bisazo pigments, electrophotographic sensitivity (Japanese) 7-38611
- fluoroform-d, Coriolis splitting parameter, vibr. depend., IR double-reson. spectra anal. 7-42616
- fluoromethane, optically pumped laser, FIR laser line meas. 7-57306
- fluoromethane, Rabi oscillations, Ramsey fringes, using CO_2 laser spectroscopy 7-10590
- fluorophenols, torsional far IR spectra, tilt influence, use of CNDO/2 method 7-56982
- p-fluorophenyltin, Raman and IR vibr. spectra 7-57058
- formate anion, isotopic species, vibr. anal., valence force fields calcs. 7-36577
- formic acid- d_1 , stretching vibr. Raman spectra 7-19866
- Fourier and computerised IR spectroscopy, Ottawa, Ont., Canada (June 1985) 7-48160
- free radicals from polyacetylene breakdown, IR colour centre laser spectroscopy 7-18890
- gallstone and bezoar, FTIR spectra, protein bands and secondary struct. 7-54473
- glycolic acid, Ar gas matrix, rot. isomerisation, ab initio SCF calcs. 7-19851
- graphite fibre reinforced epoxy composite, characterisation by diffuse reflectance Fourier transform IR 7-53332
- guanine, matrix isolated, IR spectra, keto-enol tautomerism 7-50126
- heptafluoriodobutane, pulse depend. IR absorpt. spectrum 7-19843
- hexabromomethane, vibrational spectra, crystal dynamics and phase transitions 7-38132
- hexafluoroethane, IR multiphoton dissociation, IR absorpt. spectra 7-42710
- hexamethyldisilylchalcogenides, Raman, IR and ^1H NMR spectral charact. 7-15615
- (hexamethylene-1,6)-bisdecylurethane, polymer chain fragment model, IR spectroscopic and X-ray studies (Russian) 7-19864
- (hexamethylene-1,6)-bisethylurethane, polymer chain fragment model, IR spectroscopic and X-ray studies (Russian) 7-19864
- hexanitroethane, crystallographic and vibrational study 7-38131
- hydrocarbon systems, gas and liq. phase, in situ modelling using FTIR at high press. 7-54221
- hydroxides, solid, OH stretching freq., ionic influences 7-50129
- 4'-hydroxy-1-methylstilbazolium, solvatochromism, spectra study, solvatochromic comparison method anal. 7-25519
- indole, cryst. and melt, vibr., IR and Raman obs. 7-3049
- indole, valence force const. IR and Raman freqs., normal coordinate anal. 7-914
- iodomethane, ν_4 band, high resolution IR spectra 7-5681
- iodomethane, IR spectrum, rot. anal. and interaction mechanism 7-57063
- iodomethane- d_1 , IR and NQR spectra 7-5706
- isoformyl cation, difference freq. laser IR spectroscopy 7-62366

infrared spectra of organic molecules and substances continued

- isolecine, homooligo peptide, conformational anal. by singlet-singlet energy transfer method 7-46998
 isooctane, in organic cpds. background mixture, IR spectra anal., max. difference method 7-46911
 cis-1,4-isoprene, mol. orientation, FT IR dichroism 7-17322
 Kevlar 49 fibres, N-H groups, photoacoustic Fourier transform IR spectra 7-39118
 Kevlar fibre surface, diffuse reflectance FTIR spectroscopy, fibre accessibility and water absorption 7-46040
 lanthanide thenoyltrifluoroacetate pyridine, Raman and FTIR spectra 7-57061
 layered structures, Raman and IR spectroscopy 7-3059
 lipid A, free, multibilayer, phase transition behaviour, FTIR, endotoxic principle of gram-negative bacteria outer barrier 7-54500
 liquid crystalline polymer, electric field FT-IR reflectance spectra 7-25688
 liquids, IR and anisotropic Raman band profiles theory, mol. interactions 7-31040
 liquids, non-polarised spectra, electric field effects, transparent capacitor spectroscopic cell 7-35607
 lithium phthalocyanine radical, optical and mag. props. 7-62417
 long-chain amphiphile on solid substrate, thermally induced disorder, Fourier transform IR spectra 7-12467
 lumiflavin vibr., isotope freq. shift, IR spectra 7-918
 m-dinitrotetramethylbenzene, single cryst., vibr. study, IR reflectance and transmission and polarised Raman spectra 7-25512
 mercaptopyrimidines, substituted, vibr. IR, Raman and UV spectra 7-31043
 methacrylic acid copolymers, struct. analysis using Fourier self-convolution of IR spectra 7-53337
 methane, absolute strengths and self-broadened widths in IR spectra 7-36622
 methane, Ar(Kr)(Xe) solid trapped, site struct. and hindered rot., IR spectra 7-5675
 methane, gaseous, low temp. collision-induced IR absorpt. 7-10562
 methane, IR band intensities 7-10579
 methane, solid to matrix, IR ν_4 band obs. 7-42608
 methane, vibr. anal. IR and Raman spectra, MNDO calcs. 7-10543
 methane $-d_0$ ($-d_4$), integrated IR intensities 7-50132
 methane- d_1 (d_3), bending mode triad, anal. model, IR spectra 7-19822
 methane- d_4 , pentad rovibr. levels, line parameters study, Fourier transform IR spectra anal. 7-50115
 methane- H_2 , gaseous mixture, far-IR absorpt. spectrum 7-10577
 methanol, adsorpt. on Al_2O_3 , Fourier transform IR spectra 7-38345
 methanol, C-O stretching band, transition dipole moment, laser Stark spectroscopy 7-57106
 methanol, FIR laser transitions, FIR and IR spectroscopic studies 7-36625
 methanol, in freons, ν (OH) IR band temp. variations 7-42610
 methionine, vibr. anal. IR and Raman spectra, MNDO calcs. 7-10543
 2-methoxy-2-oxo-1,3,2-oxazaphosphorinane, conformer struct. and populations, IR, NMR and X-ray spectra anal. 7-25509
 5-methoxyindole, IR and electronic absorpt. spectra 7-50103
 methyl(difluorophosphineborane), vibrational assignment, normal coordinate anal., Raman and IR spectra 7-62384
 methyl chloride, Fourier transform IR spectra, rot.-vibr. anal. 7-10571
 methyl cyanide- d_0 (d_3), lattice vibrs., Raman and IR spectra study 7-46019
 2-methyl oxetan, vibr. circular dichroism spectra, expt. and theoretical results 7-50208
 methyl silane, rot.-vibr. anal., Fourier transform IR spectra 7-19846
 methyl silane, torsional dipole consts., rot.-vibr. anal., microwave and IR spectra 7-19829
 methyl vinyl ketone, mol. torsional interactions, flexible model, far-IR spectra anal. 7-50101
 4-methyl-pyridine($-d_7$), phase transitions, mol. mechanism, IR and Raman spectra 7-32637
 methyl-substituted amine-HF complexes, methylation effect, IR spectra anal. 7-19855
 N-methylacetamide-formamide, varying H bond geometry, N-H bond vibr. properties, ab initio calcs. 7-10407
 methylene, triplet, ν_2 fundamental band, IR spectra 7-10568
 methylene, X^3B_1 , IR rot. transitions, diode laser absorpt. obs. 7-10567
 methylene chloride, high resol. vibr.-rot. anal., IR spectra 7-31019
 9-methylguanine, matrix isolated, IR spectra, keto-enol tautomerism 7-50126
 methylnitrene, matrix-isolated, IR and UV absorpt. spectra 7-42637
 methylphosphine, CO_2 laser irradiation, IT multiphoton absorpt. spectra 7-62474
 methylthiirane, vibr. spectra and ab initio calcs. 7-50147
 monolayer at liquid/solid and gas/solid interfaces, IR external refl. spectroscopy optimisation 7-48883
 multi- Σ donor and π -acceptor charge transfer complexes, struct., elec. and optical props. 7-44513
 nematic liquid crystals, IR dichroism, mol. interactions effects 7-45981
 neopentane, plastic phase orientational motion, Raman and IR spectra anal. 7-57067
 nitrile ylides, matrix photolysis of phenyl and azidostyrenes, isotopic shift, mol. struct. FT IR spectra anal. 7-31035
 nonadecane, liq., energy difference between specific and localised conform. isomers, FTIR spectra 7-42615
 olefin- H_2O complexes, matrix isolation study, IR spectra, H-bonds 7-31032
 oleic acid, polymorphism, order-disorder phase transition, IR and Raman spectra anal. 7-33379
 organic conductors, IR absorption spectra and electron-electron interactions 7-46032
 organic films, on inorganic substrates, FT IR reflection spectrosc. 7-39097
 organic fusion reactor coolant, radiation stability 7-62059
 organic linear chain conductors, IR and near IR props. 7-22247
 organic molecule conformational anal., vapour phase IR spectra study 7-57069
 organometallic adduct formation during MOCVD growth of InGaAs films 7-33588
 peak-separation algorithm for personal computer, appl. to visible emission and IR absorpt. spectra (Japanese) 7-31015
 penanthrene-TCNQ complex, physical props. 7-52622
 pentachlorophenol-hexachlorobenzene, solid soln., H-bonding and phase transitions 7-17310

infrared spectra of organic molecules and substances continued

- 1,3-pentadiyne, IR band intensities prediction using bond polar parameter method 7-50110
 1-pentyne, vibr. anal., IR and Raman spectra 7-19852
 perfluorotrimethylgermyl anion, vibr., IR and Raman spectra (German) 7-31048
 peroxide urea-formaldehyde oligomers, structuration, IR spectra 7-39126
 perylene red film coated on Ge, ATR and refl.-absorpt. IR spectroscopic analysis 7-41510
 PET, films, depth-profiling, FTIR photoacoustic spectroscopy 7-25686
 PET, three-dimens. IR spectroscopy 7-46041
 PET film, trichroic IR absorpt. analysis, methods description 7-33380
 PET films, one-way drawn, trichroic IR absorpt. spectra 7-33381
 phenols, vibr. spectra, calc. and interpretation 7-42596
 phenyl compounds, vibr. studies, IR and Raman spectra 7-63758
 phenylalkynes, conform. in soln. and solid, vibr. anal., Raman and IR spectra study, valence force field calcs. 7-36612
 phthalocyanine metallamacrocyclic assemblies, $[Si(Pc)O]_n$, molecular metals, conduction props. 7-2585
 pivalic acid in dil. solution, dimerisation, IR spectroscopy 7-65313
 plasma film polymerisation, ion bombardment effects, deposition rates, IR, UV and visible absorpt. spectra studies 7-28312
 platinum-cyanoalkene complexes, mol. vibr. study, Raman and IR spectra anal. 7-42626
 PMMA film on glassy C, IR external refl. spectroscopy obs. 7-41509
 polar fluids, FIR power absorpt., maximum freq. decrease with temp. 7-53319
 poly(4-(3-pyridyl), 8-methyl, 2,3-6,7-quinolino), soluble aromatic ladder polymer, preparation and props. 7-2593
 poly(C) and poly(I).poly(C) complexes with model phospholipid membranes, IR spectroscopic obs. 7-40094
 poly(ethylene oxide)- $LiClF_4SO_3$ evaporated electrolyte films, struct. and ionic cond. characts. 7-64002
 poly(p-phenylene terephthalamide), single cryst. and spherulites, morphology and struct. investig. 7-11949
 poly(phenylene vinylene), oriented films, IR spectra 7-37896
 poly(vinyl acetate) film on Cu, FTIR surface EM wave spectroscopy, Otto config. 7-46162
 poly m-phenylene sulphide, SbF_5 doping, elec. cond., IR spectra 7-17006
 poly-L-lysine, deuterated, Fourier transform vibr. circular dichroism in amide I bands 7-54475
 poly-p-decylstyrene solns., optical and hydrodynamic investig. (Russian) 7-13167
 poly-p-phenylene sulphide, SO_3 -doped, mol. structure, 1H NMR, ^{13}C CP/MAS NMR and IR studies 7-2939
 poly-peri-naphthalene, 1D graphite polymer, morphology and struct. 7-44400
 poly-vinylacetate-Cu, thin polymer films, Fourier transform IR ellipsometry 7-53334
 polyacetylene:I, photoexcitation spectra 7-64657
 polyacetylene:I films, liquid crystal polymerisation synthesis under mag. fields 7-65318
 polyacetylene, cond., fast FTIR and IR intensity spectra, struct. and electronic props. 7-53335
 trans-polyacetylene, doped, in soln., IR spectral props., conjugation lengths depend. 7-64655
 polyacetylene, dynamical cond. of soliton lattice and polaron lattice, continuum model 7-45174
 polyacetylene, dynamical phonon conductivity, determ. 7-64111
 trans-polyacetylene, highly oriented, photoexcitations and photocond. response 7-64292
 polyacetylene, I_2 -doped, quantitative optical study 7-53380
 trans-polyacetylene, IR activity of phonons around a soliton 7-64107
 polyacetylene, localised modes of soliton, IR absorpt. 7-64108
 polyacetylene, p-type doped, reaction with H_2O 7-65316
 polyacetylene, solitons and IR-active localised vibrational states, Schrieffer-Heeger model calcs. 7-2134
 polyacetylene films, oxygen-exposed, IR transmission spectra 7-13181
 polyacetylene partially isomerized, detection of soliton shape modes 7-38469
 polyacrylonitrile fibres, shrinkage, IR spectra investig. 7-59206
 polyamide acids, dil. soln., structuration (Russian) 7-42810
 polyamide hydrazides, aromatic, p- and m-phenylene units effects on struct.-prop. rels. 7-51604
 polyaniline and aniline oligomers, spectroscopic and elec. props. 7-64653
 polyatomic molecules, jet-cooled IR laser spectroscopy 7-41495
 polyatomic mols., IR spectra, rot. reson. 7-25514
 polybutadiene, sequence distribts., polymerisation kinetics, IR spectra, NMR 7-16444
 polybutadienes, high-temp, struct. transition obs. (Russian) 7-63820
 polycyclic aromatic hydrocarbon cations, doubly-charged, form. and destruction, IR and visible spectra 7-55774
 polydiacetylene, conductivity enhancement by chemical doping and ion implantation 7-21957
 polydiacetylene, IR photoinduced absorpt., bipolarons 7-53313
 polydimethylsiloxane oligomers, FT-IR spectra, Fourier self-deconvolution appl. 7-25687
 polyesteramideurethane, segmented, struct., polar low mol. wt. cpds. effects (Russian) 7-26673
 polyethylene, low density, IR spectroscopy under high elec. stresses 7-39129
 polyethylene film, low density, diffusion and sorption of liquids, IR ATR spectrosc. obs. (German) 7-53302
 polyethylene films, picosecond Raman scatt. after IR excitation, ultrafast vibr. energy transfer 7-64621
 polyethylene IR absorption spectra modification by elec. fields 7-53352
 polyethylene oxide-disubstituted benzene intercalates, Fourier transform IR spectra 7-13153
 polyethylenes, supermol. struct., glow-discharge induced transformations (Russian) 7-63523
 polyimides, dil. soln., structuration (Russian) 7-42810
 cis-1,4-polyisoprene, mol. orientation, FT IR dichroism 7-13159
 polyisoprene, sequence distribts., polymerisation kinetics, IR spectra, NMR 7-16444
 polymer, three-dimens. IR spectroscopy 7-46041
 polymer blend, intensity spectroscopy and FTIR as tool for struct. and inter mol. interactions determ. 7-53338
 polymer blend films, Fourier transform IR/ATR spectroscopy studies 7-53333

infrared spectra of organic molecules and substances continued

- polymer film on metal substrate, FTIR surface EM wave spectroscopy, Otto config. 7-46162
- polymer mixtures, H bonding, enthalpy-IR freq. shift correl., acid-base interaction 7-51667
- polymer-metal system, enhanced ATR spectra of polymer surface layers 7-22266
- polymers, deformation, elastic and plastic, IR spectrosc. obs. (Russian) 7-64659
- polymers, gas-filled, action as cutoff optical filters in the IR region 7-57529
- polymers and related cpds., electronic props., Winter School, Kirchberg, Austria (March 1985) 7-4613
- polyoxy-(allyl)phenylene electrochemically prepared film, elec. props., permittivity and solubility 7-27665
- polyoxyethylene, conformation, vibrational spectra, normal coordinate analysis 7-53317
- polyoxyethylene-p-dihalogenbenzene intercalates, struct. 7-13154
- polypeptides, vibr. circular dichroism, 3_{10} -helix form., chain length depend., IR spectra, PMR 7-15633
- polyphenylene sulphide coatings, internal struct., curing effect 7-22861
- polyphenyls, phase transitions and IR spectra under press. 7-6725
- polypropylene, high-oriented, struct. rel. to physico-mech. props. (Russian) 7-26672
- polypropylene, IR spectroscopy under high elec. stresses 7-39129
- polypropylene, isotactic, polymorphic forms, FTIR far-IR obs. 7-53339
- polypropylene IR absorption spectra modification by elec. fields 7-53352
- polyethylene films, ion bombarded, primary chemical events, IR study 7-26809
- polythiophene, IR activity of photoexcitations 7-7703
- polythiophene, vibrational spectra and elec. conductivity 7-2598
- polythiophene films, electrochemically polymerised, optical studies 7-51670
- polyurethane insulation, thermal and elec. aging, prebreakdown phenomena, FTIR spectra study 7-39568
- polyurethanes, molecular struct., morphology, phase mixing, mech. props. 7-51664
- polyvinyl acetate film, trichroic IR absorpt. analysis, methods description 7-33380
- polyvinyl carbazole plasma CVD thin films, photoconductive props. study, IR and UV spectra meas., electrode effects 7-27367
- polyvinylidene film, oriented phase I, trichroic IR absorpt. 7-33382
- polyvinylidene fluoride, three-dims., FTIR spectroscopy 7-46041
- polyvinylidene fluoride/PZT, composites, dielec. behaviour 7-38992
- polyvinylidene fluoride, films, depth-profiling, FTIR photoacoustic spectroscopy 7-25686
- porphyrin coordination polymers, pyrazine-bridged, optical and conductive props. 7-2586
- potassium saccharinate, single cryst., elemental anal. IR spectra 7-22235
- proline, stabilising solute, calorimetric and IR spectroscopic study 7-8492
- propane, vibr. anal. IR and Raman spectra, MNDO calcs. 7-10543
- propanes, ^1H labelled, IR and Raman spectra, vibr. analysis, D substitution effect 7-50141
- propyne, $2\nu_9$ band study, Fourier transform IR spectra anal. 7-50119
- propyne, ν_3 and $2\nu_9$ bands study, Fermi reson., IR spectra anal. 7-50120
- protein in aqueous solution, FTIR spectra, automatic water subtraction procedure 7-54836
- protein structure by FTIR self-deconvolution 7-54476
- protein structure determination by FTIR 7-54471
- protein structure-spectra correlations, nonaqueous solvent effects using FTIR and ATR flow cell 7-54472
- proteins and lipids, FTIR spectra, water subtraction procedure 7-54834
- PTFE, chem. modified, humidity sensor appls. 7-9839
- PVC, pure and plasticized, orientation, Fourier transform IR study 7-44661
- pyridine, on Ag surface, IR laser stimulated desorption mol. spectroscopy 7-58614
- pyrozone, triplet lifetime, temp dependence, visible and IR phosphorescence spectra 7-22328
- trans-retinylidene Schiff base, protonation on crystal surfaces, attenuated total refl. IR study 7-50102
- rhodopsin refolding during Meta II decay, Fourier transform IR difference spectroscopy obs. 7-59926
- riboflavin, and derivatives, vibr., isotope freq. shift, IR spectra 7-918
- ribonuclease, FTIR obs. of folding 7-54470
- rubber, natural, mol. orientation, FT IR dichroism 7-13159
- rubber, natural, mol. orientation, FT IR dichroism 7-17322
- salicylidenamines, thermochromic and photochromic, IR spectra, conformational influence 7-53310
- semirigid macromolecules, conc. solns., liq.-cryst. order form. (Russian) 7-36833
- silaethylene, harmonic vibr. freqs., IR spectra, ab initio SCF CI calcs. 7-15600
- skatole, valence force const. IR and Raman freqs., normal coordinate anal. 7-914
- sodium saccharinate single cryst., elemental anal. IR spectra 7-22235
- stearic acid mono- and bi-layers on Al and Au, refl.-absorpt. IR spectra, order-disorder transitions 7-46165
- superconductors, FIR spectroscopy 7-38816
- surface, cadmium stearate Langmuir-Blodgett films, thermal disordering, optoacoustic IR spectra anal. 7-52236
- surface EM wave FTIR spectroscopy of very thin films 7-41506
- surface FTIR-ATR spectroscopy, lower limit of thickness of measurable surface layer 7-41508
- surface IR external reflection spectroscopy of thin films on glassy C electrodes 7-41509
- surface molecules, Fourier transform IR studies 7-54220
- TCNQ salt, MPHT(TCNQ) $_2$, ion-radical salt, spin ordering 7-64442
- TCNQ salts, quarter-filled band, optical absorption studies 7-46033
- tetrachlorodibenzodioxins, isomers, identification, micro-diffuse reflectance and matrix isolation FT-IR techniques 7-25502
- tetracyanoethylene-methylated [2.2]paracyclophanes charge transfer complexes, IR and mass spectroscopy 7-25523
- tetradecafluorohexane, rot. isomerism and vibro spectra calc. 7-5682
- tetramethyl-phenylene-diamine chloranil, mixed-stack cpds., spectroscopy of dimerisation 7-22260
- tetraphenylmethane, vibr., dichroism, IR and Raman spectra 7-31042
- 2-thio-1,3,2-oxazaphosphorinane, conformer struct. and populations, IR, NMR and X-ray spectra anal. 7-25509
- thioformaldehyde, RF discharge, optogalvanic detected IR spectra 7-20970

infrared spectra of organic molecules and substances continued

- thiopyrrolycyanine dyes, in polymer matrix, hypsochromic shift, solvation, IR spectra 7-42611
- (TMN) $_3\text{X}_2$, (X=ClO $_4$, AsF $_6$), cation radical salts of tetramethoxynaphthalene, EPR, optical absorpt. and conductivity studies 7-53113
- TMTCT salts, electronic and vibr. absorption spectra, electronic correlations 7-46034
- (TMTSF) $_2\text{AsF}_6$ and (TMTSF) $_2\text{SbF}_6$, SDW state, far IR spectra 7-33388
- (TMTTF) $_2\text{Mo}_2\text{Cl}_4$, prep. by electrocrystallisation, struct. and spectroscopic characterisation 7-46295
- toluene adsorbed on activated C, IR spectra 7-10573
- s-triazine, gas phase, mol. struct., GPED anal., ab initio force field calcs. 7-36457
- trichloromethanesulphenyl chloride, mol. vibr. and config., Raman and IR spectra anal. 7-42622
- 2,4,6-trichloropyrimidine, liq. and vapour, electronic and vibr. spectra, UV and IR obs. 7-19859
- trifluoroacetic acid, H-bonded complex with esters, lifetimes, IR absorpt. spectra 7-50133
- trifluoromethane, interacting states, high resolution FTIR absorpt. spectra 7-57065
- 3,3,3-trifluoropropylene, intracavity dye laser photoacoustic spectra for overtone excitation, IR spectra 7-10575
- trimethyl-d $_5$ -pyrazine, normal vibr., Raman and IR parameters investig. 7-50074
- trimethylammonium hexachloroantimonate, mol. vibr., Raman and IR spectra anal. 7-53347
- 3,3,4-trimethylhexane, config. anal., IR and Raman spectra 7-19861
- 2,3,3-trimethylhexane, conformational anal., Raman and IR spectral obs. and vibr. assignments 7-15614
- trimethyloxonium hexachloroantimonate, mol. vibr., Raman and IR spectra anal. 7-53347
- trimethylpyrazine, normal vibr., Raman and IR parameters investig. 7-50074
- trimethylsulfonium iodide-d $_0$ (-d $_9$), vibr. spectrum, normal coord. calcs. 7-50077
- trimethylsulfonium-d $_9$ (-d $_9$), vibr. spectrum, normal coord. calcs. 7-50077
- two-configuration SCF wave functions, IR intensities and polarisabilities evaluation 7-10582
- unimolecular reaction, kinetic data eval. from freq. shifts of IR absorpt. bands 7-33911
- N-urethanyl- α -amino acids, Fourier transform vibr. circular dichroism of carbonyl stretching modes 7-50207
- vibrationally excited mol. IR absorpt. red shift for CO $_2$ laser pulse duration control 7-43174
- vinyl chloride, vibr. distrib., time-resolved FTIR photofragment emission spectroscopy 7-25508
- vinyl formate, gas phase structure anal., ab initio calcs., molecular mechanics calcs., IR spectra 7-19691
- violacein, thin layer chromatography and FTIR analysis 7-54469
- VPE, organometallic, in-situ, real-time diagnostics using IR-diode laser spectroscopy 7-22537
- BrO $_2$ RF discharge, optogalvanic detected IR spectra 7-20970
- CCl $_4^+$, Born-Oppenheimer pot. fn., mol. rot.-vibr. study, IR spectra anal. 7-36604
- CoCl $_2$ dipyrindine quasi-1D Ising system, far IR magnetic excitation spectrum 7-59040
- D $_2\text{O}$, optically pumped laser, FIR laser line meas. 7-57306
- Ga(CO) $_2$, form. in hydrocarbon matrices, magnetic parameters, EPR and IR spectra anal. 7-19906
- H-bonds in molecular biology, FTIR spectra, strongly anharmonically coupled vibr. 7-47009
- H $_2$ -methane pairs, rototranslational far IR absorpt. spectra 7-15601
- Li(ethylene) $_n$, in solid Ar, IR spectra and struct. 7-36614
- γ -methacryloxypropyltrimethoxysilane, chem. reaction on PbO surface, Fourier transform IR spectra 7-53308
- Mo complex, Mo phthalocyanine, struct., IR spectra, powder and liq. soln. EPR spectra study 7-64509
- OH(OD), stretching vibr. in alcohols and silanols, pop. lifetimes, IR spectra 7-19844
- PrCl $_3$ organic complexes, spectral energies and oscillator strengths 7-3067

infrared spectra of polyatomic inorganic molecules

- adsorption of H $_2\text{O}$ and pyridine on (VO) $_2\text{P}_2\text{O}_7$, IR spectra 7-17818
- alkali halides, neutral molecule incorporation, composite form. at room temp. 7-54101
- alkali metal chlorate ion pairs, coord. structs., FT IR matrix isolation spectra 7-62367
- alkali metal perchlorate vitrified dil. solns., IR spectra anal. 7-19857
- astrophysical molecules, theoretical predictions of the infrared and microwave spectra of small molecules 7-10561
- CO $_2$, isotopic species, vibr. transition const., IR emission spectra 7-19849
- electrooptic parameters, valence optical theory 7-31088
- hydroxides, solid, OH stretching freq., interionic influences 7-50129
- matrix-isolated molecules, FTIR vibr. circular dichroism 7-50104
- peak-separation algorithm for personal computer, appl. to visible emission and IR absorpt. spectra (Japanese) 7-31015
- rare earth naphthenate complexes, extract phase, FTIR and subtraction spectra 7-50142
- salt/water/aprotic solvent mixtures, alkali cation influence, IR spectra anal. 7-19856
- simple molecules, superfine, hyperfine struct., from IR spectra 7-10586
- thiometallato complexes, mol. vibr., electronic struct., IR and Raman spectra study 7-57068
- transition metal complexes, IR and Raman spectra 7-50128
- two-configuration SCF wave functions, IR intensities and polarisabilities evaluation 7-10582
- vibrationally excited mol. IR absorpt. red shift for CO $_2$ laser pulse duration control 7-43174
- vittrified dil. alkali metal nitrate solns., IR spectra anal. 7-19857
- water, liquid, OH stretching vibr. spectrum, mol. dynamics study, IR, Raman and neutron diff. spectra 7-44329
- water vapour abundance and distrib. in Jupiter atmosphere, IR obs. 7-60594
- AlBr $_3\text{NH}_3$, vapour phase, vibr. anal., high temp. IR spectra 7-31050
- Ar-HCl van der Waals complexes, IR spectra, secular eqn. calc. 7-31031
- Ar-HF binary complex, long-lived metastable systems 7-36515
- Ar-N $_2\text{O}$ van der Waals complex, mol. beam IR spectra 7-31030

infrared spectra of polyatomic inorganic molecules continued

- ArHCl, intracavity for IR laser spectroscopy, van der Waals bonds, vibr. motions 7-10589
 ArHF van der Waals complexes in supersonic jets, IR laser spectra 7-19842
 C_2N_2 -Ar gaseous mixture, collision-induced absorpt., quadrupole moments, IR and microwave spectra 7-50098
 CO, IR active gas at high press., absorpt. props. 7-10578
 CO₂, and mixtures, line interaction effects in IR absorpt. spectra 7-31038
 CO₂ FTIR spectra, band intensities 7-50264
 CO₂, gas mixtures, ν_3 band, rot. relax., IR spectra 7-42613
 CO₂, IR absorption spectrum, 2.7 μ m and 4.8 μ m band intensities 7-50130
 CO₂ mixtures, gas density effect on Q branch in IR spectra 7-42612
 $^{13}CO_2/^{12}CO_2$, abundance meas. by nondispersive IR heterodyne ratio-metry 7-15731
 CO₂-Ar gaseous mixture, collision-induced absorpt., quadrupole moments, IR and microwave spectra 7-50098
 Ca salts, ion-molecule interactions in DMF, IR spectrosc. obs. 7-10584
 ClH_3^+ ion, ν_2 band, mag. field modulated IR laser spectrosc. 7-36605
 CO₂, intensity and press. broadening meas. in ν_3 fund. 7-50265
 COCl₂, electronic transitions, IETS 7-50099
 CsH₂PO₄(d₂), polarised IR and Raman spectra, internal vibr. 7-50125
 CsH₂PO₄(d₄), polarised IR and Raman spectra, transition dipole moments, orientation calcs. 7-50124
 Cu complex, 2-acetylpyridine thiosemicarbazone copper(II) complex, mag. moment meas., ESR and spectra investig. 7-57105
 Cu complex, pyridine 2-aldehyde thiosemicarbazone copper(II) complex, mag. moment meas., ESR and spectra investig. 7-57105
 D₂O, H- and D-bonded dimers, relative stabilities, IR spectra 7-62364
 DOCl, FTIR spectrum, band origins 7-50140
 F₂+CS₂, reaction, mol. electronic emission spectrum 7-3577
 FDF⁻, IR spectrum, ab initio calcs. 7-25506
 FHF⁻, IR spectrum, ab initio calcs. 7-25506
 Fe complex, oxy(tetraphenylporphyrinate), Iron II, cocondensation products, struct. and bonding, IR spectra 7-10572
 Fe oxide coatings on Invar, IR emission, absorpt. modes effect 7-27708
 Fe oxides, coatings on Fe, IR emission, absorpt. modes effect 7-27708
 Fe₂O₃, adsorpt. of pyridine, gas chromatography and IR spectro study 7-39917
 Fe(OH)₃, adsorpt. of pyridine, gas chromatography and IR spectro study 7-39917
 GaBr₃, vapour phase, vibr. anal., high temp. IR spectra 7-31050
 GeH₄, CO₂ laser irradiation, IT multiphoton absorpt. spectra 7-62474
 GeH₃D(GeD₃H), bending mode triad, anal. model, IR spectra 7-19822
 H+CO₂, rot. resolved hot atom collisional excitation by time-resolved diode laser spectra 7-10731
 H₂¹⁸O, hot band, IR spectral line positions and intensities 7-36623
 H₂-Ar pairs collision-induced rototranslational spectra, ab initio dipole-moment surface 7-15493
 H₂-He collision complexes, rotovibr. spectra. SCF CEPA calcs. 7-42478
 H₃⁺ and isotopomers, IR spectra, ab initio calcs. 7-30929
 H₃⁺, vibr.-rot., IR photodissociation spectra 7-31009
 H_n⁺ cluster ions, (n=5,7,9,11,13,15), vibrational predissociation spectroscopy 7-10588
 HBO detection by discharge modulated IR diode laser spectroscopy 7-25505
 HCN cluster form. in carbon tetrachloride matrix, IR spectra 7-19841
 HCN-HF, excited vibr. states, gas-phase IR spectrum 7-50108
 HCN-HF H bonded complexes, hot bands Doppler limited laser spectroscopy 7-19835
 (HCN)_n microcluster selective formation in cryogenic matrices, FTIR spectroscopy obs. 7-48895
 HDO and D₂O, IR spectra, vibro-rot. transitions, line intensity meas. 7-50109
 HDO, H- and D-bonded dimers, relative stabilities, IR spectra 7-62364
 HDO, $\nu_1 + \nu_2$ and $3\nu_2$ bands, energy level and intensity calcs. 7-5654
 HDO, vibr. modes, rot. decoupling 7-57042
 (HF)₂, IR and Raman spectra, vibr. calcs., secondary basis set superposition error 7-25478
 (HF)₃, vibr. predissoc. IR spectra 7-19971
 H₂GeD, Fourier transform IR spectra, rovibr. anal. 7-25516
 HI and DI in solid N₂, IR spectra in temp. range 9 to 30 K 7-50127
 HN₃, rot. anal. for ground, ν_2 and ν_6 states, IR spectra 7-19850
 HNC, 2100 cm⁻¹ bands, IR Fourier transform spectra anal. 7-50117
 H₂O, absorpt. of 2.3 μ m radiation 7-57060
 H₂O biological charge transfer processes, IR and microwave spectra 7-3749
 H₂O dimer, far IR absorpt. spectra 7-47539
 H₂O, H- and D-bonded dimers, relative stabilities, IR spectra 7-62364
 H₂O in P/Comet Halley (1982i), post-perihelion obs. from KAO 7-47786
 H₂O mol., IR absorpt. spectra, anharmonicity effects, contact trans-formational and quantum chemical calcs. 7-25385
 H₂O, submm rotational lines, use for cometary spectroscopy 7-47795
 H₂¹⁸O, energy levels, line intensities, Fourier transform IR spectra 7-5674
 H₃O⁺, ν_3 fundamental band meas. with colour centre laser 7-57064
 HOCl, FTIR spectra, vibr. rot. const. and harmonic force field 7-50140
 HOCl, IR spectra, ν_2 and ν_3 bands, a-type and b-type transitions 7-50112
 H₂S adsorbed on SiO₂/Na, FTIR and Raman spectra obs., Na promotion of Claus process 7-46869
 H₂S, in O₂ matrix, FT IR spectra 7-36606
 (H₂S)₂ in O₂ matrix, FT IR spectra 7-36606
 HSOH, Cl analytic energy second derivatives, IR intensities and vibr. freqs. prediction 7-5608
 H₂SiD, Fourier transform IR spectra, rovibr. anal. 7-25516
 H₂SiF, Coriolis coupling, FT IR spectrum, rovibr. anal. 7-5679
 H₂SnBr, rovibr. anal., harmonic force field calc., Fourier transform IR spectra study 7-50122
 H₃¹¹⁶Sn⁷⁹Br, FT IR spectra, rovibr. investig. 7-921
 H₃SnCl, rovibr. anal., harmonic force field calc., Fourier transform IR spectra study 7-50122
 H₃¹¹⁸Sn³⁵Cl, FT IR spectra, rovibr. investig. 7-921
 H₃SnI, rovibr. anal., harmonic force field calc., Fourier transform IR spectra study 7-50122
 H₃¹¹⁶SnI, FT IR spectra, rovibr. investig. 7-921
 HTO, mol. vibr.-rot., IR spectra anal. 7-50116
 KSFO₃, vibr., force const., IR spectra 7-19837

infrared spectra of polyatomic inorganic molecules continued

- Li cpds., energy stability, struct., vibr. spectra, MO LCAO SCF calcs. 7-15512
 Li salts, ion-molecule interactions in DMF, IR spectrosc. obs. 7-10584
 Mg salts, ion-molecule interactions in DMF, IR spectrosc. obs. 7-10584
 MgH₂, collisional redistrib. profiles meas. 7-42525
 Mn₂(CO)₁₀, photolysis, thermal chem., photofragment vibr. excitation 7-23047
 Mo complex, tetraacetomolybdenum, metal-metal quadruple bonds, normal coordinate anal. 7-42578
 Mo complexes, isopropylammonium dihydrogenoctamolybdate dihydrate, vibr. spectrum 7-36628
 Mo complexes, with dioxo ligands, mol. vibr., IR and Raman spectra anal. 7-50151
 Mo₂Cl₈⁴⁻, metal-metal quadruple bonds, normal coordinate anal. 7-42578
 N₂-H₂, gaseous mixture, far IR absorpt. spectrum 7-19858
 N₂-HF, IR spectrum and vibr. predissoc. 7-50106
 N₂-methane gaseous mixture, collision-induced absorpt., IR and microwave Fourier transform spectra anal. 7-50097
 NF₃, integrated intensities and IR absorpt. bands, ab initio (3.1) calcs. 7-56953
 NH₂ + NO reaction, kinetic spectroscopy using a color center laser 7-9901
 NH₂⁻ struct., velocity modulation IR laser spectroscopy 7-15599
 NH₃, adsorpt. complexes with heterogeneous catalysts, vibr. study, IR spectra anal. 7-36607
 NH₃ CW MIR laser, intensity and half-widths, absorpt. meas. 7-36941
 NH₃, integrated intensities and IR absorpt. bands, ab initio (3.1) calcs. 7-56953
 NH₃, ν_2 band, vibr.-rot. transitions, press. broadening coeffs., IR spectra anal. 7-50121
 NH₃ S₂ bands, isotope shift, diode laser spectra 7-19845
 NH₂D and ND₂H, IR spectra, vibr.-rot. band, inversion doubling 7-25517
 NH₂D, IR and microwave spectra, rot. anal. 7-25518
 NH₃⁺, ν_4 fundamental band, IR difference-freq. laser spectra 7-50096
 NO+NO₂=N₂O₃, kinetic meas., time-resolved IR laser absorpt. 7-17771
 NO₃⁻, aq. soln., band shape anal., Raman and IR spectra 7-57067
 N₂O, band intensities, IR absorpt. 7-36619
 N₂O IR transmittance, band models comparison 7-19860
 N₂O, protonated, IR spectra, vibr. and rot. anal., struct. 7-10566
 N₂O, submm spectroscopy 7-31041
 Na salts, ion-molecule interactions in DMF, IR spectrosc. obs. 7-10584
 Ne-OCS, mol. beams, IR absorpt. and microwave-IR double reson. spectra 7-62427
 Ni complex, tetrakis(trimethylphosphine) Ni(0), synthesis and mol. vibr. study, Raman and IR spectra anal. 7-42627
 NiO, adsorpt. of pyridine, gas chromatography and IR spectro study 7-39917
 Ni(OH)₂, adsorpt. of pyridine, gas chromatography and IR spectro study 7-39917
 O₃ absorption of high-power IR radiation 7-1237
 O₃, IR multiphoton excitation probed by CARs, vibr. population distrib. 7-10591
 OCS, line strengths and collisional half-widths, IR spectra 7-36620
 OCS, rot.-vibr. anal., electronic ground state, MW, IR and Raman spectra 7-19820
 OF₂, ν_2 fundamental, rovibr. study, Fourier transform IR spectra anal. 7-50123
 PF₃, integrated intensities and IR absorpt. bands, ab initio (3.1) calcs. 7-56953
 PF₃ molecules, jet-cooled IR laser spectroscopy 7-41495
 PH₃, integrated intensities and IR absorpt. bands, ab initio (3.1) calcs. 7-56953
 POBr, gaseous, form., mass spectrometric and matrix IR investig. 7-39908
 Pd complexes, bivalent, mutual influence of ligands, vibr. spectrosc. investig. 7-10585
 Pd(CN)_x (x=1 to 4), liq. NH₃ solns., Raman and IR vibr. spectra 7-57076
 Pt complex, tetrakis(trimethylphosphine) Pt(0), synthesis and mol. vibr. study, Raman and IR spectra anal. 7-42627
 Re complex, tetraacetodichlororehenium, metal-metal quadruple bonds, normal coordinate anal. 7-42578
 Re₂Cl₈²⁻, metal-metal quadruple bonds, normal coordinate anal. 7-42578
 Rh, Al₂O₃ supported, CO-induced struct. changes, H₂ effect, IR study 7-23063
 SCN⁻, aq. soln., band shape anal., Raman and IR spectra 7-57067
 (SF₆)₂, mol. beam IR laser photodissoc. 7-10576
 SF₆ clusters, supersonic jet, Fourier transform IR spectra 7-15598
 SF₆, dimer dissoc., dimer conc., isotope effect, model and bolometer IR spectra anal. 7-19977
 SF₆, IR multiphoton excitation probed by CARs, vibr. population distrib. 7-10591
 SF₆ in Ar soln., IR absorpt. spectra 7-25522
 SF₆, mol. vibr.-rot. const., IR saturated absorpt. spectra anal. 7-50118
 SF₆-Ar mixtures vibr. relax. time resolved IR multiphoton absorpt. 7-5752
 SF₆-Ar₂ clusters, spectroscopic obs. of phase coexistence 7-36842
 SF₆+N₂O, vibr. energy transfer and relax. study, kinetic model, IR fluorescence spectra 7-50227
 SF₆Ar, mol. beam IR laser photodissoc. 7-10576
 SO₂ adsorbed on SiO₂/Na, FTIR and Raman spectra obs., Na promotion of Claus process 7-46869
 SO₃ complexes with selected O₂-containing bases, matrix isolation IR spectra 7-36615
 SiF₄, CO₂ laser irradiation, IT multiphoton absorpt. spectra 7-62474
 SiF₄, dimer dissoc., dimer conc., isotope effect, model and bolometer IR spectra anal. 7-19977
 SiF₄ in Ar soln., IR absorpt. spectra 7-25522
 SiF₄, saturation spectrum at P(30) line of 9.4 μ m band of CO₂ laser 7-50134
 SiH₂, geometric structs., force const. and vibr. spectra, SCF CI calcs. 7-19713
 SiH₃, geometric structs., force const. and vibr. spectra, SCF CI calcs. 7-19713
 SiH₄, CO₂ laser irradiation, IT multiphoton absorpt. spectra 7-62474

infrared spectra of polyatomic inorganic molecules continued

- SiH₄, dimer dissociation, dimer concentration, isotope effect, model and bolometer IR spectra anal. 7-19977
 SiH₄, geometric structures, force constants and vibr. spectra, SCF CI calcs. 7-19713
 SiH₃D(SiD₃H), bending mode triad, anal. model, IR spectra 7-19822
 Si₃N₄, films, IR character., optical dispersion induced freq. shifts 7-27709
 Sn complexes, ESCA, Mossbauer and IR spectrosc. investig. 7-5678
 SnH₃D(SnD₃H), bending mode triad, anal. model, IR spectra 7-19822
 T₂O, IR spectra, ν_3 mode, rot. and quartic distortion consts. 7-50111
 TeF₆, ν_3 bond, free jet IR absorpt. spectroscopy 7-10569
 UF₆, diode laser absorption at room temp. around 16 μ m 7-25521
 UO₂Cl₂·2H₂O, IR spectra, complex effect, isotope shift, extraction anal. 7-25058
 W complex, W(VI)-mannitol, IR and NMR spectrosc. 7-50136
 W complex, W(VI)-sorbitol, IR and NMR spectrosc. 7-50136

infrared telescopes *see telescopes***infrared thermography** *see infrared imaging***infrared transmitters** *see infrared sources***infrasonic waves** *see acoustic waves***initial value problems**

- 3D 2-phase immiscible flow displacement, finite element analysis and error analysis (*Chinese*) 7-16229
 abstract time-dependent transport equations, initial-boundary value evolution problem 7-56190
 astrophysical flows, initial value problems, simple adaptive grids in 1D 7-66457
 asymptotic behavior of solution to the Cahn-Hilliard equation 7-55966
 asymptotic expansions and boundary conditions for time-dependent problems 7-35247
 Burger's eqn., convergence to steady-state of solns. 7-26234
 cylindrical waveguides, aperiodic EM wave processes 7-50464
 cylindrical waveguides, resonance phenomena and aperiodic wave processes 7-50463
 differential equation, numerical soln. using interval methods 7-41079
 differential equations, singularity perturbed, dichotomies and stability 7-55995
 Einstein-scalar eqns., spherically symmetric, solns. in large data limit. 7-9712
 elastic body containing moving crack, dynamics 7-43788
 ferroelectric ceramic bar, normal mode responses, influences of domain switching and dipole dynamics 7-45945
 hyperbolic conservation law approx., nonoscillatory shock capturing methods 7-26318
 hyperbolic differential equations, soln. of boundary-value problem, optimal control appl. 7-35220
 incompressible viscous fluid with density, initial boundary value problem, weak soln. 7-61112
 initial-boundary value problems, pseudospectral method of soln. (*Russian*) 7-56006
 integration error controls for a finite element viscoelastic analysis 7-20601
 internal waves, nonstationary theory, existence theorems (*Russian*) 7-61130
 isentropic gas dynamics, rarefaction waves, vacuum state 7-57871
 Lamb's initial and boundary value problem, elastic medium with memory 7-41103
 Langmuir turbulence, Zakharov eqns., nonlinear Schrodinger limit 7-11647
 linear thermo-microelasticity, first boundary initial value problem 7-57686
 linearised compressible and resistive MHD equations, finite element semi-discretisation 7-11623
 liquid filled viscoelastic tubes, wave propag., 2D initial boundary value problem, transform soln. 7-37477
 Marangoni convection, surface deformation, nonlinear diffusion eqn. 7-51130
 Maxwell eqns. independency (*Hungarian*) 7-50441
 multiple steady states for characteristic initial value problems 7-26330
 nonlinear higher order parabolic eqns. with absorption, finite speed of propagation and asymptotic rates 7-61038
 nonlinear initial-boundary value problems 7-55987
 numerical integration for small-parameter system in presence of derivative (*Russian*) 7-61081
 operational calculus, application to initial and boundary value problems 7-55984
 ordinary differential equations in locally convex spaces 7-48316
 perfect elastoplasticity, dynamic problem, generalized solns. 7-24429
 plate analysis using initial-value method 7-20600
 plate bending, stability regions 7-16080
 polytropic ideal gas, nonfixed on the boundary, 1D motion 7-11449
 reaction-diffusion eqn., numerical solns. asymptotic behaviour 7-61284
 Riccati transformation in the solution of boundary value problems 7-35249
 Schrodinger equations, $L^\infty(R^n)$ decay of classical solns. 7-56085
 shells, spherical, and circular membranes, flexure theory, stochastic bifurcation 7-26151
 superconvergent integration for dynamics systems and other problems of m -th order (*German*) 7-14753
 time-dependent partial differential eqns., 2D mesh moving technique 7-18573
 unsteady boundary value problems, operator splitting 7-29695
 van der Waals fluid, Riemann problem, numerical integration 7-38153
 viscous heat-conductive gas, asymptotic behaviour of initial value problem solns. 7-50913
 viscous stratified flow, dynamics, initial boundary value problem soln. (*Russian*) 7-9675
 Vlasov-Maxwell equation, initial value problem, local solns. 7-9683

injection lasers *see semiconductor junction lasers***injury by radiation** *see biological effects of radiation***ink jet printers**

- drop formation in ink jet through theoretical analysis of one-dimensional model and experimental scale-up nozzles 7-26328

inorganic insulators *see insulating materials***inorganic molecule configurations***see also isomerism*

- 3d metal compounds, equilib. geometry, pot. surface, ab initio calcs. 7-15511

inorganic molecule configurations continued

- alkali metal chlorate ion pairs, coord. structs., FT IR matrix isolation spectra 7-62367
 alkali metals ionic clusters, stability and struct. $X\alpha$ and ab initio methods 7-10421
 borosilicate glass leaching behaviour, mol. struct. effects 7-21530
 CN⁻-H₂O, quantum-chem. MO SCF calcs. 7-5597
 compound metal clusters, struct. and electronic structs. calcs. 7-15783
 fluorosilanes, protonated, structs., energetics, ab initio MO calcs. 7-56956
 formaldehyde, optimised geometries and harmonic freqs., MP2 calcs. 7-62255
 HBF₄⁺, Γ_8 struct., bond lengths, microwave spectra 7-62357
 hydrides, relative energy characts., electronic correl. in ab initio calcs. 7-15528
 layered cpds. reactivity, conf., New York, NY, USA (Apr. 1986) 7-41003
 metal clusters, geometrical structure 7-15774
 metal-metal multiple bonding, cluster electron count and geometries, HMO calcs. 7-25410
 orthophosphates, ³¹P NMR chem. shift, anisotropies, struct. and cation effects 7-50187
 planar four-coordinated metal complexes, symm. effects, RHF MO SCF calcs. 7-56963
 small clusters, electronic and geometrical structs. 7-15773
 thiazyl compounds, struct. and bonding investigated at SCF level, electron correl. effects 7-10439
 trifluoromethyl imino sulphur difluoride, ab initio calcs. at SCF level, equilib. geometries and population anal. 7-10382
 tris(tetrahydroborato)titanium(II)-dimethoxyethane, cryst., X-ray structural investig. 7-51730
 zirconia transparent gel-monolith from Zr alkoxide, controlled hydrolysis prep. 7-8313
 (AgO₂)_x complexes, ($x=1,2$), bonding and configuration, matrix isolation ESR spectra anal. 7-19905
 AgOH, metal-OH bonding study 7-52240
 Ar clusters, mass distrib. meas. and struct. model 7-15762
 Ar-NO van der Waals molcs., microwave and RF spectra, hyperfine parameters 7-31026
 Ar₂-HF(DF) trimers, mol. rot., hyperfine struct., spectra anal. and calcs. 7-50060
 (ArH)⁺, short-range pot. curves, Lyman- α line blue wing (*French*) 7-10463
 Au(O₂)_x complexes, bonding and configuration, matrix isolation ESR spectra anal. 7-19905
 B(OH)₃, electron density, X-ray diffr. determ. at 105 K, ab initio calcs. 7-44458
 Be²⁺-H₂O, geometry and vibr. freqs., ab initio HF calcs. 7-49881
 C cage molecules of icosahedral symmetry, stability anal. 7-20088
 C₄, struct., energies, single reference CI calcs. 7-19720
 C₆, cyclic ground state, struct., ab initio calcs. 7-42819
 C₆₀ and similar substances, inert gas trapping, possible occurrence in meteorites 7-50436
 C₆₀, cage-like struct., HMO calcs. 7-15520
 C₆₀ cluster, electronic structure, LMTO calcs. 7-19682
 C₆₀, localised mol. orbitals and electronic struct., PRDDO calcs. 7-49925
 C₆₀ icosahedral clusters, struct. anal. and magic numbers 7-31202
 CBe₂, struct., stability and bonding 7-10392
 C₂Be₂, struct., stability and bonding 7-10392
 ((CO)₅-W-H-W(CO)₅)₂, struct., H atom dynamics, spectrosc. investig. 7-15613
 Co complex, CO(II)-5' IMP, struct., hydration, mag. suscept. and Mossbauer emission obs. 7-36660
 Co complex, Co(II) nonamethylimidodiphosphoramidate, struct., mag. props., NMR 7-50197
 Co complex, Co(II) octamethylpyrophosphoramidate, struct., mag. props., NMR 7-50197
 Co complexes, dimeric, bonding and struct. 7-56939
 Co-O cluster ions, collision-induced dissociation, struct. calcs., mass spectral anal. 7-54107
 Cr(NH₃)₆ ligands, trigonally distorted, ⁴A_{2g}-²E_g, ²T_{1g} spectra and ligand field calcs. 7-57077
 CsAlF₄, struct., GPED automatic background subtraction 7-15710
 Cu(II) complexes, bis(β -diketonato) and β -diketonate ligands, double melting, mesomorphism, long chain substituent effect 7-1862
 Cu complex, bis(diisopropylsalicylato)copper(II) pyridyl nitronyl nitroxide, mol. conform., ESR study 7-57103
 Cu complex, bis(dithiocarbamate) copper(II), struct., NDDO calcs. 7-15515
 Cu complex, sulphato aquotris(benzotriazole) Cu(II) benzotriazole, cryst. and mol. struct. 7-21181
 Cu complexes, glutamic acid, struct., EXAFS study 7-19882
 Cu complexes, with ethanolate, mol. and electronic struct., EPR study 7-19901
 Cu(II)-alkyl persulphide complex prod., mol. and electronic struct. 7-15590
 (CuO₂)_x complexes, ($x=1,2$), bonding and configuration, matrix isolation ESR spectra anal. 7-19905
 CuOH, metal-OH bonding study 7-52240
 DO₂, third-order anharmonic pot. consts. equilib. structure parameters, calc. procedure 7-10544
 Eu complexes, Eu(NO₃)₃(triphenylphosphine oxide)₃ systems, cryst. and mol. structs. 7-51723
 Fe complex, oxy(tetraphenylporphyrinate), Iron(II), cocondensation products, struct. and bonding, IR spectra 7-10572
 Fe complex ((ethyl)₄N)₆[Tl₆Fe₁₀(CO)₃₆], struct. and bonding study, HMO calcs. 7-25411
 Fe complex Fe(II) trans-bis(dimethyl-glyoximate)bis(dibutyl phenylarsine) cryst. and mol. struct. 7-51711
 Fe complexes, Fe(II)-neutral N bases, reactivity, basket-handle super-struct. effects 7-54100
 GeH₄⁺, Jahn-Teller, struct. and energy distortions ab initio CI calcs., HF calcs. 7-15523
 H₂-HF complex, struct., bonding, vibr. freq. shift 7-19817
 HBeOH (HBOH) (HCOH) (HMgOH) (HAlOH) (HSiOH), struct. and vibr. freqs., SCF calcs. 7-10386
 HCN, optimised geometries and harmonic freqs., MP2 calcs. 7-62255
 HCl BF₃, struct. determ. mol. beam electric reson. spectroscopy 7-15591
 H₂GeX (X=F, Cl, Br, I), harmonic force fields and vibr. spectra, ab initio HF calc. 7-50064

inorganic molecule configurations continued

- H₃N-HF-HF, H bond cooperativity, structural and energetic props., ab initio calcs. 7-19697
H⁻(NH₃)₂ cluster, struct., stability, ab initio MO calcs. 7-56965
H⁻(NH₃)₂ cluster, struct., stability, ab initio MO calcs. 7-56965
HO₂ radical, third-order anharmonic pot. consts. equilib. structure parameters, calc. procedure 7-10544
H₂O, mol. struct., density functional anal. 7-62272
H₂O, optimised geometries and harmonic freqs., MP2 calcs. 7-62255
H₂O, pot. energy surfaces 7-10468
H₂O-H₃O⁺ molecule, intermolecular energy anal. SCF calcs. 7-15479
(H₂O)_n, n=4 to 8, geometries and relative energies, Monte Carlo energy minimisation study, ab initio SCF calcs. 7-30921
HOCl, FTIR spectra, equil. struct. 7-50140
H₂P₂ isomers, electronic states, ab initio mol. electronic struct. theory 7-56934
H₃P-HF-HF, H bond cooperativity, structural and energetic props., ab initio calcs. 7-19697
H₂S, pot. energy surfaces, spectroscopic props., ab initio CEPA calcs. 7-19686
H₃S⁺, pot. energy surfaces, spectroscopic props., ab initio CEPA calcs. 7-19686
H₂Se, pot. energy surfaces 7-10468
H₂SeO, geometry and energy, role of optimum supplementary d-orbitals 7-25344
H₂Si-B₂H₆, form., geometry, ab initio calcs. 7-25376
H₂SiO₄, force fields, ab initio MO calcs. 7-25375
H₂SiX (X=F, Cl, Br, I), harmonic force fields and vibr. spectra, ab initio HF calc. 7-50064
H₂SnX (X=F, Cl, Br, I), harmonic force fields and vibr. spectra, ab initio HF calc. 7-50064
HgBr₂ struct., GPED automatic background subtraction 7-15710
IBr, ion-pair states, spectral anal. 7-19873
INl, spectra and struct., AO⁺ state, rot. and vibr. consts. 7-50081
K₂(Fe(CN)₅NO).1.25 H₂O, DTA-TGA, cryst. and mol. struct. and vibr. props. 7-6597
Li cpds., energy stability, struct., vibr. spectra, MO LCAO SCF calcs. 7-15512
LiCN(LiNC), struct., electron correl. calcs. 7-30956
(LiH)_n linear infinite chains study, pseudo-lattice method, ab initio SCF calcs. 7-36470
Li(LiF)₄⁺, conform. energies, LCGTO Xα method anal. 7-25393
Mg-B₁₂H₁₂, stable conform., SCF-MO calcs. 7-15477
Mo₄Cl₈(PEt₃)₄, metal-metal multiple bonding, cluster electron count and geometries, HMO calcs. 7-25410
Mo₄L₄L'₆ (L, L' = S, Se, Cl, Br), cluster compounds, electronic struct., 3-band model, tight-binding and extended Huckel method calcs. 7-32913
N₂BH₃, struct., ab initio calcs. 7-49887
NH₂⁻ struct., velocity modulation IR laser spectroscopy 7-15599
NH₃ dimer, geometry and energy calcs. SCF calcs. 7-15499
NH₃, optimised geometries and harmonic freqs., MP2 calcs. 7-62255
NH₃ unimolecular dissociation, pot. energy surface, classical trajectory study 7-13745
(NH₃)₂, dimer struct., electron spectra anal., HF calcs. 7-36686
N₂H, MCSCF equilib., transition struct. and reaction path determ. 7-8251
N₂H₂, MCSCF equilib., transition struct. and reaction path determ. 7-8251
NH₂NO, struct. and vibr. freqs. calc. using basis sets ranging from STO-3G to 6-311G** 7-10385
NH₂NO₂, electronic ground and first triplet states struct., SCF calcs. (French) 7-15498
NO₂ and ions, deform. densities, d function role in ab initio calcs. 7-62260
N₂O, protonated, IR spectra, vibr. and rot. anal., struct. 7-10566
N₂O, protonated, struct. determ. by ab initio MP2 gradient method 7-25343
N₂OH⁺ isomers, struct. and energy levels, ab initio MO, SCF and CI calcs. 7-15481
N₂OH⁺, struct., protonation site and energies, ab initio MO calcs., SCF calcs., CI calcs. 7-15480
NSCl₃, NSOF and NSF₃ and their isomers, ab initio calcs. at SCF level, equilib. geometries and population anal. 7-10382
Na₂Cl, microclusters, ionisation induced structural transitions, pseudo-potential, HF calcs. 7-25379
Na₁₀(H₂W₁₂O₄₂), cryst. and mol. struct. studies 7-6596
NbCl₅(Br₅), vibr. anal., GF matrix method calcs. 7-42593
Ni complex, bis (S-ethylthiosemicarbazide) nickel (II) iodide, cryst. and mol. struct., X-ray diff. study 7-2005
Ni complex, bis(dithiocarbamate) nickel II, struct., NDDO calcs. 7-15515
Ni complex, tris(ethylenediamine)ethylenediaminetetraacetic acid nickel(II), X-ray structural anal. 7-15728
No₂Cl₂ microclusters, ionisation induced structural transitions, pseudo-potential, HF calcs. 7-25379
Pt complex, platinum(II) diiodo-L-histidine, cryst. and mol. struct. determ. 7-12032
Re₆L₆L'₆ (L, L' = S, Se, Cl, Br), cluster compounds, electronic struct., 3-band model, tight-binding and extended Huckel method calcs. 7-32913
S₈, crown struct., pot. hypersurface, EHT calcs. 7-36483
(SN₂)_n molecular orbits, various chain sizes, MNDO calcs. 7-15517
Si₄N₄⁴⁺ dication, HF instabilities 7-15508
S₂ and ions, deform. densities, d function role in ab initio calcs. 7-62260
SO₂-H₂S complex, microwave spectrum, rot. transitions 7-42601
SO₂-HF(DF), mol. geometry, ¹⁹F spin-spin and D-nucl. quadrupole coupling consts., rot. spectrum 7-5666
S₂¹⁸O, equilib. struct., diode laser spectrosc. obs. 7-5661
S₂¹⁸O, equilib. struct., diode laser spectrosc. obs. 7-5661
SO₂HCN (SO₂DCN) dimers, anti-H-bonded, rot. spectrum, mol. geometry 7-36592
SbCl₃, struct., GPED automatic background subtraction 7-15710
SiF₄, force fields, ab initio MO calcs. 7-25375
SiH₄, geometric structs., force consts. and vibr. spectra, SCF CI calcs. 7-19713
SiH₂, ¹A₁, ¹B₁ and ³B₁ states equilib. and stretched SiH bonds SCF CI calcs. 7-49944
SiH₂, geometric structs., force consts. and vibr. spectra, SCF CI calcs. 7-19713

inorganic molecule configurations continued

- SiH₃, geometric structs., force consts. and vibr. spectra, SCF CI calcs. 7-19713
SiH₄, geometric structs., force consts. and vibr. spectra, SCF CI calcs. 7-19713
SiH₄⁺, Jahn-Teller, struct. and energy distortions ab initio CI calcs., HF calcs. 7-15523
Si₂H₄, struct. and stability, ab initio calcs., heat of form. 7-10441
SiH₃(D₃), ions and radicals, pot. energy curves and electron affinities determ., photoelectron spectra anal. 7-25603
(SiH₃)₂O mol. struct., hydrolysis of Si-O bonds, density functional anal. 7-62272
Si₂H₆O, polarisation functions, ab initio MO calcs. 7-62263
SiH₃OH, mol. struct., density functional anal. 7-62272
SnH₄⁺, Jahn-Teller, struct. and energy distortions ab initio CI calcs., HF calcs. 7-15523
(SnH₃) groups containing inorganic compounds, struct. and acid-base props. MNDO calcs. 7-10424
Tc₂Br₁₂, metal-metal multiple bonding, cluster electron count and geometries, HMO calcs. 7-25410
UC₂, gaseous molecular forms, discrete variational Xα molecular orbital calcs. 7-10420
W complexes, W (VI) isopropylimido, cryst. and mol. structs. 7-51722
WCl₃, struct. parameters, GPED statistical anal. 7-51714
W₂Cl₆, mol. struct., GPED 7-5770

inorganic molecule electronic structure *see molecular electronic states***insolubility** *see solubility***inspection**

- see also quality control; reliability; testing*
ASME code for nuclear plant component in-service inspection, 1984-5 revisions 7-5404
biomedical electronic instruments safety and testing Electrotechnical Testing Institute practices (Czech) 7-18090
Calder Hall, safety, inspection and maintenance 1956-86, review 7-56809
Calder Hall and Chapelcross reactor pressure circuits, in-service inspection 7-56810
coatings, thickness meas., thermo-EMF obs., method of division 7-48687
composite material, nondestructive meas. of dielec. permeability by non-steady frequency-phase method 7-33888
Creys-Malville (France) nuclear power station maintenance QA (French) 7-25127
CT methods use for nondestructive inspection under conditions of insufficient data 7-39818
dielectric material, radiation diagnostics of electric potentials, sensitivity and resolution 7-8233
dielectric waveguides use as sensors for dielec. consts. 7-4863
echo inspection of articles with coarse-grained struct. and rough surface, max. attainable sensitivity calc. 7-65255
eddy current electrical cond. meters, inspection errors rel. to geometric parameters 7-28244
eddy current inspection problems of weakly cond. weakly mag. media, EM field calcs. 7-39821
electroradiography inspection method for castings 7-65262
fibre reinforced polymer composites, binder content in impregnated reinforcement, contactless US inspection use 7-3565
fluorescent dye penetrant inspection, UV radiation safety and visual enhancement 7-40311
high-quality quartz crystals impurities assessment, production development results 7-59823
hologrammetry for automatic inspection in hostile environments 7-31280
holographic NDT, conf., Los Angeles, CA, USA (Jan. 1986) 7-35090
integrated circuit subsurface features, detect. by photoacoustic microscopy 7-50873
laminated dielectric, parameters determ. near min. of absolute refl. coeffs., variable freq. radio-interference method 7-65264
laminated dielectric with losses, parameters determ. in broad freq. range, inspection method 7-65263
laser ultrasonic generation and optical detection with a confocal Fabry-Perot interferometer 7-28250
magnetic and thermoelec. methods of phase analysis 7-28240
magnetic inspection of internal defects in components using combined magnetization 7-28242
magnetic particle inspection, visibility and magnetisation (German) 7-8239
metals and semiconductor objects, contactless quasioptical resonator inspection 7-54052
NDT, elec. current methods, numerical modelling, appl. to weld testing 7-33882
nondestructive inspection of case hardened parts using resistivity 7-39842
nuclear fuel plant, use of portable counter for in-plant fuel inventory verification 7-30587
nuclear NDT development at Harwell, review 7-65270
nuclear power plant in-service inspection and reliability programme 7-15292
nuclear power plants, reinspection methods implemented for quality 7-36231
nuclear reactors, risk assessment application to NRC inspection 7-49594
ocean research and underwater exploration vehicles, SAR, NAUTILE, SAGA and ELIT systems 7-9201
optical components microscopic inclusions location, automatic inspection device using Q-switched YAG laser 7-31544
optical fibre cut-end inspection method using acoustic emission sensor (Japanese) 7-11189
optical nondestructive evaluation at the National Bureau of Standards 7-39835
PCB, using laser scanner 7-57601
permeable fibre materials, thin sheets, determ. of ave. pore size by optical method 7-22961
plane parallel components, US inspection, shear wave beam multiple reflection 7-54055
power range monitoring systems and neutron channels, in situ detection of channel degradation 7-36214
production line NDT appls., holographic and visual inspection methods 7-39837
radiowave diffraction method of complex quality control of cond. surfaces and dielec. coatings 7-39820
robotic inspection of irradiated components from decommissioned nuclear plant 7-19420
robotics in US NDT, conf., London, England, 1986 7-18505

inspection continued

- seismometers certification, infrared-frequency vibration parameters meas. using microcomputers 7-4208
- SEM, low voltage, inspections of ICs, charging effects 7-56388
- semiconductor device inspection using Leitz ELSAM acoustic microscope (*German*) 7-31591
- SIAM, microcomputer aided crack detection system (*French*) 7-13713
- sound level meters, Japanese testing and calibration methods 7-1334
- spatially resolved XPS studies for semicond. device appls. 7-23087
- steel, rail, US inspection signal rel. to microstruct. and surface condition 7-3556
- steel, stainless, type 304, tubes, surface stress meas. using blind-hole strain gauge method, calibration 7-65249
- steel reinforcement, hot-rolled, strength characts. eval. using mag. method 7-39824
- steel rolled sheet, distorted form effect on inspection results by shadow method 7-39815
- tomograms of moving object, dynamic synthesis method and equipment 7-8235
- US inspection, horizontally polarised transverse waves appl. 7-28247
- US inspection instruments, improved sensitivity 7-65256
- US shadow method of inspection of rolled sheets, distorted form effect 7-39815
- US thickness measurement, standardless, of objects having variable sound vel. with depth 7-65257
- welded joints, US inspection equipment appl. 7-28245
- WVER-440 type pressure vessel, manual and mechanized inspection (*German*) 7-56784
- X-ray real-time imaging for weld inspection, methods and equipment 7-54045
- Fe-Si, thermoelec. rapid inspection, contacts temp. effect 7-2580
- GaAs semiinsulating slices, spatial inhomogeneities, near IR transmission imaging techniques 7-33400
- Nb, supercond., nondestructive inspection by scanning laser acoustic microscope 7-3566
- Zr-Nb (2.5 wt.%) pressure tubes, remote field through wall EM inspection 7-46759

instability *see stability***installation**

- see also commissioning*
- vertical ground coupled heat pump system design and performance 7-8431

installation management (computers) *see DP management***instrument landing systems** *see aerospace instrumentation; aircraft instrumentation***instrumentation**

- see also aerospace instrumentation; computerised instrumentation; digital instrumentation; digital readout; display instrumentation; nuclear instrumentation; physical instrumentation control; signal generators; signal sources*
- accuracy verification of meas. instrument scales, member of check points determ. 7-4804
- AES, instrumentation, data reduction, depth profiles 7-22390

instrumentation amplifiers

- lock-in-phase amplifier for IETs operating at 200 kHz 7-24734

instruments

- see also individual types of instruments, e.g. astronomical instruments, bridge instruments, optical instruments*
- see also meters*
- No entries

insulated gate field effect transistors

- DC motors in wheelchairs and prostheses, switching converters for efficient control 7-34355
- dielectric films, on compound semiconductors, conf., Las Vegas, USA (Oct. 1985) 7-35108
- MIS structure, carriers in insulator and at semiconductor-insulator interface, EEPROM appl. 7-2730
- MOSFET, Pt-gate, ammonia sensitivity, dependence on gate electrode morphology 7-61330
- MOSFET, substrate hole current, oxide breakdown 7-12863
- MOSFET chopper amplifier based signal source, brain voltage changes meas. appl. 7-23480
- MOSFET power switches for diagnostic neutral beam decelerating supply 7-19480
- MOSFETs, quasi one-dimensional inversion layers, hopping magnetoconductance fluctuations 7-12868
- MOSFETs, weak localisation in isotropic and anisotropic 2D electron gases 7-64172
- NMR field cycling device using GTOs and MOSFETs 7-35546
- pMOS dosimeters, long-term annealing and neutron response 7-56880
- semiconductor electrical characterisation, non-contacting methods, book contrib. 7-45335
- SOI lateral solid phase epitaxy, selective P ion implantation 7-52359
- split-drain MOS magnetic field sensor 7-4875
- α -As₂Te₃ films, hole transport investigation by transient field-effect and time-of-flight methods 7-22040
- CaF₂-Si structure with epitaxial CaF₂, electronic characteris 7-22026
- GaAs MESFET and JFET devices, elec. resist., Hall effect, influence of electronic subband mag. depopulation 7-38740
- n-GaAs metal-dielectric-semiconductor system, field effect, transistor studies 7-52841
- GaAs/GaAlAs TEGFET, resistance laboratory unit determ., using quantum Hall effect 7-18812
- Ga_{0.47}In_{0.53}As-Si₃N₄ interface, elec. charact., appl. to depletion-mode MISFET 7-38752
- InP-SiO₂ MISFET, electron tunnelling into oxide traps 7-38764
- Si, low-energy ion beam oxidation, appl. to n-channel MOSFET fabrication 7-3529
- Si MOSFET, resistance laboratory unit determ., using quantum Hall effect 7-18812
- Si MOSFETs, laser-recrystallized, grain boundary location using antireflection cap 7-46312
- Si MOSFETs, weak localisation magnetoresist. in almost quantising mag. fields 7-22024
- Si, quantum Hall resistance meas., using improved Josephson potentiometer 7-18810
- Si, quantum Hall resistance standard realisation at BIPM 7-18811
- a-Si:P, selective doping and solid phase epitaxial growth, MOSFET appls. 7-27893

insulated gate field effect transistors continued

- Si-CaF₂ SOI technology by heteroepitaxial growth 7-22022
- Si-CaF₂-Si MOSFET structures, heteroepitaxial growth, struct., elec. props. 7-12567
- Si-SiO₂, lateral solid phase epitaxial growth, SOI transistors fabrication 7-2399
- SiO₂ film MOSFET, excimer laser beam irradiation and RIE, radiation damage 7-2056

insulating coatings

- see also varnish; waxes*
- ceramic electrical insulators for liquid metal blankets 7-49624
- Fe-Si (3 wt.%), domain structure and mag. props., influence of plane tension and insulating coatings 7-12991

insulating materials

- see also asbestos; ceramics; composite insulating materials; dielectric materials; gaseous insulation; glass; insulating thin films; mica; organic insulating materials; thermal insulating materials*
- ceramic electrical insulators for liquid metal blankets 7-49624
- data compilation for radiation effects on ceramic insulators 7-58350
- inception voltage of discharges in voids 7-53236
- porcelain, sintering kinetics, struct. evolution 7-28004
- Si₃N₄, hot pressed, elec. cond., microstruct., fusion reactor insulator appl. 7-52619
- ZrO₂, partially stabilised, phase stability, elec. cond., fusion reactor elec. insulator appl. 7-52618

insulating materials, acoustic *see noise abatement***insulating materials, thermal** *see thermal insulating materials***insulating oils**

- electrokinetic phenomena in dielectric liquids 7-51542
- electrostatic charge generation in the insulating systems of transformers (*Polish*) 7-37431
- gamma-ray effects on elec. props. 7-48829
- silicone oils, air bubbles attached to point electrodes 7-37779
- streamer mechanisms under AC voltage conditions 7-51543

insulating thin films

- see also dielectric thin films; electronic conduction in insulating thin films*
- conference, Toulouse, France (April 1985) 7-35103
- ion beam deposition on insulating substrate, space charge effects 7-7895
- pentacene, vacuum deposited amorphous films, X-ray diffr. and photoelectron spectra anal. 7-22434
- photoformation of dielectric materials, review 7-53633
- polyethylene films, high field dielectric loss meas. 7-17264
- polyiodide chain complexes, thin films, optical absorpt. spectra meas. 7-22366
- specific breakdown field concept 7-39035
- stearic acid films, dielec. breakdown field meas. 7-27661
- tetrabenzofulvalene, polycrystalline thin films, TOF expts. 7-45333
- thermal resistance of a system of two insulating films held between metallic plates 7-21781
- thickness meas. using contact instrument, surface geometry effects 7-4811
- AgBr thin films and microcrystals, surface pot., ionic cond. data anal. 7-58534
- Al/Al₂O₃/Au thin film struct., dielec. props. meas. and equivalent circuit anal. 7-17115
- AlN corrosion protective coating for TbFe magneto-optical media 7-53953
- Al₂O₃ coating, thickness meas. and control during thermal spraying 7-61315
- Al₂O₃ coatings made by sol-gel process, mechanical props. 7-22867
- Al₂O₃, film, prep. by pyrolysis of Al isopropylate 7-17448
- Al₂O₃ films, ion secondary electron emission 7-22416
- Al₂O₃ films, optical props., stoichiometry depend. 7-53421
- Al₂O₃, substrate on NiO, NiAl₂O₄ form. investig. 7-16877
- Al₂O₃ thin films, electron emission characts., continuous dynode appl. 7-17376
- Al₂O₃ thin films, spectral ellipsometric TEM and electron spectra studies 7-27208
- Al₂O₃, transparent, growth from ultrafine alumina sol characteris. 7-13395
- Al₂O₃-TiO₂ amorphous films, thermal expansion and coordination state of cations 7-44860
- AlPO₄ dielectric films for Ge MIS structures, inversion layers obs. 7-45502
- Ar solid crystalline films, electron stimulated desorption, exciton mechanism calcs. (*Russian*) 7-27096
- BN, optical energy gap, density, hardness 7-39204
- BN protective coating on ZnS and ZnSe IR transmitting windows 7-46731
- BaO MBE on W (110) 7-16886
- C, amorphous film, modification by inert gas ion irradiation 7-64018
- C amorphous films for InP MIS structs., ion-beam sputtering and plasma deposition 7-7400
- C diamondlike coatings, ion beam induced conductivity and structural changes 7-22053
- C films, plasma deposited from methane, elec. conductivity, optical absorpt. 7-38786
- C, for MIS struct., interfacial characts. 7-2732
- a-C:H, optical and electronic props. rel. to deposition parameters 7-38406
- a-C:H, optical energy gap, density, hardness 7-39204
- a-C:H, plasma deposition, characterisation of hydrocarbons used 7-39422
- a-C:H, plasma emission spectroscopy, chem. anal. 7-38407
- a-C:H films, plasma deposited, optical props. 7-27799
- CaF₂, crack-free epitaxial film, on GaAs (100), surface morphology, elec. props. 7-39392
- CaF₂ epitaxial films on Si, structural and electrical props. improvement by rapid thermal annealing 7-38400
- CaF₂, MBE growth of epitaxial insulator-metal-semicond. struct., CaF₂-CoSi₂-Si 7-22496
- CaF₂, MBE on Si and overgrowth with Si or Ge, characts. 7-22495
- CaF₂, on GaAs films, optical energy gap, density, hardness 7-39204
- CaF₂, optical energy gap, density, hardness 7-39204
- CaF₂-Si, heteroepitaxy of Si and Ge 7-22497
- CaF₂-Si interface, strains in MBE grown insulator films, MeV ion channeling meas. 7-7080
- CaF₂-Si interface, with epitaxially grown insulator, post-growth annealing treatments 7-7074

insulating thin films continued

- CaF₂-Si interface, with MBE grown insulator, trap states, I-V, C-V meas. 7-7407
- Ca,Sr_{1-x}F₂ layers, epitaxial growth on CaF₂ by vac. evap. 7-22498
- CoO₂ films, optical absorption edge and energy gap 7-33471
- CuCl single cryst. thin films, resonant two-photon absorption and emission 7-22310
- Fe oxide passive film composition and growth, atom probe depth profiling anal. 7-32869
- Fe-Cr oxide film struct., in- and ex-situ fluorescence EXAFS study 7-64007
- Ga₂Se₃ films on GaAs substrates, insulating coating, stoichiometric vacancies, carrier mobility 7-52846
- Ge₃N₄ native insulator layer on Ge single cryst., microstruct. and props. studies 7-12574
- GeO₂ native insulator layer on Ge single cryst., microstruct. and props. studies 7-12574
- KCl, films, CO adsorpt., IR investig. 7-63945
- KP, thin films, composition and thickness determ. 7-21785
- La₂O₃, amorphous, DC cond. mechanism 7-22055
- Li₂WO₃ films, free-electron electrochromic modulation 7-22359
- MgO films, ion secondary electron emission 7-22416
- MgO,Al₂O₃ epitaxial film substrate for Si solid phase epitaxy 7-38399
- Nb-Ti-O ceramic coatings, synthesis by reactive ion plating and sputter deposition, struct., electrophysical props. 7-64031
- Nd₂O₃ films epitaxial growth by a reactive-evaporation method 7-59429
- Ne solid crystalline films, electron stimulated desorption, exciton mechanism calcs. (*Russian*) 7-27096
- Ru-Ti-O ceramic coatings, synthesis by reactive ion plating, struct., electrophysical props. 7-64031
- S, MeV He⁺ beam erosion, temp. depend. yield meas. 7-27847
- Si oxides, native and thermal films and Si/oxide interfaces, stoichiometry and interface transition layer, atom probe FIM study 7-32844
- Si-O amorphous films, structure and defects 7-58700
- Si₃N₄ insulating thin film deposition, remote plasma enhanced low temp. CVD process 7-13389
- SiN films, Auger line, influence of Ar⁺ ion bombardment 7-39339
- SiN films, H-free, ion beam sputter deposition 7-13353
- SiN films, plasma CVD deposition and props. (*Japanese*) 7-13381
- SiN, microwave plasma deposition, fabrication and characterisation 7-39421
- Si₃N₄ amorphous insulator thin films, defect-enhanced UV etching damage studies 7-26797
- Si₃N₄ CVD film, prep. and props. 7-64337
- Si₃N₄ CVD on Si surface, RIE 7-59691
- Si₃N₄ film CVD, glow-discharge electron beams appl. (*Czech*) 7-56373
- Si₃N₄ films, excimer laser-induced CVD 7-59441
- Si₃N₄ films, IR charactn., optical dispersion induced freq. shifts 7-27709
- Si₃N₄ films, photo-ionisation assisted photo-CVD 7-17442
- Si₃N₄ films, plasma deposited, bonds and defects 7-17437
- Si₃N₄ films, plasma-enhanced CVD deposition from SiH₄/NH₃/N₂ mixtures 7-39414
- Si₃N₄ films on GaAs:Te, annealing-encapsulation props. investigated by nuclear analysis techniques 7-8030
- Si₃N₄ LPCVD films, bombardment induced H redistrib. 7-38404
- Si₃N₄ localised films on Si substrate, laser deposition 7-39418
- Si₃N₄ MNOS struct., CVD, elec. props., effects of deposition variables 7-52843
- Si₃N₄ surface structure and chemisorption, XPS, AES and direct recoiling studies 7-32790
- Si₃N₄ thin films, electronic conduction 7-58932
- Si₃N₄ thin films, reactively sputtered, hopping cond., defect states 7-52620
- a-Si₃N₄:H films, plasma enhanced CVD, chemical and mech. props. 7-38420
- a-Si₃N₄:H films deposited by plasma enhanced CVD, optical and elec. props. 7-39205
- Si₃N₄/GaAs buried interface, EXAFS studies in total reflection and dispersive modes 7-64765
- Si₃N₄-SiO₂-Si struct., injector props. 7-38763
- Si₃N₄ film form. and charact., ion and vapour deposition method 7-13370
- Si₃N₄H_x films, synchrotron radiation excited CVD, deposition mechanisms and H content 7-52369
- Si₃N₄O₂ films on GaAs:Te, annealing-encapsulation props. investigated by nuclear analysis techniques 7-8030
- SiO films, local field-enhanced electronic conduction, activation energy and Poole-Frenkel const. calcs. 7-38570
- SiO, stress meas. techniques 7-52380
- SiO₂ : N ultrathin films, carrier conduction, nitriding effects obs. 7-38790
- SiO₂ amorphous film, ionic character, HEED study 7-63468
- SiO₂ deposition from SiH₄-N₂O, role of adsorption shapes 7-17447
- SiO₂ film CVD, glow-discharge electron beams appl. (*Czech*) 7-56373
- SiO₂ film MOSFET, excimer laser beam irradiation and RIE, radiation damage 7-2056
- SiO₂ film on Si produced by thermal oxidation 7-65228
- SiO₂ films, ballistic electron transport 7-45531
- SiO₂ films, effects of nitridation press. on props. 7-33818
- SiO₂ films, energy levels of electron traps (*Japanese*) 7-64148
- SiO₂ films, hydrogenation during thermal nitridation in NH₃ 7-13763
- SiO₂ films, interface states, charge trapping (*Spanish*) 7-17110
- SiO₂ films, low-temperature plasma-enhanced CVD deposition 7-33581
- SiO₂ films in MOS capacitors, ion implantation induced electron traps 7-38589
- SiO₂ films on GaAs:Te, annealing-encapsulation props. investigated by nuclear analysis techniques 7-8030
- SiO₂ films on Si, low-temperature annealing, interfacial props. of MOS structures 7-46526
- SiO₂ films on Si produced by surface oxidation, stresses and defects 7-65230
- SiO₂ films on Si substrates, plasma etching parameter variation effects, response-surface methodology study 7-22854
- SiO₂ films thermally grown on Si, decomposition acceleration factors 7-63999
- SiO₂, glassy and thermal films, cathodoluminescence of intrinsic defects 7-7766
- SiO₂, growth on Si, annealing by lamp heating 7-22930
- SiO₂ insulating thin film deposition, remote plasma enhanced low temp. CVD process 7-13389
- SiO₂ layers, thermally nitrided, charge transport 7-38791

insulating thin films continued

- SiO₂ MIS structures, trap generation under charge injection stress 7-7392
- SiO₂, microporous thin films, thermochemical nitridation in NH₃ 7-46726
- SiO₂, natural oxide on a-Si, structure, HEED study 7-63469
- SiO₂, plasma deposition rates, influence of insulating film 7-3203
- SiO₂ protection layer on the surface of V/Si during silicide formation 7-58662
- SiO₂, thermal films, defect formation by high temp. annealing 7-45035
- SiO₂, thermal films, nitridation 7-58680
- SiO₂, thermal oxidation of Si, effects of GeCl₄ 7-65238
- SiO₂, thermal oxide films on Si, X-ray scattering studies 7-52326
- SiO₂ thin films, constant current stressed voltage-time charact., dynamic trapping effects 7-45529
- SiO₂ thin films, intrinsic bonding defects and impurities, EPR studies 7-13034
- SiO₂ thin films in MOS capacitors, wear-out charactn., processing depend. 7-38756
- SiO₂ ultrathin films, structure, IR study 7-58674
- SiO₂ ultrathin gate oxide films, breakdown props., post-oxidation annealing effects 7-22187
- SiO₂/Cl, ion implanted, Cl ion redistrib., SIMS studies 7-21249
- SiO₂/F layers, modified CVD 7-53608
- SiO₂/Hg films, Hg-sensitized photo-CVD, X-ray fluorescence anal. 7-17440
- SiO₂/V amorphous films, Rf-sputtered, SCL conduction 7-64380
- SiO₂-GeO₂ film, oxide flow during H₂ treatment, planarization technique 7-2426
- SiO_x amorphous insulator thin films, defect-enhanced UV etching damage studies 7-26797
- SiO_x evaporated thin films, struct. study 7-58699
- SiO_x films, vibrational spectra and structure (*Russian*) 7-64709
- SiO_x films deposited by reactive evaporation, characterisation 7-64013
- SiO_x/P films, pure and doped, low press. CVD growth, structural, optical, elec. props. 7-27186
- SiON-GaAs interface, plasma enhanced CVD deposited SiON, NH₃ plasma pretreatment effects 7-7874
- SiO_xN_y films, deposited by plasma-enhanced CVD, charact. 7-2413
- SiO_xN_y films, IR optical props. 7-7777
- SiO_xN_y films, low press. CVD and composition analysis 7-12554
- SiO_xN_y films, PECVD deposited, props. as selective diffusion barrier 7-2440
- SiO_xN_y films, plasma-enhanced CVD growth 7-22514
- SiO_xN_y films, plasma-enhanced CVD deposited, annealing 7-32861
- SiO_xN_y plasma-enhanced CVD films as selective Zn diffusion barriers 7-12539
- Si_{1-x}Sn_xO_{1+x} amorphous thin films, optical and structural studies 7-64714
- SnO₂ films, CVD deposition, elec. and optical props. 7-7429
- SnO₂:F thin film, uses for a-Si:H/a-Si_{1-x}C_x:H solar cells 7-46952
- TaO₅ layer on Ta, SIMS depth profiling 7-13314
- Ta₂O₅:H films, NPL standard, distrib. of H, AES and SIMS 7-26789
- Ta₂O₅ film, photocurrent and elec. cond. mechanism, electrode interface effects studies 7-27366
- TeO₂ films, nanosecond pulsed laser-induced segregation 7-44610
- TiN films, deposition by arc evaporation 7-63392
- TiN thin film, adhesion on PBI plastic produced by large-current ion implantation machine (*Japanese*) 7-8149
- TiO₂ films, low temp. CVD for Si/TiO₂ MIS structures 7-17105
- TiO₂-SiO₂ dielectric multilayer stacks, absorption meas. by photoacoustic technique 7-17331
- TiO₂ films, CVD 7-53620
- VO₂ film, cond., magnetoresist. and nonlinear resist. in strong elec. field, metal-insulator transition study 7-52706

insulation

see also cable insulation; electric breakdown; insulating coatings; insulating materials; insulators; machine insulation; transformer insulation

surface flashover in insulator with reduced E-field 7-64569

insulation, thermal see thermal insulation**insulation co-ordination**

double impulse tests of long airgaps, leader decay and reactivation 7-20975

insulation testing

double impulse tests of long airgaps, voltage front perturbation effects 7-20976

electric and mechanical breakdown, space environment effects simulation 7-39013

electrical damage, fluorescence probes 7-51525

epoxy insulation study using X-ray computing tomograph 7-13679

flat layer insulators, RF flaw detection, diff. 7-54053

glass fibre reinforced epoxy resin insulator, interface treeing phenomena study 7-39012

organic insulating materials tracking breakdown, associated discharge light emission characts. 7-44274

polyurethane insulation, thermal and elec. aging, prebreakdown phenomena, FTIR spectra study 7-39568

insulator-metal boundaries see metal-insulator boundaries**insulator-semiconductor boundaries see semiconductor-insulator boundaries****insulators**

i.e. insulating devices. For materials see insulating materials

see also bushings; insulation

contamination from industrial plant precipitated pollution (*Russian*) 7-59891

laser breakdown due to nonequilib. changes in their optical characts. near absorbing inclusions 7-53233

long-spindle insulator damage by shotgun (*Japanese*) 7-22787

materials modification with ion beams, review 7-16647

Miyazaki Prefecture, effect of typhoons on sea salt deposition on insulators (*Japanese*) 7-66248

PBFA II vacuum magnetically insulated transmission line redesign to inductive energy store 7-30755

PBFA-II vacuum insulator stack design engineering viewpoint 7-30774

Proto II accelerator, low inductance diode design for imploding plasma loads, insulator breakdown 7-30760

PROTO II accelerator power flow modification in insulator stack 7-30669

Supermite accelerator water-plastic-vacuum interface design 7-30748

integral equations

- see also *integro-differential equations*
- 2D anisotropic rod scatt., plane-wave integral eqn. 7-57219
- 2D elastostatics, stress computation by BEM 7-37330
- 3D crack, surface and through, integral eqns. method 7-1504
- acoustical transformation technique as a practical tool 7-37257
- asymptotic behaviour of resolvents of abstract Volterra equations 7-61022
- Banach spaces, nonlinear integral operators and chaos 7-24543
- Bartn's integral generalisation, related integrals of complete elliptic integrals 7-29715
- bivariational methods for linear integral equations with nonsymmetric kernels 7-48324
- boundary element method for elastostatics with internal constraints 7-29758
- boundary integral equation on polygonal domains, superconvergent approx. to soln. 7-48323
- boundary-integral-equation and finite-element methods, combined scheme for elasticity theory problems 7-56041
- conducting circular torus with dielectric sleeve, electrostatic problem 7-57204
- crack tip stress intensity factors, boundary integral method 7-16129
- cubic cylindrical single crystals, stress determ., Abel inversion (*Russian*) 7-16672
- cylinder, circular, sliding over dissimilar thermally conducting half-plane 7-20666
- cylinder, composite with penny-shaped crack, impact response 7-37384
- dielectric cylinders embedded in two-layer lossy medium, EM scatt. anal. 7-1009
- dielectrically-loaded conducting spheres, FEM for scattering 7-15808
- diffraction magnetodielectrics 7-36846
- droplet vaporisation, internal circulation integral eqn. formulation 7-37530
- dyadic Green's function, improper integrals evaluation 7-31216
- dyadic Green's function as an inverse operator 7-36851
- eddy current flow inversion algorithm, experimental verification 7-54059
- elastic half-space, separating inclusion 7-43678
- elastic layer on rigid flat supports, contact problem 7-31709
- elastoplastic boundary value problem, Galerkin approach 7-50956
- elastostatics, linearised, existence and uniqueness theorems for boundary integral equations 7-61102
- electrostatic problems, integral eqns. for thin dielec or conducting layers 7-31209
- elliptical equations, numerical procedures, capacitance matrix method (*Russian*) 7-56008
- EM fields in cavities with current normal to walls, monochromatic solns. 7-42849
- evolution equations, integrable solns. 7-60963
- Fermi-Dirac functions, high-precision analytic approx. by elementary fns. 7-29880
- ferrofluid, mag. saturated, particle pair correlation 7-59102
- Feynman path integral, new formulation 7-35302
- finite plane isotropic elastic medium, straight crack, complex path independent integrals 7-43792
- flat laminae, capacity anal. 7-62565
- Fokker-Planck equation solns., polynomial expansion and integral eqn. methods 7-61291
- fully symmetric interpolatory rules for multiple integrals 7-48327
- generalised Noether identities and appls. 7-48933
- geophysical prospecting, network theory appls. in Euclidean space (*French*) 7-23647
- ideal fluid, shear flow stability, effect of stratification 7-26249
- inhomogeneous elastic body with circular crack, equil. problem 7-16127
- interpolatory product integration rules, extension of results to noninterpolatory rules 7-48328
- kinked crack solved by Mellin transform 7-43789
- Lippmann-Schwinger equation solution for short-range potentials 7-19034
- liquid hard sphere model, binary correl. function integral eqn., analytic soln. (*Russian*) 7-32252
- macrocrack-microdefect interaction, stress field anal. 7-43797
- Maxwell and integral eqn. equivalency for 3D and 7D scatt. problems 7-57220
- Meixner multinomials, use in the approximate calculation of integrals 7-61001
- metallic electrons, pair correl. functions, real space variational calcs. 7-52479
- minimisers, near singular points, behaviour of derivatives 7-41057
- multicomponent generalizations of integrable nonlinear partial differential eqns. 7-74
- multiple positive solutions of nonlinear integral equations and applications 7-29686
- nonlinear 3D fracture dynamics, path-independent integrals 7-63069
- nonlinear fracture problems, path-independent integral, finite element approach 7-63068
- nonlinear Volterra integral equations with several kernels, construction method 7-29706
- off-shell two-particle scatt. function, three-body problem, phase function method generalization (*Russian*) 7-41163
- open boundary problems, differential and integral methods 7-50454
- open quantum systems and Feynman integrals, problems 7-29781
- open resonators, Huygens-Fresnel principle and integral eqns. 7-31244
- optical bistability, thermally induced, nonlinear integrated eqn. 7-50617
- parametric magnetic head field eqns., generalised Poisson integral approach 7-42839
- path integrals, semiclassically based Monte Carlo evaluation 7-41069
- path-independent integrals for the direct determination of stress intensity factors in certain classical crack problems 7-43791
- periodic boundaries between isotopic dielectrics, EM waves diff. 7-57212
- periodic metal-semicond. array, depletion layer profile calc. 7-22010
- periodic solutions of wave eqn., iteration method 7-108
- phase problem, complex coherence function, nonlinear integral eqns. 7-9710
- physical optics, fields, perfectly conducting screen aperture, line integrals 7-15802
- plane, elastic, hole-defect interaction, stress distrib., integral eqn. method 7-37964
- plane wave diffraction by dielectric cylinder, oblique incidence 7-50461
- Poisson integral, spherical expansion for determ. of gravit. pot. of arbitrary mass distrib. 7-66447
- polyatomic systems, integral eqn. rational closures 7-25626

integral equations continued

- polymer melt struct., nonperturbative integral eqn. theory calcs. 7-44345
- radiative transfer, time-dependent, theory 7-48646
- reinforcement problems, formulation in terms of boundary integral equations 7-1410
- Reissner plates, simply supported, integral equation system 7-94
- reissner-Sagoci problem for a non-homogeneous elastic solid 7-43680
- relative error minimisation, associated nonlinear integral eqn., harmonic mean 7-61014
- resonators, high frequency, boundary-integral eqns. calcs. (*Russian*) 7-56007
- resonators, stable, approx. method for solving integral equations 7-20382
- rod-type vibr.-freq. transducers, resonator shape optimisation 7-1482
- scattering problems, hybrid iterative method 7-20099
- Schrodinger integral equation, collocation method soln. 7-116
- shells, shallow, boundary/interior element method for quasi-static and transient response analyses 7-6090
- short magnetic cylinder in transverse time-harmonic mag. field, 7-62574
- signal processing, integral equations in diagnosis problems (*Russian*) 7-34234
- sine-Gordon model, exact Bethe-ansatz thermodynamics, long string effects 7-35393
- solar oscillations frequencies, integral formula for solar rot. as function of depth and latit. 7-55599
- sound scattering, Helmholtz integral eqn. method 7-50812
- space with two hyperboloidal cuts under the action of a uniformly distributed pressure 7-97
- special function calcs. from two complex variables (*Russian*) 7-56022
- square specimen, compressed, with longit. or diagonal crack, stress intensity factors calc. 7-16118
- Stokes problem, stationary, boundary integral eqn. method (*Chinese*) 7-14779
- stream suction problem, singular integral eqn. of singular function type, numerical soln. (*Russian*) 7-26305
- strip, infinite, with cracks and holes, singular integral eqn. soln. 7-26219
- strip with circular hole, stress concentration calc. by singular integral equations 7-16123
- strongly scattering particles, high density medium, integral equations for first two statistical moments of field 7-10828
- synchrotron radiation, corrections in derivation of formulae 7-55442
- transport in semi-infinite ducts, singular integral eqn. formulation 7-48641
- two-dimensional slow viscous flows past obstacles in a half-plane 7-57788
- viscous fluid, flow transition, Orr-Sommerfeld eqn. soln. (*Russian*) 7-43850
- Volterra type partial integral inequalities as solns. to partial integral eqns. 7-29709
- weakly singular discrete Gronwall inequalities 7-41081
- Wood-Saxon pot. radial path integral, path integration over SU(2) manifold 7-35958
- H, multiphoton ionisation by intense laser field, integral eqn. approach 7-62339

integral transforms see *transforms***integrated circuit manufacture**

- Used for commercial manufacture only
- see also *masks; photolithography*
- 3D holographic miniprojector, integrated circuits assembly and quality control appl. 7-25763
- holographic microscope, projection type, for microcircuits assembly and QC 7-62650
- mass spectrometry in IC fabrication 7-39940

integrated circuit technology

- See also under *specific integrated circuit headings*
- see also *integrated optoelectronics; resists; semiconductor technology*
- 3D, SOI rapid-zone recrystallisation using pulsed Xe arc lamp, elec. and physical props. 7-53776
- amorphous semiconductors for microelectronics appls., conf., Los Angeles, CA, USA (Jan. 1986) 7-24282
- Auger sputter depth profiling applied to advanced semiconductor device structures 7-21254
- conference on semiconductors, Jevnaker, Norway (June 1986) 7-14705
- contact resist., four-terminal meas. techniques 7-35537
- corrosion of electronic materials and devices, causes and prevention 7-33815
- HF measurements on chip components (*German*) 7-45368
- high resolution scanning thermal profiler 7-48693
- insulating films on semiconductors, conf., Toulouse, France (April 1985) 7-35103
- laser induced etching of polyimide encapsulants in IC evaluation 7-53941
- laser materials processing developments at GEC Hirst Research Centre (UK) 7-53581
- laser processing of materials, conf., London, England (Dec. 1986) 7-48185
- metal nitride films, prep., props., microelectronics appls. 7-33557
- metallic glasses as diffusion barriers 7-52144
- micro-mechanics, Si-beams rectangular cross-section for atomic force sensing 7-51590
- microdevices and superlattices, MBE growth, quasi-gas transition layers 7-38379
- microelectronic devices and materials, characterisation methods, book 7-41028
- microstructures and microdevices, conf., Goteborg, Sweden (Aug. 1986) 7-35097
- multi-level SOI recrystallization using a novel seed structure 7-53778
- nuclear and space radiation effects in electronics, conf., Providence, RI, USA (July 1986) 7-55875
- photoformation of dielectric materials, review 7-53633
- polyamic acid films, vapour deposition technique 7-7855
- pre-oxidation treatment, appl. of UV radiation 7-33862
- reactive magnetron sputtering, microelectronics appl. 7-33556
- SAW accelerometers using integrated thick and thin film technologies 7-301
- semiconductor device physics, conf., Madras, India (Nov.-Dec. 1985) 7-35102
- semiconductors and metals study 7-51591
- SOI formation, high dose O⁺ ion implantation, lamp annealing 7-32527
- SOI lateral solid phase epitaxy, selective P ion implantation 7-52359
- sputter deposited coatings, microstructure, IC appls. microstructure of sputter deposited coatings, IC appls. 7-52338
- submicron backscattered electron microanalysis in SEM 7-23113

integrated circuit technology continued

- submicron pattern generation by electron-beam decomposition of carbonyls 7-53597
- thin films, interfaces and phenomena, conf., Boston, MA, USA (Dec 1985) 7-18502
- Ag/AgCl electrodes fabricated with IC-compatible technologies, chemical sensor reference appl. 7-8343
- Al film, laser deposition for metallisation 7-53631
- Al/TiN/Si contacts for VLSI, analytical electron microscopy 7-58651
- Al-Si/MoSi₂ stable contacts to shallow junctions 7-52847
- As₂S₃ amorphous chalcogenide optical grid, submicron resolution, VLSI appls. 7-48899
- GaAs, LEC growth for IC technology appls. 7-64894
- GaAs, large dislocation-free cryst. growth for LSI appls. 7-64895
- LiNbO₃, optoelectronic material, radiation effects 7-26811
- Si doped, laser deposition for interconnections 7-53632
- Si LOCOS substrates, nucleation of dislocations at thin film edges 7-51597
- Si, low pressure epitaxial growth, appl. to dielec. isolation technology 7-53624
- Si materials science and technology, conf., Boston, MA, USA (May 1986) 7-29598
- Si materials science issues in IC processing 7-35115
- Si, photon enhanced oxidation mechanisms 7-54032
- Si, rapid thermal oxidation and nitridation 7-33861
- Si substrate, insulator growth by rapid thermal processing 7-22921
- Si, surface nitridation, current status 7-33866
- Si:B(As)-Co, silicide formation using rapid thermal processing, defect behaviour 7-32726
- Si:B(P), lateral diffusion, modeling LOCOS effects 7-33865
- Si:O, P, Sb wafers, O precipitation during simulated CMOS cycles 7-38218
- SiO₂ films, effects of nitridation press. on props. 7-33818
- SiO₂, optoelectronic material, radiation effects 7-26811
- SiO₂, surface nitridation, current status 7-33866
- SiO₂:N thin films on Si, surface nitridation in low NH₃ press. 7-46721
- Ta₂O₅ films for MOS DRAMs using ultra-high purity Ta sputtering target 7-59423
- TiN-TiSi₂ bilayers and selectivity doped thin films, material characterisation 7-33817
- W and refractory metals, VLSI appls., conf., Albuquerque, NM, USA (Nov. 1984 and Oct. 1985) 7-14715
- W LPCVD film struct., IC appls. 7-58692
- W, selective CVD for VLSI device appls. 7-17455
- W, selective CVD for VLSI appls. 7-17457
- W, selective LPCVD for MOS VLSI appls. 7-17456
- W, selective LPCVD for CMOS VLSI, appls. 7-17471
- W, selective LPCVD on self-aligned Ti and PtNi silicides 7-17458
- WF₆, physicochemical props. rel. to CVD for VLSI appls. 7-17462

integrated circuit testing

- cameras, automatic focusing systems, IC testing 7-41517
- HF measurements on chip components (*German*) 7-45368
- microelectric photoresists, uncoated, SEM inspection, low-loss electron images 7-9927
- optical filtering, noncoherent, for automating testing of semiconductor structures 7-20153
- SEM, low voltage, inspections of ICs, charging effects 7-56388
- SEM-based characterisation techniques, review 7-51598

integrated circuits

- see also digital integrated circuits; hybrid integrated circuits; large scale integration; linear integrated circuits; masks; monolithic integrated circuits; substrates; thick film circuits; thin film circuits*
- III-V semiconductors, defect recognition and image processing, conf., Montpellier, France (July 1985) 7-29596
- physical processes of semiconductor devices, book 7-35
- semiconductor wafers, integrated circuit metrology with confocal optical microscopy 7-46773
- thermal sensors based on transistors and ICs review 7-48743

integrated logic circuits

- gate array appls. in implants for nerve stimulation in paraplegic patients 7-34339

integrated optics

- see also fibre optics; integrated optoelectronics; optical films; optical modulation; optical waveguides; semiconductor junction lasers*
- acousto-optic cell appls. of optical waveguides 7-1264
- acousto-optic device modules for communication, signal processing and computing 7-31526
- acousto-optical waveguide-type optical separators 7-62825
- acoustooptical Bragg diffraction, devices and appls. 7-45983
- active guided wave devices, coupled mode anal. 7-62829
- aspheric figure generation using feedback from IR phase-shifting interferometer 7-37219
- batch processed optical scanner using Si micromechanic techniques 7-20473
- branching waveguides, distrib.-index, phase space evaluation 7-31453
- branching/combining optical circuit, low radiation loss, using high SiO₂ channel waveguides 7-31458
- chalcogenide glass grating couplers, fabrication using electron beam induced Ag doping (*Japanese*) 7-62817
- chalcogenide glasses in integrated and fibre optics, review 7-31412
- channel waveguides intersecting at right angle, Bragg grating coupling analysis 7-6023
- comparison of optical and acoustical signalprocessing techniques 7-1317
- conference, Cambridge, MA, USA (Sept. 1985) 7-24278
- corrugated waveguide diffraction gratings in integrated optics, TE-TE and TM-TM coupling coeffs. 7-26035
- coupled lightguides, filter operation, parameters choice 7-37111
- coupling elements based on 2D refractive-index gradient 7-20411
- desorption, light induced, bistability mechanism in integrated optical devices 7-57424
- developments (*German*) 7-57608
- developments in integrated optical components (*German*) 7-50789
- DFB laser deficiencies and proposed alternatives 7-1194
- DFB lasers, fibre optic technology advances 7-1193
- dielectric guides in integrated optics (*German*) 7-62848
- diffuser with controlled divergence 7-5969
- directional coherent coupler, nonlinear, instabilities, all-optical phase-controlled switching 7-11027
- directional coupler switches, $\Delta\beta$ phase reversal, crosstalk characts. 7-26037

integrated optics continued

- distributed-index planar microlens and stacked planar optics: a review of progress 7-31416
- doublelayer waveguide, parameter determ. 7-50736
- electro-optic Bragg gratings for integrated optical combinatorial logic 7-26040
- electro-optic directional coupler switches, crosstalk due to reversed- $\Delta\beta$ electrode misalignment 7-20471
- electrooptic modulators, digital and quasi-linear, synthesized from directional couplers 7-50727
- ferromagnetic garnets, magneto-optical effects and appls. (*French*) 7-59190
- fibre laser Doppler velocimeter, integrated optic device 7-6022
- fibre optical sensors, semiconductor laser and integrated optics use 7-25998
- fibre sensors, integrated optical components 7-26042
- finite element modelling of integrated optical waveguides 7-43362
- frequency domain reflectometry for fibre/integrated optic systems, high resolution distrib. fibre optic sensing 7-25987
- Fresnel lenses, proton exchanged, in LiNbO₃:Ti waveguides, integrated optic RF spectrum analyser 7-31522
- geodesic lens family design, theoretical analysis 7-57507
- glass photochromic diffusion waveguides, absorbing-mask mode selectors automatically matched to mode field 7-50739
- glass waveguides, Ag film diffused, diffusion process and optical props. 7-50737
- glass waveguides, ion-exchanged, stress 7-31454
- gradient index imaging systems, conf., Palermo, Sicily, Italy (Sept. 1985) 7-29570
- gradient-index slab lens with high numerical aperture, indiffusion ion exchange and cementing fabrication 7-31415
- grating coupler on optical fibre 7-26004
- grating element for the entry and focusing of radiation in a planar waveguide 7-37126
- guided-wave devices for telecommunication systems 7-62830
- holographic grating fabrication by tunable pulsed dye laser 7-5983
- holographic interferometer with monomode fibres, appl. to integrated optic grating device manufacture 7-25757
- III-V semiconductor integrated waveguides as all-optical logic devices 7-25869
- integrated coupled-cavity lasers, design and fabrication 7-25843
- intensity-dependent guided wave phenomena 7-25872
- IR light modulator using free carrier absorpt. effects (*Japanese*) 7-5991
- LAN, ultra-high speed fibre optic, integrated optical circuits 7-26038
- laser diode linear arrays, quasi-CW, high-power operation 7-43137
- lens design using GRIN lens techniques 7-43449
- LV optical modulator and self-biased self electro-optic-effect device 7-43445
- matrix switches, integrated optical, laser diode gain guides 7-37209
- merocyanine dye Langmuir-Blodgett films, optical third-harmonic generation 7-20329
- microlens, planar distributed index highly integrated, characts 7-43448
- microoptic components formed by local modification of the structure of porous glasses 7-43451
- mirror with corrugated waveguide on surface, spectral and laser characts. 7-43291
- multicomponent integrated optical system development, the shape of things to come 7-50791
- multimode branching waveguide, distrib.-index, evaluation by phase space 7-31451
- multimode waveguide systems, coupled-mode eqns. 7-37149
- multiple scattering problems, path-integral formulation 7-50787
- multiwaveguide systems with non-parallel guides, appl. of coupled-mode theory 7-20410
- noncollinear light propag. in rippled waveguide, geometrical optics approach 7-50742
- nonlinear directional coupler, beam-propag. method anal. 7-37148
- nonlinear planar waveguide, self-interaction and bistability 7-43375
- organic materials for integrated optics 7-25911
- phase diff. grating parameter control, computational technique 7-43338
- phase reversal travelling wave integrated optic modulators, time-domain anal. 7-5988
- phased-array diode lasers coupled-mode anal. 7-43095
- photochromic conversion effect in case of light modulator (*German*) 7-57609
- photorefractive polymer for optical recording of waveguide gratings 7-5963
- photoreist gratings on reflecting substrates interference pattern 7-1042
- planar corrugated waveguides, rigorous EM treatment 7-43366
- planar graded waveguides, parameters meas. in near IR, refractometric method 7-37150
- planar microlens fabrication by ion exchange/diffusion, distrib. index profile 7-31417
- planar optical waveguides, stability and instability of nonlinear standing waves 7-57554
- planar waveguide losses meas. using coherent fibre bundle 7-50734
- polydiacetylenes as nonlinear waveguide materials 7-25871
- prism coupling efficiencies by direct meas. of coupling gap in integrated optical structures 7-6021
- quantum well self-electro-optic effect device using 2X2 array of optically bistable switches 7-11176
- quantum well structures, linear optical props. elec. field depend. waveguide electroabsorpt. and sum rules 7-13133
- review (*Spanish*) 7-37208
- rough surface bounding layered medium, equiv. impedance, appl. to integrated optical waveguide 7-57239
- semiconductor doped glass, integrated nonlinear optical device fabrication 7-25873
- semiconductor for integrated optics in optical fibre communication systems, props., review 7-11178
- semiconductor laser amplifier, 1.3 μm , with integrated passive waveguides 7-20278
- semiconductors, morphological stability in epitaxy, appl. to optoelectronic monolithically integrated structures 7-27172
- spatial sampler using integrated optic techniques, electrooptic directional couplers 7-31524
- surfaces with adsorbed molecules, surface coherent antiStokes Raman spectroscopy as analytical tool 7-1233
- swept wavelength reflectometer for integrated-optic measurements 7-41432

integrated optics continued

- taper coupler for integrated optics formed by ion-exchange under nonuniform electric field 7-50740
 tapered waveguide beam radiation 7-5995
 telecommunications appl. (*German*) 7-43446
 telecommunications using integrated optics including wave conductors and electro-optical couplers (*German*) 7-50790
 thin-film phase shifters, nonreciprocal TM-mode 7-11103
 travelling-wave modulators, ultrafast, with reduced vel. mismatch 7-50730
 wave propagation obs. in integrated optical waveguides and circuits 7-31523
 wavefront sensor, lens focusing onto detector array 7-26041
 waveguide, tapered slab type, spectrum anal. using mode cutoff effect 7-37158
 waveguide, TM-mode selective filter using a high refractiveindex lossy layer cladded optical waveguide 7-5997
 waveguide attenuation meas. by prism coupling and scattered light techniques 7-43363
 waveguide Bragg mirror with negative differential characteristic 7-43447
 waveguide horn-grating demultiplexer circuit, single-mode operation 7-62846
 waveguide mode field and propagation consts., calc. by numerical method 7-31455
 waveguide-bend configuration with low-loss characteristics 7-37147
 waveguides, electrooptic light modulation by fringing field of Gunn domain 7-57534
 waveguides, finite difference anal. without spurious mode solns. 7-1262
 X-ray Bragg optics 7-21043
 Ag-AgCl-ZnS photoinduced periodic struct. for planar waveguide study 7-43371
 AlGaAs integrated-hybrid Bragg heterostruct. laser thermal stability of distributed-refl. spectral bands 7-57393
 AlGaAs-GaAs MQW CCD spatial light modulators using electroabsorption effects 7-20407
 Al_xGa_{1-x}As, AlAs and GaAs epitaxial multilayers as optical interferometric elements 7-342
 CS₂, use in nonlinear light guides of nonresonant type (*German*) 7-57609
 CdSe_{1-x}S_x crystal waveguide Bragg light modulators 7-1288
 GaAs-GaAlAs MQW waveguides, nonlinear propag. 7-26033
 (GaAl)As monolithic composite-cavity laser, chem. etching technique 7-50579
 GaAlAs-GaAs multi-heterostructures, MOCVD growth for surface emitting lasers 7-59440
 GaAs, direct maskless fabrication of submicrometre gratings 7-62855
 GaAs Fresnel waveguide grating lenses, aberration corrected, simulation 7-26036
 GaAs inverted rib, phase modulators grown by VPE, optical and electrooptical anal. 7-31450
 GaAs monolithic integrated optics, performance in space environment 7-26028
 GaAs, n-type, proton irradiated, effects of annealing on optical properties 7-28155
 GaAs PIN electro-optic travelling-wave modulator at 1.3 μ m 7-1287
 GaAs waveguide, thermal index changes by optical absorpt., all-optical signal processing 7-31381
 GaAs/Al_xGa_{1-x}As 3D ICs, selection rule for epitaxial growth techniques, LPE, MOVPE and MBE 7-46326
 GaAs-AlGaAs quantum wells in waveguides, physics and appls. 7-26034
 GaAs-GaAlAs MQW optical waveguides, nonlinear props. 7-37027
 GaAs-GaAlAs monolithic laser amplifier, C³, with bistable characts. 7-25842
 GaInAsP integrated coupled-cavity lasers, design and fabrication 7-25843
 GaInAsP strip-loaded planar waveguide for high-speed electroabsorpt. modulator 7-31449
 InGaAs/InP multiple quantum well waveguides, low loss, MOCVD growth 7-43358
 InGaAsP 1.55 μ m mode-locked laser with single-mode fibre output 7-50600
 InGaAsP-InP DFB laser monolithically integrated with tunable external cavity, linewidth and FM characts. 7-57316
 InGaAsP-InP optical switches, carrier induced refractive index change 7-57606
 InGaAsP-InP waveguides, optical parameters 7-62831
 InP dry etching at room temp. 7-28227
 InP waveguide, thermal index changes by optical absorpt., all-optical signal processing 7-31381
 LiNbO₃ (001), z-cut, surface struct., RHEED studies 7-2308
 LiNbO₃ based integrated light conductor (*German*) 7-57609
 LiNbO₃ blazed grating couplers and appl. to integrated optics 7-15969
 LiNbO₃ coded phase-reversal modulator with 20 GHz bandwidth at 1.3 μ m wavelength 7-57533
 LiNbO₃ integrated optics, review of theory and technology 7-20470
 LiNbO₃ integrated optical components for fibre gyroscopes 7-20472
 LiNbO₃ integrated optical substrates, Maker fringe anal. 7-26026
 LiNbO₃ integrated optical substrates, refractive index meas. by total internal reflection 7-26027
 LiNbO₃ integrated optical components for optical communication appls. (*German*) 7-37210
 LiNbO₃ integrated optic devices, Ti film charactn. 7-57607
 LiNbO₃ optical components for modulation and switching 7-15996
 LiNbO₃ optoelectronic material, radiation effects 7-26811
 LiNbO₃ substrates, growth and composition effects 7-26025
 LiNbO₃ traveling-wave optical couplers and interferometric modulators, power requirements 7-57539
 LiNbO₃ waveguide mode extinction modulators, design 7-26030
 LiNbO₃ z-cut interferometers, thermal instability, electrostatic mechanism 7-37207
 LiNbO₃:H channel waveguides, anal. 7-26023
 LiNbO₃:H optical waveguides, devices, charactn. and future prospects 7-26022
 LiNbO₃:H ring resonators, operation at 0.79 μ m and 1.3 μ m 7-26029
 LiNbO₃:H waveguides, anomalous side-shifted multimode spectra 7-37140
 LiNbO₃:He⁺ implanted waveguide stability 7-43364
 LiNbO₃:MgO, melt growth and charactn. 7-58170
 LiNbO₃:Ti, low-loss TM-pass polariser fabricated by proton exchange in z-cut waveguides 7-43444
 LiNbO₃:Ti 4×4 nonblocking interconnection network for test bed, video switching 7-26039
 LiNbO₃:Ti channel waveguide electro-optic cutoff modulator 7-43353

integrated optics continued

- LiNbO₃:Ti guided-wave optical switch, 1×16, polarisation-independent 7-31525
 LiNbO₃:Ti integrated electro-optic devices, modelling and beam propag. anal. 7-11177
 LiNbO₃:Ti integrated optical parametric oscillators, numerical model 7-57459
 LiNbO₃:Ti integrated optical devices, domain inversion effects 7-62849
 LiNbO₃:Ti intersecting optical waveguides 7-43359
 LiNbO₃:Ti modified 1×2 directional coupler waveguide modulator 7-1259
 LiNbO₃:Ti three-waveguide polarisation splitter 7-50788
 LiNbO₃:Ti(H) waveguides, photorefractive susceptibility, charactn. methods 7-26024
 LiTaO₃ substrates, growth and composition effects 7-26025
 Nd:YAG laser, SHG in four-layer waveguide struct. using 2-methyl-4-nitroaniline in high index top layer (*Japanese*) 7-43240
 PLZT/Si spatial light modulators, technology 7-20408
 Si, etching V-groove structures 7-26031
 SiO₂ optical waveguides, low-loss planar, fabrication using thermal nitridation and charactn. 7-26032
 SiO₂, optoelectronic material, radiation effects 7-26811
 SiO₂:Ge integrated optical waveguides, plasma CVD 7-27941
 SiO₂:GeO₂ optical waveguides, laser heating effect on opt. props. 7-50792
 ZnS, ZnSe nonlinear planar waveguides, bistability and self-pulsing using prism couplers 7-57427
- integrating optoelectronic circuits** *see integrated optoelectronics*
- integrated optoelectronics**
 cameras, automatic focusing systems, IC testing 7-41517
 carrier-injected bipolar transistor optical modulators and switches 7-50732
 fibre-optic hybrid receiver uses thick film technology 7-26021
 holographic grating fabrication by tunable pulsed dye laser 7-5983
 hybrid integrated components for optical fibre communication and instrumentation systems 7-25997
 III-V semiconductor, integrated optoelectronics, micrograting form. by HV electron beam lithography 7-31443
 manufacturing micro-optic devices with low insertion loss using autocollimated imaging 7-37205
 picosecond electronics and optoelectronics, topical meeting, Lake Tahoe, NV, USA (Mar. 85) 7-41007
 review (*Spanish*) 7-37208
 semiconductor multiple quantum wells, optoelectronics for optical modulation and bistability 7-25952
 semiconductors, morphological stability in epitaxy, appl. to optoelectronic monolithically integrated structures 7-27172
 semiconductors for integrated optoelectronics in optical fibre communication systems, props., review 7-11178
 AlGaAs injection heterolasers and integrated laser-photodetector pairs, prepared by microcleaving 7-31343
 FeSi₂ thin films, appl. to electro-optic VLSI interconnects 7-53427
 GaAs films, dense electron-hole plasmas, picosecond dynamics, acoustic phonon generation 7-45373
 GaAs monolithic optoelectronic ICs for high-speed fibre optic transmission 7-37203
 GaAs-GaAlAs monolithic laser amplifier, C³, with bistable characts. 7-25842
 Ge₂Si_{1-x}Si strained-layer heterostructure, transport, optical props. and appls. 7-7349
 InGaAsP films, dense electron-hole plasmas, picosecond dynamics, acoustic phonon generation 7-45373
 InP dry etching at room temp. 7-28227
 LiNbO₃, optoelectronic material, radiation effects 7-26811
 PLZT/Si spatial light modulators, technology 7-20408
 SiO₂, optoelectronic material, radiation effects 7-26811
- integrating circuits**
 radiation logging curves, recording scale automatic displacement (*Russian*) 7-34710
 voltage-to-time converter for thermometer 7-30011
- integrating spheres** *see photometry*
- integration**
 air pollution transport eqns., multistep/multigrid implicit technique 7-54402
 Airy functions, use of in integral evaluation 7-70
 apparatus cooldown using He or N cooling systems, mass flow requirements calc. 7-56281
 Bloch density matrix for oscillator in electric and mag. field, path integral formulation 7-62605
 Born partial wave integrals, numerical evaluation 7-48462
 closed form expressions for integral involving Coulomb potential 7-29738
 crystallography, 3D intensity data from single crystal reflections, graphical display 7-11829
 damage model, 3-D finite strain viscoelastic 7-50955
 damped quantum oscillator, functional integration method anal. 7-24479
 dielectric cylinders embedded in two-layer lossy medium, EM scatt. anal. 7-1009
 differential equations, nonlinear, Painlevé test and integrability 7-48309
 eigenvalue interpolation, integration scheme 7-32894
 Einstein's equations, integration using the Bondi metric 7-61172
 elastic-plastic eqn. analysis and numerical soln. (*French*) 7-41101
 essentially nonlinear systems, simplified asymptotic integration algorithm 7-41091
 exponential integral, numerical evaluation throughout complex plane 7-24399
 Feynman histories, functional contour integration summing technique 7-24456
 finite element viscoelastic analysis, integration error controls 7-20601
 first integrals for π -systems, DISSYS program 7-48299
 fully symmetric interpolatory rules for multiple integrals 7-48327
 functional integration, measure and support 7-9655
 gravitational potential in spherical coordinates, Poisson integral radial recursive integration 7-9367
 gyrocompass, integration of eqns. of motion 7-43652
 Hamiltonians and quantum integrability 7-9694
 initial-value problems, numerical integration for small-parameter system in presence of derivative (*Russian*) 7-61081
 integrability conditions for systems for two equations of the form $u_t = A(u)u_{xx} + F(u, u_x)$ 7-4662

integration continued

- integrable multiwave interaction systems of ordinary differential equations 7-4671
 integral involving powers of $(1-x^2)$, evaluation 7-69
 interpolatory product integration rules, extension of results to noninterpolatory rules 7-48328
 Legendre functions, closed analytical expressions and integrals 7-61005
 magnetisation analysis, mesh partitions 7-5813
 multi-layered elastic half space, seismic waves due to horizontally propag. vertical fault (*Chinese*) 7-47340
 multivalued differential systems, integral equivalence 7-18564
 Navier-Stokes eqns., arbitrarily convex quadrilateral elements (*Chinese*) 7-16144
 Navier-Stokes eqns., pseudo-time algorithm for integration to steady state 7-26302
 Neveu Schwarz model, scattering amplitude calcs. using supersheet functional integration 7-442
 nonlinear hydrodynamic eqns., integrability, gradient algorithm and Lax representation 7-61114
 nonlinear integrable classical Hamiltonian, quantisation and quantum integrability 7-24470
 nuclear power station simulation, parallel-processing modular system 7-10197
 Painleve analysis, Yoshida's theorems and direct methods in the search for integrable Hamiltonians 7-61030
 Painleve integrability test for nonlinear partial differential eqns. 7-41071
 plasticity equations, numerical integration scheme 7-63004
 plates, inelastic, bending problems, influence functions use (*German*) 7-20606
 polydyadic structure, near-integrability 7-29726
 pyramid finite elements, basis functions and numerical integration 7-24406
 quantum oscillator in radiation field, interaction energy 7-29806
 Riemann derivatives and general integrals 7-24372
 rigid body dynamics, general integrable cases for problems with no axial symmetry 7-24413
 rigid body in resistive medium, eqns. of free motion, stability control of numerical integration 7-41088
 Schrodinger equation, nonlinear, numerical integration 7-29794
 second-order differential equations, integrals of soln. combinations 7-35231
 SETI, time and space acousto-optic folded spectrum processing 7-26080
 stochastic differential equations with variable diffusivity, numerical integration 7-35233
 superconvergent integration for dynamics systems and other problems of m-th order (*German*) 7-14753
 uniformly asymptotic expansion for integral with large and small parameter 7-48314
 van der Waals fluid, Riemann problem, numerical integration 7-38153
 variable coefficient KdV equation, similarity anal. and exact soln. 7-29771
 Hg electrode-soln. interface, 2-anion simultaneous adsorpt., elec. double laser parameters algorithm 7-54132

integro-differential equations

- see also Boltzmann equation; Fokker-Planck equation; Liouville equation; master equation; Vlasov equation
 asymptotic behaviour of resolvents of abstract Volterra equations 7-61022
 Benjamin-Ono eqns., interacting soliton solns. 7-24433
 dendritic crystal stability integro-differential operator formulations 7-38422
 elasticity with deformations, inhomogeneous theory 7-9672
 ferromagnetic thin film, precession soliton, nonlinear integro-differential eqn. soln. 7-64500
 flight vehicle aeroelasticity, 3D motion, nonlinear integrodifferential eqns. 7-43737
 jet calculus, inclusion of coherence effects 7-61764
 linear hyperbolic partial differential integral eqns., propag. of singularities 7-29700
 magnetic quadrupole, short wavelength drift waves, linear theory 7-44228
 mode convertors, optimised overmoded TE01 to TM11, high power appls. at 70, 140 GHz 7-37708
 muscle contraction, analysis using integro-differential equation 7-59911
 nonlinear integro-differential eqns., method of freezing for appl. to elasticity problems 7-48359
 nonlinear maps with memory 7-41070
 nonlinear singular integro-differential equation, existence and uniqueness analysis 7-35242
 nonlocal equations of motion and their balance laws 7-35214
 parabolic type integro-differential eqn., time discretisation 7-35251
 plane problems of thermoelasticity, thermal stress components, integro-differential correlations (*Ukrainian*) 7-11281
 potential flow, vortex filament motion and decay 7-11424
 resonant optical medium surface, nonlinear refl. and refraction of scanning laser beam, integrodifferential eqns. method calcs. 7-43209
 semiconductor double heterostructures, luminescence radiation photon recycling 7-13208
 shear wave bundles in nonlin. hereditary medium, quasioptical approx. 7-31654
 simultaneous integro-differential eqns., soln. using Kontorovich-Lebedev transform 7-55968
 space-charge currents, transient decay, description using integro-differential eqns. 7-7643
 unsteady compressible viscous flow over airfoils, integro-differential and finite-difference methods 7-31821
 Volterra type integro-diff. eqns., periodic boundary value problems 7-29718
 water waves, large amplitude, num. computation 7-18326

intelligence, artificial see artificial intelligence**intelligibility, speech see speech intelligibility****intensification see amplification****intensity measurement****see also acoustic intensity measurement**

No entries

interacting binary stars see binary stars; cataclysmic binary stars; eclipsing binary stars; X-ray binary stars**interacting boson approximation**

- ¹²⁸Xe, M1 transitions between collective levels, proton-neutron IBM anal. 7-19197

interacting boson approximation continued

- ^AAu, A=189-195, $h_{11/2}$ bands, particle-core coupling calcs., IBM core testing and negative parity states 7-56590
 B(E2), IBM expressions for inter-representation transitions in deformed nuclei (*Chinese*) 7-24960
 band sequences and interbandhead E2 transitions, IBM SU(3) limit 7-10122
 boson mapping of the shell model algebra obtained from a seniority-dictated similarity transformation 7-49265
 boson states with Dyson's description, truncation schemes 7-49264
 boson-fermion hybrid representation for antisymmetrizer, many-body forces 7-61817
 collective shell model states, IBM-2 boson state mapping 7-19150
 collective states, F-spin analysis, global study of groups of nuclei, IBM analysis 7-49223
 correspondence with fermion dynamical symmetry model 7-49262
 developments and applications 7-41910
 diagonalization procedure and E2 transition probability calcs. 7-49261
 dynamical symmetries in non-U(6) formalism 7-41918
 exchange term in the IBFM Hamiltonian, shell-model origin 7-41916
 heavy-ion spectroscopy viewed from the IBM 7-35931
 IBM4, dynamical symmetry in light nuclei 7-56625
 IBM with boson surface-dealt interaction 7-15193
 interacting boson-fermion approximation, inertial parameters 7-41913
 interacting vector boson model, boson representations of symplectic algebras 7-41912
 Majorana force calcs. from M1 mode anal. 7-49299
 medium and heavy weight nuclei, two-boson spectra 7-41898
 microscopic three-boson force in a six-fermion system 7-41915
 N_pN_n scheme, global IBA calc. 7-49266
 negative parity bands in collective pair approach 7-24930
 quadrupole sum rule violation and E2 matrix elements 7-61819
 rare earths, octupole states and bandhead energies in deformed nuclei, IBM calc. 7-30312
 transition operators and Hamiltonian of interacting quasiparticles and quadrupole bosons 7-30356
 U(12) systematics in IBA Hamiltonian, level energies and B(E2) ratios 7-41914
 g boson signature from g-factor variations 7-41917
 Ag, odd-A nuclei, low-lying $7/2^+$ states, quadrupole interaction calcs. 7-19167
¹²⁸Ba, band crossings, IBM calcs. 7-10096
¹⁴²Ba, 2_1^+ state g-factor, hydrodynamic model and IBA-2 anal. 7-30332
^ACa, A=40, 48 relativistic self-consistent field calculations for some closed-nuclei 7-56627
 Ce, odd-mass isotopes, backbending, IBA anal. 7-19149
^AFe(n,n'), A=54, 56, 58, gamma distrib., excited level schemes, B(E2) values 7-30419
 Ge, high spin states, B(E2) values, g-factors IBM coupled calcs. 7-35930
⁶⁶Ge, g-factor meas., evidence for higher multipole forces and states 7-49240
 Hf, generalisation of $\hat{Q}\hat{Q}$ Hamiltonian for IBM 7-61816
¹⁹⁵Ir low-spin positive-parity states identification U(6/4) supersymm. representations 7-41869
^AKr, A=78, 80, negative-parity states, E2 transition probabilities, IBM anal. 7-30340
^ANd, A=even 142-150, effective charges in IBM, mass depend., B(E2) values 7-30321
¹⁶O, relativistic self-consistent field calculations for some closed-nuclei 7-56627
³⁰P, occurrence in O(6) multiplet with ³⁰Si, IBM4 dynamical symmetry anal. 7-56625
 Pd, A≈100 isotopes, positive parity states in IBA-1 model (*Rumanian*) 7-15189
¹⁹⁵Pt(³²S, ³²S'), 125 MeV, levels and transitions, B(E2) values, SUSY classification in IBFM 7-30310
 Rh, odd-A nuclei, low-lying $7/2^+$ states, quadrupole interaction calcs. 7-19167
¹⁰⁷Rh, level scheme study via γ -ray spectrum following β -decay, IBM comparison 7-41944
 Ru, A≈100 isotopes, positive parity states in IBA-1 model (*Rumanian*) 7-15189
^ASe, A=76, 78, negative-parity states, E2 transition probabilities, IBM anal. 7-30340
³⁰Si, occurrence in O(6) multiplet with ³⁰P, IBM4 dynamical symmetry anal. 7-56625
¹⁵⁴Sm(p,p'), 800 MeV, collective state excitations, Glauber model, IBM anal. 7-24981
 Tc, odd-A nuclei, low-lying $7/2^+$ states, quadrupole interaction calcs. 7-19167
^ATi, A=44, 46, 48, IBM description of energy spectra (*Chinese*) 7-10115
^ATi, A=191-197, $h_{9/2}$ bands, particle-core coupling calcs., IBM core testing and negative parity states 7-56590
¹²⁸Xe, excitation energies and branching ratios, F-spin structure of eigenstates, IBM-2 appl. 7-49300
^AZn(n,n'), A=64, 66, 68, 70, gamma distrib., excited level schemes, B(E2) values 7-30419

interacting boson model see interacting boson approximation**interacting control systems see multivariable control systems****interactive systems****see also online operation**

- 3D CT image reconstruction and display (*Chinese*) 7-60118
 BWR nuclear power plant simulation 7-49530
 chemical graph theory 7-30916
 discontinuous flows, teaching using interactive techniques and windowing 7-60923
 diverse experimental data preliminary processing 7-4825
 gas turbine CAD system with Denton scheme for flow program, comparison with expt. results 7-63177
 gas turbine computer-aided interactive design system, Denton scheme for flow program 7-63176
 IUE spectra, VIRIS-VAX interactive reduction 7-40720
 lens design, interactive computer program 7-50693
 lens design software, human dimension 7-50675
 optical system design, interactive ray-tracing program integrated with solid-modelling CAD system 7-50679
 terrain data interactive image processing, digital SM-4 Omega system 7-66334
 X-ray CT image, 3D display of cerebral ventricle 7-47280

interatomic potentials *see potential energy functions*

intercalation compounds

- alkali halides, neutral molecule incorporation, composite form. at room temp. 7-54101
 alkylamines, interaction with layered compounds 7-46838
 alkylamines intercalation into $\text{HfCa}_2\text{Nb}_3\text{O}_{12}$, structural studies 7-65306
 chalcogenide intercalation compounds with NH_3 guest species, NMR 7-53160
 CoCl_2 -graphite, obs. of magnetic state, high magnetic field 7-59008
 coke, metallurgical, microstruct. analysis and intercalated species 7-28008
 2,9-dimethyl-1,10-phenanthroline intercalated into $\alpha\text{-Zr}(\text{HPO}_4)_2$, ion exchange with Co^{2+} , Ni^{2+} and Cu^{2+} , dimer formation 7-65305
 electronic struct., initial stages of intercalation 7-53503
 energy conversion and storage using insertion materials 7-28391
 graphite:B-Na, Fermi level displacement, diamag. anisotropy and Hall effect meas. 7-16933
 graphite, intercalated fibre elec. conductors, passivating coatings 7-8140
 graphite, pyrolytic, highly oriented, intercalation reaction with K vapour, neutron diffr. study 7-1999
 graphite, stage transformation, stochastic model 7-21433
 graphite, staging, struct., dynamical and magnetic props., review 7-1966
 graphite, staging walls charge profile, Thomas-Fermi description 7-12687
 graphite fibre, benzene-derived, exfoliation and characters. 7-46663
 graphite intercalated with alkali metals, electron struct., soft X-ray emission spectroscopy 7-45117
 graphite intercalated with Br, struct. and phase transitions, review 7-52041
 graphite intercalation compound, 2D Rb liquid, modulation potential, X-ray study 7-44639
 graphite intercalation compound, C_{1-x}F_x , resistivity and ESR study 7-64197
 graphite intercalation compound with H_2SO_4 , optical study of K-point π -band dispersion 7-17317
 graphite intercalation compound with HNO_3 , diffusion, charge transfer and strain fields, ESR study 7-53117
 graphite intercalation compounds, first stage, with heavy alkali metals, electronic props. 7-2463
 graphite intercalation cpds., 2D magnetism, review 7-59033
 graphite intercalation cpds., staging dislocation electronic struct., electron scatt. rates, residual resist. 7-52558
 graphite surface (0001)-(2 \times 2)K intercalated structure, LEED calcs. 7-6952
 graphite- AlCl_3 , phases and phase transform., X-ray crystallography (French) 7-44783
 graphite- AsF_5 , galvanomag. props. 7-58822
 graphite- AsF_5 , stage 1, nonresonant intercalant modes, Raman scatt. studies 7-38136
 graphite-Br, electromech. effect on heating 7-45414
 graphite-Br intercalation cpds., 2D stripe-domain system, melting transition 7-58449
 graphite- ClF_3 , electrical conductivity 7-7295
 graphite-Cs, $\text{C}_{24}\text{Cs}(\text{H}_2)$, domain mobility and rot. tunnelling spectrum 7-63525
 graphite- CuCl_2 , ideal resistivity studies 7-32976
 graphite-Fe, atomic structure, EXAFS studies 7-12011
 graphite- FeCl_3 , mag. suscept. and low temp. transition meas. 7-58993
 graphite- FeCl_3 , spin-lattice relax. time meas., AC suscept. bridge techniques 7-13054
 graphite- HNO_3 , absolute Pauli spin suscept. meas., Fermi level density of states determ., ESR/NMR method 7-12940
 graphite- HNO_3 , $\text{C}_{20}\text{HNO}_3$, low-temp. struct. 7-51721
 graphite- H_2SO_4 , $2\text{H}_2\text{SO}_4$, $\text{C}_{24}\text{H}_2\text{SO}_4$, quasi-2D, cond. electron state transform. in microwave field, ESR meas. 7-64508
 graphite-K, C_6K , anisotropic binding of K, nuclear resonance photon scatt. of bremsstrahlung 7-51695
 graphite-K, C_8K , density of states, interlayer band occurrence 7-2454
 graphite-K, C_8K , electronic band struct., angle resolved UPS study 7-27232
 graphite-K, C_8K , positron annihilation spectra, effect of H absorption 7-39270
 graphite-K, high-stage struct., temp. depend., X-ray diffr. study 7-63592
 graphite-K, KC_{24} , 2D layer melting dynamics, neutron scatt. meas. 7-21420
 graphite-K, KC_{24} , kinetically-hindered low-temp. staging transition, P-T phase diagram, resist. anomaly meas. 7-6786
 graphite-K, positron localisation 7-39271
 graphite-KHg, KHgC_4 and KHgC_8 , valence bands, XPS studies 7-16932
 graphite-KHg, supercond. props., density of states model 7-27457
 graphite- Li , Li_xC_6 , elastic effects, comp. depend. staging studies 7-63707
 graphite-Rb, RbC_{24} , 2D layer melting dynamics, neutron scatt. meas. 7-21420
 inorganic layered cpds., reactivity, conf., New York, NY, USA (Apr. 1986) 7-41003
 Lamellar cpds., X-ray absorpt. studies 7-59286
 material modification, controlled prop. prod. (Czech) 7-7909
 polyethylene oxide-disubstituted benzene intercalates, Fourier transform IR spectra 7-13153
 polyoxyethylene-p-dihalogenobenzene intercalates, struct. 7-13154
 rhodamine dye intercalated smectite, fluorescence props. 7-22325
 transition metal dichalcogenides, low-dimens., as secondary cathodic materials, book contrib. 7-28394
 transition metal phosphorous trisulphides, electronic, structural and mag. props., intercalation cpds. and chemical props. 7-44499
 $\text{Ag}_{0.25}\text{NbSe}_2$:Li, Li diffusion and intercalation 7-16806
 Ag_xNbSe_2 intercalation cpds., crystal structures and staging 7-12023
 $\text{Ag}_x\text{Ti}_{23}$, stage-2 interaction cpd., order-disorder phase transition 7-12255
 $\text{Ag}_{1/3}\text{TiS}_2$ intercalation cpd., transport and mag. props. 7-52572
 AsF_5 -graphite, intercalation compounds, staging phenomenon studied using Ising model 7-58464
 BN:Cs(Br), intercalation cpd. formation 7-44574
 C fibres, high electrical conductivity intercalation treatment (French) 7-59646
 C- AsF_6 intercalation cpd., Raman scatt., coupled electron-phonon excitation 7-46045
 C_{28}Br_2 intercalation cpd., 2-D system with competing interactions, phase transitions 7-6791
 C_6S_8 , first stage intercalation cpd., self-consistent band struct. calc. 7-52395

intercalation compounds continued

- $\text{C}_{10}\text{CuCl}_2$, Shubnikov-de Hass effect, amplitude behaviour (Russian) 7-52571
 C_{16}ICl , intercalation cpd., Shubnikov-de Hass effect, amplitude behaviour (Russian) 7-52571
 C_8K and C_{24}K intercalation cpds., angle-depend. X-ray emission bands 7-46248
 C_8K first stage intercalation cpd., self-consistent band struct. calc. 7-52395
 C_8K type graphite intercalation cpds., mol. dynamics study of model system 7-63430
 $\text{C}_5\text{MnCl}_2 \cdot 2.4\text{NH}_3 + 4.8\text{NH}_3$, thermochemical energy storage, kinetic study (French) 7-17782
 C_8Rb , first stage intercalation cpd., self-consistent band struct. calc. 7-52395
 $\text{C}_5\text{SO}_3\text{F}$ fibre intercalation cpds., enhanced elec. cond. 7-33927
 $\text{Cd}_2\text{P}_2\text{S}_6$ intercalated with pyridine, D NMR study 7-33279
 $\text{Cd}_2\text{P}_2\text{S}_6$ intercalated with pyridine complexes of ferric ion, spectroscopic and ESR studies 7-64519
 CoCl_2 -graphite intercalation cpds., mag. susceptibility meas. 7-45638
 Cr_2TiS_2 , intercalated dichalcogenide, electronic struct. 7-52387
 Cs , in graphite monolayer on Re surface, struct. and props., AES, TDS and thermionic emission anal. 7-45017
 CsBi_2 -graphite intercalation cpds., stage 1, α and β phases, X-ray diffr. study 7-58226
 CsC_x ($x=8,24$), intercalation cpds., XANES studies, polarisation effects 7-59294
 Cu_xNbSe_2 intercalation cpds., crystal structures and staging 7-12023
 Eu_2TiS_2 mixed valence intercalation cpd., low-temp. synthesis and mag. props. 7-17779
 FeCl_3 -graphite intercalates, high resolution electron microscopy 7-16433
 Fe_2TiS_2 , intercalated dichalcogenide, electronic struct. 7-52387
 Fe_2ZrSe_2 , intercalated layered cpd., thermopower and low DC field magnetisation study 7-17199
 GaSe laminar semicond. intercalation cpds., phase equilibria and stability studies (Russian) 7-21409
 GaSe layered intercalated crystals, formation of electric state 7-38994
 GaSe-Li , intercalated layer compounds, conc. depend. of electrode potential 7-7230
 graphite- KH_2 , struct. and electronic props. 7-27234
 $\text{H}_{0.33}\text{TaS}_2$, host lattice-intercalant strong interaction, proton mobility hysteresis, PMR study 7-53159
 $\text{H}_2\text{O}_2\text{PO}_4 \cdot 4\text{H}_2\text{O}$ intercalation with piperidine, hydrazine, pyridine, pyrazine or (dimethylaminomethyl) ferrocene 7-65304
 InSe laminar semicond. intercalation cpds., phase equilibria and stability studies (Russian) 7-21409
 InSe-Ag intercalation cpd., prep. 7-54146
 InSe-Li , intercalated layer compounds, conc. depend. of electrode potential 7-7230
 $\text{In}_2\text{Se}_3\text{-Ag}$ intercalation cpd., prep. 7-54146
 KC_{24} intercalation cpd., low temp. structural transition 7-21431
 KC_8 intercalation cpd., polarisation depend. XANES study 7-59298
 $\text{KC}_8/\text{D}_2\text{O}$ intercalation cpd., X-ray diffr., NMR, EPR and gas phase mass spectra anal. 7-46843
 KC_x ($x=8,24$), intercalation cpds., XANES studies, polarisation effects 7-59294
 $\text{KH}_{0.8}\text{C}_x$, polarisation depend. XANES study 7-59298
 $\text{K}(\text{NH}_3)_2\text{C}_{24}$, intercalation cpd., 2D diffusion-limited kinetics 7-58552
 K_2TiO_9 , layered, synthesis and struct. 7-32406
 Li/MoX_2 and Li/WX_2 ($\text{X}=\text{S,Se,Te}$) electrochemical cells at low voltages, dichalcogenide decomposition 7-65436
 Li-TaS_2 , room temp. optical transmission spectra, charge transfer and band struct. modification 7-45962
 LiC_6 intercalation cpd., phonon dispersion, two-body pot. 7-44715
 LiFeClMoO_4 , synthesis, struct. and low temp. magnetism 7-21172
 Li_2GaSe intercalation cpd., elec. resist. and Hall effect meas. 7-12719
 $\text{Li}_{1+x}\text{Mn}_{1-x}\text{SgRu}_{1-x}\text{O}_4$, Li insertion cpd., prep. and characterisation (German) 7-26720
 LiMoS_3 , synthesis, electrochemistry and struct. 7-33619
 $\text{Li}_x\text{Mo}_6\text{Se}_8$ intercalation cpd., entropy and struct. transition, lattice gas model 7-6832
 $\text{Li}_x\text{Mo}_6\text{Se}_8$ intercalation cpd., entropy, electrochem. cell calorimetry studies 7-6833
 $\text{Li}_x\text{Mo}_6\text{Se}_{8-y}\text{I}_y$, Li electrochemical insertion, struct. studies 7-37947
 $\text{Li}_x^+(\text{NH}_4)_y(\text{NH}_3)_z\text{TiS}_2^{(x+y)-}$ intercalation cpd., NH_3 oxidation, charge compensation 7-32354
 $\text{Li}_2\text{Na}_2\text{TiS}_2$ intercalated dichalcogenides, struct., electrochem. and thermodynamic props. studies 7-21167
 Li_2TiS_2 , intercalation in solid-state battery cathode, TEM study 7-17854
 Li_xTiSi_2 , elastic effects, comp. depend. staging studies 7-63707
 $\text{Li}_x\text{TiGaSe}_2$, ion intercalated, dark current and photocurrent relax. meas. 7-38622
 LiV_2O_5 , Li inserted, struct., neutron and X-ray powder diffr. anal. 7-32391
 $\text{Li}_x\text{V}_6\text{O}_{13+y}$ nonstoichiometric intercalation cpd., phase stability and elec. cond. studies 7-12723
 MnCl_2 -graphite intercalation cpds., mag. susceptibility meas. 7-45638
 MoS_2 , intercalated with Fe, Ni and Pd, AES, sputtering studies 7-63867
 MoS_2 , surface chemistry and props., photoemission, SIMS and SEM anal. 7-44971
 $(\text{NH}_3)_{0.23}\text{H}_{0.31}\text{MoO}_3$, intercalation cpd. struct., enthalpy of reaction 7-46841
 $(\text{NH}_4)_{0.32}\text{H}_{0.16}\text{WO}_3$, intercalation cpd. struct., enthalpy of reaction 7-46841
 $(\text{NH}_4)^+_{0.22}\text{TiS}_2^{0.22-}$ ionic intercalation cpd., synthesis, characterisation by thermal anal., mag. 7-45244
 $(\text{NH}_4)_{0.84}\text{V}_3\text{O}_8$, intercalation cpd. struct., enthalpy of reaction 7-46841
 NaFeClMoO_4 , synthesis, struct. and low temp. magnetism 7-21172
 $\text{Na}_x\text{Mo}_2\text{O}_4$ intercalation cpd., struct., mag. suscept., X-ray diffr. and electrochemical anal. 7-46842
 $\text{Nb}_2\text{Pd}_{0.74}\text{Cu}_{0.22}\text{S}_2$, reactivity, intercalation structural changes, X-ray diffr. exam. 7-46839
 $\text{NbS}_2(\text{Se}_2)$ -transition metal intercalation cpds., EXAFS 7-53446
 NbSe_2 :Li, Li diffusion and intercalation 7-16806
 Ni hydroxy-psica intercalation complexes, mag. props. 7-17162
 Ni , $\text{M}_{1-x}\text{Zn}_x$ where $\text{M} = \text{Cd, Zn, Mg}$, IR, visible and UV spectra, dilution and intercalation effects 7-13175
 PbLiInSe , intercalation-layer compound, dielectric-metal cond. transition 7-7230
 RbC_8 , 2D graphite intercalation cpds., bond angle determ. EXAFS study, Debye-Waller anisotropy. 7-59293

intercalation compounds continued

- RbC₂₄ (x=8, 24), intercalation cpds., XANES studies, polarisation effects 7-59294
- Ru complex, Creutz-Taube complex with HUO₂PO₄, synthesis, struct. and oxidation, IR and X-ray spectra anal. 7-46840
- α -RuCl₃, intercalation reactions, electron/ion transfer and exchange reactions 7-46837
- SbCl₅ intercalated graphite, stage 2, basal plane resistivity and phase diagram 7-45258
- SbCl₅F_{3-m} graphite intercalation cpds., struct., X-ray diffr. studies 7-12008
- TaS₂, electrochem. intercalation reactions with Li, K, H, In, Ga, In_{0.17}Ga_{0.83}, nucl. quadrupole interactions, TDPAC meas. 7-17245
- TiO₂(B) open metastable structure, layered, synthesis and struct. 7-32406
- TiS₂ intercalation cpd. with Mn, Fe, Co, Ni elec. resist. and thermopower studies 7-45331
- To₂NiSe₆, reactivity, intercalation structural changes, X-ray diffr. exam. 7-46839
- To₂PdSe₆, reactivity, intercalation structural changes, X-ray diffr. exam. 7-46839
- Yb₂TiS₂ mixed valence intercalation cpd., low-temp. synthesis and mag. props. 7-17779
- α -ZrP-propylamine, intercalation cpd., amine loading, protonic cond., admittance meas. 7-44909

interconnected systems see large-scale systems

interdiffusion see diffusion

interface electron states

- 2D systems, proceedings of Winter School, Mauterndorf, Austria (Feb. 1986) 7-48131
- arbitrary continuous superlattices, general anal. 7-7322
- conference, Oconomowoc, WI, USA (April-May 1985) 7-18468
- continuous composite materials, interface response theory 7-64039
- Coulomb interaction in presence of surface 7-38794
- curved interface, quasi-2D quantum electron states 7-17066
- disordered interfaces, electronic struct. calcs., Lloyd model 7-2657
- disordered multilayered systems, local density of states determ., recursion method 7-52528
- disordered oxide-semiconductor interface, inversion layer electronic density of states 7-58852
- double layer dielec. films, X-ray irradi. effects 7-58332
- dynamical phenomena at surfaces, interfaces and superlattices, summer school, Erice, Italy, (July 1984) 7-1
- electrolyte near critical point elec. struct. of interface, elec. double layer 7-33063
- electronic structure of surfaces, interfaces and superlattices 7-2665
- fractional quantum Hall states, hierarchy termination and impurity effect scaling 7-21978
- heterojunction band lineups and interface dipoles, tight binding theory 7-7368
- III-V semiconductor superlattices and quantum well structures, electronic props. 7-52817
- image charges and their influence on the growth and the nature of thin oxide films 7-64312
- insulator-semiconductor interface, unified disorder induced gap state model 7-2656
- integer quantum Hall effect, theory 7-52824
- interfacial diffusion effect on superlattice electronic structure (Chinese) 7-7303
- ionic cryst.-semicond. superlattice interface excitations, classical anal. 7-52845
- magnetism and electronic struct. at surfaces and interfaces, ab initio calcs. 7-58854
- metal-Al₂O₃-InP structs., improved elec. props. with heat resist. interface 7-38753
- metal-insulator-semicond. structs., interface state density profile determ., DLTS spectra interpretation 7-38733
- metal-p⁺-n structures, Schottky barrier height enhancement, calcs. including free carriers 7-2709
- metal-semiconductor interface, unified disorder induced gap state model 7-2656
- metal-semiconductor Schottky diodes, interface state form. and barrier height control 7-52839
- metal-SiO_xN_y-SiO₂-Si system, plasma oxynitride effect on interface charge 7-38761
- MIS structure, small-signal DLTS response from insulator semiconductor interfacial traps, model anal. 7-64147
- modulated semicond. structs., conf., Kyoto, Japan (Sept. 1985) 7-4630
- MOS capacitors, interface state generation by ionising radiation, oxide thickness depend. 7-58900
- MOS capacitors, radiation-induced interface state generation 7-58899
- MOS interface charge state transient spectroscopy 7-45506
- MOS structure, gamma irradi. effects, mech. stress depend. 7-58903
- MOS structure, X-ray irradi., interface trap annealing, two-reaction model 7-58901
- MOS structures, interface and bulk traps, effect of processing steps 7-38758
- MOS systems, freq. spectrum of reciprocal capacitance 7-38741
- MOS systems, interface state generation upon carrier injection 7-38759
- multiple-scattering treatment of surfaces and interfaces 7-45420
- p-n junction, boundary conditions at high injection level in space charge region 7-17091
- quantum well structures, localised states, strain depend. 7-7312
- quantum wells, electronic struct., interface disorder effects 7-45476
- Schottky barrier, models and elec. charactn. methods 7-52738
- Schottky barrier diodes, interface density meas. using I-V characteristics 7-58857
- semiconducting materials, cryst., and device appls., book 7-60894
- semiconductor doping superlattices, physics and applications 7-52826
- semiconductor heterojunction band line-ups, tight-binding theory 7-52813
- semiconductor heterojunctions, interface states, 1D relativistic models 7-52753
- semiconductor heterostructures, band-edge discontinuities, heuristic approach 7-52815
- semiconductor heterostructures, electronic states, valence subbands 7-7307
- semiconductor heterostructures, inelastic light scatt. by electronic excitations 7-13171
- semiconductor interface physics and chem., conf., Pasadena, CA, USA (Jan. 1986) 7-4

interface electron states continued

- semiconductor strained layer superlattices, electronic and optical props. 7-7359
- semiconductor structures, 2D localisation and interaction effects 7-52531
- semiconductor superlattice, 3D anisotropic system, surface states and quantum Hall effect 7-38700
- semiconductor superlattice, boundary surface collective charge-density excitations 7-52776
- semiconductor superlattices, surface plasmons obs. 7-52777
- semiconductor-dielectric boundary, surface state density spectrum determ. using equivalent three element circuit (Russian) 7-27434
- semiconductor-electrolyte interface photoelectrochemical system, quantum yield interpretation and surface state model calcs. 7-23036
- semiconductors, cryst. and amorphous, and heterojunctions, electronic struct. using bremsstrahlung isochromat spectroscopy 7-52795
- semiconductors, MBE growth, RHEED and photoemission studies 7-2438
- steel, electrospray alloying with carbides, electron nature of interaction, phase comp. 7-8182
- superlattices, surfaces and interfaces, structural, electronic and mag. props. 7-16849
- system, silicide form., struct. and electronic props. 7-38363
- tight-binding muffin-tin orbital Green's function method 7-52721
- transition metal surfaces and interfaces, hyperfine fields 7-58847
- two-dimensional carrier systems, parallel transport 7-52827
- two-dimensional electronic systems, plasmons and intersubband resonances 7-52730
- AgBr/AgCl interface, photocarrier transfer and energy band location studies 7-45433
- Al-ethyl alcohol interface, surface polaritons, four-wave mixing 7-43244
- Al-polyacrylic acid interface, reactivity, comp., XPS 7-28334
- Al-polyethylene interface, reactivity, comp., XPS 7-28334
- Al-Si:Ar,H, ion implanted ultrahigh Schottky barriers, interfacial traps, DLTS study 7-45489
- Al-SiO₂-Si MOS capacitors, optical and thermal cross-section of interface states, photocapacitance meas. 7-38742
- Al_{1-x}Ga_xAs multiple quantum wells, photoluminescence studies, press. depend. (Chinese) 7-13194
- AlGaAs/AlAs multiquantum-well structs., staggered band alignments 7-7361
- AlGaAs/GaAs heterostruct., quasicrystalline system, electronic struct. studies 7-38699
- AlGaAs-GaAs, modulation doped heterostructs., high field transient transport 7-12836
- AlGaAs-GaAs heterointerface, ballistic transport of quasi-2D electron gas 7-52788
- AlGaAs-GeAs n-n heterojunction, thermionic current and capacitance, effect of subband quantisation in 2D electron gas 7-17090
- Al_{0.9}Ga_{0.7}As/GaAs quantum wells, photocond. of confined donors 7-7282
- Al_{1-x}Ga_xAs/GaAs quantum wells, photolum., periodic variation investig. 7-2688
- Al_{1-x}Ga_xAs-GaAs heterointerface, 2D electron gas density 7-45448
- AlInAs-GaInAs superlattices, electronic transport and depletion by tunnelling 7-27395
- Au-GaAs, interface state meas. at Schottky contacts, admittance characterisation technique 7-2718
- Au-GaAs, Schottky contact, interface states, trap characterisation 7-27421
- Au-GaAs_{1-x}Sb_x Schottky barriers, I-V characts., temp. depend. 7-64344
- CaF₂ epitaxial films on Si, structural and electrical props. improvement by rapid thermal annealing 7-38400
- CaF₂-Si (111), interface form., photoemission study 7-2395
- CaF₂-Si (111), MBE grown, electronic struct. 7-2725
- CaF₂-Si (111) interface, electronic struct. 7-38737
- CaF₂-Si interface, with MBE grown insulator, trap states, I-V, C-V meas. 7-7407
- CdI₂-Ag interface, absorpt. and luminesc. spectra studies (Russian) 7-59224
- CdS thin film MIS structs., band bending and interface state density 7-7402
- a-CdS/n-Si heterojunctions, elec. props. 7-64342
- CdTe films on InSb, interface struct. and band offsets 7-58664
- CdTe/GaAs heterojunction, defect and impurity states, photovoltage meas. 7-17065
- CdTe-(Cd,Mn)Te MQW, optical and magneto-optical props. 7-13137
- n-CdZnS/p-CuInSe₂ polycrystalline solar cells, open circuit voltage 7-17889
- CoSi₂-Si heterostructures, MBE or solid phase epitaxially grown, Schottky barrier heights, DLTS spectra 7-12859
- CoSi₂-Si Schottky barriers, epitaxially grown, supercond. below 1.05K, tunnelling spectra 7-12860
- Cu-CdTe interface form., effect of different cation-anion bond strengths 7-27149
- Cu-Cu₂O Schottky barrier solar cells, interfacial layer effects investig. using n-V_∞ diagram 7-54304
- Cu-GaAs (110), electron struct., synchrotron radiation photoelectron spectroscopy 7-27420
- Cu-Hg_{0.75}Cd_{0.25}Te interface form., effect of different cation-anion bond strengths 7-27149
- CuInSe₂-CdS solar cells, capacitance determ. of interfacial states 7-13916
- Fe overlayers or sandwiches with Cu (001), electronic and mag. props. 7-64499
- Fe-Ge (110) interface, electronic struct. calc., mag. effects 7-45496
- GaAlAs/GaAs:C quantum wells interface struct. and luminesc. efficiency 7-7735
- Ga_{1-x}Al_xAs-GaAs-Ga_{1-x}Al_xAs quantum well, donor ion dielec. response 7-45417
- GaAs (110) with Sb overlayers, electronic band bending at interface 7-58895
- n-GaAs, cleaved clean (110) surface initial band bending cause, noble metal deposition 7-22017
- GaAs heterostructures, valence subbands, excitons and luminescence 7-7321
- GaAs MESFET and JFET devices, elec. resist., Hall effect, influence of electronic subband mag. depopulation 7-38740
- GaAs quantum wells, electron interference effects, obs. of bound and reson. states 7-64334
- GaAs sawtooth doping superlattices, photoluminescence, transport props. 7-52825
- GaAs Schottky-barrier formation and microscopic metal clusters 7-45497

interface electron states continued

- GaAs/Al_{1-x}Ga_xAs heterostructure interfaces, band discontinuities, electrical meas. 7-52814
- GaAs/Al_{1-x}Ga_xAs quantum-well bound states, valence-band offsets 7-7313
- GaAs/AlAs superlattices, electronic band structure, pseudopot. method calc. 7-17084
- GaAs/AlAs/GaAs:Se heterojunctions, elec. behaviour, DLTS studies 7-7360
- GaAs/AlGaAs quantum wells, MBE growth and energy levels, photoluminescence meas. 7-7067
- GaAs/Ga_{1-x}Al_xAs graded interface superlattice band struct. calcs. 7-58879
- GaAs/GaAlAs disordered superlattices, carrier localisation obs. 7-12818
- GaAs/GaInAs interface, EELS near a single misfit dislocation 7-33497
- GaAs-(AlGa)As heterostructure, modulation-doped, valence band mixing, and optical emission 7-7344
- GaAs-Al junction, interface states, DLTS study 7-58892
- GaAs-Al_{0.44}Ga_{0.56}As quantum wells, MBE grown, tunnelling assisted photon emission, photoluminescence meas. 7-46120
- GaAs-Al_xGa_{1-x}As (001) superlattices, periodicity, charge density and zone folding effects 7-2685
- GaAs-Al_{1-x}Ga_xAs MOCVD quantum well structures, time-resolved photolum. 7-53410
- GaAs-Al_{1-x}Ga_xAs quantum well structure, recomb. dynamics, photolum. obs. 7-12809
- GaAs-Al_{1-x}Ga_xAs superlattice, hole subbands (*Chinese*) 7-58873
- GaAs-Al_{1-x}Ga_xAs superlattices, electronic and optical props., alloying and press. effects 7-64327
- GaAs-Al_{1-x}Ga_xAs type I superlattices, electronic struct., tight binding calcs. 7-45475
- GaAs-AlAs multiple quantum wells, photoconductivity, photorefectance and photolum. meas. 7-27368
- GaAs-AlAs superlattice, energy bands, cohesive energy, form. energy, self-consistent calcs. 7-21995
- GaAs-AlAs superlattices, folded acoustic branches, leakage-induced and disorder-activated modes 7-33389
- GaAs-AlAs pseudoheterostructure, tunnelling transmission probability, many-band pseudopotential model 7-38701
- GaAs-AlGaAs extended state superlattices, shallow donor state transition energies 7-33082
- GaAs-AlGaAs heterointerface, band offsets, overview 7-12831
- GaAs-AlGaAs heterostruct., band discontinuity determ., DLTS, interface charge density, trap conc. 7-12833
- GaAs-AlGaAs heterostructures, zero mag. field thermopower meas., temp. var. 7-33075
- GaAs-AlGaAs heterostructures, density of states of Landau levels 7-52822
- GaAs-AlGaAs MQW optical NOR gate, exciton and carrier dynamics, time resolved obs. 7-50628
- GaAs-AlGaAs superlattices, magnetotransport 7-45471
- GaAs-Ga_{0.7}Al_{0.3}As heterojunction, donor-acceptor radiative recomb. mechanism, photolum. spectra study 7-17083
- GaAs-Ga_{1-x}Al_xAs superlattices, shallow impurity state binding energies 7-45416
- GaAs-Ga_{1-x}Al_xAs 2D quantum well heterostructures, magneto-impurities, mag. field and press. effects 7-52728
- GaAs-Ga_{1-x}Al_xAs heterojunctions, electron energy levels 7-17082
- GaAs-Ga_{1-x}Al_xAs heterojunctions, impurities, optical props. 7-27396
- GaAs-Ga_{1-x}Al_xAs multiple well heterostructures, far IR absorpt. by shallow donors 7-45458
- GaAs-Ga_{1-x}Al_xAs quantum well structures, energy spectra of donors and acceptors, spatially dependent screening effects 7-45459
- GaAs-Ga_{1-x}Al_xAs quantum well, hydrogenic donor low-lying excited states, reson. states, positions and widths 7-45460
- GaAs-Ga_{1-x}Al_xAs quantum wells, with indirect gap semicond. barriers, electron tunnelling 7-64340
- GaAs-Ga_{1-x}Al_xAs superlattices, in appl. elec. field, interband optical transitions 7-53274
- GaAs-GaAlAs heterojunctions, fractional quantum Hall effect obs. 7-52821
- GaAs-GaAlAs heterostructure, LPE grown, interface photoluminescence spectra 7-53390
- GaAs-GaAlAs MQW structures, exciton-exciton interaction 7-52439
- GaAs-GaAlAs superlattices, electron states in microstructs. 7-52807
- GaAs-GaAlAs superlattices, density of states of Landau levels, sp. ht., magnetisation meas. 7-52823
- GaAs-GaAlAs:Si modulation doped quantum wells, electron mobility, temp. depend. 7-45473
- GaAs-GaAlAs-GaAs heterojunction barriers, single particle tunnelling, five level k.p theory 7-64341
- GaAs-GaAs-Al_{1-x}Ga_xAs heterostructures, photosensitivity spectra 7-64319
- GaAs-metal interfaces, Fermi level pinning 7-2714
- GaAs-Mn(V), extrinsic surface states, core level UPS study 7-2713
- GaAs-oxide interfaces, defect stabilised electronic properties 7-38748
- GaAs-Si p-n heterojunctions, interface charge polarity 7-38686
- GaAs_{1-x}Al_xAs MQW, MOCVD grown, excitons, photoluminescence spectra 7-38702
- GaAs(110)-Al, Schottky barrier form., effect of surface and interface kinetics 7-2668
- Ga_{0.3}In_{0.7}As-InP strained layer superlattice, inter-band magneto-absorption 7-45998
- Ga_{0.47}In_{0.53}As/Al_{0.7}In_{0.3}As superlattices, electronic struct., strain-induced elec. field effects 7-7358
- Ga_{0.47}In_{0.53}As-InP heterojunction, with three electron subbands, hydrostatic press. effect 7-2695
- Ga_{0.47}In_{0.53}As-Si₃N₄(SiO₂) interface, elec. charact. 7-38752
- Ga₂In_{1-x}P_{1-x}As_{1-y}InP heterojunction interfaces, electron energy band structure (*Chinese*) 7-33070
- GaP-Ga semiconductor-liquid metal contact, transition from rectifying to ohmic operation 7-52833
- GaP-In semiconductor-liquid metal contact, transition from rectifying to ohmic operation 7-52833
- GaSb/AlSb single quantum wells, electroluminescence and photoluminescence studies 7-46136
- Ge-AlPO₄ MIS structures, inversion layers obs. 7-45502
- Ge-Si superlattices, structurally induced optical transitions, electroluminescence spectra 7-59184
- Hg_{1-x}Cd_xTe heterojunctions, supersymmetry, band-inverting contact 7-52717

interface electron states continued

- HgTe-CdTe superlattice, IR magnetooptics and band struct. 7-13138
- p-HgTe-CdTe superlattices, magnetotransport props. 7-33076
- HgTe-Hg_{1-x}Cd_xTe heterojunctions, hole Hall mobility enhancement 7-33077
- InAs (110), surface electron states, effect of Al submonolayer coverage, soft XPS study 7-2653
- In_{0.53}Ga_{0.47}As-InP heterointerfaces, CV profiling 7-12834
- In_{1-x}Ga_xAs (100)-metal interfaces, Fermi level pinning and chem. interactions 7-2712
- InP electrodes, surface modified, time resolved photoelectrochemical meas. 7-27415
- InP MIS struct. with amorphous C films, interfacial electronic props. 7-7400
- InP MIS structures, prep. by RF plasma oxidation, interface elec. props. 7-2731
- InP MIS structures, thermal treatment in P overpressure 7-7394
- InP/Al UHV-cleaved and laser annealed interface, acceptor-like electron traps 7-7310
- InP/native oxide MIS structures, interface elec. props. 7-33851
- InP-aqueous electrolyte interfaces, laser induced photoelectrochemistry 7-27412
- InP-C based MIS struct., interfacial characts. 7-2732
- InP-metal interfaces, Fermi level pinning 7-2714
- InSb (110), surface electron states, effect of Al submonolayer coverage, soft XPS study 7-2653
- InSb bicrystals, n-inversion layers, pressure dependence electron states 7-45468
- InSb MOS interfaces, annealing, O diffusion and reaction 7-58665
- InSb MOS structures, heat treatment effects 7-8031
- InSb-SiO₂ MIS structures, photo-CVD fabrication 7-38739
- LiNbO₃-Si, acoustoelectronic storage, effects of illumination, temp. change, electric fields 7-7405
- Mo-Si(111)(2×1) interface, early formation stage 7-27150
- MoS₂-Co catalyst-promotor interaction, UPS, XPS, LEED studies (*Chinese*) 7-39913
- NiSi₂-Si, localised states, barrier height, Fermi level 7-27430
- NiSi₂-Si, Schottky barrier, interfacial defect states 7-27428
- Pb_{1-x}Sn_xTe heterojunctions, supersymmetry, band-inverting contact 7-52717
- Pb_{1-x}Sn_xTe-PbTe superlattice, electronic struct., envelope pn. approx. 7-45465
- Pd Frank-Van der Merwe growth on Ag (111), AES, surface reflectance spectra studies 7-32829
- PdSi₂-Si, localised states, barrier height, Fermi level 7-27430
- Si, accumulation layers, quasi-1D transport, strong localisation 7-64359
- Si p-n structures, induced current pot., temp. depend., impurity levels, SEM 7-17073
- Si, single crystal wafer, oxidation, rapid thermal processing 7-22928
- a-Si solar cells, insulator-semiconductor interface properties 7-13901
- Si solar cells, polycrystalline, interface state characterization by electric noise meas. 7-13920
- Si:Au,Fe-SiO₂, MOS struct., trap centres 7-7388
- a-Si:H/P multilayer films, plasma CVD and elec. cond. studies 7-39428
- a-Si:H films, metal-semiconductor contacts, characterisation 7-38724
- a-Si:H multilayer films, charge transfer doping, cond., photocond. meas. 7-38735
- a-Si:H ultrathin layers, photoluminescence characts., layer thickness depend. in variety of sample configurations 7-46123
- a-Si:H/SiN_x interface, slow states, transient photoconductivity studies 7-38670
- a-Si:H/SiO₂/metallic gate struct., capacitance-volt. characts. 7-45515
- a-Si:H/a-SiN_x:H interface system, struct. and electronic props. 7-38361
- a-Si:H/a-SiN_x:H interface, deep states and photoluminescence spectra, transistor characts. 7-39186
- a-Si:H/c-Si heterojunctions, reverse current characteristics 7-58887
- a-Si:H/metal junction, pot. profile determ. 7-2715
- Si:Na MOSFET struct., hopping cond. in 2D impurity band 7-45512
- Si/NiSi₂ heterojunction, interface states, DLTS and hydrogenation studies 7-12777
- Si/NiSi₂(111), intrinsic interface states and defect states 7-22011
- Si/Si₃Ge_{1-x} superlattices, strain induced confined electron states 7-7311
- Si/SiO₂, ion implantation-induced interface states generation and charge trapping study 7-12874
- Si/SiO₂, two-step oxidation of thin gate oxides, trapping characts., hot electron effect study 7-64351
- Si/SiO₂ interface, oxide trap capture cross section and tunnelling emission, DLTS stud. 7-12875
- Si/SiO₂/TiSi₂(WSi₂) MOS capacitors, radiation-induced interface traps 7-58897
- Si-Au interface, atomic bonding 7-58663
- Si-C based MIS struct., interfacial characts. 7-2732
- Si-Cu interface, atomic bonding 7-58663
- Si-Ge heterojunction, structural and electronic props. 7-21997
- Si-InP (110) heterojunction, characterisation 7-33079
- Si-NiSi₂(Pd,Si)(Pt,Si), interface electronic states (*Chinese*) 7-58845
- Si-PtSi thin film Schottky diodes, barrier height meas. 7-64308
- Si-SiGe strained layer superlattices, electric subbands 7-2700
- Si-SiO₂ MIS struct., temp. stress influence (*Slovak*) 7-7389
- Si-SiO₂ (111) interface, dangling bonds, dipolar interactions investig. 7-17107
- Si-SiO₂ interface, chem. transition, density of states calcs. 7-7397
- Si-SiO₂ interface, ESR signal from P₀ centres, anisotropic props. 7-38940
- Si-SiO₂ interface, electrically active defects 7-33102
- Si-SiO₂ interface, MOS capacitance derivative freq. depend., surface state densities and capture cross section 7-45507
- Si-SiO₂ interface properties in the 10¹⁷-10¹⁹ cm⁻³ doping range 7-38762
- Si-SiO₂ interface state density effect on elec. props. of Pt-diffused MOS struct. (*Japanese*) 7-7404
- Si-SiO₂ MOS capacitors, defect struct. and interface state generation 7-7399
- Si-SiO₂ struct., interfacial charged centres, low temp. RF plasma treatment 7-2661
- Si-SiO₂ system, interface state generation by nonionizing UV radiation 7-38760
- Si-SiO_{2-x}N_{2-x}N_{2x/3}-Al structures, interface states, DLTS study 7-45513
- Si-SiO₂ interface density of localised states, C-V and G-V characts. meas. 7-38734
- Si-silicide interfaces, electronic struct. 7-21972
- Si-TiO₂ MIS structures, low temp. CVD of TiO₂ films 7-17105

interface electron states continued

- Si-Yb interfaces, mixed valence of Yb, synchrotron radiation photoemission spectra, metal coverage and annealing temp. depend. 7-32966
 Si_3N_4 films prep. by ECR plasma CVD, phys. and elec. props. 7-58716
 SiO_2 CVD photox layers, Hg-sensitised, elec. props. 7-64379
 SiO_2 films, interface states, charge trapping (*Spanish*) 7-17110
 SiO_2 layers, electrical properties 7-58931
 SiO_2 -Cs-Si MOS, semicond. flatband voltage depend. on impurity distrib. 7-27433
 SiO_2 /SiC interface, elec. characts., MOS conductance technique meas. 7-12873
 SiO_2 -Si interface, chem. struct., XPS determ., suboxide distrib. and interface state form. 7-38358
 SiO_2 -Si interface, electronic state charactn. 7-38747
 SiO_2 -Si interface, insulator props. after exposure to $\text{H}_2 + \text{N}_2$ and NH_3 . 7-59693
W-vacuum-Au junctions, quasi-self-consistent barrier calc. 7-33065
ZnO-electrolyte interface, electrolum. under cathodic and anodic pulsed polarisation 7-13235
ZnO-electrolyte interface, photoconductivity and photocurrent spectra, influence of exciton absorption 7-45486
 $\text{ZnSe}/(\text{Zn}_{1-x}\text{Mn}_x\text{Se})$ strained layer superlattices, electronic energy states and relax. 7-45425

interface phenomena

- see also adsorption; composite material interfaces; crystal surface and interface vibrations; interface structure; Kapitza resistance; semiconductor-electrolyte boundaries; surface phenomena
air-water interface, mass transfer in eddies 7-11493
amphiphilic molecules, adsorpt. and orientation, liq.-liq. interface 7-12403
bimetallic film couples, interfacial phase form., in situ annealing X-ray diff. obs. 7-21705
binary alloys, directional solidification, morphological and thermosolutal instabilities, perturbation anal. 7-58446
binary mixture with diffusion, mass transfer across moving interface, boundary condition 7-58436
binary semiconductor alloys, directional solidification, convection, segregation, ampoule and furnace design 7-59501
brass plated steel cords, mech. and cohesion props. in sulphurising environment 7-39740
Bridgman growth, interface temp. distrib., furnace stability, computer calc. 7-53546
ceramics, props. meas., conf., Soverato, Italy (Sept. 1986) 7-9582
charge-induced effect on creep and hardness 7-21598
charged solid-liq., interfaces, dipolar hard spheres, density functional theory study 7-63414
coating-solid interface, nonlinear mechano diffusion 7-17669
cohesive-frictional material, approx. statistical soln. of elastoplastic interface for Galin problem 7-43707
colloids, interfacial particles, electrostatic trapping mechanism 7-13828
Coulomb interaction in presence of surface 7-38794
crack problems, appl. of conservation integrals 7-37387
crystal growth, closed-tube chem. vapour transport, interface kinetical limitations, semiempirical calcs. 7-27878
crystal growth, interfacial, surface angles at three phase line, melt solidification conditions, thermodynamic analysis 7-27889
crystal growth from solution, α -factor of Jackson 7-44425
crystal-melt interface, diffusional light scatt. 7-39137
diffusion layer growth kinetics, effects of metal-gas interface 7-26911
diffusion-controlled interfacial growth, dense branching morphology form. 7-21147
dimethyl sulphoxide, dendritic solidification and surface-pressure-induced wetting transition in narrow gaps 7-27223
disequilibrium and self-organisation, book 7-24328
dosimetry, interface phenomena, Monte Carlo prediction 7-56878
drops on planar surface, dislodgment due to surrounding fluid motion 7-52190
dynamic scaling of Eden-cluster surfaces 7-14888
effect of ion irradi., 7-28160
electrical properties of interfaces (*Japanese*) 7-64309
electrochemical processes, low freq. dispersion 7-39904
epitaxial films, multilayer, X-ray diff. determ. of elastic stresses and misalignment (*Russian*) 7-38371
fluid-liquid interface, multicomponent mass transfer 7-8255
fluid-solid interface, one order parameter theory 7-27098
fluid-wall interface, wetting, computer simulation and statistical sum rules 7-32753
freezing and interfaces, appl. of density functional theories in 2D and 3D 7-32621
gas-liquid contact in Karr columns, press. drop, gas holdup and interfacial area 7-6284
grain boundary, unstable spreading of fluid inclusion under normal stress 7-26761
growth instability, scaling, simulation 7-44746
HCL, condensation on charged CO_2 walls, Stockmayer model calcs. 7-63784
 $\text{Hg}/\text{H}_2\text{O}$, polarised interface, interfacial tension 7-27056
high-multiplicity, optical density as a fn. of interface structure 7-39923
ice, melting in porous media, solid-liq. interface motion, temp. distrib. 7-50926
incomplete crystals, surfaces, defects, interfaces and layered structures, theory 7-16926
insulating polymers, elec. cond. and breakdown phenomena 7-45306
insulators, radiation effects, conf., Guildford, England (July 1985) 7-29590
interfacial bonding and adhesion, conf., Aspen, CO, USA (Aug. 1985) 7-24269
interfacial monolayer between surfactants, rheological anal. of the Marangoni effect. 7-38233
interfacial turbulence and mass transfer, importance of surface compressional elasticity modulus and Reynolds number 7-63128
intergranular phase, continuous, morphological stability 7-63772
internal damage in struct. solid, stochastic approach 7-37965
interphase solute transport, interfacial resistance, surfactant effects 7-52188
ion transfer across interfaces between two media, kinetics 7-32687
joints of dissimilar metals, adhesively bonded strength evaluation 7-46791
laminar natural convection flow in square enclosure thermal cond. effect 7-51115

interface phenomena continued

- layered structures, growth kinetics in various diffusion couples 7-21678
liquid, axisymm., spreading over surface of solid, thermal stresses 7-63916
liquid bridge between two spheres, gravity effects 7-6919
liquid surfaces, stabilisation by application of variable force fields 7-63907
liquid-gas interface, asymptotics from nonlocal van der Waals theory 7-52187
liquid-vapour interface, density fluctuations, gravity effects close to critical temp. 7-32626
metal-ceramic interfacial props., thermodynamics 7-12506
metal-metal interface, barrier pot. calc. for tunnelling electrons 7-52746
metal-solid electrolyte boundary, self-consistent electron theory, double layer, parametric instability, capacitance anomalies 7-52832
metal/electrolyte interface electrodynamics, surface soliton form. 7-21958
metal/solid electrolyte interface, elec. simulation 7-52122
microemulsions, interfacial phase transitions 7-33970
microemulsions, interfacial props., critical roughening composition, disordered struct. 7-11893
microstructure of organic mono- and multilayers 7-52296
modelling of interfacial reactions 7-21698
molecular dynamics simulations 7-16875
molecular fluids and multicomponent mixtures, interfacial phase transitions 7-32755
monolayer at liquid/solid and gas/solid interfaces, IR external refl. spectroscopy optimisation 7-48883
morphological stability, weakly nonlinear, effect of latent heat 7-59497
multiphase interface and interaction problems, probabilistic modelling and simulation 7-52219
nematic liquid-substrate interface, orientational transitions, wetting, Landau-de Gennes theory 7-63914
nucleation, sympathetic, morphology, crystallography and kinetics 7-65035
partially molten systems, connectivity of melt systems in partially molten peridotite 7-8924
partially molten systems, distrib. of apparent dihedral angles on random sections 7-8927
partially molten systems, effect of water saturation on partial melt distrib. in olivine-pyroxene-plagioclase system 7-8925
partially molten systems, permeabilities and interfacial areas and curvatures 7-8926
pearlite-austenite interface, SEM obs. 7-39505
pearlite-martensite interface, SEM obs. 7-39505
phase interfaces, boundary-layer theory for dynamics and thermodynamics 7-26909
piezoelectric substrates, Stoneley waves propag. along interface between same materials, theoretical anal. (*Japanese*) 7-32781
planar interface, reflection and transmission of ultrasound 7-63967
plasma MHD surface waves, mag. field direction variation effects 7-31963
plate oscils. across liquid interface, contact-angle hysteresis effects 7-52189
polyampholytes acrylic acid-2-methyl-5-vinylpyridine, surface activity at liq.-gas interface determ. 7-6924
polymer blending microrheology, blend morphology origination, influence of coalescence 7-43828
polymers, glassy, bimaterial interface, cracks, incipient plastic zone shape, elastic const. effect 7-53874
powder densification by interface-reaction controlled grain boundary diffusion 7-64950
PTCR, high temp., interaction with O models 7-58861
PVC-polycaprolactone interface, diffusion, temp. and time depend. 7-32723
PVC-polyvinyl butyral (phenolformaldehyde resin), thermophys. props. (*Russian*) 7-27040
quantum liq.-quantum cryst. phase interface, hydrodynamic eqns., sound transmission calcs. 7-32746
response theory of discrete composite systems 7-38424
rippled interface between liqs. of different densities, shock wave effects 7-58572
rubber-glass interfaces, form. and rupture (*French*) 7-54072
Saffman-Taylor finger, sidebranching in interfacial dynamics, white noise effect 7-21627
salol melt-grown crystals, decanted surface markings, in situ microscope obs. 7-27068
scale adhesion and growth mechanisms, S effect 7-65206
semi-insulators, low-freq. dispersion phenomena anal. 7-38991
semipermeable membranes, wetting regimes and interfacial phenomena 7-12407
solid-liq. interface, Fourier-transform IR spectroscopy with photothermal beam deflection appl. 7-52234
solid-liq. interfacial tensions, q-state Potts lattice gas model, mean-field approx. calcs. 7-256
solid-liquid interface, light scatt. by surface ripples 7-64595
solid/liquid interface, pulse echo US study of location during solidification and melting 7-52006
solid/liquid interface struct. and elec. props. (*Japanese*) 7-63941
solid/melt interfaces, cryst. growth, computer simulation studies 7-16469
solids in contact, interfacial bonding 7-27148
statistical physics, conference, Oaxtepec, Morelos, Mexico (Aug. 1985) 7-9584
steel, stainless, duplex, austenitic-ferritic, cavitation erosion 7-65149
Stefan problem, two-phase, with interfacial energy and entropy 7-43633
steric interaction between wandering walls, mean field theory 7-27058
stratified fluids, Squire's theorem 7-11490
submicron materials characterisation, conf., Evanston, IL, USA (Oct. 1983) 7-24294
supercooled vapour condensation, phase boundary velocity 7-21399
surfactant mixtures, immiscible ideal solns., ideal interfacial layer 7-6921
tetrachloromethane, in porous SiO_2 , structural features, neutron-diff. studies 7-16536
transient stress around interface crack 7-37382
transitions, bifurcation of renormalisation-group fixed pts. 7-27062
triglycine sulphate nucleation in supersaturated solns., induction period meas. 7-26680
turbulent mass transfer at mobile interface, computer simulation 7-43865
two coupled semi-infinite systems near criticality 7-44747
two-dimensional growth models, interface dynamics, time-reversal invariance and universality 7-63532

interface phenomena continued

- two-layer and three-layer flows, three-wave resonant interactions and multiple reson. 7-11439
vapour bubble, quasistatic growth on boiling liq. surface, contact angle var. 7-44951
vapour layer on liquid surface, mathematical model 7-20843
wandering in pure and impure and bulk phases 7-32791
water and alcohol liquid-gas boundary studied by photoacoustic spectroscopy 7-51950
waves, interfacial, large-amplitude 7-11438
Ag interfacial surface energy atomistic estimation and adhesion meas. (Japanese) 7-58657
Ag particles, adsorbate light scatt., energy transfer induced interfacial optical processes 7-39109
Ag thin films on NaCl, preferred orientations, detection of complete set 7-39542
AgI, two-phase mixture, effect of dispersoid on elec. transport 7-2621
Ag₃Si-potential forming ions-solution interface, potentials calcs. (Russian) 7-27138
Al, charge-induced effect on creep and hardness 7-21598
Al/Cu friction welds, microstruct. and mech. props. (German) 7-46792
Al-Li (9.5 at.%), coarsening of δ -Al₃Li precipitates, var. of average Li content in Al matrix 7-3313
Al-semiconductor interfaces, form. of active electronic barrier, novel approach in corrosion prevention 7-65178
 α -Al₂O₃, ceramic matrices, precip. morphology 7-65049
Al₂O₃ film-stainless steel adhesion, improvement using surface precipitates (Japanese) 7-22880
Al₂O₃, joining by inducing localised reducing conditions 7-46787
Al₂O₃, mixing of metal overlayers, ion beam irradi., rapid thermal annealing, pulsed laser irradi. 7-58330
Ar-CO₂ interface, wetting, model 7-2303
Ar-CO₂ interface, wetting transitions, density functional theory and modified hypernetted chain calcs. 7-63913
Au interfacial surface energy atomistic estimation and adhesion meas. (Japanese) 7-58657
Bi thin films (111), melt growth, in-situ obs. by TEM 7-53573
C steel-cast Fe-Cr bimetal, interface bonding strength (Korean) 7-17618
CdTe, epitaxial growth on GaAs (100) 7-21779
CoSi, CoSi₂ thin films, study by ultrasoft X-ray spectroscopy (Russian) 7-52345
Cr/Ni interface broadening and topography of Auger sputtered profiles 7-53485
Cs, liq.-vap. interface, electron and ion distrib., self-consistent Monte Carlo simulation 7-52024
Cu interfacial surface energy atomistic estimation and adhesion meas. (Japanese) 7-58657
Cu-Cu₂O Schottky barrier solar cells, interfacial layer effects investig. using n-V_{oc} diagram 7-54304
Fe, Armc, diffusion bonding, precip. of Fe carbides in ferrite 7-39521
Fe, reaction with HCl-O₂-Ar mixtures at 550°C 7-17713
Fe/Sn interface, electrolyte template, determ. of reaction time during first stage of FeSn₂ growth 7-53990
Fe-based alloys, C diffusion in compound welds having intermediate layer 7-44887
Fe-Cr-Mo (9.1 wt.%), initiation of breakaway oxidation in high press. CO₂ atm. 7-33845
FeTiO₃, ceramic matrices, precip. morphology 7-65049
GaAs, LEC growth, solid-liq. interface, meniscus shape, X-ray image processing appl. 7-17406
GaAs polycrystalline solar cell, electron beam generated carriers in presence of grain boundaries 7-64262
GaAs, vapour etching, buried interface, carrier traps 7-28213
He superfluid-solid He interface, macroscopic surface oscillations, second sound and kinetic phenomenon, hydrodynamic approx. calcs. 7-32745
HgTe/ZnTe, isothermal interdiffusion expts. 7-52152
LiCl-Li₂O-B₂O₃-Al₂O₃, amorphous Li⁺ conductor, crystn. and phase separation, interface effect (Chinese) 7-38245
Ni-base superalloy, single cyst., SRR99, creep behaviour 7-17587
Ni-Cr, bonding to dental glass 7-39844
Ni-SnPbBi system, crack form. in diffusion zone 7-3397
NiO, two-phase mixture, effect of dispersoid on elec. transport 7-2621
NiTi sputtered films on glass substrates, interfacial reaction, Auger study 7-22395
Pt/H₃(PMo₁₂Mo₄₀).22H₂O-polyethylene oxide interface, audiofrequency behaviour 7-52693
Si, SiC microdefect generation, melt-interface mechanism 7-53710
Si/Zn, amorphous-crystalline interface, backscattering and channelling study 7-6663
Si-Si surfaces, direct bonding, silanol group reactions and O diffusion mechanisms 7-21791
Si-SiO₂ structs., low and high temp. oxidised, inversion electron mobility study 7-22019
a-Si-SnO₂ interface, solid state reaction, XPS study 7-22449
SiC, mixing of metal overlayers, ion beam irradi., rapid thermal annealing, pulsed laser irradi. 7-58330
SiC, wettability by Al and Al-Si 7-58569
Si₃N₄ ceramics, joining with glass solder in CuO-SiO₂-TiO₂ system 7-22974
Si₃N₄, mixing of metal overlayers, ion beam irradi., rapid thermal annealing, pulsed laser irradi. 7-58330
SiO₂, mixing of metal overlayers, ion beam irradi., rapid thermal annealing, pulsed laser irradi. 7-58330
SiO₂-polyimide interface, locus of failure, XPS study 7-28261
Sn/SnTe bilayers, electron diffr. pattern fine struct., influence of angular misorientation 7-16885
Sn-Sb, dil., planar solid-liq. interface, morphological development and stability (Korean) 7-7985
Sn-Sb (2 at.%), morphological development of planar solid-liq. interface (Korean) 7-17523
Ta/W diffusion couples, analytical electron microscopy 7-39946
Ta-Ir alloy, amorphous, rapidly solidified, high temp. oxidation 7-33841
Ta₂O₅ film, photocurrent and elec. cond. mechanism, electrode interface effects studies 7-27366
Ti-coated Be substrate, bond failure, thin film fracture 7-59600
TiC-coated cemented carbide cutting tools, role of interface development during CVD 7-53930
U/Nb diffusion couples, analytical electron microscopy 7-39946
W and refractory metals, VLSI appls., conf., Albuquerque, NM, USA (Nov. 1984 and Oct. 1985) 7-14715

interface phenomena continued

- WC-Co, TiN-coated, residual stress and strength, X-ray diffr. study (Japanese) 7-8101
ZrO₂, ceramic matrices, precip. morphology 7-65049
- interface structure
- amorphous compositionally modulated superlattices, growth and struct. 7-27168
amorphous multilayer X-ray reflectors, layer imperfections effects 7-25936
analysis, appls. conf., Veldhoven, Netherlands, (Oct. 1985) 7-24289
applied materials charact., conf., San Francisco, CA, USA (April 1985) 7-18495
atomic structure models, electron microscope images, computer simulation 7-16380
Auger depth profiling, interface resolution 7-54246
carbide/ α -Fe matrix interface, void nucleation mechanism 7-38354
ceramic grain boundaries, bonding and interfacial structure 7-26765
chalcogenide-metal contacts, interdiffusion, struct., comp., electron irradi. effects 7-21686
characterisation by optical reflectance and ellipsometry 7-45084
characterization, ion scatt. and channelling, scanning tunnelling microscopy and computer simulation (Japanese) 7-7803
coherently strained Si-like structs., critical layer thickness, atomistic Monte Carlo calc. 7-12498
composite systems, interface response and scatt. matrix theories 7-7033
composition modulated layered structs., elastic strain, X-ray diffr. studies 7-27086
compound semiconductor/metal contacts, interfacial microstruct., elec. props., phase diagrams 7-45495
conference, Oconomowoc, WI, USA (April-May 1985) 7-18468
cyclohexane-d₆-methanol mixtures, stabilised vapour-liquid interface 7-12400
directional solidification, asymptotic eqns. and solid-liquid interface struct. 7-52010
discrete crystals, layered struct. form., theory, quantum well sandwiches and superlattices appl. 7-12507
dislocation structures, low energy, in interfaces 7-63976
dynamical phenomena at surfaces, interfaces and superlattices, summer school, Erice, Italy, (July 1984) 7-1
EELS in STEM of surfaces and interfaces, dielec. theory and verification 7-18935
electron diffraction, matrix reflection fall-off, interference effects and coherence conditions depend. 7-11855
epitaxial crystals, interface struct. by CB diffraction 7-16899
epitaxial layer-substrate interface defects 7-21715
Fe-Si multilayered thin films, stacking structs., magnetostatic coupling and layer boundary interdiffusion 7-7574
figured multilayer optical element, image quality 7-37102
fluctuating, 2D solid-on-solid model, correl. function calcs. 7-2397
E-glass fibre composite interfaces, surface studies using diffuse reflectance and photoacoustic FTIR spectra 7-46044
heteroepitaxial structures, lattice parameter difference meas. using extremely asymmetrical Bragg diffr. 7-51569
heterostructure growth by MBE, growth approaches to improve interface quality 7-2421
heterostructure lattice mismatch determ. by X-ray diffr. in SEM 7-6482
high energy ion scatt., struct. anal. of surfaces and interfaces 7-22410
high-multiplicity, optical density as a fn. of interface structure 7-39923
incomplete crystals and crystalline interfaces, discrete struct. anal. 7-12508
internal, interphase, diffr. effects 7-12496
internal interfaces, diffr. effects, general considerations and grain boundary effects 7-12495
IR external reflection spectroscopy of thin films on glassy C electrodes 7-41509
kinetics and energetics studies at surface and interfaces 7-2422
liquid-solid interface, kinetics of crystal growth 7-1924
metal insulator-metal structures, field-induced hot-electron emission, energy anal. 7-30121
metal-electrolyte rough interface, AC response, inverse-Cantor-bar model anal. 7-22012
metal-metal and metal-dielectric systems, adhesion calc. 7-7023
metal-semiconductor contact, microscopic many-electron model 7-27431
metal-semiconductor interfaces, epitaxial silicide technology 7-52835
metal-semiconductor interfaces and Schottky barriers, microscopic and macroscopic props. 7-2721
metal-semiconductor junctions, formation, structural and electrical props., RBS and ESCA studies 7-38727
metal/ceramic, diffusion welded layered composites, transition zone metallography, struct., hardness (German, English) 7-8226
metallic-based layered structs., depth profile anal. using multilayer anodisation 7-27170
metals, internal interfaces, grain boundary struct., intergranular fracture 7-26766
MIM structures, electrorreflectance spectra, interface contribs. 7-53276
modulated semicond. structs., conf., Kyoto, Japan (Sept. 1985) 7-4630
MONOS structures, shaped Auger anal. 7-63980
multilayer semicond. structures, X-ray diffr. characterisation 7-51574
multilayer X-ray mirror performance, coating thickness errors and boundary roughness determ. 7-30148
multilayered structures for soft X-ray mirrors, physical charactn. 7-37098
pentadecanoic acid/H₂O, mol. monolayer at gas-liquid interface, mol. orientation, SHG 7-16839
phenol, aq. soln., liq.-vap. interface, second harmonic light phase, relation to mol. orientation 7-27057
pivalic acid directional solidification, metastable dendritic interface pattern obs. 7-63779
planar interface, cellular and dendritic struct. transitions during rapid solidification 7-22666
PMMA film on glassy C, IR external refl. spectroscopy obs. 7-41509
polymer interfaces, bonding and adhesion 7-28265
quartz crystal microbalance, use for surface anal. in combination with surface sensitive spectroscopies 7-27076
semiconductor characterisation, Raman spectroscopy, review 7-53354
semiconductor heterojunctions, microscopic many-electron model 7-27431
semiconductor interface physics and chem., conf., Pasadena, CA, USA (Jan. 1986) 7-4
semiconductor materials, high resolution microstruct. studies using TEM 7-21055

interface structure continued

- semiconductor microelectronic structures, depth profiling by SIMS and AES 7-26790
- semiconductor superlattices and heterostructures, structure, EXAFS studies 7-12509
- semiconductors, MBE growth, RHEED and photoemission studies 7-2438
- semiconductors, polycrystalline, extended interfacial defects, geometrical character 7-6640
- semiconductors, SEM three-dimensional characterisation 7-52312
- semiconductors, solid-phase epitaxial regrowth, amorphous-crystalline interface evolution 7-12568
- Si-SiGe strained superlattices on Si substrates, MBE growth, characterisation, appl. for HEMT 7-27218
- slowly decaying interfacial profiles, correspondence with reflectivity 7-45967
- small particle or interface charact., appl. of parallel detection EELS 7-33499
- sodium dodecylphenanthrene sulphonate/H₂O, mol. monolayer at gas-liquid interface, mol. orientation, SHG 7-16839
- SOI films, lamp zone melting recrystallisation, liquid-solid interface 7-38419
- SOI formation, high dose O⁺ ion implantation, lamp annealing 7-32527
- SOI thin films, props. after laser focused beam processing 7-32497
- solid surface, physics, conf., Smolenice, Czechoslovakia (Sept. 1984) 7-48170
- solid-fluid interface, FCC (111) cryst., layerwise struct., mol. dynamics simulation 7-2367
- solid/liquid interface struct. and elec. props. (*Japanese*) 7-63941
- SOS, crystalline quality improvement by ion beam technique 7-16651
- steel, boronised, boride-substrate interface morphology 7-53984
- strained layer superlattice interfaces, Monte Carlo stability anal. 7-27165
- strained layer superlattices, symposium, Annandale, NJ, USA (June 1986) 7-48150
- submicrometer layer heterostructures, X-ray crystallographic techniques 7-6481
- superlattice interfaces, two-dimensional Lennard-Jones strained layer systems, Monte Carlo stability anal. 7-2398
- superlattices, surfaces and interfaces, structural, electronic and mag. props. 7-16849
- surface analysis, AES, XPS, ISS and SIMS, review 7-28372
- surface behaviour diagrams, for surface and interfacial reactions 7-27077
- TEM imaging using inner potential differences 7-52299
- thin film multilayered structures, microcleavage TEM charactn. 7-38375
- vertical interfaces, solid, photothermal beam-deflection imaging 7-48721
- X-ray photoelectron diffraction, submonolayer interface struct. determ. appls. (*Japanese*) 7-11852
- Ag/In thin film couples, interface AgIn₂ cpd. form. and props., gamma ray spectra 7-21688
- Ag-Au, thin interface regions, EXAFS studies 7-59285
- Ag-Au bilayers, EXAFS and X-ray reflectivity meas. 7-27821
- Ag-Si interfaces, micro-quantitative AES anal. using SEM-SAM apparatus 7-27147
- Al/a-SiC films, RF sputtered, interfacial struct. and reactions, 573-773K (*Japanese*) 7-53583
- Al/III-V semiconductor interfaces, laser-induced chem. reactions 7-7017
- Al/Nb sputter deposited multilayer VUV mirrors, design and fabrication 7-31424
- Al-Cu, thin interface regions, EXAFS studies 7-59285
- Al-Cu interface, grazing incidence X-ray study of interfacial reactions 7-21543
- Al-GaAs, pure and Si or Zn doped interfaces, composition depth profile, pulsed laser atom probe study 7-32842
- Al-GaAs interfaces, convergent beam electron diffr. patterns 7-27156
- Al-GaAs Schottky barrier contacts, MBE grown, interface reactions, vacuum annealing effects 7-45022
- Al-Mo multilayered films, struct., elec. props. 7-58863
- Al-Ni multilayered films, struct., elec. props. 7-58863
- Al-polyacrylic acid interface, reactivity, comp., XPS 7-28334
- Al-polyethylene interface, reactivity, comp., XPS 7-28334
- Al-Si/Ti/Al-Si VLSI metallisation, electromigration and microstruct. props. 7-21550
- AlAs/GaAs modulated struct., high resolution double-cryst. X-ray diffr. studies 7-7029
- AlAs-GaAs superlattice waveguides in separate confinement heterostructure laser diodes, threshold current density 7-20267
- AlAs-GaAs superlattices, phase transitions under high press. 7-64016
- Al_{0.5}Ga_{0.5}As-GaAs layered structures, metal organic VPE grown, depth profiles, SIMS anal. 7-21684
- Al₂O₃, spinel growth, interface struct. investig. 7-16566
- Al₂O₃-NiO thin-film reactions, NiAl₂O₄ form. investig. 7-16877
- Al₂O₃-Ti interface reactions studied by AES and UPS 7-21702
- Al₂O₃-transition metal film interfaces, thermal reaction, backscattering spectra, X-ray diffr. studies 7-52304
- Au layer on GaP, emission spectrochemical anal. using glow discharge, appl. to in-depth anal. (*Japanese*) 7-63886
- Au/In thin film couples, interface AuIn₂ cpd. form. and props., gamma-ray spectra 7-21688
- Au-GaAs, annealed, interface erosion 7-21683
- Au-GaAs, contact, structural and elec. props. 7-27424
- Au-GaAs contacts, elec. and struct. props. 7-2711
- Au-Ge-GaAs, interfacial reactions, struct. after annealing 7-27154
- Au-Ge-Ni-GaAs, non-alloyed ohmic contact, solid phase epitaxy 7-27423
- AuGa_{1-x}As (001), chemically unreactive interfaces formation 7-7050
- AuGe-GaAs, ion beam induced phenomena 7-12166
- AuNiGe-GaAs ohmic contacts, microstruct. anal. and contact resist. meas. 7-29393
- AuZn layer on GaP, emission spectrochemical anal. using glow discharge, appl. to in-depth anal. (*Japanese*) 7-63886
- Be-Ti multilayer interference system, struct. and phase composition, electron microscopy, X-ray and neutron diffr. meas. 7-63984
- a-C-Ag thin multilayer struct., vacuum condensation, interface development, sheet cond., thickness 7-21681
- a-C-Au thin multilayer struct., vacuum condensation, interface development, sheet cond., thickness 7-21681
- C-W multilayers, sputtered, ellipsometry monitoring, X-ray refl., XPS 7-39376
- CaF₂-Si, interface struct., high resolution TEM study 7-2394
- CaF₂-Si (111), interface form., photoemission study 7-2395
- CaF₂-Si (111) interface, electronic struct. 7-38377

interface structure continued

- CaF₂-Si interface, with epitaxially grown insulator, post-growth annealing treatments 7-7074
- CaF₂-Si(111), tensile strain, interfacial disorder, reordering 7-27163
- Cd_{0.8}Hg_{0.2}Te, abrupt interfaces using thermal and photo-MOVPE, Hall meas. 7-27917
- CdTe films on InSb, interface struct. and band offsets 7-58664
- CdTe-GaAs heteroepitaxial interface, at. resolution HVEM study 7-2392
- Co/Ag, compositionally modulated layered films, saturation magnetisation and FMR, thickness depend. 7-7565
- Co/Cr compositionally modulated layered films, saturation magnetisation and FMR, thickness depend. 7-7565
- Co-Sn multilayers, amorphisation and interdiffusion, EXAFS and XANES studies 7-64812
- CoSi₂-Si epitaxial heterostructures, growth and characterisation 7-27212
- CoTi-CoNb amorphous alternating layers, magnetic and diffusional props. study 7-7563
- Cr/Cu multilayer structs., scanning Auger microprobe depth profiling, sputtering effects 7-58659
- Cr-Ge thin film interface, interdiffusion, reaction and intermixing, soft X-ray photoemission study 7-27028
- Cu, crystal surface and interface, heterophase fluctuations (*Russian*) 7-58650
- Cu/In thin film couples, interface CuIn₂ cpd. form. and props., gamma ray spectra 7-21688
- Cu-Al bilayers, EXAFS and X-ray reflectivity meas. 7-27821
- Cu-Al interfacial interaction, struct., synchrotron radiation photoemission study 7-22444
- Cu-Al₂O₃, interaction, X-ray photoelectron spectroscopy, Auger electron spectroscopy 7-58669
- Cu-CdTe interface form., effect of different cation-anion bond strengths 7-27149
- Cu-Hf multilayers, interface EXAFS study 7-64811
- Cu-Hg_{0.75}Cd_{0.25}Te interface form., effect of different cation-anion bond strengths 7-27149
- Cu-Ni interface, emission spectrochemical anal. using glow discharge, appl. to in-depth anal. (*Japanese*) 7-63886
- Cu-Si interface, surface struct., angle resolved Auger electron emission determ. 7-21672
- Cu-W, layered, ion beam mixing, energy and dose depend., RBS 7-38075
- EuS-SrS mag. superlattices grown on Si(111), strain, study by He ion channelling 7-27215
- Fe/Cu multilayered samples, ion beam mixing-induced metastable phases 7-58377
- Fe/Fe oxide passive film interface composition and growth, atom probe depth profiling anal. 7-32869
- Fe/Fe-O/Al₂O₃ systems, diffusion bonded, interface chemistry, bonding strength 7-28079
- Fe-graphite structures, ion induced mixing, sputtering yield, fluoresc., RBS depth profile meas. 7-64844
- Fe-Ti multilayered films, ion bombard., microstructure, TEM obs. 7-12165
- Fe-Ti-C multilayered films, ion bombard., microstructure, TEM obs. 7-12165
- Fe-Zr alloy formation at Fe/Zr thin film interfaces, Mossbauer study 7-63975
- Fe₈₀C₂₀Si compositionally modulated amorphous struct., mag. and diffusional props. study 7-7564
- (FeMg)₂SiO₄, spinel growth, interface struct. investig. 7-16566
- FeSi oxidised interface system, XPS, XAES and Auger parameter studies 7-7025
- GaAlAs/GaAs:C quantum wells interface struct. and luminesc. efficiency 7-7735
- GaAlSb/GaSb (111) heterostructures, signs of misfit dislocations, X-ray topographic determ. 7-38349
- GaAs device structures, γ -ray effects, surface generation-recombination processes 7-64349
- GaAs epitaxial films, domain form., crystallographic analysis 7-58690
- GaAs high quality layers grown on Si by MOCVD, misfit dislocations at interface 7-27922
- GaAs MOCVD growth on Si with superlattice intermediate layers, material props. 7-27923
- GaAs, nucleation and growth on Ge, antiphase boundary struct. 7-2420
- GaAs, solid-phase-epitaxy, interface structure and impurity effects 7-2407
- GaAs/Al quantum wells, MBE growth, photoluminescence and absorption linewidth studies 7-7749
- GaAs/AlAs 1-D MBE superlattice, struct. parameters, X-ray double cryst. diffr. studies (*Chinese*) 7-12503
- GaAs/AlAs heterostruct., transition layer form. during LPE 7-45074
- GaAs/AlAs superlattice, optical phonons and interface thickness, Raman scatt. studies 7-7705
- GaAs/AlGaAs quantum wells, MBE growth, interface disorder studies 7-7026
- GaAs/AlGaAs superlattice, compositional disordering by focused ion beams 7-6695
- GaAs/Au contacts, interface morphology 7-45020
- GaAs/GaAlAs superlattice, optical phonons and interface thickness, Raman scatt. studies 7-7705
- GaAs/GaAlAs ultrathin layer systems, MOCVD growth and struct. props. 7-7063
- GaAs/GaInAs interface, EELS near a single misfit dislocation 7-33497
- GaAs/GaPAsSb, double heterostruct., LPE, lattice matching, X-ray diffr., luminesc. 7-58884
- GaAs/metal interface microstruct. and reactions, stability and elec. props., TEM and STEM studies 7-12515
- GaAs-(Ca,Sr)F₂ heterostructure interfaces, twinning, Raman spectra 7-13148
- GaAs-Al_{0.3}Ga_{0.7}As, thin single quantum well, MBE growth kinetics, normal and inverted interfaces 7-45045
- GaAs-Al₂O₃, dielectric film mol. beam epitaxial growth 7-38360
- GaAs-Al_{0.5}Ga_{0.5}As, heterojunction form. anal. 7-39436
- GaAs-Al_{0.5}Ga_{0.5}As superlattice, composition anal., electron microscopy studies 7-7028
- GaAs-AlGaAs superlattice, surface and interface optical phonons, EELS studies 7-6955
- GaAs-AlGaAs superlattice, lattice images, high contrast TEM obs. 7-7027
- GaAs-AlGaAs superlattices and superstructures, growth by metal organic CVD (*Japanese*) 7-13386

interface structure continued

- GaAs-anodic oxide interfaces, annealing, As enrichment, photoluminescence, Rutherford backscattering anal. 7-21687
 GaAs-AuGeNi contacts, interface composition and barrier heights 7-58891
 GaAs-AuNiGe (TiSi₂)(Au) interfaces, struct. and elec. props. 7-22013
 GaAs-CaF₂, dielectric film mol. beam epitaxial growth 7-38360
 GaAs-GaAlAs interface dislocations, stereographic obs. by IR light scatt. 7-32235
 GaAs-GaAlAs quantum well excitons, interface disorder and mobility 7-52808
 GaAs-GaAs:Cr(Te), VPE grown, photoluminescence study, effect of substrate doping 7-27771
 GaAs-Ge epitaxial interface, extended defects, geometrical character 7-6640
 GaAs-Mo Schottky diodes, elec. characts. and microstruct. study 7-22015
 GaAs-Si heteroepitaxial interface, at. resolution HVEM study 7-2392
 GaAs-Si heteroepitaxial interface, atomic structure 7-52298
 GaAs-Si₃N₄ interface, multipolar plasma deposition, high resolution electron microscopy study 7-12499
 GaAsP-GaAs(P) strained-layer superlattices, MOCVD and device prep. 7-7876
 GaAs(110)-Al, Schottky barrier form., effect of surface and interface kinetics 7-2668
 GaInAs/InP quantum wells, atmospheric organometallic vapour phase epitaxial growth 7-27912
 Ga_{0.47}In_{0.53}As/Al_{0.48}In_{0.52}As modulated struct., high resolution double-cryst. X-ray diffr. studies 7-7029
 Ga_{1-x}In_xAs-Al_{1-y}In_yAs superlattices, electronic struct., depend. on growth axis 7-64329
 GaInAsP/InP heterojunctions, atmospheric press. MOVPE growth TEM studies 7-3196
 GaP epitaxial layers, MOCVD growth on Si, TEM and SEM 7-38416
 GaP on Si substrate, MOCVD growth and characterisation 7-27926
 GaP/GaAsP epitaxial layers, MOCVD growth on Si, TEM and SEM 7-38416
 GaSb/GaSb:Si (111) autoepitaxial structures, signs of misfit dislocations, X-ray topographic determ. 7-38349
 Ge ion beam deposition on (100) single cryst. substrate, interface, thin film and damage form. 7-17423
 Ge, MBE on Si, role of surface reconstruction, LEED, Rutherford backscattering, channelling meas. 7-7034
 Ge:H, H composition at surfaces and interfaces 7-27083
 a-Ge/au interfaces, atomic intermixing, asymmetries 7-21682
 Ge-CaF₂-Si heteroepitaxial structures, MBE grown, twinning, topography, channelling, TEM, SEM 7-12566
 Ge-metal interfacial atomic struct. and cpd. form., FIM studies 7-32846
 Ge-Si(111) interface, geometrical struct. 7-38310
 GeSi-Si heterostructures, MBE grown, structural props., quality, electron diffr., imaging obs. 7-7036
 GeSi_{1-x}Si_x multilayers, MBE grown, thermally annealed, Ge diffusion, strain relax., ion channelling, backscattering anal. 7-6896
 Hf-Si multilayers, X-ray optical props. rel. to layer imperfections 7-37097
 HgCdTe-CdZnTe heterojunctions, lattice matching 7-21717
 Hg_{1-x}Cd_xTe/Ag(Cu)(Al) interfaces, morphology, Hg bonding effects 7-7021
 HgTe-CdTe superlattices, struct. characterisation 7-27164
 In adatom on Si (100), bonding coordination number, synchrotron photoemission studies 7-45071
 In-GaAs reactions, interfacial native oxide layer effects 7-12501
 In-glass, glow discharge induced changes 7-12577
 In-Pt-GaAs, heterojunction ohmic contacts, elec. and morphological props. 7-27155
 InAs-GaAs superlattices grown by beam-separation MBE, surface morphology and elastic strain 7-7031
 InGaAs/InP heterostructures, chloride VPE, interface form. control 7-58656
 InGaAsP layers on InP (001), origin of grown-in dislocations 7-38415
 InGaAsP-InP buried heterostructure lasers, internal thermal stress distrib. 7-10931
 InP:Sn substrate/epilayer interface, Sn depth profiling, AES and SIMS studies 7-27146
 InP/SrF₂ lattice mismatch, temp. depend. 7-63849
 InSb, anodic native oxide, interface width, AES profiles 7-22911
 KH₂ graphite intercalation cpd., struct. and electronic props. 7-27234
 LaB₆-GaAs interfaces, thermal stability, high energy ion scattering studies 7-21680
 LiNbO₃:Y single crystal, Czochralski growth, crystal-melt interface stability (Chinese) 7-58168
 Mo/C multilayered structs., high resolution electron microscopy studies 7-63968
 Mo/Ni superlattice, sputtered, struct. anal. 7-45030
 Mo/Si multilayered structs., high resolution electron microscopy studies 7-63968
 Mo/V quasiperiodic multilayers, growth and superconductivity 7-12927
 Mo-Si(111)(2X1) interface, early formation stage 7-27150
 MoSe₂-MoS₂ ultrasharp interfaces grown with van der Waals epitaxy 7-13367
 Nb/Cu Fibonacci 1D quasiperiodic superlattice struct., X-ray diffr. meas. 7-52307
 Nb-Al₂O₃, diffusion processes and interphase boundary morphology 7-16817
 Nb-Al₂O₃ interface, grain boundary struct., elemental comp. determ., TEM obs. 7-21225
 NbN-Nb₂O₅-NbN trilayer structure, TEM studies 7-7018
 Ni/Al/Si system, contact structure formation by rapid thermal melting 7-45019
 Ni/Cr(Nb) alternating layers, ion beam mixing 7-21303
 Ni-Ag(001), Au doped, thin films, interphase boundaries, struct. and composition 7-27158
 Ni-Al₂O₃, diffusion processes and interphase boundary morphology 7-16817
 Ni-AuGe-GaAs, ion beam induced phenomena 7-12166
 Ni-AuGe-GaAs, ohmic contacts, interface reactions, elec. behaviour 7-27031
 Ni-Fe (100), layered struct. reflectivity and EXAFS study 7-59292
 Ni-GaAs, interphase contact and interaction 7-16880
 Ni-GaAs interfacial reactions, contact elec. props. 7-12504

interface structure continued

- Ni-MgO, diffusion processes and interphase boundary morphology 7-16817
 Ni-Nb amorphous films, early stages of reaction with cryst. Au films 7-21703
 Ni-NiO interface struct., TEM study 7-21692
 Ni-P contacts, phase formation 7-63983
 Ni-Si, interphase contact and interaction 7-16880
 Ni-Si interface, struct., RHEED, Rutherford backscattering spectrometry 7-27143
 Ni-Ti(Ta)(Cr), amorphous and cryst. reaction with Si studied by RBS and TEM 7-21704
 NiAl₂O₄, spinel growth, thin film Al₂O₃ substrate, topotactic relationships 7-58717
 NiFe₂O₄-MgO sputtered films, struct., comp., AES study 7-22478
 NiO, spinel growth, interface struct. investig. 7-16566
 NiSi₂-Si, Schottky barrier height, structural characterisation 7-27429
 NiSi₂-Si (111) epitaxial interface, strain meas. by MeV ion channelling 7-27157
 NiSi₂-Si (111) interface struct., X-ray standing-wave analysis 7-58661
 NiSi₂-Si epitaxial interface, extended defects, geometrical character 7-6640
 NiSi₂-Si interfaces, convergent beam electron diffr. patterns 7-27156
 NiSi₂-Si(111) interface struct. charactn. by X-ray diffr. (Japanese) 7-63399
 Ni₂Si growth kinetics from Ni and Ni-V films on Si surfaces, TEM, AES, X-ray diffr. and backscatt. studies 7-45032
 NiTa-GaAs, phase separation, cross-sectional TEM 7-27152
 Pb-Ge multilayers, cumulative disorder and X-ray line broadening 7-32847
 PbSe-SnSe strained layer superlattice, prep. and struct. anal. 7-52301
 Pd Frank-Van der Merwe growth on Ag (111), AES, surface reflectance spectra studies 7-32829
 Pd/Si interface composition and silicide form., atom probe FIM study 7-32845
 Pd-Si interface, compositional depth profiles and intermixing, atom probe FIM study 7-32843
 PdSi on Si, phase transform. to Pd₂Si, kinetics 7-16795
 Pd₂Si polycryst. film on Si, ion sputtering effects, XPS, UPS and scanning tunnelling microscopy studies 7-59357
 Pd₂Si-Si interface, at. struct., TEM obs. 7-63977
 Pt on Si, struct. and comp. of silicides formed in photon annealing, Auger obs. 7-2402
 Pt/SiN₂/Si structure, nucleation kinetics and spatial distribution of spherulitic PtSi clusters 7-21675
 Pt-Si interfacial growth following Si chemisorption, intermixing, SEXAFS obs. 7-64772
 PtSi/p-Si thin Schottky diodes, TEM, TED, I-V curve and photoemission characts. 7-12861
 PtSi/Si heterogeneous interface struct., defects, and coherency, HRTEM meas. (Japanese) 7-7019
 PtSi-Si, interfacial metallurgical interactions, elec. characts., effect of H 7-52834
 RSi_{2-x}Si (R=Sc, Y, Gd, Ho, Tb, Dy, Er, Tm, Yb, Lu), silicide thin films, phase composition, conductance, surface morphology 7-7072
 Rh/GaAs Schottky contact, correlation between solid-state reaction and electrical props. 7-58655
 RuO₂/Ti interface, struct. study using LEED, AES and XPS 7-63981
 Si (111), ordered Au, Ag, Cu overlayers, surface states, inverse photoemission studies 7-2660
 Si (111)/Au interfaces, structural and electronic props., annealing effects 7-21679
 Si (111)/CaF₂ interface and surface phonons, high resolution EELS study 7-38319
 Si bicrystals obtained by solid-phase intergrowth, interface region struct., electron microscopy 7-45023
 Si, CVD thin film backside gettering effectiveness 7-38217
 Si, defect diagnostics for submicrometer VLSI, book contrib. 7-44562
 Si films, laser beam melted, facet formation at solid-melt interface 7-38418
 a-Si high quality films and superlattice solar cells, prep. method 7-46346
 Si ion beam deposition on (100) single cryst. substrate, interface, thin film and damage form. 7-17423
 Si MBE growth on Si (100) and (111), interface formation 7-21773
 Si MBE layers, defects 7-21772
 Si, MBE on Si, role of surface reconstruction, LEED, Rutherford backscattering, channelling meas. 7-7034
 Si multilayers, LPE growth, DEM, TEM obs. 7-12565
 Si oxidation, Si/oxide interface struct. 7-65231
 Si, self-implantation-induced temp. depend. amorphisation, TEM and Monte Carlo simulation studies 7-16595
 Si solar cells, polycrystalline, junction formation by light induced diffusion 7-13919
 Si, substrate for CVD of W, effects of dopants and cryst. perfection 7-16912
 Si surface studies with a high resolution transmission electron microscope 7-21595
 Si-B-Si polycrystal-single cryst. interface, impurity diffusion across boundary 7-27013
 Si:B(As)-Ti(Co), silicide formation using rapid thermal processing, defect behaviour 7-32726
 Si:H, H composition at surfaces and interfaces 7-27083
 a-Si:H doping superlattice interface struct. charactn. 7-58652
 a-Si:H films, growth habit, influence of substrate struct., ellipsometry study 7-45055
 a-Si:H surfaces and interfaces, microstruct., ellipsometry studies 7-38362
 a-Si:H thin films, bulk and interface struct., in situ ellipsometry study 7-27200
 a-Si:H/Pd system, silicide form., struct. and electronic props. 7-38363
 a-Si:H/a-Si₃N₄:H superlattices, plasma deposition methods 7-39439
 a-Si:H/a-SiN_x:H heterostructures, interface formation and microstructural evolution 7-2389
 a-Si:H/a-SiN_x:H interface system, struct. and electronic props. 7-38361
 a-Si:H/a-SiN_x:H superlattices, interface struct., optical reflectance determ. 7-12497
 a-Si:H/a-SiN_x:H superlattices, interface defects and disorder 7-52306
 a-Si:H/a-SiN_x:H superlattice interface struct. charactn. 7-58652
 a-Si:H-SiN_x:H interface, compositional profile, Rutherford backscatt. study 7-13292
 Si:P/Ti, enhanced grain growth by silicide form. 7-27142

interface structure continued

- Si:P(As)/SiO₂ interface, oxidation rates and oxide props., dopant effects determ. 7-12514
- Si/Au buried interface struct. determ., optical second harmonic generation studies 7-63982
- a-Si/c-Si interface, microcrystallites and orientational proximity effect, HREM image interpretation, comment and reply 7-45028
- Si/metal interfaces, silicide form. kinetics during thermal annealing 7-16897
- Si/oxide interfaces, native and thermal, stoichiometry and interface transition layer, atom probe FIM study 7-32844
- a-Si/Si (111) interface ordering, X-ray diffr. 7-32848
- Si/Si₃N₄ interfaces, phase separated structures, Ar⁺ ion bombardment effects, ZPS studies 7-22439
- Si/SiO₂ interface struct., suboxide states, localisation and crystallographic depend., XPS study 7-58653
- Si/SiO₂ system, dielec., elec. and struct. props. 7-7040
- Si/SiO₂ system, two-step oxidation and interface structs. 7-3542
- Si/Ti selectively sputter deposited interface, Auger and Rutherford backscatt. studies 7-21690
- Si-Al₂O₃, SOS struct., UV reflectance meas., ellipsometry study 7-33414
- Si-alkaline earth fluoride structures, heteroepitaxial growth, struct., elec. props. 7-12567
- Si-Au interface, atomic bonding 7-58663
- Si-Au-Pt interfaces, PtSi formation, RBS studies 7-58547
- Si-binary alloy interfacial interactions, Rutherford backscattering spectrometry, TEM 7-12505
- Si-CaF₂-Si heteroepitaxial structures, MBE grown, twinning, topography, channelling, TEM, SEM 7-12566
- Si-Cu interface, atomic bonding 7-58663
- Si-Cu-Au layered struct. reflectivity and EXAFS study 7-59292
- Si-Ge heterojunction, structural and electronic props. 7-21997
- Si-Ge interface, solid phase epitaxy, intermixing, EXAFS, AES, LEED obs. 7-63973
- a-Si-Ge multilayer interfaces, Raman scatt., X-ray diffr. characterisation 7-27167
- Si-Ge multilayered structures, Bi ion implanted, projected range distrib., glancing angle RBS anal. 7-63689
- Si-Ge-Si epitaxial layer structs., particle channelling study, statistical equilib. 7-58386
- Si-InP (110) heterojunction, characterisation 7-33079
- Si-metal complexes on W(110), atomic interactions, FIM study 7-21691
- Si-metal interfacial atomic struct. and epd. form., FIM studies 7-32846
- Si-Si homoepitaxial interfaces, MBE grown, oxygen trapping 7-32855
- Si-Si interfaces, MBE grown, sputter cleaned, microstructure, electron microscopy obs. 7-12512
- Si-Si₃N₄, SOI, N⁺ implanted, microstructural characterisation 7-52300
- Si-Si₃N₄ SOI structs., formation by N⁺ implantation 7-32532
- Si-SiO₂, Si oxidation kinetics, interface width determ. 7-39764
- Si-SiO₂ (111) interface, dangling bonds, dipolar interactions investig. 7-17107
- Si-SiO₂ interface, AES depth profiling during sample rotation 7-27829
- Si-SiO₂ interface, chem. transition, density of states calcs. 7-7397
- Si-SiO₂ interface, computer simulation of high-resolution TEM images 7-44318
- Si-SiO₂ interface, ESR signal from P₀ centres, anisotropic props. 7-38940
- Si-SiO₂ interface, microchemistry 7-32850
- Si-SiO₂ interface, struct. models 7-58658
- Si-SiO₂ interface, study using variable energy positron beam 7-38063
- Si-SiO₂ interface relief study using scanning tunnelling microscopy 7-63978
- Si-SiO₂ interface roughness, evolution, characterisation 7-32852
- Si-SiO₂ interface struct., ellipsometric charactn., rel. to elec. props. 7-63985
- Si-SiO₂ interfaces, microstruct. and electronic props. 7-38359
- Si-SiO₂ SOI struct. formed by high dose ion implantation, high resolution TEM study 7-59690
- Si-SiO₂ SOI structure, lateral solid phase epitaxial growth, TEM study 7-38369
- Si-SiO₂ structures, prod. by recrystallisation, subgrain boundaries, barrier effects 7-52305
- Si-Ta interface, depth profile, Ar⁺ ion bombard., Auger electron spectra anal. 7-46261
- Si-TiSi₂, TiSi₂ local epitaxial growth on Si (111), rapid thermal annealing, annealing ambient 7-33856
- Si-Ti(TiSi₂), Schottky barrier height investig. 7-2716
- Si-Yb interfaces, mixed valence of Yb, synchrotron radiation photoemission spectra, metal coverage and annealing temp. depend. 7-32966
- β-SiC films on substrates, CVD, X-ray topography 7-63998
- βSiC single cryst., wet and dry oxidation kinetics and interface characts. 7-13674
- SiC-Si, reaction bonded composite, mech. props. and microstruct. anisotropy 7-65146
- SiC-Si reaction bonded composite ceramics, interface struct., grain boundaries 7-64995
- SiC-based ceramics, sintered and hot isostatically pressed, microanalytical investigation 7-27991
- SiC-Si, interface struct. study 7-45021
- SiGe superlattice structures, Sb doped, MBE grown, comp., doping profiles, SIMS, Rutherford backscattering spectra 7-7035
- SiGe-Si structures, MBE growth mode and interface structure 7-52311
- Si₃N₄ films prep. by plasma anodisation, XPS depth profiling 7-58667
- SiO₂ films on Si, low-temperature annealing, interfacial props. of MOS structures 7-46526
- SiO₂/Si (111) interface ordering, X-ray diffr. 7-32848
- SiO₂-Si interface, chem. struct., XPS determ., suboxide distrib. and interface state form. 7-38358
- SiO₂-Si interface, roughening induced during AES depth profiling 7-21685
- SiO₂ window on Pb-In-Au alloy films, hillock growth mech. of alloy films 7-16893
- SiON-GaAs interface, plasma enhanced CVD deposited SiON, NH₃ plasma pretreatment effects 7-7874
- SiO₂N_x plasma-enhanced CVD films as selective Zn diffusion barriers 7-12539
- Si(111) substrates, MBE growth of non-lattice-matched (Ba,Ca)F₂, (Pb,Sn)Se-(Ba,Ca)F₂ and CdTe-(Ba,Ca)F₂ layers 7-27216
- Sm-Si Schottky barriers, elec. and struct. characts., 7-38675
- Sn-Ge interface form., growth mode, AES, RBS studies 7-58666

interface structure continued

- Ta-Cu, multilayer systems, temp. depend. of ion beam mixing, 77-book (*Chinese*) 7-51884
- TbFeCo/dielectric interface, chemical stability, interdiffusion and oxidation, AES, XPS and RBS depth profile studies 7-12513
- Ti/Si (111) interface, diffusion and silicide form. kinetics, XPS meas. 7-52308
- Ti-Cu thin films, reaction kinetics, stress, and microstruct. 7-21764
- Ti-N films deposited by ion plating, intermediate layers, TEM study 7-46350
- Ti-Si interface, silicide form., Auger and appearance pot. spectra studies 7-45031
- Ti-SiC interface, compositional depth profiles and intermixing, atom probe FIM study 7-32843
- Ti-SiO₂-TiSi₂-Si, high temp. reaction between Ti and SiO₂, XPS, sputtering (*Japanese*) 7-7022
- TiN films on tool steel, plasma-assisted CVD deposited, interfacial composition 7-52303
- TiO₂ films, reactive ion plating on PET substrates, interface structure, ESCA studies 7-7897
- TiSi₂:B(P)(As) films on Si, impurity diffusion 7-7077
- V/Ni multilayered superlattice, microstruct., X-ray and neutron diffr. 7-32849
- V₃Si/V₂Si₃ interface, crystallography of matrix-precip. interface and elastic strain field (*French*) 7-65036
- W selective LPCVD layers on Si substrate, interfacial struct. 7-16883
- W selective low press. CVD growth on Ti, TiSi₂ and PtNiSi, surface reactions, struct. 7-27183
- W/C multilayer films, thermal stability, X-ray diffr. studies 7-27169
- W/C multilayered structs., high resolution electron microscopy studies 7-63968
- W/polyethylene interface struct. and defects, FIM obs. 7-27151
- W/Si multilayered structs., high resolution electron microscopy studies 7-63968
- W-Cu, multilayer systems, temp. depend. of ion beam mixing, 77-book (*Chinese*) 7-51884
- W-Si interfaces, microstruct. charactn. 7-16882
- W-Si multilayers, X-ray optical props. rel. to layer imperfections 7-37097
- W-Si system, selective deposition of W films on Si wafers, WSi₂ formation 7-21748
- W-Ti-Si interface, WSi_x form. by rapid thermal annealing, growth kinetics, Ti film effects 7-63969
- WSi_x CVD films on Si and Si₃N₄ coated Si, excess Si redistribution upon annealing 7-21723
- WSi_x-GaAs interface, thermal stability 7-52302
- W₂Si₃, reactively sputtered films, metastable phase form. 7-52340
- Zn₃(PO₄)₂ coating, deposited on cold rolled steel surface, Fe dissolution, X-ray fluoresc. anal. 7-28168
- ZnSe MBE layers on GaAs, lattice mismatch effects, TEM, photolum. and X-ray diffr. studies 7-45042
- ZnSe/GaAs interface, MOCVD grown, ZnSe film stoichiometry 7-39415
- ZnSe:Ga:Cr heterostructure, interface stress 7-38352
- ZnSe-In₂-Sn₂O₃-y junctions, microstruct. optical props., influence of deposition method 7-21689
- ZrO₂-Sc₂O₃, cubic to β martensitic transform. 7-22681
- ZrO₂-Y₂O₃/(U, M)O_{2±x}, M=Sc or Y, interface charactn. 7-21677
- interface tension** *see surface tension*
- interface vibrations** *see crystal surface and interface vibrations*
- interfaces, computer** *see computer interfaces*
- interfaces, mechanical** *see mechanical contact*
- interfacial energy** *see surface energy*
- interfacial tension** *see surface tension*
- interfacial waves** *see surface waves (fluid)*
- interference**
see also interference (signal); interference (wave)
 double edge cracks, interference effect on limit moment 7-26203
 magnetic flaw detection of pipelines, eddy currents as interfering factor 7-39822
- interference (signal)**
see also crosstalk; electromagnetic interference
 atmospheric transmission losses use for interference resistant communications 7-34585
 cosmic and geophysical noise in measurements of small displacements 7-4757
 fibre optic gyroscope, noise due to birefringence modulation 7-31479
 length measurement, improving sensitivity, noise removal (*Japanese*) 7-48690
- interference (wave)**
see also acoustic wave interference; electromagnetic wave interference
 multidimensional spectral anal., ionospheric mode structs. decomposition 7-40641
 multilayer interference systems, layer thickness dispersion effects 7-4698
 partial determinacy of wave fields 7-41107
 Young's double hole interference experiments with hairpin cathode electron gun 7-1020
- interference nulling** *see interference suppression*
- interference spectrometers**
 astronomical instrumentation and techniques, conf., Tucson, AZ, USA (March 1986) 7-48162
 Fabry-Perot multichannel spectrometer for infrared astronomy 7-55474
 Fourier spectrometer, phase correction, computational algorithm 7-41504
 Fourier transform, near-IR, with IR vidicon 7-48889
 Fourier transform, spectrometer, microcomputer-controlled, path difference control 7-48861
 Fourier transform IR, dual beam dynamic range considerations in ultimate sensitivity 7-48890
 Fourier transform IR spectrometer, research grade, Digilab FTS 60, design and performance 7-48892
 Fourier transform IR spectrophotometer, rotary scanning, props. and performance 7-48893
 Fourier transform spectrometer, Los Alamos design with microprocessor control 7-48860
 FTIR spectrometer, high resolution, for atomic, mol. and cryst. spectroscopy 7-41505
 FTIR spectrometer sample cell, Invar, thermal calibration 7-41507
 gas chromatograph/FTIR system, optimal design 7-48891
 hazardous gas monitoring system in chem. manufacturing facility, open path FTIR air monitor 7-54416

interference spectrometers continued

- IR emission accessory for surface analysis, ellipsoidal mirror 7-54225
 Michelson interferometer, hand-held, design and sensitivity for Space Shuttle glow obs. 7-55421
 Michelson interferometer, slightly-cooled high-resolution, for limb emission meas. from space 7-55317
 Michelson spectrometer, corner cube reflector for cryogenic appl. 7-41491
 one-sided interferograms in Fourier spectrometers, recovery of linear phase errors 7-35581
 optical data processed Fourier transform spectrometer 7-24707
 PEPSIOS, Polyetalon Pressure Scanned Interferometric Optical Spectrometer 7-18377
 PEPSIOS system, modifications and Periodic Comet Halley (1982i) imaging 7-18356
 SCRIBE interferometer atmospheric emission spectra 7-55319

interference spectroscopy

see also *Fourier transform spectroscopy*

No entries

interference suppression

see also *echo suppression*

- 2D target reconstruction using normalisation and autocorrelation, noise elimination 7-36908
 acoustic noise cancellation 7-37259
 adaptive microphone-array system for noise reduction 7-31609
 AM noise in FM spectroscopy, shot-noise limited meas. of H₂O vapour pressure broadening 7-18888
 biomedical electronic instruments safety and testing Electrotechnical Testing Institute practices (Czech) 7-18090
 cosmic and geophysical noise in measurements of small displacements 7-4757
 ECG, power line interference estimation and removal 7-65863
 electro-optic directional coupler switches, crosstalk due to reversed- $\Delta\beta$ electrode misalignment 7-20471
 EM flowmeters, noise reduction 7-37599
 frequency domain acoustic noise canceller, frequency bin adaptive filtering 7-37247
 hearing aids, noise cancellation 7-40175
 IR film thickness gauging, optical interference suppression 7-33472
 laser FM measurement technique, suppression of residual AM 7-15919
 NMR magnetic field meter, high-field meas. at liquid He temp. 7-18849
 REDMASK noise reduction filtering for the hearing-impaired 7-34162
 SAW filters, method for false signal level reduction 7-57640
 semiconductor DFB lasers, spectral chirping suppression 7-20220
 US pulse echo signals, processing for electro-acoustic conversion distortion removal (Japanese) 7-43540
 AlGaAs laser diode, HF stabilisation 7-15864
 He-Cd laser, noise reduction by discharge current modulation 7-31348

interferometers

see also *acoustic wave interferometers; electromagnetic wave interferometers; interferometry*
 gravitational wave detectors, antenna patterns of interferometric detectors for linearly polarised waves 7-55453

interferometry

see also *acoustic wave interferometry; electromagnetic wave interferometry; holographic interferometry; interferometers*
 COW experiment, nonrelativistic, in uniformly accelerated reference frame 7-41143
 DIII-D, plasma diagnostic set, design, installation and operation, eng. and physics problems 7-25217
 neutron, wave field calcs. in accelerated interferometers 7-48439
 neutron interferometric double-resonance experiment 7-15046
 neutron Laue-Laue interferometry 7-11831

intergalactic matter

see also *clusters of galaxies; galaxies*

- 1759+211, nearby radio galaxy, contrib. of ram-pressure bending to oscillating radio jet 7-55820
 Abell 370, arc structure in cluster of galaxies 7-60815
 absorption clouds number density, evidence for redshift evolution from quasars UV spectra 7-55829
 B2 1225+317, quasar, Lyman-alpha forest from 3140 Å to 3940 Å 7-48097
 B2 1320+299, quasar with asymmetric radio struct., mag. field lines distrib. 7-35065
 Bootes void, spectroscopic survey of Case emission-line galaxies 7-29534
 clusters of galaxies, core self-regulated cooling flows and low-mass star form. 7-66741
 Coma/A 1367 Supercluster, dynamical interaction with galaxies rel. to radio continuum props. 7-29547
 cooling flows, narrow absorption lines 7-66761
 cooling flows in southern clusters, relation to star form. in central galaxies 7-55821
 cooling gas, column densities and UV lines of highly ionized atoms 7-23992
 galaxies radio trails, bending by galactic winds and rot. 7-35045
 GC 1556+335, quasar, intervening cluster model for absorpt. line spectrum 7-29552
 hot intracluster gas in poor galaxy clusters, relation to luminosities of first-ranked galaxies 7-55843
 intracluster medium, equilib. of gas in gravit. field of cD-type galaxies 7-24204
 Lyman-alpha absorbing clouds, nonspherical clouds model 7-60805
 Magellanic H I bridge, 160 pc shell feature characts., stellar wind or SNR origin 7-35049
 Magellanic Stream, dust content 7-66721
 molecular astrophysics, NATO conf., Bad Windsheim, Germany (1984 July) 7-9589
 molecular gas mass in Galaxy, review 7-9530
 photoionisation by high-redshift quasars, dynamics of cosmological H II regions 7-40938
 pressure variations, determ. using extragalactic jets as probes of surrounding medium 7-55822
 pressure-confined polytropic intergalactic clouds within homogeneous dark matter, equilibria and instabilities 7-4316
 primordial clouds, fragmentation rel. to form. of primordial stars 7-47999
 primordial intergalactic gas, heating by background radiation in presence of H₂ 7-24205
 protoclusters of galaxies, gas IR emission 7-4600

intergalactic matter continued

- Q0800+608, quasar, jet speed determ. from interaction with intergalactic model 7-9555
 SN 1987A in LMC, line-of-sight interstellar-intergalactic material 7-66632
 Virgo Cluster, spiral galaxies interaction with intracluster medium from 2.8 cm continuum obs. 7-9540
 Virgo cluster core, intracluster medium rel. to orbital motion of H I deficient spiral galaxies 7-24230
 voiding scales, implications of two-dimensional covariance function for IRAS sources 7-14677
 voids, evidence from large-scale structure probes in Corona Borealis region 7-40922
 voids at high redshifts, constraints from QSO Ly α absorbers 7-55823
 CO absorption line towards M82, obs. rel. to large mol. halo or intergalactic mol. gas 7-24223

intergranular fracture see brittle fracture**intermediate boson decay**

- two and three jet decays, Monte Carlo simulation of e^+e^- -intermediate bosons 7-30268
 $e^+e^- \rightarrow W^+W^-$, probing the weak boson sector, anomalous couplings search, helicity amps. 7-56533
 $e^+e^- \rightarrow Z^0 \rightarrow b\bar{b}$, unpolarized and polarized forward-backward asymmetries, properties 7-538
 $\gamma e^- \rightarrow W e^-$, W prod. and decay diff. cross sections, beam pol. and anomalous mag. moment effects (Russian) 7-30299
 W decays, W, Z mass limits, SUSY signals 7-61682
 W $\rightarrow e\bar{\nu}$, single electron search expt., sparticle mass limits 7-49142
 W $\rightarrow e\nu(\mu\nu)$, $e-\mu$ universality test of weak couplings, g_{τ}/g_e , g_{μ}/g_e meas. large missing energy events 7-61679
 W $\rightarrow b\bar{\nu}$, supersymmetric signals in leptonic decays 7-41808
 W $\rightarrow l\bar{\nu}$ ($l=d,s$), electroweak one-loop corrections, form factor, calc. scheme 7-5091
 W $\rightarrow \nu\bar{\nu}$, τ -observation from missing transverse energy events 7-61679
 W $\rightarrow u\bar{u}$, rate and energy distribution for hyperphoton production 7-35875
 W $\rightarrow WZ$, W and Z decays, W, Z mass limits 7-61682
 W $\rightarrow \gamma l^+\bar{l}$, $\mu\mu$ meas. proposals as electroweak model test 7-15156
 W $\rightarrow l^+\bar{l}$, $\mu\mu$ meas. proposals as electroweak model test 7-15156
 W $\rightarrow l^+\bar{l}$ (b), branching ratio comparisons, CP nonconservation 7-10061
 W $\rightarrow L^+\bar{L}$ (L=heavy lepton), event search at CERN collider 7-61680
 W' decay, generalized vector-boson dominance anal. 7-61681
 Z $\rightarrow b\bar{b}$ (bs), branching ratio comparisons, CP nonconservation 7-10061
 Z decays, W, Z mass limits, SUSY signals 7-61682
 Z $\rightarrow g\bar{g}$, $gq\bar{q}$, $l^+l^- \gamma$, preon-composed bosons 7-24885
 Z $\rightarrow H\gamma$ (HH γ), composite model study 7-24886
 Z $\rightarrow h\bar{h}$, Higgs boson signature 7-61678
 Z $\rightarrow l^+\bar{l}$, supersymmetric signals in leptonic decays 7-41808
 Z $\rightarrow \nu\bar{\nu}$, composite model study 7-24886
 Z $\rightarrow \nu\bar{\nu}$, CP nonconservation effects in the standard model 7-5090
 Z $\rightarrow f\bar{f}$, branching ratios in SU₈ multigenerational grand unification 7-30267
 Z $\rightarrow l\bar{l}$, investigation of weak neutral currents in $h_1h_2 \rightarrow V(t\bar{t})$, $V(t\bar{t}) \rightarrow \gamma$, Z $\rightarrow \gamma$ 7-5098
 Z $\rightarrow l\bar{l}\gamma$, Stokes parameter calcs. and anomalous mag. moment 7-41807
 Z \rightarrow neutralinos in supersymmetric SU(2) \times U(1) model 7-519
 Z $\rightarrow \nu\bar{\nu}$ (ν =new neutrino species), event search at CERN collider 7-61680
 Z $\rightarrow q\bar{q}\gamma$, Stokes parameter calcs. and anomalous mag. moment 7-41807
 Z $\rightarrow q\bar{q}\nu$, minimal standard model anal. 7-19120
 Z $\rightarrow W^+ + \text{anti-}W^-$ and Z decays, W, Z mass limits 7-61682
 Z $\rightarrow ZH$ from $gg \rightarrow Z$, cross section calcs., fourth generation quarks 7-10082
 Z $\rightarrow ZH$ from $q\bar{q} \rightarrow Z^*$, cross section calcs., fourth generation quarks 7-10082
 Z $\rightarrow W^+l^+\bar{\nu}_l$, test for γW^+W^- , Z $^0W^+W^-$ structure, W-magnetic moment anal. 7-24870
 H $\rightarrow W^+W^- \gamma$, decay width determ. 7-15155
 W $\rightarrow q\bar{q}$, reconstructing jet-jet invariant masses 7-10060
 Z $\rightarrow \nu\bar{\nu}H$, composite model study 7-24886

intermediate bosons

- see also *intermediate boson decay; W bosons; Z bosons*
 Abelian composite vector boson model, spontaneous symmetry breaking 7-41754
 anomalous high-energy behaviour in boson fusion 7-35761
 axion, 1.7 MeV, restrictions from nuclear intermetal-pair-transitions 7-19200
 axion production in 800 GeV hadronic showers 7-19139
 axion-EM coupling, implications for cosmic background radiation 7-439
 axions, rest mass and Universe dark matter 7-60524
 composite models, leptogluons and exotic coloured vector bosons 7-41756
 cosmic axion string decays, constraint on Peccei-Quinn symm. breaking scale 7-24517
 cosmic strings, radiation of Goldstone bosons 7-56129
 dark matter candidates, scatt. and annihilation cross sections 7-15089
 dark matter in Universe 7-9560
 dilaton, technicolour model, mass and lifetime estimates 7-41712
 E₈ supergravity GUT with SU(N,1) invariant Kahler potential, strong CP violation elimination via invisible axion 7-61524
 electroweak bosons, leptons and Han-Nambu quarks in a unified spinor-isospinor preon field model 7-49102
 gauge hierarchy problem, mass generation by nonperturbative quantum effects 7-19007
 Higgs boson, props. 7-49039
 Higgs boson, statistical analysis techniques applied to new-particle searches 7-61784
 Higgs boson mass upper bounds in electroweak interaction models 7-19054
 Higgs boson masses, perturbative calcs. 7-61452
 Higgs boson production at heavy Z-resonance 7-35759
 Higgs boson-quarks composite model 7-10008
 Higgs bosons in softly broken two-doublet supersymmetry model 7-35731
 Higgs detection via Z 0 polarisation in pp interactions 7-24914
 Higgs doublet models, bounds on masses 7-61537
 Higgs field mass parameter, perturbative evolution in SUSY gauge theory 7-408
 Higgs-boson doublets, model, with no increase in parameters 7-15110
 high mass dilepton production in hadron collisions, review 7-56574
 Kaluza-Klein theory, symm. breaking and vector boson masses 7-41192

intermediate bosons continued

Kerr-Newman metric, charged boson bound states (*Chinese*) 7-9729
left-right symmetric models, light scalar indications 7-15099
light Higgs scalar boson searches, prospect for next generation e^+e^- collider 7-24807
light neutral Higgs bosons, prod. rates in $N=1$ supergravity theories 7-29858
luminous axion clusters, photon decay, measurable luminosities 7-47694
mass limits in left-right symmetric models 7-56498
open superstring with $O(32)$ massless gauge bosons, principal-part regularization 7-19046
parity invariance, strong and electromagnetic interactions 7-9995
preon-composed bosons, spectrum, decay props. 7-24885
radiative corrections to vector boson masses for heavy Higgs bosons 7-30272
scalar boson emission by electrons in a steady magnetic field in the Weinberg-Salam theory 7-10003
sextet quarks and light pseudoscalars 7-5047
solar axions, ultralow background search 7-55393
stellar axion emission rates in nonrelativistic degenerate regime 7-55458
strongly interacting Higgs sector, σ -model simulation 7-48975
 $SU(2) \times U(1)$ radiative corrections, nonstandard Higgs bosons 7-10005
superstring models, neutral E_6 gauge boson 7-61196
superstring models on Calabi-Yau manifolds, gauginos and Higgs particles 7-61514
technicolour theory with pseudo-Goldstone bosons, one-loop corrections 7-56525
type-I $SO(32)$ superstring theory, proof of one-loop finiteness, response to comment 7-41224
type-I $SO(32)$ superstring theory, proof of one-loop finiteness, comment 7-41223
UA2 jets, W and Z associated production meas. 7-61776
variant axion models, constraints 7-30237
vector boson mass generation in two-dimensional gauge theories 7-426
vector bosons, renormalisation scheme depend. of electroweak parameter shifts 7-19053
Weinberg, chiral model, saddle points and skyrmion solns. 7-15100
(e^- axion), stellar axion production mechanism 7-24974
 $e^+e^- \rightarrow f\bar{f}$, asymmetries and cross section, superstring gauge boson effects 7-499
 e^+e^- annihilations, joint quarkonium and neutral Higgs boson production anal. 7-15168
 $\tilde{e}^+\tilde{e}^- \rightarrow \gamma X$, identification of missing neutrals using long. pol., ν , $\bar{\nu}$, $\tilde{\gamma}$ and \tilde{H}^0 7-49127
 $e^+e^- \rightarrow \gamma\gamma\gamma$, heavy flavor production with gluon bremsstrahlung 7-15125
 $e^+e^- \rightarrow H^\pm tb$, Higgs boson prod. cross sections, standard model comparison 7-19124
 $eN \rightarrow eN$, production in heavy targets 7-49155
 $eN \rightarrow eN$ + axion, search for axion-like particles in electron bremsstrahlung 7-24891
 $ep \rightarrow ep$, scattering asymmetries, superstring gauge boson effects 7-499
 $\eta \rightarrow H^+X$, production mechanism, differential characteristics 7-41796
 η effects and instanton physics in low energy axion dynamics 7-30191
 $gg \rightarrow Q\bar{Q}g(\bar{g}g)$, heavy flavor production with gluon bremsstrahlung 7-15125
 $K \rightarrow e\bar{\nu}H$, Higgs production phenomenological limits 7-513
 $NN \rightarrow NN\phi$, low-mass pseudoscalar boson production 7-41845
 $\tilde{\nu}e \rightarrow$ gaugino + X, poss. μ prod. from $Cy\ X-3$ 7-23962
 pp , one-jet events, colour scalar bosons as source of jets 7-5134
 $pp \rightarrow H^+H^-$, SUSY Higgs production, SUSY standard model calcs. 7-61763
 $pp \rightarrow W^\pm \nu_\ell (Z^0(W^\pm\gamma) \rightarrow L^\pm\bar{\nu}_\ell)$, heavy lepton production through vector boson fusion processes 7-10078
 $\pi^+ \rightarrow a e^+ \nu$, $a =$ axion, branching ratio calc., chiral Lagrangian anal. 7-511
 $\tilde{t} \rightarrow \gamma H$, minimal and two-doublet Higgs prod., standard model 7-35762
 $\tilde{t} \rightarrow ZH$, minimal and two-doublet Higgs prod., standard model 7-35762
 $V \rightarrow H\gamma$ radiative decay, relativistic effects calcs. 7-49094
W and Z production properties 7-61777
Y bosons, signatures in pp and $p\bar{p}$ colliders 7-24851
 Z' , experimental consequences of unification group symmetry breaking 7-49038

intermediate state

ferromagnetic superconductors, intermediate state 7-52915
intermediate valence and heavy fermion model systems 7-33122

intermediate valence compounds see mixed valence compounds

intermetallic compounds see alloys

intermodulation

acousto-optic signal processing system intermodulation products 7-1041

intermodulation measurement

No entries

intermolecular forces

see also Van der Waals forces
aniliniums, long range interactions, near UV spectra, MNDO and CNDO calcs. 7-19879
dimers, H bonded, intermol. interactions, quantitative model 7-36721
formamide, atomic multipoles, molecular potentials, interaction energies SCF MO calcs., atomic multipole expansion 7-19696
formate ion, atomic multipoles, molecular potentials, interaction energies SCF MO calcs., atomic multipole expansion 7-19696
gas, spherically symmetric pair-pot. energy fn., second acoustic virial coeff. method calc. 7-62481
intermolecular interaction energies, SCF calcs., variation-perturbation procedure 7-15505
lysophosphatidyl ethanolamine, energetics, hydration struct., ab initio pots. 7-65300
macromolecular systems, pressure equation generalisation 7-10784
magnetic lattice gas of molecules in transverse field, molecular field approx. 7-2802
methyl group motion, rotation barrier and spin-lattice relax. time meas. 7-50291
micellar and microemulsion globules solvent induced attractions 7-54195
model suspensions, 2D, interactive and non-interactive rigid spherical particles, hydrodynamic interactions (*French*) 7-8306
molecular interactions, theoretical aspects, book 7-48213
molecule + molecule vibr.-rot. energy transfer, collision time-correl. functions 7-50315
monomer orientation in H bonded and weakly bonded complexes, elec. influence 7-954
N-molecule system, long-range dispersion interactions, spherical tensor theory 7-42723

intermolecular forces continued

N-molecule system, long-range induction interactions, spherical tensor theory 7-42722
N-molecule system, long-range isotropic interactions, spherical tensor theory 7-42724
nitromethane, solid, methyl group rot., pot. surface calcs. 7-11972
poly(α -methylstyrene) adsorbed monolayer on mica, intermolecular force meas. 7-21623
poly-1,4-phenylenesulphide, struct., comparative analysis with small mol. model 7-44419
simple gas, free expansion anal. by use of first law of thermodynamics 7-16293
spherical mols. model mixtures, phase equilib. 7-38203
three particle loosely bound states, adiabatic hyperspherical approx. 7-10702
 H_2 -HF complex, struct., bonding, vibr. freq. shift 7-19817
 $(H_2)_2$ dimer, MP4 interaction energies and basis set superposition errors 7-62479
 H_2O , atomic multipoles, molecular potentials, interaction energies SCF MO calcs., atomic multipole expansion 7-19696
 H_2O -Cu(Ni), complexes, bonding, intermolecular electron correl. 7-10449
 $H_2O^+(H_2O)_2$, SCF interaction energies, nonadditivity 7-57143
NF-IF, electronic energy transfer, long-range interaction model 7-62478
 NH_4^+ , atomic multipoles, molecular potentials, interaction energies SCF MO calcs., atomic multipole expansion 7-19696

intermolecular mechanics

see also association; intermolecular forces; kinetic theory of gases; liquid structure; liquid theory; Morse potential; potential energy functions
alkane chains, internal rot. in anisotropic environment 7-956
carbon tetrachloride, neutron diffr. intermol. scatt. functions and RISM partial scatt. functions 7-31145
P-carborane, plastic cryst. phases, mol. notions 7-63528
chlorophyll forms, vib. state and struct. anal., Raman spectra 7-19867
chlorophyll- H_2O system, ab initio LCAO SCF MO calcs., ionisation pot., electron affinity, intermol. mechanics 7-8520
collisional time-correlation functions for molecular interactions 7-36719
conjugated systems, computer reaction simulation, hybrid model 7-49874
diacyl peroxides, low temp. photolysis, vib. anal. for CO_2 dimer, IR spectra 7-15597
fluids of optically isotropic mols., collision-induced light scatt. 7-33405
fluorescence, diffusion-enhanced intermol. energy transfer, simulation method 7-10660
graphics system for molecular structures and properties, display system, Winchester Graphical System 7-49875
hard sphere fluids, bridge fn. calc. 7-63418
hydrophobicity parameters from partition coeffs. 7-13954
Kleinman symmetry in molecules, information from SHG meas. 7-25609
liquids, IR and anisotropic Raman band profiles theory, mol. interactions 7-31040
long-range energy transfer for inhomogeneous spatial distrib. and indirect donor-donor interaction 7-33419
methyl alcohol, ^{13}C NMR chem. shifts, intermol. interactions effects 7-50193
molecular H-bonded systems, interaction energies, polarisation counterpoise corrections 7-62262
nematic liquid crystals, IR dichroism, mol. interactions effects 7-45981
nonempirical atom-atom potential for main components of intermolecular interaction energy 7-31139
polymer interaction with small mol., iterative transfer perturbation method 7-19709
projection operator formalism, alternative derivation of perturbation expansions 7-5580
salicylidenamides, thermochromic and photochromic, IR spectra, conformational influence 7-53310
smectic C^* twisted phase, induced, helical twisting power 7-58130
tetramethyl tin isolated in Ar, inelastic neutron scatt., intermol. interaction, rot. tunnelling 7-20067
Tween 81-hexadecane- H_2O , props. in low-temp. region, struct., 1H , 2H and ^{13}C NMR 7-8318
wetting layer thickness, equilibrium, dispersion forces calcs. 7-32754
Ge Cl_4 , neutron diffr. intermol. scatt. functions and RISM partial scatt. functions 7-31145
HF-He, mol. interactions, nonexpanded dispersion and induction energies, damping functions 7-42474
 H_2O dimer, MBPT, coupled cluster study 7-49892
 H_2O , long-range intermol. interaction energies using RPA/moment function methods 7-10698
 H_2O - H_2O_2 mixtures, long-range intermol. interaction energies using RPA/moment function methods 7-10698
 H_2O_2 , long-range intermol. interaction energies using RPA/moment function methods 7-10698
 $SiCl_4$, neutron diffr. intermol. scatt. functions and RISM partial scatt. functions 7-31145
 $SnCl_4$, neutron diffr. intermol. scatt. functions and RISM partial scatt. functions 7-31145
 $TiCl_4$, neutron diffr. intermol. scatt. functions and RISM partial scatt. functions 7-31145
 VCl_4 , neutron diffr. intermol. scatt. functions and RISM partial scatt. functions 7-31145

intermolecular vibrations see molecular rotational-vibrational energy transfer

intermolecular vibrations (molecular crystals) see lattice dynamics of molecular crystals

internal combustion engines

2D intake manifold flow digital simulation of 4-cylinder internal combustion engine 7-63170
adiabatic diesel engine, combustion characts. of powdered coal fuel 7-65596
ceramics, powder prep., sintering and compaction, internal combustion engine appl. 7-3240
ceramics, reciprocating engine requirements 7-3242
diesel engine, Miller supercharging system appl. 7-65597
diesel engine, partial adiabatic cycle heat loss 7-65522
diesel engine with exhaust heat recovery, combustion chamber insulation effect 7-65599
flow field using Lagrangian-Eulerian method (*Chinese*) 7-20813
Mazda rotary engine technology, combustion characts. 7-65598
optimization rules in thermal cycle models 7-65520

internal conversion

- see also *conversion electron spectra*
 conf., Leningrad, USSR, April 1985 7-29574
 electron shell rearrangement effect on internal conversion coeffs. 7-30376
 field-enhanced internal conversion, appl. to γ -ray laser 7-10125
 nuclear data sheets, recent refs. Jan. to April 1986 7-31
 transition probability of K-shell internal conversion in intense radiation field 7-5193
 $^0_{-}e^+e^-$ branching ratio meas. 7-49131
 ^{145}Cs , β -decay study and internal conversion coefficient meas. 7-5198
 ^{152}Dy , quasicontinuum γ -rays from collective high-spin states, internal conversion coeff., multipolarity meas. 7-56639
 ^{139}Eu decay props., γ -ray and internal conversion meas. 7-49306
 $^{57}\text{FeF}_3\cdot 3\text{H}_2\text{O}$, resonance scintillators for recoilless 14.4 keV γ -quanta 7-62202
 ^{54}Fe , internal pair conversion probability ratios for E0 transitions from K-shell 7-30379
 ^{70}Ge , internal pair conversion probability ratios for E0 transitions from K-shell 7-30379
 ^{177}Hf , K-allowed E1 transitions ICC anomalies and penetration matrix elements (*Russian*) 7-597
 ^{180}Hf , longitudinal conversion-electron polarization 7-30377
 ^{127}I , M1 transitions, internal conversion coefficient/electron density correlations 7-24961
 ^{129}I , M1 transitions, internal conversion coefficient/electron density correlations 7-24961
 ^{114}In , internal conversion coefficients, many-electron and solid-state effects 7-30378
 $\text{K}_4^{40}\text{Fe}(\text{CN})_6\cdot 3\text{H}_2\text{O}$, resonance scintillators for recoilless 14.4 keV γ -quanta 7-62202
 $^{\text{A}}\text{Lu}$, A=175,177, K-allowed E1 transitions ICC anomalies and penetration matrix elements (*Russian*) 7-597
 ^{175}Lu , longitudinal conversion-electron polarization 7-30377
 ^{60}Ni , internal pair conversion probability ratios for E0 transitions from K-shell 7-30379
 $^{\text{A}}\text{Pb}$, A=194-196, energy level conversion coeff. meas. from ^{184}W (^{16}O , xn) 7-19206
 ^{47}Sc decay: half-life, γ -emission probability, transition probability, end-point energy and internal conversion coeff. 7-24959
 ^{76}Se electric monopole transitions, IC electrons, level lifetimes from ^{76}Br EC decay 7-19202
 ^{139}Sm decay props., γ -ray and internal conversion meas. 7-49306
 ^{119}Sn , internal conversion rate changes due to lower multipole admixtures 7-10126
 ^{119}Sn , M1 transitions, internal conversion coefficient/electron density correlations 7-24961
 $^{\text{A}}\text{Ta}$, A=179,181, K-allowed E1 transitions ICC anomalies and penetration matrix elements (*Russian*) 7-597
 ^{125}Te , M1 transitions, internal conversion coefficient/electron density correlations 7-24961
 ^{125}Te , valence electron contact density 7-25457
 $^{\text{A}}\text{Tm}$, A=167,169,171, K-forbidden E1 transitions, ICC anomalies and penetration matrix elements (*Russian*) 7-597
 ^{171}Yb , K-forbidden E1 transitions, ICC anomalies and penetration matrix elements (*Russian*) 7-597
 ^{64}Zn , internal pair conversion probability ratios for E0 transitions from K-shell 7-30379

internal conversion in atoms see *Auger effect*

internal conversion in molecules see *nonradiative transitions*

internal fields, crystal see *crystal field interactions*

internal friction

- see also *Bordoni effect; damping; Snoek effect; Zener relaxation*
 alkali silicate glasses; internal friction, amplitude depend., cooperative movement parameter near the glass transition temp. 7-2099
 alloy, nonuniformly distrib., internal friction rel. to diffusion (*Russian*) 7-65074
 alloys, FCC, internal friction, interaction between dislocation kinks and substitutional solute atoms 7-51935
 Au, internal friction background, low-frequency 7-38113
 bar, bending vibr., amplitude-dependent internal friction, influence of non-uniformly stressed condition (*Russian*) 7-58410
 CDW elasticity model 7-52472
 Collette torsion pendulum theory 7-14934
 crystal with dislocations, first-order phase transitions 7-38178
 epoxy, Al particle filled, damping charact., dynamic structural model appl. 7-33709
 frictional materials, theoretical framework for modelling behaviour 7-43706
 glass ceramics, development in China, review 7-6527
 mammalian tissues and bones, shock-absorbing props. 7-3829
 metals, polycrystalline, internal friction temp. spectrum and microplasticity (*Russian*) 7-16684
 oxide glass, low-temp. internal friction, longitud. and transverse two-well systems rel. contrib. 7-12202
 polycrystals, high temp. internal friction, rel. to grain boundary diffusion 7-63743
 polymers, internal friction, amplitude depend., cooperative movement parameter near the glass transition temp. 7-2099
 solids, review 7-6720
 steel, austenitic, martensite transform. start temp. increase in electrolytic H impregnation, internal microstresses role 7-17690
 steel, austenitic stainless, high cycle fatigue props., age hardening 7-13598
 steel, Cr type, dislocation struct. after hydraulic pressing followed by austempering 7-3334
 steel, maraging, low-temp. internal friction, H effects (*Russian*) 7-33710
 steel, Ni-Cr, anelastic props. of grain boundaries and transition temp., effect of temper embrittlement 7-22815
 steel, stainless, ferrite, high-Cr, solubility of Ti and Nb carbides, temp. depend. of internal friction obs. 7-53740
 steel, stainless, martensitic and austenitic, amplitude depend. damping rel. to annealing and tempering (*German*) 7-13498
 steel foils, H charged, internal friction, quasi-molecular state (*Russian*) 7-59561
 zircaloy-4, polycryst., high temp. internal friction 7-17571
 Al, high purity macrocrystalline, internal friction peak, contrib. of bamboo boundaries 7-8037
 Al, hysteresis behaviour of medium temp. peaks (*French*) 7-63742
 Al internal friction peak obs., dislocation configurations 7-38115

internal friction continued

- Al sheet, dislocation relax. contrib. to deform., internal friction and dynamic modulus meas. during creep 7-63626
 Al-Ag, anelastic effects due to precip. and dissoln. 7-13487
 Al-Ag (5 wt.%), anelastic effects, quench sensitivity, precip. and dissolution 7-53784
 Al-Si, cold worked, damping characts. 7-28064
 $\beta''/\beta\text{-Al}_2\text{O}_3\text{-(Na}_{0.6}\text{K}_{0.4})_2\text{O}$, mixed-alkali-mixed phase cpds., acoustic study 7-63749
 BW alloy fibre, torsional pendulum, shear modulus and internal friction meas. 7-48232
 BaO-Mg(Zn)O-P₂O₅ glasses, internal friction investig. 7-6721
 CaO-Sr(Ba)(Mg)(Zn)O-P₂O₅ glasses, internal friction investig. 7-6721
 Co, internal friction and linear expansion coeff. in phase transition region 7-44857
 CsI, internal friction, plastic deformation, crystallographic orientation 7-12205
 CsI single crystals, dislocation internal friction mechanisms study 7-63625
 Cu based alloys, internal friction, Young's modulus, amplitude relationship (*Russian*) 7-65075
 Cu-Zn-Al, dislocation density and mobility during reversible martensitic transforms. 7-26759
 CuAlNi deformed single cryst., internal friction amplitude depend. (*Russian*) 7-13491
 Fe, Armco, mag. internal friction, cathodic charging effect 7-17212
 Fe foils, H charged, internal friction, quasi-molecular state (*Russian*) 7-59561
 Fe, magnetic domain walls, low freq. internal friction (*Chinese*) 7-38898
 Fe-N, Snoek-Koster relax., dislocation effects (*Russian*) 7-44686
 Fe-Ti-N, mech. props. rel. to cold working 7-28089
 GaAs:B, internal friction temp. depend. studies 7-38112
 GaP:B, internal friction temp. depend. studies 7-38112
 InAs:B, internal friction temp. depend. studies 7-38112
 InP:B, internal friction temp. depend. studies 7-38112
 (KBr)_x(KCN)_x mixed crystals, elastic shear const. and internal friction, torsion pendulum resonance meas. 7-26829
 KCl:CaCl₂, internal friction 7-38114
 K_{0.3}MoO₃, CDW conductor, elastic anomalies 7-44652
 Mg, dislocations, interaction with pinning centres, 4.2 to 295K 7-44558
 MoO₃-P₂O₅ glass, low-temp. internal friction, longitud. and transverse two-well systems rel. contrib. 7-12202
 Nb-based alloys, grain boundary internal friction investig. (*Russian*) 7-13490
 Nb-Mo-O alloys, internal friction and yield point (*Russian*) 7-59563
 Nb-N, internal friction rel. to quenching temp. (*Russian*) 7-46543
 Nb-Ti-O alloy, struct. state obs. by internal friction, oxide precip. (*French*) 7-13494
 Ni and Ni-Cu, gamma-irradiated, point defect migration 7-6893
 Ni foils, H charged, internal friction, quasi-molecular state (*Russian*) 7-59561
 Ni₄₀Pd₆₀P₂₀, glass transition, internal friction by Collette torsion pendulum 7-38199
 Ni₃₅Ti₆₅, amorphous, internal friction of H 7-39577
 Pb-Tl alloy single crystals, plasticity and internal friction changes at supercond. transition (*Russian*) 7-26832
 Pd-B-H alloys, internal friction, elastic consts. 7-26857
 Pd-H alloys, low freq. internal friction meas., precipitation peak obs. 7-51933
 PdH_x, H diffusion by tunnelling 7-6880
 Sb alloys, polycrystalline, elastic consts. meas. 7-21319
 Sb single crystals, dislocation thermoactivated amplitude-dependent internal friction (*Russian*) 7-51934
 Si:Pd, inelastic relax., neutron irradiation effects 7-44689
 SiC fibre reinforced Al composite wires, neutron irradiation, mech. props., fusion reactor appl. 7-49628
 SrO-Ba(Mg)(Zn)O-P₂O₅ glasses, internal friction investig. 7-6721
 Ta, diffusion of H, internal friction 100-400K (*Chinese*) 7-6872
 Ta wire, cold worked, internal friction, hydride precip. (*Chinese*) 7-8034
 TiNi, mono- and polycryst., elastic props. and internal friction, premartensitic anomalies (*Russian*) 7-59564
 Zn, amplitude-dependent internal friction, press. depend. (*Russian*) 7-58409
 Zn polycrystalline, internal friction, temp., time and amplitude depend., heat expansion anisotropy effects (*Russian*) 7-16687
 Zr, internal friction and linear expansion coeff. in phase transition region 7-44857
 Zr, internal friction due to grain boundary relax. 7-65076

internal friction of liquids see *viscosity of liquids*

internal mechanics, molecular see *molecular vibration*

internal mechanics of atoms see *atomic structure*

internal modes see *molecular vibration in solids*

internal strains see *internal stresses*

internal stresses

- 2D elastostatics, stress computation by BEM 7-37330
 alkali halide crystals, dislocation displacements distrib. characts., local dislocation density effects (*Russian*) 7-21214
 alkali metal halides, hardening, effect of dislocation elec. charge 7-51816
 alloy, structural, creep and stress relax. mechanism 7-46571
 amorphous ribbons, magnetostriction meas., SAMR method, anisotropy effects study 7-7580
 antireflection coating stress in Fabry-Perot etalons 7-30064
 axisymmetric 3D residual stresses, new meas. method using inherent strains as parameters 7-51013
 bearing type, austenite transform. kinetics and internal stresses in bainitic hardening 7-39563
 bicrystals, shear incompatible, approx. evaluation method for elastic stresses by virtual array of dislocations (*Japanese*) 7-32841
 bimetal cylinder, temp. fields and residual stresses in cooling 7-33705
 biomechanics dynamic problems, deformable solid model with reaction 7-47140
 β -brass bicrystals, Bauschinger effect, grain boundary contrib. 7-46574
 complex bodies, residual stresses, investig. by photoelastic methods (*Polish*) 7-43683
 composite materials, mode I edge delamination, stress distrib. ahead of crack, thermal residual stress 7-6151
 composition modulated layered structures, elastic strain, X-ray diffraction studies 7-27086
 crack parameter, finite element modelling of grinding residual stress effects 7-16113

internal stresses continued

critical resolved shear stress for systems with general periodic stress fields 7-38085
crystal internal strains, acousto-optical study (French) 7-7671
cubic cylindrical single crystals, stress determ., Abel inversion (Russian) 7-16672
CVD and PVD coatings, structural, mechanical and tribological props. and applications 7-53935
cylinder, hollow, surface compression strengthened, stable crack growth 7-37385
discs and rings, subjected to rolling contact, stress intensity factors for small cracks in rim 7-57761
Elinvar alloys, dispersion hardening and softening, elastic limit studies (Russian) 7-59539
epoxy polymers, compact tension specimen casting, fatigue crack growth rate testing 7-13681
fatigue failure at stresses below fatigue limit 7-38102
fibre reinforced composites with internal stresses under control 7-3383
films, decohesion from ceramic or semiconductor substrates 7-21711
gels, drying induced shrinkage, liquid flow and chem. reactions 7-23069
glass, helicopter windshield, chemically tempered impact fracture 7-28108
grain boundary cavity-growth kinetics determ. from cavity-size distrib. during creep and continuous nucleation 7-26767
graphite fibre reinforced Al matrix composites, interface charactn., TEM obs. 7-44554
Hertzian contact, internal stresses, influence on material stresses, calc. with different stress hypotheses 7-16134
Hertzian contact, stress hypotheses and material stresses 7-1521
III-V semiconductor strained-layer effective-mass superlattices 7-7378
ion implantation, elastic vibrations 7-12094
magnetoacoustic emission meas. of residual stresses 7-45749
materials fatigue behaviour, influencing factors (Japanese) 7-39642
mean stress dependence of the thermoelastic constant 7-65248
metal, structural, creep and stress relax. mechanism 7-46571
metal matrix composites, thermal residual stress 7-63848
metal sheets, rolled, US SH wave vel., ang. depend. 7-38126
metal-SiO₂-N₂-SiO₂-Si system, plasma oxynitride effect on interface charge 7-3761
metallic and compound films, mech. props., relation between different quantities 7-8041
metals, deformed, heterogeneous dislocation distrib., two-parameter description 7-44547
metals, deuteron irradi., multiple fracture planes, bubble growth 7-58372
metals, irradiated, deformation rate, impurity atmosphere effects (Russian) 7-33727
metals, irradiated, internal stress, diffusion relaxation 7-58133
metals, nonelastic deformation, modelling internal stresses 7-51924
metals, steady state creep, strain response to complete unloading 7-59568
metals, texture and internal stress determ. using ultrasonic Rayleigh waves and neutron diffraction 7-46767
monolithic fuel cell tapes, three-layer ceramic composite, stress and fracture analysis 7-3407
MOS structure, gamma irradi. effects, mech. stress depend. 7-58903
nickel phthalocyanine films, vacuum deposited, illum. at substrate and nonsubstrate surfaces, asymmetries in optical props. 7-59277
pentacene films, vacuum deposited, illum. at substrate and nonsubstrate surfaces, asymmetries in optical props. 7-59277
phase transformations in solids, plastic deformation and thermodynamic hysteresis 7-16714
plate, epoxy, subjected to rapid cooling on both surfaces, residual stress anal. 7-63007
polyacrylonitrile fibres, shrinkage, IR spectra investig. 7-59206
polyethylene, medium-density, noncontact monitoring of cyclic loading and stress relax. by US backscatter 7-59724
polyimide adhered films, solvent induced crack-like defects 7-46653
polymer crystallisation, assoc. acoustic emission due to stress release 7-44704
polyoxymethylene, ageing, residual stress, crystallinity, WAXS 7-39550
positron annihilation at the grain boundaries of polycrystals 7-46196
probing method for investig. of rules of change in stressed and strained state 7-59714
refractory metal nitride, sputtered coatings, wear and friction 7-33800
residual stress analysis, US techniques 7-65273
residual stress determination through combined use of holographic interferometry and blind-hole drilling 7-63087
residual stress meas. by speckle multiple image shearing camera 7-31720
sapphire, ion implantation, mechanical surface property modifications 7-32473
semiconductor crystals, point defect behaviour, influence of isovalent impurities as sources of elastic stresses 7-51756
shape memory alloy, intrinsic stresses evaluation by AE 7-39829
SOI films, thermal stresses during zone melting recrystallisation, sub-boundaries, in-plane orientation 7-33554
SOI technology by zone-melting recrystn. on quartz substrates 7-21736
SOS epitaxial layers, strain meas., using X-ray diff. 7-44305
stainless steel plate, thermoviscoelastic stress analysis 7-2092
steel, austenitic, martensite transform. start temp. increase in electrolytic H impregnation, internal microstresses role 7-17690
steel, austenitic stainless, residual stress meas. SEM/ASTM round robin study 7-13680
steel, C, creep, glide plane stresses, yield point, dislocation theory (Russian) 7-59580
steel, C, inverse magnetostrictive effect and electromagnetic non-destructive testing methods 7-13714
steel, Cr-Mo-V, creep crack growth at 838 K, displacement-controlled loading behaviour 7-17626
steel, Cr-Ni-Cu, welded specimens, residual stress meas. mag. induced US vel. obs. 7-46761
steel, dual phase, work hardening, accommodation strains in ferrite phase, finite element analysis 7-17550
steel, fatigue fracture surface at elevated temps., X-ray fractographic study (Japanese) 7-8098
steel, ferromag., magnetic state inspection, elastic stresses in trans-Rayleigh region 7-3558
steel, high strength structural, finishing monitoring by magnetic structure-scope based on the Barkhausen effect 7-28241
steel, HSLA, rolled sheets, residual surface stresses, corrosion pot., X-ray obs. 7-39704
steel, low alloy, B-containing, near-threshold fatigue cracks 7-46605

internal stresses continued

steel, low alloy, fatigue fracture in air and 3.5% NaCl soln., X-ray fractography (Japanese) 7-8099
steel, low alloy, retarded brittle fracture, crack nucleation stress and internal microstresses (Russian) 7-8084
steel, low C, strain ageing, internal stress, Bauschinger effect 7-39612
steel, low-alloy, H-beams, controlled rolling effect on mech. props. 7-39562
steel, martensitic transformation, residual stresses establishment 7-33657
steel, mild, crit. stress intensity factor, influences of grain size and pre-racking load 7-59607
steel, Ni-Co-Mo, maraging, ultrahigh strength, H embrittlement rel. to Ni or Cu coating 7-28137
steel, Ni-Cr-Mo, autofrettaged tubes, residual stress determ. by neutron and X-ray diff. 7-33743
steel, plain C, cold-rolled, texture and lattice deform. states (German) 7-53765
steel, pressure vessel with surface fatigue cracks, leak-before-break failures analysis 7-65141
steel, quenching, effect of martempering on thermal stress and strain 7-46532
steel, quenching stresses interaction with structural transforms. 7-22727
steel, spring, residual stress meas., effect of decarburisation, shot peening and cyclic torsion loading (German) 7-22904
steel, stainless, laser surface melted, residual stresses 7-3506
steel XC 80, pearlitic transformation in continuous cooling calc., thermal stresses contrib. (French) 7-46410
structural tension relax. in small particles 7-6708
tetracene films, vacuum deposited, illum. at substrate and nonsubstrate surfaces, asymmetries in optical props. 7-59277
thermal stress generation during quenching, effect of stress relax. rate 7-17590
thin films, during deposition, review 7-52380
two-phase solid, cyclically loaded, residual stresses 7-63010
X-ray stress measurement by use of synchrotron rad. source (Japanese) 7-8213
Ag thin film growth, in situ study by internal stress meas. 7-16890
AgX (X=Cl,Br), extruded fibres, optical and material props. 7-37184
Al, lattice sparring of interstitial solid solns. of B and C, deform. interaction, pseudopotential method (Russian) 7-58271
Al recrystallisation, cryst. boundary stresses, synchrotron X-ray topography study 7-26684
Al, relaxation process studied by positron annihilation 7-6698
Al surfaces (111) and (110), surface tensile stress tensor calcs. 7-44982
Al thin films, stress relax. mechanisms 7-21784
Al-Mg (5 at.%), creep, interpretation of internal stress determ. from dip tests 7-65091
Al₂O₃ coatings made by sol-gel process, mechanical props. 7-22867
Al₂O₃, profiled crystals, bubble distrib., cellular struct., residual stresses 7-32422
Al₂O₃, sintered, X-ray stress meas. (Japanese) 7-8169
BN, ion-plated, prep. and charact. 7-17477
C diamond-like films, stresses, energy depend. 7-45097
C fibre reinforced C, 3D, residual stress 7-52090
C fibre reinforced polymer cracks, lightweight construction appl. (German) 7-22825
a-C films, crystallisation, influence of residual stresses and density fluctuations 7-21750
C films, diamond-like, intrinsic stress, depend. on deposition parameters 7-58721
C films, transparent, sputter- and plasma-deposition 7-22474
CaF₂, fluoride residual stress fields in cylindrical Bridgeman-Stockbarger crystals 7-11976
CaF₂-BaF₂ epitaxial bilayers on Si (111), characterisation 7-12521
Cd, polycrystalline, steady-state creep, internal and effective stresses 7-38100
Co-Ni-Ti-based alloys, critical shear stress asymmetry during stretching and compression (Russian) 7-8054
CoCr evaporated films, mag. props. 7-33225
CoSi₂ films, structural analysis by X-ray diff. in the grazing Bragg-Laue geometry 7-7042
Cr evaporated and ion assisted deposited coatings, microstruct., electron microscope obs. 7-52335
Cr, low alloyed, elastobrittle failure under thermal loading stresses 7-33790
Cr, residual macrostress distrib. after cyclic heat treatment, US and X-ray study (Russian) 7-53772
Cr thin films, intrinsic stress, elasticity modulus, thermal expansion and struct. 7-16889
Cr-Ta-C, ageing, hardening processes, carbide separation and dissolving (Russian) 7-59541
CrC coatings on high speed steel, deposition process and mechanical props. 7-64011
Cu current collecting grid on Si solar cells, oxidation and spalling 7-22910
Cu, fatigue near surface indentations and pits, deform. 7-46628
Cu single crystal, deformed, lattice parameter changes through long-range internal stresses (German) 7-16673
Cu thin film growth, in situ study by internal stress meas. 7-16890
Cu-He system, closed swelling layer, internal stress distrib. (Russian) 7-59571
Cu-Zn alloy, cyclic BCC-9R martensitic transform-induced dislocations Burgess vector, electron microscopy studies 7-51775
Cu₄₈Si₅₂, amorphous, crystallisation, intermediate long period superlattice phase form. 7-21098
Fe alloys, high-temp. creep, rel. between dislocation density and internal stress 7-13524
Fe, creep, glide plane stresses, yield point, dislocation theory (Russian) 7-59580
Fe, single crystals, flow stress at 225, 250 and 273 K, orientation depend. 7-53832
Fe, surface damage, plastic deform., 4-293 K (Russian) 7-59581
Fe thin films, stress development during oxidation 7-45096
Fe-Co-Mn(V) films, ion beam sputtered, soft mag. props. 7-33237
Fe-Cr-C, martensite nucleation, dislocations, grain boundaries, plastic accommodation 7-28040
Fe-Ni(-C), martensite nucleation, dislocations, grain boundaries, plastic accommodation 7-28040
Fe-Si (3 wt.%), mag. props., influence of elastic-stress state produced by coatings 7-12990

internal stresses continued

- Fe-Si (3 wt.%), secondary recrystallisation, seed grain formation, influence of elastic anisotropy energy 7-13470
- GaAs, epitaxial film on (001) oriented Si and Ge substrates, structural props. 7-58687
- GaAs, LEC-grown wafer, EL2 conc., stress distrib., near-IR absorption mapping 7-52522
- GaAs MBE heteroepitaxial layers, lattice distortions, X-ray diffr. and Raman studies (*Japanese*) 7-27219
- GaAs, MOCVD growth on Si, band gap energy and stress 7-38368
- GaAs:Cr, meas. of residual stress by Cr-related luminesc. lines 7-7726
- GaAs:In, LEC growth, annealing, solid soln. hardening, dislocation density, elec. props. 7-17404
- GaAs-InAs strain layer modulated structures, MBE grown, cross-sectional TEM 7-7032
- GaAs-InAs superlattice, reflection electron diffraction intensity oscillation 7-7030
- GaInAsP/InP stressed heterostructure lasers, lifetimes meas. 7-5890
- GaInAsP-InP laser, anisotropic deform. influence on radiative characts., threshold, polarisation and watt-ampere charact. 7-43100
- GaInAsP-InP laser, anisotropic deform. influence on radiative characts., spectral characts. 7-43101
- GaN, X-ray phase anal., elastic props. 7-45050
- GaP MBE heteroepitaxial layers, lattice distortions, X-ray diffr. and Raman studies (*Japanese*) 7-27219
- Ge, dislocation transmission through $\Sigma=9$ symm. tilt boundaries, dynamic and crystallographic anal. 7-63647
- Ge, uniaxially stressed, internal strain parameters, surface effects 7-44980
- Ge-GeO₂, defect formation, during thermal oxidation 7-65237
- In As_{1-x}Sb_x epitaxial layers, MOCVD, strained-layer superlattices 7-39407
- InAs-GaAs superlattices grown by beam-separation MBE, surface morphology and elastic strain 7-7031
- InAs₂P_{1-x}, LEC-grown single crystals, growth defects and lattice strains 7-38001
- In_{0.49}Ga_{0.31}As-InP strained-layer effective-mass superlattices 7-7378
- InGaAsP film, defect struct. and strain anal., X-ray topography 7-52344
- InGaAsP-InP buried heterostructure lasers, internal thermal stress distrib. 7-10931
- InGaPAs/GaAs interface stress, Cr-related luminescence study 7-46101
- InP single crystals, thermal activation of glide 7-21213
- LiF:C⁺, ion implanted, impurity defects outside implantation zone 7-7773
- Mg, high purity polycryst., creep behaviour, recovery, and stress exponent determ. 7-26840
- Mg-Mn-Al-Zn, MA8, superplastic deform., effective stresses (*Russian*) 7-53811
- MgAl₂O₄ stoichiometric spinel, electron beam-induced diffusion, cracking and phase separation 7-16641
- MgF₂ films deposited on fused SiO₂ with ion beam assistance, adhesion, internal stresses 7-21749
- MgO:Fe, small angle [001] twist boundaries, Fe solute effect 7-32459
- MnO₂, crystallite size, strain, X-ray diff. study 7-2221
- Mo-Ni-Co-Sn, liq. phase sintering, grain boundary migration, coherency strain effect 7-22604
- Mo(100), pulsed laser irradiated, use of LEED for surface damage charact. 7-21592
- NaCl whisker crystals, strength, depend. on dislocation struct. 7-45101
- Nb epitaxial film (110), elastic strain generation and relax. (*Russian*) 7-16916
- NbC_{0.97}, single cryst., mechanical stresses, thermo-EMF 7-21944
- Ni binary alloys, solid soln. hardening, flow stress, Young's modulus 7-13465
- Ni, magnetic biaxial anisotropy induced by plastic deformation 7-59006
- Ni-Cu diffusion contact, mass transfer at grain boundaries in fields of diffusion-concentration stresses 7-2272
- Ni-Fe-In ternary Permalloy electroplated films, mag. props. and thermal stability 7-33236
- Ni₃Al, solid soln. hardening with ternary additions, Young's modulus 7-13464
- NiSn-SiC composite coatings, electrodeposition, wear resist., hardness, porosity 7-33613
- PZT, shock-recovery expts. 7-38119
- Pt, sputtered film, microstruct., thickness effect studied by X-ray diffr. method 7-21756
- Si, dislocation transmission through $\Sigma=9$ symm. tilt boundaries, dynamic and crystallographic anal. 7-63647
- Si, epitaxial growth using dual heating, slip dislocations and radial temp. gradient 7-38366
- Si, heteroepitaxial film, on Ge, Al-Mg spinel and sapphire substrates, resonance Raman scattering 7-64017
- Si, ion implanted, mech. stresses, laser interferometer studies 7-6657
- Si, low temp. oxidation studies, internal stress 7-33864
- Si, microarea stress study by microprobe Raman spectroscopy 7-63708
- Si, oxidation 7-65227
- Si oxidation models calcs., oxide thickness time depend. and stress effects 7-22916
- Si, selectively epitaxial, origin of lattice defects 7-32881
- Si, twinning partial dislocations, velocity 7-63629
- Si, twinning partial dislocations, effective stresses, anal. 7-63630
- Si, uniaxially stressed, internal strain parameters, surface effects 7-44980
- Si:B, ion implanted, strain profile, double cryst. X-ray rocking curve simulation 7-2060
- a-Si:H films, annealing, compressive stress, H evolution 7-28059
- a-Si:H films, light-induced defects and internal stresses 7-12751
- a-Si:H sputtered films, intrinsic stress, H effects 7-7078
- SiO, dendritic web growth, plastic flow, O effects 7-16471
- Si/Si_{0.5}Ge_{0.5} strained layer superlattices, 2D electron systems 7-7380
- Si/SiO₂/TiSi_x(WSi_x) MOS capacitors, radiation-induced interface traps 7-58897
- Si-SiO₂ interface roughness, evolution, characterisation 7-32852
- SiC whisker or particle reinforced Al composites, deform. thermal expansion, strengthening mechanisms 7-3373
- Si₃N₄ ceramics, hot pressed, fatigue test with Knoop indentation, residual stress effects (*Japanese*) 7-17640
- a-Si₃N₄:H films, plasma enhanced CVD, chemical and mech. props. 7-38420
- Si₃N₄/ferritic stainless steel, joining with soft metal interlayers, tensile strength 7-28266

internal stresses continued

- Si₃N₄-SiC film, hybrid material prepared by plasma CVD, microhardness and internal stress 7-13616
- SiO₂ evaporated and ion assisted deposited coatings, microstruct., electron microscope obs. 7-52335
- SiO₂ film on Si produced by thermal oxidation 7-65228
- SiO₂ films, LPCVD from diacetoxyditertiarybutoxysilane in temp. range 450 to 600°C 7-53622
- SiO₂ films on Si produced by surface oxidation, stresses and defects 7-65230
- SiO₂-GeO₂ optical fibre surfaces, formation mechanism, of H-associated defect centre 7-65158
- SiO₂-P₂O₅ glass films, deposited by different CVD methods, phys. props. 7-27220
- SiO₂N₂ films, plasma-enhanced CVD growth 7-22514
- SmCo₅ fine particles, produced by ball milling, strain and domain wall energy (*Japanese*) 7-7556
- TaH_{0.07}, lattice location of H by channeling method 7-1975
- Ta₂O₅ evaporated and ion assisted deposited coatings, microstruct., electron microscope obs. 7-52335
- TbCo, amorphous sputtered films, mag. props., film struct., comp., internal stress meas. (*Japanese*) 7-7570
- (Ti,Cr)B₂ sintered electrode exposed to liq. Al, degradation, effect of segregated Cr 7-28045
- Ti alloy, heat cycling regimes and effects 7-8028
- Ti-Cu-Ti thin films, reaction kinetics, stress, and microstruct. 7-21764
- Ti(C,N) films on steel substrates, residual stress 7-52373
- TiC coatings on high speed steel, deposition process and mechanical props. 7-64011
- TiC_{0.98}, single cryst., mechanical stresses, thermo-EMF 7-21944
- TiN coatings, internal stress and adherence 7-52374
- TiN films, RF ion plating, residual stress, bias voltage effect (*Japanese*) 7-16917
- TiN films as diffusion barriers in high temp. metallisation (*Japanese*) 7-46319
- TiN ion plated films, tempering effects 7-59461
- Ti_{1-x}Nb_xCo_{0.5}N_{0.5} solid solns., prod. factors influence on struct. parameters of variable comp. phases 7-7940
- TiO₂ evaporated and ion assisted deposited coatings, microstruct., electron microscope obs. 7-52335
- TiO₂ films, pulse laser irradiated, Raman studies of phase transformations 7-12569
- V epitaxial film (110), elastic strain generation and relax. (*Russian*) 7-16916
- W CVD films, high temp. stress meas. 7-58718
- W film deposition by photolytic dissociation, charact. 7-17466
- W films, magnetron sputtering prep., elec. and mech. props. 7-16913
- W LPCVD film struct., IC appls. 7-58692
- W-Re, damage mechanisms, cold brittleness, dislocation motion (*Russian*) 7-59619
- WC coatings on high speed steel, deposition process and mechanical props. 7-64011
- WC-Co, TiN-coated, residual stress and strength, X-ray diffr. study (*Japanese*) 7-8101
- WC-Co sintered carbides, X-ray diffr. obs. of microstruct. after hardening, optimum heat treatment cycle 7-65063
- WSi₂ CVD films, high temp. stress meas. 7-58718
- (YSmLuGd)₃(FeGa)₅O₁₂ garnet film struct. and mag. props., mag. bubble memory appls. (*Japanese*) 7-7575
- ZnSe/GaAs:Cr heterostructure, interface stress 7-38352
- ZnSe-GaAs:Cr, meas. of residual stress by Cr-related luminesc. lines 7-7726
- ZnSe-ZnTe strained-layer superlattices, lattice strain and lattice dynamics 7-58654
- ZrC_{0.95}, single cryst., mechanical stresses, thermo-EMF 7-21944
- ZrO₂ (partially stabilised)/steel system, solid state bonding with Ti interlayer 7-28264
- ZrO₂ films, pulse laser irradiated, Raman studies of phase transformations 7-12569
- ZrO₂ transform. toughened ceramics, fracture toughness rel. to transform. temp. 7-46614

internuclear double resonance *see* INDORinterpenetrating networks *see* polymer blends

interplanetary magnetic fields

- B_z-component orientation, relation to longit. elec. currents in ionosphere cusp region 7-4261
- B_z component, effect on ionospheric polar plasma convection and auroral emissions 7-34777
- B_z-component, relation to plasma concentration vars. in main ionospheric trough during mag. storm 7-34780
- By-component, effect on north-south asymmetry of geomag. activity 7-9336
- P/Comet Halley (1982i), coma mag. field characts., Vega obs. (*Russian*) 7-4381
- P/Comet Halley (1982i), magnetic field free cavity form. 7-60606
- P/Comet Halley (1982i), Pioneer Venus obs. during inferior conjunction 7-18382
- comet plasma-solar wind interaction, laboratory simulation expt. 7-9434
- corotating interaction region determ. method, using solar wind velocity data 7-55402
- cosmic rays transport parameters, implications of diurnal anisotropy long-term vars. 7-66408
- Earth magnetosheath, MHD turbulence obs. 7-34786
- flare-generated shock waves, mag. cloud chamber effects rel. to He-enriched plasma cloud 7-4282
- fluctuations in 3×10^{-4} to 10^{-2} Hz range 7-40662
- general solution for field produced from stationary solar sources 7-55411
- geomagnetic indices rel. to interplanetary parameters (1966-75) (*Chinese*) 7-18336
- heliosphere magnetic fields 7-4428
- loop structure behind travelling shock event, props. 7-60501
- magnetosphere interaction, generation and propag. mechanisms of low-latit. mag. pulsations 7-55370
- magnetosphere interaction, interplanetary magnetic field effects on solar wind plasma entry 7-29370
- magnetosphere interaction, limits on energy transfer through dayside merging 7-47636
- magnetosphere interaction, mag. field magnitude rel. to low latit. geomag. pulsations 7-55371

interplanetary magnetic fields continued

- magnetosphere interaction, Prindahl-Spanglev hypotheses definitive test 7-14420
- magnetotail reconnection, effect of external elec. field 7-9323
- March 1979 solar wind conditions, interplanetary scintillation observations 7-23963
- MHD turbulence in Comet Halley environment, relation to energetic particles obs. 7-14529
- nonrelativistic particles propagation, generalised Compton-Getting transformation 7-34810
- quasi-parallel interplanetary shocks, mag. field structs. 7-9353
- sector structure, relation to magnetosheath energetic electron fluxes during geomag. disturbances 7-4273
- sector structure effects on winter ionosphere 7-40664
- solar energetic particles scattering, implications of pitch angle distrib. for mag. field fluctuations model 7-55392
- solar flare region magnetic field rel. to IMF B_z at 1 AU 7-55404
- solar wind, compound stream formation, effects on solar energetic particles and galactic cosmic rays 7-47656
- solar wind, directional discontinuities (0.46 to 1.0 AU) 7-9351
- solar wind, effect on plasma sheet 7-14419
- solar wind, field annihilation region and assoc. galactic cosmic rays intensity enhancement 7-23960
- solar wind, field effect on high-latitude ionosphere 7-14421
- solar wind, ion accel. through drift and diffusion at interplanetary shocks 7-47658
- solar wind, mag. and elec. fields meas. near Periodic Comet Halley (1982i) 7-14522
- solar wind, merged interaction regions, coalescence between 6.2 and 9.5 AU 7-47657
- solar wind, shocks fine struct., BIFRAM plasma spectrometer meas. 7-55405
- solar wind, velocity variations around Hale type sector boundaries 7-47662
- solar wind anisotropy, effect on cosmic ray var. (*Japanese*) 7-40658
- solar wind characteristics at 1 AU rel. to Hale sector boundaries 7-47661
- solar wind characts. (*Italian*) 7-60622
- solar wind cosmic ray aspects 7-35124
- solar wind effects on winter north polar currents 7-60450
- solar wind field characts. (book) 7-48216
- solar wind field conditions and Pc 3-4 energy densities 7-60493
- solar wind field merging with geomag. field 7-47633
- solar wind interactions, conf., Toulouse, France (1986 June-July) 7-55873
- solar wind interactions, review (*Russian*) 7-40663
- solar wind magnetic clouds influence on cosmic ray intensity var. 7-23959
- solar wind perturbation in foreshock 7-9322
- solar wind props., correl. with Jupiter MF and HF emission 7-4362
- solar wind shocks, subcritical and supercritical, mag. field and energetic particle obs. 7-34820
- solar wind-comet interactions 7-9437
- solar wind-magnetosphere interaction, implications for 1972 August 4 mag. storm 7-29364
- solar probes for solar wind and magnetic field structure examination 7-47663
- tangential discontinuities of solar wind and Kelvin-Helmholtz instability 7-55403
- three-dimensional heliospheric current sheet struct., solar cycle variations 7-55401
- weak magnetic fields meas. in diffuse media, appl. of reson. scatt. spectra 7-23991

interplanetary matter

- see also interplanetary magnetic fields*
- circumsolar dust, interferometric obs. of F-corona radial vel. field between 3 and 7 solar radii 7-66535
- P/Comet Giacobina-Zinner (1984e), origin of metal ions in cometary coma 7-9415
- P/Comet Halley (1982i) environment, wave and plasma meas. on Vega-1 and Vega-2 spacecraft 7-14524
- P/Comet Halley (1982i) plasma tail, electron density irregularities from radio source scintillation obs. 7-66516
- cometary dust, coma morphology and dust emission pattern modelling for P/Halley (1982i) 7-14526
- cometary dust grains from P/Halley (1982i), results from Vega-1 secondary electron currents meas. 7-14521
- cometary ions in environment of P/Halley (1982i), obs. at and within cometopause region 7-14530
- cometary plasma tails and tail rays, stability anal. 7-24076
- compositional model rel. to interstellar grains 7-60596
- conductor motion through magnetoplasma, assoc. Alfvén wings struct. 7-23989
- dust, refractory minerals comp. 7-34823
- dust grains, scatt. phase function determ. from blue light survey of gegenschein 7-24065
- dust particles, solar flare track densities rel. to asteroidal or cometary source for zodiacal dust cloud 7-55531
- Earth bow shock, electrostatic potential jump determ. from solar wind ion components meas. 7-34821
- Earth magnetosheath, MHD turbulence obs. 7-34786
- electric fields, E_y -vars. rel. to ionospheric plasma concentration vars. in main ionospheric trough 7-34780
- energetic particles in environment of Periodic Comet Halley (1982i), Giotto obs. 7-14529
- flare-associated interplanetary shock-wave, 3D morphology 7-18343
- flare-generated shock waves, mag. cloud chamber effects rel. to He-enriched plasma cloud 7-4282
- Giotto spacecraft, charging effects in cometary environment of P/Halley (1982i) 7-14473
- heliosphere gas, heating and frictional drag due to solar wind 7-14471
- icy grains, optical consts. of H_2O-NH_3 ice mixtures 7-23993
- interstellar neutral atoms (H and He) 7-47654
- magnetosheath, characts. of energetic electron fluxes during enhanced geomag. activity 7-4273
- magnetosphere interaction, contrib. of solar wind to low-latit. geomag. pulsations 7-55371
- magnetosphere interaction, generation and propag. mechanisms of low-latit. mag. pulsations 7-55370

interplanetary matter continued

- micro-organisms, heat exposure expt. rel. to entry into planetary atmosphere 7-9275
- nonrelativistic particles propagation, generalised Compton-Getting transformation 7-34810
- particle interaction with Alfvén solitons, contrib. to proton heating 7-66418
- plasma wave events assoc. with type III radio bursts, ISEE-3 obs. rel. to electron speeds determ. 7-66533
- resonant scattering rel. to far-UV diffuse background, Voyager 2 obs. for NGP 7-60839
- shock waves from solar wind rel. waves, relation to cometary flares 7-4371
- solar cosmic rays propagation, Monte Carlo calcs. for interplanetary propag. of relativistic protons 7-66405
- solar energetic particles propag., local scatt. props. of interplanetary medium from particle pitch angle distrib. 7-55392
- solar wind, Helios obs. rel. to generation and propag. of Type III radio bursts 7-47801
- solar wind-magnetosphere interaction, interplanetary magnetic field effects on plasma exchange 7-29370
- type III radio bursts, implications of 169 MHz obs. of solar type III burst sources 7-66562
- zodiacal dust, IR and visible obs. anal. 7-47762
- zodiacal dust cloud, relation to nature of cometary nuclei 7-34936
- zodiacal dust cloud structure, comparative study of 3D models 7-55532

interplanetary medium *see interplanetary matter***interpolation**

- see also function approximation*
- 2D viscous flows, time-dependent, incompressible, finite element anal. 7-26165
- atmosphere, press. and temp. vertical profiles reconstruction by interpolation methods 7-34730
- automatic interpolation methods for mapping piezometric surfaces, appl. to groundwater reservoirs 7-40574
- eigenvalue interpolation, integration scheme 7-32894
- elastoplastic problems at finite strain, FEM solution 7-43694
- electric field computation, finite-element and boundary-element methods combined (*Chinese*) 7-10822
- equal order velocity-pressure formulation 7-16142
- eyepiece, two-component, design and correction, calc. process 7-25921
- hyperbolic conservation law approx., nonoscillatory shock capturing methods 7-26318
- image processing, resolution and robustness, regularization principle 7-42968
- magnetic field computation, C^1 quadratic interpolant 7-50445
- mandibular kinesiographic meas., distorted, signal restoration 7-47149
- monofrequency laser interferometer with fine resolution 7-18753
- panel method based on special interpolation functions for flow anal. 7-14780
- pixel-selected ray-tracing for image generation (*Japanese*) 7-57264
- plates, laminated composite, 3D hybrid stress isoparametric element 7-56020
- scanning electron microscopy, online digital recording system 7-4933
- sea bed contour map construction from random data, iterative method 7-34725
- sea bed contour map construction from random data, spline method 7-34726
- sea bed contour map construction from random data, spline method 7-34728
- sea bed contour map construction from random data by interpolation 7-34727
- semiclassical scattering, curve crossing, interpolation procedure for numerical adiabatic pot. 7-24458
- statistical interpolation by means of successive corrections for meteorological data, statistical interpolation by means of successive corrections 7-47519
- water level computation between high and low tides, FORTRAN program 7-55077
- Hg electrode-soln. interface, 2-anion simultaneous adsorpt., elec. double laser parameters algorithm 7-54132

interstellar dust *see cosmic dust***interstellar magnetic fields***see also interstellar matter*

- 0133+476, 0235+164, 1749+096, 2131-021, variable quasars, mag. field directions from multifreq. polarisation obs. 7-40955
- Barnard 335, dense mol. cloud, mag. field characts. and polarimetric anal. 7-14625
- 3C 273, quasar, particle accel. and mag. field strength in jet hotspot 7-14676
- Cas A, mag. field enhancements model for compact nonthermal radio knots 7-66691
- Faraday rotation meas. on 163 pulsars 7-66648
- G7.7-3.7, highly-polarised radio supernova remnant, mag. field directions from polarisation obs. 7-48045
- galactic centre region, prominent polarised plumes and their mag. field, linear polarisation obs. 7-14656
- galactic field struct. 7-40963
- galactic nuclei, bipolar jets prod by turbulent Alfvén waves 7-60523
- Galactic wind and termination shock, accel. and transport of ultra-high-energy cosmic rays 7-66403
- general aspects (book) 7-48216
- Heiles Cloud 2, magnetic field structure from K-band polarimetry 7-60762
- IC 443, supernova remnant, mag. fields from multiwavelength investigation 7-40896
- LDN 723, dense mol. cloud, mag. field characts., polarimetric anal. 7-14625
- M51, spiral mag. field config., visible polarimetric obs. 7-60800
- M87 halo, mag. field strength from Compton model for X-ray emission 7-66752
- molecular clouds, effects of oblique mag. fields on MHD shocks propag. 7-66454
- Mon R2 star form. region, IR sources and polarisation obs. 7-60753
- NGC 1068, Seyfert galaxy, mag. field strength from radio struct. in inner 1 arcsecond 7-48068
- paramagnetic grain alignment associated with internal friction and the polarization efficiency 7-48053
- radio galaxies, role of magnetic energy dissipation in force-free jets 7-29391

interstellar magnetic fields continued

- Sco X-1, lobe characts. determ., VLA obs. 7-60721
- small-scale variations in galactic mag. field, rot. measure vars. across extragalactic radio sources 7-29524
- SN 1006 remnant, mag. field characts. 7-35025
- transverse magnetic fields, time-depend. plasma interaction 7-60527
- weak magnetic fields meas. in diffuse media, appl. of reson. scatt. spectra 7-23991

interstellar matter

see also H I regions; H II regions; interstellar magnetic fields; interstellar molecules; nebulae

- 217 nm band, catalogue of equivalent widths 7-66479
- 220 nm extinction feature, charge transfer model 7-55787
- 220 nm extinction feature, interpretation 7-48018
- 443-nm diffuse absorption band, equivalent width obs. 7-24187
- abundances of S and Zn in high density sight-lines 7-66730
- accretion onto pulsars, implications for activation 7-66645
- active galactic nuclei, dense gas clouds characts. 7-66770
- active galactic nuclei, narrow emission line region O III 500.7 nm forbidden line 7-40933
- active galaxies, matter inflow to nucleus triggered by companion galaxies 7-55788
- amorphous C submicron grains, extinction spectra in UV-visible range 7-35023
- anomalous interstellar dust in open cluster Trumpler 37, evidence from UV extinction curves 7-48010
- B5, interstellar dark cloud, evidence for large dust grains 7-9529
- Barnard 335, dense mol. cloud, mag. field characts. and polarimetric anal. 7-14625
- Barnard 62, Bok globule, optical and IR evidence for star form. 7-9527
- bipolar molecular outflows, nature of collimating mechanism 7-40816
- bipolar sources formation in dense mol. clouds, isotropic wind collimation models 7-24182
- broad-line clouds in active galactic nuclei, computational methods for emission-line spectrum 7-9534
- broad-line clouds in active galactic nuclei, emission spectrum of low-ionisation lines 7-9535
- bubbles, wind driven, soft X-ray spectra 7-4545
- bubbles structure and evolution is multiphase interstellar medium, physical model 7-60764
- cataclysmic binary stars, interstellar absorpt. rel. to observational selection in magnitude-limited sample 7-29479
- in CD-type galaxies, equilb. of gas in galaxy gravit. field 7-24204
- chemical characts. 7-40900
- chemical composition and molecular abundances of molecular clouds 7-14635
- chemical evolution, He and heavy-element enrichment of interstellar medium 7-40905
- chemical evolution models construction techniques 7-40721
- chemistry of interstellar clouds, dynamical perspective 7-24194
- cloud-cloud collisions, contrib. to high-mass stars formation 7-55610
- clouds, chem. processes and submm astronomy 7-48060
- clouds collisions, contrib. to damping of spiral density waves in galaxies 7-66755
- Clump 1, unusual mol. cloud complex near galactic centre, ^{12}CO and ^{13}CO obs. 7-48044
- EZ CMa (HD 50896), UV spectrum and interstellar environment 7-18422
- cold clouds, CO radio-line profiles interpretation 7-4544
- cold dark clouds, C_2H_2 $2_{20}-2_{11}$ absorpt. line obs. 7-66716
- cold dust grains, sub-millimetre emission from galactic disk ($l=150^\circ$ to $l=82^\circ$) 7-4558
- collapsing gas clouds, cosmic ray accel. 7-55390
- collimated outflows in interstellar mol. clouds, model for Herbig-Haro objects (HH 7-11) 7-55775
- comets in Oort Cloud, impact by interstellar grains and debris formation 7-40783
- compact blue dwarf galaxies, dust content 7-48078
- compact galactic H II regions, extinction and reddening anal. 7-60747
- complex molecule production in dense interstellar clouds 7-14640
- compositional model based on interplanetary dust and ordinary chondrites 7-60596
- Conference on nebulae and abundances, Austin, TX, USA (April 1986) 7-35096
- cooling flows in normal elliptical and S0 galaxies, contrib. to related radio and X-ray props. 7-66753
- cooling gas, column densities and UV lines of highly ionized atoms 7-23992
- Cygnus superbubble characts. 7-66776
- cold dark clouds, chemical model 7-24195
- dark globules in Cep OB2 association, CO obs. of radial globule systems 7-24172
- dark globules radial systems 7-4536
- dark matter in the Universe 7-60851
- dark matter nature 7-60658
- dense molecular cloud cores, formyl radical and formyl ion obs. 7-48064
- dense molecular clouds, elemental abundances, influence of initial conditions 7-35029
- dense molecular clouds, ion-molecule calc. of CCD/CCH abundance ratio 7-66712
- dense molecular clouds, upper limits to the PO abundances 7-66713
- diffuse absorption features, charge transfer model 7-55787
- diffuse clouds, chemical reactions 7-14641
- diffuse collisionally ionised C IV and Si IV below $Z=1$ kpc, evidence from IUE obs. 7-55783
- diffuse galactic 380 μm emission 7-48090
- diffuse interstellar bands, C molecules as possible carriers 7-48020
- diffuse interstellar bands, constraints on dust grain hypothesis 7-55762
- diffuse interstellar bands in LMC, obs. at 637.6 and 637.9 nm. 7-55758
- diffuse interstellar lines, astrophysical influences on line strengths 7-48021
- disk galaxies, gas flow simulation, tilts and corrugation waves evol. 7-60806
- in disk galaxies, phenomena arising from nonstationary central black hole 7-60795
- dispersion measure of pulsar PSR 0809+74, determ. from decametric wavelength obs. (Russian) 7-55697
- DR-21 molecular cloud, density struct. from HC_3N $J=4-3$ line obs. (Russian) 7-55777
- dust, light extinction and polarisation 7-40888

interstellar matter continued

- dust, review (Russian) 7-40899
- dust, submm characts. 7-48059
- dust grain models, comparison with obs. 7-48013
- dust grains, appl. of EXAFS studies 7-24185
- dust grains, SiC and amorphous C, laboratory expts. 7-47699
- dust grains composition, IR signatures of refractory grain processing in circumstellar shells 7-55611
- dust in dense regions of interstellar matter, Jena workshop, Georgenthal, DDR (March 1986) Jena workshop, Georgenthal 7-40981
- dust-mol. excitation interaction in submm astronomy 7-47698
- early-type galaxies, gas characts. determ. from X-ray meas. 7-55799
- in early-type galaxies, prevalence of cooling flows from interstellar gas density profiles 7-14664
- early-type galaxies with emission lines, central region ionised gas 7-60578
- electron density of local interstellar medium, Voyager heliospheric shock obs. (Russian) 7-14634
- elliptical galaxies, self-regulated cooling flows and low-mass star form. 7-66741
- elliptical galaxies, wind model, chem. and photometric props. 7-66733
- enrichment by mass losing stars 7-47842
- expanding H I supershells around OB associations, nature 7-4527
- extinction curve, very broad struct. profile 7-14645
- galactic 511 keV line and positronium beams 7-62547
- galactic centre, nonthermal radio emission from continuum arc 7-55844
- galactic corona, IUE obs. rel. to kinematics, ionisation, and abundances 7-48054
- galactic disk, evidence for local chemical inhomogeneities from classical Cepheids 7-34997
- in galactic disks, tidal perturbations rel. to triggering of Seyfert galaxies and quasars 7-9537
- galactic Faraday rotation, arc-minute scale var. 7-35038
- galactic halo, search for million degree gas through [Fe X] 637.5 nm absorpt. 7-55758
- galactic halo and disk, mass constraints on objects constituting missing mass 7-14650
- galactic halo gas properties, form. of C IV and Si IV ions 7-24171
- galactic IR absorption var. with latitude 7-48089
- galactic nucleus explosion and hot interstellar matter effects on galactic ridge X-ray emission 7-40962
- galactic ridge radio recombination lines, origin from H272 α lines survey 7-66718
- in galactic spiral arms, vertical vel. struct. rel. to energetics of vel. active regions 7-24220
- galactic warped disks, haloes and gravity 7-66744
- galactic wind, role in cosmic rays origin and accel. 7-55390
- Galactic wind and termination shock, accel. and transport of ultra-high-energy cosmic rays 7-66403
- galactic winds, contrib. to radio trails bending 7-35045
- galaxies active nuclei, distrib. function description of cloud props. 7-29535
- gamma-ray line emission, constraint on origin of mass 22 nuclei in astro-physical environments 7-35069
- gas, isotope fractionation chemistry 7-14641
- gas clouds orbits in galactic bulges, cloud stability anal. 7-66707
- gas flow in spiral galaxies: effects of rotation, thermal processes, and self-gravitation 7-29531
- gas-phase chemistry in dense clouds, complex molecule synthesis 7-18444
- gas-phase depletions, relations to dust polarisation parameters 7-48015
- giant molecular clouds, dynamical effects of encounters with wide binaries in solar neighbourhood 7-66663
- giant molecular clouds, star form. model 7-29525
- giant molecular clouds in galaxies, N-body simulation of random vel. generation and accel. 7-18445
- grains in Cyg X-3 halo, observational props. X-ray scattering effects 7-47977
- graphite spheres (C_{60} structure), effect of cavities and mantles on UV extinction peak 7-4546
- Hd 144941, H-deficient star, UV spectroscopy rel. to peculiar interstellar reddening 7-47887
- high-latitude molecular clouds, distances and extinctions 7-35022
- high-temperature plasma in Orion Nebula, detect. of intense 6.7-keV Fe X-ray emission line 7-55780
- high-velocity clouds, collisions with galactic disks 7-48065
- high-velocity clouds, search for dust, IR emission search 7-48093
- high-velocity gas detect. towards WR star HD 50896, possible SNR 7-14627
- hot molecular cloud cores, torsionally-excited methanol obs. 7-48005
- IC 2944 stellar aggregate as apparent conc. of stars, reddening characts. 7-14617
- IC 443, supernova remnant, interaction with multiphase interstellar medium 7-40896
- IC 4499, globular cluster, reddening and distance 7-14616
- in intervening galaxy towards QSO B2 1225+317, high-resolution spectroscopy of $z=1.79$ absorpt. line system 7-66782
- ion molecule reactions in interstellar molecular clouds 7-13765
- ion-molecule reactions at low temperatures 7-13764
- ionised gas towards galactic centre, constraints from low-freq. radio recomb. lines 7-66719
- IR spectroscopy 7-14638
- IRAS galaxies, total gas masses from sub-millimetre obs. 7-9532
- IRAS low-temp. unidentified print sources, ^{13}CO and ^{12}CO obs. 7-48006
- IRAS sources in mol. clouds, search for H_2O masers 7-35066
- isolated T Tau stars, form. from very small interstellar clouds with almost no residuals 7-47869
- isothermal spherical gas clouds, condensation, similarity solns. 7-35028
- Jeans collapse in a turbulent medium 7-60752
- L134 dark cloud, search for interstellar CH abundance vars. 7-66701
- L1551, extended far-IR emission obs. assoc. with mass outflow from young star (IRS 5) 7-66715
- L1551 IRS 5, IR polarimetry of nearby refl. nebula 7-24186
- L1551 molecular cloud, VLA obs. of 4.8 GHz H_2CO transition 7-60765
- L183, cold dark cloud, chemical model 7-24195
- large-amplitude wave in gas disk, stationary periodic wave theory 7-23987
- LDN 1551, bipolar nebula IR emission characts. 7-48061
- LDN 1642, high-latitude cloud, IRAS mapping, visible surface brightness and extinction 7-48062
- LDN 723, dense mol. cloud, mag. field characts., polarimetric anal. 7-14625

interstellar matter continued

- light nuclide production from interstellar matter-cosmic ray interactions 7-47836
- LMC, average interstellar UV extinction curve 7-35042
- in LMC, kinematics of H I gas and old long-period variable stars 7-55605
- LMC search for million degree gas through [Fe X] 637.5 nm absorpt. 7-55758
- Local Group Sb and Sbc galaxies, physical and star form. props., H I obs. 7-60809
- local interstellar medium, evidence for C IV and Si IV from IUE obs. of late B-type stars 7-60771
- local interstellar medium, limits on 'local fluff' from IUE Mg I data 7-55782
- local interstellar medium, multi-component vel. struct. 7-35018
- local interstellar medium processes from UV space astronomy, symposium, Toulouse, France (June-July 1986) 7-48132
- Lupus dark clouds complex, CO obs. rel. to low-mass stars form. 7-29523
- Lynds 1457, nearest mol. cloud, discovery of assoc. hard X-ray source (H0253+193) 7-66789
- Lynds 810, large interstellar globule, distance determ. rel. to membership of Vul OB1 complex 7-24178
- M16, star-forming complex, obs. of giant stellar wind shell assoc. with H I region 7-18446
- M17SSW, molecular cloud, CO submm mapping 7-60748
- M17 molecular cloud, density struct. from HC₃N J=4-3 line obs. (*Russian*) 7-55777
- M17 molecular cloud, vel. struct. anal., CO mapping 7-60745
- M17 SW molecular cloud, submillimetre molecular spectroscopy with Texas MWO radio telescope 7-55763
- M31, interstellar H I holes and supernova rate 7-35036
- in M31, M33, UV interstellar extinction from IUE obs. of massive stars 7-47881
- in M31 nucleus, near-UV obs. with ESA Photon Counting Detector 7-4562
- in M81, global spiral struct. and nonthermal emission 7-55798
- M82, interstellar medium in central 1 kpc of active galaxy 7-55816
- M87, X-ray emission obs. from hot halo gas 7-66752
- Magellanic H I bridge, 160 pc shell feature characts. 7-35049
- Markarian 3, Seyfert 2 galaxy, dust in emission-line gas 7-66746
- MHD shock waves in interstellar mol. clouds, theory for oblique mag. fields for oblique mag. fields 7-66454
- MHD turbulence and density fluctuation in interplanetary and interstellar space 7-60529
- MKN 739, multiple nucleus galaxy, interstellar characts. and obs. 7-55790
- mm and sub-mm spectroscopy 7-14644
- molecular astrophysics, NATO conf., Bad Windsheim, Germany (1984 July) 7-9589
- molecular chemical evolution, role of dust grains 7-48014
- molecular cloud cores, candidate solar-type protostars from IRAS survey 7-47853
- molecular clouds, Cherenkov microwave emission-line mechanism (*Chinese*) 7-66690
- molecular clouds, nonequilib. excitation of rot. levels of cyanoacetylene 7-60743
- molecular clouds, possible connection with optical H II regions 7-40887
- molecular clouds, shock waves, theoretical models 7-14643
- molecular clouds, sub-mm astronomy and astrophysics 7-14637
- molecular clouds, submillimetre spectral lines obs. in very dense regions 7-66711
- molecular clouds form. in galaxies with different Z, opacity-driven fragmentation of diffuse clouds 7-40908
- molecular clouds fragmentation, implications of mass-radius-vel. dispersion relations 7-55753
- molecular clouds in outer Galaxy, far-IR characts. and star form. 7-66709
- molecular clouds towards Cas A, VLA obs. of 1667 MHz OH absorpt. 7-55761
- molecular gas mass in Galaxy, review 7-9530
- molecular J-type shocks as initial value problem 7-60761
- molecules, radio observations, review 7-14636
- molecules, visible and UV studies/1980-4 7-14639
- in nearby galaxies, studies using background QSOs as probes 7-18461
- nearby gas, IUE and optical spectral meas. 7-66729
- nearby molecular clouds, proceedings, Toulouse, France (September 1984) 7-24299
- neutral atoms (H and He), elastic collisions with solar wind protons inside heliosphere 7-47654
- neutral gas shell surrounding H II region, dynamical evolution 7-66692
- in NGC 1566, barred spiral galaxy, extinction maps from imaging spectroscopy of spiral arm 7-24214
- NGC 1960, open cluster, interstellar extinction 7-4532
- NGC 2539, open cluster, interstellar reddening and distance 7-29521
- NGC 3448, amorphous galaxy, photometry and H I dynamics 7-35041
- in NGC 4594, mass distrib. 7-40914
- NGC 6357 molecular cloud, IR obs. rel. to star form. 7-48009
- NGC 7039, northern open cluster, evidence for variable reddening from Stromgren and H β photometry 7-66687
- OB supergiant stars, polarisation characts., interstellar contrib. 7-47845
- observational physics and astrophysics, book 7-55916
- observations and models review 7-66725
- OMC-1, NH₃ line emission, search for linear polarisation 7-48011
- OMC-1, submillimetre molecular spectroscopy with Texas MWO radio telescope 7-55763
- optically thick dust, effect of intervening galaxies on quasar counts and colors 7-55847
- FU Ori stars, effects on interstellar medium 7-66580
- Orion Association, absorpt. anal. 7-55477
- Orion bright bar and the associated shocks (*Japanese*) 7-4543
- Orion IRC 2, vibr. excited cyanoacetylene obs. 7-48063
- Orion Molecular Cloud 2, IR refl. nebulae obs. 7-55765
- Orion region, extinction and dust characts. 7-66728
- Orion-KL region, maps of high-vel. CO outflow 7-29522
- Palomar-Westerbork survey of northern spiral galaxies 7-40724
- paramagnetic grain alignment associated with internal friction and the polarization efficiency 7-48053
- Per A, cool gas content, CO and H I obs. 7-60774
- Pleiades, interstellar dust grains IRAS obs. 7-48003
- polarization standard stars, position angle wavelength dependence 7-9473

interstellar matter continued

- polycyclic aromatic hydrocarbons, possible visible luminesc. from Red Rectangle (HD 44179) 7-48008
- Population III, heating of dust and radiative spectrum (*Chinese*) 7-66680
- protostar formation regions, submm astronomy with FIRST 7-47890
- pulsars, dispersion measures determ. 7-66646
- pulsars, multiple imaging by refl. in interstellar medium 7-40856
- QSOs, emission line profiles from Keplerian cloud ensembles 7-4586
- quasars, effects of reddening on broad line region energetics 7-9553
- radiative shocks, dynamical models and line spectra of steady shocks 7-55454
- radio aspects (book) 7-55914
- radio wave propagation, refractive and diffractive scatt. effects 7-55759
- radiowave refraction, meas. with Quasat-Earth based VLBI system 7-60576
- RCW 103, young supernova remnant, obs. of expanding shells in filamentary edge of remnant 7-14632
- reflection nebulae, CCD surface photometry of bright nebulae 7-55773
- refractive interstellar scintillation, obs. in quasar (1741-038) 7-55845
- refractive interstellar scintillation of radio sources 7-66777
- S140 IRS molecular cloud, obs. of bipolar outflow assoc. with S140 (IRS 1) 7-66710
- S235B region, mol. line obs. of young stellar object 7-24188
- scintillation, use for meas. of pulsar space vel. 7-60698
- Sco X-1, reddening and distance 7-60708
- in Seyfert galaxy nuclei, near-UV spectroscopy rel. to reddening and Bowen fluoresc. 7-55801
- Sgr A West region, ionised gas dynamics and comp. 7-40935
- Sgr B2, vibr. excited cyanoacetylene obs. 7-48063
- Sh2-235, mol. cloud-ionised emission nebula interface modelling, C recomb. lines obs. anal. 7-48012
- in Shapley-Ames elliptical galaxies, interstellar dust content from IRAS obs. 7-66758
- shells around elliptical galaxies, tests for mass distrib. and 3-D shape 7-9536
- shock waves, limits of validity of isothermal approximation 7-60742
- shocked gas chemistry 7-14642
- small spherical non-gravitationally bound cool clouds, condensation 7-60751
- small-scale interstellar dust distrib. towards NGC 2516 open cluster 7-35043
- SN 1987A in LMC, line of sight interstellar spectral features 7-66629
- SN 1987A in LMC, line-of-sight interstellar-intergalactic material 7-66632
- SN 1987A in LMC, vel. systems of interstellar absorpt. lines 7-66637
- solar neighbourhood, extinction distrib. 7-18443
- solar wind interaction review (*Russian*) 7-40663
- solar wind interaction with interstellar neutral H, three-fluid model 7-9354
- South Galactic Pole and Magellanic Stream, dust and H I distrib. 7-66721
- spherical grains, polarization, props., light scattering. 7-14631
- spiral galaxies, star form characts., far-IR lumin. and CO line obs. anal. 7-4563
- spiral galaxies, very small dust particles and IR emission characts. 7-24209
- star formation regions, far IR, submm and mm dust emission spectra 7-24180
- sub-millimetre/far-IR emission from warm and cold dust clouds, observational review 7-48022
- submm obs. 7-48058
- Sun interactions, effect on Earth climate 7-4547
- superbubbles, evolution through sequential supernova explosions in plane-stratified gas distrib. 7-55778
- supernova shock wave propag. into interstellar medium 7-4537
- Taurus dark clouds region, photometric study of flare stars 7-24136
- terminal velocities, determ. of inner galactic rot. curve shape 7-35050
- time-dependent chemistry in dense mol. clouds, interstellar grain surface reactions 7-24179
- TMC-1, cold dark cloud, chemical model 7-24195
- TMC-1, density struct. from HC₃N J=4-3 line obs. (*Russian*) 7-55777
- Trifid reflection nebulae, dust grain characts. 7-35024
- turbulence, small-scale mag. field vars. from rot. measure vars. across extragalactic radio sources 7-29524
- 4U 1907+09, X-ray binary pulsar, interstellar reddening determ. for optical counterpart 7-18440
- unipolar bubbles in star-forming regions 7-55770
- Ursa Major I(S) group galaxies, far-IR obs. rel. to dust and H II regions heating 7-29548
- UV absorption lines, equivalent width data: statistics and new oscillator strengths for Si II, Fe II and Mn II 7-55444
- UV absorption lines towards A0 V star HD 119921, C IV and Si IV lines obs. 7-48057
- UV extinction curves shapes, IUE anal. of 2175 Å bump 7-48039
- UV extinction curves towards OB associations, statistical anal. of IUE obs. 7-55785
- UV extinctions towards OB associations and star-forming regions, IUE obs. 7-55786
- Vela Star Cloud, foreground reddening struct., photometry obs. 7-35015
- velocity gradients perpendicular to the galactic plane in the solar vicinity 7-60755
- very broad-band extinction structure, obs. by combined uvby and UVB photometry 7-48019
- very local gas, ionisation characts. 7-14628
- very local interstellar medium, IUE study 7-66727
- Vir A, cool gas content, CO and H I obs. 7-60774
- in Virgo cluster spiral galaxies, orbital motion rel. to interstellar gas stripping 7-24230
- S Vul cluster (C 1947+272), UVB photometry rel. to reddening, distance and age 7-14620
- W3 molecular cloud complex, dust clouds distrib. from stellar colour excesses 7-48004
- W51 IRS 2, star-forming region, NH₃ maser and thermal emission obs. 7-66702
- W51A, vibr. excited cyanoacetylene obs. 7-48063
- Wolf-Rayet stars, extinction anal. 7-66624
- Wolf-Rayet stars winds effects, implications of revised mass loss rates 7-29480
- X-ray emission from a galactic ridge, contrib. from supernova remnants 7-24221
- ²⁶Al, gamma-ray line emissivity from Wolf-Rayet star prod. 7-47830

interstellar matter continued

- ²⁶Al in the interstellar medium, review 7-48050
²⁶Al near galactic centre, common origin for gamma-ray lines at 0.51 and 1.81 MeV 7-24238
 C abundance, determ. toward ρ Oph and β^1 Sco. 7-9531
 C I, 809 GHz fine-structure line obs. in dense mol. clouds 7-66717
 D chemistry within broad model 7-35030
 H dust particles, quasi-2D quantum electron states 7-17066
 H I bubble around O7 star (HD 91824) in Carina region, prod. by stellar wind of O-type star 7-60760
 H I bubble related to HD 88500, WC star 7-40808
 H I content of lenticular and early-type galaxies, comparison between field and Virgo cluster samples 7-4559
 H I in halo and LMC 7-60768
 H I layer in edge-on dwarf galaxy NGC 5023, thickness determ. from synthesis obs. 7-24208
 H I Lyman alpha absorption, correction for effects on observed stellar Lyman alpha profiles 7-60637
 H I small-scale structure and soft X-ray background 7-55769
 H I spectral characts. of galaxy pairs and small groups 7-14669
 H I survey of Southern Milky Way, 21-cm obs. 7-40894
 H₂ line emission from centre of Galaxy, spatial distrib. and vel. field 7-9528
 Li differential depletion in diffuse interstellar clouds 7-66706
 Mg II absorption lines, influence on stellar chromospheric Mg II emission lines 7-47840
²⁶Mg fossil anomaly rel. to excess in meteorites 7-48036
 Na I line strength versus reddening relation, influence on stellar population synthesis 7-9526
 OH clouds vel., use for Sun-galactic centre distance determ. 7-4554
 OH IIa sources, nonthermal emission lines (*Chinese*) 7-66690

interstellar molecules

- B335, Bok globule, cyanoacetylene obs. 7-18448
 bipolar molecular outflows, nature of collimating mechanism 7-40816
 bipolar outflow from young star L1551 IRS 5, extended far-IR emission obs. 7-66715
 charge transfer reactions, contrib. to diffuse interstellar bands 7-55787
 chemical evolution of molecules, role of dust grains 7-48014
 chemical processes and submm astronomy 7-48060
 cyanoacetylene, nonequilibrium excitation of rot. levels 7-60743
 cyanoacetylene, vibr. excited, detect. in star form. regions 7-48063
 cyanopolyacetylene, rot. const., MINDO/3 calcs. 7-60770
 cyclopropenylidene, ¹³C-substituted, $2_{12}-1_{01}$ transition obs. 7-55768
 cyclopropenylidene, detection of ¹³C isotopes 7-40891
 cyclopropenylidene, deuterated, TMC-1 detection at 19.4 GHz 7-55772
 cyclopropenylidene (C₃H₂), $2_{20}-2_{11}$ absorpt. line obs. in cold dark clouds 7-66716
 cyclopropenylidene-d, detect. and implications 7-66693
 diffuse bands in reddened OB stars, molecular origins 7-66697
 Far Infrared Submillimetre Space Telescope mission 7-34866
 formaldehyde, protonated, rot. const., ab initio MO calcs. 7-25349
 formaldehyde, VLA maps of line absorpt. towards NGC 2024 H II region 7-48041
 formaldehyde (H₂CO) in L1551 mol. cloud, VLA obs. of 4.8 GHz transition 7-60765
 formyl ion, dissociative recombination of interstellar ion, electronic struct. calc. 7-20064
 formyl radical and cation in dense molecular cloud cores 7-48064
 G24.6+0.0 (Scutum ring), obs. of ring of H II regions assoc. with CO and H I shells 7-18447
 G34.3+0.2, compact H II region, NH₃ obs. of warm molecular core 7-24173
 galactic centre, mol. obs. with University of Cologne 3 m telescope at Gornegrat Observatory 7-60557
 galactic centre neutral disk, CO and CS obs. 7-35040
 giant molecular clouds, search 7-4539
 ion+molecule reaction rates at low temp. 7-23006
 ion-polar neutral reactions, dense interstellar cloud chemical models 7-48032
 IRAS sources in mol. clouds, search for H₂O masers 7-35066
 isoformyl cation, difference freq. laser IR spectroscopy 7-62366
 J-type shocks as initial value problem 7-60761
 large interstellar molecules, thermal props., absorpt. bands, and chemical stability 7-24189
 LDN 1641, second mol. cloud core discovery, EHF obs., HCN and H₂ mapping 7-14622
 M31, NE spiral arm mol. complex, CO mapping 7-66734
 maser source involving H₂O and cold dust, theoretical study 7-24197
 methane ion+H₂→CH₃⁺+H, ion reaction at interstellar cloud conditions 7-23008
 methanol, torsionally excited, in hot mol. cloud cores, centimetre-wave lines obs. 7-48005
 methanol-¹³C, laboratory microwave spectrum, Ori A identification 7-57053
 methyl cyanide in Orion hot core, excitation, 1.3 mm obs. 7-60758
 methyl ion+H₂→CH₃⁺+h ν , rate coeffs. rel. to role of electronic transitions in radiative assoc. processes 7-66714
 methyliidene (CH), rotationally excited interstellar molecule in direction of W51 H II region 7-24193
 methyliidene ion+H, ion reaction at interstellar cloud conditions 7-23008
 mm wave spectra of molecules 7-24196
 molecule study method, by laboratory photofragment spectroscopy 7-24017
 N-mer growth model, geometrical cross-section 7-48016
 NGC 2071, refl. nebula, nearby bipolar flow source NH₃ obs. 7-24181
 NGC 7023, outflow source, CO mapping 7-60772
 observations with Cologne University 3-m radio telescope 7-24004
 OMC-1, obs. of P(2,1) line of H₂O⁺ 7-9524
 Ori A, monitoring obs. of SiO maser emission at 7 mm wavelength (1977 to 1979) 7-4449
 Orion KL, NH₂D detect. and abundance 7-60754
 Orion Molecular Cloud 1, IR polarisation obs. and discovery of H₂ refl. nebula 7-14633
 outflow sources, NH₃ obs. anal. 7-66576
 pentynylidyne radical (C₅H), in interstellar space, hyperfine struct. obs. 7-60749
 Perseus dark clouds, visual extinction and CO emission 7-14623
 Perseus globules, physical and chem. conditions, NH₃ and cyanoacetylene obs. 7-35021
 photoionization by UV and X-ray radiation 7-24001

interstellar molecules continued

- polycyclic aromatic hydrocarbon cations, doubly-charged, form. and destruction, IR and visible spectra 7-55774
 polyynes and related species 7-48031
 production by MHD shocks in diffuse interstellar clouds 7-48034
 radioastronomical spectra (book) 7-35140
 S235B region, mol. line obs. of young stellar object 7-24188
 Schmidt law for the molecular gas profiles of disk galaxies 7-55814
 Sgr B2, obs. of P(2,1) line of H₂O⁺ 7-9524
 Sharpless 252, assoc. dust and gas, UVRI polarimetry and molecular line obs. 7-48023
 submillimetre spectral lines obs. in very dense regions, results from Cs, H₂CO and HCN 7-66711
 submillimetre astronomy, conf., Segovia, Spain (June 1986) 7-41013
 submillimetre molecular spectroscopy with Texas MWO radio telescope, results from OMC-1 and M17 SW mol. clouds 7-55763
 submm transitions, characts. 7-47698
 Taurus Molecular Cloud-1, observations of pentynylidyne radical hyperfine struct. 7-60749
 urea, rot. transition, appl. to interstellar studies 7-10559
 e⁺e⁻ annihilation in interstellar H₂ gas, laboratory simulation 7-14426
 C₂, (3,0) Phillips band detect. towards ζ Oph 7-48043
 C₂, molecular rotational excitation processes 7-24198
 C₃, C₃, C₃, possible carriers of diffuse interstellar bands 7-48020
 CCD/CCH abundance ratio in dense interstellar clouds, ion-molecule calc. 7-66712
 CH, search for abundance vars. towards L134 dark cloud 7-66701
 CH⁺, interstellar mol., high resol. laser photofragment spectra 7-31063
 CH₃⁺+H→methane ion+H₂, ion reaction at interstellar cloud conditions 7-23008
 CNH₂⁺, laboratory generation, mass spectra 7-46811
 CO, absorpt. lines obs. in IR spectrum of M8 E 7-48040
 CO absorption line towards M82, obs. rel. to large mol. halo or intergalactic mol. gas 7-24223
 CO, bipolar mol. outflow obs. assoc. with S140 (IRS 1) 7-66710
 CO in Arp 220, the molecular gas, mm interferometry of galaxy nucleus 7-55815
 CO in barred spiral galaxy NGC 5383, J=1-0 transition obs. 7-55827
 CO in interacting and isolated galaxies, star formation efficiency rel. to molecular content 7-55812
 CO in Seyfert galaxies, spatial distrib. and central source 7-55808
 CO in Virgo Cluster spiral galaxies 7-55800
 CO, isotopic species, B¹²C⁺-X¹²C⁺ transition, vacuum UV obs. 7-62401
 CO, J=1-0 emission detect. in Seyfert galaxy/QSO (Markarian 231) 7-66757
 CO, J=2-1 obs. of three southern star form. regions 7-18441
 CO line formation in bipolar flows, line profiles in accelerated outflows 7-48042
 CO measurements with submm heterodyne spectrometer 7-60562
 CO, obs. in Clump 1, unusual mol. cloud complex near galactic centre 7-48044
 CO, obs. in dark clouds in Lupus 7-29523
 CO, obs. of high-vel. outflow in Orion-KL region 7-29522
 CO, obs. of radial systems of dark globules in Cep OB2 association 7-24172
 CO peak in nearby mol. cloud Lynds 1457, discovery of assoc. hard X-ray source (H0253+193) 7-66789
 CO survey of molecular clouds, implications for high-mass stars formation due to cloud-cloud collisions 7-55610
 CO towards quasar PHL 61, EHF obs. (*Russian*) 7-40957
 CO⁺+H, ion reaction at interstellar cloud conditions 7-23008
 CS⁺, upper limits in diffuse interstellar clouds 7-35020
¹²CO, A=12,13, in mol. clouds, detect. with submillimetre heterodyne spectrometer 7-353
¹²CO (A = 12, 13), obs. in unidentified cold IRAS print sources 7-48006
¹²CO, obs. in Ursa Major I(S) group galaxies 7-29548
¹²CO in dwarf irregular galaxies, search for J=1-0 emission in twelve objects 7-35033
 DCO⁺+H→HCO⁺+D, ion reaction at interstellar cloud conditions 7-23008
 H₂, 2 mm emission in star-forming clouds, S(1) line mapping rel. to shock waves and jets 7-55760
 H₂, form. on amorphous silicate grains 7-24184
 H₂ formation in molecular clouds, implications of mass-radius-vel. dispersion relations 7-55753
 H₂+H, collision-induced dissociation at interstellar densities 7-55448
 HCN/HNC abundance ratio vars. in Orion molecular cloud 7-48033
 HC₃N, J=4-3 line obs. in TMC-1, DR-21 and M17 rel. to mol. clouds struct. (*Russian*) 7-55777
 H₂NC⁺, interstellar mol., pot. energy surfaces, ab initio MO theory 7-19687
 HN₂O⁺, millimetre-wave spectrum and mol. const. 7-29387
 H₂O, 1.35-cm line obs. using acousto-optical spectrometer on RATAN-600 radio telescope 7-66463
 H₂O masers in nearby galaxies, luminosities and line profiles 7-14661
 H₂O⁺, obs. in interstellar medium and Periodic Comet Halley (1982i) 7-9524
 He⁺+H₂, ion-molecule reaction rate at low-temp. conditions of interstellar space 7-23007
 methanol, protonated, rot. const., ab initio MO calcs. 7-25349
 NH₃, hot emission, obs. towards H₂O masers near W3(OH) 7-9525
 NH₃ in OMC-1 and Orion Nebula, line emission, search for linear polarisation 7-48011
 NH₃ inversion line obs., molecular cloud kinetic temps. 7-66700
 NH₃, maser and thermal emission obs. toward star-forming region (W51 IRS 2) 7-66702
 NH₃⁺+H₂, ion-molecule reaction rate at low-temp. conditions of interstellar space 7-23007
 N₂H⁺+H₂, ion-molecule reaction rate at low-temp. conditions of interstellar space 7-23007
 O⁺+H→H⁺+O, ion reaction at interstellar cloud conditions 7-23008
 OH absorption in extragalactic sources, Arcetri survey 7-40895
 OH, laboratory meas. of rot. spectrum with tunable far-IR radiation 7-47691
 OH maser emission from galaxies IR 1017+08 and Zw 475.056, 1667 MHz obs. 7-29539
 OH, obs. of highly excited states towards galactic H II regions 7-24177
 OH, photodissociation processes in astrophysical environment 7-23042
 OH radical, Cherenkov microwave line emission mechanism for mol. clouds spectra (*Chinese*) 7-66690

interstellar molecules continued

- PO abundances in dense molecular clouds, upper limits from microwave obs. 7-66713
S compounds chemistry in mol. shocks 7-48048

interstitials

- see also Cottrell atmospheres; crowdions; Snoek effect
2D diffusion kinetics, influence of point defects 7-38263
alkali halide crystals, self-trapped exciton recomb. luminesc.-recomb. induced F-centre form. anticorrel. calcs. 7-13201
alloys, interstitial, order-order transitions (Russian) 7-39502
atom motion and lattice dynamics, quantum mechanical model 7-58528
close-packed crystals, imperfect, self-diffusion of impurities, thermally-activated change in mechanism (Russian) 7-58523
diamond, interstitial H or muonium, Hartree-Fock analysis 7-32947
diamond, normal muonium, lattice relax. calcs. 7-51789
diamond, type IIa, ion implanted, volume expansion 7-58298
diamond-like structure semiconductors vibrational spectra of interstitials (Chinese) 7-32592
diffusion, isotope effect, quasi-harmonic calcs., appl. to CoO and NiO 7-26996
diffusion and trapping, Monte Carlo simulations 7-32720
diffusion and trapping, Monte Carlo simulations 7-32721
diffusion in crystals, quantum theory 7-44916
electron irradi.-induced trap defects, DLTS study 7-12155
FCC pure metals, neutron irradiated, thermal stability of cascade defects, annealing expt. 7-51856
(Fe_{1-x}Ni)₉₂C₈ pseudobinary FCC alloys, magnetic phase diagram studies 7-2844
ferromagnetic materials, defect and microstructural analyses using TEM 7-37817
fusion material, irradiation, model for interstitial dislocation loop nucleation and growth kinetics 7-51817
fusion reactor materials, neutron irradi., defect struct. 7-51844
graphite, dynamic simulation of interstitial atom, self-energy and migration energy calcs. 7-2014
Group VII hydrides, high-pressure. cryst. struct. 7-21183
interstitial alloy vol. and phase diagram, order-order transition, conc. depend. calcs. (Russian) 7-32640
irradiated metals, isochronal annealing PAC monitored defect reactions anal. 7-44623
L1₂ ordered alloys, grain boundary strength and fracture, electronic and struct. studies 7-33756
Laves phases, and struct. rel. cpds., interstitial site occupancy of H atoms 7-16549
light interstitial quantum diffusion rate, strongly coupled vibr. 7-52106
metal-H systems, bonding, statistical thermodynamic aspects 7-21472
metallic glasses-H₂, mechanical relaxation behavior 7-26859
metals, hot oxidation, solute-elastic effect in interstitial solid solns. (French) 7-58478
metals, irradiated, creep mechanisms, dislocation climb and slip 7-12194
metals, irradiated, deformation, impurity atmosphere effects (Russian) 7-59569
metals, light interstitial motion, recent expts. 7-52114
metals, light particle quantum tunnelling and diffusion 7-52113
metals, point defects in thermal equilibrium, laser interferometry-neutron diff. studies 7-58274
metals, radiation swelling, vacancy-interstitial and interstitial-impurity complex form. (Russian) 7-58309
mobile interstitial atom-substitutional impurity complex form. (Russian) 7-12372
muon polarisation function and spin dynamics 7-53188
phase diagram of interstitial alloys with nonequivalent positioning of interstitial atoms (Russian) 7-38163
point defect absorption by dislocations, preference parameter temp. depend. (Russian) 7-16607
quartz, H₂ diffusional uptake and hydrolytic weakening 7-40469
solid solution, two-component, joint diffusion 7-58520
solid solution alloys, FCC and BCC lattice structs., H diffusion models 7-21532
solid solution ordering types, rel. between symm. and combinatorial methods 7-6790
solid solutions, ordering, stress-induced interactions 7-39508
solid solutions, precipitate growth under irradiation, theory 7-12296
steel, austenitic, martensite transform. start temp. increase in electrolytic H impregnation, internal microstresses role 7-17690
steel, austenitic stainless, elastic moduli at 4 K, C and N effects 7-46541
steel, austenitic stainless, strain ageing and load relax. behaviour at room temp. 7-28092
steel, Cr, ferritic, neutron irradi., isochronal annealing, elec. resist. recovery 7-58348
steel, Cr-Ni high-temp. type, N and heat treatment effect on struct. and mech. props. 7-33688
steel, pressure vessel, neutron irradi., defect microstruct., SANS and TEM studies 7-58351
steel, stainless, neutron irradiated, defect clusters, positron annihilation lifetime meas. 7-51853
steel, stainless, neutron irradiation effects on mech. props., damage and yield stress 7-51865
surfaces and interfaces, electronic states, multiple-scatt. treatment 7-45420
thermal nitridation in NH₃, atomic transport mechanisms 7-8201
transition metal impurities, interstitial, enhanced mobilities and reactivities 7-17769
transition metal oxides, impurity and defect electron struct., self-consistent local density theory 7-45208
transition metals, impurity and defect electron struct., self-consistent local density theory 7-45208
tribochemistry, chemical reaction increase by friction 7-46868
void nucleation, in ternary solid soln. of vacancies, interstitial atoms and gas, self-consistent model 7-44525
Zircaloy-2, irradi. growth under temp. cycling, solute-interstitial complex mechanism 7-44607
Ag, proton and ion irradi., self-interstitial atom interactions with defect clusters, elec. resist. meas. 7-58384
AgCl, electronic struct. of intrinsic interstitial defects 7-21852
Al (110), Ar ion damage production, mol. dynamics simulation 7-58378
Al, lattice sparing of interstitial solid solns. of B and C, deform. interaction, pseudopotential method (Russian) 7-58271
Al, nuclear quadrupole interactions in the presence of muons 7-53192
Al_xGa_{1-x}As, Ga interstitial identification by ODMR 7-33302

interstitials continued

- AlH₃, isolated H impurity vibr. spectrum, isotope depend. (Russian) 7-16703
AlZn dilute alloys, electron irradiation induced interstitial defects, EXAFS study 7-63661
Au, cascade overlap effect on defect struct. after repeated neutron irradiation 7-51859
Au, defect development from displacement cascade damage in low temp. neutron irradiation 7-51851
BaO-B₂O₃-Al₂O₃, aluminoborate glass, X-irrad., optical and thermal bleaching 7-45820
Bi, electronic structure, effect of ion implantation 7-45143
Bi, rhombohedral, lattice relax. and muon⁺ sites 7-53190
Bi₂Ni, α -irrad. and H implanted, elec. resist. and superconducting T_c 7-7202
CdS, electron beam irradiated, red flash-like luminescent centres, annealing 7-7740
Co-Cr surgical implant alloy, mech. props., effects of N additions 7-59573
Cu, cascade overlap effect on defect struct. after repeated neutron irradiation 7-51859
Cu, defect development from displacement cascade damage in low temp. neutron irradiation 7-51851
Cu, nuclear quadrupole interactions in the presence of muons 7-53192
Cu, pion decay site spectroscopy, interstitial sites 7-53191
Cu-Zn alloys, electron irradiation, interstitial cluster form., diffusion rates, resistivity 7-2013
Cu₃Au, irradiation disordering and reordering by fusion neutrons, electrical resistivity meas. 7-51864
Fe and alloys, molten, N solubility, statistical thermodynamics 7-52060
Fe, Armco, annealed and cold worked, neutron irradi. damage 7-2067
Fe based eutectic alloy powder, plasma coatings with interstitial phases, tribotechnical props. 7-17731
 α -Fe, dislocation pair jog, energy characts., mol. dynamics method anal. (Russian) 7-32440
 α -Fe, edge dislocation, zones of spontaneous absorpt. of point defects 7-44599
 α -Fe, electron irradiated, residual resistivity recovery and mag. after-effect 7-27570
Fe, neutron irradiated, defect clusters, positron annihilation lifetime meas. 7-51853
Fe, neutron irradiation effects on mech. props., damage and yield stress 7-51865
Fe, pure, diffusion of H, dislocation trapping, interstitial impurities effect (Japanese) 7-52140
Fe:He(C), distribution and migration of interstitial impurities in the field of a screw dislocation core 7-6669
Fe-Al (40 at.%), electron irradi., Huang scatt. from interstitials 7-58272
Fe-base alloys, interstitial impurity-dislocation binding energy (Russian) 7-58310
Fe-Cr, neutron irradiated, defect clusters, positron annihilation lifetime meas. 7-51853
Fe-Cr-Ni alloys, FCC, dilation by interstitial C and N 7-44451
Fe-Cu, neutron irradi., defect microstruct., SANS and TEM studies 7-58351
Fe₈₄B₁₆ amorphous alloy, interstitial element segregation during fracture (Russian) 7-53875
FeH_x cleavage strength, tight-binding model calcs., interstitial solute effects 7-59538
FeO, wustite, defect agglomeration at high temps., elec. conduction model 7-21197
Fe_{0.93}O, wustite, defect arrangement at high temps. 7-21196
Fe₂O₃- α hematite, O activity depend., high temp. Mossbauer spectra 7-38978
GaAs-GaAs:Cr(Te), VPE grown, photoluminescence study, effect of substrate doping 7-27771
Ge, ionisation-stimulated annealing of Frenkel pairs under electron or gamma irradiation 7-38061
n-InP:Zn, Zn diffusion 7-63882
InP:Zn(Cd), interstitial-substitutional diffusion, doping effects 7-6878
KBr microcrystalline powders, interstitial cluster stability 7-32485
LaNi₅, diffusion of H and D, temp. depend. 7-6874
LaNi_{4.5}AlH_x and LaNi_{4.5}Al_{0.5}H_x, dynamical disorder of H, quasi-elastic neutron scatt. study 7-21535
LaNi₅H₂O, dissociation press., O content depend. 7-63825
LaNi_{4.5}MH_x (M=Mn, Cu), dynamical disorder of H, quasi-elastic neutron scatt. study 7-21535
LiCl:Fe²⁺, X-ray irradi., EPR spin Hamiltonian parameters 7-45808
MgO(Al₂O₃)_n, electron beam irradi., point defect aggregation, screw dislocation climb 7-63662
Mo-BN sputtered films, anisotropic lattice strain and grain orientation 7-12516
Mo-N polycrystalline films, implanted, single defects, X-ray diff. data anal. 7-38372
NaCl:Co, doped and undoped, thermoluminescence and X-ray fluorescence spectra 7-22356
NaCl:Eu²⁺ crystals, γ -irradiated, colourability 7-12062
Nb, interstitial N, O, H, D, Zwischenreflex scattering 7-51766
Nb, interstitial point defects, diffuse neutron and X-ray scatt. studies 7-51765
Nb, neutron irradiated, effect of irradiation temp. and O impurity on yield strength 7-58344
Nb-Hf-Ta-O dilute alloy system, O-induced nonaxially symmetric elec. field gradient, TDPAC meas. 7-12686
Nb-Li alloys, interstitial impurity distrib., thermodynamic anal. (Russian) 7-32430
Nb-N polycrystalline films, implanted, single defects, X-ray diff. data anal. 7-38372
Nb-Ti-H(D), anomalous anelastic relax., statistical model 7-28065
Nb-Ti-H(D) alloys, anomalous anelastic relax., statistical model anal. 7-8036
Nb-Ti-O alloy, struct. state obs. by internal friction, oxide precip. (French) 7-13494
NbH_x, interstitial H total cross-section determ., localised modes and diffusion, neutron transmission meas. 7-12061
Ni defect development from displacement cascade damage in low temp. neutron irradiation 7-51851
Ni, dislocation-impurity C interstitial interaction, computer simulation studies 7-2046
Ni, nucleation and growth of He platelets, computer simulation 7-58269
Ni, single and multiple defect props., mol. dynamics simulations 7-12060

interstitials continued

- Ni-C, C-vacancy binding 7-44601
 Ni-He, electronic state or interstitial He atoms, MO calcs. of model clusters 7-16969
 Ni₃Al, thermal and elec. cond., temp. and comp. depends. 7-64200
 NiO, diffusion processes down coincident tilt boundaries 7-38253
 Pb-Sn-G solid solns., elec. transport props. and defect form. studies (French) 7-33017
 Pd-B-H dilute solutions, statistical mechanics 7-21669
 Pd-Y-H ternary solid soln., H diffusivity 7-63866
 Pd₂CeH_x, H solubility in ordered/disordered Pd alloys 7-21473
 PdH_{0.74} single cryst., local H arrangement around muons, μ SR studies 7-51788
 Pd₃MH_x (M=Fe, Mn), H solubility in: ordered/disordered Pd alloys 7-21473
 Pd₃Si formation, dopant redistrib. in Si substrate 7-21255
 Sc₂Cl₆B(N) infinite chain phases, single cryst. struct. studies 7-32385
 Sc₂Cl₂B(N) metal-metal bonded cluster phases, single cryst. struct. studies 7-32385
 ScH₃(D_{3h}), H diffusion 7-52117
 Sc₂S₃, solid, elec. cond. (Japanese) 7-33002
 Si, crystal growth, impurity effect on formation of microdefects 7-32340
 Si, Czochralski growth, relax. in point defects system 7-16468
 Si, defect reactions and atomic diffusion 7-38264
 Si, diffusion modelling, point defect interactions 7-32715
 Si, dopant diffusion under thermal nitridation conditions 7-32716
 Si float zone wafers, interstitial form. during thermal oxidation, effect of HCl 7-39789
 Si, Fourier transform photoluminescence analysis 7-53412
 Si, heavily doped crystals, behaviour of O and dopants 7-32483
 Si, impurity gettering, defect-defect interaction mechanisms 7-16585
 Si, interstitial-based intrinsic gettering process appl. to multilevel defects structs. 7-38048
 Si, ion implantation, interstitial trapping, dopant migration and epitaxial regrowth 7-12103
 Si, ionisation-stimulated annealing of Frenkel pairs under electron or gamma irradiation 7-38061
 Si, normal muonium, location and hyperfine props., Hartree-Fock cluster calcs. 7-52539
 Si, oxidation, stresses and defects 7-65230
 Si, oxidation, surface layer defect formation 7-46733
 Si, oxidation, transport processes 7-65233
 Si, radiation defect thermal ionisation, effect of dislocations on activation energy 7-6680
 Si, rapid thermal annealing of ion implanted layers, role of trapped interstitials 7-17568
 Si, self-diffusion and impurity diffusion, review 7-32713
 Si shallow p-n junctions, reactive ion etching damage, defects and leakage current studies 7-27411
 Si single crystals, dislocation-free, nature of microdefects 7-44528
 Si, thermal oxidation, growth of very thin films 7-33850
 Si, thermal oxidation, point defect kinetics modelling 7-13673
 Si:¹¹¹Cd, hyperfine interactions, temp. depend., gamma-ray spectra studies 7-64553
 Si:As, ion implantation-induced defects 7-32433
 Si:As, precipitation and cluster form., elec. resist., backscatt. and TEM studies (Chinese) 7-12285
 Si:Au, U- and W-shaped impurity diffusion profiles investigation 7-16805
 Si:B, amorphisation by ion implantation 7-38080
 Si:B, O, heavily doped, O precipitation, diffuse X-ray scatt. studies 7-32669
 Si:B, Fe, EBIC and DLTS meas., comparisons 7-7265
 Si:B(P)(As)(Sb), retarded and enhanced dopant diffusion related to implantation-induced excess vacancies and interstitials 7-63881
 Si:C, O, solubility, segregation, diffusion and precipitation 7-16777
 Si:C(C,P), C diffusion during annealing and P in-diffusion 7-16812
 Si:Fe, interstitial Fe, spin delocalisation 7-13059
 Si:Fe, interstitial impurity, superhyperfine interaction and spin-lattice relax. 7-53178
 Si:Fe,O, Fe intrinsic gettering, EPR studies 7-16553
 Si:H(Ne)(Ar), ground state one-electron energies, SCF MS X_α calcs. 7-44582
 Si:N, deep level generation and annihilation 7-16612
 Si:O, C, precipitation, microstructures, TEM studies 7-32668
 Si:O, conf., Boston, MA, USA (Dec. 1985) 7-14711
 Si:O, Czochralski grown, O-related defects after annealing, IR TEM and resistivity meas. 7-32466
 Si:O, diffusivity and diffusion mechanism of O 7-16810
 Si:O, IR absorption meas. of interstitial O conc., calibration 7-33401
 Si:O, O precipitation sintering, shaping, and shrinking, precursor oxide phase roles 7-16772
 Si:O, O precipitation, numerical models 7-16775
 Si:O, O precipitation ad thermal donors 7-16767
 Si:O, positron annihilation study 7-3105
 Si:O, precipitation kinetics, interstitial diffusion 7-44837
 Si:O, self-interstitial migration, dislocation loops and elongated Frank dipoles 7-58300
 Si:O, vacancy-enhanced O diffusion 7-16811
 Si:O,C,N, precipitation phenomena, TEM studies 7-16768
 n-Si:P,C, electron-irradiated and injection-annealed, vacancies, dislocations and C interstitials 7-51815
 Si-Al, P, defect struct. and dynamics 7-16552
 SiO₂, dopant diffusion under thermal nitridation conditions 7-32716
 TaT₂, evolution of lattice spacing and damage 7-16582
 β -TbH(D)_{1.9+x}, defect study 7-37971
 (Th,U)O₂ reactor fuel, irradiation induced interstitials and vacancies 7-5331
 Ti-Al-Nb (6.2 wt.%), fusion weld, defect regions, cracking, porosity, interstitials analysis 7-28109
 Ti-Mo alloy, ordering, effect of interstitial trace elements (Russian) 7-37928
 Ti₄H₂He, interatomic bond rel. to He saturation (Russian) 7-38022
 Ti₆₀Ni₄₀Au₂, martensite, interstitial H-induced extra reflection, TEM and electron diffr. study 7-59521
 UO_{2+x}, pure and cation doped, elec. conductivity, O potentials, defect structures 7-12718
 UO_{2+x}, stoichiometry, thermodynamic analysis of point defects, 600-1400°C 7-16550
 V-H(D), elastic shear consts., temp. depend., effect of H and D 7-63711
 VB, 14 MeV neutron irradi., TEM dislocation obs. 7-56819

interstitials continued

- VD_x, force dipole tensor and elastic consts., diffuse X-ray scatt. obs. 7-26831
 VH₂, cleavage strength, tight-binding model calcs., interstitial solute effects 7-59538
 V₂Si, muon diffusion and localisation, transverse field muon spin resonance studies 7-53194
 Y₂O₃, DC cond. as function of water vap. press. 7-45317
 Y₂O₃, elec. cond. as function of O₂ partial press. in wet and dry atm. 7-45405
 Zn, neutron irradiated, yield-stress recovery 7-22720
 Zr, neutron irradiated, solute effects on damage production and recovery 7-51861
 Zr-Ti (Sn)(Dy)(Au), neutron irradiated, solute effects on damage production and recovery 7-51861
 Zr-Ti(Sn)(Au), low temp. damage prod. and recovery after fusion neutron irradiation 7-51862
 ZrF₄-BaF₂-LaF₃-AlF₃-LiF glass, X-ray radiation damage, EPR studies 7-21278
 ZrTi, ZrTi_{1.6}, ageing, TEM study 7-51773
- intersystem crossing** see nonradiative transitions
intra-molecular rotation see rotational isomerism
intramolecular forces see atomic forces
intramolecular mechanics see atomic forces
intramolecular potentials see potential energy functions
intramolecular rotation see rotational isomerism
intramolecular vibrations see molecular vibration; molecular vibration in solids
intrinsic magnetisation see spontaneous magnetisation
intrusion detectors see safety systems
- Invar**
 FTIR spectrometer sample cell, Invar, thermal calibration 7-41507
 surface, Fe oxide coatings, IR emission, absorpt. modes effect 7-27708
 Co-Fe-Ni-V alloys, Invar props. and mag. field distrib. (Russian) 7-45733
 Fe-Ni (36 at.%), Invar, oxidation, effect of annealing conditions 7-28167
 Fe-Ni Invar, high-field hysteresis and ferromag.-antiferromag. coexistence 7-22122
 Fe-Pt Invar alloys, premartensitic transform., local structural change, EXAFS study 7-63556
 Fe-Pt Invar disordered alloys, premartensitic transform., mag. anomalies 7-7495
 Fe₆₅Ni₃₅, paramagnetic spin fluctuations 7-52937
 Fe₃Pt, paramag. phase, inelastic neutron scatt. meas. 7-27493
- inverse photoemission spectroscopy**
 adsorbates on metals, struct. of inverse photoemission spectra, model Hamiltonian study 7-33478
 atoms, Z=6 to 92, bremsstrahlung double differential cross section, photon energy depend. 7-42569
 graphite, electronic band struct., unoccupied, angle-resolved inverse photoemission study 7-64725
 heavy-fermion metals, isochromat spectroscopy data interpretation, periodic Anderson model 7-7087
 intermediate-valence system, fluctuations and photoemission props. calc. in tetrahedral-cluster model 7-39354
 metal surfaces, inverse photoemission studies, review 7-59279
 polarised electrons in surface physics, book 7-29607
 pyrazine, adsorbed on Ag (111), affinity level, EELS, inverse and direct photoemission spectra studies 7-52724
 semiconductors, cryst. and amorphous, and heterojunctions, electronic struct. using bremsstrahlung isochromat spectroscopy 7-52795
 solid surfaces, chemistry and physics, book 7-60891
 solid surfaces, ferromagnetic and nonmagnetic, spin-dependent electron scatt., photoemission and inverse photoemission calcs., book contrib. 7-33493
 surface (100), unoccupied surface states, surface barrier, spectroscopy 7-2651
 surface electron states, clean and adsorbate covered surfaces 7-52719
 surfaces (111) and (110), atomic adsorption of O, inverse photoemission study 7-7783
 VUV spectrometer-detector system calibration using synchrotron radiation 7-24710
 Ag surface (100), (110) and (111), momentum-resolved isochromat spectroscopy 7-27813
 Al, bremsstrahlung isochromat spectra, electron-energy losses 7-22377
 Au (110), adsorbed Xe layers, final state screening in inverse photoemission spectra 7-3104
 Ce alloys, electronic structure, spectroscopic and thermodynamic props., impurity Anderson Hamiltonian 7-32900
 Ce cpds., many body theory for spectroscopies 7-64790
 Ce mononitrides and alloys, photoemission and bremsstrahlung isochromat spectra 7-3155
 Ce, photoelectron and bremsstrahlung isochromat spectra 7-7817
 CeCu₂, heavy fermion system, photoemission and inverse photoemission studies 7-3148
 CePd₃, electronic structure and intrinsically selective absorption 7-38444
 Cs outer-core emission spectra, many-body effects and spin-orbit partner behaviour obs. 7-53436
 Cu (001), single cryst., inverse photoemission polarisation effects study 7-27812
 Cu₂Y_{1-x}, amorphous alloys, empty and occupied electronic states, inverse and direct photoemission spectroscopies study 7-32899
 Fe itinerant ferromagnets, electronic struct. determ., spin depend. inverse photoemission studies, book contrib. 7-33479
 p-GaAsP, longitudinally polarised electron bombarded, circularly polarised recomb. radiation emission 7-27807
 GdPd₃, electronic structure and intrinsically selective absorption 7-38444
 K, outer-core emission spectra, many-body effects and spin-orbit partner behaviour obs. 7-53436
 LaPd₃, electronic structure and intrinsically selective absorption 7-38444
 Mg, bremsstrahlung isochromat spectra, electron-energy losses 7-22377
 Mo (001), unoccupied surface states, inverse photoemission study 7-46171
 Ni (110) with adsorbed CO, bremsstrahlung isochromat spectroscopy 7-27379
 Ni (110) with chemisorbed O₂ or CO, mag. props. investigated by spin-polarised electron beams 7-58994
 Ni itinerant ferromagnets, electronic struct. determ., spin depend. inverse photoemission studies, book contrib. 7-33479

inverse photoemission spectroscopy continued

- NpO₂, radioactive layers, bremsstrahlung isochromat spectroscopy 7-39210
 Pd (111), CO chemisorption, inverse photoemission spectra 7-21638
 Pd (111), high resolution inverse-photoemission study 7-17357
 Pt (111) with coadsorbed CO and K, inverse photoemission 7-52726
 Rb, outer-core emission spectra, many-body effects and spin-orbit partner behaviour obs. 7-53436
 Ru (001), adsorbed Xe multilayers, inverse photoemission spectra, final-state screening effects 7-13251
 Ru (001), CO chemisorption, inverse photoemission spectra 7-21638
 Si (111), ordered Au, Ag, Cu overlayers, surface states, inverse photoemission studies 7-2660
 Si (111) with ordered Cu, Ag and Au overlayers, inverse photoemission spectroscopy 7-59280
 Si, bremsstrahlung isochromat spectra, electron-energy losses 7-22377
 SiO₂, electronic structure, direct and inverse photoemission and soft X-ray emission spectra (*French*) 7-59374
 Ta (100), unoccupied surface states, inverse photoemission spectra 7-64302
 TiPd₃, electronic structure and intrinsically selective absorption 7-38444
 U-based heavy Fermion systems, final-state effects in inverse photoemission 7-53437
 URu₂Si₂, heavy fermion system, core levels and band struct., electron spectra studies 7-52418
 USi₃(Ir)₃ intermetallics, correlation effects, XPS and bremsstrahlung isochromat spectra 7-21844
 W(001), unoccupied surface states, inverse photoemission study 7-46171
 YPd₃, electronic structure and intrinsically selective absorption 7-38444

inversion layers

- 2D electron systems, width effect on magnetoconductivity 7-27353
 disordered oxide-semiconductor interface, inversion layer electronic density of states 7-58852
 finite temp. Coulomb electron correl., insulator-metal transition calcs. 7-52424
 magnetoresistance of 2D electron in lateral superlattice 7-38599
 metal-semiconductor Schottky diodes, interface state form. and barrier height control 7-52839
 MIS inversion layer solar cells 7-3680
 MIS struct., light scatt. from inversion layer 7-3033
 MIS tunnel struct., inversion condition 7-7401
 MOS capacitance in strong inversion at high temp., freq. depend. 7-7403
 MOS diodes, thin-oxide, equilibrium props. 7-7393
 optically induced inversion in the MIS solar cell 7-8380
 proximity systems, low-dimensional, Josephson current, field effect, appl. to Nb-InAs-Nb system 7-45573
 quasi 2D electron system, spin relax. 7-64101
 quasi one-dimensional inversion layers, hopping. magnetoconductance fluctuations 7-12868
 semiconductor, inversion bond bending at surface, generation-recombination noise 7-17067
 semiconductor, surface space charge layer, electronic self-energy calc. (*Korean*) 7-27373
 SIS layered structures with metallised surfaces, interface excitations 7-22031
 ternary chalcopyrite semiconductor, gate capacitance in n-channel inversion layers, quantising mag. field 7-2733
 AlAs/GaAs superlattice/GaAs interface, inversion holes, long term storage 7-45442
 CdGeAs₂, n-channel inversion layers, oscillatory diffusivity-mobility ratio, quantising mag. field 7-45419
 CdS inversion layers, carrier effective mass calcs. 7-64055
 CdS, photoconductivity spectrum, surface excitons, localised hole in quantum inversion layer 7-12762
 Cu-Al long-period superlattice, interface struct., TEM and HREM study 7-16499
 GaAs, inversion layers, hot free electron gas, intraband absorpt. coeff. calc. 7-33083
 GaAs quantised inversion layers, hot 2D electron gas, spectral acoustic phonon emission intensity 7-52452
 Ge-AlPO₄ MIS structures, inversion layers obs. 7-45502
 InP MIS structures, prep. by RF plasma oxidation, interface elec. props. 7-2731
 InSb bicrystals, n-inversion layers, pressure dependence electron states 7-45468
 InSb, electron inversion layers, cyclotron and electron spin resonance 7-38736
 InSb MOS structures, heat treatment effects 7-8031
 Si (001) inversion layers: in parallel mag. fields, electronic g-factor 7-12783
 Si (111) in MIS struct., Hall resistivity of 2D electron gas in strong mag. fields 7-7391
 Si, electrons and phonons in 1D and 2D in semicond. structures 7-2734
 Si films, n-channel inversion layers, piezoresist. effect studies 7-45318
 p-Si grating solar cells, 2D collection and injection 7-23163
 Si inversion layer, localisation and interaction in a strong mag. field 7-64343
 Si MOS inversion layers; high field low temp. transport props. (*Chinese*) 7-12862
 Si MOS inversion layers, quantum transport effects 7-52767
 Si, MOS inversion layers, scaling relation of cond. in strong mag. fields 7-64352
 Si n-type (100) inversion layers, valley splitting enhancement by lossless edge currents 7-7395
 Si quantised inversion layers, hot 2D electron gas, spectral acoustic phonon emission intensity 7-52452
 Si surface, electronic inversion layer, positive magnetoresist. obs. 7-38596
 p-Si wafer, minority-carrier diffusion length determ., photocurrent generation method 7-38579
 Si:Na MOSFET struct., hopping cond. in 2D impurity band 7-45512
 SiO₂/SiC interface, elec. characts., MOS conductance technique meas. 7-12873

invertors

- electronic current source of CO₂ laser, power modulation capability (*German*) 7-50601
 half-bridge invertor, HF variable voltage-fed, used for geophysical survey transmitter 7-23879
 induction motor acoustic noise reduction using optimum PWM waveforms of invertor 7-20499
 photovoltaic array I-V characteristic measurement error 7-3688

invertors continued

- PWM invertor with 20 kHz switching freq. using Bi-MOS power transistors, acoustic noise of driven induction motor 7-62934
 ultrasonic power generator using voltage-vector controlled resonant invertor 7-20535

investment

- energy conservation investment, economic efficiency 7-65380

iodine

see also nuclei with

- adsorption on Ni {100}, surface phases, SEXAFS, breakdown of Fourier filtering single shell anal. 7-59304
 adsorption on Ni {100}, surface phases, SEXAFS, multishell simulation anal. 7-59303
 arc in air, plasma comp., Gibbs free energy calcs. 7-37795
 Asterix IV I laser, design and performance 7-10913
 atom, 1315 nm forbidden emission satellite spectra 7-49999
 atom, (²P_{1/2}) state, absolute yield from I₂ photodissoc., optoacoustic spectrosc. meas. 7-49963
 atom, electron impact ionisation cross sections meas., TOF spectra 7-42770
 atom, photodissoc., initiated by laser emission 7-65339
 atom, photoemission cross-section and ang. distrib. parameters, inner and outer shell ionisation 7-15565
 atom, X-ray photoelectron and Auger electron spectrosc. 7-5647
 atomic, laser amplifier, free running operation mode 7-57307
 atoms, four-photon ionisation, three-photon resons., AC Stark broadening 7-57036
 biological materials, I determination by epithermal neutron activation analysis 7-34364
 cells for laser stabilisation, preparation and anal. 7-62718
 chemisorption by Fe surface, retention modelling, role in source term reduction, reactor accident anal. 7-33961
 chemisorption on (111) and (100) surfaces of Si 7-6979
 conference on iodine chemistry in reactor safety, Harwell, England (Sept. 1985) 7-48176
 crystal growth by phys. vap. transport, faceting and rounding during sublimation 7-58177
 detection, in atmospheric, differential reson. technique 7-40552
 dimer, n-hexane soln., Raman excitation profile 7-10596
 hyperfine spectra at 629 nm (*Chinese*) 7-5689
 impurity in lead phthalocyanine, influence on electrical props. 7-58927
 laser, solar-pumped, beam profile meas. 7-37006
 laser-induced fluoresc. appl. to temp. meas. in compressible flow 7-41383
 liquid, optical props. 7-17294
 mass transfer, I-assisted, in simulated LMFBR fuel pin 7-49537
 metallisation and struct. transform. under press. 7-44800
 molecule, absorpt. spectrum meas. by single-mode tunable pulsed ring dye laser 7-11006
 molecule, B 0_u⁺ state studied near dissociation limit, hyperfine interactions 7-25430
 molecule, B state, hyperfine interactions and u-g perturbations 7-25429
 molecule, collision-induced rot. transfer 43-0 band, B-X system, rel. intensity 7-15585
 molecule, excited state lifetime, modulated fluoresc. emission 7-19911
 molecule, F(0_u⁺) ion-pair state anal., OODR and fluoresc. excitation spectrum 7-19931
 molecule, higher electronic states, rot.-vib. anal., mol. fluoresc. study 7-19918
 molecule, in liquid Xe, vibr. relax. following geminate recombination 7-10712
 molecule, mag. predissoc., photoacoustics using RF laser optogalvanic detection 7-50273
 molecule, photodissoc., absolute I(²P_{1/2}) yield laser optoacoustic meas. 7-49963
 molecule, time behaviour of secondary emission excited by nearly-resonant light pulses 7-62445
 molecule, transfer bands, relative rot. line intensities 7-19941
 molecule, visible spectroscopy using dye laser light source 7-20275
 molecule, X state, polynomial and near-dissoc. representations for spectral data 7-5714
 molecule β(1g) ion-pair state, double-reson. spectra 7-31118
 p- 7-21010
 photodissociation laser, active mode locking, acousto-optic modulator (*Korean*) 7-25852
 photodissociation laser, solar-pumped 7-15854
 photodissociation laser using I₂+C₃F₄I and I₂+O₃ mixtures 7-50547
 photodissociation laser using pentafluoroethyl iodide, low-threshold solar-pumped laser operation 7-1091
 photodissociation laser with thermal recirculation (*Czech*) 7-57301
 polyacetylene:Br(I), polarised EXAFS and near edge spectra studies 7-64778
 polyacetylene:I₂ complexes, monosubstituted, isomerism, elec. cond., UV spectra 7-45289
 polyacetylene:I₃⁻, semicond. soliton lattice-metal phase transition, photo-modulation spectra studies 7-21819
 polyacetylene:I, DC elec. cond. studies 7-33018
 trans-polyacetylene:I, electron spin-lattice relax. and phase memory time, spin echo studies 7-64512
 polyacetylene:I, metallic, effective mass, magnetoreflexion studies 7-64056
 polyacetylene:I, photoexcitation spectra 7-64657
 trans-polyacetylene:I, polarised L₁ edge XANES anal., short range order full multiple scatt. calcs. 7-53444
 polyacetylene:I (AsF₆) films, synthesis, elec. and optical props. 7-63513
 polyacetylene:I films, liquid crystal polymerisation synthesis under mag. fields 7-65318
 polyacetylene, I₂-doped, quantitative optical study 7-53380
 polyanthracene:I, charged elementary excitations, EPR study 7-7246
 polymer films, I-doped, prep. by glow discharge polymerisation, elec. conductivity 7-22584
 polyphenylacetylene:I, conformational defects, ESR studies 7-64531
 α-quinquehiophene-stearic acid: I Langmuir-Blodgett films, elec. cond. 7-33106
 radioiodine adsorption on silica gel 7-28434
 radioisotope production, anal. and appl., conf., Banff, Canada, Sept. 1985 7-24254
 renal volume calculation using [¹²⁵I]hippuran gamma camera renography and computerised image processing 7-8680
 (SCN)_xI, prep., elec. cond. 7-52597
 solid, monatomic metallic, press. induced FCC phase 7-63805

iodine continued

- solid, UPES and EHT calcs. 7-64870
 tetraethylmethylenediamine- I_2 charge transfer complex, electronic struct. influence, electronic absorpt. spectra 7-10611
 tetramethylmethylenediamine- I_2 charge transfer complex, electronic struct. influence, electronic absorpt. spectra 7-10611
 vapour, luminescence-Raman scattering transformation (*Japanese*) 7-59219
 AgClI, impurity centre local electron states 7-45207
 CdTeI, segregation coeff., recoil implanted tracer technique 7-21461
 $Cu_{2-x}Cd_xTe-Zn_{39.5}Cd_{60.5}Te$ I, heterojunction solar cells, fabrication and characterisation (*Korean*) 7-28402
 F_2+I_2 , room-temp. reaction, obs. of I, IF chemiluminesc. 7-28289
 I^- , solns., positronium form. and hydrated positron reactions 7-17809
 I^- , solvation struct. in formamide (formamide- H_2O), NMR relax. obs. 7-15539
 $I+HI$, 3D trajectory study 7-42729
 $I+He^+$, L-subshell ionisation, X-ray prod. 7-50303
 $I+Na$, ion-pair formation collisions, model simulation of differential cross sections 7-10737
 $I+ClO_2^-$, oscillatory reaction, stirring and premixing effects 7-28278
 $I^+ + He(H_2)$, total one-electron capture cross sections 7-10754
 $I_2 + He$, bound and continuum states, excitation transfer, optical and electron spectroscopy investig. 7-36689
 I_2 , collisions with solid surfaces, dissociation, dynamics and energy transfer 7-36803
 I_2 external absorption cell stabilised He-Ne laser 7-20308
 I_2 gas phase radiation chemistry in reactor post-accident environments 7-49601
 I_2 optically pumped molecular beam lasers 7-10916
 I_2 , recombination and relaxation dynamics of diatomic molecules in condensed phases 7-10684
 I_2 saturated absorption lines identification, excited with green He-Ne laser 7-20372
 I_2 , supersonic flow study by 3D visualization and laser-induced fluorescence 7-20751
 I_2-H_2O vapour partitioning under severe reactor accident conditions 7-49602
 I_2-KI-S_8 melts, percolative cond. calcs. 7-6845
 $I_2-Sb_2S_3$ system, SbSI form. and melting diagram 7-26919
 I_2+F , reaction dynamics, quasiclassical trajectory studies 7-22998
 I_2+F , reactive collision, IF laser induced fluoresc. (*French*) 7-13727
 I_2+Xe , atom and excitation transfer, energy disposal, product rot. alignment 7-31158
 I_3^- , electrical cond. mechanism, tight-binding and ab initio pseudopot. calc. 7-52546
 ^{123}I , cyclotron prod. for positron emission tomography appl. 7-28695
 ^{123}I , cyclotron prod., excitation function and yields in $^{127}I(p,x)$ reactions 7-28694
 ^{123}I , high-purity, prod. and specific activity meas. 7-28696
 ^{123}I , production optimization from statistical calcs. for $^{124}Xe(p,x)$ reaction 7-54744
 ^{123}I , radioisotope prod. for medical appl., review 7-28693
 $[^{123}I]$ iodoamphetamine, SPECT imaging and radiopharmaceutical prod., review 7-28656
 ^{123}I and ^{60}Co in eye plaque therapy, Monte Carlo dosimetry 7-40300
 ^{123}I decay rel. to amplification of oncogenes and integrated SV40 sequences in mammalian cells 7-40224
 ^{123}I decays rel. to range of high LET effects in DNA 7-8660
 ^{125}I , high-sensitivity meas. in cyclotron prod. ^{123}I 7-28697
 $^{127}I_2$ absorption cell, improved He-Ne laser at 612 nm appl. 7-20270
 $^{127}I_2$ stabilised He-Ne laser, at 605 nm 7-20309
 ^{129}I , level decrease in rad. waste by Hg minerals 7-19537
 ^{131}I injected into rats, postirrad. changes in skeletal muscle and thyroid gland (*Russian*) 7-14059
 ^{131}I , specific activity meas. in commercial samples 7-28698
 ^{131}I treatment of thyroid cancer: absorbed dose calc. from post-therapy scans 7-65842
 I_2^*+Ar , collision, rotational energy transfer 7-36734
 I_2^*+He , collision, rotational energy transfer 7-36734
 $I_2^*+I_2$, collision, rotational energy transfer 7-36734
 $KCl:I$, electron excitation self-trapping 7-32594
 $Li-I_2$ solid state batteries, performance of polyacrylonitrile-based cathodes. 7-54282
 O_2-I chemical lasers, singlet O_2 generator 7-20217
 O_2-I_2 chemical laser, influence of water vapour on output energy 7-25808
 O_2-I_2 chemical lasers, review 7-15852
 O_2-I_2 gas dynamic lasers using microwave excitation, design and operation (*German*) 7-36986
 O_2-I_2 laser active medium, theoretical model 7-1093
 $PbTe:In,I$, Soret effect, impurity cond. distrib., thermoelec. power meas. 7-44930
 $RbCl:I$, relaxed exciton states, optical conversion 7-53397
 $S-I$ working fluid, max. heat flux transferable in thermosiphon 7-50930
 $TlBr:I$ indirect exciton transition, effects of disorder 7-2489

iodine compounds

- X-ray fluorescence anal. of K X-ray intensities 7-59805
 $IBr+He$, bound and continuum states, excitation transfer, optical and electron spectroscopy investig. 7-36689
 IBr , ion-pair states, spectral anal. 7-19873
 IBr^+ , $A^2\Pi-X^2\Pi$ electronic emission spectrum 7-25528
 $ICl+He$, bound and continuum states, excitation transfer, optical and electron spectroscopy investig. 7-36689
 ICl , $B^2\Pi_g$ state, predissoc., fluoresc. decay meas. 7-10687
 ICl , collisions with solid surfaces, dissociation, dynamics and energy transfer 7-36803
 ICl photodissociation laser at 11.35 μm , gain and energy 7-43082
 ICl , visible spectroscopy using dye laser light source 7-20275
 $ICl-Ne$, A, E and X states, binding energies, optical-optical double reson. 7-62425
 $ICl+Xe$, form. of $XeCl$ and XeI , fluoresc. 7-17773
 IF , chemiluminesc. 7-31089
 IF , $E(O^+)$ state, two-photon sequential absorpt. spectra 7-19988
 IF hybrid chemical-laser, quenching of NF singlet states 7-43081
 IF pulsed laser, flow parameters optimisation, intracavity gain detect. 7-10914
 IF reaction product, laser induced fluoresc. (*French*) 7-13727
 $IF+NF$, electronic-to-electronic energy transfer rate, temp. depend. 7-36740

iodine compounds continued

- IF_5 , chemical doping of aluminium polyfluorophthalocyanine 7-52600
 $INCO$, microwave spectrum, rot. and centrifugal distortion consts., quadrupole hyperfine struct. 7-5667
 IO_2 radical in $KClO_4$ crystals, ESR study 7-22143
 $IO_3^-+H_3AsO_3$, stirring effects and bistability, coalescence-dispersion model 7-46801
 IOF_5 , excited vibr. state, microwave spectrum, vibr. and rot. parameters 7-25498
 I_2 , acridine charge-transfer complex, reson. Raman and far-IR spectra anal. 7-42620
 I_2 , hexamethylenetetramine charge-transfer complex, reson. Raman and far-IR spectra anal. 7-42620
 I_2 , phenazine charge-transfer complex, reson. Raman and far-IR spectra anal. 7-42620
 $NF-IF$, electronic energy transfer, long-range interaction model 7-62478

ion accelerators

- 30 kV accelerator for negative ion beams 7-18916
 100 TW particle beam fusion accelerator for inertial confinement fusion program 7-30664
 Applied-B ion diode expts. on Particle Beam Fusion Accelerator-I 7-10310
 ATLAS, positive ion injector status, ECR ion source and superconducting linac 7-62134
 boil off Li vapour source for PBFA II ICF expts. 7-25293
 cluster ion accelerator using triangle-shaped accelerated waves 7-42246
 compact 2.86 GHz ECR ion source (*Japanese*) 7-19600
 convex spherical surface emitting a space charge limited ion current, imaging props. 7-5515
 CW operation of the TIT 1H-type Heavy Ion Linac (*Japanese*) 7-19564
 electrodes, energy dissipation during HV vacuum breakdown 7-30777
 fusion research, use of heavy-ion accelerators 7-10285
 heavy ion injector linac based on superconducting interdigital accelerating structs. 7-62135
 heavy-ion linear accelerator for Tokyo Institute of technology, Mitsubishi Electric designed unit (*Japanese*) 7-10311
 HERA-RFQ injector for Alvarez linac, present status 7-62130
 high-current electron beams, Buneman instability in neutral gas, ion collective acceleration 7-49749
 inhomogeneous magnetic fields with axial symmetry, 5th order ang. aberrations, corrections (*Chinese*) 7-5508
 INS RFQ linac TALL, beam test 7-10318
 KALIF ion accelerator, beam comp. investig. in anode plasma 7-30742
 large-area liquid-lithium ion source for inertial confinement fusion 7-25296
 light ion multichannel acceleration, resonator EM props. 7-5497
 linacs, high-current beam dynamics and transport, theory and experiment, review 7-62117
 linacs for medical and industrial applications 7-62110
 linear induction accelerator, HERMES III, power flow eval. 7-30761
 low- β ion acceleration with a MEQUALAC 7-15448
 magnetic quadrupole multiplet microbeam forming systems (*Chinese*) 7-10325
 magnetically insulated transmission line in PROTO II accelerator, anode and cathode joints, gap closure 7-30756
 MEQUALAC low- β in accelerator for plasma diagnostics 7-26528
 MFTF, industrially fabricated ion source, test and conditioning 7-19435
 negative ion injector extension for JAERI tandem accelerator 7-56898
 particle acceleration using lasers (*German*) 7-5495
 particle beam fusion accelerator for inertial confinement fusion program, construction projection 7-30665
 particle beam fusion accelerator I (PBFA I), automated features of control/monitor system 7-30754
 Particle Beam Fusion Accelerator II (PBFA II), computer model of vacuum system design 7-30773
 Particle Beam Fusion Accelerator II (PBFA II), energy storage system 7-30765
 Particle Beam Fusion Accelerator II (PBFA II), energy transport meas. and computer simulation 7-30764
 Particle Beam Fusion Accelerator II (PBFA II), laser triggering optical system 7-30771
 Particle Beam Fusion Accelerator II (PBFA II), laser trigger system design 7-30772
 Particle Beam Fusion Accelerator II (PBFA II), quality assurance of R&D project 7-30763
 particle beam fusion accelerator II (PBFA II), vacuum insulator stack failure mechanisms 7-30749
 particle beam fusion accelerator II (PBFA II) control/monitor system 7-30751
 Particle Beam Fusion Accelerator II (PBFA II) engineering design of pulse forming system 7-30770
 particle beam fusion accelerator II (PBFA II) high speed multi-channel data acquisition system 7-30752
 Particle Beam Fusion Accelerator II (PBFA II) Marx generator engineering and assembly line technology 7-30768
 Particle Beam Fusion Accelerator Marx generators 7-30767
 particle beam fusion accelerator-II (PBFA-II), design of applied-B ion diode 7-36343
 PBFA II accelerator assembly and characterisation 7-30762
 PBFA II Plasma Erosion Opening Switch geometry effect on current transfer 7-26543
 PBFA II vacuum magnetically insulated transmission line redesign to inductive energy store 7-30755
 PBFA-II photoactivation, fusion breakeven experiments, radiation protection problems 7-30775
 PBFA-II vacuum insulator stack design engineering viewpoint 7-30774
 plasma impulse accelerators with cylindrical electrodes 7-36340
 plasma opening switch experiments on PBFA I using flashboards 7-26542
 plasma opening switch performance on Supermite and PBFA II 7-26541
 positive ion sources and injectors for linacs 7-62126
 Proto II accelerator, low inductance diode design for imploding plasma loads, insulator breakdown 7-30760
 PROTO II accelerator power flow modification in insulator stack 7-30669
 PROTO II crossover network, time domain reflectometry meas. 7-30759
 pulsed power accelerator for fusion research, SF₆ reprocessing system 7-30769
 pulsed power accelerators, low-jitter Marx generators for reliability 7-30766

ion accelerators continued

- pulsed power research facilities, successful long-term operation, contributing factors, PBFA-I as example 7-30778
 Reiden IV, light ion beam fusion research 7-11807
 relativistic heavy ion accelerators, review 7-30787
 relativistic heavy ion collector, magnet system status 7-36347
 RF ion source, focusing system, expt. and theoretical investigs. 7-10840
 RF superconducting linac structures for heavy ions and electrons 7-62119
 RFQ linac, very heavy ion acceleration 7-10319
 RFQ-based H^- injector for BNL/FNAL 200 MeV proton linacs 7-62132
 RIKEN Ring Cyclotron and its experimental program 7-36355
 Rf 6 MV laser triggered SF_6 filled switch for PBFA II 7-30746
 super HILAC upgrade project, MEVVA ion source, beam transport line 7-62133
 superconducting linear accelerators for heavy ions, review 7-56886
 superconducting post accelerator linac for JAERI tandem 7-36371
 surface discharges as intense photon sources for light-ion fusion accelerator cleaning 7-37800
 Tohoku University Dynamitron facility 7-30818
 transverse field focusing 180 keV negative ion accelerator, design and fabrication 7-15439
 triggered cascade gas switches for PBFA I 7-30747
 vacuum system for multipurpose 14 MeV neutron source 7-35529
 voltage amplification in dense plasma focus, appl. to car spark plugs 7-63374
 voltage regulation and breakdown prevention device (Chinese) 7-5499
 H^- ion high current density accelerator, design and diagnostics 7-15429
 H^- ion source development for linac appl., review 7-62127
 H^+ , pulsed ion beam, inductive post-acceleration obs., beam energy meas. 7-11805
 Li ion source for PBFA II ICF research 7-25292
 Li plasma anode layers for PBFA II ion diode 7-25295
 Li plasma generation for large area ion diode 7-25294
 $^{20}Ne^{+}$ and $^{20}Ne^{4+}$ ion acceleration at the U-120 cyclotron (German) 7-56887
 U ion acceleration in split coaxial RFQ (Japanese) 7-19573

ion-atom collisions *see atom-ion collisions***ion beam applications**

- see also ion beam lithography; sputtering*
 cluster beam technique for thin film deposition 7-17478
 diamond-like layers deposited from C ion beams, struct. (Russian) 7-17475
 glass surface after ion-beam cleaning, ellipsometric investig. 7-43453
 III-V semiconductors, patterning using photoelectrochem. etching and focused ion beams 7-22924
 ion implanter, ion beam transport system, ion-optical characteristics (Korean) 7-24723
 ionized-cluster-beam deposition apparatus (Japanese) 7-22583
 perfluoropolyether lubricant on magnetic disc surface, ion-induced volatilisation for quantitative anal. 7-39933
 semiconductor interfaces, bonding and adhesion, characterisation techniques, electronic struct. 7-27418
 SOS, crystalline quality improvement by ion beam technique 7-16651
 SOS, ion beam improved, elec. characts. 7-17114
 steels, stainless, ion-nitrided, struct. and props. 7-22884
 surface modification by ion beam enhanced deposition and dynamic ion mixing 7-64027
 thin film deposition, film homogenization, parameter optimisation 7-7898
 thin film deposition on floating substrates in three grid microetch system 7-7896
 thin film deposition on insulating substrate, space charge effects 7-7895
 vacuum, electron and ion technologies, conf., Sozopol, Bulgaria (Oct. 1985) 7-35098
 Al_2O_3 coatings, ion beam and chemically etched, comparison 7-22868
 ArH^+ exciplex laser, pumped by electron or proton beam, active medium modelling 7-62672
 Au films, focused ion beam induced deposition 7-46334
 Ba ion beam magnetic field and space pot. diagnostic for STM plasma 7-1764
 Mo single crystals, high temp. deep following ion thermal treatment (Russian) 7-53813
 Nb-NbO₂-PbInAu Josephson junction fabrication by ion beam oxidation 7-22074
 Pd, metallisation using decomposition of palladium acetate films with microfocused ion beam 7-52314
 Si, chemically assisted ion beam etching using low energy Kaufman source 7-22931
 Si detector material, ion beam diagnostic techniques 7-46895
 Si solar cells, H passivation by ion beams 7-17867
 Si_3N_4 , amorphous thin films grown by ion beam assisted deposition, IR and ion beam anal. 7-39209
 Ta films, maskless ion beam assisted deposition 7-46342
 TiN sputtered films, mech. props., substrate ion beam pretreatment effects 7-22484
 W films, maskless ion beam assisted deposition 7-46342

ion beam effects

- see also ion beam mixing; ion-surface impact; ionoluminescence; plasma-beam interactions*
 adhesion, ion beam enhanced 7-65279
 alkali phosphates, ion bombardment-induced surface modifications, stoichiometry, core levels and valence struct., ESCA studies 7-26816
 alloy surfaces, amorphisation during nanosecond ion beam irradiation 7-6517
 alloys, ion bombardment-induced segregation and redistribution 7-58381
 alloys, surface-modified, cross-section precip. extraction replica technique 7-54042
 alloys and isotopic mixtures, preferential sputtering, isotope enrichment 7-59328
 alumina, grain boundary glassy phase, ion milling of TEM specimens 7-44327
 amorphous targets, sputtered particles, angular distrib. 7-59342
 Auger emission, ion-induced, from solid targets, review 7-59360
 ceramics, ion milling of TEM specimens, grain boundary glassy phase 7-44327
 channelling of charged particles in solids 7-38081
 charge transport between junctions rel. to ion shunt effect 7-63668
 Chinese hamster cells, modification by mesoporphyrin-IX derivatives of damage by He ions and protons (Russian) 7-14064

ion beam effects continued

- collision cascades, ionization, spikes and energytransfer 7-12170
 conducting polymer films produced by Ar^+ irradiation of HPR-204, physical and elec. props. 7-26808
 conference, Boston, MA, USA (Dec. 1985) 7-9590
 conference, Catania, Italy (9-13 June 1986) 7-60865
 damage in solids, fractal concepts 7-58380
 diacetylene, ion beam induced polymerisation 7-32525
 diamond, volume expansion during ion implantation, point defect creation and interactions 7-51890
 direct impact induced amorphisation, effect of ion beam annealing 7-58383
 dual-ion irradiation station at Tokyo Univ. for fusion materials testing 7-51875
 effect of ion irradiation, 7-28160
 eroding surface profile during ion sputtering, Huygens' construction study 7-27842
 erosion and wear of solids, ion implantation effect 7-63683
 fast ion dechannelling, electronic diffusion coeff. calc. 7-44635
 film deposition using low energy ion beam from single grid Kaufman type ion source (Japanese) 7-62156
 fluorapatite, relative defect-production efficiency for fission fragments, alpha decay and electron irradiation 7-12167
 French Metallurgy Society meeting, Paris, France (Oct. 1986) (French) 7-29579
 fusion reactor structural materials, irradiation, He effects control 7-51845
 fusion reactor structural materials, swelling after neutron and ion irradiation, comparison 7-58357
 gas bubble lattice form. and props. under light gas ion irradiation 7-63681
 glasses, surface structure minimal disturbance under ion bombardment 7-12419
 graphite, first wall thermal performance in ICF reactor 7-49634
 graphite, fusion reactor, surface erosion by D_2^+ irradiation, struct. 7-51869
 graphite, He ion irradiation, thermal desorption 7-52245
 graphite, pyrolytic, sputtering with O ions at various target temps. 7-49633
 ice, ion bombardment, classical dynamics model 7-23996
 ice films, Kr^+ bombardment, ion cluster desorption, TOF mass spectra study, astrophysical implications 7-26815
 ice thin films, ion irradiation erosion effects meas., astrophysical discussion 7-26814
 III-V semiconductors, ion beam damage-induced masking for photoelectrochem. etching 7-44628
 inert gas- O_2 -(SF_6) discharges, charged particle induced, O_3 synthesis 7-3587
 inert gases implanted in solids, model of diffusion and release behaviour (Chinese) 7-38257
 insulators, fast heavy ion impact-induced secondary ion emission studies 7-27845
 insulators, high dose radiation damage, voids and dislocations 7-32502
 ion bombardment, collision cascade momentum distrib., sputtering yield and atomic mixing, geometrical treatment 7-27846
 ion bombardment, narrow beam, surface morphological changes 7-51868
 ion implanted layers, anal. by X-ray diffraction (Chinese) 7-51801
 ion-stimulated sorption, nonequilibrium composition and struct. film growth technology 7-22585
 Kapton foil, N ion energy loss meas. and calcs. 7-63694
 low temp. solids, low energy atom and ion bombardment, sputtering and radiation damage mechanisms study 7-27844
 materials modification with ion beams, review 7-16647
 metal surfaces, oxidation, Ar^+ ion bombardment effects 7-39755
 metal wear resistance, ion implantation and ion assisted coatings 7-3513
 metallic glasses, ion irradiation, inelastic deform. induced by fast ion electronic energy loss 7-63688
 metallic thin films, amorphisation and film anal., ion beam techniques 7-37868
 metals, defect profiles, low energy positron meas. 7-64731
 metals, ion implantation of inert gases, high press. precip. phases 7-38031
 mineral powder mixtures, X-ray diffraction anal. by heavy ion bombardment 7-32223
 mutation induction in spores of *Bacillus subtilis* by accelerated very heavy ions 7-28618
 Mylar foil, N ion energy loss meas. and calcs. 7-63694
 Nb_3Ir films, superconduct. transition temp., effect of radiation induced disordering 7-45540
 non-semiconductor material, surface modification by ion beam indication (Chinese) 7-51799
 photographic plates, low energy heavy molecule ion impact model 7-15028
 plasma film polymerisation, ion bombardment effects, deposition rates, IR, UV and visible absorpt. spectra studies 7-28312
 PMMA, surface characterisation by SIMS 7-26817
 PMMA and Microdeposited 23M, As^+ ion bombardment, appl. for ion beam lithography and masking 7-26810
 polydiacetylene Langmuir-Blodgett films, ion beam irradiation 7-6690
 polyimide thin films, plasma-assisted etching, ion bombardment effects, quartz cryst. microbalance studies 7-28211
 polymer sheets, beam charged, ion spot phenomenon anal. 7-58356
 polymers, ion bombardment effects 7-32524
 polystyrene, nanosecond proton and He ion pulse radiolysis studies 7-21297
 polystyrene, tracer diffusion meas. using Si and the elastic recoil detect. 7-39337
 polystyrene films, ion bombarded, primary chemical events, IR study 7-26809
 polyvinylidene fluoride, modifications under high energy heavy ion, X-ray and electron irradiation, XPS study 7-38076
 PTFE and PVDF, aging, irradiation by X-rays, electron and ion beams, XPS study 7-32498
 quartz, fused, surface structure minimal disturbance under ion bombardment 7-12419
 radiation effects in glasses 7-32518
 radiation-stimulated diffusion during ion etching 7-38261
 range and damage 3D distrib. including recoil transport 7-63691
 rhabdomyosarcoma tumor cells, rat, pot. lethal damage repair after X-ray or Ne ions 7-18031
 semiconductor, interaction of high power pulsed ion beams, solid phase epitaxy 7-12096

ion beam effects continued

- semiconductors, ion beam induced epitaxial crystn., kinetics, mechanisms and microstruct. 7-12171
 Si-Al Schottky barriers, Ar ion implantation damage, thermal anneal recovery 7-17101
 slow ions, nonlin. energy-loss straggling, in solids 7-2075
 solids, interaction of GeV heavy ions, GANIL results 7-63678
 sphene, natural radiation damage, fission track and thermoluminescence props. 7-51889
 sputtered magnetic thin film, ion beam irradi., struct. studies 7-22588
 sputtering, high depth resolution problem 7-27849
 stainless steel, ion irradiated, X-ray microanalysis, of equilibrium and nonequilibrium segregation 7-46488
 steel, austenitic, surface blistering from pulsed H plasma, formation mechanism 7-63667
 steel, austenitic stainless, D permeability, He irradiation effects 7-2267
 steel, austenitic stainless, heavy ion bombarded, η -phase precipitate form., electron microscopy studies 7-13459
 steel, austenitic stainless, precip. stability, during heavy ion irradi. 7-58367
 steel, austenitic stainless, swelling under dual ion beam irradi. 7-44629
 steel, austenitic stainless, void stability, effect of O 7-58262
 steel, ferritic stainless, cavity form., effect of electron/He dual beam irradi. 7-58341
 steel, ferritic stainless, He-doped, microstruct. evolution following 14 MeV Ni ion irradi. 7-58363
 steel, implanted with N ions, physicochem. characters. of surfaces, wear resist. (French) 7-28209
 steel, stainless, ferritic, irradi., grain boundary segregation, STEM microanalysis 7-22701
 steel, stainless, ion irradi., positron annihilation studies 7-46219
 surface erosion by ion bombardment 7-16843
 surface fracture during He⁺ ion bombardment 7-21294
 surface modification by ion beam methods, review 7-27081
 SUS316, 40 keV Cu⁺, Fe⁺ and fission neutron irradi. effects. 7-56823
 target heating in low-energy ion beam processing 7-21293
 temperature field evolution on ion beam irradiated absorber 7-63670
 transfer conserving distribution properties (Czech) 7-5828
 vapour phase cryst. growth, ion/surface interactions, photo-induced reactions, review 7-53609
 Si, low energy ion beam damage, ellipsometric characterisation, two-film optical model 7-27680
 Ag (110), ion bombarded, He atom scatt. 7-64863
 Ag films, ion-induced microcones, TEM obs. 7-58593
 Ag, proton and ion irradi., self-interstitial atom interactions with defect clusters, elec. resist. meas. 7-58384
 Ag/Cu interface, metastable solid soln. form. by ion mixing 7-12163
 Ag-Cu(Ni) systems, amorphisation induced by ion mixing 7-21300
 Al (100), polycryst., single cryst. and amorphous, ballistic collision cascade anisotropies 7-58379
 Al (110), Ar⁺ sputtered, vacancy-type defect distrib., variable energy positrons study, mol. dynamics simulations 7-12429
 Al (110), sputtered defect profile, variable-energy positron beam meas. 7-38077
 Al, FCC cryst. struct., secondary ion emission, current density effects 7-59318
 Al film deposition from partially ionised vapour flux, fast ion interactions 7-12531
 Al surface, ion irradiated, flaking, orientation dependence 7-38074
 Al-Cd single crystals, Cd-vacancy complex disassociation under ion irradiation 7-26741
 Al-Cr(Mn)(Fe) amorphous films, quasicrystalline transformation by ion irradiation 7-2071
 Al-He ion irradi. system, bubble form., positron lifetime meas. 7-37966
 Al-Li, quenched, ageing, light ion irradi., δ -phase form. and particle growth 7-26807
 Al_{0.3}Ga_{0.7}As, thermal and ion-assisted reactions with Cl₂ 7-28349
 AlMgSc first wall materials, sputtering and radiation induced segregation 7-38072
 AlMn films, ion irradiation-induced amorphous to quasicryst. transform., comp. depend. study 7-16654
 Al₂O₃, amorphous layers, formation and annealing, ion irradiation 7-58385
 Al₂O₃, mixing of metal overlayers, ion beam irradi., rapid thermal annealing, pulsed laser irradi. 7-58330
 Ar, solid, energy transfer during ion bombard. 7-64842
 Au, cascade damage under heavy ion irradi. at high temp., in situ obs. 7-58368
 AuGe-GaAs, ion beam induced phenomena 7-12166
 BaFe₁₂O₁₉, defects created by Kr ion bombardment, HREM study 7-12168
 C, amorphous film, modification by inert gas ion irradiation 7-64018
 C diamondlike coatings, ion beam induced conductivity and structural changes 7-22053
 C foil, secondary electron emission from fast ion bombardment 7-53459
 C sputtered films, ion enhancement, struct. prop. relationships studies 7-52332
 C thin surface layers on steel substrates, anticorrosion props., ion bombardment effects study 7-27202
 C-Sn composite sputtered films, ion enhancement, struct. prop. relationships studies 7-52332
 C-Ti composite sputtered films, ion enhancement, struct. prop. relationships studies 7-52332
 CdSe lattice defects, digital struct. anal. by ion beam thinning for high resolution electron microscopy 7-6616
 Co, O₂ chemisorpt., influence of Ar⁺ ion bombardment (Russian) 7-52253
 Co single crystal foils, α - and β -phase, ion transmission and sputtering 7-59322
 CoCr evaporated films, mag. props. 7-33225
 CoSi₂, thin film, electrical transport props. 7-27442
 Cr evaporated and ion assisted deposited coatings, microstruct., electron microscope obs. 7-52335
 Cr single crystals, action of α -particles (Russian) 7-51880
 Cr/Cu multilayer structs., scanning Auger microprobe depth profiling, sputtering effects 7-58659
 Cr-C, Cr-Mo double layer films, Ar⁺, Xe⁺ ion bombardment (Chinese) 7-51885
 CrSi₂, Ar⁺ ion beam induced surface and subsurface modifications, AES study 7-64846

ion beam effects continued

- Cr₂Si, Ar⁺ ion beam induced surface and subsurface modifications, AES study 7-64846
 CsI, H_n⁺ cluster ion impact-induced Cs⁺ desorption, TOFS study 7-27843
 Cu alloys, high-strength, rad.-enhanced recrystn. 7-51871
 Cu, damage correlation of high energy neutron and ion irradiation, sub-cascades 7-51860
 Cu films, sputter deposition, effect of ion bombardment of growing film 7-64009
 Cu, ion irradi., sputtering and lattice damage, cryst. orientation effect 7-64843
 Cu, ion irradiated, mech. prop. meas. 7-51873
 Cu, O₂ chemisorpt., influence of Ar⁺ ion bombardment (Russian) 7-52253
 Cu, O₂ chemisorption kinetics as function of ion bombardment and temp. (Russian) 7-58622
 Cu surface, ion bombardment-induced microtopography 7-58588
 Cu surface, ion irradi., sputtering and lattice damage, cascade simulation 7-59327
 Cu surface, sputtering and surface topography evolution 7-58586
 Cu, surface structure minimal disturbance under ion bombardment 7-12419
 Cu wires, thin, sputter-induced cones 7-51881
 Cu-Ni-Fe, irradi., stability of periodic decomp. struct. 7-58366
 Cu-Zr, ion irradiated, mech. prop. meas. 7-51873
 Cu₃Au alloy, displacement cascade collapse at low temp. 7-51892
 CuInSe₂ polycryst. semicond. growth from melt, surface props., ion bombardment and annealing effects 7-46304
 CuPd, disordering by 14 MeV Cu ions between 296 and 823 K 7-51877
 CuZr metallic glass, blistering under He implantation, EELS anal. 7-16593
 ErSi₂, behaviour under ion bombard. and O exposure, AES, EELS 7-33506
 Fe, O₂ chemisorpt., influence of Ar⁺ ion bombardment (Russian) 7-52253
 Fe-9Cr ferritic steel, 40 keV Cu⁺, Fe⁺ and fission neutron irradi. effects. 7-56823
 Fe-Al bilayered samples, ion beam induced atomic mixing 7-6689
 Fe-Cr (12 at.%), ferritic alloy, He⁺ implantation and Fe⁺ irradi., bubble nucleation and growth 7-58362
 Fe-Ni-Cr, high-purity, irradi., void swelling and nucl.-induced phase transforms. 7-58340
 Fe-Ni-Cr-P, ion irradi., swelling suppression, effect of P modification 7-58358
 Fe-Ti multilayered films, ion bombard., microstructure, TEM obs. 7-12165
 Fe-Ti-C multilayered films, ion bombard., microstructure, TEM obs. 7-12165
 Fe₂B₅, high energy heavy-ion irradiation, electrical resistance meas., evidence for electronic energy loss effect 7-58353
 FeCrNiWMo alloys, sputtering effects on props 7-36240
 FeNiCr, strain measurement in convergent beam electron diffraction 7-16562
 GaAs, dry etching, radiation damage 7-54024
 GaAs, ion irradi. high-resistivity layer, thickness and resistance, free carrier density and cryst. orientation dependence 7-58354
 GaAs, plasma etching damage, Raman scatt. study 7-54023
 GaAs:Cs, impurity ion beam effects, SIMS depth profiling 7-22419
 GaAs:Zn, ion damage and recrystn. annealing, conversion electron EXAFS meas. 7-64821
 GaAs_{1-x}P_xBe⁺-GaP:Be⁺ strained-layer superlattices, ion implantation doping, structural study 7-38030
 GaP, Ar⁺ irradiated, damage profile, backscattering spectra, anal. by computer program 7-64840
 GaP, implanted with He ions and protons, microhardness rel. to damage density 7-51883
 GaP:He⁺, implanted, swelling, strain and radiation damage 7-6694
 Ge ion beam deposition on (100) single cryst. substrate, interface, thin film and damage form. 7-17423
 Ge:As(Sb)(Te)(Bi), implanted, heavy ion damage, TEM, annealing studies 7-63676
 Ho ionic bombardment, continuous spectrum form. 7-42528
 In foils, ion bombarded, desorbed neutral energy distrib. studies 7-22406
 InP, radiation-damaged photocond., Hertzian dipole meas. of picosecond photoresponses 7-52690
 InSb (-1-1-1) (3 × 3) reconstructed, X-ray diffr. studies 7-6951
 LiF surface, Ar⁺ and Ar²⁺ bombarded, desorption of F⁺, secondary ion mass spectra study 7-21661
 LiNbO₃, ion beam induced luminesc. 7-27793
 Li₂O, neutron and ion irradi. damage, ESR and optical absorption studies 7-32509
 MgAl₂O₄, Ar⁺ ion irradi., XPS and RBS characterisation 7-32514
 MgF₂ films deposited on fused SiO₂ with ion beam assistance, adhesion, internal stresses 7-21749
 Mo (100), ion irradiated, sub-surface defects, study by variable energy positrons 7-39286
 Mo group glasses, anomalously high bulk cond. meas. in metal-glass structs. 7-17029
 Mo, surface structure minimal disturbance under ion bombardment 7-12419
 NO₂ amorphous insulator, Ar⁺ sputtering, ang. distrib. and energy spectra study 7-27848
 Na₂O-SiO₂ glass, relative defect-production efficiency for fission fragments, alpha decay and electron irradiation 7-12167
 Nb film microstruct., nonnormal incidence ion bombardment effects 7-12174
 Nb-D, implanted, lattice distortion, channelling method 7-58382
 Nb₂Ir films, lattice-stiffness changes due to ion irradiation, Brillouin scatt. 7-52379
 NbN/Pb-In Josephson junctions, fabrication by Ar⁺ ion bombardment 7-2787
 NbN/Pb(In) Josephson junction, Ar⁺ irradi., characts. (Japanese) 7-22071
 Nb₃Sn films, superconducting critical temp., effect of ion beam irradiation 7-7430
 Ni (110), defects developed by epitaxial growth of Ni film or ion bombardment 7-63924
 Ni, defects created by low-energy ion bombardment, investig. by slow electron diffr. (Russian) 7-58374
 Ni foil, N ion energy loss meas. and calcs. 7-63694

ion beam effects continued

- Ni, ion irradiation-induced implant diffusion and segregation, synergistic effects, kinetic model calcs. 7-16658
- Ni, irradi. with energetic ions, defect prod. and recovery 7-58370
- Ni, Ne ion irradi. samples, yield stress studies (*Russian*) 7-12162
- Ni, Ni ion irradi., 14 MeV, void form., gas effects 7-58360
- Ni, Ni ion irradi., pore conc., effect of pre-implanted He (*Russian*) 7-32513
- Ni, O₂ chemisorpt., influence of Ar⁺ ion bombardment (*Russian*) 7-52253
- Ni, void stability, effect of O 7-58262
- Ni-AuGe-GaAs, ion beam induced phenomena 7-12166
- Ni-B, implanted, mech. props., disorder and amorphicity 7-53819
- Ni-Fe film, ion beam sputter deposition, ion bombardment effect on preferred orientation 7-64010
- Ni-P, implanted, mech. props., disorder and amorphicity 7-53819
- Ni-Si alloy, Ni₃Si precipitation during electron and ion irradiation 7-51876
- NiAl thin films, ion irradi. induced amorphisation studies rel. to cascade parameters 7-63671
- Ni₆₉Cr₆Si₁₃B₇Fe_{2.6}, amorphous alloy, 70 MeV Ni⁶⁺ ion irradi., surface swelling 7-16646
- a-P, sputtered, response to intense ion bombardment 7-27447
- Pd films, sputter deposition, effect of ion bombardment of growing film 7-64009
- Pt films, sputter deposition, effect of ion bombardment of growing film 7-64009
- Pt group glasses, anomalously high bulk cond. meas. in metal-glass structs. 7-17029
- Rh foils, ion bombarded, desorbed neutral energy distrib. studies 7-22406
- S thin films, MeV He⁺ beam erosion, temp. depend. yield meas. 7-27847
- Si (100), reactivity, thermal desorption of propylene, defect- and electron-enhanced chemistry 7-21660
- Si (111), Ar ion bombardment, RHEED and REM studies 7-32511
- Si, amorphisation and crystallisation 7-11914
- Si, amorphous and single cryst., etching rate, ion backscatt. and channelling meas. 7-28231
- Si cascade branching, Monte Carlo simulation 7-58376
- Si defect annealing and impurity activation during high-intensity As⁺ implantation doping 7-58295
- Si, dislocation loops, generated by ion implantation and furnace annealing, depth profiles, RBS, X-ray diffr., TEM anal. 7-51882
- Si, disorder generation by Ar⁺ implantation, Rutherford backscatt.-channelling meas. 7-63680
- Si, dry etching, radiation damage 7-54024
- Si, electron and ion irradiation induced amorphisation, point defect dispersion and mobility 7-11916
- Si homogeneous amorphisation, ion implantation energy depend. study 7-63638
- Si ion beam deposition on (100) single cryst. substrate, interface, thin film and damage form. 7-17423
- Si, ion beam induced recrystn., channelling effect 7-16650
- Si, ion bombard., damage accumulation, flux depend., RBS 7-51891
- Si, ion implantation, damage profile studies, multilayer model (*Chinese*) 7-6648
- Si, ion-induced etching, surface processes 7-59702
- Si MBE layers, defect characterisation, luminesc., TEM studies 7-13227
- Si, reactive sputter etching, damage removal methods 7-17742
- Si Schottky diodes, H₂⁺ bombarded, elec. props. 7-38677
- Si shallow p-n junctions, reactive ion etching damage, defects and leakage current studies 7-27411
- Si single crystal, reactive ion etching-induced damage, nondestructive thermal wave monitoring 7-28230
- Si substrate, anisotropic dry etching effects on surface props., XPS, ion channelling and Raman scatt. studies 7-28229
- Si surface, residue form. in trifluoromethane discharge environment 7-54020
- Si, surface damage induced by low energy ion sputtering (*Chinese*) 7-6693
- Si wafers, etching by NF₃, plasma and reagent pulse induced transients 7-3533
- Si wafers, striation prod. by grazing ion incidence 7-63684
- Si:Ar⁺, ion implanted thin film, defect form., dose depend. study 7-51793
- Si:As on sapphire, ion beam recrystallised and laser annealed, elec. props. 7-16649
- Si:As(Sb)(Bi), implanted, heavy ion damage, TEM, annealing studies 7-63676
- Si:Hg⁺, ion implant range distributions, Rutherford backscatt. studies 7-2073
- Si:In⁺, ion implanted, damage prod., incidence angle depend. 7-65242
- Si:Zn, amorphous-crystalline interface, backscattering and channelling study 7-6663
- Si-Al structures, ion mixing, effect of interfacial oxide 7-21537
- Si-Ar:Hg⁺, ion implant range distributions, Rutherford backscatt. studies 7-2073
- Si-Co(Pt)(Au), high energy density pulsed ion beam irradiation, study of reacted layers 7-52151
- SiC (4H) p-n junction, ion implanted, S-type I-V characteristic 7-64320
- Si₃N₄ CVD layers, etch rate modification by ion bombard. and annealing 7-28217
- Si₃N₄ film synthesis by ion-assisted deposition, antireflection coating use 7-37213
- Si₃N₄ LPCVD films, bombardment induced H redistrib. 7-38404
- Si₃N₄, mixing of metal overlayers, ion beam irradi., rapid thermal annealing, pulsed laser irradi. 7-58330
- SiO₂ evaporated and ion assisted deposited coatings, microstruct., electron microscope obs. 7-52335
- SiO₂ film synthesis by ion-assisted deposition, antireflection coating use 7-37213
- SiO₂, fused silica, O₂⁺ and Kr⁺ irradiated, paramagnetic defects, ESR study 7-53132
- SiO₂ glass, radiation damage 7-32520
- SiO₂, ion activated chem. etching, laser interferometer studies 7-6657
- SiO₂, ion-induced etching, surface processes 7-59702
- SiO₂, mixing of metal overlayers, ion beam irradi., rapid thermal annealing, pulsed laser irradi. 7-58330
- SiO₂, native oxide, ion and electron bombardment induced surface modifications studies 7-12175
- SiO₂-Al₂O₃-CaCO₃-Na₂CO₃ glass system, Ar⁺ ion beam effects 7-32521

ion beam effects continued

- SiO₂-Na₂O-CaO-Al₂O₃-MgO glasses, heavy ion irradiation, enhanced diffusion, preferential sputtering 7-32523
- SnO₂ (110), O deficient surface, photoemission study, comparison with TiO₂ (110) 7-46277
- Ta, BCC cryst. struct., secondary ion emission, current density effects 7-59318
- Ta-Cu, Cu₃ cluster formation, atomic mixing and demixing (*Chinese*) 7-53468
- Ta₂O₅ evaporated and ion assisted deposited coatings, microstruct., electron microscope obs. 7-52335
- Ti surface, heavy-ion-induced D desorpt. meas. 7-44990
- Ti_{1-x}B_x films deposited onto Mo by co-sputtering, D retention 7-51870
- TiC sputtered films, influence of ion bombardment 7-3171
- TiN (100) epitaxial film sputtering, defect density, ion irradi. effects, TEM study 7-58684
- TiO₂ (110), O deficient surface, photoemission study, comparison with SnO₂ (110) 7-46277
- TiO₂ evaporated and ion assisted deposited coatings, microstruct., electron microscope obs. 7-52335
- V film, B ion implementation, phase changes, electron microscopy study 7-12169
- V-Cr-Ti, ion-irradi., swelling and microstruct. evolution, effect of He 7-58359
- VCE formed by Ce ion implantation, lattice-location studies of Ce ions 7-2042
- W, polycryst. foils and single crystals, chemical etching, ion bombardment effects, AES study 7-28212
- W thin films, plasma-assisted etching, ion bombardment effects, quartz cryst. microbalance studies 7-28211
- (YEuTmCa)₃(FeGe)₂O₁₂ films, planar anisotropy and magnetisation, ion irradi. effects study 7-2906
- YIG, irradiation by high energy heavy ions, electronic stopping power effects on damage rate 7-58352
- ZnS thin films, radiation enhanced adhesion to SiO₂ substrates 7-32504
- Zr (0001) HCP to BCC phase transition He⁺ capture effects, AES, TDS and SIMS studies 7-58590
- Zr, HCP cryst. struct., secondary ion emission, current density effects 7-59318
- Zr-Fe amorphous alloys, chemical short range order, thermal relaxation and ion irradiation effects 7-44385

ion beam lithography

- conference, Catania, Italy (9-13 June 1986) 7-60865
- Delft ion beam pattern generator project progress 7-41532
- NanoFab-150, focused ion beam system 7-18913
- PMMA and Microdeposit 23M, As⁺ ion bombardment, appl. for ion beam lithography and masking 7-26810
- polystyrene, nanosecond proton and He ion pulse radiolysis studies 7-21297
- p-Si Schottky barriers, N₂ and Ar ion beam etching effects (*Korean*) 7-12858
- SiO₂ layers on Si, patterning of fine structs. by ion beam exposure and wet chemical etching 7-13656
- WO₃ amorphous films as high-contrast inorganic ion resists 7-63672

ion beam mixing

- alloy thin films, co-deposited, phase form. 7-59492
- beam-solid interactions and phase transformations, conference, Boston, MA, USA (Dec 1985) 7-9590
- collisional mixing, magnitude and mechanism 7-63677
- conference, Catania, Italy (9-13 June 1986) 7-60865
- dual-purpose machine, for ion implantation and ion beam mixing (*Chinese*) 7-51799
- layered solid, marker evolution on ion irradi., computer simulation 7-21302
- metal surfaces, ion beam and laser processing for improvement corrosion resist., surface modification program 7-65200
- metastable surface alloy form. and stability 7-16652
- Monte Carlo program, TCIS code and appl. (*Chinese*) 7-53469
- noble metal film adhesion on sapphire, ion beam induced enhancement 7-21292
- radiation-enhanced diffusion, cohesive energy correlation 7-32510
- semiconductor microelectronic structures, depth profiling by SIMS and AES 7-26790
- solid-solid interfaces, radiation-induced mixing 7-32516
- steel, high-speed, ion beam metallurgy processing, influence on surface props. (*Chinese*) 7-53764
- surface modification by ion beam enhanced deposition and dynamic ion mixing 7-64027
- surface modification by ion beam methods, review 7-27081
- thin films, interfaces and phenomena, conf., Boston, MA, USA (Dec 1985) 7-18502
- vapour phase crystal growth, ion/surface interactions, photo-induced reactions 7-53609
- Ag-brass, mixing layer, friction props., ion beam mixing (*Chinese*) 7-51888
- Al-Fe, ion induced metastable phases 7-63673
- Al-Mn surface icosahedral phase form., ion beam mixing and interdiffusion 7-16653
- Al-Pd, ion induced metastable phases 7-63673
- Al-Zn, ion induced metastable phases 7-63673
- AlAs/GaAs superlattice mixing induced by Si⁺ implantation 7-58649
- Al₂O₃/Fe interface, ion beam mixing, conversion electron Mossbauer spectra studies 7-63679
- B-Fe, ion beam mixing, effects of Xe⁺ implantation (*Chinese*) 7-51886
- B-Ni, ion beam mixing, effects of Xe⁺ implantation (*Chinese*) 7-51886
- Cu, ion mixing and thermochemical props. of markers 7-26805
- Cu-Er metallic glass, ion beam mixing, diffusion and phase separation meas. 7-16659
- Cu-W, layered, ion beam mixing, energy and dose depend., RBS 7-38075
- Fe/Cu multilayered samples, ion beam mixing-induced metastable phases 7-58377
- Fe/Ti multilayered struct., wear and friction, ion beam mixing effects 7-28141
- Fe-graphite structures, ion induced mixing, sputtering yield, fluoresc., RBS depth profile meas. 7-64844
- Fe-Ti/AISI 304 stainless steel system, ion beam mixed, wear and friction studies 7-46657
- GaAs, ohmic contact, form. using ion beam mixing 7-21299

ion beam mixing continued

- In-Sn alloy, diffusion coeffs. of In and Sn determ. by AES using Xe ion bombardment 7-22405
 Mo film ion beam mixing of marker atoms, heat of mixing effect 7-21304
 Mo film on Si, ion beam mixing, amorphous layer form. 7-21301
 MoS₂ sputtered films, tribological props., ion beam mixing effects 7-3441
 Ni/Cr(Nb) alternating layers, ion beam mixing 7-21303
 Ni-Al alloy phase transforms. during ion beam mixing, electron diff. and microscopy studies 7-16655
 Ni-Cr films, sputter deposition and ion beam mixing, microstruct. 7-44630
 Ni-Ti films, sputter deposition and ion beam mixing, microstruct. 7-44630
 Ni-Ti metallic glass, ion beam mixing, diffusion and phase separation meas. 7-16659
 Ni-TiC-Si, TiC as mixing barrier for Ni-Si ion beam mixing 7-44922
 Pd-Ti matrix-marker layer system, cascade mixing, projectile mass depend. 7-58375
 Pd_{0.67}B_{0.33}, amorphous, prep. by low temp. ion beam mixing (Chinese) 7-51887
 Ru film, ion beam mixing of marker atoms, heat of mixing effect 7-21304
 Si:P,Sb, mixing of P and Sb ions by recoil implantation, sheet resist., annealing temp. depend. 7-21291
 Si/Ni system, silicide formation, ion beam induced, embedded markers and moving species 7-21298
 Si/Pt/Si layered marker evolution on ion irradi., computer simulation 7-21302
 Si-Ta interface, depth profile, Ar⁺ ion bombard., Auger electron spectra anal. 7-46261
 SiC, mixing of metal overlayers, ion beam irradi., rapid thermal annealing, pulsed laser irradi. 7-58330
 α -SiC polycrystals, pulsed laser annealing and ion beam mixing surface modification studies 7-16657
 α -SiC, sintered, non-equilib. surface conditions and microstruct. changes following pulsed laser irradi. and ion beam mixing of Ni overlayers 7-65170
 Ta-Cu, multilayer systems, temp. depend. of ion beam mixing, 77-book (Chinese) 7-51884
 TiN, ion beam enhanced deposition on tool steel, friction and wear reduction 7-53910
 TiN thin film, adhesion on PBI plastic produced by large-current ion implantation machine (Japanese) 7-8149
 TiSi₂ formation by As⁺ ion beam mixing and rapid thermal annealing 7-52153
 W-Cu, multilayer systems, temp. depend. of ion beam mixing, 77-book (Chinese) 7-51884
 WSi₂ formation by As ion implantation, ion beam mixing (Chinese) 7-51797
 Zr, oxidation effect of Ar ion beam mixing (Chinese) 7-53997

ion beams

- see also beam-foil spectra; beam-foil spectroscopy; energy loss of particles; ion beam effects; ion optics; ion-surface impact; mass spectrometers; particle accelerators*
 canal rays to ion implantation, review article 7-55920
 charged-particle beams in cylindrical waveguide, ponderomotive confinement 7-35624
 coincidence laser spectroscopy, ultrasensitive technique for fast ionic or atomic beams 7-30100
 cyclotron resonance, phase indication 7-22144
 divergence angle of intense pulsed ion beam extracted from dual-current-feed magnetically insulated diode 7-11802
 elements, charge distrib. in ion beam produced from RF-spark ion source 7-46883
 EM ion beam instabilities, one and two dims. simulations 7-6379
 EM ion cyclotron beam anisotropy instability, contrib. to left-hand polarised mag. waves in magnetotail 7-66400
 Faraday cup to measure ion current in a strong magnetic field 7-19597
 frequency standards based on stored ions 7-14924
 gamma-ray beams produced by collision of relativistic ions with laser photons, spectrum and polarisation 7-50002
 generation and focusing from conical pinched electron beam diode 7-11806
 intense, propagation across plasma-filled magnetic cusp 7-42261
 intense light ion beams, current neutralisation in Ar gas 7-36363
 ion beam-target interaction, ablation process obs., backlighting technique 7-11793
 ionised cluster beams, form. and kinetics 7-15771
 low- β ion acceleration with a MEQALAC 7-15448
 low-energy ion beam generation from broad-beam ion sources, appl. to sputtering (German) 7-41537
 metal cluster ions, size-selected, in triple quadrupole arrangement, expts. 7-15777
 negative ion beam extraction and acceleration from low field surface produced sources 7-15445
 negative ion beam extraction and acceleration from volume prod. sources 7-15446
 pellet compression schemes, indirect irradiation by relativistic electron beam 7-11808
 plasma channels for light ion beam propag. in target development facility 7-15357
 plasma erosion switch, reflecting system 7-44268
 plasma focus device as beam source rms beam emittance 7-30807
 production, magnetically insulated diode 7-6472
 production of an ion beam from a beam focus 7-57228
 proton beam, intense, energy spectrum meas. with magnetic spectrography 7-42260
 proton beam deflection phenomena in a Pulselac post-acceleration gap 7-56892
 RF ion source, ion energy distrib., radial extraction, injected electron beam 7-30118
 self-magnetically-insulated plasma-focus diode, intense pulsed light-ion beam source 7-11803
 small-angle scatt., inverse square interaction pot. 7-53481
 strong intrabeam scattering in heavy ion and protonbeams 7-5516
 Thomson spectrometer, time-resolving for ion beam diagnosis 7-56372
 transport equation, soln. by flux decomposition method 7-20126
 transport through ideal quadrupole, hexapole and octopole operating in RF-only mode 7-41528
- ion beams continued**
 transverse field focusing matching/pumping system for beam injection 7-15440
 p beam, polarized, production technique 7-49168
 p(p) polarized beam production from Λ^0 , (Λ^0) decays 7-30796
 Ar⁺, (n=9, 13), metastable ion beams, forbidden lines, visible spectrum 7-57022
 Au ion beam, residual ranges in various media, time of flight spectra and adsorption meas. 7-25333
 Ca⁺, (n=11, 12), metastable ion beams, forbidden lines, visible spectrum 7-57022
 F³⁺, quintet transitions, beam-foil spectra anal. 7-31004
 Fe, multiply-charged ions, electron-impact ionisation cross sections, crossed-beam meas., rate coefficient calcs. 7-25660
 Fe+D(He)(C)(N)(O), thick target bombardment, X-ray production cross sections 7-20025
 H⁻, 30 kV accelerator for negative ion beams 7-18916
 H⁻ beam dynamics, mag. field studies in cyclotron 7-62168
 H⁻ extraction and electron control in multipole ion source 7-18915
 H⁺ beam, space charge compensation by pregenerated plasma 7-44200
 H⁺, pulsed ion beam, inductive post-acceleration obs., beam energy meas. 7-11805
 K⁺, (n=10, 11, 14), metastable ion beams, forbidden lines, visible spectrum 7-57022
 N₂⁺, effusive molecular beam crossed by an electron beam and the optical model of this effect 7-10738
 Nb⁺, (n=14, 15, 16), metastable ion beams, forbidden lines, visible spectrum 7-57022
¹⁴⁷Sm ion beam cross section meas. using SSNTD 7-19594
 Ti+D(He)(C)(N)(O), thick target bombardment, X-ray production cross sections 7-20025
- ion chambers** *see ionisation chambers*
ion counters *see counters*
ion cyclotron resonance heating *see plasma heating*
ion cyclotron resonance spectra *see mass spectra*
ion cyclotron resonance spectroscopy *see mass spectroscopy*
ion density
see also plasma density
 ion distribution near charged electrode, local density functional approx. 7-54131
 magnetotail plasma sheet, H⁺ and He⁺⁺ densities and temps 7-34789
 non-neutral ion plasma generation and diagnostics 7-51513
 He glow discharge, positive column, population difference and pulse-mode optogalvanic effect 7-26570
 SF₆ ions, densities, mobilities, Gerdien ion counter meas. 7-11581
- ion emission**
see also field ion emission; secondary ion emission; thermionic ion emission
 emission electronics, conf., Tashkent, USSR (Oct. 1984) 7-9575
 polyethylene, charged particle exoemission rel. to deform. and fracture 7-7827
 radiation induced electrostatic instability on surface of ionic crystals 7-46816
 GaAs, laser-induced damage and ion emission at 1.06 μ m 7-37008
 InSb, pulsed laser evaporation, neutral and charged particle emission 7-3120
 KCl:Ti, luminescence, intensive KrF laser irradiation (Russian) 7-17340
 Mg thin films, initial oxidation stages, emission phenomena 7-13629
 Si surface-barrier detector as source of slow protons 7-49777
- ion engines**
see also aerospace propulsion; rockets
 No entries
- ion etching** *see sputter etching*
- ion exchange**
 alkali metal ions, free energy, additivity rules (German) 7-2233
 borosilicate glass, dissolution method study using fission track method 7-53937
 cation-exchange resin, granulated, ionic composition, pulsed elec. field effects 7-54134
 chelate ion exchanger kinetics, equilib. and kinetic data 7-13731
 chelate ion exchanger kinetics 7-13730
 desalination ion exchange installations, meas. and control 7-28339
 2,9-dimethyl-1,10-phenanthroline intercalated into α -Zr(HPO₄)₂, ion exchange with Co²⁺, Ni²⁺ and Cu²⁺, dimer formation 7-65305
 electrodialysis, internal heat sources effects 7-13802
 fibre optic sensors, waveguide couplers, fabrication by ion exchange 7-57583
 glass, dilation by field-assisted ion exchange 7-11188
 glass, ion exchange, surface investig. by XPS and X-ray spectra studies 7-13614
 glass waveguides, ion-exchanged, stress 7-31454
 glass waveguides, semiconductor-doped and ion-exchanged 7-43357
 gradient index lens for low-loss coupling of laser diode to single-mode fibre, ion exchange fabrication 7-31465
 membrane water-electrolysis, alkaline type, for H₂ energy storage 7-3727
 membranes, MK-40, with electrodeposited basic polyelectrolyte films, permselectivity 7-13803
 membranes in organic salts, molar conductance, viscosity model 7-13801
 methyl halides, nucleophilic substitution reactions, quantum-mechanical model, HMO calcs. 7-36482
 naphthazarin, vibronic states relax., fluoresc. spectra study. 7-50221
 planar microlens fabrication by ion exchange/diffusion, distrib. index profile 7-31417
 single ions, transfer between two solvent, free energy 7-17785
 water desalination by electrochemical membrane process (German) 7-13819
 zeolite 13X, hydrophobic, generation by exchange with octadecylammonium ion 7-13809
 α -AgI ion-exchange reaction with β -Al₂O₃-Na₂O, potentiometric study 7-54230
 β -Al₂O₃:Nd³⁺, solid state laser host, optical props. 7-57343
 Al₂O₃-SiO₂ GRIN glass, delta-n control by additives in AgCl diffusion baths 7-31528
 BaSO₄ powder, solubility in water containing strong acidic ion exchange resin 7-21468
 Ca₂Si₆O₁₈·H₂O, tobermorite, ion exchange props. 7-59752
 CdS anodic film growth, initial stages, voltammetry and computer simulation studies 7-20216

ion exchange continued

- H(H₂O)₂BiO₃, prep. from KBiO₃ by ion exchange, high proton cond. 7-2260
 H₂O₂ behaviour in RBMK-1000 BWR safety control system coolant circuit 7-30631
 KCl (100), interaction of NaCl mol. beams with surface, desorption flux meas., SIMS obs. 7-33508
 KNO₃-glass, ion-exchange diffusion, planar waveguides 7-11108
 Li₃-H₂TaO₄, prep. by means of hydrothermal synthesis and protolysis 7-39449
 LiNbO₃ planar-optical waveguides, proton-exchanged, chem. and optical props. 7-57544
 LiNbO₃:Ti, low-loss TM-pass polariser fabricated by proton exchange in Z-cut waveguides 7-43444
 LiNbO₃:Ti waveguide, SHG, indiffusion proton exchange fabrication 7-25893
 LiNbO₃:Ti waveguides, proton-exchanged Fresnel lenses 7-31522
 Mn₂O₄, electrolytic preparation, phase transitions and ion exchange 7-3921
 Na-K ion-exchanged glass waveguides, swelling characts. 7-31532
 Na₂O-SiO₂-Ag₂O, Na⁺⇌Ag⁺ ion-exchanged, elec. conduction 7-27002
 α-RuCl₃, intercalation reactions, electron/ion transfer and exchange reactions 7-46837
 TiNO₃-glass, ion-exchange diffusion, planar waveguides fabrication 7-11108
 α-ZrP-propylamine, intercalation cpd., amine loading, protonic cond., admittance meas. 7-44909

ion exchanging *see* **ion exchange****ion excited X-ray emission** *see* **ion microprobe analysis****ion implantation**

- see also semiconductor doping*
 alloys, ion projection ranges and their distrib., personal computer programs (*Japanese*) 7-6659
 ball bearings, ion implanted, endurance life and fretting wear 7-13603
 bombardment-induced segregation and redistribution 7-58381
 canal rays to ion implantation, review article 7-55920
 ceramics, ion implantation and near surface microstructures, analytical electron microscopy 7-37816
 channelling contrast microscopy, He⁺ microbeam, semiconductor impurity profiles 7-51587
 conference, Catania, Italy (9-13 June 1986) 7-60865
 crystallisation dynamics of ion-implanted layers, during pulsed laser irradiation 7-44435
 depth distribution of ions implanted into singlecrystals 7-6667
 depth profiles for high fluence implantations, method of equivalent at. stopping 7-51795
 diamond, type IIa, ion implanted, volume expansion 7-58298
 diamond, volume expansion during ion implantation, point defect creation and interactions 7-51890
 dual-purpose machine, for ion implantation and ion beam mixing (*Chinese*) 7-51799
 elastic vibrations, mechanical stresses 7-12094
 erosion and wear of solids, ion implantation effect 7-63683
 Fe-D formed by D ion implantation, multiple D occupancy of vacancies 7-63643
 film, ferromag., backward bulk magnetostatic wave propag. by grating formed by ion implantation 7-53093
 fusion reactor first wall, implantation-driven permeation characts. 7-49640
 garnet bubble films, H₂⁺-implanted, thermal stability and aging 7-22124
 garnet bubble films, H₂⁺-implanted, H out-diffusion suppression of overlayers 7-38259
 garnet films, He⁺(H₂⁺) implanted, magnetisation and uniaxial anisotropy meas. 7-7576
 glass, Ar ion implantation, effect on mechanical and optical props. (*Chinese*) 7-51796
 hard coatings formed by Ti implantation on 304 stainless steel, XPS study 7-3154
 III-V semiconds., ion beam damage-induced masking for photoelectrochem. etching 7-44628
 Inconel 600, corrosion resist., effects of BF₂⁺ ion implementation 7-39734
 inert gas bubble precipitate solid in Al, defects, high resolution electron microscopy studies 7-32424
 inert gases implanted in solids, model of diffusion and release behaviour (*Chinese*) 7-38257
 inhomogeneous materials, implanted ion depth distrib. 7-21250
 InP:Si, ion implanted, rapid thermal annealing and solid phase epitaxy 7-21296
 insulators, chemical modification by ion implantation, hot atom chemistry processes, review 7-26813
 ion beam transport system, ion-optical characteristics (*Korean*) 7-24723
 kinetics of implanting accelerated gas ions in crystalline solids 7-6649
 low temperature equipment (*Chinese*) 7-61336
 magnetic bubble devices, ion-implanted, bubble generation mechanism 7-59082
 magnetic domain studies, review 7-17209
 materials modification with ion beams, review 7-16647
 metal surfaces, ion beam and laser processing for improvement corrosion resist., surface modification program 7-65200
 metal surfaces, ion implanted, durability 7-53918
 metal wear resistance, ion implantation and ion assisted coatings 7-3513
 metal-carbide composites, implantation modified, friction, surface chemistry 7-46660
 metallic glasses-H₂, prep., struct. and props. 7-26663
 metallic materials, ion implantation and near surface microstructures, analytical electron microscopy 7-37816
 metallic materials, surface refinement by ion implantation, friction, abrasive and corrosion resist. (*German*) 7-53949
 metals, H ion implants, trapping coefficients 7-6884
 metals, ion beam-induced nitride form. and phase identification, X-ray diff. study 7-12176
 metals, ion implantation of inert gases, high press. precip. phases 7-38031
 microelectronic materials processing, appl. of neutron depth profiling, book contrib. 7-44595
 Monte Carlo methods to solve theoretical problems 7-2034
 Monte Carlo program, TCIS code and appl. (*Chinese*) 7-53469
 MOS structures, ion implanted, enhanced tunnelling 7-64358
ion implantation continued
 multilayer targets, models for implementation 7-26772
 noble metal film adhesion on sapphire, ion beam induced enhancement 7-21292
 nonequilibrium surface layers, electron emission props. 7-12090
 photodisplacement techniques for defect detection 7-44865
 phthalocyanine polymer films, I₂ implantation 7-26776
 plasma source ion implantation 7-26547
 polydiacetylene, conductivity enhancement by chemical doping and ion implantation 7-21957
 polydiacetylenes, analogies to inorganic semiconductors and graphite 7-2592
 polydiacetylenes as nonlinear waveguide materials, fabrication 7-25871
 polymer films, radiation-induced implantation in metallic substrates 7-8163
 polyphenylenesulphide:As conducting polymers, ion implantation techniques 7-21923
 precision function components, improvements made by ion implantation (*Chinese*) 7-53919
 processing machines develop. (*Japanese*) 7-53637
 pulsed mixed Ti⁺ and N⁺ ion beams (*Chinese*) 7-51800
 quartz: Cu⁺(Fe³⁺)(Nb⁵⁺), ion implanted, coloration and transparency (*Japanese*) 7-7656
 quartz, ion implanted optical waveguides, refractive index profiles 7-25964
 radiation-enhanced diffusion of implanted impurities in semiconductors, calc. 7-6883
 range and damage 3D distrib. including recoil transport 7-63691
 range distributions, moment calcs. 7-2072
 rapid thermal processing, conf., Boston, MA, USA (Dec. 1985) 7-14713
 rolling bearings, friction, wear and corrosion control 7-46658
 Rutherford backscattering-particle induced X-ray emission analysis, large residual defects 7-54251
 sapphire, implanted ions recrystallisation driven migration and oriented precipitation 7-2266
 sapphire, ion implantation, mechanical surface property modifications 7-32473
 semiconducting materials, cryst., and device appls., book 7-60894
 semiconductor, interaction of high power pulsed ion beams, solid phase epitaxy 7-12096
 semiconductors, disordered, ion implanted, low power laser annealing 7-38055
 semiconductors, implanted ions diffusion redistribution, effect of radiation defects 7-51810
 semiconductors, impurity profiles, depth resolution of SIMS 7-54253
 semiconductors, ion implantation and near surface microstructures, analytical electron microscopy 7-37816
 sheet resistance low dose monitoring using the double implant technique 7-21244
 Si-Al Schottky barriers, Ar ion implantation damage, thermal anneal recovery 7-17101
 SOI, conf., Boston, MA, USA (Dec. 1985) 7-35101
 SOI buried layer form. by high dose implantation, mass transport studies 7-32479
 SOI formation, high dose O⁺ ion implantation, lamp annealing 7-32527
 SOI lateral solid phase epitaxy, selective P ion implantation 7-52359
 SOI structures, ion beam synthesised, carrier lifetime increase 7-12865
 SOI structures, ion implanted, defect EPR spectra studies 7-27603
 SOI wafers, O implantation prep., background doping effects 7-32478
 solar cell high throughput automated fabrication line 7-8417
 solids, ion-implanted impurities, steady-state concs., ultimate retained doses, determ. 7-6658
 SOS, double solid phase epitaxial regrowth, amorphous layer, self-implantation, ion energy, defect density 7-58691
 SOS films, regrowth rates of amorphous layers created by self-implantation 7-16661
 steel, austenitic, thermal desorption after high-energy d implantation 7-52232
 steel, austenitic stainless, oxide scales formed in CO₂ at 825°C, microstruct., influence of ion implantation 7-65196
 steel, implanted with N ions, physicochem. characters. of surfaces, wear resist. (*French*) 7-28209
 steel, ion implantation and thermal oxidation treatments for wear reduction 7-3481
 steel, low alloy XC06, N implanted, grazing incidence X-ray diffraction 7-16591
 steel, martensitic stainless, bearing appls., Ti and C ion implantation, enhanced lubricated sliding wear resistance 7-53916
 steel, migration-effect of N⁺ implantation, during wear (*Chinese*) 7-53998
 steel, mixed Ti⁺ and N⁺ ion beams composition and struct. changes (*Chinese*) 7-51800
 steel, N⁺ implanted layers, in 9Cr18, GCr15 steels (*Chinese*) 7-53996
 steel, stainless, ion implanted with N, fretting wear resist. 7-13636
 steel, stainless, surface deuterium recombination 7-62063
 surface engineering for corrosion protection 7-3478
 surface modification by ion beam enhanced deposition and dynamic ion mixing 7-64027
 surface modification by ion beam methods, review 7-27081
 synthetic metals science and technology, conf., Kyoto, Japan (June 1986) 7-60872
 Triotron sputtering equipment for the production of mixed Ta/Si layers (*German*) 7-33564
 uniform ion doping, beam energy calc. program 7-32477
 X-ray diffraction analysis, of structural changes (*Chinese*) 7-51801
 X-ray fluorescence, grazing incidence, for implantation profile tracing (*French*) 7-13834
 ZnO:Bi (Sb) (transition metal), Schottky-like barriers, ion implantation, annealing 7-58860
 Ag-D films, implanted, elec. resist. meas., vibr. props. 7-38775
 Al disks, He ion implanted, He re-emission ratios and surface obs. (*Japanese*) 7-12089
 Al foils, alumina form. by O₂⁺ implantation, sheet resistance and XPS meas. 7-26780
 Al, implanted, FCC solid Ar bubbles, X-ray diff. 7-2043
 Al, polycrystalline, near surface struct., simultaneous He⁺ and H⁺ implantation effects 7-58302
 Al:Bi-KCl:Bi, bilayer cpd., Bi ion implantation, thermal annealing 7-32474
 Al:Eu³⁺, ion implanted, anodization, electroluminesc. obs. 7-7761

ion implantation continued

- Al-Al₂O₃-Au sandwich struct., forming process in high elec. field (Japanese) 7-22028
 Al-Ge mixture, H implanted, evidence for metal-insulator transition in Al 7-2483
 Al-Ni-Pt, high temp. oxidation rel. to alloying additions, ion implantation, Rutherford backscatt. 7-53987
 Al-Si:Ar,H, ion implanted ultrahigh Schottky barriers, interfacial traps, DLTS study 7-45489
 Al-Si/MoSi₂ stable contacts to shallow junctions 7-52847
 Al-Xe, implanted, form. of solid precipitates and fluid bubbles, TEM obs. 7-38032
 AlAs/GaAs superlattice mixing induced by Si⁺ implantation 7-58649
 AlAs-GaAs superlattices, Si ion implantation, dose-dependent mixing 7-12500
 AlAs-GaAs superlattice, Si⁺ implantation, depth dependent mixing 7-27032
 AlAs-GaAs superlattices, disordering by Si and S implantation 7-45024
 AlAs-GaAs superlattice, compositional disordering control by Ar ion implantation 7-51806
 AlGaAs MQW lasers, index-guided, fabrication by selective disordering using Be focused ion beam implantation 7-20269
 AlGaAs multiquantum well-buried optical guide lasers, fabrication by Si-induced disordering 7-10995
 AlGaAs-GaAs superlattices, Se (Si)(Mg)(Be) ion implantation, intermixing, residual damage 7-26782
 AlGaAs-GaAs-Si, Be superlattices, correlation between Si diffusion and Si-induced disordering 7-38034
 Al_xGa_{1-x}As:Be epitaxial layers, ion implanted, rapid thermal annealing 7-21257
 Al_xGa_{1-x}As-GaAs superlattices, ion implanted, defect struct. 7-26783
 Al₂Mo precipitate microstruct. and orientation, implantation and annealing effects, electron microscopy study 7-16782
 AlN formed by N ion implantation of Al, electronic struct. 7-58926
 α-Al₂O₃, crystallisation of amorphous surface layers 7-58304
 β-Al₂O₃, diffusion of implanted ions (Chinese) 7-51798
 Al₂O₃ subsurface layers formed by O₂⁺ ion implantation into Al, O₂ bubbles obs. 7-2035
 α-Al₂O₃:Br, ion implanted, RBS and annealing studies 7-32515
 α-Al₂O₃:N⁺, ion implantation, ion-acoustic microscopy 7-51792
 Ap-Xe-Kr(Ar), ion implanted, bubble growth, lattice parameters, TEM obs. 7-51803
 Au, surface deuterium recombination 7-62063
 Au-Ge/Ni/GaAs ohmic contacts, ion implantation and metallisation prep. 7-22014
 B-Fe, ion beam mixing, effects of Xe⁺ implantation (Chinese) 7-51886
 B-Ni, ion beam mixing, effects of Xe⁺ implantation (Chinese) 7-51886
 Bi, electronic structure, effect of ion implantation 7-45143
 Bi₃Ni, α-irrad. and H implanted, elec. resist. and superconducting T_c 7-7202
 C:Au(Bi) films, ion implanted, projected ranges and range stragglings, RBS anal. 7-63690
 CaTiO₃, crystallisation of amorphous surface layers 7-58304
 Cd_{0.7}Hg_{0.3}Te:B⁺, ion implanted, photoreflection spectra in the edge absorption region 7-39099
 CdS:Ri⁺(Kr⁺)(Ar⁺)(Ne⁺), ion implantation damage 7-26812
 CdTe: B⁺(Cu⁺) ion implantation damage, rapid thermal annealing, photolum. anal. 7-39162
 CdTe, segregation coeffs. of Ag, Co, I and In, recoil implanted radioactive tracer technique 7-21461
 Co-Cr-Al-Hf(Y), high temp. oxidation rel. to alloying additions, ion implantation, Rutherford backscatt. 7-53987
 CoSi₂-Si, mesotaxy, single crystal growth of buried CoSi₂ layers 7-58671
 Cr-C, deposited on Fe, surface amorphous alloys, Ar⁺ and Xe⁺ bombardment (Chinese) 7-51885
 Cr-Mo, deposited on Fe, surface amorphous alloys, Ar⁺ and Xe⁺ bombardment (Chinese) 7-51885
 Cu mirrors, Ag⁺ implanted, laser oxidation and optical props. 7-5971
 Cu:Ar(Ne)(C), single crystal, ion implantation, damage profile anal. using Auger electron spectroscopy 7-51802
 Cu-based alloys, rapid solidified and ion implanted, struct. studies 7-21130
 Cu-Fe, implanted solid solns., Mossbauer study on thermal dynamics of Fe atoms 7-45855
 Cu-Fe host-impurity system, O ion bombarded, internal oxidation, Mossbauer spectra studies 7-59131
 CuInS₂:P, ion implanted, pulsed electron beam annealing 7-16644
 CuZr metallic glass, blistering under He implantation, EELS anal. 7-16593
 D trapping and desorption during high fluence implantation in insulators and semiconds. 7-26781
 Fe, migration-effect of N⁺ implantation, during wear (Chinese) 7-53998
 Fe single crystals, Bi ion implantation, high substitutional fractions 7-58299
 Fe:B polycrystalline films, amorphous alloy layer formation by ion implantation (Chinese) 7-6647
 Fe-Al, al alloying for oxidation resist. improvement, comparison between ion implantation and laser irrad. 7-22883
 Fe-based amorphous alloys, O₂ adsorption, ion bombardment effects 7-21637
 Fe-Br, mag. hyperfine field of ⁸²Br, NMR nuclear orientation study 7-13049
 Fe-C-N, ion implanted, C surface contamination, AES and XPS studies 7-38312
 Fe-Cr, P implanted amorphous alloys, corrosion, passivation, microstruct. 7-65180
 Fe-Cr (12 at.%), ferritic alloy, He⁺ implantation and Fe⁺ irrad., bubble nucleation and growth 7-58362
 Fe-Cr alloys in acidic electrolytes, effects of P implantation on passivity 7-59658
 Fe-N, implantation at 77 K, surface comp., microstructure, AES, HVEM, transmission HEED studies 7-38033
 Fe-Ti-C ion-implanted amorphous alloys, precipitate microstruct. studies, conc. depend. 7-16434
 FeCrAlY coatings, ion-implanted, oxidation behaviour 7-53974
 Fe₁₆N₂, high-dose ion implantation prep., mag. props. 7-59055
 Fe₃₀Ni₅₀ alloy foils, N₂⁺ implantation, oxidation behaviour, conversion electron Mossbauer spectra study 7-22877
 Ga_{1-x}Al_xAs, ion-implanted, defect creation 7-21240
 GaAs, by H⁺, He⁺, Ar⁺, elastic vibrations 7-12094

ion implantation continued

- GaAs, ion implant depth profiles, channelling, Monte Carlo simulation 7-51811
 GaAs, ion implanted, flash tube annealing 7-39551
 GaAs, ion implanted, rapid thermal annealing, review 7-58296
 GaAs, ion implanted, stoichiometry violation, electron microscopy studies 7-12303
 GaAs, ion implanted and laser irradiated, defect studies 7-32432
 GaAs, ohmic contact, form. using ion beam mixing 7-21299
 GaAs, solid-phase-epitaxy, interface structure and impurity effects 7-2407
 GaAs, transient thermal processing 7-16601
 GaAs, undoped semi-insulating, dislocations, deep trap levels, FET meas. (Chinese) 7-12643
 GaAs:Al, surface layer, degree of disordering, effect of dopant 7-63929
 GaAs:Al⁺(P⁺), ion implantation damage 7-38024
 GaAs:B, ion implanted, near-intrinsic and extrinsic photocapacitance due to the EL2 level 7-7147
 GaAs:B, ion implanted, struct. and damage distrib., TEM study 7-51893
 GaAs:B buried isolation layer form. by focused ion beam, FIBI-MBE system 7-51804
 GaAs:Be⁺, ion implanted, residual microstruct., TEM studies 7-32675
 GaAs:H, ion implanted, damaged layers, IR Raman probing 7-59191
 GaAs:Mg MBE layers, photoluminescence 7-22295
 GaAs:Mg⁺, formation of p-type layers using ion implantation and rapid thermal annealing 7-45311
 GaAs:P, ion implanted and pulse laser annealed, Raman study 7-6653
 GaAs:Se, ion implanted, annealing mechanism 7-26777
 GaAs:Si, electrical props. of p-type layer 7-12722
 GaAs:Si, ion implanted, amorphisation and epitaxial regrowth, defect depth profiles 7-12088
 GaAs:Si, ion implanted, rapid thermal annealing effects 7-21259
 GaAs:Si, ion implanted and rapid thermal annealed, activation efficiency, crystal stoichiometry effects 7-51791
 GaAs:Si, semi-insulating, ion implanted, LEC growth, elec. activation efficiency, stoichiometry dependence 7-46298
 GaAs:Si⁺ wafers, implant at. profiles, planar and residual channelling effects 7-12181
 GaAs:Si(B)-Ga_{0.25}Al_{0.75}As:Si(B) quantum wells, ion implanted, TEM and photolum. studies 7-58865
 GaAs:Zn, ion-implanted, acceptor-associated emission, selective self-optical compensation effect 7-22304
 GaAs/AlGaAs superlattice, compositional disordering by focused ion beams 7-6695
 GaAs/AlGaAs superlattices, Si implanted, compositional disordering, SIMS studies 7-12091
 GaAs-AlAs, superlattices, mixing, ion implantation, rapid thermal annealing, Raman scattering 7-53355
 GaAs-AlAs MQW structures, Ga⁺ ion implantation defects 7-44585
 GaAs-AlAs superlattices, Se implantation, effect on compositional disordering 7-26784
 GaAs-AlGaAs heterojunctions, Be⁺, O⁺ ion implantation, impurity profiles, elec. characts. meas., SIMS, annealing 7-12813
 GaAs-GaAlAs heterojunction bipolar transistors, ²⁴Mg and ⁶⁴Zn implanted profiles 7-44591
 GaAs_{1-x}P_x:Be⁺-GaP:Be⁺ strained-layer superlattices, ion implantation doping, structural study 7-38030
 GaAs_{1-x}P_x:Be⁺-GaP:Be⁺ strained layer superlattices, ion implantation doping, optical and elec. props., device appls. 7-44583
 GaInAs, pn junction formation by simultaneous implantation and diffusion annealing 7-38028
 Ga_{0.47}In_{0.53}As:Be epitaxial films, ion implanted, rapid thermal and furnace annealing 7-22729
 GaP single crystals, high energy ion implantation, damage profiles 7-16590
 GaP:He⁺ implanted, swelling, strain and radiation damage 7-6694
 (Gd,Bi)₃(FeGaAl)₂O₁₂ garnet films, selected area liq. phase epitaxy, local ion implantation effects 7-21726
 Ge, mixed group III and group V ion implantation 7-21243
 Ge ultra-thin films, self-implantation, grain growth enhancement, TEM study 7-12173
 Ge:H films, post-deposition hydrogenated, electrical props. 7-32296
 Ge:Si, ion-implanted amorphous surface layers, EXAFS 7-27823
 HgCdTe materials for infrared detectors, prep. techniques 7-64019
 HgCdTe: In, ion implanted, damage and rapid thermal annealing 7-63637
 HgCdTe:B, bulk and thin film, resonant impurity levels, magnetotransport studies 7-64162
 HgCdTe:B⁺, ion implanted n⁺p junction, lifetime and carrier conc. profile 7-45450
 Hg_{1-x}Cd_xTe:B, ion implanted, annealing, nature oxide encapsulation 7-2036
 HgGa₂Se₄, photocond., photoluminescence spectra, annealing and ion implantation effects 7-39152
 HgGa₂Se₄, single cryst., deep levels, photocond. and photolum. spectra 7-7159
 In_{0.53}Ga_{0.47}As:Be, high dose implants, rapid thermal annealing 7-16602
 InP, high resistivity layer form. by ion implantation, ohmic contact characterisation 7-38035
 InP:Be(Si), isothermal anneal techniques, comparison 7-16603
 InP:Fe, Si-implanted and rapid thermal annealed, photoluminesc. study 7-59243
 InP:Hg ion implanted at 200°C, rapid thermal annealing, carrier conc. and mobility 7-32469
 InP:Mg p-n junction waveguide fabricated by Mg ion implantation 7-64326
 InP:Zn, ion implantation and annealing, Raman studies 7-6652
 LiF, F- and F₂-centres induced by ion implantation 7-26747
 LiF, N ion implanted and X-irrad., microhardness response 7-21344
 LiF:C⁺, ion implanted, impurity defects outside implantation zone 7-7773
 LiF:Ne⁺(Ar⁺), defect and colloid production by ion implantation 7-26746
 LiH, ¹¹C and ¹³N implantation, chemical effects, radiochromatography study 7-28324
 LiMO₃ (M=Nb,Ta), ion implanted optical waveguides, refractive index profiles 7-25964
 LiNbO₃, by H⁺, He⁺, Ar⁺, elastic vibrations 7-12094
 LiNbO₃, He⁺ implantation, lattice disorder, refractive index changes 7-25966

ion implantation continued

- LiNbO₃ optical waveguides, ion-implanted, optical damage resistance 7-43360
- LiNbO₃, optoelectronic material, radiation effects 7-26811
- LiNbO₃ planar waveguides, He⁺ ion implantation, transient annealing 7-25965
- LiNbO₃:He⁺ implanted waveguide stability 7-43364
- LiNbO₃:He⁺ optical waveguides, thermal annealing 7-15983
- LiNbO₃:He⁺ optical waveguides, ion implanted, Li outdiffusion modelling 7-62832
- MgAl₂O₄:He spinel, implanted, high temp. electron irradi., structural damage 7-51829
- MgO:H, C single crystals, ion implanted, C and H diffusion behaviour, SIMS studies 7-32714
- MgO:Na, ion implanted single crystals, HREM obs. 7-12292
- Mo, He pipe diffusion along dislocations 7-58544
- Mo, thermodynamic stability in a fusion reactor environment, H, O and C implantation and diffusion 7-49658
- Mo:Cu(Re), pulsed ion implantation, surface struct. 7-51867
- Mo:D, ion implanted, impurity trapping 7-38029
- Mo-N polycrystalline films, implanted, single defects, X-ray diffr. data anal. 7-38372
- Nb:He⁺ (H⁺) films, radiation defects produced by ion implantation 7-7059
- Nb-D, implanted, lattice distortion, channelling method 7-58382
- Nb-N polycrystalline films, implanted, single defects, X-ray diffr. data anal. 7-38372
- Nb₂Si₂, N⁺ implantations, effect on A15 phase formation 7-63480
- ²⁰Ne⁺ and ²²Ne⁺, ion implantation in elemental solids, range profile, gamma-ray spectra 7-2959
- Ni, ion implantation and pulsed laser melt quenching, metastable phase and defect struct. form. studies 7-16625
- Ni, ion irradiation-induced implant diffusion and segregation, synergistic effects, kinetic model calcs. 7-16658
- Ni-B, ion implanted, high temp. oxidation, defect diffusion 7-33846
- Ni-Al(Si), aged γ/γ' alloys, He⁺ implantation studies 7-22690
- Ni-B, implanted, mech. props., disorder and amorphicity 7-53819
- Ni-B amorphous films, ion implanted and sputtered, elec. props. 7-22032
- Ni-P, implanted, mech. props., disorder and amorphicity 7-53819
- Ni-P ion-implanted and melt spun amorphous alloys, crystn., TEM, RBS and DTA meas. 7-16439
- Ni-Si-Mg, high temp. oxidation rel. to alloying additions, ion implantation, Rutherford backscatt. 7-53987
- Ni₃B, amorphisation by ion implantation, RBS/channelling studies 7-11912
- Pb_{1-x}Sn_xTe:⁵⁷Br⁺, depth profiles, SIMS meas. and theoretical calcs. 7-6662
- Pd/Si:B,As/Si:B, As ion implant redistribution during Pd₂Si formation using rapid thermal annealing 7-16816
- Pd-Fe:B(O), mag. susceptibility, impurity effects 7-27520
- Pd-H system, ion implanted, XPS and UPS studies 7-7813
- Pd 7-17871
- Si : BF₂ preamorphised implanted samples, defects and leakage currents abs. 7-38514
- Si, amorphised and rapid thermally annealed, extended defects 7-16660
- Si, amorphised films, solid phase epitaxial regrowth, TEM characterisation 7-32883
- Si, amorphous, ion implanted, picosecond laser induced crystn. 7-16621
- Si, Auger electron spectroscopy, sensitivity, contamination levels 7-54245
- Si buried oxide form. mechanisms by ion implantation 7-44580
- Si buried oxide structure formed by O ion implantation 7-12099
- Si, by H⁺, He⁺, Ar⁺, elastic vibrations 7-12094
- Si crystals, low energy Ag⁺ implantation-induced deep centre depth distrib., DLTS study 7-26820
- Si defect annealing and impurity activation during high-intensity As⁺ implantation doping 7-58295
- Si, defect diagnostics for submicrometer VLSI, book contrib. 7-44562
- Si, defects and device processing, achievements and limitations 7-32428
- Si detectors, high UV sensitivity and scintillator readout appls. 7-19666
- Si, diffusing metallic impurities, H implantation effects 7-12370
- Si, diffusion of ion-implanted impurities, modelling on IBM PC 7-38265
- Si, dislocation loops, generated by ion implantation and furnace annealing, depth profiles, RBS, X-ray diffr., TEM anal. 7-51882
- Si, disorder generation by Ar⁺ implantation, Rutherford backscatt.-channelling meas. 7-63680
- Si films, grain size and texture enhancement by seed selection through ion channelling 7-38401
- a-Si films, ion implanted device structures, solid phase epitaxy, elec. props. 7-12564
- Si films, solid epitaxial regrowth, structural and electrical characteristics 7-38403
- Si, heavily doped, thermoreflectance, study 7-45999
- Si, high dose implantation, with Co, Ni, Fe ions struct. and phase modifications 7-12095
- Si homogeneous amorphisation, ion implantation energy depend. study 7-63638
- Si, implantation damaged, transient enhanced dopant diffusion 7-44910
- Si, implanted layers, short time annealing, light source comparisons 7-21263
- Si, impurity profiles, depth resolution of SIMS 7-54253
- Si, ion beam induced recrystn., channelling effect 7-16650
- Si, ion implantation, damage profile studies, multilayer model (*Chinese*) 7-6648
- Si, ion implantation, interstitial trapping, dopant migration and epitaxial regrowth 7-12103
- Si, ion implantation-induced amorphous layer, temp. and dose depend. model calcs. 7-16594
- a-Si, ion implanted, 2D model of nucleation and regrowth 7-38408
- Si, ion implanted, amorphous phase transformation during rapid thermal annealing 7-16435
- Si, ion implanted, damage profiles, multilayer anal. by optical spectra (*Chinese*) 7-58294
- Si ion implanted, epitaxy by thermal and laser processing, review 7-33706
- Si, ion implanted, laser beam melting and resolidification 7-12126
- Si, ion implanted, mech. stresses, laser interferometer studies 7-6657
- Si ion implanted surface dopant cross-contamination, enhanced diffusion effects 7-32719
- Si, ion implanted with Ar⁺, H₂ passivation, polycrystalline phase formation 7-12087

ion implantation continued

- Si ion-implanted with MeV energy B⁺, P⁺ and As⁺ ions, annealing behaviour 7-51776
- Si masked ion-implanted devices for solar cell and optical sensor appls. 7-40006
- Si materials and process charact. for VLSI, SIMS studies 7-33988
- Si materials science and technology, conf., Boston, MA, USA (May 1986) 7-29598
- Si materials science issues in IC processing 7-35115
- Si, mixed group III and group V ion implantation 7-21243
- Si polycrystalline films, sheet resistance, rapid thermal annealing prior to and post As ion implantation 7-12886
- Si polycrystalline solar cells, passivation by low-energy H⁺ ion implantation 7-23157
- Si, rapid thermal annealing of ion implanted layers, role of trapped interstitials 7-17568
- Si, recoil implantation of O₂, characterisation by double-crystal X-ray diffraction, TEM, Monte Carlo simulation 7-51807
- Si SOI, buried oxide structures, ion implanted, ESR studies 7-59111
- Si SOI structure, high-dose O₂⁺ implanted, dopant diffusion 7-52139
- Si SOI structure, O⁺ implantation and high temp. annealing 7-44579
- Si SOI structures, implanted buried oxide, high-temp. annealing 7-6654
- Si SOI structures, O₂⁺ implanted, oxide precipitates, ordering 7-21449
- Si, self-implantation, damage production kinetics 7-21239
- Si, self-implantation-induced temp. depend. amorphisation, TEM and Monte Carlo simulation studies 7-16595
- Si, self-implanted, defects and amorphisation 7-2041
- Si, self-implanted, strain 7-51918
- Si single cryst., transition metal ion implantation, silicide form., RBS and X-ray diffr. studies 7-16656
- Si single crystals., insulating cpd. form. by ion beam synthesis, RBS, SIMS and cross-sectional TEM studies 7-26779
- Si solar cell fabrication using masked ion implantation using SiO₂ 7-23165
- Si solar cells, crystalline, metal grid optimisation and emitter tailoring, computer model extension 7-54292
- Si solar cells, low recombination p⁺ and n⁺ regions for high performance 7-3655
- Si solar cells, multicrystalline, thermal annealing for fabrication 7-17865
- Si solar-cells, loss reduction by ion implantation, laser radiation, protective coatings (*Dutch*) 7-23134
- Si, substrate for CVD of W, effects of dopants and cryst. perfection 7-16912
- Si substrate for W CVD, effect of dopants and crystal perfection 7-22576
- Si surface, effect of preoxidation annealing, ion implantation and sputtering on oxide film decomposition 7-63999
- Si wafers, self and ion beam annealing, epitaxial growth and damage layer, TEM study 7-12172
- Si:Ag, implantation damage regrowth studied via Ag depth profiling 7-22730
- Si:Ag-Ag, formation of Schottky junctions by Ag implantation in Si 7-12784
- Si:Al, atom and acceptor depth distributions of channelled Al as a function of ion energy and crystal orientation 7-21247
- Si:Al, ion implanted and annealed, Al precipitation, TEM studies 7-21238
- Si:Al implanted crystals., amorphous surface regions with crystalline impurity grains, TEM study 7-58579
- Si:Al(In), recrystallisation by pulsed electron beam, impurity profiles 7-16605
- Si:Ar, high dose implanted, thermal regrowth, RHEED studies 7-21734
- Si:Ar laminated structure formed by Ar ion doping, electroluminescence 7-7676
- Si:As, deep level spectra, ion implanted defects, laser annealing 7-21869
- Si:As, high dose implanted, defect density reduction by low temp. oxidation 7-58297
- Si:As, implanted, supersaturated soln., defect struct., TEM obs. 7-58483
- Si:As, ion implantation, damage profiles determ. by spectroscopic ellipsometry and stripping (*Chinese*) 7-32468
- Si:As, ion implantation-induced defects 7-32433
- Si:As, ion implanted, electronic transport props. 7-7233
- Si:As, ion implanted, rapid thermal annealing 7-16615
- Si:As, ion implanted, rapid thermal annealing, metastable activation 7-16616
- Si:As, Rutherford backscattering-particle induced X-ray emission analysis 7-54251
- Si:As,P, double diffused shallow junctions, rapid thermal annealing 7-22006
- Si:As (B)(BF₂⁺), p-n junction diode, rapid thermal annealing 7-22005
- Si:As films, preannealed and As ion implanted, structural changes during transient post-annealing 7-16904
- Si:As ion implanted, defect structs. generated by buried amorphous layer regrowth 7-38078
- Si:As ion implanted films, defects charactn. by AC Hall effect meas. 7-38601
- Si:As on sapphire, ion beam recrystallised and laser annealed, elec. props. 7-16649
- Si:As substrate, dopant redistrib. during silicide formation 7-21255
- Si:As⁺, heavily doped, ion implant deactivation 7-17567
- Si:As⁺(As₂⁺), ion implanted, phys. props., spreading resist., TEM, Rutherford backscattering, SIMS 7-26775
- Si:As(BF₂), ion implanted, diffusion and defects, transient scanning electron beam annealing 7-38065
- Si:As(B), ion implant redistribution, diffusion modelling 7-16814
- Si:As(B), ion implanted, pulsed laser annealing, optical reflection kinetics 7-58323
- Si:As(B) polycrystalline films, rapid thermal processing before and after ion implantation, effect on cond. 7-22046
- Si:As(P)(B)-SiO₂ interface, segregation, transport coeffs. of impurities 7-63880
- Si:Au,Fe-SiO₂, MOS struct., trap centres 7-7388
- Si:B, amorphisation by ion implantation 7-38080
- Si:B, B ion dose identification, HF C-U meas. 7-6661
- Si:B, BF₂⁺ ion implantation and rapid thermal annealing 7-21241
- Si:B, diffusion and activation of implanted B during rapid thermal annealing 7-16643
- Si:B, ion implanted, amorphous layer thickness, SIMS profiling 7-51794
- Si:B, ion implanted, B diffusion, rapid thermal annealing 7-58538
- Si:B, ion implanted, defect and dopant depth profile studies 7-2045

ion implantation continued

- Si:B, ion implanted, dopant redistrib. during rapid thermal annealing 7-38042
- Si:B, ion implanted, strain profile, double cryst. X-ray rocking curve simulation 7-2060
- Si:B, ion implanted, transient annealing and residual defect DLTS study (Chinese) 7-12642
- Si:B,P solar cells produced by pulsed excimer laser annealing of ion-implanted junctions 7-8419
- Si:B layers, preamorphised and ion implanted, structural and elec. characterisation 7-52347
- Si:B p^+-n solar cells fabricated using masked ion implantation, electro-optical characts. 7-23143
- Si:B p^+-n shallow junctions obtained by implantation into preamorphised Si, elec. charactn. 7-38703
- n-Si:B⁺(BF₃⁺), ion implanted, rapid thermal annealing, DLTS 7-16619
- Si:B⁺(BF₂⁺), ion implanted, characterisation by IR attenuated total reflection spectroscopy 7-17327
- Si:B⁺(BF₂⁺) submicron p-n junctions, ion implanted, dopant distrib., Raman study 7-21252
- Si:BF₂⁺ ion implanted, solid phase epitaxial growth, cross-sectional TEM study 7-38364
- Si:BF₂⁺ (001), ion implanted, residual defects, cross-sectional TEM study 7-32471
- Si:BF₂⁺ p^+-n diodes, BF₂⁺-implanted and rapid thermal annealed, junction leakage currents meas. 7-12814
- Si:BF_n⁺(PF_n⁺), ion implantation damage, backscattering channelling meas. 7-63675
- Si:B(Ga)(As)(Sb) 7-2040
- Si:B(P)(As)(Sb), retarded and enhanced dopant diffusion related to implantation-induced excess vacancies and interstitials 7-63881
- Si:C,N, ion implanted, C surface contamination, AES and XPS studies 7-38312
- Si:Cu, ion implantation-amorphised, direct imaging of pulsed laser-induced buried molten layers 7-12130
- Si:D, ion implanted, channelling meas. 7-16597
- Si:F, implanted, dry oxidation kinetics, impurity effects 7-13667
- Si:Fe, silicides obtained by Fe⁺ implantation 7-6655
- Si:Ga, highly cond. shallow junction layer form. by ion implantation 7-38037
- Si:Ga MBE layers, ion implantation doping using liq. metal ion source, carrier conc., spreading resist., SIMS profiles 7-12563
- Si:Ge, Ge⁺ preamorphisation implants, effect on extended defect formation during subsequent solid phase epitaxy 7-16599
- Si:Ge⁺, ion implanted and annealed, crystalline to amorphous transformation, TEM study 7-32643
- a-Si:H, gas-phase and ion-implantation doped, doping efficiencies 7-51790
- Si:H, ion implanted and annealed, H depth distrib. 7-26785
- a-Si:H(P,B) films, ion implanted, photoelectric and optical props. 7-38615
- Si:H films, ion implant redistribution 7-16921
- Si:In, substitutional ion implanted dopants, electron and positron channelling studies 7-26778
- Si:In⁺, ion implanted, damage prod., incidence angle depend. 7-65242
- Si:Li, ion implanted, impurity redistribution under pulsed laser radiation 7-12098
- Si:N, high dose implanted, swelling, saturation, and sputtering effects 7-16648
- Si:N, N incorporation and behaviour 7-16598
- Si:N, oxidation-inhibiting behaviour after N implantation, thermogravimetric anal. 7-59697
- Si:N,O, impurity interactions in optical defects 7-17348
- Si:N₂⁺, N₂⁺ implantation, local inhibition of oxidation 7-59688
- Si:N⁺, dose and dose rate of ion implantation, Si₃N₄ formation 7-32533
- Si:O, ion implanted, octahedral oxide particle nucleation and growth 7-16776
- Si:O, ion implanted, structure before and after heat-pulse annealing 7-16600
- Si:O, self-interstitial migration, dislocation loops and elongated Frank dipoles 7-58300
- Si:O,B⁺, ion implanted, reverse annealing 7-16617
- Si:O for SOI formation, ordered precipitate structure and coesite formation 7-52065
- Si:O₂⁺, Si on insulator structs., amorphous and crystalline oxide precipitates 7-13655
- Si:P, ion implanted, dynamic annealing, dose rate effects 7-12093
- Si:P, ion implanted defect structs. rel. to implant energy 7-38079
- Si:P, Ni⁺, ion implantation and annealing 7-21245
- Si:P,Sb, mixing of P and Sb ions by recoil implantation, sheet resist., annealing temp. depend. 7-21291
- Si:P⁺(PF₃⁺), ion implanted, rapid thermal annealing, solar cell appls. 7-23193
- Si:PF₃⁺ ion implanted, recrystallisation kinetics during fast thermal annealing 7-16618
- Si:P(Al), random and channelled implantation profiles and range parameters of dopants 7-21246
- Si:P(B) LPCVD films, amorphous and polycrystalline, struct., elec. resist. meas. 7-52870
- Si:Sb,As, cryst. aid amorphous, impurity band form., X-ray spectra studies 7-12650
- Si:Sb MBE layers, doping by secondary implantation 7-12102
- Si:Sn, ion implanted, annealing behaviour, channelling and conversion electron Mössbauer spectroscopy 7-13485
- Si:Sn,B, shallow junction formation, preamorphisation by Sn implantation 7-7338
- Si:Ti, ion implanted, deep level charactn. 7-38513
- Si:Ti ion implanted layers, defect form. and precipitation, electron microscopy studies 7-12097
- Si:W⁺ layers, implanted and annealed, struct., TEM, electron diff. studies 7-32858
- Si:Zn, amorphous-crystalline interface, backscattering and channelling study 7-6663
- p-Si/Al Schottky barriers, Ar⁺ implantation damage, oxidation, etching and elec. props. 7-21290
- Si/SiO₂, ion implantation-induced interface states generation and charge trapping study 7-12874
- Si-Al Schottky barrier diodes, ion implant modification 7-45498
- Si-B⁺, Ge⁺, preamorphised shallow junctions, end-of-range and mask edge lateral damage 7-38071
- Si-Fe, ion implanted, channeling/RBS studies 7-2039

ion implantation continued

- Si-Ge multilayered structures, Bi ion implanted, projected range distrib., glancing angle RBS anal. 7-63689
- Si-Si₃N₄, SOI, N⁺ implanted, microstructural characterisation 7-52300
- Si-Si₃N₄, SOI structs. formed by N⁺ implantation EPR of defects 7-33273
- Si-Si₃N₄ buried nitride SOI structs., N⁺ ion implantation, elec. and physical props. 7-33100
- Si-Si₃N₄ SOI structs., formation by N⁺ implantation 7-32532
- Si-SiO₂, buried layer SOI structs., elevated temp. high dose O⁺ implantation, effect of annealing 7-32530
- Si-SiO₂, buried oxide formation by O⁺ implantation, donor creation, enhanced conductivity 7-32529
- Si-SiO₂, buried oxide SOI struct., effects of annealing temp. on characts. 7-33099
- Si-SiO₂, buried SiO₂ formation, high dose O⁺ implantation at room and liquid N₂ temp. 7-32528
- Si-SiO₂, SOI struct., deep O⁺ implantation, strain and damage in Si 7-32531
- Si-SiO₂, SOI structs. formed by O⁺ implantation, EPR of defects 7-33272
- Si-SiO₂ SOI struct. formed by high dose ion implantation, high resolution TEM study 7-59690
- Si-SiO₂/Cs MOS, semicond. flatband voltage depend. on impurity distrib. 7-27433
- β -SiC monocryst. thin films, ion implantation and annealing, amorphisation and recrystn. processes study 7-16596
- β -SiC:Al⁺(P⁺) epitaxial films, ion implanted, rapid thermal annealing 7-16905
- SiC:B⁺(Al⁺), stoichiometric disturbances due to ion implantation 7-6651
- β -SiC:B(N) films, ion implanted, rapid thermal annealing 7-17569
- Si₃N₄, SOI formation by ion implantation 7-32526
- SiO₂ films in MOS capacitors, ion implantation induced electron traps 7-38589
- SiO₂ layers on Si, patterning of fine structs. by ion beam exposure and wet chemical etching 7-13656
- SiO₂, optoelectronic material, radiation effects 7-26811
- SiO₂, refractive index changes formed by N⁺ implantation 7-25915
- SiO₂, SOI formation by ion implantation 7-32526
- SiO₂:Au(Bi), ion implanted, projected ranges and range stragglings, RBS anal. 7-63690
- SiO₂:B(P), thermally grown, diffusion of ion-implanted dopants 7-38041
- SiO₂:Sb, ion-implanted, diffusion 7-58542
- Ta, Ne implanted, annealing behaviour of H traps 7-46506
- TaSi₂-Si interface, ion implanted, dopant diffusion, SIMS anal. 7-38271
- α -Ti:Si, ion implanted, diffusion profiles, annealing behaviour 7-12369
- Ti-Ni, crystalline to amorphous transitions, struct. anal. 7-44375
- Ti-Si:As⁺(P⁺)(BF₂⁺), TiSi₂ formation, ion implantation doping and masking oxide film effects 7-21708
- TiN coatings, ion implanted, wear resistant props. (Japanese) 7-46698
- TiN compound layer prepared by ion implantation, XPS and FTIR obs., depth profile analysis of ion etched samples 7-59373
- TiN thin film, adhesion on PBI plastic produced by large-current ion implantation machine (Japanese) 7-8149
- TiSi₂O films, quantitative SIMS analysis, in situ ion implantation of ¹⁸O reference level 7-12100
- V film, B ion implantation, phase changes, electron microscopy study 7-12169
- VCE formed by Ce ion implantation, lattice-location studies of Ce ions 7-2042
- W, thermodynamic stability in a fusion reactor environment, H, O and C implantation and diffusion 7-49658
- WSi₂, formation by As ion implantation, ion beam mixing (Chinese) 7-51797
- YIG films, low dose ion implanted, magnetostatic backward vol. waves 7-45765
- YIG:H, ion implanted, elastic recoil analysis using 44 MeV Cl ions 7-12107
- YIG:H, sp. ht. and annealing behaviour, conversion-electron Mossbauer spectroscopy study 7-17253
- YIG:Ne⁺ ferrite films, surface magnetostatic wave damping, ion implantation effects (Russian) 7-33242
- (YLuBi)₃(FeGa)₅O₁₂, Ne⁺ implanted, CEMS study (Chinese) 7-7620
- (YLuBi)₃(FeGa)₅O₁₂:Ne⁺ films, stripe domain stabilisation by ion implantation 7-53100
- Y₂O₃-ZrO₂:Fe, high dose ion implanted, profile shapes and electronic cond. 7-32472
- (YSmLuGd)₃(FeGa)₅O₁₂ garnet film struct. and mag. props., mag. bubble memory appls. (Japanese) 7-7575
- ZnO:H, quantised accumulation layers on ZnO surfaces, photoenhancement 7-7304
- ZnS(Se), IR transmitting windows, protective coatings 7-46731
- ZnSe:Er³⁺, ion implanted, identification of cathodolum. centres 7-53417
- ZrO₂:N₂⁺, ion implantation, ion-acoustic microscopy 7-51792
- ZrO₂:Ti, ion implantation, mech. props. 7-28102
- ZrO₂-YO_{1.5}, thermal behaviour of ⁵⁶Fe implantations 7-27006

ion lasers

- excitation of He-metal vapour mixture, glow-discharge electron beams appl. (Czech) 7-56373
- high-current relativistic electron beam, ionisation wavefront struct. and propag. vel. 7-51469
- highly charged ions, excited-state stability and X-ray lasers 7-31305
- metal atoms and ions, lasing mechanism and energy characts., relax. processes of metastable states 7-62673
- plasma recombination lasers similar to thermionic convertors 7-10915
- plasma X-ray lasers, Z-scaling of gain 7-20203
- radial electron distribution structure, meas. in high-current discharge, ion laser media appl. 7-44295
- soft X-ray laser program at Livermore 7-20202
- stellar envelopes, He I laser action theory 7-4438
- super-dense hollow cathode discharge, plasma light amplification (Japanese) 7-6476
- X-ray laser program at Sandia, gas puff Z-pinch implosions 7-20207
- X-ray laser research, in situ calibrations of grazing incidence vacuum monochromators 7-41570
- X-ray laser research at CEL-V 7-20209
- X-ray lasers, conf., Aussois, France (April 1986) 7-18480
- X-ray lasers pumped by photoionisation 7-20210
- XUV laser expt. survey 7-20198
- XUV laser numerical modelling 7-20213

ion lasers continued

- AR II lines, laser generation in water cooled helical hollow cathode discharge 7-57299
 Ar gas puff Z-pinch implosions, X-ray emission, appl. to X-ray lasers 7-26483
 Ar high press. discharge, X-ray initiated, laser appls., anal. 7-63385
 Ar, integrated acousto-optic mode locker design 7-37005
 Ar ion laser, high-power, with extended functional capabilities 7-25839
 Ar ion laser, wideband power regulation system 7-31347
 Ar ion lasers excited by low-energy electron beams 7-20186
 Ar laser coagulator, LAK, for ophthalmic therapy 7-8673
 Ar laser coagulator, use in ophthalmic therapy 7-8674
 Ar⁺ CW laser beam, central dark-space form. (Chinese) 7-57390
 Ar⁺ laser light, SHG in urea crystal (Chinese) 7-57458
 Ar⁺, performance assessment of laser wavemeter (Korean) 7-24692
 Ar⁺ photoionisation pumping via two-electron shakeup 7-20195
 B I isoelectronic sequence, short wavelength laser calcs. 7-20214
 Be I isoelectronic sequence, short wavelength laser calcs. 7-20214
 Be IV ion, 4f to 5g transition generation obs. in recombining laser plasma 7-57303
 C fibre, laser produced plasma, XUV expansion coded recombination lasers 7-62679
 C fibre plasma, laser produced, population inversion and gain meas. 7-26505
 C I isoelectronic sequence, short wavelength laser calcs. 7-20214
 C III vacuum arc discharge, reson. photoexcitation, fluoresc., X-ray laser prototype 7-20987
 C VI recombination laser, X-ray laser schemes 7-20206
 Cd⁺ photoionisation pumping via two-electron shakeup 7-20195
 Cs III Auger laser, XUV at 63.8 nm, proposal 7-25801
 Cu II lines, laser generation in water cooled helical hollow cathode discharge 7-57299
 Cu plasma, Ne-like, gain expt. 7-20876
 H-like Balmer alpha lines, recomb. and photo-pumping mechanisms for gain prod. 7-20212
 He⁺ photoionisation pumping via two-electron shakeup 7-20195
 He²⁺ recombination lasers in VUV excited by intense proton beams 7-25798
 He-Cd laser transitions, level width determ., double-mode lasing state 7-43080
 He-Cd⁺ white light laser, hollow cathode, power stabilisation 7-57385
 He-Kr⁺ laser operation, DC He and He-Kr discharges in Al hollow cathode tubes 7-10912
 He-N₂ laser, pulsed electric-discharge, laser props. investig. 7-62675
 He-Zn laser with transverse HF excitation 7-1090
 In plasma, laser ablated inner-shell photoionisation-pumped, optical gain at 185 nm 7-20193
 Kr II lines, laser generation in water cooled helical hollow cathode discharge 7-57299
 Kr ion laser, perturbations obs. in 0-10 kHz range 7-5871
 Li⁺ pumping by soft X-rays, EUV emission 7-20196
 N₂⁺, electron beam excitation at 391.4 and 427.8 nm, He effects 7-10917
 N₂⁺ laser, quasiperiodicity criterion of the spectral structure of pulsed radiation 7-43067
 Ne gas puff Z-pinch implosions, X-ray emission, appl. to X-ray lasers 7-26483
 Ne, imploding Z pinch for X-ray laser research 7-20918
 Se Ne-like laser, progress in anal., review 7-20194
 Se X-ray laser targets, hydrodynamic aspects 7-20208
 Se XXV plasma, laser produced, electron impact, laser transitions 7-26508
 Sr ions, Ne-like laser plasma, photoexcitation, X-ray and XUV spectra 7-26507
 Xe ion laser, short-wavelength, pumped by Auger decay, obs. 7-36938

ion lenses *see lenses***ion lithography** *see ion beam lithography***ion microanalysis**

- see also ion microprobe analysis*
 semiconductor superlattices, ion beam channelling, review 7-51902
 stigmatic ion microscope, elimination of residual image distortion 7-61403
 H pressure at solid surface layers, expt. investig. 7-18929

ion microprobe analysers *see ion microprobe analysis***ion microprobe analysis**

- see also ion microanalysis*
 CR-39 track detectors, impurity content, PIXE and neutron activation studies 7-36406
 external beam proton-induced gamma-ray emission analysis, C and O determ. 7-23088
 lunar soil sample analysis (Rumanian) 7-18363
 metallic materials, nucl. anal. (German) 7-54211
 nuclear micro-beam probe for the investigation of surfaces, microprocessor-controlled 7-8352
 PIXE analysis equipment system 7-59816
 proton bombardment elemental analysis, reliability using air mounted sample 7-59815
 radioisotope gauge apple, and development 7-61311
 rare earth elements in minerals 7-60427
 Rutherford backscattering-particle induced X-ray emission analysis, large residual defects 7-54251
 semiconductor structures, MeV He⁺ microbeam analysis 7-13315
 thick sample PIXE anal., on-demand beam pulsing system 7-56374
 tissue culture cells, imaging intracellular elemental distrib. and ion fluxes using ion microscopy, freeze-fracture 7-60139
 uterine myoma, human, quantitative PIXE anal. 7-23497
 Cu, single crystal, proton induced Kossel X-ray diffraction 7-53451
 Fe₂Ni₈₀-B₂₀, XRF and PIXE surface anal. 7-12411
 Mn_{1-x}Zn_xFe₂O₄ substrates, Auger microprobe temperature profiles of contamination residue 7-59822
 Pt, and Pt group metals, ion probe microanalysis effect of O₂ admission 7-17380
 Si, multiply ionised atom, heavy ion induced X-ray emission, post collision and processes 7-65365
 Si:As, Rutherford backscattering-particle induced X-ray emission analysis 7-54251
 Ti-Mo (15 wt.%), Young's modulus, cohesive energy, H effect (Chinese) 7-8033

ion microscopes

- see also field emission ion microscopes; ion microscopy*
 No entries

ion microscopy

- see also field emission ion microscopy; ion microscopes*
 analytical ion microscopy for cell biology and tissue studies 7-40386
 channelling contrast microscopy, He⁺ microbeam, semiconductor impurity profiles 7-51587
 stigmatic ion microscope, elimination of residual image distortion 7-61403
 stigmatic ion microscopy, high resolution imaging 7-4922
 submicron techniques, conf., Nova Scotia, Canada (July-Aug. 1984) 7-35104
 tissue culture cells, imaging intracellular elemental distrib. and ion fluxes using ion microscopy, freeze-fracture 7-60139
 Fe-V-N, Fe-Al-N, Fe-Mo-N, nitriding, surface layer struct., Mossbauer spectra (Russian) 7-59672
 Nb-Zr, mixed dislocations, nuclei atomic configs., computer modelling (Russian) 7-58281

ion mobility

- see also electrolytic ion mobility; ionic conduction in solids*
 alkali metal ions in inert gases, energy distrib. 7-20839
 gases, ion velocity distribution functions 7-26384
 ion motion in autoresonant accelerator with hollow electron beam, num. simulation 7-37620
 ionosphere, ion velocity rel. to Pc 3-5, EISCAT 1983 obs. (Chinese) 7-18329
 methane-SF₆ mixtures, negative ion drift velocities 7-11583
 transition metal impurities, interstitial, enhanced mobilities and reactivities 7-17769
 Ar⁺, mobility, temp. and field depend. 7-51380
 C₂H₅O⁺, x=3 to 5, struct. isomers, gas-phase ion mobility study, ab initio calcs. 7-36456
 Cd⁺, ion drift velocity in He glow discharge, meas. using AlGaAs laser (Japanese) 7-20294
 H⁺(H₂O)_n, mobility in water vapour, TOF mass spectra 7-11582
 He₂⁺, mobility, temp. and field depend. 7-51380
 Kr, ion mobility of Kr²⁺ at 88 K 7-63246
 (Li, K)Cl, molten, internal cation mobilities 7-2243
 Li⁺, in the, mobility and longit. diffusion 7-20834
 LiCl-KCl, molten mixture, eutectic, isotope self-exchange vels., simulation 7-57187
 N-liquid, mobility of positive ion 7-26576
 O₂, negative ion mobilities meas. 7-20838
 SF₆, charge transfer, time-resolved study 7-10748
 SF₆ ions, densities, mobilities, Gerdien ion counter meas. 7-11581
 Xe₂⁺, mobility, temp. and field depend. 7-51380

ion-molecule collisions

- see also charge exchange; ion-molecule reactions*
 atomic negative ions, electron detachment, overview 7-15563
 charge exchange, reaction dynamics, crossed mol. beam collisions 7-57167
 electron capture from molecular to partially stripped ions, Oppenheimer-Brinkman-Kramers approx. calcs. (Russian) 7-57169
 excited state prod. by negative ion detachment 7-15686
 iodomethane+NO⁺, charge exchange, ground state radiative lifetimes, ion cyclotron reson. spectra anal. 7-31114
 ion chemistry, gaseous, hybrid BEQQ mass spectrometer appls. 7-48904
 rotationally inelastic scatt., quantum close-coupled eqns., linear reference pot. algorithm 7-62477
 tetrafluoromethane+He⁺(Ne⁺)(Ar⁺)(N⁺)(N₂⁺)(O₂⁺)(H₂⁺)(H₃⁺), excitation cross sections 7-62501
 Al_n⁺ (n=2,3)+O₂(H₂O)(ethylene), absolute cross sections, meas. 7-5743
 Ar⁺+H₂, chemical reaction and charge-transfer processes, RIOSA quantum-mechanical study. 7-31159
 Ar⁺+H₂(N₂) collisions, ion energy-loss spectroscopy 7-50324
 Ar⁺+N₂, absolute spin-orbit state excitation cross sections, fine-struct. 7-42730
 Ar⁺+N₂, charge transfer collision, Franck-Condon principle at low collision energies study 7-62511
 Ar⁺+N₂, electron transfer, state-to-state study 7-10714
 Ar⁺+N₂ collisions, low energy charge transfer reactions, time-of-flight spectra studies 7-31163
 Ar⁺+Na₂MoO₄(NaNbO₃)(MoO₃)(Nb₂O₅), ion-induced decomp., metalisation channels, XPS anal. 7-57149
 Ar⁺+O₂ collisions, low energy charge transfer reactions, time-of-flight spectra studies 7-31163
 Ar^{q+}+D₂, collision parameters, energy-gain spectra meas., multichannel Landau-Zener model anal. 7-36752
 Ar₂⁺+N₂, charge-transfer, mol. dynamics study 7-50335
 B₂⁺+H₂ pot. energy surfaces, diatomics-in-molecules calcs. 7-5748
 CS₂^{q+}+atom(molecule), (q=2, 3), electron capture 7-5763
 Ca salts, ion-molecule interactions in DMF, IR spectrosc. obs. 7-10584
 Ca²⁺, reson. transfer and excitation, charge state and electron momentum distrib. depend. 7-970
 Cl⁺, charge transfer reactions with organic mols., cross section anal. 7-15701
 Cs⁺, low-energy collisions with atoms and mols., absolute total cross section meas., curve-crossing model anal. 7-36749
 H⁺, vibr. excitation by charge exchange with mols., TOF anal. (German) 7-57170
 H⁺+BH(X¹Σ⁺) charge transfer dynamics 7-50331
 H⁺+H₂, atomic data relevant to edge plasmas 7-20063
 H⁺+H₂, nondissociative and single ions., cross section meas. 7-31147
 H⁺+H₂ double capture, collisions, H⁺ ion excitation energy meas., Franck-Condon calcs. 7-36751
 H⁺+H₂(D₂), charge transfer into 2S state, differential cross sections meas. 7-36750
 H⁺+HF, charge transfer processes, ab initio calcs. 7-5744
 H⁺+HF(CO₂), rot. energy transfer, pot. energy surface 7-967
 H⁺+N₂O, collision excitation, photon emission spectra 7-15678
 H₂+Ar^{q+} (1^q), total one-electron capture cross sections 7-10754
 H₂⁺+H⁺ total ang. momentum barriers 7-50294
 H₂⁺+H₂, atomic data relevant to edge plasmas 7-20063
 H₂+H₂, electron loss to the continuum, absolute cross sections 7-50304
 H₂⁺+H₂, atomic data relevant to edge plasmas 7-20063
 He⁺+tetrafluoromethane, absolute excitation cross sections 7-20010
 He⁺, vibr. excitation by charge exchange with mols., TOF anal. (German) 7-57170

ion-molecule collisions continued

- He⁺+H₂, elastic and inelastic scatt. mechanisms, energy loss spectra 7-15671
 He⁺+H₂, electron loss to the continuum, absolute cross sections 7-50304
 He⁺+H₂, nondissociative and single ionis., cross section meas. 7-31147
 He⁺+H₂(N₂)(O₂)(CO)(NO), metastable state, collisional quenching cross section 7-62315
 He²⁺+CO₂, CO₂ gas laser preionisation study 7-62508
¹¹¹InCl and ¹¹¹InI, ion-molecule collisions in gaseous forms, cross sections 7-20006
 K⁺, scatt. by diatomic gases and spherical mols., energy transfer flight time meas. (*German*) 7-57163
 Li salts, ion-molecule interactions in DMF, IR spectrosc. obs. 7-10584
 Li⁺, scatt. by diatomic gases and spherical mols., energy transfer flight time meas. (*German*) 7-57163
 Li⁺+N₂, vibr. rot. energy transfer, collisional time-correl. functions 7-50316
 Mg salts, ion-molecule interactions in DMF, IR spectrosc. obs. 7-10584
 N₂+H-like ions projectile ionisation cross section 7-969
 N₂+N₂⁺(Ar⁺), charge transfer, crossed mol. beam study 7-57166
 N₂⁺+N₂, charge transfer reaction, calc. of vibr. levels for neutral mols. 7-42759
 Na salts, ion-molecule interactions in DMF, IR spectrosc. obs. 7-10584
 Na⁺, scatt. by diatomic gases and spherical mols., energy transfer flight time meas. (*German*) 7-57163
 Ne⁺+tetrafluoromethane, absolute excitation cross sections 7-20010
 Ne^{q+}+D₂, collision parameters, energy-gain spectra meas., multichannel Landau-Zener model anal. 7-36752
 O₂+H-like ions projectile ionisation cross section 7-969

ion-molecule reactions

- air, positive corona discharge, influence of water mols., mass spectra anal. 7-32180
 alkali metal cation-halogen anion microclusters, struct. and energetics 7-8266
 anion-water complexes, struct. and binding energy, ab initio study 7-15483
 association and clustering form., thermochemical data 7-18514
 complex molecule production in dense interstellar clouds 7-14640
 electron capture from molecular to partially stripped ions, Oppenheimer-Brinkman-Kramers approx. calcs. (*Russian*) 7-57169
 intermolecular potential functions, additivity 7-10699
 interstellar clouds, reactions at low temps. 7-13764
 interstellar clouds chemistry, ion-molecule calc. of CCD/CCH abundance ratio in dense clouds 7-66712
 interstellar ion-polar neutral reactions, chemical models 7-48032
 interstellar molecular clouds 7-13765
 low-temperature ion+molecule reaction rate coeffs. 7-23006
 metal cluster ions, size-selected, in triple quadrupole arrangement, expts. 7-15777
 methane anion+methane, internal energy depend. of cross section and mechanism branching, TESICO investig. 7-28298
 methane ion+H₂→CH₃⁺+H, ion reaction at interstellar cloud conditions 7-23008
 methyl cation+H₂ radiative assoc. rate 7-3585
 methyl ion+ethylene (acetylene) reaction, collision complexes form. 7-39867
 methyl ion+H₂→CH₃⁺+H, rate coeffs. rel. to role of electronic transitions in radiative assoc. processes 7-66714
 molecules, neutral and anionic, proton affinities, ab-initio calcs., role in ion-mol. reactions 7-5590
 rate determination meas. technique description 7-54076
 salt/water/aprotic solvent mixtures, alkali cation influence, IR spectra anal. 7-19856
 tetrafluoromethane+He⁺(Ne⁺)(Ar⁺)(N⁺)(N₂⁺)(O₂⁺)(H₃⁺), excitation cross sections 7-62501
 vinyl-d₂ cation+H₂, reaction cross-section, vibr. state depend., TESICO obs. 7-54102
 Al₃⁺+O₂ mass selected ions, reaction study 7-22993
 Ar⁺+H₂, chemical reaction and charge-transfer processes, RIOSA quantum-mechanical study. 7-31159
 Ar⁺+N₂, charge exchange reactions, TEPCO method anal. 7-20076
 C⁺+H₂(D₂), rate const. determ. 7-17774
 C₂⁺, excited state, prod., ion-mol. reactions, FT mass spectra investig. 7-54087
 CH₃⁺+H→methane ion+H₂, ion reaction at interstellar cloud conditions 7-23008
 CO⁺+CO+M, where M=CO, Ne and He, association reactions, third-order kinetics, temp. depend. 7-46817
 Cl⁺+H₂, reactive collisions, trajectory surface-hopping study 7-3576
 Cr⁺+H₂(HD)(D₂), kinetic and electronic energy effect, mass spectra 7-65293
 D⁺+H₂(D₂), trajectory surface hopping calcs. 7-59747
 H⁺+D₂, trajectory surface hopping calcs. 7-59747
 H⁺+O₂, charge transfer collisions, vibr. state resolved meas. 7-5762
 H₂⁺+H₂, H₃⁺ form., quasiclassical trajectory surface hopping method 7-59750
 H⁺+CO₂, charge transfer reaction cross section and pot. energy curve meas. 7-54086
 H₂O⁺, Fourier transform ion cyclotron reson. mass spectrometry 7-13734
 H₂O⁺, Fourier transform ion cyclotron reson. mass spectrometry 7-13734
 He+H₂⁺, reaction, quantum infinite order sudden approx. 7-54097
 He⁺+H₂, ion-molecule reaction rate at low-temp. conditions of interstellar space 7-23007
 He⁺+H₂(D₂), rate const. determ. 7-17774
 He₂⁺+N₂(CO₂), charge transfer reaction rate consts. 7-22983
 He₂⁺+Ne₂, reaction kinetics at atm. press., three-body processes 7-22984
 Kr⁺+H₂(D₂)(HD), spin-orbit state and isotope effects, pot. energy curve, cross sections meas. 7-39859
 N₃⁺+H₂, electron transfer rate const. calc. 7-33917
 N₂⁺+O₂, charge exchange reaction in temp. range 8 to 163 K, rate coeff. meas. 7-46810
 NH₃⁺+H₂, ion-molecule reaction rate at low-temp. conditions of interstellar space 7-23007
 NH₄⁺, Fourier transform ion cyclotron reson. mass spectrometry 7-13734

ion-molecule reactions continued

- N₂H⁺+H₂, ion-molecule reaction rate at low-temp. conditions of interstellar space 7-23007
 NO⁺+NO, association reactions, third-order kinetics, temp. depend. 7-46817
 Na⁺+N₂(CO)(CO₂), dissoci., rot. rainbow effect, time-of-flight spectra 7-54117
 Ne⁺+H₂(D₂), rate const. determ. 7-17774
 O₂⁺+methane-d₀(d₁)(d₂)(d₃)(d₄), reaction rate coeff. and product distrib. meas., isotope effect 7-13741
 SC⁺+H₂, endothermic reaction ab initio pot. energy surfaces 7-13746
 SF₆, charge transfer, time-resolved study 7-10748
 SiH₄ glow discharge, ion-molecule reactions and amorphous Si deposition 7-65325
 SiH₄-Ar-H₂ plasma, Si deposition 7-23011
 UO₂²⁺+2RH→R₂UO₂+2H⁺, ion exchange equilibria and kinetics 7-25071

ion optics

- see also ion beams; ion microscopes; mass spectrometers
 160 keV JET neutral beam injectors, single-beamlet system, ion optics study 7-11783
 aberration theory for electrostatic round lenses, multipole lenses and deflectors 7-1021
 Applied-B ion diode expts. on Particle Beam Fusion Accelerator-I 7-10310
 beam optical quality and plasma emittance props. (*French*) 7-62160
 charged particle motion in 2D hexapole field, stability 7-41526
 charged particle stability in 2D octopole fields 7-41527
 combined electrostatic focusing-deflection systems, asymptotic aberrations 7-10835
 ion beam transport through ideal quadrupole, hexapole and octopole operating in RF-only mode 7-41528
 ion implanter, ion beam transport system, ion-optical characteristics (*Korean*) 7-24723
 magnetic quadrupole multiplet microbeam forming systems (*Chinese*) 7-10325
 mass spectrometer, double focusing, with elec. prism, ion optics and petroleum products anal. 7-15029
 multiple-electrode ion extraction systems, design 7-42270
 multipole devices with 2D electric fields 7-41525
 negative ion beam extraction and acceleration from low field surface produced sources 7-15445
 negative ion beam extraction and acceleration from volume prod. sources 7-15446
 prism, decelerating, electric, test dispersion meas. 7-57229
 RF ion source, focusing system, expt. and theoretical investigs. 7-10840
 scanning ion beam systems, in-lens deflection 7-42889
 TEXT heavy ion beam probe system 7-1754

ion plating

- alloy thin films, co-deposited, phase form. 7-59492
 cutting tools, performance improvement through the use of ion plated coatings 7-53931
 diamond-like layers deposited from C ion beams, struct. (*Russian*) 7-17475
 processing machines develop. (*Japanese*) 7-53637
 surface engineering for corrosion protection 7-3478
 Al/Al₂O₃ films, ion plated in Ar-O₂ gas mixture, structure anal. 7-7899
 Al-Al₂O₃, ion plated coatings using pulsed O₂ process 7-22586
 Au-Si eutectic alloy liquid metallic ion source (*Chinese*) 7-33600
 B/N coatings, ion plating, amorphous struct., wear resist. 7-22580
 BN, ion-plated, prep. and charact. 7-17477
 C coatings, ion plating, amorphous struct., wear resist. 7-22580
 CoCrAlY, sputter ion plated coatings for gas turbines 7-53971
 Cr coatings on gun tubes, cylindrical geometry ion plating technique 7-53638
 Cu, on steel, deposition conditions effect on coating struct. 7-39748
 Fe-Cr, on steel, deposition conditions effect on coating struct. 7-39748
 GaN films, epitaxial growth by reactive ion plating, elec. props. 7-3206
 Mo on austenitic steel, corrosion resist. in flowing Na environment 7-59667
 Nb-Ti-O ceramic coatings, synthesis by reactive ion plating and sputter deposition, struct., electrophysical props. 7-64031
 NiCrAlTi, sputter ion plated coatings for gas turbines 7-53971
 Ru-Ti-O ceramic coatings, synthesis by reactive ion plating, struct., electrophysical props. 7-64031
 Si homoepitaxial thin film growth by ultrahigh vacuum ion beam sputter deposition 7-22582
 Si₃N₄ film form. and charact., ion and vapour deposition method 7-13370
 Ti-N films deposited by ion plating, intermediate layers, TEM study 7-46350
 Ti-N reactively ion plated coatings on high speed steel, turning performance, wear 7-46656
 TiC film ion plated on austenitic stainless steel, adherence rel. to ionisation (*Japanese*) 7-53636
 TiN coatings, ion plating, metal properties modification 7-39435
 TiN compound layer prepared by ion implantation, XPS and FTIR obs., depth profile analysis of ion etched samples 7-59373
 TiN, film, triode ion plating, influence of substrate temp. on struct. 7-39438
 TiN films, ion plated, stability anal. 7-2400
 TiN films, RF ion plating, residual stress, bias voltage effect (*Japanese*) 7-16917
 TiN, ion beam enhanced deposition on tool steel, friction and wear reduction 7-53910
 TiN ion plated films, tempering effects 7-59461
 TiN, ionisation assisted PVD processes 7-33599
 TiN thin films, activated reactive evaporation deposited, vacuum annealing, struct., mech. props. 7-8010
 TiO₂ films, reactive ion plating on PET substrates, interface structure, ESCA studies 7-7897
 ZrN films, ion plated, stability anal. 7-2400
- ion probe analysers see ion microprobe analysis
 ion probe microanalysis see ion microprobe analysis
 ion pumps
 No entries
 ion recombination
 air, ionisation by fast electron pulse, nonequib. conductivity 7-6364
 atomic ions, dielectronic recombination in elec. fields, quantum defect theory 7-62527

ion recombination continued

- elements, charge distrib. in ion beam produced from RF-spark ion source 7-46883
 formyl ion, dissociative recombination at interstellar cloud conditions 7-23009
 formyl ion, dissociative recombination of interstellar ion, electronic struct. calc. 7-20064
 methane, protonated, dissociative recombination at interstellar cloud conditions 7-23009
 2-naphtholate, H^+ recomb. and H^+ induced quenching, temp. depend. 7-57135
 photosynthetic bacteria reaction centres, recomb. kinetics, electric field depend. 7-47017
 plasma, emission characteristics, soft X-ray region, plasma diagnostics, radiative-collisional model study 7-62312
 plasma, fast heavy-ion charge states, effect of dielectronic recombination 7-16310
 plasma, high density, electron-ion recombination 7-31927
 post-arc cond., circuit breaker arc, plasma parameters meas. 7-32183
 steel, stainless, surface deuterium recombination 7-62063
 N,N,N',N' -tetramethylbenzidine in various polar solvents, monophotonic ionisation 7-12758
 ylides, neutralisation-reionisation mass spectrometry 7-10766
 Ar plasma column prod. by EM surface wave, recomb. controlled regime 7-20908
 Au, surface deuterium recombination 7-62063
 Be, isoelectronic series, dielectronic recomb. rates calcs. 7-50352
 Ca, dielectronic recomb. with K-shell excitation 7-42761
 Cr^{3+} , dielectronic recombination, photon/ion coincidence meas. 7-10756
 Fe^{21+} , dielectronic recomb., rate coeff. calc. 7-30991
 Fe^{22+} , dielectronic recomb., rate coeff. calc. 7-30991
 H. ion recomb. and level pops., role of charge exchange 7-31925
 H-like ions, dielectronic recomb. rate consts. calcs. 7-36759
 H_2 , low temp. plasma, electrode sheath, calcs. 7-37703
 H_2^+ , slow electron impact dissociation, recomb. 7-50382
 H_3^+ , dissociative recombination at interstellar cloud conditions 7-23009
 I_2 , in liquid Xe, vibr. relax. following geminate recombination 7-10712
 N_2H^+ , dissociative recombination at interstellar cloud conditions 7-23009
 Ne, $2p^23d$ level population in Hf discharge afterglow, press. depend. 7-20853
 Ne, high-frequency discharge, dissociation, recomb. of excited atoms in afterglow 7-10456
 Ne-like ion recombination in finite density plasma, rate coeff. calc. 7-57982
 Ne_2^+ glow discharge, time depend. of spectral line intensities from afterglow plasma 7-32142
 SF₆, RF breakdown and discharges, continuum modelling 7-37798
 Se XXIV and XXV plasma, dielectronic recombination calcs. 7-26510
 Se^{25+} , dielectronic recombination, density depend. 7-976
 Se^{26+} , dielectronic recombination, density depend. 7-976
 Se^{27+} , dielectronic recombination, density depend. 7-976
- ion scattering** see collision processes; ion mobility; ion-surface impact
ion scattering spectroscopy see ion-surface impact
ion solvation see solvation
ion sources
 see also ion emission
 alkaline ion source design for SIMS (French) 7-9922
 antiproton capture in Penning trap from keV source 7-25285
 ATLAS, positive ion injector status, ECR ion source and superconducting linac 7-62134
 atmospheric pressure ionisation source for Finnigan-MAT 400 mass spectrometer 7-4911
 boil off Li vapour source for PBFA II ICF expts. 7-25293
 bucket ion sources, plasma flow operation conditions obs. 7-20881
 capillary liquid metal ion sources 7-9924
 compact 2.86 GHz ECR ion source (Japanese) 7-19600
 compact multiply charged 10 GHz ion source CAPRICE for all metallic and gaseous elements (French) 7-49767
 compact sputtering PIG ion source (Chinese) 7-5523
 conf., Saskatoon, Canada, May 1986 7-29595
 convex spherical surface emitting a space charge limited ion current, imaging props. 7-5515
 corona excited supersonic expansion, for cold radicals or ions production 7-9926
 cryogenic pulsed ion source focusing, beam characteristic 7-30655
 cryogenic pulsed ion source with stirring cycle refrigerator 7-30654
 cusped magnetic field ion source, plasma props. calcs. 7-20915
 Delft ion beam pattern generator project progress 7-41532
 deuterium ion source for plasma chromatograph and mass spectrometer 7-4909
 duoplasmatron ion source, electron beam generation 7-32114
 duoplasmatron ion source, optimum operating conditions (Korean) 7-25281
 dust-impact ion source, TOF mass spectrometer 7-48907
 EXB type devices, discharge phenomena (Japanese) 7-51539
 ECR-type ion source, multipole field optimisation 7-15432
 electron bombardment ion source with small energy spread and high brightness 7-15031
 energy analyser with MCP calibrated using cellulose nitrate film 7-48914
 ethanol, photoionisation mass spectra, temp. effect 7-46818
 Fermilab antiproton source, design 7-36359
 Fermilab antiproton source, intermediate energy electron cooling 7-36357
 Fermilab Antiproton Source, physics workshop report 7-49174
 field emission, conference, Berlin, Germany (July 1986) 7-29577
 focusing system, expt. and theoretical investigs. 7-10840
 GANIL beam production 7-36375
 glow discharge ion gun, applic. to sputtering yield meas. 7-13303
 glow discharge ion source, ion energy distributions 7-4914
 glow discharge mass spectrometry 7-9916
 n-hexane, photoionisation mass spectra, temp. effect 7-46818
 hollow cathode discharge for thin film formation 7-41536
 inert gas- NH_3 ion form. by electron ionisation, mass anal. ion kinetic energy spectra 7-13736
 inverse diode computations, using stationary particle codes 7-30812
 inverse pinch diode research 7-30811
 ion implantation and ion beam mixing, dual purpose machine (Chinese) 7-51799
 ion trapped in Lamb-Dicke limit, laser-cooled, reson. fluoresc. 7-10481

ion sources continued

- ISOL study of nuclei far from stability 7-36374
 ISOLDE Users' guide 7-19598
 Kaufman source, low energy, appl. to chem. assisted ion beam etching of Si 7-22931
 KEK H-ion source development and status (Japanese) 7-19601
 large-area liquid-lithium ion source for inertial confinement fusion 7-25296
 laser spectroscopy appl. to heavy ion reaction sources 7-36373
 light ion beam extraction from diode, PIC code 7-5527
 light negative ion sources, conf., Palaiseau, France, March 1986 7-9601
 linear acceleration, conf., Tsukuba, Japan, (Sept. 1986) 7-18504
 liquid meal, mechanism 7-25275
 liquid metal ion source, residual gas and secondary electron bombardment effects 7-30800
 liquid metal ion sources, field and temp. depend. of ion emission 7-7824
 long lifetime ion source with plasma cathode 7-48913
 low energy ion beam from single grid Kaufman type ion source (Japanese) 7-62156
 low pressure arc ion source with Li vapour 7-5525
 low- β ion acceleration with a MEQALAC 7-15448
 low-energy ion beam generation from broad-beam ion sources, appl. to sputtering (German) 7-41537
 magnetically multipole line-cusp Ar^+ ion source, magnetic field effects on plasma props. (Chinese) 7-6407
 3-methylpentane, photoionisation mass spectra, temp. effect 7-46818
 MFTF, industrially fabricated ion source, test and conditioning 7-19435
 microwave, with two-grid accelerator 7-364
 miniature high current metal ion source 7-19593
 multicharged heavy ion source for the RIKEN linear accelerator (Japanese) 7-56897
 multilayer chamber, pulsed ion beam implantation, mixed Ti^+ and N^+ ion beams (Chinese) 7-51800
 multiple-electrode ion extraction systems, design 7-42270
 NanoFab-150, focused ion beam system 7-18913
 negative ion beam extraction and acceleration from low field surface produced sources 7-15445
 negative ion beam extraction and acceleration from volume prod. sources 7-15446
 negative ion sources, development 7-15437
 optical quality and plasma emittance props. (French) 7-62160
 Penning source, Dudnikov type with LaB_6 cathodes, operation 7-56375
 PIG, ion source for negative ions 7-36704
 plasma boundary-extractor electrode distance, erosion effects 7-18918
 plasma focus device, rms beam emittance 7-30807
 plasma focus particle beams, RMS emittance meas. 7-32113
 plasma source ion implantation 7-26547
 plasma-filled applied-B diode 7-25297
 point pinch diode for intensive ion beam generation, cylindrical target compression 7-10323
 positive ion sources and injectors for linacs 7-62126
 proton source, high purity, pulsed with cryogenic plasma diode 7-30815
 pulsed dye laser for KEK optically pumped polarized ion source (Japanese) 7-20280
 radial field discharge for high-flux ion extraction 7-41534
 rare-earth ionization in the ion source with surface ionization 7-30802
 RF, with metal discharge chamber 7-30114
 RF ion source, ion energy distrib., radial extraction, injected electron beam 7-30118
 SIMS equipments with primary ion mass separation (German) 7-9915
 SIMS microprobe analysis using liquid metal ion source 7-9920
 solid discharge ion source for heavy ion fusion 7-25290
 sputter ion gun based on Bayard-Alpert pressure gauge 7-18917
 super HILAC upgrade project, MEVVA ion source, beam transport line 7-62133
 tandem volume sources, extracted current density depend. on discharge parameters 7-10330
 tandem volume sources, spectroscopic meas. of atomic populations and temps. 7-10345
 TARA neutral beam injector system, ion source electrical characterisation 7-19439
 TFTR neutral beam ion source fault detector 7-15401
 thermal-equilibrium processes for radioisotopes 7-25277
 thermonuclear fusion research by sheet plasma, vol. prod. H^- and D^- ion source 7-32105
 ultrahigh vacuum ion source using Bayard-Alpert gauge 7-61400
 zeolite A ion source, emission characts. 7-49776
 p(p) polarized beam production from Δ^0 , (Δ^0) decays 7-30796
 ^{22}Ac , α -particle source, absolute energy meas. 7-42276
 Ar^+ beam, microwave ion source, beam extraction expts. 7-363
 Au liquid metal ion source, focused droplet beam 7-30801
 Au-Si eutectic alloy liquid metallic ion source (Chinese) 7-33600
 AuSi liquid ion sources, alloy composition 7-35623
 Bi liquid metal ion source study 7-30799
 C⁻ negative-ion-beam deposition system, mass-separated 7-3170
 ^{252}Cf , α -particle source, absolute energy meas. 7-42276
 Cs, laser initiation of discharge channels for pulsed ion beam research 7-25291
 Cu-P alloy liquid metal ion sources, ion formation 7-64878
 Cu-P-Pt-B liquid metal ion source, B^+ and P^{2+} ion emissions 7-41531
 Ga, liquid, electrohydrodynamics, ion source appls. 7-31887
 Ga liquid ion source at low emission currents 7-30798
 Ga liquid metal ion source, influence of substrate geometry on emission props. 7-53508
 Ga⁺ ultra-fine ion probes for SIMS imaging microanalysis 7-4908
 H⁻ ion prod., dependence on plasma and wall parameters 7-25288
 H⁻ multicusp ion source, wall effect on volume prod. 7-25289
 H⁻ duoplasmatron arc, plasma emission mechanism 7-26532
 H⁻, 30 kV accelerator for negative ion beams 7-18916
 H⁻ and D⁻ extraction from large magnetic multipole source 7-58037
 H⁻ beam from pulsed magnetically insulated diodes 7-10343
 H⁻ charge-exchange injection into synchrotron, stripping C foil 7-62159
 H⁻, D⁻ vol. prod. ion source by sheet plasma, proton accelerator and thermonuclear fusion research applications (Japanese) 7-5511
 H⁻ density in large mag. multipole source 7-10329
 H⁻ extraction, effect of weak mag. field in front of plasma electrode 7-10341
 H⁻ extraction and electron control in multipole ion source 7-18915
 H⁻ extraction from volume sources 7-15447
 H⁻ generation and cathode plasma formation in magnetically insulated diode 7-10342

ion sources continued

- H⁻ hybrid and tandem sources, high resolution VUV light emission meas. 7-10346
- H⁻ hybrid volume source, ion and electron density profiles 7-10340
- H⁻ ion beam, steady-state, production from plasma source 7-36365
- H⁻ ion extraction from mirror ECR source 7-10334
- H⁻ ion form. on low work function surfaces 7-15444
- H⁻ ion source, effect of magnetic filter on volume production typenegative ion source 7-5526
- H⁻ ion source, generation using tandem multicusp plasma generator 7-15438
- H⁻ ion source development for linac appl., review 7-62127
- H⁻ ion volume prod., effect of chamber volume and gas pressure 7-10347
- H⁻ ion volume prod. in hybrid multicusp sources 7-10331
- H⁻ magnetic multicusp discharges, e⁻ energy distrib. function modelling 7-10337
- H⁻ multipole plasma source, neutral H level populations, spectroscopic meas. 7-817
- H⁻ plasma ion source, wall material effects 7-62155
- H⁻ production in multicusp source, effect of gas mixing 7-10332
- H⁻ source, H₂ rovibrational population; CARS time-resolved meas. 7-10605
- H⁻ source development at BNL 7-10333
- H⁻ surface conversion source with hot walls 7-15443
- H⁻ tandem multipole ion source, Langmuir probe meas. 7-10336
- H⁻ tandem multipole ion source, plasma parameter meas. by Langmuir probe anal. 7-10339
- H⁻ tandem multipole source, plasma parameter meas. using Langmuir probe technique 7-10338
- H⁻ volume ion sources, modelling of vibrational population distrib. 7-10344
- H⁻ volume prod. ion source, model 7-10335
- H⁺ beam, heating of the plasma, spectrosc. appls. 7-48864
- H⁺ polarised source ETH, cooling intense atomic beam 7-5521
- H⁺ sources, optically pumped, tensor polarised 7-62171
- He production and accumulation system 7-30828
- He⁻ tandem multipole ion source, Langmuir probe meas. 7-10336
- He-jet fed ISOL facility KUR-ISOL at the Kyoto University reactor 7-30822
- Li flashover ion source development 7-30652
- Li ion source for PBFA II ICF research 7-25292
- Li, laser-produced plasma for pulsed ion beam research 7-25291
- Li, liquid ion source, nonlinear behaviour of liq. surface in electric fields 7-42259
- Li plasma anode layers for PBFA II ion diode 7-25295
- Li plasma generation for large area ion diode 7-25294
- Li, plasma generation for PBFA-II ion diodes 7-20962
- Li, spin polarised beams, production and acceleration 7-49766
- Li⁻ ion form. on low work function surfaces 7-15444
- Li⁺ triode ion gun, thermal emission, characts. meas. 7-39345
- Na⁺ spin polarised beams, production and acceleration 7-49766
- Na⁺ ion production, microwave discharge ion source 7-15030
- Ni-B-Si alloy liquid metal ion sources, ion formation 7-64878
- O⁺ ion beams, low-energy, from microwave ion source 7-30113
- ²¹⁰Po α -source, use in determining Al, F, N content in samples 7-65360
- Pt-P alloy liquid metal ion sources, ion formation 7-64878
- S⁺ surface-barrier detector as source of slow protons 7-49777
- ¹⁴⁷Sm ion beam cross section meas. using SSNTD 7-19594
- Xe ions, prod. by saddle-field neutral beam source, distrib. 7-35622

ion-surface impact

- see also particle backscattering; sputtering
- alkali chlorides, particle bombardment-induced secondary photon emission 7-59264
- alkali halides, electron- and ion-induced sputtering, atomic excitation 7-59348
- alkali phosphates, ion bombardment-induced surface modifications, stoichiometry, core levels and valence struct., ESCA studies 7-26816
- amorphous solids, mean scatt. angle, first moments of longit. distrib., elastic losses of ion energy 7-26806
- binary compounds, H ion bombarded, secondary ion emission (Russian) 7-59321
- charged particle, interaction with solid surface, general formalism, spherical geometry 7-2652
- contrast mechanisms in electron and ion induced secondary electron images 7-27834
- conversion layers on Al, struct., TEM, LAMMA, AES, XPS, SIMS, ion scatt. spectra 7-23094
- desorption, electronic transition induces, workshop, Schloss Elmau, Bavaria, Germany (Oct. 1984) 7-20
- electron capture spectroscopy as a probe of surface electron-spin polarisation 7-59368
- energy cost to sputter an atom from a surface in keV ion bombardment processes 7-64862
- eroding surface profile during ion sputtering, Huygens' construction study 7-27842
- erosion by ion bombardment 7-16843
- excited state form. dist., reson. charge exchange, multichannel theory 7-46266
- glass, surface recomb. of electrons and ions, kinetic theory 7-46263
- graphite, pyrolytic, sputtering with O ions at various target temps. 7-49633
- heavy ion induced desorption from surfaces, thermal spike model 7-44996
- heavy-ion induced desorption, ion form. studies 7-46259
- high energy ion scatt., struct. anal. of surfaces and interfaces 7-22410
- impact-collision ion scatt. spectroscopy for surface at. struct. anal. 7-63931
- inelastic energy loss and electron emission 7-17384
- insulators, fast heavy ion impact-induced secondary ion emission studies 7-27845
- interface and surface struct. characterization, ion scatt. and channelling, scanning tunnelling microscopy and computer simulation (Japanese) 7-7803
- interface struct., dielectric film mol. beam epitaxial growth 7-38360
- ion bombardment, collision cascade momentum distrib., sputtering yield and atomic mixing, geometrical treatment 7-27846
- ion bombardment of thin films, secondary emission yield, incident charge state depend. 7-59319
- ion scattering techniques, atomic arrangement (Japanese) 7-27838

ion-surface impact continued

- ion-scattering spectroscopy, shadowing and focusing effects 7-53491
- ionised gas physics, conf., Sibenik, Yugoslavia, (Sept. 1986) 7-24307
- ISS, sputter depth profile analysis, hybrid electron-ion gun and CMA spectrometer 7-39941
- low temp. solids, low energy atom and ion bombardment, sputtering and radiation damage mechanisms study 7-27844
- materials modification with ion beams, review 7-16647
- metal clean surfaces, ion-induced secondary electron spectra 7-59346
- metal surfaces, ionic slow collisions, Auger neutralisation 7-53482
- metal-polyethylene, adhesion of metal films, effects of Ar⁺ bombardment 7-28267
- metals, ion bombarded, continuous spectrum optical emission 7-13295
- metals, sputtering by ion bombardment, excited states of sputtered atoms 7-7807
- molecule sputtering, atom- and ion-induced, collision mechanisms 7-59349
- Monte Carlo program, TCIS code and appl. (Chinese) 7-53469
- non-dissociative scattering, processing effect 7-13309
- oxide layer on chemically polished and etched InP (111), ion scatt. spectra, AES, ESCA 7-22925
- oxides, sputtering by inter gas ions, depletion layer study, Sigmund's sputtering theory 7-46262
- plasma-surface interactions in plasma-enhanced CVD, book contrib. 7-27943
- polystyrene, tracer diffusion meas. using Si and the elastic recoil detect. 7-39337
- position sensitive detector, 2D, design and testing 7-49833
- Rosen-Zener approximation in surface-ion scattering theory 7-33502
- scattered ion energy spectra under mol. bombardment 7-13294
- secondary electrons emitted from foil, diffraction obs. 7-13307
- secondary ion emission, oxygen pressure dependence 7-64859
- secondary ion energy distrib., surface chem. anal. 7-53486
- shadow cones, form. by target atoms bombard. by ions, classical scatt. theory calcs. 7-36731
- slow collision, neutralisation probability, complex energy Demkov model 7-22432
- small-angle scatt., inverse square interaction pot. 7-53481
- solid surface exam. by ion and electron spectroscopy, with angular resolution 2-6° 7-32773
- solid surfaces, chemistry and physics, book 7-60891
- sputtering, preferential, collisional aspects using Monte Carlo method 7-53464
- steel, austenitic stainless, materials erosion and redeposition studies at PISCES facility, net erosion under redeposition 7-49637
- steel, stainless, ion trapping of D⁺, mechanisms 7-64857
- stopping powers for ion bombardment using EDEP1 program 7-51895
- surface analysis, AES, XPS, ISS and SIMS, review 7-28372
- surface science, modern techniques, book 7-60911
- swift ion total backscattering from solid targets at grazing incidence 7-53483
- techniques for surface studies, book 7-60888
- UHV apparatus for heavy ion induced electron spectroscopy (Japanese) 7-56381
- vacuum symposium, Tokyo, Japan (1985) (Japanese) 7-14698
- X-ray emission spectra, excitation of atoms 7-13310
- Ag surface, low energy K⁺ small angle scatt. 7-53484
- Al (110), Ar-induced Auger electron emission, Doppler broadening 7-59345
- Al (110), H₂⁺ scatt., charge exchange 7-3133
- Al (110), scatt. of H₂⁺ ions, resonant transition rates for charge transfer 7-3134
- Al Auger electron emission by Ar bombardment, Monte Carlo simulations 7-53470
- Al, FCC cryst. struct., secondary ion emission, current density effects 7-59318
- Al foil, H⁺ induced ridge electrons emission 7-46270
- Al, heavy ion impact, secondary electron energy spectra 7-46265
- Al, ion trapping of D⁺, mechanisms 7-64857
- Al surface, H⁺ Auger and resonant neutralisation, charge capture probability, parameter-free perturbation theory calcs. 7-3141
- Al surface, H⁺ Auger neutralisation, transition rate calcs. 7-3140
- Al surface, ion induced secondary electrons, surface topography effects 7-13280
- Al, surface oxidation, diffusion of Au atoms through oxide layers 7-8200
- Al₂O₃ films, ion secondary electron emission 7-22416
- Ar, solid, electronic sputtering by keV H ions 7-59353
- Ar⁺ solid, sputtering mechanism by keV ions 7-59354
- Ar⁺ average equilb. charge state determ., H⁺ secondary ion yield meas. on Au and C target surfaces 7-42757
- Ar⁺ collision with surface, direct recoil ion fractions, kinetic energy depend. 7-13302
- Ar⁺, target sputtering, surface analysis, glow discharge optical spectroscopy (French) 7-20998
- Au (110), electron emission, interaction of multiply charged ions with surface 7-53473
- Au crystal, H⁺ ion channelling, catastrophe theory 7-21312
- Au film, (H₂O)₂H⁺ energetic cluster impact, transmission electron microscopy 7-13304
- Au foil, H⁺ induced ridge electrons emission 7-46270
- Au surface, H⁺ Auger neutralisation, transition rate calcs. 7-3140
- Au surface, low energy K⁺ small angle scatt. 7-53484
- Au-Pd, preferential sputtering and surface segregation 7-59339
- C foil, H⁺ induced ridge electrons emission 7-46270
- C thin surface layers on steel substrates, anticorrosion props., ion bombardment effects study 7-27202
- C⁺ projectile on C foil, convoy electron yield, target thickness depend. 7-27839
- CO, chemisorbed on Pt (111), adsorbate vibr. modes, inelastic He atom scatt. obs. 7-32782
- CaF₂ (111), surface at. struct. anal., impact-collision ion scatt. spectroscopy 7-63931
- CdTe, ion milling, TEM 7-39344
- p-CdTe, single crystal and thin film, chemical etching study 7-46724
- Cr single crystals, action of α -particles (Russian) 7-51880
- CsI, H₂⁺ cluster ion impact-induced Cs⁺ desorption, TOFS study 7-27843
- Cu (115), low temp. behaviour of surface roughness 7-6941
- Cu electrode-electrolyte interface, surface anal., XPS, ion scatt. spectra 7-22895

ion-surface impact continued

- Cu, materials erosion and redeposition studies at PISCES facility, net erosion under redeposition 7-49637
 Cu single cryst. target, atomic and mol. ion surface semichannelling, Lindhard atomic string model calcs. 7-63697
 Cu surface, ion irradi., sputtering and lattice damage, cascade simulation 7-59327
 Cu surface, low energy O^+ ion bombardment, atom and mol. ejection 7-59325
 Cu/Pd metallic superlattices, UPS, LEED, AES and ISS studies 7-3153
 Cu-Ni alloy surfaces, composition, low energy ion scatt. study 7-32771
 Fe (100) 7-8154
 Fe, passive anodic oxide form., surface anal., XPS, ion scatt. spectra 7-22895
 Fe-Cr, passive anodic oxide form., surface anal., XPS, ion scatt. spectra 7-22895
 Fe-Sn (001), surface segregation of Sn, surface struct. anal. 7-58594
 Fe₃₀B₂₀ ribbons, amorphous and crystallised, surface comp., electronic props., topography, AES, XPS, ion scatt. studies 7-27065
 Fe₃O₄, surface magnetism, ion bombardment effects 7-12949
 GaAs, multilayer struct., calc. elastic scattering spectra 7-13311
 GaAs, near-surface structure, analysing He^+ ion beam effects 7-7808
 GaAs, surface oxidation, effect of anodizing conditions 7-13669
 GaAs-Al₂O₃, interface struct., dielectric film mol. beam epitaxial growth 7-38360
 GaAs(100), thermal and ion-assisted reactions with Cl₂ 7-3537
 GaP, ion-induced Auger electron emission under shadowing conditions 7-64841
 Ge, vibrational correlation functions 7-51966
 Ge:H, H composition at surfaces and interfaces 7-27083
 H⁺ surface collisions, H⁻ formation process 7-17389
 He scatt. ion yields from neutral or ion bombard. of solids 7-13313
 He⁺ low energy ion-surface scatt., reionisation process theory 7-22413
 He⁹⁺+Ag(Cd)(In)(Sn)(Sb)(Te)(I), L-subshell ionisation, X-ray prod. 7-50303
 HeH⁺+C, fast mol. ion dissoc., charged fragment wake effects (French) 7-50345
 Ho surface, ion sputtering, emission spectra studies 7-64853
 InP(Sb), ion milling, TEM 7-39344
 Kr, solid, electronic sputtering by keV H ions 7-59353
 Kr, solid, sputtering mechanism by keV ions 7-59354
 Kr⁺ average equil. charge state determ., H⁺ secondary ion yield meas. on Au and C target surfaces 7-42757
 Kr³⁶⁺, emerging from solid foils, anomalous population of deep capture states 7-42758
 LaB₆-GaAs interfaces, thermal stability, high energy ion scattering studies 7-21680
 LiF surfaces, preferential sputtering, XPS and direct recoil spectrometry study 7-22422
 MgO, energy spectra meas. of secondary electrons for controlled emission 7-39340
 MgO films, ion secondary electron emission 7-22416
 MgO, ion-induced Auger electron emission under shadowing conditions 7-64841
 Mo (100), Na⁺ ion elastic scatt., interaction pot. determ. 7-13299
 Mo (111) surface layer relax., low energy Li⁺ ion scatt. study 7-6943
 Mo, ion trapping of D⁺, mechanisms 7-64857
 N⁺ and N₂⁺ scatt. from Cu (001), 2D pattern obs. 7-46269
 NH⁺+C, fast mol. ion dissoc., charged fragment wake effects (French) 7-50345
 NO₂ amorphous insulator, Ar⁺ sputtering, ang. distrib. and energy spectra study 7-27848
 Nb, ion trapping of D⁺, mechanisms 7-64857
 Ni (100), adsorption of ethylene, determ. of adatom abundance using elastic recoil detect. anal. 7-33984
 Ni (111), coadsorption of NH₃ and CO, multilayer formation studied by metastable quenching spectroscopy 7-21639
 Ni (111), secondary ion emission, temp. depend., under Ne⁺ bombardment 7-64856
 Ni, adsorption of Si, surface geometry, low energy ion scatt. determ. 7-53474
 Ni, energy distrib. surface peak of scattered He ions and atoms 7-64855
 Ni, polycrystalline, electron emission and projectile scatt. during Ne⁺ ion bombardment, coincidence method 7-7806
 Ni surface, (100) and (110), He⁺ Rutherford backscatt., continuum approx. parameter effects 7-46271
 Ni surface, ion desorbed D charge state fractions study 7-46268
 NiSi₂ epitaxial layer on Si (001), surface struct., ion-scatt. studies 7-27075
 O adsorbed layer on Ni (110), struct. anal., low energy ion recoil spectra study 7-2384
 O₂⁺ scattering from Ag(111), harpooning transitions, O₂⁻ formation 7-36805
 Pb (110), surface initiated melting, ion shadowing and blocking meas., RHEED 7-44769
 Pd (110), adsorbed H, row pairing model 7-2370
 Pt (111), O adsorbate-induced surface-phonon softening 7-58600
 Pt-Ni alloys, surface segregation, ISS study 7-52208
 Pt-Si₃N₄-n-GaAs contacts, elec. and metallurgical characs. 7-64345
 Pt/Ti (111), chemisorption of CO and O₂ 7-27131
 Rh (111), clean and with adsorbed O, ion bombarded, desorbed atoms distributions 7-22420
 S thin films, MeV He⁺ beam erosion, temp. depend. yield meas. 7-27847
 S thin layers, sputter erosion by 1.0 MeV He⁺, induced X-ray emission meas. 7-64860
 Si, chemical sputtering by ions, electrons and photons 7-59355
 Si, chemically assisted ion beam etching using low energy Kaufman source 7-22931
 Si, HF passivated, surface chemistry, XPS and ion scatt. spectra 7-33857
 Si, ion bombarded with H ions, refractive index variations in the near-surface region 7-17299
 Si, low-energy ion beam oxidation, appl. to n-channel MOSFET fabrication 7-3529
 Si MBE growth on Si (100) and (111), interface formation 7-21773
 Si surface, Ar⁺ ion impact, LMM and LVV Auger electron emission 7-59320
 Si surface damage caused by H ions, review 7-16813
 n-Si, surface potential, stabilisation by ion bombardment 7-12782
 Si surface study after Ar ion-assisted Cl₂ etching 7-3538

ion-surface impact continued

- Si surfaces, passivated by H/hydrogen mixtures, surface dielectric layers characterisation 7-17746
 Si, vibrational correlation functions 7-51966
 Si:H, H composition at surfaces and interfaces 7-27083
 Si-Ta interface, depth profile, Ar⁺ ion bombard., Auger electron spectra anal. 7-46261
 SiN films, Auger line, influence of Ar⁺ ion bombardment 7-39339
 Si₃N₄ films on GaAs:Te, annealing-encapsulation props. investigated by nuclear analysis techniques 7-8030
 Si_xN_yO_z films on GaAs:Te, annealing-encapsulation props. investigated by nuclear analysis techniques 7-8030
 SiO₂, chemical sputtering by ions, electrons and photons 7-59355
 SiO₂ films on GaAs:Te, annealing-encapsulation props. investigated by nuclear analysis techniques 7-8030
 SiO₂, sputtering in XeF₂ and Cl₂ atms. 7-53465
 SiO₂ surface interaction with CF₃⁺ and CH₄⁺, mol. sputtering model calcs., AES meas. 7-27854
 Si(111) with adsorbed Ag layers, struct. anal. by impact collision ion scatt. spectroscopy 7-6999
 Ta, BCC cryst. struct., secondary ion emission, current density effects 7-59318
 Ta films, (H₂O)₂H⁺ energetic cluster impact, transmission electron microscopy 7-13304
 TaC (001), multiple scatt. of low energy He⁺, Ne⁺, Ar⁺ ions 7-22426
 Ti surface, heavy-ion-induced D desorpt. meas. 7-44990
 Ti-D, D stopping cross sections, deviations from Bragg's rule 7-51903
 TiN sputtered films, mech. props., substrate ion beam pretreatment effects 7-22484
 TiSi₂:As(Sb) layers, dopant redistribution during silicidation by rapid thermal annealing, ion scatt. spectra study 7-21253
 U⁺+Al(C)(Be)(Mylar), electron stripping, cross section meas. 7-64849
 W (100), surface reconstruction investig., He diff. studies 7-2320
 W (110), hyperthermal K⁺ scattering, HFS-LCAO pair potential 7-22412
 W, polycryst. foils and single crystals, chemical etching, ion bombardment effects, AES study 7-28212
 W surface, cesiated, H⁻ form. by H⁺ bombardment 7-17390
 W surface, work function reduction due to Cs⁺ ion bombardment 7-45430
 WTi-Si barriers, modification by low energy Ar⁺ ions 7-22433
 Xe, solid, sputtering mechanism by keV ions 7-59354
 Xe³⁵⁺+Al(C)(Be)(Mylar), electron stripping, cross section meas. 7-64849
 YIG:H, ion implanted, elastic recoil analysis using 44 MeV Cl ions 7-12107
 ZnS(Se), ion milling, TEM 7-39344
 Zr, HCP cryst. struct., secondary ion emission, current density effects 7-59318
 Zr-D D stopping cross sections, deviations from Bragg's rule 7-51903

ion thrusters see ion engines**ionic conduction in liquids see electrical conductivity of electrolytic liquids; electrical conductivity of liquids****ionic conduction in solids**

- see also superionic conducting materials
 apatite ceramics, with microstruct. controlled by Y³⁺ substitution, elec. props. 7-21523
 binary systems, ionic conductivity, freq. dependence 7-52108
 ceramics, elec. resist. meas. by impedance spectroscopy 7-9844
 dielectrics, conference, Erlangen, W.Germany (July 86) 7-35099
 dispersed ionic conductor, conductivity, percolation model 7-6856
 dispersed solid electrolyte systems, mode of ionic cond. 7-2262
 glass ionic conductivity mechanism 7-44902
 ice, cubic, proton transport, FTIR obs. 7-53340
 impedance studies, bridge balance conditions and error corrections (German) 7-30033
 interaction energies, relativistic ab initio calc., review 7-52109
 mass transport in solids 7-26995
 oxides; perovskite-type, activation energy for proton conduction 7-52130
 oxides, defect behaviour, computer-based atomistic simulation studies 7-16548
 poly(ethylene oxide)-KAg₄I₅, room temp. ionic cond. comp. depend. meas. 7-12363
 poly(ethylene oxide)-LiAg₄I₅, room temp. ionic cond. comp. depend. meas. 7-12363
 poly(ethylene oxide)-NaSCN mixture, ionic conductivity and phase behaviour studies 7-32704
 poly(propylene oxide)-Li salt complexes, ionic cond., high press. effects study 7-32703
 polyepoxide co sulphide, elec. cond., press. and temp. depend. 7-21516
 polymer electrolyte developments, book contrib. 7-27008
 polyphosphazene salt complexes with LiSO₃CF₃, ionic conductors, dimensional stability 7-63872
 polystyrene plasma deposited thin films, ionic cond., free vol. model calcs. and meas., press. depend. 7-27009
 proton conductivity of hydrogen-bonded chain, light and ultrasonic effects 7-44891
 quartz, as-grown or Li-, Na-, Cu- electrodiffused, radiation-induced conductivity 7-6691
 relativistic ab initio calcs., review 7-52110
 silicate glasses containing alkali and alkaline earth metals, alkali ion mobility (Japanese) 7-27007
 small-signal AC frequency response functions 7-63869
 tracer diffusion and ionic cond., correlation effects 7-6857
 triorthophosphates, superionic, synthesis and charactn. 7-53530
 zeolites, ion selectivity, appl. to chabazite 7-63874
 Ag halide emulsion microcrystals, Maxwell-Wagner effect 7-16800
 Ag-AgI-Ag 2D ionic cond. system, fractional dimensionality of Ag dendrites 7-45100
 Ag-As-Se glasses, electrical conductivity studies 7-27369
 Ag_{0.15}As_{0.425}Se_{0.425-x}Te_x chalcogenide glasses, ionic and electronic cond., comp. depend. study 7-12768
 AgBr films with optical absorpt., sensitizing dyes effect on ionic cond. 7-26999
 AgBr thin films and microcrystals, surface pot., ionic cond. data anal. 7-58534
 AgI, two-phase mixture, effect of dispersoid on elec. transport 7-2621
 AgI-Ag₂MoO₄ glasses, ionic conductors, mechanical and electrical relax. 7-44687

ionic conduction in solids continued

- AgI-Ag₂MoO₄ glasses, ionic conductivity, effect of structural relax. 7-44903
- AgI-Ag₂MoO₄ system, conductivity in the liquid and glassy states 7-44881
- AgN₃, elec. cond. under high press., decomp. by dielec. breakdown 7-27010
- (Ag₂O)₂(B₂O₃)_{100-x} glasses, microstruct. and electronic cond. studies 7-6534
- AgPO₃-based glasses, struct. and elec. props., Raman spectra and ionic cond. meas. 7-6550
- AgSbTeO₆, ionic conductivity and powder X-ray diffr. characterisation 7-12362
- β'-Al₂O₃-K₂O-NaO, ionic conductivity, mixed alkali effect 7-52131
- Al₂O₃-Na₂O, beta-type ionic cond., mixed alkali effects, percolation model 7-12355
- B²⁺-Al₂O₃-Na₂O-ZrO₂ ceramics, transform toughened, fabrication, mech. props. ionic resist. 7-65143
- Al₂O₃-SiO₂-CaO glasses containing rare alkali oxides, struct. and elec. props 7-6528
- BaO-B₂O₃-Fe₂O₃ glasses, γ-irradiated and heat treated, elec. conductivity and crystn. 7-21510
- BaZrF₆, ionic conductivity 7-52129
- Bi₂O₃, ionic cond., w.r.t. lone pair separation and cryst. symm. 7-12361
- Bi₂O₃-ZrO₂-Y₂O₃ system, O ion conduction 7-44905
- BiVO₄, pure and CaO doped polycryst. samples, sheelite struct., elec. cond., anion vacancy motion investigation 7-32712
- CaF₂-Nd single crystals, ionic conductivity study 7-21521
- CeO₂, doped with trivalent cations, grain boundary effect, microstruct. and microanal. 7-38249
- CeO₂-Y³⁺(Gd³⁺)(La³⁺), grain boundary effect, elec. meas. 7-38248
- CeO₂-CaO, ceria-calcia ceramics, ionic cond., effect of microstruct. 7-38250
- CsPbBr₃ and CsPbCl₃, ionic cond. and phase transforms., 30 to 380°C 7-58457
- CsSbTeO₆, ionic conductivity and powder X-ray diffr. characterisation 7-12362
- CsSn₂F₆, F⁻ motion, NMR and electrical conduction 7-52132
- β-Cs₂ZrF₆, ionic conductivity 7-52129
- CuBr-Cu₂S solid solns., fast Cu ion transport 7-52121
- Gd_{1-x}Sr_xCrO₃, coordination number and elec. cond., EXAFS and XANES studies 7-64785
- H(H₂O)₂BiO₃, prep. from KBiO₃ by ion exchange, high proton cond. 7-2260
- HNbO₃, electrical conductivity meas. 7-16802
- H₃PMo₃O₄₀·nH₂O, polycryst., NMR and H⁺ conductivity investig. 7-17230
- In_{1-x}Li_xVO₄ solid solutions, characterisation, ionic conductivity (French) 7-44833
- K halides, injection of charge carriers from a point contact 7-6868
- KBr:Se²⁺, mag. circular dichroism, electric conductivity, mobility of anion vacancies 7-3024
- KCl:Sr, quenched and as-grown crystals, ionic cond., impurity dispersion state effects study 7-26786
- K₂(Ga₂Ga₈+Ti_{16-x}O₅₆), synthesis of new cpd. by flux method 7-27883
- KH₂(IO₃)₃, proton cond. and cryst. struct., X-ray and neutron diffr. studies 7-12026
- KH₂PO₄ pellets, protonic conductivity, complex impedance study 7-2261
- K₂O-B₂O₃, elec. cond., molar volume 7-58535
- K₂O-Fe₂O₃-TiO₂ system, cryst. growth of titanates, morphology, ionic cond. 7-53523
- KSbTeO₆, ionic conductivity and powder X-ray diffr. characterisation 7-12362
- KSn₂F₆, F⁻ motion, NMR and electrical conduction 7-52132
- KTaWO₆·H₂O, pyrochlore-type cpd., characterisation 7-1989
- K₂TiF₆, ion motions and cond., NMR relax. time meas. 7-38246
- KZnF₃, high temp. mean square ionic displacements 7-2259
- La_{1-x}Ca_{0.5x}Ba_{0.45x}FeO_{3-α}, elec. cond. props. rel. to struct. 7-63871
- La_{1-x}Sr_xFeO_{3-α}, elec. cond. props. rel. to struct. 7-63871
- Li spinel insertion compounds, reactions, mag. and elec. props. 7-33920
- Li₂-WO₃-Nb₂O₅ sputtered amorphous films, electrochromic props. study 7-22221
- LiAlSi₂O₆, β-spodumene, ionic conductivity 7-52133
- Li₃BN₂, synthesis, polymorph struct., ionic cond. meas. 7-32388
- LiD:Mg²⁺, elec. props., X-irradiation effects, DC cond., dielec. loss and ionic thermocurrent meas. 7-27341
- Li₂+Ga_{1-x}Mg(Zn)_xO₄, solid solns., ionic cond. comp. depend. meas. 7-12366
- LiH:Ca²⁺, elec. props., X-irradiation effects, DC cond., dielec. loss and ionic thermocurrent meas. 7-27341
- LiKSO₄ crystals, elec. conductivity anisotropy 7-21509
- Li₂+₄(Li₁Mg_{1-x}Sn_x)O₈, ramsdellite type cpds., ionic conductivity and cryst. chemistry 7-32708
- Li₂Mg_{1-x}Fe_{2x}Sn_{3-2x}O₈, ramsdellite type cpds., ionic conductivity and cryst. chemistry 7-32708
- Li₃N:H, doped and undoped fast ionic conductor, positron annihilation 7-39276
- LiNaSO₄, BCC, rotator phase, solid electrolyte behaviour, thermodynamic props. 7-21139
- LiNbO₃, prod. by Czochralski and Stepanov methods, elec. phenomena accompanying growth 7-32332
- Li₂O-B₂O₃, ion conducting glass, effect of CaO substitutions on transport and physical props. 7-58535
- Li₂V₆O₁₃ single cryst., Li transport props. and partial molar entropy 7-6871
- Li₂WO₄, elec. transport mechanism, superionic phase 7-12359
- Li_{2-2x}Zn_xGaO₄, solid solns., ionic cond. comp. depend. meas. 7-12366
- Li_{2-4x}Zr_{1+x}(PO₄)₂ solid solns., ionic cond. meas. 7-44906
- Li_{1-x}Zr_x[PO₄]₃ ionic cond. comp. depend., X-ray diffr., prep. method depend. 7-12365
- NH₄Cl, phase transitions, elec. props. study 7-17257
- NH₄H₂(IO₃)₃, proton cond. and cryst. struct., X-ray and neutron diffr. studies 7-12026
- NH₄Sn₂F₆, F⁻ motion, NMR and electrical conduction 7-52132
- (Na,Rb)-O-GeO₂ glasses, mixed alkali effect 7-12367
- 20(NaK)₂O-xGa₂O₃-(80-x)SiO₂ glasses, elec. conductivity, mixed alkali effect 7-27001
- NaLa(MoO₄)₂ single crystals and ceramic, elec. cond. meas., disordering mechanisms 7-6863
- Na₂MoO₄, on Mo porous electrodes for alkali metal thermoelec. converter, voltammetric studies 7-28405

ionic conduction in solids continued

- β-Na₂O-Al₂O₃ ionic conductors, mechanical and electrical relax. 7-44687
- Na₂O-Al₂O₃-GeO₂ glasses, ionic transport meas., packing density depend. 7-32710
- Na₂O-B₂O₃-SiO₂ glass, Na⁺ self-diffusion and elec. cond. studies 7-21515
- Na₂O-GeO₂ glasses, ionic transport studies 7-6864
- Na₂O-P₂O₅ thin films, elec. resist., effect of sorbed water 7-21514
- Na₂O-SiO₂-Ag₂O, Na⁺⇌Ag⁺ ion-exchanged, elec. conduction 7-27002
- Na₂O-Y₂O₃-MO-SiO₂ glass, (M=Mg, Sr, Ca), Na⁺ conductivity 7-52134
- Na₂O-Y₂O₃-SnO₂-SiO₂ glass, Na⁺ conductivity 7-52134
- NaSn₂F₆, F⁻ motion, NMR and electrical conduction 7-52132
- Na₂Ti_{0.75}Si_{2.25}P₂O₁₂, NASICON-based glass and glass ceramics, synthesis and characterisation 7-44908
- Na₂YSi₄O₁₂, twinning, crystal struct. 7-21226
- Na₂Zr_{2-x}In_xSi_{2-x}P_{1+x}O₁₂ system, chem. composition, cryst. struct. and ionic cond. (Chinese) 7-12006
- Na_{1+x}Zr_{2-x(x/2)}Mg_(x/2)(PO₄)₃ solid soln., cryst. chemistry and ionic cond. studies 7-32408
- PVDF films, elec. field-induced gas emission meas., ionic charge transport study 7-27872
- Pb-Sn-G solid solns., elec. transport props. and defect form. studies (French) 7-33017
- PbBr₂ layers, vacuum deposited, elec. cond. temp. depend. 7-27000
- PbF₂-MnF₂-Al(PO₃)₃ glasses, conductivity and mechanical relax 7-16803
- α-PgZrF₆, ionic conductivity 7-52129
- poly(ethylene oxide)-RbAg₄I₅, room temp. ionic cond. comp. depend. meas. 7-12363
- RbAg₄I₅, electrodeless meas. method 7-48777
- Rb₂Cu₃Cl₁₃, solid electrolyte, elec. cond. and cryst. struct. 7-2257
- RbSbTeO₆, ionic conductivity and powder X-ray diffr. characterisation 7-12362
- RbSn₂F₆, F⁻ motion, NMR and electrical conduction 7-52132
- SrCl₂-Al₂O₃ system, enhancement of ionic conductivity 7-2256
- Sr(NO₃)₂, ionic cond. study as function of pelletizing press. 7-12358
- α-SrZrF₆, ionic conductivity 7-52129
- TiCl:Al₂O₃, ionic transport investig. 7-16798
- TiSbTeO₆, ionic conductivity and powder X-ray diffr. characterisation 7-12362
- TiSn₂F₆, F⁻ motion, NMR and electrical conduction 7-52132
- WO₃ based electrochromic windows, recent R&D 7-37122
- Y₂O₃, elec. cond. as function of O₂ partial press. in wet and dry atm. 7-45405
- Zn(PO₃)₂-CdCl₂-KCl glasses, electrical conductivity and IR spectra 7-2253
- ZrF₄-BaF₂-CsF glasses, ionic conductivity 7-52129
- ZrF₄-BaF₂-ThF₄-LiF quaternary glasses, ionic cond. and NMR studies 7-6865
- ZrF₄-PbF₂-AlF₃-LiF-NaF glasses, mixed alkali effect, DC cond. 7-63873
- ZrF₄-PbF₂-AlF₃-NaF-KF glasses, mixed alkali effect, DC cond. 7-63873
- ZrO₂, solid electrolytes, effect of admixture cation radius on sintering 7-13398
- ZrO₂-YO_{1.5}, thermal behaviour of ⁵⁶Fe implantations 7-27006
- α-ZrP-propylamine, intercalation cpd., amine loading, protonic cond., admittance meas. 7-44909

ionic conductivity in solids see ionic conduction in solids

ionic thermocurrents see thermally stimulated currents

ionisation

- see also associative ionisation; autoionisation; charge exchange; electron attachment; electron capture; field ionisation; ion recombination; ionisation of atoms; ionisation of gases; ionisation of liquids; ionisation of molecules; ionisation of solids; ionisation potential; Penning ionisation; photoionisation; surface ionisation
- galactic corona, IUE obs. rel. to kinematics, ionisation, and abundances 7-48054
- interstellar medium, IUE evidence for diffuse collisionally ionised C IV and Si IV below Z=1 kpc 7-55783
- interstellar radiative shocks, ionisation struct. and line spectra of steady shocks 7-55454
- stellar winds, ionisation of radiation-driven winds of hot luminous stars 7-47841
- H II regions, extragalactic, ionisation parameter vars. rel. to O abundances calibration 7-40903
- H II regions, extragalactic, He ionisation struct. rel. to He/H abundance ratio 7-40906

ionisation chambers

- angular response compensation 7-42279
- aromatic seeding agents for laser ionization in counting gases 7-42294
- beta radiation unit of absorbed dose rate to tissue, PTB National Primary Standard 7-28717
- calibration factors for radionuclide calibration 7-30894
- calibration of soft X-ray sources and instruments, 1986 status 7-25322
- collection efficiency in a pulsed swept beam: chamber size effects 7-14134
- collection efficiency in a pulsed swept beam: collimator scatt. effects. 7-14135
- conf., Vienna, Austria, February 1986 7-40989
- CP violation experiment, detector configuration and trigger 7-41786
- cylindrical chamber dimensions and the corresponding values of A_{wall} and N_{gas}/(N_Aion) 7-40304
- dose calibrator ionisation chamber standards for radionuclide assay 7-40310
- dose calibrators meas., evaluation 7-30891
- double needle gas counter arrangement for measurements of low beta radioactivity solid emitters 7-19641
- Eberline RO2 ionisation chamber survey instrument, modifications for the quantities ambient and directional dose equiv. 7-54758
- electret pulse chamber, detection props. 7-5555
- electric generator overheating, early diagnostics using data for release of aerosols in insulation (Russian) 7-59787
- electron yield detectors for near surface EXAFS 7-61414
- extrapolation chamber for β-ray detect., performance characts. 7-25302
- high resolution β⁻ digital autoradiography using a single step parallel plate chamber 7-5573
- high-pressure ionisation chamber, appl. to meas. mean neutron energy or γ-ray dose fraction in a mixed neutron-γ field 7-34280
- high-pressure ionisation chamber to meas. mean neutron energy and γ-ray dose fraction 7-34281

ionisation chambers continued

- laser induced two-photon ionisation absorption, seeding agents for particle track simulation 7-5540
 liquid Ar-methane image chambers, drifting electrons over large distances 7-49800
 liquid TMS track chamber 7-62209
 low pressure multistep detectors, high energy particle identification appl. 7-42290
 LTD, FASTBUS time digitiser for LEP detectors 7-42307
 measurement assurance, manufacturer's view 7-30892
 modified Bragg-curve centroid detection, particle identification 7-62228
 Monte Carlo computer code system for ionization chamber response analysis, development and testing 7-42433
 multiwire proportional chambers for time-resolved studies on muscle 7-47144
 MWPC based system for digitizing electrophoretic gels 7-47296
 NBS measurements of sample geometry effects on ionization chamber calibrations 7-30893
 NBS pressurized ^{40}Ar ionisation chamber A, calibration uncertainties 7-30895
 NBS Radioactivity Group, instrumentation calibration 7-30890
 neutron absorbed dose component determ. in mixed field (Chinese) 7-5560
 on-line system for rare spontaneous fission events 7-19634
 Oxford MDM-2 spectrometer, hybrid focal plane detector 7-5551
 parallel plate avalanche counter for high resolution minimum ionizing particle detection 7-30853
 parallel-plate ion chamber, N_{gas} determ., dosimetry appl. 7-40299
 proportional chamber, multielement, for ^{136}Xe $\beta\beta$ decay 7-42287
 proportional counter, use in muon identification system 7-15466
 pulse ionisation chamber for ^{136}Xe double β -decay expt. 7-19631
 SIR ionisation chamber, energy response functions 7-49790
 thin multiwire chamber working at high amplification, gas comp., cathode and parameter effects 7-49799
 UVVVR ionisation chamber, energy response functions 7-49790
 VENUS central drift chamber, charged particles, pattern recognition algorithm 7-822
 X-ray position detection, 6 μm position resolution, use of wire proportional chambers 7-42288
 Ar gas, laser induced multiplication and visualisation of free electrons 7-49812
 Mg/Ar ionisation chambers used as γ -ray dosimeters in mixed neutron-photon fields, characts. 7-34282
 Na ionization detector for FBR sodium leak detection system 7-5355
 Si drift chambers, electron dynamics 7-42329
 Xe, compressed, for gamma-ray spectroscopy 7-10350
 Xe-filled compensated ionisation chamber, transient anal. to quantify sensor degradation 7-42134

ionisation gauges

- Bayard-Alpert gauge, low pressure limit 7-18798
 controller with logarithmic response for Bayard-Alpert vacuum gauge 7-14959
 hot filament ionization gauges for high pressures in the vacuum range 7-35530
 modulated Bayard-Alpert gauge, residual current studies 7-35533
 plasma measurements in mag. field 7-20933
 sputter ion gun based on Bayard-Alpert pressure gauge 7-18917
 total and partial press. meas., vacuum metrology 7-35531

ionisation of atoms

- see also *atomic electron impact ionisation*
 above-threshold ionisation and electron scattering in intense laser fields 7-30992
 alkali earth metals, photoionisation cross sections 7-50039
 alkali metal mixtures, collisional ionisation study (French) 7-10729
 alkali-metal atoms, photoionisation cross sections, ab initio RRPA calcs. 7-36462
 atom-ion collisions, $Z=32$ to 54, L-shell ionisation, X-ray yield, threshold behaviour 7-10734
 atom-ion collisions L subshell ionisation probabilities vacancy sharing 7-15697
 atomic impurities in Ne, optogalvanic effect 7-30970
 atomic multipole transitions, positions of minima in multipole matrix elements 7-36550
 atoms in a low field, review 7-898
 autoionising states, complementary branching ratios by satellite excitation 7-19786
 bound state existence confirmation for atomic and mol. projectiles inside solid targets, expt. investig. (French) 7-22427
 clusters in beams, review 7-31204
 collinear laser-fast-beam spectroscopy, collisional ionisation detection scheme 7-18882
 discrete states in the continuum, generation by coupling of bound states 7-36509
 electric fields effect on autoionising resonances 7-10520
 electronic chemical potential calc. 7-25336
 element, single, ionisation equilib. theory, approximate soln. 7-19787
 final-state effects in above-threshold ionisation 7-31167
 heavy atoms, photoionisation, Cooper minima, relativistic effects 7-36561
 high-Z elements, Li, La, L β and L γ X-ray prod. cross sections, meas. 7-19801
 highly charged ions, multiple-electron capture, classical over-barrier model 7-10744
 inert gas + H^+ , electron transfer and ionis., δ -electron spectrosc. 7-42685
 inert gas atoms, multiple ionisation by intense laser pulse 7-62332
 inert gas atoms ionisation by CO_2 laser, nonlinearity 7-62335
 inert gases, multiphoton ionisation study 7-19798
 inert gases multiphoton ionization in intense ultraviolet laser fields 7-19797
 inner-shell ionisation by H^+ collisions 7-42750
 ion bombardment induced X-ray emission spectra 7-13310
 ion chemistry, gaseous, hybrid BEQQ mass spectrometer appls. 7-48904
 ion-pair formation collisions, model simulation of differential cross sections 7-10737
 ionised gases, atomic and mol. physics, conf. Greifswald, Germany (Aug. 1986) 7-18499
 laser field ionisation, quantum model calcs. 7-50032
 laser ultrasensitive high-resolution spectroscopy of short-lived radioactive atoms 7-10522
 laser-induced autoionization from a double Fano system 7-57034
 light negative ion prod., conf., Palaiseau, France, March 1986 7-9601

ionisation of atoms continued

- light rare earths, $\text{L}\gamma_{2,3}$ satellite, X-ray emission spectra anal. 7-36523
 line profiles influenced by selective ionization in low pressure discharges 7-21002
 medium and heavy elements, L-subshell ionisation cross sections, X-ray spectra anal. 7-30977
 multielectron atoms, multiphoton excitation and ionisation 7-19796
 multiphoton autoionisation by smooth laser pulses 7-15577
 multiphoton excitation techniques for combustion diagnostics 7-17789
 multiphoton ionisation, continuum struct., high optical. harmonics 7-50046
 multiphoton ionisation theory, review 7-19793
 multiphoton ionization study of nonlinear processes in atoms 7-10510
 multiphoton stripping of atoms, review 7-42576
 multiple core holes, electronic system response and spectra prod., many-body theory 7-42477
 Ni+Ni collisions, quasimol. form., X-ray spectra study 7-31157
 noble gas metastable atoms, interaction with transition metal surface 7-64852
 nonlinear atomic, multi-quantum, interactions at high electric field strengths 7-20165
 nonlinear processes, high order, multiphoton ionis. investig. 7-10528
 nuclear excitation by laser driven coherent outer shell electron oscillation, gamma-ray laser appl. 7-10121
 open-shell atoms, ions and excited states, photoionisation 7-36562
 photoionisation, ang. depend. electronic Green's fn., finite basis-sets 7-42570
 photoionisation, by strong elec. fields, 1D model 7-36804
 photoionisation, relativistic Cooper minima for ground-state atoms, independent-particle approx. calcs. 7-62275
 photoionisation, threshold effects in strong-field, non-perturbative realistic model 7-36563
 photoionisation of ions, ionic and point-Coulomb relativistic Cooper minima, independent particle approx. calcs. 7-62276
 plasma, emission characteristics, soft X-ray region, plasma diagnostics, radiative-collisional model study 7-62312
 ponderomotive potential, effect in above-threshold ionisation processes 7-19800
 satellite excitation, complementary branching ratios 7-10519
 short wavelength coherent radiation generation and production conf. Monterey, CA, USA (March 1986) 7-18467
 Si II, autoionizing levels and identification of 1400 Å feature in Ap-Si stars 7-40821
 space charge effect on electron angular distribution after multiphoton ionisation 7-15568
 sputtered atoms, ionisation probability studies 7-20068
 stimulated Raman scattering, off-resonant enhancement investig. 7-50148
 symmetric heavy ion collisions, K X-ray prod., target thickness fn., X-ray spectra anal. 7-30978
 three- and four-level systems, strong field and ionisation dynamics 7-10525
 transition and ionisation energies, g-Hartree ab initio calcs. 7-15488
 two-laser multiphoton ionisation, Raman-type resons. 7-50035
 two-level atom, internal relax. effect on quantum fields 7-1048
 two-photon two-level interactions, ionisation and cascade decay effects 7-15574
 Ag clusters, small, photolytic, oscill. of photoionisation thresholds on AgBr grain surface 7-36841
 Ar, Auger emission, electron-electron coincidence investig. 7-30996
 Ar, dipole ($e,2e$) cross sections, plane-wave Born calcs. 7-30935
 Ar, double ionisation by single electron impact 7-62526
 Ar, ionis. behind normal plasma shock waves, conservation eqns. 7-31980
 Ar, photoionis. with synchrotron radiation, angle-resolved electron spectra 7-905
 Ar, photoionisation, photoelectron and electron momentum spectroscopy 7-36560
 Ar $^{+}$ photoionisation pumping via two-electron shakeup 7-20195
 Ar+ H^+ (He^{2+}), electron emission, impact parameter depend., TOF, coincidence spectra anal. 7-42747
 Ar+He, 2^3P , state quenching 7-62319
 Au $^{51+}$, Ni-like, population inversion, ionisation model 7-25462
 Ba, singly and doubly charged ion form. by nonlinear laser induced ionisation 7-42573
 Ba atoms, multistep photoionisation, total angular momenta of autoionisation steps 7-50031
 Ba autoionising states, internal conversion and fluoresc. two-step process 7-25467
 Ba, double Rydberg states, ionisation, two-photon and TOF mass spectra 7-19809
 Ba neutral atoms, high-lying states, laser pumped, two-photon spectra 7-19811
 Ba $^{+}$, metastable autoionising state, lifetime meas. 7-19788
 Ba $^{+}$, photoionisation absolute cross section meas. 7-50034
 $^{138}\text{Ba}+\text{H}^+$, elastic backscatt., K-shell ionis. probability, reson. effect 7-42748
 Be, 3^3P^0 and 1^3P^0 Rydberg series, autoionising states, complex eigenvalue Schrodinger eqn. soln. 7-62329
 Bi II, $6s^26p^2$ 3^3P - $6s^26p^2$ 3^3D , series in photoabsorption 7-25469
 Br XXV to XXI, spectra and energy levels 7-25444
 C, double excitation and ionisation by strong pulsed laser 7-42571
 C IV in OB-type stars, ionisation fraction determ. from UV line profiles and IR excesses 7-47884
 C, photoionis. cross section, generalised RPAE calcs. 7-42574
 C $^{4+}$ projectile on C foil, convoy electron yield, target thickness depend. 7-27839
 Ca, electronic struct. calcs., relativistic effects 7-36504
 Ca, laser-XUV excited state spectroscopy 7-19746
 C $_n^+(a=+or-)$, abundance distrib., magic numbers, photoionis. mass spectroscopic investig. 7-15759
 Cd, autoionisation widths, calcs. and optogalvanic spectra 7-36521
 Cd $^{+}$, alignment after photoionis., fluoresc. radiation polarisation meas. 7-890
 Cd $^{+}$, autoionising states, picosecond soft-X-ray ionis. spectroscopy 7-10521
 Cd $^{+}$ photoionisation pumping via two-electron shakeup 7-20195
 Cl, photodissoc., third harmonic interference, polarisation effects, MPI spectra 7-50045
 Cl, photoionisation cross section at 584 Å 7-36702
 Cl plasma, photo-excitation and ionisation, transition energies, orbital relax. effect 7-37651
 Cs, 5s ionisation, PES satellite struct., CI approach 7-62296

ionisation of atoms continued

- Cs, gas phase atoms, detect. by 2-photon resonant ionisation spectroscopy 7-42533
 Cs, photoionisation in 650 to 760 Å UV spectra 7-50033
 Cs, resonance ionisation in presence of buffer gas collisions 7-10527
 Cs vapour, comp. study, reson. doublet absorpt. meas. 7-36518
 Cs, vapour, two-photon reson. four-wave mixing and multiphoton ionis. in heat pipe oven 7-901
 Cs⁻, low-energy collisions with atoms and mol., absolute total cross section meas., curve-crossing model anal. 7-36749
 D, large angle scattering, from Cu, Au and Ni, energy spectrum 7-64854
 D, resonant IR two-photon ionisation 7-15573
 Dy, L subshell ionis. by deuteron impact, cross section determ. 7-51878
 F I, excited levels, photoionisation cross-sections, Thomas-Fermi calcs. 7-10423
 F, multiphoton ionisation spectroscopy 7-10534
 F+Au, X-ray emission from multiply ionized atoms (Rumanian) 7-15699
 Fe, multiply charged ions, electron-impact ionisation, excitation energies and cross section calcs. 7-25425
 Fe, multiply-charged ions, electron-impact ionisation cross sections, crossed-beam meas., rate coefficient calcs. 7-25660
 Fe⁺, excited state selected, one-colour UV multiphoton ionis. 7-36506
 Fe²¹⁺, dielectronic recomb., rate coeff. calc. 7-30991
 Fe²²⁺, dielectronic recomb., rate coeff. calc. 7-30991
 Fe+D(He)(C)(N)(O), thick target bombardment, X-ray production cross sections 7-20025
²²¹Fr, radioactive isotope detection, laser resonant photoionisation method 7-42572
 Ga, reference sample, absolute isotropic abundance ratio and at. weight 7-42779
 Ga, resonant state, autoionis., electron spectra 7-900
 Gd, autoionising states, electric field effects, UV spectra anal. 7-42531
 H, 1D atom, ionis. by reson. elec. field 7-5780
 H discharge, at. and mol. meas. using reson. multiphoton ionisation 7-20955
 H excited states, photoionisation in strong elec. fields 7-10526
 H, highly excited, quasi-Landau struct. 7-36510
 H, ideal gas, modified Gibbs state 7-44087
 H, large angle scattering, from Cu, Au and Ni, energy spectrum 7-64854
 H, microwave ionisation below classical chaos border 7-57142
 H, microwave ionisation of highly excited states, stochastic effects 7-15562
 H, multiphoton absorption above ionisation threshold, Sturmian expansion appl. 7-36565
 H, multiphoton excitation techniques for combustion diagnostics 7-17789
 H, multiphoton ionisation, time-depend. theory 7-42568
 H, multiphoton ionisation by intense laser field, integral eqn. approach 7-62339
 H, Stark effect and field ionis. 7-5628
 H, Stark ionisation multichannel reson. quantisation 7-50005
 H⁺, ¹p⁰ symmetry, Wannier two-electron ionis. ladder, wave fn. calc. 7-62274
 H-Like ions+Ar(Ne)(N₂)(O₂) targets, projectile ionisation cross section 7-969
 H+C³⁺, pot. energy curves, spin-coupled VB theory 7-957
 H+He, single-electron detachment, time correlated electron spectrum study. 7-36741
 H⁺+Al⁺(Ga⁺)(In⁺)(Ti⁺), charge transfer and ionis. 7-31162
 H⁺+Ar, p state ionisation, density matrix parameters meas., DWBA calcs. 7-36743
 H⁺+Dy(Yb), L-subshell ionisation cross section, X-ray emission 7-50327
 H⁺+K, ionisation and charge transfer collisions, cross section meas. 7-20031
 H⁺+Nd(Sm)(Tm), K-shell ionisation cross sections 7-50326
 H⁺+Ne(Na)(Mg), multiple ionisation, charge transfer cross sections 7-15706
 H⁺+He, elastic and inelastic scatt. mechanisms, energy loss spectra 7-15671
 H⁺L(Cr,Fe,Co,Zn), k-shell ionization cross sections and theoretical models 7-5627
 He, ¹p⁰ symmetry, Wannier two-electron ionis. ladder, wave fn. calc. 7-62274
 He + H⁺(H⁺), single and double ionisation by fast antiproton and proton impact 7-20027
 He, atom, with turbulent flow, two electron group model for RF ionisation 7-31921
 He autoionising states, laser-induced transition 7-42566
 He, collisions with fast, highly charged ions, electron capture to the continuum meas. 7-20026
 He, double excited states, correl. wavefunction calcs. (French) 7-10454
 He, doubly excited autoionising resonance states, Hylleraas-type wave fn. calcs. 7-30940
 He, ground state, one-electron loss cross section in H₂ gas 7-50338
 He, in Wolf-Rayet stars, ionisation state rel. to mass loss rates 7-9475
 He ionisation structure in H II region complexes, implications for He/H abundance ratio 7-40906
 He, large angle scattering, from Cu, Au and Ni, energy spectrum 7-64854
 He multielectron multiphoton ionisation 7-19795
 He, multiply charged ions collisions, semiclassical model, double electron transitions 7-10733
 He, photoelectron satellites at threshold, photoelectron spectra anal. 7-36564
 He, photoelectron satellite branching ratios, asymmetry parameters, UV PES anal. 7-62333
 He, photoionisation, partial cross-sections and Rydberg series resons. 7-903
 He Rydberg state, absolute photoionisation cross section 7-62331
 He, surface peak in energy distrib. 7-64855
 He, threshold double photoionisation 7-19804
 He⁺ + light target atoms (28 ≤ Z ≤ 46), L shell X-ray prod. cross sections meas., first Born approx. and ECPSR theory anal. 7-36526
 He⁺ low energy ion-surface scatt., reionisation process theory 7-22413
 He⁺, photoionisation production and fluorescence angular distrib. 7-25451
 He⁺ photoionisation pumping via two-electron shakeup 7-20195

ionisation of atoms continued

- He-like ions, energy level population autoionisation states (French) 7-10518
 He+B²⁺(Oⁿ⁺)(Siⁿ⁺), double- and single-electron capture and loss cross section meas., OBK scaling calcs. 7-42756
 He+C²⁺(Ne¹⁰⁺) electron capture, bound and continuum states, impulse approx. 7-50329
 He+H⁺, electron ejection, double differential cross section meas. 7-20024
 He+H⁺(H⁺), double ionisation, ab initio calcs. 7-42737
 He+He, ionis. cross section meas. 7-62494
 He+He⁺, single and double ionis., cross section meas. 7-31148
 He+NH₃, Rydberg atom ionis., rot. deexcitation 7-36737
 He+Rb, afterglow, inelastic collisions quenching cross sections 7-42746
 He⁺+Ca(Cr)(Cu), target K-shell ionis., cross-sections and probabilities 7-50343
 He⁺+H⁺, ionis., beam-pulsing expt. 7-31160
 He⁺+He collisions, projectile ionization, doubly differential cross section study 7-971
 He⁺+Ne(Na)(Mg), multiple ionisation, charge transfer cross sections 7-15706
 He²⁺+K, ionisation and charge transfer collisions, cross section meas. 7-20031
 He⁺+Ag(Cd)(In)(Sn)(Sb)(Te)(I), L-subshell ionisation, X-ray prod. 7-50303
³He²⁺ electron capture and stripping cross section in Al, Ni, Ag and Au targets 7-10753
¹⁹⁷Hg, nuclear isomer separation, for gamma-ray laser 7-10091
 I, four-photon ionisation, three-photon resons., AC Stark broadening 7-57036
 I, photoemission cross-section and ang. distrib. parameters, inner and outer shell ionisation 7-15565
 I+Na, ion-pair formation collisions, model simulation of differential cross sections 7-10737
 In plasma, laser ablated inner-shell photoionisation-pumped, optical gain at 185 nm 7-20193
 In, resonant state, autoionis., electron spectra 7-900
 In sputtered excited neutral atoms vel. distrib. meas. and deexcitation model calcs. 7-875
 K, two- and three-photon ionis. 7-30993
 Kr, 3p excitation, multiple photoionisation cross sections, TOF mass spectrometer anal. 7-19802
 Kr autoionising region, multiphoton ionisation study 7-62336
 Kr, Rydberg states, four-photon excitation 7-62328
 Kr, ultrasensitive laser isotope anal. 7-19803
 Kr, visible transitions, autoionis. obs., optogalvanic spectra 7-57035
 Kr³⁶⁺, emerging from solid foils, anomalous population of deep capture states 7-42758
 Kr+Kr ions, quasimolecular Auger emission, impact energy depend. 7-25645
 Li, ²p₁ levels, relativistic autoionisation, threshold phenomena, CI mechs. 7-49950
 Li, ²p₁ level, relativistic autoionisation, CI mechs. 7-49949
 Li, two-photon resonant three photon ionisation, power broadening, laser bandwidth and interaction time effect 7-36571
 Li⁺, ¹p⁰ symmetry, Wannier two-electron ionis. ladder, wave fn. calc. 7-62274
 Li⁺ pumping by soft X-rays, EUV emission 7-20196
¹⁷¹Lu, A-173-6, resonance ionization mass spectrometry for high resolution optical spectra 7-19744
 Mg, ¹P doubly excited autoionisation states, CI calcs. 7-36497
 Mg, autoionising Rydberg states, reson. ionisation mass spectrometry 7-19785
 Mg, multiphoton ionis. investig. 7-30994
 Mg, multiphoton ionisation, DC elec. field effects 7-62337
 N, high freq. excitation, vac. UV spectra 7-10476
 N, threshold double photoionisation 7-19804
 N⁺+Ar, transfer ionisation, differential cross section meas. 7-50325
 N₂⁺ + Au, impact ionisation, L₃ subshell alignment, coupled states anal. 7-25643
 Na, 3P state, photoionization polarization and correlation characteristics, energy dependence 7-5648
 Na ion beam generation, field ionisation of laser-excited Rydberg atoms 7-57186
 Na ion formation in vapour containing laser selected Rydberg atoms 7-10462
 Na, laser excitation, competition between photoionization and two-photon Raman coupling 7-10529
 Na, vapour ionization by laser resonance saturation 7-19791
 Na+electronegative molecule, thermal collisions, laser-induced ionis. mechanism 7-62488
 Na+Na, associative ionis. cross section meas., spin-selected velocity depend. 7-42736
 Na+Na(Na⁺), ion pair prod., laser excitation effect 7-62507
 Na+Ne⁺(Ar⁺)(Xe⁺), Rydberg electrons removal, cross section meas. 7-36742
 Nd, reson. ionisation photoelectron spectroscopy 7-19799
 Ne, dipole (e,2e) cross sections, plane-wave Born calcs. 7-30935
 Ne discharges, optogalvanic spectra using tunable laser radiation 7-61389
 Ne, electron impact induced post-collisional KL_{2,3}L_{2,3} Auger decay 7-5773
 Ne, ionisation cross section determ., correction factor 7-19701
 Ne, photoelectron satellites at threshold, photoelectron spectra anal. 7-36564
 Ne, photoionis. with synchrotron radiation, angle-resolved electron spectra 7-905
 Ne⁺ + Au, impact ionisation, L₃ subshell alignment, coupled states anal. 7-25643
 Ni_n (n=1 to 6) clusters, electronic struct., ab initio SCF and CI calcs. 7-10446
¹⁶O, collisions with wide range of targets, K-shell ionisation, polarisation and binding effects 7-31165
 O, photoionis. cross section, generalised RPAE calcs. 7-42574
 Pb, 6p subshell, admixed state effect on photoionisation 7-25470
 Pb, resonant state, autoionis., electron spectra 7-900
 Pb(Pb,X), 5.7 MeV/n, e⁻ and e⁺ spectra, sudden rearrangements of electronic shells 7-49441
 Pd isoelectronic series, ⁴f¹⁰ subshell, photoionis. and electron impact ionis. 7-902
 Pr, reson. ionisation photoelectron spectroscopy 7-19799

ionisation of atoms continued

- Ra relativistic splittings of Cooper minima, RPPA study 7-862
 Rb, collisional ionisation study (*French*) 7-10729
 Rb transient excitation produced by nonresonant laser pulses 7-15569
 Rb+Rb, collisional ion-pair form., Coulomb pot. 7-15698
 Rh (111), clean and with adsorbed O, ion bombarded, desorbed atoms distributions 7-22420
³²S, collisions with wide range of targets, K-shell ionisation, polarisation and binding effects 7-31165
 S, UV photoionisation and autoionisation 7-10523
 S+Au, X-ray emission from multiply ionized atoms (*Rumanian*) 7-15699
 Se, photoionisation and autoionisation, UV spectra 7-10524
 Se⁺, resolved Zeeman thresholds in photodetachment in mag. field 7-42549
 Si⁺, sputtered, ionisation and bond breaking 7-13306
 Si/Fe, low damage surface anal., sputtered atom resonance ionisation method 7-58584
 Sm, reson. ionisation photoelectron spectroscopy 7-19799
 Sm+H⁺, 4 MeV collisions, L-subshell ionisation probabilities, impact parameter depend. 7-42749
 Sr, autoionising series, multichannel quantum-defect theory model data fit, UV PES study 7-62334
 Sr, autoionizing levels meas. (*Chinese*) 7-5645
 Sr ions, in air-acetylene flame, time decay, laser-induced ionis. detect. 7-62316
 Sr, singly and doubly charged ion form. by nonlinear laser induced ionisation 7-42573
 Sr, two-photon resonant three photon ionisation, power broadening, laser bandwidth and interaction time effect 7-36571
 Sr⁺+Ba, laser-induced charge exchange, quasi-mol. model, fluores. anal. 7-36748
 Ta, L-subshell ionis., proton deuteron and alpha impact induced, low-velocity effects 7-51879
 Ti⁺ excited state selected, one-colour UV multiphoton ionis. 7-36506
 Ti+D(He)(C)(N)(O), thick target bombardment, X-ray production cross sections 7-20025
 Ti+He⁺(Li⁺)(H⁺), inner-shell ionis. polarisation effect, variational wave fn. calc. 7-62491
 Ti atoms, detection using resonance ionisation 7-15570
 Ti II, electron impact, 6¹S₀-6³P₁ intercombination transition excitation resonance obs. 7-36778
 U⁺+Al(C)(Be)(Mylar), electron stripping, cross section meas. 7-64849
 V⁺, excited state selected, one-colour UV multiphoton ionis. 7-36506
 W, L-subshell ionis., proton deuteron and alpha impact induced, low-velocity effects 7-51879
 Xe, 5p photoionis., angle- and spin-resolved photoelectron spectroscopy, expt. charactn. 7-904
 Xe, 6s state, three-photon excitation and four-wave-mixing, two-colour interference effect 7-19812
 Xe, above-threshold multiphoton ionisation, circularly and linearly polarised light, PES spectra study 7-62338
 Xe atoms, J=1 even-parity autoionisation 7-50029
 Xe, autoionisation under two- and three-phonon excitation 7-15561
 Xe ionisation, photoelectron angular distrib. 7-19794
 Xe, J=0 autoionisation, multichannel-quantum-defect theory anal. 7-36559
 Xe multielectron multiphoton ionisation 7-19795
 Xe multiphoton ionisation, suppression with circularly polarisation coherent light 7-19792
 Xe, multiphoton ionisation, final state redistribution, electron energy spectra anal. 7-25468
 Xe, multiphoton ionisation spectrum, space charge elimination pulse polarisation effects 7-15567
 Xe, multiphoton ionisation study 7-19798
 Xe, multiphoton ionisation 7-62330
 Xe, multiple photoionisation, charge state of ions, TOF mass spectra anal. 7-50036
 Xe, photoelectron angular distributions, ponderomotive effects 7-50037
 Xe, photoionis. with synchrotron radiation, angle-resolved electron spectra 7-905
 Xe photoionisation, photoelectron and electron momentum spectroscopy 7-36560
 Xe, Rydberg states, four-photon excitation 7-62328
 Xe, two-photon one-electron ionisation cross. sections, RPA, LDA HF calcs. 7-49912
 Xe vacancy cascade following inner-shell ionisation, Monte Carlo simulation 7-30998
 Xe-Ar, laser-induced collisional energy transfer, multiphoton ionisation study 7-57152
 Xe+N⁷⁺, transfer ionization, differential cross section meas. 7-50325
 Xe⁶⁺+Al(C)(Be)(Mylar), electron stripping, cross section meas. 7-64849
 Yb, L subshell ionis. by deuteron impact, cross section determ. 7-51878
 Yb, photoionisation, relativistic RPA calcs. 7-42567
 Zn, detection and study by laser-enhanced ions. spectrometry 7-54202
 Zn⁺, alignment after photoionis., fluoresc. radiation polarisation meas. 7-890
 Zr, ionis. pot. determ., two laser field-ionis. spectroscopy 7-5650
 Zr, metal beam, laser prod. and diagnostics, rel. to isotope separation 7-42783

ionisation of gases

- see also *atmospheric ionisation; electron avalanches; Townsend discharge*
 aerosol mixtures, ion formation from neutral molecule surface absorption 7-11580
 air, ionisation by fast electron pulse, nonequilib. conductivity 7-6364
 binary gas mixtures, electron transport, collision cross section and dielectric strength 7-63244
 cosmic ray induced ionisation intensity meas. 7-40308
 critical ionisation velocity process 7-31924
 dusty weak ionised gas, phys. and physicochem. props. 7-20841
 electrons in dry air, W value re-eval. 7-62242
 ethane, ionisation by X-rays, effect of fluid density on energy absorpt. 7-31920
 hexafluoropropylene, mol. gas, γ -ray induced ionis. 7-63247
 hexane, gas, high density, Townsend ionis. coeff. and breakdown voltage 7-20842
 high-current relativistic electron beam, ionisation wavefront struct. and propag. vel. 7-51469
 hygrometer, gas, ionisation type, charge carrier mobility meas. 7-56295

ionisation of gases continued

- inert gas, hollow cathode discharge, at. energy level excitation, laser lines 7-1804
 ionised gases, atomic and mol. physics, conf. Greifswald, Germany (Aug. 1986) 7-18499
 laser induced two-photon ionisation absorption, seeding agents for particle track simulation 7-5540
 methane, deposition plasma, homogeneous and heterogeneous chemistry, deposition of C:H 7-39424
 methane, ionisation by X-rays, effect of fluid density on energy absorpt. 7-31920
 partially dissociated and ionised gas mixtures, chem. equilib., flow, effective transport coeffs. calcs. 7-31917
 perfluorocyclobutane, mol. gas, γ -ray induced ionis. 7-63247
 photoionisation method for at. and mol. concs. determ. 7-39937
 plasma atomic kinetics, evolutionary problems soln. by Monte Carlo method 7-20864
 RF plasma electron kinetics, attachment and ionis., self-consistent treatment 7-20850
 stepwise discharge and ionisation, kinetic eqns. 7-32143
 streamer plasma polarisation behind an ionisation wavefront 7-1799
 tetramethylsilane, mol. gas, γ -ray induced ionis. 7-63247
 uV-sustained glow discharge opening switch experiments 7-32132
 viscous shock layer, ionisation of gas modelling 7-11466
 weakly ionised gases, kinetic theory 7-20826
 Ar discharge, pulsed electron beam injection, potential profile, temporal evolution 7-51534
 Ar, metastable population meas. and flow instability due to shock wave, comparison with models 7-16207
 Ar plasma, DC pulse generation, creation and stabilisation processes study 7-32098
 Ar, w for 150 MeV protons, dosimetry appl. 7-14133
 Ar/C₂F₆ mixtures, Penning ionisation for diffuse discharge switching appls. 7-37622
 CO-Xe(NH₃) mixtures, photoionis. discharge, energy characts. 7-21027
 CO₂ laser, continuous electronis., output characts. (*Russian*) 7-20182
 CO₂ laser, form. of self-maintained volume discharge using compact electrode system 7-63394
 CO₂-Xe(NH₃) mixtures, photoionis. discharge, energy characts. 7-21027
 Cs, vapour, two-photon reson. four-wave mixing and multiphoton ionis. in heat pipe oven 7-901
 Cs vapour in heat pipe oven, two-photon resonant four-wave mixing obs. 7-43239
 H, ideal gas, modified Gibbs state 7-44087
 He, atom, with turbulent flow, two electron group model for RF ionisation 7-31921
 He+positronium, annihilation spectrum 7-62547
 Kr, primary and secondary ionisation coeffs. meas. 7-1668
 KrF electron beam sustained discharge excimer lasers, discharge constriction, photodetachment, ionisation instabilities 7-10920
 N₂, breakdown voltage distribution meas. 7-31922
 N₂ gas breakdown by 13.56 MHz electric field 7-1806
 N₂, photoionisation discharge plasma, decay characts. 7-21038
 N₂ streamers, 2D numerical simulation 7-32190
 N₂, w for 150 MeV protons, dosimetry appl. 7-14133
 Na plasma, creation by resonant laser interaction study 7-32033
 Na, vapour, light-induced current calcs. and meas. 7-44096
 O₂, plasma, weakly ionised, electron heating and ionis. by RF fields 7-20862
 SF₆, mol. gas, γ -ray induced ionis. 7-63247
 SF₆ plasma, electrostatic interaction effect on composition 7-37632
 SF₆, RF breakdown and discharges, continuum modelling 7-37798
 Xe, 4p excitation, multiple photoionisation cross sections, TOF mass spectrometer anal. 7-19802
 Xe, primary and secondary ionisation coeffs. meas. 7-1668
 Xe-Ar, H₂, plasma, comp. eval. 7-1733
 XeCl laser, UV-preionised, long optical pulse duration, preionisation and discharge stability 7-1080

ionisation of liquids

- dicarboxylic acids undergoing conformational transitions, ionisation equilibria, ¹H NMR 7-13757
 micelles, spherical and nonspherical, asymmetrisation, free energy, conc. depend. 7-8321
 N,N,N',N'-tetramethylbenzidine in various polar solvents, monophotonic ionisation 7-12758

ionisation of molecules

- see also *molecular electron impact ionisation*
 ab initio wave functions 7-36444
 acetylene, binding energies, ab initio HF calcs. 7-49894
 acetylene, vap., REMPI and third harmonic generation 7-25612
 acetylene, X-ray photoelectron spectrum study, diabatic model anal. 7-36448
 alignment parameters, circular dichroic photoelectron angular distrib. meas. 7-36687
 alkali cluster beams, photoionis. mass spectra, abundance distrib. 7-15768
 n-alkyl benzene chromium tricarbonyls intramolecular vibr. relax. 7-5728
 alkylamines, surface ionis. mass spectra 7-10763
 aminoalcohols, surface ionis. mass spectra 7-10763
 aniline, excited vibronic states, ion dip spectroscopy 7-19990
 anthracene single and triplet states in liq. soln. photoionisation cross sections 7-25616
 autoionising states, avoided crossings 7-950
 benzene, ¹B₁ state, photoionis., mass and photoelectron spectra 7-42681
 benzene, ionization-Raman double-resonance spectroscopy 7-10604
 benzene, pulse elec. discharge, triplet state and radical prod., multiphoton ionisation spectra 7-19958
 (benzene)_n, multiphoton ionis. by laser, dynamics and spectroscopy (*French*) 7-5730
 benzene cations, energy-selected, multiphoton ionisation, TOFMS 7-10680
 benzene chromium tricarbonyl-d₀(d₆) deuteration effect on multiphoton dissociation 7-5727
 benzene like molecules, complete valence ionisation spectra with ab initio many body Green's function method 7-50247
 biphenyl, mol. vibr., supersonic jet spectroscopy, mol. fluoresc. and multiphoton ionisation spectra anal. 7-57129
 bound state existence confirmation for atomic and mol. projectiles inside solid targets, expt. investig. (*French*) 7-22427

ionisation of molecules continued

- 1,3-butadiene ions, photodissoc., photoelectron photoion coincidence study, isomerisation barrier meas. 7-36711
 carbon tetrafluoride, extreme UV photoexcitation study, UV fluoresc. anal. 7-36637
 chlorotrifluoromethane, partial photoionis. cross sections, 27-70 eV 7-36708
 chrysene, single and triplet states in liq. soln. photoionisation cross sections 7-25616
 cluster dissociation dynamics following multiphoton ionisation 7-20082
 clusters in beams, review 7-31204
 η -cyclopentadienylnickel nitrosyl, dissoc. and multiphoton ionis., photofragment spectroscopy 7-50281
 diatomic molecules, photoemission processes, ab initio calcs. 7-19676
 1,4-dichlorobenzene, unimol. ionic form. rates, determ., pulsed laser-line. reflection TOF mass spectrometry 7-15667
 dichlorodifluoromethane, partial photoionis. cross sections, 27-70 eV 7-36708
 dimers, first row homonuclear, orbital forces and chemical bonding in density functional theory 7-5595
 dimethyltelluride, excimer laser photolysis, laser mass spectroscopy 7-22547
 discrete states in the continuum, generation by coupling of bound states 7-36509
 ethylene photoionisation, ground state inversion pot., multicentre diff. effects 7-947
 ethylene-HCl van der Waals mol., dissociation energies and heats of formation, photoionisation study 7-19966
 fluorene, single and triplet states in liq. soln. photoionisation cross sections 7-25616
 fluoroform, partial photoionis. cross sections, 27-70 eV 7-36708
 fluoromethane, dissociative photoionis., translational energy disposal and mechanisms 7-10663
 FT photoelectron spectroscopy, correl. fn. and harmonic oscillator approx. 7-10665
 halogenated aromatic hydrocarbons, resonant two photon ionization in supersonic beams 7-19961
 highly symmetric mols., two-photon transitions, molecules, magneto-optical interaction 7-10691
 hydrazines, surface ionis. mass spectra 7-10763
 inert gas clusters, ionis. energies, lin. correl. plot 7-25697
 iodomethane, multiphoton ionisation mass spectra 7-19960
 ion chemistry, gaseous, hybrid BEQQ mass spectrometer appls. 7-48904
 ionised gases, atomic and mol. physics, conf. Greifswald, Germany (Aug. 1986) 7-18499
 large interstellar molecules, ionisation potentials and photodecomposition 7-24189
 laser induced two-photon ionisation absorption, seeding agents for particle track simulation 7-5540
 Meldrum's acid, ionisation rot. barriers 7-62307
 metal β -diketonate, multiphoton ionisation mass spectra 7-19960
 metal clusters, ionisation phenomena, ab initio wave functions 7-36444
 metal clusters, ionisation threshold, photoionisation TOF mass spectra 7-20085
 methane, binding energies, ab initio HF calcs. 7-49894
 methane, electron scatt. cross sections, 0.1 to 500 eV, complex optical pot. calcs. 7-25382
 methane, fine struct. near C-K edge region in photon W-value 7-19962
 methane, photoionisation cross section, ground state inversion pot. method/diff. theory 7-945
 methane- d_0 (d_4), ionisation potential, photoionis. mass spectrosc. obs. 7-50271
 methanol, multiphoton ionis., IR laser study 7-62475
 methyl fluoride, dissociative ionis., methylene and methyl ions, form., photoelectron spectra 7-10662
 methyl iodide fragmentation and multiphoton ionization 7-10689
 2-methylpyrazine singlet-triplet transitions in supersonic jet, multiphoton ionis. detect. 7-948
 molecular threshold electron spectra, TEPISCO-II apparatus 7-18907
 monohalobenzenes, electron struct., mol. reactivities, He Penning ionisation spectra and UV photoelectron spectra anal. 7-25642
 multiple core holes, electronic system response and spectra prod., many-body theory 7-42477
 naphthalene single and triplet states in liq. soln. photoionisation cross sections 7-25616
 Ni+Ni collisions, quasimol. form., X-ray spectra study 7-31157
 organic vapours, photoionisation, average energy per photon 7-19970
 pentane isomers, ionis. and electron thermalisation distances, mol. shape and density effects 7-50347
 perfluoroalkanes, electron attachment and ionisation processes 7-50348
 phenetole cations, laser-induced dissoc., REMPI obs. 7-42711
 phenylsilane vapour, VUV spectra and multiphoton ionisation study, photolysis prod. of Si 7-50172
 photoionisation, ground state inversion pot., multicentre diff. effects 7-947
 polyatomic molecules and ions, laser-induced dissoc., REMPI obs. 7-42711
 positronium molecule, autoionisation state, complex coordinate rot. 7-994
 pyrazine, singlet-triplet transitions in supersonic jet, multiphoton ionis. detect. 7-948
 pyridine- I_2 complex, ionic dissoc., electrochem. investig. 7-54209
 quaternary ammonium salts, surface ionis. mass spectra 7-10763
 quinone like molecules, complete valence ionisation spectra with ab initio many body Green's function method 7-50247
 resonant multiphoton ionisation, plasma diagnostics appls. 7-20954
 single-and multi-photon ionisation process dynamics 7-36701
 spectra calc., Green's function method 7-36684
 trans-stilbene, ground state, torsional motion, two-colour stimulated emission spectroscopy 7-50322
 stimulated Raman scattering, off-resonant enhancement investig. 7-50148
 tetrafluoromethane, ionisation cross section determ., correction factor 7-19701
 tetrafluoromethane ion, lifetime, mass spectra 7-19969
 tetraphenylporphyrin metal complexes, multiphoton ionisation mass spectra 7-19960
 tissue-equivalent gas mixtures, photoionisation, average energy per photon 7-19970
 transient species in supersonic, free jet expansion, laser induced fluoresc. 7-31099
 transition dipole-solvent interaction in photoionization 7-50270

ionisation of molecules continued

- trimethylgallium decomposition during CVD, effect of added hydrazine, multiphoton and electron ionisation mass analysis 7-23010
 van der Waals species, multiphoton ionis. 7-10694
 vibrationally excited molecules, ions, by UV irradi. or electron impact, stochastic dynamics 7-19734
 X-ray and UV induced ionisation of molecules 7-24001
 p-xylene, resonant multiphoton ionisation dissoc. mechanism 7-8295
 ylides, neutralisation-reionisation mass spectrometry 7-10766
 AlF, photoionis., laser sputtering and high-temp. vaporisation reactions 7-15629
 Ar₂, excimer states, photoionisation cross sections 7-57137
 ArXe, excited states, photoionisation and predissoc. 7-19959
 ArXe⁺, DC discharge in supersonic jet, UV-visible emission spectra anal. 7-19874
 Bi, cluster, laser vaporisation and photoionis., TOF mass spectrometry 7-31201
 C₂, photoionisation cross section, ground state inversion pot. method/diff. theory 7-944
 CCl, pulse elec. discharge, triplet state and radical prod., multiphoton ionisation spectra 7-19958
 CH radical, electronic struct., reson. multiphoton ionisation spectra anal. 7-50240
 CO, 5σ photoionis., reson. effects calcs. 7-36705
 CO, B²⁺ state, electronic autoionis., cross section calc. 7-15656
 CO, chemisorbed, ionisation phenomena, ab initio wave functions 7-36444
 CO, electrostatic autoionis., review 7-951
 CO, photoionisation cross sections, ground state inversion pot./diff. theory 7-946
 CO, soft X-ray induced fragmentation, Auger electron-ion coincidence study 7-36700
 CO₂, autoionisation and isotope effect in threshold UPS 7-19948
 CO₂ gas laser, preionisation using α particles study 7-62508
 CO₂, photoionisation cross sections, ground state inversion pot./diff. theory 7-946
 CS, $3s^2 + a^3\Pi$ band system, reson. enhanced multiphoton ionis. detect. 7-5663
 CS₂, photoabsorpt. and photofragmentation meas. 7-62460
 Cl₂, photoionis. cross section meas. 7-62461
 Cl₂, photoionisation cross section at 584 Å 7-36702
 D₂O, quantum state selective detection by (2+1) REMPI 7-36706
 F₂, photoionisation cross section, ground state inversion pot. method/diff. theory 7-944
 Ga₂O, He I photoelectron spectra, relativistic DVM SCC Xalpha calcs. 7-50252
 H discharge, at. and mol. meas. using reson. multiphoton ionisation 7-20955
 H⁺+H₂ double capture, collisions, H⁺ ion excitation energy meas., Franck-Condon calcs. 7-36751
 H₂, atomic data relevant to edge plasmas 7-20063
 H₂, autoionising $1^2\Sigma_g^+$ and $1^2\Pi_g$ states, theory 7-5646
 H₂, B¹ Σ_g^+ and D¹ Π_g states, REMPI, photoelectron spectra 7-62469
 H₂ discharge, diagnostics by resonant multiphoton ionization 7-15657
 H₂, double photoionisation cross sections and electron energies, ab initio calcs. 7-15654
 H₂, E,F¹ Σ_g^+ state, REMPI, ab initio calcs. 7-62470
 H₂ excited states, rot. and vibr. branching ratios, UPS 7-5725
 H₂, low temp. plasma, electrode sheath, calcs. 7-37703
 H₂, metastable, discharge rotational temp. and density determ., resonant multiphoton ionisation method 7-44105
 H₂, photodissociation of doubly excited states, Lyman- α fluoresc. spectra anal. 7-19945
 H₂, photoionisation and photodissociation, six photon ionisation, vibrational levels 7-10682
 H₂, resonantly enhanced multiphoton dissociative ionisation, photoelectron spectroscopy 7-15645
 H₂, resonantly enhanced multiphoton dissociative ionis. meas. 7-19968
 H₂, Rydberg states, nonpenetrating, autoionis., energy-level struct. calcs. 7-15492
 H₂, single- and multi-photon ionisation process dynamics 7-36701
 H₂, stepwise two-photon ion-pair production, mol. spectroscopy 7-10683
 H₂, vibrationally excited, rot. excitation and dissoc. meas. using resonant multiphoton ionization 7-15658
 H₂⁺, electron impact, autoionising states, avoided crossings 7-950
 H₂+H⁺(He⁺), nondissociative and single ionis., cross section meas. 7-31147
 HBr, d shell photoionisation, shape resonances study 7-19964
 HCl, photoionisation cross section, ground state inversion pot. method/diff. theory 7-944
 HI, d shell photoionisation, shape resonances study 7-19964
 H₂O, photoionis. cross-sections and asymm. parameters 7-36707
 H₂O, photoionisation cross section, ground state inversion pot. method/diff. theory 7-945
 H₂O, quantum state selective detection by (2+1) REMPI 7-36706
 H₂O, vap., differential cross sections, semiempirical model 7-42695
 HPNH, photoionisation cross-sections, MS X α calcs. (French) 7-5599
 H₂Se, photoionisation, ionisation pot. and bond energies 7-19979
 H₂Se, photoionisation and autoionisation, UV spectra 7-10524
 He + Br₂(I₂)(Cl)(IBr), bound and continuum states, excitation transfer, optical and electron spectroscopy investig. 7-36689
 He⁺+H₂, elastic and inelastic scatt. mechanisms, energy loss spectra 7-15671
 HeN⁺, quasi-molecule, autoionisation 7-62459
 InO₂, He I photoelectron spectra, relativistic DVM SCC Xalpha calcs. 7-50252
 K_N, laser photoionisation of clusters containing up to 101 atoms 7-42822
 Kr₂, excimer states, photoionisation cross sections 7-57137
 KrXe, excited states, photoionisation and predissoc. 7-19959
 Li₂, isotopes, laser separation, double REMPI spectra 7-42694
 Li₂, optical-optical double reson. and double reson. multiphoton ionis. 7-42742
 Li₂, photoionisation and Auger electron emission, HF calcs. 7-36703
 Li₂, vibr. excited by optical pumping, electron impact ionisation cross sections 7-62536
 N₂, $a^1\Pi_g$ state, REMPI 7-31121
 N₂, electron and photon collision cross section 7-18513
 N₂, Hopfield series, ab initio theory 7-10408
 N₂, photoionis. cross section, HF calcs. 7-42693
 N₂ pulse elec. discharge, triplet state and radical prod., multiphoton ionisation spectra 7-19958

ionisation of molecules continued

- N_2 , soft X-ray absorpt., at. ion yield 7-949
 N_2 , soft X-ray-induced fragmentation, Auger electron-ion coincidence studies 7-42697
 N_2 , triplet Rydberg state, autoionis., TOF mass spectra 7-19963
 N_2^+ , photoion, resonant excitation, rot. distrib. 7-31122
 N_2 +Ar, electron transfer, state-to-state study 7-10714
 NH_3 dimer, ionis., proton transfer, ab initio pot. energy surface calc. 7-42518
 NH_3 , photoionisation cross section, ground state inversion pot. method/diff. theory 7-945
 NH_3 , quantum resolved molecular-beam scattering 7-15695
 NH_3^+ +NO, cross section as a fn. of ion vibr. level, REMPI time of flight spectra, mass spectra 7-20028
 $(NH_3)_2$, dimer struct., electron spectra anal., HF calcs. 7-36686
 $(NH_3)_n$ ($n=2$ to 5), clusters, electronically excited \bar{A} states, two-photon ionis. mass spectroscopy 7-15761
 NO , $A(^2\Sigma^+)$ state, two-photon ionis., non-Franck-Condon behaviour 7-25615
 NO , autoionisation of $v=3$ Rydberg states, branching ratios, multiphoton spectra anal. 7-36718
 NO , autoionising levels, two-photon spectra 7-10688
 NO dimer, ionisation phenomena, ab initio wave functions 7-36444
 NO , excited state, circular dichroism in photoelectron ang. distrib. 7-19909
 NO molecule scatt. from graphite surface 7-13316
 NO , photoexcitation and ionisation cross sections, Stieltjes-orbital representations, HF calcs. 7-19677
 NO , photofragment, REMPI and TOF mass spectra 7-25613
 NO -Kr, van der Waals species, multiphoton ionis. 7-10694
 NO -Ne, van der Waals species, multiphoton ionis. 7-10694
 NO^+ + NH_3 , cross section as a fn. of ion vibr. level, REMPI time of flight spectra, mass spectra 7-20028
 NO_2 , photodissoc. REMPI study of photofragment energy 7-42709
 N_2O , photoionis. dynamics and vibr. branching ratios, fluoresc. spectra 7-15653
 N_2O , photoionisation cross sections, ground state inversion pot./diff. theory 7-946
 Na_2Cl , microclusters, ionisation induced structural transitions, pseudopotential, HF calcs. 7-25379
 Ne_2 , excimer states, photoionisation cross sections 7-57137
 $NeXe$ excited states, photoionisation and predissoc. 7-19959
 $NiCO$, single- and multi-photon ionisation process dynamics 7-36701
 NO_2Cl_2 microclusters, ionisation induced structural transitions, pseudopotential, HF calcs. 7-25379
 O_2 , autoionisation states, vibr. assignments 7-50073
 O_2 , photoionis. cross section, HF calcs. 7-42693
 O_2 , photoproduction cross sections, mass spectrometry, photoionisation and photodissociation 7-10681
 O_2^+ predissociative photoionisation, triple coincidence, double time-of-flight study 7-36709
 O_2^+ , $X^2\Pi_g$ vibr. branching ratios, 905-1000 Å, autoionis. effect 7-50272
 SF_6 , charge transfer, time-resolved study 7-10748
 SF_6 , dissociative photoionisation, triple coincidence, double time-of-flight study 7-36709
 SF_6 , thermal attachment rate constants, 200-600K 7-975
 SO_2 , super-excited molecule, quantum defect theory ionisation channels 7-30962
 Sb_x cluster, laser vaporisation and photoionis., TOF mass spectrometry 7-31201
 Sb_3Bi_3 cluster, laser vaporisation and photoionis., TOF mass spectrometry 7-31201
 SeH , photoionisation, ionisation pot. and bond energies 7-19979
 SiH_n ($n=1$ to 4), photoion yield and thresholds, photoionisation mass spectra study 7-50242
 $SiH_3(D_3)$, ions and radicals, pot. energy curves and electron affinities determ., photoelectron spectra anal. 7-25603
 Te_2 , isotope selective ionization 7-36699
 TiO_2 , He I photoelectron spectra, relativistic DVM SCC Xalpha calcs. 7-50252
 U complex, bis(acetylacetonato)dioxouranium(VI), electron ionis. mass spectra 7-10762
 Xe_2 , excited states, photoionisation and predissoc. 7-19959

ionisation of solids

- fast dust particle impact and related techniques, ion form. studies 7-46259
 fine structure in ionisation cross sections, surface science appl., review 7-27074
 semiconductors, crystal excitation by electric discharges, point defect ionisation 7-33331

ionisation potential

see also work function

- acetylene, optical transition energies and ionisation pot., DVM-Xa calcs. 7-25391
 aldehydes, ionisation pot., calc. based on interactions between struct. units 7-15738
 α -aminoalkyl radicals, electrochemical detection, bond dissoc. energies determ. using oxidation pots. 7-28286
 aqueous soln., free energies of hydration, ionisation pots., electron affinities 7-65292
 atomic ionisation energy and electron affinity, correl. energy estimation by local approx. 7-56991
 atomic systems, electronic chemical potential calc. 7-25336
 atomic transition and ionisation energies, g-Hartree ab initio calcs. 7-15488
 atoms and ions, Stark width and shift regularities 7-36539
 azoles, protonation energies and tautomerism, basis set effects 7-25374
 benzenes, substituted, ionisation pots., electron affinity, HAM/3 study 7-19710
 o-benzyne, valence ionis. energy and mol. geometry, green fn. method, CI and GVB calcs. 7-62290
 trans-butadiene, optical transition energies and ionisation pot., DVM-Xa calcs. 7-25391
 calculation using interactions between structure units (Russian) 7-10776
 chloroferrocenes, ionisation pot., electron impact study 7-20062
 chlorophyll- H_2O system, ab initio LCAO SCF MO calcs., ionisation pot., electron affinity, intermol. mechanics 7-8520
 cluster dissociation dynamics following multiphoton ionisation 7-20082
 cyanomethanes, He(I) photoelectron spectrum; vertical ionisation energies, LBCO-MO model 7-50249

ionisation potential continued

- diamond, stopping cross section of ^{12}C projectiles 7-51899
 diatomic inert gas dications, dissoci., detect. and charactn. 7-46804
 2-dicyanomethylene-1,3-indanedione-methylated [2.2]paracyclophanes charge transfer complexes, IR and mass spectroscopy 7-25523
 dimethyl ether, isomers, VUV-optical oscillator strength distrib. 7-15650
 dipole polarisability of atoms and ions, ionis. pot. correl. 7-42529
 ethanol, photoionisation mass spectra, temp. effect 7-46818
 ethenone, dissoci., nonlin. UV excitation 7-19981
 ethyl alcohol, isomers, VUV-optical oscillator strength distrib. 7-15650
 ethyl methyl ether, isomers, VUV-optical oscillator strength distrib. 7-15650
 ethylene, optical transition energies and ionisation pot., DVM-Xa calcs. 7-25391
 ethylene dications, F-substituted, geometries and energies, ab initio calcs. 7-10401
 ethylene propylene, fluorinated, ionis. pot. and work function meas. using low-energy electron beam 7-22397
 flavins, struct. and REDOX props., electron distrib., MINDO/3 calcs. 7-56977
 graphite stopping cross section of ^{12}C projectiles 7-51899
 halogen thiocyanates (isothiocyanates), ionis. pots., photoelectron spectrosc. and ab initio calcs. 7-25601
 n-hexane, photoionisation mass spectra, temp. effect 7-46818
 8-hydroxyquinoline, intramol. H bonding, UV photoelectron spectra and MO calcs. 7-25367
 8-hydroxyquinoline-N-oxide, intramol. H bonding, UV photoelectron spectra and MO calcs. 7-25367
 ionic cpds., struct., ionisation pot., stark shift 7-15634
 ketones, ionisation pot., calc. based on interactions between struct. units 7-15738
 metal clusters, ionisation threshold, photoionisation TOF mass spectra 7-20085
 metal clusters, photoionisation spectra, evolution, rel. to size 7-15769
 metal clusters, shell structure and response props. 7-15767
 metal trimer clusters photodissoc., bound-free transitions fluoresc. study 7-23045
 methane- d_0 (- d_4), ionisation potential, photoionis. mass spectrosc. obs. 7-50271
 methyl chalcogenides, UV photoelectron spectrosc. investig. 7-5721
 methyl fluoride clusters, photodissoc., photoionisation efficiency curves, appearance pots. 7-50435
 1-methylallyl cation, photoionisation mass spectrometry, heat of form., ionisation energies, ab initio MO calcs. 7-13798
 3-methylpentane, photoionisation mass spectra, temp. effect 7-46818
 molecules, electronic struct. calcs., basis sets correl. balance 7-56928
 monohalobenzenes, electron struct., mol. reactivities, He Penning ionisation spectra and UV photoelectron spectra anal. 7-25642
 orbital electronegativity and ionisation pot., physical significance of local density functional theory eigenvalues 7-62245
 orbital systems, fractionally occupied, density functional theory, appl. to ionisation and transition energies 7-42451
 pentacene, vacuum deposited amorphous films, X-ray diffr. and photoelectron spectra anal. 7-22434
 poly(p-phenylene sulfide), UV photoelectron spectra 7-15748
 polyaniline, conducting polymer, electronic and electrochem. props., MNDO calc. 7-2462
 polyaniline, geometries, bond struct., electrochemistry, MNDO calcs. 7-15750
 polydiacetylenes, electronic struct., substituent-induced strain effect, MNDO calcs. 7-10427
 trans-polyenes, electronic struct., DVM-Xa calcs. 7-25392
 polyfuran and copolymers, electronic struct., cond. props., ab initio cryst. orbital calcs. 7-52410
 polyhalomethanes, X-ray photoelectron spectra, chem. shifts 7-15648
 polypropylene, ionis. pot. and work function meas. using low-energy electron beam 7-22397
 polypyrrole and copolymers, electronic struct., cond. props., ab initio cryst. orbital calcs. 7-52410
 polythiophene and copolymers, electronic struct., cond. props., ab initio cryst. orbital calcs. 7-52410
 propyl alcohol, n- and iso-, isomers, VUV-optical oscillator strength distrib. 7-15650
 rare earths, 4f levels, appearance pot. spectrosc. 7-39324
 semiconductor heterojunction band discontinuities, dielec. electronegativity anal. 7-2699
 sputtered atoms, ionisation probability studies 7-20068
 tetracyanoethylene-methylated [2.2]paracyclophanes charge transfer complexes, IR and mass spectroscopy 7-25523
 thiouracil, tautomers, MNDO calcs. 7-56984
 transition elements, first row, energy-adjusted ab initio pseudopot. 7-49898
 transition metal clusters, chemisorpt. patterns, charge depend. 7-15763
 tribromomethane, one electron transition, VUV spectra 7-10612
 tribromomethyl radical, geometry and electronic struct., SWXa calcs., ab initio UHF calcs. 7-19703
 trichloromethane, one electron transition, VUV spectra 7-10612
 trichloromethyl radical, struct. and electronic states, ab initio UHF SWXa calcs. 7-30949
 triiodomethane, one electron transition, VUV spectra 7-10612
 Ag_s^{8+} , electronic struct., Dirac scattered wave study 7-42818
 $AlOH$, enthalpy of form., mass spectrometric determ., equilib. const., ionisation pot. 7-59777
 Ar, 3s-subshell excitation, photoabsorption spectra anal., HF calcs., config. interaction calcs. 7-30947
 Ar, excitation energies, coupled cluster method calcs. 7-49893
 AsO_4^{3-} , electronic struct., ionisation pot. MS-Xa calcs. (French) 7-856
 Be_{13} and Be_{55} , stability and struct., binding energy, ionisation pot. 7-11988
 Bi II, $6s^26p^2$ $3P_0$ - $6s^26pnd$ $3D_1$ series in photoabsorption 7-25469
 C glassy state, stopping cross section of ^{12}C projectiles 7-51899
 C_{60} cluster, spherical, DV-Xa electronic struct. 7-10806
 C_{60} , localised mol. orbitals and electronic struct., PRDDO calcs. 7-49925
 $CH_3N_2^+$, pot. energy surface, ab initio MO calcs. 7-10390
 Cs vapour, comp. study, reson. doublet absorpt. meas. 7-36518
 $CsUO_2(NO_3)_3$, charge transfer bands position, ionisation pot. effects, luminesc. spectra anal. 7-46146
 D_2 , Te, Rydberg states, high resol. VUV spectra 7-50173
 F-like ions, energy level distances, relativistic perturbation theory calcs. 7-866
 FNO_2 , semi-empirical MO-LCAO method validity eval. 7-15482

ionisation potential continued

- FeC₄H₆⁺ isomers, gas-phase photodissoc., bond energy and struct. determ. 7-15661
- ²²³Rn, radioactive isotope detection; laser resonant photoionisation method 7-42572
- GeSe₂, vitreous and crystalline states, energy difference, bond energy, calorimetry study 7-59775
- H-like ions, Sommerfeld-Dirac expression in diffusional quantum theory 7-35323
- HO₂⁺, electronic struct., MRD-CI calcs. 7-10450
- HSCN (HNCS), ionis. pots., photoelectron spectrosc. and ab initio calcs. 7-25601
- H₂Se, photoionisation, ionisation pot. and bond energies 7-19979
- H₂Te, Rydberg states, high resol. VUV spectra 7-50173
- Hg clusters, photoionisation spectra, evolution, rel. to size 7-15769
- KUO₂(NO₃)₃, charge transfer bands position, ionisation pot. effects, luminesc. spectra anal. 7-46146
- Kr, Rydberg states, four-photon excitation 7-62328
- Mg, excitation energies, coupled cluster method calcs. 7-49893
- Mo (100), chemically modified, chemisorption bond energies of Lewis acids and bases 7-23056
- Mo V, HF calcs. and spectra 7-10477
- NH₃ dimer, ionis., proton transfer, ab initio pot. energy surface calc. 7-42518
- NH₄UO₂(NO₃)₃, charge transfer bands position, ionisation pot. effects, luminesc. spectra anal. 7-46146
- Na atoms, desorption from hot W surface, resonance ionisation study 7-63966
- Na₂Cl, microclusters, ionisation induced structural transitions, pseudopotential, HF calcs. 7-25379
- NaOH₂, ionization potential determ. 7-10808
- Ne-like ions, energy level distances, relativistic perturbation theory calcs. 7-866
- Ni_n (n=1 to 6) clusters, electronic struct., ab initio SCF and CI calcs. 7-10446
- NiC₄H₆⁺ isomers, gas-phase photodissoc., bond energy and struct. determ. 7-15661
- No₂Cl₂, microclusters, ionisation induced structural transitions, pseudopotential, HF calcs. 7-25379
- O+unsaturated hydrocarbon, relative rate consts. at room temp. 7-28283
- PO₄ⁿ⁻, electronic struct., ionisation pot. MS-Xα calcs. (French) 7-856
- PuF₆ and PuF₃ mols., ionisation and appearance pots. meas. bond dissociation energy calcs. 7-10765
- RbUO₂(NO₃)₃, charge transfer bands position, ionisation pot. effects, luminesc. spectra anal. 7-46146
- SO₄ⁿ⁻, electronic struct., ionisation pot. MS-Xα calcs. (French) 7-856
- SeH, photoionisation, ionisation pot. and bond energies 7-19979
- SeO₄ⁿ⁻, electronic struct., ionisation pot. MS-Xα calcs. (French) 7-856
- SiH_n (n=1 to 4), photoion yield and thresholds, photoionisation mass spectra study 7-50242
- Xe, Rydberg states, four-photon excitation 7-62328
- Zn, detection and study by laser-enhanced ions. spectrometry 7-54202
- Zr, ionis. pot. determ., two laser field-ionis. spectroscopy 7-5650

ionisation time *see* **ionisation****ionogen** *see* **electrolytes****ionoluminescence**

- alkali chlorides, particle bombardment-induced secondary photon emission 7-59264
- 9,10-dichloroanthracene monocrystals, alpha scintillations, decay kinetics 7-7769
- Cu, photon emission from sputtered atoms, temp. effects 7-13312
- Ga-In, liq. surface segregation, ion bombard. photon emission study 7-32265
- LiNbO₃, exciton lumin., ion beam induced 7-53418
- LiNbO₃, ion beam induced luminesc. 7-27793
- Ni, cryst., anomalous ion-photon and secondary ion emission mean Curie pt. 7-39343

ionosondes *see* **ionospheric measuring apparatus****ionosphere**

- see also D-region; E-region; F-region; ionospheric electromagnetic wave propagation; ionospheric techniques; sporadic-E layer*
- 3D ionospheric plasma cloud dynamics, self-consistent anal. 7-47629
- abrupt mag. field changes over polar ionosphere, MAGSAT observations 7-47622
- aerodynamics of spacecraft in the ionosphere, collisionless plasma expansion study 7-31950
- Alfven wave stimulated Brillouin scatt. in low-density plasmas in ionospheric conditions 7-44146
- anomalously weakly damped plasma waves excited by the finite amplitude ballistic process 7-55353
- auroral arc electrodynamics correlation with neutral winds 7-47609
- auroral electrons and HF waves generation 7-34775
- auroral kilometeric radiation, relativistic plasma maser instability theory 7-11694
- auroral LHR noise, obs. by S-310JA-6 sounding rocket (1978 August 27) 7-66393
- auroral radar spectra obtained with SABRE, statistical study 7-47627
- auroral zone, ion-acoustic double layers, finite amplitude theory 7-37702
- beam-generated electrostatic electron waves 7-47645
- Birkeland currents correlated with d.c. elec. fields 7-55347
- charged particle fluctuations in lower ionosphere, assoc. scale times and scale lengths 7-29359
- charged particle fluxes in S Atlantic mag. anomaly effect of plasma pitch-angle and radial diffusion 7-4275
- Cherenkov radiation due to ionospheric plasma 7-9286
- conducting body moving through magnetoplasma, plasma wave generation 7-9369
- conductivity non-uniformity effects on magnetospheric Alfven waves 7-55381
- conjugate ionosphere thermal coupling at mid-latitudes and tilt of geomagnetic field 7-9301
- convection electric field empirical model with IMF dependence 7-29352
- convection electric field large scale structures 7-29342
- convection morphology and particle precipitation assoc. with dayside aurora 7-55352
- critical ionization phenomena and dissociative electron-ion recombination 7-55377
- critical ionization velocity, proposal for Space Shuttle expt. to verify hypothesis 7-9312
- critical velocity phenomena, anomalous ionization 7-66388

ionosphere continued

- current systems, mag. field contrib. to crust meas. 7-14191
- current-voltage relation in auroral current sheets 7-60456
- day-night inhomogeneity, effects on ELF fields 7-66219
- dayside auroral ionosphere, ion convection and elec. fields 7-55348
- deuteron whistlers in outer ionosphere, charact. freqs. in five-component plasma 7-18335
- diagnostics of small-scale nonuniform structure, digital ionosonde data 7-40627
- diffuse plasma resonances, theory of force-free EM oscils. 7-60466
- discrete auroral arcs elec. potential, effects of anomalous potential 7-23927
- disturbance due to 1983 June 11 total solar eclipse over Papua New Guinea, mag. field effects (Chinese) 7-55346
- disturbance due to lower atm. nucl. explosion (Chinese) 7-29257
- double layers simulation, model of auroral circuit 7-9297
- duct propagation of short-period MHD wave, anal. using International Reference Ionosphere model 7-66392
- eddy currents and generation of Pc 3 at very low latitudes 7-55385
- EISCAT ionospheric sounding facility 7-29377
- electric currents associated with abnormal quiet days in Sq(H) 7-47610
- electric dipole field in inhomogeneous ionosphere, Maxwell's eqns. soln. 7-29330
- electric field and current determ. method using ground mag. variations (Chinese) 7-4250
- electric field disturbances and the evolution of ionosphere inhomogeneities 7-40626
- electric field source identified by spectral studies 7-60458
- electric fields and currents during substorms, modelling study 7-29350
- electrical and electrothermal conductivities of planetary ionospheres, determ. for Earth, Mars and Venus 7-34781
- electron and ion temperatures, empirical model 7-9314
- electron beam injection experiment, wave generation study 7-29354
- electron beams, effect on radiowave propagation 7-55354
- electron concentration profile near max. of ionosphere, analytic extrapolation 7-9293
- electron content, solar flare effects (Chinese) 7-18394
- electron density charact. determ. from VHF transionospheric signal time delay at subauroral latitudes 7-23933
- electron density of sub-auroral ionosphere, height-latitude distrib. 7-40624
- electron distribution function and radial diffusion coeff., meas. at L=1.2 to 1.4 from Interkosmos-19 data 7-34805
- electron distributions of north and south polar cap regions, electron precipitation processes 7-9300
- electron energy spectra and electrostatic cyclotron waves during diffuse auroras, coordinated obs. 7-34763
- electron flow spatial component derived from 2D drift observations 7-60464
- electron resonance with coherent whistler mode waves 7-60460
- electron temperature enhancement in subauroral zone, DE 2 satellite obs. 7-29351
- electrostatic potential at large-scale in auroral plasma, numerical BGK calcs. 7-23945
- electrostatic shocks as nonlinear ion acoustic waves, model 7-29365
- ELF wave generation in lower ionosphere 7-9307
- EM disturbances, IKB-1300 meas. at auroral latitudes 7-66389
- EM ion drifts, relationship between meridional and longit. components at mid and low latits. 7-9315
- emission layer for dayside aurora, EUV-near IR O emission features obs. 7-55345
- equatorial electrojet, drift speeds of irregularities of kilometre and metre sizes 7-4257
- equatorial electrojet, effect of source-field geometry on EM induction Earth 7-28821
- equatorial electrojet, type II irregularities modification by finite amplitude type I waves 7-34778
- faint auroral arc, study of elec. field configuration and plasma parameters 7-29337
- flux transfer events at magnetopause, influence on polar ionosphere 7-40632
- geomagnetic activity, connection between characteristic parameters of solar and geomag. 11-year cycles 7-18114
- geomagnetic activity, contrib. of By-component of interplanetary mag. field to north-south asymmetry 7-9336
- geomagnetic activity, longit. distrib. of C9 index rel. to solar mag. field 7-18400
- gravity waves in ionosphere, radiointerferometric obs. 7-4253
- harmonic waves above and below lower hybrid freq. 7-55351
- HF modification, small scale plasma density depletions form. 7-4263
- high-latitude ionosphere, elec. fields and pot. patterns for different interplanetary conditions 7-14421
- high-latitude ionosphere observed simultaneously with IMF 7-29343
- inhomogeneity dynamics by numerical model 7-9296
- interhemispheric coupling during low solar activity, numerical model 7-23931
- interhemispheric plasma transport 7-14409
- ion acoustic double layers in auroral plasma 7-66387
- ion cloud release experiment, Star of Lima Ba and Sr shaped charge explosion expts. 7-9302
- ion cloud release expt., electric field pulse associated with Star of Condor Ba explosion 7-9304
- ion cloud release expt., Star of Condor critical velocity experiment 7-9303
- ion cloud release expt. Star of Lima, particle results 7-9305
- ion heating by waves with freqs. below the ion gyrofrequency 7-40633
- ion transport to plasma sheet, acceleration of polar ionosphere ions 7-23928
- ion velocity rel. to Pc 3-5 EISCAT 1983 obs. (Chinese) 7-18329
- ion-cyclotron instabilities excited by high power radio waves 7-47619
- ionisation enhancements due to electron precipitation, effect on VLF waves in Earth-ionosphere waveguide 7-47626
- IRI-79, electron content prediction of International Reference ionosphere (Chinese) 7-4252
- ISIS-II spacecraft, discharge of RF-induced DC potential by positive ions 7-66427
- Joule and particle heating rates, latitudinal variations 7-29340
- Langmuir probe measurements in sheath of highly charged body, model study 7-37744
- longitudinal currents in dayside cusp, charact. as function of interplanetary mag. field orientation 7-4261

ionosphere continued

- longitudinal electrostatic field formation on auroral lines of force, role of cold ionospheric plasma 7-34766
- low latitude discrete chorus emissions and VLF hiss 7-55355
- low-latitude disturbances during substorms 7-60442
- lower ionosphere diagnostics, appl. of radio waves resonance scattering method 7-47613
- lunar geomagnetic tide at night 7-60159
- magnetic flux tube emptying by upward-flowing current 7-14418
- magnetosphere-ionosphere coupling studies recent advances 7-23939
- meteor showers in low ionosphere, local and long-distance effects 7-4256
- mid-latitude medium scale traveling ionospheric disturbances, source regions characts. 7-60446
- midday auroral oval, rocket meas. of electron influx 7-55349
- molecular photoionization by UV and X-ray radiation 7-24001
- multiple auroral arcs and Birkeland currents, evidence for plasma sheet boundary waves 7-9320
- narrow electron beam precipitation associated with narrow auroral arc 7-47607
- near-Earth space environment, spaceglow and material erosion 7-60506
- negative ionic species, effects on use of whistlers as diagnostic technique in lower ionosphere 7-66381
- nonlinear wave structures in the ionosphere, role of plasma instabilities 7-66386
- north polar currents in winter, geomag. activity effects 7-60450
- Pc 4 responsible for large fluctuating elec. fields 7-29339
- perpendicular ion acceleration regions, observations of plasma waves 7-40634
- photoelectronic lines at 22.2 to 27.2 eV, energy spectra depend. on ionospheric parameters 7-9290
- plasma, auroral, ion cyclotron wave explosive instability effects 7-1684
- plasma, newly-born ion effect and thermal effect on whistlers 7-40572
- plasma characteristics meas. by Space Shuttle plasma diagnostics package, Shuttle-induced perturbations 7-47625
- plasma clouds, stability criterion for large-scale structuring 7-9308
- plasma concentration vars. in main ionospheric trough during mag. storm, relation to interplanetary mag. field 7-34780
- plasma convection patterns at high latitude, empirical models 7-60457
- plasma depletion experiment (due to Spacelab-2), prod. of window for galactic background radioemission obs. 7-60469
- plasma fluctuations during radio sounding, 3D spectrum 7-40628
- plasma jet from sounding rocket, ion beam adiabatic coding 7-60461
- plasma jet injection into ionosphere elec. field eqns. 7-51416
- plasma parameters measurements in vicinity of Space Shuttle, Langmuir probe results 7-29360
- plasma parametric turbulence in mag. field 7-1697
- plasma trough at high latitude, study of plasma flow 7-29338
- plasma velocity determ. by EISCAT radar method 7-29285
- plasma wave beam effect on lower ionosphere plasma, nonlinear effects 7-14411
- plasma waves in ionosphere, energy balance between plasma and plasma waves 7-60445
- plasma pause and F-region and mid-latitude trough, simultaneous observations 7-47618
- plasma sphere, electron temp. vars. along geomag. field lines rel. to electron density profiles and VLF paths 7-4258
- plasma sphere-ionosphere coupling, nearly conjugate dual-spacecraft measurements 7-29348
- inner plasmasphere, substorm introduction of 1 keV magnetospheric ions 7-23941
- polar cleft topside region, plasma flow 7-60455
- intense polar rain occurring symmetrically in both hemispheres and solar wind interaction 7-29356
- polar region, convection and auroral emissions and interplanetary mag. field B_z component 7-34777
- Porcupine artificial plasma jet experiment, Xe ion beam behaviour 7-9311
- post-noon auroral oval dynamics 7-55350
- prereversal enhancement of zonal electric field, due to F-region dynamo 7-55359
- radiowave heating experiment at Tromsø, 1-metre irregularity production 7-29353
- radiowave heating expts., excitation of electrostatic fluctuations by thermal modulation of whistlers 7-29358
- radiowave heating expts., ionosphere response involving plasma instabilities 7-29344
- radiowave modification of electron distrib. function, due to resonant HF absorpt. 7-60459
- rapid plasma flow bursts at high-latitude, EISCAT dayside obs. 7-23930
- RF emissions from pulsed electron beams in space, near-field radiation anal. 7-66391
- seismic-ionospheric electrical interaction, resonant phenomena 7-28890
- SHF radiation energy dissipation, effect of anomalous absorpt. 7-4262
- Shuttle glow, chemilum. processes 7-47602
- Shuttle glow, rammed surface temp. dependence 7-9284
- slab thickness at Delhi, lunar and solar daily variations 7-60441
- solar flare induced changes in total electron content, 24 April 1984 flare (Chinese) 7-4251
- Space Shuttle bay area, ion species observations 7-60462
- spacecraft glows, surface-catalysed reactions role 7-14401
- spacelab-2 experiments 7-23973
- spiky parallel DC electric fields in the aurora 7-60463
- Sq day-to-day var. in geomag. conjugate areas; current effects 7-60452
- storm disturbances of F_2 -layer, review 7-9288
- storm sudden commencement elec. fields 7-60492
- storm time current systems and low-latitude aurora 7-29327
- storm-time disturbance of F_2 -layer, positive phase 7-9295
- structure formation of outer ionosphere 7-9287
- tethered satellite (on end of cable from larger satellite), electric current behaviour 7-9360
- thermal electron quenching of $N(^2D)$, implications for photoelectron flux and thermal electron temp. 7-14412
- TID at medium-scale, observations of 2-types 7-29346
- TID of medium scale, radiotelescope differential Doppler meas. method and obs. 7-47615
- topside, preferential O^+ heating observed by sounding rocket 7-23929
- topside thermal structure, bi-Maxwellian transport eqns. for SAR arcs 7-55365
- transverse magnetic fields, time-depend. plasma interaction 7-60527
- turbulence associated with 2D magnetised Rayleigh-Taylor instability, spectral characts. 7-44170

ionosphere continued

- typhoons over Japan causing disturbances in ionosphere 7-4259
- ULF wave filter model 7-40640
- upgoing auroral H^+ and O^+ ion beams, wave-particle interactions 7-9306
- VLF pulsations (type 2QP) observed on the ground and associated mag. pulsations 7-23955
- VLF signals reflection height, assoc. electron density var. 7-60448
- wave processes (Russian) 7-9298
- waves generated by electron beams 7-34774
- wintertime effects of interplanetary magnetic field sector structure 7-40664
- zonal plasma flow, geomagnetic signature in equatorial ionosphere 7-60465
- CO_2 , molecule, vibr. relax. during injection from spacecraft 7-34087
- H^+ outflow, effects on comp and plasma props. of magnetotail plasma sheet 7-34789
- O_2^+ in dayside ionosphere, vibrational distrib. 7-55363
- SF_6 release expt. at F-region altitudes, excitation of O permitted lines 7-9282
- ionospheric electromagnetic wave propagation**
see also atmospheric
- 250 MHz/GHz scintillation parameters, equatorial, polar and auroral environments 7-66384
- absorption of cosmic radio noise at high latitudes, spectrum 7-14405
- Alfvén wave stimulated Brillouin scatt. in low-density plasmas in ionospheric conditions 7-44146
- Antarctica multiple VLF propag. paths, burst precipitation induced perturbations 7-66379
- auroral E-region, radar irregularities, propag. angle depend. 7-60447
- auroral ionosphere, electric field and electron flux effects on SW radio signals 7-40630
- auroral LHR noise, obs. by S-310JA-6 sounding rocket (1978 August 27) 7-66393
- C-band scintillations due to disturbances 7-60442
- collision frequency, vertical distrib., multifrequency radioabsorpt. meas. 7-55278
- cyclotron harmonic waves, propagation paths in mag. meridian plane 7-9313
- D-region, artificial periodic inhomogeneities formation, attachment and recombination processes 7-60443
- D-region, winter-time, electron densities and wind vels. from partial refl. radar obs. 7-47612
- decametric propagation, large-scale inhomogeneities effect 7-40629
- delay measurement for signal traversing dispersely inhomogeneous ionosphere layer, accuracy 7-23934
- deuteron whistlers in outer ionosphere, charact. freqs. in five-component plasma 7-18335
- E-region, SABRE backscatter meas. rel. to vertical velocity structures 7-4254
- Earth's atmosphere radio transillumination, signal parameters, ionosphere effect 7-55367
- Earth-ionosphere waveguide, ELF mode constants calc., noniterative procedure 7-40636
- electron-ion collision frequency dependence of plasma parameters 7-66382
- ELF propagation variations at mid and high latitudes 7-60471
- ELF radio wave scattering on global inhomogeneities of earth-ionosphere cavity 7-29332
- eLF/VLF/LF propagation and system design 7-40642
- equatorial electrojets, small scale plasma motions, HF Doppler obs. 7-55361
- equatorial scintillations, effect of mag activity 7-34762
- Es-layer, effect on astron. VHF aperture synthesis observations (Chinese) 7-66471
- F_2 -layer, hourly variability estimation at low latitude station 7-60472
- F_2 -layer nighttime penetration freq. rel. to cold front passage (Chinese) 7-18331
- F_2 -layer visualisation, eleven years of ionospheric chronograms 7-23848
- F-region, HF-enhanced plasma line temporal evol. 7-34776
- F-region irregularities of small-scale, HF backscattering study indicating strong sub-auroral ion flow 7-29397
- F-region parameters determ., resonance scattering method 7-55356
- far zone radio signal struct. and dispersion distortion peculiarities 7-34765
- forecasting, short-term ionospheric, problems 7-40645
- HF groundwave and skywave propagation 7-40643
- HF modification, small scale plasma density depletions form. 7-4263
- HF propag. through the ionosphere 7-55366
- HF propagation modelling, and RF prediction 7-23942
- HF propagation problems in ionosphere 7-23943
- HF refraction insertion into ionospheric waveguide 7-14406
- HF sky wave paths, maximum usable frequencies, sounder updates for statistical model predictions 7-40638
- HF skywave remote sensing, frequency management 7-40646
- HF-produced medium-scale inhomogeneities, propagation effects 7-14404
- high power radiowave interactions with ionospheric plasmas 7-29362
- trans-ionospheric UHF signals, multipath effects in angle-of-arrival measurements 7-47621
- LF (40 kHz) radio waves propagation, influence of winter anomaly 7-47611
- long-distance 40 kHz signals propag., effects of geomag. storms on sunrise fading 7-55360
- Loran-C 100 kHz sky wave vars. (Chinese) 7-18333
- meteor bursts for communication links, database anal. approach 7-60607
- metre-wave propagation, effect of gravity waves 7-4253
- MF sky waves, measured and predicted field strengths comparison in Japan 7-23932
- multidimensional spectral anal., ionospheric mode structs. decomposition 7-40641
- nonstandard normalization of ionospheric radio signals 7-34764
- perturbed reflection layer, electric field calc. 7-40637
- plasma, upper hybrid resonance and turbulence excitation by intense radio wave 7-55362
- plasma depletion experiment (due to Spacelab-2), prod. of window for galactic background radioemission obs. 7-60469
- plasmasphere, electron temp. vars. along geomag. field lines rel. to electron density profiles and VLF paths 7-4258
- post-storm event radiowave absorpt., separation into three phases 7-29329

ionospheric electromagnetic wave propagation continued

- radio disturbances prediction service, outline (*Japanese*) 7-23844
- radio propagation models and prediction, review 7-18334
- radio signal distortion near 3D caustic 7-40631
- radio waves absorpt. during solar eclipse, 1.8 and 2.2 MHz obs. 7-29361
- radio waves resonance scattering, appl. to diagnostics of lower ionosphere 7-47613
- radio waves scattering from underdense meteor trains, electron volume density formulae 7-4383
- radio windows in ionosphere and magnetosphere, theory 7-4255
- radioaltimeters, regular ionospheric errors compensation possibility 7-34784
- radiowave, role in Quasat-Earth based VLBI system operation 7-60576
- radiowave heating expts., excitation of electrostatic fluctuations by thermal modulation of whistlers 7-29358
- radiowave heating expts., ionosphere response involving plasma instabilities 7-29344
- radiowaves, electron beam effects 7-55354
- ray scattering in gyrotropic medium, theory 7-9294
- satellite phase links, ionospheric dispersion effects on operation 7-60473
- scintillation of transionospheric VHF signals at mid-latitude 7-4260
- SHF radiation, energy dissipation in ionosphere 7-4262
- short wave multiple scattering in ionosphere, effect on fluctuations 7-60444
- short wave range operating frequency selection w.r.t. atmospheric disturbances (*Czech*) 7-60474
- solar activity cycle influencing MF radioabsorption 7-34767
- stimulated radio emission of the ionospheric plasma at the second harmonic of the pump wave frequency 7-29331
- topside and bottom-side data above Haikou region, China (*Chinese*) 7-18332
- transient field of atmospheric surface duct 7-14413
- transionospheric 140 MHz signal scintillation due to equatorial F-region irregularities 7-29357
- TV signal propagation at VHF, far beyond primary service zone 7-34768
- UHF/SHF SATCOM propagation and system design 7-40555
- VHF propagation, appl. to drift speed determ. for equatorial electrojet irregularities 7-4257
- VHF transionospheric signal time delay at subauroral latitudes, electron density characts. determ. 7-23933
- VHF-FM broadcast Es propagated signal polarisation obs. 7-60468
- VLF propagation at high southern latitudes, from sferics observations 7-47617
- VLF reflection in low ionosphere, local and long-distance effects of meteor showers 7-4256
- VLF signals reflection height, assoc. electron density var. 7-60448
- VLF waves in Earth-ionosphere waveguide, perturbations due to electron precipitation-induced ionisation enhancement 7-47626
- VLF waves use for D-region electron density determ. (*Japanese*) 7-66394
- whistler dispersion, semi-annual and annual vars. meas. 7-14410
- whistlers, newly-born ion effect and thermal effect 7-40572
- whistlers, nonlinear shift of wave parameters in ionosphere 7-66380
- whistlers, wintertime propagation characts., for N China observations (*Chinese*) 7-4265
- whistlers propagation, new plasma model rel. to diagnostic techniques in lower ionosphere 7-66381
- winter anomaly of D-region, numerical calcs. 7-47620

ionospheric measuring apparatus

- tethered satellite (on end of cable from larger satellite), electric current behaviour 7-9360

ionospheric measuring instruments *see ionospheric measuring apparatus***ionospheric propagation** *see ionospheric electromagnetic wave propagation***ionospheric techniques**

- chirped incoherent scatter radar measurement method for plasma line spectrum 7-29286
- collision frequency, vertical distrib., multifrequency radioabsorpt. meas. 7-55278
- conductivity models generation method 7-14395
- critical ionization velocity, proposal for Space Shuttle expt. to verify hypothesis 7-9312
- delay measurement for signal traversing dispersely inhomogeneous ionosphere layer, accuracy 7-23934
- EISCAT ionospheric sounding facility 7-29377
- EISCAT radar sounding, GEN-SYSTEM correlator algorithms 7-29333
- electric field and current determ. method using ground mag. variations (*Chinese*) 7-4250
- electron density determ. accuracy of EISCAT radar facility 7-29281
- F₂-layer visualisation, eleven years of ionospheric chronograms 7-23848
- HF backscatter use to determine nucl. explosion effect on ionosphere (*Chinese*) 7-29257
- HF sky wave paths, maximum usable frequencies, sounder updates for statistical model predictions 7-40638
- incoherent radar scatter line in presence of auroral electron precipitation 7-29287
- incoherent scatter radar probing of GP-100 km atm. and ionosphere 7-9211
- ionogram profile reduction method (*Chinese*) 7-18307
- LF whistlers group travel time use for ionosphere diagnostics 7-40572
- nose extension method use for whistler duct electron content determ. (*Chinese*) 7-29258
- plasma pot. calcs. from meas. Langmuir probe characts. 7-18306
- plasma velocity determ. by EISCAT radar method 7-29285
- prediction of ionospheric conditions, book 7-55909
- radio waves resonance scattering, appl. to diagnostics of lower ionosphere 7-47613
- radiointerferometric sounding, appl. to gravity waves obs. 7-4253
- radiowave incoherent scatter sounding for temperature and ion composition 7-29284
- radiowave sounding, multipulse zero lag for better incoherent scatter profile accuracy 7-29282
- radiowave sounding using EISCAT incoherent scatter, deconvolution of altitude smearing 7-29283
- resonance scattering method for F-region parameters determ. 7-55356
- SABRE radar use for ionosphere investigation 7-47627
- short-term HF propagation forecasting, problems 7-40645
- signal processing, use of communications techniques 7-29411
- tethered satellite (on end of cable from larger satellite), electric current behaviour 7-9360
- TID of medium scale, radiotelescope differential Doppler meas. method and obs. 7-47615

ionospheric techniques continued

- VHF radar use for equatorial electrojet elec. fields determ. 7-60414
- VLF waves use for D-region electron density determ. (*Japanese*) 7-66394
- whistler diagnostics, new plasma model rel. to diagnostic techniques in lower ionosphere 7-66381

iontophoresis *see electrophoresis***ions**

- see also atoms; electrolytic ions; hydrogen ions; negative ions*
- No entries

IR astronomy *see infrared astronomy***IR detectors** *see infrared detectors***IR drop** *see electric potential***IR focal plane arrays** *see image sensors; infrared imaging***IR imaging** *see infrared imaging***IR sources** *see infrared sources***IR spectra of diatomic inorganic molecules** *see infrared spectra of diatomic inorganic molecules***IR spectra of inorganic liquids and solutions** *see spectra of inorganic liquids and solutions***IR spectra of inorganic solids** *see infrared spectra of inorganic solids***IR spectra of organic molecules and substances** *see infrared spectra of organic molecules and substances***IR spectra of polyatomic inorganic molecules** *see infrared spectra of polyatomic inorganic molecules***IR thermography** *see infrared imaging***irasers** *see lasers***iridium***see also nuclei with*

- anodic dissolution in Cl⁻ melts, salt passivation 7-52053
 - electrodes, deposition and stripping props. of Hg 7-45058
 - etching by photochem. machining 7-22909
 - field evaporation rate, temp. depend. 7-33525
 - foil sample, Cs diffusion and surface ionisation studies 7-3138
 - itinerant electron Zeeman splitting anisotropy meas. 7-52536
 - Middle-Lower Jurassic rocks of Venetian region, N Italy, Ir anomaly detect. 7-55038
 - Ordovician-Silurian boundary stratotype, Ir abundances meas. 7-4014
 - paramagnetic suscept. temp. depend., thermal expansion effects 7-17156
 - single crystals, bulk self-diffusion, radiometric anal. (*Russian*) 7-58530
 - single-layer metallic structures obs. in EUV and VUV 7-22215
 - structural stability of reconstructed (110) surfaces 7-7326
 - surface, (100), FCC, hexagonal reconstruction 7-58591
 - surface, (100) surface reconstruction by field-ion microscopy 7-2316
 - surface (100), low temp. field evaporation of clusters, surface reconstruction, field ion microscopy studies 7-44973
 - surface (110) and (100), reconstruction, obs. in field ion microscope 7-1828
 - surface (111), adsorbed Cs atoms, photo- and electron-stimulated deformation of monolayer 7-58627
 - surface (111), spin-resolved photoemission meas. of transitions to secondary unoccupied bands 7-53501
 - surfaces, reconstructed, direct imaging using field ion microscopy 7-32767
 - Ge-Ir interfacial atomic struct. and cpd. form., FIM studies 7-32846
 - ¹⁹²Ir, accidental internal deposition, absorbed organ dose, γ -camera meas. 7-8688
 - ¹⁹²Ir dosimetry, use of simulator-based CT 7-14132
 - Ru-Ir bicrystal superlattice, stacking struct. and superconductivity 7-2432
 - Ru-Ir bicrystal superlattices, X-ray and transport studies 7-27159
 - Si-Ir, self-consistent one-electron states of 5d transition-atom impurities 7-32950
 - Si-Ir interfacial atomic struct. and cpd. form., FIM studies 7-32846
- iridium alloys**
- see also iridium compounds*
 - Nb₃Ir films, supercond. transition temp., effect of radiation induced disordering 7-45540
 - AuIr, heat of form. and cryst. struct., linear augmented STO calcs. 7-51705
 - CeIr₂, electronic structure, spectroscopic and thermodynamic props., impurity Anderson Hamiltonian 7-32900
 - EuIr₂Si₂, Eu intermediate valence 7-7188
 - Ir-Pt (2 at.%), surface segregation, AES study 7-27066
 - IrCe cathodes, thermal emission and sublimation 7-13317
 - IrLa cathodes, thermal emission and sublimation 7-13317
 - Lu-Ir, superconducting transition temp. and lattice constants 7-64387
 - Mo₃₂Ir, cryst. struct., X-ray diff. meas. at 293K and 12.5K 7-16491
 - Nb₃Ir films, lattice-stiffness changes due to ion irradiation, Brillouin scatt. 7-52379
 - Ta-Ir alloy, amorphous, rapidly solidified, high temp. oxidation 7-33841
 - Ta-Ir amorphous thin film thermal stability, crystallisation behaviour studies 7-63464
 - Ta₅₅Ir₄₅ amorphous alloy, crystallisation study 7-58145
 - TaIr, electronic struct. calcs. 7-45200
 - TaIr-GaAs Schottky barrier contacts 7-17102
 - UIr, cryst. struct., X-ray diff. study 7-37927
 - UIr₂Si₂, ThIr₂Si₂, magnetochemistry and crystal chemistry 7-58976
 - Zr-Ir, hardening by dispersed ω -phase particles, annealing effect (*Russian*) 7-65053
 - Zr-Ru-Ir system, solidus surface projection of Zr-ZrRu-ZrIr partial system 7-7972
 - Zr-ZrRu-ZrIr partial system, phase diagram and crystn. 7-22642
 - Zr₃Ir₃, crystal struct., Mn₂Si₃ deform. superstruct. type 7-11998

iridium compounds*see also iridium alloys*

- existence and electrical props. (*French*) 7-17008
- silicide, epitaxial growth on Si (111) 7-21760
- Er₃Ir₄Si₁₃, existence and electrical props. (*French*) 7-17008
- Ho(Ir_{0.7}Rh_{0.3})₄B₄, antiferromag. superconductors, upper crit. mag. field (*Russian*) 7-58963
- Ho₃Ir₄Si₁₃, existence and electrical props. (*French*) 7-17008
- In_xGa_{1-x}As pseudomorphic quantum well lasers, carrier collection and stimulated emission 7-10928
- Ir complex, (Ir(CO)₂4,4',5,5'-tetracyano-2,2'-biimidazole), anisotropic conductor, phys. props. 7-7242
- Ir complex, (NEt₄)(Ir(CO)₂4,4',5,5'-tetracyano-2,2'-biimidazole) mixed valence cpd., anisotropic conductor precursors identified by intermolecular charge transfer 7-7190

iridium compounds continued

- Ir complexes, Vaska's cpd., ^{17}O NMR study 7-10625
 IrBr_6^{2-} , in A_2MX_6 -type host crystals, near-IR absorpt. spectra 7-22232
 IrCl_6^{2-} , in A_2MX_6 -type host crystals, near-IR absorpt. spectra 7-22232
 $(\text{Ir}(\text{H}_2\text{O})_6)^{3+}$, substitution inertness, rate const. meas. 7-59742
 IrO_2 coated anode for V redox cell, eval. of electrode materials 7-54286
 Ir_2Se_3 , synthesis, powder diffraction characterisation 7-64956
 UlrGa_3 , structural chemistry, mag. behaviour 7-16513
 UlrSi_3 , mag. and elec. props. 7-45674

iron

see also nuclei with

- α -phase, activation energy of S diffusion, surface segregation, AES obs. 7-39529
 α -phase, moving edge dislocation, interaction with moving defects (*Russian*) 7-12114
 α -phase, Z 7-38016
 α -phase 7-44599
acicular particles, oxide layer morphology and mag. props. 7-52067
adsorption on Ar^+ -sputtered MoS_2 (0001), LEED, AES, EELS, and work function studies 7-52275
aggregated particles fractal dimension meas. by electron microscopy 7-26598
 $\text{Al}_2\text{O}_3/\text{Fe}$, single cryst., thermoluminesc. response 7-27794
alloying with N under high press. 7-3266
alloys, magnetic anisotropy and spin reorientations 7-38855
alpha form, H-H binding energy, lattice location and heat of formation 7-32361
alpha phase, dislocation pair jog, energy characts., mol. dynamics method anal. (*Russian*) 7-32440
alpha phase, high energy proton and alpha-particle irradiation, radiation defects (*Russian*) 7-16645
amorphous, elastic constants, relax. effects 7-51910
Armco, annealed and cold worked, neutron irradiation damage 7-2067
Armco, H charging, Rayleigh wave attenuation, mag. field effect 7-53107
Armco, mag. internal friction, cathodic charging effect 7-17212
Armco and Vacofer, yielding behaviour, H influence 7-33753
atom, inductively coupled plasma, emission, computer simulation 7-8348
atom, $\text{L}_{2,3}\text{M}_{4,5}\text{M}_{4,5}$ Auger process, meas. 7-57038
atomic beam, atom density meas., laser induced fluorescence 7-19762
atoms, transition energies, X-ray spectra, X α theory, X-ray transition energies 7-10422
Auger spectra, extended fine structures 7-64831
BCC, defects and radiation damage, computer simulation studies 7-2048
BCC, effective fracture energy assoc. with cleavage crack growth 7-44678
BCC, H-dislocation interaction mechanism, embrittlement and dislocation motion 7-44600
BCC, mag. ordering and electronic struct. (*Russian*) 7-33170
BCC and FCC forms, ferromag. phases investig. 7-2851
cast Fe, (*German, English*) 7-59641
catalyst on $\gamma\text{-Al}_2\text{O}_3$ surfaces, reaction, studies by positron annihilation 7-39309
cathode surface, plasma nitriding, N conc. profile modelling 7-54188
cathodic charging, H trapping 7-21256
cementation layer struct., Mossbauer spectra, radioisotope method, microhardness obs. (*Russian*) 7-39741
circularly polarised X-ray absorpt. 7-59302
clusters, icosahedral and cubo-octahedral coordination, electronic struct., first-principles method calcs. 7-45132
clusters ionisation threshold, photoionisation TOF mass spectra 7-20085
corrosion inhibition by H_2O_2 7-39695
corrosion thin films, laser Raman spectroscopy at 100 to 150°C in air 7-39722
creep, glide plane stresses, yield point, dislocation theory (*Russian*) 7-59580
creep, high-temp., rel. between dislocation density and internal stress 7-13524
critical mag. phenomena, results from μSR studies in paramag. and ferro-mag. $\alpha\text{-Fe}$ 7-45872
crystals, growth shape, effect of melt undercooling (*Russian*) 7-46308
cubic polycrystals, elastic consts., Young's modulus rel. to axial texture (*Russian*) 7-59562
diffusion, in GaAs, temp. depend. 7-6875
diffusion bonding, precip. of Fe carbides in ferrite 7-39521
diffusion of ^{59}Fe and ^{59}Co in Fe, mag. anomalies, quasi-chemical model 7-6862
dislocation assemblies, parameter linking change in internal energy and vol. in creation (*Russian*) 7-58279
dislocation-mechanics-based constitutive relations for material dynamics calcs. 7-63706
disperse reduced, oxidation, effect of additions 7-22888
ductility, high-temp., high temp. ductility, effects of B 7-46588
edge and screw dislocation density determ., TEM, etching and positron lifetime meas. 7-38006
electrical resistivity, high temp. and press. 7-38534
electrochemical behaviour in strongly alkaline soln. (*French*) 7-59768
electrode in NaOH, pot. modulated reflectance spectra 7-28316
electrode surface, second harmonic generation study using a picosecond laser 7-23030
electrodeposited, grain struct. and size, positron lifetime study 7-46209
electrodes, electrodisolution and passivation $\text{K}_2\text{CO}_3\text{-KHCO}_3$ solns., ionic comp. effect 7-17677
electrodes, H atom diffusion and trapping, meas. by potentiostatic double-step method 7-21525
electron irradiated α -phase, residual resistivity recovery and mag. after-effect 7-27570
epitaxial FCC $\gamma\text{-(111)p(1}\times\text{1)}$ films on Cu (111), surface ferromagnetic order 7-45773
epitaxial films, mag. size effects 7-59081
epitaxial growth on Cu (100) 7-52353
epitaxial layer on GaAs, simultaneous epitaxy and substrate out-diffusion 7-38355
epitaxial monolayers on Au (100), surface magneto-optic Kerr effect 7-59080
FCC metastable phase epitaxial films on Cu local mag. moment, XPS study 7-53504
Fermi surface change near the mag. transition 7-16935
ferritic, grain boundary segregation of P and C 7-39530

iron continued

- ferritic spent fuel casks, predrop test anal., stresses and fracture toughness 7-46651
ferromagnetic, band struct. and optical props. 7-2476
ferromagnetic, positron spin polarisation relax. study 7-46203
ferromagnetic, spin depend. Compton profile, circularly polarised synchrotron radiation study 7-33477
ferromagnetic sp. ht. meas. by pulse-heating technique 7-7513
ferromagnetic superlattices with magnetisation perpendicular to surface, collective excitations, magnetostatic theory 7-45647
ferromagnetic thin absorbing film on reflecting struct., equatorial Kerr effect 7-53287
ferromagnets, spin-resolved photoemission and bremsstrahlung calcs. and data anal., book contrib. 7-33523
field evaporation in Ne and H, temp. and field depend. 7-33526
film, electrodeposition and corrosion, piezoelec. cryst. substrate obs. 7-39707
films, ethane and ethylene adsorpt. and reaction, mass spectra, XPS, UPS, electrical resistance and work function meas. 7-32837
films, particulate, vapour deposition on Al_2O_3 growth and props. 7-17427
films on Ni substrates, magnetism and interface processes, in-situ conversion electron Mossbauer study 7-7571
fine particles magnetic props., necking config. effects study 7-53060
foil, transient mag. field effect on Si^{2+} 7-10537
foils, H charged, internal friction, quasi-molecular state (*Russian*) 7-59561
friction, solid struct. calcs. 7-51932
Hall effect, anomalous, and energy band struct. (*Russian*) 7-52414
He production in HFIR neutron irradiated pure elements 7-51852
high-luminosity non-coronal stars, Fe II emission line profiles 7-47867
high-pressure phase transitions, laboratory expts. 7-38179
high-temperature corrosion film characterization using Raman microscopy 7-46772
hot deformed, metadynamic recryst. 7-3335
Hubbard model, degeneracy and quantum effects 7-7469
I-line excitation processes, investig. 7-19775
impurities in Ge-Sb-Te system, diffusion 7-21527
 $\text{In}_{0.5}\text{Ga}_{0.47}\text{As}$:Fe metalorganic CVD epitaxial growth and elec. props. 7-63993
inelastic electron scatt., spin-depend. energy loss processes, book contrib. 7-33500
intergranular corrosion, inhibition mechanism of S-containing additives 7-53946
inverse magnetostrictive effect and electromagnetic non-destructive testing methods 7-13714
ion implantation, of Si, struct. and phase modifications 7-12095
ionised atom miscibility in H-plasmas under solar interior conditions 7-14555
ions, energy levels, radiation effects and corrections 7-49960
itinerant electron ferromagnetism, mag. susceptibility, Curie-Weiss law, temp. depend. 7-27501
itinerant ferromagnets, electronic struct. determ., spin depend. inverse photoemission studies, book contrib. 7-33479
Kamchiba River mouth, Bulgaria, Fe in sediments, river and sea water 7-29085
laser glazing and boronizing 7-39753
laser irradiation, Nb surface alloying, Mossbauer spectra (*Russian*) 7-58580
late-type supergiant eclipsing binaries, chromospheric ionisation and opacity, UV, spectra 7-40869
layer growth on polysiloxane surface in stream of $\text{H}_2\text{-Cl}_2$ mixture (*Russian*) 7-65353
liquid, surface comp. and surface tension, effect of S and Mn (*Chinese*) 7-6916
liquid and solid states, mag. susceptibility effect of O content (*Russian*) 7-52953
low energy ^4He ion range and damage distrib. 7-63674
low-field mag. hysteresis 7-64483
magnetic domain walls, low freq. internal friction (*Chinese*) 7-38898
magnetic domains, spin-polarised SEM studies 7-56376
magnetic field effect on wear 7-7582
magnetic films, MBE growth on GaAs, interface effects 7-27584
magnetic properties of different phases, modelling using Monte Carlo method (*Russian*) 7-58992
magnetic surfaces, spin polarised Auger electrons 7-53456
matrix, interface with carbide particle, void nucleation mechanism 7-38354
melting curve at high pressure, implications for temps. in Earth's outer core 7-23614
metal films, mech. props., relation between different quantities 7-8041
metal surfaces immersed in liquid media, pulsed laser oxidation and nitridation 7-59656
microcrystals, diffusive motion studied by Mossbauer spectroscopy 7-45857
microcrystals on SiO_2 , adsorption of H_2 , positron annihilation studies 7-39311
microhardness correction procedures evaluation 7-3550
Mossbauer effect, inhomogeneous magnetic hyperfine line broadening, nonlinear RF spectra 7-45858
multiply charged ions, electron-impact ionisation, excitation energies and cross section calcs. 7-25425
multiply-charged ions, electron-impact ionisation cross sections, crossed-beam meas., rate coefficient calcs. 7-25660
muon arrhenius jump rates, neutrino emission 7-27643
muon spin precession and the hyperfine anomaly 7-45906
nanocrystalline, positron lifetime spectroscopy 7-46177
negative muon spin precession and hyperfine field anomaly study 7-45894
neutron irradiated, defect clusters, positron annihilation lifetime meas. 7-51853
neutron irradiation effects on mech. props., damage and yield stress 7-51865
NGC 4151, Seyfert galaxy, detect. of intense Fe line emission at 6.4 keV 7-18452
ore fields, inhomogeneously magnetised models selection optimisation 7-23526
overlayers or sandwiches with Cu (001), electronic and mag. props. 7-64499
oxidation, multilayer scale form. 7-33838
oxidation, twinning and precipitation reactions 7-17733
oxygen corrosion in neutral aerated sulphate solns., dynamic systems analysis (*German*) 7-8192

iron continued

- paramagnetic ground state props. and pair potentials 7-32352
particle filled epoxy matrix, dynamic mech. props., storage and loss moduli 7-3349
particles, ultra fine, ferromag., growth rel. to mag. field 7-53515
particles on planar Al_2O_3 supports, low rate growth 7-32779
passivated, comp., electron backscattering Mossbauer spectra, XPS studies 7-28193
passivation and spontaneous dissolution in presence of O_2 7-22872
passive, adsorption and absorpt. of Cl^- ions 7-28340
passive anodic oxide form., surface anal., XPS, ion scatt. spectra 7-22895
passive layer, critical thickness at Flade pot. 7-39757
permeation of $\text{H}(\text{D})$, oscill. press. effects 7-27025
phase diagrams, appl. for online press. and temp. calibration 7-4853
photoemission study, existence of valence band satellite 7-46274
photoemission study of valence band satellite, comment 7-46273
pitting corrosion, role of Cl^- ions (Japanese) 7-33829
plastic deform., H permeation, dislocation traps 7-65082
point defect and edge dislocation interaction simulation and radiation creep rate estimation in α -Fe crystal 7-21216
polymorphic forms stability, elastic consts. in 20 to 1470°C range, enthalpy of fusion rel. to self-diffusion activation energy 7-6781
porous, segregation of impurity elements, alloying elements selection and activated sintering 7-53742
positive muon diffusion and hopping rate 7-52111
positive muon studies in mono- and poly-crystalline Fe, low temp., dipolar fields, jump freqs. 7-45861
positron annihilation, high press. Doppler broadening expts. in diamond anvil 7-46189
powder, development of new type with unusual props. (German) 7-3227
powder, fine, corrosion resist. and mag. prop. changes, surface-active agent use in prep. 7-54001
powder, force characts. of powder compaction process 7-7912
powder, quality assessment method 7-53671
powder, ultrafine, and hot forged specimens, reduction temp. effect on struct. form. and props. 7-53670
powders, hot pressing, fracture toughness, intergranular failure rel. to porosity 7-13596
powders, sintering, densification, grain growth (Japanese) 7-53662
proton irradiation behaviour, 11 MeV 7-58369
pulsed laser irradiated, spin-polarised photoemission 7-39360
pure, diffusion of H, dislocation trapping, interstitial impurities effect (Japanese) 7-52140
pure, solid/liquid interface, pulse echo US study of location during solidification and melting 7-52006
PVC-Fe powder mixtures, shock consolidation, densification, industrial appls. 7-39473
quartz: Fe^{2+} , ion implanted, coloration and transparency (Japanese) 7-7656
reaction with $\text{HCl-O}_2\text{-Ar}$ mixtures at 550°C 7-17713
recrystallisation, deform. threshold, annealing temp. depend. (Russian) 7-59546
rolling texture, effect of parity 7-59548
seafloor hydrothermal plumes of E Pacific Rise, Fe, He, Mn obs. showing Fe enrichment 7-9028
single crystal, (001) oriented, hydrogen induced cracking and hydrogen embrittlement (Japanese) 7-33782
single crystals, Bi ion implantation, high substitutional fractions 7-58299
single crystals, flow stress at 225, 250 and 273 K, orientation depend. 7-53832
small ferromag. particles in Al_2O_3 matrix, mag. props., comparison with spin glasses 7-7557
solid and molten, X-ray $K\alpha_1$ and $K\beta_1$ lines (Russian) 7-39211
solubility of Nd, positron annihilation study 7-46208
solution kinetics in molten Zn 7-16752
spherical inclusion filled PMMA, techniques and models for elastic moduli, US evaluation 7-39833
spin wave excitations and magnetisation temp. depend. 7-45642
sputtered films, mag. perpendicular anisotropy, Mossbauer studies 7-59076
sputtered magnetic thin film, ion beam irradiat., struct. studies 7-22588
static paramag. spin susceptibility at finite temps. 7-33138
Stoner excitations, free-electronlike, spin-polarised EELS 7-45648
Sun, chromosphere limb spectra, Fe II emission curve of growth 7-24116
Sun, Fe I, 532.419 nm line form. depth in photosphere mag. field (Chinese) 7-66525
Sun, inner corona, spectral obs. during 1973 June 30 total eclipse 7-24117
surface, (001), hyperfine fields 7-58847
surface, (100), with adsorbed CO, UPS characterisation of a and b adsorption states 7-27126
surface, (100) with adsorbed CO, adsorbate, tilted dissociation precursor 7-58642
surface, (110), clean and O-covered, struct., surface extended energy loss fine struct., spectra obs. 7-12481
surface, (111), CO_2 adsorption and dissociation, ARUPS 7-63961
surface, (111), electron capture spectroscopy 7-59368
surface, (111), K precovered, promotion of surface reactions with N_2 7-13807
surface, adsorpt. and dissoc. of N_2 , EHT calcs. 7-56988
surface, Fe oxide coatings, IR emission, absorpt. modes effect 7-27708
surface, H_2 and N_2 interactions, pulsed laser atom probe studies 7-32811
surface, N^+ implantation, migration effect during wear (Chinese) 7-53998
surface, oxidised, chemisorption of pyridine and pyrrole, XPS 7-27128
surface, polycryst., interaction with $\text{O}_2(\text{N}_2)$, electron spectrosc. obs. 7-7794
surface (001), Ni film epitaxial growth, LEED and AES studies 7-64022
surface (100), oxidation and reconstruction, AES, LEED, ellipsometry and ion scatt. studies 7-8154
surface (100), resonant photoemission near 3p-electron excitation threshold 7-64876
surface (100) finite temp. surface magnetism 7-52949
surface (100) with surface C, gasification by O, CO desorption 7-6993
surface (110), chemisorptive bonding of CO, pseudofunctional electron muffin-tin approach 7-2348
surface (110), clean and Ag coated, magnetic hyperfine field, local structure 7-21878
surface (111) chemisorbed N_2 , adsorbate geometry, angle resolved XPES anal. 7-45009

iron continued

- surface damage, plastic deform., 4-293 K (Russian) 7-59581
surface friction layers, study by AES method (Russian) 7-59674
surface I retention modelling, role in source term reduction, reactor accident anal. 7-33961
surface layers under toluene, laser irradiated, supersaturation with C 7-51820
surface magnetism, effect of adsorbed O 7-58973
surface magnetism 7-27528
surface oxide films, spectral polarised directional emissivity meas., stratified media theory interpretation 7-17291
surfaces, chemical cleaning by NO 7-22886
surfaces, fluorination, XPS study 7-22887
surfaces, smooth (110), (111) and stepped (110), adsorption of CO_2 , UPS, work function meas. 7-12484
surfaces (100) and (110), Stoner excitation spectrum, spin-polarised electron energy loss spectroscopy 7-53463
surfaces and overlayers, mag. and electronic props. 7-58985
TGS: Fe^{2+} crystals, spatially distributed defects, luminescence studies 7-26770
thermal equilibrium vacancies, muon spin resonance studies 7-51757
thermal expansion, electron correl. effects 7-2238
thermodynamic props., data tables and reviews 7-18512
thin films, formed by laser breakdown CVD, metastable phase form. 7-38377
thin films, sputter deposited at oblique incidence, microstruct. and mag. props. (Japanese) 7-33560
thin films, stress development during oxidation 7-45096
thin films, surface plasma waves, optical and magneto-optical effects 7-27704
total angular momentum, atomic mag. moments, calc. 7-62540
ultra thin films, Brillouin scatt. 7-27728
ultrathin films on Pd (111), photoemission, LEED and AES studies 7-45068
Vega, Fe comp. and atm. microturbulence characts. 7-4445
whisker, ferromag. domain struct. obs. 7-7536
whiskers, (011), Neel's domain struct. in weak and zero applied fields 7-2888
whiskers, mag. domain obs. by colloidal-SEM method (Japanese) 7-7533
X-ray Compton-Raman scatt. from atomic inner shell electrons 7-13257
X-ray emission $K\alpha_{1,2}$ spectra 7-64825
X-ray photoabsorption cross sections 7-46240
zone refined, radiation hardening by 14 MeV neutrons, temp. depend. 7-51857
Ag/Fe (001) interface, hyperfine fields 7-58847
Al diffusion into Fe, influence of mag. field, radioactive isotope study (Russian) 7-52157
 Al_2O_3 :Fe:Y, high temp. DC elec. cond. rel. to superalloy oxide scale adherence 7-52615
 Al_2O_3 :Fe spheroids, Norton Masterbeads for solid particle solar receiver, optical props. 7-40043
 Al_2O_3 :Fe spheroids, Norton Masterbeads for solid particle solar receiver, optical props. 7-40044
 Al_2O_3 -Fe particle dispersed system, cosputtered films, EXAFS study 7-64810
 $\beta''\text{-Al}_2\text{O}_3\text{:Na}_2\text{O:Fe}^{2+}$, luminesc. thermal effects 7-33444
 $\text{BaTiO}_3\text{:}^{57}\text{Fe}$, multiphonon transitions from modulated hyperfine electric field gradients 7-27633
 $\text{BaTiO}_3\text{:Fe}^{2+}$, ferroelectric transition, EPR 7-33343
C deposition in vacuum carburising (Japanese) 7-33827
 $\text{CaFe}_2\text{:}^{57}\text{Fe}$, Mossbauer absorption and emission expts., relax. and after-effect study 7-27635
 CdTe:Fe^{2+} , impurity vibronic coupling and near IR spectra characts. 7-26889
Co-Fe bilayer thin films, annealing behaviour, mag. props. 7-59079
 $\text{Cs}_2\text{NaAlF}_6\text{:Fe}^{2+}$, impurity ion spin Hamiltonian parameters, EPR determ. 7-64523
Fe clusters+ NH_3 , reaction kinetics, cluster binding sites and adsorbate binding energies 7-54106
Fe electrodes, passivated, capacitance under simulated erosion-corrosion conditions 7-3514
Fe films on insulators, H^+ bombardment, Mossbauer and adhesion study 7-32517
Fe I, cascade Zeeman quantum beats, stepwise pulsed-laser excitation, fluoresc. anal. 7-49997
Fe I, II, excited state level populations in ICP discharge 7-30963
Fe I 1564.854 nm line diagnostics of solar magnetic flux tubes 7-66531
Fe I lines in solar facular areas, shifts and asymmetries 7-66529
Fe I solar photospheric lines, 5-min oscill. in wings and bisectors 7-66530
Fe II, electron impact excitation, collision strengths, R matrix method, CI calcs. 7-25424
Fe II 396.94 nm solar line in Ca II H and K wings 7-4398
Fe II oscillator strengths and lifetimes 7-57019
Fe III forbidden emission lines, identification in UV spectrum of Sun 7-47813
 α -Fe, plastic deformation, magnetoacoustic and Barkhausen emission study 7-45749
Fe polymorphism interpretation 7-51700
 α -Fe surfaces, segregated elements, bonding state 7-16763
Fe XIX-XXI, tokamak plasmas, inner-shell X-ray line spectra 7-6371
Fe XV, allowed transitions, Hartree-Fock and Dirac-Fock calcs. 7-15494
Fe XXII line intensity ratios for plasma electron density diagnostics 7-26516
 Fe^{2+} excited state selected, one-colour UV multiphoton ionis. 7-36506
 Fe^{2+} aq. solvation, Monte Carlo simulation 7-54154
 Fe^{2+} , dielectronic recomb., rate coeff. calc. 7-30991
 Fe^{2+} , dielectronic recomb., rate coeff. calc. 7-30991
Fe:B polycrystalline films, amorphous alloy layer formation by ion implantation (Chinese) 7-6647
 α -Fe:H, H induced softening, yield stress reduction 7-39607
Fe:H(D), lattice strains, meas. 7-2268
Fe:He(C), distribution and migration of interstitial impurities in the field of a screw dislocation core 7-6669
Fe/ Al_2O_3 interface, ion beam mixing, conversion electron Mossbauer spectra studies 7-63679
Fe/Cu microlaminate condensates, creep and struct. investig. (Russian) 7-33749
Fe/Cu multilayered samples, ion beam mixing-induced metastable phases 7-58377

iron continued

- Fe/Fe oxide passive film interface composition and growth, atom probe depth profiling anal. 7-32869
 Fe/Fe-FeO/Al₂O₃ systems, diffusion bonded, interface chemistry, bonding strength 7-28079
 Fe/H₂O interface, pulsed-laser-induced reactive quenching, FeO metastable phase form. studies 7-45005
 Fe/O in metal-poor late-type stars 7-40803
 Fe/Sn interface, electrolyte tinplate, determ. of reaction time during first stage of FeSn₂ growth 7-53990
 Fe/Ti multilayered struct., wear and friction, ion beam mixing effects 7-28141
 Fe/Zn diffusion couple, anomalously fast diffusion 7-16818
 Fe-air alkaline batteries, thermodynamic framework for efficiency estimation 7-3636
 Fe-Al bilayered samples, ion beam induced atomic mixing 7-6689
 Fe-Al₂O₃ melt, steam explosion suppression by coolant viscosity increase 7-8284
 Fe-Au compositionally modulated multilayered films, magneto-optical Kerr rot., wavelength depend. 7-3100
 Fe-Au-Fe double layers, exchange coupling 7-27510
 Fe-Br, mag. hyperfine field of ⁸¹Br, NMR nuclear orientation study 7-13049
 Fe-Cr-Fe double layers, exchange coupling 7-27510
 Fe-Cu, epitaxially grown Fe films, electronic and crystallographic struct. 7-27214
 Fe-Cu compositionally modulated multilayered films, magneto-optical Kerr rot., wavelength depend. 7-3100
 Fe-Cu multilayer films, layered mag. domains, Schlieren-Lorentz TEM studies 7-38916
 Fe-Ge (110) interface, electronic struct. calc., mag. effects 7-45496
 Fe-graphite diffusion chromised materials, high-temp. interaction in hydrogen 7-17671
 Fe-graphite structures, ion induced mixing, sputtering yield, fluoresc., RBS depth profile meas. 7-64844
 Fe-H system, dislocated single crystals, positron trapping reduction on H charging 7-39262
 Fe-H system, H-defect interactions study by positron annihilation 7-38046
 Fe-H₂O reaction under high pressure, implications for evolution of Earth 7-8887
 Fe-Mg superlattices, mag. props. (*Japanese*) 7-12950
 Fe-Mn superlattices, NMR study (*Japanese*) 7-13046
 Fe-N, implantation at 77 K, surface comp., microstructure, AES, HVEM, transmission HEED studies 7-38033
 Fe-Ni alkaline batteries, thermodynamic framework for efficiency estimation 7-3636
 Fe-Ni-Au trilayer film, structural depth profiling by glancing angle X-ray diffraction 7-26593
 Fe-Pd multilayer struct., localised phonon modes 7-46061
 Fe-Pd multilayer structures, collective spin waves 7-46060
 Fe-SiO₂ compositionally modulated mag. film props. study 7-7566
 Fe-SiO₂ granular films, mag. relax., DC SQUID magnetometry, Mossbauer spectra 7-45761
 Fe-Ti multilayered films, ion bombard., microstructure, TEM obs. 7-12165
 Fe-Ti-C multilayered films, ion bombard., microstructure, TEM obs. 7-12165
 Fe-V superlattices, NMR study (*Japanese*) 7-13046
 Fe-V superlattices and alloys, magnetism study 7-64436
 Fe-W, multilayer structures, collective spin waves 7-46060
 Fe-W (110), spin-resolved photoemission spectra of epitaxial Fe layers 7-46276
 Fe+D(He)(C)(N)(O), thick target bombardment, X-ray production cross sections 7-20025
 Fe²³⁺+H⁺, Fine-struct. excitation, plasma screening effects, ion-sphere and Debye-Huckel models 7-62509
 Fe₂, diatomic molecules, electronic configuration, ⁵⁷Fe Mossbauer data 7-10640
 Fe₃ cluster, vibr. photodissoc. spectra, IR laser study 7-62475
 Fe_n⁺ (n=6 to 16), cluster ions, mass selected, prod., continuous source 7-10805
 Fe(CO)₄, IR laser-induced photochem. 7-65334
 Fe(0) microclusters, in A-type zeolites, mag. props. meas. 7-17256
⁵⁶Fe, implanted in ZrO₂-YO_{1.5}, ion conducting material, thermal behaviour 7-27006
 Ga_{0.4}In_{0.53}As-InP:Fe(S), deep defect levels, photoluminescence, DLTS meas. 7-33457
 β-Ga₂O₃:Fe³⁺(Cr³⁺), zero-field splittings and site distortions 7-59119
 GaP:Fe, deep levels formed by Fe complexes 7-12657
 H pumping and compression by superpermeation 7-58543
 H⁺+Fe, k-shell ionization cross sections and theoretical models 7-5627
 InP:Fe, Czochralski-grown, stoichiometric-related faulted loops, struct. and lumin. props. 7-51772
 InP:Fe, deep levels formed by Fe complexes 7-12657
 InP:Fe, epitaxial layers, MOCVD, doping profiles, SIMS, resist., temp. depend. 7-21248
 InP:Fe, LPE growth, SIMS 7-52363
 InP:Fe, midgap impurity levels, isomer shift and charge state calcs. 7-2538
 InP:Fe, OMVPE grown, electronic and optical props. 7-52868
 InP:Fe, optical spectra 7-53372
 InP:Fe, photoconducting flat response detectors from UV to X-ray region 7-5563
 InP:Fe, programmed magnetic field applied LEC crystal growth 7-59399
 InP:Fe, Si-implanted and rapid thermal annealed, photoluminesc. study 7-59243
 InP:Fe, transient photoconductive response 7-52681
 InP:Fe,Ga,Sb, LEC growth, dislocation density, resistivity, SIMS obs. 7-53552
 InP:Fe photoconductive detectors for VUV and soft X-ray regions 7-30084
 InP:Fe semi-insulating layers, MOVPE growth and elec. characts. 7-22511
 InP:Fe wafer, semi-insulating, elec. characteristics 7-45323
 In₂Te₂:Fe, Fe²⁺ elec. inactivity study, mag. suscept., Mossbauer spectra and XPS anal. 7-52494
 KAlSi₃O₈:Fe³⁺, orthoclase, absorpt. and luminesc. spectra 7-53383
 K₂MoO₄:Fe, CDW state, Mossbauer studies 7-53112
 KTaO₃:Fe³⁺, EPR of Fe³⁺ centres, electric field effect 7-38926
 KTaO₃:Fe³⁺, ESR, effect of external electric field 7-38933

iron continued

- LiAlO₂:Fe³⁺, Mossbauer relaxation spectrum, electric quadrupole shifts dependency on mag. field 7-7182
 LiAlO₂:Fe³⁺, spin-lattice relax. times, Mossbauer spectroscopy 7-45848
 LiCl:Fe³⁺, X-ray irradi., EPR spin Hamiltonian parameters 7-45808
 LiNbO₃:Mg, Fe crystals, photoconductivity props. studies 7-38624
 LiNbO₃:Fe, and undoped crystals, decay of γ-centres 7-7658
 LiNbO₃:Fe, asymmetric photoinduced scattering of light 7-17282
 LiNbO₃:Fe, Czochralski growth and holography appl. 7-59404
 LiNbO₃:Fe, linear electro-optic effect, optical damage by He-Ne laser (*Korean*) 7-27698
 LiNbO₃:Fe, speckle size depend. on laser beam size via photo-induced light scattering 7-5840
 LiNbO₃:Fe cryst., Raman spectra, photo-induced refractive index change effects 7-53300
 LiNbO₃:Fe crystal, white-light information processing, coupled wave theory 7-25728
 LiNbO₃:Fe crystals, refractive index gratings, microphotometric study 7-62649
 LiNbO₃:Fe crystals, biharmonic pumping, photoinduced light dispersion (*Russian*) 7-31391
 LiNbO₃:Fe planar optical waveguide, hologram recording, dopant conc. depend. 7-15828
 LiNbO₃:Fe²⁺, anomalous phase transitions, Mossbauer spectroscopy studies 7-2992
 LiNbO₃:Fe³⁺, EPR of axial and low-symmetry paramagnetic centres 7-38925
 LiNbO₃:Fe³⁺, Mossbauer spectroscopic evidence of angle-depend. intersystem crossing 7-33312
 MgO:Fe, gamma irradi., thermoluminescence and TSC studies 7-33464
 MgO:Fe, gamma-ray and electron radiation-induced conductivity 7-33015
 MgO:Fe, positron lifetime spectra, impurity effects 7-39278
 MgO:Fe, small angle [001] twist boundaries, Fe solute effect 7-32459
 Mn²⁺Mn³⁺SiO₂:Fe(Ca)(Al), antiferromagnetism and spin glass order, mag. meas. 7-27518
 Mo fibre reinforced Fe composites, extruded, struct. and fractography 7-13595
 Na₂O-Fe₂O₃-Al₂O₃-SiO₂ glasses, Fe³⁺ ESR spectra, valence-coord. state 7-45813
 Ni-Fe (100), layered struct. reflectivity and EXAFS study 7-59292
 Ni-Fe alkaline accumulator develop. in Hungary (*Hungarian*) 7-17855
 O₂ chemisorpt., influence of Ar⁺ ion bombardment (*Russian*) 7-52253
 PbTiO₃:Fe³⁺, F⁻ charge compensating cluster form., EPR spectra studies 7-64518
 Si:Al,Fe-SiO₂, MOS struct., trap centres 7-7388
 Si:B,Fe, EBIC and DLTS meas., comparisons 7-7265
 Si:Fe, Czochralski grown, interdependence of contamination and defect formation 7-32467
 Si:Fe, interstitial Fe, spin delocalisation 7-13059
 Si:Fe, interstitial impurity, superhyperfine interaction and spin-lattice relax. 7-53178
 Si:Fe, intrinsic gettering, EPR and TEM study 7-38216
 Si:Fe, low damage surface anal., sputtered atom resonance ionisation method 7-58584
 Si:Fe, MOS capacitor elec. parameters, effects of process chemical purity 7-33103
 Si:Fe, silicides obtained by Fe⁺ implantation 7-6655
 Si:Fe,O, Fe intrinsic gettering, EPR studies 7-16553
 Si:Fe polycrystalline solar cells, structural, elec., photovoltaic props., impurity effects 7-39990
 Si:Fe, ion implanted, channeling/RBS studies 7-2039
 Sr_{0.8}Ba_{0.4}Nb₂O₆:Ce(Fe), photorefractive props. 7-45955
 SrTiO₃:Fe³⁺, impurity energy levels, tight binding model, Green's function method calcs. 7-21856
 Ta₂O₅-Fe-Fe₂O₃ system, equilibria at 1200°C 7-12301
 Ti/Fe multicomponent films on steel, sputter deposition and characteris. (*Japanese*) 7-3167
 YAG:Fe, defect and optical props. 7-59258
 Y₂O₃-ZrO₂:Fe, high dose ion implanted, profile shapes and electronic cond. 7-32472
 ZnCO₃:Fe²⁺, mixed spin relax. processes 7-64522
 ZnS:Al, Cr, Fe crystals, recomb. luminesc., EPR and photocond. meas. 7-3076
 ZnS:Cr³⁺, Fe³⁺ single crystals, impurity centre charge exchange, plastic deform. effects, ESR spectra studies 7-16984
 ZnS:Fe,Cu, three-centre Auger recombination, EPR study 7-45806
 ZnS:Fe electronic struct., K-edge EXAFS study 7-64079
 ZnS:Fe²⁺, impurity vibronic coupling and near IR spectra characts. 7-26889
 ZnSe:Cu,Al,Fe crystals, melt-grown, absorpt. coeff., impurity effects 7-3070
 ZnSe:Fe, impurity ion photoionisation, EPR, photoconductivity spectra 7-52495
 ZnWO₄:Fe single crystals, spectroscopic props. 7-7725
 ZrF₄-based fluoride glasses, Fe ions anal. 7-64672

iron alloys

- see also Elinvar; Invar; iron compounds; Permalloy; steel
 Alloy 600, intergranular SCC, in aq. soln. containing dissolved H₂, activation energy 7-59683
 Alloy 600, reactor steam generator material, properties and performance 7-30556
 alloy 600 nuclear steam generator tubes, local pitting conditions using Pourbaix diagrams 7-46716
 Alloy 600 PWR steam generator tubing, intergranular attack and SCC remedial methods 7-8199
 alloy 600 tubes, intergranular attack, cause evaluation 7-59685
 alloy 600 tubes in PWR steam generators, localised electrochem. corrosion 7-39760
 alloy 600 tubing in nuclear steam generators, intergranular attack, environmental effects eval. 7-39761
 Alloy 718, Ni-base superalloy, fatigue crack propag. under hold-time cycling, effect of grain size 7-28106
 Alloy 800 H, high temp. fatigue, damage mechanism (*German*) 7-17604
 Alnico 5, Fe-Co-Ni-Al-Cu, microstruct. and mag. props., effects of heat treatment (*Korean*) 7-8138
 amorphous alloys, cold shortness (*Russian*) 7-39649
 amorphous alloys, O₂ adsorption, ion bombardment effects 7-21637
 bimetal of C steel-cast Fe-Cr, interface bonding strength (*Korean*) 7-17618

iron alloys continued

- bronze BrAZh, elec. discharge sintering of powder from swarf, electro-phys. and mech. props., microstruct. 7-27974
 cast, surface melting, composition and impurity effects 7-21423
 cast Fe, 7-27317
 cast Fe, alloyed, pearlite, flake graphite, thermal fatigue resist. 7-46606
 cast Fe, bainitic ductile, microstruct. rel. to comp. and heat treatment 7-39579
 cast Fe, chem. analysis with VRA-30 sequential X-ray fluoresc. spectrometer 7-8333
 cast Fe, Cr-type, duplex nature of eutectic carbides 7-13440
 cast Fe, diffusion bonding, precip. of Fe carbides in ferrite 7-39521
 cast Fe, diffusion interaction with steel in forging, explosive treatment and thermal cycling 7-28070
 cast Fe, ductile, austempering techniques 7-59552
 cast Fe, ductile and grey, laser surface hardened, sliding wear 7-17650
 cast Fe, flake and nodular graphite, breaking behaviour of perforated notched specimens 7-17606
 cast Fe, graphite, directionally solidified, struct. transitions 7-13443
 cast Fe, graphite morphology and growth kinetics (*Chinese*) 7-65017
 cast Fe, grey, skin casting under microgravity conditions 7-22661
 cast Fe, high Cr, grinding balls, jet slurry corrosive wear 7-39676
 cast Fe, high-Cr, wear-resistance, laser and heat treatment effect on struct. and props. 7-8174
 cast Fe, high-strength, form. of wear resistant structs. corresponding to Charpy principle 7-28180
 cast Fe, laser surface hardening, optimisation of process variables 7-13645
 cast Fe, metastable austenite form. rel. to initial treatment and struct. 7-46455
 cast Fe, nodular, ferritising action of increased Mg content on struct. 7-3292
 cast Fe, nodular graphite, fatigue crack propag. rel. to microstruct., SEM obs. (*Chinese*) 7-13542
 cast Fe, pearlitic, flake graphite, alloyed, thermal expansion 7-52094
 cast Fe, pearlitic, nodular, fractographic anal. 7-53882
 cast Fe, Sn plating, heat diffusion method, corrosion resist in H_2SO_4 (*Japanese*) 7-53956
 cast Fe, vermicular graphite, elastic props. 7-13493
 cast Fe, white, Cr-Mo, unidirectionally solidified, sclerometric study 7-3455
 cast Fe, with lamellar graphite, mech. props. and morphology (*German*) 7-21160
 cast Fe/stainless steel couple, galvanic corrosion NaCl soln., boundary element prediction (*Japanese*) 7-13635
 Cr-MoVW ferritic steel, ductile-brittle transition temp., irradi. flux depend. 7-56825
 creep, high-temp., rel. between dislocation density and internal stress 7-13524
 dilute, with 3d impurities, X-ray absorpt. edges (*German*) 7-46241
 dilute alloys, electron irradi., positron lifetime meas. 7-39250
 dilute alloys with 3d elements, electronic struct., K-edge XAS study 7-64066
 $(Fe_{1-x}Ni_x)_{92}C_8$ pseudobinary FCC alloys, magnetic phase diagram studies 7-2844
 Fe-D formed by D ion implantation, multiple D occupancy of vacancies 7-63643
 Fe-Ni-B metallic glasses, struct. and crystn. kinetics, DSC and X-ray diff. meas. 7-16436
 Fe-Si multilayered thin films, stacking structs., magnetostatic coupling and layer boundary interdiffusion 7-7574
 FeB, amorphous alloy, metallic glass ribbon, thermal diffusivity, photoacoustic study 7-45262
 FeCrAlloy, interaction with $Na_2O \cdot 2SiO_2$ glass 7-3501
 first wall candidate alloys, HFIR irradi. microstruct. development 7-56824
 first wall candidate ferrite alloys, Ni doped, postirrad. tensile behaviour 7-56827
 friction and wear characteristics of asbopolymer material 7-28153
 graphite fibre reinforced Al-Mg-Fe, unidirectional and angle-ply, strength and fracture anal. 7-59605
 Hastelloy B-2 and G-3, polarization effects in galvanic corrosion 7-39706
 Hastelloy X, H_2 permeation in high temp. alloys, oxide layer effects (*German*) 7-30568
 Hastelloy X, thermomech. response, viscoplastic constitutive model 7-8059
 HT-9 martensitic steel, radiation induced segregation 7-56830
 HTR alloys, carburisation behaviour 7-10234
 Incoloy 800 H, oxidation, EMPA profiles in depletion zone 7-17727
 Incoloy 800 H, permeability of 3H and H in heat exchanger tubes (*German*) 7-56759
 Incoloy 800H, corrosion protection by plasma assisted vapour deposited and laser fused silica coatings 7-28208
 Incoloy 800H, multilayer oxide scales in gas atmosphere, Ti distribution 7-53972
 Incoloy 904, precipitate size, magnetoacoustic and Barkhausen emission study 7-45749
 Inconel 600, corrosion resist., effects of BF_4^+ ion implementation 7-39734
 Inconel 600, H permeation studies for fusion reaction 7-5435
 Inconel 600, recovery kinetics, X-ray determ. 7-22722
 Inconel 600 and 690, SCC under high temp. NaOH, comp. and annealing effect 7-39710
 Inconel 600 in direct absorption received, optical props. at high temp. 7-40042
 Inconel 718, Ni-base superalloy, creep deform., back stress determ. 7-46564
 Inconel X-750, air environment/creep interactions, prior exposure times effect 7-13499
 Inconel X-750, Ni-base superalloy, SCC susceptibility in high-temp. water, effect of chloride 7-39729
 laminated composite with unique microstruct., development by C diffusion control 7-17501
 magnetic texture and inhomogeneity, muon polarisation and spin relax. rate meas. 7-45895
 martensitic transformations, effect of stresses and mag. fields 7-53731
 misch metal-Fe-B melt-spun magnets, mag. and structural props. 7-53032
 Nimonic 86, carburised, heat treatment, creep behaviour rel. to carbide precip. (*Korean*) 7-46560

iron alloys continued

- Nimonic PE 16, Ni-base superalloy, duplex γ' particle hardening 7-28053
 oxidation studies using EELS and EDX in the TEM 7-17734
 $Pd(Fe,Co,Ni)_{0.05-0.15}Si_{0.17}$ metallic glasses, crystallization kinetics, elec. resist. obs. (*Chinese*) 7-11919
 rare earth alloys, $R_2(Fe,Al,Co)_{14}B$, mag. props., composition depend. 7-53030
 rare earth alloys, $R_2Fe_{14}B$, $R=La-Nd, Sm, Gd-Tm, Lu$ and Y , ^{57}Fe Mossbauer spectra 7-64551
 rare earth alloys, R-Co-Fe system between 2:17 and 2:7 phase regions, phase equilibria, metallography, X-ray diff., thermomagnetic anal. 7-17511
 rare earth-iron-boron permanent magnet materials, prep. and props., book contrib. 7-27981
 spin wave excitations and magnetisation temp. depend. 7-45642
 steel, $X8CrNiTi18.10$, corrosion product layers in PWRs at pH 7 (*German*) 7-19356
 Super Invar- $Ta_{16}W_{18}O_{94}$ composite, thermal expansion coeff. 7-12331
 surfaces and overlayers, mag. and electronic props. 7-58985
 two-component liq. alloys, density of electron states, calc. (*Russian*) 7-45110
 Al-Fe, ion induced metastable phases 7-63673
 Al-Fe, quasicrystals, diffraction pattern simulations 7-6585
 Al-Fe, rapidly cooled, $Al_{13}Fe_4$ tenfold twins, TEM obs. 7-63631
 Al-Fe amorphous films, quasicrystalline transformation by ion irradiation 7-2071
 Al-Fe system, phase diagram, DTA obs. 7-39485
 Al-Fe-Ce, quasicrystalline decagonal phase, TEM 7-46492
 Al-Fe-Ce-La-Nd-Rr alloys rapidly quenched, positron annihilation studies 7-46184
 Al-Fe-Mg, solidified from liq. phase, struct. (*Russian*) 7-39498
 Al-Fe-Mn icosahedral alloys, elec. resist. and Hall coeff. studies 7-27316
 Al-Fe-Mn powder, rapidly solidified, microstruct. 7-46445
 Al-Fe-R, $R=Ce, Er, Nd$ or Gd , rapidly solidified microstruct. 7-59502
 Al-Fe-Si, 1060 alloy, corrosion in p-quinone and acetic acid 7-28170
 Al-Fe-Si, dil., solidification, intermetallic cpd. form. 7-13442
 Al-Fe-Si, quasicrystalline phases and amorphous structure 7-51637
 Al-Fe-Si, TEM geometric projection of crystal struct. 7-16501
 Al-Fe-Si system, intermetallic phases, electron probe microanalysis, X-ray diff. 7-59491
 Al-Fe-Si-TiO₂, dispersion hardened, strength props., effect of matrix particle size and oxide vol. fraction 7-17544
 Al-Fe-V rapidly solidified sheets, mech. props., hot rolling effects 7-22838
 Al-Fe-Zr, Al-Mn-Fe and Al-Fe-Mischmetal, wear, comparative investigations. and prep. method role 7-13605
 Al-Ge-Fe and Al-Si-Fe, amorphous ductile, with two separate phases 7-59493
 Al-Mn-Fe alloy, aging characteristics, pre-cold working effects 7-53758
 Al-Ni-Fe(Co) powders, cold sintering 7-64972
 Al-Si-Fe, RR 58, electrolasg refined, creep 7-39582
 Al-Si-Mn-Fe, intermetallic phases, TEM obs., extraction replica technique 7-39807
 Al-Zn-Mg-Zr-Fe, superplasticity rel. to grain refining addition elements 7-46561
 $Al_{13}Fe$ tenfold twins in rapidly cooled Al-Fe alloy, TEM obs. 7-63631
 $Al_6Mn_{1-x}Fe_x$, rapidly quenched, crystn. process, high temp. X-ray studies 7-1922
 $Al_{86}Mn_7Fe_7$, $Al_{86}Mn_{14}$, icosahedral alloys, obs. of mirror-related grains 7-37867
 $AlNiFe_{0.5}$, reactor fuel cladding, corrosion resistance, rupture strength, neutron irradiation effects testing 7-59670
 Au-Fe, dil., Kondo system, mag. scatt. time of conduction electrons meas. 7-21902
 Au-Fe, mag. hyperfine field, temp. and composition depend. 7-45243
 Au-Fe (10 to 35 at.%), early stage clustering struct. 7-59536
 AuFe re-entrant spin glass, magnetoelastic. and AC susceptibility studies 7-7518
 $Ba_2CaCuFe_2F_{14}$, heteronuclear trimers with ferrimag. behavior (*French*) 7-64448
 C diffusion in compound welds having intermediate layer 7-44887
 Ce ($Fe_{1-x}Al_x$)₂, Fe-rich intermetallics, mag. and elec. props. 7-45621
 Ce-(Fe,Co)-(B,Si) system alloys, melt spun ribbons, mag. props. (*Japanese*) 7-53052
 Ce-Fe-Si system, electron struct. of ternary intermetallic cpds. (*Russian*) 7-38525
 Ce(Co,Cu,Fe)₆, magnetically hard, heat treatment effects on struct. and mag. characts. 7-27564
 $Ce_2Fe_{14}B$, anisotropy constants, temp. depend. (*Chinese*) 7-59003
 $CeNi_{1-x}Fe_x$, mag. and cryst. props., effect of H absorpt. 7-33168
 Co-Al-Fe, B2, slow plastic flow props. between 1100 and 1400 K 7-46565
 Co-Au-Fe, dil., local structural and mag. environments of Fe 7-26965
 Co-based amorphous alloys, anisotropic electrical magnetoresistivity at 295 K 7-58796
 Co-Cr-Fe sputtered films, dilute, Mossbauer effect 7-22167
 Co-Fe-B amorphous powders, flame-spray quenching process for continuous prod. 7-53679
 Co-Fe-Ni-V alloys, Invar props. and mag. field distrib. (*Russian*) 7-45733
 Co-Fe-V-Si-B metallic glass, Co-rich, temp. and annealing dependences of magnetostriction const. 7-33255
 Co-Ni-Fe underlayer for double-layer perpendicular media, vacuum deposition and mag. props. 7-27577
 $Co_{0.92}Fe_{0.08}$, FCC, Fermi surface, de Haas-van Alphen studies 7-52406
 $Co_{74}Fe_6B_{20}$ amorphous sputtered thin films, magnetic anisotropy origins 7-27583
 CoFeCr sputtered films, struct. and mag. props. 7-27175
 $Co_{69}Fe_{45}Cr_7Si_{22}B_{22}$ metallic glasses, long-time tunnelling heat relaxation meas. 7-38223
 CoFeMoB amorphous thin films, prep. and high-freq. impedance studies 7-53585
 $(Co_{0.85}Fe_{0.06}Ni_{0.08}Nb_{0.01})_{75}Si_{10}B_{15}$ amorphous alloys, structural relax. and crystn., positron annihilation studies 7-37869
 $Co_{57}Fe_{10}Ni_{11}B_{17}$, metallic glasses, superplastic deform. (*Russian*) 7-39599
 $Co_{58}Fe_{10}Ni_{10}Si_{11}B_{16}$, metallic glasses, multiplet splitting, XPS study 7-27858
 $Co_{68}Fe_7Ni_{13}Si_7B_5$, amorphous alloy, superplasticity 7-3368

iron alloys continued

- CoFeSiB inhomogeneous magnetic alloys, anomalous Hall effect—magnetic polarisation correl. 7-7208
 (Co_{0.95}Fe_{0.05})₇₅Si₁₅B₁₀ amorphous alloy, mag. saturation 7-45632
 Co₇₀Fe₄Si₁₅B₁₀, amorphous alloy, mag. props. rel. to mag. coating 7-22123
 Co₇₁Fe₂₈Si₁₅B₁₀ amorphous alloys, mag. props., stress and annealing depend. 7-33250
 Co₈₅Fe₅Si₈B₂ amorphous alloys, annealing, positron annihilation parameters anal. 7-39303
 Co₈₅Fe₅Si_{7.5}Ge_{1.5}B_{2.5}, amorphous alloy, struct. changes after γ -irrad. (Russian) 7-58336
 Co₅₈Ni₁₀Fe₃B₁₆Si₁₁, metallic glass, reversible struct. transformation 7-1907
 Co₅₈Ni₁₀Fe₃B₁₆Si₁₁ amorphous ferromag. alloy struct., shock loading effects, mag. struct. anal. 7-2100
 Co₅₈Ni₁₀Fe₃B₁₆Si₁₁ amorphous ferromagnet, prep. and struct. 7-22605
 Cr-Fe (28.5 at.%) superparamag. particles formed during solid soln. decomp., mag., transitions (Russian) 7-33220
 CrMoV ferritic steels, He containing, fatigue behaviour in fusion reactor 7-56828
 Cu (111)-Fe crystal, CO adsorption 7-21616
 Cu (111)-Fe surface alloys, prep. and oxidation 7-22870
 Cu-Al-Fe, Al bronze, superplasticity, effect of Fe content 7-65109
 Cu-Al-Fe, stacking fault energy determ. (Russian) 7-12082
 Cu-Al-Fe-Mn (Ni) bronzes, microstruct., corrosion 7-39697
 Cu-Al-Ni-Fe bronze, laser glazing, microstruct. 7-52197
 Cu-Al-Ni-Fe-Mn bronze, cast, laser surfacing, improved corrosion resist., microstruct. characteris. 7-13651
 Cu-Fe, diffusion of Fe studied by Mossbauer spectroscopy 7-2252
 Cu-Fe, dil., local structural and mag. environments of Fe 7-26965
 Cu-Fe, implanted solid solns., Mossbauer study on thermal dynamics of Fe atoms 7-45855
 Cu-Fe, thermomech. treatment, softening rel. to disperse α -Fe particle, size and orientation 7-28054
 Cu-Fe (0.6 to 2.2 at.%) solid solns., decomp. processes, effect of O₂ (Russian) 7-33681
 Cu-Fe alloy, BCC and FCC Fe particles, field ion microscopy studies 7-33667
 Cu-Fe alloys, electronic structure and impurity states, optical investigations (Russian) 7-32943
 Cu-Fe host-impurity system, O ion bombarded, internal oxidation, Mossbauer spectra studies 7-59131
 Cu-Fe system, diffusion of positive muons, detection by zero-field muon spin resonance 7-45862
 Cu-Fe-Al, cold rolled, γ to α transform. of fine α -Fe precipitates, mag. props. 7-3300
 Cu-Fe-Al alloys, thermoelec. power temp. depend. (Russian) 7-12706
 Cu-Fe-Mg-Ni-Al alloy, stress relaxation in tension and creep in torsion 7-44667
 Cu-Ni-Fe, alloy decomposition and periodic struct. coarsening 7-53735
 Cu-Ni-Fe, irrad., stability of periodic decomp. struct. 7-58366
 Cu-Ni-Fe, specific heat capacities (German) 7-2228
 Cu-Ni-Fe-Mn, physical props. rel. to precip. and thermal treatment (German) 7-12698
 CuFe alloys, anomalous Hall effect 7-52577
 CuFe dilute alloys, electron struct., X-ray $L\alpha$ emission spectra studies 7-12598
 CuFe-NiCr thermocouple, mag. field effects (Chinese) 7-24646
 Cu_{100-x}Fe_x alloys rapidly quenched, spin glass state 7-12979
 Cu₈₈Fe₂, antiferromagnetic interactions, EXAFS and XANES anal. of Fe atom environment and clustering 7-64808
 CuNiFe, electron irrad., decomposition kinetics and morphology 7-58491
 Dy_{0.73}Tb_{0.27}Fe₂ alloys, magnetomechanical coupling 7-45788
 Dy-Fe-Re, intermetallic-based solid solns., phase equilib. and mag. props. 7-22639
 DyFe alloys, amorphous thin films, thermomag. recording, magnetisation reversal, coercivity 7-64459
 DyFe amorphous alloys, local mag. anisotropy energy estimation 7-7503
 Er₂(Fe,Co)₁₄B, struct., composition depend. 7-51701
 Er₂(Fe,Mn)₁₄B, struct., composition depend. 7-51701
 Er_{0.135}Fe_{0.815}B_{0.052} melt spun ribbons, mag. and struct. props. 7-59059
 Er₂Fe₁₄B alloys, magnetic anisotropy and spin reorientations 7-38855
 EuCo_{2-x}Fe₂Si₂, Eu valency 7-58787
 Fe-Cr coatings for gun bores, morphology and erosive wear 7-46697
 (Fe,Co,Ni)-P layers, electrochemical deposition, struct. (Chinese) 7-7037
 Fe base alloys, rapid solidification technology 7-39493
 Fe based eutectic alloy powder, plasma coatings with interstitial phases, tribotechnical props. 7-17731
 Fe/FeZn₁₃/Fe-Si composite diffusion couples, effect of Si on stability and growth of Fe-Zn phases 7-54011
 Fe/Ni Reed blades, Au coated, AES/SEM study 7-44972
 Fe-9Cr ferritic steel, 40 keV Cu⁺, Fe⁺ and fission neutron irrad. effects. 7-56823
 Fe-Ag sputtered films, thermal stability, X-ray diffr. and Mossbauer studies 7-58679
 Fe-Al, ²⁶Al diffusion, radioactive isotope meas. (Russian) 7-32700
 Fe-Al, alloying for oxidation resist. improvement, comparison between ion implantation and laser irrad. 7-22883
 Fe-Al, atomic radial distrib. function, close order sorting parameter (Russian) 7-58206
 Fe-Al, B2-ordered alloys, dislocation energies and mobilities 7-58283
 Fe-Al, disordered, phonon dispersion curves 7-2124
 Fe-Al, thin foil, interfacial migration, velocity-driving force relations 7-46411
 Fe-Al (40 at.%), electron irrad., Huang scatt. from interstitials 7-58272
 Fe-Al cold-rolled nonbrittle powder strip prep., texture and mag. props. 7-46370
 Fe-Al disordered alloys, electronic struct., mag. props. and Mossbauer spectra 7-64073
 Fe-Al disordered alloys, mag. props., site-diluted Ising model calcs. 7-2873
 Fe-Al metastable alloy sputtered film, mag. props., comp. depend., X-ray diffr. and Mossbauer meas. 7-7559
 Fe-Al quasicrystalline alloys, isomorphism, neutron diffr. meas. 7-51638
 Fe-Al-C (3.8, 1.8 wt.%), martensite crystallostruct. changes, effect of temp. and heating/cooling rates (Russian) 7-53727
 Fe-Al-Co ordering alloys, phase separations 7-33634
 Fe-Al-Mn, austenitic, SCC in NaCl soln. 7-8195
 Fe-Al-Mn, fatigue crack growth 7-65130

iron alloys continued

- Fe-Al-N, nitriding, surface layer struct., Mossbauer spectra (Russian) 7-59672
 Fe-Al-Si, Sendust, magnetocrystalline anisotropy 7-33165
 Fe-Al-Si system, electronic struct. interatomic bonding, X-ray emission spectra analysis (Russian) 7-39320
 Fe-Au, solute segregation, grain boundary structural transform. 7-22687
 Fe-Au system, low Au conc., low temp. nucl. orientation and NMR-ON studies 7-2936
 Fe-Au(Sb)(Cu), dilute alloys, electron irradiated, vacancy-solute interaction, positron lifetime, muon spin rotation studies 7-39288
 Fe-B, amorphous, structural characterisation by laboratory EXAFS spectrometer 7-1911
 Fe-B, amorphous alloys, crystallisation, morphology rel. to sample thickness (Russian) 7-37861
 Fe-B, amorphous metallic films, SAX investig. (Russian) 7-51576
 Fe-B, atomic radial distrib. function, close order sorting parameter (Russian) 7-58206
 Fe-B, B solubility in Fe 7-7971
 Fe-B, metallic glasses, photoemission investig. (Slovak) 7-59369
 Fe-B (15 at.%), amorphous powder and strip, struct., mag. props., thermal stability (Russian) 7-63470
 Fe-B alloys, metastable crystalline, Mossbauer study of local atomic environments 7-17252
 Fe-B amorphous sandwich films, concentration-dependent diffusion 7-45027
 Fe-B based metallic glasses, corrosion in H₂SO₄, alloying effect 7-28201
 Fe-B based metallic glasses, embrittlement, formation of B-rich zones 7-59598
 Fe-B liq. and amorphous alloys, interference functions, X-ray diffr. study and cluster calcs. 7-26656
 Fe-B metallic glasses, atomic radial distrib. functions, ultradispersed eutectic structural model 7-11923
 Fe-B metallic glasses, imperfection struct., positron annihilation studies 7-37885
 Fe-B metallic glasses, struct. relax., Curie temp. meas. 7-21124
 Fe-B rapidly quenched cryst. alloys, local atomic environments, spin echo NMR studies 7-7606
 Fe-B-Ce-based metallic glasses, mag. domain structs. and annealing embrittlement 7-27586
 Fe-B-Si and Fe-B-Si-Cr-Mo-W, finely cryst. and amorphous structs. on surface by laser treatment 7-8175
 Fe-B-based amorphous alloys, struct. evolution during heating (Russian) 7-16418
 Fe-base alloys, grain boundary internal adsorption of C and P, segregation study (Russian) 7-6961
 Fe-base alloys, interstitial impurity-dislocation binding energy (Russian) 7-58310
 Fe-base alloys, N and H solubility, equivalent influence of alloying elements 7-59495
 Fe-based, Co-free alloys for valve hard facings in nuclear plants, 1985 progress 7-49551
 Fe-based amorphous alloys, secondary ion emission during heating (Russian) 7-51656
 Fe-based metallic glasses, secondary ion emission and sputtering 7-3137
 Fe-based metallic glasses, magnetic aftereffect and magnetostriction studies 7-27571
 Fe-based thin films, saturation magnetisation and coercive force 7-59074
 Fe-Bi, ion implanted, high substitutional fractions 7-58299
 Fe-C, ferrite and cementite refl., polishing conditions effect (German, English) 7-22938
 Fe-C, ferrite nucleation at austenite grain edges, kinetics 7-7991
 Fe-C, friction, solid struct. calcs. 7-51932
 Fe-C, solidification in mag. fields (Russian) 7-59508
 Fe-C austenite, binary, C diffusivity, revised expression 7-38238
 Fe-C base ternary and multicomponent alloys, eutectic temp. and comp., theoretical calc. 7-59504
 Fe-C hypoeutectic melt struct., temp. and holding time depend., X-ray studies (Russian) 7-16396
 Fe-C martensite, struct. in transition state from first to third stage of tempering, electron microscopy and diffr. study 7-46528
 Fe-C system, elastic anal. of deform near spherical C particle embedded in Fe matrix 7-63709
 Fe-C system, phase diagrams, thermodynamic modelling, direct use of chem. pot. function 7-7970
 Fe-C-H system, H charged, methane bubble form., positron studies 7-37967
 Fe-C-Mn(Ni)(Co)(Si), ferrite nucleation at austenite grain edges, kinetics 7-7991
 Fe-C-Mn(Ni)(Co)(Si)(Mo), nucleation of proeutectoid ferrite at austenite grain boundaries 7-8003
 Fe-C-N, ion implanted, C surface contamination, AES and XPS studies 7-38312
 Fe-C-based alloys, high C, rapidly solidified, mech. props. 7-22673
 Fe-Ce amorphous alloys, mag. props. and elec. resist. 7-59010
 Fe-Ce(Pr) liquid alloys, variable valency investig. 7-7192
 Fe-cementite alloy castings, Young's modulus and thermal expansion 7-65068
 Fe-Co, liq., thermodynamic mixing functions, Knudsen cell mass spectrometry (German) 7-21470
 Fe-Co, thermal equilibrium vacancies, muon spin resonance studies 7-51757
 Fe-Co alloys, powder and thin film samples, nuclear spin-lattice relax. studies 7-38955
 Fe-Co alloys, powder metallurgy produced, mag. props. 7-33211
 Fe-Co dil. alloy, ^{56,57,60}Co isotopes, hyperfine anomalies, α -factors NMR/ON obs. 7-33278
 Fe-Co-As mixtures, phase diagram isothermal sections, binding 7-46418
 Fe-Co-B films, phase transition, microstruct. 7-33568
 Fe-Co-B powders, amorphous mag. state, Mossbauer spectra study 7-45846
 Fe-Co-Cr-Mo alloys, electronic struct. and mag. props., X-ray spectra studies (Russian) 7-32902
 Fe-Co-Mn(V) films, ion beam sputtered, soft mag. props. 7-33237
 Fe-Co-Mo alloys, liq., H solubility meas. and estimates (German) 7-58487
 Fe-Co-Ni amorphous alloys, anisotropic magnetoresist. studies 7-58793
 Fe-Co-Ni based alloys, crystalline and amorphous, magnetoresistance 7-38538
 Fe-Co-Ni cryst. alloys, anisotropic magnetoresist. studies 7-58794

iron alloys continued

- Fe-Co-Ni powder, fine, corrosion resist. and mag. prop. changes, surface-active agent use in prep. 7-54001
 Fe-Co-Ni-Al-Cu metallic alloy ordering and spinodal decomposition, atom probe FIM study 7-33676
 Fe-Co-Ni-Ti (34.9, 20.0, 10.2 wt.%), thermoclastic martensite transformation 7-52032
 Fe-Co-Si-B glass, liq.-quenched, cooling condition depend. of saturated mag. flux density 7-58991
 Fe-Co-V, atomic ordering mechanism, neutron diffr. study (*Russian*) 7-46459
 Fe-Co-V, ordered alloy, plastic deform., antiphase boundaries (*Russian*) 7-39596
 Fe-Co-based ternary alloys, atomic and mag. moment mutual ordering (*Russian*) 7-33169
 Fe-Co(V) alloys 7-51708
 Fe-Cr, high temp. oxidation, effect of various amounts of Ce and CeO₂ 7-53945
 Fe-Cr, high-temp. air corrosion products, distrib. and charactn. by Raman microscopy 7-65205
 Fe-Cr, intergranular corrosion, inhibition mechanism of S-containing additives 7-53946
 Fe-Cr, liquid alloy, N activity coeff., soln. model for nonmetallic solutes 7-65043
 Fe-Cr, neutron irradiated, defect clusters, positron annihilation lifetime meas. 7-51853
 Fe-Cr, oxide film form., FTIR reflectance spectroscopy characteris. 7-46043
 Fe-Cr, P implanted amorphous alloys, corrosion, passivation, microstruct. 7-65180
 Fe-Cr, passive anodic oxide form., surface anal., XPS, ion scatt. spectra 7-22895
 Fe-Cr, passive current fluctuations, statistical anal. 7-28190
 Fe-Cr, thin oxide film form., XPS study 7-22898
 Fe-Cr (12 at.%), ferritic alloy, He⁺ implantation and Fe⁺ irradi., bubble nucleation and growth 7-58362
 Fe-Cr (3 wt.%), oxidation behaviour 7-17716
 Fe-Cr alloy films, oxide film form. by aqueous corrosion, EXAFS study 7-64007
 Fe-Cr alloys, H diffusion and trapping 7-27018
 Fe-Cr alloys in acidic electrolytes, effects of P implantation on passivity 7-59658
 Fe-Cr coating, ion plating on steel, deposition conditions effect on coating struct. 7-39748
 Fe-Cr surface oxide scales, XANES 7-65193
 Fe-Cr system, thermodynamic charactn., mass spectrometry 7-53736
 Fe-Cr-Al, C solubility, influence of Ti and Nb, high-temp. oxidation resist. 7-22876
 Fe-Cr-Al alloys, Al₂O₃ scale growth 7-65214
 Fe-Cr-Al-Ce, microstruct., high temp. corrosion rel. to Ce additions 7-13648
 Fe-Cr-B, amorphous, Cr redistribution between phases during crystallisation, Mossbauer spectroscopy 7-21100
 Fe-Cr-B metallic glasses, imperfection struct., positron annihilation studies 7-37885
 Fe-Cr-B-Si, amorphous, annealing effects on Curie temp. 7-45675
 Fe-Cr-C, martensite nucleation, dislocations, grain boundaries, plastic accommodation 7-28040
 Fe-Cr-C steels, martensite and bainite transforms. (*Russian*) 7-13448
 Fe-Cr-C system, phase diagrams, thermodynamic modelling, direct use of chem. pot. function 7-7970
 Fe-Cr-C-B hard surfacing weld deposits, abrasive wear resist. and microstruct. 7-22847
 Fe-Cr-Co permanent magnetic alloys, casting 7-53051
 Fe-Cr-Co solid soln., uniaxial tensile stress in spinodal decomp. effect on coercive force, thermomag. treatment effects 7-7555
 Fe-Cr-Co-Mo alloy struct., 2D scatt. X-ray intensity distrib. patterns, anal. by direct variation method 7-64734
 Fe-Cr-Co-Mo permanent magnet ribbons, mag. props., influence of modulated structure 7-53043
 Fe-Cr-Co-Si-Ti, permanent mag. alloy, ductile, effect of heat treatment on mag. props. (*Korean*) 7-8137
 Fe-Cr-Co(Si), permanent magnet alloys, microstruct., mag. props., Si content effect 7-22117
 Fe-Cr-Mn, mag. susceptibility and elec. resist. (*Russian*) 7-52952
 Fe-Cr-Mn-C, laser clad, microstruct. and wear props. 7-13652
 Fe-Cr-Mn-Ni-C system, phase relationships at solidification temps. 7-28014
 Fe-Cr-Mo, oxidation, boric acid coatings effect 7-65197
 Fe-Cr-Mo, surface segregation, Auger anal. 7-16844
 Fe-Cr-Mo (9.1 wt.%), initiation of breakaway oxidation in high press. CO₂ atm. 7-33845
 Fe-Cr-Mo system, phase boundaries of intermetallic compounds (*Japanese*) 7-53697
 Fe-Cr-Mo-Mn-C-P, sintered, ageing and steam oxidation, effect of P 7-7930
 Fe-Cr-Mo-Zr amorphous alloys, corrosion resistance (*Japanese*) 7-65194
 Fe-Cr-Ni, austenitic, electron irradi., conversion of stacking fault tetrahedra to voids 7-58342
 Fe-Cr-Ni, Ferralium 255, polarization effects in galvanic corrosion 7-39706
 Fe-Cr-Ni, hardening at low temp. (*Russian*) 7-39554
 Fe-Cr-Ni, intergranular corrosion, inhibition mechanism of S-containing additives 7-53946
 Fe-Cr-Ni, low temp. mag. susceptibility and mag. transitions (*Russian*) 7-45628
 Fe-Cr-Ni alloys, FCC, dilation by interstitial C and N 7-44451
 Fe-Cr-Ni alloys, local ordering, neutron irradi. effects, elec. resist. meas. 7-2070
 Fe-Cr-Ni-Al-Si-Mn, oxidation from 700 to 1000°C 7-65207
 Fe-Cr-Ni-C system, phase relationships at solidification temps. 7-7969
 Fe-Cr-Re system, interaction of intermediate phases, phase equilibria 7-17514
 Fe-Cr-Si-B metallic glass wires, corrosion rel. to crystallinity and comp. 7-46701
 Fe-Cr(Al), high temp. corrosion in sulphidising/oxidising environments, review 7-39737
 Fe-Cu, neutron irradi., defect microstruct., SANS and TEM studies 7-58351
 Fe-Cu, pore form. during sintering, effect on mech. props. 7-64970
 Fe-Cu, sintering, form. of Cu pockets in Fe grains 7-7922

iron alloys continued

- Fe-Cu alloy, neutron irradiation, magnetoacoustic and Barkhausen emission study 7-45749
 Fe-Cu alloys, phase transformations, SANS studies 7-53747
 Fe-Cu evaporated film, composition distrib. and mag. props., Mossbauer meas. 7-7561
 Fe-Cu films, obliquely evaporated, inhomogeneous conc. distrib. 7-38367
 Fe-Cu metastable alloy sputtered films, mag. props., X-ray diffr. and Mossbauer meas. 7-7560
 Fe-Cu powder, contact form. during liq. phase sintering 7-7925
 Fe-Cu sputtered films, thermal stability, X-ray diffr. and Mossbauer studies 7-58679
 Fe-Cu-Ag amorphous alloys produced by vapor quenching 7-7849
 Fe-Cu-C, C activity, effect of Cu 7-13432
 Fe-Cu-Ni, FCC ternary alloys, mag. props. 7-22852
 Fe-Cu-P, sintered, ageing and steam oxidation, effect of P 7-7930
 Fe-Dy-C high coercivity permanent magnet materials 7-2903
 Fe-Ge amorphous and cryst. layers, short range order and valence bands 7-13266
 Fe-graphite compacts, sintering, alloying, mech. props. 7-39455
 Fe-H system, electron and neutron irradi., positron lifetime meas. 7-44603
 Fe-La amorphous alloys, high-field susceptibility and Curie temp. 7-58989
 Fe-M-B metallic glasses (M=Ti,V,Cr,Mn,Co,Ni,Cu,Pd,C,Si,Ge,Sn), formation kinetics, thermal stability 7-58474
 Fe-Mn, alloying with N under high press. 7-3266
 Fe-Mn, FCC alloys, H-induced martensitic transform. (*Japanese*) 7-33655
 Fe-Mn, friction, solid struct. calcs. 7-51932
 Fe-Mn, kinetics of α -phase form. and role in shape memory effect (*Russian*) 7-46581
 Fe-Mn, p/m type, martensitic transform. and struct. form. mechanisms 7-33658
 Fe-Mn-Al, mag. props., struct. and deform. texture 7-2892
 Fe-Mn-Al, plasma nitriding, sputtering and redeposition of cathode material 7-39752
 Fe-Mn-Al, processing and props., effect of Si and C additions 7-17707
 Fe-Mn-Al-Cr system, rel. between γ - α transform. temp. and comp. of metastable austenite region (*Chinese*) 7-7993
 Fe-Mn-C, FCC, energy of complex packing defects, calc. (*Russian*) 7-58263
 Fe-Mn-C, local instability in FCC struct. (*Russian*) 7-58208
 Fe-Mn-C critical nucleus comp. of ferrite 7-7967
 Fe-Mn-Ni system, melting diagram 7-3278
 Fe-Mo (14.5 wt.%), ageing, discontinuous dislocational transform., coercivity obs. 7-3305
 Fe-Mo-N, nitriding, surface layer struct., Mossbauer spectra (*Russian*) 7-59672
 Fe-N alloys, phase state and precipitation, plastic deformation effects (*Russian*) 7-46551
 Fe-N martensite, transform. kinetics, anal. by nonisothermal dilatometry 7-8004
 Fe-N system, phase diagram, thermodynamic calc. 7-7973
 Fe-Nb-C system, austenite-nonstoichiometric precip. equilib. 7-3303
 Fe-Nd-B magnets, microstructure and mag. props. 7-53049
 Fe-Nd-B permanent magnets, prep. by liquid dynamic compaction 7-53661
 Fe-Nd-B system, phase relations 7-46422
 Fe-Nd-B-Al sintered magnets, TEM studies 7-51999
 Fe-Ni, austenite form. during continuous heating (*Russian*) 7-17557
 Fe-Ni, austenitic, Mag. ordering and mech. props. (*Russian*) 7-58280
 Fe-Ni, austenitic crystals, nitrided, phase comp. of diffusion layers (*Russian*) 7-63922
 Fe-Ni, creep in vacuum and air, relationships governing deform. and failure 7-28097
 Fe-Ni, electron irradi., low temp. phase transitions (*Russian*) 7-51832
 Fe-Ni, hyperfine mag. fields, temp. dependence 7-12683
 Fe-Ni, intergranular corrosion, inhibition mechanism of S-containing additives 7-53946
 Fe-Ni, liquid alloy, N activity coeff., soln. model for nonmetallic solutes 7-65043
 Fe-Ni, martensitic transform., defect form., positron annihilation study (*Chinese*) 7-39213
 Fe-Ni, thin oxide film form., XPS study 7-22898
 Fe-Ni alloy, mag. remanence at low-temperature 7-24088
 Fe-Ni alloy, X-ray fluoresc. determ. using NRLXRF programme 7-59800
 Fe-Ni alloy surfaces, sputter-cleaned, work function and dipole barrier 7-38673
 Fe-Ni alloys, diffusion, plastic deformation effects (*Russian*) 7-58531
 Fe-Ni alloys, martensitic transform., positron annihilation study of defects 7-39266
 Fe-Ni austenitic alloys, martensitic transformations, grain size effects (*Russian*) 7-46465
 Fe-Ni based metallic glasses, quenched in excess vol. and structural relax. 7-6531
 Fe-Ni conc. determ. by electron probe microanal. in energy dispersive system, ZAF factor approx. 7-28369
 Fe-Ni evaporated films for a back layer of perpendicular mag. recording media, prep. 7-27908
 Fe-Ni FCC alloys, low temp. phase equilib., mag. effects 7-26914
 Fe-Ni films, γ -phase low temp. precipitation investig. (*Russian*) 7-33666
 Fe-Ni glassy alloys magnetostriction values from stress depend. of Young's modulus 7-33251
 Fe-Ni martensite crystals, positions, external stress effects (*Russian*) 7-46409
 Fe-Ni soft magnetic film single-pole readout head, induced RF permeability variation 7-53072
 Fe-Ni system, liq. phase equilib., above 1200K, mag. contrib., thermodynamic analysis 7-7966
 Fe-Ni system, phase equilibria, mag. contrib. to thermodynamic functions, below 1200K 7-7965
 Fe-Ni thin films, α to γ transform, redistrib. of atoms in submicrostruct. (*Russian*) 7-53722
 Fe-Ni-Al, sintered, ageing, precip. strengthening, tensile strength 7-39536
 Fe-Ni-Al-C (22, 8, 2.4 wt.%), rapidly quenched, metastable modulated struct., analytical STEM study 7-46450
 Fe-Ni-Al-Co system, miscibility gap, phase decomp. in Alnico mag. alloys 7-17537

iron alloys continued

- Fe-Ni-B, amorphous, shock loading, inclusions dissolving, domain struct. (Russian) 7-63487
- Fe-Ni-B metallic glasses, crystallisation, microhardness (Russian) 7-59617
- Fe-Ni-B system, distrib. equil. in two-phase fields 7-22641
- Fe-Ni-C alloys, martensitic transform., effect of soln. strengthening of austenite 7-53728
- Fe-Ni-C and Fe-C, bainite reaction kinetics, austenitising temp. effect 7-13453
- Fe-Ni-Co alloy, H damage, lattice distortion, defect and crack generation, positron lifetime study 7-39675
- Fe-Ni-Cr, high-purity, irradi., void swelling and nucl.-induced phase transforms. 7-58340
- Fe-Ni-Cr, oxidation, TEM study, nonprotective oxide growth 7-8180
- Fe-Ni-Cr, oxidation study, protective oxide growth 7-8179
- Fe-Ni-Cr, reactor bolting material A-286, failure analysis 7-30536
- Fe-Ni-Cr, structural materials, swelling after neutron and ion irradi., comparison 7-58357
- Fe-Ni-Cr (25.15 wt.%), MC stabilized, fatigue life, effects of implanted He 7-53852
- Fe-Ni-Cr alloys, internal carburisation, effect of S 7-33839
- Fe-Ni-Cr-Mo-Ti-C, JPCA, He injected and creep ruptured, microstruct. obs. 7-53853
- Fe-Ni-Cr-P, ion irradi., swelling suppression, effect of P modification 7-58358
- Fe-Ni-Cr-Ti-B, constant elastic alloy, torsion reson. freq. temp. coeff. rel. to B content (Chinese) 7-13488
- Fe-Ni-Nb, martensitic transform. and shape memory effect (Russian) 7-46470
- Fe-Ni-Nb alloys, shape memory effect, effect of phase hardening (Russian) 7-53809
- Fe-Ni-P-B amorphous powders, flame-spray quenching process for continuous prod. 7-53679
- Fe-Ni-P-C, amorphisation under action of high press. and shear deform. (Russian) 7-58163
- Fe-Ni-Sb, grain boundary segregation of Ni and Sb 7-22689
- Fe-Ni-Si-B glass, liq.-quenched, cooling condition depend. of saturated mag. flux density 7-58991
- Fe-Ni-Si-B glass alloy, liq. quenched, saturated mag. flux density, effect of peening 7-13611
- Fe-Ni-Si-B metallic glasses, imperfection struct., positron annihilation studies 7-37885
- Fe-Ni-Ti, austenitic crystals, nitrided, phase comp. of diffusion layers (Russian) 7-63922
- Fe-Ni-Ti(Al)(Cr), nitrided layers, struct. investig. using Mossbauer spectroscopy (Russian) 7-53992
- Fe-Ni-V, alloying with N under high press. 7-3266
- Fe-Ni-W system, phase equil., expt. and theoretical study 7-28013
- Fe-Ni-Zr metallic glasses, Ni contrib. to magnetism 7-53183
- Fe-Ni-based alloys, amorphous and crystalline, mag. phase transitions 7-52983
- Fe-Ni-based amorphous alloys, relax. spectra, effect of pulse treatment 7-46536
- Fe-Ni(-C), martensite nucleation, dislocations, grain boundaries, plastic accommodation 7-28040
- Fe-P, amorphous alloys, electrodeposition and melt spinning prep., struct. anal. 7-11934
- Fe-P, sintered compacts, struct. and mech. props., effect of P addition 7-7917
- Fe-P amorphous alloy preparation by electroplating 7-17489
- Fe-P system, sintering at atm. press. 7-64971
- Fe-P-C system, ferritic, grain boundary segregation of P and C 7-39530
- Fe-P-Cu(Ni)(Mo), sintered atomised powder premixes, mech. props. 7-7931
- Fe-Pd, thermoelastic FCC-FCT martensitic transform. mechanism, TEM obs. 7-28041
- Fe-Pd-N austenite, thermodynamics, 1315-1538K 7-13429
- Fe-Pd-S system, phase equil. 7-3272
- Fe-Pt, dilute alloys, ferromagnetic, internal mag. fields, impurity conc. dependence 7-38858
- Fe-Pt (36 at.%), cryst. struct., permanent mag. props. (Japanese) 7-53036
- Fe-Pt Invar alloys, premartensitic transform., local structural change, EXAFS study 7-63556
- Fe-Pt-N austenites, thermodynamics 7-63844
- Fe-R intermetallics, (R=rare earth), intersublattice mol. field studies 7-27306
- Fe-R-B (R=rare earth) metallic glass permanent magnets, TEM studies 7-26661
- Fe-R-B (R=rare earth) metallic glass permanent magnets, struct. and mag. props. 7-27565
- Fe-Sc alloys, struct. and mag. props., NMR and X-ray diffr. studies (Russian) 7-6578
- Fe-Sc amorphous alloys, Curie temp., mag. moment and magnetovolume effects 7-33172
- Fe-Si, deform. behaviour, influence of mech. twinning (German) 7-17603
- Fe-Si, electrical steels, physical metallurgy, conf., New York, USA (Feb. 1985) 7-4626
- Fe-Si, electrical steels and alloys, conf., Vladimir, USSR (Dec. 1984) 7-9576
- Fe-Si, grain oriented, hot rolling texture, thickness variations 7-8009
- Fe-Si, H-induced grain boundary migration 7-21230
- Fe-Si, high-Si, alloy elements influence on plasticity and mag. props. 7-8067
- Fe-Si, melt quenched, struct. formation 7-13480
- Fe-Si, plasticity, influence of thermomechanical parameters 7-13512
- Fe-Si, polycrystalline, magnetisation, domain struct. and magnetostriction (Russian) 7-59051
- Fe-Si, rapidly quenched ribbons, grain growth, mag. props. 7-8017
- Fe-Si, structure, texture and mag. props. 7-12995
- Fe-Si, thermoelec. rapid inspection, contacts temp. effect 7-2580
- α -Fe-Si, Zn vapour induced cracking phenomena (French) 7-3394
- Fe-Si (2 wt.%), microstruct., mag. props., thermomech. history effect 7-7551
- Fe-Si (3 at.%), grain-oriented, fatigue crack growth, direct, real-time obs. (Japanese) 7-59615
- Fe-Si (3 wt.%), continuously cast slabs, high temp. grain growth during reheating 7-8019
- Fe-Si (3 wt.%), denitriding in solid state on heating in vac. 7-8159

iron alloys continued

- Fe-Si (3 wt.%), domain structure and mag. props., influence of plane tension and insulating coatings 7-12991
- Fe-Si (3 wt.%), dynamic remagnetisation, structural depend. of losses 7-12994
- Fe-Si (3 wt.%), Goss orientation rel. to hot rolling conditions 7-8018
- Fe-Si (3 wt.%), grain oriented, desulphurisation kinetics, 899-1171°C 7-8002
- Fe-Si (3 wt.%), grain oriented, texture development for regular and high permeability 7-8008
- Fe-Si (3 wt.%), hot rolling, austenite formation 7-13481
- Fe-Si (3 wt.%), microstruct., mag. props., influence of elastic-stress state produced by coatings 7-12990
- Fe-Si (3 wt.%), mag. props. and domain struct., influence of laser treatment 7-12993
- Fe-Si (3 wt.%), mag. texture of surface layers 7-13062
- Fe-Si (3 wt.%), microstructure, change in stereological characteristics on secondary recrystallisation 7-13468
- Fe-Si (3 wt.%), noncrystalline lamination, Bloch wall bowing anomaly, wall surface pinning 7-33196
- Fe-Si (3 wt.%), recrystallisation texture regulation using small deformations 7-13472
- Fe-Si (3 wt.%), secondary recrystallisation, sharp ribbed texture formation 7-13469
- Fe-Si (3 wt.%), secondary recrystallisation, seed grain formation, influence of elastic anisotropy energy 7-13470
- Fe-Si (3 wt.%), secondary recrystallisation grains, subboundaries formation and their influence on mag. domain struct. 7-13471
- Fe-Si (3 wt.%), specific magnetic loss meas. at remagnetisation freq. 50 Hz to 200 kHz 7-9850
- Fe-Si (3 wt.%) bicrystals, domain struct. and magnetisation 7-12992
- Fe-Si (33 at.%), amorphous films, mag. anisotropy, effect of crystn. and deform. (Russian) 7-53088
- Fe-Si (3.2 wt.%), mag. props., influence of substructural features 7-12996
- Fe-Si (3.3 wt.%), grain-oriented, domain refined, core losses 7-33692
- Fe-Si (4.5 to 7.5 wt.%), melt-spun, ordered struct. 7-1951
- Fe-Si (5.8 at.%) bicrystals, plastic deform., coincident twin boundaries 7-13502
- Fe-Si alloy wires, rapidly solidified by in-rotating-water-spinning method, prod. and props. (Japanese) 7-22654
- Fe-Si amorphous magnetic thin films, sputter deposition methods 7-22483
- Fe-Si anisotropic elec. engineering steels, EM losses, thermomechanical treatment effects (Russian) 7-59550
- Fe-Si cold-rolled nonbrittle powder strip prep., texture and mag. props. 7-46370
- Fe-Si electric steel, X-ray texture analysis using TZ-6 texture attachment 7-8214
- Fe-Si electrical sheet steel, magnetostriction variations meas., ponderomotive force influence 7-13012
- Fe-Si electrical steels, anisotropic cold-rolled, magnetisation characts. 7-12966
- Fe-Si powders, grain size, influence of α - γ transform. 7-7992
- Fe-Si sheets, grain oriented, orientation of individual grains by means of Kossel patterns (Japanese) 7-22716
- Fe-Si sheets, grain oriented, generation of secondary nuclei (Japanese) 7-22717
- Fe-Si single crystals, deformed, dipole drift mechanism of early stages of dislocation pattern 7-38098
- Fe-Si-Al, carbide precip. kinetics, core loss 7-8001
- Fe-Si-Al, electrical steel sheet, rollability, core losses (German) 7-59549
- Fe-Si-Al, Sendust films, DC opposite sputtered, mag. and crystallographic characteristics 7-7847
- Fe-Si-Al alloy single crystals, mag. props. (Japanese) 7-22104
- Fe-Si-Al films, magnetoelastic effect and anisotropy fields 7-59071
- Fe-Si-Al(Ga)(Al)(Ni)(Co)(Cr)(Mn)(Nb), atomic ordering and mechanical props. 7-11990
- Fe-Si-B, amorphous alloys, crystallisation, morphology rel. to sample thickness (Russian) 7-37861
- Fe-Si-B, normalising, decarburisation, secondary recrystallisation, mag. induction obs. 7-8020
- Fe-Si-B, solidification in mag. fields (Russian) 7-59508
- Fe-Si-B (10, 15 at.%), metallic glass, plastic deform. resist. 7-13521
- Fe-Si-B (10, 15 at.%) alloy glass, ion milling rate, cooling condition depend. 7-46690
- Fe-Si-B alloy glass, crystn., effect of solid-liq. interfacial energy 7-16437
- Fe-Si-B amorphous alloys, hypoeutectic, thermal stability and soft mag. props. 7-11928
- Fe-Si-B amorphous alloys, electron momentum distrib. and Fermi energy, Doppler broadening positron annihilation 7-39220
- Fe-Si-B mag. film, magnetoelastic wave generation and detection 7-59070
- Fe-Si-B metallic glasses, wear resist. 7-13604
- Fe-Si-B metallic glasses, struct. relax. (Chinese) 7-65070
- Fe-Si-C single cryst., surface segregation and interactions 7-2322
- Fe-Si-Cr system, ordering process, thermal expansion studies (Russian) 7-1932
- Fe-Si-Ni (6.5, 2 wt.%), development of Goss texture, lowering of core loss 7-33693
- Fe-Sn amorphous alloys, crystn. behavior, DTA, magnetisation and X-ray diffr. meas. 7-44372
- Fe-Sn (001), surface segregation of Sn, surface struct. anal. 7-58594
- Fe-Sn (100), surface structural transitions during Sn surface segregation 7-52210
- Fe-Sn mixed powder compacts, activated sintering (Korean) 7-3221
- Fe-Tb amorphous alloys, film and bulk mag. props. and thermal expansion meas. 7-7540
- Fe-Tb amorphous thin films, RF sputtered, struct. and elec. meas. 7-12534
- Fe-Tb cluster, localised props., multiple scatt. $X\alpha$ SCF method 7-21848
- Fe-Te sputtered films, CsCl-type ordering and amorphisation 7-64021
- Fe-Ti compositionally modulated amorphous films, sputter deposition prep. 7-22482
- Fe-Ti/AISI 304 stainless steel system, ion beam mixed, wear and friction studies 7-46657
- Fe-Ti-C ion-implanted amorphous alloys, precipitate microstruct. studies, conc. depend. 7-16434
- Fe-Ti-C system, austenite-nonstoichiometric precip. equil. 7-3303
- Fe-Ti-N, mech. props. rel. to cold working 7-28089

iron alloys continued

- Fe-TiB₂ eutectic system, microhardness, modulus of elasticity (*Russian*) 7-39648
 Fe-V, amorphous and metastable cryst. alloys prod. by vap. quenching 7-46420
 Fe-V-N, nitriding, surface layer struct., Mossbauer spectra (*Russian*) 7-59672
 Fe-VC composites, cold sintered, mech. props., bonding integrity 7-39471
 Fe-W-B metallic glasses, imperfection struct., positron annihilation studies 7-37885
 Fe-W-based alloys, amorphous and crystalline, mag. phase transitions 7-52983
 Fe-X, X=Al, Si, Nb, Ti, Zr, coercive field measurements 7-64491
 Fe-Zn, intermetallic phase, reversible electrode 7-17802
 Fe-Zn alloys, sputtered, X-ray diffr., magnetisation and Mossbauer studies 7-59075
 Fe-Zr, amorphous, high-field magnetisation hysteresis, spin glass clusters 7-2898
 Fe-Zr, amorphous, superparamagnetic behaviour 7-2904
 Fe-Zr, amorphous and microcrystalline, exchange interaction and saturation magnetisation 7-45651
 Fe-Zr, mechanically alloyed, glass forming ability 7-21110
 Fe-Zr alloy formation at Fe/Zr thin film interfaces, Mossbauer study 7-63975
 Fe-Zr-B, amorphous, meas. of Curie temp. 7-2853
 Fe₅₀Ni₂₂Cr₁₀P₁₈ and Fe₄₈Ni₃₄P₁₈ metallic glasses, spin waves, study by polarised neutron scatt. 7-12962
 Fe_{70.4}Al_{29.6}, reentrant spin glass, field induced modulated spin structure 7-38882
 (Fe-B)₈₅Nd₁₅ amorphous films, soft mag. props. 7-53077
 FeAl, B2-structured, annealed and slow cooled, occurrence of displacement fringes 7-6808
 FeAl, electronic struct. of vacancies 7-16975
 FeAl, ordered B2 polycryst., Young's modulus, temp. and comp. depend. 7-33716
 FeAl, short-range order-induced equilib. resist. conc. depend. meas. 7-26700
 FeAl, X-ray emission and absorpt., ab initio self-consistent band struct. calcs., LMTO method 7-64826
 FeAl₃, Fe₂Al₃, combustive synthesis, physicochemical props. 7-7918
 FeAl₃ phases, binding anal. 7-44445
 Fe₃Al, near surface atomic correlations depth profiling, total reflection of synchrotron radiation 7-52214
 FeAlNiCoCu permanent magnetic material, phase decomposition kinetics, atom probe FIM study 7-33669
 FeB amorphous magnetic thin films, spin wave mode linewidth meas. 7-45826
 Fe_{100-x}B_x amorphous alloy, temp. depend. of the resistivity (*Chinese*) 7-27314
 Fe_{100-x}B_x metallic glass system, elec. resist. under press. 7-7200
 Fe₅₀B₅₀ amorphous film, energy-dispersive X-ray diffr. meas. 7-63401
 Fe₇₅B₂₅, polymorphous crystallisation into Fe₃B orthorhombic phase 7-37874
 Fe₇₉B₂₁, amorphous alloy, elec. resist. and crystn. on hardening from different temps. 7-44380
 Fe₈₀B₂₀, amorphous, partial pair distribution function determ. 7-51640
 Fe₈₀B₂₀ amorphous alloy, differential AC method of thermopower measurement 7-48776
 Fe₈₀B₂₀ amorphous alloys, EXAFS meas. at B k-edge 7-64807
 Fe₈₀B₂₀, amorphous surface layer produced laser irradiation, thickness meas. using X-ray diffr. 7-44304
 Fe₈₀B₂₀, glass metals, temp. depend. of positron trapping effect 7-39292
 Fe₈₀B₂₀, metallic glasses, multiplet splitting, XPS study 7-27858
 Fe₈₀B₂₀ metallic glasses, retardation of annealing embrittlement by Ce microadditions 7-65118
 Fe₈₀B₂₀ ribbons, amorphous and crystallised, surface comp., electronic props., topography, AES, XPS, ion scatt. studies 7-27065
 Fe₈₁B₁₉ amorphous alloy, thermally activated time fluctuations of nucl. spin orientation 7-7622
 Fe₈₁B₁₉ amorphous ribbon, averaged spin orientation under uniaxial compression, Mossbauer spectra study 7-45792
 Fe₈₁B₁₇, amorphous powder, surface struct. rearrangement by pulverisation, CEMS obs. 7-13065
 Fe₈₃B₁₇, metallic glass, struct. relax. X-ray and neutron diffr. study 7-6521
 Fe₈₃B₁₇ with V, Cr, Mn or Nb, amorphous, mag. contrib. to thermopower 7-45287
 Fe₈₄B₁₆ amorphous alloy, heterogeneous surface struct., Mossbauer differential conversion electron spectra anal. 7-2319
 Fe₈₄B₁₆ amorphous alloy, layer-by-layer phase anal., depth-selective conversion-electron Mossbauer spectroscopy 7-17255
 Fe₈₄B₁₆ amorphous alloy, interstitial element segregation during fracture (*Russian*) 7-53875
 Fe₈₅B₁₅, high energy heavy-ion irradiation, electrical resistance meas., evidence for electronic energy loss effect 7-58353
 Fe₇₅B₁₅Si₁₀, amorphous alloy powders, rapid quenching water atomisation process 7-46371
 Fe₇₈B₁₂Si₁₀, amorphous, very small angle neutron scatt. 7-44392
 Fe₇₈B₁₃Si₉ amorphous and partially crystalline alloy, high resolution TEM studies 7-21127
 Fe₇₈B₁₃Si₉, amorphous alloys, mag. losses, aging kinetics 7-59056
 Fe₇₈B₁₃Si₉ amorphous ribbons, ferromag. resonance 7-27606
 Fe₇₈B₁₃Si₉ glass reinforced Al composite, fabrication by multi-lamina explosive compaction 7-59482
 Fe₇₈B₁₃Si₉, magnetron sputtered amorphous alloys, thermal, mag. and magnetomechanical props. 7-33249
 Fe₇₈B₁₃Si₉ metallic glasses, retardation of annealing embrittlement by Ce microadditions 7-65118
 Fe₈₀B₁₂Si₈, amorphous alloy ribbons, processing conditions rel. to mag. prop. changes (*Korean*) 7-7919
 Fe₈₀B₁₄Si₆ amorphous ribbons, anisotropy of losses 7-45658
 Fe₈₀B₁₄Si₆ metallic glasses, long-time tunnelling heat relaxation meas. 7-32223
 Fe_{81.5}B_{14.5}Si₄, amorphous, mag. hyperfine fields under stress, Mossbauer study 7-22166
 Fe₈₂B₁₂Si₆, amorphous, initial crystallisation 7-44387
 Fe₈₂B₁₂Si₆ metallic glasses, crystn., magnetisation, scaling, mag. relax. meas. 7-63496
 Fe₈₀B_{14.5}Si_{3.5}C₂ metallic glass, laser beam irradiation, high energy, shear band form. and cracking 7-59606

iron alloys continued

- Fe₈₀B₁₆Si₂C₂ metallic glasses, retardation of annealing embrittlement by Ce microadditions 7-65118
 Fe₈₁B_{13.5}Si_{3.5}C₂ amorphous and cryst. alloy, Si diffusion and segregation 7-6859
 Fe₈₁B_{13.5}Si_{3.5}C₂, Metglass 2605 SC, surface crystn. behaviour 7-58154
 Fe_{81.5}B_{13.5}Si_{3.5}C₂, amorphous ferromag. alloy, acoustic waves, mag. field induced changes 7-2917
 Fe₇₇B₁₆Si₇Cr₂ metallic glass, crystallisation, DSC and X-ray diffr. studies 7-11932
 Fe_{90-x}B_xZr₁₀, amorphous, B addition effect on mag. props., elec. resistivity, crystallisation (*Chinese*) 7-7487
 Fe₈₁Be_{13.5}Si_{3.5}C₂ soft ferromag. metallic glasses, domain wall motion and energy dissipation studies 7-64478
 Fe₈₀C₂₀-Si compositionally modulated amorphous struct., mag. and diffusional props. study 7-7564
 FeCSiP alloys, cast, graphite nodule shape effects, ultrasound vel. meas., comp. depend. 7-3285
 Fe₇₀(CeNdPr)₂₀B₁₀, rapidly quenched ribbons, hard mag. props. 7-27562
 FeCo alloy, electronic struct., effect of ordering, positron annihilation and Mossbauer effect study 7-45142
 FeCo alloys, critical mag. phenomena, results from μ SR studies 7-45872
 Fe_{1-x}Co_x, spin-polarised positron annihilation and mag. moments 7-53439
 Fe₇₀Co₃₀-SiO₂ compositionally modulated mag. film props. study 7-7566
 (FeCo)₈₀B₂₀ amorphous ultrafine particles, mag. props. 7-53063
 (Fe_{1-x}Co_x)₈₀B₂₀, amorphous alloy, crystallisation kinetics (*Korean*) 7-26638
 (Fe_{1-x}Co_x)₈₄B₁₆ amorphous alloy, temp. depend. of the resistivity (*Chinese*) 7-27314
 Fe₆₇Co₁₈B₁₅S metallic glass, magnetic aftereffect, thermal treatment, positron lifetime study 7-38907
 (Fe_{1-x}Co_x)₇₇B₁₃Si₁₀ amorphous alloys, Mossbauer study 7-7623
 Fe₆₇Co₁₈B₁₅Si, amorphous mag. alloy, crystallisation, elec. resist., TEM obs. 7-11927
 Fe₇₄Co_{10-x}Cr_xB₁₆ amorphous alloys, form. and crystn. 7-11930
 Fe₇₄Co_{10-x}Cr_xB₁₆, amorphous, prep. by melt spinning, X-ray diffr., DSC, Mossbauer studies 7-46369
 Fe₃Co_{70-x}Cr_xSi₁₀B₁₅, x=0, 3, 6, 9, amorphous ferromagnet, 180° domain wall (*Korean*) 7-33198
 Fe_{5.85}Co_{72.15}Mo₂B₁₅Si₅ amorphous ribbons traversed by DC electric currents excess resistance, collective motion of ferromag. domain walls 7-32989
 (Fe_{1-x}Co_x)₇₈Si_{9.5}B_{12.5} amorphous alloys, density of states, XPS studies (*Chinese*) 7-13320
 Fe₆₇Co₁₈Si₁₄, mean positron lifetimes after annealing (*Chinese*) 7-27814
 Fe₉₂Cr₈O_{0.08}, near surface layer conc. profile, XPS (*Russian*) 7-58582
 FeCrAlY, Al₂O₃ adhesion mechanism 7-33843
 FeCrAlY coatings, ion-implanted, oxidation behaviour 7-53974
 Fe_{80-x}Cr_xB₂₀ metallic glasses, electron transport props., disorder and mag. effects 7-52563
 Fe_{85-x}Cr_xB₁₅(Ni₁₅) metallic glasses, mag. and elec. props. 7-13002
 FeCrNi, oxide film thin overlayers, quantitative AES depth profiling studies 7-7796
 Fe_{82-x}Cr_xNi₁₈, single cryst. alloys, short range atomic ordering (*Russian*) 7-63558
 Fe₄₃Cr₂₅Ni₂₀B₁₂ glass, devitrification, mag. meas. and X-ray diffr. studies 7-21128
 FeCrNiW amorphous alloys SCC behaviour 7-39727
 FeCrNiWMo alloys, sputtering effects on props 7-36240
 Fe₇₀Pi₃C₇ amorphous alloy, surface layer chemical bonds, XPS studies 7-12417
 Fe₇₆Cr₄P₈C₁₂, amorphous alloy, mag. short range order above T_c, paramag. phase 7-45623
 Fe₇₀Cr₂Si₁₀B₁₅ metallic glass, field electron emission 7-33530
 Fe_{75-x}Cr_xSi₁₀B₁₅, x=0, 2, 4, 6, amorphous ferromagnet, 180° domain wall (*Korean*) 7-33198
 Fe_{80-x}Cr_x(SiB)₂₀ amorphous alloy, induced anisotropy, melt spinning effects (*Russian*) 7-59004
 FeGe single cryst., magnetisation, temp. depend. (*Russian*) 7-2891
 Fe₂Ge_{1-x} amorphous magnetic alloys, d-band occupancy, EELS study 7-64059
 FeH_x cleavage strength, tight-binding model calcs., interstitial solute effects 7-59538
 (Fe_{1-x}M_x)₈₄B₁₆ (M=Co,Ni) thermoelectric power, influence of Cu(Ni) additives 7-32995
 (FeM)₈₀B₁₄Si₆, M=Mn, Mo, V, glass, magnetoresistance 7-64203
 FeMnAl, low temperature specific heat (*Chinese*) 7-12306
 (Fe_{1-x}Mn_x)₇₈B₂₂, amorphous alloys, lattice parameters, annealing, X-ray diffr., elec. resist. 7-37878
 (Fe_{1-x}Mn_x)₈₄B₁₆, amorphous, Mn content effect on elec. resistivity (*Chinese*) 7-12692
 (Fe_{1-x}Mn_x)Pt alloys, mag. phase diagram 7-64434
 Fe₇₅Mo₃Si₉B₁₃, amorphous, structural relax. and quasi-texture 7-11925
 Fe₁₄Nd₂B magnets, high-field magnetostriction 7-53104
 Fe₁₄Nd₂B permanent magnet, Dy substituted positron annihilation studies 7-3108
 Fe₇₆Nd₁₆B₈ plasma sprayed permanent magnets, characs. 7-45754
 Fe₇₇Nd₁₅B₈, sintered permanent magnets, domain wall obs. 7-27544
 Fe₇₇Nd₁₅B₈-based melt spun ribbons, crystallisation and mag. props. 7-26662
 Fe₁₄Nd(Y)(Ce)₂B fine particles prep. by hydriding, mag. props., recording appls. 7-53660
 FeNi metallic mag. film, mag. anisotropy field freq. dispersion 7-33240
 (Fe_{0.15}Ni_{0.85})₇₅P₁₆BeAl₃, static scaling in an amorphous metallic spin glass 7-38871
 Fe_{1-x}Ni_x bulk melts, containerless undercooling, solidification 7-26916
 Fe₅₀Ni₅₀ alloy foils, N₂⁺ implantation, oxidation behaviour, conversion electron Mossbauer spectra study 7-22877
 Fe₅₀Ni₅₀, Deltamag, magnetic ribbons, inverse Wiedemann effect for very low torsions 7-45786
 (Fe₆₅Ni₃₅)-x (Fe₆₅Mn₁₅)_x alloys, low field magnetisation and Mossbauer effect studies 7-33311
 FeNiAlCoTiCuS permanent magnetic material, phase comp. and ordering, atom probe FIM and TEM studies 7-33635
 (Fe_{1-x}Ni_x)₈₀B₂₀, amorphous, contribution of Ni to hyperfine fields (*Korean*) 7-27636
 (Fe_{1-x}Ni_x)₈₄B₁₆, amorphous alloy, temp. depend. of the resistivity (*Chinese*) 7-27314
 Fe₄₀Ni₄₀B₁₀, Fe₃₀Cr₁₀Ni₄₀B₂₀ metallic glass, fracture toughness rel. to prep. and struct. 7-53870

iron alloys continued

- Fe₄₀Ni₄₀B₂₀, amorphous, positron annihilation studies 7-45859
 Fe₄₀Ni₄₀B₂₀, amorphous thin films, coercive field, annealing effects 7-7553
 Fe₄₀Ni₄₀B₂₀, amorphous and crystalline, elec. resistivity, temp. dependence 7-21892
 Fe₄₀Ni₄₀B₂₀, amorphous metallic films, SAX investig. (Russian) 7-51576
 Fe₄₀Ni₄₀B₂₀, amorphous alloys, domain wall motion, SEM obs. 7-52978
 Fe₄₀Ni₄₀B₂₀, amorphous alloy, Barkhausen noise, neutron irradiation effect 7-53029
 Fe₄₀Ni₄₀B₂₀, amorphous alloy, effect of plastic deform. on mech. and mag. props. (Russian) 7-53810
 Fe₄₀Ni₄₀B₂₀, concentration dependence of surface insulating coating, influence on magnetic props. 7-64479
 Fe₄₀Ni₄₀B₂₀, metallic glass ribbon, failure mechanics and atom probe study correlations 7-28139
 Fe₄₀Ni₄₀B₂₀, metallic glass, neutron diffr. struct. factors determ. 7-51654
 Fe₄₅Ni₄₅B₁₀, amorphous, internal friction, thermo-EMF struct., annealing effect (Russian) 7-59560
 Fe₅₀Ni₃₀B₂₀, amorphous alloys, domain wall motion, SEM obs. 7-52978
 Fe₅₀Ni₃₀B₂₀, amorphous ferromagnets, elec. resist. and thermopower meas., comp. and temp. depend. 7-45263
 Fe₅₀Ni₃₀-x B₂₀, XRF and PIXE surface anal. 7-12411
 Fe₄₀Ni₃₈B₁₈Mo₄, Metglass 2826 MB, surface crystn. behaviour 7-58154
 Fe₄₀Ni₃₈B₁₈Si₂, glassy alloys, variation of mag. inhomogeneity 7-45634
 (Fe_{1-x}Ni_x)₉₂C₈ pseudobinary FCC alloys, ferromagnetism onset, magneto-volume effect study 7-2845
 FeNiCr disordered FCC alloys, paramagnetic-antiferromagnetic-spin glass reentrant transition obs. 7-17175
 FeNiCr, grain boundary solute segregation 7-56833
 FeNiCr spin glass, Edwards-Anderson order parameter temp. depend. meas. (Russian) 7-2866
 FeNiCr, strain measurement in convergent beam electron diffraction 7-16562
 FeNiCr:SiB₂P, grain boundary segregation, Auger and energy dispersive X-ray mapping 7-16571
 FeNiCr₂₀, spin glass, phase transition, mag. suscept. study 7-53004
 Fe₅₀Ni₄₈-x Cr₂ spin glasses, critical dynamics 7-45683
 FeNiCr(Mn) spin glasses, nonlinear mag. suscept. study 7-52991
 Fe₃₀Ni₃₆Cr₁₂Mo₂Si₂B₁₅, amorphous alloy, Curie temp., press. effect 7-52976
 FeNiMn_{0.15}, spin glass, phase transition, mag. suscept. study 7-53004
 Fe₅₀Ni₄₅-x Mn₁₅, low temp. sp. ht. near ferromag.-antiferromag. transition (Russian) 7-7512
 Fe₃₈Ni₄₀Mo₄B₁₈, metallic glass, positron annihilation (Chinese) 7-64726
 Fe₄₀Ni₃₈Mo₄B₁₈, amorphous, positron annihilation studies 7-45859
 Fe₄₀Ni₃₈Mo₄B₁₈, amorphous alloys, thermal devitrification kinetics 7-51651
 Fe₄₀Ni₃₈Mo₄B₁₈, metallic glass, conversion electron Mossbauer spectra 7-48926
 Fe₄₀Ni₃₈Mo₄B₁₈, soft ferromag. metallic glasses, domain wall motion and energy dissipation studies 7-64478
 Fe₄₀Ni₄₀Mo₄B₁₆, amorphous alloys, positron annihilation peakrate temp. depend. meas. 7-39302
 (FeNi)₇₈Mo₄B₇Si metallic glass, mag. shielding props., composition depend. 7-27558
 Fe₄₀Ni₃₈Mo₄B₁₆Si₂, ferromag. amorphous ribbons by field quenching technique, mag. anisotropy 7-33164
 Fe₄₀Ni₄₀P₂₀, amorphous alloy, electron struct. and surface struct., XPS and UPS studies 7-27238
 Fe₄₈-x Ni₄₈P_{17.5}, small-angle polarized neutron scattering study 7-52939
 Fe₄₀Ni₄₀P₁₄B₆, amorphous alloy, relax. struct. transforms., 80 to 300K 7-1890
 Fe₄₀Ni₄₀P₁₄B₆, amorphous material behaviour in friction 7-28151
 Fe₄₀Ni₄₀P₁₄B₆, amorphous alloys, annealing, positron annihilation parameters anal. 7-39303
 Fe₄₀Ni₄₀P₁₄B₆, amorphous ribbon, magnetoelastic, Matteucci effect meas. (Spanish) 7-53103
 Fe₄₀Ni₄₀P₁₄B₆, ferromag. amorphous alloy, struct. relax., effect of surface 7-28062
 Fe₄₀Ni₄₀P₁₄B₆, metallic glass, heterogeneous struct., EXAFS study 7-27816
 Fe₄₀Ni₄₀P₁₄B₆, metallic glasses, multiplet splitting, XPS study 7-27858
 Fe₄₀Ni₄₀P₁₄B₆, metallic glasses, superplastic deform. (Russian) 7-39599
 Fe₄₀Ni₄₀P₁₄B₆, Metglas 2826, magnetic ribbons, inverse Wiedemann effect for very low torsions 7-45786
 Fe₄₀Ni₄₀P₁₄B₆, Metglass 2826, crystn. behaviour, influence of annealing atm. 7-53768
 Fe₄₀Ni₄₀P₁₄B₆, amorphous and crystallised alloys, surface oxidation behaviour 7-59666
 (Fe_{0.15}Ni_{0.85})₇₅P₁₆B₆Al₃, amorphous spin glasses, relaxation 7-53000
 (Fe_{0.15}Ni_{0.85})₇₅P₁₆B₆Al₃, metallic spin glass, time decay of saturated remanent magnetisation 7-59058
 (Fe_{0.5}Ni_{0.5})₇₅P₁₆B₆Al₃, metallic glass, struct. relax., theory (Russian) 7-44397
 Fe₇₀Ni₁₀P₁₃C₇, amorphous powder, crystallisation (Russian) 7-58162
 (FeNi)₁Pd_{1-x}, atomic mag. moments, magnetisation meas. (Russian) 7-17198
 Fe₅₀Ni₃₅Pd₂₅, surface oxidation, X-ray α , β emission spectra studies 7-13265
 Fe₇₀Ni₁₀Si₁₀B₁₂, amorphous and cryst. states., oxidation (Russian) 7-53993
 Fe₂₀Ni₄₀Si₁₀Si_{0.98}B_{0.14}, amorphous viscoelastic behaviour 7-21348
 (Fe_{0.6}Ni_{0.4})₈₂Si₈B₁₀, amorphous alloys, structural relax. and crystn., positron annihilation studies 7-37869
 (Fe_{1-x}Ni_x)₇₇Si₀B₁₃, amorphous, structural anal. (Korean) 7-26655
 (Fe_{1-x}Ni_x)₇₇Si₀B₁₃, amorphous, effective mag. moment, Curie temp. (Korean) 7-27503
 Fe₁₀Ni₅₅Si₀B₁₅, spin glass, amorphous, effect of phase segregation during struct. relax. 7-39517
 Fe₄₀Ni₄₀Si₆B₄, metallic glass, positron trap depth distrib. determ., lifetime and Doppler effect meas. 7-39304
 Fe₇₀Ni₁₀Si₁₀B₁₂, amorphous alloys, thermal devitrification kinetics 7-51651
 Fe₇₅Ni₃₅B₁₃, amorphous, structural relax. and quasi-texture 7-11925
 (Fe_{0.93}Ni_{0.07})₇₇Si₀B₁₃, amorphous spin glass, dynamic mag. susceptibility and critical phenomena (Russian) 7-7511
 Fe₄₄Ni₅₆Si_{7.88}B_{14.56}C_{0.25}, amorphous filler metal, struct. props. (Korean) 7-32292
 Fe₂P, electronic struct., mag. props., KKR, LMTO methods, LSD approx. 7-64070

iron alloys continued

- Fe₂P, mag. props. under high press., competing magnetic interactions 7-7542
 Fe₈₀P₂₀, amorphous ribbons, structural relax., crystallisation, Mossbauer spectra (Chinese) 7-11918
 Fe₈₂P₁₈B₇, metallic glass, mag. anisotropy and correlated hyperfine interactions 7-7505
 Fe₈₀P₁₃C₇ alloy, metallic glass surface layers by rapid quenching, micro-hardness 7-3512
 Fe₈₀P₁₃C₇, amorphous alloy powders, rapid quenching water atomisation process 7-46371
 FeP_{GA}, amorphous, magnetoelastic props. 7-27591
 FePd, annealed, transport and thermal expansion props. 7-46512
 FePd, thermal expansion and α - γ phase boundary lines 7-2239
 Fe(Pd_{1-x}Au_x)₃, disordered alloys, atomic and mag. structs., Mossbauer studies (Russian) 7-17247
 FeR alloys, R=rare earth, permanent quadrupole magnets, construction and calcs. 7-19578
 FeRh, X-ray emission and absorpt., ab initio self-consistent band struct. calcs., LMTO method 7-64826
 Fe_{0.1}Rh_{0.9}, saturated absorpt. of gamma radiation, ⁵⁷Fe Mossbauer study 7-7621
 Fe₂Sb_{100-x}, amorphous, metal-insulator transition and effects of localisation and correlation 7-45407
 FeSi, low temp. magnetostriction meas. 7-45790
 FeSi oxidised interface system, XPS, XAES and Auger parameter studies 7-7025
 FeSi₂, epitaxial growth on Si, effects of thin interposing layers 7-22471
 Fe_{1-x}Si_x, amorphous films, Hall effect and mag. anisotropy 7-2911
 Fe₃Si, electronic struct. and X-ray spectra, disorder effects (Russian) 7-32903
 Fe₃Si, near-stoichiometric high temp. creep and struct. investig. 7-22762
 Fe₃Si, transition metal impurities, electronic struct. and site preference 7-12653
 Fe₆₇Si₃₃ (Russian) 7-59078
 Fe₆₇Si₃₃, amorphous films, ferromag., induced mag. anisotropy (Russian) 7-52974
 Fe₆₇Si₃₃, thin amorphous films, plastic deform. (Russian) 7-59585
 Fe₆₇Si₃₃, magnetoelastic acoustic emission 7-33257
 Fe₂Si_{1-x}, amorphous magnetic alloys, d-band occupancy, EELS study 7-64059
 FeSiB amorphous alloy, double-layer struct. unit model 7-16423
 Fe₇₇Si₀B₁₃, amorphous, structural anal. (Korean) 7-26637
 Fe₇₀Si₀B₁₃, as-quenched and cold-rolled amorphous alloy, mag. props. 7-33219
 Fe₇₈Si₀B₁₂, amorphous ribbons, X-band ferromag. resonance, transmission of microwaves 7-27607
 Fe₇₈Si₀B₁₂, amorphous alloys, surface crystallisation and mag. props. 7-51649
 Fe₇₈Si₀B₁₃, amorphous, tensile strength, elastic stiffness (Japanese) 7-3346
 Fe₇₈Si₀B₁₃, amorphous ribbons, magnetoelastic effects on practical props. 7-33252
 Fe_{90-x}Si₁₀B₁₀, amorphous alloys, multistep-micro-crystallisation studies 7-21129
 Fe₈₀Si₁₀P_{20-x}, amorphous alloys, struct., mag. and elec. props. (Korean) 7-2893
 FeSnSb dilute alloys, local lattice relax. around impurity, K-edge EXAFS study 7-64159
 Fe_{0.74}Tb_{0.26}, amorphous, oxidation 7-65192
 Fe₇₃Ti₁₇H₄, amorphous alloys, Mossbauer spectra 7-33308
 Fe_{1-x}V_x, polarised neutron study 7-52940
 (Fe_{1-x}Ni_x)₈₄B₁₆, amorphous, low temp. resistivity anomaly (Chinese) 7-64198
 Fe_{84-x}V_xB₁₆, amorphous alloys, crystn., products and kinetics 7-51677
 (Fe_{1-x}W_x)_{84.5}B_{15.5}, amorphous alloys, elec. and mag. props. (Chinese) 7-12969
 FeZr, amorphous and microcryst., exchange interaction and saturation magnetisation (Russian) 7-12963
 Fe₉₁Zr_{0.9}, amorphous alloys, critical mag. phenomena, results from μ SR studies 7-45872
 Fe₉₀Zr₁₀, amorphous alloy, differential AC method of thermopower measurement 7-48776
 Fe₉₀Zr₁₀, amorphous powder, surface struct. rearrangement by pulverisation, CEMS obs. 7-13065
 Fe₉₀Zr₁₀, glasses, crystallisation characteristics 7-51647
 Fe₉₀Zr₁₀, glasses, crystallisation characteristics 7-51648
 Fe₉₁Zr₉, amorphous, long-range mag. order, neutron scatt. and AC susceptibility studies 7-58979
 Fe₉₁Zr₉, amorphous, long-range mag. order, small-angle neutron scatt. 7-58980
 Fe₉₀Zr₈, mag. susceptibility, elec. resist., magnetoresistance meas. 7-52954
 Fe_xZr_{100-x}, amorphous alloys, Kohlrausch thermal relax., sp. ht. meas. 7-59027
 Fe_{77.5}Si_{7.5}B₁₅, amorphous wires, Barkhausen and Matteucci effects, influence of tensile and compressive stress 7-33254
 Fe_{0.65}Si_{0.35} thin films, amorphous and crystalline, magnetisation rotational processes 7-53085
 Gd-Fe, amorphous Faraday rotation 7-64612
 Gd-Fe evaporated amorphous alloy films, mag. props. and FMR behaviour studies 7-45825
 Gd-Fe sputtered amorphous films, structural relax., positron lifetime meas. 7-37870
 Gd-Fe-Co, amorphous Faraday rotation 7-64612
 Gd-Tb-Co-Fe sputtered amorphous films, Kerr magneto-optical effect, anisotropy dispersion effects 7-38913
 GdFe amorphous films with perpendicular anisotropy, Hall loop meas., mag. struct. studies 7-7205
 GdFe amorphous thin films, electrical conductivity, influence of mag. order 7-7409
 Gd₂Fe₁₄B alloys, magnetic anisotropy and spin reorientations 7-38855
 Gd₂TbFe, corrosion resistance improvement by metal coatings 7-53952
 Ge₈₀-Mn₂₀, amorphous alloy, Curie point and crystallisation temp. 7-17173
 HfFe₂, electronic struct. and mag. props., tight-binding approx. calcs. 7-2475
 Ho₂(CoFe)₁₇, intermetallics, high field magnetisation studies 7-53038
 Ho₂Fe₁₄B alloys, magnetic anisotropy and spin reorientations 7-38855
 Ho₂Fe₁₄B single crystals, mag. anisotropy and magnetisation 7-27547
 Ho₂Fe₁₄B spin reorientation, NQR meas. 7-52960

iron alloys continued

- (La_{1-x}Ce_x)₂Fe₁₄B rapidly quenched ribbons, hard mag. props. 7-27549
 La(Fe_xAl_{1-x})₁₃, mag. props. determined via neutron scatt. and Mossbauer spectroscopy 7-2820
 LaNi_{5-x}Fe_x, spin freezing props. 7-64464
 LuFe₂, electronic struct. and mag. props., tight-binding approx. calcs. 7-2475
 Mg-Fe, dil., Kondo system, mag. scatt. time of conduction electrons meas. 7-21902
 Mg-Fe dilute thin film, mag. screening and Kondo-type behaviour 7-12944
 Mn_{1-x}Fe_x, sputtered films, mag. props. 7-38915
 (Mn_mFe_{1-m})_{100-x}Bi_x films, evaporated, structure and mag. props. (Japanese) 7-59077
 Mn₂Fe_{1-x}Si solid solns., thermal expansion 7-6835
 Mo-Fe dilute alloy, Fe solute atom-screw dislocation interaction force, modified tight-binding recursion method calcs. 7-51814
 Nb₆Au_{24-x}Fe_x, A-15 supercond., transition temp. and mag. susceptibility 7-2768
 (Nd,Tb)_{16.7}Fe_{75.5}B_{7.8}, magnetisation meas., spin reorientation temp. 7-17161
 Nd-Dy-Fe-B-based sintered magnet, microstruct., heat treatment effects 7-53767
 Nd-Fe-B, metastable amorphous alloys, crystn., thermal stability 7-39482
 Nd-Fe-B, microstructure, scanning tunnelling microscopic studies 7-58494
 Nd-Fe-B, permanent mag. alloy, Mossbauer spectroscopic study (Chinese) 7-7613
 Nd-Fe-B, phase diagram, permanent mag. anal. 7-39486
 Nd-Fe-B amorphous ribbons, effect of crystallisation conditions on hard mag. props. 7-27561
 Nd-Fe-B based permanent magnets, hysteresis loop and mag. anisotropy 7-53031
 Nd-Fe-B liquid-quenched alloys, mag. props. 7-27550
 Nd-Fe-B permanent magnet, microstructure and coercivity 7-27559
 Nd-Fe-B permanent magnets, prod. by hydrogen decrepitation/attritor milling route 7-22606
 Nd-Fe-B permanent magnets, BCC phase mag. props. at grain boundaries 7-53044
 Nd-Fe-B rapidly solidified permanent magnet materials, magnetisation processes and domain wall motion 7-38902
 Nd-Fe-B rapidly solidified ribbons, magnetisation, quench rate depend. 7-53034
 Nd-Fe-B sintered magnets, hysteresis loops, anal. 7-33215
 Nd-Fe-B system, permanent magnet, mag. props. (Korean) 7-7554
 Nd-Fe-B system, temp. depend. of coercive force, effect of annealing, aging and sintering 7-27560
 Nd-Fe-B-Co-Al based permanent magnets, mag. props. and temp. characts. 7-53045
 Nd-Fe-C(Si)(Ge)(Pb)(Sn) ternary phase studies. X-ray anal. and Curie temp. meas. 7-7508
 Nd-Fe-Co, amorphous films, perpendicular magnetic, mag. and magneto-optical props. 7-64496
 Nd₂(Co₂Fe_{1-x})₁₄B alloys, mag. struct., preferential site occupation 7-45619
 NdDyFe₁₄B spin orientation and preferential 4f site occupation, powder neutron diff. study 7-22100
 NdFe alloys, magnetic moment irreversibility from temperature cycling 7-33194
 NdFe-stee hybrid permanent magnet wiggler development for SPEAR ring 7-42250
 Nd₂(Fe_{0.5}Al_{0.33})₁₄B, reduction of mag. hyperfine fields and Curie temp. on Al substitution, Mossbauer spectra 7-38859
 NdFeB, anisotropic permanent magnet, prep. and investig. 7-52969
 Nd_{1.5}Fe_{7.5}B₈ based pseudobinary alloys, sintered permanent magnets, depend. of coercivity on anisotropy field 7-45744
 Nd_{1.5}Fe_{7.5}B₈ permanent mag., rotational hysteresis energy and magnetisation reversal 7-64492
 Nd₂Fe₁₄B alloys, magnetic anisotropy and spin reorientations 7-38855
 Nd₂Fe₁₄B, cryst. field effects 7-45598
 Nd₂Fe₁₄B, EFG tensor for interpretation of Mossbauer effect meas. near spin reorientation temp. 7-38968
 Nd₂Fe₁₄B, elastic props. between 120 to 300K 7-27529
 Nd₂Fe₁₄B, magnetic props., H₂ absorption effects 7-38906
 Nd₂Fe₁₄B permanent magnet materials, prep. and props., book contrib. 7-27981
 Nd₂Fe₁₄B permanent magnet, magnetic anisotropy consts. determ. from unsaturated torque curves 7-52973
 Nd₂Fe₁₄B single crystals, mag. anisotropy and magnetisation 7-27547
 Nd₂Fe₁₄B sputtered films, perpendicular anisotropy 7-53073
 Nd₂Fe₁₄B untextured polycrystals, magnetic hyperfine fields, Mossbauer spectra anal. 7-12682
 Nd₂Fe₂₃B₃, struct., Curie temp., X-ray diffraction anal. 7-11994
 NdFeBCoAl magnets, Curie temp., coercive force and magnetisation 7-52982
 Nd₂Fe_{14-x}Co_xAl₁₀B alloys, permanent mag. props. 7-45755
 Nd₂Fe_{14-x}Co_xB system, mag. phase transitions and anisotropy 7-27524
 Nd₂Fe_{14-x}M_xB, (M=Co,Ni,Cu,V,Al,Cr,Mn), crystallographic and mag. props. 7-27522
 Nd₂Fe_{12-x}Mn_xCo₂B, mag. props. 7-52946
 Nd₂Fe_{14-x}Ru_xB alloys, mag. props., comp. depend. study 7-7547
 Nd₂(Fe_{0.6}Si_{0.33})₁₄B, reduction of mag. hyperfine fields and Curie temp. on Si substitution, Mossbauer spectra 7-38859
 NdHoDyFeB permanent magnets with zero temp. coeff. of induction 7-53047
 Nd_{2-x}R_xFe₁₂Co₂B, mag. characts. 7-45670
 Nd₂(Y₂(Fe_{1-x}Al_x)₁₄B, intrinsic and permanent mag. props. (Chinese) 7-13003
 Ni-Al-Fe system, phase equilibria in the Ni-rich region 7-39487
 Ni-base alloy 718, cast, weld heat-affected zone liquation morphology 7-53715
 Ni-Cr-Mo-Fe system, pitting corrosion, temp. depend. 7-65186
 Ni-Fe (100) surface, break-up of oxide films by S₂ impingement, LEED and AES meas. 7-46260
 Ni-Fe film, ion beam sputter deposition, ion bombardment effect on preferred orientation 7-64010
 Ni-Fe films, ion beam sputtered, magnetoresistance props. 7-22033
 Ni-Fe-Cr, age hardenable, SCC in PWR coolant water, heat treatment and Zr additions effect 7-39708
 Ni-Fe-Cr, Inconel 600 and Incoloy 800, fracture toughness 7-59596

iron alloys continued

- Ni-Fe-Cu, mag. props., hardness, elec. resist., V, Nb and Ta additions effect (Japanese) 7-12998
 Ni-Mo-Cu-Fe-Mg, coarse-grained PC permalloys, annealing-twin density (Japanese) 7-3330
 Ni-Mo-Fe-Cr alloy, transient phase obs during long range ordering to Ni₄Mo, electron diff. study 7-63806
 Ni₇₀Cr₇Fe₃Si₁₂B₁₂ ribbon, rapidly quenched from melt, struct. inhomogeneity and crystallised metastable phase (Chinese) 7-63477
 Ni₈₃Cr₇Fe₃Si₄B₃, amorphous alloy, crystallisation (Chinese) 7-6518
 Ni_{69.2}Cr_{4.6}Si_{13.7}B_{7.5}Fe_{2.6}, amorphous alloy, 70 MeV Ni¹⁶⁺ ion irradi., surface swelling 7-16646
 Ni₃(FeM) alloys, (M=Nb, V, Ta), atomic short range order, pseudopot. calcs. (Russian) 7-44448
 Ni₃(Fe,M) (M=Cr, Mn, W, Mo), atom pair interaction energy and Kurnakov temp. (Russian) 7-1938
 Ni₃(Fe,Nb), order-disorder transformation, positron annihilation study 7-39509
 NiFe-Co-Au trilayer film, structural depth profiling by glancing angle X-ray diffraction 7-26593
 Ni_{0.64}Fe_{0.36} intermetallic cpds., charge redistrib., L-edge XANES study 7-64816
 Ni₃Fe, dislocation annihilation and strain hardening (Russian) 7-46500
 Ni₃Fe, order-disorder transformation, positron annihilation study 7-39509
 Ni₃Fe, ordered alloy, antiphase boundary form. energy, atomic config., Morse pot. approx. (Russian) 7-46419
 Ni₃Fe, ordered and disordered, mag. permeability studies 7-59053
 Ni₅₀Fe₅₀ (100) alloy, segregation and adsorption of S 7-21617
 Ni₆₀Fe₄₀ (100), initial oxidation and sulphidation, LEED study 7-58641
 Ni₇₇Fe₂₃, amorphous, mag. scatt. influence on transport props. 7-33001
 (Ni₃Fe)_{1-x}Cr_x alloys, ordering study, comp. depend., electron diff. and Mossbauer meas. 7-51690
 Ni₃(Fe_{1-x}Mn_x) magnetic alloys, impurities, ordering 7-51995
 Ni_{1-x}Fe_xMnSb, half-metallic ferrimag., mag. and crystallographic props. 7-45672
 Ni_{41.5}Fe_{58.5}R-Al matrix, (R = Mischmetal), H sorption, nonequilib. parameter 7-32836
 NpFe₂Al_{8-x}, mag. props., Mossbauer effect and neutron diff. 7-59127
 Pd-Ag-Fe (1 and 2 at.%), plastically deformed, elec. resist., short range order effects 7-27318
 Pd-Fe dilute alloys, Fermi surface exchange splitting, de Haas-van Alphen effect studies 7-52405
 Pd-Fe(B,O), mag. susceptibility, impurity effects 7-27520
 PdFe, drawing effects on elec. resist. and mech. props. (Russian) 7-17584
 PdFe ordered alloy, discontinuous domain coalescence (Russian) 7-2025
 Pd₃Fe disordered alloy, low-energy spin-wave excitations, Heisenberg model calcs. 7-2829
 Pd₃Fe, disordered phase, electronic struct. anal. 7-58735
 Pd₃Fe, electronic struct. 7-52415
 Pd₃Fe hydrated ordered alloy, mag. behaviour, Mossbauer studies (Russian) 7-2890
 Pd_{1-x}Fe_xH₂ system, isomeric shift, fluctuations of hyperfine interaction, Mossbauer study 7-45843
 Pd₃FeH₂, H solubility in ordered/disordered Pd alloys 7-21473
 PdFeMn₂, reentrant alloy, ferromagnetism investig. 7-2860
 Pd₇₅Fe₂₅(P₂₀) amorphous spin glasses, muon spin relax., temp. depend. meas. 7-45882
 Pr-Fe, amorphous films, perpendicular magnetic, mag. and magneto-optical props. 7-64496
 Pr₂Fe_{14-x}Co_xB system, struct. and magnetism 7-45631
 PrCo_{4-x}Fe_xB, crystallographic and mag. props. 7-45671
 Pr_{1.5}Fe_{7.5}B₈, sintered permanent magnets, depend. of coercivity on anisotropy field 7-45744
 Pr₂Fe₁₄B, anisotropy constants, temp. depend. (Chinese) 7-59003
 Pr₂Fe₁₄B permanent magnet materials, prep. and props., book contrib. 7-27981
 Pr₂(Fe_{1-x}Co_x)₁₄B, mag. props. 7-64549
 Pr_{2-x}R_xFe₁₂Co₂B, (R=Dy, Tb), mag. characts. 7-45670
 Pt₁Mn₁Fe_{1-x}, mag. state near critical composition (Russian) 7-17170
 Pu-Fe alloys, formation amorphous or metastable structures 7-16421
 R₂Fe₁₄B, cryst. field effects at rare-earth sites 7-45598
 R₂Fe₁₄B, permanent magnet, props. and struct. 7-53053
 R₂Fe_{14-x}Co_xB, spin reorientations 7-64484
 R₂Fe_{14-x}Mn_xB (R=Pr, Gd, Nd, Pr, Gd), mag. characts. 7-27523
 R₂Fe_{12-x}Mn_xCo₂B (R=Pr, Gd), mag. props. 7-27500
 RGa₂Fe₂ (R=La, Ce, Pr, Nd, Sm), cryst. struct., mag. props. 7-45614
 Rh-Fe wires as resistance thermometers 7-307
 Ru₂Fe_{90-x}B₁₀ amorphous alloys, magnetic phase diagram, magnetisation and Mossbauer studies 7-53042
 Si-Fe BCC alloy, struct. and mag. props., order-disorder transition effects (Russian) 7-32346
 SiFe, grain oriented, Barkhausen noise behaviour, effect of local strain 7-33205
 Si₃N₄/Al/Invar ceramic/metal joints, rel. between tensile and three-point bending strengths 7-39583
 Sm-Co-Fe-transition metal permanent magnets, magnetisation 7-53033
 Sm-Fe amorphous thin films, low temp. mag. props. (Chinese) 7-38910
 Sm-Fe-Co-B-Si melt-spun alloys, mag. props. 7-27553
 Sm₂(Co, Fe, Cu, Zr)₁₇ sintered compact permanent magnet, mag. props., comp. and heat treatment effects (Korean) 7-2894
 Sm₂(Co_{1-x}Fe_x)₁₇, rapidly quenched ribbons, mag. props. 7-27552
 a-Tb-Fe/Ni-Fe-Mo bilayer films, unidirectional anisotropy 7-59065
 Tb_{0.3}Dy_{0.7}Er_{0.2}Fe₂, spin reorientation, Mossbauer study 7-13068
 Tb_{0.27}Dy_{0.73}Fe₂, Terfenol, polycrystalline, domain structures and magneto-mech. coupling 7-53025
 Tb_{0.27}Dy_{0.73}Fe₂, twinned [112] crystals, magnetostriction 7-53105
 TbFe amorphous alloys, local mag. anisotropy energy estimation 7-7503
 TbFe amorphous alloys, magneto-optical props. and mag. anisotropy 7-27706
 TbFe and GdTbFeCo alloys, amorphous thin films, thermomag. recording, magnetisation reversal, coercivity 7-64459
 TbFe films, micron-size laser-written mag. domains, Lorentz microscopy 7-2913
 TbFe magneto-optical layer, AlN corrosion protective coating 7-53953
 Tb₂₁Fe₇₉ amorphous films, radial distribution function 7-37860
 Tb₃₁Fe₆₉ amorphous films, mag. props. and domains, substrate temp. effects 7-13011
 TbFeCo amorphous film sputtered onto polycarbonate substrate, depth profile, XPS 7-65362

iron alloys continued

- TbFeCo/dielectric interface, chemical stability, interdiffusion and oxidation, AES, XPS and RBS depth profile studies 7-12513
 TbFeCo-based amorphous films, magneto-optical recording appls. 7-53074
 Tb(Fe_{1-x}Co_x)₃, struct. and mag. props. 7-1950
 a-Tb₆₄Fe₂₀Ga₁₆, mag. phase transition behaviour in random anisotropy system 7-2864
 (Tb_{1-x}Fe_x)_{1-y}U_y, amorphous, magneto-optical effects 7-59187
 Ti-Al-Cr-FeSi, AT3 alloy, corrosion resist. and hydrogenation susceptibility in dil. H₂SO₄ soln. 7-17685
 Ti-Al-Fe, mech. props., investg. as implant material (*German*) 7-46647
 Ti-Al-Mo-Fe, struct. changes during phase transitions (*Russian*) 7-53721
 Ti-Fe, amorphous phases, mechanical alloying 7-27972
 Ti-Fe, electronic, mag., supercond. and glass forming ability rel. to stability 7-38846
 Ti-Fe, metastable β -phase alloys, mech. twinning TEM obs. 7-6633
 Ti-Fe H storage, theory 7-34074
 Ti-Fe powder mixture compacts, sintering behaviour in H atm., TiFe synthesis 7-53672
 α -Ti-Fe system, Fe solubility, 360 to 580°C, Mossbauer studies 7-32656
 Ti-Fe-Mn, sintering, dilatometry, thermographic obs. 7-13404
 Ti-Fe-Mn compacts, vol. changes in sintering, Mn Influence 7-7926
 TiC-Fe-Cr alloyed with Si, high-Cr, sinterability and mech. props. improvement 7-64986
 TiCr_{2-x}Fe_x alloys, H absorption and storage investg. 7-32832
 TiFe, adsorption of O, AES study 7-59312
 TiFe, H absorpt., Mossbauer obs. 7-27642
 TiFe, oxidised, bulk and surface phase composition 7-46700
 Ti₄Fe₂O, H absorpt., Mossbauer obs. 7-27642
 TiN-Fe sputtered binary coatings on steel substrates (*Japanese*) 7-59419
 TiNi-Fe alloys, martensitic transform. and props. (*Russian*) 7-39511
 TiNiFe, premartensitic state investg., Mossbauer effect studies (*Russian*) 7-3298
 Ti₅₀Ni₄₇Fe₃, intermetallic cpd., martensitic transform. at high press. (*Russian*) 7-59520
 Ti_{75-x}Sb₂₅Fe_x, A-15 supercond., transition temp. and mag. susceptibility 7-2768
 U-Si-Fe, β to α phase transform., dilatometry, metallography 7-28036
 UFe₂, spin-polarised energy bands, density of states and eqn. of state 7-58734
 U₂Fe, heavy fermion superconductor, penetration depth rel. to saturation spin moment 7-52893
 UFe₂Al_{12-x}, ferromagnetic suscept. meas. 7-12954
 V-Cr-Fe, corrosion in pressurised water, 288°C 7-53967
 V-Fe-H alloys, positron annihilation near crit. electron conc. 7-46199
 V-Ti-Fe-H₂ system, V-rich, dihydride form., lattice parameters, thermodynamics 7-32369
 VFeSi, VFeGe, solid solns., elec. resist. (*Russian*) 7-45273
 W fibre reinforced Fe-Cr-Al superalloy, surface cladding and matrix deform., thermomech. loading 7-46568
 W-Fe-Co-Ni system, isotherms of solidus and phase comp. above 1200°C 7-65006
 W-Fe-Co-Ni system, phase equil., peritectic transform. 7-53701
 W-Ni-Fe, sintered, ductility and precip. 7-17589
 W-Ni-Fe system, matrix and interfacial precip. 7-46478
 WC-FeNi cemented carbides, abrasion, controlling mechanism 7-3460
 Y-Fe sputtered amorphous films, mag. props. 7-53083
 Y-Fe-B system alloys, mag. props. 7-27563
 Y-Pd-Fe, intermetallics, interaction characts. and props. 7-46414
 Y(Dy)(Er)_{2-x}Th_xFe₁₄B alloys, mag. props., comp. depend. study 7-7492
 Y₂(Fe,Al,Co)₁₄B, mag. props., composition depend. 7-53030
 Y₂Fe₁₄B, electronic struct. and mag. props. recursion method calcs. 7-2452
 Y₂Fe₁₄B, magnetic props., H₂ absorption effects 7-38906
 Y_{100-x}Fe_xH_y metallic glasses, mag. props., H content effects 7-33155
 Y₂Fe_{14-x}Si(Cu)B alloys, mag. props. 7-45681
 YbFe₂, YCrB₂-type structure, formation in Yb-Fe-B ternary systems 7-6581
 Yb₂Fe₁₄B, exchange and cryst. field interactions 7-27512
 Zn-Fe alloys, high-current density electroplating 7-17485
 Zr-Cr-Fe, polytype structures, TEM, electron diff. obs. 7-37925
 Zr-Fe amorphous alloys, chemical short range order, thermal relaxation and ion irradiation effects 7-44385
 Zr-Fe compounds, electronic, lattice and supercond. props., rel. to amorphous alloys 7-17133
 ZrFe₂, electronic struct. and mag. props., tight-binding approx. calcs. 7-2475
 Zr₇₅Fe₂₅, hydrogenised, positron lifetime and Mossbauer study 7-46198
 Zr₇₆Fe₂₄, metallic glass, interaction of O, XPS study 7-39350
 ZrMnFe₂ system, H storage material, effect of hyperstoichiometric Fe 7-45000

iron compounds

- see also ferrites; iron alloys
 chemical bond, struct., short range order 7-32350
 complexes, spin transition induced by heat, pressure, light and nuclear decay 7-58785
 ferrichromites, coordination and oxidation states, XPS and XANES studies 7-63583
 ferrous spinel, oxidation kinetics and mechanism, elec. cond., thermogravimetry 7-27326
 garnet epitaxial films, near a nonmagnetic metallic disk, domain struct., mech. stress effects 7-38922
 garnet film, epitaxial growth from weakly dissociated molten soln. 7-64944
 garnet films containing Bi, comp. study, XPS and chemical etching anal. 7-45083
 haematite, Fe₂O₃, microhardness meas. up to 900°C 7-21343
 intercalation cpd. with graphite, atomic structure, EXAFS studies 7-12011
 intercalation cpd. with MOS₂, AES, sputtering studies 7-63867
 minerals, Fe sites, electronic struct., iterative EHT, multiple scatt. X α calcs. and Mossbauer meas. 7-17244
 nitrides, decomposition on surface treated steel 7-17736
 ores, saturation magnetisation, temp. depend., Backer's chem. reaction (*Korean*) 7-33263
 oxalate (2,2'-bipyridine) iron polymer, slow paramag. relax., Mossbauer spectra 7-27638
 oxide coatings on Invar, IR emission, absorpt. modes effect 7-27708

iron compounds continued

- oxide passive film composition and growth, atom probe depth profiling anal. 7-32869
 oxide surfaces, chemisorption of pyridine and pyrrole, XPS 7-27128
 oxides, coatings on Fe, IR emission, absorpt. modes effect 7-27708
 phthalocyanines, spontaneous pyroelec. current obs. 7-27669
 polyacetylene:AsF₆⁻ (ClSO₃)⁻ (FeCl₄)⁻ metallic elec. cond. studies 7-64231
 polyacetylene:FeCl₃, DC elec. cond. studies 7-33018
 silicate minerals and glasses, Fe K-edge EXAFS studies, Fe coordination 7-59287
 sputtered atom excitation, optical spectra studies 7-59347
 surface friction layers, study by AES method (*Russian*) 7-59674
 surface oxide layer, reduction by H adsorption, AES and LEED studies 7-8297
 YIG, ⁵⁷Fe enriched, quantum beats from synchrotron radiation pulses 7-2960
 Al₂O₃-SiO₂-Fe₂O₃-CaO-MgO-Na₂O-K₂O glass batch melting, interaction between solid, liq. and gas 7-7946
 B-Fe, ion beam mixing, effects of Xe⁺ implantation (*Chinese*) 7-51886
 Ba₂CaCu₂Fe₂F₁₄, exchange interactions, mag. susceptibility meas. 7-45654
 BaCo₂Fe₁₆O₂₇, hexagonal ferrites, neutron diff. studies 7-45622
 BaFe₂ZrF₄-FeF₂ glasses, Raman scatt. study 7-27713
 BaFe_{12-x}Mn_xO₁₉, Mn substitution effects on mag. props. (*Chinese*) 7-7486
 BaFe₁₂O₁₉, hexagonal ferrites, neutron diff. studies 7-45622
 BaMg₂Fe₁₆O₂₇, hexagonal ferrites, neutron diff. studies 7-45622
 BaO-B₂O₃-Fe₂O₃ glasses, γ -irradiated and heat treated, elec. conductivity and crystn. 7-21510
 BaO-Fe₂O₃-B₂O₃-based glasses, crystallisation behaviour, nucleating agent effects 7-51650
 BaO-RuO₂-Fe₂O₃ system, equilibria description 7-65340
 BaO-V₂O₅-Fe₂O₃ semiconducting glasses, elec. props., Mossbauer, EPR and X-ray diff. studies 7-7236
 Bi-Zn-Fe-O amorphous films, struct. and mag. props. 7-51645
 Ca₃Fe₂TiO_{8+x}, perovskites, microdomains, electron microscopy 7-16533
 (Ca₁₁Mg₈Fe₃Mn₁₁)(CO₃)₂, ankerite, ⁵⁷Mossbauer spectra relax. rates 7-27640
 CaMgSi₂O₆ - CaFeSi₂O₆, solid solns. short range order parameters, determ. from EXAFS pair distrib. fns. 7-59289
 CoAlFeO₄, cubic spinel, Mossbauer anal. 7-33304
 Co_{1-x}Fe_xCr₂S₄, paramag. susceptibility study 7-52934
 Co₄Fe_{1-x}Cr₂S₄ mixed spinel system, temp. depend. Mossbauer studies 7-38976
 CoO_x-Fe₂O₃ selective coatings, spray pyrolysis for high temp. appls. 7-5974
 Cr-Fe-C system, EELS fine struct. 7-39333
 Cs₃FeCl₄·H₂O, antiferromagnet, mag. phase diagram, spin wave excitations, Mossbauer spectra 7-45676
 Cs₃Fe₂F₉, precise struct. determ. and ferromag. props. anal. 7-1981
 Cs₃Fe(SO₄)₃, columnar cpds., vibr. spectra and phase transitions 7-17314
 CuFe₂S₃, EXAFS meas. under high press. by diamond anvil cell 7-64754
 Cu_{1.80}Fe_{0.05}S₃, structural phase transitions, X-ray diff. study 7-1935
 Cu_{0.96}Fe_{0.04}SiF₆·6H₂O Jahn-Teller cryst., glass transition, calorimetry and Mossbauer studies (*Russian*) 7-26952
 Cu₂FeSnS₄, stannite, melting, polymorphic transition temp. 7-44764
 Fe (III) complexes, spin-exchange processes 7-12677
 Fe (II) complexes, spin-exchange processes 7-12677
 Fe (OH)₃ as colloidal barrier in aquifer for seasonal thermal energy storage 7-65610
 Fe complex, Fe(hexaphenyl-1,4,7,10-tetraphosphadecane), tetraphenylborate, electronic relax. 7-25578
 Fe complex, ferric acetyl acetate, EPR studies 7-13024
 Fe complex, nucleophilic attack, activation mechanism, EHT and INDO calcs. 7-39847
 Fe complex, oxy(tetraphenylporphyrinate), Iron II, cocondensation products, struct. and bonding, IR spectra 7-10572
 Fe complex [(Fe(PH₃)₃(C₆H₁₃))⁺, localised INDO calcs. 7-49927
 Fe complex [(ethyl)₄N]₆[Ti₆Fe₁₀(CO)₃₆], struct. and bonding study, HMO calcs. 7-25411
 Fe complex Fe(II) trans-bis(dimethyl-glyoximate)bis(dibutyl phenylarsine) cryst. and mol. struct. 7-51711
 Fe complexes, (Fe₂O(acetate)₆(pyridine)₃)(pyridine), intramol. electron transfer, phase transition mechanism 7-10742
 Fe complexes, Fe(II)-neutral N bases, reactivity, basket-handle superstruct. effects 7-54100
 Fe complexes of pyrazolone derivatives, biological activity, Mossbauer spectra study 7-40098
 Fe oxide layer on Fe acicular particles morphology and mag. props. 7-52067
 Fe phthalocyanine, local electron distrib., Penning ionis. electron spectrosc. 7-62521
 Fe Si₂ form. by ion implantation in Si, RBS and X-ray diff. studies 7-16656
 Fe/Fe₂O₃/Al₂O₃ systems, diffusion bonded, interface chemistry, bonding strength 7-28079
 Fe-Cr oxide film struct., in- and ex-situ fluorescence EXAFS study 7-64007
 Fe-Ge-Te, compound formation, microstructure, X-ray diffraction, dilatometry studies 7-7980
 Fe-Mg-Si-O system, phase equilibria at high press. and temp., thermochemical data base 7-21407
 Fe-Mo(W) complexes, dinuclear clusters, fine and hyperfine struct. 7-36659
 Fe-N, Snoek-Koster relax., dislocation effects (*Russian*) 7-44686
 Fe-N binary solid solns., interstitial atom ordering, Mossbauer study 7-38974
 Fe-N mag. moments and bulk prep. by reduction-sintering method with heat treatment 7-7936
 Fe-N system, phase diagram, thermodynamic calc. 7-7973
 Fe-O system, struct. transitions, cryst. struct. formation 7-58459
 Fe-Si thin films, silicide formation, AES and EELS studies 7-32862
 Fe-Te sputtered films, metastable phases 7-38370
 Fe-tetrasulphonated phthalocyanines, photography, SERS and electrochemical studies 7-13155
 Fe_{2-x}Al₂O₃·1-8 H₂O substituted ferrihydride, Mossbauer, X-ray diff. and electron microscopy studies 7-7617
 FeAsS, arsenopyrite, X-ray chemical shift, K absorpt. spectra anal. 7-46239
 Fe₂B-Ni₂B, distrib. equil. in two-phase fields 7-22641

iron compounds continued

- FeBO₃, antiferromagnet, parametric excitation of magnons with a decay spectrum 7-52966
 FeBO₃, NMR of ⁵⁷Fe domains and domain walls 7-7593
 Fe₂BO₆ crystals, Laue diffracted Mossbauer spectra near spin-reversal phase transition 7-38975
 FeCN ion, mass transfer of submerged jet impinging on cylindrical surface 7-26325
 FeCO colloids, anisotropy in elec. cond. induced by external field 7-39924
 FeCO₃, antiferromag., magneto-optical determ. of exchange parameters (Russian) 7-53283
 Fe(CO)₅, laser stimulated CVD, kinetics 7-64925
 Fe(CO)₅, photofragmentation dynamics using coherent VUV for product detect. 7-19976
 Fe(CO)₅+He, dissociation, excitation, mol. orbital correls. 7-10735
 FeCl₂ 3p-3d hybridisation eval., valence band photoelectron spectra meas. 7-53495
 FeCl₂, magnetostriction, X-ray diff. meas. 7-33258
 FeCl₂ metamagnet, spin-lattice coupling and tricritical behaviour 7-2849
 FeCl₃ intercalation cpd. with graphite, mag. suscept. and low temp. transition meas. 7-58993
 FeCl₃, interphase transport investig. 7-57006
 FeCl₃, layer struct., IR vibr. spectra 7-13151
 FeCl₃, vac. deposited, effect on cathodic charact. of Cl₂-H₂ cells (Japanese) 7-13850
 FeCl₃-graphite intercalation cpd., spin-lattice relax. time meas., AC suscept. bridge techniques 7-13054
 FeCl₃-graphite intercalates, high resolution electron microscopy 7-16433
 FeClMoO₄ layered compound, struct. and mag. props., Mossbauer effect, mag. suscept., and neutron diff. studies 7-58981
 Fe(ClO₄)₃, frozen aq. solns., short-range order, Mossbauer obs. 7-45844
 FeCo oxides, oxidation state and site symmetry, EXAFS and XANES studies 7-63584
 Fe_{1-x}Co_xCl₂, Fe²⁺ localised excitation and spin orientation, ESR studies 7-64524
 Fe_{1-x}Co_xCl₂, random-field and competing-anisotropy effects, sp. ht. study 7-2872
 FeCoCrS₈, crystallographic and mag. props., Mossbauer study (Korean) 7-33310
 FeCo₂O₄, fine-particles, low temp. prep. by solid solution precursor method 7-59486
 Fe₃₀Co₃₀Si₁₀B₁₂, magnetic induced anisotropy, crossover effect 7-17169
 FeF₂-FeF₃, ion-molecule equilibria, mass spectra, heat of form., electron affinity 7-46862
 FeF₃, pyrochlore struct., soft chemistry synthesis and thermal transitions 7-17396
⁵⁷FeF₃·3H₂O, resonance scintillators for recoilless 14.4 keV γ -quanta 7-62202
 (Fe²⁺_{2-x}Fe³⁺_xTi⁴⁺_x)O₄²⁻, submicron synthetic titanomagnetites, oxidation products, IR spectra 7-27716
 x-FeGa₂S₄ layer cpd. mag. props. and ionic distrib., 2D magnetic system models 7-38880
 (Fe_{0.8}Ga_{0.2})₂TiO₅ spin glass, remanent magnetization reduction, Heisenberg and Ising comparison 7-53019
 Fe₂Ge, chemical bond, struct., short range order 7-32350
 FeH₂, prep. under high press., Mossbauer obs. 7-33313
 Fe(H₂O)₆²⁺ clusters, intermol. pot. fn. and pot. energy surface, ab initio UHF calcs. 7-25354
 FeH₃(PO₄)₂·2.5H₂O, pyrite-phosphate mixtures, X-ray phase and electron microscopic studies 7-33652
 Fe(II) tetraphenylporphyrin bis(tetrahydrofuran), electronic ground state, electron density meas. 7-51716
 Fe_{3-x}M_xO₄ (M=Ti, Cr, Mn, Al), substituted magnetite, reactivity in O₂, relation with cation distrib. (French) 7-46829
 (FeMg)₂SiO₄, oligoclase, high fluence D implantation, trapping and desorption, saturation conc. studies 7-26781
 (FeMg)₂SiO₄, spinel growth, interface struct. investig. 7-16566
 (FeMn)₈₀B₁₄Si₆ glass, magnetoresistance and magnetisation 7-45354
 (Fe_{1-x}Mn_x)₂P system, Mossbauer study 7-53180
 Fe₂Mn_{1-x}S, high temp. metal-nonmetal transition 7-7117
 (FeMo)₈₀B₁₄Si₆ glass, magnetoresistance and magnetisation 7-45354
 Fe₁₆N₂, high-dose ion implantation prep., mag. props. 7-59055
 Fe_{3-x}N film, hexagonal, prep. by plasma reaction, mag. charact. 7-13380
 γ -Fe₂N, Auger spectra, electronic struct. (Russian) 7-64832
 Fe₂N thin films, ion beam deposited, mag. props. and corrosion resistance 7-33231
 Fe(NH₄)₂(SO₄)₂·6H₂O, EPR of Mn²⁺, Mn²⁺-Fe²⁺ exchange interaction 7-2924
 Fe(NO₃)₃ reactions with catechol and Na₂S₂O₄, dispersive mode stopped flow X-ray absorption spectroscopy 7-61416
 FeNb₂O₆, cryst. struct., determ. by neutron diff. 7-6599
 Fe_{1+x}Nb_{1-x}Se₁₀, resistivity, mag. susceptibility, influence of stoichiometry 7-52426
 Fe_{1+x}Nb_{1-x}Se₁₀-yS_y, struct. mag. suscept. and ESR meas. 7-58228
 Fe_{3-x}Ni_xC₂, prep. and characterisation 7-17490
 (Fe_{0.15}Ni_{0.85})₇₅P₁₆B₆Al₃, magnetic susceptibility appl. of dynamic scaling 7-59019
 (Fe_{1-x}Ni_x)TiH_x, critical study of β -region 7-27634
 FeO, high-pressure, metallisation obs. and implications for Earth's core 7-66101
 FeO, wustite, defect agglomeration at high temps., elec. conduction model 7-21197
 FeO⁻, rot., autodetachment spectroscopy 7-62462
 FeO-PbO-P₂O₅ glasses, atomic environments, EXAFS studies 7-64787
 Fe₂O₃-CaO-MgO-BaO-Na₂O, wustite solid solns., interdiffusion coeffs., 1073-1473K (Japanese) 7-12357
 FeO_x fine particles, magnetic and morphological props., annealing effects study 7-53766
 FeO_x, wustite, molar thermodynamic properties, thermogravimetric anal. (French) 7-26981
 Fe_{0.93}O, wustite, defect arrangement at high temps. 7-21196
 Fe_{0.84}O, metallisation at elevated press. and temp., shock wave elec. resist. meas. 7-7297
 Fe_{1-x}O, defect cluster energies, MO calc. 7-2010
 Fe_{1-x}O, dopant cations interaction with 4:1 defect clusters, theoretical study 7-63644
 Fe_{1-x}O, double electron exchange, Mossbauer spectroscopy 7-17168
 Fe_{1-x}O, wustite, electronic struct. and X-ray absorption spectra 7-2479
 Fe_{1-y}O, wustite, defect clustering 7-51787

iron compounds continued

- γ -Fe₂O₃ acicular particles, magnetisation reversal by flipping mechanism 7-7545
 Fe₂O₃, adsorpt. of pyridine, gas chromatography and IR spectro study 7-39917
 Fe₂O₃ amorphous film deposition by laser CVD 7-39416
 α -Fe₂O₃ crystals, mag. phase transition, Mossbauer study 7-45850
 γ -Fe₂O₃, dispersion and particle packing of mag. oxide powders 7-3233
 γ -Fe₂O₃ films, CVD deposited, uniaxial mag. anisotropy 7-33234
 Fe₂O₃, haematite, prep. from δ -FeOOH by thermal decomp. on grinding, X-ray diff. line broadening 7-46390
 α -Fe₂O₃, hematite, magnetoelastic wave, parametric amplification in reversal of wavefront 7-7578
 Fe₂O₃, hematite, magnetoelastic wave propagation, polarisation effects 7-7581
 α -Fe₂O₃, hyperfine field changes obs., selective Mossbauer refl. spectrum detection 7-64554
 α -Fe₂O₃ microcrystals, IR spectra calc. 7-53315
 γ -Fe₂O₃ particles, colloidal suspension, mag. props. of ionic ferrofluids 7-45758
 γ -Fe₂O₃ particles, pure and Co-modified, microstructural defects 7-58497
 α -Fe₂O₃ particles in silicone oil, mag. suspension, rheology 7-37408
 α -Fe₂O₃, photoemission satellites, electronic struct. 7-39358
 α -Fe₂O₃ powder compacts, shock-modified, Morin transition, Mossbauer and magnetisation studies 7-2852
 Fe₂O₃ powder type audio tapes, mag. domain obs. by colloid-SEM method (Japanese) 7-7533
 γ -Fe₂O₃ preparation by mechanochem. transform. of γ -FeOOH in presence of Li₂CO₃ 7-59478
 γ -Fe₂O₃ reactive RF sputter deposition, struct., elec. and mag. props. studies 7-17421
 Fe₂O₃ reactivity, decomposition mechanism depend., reaction vol. and densification meas. 7-28308
 α -Fe₂O₃, reduction-sintering prep., mag. props. 7-59054
 Fe₂O₃ silica coated particle dispersions, magnetic recording appls. 7-53057
 α -Fe₂O₃ single crystal, backward surface wave, parametric instability and amplification 7-22128
 γ -Fe₂O₃ sputtered thin films, CoCr-doped, stress-induced perpendicular mag. anisotropy 7-33232
 γ -Fe₂O₃ superfine powder, prep. and gas sensitive props. (Chinese) 7-59484
 γ -Fe₂O₃ thin films, mag. props. 7-33233
 Fe₂O₃:Co particles, coercivity time-scale depend., magnetic switching units vol. determ. 7-53059
 Fe₂O₃:Co sputtered films, X-ray diffraction anal. 7-58675
 γ -Fe₂O₃:H, H content, DTA, mag. anal. and Mossbauer studies (Chinese) 7-12104
 γ -Fe₂O₃:H, hydrogen probe using thermal neutron transmission gauge (Chinese) 7-6666
 Fe₂O₃:Ti(Sn,Nb), γ -ray damage, impurity effects on annealing 7-6679
 α -Fe₂O₃/AgI composite electrolytes, phase transition temperatures (Chinese) 7-38244
 Fe₂O₃/o-toluidine photoelectrochemical imaging system (Japanese) 7-35590
 Fe₂O₃-BaO-B₂O₃-V₂O₅ glasses, Fe³⁺ site occupancy, Mossbauer studies 7-6541
 Fe₂O₃-Na₂O-B₂O₃ glasses, Mossbauer study 7-7619
 Fe₂O₃-P₂O₅-K₂O glasses, mixed valence, EXAFS studies 7-64786
 Fe₂O₃-SrO system, glass ribbon prep. by melt spinning, charact. 7-53690
 Fe₂O₃, hematite, O activity depend., high temp. Mossbauer spectra 7-38978
 Fe_{3-x}O₄, diffusion-controlled form. during reactions, defects effects 7-17768
 Fe_{3-x}O₄, magnetite, O activity depend., Mossbauer spectra 7-38977
 Fe₃O₄, dispersion and particle packing of mag. oxide powders 7-3233
 Fe₃O₄ films, mag. anisotropy and magneto-optical props. 7-2910
 Fe₃O₄, magnetite, cryst. struct. under press. 7-16524
 Fe₃O₄, magnetite, Fe and impurity cations, migration enthalpies meas. 7-58541
 Fe₃O₄, magnetite, high press. cryst. chemistry 7-16521
 Fe₃O₄, magnetite, hysteresis props. rel. to particle size 7-14268
 Fe₃O₄, magnetite, mag. after-effects at room temp. 7-64493
 Fe₃O₄, magnetite-laced microspheres, mag. moment meas. 7-53064
 Fe₃O₄, Mott-Wigner glass, polaronic order-disorder transition, muon spin rot. meas. 7-44787
 Fe₃O₄ particles in magnetic fluid, surface mag. props., Mossbauer spectra study 7-45756
 Fe₃O₄ single cryst., dielec. and conducting props. study below Verwey point 7-53230
 Fe₃O₄, small polaron conduction and short-range order 7-7239
 Fe₃O₄, surface magnetism, ion bombardment effects 7-12949
 Fe₃O₄-CaO-SiO₂ amorphous oxides, magnetic props. and struct., Mossbauer spectra study 7-7538
 Fe₃O₄-ZnFe₂O₄ system, thermodynamic props., EMF obs., X-ray diff. 7-22646
 Fe_xO·Li₂O(CaO)(Al₂O₃)(SiO₂), synthetic wustite, elec. cond., doping elements effect (Korean) 7-2609
 FeOCl, anisotropic layer cpd., hyperfine interactions, Mossbauer spectra 7-58786
 Fe(OH)₃, adsorpt. of pyridine, gas chromatography and IR spectro study 7-39917
 FeOOH, poorly-ordered precursors, local struct., EXAFS studies 7-63577
 FeOOH sols, crystallisation, Mossbauer study 7-38970
 FeOOH thin films, precipitated, structure anal. 7-32860
 γ -FeOOH-LiCO₃, mixture, mechanochem. transform. and γ -Fe₂O₃ form. 7-59478
 FeP(As)O(S)₄, dielec. const. meas. w.r.t. bond ionicity (French) 7-38988
 FePO₄-II, high press. phase, mag. props. 7-45852
 FePS₃, absorpt. spectra of transition metal ion 7-33411
 FePS₃, layered cpd., valence and conduction bands studied by synchrotron radiation 7-38450
 FePS₃, optical absorption in near IR, visible and near UV regions 7-46070
 FeS containing Cr and Mn, cation vacancy conc. 7-16551
 FeS₂ polycryst. photoactive MOCVD films, photocond. and time-resolved microwave cond. meas. 7-45386
 FeS₂, pyrite cryst., chemical vapour transport with halogens 7-53513
 FeS₂ pyrite films, chemically deposited, interband transitions 7-13246

iron compounds continued

- FeS₂-Al secondary cell, characts. of AlCl₃/1-butylpyridinium chloride electrolyte (*Japanese*) 7-8371
- FeS₂-Al secondary cell, positive electrode reaction kinetics, AC impedance study 7-8372
- FeS₂-Al secondary cell performance develop. using AlCl₃/1-butylpyridinium chloride electrolyte 7-8370
- FeS₂-Al secondary cell with basic AlCl₃-NaCl melt, cell performance and positive electrode reaction (*Japanese*) 7-13852
- FeS₂-electrolyte photoactive interface, electronic props. 7-33086
- FeSb₂O₄, thermodynamics studies, 10 to 300K 7-2231
- Fe₂Se₃ and As₂Se₃-Fe₂ films, electronic props. 7-58922
- FeSi, heat of form. evaluation from X-ray emission spectra (*Russian*) 7-59776
- FeSi₂ thin films, appl. to electro-optic VLSI interconnects 7-53427
- Fe₂(SiO₄), defects, Fe³⁺ conc., microscope-spectrometric method 7-17330
- Fe₂SiO₄, fayalite, electron density and polarised absorption spectra 7-22280
- Fe₂SiO₄, spinels, cryst. struct. as function of temp. and heating duration 7-16522
- Fe₂SiO₄-Zn₂SiO₄, limited solid soln., cation ordering 7-51709
- Fe₂Si₂O₇(OH)₂, grunerite, mag. order, quasi-one dimensional antiferromag. with spin canting transition 7-58983
- Fe_{0.458}Sn_{0.088}O_{0.454} film, mag. props., appl. in perpendicular mag. recording 7-59005
- Fe₂Ta₂S₆, channel structs., 3d metal pairing 7-26719
- FeTiO₃, ceramic matrices, precip. morphology 7-65049
- FeTiO₃, mag. struct. 7-7484
- FeTiO₃, oblique easy-axis antiferromag. neutron scatt. study of mag. excitations 7-45643
- FeTiO₃, olivine, high fluence D implantation, trapping and desorption, saturation conc. studies 7-26781
- Fe_{2-x}Ti_{1+x}O₅, pseudo-brookite, anisotropic spin-glass transition, transverse spin ordering, μ SR study 7-45688
- Fe₂Ti_{0.6}O₄, magnetisation in 1 to 30 microns particle size range 7-47425
- Fe₂TiS₂, intercalated dichalcogenide, electronic struct. 7-52387
- Fe₂TiS₂, intercalation cpd., elec. resist. and thermopower studies 7-45331
- (FeV)₁₀B₁₄Si₆ glass, magnetoresistance and magnetisation 7-45354
- Fe₂V_{4-x}Mo_xO₁₃ type phases, Mossbauer spectra 7-38969
- FeVO₄, magnetic phase transitions, mag. suscept. and sp. ht. meas. 7-2842
- Fe_{1-x}Zn_xF₂ diluted Ising antiferromagnet, magnetisation critical exponent crossover, Mossbauer meas. 7-7529
- Fe₂ZrSe₂, intercalated layered cpd., thermopower and low DC field magnetisation study 7-17199
- Fe₃(1- δ)O₄, magnetite, synthesis, crystal growth and characterisation 7-2647
- Fe_{1-x}Cr_xBO₃, weak ferrimagnetism, antisymmetric exchange 7-45741
- Ga_{2-x}Fe_xO₃, precipitation in MgO-Ga₂O₃-Fe₂O₃ (*French*) 7-6798
- Hg_{1-x}Fe_xSe, ionised resonant donor and acceptor superlattice form., screened Coulomb interaction, carrier scatt. effects 7-16981
- K₂CoFe_{1-x}F_x, oblique antiferromag. phase, spin waves, inelastic neutron scatt. study 7-64443
- KFe₂O₅, ceramic, radiation induced products STEM microanalysis 7-16639
- KFeS₃, hydrogenated, ESR meas. in 100 to 320K range 7-13016
- K₂LiFe₂S₆Cl, djerfisherite, electrochemically synthesised, cryst. struct., neutron diff. study 7-58224
- K₂Ni_{1-x}Fe_xF₄, 2D random mixture with competing spin anisotropies, Mossbauer spectroscopy 7-59021
- K₂O-Al₂O₃-B₂O₃-Fe₂O₃-Gd₂O₃ glasses, mag. props., composition dependences 7-2823
- K₂O-Ga₂O₃-SiO₂-Al₂O₃-Fe₂O₃-FeO melts, struct. role of Fe³⁺, Ga³⁺, Al³⁺, Fe redox ratio 7-26635
- Li-Al/FeS₂ cell with LiCl-LiBr-KBr molten electrolyte 7-65439
- LiFe_{0.5}Al_{0.5}Ga_{0.8}O₈, magnetisation and lattice parameter, role of Al and Ga ions 7-22097
- Li_{1+x}FeCl₄, ionic conductors, Mossbauer spectra studies (*French*) 7-2955
- LiFeClMoO₄, synthesis, struct. and low temp. magnetism 7-21172
- Li₂Fe(MoO₄)₃, insertion cpd., struct., from neutron powder diff. data 7-1985
- LiFeP₂O₇, cryst. synthesis, at. struct., DTA, X-ray diff. study 7-26708
- Li₂Fe₂(PO₄)₃, microtwinning, X-ray struct. investig. 7-44567
- Li₂Mg_{1-x}Fe_xSn_{1-x}O₈, ramdellite type cpds., ionic conductivity and cryst. chemistry 7-32708
- (Mg,Fe)SiO₃, hypersthene, Mossbauer spectra of Fe²⁺, electronic spin relax. 7-33307
- MgO-FeO, solid solns. short range order parameters, determ. from EXAFS pair distrib. fns. 7-59289
- MgO-Ga₂O₃-Fe₂O₃ system, precipitation of Ga_{2-x}Fe_xO₃ (*French*) 7-6798
- MgO-LiFeO₂, solid solns. short range order parameters, determ. from EXAFS pair distrib. fns. 7-59289
- Mn_{1-x}Fe_xAs, phase transitions, effect of external press. and chemical substitutions 7-63798
- MnFeF₆(H₂O)₂, ferrimag., mag. and Mossbauer study 7-45845
- Mn_{0.35}Zn_{0.35}Fe_{2.12}O₄, single cryst. surface damage depth meas. 7-52979
- Mn_{0.61}Zn_{0.33}Fe_{2.04}O₄ single cryst., low temp. acoustic props. anomalies, spin-reorientation transitions 7-51957
- NH₄Fe₂F₆, topotactic oxidation for FeF₃ synthesis 7-17396
- NaFeClMoO₄, synthesis, struct. and low temp. magnetism 7-21172
- Na₂O-B₂O₃-Fe₂O₃ glass, hyperfine parameter distrib., ⁵⁷Fe Mossbauer study 7-22170
- Na₂O-Fe₂O₃-Al₂O₃-SiO₂ glasses, Fe³⁺ ESR spectra, valence-coord. state 7-45813
- Na₂O-Fe₂O₃-SiO₂ systems, glass formation and props. 7-2203
- Na₂O-FeO-SiO₂ systems, glass formation and props. 7-2203
- Na₂O-SiO₂-FeCO₃-Fe₂O₃ glass system, prep., props and struct. 7-1900
- (Na₂O.2SiO₂)_{1-x}(Fe₂O₃)_x glasses, Fe ions, ionic state and coordination geometry 7-63492
- NiCoFe ferrite, perminvar, wall displacements, induced anisotropy effect. 7-52968
- PbFe₂O₉, cryst., complex magneto-optical polar Kerr effect spectra 7-53280
- PbO-B₂O₃-Fe₂O₃ glass, ESCA study 7-26651
- PbO-Fe₂O₃-B₂O₃ glass ceramics, mag. props. and EPR spectra of precipitated mag. phases 7-45748
- PbO-Fe₂O₃-P₂O₅ glasses, liquid chromatography and Raman scattering studies 7-11946
- Pb(PO₃)₂-Fe₂O₃ glass, struct. props., chromatography and Raman spectra studies 7-21112

iron compounds continued

- Pb(Zr_{0.38}Fe_{0.20}Nb_{0.20}Ti_{0.02})_{0.995}U_{0.005}O₃ ferroelec. ceramic, TEM study 7-17272
- RbFeF₄ layer cpd., structural phase transitions studies 7-26942
- Rb₂KFeF₆, structural phase transitions 7-52044
- Rb₂KFeF₆, structural phase transition, Raman scatt. and group-theoretical studies 7-52045
- SiO₂-Na₂O-Al₂O₃-ZnO-Fe₂O₄-Si glass system, Fe behaviour at various compositions and reducing conditions 7-1899
- SiO₂-Na₂O-CaO-MgO-Al₂O₃-BaO-FeO₃ glass, elec. field stimulated Na depletion 7-6897
- SnFe_{0.95}Mo_{0.05}S₈, Chevrel-phase superconductor, collinear ordering, EXAFS studies 7-13258
- Sr₂FeTiO_{6-x}, defect struct. 7-1992
- Ta₂O₅-Fe-Fe₂O₃ system, equilibria at 1200°C 7-12301
- TiFe(CN)₆ microsphere production by sol-gel process 7-30679
- Ti₄Fe₂O₉, adsorption of O, AES study 7-59312
- Ti₃Fe(SO₄)₃, columnar cpds., vibr. spectra and phase transitions 7-17314
- TiFe₂-Se₂ layered cpd., single cryst., magnetic and structural props., Mossbauer and X-ray diff. studies 7-2848
- UF₆Gas, structural chemistry, mag. behaviour 7-16513
- YFeO₃-Fe₂O₃ mixed phase system microcryst., anomalous behaviour of mag. hyperfine field 7-45760
- YIG, small thin-film samples, magnetic resonances anal. 7-53090
- Zn_{1-x}Fe_xCr₂S₄, paramag. susceptibility study 7-52934
- ZnFeF₆(H₂O)₂, cryst. struct., mag. and Mossbauer study 7-45845
- ZnO-Fe₂O₃ powder mixtures, shock synthesis of Zn_{1-x}Fe_{2+x}O₄ 7-37955
- ZnO₂-Fe₂O₃ powder mixtures, shock synthesis of Zn_{1-x}Fe_{2+x}O₄ 7-39899
- ZrF₄-BaF₂-GdF₃-AlF₃-NaF-FeF₃, optical fibre glasses, trace amounts of Fe, characterisation 7-2956
- iron phosphate semiconductor glasses** see *amorphous semiconductors*
- irradiation effects** see *radiation effects*
- irradiation induced creep**
- FACSIMILE code for void swelling calc. 7-25037
- metals, irradiation-induced transient creep during pulsed irradiation 7-13528
- polymer, radiation-induced stress change during electron irradiation 7-16631
- spent fuel rods, accelerated high-temperature tests under dry storage conditions, creep deformation meas. 7-36153
- steel, austenitic stainless, in-reactor deform. 7-56826
- steel, austenitic stainless, Ti-stabilised, high temp. embrittlement modification of rad. induced He distrib. by thermo mech. pretreatment (*German*) 7-17643
- steel, stainless, type 316, neutron damage USA-Japan studies 7-56834
- Zircaloy-2, irradi. growth under temp. cycling, solute-interstitial complex mechanism 7-44607
- α -Fe, cryst., point defect and edge dislocation interaction simulation and radiation creep rate estimation 7-21216
- Ni, electron bombardment effect, 200 to 500°C 7-8062
- V-20Ti pressurized tubes, creep response to neutron irradiation 7-56831
- Ising lattices** see *Ising model*
- Ising model**
- (1+1)-dimensional, correl. length, finite-size scaling universality and boundary conditions, comment and reply 7-41293
- 1D Ising ferromagnet, multi-spin flip critical dynamics 7-38888
- 2D, logarithmic singularities of Q-depend. susceptibility 7-27484
- 2D, uniaxial anisotropy and next-nearest-neighbour 7-41298
- 2D, with competing interactions, Monte Carlo studies, review 7-59043
- 2D model on square superlattice, critical props., real space renormalisation group calcs. (*Chinese*) 7-27532
- 2D random field, correlations 7-6754
- 3D Ising model program, vectorisation on the CDC CYBER 205 7-41281
- $\pm J$, on arbitrary lattice, geometry-induced ferromagnetic-nonferromagnetic phase transition 7-27535
- Φ^4 field theory on square lattice, finite size scaling anal. 7-9945
- Φ^4 theory, nonuniversal power laws and critical-to-classical crossover 7-41297
- alloys, order-disorder phenomena, Ising model calcs. allowing for atomic vibrations 7-21400
- amorphous Ising ferromagnet, transverse suscept. investig. 7-2870
- analyticity of correlation functions in 2D 7-235
- anisotropic, mean-field renormalisation approach 7-4775
- anisotropic cubic spin-1 Ising model, linear chain approx. 7-2876
- anisotropic interface tension, scaled interface width and equilib. shape in 2D, relationships 7-12401
- ANNI model, two-dimensional, ring recurrence method anal. 7-48609
- ANNI model, two-dimensional, wetting phenomena 7-27064
- antiferromagnet, ground-state entropies in two and three dimensions 7-45717
- antiferromagnet with site-diluted free surface, surface phase diagram 7-45718
- antiferromagnetic quantum spin chains, random exchange effects, Monte Carlo study 7-64475
- antiferromagnets in maximum critical fields 7-17185
- axial decorated Ising model with competing interaction, phase diagram and thermodynamics 7-14875
- Bethe lattice, Ising model with competing interactions up to third-nearest-neighbour generation 7-41288
- binary alloy, FCC Ising, multiaut interactions, low temp. behaviour and Monte Carlo simulations 7-6755
- binary crystals, FCC, ordering, Monte Carlo simulation 7-38154
- C* algebra approach to analyticity in quantum statistical mechanical models 7-56148
- Cayley tree, S=1, generalization of Falk's theorem and i- δ relations 7-7466
- Cayley trees, randomly closed, and fractal dimensionality 7-4784
- chain with nonconstant external field 7-29929
- chaotic spin-glass phase, description in terms of T=0 fixed point 7-45716
- charge transfer compounds, thermodynamic and dynamic props. 7-59048
- cluster size distrib. probabilities in Ising model with four-spin interactions 7-64424
- complex dynamical systems, phase transform. 7-29954
- critical exponents in non-integer dimensions 7-56172
- crystal-field effect on the transverse susceptibility in spin-S Ising chains 7-45601
- Curie-Weiss-Ising model, limit Gibbs states 7-7467
- desorption from a linear chain of adsorption sites, kinetic Ising model 7-21649

Ising model continued

diamond lattice, renormalisation anal. and spin observables 7-48632
 dilute antiferromagnet, random-field Ising model 7-7528
 dilute random-field Ising model, domain growth, self-similar dynamical scaling breakdown 7-35430
 dipolar, critical relax. at marginal dimension 7-52925
 disorder fields in two-dimensional conformal quantum-field theory and $N=2$ extended supersymmetry 7-41161
 disordered ferromag. binary system, phase diagram 7-59041
 disordered systems, thermodynamic props., renormalisation group calcs. 7-56185
 n-dodecyl-octaoxyethylene glycol monoether micellar solns., long-range crossover 7-21068
 domain-wall interactions and spatially modulated phases 7-2146
 dynamical planar random lattice, Ising model, exact soln. 7-41286
 eight-vertex model, elec. correlation function in scaling limit to first order in four-spin coupling 7-24595
 elastic Ising antiferromagnets on a triangular lattice 7-33185
 exact equilibrium shapes of Ising crystals on triangular/honeycomb lattices 7-53014
 exclusion process and droplet shape, isomorphism with stochastic Ising model 7-29922
 factorization of the kinetic Ising model 7-56169
 FCC binary alloys, phase diagrams, frustration effects 7-22114
 ferroelectrics, thermodynamics equilib. critical exponents and stability 7-12237
 ferromagnet, fixed spin influence on thermodynamic behaviour 7-38887
 ferromagnet, ground state magnetic struct., antiferromag. impurity effects (Russian) 7-22086
 ferromagnet, magnetism at site-bond diluted anisotropic free surface 7-2800
 ferromagnet, surface effects, mean field renormalisation group study 7-12982
 ferromagnet, with biquadratic exchange interaction and uniaxial anisotropy 7-17189
 ferromagnetic, 3 D, with quenched random nonmagnetic impurities 7-17190
 ferromagnetic, transverse mag. field effects, Monte Carlo simulation 7-64473
 ferromagnetic fluid, phase transition for Ising-like spins 7-17174
 ferromagnetic Ising model, upper bounds on critical temp. 7-17183
 ferromagnetic thin films, magnetisation calcs., differential operator method 7-45774
 ferromagnets, dilute, lines and domain walls 7-33109
 ferromagnets on triangular lattice, bond- and site-diluted model, critical props. 7-12983
 finite model on torus, partition function 7-35443
 four-state Potts models equivalence of Ising model with two- and three-spin interactions 7-48600
 fractal clusters, scaling, distrib. fn. 7-35462
 frustrated spin clusters, dynamical susceptibility anal. 7-7526
 fully frustrated, X-Y nature on triangular lattice, Monte Carlo simulation 7-24591
 generalised mixed spin model, renormalisation group approach (Chinese) 7-9779
 Glauber spin dynamics on fractal lattices, numerical simulation 7-64472
 graphical enumeration of the 2D Ising problem 7-14897
 ground state props. for model with general spin S 7-58968
 Heisenberg Ising-like antiferromagnets on a triangular lattice, mag. props. 7-27540
 high dimensional Ising models, magnetisation critical behavior 7-33187
 homogeneous lattices embedded in varieties of genus O 7-35421
 Hopfield model, metastable state structure 7-24576
 hypercubic lattice, critical conditions 7-29941
 ID, in a variety of random fields 7-33188
 ID random field Ising model, characteristic fractal dimension calc. 7-45719
 infinite-range Ising model, complex temp. plane zeros in mean-field approx. 7-35454
 inhomogeneous one-dimens. models, construction of exact solns. 7-35453
 interface wandering in pure and impure and bulk phases 7-32791
 interfacial growth instability, scaling, simulation 7-44746
 Ising spin 1/2 lattice model, magnetic susceptibility, critical parameters, shifted ratio method 7-14890
 Kauffman's model, multivalley structure, analogy with spin glasses 7-24571
 kinetic, exponents far from T_c for relax 7-52926
 kinetic, microscopic obs. 7-35178
 kinetic dynamics, Monte-Carlo renormalization group study 7-259
 kinetic two-spin facilitated model on square lattice, Monte Carlo simulation 7-24598
 lattice models, iterative method of soln. in mag. field 7-45600
 layered frustration models, susceptibility, high temp. series expansions 7-22085
 layered Ising magnets, quasi-1D kinetics of ordering processes 7-2887
 loop gas model, square lattice, critical behaviour, equivalence to Ising model 7-216
 magnetic chains, anisotropic, of arbitrary spin, Bethe ansatz for two-magnon bound states 7-53015
 magnetic hard-square lattice gas, multicritical scaling 7-48607
 magnetic lattice gas of molecules in transverse field, molecular field approx. 7-2802
 magnetic phase diagram, Ising model on 2D triangular lattice, antiferromag. interactions 7-53012
 magnetisation of thin ferromag. film, Ising approx. 7-64425
 mass transport along surfaces, computer modelling, book contrib. 7-27082
 mean field kinetic Ising model, microscopic approach using Liouville formalism 7-2801
 mean field theory using random chessboard model 7-14889
 mean-field renormalisation group, unified approach to bulk and surface critical behaviour 7-48665
 metamagnet, phase diagrams based on model interactions 7-21650
 methane monolayer on graphite, thermodynamic study 7-16863
 micellar solutions, origin of nonuniversality 7-46879
 microcanonical simulation of 3D random-field Ising model 7-38892
 Migdal-Kadanoff renormalisation, appl. to Potts model 7-24600
 mixed phase transition for hierarchical Ising spin glass model 7-38886
 mode condensation in a hierarchical system 7-45714
 model microemulsion, phase equilibria and critical endpoints 7-17828

Ising model continued

multicomponent Ising model with complex thermodynamic parameters, phase coexistence 7-29942
 multicomponent solid solutions, atomic distribution functions, Ising model 7-44753
 multicritical points in an Ising random-field model 7-17187
 multilattice microcanonical simulation algorithm, 2D Ising model calcs. 7-24597
 multiorientational Ising-type dipoles in transverse tunnelling field, partition function calcs. 7-263
 multispin correls., multiparticle entropy method calcs. 7-45708
 multispin interaction system, phase transition order, Monte Carlo simulation 7-18719
 nearest neighbour Ising spin glass, low temp. phase, heuristic theory 7-33186
 neural network, spin-glass model with Monte Carlo dynamics 7-23292
 one-dimensional ferromag. $1/n^2$ Ising chain, crit. temp. 7-7527
 one-dimensional Ising bridge model, general solution 7-61274
 one-dimensional random field Ising model, characteristic fractal dimension calc. 7-18724
 paramagnet-spin glass transition in transverse field 7-53017
 pattern recognition, chopper model 7-253
 phase diagram and decay of spin-spin correlations 7-24565
 phase transitions in two-dimensional uniformly frustrated XY spin systems 7-2875
 planar Ising ferromagnet, Yang-Lee zeros 7-52924
 quantum Hamiltonian rel. to one-spin transfer-matrix descriptions 7-56180
 quantum transverse Ising spin-glass model, mean field approx. 7-22116
 quasicrystal, eight-vertex model 7-26689
 quasicrystals, magnetic phase structure on the Penrose lattice 7-53013
 random 2D lattice, phase transitions 7-61275
 random band Ising model on Bethe lattice 7-38885
 random field Ising model, higher-order cumulants 7-53016
 random field problem, critical behaviour, Fisher renormalisation 7-41289
 random field systems, static and dynamic props. 7-45710
 random lattices versus regular lattices, Ising model, fermions on random lattices 7-35466
 random-bond model, three-dimensional, phase diagram and crit. props. 7-45715
 random-field, formation of domains 7-45602
 random-field, with trimodal distrib., phase diagram 7-56182
 random-field Ising model, high temp. series 7-2869
 random-field systems, integer optimization and zero-temperature fixed point 7-7530
 reaction-diffusion, nonequilib. phase transforms, critical behaviour, Monte Carlo scaling 7-61304
 real-space normalisation, Kakutani metric appls. to small Ising systems and gauge-field quantisation 7-41294
 reentrant wetting phenomena and crit. behaviour near bulk critical points 7-44956
 roughening transition at low temps. 7-2144
 scale-invariant description of critical region, Percus-Lebowitz method 7-29962
 semi-infinite Ising systems, critical and multicritical phenomena 7-59044
 simple cubic lattice, fully frustrated, Monte Carlo simulations 7-53011
 simple magnets and spin glasses, zero field muon spin relax. 7-53193
 simulation using microcanonical algorithm 7-29932
 spin correlations of Ising model, Langevin simulation 7-4778
 spin dynamics on 2 D fractal lattice, Monte Carlo study 7-2874
 spin glass, finite dimensional, internal field distn. fns., internal energy calcs. 7-12985
 spin glass, phase diagram and replica momenta, n-colour Ashkin-Teller model 7-59039
 spin glass, replica symmetric solns. in tree approx. 7-53007
 spin glass, short range, ultrametricity and zero modes 7-22115
 spin glass, stability, replica symm., toy model 7-27534
 spin glass, three-dimensional, entropy and free energy, Monte Carlo simulation 7-17184
 spin glass on a Bethe lattice of infinite coordination, symmetry breaking 7-45712
 spin glass relax., numerical calcs. 7-56175
 spin glasses, absence of phase transitions and cluster props. 7-59038
 spin glasses, anisotropy-induced Heisenberg-Ising crossover 7-38890
 spin glasses, naive mean field equations 7-33184
 spin glasses, replica Monte Carlo simulation 7-45713
 spin glasses, zero temp. internal magnetic field distrib. calcs. (Russian) 7-27533
 spin-1, on Bethe lattice, statistical mechanics calcs. 7-2877
 spin-1 model, with bilinear and biquadratic exchange interactions, renormalisation group calcs. 7-53010
 spin-1 model with pair correlation, dynamics 7-41283
 spin-1/2 Heisenberg antiferromagnet, triangular lattice, Ising-like exchange anisotropy, magnetisation process 7-53021
 spin-glass states, invariant geometry 7-45711
 spin-glass transition, domain wall scaling, energy and free energy distrib. calcs. 7-38891
 spinodal decomposition, diffusion limited, corrections to late-stage behaviour, Lifshitz-Slyozov scaling and Monte Carlo study 7-38206
 spontaneous magnetisation on 3-12 lattice 7-7465
 square lattice Ising model, antiferromagnetic susceptibility and short-range correlation function 7-38893
 square lattice Ising model, pair correlation function 7-35465
 stability of the isotropic fixed point near one dimension 7-9787
 statistical methods, conf., Oaxtepec, Mexico, Jan. 1986 7-24268
 strips, correl. lengths universal scaling form calcs., boundary conditions depend. 7-56177
 thermodynamic behaviour in generalized spherical model 7-27536
 thermodynamic functions of the three-dimensional Ising model at $T>T_c$ (Ukrainian) 7-9781
 thermodynamics, Monte Carlo simulation 7-29939
 three dimensional Ising model, simulation on Cyber 205, fast algorithm 7-9794
 three-dimensional Ising model, partition fn. calcs. 7-61264
 three-spin interaction Ising model with a nondegenerate ground state at zero applied field 7-29930
 three-spin interaction model, phase transition order 7-18718
 three-spin Ising model, conformal invariance and critical behaviour 7-53009
 (TMTSF)₂ClO₄, anion ordering and lattice expansion 7-58511

Ising model continued

- transverse, fermionic representation and functional integral approach 7-45709
 transverse, random forces, relax. and memory functions, dynamical behaviour calcs. in high-temp. limit 7-56178
 transverse Ising model in random parallel field, internal energy expansion 7-33189
 transverse susceptibility, direct calc. from local mag. field distrib. 7-17149
 triangular, two- and three-spin interactions, ground state spin config. studies 7-9802
 triangular lattice, 2×1 and 2×2 structures, phase transitions 7-63765
 tricritical point, Ising models with random bonds and crystal field interactions 7-2868
 trimodal random-field, on Bethe lattice and tricritical point 7-56181
 two and three dimensional, biquadratic exchange interactions, reentrant behaviour, Monte Carlo study 7-12986
 two dimensional Ising model with crossing and 4 spin interactions, soln. for mag. field 7-33135
 two dimensional Ising model with layered exchange interactions and alternate surface magnetic fields 7-2836
 two-dimensional, wetting transition calcs. with axially competing interactions 7-6928
 two-dimensional antiferromagnetic Blume-Capel model, Monte Carlo simulation 7-64471
 two-dimensional conformally invariant theory, operator content, effect of boundary conditions 7-4776
 two-dimensional growth models, interface dynamics, time-reversal invariance and universality 7-63532
 two-dimensional Ising model, large block spin interaction 7-41285
 two-dimensional Ising model, Yang-Lee zeros 7-238
 two-dimensional lattice gas phase diagrams, multi-critical point positions 7-2142
 two-dimensional with layered quenched bond randomness, free energy and specific heat calcs. 7-7531
 two-sublattice temp.-induced metamagnets, dipol-octopole interaction calcs. 7-17191
 viscous liquids, defects and relaxation 7-11877
 wetting transitions near bulk critical temps., long-range forces effects calcs. 7-58573
 Yang-Lee edge singularity on fractals 7-18722
 Z_2 gauge theory, finite lattice effects 7-389
 Z_2 Ising models, equivalence to $N=2$ nonlocal $SU(3)$ current algebra 7-56470
 Ag-Mn-Sb, dilute metallic spin glasses, response time, temp. depend. study 7-2896
 AgMnAu spin glasses, crit. behaviour, Dzyaloshinsky-Moriya interactions 7-7525
 AsF_6 -graphite, intercalation compounds, staging phenomenon studied using Ising model 7-58464
 Au (110) (1×2) , sp. ht. anomaly for order-disorder transition, LEED study 7-12310
 AuCr spin glass, remanent magnetization reduction, Heisenberg and Ising comparison 7-53019
 $CoCl_2$ dipyrindine quasi-1D Ising system, far IR magnetic excitation spectrum 7-59040
 $CsH_2(D_2)PO_4$, ferroelectrics, electrostrictive corrections to pseudo 1D Ising model 7-59158
 $CuCl_2 \cdot 2DMSO$, paramagnetic susceptibility of antiferromagnetic quantum chain 7-52997
 CuMn spin glass, remanent magnetization reduction, Heisenberg and Ising comparison 7-53019
 CuMnAu spin glasses, crit. behaviour, Dzyaloshinsky-Moriya interactions 7-7525
 $Dy(As_{1-x}V_x)_2O_4$, random-field effects on Ising Jahn-Teller phase transition 7-58461
 Fe, mag. props., of different phases, modelling using Monte Carlo method (Russian) 7-58992
 Fe-Al disordered alloys, mag. props., site-diluted Ising model calcs. 7-2873
 $FeCl_2$ magnet, spin-lattice coupling and tricritical behaviour 7-2849
 $(Fe_{0.8}Ga_{0.2})_2TiO_5$ spin glass, remanent magnetization reduction, Heisenberg and Ising comparison 7-53019
 $Fe_{1-x}Zn_xF_2$ diluted Ising antiferromagnet, magnetisation critical exponent crossover, Mossbauer meas. 7-7529
 $K_2Ba(NO_2)_4$, successive phase transitions, dipolar frustration 7-53247
 KD_2PO_4 -type ferroelectrics, central peak, deuteration effects 7-64586
 $LiMo_2Li_{1-x}F_x$, dilute dipolar-coupled magnet, ferromagnetism, glassiness, metastability 7-22098
 $Mn_{0.5}Zn_{0.5}F_2$, sp. ht. meas. in random fields 7-33178
 $Mn_xZn_{1-x}F_2$, 3D site-random Ising magnet, crit. behaviour 7-17186
 $Rb_2MnO_7 \cdot CrO_3Cl_4$, randomly disordered mag. system, mag. cluster excitations and wave-like magnons 7-38881
 Si:As, highly doped, spinodal decomposition and clustering 7-52063
 $YIG:Ho^{3+}$, laser mag. reson. study, quasi-Ising model 7-53147
 ZnMn, Ising-type spin glass, uniaxially anisotropic, successive transitions 7-17188

island-like metallic thin films *see discontinuous metallic thin films*

islet-like metallic thin films *see discontinuous metallic thin films*

isobaric analogue resonances

- see also nuclear collective states and giant resonances*
 particle decay of resonant state generated by direct reaction 7-49366
 relaxation parameters, shell optical approach 7-35957
 $^{138}Ba(p,p')$, K-shell ionization probability, nuclear reaction effect 7-42748
 ^{57}Co $d_{5/2}$ isobaric analogue resonance fragments, γ -decay schemes, M1 strength from (p,γ) and $(p,p'\gamma)$ 7-35987

isobaric analogue states

- see also isobaric analogue resonances*
 $^7Li(p,\pi^-)^8B$, $E_p=200$ MeV, cross section, analyzing power angular distrib. meas. 7-56677
 first-forbidden β -decays, constraints on parity mixing matrix elements from hard pion exchange 7-61836
 $^{14}C(\pi^+,\pi^-)^{14}O$, sequential nature of charge exchange, multiple scatt. anal. 7-36055
 $^{14}C(\pi^+,\pi^0)^{14}N$, sequential nature of charge exchange, multiple scatt. anal. 7-36055
 ^{66}Ge , beta-delayed proton decay 7-41946

isobaric analogue states continued

- $^7Li(p,\pi^-)^8Li$, $E_p=200$ MeV, cross section, analyzing power angular distrib. meas. 7-56677
 ^{208}Pb , isobaric analogue state width determ. using TDA Green function 7-61848

isobars *see atmospheric pressure and density*

isoelectronic series

- atomic momentum expectation value ratios upper bounds Drescher's inequality 7-15473
 atoms, total energy, nucl. attraction energy and interelectron interaction 7-50287
 closed shell ions, electric field gradient Sternheimer function 7-12681
 dipole polarisability of atoms and ions, ionis. pot. correl. 7-42529
 H-like ions, proton impact Fine-struct. excitation, plasma screening effects, ion-sphere and Debye-Huckel models 7-62509
 heavy Ni-like ions, X-ray transition energies 7-19749
 hydrogenic atoms in potential $V(r)=gr+\lambda r^2$, exact solns., ground-state eigenvalue bounds, moment calcs. 7-49910
 hydrogenic ions in mag. field, centre-of-mass energy 7-50011
 hydrogenic species, relativistic atomic struct. calcs., momentum space approach 7-42461
 hydrogenic Zeeman effect, second-order perturbation calc. 7-50012
 many-electron atoms, quantum-mechanical model 7-25338
 Al isoelectronic series highly ionised atoms injected into PLT and TFTR discharges, spectra 7-19748
 Au, spectral obs. of highly charged ions belonging to Fe, Co, Cu and Zn isoelectronic sequences 7-37747
 B I isoelectronic sequence, short wavelength laser calcs. 7-20214
 B-like ion plasma, dielectronic satellites 7-58054
 Be I isoelectronic sequence, short wavelength laser calcs. 7-20214
 Be I isoelectronic series, atomic and spectral data for typical tokamak plasma conditions 7-24322
 Be, isoelectronic series, dielectronic recomb. rates calcs. 7-50352
 Be isoelectronic series, fine struct. multiconfigurational DF calcs. 7-62266
 Be-like ions, electron impact excitation rates 7-10760
 Be-like ions, excitation cross sections, Coulomb-Born approx. 7-25658
 Be-like ions, transition probabilities, line strength 7-15548
 Bi spectral obs. of highly charged ions belonging to Fe, Co, Cu and Zn isoelectronic sequences 7-37747
 C I isoelectronic sequence, short wavelength laser calcs. 7-20214
 C isoelectronic series, intercombination transition probabilities, CI calcs. 7-36489
 Cl isoelectronic sequence, allowed 3-3 transitions, Slater parameter optimisation, HF CI calcs. 7-48205
 Cu-like heavy positive ions, binding energy and electron density, relativistic Thomas-Fermi theory 7-49923
 F-like ions, energy level distances, relativistic perturbation theory calcs. 7-866
 F-like ions, Zr^{31+} to Sn^{41+} , X-ray transitions 7-25445
 FI isoelectronic series X-ray lines, wavelengths and identifications 7-5626
 Fe XV, allowed transitions, Hartree-Fock and Dirac-Fock calcs. 7-15494
 Fe^{21+} , dielectronic recomb., rate coeff. calc. 7-30991
 Fe^{22+} , dielectronic recomb., rate coeff. calc. 7-30991
 H-like atom, spectrum in high-frequency EM field analytic solution 7-42483
 H-like atom, transition-matrix elements determ. 7-56944
 H-like atoms, spectral restructuring in magnetised plasma in quasimonochromatic elec. field 7-19776
 H-like atoms, stability, particle in a spherical box theory 7-9629
 H-like ion plasma, laser interaction, X-ray line emission self absorpt. and escape factors 7-37689
 H-like ions, dielectronic recomb. rate consts. calcs. 7-36759
 H-like ions, nucl. quadrupole moment, HFS 7-49914
 H-like ions, spontaneous emission spectral line, natural broadening shape 7-42541
 H-like ions, spontaneous two-photon decay rates 7-15530
 H-like ions in laser plasma, freq. redistrib., Stark broadening of lines 7-44203
 H-Like ions + $Ar(Ne)(N_2)(O_2)$ targets, projectile ionisation cross section 7-969
 H-like systems in arbitrary mag. fields, ground and excited states wave functions expansion calcs. 7-2519
 HXCHY where $X,Y=CH_2, NH$ and O , 1,3 shift, SCF and CI study 7-10448
 He, ground state, correl. energy eval., correl. fn. influence 7-36447
 He isoelectronic sequence, relativistic second-order many-body corrections 7-870
 He, isoelectronic series, application of a variational fn. to ground-state energies 7-15485
 He isoelectronic series, binding energies and radiative lifetimes, Dirac Hamiltonian, relativistic variational soln. 7-25456
 He isoelectronic series, correl. effects, local level, CI partitions 7-49940
 He isoelectronic series, electron scatt., plasma screening effect, distorted wave approach study 7-62532
 He-like atoms, bound states, least-squares calc. 7-49883
 He-like ions, double-excited, electron correl. 7-19722
 He-like ions, electron excitation, distorted-wave polarised orbital approach 7-62531
 He-like ions, energy level population autoionisation states (French) 7-10518
 He-like ions, multiconfiguration DF study 7-62298
 He-like ions, plasma, laser interaction, X-ray line emission self absorpt. and escape factors 7-37689
 He-like ions, radiative corrections, multiconfigurational DF study 7-62299
 He-like ions, spontaneous two-photon decay rates 7-15530
 He-like systems, energies and widths of singlet and triplet S resonances 7-36508
 Li, quantum defect determ. from negative-energy reaction matrix 7-42480
 Li-like ions, electron-impact ionisation, excitation-autoionisation contrib. 7-978
 Li-like ions, first excited state, intra- and inter-shell correl. effects 7-62295
 Li-like multicharge ions, ultrafine structure, nonrelativistic approx. 7-5612
 Mg isoelectronic series, energy levels, multiconfig. optimised pot. model calcs. 7-19723

isoelectronic series continued

- Mg-like ions, electron impact excitation, LS coupling, distorted wave approx. 7-42767
 Mg-like ions, energy levels, model-pot. relativistic perturbation calcs. 7-24320
 N I like ions, identification of forbidden lines of Si VIII, S X and Ar XII in solar spectrum 7-66441
 Na-like ions, relative emission-line strengths for Al III and Si IV in Sun 7-47799
 Na-like ions, Rydberg states, dynamic polarisability, HF calcs. 7-62273
 S isoelectronic series, Ca XI to Mn XVI, laser plasma, spectra 7-49989
 Ne-like ions, energy level distances, relativistic perturbation theory calcs. 7-866
 Ne-like ions, in laser-prod. plasma, density-sensitive line emission 7-6448
 Pb, spectral obs. of highly charged ions belonging to Fe, Co, Cu and Zn isoelectronic sequences 7-37747
 Pd, 4¹⁰ subshell, photoionis. and electron impact ionis. 7-902
 S isoelectronic series, transition probabilities and wavelengths 7-15550
 Si isoelectronic sequence, allowed 3-3 transitions, Slater parameter optimisation, HF CI calcs. 7-48206
 Th, spectral obs. of highly charged ions belonging to Fe, Co, Cu and Zn isoelectronic sequences 7-37747
 Ti, H-like, dielectronic satellite spectra 7-19741
 U, spectral obs. of highly charged ions belonging to Fe, Co, Cu and Zn isoelectronic sequences 7-37747

isomer shift

- alkyl nitriles, conformational kinetics calcs., gas and liquid phases, MR spectra 7-19896
 alkyl nitriles gas and liquid phases, syn-anti conformer equilib., MR chem. shift study 7-19895
 cubic lattices, diffusing atoms, Mossbauer spectrum studies 7-64552
 Co-Cr-Fe sputtered films, dilute, Mossbauer effect 7-22167
 CoAlFeO₄, cubic spinel, Mossbauer anal. 7-33304
 Co₂Fe_{1-x}Cr_{2x}S₄ mixed spinel system, temp. depend. Mossbauer studies 7-38976
 CuTaS₃, isomer shift of elec. split 6.2 keV nucl. transition of ¹⁸¹Ta 7-7624
 EuCu₂Si₂, Eu valency, effect of Cu or Si replacement by other ions 7-58787
 Fe complex, Fe(hexaphenyl-1,4,7,10-tetraphosphadecane), tetraphenylborate, electronic relax. 7-25578
 Fe sites in minerals, electronic struct., iterative EHT, multiple scatt. Xα calcs. and Mossbauer meas. 7-17244
 Fe-Al disordered alloys, electronic struct., mag. props. and Mossbauer spectra 7-64073
 Fe-Te cluster, localised props., multiple scatt. Xα SCF method 7-21848
 Fe₂, diatomic molecules, electronic configuration, ⁵⁷Fe Mossbauer data 7-10640
 FeCoCr₄S₈, crystallographic and mag. props., Mossbauer study (Korean) 7-33310
 FeH_x, prep. under high press., Mossbauer obs. 7-33313
 (Fe_{1-y}Ni_y)TiH_x, critical study of β-region 7-27634
 Fe₂O₃-Na₂O-B₂O₃ glasses, Mossbauer study 7-7619
 Fe₂P₁₁B₇ metallic glass, mag. anisotropy and correlated hyperfine interactions 7-7505
 Fe₂Ti₂₇H₄, amorphous alloys, Mossbauer spectra 7-33308
 Fe₂V_{4-x}Mo_xO₁₃ type phases, Mossbauer spectra 7-38969
⁵⁷Fe isomer shifts and the problem of calibration 7-61310
 InP:Fe, midgap impurity levels, isomer shift and charge state calcs. 7-2538
 Np cpds., Mossbauer spectroscopy, appl. to solid state chemistry 7-17248
 NpM₄Al_{8-x} (M=Cr, Fe, Cu), mag. props., Mossbauer effect and neutron diff. 7-59127
 NpO₂CO₃, crystal chemistry, Mossbauer studies 7-17249
 NpOS, mag. props. 7-13064
 Pd_{1-x}Fe_xH_n system, isomeric shift, fluctuations of hyperfine interaction, Mossbauer study 7-45843
⁸⁷Rb^m, isomer shift, mag. moment, laser induced nuc. orientation 7-10106
 Sb cpds., Mossbauer isomer shifts, first-principles scalar-relativistic linear muffin-tin orbital method calcs. 7-2957
 Sn complexes, ESCA, Mossbauer and IR spectrosc. investig. 7-5678
 Sn cpds., Mossbauer isomer shifts, first-principles scalar-relativistic linear muffin-tin orbital method calcs. 7-2957
 SnF₂-SnF₄ system, Mossbauer reson. studies 7-7625
 α-SnF₆, Mossbauer lattice parameters 7-17251
 α-SnF₆, Mossbauer resonance 7-45854
 SnS(Se)(Te), electronic props., ionicity and isomeric shift correl. 7-7114
 SnTe, Mossbauer spectra and microhardness, stoichiometry deviation effects, vacancy conc. and distrib. 7-26973
¹¹⁹Sn compounds, Mossbauer spectra interpretation SCC-Xα-MO calcs. 7-36474
¹²⁵Te, Mossbauer isomer shifts and contact densities 7-38966
¹²⁵Te, valence electron contact density 7-25457
 α-Ti-Fe system, Fe solubility, 360 to 580°C, Mossbauer studies 7-32656
 Y_{100-x}Fe_xH₄ metallic glasses, mag. props., H content effects 7-33155
 Zn cpds., Mossbauer isomer shifts, first-principles scalar-relativistic linear muffin-tin orbital method calcs. 7-2957
 Zn ferrite, shock-synthesised, Mossbauer spectroscopy 7-38979

isomerisation

- acetylacetone enolate anions, collision-induced losses of ketene, mass spectra 7-13839
 allyl phenyl ether, photoisomerisation reaction mechanisms, IR multiphoton excitation study 7-62372
 Δ^{2,2'}-bi-(2H-1,4-benzothiazine), photochromism and thermochromism, quantum yield 7-46859
 3,3-bis(nitratomethyl)oxetane, solid and soln., IR lineshape 7-3047
 1,3-butadiene ions, photodissoc., photoelectron photoion coincidence study, isomerisation barrier meas. 7-36711
 cycloheptatriene, isomerisations, kinetic CARS appls. 7-36630
 cyclopropane-1,1-d₂, thermal isomerisation, master eqn. iterative soon., variable successive overrelaxation method 7-33914
 dicarboxylic acids undergoing conformational transitions, ionisation equilibria, ¹H NMR 7-13757
 6b,8a-dihydrocyclobut(a)acenaphthylene, photoisomerisation, solvent and irradiation parameter effects, visible and UV spectra study. 7-33947
 9,9-dimethyl-1,5-dihetero-spiro (5.5) undecanes, conformational dynamics, 3D topological approach 7-10402
 diphenylbutadiene, soln., rot. reorientation dynamics and picosecond photoisomerisation 7-15592

isomerisation continued

- 1,3-diphenylthioureas, ¹³C NMR spectra, chemical shifts and mol. conform. study 7-42650
 1,3-dipyridyl thioureas, ¹³C NMR spectra, chemical shifts and mol. conform. study 7-42650
 elastomer gels, swollen cis-trans isomerisation, network density effects 7-8273
 ethyl, ethenyl and ethynyl anions, structs. and rearrangement processes, ab initio MO calcs. 7-59757
 ethylene in Ar and water, photo-isomerisation, trajectory study 7-8264
 glycolic acid, rot. isomerisation, ab initio SCF calcs., IR Ar matrix spectra 7-19851
 hexakis(dimethylsilyl)benzene, rot. isomerisation mechanism and barriers, ¹H and ¹³C NMR spectra anal., EFF calcs. 7-25359
 hydrocarbons, adsorption and reactions on clean and S or C covered Mo (100) 7-28345
 2,4-methanoprolin, L-proline analogue in small peptides study, ¹H NMR and NOE spectra anal. 7-25545
 methyl ethyl ketone, pyrolysis, reaction mechanisms (French) 7-54112
 methyl isocyanide, overtone-induced isomerisation, master eqn. formalism 7-13750
 1-methylcyclohexyl cation to 1,2-dimethylcyclopentyl cation, rearrangement, MINDO/3 study 7-10428
 cis, cis-octatetraene, excited 2¹A_g state pot., isomerisation study 7-13747
 organic cpds. excited state H⁺ transfer, state orbital correls. 7-13760
 organorhenium hydrides and alkyls, mass spectra, electron impact induced H-rearrangements 7-42773
 oxalic acid, isomerisation and unimol. dissociation channels, MO calcs. 7-28295
 phase space bottlenecks, statistical theories 7-65298
 phospholipid membranes, multipulse dynamic NMR 7-17956
 polyacetylene, cond., fast FTIR and IR intensity spectra, struct. and electronic props. 7-53335
 polyacetylene, Durham, isomerisation and doping, ESR study 7-64510
 polyacetylene, Durham, struct., X-ray scatt. 7-37898
 polyacetylene, undoped, elec. props., thermal isomerisation and impurity effects 7-64232
 polyacetylene partially isomerized, detection of soliton shape modes 7-38469
 polymethine dyes, photoisomer transform. schemes 7-39878
 polyphenylmethylsiloxane, cyclic, preparation and fractionation 7-23013
 (1.1.1) propellane, rearrangement to 3-methylene-cyclobutene, quasi ab initio PRDDO study 7-25404
 1,3-pyridylphenylthioureas, ¹³C NMR spectra, chemical shifts and mol. conform. study 7-42650
 salicylidenamides, thermochromic and photochromic, IR spectra, conformational influence 7-53310
 sigmatropic rearrangement, potential energy surface homology 7-13725
 solvent, dissociation, isomerisation and diffusion in double-well potential 7-33922
 trans-stilbene, soln., rot. reorientation dynamics and picosecond photoisomerisation 7-15592
 triaryl-substituted keto/enol pairs, gas-phase ion chemistry, mass spectra 7-13737
 two-state system, strong nonadiabatic interactions and fast radiationless transitions 7-57128
 unimolecular reactions induced by vibr. overtone excitation, collisional energy transfer 7-39863
 unimolecular reactions of isolated collisional gas phase and solvated molecules 7-13792
 vinyl alcohol, aq. soln., ketonization, ab initio STO-3G calcs. 7-22988
 Ag dimers and clusters, matrix isolated, guest-host interaction and photochem. transform. 7-15786
 Ag₃ clusters isolated in solid Xe matrices, reson. Raman scatt. and photoisomerisation process 7-25696
 Ar₇, melting transition and nonrigid dynamics onset, mol. dynamics simulation study 7-26920
 N-aryl-4-t-butyl-thiazoline-2-thiones, rot. barrier, enantiomer separation 7-13759
 CH₃NO₂, potential energy surface, rearrangements, ab initio calcs. 7-10465
 CINC isomerisation to C1CN, MINDO calcs. 7-56979
 FNC isomerisation to FCN, MINDO calcs. 7-56979
 H₂, ortho-para conversion, non-dissociative, on mag. surfaces, theory review 7-17781
 Ru(NH₃)₅-bipyridylbutadiene-Ru(NH₃)₅ compound photoisomerisation mol. switching, electronic coupling parameter calc. 7-19678

isomerism

- see also isomerisation; rotational isomerism
 aliphatic bis-phenylhydrazones, stereoisomerism 7-50183
 alkanes, isomers study, depolarised Rayleigh-Brillouin scatt. investig. 7-62386
 n-alkanes, liq., energy difference between specific and localised conform. isomers, FTIR spectra 7-42615
 alkene nitrite isomers, radicals, EPR investig. 7-36653
 alkyl groups, saturated, undoped, substituent consts., structural and polarity effects (German) 7-36471
 alkyne isomer groups, chemical thermodynamic props. data 7-60901
 amino acids in Murchison meteorite 7-40786
 aziridine, bond inversion rate determ., PMR line shape anal. 7-19892
 azoles, protonation energies and tautomerism, basis set effects 7-25374
 azoles, UV photoelectron spectral assignment, ab initio. MRD CI calcs. 7-50239
 benzene+ethylene, isomer group equilib. mole fractions, calcs. 7-13738
 benzenoid hydrocarbons, Kekule structs., rel. to no. of hexagons 7-878
 benzenoid hydrocarbons, number rel. to number of hexagons 7-879
 benzofurans, UV spectra, substituent influence 7-50170
 benzoic acid, fluoresc. and phosphoresc., acetic acid effect 7-57114
 benzonitriles, substituted, thermodynamic functions 7-52082
 substituted benzoylaminopropionic acid esters, conformational equilib., IR spectra, steric effects 7-57066
 bis (trihalomethyl) ether, conformer struct. and stability, rot. barriers, torsional force consts., mol. mechanics calcs. 7-19998
 bis (trihalomethyl) thioether, conformer struct. and stability, rot. barriers, torsional force consts., mol. mechanics calcs. 7-19998
 borane tetrahydrofuran, form. of borane adducts, ¹¹B NMR study. 7-50199
 1-bromo-2-methylpropane, gaseous phase, conformational stability, for IR and LF Raman spectra 7-10602

isomerism continued

- 1,3-butadiene ions, photodissoc., photoelectron photoion coincidence study, isomerisation barrier meas. 7-36711
 Cahn-Ingold-Prelog assignment of R and S configs., hand method 7-14737
 chlorin, photoisomer, in n-octane, emission anisotropy 7-57052
 trans-1-chloro-2-butene, conformation and mol. struct. determ. by gas phase electron diff. 7-50356
 5-chloro-2-hydroxypropidine, tautomerism, IR and UV spectra 7-31047
 1-chloro-2-methylpropane, gaseous phase, conformational stability, for IR and LF Raman spectra 7-10602
 cyclohexyl halides, thiourea inclusion compounds, substituted cyclohexane conform., ^{13}C CP/MAS NMR spectra 7-19889
 cytosine, metal stabilised iminoxo form, form. and geometry 7-26710
 cytosine and thio derivatives, tautomerism, ab initio study 7-837
 demethyl porphyrins, monosubstituted free-base series, MCD study, INDO and CI calcs. 7-25401
 2,4-di(2-pyrenyl)pentane, meso and racemic diastereoisomers, absorpt. and fluoresc. spectra 7-62434
 diazoethenes, ground state geometries, semi-empirical MINDO/3 and MNDO calcs. 7-56975
 1,2-dichloroethene, isomeric mixtures, determ. of struct. and comp., GPED spectra anal. 7-36763
 dicyclohexyl-18-crown-6, A and C isomers, struct., X-ray diff. study 7-42799
 2,3-dihydrofuran, ring puckering vibr. and centrifugal distortion, microwave spectra anal. 7-36596
 2,4-dihydroxyquinoline, gas phase, prototropic equil., electron impact fragmentation spectra anal., LCAO-CNDO calcs. 7-36479
 dimedone Schiff bases, stretching vibr., IR spectra, solvent effects 7-57057
 1-(3,4-dimethoxyphenyl)-4-methyl-5-ethyl-7,8-dimethoxy-5H-2,3-benzodiazepine, config., X-ray anal. 7-21186
 dimethyl ether, isomers, VUV-optical oscillator strength distrib. 7-15650
 12,2-dimethyl-1,3-dioxolane-4-methanol, OH stretching band, free and H bonded species equil., dichroism and IR spectra 7-10641
 1,5-dimethyl-1,5-divinyl-3,3,7,7-tetraphenylcyclotetrasiloxane, disordered cryst. struct. investig. 7-51745
 N,N'-dimethyl-4,4'-bipyridine, oxidation states, electronic struct. and conform. anal. 7-25383
 dimethylbenzonitriles, IR and Raman spectra 7-25501
 12-(2',4'-dinitrobenzyl)pyridine, photochromism, nature and decay time of transient species, Raman spectroscopy 7-10599
 3,4-diphenyl-2,5-dimethyl-2,4-hexadiene, free radicals, γ -irradiation generated, visible absorpt. and EPR spectra 7-57100
 1,2-diphenyl-3,3,4,4-tetramethylcyclobutene, free radicals, γ -irradiation generated, visible absorpt. and EPR spectra 7-57100
 2,5-diphenylfuran, low-freq. modes, fluoresc. excitation spectra 7-57117
 n-dodecane-hexane isomer mixtures, ultrasonic speeds and isentropic compressibilities 7-51943
 enantiomers, R, S labels assignment method 7-14736
 ethyl alcohol, isomers, VUV-optical oscillator strength distrib. 7-15650
 ethyl methyl ether, isomers, VUV-optical oscillator strength distrib. 7-15650
 etioporphyrin metal complexes, isomers, vibr. spectra interpretation 7-42617
 europium carboxylate, luminescence props. calcs. 7-42667
 flavins, mol. geometry and REDOX props., MINDO/3 calcs. 7-56976
 fluorocyclohexane, thiourea inclusion compounds, substituted cyclohexane conform., ^{13}C CP/MAS NMR spectra 7-19889
 fluoromethane, conversion of different nuclear spin modifications, isotopic effect 7-50400
 D-glucopyranose, struct. stereochemistry, solvation props. PCIO calcs. 7-15518
 guanine, matrix isolated, IR spectra, keto-enol tautomerism 7-50126
 halogen thiocyanates (isothiocyanates), ionis. pots., photoelectron spectroscopy and ab initio calcs. 7-25601
 3-hydroxyflavone, ground state tautomer, proton transfer relax., laser fluore. spectroscopy 7-15640
 L-iduronic acid, sulphated residue in heparins, conformer struct. and population study, ^1H NMR spectra anal., force field calcs. 7-25546
 [N-(2-l) furylidene]- β -(z-furyl)serine methyl ester, diastereomeric forms, tautomeric equil., solvent effects ^1H and ^{13}C NMR spectra 7-19893
 isocytosine, and thio derivatives, tautomerism, ab initio study 7-837
 mercaptoprimidines, substituted, vibr. IR, Raman and UV spectra 7-31043
 metal-phosphine complexes, stereodynamics, equil. conformations, DNMR 7-31083
 methyl fluoride, pot. surface studied using ab initio MO theory with electron correl. energy 7-42494
 methyl imino sulphur difluoride, ab initio calcs. at SCF level, equil. geometries and population anal. 7-10382
 N-methyl-N'-nitro-N-nitrosoguanidine, conform. struct. and stability, ab initio MNDO calcs. 7-25406
 2-methylaziridine, bond inversion rate determ., PMR line shape anal. 7-19892
 methylcyclobutane- d_3 , conformational stability, low freq. Raman spectra anal. 7-50146
 methylcyclohexane, thiourea inclusion compounds, substituted cyclohexane conform., ^{13}C CP/MAS NMR spectra 7-19889
 methylenefluoronium ylide, pot. surface studied using ab initio MO theory with electron correl. energy 7-42494
 9-methylguanine, matrix isolated, IR spectra, keto-enol tautomerism 7-50126
 nitroimidazoles, UV spectra, CNDO/S calcs. 7-19878
 nitromethane, isomers, struct., quantum mech. harmonic force field calcs. 7-56952
 nonadecane, liq., energy difference between specific and localised conform. isomers, FTIR spectra 7-42615
 nonequilibrium selecting system, quantum-mechanical model, asymmetric interactions 7-19991
 oligosaccharide structures, containing hexopyranose units, graphic representation 7-14734
 parity violating energy difference between enantiomers, meas. 7-42781
 pentane isomers, ionis. and electron thermalisation distances, mol. shape and density effects 7-50347
 1-pentyne, vibr. anal., IR and Raman spectra 7-19852
 phenol-formaldehyde resins, sequence struct. anal., NMR spectra 7-50177
 phosphates, ^{17}O , ^{31}P , ^1H and ^{13}C NMR spectra study 7-25544
 phosphites, ^{17}O , ^{31}P , ^1H and ^{13}C NMR spectra study 7-25544

isomerism continued

- N-phthalyl-4-bromo-L-glutamic acid, dimethylester, struct. and absolute configuration 7-40092
 polyacetylene:1, complexes, monosubstituted, isomerism, elec. cond., UV spectra 7-45289
 polymethine dyes, isomers, hidden struct. in visible-UV absorpt. spectra 7-50166
 polysaccharide structures, containing hexopyranose units, graphic representation 7-14734
 propyl alcohol, n- and iso-, isomers, VUV-optical oscillator strength distrib. 7-15650
 purines, tautomeric equil., gas phase and aq. soln., HF calcs., MNDO calcs. 7-25403
 purines in ground and lowest excited singlet states, dipole moments 7-54466
 pyrimidines, tautomeric equil., gas phase and aq. soln., HF calcs., MNDO calcs. 7-25403
 specific heat extremum behaviour, 2-state isomerism model 7-16058
 terbium carboxylate, luminescence props. calcs. 7-42667
 tetrachlorodibenzodioxins, isomers, identification, micro-diffuse reflectance and matrix isolation FT-IR techniques 7-25502
 tetrachloromethane dication, isomers, mass spectrometry and ab initio calcs. investig. 7-36513
 tetrahydrofuran, parity violating energy differences between chiral conformations 7-10777
 thiophosphates, ^{17}O , ^{31}P , ^1H and ^{13}C NMR spectra study 7-25544
 thiouracil, tautomers, MNDO calcs. 7-56984
 toluene, mixed acid nitration, isomer distrib., mass transfer effects on selectivity 7-54094
 trichloromethyl radical, struct. and electronic states, ab initio UHF SWX_α calcs. 7-30949
 trifluoroacetone nitrile, isomers, anion form. and dissoc., electron attachment 7-10740
 trifluoroisocyanide, isomers, anion form. and dissoc., electron attachment 7-10740
 trifluoromethyl, inversion barrier heights, SCF and CI calcs. 7-62289
 trifluoromethyl imino sulphur difluoride, ab initio calcs. at SCF level, equil. geometries and population anal. 7-10382
 uracil and thio derivatives, tautomerism, ab initio study 7-837
 weak molecular complexes, isomerism, molar heat capacity at const. press. investig. 7-28305
 1-aminocyclopropane-1-carboxylic acid, chem. shifts, PMR 7-19902
 AsH₃, isotopic species, mol. vibr., inversion splitting calcs. 7-19997
 C₅, geometric isomers, ab initio calc. of equil. struct. 7-62291
 CH₃N₂⁺, pot. energy surface, ab initio MO calcs. 7-10390
 C₂H₅O⁺, x=3 to 5, struct. isomers, gas-phase ion mobility study, ab initio calcs. 7-36456
 ClOO, low-lying electronic states, SCF-X_α-MS calcs. 7-49922
 FCP and higher-lying isomer, struct., stabilities, ab initio study 7-864
 FeC₄H₄⁺ isomers, gas-phase photodissoc., bond energy and struct. determ. 7-15661
 H₂ cluster detection at 4.2K 7-36843
 H₂, ortho to para transition, decay rate, quantum electrodynamic method 7-10674
 HCP and higher-lying isomer, struct., stabilities, ab initio study 7-864
 H₂P₂ isomers, electronic states, ab initio mol. electronic struct. theory 7-56934
 HSCN (HNCS), ionis. pots., photoelectron spectrosc. and ab initio calcs. 7-25601
 HXCHY where X,Y=CH₂, NH and O, 1,3 shift, SCF and CI study 7-10448
 KF.xHF (x=2.5, 3), homologous anions, crystal struct. anal. 7-26711
 NF₃⁺, inversion barrier heights, SCF and CI calcs. 7-62289
 NSCl₃, NSOF and NSF₃ and their isomers, ab initio calcs. at SCF level, equil. geometries and population anal. 7-10382
 NiC₄H₃⁺ isomers, gas-phase photodissoc., bond energy and struct. determ. 7-15661
 OCIO, low-lying electronic states, SCF-X_α-MS calcs. 7-49922
 PH₃, isotopic species, mol. vibr., inversion splitting calcs. 7-19997
 Pd(CN)_x (x=1 to 4), liq. NH₃ solns., Raman and IR vibr. spectra 7-57076
 SbH₃, isotopic species, mol. vibr., inversion splitting calcs. 7-19997
 Si₃, gas isomers, thermodynamics 7-25350
 SiC₂, protonated isomers, struct. and proton affinity, ab initio HF MO calcs. 7-25384
 Sn complex, Sn (IV) meso-tetraphenylporphyrins spectrosc. cis-influences 7-50159
 s-tetrazine clusters, photophysics and photochemistry, laser induced fluoresc. 7-31098

isomorphism

- crystals, numerical vector representation 7-11978
 heavy atom sites in isomorphous derivatives, vector search and feedback methods 7-11820
 Maxwell-Dirac isomorphism 7-48447
 polyaryl ether ketone blends, isomorphic behaviour, miscibility, glass transition and melting temps. 7-44416
 Al-transition metal quasicrystalline alloys, isomorphism, neutron diff. meas. 7-51638
 CaMnGe₂O₆-Ca_{0.5}Mn_{0.5}SiO₃ cross section of CaSiO₃-MnSiO₃-MnGeO₃-CaGeO₃ system 7-2213
 CrNH₄P₂O₇ and α- and β-CrNH₄HP₃O₁₀, preparation and characts. 7-3161

isothermal transformations

- pearlite spacings, meas. of spread 7-39804
 phase change models for freezing and thawing soils 7-8456
 phase change models for freezing and thawing soils 7-8457
 single cryst., isothermal phase transformation, linear analytical theory 7-44790
 steel, constructional, struct. and props. after high-temp thermomech. isothermal working 7-46522
 steel, Cr-Ni-Mo type, austenitisation conditions effect on austenite decomp. kinetics and mech. characts. 7-39557
 steel, eutectoid, microstruct. obs. of bainite stars 7-53695
 steel, hardening process modelling, stresses effect on struct. transform 7-39555
 steel, high-C, hardened, mech. prop. changes on tempering, martensite decomp. role 7-3375
 steel, low-alloy, bainitic transform., kinetics and mechanism 7-13447
 steel, low-C, polymorphic transform., kinetics 7-33653

isothermal transformations continued

- steel, low-C, wrought, thermal strengthening methods effectiveness 7-46524
 steel, pearlite-austenite transformation during heating, kinetics problems 7-33633
 steel, plain C, eutectoid, continuous cooling austenite-to-pearlite transform. kinetics, prediction using isothermal data 7-17524
 steel, superhardenable treated, transform kinetics 7-39535
 steel XC 80, pearlitic transformation in continuous cooling calc., thermal stresses contrib. (*French*) 7-46410
 steels, transformation, improved calc. 7-28009
 CaTiO_3 (perovskite), high press. phase transformations and isothermal compressibility 7-14269
 Fe-Al-C (3.8, 1.8 wt.%), martensite crystallostruct. changes, effect of temp. and heating/cooling rates (*Russian*) 7-53727
 Ni alloy, heat-resisting, supersaturated solid soln., isothermal decomp. kinetics 7-33682

isotope detection

- see also mass spectra
 ^{221}Fr , radioactive isotope detection, laser resonant photoionisation method 7-42572
 Li, isotopic anal., SES-ICP investig. 7-46908

isotope effects

- see also isotope shifts
 acetonitrile, anharmonic force consts., Fermi coupling, IR and Raman spectra 7-920
 acetonitrile- d_3 , ^2H and ^{14}N spin-lattice relaxation rates, solvent effects 7-19897
 alkali halides, trapped atomic H and muonium 7-45900
 alkali metal atoms, orientation, alignment and HFS 7-50278
 alkali metal isotopes, radioactive, ground state hyperfine struct. determ. by RF mag. reson. and laser optical pumping 7-25681
 alkane molecules, T beta-decay, molecular final-state interactions 7-49311
 allene- d_2 (-1,1- d_2), pure rot. spectra, microwave FT spectrosc. 7-5669
 benzene, ^1H chem. shift; D isotope effects, conc. depend. additivity rule 7-50196
 benzene, isotopic mixture in liq. crystals, dipolar coupling consts., 2D multiple quantum NMR 7-57090
 benzene chromium tricarboxyl- d_6 (d_6) deuteration effect on multiphoton dissociation 7-5727
 benzene clusters, vibr. predissoc. spectra assignment, isotope use in mass spectroscopic detect. 7-31125
 benzene liquid, intermolecular resonance vibrations, IR absorpt. spectra, isotropic dilution (*Russian*) 7-59215
 benzene- d_6 (d_6), vap., vibr. levels, fluoresc. spectra 7-10651
 benzenes, soln. electron affinities, isotope enrichments 7-10770
 bicyclo[1.1.1]pentanone, struct. and microwave spectrum 7-50094
 carbohydrate solns., aqs., molar vols., isobaric expansion coeffs. and compressibilities 7-12183
 o-carborane, B quadrupole coupling, NMR study 7-5704
 N-chloro-N-methylmethanamine, microwave spectrum, struct., quadrupole coupling consts. 7-50085
 chloroform- d_3 , ^3H spin-lattice relaxation rates, solvent effects 7-19897
 chlorotrifluoroethene, IR multiphoton dissociation, press. depend. calc. 7-62467
 cycloheptatriene, muonium addition, ring inversion kinetics of radicals 7-42792
 deuterio-isobutyric acid (coax)- D_2O , critical mixtures, isotope effects 7-12253
 deuterio-isobutyric acid (COOH)- H_2O , critical mixtures, isotope effects 7-12253
 deuterobenzenes, first excited singlet state vibr. level, fluoresc. lifetime meas. 7-50214
 1,2-dichlorobenzene- d_3 (d_3), isotopic species, r_0 structure calcs., microwave spectra 7-19834
 dichloromethane- d_2 -dichloromethane- d_2 , γ , mode vibr. linebroadening, Raman spectra 7-5685
 diffusion, isotope effect, quasi-harmonic calcs., appl. to CoO and NiO 7-26996
 difluorodichloromethane, mol. consts., force field study, thermodynamics props. 7-57088
 dimethylthallium(II) cation, aq. soln., mol. motion, NMR spin relax. time meas. 7-57088
 ethane- d_6 (d_6), intensity parameters, Raman trace scatt. 7-15608
 ethanol- d_3 (d_3)- d_3 , rot. correl. function, group struct. 7-15627
 ethylene, chemisorption and decomposition on Ni (100) 7-59785
 FCC solids, vacancy diffusion, jump dynamics and isotope effect calcs. 7-44890
 fluoromethane, conversion of different nuclear spin modifications, isotopic effect 7-50400
 formate anion, isotopic species, vibr. anal., valence force fields calcs. 7-36577
 four EM wave interaction in two-isotope gas medium (*Russian*) 7-25906
 free radicals, muon spin rotation spectroscopy, compliment to ESR spectroscopy 7-42787
 gas ring lasers, asymmetry in wave interaction 7-36995
 germinalacetylene- d_6 (d_6), vibr. anal., mol. consts. study, F-G matrix technique calcs. 7-36578
 hexane- d_6 , oriented, proton multiple quantum NMR spectra 7-19887
 homoamantane, ionised, methyl elimination, field ionisation kinetics and ^2H and ^{13}C labelling 7-42775
 homonuclear diatomic mols., asymm. isotopic modifications, energy limits calcs. 7-10415
 hydrates, solid, mol. stretching freq. versus H bond distance correlation anal. 7-21370
 isoformyl cation, rot.-vibr. energies, ab initio pot. surfaces 7-62264
 metals, electrochemical desorption step, rel. to isotope effect 7-13782
 methane, proton-proton spin-spin coupling surface 7-42645
 methane - d_6 (- d_6), integrated IR intensities 7-50132
 methane anion+methane, internal energy depend. of cross section and mechanism branching, TESICO investig. 7-28298
 methane monolayer on graphite, thermodynamic study 7-16863
 methane- t_1 , triton β decay, effect on neutrino mass determ. 7-49310
 methanol- d_6 (d_6)-cyclohexane- d_6 (d_6), critical mixtures, isotope effects 7-12253
 methyl radical+H(D), rate const. determ., laser photolysis and reson. fluoresc. 7-8250
 methylsilanethiol, gauche and trans isomers, struct., dipole moments, internal rot. obs. 7-5668

isotope effects continued

- 1-methyluracil, isotopic derivatives vibr. spectra, ab initio Hartree-Fock SCF calcs. 7-15589
 multicomponent mixtures, thermal diffusion, Enskog theory 7-51364
 muonium+benzoic acid derivatives, addition reaction in aq. solns., Hammett free energy 7-15744
 muonium+diatomic molecule, gas-phase reaction dynamics 7-54092
 naphthalene, isotopically mixed cryst., resonant secondary emission and spectral diffusion 7-42665
 nitril halides and their isotopes, vibr. anal. 7-50051
 organic radicals, muonium-containing, H^+ -Mu isotope effects 7-15745
 phenanthrene- d_6 (d_6), in supersonic free jet, electronic spectra, intramol. dynamics 7-42672
 phenol- d_6 - D_2O , critical mixtures, isotope effects 7-12253
 PMMA, plastic optical fibres, for near IR transmission, prep. 7-62834
 polystyrene, normal and deuterated blends, isotope effects on interdiffusion 7-27029
 polystyrene, plastic optical fibres, for near IR transmission, prep. 7-62834
 propane- t_1 , triton β decay, effect on neutrino mass determ. 7-49310
 propanes, ^1H labelled, IR and Raman spectra, vibr. analysis, D substitution effect 7-50141
 propyl fluoride, r_e struct., rot. isomerism, microwave spectra and moments of inertia meas. 7-10556
 pulsed laser field desorption TOF spectroscopy, ultrafast ion reaction time meas. 7-20072
 pyrazine- d_4 , spectral anal., Lennard-Jones-H-bonding pot. energy calcs. 7-5734
 pyrazine- d_4 -pyrimidine, spectral anal., Lennard-Jones-H-bonding pot. energy calcs. 7-5734
 pyrazine- h_4 -pyrazine- d_4 , spectral anal., Lennard-Jones-H-bonding pot. energy calcs. 7-5734
 pyrene- d_6 (d_6), vibronic coupling and two-photon spectra 7-42712
 pyridine-chloroform complex, D NQR meas. 7-50194
 rotational anal., use of isotopic effects 7-15587
 secondary ion emission, isotope fractionation, velocity-dependent 7-53472
 small molecules, multiple photoionisation and photodissociation, mass spectrometer and coincidence studies 7-19965
 superconducting state parameters, pseudopot. depend. 7-12896
 tetraphenylporphyrin metal complexes, reson. Raman spectra 7-19862
 trimethyl- d_3 -pyrazine, normal vibr., Raman and IR parameters investig. 7-50074
 trimethylamine- d_3 , solid, mol. reorientation, NMR quadrupole echo spectra 7-62411
 trimethylpyrazine, normal vibr., Raman and IR parameters investig. 7-50074
 trimethylsulfonium iodide- d_6 (d_6), vibr. spectrum, normal coord. calcs. 7-50077
 trimethylsulfonium- d_6 (d_6), vibr. spectrum, normal coord. calcs. 7-50077
 A/O ($\text{B}^2\Sigma^+-\text{X}^2\Sigma^+$) system, Franck-Condon factors, isotope effect 7-10671
 AgI, mol. consts. and millimeter-wave rot. transitions, meas. 7-10555
 AlH_3 , isolated H impurity vibr. spectrum, isotope depend. (*Russian*) 7-16703
 BHF_2 (BDF_2), mol. consts., vibr. anal. 7-50058
 $\text{Bi}_{12}\text{SiO}_{20}$ crystals, local vibr. of Si isotopes, Raman spectra 7-7689
 CHe^+ , mass spectrometric obs. 7-49956
 C_2He_2^+ , mass spectrometric obs. 7-49956
 $^{12}\text{CO}_2$ - $^{13}\text{CO}_2$ isotope laser 7-31299
 CS_2 , liq., isotopic thermal diffusion meas. 7-44880
 $\text{Ca}+\text{H}_2$ (D_2), collisional quenching, time-resolved emission spectra anal. 7-36528
 ClO_2 , struct., pot. functions, electron diffraction and spectroscopic data 7-15708
 Cr^++H_2 (HD) (D_2), kinetic and electronic energy effect, mass spectra 7-65293
 CsH_2PO_4 (d_2), polarised IR and Raman spectra, internal vibr. 7-50125
 D, Rydberg const. meas. via Balmer- α wavelength single-photon determ. 7-36516
 D^++H_2 (D_2) trajectory surface hopping calcs. 7-59747
 D_2^++Cs , dissociative charge exchange, D_2 predissociation spectra anal. 7-36753
 DF dimer+DF(HF), collisional vibr. relax., rate consts. meas. 7-50320
 D_2O , H- and D-bonded dimers, relative stabilities, IR spectra 7-62364
 D_2O^+ , $\text{B}^2\Sigma$ state predissoc., intramol. dynamics, photoelectron spectroscopy 7-42699
 F+ H_2 (HD) (D_2), quantum reaction probabilities, hyperspherical coordinates 7-13754
 FDF $^+$, IR spectrum, ab initio calcs. 7-25506
 Fe II complexes, spin transition induced by heat, pressure, light and nuclear decay 7-58785
 Fe:H(D), lattice strains, meas. 7-2268
 Ge:CuH(D_2), acceptor electronic state symm., isotope effects study 7-21863
 Ge:Ga single crystals, tracer diffusion coeff. and isotope effect, SIMS meas. 7-27019
 H, Rydberg const. meas. via Balmer- α wavelength single-photon determ. 7-36516
 H+ F_2 (Cl_2), kinetic isotope effects, dynamics calcs. 7-54098
 H+ H_2 , and isotropic analogs, reactive scatt. 7-17776
 H^++D_2 , trajectory surface hopping calcs. 7-59747
 H_3^+ and isotopes, semiclassical vibr. eigenvalues, adiabatic switching method 7-57043
 H_n^+ , even cluster ions, form., reactivity collision-induced dissociation, isotope effects, mass spectra anal. 7-50434
 HCN isotopes, quartic approx. of pot. function, mech. spectroscopic problem 7-50288
 HCl BF $_3$, struct. determ. mol. beam electric reson. spectroscopy 7-15591
 HD Tokamak plasma, fast Alfvén wave propag., expt. meas. 7-58014
 HD $^+$, electrical props. adiabatic calcs. 7-56927
 HDO, H- and D-bonded dimers, relative stabilities, IR spectra 7-62364
 HI-HF complexes, struct. and microwave spectra 7-50087
 H_2O , rot. levels, isotope effects, three-parameter model 7-31018
 H_2O^+ , $\text{B}^2\Sigma$ state predissoc., intramol. dynamics, photoelectron spectroscopy 7-42699
 H_2O -DMSO, mol. dynamics, PMR relax. study 7-36651
 He-hydrogenic trace mixtures, temp. depend. of thermal diffusion factor, role of column calibration factor 7-63240
 $^3\text{He}+^4\text{He}$ (^4He), elastic scatt. cross section ratio, nucl. spin lattice relax. time anal. 7-42652
 He_2H^+ (He_2D^+), rot.-vibr. states calcs. 7-36576

isotope effects continued

- HeRh²⁺ adsorbed compound ion, field dissociation by atomic tunnelling 7-33919
 HeRh²⁺, cpd. ion, dissoc. in high elec. field, at. tunnelling, orientational and isotope effects 7-42777
 Hg-Ar, low press. electrical discharge, isotope effects, hyperfine struct. 7-37786
 I⁻, solvation struct. in formamide (formamide-H₂O), NMR relax. obs. 7-15539
 InBr, A-X system, rot. struct., dissoc. energy 7-50071
 InBr, rot. anal., use of isotopic effects 7-15587
 KH₂PO₄ (KD₂PO₄), low freq. optical vibr. interaction, Raman spectra 7-46026
 Kr⁺+H₂(D₂)(HD), spin-orbit state and isotope effects, pot. energy curve, cross sections meas. 7-39859
 Li + XF (where X = Mu, ¹H, ³H, ¹⁰H), quasiclassical trajectory calcs., isotopic and orientational study 7-33923
 (Li, K)Cl, molten, internal cation mobilities 7-2243
 Li, self-diffusion and isotopic effects, pseudopot. formulation 7-26990
⁶Li₂, ²Σ⁺ state, isotope effect, Fourier transform spectroscopy 7-5660
⁶Li₂, ²Σ⁺ state pot. energy curves, adiabatic corrections 7-36514
⁶LiD, X¹Σ⁺ and A¹Σ⁺ states, pot. energy curves 7-5622
⁶LiH, X¹Σ⁺ state pot. energy curves, adiabatic corrections 7-36514
⁶LiH, X¹Σ⁺ and A¹Σ⁺ states, pot. energy curves 7-5622
 LiH(D), pot.-energy curves, PMO-RKR-van der Waals pot., Pade approx. method 7-30965
 Mu + F₂(Cl₂), kinetic isotope effects, dynamics calcs. 7-54098
 ND₂ReO₄, heat capacity anal. 7-26984
 ND₂SCN, phase transitions, spin lattice relax. study 7-33286
 NH₃ unimolecular dissoc., pot. energy surface, classical trajectory study 7-13745
 NH₃(ND₃), predissociation, dissoc. attachment cross section 7-50279
 N₂O spectra in 1100 to 1440 cm⁻¹ region 7-19854
 Na⁺, solvation struct. in formamide (formamide-H₂O), NMR relax. obs. 7-15539
 Na₂O.3SiO₂ glass, Na leaching rates in H₂O and D₂O, comparison 7-63885
 NbO₂H₂(D₂), H tunnelling, isotope and temp. depend. 7-27474
 Ni, polycryst., adsorption-desorption of CO, kinetics 7-16873
 O + H₂(HD)(D₂), trajectory isotope effects, pot. energy surfaces 7-65296
 O + HD reaction rates, variational transition state theory 7-59749
 O₂, electron impact, vibr. excitation, three-body electron attachment, isotope effect 7-57185
¹⁸O₂, Schumann-Runge bands, oscillator strengths meas. 7-62455
¹⁸O₂, Schumann-Runge bands, predissoc. linewidths meas. 7-62464
 O₂⁺ + methane-d₀(d₁)(d₂)(d₃)(d₄), reaction rate coeff. and product distrib. meas., isotope effect 7-13741
 OCS, vibr. excited, photodissoc. cross section meas. 7-15662
 OH + HCl (DCl), reaction rates, vibr. excitation and isotopic substitution effect 7-22996
¹⁶O¹⁸O, Schumann-Runge bands, oscillator strengths meas. 7-62454
¹⁶O¹⁸O, Schumann-Runge bands, predissoc. linewidths meas. 7-62465
 Pd-T system, solubility meas., comparison with Pd-D and PdH systems 7-21474
 Pd_{0.8}Ag_{0.2}-T systems, solubility meas., comparison with Pd_{0.8}Ag_{0.2}-D and Pd_{0.8}Ag_{0.2}-H systems 7-21474
 PdT_{0.7}, quasi-harmonic phonon dispersion relation, coherent neutron scatt. study 7-38141
 Rb + H₂(D₂), fine-structure transition cross-sections, quantum-mechanical calcs., importance of perturber rotational levels 7-57161
 SO₂-HF(DF), mol. geometry, ¹⁹F spin-spin and D-nucl. quadrupole coupling consts., rot. spectrum 7-5666
 SeO₂, struct., pot. functions, electron diff. and spectroscopic data 7-15708
 Si³⁵Cl₄H, mm wave rot. spectra, centrifugal distortion const. and harmonic force field anal. 7-25496
 SnH⁺ (SnD⁺), ⁵Π_g(¹Π_g), X¹Σ⁺ visible emission spectra 7-5688
 SnH₄, rot. spectrum in vibr. ground state obs. by IR-RF double reson. 7-25573
 Ta-H(D)(T), heat of transport, isotope and temp. depend. 7-27024
 TeF₆, ν₃ bond, free jet IR absorpt. spectroscopy 7-10569
 UF₆, diode laser absorption at room temp. around 16 μm 7-25521
 β-V₂D, single cryst., neutron diffraction investig. 7-32415
 β₁-V₂H, single cryst., neutron diffraction investig. 7-32415
 W (211), activated chemisorption of methane 7-52279
 YH_{0.18}(D_{0.18}), H pairing and anisotropic pot. for H isotopes, neutron spectroscopy study 7-38144

isotope exchanges

- ice, cubic, proton transport, FTIR obs. 7-53340
 interstellar clouds, reactions at low temps. 7-13764
 Kevlar 49 fibres, N-H groups, photoacoustic Fourier transform IR spectra 7-39118
 D + H₂ - HD + H, quantum mech. reactive scatt. problem, L² soln. 7-62485
 H⁺/D⁺ fractionation, NMR investig. with various probe nuclei 7-56312
 H-D exchange, fast atom bombardment mass spectrometric obs. 7-50392
 H + muonic H, low energy collisions, isotopic derivatives, cross sections, electron screening effect 7-31143
 H + H₂, collision theory thermal rate consts., on SLTH pot. surface 7-54085
 HD-H₂O, sonolysis, H₂ and D₂ form., H/D isotope exchange 7-13755
 LiCl-KCl, molten mixture, eutectic, isotope self-exchange vels., simulation 7-57187
 O₂ 7-3608
 OH + NO(NO₂)(N₂O), isotope exchange reactions, LMR detection, rate const. meas. 7-39882
 OH + O₂, isotope exchange reactions, LMR detection, rate const. meas. 7-39882
 UF₆ + UF₅, isotope exchange and separation 7-15733

isotope relative abundance

- see also element relative abundance
 Allende meteorite, Hg isotope ratios 7-55583
 Amazon River, continental shelf organic C accumulation, stable isotope characts. 7-34463
 Amazon River, continental shelf sediment accumulation and transport ²¹⁰Pb anal. 7-34462
 Amitsoq gneisses (early Archaean) of Isukasia area, W Greenland, geochronology and isotopic var. 7-34485
 N Apennines, deformation phases dating using K-Ar and ⁴⁰Ar/³⁹Ar techniques 7-40459

isotope relative abundance continued

- upper atmosphere, O isotope composition, deep-sea spherule evidence 7-9441
 atmospheric methane, stable C isotope ratios 7-29167
 atom probe mass analysis with a signal height discriminating timer 7-30127
 basalts from S Atlantic hotspots, geochemical correl. with southern African kimberlites 7-34409
 basalts of mid-ocean ridges, inert gas abundances 7-60198
 Bencubbin, stony-Fe meteorite, ¹⁵N enrichment 7-4387
 benzenes, soln. electron affinities, isotope enrichments 7-10770
 Black Hills of S Dakota, USA, Precambrian rock origin, isotope geochemical constraints 7-60205
 Cainozoic basalts of E China, Pb, Sr and Nd isotope systematics and chemical characts. 7-29011
 carbonaceous chondrites, O and H isotopic relations in water and acid residues 7-9443
 chondritic meteorites, comp. rel. to solid materials form. in preplanetary nebula 7-24024
 Colorado Peaks volcanic rocks, USA, isotope and trace element geochemistry 7-60203
 conf., Erice, Italy (April 1986) 7-41001
 cosmic ray ³He/⁴He ratio at high energies, implications of rigidity spectrum of He nuclei 7-66410
 cosmology, primordial ³He abundances 7-60840
 Cretaceous-Tertiary extinction event, palaeoceanography characts., isotopic and geochem. anal. 7-18104
 data multidimensional treatment method 7-66315
 deep-sea sediments, O isotope stratigraphy, graphic correl., appl. to Late Quaternary 7-23894
 Dhajala chondrite, radionuclide depth profiles determ. 7-29439
 Dhurmsala, LL-chondrite, cosmic ray records 7-9442
 early solar system and isotope abundance anomalies 7-47739
 East Pacific Rise and Guaymas Basin, hot springs U-Th-Pb systematics 7-40462
 Eifel periodotite xenoliths, trace element and isotope geochemistry rel. to subcontinental lithosphere 7-34484
 ethanol from Bulgarian wines, liquid scintillation meas. 7-20071
 galactic cosmic radiation, H and He isotopes rel. to source abundances and interstellar propag. 7-55394
 geochemistry of well gases in Harding County, New Mexico, USA 7-60226
 glaciolacustrine sediments of Yukon Territory O isotope evidence for early Holocene thaw unconformity 7-9034
 glassy submarine basalts dating and He isotope disequilibrium 7-66352
 Great Artesian Basin, Australia, very old groundwater ³⁶Cl dating and chem. 7-66194
 Grenville Front, Labrador, Canada, Sr, Nd, Pb isotope geochemistry 7-60199
 SW India, monsoon fluctuations in 20000 yr BP O isotope/pollen records 7-47532
 inert gases, systematics in basalts and dunite from Reunion and Grand Comore 7-29012
 inert gases in planetary atmospheres, effects of mass fractionation during transonic escape 7-55508
 kimberlites from southern Africa, geochemical correlation with S Atlantic hotspots 7-34409
 Kraternaya Bay region, Yankicha Island, Kuril Islands, water chem. and isotopic comp. 7-29078
 late-type Population I dwarf stars, Li abundances and ⁷Li/⁶Li ratios 7-14562
 low-level counting techniques 7-29296
 mantle isotopic heterogeneity with different size scales 7-8889
 Mariana Trough basalt glasses, light noble gases comp. anal. 7-40436
 Marydale Group, southern Africa, metamorphosed banded Fe formation, Pb-Pb dating and assoc. geochem. 7-60189
 meteorites, carbonaceous chondrite C isotopes and element abundances 7-24086
 meteorites, cosmogenic isotope and track records rel. to cosmic ray fluxes 7-29440
 meteorites, Si isotopic composition 7-60609
 meteorites (irons), ¹⁰⁷Ag anomalies, and petrology 7-14545
 micrometeorites, O isotopes in deep-sea spherules 7-9441
 milk River aquifer, Canada, old groundwater ³⁶Cl dating and chem. 7-66195
 minerals, ⁴⁰Ar/³⁹Ar dating, errors due to ³⁹Ar loss during neutron activation 7-60390
 Mont Saint Hilaire plutonic complex, Quebec, Canada, Ar isotopes and emplacement history 7-4007
 Nagano, Japan, ³He/⁴He ratio anomalies in hot spring gases, assoc. with 1984 September 14 earthquake 7-40422
 natural gas wells in Sacramento basin, California, He isotope and mantle origin 7-60206
 ocean chemical composition, ²¹⁰Po and ²¹⁰Pb in Gulf of Mexico seawater 7-34552
 oceanic basalts of Oceanographer transform, Mid-Atlantic Ridge, three-component isotopic heterogeneity 7-54956
 oceanic crust, O isotopic profile through upper kilometer at DSDP Hole 504B 7-34467
 Outer Hebrides, evidence for enriched lithospheric keel, mantle xenoliths comp. anal. 7-47407
 SW Pacific islands, Pb, Sr, Nd isotope and element abundances study 7-8874
 peat dating by U-Th disequilibrium, geochem. aspects 7-60392
 Phanerozoic, seawater, SR isotopic comp. var. 7-60273
 Population II giant stars, C isotopic ratios determ. 7-60654
 primary lavas from Okmok volcano, central Aleutians, geochemistry rel. to arc magmatogenesis 7-28949
 Quelccaya Ice Cap, Peru, ^{δ18}O stratigraphy rel. to Little Ice Age record 7-34670
 Ragland meteorite, LL 3.4 chondrite find from New Mexico, O isotopic comp. 7-9450
 Rainy Lake area, Ontario, Canada, geochemical study of mantle heterogeneity and crustal cycling 7-60202
 Roberts Victor eclogites, ¹⁸O/¹⁶O ratios rel. to ancient oceanic crust hypothesis 7-55042
 Rockall Plateau, dipping-reflector passive margin struct., Pb isotopic evidence 7-66037
 Scotland, Caledonian Pb isotope geochemistry and mantle source 7-23590

isotope relative abundance continued

- marine sediment Th, U, ^{226}Ra , ^{230}Th , ^{231}Pa conc. determination, alpha scintillation method 7-4199
- Seychelles microcontinent, younger igneous rocks isotopic and geochronological anal. 7-40452
- Sharyzhalgai complex, Baikal region, USSR, ultrabasics Rb-Sr isochrone anal. 7-23603
- Central Sierra Nevada, United States Winter storms ice-phase water capture regions identification, use of snow O isotopic comp. 7-4084
- SNC meteorites, ^{10}Be contents determ. 7-40785
- South China Sea, palaeoclimate and palaeoceanography during Holocene, sediment O isotopic anal. (Chinese) 7-55264
- stable isotopes in high-temp. geological processes, book 7-35126
- stratosphere, O_3 isotope measurements at Texas, USA, ^{49}O and ^{50}O observations 7-66209
- sulphate deposits in S Alberta fractured till, $\delta^{18}\text{O}$ and $\delta^{34}\text{S}$ anals. rel. to origin 7-23726
- super metal rich stars, Mg isotopic characts. determ. from MgH spectral obs. 7-60645
- Tariat Depression, Mongolia, Nd, Sr isotope study and subcontinental lithosphere evolution 7-60201
- Wethersfield (1982) chondrite, abundances of cosmogenic radionuclides and noble gases 7-34952
- ^{26}Al production by Wolf-Rayet stars, galactic yield and gamma-ray line emissivity 7-47830
- ^{27}Al in red giants, effect of ($^3\text{He}, d$), (α, t) and (p, γ) reactions 7-19267
- Ar in Allende meteorite, determ. by laser microprobe 7-55584
- $^{40}\text{Ar}/^{39}\text{Ar}$ ages from Aileu Formation, East Timor, Indonesia, implications for retrogressive metamorphism 7-28916
- $^{10}\text{B}/^{11}\text{B}$ ratio, determ. in nucl. reactor moderator 7-56753
- ^{10}Be , conc. in meteorite, AMS meas. 7-66524
- C in Palaeozoic ocean, isotopic characts. 7-9029
- C stable isotopes meas. at nanomole level, using static mass spectrometer 7-17842
- CCD/CCH abundance ratio in dense interstellar clouds, ion-molecule calc. 7-66712
- $^{13}\text{CO}_2/^{12}\text{CO}_2$, abundance meas. by nondispersive IR heterodyne ratiometry 7-15731
- $^{12}\text{C}/^{13}\text{C}$ for interstellar cyclopropenylidene 7-40891
- $^{12}\text{C}/^{13}\text{C}$ ratio in comets, implications of synthetic Swan band profiles of $^{12}\text{C}/^{12}\text{C}$ and $^{12}\text{C}/^{13}\text{C}$ 7-60532
- $^{12}\text{C}/^{13}\text{C}$ ratio in solar photosphere, determ. from CO vibr.-rot. bands 7-55598
- $^{13}\text{C}/^{12}\text{C}$ ratio of atmospheric CO_2 , ice core record for past two centuries 7-34637
- $^{13}\text{C}/^{12}\text{C}$ ratios, stratigraphic tool in East Mediterranean (French) 7-60190
- $^{13}\text{C}/^{12}\text{C}$ rel. to long-range transport of continental particulate C in marine atmosphere 7-55221
- $^{13}\text{C}/^{13}\text{C}$ ratio in Lake Karewa sediment, India, palaeoclimate characts. determ. 7-4175
- ^{14}C in atmosphere, seasonal vars. 7-23256
- ^{14}C , T corrected, use for mixed groundwaters dating 7-9044
- Ca-Ti-Cr isotopic anomalies in Allende meteorite, correlation with solar $^{48}\text{Ca}/^{46}\text{Ca}$ abundance 7-55586
- ^{48}Ca anomalies in carbonaceous chondrite hibonites 7-55579
- $^{48}\text{Ca}/^{46}\text{Ca}$, solar abundance ratio, correlation with Ca-Ti-Cr isotopic anomalies in Allende meteorite 7-55586
- ^{36}Cl , conc. in meteorite, AMS meas. 7-66524
- D/H galactic ratio 7-35030
- D/H ratio in atmosphere of Uranus implications of methane- d_1 detect at $1.6\text{ }\mu\text{m}$ wavelength 7-55529
- Ga, reference sample, absolute isotopic abundance ratio and at. weight 7-42779
- H_n^+ , isotopes, relative abundance, mass spectrometric meas., computer-assisted null point method 7-25489
- ^3H , environmental, appl. to meas. of water movement in unsaturated zone under irrigated area 7-23757
- He isotopes in sedimentary basins, relation to form. mechanism 7-47405
- He-H, isotope composition, spectrosc. determ. 7-50395
- ^4He , atm. inert gases corrected, use for mixed groundwaters dating 7-9044
- $^{40}\text{K}/^{39}\text{K}$ ratio in Earth lower mantle, implications of K-Ar isochron dating of Zaire cubic diamonds 7-23612
- $^{26}\text{Mg}/^{24}\text{Mg}$ in interstellar medium rel. to ^{26}Mg excess in meteorites 7-48036
- ^{53}Mn , evidence of existence in solar nebula 7-34891
- N_2 , isotope abundance ratio determ., mol. emission spectrometry 7-17835
- $^{15}\text{N}/^{14}\text{N}$ in basaltic glasses rel. to mantle degassing and structure 7-60193
- $^{15}\text{N}/^{14}\text{N}$ ratios, appl. to detect. of N pollution in hydrosphere and atmosphere 7-28422
- ^{22}Na , gamma-ray constraint on interstellar abundance rel. to origin of mass 22 nuclei 7-35069
- O in Palaeozoic ocean, isotopic characts. 7-9029
- O isotopic records in deep-sea sediments and Holstein interglaciation 7-47529
- $^{16}\text{O}/^{18}\text{O}$ ratio in solar photosphere, determ. from CO vibr.-rot. bands 7-55598
- Os, isotopic composition in terrestrial samples from accelerator mass spectrometry meas. 7-23611
- Pb isotope evolution rel. to Earth core growth, implications of siderophile and chalcophile abundances in oceanic basalts 7-34397
- Pb-Pb isochron dating method for deeply weathered terrains geochronology 7-60391
- ^{207}Pb ($A=204, 206, 207, 208$) in Bo Country chondrite (Chinese) 7-18391
- Ra isotopes in groundwater, porous flow model for steady state transport 7-23725
- ^{222}Rn in Gulf Coast geopressured-geothermal reservoirs, United States 7-8881
- $^{28}\text{Si}/^{29}\text{Si}/^{30}\text{Si}$, in IRC+10216, determ. from obs. of $^{29}\text{SiC}_2$ and $^{30}\text{SiC}_2$ 7-29474
- ^{232}Th concentrations in seawater, meas. techniques and results 7-34554
- ^{50}Ti anomalies in carbonaceous chondrite hibonites 7-55579
- U, determ. of isotope ratio, simultaneous anal. with Th, delayed neutron counting method 7-3615
- $^{234}\text{U}/^{238}\text{U}$ ratio in seawater, meas. techniques and results 7-34554
- $^{234}\text{U}/^{238}\text{U}$ activity ratios in geological materials, determ. by α spectrometry 7-60255

isotope relative abundance continued

- ^{238}U decay series nuclides, evidence for recent migration in granite pluton 7-28917
- ^{238}U , isotopic composition, determ., nuclear spectrometric method 7-62198
- isotope separation**
- see also isotope exchanges; laser isotope separation; radiochemistry
- benzenes, soln. electron affinities, isotope enrichments 7-10770
- binary mixtures, separation, nonstationary mass transfer 7-42778
- dye laser pumping by Cu vapour laser for U isotope separation 7-50553
- edge dislocation, pipe diffusion, isotope separation 7-58521
- energetic requirements for isotope separation by plasma methods 7-63359
- exotic nuclei far from stability, fast separation system (French) 7-19192
- heavy ion fragmentation isotope production at intermediate energies, GANIL expts., overview 7-5783
- interstellar gas, isotope fractionation chemistry 7-14641
- ion exchange separation of short-lived transplutonium nuclides 7-36806
- ISOL study of nuclei far from stability 7-36374
- ISOLDE, intense unstable-nuclei beam production 7-48908
- ISOLDE Users' guide 7-19598
- laser spectroscopy appl. to heavy ion reaction sources 7-36373
- metals, electrochemical desorption step, rel. to isotope effect 7-13782
- multi-fluid, steady state model for rotation and separation in a fully ionized, magnetized plasma column 7-26548
- on-line chemical separation for nuclear studies 7-50394
- radioisotope production, anal. and appl., conf., Banff, Canada, Sept. 1985 7-24254
- RIKEN He jet transport system, IGISOL appl. 7-36372
- thermal diffusion column for isotope separation, cut and feed rate effects on circulating flow 7-50393
- tritiated water, enrichment and vol. reduction using an electrolysis cell with a permeable cathode 7-49668
- Am separation and activity meas. in sea algae 7-54370
- ^{47}Br , $A=75-7$, radioisotope prod. for medical appl., review 7-28693
- C stable isotopes meas. at nanomole level, using static mass spectrometer 7-17842
- ^{64}Cu , radioisotope enrichment, nuclear recoil appl. 7-62539
- ^{18}F , radioisotope prod. for medical appl., review 7-28693
- H^+/D^+ fractionation, NMR investig. with various probe nuclei 7-56312
- HDO, vibr. modes, rot. decoupling 7-57042
- He-jet fed ISOL facility KUR-ISOL at the Kyoto University reactor 7-30822
- ^{123}I , radioisotope prod. for medical appl., review 7-28693
- Li_2 , isotopes, laser separation, double REMPI spectra 7-42694
- ^6Li , enrichment by electromigration in molten LiNO_3 7-2244
- N, isotope separation by nitric acid method 7-25677
- ^{239}Np , $A=243, 244$, separation and identification by centrifuge system 7-24995
- ^{239}Pu , ^{240}Pu and ^{242}Pu , conc. determ. by isotope dilution-thermal ionisation mass spectrometry 7-10769
- U accountancy in atomic vapour laser isotope separation 7-30520
- U isotope separation using nozzle effects, fluid dynamic analysis 7-61975
- U laser isotope separation in the UK, development and policy implications 7-49553
- UF_6+UF_5 , isotope exchange and separation 7-15733
- Zn isotopes, separation by liq. phase thermal diffusion 7-15732
- isotope shifts**
- see also atomic spectra
- $^{14}\text{CO}^+$, rot.-vibr. anal., UV spectra 7-19821
- acetone- $d_0(d_1)(d_6)$, mol. torsion, semirigid rotor model, far-IR spectra anal. 7-50105
- alkali metal perchlorate vitrified dil. solns., IR spectra anal. 7-19857
- benzene, substituent effects on vibr. modes 7-19824
- $\beta\text{-BoB}_2\text{O}_4$, crystal vibr. assignment, Raman and IR spectra anal. 7-53346
- n-butane- d_6 , C-H bonds, vibr. anal. gas phase IR spectra simulation 7-19825
- carbonyl oxide, IR spectra, harmonic freq. and ^{18}O isotopic shifts 7-62361
- cellulose acetates, units distrib., NMR spectrosc. obs. (Russian) 7-15757
- CO_2 , isotopic species, vib. transition const., IR emission spectra 7-19849
- cyclohexylphosphine, chair conform. identification in the gas phase, microwave spectra anal. 7-36597
- diacyl peroxides, low temp. photolysis, vibr. anal. for CO_2 dimer, IR spectra 7-15597
- dichloromethylbenzene- $d_0(d_1)(d_6)$, internal rot., ^{13}C spin-lattice relax. times and NOE factors 7-50189
- 2,2-dichloropropane- $d_0(d_3)$, vibr. anal. IR and Raman obs. 7-919
- dioxirane, IR spectra, harmonic freq. and ^{18}O isotopic shifts 7-62361
- field shift and generalised moments of nuclear chargedistribution 7-10105
- fluoroform- d , Coriolis splitting parameter, vibr. depend., IR double-reson. spectra anal. 7-42616
- glycolic acid, ^{13}C and ^{18}O isotope shifts, rot. isomerisation, ab initio SCF calcs., IR Ar matrix spectra 7-19851
- HBF_4 , Γ_8 struct., bond lengths, microwave spectra 7-62357
- heavy atoms, hyperfine struct., isotope shift nucl. struct. effects optical spectra 7-19768
- hexafluoride mols., vibr. isotope shifts 7-943
- 1,3,5-hexatriene, conform. struct, vibr. anal., ^2H substitution effects, RHF calcs. 7-25386
- 9-hydroxyphenalenone- d (di) Shpol'skii matrix isolated, H bonding, phosphoresc. 7-19926
- indole, valence force const. IR and Raman freqs., normal coordinate anal. 7-914
- lumiflavin vibr., isotope freq. shift, IR spectra 7-918
- methyl(difluorophosphineborane), vibrational assignment, normal coordinate anal., Raman and IR spectra 7-62384
- methyl chloride, Fourier transform IR spectra, rot.-vibr. anal. 7-10571
- methyl chloride, rot. transitions, isotope shifts, microwave spectra anal. 7-42606
- methyl-substituted amine-HF complexes, methylation effect, IR spectra anal. 7-19855
- methylene chloride, isotope effect, empirical general harmonic force field 7-62346
- nitrile ylides, matrix photolysis of phenyl and azidostyrenes, isotopic shift, mol. struct. FT IR spectra anal. 7-31035
- phosphates, ^{17}O , ^{31}P , ^1H and ^{13}C NMR spectra study 7-25544
- phosphites, ^{17}O , ^{31}P , ^1H and ^{13}C NMR spectra study 7-25544
- polyaniline, ^{15}N - and ^2H -substituted derivatives, vibrational spectra 7-53351

isotope shifts continued

- potassium hydrogen malonate, crystn., inelastic neutron scatt. 7-32419
 protoporphyinato nickel (II), isotope shifts, vibr., LF reson. Raman spectra 7-19868
 radioactive atoms, HFS, isotope shift using computer controlled dye laser 7-20249
 radioactive atoms, laser spectroscopy photon correl. technique 7-19769
 resonance ionisation mass spectrometry and photon burst anal., isotopically selective laser measurements 7-54213
 riboflavin, and derivatives, vibr., isotope freq. shift, IR spectra 7-918
 SeS₂, rot. anal., isotropic shifts, mol. moments, IR Fourier transform spectra 7-62370
 skatole, valence force const. IR and Raman freqs., normal coordinate anal. 7-914
 thiophosphates, ¹⁷O, ³¹P, ¹H and ¹³C NMR spectra study 7-25544
 toluene, vib. anal., isotropic species, comparison with benzene 7-19824
 tribromacetamide, ¹⁵N isotope effects, Raman spectra, ab initio calcs. 7-19871
 tribromoacetonitrile, force field and thermodynamic fns. 7-30960
 trimethylchlorogermane, liq., vibr. anal., isotope effects, Raman bandshape anal. 7-33371
 vitrified dil. alkali metal nitrate solns., IR spectra anal. 7-19857
 AgBr, vibr. states, rot. transitions, isotope shifts, Dunham pot., microwave spectra anal. 7-42605
 AsH₃, isotopic species, mol. vibrs., inversion splitting calcs. 7-19997
 Ba II, isotope shift, hyperfine struct., fast ion beam spectra 7-19743
 CCl₄⁺, Born-Oppenheimer pot. fn., mol. rot.-vibr. study, IR spectra anal. 7-36604
 CO, b²Σ⁺-a²Π, system, Kaplan bands, UV obs. 7-62395
 CO, isotopic species, B²Σ⁺-X²Σ⁺ transition, vacuum UV obs. 7-62401
 CO₂, amorphous solid, mol. vibr., IR spectra anal. 7-53307
 CO₂, autoionisation and isotope effect in threshold UPS 7-19948
 CaF₂:Er³⁺, H⁺(D⁺), IR excitation and absorpt. spectra anal. of sites 7-53306
 CaO-SiO₂ polycryst. silicates, FTIR and Raman spectra, isotopic shifts and force consts. 7-53341
 Cd isotopes, hyperfine structure splitting, isotope shift meas. 7-41885
 CdD, B²Σ⁺-X²Σ⁺ system study, near-UV spectra anal. 7-50164
 Cs, isotope shifts, relativistic DF contrib., reson. doublet, UV laser spectroscopy 7-10475
 DBr⁺, X²Π_{3/2} ground state, mol. rot.-vibr., isotope shifts, double modulation Faraday LMR IR spectra 7-62369
 DI, Ar matrix, conc. effects, binary complexes with impurities, IR spectra anal. 7-31034
 Er, low-lying states electronic density, ab initio multiconfiguration DF calcs. 7-15486
 Fe complex, oxy(tetraphenylporphyrinate), Iron II, cocondensation products, struct. and bonding, IR spectra 7-10572
 Fr, isotope shifts, relativistic DF contrib., reson. doublet, UV laser spectroscopy 7-10475
 Fr, second resonance doublet, wavelength meas. fine-, hyperfine structure, isotope shifts 7-57020
 Ga, isotope shift, hyperfine struct., magnetic-dipole- and electric quadrupole coupling consts., atomic fluoresc., MCHF method 7-30985
 Ga(CO)₂, form. in hydrocarbon matrices, magnetic parameters, EPR and IR spectra anal. 7-19906
 GaCl, isotopic derivatives, Dunham pot. for electronic ground state, microwave spectra anal. 7-31029
 GeH⁺(GeD⁺) in He afterglow, a³Π₀₊₁-X¹Σ⁺ visible band system 7-50152
 H₂, line width, isotope shift and Rydberg constant determ. 7-25433
 H⁺/D⁺ fractionation, NMR investig. with various probe nuclei 7-56312
 H₂ and isotopes, nonadiabatic eigenvalues and adiabatic matrix elements 7-62381
 H₂ and isotopomers, rot. transition, Raman line position 7-62380
 HCN, isotopic species, electronic states, pot. surface, dissoci. vibr. anal., CI calcs. 7-62297
 H(D), T-tube plasma, β-line. central dip, ion dynamic effects anal. 7-36542
 HI, Ar matrix, conc. effects, binary complexes with impurities, IR spectra anal. 7-31034
 HNC, 2100 cm⁻¹ bands, IR Fourier transform spectra anal. 7-50117
 HOCl, FTIR spectra, vibr. rot. consts. and harmonic force field 7-50140
 Hg, 6¹S₀-6³P₁ transition isotope shift in UV absorpt. spectra 7-19770
 Hg UV spectra, isotopic shifts and hyperfine splittings 7-49987
 IBr, ion-pair states, spectral anal. 7-19873
 InBr, isotope shift, rot. anal., UV spectra 7-19876
 Li, ⁶Li ground state, specific mass shift, isotope shift, ab initio calcs. 7-36495
 Li, excited states, quantum defect and isotopic shift meas., millimeter wave ODR spectroscopy 7-15538
⁷Li II, absolute wavelength determination, fine struct. determ. 7-10771
⁶Lu, A-173-6, resonance ionization mass spectrometry for high resolution optical spectra 7-19744
⁶Lu, A=173,174, high resolution mass resolved spectra 7-15552
 Mg, spectra struct. and isotope shifts, many-body perturbation theory calcs. 7-50019
 Mo complex, Mo phthalocyanine, struct., IR spectra, powder and liq. soln. EPR spectra study 7-64509
 Mo complexes, with dioxo ligands, mol. vibr., IR and Raman spectra anal. 7-50151
 ND₃, elastic consts. and elasto-optic coeffs., Brillouin spectra anal. 7-53359
¹⁵NH⁺, X²Π state, IR rot.-vibr. spectrum, isotopic shifts and equilib. consts. 7-50107
 NH₃ S₂ bands, isotope shift, diode laser spectra 7-19845
 NH₄H₂PO₄:SeO₄²⁻, partially deuterated, D concentrations in H₂PO₄⁻ and NH₄⁺ radicals, ESR spectra 7-27671
 NH₃(ND₃) band intensity and symmetry effect on absorpt. spectrum 7-57049
^{20,22}Ne, specific mass isotope shift, laser optogalvanic spectra 7-19771
 O₂, UV Huggins bands, isotope shift obs. 7-19819
 PH₃, isotopic species, mol. vibrs., inversion splitting calcs. 7-19997
 Ra I and II, HFS, isotope shift fast-beam laser spectroscopy 7-42534
 S₂, b²Σ⁺-X²Σ⁺ system consts., IR and microwave spectra anal. 7-19848
 SF₆, dimer dissoci., dimer conc., isotope effect, model and bolometer IR spectra anal. 7-19977
 SBH₃, isotopic species, mol. vibrs., inversion splitting calcs. 7-19997
 Si:N, deep level generation and annihilation 7-16612
 Si:N,O, impurity interactions in optical defects 7-17348

isotope shifts continued

- SiF₄, dimer dissoci., dimer conc., isotope effect, model and bolometer IR spectra anal. 7-19977
 SiH₄, dimer dissoci., dimer conc., isotope effect, model and bolometer IR spectra anal. 7-19977
 SiH₃(D₃), ions and radicals, pot. energy curves and electron affinities determ., photoelectron spectra anal. 7-25603
 Sr, isotope shift and hyperfine struct., atomic fluoresc. anal. 7-30987
⁸⁸Sr, optical isotope shift in 6s²-6s6p resonance transition 7-5635
 Th, plasma, XUV spectra, isotope line identification, HF and DF calcs. 7-15487
 UO₂Cl₂·2H₂O, IR spectra, complex effect, isotope shift, extraction anal. 7-25058
²³⁵U, spectral line classification, isotope shifts, Lande g factors, pattern-recognition technique 7-62309
 WO, vibr. consts. determ. 7-15586

isotopes

see also radioisotopes

- H₂ adsorption on Ni (111), isotope effects, kinetic investig. 7-21624
 Li, isotopic anal., SES-ICP investig. 7-46908

isotopic generators see radioactive sources

isotopic spin (elementary particles)

see also baryon spin and parity; elementary particle spin and parity

- Dirac equation, generalisation admitting isospin and colour symmetries 7-9941
 Dirac equations, exact solutions in constant chromomagnetic fields 7-61434
 EM and isospin breaking effects on e⁻/e, standard model predictions 7-24816
 hedgehog chiral soliton bags, spin-isospin projection using collective coordinates, nucleons 7-19074
 technicolour theory with pseudo-Goldstone bosons, one-loop corrections 7-56525
 NN scattering, radial excitations, RGM and constituent quark model calcs. 7-19125
 NN symmetric Lorentz invariant scatt. amplitude, Yukawa representation 7-41830
 np scattering, spin and isospin nonconservation by a colour force 7-30285
 πN→πN, isospin-even forward scatt. amplitude as low-energy QCD test 7-56572
 πN low energy scatt., isospin-even forward scatt. amplitude as QCD test 7-41835

iteration methods see iterative methods

iterative methods

see also predictor-corrector methods

- anisotropic materials, crack tip field evaluation, iterative soln. of eigenvalue problem 7-43776
 approximation by the iterative combination of exponential type operators 7-56021
 balance equations in periodic domain, numerical model, balanced turbulence 7-34604
 beams, thin-walled open, elastic nonlinear static analysis 7-62984
 Chebyshev collocation methods for parabolic eqns., heat eqn., advection-diffusion eqn. 7-48649
 continuous stochastic processes, random gaussian elements approx. (German) 7-41276
 convection, steady-state, 3D problem, numerical soln. (Russian) 7-61296
 convergence (Russian) 7-61082
 coupled natural convection and radiation in an axisymmetric cavity, finite element soln. 7-37311
 coupled-cluster approach, convergence accel., DIIS method 7-15468
 CT methods use for nondestructive inspection under conditions of insufficient data 7-39818
 deconvolution, iterative algorithm with quadratic convergence 7-42969
 defective eigenvalues, simultaneous inverse iterations 7-48344
 diffraction tomography and maximum entropy Fourier synthesis 7-65884
 diffraction tomography reconstruction, max. entropy method 7-47256
 diffusion eqn., iteration scheme convergence in nodal expansion method 7-30465
 digital correlation method, optimised appl. to deformation analysis 7-26136
 eddy current flaw inversion algorithm, experimental verification 7-54059
 eddy currents, flux reflection and flux conc. effects, 3D finite element anal. 7-42845
 elastic-plastic problem soln. with increasing strain hardening of material 7-11304
 electrodynamics, iterative method of problem soln. (Russian) 7-62609
 elliptic boundary value problems, Schwarz alternation method in a sub-space 7-18569
 elliptic finite element problems on regions partitioned into substructures, iterative methods 7-48341
 elliptic partial differential eqns., iterative soln. by local discrete Fourier anal. 7-18572
 EM wave scattering, spectral iterative technique appls. 7-62590
 equal order velocity-pressure formulation 7-16142
 Fornberg's numerical method for conformal mapping 7-48342
 free and forced convective heat transfer, FEM 7-51117
 gravitational potential determ. for axisymmetric mass distrib., hydrodynamic test results 7-66446
 ignorance-based signal estimation given multiple noisy realizations 7-47264
 image processing of Fourier magnitudes, continuous object distributions reconstruction 7-42959
 image processing of Fourier transform, complex-valued objects reconstruction 7-42960
 image reconstruction, constrained, of complex waveforms 7-42971
 image reconstruction, Fresnel zone transforms, stationary phase approx. 7-42963
 image restoration, linear degradation effects, iterative algorithm 7-42970
 incompressible flow, viscous, variational formulation 7-37422
 intramolecular dynamics calculations, effective Hamiltonians 7-19995
 Ising lattice models, iterative method of soln. in mag. field 7-45600
 Kepler's equation solution, procedures using FORTRAN 7-24018
 Langmuir probe technique for plasma parameter measurement in a medium density discharge 7-11782
 lattice fermion, incomplete LDU decomposition, appl. to conjugate residual methods 7-41082
 lattice gauge theory, heat bath method for vectorized processing 7-18974
 lidar, range-height indication measurements, data anal. 7-57394

iterative methods continued

- linear transport equation, inner iteration convergence for finite difference approx. 7-35482
 Lippmann-Schwinger equation, iterative solution 7-48461
 Lippmann-Schwinger-type eqns. iterative soln. 7-15669
 liquid-vapour mixing flow, 1D calcs. 7-63199
 many-electron systems, symmetric group approach, spin-depend. operators 7-15475
 mechanical contact problems with friction, 3D, static and dynamic analysis 7-43804
 monotone iterative technique for boundary value problems (*German*) 7-14754
 monotone techniques for first order boundary value problem 7-55969
 multi-level finite element solution algorithms, correction procedure use 7-35261
 Navier-Stokes equations, iterative solutions 7-37425
 Navier-Stokes equations, penalty FEM, iterative methods convergence 7-51024
 neutron spectra, error analysis for iterative algorithm 7-49493
 nonstationary iteration methods of solving nonlinear operator equations 7-60999
 nuclear medicine images, digital restoration by two-step procedure 7-14121
 one-dimensional random field Ising model, characteristic fractal dimension calc. 7-18724
 open-channel network flow model (*Japanese*) 7-35285
 operational calculus, application to initial and boundary value problems 7-55984
 optical-electronic hybrid system with feedback, iterative image reconstruction 7-57252
 path integral convergence, quantum propagator evaluation using iterative technique 7-112
 periodic solutions of wave eqn., iteration method 7-108
 pipe flow, unsteady, attenuation prediction, num. method appl. 7-31732
 plane wave, E- and H-polarised, transient scatt. by flat strip, spectral iteration scheme 7-56048
 plasma, spectral intensities, steepest descent inversion calcs. 7-51510
 plates and envelopes, nonlinear theory and net approx. 7-18597
 projection methods and self-regularization in ill-posed problems 7-18586
 s-orthogonal polynomials, coeffs. computation by iterative process 7-48291
 scattering problems, hybrid iterative method 7-20099
 sea bed contour map construction from random data, iterative method 7-34725
 sea-bed-structure interaction in the presence of frictional effects for submarine pipelines 7-20664
 shallow water eqns., two-stage FEM Fortran program, FEUDX 7-55080
 soil, infiltration from cavities; num. soln. 7-18254
 steady Euler eqns., multiple-grid and Osher's scheme 7-51021
 steady flow problems, press-vel. components, algorithm comparison 7-37417
 thermal radiation, transfer eqns., implicit difference eqns. (*Russian*) 7-43642
 tomographic reconstruction consistency by iterative methods 7-47253
 tomography, computer assisted, detector width artifact correction 7-47255
 transonic flows with mixed finite elements, vector potential formulation 7-43966
 unitary quantum time evolution by iterative Lanczos reduction 7-24451
 vortex breakdown simulation, multigrid method 7-26284
 X-ray double crystal diffractometry, semiconductor materials anal. 7-51577
 X-ray microanalysis, quantitative models (*French*) 7-46887
 Fe sites in minerals, electronic struct., iterative EHT, multiple scatt. α calcs. and Mossbauer meas. 7-17244
 H₂-Ar, rot. line broadening calc., projection operator algebra and linked cluster theorem 7-42687

itinerant model of magnetism see band model of magnetism

IV-VI semiconductors

- dipole-dipole interactions and ferroelectric props. 7-39046
 IR coating materials, physical effects 7-37065
 refractive indices of some narrow and wide bandgap materials 7-13118
 vibronic theory of struct. phase transition and tricritical point 7-38187
 GeS single cryst., absorpt. coeff. meas., optical energy gap determ., 2D and 3D model anal. 7-17289
 GeSe, cryst. growth in Xe atmosphere, expts. performed on Spacelab D1 mission 7-21145
 GeTe, α - γ phase transformation kinetics, effect of heat treatment 7-63795
 GeTe, dipole-dipole interactions and ferroelectric props. 7-39046
 GeTe, energy bands, relativistic empirical tight binding theory 7-45149
 GeTe, ferroelec. phase transition, electron-phonon interaction 7-13106
 GeTe, slight nonstoichiometry and high free carrier density, phase diagram study (*Russian*) 7-2191
 GeTe, solid and liquid states, electrophysical props. 7-52654
 GeTe, valence and energy spectrum, supercond. state 7-45534
 GeTe: Cd(In)(Sb), solution mechanism of impurities, effect of heat treatment 7-21455
 GeTe-PbSe, phase transformations, cation-anion substitution, electrophysical props. 7-7978
 (Pb,Sn)Se IR detector arrays, heteroepitaxial growth on fluoride-covered Si substrates 7-39429
 (Pb,Sn)Te-(Ba,Ca)F₂ layers, MBE growth on non-lattice-matched Si substrates 7-27216
 Pb salt tunable diode laser for two-tone optical heterodyne spectroscopy 7-30102
 Pb_{1-x}Cr_xTe, prep. and electrical props. 7-12721
 PbGeTe, thermal cond. minimum, thermoelectric appl. 7-38276
 Pb_{0.93}Ge_{0.07}Te, glassy and cryst., defect struct., positron annihilation studies 7-46221
 PbS, density of states and effective mass determ. 7-38433
 PbS, epitaxial film, weak-field magnetoresistance, multi-valley model (*Korean*) 7-33114
 PbS polycryst. semicond. films, laser annealing effects 7-58317
 PbS/PbSe heterostructure, band offsets, photovoltaic study 7-58872
 PbS/PbTe 1D superlattice struct., X-ray diff. patterns, coherent and incoherent phase scatt. 7-64733
 Pb_{1-y}(S_{1-x}Te_{1-x})_y, solid solution, growth from vapour, region of homogeneity 7-46285
 PbSe and other IV-VI cpds., acoustic mode vibr. anharmonicity 7-63751

IV-VI semiconductors continued

- PbSe, energy band structure, thermorefectance study 7-3028
 PbSe films, elec. cond. and thermoelec. power, dynamic behaviour 7-2750
 PbSe films, photosensitivity mechanism 7-58923
 PbSe:Ag, electron irradi. stimulated impurity diffusion 7-63878
 PbSe: Cd, crystal growth and impurity distrib., electron probe X-ray microanal. studies 7-63639
 PbSe-PbS(Pb_{1-x}Sn_xSe)(Pb_{1-x}Eu_xSe) DH lasers with remote p-n junctions 7-57333
 PbSe-SnSe strained layer superlattice, prep. and struct. anal. 7-52301
 PbSe_{1-x}S_x epitaxial films, absorpt. edge, band gap, comp. depend., 77-300K 7-39063
 PbSe_{1-x}Te_x, optical absorpt. edge slope increase, comp. depend 7-39064
 PbSe_{1-x}Te_x thin films, localised defect states and Hall effect 7-2752
 Pb_{0.8}Sn_{0.2}Te epitaxial films, vacuum deposition growth in a quasiclosed vol. 7-46329
 Pb_{0.88}Sn_{0.12}Te cryst., annealing characts. and laser fabrication (*Chinese*) 7-10933
 Pb_{1-x}Sn_xS films, phase composition, fast-electron diff. 7-63990
 PbSnSe, IR optical bistability at mW powers 7-57436
 Pb_{0.91}Sn_{0.07}Se, ferroelec. phase transition, electron-phonon interaction 7-13106
 PbSnTe as IR sensor material, characts. (*Japanese*) 7-56339
 PbSnTe BH laser reflectivity, lateral confinement effects 7-43090
 PbSnTe laser, single-mode, 8 μ m with buried heterostructure, design 7-36980
 PbSnTe, thermal cond. minimum, thermoelectric appl. 7-38276
 PbSnTe-TAGS and PbTe materials testing for PU238 special applications radioisotope thermoelectric generators 7-65500
 Pb_{0.75}Sn_{0.25}Te:In, Ge(S)(Se), elec. resist., photocond., Hall effect meas. 7-17050
 Pb_{0.8}Sn_{0.2}Te thin films, structural and elec. props., pulsed laser-irrad. effects study 7-21270
 Pb_{0.8}Sn_{0.2}Te:Ga solid solns., diffusion coeff., temp. depend. study 7-2254
 Pb_{0.8}Sn_{0.2}Te:In, impurity diffusion, thermoelec. probe meas. 7-63879
 Pb_{0.8}Sn_{0.2}Te-PbSe_{0.08}Te_{0.92} heterostruct., LPE prepared, characts. 7-52759
 Pb_{1-x}Sn_xTe films prepared by MOCVD, elec. props. 7-27919
 Pb_{1-x}Sn_xTe heterojunctions, supersymmetry, band-inverting contact 7-52717
 Pb_{1-x}Sn_xTe narrow-gap semicond., electron-electron interaction, effect on permit., two-band model 7-52420
 Pb_{1-x}Sn_xTe quantum oscills. spectrum anal., two-window Fourier transform technique 7-52404
 Pb_{1-x}Sn_xTe solid solns., intrinsic defect donor states characts. Hall effect temp. depend. meas. 7-58762
 Pb_{1-x}Sn_xTe surfaces, AES, LEED and Kikuchi pattern obs. 7-52200
 Pb_{1-x}Sn_xTe:Bi, free carrier density 7-38572
 Pb_{1-x}Sn_xTe:In, impurity levels, covalent defect theory 7-52515
 Pb_{1-x}Sn_xTe-PbTe graded-gap heterostruct., spectral photoelec. quantum efficiency 7-36961
 Pb_{1-x}Sn_xTe_{1-y}Se_y solid soln. single crystals, density, comp., lattice const. and galvanomag. props. (*Russian*) 7-44500
 Pb_{1-x}Sn_xTe:Se IR photodiodes for 3 to 14 μ m, comparison 7-41466
 PbTe crystals, Bridgman growth in centrifuge, convection effects (*French*) 7-53542
 PbTe, diffusion controlled travelling heater method growth, thermal diffusion effect 7-53527
 PbTe doping superlattices, transport and magneto-optical props. 7-12852
 PbTe, epitaxial film, weak-field magnetoresistance, multi-valley model (*Korean*) 7-33114
 PbTe, ferroelec. phase transition, electron-phonon interaction 7-13106
 PbTe films and electrical contacts with Au, Al and Ag, photothermal deflection meas. 7-38784
 PbTe films prepared by MOCVD, elec. props. 7-27919
 PbTe heteroepitaxial films, low temp. lumin. 7-39157
 PbTe IR detector arrays, heteroepitaxial growth on fluoride-covered Si substrates 7-39429
 PbTe, impurity levels, covalent defect theory 7-52515
 PbTe, interband absorption in a mag. field, exciton states 7-22227
 PbTe, low-voltage electroabsorpt., exciton states, magnetoabsorpt. spectra 7-2501
 PbTe, mag. susceptibility, optical absorpt. spectra, effect of intrinsic defects 7-64670
 PbTe, narrow gap semiconductors, Knight shift 7-53166
 PbTe oxidised disordered films, magnetoresist. quantum oscills. obs. 7-64271
 PbTe single-cryst. films, negative photocond., slow relax. and photomemory 7-58832
 PbTe, solid and liquid states, electrophysical props. 7-52654
 PbTe, thermoelectric props., effect of dielectric inclusions 7-12746
 PbTe whisker crystals, Gunn-type oscills. 7-52626
 PbTe:Ga, doping during vapour phase growth, elec. props. 7-26774
 PbTe:In, MIS struct., tunneling spectra of quasilocal impurity states 7-12869
 PbTe:In₂I₃ Soret effect, impurity cond. distrib., thermoelec. power meas. 7-44930
 PbTe:Mn²⁺, superhyperfine struct., EPR spectra 7-27595
 PbTe:O films, O diffusion to bulk and crystallite boundaries 7-63884
 PbTe:Ti, Na, carrier reson. scatt., effect on transport coeffs. 7-38602
 PbTe:Ti(Tl,Na) films, superconducting transition 7-38797
 PbTe/PbEuSe single quantum well diode laser with side optical cavity 7-43105
 PbTe-EuTe short period superlattices, props., appl. to laser diodes 7-52785
 PbTe-Pb_{1-x}Sn_xTe superlattice, quantum Hall effect 7-2682
 PbTe-Pb_{1-x}Sn_xTe superlattice, electronic structs., envelope pn. approx. 7-45465
 PbTe-PbEuSeTe, compositional and doping superlattices, struct., electronic, optical and magneto-optical studies 7-53290
 PbTe-PbEuSeTe multiquantum wells, electron-hole recomb., photolum. 7-13216
 PbTe-PbSnTe compositional and doping superlattices, struct., electronic, optical and magneto-optical studies 7-53290
 Pb_{1+x}Te:Ti, quasilocal level and transport props. 7-38492
 PbTe_{1-x}S_x epitaxial films, absorpt. edge, band gap, comp. depend., 77-300K 7-39063
 PbTe_{1-x}S_x, free carrier scatt. near a phase transition 7-38557
 PbTeSe layers, LPE growth on nonplanar (100) and (110) oriented substrates, laser appl. 7-17479

IV-VI semiconductors continued

- PbTe_{0.97}Se_{0.03} Ga solid solns., diffusion coeff., temp. depend. study 7-2254
 PbTe(Se)(S), energy bands, relativistic empirical tight binding theory 7-45149
 PdTe: Cd, free charge carrier conc., donor action and Te precipitates effects (*Russian*) 7-16592
 Sn/SnTe bilayers, electron diff. pattern fine struct., influence of angular misorientation 7-16885
 SnS, photoacoustic response and transmission spectra, thermoacoustic meas. 7-46014
 SnS(Se)(Te), electronic props., ionicity and isomeric shift correl. 7-7114
 SnSe, high temp. oxidation mechanism 7-3536
 SnSe, IR absorpt. edge, transition temp. coeffs. 7-27721
 SnSe thin films, vacuum deposited, high temp. phase form., X-ray diff. study 7-32873
 SnSe(S), second order displacive transition and soft mode behaviour, neutron diff. study 7-26895
 SnTe, conc. depend. props. in region of homogeneity 7-45366
 SnTe, dipole-dipole interactions and ferroelectric props. 7-39046
 SnTe, energy bands, relativistic empirical tight binding theory 7-45149
 SnTe, Mossbauer spectra and microhardness, stoichiometry deviation effects, vacancy conc. and distrib. 7-26973
 SnTe, optical anisotropy due to spatial dispersion 7-53266
 SnTe, solid and liquid states, electrophysical props. 7-52654
 SnTe: Bi epitaxial layers, vacuum deposition, optical and electrical props. 7-59430
 SnTe: Cd(In)(Sb), solution mechanism of impurities, effect of heat treatment 7-21455
 SnTe: In, superconducting transition 7-38798

izod testing see dynamic testing

J particles see psi mesons

Jahn-Teller effect

- A15 cpds., supercond. rel. to martensitic transition, microscopic theoretical model 7-2767
 1,4-anthraquinone, T₁ state, Jahn-Teller distortion, phosphoresc. 7-42677
 1,4-anthraquinone phosphoresc. depend. on polycryst. matrix, Jahn-Teller pseudoeffect 7-50236
 aromatic carbonyl cpds., mol. photophysics, proximity effect and pseudo-Jahn-Teller interaction 7-62457
 benzene, Jahn-Teller spectra, MQDT anal. 7-57009
 Berry's geometrical phase and the sequence of states 7-58779
 bis arene sandwiches, C₂R₂FeC₆R₂ where R=H or CH₃, and (C₆(CH₃)₆)₂Fe⁺, hyperfine and mag. props. 7-12680
 decamethylcobaltocene, electronic struct. and dynamic Jahn-Teller effect EPR 7-59104
 decamethylnickelocenium, electronic struct. and dynamic Jahn-Teller effect EPR 7-59104
 dynamic Jahn-Teller effect for orbital doublet with centre of tetragonal symmetry 7-27303
 four-sublattice Jahn-Teller crystals, phase transitions, free energy and symm. props. calcs. 7-2544
 hexahalo complexes, vibronic coupling and state Jahn-Teller effect 7-19725
 II-VI semiconductors, Jahn-Teller interaction, influence of mag. field 7-16995
 metal-H systems, Jahn-Teller relax. effects in inelastic neutron scatt. spectra 7-58781
 metals, degenerate excited H states, Jahn-Teller effects calcs. 7-52535
 methane ion, photoelectron spectrum, Jahn-Teller effect, ab initio SCF and CI calcs. 7-42683
 orthorhombic paramagnet, J=1, external field induced Jahn-Teller effect (*Polish*) 7-7179
 polar semiconductors, LO-phonon modes bound to neutral impurities 7-45178
 quartz, E'₂-centres, conversion rate into E'₂-centres 7-52517
 radial oscillator states in polar coordinates 7-36501
 structural and magnetic instabilities in low-dimensional systems 7-59034
 tetrahedral mols., T₂ electronic state vibronic wavefunctions 7-19731
 transition metal layered compounds, structural phase transitions, microscopic theory 7-44807
 tunnelling states of off-centre impurities and Jahn-Teller systems, 3D harmonic oscillator function calcs. 7-2537
 unitary transformations in solid state physics, book 7-24310
 Ag_{0.5}V_{0.5}PS₃, struct., metal ordering and mag. props. 7-16517
 Ba₂CaCu₂Fe₂F₁₄, exchange interactions, mag. susceptibility meas. 7-45654
 α-Ba₂Cu₃F₁₄, crystalline structure (*French*) 7-26730
 BaTiO₃: Mn, Mn oxidation state change near phase transitions 7-16974
 Ca₃Mn₂Ge₃O₁₂ single domain crystals, birefringence and spontaneous phase transitions 7-17303
 CdTe: Co, Jahn-Teller interaction, influence of mag. field 7-16995
 CdTe: Fe²⁺, impurity vibronic coupling and near IR spectra characts. 7-26889
 CeAg_{1-x}In_x, magnetisation process, strain effects 7-64488
 CsCuCl₃, dynamic Jahn-Teller effects, mag. susceptibility study 7-45613
 CsCuCl₃, Jahn-Teller induced helical deformations 7-7178
 CsMCl₃ (M=Cu, Cr), hexagonal Jahn-Teller crystals, struct. phase transitions, face-sharing coupling, ground-state configuration 7-2180
 CsMCl₃ (M=Cu, Cr), hexagonal Jahn-Teller crystals, struct. phase transitions, mean-field approx. 7-2181
 Cs₂NaInCl₆: Cr³⁺, elpasolite lattice, broadband near-IR luminesc. 7-17338
 Cs₂NaYBr₆: Cr³⁺, elpasolite lattice, broadband near-IR luminesc. 7-17338
 Cs₂NaYCl₆: Cr³⁺, elpasolite lattice, broadband near-IR luminesc. 7-17338
 Cu complex, hexakis (1-methyltetrazole) copper II bis(tetrafluoroborate), Cu(II) sites, Jahn-Teller behaviour, ESR spectra anal. 7-21163
 Cu²⁺ complexes with phenanthroline, struct., ESR 7-31080
 Cu²⁺ impurity ion in octahedral environment, EPR spectrum, MM field freq. and temp. depend. 7-27596
 Cu_{0.96}Fe_{0.04}SiF₆·6H₂O Jahn-Teller cryst., glass transition, calorimetry and Mossbauer studies (*Russian*) 7-26952
 Cu_{1-x}Ni_xCr₂O₄, heat capacity anomalies, cooperative Jahn-Teller effect 7-6823
 Cu_{0.5}Ti₂(PO₄)₃, Nasicon-type phase, struct. and physical props. 7-45804
 Dy(As_{1-x}V_{1-x})O₄, random-field effects on Ising Jahn-Teller phase transition 7-58461

Jahn-Teller effect continued

- FeCoCr₂S₈, crystallographic and mag. props., Mossbauer study (*Korean*) 7-33310
 p-GaAs: Cr, excited and metastable states of Cr-related double centres 7-7153
 GaAs: Cu, neutral state of deep acceptors, photoluminescence spectra, Jahn-Teller effect 7-64149
 GaP: Cr, impurity ion-lattice coupling, reson. phonon scatt. spectra 7-58420
 GeH₄⁺, Jahn-Teller, struct. and energy distortions ab initio CI calcs., HF calcs. 7-15523
 InP: Cr, impurity ion-lattice coupling, reson. phonon scatt. spectra 7-58420
 InP: Mn³⁺, Jahn-Teller effect, mag. suscept. and ESR spectra anal. 7-52534
 KBr: MnO₄, low temp. resonance Raman scatt. and luminescence 7-39101
 KCl: Ti⁴⁺-type phosphors, Jahn-Teller-induced A-absorption and A-emission bands 7-53398
 LiNbO₃: Ni(Cu), γ-irradiated, ESR spectra of impurity centres 7-17218
 MnZnFe₂O₄, struct., Mossbauer, X-ray, and mag. meas. 7-1971
 N heterocyclic cpds., mol. photophysics, proximity effect and pseudo-Jahn-Teller interaction 7-62457
 NaCl: Cu, nuclear quadrupole spin-phonon interaction 7-22155
 NaF: Cu, nuclear quadrupole spin-phonon interaction 7-22155
 Nb₂Sn_{1-x}Sb_x, A15 pseudobinary alloy, structural transitions and related anomalies 7-38182
 Ni₂Cd_{1-x}Mn₂O₄ spinels, cation distrib., structural transitions and Jahn-Teller distortion 7-58227
 RbMCl₃ (M=Cu, Cr), hexagonal Jahn-Teller crystals, struct. phase transitions, face-sharing coupling, ground-state configuration 7-2180
 RbMCl₃ (M=Cu, Cr), hexagonal Jahn-Teller crystals, struct. phase transitions, mean-field approx. 7-2181
 Si, Jahn-Teller vibronic state of the neutral vacancy 7-16705
 Si: N(O), pseudo Jahn-Teller effect and chemical rebonding 7-16992
 SiH₄⁺, struct. and energy distortions, ab initio CI calcs., HF calcs. 7-15523
 SiH_n⁺ (n=1 to 4), photoion yield and thresholds, photoionisation mass spectra study 7-50242
 SnB₆: Er³⁺, Jahn-Teller phenomena in valency-mixing surroundings 7-5240
 SnH₄⁺, Jahn-Teller, struct. and energy distortions ab initio CI calcs., HF calcs. 7-15523
 SrTiO₃: Mn, Mn oxidation state change near phase transitions 7-16974
 Tb₂Ti₂O₇, elastic modulus, low temp. anomalies 7-44651
 TbVO₄ coherent vibr. and electronic excitation, time resolved spectra 7-22230
 Ti_{1-x}V_xH₂, FCC-FCT transition, positron annihilation obs. 7-32641
 (Y,Gd)₃Fe₅O₁₂: Mn, thin films, noncubic mag. anisotropy origin 7-53068
 Zn complexes, zinc(II)-bis-histidine: Cu, Jahn-Teller effect induced phase transition, ESR detect. 7-53122
 ZnS: Cu²⁺, Cr excitation spectrum interpretation 7-58775
 ZnS: Cu²⁺, multimode Jahn-Teller effect in the luminescence spectrum 7-12675
 ZnS: Fe²⁺, impurity vibronic coupling and near IR spectra characts. 7-26889
 ZnSe: Mn, ⁴E states, spin-orbit interactions and dynamical Jahn-Teller effect 7-21875
 ZnTiF₆: Cu²⁺·6H₂O, Jahn-Teller effect and phase transitions, powder EPR study 7-13023

jellies see gels

jellium

- deformable jellium model, electronic density of states calcs. 7-64044
 diffuse jellium-metal film surface, electrodynamic response, microscopic theory RPA calcs. 7-52458
 electromigration in jellium metal, electron wind force 7-32728
 electron-positron systems, two-component density-functional theory, self-consistent density calcs. 7-27277
 Fresnel optics, nonlocal corrections calcs. 7-45957
 gravitationally-induced supercurrents in Schwarzschild fields appl. of jellium model 7-45595
 magnetised plasma, neutron excitation of Landau and collective modes 7-7134
 metal surface, interaction with dipole, electronic struct. calcs. 7-2663
 metal surface, pot. change with charge, Thomas-Fermi-Dirac-jellium model 7-52715
 metal surface, self-consistent image pot. 7-38662
 metal surface state positron annihilation 2D ang. correl., jellium model calcs. 7-3106
 metal surfaces, jellium model, nonlocal exchange and correlation 7-52736
 metallic superlattices, electron scatt. by plasmons 7-32931
 metallic superlattices, plasmon spectra 7-64137
 metallic surface, pseudopotentials and dynamical props. 7-2341
 simple liquid metals, pseudoclassical approach to electron and ion density correlations 7-6503
 simple metals Auger energy, Slater transition state calcs., metallic and atomic states, jellium model 7-38475
 small metal particles, dynamic polarisability, jellium model, RPA calcs. 7-52460
 small metal particles, surface excitations by fast electron scatt. 7-7140
 surface, physisorbed positronium, positron states model anal. 7-38347
 van der Waals interaction between atom and metal surface, response function approach 7-21964
 Al (110), scatt. of H₂⁺ ions, resonant transition rates for charge transfer 7-3134
 H₂-metal impact, density functional approach, dynamic response at metal surfaces, van der Waals interaction, excitation of electron-hole pairs 7-3129
 He-metal impact, density functional approach, dynamic response at metal surfaces, van der Waals interaction, excitation of electron-hole pairs 7-3129
 Na overlayer on Al, two step pot. model, nonlocal corrections to Fresnel optics cal. 7-64716
 Ni₂H clusters, charge distrib., Hartree-Fock SCF INDO calcs. 7-52411
 Pd (111), high resolution inverse-photoemission study 7-17357
 W, He field adsorption and evaporation 7-32802
 W surface, field adsorption of He 7-32816

jet stream *see atmospheric movements*

jets

see also plasma jets; sprays
 2D jet impinging on a wedge, mean flow props., skin friction coeffs. 7-16224
 adiabatic curvilinear surface, turbulent wall jets, integral relations 7-11488
 aerodynamic noise principles (*Chinese*) 7-11208
 air, development and breakaway, coanda effect, interferometric, Schlieren and shadowgraph investigs. 7-51358
 air-water/steam-water jets, confined two phase, analytical entrainment model (*Chinese*) 7-1596
 airfoils, intersection of jets 7-37238
 alkoxy radicals, electronic struct., rot. resolved spectra 7-62352
 annular jet, wake and wake-induced shear layer excitation 7-37508
 annular jet mixing regions, flow struct., press. fluctuations 7-20766
 anthracene-NH₃, jet-cooled clusters, van der Waals complexes, exciplexes, visible fluoresc. spectra 7-19936
 V1343 Aql (SS 433), evidence for relativistic beaming from VLBI obs. 7-9476
 V1343 Aquilae (SS 433), Doppler-shifted X-ray line emission assoc. with high-speed jets 7-9493
 astrophysical, numerical calcs. on viscous jets 7-4565
 attachment process of switching of a jet in a wall-attachment device 7-26327
 axisymmetric free jets having parabolic profiles at nozzle exit, hot-wire turbulence meas. 7-51260
 axisymmetric opposed turbulent jet study 7-43995
 axisymmetric wall jet on circular cylinder, boundary layer flows 7-57892
 broadband sock-associated noise and screech tones 7-20502
 bromotrifluoromethane in supersonic free jet, isotope-selective IR multi-photon dissociation 7-5781
 buoyant vapour bubbles modelling growth and collapse, rigid boundary, stagnation flow 7-16220
 4C 18.68, quasar, jet struct. near QSO core rel. to precessing twin-jet model 7-4588
 chemically reacting transverse turbulent jet, flame struct. and vorticity 7-20809
 circular jet with initially laminar boundary layers, turbulent interaction region 7-11486
 coaxial supersonic jet, interaction with vortex ring 7-51259
 collapse of MRL 38 mm shaped charge, database for computer modelling 7-63192
 collision of multiple supersonic jets related to pip noise generation in cage valve 7-26316
 P/ Comet Halley (1982i), coma morphology and dust emission pattern modelling 7-14526
 P/ Comet Halley (1982i), dust and gas jet detect. from Vega-1 secondary electron currents meas. 7-14521
 P/ Comet Halley (1982i), jets visible and near-UV spectra from Vega three-channel obs. 7-14519
 P/Comet Halley (1982i), obs. of nucleus and jets by Vega missions 7-9438
 P/ Comet Halley (1982i), Vega-2 near-IR obs. of dust and gas jets 7-14520
 condensation, turbulent gas jets, elec. field control 7-11485
 conference, Cambridge, England (March 1986) 7-40987
 confined, mixing 7-6263
 confined air-water jets flow-field measurements and physical processes 7-37527
 confined swirling coaxial jet flow multiple-scale turbulence model 7-31813
 constrained gas-liquid jet in isothermal cocurrent flow, hydrodynamics 7-44015
 current-carrying, deformation by nonviscous elec. cond. liquid 7-51257
 9-cyanoanthracene, fluoresc. lifetimes in bulb and supersonic free jet 7-36670
 diffusion flame in co-flowing air stream, turbulence struct. 7-43996
 diffusion flames, flow visualisation using Mie scatt. method 7-11566
 diffusion flames, swirl effect on stability 7-23017
 drop formation in ink jet through theoretical analysis of one-dimensional model and experimental scale-up nozzles 7-26328
 dye jet laser, continuous, liquid-circulation systems 7-31312
 dye laser, tunable, CW, Ar⁺ laser-pumped, spectral props. 7-1096
 dye ring laser, 580 nm, CW, single-mode, dye circulation system 7-1201
 ferrofluid jet in mag. field, droplet form. using capillary nozzles 7-37553
 flow development and control, shear layer growth 7-11482
 flow sensor, swirling jet type, and flow field 7-37562
 flow visualisation, image processing using streamline coordinates 7-37572
 fluidic watering device consisting of vortex chamber, self-oscills. 7-37467
 force reduction, Coanda effect appl. 7-43998
 free jet spectroscopy by coherent Raman methods 7-15003
 free-vortex nozzle, supersonic jet struct. study using pulse holographic interferometry 7-51256
 gas concentration and gradient meas. in photoacoustically perturbed jet 7-37560
 gas flow, nonequilib. processes on free boundary 7-57940
 gas jet impacting a cavity, temp. and velocity meas., flow anal. 7-43999
 gas jets, internal collisions 7-57888
 gas transport during oscill. flow, effect of turbulent jet 7-8635
 gasdynamic focusing in supersonic jets, chemical anal. appl. 7-20752
 gases, premixed turbulent combustion, second-order closure prediction 7-57942
 glass, molten, jet formation during absorpt. wave propag. 7-46251
 glass fibre processing, spinning process in liq. state 7-3258
 high temperature pulsed nozzle for supersonic jet spectrometry, gas chromatographic appls. 7-15005
 hydrodynamic losses in the radiation of sound 7-50891
 impingement on wedge, edge-tone flowfield 7-11483
 incompressible 2D jet reattachment, augmented thrust and mass flow 7-51248
 inert gases, condensation in free jets, scaling laws, similarity relations 7-42825
 initial turbulence vel. distrib. function in bounded jet flow 7-26323
 IR laser spectroscopy, jet-cooled, for polyatomic molecules 7-41495
 jets, Raman scatt., Franck-Condon and double reson. study 7-31082
 laminar jet, in narrow slot at large Reynolds number 7-1599
 Landau-Square jet flow, momentum-flux condition 7-31852
 laser Doppler velocimetry, multi-pt. system using phase diffraction grating 7-37605

jets continued

laser excitation dynamics of at. and mol. clusters in free jets 7-42823
 liquid drop, instability development in elec. field 7-31850
 liquid jets, breakup and atomisation, transient behaviour 7-51249
 liquid metal turbulent jet, mixing and solidification in co-flowing stream 7-51250
 liquid-solid impact, shock structs. and jetting conditions 7-32573
 liquids, mixing, conc. meas. by fluoresc. technique 7-65366
 local separation zones in viscous jets, existence and nonuniqueness 7-1595
 mass transfer of submerged jet impinging on cylindrical surface 7-26325
 medical jet injector, some phys. aspects 7-65887
 metals, condensation in free jets, scaling laws, similarity relations 7-42825
 methane, turbulent jet discharge, planar imaging 7-20767
 methane-air turbulent diffusion flames laminar-flamelet modelling 7-57938
 2-methylpyrazine singlet-triplet transitions in supersonic jet, multiphoton ionis. detect. 7-948
 modulated water jets, numerical modeling 7-63190
 molecular gas flow, low density, collisional stimulation, intramol. motion and relax., macroscopic quantum effects 7-15693
 multi-spark visualization of typical combustor flowfields 7-26372
 mushroom-like currents (vortex dipoles), obs. in ocean and laboratory tank 7-29033
 noise, effect of upstream disturbance (*Chinese*) 7-57630
 nonisothermal plane point jet, single-parameter self-similar problem 7-44002
 nonuniform subsonic jet collision with plane obstacle 7-57889
 oceans, steady wind-driven upwelling in presence of baroclinic coastally trapped jet 7-8984
 one-dimensional fluid jet models, numerical comparisons appl. to drop-on-demand ink-jet printing 7-31851
 perylene-NH₃, jet-cooled clusters, van der Waals complexes, exciplexes, visible fluoresc. spectra 7-19936
 phenanthrene-d₉(-d₁₀), in supersonic free jet, electronic spectra, intramol. dynamics 7-42672
 plane jet at low Reynolds number confined in rectangular channel, numerical analysis 7-37507
 plane jets, of ideal incompressible fluid, nonsymm. collision 7-31853
 plane turbulent jet propagating in transverse flow, rarefaction 7-11487
 plate with jet impingement, holographic visualisation of pressure distrib. 7-37569
 pouring liquid flow from container, free surface study 7-51258
 pressure losses in channel with injection of jet system (*Ukrainian*) 7-11542
 pressure-wave and microjet cavitation damage, rotating-disc expts. 7-26225
 propane jet flames, near-nozzle region, flow struct. 7-8280
 proximity sensors, flow meas. with beam-scanning LDV 7-37604
 pseudo-sound field and feedback mechanism (*Chinese*) 7-51246
 pulse jet structure, energy balance in transient zone, turbulence 7-20768
 pulsed gaseous free jets for UPS 7-36685
 pulsed supersonic He free-jet expansions, time-of-flight characterisation 7-11457
 pyrazine, singlet-triplet transitions in supersonic jet, multiphoton ionis. detect. 7-948
 Q0800+608, quasar, VLA obs. of remarkable one-sided jet 7-9555
 radial attaching jet flow control, flow before reattachment point 7-20769
 radial reattachment turbulent jet flow, press. distrib. 7-26324
 radial swirling free jet flow (*French*) 7-63157
 rectangular 3D jet, reattachment to side wall, oscillations from nozzle 7-20770
 rotating fluids, unsteady jets, similarity solns. 7-6217
 round jets, turbulent and heated, similarity solns. 7-1598
 self-preserving, variable-density, turbulent free jets 7-1597
 similarity solns., local equilib. assumption 7-11484
 simulation in 3D of very strong shock waves 7-6247
 single capillaries, droplet formation in the jet regime of a liquid/liquid system (*German*) 7-16227
 single unsteady supersonic jet, interaction with moving obstacle of finite dims. 7-51255
 slot, 2D with inclined walls, steady pot. flow, contraction coeff., capillarity effect 7-57891
 solids circulation pattern and particle mixing in large jetting fluidised bed 7-63208
 sound freq. in resonant pipe, displacement meas. 7-24622
 spreading rate, instability waves, phase difference effect 7-51247
 steady liquid compound jet flow, num. treatment 7-37506
 steam jet impingement on high temp. ZrO₂ surface to produce H₂ 7-54362
 submerged supersonic jets, compressibility effects 7-51254
 supersonic air ejector, primary flow oscill. 7-37492
 supersonic and subsonic mixing, parabolised Navier-Stokes anal. 7-11481
 supersonic jet, light amplification coefficient and intensity, spasmodic increase during metastable atom and mol. condensation (*Russian*) 7-50523
 supersonic jet spectroscopy, appl. to mol. dynamics 7-57129
 surface pressure in 3D turbulent jet/boundary interaction 7-6262
 swirling jet, self-similar solns. 7-51253
 thermal plume, turbulent struct., vel. field (*French*) 7-31762
 transient species in supersonic, free jet expansion, laser induced fluoresc. 7-31099
 turbulence, coherent struct., spatial details 7-43870
 turbulent, 2D, acoustic enhancement of widening rate and turbulence intensity 7-51261
 turbulent, carrier phase temp. and momentum distrib., num. and expt. investig. 7-51251
 turbulent, influence of mode composition of acoustic perturbations 7-62945
 turbulent, mixing in 2D ducts with transverse jets 7-31757
 turbulent afterburning jets, temp. and conc. fluctuations, num. investig. 7-26362
 turbulent jet flow perpendicular to flat plate, shear stress meas. by erosion technique 7-31898
 turbulent mixing of coaxial jets between H₂ and air 7-37505
 turbulent plane jet, organised struct., role in momentum and heat transport 7-44000
 turbulent Reynolds stresses in the swirling radial free jet flow (*French*) 7-63191
 turbulent transfer in an axisymmetric agitated jet, expt. study 7-26259

jets continued

- two-dimensional turbulent jet, discrete vortex simulation, shear layers 7-16225
 two-phase, crossed electric and magnetic fields effects (*Russian*) 7-26326
 two-point pressure-velocity correlations, conditional average and linear estimation in a round jet flow 7-26329
 underexpanded jet flow into subsonic counterflow, propag. laws 7-57890
 unimolecular reactions of isolated collisional gas phase and solvated molecules 7-13792
 unsteady jets, 3D surface shape estimation by image processing 7-37573
 vertical entry of solids into water 7-31849
 vertical liquid jet system with downcomers, flow characts. 7-16226
 viscoelastic fluids, flow phenomena, statistical study 7-31845
 viscous gas jet flowing from a conical nozzle, density fluid, num. soln. 7-51252
 viscous incompressible fluid jet, starting vortex, transient motion 7-44001
 vortex growth in bounded rectangular jet, numerical anal. 7-37469
 wall jet diffusion combustion, heat exchange process, num. investig. 7-26266
 wall jet with turbulent boundary layer, 3D mixing 7-37503
 water-air ejector, free-rotating three-slot feedwater nozzle, expt. investig. 7-43997
 wave struct., Rayleigh linear inviscid instability anal., 7-51054
 weakly swirled turbulent jet aerodynamics 7-20771
 Ar clusters, mass distrib. meas. and struct. model 7-15762
 ArHF van der Waals complexes in supersonic jets, IR laser spectra 7-19842
 ArXe⁺, DC discharge in supersonic jet, UV-visible emission spectra anal. 7-19874
 H flame-out in air flow, gas dynamic struct., interaction effect 7-26315
 H₂, jets, ignition behind reflected shock waves 7-37504
 H₂, turbulent jet diffusion flame, conserved scale probability density functions 7-26260
 HCl, soln., elec. surface pot. change with conc. and surface age (*Russian*) 7-27063
 He+H⁺, electron ejection, double differential cross section meas. 7-20024
 N, horizontal gas jet submerged in liq., penetration study 7-62052
 N₂, fuse jets, high-temp., rot. relax. 7-62500
 N₂, vibrationally nonequilibrium jet, Na impurity radiation 7-42744
 NH₃, jets, Raman scatt., Franck-Condon and double reson. study 7-31082
 NO₂, excited state rot.-vibr. anal., supersonic jet fluoresc. excitation spectra 7-19919
 NaOH, molten, hot N submerged impinging jets study 7-62051
 OCS, jet-cooled, $^1\Sigma^+ \rightarrow \Pi$ transition, spectrosc.-investig. 7-62400
 SF₆ clusters, supersonic jet, Fourier transform IR spectra 7-15598
 SF₆ jets, Raman scatt., Franck-Condon and double reson. study 7-31082
 s-tetrazine clusters, photophysics and photochemistry, laser induced fluoresc. 7-31098
 UF₆, multiphoton dissoc. in supersonic jets 7-42706

JJFT see junction gate field effect transistors

Johnsen-Rahbek effect see adhesion; electrostatics

Johnson noise see thermal noise

joining processes

see also brazing; cable jointing; soldering; welding

optical fibre characteristics and industrial production techniques (*French*)

7-1282

Al₂O₃, joining by inducing localised reducing conditions 7-46787

C fibre reinforced plastic, cemented lap joint, stress-strain state and strength 7-33794

Cu, diffusion bonding, strain-free mounting appl. 7-3572

Fe, Armo, diffusion bonding, precip. of Fe carbides in ferrite 7-39521

SiC ceramics, joining with Si₃N₄-Y₂O₃-La₂O₃-MgO mixture (*Japanese*)

7-65280

Si₃N₄/ferritic stainless steel, joining with soft metal interlayers, tensile strength 7-28266

Ti alloys, superplastic forming and diffusion bonding 7-8048

jointing, cable see cable jointing

jointing (electric connectors) see electric connectors

Josephson effect

I-V characteristics of anomalous Josephson tunneling junction (*Chinese*)

7-64404

AC Josephson effect, voltage bias studies at high freqs. 7-38822

AC Josephson effect for dynamic mag. susceptibility and ESR measurements 7-12917

analog simulation, junction in microwave field, devil's staircase, fractal dimension and decay constants 7-38821

annular junctions, soliton dynamics 7-2784

chaos, quantum effects 7-52905

chaos in a superconducting quantum interferometer 7-18873

coherent oscillations in small tunnel junctions 7-33067

computer controlled Josephson voltage standard 7-14970

conf., Neuchatel, Switzerland, April 1986 7-40984

contacts, critical current quantum renormalisation 7-12921

coupled superconducting array in a mag. field, quantum effects 7-64409

cross-strip junction, elementary pinning force for a superconducting vortex

7-45592

current biased junction, macroscopic quantum phenomena 7-45569

current-biased Josephson junction, in parallel with arbitrary dissipative circuit, quantum energy levels and tunnelling 7-2788

DC driven damped Josephson junctions, fluxon collisions, radiative losses, perturbation calcs. 7-12915

DC driven junctions, inhomogeneous damped, many-fluxon kinetics

7-45571

DC SQUID, macroscopic quantum tunnelling 7-38820

disordered granular superconductor near percolation, phase transitions

7-17140

dynamic state stability, perturbed sine-Gordon model 7-52911

fluxon-antifluxon collision in a Josephson transmission line 7-2790

frustrated XY model for Josephson- or proximity-coupled superconducting arrays, screening length calcs. 7-64391

granular superconductor resistively shunted Josephson junction arrays, phase diagram, self-charging model calcs. 7-7451

Josephson junction with time-independent driving current, chaotic behaviour 7-52904

junction, critical temp., ordered magnetic impurity effects calcs. (*Russian*)

7-22072

junction, quantum dynamics, phase periodicity effects 7-27473

junction, sine-Gordon solitons in external fields 7-61263

Josephson effect continued

- junction array, positional disorder 7-64408
 junction fluxon props. in presence of surface and shunt losses, analytic solns. 7-7452
 junctions, I-V characts., fluctuation effects 7-52902
 junctions, phase fluctuations, thermal excitation and zero-point motion effects calcs. 7-7450
 junctions, tunnelling spectroscopy of a macroscopic variable 7-45435
 junctions with microinhomogeneities attracting solitons, crit. currents 7-64406
 Kosterlitz-Thouless transition in Josephson junction arrays 7-45570
 large area junction, appl. RF signal effects, nonlinearity and hysteresis loop calcs. 7-7453
 long junction, fluxon collisions, radiated energy study 7-52913
 loop containing single Josephson junction, multiple-quantum-flux penetration 7-64407
 macroscopic current states decay rate determ. 7-52912
 macroscopic quantum systems, weakly coupled, limiting Gibbs state calcs., appl. to Josephson oscillator 7-45582
 NBS Josephson array voltage standard 7-18824
 networks of superconducting islands loose coupled via Josephson junctions (*Dutch*) 7-52907
 nonlinear transport due to driven collective modes 7-52473
 ordered magnetic impurities in barrier region near critical temp. 7-58961
 point-contact-type Josephson harmonic mixer, frequency meas. of FIR lasers 7-20310
 proximity systems, low-dimensional, Josephson current, field effect, appl. to Nb-InAs-Nb system 7-45573
 quantum effects in Josephson circuits 7-17138
 quantum Hall resistance meas., using improved Josephson potentiometer 7-18810
 refractory material end-type junctions, detection props. 7-64411
 resistance oscillations in a Josephson-junction array in a magnetic field 7-2789
 resistivity shunted junctions, steps anal., modified Kepler transform. 7-38823
 spatio-temporal coherence and chaos, conf. Los Alamos, USA, Jan. 1986 7-48158
 superconducting junction arrays development, for high-precision voltage standards 7-18823
 superconductor-ferromagnet-superconductor contacts, steady state Josephson effect (*Russian*) 7-7446
 superconductors with heavy fermions, Josephson effect 7-33131
 switching behaviour, Werthamer model calcs. (*Russian*) 7-52901
 thermal activation energy, appl. to Josephson effect 7-33129
 thin-film junctions, series array, subharmonic gap structure obs. 7-12914
 triplet pair states, superconductive tunnelling 7-38825
 tunnel junction, β -particle detection by DC Josephson effect 7-30832
 tunnel junction, electric and mag. coupling, applied microwave (*Chinese*) 7-12913
 tunnel junction with inverted population, Josephson effect (*Chinese*) 7-27471
 tunnel junctions, microwave-driven, one-third harmonic generation 7-52899
 tunnel junctions, microwave-soliton or microwave-antisoliton interaction 7-33130
 tunnelling junctions for α -particle detection 7-56910
 volt realisation using integrated Josephson ccts. 7-14971
 voltage and resistance, US legal units 7-41329
 voltage meas. appl., Josephson standard establishment at NPL, India 7-18826
 voltage measurement appl., Chinese Josephson standard, $2e/h$ precision determ. 7-18825
 voltage-current characts., long Josephson junction with periodic inhomogeneities 7-58960
 weak links, superconductive-controlled 7-17139
 BaPb_{1-x}Bi_xO₃ bicrystals, nature of Josephson tunnel barrier 7-45568
³He superfluid flowing in narrow aperture, Josephson effect calcs. 7-52177
⁴He, superfluid, search for Josephson effect using low freq. acoustic resonator 7-44936
 Nb, point contact Josephson junction, I-V characteristics (*Rumanian*) 7-17141
 Nb/a-Si/Nb structures, AC Josephson effect 7-12919
 Nb/Nb₂O₃/Pb film struct., Josephson and tunnel junctions, scanning tunnelling microscope study 7-64410
 Nb/NbO_x/Pb system, pseudo-inverse AC Josephson effect 7-7454
 Nb/Yb-YbO_x/Nb all-refractory Josephson junction 7-38818
 Nb-a-Si-Nb Josephson junctions, for IR laser radiation response near plasma reson. freq. 7-58958
 Nb-In point contact, observation of chaotic noise 7-7445
 Nb-NbO_x/Pb Josephson tunnel junctions, bifurcations, noise and near-reson. perturbations influence 7-58957
 Nb-NbO_x-PbInAu, Josephson tunnelling current depend. on normal state tunnelling resist. 7-22073
 Nb-NbO_x-PbInAu Josephson junction fabrication by ion beam oxidation 7-22074
 Nb-Si⁺-Nb high quality Josephson end junctions, characts. 7-12920
 Nb₂Al(Ge)/Pb magnetron sputtered Josephson tunnel junction props., film deposition conditions dependence 7-58955
 NbN Josephson tunnel junctions, appl. to DC-SQUIDS 7-7449
 NbN/Pb-In Josephson junctions, fabrication by Ar⁺ ion bombardment 7-2787
 NbN/Pb(In) Josephson junction, Ar⁺ irr., characts. (*Japanese*) 7-22071
 NbN-Nb₂O₃-NbN trilayer structure, TEM studies 7-7018
 Pb alloy base electrode Josephson junction, self-positioned, fabrication 7-52906
 Pb-In films, Josephson junction, thermal stress cycles, hillock form. (*Japanese*) 7-12536
 Pb-In-Au fine-grained codeposited alloy films, RF plasma oxidation 7-53970
 Si-B, critical supercond. current induced by proximity effect, mag. field depend. 7-22069
 Sn granular films, superconductivity and metal-insulator transition (*Chinese*) 7-12923

Joshi effect see glow discharges

Joule-Thomson effect

- ethane dilute gas thermophysical props. correl. and extrapolation, SSR-MPA pot. model calcs. 7-16294

Joule-Thomson effect continued

- hybrid closed-cycle cryocooler, for DC SQUID use 7-56278
- monatomic gases and their mixtures, dilute gas props. 3 parameter MSK pot. calcs. 7-16285
- He II, liquid, Joule-Thomson effect 7-2287
- N₂ dilute gas thermophysical props. correl. and extrapolation, SSR-MPA pot. model calcs. 7-16294
- O₂ dilute gas thermophysical props. correl. and extrapolation, SSR-MPA pot. model calcs. 7-16294

joysticks *see computer graphic equipment*

junction gate field effect transistors

- GaAs JFET devices, elec. resist., Hall effect, influence of electronic sub-band gap depopulation 7-38740

junction lasers *see semiconductor junction lasers*

junctions, waveguide *see waveguide couplers*

Jupiter

- asteroid orbits perturbations, effects of secular resonances ν_{16} and ν_5 7-47748
- atmosphere, NH₃ abundance and cloud opacities determ. from Voyager IRIS data 7-24051
- atmosphere, semiannual oscillations 7-29418
- continuum radiation, periodic amplitude var. 7-47756
- decametric radio emission, localisation of S-component sources 7-24049
- decametric radio spectra, origin of Io-phase-dependent S-bursts 7-47753
- Europa, tidal heating in internal ocean model 7-47757
- formation, planetary growth rate around 1 solar mass star 7-55497
- Galilean satellite eclipse timings: 1983/5 report. I 7-18368
- Galilean satellite eclipse timings, for AD 1983 to 1985 period 7-55524
- Galilean satellite system, energy budget and orbital accel. 7-29423
- Galilean satellites, anal. of occultation obs. and comparison with theories 7-47754
- Galilean satellites, compact ephemerides (August 1987 to February 1988) 7-4295
- Galilean satellites, heliometer obs. (1891 to 1906) comparison with modern ephemerides 7-24048
- Galilean satellites, photometric obs. of mutual events (Project Omega 1985/86) 7-18370
- Galilean satellites mutual phenomena, conf., Bagnères de Bigorre, France (April 1986) 7-60856
- Galileo planetary exploration mission 7-55428
- Ganymede, early thermal profiles and strength of lithosphere 7-40748
- Ganymede, geology and surface features 7-34917
- Ganymede, tectonic framework of grooved terrain 7-24050
- Ganymede, terrain types and local-style stratigraphy of grooved terrain 7-55525
- Great Red Spot, Rossby autosoliton and stationary physical model 7-40750
- Great Red Spot, simulation (Russian) 7-47695
- HF and MF emission, correl. with solar wind plasma and mag. field characts. 7-4362
- HF emissions, control by Io 7-40752
- HF radiation from northern and southern hemispheres, ray-tracing 7-60595
- icy satellites, radar glory from buried craters 7-34913
- In torus, O I and S I densities from UV spectra 7-55522
- Io, ground-based IR obs. anal. 7-34916
- Io cold plasma torus, mass and energy balance model 7-9403
- Io plasma ribbon model 7-24053
- Io plasma torus, stability study 7-9406
- Io plasma torus and the source of Jovian kilometric radiation (bKOM) 7-34912
- Io plasma torus boundaries, radio emission 7-40751
- Io surface materials, phase curves interpretation in terms of Hapke's function 7-55523
- lightning in water clouds 7-18369
- magnetodisk total meas, estimate from partially open magnetosphere models 7-55443
- magnetosphere, Iogenic ions outward diffusion and associated heating 7-9405
- magnetosphere, two-dimensional radial plasma outflow model 7-66498
- magnetosphere dominated by corotation study of steady state plasma transport 7-40728
- magnetosphere fast neutral atoms emission and effects on solar wind, cometary exosphere analogue 7-55521
- magnetosphere flow features, similarity model illustrating effects of toroidal mag. field and rotation 7-9407
- magnetosphere IMF control and convection 7-29422
- magnetosphere inner region, observational constraints on interchange models 7-66497
- magnetosphere trapped particles affected by Ganymede and Callisto 7-24054
- magnetosphere-Io torus system characts. 7-47758
- magnetospheres, struct. of Alfvén wings assoc. with conductor moving through magnetoplasma 7-23989
- Mercury magnetosphere, Jupiter as source of electron bursts 7-9391
- mutual satellite phenomena, longitude discrepancy resolution 7-40747
- planetary satellites, cratering in icy targets 7-34863
- protosatellite accretion disks, global characts. 7-34914
- radio wavelength zone-belt struct. of atmos. 7-40749
- radio wave emission at 1.2 kHz, magnetosphere source region 7-9404
- satellite positions and flux density meas. by VLA in SHF 7-40746
- satellite system, exponential distance law (French) 7-34911
- satellites, conf., Vulcano, Italy (September 1985) 7-29597
- satellites, cratering characts. rel. to Saturn satellites 7-34920
- satellites geological mapping 7-34915
- simulation for film '2010' 7-34910
- South Tropical Dislocation in 1983-4 period 7-47755
- spherical albedo, relation to observable characts. of planetary atmosphere 7-24031
- upper troposphere, zonal mean characts., Voyager IR obs. anal. 7-24052
- water vapour in atmosphere, abundance and distrib. 7-60594

K-capture *see nuclear electron capture*

K mesons *see kaons*

K-N interactions *see kaon-nucleon interactions*

Kalman filters

- extended Kalman filter for automatic target following of lunar reflectors (German) 7-23521
- Extended Semianalytical Kalman Filter and its application to synchronous orbits 7-29386

Kalman filters continued

- flow, transient velocity profiles, real-time estimation using Kalman filtering techniques 7-37582
- implicit Kalman filter algorithm for nuclear reactor analysis 7-30488
- LOFT pressurizer, on-line instrument failure detection, Kalman gain approach 7-5354
- monochrome still image noise reduction by a hybrid method based on an anisotropic stochastic model (Japanese) 7-42998
- moving sound source analysis, orbit determ. using linear sensor array 7-43492
- multi-channel, for epileptic EEG structural anal. 7-54793
- nuclear reactor control information, provision in presence of instrument failures 7-5367
- optimal estimation theory in data analysis and signal processing 7-35500
- plasma diagnostics, Kalman filter-based signal processor 7-1761
- radioastronomical images, very large array phase data modelling by Box-Jenkins method 7-14504
- underwater acoustic exploration, appl. of array processing for parallel linear recursive Kalman filtering 7-65986
- underwater tracking, 3D, that considers acoustic medium effects 7-43544
- use of Kalman filters in data compression of gastransmission pipeline data 7-11553

kaon-baryon interactions

- see also kaon-baryon scattering; kaon-hyperon interactions; kaon-nucleon interactions*
- No entries

kaon-baryon scattering

- see also kaon-baryon interactions; kaon-hyperon scattering; kaon-nucleon scattering*
- No entries

kaon decay

- see also kaon hadronic decay; kaon leptonic decay*
- CP nonconservation, time depend. perturbation theory for quaternionic quantum mech. 7-5087
- rare kaon decay, present and future high intensity machines 7-49133
- K decay, conference summary 7-35853
- K \rightarrow e $\bar{\nu}$ H, Higgs production phenomenological limits 7-513
- K \rightarrow $\pi^0\gamma e\bar{\nu}$, decay probability, dependence on γ -detection threshold, T violation asymmetry 7-56538
- K \rightarrow $\pi^0\pi^0 e\bar{\nu}$, decay probability, form factor meas. 7-56538
- K⁰(K[±]) decay, meas. possibilities for T-, CP-, CPT-violation parameters 7-10053
- K⁺ \rightarrow $\pi^+ e e^-$, effect of nonstandard vector boson couplings 7-35856
- K⁺ \rightarrow $\pi^+ \pi^- e^+ \nu$, gauged nonlinear σ model with Wess-Zumino condition 7-41790
- K⁺ \rightarrow $\pi^+ \nu \bar{\nu}$, branching ratio, KMC predictions, fourth generation mixing effects 7-41785
- K⁺ \rightarrow $\pi^+ \nu \bar{\nu}$, experimental BNL787, status, anal. of generation problem 7-41979
- K⁰ \rightarrow $\gamma\gamma$, chiral perturbation theory corrections to SU(3) terms 7-15160
- K⁰ \rightarrow $\pi^+ l^+ \nu$, l⁺ polarization, effects of heavy subdominantly coupled neutrino mixing 7-61652
- K⁰ \rightarrow e $^+ \pi^+ \nu$, search for T and CPT violation 7-41787
- K⁰ \rightarrow e $^+ \pi^- \nu$, search for T and CPT violation 7-41787
- K_S \rightarrow $\gamma\gamma$, branching ratio upper limit determ. 7-35878
- K⁰ decay, CP violation, experimental anal. 7-41786

kaon hadronic decay

- see also kaon regeneration*
- nonleptonic K decays in broken SU(3)×SU(3) 7-49134
- K \rightarrow 2 π , CP violation in six-quark standard model 7-35740
- K \rightarrow 2 π , vacuum insertion and nonperturbative effects 7-10057
- K \rightarrow $\pi\pi$, $\Delta I=1/2$ rule in the large-N limit 7-24881
- K \rightarrow $\pi\pi$ amplitude, kaon-to-vacuum weak matrix element, soft pion techniques 7-49135
- K \rightarrow $\pi\pi$ amplitudes in QCD duality approach, $|\Delta I|=1/2$ rule problems in standard model 7-10056
- K \rightarrow $\pi^+ \pi^0 \pi^0$, matrix element determ., confirmation of $\Delta T=1/2$ rule 7-56540
- K⁰ \rightarrow $\pi\pi$, effective dynamical model for $\Delta I=1/2$ rule, quark wave functions 7-15146
- K⁺ \rightarrow $\pi^+ \pi^+ \pi^-$, amplitude in quenched approx., lattice calculation 7-35857
- K⁺ \rightarrow $\pi^+ a$, branching ratio 7-15147

kaon-hyperon interactions

- see also kaon-hyperon scattering*

No entries

kaon-hyperon scattering

- see also kaon-hyperon interactions*

No entries

kaon interactions *see kaon-baryon interactions; kaon-nucleus reactions; meson-meson interactions*

kaon leptonic decay

- K $\rightarrow\mu e$, anal. in CP violation models 7-436
- K_L $\rightarrow\mu^+ \mu^-$, CP-nonconservation with four generations 7-24875
- K_L $\rightarrow\mu^+ \mu^-$, muon polarization, effect of left-right squark flavour mixing 7-35737

kaon-nucleon interactions

- see also kaon-nucleon scattering; kaon-proton interactions*
- K⁺d \rightarrow ηX , $\eta\rightarrow 2\gamma$, 10 GeV, differential cross section meas., quark-fusion model anal. 7-5124
- KN $\rightarrow\phi B$, partial wave anal., Skyrme model comparison 7-15171
- NK $\rightarrow\phi X$, joint hadron prod., parton model comparison 7-19143
- NK $\rightarrow\phi X$, low p_T interactions, Lund model comparison 7-19142
- K⁺N channel coupling, quark pot. model with resonating group method 7-41705

kaon-nucleon scattering

- see also kaon-nucleon interactions; kaon-proton scattering*
- K(K)N scattering, cloudy bag model $\Lambda(1405)$ anal. 7-35905
- K⁺N, elastic scattering, partial wave anal., SAID computer package 7-550

kaon-nucleus reactions

- for inelastic kaon-nucleus scattering, see "kaon-nucleus scattering"*
- see also kaon-nucleon interactions*
- A=12-40, strangeness exchange reactions with the recoil corrected continuum shell model 7-19190
- (K_LK_S), differential K_S regeneration cross sections, inelastic screening effects, diffractive model anal. 7-10175
- (K⁺ π), stopped-K hypernuclear expt. at KEK 7-41930
- (K⁺, π^-) reaction, hypernuclei and spin-orbit interaction 7-49473
- (K⁺ π^0), hypernuclear formation, pole graph method anal. 7-42074

kaon-nucleus reactions continued

- $^{12}\text{C}(\text{K}^-, \pi^-)$, hypernuclear yield calcs. using DWIA 7-5184
 $^{13}\text{C}(\text{K}^-, \pi^-)$, $s^+p^0s_{\text{A}}$, $s^+p^0p_{\text{A}}$ state spectra, baryon decays, neutron spectra, nuclear and hypernuclear γ -spectra 7-56634
 $^2\text{H}(\text{K}^-, \text{N}, \Delta(\Sigma))$, three-body multichannel, two body interaction anal. 7-36057
 $^3\text{He}(\text{K}^-, \pi^-, \text{nD}_2)$, strangeness-1 dibaryon search expt. 7-36056
 $^4\text{He}(\text{K}^-, \pi^-)$, hypernucleus production cross section calcs., PWIA anal. 7-10118

kaon-nucleus scattering

- see also *kaon-nucleon scattering*
 (K^+, K^+) , elastic and inelastic scatt. on deformed nuclei 7-61922

kaon production

- heavy ion collisions, relativistic subthreshold antikaon production 7-36018
 P_T dependence of π^+ , K^+ , p and $\bar{\text{p}}$ prod. in central rapidity region of e^+e^- and pp 7-61757
relativistic heavy-ion collisions, subthreshold kaon production and compression effects 7-49448
 $\text{D}^0 \rightarrow \text{K}^- \pi^+$ lifetime meas. 7-41795
 $\text{D}^0 \rightarrow \text{K}^- \pi^+ \pi^- \pi^+$ lifetime meas. 7-41795
 $\text{D}^0 \rightarrow \text{K}^0 \phi$, branching ratio meas. 7-61661
 $\text{D}^0 \rightarrow \phi \text{K}^0$, anal. using algebraic method with hard-meson extrapolation 7-19103
 $\text{D}^+ \rightarrow \text{K}^- \pi^+ \pi^+$ lifetime meas. 7-41795
 $\text{e}^+ \text{e}^- \rightarrow \text{e}^+ \text{e}^- \text{K}_S^0 \text{K}^+ \pi^+$, two photon spin-1 meson production obs. 7-24900
 $\text{e}^+ \text{e}^-$ jets, pion and kaon multiplicities 7-61705
 (γ, K^+) , anal. with Coulomb, optical distortions, hypernuclear excitations 7-41973
 $\gamma\gamma \rightarrow \text{M}^+ \text{M}^-$ ($\text{M} = \pi, \text{K}$), next-to-leading-order perturbative QCD calcs. 7-61591
 $\text{K}^+ \text{p} \rightarrow \phi \text{K}^+ \text{p}$, $\phi \rightarrow \text{K}^+ \text{K}^-$, 13 GeV/c, ϕK^+ mass spectrum, spin-parity anal. 7-554
 $\Lambda_c^+ \rightarrow \text{K}^0 \text{p} \pi^+ \pi^-$, Λ_c^+ polarization meas. from $^{12}\text{C}(\text{n}, \Delta^+)$, 40-70 GeV/c 7-5088
 $\nu, \bar{\nu} \rightarrow \text{KX}$, 1-5 GeV, nucleon decay search implications 7-19116
 $\nu, \bar{\nu} \rightarrow$ strange particles, inclusive production rates 7-528
 $\bar{\nu} \rightarrow \text{K}^0 \text{X}$, low-energy annihilation, cross section meas. 7-15169
 $\bar{\text{p}} \text{p} \rightarrow \text{K}_L \text{K}_S (\text{K}_S \text{K}_S) (\text{K}^- \text{K}^+)$, baryon exchange model anal., cross sections, resonances 7-30287
 $\bar{\text{p}} \text{p} \rightarrow \text{K}_S \text{K}_S$, proposed $\xi(2230)$ search expt. 7-49167
 $\bar{\text{p}} \text{p} \rightarrow \text{K}^0 (\text{K}^0) \text{K}^+ \pi^-$, meas. possibilities for T-, CP-, CPT-violation parameters in $\text{K}^0 (\text{K}^0)$ decay 7-10053
 $\bar{\text{p}} \text{p} \rightarrow \text{KX}$, charged particle multiplicity, dual parton and quark fragmentation models 7-19135
 $\bar{\text{p}} \text{p} \rightarrow$ kaons, kaon-pion branching ratio anal. 7-49171
 $\bar{\text{p}} \text{p} \rightarrow \text{K} \pi \text{NX}$, inclusive spectra, quark-gluon string model anal. 7-61769
 $\bar{\text{p}} \text{p} \rightarrow \bar{\text{p}} \text{p}, \pi^+ \pi^-, \text{K}^+ \text{K}^-$, antiproton spin physics expt. at LEAR 7-49170
 (π^+, K^+) , hypernuclear experiment at KEK 7-41930
 $\bar{\text{p}} \text{p} \rightarrow \text{K} \pi \text{NX}$, inclusive spectra, quark-gluon string model anal. 7-61769
 $\pi^- \text{p} \rightarrow \text{K}^0 \text{K}^0 \text{n}$, amplitude anal. at 40 GeV/c 7-41847
 $\pi^- \text{p} \rightarrow \text{K}^0 \text{K}^0 \text{n}$, systematic study of 2^{++} meson spectrum 7-555
 $\pi^- \text{p} \rightarrow \text{K} \text{K} \pi$, Dalitz plot anal. 7-61737
 $\pi^- \text{p} \rightarrow \text{K}^+ \Sigma^+$, 5-140 GeV, extensive reaction anal., strange Regge trajectory props. 7-61747
 $\pi^+ \text{p} \rightarrow \text{K}^+ \Sigma^+$, pole plus cut model anal. 7-15174
 $\psi \rightarrow \gamma \phi \phi \rightarrow \gamma \text{K}^+ \text{K}^- \text{K}^+ \text{K}^-$, glueball search 7-24879
 $\tau \rightarrow \nu \nu, \text{K}^0 \nu$, branching ratios, effects of asymptotic flavour symmetry, QCD anal. 7-49143
 $^{20}\text{Ne}(\text{p}, \Delta \text{K}_L^+)$, strange particle production expt. 7-49392

kaon-proton interactions

- see also *kaon-proton scattering*
 $\text{K}^- \text{p} \rightarrow \text{K}^0 \text{K}_L^0 \text{Y}^*$, source of $s\bar{s}$ states with even spin 7-41857
 $\text{K}^- \text{p} \rightarrow \text{K}^0 \text{n}$, bounds on EKN^2 from positivity and charge-exchange data 7-61738
 $\text{K}^- \text{p} \rightarrow \Delta^0 \text{X}$, 150-350 MeV/c, analysis of two-body channels 7-24905
 $\text{K}^- \text{p} \rightarrow \Delta \pi (\Sigma \pi)$, quark contribution to nuclear force 7-551
 $\text{K}^- \text{p} \rightarrow \pi^+ \Sigma^+$, 5-140 GeV, extensive reaction anal., strange Regge trajectory props. 7-61747
 $\text{K}^- \text{p} \rightarrow \pi^- \Sigma^+$, pole plus cut model anal. 7-15174
 $\text{K}^+ \text{p}$, 250 GeV/c, maximum particle densities in rapidity space 7-61752
 $\text{K}^+ \text{p}$, 250 GeV/c, cross sections and charged multiplicity distrib. 7-24909
 $\text{K}^+ \text{p} \rightarrow \Delta \text{pX}$, hyperon inclusive production 7-41855
 $\text{K}^+ \text{p} \rightarrow \phi \text{K}^+ \text{p}$, $\phi \rightarrow \text{K}^+ \text{K}^-$, 13 GeV/c, ϕK^+ mass spectrum, spin-parity anal. 7-554
 $\text{K}^- \text{p} \rightarrow \text{K}^- \pi^+ \text{n}, \text{K}^* \text{L}$ -excitation series obs., spherical harmonic moments anal. 7-24915
 $\text{K}^- \text{p} \rightarrow \Delta \text{X}$, Δ polarization, energy dependence and p_T variance, QCD comparisons 7-61754

kaon-proton scattering

- see also *kaon-proton interactions*
forward elastic amplitude, Stieltjes extrapolation to unphysical cut 7-15172
 πn elastic partial wave scatt. anal. 7-41836

kaon regeneration

No entries

kaon resonances see *meson resonances***kaon scattering** see *kaon-baryon scattering; kaon-nucleus scattering; meson-meson scattering***kaons**

- see also *kaon regeneration*
charge radius meas. by direct scatt. 7-10063
K-balls in chiral lagrangian 7-35692
low energy meson physics in the superconducting quark model 7-35811
micrononcausal Euclidean wave functions assuming Yukawa type couplings 7-41596
 $\text{K} \rightarrow \text{e} \nu \text{H}$, Higgs production phenomenological limits 7-513
 $\text{K} \rightarrow \mu \text{e}$, anal. in CP violation models 7-436
 $\text{K} \rightarrow \pi \pi^0$, matrix element determ., confirmation of $\Delta T = 1/2$ rule 7-56540
 $\text{K} \rightarrow \pi^0 \gamma \text{e} \nu$, decay probability, dependence on γ -detection threshold, T violation asymmetry 7-56538
 $\text{K}^0 \text{K}^0$ mixing, double penguin-like diagrams for ϵ parameter 7-5028
 $\text{K}^0 \text{K}^0$ mixing, short-distance contrib. from QCD sum rules 7-15122
 $\text{K}^0 \text{K}^0$ system, CP and CPT violation 7-30206
 $\text{K}^0 \text{K}^0$ system, CP violation, anal. using Kobayashi-Maskawa matrix 7-61497

kaons continued

- $\text{K}^+ \rightarrow \pi^+ \nu \mu$, branching ratio, KMC predictions, fourth generation mixing effects 7-41785
 $\text{K}^- \rightarrow \pi^+ \nu \mu$, experimental BNL787, status, anal. of generation problem 7-41979
 $\text{K}_L^0 \rightarrow \pi^+ \pi^- \nu \mu$, 1^+ polarization, effects of heavy subdominantly coupled neutrino mixing 7-61652
 $\text{K}^0 \rightarrow \text{e}^+ \pi^+ \nu$, search for T and CPT violation 7-41787
 $\text{K}^0 \rightarrow \text{e}^+ \pi^+ \nu$, search for T and CPT violation 7-41787
 $\text{K}_L - \text{K}_S$ mass difference in the chiral quark-loop model 7-61684
 $\text{K}^0 \rightarrow \text{K}^0$ transitions in matter 7-61498
 K^0 decay, CP violation, experimental anal. 7-41786
 $\gamma \gamma \rightarrow \text{K}^+ \text{K}^- \pi^+ \pi^-$, vector meson prod., $\phi(1020)$ and $\text{K}^*(890)$ signals 7-5136

Kapitza-Dirac effect

- see also *Schwarz-Hora effect*
No entries

Kapitza resistance

- $\text{Gd}_3\text{Ga}_2\text{O}_{12}$, sintered, mag. refrigerant, Kapitza conductance to He II 7-58603
 ^3He , superfluid, hydrodynamic boundary conditions and cooling 7-63897
 $^3\text{He}-\text{CuK}_2(\text{SO}_4)_2 \cdot 6\text{H}_2\text{O}$, thermal resist., surface mag. coupling, effect of ^4He addition 7-52173
 $^4\text{He}/\text{Au}$ system, Kapitza resistance between Au and superfluid, singularity 7-58559
Si laser annealed surface, Au submonolayer coverage, Kapitza anomaly reentry obs. 7-38318

KDP see *potassium compounds***KdV equation** see *wave equations***Kelvin-Helmholtz instability** see *flow instability***keratin** see *proteins***kerma** see *dosimetry***Kerr effect (optical)** see *optical Kerr effect***Kerr electro-optical effect**

- see also *optical Kerr effect*
alkylene-aromatic polyester, thermotropically mesogenic, solns., Kerr effect 7-7674
artificial Kerr medium, microspheres suspension, moving electromag. gratings, response study, Planck-Nernst eqn. 7-64605
benzene, anisotropic mol. liq., Kerr consts. and anisotropic electronic polarisability calcs. 7-53273
binary liquid mixtures, Kerr effect 7-53271
double injection charge transport in dielectrics 7-33334
droplet clustering in microemulsions, electric birefringence study 7-28354
4-n-hexylphenyl-4-butylbenzoate liq. cryst., isotropic phase, Kerr effect studies 7-33364
hexylphenylbutylbenzoate nematic, isotropic phase, Kerr effect dispersion, mol. dipole relax. study 7-63448
molecular Kerr relaxation theory for liquids in reorienting pulse fields 7-36663
nitrobenzene, polar mol. liq., Kerr consts. and anisotropic electronic polarisability calcs. 7-53273
nitrobenzene, radiation-induced Kerr electro-optic effect 7-53272
pentanol isomers, n-heptane solvent, mol. assoc., optical Kerr effect study 7-62429
ternary microemulsion system, phase electric birefringence meas. 7-27699
voltage measurements on multimegavolt pulsed power accelerators 7-25286
water, polar mol. liq., Kerr consts. and anisotropic electronic polarisability calcs. 7-53273

Kerr magneto-optical effect

- ferromagnetic thin absorbing film on reflecting struct., equatorial Kerr effect 7-53287
film-substrate system, magneto-optical longit. Kerr effect 7-13136
magnetic domain imaging with scanning Kerr effect microscope 7-45725
magnetic domains, obs. by magneto-optical Kerr effect 7-64618
magnetic film-magnetic substrate system, magneto-optical transverse Kerr effect 7-22226
metallic crystals, magneto-optical Kerr effect, charge carrier plasma reson. enhancement calcs. 7-45997
particulate recording media, magneto-optic Kerr effect hysteresis loop meas. 7-48782
AlN sputtered film, Kerr effect enhancement 7-64610
Co-Au compositionally modulated multilayered films, magneto-optical Kerr rot., wavelength depend. 7-3100
Co-Cu compositionally modulated multilayered films, magneto-optical Kerr rot., wavelength depend. 7-3100
CoCr layers, domain obs. with digitally enhanced Kerr-microscope 7-45726
Fe epitaxial monolayers on the Au (100), surface magneto-optic Kerr effect 7-59080
Fe thin films, surface plasma waves, optical and magneto-optical effects 7-27704
Fe-Au compositionally modulated multilayered films, magneto-optical Kerr rot., wavelength depend. 7-3100
Fe-Cu compositionally modulated multilayered films, magneto-optical Kerr rot., wavelength depend. 7-3100
Gd-Tb-Co-Fe sputtered amorphous films, Kerr magneto-optical effect, anisotropy dispersion effects 7-38913
 $\text{Li}_{1-x}\text{Zn}_x\text{Fe}_2\text{O}_4$, outside spin wave manifold effective linewidth values, effect of dimensional reson. 7-53146
 $\text{Mg}_{1-x}\text{Mn}_x\text{Fe}_2\text{O}_4$, outside spin wave manifold effective linewidth values, effect of dimensional reson. 7-53146
Nd-Fe-Co, amorphous films, perpendicular magnetic, mag. and magneto-optical props. 7-64496
 $\text{PbFe}_{12}\text{Ga}_4\text{O}_{19}$ ($x=0, 1, 3, 4$), magneto-optical props. 7-53281
 $\text{PbFe}_{12}\text{O}_{19}$, cryst., complex magneto-optical polar Kerr effect spectra 7-53280
Pr-Fe, amorphous films, perpendicular magnetic, mag. and magneto-optical props. 7-64496
SiO sputtered film, Kerr effect enhancement 7-64610
TbCo film, optical disc memory struct., mag. props., underlayer film treatment effect 7-45767
TbFe amorphous alloys, magneto-optical props. and mag. anisotropy 7-27706
TbFeCo-based amorphous films, magneto-optical recording appls. 7-53074
 $(\text{Tb}_x\text{Fe}_{1-x})_2\text{U}$, amorphous, magneto-optical effects 7-59187

kicksorters *see counting circuits***kidney**

artificial, press. losses in apparatus with capillary channels made of semipermeable film 7-28772
 ascending limb of Henle's loop, active transport and steady state distrib. of Na^+ (*Chinese*) 7-28485
 cancerous and normal tissues, fluoresc. polarisation spectroscopy and time-resolved fluoresc. kinetics, rat obs. 7-8646
 computerised image processing for renal volume calculation using ^{125}I hippuran gamma camera renography 7-8680
 filter control, system dynamics model 7-40201
 fluid waves in renal tubules 7-28547
 hollow-fibre modules, flow distrib. study 7-65783
 nuclear techniques in diagnostic medicine, book 7-24312
 proton relaxation times in mouse liver, heart and kidney, temporal fluctuations 7-47005
 radiographic images, digitally subtracted, diagnostic effects of edge sharpening filtration and magnification 7-54722
 radionuclide renogram, renal retention function calc., deconvolution technique based on total linear squares 7-65846
 rat tissue, mag. field effects, phase-contrast microscopy obs. 7-8645
 selenoproteins in bovine kidneys, anal. using gel chromatography and neutron activation 7-34363
 slow flow system in long permeable tubule, one- and two-dimensional models 7-47142
 US kidney images recognition by 2D dynamic programming method 7-18034

Kikuchi lines *see electron diffraction crystallography*killed steel *see alloy steel*kinematic viscosity *see viscosity***kinematics**

see also acceleration; ballistics
 Clump 1, unusual mol. cloud complex near galactic centre, ^{12}CO and ^{13}CO obs. 7-48044
 Coma cluster galaxies, vel. dispersion profile rel. to cluster mass 7-40945
 curved beam elements with penalty relaxation 7-37335
 femoropatellar joint, trajectory pattern and load-bearing capacity when diseased (*Japanese*) 7-8638
 galactic corona, IUE obs. rel. to kinematics, ionisation, and abundances 7-48054
 galactic disks, solitary vortices theory 7-14657
 globular cluster system of M87, vel. dispersion from spectroscopic obs. 7-48001
 human spinal cord effects of impact loads, full-scale and computational expts. 7-34294
 instruction using microcomputers 7-14732
 interstellar absorption lines' towards SN 1987A in LMC, radial vel. systems identification 7-66637
 interstellar molecular clouds, mass-radius-vel. dispersion relations rel. to cloud fragmentation 7-55753
 Newton's laws of rigid body mechanics, proof using stroboscopic photograph 7-55927
 NGC 4151, Seyfert 1 galaxy, C IV 155 nm line profile obs. (1978 to 1983) 7-60814
 NGC 4214, 4449, blue irregular, galaxies, kinematics of H II regions 7-40925
 planetary nebulae, internal motions in 32 genuine PNe and misclassified object 7-4541
 plates and shells, finite strain large deformation, nonlinear theory 7-20602
 shells, elastic-viscoelastic layered, multi-director formulation 7-37347
 shoulder complex, human, statistical database for biomech. props., kinematics 7-8632
 supernova remnants, colliding, oblique shock refls. rel. to anomalous H I vel. features 7-24175
 Virgo galaxy cluster, orbits of H I deficient spiral galaxies 7-24230

kinematography *see cinematography*kinerecording *see video recording***kinetic theory**

see also Boltzmann equation; collision processes; intermolecular mechanics; kinetic theory of gases
 aggregation phenomena and fractal aggregates (*French*) 7-9757
 binary fluid mixtures, comparative anal. by extended irreversible thermodynamics and kinetic theory 7-16290
 charged particles motion, bounded systems with collisions 7-48521
 dense fluids, viscosity and mutual diffusion coeff. calcs. 7-26379
 developing simplified models of combustion chemistry bysimulation with detailed chemical kinetics models 7-13779
 Enskog equation in two space variables 7-4799
 glass, surface recomb. of electrons and ions, kinetic theory 7-46263
 inhomogeneous fluid, tracer diffusion, kinetic theory 7-58111
 maximum entropy ensembles and equilib. soln., in kinetic theory of liquids 7-26605
 mechanics of continuous media, kinetic theory and material frame-indifference principle 7-24422
 mineral waste dil. suspensions, interacting particles, kinetic theory 7-46880
 mixtures, continuum theory, motivation from discrete considerations 7-57680
 polymer solutions, structural approach, dumbbell model, vector model (*French*) 7-6259
 quantum dynamical systems, Bogolyubov kinetic eqn. 7-24442
 self-consistent kinetic equations, soln. method (*Russian*) 7-56141
 SOKIRK-simulation of kinetic data by Runge-Kuttamethod 7-11876
 statistical methods, conf., Oaxtepec, Mexico, Jan. 1986 7-24268
 two-level atom, Brownian motion in light wave 7-897
 Ag thin film form., nucleation and growth processes 7-2419

kinetic theory of gases

see also Brownian motion; collision processes; equations of state; intermolecular mechanics; Joule-Thomson effect
 Boltzmann-Fokker-Planck eqn., kinetic gas theory formulation 7-63239
 charged particle transport, influence of finite mass-ratio 7-1661
 complex molecules, effective kinetic diameter determ. 7-26376
 dense gases, transport processes, kinetic theory 7-6342
 dilute diatomic gas, equilibrium eigenmodes 7-16291
 dilute gases, chem. reaction rate, viscous flow and thermal flux effect calcs. 7-28268
 electron swarm in a model gas, diffusion coeffs., Monte Carlo simulation 7-1662

kinetic theory of gases continued

electron swarms in gases, vel. distrib. function and transport coeffs. 7-1663
 Enskog equation, global existence theorem 7-31911
 first order conserved densities 7-51365
 gaseous swarms, reactive phenomena theory 7-13749
 heavy target, boundary layers arising when intermediate energy beam is stopped 7-16292
 hyperbolic conservation laws with relaxation 7-48373
 isothermal mol. gas, Maxwellian versus Rayleigh distrib. 7-18535
 light induced drift of gas particles, kinetic theory 7-16289
 Maxwellian gas, relax. to quasiequilibrium state 7-44085
 Maxwellian particle gas mixtures, coupled linearised Boltzmann eqn. 7-1664
 metal vapours and vapour-gas mixtures, atomic interactions and transport coeffs. 7-11575
 molecular Knudsen gas, cross effect between heat and momentum transport 7-26380
 monatomic gases, Chapman-Enskog approx. and Boltzmann eqn. calcs. 7-37615
 multiatomic gases, kinetic eqns. for relaxation processes 7-31915
 multiatomic gases, relaxation processes 7-31916
 non-stationary gas flows, hydrodynamic fields, dynamics of space-time correlations 7-26243
 noncondensable gas behaviour in vapour, macroscopic eqns., boundary conditions and Knudsen layer corrections calcs. 7-31840
 nonequilibrium gas-solid system, transport processes, kinetic theory calcs. 7-16254
 nonideal gas, quantum kinetic equation in three-particle approximation 7-24536
 nonmonotonic relaxation in an atomic gas and the kinetics of threshold processes 7-1665
 particles diffusion and heat flux in the initial stage of the transport process 7-20589
 polyatomic molecular gas, kinetics, classical theory 7-6345
 rarefied gas, thermally induced flow, thermal force on high thermal cond. spherical particle, kinetic model eqns. calcs. 7-51232
 reaction threshold, rel. to gas dynamics eqns. (*Russian*) 7-26381
 rigid molecules, new rigid motion algorithm for MD simulations 7-50284
 rough sphere dense gas kinetic theory 7-31910
 statistical thermodynamics, theory and appls. 7-29864
 thermal relaxation, model problem 7-57974
 thermally conducting gas, isothermal phase discontinuity 7-31909
 transport theory conf., Montecatini Terme, Italy, June 1985 7-60874
 weakly ionised gases, kinetic theory 7-20826
 H, ideal gas, modified Gibbs state 7-44087
 HCl/Xe/He gas mixture, kinetic model of discharge (*Russian*) 7-11577
 He- N_2 mixture, calc. of classical cross sections related to the Senftleben-Beenakker effect on physical parameters 7-16287
 Li monatomic vapour, transport props., depend. on two body atom-atom interaction pot. 7-6343
 N_2 , glow discharge, electron kinetics, Boltzmann and vibr. rate balance eqns., self-consistent solns. 7-21035

kinetic theory of liquids *see kinetic theory; liquid theory*kinetics of chemical reactions *see reaction kinetics***kink bands**

dynamic kinks on dislocations 7-2016
 metals, electronic structures of lattice defects, tight binding recursion method 7-27289
 Al_2O_3 fibre reinforced Al composites, compressive failure modes, dead weight or machine loading 7-39663
 Fe, Armooc and Vacofer, yielding behaviour, H influence 7-33753
 InSb, α dislocations, motion, small shear stresses 7-44553
 Si 7-26753
 Si single cryst., dislocation line kink mobility and double kink form. kinetics 7-26760

kinoforms *see computer-generated holography*Kirkendall effect *see diffusion in solids*kitchen appliances *see domestic appliances***KKR calculations**

alloys, ternary substitutional, electronic structure, KKR-CPA method 7-64074
 crystal lattice, spiral mag. struct., band struct. calcs. 7-7096
 Kondo lattice, heavy fermion band form., effective magnetic moments, and Wilson ratio, relativistic KKR calcs. 7-22091
 noble metal alloys, Al- K_α XPS intensities 7-27870
 non-muffin-tin potentials in multiple-scattering theory 7-32895
 surfaces and interfaces, electronic states, multiple-scatt. treatment 7-45420
 Ag-based dilute alloys, low temp. elec. resist. 7-52565
 Ag-Pd, random alloys, residual electrical resistivity, first-principles calc. 7-2569
 AgCd, electronic structure, disordering effects (*Russian*) 7-32901
 Au, Pt $_{1-x}$, mag. susceptibility, 77 to 450K 7-17164
 CoAl, electronic struct. of antistructure Co atoms and Co-vacancies 7-7165
 Cu-based dilute alloys, low temp. elec. resist. 7-52565
 Cu-Zn (Ga)(Ge), random alloys, residual electrical resistivity, first-principles calc. 7-2569
 Fe $_2$ P, electronic struct., mag. props., KKR, LMTO methods, LSD approx. 7-64070
 HfB, electronic struct., chem. bonding, Green's function methods 7-58741
 Mn $_2$ P, electronic struct., mag. props., KKR, LMTO methods, LSD approx. 7-64070
 Mo, electronic struct. of mag. 3d impurities, local density approx. 7-64432
 Nb, electronic struct. of mag. 3d impurities, local density approx. 7-64432
 Nb, Fermi surface, Fermi vel., many-body enhancement and supercond. energy gap anisotropies calcs. 7-58729
 Ni-Mo, random alloys, residual electrical resistivity, first-principles calc. 7-2569
 Ni $_2$ P, electronic struct., mag. props., KKR, LMTO methods, LSD approx. 7-64070
 PdFe, disordered phase, electronic struct. anal. 7-58735
 TiB, electronic struct., chem. bonding, Green's function methods 7-58741
 Y electronic struct., electron-phonon matrix and superconductivity, high press. effects, KKR calcs. 7-21805

KKR calculations continued

- ZrB, electronic struct., chem. bonding, Green's function methods 7-58741
 ZrN, electronic struct., metal vacancy effects, KKR-CPA method anal. 7-12606

klystrons

- see also reflex klystrons*
 insertion devices for synchrotron sources, conf., Stanford, CA, USA (Oct. 1985) 7-29584
 maximum efficiency of a conventional klystron output cavity 7-62186
 operational experience with SLAC energy upgrade 7-62111
 optical, free electron laser props. (*Japanese*) 7-11177
 optical klystron, theory 7-360
 optical klystron, VUV harmonic generation on storage ring 7-1229
 optical klystron, XXUV laser harmonic generation, effects of wiggler errors 7-1127
 optical klystrons, optimisation criteria 7-36972
 plasma lower hybrid resonance heating, 500 kW klystron design 7-26452

Knight shift

- see also nuclear magnetic resonance*
 metal particles, quantum size effects 7-7597
 muons in metals, valence-electron-only molecular orbital calcs. of Knight shift 7-2961
 (TMTSF)₂ClO₄, NMR study of molecular motion, anion ordering 7-53175
 transition metals, Knight shift spin and orbital contribs., real-space formulation, Green's function method 7-2940
 transition metals-H₂, disordered, NMR studies 7-27618
 AgSn(Sb), impurity-vacancy and impurity-impurity interactions calc. from diffusion enhancement 7-6672
 Bi, muon Knight shift anisotropy study 7-45893
 CdMg dilute alloys, muon Knight shift temp. depend. study 7-45892
 CeB₆ heavy fermion system, muon Knight shift study 7-45886
 CeCu₂Si₂ heavy fermion superconductor, magnetic field penetration, muon spin relax. studies 7-45886
 CeH_{2.7} heavy electron system, muon spin rot., Knight shift and relax. studies 7-45885
 CeNi₂P₂, 4f-magnetism study by susceptibility and NMR 7-22154
 CePb(Al)₃ heavy fermion system, muon Knight shift study 7-45886
 EuNi₂P₂, 4f-magnetism study by susceptibility and NMR 7-22154
 Gd, μ SR studies, Knight shifts and relax. above Curie temp. 7-45877
 LiAl(Ga)(In)(Zn)(Cd) B32-type Zintl phases, mag. props., exchange enhancement, APW calcs. 7-27504
 Mo₅Si(Ge), neutron irradi., NMR and mag. suscept. studies (*Russian*) 7-13051
 NaIn B32-type Zintl phases, mag. props., exchange enhancement, APW calcs. 7-27504
 Na₂Ta₂W₁₀O₃₂, NMR study of metal-insulator transition 7-2484
 NbH₄, mag. spin susceptibility and Knight shift 7-33141
 PbTe, narrow gap semiconductors, Knight shift 7-53166
 Pt (001), hyperfine fields 7-58847
 Sb, muon Knight shift press. depend. meas. and mol. cluster calcs. 7-45890
 SbSn dilute alloys, muon Knight shift and trapping, comp. and temp. depend. 7-45889
 Sm intermetallic cpds., Knight shift, density matrix perturbational approach 7-33283
 Ti, HCP, ⁴⁷Ti and ⁴⁹Ti NMR studies, spin-echo profiles 7-7599
 TiH₃, Ti Knight shift meas. 7-38954
 UBe₁₃ heavy-fermion superconductor, muon Knight shift study 7-7628
 UBe₁₃-Gd, EPR in superconducting phase 7-33269
 UCu₅ magnetic heavy electron materials, muon spin rotation studies 7-45884
 UPt₃ heavy fermion supercond., muon spin relax. and Knight shift meas. 7-45888
 UPt₃ heavy fermion system, muon Knight shift study 7-45886
 U_{1-x}Th_xBe₁₃ heavy fermion superconds., muon Knight shift and zero-field relax. meas. 7-45887
 U₂Zn₁₇ magnetic heavy electron materials, muon spin rotation studies 7-45884
 Yb_{1-x}In_xCu₂, Yb valence transition 7-45245
 YbNi₂P₂, 4f-magnetism study by susceptibility and NMR 7-22154
 Zn, electric quadrupole interaction of ⁶⁷Zn, mag. reson. meas. 7-53167

knockout reactions *see direct nuclear reactions and scattering***knowledge based systems** *see expert systems***knowledge engineering**

- analogical representation of liquids in naive physics, intuitive knowledge modelling 7-26607
 protein structure, knowledge-based prediction and novel mols. design 7-65692
 speech processing appls. (*Japanese*) 7-20511

Knudsen flow

- 3D hypersonic rarefied gas flow around rotating bodies 7-20761
 aerosol particle, thermophoresis at arbitrary Knudsen numbers 7-44014
 aerosol particles, spherical, thermophoresis at arbitrary Knudsen nos. 7-63185
 aerosol spherical particles at arbitrary Knudsen no., thermophoresis, gas-kinetic eqn. 7-44030
 conductance, dependence on geometric shape of wall (*Japanese*) 7-63182
 filler evaporation from porous body with plane surface 7-51230
 heat transfer between parallel plates at arbitrary Knudsen numbers 7-57883
 Lennard-Jones fluids, thermoviscous coupling and nonlinear transport effects on plane Couette flow 7-57793
 molecular angular momentum polarization in Knudsen flow, anal. for different surfaces 7-31842
 molecular Knudsen gas, cross effect between heat and momentum transport 7-26380
 multicomponent gas mixtures, interaction with wall, Navier-Stokes boundary condition 7-51233
 noncondensable gas behaviour in vapour, macroscopic eqns., boundary conditions and Knudsen layer corrections calcs. 7-31840
 particle metallising, kinetics of vapour condensation 7-2162
 propane, fluid, thermal cond. and diffusivity meas., Knudsen-effect, line-source method 7-48727
 rarefied gas, thermally induced flow, thermal force on high thermal cond. spherical particle, kinetic model eqns. calcs. 7-51232
 rarefied gases in tubes and systems, state of the art, review 7-51234
 slow nonisothermal gas flow between parallel plates 7-11471
 sphere motion in rarefied gas, temp. variation 7-43984

Knudsen flow continued

- spherical particle surface, heat transfer investigated using mol. kinetic methods 7-63184
 thermal fluctuations in a Knudsen flow system 7-63183
 thin tubes, Knudsen flows, dynamics of test particle, diffusion approx. 7-11470
 N plasma particle-gas mass transfer, Knudsen effect 7-31937
 Na, hyperfine population relax. in wall collisions 7-62326

Knudsen number *see Knudsen flow***Kohn effect** *see lattice dynamics***Kondo effect**

- d-wave superconductivity in the large-degeneracy limit of the Anderson lattice 7-45551
 alloys, amorphous, modified mag. Kondo theory 7-33000
 Anderson impurity model, finite U, ground state and spectroscopic props. 7-2817
 Anderson Kondo lattices, heavy-fermion superconductivity 7-2775
 Anderson lattice, low temp. sp. ht., functional integral approach, boson representation 7-16788
 Anderson model, Bethe ansatz soln., cryst. field and spin-orbit coupling effects 7-2449
 Anderson model, dynamic susceptibility, freq. depend., 1/N_f expansion studies 7-2816
 Anderson periodic model, appl. of Gutzwiller method 7-45109
 Anderson-type model, two-band in 1D, mag. susceptibility and other ground-state props. 7-22092
 coexistent phase in antiferromag. Kondo lattice (*Chinese*) 7-64431
 Coqblin-Schrieffer model in large-N limit, magnetisation 7-45617
 degenerate Kondo lattice, magnetic instability and sp. ht. calcs. 7-58977
 dense Kondo heavy fermion systems, Cooper pairs attractive interactions freq. depend. 7-58951
 dense Kondo systems, coherent state and Z⁻¹ expansion 7-2603
 dilute alloys, low-temperature resistivity, transport eqn. 7-21898
 electron gas, degenerate, tunnelling atom interactions, low temp. behaviour 7-27270
 field theoretical approach to solid state physics 7-12934
 generalised Anderson model, mixed valence system modelling 7-2562
 heavy electron Fermi liquids, Hubbard model anal., similarities to ³He 7-2522
 heavy electrons, Gutzwiller method 7-27228
 heavy fermion alloys, Kondo exponent, conc. depend. 7-27495
 heavy fermion alloys, Kondo exponent, conc. depend. 7-27497
 heavy fermion liquids, superconductivity, microscopic and phenomenological aspects 7-2773
 heavy fermion state form., Kondo lattice calcs. 7-206
 heavy fermion superconductivity, conduction band and virtual bound states, Kondo-like interaction, periodic Anderson Hamiltonian calcs. 7-27460
 heavy fermion superconductivity, tight binding picture and Cooper pairs 7-2776
 heavy fermion systems, disorder and coherence 7-21888
 impurity systems, intermediate valence and kondo impurities, noncrossing approx. 7-7162
 lattices, heavy fermion band form., effective magnetic moments, and Wilson ratio, relativistic KKR calcs. 7-22091
 lattices, magnetoresistance at low temp. 7-2600
 low temp. lattice Anderson model, large-orbital-degeneracy expansion in the Kondo limit 7-64037
 metals, Kondo effect amplification by mag. field 7-52602
 periodic Anderson model, extended and localised states 7-38504
 strongly correlated Fermi systems, Gutzwiller saddle-point approx., functional integral approach 7-207
 transition metal impurities in host metals, magnetic nature, superconductivity studies, review 7-7437
 valence fluctuating lattice systems, self-consistent perturbation theory 7-2561
 weakly localised regime, effect of mag. impurity on conductivity 7-2839
 Al-Si(Ge)(Ga), low temp. diffusion and trapping of muons 7-45865
 Au-Fe, dil., Kondo system, mag. scatt. time of conduction electrons meas. 7-21902
 Ce alloys, electronic structure, spectroscopic and thermodynamic props., impurity Anderson Hamiltonian 7-32900
 Ce compounds, heavy-fermion state in the Anderson lattice 7-7476
 Ce compounds, intermediate valence and Kondo lattice models 7-2560
 Ce cpds. and alloys, kondo effect versus crystal field 7-2602
 Ce Kondo systems, thermopower, elec. resist. and cryst. field effects 7-21900
 Ce-Cu amorphous alloys, mag. and transport props., Ce-derived anomalies 7-52601
 CeAl₂, low-temp. high-field magnetoresist. meas. 7-38541
 CeAl₃ Kondo lattice, coherent regime, Hall effect temp. depend. study 7-52581
 CeAl₃ nonmagnetic Kondo lattices, coherent regime, Hall effect temp. depend. meas. 7-52582
 CeCu₆ heavy-fermion material, coherent and incoherent behaviour, Hall effect and magnetoresist. 7-32992
 CeCu_{2-x}Ni_xSi₂ Kondo-lattice system, resist. anomalies 7-58799
 CeCu₂Si₂ Kondo lattice heavy fermion system, quasi-particle-phonon interactions 7-2521
 CeCu₂Si₂ nonmagnetic Kondo lattices, coherent regime, Hall effect temp. depend. meas. 7-52582
 Ce_{0.8}La_{0.2}Al₃ nonmagnetic Kondo lattices, coherent regime, Hall effect temp. depend. meas. 7-52582
 Ce(Rh_{1-x}Co_x)₂B₂ ferromag. Kondo system, anomalous elec. resist. temp. depend. 7-2601
 CeSi₃, galvanomag. and thermoelec. props. 7-38537
 CeZn₂ Kondo anomaly and metamagnetism 7-64234
 Eu₂Ce_{1-x}Cu_xSi₂ cryst., mixed valence state and Kondo system coexistence (*Russian*) 7-7185
 Fe_{100-x}B_x amorphous alloy, temp. depend. of the resistivity (*Chinese*) 7-27314
 (Fe_{1-x}Co_x)₈₄B₁₆ amorphous alloy, temp. depend. of the resistivity (*Chinese*) 7-27314
 Fe_{80-x}Cr_xB₂₀ metallic glasses, electron transport props., disorder and mag. effects 7-52563
 (Fe_{1-x}Ni_x)₈₄B₁₆ amorphous alloy, temp. depend. of the resistivity (*Chinese*) 7-27314
 (Fe_{1-x}V_x)₈₄B₁₆ amorphous, low temp. resistivity anomaly (*Chinese*) 7-64198

Kondo effect continued

- La_{1-x}Ce_xNi, Kondo lattice form., elec. resist. and susceptibility meas. 7-21899
 Mg-Fe, dil., Kondo system, mag. scatt. time of conduction electrons meas. 7-21902
 Mg-Fe dilute thin film, mag. screening and Kondo-type behaviour 7-12944
 Ni-B alloy with transition metal additives, amorphous, mag. scatt. influence on transport props. 7-33001
 U compounds, heavy-fermion state in the Anderson lattice 7-7476
 UBe₁₃ coherent Kondo state, upper critical field calcs. 7-2793
 U₂La_{1-x}Te single crystals, elect. resist. temp. depend. Kondo effect and ferromagnetic ordering 7-13119
 UPd₃Sn, heavy electron behaviour, elec. resist., mag. susceptibility, sp. ht. meas. 7-32679
 U(Pt,Pd)₃, heavy-fermion alloys, resistivity 7-17012
 UPt₃ Kondo lattice, low-temp. sp. ht., suscept. and resist. meas., press. depend. anal. 7-7220
 Yb compounds, intermediate valence and Kondo lattice models 7-2560
 YbBe₁₃, low temp. Mossbauer study 7-33309

Korringa-Kohn-Rostoker calculations *see* KKR calculations**Korteweg-de Vries equation** *see* wave equations**Koster effect** *see* dislocation damping**k.p. calculations**

- binary compound polar semiconductors with nonparabolic energy bands, electronic struct. 7-2478
 graphite intercalation cpds., staging dislocation electronic struct., electron scatt. rates, residual resist. 7-52558
 momentum Bloch functions, closure property 7-45123
 quantum well structures, localised states, strain depend. 7-7312
 AlAs/GaAs/AlAs quantum wells, eigenvalues calcs. 7-12820
 p-CdGeAs₂ semicond., hole mobility and scatt., temp. depend. study 7-52609
 GaAs-GaAlAs-GaAs heterojunction barriers, single particle tunnelling, five level k.p. theory 7-64341
 InSb conduction band spin splitting, spin reson. interaction obs., LMTO and k.p. perturbation calcs. 7-12676
 Pb_{0.98}Yb_{0.02}Te, cyclotron resonance meas., k.p. model calcs. 7-27605

Kramers-Kronig relations

- n-alcohols, IR intensities in liq. phase, OH vibrs., assoc. model 7-53336
 cytochrome c, nonradiative decay, absorpt. and reson. light scatt. 7-62440
 linear causal system, Kramers-Kronig relations, asymptotic consequences 7-51190
 picolytricyanoquinodimethane, mol. cryst., charge transfer transitions, electronic spectra 7-22279
 polyacetylene, I₂-doped, quantitative optical study 7-53380
 CO₂ ice, absorpt. coeff. and refr. index, laboratory meas. UV to microwave, review 7-3008
 CrCl₃, ionic crystals, optical and electron energy loss studies 7-3066
 GaAs, nonlinear refractive index, dispersive nonlinearities meas. 7-43192
 Ge, holes optical effective mass, determ. by interf. method 7-17290
 KClO₄ single crystals, vibr. anal., optical modes, IR spectra studies 7-22245
 LaS, NaCl type lattice, current carriers and cond. 7-45346
 Pb_{1-x}Cd_xSe, inter-band transitions, thermoreflectance study 7-3029
 PbSe, energy band structure, thermoreflectance study 7-3028
 ScN compensated semimetal single crystals, electronic struct., reflectivity and elec. props. meas. 7-27253
 Si, electrooptical effects 7-59182
 a-Si:H, optical dispersion relations, determ. 7-33353
 Si₃N₄, amorphous, optical dispersion relations, determ. 7-33353
 YIG, optical reflectivity meas. by synchrotron radiation spectroscopy 7-59135
 Y₂O₃, single crystals, optical spectra in VUV 7-53363

Kramers systems *see* determinants**Kromayer lamps** *see* mercury vapour lamps**Kronig-Penney model**

- dimerised Kronig-Penney model, band struct. 7-18530
 metals, elec. resist. saturation, 1D Kronig-Penney model 7-38533
 multi-photon transitions in solids, dressed bands approach 7-22327
 random Kronig-Penney pots., resist. and phase-disrupting collisions 7-7095
 relativistic surface states of distorted surfaces, relativistic Kronig-Penney eqn. 7-7319
 GaAs/AlAs superlattice, optical phonons and interface thickness, Raman scatt. studies 7-7705
 GaAs/GaAlAs superlattice, optical phonons and interface thickness, Raman scatt. studies 7-7705
 GaAs-Al_xGa_{1-x}As superlattice, hole subbands (*Chinese*) 7-58873
 In_{0.69}Ga_{0.31}As-InP strained-layer effective-mass superlattices 7-7378

krypton*see also* nuclei with

- acousto-optic interaction in FIR 7-37623
 adsorbate, excited states assignment 7-52725
 adsorbed on Au (111), He atom-surface scatt. 7-27851
 adsorbed on graphite, adsorption isotherm meas. near commensurate-incommensurate transition 7-38337
 adsorbed on graphite, incommensurate phase, computer simulation studies 7-7009
 adsorbed on Pt (111), adsorbate-substrate vibr. coupling 7-52221
 adsorption on SF₆ covered graphite (*French*) 7-32799
 atom, 3p excitation, multiple photoionisation cross sections, TOF mass spectrometer anal. 7-19802
 atom, autoionising region, multiphoton ionisation study 7-62336
 atom, Coulomb and exchange operators, valence electron only SCF calcs. 7-15507
 atom, electron impact, low energy, in afterglow 7-20060
 atom, electron impact excitation into metastable states effective cross sections 7-36775
 atom, electron impact ionisation, cross sections, fast-neutral beam method, TOF spectra 7-42769
 atom, electron scatt., cross section meas. 7-31171
 atom, electron scatt., intermediate energy, elastic and inelastic, differential cross-sections 7-25648
 atom, kinetic energy density, nonlocal correl. fn., CI wave fns. and HF calcs. 7-42496
 atom, multielectron photoelectron meas. 7-5643

krypton continued

- atom, photoionization cross sections of excited states, UPES anal. 7-50241
 atom, relativistic electron (positron) elastic scatt. 7-36767
 atom, Rydberg states, four-photon excitation 7-62328
 atom, self-consistent exchange parameters, radial depend. anal. 7-49920
 atom, small angle differential cross sections for electron elastic scatt. 7-15713
 atom, two-electron-one-photon excitations, X-ray photoabsorpt. studies 7-36527
 atom, ultrasensitive laser isotope anal. 7-19803
 atom, visible transitions, autoionis. obs., optogalvanic spectra 7-57035
 atoms, multiple ionisation by intense laser pulse 7-62332
 coadsorbed with NO₂ on Ag (110), magnetic resonance 7-59113
 cryogenic crystals, exciton diffusion and energy transport studies 7-52438
 defect props. in condensed two-dimensional lattice 7-2018
 dense plasmas, continuum ξ -factor determ. 7-20865
 diffusion in liquid Ar, cryogenic temp. controller 7-30020
 dimer, spectroscopic consts., coherent VUV and XUV radiation sources 7-10472
 electron thermalisation processes obs. by pulse-radiolysis microwave cond. method 7-20051
 excimer states, photoionisation cross sections 7-57137
 fluid, collective modes 7-1833
 Fourier transform EXAFS spectra, nonstructural low-R peak 7-64744
 gas, doubly-ionised by electron impact, spectral line Stark broadening meas. 7-62320
 gas, electron beam deposition 7-5771
 gas, primary and secondary ionisation coeffs. meas. 7-1668
 gas, supercontinuum generation with femtosecond pulses 7-25908
 gas, transport phenomena, multiparametric potential models 7-6344
 implanted systems, local environment, K-edge XANES and Rutherford backscatt. spectra studies 7-64809
 ion, O-like, electron impact excitation, coupling effects 7-982
 ion average equilb. charge state determ., H⁺ secondary ion yield meas. on Au and C target surfaces 7-42757
 ion bombardment of thin films, secondary emission yield, incident charge state depend. 7-59319
 ion laser, perturbations obs. in 0-10 kHz range 7-5871
 ion mobility of Kr²⁺ at 88 K 7-63246
 ions, energy levels, radiation effects and corrections 7-49960
 Kr, elastic scatt. of electrons, phaseshifts and differential cross sections, local-density approx. 7-19695
 laser action, output pulse lengths achieved with electron beam pumping 7-15843
 laser action of Cs in Kr 7-15855
 liquid, electron mobility meas. 7-2614
 matrix isolation of NH(ND), radiative decay and radiationless relax., lifetime meas. 7-10653
 monolayer adsorbed on graphite surface, dislocation interactions 7-2357
 monolayers adsorbed on ionic crystals, critical temps. 7-21666
 monolayers on graphite, domain wall modes 7-38333
 physisorbed films on Pt (111), impurity-quenched orientational epitaxy 7-45003
 physisorbed on Ag (110), adsorption of NO₂, EPR, LEED AES studies 7-53116
 proportional counter avalanche growth, concentration depend. in Kr+cyclohexane mixtures 7-826
 rare gas floating monolayers, dynamics in self-consistent phonon theory 7-2362
 solar Kr abundance determ. from anal. of s-process branching at ⁷⁹Se 7-23990
 solid, electronic sputtering by keV H ions 7-59353
 solid, sputtering mechanism by keV ions 7-59354
 spin-orbit splitting, determ. from ab initio pseudopotential 7-2547
 submonolayer film on graphite, phase diagram, relax. mechanisms, density functional theory calcs. 7-63953
 surface tension at low temps. 7-58566
⁷⁹Kr: a new radionuclide for nuclear medicine 7-40290
 Al-Xe-Kr, ion implanted, bubble growth, lattice parameters, TEM obs. 7-51803
 Ar-Kr liquid mixtures, diffusion coeffs., simulation 7-44344
 CdS:Kr⁺, ion implantation damage 7-26812
 HCl-Kr, mixture, vibr. relax., rate const. meas. 7-15687
 He-Kr⁺ laser operation, DC He and He-Kr discharges in Al hollow cathode tubes 7-10912
 Kr II lines, laser generation in water cooled helical hollow cathode discharge 7-57299
 Kr XXIX 2s²2pⁿ-2s2pⁿ⁺¹ transition meas. 7-880
 Kr XXVIII 2s²2pⁿ-2s2pⁿ⁺¹ transition meas. 7-880
 Kr²⁺, energy level radiation lifetime calcs. 7-25455
 Kr²⁸⁺, electron impact excitation cross sections, CI calcs. 7-36493
 Kr³⁺, spontaneous two-photon decay rates 7-15530
 Kr³⁶⁺, emerging from solid foils, anomalous population of deep capture states 7-42758
 Kr²⁺, effective charge, around 4 MeV per nucleon 7-50297
 Kr-Cd mixture, Cd reson. line broadening, interaction pot. anal. 7-36520
 Kr-halide excimers, interaction with simple cryogenic liquids 7-42776
 Kr-He-H₂ mixtures, self-quenching streamer or Geiger-Muller region 7-19669
 Kr-TEA gas mixtures, emission spectra in proportional counter 7-62226
 Kr+Ar₂, van der Waals bond exchange, mol. beam study, ang. and vel. distrib. 7-23000
 Kr+Ar⁺, charge exchange cross-sections meas. 7-62519
 Kr+Cs⁺, low-energy collisions, absolute total cross section meas., curve-crossing model anal. 7-36749
 Kr+H₂, electron capture cross sections 7-10747
 Kr+H⁺, recoil ion prod. from zero-impact-parameter 7-50310
 Kr+He⁺, analytic repulsive pot. calc. 7-50308
 Kr+Kr ions, quasimolecular Auger emission, impact energy depend. 7-25645
 Kr+Kr²⁺, L-shell ionisation, X-ray yield, threshold behaviour 7-10734
 Kr+Li₂, total integral scatt. cross-sections 7-36728
 Kr+N₂²⁺, energy loss spectra 7-50334
 Kr+Na, fine-struct. branching ratios, meas. 7-15676
 Kr+Xe₂, van der Waals bond exchange, mol. beam study, ang. and vel. distrib. 7-23000
 Kr⁺+H₂(D₂)(HD), spin-orbit state and isotope effects, pot. energy curve, cross sections meas. 7-39859
 Kr⁴⁺+He(Ne), state-selective electron capture, translational energy spectra 7-50337

krypton continued

- Kr₂, diatomic molecule sputtering, independent binary collision approx. 7-59350
 Kr₂, photoionization cross sections of excited states, UPES anal. 7-50241
 Kr₂, radiative lifetime of Al_n states, time-resolved fluoresc. 7-19952
⁸¹Kr, A=89.91 double filter method for meas. 7-40317
⁸⁰Kr, sedimentary processes and metal depth profiles 7-55010
⁸¹Kr, analysis in groundwater using laser resonance ionisation spectroscopy 7-29095
⁸⁵Kr, atmospheric activity monitoring 7-23259
⁸⁵Kr, concentration meas. in atm. around nuclear power reactors 7-23257
⁸⁵Kr, sampling unit for air sample 7-23258
 NO-Kr, van der Waals species, multiphoton ionis. 7-10694
 Na+Rg optical collisions, (Rg = He, Ne, Ar, Kr, Xe), fine struct. branching ratio determ. 7-10704
 Ne:Kr, solid, local phase transition near impurity center 7-26945
 Xe-Kr mixtures adsorbed on graphite, X-ray diffraction studies 7-6966

krypton compounds

- Kr clathrate hydrates, sp. heat, compositions and heat of dissoc. in range 85 to 270K, calorimetric determ. 7-26974
 KrCl laser spectrum, absorption lines and spontaneous emission 7-36947
 KrCl-XeCl, double laser oscill., quenching effect 7-57304
 KrCl* discharge laser, 0.6J output energy 7-43079
 KrF amplifiers, dynamic absorption effects 7-43062
 KrF Aurora laser system, design and performance of large area monolithic electron guns 7-36987
 KrF discharge excimer laser, capacitor-transfer-type with automatic preionisation, efficiency 7-20201
 KrF e-beam sustained discharge laser, efficiency 7-31307
 KrF electron beam pumped laser mixtures, electron density meas. 7-57300
 KrF electron beam sustained discharge excimer lasers, discharge constriction, photodetachment, ionisation instabilities 7-10920
 KrF, excimer laser amplifiers VUV anti-Stokes Raman line generation 7-57450
 KrF excimer laser excitation, low impedance electron beam system 7-36989
 KrF laser cavity, multipass grating interferometer appl. to line narrowing 7-35573
 KrF, laser excitation of luminescence, in KCl:Ti (*Russian*) 7-17340
 KrF laser gain meas. system 7-62717
 KrF laser system, Aurora, for inertial confinement fusion studies 7-15894
 KrF multicomponent laser operating above atm. press. 7-31302
 KrF, picosecond high power laser system characts. 7-62676
 KrF-SF₆ mixtures, excimer mol. excitation in steady-state plasma jet 7-58070
 KrF* amplifiers for UV laser system 7-62724
 KrF* and Kr₂F*, formation kinetics in He/Ar/Kr/F₂ mixtures (*Chinese*) 7-39892
 KrF*, high power subpicosecond laser system 7-62677
 KrXe, excited states, photoionisation and predissoc. 7-19959

Kuhn-Thomas sum rule see *molecular energy levels*

Kurie plots see *beta-decay theory*

kymography see *diagnostic radiography*

Kypoulous method see *crystal growth from melt*

labelled atoms see *radioactive tracers*

labelled compounds see *radioactive tracers*

labelled molecules see *radioactive tracers*

laboratories

see also *acoustical laboratories*

- accreditation in UK 7-14911
 activation analysis, high sensitivity, using underground laboratory for gamma spectroscopy 7-24743
 APL Bioelectromagnetics Laboratory 7-47263
 computerized perception laboratory, problems encountered 7-60008
 course construction 7-18519
 low-level counting, conference, Bratislava, Czechoslovakia (Oct. 1985) 7-24272
 low-level measurement laboratory construction and shielding 7-24335
 neurofunction laboratory for quantitative assessment of movement disorders for spastic cerebral palsy patients 7-3918
 physics laboratory, undergraduate, computer management system 7-48223
 underground laboratory in Freiberg, GDR 7-24334
 underground low background laboratories of the Baksan Neutrino Observatory 7-24333

laboratory apparatus and techniques

- see also *specific instruments and techniques, e.g. balances, plasma probes, vacuum techniques*
 see also *instrumentation; instruments; measurement; student laboratory apparatus; test equipment; test facilities; testing*
 accreditation in UK 7-14911
 active anti-vibration platform, multivariable control 7-29991
 advanced laboratory data analysis systems 7-18767
 analytical software in laboratory research 7-24632
 articulated arm for laser beam delivery, in use and construction 7-50613
 automatic manipulation of microlitre volumes of liquid reagents 7-41362
 cooldown using He or N cooling systems, mass flow requirements calc. 7-56281
 facilities in Milton S. Eisenhower Research Center 7-4827
 frictional sliding guides, dovetail type, construction for use in optical instruments 7-41364
 information management, IBM PC package 7-24631
 IR imaging of camouflage materials, laboratory test facility 7-4850
 magnetometer bench with shield and regulator 7-30049
 MBE simultaneous growth on multiple Si substrates, apparatus 7-7867
 MOCVD laboratory, integrated safety system 7-22528
 robot, decision criteria for purchasing 7-24637
 robot for analytical samples preparation 7-29990
 sample transfer system for surface studies over pressure range 10⁻⁷ to 10⁶ Pa 7-61323
 semi-automatic device for corrosion pit depth and position meas. 7-54035
 separation of fine particles, using rotating tube with alternate flow 7-35502
 shock tube powder dispersal unit 7-56241
 soil testing, BASIC program 7-34735
 solar insolation simulation by compact-source iodide lamps 7-23122

laboratory apparatus and techniques continued

- solar pumps, water cooled, expt. laboratory study of dimensioning principles (*Rumanian*) 7-13930
 solitons, demonstration of behaviour using nonlinear electrical transmission line 7-55932
 sound-reducing enclosure 7-18770
 synergistic relationship between computers and robotics 7-24638
 thermophysical laboratory database formation, using pulse heat method 7-4828
 thermophysical research automation at BSSR Institute of Heat and Mass Transfer 7-4823
 uniaxial pressure device for neutron scattering experiments 7-41399
 workload management system for microcomputers 7-24630

labryrith speakers see *loudspeakers*

Lacertids see *BL Lac-type objects*

ladder filters see *filters*

lakes

see also *rivers*

- acidic precipitation, conf., Muskoka, Ontario, Canada (Sept. 1985) 7-48167
 acidification delay, role of groundwater 7-23247
 acidification meas., integrated palaeoecological approach 7-65658
 acidification of lakes, regional direct distribution model 7-60291
 Adirondack lake, NE USA, Zn water chemistry in acidified lake 7-65656
 air flow changes due to construction of reservoir 7-14346
 Anambra Basin, Nigeria, water supply of Njikoka and Awka areas 7-18218
 Arenal Reservoir, Costa Rica, air flow modification due to reservoir construction 7-14346
 Baikal, USSR, underwater optics (*Russian*) 7-60283
 Balaton Lake, Hungary, subsatellite remote sensing expts. 7-66185
 Balaton Lake region, water quality management, methodology and appl. 7-60281
 Balkhash, USSR, macrocirculation movements arising from seiche action 7-9051
 Banff National Park, Alberta, Canada, lake sediments and Holocene glaciation 7-23721
 blue ice lakes of Greenland, cosmic dust placers discovery 7-14548
 boundary layer breeze over lake and land (*Chinese*) 7-55209
 circulation, trajectory calculation in finite difference model 7-60285
 currents, finite difference method 7-60284
 Dead Sea, high level of lake at 6700 yr BP, salt deposit evidence 7-55087
 drift currents, conservation of vol. global constraints (*French*) 7-47472
 earthquake record in lake sediments 7-3993
 surface energy balance modelling, review 7-23722
 Eyre, surface emissivity, NOAA-7 AVHRR meas. 7-14287
 SW Finland, generalisation of Landsat MSS interpretations of aquatic areas 7-9035
 Finland, lake ice freeze-up and break-up dates rel. to air temp. climate 7-14342
 gravel pits in Rhine Valley north of Strasbourg, hydrological balance with groundwater (*French*) 7-47468
 Lake Hoare, Antarctica N₂ supersaturation in lakewater 7-55103
 Huron, USA, lake levels during Holocene, Lake Nipissing transgression 7-66174
 ice cover on sea and lakes, remote sensing method based on nonthermal radiowave emission 7-66141
 ice pump mechanism for melting of ice and refreezing at a greater height 7-29056
 infiltration through bed of shallow ponds, theory 7-18251
 Integrated Lake-Watershed Acidification Study database documentation 7-46976
 International Association for Great Lakes Research, 29th conference, Scarborough, Ontario (May 1986) 7-18507
 Karewa, India, sediments ¹³C/¹²C and C/N ratios, palaeoclimate characts. determ. 7-4175
 La Grande-2 Reservoir, Quebec, gravity var. due to water transport 7-8793
 lacustrine levels and neotectonic around Lake Faguibine (Mali) (*French*) 7-18164
 Lake Arakhlai, USSR, ice gas inclusions and ice sheet radioluminescent temp. 7-23709
 Lake Norman, NC (USA) application of ecosystem assessment model 7-65654
 Lake Sevan, determ. of organic matter and chlorophyll using laser fluorescence 7-23713
 Lippajarvi, Finland, cultural eutrophication and related restoration problems 7-34559
 McCloud Lake, soft water acidic lake in Florida, ions sources and sinks 7-23763
 Michigan, USA, polychlorinated biphenyls contrib. and losses, atm. and nonatmospheric 7-8459
 Michigan, USA, Southern basin sediments, pollutant polycyclic aromatic hydrocarbons 7-29089
 Michigan, USA, toxaphene pollutant 7-34084
 Michigan, water quality modelling, use of Thematic Mapper data 7-34697
 Mono Lake sediments, California, record of Pleistocene geomagnetic variation and atmospheric ¹⁰Be 7-23842
 Okanagan lake tributaries, BC, Canada, P content of suspended sediment and bioavailability 7-4070
 Ontario, Canada, pollutant transport in coastal zone 7-9047
 Ostrovo (Lake Vegoritis), Greece, model of thermal stratification 7-29116
 periodic wave propagation 7-6230
 pollution, computer assessment of eutrophication countermeasures 7-55112
 Port Hope Harbour, Lake Ontario, sediment quality assessment and benthic community 7-28423
 Poyang Lake, China, Quaternary evol., sediment anal. (*Chinese*) 7-55105
 Qinghai lake, Qi-Lian mountain area, Nanshan, China, lake freezing and weather (*Chinese*) 7-18299
 Qinghai-Xizang (Tibet) Plateau, Quaternary lakes retreat and climatic significance (*Chinese*) 7-55104
 Quebec, Canada, reservoir induced seismicity at several hydroelectric sites (*French*) 7-18118
 radionuclide spills and discharge plumes, Lake Ontario, microcomputer-based model 7-13942

lakes continued

- reservoirs, upwelling response to surface shear stress 7-29088
- resources management master planning, GIS and remote sensing role 7-4072
- river reservoir simulation, linear dynamical system integral invariant approach 7-18214
- seasonal anoxia, actinide release 7-60286
- sediment cores, distributed parameter models for vertical mixing 7-66183
- sediment suspended load in lakes, Landsat remote sensing technique 7-29303
- seismicity induced at hydroelectric reservoirs in Canada (*French*) 7-18118
- shallow, unsteady flow around spherical bodies 7-6227
- smart acoustic current meters, experiences in Lake St. Clair, Canada/USA 7-9255
- Tai, China, storm deposition study 7-55097
- Tatayema volcano, Japan, crater lake sulphur sedimentation history 7-34421
- temperature gradients in lake sediments 7-65993
- thermal stratification, 1D models for lakes and oceans 7-55076
- topographic Rossby waves, 1D models, elongated basins, various lake cross sectional distributions 7-18220
- topographic waves in elliptical basins, analytical solns. 7-66180
- underwater noise due to rain, hail, and snow 7-50830
- unstratified water bodies, mean circulation driven by wind 7-4066
- USA, August 1986 hydrological conditions 7-23718
- USA, October 1986 hydrological conditions 7-55101
- variable head multireservoir power system, optimisation for long term regulation 7-23119
- water level measurement system, management information systems 7-66162
- wind-driven circulation 7-9046
- wind-induced free surface flow anal., 3D, FEM 7-43839
- wind-induced sediment resuspension, model 7-9042
- $\text{Li}_2\text{B}_2\text{O}_7\text{-Li}_2\text{SO}_4\text{-LiCl-H}_2\text{O}$, saturated soln., phase equilibrium, props. 7-40507
- N_2 supersaturation in Lake Hoare, Antarctica 7-55103
- T concentration in lake water, variations 7-55099
- T, reactor produced, migration in Lake Huron 7-13938
- Zn water chemistry in acidified lake 7-65656

Lamb shift

- atomic-level shifts in a squeezed vacuum 7-43032
- atoms, quantum optics absorber theory 7-1046
- excited atom, radiative process fluctuations 7-889
- lasers with plane-parallel resonators, Lamb dip asymmetry 7-5917
- QED, Lamb shift and spontaneous emission without field quantisation 7-19057
- quantised atom, spontaneous emission phenomenon 7-1045
- Rydberg atoms, props. and quantum optics 7-1064
- CO_2 laser, optogalvanic Lamb dip freq. stabilisation 7-31301
- H, Lamb shift, proton mass corrections 7-42510
- H Rydberg atom, Lamb shift in waveguides 7-10458
- H Rydberg states, Doppler-free two-photon spectra 7-10533
- He energy levels, relativistic correction, variational calcs. 7-869
- He-Ne laser stabilised by Lamb dip, emission frequency scatter, causes 7-62667
- ^4He , muonic, Lamb shift at low temps. 7-57192
- Li^{25} ground state, specific mass shift, isotope shift, ab initio calcs. 7-36495
- U^{90+} , He-like, Lamb shift from beam-foil time of flight meas. 7-36551

Lamb waves see surface acoustic waves**lambda point** see superfluid helium-4**laminar flow**

see also laminar to turbulent transitions

- abrupt expansions, planar and axisymm., finite element anal. 7-37428
- air, laminar flow and heat transfer in tube bank, finite element calcs. 7-51313
- air boundary layer, active transition fixing and control 7-31740
- air flow visualisation in clean rooms using laser light sheet method (*Japanese*) 7-57966
- annular duct, convective heat transfer, turbulent to laminar reverse transition (*Japanese*) 7-11543
- annular thermal entry problem, num. solns. 7-16180
- arbitrary obstacle, 3-D boundary layer calc. (*French*) 7-11382
- arch-type vortex, form. behind normal plate in laminar boundary layer 7-26288
- asymptotic laminar boundary layer, mass transfer effects on transient behaviour 7-4323
- atmospheric gliding entry, heating, scaling relations 7-51200
- axisymmetric laminar plume, asymptotic soln. for large Prandtl no. 7-26275
- blunt cone lateral surface heat exchange in boundary layer flow 7-1529
- boundary layer, heat and mass transfer, external turbulence effects 7-1541
- boundary layer, separation point determ. 7-31741
- boundary layer, transverse flow, num. solns. 7-57798
- boundary layer flow, MHD with heat and mass transfer 7-20806
- boundary layer on cylinder, Dorodnitsyn's method calcs. (*Russian*) 7-20685
- boundary layer swirling flow on permeable surface 7-31815
- boundary layers, active stabilisation, turbulence transition, drag reduction 7-20683
- boundary layers on continuous moving surface, momentum and heat transfer 7-63111
- boundary-layer flow past a cylinder with massive blowing 7-31742
- buoyancy-driven convection flow in settling vessels having inclined walls 7-51135
- capillary waves, sheets of fluid, highest waves criteria study 7-43953
- cavity flows, 2D laminar and chaotic mixing 7-16263
- channel, vertical, partially blocked, laminar mixed convection 7-43842
- channel flow with stepwise variations of wall temp., transient forced convection 7-37426
- circular channels, variable cross section, momentum, energy and mass transfer (*Russian*) 7-11549
- circular jet with initially laminar boundary layers, turbulent interaction region 7-11486
- coherent struct. in reattaching laminar and turbulent shear layers 7-51079
- combined free and forced laminar convection in thermal entrance region of channel, Prandtl no. effect 7-37453
- compressible flow, boundary layer excitation by surface heating or cooling, numerical simulation 7-6181
- compressible laminar boundary layer eqn's., stream function numerical soln. 7-6183
- compressible laminar boundary layer flow with heat transfer, quasi-linearization technique 7-26247
- compressible MHD boundary layer at wedge 7-6325
- compressible turbulent flows, 2D, Navier Stokes eqns. solved using finite element method 7-43960
- condensation of flowing vapour on horizontal elliptic cylinder 7-58452
- conical three-D diffusor or confusor, mass transport, numerical soln. 7-26353
- convection, finite-amplitude axisymmetric, between rigid rotating planes 7-26272
- convective gas flow in vertical slots, steady Navier-Stokes eqns. 7-37461
- convergent tube, oscillatory incompressible fluid laminar flow 7-20794
- corner flow, incompressible fluid with suction, heat transfer eval. 7-26277
- Couette flow, axial laminar, characteristics in concentric and eccentric double tube models (*Japanese*) 7-11379
- Couette flow, axial laminar, characteristics in concentric circular double tube model (*Japanese*) 7-11378
- Couette flow, axial laminar, characteristics in eccentric circular double tube model (*Japanese*) 7-11377
- Couette-Taylor instability, hydrodynamic and phase-transition descriptions, expt. study of connection 7-20691
- curved pipes, multiple laminar flows 7-26343
- cylinders subject to transverse streamline flow, turbulent boundary layer separation (*Russian*) 7-11400
- dissipative systems, stationary soliton soln. investig. 7-51034
- duct, cross shaped cross section, parametric study of friction and heat transfer 7-26276
- duct flow, 3D laminar use of curvilinear coordinates 7-16269
- duct flow, heat cond., numerical soln. 7-57790
- duct flow subjected to axial variation of heat transfer coeff. 7-51111
- ducts, finned, triangular, fully developed flow, friction factors 7-63224
- dusty gas, conducting, channel flow, graphical anal. 7-63214
- eddies, large-scale separated, inviscid solutions 7-16189
- electrostatic effect on small perturbation development in the boundary layer on thin airfoil 7-1641
- electrostatic charge generation in the insulating systems of transformers (*Polish*) 7-37431
- end-wall vortex and boundary layer, numerical simulation 7-51181
- equal order velocity-pressure formulation 7-16142
- falling liquid film, heat transfer from horizontal smooth tube 7-63131
- fibre laser Doppler anemometer and boundary-layer meas. appl. 7-37609
- film, pool boiling from curved surfaces, integral method calcs. 7-1568
- film condensation instability at surface of a cylinder 7-37526
- flame, premixed, struct. and extinction limit, Lewis no. effects (*Chinese*) 7-11559
- flow past sudden expansions, Navier-Stokes solns. 7-43846
- flow/pressure meas. using oscillating fluidic LPA 7-37563
- fluid flow past short, heated cylinder, finite element soln. 7-57789
- forced convection inside ducts with temp. periodic variation 7-31736
- forced Rayleigh scattering appl. to hydrodynamic meas. 7-11572
- free convective heat transfer, temp. factor effect 7-63143
- free convective heat transfer in vertical uniform heat flux ducts 7-43891
- front motion, metastability and subcritical bifurcations 7-51056
- fully developed flow in plate fin passages, heat transfer, fin shape effect 7-63110
- gas absorption with instantaneous chemical reaction in a laminar falling film 7-37558
- gas concentration and gradient meas. in photoacoustically perturbed jet 7-37560
- gas velocity imaging using photothermal deflection effect 7-20817
- Görtler vortices spacing on concave walls 7-31812
- gravity current on sloping bottom, rot. flow interaction, shelf wave generation, flow visualisation expts. 7-43947
- gravity influenced free surface flows, iteration method for integral equations (*Chinese*) 7-26246
- hairpin vortices, generation in laminar boundary layer, obs. 7-57796
- hairpin vortices, generation in laminar boundary layers, obs. 7-57797
- heat transfer and flow in curved square channels, elliptic nature, numerical visualisation 7-37432
- Hele-Shaw cells, imperfect, flow properties 7-6184
- horizontal fluid flow near vertical heated surface, mixed convection study 7-51133
- hydrodynamically developed flow through doubly connected ducts 7-51314
- hydrostatic circular thrust bearings: a study of inertia effects 7-51003
- ideal fluid, shear flow stability, effect of stratification 7-26249
- idealised spiral wound membrane module, fluid flow 7-6312
- incompressible 2D boundary layer eqns. similarity solns. 7-51042
- incompressible flow in forward-facing step geometries, Navier-Stokes solns. 7-6180
- incompressible flow with large negative long. press. gradient, friction and heat transfer 7-51047
- incompressible laminar boundary layer, MHD flow past non-isothermal cone 7-11554
- incompressible oscillating flow, mean-parameter modeling 7-63109
- incompressible separated flows, iterative boundary-layer-type solver 7-11380
- interfacial wave generation, investigation through flow visualisation and LDA 7-37438
- jet, in narrow slot at large Reynolds number 7-1599
- jet diffusion flame in co-flowing air stream, turbulence struct. 7-43996
- junction flow, unsteady characteristics, visualisation 7-57799
- laminar boundary layer eqns. fast approx. soln. 7-16155
- laminar plasmatron cathodic jet, optospectroscopic studies 7-26535
- laminarisation and reversion to turbulence of low Reynolds no. flow 7-51039
- line plume, laminar, falling in fluid, stability investig. 7-57807
- liquid film, laminar downflow over cylindrical surface, thermal entry region, heat transfer 7-51096
- liquid flow in coaxial pipes, heat transfer study 7-63137
- liquid metal flow in cylindrical induction pump with inductors producing travelling mag. field, anal. (*German*) 7-63107
- methane-air laminar counterflow diffusion flames, struct., CARS meas. 7-57939
- methane-air laminar diffusion flames, struct. 7-65327

laminar flow continued

laminar flow continued

- methane-air turbulent diffusion flames laminar-flamelet modelling 7-57938
 MHD channel flow through porous medium 7-57932
 MHD laminar flow, vortex behaviour 7-63228
 micropolar fluid in magnetic field, laminar free convective heat transfer, suction/injection effects 7-57824
 mixed convection flow about horizontal cylinder (*French*) 7-1552
 mixed laminar convection in entrance region of inclined rectangular channels 7-63148
 mixing layer developing region, skew laminar wake initial condition 7-31808
 mixing layer in longit. mag. field 7-51048
 momentumless wakes, self-similar solns. 7-51151
 natural convection flow in square enclosure thermal cond. effect 7-51115
 natural convection flow on inclined flat plates with uniform surface heat flux, wave instability 7-20725
 natural convection in an enclosure 7-20710
 natural convection in annuli between concentric and eccentric cylinders 7-37546
 natural convection in square channel, penalty FEM 7-51132
 natural convection on plates with variable surface temp. or heat flux 7-31743
 natural convective flow along isothermal vertical surface, stability 7-31744
 Newtonian fluids in curved rectangular ducts, bifurcation phenomena 7-16154
 non-Newtonian flow in helical channels with constant pitch, var. calcs. 7-43988
 non-Newtonian fluids, 3D boundary layer eqns., similarity solns. 7-37497
 non-Newtonian laminar falling liquid film, thermal entrance region, heating and evaporation 7-51235
 oscillatory rectangular duct flows with turbulence transition, laminar phase vel. distribts. 7-16257
 Oseen flow past sphere as function of Reynolds number 7-51038
 oval twisted tubes, transverse streamline gas flow, characts. (*Russian*) 7-11548
 particle deposition from gas-disperse flow in vicinity of stagnation point 7-63206
 penalty finite-element analysis of coupled fluid flow and heat transfer for in-line bundle of cylinders in cross flow 7-31792
 perturbation propag. in boundary layer on flat channel walls 7-51045
 phase flow regimes, heat exchange with vapour condensation in horizontal tubes 7-31858
 pipe laminar thermal energy region, transient unsteady convective heat transfer 7-31775
 plate, flat, with vectored surface mass transfer, heat transfer characts. (*Chinese*) 7-11398
 plate array aligned in rectangular duct flow, heat transfer, press. drop 7-31788
 plate-fin and tube heat exchanger, fluid flow and heat transfer 7-20703
 porous medium with crack, elastic-hydrodynamic problem of fluid inflow 7-11534
 power-law fluid in horizontal ducts, laminar mixed convection heat transfer 7-37427
 pulsating flow in curved pipes, axial vel. profiles 7-37543
 recirculating flow, vortex simulation 7-57851
 rectilinear pipes with multiply connected cross sections, laminar vel. distribts. 7-57920
 rotating concentric cylinders, same or opposite directions, turbulence and vortices 7-16255
 separated laminar natural convection above horizontal isothermal square cylinder 7-31783
 shear layer instabilities obs. in flow through axisymmetric sudden expansions 7-11376
 ships, flow around aft section, static pressure meas. 7-37594
 slurries, laminar pulsatile flow, numerical study 7-51035
 space-charge flow form., relativistic theory 7-51040
 stability criteria and lower critical Reynolds number 7-1530
 stagnant zone, form. at different Bernoulli numbers, nonlin. num. soln. 7-51241
 steady flow dispersion, gently curving tube, low Dean number, Monte Carlo and num. solns. 7-44053
 steady laminar flow through a twisted pipe of elliptical cross-section 7-37429
 steady liquid compound jet flow, num. treatment 7-37506
 steady-state freezing of liquids in laminar flow between two parallel plates 7-51036
 stirrers and induction pumps, liquid metal velocity distrib. effects on electrodynamic forces (*Polish*) 7-63231
 Stokes flow, chaotic advection 7-31737
 stratified fluids, stationary closed streamlines, laminar flow theory of vortices 7-6267
 stratified shear layer, stability 7-43849
 streamline routing through fracture junctions 7-55028
 supercritical fluid, diffusion and mass transfer 7-63106
 supersonic laminar flow with strong viscous-inviscid interaction 7-51212
 surfactant systems, drag reduction, physico-chem. props., rheology 7-43992
 Sutterby fluid, steady laminar flow in rectangular duct inlet region 7-43990
 swirling jet, self-similar solns. 7-51253
 symmetric sudden expansion flow boundary layer eqn. limitation 7-16156
 three-dimensional boundary layer eqns. in streamline coordinates, numerical soln. 7-51041
 toluene, laminar flow, heat transfer in thermal inlet region 7-43895
 twisted circular-sector ducts, fluid flow and heat transfer anal. 7-11374
 unsteady free-convection flow past accelerated plate, skin friction 7-4321
 unsteady laminar forced convection from impulsively started sphere, temp. field 7-43852
 vapour condensation in cylindrical borehole, heat transfer 7-11408
 vapour flow characts. of slender cylindrical heat pipes 7-11375
 vapour flow in low temp. heat pipes, effect of evaporation and condensation zones 7-63136
 velocimetry in laminar and turbulent flows using the photothermal deflection effect with a transient grating 7-31901
 viscoelastic fingering, time effects 7-57800
 viscoelastic fluid, laminar flow in curved pipe of circular cross section with varying curvature 7-16215
 viscous incompressible flow in a narrow channel with one free wall and fluid supply through a porous insert 7-1636

laminar flow continued

- viscous incompressible laminar flow, drag reduction, optimal control 7-57794
 viscous laminar small Reynolds-number flow over wavy walls 7-43840
 volume cycling in tapered pipe, dye streak meas., Eulerian and Lagrangian velocity profiles 7-44051
 water, pure and saline, thermal buoyancy induced flow stability 7-1532
 water flow in capillary, surface and kinetic energy, laboratory exercise 7-18528
 wing, rotating, laminar boundary layer eqns. 7-11381
 wing, stationary turbulent boundary layer anal. 7-11397
 CO₂-H₂O-N₂ laminar and turbulent mixing, vibr. relax. 7-11459
 GaAs, LPE from soln. in laminar flow, high growth rates 7-33605
 GaAs, MOCVD, gas phase depletion and flow dynamics in horizontal reactors 7-17433
 H₂-O₂-N₂ flames, one-dimensional simulation, mathematical and numerical aspects 7-39893

laminar to turbulent transitions

- annular duct, convective heat transfer, turbulent to laminar reverse transition (*Japanese*) 7-11543
 boundary layer, wall vibr. effect 7-43880
 boundary layer turbulence transition mechanisms interchange 7-57795
 boundary layers, surface roughness effects and transition modelling 7-31769
 boundary layers transition on cone 7-31745
 boundary-layer transition, roughness trips with rows of spherical elements 7-51050
 cavity flows, 2D laminar and chaotic mixing 7-16263
 circular cylinder in cross flow, tripping wire effect on boundary layer transition 7-43847
 circular cylinder in fluid flow, turbulence transition, wakes 7-6191
 coherent struct., spatial details 7-43870
 compressible boundary-layer transition, first and second role modes 7-11452
 convection transition, 3D spectra evolution 7-57831
 cubic cavity, convection at high Rayleigh number, inclination influence 7-16178
 distributed roughness effect on transition enhancement 7-37433
 external turbulence effect on boundary layer flow in nozzle 7-1542
 flow around a circular cylinder, oil-flow photographs anal. 7-43848
 heat transfer, local coefficients from staggered bundles of rough tubes in crossflow, expt. 7-43894
 intermittent chaos, global spectral structs. for periodic laminar motions with turbulence 7-41271
 intermittent flow, 2-fluid model of acoustic noise 7-11212
 laminar boundary layers, active stabilisation, turbulence transition, drag reduction 7-20683
 laser-induced convection, instability, laminar to turbulent transition 7-37464
 meandering rivulet flow transition in vertical parallel plate channels 7-16268
 MOVPE growth, flow patterns in vertical reactors 7-22535
 Newtonian liquid-gas stratified flow, interfacial level gradient effects 7-37509
 oscillation excitation is supersonic boundary layer by external acoustic field 7-51046
 oscillatory rectangular duct flows with turbulence transition, laminar phase vel. distribts. 7-16257
 pipe flow, sinusoidal flow modulation 7-16262
 sensors with hydrodynamic smoothing for conductometry of turbulent flows 7-57961
 separation flow around a cylinder near a plane screen, num. modeling 7-63123
 steady-state flow in channels, heat transfer calcs., three-parameter model 7-51123
 supersonic turbulent flow, rapid expansion, bulk dilation role 7-51087
 thermal lens oscills. on liq. surface produced by laser beam 7-11403
 transition via spatiotemporal intermittency 7-43861
 viscous fluid, flow transition, Orr-Sommerfeld eqn. soln. (*Russian*) 7-43850
 vortex streets, circular cylinder wake, effect of cylinder vibr. 7-51173
 wedges with leading edge sweep, heat transfer, premature transition 7-6211
 wing, stationary turbulent boundary layer anal. 7-11397

laminates

- see also delamination*
 beams, symmetric laminated, optimal design considering damping 7-31639
 cellulose fibre reinforced polyester, prep., and props. 7-3265
 centrally notched laminates, residual strength determ. (*Chinese*) 7-13557
 composite, stress singularity by FEM 7-1401
 composite laminates, fatigue and residual strength 7-44672
 composite laminates, first ply failure anal. 7-44670
 composite laminates, with matrix cracking and interior delamination, stiffness props. 7-44669
 composite materials, method for predicting nonlinear viscoelastic props. 7-63020
 composite plate theory, laminated with improved in-plane response 7-37354
 composite wedges, laminated, stress singularities 7-43659
 composites, compressive failure modes 7-6717
 contactless testing, RF method, linear antennas impedance meas. 7-54054
 cracked cross-ply laminates, stiffness reduction anal. 7-44644
 cracked-lap shear specimen thickness for interlaminar fracture toughness determ., delamination vs. adhering failure 7-1510
 cross-ply flat specimens, interlaminar edge stress analysis 7-57694
 cross-ply plates, micromech. initial failure anal. 7-62975
 curvilinear structure, stress distribution (*Russian*) 7-63012
 dielectric, parameters determ. near min. of absolute refl. coeffs., variable freq. radio-interference method 7-65264
 dielectric with losses, parameters determ. in broad freq. range, inspection method 7-65263
 digital image correlation methodology use for deform. quantification 7-59718
 dynamic moire interferometry of stress wave propag. 7-59717
 elastic, twinned crystal, linear response 7-43665
 end-notch flexure specimen, mode II interlaminar fracture toughness, finite element anal. 7-1509
 failure in compression, surface delamination along macrocrack 7-6155

laminates continued

- ferrous laminated composite with unique microstruct., development by C diffusion control 7-17501
- fibre reinforced composite, struct.-performance maps 7-17574
- fibre reinforced composite laminates, yield and ultimate strengths 7-22785
- fibre reinforced composites, strength of pin loaded holes, effect of pin load distrib. 7-1403
- fibre reinforced laminate plate, wave propag. 7-63051
- fibre reinforced laminates, transverse ply cracking strains 7-39637
- fibre reinforced polyester resin, glass sphere filled, Young's and flexural moduli 7-3350
- fibrous, energy dissipation properties, anisotropy 7-6143
- flaw detection, signal recognition automation using linear prediction model 7-3561
- flaws, pulsed photothermoelastic quantitative eval. 7-54048
- flexure specimen, end-notched, for mode II testing, design and anal. 7-51005
- glass and C fibre reinforced epoxy, cross-ply cracking 7-39617
- glass fibre reinforced polyester laminate, hydrothermal ageing, degradation, US obs. 7-13708
- glass fibre reinforced polyester laminates, fatigue tests 7-3428
- glass-copper laminate, one-dimens. unsteady heat cond., appl. to thermal diffusivity meas. 7-31624
- graphite fibre reinforce epoxy, holographic investigation of stressing techniques for detecting flaws 7-59732
- graphite fibre reinforced borosilicate glass matrix composites, thermal expansion, laminate theory anal. 7-52087
- graphite fibre reinforced epoxy, dynamic moire interferometry of stress wave propag. 7-59717
- graphite fibre reinforced epoxy, holographic interferometry analysis of bending rigidity loss 7-59733
- graphite fibre reinforced epoxy, NDT by OTDR in embedded optical fibres 7-28255
- graphite fibre reinforced epoxy, subjected to cyclic thermal loading, damage-induced prop. changes 7-46600
- graphite fibre reinforced epoxy and polyamide matrix composites, thermal expansion, laminate theory anal. 7-52087
- graphite fibre reinforced epoxy laminates, dynamic response at high shear strain rates 7-3371
- graphite fibre reinforced epoxy laminates, fatigue damage mechanisms and residual props. 7-44671
- graphite fibre reinforced epoxy laminates static or fatigue loading, fracture surface anal. (German) 7-22826
- graphite fibre reinforced PEEK, quasi-isotropic laminate, shear strain meas. by moire interferometry 7-65253
- graphite fibre reinforced polyethersulphone, laminates, temp.-dependent behaviour of matrix 7-17620
- graphite fibre reinforced polyimide, laminates, temp.-dependent mech. behaviour of matrix 7-17620
- holographic investigation of stressing techniques for detecting flaws 7-59732
- hyperelastic multilayered bodies, micromorphic effects, nonstandard anal. 7-56037
- layered media with dissimilar materials, elastoplastic anal. 7-26160
- mechanics of damage and fatigue, conf., Haifa, Israel (Jul. 1985) 7-48139
- membranes consisting of alloy and oxide layers, non-steady-state H permeation 7-6889
- metal-polymer two-layer plates under bending load, strength and stiffness calc. 7-57713
- metallic glass reinforced Al composite fabrication by multi-lamina explosive compaction 7-59482
- multilayer composite material for X-, γ - and β -ray detector windows 7-5570
- multilayered plate, acoustic material signature calc. 7-37300
- Neoprene/styrene-butadiene rubber laminates, water permeation study 7-12374
- panel, in situ testing of mech. props., flexural wave phase changes obs. 7-63095
- plastic composites, layered, periodic necking instability 7-43709
- plate, multilayer reinforced, with through crack, stress state and limiting equil. 7-11344
- plate/shell element, field-consistent four-noded laminated anisotropic 7-62983
- plates, anisotropic laminated elastic, finite deflections 7-37336
- plates, first-ply failure analysis of composite laminates 7-63053
- plates, laminated, boundary layer approach to free-edge stress concentration 7-26158
- plates, laminated, non-classical approx. bending theory (Chinese) 7-43692
- plates, laminated composite, 3D hybrid stress isoparametric element 7-56020
- plates, laminated thick composite, buckling, hygrothermal effects 7-11321
- plates, rectangular laminated composite, dynamic stability analysis using finite strip method 7-6118
- plates with metal bearing layers, use in compressed elements, equil. mode stability 7-31667
- rare earth aluminium RAI_2 layered structural sintered composite, mag. entropy 7-59016
- shell, applied theory development 7-1413
- shell, cylindrical, three-layer, spectrum of regions of dynamic instability 7-16085
- shell, flat, multiply, nonlinear variant of elasticity theory 7-1414
- shell, inclined Timoshenko-type, triangular finite element construct. 7-1415
- shell, multilayered, coiled, unidirectional buckling 7-16088
- shells, layered composite, thermoelasticity 7-31649
- shells, three-layered cylindrical, stability under external press. on basis of 3D formulation 7-31666
- shells laminated, buckling problems, nonlinear first order theory (German) 7-20614
- stress state analysis using orthotropic photoelasticity 7-57778
- textile structural composites, 3D, fibre inclination model 7-32545
- two-layered, subjected to impact load, dynamic response (Japanese) 7-50946
- Al-epoxy laminated composites, US dispersion studies 7-26871
- C fibre reinforced epoxy, laminates, quasi-isotropic, response to biaxial stress 7-33732
- C fibre reinforced epoxy laminates, matrix splitting, K_1 - K_2 interaction (German) 7-22829

laminates continued

- C fibre reinforced epoxy resin laminates, curing characts., fibre kinking 7-39474
- C fibre reinforced plastic laminates, ply failure under moisture and temp. influences (German) 7-22744
- C fibre reinforced plastic laminate; impeding edge-delamination development effect on tension-tension loading (German) 7-22827
- C fibre reinforced plastic, damage states, US and acoustic emission study (German) 7-22828
- C fibre reinforced thermoplastic laminates, compressive strength 7-39580
- C fibre/glass fibre reinforced polyester hybrid laminates, impact and perforation props. (Japanese) 7-13569
- Fe/Cu microlaminate condensates, creep and struct. investig. (Russian) 7-33749

lamps

- see also discharge lamps; filament lamps; light sources
- ophthalmological laser slit lamp 7-47202
- radiating atoms on lamp filament, photography (French) 7-37080

Landau levels

- 2D systems, proceedings of Winter School, Mauterndorf, Austria (Feb. 1986) 7-48131
- broadening, 2D electron gas in strong electric field 7-52455
- disordered two-dimensional system in strong magnetic field and random potential, conductivity calcs. 7-58788
- electrical conductivity, interacting 2D electrons in a mag. field 7-52573
- electron gas, 2-D, background density of states between Landau levels 7-2456
- electron gas, 2D, density of states for high Landau levels and random potential 7-58753
- electron gas, galvanomag. props., interaction effects, applied electric and mag. fields 7-52477
- electron plasma, pure, strong mag. field states 7-45185
- fermion system, two component, fractional quantum Hall effect, excitation spectrum 7-52656
- fractional quantum Hall effect, energy gaps 7-27272
- fractional quantum Hall effect, quasiparticle states 7-21979
- fractional quantum Hall effect, theory 7-52658
- fractional quantum Hall states, hierarchy termination and impurity effect scaling 7-21978
- fractional quantum Hall states, size depend. in small system calcs. 7-2517
- free electron distrib., parabolic band, Landau level population inversion in crossed elec. and quantising mag. fields 7-38472
- integer quantum Hall effect, theory 7-52824
- localised Landau orbits, completeness 7-7133
- magnetised plasma, neutron excitation of Landau and collective modes 7-7134
- quantum Hall effect, fractional, spin-reversed quasi-particles, many-body approach 7-2629
- quasi 2D quantum wells, linear and nonlinear electrical conduction 7-64331
- semiconductor, excitonic trions, Landau level oscills., mag. field effect study 7-21820
- semiconductor heterostructures, electronic states, valence subbands 7-7307
- semiconductor superlattice, 3D anisotropic system, surface states and quantum Hall effect 7-38700
- semiconductors, photoelectrons subjected to parallel elec. and quantising mag. fields 7-64280
- (TMTSF) $_x$ Bechgaard salts, mag. field induced SDW phases 7-45703
- two dimensional, electron gas, partially occupied Landau level, dielec. const. RPA calcs. 7-64139
- two-dimensional polaron, cyclotron reson. spectrum calc. 7-45175
- AlGaAs-GaAs heterostructures, dissipationless quantum Hall effect, size-depend. quantised breakdown 7-45469
- GaAs $n^+n^-n^+$ structs., quasi-elastic inter-Landau-level scattering processes 7-17086
- GaAs/Si/AlGa $_{1-x}$ As quantum wells, photolum. studies 7-39178
- n^- -GaAs/AlGa $_{1-x}$ As/ n^+ -GaAs capacitors, accumulation layers magnetotunnelling obs. 7-12880
- GaAs-AlGa $_{1-x}$ As heterojunctions, subband Landau-level spectroscopy 7-21996
- GaAs-AlGa $_{1-x}$ As heterostructures, voltage-controlled dissipation in the quantum Hall effect 7-27393
- GaAs-AlGa $_{1-x}$ As multiple quantum well, electron-phonon interaction 7-2684
- GaAs-AlGaAs DH injection laser, optical and transport props., emission energy shift, threshold current meas. 7-1101
- GaAs-AlGaAs heterostructures, density of states of Landau levels 7-52822
- GaAs-AlGaAs modulation-doped quantum wells, photolum., giant oscillations, influence of mag. fields 7-7751
- GaAs-Ga $_{1-x}$ Al $_x$ As quantum wells, interband photocond. and excitonic Landau level transitions in mag. field 7-27390
- GaAs-GaAlAs heterojunction, 2D system, high order fractional quantisation obs. 7-27397
- GaAs-GaAlAs heterojunctions, fractional quantum Hall effect obs. 7-52821
- GaAs-GaAlAs superlattice, mag. levels 7-52476
- GaAs-GaAlAs superlattices, density of states of Landau levels, sp. ht., magnetisation meas. 7-52823
- Ga $_{0.3}$ In $_{0.7}$ As-InP strained layer superlattice, inter-band magneto-absorption 7-45998
- Ga $_{0.47}$ In $_{0.53}$ As/Al $_{0.49}$ In $_{0.51}$ As quantum well, interband magnetoabsorpt. meas., effective mass determ. 7-17088
- Ga $_{0.47}$ In $_{0.53}$ As-InP heterojunction, chem. beam epitaxy grown, 2D electron gas 7-12803
- Ge, heavy holes, Landau level spectrum, optical gap form. 7-45191
- Ge light hole Landau level inversion, light amplification in crossed elec. and mag. fields 7-31293
- H-like systems in arbitrary mag. fields, ground and excited states wave functions expansion calcs. 7-2519
- Hg $_{0.8}$ Cd $_{0.2}$ Te, low temp. hot electron energy relax. time in extreme quantum limit mag. fields 7-33035
- Hg $_{1-x}$ Mn $_x$ Te LPE crystals, magnetophonon reson. recomb. with phonon emission 7-63755
- Hg $_{1-x}$ Mn $_x$ Te, magnetoresist. meas., effect of valence band spectrum quantisation at low temps. 7-52653
- InAs/GaSb quantum well, 2D electron gas, cyclotron reson. oscills. meas. 7-38944

Landau levels continued

- InP n^+n^+ struct., space-charge limited magnetoconductivity 7-45472
 InSb, resonant states, strong mag. field, Coulombic impurity pot. 7-32925
 PbTe-PbEuTeSe multiquantum wells, electron-hole recomb., photolum. 7-13216
 Si (100) MIS structs., state density of 2D electrons in transverse mag. field 7-12870
 Si, excitonic absorpt., MCD spectra, low mag. fields 7-27257
 Si MIS structs., quantum Hall resistance, localised and mobile electron states 7-38744
 Si, MOS inversion layers, scaling relation of cond. in strong mag. fields 7-64352
 Si n-type (100) inversion layers, valley splitting enhancement by lossless edge currents 7-7395

Lande g-factor *see g-factor***Lande splitting factor** *see g-factor***Langmuir-Blodgett films**

- acentric mol. assemblies, fabrication, structural and electrical characts. 7-58648
 arachidic acid, Langmuir-Blodgett mono-mol. layers, surface-enhanced SHG 7-17355
 arachidic acid Langmuir-Blodgett films, SIMS depth profiling 7-59356
 arachidic acid Langmuir-Blodgett multilayers, profile structs., X-ray diff. studies 7-21630
 cadmium arachidate, Langmuir-Blodgett films, angle-resolved photoemission with synchrotron radiation (*Japanese*) 7-3152
 cadmium arachidate, Langmuir-Blodgett multilayers, order-disorder transitions, Raman spectra 7-53309
 cadmium arachidate, struct. disorder and polymerisation competition at elevated temp., IR spectra obs. 7-46163
 cadmium arachidate Langmuir-Blodgett films, elastic props., Brillouin scatt. study 7-32885
 cadmium stearate Langmuir-Blodgett films on sapphire, thermal disordering, optoacoustic IR spectra anal. 7-52236
 copper phthalocyanine Langmuir Blodgett film/GaAs MIS devices 7-55918
 cyanine dye J aggregates, Langmuir-Blodgett films, multiple wavelength optical recording 7-50666
 cyanine dyes, Scheibe aggregate monolayers, without long alkyl chains, spectra, dichroism 7-59221
 deposition system, hydraulic with adjustable speed 7-59415
 dihematoporphyrin ether, cancer therapy drug, Langmuir-Blodgett films at water-air interfaces 7-65699
 dye deposited on glass and Ag substrate, nonlinear Langmuir-Blodgett films, struct. and optical props. 7-53259
 dyes, mol. sublattice form., linear Stark effect study 7-57108
 fatty acid Langmuir-Blodgett monolayers, structural study of conducting defects 7-52325
 hemicyanine dye monolayer, surface plasmon enhanced SHG 7-25881
 henecosulfurundecanoic acid, multilayered Langmuir-Blodgett films, prep. 7-6996
 hydrophobic water-stable monolayers on mica, interaction meas. 7-32759
 layered structures, Raman and IR spectroscopy 7-3059
 linear Pockels response of a monolayer Langmuir-Blodgett film 7-13131
 long-chain amphiphile on solid substrate, thermally induced disorder, Fourier transform IR spectra 7-12467
 merocyanine dye films, optical third-harmonic generation 7-20329
 merocyanine dyes, J aggregate form. in mixed monolayers, visible spectra and surface pressure-area isotherms anal. 7-31059
 merocyanine Langmuir-Blodgett layers, optical props. 7-17351
 1-methyl-1'-octadecyl-2,2'-cyanine perchlorate dye, Langmuir-Blodgett multilayers, Ag/glass substrate, distance depend of SERS 7-32801
 microstructure of organic mono- and multilayers 7-52296
 molecular electronics materials, Langmuir-Blodgett technique, microlithography resist appls. (*Japanese*) 7-6964
 molecular films, small angle X-ray studies 7-58620
 monolayer films, exposed mol. ends, Penning ionis. electron spectrosc. 7-63991
 monolayers, phase transitions, fluoresc. microscopy 7-32867
 multilayer thin films, overlayer-induced surface monolayer ordering 7-32868
 optically nonlinear, hemicyanine Langmuir-Blodgett films, electron diff. study 7-51584
 organic Langmuir-Blodgett films, molecular design (*Japanese*) 7-21742
 PMMA-merocyanine dye Langmuir-Blodgett multilayer mixtures, deposition studies, SHG obs. 7-58715
 polydiacetylene Langmuir-Blodgett films, ion beam irradiation 7-6690
 polymer films as nonlinear optical materials 7-37021
 pyroelectric devices, optimisation of thermal performance 7-59155
 α -quinque thiophene-stearic acid: I Langmuir-Blodgett films, elec. cond. 7-33106
 SEM monitoring of internal structure 7-45015
 stearic acid mono- and bi-layers on Al and Au, refl.-absorpt. IR spectra, order-disorder transitions 7-46165
 stearic acid-Langmuir-Blodgett films, boundary lubricant efficiency (*Japanese*) 7-8118
 surface EM wave FTIR spectroscopy of very thin films 7-41506
 surface FTIR-ATR spectroscopy, lower limit of thickness of measurable surface layer 7-41508
 surface study using electron microscopy and X-ray reflectivity 7-58677
 surface-plasmon-polaritons, antisymmetric coupled, in Langmuir Blodgett-Ag-Langmuir Blodgett struct. 7-22364
 TCNQ salt, conducting Langmuir-Blodgett film, electronic transport props. 7-38782
 TCNQ salt, mixed-valence, conducting Langmuir-Blodgett films form. (*French*) 7-52323
 thermal desorption, quartz-crystal microbalance studies 7-63949
 2-tricosenoic acid, guided optical waves in ATR geometry 7-31462
 ω -tricosenoic acid Langmuir Blodgett film/GaAs MIS devices 7-55918
 ω -tricosenoic acid Langmuir-Blodgett films, RHEED 7-16887
 2-tricosenoic acid multilayers, optical const. 7-22372
 trough with four movable barriers for film deposition 7-59416
 Al-Langmuir film-SnO₂, photovoltage spectra 7-64354
 GaAs/Langmuir-Blodgett MISS devices, switching characts. 7-38751

Langmuir probes

- see also plasma diagnostics*
 actively cooled Langmuir probe for long pulse appls., design and fabrication 7-26517
 Alcator C edge plasma, directional asymmetries 7-63300

Langmuir probes continued

- aperture limiter shadow of T-10 tokamak, Langmuir probe meas. 7-51394
 automatic Langmuir probe plasma diagnostic 7-58063
 boundary parameter meas. using Langmuir probes in JET 7-51395
 calorimeter probe heads in TFTR, use of graphite 7-1768
 cylindrical Langmuir probe technique for plasma parameter measurement in a medium density discharge 7-11782
 DENSEPACK array of Langmuir probes, Alcator C Tokamak fusion expt. appl. 7-20940
 electrical characts. of Langmuir probe moving in field of highly charged body 7-37744
 elementary process determ. by Langmuir probes 7-20945
 ion-acoustic wave reflection from discharge-tube walls, expt. obs. 7-26411
 Janus, a bidirectional, multifunctional plasmadiagnostic for Alcator C Tokamak 7-1739
 JET, edge phenomena, probe diagnostics 7-63334
 JET tokamak, single Langmuir probes, spurious values of electron temp. 7-49677
 magnetically confined vacuum arcs, plasma parameter meas. 7-32163
 non-neutral ion plasma generation and diagnostics 7-51513
 plasma channel, relativistic electron beam propagation, ion density model, Langmuir probe and beam transport meas. 7-31997
 plasma deposition, negative ion form. 7-7887
 plasma pot. calcs. from meas. Langmuir probe characts. 7-18306
 Plasma-Materials Interactions Test Facility electron cyclotron resonance microwave plasma system 7-51477
 probes for edge plasma studies in TFTR 7-1779
 reversed field pinch, behaviour of peripheral plasma 7-51509
 RF etching plasma parameters and the use of Langmuir probes 7-32100
 TEXTOR, plasma-wall interactions, heating, review 7-63289
 tokamak plasma scrape-off layer particle flux penetration 7-16298
 trifluoromethane plasma in planar reactor, probe meas. 7-37750
 Ar, flowing afterglow, metastable influence, expt. apparatus description 7-58073
 Ar plasma, DC pulse generation, creation and stabilisation processes study 7-32098
 H⁻ tandem multipole ion source, Langmuir probe meas. 7-10336
 H⁻ tandem multipole ion source, plasma parameter meas. by Langmuir probe anal. 7-10339
 H⁻ tandem multipole source, plasma parameter meas. using Langmuir probe technique 7-10338
 He⁻ tandem multipole ion source, Langmuir probe meas. 7-10336
- lanthanides** *see rare earth metals*
lanthanons *see rare earth metals*
lanthanum
see also nuclei with
 atom, fast electron bremsstrahlung cross sections 7-36780
 atom, resonant UPS, 5p valence band interaction, photoionisation cross section 7-15564
 crystal electronic struct., electron-phonon interactions and superconducting transition temp. calcs. (*Chinese*) 7-27261
 epitaxial layer on W field emitter, surface self-diffusion studies 7-32702
 ions, Ne-like, precision wavelength meas. in X-ray spectra 7-36525
 L_{γ2,3} satellite, X-ray emission spectra anal. 7-36523
 oxidation kinetics 7-65190
 X-ray M_{4,5} fluorescent emission spectrum, hole-induced shakedown processes. 7-53450
 Ba_{0.1}Fe_{1.1}Ca_{0.8}Fe₁₂O₁₉-La₂O₃, hexagonal ferrites, influence of electric field on struct. and props., Mossbauer study 7-7616
 CeO₂:La³⁺, grain boundary effect, elec. meas. 7-38248
 LaNi₅ oxide surface layers, H₂ adsorpt. kinetics 7-32833
 La₂O₃, reflection spectra, 4d ionisation threshold 7-46234
 Nb-La-Nb epitaxial film sandwiches, metastable phases 7-32857
 PbTiO₃:La piezoelectric ceramics, vacancies, positron lifetimes 7-37980
 UO₂-La(OH)₃, radionuclide coprecipitation solid solution formation 7-5475
 YIG:La-Ga-YIG:La double layered film, different magnetisation and anisotropy, magnetostatic mode spectra 7-64498
- lanthanum alloys**
see also lanthanum compounds
 Al-Ba-La system, phase equilb. study 7-3279
 Al-Fe-Ce-La-Nd-Rr alloys rapidly quenched, positron annihilation studies 7-46184
 Al-Fe-Mischmetal, wear, comparative investigs. and prep. method role 7-13605
 Al-La, oxidation kinetics 7-65190
 Ce_{0.8}La_{0.2}Al₃ nonmagnetic Kondo lattices, coherent regime, Hall effect temp. depend. meas. 7-52582
 Ce₂La_{1-x}Al₃ solid solns., magnetic and thermoelectric props. 7-7212
 Ce₂La_{1-x}Cu₆ electronic states, resonant photoemission study 7-53496
 (Ce_{1-x}La_x)In₃ antiferromagnetic alloys, thermoelec. power meas., band gap form. 7-38543
 Cr-Os-Ta-La system, anomalous elastic and thermal props. in region of phase transform. (*Russian*) 7-53783
 Cu-La, thermodynamic props. rel. to glass forming ability 7-38204
 Fe-La amorphous alloys, high-field susceptibility and Curie temp. 7-58989
 Gd_{2-x}La_xAl₃ pseudobinary cpd., mag. props., disorder effects 7-7523
 Gd₂La_{0.5}-Co₂B₁₀ mixed glasses, mag. props., phase transitions, microstruct. effects 7-64465
 Ir-La, cathodes, thermal emission and sublimation 7-13317
 La-Al, glass, short-range struct., pulsed neutron and X-ray diffraction 7-1912
 La-Mg alloy, H adsorpt., H storage investig. 7-52241
 La-Mg system, phase equilb. study 7-26935
 La-Si, glass, short-range struct., pulsed neutron and X-ray diffraction 7-1912
 LaAg, nonmag. cpds., transport props. and electronic struct. 7-2575
 La_{100-x}Al_x metallic glasses, electron transport 7-45265
 LaAl(Si)(Ag)(Au) nonmagnetic metallic glasses, negative TCR and electronic struct. studies 7-52562
 LaB₆, Fermi surface, 2D angular correlation of positron annihilation radiation 7-39241
 LaBe₁₃, band struct. calc. 7-32905
 La_{2-x}Ca_xMg₁₇, H₂ storage appl. 7-40052
 La₂Ce_{1-x}B₆, Zeeman splitting, thermodynamics of Coqblin-Schrieffer model 7-58783
 (La_{1-x}Ce_x)₂Fe₁₄B rapidly quenched ribbons, hard mag. props. 7-27549

lanthanum alloys continued

- La_{1-x}Ce_xNi, Kondo lattice form., elec. resist. and susceptibility meas. 7-21899
 La(Cr,Mn_{1-x})₂Ge₂, layer struct. intermetallic cpd., mag. props. comp. depend. studies 7-7489
 La(Fe₂Al_{1-x})₁₃, mag. props. determined via neutron scatt. and Mossbauer spectroscopy 7-2820
 La_{0.9}Nd_{0.1}Ni_{2.5}Co_{2.4}Si_{0.1}, electrode, storage capacity investig. 7-33946
 LaNi₅, adsorpt. rate at H₂-LaNi₅ interphase, diffusion coeff. eval. 7-32696
 LaNi₅, amorphous, short range order 7-37858
 LaNi₅, anisotropic H migration, deposition potentials, hardness, brittleness meas. 7-6873
 LaNi₅, diffusion of H and D, temp. depend. 7-6874
 LaNi₅:H films, resist. rel. to hydrogenation 7-58910
 α-LaNi₅-H, multiply cycled, inelastic neutron scatt. 7-32835
 LaNi_{4.77}Al_{0.22}-LaNi₅, hydride chem. heat pump, thermodynamics 7-13926
 LaNi_{4.7}Al_{0.3}H_x-n-undecane suspension, H₂ absorpt. kinetics 7-33966
 LaNi₅-Fe_x, spin freezing props. 7-64464
 La₁₁Ni₄Ge₆, cryst. struct., trigonal-prismatic coordination of atoms 7-21159
 LaNi₅H₂O, dissociation press., O content depend. 7-63825
 LaNi₅H₂-n-octane suspension, H₂ absorpt. kinetics 7-33966
 LaPd₃, electronic structure and intrinsically selective absorption 7-38444
 LaPd₃Si₂ single crystal, Czochralski growth, charactn. 7-53557
 LaPd₃Si₂(Rh₂Si₂) ternary compounds, superconductivity 7-12901
 LaRh₂Si₂ single crystal, Czochralski growth, charactn. 7-53557
 LaRuSn₃, cage-like void structures (*German*) 7-32365
 Ni-Al-La, defect form., disordering, strengthening effect of La addition 7-22708
 Sn-La binary system, phase diagram and equilib. 7-7961
 Sn(La-Gd)₃Rh₂Sn₁₂ crystals., structural distortion and chem. bonding, X-ray diff. studies 7-1947
 U-La_{1-x}-Te single crystals., elect. resist. temp. depend. Kondo effect and ferromagnetic ordering 7-13119

lanthanum compounds

- see also lanthanum alloys
 fluorozirconate glass, chem. durability, reaction with water 7-39682
 X-ray absorpt. edges, many body effects, determ. 7-64789
 Al₂O₃-La₂O₃-NiO(CuO), phase transformations and solid soln. form. 7-2176
 Ba-La-Cu-O system, possible high T_c superconductivity 7-2770
 BaLaCuO, magnetic susceptibility meas., indication of high-T_c superconductivity 7-58953
 Ba_{1-x}La_xF_{2+x} solid solutions, thermally stimulated depolarisation currents 7-53226
 BaLaFeO₄, layered cpds., bidimensional mag. coupling, Mossbauer spectra 7-27637
 BaLaFeO₄, prep. and characterisation 7-1987
 BaLaGa₃O₇, luminescence props. 7-27768
 BaLa₂O₄-TiO₂, phase props., X-ray and elec. meas. 7-2220
 BaLa₂Ti₄O₁₂, dielectric props. at low temps. 7-45909
 (Ba_{1-x}La_x)TiO₃ semiconducting ceramic props., grain boundary and dopant effects (*Japanese*) 7-6631
 (Ba_{1-x}La_x)(Ti_{1-y}Zr_y)_{1-x/4}O₃ ceramics, electrostrictive effect 7-53240
 BaO-La₂O₃-Al₂O₃ system, synthesis, characterisation and spectroscopic investigations of mixed hexa-aluminates 7-63827
 BaO-La₂O₃-Nd₂O₃-Al₂O₃ systems, synthesis, characterisation and spectroscopic investigations of mixed hexa-aluminates 7-63827
 BaTiO₃-La₂O₃, semiconductor props., influence of dopant oxides 7-6650
 CaLaAlO₄ crystals, growth by Czochralski method 7-22460
 CaLaFeO₄, layered cpds., bidimensional mag. coupling, Mossbauer spectra 7-27637
 CaLa₂S₄ optical ceramic, powder synthesis 7-37067
 CeLaRu₂Si₃, high energy EXAFS and XPS studies 7-64801
 Cr,Nd:LaMgAl₁₁O₁₉ laser material, optical props. 7-10958
 (Eu, Lu, La)₃Fe₅O₁₂ films, gyromagnetic ratio, damping parameter and mag. anisotropy 7-45777
 KPbLaF₆ solid soln. twinned cryst. struct., lattice parameters and point group, X-ray diff. studies (*French*) 7-58231
 (La,Ca)(Co,Mn)O₃, sinterability, phase composition and microstructure 7-33622
 La complex, Ln(NO₃)₃·1,1-bis(quinol-8-oxo)-3,5,9-trioxadecane, XPS 7-57133
 La complexes, (hexaaquadodecapropionate)tetralanthanum(III) dithiocarbamate dihydrate, cryst. struct. 7-12030
 La-Ba-Cu-O system, superconducting transition above 40 K, high press. 7-58946
 La-Co-O system, nonstoichiometric K₂NiF₄-type phases 7-37936
 La-Mn-O system, solid state equilibrium relationships 7-38160
 LaB₆ (001), adsorption of Cs, surface structure and work function 7-6977
 LaB₆ (001), field evaporation in the presence of H₂, atom probe FIM 7-21652
 LaB₆ cathodes in Dudnikov type Penning source 7-56375
 LaB₆, cryst. struct. determ., defect content 7-58245
 LaB₆ crystals, floating zone growth using Xe arc image furnace, dislocation density 7-33552
 LaB₆, crystals grown with Xe arc image furnace, subgrains 7-59411
 LaB₆ dispersed powders and compact specimens, struct. and morphology 7-64976
 LaB₆, lattice dynamics studied by ion channelling, La in Einstein model 7-44710
 LaB₆, optical props. and band struct., spectroscopic ellipsometry meas. 7-13157
 LaB₆, orientational effects of interactions of electrons in APS spectra 7-46243
 LaB₆ pulsed hot cathode discharge, for uniform plasma production 7-32006
 LaB₆, radiative decay of 4d⁹4fⁿ⁺¹ excited states 7-39321
 LaB₆ space-charge-limited electron gun analysis 7-56380
 LaB₆-GaAs interfaces, thermal stability, high energy ion scattering studies 7-21680
 LaBO₃, luminesc. of Sb³⁺ 7-33442
 LaCO₃OH polymorphs, prep., cryst. data, X-ray powder diff., IR spectra, TGA curves 7-32392
 La_{1-x}Ca_{0.55}Ba_{0.45}FeO_{3-δ}, elec. cond. props. rel. to struct. 7-63871
 La_{1-x}Ca_xCr_{1-y}Ni_yO₃, production and elec. parameters 7-33007

lanthanum compounds continued

- La₃₀Ce₆Li₂₄O₆₉, Li₂₄Ce₁₂Li₂₄O₇₂ and La₃₀Th₆Li₂₄O₆₉, cubic and tetragonal phases, structures 7-26725
 La₂Co₄P₁₂, synthesis, cryst. struct., X-ray diff. study 7-32387
 LaCrO₃-Cr cermet, mech. props., interparticle welding 7-39630
 La₂CuO₄, thermal cond. meas. in semiconducting and metallic phases 7-16830
 LaF₃, broadband VUV reflectance coatings for Al mirrors 7-57520
 LaF₃, epitaxial growth on Si (111), photoluminescence, Raman scattering Rutherford backscattering/channeling 7-59437
 LaF₃, lattice phonons, high temp. Brillouin scatt. studies 7-46059
 LaF₃, spectral parameters, lattice defects effects, X_α discrete-variation method calcs. 7-7170
 LaF₃:Dy³⁺(Ho³⁺)(Er³⁺), surface temp. meas., fluoresc. appl. 7-19947
 LaF₃:Nd³⁺, energy value calc. of Stark sublevels (*Chinese*) 7-38519
 LaF₃:Pr³⁺, ³¹P fluorescence quenching processes 7-22314
 LaF₃:Pr³⁺, laser action, relax., photon echo technique 7-20229
 LaF₃:Pr³⁺, spin Hamiltonian spectroscopy, spin-spin cross relax. by optical pumping 7-22228
 LaF₃:Pr³⁺,Nd³⁺, energy up-conversion, UV fluoresc. obs. 7-53401
 LaF₃:Pr³⁺, crystal photon echo effect, use in contemporary electronics 7-15820
 LaF₃:Pr³⁺Gd³⁺, two-photon excitation and interconfigurational energy transfer 7-3083
 La₂Ga₅Ta_{0.5}O₁₄:Nd³⁺, luminescence and absorption spectra and low-threshold stimulated emission 7-7731
 La₂Li_{0.5}Co_{0.5}O₄:⁵⁷Co, Ti, ⁵⁷Fe³⁺ anomalous charge state obs., ⁵⁷Co³⁺ nuclear decay studies 7-21881
 LaLiGe₂, crystal structure (*Ukrainian*) 7-12009
 LaMgAl₁₁O₁₉, elastic and anharmonic props., acoustic meas. 7-44706
 LaMgAl₁₁O₁₉:Nd(Eu), single cryst., phys. chem. and spectrosc. props. 7-13185
 LaMgAl₁₁O₁₉-LaMgGa₁₁O₁₉-LaMgFe₁₁O₁₉ system, solid solns. 7-39491
 LaMn(Fe)Si₂, struct. and mag. props. studies (*French*) 7-37950
 La₂Mo₂O₇, quasi-2D single cryst. struct. and electronic props. studies 7-58238
 LaNbO₄, single crystal, elastic props. 7-51915
 LaNi₅-H₂ system, γ-phase hydride, in situ X-ray diffractometry study 7-26712
 LaNi₄AlH₂ and LaNi_{4.5}Al_{0.5}H₂, dynamical disorder of H, quasi-elastic neutron scatt. study 7-21535
 LaNiAl₁₁O₁₉, magnetoplumbite type cpd., synthesis, cryst. growth and struct., electronic spectra 7-44476
 LaNi₂H₂, stoichiometry deviation and structural disorder, H content depend., EXAFS study 7-68415
 LaNi₄MH₂ (M=Mn, Cu), dynamical disorder of H, quasi-elastic neutron scatt. study 7-21535
 La₂NiO₄, quasi-2D, canted antiferromag. order studies 7-33153
 La₂NiO₄, struct. characterisation of orthorhombic form 7-1990
 La₂NiO₄, thermal cond. meas. in semiconducting and metallic phases 7-16830
 La₂Ni₄P₁₇, bonding relationships and electronic struct. calcs. 7-16941
 LaO, X²⁺ and B^Σ states, spin-rot. and hyperfine interactions 7-5715
 La₂O₃ cryst., Auger spectra, electron polarisation effect 7-59313
 La₂O₃ dielectric system, Auger and photoelectron spectra, fine structures 7-13322
 La₂O₃ film, amorphous, DC cond. mechanism 7-22055
 La₂O₃, radioactivity removal 7-28325
 La₂O₃, thermal expansion coeff. below room temp. 7-12332
 La₂O₃-SiO₂ systems, liq. immiscibility 7-6807
 LaOBr, single cryst. growth, struct., X-ray diff. study 7-44431
 La(OH)Br·nH₂O, prep. and characterisation 7-12018
 La₂O₅:S:Er, Nd, mag. susceptibility, dielec. const. and dielec. losses 7-2810
 La₂O₄:Nd³⁺ degenerate four-wave mixing spectroscopy 7-11039
 La_{0.6}Pb_{0.4}Co_{0.1}Mn_{0.9}O₃, elec. conductivity, influence of Co ion substitution for Mn 7-45314
 LaS, NaCl type lattice, current carriers and cond. 7-45346
 La₂S₃-La₂O₃-Ga₂O₃-Ga₂S₃ glassy and crystalline chalcogenides, EXAFS structural study 7-63481
 La_{0.7}Sr_{0.3}CoO₃ cathodes for CO₂ waveguide lasers, electrical and emission charact. 7-59383
 La_{1-x}Sr_xCoO₃, local struct., EXAFS and XANES studies 7-63582
 La_{1-x}Sr_xCoO₄, superconducting transition at 36.2 K 7-58947
 La_{1-x}Sr_xFeO_{3-δ}, elec. cond. props. rel. to struct. 7-63871
 La_{1-x}Sr_xMO₃ (M=Cr, Mn, Fe, Co), electrodes for high temp. oxide fuel cells 7-54291
 La₂TiMo₆ (M=Fe, Ni, Cu, Zn), synthesis, struct. and elec. props. 7-2619
 LaTiO₃-based perovskites, IR vibr. spectra studies 7-39102
 LaZnFe₁₁O₁₉, cation distribution and random spin canting 7-37945
 LiLaP₄O₁₂:Nd³⁺, Yb³⁺, metaphosphate glasses, Nd³⁺ to Yb³⁺ energy transfer, luminesc. study 7-22323
 MgH₂-LaH_{2.8} hydrides, H diffusion coeff., NMR studies 7-32705
 Na₂(La,Co)TiP₂O₁₂, Nasicon analogues, cryst. data 7-12014
 NaLa(MoO₄)₂ single crystals and ceramic, elec. cond. meas., disordering mechanisms 7-6863
 NaLa(MoO₄)₂:Nd³⁺, Raman and IR spectra study 7-46046
 Na₂LaZrP₂O₁₂ crystals, X-ray powder diff. data 7-26722
 Nd:La₂Be₂O₇ laser rods with greatly reduced thermal lensing 7-10959
 Nd³⁺:La₂Lu₂Ga₃O₁₂ZZ 7-10957
 PLZT ceramics, hot pressed, chemically induced grain boundary migration and recrystallisation 7-27027
 PLZT ceramics (*Japanese*) 7-2981
 PLZT, elastic-plastic contact damage 7-39627
 PLZT, ferroelec. ceramic, laser-induced surface metallisation 7-53924
 PLZT, ferroelectric films, properties and applications 7-59156
 PLZT hot pressed ceramic, polarisation reversal studies under hydrostatic press. 7-59160
 PLZT light shutter for color viewfinder and video projector appl. (*Japanese*) 7-20398
 PLZT, piezoelec. ceramics, prep. and industrial appls. 7-13096
 PLZT transparencies contrast increase, using electrically controlled light scattering 7-25909
 PLZT, transparent ferroelectric ceramic, surface composition and structure 7-32765
 PLZT, transparent ferroelectric ceramic, irradiation effects 7-59157
 PLZT-PZN electro-optic ceramics, elec., opt. and switching props. 7-7646

lanthanum compounds continued

- Pb_{1-x}La_xTi_{1-(x/4)}O₃ sputtered film struct., dielec., and pyroelec. props. studies 7-21724
 Pb_{1-x}La_xTi_{1-x/4}O₃ thin film pyroelectric infrared sensors 7-56338
 Pr:LaCl₃ photon avalanche laser at 4.9 μ m 7-15869
 Pr³⁺:LaF₃, spin-spin reservoir cross-relax. via optical pumping 7-15652
 Si₃N₄-Al₂O₃-La₂O₃ ceramics, sintered, IR absorpt. and Raman spectra 7-46000
 Sr_{0.69}La_{0.31}F_{2.31}, nonstoichiometric phase, atomic struct. 7-21175
 SrLaFeO₄, layered cpds., bidimensional mag. coupling, Mossbauer spectra 7-27637
 (YEuTmCa)₃(FeGe)₅O₁₂/(YLa)₃Fe₅O₁₂ ferrite/garnet layered struct., domain wall and ferromag. reson. props. (*Russian*) 7-45828
 ZrF₄-BaF₂-LaF₃, mid-IR glass and optical fibres, dispersion characts. 7-37178
 ZrF₄-BaF₂-LaF₃-AlF₃ glass, etching method for prep. of IR fibres with high tensile strength 7-1243
 ZrF₄-BaF₂-LaF₃-AlF₃-NaF glass, crystal growth and microstruct. 7-1896
 ZrF₄-BaF₂-LaF₃-AlF₃ optical fibres, gamma irradiation, EPR and IR studies 7-37183
 ZrF₄-BaF₂-LaF₃-AlF₃, heavy metal fluoride glass system, viscosity and crystallisation 7-37883
 ZrF₄-BaF₂-NaF-AlF₃-LaF₃ glasses, crystallisation study 7-63491
 ZrF₄-LaF₃-BaF₂-NaF glasses, EPR of Cu²⁺ ions 7-27593

Laplace transforms

- analysis of structures produced from visco-elastic materials by the aid of ADINA-program 7-1453
 boundary element method applied to some inverse problems 7-1436
 convex cylinder, EM wave scattering, anal. using multiple Laplace transform 7-5819
 cylinder, composite with penny-shaped crack, impact response 7-37384
 thermal conductivity and diffusivity for arbitrary heat input, meas. method (*Japanese*) 7-16832

Large Magellanic Cloud

- average interstellar UV extinction curve 7-35042
 B-type supergiants, energy distrib. and model atm. 7-55635
 diffuse interstellar bands in LMC, obs. at 637.6 and 637.9 nm 7-55758
 30 Dor, area spectroscopy of northern part of core 7-66698
 E2, intermediate-age LMC cluster, colour-magnitude diagram rel. to age and metallicity 7-40883
 E2, LMC halo cluster, deep CCD photometry and colour-magnitude diagram 7-66685
 ESO 121-SC03, CCD BV photometry of remote cluster in LMC 7-55745
 globular clusters, age determ., metallicity-age relation and AGB stars luminosity function 7-4561
 H₂O masers in LMC, 22-GHz obs. 7-14661
 HV 12714, eclipsing and possible LMC membership, spectral obs. binary star, lumin. 7-47981
 interstellar H I obs. 7-60768
 interstellar [Fe X] 637.5 nm absorpt. in galactic halo and LMC, implications for million degree gas 7-55758
 LH 39, OB association in LMC, spectroscopic obs. rel. to age and initial mass of Wolf-Rayet member 7-66684
 LMC X-3, UV obs. and V, JHK photometry 7-55715
 LMC X-3, X-ray binary containing black hole, for-UV obs. by IUE 7-55733
 RR Lyr stars in LMC, B and V magnitudes 7-47924
 MG 4 and 5, WR stars in LMC near 30 Dor, spectrophotometry 7-60691
 N44C1, H II region, exciting star characts. 7-40892
 NS 105-67, massive double-lined O-type binary in LMC, spectroscopic obs. 7-55711
 old long-period variable stars in LMC, vel. dispersion determ. 7-55605
 quasar in direction of LMC (0557-672), V-magnitude and redshift 7-4592
 R136a, group of 8 massive stars within Tarantula Nebula 7-55749
 Sanduleak -69°202, SN 1987A progenitor, RI photometry 7-66640
 SN 1987A, in LMC, discovery, precise position, possible progenitor, photometry, and spectrum 7-66628
 SN 1987A, neutrino signal obs. and interstellar absorpt. lines vel. systems 7-66637
 SN 1987A, photometric and spectral obs. (1987 February 24-26) 7-66632
 SN 1987A, photometric and spectral obs. and evidence for companion to progenitor 7-66630
 SN 1987A, photometry and spectral characts. (1987 February) 7-66640
 SN 1987A, Type II SN, astrometry, spectral and photometric obs. and progenitor characts. 7-66629
 SN 1987A in LMC, astrometric obs., UV photometry and spectrum, and visual magnitude estimates 7-66642
 SN 1987A in LMC, IUE obs. of UV spectra and light curve 7-66638
 SN 1987A in LMC, multiple nature of progenitor star, (Sanduleak -69°202) 7-66636
 SN 1987A in LMC, optical spectra, radiobrightness and double nature of progenitor 7-66634
 SN 1987A in LMC, progenitor position, photometry, and polarization 7-66631
 SN 1987A in LMC, spectral evolution (1987 Feb. 25-Mar. 1) 7-66641
 very low excitation compact nebulae, UV and optical spectra of exciting stars 7-47883

large scale integration

- CMOS/SOI devices, laser recrystallisation 7-8014
 position sensitive LSI detector for low energy ESCA electrons 7-19668
 radio astronomy, wideband very fast FFT spectrum analyzer 7-47710
 GaAs, large dislocation-free cryst. growth for LSI appls. 7-64895

large-scale systems

- see also *hierarchical systems*
 heart's pathological sinus mode modelled by system of interconnected pacemaker cells 7-54518
 hydraulic network, large-scale, nonlinear conservation laws 7-10196
 system theory, conf., Knoxville, TN, USA (Apr. 1986) 7-14714

laser accessories

- acousto-optic mode locker, appl. to Ar ion laser 7-37005
 acousto-optic modulators, deflectors and Q-switches, basics 7-50605
 ALGOCS II He-Ne laser alignment equipment (*Rumanian*) 7-11001
 aspherical focusing lenses for high-power multi-wavelength laser systems 7-62808
 Aurora KrF laser system, design and performance of large area monolithic electron guns 7-36987

laser accessories continued

- autocorrelator based on multiphoton ionisation, for UV and visible regions 7-43133
 birefringent filter design for CW dye laser resonator, spectral tuning band 7-50720
 capillary design for Ar milliwatt laser (*German*) 7-20274
 chemiluminescence based F₂ detector, excimer laser monitor appl. 7-20216
 cholesteric liquid crystal device for laser tuning 7-15858
 coatings for multiwavelength solid state lasers, laser beam testing expts. 7-57522
 coaxial ceramic pulse-forming line for XeCl laser 7-43061
 cylinder lens design for X-ray laser 7-43317
 deflecting focusing kinoform 7-25736
 dielectric coatings for laser mirrors, fabrication 7-15965
 dispersive resonator with Gaussian stop and telescopic system, emission spectra study 7-62731
 dye jet laser, continuous, liquid-circulation systems 7-31312
 electro-optic devices, Pockels cell, review 7-50729
 electro-optical shutter, large-aperture, with liquid electrodes 7-20248
 electrode design for gas discharge laser using finite difference method 7-1178
 electromechanical laser-beam modulator with high-frequency stability 7-31372
 electrooptic modulator, CW laser power stabilisation 7-1203
 ENEA free electron laser, linearly polarized EM undulator, design parameters 7-1137
 excimer laser amplifiers, scalability, double-pass and expanding beam geometries calcs. 7-43143
 excimer laser excitation, using low impedance electron beam system 7-36989
 excimer lasers, use of low-power ionisers in the excitation of active media 7-1184
 Fabry-Perot fibre optic sensor and its appls. 7-43424
 Faraday isolator, simple compact high performance permanent magnet 7-31437
 focusing element development for materials processing 7-11023
 free electron laser, mirror degradation and performance requirements 7-43152
 glass plate stack mirror for laser resonator, refl. coeff. 7-57508
 glass series, active, material selection for acousto-optic mode-lockers 7-57493
 holographic lens for laser beam expansion, design 7-62812
 hypocycloidal pinch device development for dye laser pumping (*Korean*) 7-62719
 inert-gas halide lasers with water dielectric pulse power driver 7-36988
 injection-laser modulation measuring apparatus 7-5929
 IR radiation ultrafast switching by laser produced Ge plasma 7-11020
 LELA experiment, piezoelectric translators, performance 7-1135
 LELA experiment, UV induced mirror damage, prelim. results 7-1135
 lensless holographic line scanner 7-25784
 liquid crystal devices for laser systems 7-10979
 liquid crystal modulator for CO₂ laser light modulation 7-62745
 metal strip gratings as submillimetre laser output couplers, power transmission theory 7-43339
 methanol pumping sources, differ free stabilisation using absorption cell 7-11756
 microminiature cryogenic refrigerator for compact CdSe laser 7-43153
 microsecond discharges in flash lamps, elec. cct. matching 7-10978
 mirror, external, for Bragg injection semicond. laser with distrib. feedback 7-36985
 mirror using degenerate four-wave mixing in saturable amplifier 7-20246
 mirror with corrugated waveguide on surface, spectral and laser characts. 7-43291
 mirrors, spectral characts. 7-20247
 multilayer coatings, for excimer laser, reflectivity calcs. 7-57521
 multilayer components for soft X-ray laser cavities 7-25844
 optical coatings, preparation and testing for high power lasers at 1.06 μ m 7-1249
 optical pump sources, incoherent, based on surface discharges 7-15883
 optical silicate glass melt, fracture in laser beam 7-43278
 Particle Beam Fusion Accelerator II (PBFA II), laser triggering optical system 7-30771
 Particle Beam Fusion Accelerator II (PBFA II), laser trigger system design 7-30772
 permanent magnet field source for circularly polarised radiation production via helical FEL 7-31349
 photoplaters for optical elements fabrication, circular scales structure synthesis 7-26044
 photoploters for phototemplates fabrication, optical radiation control 7-25834
 polymethine dye grazing-incidence laser (*Russian*) 7-50583
 power stabilizers for turning down laser noise 7-5900
 pulse generator supply for CO₂ laser 7-1195
 quartz ceramic reflectors, γ -irrad. effects on Nd:YAG laser energy characts. 7-50575
 radiation detectors classification and characts. (*Czech*) 7-61367
 semiconductor laser, narrow linewidth, single frequency, with phase conjugate external cavity mirror 7-43157
 semiconductor laser, pulsed, signal spectrum variation, expt. study and input signal cct. design 7-36966
 sparks, sliding, schlieren method investig. 7-32158
 storage ring for high power XUV FEL 7-31351
 undulator, linear, variable gap permanent magnet, for ENEA free electron laser expt 7-43151
 variable gap permanent magnet linear undulator for ENEA-FEL expt. 7-1191
 wiggler for IR FEL and coherent harmonic generation 7-31352
 window heating by pulsed laser, focal lengths and rise times 7-43179
 XUV laser cavities and pumping optics 7-25845
 Ar ion laser, wideband power regulation system 7-31347
 BaTiO₃ double phase conjugation mirror, anal., demonstration and laser appl. 7-43252
 CO₂ laser, electronic current source, power modulation capability (*German*) 7-50601
 CO₂ laser amplifier, multiatmosphere high gain, characts. and gain at 9.294 μ m 7-57366
 CO₂ laser cathode systems, characts 7-15900
 CO₂ laser detection, using CdHgTe detector 7-5915
 CO₂ laser gas transport system, compact axial flow 7-57367
 CO₂ laser spectrum monitoring and displaying instrument 7-5935

laser accessories continued

- CdS waveplates for IR lasers, reproducible volume manufacture 7-37138
 Cu mirrors, Ag⁺ implanted, laser oxidation and optical props. 7-5971
 GaAlAs/GaAs surface-emitting linear laser arrays with etched mirrors 7-20255
 He-Cd laser, noise reduction by discharge current modulation 7-31348
 He-Ne laser, internal mirror, freq. and power stabilisation using fan (Korean) 7-25849
 He-Ne laser, standardisation for metrological purposes 7-5909
 I₂ cells for laser stabilisation, preparation and anal. 7-62718
 La_{0.7}Sr_{0.3}CoO₃ cathodes for CO₂ waveguide lasers, electrical and emission characts. 7-59383
 Nd:YAG laser unstable resonator output coupler based on Fabry-Perot interferometer 7-43166
 Nd_{0.7}Sr_{0.3}CoO₃ cathodes for CO₂ waveguide lasers, electrical and emission characts. 7-59383
 O₃ saturable absorber for KrF laser 7-20369
 Xe lamp, double discharge, for Nd laser pumping 7-11002
 ZnSe photoelastic modulator for IR 7-43348

laser annealing *see laser beam annealing***laser applications** *see laser beam applications***laser applications in medicine**

- 3D human body segmental motion meas. using laser scanning system 7-28568
 π -laser, biomedical experiences 7-47208
 angioplasty with a laser and fibre optics at 2.94 μ m 7-34221
 arterial anastomoses, laser-assisted and sutured, mech. props. under axial loading, rabbit obs. 7-23374
 articulated arm for laser beam delivery, surgical appl. 7-50613
 biliary calculi, gallstones, pulsed-laser fragmentation, optical study 7-60036
 cancer therapy, optimum wavelength, cell components and mucous membrane absorptive spectrograms (Chinese) 7-28641
 conference, laser science advances, Dallas, TX, USA (Nov. 1985) 7-9573
 conference on optical and laser technology in medicine, Los Angeles, CA, USA (Jan. 1986) 7-29587
 conference on optical instrumentation for biomedical laser appls., Innsbruck, Austria (April 1986) 7-40994
 dentistry applications 7-40242
 dermatology appls. of lasers, overview 7-34223
 development trends and market pot. of biomedical lasers 7-47196
 dye laser surgical successes 7-34217
 endarterectomy of expt. atheromas, fibre optic laser delivery 7-34220
 endoscopes, fibre optics, diagnostic and surgical appl. 7-40243
 excimer laser technology developments and appls. 7-25840
 excimer lasers in medicine, surgical appls. 7-60073
 fibre optic beam delivery systems in high power laser surgery 7-47201
 fibre optic cable for CO₂ laser scalpel 7-14086
 fibre optic laser beam delivery system for medical appls. 7-47200
 flexible waveguide for CO₂ laser surgery 7-34226
 haematoporphyrin derivative, laser-induced fluoresc., tumour localisation 7-23431
 hand-held surgical CO₂ lasers, advanced appls. 7-34219
 holographic endoscopy with gradient-index optical imaging systems and optical fibres 7-31271
 IR fibres, appl. for laser surgery in medicine 7-40248
 medical electronics developments, review (Italian) 7-18094
 medical fiberoptic laser probe for treatment of occlusive vessel disease 7-34227
 nerve anastomosis with low-power CO₂ laser, rat model 7-23421
 nerves, severed, repair by Ar laser 7-23420
 ocular lenses, human, diagnostic evaluation using quasi-elastic light scatt. spectroscopy 7-34230
 ophthalmic combined Ar YAG-laser system 7-47197
 ophthalmic laser interferometry 7-47204
 ophthalmic therapy, argon laser coagulator use 7-8674
 ophthalmic therapy, LAK argon laser coagulator design and use 7-8673
 ophthalmological laser slit lamp 7-47202
 ophthalmology, Nd:YAG Q-switched laser, obs. on optical construction 7-47203
 oral and oesophageal cancer, human, selective effect of YAG laser (Chinese) 7-28642
 otorhinolaryngology, low-power laser therapy using fiberoptic instruments 7-28648
 overview of optics and lasers in medicine 7-29567
 pulsed UV laser for surgery 7-34232
 retinal blood flow visualisation and meas. by laser speckle photography 7-47212
 retinal therapy, preselectable intensity distrib. in large-area laser coagulation by electronically controlled beam deflection 7-47207
 surgery using CO₂ laser, speculum surface finish effect on beam refl. 7-65830
 surgical instruments, diffuse laser light refl. from surfaces 7-47205
 surgical instruments, surface treatment for improved safety 7-34328
 surgical pulsed CO₂ lasers, asymptotic and dimensionless anal. of living tissue response 7-65813
 therapeutic laser, CO₂ scanning, thermal effect on tissues 7-47162
 therapeutic laser instrument for ophthalmology, the VISULAS YAG 7-54709
 tissue morphological anal. and ablation rates in the UV and visible for laser angioplasty 7-23399
 tissue-laser interaction, thermal and biological aspects of medical laser appl. 7-60037
 vascular anastomosis, rat expts. 7-23422
 vascular tissue: CO₂, Nd:YAG, and Ar laser welding 7-34225
 wound healing stimulation by lasers, mouse obs. 7-34224
 wound repair by laser welding 7-34222
 Nd:YAG, CO₂ dual wavelength laser system for surgery 7-47198
 Nd:YAG laser, multidisciplinary use 7-47199
 Nd:YAG laser and sapphire contact probe, surgical appls. 7-34228
 ZnSe IR optical fibres, development, appls. 7-37190

laser beam annealing

- Au_n(TeO₂)_{n-1} thin films, nanosecond laser annealing, Au cluster redistribution, growth and coalescence 7-12145
 channelling contrast microscopy, He⁺ microbeam, semiconductor impurity profiles 7-51587
 CMOS/SOI devices, laser recrystallisation 7-8014
 crystal-to-amorphous phase transition under laser annealing, model 7-16424
 high-technology materials processing, review 7-13342

laser beam annealing continued

- materials processing, welding and machining, conf., San Francisco, USA (Nov. 1985) 7-9597
 materials processing developments at GEC Hirst Research Centre (UK) 7-53581
 metallic glasses, laser annealed struct. and magnetoelastic props., effects of surface characts. 7-45785
 nonequilibrium effects in semiconductor and metal surfaces under laser annealing 7-2061
 photoformation of dielectric materials, review 7-53633
 pulsed, surface structure formation 7-58322
 ω -(1-pyrenyl)alkanoic acids, vac.-deposited film, fluoresc. spectral changes 7-58316
 semiconductors, disordered, ion implanted, low power laser annealing 7-38055
 semiconductors, laser annealing dynamics, thermal model 7-21272
 semiconductors, laser machining, physical processes in surface erosion 7-2053
 semiconductors, solid-phase epitaxial regrowth, amorphous-crystalline interface evolution 7-12568
 SOI film, two-beam laser recrystallisation 7-38393
 SOI films, laser recrystallisation, agglomeration, surface roughness and crystal imperfection 7-38389
 thermal processing of materials using CO₂ and solid state lasers (Rumanian) 7-16624
 Al/III-V semiconductor interfaces, laser-induced chem. reactions 7-7017
 Bi₂-Sb₂Te₃ polycryst. semicond. films, laser annealing effects 7-58317
 CdS films, spray deposited, laser annealing, struct., carrier mobility 7-58318
 Cu-Zr amorphous alloy, induced recrystallisation by electron and laser beam irradiation 7-12152
 GaAs-Ag (Au), excimer laser annealed Au(Ag) contacts 7-12857
 a-GaAs films, dynamics of laser annealing by transient grating method 7-12122
 GaAs films on amorphous insulating substrates, laser recrystallisation 7-38397
 GaAs:P, ion implanted and pulse laser annealed, Raman study 7-6653
 a-GaAs-Si (100), epitaxial regrowth by excimer laser annealing, FET fabrication 7-32875
 a-Ge films, dynamics of laser annealing by transient grating method 7-12122
 a-Ge films, laser-induced phase transitions, time resolved TEM study 7-38056
 Ge, pulsed laser melting, time-resolved reflectivity meas. 7-2158
 InP films on oxidised Si substrate, laser recrystallisation 7-38398
 InP/Al UHV-cleaved and laser annealed interface, acceptor-like electron traps 7-7310
 Mn allotropic phases nucleation during laser annealing, melting, solidification and regrowth 7-12143
 PbS polycryst. semicond. films, laser annealing effects 7-58317
 Pd₇₇Si₂₃ metallic glasses, picosecond laser annealing 7-44613
 Si (111) surfaces, reconstruction study 7-2315
 Si, amorphous, pulsed laser irradi., time-resolved X-ray absorption studies 7-3115
 Si, complex refractive index meas. during pulsed laser annealing 7-45970
 Si films on fused quartz, laser annealing and Raman spectra 7-58708
 Si films on glass substrates, laser recrystallisation 7-38395
 a-Si foils, pulsed laser irradi., clusters and plasmas, time resolved X-ray absorpt. meas. 7-64755
 Si, heavily doped, thermoreflectance, study 7-45999
 Si ion implanted, epitaxy by thermal and laser processing, review 7-33706
 Si, polycrystalline film SOI structures, recrystn. by laser irradiation 7-32856
 Si, pulsed laser melting, time-resolved reflectivity meas. 7-2158
 Si solar cells, passivated, laser processed, 18% efficiency 7-59837
 Si, surface, laser beam melting and recrystallisation 7-12431
 Si wafer, laser and energy-beam annealing of mechanical damage, melting and recrystallisation 7-46516
 Si:As, deep level spectra, ion implanted defects, laser annealing 7-21869
 Si:As, implanted, supersaturated soln., defect struct., TEM obs. 7-58483
 Si:As on sapphire, ion beam recrystallised and laser annealed, elec. props. 7-16649
 Si:As⁺, epitaxial regrowth, CW Ar laser annealing (Korean) 7-27197
 Si:As(B), ion implanted, pulsed laser annealing, optical reflection kinetics 7-58323
 Si:B, ion implanted, strain profile, double cryst. X-ray rocking curve simulation 7-2060
 Si:B:P solar cells produced by pulsed excimer laser annealing of ion-implanted junctions 7-8419
 Si:Li, ion implanted, impurity redistribution under pulsed laser radiation 7-12098
 Si:N, N incorporation and behaviour 7-16598
 Si:P, pulsed laser annealing, molten phase local nucleation study 7-63655
 Si:P, pulsed laser processing via free carrier absorpt. 7-21273
 a-Si/Al films, laser-induced phase transitions, time resolved TEM study 7-38056
 poly-Si-SiO₂, Ar⁺ laser recrystallised interface characts., effects of technological parameters (Chinese) 7-33092
 α -SiC polycrysts., pulsed laser annealing and ion beam mixing surface modification studies 7-16657

laser beam applications

- see also holography; integrated optics; laser applications in medicine; laser beam annealing; laser beam machining; laser beam welding; laser isotope separation; laser printers; matrix isolation spectroscopy; measurement by laser beam; modulation spectroscopy; optical communication; optical radar; plasma production and heating by laser beam; Raman spectroscopy; remote sensing by laser beam; spectroscopy; two-photon spectroscopy*
 2-GHz frequency-domain fluorometer 7-23091
 aerosol flow and vapour characterisation by photothermal methods 7-51345
 air flow visualisation in clean rooms using laser light sheet method (Japanese) 7-57966
 articulated arm for laser beam delivery, in use and construction 7-50613
 atomic beam deflection by multiple laser beam, photon statistics test 7-10902
 atomic beams, collimation and decollimation by laser radiation 7-42782
 atomic beams, collimation and decollimation by laser radiation pressure 7-42785

laser beam applications continued

cladding of metallic surfaces (*Chinese*) 7-8155
 communication, picosecond laser pulses, transformation by multiple scattering media 7-42944
 conf., Rochester, NY, USA 7-9595
 conference, laser science advances, Dallas, TX, USA (Nov. 1985) 7-9573
 conference on laser appls. in chem. and biophys., Los Angeles, CA, USA (Jan. 1986) 7-40993
 CVD of Si films, photolytic or pyrolytic dissoc. of SiH_4 7-13388
 diamond, synthesis by laser induced CVD, low press. 7-13371
 diamond layers, growth in laser heated substrate (*Russian*) 7-22507
 distance measurements using two-mode Zeeman laser system (*Japanese*) 7-24623
 drift chamber calibration using lasers, review 7-42284
 dye laser spectrometer with ultra-high-resolution, using passive reference resonator 7-18889
 electrically conductive laser waveguide for in-situ spectroscopic study of rotating electrochem. electrode 7-5994
 electron acceleration in vacuum by two laser beams 7-50480
 electrophotographic color printing using elliptical laser beam scanning 7-56362
 erasable recording, overcoated organic dye-binder optical disc medium 7-20148
 etching and deposition, basic mechanisms, review 7-53923
 etching of electronic materials 7-28162
 etching of polyimide encapsulants in IC eval. 7-53941
 excimer laser applications in imaging technology (*Japanese*) 7-56367
 excimer laser physics, props. and appls. 7-50544
 excimer laser technology developments and appls. 7-25840
 fiber-optic gyro for space applications 7-30005
 fibre optic gyroscope, passive ring cavity-type, 1.5- μm DFB InGaAsP laser appl. 7-57562
 fibre optic interferometer using FM laser diodes 7-31470
 fibre optic system using laser source with arbitrary coherence time, phase noise anal. 7-15979
 films, laser-assisted CVD, surface undulations, Raman microprobe analysis 7-12430
 forensic science laser usage in lab. and crime scene environments, design issues 7-11022
 free radicals colour centre laser spectroscopy 7-18890
 free-space laser communications system design, SNR impact 7-34676
 gas-phase alkali compound photodissociation, photofragment fluoresc. anal. 7-19974
 gasdynamic focusing in supersonic jets, chemical anal. appl. 7-20752
 gyroscope, correlated emission laser type 7-41368
 gyroscope, ring laser type, skewed probability densities, coloured noise effect 7-41369
 gyroscope reliability for inertial navigation platforms (*Italian*) 7-25860
 heat conduction in a moving semi-infinite solid subjected to pulsed laser irradiation 7-62964
 heterodyne three-level spectroscopy 7-9907
 high power lasers and their applications (*French*) 7-15890
 high-technology materials processing, review 7-13342
 holographic grating fabrication by tunable pulsed dye laser 7-5983
 industrial laser annual handbook 7-24316
 intracavity optical-optical double resonance spectroscopy technique 7-50552
 KEK TOPAZ barrel TOF counters, laser calibration system 7-62214
 laser applications in chemistry, conf., Quebec City, Canada (June 1986) 7-41000
 laser enhanced plating and etching using photothermal effects 7-59651
 laser heating for chemical conversions: unique features and limitations 7-65307
 laser microprobe mass analysis, quantitative 7-54250
 laser tomography, appl. in obs. of crystal defects (*Japanese*) 7-51750
 laser-assisted metallisation for low-cost high-efficiency solar cells 7-8415
 laser-driven flyers backed by high impedance windows, vel. meas. 7-30029
 lensless holographic line scanner 7-25784
 levelling device for adjustment of RATAN-600 radio telescope, design and performance 7-66468
 light source, spectrally-broad picosecond for calibrating photonics equipment 7-20378
 $\text{LiNbO}_3\cdot\text{Cu}(\text{Er})(\text{Mg})(\text{H})$, laser-induced grating characteristics 7-62746
 lunar laser ranging data, appl. to determ. of Earth rotation parameters (*Chinese*) 7-3959
 lunar laser ranging measurements, implications for tidal energy dissipation 7-14301
 mass analyzer, laser microprobe, LAMMA 1000 7-8341
 mass spectrometry, laser ionisation, appl. to thin film and near-surface layer studies 7-28374
 materials processing, conf., London, England (Dec. 1986) 7-48185
 materials processing, focusing element development 7-11023
 materials processing, temp. distrib. meas. in laser-heated materials 7-9837
 materials processing, welding and machining, conf., San Francisco, USA (Nov. 1985) 7-9597
 materials processing developments at GEC Hirst Research Centre (UK) 7-53581
 materials-processing using YAG laser, plume generation, influence on processing variables 7-12148
 metal surfaces, ion beam and laser processing for improvement corrosion resist., surface modification program 7-65200
 metallic and ceramic ultrafine particles, laser prod. 7-13406
 metallic materials, nucl. anal. (*German*) 7-54211
 metals, surface-breaking defect characterization using laser-generated ultrasound 7-46774
 molecular absorption, automated laser system for IR-IR, UV excitation anal. 7-6354
 moving-mirror laser-beam scanner enhancement by multipath reflection 7-15963
 NDT applications of laser-generated focused acoustic waves 7-17754
 NMR laser, modulated near to bifurcation used as small signal detector 7-15911
 nonlinear polarisation spectroscopy, normal waves, light-induced anisotropy 7-48858
 nonstationary active spectroscopy, laser pulse incoherence effect 7-48857
 optical correlation design, wavelength-angle multiplexing appl. 7-25939
 optical disc memory light source, ML6000 series of high-power laser diodes (*Japanese*) 7-20271

laser beam applications continued

optical fibres, single crystal pulling, laser heated pedestal growth technique 7-53578
 optically excited resonant diaphragm pressure sensor 7-56243
 optogalvanic spectroscopy, system design and optimisation, use in discharge studies 7-61389
 organometallic compounds, laser mass spectroscopy, laser CVD appl. 7-22573
 particle acceleration using lasers (*German*) 7-5495
 particle accelerators, IR laser driven, with oversized DBR and HFB waveguides 7-10309
 Particle Beam Fusion Accelerator II (PBFA II), laser triggering optical system 7-30771
 Particle Beam Fusion Accelerator II (PBFA II), laser trigger system design 7-30772
 photodisplacement techniques for defect detection 7-44865
 photoformation of dielectric materials, review 7-53633
 photon correlation spectroscopy, laser fluctuation compensation 7-41487
 photoplaters for optical elements fabrication, circular scales structure synthesis 7-26044
 photoplotter for phototemplates fabrication, optical radiation control 7-25834
 photothermal generation of Rayleigh waves 7-43621
 photothermal imaging, spatial resolution of subsurface structure 7-26110
 picosecond Raman studies using 5 kHz tunable dye laser system 7-18881
 Planck radiation, intense, laser generation 7-16056
 plasma and gas spectroscopy with tunable lasers 7-48862
 plotter for high-information-density images recording 7-26043
 polyimide encapsulants, laser induced etching 7-53941
 polymer film, excimer laser micromachining and surface microstruct. modification 7-53940
 polymeric films, prep. on solid surfaces in vacuum, use of laser radiation 7-7862
 polyvinylcarbazole film based photoreceptor, photoinduced memory effect, appl. to laser recording (*Japanese*) 7-37076
 pulsed dye laser for KEK optically pumped polarized ion source (*Japanese*) 7-20280
 pulsed laser field desorption TOF spectroscopy, ultrafast ion reaction time meas. 7-20072
 pyridine, on Ag surface, sub-monolayer adsorbate, SHG, CW diode laser-Maui surface expt. 7-16874
 radiation therapy, fibre optic position verification device 7-47213
 refractometry, combined qualitative and quantitative methods 7-41434
 refractory substances, apparatus for examining sublimation and evaporation 7-41374
 relativistic electron beam generation in laser-based foilless diode 7-42267
 Rimfire 6 MV laser triggered SF_6 filled switch for PBFA II 7-30746
 ring-laser gyroscope, random dither modulation 7-57376
 satellite datalink using hologram laser beam corrector-collimator 7-25754
 satellite laser ranging, chord and relative height estimation from single data passes (*Chinese*) 7-3961
 scanner, image capture capabilities and inspection applic. 7-57601
 scanner, spinning polygon, design 7-50705
 scanner using stacked piezoelectric ceramic actuators 7-20312
 scanning laser acoustic microscope high-resolution imaging with digital processing 7-1318
 scanning laser acoustic microscope image reconstruction theory 7-1338
 scanning laser photoacoustic microscopy, phase transition studies 7-20582
 scanning optical fibre microscope, laser beam induced current images, of semiconductor materials 7-48846
 SDI driving optics development 7-48824
 semiconductor chalcogenide layers, optical recording physical basis (*Russian*) 7-50667
 semiconductor laser linewidth reduction for spectroscopic source 7-10924
 semiconductors, MOCVD, organometallic precursors monitoring by laser mass spectroscopy 7-22547
 simulating chaos in lasers 7-61253
 slightly slanting impact on an elastic cantilever column—an experimental study 7-51008
 sound reproduction from old wax phonographic cylinders, laser beam reflection method use 7-37014
 spatial-frequency image filtering in laser scanning microscopes (*Russian*) 7-41458
 spectroscopy, principles and appls. (*Slovak*) 7-24706
 steel, boride layers, obtained by laser irrada., wear 7-28150
 steel, high-speed tool, laser glazing and boronizing 7-39753
 steel, stainless, laser surface melted, residual stresses 7-3506
 steel, structural, Cr surface alloyed layer, form. by CO_2 laser (*Korean*) 7-28196
 steel, tool, laser surface quenching, comparative anal. of two- and three-stage thermal cycles 7-28178
 steel, V, W2, laser surface melting, effects of prior heat treatment 7-65195
 strategic defense application of chemical lasers 7-10980
 surface analysis by laser ionisation, review 7-52213
 surface analysis with second harmonic generation 7-16848
 surface treatment, recent developments 7-21274
 TEXT, ECRH absorption and propagation studies via collective Thomson scattering 7-11749
 thermal diffusivity, laser flash meas. method (*Japanese*) 7-16831
 thermal lens formation speed meas. (*Japanese*) 7-50614
 thermal shock testing of ceramics with pulsed laser irradiation 7-32491
 thin hard coatings, adhesion test methods, review 7-46741
 thin-film recording medium perforation by sharply focused laser radiation 7-36890
 trace gas analysis, by intracavity He-Ne laser thermal deflection 7-61381
 transient IR absorption measurement, bulk free-carrier lifetime in Si 7-52650
 transmission thermoacoustic imaging without contact 7-31601
 turbulence, laser homodyne technique meas. 7-26254
 ultra-high pressure shock generation using UV high power lasers 7-30028
 ultracoherent transient spectroscopy using phase and amplitude modulated laser pulses 7-18880
 ultrasonic pulse propag. using laser generation and electromagnetic acoustic transducer detection 7-26114
 Van de Graaff 3 MV accelerator, using laser photoelectron emission from cold Y_2O_3 cathode 7-10314
 vapour phase cryst. growth, ion/surface interactions, photo-induced reactions, review 7-53609
 writing for optical data storage on $\text{Te}_{80}\text{S}_{19}\text{As}$ overcoated trilayer struct. 7-20149

laser beam applications continued

- Al film, laser deposition for metallisation 7-53631
 Al thin films, corrective trimming by laser controlled wet chem. etching 7-28195
 AlGaAs, laser-assisted MOVPE growth 7-64928
 AlGaAs, MOVPE, laser assisted, selective area irradi., carrier conc. 7-22545
 Al_{0.9}Ga_{0.1}As film formation by laser beam interaction with AlAs/GaAs multilayer structure 7-12570
 Ar gas, laser induced multiplication and visualisation of free electrons 7-49812
 Au CVD by laser induction 7-22564
 CO₂ lasers, unconventional material processing appl. 7-17759
 CO₂ pulsed laser, medium repetition rate, materials processing appls. 7-20184
 CaCO₃ marble rock, laser treatment 7-51821
 CdS-Si and CdS-CuInSe₂ heterojunctions, struct., elec. and photoelectric props. 7-22001
 CdTe homoepitaxy on CdTe (111) by laser MBE, nucleation kinetics 7-22499
 Cs atomic beam, cooling using laser 7-10897
 Cu foil, excimer laser assisted gas phase etching 7-54015
 CuCl, excitonic particle study by laser spectroscopy 7-16953
 Fe, cast, laser surface hardening, optimisation of process variables 7-13645
 Fe, ductile and grey cast, laser surface hardened, sliding wear 7-17650
 Fe, laser glazing and boronizing 7-39753
 Fe-Al, alloying for oxidation resist. improvement, comparison between ion implantation and laser irradi. 7-22883
 GaAlAs MOCVD layers, stoichiometry variation determ., pulsed laser atom probe anal. 7-12305
 GaAs, laser-assisted MOVPE growth 7-64928
 GaAs, CVD, laser selective deposition on GaAs and Si substrates 7-22546
 GaAs excimer-laser-stimulated CVD, polycryst. thin film growth and props. 7-64912
 GaAs laser induced etching in carbon tetrachloride atm., fluoresc. 7-59700
 GaAs, MOVPE, laser assisted, selective area irradi., carrier conc. 7-22545
 GaAs, Raman phonon piezospectroscopy, IR meas. 7-64647
 GaAs, stepwise monolayer growth by switched laser MO-VPE 7-53626
 GaAs substrates, laser-induced metal and alloy plating, silicide form. 7-39448
 GaAsP, CVD, laser selective deposition on GaAs and Si substrates 7-22546
 H, electron scatt. in chaotic laser field 7-10703
 H₂O vapour, kinetic cooling by CO laser radiation 7-16297
 He-Ne laser for optical fibres fault location 7-31545
 HgCdTe anodic oxide surface analysis by laser ionisation 7-13275
 InGaAs, CVD, laser selective deposition on GaAs and Si substrates 7-22546
 InP, optical generation and phase-sensitive detection of SAWs 7-58598
 Krf lasers, inertial confinement fusion appl. 7-10288
 MO, micrometer-scale line deposition using near UV laser light 7-59438
 Nb, supercond., nondestructive inspection by scanning laser acoustic microscope 7-3566
 Nb₃Al superconducting tape prepared by CO₂ laser beam irradiation 7-17145
 Nd:YAG injection-seeded laser, polarisation feedback stabilisation, spectroscopy appls. 7-57338
 Nd:YAG laser, synchronously operated streak camera appl. 7-18903
 Ni-Cr, oxidation, laser surface treatment and its influence on development of healing Cr₂O₃ scales 7-65204
 Np, valence state adjustment using laser photochem. in nucl. fuel reprocessing (*Japanese*) 7-61971
 O atom, flame diagnostics by two-photon fluoresc., UV laser appl. 7-23015
 PLZT, ferroelec. ceramic, laser-induced surface metallisation 7-53924
 Pd electrodeposition assisted by laser beam (*German*) 7-39440
 Pd-Ag alloy electrodeposition assisted by laser beam (*German*) 7-39440
 PdRhPSi(SiNi), amorphous laser processed surface alloy on cryst. Ni in NaOH soln., anodic charact. 7-28317
 Pt, micrometer-scale line deposition using near UV laser light 7-59438
 Si doped, laser deposition for interconnections 7-53632
 Si, film deposition by radical jet laser-induced CVD 7-59457
 Si powders, prod. from laser-heated silane, cryst. struct. 7-46362
 Si, solar cell fabrication using laser groove technique, commercial viability 7-59862
 a-Si solar cell submodules, integrated type, laser patterning method 7-65470
 a-Si solar cells, fabrication methods using UHV reaction chamber system, high conversion efficiency 7-54293
 Si solar cells, loss reduction by ion implantation, laser radiation, protective coatings (*Dutch*) 7-23134
 Si substrates, laser-induced metal and alloy plating, silicide form. 7-39448
 Si-B, excimer laser-induced shallow diffusion, junction form. 7-38038
 Si(BP), doping by XeCl excimer laser irradi., ultra-shallow junction fabrication 7-58303
 a-Si:H film, photo-assisted plasma CVD 7-33593
 a-Si:H heterojunction solar cell modules, fabrication by laser scribing 7-13900
 Si-Si₃N₄ and Si-Si₃N₄-SiO₂ SOI structures, laser recrystallisation, effects of different capping layers, characterisation 7-45511
 SiC film, laser deposition for solar cell use 7-53634
 α-SiC, sintered, non-equilib. surface conditions and microstruct. changes following pulsed laser irradi. and ion beam mixing of Ni overlayers 7-65170
 Si₃N₄, laser activated CVD, deposition rate, refractive index 7-33591
 Si₃N₄ localised films on Si substrate, laser deposition 7-39418
 SiO₂ glass, surface analysis by laser ionisation 7-13275
 SiO₂, laser activated CVD, deposition rate, refractive index 7-33591
 SiO₂:GeO₂ integrated optical waveguides, laser heating effect on opt. props. 7-50792
 Ti, thermochemical surface treatment using lasers, wear and corrosion resist. 7-22908
 U, chemistry, laser appl. 7-19365
 V, IR laser induced oxidation obs. 7-65215

laser beam applications continued

- W, micrometer-scale line deposition using near UV laser light 7-59438
 ZnSe laser-induced epitaxial growth on GaAs using organic compounds 7-52366
- laser beam applications in medicine** *see laser applications in medicine*
- laser beam effects**
see also biological effects of laser radiation; laser beam annealing; plasma-beam interactions; plasma production and heating by laser beam
 7-39389
 ablation studies, planar multilayered targets preparation 7-19426
 acoustic tomography of pulsed laser beams 7-62944
 adlayer photostimulated phase transitions on semicond. surface, reson. conditions calcs. (*Russian*) 7-45016
 ad-molecular processes, laser induced, energy and phase relax. 7-21610
 adsorbed atoms, thermal relax. in an intense laser field 7-38330
 adsorbed atoms on coated transparent crystal, laser heating 7-63654
 adsorbed layers, laser-induced photodesorption 7-52281
 adsorbed molecules photodesorption by IR laser-adsorbate coupling 7-58616
 adspecies, anharmonic, transient excitation by pulsed laser radiation 7-21611
 aerosol drops, explosive vaporization under CO₂ laser beam irradiation 7-57388
 aerosol particle, transverse motion in a laser radiation field 7-46881
 AgCl-Ag films, photo-induced gratings due to radiative TE modes 7-22363
 air, atmospheric, optical breakdown during axicon laser focusing 7-44288
 air, breakdown by laser radiation, mechanism modelling 7-20996
 air, optical breakdown near solid rough surface, time of appearance 7-26386
 alkali halide crystals, F-centre formation threshold by two-photon absorpt. 7-32437
 alkali halide crystals, optical breakdown threshold, size depend. 7-44615
 alkali metal halides, desorption, UV-photon-stimulated, laser-synchrotron studies of dynamics 7-21612
 alumina, UV laser sputter etching effects, laser-induced fluorescence and interferometry studies 7-26798
 As-S, amorphous semicond. films, laser action on light sensitivity (*Russian*) 7-64713
 atom, laser beam excited, collisional and radiative relax. 7-5637
 atom, Yukawa pot. model, electron elastic scatt., laser modified 7-25654
 atomic and mol. clusters in free jets, laser excitation dynamics 7-42823
 atomic beam, deflection and focusing by reson. light field 7-42786
 atomic beam laser cooling, reson. radiation press., simulation approach 7-15555
 atomic beams, stopping with laser light, entropy prod. 7-42556
 atomic cooling, stopping and trapping 7-10504
 atomic electron scattering, nonreson., in low-freq. laser field 7-20050
 atomic gases, ultracold, collective quantum effects by laser-cooling techniques 7-30989
 atomic systems, transient temporally modulated laser radiation interaction 7-20296
 atoms, 3D confinement and cooling by reson. radiation press. 7-10505
 book, laser damage in optical materials 7-24311
 book, laser-induced dynamic gratings 7-9605
 bromotrifluoromethane, CW CO₂ laser induced reaction, frequency depend. kinetics 7-953
 1,3-butadiene, laser powered homogeneous pyrolysis, kinetics investig. 7-65309
 cellular growth structures, rapid solidification, compositional profiling 7-46453
 cluster beams, refractory, laser spectroscopy 7-15794
 coating defects, correlation between pulsed laser damage and probe laser scatter 7-38049
 coatings for multiwavelength solid state lasers, laser beam testing expts., damage threshold 7-57522
 collision dynamics, laser effects, overview 7-20002
 compound semiconductors, laser stimulated desorption, dimerisation enhanced phase transition 7-58619
 compressible liq., localised laser thermooptical volume source surface wave excitation, numerical estimates 7-31818
 conference, Boston, MA, USA (Dec. 1985) 7-9590
 conference, laser science advances, Dallas, TX, USA (Nov. 1985) 7-9573
 continuous IR laser excitation, chem. kinetics appl. 7-65310
 cooling, semiclassical theory 7-5640
 coulomb screened potential, charged particle scatt., multiphoton free-free transitions 7-18641
 cubic crystals, nonlinear phonon generation via localised modes 7-51978
 damage in solids, review 7-38054
 damage research at LANL (USA) 7-57392
 desorption, electronic transition induces, workshop, Schloss Elmau, Bavaria, Germany (Oct. 1984) 7-20
 desorption, laser-stimulated, desorption mode instability 7-21634
 desorption from surfaces, nonequilib. infrequent events, mol. dynamics 7-38322
 diatomic mol. on substrate, reson. laser induced desorption, classical and quantum models 7-58618
 difluoroethane resonant mols., capillary flow, laser light effects in transitional flow regions 7-57927
 dimethylnitramine, pulsed laser pyrolysis GC/MS anal. 7-65308
 dimethylnitrosamine, pulsed laser pyrolysis GC/MS anal. 7-65308
 dressed-atoms, stimulated pair transition in strong light fields 7-62327
 drops, surface tension dynamics, laser-induced modification 7-58570
 dye solutions, quantum efficiency of fluoresc., determ. by diffraction at laser induced phase grating 7-3081
 elastomers, impurity containing, exposed to laser pulses, thermooptic lenses, form. kinetics 7-51671
 electric voltage and current pulse generation by laser interaction with target 7-44611
 electron scatt. in a laser field, modified perturbation theory 7-36572
 electron scattering in nonMarkovian fluctuating fields, high intensity effects 7-25472
 electron-atom collisions in external laser field, n-phonon processes 7-50038
 electron-atom collisions in presence of strong laser field, Kroll-Watson formula 7-5638
 etching of polyimide encapsulants in IC eval. 7-53941
 ethene, gas, CO₂ laser irradiation, end-point anal., IR spectroscopy detect. 7-65335
 ferromagnets heated with a short intense laser pulse 7-64460

laser beam effects continued

fibre-reinforced composites, mechanical effects of Nd:glass laser 7-6676
 French Metallurgy Society meeting, Paris, France (Oct. 1986) (*French*) 7-29579
 fused quartz, surface periodic struct. formation during vaporisation by CO₂ laser radiation 7-6936
 fused silica, laser-driven shock wave dynamics study 7-44691
 gas, laser beam configs. for cumulative interaction with electrons 7-11584
 gas mixture-laser interaction model, appl. to thermally activated laser-induced CVD 7-46333
 gas-solid interface, photon-phonon conversion, laser-linewidth effects 7-58599
 Gaussian laser mode absorpt. in mol. beam 7-57484
 glass, fused spots formed by laser radiation, interferometric study 7-2054
 glass, laser damage initial stage, luminesc. and microwave absorpt. obs. 7-31375
 glass, laser exposure, repeated, absence of below-threshold ionisation and cumulation effect 7-63653
 glass, laser irradiated with picosecond high-power pulses, long-range structural changes 7-12123
 glass, microdefect accumulation kinetics during optical irradiation 7-38050
 glass, molten, jet formation during absorpt. wave propag. 7-46251
 graphite, first wall thermal performance in ICF reactor 7-49634
 graphite, laser ablation, small-scale expts. 7-61517
 graphite, laser excitation effects, time resolved picosecond reflectivity study 7-12136
 graphite, laser heated, optical characts. 7-32686
 graphite, pulsed laser melting, impurity redistrib., RBS channelling, Raman scatt. and TEM meas. 7-12135
 graphite fibre reinforced epoxy, reflectance and thermal response during high-power CO₂ laser irradi. 7-32496
 graphite surface laser irradiation, ionic cluster desorption, time-of-flight meas. 7-12138
 graphite surface pulsed laser irradiation, SEM, TEM and STEM microstructural studies 7-12139
 graphite surface pulsed laser melting, cluster form. and evaporative loss, nanosecond time resolved reflectivity meas. 7-12137
 gratings written with single laser beam, laser-induced surface ripples, Raman microprobe obs. 7-20400
 half-space heated by laser radiation, thermoelasticity generalised dynamic problem 7-1476
 hardening of instrument parts, holographic evaluation 7-5857
 heat conduction in a moving semi-infinite solid subjected to pulsed laser irradiation 7-62964
 heating of slab by time-dependent irradiation 7-21266
 high-technology materials processing, review 7-13342
 homogeneous medium, selective laser heating and nonlinear light scattering 7-5938
 insulators, excimer laser irradiated, surface deformation 7-21596
 insulators, laser breakdown due to nonequilib. changes in their optical characts. near absorbing inclusions 7-53233
 intense incoherent light flashes, optohydraulic effect 7-20760
 interference filters, laser-induced heat flow 7-43333
 ion-implanted layers, crystallisation dynamics, during pulsed laser irradi. 7-44435
 laser created X-ray source, study and appls. 7-61418
 laser direct writing and laser-assisted CVD of III-V cpds. on GaAs 7-1373
 laser spectroscopy, conf., Maui, HI, USA, June 1985 7-9586
 laser-generated ultrasound, detect. using confocal Fabry-Perot interferometer 7-50893
 laser-hardened layer thickness, influence of laser pulse time profile 7-44612
 laser-induced convection, instability, laminar to turbulent transition 7-37464
 laser-irradiated materials, nonequilib. melting and solidification, computational modeling 7-2059
 laser-plasma ablation, steady-state theory, self-regulating flow 7-58024
 laser-stimulated desorption of adsorbed molecules via electronic excitation 7-59309
 laser-stimulated phase transition kinetics, theory 7-6775
 laser-triggered electrical breakdown of gases, unconventional geometries 7-44095
 LiF, physisorbed bromomethane, laser photofragmentation and photodesorp. 7-50275
 LIMA analysis, performance assessment and applications 7-28375
 liquid aerosols, laser-induced breakdown, droplet size effects 7-44272
 liquids, natural convection caused by laser radiation absorpt. 7-26274
 magneto-optical thin films, under laser irradiation, thermal anal. 7-45995
 materials processing, conf., London, England (Dec. 1986) 7-48185
 materials processing, temp. distrib. meas. in laser-heated materials 7-9837
 materials processing, welding and machining, conf., San Francisco, USA (Nov. 1985) 7-9597
 melting of solids, theory 7-21267
 melting of solids, theory 7-21268
 metal, intense laser irradiation melting in high vel. gas flow, interaction model calcs. 7-58321
 metal, kinetics of equilibrium oxidation, CW laser irradiation 7-17721
 metal, nitriding, laser-plasma synthesis, melting processes calc. 7-28176
 metal bulk sample, laser heating and combustion by obliquely incident radiation 7-26795
 metal processing by pulse-periodic CO₂ laser radiation, physical laws 7-51824
 metal surface, field adsorbed He and Ne, atom-probe spectroscopy studies 7-32803
 metal surface, pulsed laser induced desorption 7-58617
 metal surfaces, opaque, ablation due to laser irradiation 7-2055
 metal surfaces, pulsed laser irradiation, thermomechanical effects, interferometric study 7-20303
 metal target, elec. charged, pot. change under laser irradi. 7-44616
 metallic and ceramic ultrafine particles, laser prod. 7-13406
 metallic films, growth by laser photolysis of carbonyls, C and O incorporation mechanisms 7-58685
 metallic glasses, metastable struct., surface melting, by plasma, laser or electron beams 7-63495
 metals, heating at free surface by laser irradiation, electron kinetic theory 7-6073
 metals, laser oxidation, absorptivity meas. 7-59682

laser beam effects continued

metals, laser radiation absorption, dependence on shape 7-26794
 metals, laser radiation screening by damage products 7-32493
 metals, scanned CW laser beam, surface EM wave rule 7-45172
 metals, vaporisation by laser radiation, vapour emission (*Russian*) 7-44782
 metals laser radiation, nature of mass transfer (*Russian*) 7-32494
 microoptic components formed by local modification of the structure of porous glasses 7-43451
 molecules, explosive absorption of finite-diameter laser beam 7-50269
 MOSFET, excimer laser beam irradiation and RIE, radiation damage 7-2056
 multilayer components for soft X-ray laser cavities, damage threshold 7-25844
 nematic films, collective rotation of molecules driven by the angular momentum of light 7-27686
 nematic liq. cryst., laser-induced mol. reorientation, nonlocal radial depend. 7-58131
 nematic liquid crystals, dynamic self-diffraction effects 7-11033
 neutral atoms laser coding and EM trapping 7-19777
 nitroaromatic crystals, resonance UV laser radiation interaction, characts. 7-25618
 nitrocellulose film, on Cu, BaF₂ or K8 glass, periodic microrelief, laser irradiation 7-63927
 noble metal surfaces, laser stimulated desorption during Cl₂ reactions 7-53453
 nonlinear optics, surface probe appls. 7-11064
 nonreactive systems, laser excitation and collisional energy transfer 7-42688
 oil surface deformation by laser heating, laser-beam self-focusing and capillary wave generation 7-50656
 optical silicate glass melt, fracture in laser beam 7-43278
 optical surface defect characts. using pulsed laser damage methods 7-37010
 oxide, laser reduction to metal, effect of heat conduction 7-17674
 periodic surface structure formation on film coatings 7-38051
 phonon pumping of superconductors 7-33125
 photodesorption, laser-induced, effect of resonant vibrational energy transfer 7-52293
 photodesorption via stimulated Raman emission of coherent surface phonons 7-16865
 piezoelectric material, with strain depend. dielec. const., modulational instability of laser beam 7-27677
 planar targets irradiated by 0.27 μ m laser, mass ablation rate and pressure meas. 7-46250
 plasma wave generation, laser interactions and particle acceleration, review (*French*) 7-31954
 plexiglass, laser-driven shock waves using dye laser irradi. 7-32569
 plume generation, influence on processing phenomena in YAG laser materials processing 7-12148
 PMMA, microdefect accumulation kinetics during optical irradiation 7-38050
 PMMA, UV laser photoablation, mass spectroscopic studies 7-22853
 PMMA films, transparent, radiation strength, low-molecular-weight additives effects 7-43273
 PMMA surfaces, excimer laser irradiated, XPS studies 7-51822
 poly(α -methylstyrene) surfaces, excimer laser irradiated, XPS studies 7-51822
 polyimide, XeCl laser ablated, conical structures obs. 7-3467
 polyimide encapsulants, laser induced etching 7-53941
 polyimide films, laser ablation in pressurized gas ambients 7-46661
 polyimide films, UV laser ablation 7-59648
 polymer film, excimer laser micromachining and surface microstruct. modification 7-53940
 polymer films, patterning by dry photoetching technique involving UV laser 7-34232
 polymer surfaces, IR laser irradiation, physico-chem. and chem. transforms 7-65350
 polymer surfaces, UV laser ablation dynamics 7-39684
 polyphenylene oxide article surface, nonstationary thermal field created by IR laser radiation, chem. processes control 7-16622
 potential scattering, resonant, in low-freq. laser field 7-18642
 probe beam diffraction at laser induced thermal lens 7-20135
 pulsed laser interactions with condensed matter, review 7-12125
 pulsed photoacoustic generation mechanisms 7-50892
 pulsed power considerations for laser guided discharges and appls. 7-37801
 pulsed power handling capability of optical fibers 7-20464
 pyridine, on Ag surface, IR laser stimulated desorption mol. spectroscopy 7-58614
 quantum optics, conf., Copenhagen, Denmark (Nov. 1985) 7-7
 quartz glass, microdefect accumulation kinetics during optical irradiation 7-38050
 radiation hydrodynamics of laser-irradiated foils 7-1649
 Raman microprobe appl. to mapping solid surfaces 7-56333
 random telegraph noise in laser-assisted collisions 7-50044
 resonance interaction of phonons with bichromatic laser radiation 7-21369
 rhodamine 590 droplet, micrometer size, high intensity laser interaction 7-43210
 Rydberg state prod. classical limit 7-876
 sapphire, filaments, CO₂ laser heating, evaporation and chlorination 7-58331
 semiconducting crystals, surface reconstruction model calcs. 7-32780
 semiconductor, surface undulations produced by pulsed laser illumination, Raman microprobe analysis 7-12430
 semiconductor chalcogenide layers, optical recording physical basis (*Russian*) 7-50667
 semiconductor rod, laser irradiated, photoacoustic wave forms, temp. depend. 7-6728
 semiconductors, laser damage of solid targets 7-58326
 semiconductors, nonlinear excitation, picosecond laser induced 7-11024
 semiconductors, ultrashort strain pulse excitation due to optical radiation absorpt. 7-32579
 sensitised organic reactions, IR-laser induced, vibr. energy transfer rate control 7-65336
 shock waves initiated by gigawatt CO₂ laser pulse in transparent target, holographic interferometry 7-38052
 slow electrons, pot. scatt. in laser field 7-18639
 SOI thin films, props. after laser focused beam processing 7-32497

laser beam effects continued

- solid surfaces, pulsed laser irradiation, energy dissipation, ion formation studies 7-46259
- solid surfaces after laser irradiation, Raman microscopy 7-21264
- SOS films, pulsed laser beam excitation, femtosecond dynamics 7-13249
- special relativity, fast beam laser spectroscopy tests 7-9666
- spectroscopy, isotope separation and photochemistry, laser-induced processes, review 7-36554
- stearic acid, evaporated thin layer, effect of laser irradiation 7-58328
- steel, C, laser treatment on fatigue and wear resistance 7-39672
- steel, high-speed, thermal stability improvement by laser alloying 7-8170
- steel, line hardening by low-power CO₂ lasers 7-13653
- steel, low C, alloying using high-intensity sources 7-28179
- steel, mild and Cr, surface saturation with B by laser radiation 7-8172
- steel, Ni alloy, laser-induced C atom directional motion 7-44894
- steel, stainless, CO and SO₂ adsorption, kinetics and laser-stimulated surface oxidation 7-63958
- steel, stainless, laser alloying with Au(Mo), Rutherford backscattering and channelling studies 7-28206
- steel, stainless, type 302, ignition of bulk by laser heating 7-3516
- steel, surface oxidation through laser beam treatment, oxide film, struct. and wettability 7-8158
- steel, TiN coating, ion-plasma appl., laser alloying, dynamic surface strength 7-17730
- steel, tool, laser surface glazing, microstruct. rel. to melt depth 7-46691
- steel 45, boronising the heating by laser radiation 7-8173
- steel surfaces, heat hardening with scanning laser beam 7-13634
- steel U6, laser alloying with W base facing powder, SiO₂ and B₄C additions effect 7-8171
- stimulated Wood's anomalies on laser-illuminated surfaces 7-11040
- submicrosecond elastic loading, material relax. phenomena 7-12186
- surface analysis by laser induced thermal waves (German) 7-8334
- surface contaminants identification, using electron spectroscopy and SEM techniques 7-4935
- surface engineering for corrosion protection, electron beam and laser glazing 7-3478
- surface modelling and absorption 7-58325
- surfaces, energy coupling during laser matter interaction 7-58327
- surfaces, laser-induced molecular processes 7-53452
- switch, all-optical, using interaction between low power light beams in liquid film 7-25864
- Te elemental and alloy thin films, laser irradiation effects, refl. meas., optical data storage appl. 7-12144
- thermal lens oscills. on liq. surface produced by laser beam 7-11403
- thermoacoustic radiation of sound by a moving laser source 7-62947
- thermo-optical sound generation in a metal 7-16052
- thin layered interference mirrors, radiation damage reduction 7-31433
- thin layers, laser sputtering, struct-form., Monte Carlo modelling 7-27901
- transparent liquid, laser-induced absorption wave propag., hydrodynamic mechanism 7-43945
- tunable-laser-induced gratings for the measurement of ultrafast phenomena 7-11041
- two-layer system, laser beam heated, transient temperature response 7-39190
- two-level atom, Brownian motion in light wave 7-897
- two-level atomic gaseous medium, light beam reson. interaction, radiation trapping effect 7-42559
- two-level atoms, beam compression by laser radiation press. 7-42555
- two-level atoms on conventional and phase conjugated surfaces, laser induced phenomena 7-57025
- two-step photoburning of spectral hole (Russian) 7-20306
- window heating by pulsed laser, focal lengths and rise times 7-43179
- Al alloy surface, UV laser pulse irradiation, microscopic crater form. 7-12124
- Al surface, impulse coupling coeff. and Nd:glass laser irradiation-induced material removal study 7-64828
- Al thin films, pulsed laser melting, transient elec. resist. and reflectance meas. 7-12141
- Al/SiO₂/Si₃N₄/Si illuminated struct., nonlinear capacitance props. study 7-38731
- Al-Cu (4.5 wt.%), laser treated, surface solidification with moving heat source 7-22648
- Al-Mn icosahedral alloy form. by pulsed electron beam and laser beam surface melting 7-26924
- Al₂O₃, laser ablation, laser-induced fluorescence study 7-46249
- Al₂O₃, mixing of metal overlayers, ion beam irradiation, rapid thermal annealing, pulsed laser irradiation. 7-58330
- Al₂O₃/Fe interface, ion beam mixing, conversion electron Mossbauer spectra studies 7-63679
- Ar, breakdown, ruby laser induced 7-11579
- Ar, laser-induced discharges, electron distribution function, collision frequency effects 7-63387
- As (0001), laser pulsed oxidation modification 7-58320
- As-S, amorphous semicond. films, laser action on light sensitivity (Russian) 7-64713
- As₂Se₃ amorphous films used for optical recording, structural transformation mechanisms (Russian) 7-51823
- Au films, rapid crystal kinetics under laser irradiation, picosec. transient reflectance meas. 7-11915
- BaF₂ (111), laser sputtering, layer-dependent 7-13274
- BaF₂ (111) surface, laser-induced sputtering, wavelength dependence 7-13273
- Br, photodissociation, initiated by laser emission 7-65339
- C atoms, double excitation and ionisation by strong pulsed laser 7-42571
- C films, amorphous, laser generated, struct. and bonding, Raman and electron energy loss spectra study 7-27800
- a-C films, crystallisation, influence of residual stresses and density fluctuations 7-21750
- CaF₂, optical damage, laser mass spectrometric study 7-58319
- Cd films, laser-assisted oxidation 7-65208
- CdS excited state dynamics studied by transient grating techniques 7-12616
- CdS resonant self-diffraction from dynamic laser-induced gratings 7-11036
- CdS single crystals, subsurface region comp., laser radiation effects, AES study (Russian) 7-58329
- Co, oxidation kinetics, laser control 7-28174
- Cr films, thin polycrystalline sputtered, oxidation by CW CO₂ laser irradiation 7-13642
- Cr single crystals, surface and deeper layers, struct. changes due to laser irradiation 7-6937

laser beam effects continued

- Cr-Ni (45 wt.%) amorphous free-standing thin films, struct. transformations, pulse laser irradiation 7-38382
- Cs, stopping with diode laser beam 7-10507
- CsI, surface stoichiometry, changes under electron and laser radiation 7-44961
- Cu, chlorinated surface, laser-induced desorption and etching processes 7-27092
- Cu films, laser-assisted oxidation 7-65208
- Cu films, rapid crystal kinetics under laser irradiation, picosec. transient reflectance meas. 7-11915
- Cu foil, excimer laser assisted gas phase etching 7-54015
- Cu mirrors, Ag⁺ implanted, laser oxidation and optical props. 7-5971
- Cu, oxidation kinetics, laser control 7-28174
- Cu thin films, CW Ar⁺ laser-induced oxidation 7-39694
- Cu-Al-Ni-Fe bronze, laser glazing, microstruct. 7-52197
- Cu-Al-Ni-Fe-Mn bronze, cast, laser surfacing, improved corrosion resist., microstruct. characteris. 7-13651
- Cu-Cr multilayers, laser alloying 7-45025
- Cu-O, laser reduction to metal, effect of heat conduction 7-17674
- CuCl excited state dynamics studied by transient grating techniques 7-12616
- CuCl nanosec. laser etching, time-of-flight study 7-39687
- CuI solid surface, laser-induced desorption and etching processes 7-27092
- Fe based eutectic alloy powder, plasma coatings with interstitial phases, tribotechnical props. 7-17731
- Fe, cast, high-Cr, wear-resistance, laser and heat treatment effect on struct. and props. 7-8174
- Fe, laser irradiation, Nb surface alloying, Mossbauer spectra (Russian) 7-58580
- Fe, metal surfaces immersed in liquid media, pulsed laser oxidation and nitridation 7-59656
- Fe, pulsed laser irradiated, spin-polarised photoemission 7-39360
- Fe, surface, H₂ and N₂ interactions, pulsed laser atom probe studies 7-32811
- Fe surface layers under toluene, laser irradiated, supersaturation with C 7-51820
- Fe thin films, formed by laser breakdown CVD, metastable phase form. 7-38377
- Fe/H₂O interface, pulsed-laser-induced reactive quenching, FeO metastable phase form. studies 7-45005
- Fe-B-Si and Fe-B-Si-Cr-Mo-W alloys, finely crystalline and amorphous structures, on surface by laser treatment 7-8175
- Fe-Cr-Mn-C alloy, laser clad, microstruct. and wear props. 7-13652
- Fe-Si (3 wt.%), mag. props. and domain struct., influence of laser treatment 7-12993
- Fe₈ cluster, vibr. photodissociation spectra, IR laser study 7-62475
- Fe₈₀B₁₄Si₃C₂ metallic glass, laser beam irradiation, high energy, shear band form. and cracking 7-59606
- Fe(CO)₅, laser stimulated CVD, kinetics 7-64925
- Ga crystalline film amorphisation by pulsed excimer laser irradiation, residual resist. and T_g meas. 7-12140
- Ga-As-AlGaAs superlattice, laser induced disordering and Si impurity incorporation 7-45018
- Ga-Se-Te, phase change optical recording, write erase characteristics 7-57491
- GaAlAs, LIMA anal., effect of alloy composition on secondary ion yields 7-28376
- GaAs, excimer laser projection etching 7-13662
- GaAs excimer-laser-stimulated CVD, polycryst. thin film growth and props. 7-64912
- GaAs, ion implanted and laser irradiated, defect studies 7-32432
- GaAs, laser-induced damage and ion emission at 1.06 μm 7-37008
- GaAs, laser-induced melting and nonlinear optical studies 7-12432
- GaAs, superheating during picosecond laser melting 7-12246
- GaAs surface, formation of gratings in laser photoemission wet etching 7-8205
- GaAs surfaces, picosecond laser melting and evaporation 7-12120
- GaAs surfaces, picosecond laser interactions, time-resolved optical studies 7-12134
- GaAsP, MOCVD growth, IR laser assisted grading 7-27945
- GaP, coherent optical phonon generation and decay 7-33040
- GaP, phonon shifts due to temp. and pressure rise induced by a laser beam 7-2125
- Ge, amorphous films, laser induced image storage 7-11078
- Ge, laser heated, time-dependent X-ray reflectivity 7-26796
- Ge, laser irradiated, electron-hole plasma dynamics investigated by time-resolved spectroscopy 7-13276
- Ge, periodic surface microrelief, determ. optical constants of laser-irradiated material 7-63926
- Ge, reflectivity meas. during pulsed laser irradiation 7-12132
- Ge surface, GeO stabilisation on laser irradiation, X-ray photoelectron spectra anal. 7-46723
- Ge surface laser irradiation, ionic cluster desorption, time-of-flight meas. 7-12138
- H, laser-assisted electron. elastic scatt., differential cross sections, exchange and dressing study 7-20046
- H₂, electron impact, in laser field, one-photon free-free transitions 7-980
- H₂O droplet, vaporisation by laser beam, electrohydrodynamics self-similar study 7-1645
- H₂O droplets, laser-induced explosion, spatially resolved spectra 7-42632
- Hf, surface nitridation by powerful CW CO₂ laser irradiation in air 7-2051
- HgCdTe, ambipolar diffusion and free carrier recombination studied by transient grating technique 7-12731
- I, photodissociation, initiated by laser emission 7-65339
- I₂, supersonic flow study by 3D visualization and laser-induced fluorescence 7-20751
- InP, laser enhanced low temp. oxidation, dissociation of N₂O 7-39780
- InSb, pulsed laser evaporation, neutral and charged particle emission 7-3120
- InSb, transient grating formation under two-photon excitation 7-11037
- In₂Se₃ films, laser synthesized, optical props. 7-59276
- In₂Se₃ films, synthesis with pulsed ruby laser 7-58707
- K, laser radiation effects in trapping 7-15554
- K_N, laser photoionisation of clusters containing up to 101 atoms 7-42822
- KBr N₂⁺ centre, selective two-step photoionisation using 1.06 μm radiation 7-38053
- KBr single crystals, X-ray irradiation, F-band absorption and thermolum., effect of laser excitation 7-21277

laser beam effects continued

- KCl(Br), radiation defects created by decay of electronic excitations 7-16626
 KLi (F_2^+)_A centre, selective two-step photoionisation using 1.06 μ m radiation 7-38053
 KTiOPO₄ crystal and optical props. 7-17403
 LaF₃:Pr³⁺,Nd³⁺, energy up-conversion, UV fluoresc. obs. 7-53401
 Li+Na, ion-pair production, laser excitation effect 7-62502
 LiF:Mg,Ti phosphor layer on borosilicate glass substrate, laser stimulated thermolum. 7-64703
 LiNbO₃, etching, laser-driven chem. reactions 7-3468
 LiNbO₃:Fe, linear electro-optic effect, optical damage by He-Ne laser (Korean) 7-27698
 LiNbO₃:Fe, speckle size depend. on laser beam size via photo-induced light scattering 7-5840
 LiNbO₄ crystal, surface photorefractive effect under UV laser irradiation 7-2057
 LiTaO₃, Czochralski grown with modulated struct., periodic laminar ferroelec. domains, SHG, optical damage threshold 7-59405
 Mg⁺ cooling by laser beam 7-25458
 Mg₂SiO₄, laser-heated, temp. distrib. meas. 7-9837
 MnCO₃, decomp. to Mn₂O₄, kinetic evol. for laser/thermal prep. 7-39870
 Mo field evaporated ions, energy distrib. obs. and evidence for post field ionisation 7-46281
 Mo, laser photochemical etching by surface halogenation 7-46676
 Mo, polycryst., dynamic recovery during rapid dumping of energy from pulsed laser (Russian) 7-32495
 Mo(100), pulsed laser irradiated, use of LEED for surface damage charact. 7-21592
 N₂O, laser dissociation, laser enhanced oxidation of InP 7-39780
 Na ion beam generation, field ionisation of laser-excited Rydberg atoms 7-57186
 Na, laser cooling to temp. of 10⁻⁶K 7-10506
 Na, optical piston dynamics using light-induced drift 7-10508
 Na+Na collisions, Rydberg state forbidden transitions in laser-assisted processes 7-5617
 NaCl crystal, surface optical breakdown, exoelectronic emission with laser irradiation, impurity effects 7-59384
 NaCl, prebreakdown nonlinear energy deposition from intense photon fields 7-51825
 Nb-a-Si-Nb Josephson junctions, for IR laser radiation response near plasma reson. freq. 7-58958
 Nb-W, superconductor-normal metal point contacts in field of CO₂ laser 7-38684
 Ni (100), chemisorption and decomposition of ethylene 7-59785
 Ni (111), desorption of CO and CO₂ molecules, Ni atom evaporation during laser bombardment 7-58628
 Ni, ion implantation and pulsed laser melt quenching, metastable phase and defect struct. form. studies 7-16625
 Ni, thermoelectric amplification of acoustic waves, CO₂ laser irradiation 7-33055
 Ni thin films, formed by laser breakdown CVD, metastable phase form. 7-38377
 Ni-base wrought superalloy, thermal fatigue resist. improvement by laser-glaze 7-22840
 P₂O₅-SiO₂ glass in multilayer struct., laser-induced flow modelling 7-38057
 PZT ceramics, pulsed TEA CO₂ laser irradi., signal generation 7-16623
 Pb_{1-x}Cd_xSe films, laser deposition 7-59422
 Pb_{0.8}Sn_{0.2}Te thin films, structural and elec. props., pulsed laser-irrad. effects study 7-21270
 Pd-Rh-P-Si, surface alloy vitrification by laser treatment 7-21271
 Pt (111), adsorption and desorption of NO, CO or H₂ 7-21643
 SF₆ resonant mols., capillary flow, laser light effects in transitional flow regions 7-57927
 Se, thin film formation by pulsed laser evaporation 7-59426
 Si (100), laser irradi., matrix atomic losses and impurity incorporation 7-2058
 Si (111), adsorbed Mo(CO)₆, laser induced electronic excitation followed by CO desorption 7-12470
 Si (111), surface ripples, depend. on laser pulse width 7-12445
 Si, amorphous, ion implanted, picosecond laser induced crystn. 7-16621
 Si, amorphous foil, time-resolved X-ray absorption during pulsed laser irradiation 7-12128
 Si, chemical sputtering by ions, electrons and photons 7-59355
 Si, crystal growth and solidification, high speed laser heating technique 7-53566
 Si, excimer laser photoablation, spectroscopic characts. of plasma 7-54019
 Si exciton transport, optical time-of-flight investigation 7-64244
 Si films, laser beam melted, facet formation at solid-melt interface 7-38418
 Si films, laser-induced melting and recrystn., heat transfer algorithm 7-21269
 Si films, phase diagram of laser induced melt morphologies 7-12131
 a-Si foils, pulsed laser irradi., clusters and plasmas, time resolved X-ray absorpt. meas. 7-64755
 Si, ion implanted, laser beam melting and resolidification 7-12126
 Si, laser ablation, cluster and plasma formation, time-resolved X-ray monitoring 7-37710
 Si, laser induced defects, rapid and classical thermal processing, annealing kinetics 7-44609
 Si, laser irradiated, electron-hole plasma dynamics investigated by time-resolved spectroscopy 7-13276
 Si, laser irradiated, surface morphology and phase transitions 7-12121
 Si, laser oxidation, electrophysical parameters of films produced 7-17741
 Si, laser-induced etching with Cl₂ 7-22915
 Si, melting induced by picosecond laser pulses 7-38166
 Si monocrystalline, light-induced grating measurements 7-11035
 Si optical phonon spectrum transform. obs. under laser pulse bombardment, CARS study 7-51967
 Si, overheating during pulsed laser irradiation 7-12127
 Si, oxidation, UV laser-induced 7-65234
 Si, periodic surface microrelief, determ. optical constants of laser-irradiated material 7-63926
 Si, photon enhanced oxidation mechanisms 7-54032
 Si, polycrystalline films, laser-recrystallized, grain boundary location using antireflection cap 7-46312
 Si, reflectivity meas. during pulsed laser irradiation 7-12132

laser beam effects continued

- Si SOI structures, polycrystalline Si films, seeding laser recrystn. 7-58706
 Si single cryst., laser-driven shock induced damage study 7-64829
 Si, structural changes produced by one micron picosecond laser pulses, TEM characterisation 7-12133
 Si surface, cellular structures formation due to interaction with picosecond light pulses 7-44960
 Si, surface, periodic struct. form. by millisecond pulsed laser light 7-44975
 Si surface laser irradiation, ionic cluster desorption, time-of-flight meas. 7-12138
 Si, thermal oxidation, UV light stimulated 7-59687
 Si thin film, laser-irradiated melt morphology and order-disorder transitions studies 7-44614
 Si:As(Sb)(In), heavily doped, laser induced oxidation 7-13672
 Si:Au, laser radiation effects on impurity levels 7-12645
 Si:Bi, solute trapping by lateral motion of {111} ledges 7-44592
 Si:Cu, amorphous, explosive crystn., RBS and time-resolved reflectivity studies 7-21265
 Si:Cu, ion implantation-amorphised, direct imaging of pulsed laser-induced buried molten layers 7-12130
 Si:In, nucleation of internal melt during pulsed laser irradiation 7-12129
 Si:P, polycrystalline, excimer laser photochemical directional etching 7-65226
 Si:P, pulsed laser annealing, molten phase local nucleation study 7-63655
 Si:Al optically excited diaphragms, reson. freq., temp. depend. 7-18971
 Si-Ti interface, laser irradiated, silicide formation 7-45079
 SiC, mixing of metal overlayers, ion beam irradi., rapid thermal annealing, pulsed laser irradi. 7-58330
 Si₃₀Ge₇₀, model alloy system, liquid-solid interface dynamics, rapid solidification 7-6761
 SiH₄, photolytic or pyrolytic dissoc. under laser irradi., Si film deposition 7-13388
 Si₃N₄, amorphous, pulsed laser excited photolum. intensity and decay meas. 7-17344
 Si₃N₄ amorphous insulator thin films, defect-enhanced UV etching damage studies 7-26797
 Si₃N₄, mixing of metal overlayers, ion beam irradi., rapid thermal annealing, pulsed laser irradi. 7-58330
 SiO, oxidation, UV laser-induced 7-65234
 SiO₂, amorphous, thermal, UV irradiation induced compaction and photoetching 7-12146
 SiO₂, chemical sputtering by ions, electrons and photons 7-59355
 SiO₂, dry silica, UV induced defect creation, ESR study 7-13032
 SiO₂, laser-induced breakdown, radiation induced defects 7-12147
 SiO₂, mixing of metal overlayers, ion beam irradi., rapid thermal annealing, pulsed laser irradi. 7-58330
 SiO₂:GeO₂ integrated optical waveguides, laser heating effect on opt. props. 7-50792
 SiO_x, amorphous, photoassisted oxidation 7-46662
 SiO_x amorphous insulator thin films, defect-enhanced UV etching damage studies 7-26797
 Sn superconducting films, resistive state visualisation using laser beam scanning 7-17142
 β -Sn surface laser irradiation, ionic cluster desorption, time-of-flight meas. 7-12138
 Sr, scattered light obs. with laser excitation 7-30968
 TbFe films, micron-size laser-written mag. domains, Lorentz microscopy 7-2913
 Te crystalline thin films, laser-induced transform., transient conductance and optical meas. 7-12142
 Te_{1-x}Ge_x amorphous films as reversible phase-change optical data storage materials 7-1242
 TeO₂ films, nanosecond pulsed laser-induced segregation 7-44610
 Ti, film, periodic microrelief, laser irradiation 7-63927
 Ti, metal surfaces immersed in liquid media, pulsed laser oxidation and nitridation 7-59656
 Ti nitridation by breakdown plasma in N₂ due to TEA CO₂ laser irradi. 7-2052
 Ti plate, ignition in air under CW laser radiation action 7-32492
 Ti thin films, laser-induced damage, parameters effects 7-21275
 TiO₂ films, pulse laser irradiated, Raman studies of phase transformations 7-12569
 V films, laser-induced oxidation kinetics 7-59681
 V, laser photochemical etching by surface halogenation 7-46676
 ZnO resonant self-diffraction from dynamic laser-induced gratings 7-11036
 ZnSe, cryst., spectral broadening about second harmonic generated by laser pulse 7-43236
 ZnSe optical films, molecular beam fabrication and laser damage props. 7-39389
 Zr nitridation by breakdown plasma in N₂ due to TEA CO₂ laser irradi. 7-2052
 Zr surface, N₂ laser irradi., at. beam prod. 7-21276
 Zr, surface nitridation by powerful CW CO₂ laser irradi. in air 7-2051
 Zr-Nb (1 wt.%), laser irradi., hardness, struct., corrosion resist. 7-3400
 ZrO₂ films, pulse laser irradiated, Raman studies of phase transformations 7-12569
- laser beam machining**
 drilling in subatmospheric press. atms. of air, plasma transients 7-20914
 high-technology materials processing, review 7-13342
 industrial laser annual handbook 7-24316
 materials processing, welding and machining, conf., San Francisco, USA (Nov. 1985) 7-9597
 metal processing by pulse-periodic CO₂ laser radiation, physical laws 7-51824
 meter for radiation parameters of engineering lasers 7-56316
 nuclear fuel disassembly, laser cutting system 7-10235
 semiconductors, laser machining, physical processes in surface erosion 7-2053
 CO₂ laser, high-power transverse-flow, props. 7-36935
 SiO₂ fibre, V-grooves fabrication using CO₂ laser 7-50783
- laser beam modulation** see optical modulation
laser beam properties see laser beams
laser beam variables measurement see laser beams; laser variables measurement
laser beam welding
 dentistry applications of lasers 7-40242
 high-technology materials processing, review 7-13342

laser beam welding continued

- industrial laser annual handbook 7-24316
- materials processing, welding and machining, conf., San Francisco, USA (Nov. 1985) 7-9597
- metal processing by pulse-periodic CO₂ laser radiation, physical laws 7-51824
- meter for radiation parameters of engineering lasers 7-56316
- plume generation, influence on processing phenomena in YAG laser materials processing 7-12148
- steel, HY series, laser weldments, S and Ni effects on mech. props. 7-13602
- steel, stainless, pulsed and continuous laser welded, solidification behaviour and microstruct. characts. 7-13444
- Al alloy, pulsed laser weldability 7-13702
- CO₂ laser, high-power transverse-flow, props. 7-36935
- CO₂, nuclear reactor fuel cladding repair (*Japanese*) 7-15243

laser beams

- see also holography; laser frequency stability; laser variables measurement; Schwarz-Hora effect*
- almost concentric resonators for low gain FEL, alignment and performance 7-43155
- apodisation with graded random phase window 7-31369
- array, randomly phased geometrical 7-36975
- articulated arm for laser beam delivery, in use and construction 7-50613
- astigmatism in laser beam optical systems 7-5829
- atmospheric correlation-time measurements and effects on coherent Doppler lidar 7-60385
- atmospheric near-mm wave propag., instrumentation for study 7-4219
- coherence of diffusely scattered radiation and its meas. 7-20134
- coherence props. control with plasma filter 7-1209
- complex optical systems, optical beam wave propag. 7-50492
- diaphragmed laser near field (*French*) 7-43180
- dispersive resonator with Gaussian stop and telescopic system, emission spectra study 7-62731
- dye CW lasers, three state pulse amplifier, temporal pulse shape 7-31344
- dye laser, short-cavity, tunable near IR picosec. pulse generation 7-50550
- dye laser, synchronously excited, with additional ultrathin resonator, picosecond pulse generation 7-31365
- dye laser radiation, polarisation modulation using intracavity method 7-62740
- external nonlinear focusing, appls. to ultrafast optical power limiting 7-50659
- far-field analytical model for laser arrays 7-11018
- femtosecond optical pulses use for investigating ultrafast phenomena 7-24640
- FIR laser beams, precision broadband attenuator 7-37012
- focusing of multimode laser beams with variable beam parameters 7-11021
- focusing system, dimensioning (*German*) 7-31378
- free electron laser, optical mode gain and evolution 7-43126
- gamma-ray beams produced by collision of relativistic ions with laser photons, spectrum and polarisation 7-50002
- Gaussian beam divergence meas. using SAW modulation 7-20297
- Gaussian beam focusing through hemispherical microlens 7-11090
- Gaussian beam transformation by Winkelmann-Abbe bi-prism 7-42904
- Gaussian beam transmission through circular aperture 7-50610
- Gaussian beams, generally astigmatic, propag. along skew ray paths 7-62623
- Gaussian beams, oscillations and discontinuity in focal shift 7-31374
- Hermite-Gaussian beam transformation by shifted spherical lens 7-42891
- index guided laser diodes, 1.3 μ m, far-field fine struct. study 7-57389
- intracavity SHG, mode-locked laser pulse temporal and spectral characts. 7-31393
- IR laser radiation propag. in weak atmosphere, phase fluctuations 7-40565
- IR radiation ultrafast switching by laser produced Ge plasma 7-11020
- light amplification due to nonlinear interaction of counterpropagating waves in a single-mode optical fiber 7-50646
- lightguides, time coherence effects of transverse laser modes 7-37009
- magnetic domain structure determ. using light diff., inverse problem (*Russian*) 7-53286
- methane, XeF laser pumped, high-efficiency first-Stokes generation 7-20347
- methane, XeF laser pumped, Stokes generation, beam parameters 7-20346
- multimode Gaussian beam photoreceiver recording 7-50612
- multimode Stokes conversion efficiency and output wavefront, off-reson. Raman interactions effect 7-20333
- multiple equivalent incoherent multiaxial-mode laser beams, Raman scatt. eqns. soln. 7-20338
- non-Gaussian laser beam form., laser with multilayer dielec. exit mirror 7-50611
- nonlinear distortion compensation of light beams with restricted deform. of control mirror 7-50622
- nonlinear resonator mode behaviour radiation power depend. on geometry 7-43160
- optical system calibration for laser beam divergence measurement (*Russian*) 7-20305
- optically thick medium exposed to laser beam, anisotropic back scatt. 7-62629
- phase conjugation of laser beam 7-25904
- phase conjugation of laser beams 7-25903
- phase conjugation reversing laser aberrations 7-50653
- phase conjugators, passive, abilities to perform aberration correction on laser beam 7-20362
- phase-coupled high power laser arrays, diff. limited output beams 7-50586
- phased-array laser, single-lobe radiation pattern generation using variable phase-shift zone plate 7-43182
- picosecond light pulse changes in a GaAs filled nonlin. Fabry-Perot resonator (*Russian*) 7-50620
- propagation in saturable absorbers, calc. 7-15953
- pulse compression by spectral hole in amplifier inhomogeneously broadened line 7-57483
- pulse duration selection using SHG, picosecond absorption spectrometer time resolution enhancement 7-61387
- pulse narrowing by backward stimulated Brillouin scattering 7-15936
- pyroelectric detection of laser radiation 7-56341
- Raman amplifier, phase correlation, pump beam temporal struct. effects 7-20343

laser beams continued

- Raman beam combining with multiaxial mode lasers 7-15939
- Raman oscillator, synchronously pumped, picosecond Stokes pulse generation 7-15933
- reflection in turbulent atmosphere under induced temperature nonuniformity of refractive index 7-60384
- rhodamine 6G ring dye laser, flashlamp pumped, short pulse generation using colliding pulse mode locking 7-43170
- ruby laser, Q-switched, pulse stretching for bubble chamber holography 7-43169
- ruby laser pulse compression and amplification, stimulated Brillouin scatt. in acetone (*Chinese*) 7-57455
- semiconductor laser, phase-locked controlled filament, far field pattern 7-10925
- semiconductor laser, pulsed, signal spectrum variation, expt. study and input signal cct. design 7-36966
- semiconductor laser, single-mode operation, influence of external resonator on emission spectrum 7-62695
- semiconductor laser, transverse beam deflection 7-5933
- semiconductor lasers, beam location and focusing using computer-controlled spot-centring technique 7-5934
- short pulse amplification in presence of absorpt. 7-57291
- soft X-ray laser beam, divergence meas. 7-1210
- soft X-ray laser development at Princeton, beam divergence meas. 7-20204
- solid-state laser pulses, spatial shaping, cavity resonator design criteria (*Polish*) 7-31363
- soliton laser stabilisation, feedback from pulse-shaping fibre 7-50602
- spatial energy distrib. determ. by Rayleigh scattering 7-43183
- stimulated Brillouin scattering for beam combination, phase conjugation 7-20348
- stimulated Raman scattering in intensity-averaging regime, beam cleanup 7-20340
- stimulated Raman scattering production of high quality laser beams 7-15930
- Stokes beams coherence props. for incoherent broadband pumps 7-20335
- transmission for laser beams using low-loss optical fibres (*German*) 7-37200
- turbulent atmosphere, thermal self-interaction of partially coherent laser beam 7-31376
- ultra-short pulses and intracavity dispersion compensation 7-57387
- ultrashort pulse optical freq. filter based on prisms 7-31441
- uniform and Gaussian beam diff. comparison, aberration balancing 7-62621
- unstable resonator with perforated mirror, phase struct. of radiation wavefront 7-25846
- UV laser beam profile monitor using alkali halide crystals 7-37011
- wait parameters determ. of Gaussian beam 7-37007
- wave-kinetic numerical approach to beam propag., canonical problems 7-31247
- wavefront dislocations in laser radiation field transmitted by fibre waveguide 7-25973
- weak picosecond pulse in glass, induced spectral broadening by intense picosecond pulse 7-31370
- Ar⁺ CW laser beam, central dark-space form. (*Chinese*) 7-57390
- CO₂ laser light modulation, liquid crystal cell, cholesteric-nematic phase transition 7-62745
- CO₂ laser pulse duration control by intracavity IR absorbing gas cell 7-43174
- CO₂ lidar systems, high speed tuning mechanism, spatial beam profile 7-36978
- CO₂ single and multilongit. mode laser emissions, SHG in CdGeAs₂ 7-43211
- CO₂ ultrashort laser pulse optical free induction decay, freq. spectrum 7-31405
- Cs vapour, generation of tunable IR ultrashort light pulses by nonlinear frequency conversion 7-1227
- Cu vapour laser with unstable resonator, background radiation influence on dye lasing 7-25856
- H₂ amplifiers, efficient high-gain, beam cleanup and low-distortion amplification 7-20341
- H₂ Raman amplifier, Stokes phase preservation 7-20342
- H₂, Raman beam combination of two-line XeF laser sources 7-20336
- He-N₂ laser, pulsed electric-discharge, laser props. investg. 7-62675
- I laser, solar-pumped, beam profile meas. 7-37006
- NH₃ superradiant Raman FIR laser with nonlinear reson. four-wave mixing generation of medium IR emission 7-50657
- Nd:glass laser amplifying system, pulse profile by saturable filters 7-43184
- Nd³⁺:YAG laser passively mode-locked by saturable absorpt. filter, ultra-short pulse generation 7-31368
- OD-CO₂ chemical laser, energy capabilities study 7-62683
- Si, photon enhanced oxidation mechanisms 7-54032
- XeCl excimer laser, amplification of UV ultrashort light pulses 7-62674
- XeCl excimer laser, generation and amplification of sub-ps UV pulses 7-62722

laser cavity resonators

- 1.5 μ m laser with high external quantum efficiency and controlled emission wavelength 7-57323
- acousto-optic mode locker, appl. to Ar ion laser 7-37005
- almost concentric resonators for low gain FEL, alignment and performance 7-43155
- anisotropic lasers, natural linewidth 7-43047
- annular reflectors for an FEL resonator 7-1146
- axial-symmetric optical passive resonators, transverse modes, series calc. (*Chinese*) 7-11003
- birefringent filter design for CW dye laser resonator, spectral tuning band 7-50720
- Bragg reflectors, overmoded cylindrical metal waveguides, coupled mode theory 7-57541
- cavity construction for single-mode tunable pulsed ring dye laser 7-11006
- cleaved coupled cavity lasers, multilongit. mode model 7-57372
- composite cavity waveguide complementary semiconductor lasers, low threshold current, large output power 7-62727
- coupled lasers, composite-resonator mode description 7-11007
- coupled optical resonators, local-field rate eqns. 7-1071
- DFB laser deficiencies and proposed alternatives 7-1194
- DFB lasers, fibre-extended-cavity, oscillation frequency tuning 7-57381
- diaphragmed laser near field (*French*) 7-43180
- diode compact linear array external cavity laser 7-43154

laser cavity resonators continued

diode discrete laser ensemble, external cavity, high spectral purity single mode CW and pulse output 7-43091
 diode element compact linear array external cavity laser, wavelength control 7-36992
 diode laser, V-grooved inner group, LPE grown, 100 mW 1.5 μm operation 7-57354
 dispersive resonator with Gaussian stop and telescopic system, emission spectra study 7-62731
 distributed feedback in optical waveguide, theory 7-57550
 double-channel planar BH multimode laser, 1.55 μm fibre grating external cavity, single-mode behaviour 7-15908
 double-pass amplifier with phase conjugate mirror, different frequencies counterpropagating waves amplification 7-50598
 dye laser, CW, with intracavity photorefractive element, mode selection 7-43167
 dye laser, short-cavity, tunable near IR picosec. pulse generation 7-50550
 dye laser, synchronously excited, with additional ultrathin resonator, picosecond pulse generation 7-31365
 dye laser, synchronously pumped, periodicity multiplication obs. with cavity length tuning 7-31311
 dye laser, synchronously pumped femtosecond CW, variable intracavity spectral windowing 7-36998
 dye laser, tunable with electro-optic Q-switching of coupled laser, characteristics 7-1197
 dye laser radiation, polarisation modulation using intracavity method 7-62740
 dye laser spectral condensation in intracavity spectroscopy, steady-state waves 7-50551
 dye laser with diffraction grating in resonator for holographic interferometry 7-43159
 dye lasers, multimode CW, dynamical instabilities, stimulated Brillouin scatt. 7-50552
 dye lasers, pulsed, intracavity, absorpt. kinetics 7-50554
 dye lasers, tuning by a cholesteric liquid crystal device 7-15858
 dye lasers using aqueous micellar solns., flashlamp pumped, efficiency and photostability 7-43084
 external-cavity laser diode, stabilisation of spectral linewidth and oscill. freq. using fibre-optic ring resonators (*Japanese*) 7-5921
 $\text{F}_a(\text{II})$ colour centre laser at 2.653 μm , synchronously pumped, mode-locked, cavity length meas. 7-5920
 Fabry-Perot interferometer, mirror random phase inhomogeneity influence, resonator use 7-24689
 Fabry-Perot resonator, confocal 4.5 m long for storage of megawatt laser pulses 7-1200
 Fabry-Perot resonators, for length reduction of tunable CW CO_2 lasers 7-11010
 Fabry-Perot resonators with active medium, large Fresnel numbers, asymptotic theory 7-11011
 fast frequency-tunable external-cavity laser, FSK modulation, 100 Mbits/s 7-57383
 FEL optical cavities, alignment, tuning 7-1143
 FEL ring resonators, mode rotation, intracavity beam divergence, alignment sensitivity 7-1144
 FEL two-stage, quasioptical cavity, cold testing 7-1145
 FIR waveguide laser cavity, quality factor 7-57379
 focusing of multimode laser beams with variable beamparameters 7-11021
 free electron laser, optical mode gain and evolution 7-43126
 frequency pulling and anomalous dispersion, aberration and perturbation effect 7-11004
 gain-guided laser arrays, excess modes 7-31316
 gas laser excitation, RF cavity design 7-57378
 gas waveguide lasers with diffraction grating, frequency selectivity and resonator losses 7-43158
 Gaussian mode calcs. for cavity filled with inhomogeneous lens-like medium 7-20283
 glass plates stack mirror, refl. coeff., temp. depend. study 7-57508
 grating resonator, selective props., appl. to lasers 7-50596
 hypersonic wavefront-reversing mirror operating in master-oscillator-amplifier config. 7-31399
 induced resonance electron cyclotron quasi-optical maser in an open resonator 7-20176
 injection heterolasers with crescent-shaped active region, spectroscopic props. 7-36962
 injection laser with external selective resonator, wide tuning range 7-43099
 injection lasers, external cavity, resonant self-pulsing, instabilities 7-43156
 integrated coupled-cavity lasers, design and fabrication 7-25843
 intracavity laser absorption spectroscopy lineshapes 7-18883
 intracavity laser spectroscopy sensitivity enhancement, use of saturable filter 7-62794
 intracavity SHG, mode-locked laser pulse temporal and spectral characts. 7-31393
 intracavity transformation of fields for flat wide-aperture resonators 7-43168
 Lamb dip asymmetry in lasers with plane-parallel resonators 7-5917
 LELA experiment, cavity alignment tests and status 7-1135
 Lorenz-type chaos in laser 7-36932
 losses, radiation spectrum locking, phase polaris. method 7-11012
 methanol, FIR lasers, intracavity triple reson. spectroscopy 7-10560
 methanol high power FIR cavity laser system with long-term stability 7-36982
 methanol- d_4 lasing lines on IR pumping by CW CO_2 laser 7-1082
 methanol- d_4 lasing lines on IR pumping by CW CO_2 laser 7-1082
 microwave excited flow lasers, configs. and operation (*German*) 7-36986
 mirror with corrugated waveguide on surface, spectral and laser characts. 7-43291
 multilayer components for soft X-ray laser cavities 7-25844
 multilayer structures for X-ray laser cavities 7-37001
 multipass grating interferometer applied to line narrowing in excimer lasers 7-35573
 multiple-stripe-geometry laser arrays, chirped and unchirped, modal eigenfunctions 7-57335
 non-Gaussian laser beam form., laser with multilayer dielec. exit mirror 7-50611
 nonlinear resonator mode behaviour radiation power depend. on geometry 7-43160
 nonsymmetrical five-layer LOC, DFB and DBR lasers, waveguiding props. 7-57319

laser cavity resonators continued

open laser resonators with tilted mirrors, losses 7-62730
 oscillation with photorefractive gain, review 7-11008
 oxazine 1 laser CW, pumped by He-Ne laser 7-36958
 parametric oscillation with aid of dynamic gratings, threshold conditions 7-1228
 parametric oscillations in semiconductor lasers 7-50647
 passive modulation laser of resonator Q-factor (*Russian*) 7-43172
 picosecond light pulse changes in a GaAs filled nonlin. Fabry-Perot resonator (*Russian*) 7-50620
 polarisation coupled resonators, spatial hole burning suppression 7-11074
 polished glass surfaces, ellipsometric obs. rel. to losses in laser cavity 7-17297
 pulsed multifrequency lasers with isotropic resonators, radiation polarisation 7-62659
 pump injection into FIR laser resonator using Al_2O_3 waveguide 7-43356
 Q-factor modulation using methods of adaptive nonlinear optics (*Russian*) 7-50604
 ray matrices for tilted interfaces 7-57370
 ray matrix method for analysis of opt. resonators with image rot. 7-50599
 retroreflector elements, partial phase self-locking possibility 7-36994
 rhodamine 590/water soln, droplet whispering-gallery-mode laser characts. 7-31310
 rhodamine 6G dye laser, 580 nm, small line width, cavity arrangement 7-62728
 rhodamine 6G laser with Brewster prisms, hybridly mode-locked 7-15913
 rhodamine 6G-DODCI femtosec. dye laser synchronously pumped by Nd:YAG laser, stabilisation 7-31346
 ring cavity, twin photon beam generation, intracavity four-wave mixing 7-62733
 ring dye laser, CW multimode, spontaneous oscillations of emission spectrum 7-43085
 ring dye laser for probing trapped ions, optical frequency standard appl. 7-20285
 ring laser, transverse mode generation 1D diaphragm effect 7-43163
 ruby laser, fabrication, output characts. (*Korean*) 7-31332
 ruby laser pulses, 1.6 ns, generation by passive Q-switching 7-25854
 ruby lasers using low-magnification unstable resonators 7-36997
 self-focused coupled cavity laser, optical bistability in semiconductor injection lasers 7-57325
 semiconductor laser, Bragg injection with external mirror, DFB 7-36985
 semiconductor laser, narrow linewidth, single frequency, with phase conjugate external cavity mirror 7-43157
 semiconductor laser, single-mode operation, influence of external resonator on emission spectrum 7-62695
 semiconductor laser, unstable resonator, phase-locked arrays 7-1196
 semiconductor laser electron-beam-pumped, single longitudinal mode operation 7-10938
 semiconductor laser with transmission grating feedback, tunable narrow-band emission 7-1099
 single-mode laser with unstable ring resonator 7-1198
 solid-state lasers, spatial shaping of pulsed beam, cavity resonator design criteria (*Polish*) 7-31363
 solid-state ring and linear lasers with electro-optic Q-switching, numerical modelling 7-36999
 soliton laser stabilisation, feedback from pulse-shaping fibre 7-50602
 stimulated scattering of light in unstable resonators 7-43225
 superdense hollow cathode discharge, plasma light amplification (*Japanese*) 7-6476
 three-level atoms in laser cavity, dual-frequency radio optical resonance with nonlinear optical indication, line profile 7-57024
 transverse modes of a laser resonator with Gaussian mirrors 7-5919
 two-atom spontaneous emission in a detuned damped cavity 7-57288
 ultra-short pulses and intracavity dispersion compensation 7-57387
 unstable confocal resonator, output characts., reson. mirror deform. and angular deflection effect (*Chinese*) 7-57371
 unstable resonator semiconductor lasers, expt. 7-57374
 unstable resonator semiconductor lasers, theory 7-57373
 unstable resonator with dihedral corner reflector in gasdynamic laser, props. 7-62729
 unstable resonator with perforated mirror, phase struct. of radiation wavefront 7-25846
 unstable resonators with 90° beam rotation 7-5918
 unstable-resonator-mode derivation using virtual-source theory 7-31364
 water vapour-He laser, pulsed and CW operation at 28 μm 7-36939
 XUV laser cavities and pumping optics 7-25845
 AlGaAs injection heterolasers and integrated laser-photodetector pairs, prepared by microcleaving 7-31343
 AlGaAs laser rib-waveguide, gain- to index-guiding transition 7-31315
 AlGaAs/GaAs long cavity ridge waveguide DFB lasers, spectral linewidth reduction 7-1179
 AlGaAs-GaAs DFB-TJS external-cavity laser with optical phase control loop, spectral linewidth 7-20222
 $\text{Al}_{0.3}\text{Ga}_{0.7}\text{As}$ -GaAs optically-pumped multiple quantum well laser 7-5922
 $\text{Al}_x\text{Ga}_{1-x}\text{As}$ -GaAs double heterostruct. injection laser, power-current characteristics study 7-62704
 $\text{Al}_x\text{Ga}_{1-x}\text{As}$ -GaAs heterostruct. injection laser with coupled cavity, dynamic stability 7-62705
 $\text{Al}_x\text{Ga}_{1-x}\text{As}$ -GaAs LOC lasers for high power low threshold current density operation, optimisation 7-10934
 $\text{Ba}(\text{NO}_3)_2$, radiation generation in resonator under stimulated Raman scatt. conditions 7-43222
 BaTiO_3 double phase conjugation mirror, anal., demonstration and laser appl. 7-43252
 CO lasers, electroionisation radiation, spectral brightness increase using multiresonator systems 7-5875
 CO_2 amplifier with mirror utilizing degenerate four-wave interaction 7-25837
 CO_2 annular gain laser, multiple pass unstable resonator 7-36991
 CO_2 , CW laser, unsaturated gain coeffs., saturation intensity (*Korean*) 7-25797
 CO_2 compact wide-aperture single-mode TE laser with low chirp rate, Cassegrain resonator 7-50580
 CO_2 continuous-flow laser with unstable resonator, acoustic vibrs. 7-25796
 CO_2 high-pressure laser, direct optical pumping with pulsed HF pump laser, low-loss resonator 7-50533
 CO_2 laser, intracavity optically controlled cryst. modulators 7-10911
 CO_2 laser, synchronisable, injection locked, Q-switched, mode-locked, cavity dumped 10 atmosphere 7-62736

laser cavity resonators continued

- CO₂ laser, TEA, with three cavity mirrors, two-line operation 7-5869
 CO₂ laser, TEA, with unstable resonator, influence of external radiation injection 7-36936
 CO₂ laser emission freq. continuous tuning band, widening using combined resonators 7-25847
 CO₂ laser pulse duration control by intracavity IR absorbing gas cell 7-43174
 CO₂ laser TE, tunable using near grazing incidence grating, performance 7-43052
 CO₂ pulsed laser freq. dynamic tuning, multispike lasing using intracavity cell with IR absorbing gas 7-62663
 CO₂ TEA laser, characteristics of confocal unstable resonator (*Korean*) 7-25848
 CO₂ TEA laser, single-mode, using self filtering unstable resonator configuration 7-25850
 CO₂ TEA laser, tunable travelling-wave, single mode operation 7-15840
 CO₂ thin-film-coated waveguide laser, RF excited 7-5908
 CaCO₃ radiation generation in resonator under stimulated Raman scatt. conditions 7-43222
 Cr³⁺:BeAl₂O₄, alexandrite, lasers using low-magnification unstable resonators 7-36997
 Cr³⁺:Gd₃Sc₂Ga₂₋₃O₁₂ garnet, laser spectral analyser 7-31362
 Cu vapour laser with unstable resonator, background radiation influence on dye lasing 7-25856
 Cu vapour laser with wavefront-reversing mirror induced in active medium 7-1199
 GaAlAs laser, collinear nearly degenerate four-wave mixing in amplifying media 7-11071
 (GaAl)As monolithic composite-cavity laser, chem. etching technique 7-50579
 GaAlAs, semiconductor laser coupled with short external cavity, stable single longitudinal mode operation 7-62737
 GaAs, refractive index dispersion, Fabry-Perot cavity oscillations obs. 7-59171
 GaAs/(GaAl)As LOC lasers, MOCVD growth and characts. 7-25835
 GaAs-AlGaAs DH injection laser, optical and transport props., emission energy shift, threshold current meas. 7-1101
 GaAs-AlGaAs large optical cavity semicond. laser arrays 7-10989
 GaAs-AlGaAs short cavity multiquantum well lasers, dry etching, threshold current and single mode operation 7-20253
 GaAs-GaAlAs diode laser array, diffraction-limited emission, aperture graded-index lens external cavity 7-11005
 GaInAsP integrated coupled-cavity lasers, design and fabrication 7-25843
 He-Ne laser, internal mirror, freq. and power stabilisation using fan (*Korean*) 7-25849
 He-Ne laser, photothermal deflection, trace gas anal. appls. 7-61381
 He-Ne laser with high specific output power (*German*) 7-20187
 I, photodissociation laser, active mode locking, acousto-optic modulator (*Korean*) 7-25852
 IF pulsed laser, flow parameters optimisation, intracavity gain detect. 7-10914
 InGaAsP 1.55 μ m mode-locked laser with single-mode fibre output 7-50600
 InGaAsP-InP, integrated external cavity laser 7-36993
 InGaAsP-InP DFB lasers with monolithic external cavity, spectral characts. for 1.3 μ m 7-20281
 InGaAsP-InP DFB laser monolithically integrated with tunable external cavity, linewidth and FM characts. 7-57316
 LiF:F₂ laser, room temperature, active element, thermal effects 7-62714
 LiNbO₃:H ring resonators, operation at 0.79 μ m and 1.3 μ m 7-26029
 NH₃ laser, compact high-power finite-impulse-response, pumped in CO₂ laser cavity 7-5907
 N₂O high-pressure laser, direct optical pumping with pulsed HF pump laser, low-loss resonator 7-50533
 NaF:F₂⁺, F₃⁺, intracavity spectrum analyser, long-wavelength IR region 7-48897
 NaNO₃ radiation generation in resonator under stimulated Raman scatt. conditions 7-43222
 Nd:glass laser system, appl. of diffraction grating to increase tuning range 7-5916
 Nd:YAG laser, mode-locked, CW, design 7-43164
 Nd:YAG laser, passively mode-locked using half-symmetric unstable resonator 7-20282
 Nd:YAG laser, Q-switching by PTM method (*Korean*) 7-25853
 Nd:YAG laser resonator, phase-conjugate using stimulated Brillouin scattering 7-43165
 Nd:YAG laser unstable resonator output coupler based on Fabry-Perot interferometer 7-43166
 Nd:YAlO₃ laser, CW, tuning characts. of 1079.5 and 1084.5 nm lines 7-15871
 O₂ compressed, intracavity Raman scattering characts. 7-37032
 PbEuSeTe/PbTe single quantum well diode laser with side optical cavity 7-43105
 Ti³⁺:Al₂O₃ coherently pumped laser, output characts., nonselective resonator 7-31331
 XeCl low divergence laser, excitation of stimulated Raman scatt. in compressed H₂ 7-57468
 YAlO₃ laser with controlled resonator Q factor, ultrashort radiation pulse generation 7-43115

laser communication see *laser beam applications; optical communication; optical communication equipment; optical links*

laser damage see *laser beam effects*

laser diodes see *semiconductor junction lasers*

laser effects see *laser beam effects*

laser frequency measurement see *frequency measurement; laser variables measurement*

laser frequency stability

- combined laser interference system for the meas. of motion 7-41443
 DFB lasers, fibre-extended-cavity, oscillation frequency tuning 7-57381
 diode tunable laser control by stepping Michelson interferometer 7-43135
 division and stabilization by dual freq. modulation method 7-15916
 dye laser, high resolution computer controlled 7-20249
 electromechanical laser-beam modulator with high-frequency stability 7-31372
 external-cavity laser diode, stabilisation of spectral linewidth and oscill. freq. using fibre-optic ring resonators (*Japanese*) 7-5921
 Fabry-Perot fibre optic sensor and its appls. 7-43424
 free-electron laser, MM-wave, sideband control 7-62716

laser frequency stability continued

- He-Ne lasers, single frequency, anal. (*Chinese*) 7-5870
 He-Ne lasers stabilized to ¹²⁷I₂ at 605 nm 7-20309
 He-Ne/ZZ 7-18761
 injection laser with external selective resonator, wide tuning range 7-43099
 integrated coupled-cavity lasers, design and fabrication 7-25843
 interferometric laser frequency division and stabilization, meas. appls. 7-20314
 measurement techniques and standards operation for freq. (*French*) 7-29983
 methane stabilised He-Ne laser, frequency meas. of methane hyperfine line 7-20190
 review of laser frequency standards 7-36977
 rhodamine 6G-DODCI femtosec. dye laser synchronously pumped by Nd:YAG laser, stabilisation 7-31346
 ring dye laser for probing trapped ions, optical frequency standard appl. 7-20285
 schlieren optics methods, comparison of light sources 7-57503
 semiconductor, digital control using microcomputer, freq. stabilisation (*Japanese*) 7-5912
 semiconductor laser, narrow linewidth, single frequency, with phase conjugate external cavity mirror 7-43157
 servo-controlled lasers progress and appls. 7-20307
 wavelength stabilization of tunable diode lasers using an internally-coupled Fabry-Perot interferometer 7-31353
 AlGaAs laser diode, HF stabilisation 7-15864
 AlGaAs-GaAs DFB-TJS external-cavity laser with optical phase control loop, spectral linewidth 7-20222
 Al_xGa_{1-x}As-GaAs heterostruct. injection laser with coupled cavity, dynamic stability 7-62705
 Ar⁺ laser, 514 and 458 nm, for use in holography 7-62721
 CO₂ laser, chaotic attractors in crisis 7-43178
 CO₂ laser, optogalvanic Lamb dip freq. stabilisation 7-31301
 CO₂ laser pumping source for CH₂F₂ laser, Stark cell stabilisation 7-43134
 GaAlAs laser diode, extremely weak feedback, lasing wavelength shift anal. 7-31325
 GaAlAs laser-diode array, high-speed electronic beam steering 7-43185
 GaInAsP integrated coupled-cavity lasers, design and fabrication 7-25843
 GaInAsP:Er semiconductor injection laser, single longitudinal model operation at 1.5 μ m 7-50558
 He-Ne laser, internal mirror, freq. and power stabilisation using fan (*Korean*) 7-25849
 He-Ne laser, stabilised by saturated absorption of methane, frequency shifts obs. 7-20192
 He-Ne laser, stabilised by external absorption cell 7-20270
 He-Ne laser, stabilised by I₂ external absorption cell 7-20308
 He-Ne laser, three-mode, frequency resonance 7-36937
 He-Ne laser, transportable, methane stabilized 7-20191
 He-Ne laser at 0.633 μ m, frequency stabilisation, using polarisation modulation 7-20295
 He-Ne laser stabilised by methane saturable absorption, effects leading to frequency shifts 7-50540
 He-Ne laser stabilised by Lamb dip, emission frequency scatter, causes 7-62667
 He-Ne/methane ring lasers stabilised using FM resonances, frequency reproducibility 7-1206
 HeNe/methane laser, absolute frequency meas. at 88 THz 7-18762
 In_{1-x}Ga_xAs_{1-y}P_y-InP quarter-wavelength-shifted DFB laser source for 1.55 μ m underwater optical cable system (*Japanese*) 7-62720
 Nd:YAG injection-seeded laser, polarisation feedback stabilisation, spectroscopy appls. 7-57338
 Nd:YAG laser, 1.06 μ m Cs₂ reference for freq. stabilisation 7-57403

laser hardening see *laser beam effects; radiation hardening; surface hardening*

laser induced breakdown see *laser beam effects*

laser induced damage see *laser beam effects*

laser isotope separation

- adsorbed species on solid surfaces, laser/surface-enhanced isotope separation 7-20070
 benzene isotopic mol. separation, laser illumination of metal-covered fine-pore diffusion membrane 7-15734
 bromotrifluoromethane in supersonic free jet, isotope-selective IR multiphoton dissociation 7-5781
 bromotrifluoromethane-¹³C, multiphoton dissociation under CO₂ laser pulses 7-42708
 chlorotrifluoromethane, Ir multiphoton dissociation induced by CO₂ laser pulses 7-992
 chlorotrifluoromethane-¹³C, multiphoton dissociation under CO₂ laser pulses 7-42708
 laser applications in chemistry, conf., Quebec City, Canada (June 1986) 7-41000
 molecular absorption, automated laser system for IR-IR, UV excitation anal. 7-6354
 review of laser-induced processes in spectroscopy, isotope separation, and photochemistry 7-36554
¹³C laser isotope separation using reactor for IR multiphoton dissociation 7-991
 Cu vapour laser for U isotope separation 7-50546
 H isotope separation by selective multiphoton dissociation 7-42780
 Kr, ultrasensitive laser isotope anal. 7-19803
 N₂ afterglow, U cpd. interaction appl. to laser isotope separation 7-39898
 T isotope separation using CO₂ laser, optimisation 7-42707
 Te₂ isotope selective ionization 7-36699
 U atomic vapour laser isotope separation data acquisition and control system 7-15735
 U enrichment using atomic vapour laser isotope separation 7-19367
 U, hyperfine structure of 2 and 4 eV levels, laser induced fluorescence study 7-25679
 UF₆, multiphoton dissociation in supersonic jets 7-42706
 Zr, metal beam, laser prod. and diagnostics, rel. to isotope separation 7-42783

laser magnetic resonance

- CF radical, far IR laser mag. reson. spectrum 7-50202
 Cl, Rydberg states transition, 6.7 μ m, obs. 7-42538
 OH+NO(NO₂)(N₂O), isotope exchange reactions, LMR detection, rate const. meas. 7-39882

laser magnetic resonance continued

- OH+O₂, isotope exchange reactions, LMR detection, rate const. meas. 7-39882
 YIG:Ho³⁺, laser mag. reson. study, quasi-Ising model 7-53147

laser mirrors *see laser accessories; mirrors***laser mode locking**

- acousto-optic loss modulators for laser mode-locking characts. 7-37129
 acousto-optic mode locker, appl. to Ar ion laser 7-37005
 DCM dye laser, CW, passive mode locking 7-1202
 dye laser, synchronously pumped, generation of high-power tunable picosecond pulses (*Chinese*) 7-5923
 dye laser mode-locked, amplification by KrF* laser 7-62724
 dye laser synchronously pumped, picosecond pulse formation 7-25811
 dye lasers, injection locked, generation of optical pulse sequence with phase control 7-43087
 F₄(II) colour centre laser at 2.653 μ m, synchronously pumped, mode-locked, cavity length meas. 7-5920
 glass series, active material selection for acousto-optic mode-lockers 7-57493
 intracavity SHG, mode-locked laser pulse temporal and spectral characts. 7-31393
 phased-array diode lasers coupled-mode anal. 7-43095
 phased-array laser, single-lobe radiation pattern generation using variable phase-shift zone plate 7-43182
 pulse shaping and passive mode-locking with nonlinear Michelson interferometer 7-15914
 rhodamine 110 dye laser, passive mode locking and dispersion compensation 7-62742
 rhodamine 6G laser, CW, combined mode locking using triphenylmethane dyes 7-37003
 rhodamine 6G laser, synchronously pumped, characts. (*Chinese*) 7-5880
 rhodamine 6G laser with Brewster prisms, hybridly mode-locked 7-15913
 rhodamine 6G ring dye laser, flashlamp pumped, short pulse generation using colliding pulse mode locking 7-43170
 rhodamine 6G-sulphur rhodamine 101 laser, CW, passive mode locking 7-11015
 rhodamine B laser, femtosecond, synchronously mode locked, spectral optimisation 7-37004
 rhodamine B laser, femtosecond hybrid mode locked 7-5927
 ring-laser gyroscope, random dither modulation 7-57376
 ruby laser, ultrashort pulse generation by passive mode locking 7-1205
 sectional constricted planar co-cavity laser diode, longitudinal mode-temp. locking study (*Chinese*) 7-10932
 semiconductor laser, actively mode-locked, diode facet reflectivity influence on dynamics 7-36959
 semiconductor laser, Bragg injection with external mirror, DFB 7-36985
 semiconductor laser, linewidth caused by spontaneous emission, comparison of mode-locked and single-mode operation 7-20224
 semiconductor laser, mode locked, suppression of timing and energy fluctuations by CW injection 7-50609
 semiconductor laser, using fast multiple quantum well absorber 7-50655
 semiconductor lasers, injection locked, freq. chirping, small signal analysis 7-50562
 semiconductor lasers, polarisation switching, injection locking mechanism 7-57380
 solid lasers with passive mode locking, stationary ultrashort pulse theory 7-43175
 solid ring laser with active mode locking, amplitude characts. 7-62739
 soliton laser stabilisation, feedback from pulse-shaping fibre, passive mode locking 7-50602
 synchronous pumping, spontaneous emission role in mode locking dynamics 7-5925
 ultra-short pulses and intracavity dispersion compensation 7-57387
 ultrafast phenomena conf., Snowmass, CO, USA (June 1986) 7-24
 AlGaAs laser diode array travelling-wave amplifier, high peak power, gateable picosec. optical pulses 7-20252
 AlGaAs-GaAs GRIN-SCH SQW laser, wide-stripe, injection locking 7-20290
 Al_{0.3}Ga_{0.7}As-GaAs optically-pumped multiple quantum well laser 7-5922
 Al_{0.3}Ga_{0.7}As-GaAs double heterostruct. injection laser, power-current characteristics study 7-62704
 Ar fibre laser, stimulated Brillouin scattering, single-mode and multimode pumped, spontaneous mode locking 7-1079
 Ar ion laser, high-power, with extended functional capabilities, mode selection and locking 7-25839
 CO₂ laser, synchronisable, injection locked, Q-switched, mode-locked, cavity dumped 10 atmosphere 7-62736
 CO₂ laser, ultrashort pulse generation by square-wave mode locking and cavity dumping 7-43177
 CO₂ laser array, 2D effective phase locking studies 7-50607
 Co:MgF₂ laser, mode locking and Q-switching by loss-modulation freq. detuning 7-62711
 Cr³⁺:BeAl₂O₄ tunable laser output pulse kinetics, spectral condensation characts. 7-50570
 GaAlAs, semiconductor laser coupled with short external cavity, stable single longitudinal mode operation 7-62737
 GaAs/GaAlAs double-well superlattice, ultra-fast optical modulator 7-52801
 GaAs-AlGaAs high-power laser array of phase-locking free struct. 7-62725
 He-Ne laser, mode-crossing reson., intracavity distance and mode-locking quality anal. 7-31373
 He-Ne lasers as sources of stable subnanosecond pulses 7-43060
 I, photodissociation laser, active mode locking, acousto-optic modulator (*Korean*) 7-25852
 InGaAsP 1.55 μ m mode-locked laser with single-mode fibre output 7-50600
 InGaAsP injection lasers, mode-locked and gain-switched, timing jitter 7-11013
 KCl:Li,F₄(II) colour centre laser, synchronously pumped, mode locking 7-62710
 LiIO₃ Raman laser for optical range, quasi-CW high power 7-25829
 Nd laser with positive electro-optic feedback, mode-locked generation of transverse modes 7-1204
 Nd:phosphate glass, colliding pulse mode locking study 7-20286
 Nd:YAG, colliding pulse mode locking study 7-20286
 Nd:YAG, regenerative amplification of temporarily compressed picosecond pulses at 2 kHz 7-43108
 Nd:YAG frequency-doubled mode locked laser, synchronous pumping of femtosec. dye laser 7-31346

laser mode locking continued

- Nd:YAG laser, actively mode locked Q-switched as stimulated Raman source at 1.54 μ m 7-20350
 Nd:YAG laser, CW mode-locked, modulator freq. detuning effects 7-62712
 Nd:YAG laser, mode locked, with intracavity phase conjugate mirror 7-50606
 Nd:YAG laser, mode-locked, CW, design 7-43164
 Nd:YAG laser, passively mode-locked using half-symmetric unstable resonator 7-20282
 Nd:YAG laser pulse narrowing by spectral windowing of self-phase modulated picosecond pulses 7-5928
 Nd:YAG mode locked laser, timing fluctuations reduction by electronic feedback 7-31371
 Nd:YLiF₄ laser, ultrashort pulse active/passive mode-locking 7-62741
 Nd³⁺:YAG laser, reproducible generation of ultrashort pulses 7-11016
 Nd³⁺:YAG laser passively mode-locked by saturable absorpt. filter, ultrashort pulse generation 7-31368
 O₂ compressed, intracavity Raman scattering characts. 7-37032
 XeCl laser, dye laser pumped, single picosecond UV pulse generation by mode-locking 7-1095
 YAlO₃ laser with controlled resonator Q factor, ultrashort radiation pulse generation 7-43115

laser modes*see also laser mode locking*

- almost concentric resonators for low gain FEL, alignment and performance 7-43155
 axial-symmetric optical passive resonators, transverse modes, series calc. (*Chinese*) 7-11003
 cleaved coupled cavity lasers, multilongit. mode model 7-57372
 composite cavity waveguide complementary semiconductor lasers, low threshold current, large output power 7-62727
 cooperative atomic interactions in a single-mode laser 7-43049
 coupled lasers, composite-resonator mode description 7-11007
 DFB laser, single longitudinal mode operation considering light refl. from optical fibre facet (*Japanese*) 7-20284
 DFB laser, V-groove, 1.3 to 1.55 μ m operation 7-20257
 diaphragmed laser near field (*French*) 7-43180
 diode laser arrays, gain-guided, ten-stripe, high-order eigenmodes 7-10986
 diode laser arrays, phase-locked, supermode structure 7-57362
 discrete diode lasers ensemble, high spectral purity single mode CW and pulse output 7-43091
 double-channel planar BH multimode laser, 1.55 μ m fibre grating external cavity, single-mode behaviour 7-15908
 dye laser, coloured noise induced first-order phase transition 7-57309
 dye laser, CW, with intracavity photorefractive element, mode selection 7-43167
 dye lasers, multimode CW, dynamical instabilities, stimulated Brillouin scatt. 7-50552
 dye lasers, two-mode, first-passage-time problems 7-1097
 dye ring laser, 580 nm, CW, single-mode, dye circulation system 7-1201
 Fabry-Perot resonators with active medium, large Fresnel numbers, asymptotic theory 7-11011
 FEL active guiding in small signal regime 7-1167
 FEL gain maximization modes in low gain-small signal regime 7-1166
 fluoromethane laser, helical feedback, higher modes 7-15844
 focusing of multimode laser beams with variable beamparameters 7-11021
 free electron laser, optical mode gain and evolution 7-43126
 free electron laser, small signal performance with two waveguide modes 7-1131
 free electron laser multimode oscillator, electron energy drift effect, instability 7-15880
 free electron laser oscillators, high gain, spatial and temporal evolution of multiple modes 7-1129
 free-electron lasers with distributed feedback, dynamics 7-50588
 gain-guided diode laser arrays, eigenmodes, junction-heating effects 7-62688
 gas laser single-mode operation, inertial props. 7-62660
 gas lasers, multimode, total electric field strength, temporal evolution 7-15848
 grating resonator, selective props., appl. to lasers 7-50596
 high-power single mode operation of index-guided inner stripe (I²S) laser by MOCVD 7-50592
 injection heterolasers with crescent-shaped active region, spectroscopic props. 7-36962
 integrated coupled-cavity lasers, design and fabrication 7-25843
 intensity correlations; effective eigenvalue charact. 7-50531
 laser pulse spatial modes, direct measurement 7-5931
 lightguides, time coherence effects of transverse laser modes 7-37009
 multi-mode laser with modulated inversion, dynamic props. 7-50530
 multielectrode DFB laser, broad wavelength tuning under single-mode oscillation 7-20258
 multimode dynamics in a free electron laser with energy shift 7-1169
 multimode Gaussian beam photoreceiver recording 7-50612
 multimode lasers, bifurcation successions 7-57294
 multimode Stokes conversion efficiency and output wavefront, off-reson. Raman interactions effect 7-20333
 multiple equivalent incoherent multiaxial-mode laser beams, Raman scatt. eqns. soln. 7-20338
 multiple-stripe-geometry laser arrays, chirped and unchirped, modal eigenfunctions 7-57335
 non-Gaussian laser beam form., laser with multilayer dielec. exit mirror 7-50611
 nonlinear resonator mode behaviour radiation power depend. on geometry 7-43160
 optical ring resonator, photorefractive gain, multimode operation 7-57377
 periodically modulated laser subharmonic bifurcation and bistability, periodic solns. study 7-62662
 phase conjugation of laser beams, single mode Q-switched ruby laser development 7-25903
 phase-locked injection laser arrays with variable stripe spacing, coupled-mode analysis 7-50581
 phased array diode lasers, far-field wavefront props., coupled mode anal. 7-31318
 picosecond light pulse changes in a GaAs filled nonlin. Fabry-Perot resonator (*Russian*) 7-50620
 quantum electronics, conf., Bucharest, Rumania (Sept. 1985) 7-55888

laser modes continued

- quantum well lasers, graded barrier, pulsed operation, near- and far-field obs. 7-31319
 quantum-beat laser theory, Fokker-Planck approach 7-57292
 Raman beam combining with multiaxial mode lasers 7-15939
 relaxation process analysis for lasers with optical pumping (*Russian*) 7-50528
 resonator, frequency pulling and anomalous dispersion, aberration and perturbation effect 7-11004
 rhodamine 590/water soln, droplet whispering-gallery-mode laser characts. 7-31310
 ring dye laser, CW multimode, spontaneous oscillations of emission spectrum 7-43085
 ring laser, homogeneously broadened, optical bistability and instabilities due to mode-mode competition 7-62735
 ring laser, homogeneously broadened, single-mode, periodic and chaotic output pulsations 7-11009
 ring laser, transverse mode generation 1D diaphragm effect 7-43163
 ring laser, two-mode, with backscatter, freq. depend. 7-37000
 ring laser single-mode model 7-20179
 ring lasers, two-mode, with controlled phase anisotropy, EM wave interaction theory 7-43161
 ruby laser, single mode Q-switched, phase conjugation of laser beam 7-25904
 ruby laser pulses, 1.6 ns, generation by passive Q-switching 7-25854
 semiconductor active waveguides, gain-guided modes 7-50563
 semiconductor complementary self-aligned laser arrays, MOCVD growth 7-31339
 semiconductor DFB lasers, single longitudinal-mode high-power type, design, theoretical aspects 7-10987
 semiconductor laser, linewidth caused by spontaneous emission, comparison of mode-locked and single-mode operation 7-20224
 semiconductor laser, multimode rate-equation anal. appl. to longitudinal mode modulation 7-20292
 semiconductor laser, narrow linewidth, single frequency, with phase conjugate external cavity mirror 7-43157
 semiconductor laser, phased-array with uniform stable supermode 7-43139
 semiconductor laser, single-mode operation, influence of external resonator on emission spectrum 7-62695
 semiconductor laser, unstable resonator, phase-locked arrays 7-1196
 semiconductor laser arrays, phase locked, injection current tailoring 7-57327
 semiconductor laser electron-beam-pumped, single longitudinal mode operation 7-10938
 semiconductor laser natural linewidth, single mode operation 7-57318
 semiconductor lasers, electron-beam-excited, nonaxial excitation modes 7-43102
 semiconductor lasers, index-guided, self stabilisation of fundamental lateral mode 7-57320
 semiconductor lasers, mode partition noise in CW and pulsed operation 7-57331
 semiconductor lasers, polarisation and wavelength control, TE, TM mode operation (*Japanese*) 7-25858
 single-mode laser with unstable ring resonator 7-1198
 stimulated Brillouin gain, depend. on pump laser mode structure 7-20354
 stimulated Brillouin scattering, effect of laser mode structure 7-20330
 transverse modes of a laser resonator with Gaussian mirrors 7-5919
 two-photon laser, single-mode, off-diagonal elements calcs. 7-62661
 unstable resonator semiconductor lasers, theory 7-57373
 unstable resonators with 90° beam rotation 7-5918
 unstable-resonator mode derivation using virtual-source theory 7-31364
 AlGaAs BH laser with flared waveguides, high power operation 7-57352
 AlGaAs laser, mode hopping suppression by saturable absorber 7-62696
 AlGaAs laser, tunability and mode-transition characteristics 7-20293
 (AlGa)As lasers, separately pumped, continuous control 7-20287
 AlGaAs multiquantum well-buried optical guide lasers, fabrication by Si-induced disordering 7-10995
 AlGaAs/GaAs DBR laser with multiquantum well active/passive waveguides 7-57350
 AlGaAs-GaAs, DFB lasers, low threshold, 0.88 μm emission, MOCVD fabricated with ridge waveguide struct. 7-5906
 AlGaAs-GaAs index-guided lasers with mode filter, props. study 7-5905
 Al_{0.1}Ga_{0.9}As:Mg/GaAs:Se quantum well heterostruct., photopumped laser operation 7-25818
 Al_{0.1}Ga_{0.9}As-GaAs broad area quantum well lasers, single-mode single-lobe operation 7-10930
 Ar fibre laser, stimulated Brillouin scattering, single-mode and multimode pumped, spontaneous mode locking 7-1079
 Ar ion laser, high-power, with extended functional capabilities, mode selection and locking 7-25839
 CO₂ compact wide-aperture single-mode TE laser with low chirp rate 7-50580
 CO₂ homogeneously broadened ring laser, optical bistability and instabilities due to mode-mode competition 7-62735
 CO₂ hybrid laser, longitudinal mode selection for subthreshold operation 7-25795
 CO₂ laser, chaotic attractors in crisis 7-43178
 CO₂ laser, single-mode operation, inertial props. effect 7-62660
 CO₂ laser emission freq. continuous tuning band, widening using combined resonators 7-25847
 CO₂ single and multilongit. mode laser emissions, SHG in CdGeAs₂ 7-43211
 CO₂ TEA laser, high-power modulation by injection-locked mode-beating 7-62738
 CO₂ TEA laser, single-mode, using self filtering unstable resonator configuration 7-25850
 CO₂ TEA laser, tunable travelling-wave, single mode operation 7-15840
 CdS laser excited with several electron beams, light pulse formation 7-43098
 GaAlAs laser diode, extremely weak feedback, lasing wavelength shift anal. 7-31325
 GaAlAs lasers, polarisation-resolved low-frequency noise 7-15863
 GaAlAs-GaAs DFB lasers with double channel planar buried heterostructure, low threshold operation 7-20256
 GaAlAs-GaAs DFB laser with double-channel planar BH 7-50594
 GaAs laser excited with several electron beams, light pulse formation 7-43098
 GaAs-AlGaAs short cavity multiquantum well lasers, dry etching, threshold current and single mode operation 7-20253

laser modes continued

- GaInAsP DFB lasers, 1.3 μm , single-mode, realisation and characts. (*German*) 7-57357
 GaInAsP integrated coupled-cavity lasers, design and fabrication 7-25843
 GaInAsP:Er semiconductor injection laser, single longitudinal mode operation at 1.5 μm 7-50558
 GaInAsP-InP surface-emitting laser with circular BH, low temp, CW operation 7-31337
 H₂ Raman generators, spatial mode struct. of stimulated Stokes emission 7-20345
 He-Cd laser transitions, level width determ., double-mode lasing state 7-43080
 He-Ne laser, mode-crossing reson., intracavity distance and mode-quality quality anal. 7-31373
 He-Ne laser, three-mode, frequency resonance 7-36937
 He-Ne laser beam divergence meas. using LiNbO₃ SAW interaction 7-1211
 He-Ne laser tuned by axial mag. field, mode competition 7-50539
 I, laser amplifier, free running operation mode 7-57307
 InGaAsP buried heterostructure lasers, polarisation, effect of stress relax. caused by repetitive temp. change 7-62690
 InGaAsP DFB lasers, extremely low-noise facet-reflectivity-controlled 7-31320
 InGaAsP ridge waveguide laser threshold current optimisation, simplified hybrid optical model 7-57321
 InGaAsP/InP DFB lasers, DFB mode oscillation, temp. range 7-5910
 InGaAsP-InP, 1.5 μm laser with high external quantum efficiency and controlled emission wavelength 7-57323
 InGaAsP-InP laser, single-mode, 1.3 μm , analog FM 7-37002
 InGaAsP-InP planar surface BH lasers with hydride VPE-grown Fe-doped current blocking layers 7-20261
 InGaAsP-InP-ridge waveguide lasers, LPE fabricated, design and 1.5 μm low-threshold operation 7-15897
 NH₃ Raman laser, single-mode homogeneously broadened, self-pulsing instabilities 7-10922
 Nd laser with positive electro-optic feedback, mode-locked generation of transverse modes 7-1204
 Nd:glass laser, passively Q-switched, output-parameter control 7-1104
 Nd:YAG CW laser, high power 1.34 μm , oscillation eigenmode 7-43112
 Nd:YAG laser, diode-pumped intracavity doubled, large amplitude fluctuations due to longitudinal mode coupling 7-5894
 Nd:YAG laser, mode-locked, CW, design 7-43164
 Nd:YAG lasers, injection-seeded, fast resonance-detection technique for single-frequency operation 7-36969
 Pb salt diode laser calibration, wavemeter 7-5930
 PbSnTe laser, single-mode, 8 μm with buried heterostructure, design 7-36980
- laser phototherapy** see laser applications in medicine; radiation therapy
laser power measurement see laser variables measurement; power measurement
laser printers
 computer generated hologram recording using a laser printer 7-43002
 α -titanylphthalocyanine photoreceptors for solid-state laser beam printers (*Japanese*) 7-37077
- laser pulse variables measurement** see laser beams; laser variables measurement
laser Q-switching see Q-switching
laser radar see optical radar
laser surgery see laser applications in medicine; surgery
laser theory
 see also laser transitions; population inversion; stimulated emission
 1.5 μm laser with high external quantum efficiency and controlled emission wavelength 7-57323
 amplifier spontaneous emission effects in laser oscillators and amplifiers, small aspect ratio, 3D calc. 7-10894
 anisotropic lasers, natural linewidth 7-43047
 autoresonant electron laser nonlinear theory 7-10976
 BH laser diodes, thermal props. 7-57328
 chaotic dynamical behavior in lasers 7-10907
 circular free electron lasers, theoretical and expt. aspects (*Japanese*) 7-20242
 cleaved coupled cavity lasers, multilongit. mode model 7-57372
 collective effects in elements and compounds 7-58433
 cooperative atomic interactions in a single-mode laser 7-43049
 coupled lasers, composite-resonator mode description 7-11007
 coupled optical resonators, local-field rate eqns. 7-1071
 coupled ring laser Lorenz systems, periodic-chaotic transition, stability anal. 7-62732
 DFB and DBR waveguide lasers, anomalous modal spectrum 7-15888
 DFB laser, stimulated scattering, nonstationary mechanism 7-5867
 DFB lasers numerical matrix method for anal. of structure 7-57349
 DFB semiconductor lasers, external optical feedback 7-57332
 diffusion limited optically pumped far-infrared laser model 7-20197
 diode laser arrays with heat sinks, temperature profile model 7-20221
 directly modulated semicond. lasers, gain nonlinearity effects calcs. 7-20218
 dye laser, IR, action in traveling-wave pumping geometry 7-25809
 dye lasers, injection locked, generation of optical pulse sequence with phase control 7-43087
 dye lasers, spectral evolution and relaxation oscillations 7-15859
 dye lasers, two-mode, first-passage-time problems 7-1097
 dye solution travelling wave laser with two photon picosec. optical pumping, time characts. 7-62685
 electric field, Brownian motion, obs. in laser 7-57293
 Fabry-Perot resonators with active medium, large Fresnel numbers, asymptotic theory 7-11011
 FEL in long undulator regime, off-axis gain enhancement 7-25833
 fibre lasers, superfluorescent, anal. 7-31329
 field fluctuations of laser oscillator, electrical circuit theory 7-15886
 field fluctuations of laser oscillator, quantum mechanical Langevin treatment 7-15885
 free electron laser, Compton and Raman regimes, Hamiltonian model 7-57348
 free electron laser, electron beam modulation in corrugated waveguide 7-10839
 free electron laser, helical wiggler mag. field, sideband instability, kinetic anal. 7-15879
 free electron laser, induced magnetobremstrahlung of electrons in an undulator field and an axial guide field 7-50574

laser theory continued

- free electron laser, microtron Cherenkov 7-10970
 free electron laser, optical mode gain and evolution 7-43126
 free electron laser, particle dynamics and beam energy with planar undulator 7-10975
 free electron laser, quantum theory, intrinsic linewidth and photon statistics 7-43130
 free electron laser, quantum-mechanical equations transition probabilities 7-1105
 free electron laser, wiggler and alternating-gradient quadrupole field, electron beam envelopes and matching conditions 7-1128
 free electron laser amplification, freq. spectrum oscillating phenomenon 7-43122
 free electron laser amplifier, kinetic energy injection 7-15878
 free electron laser energy model (Chinese) 7-5896
 free electron laser gain, radiation force effects 7-57347
 free electron laser multimode oscillator, electron energy drift effect, instability 7-15880
 free electron laser operational conditions using a standing wave wiggler 7-43123
 free electron laser oscillators, VUV/soft X-ray, options for development 7-31333
 free electron laser small signal theory, particle simulations 7-10971
 free electron laser soft X-ray overtone production 7-20234
 free electron laser transverse correlations in start-up from noise 7-20236
 free electron laser working state anal. (Chinese) 7-5897
 free electron lasers, AC, using relativistic electron beams 7-10973
 free electron lasers, FIR, review 7-36974
 free electron lasers, Hamiltonian model 7-50572
 free electron lasers, high gain as generators of short wavelength coherent radiation 7-20232
 free electron lasers, noncollinear, off-axis schemes 7-15877
 free electron lasers, planar metal grating 7-10969
 free electron lasers, superradiant harmonic radiation, 3D model 7-20233
 free electron lasers even-harmonic generation mechanism 7-43127
 free electron parametric laser theory 7-43125
 Free-electron laser amplifiers, stimulated head-on scatt., self-modulation study 7-43132
 free-electron lasers, gain props., gradient magnetic field effect calcs. 7-20238
 free-electron lasers, tapered, beam density, deceleration and spatial exponentiation rate limits calc. 7-43129
 frequency pushing in lasers with injected signal 7-36931
 gain-guided triple stripe lasers, self-consistent anal. 7-62702
 gamma-ray lasers, proposals, critical review 7-10945
 gas laser single-mode operation, inertial props. 7-62660
 gas laser with nonlinearly absorbing cell, statistical characteristics of emission 7-20215
 gas lasers, multimode, total electric field strength, temporal evolution 7-15848
 gas lasers, positive P representation and the laser equations 7-10909
 gas waveguide lasers with diffraction grating, frequency selectivity and resonator losses 7-43158
 graded-index separate-confinement heterostruct. laser, carrier capture time 7-1100
 He-Ne lasers, single frequency, anal. (Chinese) 7-5870
 induced resonance electron cyclotron quasi-optical maser in an open resonator 7-20176
 inhomogeneously broadened laser with a saturable absorber 7-43050
 injection laser photosensitive props., effective gain method 7-62693
 injection lasers, bistable, instability studies (Chinese) 7-10923
 instabilities, semiclassical models, review 7-15921
 intensity correlations; effective eigenvalue charactn. 7-50531
 inversion filament form, in laser media due to interatomic interactions via superradiation field 7-50529
 laser electron acceleration in stimulated Compton scatt. 7-50645
 laser transients, statistical fluctuations meas. 7-31297
 Lorenz equation with symmetry breaking, quantum chaos for laser model 7-50525
 Lorenz laser, time averaged output power in self-pulsing and chaotic regime 7-62652
 Lorenz-type chaos in laser 7-36932
 macroscopic scale systems, electron, positron and radiation quasi-channelling 7-63695
 MQW DFB laser, theoretical anal. 7-20223
 multi-mode laser with modulated inversion, dynamic props. 7-50530
 multimode lasers, bifurcation successions 7-57294
 multiple-stripe-geometry laser arrays, chirped and unchirped, modal eigenfunctions 7-57335
 narrow stripe geometry lasers, nonlinear light-current characts. 7-15866
 noise, coherence and photon statistics, review 7-1072
 noise anal. by first-passage-time techniques 7-20178
 nonlinear optical amplifier, resolution method for moment eqns. 7-43254
 nonsymmetrical five-layer LOC, DFB and DBR lasers, waveguiding props. 7-57319
 nuclear structure properties for gamma-ray lasers 7-10946
 open laser resonators with tilted mirrors, losses 7-62730
 optical klystrons, optimisation criteria 7-36972
 optical ring resonator, photorefractive gain, multimode operation 7-57377
 optical transitions in vibronic systems, generalized Rabi eqns., exact solns. in rotating wave approx. 7-20171
 periodically modulated laser subharmonic bifurcation and bistability, periodic solns. study 7-62662
 phase-locked injection laser arrays with variable stripe spacing, coupled-mode analysis 7-50581
 phased array diode lasers, far-field wavefront props., coupled mode anal. 7-31318
 pulse amplification, transient and asymptotic small signal gain 7-43048
 pulse lasers, short period loss modulation anal. (Russian) 7-50527
 pulse shortening in nonlinear amplifier 7-43196
 pulsed laser operation with saturable absorber, planar codimension four singularity universal unfolding, 5D Lorenz eqns. phase portraits 7-10910
 pulsed multifrequency lasers with isotropic resonators, radiation polarisation 7-62659
 pump-noise suppressed laser oscillator, amplitude squeezing 7-36928
 quantum electronics, conf., Bucharest, Rumania (Sept. 1985) 7-55888
 quantum well lasers, resonant injection 7-10927
 quantum well lasers—gain, spectra, dynamics 7-10935
 quantum-beat laser theory, Fokker-Planck approach 7-57292
 quantum-box lasers, 3D, gain and threshold current density 7-10937

laser theory continued

- Raman laser, fibre, synchronously pumped, anal. 7-15873
 relaxation process analysis for lasers with optical pumping (Russian) 7-50528
 ring laser, two-mode, with backscatter, freq. depend. 7-37000
 ring laser dynamic frequency characteristic, Floquet theory 7-43162
 ring laser model with additive white noise, postponed bifurcations 7-62734
 ring laser plane wave Maxwell-Bloch eqns. linear stability anal. 7-15910
 ring laser single-mode model 7-20179
 ring laser with two-anode element, reactive oscillations 7-50589
 saturation effects in coupled lasers with homogeneous gain 7-43046
 semiconductor active waveguides, gain-guided modes 7-50563
 semiconductor DFB laser amplifiers, optical bistability 7-57324
 semiconductor DFB lasers, single longitudinal-mode high-power type, design, theoretical aspects 7-10987
 semiconductor laser, dynamic spectra and propag. in single model fibres 7-20225
 semiconductor laser, multimode rate-equation anal. appl. to longitudinal mode modulation 7-20292
 semiconductor laser, phase and frequency noise, probability density function 7-20266
 semiconductor laser arrays, phase locked, injection current tailoring 7-57327
 semiconductor laser natural linewidth 7-57318
 semiconductor lasers, electron-beam-excited, nonaxial excitation modes 7-43102
 semiconductor lasers, injection locked, freq. chirping, small signal analysis 7-50562
 semiconductor lasers, mode partition noise in CW and pulsed operation 7-57331
 semiconductor lasers, nonlinear system modeling based on Volterra series 7-20226
 semiconductor lasers, travelling-wave rate eqn. anal. 7-62701
 semiconductor twin-stripe lasers, optical and electronic control of Hopf bifurcation 7-57326
 sensitized media, lasing efficiency, excitation summation influence 7-25828
 short pulse amplification in presence of absorpt. 7-57291
 single quantum well laser, current pumped, second quantised state lasing 7-50559
 solid FEL, possibility of obtaining coherent short wave radiation 7-20237
 solid lasers with passive mode locking, stationary ultrashort pulse theory 7-43175
 solid-state ring and linear lasers with electro-optic Q-switching, numerical modelling 7-36999
 soliton laser, numerical model 7-43051
 soliton laser, theory (Japanese) 7-20180
 soliton laser model, spatio-temporal coherence and chaos, conf. Los Alamos, USA, Jan. 1986 7-48158
 spatial effects and Eckhaus instability, Lorenz eqns. 7-50532
 stripe-geometry injection laser model (Czech) 7-5882
 super-dense hollow cathode discharge, plasma light amplification (Japanese) 7-6476
 superluminescent diodes, high frequency modulation 7-62744
 superradiance generated in lasers with filamentary plasma active medium 7-1044
 synchronous pumping, spontaneous emission role 7-5925
 transfer levels for isomeric deexcitation in γ -ray lasers 7-10908
 twin-channel lasers, optical characts. modelling 7-20302
 two-photon laser, single-mode, off-diagonal elements calcs. 7-62661
 unstable resonator semiconductor lasers, theory 7-57373
 upside down mounted ridge-waveguide lasers, thermal resistance, device model anal. 7-43092
 X-ray laser expts. 7-62678
 XUV, RF-linac-driven, gain physics 7-20235
 XUV laser numerical modelling 7-20213
 ArH⁺ exciplex laser, active medium modelling 7-62672
 B I isoelectronic sequence, short wavelength laser calcs. 7-20214
 Be I isoelectronic sequence, short wavelength laser calcs. 7-20214
 C I isoelectronic sequence, short wavelength laser calcs. 7-20214
 CO₂ gas laser, preionisation using α particles study 7-62508
 CO₂, intramode and Fermi relax. influence on multiple-pass short pulse energy extraction 7-57156
 CO₂ laser, single-mode operation, inertial props. effect 7-62660
 CO₂ laser array, 2D effective phase locking studies 7-50607
 CO₂-N₂-H₂ gasdynamic laser with 2D nozzles, gain optimisation 7-50541
 CO₂-N₂-H₂O gasdynamic lasers, collisional relaxation mechanisms 7-20181
 Er:YAG laser, quasistationary generation, cross-relax. mechanisms 7-57339
 GaAs injection laser, twin-stripe, lateral behaviour, self-consistent model 7-15861
 HF, chem. laser, modeling based on standing detonation wave 7-62681
 He-N₂ laser, pulsed electric-discharge, laser props. investig. 7-62675
 He-Ne Zeeman laser, nearly degenerate four wave mixing and high order effects 7-1078
 InGaAsP 1.3 μ m diode laser, ultra-high-speed modulation 7-5924
 InGaAsP ridge waveguide laser threshold current optimisation, simplified hybrid optical model 7-57321
 InGaAsP-InP bistable lasers, temp. depend. 7-5887
 KrF e-beam sustained discharge laser, efficiency 7-31307
 NH₃ lasers, FIR, instabilities and chaotic emission 7-15849
 Nd laser with positive electro-optic feedback, mode-locked generation of transverse modes 7-1204
 Nd:YAG fibre lasers, superfluorescent, anal. 7-31329
 O₂-I₂ laser active medium, theoretical model 7-1093
 OD-CO₂ chemical laser, energy capabilities study 7-62683
 Se Ne-like laser, progress in anal., review 7-20194

laser transitions

- see also laser theory
 azacoumarin dyes, fluorinated, laser dye stability, lifetimes, fluoresc. 7-59237
 BH laser diodes, very low threshold high reliability 1.30 μ m high yield manufacturer by MOCVD 7-31340
 carbonyl fluoride, laser lines, optically pumped, heterodyne freq. meas. 7-36943
 15-N cyanogen fluoride FIR laser lines, CW optically pumped 7-25799
 DFB lasers, phase tunable type, 1.5 μ m operation, FM and spectral characts. study 7-43171

laser transitions continued

- dibromomethane, optically pumped laser, FIR laser line meas. 7-57306
difluoromethane, CO₂ laser pumped, freq. meas. on FIR laser emissions 7-1084
difluoromethane pumped by ¹²C¹⁶O₂, ¹²C¹⁸O₂ lasers, submillimetre emission assignment 7-36944
diiodomethane, optically pumped laser, FIR laser line meas. 7-57306
diode laser, single quantum well, wavelength switching by injection-current control 7-50556
double-channel planar BH multimode laser, 1.55 μm fibre grating external cavity, single-mode behaviour 7-15908
dye laser, high power, synchronously pumped operating at 410 to 550 nm 7-25841
dye ring laser, 580 nm, CW, single-mode, dye circulation system 7-1201
ethyl iodide, laser lines, optically pumped, heterodyne freq. meas. 7-36943
F₄(II) colour centre laser at 2.653 μm, synchronously pumped, mode-locked, cavity length meas. 7-5920
FIR molecular lasers, optically pumped, freq. meas., 0.1 to 8 THz, review 7-43068
fluoromethane, optically pumped laser, FIR laser line meas. 7-57306
fluoromethane laser, helical feedback, higher modes 7-15844
He-Ne lasers stabilized to ¹²⁷I₂ at 605 nm 7-20309
index guided laser diodes, 1.3 μm, far-field fine struct. study 7-57389
inert gas, hollow cathode discharge, at. energy level excitation, laser lines 7-1804
metal atoms and ions, lasing mechanism and energy characts., relax. processes of metastable states 7-62673
methane-d₂ laser, submillimetre molecular, new emission lines 7-1089
methanol, FIR laser transitions, FIR and IR spectroscopic studies 7-36625
methanol, FIR lasers, intracavity triple reson. spectroscopy 7-10560
methanol high power FIR cavity laser system with long-term stability 7-36982
methanol laser lines from torsionally excited CO stretch states, and from OH-bend, CH₃-rock, and CH₃-deformation states 7-36942
methanol-d₁ lasing lines on IR pumping by CW CO₂ laser 7-1082
methanol-d₄ lasing lines on IR pumping by CW CO₂ laser 7-1082
methyl chloride, CO₂ laser pumped, freq. meas. on FIR laser emissions 7-1084
methyl fluoride-d₃, and isotopic, laser lines, optically pumped, heterodyne freq. meas. 7-36943
methylene chloride, far IR laser, optically pumped by CO₂ laser 7-62670
propargyl fluoride FIR laser lines, CW optically pumped 7-25799
relaxation process analysis for lasers with optical pumping (Russian) 7-50528
rhodamine 6G dye laser, 580 nm, small line width, cavity arrangement 7-62728
ridge waveguide lasers, 1.55 μm bridge contacted, gain guiding to index guiding transition 7-57322
semiconductor DFB laser, 1.5 μm, feedback effects on spectra 7-31321
soft X-ray laser development at Princeton, gain at 182 Å 7-20204
soft X-ray laser development at Princeton, progress 7-20251
soft X-ray laser program at Livermore 7-20202
soft X-ray laser research at Palaiseau 7-20205
solid-state lasers, broad-band, conc. of emission spectrum in near IR 7-43114
vinyl chloride FIR laser lines, CW optically pumped 7-25799
water vapour-He laser, pulsed and CW operation at 28 μm 7-36939
AlGaAs-GaAs, DFB lasers, low threshold, 0.88 μm emission, MOCVD fabricated with ridge waveguide struct. 7-5906
AlGaInP visible semicond. lasers, mesa stripe struct., MOVPE grown, 621 nm CW operation at 0°C 7-20262
Al_{0.4}Ga_{0.6}Sb-GaSb-Al_{0.4}Ga_{0.6}Sb MBE strained layer DH, optically pumped laser oscill. 1.6 to 1.8 μm 7-5888
Ar ion laser, high-power, with extended functional capabilities, visible and UV transitions 7-25839
Ar⁺ laser, 514 and 458 nm, for use in holography 7-62721
Ar⁺ photoionisation pumping via two-electron shakeup 7-20195
Ar-Xe laser at 1.73 μm, electron beam and electric field pumped 7-1077
Ar-Xe pulse-periodic large-volume electron beam-controlled laser, IR transitions in Xe atom 7-43059
Au I vapor laser, room temperature operation 7-10919
Au vapor laser, design, construction and performance (Chinese) 7-5903
Be IV ion, 4f to 5g transition generation obs. in recombining laser plasma 7-57303
C fibre, laser produced plasma, XUV expansion coded recombination lasers 7-62679
CO₂, high intensity absorpt., mod. rot. effect, lasing transitions 7-62473
CO₂ laser, 4.3 μm, longitudinal-discharge output parameters 7-43056
CO₂ laser, hot-cell-free, at 4.3 μm 7-15891
CO₂ laser, TEA, tunable multiline and single line operation at 10.6 μm and 9.4 μm 7-31300
CO₂ laser, TEA, with three cavity mirrors, two-line operation 7-5869
CO₂ laser amplifier, multiatmosphere high gain, characts. and gain at 9.294 μm 7-57366
CO₂ laser P(16) transition, temp. variation of linewidth 7-36934
CO₂ lasers, high energy picosecond 10 μm pulses 7-62665
CO₂ TEA laser emitting in 11 μm region, gain and output parameters 7-1073
¹⁴CO₂-¹²CO₂ isotope laser 7-31299
CO₂ laser emitting in 4.2 μm range, construction and props. 7-1186
Cd⁺ photoionisation pumping via two-electron shakeup 7-20195
Co:MgF₂ laser, mode locking and Q-switching by loss-modulation freq. detuning 7-62711
Cr, Tm:GdScGa₅O₁₂ laser, dual freq. study 7-43117
Cr:ScBO₃ laser, tunable over 785 to 892 nm 7-15872
Cr³⁺:BeAl₂O₄, alexandrite, nonradiative transition dynamics 7-1102
Cr³⁺:BeAl₂O₄ crystals, growth and laser performance 7-15870
Cr³⁺:SrAlF₅ laser emission tunable from 825 to 1010 nm 7-10964
Cs, atom, lasing action in Kr gas 7-15855
Cs III Auger laser, XUV at 63.8 nm, proposal 7-25801
Cu halides, vapour lasers, resonance radiation trapping effects 7-62669
Cu I vapor laser, room temperature operation 7-10919
Cu II laser with tulip shaped hollow cathode 7-43145
Cu vapor lasers, resonance radiation trapping effects 7-62669
CuCl laser radiation at 510 nm, internal attenuation 7-36949
D₂O, optically pumped laser, FIR laser line meas. 7-57306
Er:BaYb₂FSF₈ active medium optimisation, lasing parameters at 1.96 μm 7-31330
Er³⁺:CaF₂ IR laser, Q-switched, CW operation 7-43107

laser transitions continued

- Er³⁺:CaF₂ IR lasers, upconversion pumping 7-43111
Er³⁺:glass, lasing props. 7-43109
F₂ laser at 157.6 nm excited by electric discharge 7-25803
GaAs-AlGaAs DH injection laser, optical and transport props., emission energy shift, threshold current meas. 7-1101
GaInAsP DFB lasers, 1.3 μm, single-mode, realisation and characts. (German) 7-57357
GaInAsP:Er semiconductor injection laser, single longitudinal mode operation at 1.5 μm 7-50558
GaInAsP-InP double heterostructure lasers, 1.5 μm, chemical beam epitaxial growth 7-57310
Gd_{2.813}Tm_{0.17}Ho_{0.017}Sc_{0.05}Ga_{4.95}O₁₂ laser active medium operating in 2 μm range 7-50568
He⁺ photoionisation pumping via two-electron shakeup 7-20195
He²⁺ recombination lasers in VUV excited by intense proton beams 7-25798
He-Cd laser transitions, level width determ., double-mode lasing state 7-43080
He-Cd positive column discharge 441.6 nm laser level (French) 7-11811
He-Kr⁺ laser operation, DC He and He-Kr discharges in Al hollow cathode tubes 7-10912
He-N₂ laser, pulsed electric-discharge, laser props. investig. 7-62675
He-Ne laser, stabilised by external absorption cell 7-20270
He-Ne laser at 0.633 μm, frequency stabilisation, using polarisation modulation 7-20295
He-Ne laser at 612 nm stabilised by I₂ external absorption cell 7-20308
He-Zn laser with transverse HF excitation 7-1090
Hg halide photodissociation laser pumped by wide-band optical radiation, three-colour emission 7-50548
Hg₃, superfluorescent laser action around 495 nm 7-15856
HgCl laser pumped by wide-band optical radiation emitting at 558 and 559 nm; 7-36955
HgI/HgI₂ laser at 442, 443, 444 nm with wide-band optical pumping 7-25806
Ho,Cr,Tm:YAG laser spectroscopic pumping scheme for 2 μm band 7-36968
I₂ photodissociation laser using I₂+C₂F₄I and I₂+O₂ mixtures 7-50547
I₂ saturated absorption lines identification, excited with green He-Ne laser 7-20372
ICl photodissociation laser at 11.35 μm, gain and energy 7-43082
In plasma, laser ablated inner-shell photoionisation-pumped, optical gain at 185 nm 7-20193
InGaAsP 1.3 μm diode laser, ultra-high-speed modulation 7-5924
InGaAsP laser amplifiers, recombination, gain and bandwidth characts. 7-57334
InGaAsP-InP, 1.5 μm laser with high external quantum efficiency and controlled emission wavelength 7-57323
InGaAsP-InP DFB laser with modified double-channel planar BH struct., 1.3 μm high-speed operation 7-15896
InGaAsP-InP DFB lasers with monolithic external cavity, spectral characts. for 1.3 μm 7-20281
InGaAsP-InP laser, ridge waveguide, threshold current anal. at 1.3 and 1.55 μm 7-31338
InGaAsP-InP laser, single-mode, 1.3 μm, analog FM 7-37002
InGaAsP-InP low-threshold separate-confinement heterostruct. laser characts. 7-31324
InGaAsP-InP ridge waveguide lasers, LPE fabricated, design and 1.5 μm low-threshold operation 7-15897
KCl:Li,F₂(II) colour centre laser, synchronously pumped, mode locking 7-62710
KX:O₂⁻ (X=Cl, Br), tunable CW laser operation in 1.45 to 2.16 μm range 7-62707
Kr lasing action, output pulse lengths achieved with electron beam pumping 7-15843
KrCl-XeCl, double laser oscill., quenching effect 7-57304
KrF laser system, Aurora, for inertial confinement fusion studies 7-15894
Mn halides, vapour lasers, resonance radiation trapping effects 7-62669
Mn vapour laser, emission spectrum and its time evolution 7-1088
Mn vapour lasers, resonance radiation trapping effects 7-62669
N₂ laser at 337.1 nm, design 7-36979
N₂⁺, electron beam excitation at 391.4 and 427.8 nm, He effects 7-10917
NH₃ lasers, line-tunable operating at wavelengths of 11 to 14 μm 7-5872
NH₃ lasers, optically pumped, CW operation in mid-IR 7-36950
Na₂, optically pumped excimer laser action, expt. obs. 7-57305
Na₂ photoionisation pumping via two-electron shakeup 7-20195
Na₂ violet bands, electronic assignments 7-15846
NaCl:O₂⁻, tunable CW laser operation in 1.45 to 2.16 μm range 7-62707
Nd:LiYF₄, two-step excitation and fluoresc. at 587.4 nm under CW pumping 7-25824
Nd:Ln₂(AlO₃)₆ laser CW tunable in 1.05 to 1.08 μm region 7-10985
Nd:YAG laser at 1.06 μm, high average power, design and charactn. 7-20265
Nd:YAlO₃ laser, CW, tuning characts. of 1079.5 and 1084.5 nm lines 7-15871
Nd³⁺:silica fibre laser, tunable CW at 0.900 to 0.945 and 1.070 to 1.135 μm 7-36983
Ne laser at 614.3 nm, superradiance under delayed excitation, asymmetry 7-1076
Ne lasing action, output pulse lengths achieved with electron beam pumping 7-15843
Ne like soft X-ray laser driven by high power optical lasers 7-62680
Ne pulsed transverse discharge, population inversion, secondary process influence 7-58084
Pb²⁺:KMgF₃ colour centre laser, tunable for 855 to 965 nm 7-15874
PbSnTe laser, single-mode, 8 μm with buried heterostructure, design 7-36980
Pr:LaCl₃ photon avalanche laser at 4.9 μm 7-15869
Pr³⁺:BaY₂F₈, stimulated emission spectra, laser action excitation 7-27745
S atomic laser, VUV, antiStokes Raman 7-15850
Se anti-Stokes Raman laser, high-power, radiating at 169 and 146 nm 7-43076
Se atomic laser, VUV, antiStokes Raman 7-15850
Se XXV plasma, laser produced, electron impact, laser transitions 7-26508
Tisapphire laser, 750 to 790 nm, pulsed injection control 7-36984

laser transitions continued

- Ti³⁺:Al₂O₃ coherently pumped laser, output characts., 675 to 945 nm tunable 7-31331
 Ti³⁺:BeAl₂O₄ chrysoberyl crystal tunable laser, 0.7 to 0.9 μ m 7-25826
 Xe lasing action, output pulse lengths achieved with electron beam pumping 7-15843
 Xe-He active medium, HF H-discharge excited, characts. investig. 7-20189
 XeF discharge laser, spectral anal. over wide range of press. (*Russian*) 7-50543
 XeF laser, electron-beam-excited, injection-controlled tuning at 435 to 535 nm 7-20199
 XeF laser, gain of ³He/Xe/NF₃ mixtures pumped by ³He(n,p)³H reaction 7-1083
 XeF* pumped by excimer radiation, near UV lasing on electronic-vibr. transitions 7-62671

laser trimming see *laser beam machining***laser tuning**

- birefringent filter design for CW dye laser resonator, spectral tuning band 7-50720
 Cr³⁺:K₂NaScF₆ laser material, tunable, crystal growth and spectroscopy 7-13347
 DFB lasers, fibre-extended-cavity, oscillation frequency tuning 7-57381
 DFB lasers, phase tunable type, 1.5 μ m operation, FM and spectral characts. study 7-43171
 diode compact linear array external cavity laser, 15 nm range tunable 7-43154
 diode element compact linear array external cavity laser, wavelength control 7-36992
 diode tunable laser control by stepping Michelson interferometer 7-43135
 distributed feedback dye laser, picosecond, excimer laser pumped 7-43086
 dye DFB picosecond freq.-tunable laser source for time-resolved meas. 7-50584
 dye laser, DFB oscillation in slab-type optical waveguide 7-15904
 dye laser, DFB producing tunable picosecond pulses, review 7-10992
 dye laser, high power, synchronously pumped operating at 410 to 550 nm 7-25841
 dye laser, short-cavity, tunable near IR picosec. pulse generation 7-50550
 dye laser, synchronously excited, with additional ultrathin resonator, picosecond pulse generation 7-31365
 dye laser, synchronously pumped, generation of high-power tunable picosecond pulses (*Chinese*) 7-5923
 dye laser, synchronously pumped, periodicity multiplication obs. with cavity length tuning 7-31311
 dye laser, synchronously pumped femtosecond CW, variable intracavity spectral windowing 7-36998
 dye laser, tunable, CW, Ar⁺ laser-pumped, spectral props. 7-1096
 dye laser, tunable with electro-optic Q-switching of coupled laser, characts. 7-1197
 dye laser DFB, achromatic pumping condition using grating 7-10999
 dye laser radiation, frequency conversion and surface spectroscopy appl. 7-15931
 dye laser system, high resolution computer controlled 7-20249
 dye lasers, tuning by a cholesteric liquid crystal device 7-15858
 dye multicomponent solution tunable lasers, electronic excitation energy migration 7-31308
 dyes, laser operation in near UV range 7-5881
 fluoromethane, FIR laser, simultaneous tunable Raman and fixed frequency oscillations 7-57302
 fluoromethanes, ¹²CH₃F and ¹³CH₃F, tunable far-infrared lasers 7-36951
 free electron laser research using 35 MeV linac at NERL (*Japanese*) 7-20243
 injection laser with external selective resonator, wide tuning range 7-43099
 integrated coupled-cavity lasers, design and fabrication 7-25843
 IR laser developments with tunable crystals and diodes 7-15887
 Lorenz-type chaos in laser 7-36932
 MQW DFB laser, theoretical anal. 7-20223
 multielectrode DFB laser, broad wavelength tuning under single-mode oscillation 7-20258
 multiwavenumber linearized diode laser spectra by overlapping frequency scans 7-41492
 polymethine dye grazing-incidence laser (*Russian*) 7-50583
 Raman dye laser, Nd:YAG pumped, pulsed tunable for spectroscopy (*French*) 7-25814
 rhodamine 6G laser, CW, combined mode locking using triphenylmethane dyes 7-37003
 rhodamine B laser, femtosecond, synchronously mode locked, spectral optimisation 7-37004
 semiconductor laser diodes, relevant to IR fibreoptics technology, new developments 7-36963
 semiconductor laser with transmission grating feedback, tunable narrow-band emission 7-1099
 semiconductor lasers, polarisation and wavelength control, TE, TM mode operation (*Japanese*) 7-25858
 SHG, critically phase matched, electrooptic tuning 7-43213
 small optically pumped CW far-infrared laser tunability and dynamics in high press. regime 7-20197
 Ti³⁺:sapphire laser material, scattering centre formation mechanism 7-10960
 two-atom spontaneous emission in a detuned damped cavity 7-57288
 wavelength stabilization of tunable diode lasers using an internally-coupled Fabry-Perot interferometer 7-31353
 wavelength-tunable single-mode fibre grating reflector 7-31442
 AlGaAs laser, tunability and mode-transition characteristics 7-20293
 AlGaAs laser, tunability, appl. to Cd²⁺ ion drift velocity meas. (*Japanese*) 7-20294
 Ar₂ excimer laser, tunable intense coherent radiation generation around 126 nm, stimulated Raman scatt. in H₂ 7-20328
 ArF, excimer laser amplifiers VUV anti-Stokes Raman line generation 7-57450
 CO lasers, CW, tunable, length reduction using Fabry-Perot resonators 7-11010
 CO₂ high-pressure laser, direct optical pumping with pulsed HF pump laser 7-50533
 CO₂ laser, gain-modulated single mode CW laser instabilities and chaos 7-43057
 CO₂ laser, TEA, tunable multiline and single line operation at 10.6 μ m and 9.4 μ m 7-31300

laser tuning continued

- CO₂ laser emission freq. continuous tuning band, widening using combined resonators 7-25847
 CO₂ laser pumping source for CH₂F₂ laser, Stark cell stabilisation 7-43134
 CO₂ laser TE, tunable using near grazing incidence grating, performance 7-43052
 CO₂ lidar systems, high speed tuning mechanism 7-36978
 CO₂ pulsed laser freq. dynamic tuning, multispike lasing using intracavity cell with IR absorbing gas 7-62663
 CO₂ TEA laser, tunable travelling-wave, single mode operation 7-15840
 CO₂ tunable waveguide laser with expanded tuning range 7-36981
 CO₂ waveguide laser, tunable, for optical pumping 7-20263
 CO₂ waveguide laser as tunable IR radiation source 7-31298
 CO₂ waveguide lasers with RF excitation, emission freq. tuning 7-43147
 CO₂ laser emitting in 4.2 μ m range, construction and props. 7-1186
 Co:MgF₂ laser, mode locking and Q-switching by loss-modulation freq. detuning 7-62711
 Cr:ScBO₃ laser, tunable over 785 to 892 nm 7-15872
 Cr³⁺:BeAl₂O₄ crystals, growth and laser performance 7-15870
 Cr³⁺:BeAl₂O₄ laser, tunable, characts. (*Chinese*) 7-5902
 Cr³⁺:BeAl₂O₄ tunable laser output pulse kinetics, spectral condensation characts. 7-50570
 Cr³⁺:Gd₂Sc₂Al₃O₁₂ laser, flash-lamp pumped 7-15902
 Cr³⁺:KZnF₃ tunable laser with nonselective pumping 7-43113
 Cr³⁺:SrAlF₃ laser emission tunable from 825 to 1010 nm 7-10964
 Cs vapour, generation of tunable IR ultrashort light pulses by nonlinear frequency conversion 7-1227
 GaInAsP integrated coupled-cavity lasers, design and fabrication 7-25843
 He-Ne laser tuned by axial mag. field, mode competition 7-50539
 KH₂PO₄ type crystals, tunable laser source down to 218.3 nm, freq. doubling and summing (*Chinese*) 7-57456
 KX:O₂⁻ (X=Cl, Br), tunable CW laser operation in 1.45 to 2.16 μ m range 7-62707
 KrF, excimer laser amplifiers VUV anti-Stokes Raman line generation 7-57450
 NH₃ lasers, line-tunable operating at wavelengths of 11 to 14 μ m 7-5872
 NH₃ lasers, optically pumped, CW operation in mid-IR 7-36950
¹⁴NH₃ and ¹⁵NH₃ laser pumped transversely by CO₂ laser 7-1085
¹⁵NH₃ laser, optical pumping, spectroscopic schemes 7-43073
 N₂O high-pressure laser, direct optical pumping with pulsed HF pump laser 7-50533
 NaClO₂·xH₂O, tunable CW laser operation in 1.45 to 2.16 μ m range 7-62707
 Nd:glass laser system, appl. of diffraction grating to increase tuning range 7-5916
 Nd:Ln₂(AlO₃)₃ laser CW tunable in 1.05 to 1.08 μ m region 7-10985
 Nd:YAG injection-seeded laser, polarisation feedback stabilisation, spectroscopy appls. 7-57338
 Nd:YAG laser, CW mode-locked, modulator freq. detuning effects 7-62712
 Nd:YAlO₃ laser, CW, tuning characts. of 1079.5 and 1084.5 nm lines 7-15871
 Nd³⁺:silica fibre laser, tunable CW at 0.900 to 0.945 and 1.070 to 1.135 μ m 7-36983
 Ni²⁺:MgAl₂O₄, Czochralski growth, stimulated emission tuning range 1.2 to 1.4 μ m 7-59406
 Pb salt tunable diode laser for two-tone optical heterodyne spectroscopy 7-30102
 Pb²⁺:KMgF₃ colour centre laser, tunable for 855 to 965 nm 7-15874
 Pb_{0.88}Sn_{0.12} Te cryst., annealing characts. and laser fabrication (*Chinese*) 7-10933
 Ti³⁺:Al₂O₃ coherently pumped laser, output characts., 675 to 945 nm tunable 7-31331
 Ti³⁺:BeAl₂O₄ chrysoberyl crystal tunable laser, 0.7 to 0.9 μ m 7-25826
 XeF laser, electron-beam-excited, injection-controlled tuning at 435 to 535 nm 7-20199
 ZnCdSe, electron beam pumped, cathodolum., gain and stimulated emission 7-64701

laser variables measurement

- absolute frequency meas., NRLM work relating to precision meas. and fundamental constants 7-14915
 automatic calibration system for laser power standard, expt. and performance eval. (*Japanese*) 7-11019
 beam profile meas., by thermographic technique 7-31377
 carbonyl fluoride, laser lines, optically pumped, heterodyne freq. meas. 7-36943
 DFB laser spectral linewidth meas. using fibre-optic gyroscope 7-1279
 diameter measurement of beams of about 1 μ m 7-5932
 difluoromethane, CO₂ laser pumped, freq. meas. on FIR laser emissions 7-1084
 diode laser array, radiation patterns, phase measurement 7-1207
 diode lasers, high power, for optical systems, phase front meas. 7-20301
 dye laser, tunable, CW, Ar⁺ laser-pumped, spectral props. 7-1096
 dye lasers, pulsed, expression for small signal gain 7-15889
 electro-optic voltage measurement in a high-power excimer laser 7-10977
 ethyl iodide, laser lines, optically pumped, heterodyne freq. meas. 7-36943
 Fizeau wavemeter, wavefront curvature compensation 7-35571
 frequency meas. of FIR lasers, using point-contact-type Josephson harmonic mixer 7-20310
 frequency measurement techniques and standards operation (*French*) 7-29983
 frequency standard, metrological certification of radiooptical freq. bridge 7-56210
 gas laser with high reliability, anal. methods (*German*) 7-20188
 Gaussian beam divergence meas. using SAW modulation 7-20297
 Gaussian laser-beam-diameter measurement using sinusoidal and triangular rulings 7-43186
 meter for radiation parameters of engineering lasers 7-56316
 methyl chloride, CO₂ laser pumped, freq. meas. on FIR laser emissions 7-1084
 methyl fluoride-d₃, and isotopic, laser lines, optically pumped, heterodyne freq. meas. 7-36943
 phase space-time distrib. meas. of coherent signal 7-25855
 photometer calibration, stable source of IR radiation 7-56317
 power meas. in μ W range, sensitive calorimeter with isothermal temp. control 7-15918
 power meas. standards scales intercomparison 7-15917

laser variables measurement continued

- power measurements, high precision absolute laser, using mag. suspended rotor 7-20298
- pulse spatial modes, direct measurement 7-5931
- pyroelectric detection of laser radiation 7-56341
- pyromagnetic detector, pulsed-periodic radiation behavior (*Russian*) 7-35509
- radiation detectors classification and characts. (*Czech*) 7-61367
- semiconductor junction DFB laser direct FM characts. meas. using delayed self-homodyne technique 7-11014
- semiconductor laser, linewidth determination from self-heterodyne meas. with subcoherence delay times 7-20300
- soft X-ray laser beam, divergence meas. 7-1210
- solid laser rods losses and efficiency meas. 7-43106
- spatial energy distrib. determ. by Rayleigh scattering 7-43183
- subpicosecond pulse duration meas. with two-photon fluore. of Xe_2 excimers 7-43187
- ultra-short laser pulse characts., microprocessor-based meas. system 7-41360
- ultrashort laser pulses, intensity profile anal. using four-wave mixing or third harmonic generation 7-25891
- UV laser beam profile monitor using alkali halide crystals 7-37011
- waist parameters determ. of Gaussian beam 7-37007
- wavelength comparison, using Fourier transform spectrometer 7-20311
- wavelength meas. using $0.63 \mu\text{m}$ transition 7-1208
- wavemeter, compact, automatic, for tunable IR diode lasers 7-43181
- wavemeter, single mode fibre used for accurate optical alignment 7-11112
- wavemeter, Twyman-Green type, performance assessment (*Korean*) 7-24692
- X-ray laser research, in situ calibrations of grazing incidence vacuum monochromators 7-41570
- CO_2 laser spectrum monitoring and displaying instrument 7-5935
- He-Ne laser beam divergence meas. using LiNbO_3 SAW interaction 7-1211
- He-Ne laser stabilised by methane saturable absorption, effects leading to frequency shifts 7-50540
- HeNe/methane laser, absolute frequency meas. at 88 THz 7-18762
- I laser, solar-pumped, beam profile meas. 7-37006
- ICl photodissociation laser at $11.35 \mu\text{m}$, gain and energy 7-43082
- KrF laser gain meas. system 7-62717
- Pb salt diode laser calibration, wavemeter 7-5930

laser velocimeters

- anemometer arrangement measurements (*Polish*) 7-57965
- bubble diameter meas. by fringe method, using laser Doppler anemometer 7-16278
- differential Doppler gauge for contactless meas. of speed and length 7-24628
- directional laser Doppler velocimeter, dual sinusoidal modulation 7-56228
- Doppler anemometer, two-colour four-beam system, two-phase mist flow meas. 7-37581
- Doppler anemometer for vel. meas. in enclosed flames (*German*) 7-18765
- Doppler flowmeters, differential, with single-mode fibre waveguides 7-44079
- fibre laser Doppler anemometer and boundary-layer meas. appl. 7-37609
- fibre optic LDV, semiconductor laser and integrated optics use 7-25998
- fluorescence signal flow-induced variation technique 7-44068
- multi-pt. system using phase diffraction grating 7-37605
- proximity sensors, flow meas. with beam-scanning LDV 7-37604
- scanning three-velocity-component laser Doppler anemometer 7-16277
- LiNbO_3/Ti integrated optic device for fibre laser Doppler velocimeter 7-6022

laser velocimetry

- anemometer meas. corrections for curved channel flow 7-37608
- coherent struct. in reattaching laminar and turbulent shear layers 7-51079
- complex flow measurement, two component LDV system (*Chinese*) 7-26366
- compressible separated turbulent shear flow, mixing, flow meas. 7-51080
- compressible turbulent free shear layer interaction 7-51078
- curved square duct with different Reynolds nos., press. loss and mean velocity field meas. (*Chinese*) 7-11545
- Doppler anemometer for superlow velocity meas. 7-43812
- Doppler anemometry, counter based in wet steam flow 7-57969
- Doppler effect methods for solid surfaces, using specular reflection (*Japanese*) 7-41359
- Doppler interferometry methods for highly accurate flow meas. 7-44073
- double-pulsed velocimetry, image shifting technique to resolve directional ambiguity 7-37559
- droplet sizing techniques, laser interferometric, performance comparison 7-30071
- fibre optic sensors, extrinsic, for remote meas., impact on meas. techniques 7-11154
- fibre optic sensors for remote measurement 7-43394
- fibre optics in laser Doppler velocimetry 7-50771
- flow acceleration measurements using laser Doppler anemometry 7-31904
- flowing two-phase dispersed particles, metrology using optical diffusion (*French*) 7-31895
- fluidised beds, freeboard, vel. meas. using laser Doppler anemometer 7-11527
- gas velocity imaging using photothermal deflection effect 7-20817
- gas-solid fluidised bed, freeboard region, two-phase flow behaviour 7-63209
- inviscid axial flow in compressor rotor, leading-edge effects, flowfield meas. 7-11562
- laminar pulsating flow in curved pipes, axial vel. profiles 7-37543
- laser-Doppler anemometer, bubble-driven flow, fluid and bubble meas., numerical soln. 7-16237
- laser-Doppler anemometry, MHD channel flow, secondary flow meas. 7-16302
- multi-point vector measurement by pulsed laser velocimetry with image compression 7-37610
- particle image displacement velocimetry for 2D flow visualisation 7-31893
- particle siting with phase Doppler spray analyser, nonspherical drops effect 7-29969
- particle size and velocity measurement using phase Doppler particle analyser 7-29968
- particles in flows, simultaneous velocity and size meas. using laser technique 7-9814

laser velocimetry continued

- photothermal deflection spectroscopy with transient grating, velocimetry in laminar and turbulent flows 7-31901
- pipeline flow meas. in flow straightener/flowmeter package 7-57948
- plunging breaking waves, velocity and force measurements in the splash zone, laser anemometry 7-63237
- Rayleigh-Benard convection, laser speckle velocimetry 7-31902
- solid-liquid two-phase flow, laser Doppler velocimeter meas. and turbulence props. 7-37533
- swirling flow, axisymmetric vortex breakdown in circular pipe 7-26286
- turbulence measurement using a laser-2-focus velocimeter 7-57967
- turbulent flow meas. in ribbed-wall flow channel and comparison with model 7-57947
- underwater optical probe for laser Doppler anemometry 7-16279
- unstationary flow, particle behaviour in Basset-Boussinesq-Oseen eqn. 7-11404
- vibration measurement, laser Doppler velocimeter and laser torsional vibrometer, comparison 7-31721
- H, swirling turbulent diffusion flames, turbulence intensity study 7-26287

laser wavelength measurement see *laser variables measurement*

laser windows see *laser accessories; optical elements*

lasers

- see also *chemical lasers; distributed Bragg reflector lasers; distributed feedback lasers; dye lasers; excimer lasers; free electron lasers; gas lasers; laser beams; laser frequency stability; laser tuning; liquid lasers; nuclear pumped lasers; Raman lasers; ring lasers; solid lasers; X-ray lasers*
- conference, laser science advances, Dallas, TX, USA (Nov. 1985) 7-9573
- electricity and modern techniques, conf., Bordeaux, France (Oct. 1985) 7-14708
- femtosecond laser pulse generation and appls. 7-15884
- high power lasers and their applications (*French*) 7-15890
- industrial laser annual handbook 7-24316
- Optical Society of America annual meeting, Seattle, WA, USA (Oct. 1986) 7-48146
- quantum electronics, conf., San Francisco, CA, USA (June 1986) 7-48147
- Romanian, history and state of the art 7-14747

latches see *flip-flops*

latent heat

- see also *heat of fusion; heat of sublimation; heat of vaporisation*
- contact melting, latent heat thermal energy storage 7-43646
- greenhouse solar system, transient response of latent heat storage 7-23227
- heat transfer characts. for latent heat storage unit with finned tube 7-43647
- low temperature thermal storage using latent heat and direct contact heat transfer 7-65618
- measurement and meaning, elementary formalism 7-29625
- morphological stability, weakly nonlinear, effect of latent heat 7-59497
- phase change problems, curved interface straightening, isoparametric finite elements 7-62963
- solidification, heat transfer characts., latent heat storage unit with finned tube 7-43648
- thermal storage using pentaerythritol slurry, storage systems eval. 7-65616
- FEMs for solidification problems, comparison 7-14759
- He, liq., in Vycor glass, thermodynamics of freezing and melting 7-52169
- Li-Na-K- CO_3/MgO salt/ceramic phase change material for high temp. thermal storage, thermoanalytic investigation 7-65631

latent heat of adsorption see *heat of adsorption*

latent heat of combustion see *heat of combustion*

latent heat of crystallisation see *heat of crystallisation*

latent heat of dissociation see *heat of dissociation*

latent heat of formation see *heat of formation*

latent heat of fusion see *heat of fusion*

latent heat of mixing see *heat of mixing*

latent heat of reaction see *heat of reaction*

latent heat of solution see *heat of solution*

latent heat of sublimation see *heat of sublimation*

latent heat of transformation see *heat of transformation*

latent heat of vaporisation see *heat of vaporisation*

latent image see *photographic process*

lattice constants

- see also *crystal atomic structure*
- alkali halide mixed crystals, phys. props., review 7-37943
- alkali halides, interionic potentials based on charge transfer model 7-58197
- austenitic steels, small precip., moire imaging in TEM 7-46490
- BAs, structural and electronic props., pseudopotential method, local density approx. 7-32353
- β -(BEDT-TTF) $_2(\text{I}_3)_{1-x}(\text{AuI}_2)_x$, thermal expansion and stepwise superconducting transition 7-27469
- B-(BEDT-TTF) $_x$ organic metal, high T_c supercond. state 7-45542
- brass, Sn alloyed, disordered areas in three component solid solns. 7-21157
- composition modulated layered structs., elastic strain, X-ray diffr. studies 7-27086
- diamond, type Ia, voidites, evidence for crystalline phase containing nitrogen, cell constant determ. 7-2011
- disordered sublattice cpds., supersonic conductivity and lattice parameters 7-38247
- Fischer-Tropsch waxes, cell parameters, temp. dependence 7-12043
- gadolinium aluminum pentafluoride dihydrate single crystals, struct. and symm. determ., X-ray diffr. study (*French*) 7-37960
- heteroepitaxial structures, lattice parameter difference meas. using extremely asymmetrical Bragg diffr. 7-51569
- II-VI semiconductors, low-temperature epitaxial growth, MBE and MOCVD 7-64906
- III-V semiconds., electronic struct. calcs. 7-12608
- kaolin-mullite, charactn. of spinel phase formed in thermal sequence 7-37937
- methane adsorbed on graphite, heat capacity calcs., quantum cell model 7-52076
- mullite powders, props. and microstruct. of fired bodies (*Japanese*) 7-22626

lattice constants continued

- ordered substitution alloys, lattice parameters, elasticity modulus (*Russian*) 7-46542
- organic conducting single crystals, electron irradiation, Bragg spot fading 7-12158
- oxides; perovskite-type, activation energy for proton conduction 7-52130
- pressure-induced phase transitions of $\text{A}^n\text{B}^{n-1}\text{C}$ compounds 7-52039
- propylammonium tetrachloromanganate, incommensurate γ phase, elastic neutron and X-ray scattering 7-16538
- rare earth metals, ground and excited state properties, local density total energy calculations 7-7141
- semiconductors, insulators and metals, structural, electronic and vibrational properties, pseudopotential calculations 7-16484
- steel, Cr-Ni-Mn, decomposition, martensite structure. rel. to alloying composition (*Russian*) 7-59531
- ternary intermetallic compounds, single crystal, Czochralski growth, characterization 7-53557
- TTF(Ni(dmit)₂)₂ molecular superconductor, BCS and small superconductor, lattice parameters (*French*) 7-2759
- unit cell dimensions and positional parameters, powder X-ray and neutron diffraction studies 7-16527
- YIG:Ca films, magneto-optical properties, reducing treatment effects 7-64617
- $\text{Ag}_{1/2}\text{In}_{1/2}\text{PS}_3$ lamellar compound, crystal structure refinement studies 7-58235
- Al, lattice spacing of interstitial solid solutions of B and C, deformation interaction, pseudopotential method (*Russian*) 7-58271
- Al-Mo (11 at.%), rapidly solidified, equilibrium phase development 7-46436
- Al-Xe, implanted, form of solid precipitates and fluid bubbles, TEM observations 7-38032
- Al-Zr-V, rapid solidification, age hardening, solid solution form. (*Korean*) 7-46475
- AlAs/GaAs modulated structure, high resolution double-crystal X-ray diffraction studies 7-7029
- $\text{Al}_x\text{Ga}_{1-x}\text{N}$ MOVPE growth, structure and electronic properties 7-21729
- AlN , electronic structure, first principles LCAO calculation 7-21813
- $\alpha\text{-Al}_2\text{O}_3$, ceramic matrices, precipitate morphology 7-65049
- Al_2O_3 ceramics, sintering, effect of TiO_2 (*Japanese*) 7-3248
- $\text{Al}_2\text{O}_3\text{-SiO}_2$, mullite ceramics, sol mixture preparation, drying method effect (*Japanese*) 7-7944
- Ap-Xe-Kr(Ar), ion implanted, bubble growth, lattice parameters, TEM observations 7-51803
- As, structural calculations 7-7143
- As_2Te_3 , metastable state, rhombohedral structure study (*French*) 7-44496
- Au_3Cr , atomic ordering, X-ray structure analysis (*Russian*) 7-1933
- BN, wurtzite-type and zincblende-type, structure changes by shock treatments 7-22676
- $\text{Ba}(\text{Bi,Pb})\text{O}_3$, semiconducting properties, X-ray powder diffraction and transport measurements (*Japanese*) 7-64237
- BaF_2 , thermal expansion from 296 to 1173 K 7-12327
- BaO , self-consistent electronic structures 7-32910
- $\text{Bi}_2\text{O}_3\text{-ZrO}_2\text{-Y}_2\text{O}_3$ system, O ion conduction 7-44905
- CaF_2 , lattice constant, force calculation in molecular dynamics simulations 7-51710
- $\text{CaMg}(\text{B}_3\text{O}_4(\text{OH})_3)_2 \cdot 3\text{H}_2\text{O}$, hydroboracite, thermal expansion 7-63850
- CaO , self-consistent electronic structures 7-32910
- $\text{Ca}_{10}(\text{PO}_4)_6(\text{OH})_2$, thermal lattice expansion, 20-600 °C 7-58510
- Cd-Hg, ω -phase lattice parameters, influence of temperature and pressure (*Russian*) 7-51704
- $\text{CdO-Bi}_2\text{O}_3$, crystallographic state of CdO lattice during sintering with Bi_2O_3 addition 7-37944
- CdTe epitaxial layers on GaAs substrates, X-ray diffraction 7-27201
- CdZnTe, epitaxial growth via low pressure CVD, IR detector applications 7-64926
- $\text{Cd}_{1-x}\text{Zn}_x\text{Te}$ mixed compound, semiconductor, lattice constants. comp. depend., X-ray diffraction study 7-58246
- Co-Si bilayered films, chemical, electronic, and structural charges upon annealing 7-22037
- $\text{Co}_{0.35}\text{Cu}_{0.45}\text{Cr}_2\text{S}_4\text{-ySe}_y$ spinels, X-ray diffraction study 7-44475
- CsCl-CsBr solid solutions, lattice parameter measurements by X-ray diffraction 7-58249
- $\text{Cs}_2\text{Na}_{10}(\text{FeO}_3)_4$ single crystal, preparation and structural characterization (*German*) 7-37951
- CsPbBr_3 , lattice thermal expansion, 140-400 °C, X-ray observations 7-44859
- CsV_2O_7 , crystals, structure, cathodic reduction from melt, and electronic properties studies 7-58236
- Cu films, sputter deposition, effect of ion bombardment of growing film 7-64009
- Cu single crystal, deformed, lattice parameter changes through long-range internal stresses (*German*) 7-16673
- $\text{Cu}_x\text{Cd}_{1-x}\text{Fe}_2\text{O}_4$ system, electronic resistance and cation distribution 7-7256
- $\text{Cu}_2\text{Cl}(\text{OH})_3$, atacamite, structure refinement, X-ray diffraction study 7-32371
- $\text{CuCo}_5\text{Ti}_5\text{O}_{12}$, delafossite type structure, compound lattice constant (*French*) 7-63572
- CuGaTe_2 , lattice thermal expansion, 80 to 650 K 7-12326
- CuInTe_2 , lattice thermal expansion, 80 to 650 K 7-12326
- Cu_2MnAl , high pressure phase transition, electronic resistance, saturation magnetization, lattice parameters (*Russian*) 7-46457
- $\text{CuNi}_5\text{S}_5\text{O}_{12}$, delafossite type structure, compound lattice constant (*French*) 7-63572
- $\text{CuNi}_5\text{S}_5\text{Ti}_5\text{O}_{12}$, delafossite type structure, compound lattice constant (*French*) 7-63572
- CuSeO_2 , delafossite type structure, compound lattice constant (*French*) 7-63572
- CuSeO_3 structure, determination and refinement, X-ray diffraction study 7-32373
- Dy-Re-Fe(CO)(Ni), intermetallic-based solid solutions, phase equilibrium and magnetic properties 7-22639
- Fe-Al disordered alloys, electronic structure, magnetic properties and Mossbauer spectra 7-64073
- Fe-C martensite, structure in transition state from first to third stage of tempering, electron microscopy and diffraction study 7-46528
- Fe-Cr-Ni alloys, FCC, dilation by interstitial C and N 7-44451
- Fe-Ni-B system, distribution, equilibrium in two-phase fields 7-22641
- Fe-Si alloy wires, rapidly solidified by in-rotating-water-spinning method, production and properties (*Japanese*) 7-22654
- Fe-Si-Cr system, ordering process, thermal expansion studies (*Russian*) 7-1932
- FeCl_2 , magnetostriction, X-ray diffraction measurements 7-33258
- $\gamma\text{-Fe}_2\text{O}_3$ reactive RF sputter deposition, structure, electronic and magnetic properties studies 7-17421
- FeTiO_3 , ceramic matrices, precipitate morphology 7-65049
- GaAs MOCVD growth on Si with superlattice intermediate layers, material properties 7-27923

lattice constants continued

- GaAs, semi-insulating, nonstoichiometry study, lattice parameter measurements 7-38220
- GaAs:Si, semi-insulating, ion implanted, LEC growth, electronic activation efficiency, stoichiometry dependence 7-46298
- $\text{Ga}_{0.47}\text{In}_{0.53}\text{As}/\text{Al}_{0.48}\text{In}_{0.52}\text{As}$ modulated structure, high resolution double-crystal X-ray diffraction studies 7-7029
- $\text{Ga}_{1-x}\text{In}_x\text{AsSb}_{1-y}$ system, low temperature phase equilibrium 7-52001
- GaN, X-ray phase analysis, elastic properties 7-45050
- GaP crystal, low temperature negative thermal expansion coefficient 7-6837
- GaSb single crystals, intrinsic point defects and microdefects, TEM studies 7-44529
- $\text{Ga}_2\text{Te}_3\text{-In}_2\text{Se}_3$ solid solutions, crystal structure, X-ray powder diffraction studies 7-16526
- $\text{Gd}(\text{Cu}_{1-x}\text{Co}_x)_2$, magnetic and crystallographic properties 7-38903
- $\text{Gd}_{2.957}\text{Se}_{1.905}\text{Ga}_{3.138}\text{O}_{12}$ garnet, congruent melting, crystal growth 7-59412
- HfN(C) reactively sputtered wear resistant coatings, structure, hardness and adhesion properties study 7-52330
- $\text{HfO}_2\text{-Ln}_2\text{O}_3$ ($\text{Ln}=\text{Y,Gd,Tb,Er,Yb}$), solid solution single crystals, physicochemical properties 7-2097
- HfTe₂, unit cell dimensions and positional parameters, powder X-ray and neutron diffraction studies 7-16527
- $\text{InAs}_x\text{P}_{1-x}$, LEC-grown single crystals, growth defects and lattice strains 7-38001
- InGaAs and InGaAsP, nonuniform, dynamical X-ray rocking curve simulations 7-2408
- InGaAsP, layers on InP, relative lattice parameter measurements, convergent beam electron diffraction 7-52371
- InGaAsP/InP multiquantum well layers, LPE, photoluminescence, X-ray diffraction 7-53640
- $\text{In}_{1-x}\text{Ga}_x\text{As}_y\text{P}_{1-y}$ compound, semiconductor alloys, lattice and band structure properties, review (*Japanese*) 7-7109
- $\text{In}_x\text{As}_{1-x}$ solid solutions, temperature dependence of lattice constants and thermal expansion coefficients 7-21165
- InSe crystals, melt-grown, electron diffraction study 7-1994
- $\text{Cl}(\text{Br})$ γ -irradiated single crystals, piezoluminescence and thermoluminescence spectral shift measurements 7-27796
- $\text{K}_2\text{O-Fe}_2\text{O}_3\text{-TiO}_2$ system, crystal growth of titanates, morphology, ionic conduction 7-53523
- K_2SbPO_6 , solid-state reaction preparation and crystal structure determination, X-ray diffraction study 7-1980
- KTiOAsO_4 structure and nonlinear optical properties studies (*French*) 7-37948
- La-Co-O system, nonstoichiometric K_2NiF_4 -type phases 7-37936
- $\text{La}_{1-x}\text{Ca}_{0.55x}\text{Ba}_{0.45x}\text{FeO}_{3-x}$, electronic conduction properties. rel. to structure 7-63871
- $\text{LaMgAl}_{11}\text{O}_{19}\text{-LaMgGa}_{11}\text{O}_{19}\text{-LaMgFe}_{11}\text{O}_{19}$ system, solid solutions, 7-39491
- $\text{La}_2\text{Mo}_2\text{O}_7$, quasi-2D single crystal structure and electronic properties studies 7-58238
- $\text{La}_{1-x}\text{Sr}_x\text{FeO}_{3-x}$, electronic conduction properties. rel. to structure 7-63871
- $\text{LiFe}_4\text{Al}_3\text{Ga}_8\text{O}_{28}$, magnetization and lattice parameter, role of Al and Ga ions 7-22097
- LiH, electronic structure, molecular cluster calculations 7-7110
- $\text{Li}_3\text{-H}_2\text{TaO}_4$, preparation by means of hydrothermal synthesis and protolysis 7-39449
- $\text{Li}_9\text{Mo}_6\text{O}_{17}$ purple bronze, crystal structure determination 7-58239
- LiNbO_3 , anomaly study by X-ray diffraction 7-6588
- LiNbO_3 proton-exchanged single crystal, optical waveguides, electro-optic effects, lattice constant and refractive index changes measurements 7-22220
- $\text{LiNbO}_3\text{-MgO}$, melt growth and characteristics 7-58170
- $\text{Li}_2\text{SO}_4\text{-H}_2\text{O}$, charge density at 80 and 298 K, X-ray and neutron diffraction 7-21166
- $\text{LiY}_{1-x}\text{Yb}_x\text{F}_4$ single crystal, growth, lattice constant and thermal expansion coefficient. temperature dependence studies 7-27891
- LiZnF_3 preparation and X-ray and NMR structural study 7-37953
- Mg-Ir, superconducting transition temperature and lattice constants 7-64387
- $\text{Mg}_2\text{Al}_3\text{Si}_5\text{O}_{18}$ and solid solutions, thermal expansion (*Japanese*) 7-21496
- Mg_2Si antiferroelectric semiconductor, electronic structure calculations 7-12608
- Mn-Cu alloy, nonlinear anelasticity and temperature dependence lattice constants, nonlinear resonance curve measurements 7-63741
- $\text{Mn}_3\text{Cr}_2\text{Ge}_5\text{O}_{12}$ garnets, crystal growth, chemical vapour transport, structure 7-53518
- $\text{Mn}_3\text{Fe}_2\text{Ge}_5\text{O}_{12}$ garnets, crystal growth, chemical vapour transport, structure 7-53518
- $\text{Mn}_3\text{Ga}_2\text{Ge}_5\text{O}_{12}$ garnets, crystal growth, chemical vapour transport, structure 7-53518
- $\text{MnNa}(\text{H}_2\text{PO}_3)_2 \cdot \text{H}_2\text{O}$ orthorhombic structure, bond lengths and angles, X-ray diffraction study 7-32372
- $\text{Mn}_2\text{Sb}_2\text{O}_7$, synthesis and crystal structure, X-ray powder diffraction measurements 7-58240
- $\text{Mn}_3\text{Si}_2\text{Te}_6$ ferrimagnetic semiconductor, crystal structure, X-ray diffraction study 7-1977
- Mo/Ni superlattice, sputtered, structure analysis 7-45030
- $\text{NaLi}_3\text{Si}(\text{Ge})(\text{Ti})\text{O}_4$ isotopic oxides, crystal structure determination, lattice energy calculations (*German*) 7-37952
- $\text{Na}_{1.7}\text{P}_4\text{W}_{14}\text{O}_{50}$ structure, refinement, single crystal, X-ray analysis study 7-58233
- Nb_3Ge films, obtained by joint evaporation technique, microstructure (*Russian*) 7-59435
- NbH , β - and γ -phases, electronic structure and phonon anharmonicity 7-45199
- $\text{Nb}_{0.94}\text{O}_2$ form. by shock reduction of Nb_2O_5 powder, rutile structure study 7-2102
- $\text{NbSe}_{10.33}$, vapour grown, crystal growth by microsteps 7-58176
- Nd-Fe-B permanent magnets, BCC phase magnetic properties at grain boundaries 7-53044
- Ni binary alloys, solid solution hardening, flow stress, Young's modulus 7-13465
- Ni epitaxial growth on Fe (001), LEED and AES studies 7-64022
- Ni-B-C-based alloys, γ phase, prolonged ageing effects (*Russian*) 7-59551
- Ni-Fe film, ion beam sputter deposition, ion bombardment effect on preferred orientation 7-64010
- Ni-H system, band structure calculations 7-45140
- Ni-Si bilayered films, chemical, electronic, and structural charges upon annealing 7-22037
- Ni-Ti-H, α/β miscibility gaps, X-ray diffraction study 7-13430
- Ni-V-H, α/β miscibility gaps, X-ray diffraction study 7-13430
- Ni_3Al , solid solution hardening with ternary additions, Young's modulus 7-13464
- NiCoGa , thermal vacancies 7-51764
- $\text{Ni}_{1-x}\text{Fe}_x\text{MnSb}$, half-metallic ferrimagnetic, magnetic and crystallographic properties 7-45672

lattice constants continued

- NiS_{1-x}Se_x, effect of Se substitution on mag. and electrical transition 7-2846
 PbIn_{1/3}Nb_{1/3}O₃, antiferroelec., phase transition, B-site cation order effects 7-7651
 Pb_{1-x}Sn_xTe_{1-x}Se_x solid soln. single crystals, density, comp., lattice const. and galvanomag. props. (*Russian*) 7-44500
 PbTiO₃, spontaneous strain, anomalous press. depend. 7-26833
 PbTiO₃-PbZrO₃-Pb(Mg_{1/3}Nb_{2/3})O₃ system, comp. fluctuation in solid soln. (*Japanese*) 7-28025
 Pb₃UO₆ struct. refinement, neutron powder diff. study 7-32370
 Pd films, sputter deposition, effect of ion bombardment of growing film 7-64009
 Pd-Ni alloys, formation enthalpies and lattice parameters, embedded atom calc. 7-44455
 PrCo_{4-x}Fe_xB, crystallographic and mag. props. 7-45671
 Pt films, sputter deposition, effect of ion bombardment of growing film 7-64009
 RbCl-RbBr mixed crystals, X-ray diffraction and color centres 7-58258
 Rb_{1-x}(NH₄)_xH₂PO₄, lattice constants, temp. and concentration dependence, X-ray diffraction anal. 7-1976
 RbV₂O₆ crystals, struct., cathodic reduction from melt, and elec. props. studies 7-58236
 Ru, electronic, structural and cohesive props., theoretical study 7-37922
 Si, charge carrier-lattice interaction, X-ray diff. study 7-51975
 SiO₂-Al₂O₃, mullite form. from xerogels, X-ray and IR obs. 7-46391
 Sr₆Nb₃O₉ single cryst., bronze-type struct., X-ray diff. study (*German*) 7-37949
 SrNd₂S₂-Nd₂S₃ solid solns., vacancy disorder charactn., Raman spectra study 7-58270
 Ta-T system, distortion by Hc form. 7-51717
 TaTe₃, evolution of lattice spacing and damage 7-16582
 TaTe₃, lattice deformation due to ³He production 7-21237
 (Tb_{1-x}Y_x)₂Co, magnetoelastic interactions and thermal expansion (*Russian*) 7-17211
 Te₂P₃ twinned cryst., space group and lattice constant, X-ray diff. determ. 7-1979
 Ti alloy metastable phases, plasticity (*Russian*) 7-33729
 TiH_x, X-ray diff., lattice parameter change, density of states 7-44469
 TiN(C) 7-52330
 TiCl_{0.7}Br_{0.3}, Debye temp., Debye-Waller factor and mean vibr. amplitude, X-ray determ. 7-26893
 TiFe_{2-x}Se₂ layered cpd. single cryst., magnetic and structural props., Mossbauer and X-ray diff. studies 7-2848
 UFe₂, spin-polarised energy bands, density of states and eqn. of state 7-58734
 UO₂-Gd₂O₃, solid solution, lattice parameters, O/U thermal conductivity meas. 7-21180
 β-V-B, rhombohedral phase, struct. and solid solubility, X-ray single cryst. diff. study 7-1948
 V-Si-N system at reduced N press., phase relations at 1273K, absence of supercond. 7-17518
 V_{3-x}Mo_xS₄, struct. and phase relations, comp. depend., X-ray powder diff. study 7-1978
 n-WSe₂ single crystal, growth, struct. and photoelectrochem. props. 7-27879
 Y₂O₃-TiO₂ system, fluorite type solid soln. crystallisation 7-1882
 Yb_{1-x}Tm_xSe, anomalous Tm valence, lattice parameters, diamag. suscept. and Hall effect meas. 7-16998
 Zn_{1-x}Cd_xS thin films, struct. and electrical props. 7-64372
 ZnMoO₄, synthesis and struct., orthogonal nonintersecting octahedral cluster chains 7-32386
 ZnO crystals, real struct. during growth process, effect of plastic deform. 7-11974
 ZnO-Bi₂O₃ mixtures, lattice parameters, depend. on Bi₂O₃ conc. 7-1974
 ZnSe, heteroepitaxial growth on GaAs, energy band gap, elastic strain effects 7-59242
 ZnSeO₃ struct. determ. and refinement, X-ray diff. study 7-32373
 Zr, α and β phases, differential heat of H absorption, isoperibol calorimetry studies 7-6967
 ZrN(C) reactively sputtered wear resistant coatings, struct., hardness and adhesion props. study 7-52330
 ZrO₂, ceramic matrices, precip. morphology 7-65049

lattice defects see crystal defects

lattice diffusion see diffusion in solids

lattice dynamics

- see also crystal surface and interface vibrations; displacive transformations; Gruneisen coefficient; lattice dynamics of covalent crystals; lattice dynamics of ferroelectric crystals; lattice dynamics of ionic crystals; lattice dynamics of metallic crystals; lattice dynamics of molecular crystals; lattice localised modes; lattice phonons; soft modes; vibrational states in disordered systems
 alkali cyanides, multipole interaction effects on cohesive and anharmonic props. 7-1942
 alloys, order-disorder phenomena, Ising model calcs. allowing for atomic vibrations 7-21400
 crystal instability, defect-phonon interactions 7-44722
 disordered crystals with nonanalytic spectrum, density of states tails 7-44713
 graphite-K intercalation cpd., C₈K, anisotropic binding of K, nuclear resonance photon scatt. of bremsstrahlung 7-51695
 insulators, indirect short-range interactions and lattice vibr. 7-21154
 interstitial atom motion and lattice dynamics, quantum mechanical model 7-58528
 IV-VI compounds, vibronic theory of struct. phase transition and tricritical point 7-38187
 Jahn-Teller effect, Berry's geometrical phase and the sequence of states 7-58779
 lanthanide oxysulphides (oxyhalides), Eu³⁺-doped, vibronic spectra 7-51968
 latt. dynamics, phonon line shapes at high temp. 7-2122
 mechanical rupture of a defective chain of atoms 7-996
 metal nitrides, vibrational entropy 7-6745
 modulated structures, lattice dynamics, appl. to superlattices 7-52220
 molecular chains, strong EM field driven, with optical type vibr. spectra, nonlinear waves and bistability 7-25865
 neutron scattering studies of dynamic props., book contrib. 7-26897
 organic crystals, chem. transformations, phase transition effects (*Russian*) 7-28309
 parametric resonance in crystals, dynamic bistability 7-1216

lattice dynamics continued

- Penrose chain, 1d, vibr. spectrum and spectral dimension: 7-32582
 periodic harmonic lattices, mechanical power transfer and energy-current density calcs. 7-9801
 polyacetylene, order parameter and optical absorption, quantum fluctuations 7-63750
 PTFE, oriented, annealing, crystn. lattice temp. behaviour (*Russian*) 7-6840
 quantum field theory of lattice dynamics and melting in sphalerite and diamond structure crystals 7-26876
 quartz, incommensurate phase, temperature dependent low-frequency modes 7-6737
 α-quartz, thermal expansion, internal strain below room temp., lattice dynamical model 7-52092
 quasicrystals, 1D, acoustic and electronic props. 7-6730
 Raman spin-lattice relax. rates, long wave approx. 7-33378
 soliton dynamics of finite 1D H-bonded system 7-2112
 structural phase transitions in highly anisotropic systems, dynamics 7-32605
 surfaces, force sum rules, Hellmann-Feynman theory 7-44989
 transition metal layered compounds, structural phase transitions, microscopic theory 7-44807
 transition metals, lattice dynamics 7-51972
 unitary transformations in solid state physics, book 7-24310
 vibrational modes of solids, nuclear reaction spectroscopy 7-21371
 Ag dimers and clusters, matrix isolated, guest-host interaction and photochem. transform. 7-15786
 As, crystalline, bond strength anal., EXAFS temp. depend. study 7-64763
 As₂S₃, crystalline, bond strength anal., EXAFS temp. depend. study 7-64763
 Ba(NO₂)₂D₂O, lattice vibr., mol. contrib., Raman spectra 7-46007
 Ba_{0.73}Pr_{0.27}F_{2.27} nonstoichiometric phase struct., neutron diff. study 7-63587
 BiLiF₄, lattice vibr., Raman study 7-53329
 Bi₁₂MO₂₀V, (M=Si,Ge,Ti), sillenite struct., local vibr. of impurities, spectral study 7-7718
 Bi₁₂Si₂₀ crystals, local vibr. of Si isotopes, Raman spectra 7-7689
 Bi₁₂XO₂₀ (X=Si,Ge,Ti), simultaneous anal. of vibr. spectra 7-46006
 CO solid films, Fourier transform IR spectra 7-59214
 CaSiO₃, perovskite type, cryst. struct., lattice dynamics and eqn. of state 7-58248
 CdS(Se), X-ray graphic elastic constants and lattice spectrum 7-32546
 CdTe:Fe²⁺, impurity vibronic coupling and near IR spectra characts. 7-26889
 CuGeF₃, semicond., elastic const., anharmonic props. 7-26830
 Cu₂OC₆(C₆H₅)₃PO₄·0.70CH₃NO₂ crystals, anharmonic atomic thermal vibr. and pots. X-ray diff. struct. study 7-63762
 GaAs interatomic force const. and normal modes, group theoretical method calcs. 7-32588
 Ge, vibrational correlation functions 7-51966
 Ge_{0.08}Sn_{0.92}Te, acoustic mode vibr. anharmonicity 7-63751
 H transfer in double minimum potential, kinetic props. and quantum dynamics 7-54104
 K₃CO(CN)₆, polytypism and phase transition, lattice dynamical calcs. 7-12262
 KSCN, vibr. spectrum in a phase with nonrigid-motion elements 7-17312
 LaB₆, lattice dynamics studied by ion channelling, La in Einstein model 7-44710
 LaTiO₃-based perovskites, IR vibr. spectra studies 7-39102
 LiGaO₂, lattice vibr. spectrum, correlation method anal. 7-26881
 LiInS₂, lattice vibr. and interatomic forces, IR reflectivity spectra anal. 7-26882
 MgSiO₃, perovskite type, cryst. struct., lattice dynamics and eqn. of state 7-58248
 N₂ solid films, Fourier transform IR spectra 7-59214
 (NH₄)₂ZnBr₄, thermosensitive photo-selective phenomenon is single crystals, Raman scatt. obs 7-46038
 Na₂P₂Se₆, isomeric forms, P₂Se₆⁴⁻ vibr. spectra, normal coordinate anal. (*German*) 7-22270
 NbC_{0.72}, atomic displacements, X-ray determ. 7-32584
 (NbSe₄)₂I, lattice vibr. at CDW transitions 7-51973
 Nb₂Sn, phonon spectrum, temp. depend. (*Chinese*) 7-64413
 Ni-B amorphous and crystalline alloys, vibr. density of states 7-38146
 O₂ solid films, Fourier transform IR spectra 7-59214
 PbSe, acoustic mode vibr. anharmonicity 7-63751
 PbSe and other IV-VI cpds, acoustic mode vibr. anharmonicity 7-63751
 PbTe, acoustic mode vibr. anharmonicity 7-63751
 Rb_{1-x}(NH₄)_xH₂(P,As)O₄, mixed system, proton localisation, obs. by incoherent neutron scatt. 7-12224
 Si, Raman mode, anharmonic damping and freq. shift 7-27718
 Si, vibrational correlation functions 7-51966
 Si:H, Si-H IR stretching bands, models, CNDO calc. 7-53314
 SiO_x thin films, plasma enhanced CVD deposited, Si chem. states, IR spectra, XPS, AES 7-21721
 SiO₂-TiO₂ solid solutions, phase relationships and spectroscopic features 7-63826
 SmAsO₄, vibrational spectra, IR and Raman obs., X-ray and thermal analysis 7-59198
 α-Sn₂F₆, Mossbauer lattice parameters 7-17251
 α-Sn₃F₈, Mossbauer resonance 7-45854
 SnTe, acoustic mode vibr. anharmonicity 7-63751
 (TaSe₄)₂I, lattice vibr. at CDW transitions 7-51973
 TiCl₃, α and δ forms, vibr. anal., IR spectra study 7-46049
 Ti₄P₂Se₆, isomeric forms, P₂Se₆⁴⁻ vibr. spectra, normal coordinate anal. (*German*) 7-22270
 UB₁₃, heavy fermion cpd., lattice dynamics, EXAFS study 7-64792
 V₃Si, anharmonicity and X-ray forbidden reflections 7-1995
 YLiF₄, lattice vibr., Raman study 7-53329
 ZnO, X-ray graphic elastic constants and lattice spectrum 7-32546
 ZnS:Fe²⁺, impurity vibronic coupling and near IR spectra characts. 7-26889
 ZrO₂-Y₂O₃ solid solutions, vibrational spectra 7-6738

lattice dynamics of covalent crystals

- diamond, brown, vibronic coupling to nearly localised modes in luminescing bands 7-51980
 diamond, radiation damage prod. of SRL centres, phonons, absorpt. spectra, cathodoluminescence studies 7-33461
 diamond-like structure semiconductors vibrational spectra of interstitials (*Chinese*) 7-32592

lattice dynamics of covalent crystals continued

- graphite, mol. dynamics simulation and Raman spectrum, atom configs. and interactions, honeycomb struct. 7-58200
 quadrupolar charge deform., adiabatic formulation 7-26879
 Cd_{1-x}Mn_xTe mixed cryst., far IR Fourier transform spectra, acoustic local mode and TA band mode 7-53378
 CdTe (100)-oriented single crystals, lattice dynamics temp. depend., X-ray studies 7-26880
 GaAs, FTIR spectra of acceptors, electronic intrasite transitions and local vibr. modes 7-53377
 GaAs, lattice dynamics and electron-phonon interactions, quasi-ion approach calcs. 7-58422
 Ge crystal, exciton gas-electron-hole liq. interactions, phase diagram, nuclei drift effects 7-2488
 Ge, fourth-order thermal expansion coeff. fn. 7-44868
 p-Ge, hot electron transport, perturbed acoustic phonon distrib. effects, Monte Carlo anal. 7-64254
 Ge, lattice dynamics, real-space force consts., adiabatic bond-charge model 7-32589
 Ge, lattice dynamics and electron-phonon interactions, quasi-ion approach calcs. 7-58422
 Mg₂Si(Ge)(Sn), anharmonic effects, first order Raman scatt. studies 7-58429
 Si, fourth-order thermal expansion coeff. fn. 7-44868
 Si, Jahn-Teller vibronic state of the neutral vacancy 7-16705
 Si, lattice dynamics, real-space force consts., adiabatic bond-charge model 7-32589
 Si, lattice dynamics and electron-phonon interactions, quasi-ion approach calcs. 7-58422
 Si optical phonon spectrum transform. obs. under laser pulse bombardment, CARS study 7-51967
 SiAs, laser annealed, Raman scatt. study 7-53325
 Si:H, impurity effects on IR absorpt. bands of Si-H centres, irradi. and unirrad. crystals. 7-53379

lattice dynamics of ferroelectric crystals

- see also displacive transformations; soft modes*
 ferromagnetic ferroelectrics, dynamic characteristics, soft modes saturation (Russian) 7-27672
 IV-VI compounds, dipole-dipole interactions and ferroelectric props. 7-39046
 Rochelle salt, phase transition dynamics 7-21367
 BaTiO₃, cryst. dynamics near T_c, Mossbauer diff. study 7-6733
 CsCaF₃, fluoroperovskites, IR refl. spectra, temp. depend. 7-22248
 EuAsO₄ crystal, vibr. spectra and optical absorption studies 7-13145
 KTa_{1-x}Nb_xO₃, lattice dynamics, nonlinear shell model 7-51971
 KZnF₃, fluoroperovskites, IR refl. spectra, temp. depend. 7-22248
 LiNbO₃, freq. temp. coeffs. of vibration modes (Chinese) 7-13093
 LiNbO₃, ilmenite modifications, vibr. spectra 7-22243
 LiNbO₃:Fe²⁺, anomalous phase transitions, Mossbauer spectroscopy studies 7-2992
 NaNO₂, solid ferroelectric and paraelectric phases, lattice vibrs., Raman and IR spectra anal., mol. dynamics calcs. 7-21373
 NaNbO₃, ilmenite modifications, vibr. spectra 7-22243
 Pb₄Ba₃Ge₃O₁₁, rhombohedral, acoustic symmetry and vibr. anharmonicity 7-16695
 Pb₂Ge₃O₁₁, rhombohedral, acoustic symmetry and vibr. anharmonicity 7-16695
 RbCaF₃, fluoroperovskites, IR refl. spectra, temp. depend. 7-22248

lattice dynamics of ionic crystals

- alkali halides, refractive index, Szigeti charge, dielec. parameters ab initio calcs. 7-13082
 alkali metal cyanide-halide mixed crystals., orientational glass state static props., microscopic model calcs. 7-63591
 alkali metal cyanide-halide mixed crystals., orientational glass state dynamic props., microscopic model calcs. 7-63756
 alumina, ion-rich β- and β'-phases, superionic props., local and long-range order determ. 7-21519
 ferrite crystals., normal lattice vibr. modes determ., nuclear site group anal. 7-16701
 β-AgI, anharmonic thermal vibrs., X-ray diff. 7-51982
 BaFCl, IR lattice vibr., dielectric dispersion and lattice dynamics 7-3044
 BiX₂-GaX₄ complex; X=Cl, Br; struct. Raman spectra study 7-46020
 C RbCrO₃Cl, CrO₃Cl⁻ vibronic anal., phosphorescence and Raman spectra 7-15605
 CdCl₂(1-x)Br_{2x} layered mixed crystals., Raman-active phonon mode study 7-51970
 3CdSO₄·8H₂O, site symm. of SO₄²⁻ ion, IR absorpt. spectra 7-33374
 CsCrO₃Cl, CrO₃Cl⁻ vibronic anal., phosphorescence and Raman spectra 7-15605
 KClO₄ single crystals, vibr. anal., optical modes, IR spectra studies 7-22245
 KCl-KBr mixed crystals., cohesion, harmonic and anharmonic props. calcs. 7-51907
 KCl_{1-x}Br_x mixed powder crystals, long wavelength optical phonons; 7-12220
 KrCrO₃Cl, CrO₃Cl⁻ vibronic anal., phosphorescence and Raman spectra 7-15605
 LiF crystals, phonon-dislocation scattering anal. 7-2131
 NaCl-type crystal, Green's fn. calc. in Montrose-Potts model 7-58419
 NaCl-type lattices, (100) surface, surface atomic vibr. modes 7-2337
 (PBr₄)⁺(MBr₄)⁻¹ complex, M=B, Al, Ga, In, mol. vibr., Raman and IR spectra anal. 7-46021
 SbBr₂-AlBr₄ complex, struct. Raman spectra study 7-46020
 SbX₂-GaX₄ complex; X=Cl, Br; struct. Raman spectra study 7-46020

lattice dynamics of metallic crystals

- close-packed structure, solid-liq. phase transitions, atomic processes 7-52012
 cubic metals, phonon spectra, dynamical pseudopot. shell model calcs. 7-51965
 phonon spectra, dynamical pseudopot. shell model calcs. 7-51964
 V-Hf-Zr-Ta C-15 phase superconducting alloys, phonon props., inelastic neutron scatt. spectra 7-51969
 AU clusters and bulk samples, Debye temps., EXAFS studies 7-2136
 Al, fourth-order thermal expansion coeff. fn. 7-44868
 Al, lattice dynamics and three-body forces, phonon freq. Debye-Waller factor calcs. 7-63760
 Al, phonon density of states from heat capacity temp. depend., inverse problem 7-6736
 Al_{0.3}Mn_{0.2}, icosahedral and crystalline phases, vibr. density of states, neutron scatt. study 7-44726

lattice dynamics of metallic crystals continued

- Ba, BCC, first-principles phonon spectrum, three-ion forces and transition-metal behaviour 7-38135
 Ca, FCC and BCC, lattice dynamics 7-38134
 Ca, phonon density of states from heat capacity temp. depend., inverse problem 7-6736
 Cd single cryst., interatomic distance and thermal motion, K-shell EXAFS, temp. and orientation depend. 7-64814
 Cd single crystals, anisotropic thermal effect, first shell distance and thermal motion, EXAFS study 7-63753
 Cs BCC single cryst., lattice dynamics, coherent inelastic neutron scatt. study 7-21376
 Cu, fourth-order thermal expansion coeff. fn. 7-44868
 Cu_{1-x}Al_x, α-phase, specific heat 7-12312
 Fe, polymorphic forms stability, elastic consts. in 20 to 1470°C range, enthalpy of fusion rel. to self-diffusion activation energy 7-6781
 In, BCT, force constant models, elastic inconsistency 7-38140
 Li, lattice dynamics at low temps. 7-44716
 MoSi₃, Al₁₅ cpd., phonon dispersion and density of states, inelastic neutron spectra, electron-phonon coupling effects 7-2121
 Nb₂Ge Al₁₅ material, displacement correl. functions temp. depend. calcs. 7-51962
 Nb₂Sb Al₁₅ material, displacement correl. functions temp. depend. calcs. 7-51962
 Nb₂Sn Al₁₅ material, displacement correl. functions temp. depend. calcs. 7-51962
 Ni (100), surface vibrs., EELS, surface and bulk phonon contribs. 7-44986
 Ni-Al alloys, premartensitic behaviour, neutron scatt. study 7-44717
 Pb, phonon density of states from heat capacity temp. depend., inverse problem 7-6736
 Pd_{0.9}Ag_{0.1}D_{0.61}, lattice dynamics and phonon line shapes 7-2120
 PdD_{0.8}, β-phase, interatomic pots. and lattice distortions 7-21372
 Th, phonon density of states from heat capacity temp. depend., inverse problem 7-6736
 W, valence bands, angle resolved XPS spectra 7-22441
 Zn, phonon spectrum fine structure 7-16702

lattice dynamics of molecular crystals

- biphenyl, cryst. mol. motions, thermodynamic studies (Japanese) 7-38151
 β-BoB₂O₄, crystal vibr. assignment, Raman and IR spectra anal. 7-53346
 chloranil soft mode driven displacive transition, Raman meas. using I cell 7-59204
 2-(chloromethyl)-2-methyl-1,3-dichloropropane, conformational equilib., Raman and IR spectra study 7-46018
 hexabromomethane, vibrational spectra, crystal dynamics and phase transitions 7-38132
 layer crystals dynamics, long wavelength vibrs., factor group anal. 7-58424
 methyl cyanide-d₀(d₃), lattice vibrs., Raman and IR spectra study 7-46019
 phenazine triplet state, optical expts., temp. depend. of reson. splittings in mol. pairs 7-16700
 polyoxymethylene, polymorphism and mol. aggregation, Raman microprobe, vibr. spectra 7-13152
 p-quaterphenyl, cryst. mol. motions, thermodynamic studies (Japanese) 7-38151
 TCNQ, single cryst., lattice mode assignment, Raman spectroscopic meas. and lattice dynamical calcs. 7-26883
 p-terphenyl, cryst. mol. motions, thermodynamic studies (Japanese) 7-38151
 tetraphenylmethane, thermal motion, lattice dynamical model 7-44730
 thiourea, paraelectric phase, mol. dynamics simulation 7-37920
 (Ag₆Sn₄I₁₂)Ge₆ cluster cpd., elastic behaviour and vibr. anharmonicity 7-12223
 C CdCl₂, impurity local modes and secondary features, Raman spectra anal. 7-33372
 CS₂, dynamical model for lattice frequencies and cryst. field splittings 7-16699
 CdBr₂, impurity local modes and secondary features, Raman spectra anal. 7-33372
 CrO₂Cl₂ vibronic anal., CCl₄ and SnCl₄ matrices, emission and excitation spectra, MODOR spectra 7-15542
 p-H₂, solid, obs. of fourth vibr. overtone transition of mol. H₂ 7-12392
 LiN(H₂D₁)₄SO₄ crystals., vibr. spectra and ferroelec. transition, Raman scatt. study 7-53304
 Li₂SeO₄ single crystal, optic modes, room temp. Raman spectra study 7-53345
 N₂ crystals, molecular-to-nonmolecular transformation at high press., theory 7-21432
 N₂O, mol. solid, lattice vibr., IR active modes (Japanese) 7-6731
 Pb₂(GeO₄)_{1-x}(SiO₄)_x(VO₄)_{2x}, vibr. and impurity mode behaviour, IR spectra studies 7-64649
 α-S orthorhombic, elastic behaviour under pressure, lattice dynamics anal. 7-16667
 YAsO₄, internal and external vibrs., IR and Raman spectra studies 7-64648

lattice energy

- see also binding energy*
 acetylene, solid, high-press. props., polymerisation paths 7-58412
 alkali metal binary alloys, low temp. phase diagram, compression effects 7-33641
 binary crystals, structural stability, chem. trends 7-21153
 biochlorite complex crystals, electrostatic Ewald energies 7-11983
 bis (4-(n-heptyloxy)-N-(p-methoxyphenyl) benzaldimino-2-olate) copper (2+), cryst. struct. 7-44509
 cholesterol p-n-hexyloxybenzoate mesophase precursor cryst. struct., X-ray study 7-63597
 crystal instability, defect-phonon interactions 7-44722
 crystal lattice, internal pot. w.r.t. electron work function 7-63545
 diamond, high pressure phase transitions total energy methods 7-63802
 electrostatic Madelung and cohesive energies for crystalline solids 7-44442
 hollandites, modelling tunnel-cation displacements using struct.-energy calcs. 7-32374
 ion mixing, radiation-enhanced diffusion, cohesive energy correlation 7-32510
 Madelung constant, lattice sum definition, conditional convergence and anal. of ambiguity in summation 7-58196
 pseudobinary alloys, tetrahedrally coordinated, Coulomb energy calcs. 7-1941

lattice energy continued

- pseudopotential method, predicting near solids and superconductors 7-32358
 sapphire colour-centre crystal, laser appls. 7-43120
 semiconductors, insulators and metals, structural, electronic and vibr. props., pseudopotential calcs. 7-16484
 semipolar crystals with rocksalt struct., mean charges calc. 7-44441
 surfaces, force sum rules, Hellmann-Feynman theory 7-44989
 zinc-blende semiconductors, high pressure phase transitions total energy methods 7-63802
 AgNO₂ crystal, room temp. electronic energy band calcs. 7-7113
 Al film, quantum size effects and dimensionality 7-45521
 As, structural calcs. 7-7143
 As₂Se₃ crystal, optical props., ab initio total energy calcs. 7-45965
 Co_{0.35}Cu_{0.45}Cr₂S₄-Se₂ spinels, X-ray diffr. study 7-44475
 CoH system, ferromag., heat of formation, total energy calcs. 7-45198
 Cr, deformation interaction of incorporation and substitution atoms 7-46556
 Cs₂K₂(TeO₃)₂, coordination, cryst. structs., lattice energy (German) 7-26714
 Cs₉Na₁₀(FeO₃)₄ single cryst. prep. and structural characterisation (German) 7-37951
 Fe, paramagnetic ground state props. and pair potentials 7-32352
 Ge, structural props., ab initio pseudopotential calcs. 7-44797
³He, solid, ground-state energy calculated by a lowest-order constrained-variation method 7-32743
⁴He, solid, ground-state energy calculated by a lowest-order constrained-variation method 7-32743
 K₂Li₃TeO₆, prep., cryst. struct., Madelung lattice energy calc. (German) 7-16515
 K₂Na₂TeO₆, cryst. struct., X-ray diffr., Madelung part of lattice energy (German) 7-37941
 Li, crystal and electronic struct., ab initio HF cluster method 7-44443
 Mo, deformation interaction of incorporation and substitution atoms 7-46556
 (NH₄)₂SO₄ crystal, cryst. fields calc., Madelung energies and cryst. pots. 7-64180
 NaLi₃Si(Ge)(Ti)O₄ isotopic oxides, cryst. struct. determ. lattice energy calcs. (German) 7-37952
 NbH, β - and γ -phases, electronic struct. and phonon anharmonicity 7-45199
 Ni, paramagnetic ground state props. and pair potentials 7-32352
 Ru, electronic, structural and cohesive props., theoretical study 7-37922
 Si, molecular dynamics, classical two and three-body interatomic potentials 7-16966
 Si, total energy and superconductivity, pseudopotential method 7-32358
 SiO₂, crystalline struct., simulation based on pot. with many-body term 7-21152
 Ti-Mo (15 wt.%), Young's modulus, cohesive energy, H effect (Chinese) 7-8033
 W, deformation interaction of incorporation and substitution atoms 7-46556

lattice gas see *lattice theory and statistics*

lattice gauge theory see *axiomatic field theory; gauge field theory*

lattice localised modes

- see also *phonon-defect interactions; phonon-impurity interactions*
 alkali metal halide crystals, impurities, local and gap mode freq. calcs. 7-26888
 anharmonic solids, local modes, analogy with kondo problem 7-16704
 anthracene single crystals, dislocation photolum. study, exciton scatt. effects (Russian) 7-22343
 cubic crystals, nonlinear phonon generation via localised modes 7-51978
 diamond, brown, vibronic coupling to nearly localised modes in luminescing bands 7-51980
 diamond, radiation damage prod. of 5RL centres, phonons, absorpt. spectra, cathodoluminescence studies 7-33461
 diamond-like structure semiconductors vibrational spectra of interstitials (Chinese) 7-32592
 diffusion, isotope effect, quasi-harmonic calcs., appl. to CoO and NiO 7-26996
 graphite, resistivity at high temp. calc., anisotropy, temp. depend. 7-52556
 light interstitial quantum diffusion rate, strongly coupled vibrs. 7-52106
 local electron centre config. instability, quasilocal modes interaction-model calcs. 7-58772
 nonlinear 1D crystalline struct., localised vibration calcs., iteration method 7-51976
 trans-polyacetylene, phonon dynamical conductivity around charged soliton 7-6740
 polyacetylene, solitons and IR-active localised vibrational states, Su-Schrieffer-Heeger model calcs. 7-2134
 semiconducting materials, cryst., and device appls., book 7-60894
 surface (001)(2 \times 1), surface vibr. excitations 7-16854
 three-phonon complexes, bound, new type of states 7-44720
 transition metal fluorides, mixed, Raman scatt. by localised and magnon modes 7-46027
 two dimensional quasi-periodic Penrose lattice, electronic and vibr. modes, localised states and band struct. 7-27300
 vibrational modes of solids, nuclear reaction spectroscopy 7-21371
 Al-H system, vibr. spectrum of isolated H impurity, isotope effects (Russian) 7-32593
 AlH₃, isolated H impurity vibr. spectrum, isotope depend. (Russian) 7-16703
 C CdCl₂, impurity local modes and secondary features, Raman spectra anal. 7-33372
 CaF₂ cryst., defect-induced hyper-Raman spectra obs. 7-53324
 Cd-In alloys, vacancy-induced elec. field gradient temp. depend., PAC meas. 7-52541
 CdBr₂, impurity local modes and secondary features, Raman spectra anal. 7-33372
 Cd_{1-x}Mn_xTe mixed cryst., far IR Fourier transform spectra, acoustic local mode and TA band mode 7-53378
 CdTe:Fe²⁺, impurity vibronic coupling and near IR spectra characts. 7-26889
 Cu sintered powder, ultrasonic attenuation meas., phonon-fraction crossover 7-2105
 Cu-In alloys, vacancy-induced elec. field gradient temp. depend., PAC meas. 7-52541
 Fe-Pd multilayer structs., localised phonon modes 7-46061

lattice localised modes continued

- GaAs, FTIR spectra of acceptors, electronic intrasite transitions and local vibr. modes 7-53377
 GaAs:C, impurity content meas., IR absorpt., room temp. meas. 7-22289
 GaAs:Ge,Si, local modes, isotopic fine struct., IR spectra 7-38145
 GaAs:P, ion implanted and pulse laser annealed, Raman study 7-6653
 GaF₃:Mn cubic cryst., local lattice instability near impurity, ESR study 7-53123
 KBr:MnO₄⁻, resonance Raman scatt. spectra 7-22234
 KCl:I, electron excitation self-trapping 7-32594
 KI:Cl, electron excitation self-trapping 7-32594
 Mo_{1-x}Re_x, enhanced superconductivity by electron renormalization of directly obs. Brout-Visscher local phonon 7-38824
 NaCl:CO₂²⁻ cryst. surface, localised intramol. vibrations, IR transmission spectra study 7-2132
 NbH_x, interstitial H total cross-section determ., localised modes and diffusion, neutron transmission meas. 7-12061
 Nb₉₉Ti₁H₁(D₁), localised H vibrs., inelastic neutron scatt. studies 7-58426
 Nb_{0.93}V_{0.07} alloys, H impurity trapping, precipitation and nucleation, localised vibr. mode meas. 7-2133
 Pb₂(GeO₄)_{1-x}(SiO₄)_x(VO₄)₂, vibr. and impurity mode behaviour, IR spectra studies 7-64649
 Si, Jahn-Teller vibronic state of the neutral vacancy 7-16705
 Si, lattice distortions and vibr. modes of substitutional impurities 7-51979
 Si, vibronic band, 1018 meV, W or I, band 7-51977
 Si, with stacking faults, electron and phonon spectra, recursion method 7-32945
 Si:B⁺(BF₃)⁺ submicron p-n junctions, ion implanted, dopant distrib., Raman study 7-21252
 Si:H, impurity effects on IR absorpt. bands of Si-H centres, irradi. and unirrad. crystals. 7-53379
 SiO, IR spectra of interstitial O 7-17325
 SiO₂B, ab initio MO electronic struct. calcs. 7-38499
 SrTiO₃H(D), O-H and O-D stretching vibrs. under applied electric field and uniaxial stress 7-44723
 TaH_{0.5}(D_{0.5}), localised H vibrs., inelastic neutron scatt. studies 7-58426
 Ti₂Si₃H(D)_{1-x}, site occupation and local vibration of H isotopes (Japanese) 7-12012
 Ti₂Si₃H(D)_{1-x}, site occupation and local vibration of H isotopes 7-12028
 Y₂Co₇, resistivity and Hall effect temp. depend. meas. 7-52568
 YH_{0.18}(D_{0.18}), H pairing and anisotropic pot. for H isotopes, neutron spectroscopy study 7-38144
 Zn-In alloys, vacancy-induced elec. field gradient temp. depend., PAC meas. 7-52541
 ZnS:Fe²⁺, impurity vibronic coupling and near IR spectra characts. 7-26889
 ZnSe:Fe, impurity ion photoionisation, EPR, photoconductivity spectra 7-52495
 ZnSe:H, proton implanted, localised vibr. mode, IR transmission spectra 7-51981
 ZrO₂, cubic zirconia, defect-induced hyper-Raman spectra obs. 7-53324

lattice mechanics see *lattice dynamics*

lattice parameters see *lattice constants*

lattice phonons

- see also *electron-phonon interactions; lattice dynamics of covalent crystals; lattice dynamics of ferroelectric crystals; lattice dynamics of ionic crystals; lattice dynamics of metallic crystals; lattice dynamics of molecular crystals; lattice localised modes; phonon-defect interactions; phonon dispersion relations; phonon drag; phonon-exciton interactions; phonon-impurity interactions; phonon-magnon interactions; phonon-phonon interactions; phonon-plasmon interactions; polaritons; soft modes; spin-phonon interactions; tunnelling spectra; tunnelling spectroscopy*
 absorbing zinc-blende type material, backward Raman scatt., ang. dispersion calcs. 7-22238
 acoustic phonon scatt. from atomically irregular surfaces, intensity reflection coeffs. 7-12446
 acridine, adsorbed on Al₂O₃, tunnelling spectra study 7-52264
 alkali metal cyanide halide mixed crystals, orientational glass state 7-21140
 alkaline earth fluorite crystals, US attenuation 7-51944
 amorphous alloys with immiscible metallic particles, superconducting props. 7-2791
 anharmonic lattice, phonon freq. shifts derived via the Wigner distribution function 7-21374
 anharmonic solids, local modes, analogy with kondo problem 7-16704
 BA_s, structural and electronic props., pseudopotential method, local density approx. 7-32353
 bicyclo (222) octane, plastic phase, monomolecular reorientational dynamics, Raman scatt. study (French) 7-26675
 binary cubic cpds., mode Gruneisen parameter~phonon freqs. ratio correl. formula 7-26894
 biphonon line broadening caused by acoustic phonon interactions 7-44721
 β -BoB₂O₄, crystal vibr. assignment, Raman and IR spectra anal. 7-53346
 2-(chloromethyl)-2-methyl-1,3-dichloropropane, conformational equilib., Raman and IR spectra study 7-46018
 concentrating, catastrophe theory for caustic behaviour 7-2113
 crystal instability, defect-phonon interactions 7-44722
 crystals, form. of phonon-focusing caustics, rel. to catastrophe theory 7-2116
 density of states, determ. from sp. ht. 7-26884
 diamond, optical phonons and elasticity at megabar stresses 7-21375
 diamond, radiation damage prod. of 5RL centres, phonons, absorpt. spectra, cathodoluminescence studies 7-33461
 dimer-lattice phonon interaction, lattice relax., exciton and electron condition terms 7-7130
 dirty superconductors, strong-coupling eqns., disorder effects 7-64393
 disordered solids, effect on frequency distrib. 7-2115
 EBBA, nematogen, diffr. and spectroscopic study of solid states 7-64645
 energy transfer and lattice phonons, mutual influence 7-16977
 ferromagnetic semiconductors, spin-depend. phonon Raman scatt., theory 7-46013
 finite Hubbard model with phonon coupling 7-12582
 frequency distrib. function anal., dielec. and scatt. props., orthogonalised moments method 7-64633
 graphite dispersed powder, C atom vibr. dynamics in IR absorpt. spectrum 7-53322
 heavy fermion systems, hydrodynamic fluctuations 7-44708

lattice phonons continued

- heavy particle one-dimensional hopping motion, phonon and electron gas interactions, localisation, scaling eqn. calcs. 7-12634
- hexagonal Belorizky model, magnetoelectric interactions 7-53109
- impulsive excitation, use of femtosecond optical pulses 7-24640
- incomplete crystals, surfaces, defects, interfaces and layered structures, theory 7-16926
- insulating films with highly reflecting boundaries, thermal resistance 7-21781
- IV-VI narrow gap vibronic ferroelec., correl. length estimate (*Russian*) 7-17277
- Khrovangal alloy, phonon thermal cond., heat treatment effects 7-12696
- layer crystals dynamics, long wavelength vibrs., factor group anal. 7-58424
- light interstitial quantum diffusion rate, strongly coupled vibrs. 7-52106
- m-dinitrotetramethylbenzene, single cryst., vibr. study, IR reflectance and transmission and polarised Raman spectra 7-25512
- mean field approx. for fermion or pseudo-spin boson interaction 7-32590
- metals, EM generation of acoustic waves, theory 7-51945
- metals, light particle quantum tunnelling and diffusion 7-52113
- methyl cyanide-d₃(d₃), lattice vibrs., Raman and IR spectra study 7-46019
- molecular struct. relaxation in flat channel, thermodynamics and kinetics 7-32583
- nonequilibrium supercond. thin films, multigap state density instability, kinetic eqns. 7-52891
- Peierls instabilities, soliton lattice in the relative phase of two coupled charge-density waves 7-21816
- perylene in microcryst. n-heptane, selectively laser excited in phonon side-band, stimulated emission 7-33415
- phenazine, adsorbed on Al₂O₃, tunnelling spectra study 7-52264
- phonon conc. catastrophes in cubic crystals 7-44714
- phonon-assisted tunnelling between two quantum wells, calc. 7-33073
- picosecond interferometric technique for study of phonons in Brillouin frequency range 7-14998
- piezoelectric materials, acoustic resonance techniques for temp., stress and impurity characterization 7-45938
- polaronic states in a slab of a polar crystal 7-2512
- trans-polyacetylene, phonon dynamical conductivity around charged soliton 7-6740
- positron-phonon interaction and positron diffusion in solids, review 7-38240
- pyrene-biphenyl mixed crystals, local heating, phonon modes and Dicke optical superradiance (*Russian*) 7-13178
- quartz, FTIR spectrum of crystals, press. effects, phonon band splitting 7-46039
- quasicrystals, two-dimensional, acoustic phonon spectrum of Penrose tilings 7-26892
- quasielastic neutron scatt., nonlinear effects and lineshape calcs. 7-63403
- resonance interaction of phonons with bichromatic laser radiation 7-21369
- sapphire, single cryst., heat pulse propag. 7-27034
- semiconducting materials, cryst., and device appls., book 7-60894
- semiconductor superlattices, dynamical screening, quasi-2D electron gas, electron-phonon interactions 7-45464
- semiconductor superlattices, phonons, acoustic and optic modes 7-12455
- semiconductors, electron energy distrib. form. due to monochromatic light intraband absorpt. 7-17285
- semiconductors, insulators and metals, structural, electronic and vibr. props., pseudopotential calcs. 7-16484
- semiconductors, nonlinear excitation, picosecond laser induced 7-11024
- Si-SiGe strained superlattices on Si substrates, MBE growth, characterisation, appl. for HEMT 7-27218
- strong-coupling superconductors, energy gap eqn. inversion, electron tunnelling spectrum temp. corrections, phonon spectrum determ. 7-52900
- structural phase transitions, total condensate of normal vibrs., group theory anal. (*Russian*) 7-44740
- superlattices, bulk and surface phonons 7-2343
- superlattices, microstructures and microdevices, conf., Goteborg, Sweden (Aug. 1986) 7-35097
- surface phonon conc. 7-2335
- tetramethyl-phenylene-diamine chloranil, mixed-stack cpds., spectroscopy of dimerisation 7-22260
- thermal conductivity, molecular dynamics and anharmonic lattice dynamics 7-21552
- Toda lattice, thermodynamics as classical limit of two-component Bethe ansatz scheme 7-41304
- α -AgI, ionic motions and neutron inelastic scatt., mol. dynamics studies 7-27004
- (Ag₂Sn₂P₂)Ge₆ cluster cpd., elastic behaviour and vibr. anharmonicity 7-12223
- Al, lattice dynamics and three-body forces, phonon freq. Debye-Waller factor calcs. 7-63760
- Al, phonon density of states from heat capacity temp. depend., inverse problem 7-6736
- Al, superconducting transition temperature, press. depend. 7-22058
- Al_{0.28}Ga_{0.72}As, photoluminescence half-width and intensity, temp. depend. 7-39179
- AlN crystal, phonon energy calcs. 7-2119
- AlN, electronic struct., first principles LCAO calc. 7-21813
- AlN films, OMVPE, Hall mobilities, impurity band 7-39410
- ³⁶Ar, latt. dynamics, phonon line shapes at high temp. 7-2122
- As₂Se₃, crystalline, electronic and geometric struct., ab initio total-energy calcs. 7-12607
- Ba, BCC, first-principles phonon spectrum, three-ion forces and transition-metal behaviour 7-38135
- BaTiO₃, vibronic ferroelec., correl. length estimate (*Russian*) 7-17277
- Bi plates, magnetoelectronic instabilities, joint action of two strong electric fields 7-52694
- Bi thin films, lattice thermal cond. meas., modified Mayadas-Shatzkes model 7-21554
- (Bi_{1-x}Sb_x)₂Te₃ single crystal, optical constants, IR spectra study 7-46030
- BiX₂GaX₄ complex; X=Cl, Br; struct. Raman spectra study 7-46020
- Ca, phonon density of states from heat capacity temp. depend., inverse problem 7-6736
- Cd_{1-x}Mn_xTe mixed cryst., far IR Fourier transform spectra, acoustic local mode and TA band mode 7-53378
- CdTe_{1-x}Se_xS₂, mixed system, optical phonon frequencies 7-2123
- CeCu₂Si₂, Kondo lattice heavy fermion system, quasi-particle-phonon interactions 7-2521

lattice phonons continued

- CeCu₂Si₂, Raman scatt. study of electronic and vibr. excitations 7-33387
- CsCaF₃, fluoroperovskites, IR refl. spectra, temp. depend. 7-22248
- Cu (100), cross-section anal. of surface and bulk phonons by electron scatt. 7-2336
- CuAl_{1-x}Ga_xSe₂, mixed crystals, Raman scatt. spectra 7-13168
- CuCl, off-centre model, vibr. and struct. props. 7-17316
- Eu chalcogenides, IR optical parameters, rel. to chemical bonds 7-53291
- F₂ solid, high-press. behaviour at low temps. 7-37923
- Ga_{1-x}Al_xAs, disorder effects of Raman scatt. 7-7704
- GaAs films, dense electron-hole plasmas, picosecond dynamics, acoustic phonon generation 7-45373
- GaAs nonradiative states of optically illuminated sample, phonon detection by superconducting tunnel junction 7-3074
- GaAs, phonon and plasmon deformation potentials, FIR spectra under uniaxial stress 7-26886
- GaAs, phonon hot spot, subTHz acoustic phonon emission 7-2118
- GaAs single quantum wells, free excitons, phase coherence and line broadening 7-45170
- GaAs:P, ion implanted and pulse laser annealed, Raman study 7-6653
- GaAs/Ga_{1-x}Al_xAs(AlAs), short period superlattices, MOCVD growth, Raman scatt., AES, X-ray diffr. 7-27386
- GaAs-AlAs superlattices, folded acoustic branches, leakage-induced and disorder-activated modes 7-33389
- GaAs-AlAs superlattices, confined longitudinal and transverse phonons, phonon spectrum calc. 7-38142
- GaN films, OMVPE, Hall mobilities, impurity band 7-39410
- GaP, coherent optical phonon generation and decay 7-33040
- GaP, phonon shifts due to temp. and pressure rise induced by a laser beam 7-2125
- GaP, phonons, ps laser induced transient dynamics 7-39113
- GdS, lattice thermal cond., two-made cond. of phonons 7-27039
- Ge crystal, laser irradiated, thermal excitation 7-38137
- Ge-base crystalline alloys with immiscible metallic particles, superconducting props. 7-2791
- HF solid, elastic and photoelastic anisotropy at high press. 7-2083
- Hg_{1-x}Cd_xSe, reson. Raman Scatt. meas. 7-7701
- Hg_{1-x}Cd_xTe, low frequency absorption bands (*Chinese*) 7-39095
- β -HgI₂ crystals, phonon spectrum and vibr. mode symmetry, first-order Raman scatt. (*Russian*) 7-3056
- InGaAsP films, dense electron-hole plasmas, picosecond dynamics, acoustic phonon generation 7-45373
- KBr films, high temp. phonon anharmonicity, IR spectra study 7-33469
- KCN, cryst., Akhiezer damping 7-21360
- KCl:F⁻:Eu²⁺, optical absorpt., excitation and luminesc. spectra 7-59250
- KD₂(WO₄)₂, vibr. characts. of O bonds, IR and Raman spectra 7-32587
- K_{0.5}Rb_{0.5}I mixed crystals, phonon combination bands, far-IR spectra anal. 7-64650
- K_{1-x}Rb_xI mixed crystals, FIR props., optical phonons 7-46011
- KTaO₃:Li, time depend. phase transform., neutron diffr. meas. 7-44799
- KZnF₃, fluoroperovskites, IR refl. spectra, temp. depend. 7-22248
- LaF₃, lattice phonons, high temp. Brillouin scatt. studies 7-46059
- LaNbO₄, single crystal, elastic props. 7-51915
- LiAl₂O₈:Fe³⁺, spin-lattice relax. times, Mossbauer spectroscopy 7-45848
- LiKSO₄, phase transition, low temp. Brillouin studies 7-44806
- LiNbO₃:Fe cryst., Raman spectra, photo-induced refractive index change effects 7-53300
- Li₂SeO₄ single crystal, optic modes, room temp. Raman spectra study 7-53345
- LiTaO₃, phonon modes, quasielastic light scatt. near T_c, Raman spectra anal. 7-3039
- MnF₂, thermal behaviour of two-exciton bands 7-2497
- Mo_{1-x}Re_x, enhanced superconductivity by electron renormalization of directly obs. Brout-Visscher local phonon 7-38824
- N₂ crystals, molecular-to-nonmolecular transformation at high press., theory 7-21432
- N₂, surface layer on graphite, motion investig. 7-32792
- NaNO₂, solid ferroelectric and paraelectric phases, lattice vibrs., Raman and IR spectra anal., mol. dynamics calcs. 7-21373
- Nb₂(Al-Ge), high T_c supercond., Raman spectra studies 7-7699
- NbH₃, β - and γ -phases, electronic struct. and phonon anharmonicity 7-45199
- NbSe₂H₃, heat capacity, Debye temp., electron-phonon coupling, electronic contrib. meas. (*Russian*) 7-6820
- Ni (100), surface vibrs., EELS, surface and bulk phonon contribs. 7-44986
- Ni surface phonon generation and picosecond light pulse detection 7-12456
- (PBr₄)⁺(MBr₄)⁻¹ complex, M=B, Al, Ga, In, mol. vibr., Raman and IR spectra anal. 7-46021
- α -P₂Se₃, cryst., press. depend. of Raman spectrum 7-33376
- Pb, phonon density of states from heat capacity temp. depend., inverse problem 7-6736
- Pb₂Cd_{1-x}F₂, phonon spectra, superionic props. 7-6735
- Pb₂Ge₂O₁₁, high pressure Raman scatt., phonon modes and Gruneisen parameters 7-33391
- RbCaF₃, fluoroperovskites, IR refl. spectra, temp. depend. 7-22248
- RbMnF₃, thermal behaviour of two-exciton bands 7-2497
- SbBr₂-AlBr₃ complex, struct. Raman spectra study 7-46020
- SbX₂GaX₄ complex; X=Cl, Br; struct. Raman spectra study 7-46020
- Small particles, Raman depolarisation ratio 7-64652
- Si:B⁺(BF₃)⁺ submicron p-n junctions, ion implanted, dopant distrib., Raman study 7-21252
- Si-Ge_{1-x} superlattices, Raman scatt. involving umklapp processes 7-3043
- SiC, cubic, ab initio calc. of ground state props. 7-6751
- Sm_{0.75}Y_{0.25}S, intermediate valence cpd., charge relax. rates, determ. by phonon spectra 7-2557
- SnS, photoacoustic response and transmission spectra, thermoacoustic meas. 7-46014
- TaT₂, lattice deformation due to ³He production 7-21237
- Th, phonon density of states from heat capacity temp. depend., inverse problem 7-6736
- TlSbS₂, Raman spectra and vibr. modes, polarisation depend. 7-27725
- Y₃Si, high T_c supercond., Raman spectra studies 7-7699
- Y_{3-x}Yb_xAl₂O₁₂, thermal conductivity, temp. and composition dependences 7-38274
- Zn₂Hg_{1-x}Se, far IR spectra study 7-22262
- ZnSe, phonons, ps laser induced transient dynamics 7-39113

lattice structure, crystals *see crystal atomic structure*

lattice theory and statistics

see also Ising model; percolation; renormalisation; X-Y model
 1/f spectra in nonlinear dynamics, noise-induced trapping at attractor boundaries 7-48557
 1D periodic lattices, uniqueness of solns. of spectral problems 7-35423
 2D three-state chiral clock model, domain-growth kinetics 7-35460
 q colourings of the triangular lattice, critical $O(n)$ model soln., dramatic polynomial 7-9786
 AC properties of 2D percolation networks, transfer matrix approach 7-14882
 adsorbed layers, order-disorder phase transition, effect on rate of elementary processes 7-6976
 aggregation models, transitions in large-scale struct. 7-29907
 aggregation phenomena and fractal aggregates (*French*) 7-9757
 Anderson localisation, upper critical dimens., wave function anomalous scaling behaviour 7-38428
 anisotropic 2D square lattice, random hopping model, percolation, diffusion and conductivity 7-61282
 antiferromagnetic Potts model, simple cubic lattice, critical fluctuations and phase transitions, Monte Carlo simulations 7-35457
 Ashkin-Teller quantum chain, criticality, finite-size effects and conformal invariance 7-52993
 Ashkin-Teller quantum chain with free boundary conditions, superconformal invariance 7-24454
 asymmetric contact process generalisation 7-29923
 asymptotic phase diagrams for lattice spin systems 7-14880
 automorphisms of algebraic varieties and Yang-Baxter equations 7-35425
 axisymmetric free jets having parabolic profiles at nozzle exit, hot-wire turbulence meas. 7-51260
 Baxter model, free-energy amplitude in finite-size scaling 7-48604
 Bethe lattice, localisation transition 7-29940
 Bethe method, thermodynamics and limit states 7-61307
 biased random walk on networks 7-61267
 biased tight-binding lattice, quantum tunnelling and thermally resisted motion 7-29946
 binary alloy, FCC Ising, multiautom interactions, low temp. behaviour and Monte Carlo simulations 7-6755
 binary alloy in ID lattice, density oscillations model 7-9800
 bipartitioning of random graphs of fixed extensive valence, statistical mechanics methods 7-48523
 Blume-Capel model, effective field theory 7-33134
 bond-diluted hierarchical lattice, shortest path length distribns. 7-4785
 Boolean cellular random nets, phase transitions 7-56171
 Bose gas in 1D, equilibrium thermodynamics 7-61276
 branched polymers, asymptotic props. on a fractal lattice 7-48595
 bridge function, in simple classical fluids, universality 7-24567
 bubble columns, turbulent coalescing, gas holdup correl. 7-37516
 Cayley tree, interacting random walkers, polymer statistics 7-9792
 Cayley trees, randomly closed, and fractal dimensionality 7-4784
 cellular automaton fluid models, continuum eqns. for large-scale behaviour 7-35286
 cellular automaton, long-range effects 7-29926
 charged particles in square lattice, minimal energy configuration 7-9799
 circle mappings, renormalisation group methods 7-56168
 classical spin systems on irregular lattices, infinite coordination limit 7-18713
 classical Toda lattice, sine-Gordon thermodynamics, Bethe-ansatz eqn. anal. 7-61272
 cloud pt. and nucleation theory 7-26906
 cluster props. of lattice spin systems with vacuum 7-35468
 clustering, two-dimensional, irreversible aggregation 7-24575
 coagulation/fragmentation processes, field theoretical study beyond Smoluchowski 7-61257
 competition between stable states in spatially-distributed systems 7-41303
 competitive trapping effects in a set of partially absorbing traps 7-9793
 complexity of games and percolation on trees of winning strategies 7-48601
 computer-generated uniform disk close packing round rhomboidal seeds, orientational order 7-61271
 conformal theories, discrete symmetries and twisted boundary conditions 7-250
 continuous time random walks with momentless waiting time distributions 7-24564
 continuous-spin models, phase diagrams, Pirogov-Sinai theory 7-48668
 continuum limit of cubic lattice of classical spins 7-35422
 continuum percolating systems, transport exponents, ϵ expansion 7-4786
 continuum systems, transport props. near percolation threshold 7-41290
 Coulomb gases, 2D, hierarchical model with Kostelitz-Thouless fixed point 7-9797
 coupled quadratic maps on 1D lattice, robust space-time intermittency and 1/f noise 7-41300
 coupled Toda lattice, soliton propag., equivalent nonlinear LC circuit study 7-29920
 critical points and intermediate phases on wedges of Z^d 7-14874
 cubic lattice, quantum mech. particle behaviour, stochastic quantisation 7-61235
 cubic lattices, regular and optimal subdivisions into sublattices 7-16456
 cubic subcomplexes in regular lattices (*Russian*) 7-48594
 decay times in one-dimensional chains 7-48618
 Delaunay percolation networks with topological disorder, renormalisation group approach 7-35434
 dense polymers, two-dimensional, exact critical exponents 7-24572
 density of states for quantum percolation problem 7-35391
 Devil's staircase 7-48574
 diagonals group and lattice coverings in n -dimensional Euclidean space 7-56009
 diffusing interacting particles in concentration gradient, Monte Carlo simulation 7-48596
 diffusion limited aggregation, maximal arm length 7-48599
 diffusion on a quasiperiodic chain 7-48611
 diffusion on fractals, combinatorial algebra 7-269
 diffusion-limited aggregation, anisotropic sticking probability on 2D square lattice, computer simulation 7-24590
 diffusion-limited aggregation, anomalous diffusion for regular and random models 7-239
 diffusion-limited aggregation, diverging length scales 7-254
 diffusion-limited aggregation, generalization and fractal dimensions 7-247
 diffusion-limited aggregation, singularities, asymptotics and scaling anal., comment and reply 7-44834

lattice theory and statistics continued

diffusion-limited aggregation with tunable lattice anisotropy 7-245
 diffusion-limited aggregation without branching, continuum approx. model 7-41287
 diffusion-limited aggregation without branching, Monte Carlo group anal. 7-61269
 diffusion-limited-aggregation in porous medium, effect of morphological disorder on viscous fingers 7-56173
 dilute magnetic systems, environmental percolation, large-cell Monte Carlo renormalisation-group calcs. 7-2861
 diluted Cayley trees, minimum gap 7-35448
 dimer model on square-, bathroom tile lattices, entropy calcs. 7-61262
 dimer pair correlations on the brick lattice, commensurate-incommensurate transitions 7-9789
 dimer problem, Kirchhoff theorem application 7-265
 directed compact site animals in two dimensions 7-24577
 disordered chain problem, integrable system canonical variables approach 7-35401
 disordered polymer chain, configurational statistics, random monomers 7-35433
 disordered systems, finite-size scaling and correlation lengths 7-35464
 disordered systems, relaxation processes, Fourier acceleration method 7-262
 disordered ultrametric models, relaxational dynamics, eigenvalue and eigenmode determ. 7-4789
 distribution and entropy of clusters in growth models 7-29915
 distributive lattices, equivalence systems and congruence systems 7-29916
 domain-wall interactions and spatially modulated phases 7-2146
 double sine-Gordon kink, Hamiltonian dynamics calcs. 7-61273
 double-sine-Gordon chain, internal dynamics calcs., nonlinear effects 7-35456
 driven diffusive systems, fast rate limit for lattice gas 7-29948
 dynamic scaling of Eden-cluster surfaces 7-14888
 dynamic systems, generalized Caratheodory's construction for dimens. characts. 7-48633
 dynamical system, time ordering and thermodynamics of fractal invariant measure 7-4790
 dynamical systems and statistical physics conf., Koszeg, Hungary, Aug.-Sept. 1984 7-48194
 Eden trees on square lattice, deterministic fractal model 7-14885
 Eden trees on the Sierpinski gasket 7-14886
 eight vertex SOS model, fusion 7-29935
 Einstein relation and exact Gell-Mann-Low function for random walks in media with random drifts 7-41251
 elastic Ising antiferromagnets on a triangular lattice 7-33185
 electronic wave functions, localisation due to local topology 7-21847
 ergodic props. of colour sequence for random walker on black-white lattice 7-14894
 ergodic symmetrically distributed random field, nonadmission of percolation 7-56186
 exactly solvable IRF model, Gordon-generalisation hierarchy, free energy parameterisation 7-24592
 exactly solvable IRF models 7-194
 Fibonacci chain eigenstates study 7-35459
 finite size scaling, systems with logarithmic specific heat 7-35447
 finite-size scaling in strips, log. corrections, Potts model appl. 7-35429
 firm closure, lattice models, percolation on interstices of BCC lattice, bubble age 7-14320
 first passage time in 2D, critical behaviour 7-48616
 fluids at liq-vapour critical point, many-body interaction effects calcs. and meas. 7-44750
 fractal clusters and percolation clusters, diffusion noise 7-35415
 fractal dimensions at percolation threshold, position space renormalisation group approach 7-48605
 fractal property of two-dimensional continuum percolation clusters 7-18716
 fractal singularities on a measure, singularity meas. on a fractal 7-35467
 frontier generating walk in gradient, determination of percolation threshold 7-35440
 frustration models, two-dimensional, ordering and phase transitions due to entropy gains 7-246
 functional integrals, renormalized expansions, coherent pot. to lattice model 7-18706
 gas model, Monte Carlo study of propagating fronts 7-48615
 gelation, 3D kinetic model, critical behaviour 7-14904
 gelation transition in Smoluchowski's coagulation eqn. 7-9790
 generalised cell mapping, largest Lyapunov exponent 7-29927
 generalised planar model, chiral and algebraic order, new phase transition scenario, Monte Carlo simulations 7-38877
 generalised random walks in 1D, fractal props. 7-9785
 generalized diffusion limited aggregation model, Monte Carlo simulations 7-244
 generalized dimensions and entropies from a measured time series 7-41256
 generating functions for connected embeddings in simple cubic, BCC lattices, percolation problem 7-24584
 genuine self-avoiding walks, trapping 7-9771
 Gibbs field uniqueness in d -dimensional lattice systems 7-48671
 graph partitioning and statistical mechanics, Monte Carlo simulation 7-48522
 Green-Kubo formalism for lattice gas hydrodynamics (*French*) 7-29912
 growth oscillations; deterministic models 7-48571
 growth probability and harmonic measure, fractal struct., scaling props. 7-61268
 growth probability distribution in kinetic aggregation processes 7-2145
 hard hexagon model, lattice gas generalisation, local densities as elliptic functions 7-9788
 hard square lattice gas, branch point singularity location, discrepancy in position 7-48612
 Hausdorff dimension as intrinsic metric prop. of fractals 7-24566
 heavy electrons, Gutzwiller method 7-27228
 height probabilities in SOS models 7-18710
 hierarchical fermion model, renormalisation on square lattice in 2D 7-56153
 hierarchical lattices, geometrical phase transitions and universality 7-41321
 hierarchical low-temperature behaviour of one-dimensional incommensurate structures 7-29914
 hierarchical scalar lattice field theories, non-Gaussian renormalisation group fixed point 7-9938

lattice theory and statistics continued

- hierarchical vector-valued ϕ^4 model, Maxwell rule and phase separation 7-48634
- Hilbert spaces, characterisation of projection lattices 7-29793
- hole distribution in Eden clusters, computer simulation 7-35450
- honeycomb lattice, exact solution of three-component system 7-29931
- Hopfield model, metastable state structure 7-24576
- hopping on hierarchical structures, mapping to diffusion on fractals 7-24574
- Hubbard model, world-line and determinantal functional-integral formulations 7-4781
- hypercube vertices random-walk diffusion, stretched exponential relax., numerical calcs. 7-56175
- incompressible motion on 2D and 3D lattices, appl. to turbulence 7-4772
- infinite cluster at percolation threshold, Monte Carlo renormalisation approach to fractal dimensions 7-35439
- infinite quasi-periodic 2D Penrose lattice, self-similar ground-state wave function calcs. 7-24599
- infinite strips with periodic boundaries, critical point structure fns., correlation lengths and susceptibility 7-24580
- inhomogeneous cellular automata, annealed and quenched, phase transitions 7-48613
- inhomogeneous eight-vertex SOS model and solvable IRF hierarchies 7-29918
- interaction round a face model, free energy expression 7-196
- interfacial growth instability, scaling, simulation 7-44746
- intersecting string model, star-triangle eqn., inversion relation and exact soln. 7-14892
- inverse semigroups, recurrence and nonrecurrence of random walk 7-61233
- Ising disordered systems, thermodynamic props., renormalisation group calcs. 7-56185
- Ising model, three dimensional, partition fn. calcs. 7-61264
- Ising model, trimodal random-field, on Bethe lattice and tricritical point 7-56181
- Ising model, two-dimensional, large block spin interaction 7-41285
- Ising model, two-dimensional, Yang-Lee zeros 7-238
- Ising model on dynamical planar random lattice, exact soln. 7-41286
- Ising model on homogeneous lattices embedded in varieties of genus O 7-35421
- Ising model spin correlations Langevin simulation 7-4778
- Ising model with general spin S, ground state props. 7-58968
- Ising model with two- and three-spin interactions, equivalence of four-state Potts model 7-48600
- Ising models with random bonds and crystal field interactions, tricritical point 7-2868
- Ising square lattice, antiferromagnetic susceptibility and short-range correlation function 7-38893
- Ising square lattice, pair correlation function 7-35465
- Ising triangular lattice, 2×1 and 2×2 structures, phase transitions 7-63765
- Kauffman's model, multivalley structure, analogy with spin glasses 7-24571
- Kauffman's random Boolean network, approach to the stationary state 7-56155
- Kauffman cellular automata, two-dimens., phase transitions 7-35400
- kinetic gelation, spatial correlations 7-35446
- kinetic gelation clusters in 3D anomalous diffusion, random walks 7-61279
- Laplacian random walk, reflecting and absorbing boundary conditions 7-18709
- large-N Heisenberg model, improved block-spin transformations and redundant operators 7-4777
- lattice animals, collapse transition and asymptotic scaling behaviour, low temp. expansion 7-29921
- lattice animals, three-dimensional, anal. using partial generating function method 7-24587
- lattice animals in d dimensions, Monte Carlo methods 7-251
- lattice systems, nonequilibrium steady state, hopping model 7-61270
- layered frustration models, susceptibility, high temp. series expansions 7-22085
- layering transitions at an interface 7-14883
- Lebowitz-Lasher lattice model, inhomogeneous, Monte Carlo simulation 7-61261
- linear polymers, collapse transition, lattice self-avoiding walk model 7-35452
- linear polymers, collapse transition on fractal lattices, interacting self-avoiding walk model 7-48603
- linear quasiperiodic arrays, diffraction spectrum 7-24579
- linear systems with strong relax., transition to aperiodic motion 7-29937
- linearised Toda lattice, gauge field-Toda amplitude duality 7-48621
- local generating functions for calc. of connected embeddings in lattice 7-24586
- locally interacting system, complexity 7-18708
- loop gas model, square lattice, critical behaviour 7-216
- Lyapunov analysis and information flow in coupled map lattices 7-41301
- macroscopic quantum systems, weakly coupled, limiting Gibbs state calcs., appl. to Josephson oscillator 7-45582
- magnetic hard-square lattice gas, multicritical scaling 7-48607
- many phases in systems without periodic ground states 7-48591
- matchings ad Random transforms in lattices, concordant sets 7-48619
- mean field renormalisation group, length scaling, critical indices 7-61260
- mean field spin-glass models with random sites 7-38874
- mean-field equations for the matching and the travelling salesman problems 7-24546
- mean-field renormalisation group, unified approach to bulk and surface critical behaviour 7-48665
- microscopic system, high press. effects, P,T thermodynamic description 7-48655
- microscopic system, high press. effects, P,T thermodynamic description, appls. 7-48656
- Migdal-Kadanoff renormalisation, appl. to Potts model 7-24600
- Monte Carlo simulations with multispin updatings, effective dynamics 7-18717
- multi-dimensional intertwined basin boundaries and kicked double rotor 7-29902
- multicomponent lattice Kadomtsev-Petviashvili eqn., linearizing integral transform 7-14891
- multiparticle diffusion, fractal kinetics 7-24604
- N-city travelling salesman problem, optimisation by simulated annealing 7-48614

lattice theory and statistics continued

- N-layer systems, asymptotic dispersion of particles, periodic boundary conditions 7-41284
- nematic liq. cryst. films, disinclinations, textures, four-state clock model description 7-257
- nonequilibrium kinetic growth oscillations 7-24569
- nonlinear lattice with long-range interaction, wave propag. (Russian) 7-109
- nonlinear response in percolation systems 7-18711
- nonlinear Schrodinger equation on lattice, classical and quantum variants 7-29817
- nonuniform lattices, classical orthogonal polynomials of discrete variable (Russian) 7-56170
- nuclear fragmentation, cluster distributions, lattice model anal. 7-24950
- occupation statistics for variously shaped particles on a rectangular $2 \times N$ lattice space 7-48598
- off lattice diffusion-limited aggregation with radial bias, liquid crystal fingering 7-63412
- one-dimensional degenerate Hubbard model, Monte Carlo simulations 7-45609
- one-dimensional Ising bridge model, general solution 7-61274
- one-dimensional lattice, charged particle motion, dynamic localisation in elec. field 7-16924
- one-dimensional quasiperiodic systems, electron spectral clustering and wave-function scaling, renormalisation-group calcs. 7-18723
- one-dimensional quasiperiodic systems, quantum energy spectra 7-35458
- oscillator, random walk on finite 1D lattice 7-252
- parallel computations in physics 7-48593
- particle diffusion and trapping, arbitrary trap size and conc. 7-9761
- particle order and disorder, minimal spanning tree, appl. to Li thin aggregated films 7-4788
- partition function, analytic props. for statistical mechanical models, Potts model anal. 7-24578
- partition function zeroes on regular and hierarchical lattices 7-48628
- pattern dynamics and optimization by reaction diffusion systems 7-54078
- pattern formation in reversible cellular automata 7-18712
- pattern recognition, chopper model 7-253
- Penrose chain, 1d, vibr. spectrum and spectral dimension. 7-32582
- percolation, series expansion derivation 7-24585
- percolation, thresholds and critical indices 7-29913
- percolation at surface, fractal dimension 7-14867
- percolation backbone, three-dimensional, single-connected links, distribution fn. anal. 7-56174
- percolation clusters, two-dimensional, fractal dimension of hull, Monte Carlo calcs. 7-241
- percolation models, critical behaviour and random walk representations 7-48532
- percolation models, critical exponent inequalities 7-35451
- percolation threshold in the continuum problem 7-41282
- percolation with trapping 7-14881
- periodic harmonic lattices, mechanical power transfer and energy-current density calcs. 7-9801
- perturbed periodic Toda chain, chaos upon soliton decay 7-41299
- phase separation on regular and fractal lattices in two dimensions 7-14887
- phase transition, sharpness in percolation models 7-61255
- phase transitions on fractal lattices with long-range interactions 7-29928
- physisorbed atoms on anisotropic rectangular lattice, struct. factor of incommensurate phases 7-52250
- piecewise linear map, mode locking, exact treatment 7-35420
- Pirogov-Sinai, theory, low temp. continuous spin Gibbs states on a lattice 7-59035
- planar convex sets containing many lattice points, van der Corput's theorem 7-56010
- planar random surfaces with extrinsic action, critical exponents 7-29938
- planar XY-model on a 2D random lattice, numerical simulation 7-24594
- polymer chain dynamics, temp. depend. cubic lattice model simulation 7-998
- polymer chain interacting with interface, critical exponents 7-14878
- polymer chains, four-dimensional, asymptotic logarithmic behaviour renormalization anal. 7-4779
- polymer self-avoiding network of fixed topology, renormalisation and exact critical exponent 7-260
- polymers, branched, corrections to scaling 7-1921
- polymers, branched, Monte Carlo and exact series anal. of lattice animals 7-48622
- polymers, randomly coiled, endpoint distrib. for neighbor avoiding walks 7-48597
- polymers and percolation, conformed invariance props. 7-48608
- Potts model, 2D, critical dynamics 7-18714
- Potts model, 2D, renormalisation by substitution 7-24568
- Potts model, antiferromagnetic, critical phases on fractals 7-24583
- Potts model, cluster-size distrib. and mag. props. 7-33136
- Potts model, dynamic critical exponent for $q=3$ and $q=4$ 7-35441
- Potts model, infinite range soln. and free energy calcs. 7-24593
- Potts model, one dimensional, critical dynamics 7-240
- Potts model, q-state, anisotropic hypercubic lattice, critical condition 7-24573
- Potts model, q-state, geometrical factor and thermal props. 7-14876
- Potts model, renormalisation and phase transitions, symmetry breaking 7-284
- Potts model, three-state, two-dimensional conformally invariant theory, operator content, effect of boundary conditions 7-4776
- Potts model, triangular, with 2- and 3- site interactions, crit. line 7-24596
- Potts model on Koch curve, renormalisation group approach 7-14884
- Potts model on Sierpinski carpets, Migdal-Kadanoff bond-moving renormalisation anal. 7-24588
- Potts models, crit. dynamics at percolation threshold 7-29917
- proteins, fractons and fractal dimension self-avoiding walk model 7-48590
- q-series, expansion into infinite products 7-48308
- q-state Potts model operator algebra representations, transfer matrix spectrum 7-35436
- q-state vertex model, soluble case 7-4780
- quantum Markov chains, translation-invariant distrib. 7-61265
- quantum spectral transform 7-48630
- quantum spin model on triangular lattice, zero-temp. props. 7-27486
- quantum systems, Langevin simulations 7-48544
- quantum XYZ models, critical props. in 2D 7-29933
- quasicrystalline alloys, unstable chemical struct. 7-44453

lattice theory and statistics continued

- quasiperiodic tiling in two and three dimensions 7-35432
 random cellular networks, struct. and evolution 7-48625
 random lattices versus regular lattices, Ising model, fermions on random lattices 7-35466
 random matrices, rigorous bounds and the replica method for products 7-35437
 random nonpercolating conductor networks, insulation breakdown calcs. 7-58744
 random resistor-fractal networks, infinite set of exponents 7-236
 random surfaces on cubic lattice, critical behaviour, phase diagram 7-24582
 random walk, correlated, on a BCC lattice with next-nearest-neighbour hops, self-consistent decoupling approx. 7-41259
 random walk, size of local time increments 7-48620
 random walk and diffusion in a stochastic lattice gas model 7-41274
 random walk motion, disorder induced transport on simple cubic lattice 7-35449
 random walker on fractal lattice, superuniversality of acceleration correl. 7-61258
 random walks, transverse spin rotation depolarisation 7-48558
 random walks on cubic lattices with bond disorder 7-48617
 random walks on trapped lattices, statistical behaviour 7-4763
 randomly diluted nonlinear resistor networks, series anal. 7-4787
 reaction-diffusion equation, microscopic selection principle 7-54079
 reaction-diffusion equations for interacting particle systems 7-29924
 reactive solid, pore growth, scaling theory 7-255
 regular-random fractal model for cluster numbers and structure in percolation 7-35427
 resistor-diode percolation on the hierarchical diamond lattice, real space renormalization group anal. 7-243
 rigid clusters enumeration, animal counting techniques 7-35444
 rigid surface in high-dimensional space 7-18707
 scaling at the conformational rod-to-coil transition 7-35442
 scaling method for asymptotic analysis of power series 7-14877
 scaling properties for the surfaces of fractal and nonfractal objects: an infinite hierarchy of critical exponents 7-18715
 schauder bases in locally solid lattice Banach spaces 7-29936
 self dual quantum $Z(5)$ model, finite-size scaling and conformal invariance 7-35428
 self-affine clusters and generalised Cantor bars generation, spatial convolution techniques 7-9796
 self-avoiding chain molecules, generic model 7-24552
 self-avoiding random walks on the hexagonal lattice, critical exponent calcs. 7-35405
 self-avoiding walk, Monte Carlo algorithms, dynamic critical exponents 7-213
 self-avoiding walk, spiral, triangular lattice analysis 7-48610
 self-avoiding walk, triangular lattice, θ point anal. 7-24551
 self-avoiding walk, triangular lattice, connective constant, Monte Carlo anal. 7-215
 self-avoiding walk, two-dimensional, exact exponents 7-214
 self-avoiding walks on random lattices, scaling theory 7-48563
 self-trapping on a dimer, discrete nonlinear Schrödinger eqn., time-depend. solns. 7-18721
 semi-infinite ferromagnetic q-state Potts bulks separated by bond diluted interface, criticality 7-33179
 semiflexible chains, solution, statistical mechanics, path integral formulation 7-41232
 Sierpinski carpet, random walk problem, spectral dimensionality and hyperscaling 7-18720
 Sierpinski carpets, classification and universal props., Potts model critical points 7-61259
 Sierpinski gasket, duality construction 7-48606
 Sierpinski gasket, random walk generating functions 7-29892
 Sierpinski gasket, self-similarity and Hilbert curve self affinity 7-24570
 Sierpinski gasket, two-dimensional with anisotropic interactions, density of states calcs. 7-242
 Sierpinski gasket fractals, hierarchical model relaxation, diffusion generalisation 7-9784
 simple cubic lattice, 3D percolation threshold estimates, Monte Carlo simulation 7-35435
 sine-Gordon chain, driven, bispectral anal. 7-29773
 sine-Gordon solitons in external fields 7-61263
 single linear chain, struct. factor calcs., finite size effects 7-48623
 site animals on square lattice, series expansions using Monte Carlo method 7-35426
 site percolation in a honeycomb lattice, renormalisation group calcs. 7-9798
 solid-liq. interfacial tensions, q-state Potts lattice gas model, mean-field approx. calcs. 7-256
 solid-on-solid models, integrable, automorphic props. of local height probabilities 7-56184
 solvable lattice models with broken Z_N symmetry and Hecke's indefinite modular forms 7-24773
 spaces of long range interactions on lattice systems, generic triviality of phase diagrams 7-9780
 spatio-temporal coherence and chaos, conf. Los Alamos, USA, Jan. 1986 7-48158
 spectrum analysis and scattering theory for a three-particle cluster operator 7-48627
 spin glass, superalgebras and random spherical model 7-53008
 spin glass model on hierarchical lattice, Parisi overlap function 7-12984
 spin models, phase transitions, cluster size distrib., geometrical factors 7-41280
 spin system, microscopic anisotropy influence on phase boundary macroscopic behaviour 7-18730
 spin-1 model on honeycomb lattice in mag. field, solvable case 7-249
 spinodal decomposition, diffusion limited, corrections to late-stage behaviour, Lifshitz-Slyozov scaling and Monte Carlo study 7-38206
 spiral avoiding loops on triangular lattice 7-14879
 spiral lattice site animals, exact enumeration theory 7-56183
 spreading phenomena in which growth sites have a distribution of lifetimes 7-35438
 square lattice, minimal-energy config. of charged particles 7-9782
 square lattice, site percolation and elastic props. 7-261
 square lattice, truly kinetic random walks, multifractal nature 7-56161
 square lattice gas with extended hard core interactions, tracer correlation factor 7-35463
 square-lattice-gas model with anisotropic repulsive interactions, multicritical behaviour, transfer-matrix scaling 7-41291

lattice theory and statistics continued

- stability of the isotropic fixed point near one dimension 7-9787
 star-triangle and inversion relations in statistical mechanics 7-48528
 star-triangle relation, class of elliptic solns. 7-248
 statistical methods, conf., Oaxtepec, Mexico, Jan. 1986 7-24268
 statistical physics, conference, Oaxtepec, Morelos, Mexico (Aug. 1985) 7-9584
 statistical physics and field theory conf., Groningen, Netherlands, Aug. 1985 7-55899
 steady-state chemical kinetics on fractals, segregation of reactants 7-41295
 stirred percolation, annealed disorder, diffusion, continuous time random walk 7-61266
 stochastic particle systems, equilibrium fluctuations in lattice gases 7-48586
 strange attractors in two-dimensional maps, dimensionality calcs. 7-9772
 subdirectly irreducible modal lattices, varieties and subvarieties 7-61256
 submonolayer ordering and multilayer adsorption, simple lattice gas models 7-12490
 surface and interface magnetism, dilution effects and influence of nature of interaction 7-59032
 temperature-driven first-order transitions, finite-size effects, Potts model, Monte Carlo calcs. 7-258
 thermal desorption spectra, simple rate eqn. derivation 7-21646
 thermally activated random walkers on ultrametric spaces, low temp. patterns 7-9783
 thin-film layering transitions, quenched disorder effects 7-27195
 three-state Potts chain with competing interactions, general kinetic model 7-29934
 threshold percolation density in strongly correlated lattice systems 7-14895
 Toda lattice, bijections and linear wave eqns. 7-48602
 Toda lattice, thermodynamics as classical limit of two-component Bethe ansatz scheme 7-41304
 Toda lattice eqn. from homogeneous realisation of $A_1^{(1)}$ basic representation 7-9795
 Toda lattice with mass interface, soliton scatt., equivalent nonlinear LC circuit study 7-29919
 trap-controlled random lattices, continuous time random walk calcs. 7-48551
 trapping of genuine self-avoiding walks 7-24563
 travelling salesman problem, numerical simulation 7-24547
 travelling salesman problem, statistical mechanics 7-29925
 triangular lattice gas automaton, nature of turbulence 7-41302
 tubes and channels, porous-walled, injection-induced flows 7-31876
 two coupled semi-infinite systems near criticality 7-44747
 two-dimensional lattice gas on triangular net, order-disorder transitions, struct. factors, Monte Carlo simulation 7-56176
 two-dimensional site-percolation model, diffusion and long-time tails, vel. autocorrel. function calcs. 7-24606
 two-sublattice systems, correlated random walks, Monte Carlo simulations 7-4783
 two-sublattice systems, correlated random walks 7-4782
 uniform branched polymers, lattice models, uniform combs in two-dimensions 7-237
 universality in phase transitions on inhomogeneous structs. 7-41279
 Virasoro algebra, von Neumann Algebra and critical eight-vertex SOS models 7-24589
 viscous fingers and diffusion limited aggregates near percolation 7-16252
 waiting time distrib. function, asymptotic solns. of continuous time random walk problems (Chinese) 7-35398
 XXZ chain, conformal invariance and spectrum 7-63768
 Yang-Lee edge singularity on fractals 7-18722
 Z_n model, infinite range soln. and free energy calcs. 7-24593
 $Z(N)$ symmetric quantum spin models, conservation laws and exact ground state energies 7-27487
 Zamolodchikov model, 3D, free energy, partition function per site 7-35424
 $Ba_2NaNb_2O_{15}$ incommensurate ferroelec. thin films, disclinations, textures, four-state clock model description 7-257
 Ge, (111) surface structure, lattice gas model anal., DAS structure 7-2309
 H_2 - D_2 mixtures adsorbed on graphite, phase diagrams 7-52180
 4He - 4He mixtures adsorbed on graphite, phase diagrams 7-52180
 $Nb_{1-x}V_x(Mo)_x$ random field system, disorder-disorder phase transition, cluster variation calcs. 7-63803
 Ni (111) with adsorbed H, phase diagrams based on model interactions 7-21650
 Si, (111) surface structure, lattice gas model anal., DAS structure 7-2309
 Xe monolayers on graphite, low temp. phase diagram, striped helical Potts model calcs. 7-38327
- lattice vibrations** see *lattice dynamics*
launchers, electromagnetic see *electromagnetic launchers*
Laves phases see *alloys*
lawrencium
 No entries
lawrencium compounds
 No entries
laying, cable see *cable laying*
LB films see *Langmuir-Blodgett films*
LCAO calculations
 acidic and basic sites on surface, electronic absorpt. spectrosc. appls. calcs. 7-36473
 alkali halides, colour centres, Hartree-Fock cluster computations 7-16985
 alkaline earth oxides, colour centres, Hartree-Fock cluster computations 7-16985
 allenes, monosubstitution, stabilisation energies, isodemic methyl exchange reaction study, ab initio LCAO SCF calcs. 7-25389
 p-aminobenzene, electronic absorpt. spectra, quantum chem. calcs. 7-36473
 atomic diabatic states, nonadiabatic interactions, CI wave fns. expansion, ab initio LCAO SCF CI calcs. 7-49945
 chemical reactivity, potential energy surfaces, LCAO, MO and SCF calcs. 7-17764
 chlorophyll- H_2O system, ab initio LCAO SCF MO calcs., ionisation pot., electron affinity, intermol. mechanics 7-8520
 compound metal clusters, struct. and electronic structs. calcs. 7-15783

LCAO calculations continued

- diamond (111) surface reconstruction, energy minimisation calculations 7-12434
 diatomic molecules, potential energy curves, numerical basis function calcs. 7-25438
 2,4-dihydroxyquinoline, gas phase, prototropic equilib., electron impact fragmentation spectra anal., LCAO-CNDO calcs. 7-36479
 electronic structure of micro-clusters, ab initio studies 7-31203
 energy-optimised GTO basis sets for LCAO calcs., gradient approach 7-10376
 ethylene, C-C bond description, HF and VB LCAO calcs. 7-25415
 hexahalo complexes, vibronic coupling and state Jahn-Teller effect 7-19725
 multicentre quantum chemical integrals, hydrogenic AO basis calcs. 7-5598
 narrow full core levels press. contrib. estimates, atomic-sphere and LCAO calcs. 7-64036
 overlap integrals calc. using recursion formulae 7-62246
 porphyrin dimers, free-base, electronic spectra, quantum chem. calcs. 7-10416
 porphyrins, proton motion, electrostatic pot. distrib., SCF-MO-LCAO calcs. 7-57147
 singly excited configurations, MCSCF method based on superposition 7-5611
 soft-core Thomas-Fermi pseudopot. for total energy calcs. 7-21845
 tetrahedral solids, semicond., dispersion of linear optical props., empirical tight-binding calc. 7-45966
 transition metal thin films, ferromagnetic, surface spin waves, multiband model 7-2834
 troxidone, antiepileptic drug, electrostatic pot., ab initio SCF-MO-LCA. study 7-855
 AgNO₂ crystal, room temp. electronic energy band calcs. 7-7113
 Al_n clusters, (n=5,9,13), electronic struct. and bonding 7-15775
 Al_n, electronic struct., first principles LCAO calc. 7-21813
 C₂CS, first stage intercalation cpd., self-consistent band struct. calc. 7-52395
 C₂K first stage intercalation cpd., self-consistent band struct. calc. 7-52395
 CO, potential energy curves, numerical basis function calcs. 7-25438
 C₂Rb, first stage intercalation cpd., self-consistent band struct. calc. 7-52395
 CaF₂, directional gamma ray Compton profile meas. and LCAO calcs. 7-2063
 CdSb crystals, band struct., LCAO calcs. 7-58737
 Co clusters, small, reactivity 7-15781
 Cu:Mn(Cr) matrix, electronic struct. calcs. 7-16976
 CuNi, substitutionally disordered, electronic struct., LCAO-CPA calcs. 7-64067
 FNO₂, semi-empirical MO-LCAO method validity eval. 7-15482
 H₂⁺ scattering from Al (110), resonant transition rates for charge transfer 7-3134
 H₂O dimer, transition from trapped to solvated electrons, ab initio calcs. 7-19700
 Li cpds., energy stability, struct., vibr. spectra, MO LCAO SCF calcs. 7-15512
 Li₂, low-lying $1\Sigma^+$ states, orbital exponent calcs. using LCAO MO CI method 7-56971
 Li_n clusters, n=2 to 13, electronic struct. and magic numbers, LCAO-X α calcs. 7-31206
 MgO (001), ab initio Hartree-Fock calcs. 7-27378
 MnO, band struct., optical props. 7-32912
 MOO⁺ (n=6,5,4), surface centres, electronic struct. anal., MO-LCAO calcs. 7-7324
 N₂ metastable states, HFS, laser-induced fluoresc. study 7-42678
 N₂, potential energy curves, numerical basis function calcs. 7-25438
 NaNO₂, cryst., piezoelec. strain consts., calcs. 7-53238
 Ni_{1-x}P_x, amorphous glasses, electronic structure, calcs. 7-7101
 Pb_{1-x}Mn_xTe, indirect exchange interaction between Mn²⁺ ions 7-27509
 Si, vacancies, hyperfine interactions, ENDOR and EPR studies 7-63609
 Si:Fe, interstitial Fe, spin delocalisation 7-13059
 a-Si:H, configurational models and adiabatic potentials of H 7-51632
 a-Si:H, Si-H-Si three centre bonds IR spectra, LCAO-MO-SCF-STO-3G calcs. 7-6741
 SiO₂:F, vitreous, substitutional impurity, semiempirical calcs. 7-32464
 SiO₂-related materials, cryst. and amorphous, electronic struct. calcs. 7-64081
 W (110), hyperthermal K⁺ scattering, HFS-LCAO pair potential 7-22412

LCD see liquid crystal displays

lead

- see also nuclei with
 1.43 MeV γ -ray penetration of shields, benchmark data 7-5487
 acid batteries, maintenance free design 7-59833
 adsorption on Cu (100), epitaxial growth, thermal He atom scattering 7-52351
 adsorption on Cu (10,10) and (510) surfaces, faceting, LEED, AES studies 7-32828
 air pollution, conc. changes in Antarctic ice during Wisconsin/Holocene transition 7-40074
 Amazon River, continental shelf sediment accumulation and transport ²¹⁰Pb anal. 7-34462
 apron for radiation protection, design improvement 7-60093
 atom, 6p subshell, admixed state effect on photoionisation 7-25470
 atom, electron scatt., relativistic effects, Kohn-Sham theory 7-42765
 atom, valence energy and polarisability, semiempirical pseudopot. calcs. 7-56926
 atoms, elastic scatt. of electrons, spin polarisation meas. 7-50364
 atoms, low-energy electron elastic scatt. calcs. 7-50362
 bar, collision with C steel bar, contact duration study 7-37393
 bone Pb anal., comparison of 2 in vitro methods 7-23499
 buildup factors and spectra for point isotropic γ -sources near the K-edge 7-36301
 chemisorbed on Ge (111), atomic geometry, surface X-ray diffr. 7-52277
 cladding on radwaste containers, corrosion study (Spanish) 7-54013
 coal fly ash radionuclides chemical anal. using alpha, gamma and X-ray fluorescence spectroscopy 7-23266
 Colorado Peaks volcanic rocks, USA, isotope and trace element geochemistry 7-60203
 cooldown mass flow requirements for He or N cooling systems 7-56281

lead continued

- deforming stress and defect struct. in low temp. anomaly region (Russian) 7-38093
 dense monolayer on Cu (100), LEED anal. 7-6989
 dissolution in HNO₃, thermometric obs. 7-8189
 East Pacific Rise and Guaymas Basin, hot springs U-Th-Pb systematics 7-40462
 electrical conductivity meas., high pressure, in diamond anvil cells at cryogenic temp. 7-56299
 electrical resistivity, temp. depend. 7-58792
 electrodeposition from aq. HCl soln. onto Pt (111) 7-27954
 electrodeposition kinetics, stripping voltammetric technique 7-27949
 film, etching by methyl radicals in discharges 7-3507
 films, breakdown, nodule form., thermal expansion effect (Russian) 7-45067
 foils, electron absorpt. and scatt. energy spectra, Monte Carlo calcs. 7-22399
 gamma-ray attenuation coeff. obs. incorporating detector resolution 7-63656
 Grenville Front, Labrador, Canada, Sr, Nd, Pb isotope geochemistry 7-60199
 ionised atomic clusters, fragmentation, TOF mass spectroscopic study 7-10807
 ions, energy levels, radiation effects and corrections 7-49960
 ions, laser produced spectra and QED effects 7-37747
 isotope evolution rel. to Earth core growth, implications of siderophile and chalcophile abundances in oceanic basalts 7-34397
 laser mechanism and energy characts., relax. processes of metastable states 7-62673
 magnetic refrigerator use, regenerator and working material heat transfer process 7-56284
 Marydale Group, southern Africa, metamorphosed banded Fe formation, Pb-Pb dating and assoc. geochem. 7-60189
 molecule, glow discharge sputtering, laser-excited fluoresc. 7-10647
 monolayer on Cu (110), struct. and melting, X-ray scatt. studies 7-7016
 monolayer on Ge (111), photoelectron scatt., temp. depend. 7-13328
 Newark Bay, New Jersey, USA, heavy metals in water column of estuary 7-55084
 normal potentials in liq. NH₃ 7-39903
 ocean chemical composition, ²¹⁰Po and ²¹⁰Pb in Gulf of Mexico seawater 7-34552
 overlayer on Cu (100), growth, phase transitions and struct., thermal energy He atom scatt. study 7-63943
 overlayer on Pt (100), underpotential deposited 7-58646
 overlayers on Cu (111), spot profile anal. of LEED 7-51586
 SW Pacific islands, Pb, Sr, Nd isotope and element abundances study 7-8874
 particulate and gaseous, in exhaust gas determ., plasma emission and atomic absorpt. spectrometry 7-59803
 phase diagrams, appl. for online press. and temp. calibration 7-4853
 phonon density of states from heat capacity temp. depend., inverse problem 7-6736
 phonon spectra, dynamical pseudopot. shell model calcs. 7-51965
 pollution in river sediments, Christchurch, New Zealand 7-13934
 positronium work function, temp. depend. 7-58859
 powders, hot isostatic pressing, empirical model 7-46365
 resonant atomic state, autoionis., electron spectra 7-900
 Rockall Plateau, dipping-reflector passive margin struct., Pb isotopic evidence 7-66037
 Scotland, Caledonian Pb isotope geochemistry and mantle source 7-23590
 seawater isotope chemistry for N Pacific bottom water 7-23703
 self-consistent relativistic band struct., normal and high press. 7-52413
 Severn Estuary, UK, sediment trace metal record for last 2000 years 7-18211
 shielding effect on 14 MeV neutrons, meas. and calcs. 7-42104
 shielding slabs, penetration of 2.75 MeV γ -rays 7-30712
 shock adiabats, shell effects 7-2104
 stainless steel-Pb particle mixture, mixing model with particles of different elec. resist. (Japanese) 7-44831
 structural elements, corrosion in contact with building materials (German) 7-3522
 submicrosecond elastic loading, material relax. phenomena 7-12186
 substrate, ⁵⁷Co Mossbauer spectra area meas., use of internal standard 7-36426
 superconducting films, 2D superconductivity, disorder effects, Eliashberg theory 7-22070
 superconducting granular film SAW attenuation, percolation model 7-2781
 superconducting transition, deform. strengthening, dislocation density (Russian) 7-58939
 surface, (110), melting, ion shadowing and blocking meas., RHEED 7-44769
 surface, anomalous thermal expansion, ion shadowing meas. 7-58512
 tetrahedral bonding and crystal struct., first-principles theory 7-32355
 thin film, optical consts. in visible region 7-7662
 thin films, surface plasmon detection, attenuated total refl. meas. 7-16961
 unstable plastic deformation at low temp., superconducting transition effects (Russian) 7-6709
 vapour, electron momentum spectra, multiconfiguration DF wavefunction 7-50351
 vapour pulsed laser operating at high excitation pulse repetition freqs. 7-43072
 work fn., temp. depend., anal. 7-52737
 X-ray photoabsorption cross sections 7-46240
 Al-AlO₂-Pb tunnel diode, NiCl₂·6H₂O soln. phase adsorpt., inelastic electron tunnelling spectra 7-12877
 a-Ge/Pb-a-Ge trilayers, melting transition of Pb 7-32884
 LiCl:Pb²⁺, absorpt. and luminesc. spectra studies (Russian) 7-46141
 Nb/Nb₂O₃/Pb film struct., Josephson and tunnel junctions, scanning tunnelling microscope study 7-64410
 Nb-NbO₂-Pb Josephson tunnel junctions, bifurcations, noise and near-reson. perturbations influence 7-58957
 Nb₃Al(Ge)/Pb magnetron sputtered Josephson tunnel junction props., film deposition conditions dependence 7-58955
 NbN/Pb(In) Josephson junction, Ar⁺ irradiat., characts. (Japanese) 7-22071
 NbSe₂-I-Pb, tunnel junctions under press. 7-52594
 Pb acid battery initial short-circuit current prediction and obs. 7-3634

lead continued

- Pb²⁺ in alkali halide crystals, polarised luminesc., model of impurity centre 7-27753
 Pb²⁺:KMgF₃ colour centre laser, tunable for 855 to 965 nm 7-15874
 Pb/bronze composite matrix for small closed cycle refrigerators 7-61340
 Pb/Nb₂O₅/Nb/Nb/Cu junction, 2D superconductor, pair tunnelling study 7-12916
 Pb/NbN/Pb sputtered thin film system, tunnelling charact., reply to comment 7-45576
 Pb/NbO_x/Nb system, pseudo-inverse AC Josephson effect 7-7454
 Pb/PbSn, chem. diffusivity of Sn in Pb, expt. determ. 7-63887
 Pb-acid batteries, mass transport during plate formation 7-39985
 Pb-acid battery, effect of chemisorbed H₂O on positive plate elec. capacity 7-54284
 Pb-acid battery, stability of SnO₂ conductor at PbO₂ cathodes 7-65440
 Pb-acid battery, study of positive plates by photoacoustic spectrophotometry 7-54283
 Pb-acid cell failure mechanism and rate, reliability studies using Weibull statistics 7-65450
 Pb-acid cells, dissolution and immobilisation of Sb, cell design 7-54289
 Pb-acid flexible sealed battery (*Japanese*) 7-65431
 Pb-acid medium-capacity sealed battery series (*Japanese*) 7-65432
 Pb-acid stationary battery crevice corrosion cracking and counter measures 7-46930
 Pb-acid storage batteries, role of transport phenomena (*Hungarian*) 7-17856
 Pb-Ag supercond.-normal conducting film structures, Andreev scatt. 7-45572
 Pb-Al disordered 3D superconductor-normal metal composite, elec. transport, magnetisation meas. 7-64383
 Pb-Ge multilayers, cumulative disorder and X-ray line broadening 7-32847
 Pb-Pb and Pb-Sn, superconducting point microcontacts, electron-phonon interaction 7-2509
 Pb-Pb isochron dating method for deeply weathered terrains geochronology 7-60391
 Pb-PbO_x-Pb tunnel junction I-V charact., Pb film quasi-particle effective chem. pot. calcs. 7-22065
 Pb-Pt composite films oxidation, KPS 7-27867
 Pb+He, inelastic collisions at thermal energies 7-983
 Pb²⁶⁺+Sn(Xe), impact parameter depend. target K X-ray emission, XES spectra anal. 7-62314
 Pb⁸¹⁺+Ag, electron capture, K X-ray emission spectra study 7-36524
²⁰⁸Pb(A=204, 206, 207, 208) in Bo Country chondrite (*Chinese*) 7-18391
²¹⁰Pb concs. and states of equilib. with ²³⁸U, ²³⁴U and ²³⁰Th in U miners' lungs 7-28724
²¹⁰Pb in air and soil, use to meas. aerosol scavenging rate and vertical profile 7-55188
²¹⁰Pb, sedimentary processes and metal depth profiles 7-55010
 Pb(n,X), 14 MeV, neutron multiplication, leakage rate from sphere, fusion reactor appls. 7-62061

lead alloys

see also lead compounds

- Bi-Pb-Sn-Cd alloy negative electrode for secondary Li batteries (*Japanese*) 7-65435
 creep crack growth parameters of model materials 7-39674
 superconducting, base electrode Josephson junction, self-positioned, fabrication 7-52906
 ternary plumbides, M-M'-Pb, (M=Ca,Sr,Sc,Y,La-Lu; M'=Co,Rh,Ir), structural and superconducting props. (*French*) 7-44491
 tunnel junction, quasiparticle RF-induced steps (*Chinese*) 7-27472
 Al-base bearing alloyed, leaded, wear charact. 7-33808
 Al-Pb, monotectic alloy, section prep., micromilling, polishing (*German, English*) 7-22937
 Al-Si-Pb-Bi, duplex alloys, melt quenching, microstruct. supercond. props. 7-45593
 Bi-Pb, superconducting transition temp., effect of plastic deform. 7-52879
 Bi-Pb alloys, supercond. and normal state, thermal cond., effect of plastic deform., 1.5-300K 7-17132
 Cd-Sn-Pb, phase diagrams, thermodynamic formalism, computer calcs. 7-3269
 CePb₃ heavy fermion material, magnetism and superconductivity 7-52880
 CePb₃ heavy fermion system, theory of mag. field induced supercond. state 7-45546
 CePb₃ heavy fermion system, muon Knight shift study 7-45886
 CePb₃, possible superconductivity in nearly antiferromagnetic itinerant fermion systems 7-38802
 Cu-Ag-Pb system, thermodynamic optimisation 7-46421
 Cu-Pb, resistance to wear and cavitation erosion of bearingalloys 7-8129
 Cu-Pb-Sn leaded bronze, resistance to wear and cavitation erosion of bearingalloys 7-8129
 Cu-Sn-Pb system, struct. form. during sintering 7-64967
 In-Pb, liq., activities, temp. depend., EMF obs. (*Japanese*) 7-12320
 In-Pb whiskers, critical currents and Ginzburg-Landau parameters 7-17144
 In-Pb whiskers, quasi 1D supercond., weak to strong coupling transition, I-V charact. study 7-38835
 K-Pb liquid alloys, excess stability, entropy 7-26975
 Li_{0.8}Pb_{0.2} liq. mixture, fast sound computer simulation, Mori-Zwanzig formalism 7-44696
 Li-Pb, fusion reactor breeder blanket fluids, T extraction, Pd catalyzed oxidative diffusion 7-49641
 Li-Pb, liq., sp. ht. calc. from expt. density and temp depend. press. data 7-63839
 Li-Pb, liq., T breeder material, compatibility with austenitic stainless steel 7-53966
 Li-Pb, liq. fusion reactor blanket, mass transfer in dynamic environment, corrosion damage 7-49659
 Li₂Pb liquid, static struct., temp. depend., screened Coulomb model anal. 7-21076
 (Mg₇₀Zn₃₀)₉₅Pb₅, metallic glasses, impurity vibr. states, influence on thermodynamic and superconducting props. 7-38148
 Na-Pb liq. alloy, thermodynamic prop. and transport coeff. 7-64199
 Nb-NbO_x-PbInAu, Josephson tunnelling current depend. on normal state tunnelling resist. 7-22073
 Nb-NbO_x-PbInAu Josephson junction fabrication by ion beam oxidation 7-22074
 Nb-Pb film couples, interfacial phase form., in situ annealing X-ray diffr. obs. 7-21705

lead alloys continued

- NbN/Pb-In Josephson junctions, fabrication by Ar⁺ ion bombardment 7-2787
 Ni-Sn-PbBi system, crack form. in diffusion zone 7-3397
 Pb based white metal, resistance to wear and cavitation erosion of bearingalloys 7-8129
 Pb In type II cylindrical superconductor, AC losses, circular magnetic field effects 7-52895
 Pb/PbSn, chem. diffusivity of Sn in Pb, expt. determ. 7-63887
 Pb-Al-Mg-Sn-Li, strength and microstruct. 7-8047
 Pb-Bi superconducting alloys with Bi precipitates, critical current density 7-17146
 Pb-Bi system, heat of fusion (*Russian*) 7-44766
 Pb-Bi system, peritectic crystallisation, cooling rate effect 7-46440
 Pb-Bi-Hg, liq., struct. microheterogeneity 7-11895
 Pb-Bi-Sn(In), alloy filaments, prod. by glass-coated melt spinning, enhancement of supercond. 7-58937
 Pb-In films, Josephson junction, thermal stress cycles, hillock form. (*Japanese*) 7-12536
 Pb-In-Au alloy films, hillock growth during heat treatment 7-16893
 Pb-In-Au fine-grained codeposited alloy films, RF plasma oxidation 7-53970
 Pb-In-Au thin films, hillock growth kinetics, grain boundary diffusion, SEM study 7-27221
 Pb-Li, flowing environment, corrosion of fusion reactor structural steels 7-53959
 Pb-Li, molten, thermally convective, corrosion of austenitic stainless and Cr-Mo steels 7-53962
 Pb-Li, strength and microstruct. 7-8047
 Pb-Sb, grain refinement, effect of solute content 7-59503
 Pb-Sn, cellular transform., directional invariance of grain boundary migration 7-22695
 Pb-Sn (2 wt.%), high temp. fatigue, dynamic recrystallisation 7-39667
 Pb-Sn (9 wt.%), solid soln. alloy 7-8066
 Pb-Sn α-phase alloys, cold-worked and splat-cooled, X-ray diffraction line anal. 7-46502
 Pb-Sn eutectic, spiral structures, convection influence 7-22653
 Pb-Sn eutectic, superplasticity, investig. by impression creep testing 7-3372
 Pb-Sn solder, deform. props. 7-46590
 Pb-Sn solder/Cu interfacial reactions, Cu₃Sn intermetallic formation 7-44924
 Pb-Sn-Ag solder alloys, phase equilibria 7-46426
 Pb-Sn-Ag system, eutectic temp. rel. to Ag content, phase diagram, thermodynamic props. 7-65005
 Pb-Te system, phase equilib., optimisation and calc. 7-3270
 Pb-Tl, Bridgman growth, pattern generation at solidification front, forbidden cells 7-22651
 Pb-Tl alloy single crystals., plasticity and internal friction changes at supercond. transition (*Russian*) 7-26832
 PbCaSn, rolling deform. texture, shear band angles 7-33724
 PbGeTe, thermal cond. minimum, thermoelectric appl. 7-38276
 PbLi eutectic, flowing, corrosion of stainless steel 7-53958
 PbSn liquid alloys, wetting and spreading, surface composition effects 7-16837
 Pb₇₄Sn₂₆ alloy surface, sputtering related phenomena (*Chinese*) 7-59316
 PbSnTe, thermal cond. minimum, thermoelectric appl. 7-38276
 Pd-Si, metallic glasses, photoemission investig. (*Slovak*) 7-59369
 Pt-Bi (22 wt.%), supercond. films, pinning in appl. mag. field (*Russian*) 7-64418
 Pt-Pb bimetallic systems, Fermi level density of states, XPS studies 7-46278
 Sn-Pb, electrodeposition kinetics, stripping voltammetric technique 7-27949
 Sn-Pb eutectic alloys, low temp. plasticity and morphology (*Russian*) 7-13510
 Sn-Pb system, metastable quasi-eutectic struct., existence range 7-3275
 Zn-Pb, monotectic alloy, section prep., micromilling, polishing (*German, English*) 7-22937
 Zr₂Pb₃, fusion blanket neutron multiplier, fabrication and props. 7-49656

lead compounds

see also lead alloys

- carboxylates, thermotropic phase transitions, DSC meas. 7-21441
 9,10-dihydroxyoctadecanoate, and binary mixtures, molten elec. cond. 7-38231
 glaze glass system, local coordination, EXAFS studies 7-63484
 (LuYBiPb₃)(FeGa₃)₂O₁₂, crystn. from soln. melt, component distrib. 7-21149
 orthovanadates and orthophosphates, diffuse satellites in electron diffr. patterns 7-26595
 PZT piezoceramics, reorientational polarization effects on stability and isotropy (*French*) 7-59153
 PZT/polyvinylidene fluoride, composites, dielec. behaviour 7-38992
 solid diode laser calibration, wavemeter 7-5930
 Ag₂Pb₃Nb₁₀O₃₀, ferroelectric with tetragonal W-bronze struct., first-order transition 7-39048
 Ba(Ca_{1/3}Nb_{2/3})₂O₃-PbZrO₃-PbTiO₃ ceramics, hot-pressed, ferroelectric phase transitions 7-7652
 BaPb β(II)-alumina, superstructure, high resolution electron microscopy study 7-12021
 BaPb_{1-x}Bi_xO₃, semicond. phase, CDW gap, optical meas. 7-53328
 BaPb_{1-x}Bi_xO₃ soln.-grown single crystals., crystallographic symmetries, effect on supercond. props. 7-37916
 BaPb_{1-x}Bi_xO₃, supercond. props., press. effects 7-45533
 BaPb_{1-x}Bi_xO₃, supercond. crystals., hydrothermal synthesis and props. 7-53532
 CdF₂-LiF-AlF₃-PbF₂ glasses, potential as a practical glass 7-37074
 CdSnO₄-PbO highly conducting films, characterisation 7-22049
 CsPbBr₃ and CsPbCl₃, ionic cond. and phase transforms., 30 to 380°C 7-58457
 FeO-PbO-P₂O₅ glasses, atomic environments, EXAFS studies 7-64787
 Ge₂₈Sb₇₂Pb₁₅₆ glasses, surface pot. relax., TSC meas. 7-64261
 GeTe-PbSe, phase transformations, cation-anion substitution, electrophysical props. 7-7978
 InF₂-PbF₂-BaF₂-SrF₂-YF₃-AlF₃-UO₂F₂, luminesc., lifetime meas. 7-27750
 K₂O-PbO-SiO₂, glass, props. rel. to phase diagram 7-13117
 K₂O-PbO-SiO₂ glasses, chemically nonuniform struct., Rayleigh and Mandelstam-Brillouin scatt. 7-1891
 K₂O-PbO-SiO₂ glasses 7-3036

lead compounds continued

- KPbBr₂·H₂O, synthesis, cryst. struct., X-ray diffr. study (*German*) 7-37940
- KPbLaF₆ solid soln. twinned cryst. struct., lattice parameters and point group, X-ray diffr. studies (*French*) 7-58231
- K₂Pb₄Nb₁₀O₃₀, ferroelectric with tetragonal W-bronze struct., first-order transition 7-39048
- K₂Pb₄Nb₁₀O₃₀·K₆Li₂Nb₁₀O₃₀ solid soln., density and struct. studies 7-1973
- La_{0.6}Pb_{0.4}Co_{0.4}Mn_{0.6}O₃, elec. conductivity, influence of Co ion substitution for Mn 7-45314
- Na₂B₂O₇·Pb₂O₄·CuO glasses, elec. props., effect of added CuO 7-2605
- Ni₈Pb(P₂O₇)₂, cryst. struct. determ. 7-1970
- PLTZ ceramics, grain growth during hot pressing 7-3232
- PLTZ ceramics, hot pressed, chemically induced grain boundary migration and recrystallisation 7-27027
- PLTZ ceramics, mechanical strength, composition and polarisation depend., microindentation meas. 7-6697
- PLTZ ceramics, optical second harmonics, temp. and elec. field depend. meas. 7-5952
- PLTZ ceramics (*Japanese*) 7-2981
- PLTZ, elastic-plastic contact damage 7-39627
- PLTZ, electrically excitable mechanical resonant mode shapes 7-26854
- PLTZ electro-optical ceramics, electron pulse irradiation-induced transient optical absorpt. study 7-6682
- PLTZ ferroelec. ceramics, IR optical and electrooptical props. studies 7-7675
- PLTZ, ferroelec. ceramic, laser-induced surface metallisation 7-53924
- PLTZ ferroelec. polycrystalline oxides, controllable powder synthesis, HP and PHP methods 7-7935
- PLTZ ferroelectric ceramics, gamma, electron and neutron irradiation effects study 7-6677
- PLTZ, ferroelectric films, properties and applications 7-59156
- PLTZ hot pressed ceramic, polarisation reversal studies under hydrostatic press. 7-59160
- PLTZ light shutter for color viewfinder and video projector appl. (*Japanese*) 7-20398
- PLTZ, piezoelec. ceramics, prep. and industrial appls. 7-13096
- PLTZ polarised ceramics, electroconductivity asymmetry obs. 7-7225
- PLTZ rhombohedral ceramics, electrocaloric effect study, diffuse phase transition intermediate state 7-7645
- PLTZ transparencies contrast increase, using electrically controlled light scattering 7-25909
- PLTZ transparent ceramic modulator, visual classroom demonstrations appl. 7-4647
- PLTZ transparent ferroelec. ceramic, hologram recording energy transfer, light scatt. effects study 7-5855
- PLTZ transparent ceramics, laser beam self-deflection and self-focusing meas. 7-5960
- PLTZ transparent ferroelec. ceramics, low freq. dielec. props. study 7-7630
- PLTZ, transparent ferroelectric ceramic, surface composition and structure 7-32765
- PLTZ, transparent ferroelectric ceramic, irradiation effects 7-59157
- PLTZ/Si spatial light modulators, technology 7-20408
- PLTZ-PZN electro-optic ceramics, elec., opt. and switching props. 7-7646
- PZT ceramic, pressure induced ferroelectric-antiferroelectric transition 7-22201
- PZT ceramic SAW interdigital transducers, anal., validity of model of Tancrell and Holland 7-6068
- PZT ceramics, ordered void struct., dielec. const., flexure strength 7-63607
- PZT ceramics, pulsed TEA CO₂ laser irradiation, signal generation 7-16623
- PZT composites, hydrostatic piezoelec. response, finite element modelling 7-64574
- PZT disc, elec. excitable mech. reson. modes 7-39042
- PZT films, crystn. kinetics 7-45090
- PZT, paraelectric phase transition broadening due to coexistence of ferroelectric and antiferroelectric phases 7-45942
- PZT, piezoelec. ceramics, prep. and industrial appls. 7-13096
- PZT powders, oxalate method prep., particle size (*Japanese*) 7-7941
- PZT, prep. by oxalate method in ethanol soln. (*Japanese*) 7-3245
- PZT, shock-recovery expts. 7-38119
- PZT solid solutions, p-t-x diagram 7-64581
- PZT:Bi piezoelectric ceramics, vacancies, positron lifetimes 7-37980
- PZT:Mn, dielec. dispersion 7-13076
- PZT:Nb ceramics, sintering, pair doping, elec. characts. 7-39469
- PZT-adhesive-PZT (glass), acoustic boundary waves propag. along thin layer between two bonded substrates 7-21602
- PZT-epoxy composites, thinning, ceramic width, acoustic impedance study 7-51954
- (Pb,Sn)Se IR detector arrays, heteroepitaxial growth on fluoride-covered Si substrates 7-39429
- (Pb,Sn)Te-(Ba,Ca)F₂ layers, MBE growth on non-lattice-matched Si substrates 7-27216
- Pb chalcogenides, mechanisms of electron scatt. 7-52611
- Pb salt tunable diode laser for two-tone optical heterodyne spectroscopy 7-30102
- Pb-glass detectors, removal of phototubes 7-49834
- Pb-PbO₂-Pb tunnel junction I-V characts., Pb film quasi-particle effective chem. pot. calcs. 7-22065
- Pb-Sn-G solid solns., elec. transport props. and defect form. studies (*French*) 7-33017
- Pb₄Te₃Ge₂O₁₁, rhombohedral, acoustic symmetry and vibr. anharmonicity 7-16695
- (Pb,Ba_{1-x})TiO₃, ferroelec. solid solns., dielectric and hysteresis props. 7-64588
- PbBi₂S₄-Bi₂S₃ system, chemically twinned phases, X-ray diffr., TEM obs. 7-32462
- Pb₂BiS₂, films, superconducting props. 7-22060
- PbBiTe₂, synthesis and physicochemical props. 7-13349
- PbBr₂ layers, vacuum deposited, elec. cond. temp. depend. 7-27000
- Pb₂Ca₂(PO₄)₆(OH)₂, apatite struct., Pb substitution, HREM study 7-16530
- Pb₂Ca₂(Si₂O₇)Cl₂, apatite struct., Pb substitution, HREM study 7-16530
- Pb₂Cd_{1-x}F₂, phonon spectra, superionic props. 7-6735
- Pb_{1-x}Cd_xSe films, laser deposition 7-59422
- Pb_{1-x}Cd_xSe, inter-band transitions, thermoreflectance study 7-3029
- PbCl₂ solid electrolyte for Cl₂-H₂ cells, cathodic characts. (*Japanese*) 7-13850

lead compounds continued

- PbCl₂-Sb₂O₃ glass system, structural aspects 7-44389
- Pb₃Cr₃F₁₉, nonlinear optic, lattice const., ferroelec. Curie temp., phase transition obs. at 555K 7-17275
- Pb_{1-x}Cr_xTe, prep. and electrical props. 7-12721
- Pb_{1-x}Eu_xSe, MBE growth for IR device appls. 7-64908
- PbEuSeTe/PbTe single quantum well diode laser with side optical cavity 7-43105
- Pb_{1-x}Eu_xTe epitaxial layers, mag. props. 7-45772
- PbF₂, environmentally nonpolluting antireflective coating of ZnSe optics 7-11097
- PbF₂, laser evaporation, luminescence of generated plasma 7-63354
- PbF₂, linear thermal expansion meas. 7-44863
- PbF₂, phys. props., effective pot. calcs. 7-26692
- PbF₂, US attenuation 7-51944
- PbF₂-GaF₃ glass films, vacuum deposition 7-64905
- PbF₂-MnF₂-Al(PO₃)₃ glasses, conductivity and mechanical relax 7-16803
- PbF₂-ZnF₂-GaF₃-AlF₃-YF₃-LaF₃:Mn II, Nd III, energy transfer 7-1889
- PbFe₂O₇·Ga₂O₃ (x=0, 1, 3, 4), magneto-optical props. 7-53281
- PbFe₂O₇, cryst., complex magneto-optical polar Kerr effect spectra 7-53280
- PbGa₂S₄ single cryst., optical absorption and photocond. studies 7-2635
- Pb_{0.95}Gd_{0.05}Te, antiferromag. exchange constant between nearest-neighbour Gd³⁺ ions 7-59002
- PbGeO₃, ferroelec. domain struct. and diffuse phase transition, permittivity meas. 7-13108
- Pb₂Ge₃O₁₁, acoustic devices, appl. of regular domain structs. 7-20567
- Pb₂Ge₃O₁₁, ferroelec. domain-struct. dynamics visualisation using a nematic liq. cryst. 7-53250
- Pb₂Ge₃O₁₁, high pressure Raman scatt., phonon modes and Gruneisen parameters 7-33391
- Pb₂Ge₃O₁₁, Mn²⁺ ESR study, pulsed saturation effects 7-64515
- Pb₂Ge₃O₁₁, rhombohedral, acoustic symmetry and vibr. anharmonicity 7-16695
- Pb₂Ge₃O₁₁, sound velocity discontinuities at the phase transition 7-17274
- Pb₂Ge₃O₁₁, surface segregation of Pb upon heating to the melting pt. 7-6931
- Pb₂Ge₃O₁₁:Gd³⁺, impurity ion reorientation kinetics 7-45940
- Pb₂(GeO₄)_{1-x}(SiO₄)_x(VO₄)₂, vibr. and impurity mode behaviour, IR spectra studies 7-64649
- PbGeS₃, vibr. props., spectral study 7-3032
- Pb_{0.93}Gd_{0.07}Te, glassy and cryst., defect struct., positron annihilation studies 7-46221
- PbH₄, equilb. bond lengths, relativistic corrections 7-36477
- PbHASO₄, ferroelec. phase transitions, proton tunnelling effect, NQR study 7-53172
- PbHPO₄, phase transition, thermal expansion meas. 7-44861
- PbHPO₄, photostimulated luminescence near ferroelec. Curie temp. 7-64697
- PbI₂, aggregated microcrystallites, Raman scatt. 7-22233
- PbI₂, layered semicond. with hexagonal end honeycomb structs., growth and optical props. 7-22277
- PbI₂:Zn, single crystals, growth and semicond. behaviour 7-53577
- PbI₂(Br)₂(Cl)₂-AgPO₃ glasses, struct. and elec. props., Raman spectra and ionic cond. meas. 7-6550
- PbIn₂Bi₂S₁₃, cryst. struct. determ. 7-1962
- PbIn_{1/2}Nb_{1/2}O₃, antiferroelec., phase transition, B-site cation order effects 7-7651
- Pb_{2-x}K_{1+x}Li₂Nb₂O₁₅, tetragonal tungsten bronzes, ferroelastic-ferroelectric coupling (*French*) 7-27674
- Pb_{1-x}La_xTi_{1-x/4}O₃ sputtered film struct., dielec., and pyroelec. props. studies 7-21724
- Pb_{1-x}La_xTi_{1-x/4}O₃ thin film pyroelectric infrared sensors 7-56338
- PbLaZrO₃TiO₃, electrostrictive ceramics, SAW transduction, electronic control 7-12450
- PbLiInSe, intercalation-layer compound, dielectric-metal cond. transition 7-7230
- Pb(M_{1/2}Sb_{1/2})O₃, perovskite type antiferroelectrics, (M=Sc, Ho-Lu), X-ray and dielec. characts. 7-7649
- Pb₂(MSb)O₆, M=Ti, Zr, Sn, Hf, pyrochlores, cryst. data 7-21171
- Pb(Mg_{1/3}Nb_{2/3})O₃ perovskite, prep. using Pb₂Nb₂O₃ and MgO 7-39468
- Pb(Mg_{1/3}Nb_{2/3})O₃ ceramics for microdisplacement actuators, electrostrictive characts. (*Japanese*) 7-17270
- Pb(Mg_{1/3}Nb_{2/3})O₃ ceramics, dielec. props. 7-46382
- PbMg_{1/3}Nb_{2/3}O₃ ceramic, elastic moduli and diffuse ferroelec. phase transition, press. depend. 7-63717
- PbMg_{1/3}Nb_{2/3}O₃, cryst. struct., electrocaloric effect, diffuse phase transition 7-22194
- PbMg_{1/3}Nb_{2/3}O₃, dynamic thermopolarisation effects 7-45922
- PbMg_{1/3}Nb_{2/3}O₃, ferroelectric, electrooptic props. 7-59180
- PbMg_{1/3}Nb_{2/3}O₃, single cryst. and ceramic samples, isotropic elastic moduli 7-6701
- PbMg_{1/3}Nb_{2/3}O₃, thermal expansion, effect of Mg and Nb substitution by divalent, trivalent, tetravalent and W⁶⁺ ions 7-63851
- PbMg_{1/3}Nb_{2/3}O₃-PbTiO₃, MnO doped, relaxor ferroelec. ceramics, dielec. ageing effects 7-22195
- Pb(Mg_{1/3}Nb_{2/3})O₃-Pb(Zn_{1/3}Nb_{2/3})O₃, ferroelec. powder, prep., solid solubility, Curie point (*Japanese*) 7-7945
- PbMgO₃NbO₃, electrostrictive ceramics, SAW transduction, electronic control 7-12450
- PbMn_{2/3}MO₃, perovskite-type cpds., (M=Mo, Te, Re), dielec. and mag. props. 7-7650
- Pb_{1-x}Mn_xTe, indirect exchange interaction between Mn²⁺ ions 7-27509
- PbMoO₄ crystals, point defects, absorpt. and fluoresc. props. 7-64674
- PbMoO₄, Czochevski grown, crystallisation front rel. to cryst. quality 7-59402
- PbMoO₄, optical radiation modulation by coherent ultrasonic excitation 7-27692
- Pb(NO₃)₂, phys. props., effective pot. calcs. 7-26692
- PbNb₂O₆-BiTiMO₆ (M=Nb, Sb), solid soln. ceramics, piezoelec. const. studies 7-2980
- PbO adsorbed γ-methacryloxypropyltrimethoxysilane, chem. reaction, Fourier transform IR spectra 7-53308
- β-PbO as cathode materials for voltage compatible Li cells 7-3632
- PbO chemically deposited layers, electrical props. 7-64377
- PbO, D₁-X²⁺ system, band intensities distrib. 7-50082
- PbO-B₂O₃ glass form., crystallisation 7-37875
- PbO-B₂O₃ flux, solubility of YIG, validity of anionic model 7-52062
- PbO-B₂O₃ optical glass, props. and structure, effect of heat treatment 7-20377
- PbO-B₂O₃-Fe₂O₃ glass, ESCA study 7-26651

lead compounds continued

- PbO-B₂O₃-SiO₂ glass dielec. thin films on anodised Al substrates 7-17269
- PbO-Fe₂O₃, binary phase diagram, DTA, X-ray diffr. meas. 7-46434
- PbO-Fe₂O₃-B₂O₃ glass ceramics, mag. props. and EPR spectra of precipitated mag. phases 7-45748
- PbO-Fe₂O₃-P₂O₅ glasses, liquid chromatography and Raman scattering studies 7-11946
- PbO-K₂O-Nb₂O₅, polymorphism, DTA, X-ray phase anal. 7-6782
- PbO-K₂O-Sb₂O₃-As₂O₃ flint type glasses, viscosity near annealing temp., depend. on PbO conc. 7-58151
- PbO-Nb₂O₅ oxide mixture transparent ferroelec. ceramics, phase form. during solid state reaction 7-6591
- PbO-Nb₂O₅-Sc₂O₃ oxide mixture transparent ferroelec. ceramics, phase form. during solid state reaction 7-6591
- PbO-SiO₂ glass, elastic props. and short- and medium-range structs. (Japanese) 7-65077
- PbO-SiO₂ glass, femtosecond nonlinearities using opt. Kerr effect 7-50660
- PbO-SiO₂ glass sputtered antireflection coatings on semiconductor laser facets 7-15964
- PbO-SiO₂ glasses, IR spectra 7-3036
- PbO-SiO₂ glasses, struct. anal., X-ray diffr. studies 7-6532
- PbO-SiO₂ mixtures, thermohomogenised layers, UV photoelectron spectra study 7-59370
- PbO-SiO₂-K₂O coloured and colourless glasses, near IR absorpt. temp. depend. study 7-13146
- β-PbO₂ as cathode materials for voltage compatible Li cells 7-3632
- PbO₂ at positive plates of Pb-acid battery, study using photoacoustic spectrophotometry 7-54283
- PbO₂ cathodes of Pb-acid battery, SnO₂ conductor stability 7-65440
- PbO₂, diffusion of H, electrochem. meas. 7-16807
- PbO₂ on positive plate of Pb-acid battery, effect of chemisorbed H₂O on elec. capacity 7-54284
- PbO₂-H₂O-based heterogeneous monotype systems, hardening and binding props. 7-65052
- Pb₃O₄ thin film, electronic props., electrochem. technique characterisation 7-7416
- Pb(Pb_{0.5})₂-Fe₂O₃ glass, struct. props., chromatography and Raman spectra studies 7-21112
- Pb₃P₄O₁₃, chemical prep., crystallographic study (French) 7-6589
- Pb₃P₂V₂-xO₈ mixed system, substitution defects, first order transition spreading 7-58458
- PbS, acoustic mode vibr. anharmonicity 7-63751
- PbS, density of states and effective mass determ. 7-38433
- PbS, epitaxial film, weak-field magnetoresistance, multi-valley model (Korean) 7-33114
- PbS ionised atomic clusters, fragmentation, TOF mass spectroscopic study 7-10807
- PbS polycryst. semicond. films, laser annealing effects 7-58317
- PbS/PbSe heterostructure, band offsets, photovoltaic study 7-58872
- PbS/PbTe 1D superlattice struct., X-ray diffr. patterns, coherent and heterophase scatt. 7-64733
- PbS-Bi₂S₃, chemically twinned phases, transformation to Galena struct. 7-12078
- Pb(S_{1-x}Te_x), quasibinary, phase diagram and miscibility gap calcs. 7-16764
- Pb_{1-x}(S_{1-x}Te_x)_y, solid solution, growth from vapour, region of homogeneity 7-46285
- 5PbS.2Sb₂S₃, boudangerite, elec. cond. (Korean) 7-27331
- Pb(S_{0.9}Nb_{0.5})O₃ ferroelectric ceramics, gamma, electron and neutron irradi. effects study 7-6677
- Pb(S_{0.9}Nb_{0.5})O₃ transparent ferroelec. ceramic production by hot pressing and props. 7-7934
- Pb(S_{0.9}Nb_{0.5})O₃, transparent ferroelectric ceramic, irradiation effects 7-59157
- Pb(S_{1-x}Nb_x)O₃ ferroelec. ceramics, IR optical and electrooptical props. studies 7-7675
- Pb(S_{1/2}Ta_{1/2})O₃, single crystals and hot pressed ceramics, ordering, domain struct., TEM obs. 7-26936
- PbSe and other IV-VI cpds., acoustic mode vibr. anharmonicity 7-63751
- PbSe, energy band structure, thermoelectronic study 7-3028
- PbSe films, elec. cond. and thermoelec. power, dynamic behaviour 7-2750
- PbSe films, photosensitivity mechanism 7-58923
- PbSe:Ag, electron irradi. stimulated impurity diffusion 7-63878
- PbSe:Cd, crystal growth and impurity distrib., electron probe X-ray microanal. studies 7-63639
- PbSe-PbS(Pb_{1-x}Sn_xSe)(Pb_{1-x}Eu_xSe) DH lasers with remote p-n junctions 7-57333
- PbSe-SnSe strained layer superlattice, prep. and struct. anal. 7-52301
- PbSe_{1-x}S_x epitaxial films, absorpt. edge, band gap, comp. depend., 77-300K 7-39063
- PbSe_{1-x}Te_x, optical absorpt. edge slope increase, comp. depend 7-39064
- PbSe₂Te_{1-x} thin films, localised defect states and Hall effect 7-2752
- Pb_{0.8}Sn_{0.2} Te epitaxial films, vacuum deposition growth in a quasiclosed vol. 7-46329
- Pb_{0.88}Sn_{0.12} Te cryst., annealing characts. and laser fabrication (Chinese) 7-10933
- PbSnEuTe, superlattices, prep. by hot wall epitaxy, props. (Japanese) 7-12546
- Pb_{1-x}Sn_x films, phase composition, fast-electron diffr. 7-63990
- PbSnSe, IR optical bistability at mW powers 7-57436
- Pb_{0.93}Sn_{0.07}Se, ferroelec. phase transition, electron-phonon interaction 7-13106
- PbSnTe as IR sensor material, characts. (Japanese) 7-56339
- PbSnTe BH laser reflectivity, lateral confinement effects 7-43090
- PbSnTe laser, single-mode, 8 μm with buried heterostructure, design 7-36980
- PbSnTe-TAGS and PbTe materials testing for PU238 special applications radioisotope thermoelectric generators 7-65500
- Pb_{0.75}Sn_{0.25}Te:In, Ge(S)(Se), elec. resist., photocond., Hall effect meas. 7-17050
- Pb_{0.8}Sn_{0.2}Te thin films, structural and elec. props., pulsed laser-irrad. effects study 7-21270
- Pb_{0.8}Sn_{0.2}Te:Ga solid solns., diffusion coeff., temp. depend. study 7-2254
- Pb_{0.8}Sn_{0.2}Te:In, impurity diffusion, thermoelec. probe meas. 7-63879
- Pb_{0.8}Sn_{0.2}Te-PbSe_{0.08}Te_{0.92} heterostruct., LPE prepared, characts. 7-52759
- Pb_{1-x}Sn_xTe films prepared by MOCVD, elec. props. 7-27919

lead compounds continued

- Pb_{1-x}Sn_xTe heterojunctions, supersymmetry, band-inverting contact 7-52717
- Pb_{1-x}Sn_xTe narrow-gap semicond., electron-electron interaction, effect on permitt., two-band model 7-52420
- Pb_{1-x}Sn_xTe quantum oscills. spectrum anal., two-window Fourier transform technique 7-52404
- Pb_{1-x}Sn_xTe solid solns., intrinsic defect donor states characts. Hall effect temp. depend. meas. 7-58762
- Pb_{1-x}Sn_xTe surfaces, AES, LEED and Kikuchi pattern obs. 7-52200
- Pb_{1-x}Sn_xTe:⁵⁷Br⁺, depth profiles, SIMS meas. and theoretical calcs. 7-6662
- Pb_{1-x}Sn_xTe:Bi, free carrier density 7-38572
- Pb_{1-x}Sn_xTe:In, impurity levels, covalent defect theory 7-52515
- Pb_{1-x}Sn_xTe-PbTe graded-gap heterostruct., spectral photoelec. quantum efficiency 7-36961
- Pb_{1-x}Sn_xTe_{1-x}Se solid soln. single crystals, density, comp., lattice const. and galvanomag. props. (Russian) 7-44500
- Pb_{1-x}Sn_xTe(S_{1-x}Se)IR photodiodes for 3 to 14 μm, comparison 7-41466
- (Pb_{0.9}Sr_{0.1})TiO₃, ferroelec. solid solns., dielectric and hysteresis props. 7-64588
- PbTe, acoustic mode vibr. anharmonicity 7-63751
- PbTe crystals, Bridgman growth in centrifuge, convection effects (French) 7-53542
- PbTe, diffusion controlled travelling heater method growth, thermal diffusion effect 7-53527
- PbTe doping superlattices, transport and magneto-optical props. 7-12852
- PbTe, epitaxial film, weak-field magnetoresistance, multi-valley model (Korean) 7-33114
- PbTe, ferroelec. phase transition, electron-phonon interaction 7-13106
- PbTe films and electrical contacts with Au, Al and Ag, photothermal deflection meas. 7-38784
- PbTe films grown by hot-wall epitaxy on KCl and BaF₂, TEM anal. 7-59432
- PbTe films prepared by MOCVD, elec. props. 7-27919
- PbTe heteroepitaxial films, low temp. lumin. 7-39157
- PbTe IR detector arrays, heteroepitaxial growth on fluoride-covered Si substrates 7-39429
- PbTe, impurity levels, covalent defect theory 7-52515
- PbTe, interband absorption in a mag. field, exciton states 7-22227
- PbTe, low-voltage electroabsorpt., exciton states, magnetoabsorpt. spectra 7-2501
- PbTe, mag. susceptibility, optical absorpt. spectra, effect of intrinsic defects 7-64670
- PbTe, narrow gap semiconductors, Knight shift 7-53166
- PbTe oxidised disordered films, magnetoresist. quantum oscills. obs. 7-64271
- PbTe single-cryst. films, negative photocond., slow relax. and photomemory 7-58832
- PbTe, solid and liquid states, electrophysical props. 7-52654
- PbTe, thermoelectric props., effect of dielectric inclusions 7-12746
- PbTe whisker crystals, Gunn-type oscills. 7-52626
- PbTe:Ga, doping during vapour phase growth, elec. props. 7-26774
- PbTe:Gd, mag. props. EPR study 7-53126
- PbTe:In, MIS struct., tunneling spectra of quasilocal impurity states 7-12869
- PbTe:In₁S_{0.2}, Soret effect, impurity cond. distrib., thermoelec. power meas. 7-44930
- PbTe:Mn²⁺, superhyperfine struct., EPR spectra 7-27595
- PbTe:O films, O diffusion to bulk and crystallite boundaries 7-63884
- PbTe:Ti, Na, carrier reson. scatt., effect on transport coeffs. 7-38602
- PbTe:Ti(Ti,Na) films, superconducting transition 7-38797
- PbTe/PbEuSeTe single quantum well diode laser with side optical cavity 7-43105
- PbTe-EuTe short period superlattices, props., appl. to laser diodes 7-52785
- PbTe-Gd₂Te₃ system, solid solns., synthesis and props. 7-21458
- PbTe-MnTe system, phase diagram, conductivity and thermoelectromotive force 7-63824
- PbTe-Pb_{1-x}Sn_xTe superlattice, quantum Hall effect 7-2682
- PbTe-Pb_{1-x}Sn_xTe superlattice, electronic structs., envelope pn. approx. 7-45465
- PbTe-PbEuSeTe, compositional and doping superlattices, struct., electronic, optical and magnetooptical studies 7-53290
- PbTe-PbEuTeSe multiquantum wells, electron-hole recomb., photolum. 7-13216
- PbTe-PbSnTe compositional and doping superlattices, struct., electronic, optical and magnetooptical studies 7-53290
- PbTe-Tb₂Te₃, solid solns., physicochemical anal. 7-21456
- PbTe-type narrow gap semicond., with antiphase boundary, physical realisation of parity anomaly 7-38432
- Pb_{1-x}Te:Ti, quasilocal level and transport props. 7-38492
- PbTeO₃, tetragonal phase, cryst. struct., X-ray diffr. study (French) 7-44466
- PbTe_{1-x}S_x epitaxial films, absorpt. edge, band gap, comp. depend., 77-300K 7-39063
- PbTe_{1-x}S_x, free carrier scatt. near a phase transition 7-38557
- PbTeSe layers, LPE growth on nonplanar (100) and (110) oriented substrates, laser appl. 7-17479
- PbTe_{0.92}Se_{0.08}:Ga solid solns., diffusion coeff., temp. depend. study 7-2254
- PbTe(S_{1-x}Se_x), energy bands, relativistic empirical tight binding theory 7-45149
- Pb(Ti,Zr)O₃ monolithic bimorph with internal electrodes 7-20559
- PbTiO₃, amorphous, with 10 mol.% B₂O₃, radial distrib. function determ., energy dispersive X-ray diffr. method 7-16420
- PbTiO₃ based glass ceramics piezoelectricity, pyroelectricity and ferroelectricity 7-7654
- PbTiO₃ ceramic; complex piezoelec. d₃₁ coeff., temp. behaviour 7-13097
- PbTiO₃, cryst. optical studies of precursor and spontaneous polarisation 7-45921
- PbTiO₃ crystals, ferroelec. transition, phase boundary kinetics 7-2990
- PbTiO₃, distorted cubic, crystn. and phase transform. 7-39548
- PbTiO₃, ferroelectric films, properties and applications 7-59156
- PbTiO₃, form. from metallo-organic precursors, kinetics 7-39465
- PbTiO₃ gels and films, hydrolysis conditions effect on characts. 7-46400
- PbTiO₃ piezoelectric fibres, synthesis by hydrothermal reaction (Japanese) 7-64974
- PbTiO₃, spontaneous strain, anomalous press. depend. 7-26833
- PbTiO₃:Cr³⁺, ceramic, EPR, ENDOR, ESE investigs. 7-13020

lead compounds continued

- PbTiO₃:Fe³⁺, F⁻ charge compensating cluster form., EPR spectra studies 7-64518
 PbTiO₃:La piezoelectric ceramics, vacancies, positron lifetimes 7-37980
 PbTiO₃-PbZrO₃-Pb(Mg_{1/3}Nb_{2/3})O₃ system, comp. fluctuation in solid soln. (*Japanese*) 7-28025
 PbTi_{1-x}Zr_xO₃ piezoceramic, annealing in gaseous media with controllable comp., effect on electrophysical props. 7-8012
 PbUO₄, cryst. struct. X-ray diff. study 7-44464
 Pb₃UO₆ struct. refinement, neutron powder diff. study 7-32370
 PbV₂O₆, vitreous and crystalline, mag. props. 7-7473
 Pb₃(VO₄)₂, β-γ transition, intermediate modulated struct. 7-2183
 PbWO₄, struct., X-ray, IR absorpt. and Raman spectra 7-37954
 PbWO₄:Nd³⁺(Pr³⁺), optical spectra 7-39146
 Pb₂Y₆F₃₂O₄, cryst. struct. determ. (*French*) 7-12016
 Pb_{0.98}Y_{0.02}Te, cyclotron resonance meas., k.p. model calcs. 7-27605
 Pb(Zn_{1/3}Nb_{2/3})O₃-PbTiO₃, perovskite ceramic powder, prep. dielec. and piezoelec. props. 7-46380
 Pb(Zr_{0.58}Fe_{0.20}Nb_{0.20}Ti_{0.02})_{0.995}O_{0.005} ferroelec. ceramic, TEM study 7-17272
 PbZrO₃, valence band struct., X-ray-electron spectra studies 7-12604
 PbZrO₃-based piezoelectric ceramics containing Pb(Zn_{1/3}Nb_{2/3})O₃ 7-2984
 PbZr_{1-x}Ti_xO₃-polyethylene 3-0 connected composite, dielec. and piezoelec. props. 7-45937
 Pb(Mg,Zn)_{1/3}Nb_{2/3}O₃, prep. and ferroelec. props. (*Japanese*) 7-27993
 PbTe: Cd, free charge carrier conc., donor action and Te precipitates effects (*Russian*) 7-16592
 α-PgZrF₆, ionic conductivity 7-52129
 Rb₂Pb₄Nb₁₀O₃₀, ferroelectric with tetragonal W-bronze struct., first-order transition 7-39048
 Sb₂S₃-PbS systems, non-stoichiometric phases close to Sb₂S₃, structure 7-32674
 SiO₂-K₂O-PbO glass melts, evaporation 7-2160
 Sr(La_{1/2}Nb_{1/2})O₃-PbZrO₃-PbTiO₃, hot-pressed ceramics, dielectric, piezoelectric and optical props. 7-64583
 V₂O₅-TeO₂-PbO, glass, elec. and optical props. (*Korean*) 7-27330
 (1-x)V₂O₅-xPbO, phase diagram in V₂O₅-rich region (*French*) 7-12265
 ZrF₄-PbF₂-AlF₃-LiF-KF glasses, mixed alkali effect, DC cond. 7-63873
 ZrF₄-PbF₂-AlF₃-NaF-KF glasses, mixed alkali effect, DC cond. 7-63873

leak detection

- gross leak calibration 7-18794
 JET, ⁴He leak detection in the presence of high D₂ partial pressure 7-49675
 pump gauges, leakage characteristics 7-48766
 steam turbine condenser leakage detectors (*Czech*) 7-61988
 vacuum, leak calibration using mass spectrometer 7-61348
 vacuum, leak standards, National Bureau of Standards program 7-61347
 vacuum technology survey, applications and prospects (*French*) 7-322
 He sniffing method for locating fine leaks (*Japanese*) 7-9840

leakage, electrical *see electrical faults***leakage, magnetic** *see magnetic leakage***leakage currents**

- bipolar batteries with common electrolyte paths, leakage currents 7-28392
 earth leakage circuit-breaker protection (*German*) 7-3782
 Si:BF₂⁺ p⁺-n diodes, BF₂⁺-implanted and rapid thermal annealed, junction leakage currents meas. 7-12814
 Ta₂O₅ films for MOS DRAMs using ultra-high purity Ta sputtering target 7-59423

learning systems

- see also adaptive systems; cognitive systems; self-adjusting systems*
 autoassociative neural network, influence of noise on behaviour 7-54525
 conf., Los Alamos, New Mexico, USA (May 1985) 7-48157
 evolutionary learning and intraneuronal dynamics 7-54434
 memory, associative recall by neural network, biological system appl. 7-54521
 neocognitron, biocybernetic approach to visual pattern recognition 7-57258
 neural network model, teachable, based on unorthodox neuron system 7-54435
 neural networks and optical resonators, coupled-mode theory 7-54513

least squares approximations

- chemometric analysis of multisensor arrays 7-8344
 cubic B-splines in least-squares smooth fitting for irregularly spaced data 7-47555
 detecting system response function determ. 7-62240
 diffusion theory, least squares principle to unify finite element, finite difference and nodal methods 7-56194
 digital terrain model for flat areas by least squares techniques on mini-computer 7-40410
 ECG, power line interference estimation and removal 7-65863
 eddy current flaw inversion algorithm, experimental verification 7-54059
 electrostatic membrane mirror, configuring by least-squares fitting 7-31422
 EM scattering and eigenvalue problems, numerical solution, hybrid technique 7-50478
 FEM transport methods, generalized least squares as generator of variational principles and weighted residual methods 7-19321
 Gibbs free energy calc., symmetric minimum-norm updates 7-39912
 global irradiation estimation, Angstrom equation fitted using least squares method, Italy 7-55215
 heat equation, ill-posed Cauchy problem, error estimates for numerical method 7-50932
 linear and nonlinear least squares computing for nuclear data eval. 7-606
 nuclear medicine images, digital restoration by two-step procedure 7-14121
 nuclear spectra deconvolution using the least squares method 7-19203
 object-field reconstruction, ill-posed problems, precision 7-42966
 oceanographic data analysis, least-squares method as filter and related power in spectrometry 7-40575
 overdetermined systems of linear inequalities, projection method for least squares solns. 7-61079
 plate bending element, bilinear, force evaluation 7-57707
 position-sensitive-detector data, integration of overlapping peaks by least-squares fitting 7-11843
 positron lifetime spectra, multicomponent anal., reliability tests 7-39287
 seismic tomography for 3D struct. and vel. determ. 7-29268
 superresolving deconvolution by nonnegative leastsquares method (*Japanese*) 7-10875
 Thomson scattering meas., photoelectron statistics effects 7-11800

least squares approximations continued

- transonic flows, least squares FEM for simulation 7-26309
 He-like atoms, bound states, least-squares calc. 7-49883

leather *see materials***LEC growth** *see crystal growth from melt***LED** *see light emitting diodes***LED displays** *see electroluminescent displays***ledeburitic steel** *see alloy steel***Lee model**

- Walecka and Friedberg-Lee field theory models, nonlinear coupled diff. eqn. soln. method 7-61444

LEED *see low energy electron diffraction***legislation**

- commercial satellite remote sensing 7-14398
 RF radiation regulations 7-28605

length measurement

- see also micrometry*
 best wave interferometer with Zeeman laser for measuring short range 7-18752
 F_A(II) colour centre laser at 2.653 μm, synchronously pumped, mode-locked, cavity length meas. 7-5920
 glass standards, geometrical dimens. stability with time 7-41328
 interferometers, electronic processing of interferograms 7-4886
 laser differential Doppler gauge for contactless meas. of speed and length 7-24628
 meter practical realisation, using light interferometer (*Slovak*) 7-61316
 nuclear fuel pin, dimensions determ. by neutron radiography, moments anal. method 7-25035
 optical images, scene geometry, length determ. 7-41340
 OTDR for optical fibre cable meas. 7-14994
 resolution improvement of length measuring systems with CCD arrays (*German*) 7-61312
 SEM appl. to short lengths meas. 7-4812
 sensitivity improvements (*Japanese*) 7-48690

length standards *see measurement standards***Lennard-Jones and Devonshire theory** *see liquid theory***Lennard-Jones potential**

- 2D Lennard-Jones system, determination of algebraic exponents near the melting transition 7-51992
 amorphous Lennard-Jones solid, shear deform.-induced orientational ordering, computer simulation 7-38155
 amorphous materials, vapour phase growth, mol. dynamics study 7-1886
 anharmonic cryst. stability, Lennard-Jones pairwise pot. anal. 7-32356
 atomic clusters, classical pot. energy surfaces investigated using simulated annealing method 7-62556
 binary mol. liq. mixtures, statistical mechanical local composition theory, mol. size and energy difference effects 7-32248
 binary-gas mixtures, phys. props. prediction, SSR-MPA and MSK pots. 7-51361
 crystal growth, Monte Carlo simulation 7-6568
 FCC (110) surface, cooperative premelting effects, molecular dynamics simulation 7-16852
 fluid, 2D, virial eqn. of state 7-6747
 fluid, behaviour in narrow pores 7-32250
 fluid mixtures, infinite-dilution activity coeffs., computer simulation 7-16383
 fluids of optically isotropic mols., collision-induced light scatt. 7-33405
 forward and inverse elastic scatt., cross section/potential surface dependence anal. 7-20000
 glassy order in quenched 2D Lennard-Jones systems, Monte Carlo study 7-63494
 hard-sphere mixtures interacting through attractive Yukawa tail, phase stability 7-11873
 HCL, condensation on charged CO₂ walls, Stockmayer model calcs. 7-63784
 interspecies transfer of momentum and energy in disparate-mass gas mixtures 7-42734
 Lennard-Jones crystals, free energies, mol. dynamics calc. 7-12318
 Lennard-Jones fluid, Kirkwood theory of shear viscosity 7-37821
 Lennard-Jones system, close to glass transition, dynamics 7-38198
 linear molecules, molecular dynamics with vector computer 7-50285
 lipid bilayer, mol. dynamics simulation 7-40115
 liquid, shear thinning and thickening, mol. dynamics study 7-11869
 liquids, Lennard-Jones, wavevector-depend. shear viscosity 7-58518
 methanol. liq., cross-correl. fn., diffusional dynamics study 7-37822
 mixtures, gas solubility Henry coeffs. determ., WCA-LL-GH perturbation theory calcs. 7-6799
 molecules, nonlin. multicentre with anisotropic reference system, thermodynamic perturbation theory 7-11882
 monolayer films, equilibrium configurations, molecular dynamics simulations 7-21771
 nonpolar polyatomic fluids, Lennard-Jones parameters (*French*) 7-6488
 organic sulphur cpds., liq., Monte Carlo simulations, develop. of suitable intermol. pot. fns. 7-31140
 phase transitions in adsorbed films, monolayer adsorption, perturbational approach 7-21665
 pyrazine-d₄, spectral anal., Lennard-Jones-H-bonding pot. energy calcs. 7-5734
 pyrazine-d₄-pyrimidine, spectral anal., Lennard-Jones-H-bonding pot. energy calcs. 7-5734
 pyrazine-h₄-pyrazine-d₄, spectral anal., Lennard-Jones-H-bonding pot. energy calcs. 7-5734
 pyridine-water complexes, intermolecular pot. functions 7-62480
 quasicrystal equilib. state of two-component 2D Lennard-Jones system, Monte Carlo simulations 7-58148
 repulsive Lennard-Jones fluid sound dispersion, density depend. 7-12212
 second virial coeffs., semi-theoretical correl., temp. depend. Lennard-Jones pot. calcs. 7-6749
 self-diffusion constant, Green-Kubo and nonequilib. calcs. comparison 7-52100
 shear thinning of Lennard-Jones fluid, mol. dynamics study 7-21059
 Stockmayer fluid between Lennard-Jones plates, mol. dynamics study, electric field effect, polarisation 7-21060
 superlattice interfaces, two-dimensional Lennard-Jones strained layer systems, Monte Carlo stability anal. 7-2398
 two-centre Lennard-Jones fluids, phase equilibria 7-32610
 Al (110), Ar ion damage production, mol. dynamics simulation 7-58378
 Ar-Kr liquid mixtures, diffusion coeffs., simulation 7-44344

Lennard-Jones potential continued

- Ar-Ne mixture, density meas. up to 8000 bar, Lennard-Jones comparison 7-1669
 CO₂, liq., neutron radial and partial distrib. fns., Lennard-Jones pot. 7-58126
 Cu, (100) surface self-diffusion of H isotopes, substrate motion effects 7-38237
 HBr+K(Li), elastic scatt., complex Lennard-Jones pot., WKB calcs., Regge Pole anal. 7-36724
 H₂S, liq., Monte Carlo simulations, develop. of suitable intermol. pot. fns. 7-31140
 He-Ar mixture, density meas. up to 8000 bar, Lennard-Jones comparison 7-1669
³He, liquid, binding energy, many-body correlations 7-6910
 N₂, liq. and fluid press., intermol. pots. comparison, mol. dynamics simulation 7-63419
 O₂-N₂ equimolar liq. mixture, excess props. and struct., mol. dynamics simulation 7-32246
 SO₂ vapour, second virial coeff., intermol. pair pots., mol. dynamics simulation method study 7-31908
 SO₂+Ar, intermol. energy transfer, trajectory study, rovibrational mol. energy depend. 7-31151
 SiO₂, vitreous, surface, adsorption and thermal accommodation of Pt single atoms 7-27133

lenses

- see also aberrations; aspherical lenses; contact lenses; electron lenses; electrostatic lenses; focusing; magnetic lenses; photographic lenses
 aberration characteristics of nonsymmetric systems 7-50689
 aberration coefficients, third order, target values 7-50688
 aberration field properties of simple non-axially symmetric optical systems 7-50691
 aberration-corrected systems, design principles 7-50687
 achromatic aplanatic lenses, design 7-62806
 achromatic combinations of holographic and refractive optical elements 7-50716
 achromatic mirror lens with corrected opening aberration (Czech) 7-62810
 achromatic single-component kinoform objective, with circular aberration coeff. 7-25737
 acoustic microscope, elastic wave propag. focusing props. of small-aperture lenses 7-43473
 acoustic microscope planar focusing lens design and operation 7-1341
 airspace apochromats, glass selection using Buchdahl dispersion eqn. 7-43274
 alignment of diffraction and refraction components in optical systems 7-25925
 apochromatic optical system design 7-43312
 aspheric ophthalmic lenses optimisation, Tscherning theory generalisation 7-65891
 beam deflection as a method for testing optical components 7-20475
 binocular objective design, gradient-index 7-31414
 biocular magnifiers and design methods 7-50695
 CAD, EASE development and user friendliness 7-57514
 Cartesian oval fibre-optic lens as linear to angular position converter 7-43407
 Cassegrain telescope with spherical lens corrector, image quality improvement (Chinese) 7-4331
 cement contact, heat resistance depend. on construction parameters 7-43299
 centering accuracy meas. of cylindrical lens, noncontact interferometric technique 7-15962
 ceramics NDT by acoustic microscopy with single zoom lens 7-3570
 chromatic aberration, longitudinal, pseudocolour effects, metrology appl. 7-42953
 cineform element synthesis, optical method based on multi-beam interferometry (Russian) 7-50794
 compensated spherical surfaces in optical systems 7-25924
 conic constant and paraxial radius of curvature measurements for conic surfaces 7-20474
 copying lenses, requirements for use in devices for information entry by holography 7-20383
 coupling of laser diodes to monomode elliptic core fibres using lens 7-20426
 cylinder lens design for X-ray laser 7-43317
 cylindrical kinoform lenses for monochromatic light, with long focal length 7-25923
 cylindrical microlenses with graduated refractive index, appls. (Italian) 7-15961
 design, aberration theory and the meaning of life 7-50678
 design, antirefl. coating parameters introduction in design phase 7-50680
 design, aspheres use 7-50690
 design, automatic, use of multi-image plane merit function 7-43310
 design, Brixner optimisation procedure 7-50683
 design, condition for obtaining pre-specified astigmatism 7-20384
 design, conf., Cherry Hill, USA (June 1985) 7-48161
 design, glass combinations selection method for aberration correction 7-50684
 design, interactive computer program 7-50693
 design, interactive ray-tracing program integrated with solid-modelling CAD system, Traz program 7-50679
 design, merit function construction with possible achievement of global min. 7-50682
 design innovations 7-50674
 design program, intelligent, development 7-50676
 design program by microcomputer with artificial intelligence 7-50677
 design program using simultaneous linear inequalities, improved version 7-50681
 design software, human dimension 7-50675
 dichromated gelatin transmission HOEs, reflective and refractive optics 7-25748
 diffraction, high-resolution projection objectives design 7-25922
 diffuser with controlled divergence 7-5969
 distributed-index planar microlens and stacked planar optics: a review of progress 7-31416
 elastomers, impurity containing, exposed to laser pulses, thermooptic lenses, form. kinetics 7-51671
 eye, excised crystalline lens, computer assisted scanning laser monitor for optical quality meas. 7-23507
 fibre, single-mode with wide acceptance angle, design using flat disc lens 7-43406

lenses continued

- finished lens moulding technology saving time and money 7-31535
 focus of high-numerical-aperture objectives, light distribution 7-43290
 Fresnel lenses, proton exchanged, in LiNbO₃:Ti waveguides 7-31522
 Gaussian beam diffracted through finite lens, focus 7-42893
 Gaussian beam focusing through hemispherical microlens 7-11090
 geodesic lens family design, theoretical analysis 7-57507
 geodesic, short-focus, spherical aberration 7-43295
 graded-index, light distribution near foci 7-43287
 gradient index imaging systems, conf., Palermo, Sicily, Italy (Sept. 1985) 7-29570
 gradient index lens for low-loss coupling of laser diode to single-mode fibre 7-31465
 gradient index lenses, ray tracing, computation of ray-surface intersection 7-31418
 gradient index lenses for fibre optic thin film temperature sensor 7-25992
 gradient-index slab lens with high numerical aperture, indiffusion ion exchange and cementing fabrication 7-31415
 GRIN lens with revolution symmetry, paraxial Fourier transforming and imaging props. 7-31420
 GRIN lenses, optical performance assessment 7-31538
 GRIN-rod lenses used in single-mode optical devices, aberration anal. 7-31421
 half-lenses for office copiers, comparison 7-43316
 Hermite-Gaussian beam transformation by shifted spherical lens 7-42891
 holographic diffractive optics for head-up displays 7-25749
 holographic image lens, optimal design 7-43007
 holographic lens for laser beam expansion, design 7-62812
 holographic lens using polyvinyl carbazole material, aberration correction 7-25745
 holographic lenses, on-axis, coupled-wave anal. 7-5839
 HP program to determ. centre thickness of convex spectacle lenses 7-14158
 induced thermal lens, spatial Fourier spectrum anal., for studying thermal conductivity and diffusivity 7-12379
 integrated optical lens design using GRIN lens techniques 7-43449
 ion implanter, ion beam transport system, ion-optical characteristics (Korean) 7-24723
 IR components with diamond-like coatings development, appl. and testing 7-31434
 IR Fresnel lenses design and manufacture at British Aerospace, using high-density polyethylene 7-31428
 IR imaging system, scanner lens design considerations 7-50704
 IR imaging system design, critical issues 7-50673
 IR lens elements and assemblies, spectral transmission meas. 7-31429
 IR lenses MTF determ., line-spread and interferometric results comparison 7-31430
 IR objective, use of proustite crystal in performance meas. 7-57511
 IR objective testing, holographic method using graphitised photographic emulsions 7-57513
 kinoform lens fabrication errors, effect on pupil function 7-25739
 large-F-number systems, aperture-lens separation effect on focal shift 7-57231
 laser image plotter for high-information-density images recording 7-26043
 laser-diode/multimode-fibre coupling: analysis using a planoconvex GRIN lens 7-31480
 lens decentering, speckle interference display 7-43301
 long focus objective, holographic method of testing, optimum conditions calc. 7-57512
 matrix of gradient microlenses fabricated by electrostimulated diffusion, optical connectors development 7-25967
 micro-Fresnel lens arrays, rectangular-apertured, fabrication by electron beam lithography 7-57505
 microlens, planar distributed index highly integrated, characts 7-43448
 microscope objective, four-element, design 7-43313
 microscope objectives, low-magnification, design and testing 7-43298
 MTF analyzer, microcomputer and dynamic RAM chip camera based 7-47
 multicomponent lens system, design of individual components, singlet use 7-20379
 ocular lens, radiation dose in radiology of the orbit 7-40292
 ocular lenses, human, diagnostic evaluation using quasi-elastic light scatt. spectroscopy 7-34230
 ocular lenses, human, in vivo meas. using quasielastic light scatt. 7-34231
 ophthalmic lens design using spline surfaces 7-54813
 ophthalmic spherocylindrical lenses, dioptric power in an off-axis meridian: the torsional component 7-40140
 optical lens systems, antennas explanation (German) 7-20381
 optimisation, automatic, recent improvements 7-43309
 optomechanical design, annotated bibliography 7-35142
 phase contrast objective, point spread function in spherical aberration presence 7-37084
 phase-contrast objectives, calc. of allowable aberrations 7-57510
 photovoltaic 22.5X linear Fresnel lens concentrator module using Si solar cells 7-17873
 planar microlens, fabrication by transverse electromigration method 7-62811
 planar microlens fabrication by ion exchange/diffusion, distrib. index profile 7-31417
 polarisation aberration coefficients 7-50686
 process testing of precision lenses 7-50796
 progressive addition lenses, peripheral power variations 7-34337
 projection lenses for light-valve display 7-50701
 push-broom linear array scanner, design of all-reflective flat-field objective 7-55320
 reversible lens, limitations on performance 7-50694
 Ronchi test with daylight illum. for testing mirrors and lenses 7-11180
 soft X-ray lenses for X-ray microscopy, UV-holographic lithography fabrication 7-35652
 space camera lenses, design 7-43314
 spherical gradient-index sphere lens, modified suspension polymerisation fabrication 7-31527
 standardisation of radii of curvature for lens design and fabrication 7-31413
 systems incorporating zero power corrector, design principle and appl. 7-50702
 systems incorporating zero power corrector, objectives and magnifiers for night vision appls. 7-50703

lenses continued
testing method based on boiling phenomenon of laser speckle 7-43319
tetrode lens system for Ga liquid ion source at low emission currents 7-30798
thermal-wave lens, ray diagrams, focusing 7-54046
thin linear axicon produced diffraction patterns and zone plates 7-37083
transform performance using holographic lenses, theory 7-10868
TV projection lens, wide-angle, design 7-50699
two-lens cemented objective, struct. parameters automated calc. 7-37085
variable focus, single lens, 3 CRT dichroic color graphics projector 7-25933
vector aberration theory and the design of off-axis systems 7-50685
wavefront sensor, integrated optical, lens focusing onto detector array 7-26041
Wood and GRIN rod lenses, third- and fifth-order aberrations 7-31419
Zeiss Gradal HS progressive addition lens, designs using splines, max. wearing comfort 7-50712
zoom convertor with focusing and thermal compensation functions 7-31516
zoom lens tolerances and design concepts 7-31426
zoom lens with built-in range extender, paraxial anal. 7-50696
zoom systems, four element with optomechanical compensation system, design 7-50711
GaAs Fresnel waveguide grating lenses, aberration corrected, simulation 7-26036
GaAs-GaAlAs diode laser array, diffraction-limited emission, aperture graded-index lens external cavity 7-11005
Ge lenses, diamond-machine for IR, quality and performance 7-25932
Si substrates, curved for multilayer X-ray reflective lenses 7-41566

lepton decay
see also muon decay
heavy fermion production and decay via W bosons, helicity projection techniques 7-61762
heavy leptonium, radiative corrections to one-photon annihilation leptonic decays 7-35871
single electron search expt., sparticle mass limits 7-49142
unstable heavy neutrinos, constraints from cosmology 7-34860
 α decay modes, standard electroweak model predictions 7-41804
 E^+ (heavy lepton) $\rightarrow N_{\mu}^+ + \nu_e + e^+ + \mu^+ + W^- + \nu_\tau$, preon model anal. 7-56524
 $L^- \rightarrow \text{udd}(\text{c} \nu)$ (L =heavy lepton), event search at CERN collider 7-61680
 $\nu_e \rightarrow \gamma X$, heavy ν , lifetime constraints from primordial light-element photodestruction anal. 7-10059
 $\nu_e \rightarrow \nu_\gamma$, lifetime in left-right models 7-35764
 $\nu_e \rightarrow W^+ W^- e$, massive neutrino decay probability calcs. in steady magnetic field, polarization effects 7-5089
 $\nu_e \rightarrow \mu + \text{majoron}$, Sun-Earth decay problem, triplet majoron model anal. 7-61673
 $\nu_\mu, \mu_e \rightarrow \nu_\tau$ oscillations limits, $\nu_\mu, \mu_e \rightarrow \tau^-$ direct coupling 7-35768
 $\tau \rightarrow 3\pi \nu_\tau$, 3π spectral function, implications for A_1 mass 7-49141
 $\tau \rightarrow e \bar{\nu}_e \nu_\tau$, ν_τ mass limits 7-24884
 $\tau \rightarrow \mu \nu_\tau$, branching ratio determ. 7-15142
 τ , neutrinoless decay, lepton-number and lepton-flavour violation search 7-61675
 $\tau \rightarrow \nu, \pi$, branching fraction meas. 7-49144
 $\tau \rightarrow \nu \gamma \tau(\rho)$, radiative 3-body decays 7-15152
 $\tau \rightarrow \mu \nu_\tau, K^* \nu_\tau$, branching ratios, effects of asymptotic flavour symmetry, QCD anal. 7-49143
 τ^- branching ratio meas. 7-61677
 $\tau^- \rightarrow \nu_e e^- \bar{\nu}_e, \nu_\mu \mu^- \bar{\nu}_\mu$, branching fraction meas. 7-61676
 $\tau^- \rightarrow \nu, \pi, \nu_\mu \pi^-, \nu_\mu \pi^0$ ($n\pi, n \geq 1$), branching fraction meas. 7-61676
 $\tau^- \rightarrow \nu, \pi, \pi^0 +$ neutral meson(s), inclusive branching fraction meas. 7-15154
 $\tau^- \rightarrow \nu, \pi, \pi^+ \pi^-, \nu_\mu \pi^+ \pi^-$ ($\pi^0, n \geq 0$), branching fraction meas. 7-61676
 $\tau^- \rightarrow \omega \pi^- \nu_\tau$, branching ratio meas., $e^+ e^- \rightarrow \tau^+ \tau^-$ expt. 7-61674
 $\tau^- \rightarrow \pi^+ \pi^- \pi^- \nu_\tau$, branching ratio 7-35874
 $\tau \rightarrow e \mu \nu_\tau$, branching fraction meas. 7-41805
 $\tau \rightarrow \mu \nu_\tau$, branching fraction meas. 7-41805
 $\nu_e \rightarrow \gamma$, decay rate calc. in E_8 superstrings 7-30266

lepton-deuteron interactions
see also lepton-deuteron scattering
 $\bar{e}d \rightarrow e^+ p$, neutron electric form factor 7-35880
 $ed \rightarrow e p n$, dynamics in light cone, nucleon form factors (Russian) 7-15165
 $ed \rightarrow e p n$, quantum field theory, projecting properties on the light front and suppression of loop diagrams 7-41669
 $ed \rightarrow e p n$, final state interaction effects, vertex fns., Feynman diagram anal. 7-5100
 $\nu d \rightarrow e p p(e^+ n n)$, exchange currents effects, solar neutrino problem soln. 7-56537
 $\nu_\mu d \rightarrow K X$, 1-5 GeV, nucleon decay search implications 7-19116
 $\nu_\mu d \rightarrow \mu p p$, pion exchange current effects 7-56559
 $\nu_\mu d \rightarrow \pi X$, 1.6 GeV, exclusive π production anal. 7-19117

lepton-deuteron scattering
see also lepton-deuteron interactions
 $ed \rightarrow e^+ d$, cross-section asymmetry 7-41820
 $ed \rightarrow ed$, relativistic corrections to polarisation tensor 7-41821

lepton electric moment
e electric dipole moment anal. in E_8 superstring models 7-61651
e electric dipole moment bounds in a wide class of models 7-41815
e electric dipole moment in SUSY electroweak model anal. 7-10065

lepton-hadron interactions
see also lepton-hadron scattering; lepton-nucleon interactions
deep inelastic scattering, higher-order QCD perturbative corrections, exponentiation 7-49158

lepton-hadron scattering
see also lepton-hadron interactions; lepton-nucleon scattering
 $e\pi$ scattering, $E_\pi=300$ GeV, space-like pion EM form factor meas. 7-10062

lepton interactions see lepton-deuteron interactions; lepton-hadron interactions; lepton-lepton interactions

lepton-lepton interactions
see also electron-electron interactions; electron-positron interactions; lepton-lepton scattering; neutrino-electron interactions; neutrino-neutrino interactions
 $l^+ l^- \rightarrow \gamma \gamma$, partial wave anal. QED 7-49126

lepton-lepton scattering
see also electron-electron scattering; electron-positron scattering; lepton-lepton interactions; neutrino-electron scattering; neutrino-neutrino scattering
No entries
lepton magnetic moment
electron, anomalous magnetic moment, constraint on composite weak-interaction bosons 7-523
electron, radiative mass and g-2, QED between conducting plates 7-457
family replication constraints on preonic model from lepton anomalies mag. moment 7-49098
e anomalous magnetic moment at finite temperature, mass shift, QED anal. 7-5096
 μ anomalous magnet moment meas., proposed precision expt. 7-36349
 ν , superstring-induced mass and mag. moment 7-35824
 ν_μ charge radius and dipole moment, limits from $e^- \nu_\mu \rightarrow e^- \nu_\mu$ 7-56438
 μ anomalous mag. moment, supersymmetry corrections in $N=1$ supergravity 7-35876

lepton mass
charged lepton mass, gauge field theory 7-61433
double β -decay rates and ν mass calcs. 7-41943
 $E_8 \times E_8$ superstring theory, p mass constraints 7-41686
electron, radiative mass and g-2, QED between conducting plates 7-457
fermion mass determination, Weinberg model 7-49021
fourth generation charged lepton, mass limit from missing transverse energy events W^\pm -heavy leptons 7-61680
Gelmini-Rondadelli model, one-loop renormalisation group anal., ν mass generation 7-24817
hierarchical quark-lepton masses and intermediate massscale in GUT 7-5016
large-N QED₃, dynamical mass generation 7-19061
lepton spectrum derivation using the TLVP EM model 7-61638
light Dirac neutrino in left-right-symmetric models 7-41681
minimal composite model, square root sum rule 7-49097
neutrino from ^{169}Yb , β -decay, natural widths meas. 7-49322
neutrino mass, lepton flavour and lepton number nonconservation 7-9989
neutrino mass in superstring model 7-48499
neutrino masses and mixings, review 7-61531
neutrino masses in extended Weinberg model 7-15104
neutrinoless double beta-decay, neutrino mass, interaction properties 7-41947
neutrinos in early Universe, mass and decay 7-4596
nonassociativity as the generating source of the mass levels of hadrons and leptons 7-61637
preon model with three SU_3 hypercolours and three SU_5 hyperflavours, lepton mass calcs. 7-49026
pseudo-Dirac ν as possible explanation of solar ν puzzle 7-56481
right-handed neutrinos, mass limits in left-right symmetric models 7-56498
 $SO(10)$ GUT, neutrino see-saw and mass matrix 7-24815
solar ν problem, Mikheyev-Smirnov-Wolfenstein mechanism and pseudo-Dirac ν 7-24819
 $SU(2) \times U(1)$ gauge theory, Majorana D and CP violation in leptonic sector 7-24790
superstring neutrino mass problem without high intermediate energy scale, soln. search 7-15096
unified left-right symmetric model of massive neutrinos with conserved lepton number 7-30224
unstable heavy neutrinos, constraints from cosmology 7-34860
upper mass limits in model analysis 7-19006
e anomalous magnetic moment at finite temperature, mass shift, QED anal. 7-5096
 \bar{e} mass limits in sparticle production expt. 7-49142
mass determination from T beta-decay, molecular effects in alkane cpds. 7-49310
 $\mu N \rightarrow e N$, massive neutrino bounds, $SU(2)_L \times U(1)$ anal. 7-19112
n beta-decay, mag. field effects, spin effects and ν mass 7-41800
 ν , massive, electroweak model anal. 7-56488
 ν , superstring-induced mass and mag. moment 7-35824
 ν mass, review of props. 7-30218
 ν mass and nuclear beta-strength, cosmological and astrophysical consequences 7-48129
 ν mass experiments 7-35748
 ν mass in Fritzsch-Steck quark model in $SO(10)$ 7-61547
 ν mass limits from ^{76}Ge neutrinoless double beta decay 7-49340
 ν mass matrix in E_6 model 7-56474
 ν mass measurement from ^3H bound-state β -decay 7-56643
 ν masses and mixing angles in $SO(10)$ model 7-61525
 ν masses in $SO(18)$ unified model 7-452
 ν masses in superstring models 7-453
 ν rest mass meas., anal. from ^3H beta-spectra meas. 7-5201
 $\bar{\nu}_e$ mass, upper limit determ., ^3H beta spectrum meas. 7-35975
 $\bar{\nu}_e$ mass, upper limit determ. from ^3H beta spectrum endpoint meas. 7-35976
 ν_e mass, upper limit determ. from ^3H beta spectra meas. (German) 7-35978
 ν_e mass, weak forces and oscillations (Danish) 7-440
 ν_e mass upper limit, ^{163}Ho electron capture expt. 7-56645
 ν_e mass using ^{163}Ho electron capture 7-30383
 ν_e masses and L parity in E_6 superstrings 7-19048
 ν_τ mass in E_6 superstrings 7-30266
 ν_τ mass limits 7-24884
 ν_τ Majorana type, mass limits in ^{76}Ge $0\nu\beta\beta$ -decay expts. 7-61841
 ν_e Majorana mass upper limit from ^{76}Ge double beta decay experiments 7-41942
 $\bar{\nu}_e$ mass limit in free molecular tritium decay 7-56652
 $\bar{\nu}_e$ mass upper limit from tritium beta decay 7-56651
 ν_e mass meas. using ^{163}Ho electron capture 7-56653
 ν mass limits from neutrinoless double beta decay expts. 7-49335
 T_2 β -decay energy spectra, HeT^+ electronic reson., and neutrino mass depend. 7-61840

lepton-nucleon interactions
see also electron-nucleon interactions; lepton-nucleon scattering; muon-nucleon interactions; neutrino-nucleon interactions
deep inelastic scatt., impulse approx. and scaling variable modification 7-527
deep inelastic scatt., large transverse momentum parton behaviour (Chinese) 7-24849
EMC effect, reanalysis of nucleon quark structure changes 7-61688
 LN , polarised deep inelastic scatt. from cloudy bag model 7-49159

lepton-nucleon interactions continued

- LN \rightarrow X, deep inelastic scatt., two-photon collisions 7-19115
 LN \rightarrow X, deep inelastic scatt., direct interaction hypothesis 7-49160
 LN \rightarrow X, EMC effect in terms of knock out reactions 7-49150
 LN \rightarrow X, structure functions and parity violation in supersymmetric QCD 7-61700

lepton-nucleon scattering

- see also *electron-nucleon scattering; lepton-nucleon interactions; muon-nucleon scattering; neutrino-nucleon scattering*
 e(μ , τ)N elastic scattering, nucleon form factors from polarized lepton scatt. 7-56556

lepton-nucleus reactions

- see also *electron-nucleus reactions; lepton-nucleon interactions; muon-nucleus reactions; neutrino-nucleus reactions*
 EMC effect, nuclear dependence of structure functions 7-56602
 EMC effect, QCD and Fermi gas model interpretations 7-15188
 EMC effect, quark and antiquark distrib., Q^2 rescaling approach 7-30316
 EMC effect, reanalysis of nucleon quark structure changes 7-61688
 EMC effect, SLAC data reanalysis and x rescaling 7-49233
 (I, ϕ)X, nuclear enhancement effect, colour oscillation mechanism 7-41987
 (I,X), deep inelastic scatt., quasi-elastic peak as unstable state 7-10137
 (I,X), deep inelastic scatt., two-photon collisions 7-19115

lepton-nucleus scattering

- see also *electron-nucleus scattering; lepton-nucleon scattering; muon-nucleus scattering; neutrino-nucleus scattering*
 deep-inelastic processes, nuclear binding, two body short range correlation effects 7-49386
 (I,I'), deep inelastic process, colour conductivity model anal., nuclear shadowing phenomenon and binding energy comparisons 7-49385
 $^{12}\text{C}(I,I')$, inclusion of two body short range correlation effects 7-49386

lepton production

- see also *electron pair production; muon production; neutrino production*
 Drell-Yan process, anal. of nuclear A dependence of q,q nuclear density distances 7-49423
 heavy fermion production and decay via W bosons, helicity projection techniques 7-61762
 heavy-ion collisions, relativistic, heavy lepton production, cross section calcs. using equivalent photon method 7-56695
 high mass dilepton production in hadron collisions, review 7-56574
 lepton pair angular distn. in Drell-Yan-like processes 7-24920
 low mass dilepton production in heavy ion collisions, background from quark-gluon plasma 7-35795
 mirror fermion production near Z^0 peak in e^+e^- collisions 7-49128
 nucleus-nucleus collisions, $\bar{c}c$ mass shift predictions by lepton-pair production 7-19077
 nucleus-nucleus collisions, ultrarelativistic, dilepton emission and the QCD phase transition 7-19290
 ultra-relativistic nucleus collisions, dilepton production 7-56690
 b(c)-quark $\rightarrow\mu\nu_\mu X$, semi-muonic branching ratio determ. and heavy quark fragmentation function calcs, e^+e^- , $\sqrt{s}=34.6$ GeV 7-61710
 B $\rightarrow K_1^{*0}\pi$, rates and CP violation, fourth-generation standard model anal. 7-19099
 D $\rightarrow\tau\nu_\tau(\mu\nu_\mu)$, branching ratios and ν_τ mass limits 7-24884
 $e^+e^- \rightarrow W^+L^+\nu_e$ test for γW^+W^- , $Z^0W^+W^-$ structure, W-magnetic moment anal. 7-24870
 $e^+e^- \rightarrow \tau^+\tau^-$, cross section determ. from 14 to 465.8 GeV 7-15142
 $e^+e^- \rightarrow W^+\bar{e}\nu_e$ test for γW^+W^- , $Z^0W^+W^-$ structure, W-magnetic moment anal. 7-24870
 e^+e^- , $\sqrt{s}=34.6$ GeV, semi-muonic branching ratio determ. and heavy quark fragmentation function calcs 7-61710
 $e^+e^- \rightarrow e^+\gamma\bar{e}$, longitudinally polarized beams, longitudinal and P-violating asymmetries, supergravity GUT calcs. 7-5082
 e^+e^- heavy Majorana fermions $\rightarrow I^{*+}I^-$, cross sections, tests for Majorana nature, CP, CPT-invariance 7-61702
 e^+e^- leptons, strong interaction contributions to four-lepton processes in electroweak SU(2) \times U(1) 7-61644
 $e^+e^- \rightarrow I^{*+}I^-$, forward-backward asymmetry as E_6 model probe 7-19093
 $e^+e^- \rightarrow \tau^+\tau^-$ 7-41824
 $e^+e^- \rightarrow \tau^+\tau^- \rightarrow \pi^+\pi^-\pi^+\pi^-$, branching ratio determ., evidence for $\tau \rightarrow \omega\pi$, branching ratio meas. 7-61674
 F $\rightarrow\tau\nu_\tau(\mu\nu_\mu)$, branching ratios and ν_τ mass limits 7-24884
 $\gamma\gamma \rightarrow I^{*+}I^-$, partial wave anal. 7-49193
 $h_1h_2 \rightarrow V(t)X$, $V(t) \rightarrow \gamma$, Z^0 , $Z^0 \rightarrow I^{*+}I^-$, weak neutral currents, expt. possibilities, lepton longitudinal polarization 7-5098
 $K_L \rightarrow \pi^+I^-\nu_\mu$, I^+ polarization, effects of heavy subdominantly coupled neutrino mixing 7-61652
 NN \rightarrow leptons, dileptons, low p_T and low pair mass anal. 7-35896
 (p, $I^{*+}I^-$)X, I=lepton, rescaling of parton distrib. 7-61883
 pp $\rightarrow e^+\bar{\nu}_X$, CP violation at the TeV scale 7-19145
 pp $\rightarrow e^+\bar{\nu}_X$, CP violation at the TeV scale 7-19145
 pp heavy leptons, 10-40 TeV, cross section calcs. in E_6 7-19138
 pp $\rightarrow W^\pm\nu_\tau(Z^0W^\pm\gamma) \rightarrow L^\pm\bar{\nu}_L$, heavy lepton production through vector boson fusion processes 7-10078
 $\pi^+ \rightarrow a\bar{e}^+\nu$, a=axion, branching ratio calc., chiral Lagrangian anal. 7-511
 $\pi^+ \rightarrow e^+e^-e^+\nu$, constraints on short-lived axions 7-511
 $\pi^+ \rightarrow e^+\nu_\gamma$, axial vector to vector weak π^+ form factor meas. 7-10055
 $\tau \rightarrow e\bar{\nu}_e\nu_\tau$, mass limits 7-24884
 W $\rightarrow\gamma I^-\bar{\nu}_\mu$, $\mu\nu$ meas. proposals as electroweak model test 7-15156
 W $\rightarrow I^-\bar{\nu}_\mu$, $\mu\nu$ meas. proposals as electroweak model test 7-15156
 $Z^0 \rightarrow I^{*+}I^-$, investigation of weak neutral currents in $h_1h_2 \rightarrow V(t)$, $V(t) \rightarrow \gamma$, Z^0 7-5098
 $Z^0 \rightarrow I^{*+}I^-$, Stokes parameter calcs. and anomalous mag. moment 7-41807
 $Z^0 \rightarrow W^{\pm}I^{\pm}\bar{\nu}_e$, test for γW^+W^- , $Z^0W^+W^-$ structure, W-magnetic moment anal. 7-24870

lepton scattering see lepton-deuteron scattering; lepton-hadron scattering; lepton-lepton scattering**lepton spin and parity**

- see also *electron spin*
 No entries

leptonic decays

- see also *baryon leptonic decay; meson leptonic decay; muon decay*
 heavy leptonium, radiative corrections to one-photon annihilation leptonic decays 7-35871
 single electron search expt., sparticle mass limits 7-49142
 E^+ (heavy lepton) $\rightarrow N\mu^+\nu_\mu \rightarrow e^+\mu^+W^-$, preon model anal. 7-56524
 $\mu \rightarrow 3e$, anal. in CP violation models 7-436
 $\mu \rightarrow e\gamma$, lepto-quark effects in E_6 superstring models 7-61651
 $\mu \rightarrow e\gamma(\gamma\gamma)$ (eee), electroweak case for EHF 7-49132

leptonic decays continued

- $\pi \rightarrow 3 e\nu$, electroweak case for EHF 7-49132
 $\tau \rightarrow e\bar{\nu}_e\nu_\tau$, ν_τ mass limits 7-24884
 τ neutrinoless decay, lepton-number and lepton-flavour violation search 7-61675
 τ^- branching ratio meas. 7-61677
 $\tau^- \rightarrow \nu_\mu e^- \bar{\nu}_e \nu_\mu \bar{\nu}_\mu$, branching fraction meas. 7-61676
 $\tau^\pm \rightarrow \nu_\mu e^\pm \bar{\nu}_e$, branching fraction meas. 7-41805
 $\tau^\pm \rightarrow \mu\nu_\mu \nu_\tau$, branching fraction meas. 7-41805
 $\tau^\pm \rightarrow \pi\nu_\tau$, branching fraction meas. 7-41805
 W $\rightarrow e\nu$ (single electron search expt., sparticle mass limits 7-49142
 W $\rightarrow e\nu(\mu\nu)$, e- μ - τ universality test of weak couplings, g_τ/g_e , g_μ/g_e meas. large missing energy events 7-61679
 W $\rightarrow I^{*+}I^-$, supersymmetric signals in leptonic decays 7-41808
 W $\rightarrow \tau\nu$, τ -observation from missing transverse energy events 7-61679
 $Z \rightarrow I^{*+}I^-$, supersymmetric signals in leptonic decays 7-41808
 $Z^0 \rightarrow I^{*+}I^-$, investigation of weak neutral currents in $h_1h_2 \rightarrow V(t)$, $V(t) \rightarrow \gamma$, Z^0 7-5098
 $\nu \rightarrow \nu'\gamma$, decay rate calc. in E_6 superstrings 7-30266

leptons

- see also *electrons; heavy leptons; muons; neutrinos; positrons*
 N quantum approach to symmetry breaking 7-35708
 bound state problem for quarks and leptons, spontaneous symm. breaking 7-35709
 composite models, leptogluons and exotic coloured vector bosons 7-41756
 electroweak-bosons, leptons and Han-Nambu quarks in a unified spinor-isospinor preon field model 7-49102
 fourth generation quark-lepton effects on third generation, quark-lepton mass matrices and renormalisation group eqns. 7-56482
 geometrical rishon model, quark and lepton generations 7-497
 lepton number/flavour violation, phenomenological implications of gauge theories 7-35728
 particle families as radial excitations, eigenstates of relativistic wave eqns. 7-30179
 quark-lepton generations, possible number 7-35792
 SO(10) \times SO(10) theory, composite and elementary quarks and leptons 7-9997
 symmetry tests for lepton number conservation, review 7-30205

leucocytes see blood; cellular biophysics**level control**

- electrooptic low-cost system for liquid level control 7-48683
 RATAN-600 radio telescope, adjustment using laser levelling device 7-66468

level crossing (energy) see energy level crossing**level measurement**

- fibre optic fluid level sensor 7-20447
 fibre optic level transducers, review 7-43405
 fibre optic sensors, development, configs., and appls., review 7-31485
 fibre optic sensors for chem. industry, industrial meas. of press., temp., and level 7-57579
 underground water level detector using US pulse echo technique 7-20528
 US level sensor for liquids under high pressure 7-11235
 water-level measuring system for drum separators in nuclear power-plant with RBMK-1000 reactor (Russian) 7-764

level meters

- see also *power measurement*
 laser level for adjustment of RATAN-600 radio telescope, design and performance 7-66468

levels, energy see energy states**levitation, magnetic see magnetic levitation****LIDAR see optical radar****Lie groups**

- see also *elementary particle symmetry*
 AKNS system, integrable equations, Lie algebra and nonispectral evolution equations 7-35209
 anharmonic oscillator, squeezed light interaction, SU(1,1) coherent states appl. 7-62655
 Beurling-Lax representations using Lie groups, GL(n, R), U*(2n) and SL(n, C) 7-29677
 Bochner-Riesz kernel asymptotics on compact Lie groups 7-14751
 Bogolyubov generating functions, quantum method, current Lie algebra, representations, functional eqns. 7-41240
 BRST analysis of super Kac-Moody and superconformal current algebras 7-4996
 BRST charge operator as nonlinear transformation generator of constraint superalgebra 7-61450
 Cartan-type graded Lie algebras positive and negative graded modules 7-35196
 charge-monopole interaction, O(3,1) symm. problem 7-48943
 chiral field, Bethe-ansatz soln., complete S-matrix and bootstrapping props. 7-48961
 classical dynamical systems, geometric description 7-24407
 classical limits and critical properties 7-48457
 cohomology and deformations of Lie superalgebras 7-48272
 compact semisimple Lie groups, invariant star products and representations 7-29678
 conformal Killing vectors in Robertson-Walker spacetimes 7-156
 contraction of Lie algebras 7-35194
 cotangent bundle, Lie group characterisation 7-9991
 Demazure-Weyl formulas, and generalization of the Borel-Weil-Bott theorem 7-9645
 differential equations, solution by group theoretical methods 7-61065
 Dirac and Weyl equations, maximal symmetry groups 7-24763
 electron hidden U(3) symmetry, Zitterbewegung and degrees of freedom, Dirac eqn., Lie algebra 7-19031
 Euclidean Kac-Moody algebras spanned by principal subalgebra action, highest weight representations 7-48273
 Federbush model, infinite number of infinite hierarchies of conserved quantities, Lie-Backlund transforms. 7-35671
 filtered Lie algebras, intrinsic nilpotent approx. (French) 7-24368
 finite dimensional Lie algebra, structure of PI-envelope 7-29676
 finite groups containing a TI subgroup 7-35207
 functions similar to Lie functions, algebras 7-60941
 G_2 , generalized 6-j symbols, algebraic expressions 7-432
 gauge-invariant Lagrangians, construction technique 7-35707
 generalized Campbell-Baker-Hausdorff formula, path-ordering and Bernoulli numbers 7-41668
 geometrical objects, transformation laws, supersymm., no. system of octonions 7-49009

Lie groups continued

- $gl(n+1, R)$ algebra, boson realisations 7-29871
 Hamilton-Jacobi equation, maximal symmetry group, relativistic particle in flat spacetime 7-18592
 hyper-relativistic quantum systems 7-48418
 Iwasawa and triangle decomp. eval. for Lie algebra real forms 7-18552
 Jacobi-matrix method based on $SO(2,1)$ algebra, parabolic coords., Coulomb fns. expansion in parabolic Sturmians 7-56076
 Kac-Moody algebras, exact realization 7-4995
 Kac-Moody algebras, Harish-Chandra modules of complex semisimple Lie groups (French) 7-55947
 Kac-Moody and gauge groups, nonrepresentability of cohomology classes 7-65
 KdV equation, general form, symmetries, Lie algebra props. 7-48375
 Lie algebra of second-order matrices, polynomial identities (French) 7-60969
 locally finite approximation of Lie groups 7-9648
 many-electron systems, symmetric group approach, spin-depend. operators 7-15475
 n-angelian Lie algebras (Russian) 7-60934
 N-level systems, quantum Markovian master eqn., evolution matrix in coherence vector formulation 7-48539
 nonconjugate elements of the same order in finite simple groups 7-18558
 nonlinear canonical transformations in Lie optics 7-20315
 nonlinear differential eqns. with superposition principles, complex and real Lie algebras 7-4655
 nonrelativistic Coulomb problem, vector operators 7-127
 orthogonal polynomials in Lie algebras 7-60972
 particle in various square well pots., algebraic approach 7-35332
 path integral quantisation and coherent states 7-114
 Poincaré gauge theory, diffeomorphisms, transformation laws and space-time symm. 7-4951
 Poisson Lie algebra C^∞ , deformations of subalgebras 7-48435
 prolongation theory, non-Archimedean approach 7-29679
 quadratic parametric processes, Lie algebraic approach, quantum optics, quantum acoustics 7-36923
 quantum commuting operators rel. to soliton eqns., field theoretical construction 7-56405
 relativistic hadronic mechanics of extended deformable particles 7-35300
 relativistic wave equations, invariance algebras and superalgebras 7-61440
 S-function infinite series and non-compact Lie groups 7-35229
 semisimple Lie superalgebras which are not direct sums of simple Lie superalgebras 7-48294
 $SO(6, 2)$ model of $SU(3)$ and its generalisation to $SU(n)$ 7-35730
 $SO(n)$, generalized 6-j symbols, algebraic expressions 7-432
 solvable lattice models with broken Z_N symmetry and Hecke's indefinite modular forms 7-24773
 $Sp(4)$ boson realizations from seniority-dictated similarity transformations 7-41920
 $sp(n, R)$, construction of boson realizations 7-431
 special embeddings, symmetry breaking scheme anal. 7-30232
 special relativity, velocity composition approach 7-29753
 strictly invariant Lagrangians, determ. from gauge invariant Lagrangians 7-61092
 string propagation and affine Lie algebras on group manifolds 7-35814
 $SU(n/n)$ graded Lie algebra 7-49008
 superalgebras, Casimir operators for infinite-dimens. representations 7-9647
 superalgebras, polynomial identities 7-60942
 superalgebras, principal five-dimensional subalgebras 7-41056
 superalgebras $B(0, n)$, irreducible *-representations 7-41054
 supergravity, graded exceptional algebras and symmetric spaces 7-35384
 superspace with underlying Banach stratification of connectivities, effective action supersymmetries 7-56459
 ten-dimensional real Lie algebras with space isotropy, classification 7-18556
 three-wave resonant interaction eqns. in $(2+1)$ dims., group anal., Lie algebra 7-29769
 two-level atom, mixed-state $SU(2)$ squeezing, quantum optical models 7-50521
 $U(p, q)$ and $U(n)$ Lie groups, complementarity relation, atomic physics appls. 7-10380
 unitary positive energy representations of the gauge group 7-61441
 unitary representations induced from maximal parabolic subgroups 7-24369
 vector coherent state theory in a group with non-commuting raising generators 7-60977
 vertex operator construction of the $SO(2n+1)$ KAC-Moody algebra and its spinor representation 7-15056
 vertex operators for non-simply-laced algebras 7-24367
 Whittaker's models and completely prime primitive ideals in the enveloping algebras 7-55961
 Wiener measures for path integrals with affine kinematic variables 7-48419
 Yang-Mills theory, covariant Lie variations and conformally conserved currents 7-48951
 4He , superfluid, nonrotating, Clebsch representations of symplectic two-cocycles 7-6904

life testing

- bisphenol-A-polycarbonates, outdoor lifetime depend. on terrestrial UV irradiance spectrum 7-54357
 CCDs for ROSAT star sensors, testing and characterisation 7-29401
 dynamic rechargeable battery end-of-life prediction 7-8373
 semiconductor laser aging, electronic apparatus (Czech) 7-57317
 semiconductor laser failure causes and distrib., laboratory service life tests 7-62692
 CO visible multiline laser, lifetime improvement 7-50582
 $In_{1-x}Ga_xAs-InP$ heterostructure APD for 1.55μ optical fibre communication system (Japanese) 7-62843
 $In_{1-x}Ga_xAs_{1-y}P_y-InP$ quarter-wavelength-shifted DFB laser source for 1.55μ underwater optical cable system (Japanese) 7-62120
 Li-LiNO₃ thermal battery cell discharge lifetime with soluble cathode materials 7-3630
 Ni-Cd aerospace cells, low Earth orbit life cycle characterisation testing 7-34020
 Ni-Cd aerospace cells, separator qualification testing 7-34013
 Ni-Cd aerospace cells, study of long term storage effects 7-34018
 Ni-Cd cell containing Pellon 2536 separator, life testing, satellite appl. 7-65446

life testing continued

- Ni-Cd geosynchronous orbit satellite batteries, life prediction 7-65447
 Ni-Cd lightweight space battery, reliability and life testing 7-65449
 Ni-H₂ secondary cells for low-Earth-orbit satellites, reliability and life testing 7-65451
 Si:H, amorphous, solar cells, current-induced and light-induced degradation, non-equivalence 7-17908
 a-Si:H thin film solar cells, accelerated stress testing using photodiode array 7-28403
lift-off process see integrated circuit technology
ligand field theory see bonds (chemical); crystal field interactions; molecular energy levels
light
 see also optics
 gravitational deflection, corrected Li expression for astrolabe obs. 7-66431
light absorption
 see also atmospheric optics; densitometry; light transmission; optical constants; optical films; optical filters; optical saturable absorption; pleochroism; spectra
 7-39072
 acetone, induced absorption and stimulated scattering of focused radiation 7-62780
 atmosphere extinction at Cerro Tololo Inter-American Observatory, (January to July 1984) 7-47542
 atmosphere extinction measurements at McDonald Observatory, UVB results (1960 to 1980) 7-47541
 atomic resonant medium, parametric absorpt., sub-Poisson light statistics 7-57285
 cannonball target, absorpt. of $0.53 \mu m$ laser light 7-20923
 chlorophyll-a, S₁ and T₁ spectra in visible region and S₁ bypassing relax. from two-photon excited states 7-47004
 condensed media, powerful surface EM wave generation role in intense light effect 7-33348
 cytochrome c, nonradiative decay, absorpt. and reson. light scatt. 7-62440
 diaphanography, breast cancer detect. by transillum., IR scatt. and absorpt. obs. on cell suspensions 7-47211
 dielectric slab, bent, with lossy coating, light absorption calc. 7-62620
 direct-gap semiconductor, reversible picosecond brightening during interband absorpt. of intense light pulses 7-12761
 electron wave functions in short-lived potentials, light absorption 7-61165
 electronic and transport props., coherent potential approx. 7-27241
 fibre optic modulator and logic gate using nonlinear refr. and absorpt. 7-37174
 fibre optic thermometer using temp. depend. absorpt., broadband detect. and time domain referencing 7-50751
 free-carrier absorpt. coeff., quasi-2D semiconducting superlattices 7-45968
 glass:Nd absorption thermometer with fluorescent referencing, fibre optic temp. sensor 7-25996
 glass, oxide, bond strength and characteristic temp., three-band theory 7-63500
 impurity liq. cryst. spectra, complex vibron struct., polarisation absorpt. band splitting studies 7-17332
 insulators, laser breakdown due to nonequilibrium changes in their optical chars. near absorbing inclusions 7-53233
 interstellar dust, UV-visible extinction spectra of submicron amorphous C grains 7-35023
 interstellar extinction, implications for dust grain models 7-48013
 intracavity laser spectroscopy meas., sensitivity calcs. 7-31336
 laser energy absorpt. meas. using differential joulemeter and optoacoustic cell calibration appl. 7-41500
 layer-periodic materials, stimulated Brillouin scatt. threshold, light and sound attenuation calcs. 7-3060
 living human body, spectral radiative props. study 7-18013
 luminescent solar concentrators, glass and dye absorption and luminescence obs. (Finnish) 7-28390
 metal mirrors, absorptance meas. at glancing incidence, photoacoustic calorimetry 7-20380
 metallic surfaces and small particles, relax. time effects in transverse dielectric fn., electromag. props. 7-38483
 metallic thin films, surface electron light absorpt. Green's function method study (Russian) 7-21970
 metallography, interference layer technique, phase optical constns., data collection construction (German, English) 7-4645
 metals, laser radiation absorption, dependence on shape 7-26794
 metals, laser radiation screening by damage products 7-32493
 syn-(methylmethyl)bimane aq. soln., lasing action obs., absorpt. and fluorescence spectra meas. 7-43083
 molecules, explosive absorption of finite-diameter laser beam 7-50269
 nematic liq. crystals, photoinduced chirality 7-44352
 orientationally disordered systems, optical props., CPA approx. calcs. 7-53256
 phase media with absorption holographic analysis 7-50513
 phenazine-tetracyanoquinodimethane, photoconductivity and optical absorpt. coeffs. near band edge 7-2641
 pigmented biological tissues with granular struct., selective interaction of short laser pulses 7-54678
 poly (N-benzylidiphenylaminomethane) film, synthesis, elec. and optoelectronic props. 7-45384
 poly-di-n-hexylsilane, conform. kinetics and packing, spectrosc. obs. 7-37887
 trans-polyacetylene, neutral soliton pair production, breaking of charge conjugation symmetry 7-64110
 trans-polyacetylene, optical absorpt. due to soliton lattice 7-64109
 trans-polyacetylene, within the extended tight-binding picture, interband transitions, hopping processes 7-27678
 polyacetylene films, oriented, optical props., photocond. meas. 7-64717
 polymers, quasi-one-dimensional, electron-electron interaction effects 7-64143
 polystyrene, monodisperse lattices, He-Ne laser transmission, attenuation coeff., specific turbidity meas. 7-62617
 polyvinyl alcohol films, heat treatment, light irradi., polyene mixtures, absorpt. spectra 7-53432
 polynes, strongly coupled Peierls insulators, soliton, polaron and photoexcitation props. 7-64114
 quantum well, optical absorpt. due to excitonic unbound states 7-64593
 reabsorption correction for luminophor, influence of refractive index 7-937

light absorption continued

- scheelite structure crystals, optical and elec. props. 7-33431
seawater, daylight absorption coeff. 7-14288
semiconductor films, heavily doped, optical absorption band shift 7-7776
semiconductor strained layer superlattices, electronic and optical props. 7-7359
semiconductor superlattices, excitons, optical props., size effect (*Japanese*) 7-12621
semiconductor superlattices, I-type, intersubband collective excitations (*Chinese*) 7-12804
semiconductors, electron energy distrib. form. due to monochromatic light intraband absorpt. 7-17285
semiconductors, ultrashort strain pulse excitation due to optical radiation absorpt. 7-32579
skin absorbance, differential cell design for in vivo photoacoustic meas. 7-47293
small-area pulses, coherent propagation in YAG:Nd and ruby activated crystals. 7-43038
soft spheroidal particles, absorptivity depend. on shape and orientation 7-42915
solar cell enhanced performance by front surface light scattering 7-8420
spherical particles, electromag. response, normal mode theory 7-17263
stimulated Brillouin and thermal scatt. of Nd μ s pulses 7-62777
storage phosphor system for computed radiography: screen optics 7-23445
structure-dependent optical phenomena 7-45953
synthetic metals science and technology, conf., Kyoto, Japan (June 1986) 7-60872
TCNQ salts, quarter-filled band, optical absorption studies 7-46033
TGS: $C_{3H_7NO_2}$ single crystals, valence bands and impurity levels, absorpt. edge meas. 7-33350
thin films, light grazing tunnelling, reson. absorpt. 7-42897
thin metal films, power absorpt. due to electron-hole pair production, screening pot. at surface 7-52490
tiny absorbing particle embedded within nonabsorbing particle, specific absorpt. 7-31239
tissue optical absorpt. characts., microscope for studying 7-14174
tissue phantom for phototherapy, optical dosimetry study 7-34284
turbid media, appl. of Kubelka-Munk theory to Fe oxides and colour of Triassic sediments 7-66098
Urbach optical absorpt. edge, electron band tails 7-16930
Ag contacts, transparent, for a-Si solar cells with ITO antireflection coating 7-65478
Ag oxidised granular film, optical absorpt. calcs., Gaussian broadening model 7-27802
AgBr films with optical absorpt., sensitizing dyes effect on ionic cond. 7-26999
 $Al_{0.3}Ag_{0.7}As$, femtosecond carrier dynamics 7-58829
 $AlSb:Se$, donor studies, incoherent laser saturation method 7-27298
 As_2S_3 chalcogenide glass, photoinduced gradient waveguide form. (*Russian*) 7-43374
 As_2S_3 glass, photostructural effects, EXAFS study 7-64758
 $Bi_{1-x}As_xS_2$ thin films, solution-gas interface deposition technique 7-7901
 $Bi_2Lu_{1-x}Y_{x-1}FeO_{12}$, ferrimagnetic garnets characterisation for MSW optical diff. 7-13040
 Br_2 liquid, optical props. 7-17294
C films, plasma deposited from methane, elec. conductivity, optical absorpt. 7-38786
 CO_2 laser pulse duration control by intracavity IR absorbing gas cell 7-43174
 $Ca_{2-x}Nd_xGa_{2+x}Si_{1-x}O_7$, Ga gehlenite, cryst. struct. and optical props. 7-16525
 $CdIn_2S_4Se_2$, semicond., optical and elec. props. 7-33010
CdS, absorpt. optical bistability, lattice heating study 7-43205
CdSe, highly excited, exciton dynamics, picosec. time-resolved gain-absorpt. spectra study 7-2494
CdSnO₃, fundamental absorption edge, spectral dependence 7-45964
CeO₂ films, optical absorption edge and energy gap 7-33471
 $Co_{0.2}Ga_{2.8}S_{3.2}$ single crystals, optical props. and impurity energy levels meas. 7-13122
CoO, band structure and optical absorption edge 7-45147
CoSi_{0.95} film, soln. growth, optical absorpt. coeff. 7-39446
Cu, electronic props., spectrosc. investig. 7-59216
CuBiS₂ thin films, spray pyrolytic deposition, elec. and optical props. 7-7894
CuInSe₂-based photoelectrochem. solar cells, optical and electronic props. studies 7-46958
CuSO₄ soln., double diffusive convection, conc. meas., optical technique. 7-57825
EuGa₂S₄, optical props. near fundamental absorption edge 7-17295
FeSi₃ thin films, appl. to electro-optic VLSI interconnects 7-53427
GaAs doping superlattices, optically induced absorpt. modulation 7-7713
GaAs, femtosecond carrier dynamics 7-58829
GaAs, ion implanted and laser irradiated, defect studies 7-32432
GaAs LEC semi-insulating crystals, pure and In-doped, IR absorpt. WRT resistivity 7-64629
GaAs waveguide, thermal index changes by optical absorpt., all-optical signal processing 7-31381
GaAs/Al quantum wells, MBE growth, photoluminescence and absorption linewidth studies 7-7749
GaAs/Al_xGa_{1-x}As heterostructs., 2D electron gas, polaron screening effects, optical absorpt. calcs. 7-2511
GaAs/Al_xGa_{1-x}As, modulation-doped quantum wells, photoabsorpt., electronic props. 7-64330
GaAs-Ga_{1-x}Al_xAs multiple well heterostructures, far IR absorpt. by shallow donors 7-45458
GaAs-Ga_{1-x}Al_xAs superlattices, optical props. 7-3007
GaN:Zn, pure and doped, electrophysical props., nonhomogeneous semicond. model 7-27292
GaSe, excitons, room temp. self screening 7-45166
(GdBi)₃(FeAlGa)₅O₁₂ garnet films, LPE growth 7-59463
GeO₂-PrCl₃ glasses, optical props. rel. to comp. 7-13150
GeS₂ glass, photostructural effects, EXAFS study 7-64758
GeSe₂ glass, photostructural effects, EXAFS study 7-64758
H₂, solid, surface localised electrons, photoresonances 7-63901
HgGa₂Se₄, optical props. in fundamental absorption region 7-39065
I₂ liquid, optical props. 7-17294
InGaAsP-InP waveguides, optical parameters 7-62831
In₂O₃:Sn, sputtered films prep. and optical props. 7-53587
InP waveguide, thermal index changes by optical absorpt., all-optical signal processing 7-31381

light absorption continued

- InSb:Ti, physicochemical behaviour of TI 7-21452
K atoms in Ar matrix, site modification by X-ray and light irradiation 7-51819
KCl:Li, F_A-centre crystals, diffraction efficiency of photoinduced gratings 7-62818
Kr gas, acousto-optic interaction in FIR 7-37623
LiCl:PB²⁺, absorpt. and luminesc. spectra studies (*Russian*) 7-46141
LiNbO₃:Fe, and undoped crystals, decay of γ -centres 7-7658
MgO:Fe, gamma irradi., thermoluminescence and TSC studies 7-33464
Mn₂Zn_{1-x}Se, energy gap comp. depend., photocond. and absorpt. edge meas. 7-38454
NF₃, high temperature absorpt. of laser radiation 7-51385
NH₃, high temperature absorpt. of laser radiation 7-51385
N₂O IR transmittance, band models comparison 7-19860
Na+Rg optical collisions, (Rg = He, Ne, Ar, Kr, Xe), fine struct. branching ratio determ. 7-10704
NbS₂ monolayers, optical absorption spectrum, Slater orbitals two-centre dipole matrix element calcs. 7-46158
NiS thin films, deposition by soln. growth techniques, X-ray diff., optical, elec. meas. 7-32870
NiSe thin films, deposition by soln. growth techniques, X-ray diff., optical, elec. meas. 7-32870
Os single crystal, energy band struct. and optical absorpt. studies 7-16938
PLZT electro-optical ceramics, electron pulse irradiation-induced transient optical absorpt. study 7-6682
PLZT ferroelectric ceramics, gamma, electron and neutron irradi. effects study 7-6677
PbGa₂S₄ single crystal, optical absorption and photocond. studies 7-2635
PbHPO₄, photostimulated luminescence near ferroelec. Curie temp. 7-64697
PbO-SiO₂-K₂O coloured and colourless glasses, near IR absorpt. temp. depend. study 7-13146
Pb(Sco_{0.5}Nbo_{0.5})O₃ ferroelectric ceramics, gamma, electron and neutron irradi. effects study 7-6677
PbSe_{1-x}S_x epitaxial films, absorpt. edge, band gap, comp. depend., 77-300K 7-39063
PbSe_{1-x}Te_x optical absorpt. edge slope increase, comp. depend. 7-39064
PbTe_{1-x}S_x epitaxial films, absorpt. edge, band gap, comp. depend., 77-300K 7-39063
Pd, optical constants measured by a multiple-wavelength ellipsometer 7-27683
Pd₂Si and PdSi, optical constants measured by a multiple-wavelength ellipsometer 7-27683
SF₆, high temperature absorpt. of laser radiation 7-51385
SF₆, liq., acousto-optic interaction in FIR 7-37623
Sb₂S₃ single crystal optical absorption and luminescence obs., 2 to 367K (*Japanese*) 7-39151
Si film growth for MOS-VLSI, Ti and Pt silicide form. 7-7870
a-Si films, surface passivation, study by photothermal deflection spectroscopy 7-59689
Si₃C₄ solubility, segregation, diffusion and precipitation 7-16777
a-Si:H, photoinduced absorpt., ps decay 7-27684
a-Si:H, picosecond photoinduced absorption and transmission 7-3006
a-Si:H, picosecond photoinduced absorption decays, interference effects 7-3012
a-Si:H biased activated reactive layer evaporation and charactn. 7-59428
a-Si:H thin films, elec. and optical props., thickness depend. 7-46168
a-Si:H/Ge:H superlattice struct., light absorption and photocond. studies 7-38715
a-Si:H/a-SiN_x:H, amorphous multilayer structures, optical props. 7-3014
SiC, hot pressed, IR optical absorpt. and refl. 7-59167
a-Si_{1-x}C_x films, RF sputtered, IR absorpt., X-ray diff., RHEED (*Japanese*) 7-53584
a-SiGe:H:F glow discharge films, electronic transport and density of states 7-45114
a-Si_{1-x}Ge_xH, F, light-induced degradation meas. 7-45397
 α -SiGeH, electronic and transport props., coherent potential approx. 7-27241
 α -SiH, electronic and transport props., coherent potential approx. 7-27241
a-SiN:H films, optical absorption const. evaluation by photothermal deflection spectroscopy 7-22361
SiO_x:P films, pure and doped, low press. CVD growth, structural, optical, elec. props. 7-27186
a-SiSn:Cl:H glow discharge films, elec. and optical props. (*Chinese*) 7-58805
SnSe, IR absorpt. edge, transition temp. coeffs. 7-27721
Sr_{0.61}Ba_{0.39}Nb₂O₆:Ce crystals, light emission obs. during freq.-degenerate laser pumping 7-15947
SrTiO₃ crystal, electron pulse irradiation-induced transient optical absorpt. study 7-6682
TiO₂-SiO₂ dielectric multilayer stacks, absorption meas. by photoacoustic technique 7-17331
TiO₂-SiO₂ multilayer coatings prep. by RF magnetron sputtering, interfacial optical absorpt. 7-1252
TiGaSe₂ single crystal, photolum. and edge absorpt. spectra 7-59241
TiSe, thermal expansion coeff. temp. depend. and absorpt. spectra meas. 7-58508
V₂O₅-TeO₂-PbO, glass, elec. and optical props. (*Korean*) 7-27330
Xe gas, acousto-optic interaction in FIR 7-37623
XeCl laser, laser snow in active medium 7-43070
YIG, ferrimagnetic garnets characterisation for MSW optical diff. 7-13040
ZnSiP₂ crystal, exciton absorpt. spectrum, energy gap and exciton binding energy determ. 7-2500
ZrO₂ thin films, high index, optical consts. in UV region 7-7775

light absorption spectra see spectra

light amplifiers see image intensifiers

light attenuation see light absorption; light scattering; light transmission; optical dispersion

light coherence

see also laser beams; lasers

- astronomical object image construction using coherency functions, atm. distortion compensation 7-55481
atomic metastable states produced during cooperative self-diffraction in a resonator, Maxwell eqn. solns. 7-42558
cell structure imagery, defocus and partially coherent illumination influence (*German*) 7-10845
coherent-mode propagation in spatially band-limited wave fields 7-31243

light coherence continued

- coupling efficiency analysis, LED to single-mode fibre 7-20415
- crack under mode I loading, coherent-light-shadow spot, theory and expt. 7-63089
- cryptocyanine, degenerate four-wave mixing, in saturable absorber, effects of optical coherence (*Korean*) 7-25901
- dual-aperture sampling with partially coherent illumination, fringe visibility 7-10843
- dye laser with diffraction grating in resonator for holographic interferometry 7-43159
- fibre optic gyroscope, phase modulated, coherent backscatter analysis 7-43427
- fibre optic interferometric sensors multiplexed using partially coherent light, expected noise levels 7-25982
- fibre optic system using laser source with arbitrary coherence time, phase noise anal. 7-15979
- grating sensor, moiré signal modulation depth under incoherent illum. 7-31447
- heterodyne/coherent optical fibre communications, ultimate performance 7-31490
- Holocoupler-Selfoc fibre system, coherent transfer matrix description 7-26016
- holographic sharp-focusing technique, sensitivity 7-36920
- integrated-intensity grating formation with pulsed light sources, fourth-order partial coherence effects 7-20403
- laboratory X-ray lasers, spatially coherent output 7-57289
- laser beam coherence props. control with plasma filter 7-1209
- laser resonator Q-factor modulation using methods of adaptive nonlinear optics (*Russian*) 7-50604
- Lau interferometer, coherence anal. 7-9879
- lightguides, time coherence effects of transverse laser modes 7-37009
- linear grating sensors, moiré signal quality rel. to light source coherence and grating gaps 7-31446
- mode correction for turbulent distortions of optical waves 7-42914
- monochromatic OTF, influence of spatial coherence 7-42981
- multimode waveguides, irregular, modal noise, radiation coherence effects 7-11111
- optical systems, energy transport with partially coherent light 7-43326
- parametrically generated light second-order coherence obs. 7-25892
- partial coherence phase problem, finite function spatial spectrum in 2D case, relation of components 7-50503
- partially coherent holography, props, and appls. 7-62646
- phase space-time distrib. meas. of coherent signal 7-25855
- quadratic media, longit. homogeneous, with absorpt. or amplification, correlated coherent states 7-50621
- quasi-monochromatic thermal light, spatial coherence meas. using double-exposure specklegrams 7-18870
- radiance theorem with partially coherent light 7-42900
- rainbow holography with a multimode laser source 7-25764
- random medium, edge diffraction of high-frequency coherence functions 7-42922
- resonance Raman scattering determ. by coherence function 7-36925
- reverse scatter from complex-shaped bodies, coherent multichannel effects 7-10851
- rough sphere, coherent scattering cross-section calc. 7-10857
- ruby laser, Q-switched, pulse stretching for bubble chamber holography 7-43169
- semi-transparent edge, coherent spread function symmetry 7-42994
- semiconductor laser and integrated optics for optical fibre sensors 7-25998
- sharpness function maximisation problem, object obs. in coherent light through randomly inhomogeneous medium 7-25714
- slightly inhomogeneous media, partially coherent optical field propag., density matrix formalism 7-15816
- small-area pulses, coherent propagation in YAG:Nd and ruby activated crystals. 7-43038
- split-step fast Fourier transform method, optical coherence calcs. 7-1022
- squeezed coherent states, superposition with thermal light 7-20173
- Stokes beams coherence props. for incoherent broadband pumps 7-20335
- three-level medium, ultrashort pulse train propag., population trapping and coherent bleaching calcs. 7-43263
- transparency, diff. props. in oblique incidence of light 7-50487
- turbulent atmosphere, high-resolution image form. of coherently illuminated objects 7-55261
- turbulent atmosphere, thermal self-interaction of partially coherent laser beam 7-31376
- two-beam interferometry, polarisation effects, coherency matrix anal. 7-24693
- undulator radiation, grating monochromators, wave-optical props. 7-36865
- visual acuity rel. to light coherence, influence of pupil 7-13998
- (AlGa)As lasers, separately pumped, continuous control 7-20287
- GaAs DH laser struct., external injection of spontaneous emission 7-31328
- Na, collisionally aided coherent atomic optical emission 7-42561
- Xe multiphoton ionisation, suppression with circularly polarisation coherent light 7-19792

light communication *see optical communication***light cones**

- see also current algebra*
- classical mechanics, Hamiltonian formulation with respect to an observer's light cone 7-48350
- compactified superstrings and torsion, light-cone gauge investigation 7-35816
- covariant light front perturbation theory and three-particle equations 7-41651
- covariant superstring with $N=1$ global supersymmetry, quantum geometry 7-35735
- gauge string fields from the light cone 7-48971
- glueball mass spectrum calculation by light-cone quantization (*Russian*) 7-61594
- invariant string field theory, gauge symmetry using light-cone gauge M^{-1} generator 7-5020
- massless light-cone gauge Feynman diagrams, cut-off and dims. regularization methods 7-41645
- nonlocal light-cone hadron operators, one-loop approx. 7-41649
- one-loop gluon self-energy in the light-cone gauge 7-24784
- open superstring light cone hamiltonian, supersymmetry relation and quartic vertex 7-41762
- QCD, dynamics of confinement, asymptotic freedom 7-49057

light cones continued

- QCD light cone gauge, integral equation for multiplicity distribution 7-15115
 - QED₂, discretized light-cone quantization of Schwinger models 7-56497
 - quark distribution amplitudes for the nucleon from perturbative QCD and QCD sum rules 7-41745
 - quasi-local mass for small surfaces 7-29827
 - string field theories, gauge covariant formulation 7-24859
 - string Lorentz algebras, Veneziano, Neveu-Schwarz-Ramond model anal. 7-10043
 - supersymmetric Yang-Mills theory, self dual condition 7-35660
 - (triangle) anomaly in the light-cone gauge 7-9975
 - U(n) Veneziano model, Wick-rotated light cone gauge, nonperturbative study 7-24854
 - Yang-Mills theory, general three-vertex, BRS identities and renormalizability of the light-cone gauge 7-35724
 - Yang-Mills theory, renormalisation in light cone gauge 7-61475
 - Yang-Mills theory in the light cone gauge, BRS formalism and renormalisation 7-48987
 - ed-cpn, dynamics in light cone, nucleon form factors (*Russian*) 7-15165
 - π structure function, Fock state expansion of hadronic wave function in QCD (*Chinese*) 7-24887
- light diffraction**
- see also holography; optical zone plates*
 - 3m-symmetry crystals, self-oscill. and vectorial self-diff. of orthogonal-polarised light waves (*Russian*) 7-43207
 - achromatic single-component kinoform objective, with circular aberration coeff. 7-25737
 - acousto-optic Bragg regime extension through Hamming apodisation of sound field 7-25712
 - acousto-optic light diffraction by ultrasonic beams, multiple plane-wave anal. 7-5833
 - acousto-optic signal processors, polarisation effects 7-25723
 - alignment of diffraction and refraction components in optical systems 7-25925
 - 4-n-alkyl-4'-cyanobiphenyls, nCBs, methyl red binary mass diffusion const., forced Rayleigh scatt. 7-64661
 - alloys, disordered, multi-site correlations, at. size effect 7-16347
 - annular aperture diffraction patterns, aberration analysis 7-62639
 - atomic metastable states produced during cooperative self-diffraction in a resonator, Maxwell eqn. solns. 7-42558
 - axicon, thin linear, diffraction patterns and zone plates 7-37083
 - benzene dynamic gratings, self-diffraction and reflection in degenerate four-wave interaction 7-37050
 - chiral smectic-C liq. cryst., light diff. props. in external elec. field 7-64604
 - classical grating and bigrating, light diff. 7-20129
 - coherent scatt. diff. patterns transform. from gas and cryst. systems, cryst.-chem. cluster model calcs. 7-62619
 - compensated spherical surfaces in optical systems 7-25924
 - conducting cylinder, amplitude and phase characts. of scattered light 7-20132
 - conference, diffraction phenomena in optical engineering appls., San Diego, CA, USA (Aug. 1985) 7-60870
 - conical diffraction mounting, generalisation of rigorous differential method 7-5831
 - convection effect, numerical investigation method 7-25711
 - cylinder, circular, diff. pattern behind cylinder in penumbral region 7-50465
 - cylindrical kinoform lenses for monochromatic light, with long focal length 7-25923
 - dense particle fields, laser diffraction meas. correction for multiple scatt. 7-1212
 - dielectric gratings, coated, in conical diffraction mounting, diffraction anomalies 7-5985
 - dielectric gratings, plane wave diff., finite element anal. (*Japanese*) 7-43342
 - diffraction gratings, false gratings and random rough surfaces, numerical comparison of light scattering 7-5830
 - display of diffraction patterns display using electric razor 7-35168
 - Fabry-Perot interferometer, OTF and resolving power, sequential theory 7-48836
 - focus of high-numerical-aperture objectives, light distribution 7-43290
 - four-wave mixing techniques for studying orientational relaxation, comparison 7-10779
 - Fraunhofer diffraction, Abbe transform and Maggi-Rubinowicz transformation formulae 7-5836
 - Fraunhofer diffraction pattern of Gaussian laser beam entering pinhole, numerical anal. 7-15815
 - Fresnel approx., validity and physical explanation 7-55935
 - Fresnel diff., circular aperture, method of Fresnel zone counting 7-55936
 - Fresnel diffraction at random phase screen inverse problem parameterisation, thermoplastic medium 'frost' deform. anal. (*Russian*) 7-50494
 - Fresnel diffraction computation, review 7-18521
 - Fresnel diffraction patterns, one-step white light in-line holography of 2-D transparencies 7-31270
 - Gaussian beam diffracted through finite lens, focus 7-42893
 - Gaussian beam transformation by Winkelmann-Abbe bi-prism 7-42904
 - Gaussian beams, generally astigmatic, propag. along skew ray paths 7-62623
 - geometrical optics, rel. to wave optics 7-35176
 - glass fibre, diff. pattern analysis, holography appl. 7-25762
 - grating efficiency measurement and automated scatter inspection system (GEMASIS) 7-62853
 - Hermite-Gaussian beam transformation by shifted spherical lens 7-42891
 - holographic grating production on plastic substrates, diffraction efficiency 7-43004
 - holographic gratings in media with photoinduced scatt., light diff. 7-57277
 - holographic lenses, on-axis, coupled-wave anal. 7-5839
 - hybrid pattern recognition by features extracted from object and Fraunhofer diff. patterns 7-42942
 - integrated-intensity grating formation with pulsed light sources, fourth-order partial coherence effects 7-20403
 - kinoforms phase structure synthesis 7-25738
 - large-F-number systems, aperture-lens separation effect on focal shift 7-57231
 - laser array, randomly phased geometrical 7-36975

light diffraction continued

- laser arrays, far-field analytical model 7-11018
 Lau interferometry and diffraction correlation (*Chinese*) 7-57247
 liquid crystals, Kapustin-Williams domains 7-16404
 low light level optical interference from double slit and pinhole, particle-wave duality 7-31245
 Maggi-Rubinowicz transformation for phase apertures 7-42896
 magnetic domain structure determ. using light diffr., inverse problem (*Russian*) 7-53286
 misaligned systems and interference effects of optical arrays, diffr. integral 7-5838
 multilayer dielectric cylinder diameter determ., diffraction meas. accuracy improvement 7-293
 nematic liquid crystal film, quasi-static elec. field enhanced optical propag. effects 7-27702
 nematic liquid crystals, dynamic gratings, self diffractions and wavefront conjugation processes 7-11067
 oppositely directed waves, self-diffraction in medium with nonlocal response 7-42907
 particle size measurement by laser diffraction beam stop and vignetting effects 7-9813
 particulate analysis, filtering effects in far-field in-line holography and diffr. pattern analysis 7-31279
 photorefractive cubic crystals, hologram diffraction efficiency and diffracted light polariz., optical activity effect 7-43020
 photothermoplastic film, deform. props. treatment process parameters 7-43281
 piezoelectric semiconductors, amplified acoustic noise anal., Bragg light diffr. method 7-43625
 planar corrugated waveguides, diffraction at normal incidence 7-62827
 polymer films, light scattering, struct. aspects of dichromatic laser speckle patterns 7-42931
 polystyrene latex suspensions, aq., semidilute, ordering process of colloidal crystals. 7-17829
 probe beam diffraction at laser induced thermal lens 7-20135
 pulses of different wavelengths, simultaneous propag. in three-level absorbers 7-15954
 quartz, rough surfaces, optical correl. study 7-42916
 random medium, edge diffraction of high-frequency coherence functions 7-42922
 relative phase effects, demonstrations 7-57
 retinal optical intensity profile model for computer-aided visual acuity assessment 7-59976
 reverse scatter from complex-shaped bodies, coherent multichannel effects 7-10851
 ring pattern of laser-induced thermal self-defocusing 7-62805
 semiconductors, light beam dynamic transformation by conduction electrons 7-11043
 skeletal muscle, frog, small angle equatorial reflections of diffr. pattern rel. to sarcomere length 7-40215
 speckle phase in image and diffr. fields, statistical props. 7-42934
 speckle stereograms for 3D display 7-20146
 spectral measurement for wavelength regions 400 nm to 750 nm and 700 nm to 2500 nm (*Japanese*) 7-351
 spherical aberration, diffraction intensities 7-57259
 spherical aberration, intermediate, geometric and diffractive parameters, comparison 7-42983
 stationary part of the Fresnel diffraction field of two antiparallel sound beams separated in space 7-57665
 string objects, vibr. anal. using a diffr. technique, multimode optical fibre appl. 7-11364
 telescopes, resonator diffr. losses 7-43292
 thermotropic copolyester with banded texture, optical diffraction pattern predictions 7-11888
 thin-film travelling-wave light modulator, diffraction efficiency 7-5987
 transparency, diffr. props. in oblique incidence of light 7-50487
 transparent media refractive index determ. by diffraction method 7-41435
 two-beam self-diffr. conditions stability in cubic nonlinear medium (*Russian*) 7-57407
 two-dimensional light scanning by waveguide acoustic modes of a plate 7-25944
 ultrasonic light diffraction effects 7-37307
 ultrasonic light diffraction phenomena 7-20575
 uniform and Gaussian beam diffr. comparison, aberration balancing 7-62621
 very low light intensity diffraction patterns, photon particle-wave duality study 7-31246
 volume holographic gratings diffraction efficiency calc. 7-1025
 wave-kinetic numerical approach to beam propag., canonical problems 7-31247
 wide-angle diffraction phenomena, finite beam size effects 7-62622
 Wood's anomaly effects on gratings of large amplitude 7-5986
 Ba₂NaNb₃O₁₅, parametric light scattering, nonlinear diffraction 7-37044
 BaTiO₃, photorefractive conical diffraction 7-7655
 Bi₁₂GeO₂₀, real time holographic image recording, diffraction efficiency (*Korean*) 7-25743
 Bi₂Lu_{3-2x}Fe₂O₁₂, ferrimagnetic garnets characterisation for MSW optical diffr. 7-13040
 CdS photosensitive cryst., 3D light diffr. from acoustic instability 7-33362
 CdS resonant self-diffraction from dynamic laser-induced gratings 7-11036
 NbTe₄, discommensurate state microstruct., electron diffr. pattern obs. 7-6598
 Pb orthovanadates and orthophosphates, diffuse satellites in electron diffr. patterns 7-26595
 Si, crystalline, ion-implanted and amorphous, light diffraction by transient gratings 7-11034
 α-SiC, wedgelike sample, self-diffraction, 2D character 7-5858
 YIG, ferrimagnetic garnets characterisation for MSW optical diffr. 7-13040
 ZnO resonant self-diffraction from dynamic laser-induced gratings 7-11036

light diffusion see *light scattering*

light dispersion see *optical dispersion*

light emitting devices

see also *light emitting diodes; light sources; luminescent devices*

No entries

light emitting diodes

see also *semiconductor junction lasers*

- coupler, bidirectional, active, compact for fibre optic transmission 7-6012
 coupling efficiency analysis, LED to single-mode fibre 7-20415
 current sensor for electrostatic double probes 7-63357
 domed LED coupling with multimode step-index optical fibre 7-31467
 edge-emitting, coupling sensitivity to single-mode fibre 7-57585
 information processing and communications appl. 7-1285
 IR radiation stable source for photometer calibration 7-56317
 lightwave telecommunication using optical fibres, history and current systems 7-50761
 long-haul single mode fibre attenuation meas., laser and LED source effects 7-43414
 luminescence, conference, Rovno, USSR (Nov. 1984) 7-24263
 multiquantum barrier, electron reflectance, theoretical study 7-7341
 optical long-wavelength components by VPE 7-46343
 plant stem diameter contactless measurement apparatus using LED and photodetector (*Japanese*) 7-23506
 pulse distortion in LEDs in single-mode fibres near zero-dispersion wavelength 7-6005
 schlieren optics methods, comparison of light sources 7-57503
 sources in single mode fibre system, diode lasers versus LEDs 7-62844
 sources in single mode fibre system, diode lasers versus LEDs 7-62845
 Al_{0.5}Ga_{0.5}As:Si, luminesc. props. (*Korean*) 7-27786
 GaAlAs/GaAs, junction isolated LED structures, MOCVD, characts. 7-27935
 GaAs DH laser struct., external injection of spontaneous emission 7-31328
 GaAs high quality layers grown on Si by MOCVD, FET and LED appls. 7-27922
 GaAs sawtooth doping superlattices, prep., LED and laser appls. 7-7372
 GaAs/Al_{0.5}Ga_{0.5}As graded index separate confinement LED, OMVPE growth 7-39402
 GaAs_{0.5}P_{0.5} degraded LEDs, origin of nonradiative centres, photocapacitance, electrolum. spectra 7-53413
 GaAs_{0.5}P_{0.5} LEDs, MOCVD growth on Si substrates 7-17438
 GaP and GaP:N diodes, electroluminescence, high press. effects 7-27787
 GaP LPE layers, reuse of Ga melt for LED prep., effect on electrical characts. 7-22592
 InGaAs:Si LED, electrical and luminesc. props., ultrasonically-induced changes 7-22350
 InGaAsP, double heterostructure LED, OMVPE, 1.3 μm emission 7-27931
 InP:Yb LPE layers, luminesc. and elec. props. 7-59464
 α-SiC, single cryst. growth using furnace with NbC heaters 7-27881

light filters see *optical filters*

light intensifiers see *image intensifiers*

light interference

see also *light interferometers; light interferometry; moire fringes*

- 3D surface metrology, interference microscopy, computer controlled instrumentation 7-29975
 birefringence presence, interference fringes in scattered beams 7-50491
 computer-controlled reflection and transmission meas. of semiconductor thin films 7-4902
 Danaines golden pupae, natural broad-band interference reflector microspectrophotometry 7-54676
 diagnostics of planar optical waveguides 7-25960
 disperse medium, light scatt., correl. radius estimate 7-42917
 dual-aperture sampling with partially coherent illumination, fringe visibility 7-10843
 Fabry-Perot interferometer-fringe system, integral-order no. of interf. calc. 7-56329
 filters, laser-induced heat flow 7-43333
 fringe visibility in coherent laser interferometric system 7-50492
 holographic time diagnostics with picosecond resolution 7-43014
 hybrid bistable optical device with a multilayer interference modulator 7-57405
 IR film thickness gauging, optical interference suppression 7-33472
 light wave attenuation by destructive attenuation, quantum mechanical props (*German*) 7-31290
 localisation effect on interference, intensity calcs. 7-20166
 localised photon states and interference 7-1059
 locality violation, interpretation of quantum mechanics 7-20167
 logic gate using spatial light modulator and interference fringe shifting 7-43351
 low light level optical interference from double slit and pinhole, particle-wave duality 7-31245
 misaligned systems and interference effects of optical arrays, diffr. integral 7-5838
 multilayer interference laser light modulator, optical bistability 7-25950
 nonclassical states, photon antibunching and statistics 7-1047
 optical interference coatings, synthesis, optimisation (*Russian*) 7-22375
 pattern produced on reflection at phase-conjugate mirror 7-42902
 photorefractive gratings on reflecting substrates interference pattern 7-1042
 quantum fluctuation effects, laser gravitational obs. sensitivity implications 7-43039
 range finders design principles 7-4808
 relative phase effects, demonstrations 7-57
 ring pattern of laser-induced thermal self-defocusing 7-62805
 scanning polarisation/interference contrast microscopy, linear imaging 7-9895
 single-photon interference experiment using a mechanical frequency shifter 7-57232
 SOI structures, thickness determ. using optical interf. method 7-18743
 speckle generated interference fringe intensity fluctuations 7-50497
 stimulated Raman measurements, time-resolved, interference phenomena 7-5955
 thin films, light grazing tunnelling, reson. absorpt. 7-42897
 two-beam interferometry, polarisation effects, coherency matrix anal. 7-24693
 Young array, polarisation effects 7-57233
 Al-ethyl alcohol interface, surface polaritons, four-wave mixing 7-43244
 Be-Ti multilayer interference system, struct. and phase composition, electron microscopy, X-ray and neutron diffr. meas. 7-63984
 GaAs-Ga_{1-x}Al_xAs heterostruct., light interf. meas. of thickness and comp. during epitaxial growth 7-64026
 Ge, holes optical effective mass, determ. by interf. method 7-17290
 LiNbO₃ integrated optical substrates, Maker fringe anal. 7-26026
 a-Si:H, picosecond photoinduced absorption decays, interference effects 7-3012

light interference continued

- Si₃N₄ films, optical props., multilayer interference systems 7-13248
- Si, (7s)²(S-(5s²))S transition, two-photon absorpt., quantum interference 7-881
- TiO₂ thin films, struct., Raman spectra rel. to optical interf. 7-22367
- ZnSe, bistable interference filters, nanosecond switching at room temp. 7-11028

light interferometers

- see also light interferometry*
- antireflection coating stress in Fabry-Perot etalons 7-30064
- aspheric figure generation using feedback from IR phase-shifting interferometer 7-37219
- astrometric, POINTS design 7-40712
- astronomical instrumentation and techniques, conf., Tucson, AZ, USA (March 1986) 7-48162
- astronomical IR 1D speckle interferometry system 7-55488
- ATF, FIR interferometer, development of high power FIR lasers 7-11757
- ATF, FIR interferometer system design, radial density profile determ 7-11758
- atomic interferometers, phase-dependence in multilevel atomic transitions 7-36569
- balance beam interferometer 7-9887
- best wave interferometer with Zeeman laser for measuring short range 7-18752
- boundary layer transition detector, using differential interferometer 7-20822
- circuit for simultaneous measurements of particle sizing interferometer signal characteristics 7-56220
- cross-grating interferometer, fringe formation 7-35578
- diffraction reflecting interferometer as combined resonator component, CO₂ laser continuous tuning band widening 7-25847
- diffraction null correctors, systems considerations, tight tolerances in fabrication 7-62820
- diode laser direct modulation heterodyne interferometer 7-41440
- distance meas., using continuously tunable light source 7-24621
- double twin path interferometer for thin film thickness meas. 7-344
- Fabry-Perot cavity, nonlinear birefringent, polarisation bistability 7-37017
- Fabry-Perot etalon, parallel processing optical limits 7-57266
- Fabry-Perot interferometer, incoherent, phase-induced intensity noise 7-56328
- Fabry-Perot interferometer, mirror random phase inhomogeneity influence, resonator use 7-24689
- Fabry-Perot interferometer, OTF and resolving power, sequential theory 7-48836
- Fabry-Perot interferometer combined arrangement for displacement meas. 7-48835
- Fabry-Perot interferometer-fringe system, integral-order no. of interf. calc. 7-56329
- Fabry-Perot resonator, transversely coupled fiber device 7-56325
- Fabry-Perot resonator with active Sagnac interferometer, multistable 7-50626
- Fabry-Perot system with Gaussian beam and optical system centering technology 7-30079
- fiber interferometer with 4X4 coupler quadrature outputs 7-31506
- fiber interferometer/amplitude modulator, two-mode 7-50750
- fiber optic interferometer, rotating ring, nonreciprocal effects 7-37171
- fiber optic interferometer and appl. to photographic materials testing 7-30077
- fiber optic interferometer using FM laser diodes 7-31470
- fiber optic interferometric electrically tunable filter using the thermo-optic effect 7-37113
- fiber optic interferometric sensor system, optically multiplexed 7-25986
- fiber optic interferometric sensors multiplexed using partially coherent light, expected noise levels 7-25982
- fiber optic Mach-Zehnder interferometric sensors, review 7-20432
- fiber optics, single-mode WDM systems using Fabry-Perot interferometers, wavelength-selective filters appl. 7-57557
- fiber-optic Mach-Zehnder interferometer, stabilisation as intensity modulator 7-20425
- Fizeau interferometer for testing the shape of plane surfaces of large optical elements 7-35585
- Fizeau wavemeter, wavefront curvature compensation 7-35571
- Fourier transform far IR spectroscopy with 4 m path difference interferometer 7-48887
- Fourier transform IR, dual beam dynamic range considerations in ultimate sensitivity 7-48890
- Fourier transform IR spectrophotometer, rotary scanning, props. and performance 7-48893
- Gabor filters applied to electronic speckle pattern interferometer images 7-9892
- goniometers, interference, operating reliability, effect of lateral beam displacement 7-41452
- grating shearing interferometer with variable shear and fringe orientation 7-35579
- heterodyne interferometric temp. sensor using transverse He-Ne Zeeman laser and polarisation maintaining fibre 7-25991
- heterodyne profiling, for angstrom region 7-35493
- III-V semiconductor integrated waveguides as all-optical logic devices 7-25869
- integrated optic device for fibre laser Doppler velocimeter 7-6022
- interferometric gravitational-wave detectors, radiation-pressure induced fluctuations reduction 7-35386
- IR interferometers at 10μm 7-35582
- Kerr nonlinear interferometer, number-phase minimum-uncertainty state with reduced number uncertainty. 7-35586
- large aperture interferometer with phase-conjugate self-reference beam 7-9884
- laser differentiating interferometer with hologram grating, use in mechanical vibr. meas. 7-56330
- laser Doppler vibrometer, interferometer-based 7-31722
- laser interferometer based on phase conjugation by stimulated Brillouin scattering 7-41450
- laser interferometer for recording holographic gratings 7-18867
- laser interferometer skin-friction meter, numerical and expt. study 7-16276
- laser interferometer syst. comparison and calibration 7-14997
- laser wavemeter, compact, automatic, for tunable IR diode lasers 7-43181

light interferometers continued

- Lau interferometer, coherence anal. 7-9879
- limitations and noise of interferometric systems using frequency ramped single-mode diode lasers 7-30065
- line diffraction test, modified point diff. interferometer 7-35572
- Lummer-Gehrcke interferometer, intensity distrib. 7-41444
- Lummer-Gehrcke multiinterferometer, phase function and intensity distrib. 7-9883
- Mach-Zehnder all-fibre interferometer as magnetometer with mag. feed-back compensation 7-25989
- Mach-Zehnder double sideband interferometric Y junction freq. translators for coherent optical fibre systems 7-25953
- Mach-Zehnder interferometer all single mode fibre magnetic field sensor 7-25990
- Mach-Zehnder interferometer with multimode fibers using the double phase-conjugate mirror 7-48834
- magnetometer fibre optic using Mach-Zehnder interferometer 7-18843
- Michelson interferometer, hand-held, design and sensitivity for Space Shuttle glow obs. 7-55421
- Michelson interferometer, optical system design for automated thermal expansion measurements 7-24694
- Michelson interferometer, optical three-dimensional displacement meter 7-41343
- Michelson interferometer, slightly-cooled high-resolution, for limb emission meas. from space 7-55317
- micrometer coupled to interferometer 7-56221
- microwave power detection by optical fibre arrangement 7-18865
- monofrequency laser interferometer with fine resolution 7-18753
- multichannel grating phase-shift interferometers 7-30076
- multichord, near infrared interferometers for the CTX and ZT-40M experiments 7-11753
- multicore optical fibres for sensors 7-25988
- multipass grating interferometer applied to line narrowing in excimer lasers 7-35573
- nonlinear Fabry-Perot interferometer as medium for waves travelling parallel to reflecting planes 7-62748
- nonlinear optical-fibre interferometer for photon number nondemolitional meas. 7-62653
- nonperturbing boundary-layer transition detector for hypersonic wind tunnel, based on laser interferometry 7-20821
- optical computing and logic using Sagnac interferometric switches 7-25940
- optically phase-locked electronic speckle pattern interferometer 7-56326
- parallel shear interferometer for stellar interferometry 7-29402
- particle sizing interferometer, new optical geometry 7-41437
- particle sizing interferometer use as polar nephelometer 7-30070
- PEPSIOS, Polyetalon Pressure Scanned Interferometric Optical Spectrometer 7-18377
- PEPSIOS system, modifications and Periodic Comet Halley (1982i) imaging 7-18356
- phase closure with a rotational shear interferometer 7-56324
- phase sensitive scanning optical microscope, interferometer-based design with submicron resolution 7-24698
- phase-shift interferometer, surface gauging in quality control 7-4885
- picosecond light switch, design (Japanese) 7-1257
- polarising, two-beam, millimeter wave dielectric meas. of birefringent materials 7-14978
- pressure sensor, interferometric single-fibre, aperture stop influence on S/N ratio 7-43388
- pulse shaping and passive mode-locking with nonlinear Michelson interferometer 7-15914
- real-time image processing with interferometer using self-pumped phase conjugate mirror 7-20156
- reflecting multibeam interferometer with anisotropic elements, characts. 7-9891
- rhodamine 6G dye laser, 580 nm, small line width, cavity arrangement 7-62728
- scanning Fabry-Perot interferometers for the far infrared, review 7-41453
- SCRIBE interferometer atmospheric emission spectra 7-55319
- single-mode fibre coupler, fabrication and appls. (Japanese) 7-6018
- speckle, interferometer, imaging, in space, image reconstruction by speckle masking 7-31258
- speckle interferometer based remote electro-optic displacement sensor 7-48838
- speckle interferometer for thermal expansion measurements 7-48840
- stepping Michelson interferometer control of tunable diode laser 7-43135
- super-smooth surface, roughness measurement using interference microscope (Japanese) 7-41344
- TFTR, detached plasma regime study using MIRI FIR interferometer 7-11760
- TFTR plasmas, Faraday rotation and line electron density meas. using FIR interferometer 7-11754
- thin film beam splitter and appl. to Michelson interferometer 7-31436
- tracking novelty filter using interferometer with phase conjugate mirror 7-43334
- twin-wave laser interferometer for remote meas., accuracy increasing methods 7-343
- two-beam, noise power spectra induced by laser phase noise 7-30066
- two-beam interferometric devices with in-phase outputs, optical bistability 7-62764
- wavelength stabilization of tunable diode lasers using an internally-coupled Fabry-Perot interferometer 7-31353
- wavemeter, Twyman-Green type, performance assessment (Korean) 7-24692
- wide band pass filters, multiple Fabry-Perot interference filter struct. (Korean) 7-25943
- Al_{0.5}Ga_{0.5}As, AlAs and GaAs epitaxial multilayers as optical interferometric elements 7-342
- CO₂ TEA laser, tunable travelling-wave, single mode operation using interferometer 7-15840
- GaAs etalons, pulsed optical logic 7-57412
- InSb bistable etalon, regenerative pulsations 7-20318
- LiNbO₃ traveling-wave optical couplers and interferometric modulators, power requirements 7-57539
- LiNbO₃, z-cut interferometers, thermal instability, electrostatic mechanism 7-37207
- LiNbO₃:Ti integrated optical devices, domain inversion effects in Mach-Zehnder interferometer 7-62849

light interferometers continued

- LiNbO₃:Ti(H) waveguide interferometers, response 7-26024
 Nd:YAG laser unstable resonator output coupler based on Fabry-Perot interferometer 7-43166

light interferometry

see also *holographic interferometry; moiré fringes*

- 3D object repositioning using a projected grating and photographic enlarger 7-41456
 acousto-optical interferometer using Kosters prisms for RF direction of arrival meas. 7-41445
 air, negative corona, neutral densities and temps., optical interferometric and thermocouple studies 7-26569
 air jet, development and breakaway, coanda effect, interferometric, Schlieren and shadowgraph investigs. 7-51358
 astronomical instrumentation and techniques, conf., Tucson, AZ, USA (March 1986) 7-48162
 astronomical speckle interferometry, cross-spectrum techniques appl. 7-55492
 astronomical speckle interferometry, image reconstruction by speckle masking, speckle spectroscopy, multiple-mirror interferometry 7-55484
 atmospheric temperature meas. by molecular rotational band obs. with Fabry-perot interferometer 7-47546
 automatic fringe pattern analysis, review 7-18869
 bubble diameter meas. by fringe method, using laser Doppler anemometer 7-16278
 ceramic technology appls. of interferometric meas. techniques 7-39813
 ceramics, parameter meas. by laser interferometry 7-9888
 ceramics, powder size and distrib., surface texture, thermal props., interferometric meas. 7-9818
 ceramics, props. meas., conf., Soverato, Italy (Sept. 1986) 7-9582
 cineform element synthesis, optical method based on multi-beam interferometry (Russian) 7-50794
 coherence measurement of quasi-monochromatic thermal light using double-exposure specklegrams 7-18870
 coherent image subtraction using phase conjugate interferometry 7-25727
 coil constant determ. in γ -expt. at PTB 7-18739
 column density meter, high precision technique for line-of-sight vapour densities meas. 7-48695
 combined laser interference system for the meas. of motion 7-41443
 computer complex for measurement and processing of interferograms 7-41454
 confocal scanning, microscope, complex defocus signal amplitude, interferometric meas. 7-30082
 conjugate lateral shear interferometry and its implementation 7-30067
 conjugate shear and moiré interferometry appl. to obtaining out-of-plane displacements derivative 7-9880
 crack stress intensity factor determ. 7-43816
 crack under mode I loading, coherent-light-shadow spot, theory and expt. 7-63089
 511 Davida, speckle interferometry and photometry rel. to dimensions, rot. pole and albedo 7-24045
 differential speckle imaging with the cophased Multiple Mirror Telescope 7-55490
 diffraction gratings, variably-spaced linear and circular, fabrication, interferometrically controlled rotary ruling engine 7-62854
 diffusely scatt. objects, dynamic deform. meas. by holographic moiré and speckle interferometry 7-46764
 dispersion, precise meas. with interferometric technique 7-9886
 displacement meas. from double-exposure laser photographs, fringe visibility 7-41442
 displacement meas. using laser-speckle interferometry and stimulated US stress waves 7-24624
 displacement measurement, speckle modulation methods (Korean) 7-29965
 displacement sensor with two-beam interferometry, US nondestructive evaluation of composite materials 7-13716
 distance meas., using continuously tunable light source 7-24621
 distance meas. by wavelength shift of laser diode light 7-4806
 dralon fibres of kidney cross-sectional shape, double refr. meas. 7-4882
 drop curvature meas. by differential interferometry 7-41339
 droplet sizing techniques, laser interferometric, performance comparison 7-30071
 dye laser, tunable, CW, Ar⁺ laser-pumped, spectral props. 7-1096
 electro-optic frequency shifters appl. in heterodyne interferometric systems 7-18866
 electronic speckle pattern interferometry, basic principles, configs., industrial appls. 7-35588
 engineering measurements, optical methods, review 7-30072
 ether-drift experiment nullified by resynchronization of observer's clocks 7-35275
 F₂(II) colour centre laser at 2.653 μ m, synchronously pumped, mode-locked, cavity length meas. 7-5920
 Fabry-Perot interferometry for spectral line profiles determ. 7-41446
 fibre optic displacement sensor, based on Mach Zehnder interferometry 7-43432
 fibre optic interferometric detection of slow phenomena 7-43423
 fibre sensor intermodal interference appl., fringe counting meas. technique 7-31499
 fibre-optic sensors, developments and A/D signal conversion problems (German) 7-26019
 fibres, single mode, picosec. stimulated Raman generation, pump pulse fragmentation and fragment compression 7-50635
 fibres and preform rods refractive index profile reconstruction from transverse interferometric data 7-11113
 film, transparent, thickness and absolute fringe order, interferometric determ. method 7-292
 flow parameters in presence of shock waves, interferometry 7-43982
 frequency shifters, wave-plate multipass counterrotating for heterodyne interferometry 7-35584
 fringe analysis by photodiode array digitizer 7-30073
 fringe compensation in speckle interferometry, NDT appl. 7-18864
 fringe contrast improvement in speckle photography, speckle reduction using vibr. optical fibre 7-9889
 fringe projection for study of deformations and projection 7-41438
 fusion-spliced fibres, Zeiss-Linnik interferometric exam. 7-31531
 general relativity interferometric tests, use of squeezed states 7-4329
 geological targets, penetration expts. 7-14271
 graphite fibre reinforced epoxy laminate, dynamic moiré interferometry of stress wave propag. 7-59717

light interferometry continued

- gravitational wave detection via correlated spontaneous emission lasers 7-35387
 HD 97950, central object of giant H II region NGC 3603, speckle masking obs. 7-29502
 heterodyne interferometric MTF meas. device, for visible and IR ranges 7-30080
 heterodyne interferometric profilometer 7-29980
 heterodyne interferometry phase change meas. 7-341
 high-speed photography, videography and photonics, conf., San Diego, CA, USA (Aug. 1985) 7-18486
 holographic and speckle image shearing interferometry, NDT appl. 7-30075
 holographic optical elements, powered refl., analysis and construction 7-25747
 holospecklegram orthogonal polarisation props. 7-24695
 hook method in anomalous dispersion, revised fringe eqn. 7-4883
 Hubble Space Telescope primary mirror, test and eval. 7-40708
 image reconstruction, weighted shift-and-add technique, statistical analysis 7-55489
 interferogram anal. by modified sinusoid fitting technique 7-35580
 IR imaging optical systems, two-level testing process 7-31431
 IR lenses MTF determ., line-spread and interferometric results comparison 7-31430
 laminate, dynamic moiré interferometry of stress wave propag. 7-59717
 laser diode array, radiation patterns, phase measurement by shearing interferometry 7-1207
 laser Doppler interferometry methods for highly accurate flow meas. 7-44073
 laser Doppler velocimetry for solid surfaces, using specular reflection (Japanese) 7-41359
 laser frequency division and stabilisation, meas. appls. 7-20314
 laser losses and efficiency meas. 7-43106
 laser radiation, diffusely scattered, spatial coherence and its meas. 7-20134
 Lau interferometry and diffraction correlation (Chinese) 7-57247
 length measurement, electronic processing of interferograms 7-4886
 lens decentering, speckle interference display 7-43301
 linear displacement meas. using spatial phase detection of 1D periodic pattern (Japanese) 7-56217
 localisation effect on interference, intensity calcs. 7-20166
 locality violation, interpretation of quantum mechanics 7-20167
 long-baseline optical interferometry and refr. index struct. function saturation 7-60574
 Mach-Zehnder, film thickness meas. of postwidthdrawal drainage 7-18750
 matched filtering for speckle location identification 7-55483
 materials testing, optical techniques 7-33897
 metal surfaces, pulsed laser irradiation, thermomechanical effects, interferometric study 7-20303
 metallic samples, shock loaded, mass ejection meas. techniques 7-30032
 metals, noncontact US inspection, laser and EM acoustic transducer techniques comparison 7-28252
 metals, point defects in thermal equilibrium, laser interferometry-neutron diff. studies 7-58274
 meter practical realisation, using light interferometer (Slovak) 7-61316
 Michelson stellar interferometry, pupil plane and image plane imaging 7-47727
 microcomputer-based image processing aids in optical analysis and simulation 7-36891
 moiré, with carrier fringes, shear strain meas. in graphite-PEEK beam 7-65253
 moiré deformation field quality and strain meas., effects of spatial coherence of light source and grating gap 7-61372
 moiré interferometry, crack tip displacement anal. 7-11367
 moiré interferometry, high sensitivity, for displacement meas., tutorial paper 7-56331
 moiré interferometry for out-of-plane displacement meas. 7-18871
 Multichannel far infrared interferometer, MIRI, signal processing for electron density meas. 7-25232
 multichannel FIR collective scatt. and interferometry systems for fusion diagnostics 7-25215
 multiple beam interference for birefringence measurement in anisotropic crystals 7-41455
 multiwavelength interferometry limit imposed by source freq. instability 7-41439
 NDT, laser ultrasonic generation and optical detection with a confocal Fabry-Perot interferometer 7-28250
 null detector, interference-type, for ang. position of object meas. 7-56327
 nylon bicomponent fibres, optical props., interf. determ. 7-45974
 one-sided interferograms in Fourier spectrometers, recovery of linear phase errors 7-35581
 ophthalmic laser interferometry 7-47204
 optical detection of nanosecond acoustic pulses 7-43584
 optical detection of ultrasound 7-43583
 optical fibres, refractive indices and birefringence meas., interferometric methods 7-29644
 optical methods in composites, conf., Keystone, USA (Nov. 86) 7-55894
 optical plate surface flatness meas. by phase detection technique 7-31536
 optical ranging by wavelength multiplexed interferometry 7-4813
 optical system centering by speckle interferometry (French) 7-37215
 optically excited resonant diaphragm pressure sensor 7-56243
 particle size measurement using fibre-optic dual-beam laser interferometer 7-35494
 particle sizing interferometer nephelometry 7-30070
 passive synthetic aperture imaging using achromatic grating interferometer 7-10867
 phase closure with rotational shear interferometers 7-36895
 phase meas. with subpicosecond resolution by time-domain interferometry 7-41451
 phase reversal travelling wave integrated optic modulators, time-domain anal. 7-5988
 phase-shifting speckle interferometry 7-48839
 picosecond interferometric technique for study of phonons in Brillouin frequency range 7-14998
 piezoelectric transducer, mechanical impulse response, optical probing 7-20551
 plasma diagnostics appl. of optically pumped FIR lasers 7-5877
 plates, butt-welded, residual deform. meas., white light speckle technique 7-17749

light interferometry continued

- principle strains in the plastic region, optical meas. using moiré method and interferometry 7-17580
 pupil and image plane interferometry at optical wavelengths: visibility and phase analysis 7-55491
 quantum measurements of positions and interferometric noises 7-14921
 quasi interferometric set up, pseudocolour encoding, spatial frequency domain 7-62640
 range finders design principles 7-4808
 real-time fringe contrast measurement in stellar interferometry 7-29402
 real-time shadow moiré vibr. meas., simple setup, high sensitivity and exact calibration 7-20668
 residual stress meas. by speckle multiple image shearing camera 7-31720
 Ronchi test with daylight illum. for testing mirrors and lenses 7-11180
 rough surface profile, two wavelength speckle interferometry, statistical props. 7-48837
 rough-surface interferometry, two-wavelength, absolute statistical error 7-41448
 scatter-plate interferometry, improvement by scatter-plate rotation (Korean) 7-24691
 scattered component of light wave meas., wavefront shearing interferometric methods 7-24690
 semiconductor laser, linewidth determination from self-heterodyne meas. with subcoherence delay times 7-20300
 shift-and-add imaging 7-55486
 shock experiments, velocity-interferometer data, digital image processing 7-18868
 shock wave fracture, interferometric investig. 7-44683
 shock-compressed transparent materials, refr. index meas. using laser interferometry 7-30081
 single mode fibres, interferometric meas. of chromatic dispersion 7-43413
 single-mode fibre waveguide, chromatic dispersion determ. by interf. method 7-43389
 single-mode fibres, birefr., chromatic and polarisation mode dispersion, interferometric meas. 7-57571
 sinusoidal phase modulating interferometry for surface profile measurement 7-9878
 sinusoidal phase modulating interferometry measurement accuracy anal. 7-9881
 SMC N2, planetary nebula, mass determ. by speckle interferometry 7-24183
 solar F-corona, interferometric obs. of radial vel. field between 3 and 7 solar radii 7-66535
 speckle, phase-averaging method modification 7-41447
 speckle interferometric data analysis, weighted shift-and-add algorithm 7-55485
 speckle metrology techniques, displacement and strain meas. 7-42936
 speckle pattern, partially developed, in far field, 2nd order statistics 7-42920
 speckle photography, photography, diffraction halo effect 7-35574
 speckle photography fringes, 2D digital processing, angular density. accuracy 7-41441
 speckle-shearing interferometry, compensation for rigid and deformational displacements 7-48841
 stellar amplitude interferometry, first angular diameter determ. 7-40811
 stellar angular diameters and limb darkening meas., potential accuracy of speckle interferometric obs. 7-47720
 strain meas. using fibre optic sensor 7-43433
 testing accuracy of optical components, recording arm distortion effects 7-43457
 thermoelastic props. meas. of plastic film covered steel plates 7-33713
 thin films, refr. index dispersion meas. 7-18863
 tokamak plasma, 2D density distrib. using phase imaging interferometry 7-11739
 tomography and interferometry, regularisation, expt. errors and accuracy 7-35583
 transparent media refractive index determ. by diffraction method 7-41435
 transport objects, refr. correction to phase in interferometry 7-30069
 triple shearing interferometry, high angular resolution 7-47717
 turbulent atmosphere, high-resolution image form. of coherently illuminated objects 7-55261
 two-beam interferometry, polarisation effects, coherency matrix anal. 7-24693
 Van Biesbroeck 8, IR speckle interferometry rel. to binary nature 7-66587
 vibratory structures, stroboscopic laser speckle interferometry 7-30074
 wave field calcs. in accelerated interferometer 7-48439
 Al alloy plates, crack opening after discontinuous growth, laser interferometry studies (Russian) 7-46604
 Ar, meas. of flow instability and metastable state population due to shock wave, hook interferometry 7-16207
 C plasma, nonuniform, shock wave propag. investig. 7-44174
 CO₂ waveguide laser, anomalous refr. indices of amplifying medium 7-36933
 GaAs third order elastic constants, US displacement interferometry 7-2087
 GaAs-GaAlAs passive MQW waveguide resonators, all-optical switching effects, expt. study 7-15967
 Ge third order elastic constants, US displacement interferometry 7-2087
 HCl-Ar gas mixtures, electron irradi., negative differential conductivity 7-63243
 LiNbO₃, temp. tuning coeff., meas. using SHG based interferometry 7-11051
 N₂ laser, four-channel TEA, for interferometric meas. on plasma focus 7-43188
 Si epitaxial layers, free carrier conc., optical interference determ. 7-2745
 Si, ion implanted, mech. stresses, laser interferometer studies 7-6657
 Si-Al optically excited diaphragms, reson. freq., temp. depend. 7-18971
 SiO₂, ion-activated chem. etching, laser interferometry studies 7-12424
 W (100), IR surface-wave interferometry 7-44245
 WC-Co cermet particle reinforced low alloy steel composite, elastic const., laser US technique 7-65268

light meters *see photometers***light microscopes** *see optical microscopes***light microscopy** *see optical microscopy***light modulation** *see optical modulation***light polarisation**

see also birefringence; optical rotation; photoelasticity; polarimetry
 aberration coefficients of lenses 7-50686

light polarisation continued

- accretion disk radiation, polarization and beaming 7-47688
 acousto-optic signal processors, polarisation effects 7-25723
 anisotropic magnetically active dielectric, light reflection and refraction 7-62618
 Fo Aqr (H2215-086), intermediate polar, visual and IR polarimetry rel. to origin of pulsations 7-47985
 atmosphere, polarisation-scatt. phase functions, one-parametric model (Russian) 7-29240
 atomic magnetic substates for radiative transition with arbitrary polarisation 7-5639
 atoms, oriented, light transmission, quantum polarisation changes (Russian) 7-20175
 B5, interstellar dark cloud, stellar polarisation meas. rel. to large dust grains 7-9529
 Barnard 335, dense mol. cloud, mag. field characts. and polarimetric anal. 7-14625
 beam splitters, fibre-optic polarising, anal. 7-15980
 bees, polarisation vision 7-3791
 Berry's topological phase, obs. by use of optical fibre 7-42905
 birefringent fibre waveguide with elliptic borosilicate cladding, polarisation characts. study 7-62835
 birefringent nonlinear media, polarisation instability and bistability 7-57443
 bistability criteria, formal and heuristic method 7-57411
 bistable device, hybrid, driven by light polarisation 7-50625
 bistatic rough surface scattering cross section for physical optics model, variation 7-20138
 bow-tie fibres, microbending losses 7-57572
 bow-tie fibres with const. curvature, macrobends 7-57573
 broadband metal/glass single-mode fibre polarisers 7-6007
 cataclysmic variable stars, linear and circular polarisation obs. 7-9491
 chart, planar for expressing state-of-polarisation of light 7-15813
 cholesteric liq. cryst., imperfect, reflection coeffs. and light depolarisation 7-45963
 cholesteric thin films, light propagation, beam polarisation rotation calcs. 7-13245
 coil of single-mode fibre, birefringence and polarisation mode dispersion 7-31498
 P/Comet Halley, (1982i), in situ photopolarimetric meas. of dust and gas in coma 7-14527
 P/Comet Halley (1982i), linear polarisation obs. 7-47782
 P/Comet Halley (1982i), polarimetry of visible and UV molecular bands 7-66503
 Comet Hartley-Good (1985 XVII), polarimetry of visible and UV molecular bands 7-66503
 condensed media, powerful surface EM wave generation role in intense light effect 7-33348
 connective tissue polarity: optical 2nd-harmonic microscopy, crossed-beam summation, and small-angle scatt. in rat-tail tendon 7-23394
 control of optical instruments, using fibre optics or Bragg cells 7-14992
 control of polarisation state, using fibre optic techniques 7-43421
 cornea, transmission of linearly polarised light 7-54550
 crosstalk meas. on high birefringence fibres 7-57566
 crystals, nonlinear polarisation spectroscopy, two-wave case 7-50624
 V645 Cyg-Duck Nebula complex, characts. and obs. 7-60655
 depolarising effect of polarised polychromatic beam propag. through optically active medium 7-5835
 difference resonance expt. with polarising prism 7-26385
 directional coupler, polarisation-preserving, appls. 7-1279
 dye laser radiation, polarisation modulation using intracavity method 7-62740
 electro-optic devices, Pockels cell, review 7-50729
 ellipsometric characterisation of single mode fibres 7-43428
 elliptically cored optical fibre for polarisation preservation using mode matching method, accurate numerical anal. 7-11116
 eye, corneal polarisation, biaxial model for living human eye 7-59973
 Fabry-Perot cavity, nonlinear birefringent, polarisation bistability 7-37017
 Fabry-Perot resonator, confocal 4.5 m long for storage of megawatt laser pulses 7-1200
 fibre, birefringent polarisation-maintaining, mode coupling distrib. meas. 7-31507
 fibre, polarisation maintaining with three layer elliptical cross section, transmission characts. 7-1268
 fibre interferometer/amplitude modulator, two-mode 7-50750
 fibre optic couplers, single-mode polarisation maintaining 7-26011
 fibre optic directional coupler, polarisation preserving 7-25999
 fibre optic gyroscope, noise due to birefringence modulation 7-31479
 fibre optic hydrophone with dual in-line resonant cavity 7-43600
 fibre optic monomode sensors, optical processing schemes for phase and polarisation state information recovery 7-50763
 fibre polarisation components, birefringent, for sensor appls. 7-20450
 fibre-optic acousto-optic tunable filter 7-5979
 fibres, birefringent, anal. 7-57587
 fibres, depolarisation of light in irregular anisotropic single mode fibres 7-62841
 fibres, multimode, polaris.-modulated signals transmission and holographic multiplexing 7-37199
 fibres, polarisation preserving, discharge fusion splice optimum method 7-31529
 fibres, polarisation-holding, internal rotation of birefringence axes 7-43400
 fibres, polarisation-maintaining, low-loss, low-crosstalk, design and fabrication 7-11138
 fibres, polarisation-maintaining and their appls., review 7-11136
 fibres, polarisation-maintaining birefringent, polarisation cross talk ultimate limit 7-25970
 fibres, single mode, elliptical, polarisation maintaining, effect of coatings 7-20454
 fibres polarisation rotation, path depend. 7-37172
 fibres side-tunnel type, polarisation-maintaining, vectorial wave anal. by variational finite elements 7-11137
 FIR and MM wave polarisation transforming reflectors 7-36854
 flames, cross-beam polarisation spectroscopy with pulsed dye laser 7-13771
 four wave mixing polarisation bistability, topological nature 7-31389
 four-wave mixing of polarised light, phase conjugation, saturation effect 7-37051
 four-wave mixing techniques for studying orientational relaxation, comparison 7-10779

light polarisation continued

- fused-fibre coupler as quarter-wave device, polarisation characts. in 1.55 μm wavelength region 7-20419
- Gaussian random surface, light scatt. backscattering enhancement and depolarisation 7-62627
- grating holograms, with high diff. efficiency 7-57278
- group theory and polarisation algebra 7-56319
- haemoglobin, inverse Faraday effect, mag. reson. Raman activity 7-65700
- Haro 6-5 complex, struct., polarisation obs. 7-48049
- DQ Her stars and other cataclysmic variables, polarisation obs. 7-9491
- heterodyne interferometric temp. sensor using transverse He-Ne Zeeman laser and polarisation maintaining fibre 7-25991
- high-birefringence fibres, dichroism eval. using crosstalk meas. 7-20421
- holospecklegram orthogonal polarisation props. 7-24695
- hybrid polarisation encoding shadow casting for optical computing, logic operations 7-1032
- III-V semiconductors, hot-electron photoluminescence, polarisation 7-46118
- impurity liq. cryst. spectra. complex vibron struct., polarisation absorpt. band splitting studies 7-17332
- incoherent beams, partially polarised, maximum degree of polarisation of resultant beam 7-57230
- induced rotation of light polarisation plane under one- and two-photon reson. conditions 7-50623
- inhomogeneous films, optical props., model (French) 7-59278
- interferometric strain meas. using fibre optic sensor 7-43433
- internal polarised radiation in multilayered atmospheres, computation 7-14377
- interstellar dust, light extinction and polarisation 7-40888
- interstellar paramagnetic grain alignment associated with internal friction and the polarization efficiency 7-48053
- interstellar polarisation, dust parameters rel. to gas-phase element depletions 7-48015
- interstellar polarisation, implications for dust grain models 7-48013
- interstellar spherical grains, polarization, props., light scattering 7-14631
- IR diffractive filters fabricated by electron beam lithography, spectral and polarising characts. 7-62816
- IR reflection nebulae in Orion Molecular Cloud 2, photometry, polarimetry and spectrophotometry 7-55765
- isotropic media, light reflection, polarisation characts. 7-42903
- L1551 IRS 5, IR polarimetry of nearby refl. nebula 7-24186
- laser cavity, losses, radiation spectrum locking, phase polaris. method 7-11012
- laser light anal. and polarisation using SHG 7-57453
- layered inhomogeneous uniaxial media, light prop., pseudo-Stokes parameters, geometric optics approx. 7-57244
- LDN 723, dense mol. cloud, mag. field characts., polarimetric anal. 7-14625
- lens systems, variation of polarisation structure of axial beams 7-36876
- lidar equation taking account of polarization, second order scattering and travelling time effects 7-60380
- liquid films, power reflection, variable angle 7-53424
- M51, spiral mag. field config., visible polarimetric obs. 7-60800
- magnetic control of polarization switching 7-62758
- magnetic stars, spectropolarimetry rel. to diagnostic contents of Stokes I and V line profiles 7-29484
- metal mirrors, absorbance meas. at glancing incidence, photoacoustic calorimetry 7-20380
- metals, laser radiation absorption, dependence on shape 7-26794
- MIS-liquid crystal structures, pseudocolour image synthesis 7-31252
- modal dispersion of polarisation and its recovery by phase conjugation, model 7-43250
- Mon R2 star form. region, IR sources and polarisation obs. 7-60753
- monochromatic light polarisation after reflection on planparallel plate 7-1023
- multimode optical fibre probe in Z-pinch plasma expt., Faraday rotation 7-11785
- natural polarisation, observations and regularities using polarising glasses 7-20130
- nematic films, collective rotation of molecules driven by the angular momentum of light 7-27686
- nematic guest-host liq. crystals, pretilt angle determ. 7-21081
- nematic liq. crystal, impurity-molecule luminescence, rotational depolarisation kinetics 7-51629
- nematic liq. crystals, orientational self-focusing, aberration pattern polarisation asymmetry 7-11077
- noncollinear light prop. in rippled waveguide, geometrical optics approach 7-50742
- nonlinear for polarisation meas. in ellipsometer optical nonlinear media 7-14993
- nonlinear liquid in DC electric field, polarization variations of intense optical wave 7-20317
- nonlinear p-polarised optical waves, exact calcs. 7-62802
- nonlinear polarisation spectroscopy, normal waves, light-induced anisotropy 7-48858
- nonlinear TE polarised surface plasmon polaritons guided by metal films 7-5946
- nonlinear TM-polarised nonlinear waves guided by thin dielectric films, calc. 7-5993
- NS3, NS12, possible bipolar nebulae, optical polarisation study 7-48047
- OB supergiant stars, visible and IR continuum spectropolarimetric obs. 7-47845
- one-dimensional periodic holographic lattices, point spectrum 7-43006
- optical fibre, stress-applied, with inhomogeneous core (Japanese) 7-50780
- optical fibres, polarisation-maintaining with hollow circular pits 7-31494
- α Ori, dust shell Si fractional condensation, mass loss rate and grain characts., polarisation anal. 7-34972
- α Ori, dust shell UVB polarisation meas. 7-34971
- α Ori, scatt. model for optical polarisation 7-47852
- Orion Molecular Cloud 1, IR polarisation obs. and discovery of H₂ refl. nebula 7-14633
- Orion region, extinction and dust characts. 7-66728
- partial circular polarisers, performance under partially polarised light 7-37108
- particle size distribution in multicomponent systems, polarisation intensity ratio and pointer beam techniques 7-29967
- phase conjugation by modal dispersal, polarisation recovery 7-11065
- phase shifts of light wave on reflection, method for absolute values determ. 7-50490

light polarisation continued

- photorefractive cubic crystals, hologram diffraction efficiency and diffracted light polaris., optical activity effect 7-43020
- photorefractive ferroelectric crystals, polarisation reversal of light beam wavefronts 7-1235
- plane refracting surface, displacement of a bounded light beam on reflection 7-50489
- plasma layer, overdense, total transparency 7-26434
- polarised light, radiative transfer, obs. 7-1382
- polarization moments in a state with high angular momentum 7-43025
- polyacetylene films, oriented, optical props., photocond. meas. 7-64717
- polyethylene terephthalate glycol, films, uniaxially stretched, amorphous orientation and induced crystallisation 7-16448
- pulsed multifrequency lasers with isotropic resonators, radiation polarisation 7-62659
- quantum well heterostructures, intraband photocond. 7-64318
- quartz, X-ray induced blue luminescence, polarisation studies 7-3086
- quartz single-mode three-layer ring optical fibre, intrinsic birefringence and polarisation dispersion props. 7-50777
- quasars, polarisation characts. 7-4584
- Raman processes with several resonant levels and variable wave polarization in gases 7-1230
- Rayleigh scatt. and weak localisation, polarisation effects 7-42924
- readout system using reflecting discs, effect of birefringence of protective layer 7-57234
- real-time optical image subtraction based on wave polarization 7-57260
- reflecting multibeam interferometer with anisotropic elements, characts. 7-9891
- resonance scattering spectra, polarisation diagrams rel. to diagnostics of very weak mag. fields 7-23991
- Reusch's piles, selective light reflection, multiple domains (French) 7-36875
- rhodamine 6G, aggregated, in PMMA matrix, polarisation props. in transmitted light 7-31060
- rigid probe mobility in bulk elastomer, stationary fluorescence depolarisation obs. 7-7744
- roof prisms, optical transfer fn., polarisation effects 7-57525
- rotating linearly polarised light source for optical meas., using acousto-optical filter 7-18850
- rotating-detector ellipsometer, response to partially polarised light 7-41427
- rough surfaces, ellipsometry, depolarisation and cross polarisation 7-9873
- scanning polarisation/interference contrast microscopy, linear imaging 7-9895
- scattering from conducting particles with rough surfaces, incoherent specific intensities 7-57242
- semiconductor, two-photon-biexciton resonance, polarisation instability 7-3005
- semiconductor lasers, polarisation and wavelength control, TE, TM mode operation (Japanese) 7-25858
- semiconductor lasers, polarisation switching, injection locking mechanism 7-57380
- semiconductors, electroabsorption of light by deep impurity centres 7-45988
- side-tunnel fibre for single-mode, polarisation characts. 7-31474
- single quantum well, doubly resonant LO-phonon Raman scatt. via deform. pot., polarisation obs. 7-39114
- single-mode fibre, polarisation retaining with improved coil performance 7-20451
- single-mode fibre, two modes, polarisation state preservation 7-6015
- single-mode fibres, birefr., chromatic and polarisation mode dispersion, interferometric meas. 7-57571
- single-mode fibres, circular and polarisation-maintaining, 2D index distrib. determ. from near-field meas. 7-11118
- single-mode fibres, polarisation dispersion, model and anal. 7-6008
- single-mode single-polarisation fibre using resonant absorbing effect, theoretical study 7-43381
- solar spectral line profiles, effects of finite spectral resolution on Stokes V profile 7-47803
- solar white-light corona, polarisation theory for hydrostatic density distrib. 7-47797
- spatial filtering logic based on polarisation state 7-43330
- spatial hole burning suppression in polarisation coupled resonators 7-11074
- speckle polarisation analysis by ellipsometric method 7-42938
- spectrophotometer for meas. of polarised emission and excitation spectra 7-56318
- spherical harmonics solution for radiative transfer models, polarisation effects 7-20131
- symbolic substitution logic, optical implementation using polarisation for coding 7-10860
- T Tau stars, circular polarisation due to grains 7-40810
- TCNQ salts, quasi 1D molecular crystals, optical props., Hubbard model generalization, cond. calc. 7-45952
- TM-polarized nonlinear slab-guided waves in saturable media 7-31407
- Tokamak plasma diagnostics by meas. poloidal magnetic field, using Zeeman splitting in Li 7-1740
- transfer operators, spectral props., existence and uniqueness of solns. 7-62624
- twisted birefringent media, characteristic directions 7-5834
- twisted nematic liq. cryst. cell, polarisation anal. using Poincare sphere (Japanese) 7-64603
- twisted nematic thin films, light propagation, beam polarisation rotation calcs. 7-13245
- two-beam interferometry, polarisation effects, coherency matrix anal. 7-24693
- ultrashort light pulses, polarisation change near two-photon resonance 7-10848
- vacuum UV light polarisation, freq. conversion and fluorescence studies 7-10849
- Wigner distribution function from single object transparency, optical system for efficient display, polarisation encoding 7-31259
- Wood's anomaly effects on gratings of large amplitude 7-5986
- Young array, polarisation effects 7-57233
- AlSb, hot electron luminesc. 7-46119
- BaTiO₃, hexagonal, optical props. around 222K struct. phase transition 7-27685
- Cd²⁺, alignment after photoionis., fluoresc. radiation polarisation meas. 7-890
- CdS, integral exciton absorpt. coeff., temp. depend. characts. 7-45959

light polarisation continued

- CsVF₄, layer cpd., struct. phase transitions, thermal diffusivity, polarised light scatt. and X-ray diff. studies 7-6788
 Cu (001), single cryst., inverse photoemission polarisation effects study 7-27812
 CuCl, giant two-photon excitation of excitonic molecules, nonlinear depolarisation effects 7-64594
 Fe₂SiO₄, fayalite, electron density and polarised absorption spectra 7-22280
 GaAlAs lasers, polarisation-resolved low-frequency noise 7-15863
 Ga_{1-x}Al_xAs, disorder effects of Raman scatt. 7-7704
 GaAs, highly doped, polarised hot electron photoluminescence 7-46121
 GaAs, optical reflection anisotropy due to surface band bending 7-39062
 GaAs, photoholes in the spin-split band, energy relax. and spin depolarisation 7-22301
 GaAs:Cu, neutral state of deep acceptors, photoluminescence spectra, Jahn-Teller effect 7-64149
 GaAs-AlGa_{1-x}As quantum wells, doubly reson. LO phonon Raman scatt., photoluminescence spectra 7-53327
 GaInAsP/InP heterostruct., luminescence polarisation, quantum size effects 7-13210
 GaInAsP-InP laser, anisotropic deform. influence on radiative characts., threshold, polarisation and watt-ampere charact. 7-43100
 n-Ga_{1-x}In_xP, light scatt. by free carriers 7-17328
 GaN crystals, polarisation props. of band-edge emission, dispersion theory appl. 7-64694
 GaP(As)(Sb), band structure, polarisation-dependent angle-resolved photoluminescence spectroscopy 7-21814
 He-Ne laser at 0.633 μ m, frequency stabilisation, using polarisation modulation 7-20295
 InGaAsP buried heterostructure lasers, polarisation, effect of stress relax. caused by repetitive temp. change 7-62690
 n-InP, light scatt. by free carriers 7-17328
 InP(As)(Sb), band structure, polarisation-dependent angle-resolved photoluminescence spectroscopy 7-21814
 InSb, optical reflection anisotropy due to surface band bending 7-39062
 KCl:Li, self-induced light polarisation oscils., stochastic field effects (*Russian*) 7-43208
 KCl:Li crystals, F_A-centres self-induced resonant radiation polarisation changes study (*Russian*) 7-33358
 KI:Ti⁺ crystals, luminescence polarisation of dimer centres 7-22335
 LiNbO₃:Fe, asymmetric photoinduced scattering of light 7-17282
 LiNbO₃:Ti 4×4 directional coupler switch with permanently attached polarisation maintaining fibre array, low crosstalk 7-31520
 LiNbO₃:Ti 4×4 nonblocking interconnection network for test bed, video switching 7-26039
 MnF₂, light scatt. from magnons 7-45996
 (NH₄)₂SO₄:Tl crystal, temp. depend. of optical absorption bands 7-64671
 Na vapour, continuous wave second harmonic generation 7-37038
 RbLiMoO₄, phase transitions, optical polarisation obs. 7-16732
 Si, dislocation luminescence lines, polarisation 7-39154
 Si, optical reflection anisotropy due to surface band bending 7-39062
 Si:O, electronic struct. and atomic symmetry of the thermal donor 7-16986
 Sm, polarisation switching and optical bistability in Fabry-Perot cavity 7-1218
 Sm vapour, optical bistability expts., polarisation switching 7-62759
 Sr, (7s)¹(5s²)¹S transition, two-photon absorpt., quantum interference 7-881
 SrTiO₃:H(D), O-H and O-D stretching vibrs. under applied electric field and uniaxial stress 7-44723
 Ti₂MoSe₆, 1D superconductor, polarised reflectance spectra 7-45554
 TiSb₂, Raman spectra and vibr. modes, polarisation depend. 7-27725
 Xe multiphoton ionisation, suppression with circularly polarisation coherent light 7-19792
 Y₃Fe₂O₁₂:Si, band model of photoinduced magnetic effects 7-17214
 Zn⁺, alignment after photoionis., fluoresc. radiation polarisation meas. 7-890

light propagation

- see also *atmospheric light propagation; guided light propagation; light propagation in plasma*
 aerosols, beam propagation through slab scattering media, small angle approx. 7-57237
 Anderson localisation in random array of scatterers, pseudosphere approx. calcs. 7-43490
 cholesteric thin films, light propagation, beam polarisation rotation calcs. 7-13245
 complex optical systems, optical beam wave propag. 7-50492
 convection effect, numerical investigation method 7-25711
 cubic cylindrical single crystals, stress determ., Abel inversion (*Russian*) 7-16672
 dense particle systems, light propagation, Kubelka-Munk theory 7-57236
 dielectric slab, bent, with lossy coating, light absorption calc. 7-62620
 Doppler shifting of a distant light source in a Schwarzschild gravitational field 7-4319
 Gaussian beams, generally astigmatic, propag. along skew ray paths 7-62623
 Gaussian wave packet propag. in absorbing medium 7-43029
 inhomogeneous medium, light scatt. and propag., longit. correl. fn. 7-36881
 lasers and optical fibres, technology, theory, propagation and nonlinear optical phenomena, review 7-43437
 layered inhomogeneous uniaxial media, light propag., pseudo-Stokes parameters, geometric optics approx. 7-57244
 light transversing a gravitational wave background, red-shift, rel. scatt. coherence 7-4735
 nematic liq. crystals, light scatt. and propag. characts. 7-39078
 nematic liquid crystal film, quasi-static elec. field enhanced optical propag. effects 7-27702
 noncollinear light propag. in rippled waveguide, geometrical optics approach 7-50742
 nonlinear distortion compensation of light beams with restricted deform. of control mirror 7-50622
 nonlinear medium, control of σ^+ beam propagation by a σ^- beam 7-62799
 open resonators, Huygens-Fresnel principle and integral eqns. 7-31244
 pulse velocity through transparent plate 7-42901
 quadratic media, longit. homogeneous, with absorpt. or amplification, correlated coherent states 7-50621

light propagation continued

- random medium, two-scale soln. to wave propag. 7-42921
 refraction channels characts., wave eqn. parabolic approx. 7-42898
 relativistic acoustic Doppler effect in the optically limit 7-55
 scaling formula for light propag. with multiple scattering in turbid medium 7-36882
 Scattering medium, radiative transfer eqns., boundary conditions study 7-62630
 slightly inhomogeneous media, partially coherent optical field propag., density matrix formalism 7-15816
 spherical EM waves in gyrotropic media 7-20133
 temporal-spatial radiation functional meas. 7-30060
 three-level medium, ultrashort pulse train propag., population trapping and coherent bleaching calcs. 7-43263
 twisted nematic thin films, light propagation, beam polarisation rotation calcs. 7-13245
 ultrashort optical pulse propag. in free space, pulse evolution computation 7-57235
 uniform and Gaussian beam diff. comparison, aberration balancing 7-62621
 Rb₂ZnCl₄, cryst., incommensurate modulation, light propag. 7-22196

light propagation in plasma

- ablation plasma and shock waves, laser interaction, holographic interferometry 7-31981
 beat-wave accelerator, collinear optical mixing of relativistic electron plasma waves 7-11614
 beat-wave equations, relativistic solitary-wave solutions 7-20885
 cavity-structured targets, stimulated Brillouin scatt. suppression obs. 7-43238
 cubic optical nonlinearities 7-1703
 double induced Mandelstam-Brillouin scatt., π states 7-11606
 electron acceleration in a laser-irradiated plasma 7-11651
 hot-electron generation and transport in high-intensity laser interaction 7-26431
 ICF, 2D Lagrangian simulations 7-11676
 laser acceleration of particles, strong internal elec. fields in nonlinear force produced cavitons 7-11662
 laser assisted charge exchange reactions, theoretical and expt. investig. (*French*) 7-5759
 laser beam filamentation in plasma 7-58021
 laser filamentation in a thermally unstable plasma 7-44179
 laser fusion, comment on state of the art 7-26473
 laser fusion physics, conf., Vancouver, BC, Canada (June 1986) 7-24256
 laser harmonic spectroscopy use as plasma target diagnostic 7-26503
 laser light absorption and scattering, computer simulation 7-26500
 laser plasma, electron-positron pair prod. 7-63285
 laser wiggler beat waves in plasma, HF amplification 7-20117
 laser-fusion pellet, essential features 7-26468
 laser-plasma scattering, antibunched radiation generation, SU(2) and SU(1,1) Hamiltonians 7-67
 laser-produced plasma, Raman scattered light obs. 7-26398
 laser-produced plasma fluctuations, kinetic model 7-26469
 Mandelstam-Brillouin scattering, modulation and self-focusing instabilities 7-58022
 optoacoustic effect in discharge plasmas, phenomenological approach 7-31987
 overdense plasma layer, total transparency 7-26434
 particle acceleration in localised electrostatic wave packet, electron reheating 7-26446
 plasma effects in laser fusion: past and future 7-26472
 plasma wave generation, laser interactions and particle acceleration, review (*French*) 7-31954
 plasma waves in laser fusion plasmas, review 7-26405
 Raman scatt. simulation by stimulated Brillouin scatt. 7-1702
 satellite double stimulated Brillouin scattering 7-51453
 soft X-ray laser beam, divergence meas. 7-1210
 stimulated Brillouin scatt. spectra in laser-plasma interactions (*Chinese*) 7-58016
 stimulated Raman scatt. of laser light filament 7-51454
 super-dense hollow cathode discharge, plasma light amplification (*Japanese*) 7-6476
 TEXTOR Tokamak microturbulence, CO₂ laser scatt. meas. 7-58015
 underdense coronal plasma, laser interaction physics 7-26432
 wave-particle interactions and energetic tail formation in the electron distribution 7-26433
 wavefront reversal by stimulated Brillouin scattering in laser plasma, numerical simulation 7-62784
 Au plasma laser produced, X-ray line absorpt. 7-20878
 H, ionised gas-laser interaction, dynamic Stark effect (*French*) 7-6395
 H-like ion plasma, laser interaction, X-ray line emission self absorpt. and escape factors 7-37689
 He, ionised gas-laser interaction, dynamic Stark effect (*French*) 7-6395
 He-like ions, plasma, laser interaction, X-ray line emission self absorpt. and escape factors 7-37689
 N₂, destruction and heat transfer of heat-shielding coating 7-63263
- light reflection**
 see also *mirrors; optical films*
 airflow, convective turbulent, light reflection, partial phase conjugation 7-43248
 angle meas. by multireflected autocollimation 7-35495
 anisotropic magnetically active dielectric, light reflection and refraction 7-62618
 antiscattering single layer theory, antiscatt. antirefl. coatings 7-1029
 atmospheric optics, inverse problems 7-47537
 atmospheric turbulence, effect on light reflection under induced temperature nonuniformity of refractive index 7-60384
 benzene dynamic gratings, self-diffraction and reflection in degenerate four-wave interaction 7-37050
 bidirectional reflectance spectroscopy, extinction coeff. and opposition effect in particulate medium 7-24033
 close binary systems, monochromatic refl. effect and temp. distribns. on distorted surfaces 7-18439
 corrugated dielectric waveguide, external light reflection, narrow band filter fabrication 7-5999
 crystal optics with spatial dispersion 7-45954
 decomposed granite soil thickness, spectral reflectance and surface temp. (*Japanese*) 7-40479
 detectors for industry (*German*) 7-299
 DFB laser, single longitudinal mode operation considering light refl. from optical fibre facet (*Japanese*) 7-20284

light reflection continued

- dichromated gelatin achromatic reflection display holograms 7-25750
dielectric objects, light scattering, Stokes reciprocity relations 7-42895
disperse media, diffuse radiation reflection 7-42918
dye monolayers, short- and long-range interactions, light refl. and transmission 7-22206
dyestuff, optical density determ. with multi-reflection, correction eqn. (Japanese) 7-35563
electro-optical modulators, total internal reflection, with multimode strip lightguides 7-43355
FIR and MM wave polarisation transforming reflectors 7-36854
Fresnel equations for a magnetoelectric medium 7-50444
giant planets, relations between spherical albedo and observable characts. of planetary atmosphere 7-24031
glass plate stack mirror for laser resonator, refl. coeff. 7-57508
grating, second-order, canonical equations 7-43340
high-sensitivity piezoelectric equipment for deflecting light beam (Russian) 7-6353
homogeneous sphere on a substrate, light reflection calcs. 7-1027
icy surfaces, astronomical, optical constns. of $\text{H}_2\text{O}-\text{NH}_3$ ice mixtures 7-23993
index matching materials for optical fibre connector reflection reduction 7-62839
injection laser application for measuring surfacegeometric parameters 7-4816
Io surface materials, phase curves interpretation in terms of Hapke's function 7-55523
isotropic media, light reflection, polarisation characts. 7-42903
laser diode output power fluctuation due to reflected lightwaves 7-31342
laser surgery, CO_2 , speculum surface finish effect on beam refl. 7-65830
linear-nonlinear media interface, phase-conjugated reflection in the field of surface reference waves 7-57479
metal-insulator two-phase mixtures, reflection of light, specularly 7-22214
meter practical realisation, using light interferometer (Slovak) 7-61316
mirrors, phase fluctuations due to conductivity noises 7-62809
mode correction for turbulent distortions of optical waves, refl. from trihedral corner reflector 7-42914
monochromatic light polarisation after reflection on planparallel plate 7-1023
moving-mirror laser-beam scanner enhancement by multipath reflection 7-15963
multilayer atmosphere, diffuse refl. 7-4308
nematic liq. crystal, symmetrically realigned, refl. of a plane TM wave 7-44367
optical bistability with waveguide mode for finite-width incident beam 7-5944
optical discs, reflection and scattering by pits, microwave simulation 7-36889
optical-fibre connector with index matching material, Fresnel reflection reduction methods 7-1267
phase shifts of light wave on reflection, method for absolute values determ. 7-50490
photometer meas. of transmission and reflection coeff. under optical prod. conditions 7-41421
plane refracting surface, displacement of a bounded light beam on reflection 7-50489
planetary surfaces, optical refl. as operator-eigenvalue problem 7-24032
polarized light transfer, spectral props., existence and uniqueness of solns. 7-62624
polarized light transfer, transport theory conf., Montecatini Terme, Italy, June 1985 7-60874
polyacetylene thin films, photoexcited states, ps relax. 7-64291
pseudo-Brewster angle, analytical soln. 7-31240
random layered medium, light reflection 7-5837
readout system using reflecting discs, effect of birefringence of protective layer 7-57234
resonant optical medium surface, nonlinear refl. and refraction of scanning laser beam, integrodifferential eqns. method calcs. 7-43209
retroreflective array in spectroscopic instrumentation, optical props. 7-56348
Reusch's piles, selective light reflection, multiple domains (French) 7-36875
roof prisms, optical transfer fn., polarisation effects 7-57525
saturable absorber boundary, bistability by reflection 7-62800
scattering medium, light transmission and reflection (French) 7-42913
Scattering medium, radiative transfer eqns., boundary conditions study 7-62630
secondary radiation polarisation, multiple specular reflection of light from crystal surface 7-39130
semiconducting plane-parallel slabs, normal-incidence exciton transmission and refl. spectra 7-39058
semiconductor films, absorbing, optical constants from transmission and reflection props. 7-41433
silicate surface layer of yellowed rice plant leaf, IR refl. spectra 7-3837
single-mode fibre ends, polished, reflections 7-26012
skeletal muscle, frog, small angle equatorial reflections of diffr. pattern rel. to sarcomere length 7-40215
smoothly irregular layer, plane wave refl. 7-50488
solid particle receiver materials, optical props., diffuse reflectance of Norton Masterbeads at high temp. 7-40044
sound reproduction from old wax phonographic cylinders, laser beam reflection method use 7-37014
stratified medium, output characts. in case of bilateral incidence of monochromatic waves 7-31241
sunlight transmission, passive optical element with selective angular reflection 7-57524
surgical instruments, diffuse laser light refl. from surfaces 7-47205
thin films, light grazing tunnelling, reson. absorpt. 7-42897
thin-film optical coatings, scatter from fluid patches 7-1028
transparent conducting oxides, uses in a-Si:H solar cells 7-46953
 BaTiO_3 phase-conjugate mirror, partial cancellation of specular reflection 7-5956
Cu, anodic oxidation in KOH soln., in situ spectroelectrochemical anal. 7-28192
Cu thin film, surface electromag. waves damping, deposition technique study 7-59274
Hg liq.-optical fibre interface, optoacoustic effect study 7-44698
Hg reflector geometry variation by immersed-electrode current (Spanish) 7-11095

light reflection continued

- Si, amorphous and crystalline, light reflection, optical third-harmonic generation 7-11059
 SiO_2 :P films, pure and doped, low press. CVD growth, structural, optical, elec. props. 7-27186
light reflection spectra *see reflectivity; spectra*
light reflectometry *see reflectometry*
light refraction
see also birefringence
alignment of diffraction and refraction components in optical systems 7-25925
anisotropic magnetically active dielectric, light reflection and refraction 7-62618
apparatus for measuring the refractive index profile of an optical fibre 7-37231
astrometry, internal refr. errors in USNO meridian circle 7-4333
autonomous satellite navigation using observations of starlight atmospheric refraction 7-60418
children, differential effects of various causes of deafness on eyes, refr. errors, and vision 7-8555
dralon fibres of kidney cross-sectional shape, double refr. meas. 7-4882
fibre optic modulator and logic gate using nonlinear refr. and absorpt. 7-37174
Fresnel equations for a magnetoelectric medium 7-50444
high accuracy universal polarimeter, accuracy improvement, appl. to ferroelec. tetramethylammonium tetrachlorozincate 7-17300
high-multiplicity, optical density as a fn. of interface structure 7-39923
mirage effect, 3D calcs. using personal computer 7-50484
plane refracting surface, displacement of a bounded light beam on reflection 7-50489
refraction channels characts., wave eqn. parabolic approx. 7-42898
resonant optical medium surface, nonlinear refl. and refraction of scanning laser beam, integrodifferential eqns. method calcs. 7-43209
suspended particles in Baltic Sea, refr. indices from measured and computed light scatt. 7-9024
telescope design using refr. of prism rows 7-37091
transparent biaxial crystals, nonlinear refr. in conical refr. region 7-31382
transport objects, refr. correction to phase in interferometry 7-30069
 LiNbO_3 for optical communication 7-31269
light scattering
see also Brillouin spectra; opalescence; Raman spectra; Rayleigh scattering; stimulated scattering
3D and 2D radiative transfer in the diffusion approx. 7-10853
aerosols, beam propagation through slab scattering media, small angle approx. 7-57237
aerosols, light scattering, 10.6- μm extinction coeff., forward-scatter meter 7-57238
Anderson localisation in random array of scatterers, pseudosphere approx. calcs. 7-43490
antiscattering single layer theory, antiscatt. antirefl. coatings 7-1029
arteriovenous O_2 difference, spectrophotometric meas., role of light scatt. 7-3942
atmosphere, mathematical model for predicting night-sky glow 7-9172
atmosphere extinction at Cerro Tololo Inter-American Observatory, (January to July 1984) 7-47542
atmospheric correlation-time measurements and effects on coherent Doppler lidar 7-60385
atomic metastable states produced during cooperative self-diffraction in a resonator, Maxwell eqn. solns. 7-42558
Baltic Sea, comparison of measured and computed light scatt. by suspended particles 7-9024
beam tensor, transformation during light-medium interaction 7-42906
benzene, liquid, structural transitions, light scattering 7-63791
bidirectional scattering distrib. function meas. using computer controlled facility 7-41414
bile salt-lecithin vesicles mixed, formation, temp. depend., quasielastic light scatt. meas. 7-34114
binary liquid mixture, late-stage phase separation and hydrodynamic flow, light scatt. meas. 7-58486
biological macromolecules, struct. deter., giant combination scatter of light 7-8484
birefringence presence, interference fringes in scattered beams 7-50491
bistatic rough surface scattering cross section for physical optics model, variation 7-20138
block copolymers, mol. wt. and comp. heterogeneity, determ. 7-6556
Born vs. Rytov approximations, is the debate over? 7-62593
caesium perfluoro-octanoate, lyotropic liq. cryst., press. depend. of nematic-isotropic transition 7-32647
cataclysmic variables, effect of scatt. cloud on hot spots flickering 7-55667
cavitation in large scale shear flows 7-51244
cholesteric liq. crystals, icosahedral ordering, light scatt. and Landau theory calcs. 7-51627
coated surfaces, influence of metal films on optical scatter and microroughness 7-13242
coating defects, correlation between pulsed laser damage and probe laser scatter 7-38049
coherent scatt. diffr. patterns transform. from gas and cryst. systems, cryst.-chem. cluster model calcs. 7-62619
colloidal suspensions, cross-correlation intensity fluctuation spectroscopy and laser trapping studies 7-28359
P/Comet Halley (1982), multiple light scattering near nucleus 7-40770
cometary dust grains, wavelength depend. of light scatt. 7-55535
conducting particles with rough surfaces, incoherent specific intensities 7-57242
connective tissue polarity: optical 2nd-harmonic microscopy, crossed-beam summation, and small-angle scatt. in rat-tail tendon 7-23394
cornea, effect of epithelial and stromal oedema on light scatt. props. 7-34132
cornea, effects of fibril orientations on light scattering 7-34134
cornea, transmission of linearly polarised light 7-54550
crystal-melt interface, diffusional light scatt. 7-39137
curved metal surface, roughness monitoring using laser light scattering (Japanese) 7-14918
cytochrome c, nonradiative decay, absorpt. and reson. light scatt. 7-62440
deep metallic grating, light scatt., surface plasmon dispersion 7-20128
dense particle fields, laser diffraction meas. correction for multiple scatt. 7-1212

light scattering continued

- dense particle systems, light propagation, Kubelka-Munk theory 7-57236
 deoxyhaemoglobin S, solns. and gels, quasi-elastic laser light scatt. 7-28464
 Dhahran, Saudi Arabia, insolation meas., diffuse fraction estimation 7-3625
 diaphanography, breast cancer detect. by transillum., IR scatt. and absorpt. obs. on cell suspensions 7-47211
 dielectric cryst. thin films, refl. and transmission coeffs., S-matrix method calcs. (*Russian*) 7-33473
 dielectric crysts., inelastic light scatt., chaotic behaviour 7-3062
 dielectric objects, light scattering, Stokes reciprocity relations 7-42895
 dielectric particle morphology dependent resonances 7-20127
 dielectric single layers, scattering reduction or enhancement 7-50483
 dielectric spheroids, attenuation efficiencies 7-20139
 dielectric spheroids, TE-type planar wave scatt. 7-42899
 dielectric targets composed of continuous assembly of circular discs, light scatt. 7-50482
 diffraction gratings, false gratings and random rough surfaces, numerical comparison of light scattering 7-5830
 diffractive diffusers for display applications 7-5977
 diffuse light in diffraction gratings and surfaceplasma oscillations 7-10847
 diffuse object, scattered light props. and appl. to roughness meas. 7-20140
 diffusely scattering objects image contrast, prod. by thick-layer transmission phase holograms 7-36921
 diffuser transmission functions and far-zone speckle patterns 7-42932
 diffusional light guides, synthesis, inverse spectral problems 7-62823
 dilute solutions, randomly broken chains, small angle neutron, X-ray and light scatt. data 7-10788
 diphenyl ether, liq., reorientational motion, press depend. light scatt. obs. 7-46054
 diphenyl methane, liq., reorientational motion, press depend. light scatt. obs. 7-46054
 disperse medium, light scatt., correl. radius estimate 7-42917
 droplet sizing techniques, laser interferometric, performance comparison 7-30071
 echelle spectrographs, scattered light background correction method 7-34874
 edge scattering from large metallic cylinders 7-10846
 ethane, thermal diffusivity around crit. point along liquid-gas coexistence curve, light scatt. meas. 7-52098
 EUV materials, low reflectance 7-57488
 ferroelectric ceramics, electromagnetic wave scatt. from dielec. permittivity tensor inhomogeneities 7-7629
 fibre array polar nephelometer, scattered light phase functions meas. for atmospheric particles 7-23896
 fibre optic gyroscope, phase modulated, coherent backscatter analysis 7-43427
 fibre optic particle concentration sensor 7-20443
 fibre optic sensors, extrinsic, for remote meas., impact on meas. techniques 7-11154
 fibre optic sensors for remote measurement 7-43394
 fibre OTDR, range and accuracy in backscatter measurements 7-15999
 flowing two-phase dispersed particles, metrology using optical diffusion (*French*) 7-31895
 fluid, chaotically convecting thin layer, temp. field, light scatt. meas. 7-51126
 fluid layer, critical opalescence in multiple scatt., density fluctuation higher correlation contrib. 7-33351
 fluids, differential light scatt. expts. 7-29627
 forward-scattering of light in wood smoke, depend. on electrical conductivity 7-42912
 free liquid surface, light scatt. 7-36880
 frequency cross-correlation of intensity fluctuations, multiple-scatter soln. limitations 7-42919
 Gaussian beam, radiation scatt. by cylinder, distrib. (*Russian*) 7-20136
 Gaussian random surface, light scatt. backscattering enhancement and depolarisation 7-62627
 generalised Lorenz-Mie theory, first exact values, comparisons with localised approx. 7-42892
 glasses, surface structure minimal disturbance under ion bombardment 7-12419
 glasses, turbid, for calibration and checking of nephelometers and turbidimeters 7-20141
 grating efficiency measurement and automated scatter inspection system (GEMASIS) 7-62853
 Gurevich equation derivation for reflectance from plane bounded scatt. media 7-20137
 n-heptane-perfluorohexane soln., phase separation, spinodal curves 7-13170
 highly reflecting diffusers, middle-IR region, develop. status study 7-57615
 homogeneous medium, selective laser heating and nonlinear light scattering 7-5938
 homogeneous sphere on a substrate, light scatt. using Mie's soln. and Weyl's method 7-1026
 III-V semiconductors, lattice defects detection using IR tomography 7-32234
 impenetrable object tomographic reconstruction 7-62592
 inhomogeneous medium, light scatt. and propag., longit. correl. fn. 7-36881
 integrated optical waveguide attenuation meas. by prism coupling and scattered light techniques 7-43363
 interplanetary dust, scatt. phase function determ. from blue light survey of gegenschein 7-24065
 interstellar dust scattering in Car II region 7-24153
 interstellar grains, albedo and scatt. props. from CCD surface photometry of refl. nebulae 7-55773
 interstellar spherical grains, polarization, props., light scattering 7-14631
 inverse optics, conf., San Diego, CA, USA (Aug. 1985) 7-60869
 inverse problems and the Newton-Kantorovich method 7-62596
 inverse scattering, inverse source approach 7-62594
 inverse scattering and three-wave interaction in nonlinear optics, review 7-11030
 inverse scattering problem soln. using null field method 7-62595
 Io surface materials, phase curves interpretation in terms of Hapke's function 7-55523
 isotropic fluid, FCC lattice model, Monte Carlo simulation and appl. to collision induced light scatt. 7-16384

light scattering continued

- IUE telescope, light scatt. profile determ. 7-60551
 22 Kalliope, multiple scatt. factor and phase coeff. from photoelectric photometry 7-47749
 L1551 IRS 5, dust scatt. model for IR polarisation of nearby refl. nebula 7-24186
 large particles, vectorial description of light scattering in eikonal picture 7-10858
 laser beam scattering by Mie centres, numerical results using localised approx. 7-10854
 laser communication, picosecond laser pulses, transformation by multiple scattering media 7-42944
 laser double-pulsed velocimetry, image shifting technique to resolve directional ambiguity 7-37559
 laser radiation, diffusely scattered, spatial coherence and its meas. 7-20134
 leaky wave spatial spectrum generated by guided wave scatt. from acoustic wave 7-31460
 lens, rabbit, ageing, in vivo quasielastic light scatt. obs. 7-28500
 lidar equation taking account of polarization, second order scattering and travelling time effects 7-60380
 lidar in inhomogeneous atm., backscatter/extinction ratio humidity effects 7-40562
 lipopolysaccharide-protein complex of *Yersinia pseudotuberculosis* in aq. solns., light scatt. obs. 7-54437
 liquid crysts., blue phase, light scatt. and elastic moduli, Landau theory calcs. 7-2084
 liquid metals, light scattering during evaporation under monochromatic radiation 7-13172
 living human body, spectral radiative props. study 7-18013
 Martian limb hazes, vertical struct. from scattered light profiles 7-55513
 metal surface roughness parameter measurement, diamond turned, light scattering technique 7-61318
 metals, laser radiation screening by damage products 7-32493
 methanol particle sizing with phase Doppler spray analyser 7-29969
 micellar and hard sphere solutions, concentrated, diffusion 7-8316
 microprocessor meter of radiation attenuation coefficient in solutions 7-4876
 Mie near forward scattering, variable Gaussian approx. 7-50493
 mirrors particulate contaminated, model for scattering 7-42910
 mixed crystals, light scatt. spectrum, linewidths from sum rules 7-46028
 MOCVD growth processes, in situ charactn. by light scatt. techniques 7-22539
 molecules, vibr. and orientational relax., correl. functions 7-36738
 multilayer atmosphere, diffuse refl. 7-4308
 multiple scattering correction in meas. of particle size and density by diffraction method 7-9815
 multiple scattering problems in integrated optics, path-integral formulation 7-50787
 multipoint fibre optic refractive index sensors 7-43419
 nematic droplet, light scatt. 7-22274
 nematic liq. crystals, light scatt. and. propag. characts. 7-39078
 nematic liq. crystals, molecular association, influence on dielectric and electro-optic props. 7-16407
 nematic liquid crystal, light scattering in elec. field 7-1843
 nematic liquid crystals, negative dielec. anisotropy, near IR light scatt. 7-1844
 nematic liquid crystals, orientational relax. time, light scatt. 7-51624
 nonideal systems, dynamic light scatt. and mutual diffusion 7-50485
 nonlinear problem of incoherent scattering in one-dimensional medium 7-4313
 nucleated blood cells, numerical anal. of light scattering 7-14042
 objective white light speckle method and incoherent data extraction (*Chinese*) 7-48833
 ocular lenses, human, diagnostic evaluation using quasi-elastic light scatt. spectroscopy 7-34230
 ocular lenses, human, in vivo meas. using quasielastic light scatt. 7-34231
 optical discs, reflection and scattering by pits, microwave simulation 7-36889
 optical glass, ultrasonic properties and low freq. light scattering 7-21361
 optical theorem, scatt. with a boundary 7-53356
 optical waveguide loss meas. by scattered radiation detection 7-37143
 optically heterogeneous materials, light scatt., struct. aspects of dichromatic laser speckle patterns 7-31248
 optically thick medium exposed to laser beam, anisotropic back scatt. 7-62629
 α Ori, scatt. model for optical polarisation 7-47852
 parametric scattering in short light pulse fields 7-57470
 particle, arbitrarily shaped, intrinsic optical activity in light scatt. 7-10844
 particle, coupled dipole method, physical reformulation 7-42923
 particle counters, quantitative count calibration 7-56397
 particle siting with phase Doppler spray analyser, nonspherical drops effect 7-29969
 particle size and velocity measurement using phase Doppler particle analyser 7-29968
 particle size distribution in multicomponent systems, polarisation intensity ratio and pointer beam techniques 7-29967
 particle size measurement by laser diffraction beam stop and vignetting effects 7-9813
 particle size measurement by light scattering, vignetting phenomena 7-56219
 particle size measurement by light scattering detection with fibre optic sensor 7-37160
 particle sizing, high resolution, using time-of-flight and light scatt. meas. 7-48684
 particle sizing and spray analysis, conf., San Diego, USA (Aug. 1985) 7-29583
 particle sizing interferometer nephelometry 7-30070
 passive ring resonator gyro, reson. characts. of backscatt. 7-50753
 phase differential scattering from microspheres 7-10855
 phase grating detection, speckle correl., optical inverse scatt. 7-50495
 phototactic microorganism *Haematococcus pluvialis*, transient photoreponses revealed by light scatt. 7-28481
 phytoplankton, intra- and interspecific single cell optical variability, obs. 7-47015
 picosecond light pulses scattered by optically induced gratings in semiconductors, frequency shift and spectral changes 7-1024
 plasma diagnostics, molecular origin of background light in Thomson scattering measurements 7-32089

light scattering continued

- plasma diagnostics appl. of optically pumped FIR lasers 7-5877
 PMMA, swelling caused by CS₂ imbibition, light scatt. investig. 7-62628
 PMMA-phosphate plasticizer systems, phase equilibrium and struct. (*Russian*) 7-63515
 polarisation state control using fibre optic techniques 7-43421
 poly-4-hydroxystyrene, dil. soln. props., light scatt. and viscosity meas. 7-39135
 poly- γ -benzyl-L-glutamate, cholesteric soln., elec. field effects (*Russian*) 7-11909
 polyamide acids, dil. soln., structurisation (*Russian*) 7-42810
 polyamide acids, optical anisotropy (*Russian*) 7-37837
 polyamide hydrazides, aromatic, p- and m-phenylene units effects on struct.-prop. rels. 7-51604
 polydiacetylene solutions, semidilute, rod-coil transition, aggregation 7-15752
 polydisperse polymer solution, size distrib. fn. determ., light scatt. appl. (*Russian*) 7-5806
 polyethylene blends, melting, crystallisation, DSC, X-ray diffr., Raman spectra 7-44411
 polyethylene blends, melting, crystallisation, relax., DSC, light scatt. 7-44412
 polyethylene blends, melting and crystallisation, small angle light scatt. 7-44413
 polyimides, dil. soln., structurisation (*Russian*) 7-42810
 polymer films, light scattering, struct. aspects of dichromatic laser speckle patterns 7-42931
 polymer solns., dynamic light scatt. from once broken rod molecules, initial relax. times 7-33404
 polyoxypropylene diol, solns., structs. and thermodynamics near consolute temps. (*Russian*) 7-63435
 polyphenylmethylsiloxane, cyclic, preparation and fractionation 7-23013
 polysaccharides, in coccoliths of *Emiliania huxleyi*, molar mass determ. 7-8479
 polystyrene, cryst. colloidal array filter 7-37117
 polystyrene, linear, atactic, chain size determ., rel. to intensity light scatt. 7-16388
 polystyrene, solns., static screening length behaviour 7-20078
 polystyrene, solns., structs. and thermodynamics near consolute temps. (*Russian*) 7-63435
 polystyrene interactions in bad solvent, experimental study 7-58124
 polystyrene latex spheres, aggregation kinetics, laser light scatt. 7-13827
 polystyrene latex spheres, particle size and vel. meas. using phase Doppler particle analyser 7-29968
 polystyrene lattices, soln., salt-induced aggregation kinetics, quasielastic light scatt. 7-59796
 polystyrene mixtures in benzene solns. light scatt. virial coeffs. 7-44737
 polystyrene solns., integrated intensity light scatt., conc., temp., mol. wt. depend. 7-46056
 polystyrene submicron size sphere in aq. suspensions, multiple light scatt. 7-59220
 polystyrene-poly(vinyl methyl ether), binary mixtures, spinodal decomposition 7-44822
 polystyrene-polyvinyl methyl ether, crit. mixture, late stage spinodal decomposition 7-26955
 polystyrene-polyvinylmethylether blends, phase decomp., small angle neutron scatt. 7-28021
 polystyrene/poly(vinylmethylether), spinodal decomposition, thermal fluctuation 7-21460
 powders, finely dispersed, optical consts. light scatt. 7-39138
 propagator for MTF of wide-angle scatterer 7-5851
 quartz, fused, surface structure minimal disturbance under ion bombardment 7-12419
 quartz fibres, geometrically perturbed, light scattering 7-57563
 quasar radiation polarisation, role of multiple scatt. by free electrons 7-4584
 quasi-elastic light scattering, data acquisition and evaluation 7-56239
 quasielastic light scattering microscope spectrometer 7-41478
 quasielastic-scattering linewidths and relaxation times for surface and mass fractals 7-1030
 radiation fields description on basis of invariance principle, average photon lifetime in scatt. medium 7-23986
 radiative transfer in scattering media 7-62630
 radiative transfer theory, small-angle approx. and numerical soln. 7-36878
 radiative-transfer inverse problem, time dependent, analytical error estimates 7-31242
 random medium with Kolmogorov spectrum and inner scale of turbulence, intensity covariance of point source 7-57245
 random phase screens, light scattering props. 7-57241
 randomly oriented particles, scatt. matrix 7-10856
 resonance light scattering from liquid suspension of microspheres 7-42911
 resonance scattering spectra appl. to very weak mag. fields diagnostics in diffuse media 7-23991
 retinal rod outer segment suspensions, effect of sonication on nucleotide-dependent light scatt. changes 7-23398
 reverse scatter from complex-shaped bodies, coherent multichannel effects 7-10851
 rice starch suspension, image transfer modulation transfer function 7-36884
 rough sphere, coherent scattering cross-section calc. 7-10857
 scaling formula for light propag. with multiple scattering in turbid medium 7-36882
 secondary radiation in optically anisotropic infinite crystals, general theory 7-7709
 secondary radiation polarisation, multiple specular reflection of light from crystal surface 7-39130
 semiconductor heterostructures, inelastic light scatt. by electronic excitations 7-13171
 silica, colloidal, gelation 7-46877
 Silica aerogels, ethyl versus methyl sol-gel comparison, polar nephelometry studies 7-8312
 simple fluids, interaction-induced light scatt., 1st and 2nd spectral moments 7-39133
 slab waveguides, guided modes, roughness-induced scattering and attenuation 7-43367
 solar cell enhanced performance by front surface light scattering 7-8420
 solar corona, anal. of H I Lyman-alpha line profiles in polar region (April 1979) 7-47809

light scattering continued

- solar white-light corona, polarisation theory for hydrostatic density distrib. 7-47797
 solid particle receiver materials, optical props., ang. scatt. and extinction characts. of Norton Masterbeads 7-40043
 speckle polarisation analysis by ellipsometric method 7-42938
 spectrophotometers, scattered light amplitude meas. 7-35567
 spectroscopy of 2D plasmas in semiconductor heterojunctions 7-2702
 spherical and rodlike macromolecules binary mixture, photon correlation spectroscopy 7-42909
 spherical harmonics solution for radiative transfer models, polarisation effects 7-20131
 statistical solution to light backscattering 7-50486
 storage phosphor system for computed radiography: screen optics 7-23445
 subhertz anisotropy fluctuations detection in small-angle light scatt. 7-64662
 sulphobetaine polymers, phase behaviour and soln. props. 7-38164
 surface ripples on solid-liq. interface, light scatt. theory 7-64595
 surface-enhanced spectroscopy appl. to change of optical props. of microenvironment of small scattering object 7-18852
 surfaces of small roughness, strong scatt. 7-42935
 synchronous excitation spectrofluorometry, scatt. background elimination 7-54203
 tetramethoxysilicon, light scatt., below sol-gel transition 7-46058
 thin-film optical coatings, scatter from fluid patches 7-1028
 thylakoid membrane, light scatt., photo-induced changes, surface charge effect 7-59934
 thylakoid membrane, light scatt., photo-induced changes, temp. treatment effect 7-59935
 tracer diffusion in concentrated colloidal dispersions 7-8303
 transient resonant light scatt., time-resolved spectra (*Japanese*) 7-59218
 transient resonant light scatt., time-resolved spectra (*Japanese*) 7-59219
 transmission and reflection by high scattering medium (*French*) 7-42913
 turbid media, appl. of Kubelka-Munk theory to Fe oxides and colour of Triassic sediments 7-66098
 turbulent medium, I-K distrib. for random optical fields 7-34674
 two-layer particle suspension, Rayleigh-Gans approx. in extremal illum. region 7-31249
 two-level atomic lattice models, spontaneous emission and light scatt. 7-50018
 two-phase flow, concentration and droplet size distrib., simultaneous and instantaneous meas. 7-37535
 velocimeter, fibre optic, low cost 7-20444
 water aerosol, light scattering, evaporation effect study 7-62626
 water-in-oil emulsions, adsorbed-solvated layers, optical obs. 7-59798
 water-oil-tenside microemulsion, three-phase regime 7-13826
 wave-kinetic numerical approach to beam propag., canonical problems 7-31247
 wavefront shearing interferometric methods for scattered component of light wave meas. 7-24690
 weak localization in finite slab, anisotropy effects and light-path classification 7-42925
 AgGaSe₂ crystals, light scatt. and transparency, annealing expts. 7-3338
 Al vacuum-deposited films, topography characts. by light scattering 7-9816
 Ar, inductively coupled plasma torch, gas flow dynamics, light scatt. technique 7-11795
 Ba₂NaNb₂O₁₅, parametric light scattering, nonlinear diffraction 7-37044
 BaSO₄ disordered diffuse solid scatterer, light scatt., weak localisation effects 7-22276
 BaSO₄ precip. growth, nucleation process, light scatt. obs. 7-16465
 Ba₂Si_{2-x}Nb₂O₆, poly- and single-domain samples, integrated light scatt. and polarisation 7-53361
 CsVF₄ layer cpd., struct. phase transitions, thermal diffusivity, polarised light scatt. and X-ray diffr. studies 7-6788
 Cu, surface structure minimal disturbance under ion bombardment 7-12419
 Fe-Au-Fe double layers, exchange coupling 7-27510
 Fe-Cr-Fe double layers, exchange coupling 7-27510
 GaAs, crystal defects, IR light scattering tomography and IR absorption microscopy 7-46023
 GaAs, dislocations, stereographic obs. by IR light scatt. 7-32235
 GaAs, EL2 clusters, scattering and absorpt. of IR light 7-53382
 GaAs, IR tomography and transmission images, numerical processing 7-32236
 GaAs in MIS struct., light scatt. from inversion layer 7-3033
 GaAs quantum wells, band offsets, inelastic light scatt. studies 7-7362
 GaAs wafers, subsurface structural defects, photon backscattering studies 7-12059
 GaAs:In(Cr), doped and undoped, microdefects obs. by IR light scatt. tomography 7-32662
 GaAs-AlGa_{1-x}As quantum wells, parabolic, light scatt. studies 7-64651
 GaAs-AlGaAs heterostructures, 2D electron system, collective excitations, light scatt. (*Japanese*) 7-12633
 GaAs-GaAlAs, modulation doped heterostructures, spectroscopy of 2D plasmas 7-2702
 GaAs-GaAlAs interface dislocations, stereographic obs. by IR light scatt. 7-32235
 n-Ga_{1-x}In_xP, light scatt. by free carriers 7-17328
 Ge, scattering inhomogeneities, two-wavelength probe meas. 7-46063
 Ge, single crystal, optical constants, surface polishing effects 7-59175
 H₂O vapour condensation on glass, growth of breath figures 7-12405
 n-InP, light scatt. by free carriers 7-17328
 KCl doped crystals, impurity centres, form. processes and thermoactivation solution 7-44576
 KH₂PO₄ precip. growth, nucleation process, light scatt. obs. 7-16465
 KTa_{0.991}Nb_{0.009}O₃, dipolar glass, cluster dynamics 7-22184
 LiIO₃ crystal, coherent four-photon scatt. by polaritons 7-22273
 α -LiIO₃ crystals, anomaly of optical props., 100 to 140°C, influence of growth defects 7-59172
 LiNbO₂:Fe photorefractive crystals, light-induced scattering 7-10887
 LiNbO₃, photoinduced light scatt. 7-3011
 LiNbO₃:Fe, asymmetric photoinduced scattering of light 7-17282
 LiNbO₃:Fe, speckle size depend. on laser beam size via photo-induced light scattering 7-5840
 LiNbO₃:Fe crystals, biharmonic pumping, photoinduced light dispersion (*Russian*) 7-31391
 LiTaO₃ crystals, parametric holographic-type light scatt. processes 7-1215
 Mg+H₂, reactive collision complex form., far wing laser light scatt. 7-22982

light scattering continued

- Mg+H₂, reactive collision dynamics by far using laser scatt. 7-28296
 Mo, surface structure minimal disturbance under ion bombardment 7-12419
 N₂O, thermal diffusivity around crit. point along liquid-gas coexistence curve, light scatt. meas. 7-52098
 PLZT ferroelec. ceramics, IR optical and electrooptical props. studies 7-7675
 PLZT transparencies contrast increase, using electrically controlled light scattering 7-25909
 PLZT transparent ferroelec. ceramic, hologram recording energy transfer, light scatt. effects study 7-5855
 PLZT transparent ferroelec. ceramics, low freq. dielec. props. study 7-7630
 Pb(Si_{1-x}Nb_x)O₃ ferroelec. ceramics, IR optical and electrooptical props. studies 7-7675
 RbFeF₄ layer cpd., structural phase transitions studies 7-26942
 SF₆, thermal diffusivity around crit. point along liquid-gas coexistence curve, light scatt. meas. 7-52098
 Si, scattering inhomogeneities, two-wavelength probe meas. 7-46063
 21R-SiC:N, shallow donor bound electronic transitions, light scatt. study 7-38494
 SiO₂ aggregates, fractal props., light scatt. studies 7-28358
 Sr, scattered light obs. with laser excitation 7-30968
 XeCl laser, laser snow in active medium 7-43070
 ZrF₄-based optical fibres, scattering loss meas. 7-11114
 Zr₂O₃-Y₂O₃, ionic diffusion coeffs. comp. depend., quasielastic light scatt. temp. depend. meas. 7-12364

light sensitive materials *see optical materials; photographic material sensitivity; photographic materials*

light sources

- see also infrared sources; light emitting devices; photometric light sources; spectroscopic light sources*
 coherent UV- and VUV- radiation generation, antiStokes Raman process 7-11062
 continuously tunable, absolute distance meas. using interferometers 7-24621
 detectors for industry (German) 7-299
 displacement meas. from double-exposure laser photographs, fringe visibility 7-41442
 energy measurements in vac.-UV region, use of reson. fluorescence 7-57502
 fibre optic sensors, extrinsic, for remote meas., impact on meas. techniques 7-11154
 flash lamp, low-pressure, background radiation from ablation phenomena 7-43282
 gas-liner pinch as source of blackbody-limited VUV radiation 7-9868
 gases, freq. mixing, tunable coherent VUV generation 7-11061
 high brightness ultraviolet light source 7-25920
 holograms, transmission, display with white light source 7-36913
 integral characts. determ. of light sources (Czech) 7-57501
 laser plasma, extreme UV and soft X-ray light source 7-63320
 linear grating sensors, moiré signal quality rel. to light source coherence and grating gaps 7-31446
 moiré deformation field quality and strain meas., effects of spatial coherence of light source and grating gap 7-61372
 multiwavelength interferometry limit imposed by source freq. instability 7-41439
 particle beams use in radiation generation from IR to γ -rays 7-42877
 pattern recognition using Fresnel holographic filter and extended source 7-62633
 Penning discharge source for extreme ultraviolet calibration 7-25919
 planar gaussian Schell-model sources, radiation efficiency 7-37081
 polarimeter for fibre characterisation using narrow- and broad-band sources 7-35569
 radiating atoms on lamp filament, photography (French) 7-37080
 rotating linearly polarised light source for optical meas., using acousto-optical filter 7-18850
 schlieren optics methods, comparison of light sources 7-57503
 SHG by Gaussian Schell-model source 7-5953
 spectral measurement for wavelength regions 400 nm to 750 nm and 700 nm to 2500 nm (Japanese) 7-351
 spectrally-broad picosecond light source for calibrating photonics equipment 7-20378
 spiral filament radiation approx. by radiation from cylindrical surface 7-37082
 surface discharges as intense photon sources for light-ion fusion accelerator cleaning 7-37800
 Tokamak as an X-ray/XUV light source 7-20926
 undulator sources, phase distribution of brilliance 7-31224
 VUV-soft X-ray beamline for spectroscopy and calibration 7-18966
 Ar, hollow cathode glow discharge, UV radiation and positive ions, investigation 7-21000

light transmission

- see also light absorption; optical filters*
 N,N'-bis(4-n-octyloxybenzyl)-1,4-phenylenediamine, condis crystal props. 7-37909
 C thin films, RF discharge deposition, mech., elec. and optical props. 7-22509
 cornea, transmission of linearly polarised light 7-54550
 dielectric cryst. thin films, refl. and transmission coeffs., S-matrix method calcs. (Russian) 7-33473
 dielectric objects, light scattering, Stokes reciprocity relations 7-42895
 diffuser transmission functions and far-zone speckle patterns 7-42932
 dye monolayers, short- and long-range interactions, light refl. and transmission 7-22206
 Fabry-Perot interferometer, OTF and resolving power, sequential theory 7-48836
 fibres, multimode, polaris.-modulated signals transmission and holographic multiplexing 7-37199
 FIR laser beams, precision broadband attenuator 7-37012
 Fresnel's reflectivity and transmission formula, modification for time-depend. optical parameters 7-31238
 glass, K-208, electrification effects in radiation optical props. 7-64592
 low resolution IR gas transmissivities, line-by-line approach 7-51386
 magnetic fluids, magneto-optical effects, birefringence 7-59186
 metallic wire grids, free-standing, transmission coeffs. in FIR, numerical computation 7-37109
 metals, laser radiation screening by damage products 7-32493

light transmission continued

- multimode optical fibres, periodic coherent pulse train transmission, broadening effects 7-11156
 nematic guest-host liq. crystals, pretilt angle determ. 7-21081
 nonlinear dielec. film, optical reflectivity and transmissivity power depend. calcs. 7-53429
 optical fibres, light transmission, comparison with elec. conduction 7-57594
 optical system, transmission coeff. calc. 7-43300
 optical theorem, scatt. with a boundary 7-53356
 phase change guest-host (PCGH) liquid crystal window to control solar energy 7-37123
 photometer meas. of transmission and reflection coeff. under optical prod. conditions 7-41421
 plasma layer, overdense, total transparency 7-26434
 PMMA, plastic optical fibres, for near IR transmission, prep. 7-62834
 polarized light transfer, spectral props., existence and uniqueness of solns. 7-62624
 polarized light transfer, transport theory conf., Montecatini Terme, Italy, June 1985 7-60874
 polyacetylene thin films, photoexcited states, ps relax. 7-64291
 polymer-metal composite thin films, plasma deposition, optical props. 7-27947
 polymers, gas-filled, action as cutoff optical filters in the IR region 7-57529
 polystyrene, monodisperse lattices, He-Ne laser transmission, attenuation coeff., specific turbidity meas. 7-62617
 polystyrene, plastic optical fibres, for near IR transmission, prep. 7-62834
 random layered medium, light reflection 7-5837
 rhodamine 6G, aggregated, in PMMA matrix, polarisation props. in transmitted light 7-31060
 rhodamine dyes, S₀-S_n two-photon absorption dynamics 7-42715
 scattering medium, light transmission and reflection (French) 7-42913
 semiconducting plane-parallel slabs, normal-incidence exciton transmission and refl. spectra 7-39058
 semiconductor films, absorbing, optical constants from transmission and reflection props. 7-41433
 shocked optical fibres, spectral transmission characts. 7-31466
 smectic liq. crystals, chiral, drive frequency effect on light transmission 7-21079
 solar cells, optical sheets, intensity enhancement by surface texturing 7-46940
 solar radiation transmission through random medium of water and glass 7-5841
 superlattices, gap solitons and nonlinear optical response 7-43204
 surface fabrication errors of optical systems, wavefront deformations calcs. 7-57262
 thin-film optical coatings, scatter from fluid patches 7-1028
 tinted hydrogel contact lenses, spectral transmittance obs. 7-54807
 transparent conducting oxides, uses in a-Si:H solar cells 7-46953
 transparent ferroelectric ceramics, comp., struct. and props. characts. anal. 7-7647
 water narrow band stochastic surface, laser beam transmission 7-13111
 Al₂O₃ glass, gel produced, optical transmission rel. to heat treatment 7-27733
 Au films, surface plasmon modes 7-7316
 C films, CK α spectra and interatomic bonding (Russian) 7-58705
 C films, diamond like, prep. and props. 7-22472
 CaO-Al₂O₃ glass, 3-5 μ m transmission, rain erosion resist., surface crystallisation treatment 7-37070
 CdIn₂O₄ thin films, DC reactive sputtered, elec. and optical props. 7-38788
 Cd_xSe_{1-x} mixed crystal, laser-induced probe-beam defocusing at band edge 7-7657
 Cd₃Sn₄, CVD, struct., elec. and optical props. (Korean) 7-27940
 CdZnTe, epitaxial growth via low press. CVD, IR detector appls. 7-64926
 Cu screen, transmission coeff. depend. on optical radiation incidence angle 7-57528
 CuCl polycrystalline layers, nonlinear propagation of nanosecond laser pulses 7-53263
 GaAs dislocated and In-doped dislocation free, inhomogeneities obs. by video-enhanced IR topography 7-32446
 GaAs semi-insulating thin wafers, EL2 defect and dislocation mapping, near-IR transmittance meas. 7-63605
 GaAs-Ga_{1-x}Al_xAs superlattices, optical props. 7-3007
 Ge-Se based glass films, photodarkening effect, exposure characts. (Japanese) 7-64706
 Hg_{1-x}Cd_xTe, epitaxial growth by low temp. metalorganic CVD 7-27911
 In₂O₃/Sn films, prep. by thermal decomposition of organometallic cpds., optical and electrical props. 7-17483
 In_{2-x}Sn_xO_{3-y} thin films, RF reactive sputtering prep., elec. and optical props. 7-39378
 In_{2-x}Sn_xO_{3-y}/Ag/In_{2-x}Sn_xO_{3-y} magnetron sputtered transparent heat-reflective films, thermal stability study 7-53426
 Li-TaS₂ intercalation cpds., room temp. optical transmission spectra, charge transfer and band struct. modification 7-45962
 α -LiIO₃ crystals, anomaly of optical props., 100 to 140°C, influence of growth defects 7-59172
 N₂O IR transmittance, band models comparison 7-19860
 a-Si:H, picosecond photoinduced absorption and transmission 7-3006
 Si:H microcrystalline films, glow discharge prep., elec. and optical props. 7-7415
 Si-N-H glow-discharge films, elec. and optical props., comp. depend. 7-58933
 SnO₂ films, CVD deposition, elec. and optical props. 7-7429
 SnO₂ films for solar cells, struct., elec., and optical props. 7-40003
 SnO₂:F thin film, uses for a-Si:H/a-Si_{1-x}C_xH solar cells 7-46952
 SnO₂:Sb thin films, doped and undoped, prep. by photolysis, phys. props. 7-22368
 TiO₂/Ag/TiO₂ struct., Ag thickness effect on optical transmission (Rumanian) 7-17354
 ZnO:Al films, RF reactive sputter deposition, struct., elec. and optical props. (Japanese) 7-27900
 ZnO/Ag/ZnO magnetron sputtered transparent heat-reflective films, thermal stability study 7-53426
 ZnS_{1-x}Se_x gradient IR optical material prepared by CVD 7-31408
 ZrO₂ thin films, optical consts. in UV regions, influence of evaporation parameters 7-39193

light velocity

wavelength of light in water, classroom demonstration 7-35167

light velocity measurement

streak camera and ring laser appl. 7-18766

light water *see water***lighting**

contrast rendering factors as alternatives to E/L ratios 7-11088

Defence Waste Processing facility, remotely replaceable lighting systems for hot cells 7-49695

fluorescent light, lack of effects on human muscle strength by kinesiology testing 7-23406

generators for commercial vehicles, oil cooled, heat transfer coefficients comparison (*German*) 7-37312

half-cylindrical illuminance parameter for lighting design 7-11087

nonresidential building daylighting by automated exterior louvres 7-8365

practical holography, conf., Los Angeles, CA, USA (Jan. 1986) 7-24281

lightning

1 to 20 MHz lightning radiation fields, amplitude spectra meas. 7-40549

aircraft lightning strike events, rel. to thunderstorm struct. 7-29172

atmospheric interference pulses in VLF band, statistical props. of time intervals 7-34659

ball, incandescent-breakdown multipoint emission studies 7-47477

Canada, lightning parameter meas. 7-47523

cloud to ground lightning flashes, data recording in eastern USA 7-18297

cloud-to-ground lightning, charge deposition to ground 7-29171

cloud-to-ground Lightning Position and Tracking System for electric utility weather problems 7-14371

East Coast Lightning Detection Network with computer-based display system 7-47556

electrostatic field measurements and the mechanism of intracloud discharges 7-55121

EM field horizontal and vertical fields for lightning above finitely conducting ground 7-34586

fulgurites, form., extreme reduction and metal silicate liquid immiscibility 7-47439

fulgurites of Kolyma River, USSR, struct. and location of find (*Russian*) 7-66119

ground coronae effects during lightning flashes 7-55122

ground electric field due to intracloud lightning 7-34587

holographic apparatus for studying simulated lightning in laboratory 7-26575

integral characts. determ. of light sources (*Czech*) 7-57501

leader tip modelling, introduction 7-66206

lightning discharge, current induced in aerial on buried telecom. line (*French*) 7-10817metal equipment struck by lightning, temp. distrib. anal. and heat fluxes (*Russian*) 7-43649metallic ground points beneath thunderstorm, calc. of space charge due to corona discharge (*Chinese*) 7-29222

nonvertical lightning channels, direction finding errors, effect of finite ground conductivity 7-14366

physical process and effects 7-34662

physics and effects on electronic circuits, textile industry appls., conf., Charlotte, NC, USA (May 1986) 7-29594

positive ground flashes, occurrence model 7-18294

radiation belts slot region electron precipitation, lightning as trigger mechanism 7-9325

RF radiation from lightning return strokes, influence of Earth conductivity 7-40535

source of Antarctic nitrates 7-55227

storms intensity determ. using centimetre and metre-wave radar (*Russian*) 7-47549

successive flashes, time interval 7-40511

surge and transient protection and warning systems 7-34663

United States, Florida and Colorado, lightning activity, topographic convection effects 7-34620

lightning conductors *see lightning protection***lightning protection***see also surge protection*

cloud to ground lightning flashes, data recording in eastern USA for lightning protection design 7-18297

metallic ground points beneath thunderstorm, calc. of space charge due to corona discharge (*Chinese*) 7-29222

surge and transient protection and warning systems 7-34663

textile industry, conf., Charlotte, NC, USA (May 1986) 7-29594

lightning rods *see lightning protection***limited space charge accumulation***see also Gunn effect; negative resistance effects; space-charge limited devices*

No entries

limiters

graphite, porous, effective thermal props., photoacoustic meas. 7-44239

GaAs current limiters, impact ionisation breakdown 7-52639

limiting circuits *see limiters***linear accelerators***see also collective accelerators; electrostatic accelerators*

18 MeV electron linac for picosecond and nanosecond beam prod. 7-49747

40 MeV proton linear operation (*Japanese*) 7-19563

100 TW particle beam fusion accelerator for inertial confinement fusion program 7-30664

Applied-B ion diode expts. on Particle Beam Fusion Accelerator-I 7-10310

ATLAS, positive ion injector status, ECR ion source and superconducting linac 7-62134

beam blowup scaling and accelerator struct. (*Japanese*) 7-19581

beam dynamics, efficiency and power of the SLAC lasertron-simulation results 7-62185

bipolar electric field flashover of vacuum interfaces in accelerator cavities 7-30750

CEBAF cavity cryostat 7-62183

CEBAF cryogenic system 7-62184

CEBAF facility, design, few-body research program 7-62105

CEBAF superconducting CW linac, overview 7-62120

collider constraints in the choices for wavelength and gradient scaling 7-62196

collider constraints in the choices for wavelength and gradient scaling 7-5502

linear accelerators continuedcompact 2.86 GHz ECR ion source (*Japanese*) 7-19600

conf., Tsukuba, Japan, (Sept. 1986) 7-18504

conference, linear accelerators, Stanford, CA, USA (June 1986) 7-60878

control of beam dynamics in high energy induction linacs 7-62176

cumulative beam breakup with a distribution of deflecting mode frequencies 7-62190

CW injector linac for 35 MeV double sided microtron (*Japanese*) 7-19557CW operation of the TIT 1H-type Heavy Ion Linac (*Japanese*) 7-19564double loop beam monitor study using single bunch linac (*Japanese*) 7-19617double-sided microtron, injector development (*Japanese*) 7-19558

electron linac, control system for Photon Factory 7-5498

electron linac, operation in short-beam mode 7-62143

electron linac, upgrade to high duty factor machine 7-62147

electron linac beam post-acceleration in chain of passive cavity structures 7-62146

electron linac laboratory, modification to applied radiation facility 7-62142

electron linac modifications to produce short, intense beam pulses 7-62139

electron linac with feedback, self-oscillatory mode 7-62144

electron linear colliders, beam-beam effects 7-62194

electron linear induction accelerators 7-62107

electron multipass multisection linac, feedback system anal. for beam breakup 7-62145

Electron Test Accelerator, beam injector, chopper and buncher system 7-25271

emittance growth in high-current linacs, field energy calcs. 7-62118

FEL intense low emittance beams prod. in electron linacs 7-1116

FEL spiking mode operation for a uniform-period wiggler 7-1109

focusing mechanism in the pulselac CU accelerator 7-62112

free electron laser EUV, three-dimens. simulation 7-43131

free electron laser project at JAERI, linac preparatory study 7-20244

frequency control of KEK-PS new 40 MeV linac (*Japanese*) 7-19574grid pulse generator for KEK PF linac (*Japanese*) 7-56903

heavy ion ICF, current status and future prospects 7-62081

heavy ion ICF reactor, critical system issues, linac design 7-25211

heavy ion injector linac based on superconducting interdigital accelerating structs. 7-62135

heavy-ion linear accelerator for Tokyo Institute of technology, Mitsubishi Electric designed unit (*Japanese*) 7-10311

HERA-RFQ injector for Alvarez linac, present status 7-62130

HERMES III, passive control of high-energy high-current beam 7-30809

high brightness electron injector for FEL driven by RF linacs 7-1117

High Brightness Test Stand 7-1114

high field accelerator using two port standing wave accelerator tube (*Japanese*) 7-19585

history of proton linear accelerators 7-62106

HV modulator for electrostatic kicker for proton beam switching and control 7-30776

IHQ linac, development and characts. (*Japanese*) 7-19577

IKONET, distributed accelerator and experiment control applications 7-19560

image processing system for electron linac beam diagnosis (*Japanese*) 7-19621

induction linac accelerators, current pulse shortening 7-49750

induction linac driver for inertial fusion, cost/performance analysis 7-25209

induction linacs and free electron laser amplifiers, fusion program appl. 7-10287

INS RFQ linac TALL, beam test 7-10318

internal dynamics and emittance growth in non-uniform beams 7-62181

ion and electron beams, high-current beam dynamics and transport, theory and experiment review 7-62117

JAERI linac, status (*Japanese*) 7-19567

JAERI linac TOF facility 7-30779

KALIF ion accelerator, beam comp. investig. in anode plasma 7-30742

KEK 40 MeV proton linac, design and RF tuning 7-25270

KEK e⁺ generator, magnet power supply control system (*Japanese*) 7-19580KEK e⁺ injection system, beam characts. (*Japanese*) 7-19613

KEK technology for future linacs, RF sources and structures 7-62124

Kharkov electron linac as injector for stretcher ring 7-62104

L-band amplifier for Osaka Univ., linac (*Japanese*) 7-19575

lasertron spent beam collector material desorption tests 7-62116

light ion multichannel acceleration, resonator EM props. 7-5497

linacs for medical and industrial applications 7-62110

linear colliders, beamstrahlung energy spread, quantum correction due to finite photon no. 7-5512

longitudinal trapping and particle loss of high intensity bunched beams 7-62178

Los Alamos FEL, electron micropulse diagnostics 7-1108

Los Alamos FEL, linear accelerator noise control 7-62115

Los Alamos FEL, oscillator expt. 7-1107

Los Alamos FEL, status 7-1106

low- β ion acceleration with a MEALAC 7-15448

MAFIA, 3D EM CAD system for magnets, RF structs., and transient wake-field calcs. 7-62136

magnetic linear accelerator (MAGLAC), switching studies 7-36342

maximum efficiency of a conventional klystron output cavity 7-62186

medical heavy particle accelerator, design (*Japanese*) 7-54741MEALAC low- β in accelerator for plasma diagnostics 7-26528

multi-section recirculating linac, beam breakup 7-62191

multicharged heavy ion source for the RIKEN linear accelerator (*Japanese*) 7-56897NERL 35 MeV linac, twin linac pulse radiolysis system (*Japanese*) 7-19566

neutron TOF spectrometer at KURRI electron linac 7-30831

non-destructive beam monitors for the SNQ-linac 7-62179

operational experience with SLAC energy upgrade 7-62111

particle beam fusion accelerator for inertial confinement fusion program, construction projection 7-30665

particle beam fusion accelerator I (PBFA I), automated features of control/monitor system 7-30754

Particle Beam Fusion Accelerator II (PBFA II), computer model of vacuum system design 7-30773

Particle Beam Fusion Accelerator II (PBFA II), energy storage system 7-30765

linear accelerators continued

Particle Beam Fusion Accelerator II (PBFA II), energy transport meas. and computer simulation 7-30764
Particle Beam Fusion Accelerator II (PBFA II), laser triggering optical system 7-30771
Particle Beam Fusion Accelerator II (PBFA II), laser trigger system design 7-30772
Particle Beam Fusion Accelerator II (PBFA II), quality assurance of R&D project 7-30763
particle beam fusion accelerator II (PBFA II), vacuum insulator stack failure mechanisms 7-30749
particle beam fusion accelerator II (PBFA II) control/monitor system 7-30751
particle beam fusion accelerator II (PBFA II) data acquisition system with waveform recorders 7-30753
Particle Beam Fusion Accelerator II (PBFA II) engineering design of pulse forming system 7-30770
particle beam fusion accelerator II (PBFA II) high speed multi-channel data acquisition system 7-30752
Particle Beam Fusion Accelerator II (PBFA II) Marx generator engineering and assembly line technology 7-30768
Particle Beam Fusion Accelerator Marx generators, photon diagnostics 7-30767
particle beam fusion accelerator-II (PBFA-II), design of applied-B ion diode 7-36343
particle longitudinal motion in RFQ accelerator, eqn. soln. 7-49748
PBFA II accelerator assembly and characterisation 7-30762
PBFA II vacuum magnetically insulated transmission line redesign to inductive energy store 7-30755
PBFA-II photoactivation, fusion breakeven experiments, radiation protection problems 7-30775
PBFA-II vacuum insulator stack design engineering viewpoint 7-30774
PF linac, high power klystron, permanent focusing magnets (Japanese) 7-19604
positive ion sources and injectors for linacs 7-62126
postacceleration characts. of the TIT 3.4 MeV/u ¹H booster (Japanese) 7-19576
precision alignment of permanent magnet drift tubes 7-62177
proton, filtering of transverse phase space, w.r.t. space charge and oscillation coupling 7-10313
pulsed power accelerator for fusion research, SF₆ reprocessing system 7-30769
pulsed power accelerators, low-jitter Marx generators for reliability 7-30766
pulsed power research facilities, successful long-term operation, contributing factors, PBFA-I as example 7-30778
pulsed transmission line linear accelerator, beam generation, acceleration, transport and extraction 7-62188
radiotherapy, accelerator, high-energy, determ. of source posn. for electron beams 7-54727
rE linacs for esoteric applications 7-62108
recirculating linac as an injector for small storage rings or free electron lasers 7-62103
RF accelerating cavities, 3D calcs. using the URMEL-3D code 7-62137
RF cavity design and codes 7-62128
RF drive system for the CEBAF superconducting cavities 7-62182
RF linear accelerators, use in fusion research and strategic defence 7-10317
RF power amplifier with dedicated interlock and feedback controller 7-62114
rF power sources for 1990 and beyond 7-62109
RF struts, for excitation of electrooptic transducer by beam in picosecond electron linac 7-15428
RF structure under high-gradient, limiting factors 7-62195
RF superconducting linac structures for heavy ions and electrons 7-62119
RF system for prebuncher for nanosec. beam accelerator (Japanese) 7-19570
RF tuning of the KEK 40 MeV proton linac (Japanese) 7-19602
RF window breakdown (Japanese) 7-19603
RFQ linac, very heavy ion acceleration 7-10319
RFQ linac structures, field stabilisation with resonant line couplers 7-62129
RFQ linac TALL, proton beam test 7-19571
RFQ linear accelerators in research and industry 7-62125
RFQ proton linac design (Japanese) 7-19572
RFQ-based H⁻ injector for BNL/FNAL 200 MeV proton linacs 7-62132
Rimfire 6 MV laser triggered SF₆ filled switch for PBFA II 7-30746
single gap debuncher cavity for the 40 MeV proton linac (Japanese) 7-19615
single pulse RFQ injector for high pulse current proton accelerators 7-62131
SLAC Linear Collider, linac developments 7-62123
SLAC Linear Collider, progress report 7-62122
slow positron production by the use of the ETL linac (Japanese) 7-19569
standing wave and travelling wave structures comparison for linacs 7-62121
Stanford Mark III infrared free electron laser 7-1112
super HILAC upgrade project, MEVVA ion source, beam transport line 7-62133
superconducting linear accelerators for heavy ions, review 7-56886
superconducting post accelerator linac for JAERI tandem 7-36371
Supermite accelerator water-plastic-vacuum interface design 7-30748
surface discharges as intense photon sources for light-ion fusion accelerator cleaning 7-37800
TeV e⁺e⁻ linear accelerator, DENKAI program for static field simulation (Japanese) 7-19588
TeV e⁺e⁻ linear collider, cathode life and gas desorpt. meas. (Japanese) 7-19587
TeV e⁺e⁻ linear collider, high power test of accelerating cavity (Japanese) 7-19586
TeV e⁺e⁻ linear collider, lasertron design studies (Japanese) 7-19589
thermal design of drift tubes for high-gradient linacs 7-62113
Tohoku 300 MeV e⁻ linac cooling system, trouble and warning system 7-19579
Tohoku 300 MeV linac, current status (Japanese) 7-19565
triggered cascade gas switches for PBFA I 7-30747
TRISTAN positron generator beam transport system (Japanese) 7-19568
twin linac pulse radiolysis system 7-49746
voltage breakdown at X-band and C-band frequencies 7-19582

linear accelerators continued

Wake Field calculations using the MAFIA 3D BCI code 7-62138
wakeless triple-soliton accelerator 7-10312
X-band 1 MeV linac, beam tests (Japanese) 7-19583
e⁻ injector linac design (Japanese) 7-19584
H⁻ ion source development for linac appl., review 7-62127
U ion acceleration in split coaxial RFQ (Japanese) 7-19573

linear algebra
see also determinants; eigenvalues and eigenfunctions; matrix algebra; tensors; vectors
cubic form, expression as a sum of cubes of linear forms 7-60954
genetic algebras, interpretation of derivations 7-48278
image reconstruction according to projections (Russian) 7-34235
optical linear algebra processors, conjugate gradient algorithm 7-57251
steady flow induced by a rotating circular cylinder in a rectangular tank 7-37475

linear-beam tubes see microwave tubes

linear combination of atomic orbitals calculations see LCAO calculations

linear differential equations
average condition number for solving linear equations 7-29713
collisional magnetic pumping, soln. of differential eqn. 7-32021
convection, linear 1D eqn., numerical dispersion by upwind differencing 7-26267
diffusion eqn., 1D lin., 5-pt. explicit finite difference method 7-14898
fourth order partial diff. eqns., soln. using finite element method 7-29759
infinite-order differential equation, existence of holomorphic solution 7-29691
nonautonomous delay differential eqns., stability conditions 7-24387
piecewise linear second order differential eqns., bifurcations of subharmonics 7-29891
plane elasticity, two-grid FEM method 7-6089
plasma heating by collisional magnetic pumping 7-16315
plates, rectangular laminated composite, dynamic stability analysis using finite strip method 7-6118
prolate spheroidal functions with large parameters, uniform asymptotic expansions 7-35243
pseudoparabolic equations, solution of boundary-value problems 7-35223
second order equations, Titchmarsh-Weyl m-function, asymptotic form 7-18576

linear integrated circuits
No entries

linear motors
Sawyer motors in optical scanning systems 7-57602

linear network analysis
airborne gravity gradiometer survey data analysis using isomorphic geodetic and electrical networks 7-47309

linear programming
solar ponds, performance eval. and optimal control (French) 7-59869

linear quadratic Gaussian control see optimal control; optimisation

linear rectification see rectification

linear rectifiers see rectifiers

linear systems
solar collector/heat exchanger system, differential game control 7-65578

linear vibrations see vibrations

linearisation techniques
see also piecewise-linear techniques
flow over nonuniform bottom, linearised soln. 7-1637
human gait anal. math. model, quasi-linearisation technique 7-65791
katharometer bridge circuit with linearising feedback 7-17840

linewidths (spectral) see spectral line breadth

linguistics
complementarity in linguistic observation, description and explanation 7-54616
speech synthesis, introduction, making computers talk, book 7-4646

linguistics, language see linguistics

linkages (electric connectors) see electric connectors

linking see joining processes

Liouville equation
see also Vlasov equation
classical solutions in 4D Euclidean space 7-9805
conformal Killing vectors in Robertson-Walker spacetimes 7-156
dynamic ensemble theory tested for classical 1D oscillators 7-29868
entropy evolution as a guide for replacing the Liouville equation 7-29869
fourth order elliptic equations, Liouville-type results 7-24393
irreversible processes formulated in a superspace, quantum theory, variation principle 7-14869
linearization and Painleve property of Liouville and Cheng equations 7-4657
mean field kinetic Ising model, microscopic approach using Liouville formalism 7-2801
quantum Liouville equation, Dyson-like expansion for solutions 7-18622
quantum systems, minimum uncertainty states, classical props. 7-14823
real periodic solns. in the μ -representation 7-48318
singular solutions on an interval 7-61057
slow motion extraction from nonlinear equations of motion 7-14763

lip microphones see microphones

lipid bilayers
amphiphiles with poly L-aspartic acid head groups, bilayer membranes, morphology, metamorphosis 7-8511
archaeobacteria lipid dynamics, nonlinear ESR studies 7-8508
black bilayers of egg phosphatidyl ethanolamine, thermotropic changes in cond. 7-54489
cardiac sarcoplasmic reticulum Ca channel, single-channel and ⁴⁵Ca²⁺ obs. 7-28477
deformation free energy of bilayer membrane and its effect on gramicidin channel lifetime 7-40110
dimyristoylphosphatidic acid/cholesterol bilayers, thermodynamic props. and phase transition kinetics 7-17955
dipalmitoyl phosphatidyl chloride, low temp. phase, headgroup mobility, NMR study 7-1856
DPPC, aqueous assemblies, high press. IR studies 7-54501
egg lecithin, bilayer lipid membranes, base conductance and electric breakdown, static mag. field effect 7-14030
electrical and laser absorpt. spectroscopic simultaneous meas. on bilayer lipid membranes 7-13972
free lipid A, multibilayer, phase transition behaviour, FTIR, endotoxic principle of gram-negative bacteria outer barrier 7-54500

lipid bilayers continued

- FTIR spectra, water subtraction procedure 7-54834
hole-mediated stability and permeability 7-8507
interfacial melting, 2D model, computer simulation 7-58448
lecithin, aq. soln., bilayer liposomes, radiation damage PMR relax. time determ. 7-34200
lecithin, myelin figures, morphology, growth behaviour 7-3750
lipid-water systems, X-ray diffr. meas. of phase transitions 7-26951
lipid/protein interaction, Fourier transform IR studies 7-54498
membranes, phospholipid order, benzyl alcohol effects 7-10619
molecular dynamics study 7-40115
mu-opioid receptor in lipid bilayer, single-channel obs. 7-23313
phase transition kinetics, lifetimes distrib. function 7-8510
phosphatidic acid bilayer lipid membranes, induction of capacitance and ionic currents by Ca^{2+} 7-54488
phosphatidylcholine, photoelectron spectra 7-54493
phosphatidylglycerol bilayers in aq. electrolyte solns., forces between, obs. 7-28473
phosphatidylinositol, photoelectron spectra 7-54493
phospholipid membranes, multiplex dynamic NMR 7-17956
phospholipid monolayers, translational molecular diffusion, substrate coupling and phase transitions 7-8509
photoinitiated ion movements in bilayer membranes containing Mg-octaethylporphyrin 7-8503
porphyrins, monolayers, intermolecular interactions 7-8513
sarcolemmal reticulum from rabbit skeletal muscle, single-channel Ca^{2+} and Ba^{2+} currents 7-28476
short range forces between charged lipid bilayers, theoretical model 7-28478
solvent-mediated interaction, nonlocal electrostatic theory of hydration force 7-17958
sphingomyelin bilayers, interactive forces 7-34115
synthetic bilayer, double-chain amphiphiles, phase transitions, DSC obs. 7-54496
synthetic bilayer, single- and triple-chain amphiphiles, phase transitions, DSC obs. 7-54497
thylakoid membranes and functional subunits, organisation, linear dichroism and fluoresc. polarisation obs. 7-59944
vesicles of N-acyl sphingomyelins, X-ray scatt., bilayer thickness determ. 7-40111
zwitterionic lipid bilayers, dielec. props. of polar head group region 7-8504

liquefaction of gases

- cryogenic sampler for collecting radioactive gases and aerosols 7-59902
He, condensation heat transfer enhancement for mag. refrigerator performance improvement 7-56283
He liquefier, condensing and freezing purification system 7-56280
He liquefier with turbo-expanders, prediction method for cool-down characts. 7-56276
He, refrigerant characts. of $\text{Dy}_3\text{Al}_5\text{O}_{12}$ and $\text{Gd}_3\text{Ga}_5\text{O}_{12}$ 7-56286
He, rot. mag. refrigerator design 7-56282

liquid alloys

- see also liquid metals
Bi-Pb-Sn-Cd alloy negative electrode for secondary Li batteries (Japanese) 7-65435
binary, high order perturbative effects 7-52085
binary alloy in ID lattice, density oscillations model 7-9800
binary alloys, associate model and two-sublattice model 7-44351
brazing alloys with active Ti additive, bonding of Syalon 7-39846
dense liquid metal fast breeder reactor fuels, swelling 7-19351
electrical resistivity and finite mean free paths 7-45266
internal press. kinetic component, eqn. of state calc. (Russian) 7-2139
isothermal compressibility, theoretical analysis (Russian) 7-58391
multi-component solns., interaction parameters, hard sphere model (Japanese) 7-11896
steel, stainless, molten, solubility of N_2 7-3304
structural changes, sensitive thermal analysis technique 7-9831
transition metal alloys, liquid and amorphous, chemical short-range order, electronic theory 7-44349
undercooled, dendritic growth, effect of growth rate dependent partition coeff. 7-65015
Ag-Au-Zn ternary system, thermodynamic functions (German) 7-44856
Ag-Ge liq. eutectic alloys, elec. resist. and struct., 600 to 900 K (German) 7-45334
Ag-Ge liquid alloy, structural phase transitions, photoemission studies 7-1836
Ag-In (Sn)(Sb)(Ge), liq., activity coeffs. of O 7-3284
Al binary alloys, thermodynamic props. (Korean) 7-26978
Al, molten, resistance of tool steels 7-33835
Al-Ge eutectic alloy, interaction with SiC whisker reinforced Al matrix composite 7-46689
Al-Mg, excess entropy of mixing, resist. calcs. 7-2571
Al-Si eutectic alloy interaction with SiC whisker reinforced Al matrix composites 7-46689
Al-Si LM 13 alloy with graphite particles, gravity die cast, dispersed graphite effect on freezing rate 7-59506
Al-Si melts, sorption degassing, struct. 7-3290
Al-Zr(Nb)(Mo), molten, thermodynamic props. 7-21450
An-In liq. alloys, magnetic and thermodynamic props. 7-2812
Au-Si, liq., thermodynamic analysis of conc. fluctuations and homogeneous nucleation, glass form. 7-44852
AuSi liquid ion sources, alloy composition 7-35623
Bi-Ag, struct. of 10 mole % Ag alloy, liq. and amorphous states 7-6512
Bi-Ga, liq., elec. resist. meas. 7-38532
Bi-Sn, liq., thermodynamic analysis of conc. fluctuations and homogeneous nucleation, glass form. 7-44852
Bi-Zn liquid alloys with miscibility gaps, struct. 7-51611
Cd-Sb melts, crystallisation and structural state, phase equilib. diagrams 7-46441
Co-Ce(Pr) liquid alloys, variable valency investig. 7-7192
Cu-Dy, thermodynamic props. rel. to glass forming ability 7-38204
Cu-Er, thermodynamic props. rel. to glass forming ability 7-38204
Cu-Gd, thermodynamic props. rel. to glass forming ability 7-38204
Cu-La, thermodynamic props. rel. to glass forming ability 7-38204
Cu-Zn-Al, liq. alloys, activity of Zn (Japanese) 7-53698
Cu-Zn-Ni, liq. alloys, activity of Zn (Japanese) 7-53698
CuTi molten alloys, evidence of chemical short range order 7-21077
Fe alloys, N solubility, statistical thermodynamics 7-52060
Fe-B liq. alloys, interference functions, X-ray diffr. study and cluster calcs. 7-26656

liquid alloys continued

- Fe-based liq. alloys, density of electron states, calc. (Russian) 7-45110
Fe-C hypoeutectic melt struct., temp. and holding time depend., X-ray studies (Russian) 7-16396
Fe-Ce(Pr) liquid alloys, variable valency investig. 7-7192
Fe-Co, liq., thermodynamic mixing functions, Knudsen cell mass spectrometry (German) 7-21470
Fe-Co-Mo alloys, liq., H solubility meas. and estimates (German) 7-58487
Fe-Cr, liquid alloy, N activity coeff., soln. model for nonmetallic solutes 7-65043
Fe-Mn(S), surface comp. and surface tension, effect of S and Mn (Chinese) 7-6916
Fe-Ni, liquid alloy, N activity coeff., soln. model for nonmetallic solutes 7-65043
Fe-Ni system, liq., phase equilib., above 1200K, mag. contrib., thermodynamic analysis 7-7966
Ga-In, liq., surface segregation, ion bombard. photon emission study 7-32265
Ga-In-Sn liquid alloy, electron field emission studies 7-33535
Ge-Ba, liq. alloys, enthalpy of form. 7-23050
Ge-Sr, liq. alloys, enthalpy of form. 7-23050
Hg-Cs, liq. alloy, molar mag. susceptibility, temp. depend 7-7494
Hg-In, liq., mag. susceptibility, conc. and temp. depend. 7-27492
Hg-In liquid alloys, vol. and thermal expansion coeffs., higher-order correlation effects 7-12328
Hg-Na, liq., mag. susceptibility, conc. and temp. depend. 7-27492
Hg-Sn liquid alloys, vol. and thermal expansion coeffs., higher-order correlation effects 7-12328
Hg-Tl, liq. alloy, molar mag. susceptibility, temp. depend 7-7494
Hg-In liquid alloys, volume, thermal expansion coeff. 7-56227
Hg-Sn liquid alloys, volume, thermal expansion coeff. 7-56227
In-Bi, liq., heat of mixing, calorimetric study 7-12283
In-Bi-Pb system, liq., thermodynamic props. (Japanese) 7-53699
In-Pb, liq., activities, temp. depend., EMF obs. (Japanese) 7-12320
In-Sn alloys, surface composition, Auger electron spectra study 7-12421
In-Tl, liq., activities, temp. depend., EMF obs. (Japanese) 7-12320
K-Cs, saturation vapour press. meas. 7-44780
K-Cs, triplet conc. fluctuations in long wavelength limit 7-63439
K-Pb liquid alloys, excess stability, entropy 7-26975
 $\text{Li}_0.8\text{Pb}_{0.2}$ liq. mixture, fast sound computer simulation, Mori-Zwanzig formalism 7-44696
Li-Mg, excess entropy of mixing, resist. calcs. 7-2571
Li-Na liquid alloy, ordering potential, concentration-concentration structure factor 7-32261
Li-Pb, fusion reactor breeder blanket fluids, T extraction, Pd catalyzed oxidative diffusion 7-49641
Li-Pb, liq., T breeder material, compatibility with austenitic stainless steel 7-53966
Li-Pb, liq. fusion reactor blanket, mass transfer in dynamic environment, corrosion damage 7-49659
Li-Pb, sp. ht. calc. from expt. density and temp. depend. press. data 7-63839
Li-Sn, liq. alloy, mixing enthalpies, high temp. calorimetry, EMF obs. 7-65044
 Li_2Pb liquid, static struct., temp. depend., screened Coulomb model anal. 7-21076
Mg-Cu alloys, vap. press. meas. by boiling temp. method, thermodynamic props. 7-44778
Mg-Ga liquid alloys, Hall effect, meas. 7-32991
Mg₂Si(Ge)(Sn)(Pb), Hall effect in solid and liq. states 7-38647
Na-Cs, triplet conc. fluctuations in long wavelength limit 7-63439
Na-Ga, liq., phase diagram and electrical resistivity 7-21408
Na-Pb liq. alloy, thermodynamic prop. and transport coeff. 7-64199
(Ni,Pd,Pt)-(Al,In) liq. alloys, enthalpies of mixing 7-46487
Ni-Ce(Pr) liquid alloys, variable valency investig. 7-7192
 Ni_3Al , molten, wetting of TiC-WC, compact (Ti,W)C- Ni_3Al , composites prep. 7-64987
Pb-Bi-Hg, liq., struct. microheterogeneity 7-11895
Pb-Li, flowing environment, corrosion of fusion reactor structural steels 7-53959
Pb-Li, molten, thermally convective, corrosion of austenitic stainless and Cr-Mo steels 7-53962
PbLi eutectic, flowing, corrosion of stainless steel 7-53958
PbSn liquid alloys, wetting and spreading, surface composition effects 7-16837
Sb-Ge-Zn system, thermodynamic investig. (German) 7-53703
Sb-Zn melts, crystallisation and structural state, phase equilib. diagrams 7-46441
Se-Te liquid alloys, struct. study by neutron diffr. 7-51610
Sn-Bi-Hg, liq., struct. microheterogeneity 7-11895
Sn-Sb melts, short-range order 7-63438
Ti-Co, liq.-alloys, thermodynamic props., mass spectrometry (Japanese) 7-52084
U-Th-Sn, liq. N-nitride equilib. 7-46417
Zn-Al eutectic alloy, interaction with SiC whisker reinforced Al matrix composite 7-46689
Zn-Sb melt, ordering models 7-44351

liquid crystal devices

- see also liquid crystal displays
acoustic holography, image processing using liquid crystal convertor 7-1319
cholesteric-nematic phase transition, appl. in CO_2 laser light modulation, liq. crystal cell. 7-62745
dye lasers, tuning by a cholesteric liquid crystal device 7-15858
ferroelectric liquid crystals and devices 7-21094
image information transmission, storage, and acquisition using an acousto-optic cell and optical matched filters 7-20143
laser system design, use of liquid crystal devices 7-10979
light valves for medical imaging 7-14107
liquid crystal spatial light modulators 7-37133
modulators with MIS-liquid crystal structure 7-20406
optical crossbar interconnections using variable grating mode devices 7-42949
optical fibre, liquid-crystal-clad single-mode tapered 7-37173
optical logic gates using liquid crystal optical switches 7-43327
phase change guest-host (PCGH) liquid crystal window to control solar energy 7-37123
polymer liquid crystals, synthesis, characterisation and applications 7-17508

liquid crystal devices continued

- polymers, liq. cryst., nonlinear optical processes, large non-resonant third order electronic responses 7-25874
 polysiloxane side chain liq. crystals, optical and electro-optical props. 7-16387
 spatial light modulator, a-Si FET addressed 7-37132
 spatial light modulator, a-Si photoconductor 7-43350
 spatial light modulator, coupled to image converter, expt. investig. 7-43440
 spatial light modulator, differentiating mode 7-25956
 television spatial light modulator appl. to computer-generated holography 7-36918
 thermography for wall heat transfer and flow visualisation 7-35520
 thin nematic liquid crystal cells, electro-optic behaviour 7-25957
 time-domain beam former, optical implementation using 2D spatial light modulator 7-42987
 twisted nematic liquid cryst. cell, polarisation anal. using Poincare sphere (Japanese) 7-64603
 wavefront correction by liquid-crystal devices 7-1250
 Bi₁₂SiO₂₀ MIS-liquid crystal structure, dynamic image processing 7-57532
 Si liquid crystal spatial light modulator 7-37130

liquid crystal displays

- ferroelectric smectics, alignment technique for displays 7-63454
 Freedericksz transitions in nematic liquid crystals, first- and second-order, EM fields effects 7-1839
 legibility factors for LCDs 7-8578
 nematic, heterocycles, NCS-polar groups and double bonds effects on material props. 7-1838
 nematic cell with cholesteric additive, electro-optic twist effect, structural effects 7-63449
 nematic liquid crystal displays, multiplexed twisted, elastic constants of hybrid mixtures 7-2078
 nematic twisted configurations with nonzero pretilt angles, director patterns, numerical calcs. 7-11898
 polymer encapsulated nematic liquid crystals for use in high resolution and color displays 7-6511
 portable flaw detector with built-in LCD thickness meter 7-13704
 projection lenses for light-valve display 7-50701
 SBE type, fundamental characteristics (Japanese) 7-7670
 SBE type, super-twisted nematic, display characts., effects of various parameters (Japanese) 7-7669
 stereoscopic display using LCDs 7-14017
 super-twisted transitions, theory 7-16410
 TV, low-cost appl. to white-light optical signal processing 7-31251
 TV, pocket-size, as spatial modulator for optical data processing 7-25958
 ultrasonogram displays on liq. crystal TV and fluorescent vacuum tube 7-31602
 visual performance evaluation of liquid-crystal shutter and shadow-mask CRTs 7-8579

liquid crystal phase transformations

- acetoxypolypropyl cellulose, liq. cryst. props., effect of chain length and degree of acetylation 7-44353
 acyl cholesteryl esters, mol. motions, temp. depend., ¹³C NMR obs. 7-38950
 4,4'-alkoxybenzoyloxy-4'-cyanoazobenzene, monolayer smectic A₁-nematic transition, dielec. studies 7-21085
 4-n-alkyl-4'-cyanobiphenyl, mol. conformation and orientational order, nematic-isotropic transition, reson. Raman probe 7-21082
 alkylcyanobiphenyl-phenylcyclohexanecarboxylate mesomorphic mixtures, binary phase diagrams, fluoresc. spectral determ. 7-27765
 trans-4'-alkylcyclohexylethyl- and 4'-alkylphenylethyl-4,4'-disubstituted biphenyls, liq. cryst. behaviour 7-11901
 azoxy-4,4'-diundecyl- α -methylcinnamate, smectic-A-smectic-C phase transition, heat-capacity meas. 7-58471
 biaxial particles, soln. of excluded vol. problem 7-32645
 bicyclo(2.2.2)octane esters, mesogenic, transition temps., viscosity, birefr., electro-optical characts. 7-1863
 bistable cholesteric twist cell, anisotropic domain growth 7-1865
 block copolymer macromol. liq. cryst. melt. nematic-smectic-A transition, mean-field approx. calcs. 7-16743
 blue phase, field induced, struct., Kossel diagrams 7-52048
 blue phase, frustrated, Kassel diagrams show elec. field-induced cubic-tetragonal struct. transition 7-32649
 blue phase I-cholesteric transition, electric field-induced, kinetic hindrance 7-58465
 blue-phases, orientation in an electric field, BP II transition to tetragonal phase 7-16397
 N-(p-n-butoxybenzylidene)p-n-ethylaniline, mag. susceptibility, anisotropy and order parameter 7-16416
 butoxybenzylidene phenylazoaniline, liq. cryst. transitions, density and US vel. studies 7-32266
 4'-butoxyphenylester 4-decyloxybenzoic acid, smectic-C phase liq. cryst., zigzag model, X-ray study 7-32646
 caesium pentadecafluorooctanoate-water discoid micelle solns., order-disorder transitions, X-ray scatt., elec. cond., NMR meas. 7-26949
 caesium perfluoro-octanoate, lyotropic liq. cryst., press. depend. of nematic-isotropic transition 7-32647
 chiral smectic C liq. crystals, mol. theory 7-1867
 cholesteric and nematic to isotropic phase transitions, dynamic effects of elec. fields 7-16740
 cholesteric blue phase liq. cryst., phase transition, chiral strain and reentrancy 7-58470
 cholesteric liq. cryst. mixtures, pitch, struct., phase transition point and optical props. studies 7-1881
 cholesteric liq. crystals, blue phases, molecular organisation and geometric frustration 7-16399
 cholesteric-nematic phase transition, appl. in CO₂ laser light modulation, liq. crystal cell. 7-62745
 cholesteric-nematic transition, electrooptic characteristics, control (Russian) 7-16741
 cholesterics, pretransition phenomena, circular dichroism method study 7-51628
 cholesteryl acetylferulate, liq. cryst. transitions, glass transition and cold crystn., DSC study 7-63814
 cholesteryl benzoates, smectic A phase with polar terminal groups, thermal props. studies 7-63459
 cholesteryl hydrogen phthalate, glass transition study, positron lifetimes meas. 7-38201

liquid crystal phase transformations continued

- cholesteryl myristate-cholesteryl benzoate mixtures, cholesteric/smectic A tricritical point, critical pitch exponents 7-38193
 cholesteryl oleate, isotropic-blue phase transition, nonlinear dielectric effect meas. 7-12272
 cyano derivatives, mesomorphic phases, polymorphism 7-2193
 1-cyclohexyl-phenyl-2-methyl ethylenes, synthesis and phys. props. 7-1870
 p-cynophenyl p'-n-heptylbenzoate, liq. cryst., phase transition studies 7-38195
 p-cynophenyl p'-n-heptylbenzoate-p-nitrobenzylidene-p'-n-heptyloxyaniline, liq. cryst. mixtures, phase transition studies 7-38196
 p-decyloxybenzylidene-p'-amino-1-methylpropylcinnamate, smectic-A-chiral-smectic-C transition meas. 7-58472
 di-4'-substituted phenyl-trans-cyclohexane-1,4-dicarboxylates, mesomorphic props., effect of inserting ketone groups in terminal chains 7-21088
 4,4'-di-n-alkoxy-2-hydroxybenzalazines, liq. cryst. props., effect of mol. central core geometry changes 7-1866
 4,4'-di-n-alkoxybenzalazines, liq. cryst. props., effect of mol. central core geometry changes 7-1866
 dioxans with dimethylene linking groups, liquid crystalline props. 7-1854
 dipalmitoyl phosphatidyl chloride, low temp. phase, headgroup mobility, NMR study 7-1856
 diphenyldiacetylene derivatives, liq. cryst. polymers and copolymers, props. 7-51621
 discogens, reentrant columnar mesophase and crystalline polymorphism (French) 7-63442
 discotic liq. cryst. strands, freely suspended, cross sectional shape 7-37845
 discotic liquid crystals, phase diagram 7-2197
 display, SBE type, super-twisted nematic, display characts., effects of various parameters (Japanese) 7-7669
 4,4'-disubstituted phenylbenzoates, mesomorphic props., effect of inserting ketone groups in terminal chains 7-21088
 DOBAMBC, smectic A-chiral smectic-C phase transition, tilt angle, polaris. and heat capacity 7-44361
 DOBAMBC, smectic-A-chiral smectic-C phase transition, mean field model 7-44362
 evidence of continuous evolution of smectic A₂ from smectic A_d 7-63813
 free-standing liquid crystal films, smectic A-hexatic B transition, critical exponent study 7-6819
 Freedericksz transitions in nematic liquid crystals, first- and second-order, EM fields effects 7-1839
 hard ellipsoids of revolution, phase diagrams calcs. 7-2192
 hard parallel spherocylinder fluid, smectic order and nematic-smectic transition 7-11905
 hard-core models, computer simulation 7-58468
 N-(p-n-heptyloxybenzylidene) p-n-pentylaniline, liq. cryst. transitions, density meas. 7-26821
 N-(p-n-heptyloxybenzylidene) p-n-pentylaniline, liq. cryst. phase transitions, density, US vel. meas. 7-1874
 4-n-heptyloxyphenyl-4'-(4'-cyanobenzoyloxy)benzoate, evidence of continuous evolution of smectic A₂ from smectic A_d 7-63813
 hexaethylene glycol dodecyl ether, lyotropic liquid crystal, defect-mediated phase transition, electron-microscopy obs. 7-21439
 hexatic liquid crystals, multicriticality 7-2201
 induced smectic phases, role of ratio of mol. lengths in binary mixtures 7-11897
 isotropic-nematic phase transition, crossover behaviour, renorm. group calcs. (Russian) 7-21445
 lead (II) carboxylates, thermotropic phase transitions, DSC meas. 7-21441
 Lebwohl-Lasher lattice model, inhomogeneous, Monte Carlo simulation 7-61261
 lipid-water systems, X-ray diff. meas. of phase transitions 7-26951
 liquid cryst. film, Freedericksz transition, mol.-dynamics model calcs. 7-44813
 liquid crystal models, reference hypernetted-chain theory 7-58469
 liquid crystal-polymer mixtures, phase diagrams, nematic-isotropic phase equilibria versus liq.-liq. demixing 7-16739
 lyotropic liq. crystals, high press. phase diagrams, re-entrant phenomenon obs. 7-12270
 lyotropic liquid crystal, smectic-nematic transition, electron-microscope obs. 7-32648
 lyotropic liquid crystals, reentrant isotropic-nematic transition 7-21443
 lyotropic liquid crystals studied by positron annihilation techniques 7-38194
 MBBA, isotropic-nematic phase transform., order parameter kinetics 7-26950
 MBBA, nematic liquid crystal, temp. depend. of cubic susceptibility, Raman study 7-22237
 membranes, bilayer, double-chain amphiphiles, phase transitions, DSC obs. 7-54496
 membranes, bilayer, single- and triple-chain amphiphiles, phase transitions, DSC obs. 7-54497
 mesogen nematic and isotropic phases, rotational relax. 7-44355
 micellar liq. cryst., isotropic phase, temp.-depend. supercooling limit, mag. birefringence meas. 7-63815
 micellar systems, isotropic-nematic transition temps., conc. depend. 7-2199
 micelle solutions, isotropic-nematic phase transition, micellar flexibility effects 7-58467
 monomers and polymers, mesophase behaviour, mol. structural effects study 7-63458
 nematic liq. crystals, relax. modes of order parameter fluctuations in vicinity of uniaxial-biaxial phase transition 7-26948
 nematic liq. crystals, surface anchoring energy, validity of Rapini-Papoular form 7-26625
 nematic liq. crystals, Freedericksz effect in crossed elec. and mag. fields 7-63446
 nematic liquid crystals, Frank constants, effects of compression 7-63702
 nematic liquid crystals, global phase diagrams, second-order nematic-isotropic transitions 7-12274
 nematic liquid crystals, phase transitions, mean-field theory of isotropic, uniaxial and biaxial phases 7-21440
 nematic liquid crystals, transitions of viscous fingering patterns 7-12273
 nematic solvent, induced cholesteric mesophases 7-2195
 nematic-isotropic interface, surface tension and mol. orientation, statistical theory 7-51619
 nematic-smectic A, tricrit. point, num. anal. 7-12268
 nematic-smectic A phase transition, calc. of tricritical temp. 7-12276

liquid crystal phase transformations continued

- nematic-smectic A-smectic C multicritical points, universality 7-2200
 nematics, disc-like mols. Frank consts. ratio meas. at mag. Frederiks transition to columnar phase 7-58136
 nematocholesteric mixtures with two-freq. control, electro-optical props. 7-59183
 nitrobenzoyloxy derivatives, mesomorphic phases, polymorphism 7-2193
 nonuniformly oriented liq. cryst., light wave-orientation interactions and induced Frederiks transition 7-16417
 4-nonyloxyphenyl-4'-nitrobenzoyloxybenzoate, DB_3ONO_2 , multiply reentrant polar mesogen, X-ray scatt. study 7-6505
 4'-n-octyl-4-cyanobiphenyl liq. crystal, surface polar ordering obs. by optical SHG 7-37856
 octylcyanobiphenyl, liq. cryst., elastic consts., permitt., birefr. meas. 7-21314
 octyloxybenzoyloxycyanostilbene, reentrant crystal enthalpies, frustrated spin-gas model 7-63816
 octyloxycyanobiphenyl and octylcyanobiphenyl, smectic Ad phases 7-2194
 octyloxycyanobiphenyl reentrant nematic, preferred density model, P-V-T test 7-12271
 para-azoxy-anisole-d₃-4-4'-diacetoxy-2-2'-dimethyl azoxybenzene nematic mixture, phase diagram, component order parameters, D and proton NMR study 7-21086
 4'-n-pentyl-4-cyanobiphenyl, well induced orientational order in isotropic phase, evanescent wave ellipsometry study 7-37857
 p-n-pentyl-p'-cyanobiphenyl and dil. solns. with tetraethylmethane, nematic and isotropic phases, density meas. 7-2079
 4,4'-di-n-pentyl-4-azoxybenzene, mesogenic transitions, Raman spectra 7-22241
 N-(p-n-pentyl-4-azobenzylidene) p-n-butylaniline, phase transitions, mag. susceptibility meas. 7-1873
 4-(4-n-pentyl-4-azobenzylideneamino)azobenzene, liq. cryst. transitions 7-63812
 phase change guest-host (PCGH) liquid crystal window to control solar energy 7-37123
 phenyl 4'-alkylcyclohexanecarboxylates, 4-alkoxymethylene and 4-alkoxy substituted, synthesis, phys. props. 7-1861
 phospholipid mesophases, X-ray small angle analysis 7-16402
 polar fluorodibenzoates, with smectic modifications, synthesis, transition temps. 7-32279
 poly γ -benzyl-L-glutamate, alignment, liq. cryst. phase transition, surface treatment effect 7-32644
 poly bis 2,2,2-trifluoroethoxy phosphazene, mol. motion, cryst.-mesophase transition, PMR spin echo obs. 7-17242
 poly- γ -benzyl-L-glutamate, cholesteric soln., elec. field effects (Russian) 7-11909
 polyethylene-tetrafluoroethylene, row crystallised film, deform. mechanism 7-44663
 polymer liq. cryst. solns., optical microscopy, Fredericksz transition, permitt. meas. 7-1864
 polymer liquid crystals, synthesis, characterisation and applications 7-17508
 polymer nematic-liquid-crystal cells, periodic Fredericksz transition investigation 7-32282
 polymeric nematics, external field effects and critical end point calcs. 7-37854
 polypropenyl ethers with mesogenic groups, side-chain liq. cryst. polymers 7-51622
 polyvinyl ethers with mesogenic groups, side-chain liq. cryst. polymers 7-51622
 positron annihilation, review 7-39273
 potassium laurate-1,decanol-D₂O, reentrant nematic-isotropic phase transition, pretransitional behaviour 7-21444
 n-propyl-4'-n-decyloxybiphenyl-4-carboxylate-n-butyl-4'-n-decyloxybiphenyl-4-carboxylate, smectic-A-hexatic-B-smectic-I point, existence and nature 7-2198
 pyrimidines, trinuclear, binary smectic systems with and without nematic gap 7-58141
 pyrimidines with dimethylene linking groups, liquid crystalline props. 7-1854
 reentrant-nematic-smectic C-smectic A multicritical points, universality 7-2200
 siloxane nematogenic side chain polymer, director alignment, dielec. relax. spectra study 7-63457
 β -sitosteryl benzoates, smectic A phase with polar terminal groups, thermal props. studies 7-63459
 sitosteryl chloride-cholesteryl laurate binary mixture, polymorphism 7-12267
 smectic A₁ binary mixture, nematic phase creation, phase diagram, transition enthalpy comp. depend. study 7-12269
 smectic A liquid crystals, screw dislocation dynamics 7-21090
 smectic A thin sample, thermal diffusivity determ., photoacoustic effect appl. 7-44812
 smectic A-smectic C phase transition, molecular statistical anal. 7-58466
 smectic C* twisted phase, induced, helical twisting power 7-58130
 smectic liquid crystals, ferroelectric, helical twist sense and spontaneous polarisation 7-16400
 smectic mixtures of A₁ and A₂ phases, nematic gap obs. 7-6792
 smectic-A-smectic-C phase transition, Frank consts. corrections, renormalisation-group method calcs. 7-16742
 surfactant vesicles studied by positron annihilation 7-39268
 terminal nonpolar cpd. binary systems, reentrant nematic phases, phase diagrams, X-ray diff. 7-21442
 terminal phenyl ring liq. crystals, nematic-isotropic transition, even-odd effects 7-38192
 terpenoid derivatives, ferroelec. spontaneous polarisation, steric hindrance of free rotation, optical rot. and transition temp. meas. 7-13101
 transition to isotropic liquid, dimensional effects (Russian) 7-2202
 tribenzocyclononene, hexasubstituted, pyramidal mesophases, optical anisotropy 7-12275
 4-n-undecyloxyphenyl-4'-(4'-cyanobenzoyloxy)benzoate, evidence of continuous evolution of smectic A₂ from smectic A₁ 7-63813
 Rh complex, dirhodium tetradecanoate, discotic mesophase struct., optical microscopy, DSC and X-ray diff. study 7-26627

liquid crystal polymer melts *see liquid crystal polymers***liquid crystal polymer solutions** *see liquid crystal polymers***liquid crystal polymers**

- acetoxypyrrol cellulose, liq. cryst. props., effect of chain length and degree of acetylation 7-44353

liquid crystal polymers continued

- alkylene-aromatic polyester, thermotropically mesogenic, solns., Kerr effect 7-7674
 block copolymer macromol. liq. cryst. melt. nematic-smectic-A transition, mean-field approx. calcs. 7-16743
 4-butoxycarbonylmethylurethane chains, nematic phase, induced rigidity study 7-57195
 comb-like liquid crystalline polymers, highly ordered smectic mesophase, X-ray obs. 7-6507
 copolyester, liq. cryst., low temp. thermal cond. 7-6899
 copolyester, liquid crystalline, molecular motion, NMR obs. 7-17228
 copolyesters, liq. crystalline, primary normal-stress difference determ. 7-6509
 cross linked, shape variation by elec. fields 7-32280
 diacetylenic liquid crystal polymers, derivatives of 10,12-docosadiyne-1,22-dioic acid 7-1868
 diphenyldiacetylene derivatives, liq. cryst. polymers and copolymers, props. 7-51621
 domains, are they disclination arrays 7-44359
 electric field FT-IR reflectance spectra 7-25688
 ethyl cellulose films, creep, liq. cryst. soln. casting 7-8069
 ethyl cellulose solns., lyotropic mesophase system, refractometry 7-53261
 helical biological polymers, liq. cryst. phases, columnar textures 7-34106
 hydroxypropyl cellulose solutions in N,N-dimethylacetamide and in dimethylsulphoxide, viscometric behaviour 7-32258
 linear polyester, mainchain nematic polymer, viscoelastic coeffs., meas. by NMR 7-17231
 mesophase behaviour, mol. structural effects study 7-63458
 nematic liq. crystals, generalised Fredericksz transition, weak anchoring effects 7-32273
 nematic solutions of rod-like and semi-flexible polymers, elastic constants 7-32537
 nematic-liquid-crystal cells, periodic Fredericksz transition investigation 7-32282
 nematics, giant dielectric response and hairpins 7-58140
 neutron scattering, appl. of 2D scattering distrib. anal. 7-11844
 nonlinear optical processes, large non-resonant third order electronic responses 7-25874
 nonlinear optical processes 7-37022
 nucleic acids, liq. cryst. microphases, 'external chromophores' and intense bands in circular dichroism spectra 7-54459
 poly γ -methyl-L-glutamate film, solidified, cholesteric struct., colour rel. to stretching and temp. 7-44354
 poly γ -benzyl-L-glutamate film, solidified, cholesteric struct., colour rel. to stretching and temp. 7-44354
 poly γ -benzyl-L-glutamate, alignment, liq. cryst. phase transition, surface treatment effect 7-32644
 poly bis 2,2,2-trifluoroethoxy phosphazene, mol. motion, cryst.-mesophase transition, PMR spin echo obs. 7-17242
 poly- γ -benzyl-L-glutamate, cholesteric soln., elec. field effects (Russian) 7-11909
 poly- γ -benzyl-L-glutamate, helical polymer, cholesteric liquid crystalline phases 7-6506
 polyacrylate derivatives, liq. cryst., dielectric transitions eval. (Russian) 7-39001
 polyesters, mesomorphic, synthesis by polymerisation of bifunctional monomers 7-1853
 polymeric nematics, electrohydrodynamic instabilities, comment 7-11557
 polymeric nematics, external field effects and critical end point calcs. 7-37854
 polymers with chiral phases, prep. 7-63453
 polypropenyl ethers with mesogenic groups, side-chain liq. cryst. polymers 7-51622
 polysiloxane, liq. cryst., with side chains, elec. field effects 7-11883
 polysiloxane liquid crystals, colour gamut 7-1857
 polysiloxane side chain liq. crystals, optical and electro-optical props. 7-16387
 polysiloxanes, cyano substituted side chain liq. cryst. polymers, X-ray diff. study 7-1869
 polyvinyl ethers with mesogenic groups, side-chain liq. cryst. polymers 7-51622
 PVC: cholesteryl acetate, raw and moulded, crystallinity determ., positron lifetime studies 7-46228
 rods, thermotropic, flow and orientation behaviour during extrusion 7-57887
 semirigid macromolecules, conc. solns., liq.-cryst. order form. (Russian) 7-36833
 side chain, X-ray diffraction 7-1846
 side chain polymer liq. cryst. solns., optical microscopy, Fredericksz transition, permitt. meas. 7-1864
 siloxane nematogenic side chain polymer, director alignment, dielec. relax. spectra study 7-63457
 smectic liq. cryst. polymer, comb-like macromolecule conformation, determ. from neutron scatt. data 7-26623
 stress relax., bond breaking, free vol. effects 7-22742
 synthesis, characterisation and applications 7-17508
 thermoplastic rubber/liquid crystal polyester dualcoextrusion coating system for optical fiber drawing 7-11190
 thermotropic aromatic polyesters, mesogenic and flexible fragments, order parameters (Russian) 7-16394
 thermotropic copolyester with banded texture, optical diffraction pattern predictions 7-11888
 thermotropic liq. cryst. polymers, history, prep. and charactn. 7-6508
 thermotropic polyester, press.-induced enantiotropic transition at room temp. 7-1916
 xanthan, helical polymer, cholesteric liquid crystalline phases 7-6506

liquid crystalline polymers *see liquid crystal polymers***liquid crystals**

- see also cholesteric liquid crystals; discotic liquid crystals; liquid crystal phase transformations; liquid crystal polymers; nematic liquid crystals; smectic liquid crystals*
 acyl cholesteryl esters, mol. motions, temp. depend., ¹³C NMR obs. 7-38950
 alkoxycyanobiphenyls and related cpds. optical anisotropies, depolarised Rayleigh scatt. 7-39132
 4-(4'-n-alkoxy-piperidino)-trans-styrylpyridine-N-oxides, highly polarisable mesogens, synthesis, appl. in nonlinear optics 7-63451
 alkylcyanobiphenyls and related cpds. optical anisotropies, depolarised Rayleigh scatt. 7-39132
 anisotropic matrix, energy transfer 7-64693

liquid crystals continued

- anthracene molecules in liquid crystal matrix, orientational order, tensor parameter, spectroscopic study 7-37851
 anthracene solute alignment in uniaxial liq. cryst. solvents, Saupe ordering matrix calcs. 7-11902
 benzene, isotopic mixture in liq. crystals, dipolar coupling consts., 2D multiple quantum NMR 7-57090
 bibliography for 1983 7-36
 1,2-bis(4'-pentyloxyhexyl)ethane, cryst. and mol. struct. 7-58257
 N,N'-bis(4-n-octyloxybenzyl)-1,4-phenylenediamine, condit. crystal props. 7-37909
 blue phase, field induced, struct., Kossel diagrams 7-52048
 blue phase, light scatt. and elastic moduli, Landau theory calcs. 7-2084
 Brochard-Leger wall in liquid crystals 7-37855
 N-(p-n-butoxybenzylidene)p-n-ethylaniline, mag. susceptibility, anisotropy and order parameter 7-16416
 caesium perfluoro-octanoate, lyotropic liq. cryst., press. depend. of nematic-isotropic transition 7-32647
 capillary cell, orientational and struct. effects in conical elec. field 7-44370
 carrier mobility measurement techniques 7-58800
 cholesteryl oleate, isotropic-blue phase transition, nonlinear dielectric effect meas. 7-12272
 chromonic mesophases, model for mol. arrangements 7-16411
 coupled oscillators in convective flow, neutron scatt. obs. 7-44366
 dimyristoylphosphatidic acid: cholesterol spiral liq. cryst., fluoresc. microscopic obs. 7-58129
 dipalmitoyl phosphatidyl chloride, low temp. phase, headgroup mobility, NMR study 7-1856
 1,3-dithians and dioxans, 2,5-disubstituted, liquid crystalline phases 7-1845
 DNA, 2-chain mols., spatial liq. cryst. packing for a different cation composition of the solvent 7-28448
 DNA liquid cryst. microphases in water-organic solns., optical props. 7-65709
 dyes, lyotropic liq. cryst., chromonic phases 7-32275
 ferroelectric liq. crystals, molecular orientation structure of surface stabilised states and their switching processes 7-16406
 ferroelectric liquid crystal cell, surface stabilised, homogeneous-twist transitions study 7-51620
 ferroelectric liquid crystals, solitary waves, mol. reorientation dynamics 7-21092
 ferroelectric liquid crystals with high spontaneous polarisation 7-59159
 film, Fredericksz transition, mol.-dynamics model calcs. 7-44813
 hexaethylene glycol dodecyl ether, lyotropic liquid crystal, defect-mediated phase transition, electron-microscopy obs. 7-21439
 n-hexane, partially oriented in liq. crystal, dipolar coupling consts., NMR methods study 7-25547
 hexatic liquid crystals, multicriticality 7-2201
 hydroxypropyl cellulose, lyotropic liq. crystals, capillary rheometry 7-63099
 induced thermal lens, spatial Fourier spectrum anal., for studying thermal conductivity and diffusivity 7-12379
 ionic thermotropic liquid crystals, prep. and props. 7-26630
 IR birefringent props. 7-39076
 Kapustin-Williams domains 7-16404
 lyotropic, high press. phase diagrams, re-entrant phenomenon obs. 7-12270
 lyotropic liq. crystals, spin relax., local order with cylindrical interfaces, translational diffusion, continuous diffusion model 7-64540
 lyotropic liquid crystal, lamellar phase, electron microscope observations (French) 7-32269
 lyotropic liquid crystals, reentrant isotropic-nematic transition 7-21443
 lyotropic mesophase, spinning, director distrib. in mag. field (French) 7-51616
 MBBA, Williams domain evolution process, Fourier spectrum anal. 7-32274
 MBBA liq. cryst., mol. orientational relax. times, luminescence meas. 7-44368
 mesophase, mol. statistical theory, conform. mobility effects 7-63445
 mesophases, orientational optical nonlinearity, review 7-1880
 micellar liq. cryst., isotropic phase, temp.-depend. supercooling limit, mag. birefringence meas. 7-63815
 microemulsions and liquid crystals 7-1871
 MIS-liquid crystal structures, pseudocolour image synthesis 7-31252
 models, reference hypernetted-chain theory 7-58469
 molecular materials and their appls. 7-16412
 monomers and polymers, mesophase behaviour, mol. structural effects study 7-63458
 multilayer fluid membrane system in the lyotropic phase of quaternary microemulsion system, steric interactions 7-34116
 nematic-smectic A-smectic C multicritical points, universality 7-2200
 nonlinear guided waves, optical hysteresis 7-57551
 nonlinear optical materials 7-57437
 nonuniformly oriented liq. cryst., light wave-orientation interactions and induced Fredericksz transition 7-16417
 4'-n-octyl-4-cyanobiphenyl liq. crystal, surface polar ordering obs. by optical SHG 7-37856
 4-octyloxy-4'-cyanobiphenyl, liq. crystal, vibr. dephasing, Raman spectra study 7-57067
 off lattice diffusion-limited aggregation with radial bias, liquid crystal fingering 7-63412
 optical studies by ATR technique 7-16413
 optical studies by ATR technique 7-16414
 order parameter, temp. depend., mol. asymm. effects 7-44369
 orientational order parameters, IR dichroism of mol. groups 7-44358
 petroleum derived mesophase pitches, viscosity meas., isotropic content, temp. depend. 7-21502
 phospholipid mesophases, X-ray small angle analysis 7-16402
 photoconductor-liq. crystal rectifier, liq. crystal dielectric anisotropy, low-freq. inversion effect 7-45395
 phthalocyanine derivatives, columnar mesophases, optical microscopy, X-ray diffr. obs. 7-1860
 porphyrin derivatives, mesogenic props. (French) 7-1859
 positron annihilation, review 7-39273
 potassium-laurate water, lyotropic liq. crystalline system, mol. motions, proton spin relax. study 7-64543
 reactive dyes, water soluble, lyotropic liq. cryst. mesophases and solid physical form 7-32276
 reentrant-nematic-smectic C-smectic A multicritical points, universality 7-2200

liquid crystals continued

- relaxation time meas. technique by bifurcation in optical bistability 7-11910
 review of new materials 7-1841
 screw-like orientated, EM wave propag. calc. 7-20113
 static liq. crystals, smooth equilib. configurations, stability 7-21084
 terphenyl-bis-(4-(3',4',5'-triheptyloxybenzoyloxy)-aniline), columnar liquid crystalline struct. study 7-51613
 thiophene, in liq. crystals, variable angle spinning ^1H NMR 7-929
 tribenzocyclononene, hexasubstituted, pyramidal mesophases, optical anisotropy 7-12275
 Tween 81- H_2O , props. in low-temp. region, struct., ^1H , ^2H and ^{13}C NMR 7-8318
 X-ray diffractometer for liquid surface obs. 7-18969
 Cu (II) complexes, bis (β -diketonato) and β -diketone ligands, double melting, mesomorphism, long chain substituent effect 7-1862
 Cu β -diketonate mesophases, miscibility and discogenic props. 7-63455
 4-n-hexyloxyphenyl 4'-n-decyloxybenzoate, liq. cryst. phases, dielec. relax. 7-53228
 NH_3 dipolar couplings in liq. crystals, anisotropic forces, NMR study 7-62413
 PH_3 dipolar couplings in liq. crystals, anisotropic forces, NMR study 7-62413

liquid drop model (nuclear) *see nuclear liquid drop model*

liquid encapsulated Czochralski method *see crystal growth from melt*

liquid films

- see also adsorbed layers; helium films; liquid helium; superfluidity; surface tension*
 7-44363
 adsorption on porous substrates, thermodynamic stabilities 7-12408
 air-driven, interfacial instability 7-11513
 breakup under the action of a pressure drop in the ambient gas 7-21577
 buoyancy effects in vertical open tubes, thermal and mass 7-31787
 cholesteric thin films, light propagation, beam polarisation rotation calcs. 7-13245
 condensation of flowing vapour on horizontal elliptic cylinder 7-58452
 disintegration by gas press. difference 7-52195
 downflow, Orr-Sommerfeld eqn. soln., optimal approach 7-51119
 electrically conducting film flow, rivulet in nonuniform mag. field 7-26356
 electrically conducting film flow transverse nonuniform mag. field 7-26355
 falling films, surface temp. meas., rel. to gas and vapour sorption 7-56263
 falling liq. film, vapour generation nucleate boiling, acoustic diagnostic technique 7-11502
 falling water films on vertical cylinder with downward step 7-6334
 film flow in vertical pipes with and without interfacial stress, long-wave eqn. 7-11540
 free-standing liquid crystal films, heat capacity and phase transformation study 7-6819
 gas-liq. descending annular flow, phase boundary turbulence and heat exchange 7-63201
 gravitational flow, initial velocity field 7-57784
 heat transfer coeff., surface nonisothermicity 7-11411
 4-(n-heptyloxy)benzylidene-4-(n-heptyl)aniline, surface smectic-I hexatic layers, X-ray obs. 7-63461
 horizontal soap film, transformation process (French) 7-32752
 laminar downflow over cylindrical surface, thermal entry region, heat transfer 7-51096
 laminar falling liquid film, heat transfer from horizontal smooth tube 7-63131
 laser interferometer skin-friction meter, numerical and expt. study 7-16276
 liquid cryst., Fredericksz transition, mol.-dynamics model calcs. 7-44813
 liquid-gas interface, linear stability of liq. film with counter-current gas flow (French) 7-1533
 magnetic liquid, film flow stability 7-51329
 metal, wedging press. 7-12410
 metal-liquid-optimally transparent dielec. system, acoustic radiation under dynamic changes in liq. struct. (Russian) 7-1357
 nematic films, collective rotation of molecules driven by the angular momentum of light 7-27686
 nematic liq. cryst. films, disclinations, textures, four-state clock model description 7-257
 nematic liquid crystal film, optical limiting using self-focusing and self-bending 7-20373
 nematic liquid crystal film, quasi-static elec. field enhanced optical propag. effects 7-27702
 nematic liquid crystal films, four wave mixing with gain 7-20366
 nematic liquid crystal films, power limiting and optical switching 7-43266
 nematic liquid layers, convective flow, multiple spatial periodicities, EHD instability 7-43909
 non-Newtonian films, dimpled, drainage 7-26321
 octamethylcyclotetrasiloxane, nonpolar liq. thin film, solvation and phase separation of water 7-44958
 plane, with free rims, dynamics 7-32763
 polydimethylsiloxane, liq., spreading, existence and role of thin precursor film 7-44954
 power reflection spectroscopy, variable angle 7-53424
 power reflectivity spectra 7-22208
 slip effect for liq. films on a rotating disk 7-57849
 smectic C films, phase winding and flow alignment 7-26628
 Stockmayer fluid between Lennard-Jones plates, mol. dynamics study, electric field effect, polarisation 7-21060
 subcooled liquid, film boiling in channels, heat transfer and hydraulic resistance 7-51145
 switch, all-optical, using interaction between low power light beams in liquid film 7-25864
 thermocapillary and thermogravitational convection in a horizontal liquid layer 7-63909
 thermocapillary convection and stability 7-12409
 thin film, with and without Al substrate, refl. coeffs., admittance method investig. 7-64711
 thin liquid films, thermocapillary flow 7-63908
 thin liquid layers, thermal conductance, meas. 7-16827
 transient dispersed-film flows in channels containing fuel rod bundles 7-10236
 turbulent film, freely-falling, momentum and heat transfer 7-20712

liquid films continued

- twisted nematic thin films, light propagation, beam polarisation rotation calcs. 7-13245
 upward thin-film flow in desalination unit, drag, dynamics 7-11509
 vertical annular countercurrent two-phase flow, flooding, liq. flow rate effect 7-1634
 viscoelastic films, surface driven leveling of surface irregularities 7-51017
 viscous liq. falling film, steady-state solitary wave 7-11435
 viscous liquid, prevention of waves in liq. layer undergoing vertical periodic motion 7-26299
 vortex couples, von Karman wakes, turbulence 7-43935
 water, thin liquid layers, thermal cond. and diffusivity 7-16828
 water molecular chains, orientation defects motion, kink soliton solution mechanism (*Russian*) 7-32260
 wetting films on fibres, peristaltic instability (*French*) 7-32751
 He, thinning effect at λ point, 3D XY model, direct Monte Carlo sampling 7-61305
⁴He superfluid, one-dimensional electron system, localisation, ripplons, scatt. and Coulomb interaction effects (*Russian*) 7-27050
 Hg film flow in transverse nonuniform mag. field 7-26355
 Hg, film flow rivulet in nonuniform mag. field 7-26356
 Ne film on Ag, triple-point wetting 7-32760

liquid flow coaxial cables *see* coaxial cables**liquid He** *see* liquid helium**liquid helium**

- see also* helium films; liquid helium-3; liquid helium-4; liquid helium sound propagation; ripplons; vortices
 channelled cryogenic liquids, heat transfer and hydrodynamics 7-16261
 charged surface stability, nonlinear autowave props. (*Russian*) 7-58556
 compressor, regenerative oilfree, for cryopumps 7-56298
 films, thinning effect at λ point, 3D XY model, direct Monte Carlo sampling 7-61305
 flow rate meas., IMGC calibration facilities 7-63234
 flow stability at supercrit. press., nonuniform heat flux distrib. in channel 7-51058
 free surface, surface tension (*Japanese*) 7-2291
 heat transfer tubes, construction (*Japanese*) 7-320
 heat transfer with nucleate boiling in channels 7-11524
 interacting Bose system, microscopic study of ground state props. and excitation spectrum 7-32736
 Joule-Thomson satellite refrigerator, advantages 7-48755
 liquefaction, condensation heat transfer enhancement for mag. refrigerator performance improvement 7-56283
 liquefaction, refrigerant characts. of Dy₃Al₂O₁₂ and Gd₃Ga₂O₁₂ 7-56286
 liquefaction, rot. mag. refrigerator design 7-56282
 liquefier, condensing and freezing purification system 7-56280
 liquefier with turbo-expanders, prediction method for cool-down characts. 7-56276
 low temperature bath for Cu-⁵⁷Co Mossbauer source, oscillations after heating by an RF pulse 7-59128
 refrigeration, large scale 7-48749
 refrigerator, small capacity, perforated plate heat exchanger matrices 7-56279
 satellite refrigerator efficiency, influence of heat exchanger longit. heat cond. 7-56274
 storage Dewar for ultrasmall scanning tunnelling microscope 7-20075
 superconducting equipment refrigeration technology develop. using liquid He 7-18790
 transmission acoustic microscopy with focal planedetection 7-1343

liquid helium-3

- see also* fermion systems; superfluid helium-3
 adsorbed on solid surface, magnetism (*Japanese*) 7-21564
 binding energy, many-body correlations 7-6910
 collision bracket of linearized quasiparticle Boltzmann equation 7-32740
 drops, ground states, variational Monte Carlo calcs. 7-12383
 energy and momentum distributions, long-range and elementary contributions 7-27044
 Fermi hypernetted chain calcs. 7-52174
 half-filled Hubbard model, similarity to heavy electron Fermi liquids 7-2522
 interactions via hard-core repulsive pot. and attractive tail, microscopic model calcs. 7-58561
 layer on exfoliated graphite, detection of ferromag. domains 7-38291
 magnetic properties, density functional anal. 7-21559
 melting curve thermometer, automated, pressure meas. appl. 7-14955
 melting pressure magnetisation curve 7-63900
 modified Gutzwiller theory, appl. to heavy-fermion systems 7-32915
 momentum dependent induced interaction model 7-27048
 Mossbauer spectroscopy, hydrostatic pressure effect on the minimum temperature of a helium-3 cryostat 7-18970
 nuclear ferromagnetism and surface ferromagnetic effect on Grafoil substrate 7-2296
 polarized liquid, sound velocity meas. 7-63895
 reentrant superfluidity in highly polarised liquid ³He 7-2295
 spin-polarised, general model for steady-state melting to produce polarized liq. 7-52184
 spin-polarized, evidence for viscosity reduction 7-6909
 thermodynamic props., lattice-gas anal. using heavy fermion-boson mixture 7-58505
³He liquid-fluorocarbon solid interface, ¹⁹F nuclear relax. rate, freq. depend., NMR meas. 7-38958
³He-CuK₂(SO₄)₂·6H₂O, thermal resist., surface mag. coupling, effect of ⁴He addition 7-52173
- liquid helium 3-4 mixtures**
 acoustic gas analyser for binary mixtures 7-39939
 adsorption energy of spin polarised at. H, relax. and recomb. processes 7-44949
 Benjamin-Feir turbulence in convective binary fluid mixtures 7-43916
 complete wetting 7-27049
 correcting dil. solns. of ³He in superfluid ⁴He, superfluid turbulence 7-44946
 dilute superfluid solns., ³He quasiparticle specular reflection 7-6911
 dilution refrigerator, liquid He cooled trap 7-319
 films, superfluid phase transitions 7-21565
 specific heat measurements with second-sound Helmholtz resonator 7-21566
 superfluid, critical vel. regime at low temps. 7-27042
 superfluid, phonon-impurity system kinetics, review (*Russian*) 7-52179
 superfluid, thermal transport props. study 7-38290
 surface superfluidity, vortex pair pot. energy (*Chinese*) 7-12391

liquid helium 3-4 mixtures continued

- tricritical behaviour 7-48545
³He-CuK₂(SO₄)₂·6H₂O, thermal resist., surface mag. coupling, effect of ⁴He addition 7-52173
- liquid helium-4**
see also boson systems; superfluid helium-4
 convection in variable cylindrical geometry, heat-flow meas. 7-51127
 critical first sound along λ -line 7-38281
 cryostats for storage Dewars 7-35526
 drops, ground states, variational Monte Carlo calcs. 7-12383
 elastic props., and density up to 20 GPa 7-32733
 electric permittivity, microwave meas. 7-13074
 elementary-excitation spectrum of a weakly interacting Bose system 7-29877
 energy and momentum distributions, long-range and elementary contributions 7-27044
 films, first and second sound 7-32734
 first sound velocity, rounding effects 7-6905
 first sound velocity near T _{λ} , gravity effects 7-12384
 impurities, variational theory 7-27045
 interior Clebsch representations and transformations of symplectic two-cycles 7-52170
 scaling and deep inelastic neutron scattering from quantum liquids and solids 7-58558
 structure factor, pair correl. function, X-ray scatt. intensity meas. 7-44937
 surface electron lifetime obs., short range order effects (*Russian*) 7-6903
 surface waves, quasi-periodic, phase locking effects 7-11444
 thermal transport props. study 7-38282
 thermodynamic temp. determ. of Ne triple point 7-18791
 thermodynamics of freezing and melting in Vycor glass 7-52169
- liquid helium sound propagation**
see also second sound; zero sound
 vibrating superleak transducers, vortex nucleation, critical velocity effects 7-12385
⁴H, critical first sound along λ -line 7-38281
⁴H, liq. and solid, elastic props., and density up to 20 GPa 7-32733
³He, liquid, magnetic properties, density functional anal. 7-21559
³He, polarized liquid, sound velocity meas. 7-63895
³He, superfluid B phase, autocorrelation functions and spinless oscillations 7-12389
³He, superfluid B-phase, sound wave pulse propag. in reson. medium 7-44940
³He-⁴He superfluid soln., phonon-impurity system kinetics, review (*Russian*) 7-52179
⁴He, first sound velocity near T _{λ} , gravity effects 7-12384
⁴He, liq. films, first and second sound 7-32734
⁴He liquid, first sound velocity, rounding effects 7-6905
⁴He, superfluid, critical temp. and nonzero momentum condensation 7-21557
⁴He superfluid, first and second sound, stochastic wave fields, acoustic turbulence calcs. 7-44938
⁴He, superfluid, fractal surface, third sound, capillary condensation 7-27041
- liquid lasers**
see also dye lasers
 2-(o-hydroxyphenyl)benzimidazole, excited state proton transfer, pulsed liq. lasers, pop. inversion obs. 7-50549
 sodium salicylate, excited state proton transfer, pulsed liq. lasers, pop. inversion obs. 7-50549
 Nd₂(SO₄)₃·8H₂O, soln. complex, ⁴F_{3/2} excited state lifetime 7-5614
- liquid liquid transformations**
 acyl cholesteryl esters, mol. motions, temp. depend., ¹²C NMR obs. 7-38950
 benzene, liquid, structural transitions, light scattering 7-63791
 binary liq. mixture, phase transitions, Yukawa tail pots., mean-spherical approx. soln. 7-63422
 caesium pentadecafluorooctanoate-water discoid micelle solns., order-disorder transitions, X-ray scatt., elec. cond., NMR meas. 7-26949
 n-heptane-perfluorohexane soln., phase separation, spinodal curves 7-13170
 isotope-induced quantum-phase transitions in the liquidstate 7-12295
 microemulsions, interfacial props., critical roughening composition, disordered struct. 7-11893
 multicomponent nonideal vapour-liq. and liq-liq. systems, phase equilibrium 7-6769
 α -octyl- ω -pentakis (oxyethylene), phase transition in water system, Raman spectra anal. 7-22244
 PMMA, Tg and T_u tacticity depend., DSC investig. 7-12277
 polybutadienes, high-temp. struct. transition obs. (*Russian*) 7-63820
 polymer solutions, branched, sol-gel transitions 7-12254
 polystyrene, cycloalkane and n-alkane solns., phase behaviour, cloud point curves 7-52030
 three-body forces and phase separation in micellar solutions 7-61299
- liquid metal embrittlement**
 Monel 400, embrittlement by Hg, effect of prestress 7-3431
 SCC mechanism based on surface mobility mechanism 7-53943
 steel, austenitic stainless, creep rupture, fatigue cracking in flowing liq. Na 7-53843
 steel, austenitic stainless, Mo-ion plated, corrosion resist. in flowing Na environment 7-59667
 steel, tool, corrosion resistance in molten Al alloy 7-33835
 Al, cracking behaviour during liquid Hg embrittlement 7-22816
 SiC, sintered, fracture after Li exposure 7-28103
 (Ti,Cr)B₂ sintered electrode exposed to liq. Al, degradation, effect of segregated Cr 7-28045
 TiB₂-TiC composite, hot pressed, degradation in liq. Al 7-28156
- liquid metals**
see also electron energy states of liquid metals; liquid alloys; mercury (metal)
 alkali metal atomic fluids, thermodynamic and electronic props. 7-45157
 alkali metals, one-component plasma structure factors 7-32264
 alkali metals, struct., total partition function and thermal props. calcs. 7-6502
 anodes, dissolution during low freq. current interruptions 7-12287
 approximate struct. theory, hot cryst. vacancy form. energy calcs. 7-63421
 bridge function in modified hypernetted chain approx., rel. to struct. factor 7-21078
 capillary liquid metal ion sources 7-9924

liquid metals continued

capillary wave dispersion relation modifications due to electric charge, surface Green fn. matching method 7-21575
characteristic parameters, thermodynamic similarity methods (*Russian*) 7-44848
clusters, phase investig. 7-15772
compressibility, coexistence line and critical characts. 7-44350
cooling of synchrotron beam line crit. elements 7-42255
d-band metals, binding force, effective interatomic pots., strong scatt. open shell metals 7-32262
density functional theory for a model of nonuniform liquid metal in partially ionized states 7-6504
dielectric function, neutron and X-ray scatt. methods 7-52481
drops, energy characts. 7-32762
electrical resistivity and finite mean free paths 7-45266
entropy, charged hard sphere model 7-21485
films, wedging press. 7-12410
flow in cylindrical induction pump with inductors producing travelling mag. field, anal. (*German*) 7-63107
flow rate measurement using EM flowmeter, error in correl. method 7-57954
fusion reactor self-cooled liquid metal blankets, anal. of MHD effects 7-15363
gas+liq. metal two-phase flow under transverse mag. field, modelling 7-51335
group IIB-VA liquid metal systems, Gibbs energy, composition depend. 7-52080
horizontal Bridgman growth in 2D flow 7-64885
horizontal Bridgman growth in 3D flow 7-64886
immiscible, decomp. sedimentation and precipitation in weightlessness and quasiweightlessness 7-63823
ion source, residual gas and secondary electron bombardment effects 7-30800
ion sources, field and temp. depend. of ion emission 7-7824
ion sources, liq. metal, mech. 7-25275
isothermal compressibility, theoretical analysis (*Russian*) 7-58391
jets, current-carrying, deformation by nonviscous elec. cond. liquid 7-51257
light scattering during evaporation under monochromatic radiation 7-13172
liquid metal-alumina systems, nonreactive, thermodynamic adhesion (*French*) 7-54073
MHD conversion, two-phase liquid metal gas flow in vertical pipes 7-65496
MHD flow in liquid metal blanket with nonuniform thickness liner (*Japanese*) 7-16271
MHD flow in liquid metal blankets with helical veins 7-51325
molecular dynamics simulations 7-16875
molten, flow pattern calc. in induction furnace (*German*) 7-31729
multiple scattering effects, cluster calcs. 7-7100
pure, ab initio variational thermodynamic calcs., hard-sphere Yukawa model 7-26606
rare earth metals, liquid state, kinetic characts. (*Russian*) 7-58517
simple liquid metals, pseudoclassical approach to electron and ion density correlations 7-6503
solid metal-metallic melt systems, phase interactions, interface energies 7-3273
stirrers and induction pumps, liquid metal velocity distrib. effects on electrodynamic forces (*Polish*) 7-63231
structural changes, sensitive thermal analysis technique 7-9831
surface tension, local density functional calcs., pseudopot. nonlocality effects 7-2304
thermal properties and compressibility 7-58509
transition metals, liquid and solid, thermal diffusivity and thermal conductivity meas. (*Russian*) 7-2567
transition metals, thermodynamic props. 7-12323
turbulent jet, mixing and solidification in co-flowing stream 7-51250
two-phase mixture with and without mag. field, shock waves 7-5410
ultrahigh-temperature thermionic conversion in space nuclear power, material considerations 7-65506
wettability of metals against ZrO_2 ceramics 7-52191
wetting and spreading, surface composition effects 7-16837
wetting of solids, metal matrix composites prep. 7-46372
X-ray scatt. due to cond. electrons 7-63440
Ag, liquid, thermoelectric power calc. 7-12704
Al, liquid, struct., X-ray, 800-1600°C (*Russian*) 7-58128
Al, molten, soln. kinetics of stainless steel 7-16753
Au, liquid, thermoelectric power calc. 7-12704
Au liquid metal ion source, focused droplet beam 7-30801
Bi liquid metal ion source study 7-30799
Cd-Bi(Sb), thermodynamic functions are modelled by chemical-physical theory, Gibbs energy 7-52051
Co, O solubility 7-12284
Cs, boiling liquid metal, critical heat flux (*German*) 7-49565
Cs, liquid alkali metals, temp. depend. of mag. susceptibility 7-33152
Cu, liquid, thermoelectric power calc. 7-12704
Cu liquid targets, sputtering, mol. dynamics studies 7-3130
Fe, mag. susceptibility effect of O content (*Russian*) 7-52953
Fe, N solubility, statistical thermodynamics 7-52060
Fe, surface comp. and surface tension, effect of S and Mn (*Chinese*) 7-6916
Ga, electrohydrodynamics, ion source appls. 7-31887
Ga, liq., elec. resist. meas. 7-38532
Ga, liq., electron distrib., struct. factors, neutron diff. determ. 7-26620
Ga liquid ion source at low emission currents 7-30798
Ga liquid metal ion source, influence of substrate geometry on emission props. 7-53508
Ga, solid and liquid, high press. phase transitions, EMF pulse study (*Russian*) 7-2166
Ga surface, in monolayer, sputtering, computer simulation studies 7-17387
Ga-GaP liquid metal-semiconductor contact, transition from rectifying to ohmic operation 7-52833
Hg, solid and liquid, high press. phase transitions, EMF pulse study (*Russian*) 7-2166
Hg, static structure factor, neutron diff. study and Monte Carlo simulation 7-37841
In monolayer on Ga, sputtering, computer simulation studies 7-17387
In-GaP liquid metal-semiconductor contact, transition from rectifying to ohmic operation 7-52833
K, boiling liquid metal, critical heat flux (*German*) 7-49565

liquid metals continued

K, liquid alkali metals, temp. depend. of mag. susceptibility 7-33152
Li, flowing environment, corrosion of steels 7-53961
Li, fusion reactor breeder blanket fluids, T extraction, Pd catalyzed oxidative diffusion 7-49641
Li, liq. fusion reactor blanket, mass transfer in dynamic environment, corrosion damage 7-49659
Li, liquid alkali metals, temp. depend. of mag. susceptibility 7-33152
Li, liquid ion source, nonlinear behaviour of liq. surface in electric fields 7-42259
Li, molten, corrosion resist. of Nb, alloying influence 7-17689
Li, self-diffusion and isotopic effects, pseudopot. formulation 7-26990
Na, boiling liquid metal, critical heat flux (*German*) 7-49565
Na, liquid alkali metals, temp. depend. of mag. susceptibility 7-33152
Na, one-component classical plasma, struct. factor, self-consistent approach (*Russian*) 7-58110
Na, thermoacoustic engine, MHD generator 7-65495
Ni, liquid, thermoelectric power calc. 7-12704
Ni, O solubility 7-12284
Pd, liquid, thermoelectric power calc. 7-12704
Pt, liquid, thermoelectric power calc. 7-12704
Rb, boiling liquid metal, critical heat flux (*German*) 7-49565
Rb, fluid, collective modes 7-1833
Rb, liquid alkali metals, temp. depend. of mag. susceptibility 7-33152
Rb, supercooled liquid, structural relax. 7-37840
Sb liquid droplets, undercooling and crystallisation 7-39496
Sn melt, steam explosion suppression by coolant viscosity increase 7-8284
Ti, liq., electron distrib., struct. factors, neutron diff. determ. 7-26620
Zn, molten, soln. kinetics of steel 7-16752
Zn-Sb, thermodynamic functions are modelled by chemical-physical theory, Gibbs energy 7-52051

liquid oscillations
see also liquid waves
conducting liq., MHD convection, Hall and wall temp. oscills. effect 7-6206
convergent tube, oscillatory incompressible fluid laminar flow 7-20794
coupled acoustic and vortical instability interactions 7-31809
drop, inviscid, in zero gravity environment, free and forced nonlinear oscills. (*German*) 7-20739
flow-induced surface instabilities, Kramer-type compliant surfaces, irreversible processes effects 7-16159
horizontal Bridgman growth in 3D flow 7-64886
incompressible fluid flows with free surfaces, 2 D sloshing problems 7-6232
laser-Doppler anemometer, pipe flow, laminar to turbulent flow transition, sinusoidal flow modulation 7-16262
linear causal system, Kramers-Kronig relations, asymptotic consequences 7-51190
liquid in vibrating cylindrical container, liquid surface response, turbulence, waves 7-16196
liquid metals, horizontal Bridgman growth in 2D flow 7-64885
periodic wave propagation 7-6230
plate oscills. across liquid interface, contact-angle hysteresis effects 7-52189
rectangular 3D jet, reattachment to side wall, oscillations from nozzle 7-20770
rotating viscoelastic liquid column of immiscible liquids, surface and interface oscills. 7-1583
shallow water equations, complex flow, boundary fitted grids 7-6231
steady flow in collapsible tube, flow limitation, oscills. of tube and flow velocity 7-51196
thermal lens oscills. on liq. surface produced by laser beam 7-11403
topographic Rossby waves, 1D models, elongated basins, various lake cross sectional distributions 7-18220
viscous drops, oscillations, viscosity effect 7-37500

liquid permeability see permeability

liquid phase epitaxial growth
p-AlGaAs/GaAs modulation-doped heterostruct., liq. phase epitaxy and carrier props. 7-33074
buried heterostructure laser devices, LPE growth 7-33609
Czochralski growth, mag., expt. model 7-44428
electroepitaxy, growth kinetics 7-7906
furnace, Au film, IR reflectivity (*Korean*) 7-33606
garnet LPE films, lattice relax. around cracks 7-7054
hexaferrite film growth, LPE on $Ba_3(VO_4)_2$ and $CoGa_2O_4$ substrates 7-52320
III-V semiconductor laser, effects of crystal defects on reliability 7-36960
laser diode, V-grooved inner group, LPE grown, 100 mW 1.5 μm operation 7-57354
laser diode heterostructures LPE growth on InP:S substrate, substrate quality evaluation 7-32453
macrosteps, shape of atomic steps and interface supersaturation 7-58689
rare earth silicide epitaxial formation by rapid annealing 7-21768
reactor, modelled as distributed parameter systems with two-time and two-space scales 7-59474
semiconductor compounds, liquid phase electroepitaxy 7-33607
semiconductors, morphological stability in epitaxy, appl. to optoelectronic monolithically integrated structures 7-27172
solar panels with LPE and metal organic CVD circuits, satellite power 7-65493
AlGaAs heterostructs., low temp. LPE growth 7-64939
AlGaAs high-power pulsed laser 7-10997
AlGaAs-GaAs heteroface solar cells, role of window layer 7-3695
AlGaAs-GaAs solar cell fabrication, elec. characts. and space appl. 7-54307
AlGaAs-GaAs space solar cells, LPE production and characterisation 7-3666
Al $_x$ Ga $_{1-x}$ As:Si, LEDs, luminesc. props. (*Korean*) 7-27786
AlGaInAs layers on InP, LPE growth 7-33608
(BiDySmLu) $_3$ (FeAl) $_2$ O $_2$ bubble garnet films, Bi-substituted, LPE growth rate reduction 7-45049
(BiDySmLuGd) $_3$ (FeGa) $_2$ O $_2$ bubble garnet films, Bi-substituted, LPE growth rate reduction 7-45049
(CdHg) $_2$ Te, LPE growth, use of in-situ wash melts 7-59466
Cd $_2$ Hg $_{1-x}$ Te, LPE and MOVPE grown, elec. props. and annealing 7-53512
Cu/nSi films, LPE growth 7-46359
Fe garnet film, epitaxial growth from weakly dissociated molten soln. 7-64944

liquid phase epitaxial growth continued

- GaAlAs laser, LPE grown, effect of crystal defects on reliability 7-36960
GaAlAs single freq. heterostr. injection lasers, LPE and VPE growth 7-62699
GaAlAs-GaAs heterostructure, LPE grown, interface photoluminescence spectra 7-53390
Ga_{1-x}Al_xAs:Si, electrical current induced liq. phase epitaxy 7-27955
Ga_{0.96}Al_{0.04}Sb layers, liq. phase epitaxial growth, elec. and photoelec. characterisation 7-39443
GaAs and GaAs:Te, defect study by positron annihilation (*Chinese*) 7-13254
GaAs, crystals, liquid-phase electroepitaxial growth, dislocation density reduction 7-58681
GaAs, epitaxial layers, grown in temp.-gradient field, effects on dislocation density 7-13393
GaAs, LPE from soln. in laminar flow, high growth rates 7-33605
GaAs LPE layers, heavily doped and compensated, hopping cond., density of states at Fermi level, carrier conc. determ. 7-2753
GaAs LPE on channelled (100) GaAs substrates 7-13391
GaAs layers, LPE growth from Ga-As-Bi soln., kinetics, edge growth effects 7-39444
GaAs, ultrathin layers, liquid phase epitaxial growth on GaAlAs substrate 7-53645
GaAs/AlAs heterostr., transition layer form. during LPE 7-45074
GaAs/AlGaAs separate confinement heterostructure lasers, LPE prep. 7-10940
GaAs-AlAs, solid soln., temp.- and current-controlled LPE, theoretical model 7-39447
GaAs-Bi, distrib. coeff. of Bi, crystn. from molten solns. 7-46428
GaInAsP-InP lasers, single-step LPE fabrication 7-10996
Ga_{1-x}In_xAsSb_{1-y} system, low temp. phase equilb. 7-52001
GaSb, LPE growth from Ga and Sn solns. 7-59467
(Gd,Bi)₂(FeGaAl)₂O₁₂ garnet films, selected area liq. phase epitaxy, local ion implantation effects 7-21726
(GdBi)₂(FeAlGa)₂O₁₂ garnet films, LPE growth 7-59463
HgCdTe, bulk melt growth and LPE, defect control 7-64940
HgCdTe, Hg-rich LPE growth using dipping furnace 7-64943
HgCdTe, high quality LPE on CdZnTe, IR detector anal. 7-64941
HgCdTe, LPE growth in multi-slice apparatus 7-64942
Hg_{1-x}Cd_xTe films, LPE using a semiclosed rotational boat 7-64937
H_{0.5}Sn_{0.5}Te, LPE growth, elec. characts. 7-33603
In_{0.5}Ga_{0.5}P layers, LPE, elec. and optical props. 7-17119
InGaAs, LPE diffusion-limited growth 7-21727
InGaAs layers on InP, LPE growth 7-33608
In_{0.53}Ga_{0.47}As, LPE growth on semiinsulating InP:Fe, SEM studies 7-22591
In_{0.53}Ga_{0.47}As-W-InP structures, LPE growth on structured substrates 7-46353
InGaAsP double heterostructures for laser diodes, LPE growth, influence of P vapour ambient 7-46355
InGaAsP, LPE growth on GaAs_{0.7}P_{0.3} substrate, crosshatch pattern 7-59472
InGaAsP laser, LPE grown, effect of crystal defects on reliability 7-36960
InGaAsP layers, LPE on GaAs, immiscibility region, lattice matching 7-59465
InGaAsP/InP 1.3 μm lasers grown on p-InP substrates, low threshold, high T₀ operation 7-1180
InGaAsP/InP laser wafers, pinhole defects, identification of source 7-46356
InGaAsP/InP multiquantum well layers, LPE, photolum., X-ray diffr. 7-53640
InGaAsP-InP distributed-feedback injection laser, fabrication by LPE and VPE 7-57337
InGaAsP-InP-ridge waveguide lasers, LPE fabricated, design and 1.5 μm low-threshold operation 7-15897
In_{1-x}Ga_xP epitaxial layers, LPE, surface morphology rel. to lattice mismatch 7-33604
In_{0.5}Ga_{0.5}P LPE layers lattice-matched to GaAs, Hall mobility meas. and MESFET fabrication 7-7905
InGaP, LPE growth on GaAs, immiscibility effects 7-39442
InP and InP based materials, epitaxial growth, review 7-33574
InP, submicron gratings, reactive ion beam etching and deformation-free LPE overgrowth 7-13659
InP:Fe, LPE growth, SIMS 7-52363
InP:Mn, LPE growth, carrier conc. control and appl. to buried heterostructure laser diodes 7-21774
Pb_{0.8}Sn_{0.2}Te-PbSe_{0.08}Te_{0.92} heterostr., LPE prepared, characts. 7-52759
PbTeSe layers, LPE growth on nonplanar (100) and (110) oriented substrates, laser appl. 7-17479
Si, crystal growth and solidification, high speed laser heating technique 7-53566
Si, epitaxial growth, conf., Toronto, Ont., Canada (May 1985) 7-9588
Si LPE layer form., depend. on Al₂M chem. reaction, M=refractory metal 7-7043
Si, LPE on patterned substrates, growth and characters 7-22599
Si multilayers, LPE growth, DEM, TEM obs. 7-12565
Si:Al films, LPE in a temperature-gradient field 7-64936
Si:Ga epitaxial layers, growth induced planar defects 7-38414
SiC, epitaxial layers from soln. in melt 7-22597
SiC, LPE growth by temp. gradient zone melting, solubilities 7-64934
SiC, LPE growth by temp. gradient zone melting, Tb-Si solvent 7-64935
Si_{1-x}Ge_x, epitaxial growth, struct., and elec. props. 7-52354
YIG, epilayers, SIMS anal. 7-27207
YIG mixed cryst. films, LPE, segregation 7-53641
ZnTe-ZnSe heterostructures, liq. phase epitaxially grown, luminesc. preps. 7-45477

liquid semiconductors

- see also *electron energy states of liquid semiconductors*
microscopic inhomogeneities in liquid semiconducting systems containing miscibility gaps 7-1829
N, shock compressed, elec. cond. meas. 7-33019
structural changes caused by heating, acoustic investigations 7-51942
Ag chalcogenides, molten, US vel. investig. 7-38124
Ag₂S(Se)-Ag₂Te(Se) liq. and glassy semicond., activation energy of carrier thermal generation, elec. meas. 7-17035
Ag₂S(Se)(Te)-Cu₂S(Se)(Te) liq. and glassy semicond., activation energy of carrier thermal generation, elec. meas. 7-17035
Bi, liq., elec. resist. meas. 7-38532

liquid semiconductors continued

- GaAs, molten, temp. fluctuation meas., 1125 to 937 K 7-58123
Ge liquid, structural phase transitions, photoemission studies 7-1836
Ge, pulsed laser melting, time-resolved reflectivity meas. 7-2158
Ge, thermodynamic interrelation between amorphous, diamond cubic and liquid states 7-12245
Ge-Te liq. eutectic alloys, elec. resist. and struct., 600 to 900 K (*German*) 7-45334
GeTe, solid and liquid states, electrophysical props. 7-52654
Ir complex, (NEt₄)₄(Ir(CO)₂4,4',5,5'-tetracyano-2,2'-biimidazole) mixed valence cpd., anisotropic conductor precursors identified by intermolecular charge transfer 7-7190
PbTe, solid and liquid states, electrophysical props. 7-52654
Se-Te liquid mixtures, mass density at high temp. and press. 7-63701
Se-Te-Au(Ag) liq. mixtures, electronic props. 7-64247
Se_{1-x}Te_x liq. semicond., Se-rich, optical absorpt. edge 7-22213
Si, electronic props., tight binding-mol. dynamics calcs. 7-16931
Si, liq. and solid, solubility of O 7-26961
Si, pulsed laser melting, time-resolved reflectivity meas. 7-2158
Si, thermodynamic interrelation between amorphous, diamond cubic and liquid states 7-12245
Si transiently molten layers, dielec. function, picosec. laser pulse reflectivity meas. 7-52488
SnTe, solid and liquid states, electrophysical props. 7-52654
Ti-SbTeSe₃ liq., semicond., elec., mag. and thermoelec. props. 7-58825
Ti-SbTeTe₃ liq., semicond., elec., mag. and thermoelec. props. 7-58825

liquid-solid transformations see *solid-liquid transformations***liquid structure**

- see also *classical theories of fluid structure; long-range order; neutron diffraction examination of liquids; quantum theories of fluid structure; short-range order; X-ray diffraction examination of liquids*
actinide ions in aq. soln., thermodynamic props., oxidation states, coordination number and struct., review 7-12322
alkali metals, one-component plasma structure factors 7-32264
alkali metals, struct., total partition function and thermal props. calcs. 7-6502
alloys, amorphous and liquid, internal press. kinetic component, eqn. of state calc. (*Russian*) 7-2139
alloys, liq., multi-component solns., interaction parameters, hard sphere model (*Japanese*) 7-11896
approximate dense liq. struct. theories, comparison using force correl. function 7-63420
benzene, viscosity and structural props. 7-6501
benzene-hexafluorobenzene, SS02 theory, charge symmetry model 7-58120
benzonitrile, FTIR and Raman obs. on dynamic and interaction processes 7-53344
binary alloys, associate model and two-sublattice model 7-44351
binary mixtures, excess props., predictions, Weeks-Chandler-Anderson type perturbation theory calc. 7-32247
binary mol. mixtures, statistical mechanical local composition theory, mol. size and energy difference effects 7-32248
bis(1,3-di(p-n-alkoxyphenyl) propane-1,3-dionato) copper (II), discotic liq. cryst. props. 7-37846
n-butane, liq., mol. dynamics simulations, mean square displacement and vel. autocorrel. functions 7-6497
t-butyl alcohol-H₂O mixtures, X-ray scatt., Kirkwood-Buff parameters 7-44337
carbon tetrachloride-SnCl₄ liq. mixture, struct., neutron diffr. exam., RISM integral eqn. calcs. 7-63432
chlorodifluoromethane, liq., mol. dynamics simulations with test-particle model pot. 7-32245
cholesteric liq. crystal, physical props. and mol.-statistical theories 7-37849
cholesteric-nematic mixtures, supermolecular structure, spiral pitch 7-44356
cresyl violet in polymer solution, picosecond rot. reorientation 7-44339
cyclohex. mol. in water, Monte Carlo simulation, pot. function, ab initio calcs. 7-21071
d-band metals, binding force, effective interatomic pots., strong scatt. open shell metals 7-32262
dense classical liquids, pair interaction, comment 7-58115
dense liq. departures from Joule's law near freezing w.r.t. vacancy props. of hot crystals 7-63840
dense simple liquids, transport and time correlation function simulations 7-26604
1,2-dibromomethane-alcohol mixtures, excess vol., comp. depend. meas. 7-63704
dipolar hard sphere fluid, struct. and thermodynamics, reference-hypernetted chain eqn. 7-11879
discontinuous potentials, mol. dynamics of hard dumbbells and vibr. hard dumbbells 7-41249
ethyl bromide, liq., Br interaction, X-ray scatt. investig. 7-21069
femtosecond relaxation, frequency-domain nonlinear-optical meas. 7-11048
fluids at liq.-vapour critical point, many-body interaction effects calcs. and meas. 7-44750
fused salts, nearest cation-anion distance, hard-sphere calcs. 7-21070
hard sphere model, binary correl. function integral eqn., analytic soln. (*Russian*) 7-32252
hard-core fluids, theoretical struct. factors 7-21062
hard-sphere mixtures interacting through attractive Yukawa tail, phase stability 7-11873
inert gases, liquefied, inherent structure, thermal disruption, mol. dynamics computer simulation 7-26612
inert gases, viscosity and structural props. 7-6501
Kuhnian polymer chain, geometrical props. 7-32256
lanthanide ions in aq. soln., thermodynamic props., oxidation states, coordination number and struct., review 7-12322
Lennard-Jones liquid, shear thinning and thickening, mol. dynamics study 7-11869
macromolecular charged fluids, struct. and dynamics 7-11892
mannitol, aq. solns., solvation investig. (*French*) 7-65299
McMOLDYN/H₂O computer simulation package for aqueous systems 7-44330
metal-liquid-optically transparent dielec. system, acoustic radiation under dynamic changes in liq. struct. (*Russian*) 7-1357
metals, approximate struct. theory, hot cryst. vacancy form. energy calcs. 7-63421

liquid structure continued

- metals, bridge function in modified hypernetted chain approx., rel. to struct. factor 7-21078
- metals, liq., X-ray scatt. due to cond. electrons 7-63440
- metals, nonuniform liq., in partially ionised states, density functional theory 7-6504
- metals or alloys, structural changes, sensitive thermal analysis technique 7-9831
- methane, viscosity and structural props. 7-6501
- methanol-d₄, mol. struct., pulsed neutron diff. study 7-63427
- methyl chloride dimer, liq. electrostatic induction, thermodynamic and struct. props. 7-57145
- micellar solns., intermolecular struct. factors, hypernetted chain Percus-Yevick approx. 7-3611
- microemulsions, interfacial props., critical roughening composition, disordered struct. 7-11893
- microscopic inhomogeneities in liquid semiconducting systems containing miscibility gaps 7-1829
- molten salts, microscopic struct. and dynamics, review 7-44348
- molten semiconductors, structural changes caused by heating, acoustic investigations 7-51942
- molten semimetals, structural changes caused by heating, acoustic investigations 7-51942
- nematic liquid crystals with simple curvature strain, symmetry props. 7-32268
- nematic liquid crystals, diamagnetic anisotropy meas. 7-38845
- nonelectrolyte liquids and their mixtures, eqns. of state and struct. 7-26898
- nonpolar solutes, in water, thermodynamic props., hydrophobic hydration shells struct. 7-12317
- organic sulphur cpds., liq., Monte Carlo simulations, develop. of suitable intermol. pot. fns. 7-31140
- polar hard dumbbell liq., struct. and props., site-site Ornstein-Zernike eqn. soln. 7-63417
- polyalanine fragment, solvent struct. hydration, Monte Carlo simulation 7-23299
- polydisperse Percus-Yevick fluid, struct. and scatt. function 7-63423
- polyelectrolyte solns., small-angle scatt. 7-44338
- polyethylene, melt viscosity, chain entanglement 7-6848
- polymer blends and copolymers, dynamics, RPA calcs. 7-37836
- polymer melt struct., nonperturbative integral eqn. theory calcs. 7-44345
- polymer melts, nonexponential density relax. and dynamic form factor in reptation regime 7-16395
- polymer melts, strained, chain retraction, length fluctuations, small angle neutron scatt. 7-51606
- polypropylene, melt viscosity, chain entanglement 7-6848
- polystyrene, colloidal cryst. in semidilute aq. suspension, ordering process 7-13829
- polystyrene solns., integrated intensity light scatt., conc., temp., mol. wt. depend. 7-46056
- propane, liq., X-ray diff. study near triple and boiling points 7-26611
- quantum liquids and solids, scaling and deep inelastic neutron scatt. 7-58558
- rare earth metals, liquid state, kinetic characts. (*Russian*) 7-58517
- scleroglucan solns., low temp. sol-gel transition, rheological behaviour, optical rot. 7-51018
- SiCl₄-TiCl₄, liq. mixtures, neutron diff., RISM anal. 7-44342
- simple liquid metals, pseudoclassical approach to electron and ion density correlations 7-6503
- slowly decaying interfacial profiles, correspondence with reflectivity 7-45967
- smectic liq. cryst. polymer, comb-like macromolecule conformation, determ. from neutron scatt. data 7-26623
- sorbitol, aq. solns., solvation investig. (*French*) 7-65299
- statistical methods, conf., Oaxtepec, Mexico, Jan. 1986 7-24268
- statistical physics, conference, Oaxtepec, Morelos, Mexico (Aug. 1985) 7-9584
- structure-force relations study 7-21064
- styrene-n-butyl acrylate emulsion copolymers, microstruct., ¹³C NMR 7-16390
- supercooled liquids, effect of local molecular order on viscoelastic behavior 7-38129
- suspension, dilute macro-ions, effective charge and diameter, Gibbs-Bogoliubov inequality calcs. 7-65356
- topologically disordered systems Frenkel excitons, electronic absorpt. spectra 7-17287
- transition metal alloys, liquid and amorphous, chemical short-range order, electronic theory 7-44349
- transition metal ion aqueous dilute solns., coordination geometry, XANES studies 7-63428
- 1,3,5-trimethylbenzene, melting point meas., liq. self-diffusion study, hard-spheres method 7-52003
- Tween 81-hexadecane-H₂O, props. in low-temp. region, struct., ¹H, ²H and ¹³C NMR 7-8318
- urea-formaldehyde polymer, struct. swelling and titration (*Russian*) 7-6500
- viscous liquids, defects and relaxation 7-11877
- water, hydrophobic effects in soln. chem., integral eqn., Monte Carlo study 7-59751
- water, liq., collective dynamics, sound dispersion 7-26613
- water, liq., FTIR spectra, fine struct., molar absorptivities of vibr. modes 7-53343
- water, liquid, intermolecular pot. simulation for interaction models 7-1835
- water, liquid network structure model 7-11878
- water, structure, quantum effects, gamma-ray diff. obs. 7-26609
- water between metal walls, Monte Carlo simulation, struct. and thermodynamic props. 7-11881
- water media, refractive index, macrocorrel. bond effects, polarisation-interference method studies (*Russian*) 7-59174
- water-organic mixtures, positron annihilation and compressibility 7-39227
- Ag-Ge liq. eutectic alloys, elec. resist. and struct., 600 to 900 K (*German*) 7-45334
- AgClO₄ soln. in acetonitriles, struct. of Ag^{II} and Ag^O solvates, EPR and electron spin-echo studies 7-17216
- AgTlTe, molten, struct. factors and radial distrib. functions, X-ray diff. meas. 7-26617
- Al, liquid, struct., X-ray, 800-1600°C (*Russian*) 7-58128
- Al-Si melts, sorption degassing, struct. 7-3290
- AlCl₃/1-butylpyridinium chloride electrolyte for Al-FeS₂ secondary cell, phys. and elec. characts. (*Japanese*) 7-8371

liquid structure continued

- Ar, fluid, collective modes 7-1833
- BeCl₂, aq. soln., mol. dynamics, X-ray diff. study 7-21075
- Bi, liq., elec. resist. meas. 7-38532
- Bi-Ag, struct. of 10 mole % Ag alloy, liq. and amorphous states 7-6512
- Bi-Ga, liq., elec. resist. meas. 7-38532
- Bi-Zn liquid alloys with miscibility gaps, struct. 7-51611
- C₆K type graphite intercalation cpds., mol. dynamics study of model system 7-63430
- Cd-Sb melts, crystallisation and structural state, phase equilib. diagrams 7-46441
- CuTi molten alloys, evidence of chemical short range order 7-21077
- Fe-B liq. alloys, interference functions, X-ray diff. study and cluster calcs. 7-26656
- Fe-C hypoeutectic melt struct., temp. and holding time depend., X-ray studies (*Russian*) 7-16396
- Ga, liq., elec. resist. meas. 7-38532
- Ga, liq., electron distrib., struct. factors, neutron diff. determ. 7-26620
- Ga-In, liq., surface segregation, ion bombard. photon emission study 7-32265
- GaAs, molten, temp. fluctuation meas., 1125 to 937 K 7-58123
- Ge-Te liq. eutectic alloys, elec. resist. and struct., 600 to 900 K (*German*) 7-45334
- GeCl₄, liq. struct., X-ray diff. obs. (*German*) 7-58118
- GeCl₄, liq. struct., X-ray diff. investig. (*German*) 7-58119
- HNO₃, ag. soln., Raman spectra 7-39125
- H₂S, liq., Monte Carlo simulations, develop. of suitable intermol. pot. fns. 7-31140
- ⁴He, superfluid, structure factor temp. depend. 7-2289
- ⁴He, superfluid and liq., structure factor, pair correl. function, X-ray scatt. intensity meas. 7-44937
- Hg, static structure factor, neutron diff. study and Monte Carlo simulation 7-37841
- K-Cs, triplet conc. fluctuations in long wavelength limit 7-63439
- KAl(SO₄)₂ solutions, effect of impurities on props. 7-6495
- K₂O-SiO₂, melt, degree of polymerisation, SiO₄ tetrahedra 7-11921
- K₂O-SiO₂ glass melts, structure 7-1831
- Kr, fluid, collective modes 7-1833
- Li/K Cl, molten, struct., thermodynamics, theory 7-37831
- Li-Na liquid alloy, ordering potential, concentration-concentration structure factor 7-32261
- LiCl aq. soln., supercooled, viscosity meas., power-law behaviour, structural relax. theories 7-2247
- LiCl₃H₂O, soln., struct., mol. dynamics simulation 7-58127
- Li₂Pb liquid, static struct., temp. depend., screened Coulomb model anal. 7-21076
- MoO₄²⁻ in aq. soln. struct., X-ray scatt. meas. 7-39883
- Na, one-component classical plasma, struct. factor, self-consistent approach (*Russian*) 7-58110
- Na-Cs, triplet conc. fluctuations in long wavelength limit 7-63439
- NaBeF₃, molten, struct., dynamic props., mol. dynamics calcs. 7-37834
- Na₂BeF₆, molten, struct., dynamic props., mol. dynamics calcs. 7-37834
- Na₂AlF₆, cryolite melt, struct., computer simulation (*Chinese*) 7-6494
- Na₂O-SiO₂, melt, degree of polymerisation, SiO₄ tetrahedra 7-11921
- Na₂O-SiO₂ glass melts, structure 7-1831
- Na₂O-SiO₂-TiO₂ system, struct. of glasses and melts (*Japanese*) 7-21121
- O₂ liquid, SRO, thermal and mag. props. (*Russian*) 7-32253
- O₂-N₂ equimolar liq. mixture, excess props. and struct., mol. dynamics simulation 7-32246
- Pb-Bi-Hg, liq., struct. microheterogeneity 7-11895
- Rb, fluid, collective modes 7-1833
- Rb, Voronoi polyhedra statistics, changes during rapid quenching, computer simulation 7-32263
- RbBr-Rb molten system, struct. studies, XANES anal. 7-63429
- S₈, liq., chem. reactions, mol. dynamics simulation 7-39862
- Sb-Zn melts, crystallisation and structural state, phase equilib. diagrams 7-46441
- Se, bond equilibrium theory anal. 7-63499
- Se-Te liquid alloys, struct. study by neutron diff. 7-51610
- SiCl₄, liq. struct., X-ray diff. obs. (*German*) 7-58118
- SiCl₄, liq. struct., X-ray diff. investig. (*German*) 7-58119
- Sn-Bi-Hg, liq., struct. microheterogeneity 7-11895
- Sn-Pb system, metastable quasi-eutectic struct., existence range 7-3275
- Sn-Sb melts, short-range order 7-63438
- SnCl₄, liq. struct., X-ray diff. obs. (*German*) 7-58118
- SnCl₄, liq. struct., X-ray diff. investig. (*German*) 7-58119
- SnCl₄-TiCl₄, liq. mixtures, neutron diff., RISM anal. 7-44342
- Tl, liq., electron distrib., struct. factors, neutron diff. determ. 7-26620
- WO₄²⁻ in aq. soln. struct., X-ray scatt. meas. 7-39883
- Zn-Sb melt, ordering models 7-44351
- ZnCl₂, molten, pair structure and interionic forces 7-44346
- ZnX₂ (X=Cl, Br, I), aqueous halide solns., EXAFS study of Zn²⁺ coordination 7-59282

liquid surface waves *see surface waves (fluid)***liquid theory**

- see also classical theories of fluid structure; equations of state of liquids; quantum theories of fluid structure*
- adhesive-hard-sphere model, crit. behaviour, mean spherical approx. 7-58113
- alkali metals, struct., total partition function and thermal props. calcs. 7-6502
- n-alkane binary mixtures, liq.-phase diffusivity meas. 7-6843
- analogical representation of liquids in naive physics 7-26607
- anisotropic and isotropic fluids, single-particle trajectories and isojets, fractal behaviour 7-26608
- approximate dense liq. struct. theories, comparison using force correl. function 7-63420
- axially-symmetric molecules, hard-body models comparison 7-58114
- binary hard sphere mixtures eqns. of state, van der Waals perturbation term calcs. 7-12226
- binary liq. mixture, phase transitions, Yukawa tail pots., mean-spherical approx. soln. 7-63422
- binary mixtures, excess props., predictions, Weeks-Chandler-Anderson type perturbation theory calc. 7-32247
- binary mol. mixtures, statistical mechanical local composition theory, mol. size and energy difference effects 7-32248
- carbon tetrachloride-SnCl₄ liq. mixture, struct., neutron diff. exam., RISM integral eqn. calcs. 7-63432
- charged colloidal dispersions, elastic scatt., static struct. factor, RPA calcs. 7-65357

liquid theory continued

- charged dielectric sphere, electron bound states 7-21960
 charged solid-liq., interfaces, dipolar hard spheres, density functional theory study 7-63414
 classical fluids, particle trajectories, fractal anal. 7-37828
 classical one-component plasma, surface props. 7-6490
 concentrated dispersions, shear viscosity, shear-dependent packing fraction, non-Newtonian behaviour 7-8309
 critical adsorpt. of fluid 7-21626
 dense classical liquids, pair interaction, comment 7-58115
 dense liq. departures from Joule's law near freezing w.r.t. vacancy props. of hot crysts. 7-63840
 dense simple liquids, transport and time correlation function simulations 7-26604
 dipolar fluid, effective pair pot. for orientational correls. in elec. field 7-37826
 dipolar fluids, density functional theory, orientational correls. in linear chains 7-37827
 dipolar hard sphere fluid, struct. and thermodynamics, reference-hypernetted chain eqn. 7-11879
 direct correl. function, thermodynamic characts. 7-58117
 electrolyte solutions, ionic props., mol. dynamics simulation 7-44331
 electrolyte solutions, symmetric problems, field theoretic approach 7-11874
 electrolytes near charged hard wall, local HNC/HNC approx. 7-8290
 fluids at liq.-vapour critical point, many-body interaction effects calcs. and meas. 7-44750
 fluids containing small or large mols., thermodynamics, low-density and high-density contrib. 7-52077
 fluids of optically isotropic mols., collision-induced light scatt. 7-33405
 free volume, entropy, and relaxation phenomena 7-21484
 generalised random walks in 1D, fractal props. 7-9785
 geometrical supercooling of liquids in porous glass 7-16720
 hard body fluids, eqn. of state 7-11872
 hard disks and hyperspheres, freezing 7-44768
 hard disks and spheres, power series expansions, critical point singularities 7-44333
 hard dumb-bell model, mol. dynamics study 7-63415
 hard fused spheres, geometry in arbitrary config., statistical mechanics 7-11870
 hard rod density in external field, Percus's eqn. soln. 7-37830
 hard sphere and disperse fluid mixtures, investig. 7-11867
 hard sphere correl. fn. moments 7-32249
 hard sphere diameter, temp. depend. 7-16382
 hard sphere fluids, bridge fn. calc. 7-63418
 hard sphere fluids, partitioning in microcapillaries, Monte Carlo and mol. dynamics simulations 7-63416
 hard sphere liquid, freezing into FCC against HCP structures, density functional theory 7-44765
 hard sphere mixture props., perturbation by intermol. attraction, structural integral eval. 7-37833
 hard sphere mixtures, additive and nonadditive, Monte Carlo simulation and integral eqn. results 7-11871
 hard sphere model binary correl. function integral eqn., analytic soln. (Russian) 7-32252
 hard sphere systems, background correl. fns. 7-37824
 hard spheres in the isobaric-isenthalpic ensemble 7-37823
 hard spheres with Yukawa tail, critical behaviour, mean spherical approx., finite element solns. 7-12251
 hard-sphere fluids, density functional models 7-58112
 hard-sphere mixtures interacting through attractive Yukawa tail, phase stability 7-11873
 hard-sphere Yukawa system, in uniform neutralizing background charge, exact soln. of modified mean spherical model 7-63413
 hierarchical reference theory, smooth cut-off formulation 7-6491
 inhomogeneous fluid, tracer diffusion, kinetic theory 7-58111
 inhomogeneous fluid density distribution, Yvon-Born-Green approach 7-21061
 interaction-induced dipoles in dense media, translational correl. function 7-44335
 Ising model, kinetic two-spin facilitated model on square lattice, Monte Carlo simulation 7-24598
 isotropic fluid, FCC lattice model, Monte Carlo simulation and appl. to collision induced light scatt. 7-16384
 kinetic theory of liquids, maximum entropy ensembles and equilb. soln. 7-26605
 Lennard-Jones fluid, 2D, virial eqn. of state 7-6747
 Lennard-Jones fluid, Kirkwood theory of shear viscosity 7-37821
 Lennard-Jones fluid, repulsive, sound dispersion, density depend. 7-12212
 Lennard-Jones fluid, shear thinning, mol. dynamics method calcs. 7-21059
 Lennard-Jones fluid, transport coeffs., mol. dynamics 7-12336
 Lennard-Jones fluid mixtures, infinite-dilution activity coeffs., computer simulation 7-16383
 Lennard-Jones mixtures, gas solubility Henry coeffs. determ., WCA-LL-GH perturbation theory calcs. 7-6799
 liquid-liquid dispersions, time- and event-driven Monte Carlo calcs. 7-54193
 liquids, Lennard-Jones, wavevector-depend. shear viscosity 7-58518
 lyotropic liq. crysts., spin relax., local order with cylindrical interfaces, translational diffusion, continuous diffusion model 7-64540
 McMOLDYN/H₂O computer simulation package for aqueous systems 7-44330
 metals, approximate struct. theory, hot cryst. vacancy form. energy calcs. 7-63421
 metals, bridge function in modified hypernetted chain approx., rel. to struct. factor 7-21078
 metals, liq., entropy, charged hard sphere model 7-21485
 metals, nonuniform liq., in partially ionised states, density functional theory 7-6504
 mixtures, dilute behaviour near crit. pt. of solvent 7-26979
 molecular dynamics, neutron scattering and collective oscillations under thermal fluctuations 7-16381
 molecular liquids, molecular dynamics study using CYBER 205 7-51599
 molecules, nonlin. multicentre with anisotropic reference system, thermodynamic perturbation theory 7-11882
 molten salt, interaction potential, fluid integral eqn. approach 7-20827
 molten salts MA₃X₁₀ and M₃AX₆, complexing, mol. dynamics studies 7-6496
 monatomic systems, liq. and dilute gas, thermodynamics and transport props., MSK pot. calcs. 7-6826

liquid theory continued

- MPB5 diffuse layer pot. drop 7-13785
 nonpolar polyatomic fluids, Lennard-Jones parameters (French) 7-6488
 off lattice diffusion-limited aggregation with radial bias, liquid crystal fingering 7-63412
 one-component classical plasma, struct. factor, self-consistent approach (Russian) 7-58110
 osmosis, solvent tension theory and thermodynamics 7-21063
 pair diffusion at close range 7-44878
 Percus method for equations with direct correlation functions (Russian) 7-16385
 Percus-Yevick approximation, soln. for fluids with angle-depend. pair interactions 7-44334
 phase transitions in adsorbed films, monolayer adsorption, perturbational approach 7-21665
 polar fluid, Soave-Redlich-Kwong equation of state 7-16710
 polar hard dumbbell liq., struct. and props., site-site Ornstein-Zernike eqn. soln. 7-63417
 polar molecules in v. dil. solns., dispersion curve separation, Debye contribs. 7-51603
 polar-nonpolar molecule mixtures, anal. soln. 7-44336
 polyatomic mol. fluids, site-site Ornstein-Zernike eqn., RISM-2 approx., asymptotic behaviour 7-32257
 polyelectrolyte chain in soln. containing counterions, size study 7-58122
 polyelectrolyte solns., spin relax., local order with cylindrical interfaces, translational diffusion, continuous diffusion model 7-64540
 polyelectrolytes, highly asymmetrical, spinodal curve 7-21466
 polyions, charged spherical, time depend. electrolyte friction calc. 7-21067
 polymer melt struct., nonperturbative integral eqn. theory calcs. 7-44345
 polymer melts, kinetic theory, polydispersity effects 7-51601
 polymer semidilute soln., dynamical scatt. factor, renormalisation group study 7-1834
 radial distrib. calcs. using cubic spline 7-58116
 restricted primitive model for electrical double layers: modified HNC theory of density profiles and Monte Carlo study of differential capacitance 7-11868
 rigid molecules, new rigid motion algorithm for MD simulations 7-50284
 rigid particles in external field, density functional statistical mechs. 7-44332
 rod-like particle fluid, transport props., mol. dynamics 7-42802
 rotational motion in molecular dynamics 7-32251
 simple liquid metals, pseudoclassical approach to electron and ion density correlations 7-6503
 simple molten salt, relaxation near liquid-glass transition 7-6492
 solubility and enhanced tension of solute in soln. 7-21066
 square-well fluid, percolation behaviour, num. procedure 7-26603
 statistical methods, conf., Oaxtepec, Mexico, Jan. 1986 7-24268
 statistical physics, conference, Oaxtepec, Morelos, Mexico (Aug. 1985) 7-9584
 statistical thermodynamics, theory and apps. 7-29864
 Stockmayer fluid between Lennard-Jones plates, mol. dynamics study, electric field effect, polarisation 7-21060
 structure-force relations study 7-21064
 suspension, dilute macro-ions, effective charge and diameter, Gibbs-Bogoliubov inequality calcs. 7-65356
 ternary correlations in liquids 7-6493
 tetrachloromethane, induction spectra, mol. dynamics simulation 7-1830
 three-body correlations, direct and total, rel. to Ornstein-Zernike two body function 7-21065
 1Dtriangle- and square-well fluids, perturbation theory 7-6489
 1,3,5-trimethylbenzene, melting point meas., liq. self-diffusion study, hard-spheres method 7-52003
 two-centre Lennard-Jones fluids, phase equilibria 7-32610
 water, liq., three-body forces and single-molecule dynamics 7-11880
 water, liquid, H-bonds, spatial correls., Raman spectra 7-13156
 water, liquid, OH stretching vibr. spectrum, mol. dynamics study, IR, Raman and neutron diff. spectra 7-44329
 water, radial distribution functions, consistency check 7-37832
 AlCl₃ solns., complexing, mol. dynamics studies 7-6496
³He, liq., Fermi hypernetted chain calcs. 7-52174
 Li ion pairs in tetrahydrofuran, indicator scale rel. to C acidity 7-51602
 N₂, liq., compressed, far IR absorpt. spectrum, density effects and rel. diffusion 7-39112
 N₂, liq. and fluid press., intermol. pots. comparison, mol. dynamics simulation 7-63419
 N₂O, in liq. SF₆, rot. self-correl. functions, mol. dynamics simulation 7-44343
 Rb, supercooled liquid, structural relax. 7-37840
 Rb, Voronoi polyhedra statistics, changes during rapid quenching, computer simulation 7-32263
 YF₃ solns., complexing, mol. dynamics studies 7-6496

liquid-vapour transformations

- see also boiling; condensation; evaporation; liquefaction of gases
 acetonitrile-1-propanol mixtures, vapour-liq. equilibria 7-38173
 1-alcohol-n-alkylaromatic cpd. systems, excess thermodynamic props. model (German) 7-2232
 alkali metal atomic fluids, thermodynamic and electronic props. 7-45157
 alternative binary system, two-dimensional, critical state 7-63783
 binary liq. mixture, phase transitions, Yukawa tail pots., mean-spherical approx. soln. 7-63422
 chemical process design, fluid props. and phase equilibria, conf., Lo-Skolen, Helsingør, Denmark (May 1986) 7-18473
 conference on iodine chemistry in reactor safety, Harwell, England (Sept. 1985) 7-48176
 cubic equation of state 7-38174
 cyclohexane-d₆-methanol mixtures, stabilised vapour-liquid interface 7-12400
 density distribution near gas/liquid critical points under reduced gravity 7-21426
 1,2-dichloroethane-benzene (toluene) (p-xylene) mixtures, liq.-vap. equilb. (German) 7-2161
 fluids at liq.-vapour critical point, many-body interaction effects calcs. and meas. 7-44750
 gas containing systems with cubic equations of state, phase behaviour 7-6752
 gas-vapour bubble oscillations in acoustic field, num. investig. 7-52022
 hard spheres with Yukawa tail, critical behaviour, mean spherical approx., finite element solns. 7-12251

liquid-vapour transformations continued

- infinite-pressure excess functions and VLE K values from liquid-phase activity coefficients 7-16708
 interface, density fluctuations, gravity effects close to critical temp. 7-32626
 isochoric heat capacity at the critical point under reduced gravity (*German*) 7-21478
 Langmuir monolayers, phase transitions, fluoresc. microscopy 7-32867
 Lennard-Jones fluid, behaviour in narrow pores 7-32250
 metastable region in the scaling theory of critical phenomena 7-44754
 methane, vibr. dephasing, critical density broadening, Raman spectra anal. 7-62387
 methane monolayer on graphite, thermodynamic study 7-16863
 methane-alkane mixtures, vapour-liq. equilib. Wilson-Wegner expansion, vapour press. calcs. 7-12248
 mixtures with supercritical gases, vapour-liq. equilib. calcs., excess Gibbs energy method 7-6768
 multicomponent mixtures, vapour-liq. critical points calc. using empirical method 7-38175
 multicomponent nonideal vapour-liq. and liq.-liq. systems, phase equilibrium 7-6769
 n-pentane-dichloromethane, excess thermodynamic props. 7-52079
 phase transitions in adsorbed films, monolayer adsorption, perturbational approach 7-21665
 Pirogov-Sinai theory, simple fluids and Gibbs phase rule 7-58440
 polymer soln. mixtures, vapour-liq. equilib., quartic hard chain eqn. of state calcs. 7-12228
 polymeric liquid films on energetically nonuniform substrates, stability and equilib. props. 7-6772
 supercritical fluid, nature 7-9622
 thermodynamic stability and viscosity behaviour or melting curve 7-12247
 van der Waals fluid, phase transitions, theory 7-48251
 vapor composition calculations from bubble point temp. and liq. composition meas. 7-52026
 vapour-gas-liquid systems with separate volumes of vapour and gas, limits of variation of specific vol. 7-51998
 CO₂-He dilute mixtures, liq.-vapour curve, ³He partial contrib. 7-32625
 CO₂-n-hexadecane supercritical system, phase equilib. and vapour density meas., high-press. multiproperty apparatus appl. 7-12249
 Cs, liq.-vap. interface, electron and ion distrib., self-consistent Monte Carlo simulation 7-52024
 H₂-containing mixtures, interaction parameter in Peng-Robinson eqn. of state 7-16712
 HF-H₂O, vap.-liq. equilib. and partial press. formulae 7-21427
 H₂O-CO₂(H₂S)(NH₃)(H₂SO₄)(H₃PO₄)(ZnCl₂)(CuCl₂), thermodynamic meas., bibliography of data sources 7-52070
 Hg, liquid-vapour interface, in-plane distrib. of atoms 7-52023
 I₂ volatility from evaporating PWR primary coolant films in accidents 7-49603
 I₂-H₂O vapour partitioning under severe reactor accident conditions 7-49602

liquid waves

- see also capillary waves; ocean waves; surface waves (*fluid*)
 acceleration measurements using laser Doppler anemometry 7-31904
 air-water interface wave-induced press., fluctuations, wave generation by wind 7-16198
 breaking wave, reflected wave 7-6231
 compressible liq., localised laser thermo-optical volume source surface wave excitation, numerical estimates 7-31818
 coupled acoustic and vortical instability interactions 7-31809
 diffraction, submerged cylinder of arbitrary shape, second-order num. soln. 7-51192
 diffraction by gap between two breakwaters, long waves, matched asymptotic expansions soln. 7-47446
 flow-induced surface instabilities, Kramer-type compliant surfaces, irreversible processes effects 7-16159
 gravity current on sloping bottom, rot. flow interaction, shelf wave generation, flow visualisation expts. 7-43947
 gravity currents, stratified fluids, turbulence effect, appl. to shallow sea fronts 7-43949
 incompressible liq. in wedge-shaped region, unsteady wave motion, 3D problem 7-51187
 induced mean flow accompanying a water-wave packet 7-37478
 interfacial wave measurement method involving light polarisation and optical activity 7-4201
 interfacial waves, finite amplitude stability, effect of basic current shear 7-43946
 nonlinear cross waves, Benjamin-Feir instability 7-51198
 nonlinear instability and evolution of steep water waves under wind action 7-31820
 nonlinear waves of different physico-mechanical nature in finite continua 7-18604
 prevention in liquid layer undergoing vertical periodic motion, by superposed liq. layer 7-26299
 singularities in water wave theory with inertial surface 7-51189
 surface gravity wave propag., interfacial props. influence 7-37479
 topographic Rossby waves, 1D models, elongated basins, various lake cross sectional distributions 7-18220
 variable depth shallow water, wave breaking, variable coeff. KdV eqn. 7-29770
 viscous liq. falling film, steady-state solitary wave 7-11435
 visualisation of slightly deformed, liquid surfaces, using K-Moire method 7-37483
 water, waves, maximum growth rate 7-43956
 water waves for finite and infinite depths, nonlinear theory 7-26301
 water waves over a sloping beach 7-63166
 wind generated waves, wave tank expts. 7-66151
 wind waves and low freq. oscillations of water surface 7-31819

liquids

- for generalities only; for specific aspects see appropriate headings
 see also liquid structure; liquid theory; solutions
 formulation of new materials 7-13341

literature reviews see reviews**lithium**

- see also nuclei with
 adatoms on W (110) nuclear quadrupole interactions, NMR study 7-2937
 aggregated thin film, particle order and disorder, minimal spanning tree 7-4788

lithium continued

- Am stars, Li abundance, reson. doublet obs. 7-60669
 arc in air, plasma comp., Gibbs free energy calcs. 7-37795
 atom, ²⁵S ground state, specific mass shift, isotope shift, ab initio calcs. 7-36495
 atom, ⁴P level, relativistic autoionisation, CI mechs. 7-49949
 atom, double electron excitation cross section, distorted wave approach 7-50379
 atom, electron elastic scatt., spin dependence meas. 7-15718
 atom, electron impact ionisation, positronium form. 7-31176
 atom, excited states, quantum defect and isotopic shift meas., millimeter wave ODR spectroscopy 7-15538
 atom, g-Hartree ab initio calcs. 7-15488
 atom, high-freq. Stark effect, laser-induced fluoresc. anal. 7-36529
 atom, isotopic anal., SES-ICP investig. 7-46908
 atom, photoionisation cross sections, ab initio RRPA calcs. 7-36462
 atom, positron impact, positronium form. cross-sections 7-36797
 atom, positron inelastic scatt., calc. of angular correlation parameters 7-15723
 atom, relativistic effective potentials in quantum Monte Carlo calculations 7-49902
 atom, spin density, cusped gaussian wave functions 7-42504
 atom, Stark levels, WKB calcs. and multichannel quantum-defect theory 7-15546
 atom, two-photon resonant three photon ionisation, power broadening, laser bandwidth and interaction time effect 7-36571
 atomic, excited states, electron correlation calc. (*Chinese*) 7-10438
 atomic Rydberg states, collisional line broadening, trilevel photo. echo meas. 7-19772
 atoms, ⁴P levels, relativistic autoionisation, threshold phenomena, CI mechs. 7-49950
 atoms, ultrafine structure, nonrelativistic approx. 7-5612
 batteries, electronic devices interfacing 7-59832
 batteries with confirmed reliability and safety 7-59830
 battery reliability for memory backup (*Japanese*) 7-65425
 beam, mag. field meas., Zeeman and motional-Stark effect 7-19766
 bonds, existence and nature 7-48249
 cells, semiconductor polymer electrode kinetics 7-54285
 chemisorption and rot. epitaxy on Ru (001), LEED, TDS obs. 7-12479
 coadsorption with H₂O on Ru (001) 7-21645
 column density meter, high precision technique for line-of-sight vapour densities meas. 7-48695
 crystal and electronic struct., ab initio HF cluster method 7-44443
 RS CVn stars, Li I line strengths in σ Gem, α Aur, HR 6469, and 93 Leo 7-18437
 δ Del stars, Li abundance, reson. doublet obs. 7-60669
 differential depletion in diffuse interstellar clouds 7-66706
 dimer, isotopes, laser separation, double REMPI spectra 7-42694
 dimer, optical-optical double reson. and double reson. multiphoton ionis. 7-42742
 dye laser diagnostic system for Li beam spectroscopy in a tokamak 7-1760
 electrodes, semicond. passivating film, impedance meas. 7-33111
 electron scatt., charge polarisation effect 7-63685
 electron scatt. by Li atoms in solids, polarisation and exchange 7-22401
 electron-electron scatt., elec. resistivity meas. 7-32981
 electronic band struct., interatomic distance, role of p-orbitals, EHT tight-binding calcs. 7-32906
 flowing environment, corrosion of steels 7-53961
 fusion reactor breeder blanket fluids, T extraction, Pd catalyzed oxidative diffusion 7-49641
 hollow cathode discharge, spectrosc. obs. 7-21008
 intercalated with TaS₂, room temp. optical transmission spectra, charge transfer and band struct. modification 7-45962
 ion, scatt. by diatomic gases and spherical mols., energy transfer flight time meas. (*German*) 7-57163
 ion affinities of O₂ and N₂ bases, basis set and correl. effects 7-5610
 ion pairs in tetrahydrofuran, indicator scale rel. to C acidity 7-51602
 ions, hyperfine structure, relativistic corrections, nucl. struct. effects 7-57007
 large clusters, struct., charge distribution and spin densities, semiempirical study (*French*) 7-26696
 laser-produced plasma for pulsed ion beam research 7-25291
 late-type Population I dwarf stars, Li abundances and ⁷Li/⁶Li ratios 7-14562
 lattice dynamics at low temps. 7-44716
 liquid, self-diffusion and isotopic effects, pseudopot. formulation 7-26990
 liquid alkali metals, temp. depend. of mag. susceptibility 7-33152
 liquid flow through thin walled elbow in uniform magnetic field 7-37555
 liquid fusion reactor blanket, mass transfer in dynamic environment, corrosion damage 7-49659
 liquid ion source, nonlinear behaviour of liq. surface in electric fields 7-42259
 M67, old open cluster, dwarf stars Li abundance 7-55743
 microclusters, fragmentation channels rel. to magic number studies 7-5811
 molecule, photoionisation and Auger electron emission, HF calcs. 7-36703
 molecule, vibr. excited by optical pumping, electron impact ionisation cross sections 7-62536
 molten, corrosion resist. of Nb, alloying influence 7-17689
 N-electron atom, electronic energy in a space of constant curvature (*French*) 7-36500
 neutral beam, Zeeman splitting, Tokamak plasma diagnostics appl. 7-1740
 overlayers on graphite, electronic struct., initial stages of intercalation 7-53503
 particle flux in tokamak plasma scrape-off layer 7-16298
 particles, electron spin-lattice relax. freezing-in, spin echo obs. 7-2921
 plasma generation for PBFA-II ion diodes 7-20962
 plasma Zeeman spectroscopy using high-intensity Li beam 7-6460
 positron annihilation, high-momentum components and core enhancement effects 7-46195
 positron annihilation in alkali metals 7-39231
 positron annihilation rate distrib., momentum-depend. enhancement factors 7-39221
 positronic, annihilation parameters calc. from arbitrary wave functions 7-46190
 primary cells, voltage compatible, β -PbO and β -PbO₂ as cathode materials 7-3632

lithium continued

- quartz:Li, (SiO₄/Li)⁰ centre, correlated ESR and thermoluminescence studies 7-22140
- quartz:Li, electrodiffused, radiation-induced conductivity 7-6691
- salts, ion-molecule interactions in DMF, IR spectrosc. obs. 7-10584
- seafloor geology and crustal generation since 116 Myr BP, foraminifera Li content evidence 7-23632
- secondary battery development with Bi-Pb-Sn-Cd alloy negative electrode (Japanese) 7-65435
- secondary battery using NbS₃ prep. under high press., performance 7-13853
- secondary cells with three electrodes, electrode processes at Li-polymer electrolyte interface 7-3639
- simple local pseudopotential 7-32888
- solvated electron electrode for secondary batteries 7-23130
- spectral emission line profile, laser produced plasma, polarisation shift (French) 7-6446
- spin polarised beams, production and acceleration 7-49766
- stacking faults, X-ray and neutron diffr. patterns 7-16580
- dwarf star of population II, ⁷Li abundance of G 64-12 halo star 7-60642
- stars of galactic halo, Li abundances of metal deficient halo dwarfs 7-60641
- surface, CO chemisorption, molecule-cluster interaction ab initio SCF-CI calcs. 7-45013
- tensile strength under (110) uniaxial stress (Chinese) 7-26825
- TEXT, plasma density and poloidal field meas. using injected Li beam 7-6452
- triode ion gun, thermal emission, characts. meas. 7-39345
- ultra-thin paper Li battery (Japanese) 7-65423
- vapour, monatomic, transport props., depend. on two body atom-atom interaction pot. 7-6343
- vapour, thermodynamic props. at press. 10² to 10⁷ Pa and temp. 1000 to 3000 K 7-57975
- work fn., temp. depend., anal. 7-52737
- Ag_{0.25}NbSe₂:Li, Li diffusion and intercalation 7-16806
- CaF₂:Li⁺, EPR of colour centres 7-17222
- Cr₂CdF₄:Cr³⁺, Li⁺, Cr³⁺ centres, EPR study 7-7589
- GeO, Li, IR absorption spectra and bands, Li-O complexes 7-33375
- In₂Se₃:Li, electrical transport props. 7-21917
- KCl:Li, F_A-centre crystals, diffraction efficiency of photoinduced gratings 7-62818
- KCl:Li, self-induced light polarisation oscils., stochastic field effects (Russian) 7-43208
- KCl:Li,F_A(II) colour centre laser, synchronously pumped, mode locking 7-62710
- KCl:Li crystals, F_A-centres self-induced resonant radiation polarisation changes study (Russian) 7-33358
- KCl:Li F_A(II) colour centre lasers appl. to intracavity laser spectroscopy 7-43189
- KCl:Li⁺, impurity interactions, sp. ht. and thermal expansion, pair density of state calcs. 7-63852
- KI:Li (F₂⁺)_A centre, selective two-step photoionisation using 1.06 μm radiation 7-38053
- KTaO₃:Li, quadrupole ferroelastic phase 7-6778
- KTaO₃:Li, time depend. phase transform., neutron diffr. meas. 7-44799
- KTaO₃:Li polydomain ferroelec. crystals, dipole impurity-induced ESR line broadening calcs. 7-53131
- Li + He(Ne), electric field effect, fluoresc. and radiative decay rate determ. 7-20009
- Li + XF (where X = Mu, ¹H, ³H, ¹⁰B), quasiclassical trajectory calcs., isotopic and orientational study 7-33923
- Li I, oscillator strengths, transition matrix elements, Dirac-Fock approx. 7-843
- Li I 670.7 nm line in stars in M67, Li abundance 7-55746
- Li II, transition wavelengths among doubly excited states 7-49980
- Li, large clusters, struct., charge distribution and spin densities, semiempirical study (French) 7-26696
- Li⁺ ion form. on low work function surfaces 7-15444
- Li⁺, ¹p⁰ symmetry, Wannier two-electron ionis. ladder, wave fn. calc. 7-62274
- Li⁺ bombard. of target atoms, shadow cone form. calc. 7-36731
- Li⁺, in the, mobility and longit. diffusion 7-20834
- Li⁺, in water, Stokes radius, Hubbard-Onsager's dielectric friction theory 7-33347
- Li⁺ pumping by soft X-rays, EUV emission 7-20196
- Li/amorphous V₂O₅-P₂O secondary cells, ethylene carbonate/2-methyltetrahydrofuran electrolyte 7-3635
- Li/CuO-chalcopyrite battery structure and characteristics (Japanese) 7-65424
- Li/Li_{1-x}V₃O₈ batteries, comparison with other secondary cells, influence of micro- and macro-structural alterations 7-46932
- Li/MoS₂ cell, spirally wound, inductive impedance 7-46931
- Li/MoX₂ and Li/WX₂ (X=S,Se,Te) electrochemical cells at low voltages, dichalcogenide decomposition 7-65436
- Li/SOCl₂ cell, corrosion, calorimetric study 7-46929
- Li/SOCl₂-SO₂Cl₂ cells, low temp. discharge behaviour 7-65422
- Li-(CF)_n batteries, open circuit voltage 7-8369
- Li-(CF)_n battery, complex impedance plots (Japanese) 7-23129
- Li-(CF)_n cells, improved discharge characts. at low temp. using mixed organic electrolytes 7-8368
- Li-air alkaline batteries, thermodynamic framework for efficiency estimation 7-3636
- Li-Al₂O₃-P₂O₅:Ag glasses, Ag⁰ centre thermal and photochemical conversion, spectroscopic consequences 7-39906
- Li-CO₂ complex, pot. energy surface, covalent ionic nature 7-30967
- Li-CuMoS₈-y porous film, prep. by solid-gas reaction, secondary battery appl. 7-27897
- Li-H systems, localised nature of chemisorption bond, calc. of chemisorption energies 7-2361
- Li-I₂ solid state batteries, performance of polyacrylonitrile-based cathodes 7-54282
- Li-LiH-Na systems, solubility of H, press. and temp. depend. 7-21471
- Li-LiNO₃ thermal battery cell discharge lifetime with soluble cathode materials 7-3630
- Li-like ions, first excited state, intra- and inter-shell correl. effects 7-62295
- Li-MoS₂, 65 Ah rechargeable batteries, design and testing 7-34010
- Li-MoS₂ batteries for space appls., proceeding of NASA/Goddard workshop, Greenbelt, MD, USA (Nov. 1985) 7-29578

lithium continued

- Li-SO₂, Li-SOCl₂ and Li-SO₂Cl₂ batteries for space appls., proceeding of NASA/Goddard workshop, Greenbelt, MD, USA (Nov. 1985) 7-29578
- Li-SO₂ batteries, effect of water during incineration 7-39983
- Li-SO₂ commercial cells, impedance meas. at various states of charge 7-54281
- Li-SO₂ primary cells, safety hazards during charging 7-34007
- Li-SO₂ rechargeable cell with Li(SO₂)₃AlCl₄ electrolyte and C electrodes 7-65443
- Li-SO₂Cl₂ cell battery pack fabrication, safety 7-34008
- Li-SOCl₂ cell battery pack fabrication, safety 7-34008
- Li-SOCl₂ primary cells, heat dissipation study 7-34009
- Li-TiS₂, 35 Ah ambient temperature rechargeable cells, design options 7-34011
- Li-vinylidene complex, struct., bonding, ab initio CI calcs. 7-49935
- Li+Cs, ion pair prod. cross sections, beam-gas study 7-39871
- Li+HBr, complex optical pots., large angle elastic scatt. calcs. using WKB theories 7-42728
- Li+HBr, elastic scatt., complex Lennard-Jones pot., WKB calcs., Regge Pole anal. 7-36724
- Li+HCl, laser catalysed reaction, pot. surfaces and transition dipoles 7-39861
- Li+HCl quenching reaction, electronic struct., ab initio SCF CI calcs. 7-56995
- Li+HF, 3D reaction, differential cross section calc. 7-59739
- Li+He, Penning ionisation, pot. well depth calcs., electron energy spectra anal. 7-62510
- Li+He²⁺, electron capture, Coulomb integral eval. 7-15679
- Li+Na, ion-pair production, laser excitation effect 7-62502
- Li+Na⁺, charge exchange collisions, cross sections calcs., atomic-orbital expansions method 7-36460
- Li⁺+dimethyl ether, assoc., rate consts. pot. energy surface, canonical variational transition states theory 7-54108
- Li⁺+He, n=Z levels, alignment and orientation (French) 7-10723
- Li⁺+N₂, vibr. rot. energy transfer, collisional time-correl. functions 7-50316
- Li⁺+Na, charge exchange collisions, cross sections calcs., atomic-orbital expansions method 7-36460
- Li⁺+Ti, inner-shell ionis. polarisation effect, variational wave fn. calc. 7-62491
- Li³⁺+He, electron capture, Coulomb integral eval. 7-15679
- Li₂, chem. bonding, kinetic energy anisotropy investig. 7-10396
- Li₂, low-lying ¹Σ⁺ states, orbital exponent calcs. using LCAO MO CI method 7-56971
- ⁶Li, 2¹Σ⁺ state, isotope effect, Fourier transform spectroscopy 7-5660
- Li₂+H₂, ab initio study 7-8257
- Li₂+He (Xe), rot. energy transfer cross sections, studied using polarisation ratio vel. depend. 7-42740
- Li₂+He(Kr), total integral scatt. cross-sections 7-36728
- Li₂ cluster, photodissoc., bound-free transitions fluoresc. study 7-23045
- Li_n clusters, n=2 to 13, electronic struct. and magic numbers, LCAO-Xα calcs. 7-31206
- ⁶Li, enrichment by electromigration in molten LiNO₃ 7-2244
- ⁷Li II, absolute wavelength determination, fine struct. determ. 7-10771
- ⁷Li NMR meas. spatial anisotropy limits 7-14988
- ⁷Li₂, A ¹Σ⁺-X ¹Σ⁺ and B ¹Π_u-X ¹Σ⁺ 7-36691
- Li⁺Li₂⁺, excitation and rot. transfer, rate const. determ. (French) 7-5750
- NbSe₂:Li, Li diffusion and intercalation 7-16806
- Nd:LiYF₄, two-step excitation and fluoresc. at 587.4 nm under CW pumping 7-25824
- Ni-Cd cells, General Electric 50 Ah, qualification testing of separator and positive plate processing 7-34012
- Rb₂CdF₄:Cr³⁺, Li⁺, Cr³⁺ centres, EPR study 7-7589
- Rb₂ZnF₄:Cr³⁺, Li⁺, Cr³⁺ centres, EPR study 7-7589
- Si:Al, Li, Au-Si pair paramagnetic state, EPR studies 7-45817
- Si:Li, ion implanted, impurity redistribution under pulsed laser radiation 7-12098
- Si:Li counterdoped n⁺p solar cells, proton-irradiated, DLTS studies 7-8376
- SiO₂:Li, crystalline quartz with Li-associated electron trap, electronic struct. 7-21860

lithium alloys

- Al-Li-Mg powders, mech. alloying 7-64968
- Zintl phases, binary and ternary, electron densities, sp³-bonding character, calc. 7-32907
- Al alloys containing Li, rapid solidification, bibliography 7-41029
- Al-Cu-Li, 2020, low-cycle fatigue, effect of environment and temp. 7-28117
- Al-Cu-Li, cryogenic toughness, orientation effects 7-39669
- Al-Cu-Li, liquid dynamic compaction, microstruct. and precipitation, TEM study 7-59529
- Al-Cu-Li, plastic deform. in conditions of quasihydrostatics (Russian) 7-59586
- Al-Cu-Li alloys, cyclic fracture, mechanisms 7-46634
- Al-Cu-Li-Mn-Cd, 2020, micromechanisms governing elevated temp. fracture resist. 7-22803
- Al-Li, coarsening of δ' precipitates 7-33663
- Al-Li, grain boundary precipitate free zone growth kinetics 7-33662
- Al-Li, quenched, ageing, light ion irradi., δ' phase form. and particle growth 7-26807
- Al-Li, thermal surface oxide layers, SIMS characterisation 7-13650
- Al-Li (9.5 at.%), coarsening of δ'-Al₃Li precipitates, var. of average Li content in Al matrix 7-3313
- Al-Li alloys, grain boundary fracture 7-39644
- Al-Li base alloys, deform. and fracture 7-39594
- Al-Li base system, solid-state phase transform. 7-46456
- Al-Li-Be alloys, arc-melted, microstruct. evaluation 7-22655
- Al-Li-Be alloys, rapidly solidified, microstruct. eval. 7-22656
- Al-Li-Cu, T₂ phase, icosahedral struct. 7-16425
- Al-Li-Cu-Mg quaternary alloy, initiation of voiding at second-phase particles 7-39645
- Al-Li-Cu-Mg-Zr, wear, comparative investigs. and prep. method role 7-13605
- Al-Li-Cu-Mg-Zr, yield stress, temp. and strain rate depend. (Japanese) 7-33734
- Al-Li-Cu-Mg-Zr die forgings, mech. props., microstruct. 7-46636
- Al-Li-Cu-Mg-Zr powder alloy, superplastic, high modulus and hardness 7-53816
- Al-Li-Cu-Zr, 2090, small fatigue crack growth 7-22817
- Al-Li-Cu-Zr, Al-Li-Zr, nucleation of δ' and β' precipitates 7-59527

lithium alloys continued

- Al-Li-Cu-Zr, fracture, ageing and comp. depend. 7-22784
 Al-Li-Cu-Zr, nucleation of precipitates 7-46476
 Al-Li-Cu-(Mg), fracture, effect of subgrain struct. and ageing practice 7-13563
 Al-Li-Cu-(Mg), stress corrosion resist. and mech. props. 7-33833
 Al-Li-Ge, corrosion rel. to Ge content 7-39715
 Al-Li-Mn (Cu), precip.-hardened, cyclic stress response and deform. behaviour 7-22791
 Al-Li-Sc, cast, decomp., mech. props., struct. (Russian) 7-59532
 Al-Li-Zn (Cu) icosahedral quasicrystals, solid state reaction and rapid solidification prep. comparison 7-37864
 Al-Li-Zn-Mg-Cu alloys, microstruct. evolution 7-53739
 Al-Li-Zr rapidly solidified alloy, plastic deform. characts. 7-22777
 Al-Mg-Li, 14 MeV neutron irradi., mech. props. microscopic struct. 7-56820
 AlCuLi alloys, large quasicrystalline dendrites, triacontahedral solidification morphology 7-32345
 AlCuLi quasicrystalline struct., construction 7-37929
 Cu-Li, prep. and props. 7-53663
 Li_{0.8}Pb_{0.2} liq. mixture, fast sound computer simulation, Mori-Zwanzig formalism 7-44696
 Li-Al/FeS₂ cell with LiCl-LiBr-KBr molten electrolyte 7-65439
 Li-In-Sb, ternary phase diagram, electrochem. investig. 7-58441
 Li-Mg, liq., excess entropy of mixing, resist. calcs. 7-2571
 Li-Mg disordered, phonons and martensitic phase transitions 7-58423
 Li-Na liquid alloy, ordering potential, concentration-concentration structure factor 7-32261
 Li-Pb, fusion reactor breeder blanket fluids, T extraction, Pd catalyzed oxidative diffusion 7-49641
 Li-Pb, liq., sp. ht. calc. from expt. density and temp. depend. press. data 7-63839
 Li-Pb, liq., T breeder material, compatibility with austenitic stainless steel 7-53966
 Li-Pb, liq. fusion reactor blanket, mass transfer in dynamic environment, corrosion damage 7-49659
 Li-Sn, liq. alloy, mixing enthalpies, high temp. calorimetry, EMF obs. 7-65044
 LiAl(Ga)(In)(Zn)(Cd) B32-type Zintl phases, mag. props., exchange enhancement, APW calcs. 7-27504
 LiMg, electron-electron scatt., elec. resistivity meas. 7-32981
 Li₄Pb liquid, static struct., temp. depend., screened Coulomb model anal. 7-21076
 Pb-Al-Mg-Sn-Li, strength and microstruct. 7-8047
 Pb-Li, flowing environment, corrosion of fusion reactor structural steels 7-53959
 Pb-Li, molten, thermally convective, corrosion of austenitic stainless and Cr-Mo steels 7-53962
 Pb-Li, strength and microstruct. 7-8047
 PbLi eutectic, flowing, corrosion of stainless steel 7-53958

lithium compounds

- see also **lithium alloys**
 borate glasses, density w.r.t. atomic arrangements, comp. depend. 7-6533
 chemical bonding, validity of formal electron counting rules 7-63544
 cordierite, cryst. struct. refinement and thermal expansion, 100-550K 7-6609
 ferrites, microstruct. effects on mag. props. (German) 7-59052
 first row compounds, solvation energies calc. 7-8269
 n-heptanoate, heat capacities and thermodynamic props. 7-52072
 intercalation cpd. with graphite, Li₂C₆, elastic effects, comp. depend. staging studies 7-63707
 intercalation cpd. with TiSi₂, Li₂TiSi₂, elastic effects, comp. depend. staging studies 7-63707
 intercalation with low-dimens. dichalcogenides, secondary cathodic materials, book contrib. 7-28394
 Li-exchanged Na-Y zeolite, thermal transform. to Li aluminosilicates, X-ray and NMR studies 7-44794
 LiH.Sb³⁺ single crystals, nuclear spin-lattice relax. time anisotropy anomaly studies (Russian) 7-33290
 LiKSO₄NH₃ single crystals, low temp. phase transitions, EPR study 7-27599
 LiNbO₃:Cu(Er)(Mg)(H), laser-induced grating characteristics 7-62746
 LiNbO₃ proton-exchange 128° Y-cut optical waveguides, acousto-optic interaction effects 7-62824
 (Na₂O)₂₅(Li₂O)₂₅(P₂O₅)₅₀ glass fibres, struct., birefringence, density and thermal shrinkage, drawing parameters depend. 7-6536
 n-pentanoate, heat capacities and thermodynamic props. 7-52072
 poly(ethylene oxide)-LiAgI₂, room temp. ionic cond. comp. depend. meas. 7-13263
 poly(styrenesulphonate)s, enthalpy of dilution, large dielectric constant solvent 7-21483
 rare earth tetraphosphates, LiRP₄O₁₂, flux cryst. growth 7-13345
 salt-poly(propylene oxide) complexes, ionic cond., high press. effects study 7-32703
 spinel insertion compounds, reactions, mag. and elec. props. 7-33920
 trifluoromethyl sulphite, in polymer electrolytes, ion pairs triplet form., conductance meas. 7-32690
 water-LiBr absorption cooling system thermodynamic design data 7-23208
 YZ-LiNbO₃, domain structure and lattice defects, effects of piezoelectricity, TEM anal. 7-2999
 B₂O₃-Li₂O-LiCl-Al₂O₃, amorphous ionic conductor, crystallisation, position annihilation study (Chinese) 7-37872
 B₂O₃-SiO₂-Li₂O-Na₂O-ZnO glasses, chemical durability 7-8143
 Ba(Li_{0.25}Sb_{0.75})O₃, cubic perovskite, prep. and struct. 7-63589
 BeO/Li ceramic, sphere-pac forms, T breeder materials, thermal cond. 7-52163
 BeO/LiAlO₂ blanket, neutron activation calcs. in Cascade 7-15380
 BiLiF₄, lattice vibr., Raman study 7-53329
 C-Li rechargeable batteries, characts. 7-59835
 CdF₂-LiF-AlF₃-PbF₂ glasses, potential as a practical glass 7-37074
 Cr-Li-K-C-O system, phase relationships at 650°C, appl. to corrosion processes in molten carbonate fuel cells 7-28020
 CrVO₄-Li₂VO₄ system, study for solid solns. (French) 7-44833
 CsLiCrO₄, ferroelectric phase transition 7-39047
 DyLiFeO₃, orthoferrite, mag. props. 7-2824
 Fe₂O-Li₂O, synthetic wustite, elec. cond., doping elements effect (Korean) 7-2609
 γ-FeOOH-LiCO₃, mixture, mechanochem. transform. and γ-Fe₂O₃ form. 7-59478

lithium compounds continued

- GaAs/LiNbO₃ struct., SAW parametric generation with light pumping 7-63934
 GaSe-Li, intercalated layer compounds, conc. depend. of electrode potential 7-7230
 H₂O-LiBr absorption heat pumps, thermodynamic design data, heating 7-23209
 In_{1-x}Li_xVO₄ solid solutions, characterisation, ionic conductivity (French) 7-44833
 InSe-Li, intercalated layer compounds, conc. depend. of electrode potential 7-7230
 K₂LiFe₂S₂Cl₂, djerfisherite, electrochemically synthesised, cryst. struct., neutron diff. study 7-58224
 K_{1-x}Li_xTaO₃ monocrys., polarisation jump, ferroelec. transition and domains study (Russian) 7-22200
 K_{1-x}Li_xTaO₃ single cryst., dielec. properties at 10⁻² to 10³ Hz 7-2997
 K₂Li₂TeO₆, prep., cryst. struct., Madelung lattice energy calc. (German) 7-16515
 K₂Pb₂Nb₁₀O₃₀-K₆LiNb₁₀O₃₀ solid soln., density and struct. studies 7-1973
 La₂Ga₂SiO₁₄, elastic and piezoelectric const., temp. depend. 7-53242
 La₂Ni₈Co₁₀O₄₇,³⁷Co, Ti, ⁵⁷Fe⁴⁺, anomalous charge state obs., ⁵⁷Co³⁺ nuclear decay studies 7-21881
 Li based ceramics, fusion breeder blanket, irradi., high burnup, large temp. gradients 7-49644
 Li based oxide ceramics, fusion breeders, chemical compatibility with stainless steels 7-49646
 Li ceramics, thermal stability with fusion reactor structural materials 7-38227
 Li containing ceramic, T breeder material, thermal cond. 7-10280
 Li halides, thermal parameters, cryst. struct. determ. 7-12020
 Li hydrides, (LiAlH₄, LiH, LiBH₄), cryst. imperfection obs., TEM 7-32445
 Li inorganic compounds, neutron irradiated, tritium release anal. 7-38070
 (Li, K)Cl, molten, internal cation mobilities 7-2243
 Li⁺ salts, salt/water/aprotic solvent mixtures, alkali cation influence, IR spectra anal. 7-19856
 Li/K Cl, molten, struct., thermodynamics, theory 7-37831
 Li/Li_{1-x}V_xO₆ batteries, comparison with other secondary cells, influence of micro- and macro-structural alterations 7-46932
 Li-ethylene-N₂ complexes, in solid Ar, IR spectra 7-31033
 Li-H₂ system, second derivative nonadiabatic coupling matrix elements determ. pot. energy surfaces 7-42501
 Li-LiH-Na systems, solubility of H, press. and temp. depend. 7-21471
 Li-LiNO₃ thermal battery cell discharge lifetime with soluble cathode materials 7-3630
 Li-Na-K-CO₃/MgO salt/ceramic phase change material for high temp. thermal storage, thermoanalytic investigation 7-65631
 Li-P-O-N glass, prep. and characterisation 7-26654
 Li-W-O films, electrochromic props., UV radiation effects study 7-22222
 Li₂WO₃-Nb₂O₅ sputtered amorphous films, electrochromic props. study 7-22221
 LiAlF₄, energy stability, struct., vibr. spectra, MO LCAO SCF calcs. 7-15512
 LiAlF₄, ion conducting layer in WO₃ based electrochromic windows, recent R&D 7-37122
 LiAlH₄, relative energy characts., electronic correl. in ab initio calcs. 7-15528
 γ-LiAlO₂, ceramic, T breeding material, compatibility with austenitic stainless steel 7-53966
 LiAlO₂ battery separator felt, prep. by sol-gel technique, phase transitions in gels 7-22601
 LiAlO₂, bond ionicities and structural props. calcs. 7-26691
 γ-LiAlO₂, breeder blanket, T recovery 7-49645
 LiAlO₂ ceramic breeder material, fabrication for NET programme 7-798
 LiAlO₂ ceramic breeder material, post irradi. T recovery 7-49647
 LiAlO₂ ceramics, fast neutron irradi., T and He retention, high temp. vacuum extraction 7-49649
 LiAlO₂ ceramics, near surface T depth profiling, low energy nuclear reactions 7-49653
 LiAlO₂, fabrication, irradi., in-pile T release, EXOTIC expts. 7-49648
 LiAlO₂, fusion blanket material, effects of sweep gas, extraction vessel material and ceramic props 7-49664
 LiAlO₂, fusion breeder blanket, in-situ T release 7-49652
 γ-LiAlO₂, fusion reactor breeder blanket, T transport modelling 7-49642
 γ-LiAlO₂, neutron irradi. effects 7-51841
 LiAlO₂ spheres, T release, time depend., diffusion coeff. 7-49643
 LiAlO₂, surface adsorp. isotherms, T inventory appl. 7-52246
 LiAlO₂, T ceramic breeder material, Italian fusion technology programme review 7-10279
 LiAlO₂, T extraction in and out of pile 7-49655
 LiAl₂O₃, T extraction in and out of pile 7-49655
 LiAl₂O₃:Fe³⁺, Mossbauer relaxation spectrum, electric quadrupole shifts dependency on mag. field 7-7182
 LiAl₂O₃:Fe³⁺, spin-lattice relax. times, Mossbauer spectroscopy 7-45848
 LiAlSi₂O₆, β-spodumene, ionic conductivity 7-52133
 LiBH₄, relative energy characts., electronic correl. in ab initio calcs. 7-15528
 Li₃BN₂, synthesis, polymorph struct., ionic cond. meas. 7-32388
 Li₃B₂O₇, temp. compensated piezoelectric cryst. SAW study 7-12452
 Li₃B₂O₇:Cu, TLD, thermal neutron response 7-5491
 Li₃B₂O₇:CuCl₂ crystallised glasses, pure and doped, thermally stimulated exoelectron emission, thermolum. 7-27874
 Li₃B₂O₇:Mn thermoluminescent phosphor, γ and in dosimetry using electrical conductivity 7-62095
 Li₃B₂O₇-Li₂SO₄-LiCl-H₂O, saturated soln., phase equilibrium, props. 7-40507
 Li₃B₂O₇-WO₃ glasses, dielec. behaviour, space charge effects 7-45917
 LiBeH₃ and Li₂BeH₄, cryst. struct. and IR absorption 7-51720
 LiBeH₃, relative energy characts., electronic correl. in ab initio calcs. 7-15528
 LiBnO₃, charactn. by γ-ray diff. 7-54061
 LiBr, lattice deform. around an F-centre 7-32435
 LiBr-LiCl binary mixed crystal system, critical nucleus, melt comp. 7-58445
 Li₂C intercalation cpd., phonon dispersion, two-body pot. 7-44715
 Li₂C intercalation cpd., electron struct., soft X-ray emission spectroscopy 7-45117
 LiCN, excited vibr. levels, distributed Gaussian basis study 7-15581
 LiCN(LiNC), struct., electron correl. calcs. 7-30956

lithium compounds continued

- Li₂CO₃-Na₂CO₃-K₂CO₃ molten salt in direct absorption received, optical props. at high temp. 7-40042
 LiCl aq. soln., supercooled, viscosity meas., power-law behaviour, structural relax. theories 7-2247
 LiCl, dipole-quadrupole dispersion coefficients, ab initio coupled HF calcs. 7-11986
 LiCl, electron correlation, band gaps and quasiparticle energies 7-27278
 LiCl, lattice deform. around an F-centre 7-32435
 LiCl:Fe³⁺, X-ray irradi., EPR spin Hamiltonian parameters 7-45808
 LiCl:Pb²⁺, absorpt. and luminesc. spectra studies (*Russian*) 7-46141
 LiCl-H₂O, aqueous soln. glasses, devitrification under diffusion control, theory 7-12279
 LiCl-KCl, molten mixture, eutectic, isotope self-exchange vels., simulation 7-57187
 LiCl-KCl mixture used to seal melt for CdSnAs₂ growth 7-7839
 LiCl-Li₂O-B₂O₃-Al₂O₃, amorphous, Li⁺ conductor, crystn. and phase separation, interface effect (*Chinese*) 7-38245
 LiCl-LiBr-KBr molten electrolyte in Li-Al/FeS₂ secondary cell 7-65439
 LiCl(H₂O), ion pairs, struct. and stability, H⁺ transfer reaction path, SCF-CNDO/2 calcs. 7-25400
 LiClO₄, in polymer electrolytes, ion pairs triplet form., conductance meas. 7-32690
 LiClO₄, solns., chem. shift, NMR 7-57085
 LiCl₃H₂O, soln., struct., mol. dynamics simulation 7-58127
 Li₃(Co(CN)₆)₂, soln., electronic struct., ESR investig. 7-31081
 Li₂O₂-Co₂Zn₂O₄, mixed ferrites, neutron diff. study 7-52943
 Li₂Cr(Mn)(Fe)(Co)(Ni)O₂ electrode materials, electronic and electrochemical props., ion intercalation, electronic model 7-33945
 Li₂CSO₄, dielec. props., press. effect 7-64555
 Li_{1-x}Cu_xMnRuO₄ system, prep. and characterisation (*German*) 7-26721
^{6,7}LiD, X¹Σ state pot. energy curves, adiabatic corrections 7-36514
^{6,7}LiD, X¹Σ⁺ and A¹Σ⁺ states, pot. energy curves 7-5622
 LiD:Mg²⁺, elec. props., X-irradiation effects, DC cond., dielec. loss and ionic thermocurrent meas. 7-27341
 LiF (TLD-100), thermoluminesc., 90 to 300K 7-3097
 LiF, crack tip dislocation nucleation obs. in bulk specimens 7-37996
 LiF, cryst., defect struct., high-temp. annealing effects (*German*) 7-32448
 LiF crystal, X-ray spectra rel. to electronic struct. (*Russian*) 7-39319
 LiF crystals, four wave mixing effect of F₂⁻ centres 7-31402
 LiF crystals, influence of deformation temp. on change in density 7-44655
 LiF crystals, phonon-dislocation scattering anal. 7-2131
 LiF crystals with F₂⁻ centres, inactive losses, investig. of mechanism 7-3072
 LiF, deformed crystal, lattice thermal conductivity, low temp. 7-52165
 LiF, dipole-quadrupole dispersion coefficients, ab initio coupled HF calcs. 7-11986
 LiF disk, stress determ. by photoelasticity method 7-51011
 LiF, electric breakdown due to injected electron beam. 7-64837
 LiF, electrification mechanism during cleaving 7-44621
 LiF electrolyte in Au-WO₃-LiF-Au solid-state electrochromic structures 7-53275
 LiF, electron beam irradi., desorbed ground state Li atoms, signal time depend. 7-52260
 LiF, electron stimulated desorption of Li, role of F-centre diffusion 7-16864
 LiF, electron- and photon-stimulated desorption, threshold effects 7-58623
 LiF evaporated films, surface anal., electron stimulated desorption, XPS studies 7-27173
 LiF, F₂ laser active element, optically stable component 7-43116
 LiF, F₂⁺ and F₂ colour centres optical study (*Chinese*) 7-37984
 LiF, F₂⁺-F₂ mixed centres, laser oscillations at room temp. 7-7714
 LiF, F₂⁺ and F₂ centres induced by ion implantation 7-26747
 LiF, fracture, mag. field effects 7-16675
 LiF, friction and wear, crit. transition points 7-26853
 LiF, γ-irrad., positron annihilation, temp. depend. 7-3110
 LiF, γ-irradiated, influence of plastic deformation on colour centre conc. 7-44538
 LiF γ-irradiated crystals, F-centres, positron annihilation and optical absorpt. meas. 7-44542
 LiF, highly pure single crystals, dislocation mobility 7-26754
 LiF ionic crystals, band-gap-energy positron emission, comment 7-45227
 LiF, lattice deform. around an F-centre 7-32435
 LiF, minerals, shock induced radiation 7-27694
 LiF, N ion implanted and X-irrad., microhardness response 7-21344
 LiF, orbital energies, multipole moments and electric field gradients, HF calcs. 7-62270
 LiF plastic crystals, formation of cracks at cleavage fracture front 7-44674
 LiF, pore-grain boundary configs., fracture surface, SEM obs. 7-32458
 LiF profiled crystals, growth by Stepanov's method, appl. for optical components 7-31409
 LiF profiled crystals, growth by Stepanov method, shaper material effects 7-32333
 LiF, quenched, dielectric props., effect of high AC field and X-ray irradiation 7-38985
 LiF, shielding effect on 14 MeV neutrons, meas. and calcs. 7-42104
 LiF, shock-compressed, refractive index, laser interferometric meas. 7-30081
 LiF shock-loaded single crystals., dislocation transport, impact surface sources effects calcs. 7-44543
 LiF, shocked along (111), temp. depend. of precursor amplitude 7-26836
 LiF single crystal., dielectric, charge buildup, influence on charging electron beam motion 7-44294
 LiF soft X-ray spectra, using photon excitation from synchrotron light source 7-30150
 LiF, Stepanov method growth and crystal shaping 7-32320
 LiF surface, Ar⁺ and Ar²⁺ bombarded, desorption of F⁺, secondary ion mass spectra study 7-21661
 LiF surface, long range interaction between rare gas atoms/molecules and surfaces, calc. 7-3135
 LiF surfaces, preferential sputtering, XPS and direct recoil spectrometry study 7-22422
 LiF TLDs, dose enhancement effects, comparison with 2D Monte Carlo calc. 7-56875
 LiF thermoluminescent dosimeter appl. in n-γ mixed field dosimetry in TRIGA reactors 7-49733
 LiF, US vibration, 20-300°C block boundaries effect 7-32457

lithium compounds continued

- LiF:C⁶⁺, ion implanted, impurity defects outside implantation zone 7-7773
 LiF:F₂ laser, room temperature, active element, thermal effects 7-62714
 LiF:Mg,Ti phosphor layer on borosilicate glass substrate, laser stimulated thermolum. 7-64703
 LiF:Mg²⁺ doped, elec. charge of dislocations 7-6628
 LiF:Mg(Ni)(Co) R' colour centres, spectral holeburning props., depend. on doping and irradiation 7-26743
 LiF:Ne⁺(Ar⁺), defect and colloid production by ion implantation 7-26746
 LiF:U, Ti(U), X-irradiated crystals, absorpt. bands of U⁴⁺ and U³⁺ ions 7-13183
 LiF:U⁶⁺, cryst., luminesc. excitation of impurity centres 7-13225
 LiF-H₂N, Li-bonded complex, force consts. calc. for vib. modes, correl. effects 7-19823
 LiF-NaF-KF eutectic melt, Cl⁻ effect on C electrode anode processes 7-23028
 LiF(H₂O), ion pairs, struct. and stability, H⁺ transfer reaction path, SCF-CNDO/2 calcs. 7-25400
 LiF(00), surface optical phonons, obs. by inelastic He scatt. 7-44987
 LiFe_{0.5}Al_{0.5}Ga_{0.5}O₈, magnetisation and lattice parameter, role of Al and Ga ions 7-22097
 Li_{1-x}FeCl₄, ionic conductors, Mossbauer spectra studies (*French*) 7-2955
 LiFeClMoO₄, synthesis, struct. and low temp. magnetism 7-21172
 Li₂Fe₂(MoO₄)₃, insertion cpd., struct., from neutron powder diff. data 7-1985
 LiFeP₂O₇, cryst. synthesis, at. struct., DTA, X-ray diff. study 7-26708
 Li₃Fe₂(PO₄)₃, microtwinning, X-ray struct. investig. 7-44567
 Li_{0.5}Ga_{0.5}Fe_{2.5-x}O₄, dilute ferrimagnetics, cluster spin glass state 7-38884
 Li_{3-x}Ga_{1-x}Mg(Zn)_xO₄, solid solns., ionic cond. comp. depend. meas. 7-12366
 LiGaO₂, bond ionicities and structural props. calcs. 7-26691
 LiGaO₂, lattice vibr. spectrum, correlation method anal. 7-26881
 LiGa₂O₈, Raman scatt. study 7-53316
 LiGa₂O₈:Co²⁺, photon-gated spectral hole burning 7-1240
 Li₂GaSe intercalation cpd., elec. resist. and Hall effect meas. 7-12719
 Li₂GeO₄, single cryst., nonlin. electromechanical parameter meas. 7-13094
 Li₂GeO₅, ferroelectric single crystals, pyroelectric props. 7-64576
 LiH, ⁷LiC and ¹³N implantation, chemical effects, radiochromatography study 7-28324
 LiH, constrained pure state one-electron density matrices 7-57014
 LiH, electronic energy, Green's fn. calc. 7-10445
 LiH, electronic struct., mol. cluster calcs. 7-7110
 LiH, ground and excited mol. states, long range pot. curves calcs. 7-19994
 LiH, single cryst., electron momentum density and Compton profiles 7-3113
 LiH, vibr. transition freqs. obtained from SCF and correlated wave functions, effects of basis set selection 7-25420
 LiH⁻, ground and first excited state electron affinities, extended-Koopman's-theorem, ab initio calcs. 7-25352
 LiH⁺, spin density, cusped gaussian wave functions 7-42504
^{6,7}LiH, X¹Σ state pot. energy curves, adiabatic corrections 7-36514
^{6,7}LiH, X¹Σ⁺ and A¹Σ⁺ states, pot. energy curves 7-5622
 Li⁺Al(Mg)(Zn) single crystals., secondary emission, exciton luminesc. and reson. Raman scatt. studies 7-3038
 LiH:Ca²⁺, elec. props., X-irradiation effects, DC cond., dielec. loss and ionic thermocurrent meas. 7-27341
 (LiH)_x linear infinite chains study, pseudo-lattice method, ab initio SCF calcs. 7-36470
 LiH(D), pot.-energy curves, PMO-RKR-van der Waals pot., Padé approx. method 7-30965
 Li_{1-x}H_xNbO₃, struct. and props. 7-12017
 (Li⁺(H₂O))_xMoO₄^{x-}, composition and struct. 7-16518
 Li_{3-x}H_xTaO₄, prep. by means of hydrothermal synthesis and protolysis 7-39449
 Li₂HfF₆, hyperfine interactions, temp. depend. 7-12679
 LiI, Debye-Waller factors of ¹²⁹I, Mossbauer study 7-2135
 LiI impinging Re surface, surface ionisation in high vacuum, work function increases due to adsorpt. 7-46264
 LiI, lattice deform. around an F-centre 7-32435
 LiI-Li₂S-SiS₂ glass, ionic cond. meas. 7-38251
 LiIO₃, acoustoionic interaction 7-39041
 α-LiIO₃, cryst., elastic wave attenuation, freq. and temp. depend. (*Russian*) 7-21364
 LiIO₃ crystal, coherent four-photon scatt. by polaritons 7-22273
 α-LiIO₃ crystals, acoustoelectric effects (*Chinese*) 7-20568
 α-LiIO₃ crystals, anomaly of optical props., 100 to 140°C, influence of growth defects 7-59172
 LiIO₃ crystals, iron-group doped, impurity centres, circular dichroism studies 7-45976
 α-LiIO₃ crystals, US studies (*Chinese*) 7-58417
 LiIO₃, ferroelectric, optical props., radiation effects 7-33406
 LiIO₃, noncollinear stimulated Raman scatt. by polaritons 7-43221
 LiIO₃, Raman laser for optical range, quasi-CW high power 7-25829
 α-LiIO₃ single crystals, morphology in relation to growth conditions 7-58192
 α-LiIO₃:Co²⁺, ESR and optical absorpt. studies of impurity ions 7-45803
 LiInP₂O₇, synthesis and cryst. struct. (*French*) 7-58223
 LiInS₂, lattice vibr. and interatomic forces, IR reflectivity spectra anal. 7-26882
 LiInS(Se)(Te)₂, bond ionicities and structural props. calcs. 7-26691
 LiInSe, epitaxial films on GaAs and GaP, RHEED 7-52318
 (Li_{1-x}K_x)_{0.9}Mo_{0.17}, superconductivity and CDW 7-45541
 LiKSO₄, Brillouin light scatt. between 20 and 80°C, elastic constants meas. 7-7712
 LiKSO₄ crystals, elec. conductivity anisotropy 7-21509
 LiKSO₄ crystals., low temp. phase transitions, Raman spectra and dielec. const. meas. 7-26943
 LiKSO₄, domain structures and phase transitions, SO₄²⁻ EPR study 7-38937
 LiKSO₄, high temp. phase transitions, IR spectra study 7-7698
 LiKSO₄, low temp. phase transitions, kinetics and symm. changes 7-2164
 LiKSO₄, phase diagram, critical points determ., press. depend., differential thermal anal. 7-6780
 LiKSO₄, phase transitions, domain form., optical birefr. meas. 7-3019
 LiKSO₄, phase transition, low temp. Brillouin studies 7-44806

lithium compounds continued

- LiKSO₄ single crystals, optical activity, ferroelec. and ferroelastic props. 7-27687
- LiKSO₄:NH₄⁺, EPR spectra, ⁷Li spin-flip satellites 7-64525
- LiLaP₂O₇:Nd³⁺, Yb³⁺, metaphosphate glasses, Nd³⁺ to Yb³⁺ energy transfer, luminesc. study 7-22323
- Li_{2+x}(Li_{1-x}Mg_{1-x}Sn₂)O₈, ramsdellite type cpds., ionic conductivity and cryst. chemistry 7-32708
- LiLuF₄ = Pr³⁺ (Nd³⁺) (Ho³⁺) (Er³⁺), stimulated emission spectroscopy 7-13179
- LiMO₃, M=Sc, Ti, V, Cr, Mn, Fe, Co, Ni, Cu props., review 7-64437
- LiMO₃ (M=Nb,Ta), ion implanted optical waveguides, refractive index profiles 7-25964
- LiMgF₃, energy stability, struct., vibr. spectra, MO LCAO SCF calcs. 7-15512
- Li₂Mg_{1-x}Fe_{2x}Sn_{3-2x}O₈, ramsdellite type cpds., ionic conductivity and cryst. chemistry 7-32708
- LiMgH₃, relative energy characts., electronic correl. in ab initio calcs. 7-15528
- Li_{0.6}Mg_{0.29}Ti₂O₅, crystal struct. refinement 7-44467
- Li₂Mg_{1.5-x}VO₄ solid soln. phase, synthesis, stoichiometry and struct. 7-21168
- LiMnFe₂O₄ ferrite, solid solution form. in contact diffusion pairs 7-2273
- Li_{1-x}MnRu_{1-x}Ti_xO₄ system, characterisation of different phases (German) 7-26971
- Li_{1+x}Mn_{1-x}GcRu_{1-x}O₄, Li insertion cpd., prep. and characterisation (German) 7-26720
- LiMo₂Li_{1-x}F_x, dilute dipolar-coupled magnet, ferromagnetism, glassiness, metastability 7-22098
- LiMo₈O₁₀, synthesis and struct., orthogonal nonintersecting octahedral cluster chains 7-32386
- Li_{0.33}MoO₃, stoichiometric triclinic bronze, cryst. struct. 7-6600
- Li_{0.9}Mo₆O₁₇ purple bronze, cryst. struct. determ. 7-58239
- Li_{0.9}Mo₆O₁₉ bronze, structs., sliding motion of CDW 7-64129
- Li₂MoO₄, high-pressure polymorphs, calorimetric study 7-32638
- LiMoS₃, synthesis, electrochemistry and struct. 7-33619
- Li_xMo₆Se₈ intercalation cpd., entropy and struct. transition, lattice gas model 7-6832
- Li_xMo₆Se₈ intercalation cpd., entropy, electrochem. cell calorimetry studies 7-6833
- Li_xMo₆Se_{8-y}I_y, Li electrochemical insertion, struct. studies 7-37947
- Li_{0.9}(Mo_{1-x}W_x)₆O₁₇, superconductivity and CDW 7-45541
- Li_{0.9}Mo_{6-x}W_xO₁₇, W substitutional effects on elec. resistivity and transport props. 7-45260
- Li₃N:H, doped and undoped fast ionic conductor, positron annihilation 7-39276
- LiND₂SO₄, ferroelastic and ferroelectric domain struct., SEM obs. 7-27675
- LiN(H₂D_{1-x})₂SO₄ crystals, vibr. spectra and ferroelec. transition, Raman scatt. study 7-53304
- Li_{1-x}(NH₄⁺)(NH₃)₂TiS₂(x+y)- intercalation cpd., NH₃ oxidation, charge compensation 7-32354
- LiNH₄SO₄, ferroelastic and ferroelectric domain struct., SEM obs. 7-27675
- LiNO₃, molten, ⁶Li enrichment by electromigration 7-2244
- LiNO₃, molten salt, thermal diffusivity meas. 7-44877
- LiNO₃/LiNO₂ as fusion reactor coolant fluid, thermochemical assessment 7-62073
- LiNa, orbital energies, multipole moments and electric field gradients, HF calcs. 7-62270
- LiNaF₂, energy stability, struct., vibr. spectra, MO LCAO SCF calcs. 7-15512
- (Li_{1-x}Na(K)_x)_{0.9}Mo₆O₁₇ anomalous transport props., resist., mag. suscept., sp. ht., struct. and supercond. transition temp. meas. 7-21913
- Li₂NaK(SO₄)₂, cryst. struct. determ. 7-58212
- (Li_{1-x}Na_x)_{0.9}Mo₆O₁₇, superconductivity and CDW 7-45541
- LiNaSO₄, BCC, rotator phase, solid electrolyte behaviour, thermodynamic props. 7-21139
- LiNaSO₄, trigonal, phys. props. 7-13099
- Li_xNa_{1-x}TiS₂ intercalated dichalcogenides, struct., electrochem. and thermodynamic props. studies 7-21167
- LiNbGeO₅, luminesc. and cryst. struct. 7-32403
- LiNbO₃:Fe photorefractive crystals, light-induced scattering 7-10887
- LiNbO₃: Ti waveguide collinear Bragg diff. cell, acousto-optic interaction efficiency anal. 7-37234
- LiNbO₃, 180° SAW reflectivity and vel. perturbation of thin metal dot arrays 7-2329
- LiNbO₃ (001), z-cut, surface struct., RHEED studies 7-2308
- LiNbO₃, absorption edge, composition dependence (Chinese) 7-39140
- LiNbO₃, anomaly study by X-ray diffraction 7-6588
- LiNbO₃ based integrated light conductor (German) 7-57609
- LiNbO₃ blazed grating couplers and appl. to integrated optics 7-15969
- LiNbO₃ bulk wave acousto-optic deflector beam steering by interdigital transducer 7-1255
- LiNbO₃ bulk-acoustic-wave transducer consisting of interdigital electrodes on grooved surface 7-43613
- LiNbO₃ channel-waveguide integrated optical components for fibre sensors 7-26042
- LiNbO₃ coded phase-reversal modulator with 20 GHz bandwidth at 1.3 μm wavelength 7-57533
- LiNbO₃ crystal, parametric generation of picosecond light pulses 7-37030
- LiNbO₃ crystal growth from liquid, physical consts. determ. 7-32322
- LiNbO₃ crystals, struct. defects and etch figures 7-44555
- LiNbO₃, Czochralski cryst. growth, computer control 7-27886
- LiNbO₃, Czochralski growth, physical constants of melt determ. 7-13348
- LiNbO₃, defect structure, Raman spectroscopy 7-63604
- LiNbO₃ degenerate acoustic elastic convolver, crystal orientation dependencies of figure of merit 7-62917
- YZ-LiNbO₃, dislocation electric fields and small-angle grain boundaries, ferroelectric domains 7-3000
- LiNbO₃, doped, holographic recording of gratings, microphotometric investig. 7-25735
- LiNbO₃, effect of pyroelectric and applied electric field 7-39043
- LiNbO₃, elastic and dielec. props. 7-63715
- LiNbO₃ electro-optic freq. translators for coherent optical fibre systems 7-25953
- LiNbO₃, etching, laser-driven chem. reactions 7-3468
- LiNbO₃, exciton lumin., ion beam induced 7-53418
- LiNbO₃, F⁺ centre wave function calc. 7-44540

lithium compounds continued

- LiNbO₃, ferroelec. single crystals with multi-domain layers, fabrication and SAW excitations 7-27676
- LiNbO₃ films, sputter deposition, refractive index 7-7851
- LiNbO₃ for optical communication 7-31269
- LiNbO₃, freq. temp. coeffs. of vibration modes (Chinese) 7-13093
- LiNbO₃, γ-irradiated, elastic and piezoelectric props. 7-45935
- LiNbO₃, He⁺ implantation, lattice disorder, refractive index changes 7-25966
- LiNbO₃, heterogeneous shock wave response, holographic interferometry studies 7-32571
- LiNbO₃, ilmenite modifications, vibr. spectra 7-22243
- LiNbO₃ integrated optics, review of theory and technology 7-20470
- LiNbO₃ integrated optics, conf., Cambridge, MA, USA (Sept. 1985) 7-24278
- LiNbO₃ integrated optical substrates, Maker fringe anal. 7-26026
- LiNbO₃ integrated optical substrates, refractive index meas. by total internal reflection 7-26027
- LiNbO₃ integrated optical components for optical communication appls. (German) 7-37210
- LiNbO₃ integrated optic devices, Ti film charactn. 7-57607
- LiNbO₃, ion beam induced luminesc. 7-27793
- LiNbO₃, ion implantation, H⁺, He⁺, Ar⁺, elastic vibrations 7-12094
- LiNbO₃, leakage SAW propag. characts. for new cut (Japanese) 7-44985
- LiNbO₃, natural single phase unidirectional low-loss SAW transducer 7-1359
- LiNbO₃, nonlinear elastic, piezoelectric, electrostrictive and dielectric consts. 7-64573
- LiNbO₃, optical components for modulation and switching 7-15996
- LiNbO₃, optical erasure of sinusoidal holographic gratings, kinetics 7-10886
- LiNbO₃ optical waveguides, ion-implanted, optical damage resistance 7-43360
- LiNbO₃, optoelectronic material, radiation effects 7-26811
- LiNbO₃, photoinduced light scatt. 7-3011
- LiNbO₃ photorefractive crystals, dynamic holographic recording process, microphotometric study 7-43005
- LiNbO₃, picosecond holography and four-wave mixing 7-20161
- LiNbO₃ piezoelectric photorefractive crystal, hologram writing and reconstruction 7-57268
- LiNbO₃ planar waveguides, He⁺ ion implantation, transient annealing 7-25965
- LiNbO₃ planar-optical waveguides, proton-exchanged, chem. and optical props. 7-57544
- LiNbO₃ polycrystalline films, prep. by hydrolytic decomp. of metal alkoxide alcoholic solns., SEM obs. 7-7044
- LiNbO₃ powders obtained by the alkoxy method, crystallisation and ferroelectric props. 7-7648
- LiNbO₃, prod. by Czochralski and Stepanov methods, elec. phenomena accompanying growth 7-32332
- LiNbO₃, profiled cryst. growth by Stepanov's method, regular domain struct. prod. 7-32330
- LiNbO₃, proton exchanged, SAW props. study 7-12454
- LiNbO₃, proton-exchanged, acoustic microscopic studies 7-21597
- LiNbO₃ proton-exchanged single cryst. optical waveguides, electro-optic effects, lattice const. and refractive index changes meas. 7-22220
- LiNbO₃ SAW bifurcation and chaotic state obs. 7-2333
- LiNbO₃ SAW oscillator for humidity and temp. meas. 7-4232
- LiNbO₃, shallow gratings, leaky surface waves, trapping and temp. compensation 7-12449
- LiNbO₃ single crystal, self-diffusion of Li ions 7-21512
- LiNbO₃ single crystal fibres, ferroelec. domain structs. 7-22202
- LiNbO₃ strip-type resonator 7-57657
- LiNbO₃, substitute for ZnO, acoustoelec. props. 7-38645
- LiNbO₃ substrate, acousto-optic signal processors, polarisation effects 7-25723
- LiNbO₃ substrates, growth and composition effects 7-26025
- LiNbO₃ surface wave device, frequency modulation of optical beam using ultrasonic diffraction grating 7-20405
- LiNbO₃, temp. tuning coeff., meas. using SHG based interferometry 7-11051
- LiNbO₃, Ti in-diffusion, intermediate phase structure 7-44473
- LiNbO₃, Ti indiffused H⁺ exchanged optical waveguides, fabrication and charactn. 7-62826
- LiNbO₃ traveling-wave optical couplers and interferometric modulators, power requirements 7-57539
- LiNbO₃, uniaxial crystal anisotropic acousto-optic interactions 7-3021
- LiNbO₃ waveguide, parametric fluoresc. amplification and oscill. 7-25894
- LiNbO₃ waveguide electro-optic freq. translators, appl. to coherent optical fibre systems 7-20468
- LiNbO₃ waveguide mode extinction modulators, design 7-26030
- LiNbO₃, z-cut interferometers, thermal instability, electrostatic mechanism 7-37207
- LiNbO₃:Co²⁺, ESR and optical absorpt. studies of impurity ions 7-45803
- LiNbO₃:Cr³⁺ (Fe³⁺) (Mn²⁺), EPR of axial and low-symmetry paramagnetic centres 7-38925
- LiNbO₃:Fe, and undoped crystals, decay of γ-centres 7-7658
- LiNbO₃:Fe, asymmetric photoinduced scattering of light 7-17822
- LiNbO₃:Fe, Czochralski growth and holography appl. 7-59404
- LiNbO₃:Fe, linear electro-optic effect, optical damage by He-Ne laser (Korean) 7-27698
- LiNbO₃:Fe, speckle size depend. on laser beam size via photo-induced light scattering 7-5840
- LiNbO₃:Fe cryst., Raman spectra, photo-induced refractive index change effects 7-53300
- LiNbO₃:Fe crystal, white-light information processing, coupled wave theory 7-25728
- LiNbO₃:Fe crystals, refractive index gratings, microphotometric study 7-62649
- LiNbO₃:Fe crystals, biharmonic pumping, photoinduced light dispersion (Russian) 7-31391
- LiNbO₃:Fe planar optical waveguide, hologram recording, dopant conc. depend. 7-15828
- LiNbO₃:Fe²⁺, anomalous phase transitions, Mossbauer spectroscopy studies 7-2992
- LiNbO₃:Fe³⁺, Mossbauer spectroscopic evidence of angle-depend. intersystem crossing 7-33312
- LiNbO₃:H channel waveguides, anal. 7-26023

lithium compounds continued

- LiNbO₃:H optical waveguides, devices, charactn. and future prospects 7-26022
 LiNbO₃:H ring resonators, operation at 0.79 μ m and 1.3 μ m 7-26029
 LiNbO₃:H waveguides, anomalous side-shifted multimode spectra 7-37140
 LiNbO₃:He⁺ implanted waveguide stability 7-43364
 LiNbO₃:He⁺ optical waveguides, thermal annealing 7-15983
 LiNbO₃:He⁺ optical waveguides, ion implanted, Li outdiffusion modelling 7-62832
 LiNbO₃:Mg, incorporation of H⁺, IR spectra of OH⁻ ions 7-7724
 LiNbO₃:MgO, melt growth and charactn. 7-58170
 LiNbO₃:Ni(Cu), γ -irradiated, ESR spectra of impurity centres 7-17218
 LiNbO₃:T surface, acousto-optic interaction, photoelastic and electro-optic contribs. 7-45982
 LiNbO₃:Ti, acousto-optical diff. elastic strain and electric field effects 7-45985
 LiNbO₃:Ti, low-loss TM-pass polariser fabricated by proton exchange in Z-cut waveguides 7-43444
 LiNbO₃:Ti 4×4 directional coupler switch with permanently attached polarisation maintaining fibre array, low crosstalk 7-31520
 LiNbO₃:Ti 4×4 nonblocking interconnection network for test bed, video switching 7-26039
 LiNbO₃:Ti channel waveguide electro-optic cutoff modulator 7-43353
 LiNbO₃:Ti directional couplers, appl. of coupled-mode theory to design with non-parallel sections 7-20410
 LiNbO₃:Ti electro-optic Mach-Zehnder waveguide modulators, 1.51 μ m operation, optically induced drift effects 7-20404
 LiNbO₃:Ti guided-wave optical switch, 1×16, polarisation-independent 7-31525
 LiNbO₃:Ti integrated optic device for fibre laser Doppler velocimeter 7-6022
 LiNbO₃:Ti integrated electro-optic devices, modelling and beam propag. anal. 7-11177
 LiNbO₃:Ti integrated optical parametric oscillators, numerical model 7-57459
 LiNbO₃:Ti integrated optical devices, domain inversion effects 7-62849
 LiNbO₃:Ti intersecting optical waveguides 7-43359
 LiNbO₃:Ti modified 1×2 directional coupler waveguide modulator 7-1259
 LiNbO₃:Ti strip waveguides at 1.3 μ m, field distrib. 7-25962
 LiNbO₃:Ti three-waveguide polarisation splitter 7-50788
 LiNbO₃:Ti waveguide, SHG, indiffusion proton exchange fabrication 7-25893
 LiNbO₃:Ti waveguide, swept wavelength reflectometer for integrated-optic measurements 7-41432
 LiNbO₃:Ti waveguide dispersion characts. description using generalised parameters 7-43369
 LiNbO₃:Ti waveguides, Ti diffusion, model 7-21528
 LiNbO₃:Ti waveguides, proton-exchanged Fresnel lenses 7-31522
 LiNbO₃:Ti X- and Z-cut directional coupler and BOA switches, voltage-length product 7-43352
 LiNbO₃:Ti(H) waveguides, photorefractive susceptibility, charactn. methods 7-26024
 LiNbO₃:Y single crystal, Czochralski growth, crystal-melt interface stability (Chinese) 7-58168
 LiNbO₃/CdSe multilayer struts. with ohmic contacts, electroacoustic conversion, SAW excitation 7-58839
 LiNbO₃/InSb layered struct. with transverse drift, SAW detection 7-12447
 LiNbO₄ crystal, surface photorefractive effect under UV laser irradiation 7-2057
 LiNbO₃-TiO₂ system, rutile structure solid-solution phase, Ti diffusion into LiNbO₃ 7-44473
 LiNbO₃(Ta)O₃ crystalline samples, low temp. sp. ht. meas. 7-2225
 LiNbO₃/Ta₂O₃ single cryst., piezoelec., pyroelec., dielec. and elastic const. 7-53565
 LiNbO₃, pure and Mg, Fe doped crystals, photoconductivity props. studies 7-38624
 LiNdP₄O₁₂:Yb³⁺, metaphosphate glasses, Nd³⁺ to Yb³⁺ energy transfer, luminesc. study 7-22323
 Li₂NpO₆, oxo-neptunates, Mossbauer and mag. studies 7-13063
 Li₂O, elastic and creep props., porosity and temp. depend. 7-53780
 Li₂O, spheres, T release, time depend., diffusion coeff. 7-49643
 Li₂O, ceramic breeder material, post irradi. T recovery 7-49647
 Li₂O, ceramics, fast neutron irradi., T and He retention, high temp. vacuum extraction 7-49649
 Li₂O ceramics, near surface T depth profiling, low energy nuclear reactions 7-49653
 Li₂O, F⁺-centre absorption energy calcs. 7-12658
 Li₂O, fabrication, irradi., in-pile T release, EXOTIC expts. 7-49648
 Li₂O, fusion blanket material, effects of sweep gas, extraction vessel material and ceramic props. 7-49664
 Li₂O, neutron and ion irradi. damage, ESR and optical absorption studies 7-32509
 Li₂O single crystals, compressive creep and plastic deform. at high temp. 7-51920
 Li₂O-Al₂O₃-SiO₂ glass, sputtering, SIMS depth profiling 7-13314
 Li₂O-Al₂O₃-SiO₂ glass, cryst. phase nucleation, DTA, X-ray diff. 7-58156
 Li₂O-Al₂O₃-TiO₂, synthesis and props. 7-33643
 Li₂O-B₂O₃, ion conducting glass, effect of CaO substitutions on transport and physical props. 7-58535
 Li₂O-B₂O₃ glasses, rapidly quenched, struct. investig. by Raman spectra 7-1913
 Li₂O-B₂O₃ glasses, thermodynamic props. 7-2211
 Li₂O-B₂O₃ glasses, vibr. spectra and struct. 7-59196
 Li₂O-B₂O₃-WO₃/Co(Cr) glasses, optical props. 7-46079
 Li₂O-CdO-SiO₂ glasses, thermal expansion, free volume 7-58152
 Li₂O-MO-B₂O₃:VO²⁺ (M=Ba,Ca,Mg) borate glasses, ESR of VO²⁺ ion 7-59110
 Li₂O-MgO(CaO)-Al₂O₃-SiO₂, multicomponent glasses, sequence of cryst. phases 7-26648
 Li₂O-Nb₂O₅-(TiO₂)₂ system, vicinity of LiNbO₃, solid solns., crystal chemical and ferroelectric props. 7-6805
 Li₂O-P₂O₅:Eu³⁺, laser-induced refractive-index gratings, four-wave-mixing techniques 7-11102
 Li₂O-P₂O₅-PON, nitrogen phosphate glasses, preparation from PON (French) 7-26657
 Li₂O-SiO₂ based photosensitive glass, machining without photoresist 7-22865

lithium compounds continued

- Li₂O-SiO₂ glass, critical cooling rates for nucleating agents 7-6795
 Li₂O-SiO₂ glass, phase nucleation, melting temp. depend. 7-6549
 Li₂O-SiO₂ glass, Pt catalysed crystallisation 7-6524
 Li₂O-SiO₂ glasses, intrinsic and recomb. luminesc. and fundamental absorpt. spectra 7-13195
 Li₂O-SiO₂ glasses, molecular dynamics simulation 7-1901
 Li₂O-SiO₂ glasses, struct., X-ray diff., molecular dynamics calc. 7-6551
 Li₂O-SiO₂ glasses prepared under microgravity and 1-g melting conditions, homogeneity 7-21117
 Li₂O-SiO₂-NaCl melts, alkali cation dissociation determ., solidification temp., elec. cond. and cryoscopic meas. 7-12288
 Li₂O-Ta₂O₅-(SnO₂)₂ system, vicinity of LiTaO₃, solid solns., crystal chemical and ferroelectric props. 7-6805
 Li₂O-ZnO-SiO₂ glasses, thermal expansion, free volume 7-58152
 Li₂O-ZrO₂-P₂O₅ system, phase equilb. and cpd. form. 7-28024
 Li₂O-2SiO₂ sol-gel glass, prep. and devitrification behaviour 7-58158
 xLi₂OyLi₂SO₄B₂O₃, IR- and Raman spectra, vibr. study and struct. 7-37879
 Li₃PO₄, ion bombardment-induced surface modifications, stoichiometry, core levels and valence struct., ESCA studies 7-26816
 LiRbSO₄:VO²⁺, optical absorpt. and EPR spectrum, crystal field parameters 7-59109
 Li₂S, triplet ground-state, electronic and stearic effects, ab initio calcs. 7-25419
 Li₂S₈, interaction with metal electrodes, cyclic voltammetry study 7-13786
 Li₂SO₄-Li₂CO₃ system, phase diagram and elec. cond. meas. 7-32612
 Li(SO₂)₂AlCl₄ electrolyte in Li-SO₂ rechargeable cell 7-65443
 LiSO₃CF₃ salt complexes with polyphosphazene, ionic conductors, dimensional stability 7-63872
 Li₂SO₄H₂O, charge density at 80 and 298 K, X-ray and neutron diff. 7-21166
 Li₂SO₄H₂O, supercooled melts, cryst. and mol. struct., thermal stability 7-21170
 Li₂SO₄(PO₄)₃, cryst. struct. at 573K, X-ray diff. studies 7-44487
 Li₃Sc₂(PO₄)₃, microtwinning, X-ray struct. investig. 7-44567
 Li₃Sc₂(PO₄)₃, monoclinic modification, cryst. struct. studies 7-44488
 Li₂SeO₄ single crystal, optic modes, room temp. Raman spectra study 7-53345
 Li₁₂Si₇, chemical bonding, validity of formal electron counting rules 7-63544
 Li₂Si₆, electronic struct., INDO calcs. 7-38437
 Li₂SiO₃, fabrication, irradi., in-pile T release, EXOTIC expts. 7-49648
 Li₂SiO₃, fusion breeder blanket, in-situ T release 7-49652
 Li₂SiO₃, Li₄SiO₄, Li₆SiO₅, breeder materials, prep. in alcoholic media 7-49654
 Li₂SiO₃ pellets, sintering, density, struct., porosity 7-53682
 Li₄SiO₄, fusion breeder blanket, in-situ T release 7-49652
 Li₂Sn_{1-x}Y_{2x}O₄, metal-insulator transition, Seebeck coeff. and elec. resist. studies 7-21817
 LiTa_{1-x}Mg_xO_{3-3x}F_{3x}, prep., ferroelec. Curie temp., effect of cationic substitution 7-45946
 LiTaO₃, 36°YX-cut, interaction of leaky SAW with bulk waves under metallic grating 7-2330
 LiTaO₃, cryst. strip growth and quality, prod. by Stepanov's method 7-32331
 LiTaO₃ crystals, parametric holographic-type light scatt. processes 7-1215
 LiTaO₃, Czochralski grown with modulated struct., periodic laminar ferroelec. domains, SHG 7-59405
 LiTaO₃, extremal directions of anisotropic diffraction and collinear acousto-optic interaction 7-17304
 LiTaO₃, low freq. dielec. response, charged point defect migration contrib. anal. 7-38984
 LiTaO₃, phonon modes, quasielastic light scatt. near T_c, Raman spectra anal. 7-3039
 LiTaO₃, pyroelectric X-ray detectors and X-ray pyrometers 7-10360
 LiTaO₃ single crystals, synthesis and recrystallisation under hydrothermal conditions 7-3157
 LiTaO₃ strip-type resonator 7-57657
 LiTaO₃ substrates, growth and composition effects 7-26025
 LiTaO₃:Cr crystal, photoinduced light scatt., noise holographic grating mechanism 7-62775
 Li₂Ta₂, intercalation reactions, nucl. quadrupole interactions, TDPAC meas. 7-17245
 LiTa_{1-x}Zn_xO_{3-3x}F_{3x}, prep., ferroelec. Curie temp., effect of cationic substitution 7-45946
 LiTbF₄, uniaxial dipolar ferromagnet, nonasymptotic crit. behaviour 7-64467
 Li₂TeO₄ glassy electrolyte, vibrational, thermal and elec. characts. study 7-6866
 Li₂TiO₃, shallow gratings, leaky surface waves, trapping and temp. compensation 7-12449
 Li₂TiS₂, intercalation in solid-state battery cathode, TEM study 7-17854
 Li₂TiGaSe₂, ion intercalated, dark current and photocurrent relax. meas. 7-38622
 LiTmF₄, Van Vleck paramagnet, 4f electron excitations, mag. relax. of ¹⁶⁹Tm nuclei 7-7601
 LiVO₂, phase transition near 200°C, elec. resist., mag. susceptibility, X-ray diff., IR spectra, EPR, thermal anal. 7-32914
 LiV₂O₅, Li inserted, struct., neutron and X-ray powder diff. anal. 7-32391
 Li₂V₂O₅, amorphous thin films, electrical conductivity 7-58921
 Li₂V₆O₁₃ single cryst., Li transport props. and partial molar entropy 7-6871
 Li₂V₆O_{13+y} nonstoichiometric intercalation cpd., phase stability and elec. cond. studies 7-12723
 Li₂WO₄, elec. transport mechanism, superionic phase 7-12359
 Li₂WO₄, high-pressure polymorphs, calorimetric study 7-32638
 Li₂WO₃, crystalline and amorphous, electrochromic solar attenuation 7-39090
 Li₂WO₃ films, free-electron electrochromic modulation 7-22359
 Li₂WO₃-LiClO₄-Nb₂O₅ electrochromic cells, electrochromic window development, materials and devices 7-50664
 LiW₃O₉F, ordered O-F distrib., NMR, Raman spectra, electrostatic energy, site pot. calcs. (French) 7-32390
 LiXO₃ (X=Nb,Ta,I), X-ray irradiated ferroelectrics, radioluminesc. and thermolum. 7-27797
 Li_{0.5+0.5x}Ti_{1-x}Fe_{2-1.5x}O₄, dilute ferrite spinels, spontaneous magnetisation, anomalous temp. depend. 7-45739
 LiYF₄, broadband VUV reflectance coatings for Al mirrors 7-57520

lithium compounds continued

- LiYF₄:Ho³⁺,Er³⁺,Tm³⁺, excited-state absorpt., energy transfer, fluoresce. study 7-22322
 LiYF₄:Tm³⁺ crystal, Tm optical spectrum, press. induced linear dichroism, electron-phonon interaction 7-3069
 LiY_{1-x}Yb_xF₄ single cryst. growth, lattice const. and thermal expansion coeff. temp. depend. studies 7-27891
 LiYbF₄:Er(Tm), energy levels Stark struct., crystn. field interactions 7-58782
 LiYbP₂O₁₂:Nd³⁺, metaphosphate glasses, Nd³⁺ to Yb³⁺ energy transfer, luminesc. study 7-22323
 LiZnF₃ prep. and X-ray and NMR structural study 7-37953
 Li_{1-x}Zn_xFe₂O₄, outside spin wave manifold effective linewidth values, effect of dimensional reson. 7-53146
 Li_{5-2x}Zn_xGaO₄, solid solns., ionic cond. comp. depend. meas. 7-12366
 Li_{2-4x}Zr_{1+x}(PO₄)₂ solid solns., ionic cond. meas. 7-44906
 Li₂ZrF₆, hyperfine interactions, temp. depend. 7-12679
 Li₂ZrO₃, ceramics, fast neutron irradi., T and He retention, high temp. vacuum extraction 7-49649
 Li₂Zr₂(PO₄)₃ superionic conductor, Li⁺ motion, NMR study, phase transition obs. 7-32709
 Li₂Zr₂P₂O₁₂, thermal expansion, structural model 7-44858
 Li_{1-4x}Zr_{1+x}(PO₄)₃ ionic cond. comp. depend., X-ray diffr., prep. method depend. 7-12365
 Li₂O-TiO₂-GeO₂, glass form., phase equilibria (*Russian*) 7-21118
⁶Li (n,α)³H, chemical effect in Li₂CO₃ and Li₂CO₃ mixed with iron compounds 7-21289
⁶LiD cylinder irradiated by 14 MeV neutrons, T and ⁴He prod., comparison with TART code 7-36245
 MgO-LiFeO₂, solid solns. short range order parameters, determ. from EXAFS pair distrib. fns. 7-59289
 (Na_{1-x}Li_x)_{0.9}Mo₆O₁₇, Na substitutional effects on elec. resistivity and transport props. 7-45260
 NaLi₂Si(Ge)(Ti)O₄ isotopic oxides, cryst. struct. determ. lattice energy calcs. (*German*) 7-37952
 NaLiYbF₈, isotopic cpds., cryst. struct. (*French*) 7-32397
 Na₂O-Li₂O-P₂O₅ glass fibres, stress optical studies 7-7673
 Ni reinforced LiF-NaF, matrix crystn. and sintering, role of reinforcing phase 7-33625
 Pb_{2-x}K_{1+x}Li₂Nb₂O₁₅, tetragonal tungsten bronzes, ferroelastic-ferroelectric coupling (*French*) 7-27674
 PbLiInSe, intercalation-layer compound, dielectric-metal cond. transition 7-7230
 RbLiMoO₄, phase transitions, optical polarisation obs. 7-16732
 SiC fibre reinforced Li₂O-Al₂O₃-SiO₂ glass ceramics, tensile and flexural strength 7-13520
 SiC fibre reinforced Li₂O-Al₂O₃-SiO₂ glass ceramic composite, thermomech. mismatch 7-46538
 SiO₂-Al₂O₃-Li₂O-ZnO-TiO₂-ZrO₂-As₂O₃-Cr₂O₃:Cr, glass ceramic, time resolved spectra 7-63478
 SiO₂-Al₂O₃-ZnO-Li₂O:Cr³⁺ garnet type glass ceramics, laser excited emission spectra 7-22288
 Ti:LiNbO₃ optical switch, three-electrode 7-15970
 YLiF₄, lattice vibrs., Raman study 7-53329
 YLiF₄:Nd³⁺, impurity two-photon absorpt. cross section meas. 7-53375
 YLiFeO₃, orthoferite, mag. props. 7-2824
 ZrF₄-BaF₂-ThF₄-LiF quaternary glasses, ionic cond. and NMR studies 7-6865
 ZrF₄-PbF₂-AlF₃-LiF-KF glasses, mixed alkali effect, DC cond. 7-63873

lithography

- see also electron beam lithography; ion beam lithography; photolithography
 contrast enhancement and indirect evaluation of lithographs, radiographic techniques 7-35611
 excimer laser applications in imaging technology (*Japanese*) 7-56367
 microstructures for localisation studies, vapor deposition and lithography methods 7-64175
 molecular electronics materials, Langmuir-Blodgett technique, microlithography resist appls. (*Japanese*) 7-6964
 projector image aberrations, illumination system collimator effect 7-57516
 solid-state devices and materials, conf., Tokyo, Japan (Aug. 1986) 7-48173
 Al thin films, corrective trimming by laser controlled wet chem. etching 7-28195

lithosphere see Earth crust**liver**

- acoustic attenuation estimation using zero-crossings technique 7-23397
 acoustic nonlinearity and sound speed, use for composition estimation 7-47157
 alcohol dehydrogenase, horse liver, EXAFS investigation of struct. site 7-65704
 beef liver catalase, refined struct. 7-17938
 cell nuclei, erythrocytes and hepatocytes, small angle scatt. obs. 7-17959
 enzymes of glutamic acid metabolism in rat liver and brain, influence of continuous and modulated laser radiation (*Russian*) 7-47164
 expert diagnostic US system, statistical approach 7-23415
 light intensity and temp. distrib. created by light emitted from an optical fibre embedded in tissue 7-47013
 membrane reception of prostaglandin E₂ in mouse tissues, effect of various doses of ionising radiation (*Russian*) 7-47173
 mitochondria, isolated, rat liver, effects of up to 475 Gy γ-rays 7-60043
 mouse liver, P containing metabolites, Zn powder injection, NMR obs. 7-8609
 mouse liver cells, membrane pot. stability rel. to damaging agents exposure 7-8535
 optical-digital joint Fourier-transform classification of liver echotexture 7-34209
 proton relaxation times in mouse liver, heart and kidney, temporal fluctuations 7-47005
 pulsed finite-amplitude US passing through, harmonic distortion development 7-34190
 rabbit liver, histochemical effects of US (*Chinese*) 7-60034
 rat tissue, mag. field effects, phase-contrast microscopy obs. 7-8645
 therapeutic US effects in vivo: action and possible mechanisms 7-47160
 three-dimensional morphometric cytology, pictorial pattern recognition 7-28801
 tissue characterisation from US B-scan data, liver and spleen appl. 7-14072

liver continued

- transplasmalemma electron transport changes in simian virus 40 transformed liver cells 7-59959
²¹⁰Pu, A=239,240, conc. in Japanese human tissues 7-18081
livestock see farming
living systems
 see also biocybernetics; brain models; extraterrestrial life; physiological models
 Lake Norman, NC (USA) application of ecosystem assessment model 7-65654
 vision research and image technology, human functions of information processing (*Japanese*) 7-28499
 C cycle in biosphere, impact of atmospheric disturbance of geochemical C cycle 7-40546

LMC see Large Magellanic Cloud**LME** see liquid metal embrittlement**load (electric)**

- see also load distribution; power station load
 ideal bolometer, background power effect on performance 7-56344
 nuclear power plant molten salt latent thermal energy storage for load following generation 7-65633
 superconducting magnetic energy storage plant for electric utility load leveling, design and estimated costs 7-54369

load distribution

- demand-side planning, role of Earth-Coupled Heat Pump 7-8359
 orthotropic toroidal shell stresses under axisymmetric loads (*Chinese*) 7-14774
 plastic deformation, slip line field method for load limit (*Chinese*) 7-16071
 system theory, conf., Knoxville, TN, USA (Apr. 1986) 7-14714

lobes (distribution) see antenna radiation patterns**local density approximation** see density functional theory**local moments in dilute systems**

- antiferromagnetic metals and alloys, 4f-local moments, SDW instability 7-58970
 dilute mag. alloy system, external mag. field, thermodynamic props. anomalies 7-45666
 metals, magnetic impurity spin coupling, s-d mixing interaction envelope function calcs. 7-2814
 one-dimensional periodic Anderson model, quantum Monte Carlo simulation 7-52938
 transition metal impurities in host metals, magnetic nature, superconductivity studies, review 7-7437
 Al-Mn alloys, cryst. and amorphous phases, mag. props. 7-17163
 Al-Si-Mn alloys, cryst. and amorphous phases, mag. props. 7-17163
 CoAl, electronic struct. of antistructure Co atoms and Co-vacancies, local moments 7-7165
 (FeNi)_{1-x}Pd_x, atomic mag. moments, magnetisation meas. (*Russian*) 7-17198
 Mg-Fe dilute thin film, mag. screening and Kondo-type behaviour 7-12944
 MnTe, electronic struct. in magnetically ordered and disordered phases, tight-binding calcs. 7-45145
 Mo, electronic struct. of mag. 3d impurities, local density approx. 7-64432
 Nb, electronic struct. of mag. 3d impurities, local density approx. 7-64432
 Ni-B alloy with transition metal additives, amorphous, mag. scatt. influence on transport props. 7-33001
 TbSc(V)(Cr)(Mn)(Co), dilute alloys, hyperfine fields and local moment form. 7-64433
 V-Fe-H alloys, positron annihilation near crit. electron conc. 7-46199
 Y₂Co₇, electronic struct. and mag. props. 7-7104

local spin density approximation see density functional theory**localised electron states**

- see also Anderson model; charge-ordered states; charge transfer states; Wigner crystal
 1D CDW systems, collective modes and impurity effects 7-21832
 1D weak localisation, effects of forward scatt. and incommensurate lattice 7-45202
 3D cubic system under the influence of a Gaussian random potential, electronic localisation props. 7-7176
 actinide materials, superconductivity, simple transition metal-type and heavy fermion behaviour 7-12897
 actinides, photoemission, final state multiplet, screening effects 7-39349
 actinides bulk magnetic and transport props. 7-12953
 alloys, substitutionally random, electron localisation and metal-insulator transition, CPA calcs. 7-27302
 amorphous semiconductors, photoconductivity behaviour during the approach to steady state 7-38637
 aperiodic linear atomic arrays, electron propag. 7-21891
 (BEDT-TTF)₂I₃, alpha and beta phases, electronic struct., EELS studies 7-45118
 chemical bonding, validity of formal electron counting rules 7-63544
 conducting polymers, statistical mechanics of localised states 7-64168
 conductivity oscillations and quantum Hall effect in weak mag. fields 7-64275
 conjugated polymers, impurities, nonlinear dynamics 7-64115
 conjugated polymers, self-localised excitations 7-64168
 dirty superconductors, weak localisation and supercond. fluctuations 7-64403
 dirty thin films, superconducting transition temp., weakly localised regime 7-52883
 disordered 1D systems of localised states, single-particle density of states Coulomb gap calcs. 7-58777
 disordered 2D system, AC cond., anomalous permitt. 7-45406
 disordered electronic systems, localisation, scaling theory and probability distrib. 7-12672
 disordered electronic systems, nonanalytic behaviour of ultrasonic attenuation 7-6729
 disordered multilayered systems, local density of states determ., recursion method 7-52528
 disordered systems, localised electron Coulomb gap, quantum hopping effects 7-2540
 disordered systems, two-level system ensemble, low-temp. thermal expansion anomalies 7-2234
 disordered systems with statistical correlations electronic states, self-consistent Born approx. 7-2542
 electron gas, localisation effects, Keldysh representation 7-52529

localised electron states continued

- fractionally charged states in 'quarter-filled' electron-phonon systems 7-52446
 glass, two-level systems, density of states and distrib. functions derivation 7-12583
 graphite (0001), adsorption of Cs, induced work function changes, LEED obs. 7-33064
 graphite fibres, galvanomag. props., weak localisation and carrier interaction effects calcs. (Russian) 7-27347
 III-V semiconductors, localised electron states of substantial transition metal impurities, review 7-27295
 incommensurate one-dimensional CDW systems, localised electronic state form. due to phase and single particle excitations 7-21834
 incommensurate systems, Aubry 1D tight binding model, hopping range extension, localised states generation 7-21800
 integer quantum Hall effect, theory 7-52824
 integral quantum Hall effect and localisation 7-64274
 interactions and localisation problems, review 7-64178
 inversion layer, finite temp. Coulomb electron correl., insulator-metal transition calcs. 7-52424
 Li_2 intermetallics, localised grain-boundary electronic states and intergranular fracture calcs. 7-45215
 lattice electronic wave functions, localisation due to local topology 7-21847
 light particle localisation in simple fluids, quantum kinetic theory 7-38489
 Lloyd model, localisation and phase coherence length 7-45106
 macroscopic systems, fluctuation phenomena in localisation kinetics 7-64177
 metal, universal conductance fluctuations, effects of finite temp., interactions and mag. field 7-64196
 metallic filaments strongly anisotropic 2D system, weak localisation in magnetoresistance 7-45282
 metallic films, quasi-two-dimensional, localisation and interactions 7-64171
 metallic films, weakly localised regime, interaction effects 7-64173
 metallic glasses, elec. cond. temp. and mag. field depend., localisation and electron interaction effect calcs. 7-2568
 metallic glasses, weak localisation, magnetoresistance meas. 7-52574
 metals, dirty, electron-phonon scatt., collision rates 7-64235
 metals, disordered, temp. coeff. of elec. resist., Mooij correlation nonuniversality 7-21893
 metals, impure, localisation, interactions and transport phenomena 7-64169
 microstructures for localisation studies, vapor deposition and lithography methods 7-64175
 narrow full core levels press. contrib. estimates, atomic-sphere and LCAO calcs. 7-64036
 Ni, electron core states overlap at very high compressions 7-21849
 non-interacting electron disordered systems, localisation, scaling theory anal. 7-64174
 nondestructive depth profiling using secondary emission spectroscopy 7-27836
 nonpolar liquid mixtures, fluctuon self-localised state of electrons 7-16993
 one-dimensional incommensurate systems, Stark-Wannier resonances and delocalisation in finite elec. field 7-12671
 one-dimensional random potentials, power-law localisation 7-45224
 one-dimensional tight-binding system, localisation by elec. field 7-16967
 one-dimensional wave equations in random and quasiperiodic media, localisation 7-21872
 organic conductors, IR absorption spectra and electron-electron interactions 7-46032
 particle coupled to fermionic environment, ground state static props. 7-45107
 Penrose lattice, electronic structure, local-environment depend. 7-52392
 polarons, absorption spectra, temp. effects 7-58752
 trans-polyacetylene, random soliton distrib., localisation and density of states calcs., renormalised virtual cryst. method 7-52453
 polyethylene films with Si incorporation, localized gap states, space-charge-limited current 7-52530
 polythiophene, doped, polaron and bipolaron excitations, Huckel approx. calcs. 7-52448
 polyyne infinite chain, solitons, polarons and phonon spectrum calcs. 7-12626
 quantum Hall effect, localisation theory 7-64170
 quantum well structures, localised states, strain depend. 7-7312
 quasi-1D mag. systems, impurity low lying states (Russian) 7-52975
 quasi-one-dimensional semiconductor, electron mobility investig. 7-2616
 quasicrystals, 1D, acoustic and electronic props. 7-6730
 quasicrystals, 1D, electron transmission 7-45254
 quasicrystals, electron localisation 7-21901
 random Hubbard alloys, localisation-affected conductivity, numerical studies 7-45223
 random systems, electron density of states 7-27230
 random systems with off-diagonal disorder, localisation studies 7-32959
 rare earth systems, weak correl. regime, localised 4f states, quasi-particle energy calcs. 7-52492
 rare earths, 4f levels, appearance pot. spectrosc. 7-39324
 rare-earth core-electron spectroscopy, mixed valency versus covalency 7-45246
 semiconductor structures, 2D localisation and interaction effects 7-52531
 semiconductor structures, electrons and phonons in 1D and 2D 7-2734
 semiconductors, amorphous, prepared by fast glass transition, localised states 7-63818
 semiconductors, disordered, with dispersive transport, elec. transient process 7-17074
 semiconductors, dispersive transport under conditions of maximum population of localized states 7-52605
 site-disordered d-dimensional lattices, hopping transport 7-45291
 structurally disordered systems, electron localisation, $2k_F$ scatt. theory anal. 7-7174
 superconductivity, two- and three- dimensional, interplay with electron localisation 7-64392
 synthetic metals science and technology, conf., Kyoto, Japan (June 1986) 7-60872
 transition metal alloys, disordered, localised and extended state coexistence 7-7175
 transition metal oxides, Fe group, metallic behaviour, rel. to mag. and elec. props. 7-2487

localised electron states continued

- transport phenomena, localisation and interactions, conf. Braunschweig, Germany (Aug. 1984) 7-60882
 two dimensional quasi-periodic Penrose lattice, electronic and vibr. modes, localised states and band struct. 7-27300
 two-dimensional electron systems, magnetoconductance, density and mag. field dependences 7-33033
 weakly localised electrons, transport equation 7-7195
 weakly localised regime, effect of mag. impurity on conductivity 7-2839
 Ag cylindrical films, weak localisation and oscill. magnetoresistance 7-7414
 Ag supported particles on C, Al_2O_3 and SiO_2 , XPS studies 7-27868
 Al films and wires, fluctuation and localisation effects 7-64176
 Al thin films, spin-orbit scatt., localisation and superconductive tunnelling studies 7-45242
 Al-polyacrylic acid interface, reactivity, comp., XPS 7-28334
 Al-polyethylene interface, reactivity, comp., XPS 7-28334
 AlN thin crystalline stoichiometric film, electronic struct., electron spectra studies 7-58916
 AlN_x nonstoichiometric sputtered films, electron localisation, transport props. 7-58929
 $As_{40}S_{30}Se_{30}$ glasses, surface pot. relax., TSC meas. 7-64261
 Au core holes, final-state screening, total energy calcs. 7-2526
 Au single crystal films, localisation and size effect 7-17118
 Au-Pd films, electron scatt. times, weak localisation studies 7-64367
 Au-Pd thin films and wires, localisation and electron-electron interaction effects, magnetoresist. meas. 7-52863
 Ba-La-Cu-O system, possible high T_c superconductivity 7-2770
 $BaPb_{1-x}Bi_xO_3$, supercond. struct. and elec. props. 7-58247
 BSO_4 disordered diffuse solid scatterer, light scatt., weak localisation effects 7-22276
 $BaZrO_3$, valence band struct., X-ray-electron spectra studies 7-12604
 $Bi_{2-x}Sb_xTe_3$ polycryst. semicond. films, laser annealing effects 7-58317
 $CaZrO_3$, valence band struct., X-ray-electron spectra studies 7-12604
 $CdCr_2Se_4$ thin films, ferromagnetic semicond., multielectron energy struct., absorpt. spectrum, temp. and doping depend. 7-38488
 $Cd,Hg_{1-x}Te$, galvanomag. props. after metal-insulator transition 7-52655
 CdTe, d-core transitions, reflectivity spectra 7-53364
 CoO_2 , intermediate valence state, XANES 7-52545
 $Ce(SO_4)_2 \cdot 4H_2O$, intermediate valence state, XANES 7-52545
 Cr, EELS studies of Cr- $L_{2,3}$ core levels 7-46258
 CrSi, EELS studies of Cr- $L_{2,3}$ core levels 7-46258
 Cs, positron annihilation and pressure-induced electronic s-d transition 7-22378
 Cu-Mg amorphous alloys, 2D weak localisation effects 7-21871
 Cu-Zr metallic glass, elec. cond., annealing effects 7-7198
 Cu_{13} , fragmental cluster model and electronic struct. (Ukrainian) 7-12597
 $Eu_2(MoO_4)_3$, nonresonant energy transfer between two different Eu^{3+} ion sites 7-46125
 Fe-Te cluster, localised props., multiple scatt. X α SCF method 7-21848
 $Fe_{80}B_{20}$ ribbons, amorphous and crystallised, surface comp., electronic props., topography, AES, XPS, ion scatt. studies 7-27065
 Fe_xSb_{100-x} amorphous, metal-insulator transition and effects of localisation and correlation 7-45407
 $Fe_xZr_{1-x}Se_2$, intercalated layered cpd., thermopower and low DC field magnetisation study 7-17199
 GaAs (001), chemisorption of CF_3 radicals, RHEED, photoelectron spectra, HF SCF calcs. 7-53497
 GaAs LPE layers, heavily doped and compensated, hopping cond., density of states at Fermi level, carrier conc. determ. 7-2753
 GaAs, negative magnetoresistance and electron localisation in the region of a metal-insulator transition 7-12737
 GaAs/GaAlAs disordered superlattices, carrier localisation obs. 7-12818
 GaAs-AlGaAs, noise, localised states, quantum Hall effect 7-45413
 GaAs- $Ga_{1-x}Al_xAs$ quantum well, hydrogenic donor low-lying excited states, reson. states, positions and widths 7-45460
 GaAs- $Ga_{1-x}Al_xAs$ superlattice localised states in barrier 7-17079
 GaSe, gamma irradi., photoluminescence spectra, temp. depend. 7-17336
 GaSe, photoexcited localised excitons thermalisation, stacking disorder effects, photolum. study 7-27770
 $Ge_{23.5}Pb_{15}Se_{61.5}$ glasses, surface pot. relax., TSC meas. 7-64261
 a- $Ge_{20}Se_{70}$:Bi films, n-type, electron transport props. studies 7-7422
 a- $Ge_{22}Se_{68}Bi_{10}$ thin film, photoconductivity 7-17052
 $Ge_{1-x}Sn_xSe_2$ glasses, elec. cond. rel. to Mossbauer and Raman spectra 7-64250
 H atoms, finite chains, intermediate one-particle states 7-7145
 4He superfluid films, one-dimensional electron system, localisation, ripples, scatt. and Coulomb interaction effects (Russian) 7-27050
 HfPt, electronic struct. calcs. 7-45200
 Hg-Au, core holes, final-state screening, total energy calcs. 7-2526
 HgO, core levels and valence band electronic struct. spin-orbit splitting, XPS and UPS studies 7-13330
 HgTe, d-core transitions, reflectivity spectra 7-53364
 In granular films, electron localisation, transition from weak to strong 7-64083
 InP, negative magnetoresistance and electron localisation in the region of a metal-insulator transition 7-12737
 InP- SiO_2 interface, electron localisation 7-45514
 $La_{1-x}Ce_xNi$, Kondo lattice form., elec. resist. and susceptibility meas. 7-21899
 Li_2Si_7 , chemical bonding, validity of formal electron counting rules 7-63544
 $Li_3Sn_{1-x}Y_xO_4$, metal-insulator transition, Seebeck coeff. and elec. resist. studies 7-21817
 Mg, local density of states region, determ. by core-core-valence Auger transitions 7-39325
 Mg quasi-two-dimensional films, electron localisation and interaction effects 7-7411
 $Mg, Cd_{1-x}Se$ single cryst. solid solns., local centres parameters determ. (Russian) 7-32953
 N_2 , shock-induced molecular dissociation 7-23022
 Ni-P metallic glasses, electronic struct., XPS study 7-39357
 Ni_3Ga , momentum density distrib., Compton scatt., positron annihilation, symmetrised APW method 7-64069
 $Ni_{1-x}P_x$ amorphous glasses, electronic structure, calcs. 7-7101
 $NiSi_2-Si$, interface states, barrier height, Fermi level 7-27430
 O_2 , shock-induced molecular dissociation 7-23022
 PBS polycryst. semicond. films, laser annealing effects 7-58317
 $PbZrO_3$, valence band struct., X-ray-electron spectra studies 7-12604

localised electron states continued

- Pd clusters on substrates, core-electron binding energy, photoemission initial and final state effects studies 7-27859
- Pd, optical constants measured by a multiple-wavelength ellipsometer 7-27683
- Pd supported particles on C, Al₂O₃ and SiO₂, XPS studies 7-27868
- PdSi₂-Si, interface states, barrier height, Fermi level 7-27430
- Pd₂Si and PdSi, optical constants measured by a multiple-wavelength ellipsometer 7-27683
- PrO₂, intermediate valence state, XANES 7-52545
- RbCu₄Cl₃, luminesc. band profile, localised carrier tunnel recomb. effects calcs. 7-3075
- Sb₂S₃, amorphous condensers, electroelectret state and local levels studies (*Russian*) 7-45923
- Si (100) surface, electron delocalisation in 2D electron gas 7-12779
- Si (111) anal., charge and current corrugation correls. in scanning tunnelling microscopy 7-63410
- Si, accumulation layers, quasi-1D transport, strong localisation 7-64359
- Si inversion layer, localisation and interaction in a strong mag. field 7-64343
- Si, isoelectronic bound exciton states, spin splitting, photolum. excitation spectra study 7-2493
- Si MOSFETs, weak localisation magnetoresist. in almost quantising mag. fields 7-22024
- Si Schottky diodes with dislocations, tunnelling transitions 7-52831
- Si, with stacking faults, electron and phonon spectra, recursion method 7-32945
- a-Si:H, B₂H₆(PH₃), localised density of states, electrophotography study 7-32957
- a-Si:H, extended state mobility and tail-state distrib. 7-2617
- a-Si:H, fluctuation induced gap states 7-27242
- a-Si:H, localised electronic state, light soaking and current injection 7-16994
- a-Si:H, thermal-equilib. processes, electronic transport 7-64167
- a-Si:H, B films, hole transport, time-of-flight meas. 7-45320
- a-Si:H films, density of states and photoconductivity 7-45392
- a-Si:H films, reactive deposition 7-33592
- a-Si:H n⁺-i-n⁺ struct., freq.-depend. noise studies 7-45484
- Si:P, localisation theory 7-64170
- Si:P, metallic, nearly-localised electron spin dynamics, EPR linewidth study 7-22110
- a-Si_{1-x}C_xH, B(P) films, valence band localised holes, light-induced ESR spectra studies 7-53110
- SiO₂, electron induced dissoc., AES study 7-22392
- SiO_x thin films, plasma enhanced CVD deposited, Si chem. states, IR spectra, XPS, AES 7-21721
- SrZrO₃, valence band struct., X-ray-electron spectra studies 7-12604
- TaI₃, electronic struct. calcs. 7-45200
- TbO₂, crystalline and glasses, localisation of 5f states, XANES study 7-64794
- U-based mag. alloys, mag. props. and electronic struct. (*Russian*) 7-12967
- UO₂ and U glasses, unoccupied 5f states, XANES study 7-39318
- UO₂, crystalline and glasses, localisation of 5f states, XANES study 7-64794
- UO₂, search for intermediate valence state, XANES 7-52545
- URu₂Si₂ heavy fermion system, core levels and band struct., electron spectra studies 7-52418
- V₁₅, fragmental cluster model and electronic struct. (*Ukrainian*) 7-12597
- WC electronic struct. and magnetic suscept., UV and X-ray photoelectron spectra 7-53493
- WO₃, electronic struct. calcs. 7-45200
- ZnTe, d-core transitions, reflectivity spectra 7-53364
- Zr₇₆Fe₂₄, metallic glass, interaction of O, XPS study 7-39350

localised modes in crystals *see lattice localised modes***localised states, electron** *see localised electron states***locomotives***see also railways*

railway brake squeal damping 7-57635

loggers *see data loggers; recorders***logic, formal** *see formal logic***logic arrays** *see cellular arrays***logic circuit elements** *see logic devices***logic circuits***see also combinatorial circuits; flip-flops; formal logic; integrated logic circuits; logic devices*

fiber-optic inverter repeater to cancel distortion 7-15993

logic design

optical binary coded ternary arithmetic and logic 7-10863

optical computing using hybrid encoded shadow casting 7-1032

logic devices*see also logic gates; threshold elements*

III-V semiconductor integrated waveguides as all-optical logic devices 7-25869

interferometric devices, two-beam, with in-phase outputs, optical bistability 7-62764

liquid crystal light valves for medical imaging 7-14107

MQW optical logic arrays, thermal crosstalk 7-38720

optical bistability and optical computers (*Danish*) 7-1214

optical bistable elements, Kerr-type medium device, noise-induced switching theory 7-62803

optical computing and logic using Sagnac interferometric switches 7-25940

optical logical inverter, stimulated Raman scatt. in optical fibre 7-57466

optical parallel logic operation with microchannel spatial light modulator 7-25731

optical phase conjugation for parallel optical logic operations 7-57474

spatial filtering logic based on polarisation state 7-43330

ZnSe interference filter triple bistable-element loop circuit for digital parallel all-optical computer 7-57409

logic gates

bistable optical devices and logic gates 7-50616

composite logic gate element and multiplexer for optical computing and optical communications 7-57421

direct coupled linear gate, high energy physics appls. 7-5565

fibre optic logic elements 7-57564

fibre optic modulator and logic gate using nonlinear refr. and absorpt. 7-37174

logic gates continued

- integrated optical combinatorial logic using electro-optic Bragg gratings 7-26040
- nonlinear interference filters, critical interpixel separation 7-31388
- optical bistable devices graphical anal. of dynamic response 7-15922
- optical logic gate using spatial light modulator and interference fringe shifting 7-43351
- optical logic gates using liquid crystal optical switches 7-43327
- optical parallel logic gate using Pockels effect modulators, fundamental components for optical digital computing 7-43347
- optoelectronic logic gate, non-reson., using GaAs-AlGaAs MQW electroabsorpt. modulator 7-37139
- semiconductor doped glass, integrated nonlinear optical device fabrication 7-25873
- GaAs all-optical logic gate arrays, fabrication and characterisation 7-57414
- GaAs etalons, pulsed optical logic 7-57412
- GaAs ultrafast all-optical logic gate based on MQW bistable device 7-57415
- GaAs-AlGaAs MQW optical NOR gate, exciton and carrier dynamics, time resolved obs. 7-50628
- GaAs-GaAlAs MQW ultrafast all-optical gate with subpicosecond ON and OFF response time 7-11026

logic simulation *see circuit analysis computing***long-range order***see also order-disorder transformations*

- A15 ordering compounds, long range order, irradi. effects (*Russian*) 7-32490
- alloys, dislocation annihilation and strain hardening (*Russian*) 7-46500
- alloys, FCC, binary, with nearest neighbour interactions, ordering 7-21403
- alloys, long-range order structs., diffusion of H 7-21508
- alumina, ion-rich β - and β' -phases, superionic props., local and long-range order determ. 7-21519
- amorphous semiconductors, optical absorpt., tight-binding model 7-45961
- atomic collisions, long-range terms 7-961
- (BEDT-TTF)₂, superconducting and mag. instabilities 7-45697
- binary alloys, geometrically non-equivalent nodes, ordering theory (*Russian*) 7-44744
- binary crystals, FCC, ordering, Monte Carlo simulation 7-38154
- computer-generated uniform disk close packing round rhomboidal seeds, orientational order 7-61271
- dipolar fluids computer simulation, perturbation approach 7-10700
- dipolar hard sphere fluid, struct. and thermodynamics, reference-hypernetted chain eqn. 7-11879
- HVEM, materials characterisation, critical voltage effect 7-37819
- itinerant electron model with crystalline or mag. long-range order 7-17152
- long-period superstructure formation, microscopic model 7-51994
- metallic foil, comp. modulated, mech. props., book contrib. 7-27222
- metastable states, simple model for dynamics 7-32601
- MIM junction with disordered insulator, tunnelling current, CPA calc. 7-52850
- Nb₃Ir films, supercond. transition temp., effect of radiation induced disordering 7-45540
- ordered substitution alloys, lattice parameters, elasticity modulus (*Russian*) 7-46542
- photoinduced magnetism, effects on long-range order 7-52931
- random field models with long range exchange, scaling theory, 1/n expansion 7-24553
- semiconductor alloys, band struct. and reduced local symm., virtual-cryst. approx. calcs. 7-38451
- semiconductors, amorphous tetracoordinated, long-range disorder and local order 7-63473
- spin glass models, effective decrease of long-range interactions 7-59036
- statistical physics and field theory conf., Groningen, Netherlands, Aug. 1985 7-55899
- strong coupling electron systems, CDW, supercond., effect of randomness 7-27459
- three-dimensional O(2) model, phase transition, vortex string role, Monte Carlo calcs. 7-264
- (TMTSF)₂X, superconducting and mag. instabilities 7-45697
- trimethylammonium copper decachloride, mag. suscept., linear tetramer with ferromag. coupling 7-7491
- Al-Fe-Mg, solidified from liq. phase, struct. (*Russian*) 7-39498
- Au₄Cr, atomic ordering, X-ray struct. anal. (*Russian*) 7-1933
- Bi-based metallic glasses, thermal relax. processes 7-51653
- Cu-Pt (25.7 at.%), transform. from short-range order to L1₂ and L1₂-₂ ordered states 7-53726
- Cu-Ti alloy system, electron irradi.-induced amorphisation, chemical disordering effects study 7-16640
- Cu₃Au, electron irradiation, long range ordering, recovery, vacancy migration and clustering, positron lifetime study 7-39543
- Cu₃Pd, alloys with periodic antiphase boundary struct., dislocation motion 7-63620
- (Fe,Ni)₃V, LRO alloys, mech. props., effects of strain rate and long-term ageing 7-53796
- Fe-Al, thin foil, interfacial migration, velocity-driving force relations 7-46411
- Fe-Co-based ternary alloys, atomic and mag. moment mutual ordering (*Russian*) 7-33169
- Fe₃Si, near-stoichiometric high temp. creep and struct. investig. 7-22762
- Na₂Se₂(PO₄)₃ cryst. struct., tetrahedra disorder and ion-ion correls. studies 7-26723
- NbC₂, ordering behaviour, superstruct. refl. obs. 7-3267
- (NbSe₂)₃l, long-range order formation near the second-order phase transition temp. 7-44802
- Ni (111), ordering of acetylene and ethylene, LEED, EELS 7-52269
- Ni (115), H₂ adsorpt., surface corrugation effects, He diff. study 7-2381
- Ni-Fe-Mn system, coexistence of Ni₃(FeMn) and Ni(MnFe) superstructures (*Russian*) 7-1946
- Ni-Mo-Fe-Cr alloy, transient phase obs during long range ordering to Ni₄Mo, electron diff. study 7-63806
- Ni-Ta amorphous alloy, struct. changes and crystallization during heating (*Russian*) 7-16419
- (Ni₃Fe)_{1-x}Cr_x alloys, ordering study, comp. depend., electron diff. and Mossbauer meas. 7-51690
- Ni₃Mn-NiCr tie line, disordering kinetics, neutron diff. investig. (*Russian*) 7-32347

long-range order continued

- NiO-CuO solid solutions, evidence for long-range cation order, TEM investig. 7-44757
 β -O₂ solid, rhombohedral Heisenberg antiferromag., neutron scatt. 7-7480
 Pd-Ce-H, electrical resistance meas. 7-32984
 Pd-Y system, obs. of order 7-58456
 PdFe, drawing effects on elec. resist. and mech. props. (Russian) 7-17584
 Pt-R contact, R=Gd, Tb, Dy, Ho, Tm, mag. order destruction by cold current 7-52980
 Si (111), ordered Au, Ag, Cu overlayers, surface states, inverse photoemission studies 7-2660
 Si_{1-x}Ge_x MBE crystals, ordering study 7-58709
 Ti electrodes, passivated, photoelectrochemical studies 7-12757
 Ti-Mo alloy, ordering, effect of interstitial trace elements (Russian) 7-37928
 UBr(Cl)(I)₃, magnetic transitions, antiferromag. order and cryst. field splitting, neutron scatt. study 7-12974
 V-N system, metastable ordered phases, cryst. struct. (Russian) 7-44447
 Y_{1-x}Dy_x dilute alloys, spin density wave antiferromagnetism 7-52947

long tailed pair *see differential amplifiers***lookup tables** *see table lookup***loop antennas**

- E polarisation, thin wire loop, backscattered field anal. 7-36861
 field strength meters calibration using loop antenna, conductive objects effect determ. 7-18822
 semiconductor laser in small loop antenna as sensitive HF EM field probe 7-24657

Lorentz transformation

- complex conformal rescalings and complex Lorentz transformations 7-56031
 Einstein's inertia-energy relationship, deduction using isotropic light signal 7-55931
 Einstein's interpretation and Lorentz-Poincare interpretations 7-35277
 foundations of relativity (German) 7-4681
 gravitation, Lorentz gauge theory, canonical formalism (Chinese) 7-9721
 group without Einsteins isotropy convention 7-56033
 Lorentz boost generators proportional operators, role as position operators 7-61136
 photoelasticity and classical mechanics, link, Lorentz group 7-11366
 Robertson's test theory, space-time struct. and dynamics 7-29752
 time transformation, rel. to special relativity and Lorentz-type theory 7-48354
 velocity composition approach to special relativity 7-29753

Lorenz number

- metals and alloys, thermal conductivity theory, Lorenz ratio 7-45272

Loschmidt number *see constants***loss angle**

- see also dielectric losses*
 No entries

loss angle, dielectric *see dielectric losses***loss measurement**

- fibre-optic micro-bend dark-field sensor 7-43431
 long-haul single mode fibre attenuation meas., laser and LED source effects 7-43414
 optical fibre cable connection and loss meas. methods (Japanese) 7-43435
 optical fibre cable integrated OTDR/throughput loss meas. system for environmental testing 7-43460
 optical fibre loss, automatic meas. of spectral depend., cutback method and system (Czech) 7-26052
 optical fibre loss meas. using optical time-domain reflectometer, launching and receiving conditions (Japanese) 7-31513
 optical fibre transmission loss characteristics during drawing, continuous measurement 7-6004
 optical single mode fibre splicing techniques, statistical anal., splice loss per fibre-span meas. 7-43416
 LiNbO₃, proton exchanged, SAW props. study 7-12454

loss tangent, dielectric *see dielectric losses***losses**

- see also dielectric losses; eddy current losses; heat losses; loss angle; magnetic leakage; optical losses*
 atmospheric transmission losses use for interference resistant communications 7-34585
 dielectric gratings with losses, diffraction analysis 7-5982
 fibre acoustic and optical waveguides, similarities and differences 7-1298
 heat pump system, thermoeconomic optimisation 7-23210
 multiple reflector antennas, diffraction losses calc., asymptotic transition region theory 7-50471
 piezoelectric US transducer, internal loss effects (Korean) 7-57662
 quartz, rotated Y-cut, bulk acoustic wave reflection theory and expt. 7-2107
 solar cell array loss mechanisms in electrical performance model 7-54319
 Stirling engines, moderate temp., mechanical losses in rolling seals 7-65561
 superconducting composites, AC losses, modified boil off method 7-17130
 AlPO₄, heat treated, IR meas., temp. coeff. of delay and insertion loss 7-13486
 Fe-Si (3 wt.%), dynamic remagnetisation, structural depend. of losses 7-12994
 Fe-Si (3 wt.%), mag. props., influence of elastic-stress state produced by coatings 7-12990
 LiNbO₃/Ti integrated electro-optic devices, modelling and beam propag. anal. 7-11177
 Si solar cells, loss reduction by ion implantation, laser radiation, protective coatings (Dutch) 7-23134

loudness

- see also acoustic intensity measurement*
 speech, relative loudness of third-octave bands 7-54606
 tinnitus, magnitude estimation and 'paradoxical' loudness 7-8595

loudspeakers

- acoustic resistance box appl. 7-50889
 active noise attenuators, loudspeaker operating conditions 7-20517
 baffles, edge diffraction, geometric theory of diffraction appl. 7-31612
 direct radiation, bifurcation and chaos 7-31608
 electrodynamic loudspeaker with baffle, motional impedance and radiation 7-50888

loudspeakers continued

- high-quality loudspeaking system development with acoustic signal processing (Japanese) 7-57661
 impulse response measurement using Goly codes 7-37304
 mutual radiation impedance of double-disk source, radiated power effect 7-31613
 psychoacoustic optimisation 7-50890
 room acoustics, inverse control using multiple loudspeakers and/or microphones 7-37252
 sound irradiation facilities, control of acoustic feedback (German) 7-37302

Love waves

- acoustic Love modes, cutoff conditions in stratified structures 7-57629
 ferroelastic film on deformable substrate, Love waves and domain struct. near phase transition 7-52216
 layer thickness, generalised linear inversion calcs. from phase vels. of Love waves (Russian) 7-24627
 Love-type seam-waves in washout models of coal seams 7-47366
 metal inhomogeneous surface layer, Love waves (Russian) 7-16683
 propagation in irregular dry sandy layer, phase vels. determ. 7-8825
 propagation weak variational formulation 7-8853
 scattering by surface-breaking crack 7-43753
 seismic SH waves in layered media, Green's functions-leaking modes calc. 7-60173
 seismic waves, propag. along surface of elastic body with arbitrary shape 7-28888
 teleseismic waves, amplitude, phase and path anomalies of mantle waves 7-47348

low energy electron diffraction

- (201) plane study using LEED, AES and angle-resolved UPS, Fermi wave vector determ. 7-58846
 adsorbed states on Pd (110), EELS and LEED study 7-27115
 adsorption of H(D) on Rh(110), form. of high density chemisorbed phase, LEED investigations 7-27094
 adsorption of O₂ on Pd (110) at 300K, LEED and EELS studies 7-27093
 adsorption on Ge (100), high resolution energy loss spectra study 7-38331
 adsorption states on W (112), arrangement and thermal stability 7-6975
 clean and adsorbate surfaces, nonmagnetic, elastic spin-polarised LEED studies, book contrib. 7-32233
 computer controlled LEED intensity and spot profile determination 7-11857
 crystalline substrates, disordered adsorpt., diffuse LEED intensity meas. 7-1823
 defects at surfaces, microscopy and diff. studies 7-2325
 disordered adsorbates, calc. of elastic diffuse LEED intensities 7-44315
 electron damping, space inhomogeneity effects 7-11858
 electronic struct., initial stages of intercalation 7-53503
 ethane, adsorbed on graphite, phase transitions, thermodynamics and struct. anal., LEED obs. 7-32797
 graphite, Ar+N₂+CO submonolayer mixtures physisorbed on graphite, LEED study 7-2364
 graphite (0001), adsorption of Cs, induced work function changes, LEED obs. 7-33064
 graphite surface, methane adsorption, incomplete wetting at low temps. 7-32798
 graphite surface (0001)-(2 × 2)K intercalated structure, LEED calcs. 7-6952
 graphite surface with adsorbed methane, LEED 7-27129
 heteroepitaxial systems, domain size determ. from LEED angular profiles 7-7075
 imperfect surfaces and adsorbates, short range order and correlations 7-6953
 instrument for quantitative spot profile anal. 7-51586
 intensity meas. using real-time digital video processor 7-44317
 low energy SEM combined with LEED 7-21056
 magnetic surfaces, electron scatt. and emission 7-59379
 metal surfaces, low energy positron diff. pattern calcs., scatt. processes anal. 7-39331
 methane adsorbed monolayers on MgO (100), LEED anal. (French) 7-21620
 molecular adsorbates, structure determ. using dynamic LEED and HREELS 7-12493
 noble gases adsorbed on metals, interadatom interactions, LEED studies 7-7014
 organic adsorbates, structure from elastic diffuse LEED 7-12494
 overlayer nucleation and growth, surface defects, characterisation by surface-sensitive diff. 7-21614
 polarised electrons in surface physics, book 7-29607
 pyridine, adsorbed on Ag (111) and Ag polycrystalline substrates, struct., electron bands, LEED, UPS 7-53506
 scanning LEED microscope, appl. to Si 7-56387
 segregation and adsorption on Ni₅₀Fe₅₀ (100) alloy, surface composition and struct. 7-21617
 semiconductor surfaces, interaction with H₂ 7-58632
 specific heat critical exponents, LEED meas., Monte Carlo data anal. 7-6824
 spin polarised, dynamical theory 7-44316
 spot profile anal. of Si (111) polished and etched surfaces 7-11859
 spot profile quantitative anal. 7-6483
 surface (100), dense Pb monolayer, LEED anal. 7-6989
 surface (1010) with K overlayers, struct. and energetics, chemisorption and desorption studies 7-21659
 surface (110), electron emission, interaction of multiply charged ions with surface 7-53473
 surface (111), struct., LEED data 7-6947
 surface crystallography, future of LEED intensities 7-1822
 surface magnetism, spin-polarised electron diff. and photoemission 7-59380
 surface structure, LEED techniques, review 7-12441
 surface structure determ., theory and expt., book 7-60892
 surface structures, disordered, diffuse LEED and XANES studies 7-12442
 surface studies, analytical techniques review 7-6933
 surfaces and overlayers, struct. determ. with diff. methods 7-2324
 tensor LEED, high speed surface struct. determ. technique 7-37809
 (110), O₂ dissociative chemisorpt. studies 7-2377
 Ag (100), adsorption of Cl, Auger, LEED, XPS, thermal desorption studies 7-58635

low energy electron diffraction continued

- Ag (110), adsorption of ethylene and ethylene oxide, work function, LEED, UPS, TDS meas. 7-52270
 Ag (110), with physisorbed Kr, adsorption of NO₂, EPR, LEED AES studies 7-53116
 Al (111), Pd and Ag films, growth and electronic struct., UPS, LEED and AES studies 7-52350
 Ar, on MgO (100), LEED anal. (French) 7-21620
 Au (110) (1×2), sp. ht. anomaly for order-disorder transition, LEED study 7-12310
 Au epitaxial ultra-thin films, X-ray diffr. studies 7-27204
 AuGa₂-GaAs (001), chemically unreactive interfaces formation 7-7050
 BaO MBE on W (110) 7-16886
 Bi, adsorpt. and growth modes on Pt (111), spectrosc., LEED and work function investig. 7-27102
 C on Fe (100), gasification by O, CO desorption 7-6993
 CO and K coadsorbed on Ni (111), adsorbates electrostatic interaction, IR reflection-absorption spectra, TPD, LEED obs. 7-32824
 CdTe films on InSb, interface struct. and band offsets 7-58664
 Ce (001), H₂ adsorption, initial stages of hydride form., UPS, LEED and EELS studies 7-21629
 CoO (100), LEED intensities, quasidynamical approx. calc. 7-12428
 Cr (100) surface, evidence for two O chemisorption sites, at room temp. 7-6980
 Cr (110), chemisorption of O₂ 7-21662
 Cu (10,10) and (510), adsorption of Pb, faceting, LEED, AES studies 7-32828
 Cu (100), adsorption of S, (2×2) surface struct., LEED anal. 7-32827
 Cu (100), c(2×2)N overlayer, surface phonon dispersion, LEED, AES and EELS studies 7-12459
 Cu (110), H adsorpt., adsorbate movement-induced subsurface reconstruction, LEED and atom diffr. meas. 7-27114
 Cu (110), surface energy anisotropy, surface reconstruction 7-2346
 Cu (110) stepped faces, O₂ adsorption 7-27132
 Cu (111) with Ni overlayers, CO adsorption studies 7-21658
 Cu (111) with Pb overlayers, spot profile anal. of LEED 7-51586
 Cu films on MgO, epitaxial and electronic structures, LEED, AES, and EELS studies 7-52352
 Cu/Pd metallic superlattices, UPS, LEED, AES and ISS studies 7-3153
 Cu-Al (111), S segregation, LEED and AES studies 7-2321
 Cu-CdTe interface form., effect of different cation-anion bond strengths 7-27149
 Cu-Hg_{0.75}Cd_{0.25}Te interface form., effect of different cation-anion bond strengths 7-27149
 CuInSe₂ polycryst. semicond. growth from melt, surface props., ion bombardment and annealing effects 7-46304
 EuO(S)(Se)(Te) (100) surfaces, structure and composition 7-12426
 Fe (III) surface, K precovered, promotion of surface reactions with N₂ 7-13807
 Fe (100) 7-8154
 Fe epitaxial films, mag. size effects 7-59081
 Fe, epitaxial growth on Cu (100) 7-52353
 Fe films, particulate, vapour deposition on Al₂O₃ growth and props. 7-17427
 Fe particles on planar Al₂O₃ supports, low rate growth 7-32779
 Fe surface oxide layer, reduction by H adsorption, AES and LEED studies 7-8297
 Fe ultrathin films on Pd (111), photoemission, LEED and AES studies 7-45068
 Fe-Cu, epitaxially grown Fe films, electronic and crystallographic struct. 7-27214
 Fe-GaAs(001)-c(8×2) interface, simultaneous epitaxy and substrate out-diffusion 7-38355
 Fe-Si-C single cryst., surface segregation and interactions 7-2322
 Fe-Sn (001), surface segregation of Sn, surface struct. anal. 7-58594
 Fe-Sn (100), surface structural transitions during Sn surface segregation 7-52210
 GaAs (111), alkali metal covered, adsorption of O₂ 7-63957
 GaAs (111) orderly faceted struct., LEED pattern anal. 7-21579
 GaAs (311)(1×1) surface, atomic geometry and electronic struct. 7-2311
 GaAs (511) and (711) surfaces, struct. studies using LEED AES, and EELS 7-2312
 Ge (111) pure and As doped, surface electronic struct., photoemission studies 7-2658
 Ge, MBE on Si, role of surface reconstruction, LEED, Rutherford backscattering, channelling meas. 7-7034
 H₂ on TiO₂ (110) stoichiometric and defective surfaces 7-6983
 Hg_{1-x}Cd_xTe/Ag(Cu)(Al) interfaces, morphology, Hg bonding effects 7-7021
 Hg_{1-x}Cd_xTe/Pt interface, overlayer-cation reaction, XPS, UPS and LEED studies 7-65349
 In monolayer and multilayer surface diffusion, growth mode and thermal stability on W (100), LEED, TDS and scanning AES studies 7-2386
 InP (100), prep. by P deposition and annealing, surface reconstruction, LEED, EELS studies 7-38311
 InP (111) orderly faceted struct., LEED pattern anal. 7-21579
 InSb (-1-1-1) (3 × 3) reconstructed, X-ray diffr. studies 7-6951
 InSb (110), LEED surface crystallography and R-Factors 7-26596
 K adatoms on Cu (001), two-dimensional condensation, LEED obs. 7-12478
 LaB₆ (001), adsorption of Cs, surface structure and work function 7-6977
 MgO (100), LEED intensities, quasidynamical approx. calc. 7-12428
 Mo (110) chemically modified surface, Au thin film form. study 7-12489
 MoS₂-Co catalyst-promotor interaction, UPS, XPS, LEED studies (Chinese) 7-39913
 MoS₂(0001), Ar⁺-sputtered, adsorption props., LEED, AES, EELS, and work function studies 7-52275
 Mo(100), pulsed laser irradiated, use of LEED for surface damage charact. 7-21592
 NO, adsorpt. on Rh (111), disoc., EELS and LEED study 7-16859
 NaF (001), LEED with position-sensitive detection, comparison with positron diffr. 7-26597
 Nb(100) surface, H₂ chemisorption, LEED, EELS and work function meas. 7-32815
 Ni (100), adsorbed S, segregation kinetics, AES and LEED studies (Chinese) 7-58607
 Ni (110), adsorbed H, struct. determ., LEED studies 7-45004
 Ni (110), adsorption of D₂, LEED, TDS, RBS, nucl. reaction anal., work function meas. 7-58638

low energy electron diffraction continued

- Ni (110), adsorption of O, surface phases, absolute coverages 7-12486
 Ni (110), defects developed by epitaxial growth of Ni film or ion bombardment 7-63924
 Ni (111), ordering of acetylene and ethylene, LEED, EELS 7-52269
 Ni epitaxial films and interfaces with Cu and Pd, mag. size effects 7-59081
 Ni epitaxial growth on Fe (001), LEED and AES studies 7-64022
 Ni, oxidation, oxide epitaxy depend. on growth temp., LEED, AES, ellipsometry studies 7-22869
 Ni-Au (110), Au-enriched by surface segregation, LEED 7-27080
 Ni-Fe (100) surface, break-up of oxide films by S₂ impingement, LEED and AES meas. 7-46260
 Ni₃Al, atomic struct. of alloy surface, LEED study 7-38306
 Ni₃Al surface, atomic struct., LEED study 7-38307
 Ni₄₀Fe₆₀ (100), initial oxidation and sulphidation, LEED study 7-58641
 O₂ adsorbed on Cu (110) and polycrystalline surfaces, UPS, XPS, AES, EELS, LEED studies 7-32820
 Os (0001), coexistence of mono- and diatomic steps 7-52204
 Pb electrodeposition from aq. HCl soln. onto Pt (111) 7-27954
 Pb_{1-x}Sn_xTe surfaces, AES, LEED and Kikuchi pattern obs. 7-52200
 Pd (100), clean and S covered, adsorption and desorption of NO, surface reactions, TPD, EELS, LEED 7-58639
 Pd (100) with Na (NaO) overlayers, adsorption of methanol, formaldehyde and formic acid 7-21657
 Pd (110), O₂ adsorption 7-52274
 Pd (110) with chemisorbed N₂, EELS, LEED and AES 7-63960
 Pd (111), O₂ adsorpt., EELS and LEED studies 7-2378
 Pt (100) with underpotential deposited Pb 7-58646
 Pt (110), catalytic CO oxidation, kinetic oscillations 7-28346
 Pt (110), surface energy anisotropy, surface reconstruction 7-2346
 Pt (111), coadsorption of K and CO, structural and vibrational studies 7-52266
 Pt (111) clean and CO covered, LEED structural anal. 7-2376
 Pt (111) with adsorbed S, surface crystallography using LEED and R factor analysis 7-27120
 Pt (111) with incommensurate graphite overlayer, LEED 7-63930
 Pt₃Ti (111), chemisorption of CO and O₂ 7-27131
 Rb_{0.3}MoO₃, (201) plane study using LEED, AES and angle-resolved UPS, Fermi wave vector determ. 7-58846
 Rh (100), coadsorption of CO and H₂, adsorbate-adsorbate interactions effects 7-44997
 Ru (001), chemisorption and rot. epitaxy of Li, LEED, TDS obs. 7-12479
 Ru (001), coadsorption of H₂O and Li 7-21645
 Ru (001), H adsorption sites at saturation coverage, LEED 7-58645
 Ru (001), H₂ chemisorption, effect of coadsorbed O₂, LEED spectra anal. 7-33959
 Sb (111), LEED studies using automated high-speed data acquisition system 7-21589
 Si (001), surface order-disorder transition 7-52209
 Si (001)-(2×8), clean and Ni contaminated, ordered-defect model 7-21586
 p-Si (100), chemical etching with aq. K₂Cr₂O₇, XPS, UPS, LEED and TRMC meas. 7-46719
 Si (100), nitridation kinetics in NH₃ by thermal activation or electron bombard., LEED, AES, and TDS study 7-39770
 Si (100)2×1, interaction with O₂ and N₂O 7-63962
 Si (111), thermal oxidation, initial stages, AES, LEED and photoelectron spectra studies 7-3543
 Si (111)/Au interfaces, structural and electronic props., annealing effects 7-21679
 Si (111)-(7×7), interface formation during W deposition 7-58710
 Si MBE growth on Si (100) and (111), interface formation 7-21773
 Si, MBE on Si, role of surface reconstruction, LEED, Rutherford backscattering, channelling meas. 7-7034
 Si pure and As-doped single-domain reconstructed (100) surface state dispersion and struct., LEED and photoemission studies 7-38667
 Si, surface structural phase identification, use of specular beam in LEED 7-58589
 Si surfaces, (110), clean and hydrogenated, atomic configuration, LEED studies 7-2314
 Si/Au buried interface struct. determ., optical second harmonic generation studies 7-63982
 Si-Ge interface, solid phase epitaxy, intermixing, EXAFS, AES, LEED obs. 7-63973
 Si-InP (110) heterojunction, characterisation 7-33079
 Si-SiO₂ interfaces, microstruct. and electronic props. 7-38359
 V, surface (100)p(1×1), ferromag. order, electron capture spectra studies 7-27526
 W (001), H adsorption, commensurate-incommensurate phase transitions 7-7010
 W (100), adsorbed O₂, diffuse LEED intensity meas. 7-1823
 W (100) and (110), adsorption of H, very low electron energy refl. study 7-12488
 W (110), adsorption of Eu, Gd and Tb 7-2118
 W (110), chemisorption of H, O, surface barrier structure 7-21663
 W (110), surface barrier, LEED fine-struct. anal. 7-38660
- low gravity experiments** see zero gravity experiments
low induction loss see loss angle
low-pass filters
 Landsat data, Fourier filtering for information extraction in surveying and mapping 7-47582
 optical diffractive diffusers for display applications 7-5977
low-temperature physics see cryogenics
low-temperature production
 see also Joule-Thomson effect; magnetic cooling; refrigeration
 adsorption cryocoolers with multi-stage compression and reduced void volume 7-315
 closed cycle cooler, simplified cold head design 7-56277
 cryobiology, status and outlook, review 7-54838
 Guinier high temp. camera conversion to low temp. device 7-15041
 NMR superconducting magnets, refrigerator coding systems 7-54713
 small closed-cycle refrigerators, composite Pb/bronze matrix appls. 7-61340
 two stage Gifford-McMahon cycle cryorefrigerator operating at 20K 7-14951
 He compressor, regenerative oilfree, for cryopumps 7-56298
 He liquefaction, condensation heat transfer enhancement for mag. refrigerator performance improvement 7-56283

low-temperature production continued

- He liquefaction, refrigerant characts. of $Dy_3Al_5O_{12}$ and $Gd_3Ga_5O_{12}$ 7-56286
 He liquefaction, rot. mag. refrigerator design 7-56282
 He liquefier, condensing and freezing purification system 7-56280
 He liquefier with turbo-expanders, prediction method for cool-down characts. 7-56276

low-temperature techniques

see also cryostats; refrigeration

- apparatus cooldown using He or N cooling systems, mass flow requirements calc. 7-56281
 automated cryogenic current comparator resistance bridge 7-18829
 biological tissue low-temp. embedding, for electron microscopy 7-23496
 capacitance bridge for low-temperature, high-resolution dielectric measurements 7-48778
 chemical kinetics of ion+molecule reactions, ion drift-tube method 7-23007
 computerised instruments interfaces standardisation, for thermophysical meas. 7-4857
 cooling device for operation at 10K, mounting without rot. seals on four-circle diffractometer 7-14954
 cryobiology, status and outlook, review 7-54838
 cryogenic current leads with current overloads and coolant flow interruption, temp. state 7-61341
 cryogenic engineering conf., Berlin, Germany (April 1986) 7-48183
 cryogenic optical systems and instruments, conference, Los Angeles, California, (January 1986) 7-24283
 cryopreservation of biological specimens, possibility of using exponential cooling regimes 7-54815
 cryothermometer using molecular luminesc. 7-48740
 DC SQUID for low-temperature magnetic spectroscopy 7-48780
 diamond knife edges, megavolt and cryo electron microscopy 7-41547
 diamond-anvil cell and closed-cycle refrigerator system 7-41400
 electrical conductivity meas., high pressure, in diamond anvil cells at cryogenic temp. 7-56299
 ENDOR/TRIPLE spectra of matrix-isolated molecules, appl. to methyl radical in Ar 7-30058
 flowmeter, turbine-type working with cryogenic products, conversion factor 7-57958
 four-terminal AC bridge, easy to build, for temp. down to 1K 7-14957
 FTIR spectrometer sample cell, Invar, thermal calibration 7-41507
 FTIR studies of liquefied and crystallised gas mixtures 7-48894
 galvanomagnetic studies of organic metals, at high pressures and low temp. 7-30035
 gravitational wave antenna with resonant capacitive transducer and d.c. SQUID amplifier 7-34881
 Guinier high temp. camera conversion to low temp. device 7-15041
 inertial clock based on computer controlled servo-driven corotation system with superconducting suspension 7-14927
 ion implantation equipment at liq. He temp. (Chinese) 7-61336
 magnetic field homogenisation by diamagnetic shields 7-42848
 magnetic fields, variable, meas. under cryogenic conditions 7-48787
 magnetic properties measurement, hydrostatic pressure, low temp. technique in mag. field (Japanese) 7-48790
 magnetometers for simultaneous magnetic and resistive meas. at low temp. high magnetic field 7-48788
 measurement methods, thermometers and magnetic effects (German) 7-24652
 measurement principles, thermodynamics and thermometer functions (German) 7-24651
 membranes with locatable single pores generation, obs. and testing 7-298
 metrological support to means of measuring flow rate for liquid cryogenic media 7-44074
 Michelson spectrometer, corner cube reflector for cryogenic appl. 7-41491
 Mossbauer spectroscopy, hydrostatic pressure effect on the minimum temperature of a helium-3 cryostat 7-18970
 MuSR, high pressure, low temp. system 7-49843
 NMR imaging using cryogenics 7-54710
 NMR magnetic field meter, high-field meas. at liquid He temp. 7-18849
 NMR systems, cryocooler design and use 7-54712
 Peltier effect based cryostat, for X-ray diffractometry at low temp. 7-14956
 radiometric standards comparison cryogenic radiometer vs. electron storage ring BESSY 7-18861
 resistance thermometer, low temperature measurement, errors 7-9833
 resistance thermometers comparisons, Allen-Bradley, TVO and TSKU-21 7-30022
 rotary jet expanders, isentropic efficiency, influence of transient performance in press. pulse tubes 7-14953
 sampler for collecting radioactive gases and aerosols 7-59902
 self-balancing resistance bridge 7-35539
 SQUID, DC, cooled to 4.2 K with hybrid closed-cycle cryocooler, operation 7-56278
 superconducting equipment refrigeration technology develop. using liquid He 7-18790
 superconducting magnet system superfluid He II for cooling 7-61343
 systems metrology, applied aspects 7-48745
 thermal properties measurement, hydrostatic pressure, low temp. technique in mag. field (Japanese) 7-48790
 thermodynamic temp. determ. of Ne triple point 7-18791
 thick film chip resistors as low temperature thermometers 7-316
 transmission line tunnel diode oscillator, low-temp. detection system 7-35538
 transmission mode US microscopy for low temp. work 7-20518
 ultrasmall scanning tunnelling microscope for use in a liquid-helium storage Dewar 7-20075
 US damage on biological targets obs. 7-3953
 C resistors for cryogenic thermometry 7-56267
 H, liq. and solid, cryogenic, high press. eqn. of state, laser interferometric meas. method 7-30027
 H₂ cluster detection at 4.2K 7-36843
 He, liquid, flow rate meas., IMGC calibration facilities 7-63234
 He transfer tubes, construction (Japanese) 7-320
 He-filled proportional counter for low temps. and appl. to cryogenic resonance electron Mossbauer spectroscopy 7-62234
³He-⁴He dil. mixtures, specific heat measurements with second-sound Helmholtz resonator 7-21566
 In compression feedthroughs, for superconducting or Cu wire 7-35527

low-temperature techniques continued

- InSb charge injection device arrays, IR camera for astronomical imaging 7-34872
 NH₃, cryogenic, high press. shock temp. meas. 7-32566
 Rh-Fe microwires as resistance thermometers 7-307
 TiSi₂ films on polysilicon, elec. resist., implications for low temp. appls. 7-58907
 ZrF₄ glass fibre, IR temperature measurements, 60 to 150 °C 7-56262
LPE see liquid phase epitaxial growth
LS coupling see Russell-Saunders coupling
LSA see limited space charge accumulation
LSI see large scale integration
lubrication
 see also friction
 abrasive wear mechanism, wear process successive obs. in SEM 7-8229
 AE technique for friction and wear obs. and seizure prediction (Japanese) 7-59721
 compressible Reynolds lubrication equation, existence and uniqueness of solns. 7-35288
 conference, tribology and lubrication, Tokyo, Japan (July 1985) 7-4631
 elastohydrodynamic lubrication of soft, highly deformed contacts under conditions of nonuniform motion 7-57770
 film-splitting flows in forward roll coating 7-26291
 human joint fluids, rheological characts. and lubrication props. 7-40178
 hydrostatic circular thrust bearings: a study of inertia effects 7-51003
 hydrostatic cushions (Spanish) 7-20661
 isothermal fluid film, asymptotic anal. 7-11362
 journal bearings, numerical modelling of thermal effects 7-51004
 laser interferometer skin-friction meter, numerical and expt. study 7-16276
 mercaptobenzothiazole lubricant additive, Raman microscopy study 7-46772
 multiphase interface and interaction problems, probabilistic modelling and simulation 7-52219
 nonmetallic crystals, cumulative work-hardening and wear 7-53762
 oil, spectrochem. anal. using plasma torch (French) 7-35602
 oil-water core-annular flow in pipe loop, turbulent lubricating film model 7-57922
 oxidative wear and boundary lubrication 7-13606
 perfluoropolyether lubricant on magnetic disc surface, ion-induced volatilisation for quantitative anal. 7-39933
 PET, friction and wear under water lubrication, degree of crystallinity effect 7-3454
 polydiphenylborosiloxane/aminimide-cured epoxy resin composites, friction and abrasion props. 7-39677
 polymers, dry and lubricated wear, speed effects 7-33805
 precision function components, improvements made by ion implantation (Chinese) 7-53919
 radiation effects on lubricants 7-10224
 Raman microscopy study of lubricant films in elastohydrodynamic contacts 7-46772
 reaction layers, AES depth profile anal., under different wear test conditions 7-28147
 real-time neutron radiography of lubricant dynamics 7-33902
 rolling of adsorption-plasticised strip, surface layer rheology influence on stressed and strained state 7-17582
 soap-mineral oil lubricating grease; 12 Li-hydroxysterate greases, thick film, ambient pressure, shear flow transient tests (French) 7-6169
 squeezing flow anal. 7-31728
 stearic acid-Langmuir-Blodgett films, boundary lubricant efficiency (Japanese) 7-8118
 steel, medium C, wear, influences of materials and operating parameters 7-8133
 steel, Ni-Cr-Mo, cylinder-on-disc lubricated sliding wear expts. (Chinese) 7-59639
 steel, sliding lubricated contact, wear and crit. failure load, effect of solid contamination 7-33803
 steel surfaces, lubricated flat, oil supply effect on fretting wear 7-8123
 turbulent lubrication flow in annular channel 7-16266
 vacuum translational-rotary transfer mechanism using bakable self-lubricating bearing 7-56297
 Ag in self-lubricating coatings for extreme temps. 7-3444
 Al-Si, graphitic, hot extruded powders, sintering, antifriction props. 7-13409
 Cu alloy base powder materials with MoS₂(Se₂), self-lubricating, tribotech. characts. 7-28146
 Cu-Pb, resistance to wear and cavitation erosion of bearingalloys 7-8129
 Cu-Pb-Sn leaded bronze, resistance to wear and cavitation erosion of bearingalloys 7-8129
 MoS₂, sputtered films, tribological props., ion beam mixing effects 7-3441
 Pb based white metal, resistance to wear and cavitation erosion of bearingalloys 7-8129
 Sn based white metal, resistance to wear and cavitation erosion of bearingalloys 7-8129
Luders bands
 phenomenological theory 7-21328
 steel, dual-phase, Bauschinger effect and coercivity, effect of ageing (Chinese) 7-8045
 steel, stress-strain curves, approx. functions 7-59591
Ludwig-Soret effect see diffusion in solids
lumiance see brightness
luminescence
 see also cathodoluminescence; chemiluminescence; electroluminescence; fluorescence; fluorescent screens; ionoluminescence; luminescence of gases; luminescence of liquids and solutions; luminescence of solids; luminescent devices; phosphorescence; phosphors; photoluminescence; sonoluminescence; stimulated emission; superradiance; thermoluminescence; triboluminescence
 atom, multi-level, randomly modulated, second order optical process 7-50522
 atomic array, cooperative spontaneous emission, small-sample limit 7-50047
 constant energy synchronous luminescence spectrometry, parameter selection, optimisation 7-15006
 cross correlation of recombining particles 7-33436
 detonation waves, spherical, attenuation under strong luminesc., num. soln. 7-63179
 organic cpds., optically allowed and forbidden $\pi\pi^*$ transitions, spectral luminesc. props. 7-31108

luminescence continued

- Red Rectangle (HD 44179), role of visible luminesc. from polycyclic aromatic hydrocarbons 7-48008
stationary radiative transfer eqn. with cylindrical symm., inverse problems 7-24602
tetrafluoromethane + He⁺(Ne⁺)(Ar⁺)(N⁺)(N₂⁺)(O₂⁺)(H₂⁺)(H₃⁺), excitation cross sections 7-62501

luminescence chambers see scintillation chambers

luminescence of gases

- 1-(N,N-dimethylaniline)-3-(anthryl)propane bichromophore, intramolecular exciplex, luminesc. 7-5716
light amplification coefficient and intensity, spasmodic increase during metastable atom and mol. condensation (*Russian*) 7-50523
Eu chelate complexes, luminesc., photophys. 7-36669
H₂ electron beam ionisation luminesc. in high-current discharge, vacuum-UV radiation props. 7-57183
He, electron impact excitation, Stokes' parameters, electron-photon coincidence spectra anal. 7-50377
I₂ vapour, luminescence-Raman scattering transformation (*Japanese*) 7-59219
Ti I, N₂ laser induced fluoresc. in vapour cloud, quenching 7-19763

luminescence of inorganic solids

- Al₂O₃:Cr,Ga, Cr-Ga complexes, energy transfer 7-22321
Al₂O₃:Fe, single cryst., thermoluminesc. response 7-27794
alkali chlorides, particle bombardment-induced secondary photon emission 7-59264
alkali halide crystals, polarised luminesc., model of Ga⁺, Ge²⁺, In⁺, Sn²⁺, Ti⁺, Pb²⁺ centres 7-27753
alkali halide crystals, self-trapped exciton recomb. luminesc.-recomb. induced F-centre form. anticorrel. calcs. 7-13201
alkali iodide crystals, luminesc. induced by photo-generated excitons, excitation spectra struct. 7-46103
alumina, UV laser sputter etching effects, laser-induced fluoresc. and interferometry studies 7-26798
benzene, shock decomposition products detection by chemiluminescence 7-23023
borate glass: Cr³⁺, Nd³⁺, energy transfer, emission spectra 7-33440
CdTe films, MBE growth, photoluminescence and TEM characterisation 7-22376
ceramic wear behaviour, cathodolum. mode appl. in SEM 7-8228
conference, Rovno, USSR (Nov. 1984) 7-24263
corundum:V⁴⁺, cryst., luminesc. 7-33454
diamond, brown, vibronic coupling to nearly localised modes in luminescing bands 7-51980
diamond, electron beam irradi., vacancies, photoluminescence, radiative decay time meas. 7-46107
diamond, radiation damage prod. of SRL centres, phonons, absorpt. spectra, cathodoluminescence studies 7-33461
double heterostructs., photon recycling, non-perfect optical confinement 7-33449
fluoride glass:Er³⁺, impurity luminesc. and absorpt. spectra studies 7-53386
fluorophosphate glass:Er³⁺, impurity luminesc. and absorpt. spectra studies 7-53386
free exciton diffusion and decay, lumin. 7-32918
glass:Ce(Eu), stable and metastable impurity valence states, spectral props. (*Russian*) 7-27747
glass:Nd, transition metal doped, fluorescence and absorption spectra 7-13229
glass:Nd absorption thermometer with fluorescent referencing, fibre optic temp. sensor 7-25996
glass:Yb³⁺, time resolved fluorescence line narrowing 7-13230
glass, laser damage initial stage, luminesc. and microwave absorpt. obs. 7-31375
glass, transition metal doped, optical absorpt. and luminesc. spectra 7-13186
glass with Hg ions, luminescence under strong pulsed laser irradi. 7-33427
heavy-metal fluoride glass fibres, impurity anal. using selectively excited photolum. 7-31473
hot anti-Stokes luminesc., picosecond spectroscopy 7-22336
II-VI semiconductor solid solutions, luminescence, exciton localisation 7-33429
III-V semiconductors, defect recognition and image processing, conf., Montpellier, France (July 1985) 7-29596
III-V semiconductors, hot-electron photoluminescence, polarisation 7-46118
impact excitation and Auger quenching of luminescent centres in crystals, appl. to ZnS:Mn 7-27827
inert gas crystals, surface or bulk location of self-trapped excitons, luminesc. 7-46129
InP:Cu, band-edge photolum. quenching, impurity recomb. centre effects study 7-39177
intradband luminesc., anal. 7-27759
ionic crystals, broad gap, luminescence, synchrotron radiation studies 7-33432
ionic crystals, recombination luminescence optical detection of magnetic resonance studies 7-33435
IR photoluminescence by Fourier transform spectroscopy 7-46134
laser diode heterostructures LPE growth on InP:S substrate, substrate quality evaluation 7-32453
LEC wafers, cathodolum. mapping, IR absorpt., X-ray topography obs. 7-33462
luminescence centre struct., rare earth elements in activated glasses 7-27754
metal oxides, intrinsic shortwave luminescence and electron excitation properties 7-33430
moving dislocations in II-VI semiconductors, dislocations, effect on physical props. 7-7224
natural quartz minerals, thermoluminescent emissions 7-27798
polar semiconductors, polaritons, secondary emission spectra, energy relax. 7-27755
polyethylene, low-density, near-UV emission obs. during electrical-tree initiation 7-59259
quantum well structures, linear optical props. elec. field depend. waveguide electroabsorpt. and sum rules 7-13133
quartz:Li, (SiO₄/Li)⁰ centre, correlated ESR and thermoluminescence studies 7-22140
quartz, α-phase, cathodoluminescence of intrinsic defects 7-7766

luminescence of inorganic solids continued

- quartz, as-grown or Li-, Na-, Cu- electrodiffused, radiation-induced conductivity 7-6691
quartz, luminescence of pure and Ge-activated samples 7-46152
α-quartz, synthetic, defects 7-63603
quartz, X-ray induced blue luminescence, polarisation studies 7-3086
quartz sands, natural, red and blue colouration of thermoluminescence 7-46153
rare earth cpds., RSc₂(BO₃)₄, (R=Ce,Pr,Nd,Sm), preparation, struct. and props. 7-1968
rare earth trifluorides:Nd³⁺, absorption and luminescence spectra, Stark sublevels 7-3077
RE-activated aluminate phosphors, UV stability, α-Al₂O₃ foreign phase influence (*German*) 7-27779
reactive ion etching, AES, photoluminescence, SEM obs. 7-65241
recombination channels, dislocations interaction with point defects, lumin. study 7-46094
ruby, Cr weakly coupled ions, cooperative photon emission 7-59256
ruby, fluorescence, radiative trapping effects, 77 to 300K 7-53395
ruby, luminescence R lines, wavelength shift under shock compression 7-13239
ruby, luminescent R-line emission, pressure calibration to shock wave eqn. of state of Au and Cu 7-18802
ruby, R, fluoresc. line lifetime meas., high press. conditions, modulation fluorometry technique 7-22307
scheelite structure crystals., optical and elec. props. 7-33431
semiconductor clusters, zero-dimensional excitons, optical spectra and luminesc. 7-12615
semiconductor doping superlattices, physics and applications 7-52826
semiconductor double heterostructures, luminescence radiation photon recycling 7-13208
semiconductor quantum-well structures, excitation diffusion and energy relax. 7-21792
seminsulating LEC wafers, radiative centres, local photoluminescence study 7-33458
solar concentrators, glass and dye absorption and luminescence obs. (*Finnish*) 7-28390
steel, brittle fracture induced photon emission (*Russian*) 7-33465
synthetic silica glass, X-ray induced absorpt. and luminesc., heat treatment effects study 7-7733
tetramethylammonium manganese tribromide, photoexcited crystals., exciton annihilation, luminesc. decay curves 7-53385
tetramethylammonium manganese trichloride, photoexcited crystals., exciton annihilation, luminesc. decay curves 7-53385
thin crystals, incoherent exciton migration, detector luminesc. decay rate (*Russian*) 7-2503
tunnel junctions, prism coupled light emission 7-38770
AG, hot electron luminescence 7-17337
Ag clusters, SHG enhancement by transient resonances, laser induced luminesc. 7-20325
Ag ultradisperse particles in holographic emulsion, photolum. 7-33446
Ag₂As₂ undoped proustite crystals, photolum. obs. 7-33445
AgBr:Rh³⁺, IR radiative recomb. 7-7748
AgCl-Ag clusters on Ag electrode surface, optical second harmonic generation, SERS, luminesc. 7-11057
AgNa(NO₂)₂, low temp. triplet exciton decay, photolum. decay temp. depend. meas. 7-21821
(Al, Ga)As/GaAs undoped quantum wells, Al and Ga interdiffusion, photoluminesc. study 7-2271
Al:Eu³⁺, ion implanted, anodization, electroluminesc. obs. 7-7761
Al-Al₂O₃-Ag MIM struts. biased near breakdown voltage, optical emission 7-52853
Al-Al₂O₃-Au MIM struts. biased near breakdown voltage, optical emission 7-52853
AlAs:Si MBE layers, photoluminesc. 7-39160
AlAs/GaAs superlattices, X-point excitons 7-33069
AlAs-GaAs superlattice waveguides in separate confinement heterostructure laser diodes, threshold current density 7-20267
Al_{0.25}Ga_{0.75}As multiple quantum wells, photoluminescence studies, press. depend. (*Chinese*) 7-13194
AlGaAs layers MOCVD using dimethyl aluminium hydride, C acceptors, photolum. 7-22517
AlGaAs superlattice for visible laser diode, energy band structure (*Japanese*) 7-12823
AlGaAs:Sb, MBE growth, Sb doping 7-2038
AlGaAs/AlAs multiquantum-well struts., staggered band alignments 7-7361
AlGaAs/GaAs, abrupt heterojunction structures, large area uniformity, MOVPE reactor design, photolum. studies 7-22524
AlGaAs-GaAs, band-gap discontinuity, determ. by quantum oscillations of photolum. intensity 7-13217
AlGaAs-GaAs single quantum well, MBE growth interruption, well width fluctuations 7-7865
Al_{0.25}Ga_{0.75}As, instability of electron-nuclear spin system in strong mag. field, luminesc. study 7-7729
Al_{0.25}Ga_{0.75}As, photoluminescence half-width and intensity, temp. depend. 7-39179
Al_{0.25}Ga_{0.75}As films and multilayer structures, MOCVD growth and characterisation, review 7-33586
Al_{0.25}Ga_{0.75}As MBE layers, deep electron traps, flux ratio effects 7-12641
Al_{0.25}Ga_{0.75}As:Be epitaxial layers, ion implanted, rapid thermal annealing 7-21257
Al_{0.25}Ga_{0.75}As:Mg/GaAs:Se quantum well heterostruct., photopumped laser operation 7-25818
Al_{0.25}Ga_{0.75}As:Si, deep donor centres 7-45217
Al_{0.25}Ga_{0.75}As:Te, low press. OMVPE, Te doping, Hall effect, carrier conc., photolum. 7-21242
Al_{0.25}Ga_{0.75}As/GaAs quantum wells, photolum., periodic variation investig. 7-2688
AlGaInP, MOCVD, photolum., quantum wells, double heterostruct. laser appl. 7-39405
Al_{0.25}Ga_{0.75}N, photoluminescence in the edge emission region 7-27778
Al_{0.48}In_{0.52}As:Si, MBE grown, crystalline and optical props. 7-52322
Al_{0.48}In_{0.52}As-Ga_{0.47}In_{0.53}As SQW, electron temp. depend. on well width, photolum. obs. 7-12810
Al_{0.25}In_{0.75}As-GaAs strained layer superlattices, X-ray diffraction and excitation spectroscopy studies 7-12853
AlN, undoped and control doped films, luminesc. studies 7-27790
AlNbO₄:Cr³⁺ tunable IR laser crystals, fluorescent spectra 7-43110
Al₂O₃, γ-irradiated, thermoluminescence from F and F⁺ centres (*Korean*) 7-27795

luminescence of inorganic solids continued

- Al₂O₃:Cr, ruby, spin memory, relax., luminesc. 7-39176
 Al₂O₃:V⁴⁺, UV-visible absorpt. and luminesc. study 7-33447
 Al₂O₃:B₂O₃:SiO₂:Cu₂O glass, Cu activated, photoconductivity, lumin., influence of radiation defects 7-45381
 β'-Al₂O₃:Na₂O:Fe³⁺, luminesc. thermal effects 7-33444
 Al₂O₃:SiO₂:Cr mullite transparent glass ceramics, Cr³⁺ luminesc. 7-46102
 Al₂O₃:Cr, Ga, ruby, Cr-Ga complexes, luminesc. study 7-22320
 AlPO₄, glass, dielectric, charge buildup, influence on charging electron beam motion 7-44294
 AlSb, hot electron luminesc. 7-46119
 AlTaO₄:Cr³⁺ tunable IR laser crystals, fluorescent spectra 7-43110
 Al₂(WO₄)₃:Cr³⁺, tunable IR laser crystals, fluorescent spectra 7-43110
 Ar, solid, energy transfer during ion bombard. 7-64842
 As₂Se₃ single crystals, geminate pair recomb., photocond., photoluminescence meas. 7-38581
 Au/-ZnS/n-ZnS electroluminescent device struct., electron-hole recomb. luminesc., minority carrier injection mechanism 7-59260
 BaFCl:Dy(Cu), thermolum., X-irradiated at room temp. 7-53419
 BaFCl:Sm³⁺(Eu³⁺)(Gd³⁺)(Ho³⁺)(Er³⁺)(Yb³⁺), charge transfer excitation and emission spectra 7-64688
 BaLaGa₃O₇, luminescence props. 7-27768
 Ba₃LaNb₃Nd³⁺ single crystals, spectral-luminesc. props. 7-39169
 Ba₂NaNb₃O₁₅, X-ray irradiated ferroelectrics, radioluminesc. and thermolum. 7-27797
 BaO:Al₂O₃:Eu²⁺, Mn²⁺ phosphor, luminesc. props. 7-46112
 BaO:Al₂O₃:Eu²⁺ phosphor, luminesc. props. 7-46112
 BaSO₄, barite, X-irrad., thermally stimulated luminesc., trap distrib. 7-59266
 BeAl₂O₄:Ni²⁺, chrysoberyl, laser induced fluoresc. and decay lifetime 7-46135
 BiB₃O₆ and Bi₃B₅O₁₂, luminesc. studies, optical absorpt. edge 7-13209
 Bi₂GeO₂₀, pure and doped crystals phys. props. 7-7283
 Bi₂GeO₁₂, luminescence excitation and reflection spectra 7-46090
 Bi_{3.8}PO_{11.2}:Nd³⁺, cryst. growth, spectroscopic props. of Nd³⁺ ions 7-46131
 Bi₁₂SiO₂₀, pure and doped crystals phys. props. 7-7283
 Ca₃Al₂Ge_{3-x}Si_xO₁₂:Tb, cathodoluminescence, photoluminescence props. 7-53404
 CaCrO₄, spin-triplet state, luminescence and ODMR 7-64686
 CaF₂:Ce, Mn crystals, energy transfer, optical absorpt. and luminesc. studies, X-ray irradiated effects 7-27773
 CaF₂:Ce,Mn, optically active sites, optical spectra 7-22305
 CaF₂:Er³⁺, H⁻(D⁻), IR excitation and absorpt. spectra anal. of sites 7-53306
 CaF₂:Eu, X-ray luminesc., spectral-kinetic props. 7-39184
 CaF₂:Eu³⁺, O₂⁻, quadrupole coupling and crystal-field shielding under hydrostatic press. 7-2551
 CaF₂:Mn, gamma irradiation-induced defects, absorpt. and excitation spectra studies 7-26801
 CaF₂:Nd single crystal, thermoluminescence and X-ray fluorescence studies 7-33463
 CaF₂:Nd³⁺, Sm²⁺ Lasers, Sm²⁺ luminesc. 7-10962
 CaF₂:O crystals, O-vacancy centres, optical props. 7-7722
 CaF₂:Sm²⁺, electronic Raman transitions study 7-46017
 CaF₂:Sm²⁺, Nd³⁺ energy transfer efficiency 7-7734
 CaF₂:Nd single crystals, thermolum., spectra and X-ray luminesc. spectra 7-64704
 Ca₃Ga₂Ge_{3-x}Si_xO₁₂:Tb, cathodoluminescence, photoluminescence props. 7-53404
 Ca₃Ga₂O₉:Nd³⁺, luminescence and absorption spectra and stimulated emission 7-7732
 CaMoO₄, crystal, photo-excited triplet state, EPR 7-13027
 Ca_{2-x}Nd_xGa_{2-x}Si_{1-x}O₇, Ga gehlenite, cryst. struct. and optical props. 7-16525
 CaO-TiO₂-SiO₂:Eu³⁺ sphere ceramic, impurity laser-excited site-selective fluorescence line-narrowing spectra 7-13200
 CaSO₄, thermally stimulated exoelectron emission and luminesc. 7-27873
 CaSO₄:Dy, gamma radiation damage on thermolum. 7-38059
 CaSO₄:Dy phosphor, thermoluminesc. props. of a new prep., dosimetry appl. 7-28701
 Ca₃Sc₂Ge_{3-x}Si_xO₁₂:Tb, cathodoluminescence, photoluminescence props. 7-53404
 Ca₃Y₂Ge_{3-x}Si_xO₁₂:Tb, cathodoluminescence, photoluminescence props. 7-53404
 Cd chalcogenides, cryst. growth by SSSR-zone melting method, photolum. 7-64897
 CdF₂:Eu³⁺, electrolum. studies 7-27785
 CdGa₂S₄, luminesc. associated with defect complexes 7-27757
 CdI₂, interband two-photon absorpt., freq. depend. 7-33451
 CdI₂:Br, indirect excitons, isoelectronic impurity effects, luminesc. spectra 7-27255
 CdI₂:Ag interface, absorpt. and luminesc. spectra studies (Russian) 7-59224
 CdIn₂(Ga₂)S₄ single crystals, phase transforms., photoluminesc. studies 7-2171
 CdIn₂S₄ optical props., annealing and γ-ray irradiation effects 7-13211
 Cd_{1-x}Mn_xS, crystal growth and charact. (Japanese) 7-7829
 Cd_{1-x}Mn_xTe exciton localisation, time resolved photolum. study 7-46106
 Cd_{1-x}Mn_xTe, photoluminescence position and lifetime 7-13205
 Cd_{1-x}Mn_xTe(Se), mag. field-induced exchange effects, photolum. meas. 7-27705
 CdS based ceramics, radiative recomb. at high excitation levels (Russian) 7-3090
 CdS crystal growth and charact. (Japanese) 7-7829
 CdS crystals, surface polaritons, luminescence 7-64098
 CdS, electron beam irradiated, red flash-like luminescent centres, annealing 7-7740
 CdS, electron-hole exchange interaction for donor-acceptor pairs as a function of separation distance 7-52537
 CdS evaporated films, cathodolum., effect of thermal annealing 7-22353
 CdS, film, charge transport, rel. to electrophysical props. 7-17121
 CdS, light emission under voltage pulses 7-7764
 CdS, luminesc. associated with defect complexes 7-27757
 CdS on synthetic clay, luminesc. lifetimes, UV spectra 7-22297
 CdS particles deposited on porous vycor glass electron transfer and photoluminesc. dynamics 7-64678
 CdS, photolum., exciton scatt. from defects and impurities, depend. on exciting light intensity 7-39156

luminescence of inorganic solids continued

- CdS plastically deformed cryst., reorientable defects, polarised luminesc. study 7-51749
 CdS single crystals, cathodoluminescence, memory effect 7-22352
 CdS single crystals, nonequilib. high-temp. vacuum annealing effects, intrinsic defect transform. 7-58764
 CdS, with compensated i-layer, photosimulated deep level transient spectroscopy 7-7765
 CdSb, optical energy gap and light emission (Japanese) 7-53264
 CdSe, exciton luminesc., polarisation depend. 7-59248
 CdSe, photogenerated high density electron-hole plasma, energy relax., rapid expansion 7-33039
 CdSe, stimulated photolum. 7-27776
 CdSe, strongly excited, electron-phonon interaction screening, luminesc. meas. 7-38606
 CdSe:Cu films, radiative recomb. centres form., photolum. spectra studies (Russian) 7-33453
 CdSe_{1-x}Te_x and CdSe_{1-x}Te_x:Cu films, deep local states, photosensitivity, spectral study 7-22371
 CdSe_{1-x}Te_x, bound excitons, thermal dissoci., photoluminescence, reflectivity meas. 7-46122
 CdSe_{1-x}Te_x, bowing parameter of direct band gap, press. depend. 7-38453
 n-CdSnAs₂, photoluminescence 7-53393
 CdTe: B²⁺(Cu⁺) ion implantation damage, rapid thermal annealing, photolum. anal. 7-39162
 CdTe (001) films, MBE grown on InSb substrates, low temp. photolum. studies 7-22317
 CdTe epitaxial layers, MBE growth on GaAs substrates, photoluminesc. 7-46083
 CdTe grown on Si by LPMOCVD, physical props., photolum., exciton related emission peak 7-27181
 CdTe, MBE growth on GaAs substrates, struct. and optical props. 7-64907
 CdTe, MBE growth on Si using (Ca, Ba)F₂ buffer layer 7-46325
 CdTe MOVPE growth on InSb substrate, characts. 7-27920
 CdTe, OMVPE growth on InSb substrates 7-33577
 CdTe:In, photocorrosion, vacancies, photoluminescence spectra 7-27948
 CdTe/(Cd,Mn)Te superlattice, optical props. heterointerface effects 7-7736
 CdTe/ZnTe superlattice, quasi-2-D excitons in strongly localised regime 7-12617
 CdTe-CdMnTe, quantum wells, excitons and kinetics 7-12622
 CdTe-CdMnTe superlattices, photoluminesc. props. 7-13218
 CdZnTe, MBE growth on GaAs substrates, struct. and optical props. 7-64907
 Cd_{1-x}Zn_xTe, second-order optical process, transient behavior, luminesc., Raman scatt. 7-64689
 Ce doped fluoride elpasolites, 5d-4f spectra, impact of ion-host interactions 7-39143
 Ce³⁺ in dielectric crystal, 5d-4f spectra, phenomenological cryst. field model 7-39148
 CeF₂:Ho³⁺, fluorescence decay characts. of Green emission 7-7747
 Cr complex, luminescence line narrowing, exchange parameter evaluation 7-64677
 Cr compounds, sputtering of Cr atoms, laser-induced fluorescence spectra studies 7-59334
 Cr(III) complexes coordinated with macrocyclic tetraamine ligands, low-temp. luminesc. 7-22330
 CsCl(Br)(I), luminescence quenching in F centers under pressure 7-22334
 CsI, two-photon induced luminesc. 7-64696
 CsMnBr₃, photoexcited crystals, exciton annihilation, luminesc. decay curves 7-53385
 CsMnCl₃ antiferromag. crystals, struct. deform. by exciton self-localisation, luminesc. spectra fine struct. study (Russian) 7-7752
 CsMnCl₃, photoexcited crystals, exciton annihilation, luminesc. decay curves 7-53385
 Cs₂NaHoBr₆, excitation, electronic absorpt. and luminesc. spectra, crystal field splittings 7-46088
 Cs₂NaInCl₆:Cr³⁺, elpasolite lattice, broadband near-IR luminesc. 7-17338
 Cs₂NaYBr₆:Cr³⁺, elpasolite lattice, broadband near-IR luminesc. 7-17338
 Cs₂NaYCl₆:Cr, impurity photolum. spectra and lifetimes, thermal quenching and temp. depend. studies 7-3084
 Cs₂NaYCl₆:Cr³⁺, elpasolite lattice, broadband near-IR luminesc. 7-17338
 Cs₂O-SiO₂ glasses, intrinsic and recomb. luminesc. and fundamental absorpt. spectra 7-13195
 Cs₂Rb_{1-x}UO₂(NO₃)₃, solid soln., spectral luminesc. 7-13224
 CsUO₂(NO₃)₃, charge transfer bands position, ionisation pot. effects, luminesc. spectra anal. 7-46146
 Cu/nSi films, LPE growth 7-46359
 CuCl microcrystals, excitons, size quantisation effects, luminesc. spectra anal. 7-53409
 CuCl single crystal thin films, resonant two-photon absorption and emission 7-22310
 CuGaS₂, cathodoluminescence from iodine transport method grown crystals (Japanese) 7-3096
 CuInS₂, heterogeneous, VLS growth, electronic defects, photocurrent spectra, photolum., EBIC analysis 7-27288
 CuInSe₂, polycrystalline thin film solar cells, donor-acceptor pair luminescence 7-17890
 CuO, crystals, diamagnetic excitons, valence band corrugation 7-64546
 Cu₂O films, annealing of Cu and O vacancies, cathodoluminescence study 7-59263
 Cu₂O, long-lived strain-confined paraexciton thermodynamics, recomb. luminesc. and thermalisation 7-2492
 DyP₃O₁₄, absorpt. spectra intensity parameters, fluoresc. radiative transition probabilities (Chinese) 7-39141
 Eu complexes, Eu(III)ethylenediamine tetraacetate and Eu(III)bis-citric acid, polarised luminescence studies 7-22313
 Eu(II)-β'-alumina, luminescence, order-disorder effects, optical, structural and ion transport props. 7-46114
 Eu₂(MoO₄)₃, nonresonant energy transfer between two different Eu³⁺ ion sites 7-46125
 Fe-graphite structures, ion induced mixing, sputtering yield, fluoresc., RBS depth profile meas. 7-64844
 GaAlAs/GaAs:C quantum wells interface struct. and luminesc. efficiency 7-7735

luminescence of inorganic solids continued

- GaAlAs-GaAs heterostructure, LPE grown, interface photoluminescence spectra 7-53390
- GaAlAs-GaAs laser diodes, catastrophic optical damage, electrolum., cathodolum., EBIC and TEM obs. 7-57329
- Ga_{0.69}Al_{0.40}As, electron-hole plasma diffusion, spatially resolved gain and luminesc. spectra 7-12747
- Ga_{0.65}Al_{0.35}As-GaAs quantum wells, elect. field-induced decrease of exciton lifetimes 7-45481
- Ga_{0.8}Al_{0.2}As-GaAs-Ga_{0.3}Al_{0.7}As quantum well structs., electroluminescence spectra, model 7-33365
- Ga_{1-x}Al_xAs, indirect-gap crystals, hot photolum., polarisation chars. 7-46092
- Ga_{1-x}Al_xAs-GaAs superlattice, exciton CW-photoluminesc., excitation intensity depend. 7-59252
- GaAs (100), ambient induced surface effects, O adsorption, photolum., conductivity 7-45429
- GaAs (100), surface Fermi level unpinning in air using photochem. 7-2655
- GaAs, atomic layer epitaxy growth, photolum., Hall meas. 7-22527
- GaAs, band-gap shifts 7-22333
- GaAs, conduction band, deformation splitting and intervalley scattering, hot photoluminesc. study 7-2548
- GaAs, Czochralski grown, defect. conc., spatially resolved photoluminesc. 7-22341
- GaAs, dislocation-complex defect interactions, photoluminescence studies 7-16608
- GaAs doping superlattices, efficient room temp. electroluminescence, tunability 7-27782
- GaAs doping superlattices, temp. depend. of tunable lumin. 7-39182
- GaAs doping superlattices, pulsed and CW photoluminescence obs. 7-46138
- GaAs, electron-hole plasma diffusion, spatially resolved gain and luminesc. spectra 7-12747
- GaAs, emission lines, lifetimes and ionisation energies 7-22306
- GaAs epilayers, plasma enhanced metalorganic CVD 7-46336
- GaAs epitaxial films, MOCVD growth using tertiarybutylarsine source 7-59439
- GaAs epitaxial layers, MOCVD grown, influence of growth parameters on residual impurities 7-7047
- GaAs epitaxial layers, MOCVD growth, optimisation using photoluminesc. analysis 7-39396
- GaAs epitaxial layers, MOCVD growth, boundary layer effects, photoluminesc. study 7-64923
- GaAs epitaxial layers grown directly on Si (100) by low press. MOVPE, intrinsic photolum. 7-27924
- p-GaAs, excitons bound to pairs of shallow impurities 7-45169
- n-GaAs films, electron-hole plasma stratification and blue luminesc. near static domain 7-52666
- GaAs heterostructures, valence subbands, excitons and luminescence 7-7321
- GaAs high quality layers grown on Si by MOCVD, photolum. intensity 7-27922
- GaAs, highly doped, polarised hot electron photoluminescence 7-46121
- GaAs, homoepitaxial growth, cross hatch defect structure 7-45054
- GaAs, hot optically excited carriers in a spin-split-off subband, energy relax. 7-22302
- GaAs, hydride VPE layers, deep level incorporation and background doping 7-17120
- GaAs, laser MOVPE growth 7-33580
- GaAs layers, MOVPE, Zn acceptor impurities, magnetophotolum. 7-22308
- GaAs, MBE layers, deep level defects, passivation by H₂ plasma exposure 7-21850
- GaAs MBE layers on Si (100), crystalline quality, rapid thermal annealing effects 7-12519
- GaAs MOCVD growth on Ge (100) and Si (100) substrates, antiphase and single domains 7-27925
- GaAs, magneto-optical photoluminescent spectra studies 7-46148
- GaAs n-i-p-i doping superlattices, selective contacts, MBE growth through shadow mask 7-13356
- GaAs, OMVPE, low pressure growth from trimethylgallium + AsH₃ 7-17439
- GaAs, phonon hot spot, subTHz acoustic phonon emission 7-2118
- GaAs, photoholes in the spin-split band, energy relax. and spin depolarisation 7-22301
- GaAs, photoluminescence lines, mag. and strain field splitting 7-3079
- GaAs photoluminescence rel. to Si substrate orientation 7-53411
- GaAs pure and Si, Mn or Cu doped crystals., impurity and defect props., heat treatment, photolum. studies 7-39163
- GaAs quantum wells, hot-carrier phonon interactions, steady-state and picosecond meas. 7-12837
- GaAs quantum wells, n-modulation-doped, negative absolute mobility of holes 7-7337
- GaAs quantum-well wire hydrogenic impurity state binding energy and lowest exciton state lum. efficiency calc. 7-2683
- GaAs, residual acceptor assessment, Raman and selective pair luminescence studies 7-26771
- GaAs sawtooth doping superlattices, photoluminescence, transport props. 7-52825
- GaAs, semi-insulating, photoluminescence imaging using laser scanning microscope 7-53384
- GaAs, semiconducting/semi-insulating reversibility 7-21939
- GaAs, semiinsulating LEC substrates, defect etching 7-59694
- GaAs, shallow acceptor levels, photoluminesc. study 7-45209
- GaAs, single domain epitaxial growth on Ge (100) 7-22578
- GaAs single domain layer growth on Si wafers by MOCVD/MBE, heteroepitaxy 7-52357
- GaAs, substrates, multi-technique approach to defect microstructure characterisation 7-52215
- GaAs, surface region, heat-treated, photoluminescence, antisite defect obs. 7-39167
- GaAs, VPE growth in hydride system, elec. props. 7-2751
- GaAs: S, Sn, epitaxial layers, photoluminescence spectra 7-46095
- GaAs:Cr, meas. of residual stress by Cr-related luminesc. lines 7-7726
- GaAs:Cr,Se, impurity complex, luminescence study 7-53396
- GaAs:Cu, neutral state of deep acceptors, photoluminescence spectra, Jahn-Teller effect 7-64149
- GaAs:Er MBE layer, dopant trapping level, photolum. obs. 7-44581
- GaAs:Ho, electroluminescence and injection currents 7-13232

luminescence of inorganic solids continued

- GaAs:In, semi-insulating substrates and ingots, In content, nondestructive meas. 7-58305
- GaAs:In annealed substrates, In distribution in surface region 7-44959
- GaAs:Mg MBE layers, photoluminescence 7-22295
- GaAs:Nb photolum., Zeeman spectra study 7-39175
- GaAs:O LEC crystals, deep photoluminesc. band, fine struct. 7-46110
- GaAs:Pr(Nd)(Yb), IR photoluminescence of rare earth impurities 7-64692
- GaAs:S, Si epitaxial layers, close space vapour transport growth, photoluminescence and electrical props. 7-21776
- GaAs:S surface elec. props. modification by plasma exposure 7-27346
- GaAs:Si, shallow donor neutralisation by atomic H, photoluminescence study 7-22294
- GaAs:Si,Se MOCVD epitaxial layer photolum. spectral shift and doping efficiency obs. (Japanese) 7-45076
- GaAs:Si/Al_{0.3}Ga_{0.7}As quantum wells, photolum. studies 7-39178
- GaAs:Si/AlAs multiquantum well structs., band struct. and photolum. studies 7-12843
- GaAs:Si(B)-Ga_{0.25}Al_{0.75}As:Si(B) quantum wells, ion implanted, TEM and photolum. studies 7-58865
- GaAs:Sn, epitaxial layers, current carrier distrib. 7-12530
- GaAs:Sn, photolum. spectra, line shape anal., conduction band to deep acceptor transition 7-46098
- GaAs:Sn(Te)(Zn) surface layers, luminesc., electrophys. parameters, effect of annealing 7-64680
- GaAs:Te, low press. OMVPE, Te doping, Hall effect, carrier conc., photolum. 7-21242
- GaAs:Te VPE, vacancy-impurity complex capture, photolum. study 7-58678
- GaAs:Ti, optical spectra 7-7720
- GaAs:Ti, ion-implanted, acceptor-associated emission, selective self-optical compensation effect 7-22304
- GaAs:Zn epilayers, metalorganic CVD, Zn incorporation 7-63996
- GaAs:Zn(C) epilayers, low pressure MOCVD growth, impurity incorporation 7-59442
- GaAs/Al quantum wells, MBE growth, photoluminescence and absorption linewidth studies 7-7749
- GaAs/Al_{0.3}Ga_{0.7}As multi-quantum well structs., photoluminescence studies 7-3078
- GaAs/Al_{0.3}Ga_{0.7}As quantum-well bound states, valence-band offsets 7-7313
- GaAs/Al_{0.3}Ga_{0.7}As superlattices, optical transitions involving unconfined states, barrier width depend., photolum. spectra 7-52773
- GaAs/AlAs single quantum well heterostructures confined by short-period superlattices, photoluminesc. 7-22296
- GaAs/AlGaAs heterostructs. on Si substrate, MOCVD and MBE growth 7-7883
- GaAs/AlGaAs multi-quantum well heterostructures, optical gain, well width depend 7-46130
- GaAs/AlGaAs quantum wells, MBE growth, interface disorder studies 7-7026
- GaAs/AlGaAs quantum wells, MBE growth and energy levels, photoluminescence meas. 7-7067
- GaAs/AlGaAs quantum wells and double heterostruct. lasers, chemical beam epitaxy, photolum. 7-22523
- GaAs/AlGaAs quantum well structures, MOCVD growth, photolum., TEM obs. 7-27929
- GaAs/AlGaAs single and coupled double wells, energy depend. light hole mass, photolum. spectra anal. 7-38691
- GaAs/AlGaAs single heterojunction quantum well structs., photolum. chars. 7-46085
- GaAs/AlGaAs single quantum wells, interrupted MBE growth and temperature-dependent optical spectra 7-46082
- GaAs/GaAlAs disordered superlattices, carrier localisation obs. 7-12818
- GaAs/GaAlAs single quantum wells, steady-state photoluminescence studies 7-7750
- GaAs/GaAlAs superlattice structs., metalorganic MBE growth 7-7864
- GaAs/GaAlAs ultrathin layer systems, MOCVD growth and struct. props. 7-7063
- GaAs/GaPAsSb, double heterostruct., LPE, lattice matching, X-ray diffr., luminesc. 7-58884
- GaAs-(Al,Ga)As double heterojunction lasers, dislocation control, electroluminescence 7-7046
- GaAs-(Al,Ga)As heterostructure, modulation-doped, valence band mixing, and optical emission 7-7344
- GaAs-Al_{0.37}Ga_{0.63}As quantum wells, photolum. studies, MBE growth, effect of interruption 7-39150
- GaAs-Al_{0.3}Ga_{0.7}As, thin single quantum well, MBE growth kinetics, normal and inverted interfaces 7-45045
- GaAs-Al_{0.44}Ga_{0.56}As quantum wells, MBE growth, tunnelling assisted photon emission, photoluminescence meas. 7-46120
- GaAs-Al_{0.4}Ga_{0.6}As, intraband recomb., luminesc. spectra anal. 7-53387
- GaAs-Al_{0.7}Ga_{0.3}As single quantum well, photolum., transient response to electric field, carrier lifetime 7-7757
- GaAs-Al_{0.7}Ga_{0.3}As SQW structure, photolum. switching by pulsed elec. field 7-13197
- GaAs-Al_{0.3}Ga_{0.7}As MBE superlattices, low temp. photoluminesc. spectra 7-22340
- GaAs-Al_{0.3}Ga_{0.7}As MOCVD quantum well structures, time-resolved photolum. 7-53410
- GaAs-Al_{0.3}Ga_{0.7}As quantum well structure, recomb. dynamics, photolum. obs. 7-12809
- GaAs-Al_{0.3}Ga_{0.7}As quantum wells, doubly resonant LO-phonon Raman scatt. obs. 7-27722
- GaAs-Al_{0.3}Ga_{0.7}As quantum wells, doubly reson. LO phonon Raman scatt., photoluminescence spectra 7-53327
- GaAs-AlAs Al_{0.3}Ga_{0.7}As-AlAs, multi quantum well structs., picosecond spectra, 2D excitons 7-13215
- GaAs-AlAs MBE MQW struct., photoluminesc. spectra (Chinese) 7-59240
- GaAs-AlAs multiple quantum wells, photoconductivity, photoreflectance and photolum. meas. 7-27368
- GaAs-AlAs short period superlattice, photoexcited carriers, dynamics 7-53402
- GaAs-AlGaAs, high quality MOVPE quantum wells, optical props. 7-53406
- GaAs-AlGaAs, multiple quantum well structs., 2s state, excitons, luminesc. study 7-22337
- GaAs-AlGaAs modulation-doped quantum wells, photolum., giant oscillations, influence of mag. fields 7-7751

luminescence of inorganic solids continued

- GaAs-AlGaAs modulation-doped heterointerface, photoluminescence spectra studies 7-46137
- GaAs-AlGaAs multiple quantum wells, temp. depend. of photorefectance 7-7753
- GaAs-AlGaAs multiple quantum well structs., photolum. under high laser excitation 7-13213
- GaAs-AlGaAs quantum wells, picosecond photolum. photocurrent spectra 7-13214
- GaAs-AlGaAs quantum wells, etched ultrasmall structs., photolum. excitation spectra meas. 7-22293
- GaAs-AlGaAs quantum well structs., luminesc. from 2s heavy hole exciton, low temp. 7-22338
- GaAs-AlGaAs quantum wells, MBE grown, photolum. study 7-27758
- GaAs-AlGaAs quantum wells, field-induced lifetime enhancements, ionisation of excitons 7-39181
- GaAs-AlGaAs quantum wells, electron-phonon scatt. rate reduction by total spatial quantisation 7-45482
- GaAs-AlGaAs superlattice, hot electrons, real space transfer effect, photolum. studies 7-39180
- GaAs-anodic oxide interfaces, annealing, As enrichment, photoluminescence, Rutherford backscattering anal. 7-21687
- GaAs-Ga_{0.9}Al_{0.1}As heterojunction, donor-acceptor radiative recomb. mechanism, photolum. spectra study 7-17083
- GaAs-Ga_{1-x}Al_xAs modulation-doped quantum well, photoluminesc. studies 7-2687
- GaAs-Ga_{1-x}Al_xAs multiple quantum wells, intrinsic and extrinsic photolum. 7-39183
- GaAs-Ga_{1-x}Al_xAs quantum well structures, electronic props. 7-52817
- GaAs-GaAlAs, quantum well wires and boxes, optically detected carrier confinement, cathodolum. 7-39188
- GaAs-GaAlAs modulation doped quantum wells, hot carrier energy relax., time resolved photoluminescence spectra 7-52828
- GaAs-GaAlAs multiple quantum well structs., quasi-2D electron-hole plasma, band-filling effects, band gap renormalisation 7-7754
- GaAs-GaAlAs quantum wells, extrinsic photolum. 7-7755
- GaAs-GaAlAs quantum wells, excitonic coupling in elec. field, photolum. spectra 7-64094
- GaAs-GaAs:Cr(Te), VPE grown, photoluminescence study, effect of substrate doping 7-27771
- GaAs-GaAs:In epitaxial layers, dislocation reduction, device performance effects 7-7354
- GaAs-Ge heteroepitaxy on Si substrates, recrystallised Ge-on-insulator intermediate layers 7-52358
- GaAs-Ge-SiO₂, semiconductor MBE layers on Ge islands on insulator, photolum. study 7-33455
- GaAs-InGa_{1-x}As strained layer superlattices, photolum. microimaging of dislocations 7-27161
- GaAs-ZnSe, MBE growth on GaAs epilayers, nucleation and characterisation 7-45046
- GaAs_{1-x}Al_xAs MQW, MOCVD grown, excitons, photoluminescence spectra 7-38702
- GaAs_{0.12}P_{0.88}N, Te and GaP:N, Si(Te) epitaxial layers, minority carrier lifetimes, surface and interface recombination effects 7-7424
- GaAs_{0.6}P_{0.4} degraded LEDs, origin of nonradiative centres, photocapacitance, electrolum. spectra 7-53413
- GaAs_{1-x}P_x:Be⁺-GaP:Be⁺ strained layer superlattices, ion implantation doping, optical and elec. props., device appls. 7-44583
- GaAs_{1-x}P_x solid solns., indirect band gap temp. depend., electrolum. spectra studies 7-38448
- GaAs_{1-x}P_xN, cathodoluminesc. efficiency, N-bound excitons influence 7-7768
- GaAs_{1-x}P_xN epitaxial layers, N conc. determ. 7-63989
- GaInAs, Czochralski-grown, dislocation effects investig. 7-7261
- GaInAs-InP, quantum well structures, adduct MOVPE, photolum., magnetoresist charact. 7-27388
- Ga_{0.47}In_{0.53}As:Be epitaxial films, ion implanted, rapid thermal and furnace annealing 7-22729
- Ga_{0.47}In_{0.53}As-InP superlattices, MOCVD grown, room temp. excitons 7-21986
- Ga_{0.47}In_{0.53}As, photoluminescence line shape of excitons 7-3087
- Ga_{1-x}In_xAs, low-pressure MOVPE growth 7-7873
- Ga_{1-x}In_xAs/GaAs heterostructures, low press. MOVPE, photolum., Auger profiling 7-27389
- Ga_{1-x}In_xAs-GaAs strained layer superlattices, low temp. photolum. 7-53407
- GaInAsP/InP heterostruct., luminescence polarisation, quantum size effects 7-13210
- GaInAsP-InP BH laser fabrication, MOCVD epitaxy, validation by photoluminescence imaging 7-31360
- GaInP-AlGaInP-GaAs heterostructures, MOVPE, Hall effect, photolum. 7-39401
- Ga_{1-x}In_xP epitaxial layers, MOVPE, surface morphology, photolum. 7-22557
- Ga_{1-x}In_xP layers, MOVPE, photolum., comp. and growth temp. depend. 7-39403
- Ga_{1-x}In_xP, MOVPE growth and characterisation 7-3192
- Ga_{1-x}In_xP/GaAs (Al_{1-x}Ga_x)As heterostructures, MOVPE, photolum., lattice matching 7-39402
- GaN crystals, polarisation props. of band-edge emission, dispersion theory appl. 7-64694
- GaN, undoped and control doped films, luminesc. studies 7-27790
- GaN:Zn, pure and doped, electrophysical props., nonhomogeneous semiconductor model 7-27292
- GaN:Zn films, MOVPE, electron cyclotron resonance plasma excitation, low temp. growth, photolum. 7-22549
- GaN:Zn(Cd), time-resolved photoluminescence study 7-22347
- GaP and GaP:N diodes, electroluminescence, high press. effects 7-27787
- GaP, deep level centres at excited states, study by transient optical absorpt. spectroscopy 7-13188
- GaP single crystals, anisotropic deep centres, polarised photolum. and thermolum. studies (Russian) 7-21867
- GaP:Pr(Nd)(Yb), IR photoluminescence of rare earth impurities 7-64692
- GaP:Zn, doping superlattices, growth and props. 7-64684
- GaP-GaAs_{1-x}P_x strained layer superlattices, photolum. microimaging of dislocations 7-27161
- GaS, layered, high temp. e-h liq., radiative recomb., luminesc. spectra study 7-17343
- GaSb/AlSb single quantum wells, electrophysical and photoluminescence studies 7-46136

luminescence of inorganic solids continued

- GaSb-AlSb multiple quantum well structs., size-induced direct to indirect gap transition 7-7373
- GaSb-AlSb quantum wells, optical transitions, obs. 7-46086
- GaSb-AlSb quantum-well structures, 2E_g transitions 7-46128
- GaSb_{0.1}AlSb quantum wells, nonparabolic behaviour under hydrostatic press. 7-64328
- GaSe, evidence of exciton-plasma transition in emission spectra 7-59249
- GaSe, gamma irradi., photoluminescence spectra, temp. depend. 7-17336
- GaSe, photoexcited localised excitons thermalisation, stacking disorder effects, photolum. study 7-27770
- GaSe, screening of excitons by free carriers, transmission, reflection and luminescence spectra 7-38460
- GaSe, spontaneous and stimulated photoluminescence studies 7-22315
- GaSe:Mn single crystals, optical props. 7-27777
- Gd, optical radiation generated by electrons (Russian) 7-53415
- Gd oxychlorides, phase equilib., X-ray diffr. and spectro-luminesc. anal. 7-46143
- Gd³⁺ compounds, Y-diluted energy migration, luminescence study 7-33443
- GdBO₃, luminesc. of Sb³⁺ 7-33442
- GdBO₃:Pr³⁺, Tb³⁺(Sm³⁺)(Dy³⁺), host lattice sensitisation, energy transfer and photolum. 7-46113
- Gd₂MSb₂Zn₃O₁₂ (M=Sr,Ca), rare-earth activated garnets, cathodolum. 7-7763
- Gd₂(MoO₄)₃:Eu³⁺, nonresonant energy transfer between two different Eu³⁺ ion sites 7-46125
- Gd₂O₃-P₂O₅ phosphors, Eu³⁺ activated, luminesc. spectra, cryst. symm. 7-3080
- Gd₂Te₂Li₃O₁₂:R, cathodoluminescence study (German) 7-22354
- Ge crystal, exciton gas-electron-hole liq. interactions, phase diagram, nuclei drift effects 7-2488
- Ge, electron-hole plasma transport 7-7272
- Ge:Zn, electron-hole droplet transport, suppression by deep impurities 7-58746
- Ge:Zn, photolum. spectrum, effect of (001) uniaxial stress 7-33450
- HgCdTe and HgTe-CdTe superlattices, IR photolum. by Fourier transform spectroscopy 7-46134
- HgGa₂Se₄, photocond., photoluminescence spectra, annealing and ion implantation effects 7-39152
- HgGa₂Se₄, single cryst., deep levels, photocond. and photolum. spectra 7-7159
- HgTe-CdTe superlattices, IR optical props. 7-13166
- HgTe-CdTe superlattices, IR photoluminesc. spectra 7-13219
- HoCl₆³⁻, ⁵I₅ cryst. field levels, assignment 7-27766
- In-Ga-P-As, gap width, temp. depend. 7-12602
- In_{0.53}Ga_{0.47}As-InP, epitaxial single quantum wells, spectroscopy of excited states 7-46126
- In_{0.18}Al_{0.82}As-GaAs strained layer superlattices, Raman studies 7-12854
- In_{1-x}Al_xAs/Au Schottky barrier heights, composition dependence 7-45431
- In_xAl_{1-x}As/GaAs strained-layer superlattices, effective mass reversal 7-17078
- InAs, In_xGa_{1-x}As, atomic layer epitaxy growth, photolum., Hall meas. 7-22527
- InAs/GaAs single quantum well structures grown by atomic layer epitaxy 7-22486
- InAs/GaAs strained-layer superlattices, band struct., TEM, X-ray and photolum. spectra 7-38722
- InAs-GaAs strained-layer superlattices, pseudo-alloy behaviour 7-7376
- InAs-GaAs superlattice, electronic props. 7-52817
- InAs-GaSb superlattices, transient photovoltaic effect 7-12764
- InF₂-PbF₂-BaF₂-SrF₂-YF₃-AlF₃-UO₂F₂, luminesc., lifetime meas. 7-27750
- In_{0.3}G_{0.7}P layers, LPE, elec. and optical props. 7-17119
- InGaAs:Si LED, electrical and luminesc. props., ultrasonically-induced changes 7-22350
- InGaAs/InP quantum wires and boxes, low temp. photoluminesc. 7-59238
- InGaAs-InP heterostruct., rare earth doped, elec. and photoluminescence props. 7-46133
- In_{0.53}Ga_{0.47}As/In_{0.52}Al_{0.48}As quantum wells, lamp annealing interdiffusion and optical props. 7-12502
- In_{0.53}Ga_{0.47}As-InP layers, photolum. and laser emission 7-7739
- In_{1-x}Ga_xAs, MOCVD, optical and elec. props. rel. to growth temp. 7-53613
- In_xGa_{1-x}As-GaAs single-quantum-well heterostructs., pseudomorphic, optical characterisation 7-22303
- In_xGa_{1-x}As, gas source MBE growth 7-52361
- In_xGa_{1-x}As, photoluminescence determ. of effects due to In alloying 7-46096
- In_xGa_{1-x}As/In_xGa_{1-y}As and (InAs)_m(GaAs)_n superlattices, MBE grown, optical studies 7-13221
- InGaAsP double heterostructures for laser diodes, LPE growth, influence of P vapour ambient 7-46355
- InGaAsP, optical gain spectra, effects of energy band struct. (Chinese) 7-59239
- InGaAsP/InP heterostructures, carrier lifetimes and quantum efficiencies, photoluminesc. studies 7-64675
- InGaAsP/InP multiquantum well layers, LPE, photolum., X-ray diffr. 7-53640
- InGaAsP-GaAs double heterostructures, luminescence efficiency and surface recombination velocity 7-13196
- InGaAsP-InP, heterolaser struct., distributed feedback conditions, luminesc. spectra anal. 7-50561
- InGaAsP-InP double heterostructures, luminescence efficiency and surface recombination velocity 7-13196
- In_{1-x}Ga_xAs_{1-y}P_yTe films, Fermi energy, dopant conc. depend. 7-52867
- InGaP/InGaAlP multiquantum-well laser diodes, MBE growth and characterisation 7-62689
- InGaP-InGaAlP MQW structs., room temp. excitons 7-58745
- In_{1-x}Ga_xP solid solns., indirect band gap temp. depend., electrolum. spectra studies 7-38448
- In_{1-x}Ga_xP, epitaxial films, radiative recomb. 7-59257
- InGaAs, LPE growth on GaAs, immiscibility effects 7-39442
- InGaP/GaAs interface stress, Cr-related luminescence study 7-46101
- InMgGaO₄, luminescence props. 7-17341
- InP (100), ambient induced surface effects, O adsorption, photolum., conductivity 7-45429
- InP, dislocation-complex defect interactions, photoluminescence studies 7-16608

luminescence of inorganic solids continued

- InP epitaxial films, MOCVD grown, identification of acceptors and donors 7-58688
 InP, epitaxial films, radiative recomb. 7-59257
 InP epitaxial layers, MOVPE, elec. charact., photolum. 7-22519
 InP films, hydride VPE, impurity incorporation, defect charact. 7-53614
 InP, luminesc. associated with defect complexes 7-27757
 InP, MOVPE; morphology, photolum., carrier conc. and mobility 7-22518
 InP, reactive ion etching, AES, photoluminescence, SEM obs. 7-65241
 InP room temp. band edge photolum. intensity interpretation 7-27762
 InP substrates, influence of inhomogeneities on quality of quaternary layers 7-32770
 InP surfaces, sputter etched, optoelectronic and structural props. 7-13661
 InP, ultrapure, atmospheric pressure OMVPE growth 7-13375
 InP:Bi thin film, epitaxy, impurity distrib., photoluminesc. spectra anal. 7-53388
 InP:Fe, Czochralski-grown, stoichiometric-related faulted loops, struct. and lumin. props. 7-51772
 InP:Fe, OMVPE grown, electronic and optical props. 7-52868
 InP:Fe, optical spectra 7-53372
 InP:Fe, Si-implanted and rapid thermal annealed, photoluminesc. study 7-59243
 InP:Yb LPE layers, luminesc. and elec. props. 7-59464
 InP/GaInAs/InP heterostructures, OMVPE, high speed p-i-n photodiodes, photolum., Hall meas. 7-27387
 InP-InP:As epitaxial layers, dislocation reduction, device performance effects 7-7354
 InSb, density of excited electron-hole plasma 7-38608
 InSb, galvanomagnetic luminescence 7-3095
 InSb, galvanomagnetic luminesc., radiative heat pump appls. 7-40019
 n-InSb, impact ionisation electron-hole pair generation, high power optical wave elec. field effect. luminesc. obs. 7-33025
 InSe, excitonic luminescence, influence of macroscopic inclusions 7-13204
 InSe, photoluminescence, defects effects 7-39161
 In₂Se₃, layered semicond., photolum. studies 7-7746
 InZnGaO₄, luminescence props. 7-17341
 KAlSiO₈, thermally stimulated luminesc. at low temps. 7-13238
 KA(WO₄)₂:Ho³⁺, A=Y, Gd, Lu, luminesc. kinetics, visible and UV spectra anal. 7-46144
 KAl(MoO₄)₂:Cr³⁺, tunable IR laser crystals, fluorescent spectra 7-43110
 KAlSi₃O₈:Fe³⁺, orthoclase, absorpt. and luminesc. spectra 7-53383
 K₂Bi(MoO₄)₄, palmierite-type cpd., cryst. struct. determ. 7-21174
 K_{1.5}Bi_{1-x}Nd_xNb_{0.5}O₁₅, cryst. growth, spectral props. of Nd³⁺ ions 7-53405
 KBr, aggregate colour centres, excitation and luminesc. 7-39173
 KBr crystals, resonant secondary luminescence and vibr. F-centre relax. 7-33434
 KBr single crystals, F-band absorpt., X-irrad., thermolum., mag. and elec. field effects 7-59230
 KBr:MnO₄, low temp. resonance Raman scatt. and luminescence 7-39101
 KBr:Se²⁻, electronic spectroscopy 7-22319
 K₂Cd₂(SO₄)₃:Sm, doped and undoped, thermoluminescence 7-39191
 KCl, aggregate colour centres, excitation and luminesc. 7-39173
 KCl crystals, luminescent, detection of radiation shake 7-27761
 KCl, vibronic mechanisms of excitation decay, defect formation 7-39158
 KCl X-ray and γ -irrad., F-centre destruction owing to subsequent laser light excitation, luminesc. spectral charact. 7-27772
 KCl:Ca, γ -irrad., Z₁-centre growth, effect of dislocations, thermolum. study 7-32487
 KCl:Cr(CN)₆³⁻, phosphorescence spectrum, temp. dependence 7-7742
 KCl:F:Eu²⁺, optical absorpt., excitation and luminesc. spectra 7-59250
 KCl:Ti, intensive KrF laser irradiation (Russian) 7-17340
 KCl:Ti, X-ray luminescence, grain size effects (Russian) 7-27767
 KCl:Ti crystal, luminesc. from metastable level of Ti³⁺ center 7-39170
 KCl:Ti³⁺-type phosphors, Jahn-Teller-induced A-absorption and A-emission bands 7-53398
 KCl(Br), F-centre near-surface generation by synchrotron radiation 7-26744
 KCl(Br)(I), luminescence quenching in F centers under pressure 7-22334
 KHo(MoO₄)₂, Ho³⁺, ground state, low temp. sp. ht., Stark components 7-44840
 KI, exciton self-localisation, radiation defects, lumin. studies 7-64681
 KI:Ti³⁺ crystals, luminescence polarisation of dimer centres 7-22335
 K₂NaScF₆:Cr³⁺, laser material, tunable, crystal growth and spectroscopy 7-13347
 K₂NaSc(Ga)F₆:Cr, impurity photolum. spectra and lifetimes, thermal quenching and temp. depend. studies 7-3084
 KNd₂Gd_{1-x}P_xO₁₂, isolated ion pair interaction, fluoresc. quenching study 7-46117
 K₂Nd(MoO₄)₄, palmierite-type cpd., cryst. struct. determ. 7-21174
 K₂O-SiO₂ glasses, intrinsic and recomb. luminesc. and fundamental absorpt. spectra 7-13195
 KUO₂(NO₃)₃, charge transfer bands position, ionisation pot. effects, luminesc. spectra anal. 7-46146
 K(Y, R)W₂O₈:Er³⁺ (R=Gd, Er, Lu) single crystals, stimulated emission spectra 7-7716
 K₂ZnCl₄, X-ray induced luminesc. and thermoluminesc. spectra anal. 7-46132
 La, X-ray M_{4,5} fluorescent emission spectrum, hole-induced shakedown processes. 7-53450
 LaBO₃, luminesc. of Sb³⁺ 7-33442
 LaF₃:Pr³⁺, ³P₀ fluorescence quenching processes 7-22314
 LaF₃:Pr³⁺, Nd³⁺, energy up-conversion, UV fluoresc. obs. 7-53401
 LaF₃:Pr³⁺:Gd³⁺, two-photon excitation and interconfigurational energy transfer 7-3083
 La₃Ga₅Ta_{0.5}O₁₄:Nd³⁺, luminescence and absorption spectra and low-threshold stimulated emission 7-7731
 La₃Lu₂Ga₃O₁₂:Nd³⁺ZZ 7-10957
 LaMgAl₁₁O₁₉:Cr,Nd laser material, optical props. 7-10958
 LaMgAl₁₁O₁₉:Nd(Eu), single cryst., phys. chem. and spectrosc. props. 7-13185
 Li₂B₄O₇:CuCl₂ crystallised glasses, pure and doped, thermally stimulated exoelectron emission, thermolum. 7-27874
 LiCl:PB²⁺, absorpt. and luminesc. spectra studies (Russian) 7-46141
 LiF (TLD-100), thermoluminesc., 90 to 300K 7-3097
 LiF, F₂ laser active element, optically stable component 7-43116
 LiF, F₃⁺ and F₂ colour centres optical study (Chinese) 7-37984
 LiF single cryst., dielectric, charge buildup, influence on charging electron beam motion 7-44294

luminescence of inorganic solids continued

- LiF:C⁶⁺, ion implanted, impurity defects outside implantation zone 7-7773
 LiF:U⁶⁺, cryst., luminesc. excitation of impurity centres 7-13225
 LiH:Al(Mg)(Zn) single crystals, secondary emission, exciton luminesc. and reson. Raman scatt. studies 7-3038
 LiLa₂P₂O₁₂:Nd³⁺, Yb³⁺, metaphosphate glasses, Nd³⁺ to Yb³⁺ energy transfer, luminesc. study 7-22323
 LiLuF₄=Pr³⁺(Nd³⁺)(Ho³⁺)(Er³⁺), stimulated emission spectroscopy 7-13179
 LiNbGeO₅, luminesc. and cryst. struct. 7-32403
 LiNbO₃, exciton lumin., ion beam induced 7-53418
 LiNbO₃, ion beam induced luminesc. 7-27793
 LiNbO₃ waveguide, parametric fluoresc. amplification and oscill. 7-25894
 LiNdP₄O₁₂:Yb³⁺, metaphosphate glasses, Nd³⁺ to Yb³⁺ energy transfer, luminesc. study 7-22323
 Li₂O-SiO₂ glasses, intrinsic and recomb. luminesc. and fundamental absorpt. spectra 7-13195
 LiXO₃ (X=Nb,Ta,I), X-ray irradiated ferroelectrics, radioluminesc. and thermolum. 7-27797
 LiYF₂:Nd, two-step excitation and fluoresc. at 587.4 nm under CW pumping 7-25824
 LiYF₄:Ho³⁺, Er³⁺, Tm³⁺, excited-state absorpt., energy transfer, fluoresc. study 7-22322
 LiYbP₄O₁₂:Nd³⁺, metaphosphate glasses, Nd³⁺ to Yb³⁺ energy transfer, luminesc. study 7-22323
 LuBO₃, luminesc. of Sb³⁺ 7-33442
 Lu₂Si₂O₇:Nd³⁺, spontaneous and stimulated emission 7-39171
 Mg₂Cd_{1-x}Se single cryst. solid solns., local centres parameters determ. (Russian) 7-32953
 MgF₂, colour centres, luminesc. study 7-39172
 MgF₂ cryst., electronic colour centres, UV absorpt. and luminesc. study 7-39174
 MgO, adsorption induced luminescence, O atomic and mol. beams 7-13231
 MgO, deformed and annealed, red cathodoluminescence spectrum 7-27792
 MgO:Al crystals, cathodolum., effect of heat treatment 7-7767
 MgO:Fe, gamma irradi., thermoluminescence and TSC studies 7-33464
 MnCl₂(MnBr₂), liq. solns. and cryst. hydrates, luminesc. quenching mechanism 7-53399
 MnS thin films, luminesc. and excitation spectroscopy studies 7-7741
 NH₄UO₂(NO₃)₃, charge transfer bands position, ionisation pot. effects, luminesc. spectra anal. 7-46146
 NO₂ molecular luminescence centre in nitrites and nitrates, struct. and electron-phonon interaction 7-3088
 NaAlSi₃O₈, thermally stimulated lumin., spectral anal. 7-46154
 NaBr:CN⁻, IR vibrational fluoresc. obs. 7-27775
 NaCl, pure and doped, irradi. defect, thermoluminesc. 7-3098
 NaCl, thermolum. of colloids centres 7-7772
 NaCl, X-ray and γ -irrad., F-centre destruction owing to subsequent laser light excitation, luminesc. spectral charact. 7-27772
 NaCl:Co, doped and undoped, thermoluminescence and X-ray fluorescence spectra 7-22356
 NaCl:Eu single cryst., EuCl₂ phase precipitation, fluoresc. and X-ray diffr. studies 7-46108
 NaCl:Mg, X-ray irradi., exciton interactions with impurity-vacancy dipoles, absorpt. and luminesc. spectra 7-45162
 NaF:Mg, doped and undoped, electron beam irradiated, thermoluminescence and thermally stimulated conductivity 7-7771
 NaGdF₄:Ce, Eu, UV ²H₃ and visible ³D₃ luminesc. 7-64676
 NaI crystals, bound excitation X-ray induced luminesc. spectra 7-53400
 NaI, luminescence excitation spectrum of self-localised excitons, phonon structure 7-39153
 β -Na₂O-Al₂O₃-CdO:Cr³⁺, luminescence spectra 7-33448
 Na₂O-Al₂O₃-SiO₂:Eu³⁺ glass, impurity laser-excited site-selective fluorescence line-narrowing spectra 7-13200
 Na₂O-CaO-Al₂O₃-TiO₂-SiO₂:Eu³⁺ glass ceramic, impurity laser-excited site-selective fluorescence line-narrowing spectra 7-13200
 Na₂O-SiO₂ glasses, intrinsic and recomb. luminesc. and fundamental absorpt. spectra 7-13195
 Na₂O-SiO₂:Tb³⁺ glasses, colour centre formation during UV irradiation 7-2049
 Na₂TbSi₂O₁₂, superionic cond., photoluminescence spectra 7-46093
 Nd complex, tetra dimethyl sulphoxide neodymium nitrate, vibr., Raman. IR and luminesc. study 7-33392
 Nd, in glass, energy transfer rate, luminesc. 7-13192
 Nd₂O₃-P₂O₅-GeO₂, phase equilibria, X-ray diffr., thermal anal., fluoresc. spectra 7-6758
 Nd₂Y_{1-x}PO₄, excitation energy transfer and ion-ion interaction 7-33421
 Ne, electron beam-induced luminescence, time-resolved studies 7-64702
 Ne:Ar(Kr)(Xe), solid, local phase transition near impurity center 7-26945
²³⁷Np, determ. using crystallophosphor photoluminesc. 7-33981
 P, amorphous, radiative recomb., time-resolved photolum. study 7-13212
 PbHPO₄, photostimulated luminescence near ferroelec. Curie temp. 7-64697
 PbMoO₄ crystals, point defects, absorpt. and fluoresc. props. 7-64674
 PbTe heteroepitaxial films, low temp. lumin. 7-39157
 PbTe-PbEuTeSe multiquantum wells, electron-hole recomb., photolum. 7-13216
 PbWO₄:Nd³⁺(Pr³⁺), optical spectra 7-39146
 PrCl₃ organic complexes, spectral energies and oscillator strengths 7-3067
 Pr_{1-x}Gd_x(sIO₄)₂, sensitisation of Gd³⁺ luminesc. by the Pr³⁺ ion 7-3082
 RbCl crystals, resonant secondary luminescence and vibr. F-centre relax. 7-33434
 RbCl, self-trapped excitons, excitation-induced atomic motion 7-21822
 RbCl:I, relaxed exciton states, optical conversion 7-53397
 RbCuCl₃, luminesc., band profile, localised carrier tunnel recomb. effects calcs. 7-3075
 Rb₂Gd(MoO₄)₄, palmierite-type cpd., cryst. struct. determ. 7-21174
 RbI crystals, bound excitation X-ray induced luminesc. spectra 7-53400
 RbI, exciton self-localisation, radiation defects, lumin. studies 7-64681
 RbMnCl₃, photoexcited crystals, exciton annihilation, luminesc. decay curves 7-53385
 Rb₂MnCl₄, photoexcited crystals, exciton annihilation, luminesc. decay curves 7-53385

luminescence of inorganic solids continued

- Rb₂O-SiO₂ glasses, intrinsic and recomb. luminesc. and fundamental absorpt. spectra 7-13195
- RbUO₂(NO₃)₃, charge transfer bands position, ionisation pot. effects, luminesc. spectra anal. 7-46146
- Rb₂ZnCl₄, X-ray induced luminesc. and thermoluminesc. spectra anal. 7-46132
- Ru complex, Creutz-Taube complex with H₂O₂PO₄, synthesis, struct. and oxidation, IR and X-ray spectra anal. 7-46840
- Sb₂S₃ single crystal optical absorption and luminescence obs., 2 to 367K (Japanese) 7-39151
- ScBO₃, luminesc. of Sb³⁺ 7-33442
- Sc₂Si₂O₇:Nd³⁺, spontaneous and stimulated emission 7-39171
- ScZnGaO₄, luminescence props. 7-17341
- Si, Czochralski, electron-irradiated, DLTS and photoluminesc. studies 7-7149
- Si, dislocation luminescence lines, polarisation 7-39154
- Si, dislocation photoluminescence, thermal quenching effects 7-39155
- Si, dislocations and electron-hole radiative recombination 7-13203
- Si epitaxial layers, impurity anal. by photoluminescence spectroscopy 7-7057
- Si epitaxial layers, ultrahigh-purity, photoluminesc. studies 7-45033
- n-Si, excitons bound to pairs of shallow impurities 7-45169
- Si, fast ionisation waves due to absorpt. and reemission of luminesc. 7-52627
- a-Si films, superlattice structure, photo-CVD deposition; solar cell fabrication 7-59450
- Si, Fourier transform photoluminescence analysis 7-53412
- Si, isoelectronic bound exciton states, spin splitting, photolum. excitation spectra study 7-2493
- Si MBE layers, defect characterisation, luminesc., TEM studies 7-13227
- Si, neutron-irradiated, photoluminescence study of annealing process 7-51833
- Si, ribbons, γ -irradiated, defect form., photoluminesc. investig. 7-46147
- Si shallow p-n junctions, reactive ion etching damage, defects and leakage current studies 7-27411
- Si, thermal donor-related isoelectronic centres, exciton binding, photoluminescence studies 7-21861
- Si, transition metal dopant complexes photolum., review 7-45203
- Si:B MBE layers, shallow states, photoluminescence spectra, doping level depend. 7-13228
- Si:C, impurity concentration determ. by photoluminesc. method 7-46084
- Si:C, photolum. detection of impurities introduced by dry etching processes 7-27748
- Si:C,O, luminescence props. of shallow donor centre 7-17347
- Si:C,O, photoluminescence of C-O related complex defects 7-22346
- Si:Ga, electron irradiated and annealed, photoluminescence spectra 7-13206
- Si:Ge, irradiated, photoluminescence spectra 7-13207
- a-Si:H, charge transport and relax., luminesc. long-time tail distrib. anal. 7-39185
- a-Si:H, photolum. and photoconductivity studies 7-33456
- a-Si:H, photoluminescence, high temp. annealing effects 7-7745
- a-Si:H, photoluminescence, thermal quenching 7-53389
- a-Si:H:P(B) films, ion implanted, photoelectric and optical props. 7-38615
- a-Si:H photo-CVD coatings, characterisation using TFT structure 7-38561
- a-Si:H ultrathin layers, CW photoluminescence, layer thickness depend. 7-13202
- a-Si:H ultrathin layers, photoluminescence characts., layer thickness depend. in variety of sample configurations 7-46123
- a-Si:H/a-SiN_x:H interface, deep states and photoluminescence spectra, transistor characts. 7-39186
- Si:N,O, impurity interactions in optical defects 7-17348
- Si:O, new donors, bound exciton recomb., photolum. study 7-22300
- Si:O, optical transition at thermal donors 7-17346
- Si:Sb, pot. enhanced doping during MBE growth, elec., optical props., cryst. quality 7-12112
- Si-SiC superlattice structs. prep. by photo-CVD, solar cell appl. 7-54326
- SiC, 6H polytype, defect lumins., due to excess C vacancies 7-53391
- 6H-SiC neutron-radiated crystals, green luminesc., electron-vibrational interaction study (Russian) 7-59255
- α -SiC:Al,B,O crystals, photolum. and electrolum. studies (Russian) 7-22344
- Si₃N₄, amorphous, pulsed laser excited photolum. intensity and decay meas. 7-17344
- SiO₂, amorphous layers, cathodoluminescence, kinetic effects 7-13237
- SiO₂ glass and cryst., luminescence props. 7-33428
- SiO₂, glassy and thermal films, cathodoluminescence of intrinsic defects 7-7766
- V-SiO₂ intrinsic defect electronic struct., optical transitions, cluster-Bethe lattice calcs. 7-2541
- SiO₂:Yb³⁺ glass, energy transfer among impurity ions, time resolved fluorescence, line narrowing meas. 7-46124
- SiO₂-Al₂O₃-MgO-TiO₂-Cr₂O₃ based glass ceramics, Cr³⁺ laser emission and excitation spectra 7-22299
- Sm³⁺ complexes, samarium (III) 4,7,13,16,21-pentaoxa-1,10-diazabicyclo-8,8,5-tricosane cryptand, luminesc. 7-13191
- SrBa₂O₇:Sm²⁺, fluorescence shift, pressure depend. (French) 7-4805
- Sr_{0.61}Ba_{0.39}Nb₂O₆:Ce crystals, light emission obs. during freq.-degenerate laser pumping 7-15947
- SrCrO₄, spin-triplet state, luminescence and ODMR 7-64686
- SrF₂:2YF₃:Er³⁺(Ho³⁺), interionic interaction, occupation kinetics, stimulated emission 7-46072
- SrF₂:2(Y_{1-x}Er_x)F₃ intracentre transition probabilities and luminesc. self-quenching 7-22332
- SrF₂:2(Y_{1-x}Ho_x)F₃ intracentre transition probabilities and luminesc. self-quenching 7-22332
- Tb³⁺ complexes, terbium (III) 4,7,13,16,21-pentaoxa-1,10-diazabicyclo-8,8,5-tricosane cryptand, luminesc. 7-13191
- TbCl₄:U⁴⁺ incommensurate struct., absorption and emission spectra studies 7-33439
- β -ThCl₄:Pr³⁺, site selective laser fluorescence spectroscopy 7-64687
- ThO₂:Np⁴⁺, absorption and emission spectra of Np⁴⁺ 7-27763
- ThSiO₄:Np⁴⁺, absorption and emission spectra of Np⁴⁺ 7-27763
- TiGaS₂ crystals, photolum., magneto-optical characts. study 7-46089
- TiGaSe₂ single cryst., photolum. and edge absorpt. spectra 7-59241
- TiGaSe₂(S₂):Nd³⁺, photoluminescence spectrum (Russian) 7-64682
- UO₂ thin films form by oxidation, luminesc. studies 7-22351

luminescence of inorganic solids continued

- W complex, pentacarbonylpyridino W(O), single cryst., polarised low temp. luminesc. 7-3094
- Xe, luminescence of trapped excitons, press. effects 7-64690
- (Y, R)₃Al₅O₁₂:Er³⁺ (R=Er, Lu) single crystals, stimulated emission spectra 7-7716
- (Y,Sc)₃Ga₅O₁₂:Cr³⁺,Er³⁺, spectral, luminesc. and lasing props., Stark sublevel lifetimes 7-25827
- Y oxychlorides, phase equilib., X-ray diffr. and spectro-luminesc. anal. 7-46143
- YAG:Ho, Cr, Tm, luminesc. and laser spectroscopic pumping scheme for 2 μ m band 7-36968
- YAG:Mn⁴⁺, luminesc. and fluoresc. line narrowing studies 7-46105
- YAG:Nd³⁺, luminescence decay 7-17342
- YAG:Nd(Nd,Ce) single crystals, luminesc. and laser props. 7-10967
- YAG:Ni(Ni, Zr) (Fe), defect and optical props. 7-59258
- YAG:Pr³⁺, up-conversion, stepwise photon absorpt. process 7-13193
- YAG:Tb, electron-phonon relax. in ⁴D₄ of Tb³⁺ 7-2130
- YAG:Tb cryst. field anal. of Tb³⁺, site selective polarisation spectroscopy 7-2546
- YBO₃, luminesc. of Sb³⁺ 7-33442
- YBO₃:Ho³⁺(Er³⁺), nonradiative energy transfer, activator ion interactions, laser-excited luminesc. study (Russian) 7-22345
- Y_{1-x}Er_xF₃ and Y_{1-x-y}Er_yTm_{1-y}F₃, 1.5 μ m IR excitation of visible lumins. via resonant energy transfer 7-46100
- Y₂MSb₂Zn₃O₁₂ (M=Sr,Ca), rare-earth activated garnets, cathodolum. 7-7763
- Y₂O₃-P₂O₅ phosphors, Eu³⁺ activated, luminesc. spectra, cryst. symm. 7-3080
- YOC:Er, Yb, antiStokes luminesc., 1.5 μ m region 7-13223
- Y₂O₃:S:Pr³⁺, luminescence spectra 7-7730
- Y₂O₃:S₂:Tb³⁺, phosphor, electronic struct., cathodoluminescence meas. 7-17350
- Y₂Pr_{0.03}Gd_{0.97}Al₅O₁₂, sensitisation of Gd³⁺ luminesc. by the Pr³⁺ ion 7-3082
- Y₂Si₂O₇:Nd³⁺, spontaneous and stimulated emission 7-39171
- Y₃Te₂Li₃O₁₂:R, cathodoluminescence study (German) 7-22354
- YVO₄:Eu,Ga(Sc)(La), optical props. and electronic struct. 7-33423
- Yb, in glass, energy transfer rate, luminesc. 7-13192
- ZnCdSe, electron beam pumped, cathodolum., gain and stimulated emission 7-64701
- ZnIn₂S₄, recombination kinetics, photoconductivity and photoluminesc. studies 7-2637
- Zn_{1-x}Mn_xTe, photoluminescence position and lifetime 7-13205
- ZnO varistors, electroluminescence temp. depend. and conduction mechanisms 7-17349
- ZnO:Co(Ni)(Cu), impurity electron states, optical spectroscopy 7-46127
- ZnO:Cu(Bi), phosphor electroluminescence mechanism, spectral energy distrib. 7-7760
- ZnO-electrolyte interface, electrolum. under cathodic and anodic pulsed polarisation 7-13235
- ZnS, cryst., p-type cond., luminesc. 7-13226
- ZnS, epitaxial film, TEM and photoelectron study 7-53408
- ZnS, fused polycryst. layers, photocond. and photolum. spectra, defect form. influence 7-46142
- ZnS, interband two-photon absorpt., freq. depend. 7-33451
- ZnS, MBE growth on Si(100), photoluminesc. props. 7-3174
- ZnS, rare earth impurities, electrolum. of Schottky barriers, photolum., charge compensation, and impurity electron states 7-64700
- ZnS, single crystal, annealed in O, intrinsic defects rel. to elec. and luminesc. props. 7-12649
- ZnS, ZnSe, crystal growth by chem. transport using NH₄Cl transport agent 7-59385
- ZnS:Al, Cr, Fe crystals, recomb. luminesc., EPR and photocond. meas. 7-3076
- ZnS:Al, temp. depend. of visible photolum., ESR studies 7-46099
- ZnS:Cr²⁺, Cr excitation spectrum interpretation 7-58775
- ZnS:Cu, Mn (H), electroluminesc., simultaneous action of AC and DC fields 7-64699
- ZnS:Cu,Mn films, vacuum deposition and DC electroluminescence 7-7868
- ZnS:Cu,Yb phosphor, AC electrolum. study 7-13233
- ZnS:Cu²⁺, multimode Jahn-Teller effect in the luminescence spectrum 7-12675
- ZnS:Er, impact cross section of Er³⁺ in luminesc. spectra 7-46150
- ZnS:Ho³⁺, radiative transitions and nonradiative processes (Chinese) 7-59235
- ZnS:In, photoluminescence, D-A pair emission 7-22312
- ZnS:In epitaxial films, photoluminescence, decay props. 7-39166
- ZnS:Mn, electrolum. study 7-13234
- ZnS:Mn, impact excitation and Auger quenching 7-27827
- ZnS:Mn, thin film electroluminesc. capacitors, trapping level spectra 7-12666
- ZnS:Mn electroluminescent thin films, photothermal deflection spectroscopy 7-27804
- ZnS:Mn films, struct. and electroluminescence props. (Japanese) 7-27783
- ZnS:Mn heavily doped phosphors, mechano and electroluminesc. 7-13240
- ZnS:Mn thin films, DC electrolum. and local destructive dielec. breakdown model calcs. 7-59147
- ZnS:Mn thin films, electrolum., review 7-27784
- ZnS:Mn thin films, local destructive breakdown and DC electrolum., film prep. and test conditions depend. 7-59146
- ZnS:TbF₃, sputtered thin films, electrolum. and photolum. 7-7727
- ZnS-CdS:Ag,Ni,Co phosphors, photolum., energy level model 7-59245
- ZnS:Se_{1-x}, single crystals, growth, exciton luminesc. 7-22453
- ZnSe cryst., low press. melt growth technique, photolum., laser appl. 7-33548
- ZnSe, donor-acceptor pairs, time-resolved recombination luminescence 7-39165
- ZnSe epitaxial layers, MOVPE grown, elec. and photolum. props. 7-7420
- ZnSe, heteroepitaxial growth on GaAs, energy band gap, elastic strain effects 7-59242
- ZnSe hydrothermal growth, cathodolum. props. 7-63531
- ZnSe layers on Ge(100), MBE growth and photoluminesc. 7-7858
- ZnSe MBE layers on GaAs, lattice mismatch effects, TEM, photolum. and X-ray diffr. studies 7-45042
- ZnSe, single crystals, growth, exciton luminesc. 7-22453
- ZnSe:Al, MOCVD growth, deep level characterisation 7-52519
- ZnSe:Al(Ca)(In), impurity diffusion coefficients, cathodoluminesc. study 7-27017
- ZnSe:As, MOCVD growth, exciton and deep emission bands 7-52367

luminescence of inorganic solids continued

- ZnSe:Cl layers grown by MBE, blue photoluminesc. 7-52364
 ZnSe:Er³⁺, ion implanted, identification of cathodolum. centres 7-53417
 ZnSe:N, MBE growth and doping, photoluminescence studies 7-27749
 ZnSe:Si, single crystal growth, chem. transport method (*Korean*) 7-27880
 ZnSe/(Zn,Mn)Se superlattice, optical props. heterointerface effects 7-7736
 ZnSe/GaAs:Cr heterostructure, interface stress 7-38352
 ZnSe-GaAs:Cr, meas. of residual stress by Cr-related luminesc. lines 7-7726
 ZnSe-ZnMnSe, quantum wells, excitons and kinetics 7-12622
 ZnSe-ZnMnSe strained layer superlattices, quantum confinement effects 7-27403
 ZnSe-ZnMnSe superlattices, photoluminesc. props. 7-13218
 ZnSe-ZnS strained-layer superlattice, low pressure MOVPE growth 7-53604
 ZnSe-ZnTe strained layer superlattices, MBE growth on InP substrates 7-13366
 p-ZnSnP, single cryst., recombination radiation, cryst. growth effects 7-53394
 ZnTe, cathodoluminescence, Zn-vapour and Te-vapour heat treatment effects 7-46151
 ZnTe epilayers, chemical transport growth, photoluminesc. props. 7-39413
 ZnTe, nonequilibrium carrier recomb. processes, plasmon effects, luminesc. spectra calcs. 7-58818
 ZnTe, obs. of time evolution from reson. Raman scatt. to excitonic-polariton luminesc. 7-33390
 ZnTe:Cl(Al), crystals, vacancy-impurity complexes, ODMR studies 7-2530
 ZnTe:Cu, impurity related neutral complex with bound exciton, photoluminescence, absorpt., Zeeman meas. 7-45165
 ZnTe:O, hot luminesc., reson. Raman scatt. studies 7-64695
 ZnTe:O, red cathodolum. kinetics, two-step electron capture model calcs. 7-59262
 ZnTe-ZnSe heterostructures, liq. phase epitaxially grown, luminesc. preps. 7-45477
 ZnTe-ZnSe superlattices, photoluminesc. 7-17339
 ZnTe-ZnSe(S) superlattices, hot wall epitaxial growth and photoluminesc. props. 7-13220
 ZnWO₄, Czochralski grown, quality, colour rel. to scintillation output 7-59407
 ZrF₄-BaF₂-LaF₃-AlF₃ fluoride glasses, lanthanide J-levels high yield luminesc. study 7-22309
 ZrSiO₄, rare earths, luminescence-spectra props., hydrothermal synthesis methods 7-64683

luminescence of liquids and solutions

- alkylcyanobiphenyl-phenylcyclohexanecarboxylate mesomorphic mixtures, binary phase diagrams, fluoresc. spectral determ. 7-27765
 -amino-5,6,7,8-tetrahydronaphthalene, depletion of singlet and triplet states due to external heavy-atom perturbation 7-57121
 anthracenes, aq.-micellar soln., dimethylaniline fluoresc. quenching and exciplex form. 7-36683
 aqueous cyanine solns., organic acid effect on spectral luminescent props. 7-46087
 azacoumarin dyes, fluorinated, laser dye stability, lifetimes, fluoresc. 7-59237
 β -cyclodextrin, synchronous wavelength scanning room temp. phosphoresc. 7-33452
 cyclohexane, liq., geminate electron-hole pairs, props. 7-64679
 9,10-diphenylanthracene, energy transfer from mesitylene and benzene 7-22316
 dye solutions, quantum efficiency of fluoresc., determ. by diffraction at laser induced phase grating 7-3081
 electrolyte-ZnO interface, electrolum. under cathodic and anodic pulsed polarisation 7-13235
 eosin in propanol, O₂ induction of delayed fluoresc. 7-36682
 erythrosine in propanol, O₂ induction of delayed fluoresc. 7-36682
 hematoporphyrin.2HCl, dye, energy transfer excitation (*Japanese*) 7-22342
 liquid crystal anisotropic matrix, energy transfer 7-64693
 MBBA liq. cryst., mol. orientational relax. times, luminescence meas. 7-44368
 methane, liquid, fluorescence spectra near needle electrode under divergent fields 7-7737
 3-methoxybenzanthrone in soln., picosecond spectroscopy of intermolecular proton phototransfer 7-54150
 syn-(methyl,methyl)bimane aq. soln., lasing action obs., absorpt. and fluoresc. spectra meas. 7-43083
 micelles, cylindrical, intramolecular fluoresc. quenching rate const. 7-54189
 micelles synchronous wavelength scanning room temp. phosphoresc. 7-33452
 nematic liq. crystal, impurity-molecule luminescence, rotational depolarisation kinetics 7-51629
 Nile blue, oxazine dye, luminesc. and H⁺ phototransfer in solns. 7-13762
 4-octyloxy-4'-heptyl- α -cyanostilbene, excimer fluorescence (*Russian*) 7-3093
 octyloxycyanobiphenyl and octylcyanobiphenyl, smectic Ad phases, time-resolved fluorescence studies 7-2194
 phenothiazine derivative-methylviologen systems, charge separation yield 7-28323
 phenyl alkyl ketones, ring-substituted, in soln., absorption and fluorescence spectra 7-42671
 polar compound in alcoholic solvents, time depend. fluoresc. shift, solute-solvent interaction 7-62436
 poly(ethylene oxide-propylene oxide-ethylene oxide) block copolymers, photoluminesc. probes 7-13199
 poly(N-vinylcarbazole) films and solns., localised exciton hopping, fluoresc. studies 7-52435
 polystyrene solns., excimer fluoresc., conc. depend. 7-7743
 porphyrins, asymmetric, electron spectra, oscillator model anal. 7-31095
 PVC, thermal degradation, fluoresc. study 7-33422
 pyrene substituted polyacrylic acid solns., interpolymer interactions, photophysical obs. 7-46109
 pyridylaryloxazoles, spectral-luminesc. and lasing props. study 7-43089
 reabsorption correction for luminophor, influence of refractive index 7-937
 rhodamine 6 G, polar soln., electron-excitation energy migration, fluoresc. 7-42674

luminescence of liquids and solutions continued

- rhodamine dyes, polar and nonpolar solvent mixtures, aggregation, luminesc. meas. 7-7758
 spatial dissipative structures, generated by diffusion and photochem. bistability 7-46111
 7,7,8,8-TCNQ, semicond., fluorescence spectra and electronic energy levels 7-27769
 uranyl ion in perchloric acid, luminescence decay 7-19548
 Cu(I) iodide complexes, tetrameric, photoluminesc. 7-33437
 Eu³⁺ in soln., ³D₀-⁷F₀ luminesc. line shift and broadening, temp. depend. meas. (*Russian*) 7-17345
 Eu³⁺ ions in liquid solution, luminescence, selective excitation 7-3089
 Eu(NO₃)₃.6H₂O, soln., anomalous temp. depend. of luminesc. decay 7-46116
 MnCl₂(MnBr₂), liq. solns. and cryst. hydrates, luminesc. quenching mechanism 7-53399
 Os complex, excited-state decay, glass to fluid transition effect, energy gap law appl. 7-21418
 Ru(II) complexes in solns., luminesc. behaviour, temp. depend. 7-22331
 Sm³⁺ complexes, samarium (III) 4,7,13,16,21-pentaaza-1,10-diazabicyclo-8,8,5-tricosane cryptand, luminesc. 7-13191
 Tb³⁺ complexes, terbium (III) 4,7,13,16,21-pentaaza-1,10-diazabicyclo-8,8,5-tricosane cryptand, luminesc. 7-13191
 UO₂²⁺ interaction with SO₄ ions, photoluminescence decay 7-27780
 UO₂²⁺ ion fluorimetry in nitric acid soln. 7-61974
- luminescence of organic solids**
 acridine red, frozen solns., excited singlet states fluoresc. spectra 7-42675
 anthracene, cathodoluminescence, scintillation decay laws, electron track model appl. 7-53416
 anthracene crystals., polaritons, picosecond secondary emission studies 7-21825
 anthracene-pyromellitic N,N'-dimethyldiimide, triplet exciton contact pairs 7-64093
 benzene, shock decomposition products detection by chemiluminescence 7-23023
 1,4-bis(β -pyridyl-2-vinyl)benzene-2,5-distyryl pyrazine mixed crystals., photopolymerisation kinetics, fluoresc. spectra studies 7-33928
 1,4-bis(β -pyridyl-2-vinyl)benzene and hydrochloride derivative, photopolymerisation kinetics, fluoresc. spectra studies 7-33928
 bis-tetraethylammonium manganese tetrabromide crystals, deformation-induced after-glow 7-64705
 copper phthalocyanine thin films, thermoelectroluminescence studies 7-7770
 1,4-dibromonaphthalene:acenaphthenequinone crystals., phosphorescence spectra and decay kinetics temp. depend. (*Russian*) 7-27751
 β -9,10-dichloroanthracene, triplet excitons, zero field DF ODMR 7-27631
 9,10-dichloroanthracene monocrystals, alpha scintillations, decay kinetics 7-7769
 epoxy resins, cure monitoring, fluoresc. method using organic dyes 7-22339
 hole-burning spectroscopy as a tool to eliminate inhomogeneous broadening 7-46104
 indole:naphthalene:(anthracene)(tetracene) crystals., impurity complexes, photolum., thermolum. and absorpt. spectra studies (*Russian*) 7-46139
 magdal red, frozen solns., excited singlet states fluoresc. spectra 7-42675
 bis-methylammonium tetrachloro manganese antiferromag. crystals., struct. deform. by exciton self-localisation, luminesc. spectra fine struct. study (*Russian*) 7-27752
 methylmethacrylate-dimethacrylate oxymethylantracene polymer blend, γ -irrad., recomb. luminesc. spectra anal. 7-46145
 naphthalene:pyrene, triplet excitons, prompt and delayed fluoresc. 7-22298
 naphthalene with α -bromonaphthalene or α -chloronaphthalene impurities, intercombination conversion during exciton capture 7-46091
 pentacene crystals, luminesc. spectra, 4.2 to 65K (*Russian*) 7-3092
 pentacene in naphthalene, two-level impurity fluorescence in strong resonant field 7-13222
 α -perylene, crystals., excitons, hydrostatic press. effects 7-52430
 perylene films, electroluminescence with conducting polymer anodes 7-22349
 plastic scintillators, light yield and scintillation response duration determ. 7-36416
 poly(N-vinylcarbazole) films and solns., localised exciton hopping, fluoresc. studies 7-52435
 cis-polyacetylene, photolum. quenching, lattice relax. approach 7-64698
 polyethylene, thermally stimulated luminesc. and depolarisation, electron trapping studies 7-27651
 polyethylene film, electrolum. meas., electrode work function effects 7-27789
 polyethylene naphthalate, electrolum. and electronic conduction in high DC fields 7-27788
 polystyrene, photodegradation, spectral differences, solvent effects 7-6675
 polystyrene film, electrolum. meas., electrode work function effects 7-27789
 polyvinyl alcohol films, fluorescence lifetime meas., single-photon counting technique 7-22311
 polyvinyl carbazole donor-acceptor complexes, luminesc. and photoemission spectra 7-46115
 PVC, thermal degradation, fluoresc. study 7-33422
 (10-(3-pyrenyl)decyl)dimethylmonochlorosilane, chemically bonded to silica surfaces, solvent effects on config., excimer decay profiles 7-22329
 pyrozone, triplet lifetime, temp dependence, visible and IR phosphorescence spectra 7-22328
 rhodamine B, frozen solns., excited singlet states fluoresc. spectra 7-42675
 sodium salicylate, relative fluorescent efficiency between 90 and 800 eV 7-13187
 sodium salicylate as combined fluoresc./refl. coating for broad band detector (*German*) 7-4891
 p-terphenyl aggregates, pure and doped, excitation energy transfer, spectral props. 7-2504
 tetramethylammonium manganese (II) trichloride 1D antiferromagnet, exciton trapping, luminesc. invest. 7-52434
 tetramethylammonium manganese tribromide:Cu²⁺, emission dynamics, exciton trapping 7-39164
 N,N,N',N'-tetramethylbenzidine in various polar solvents, monophotonic ionisation 7-12758
 TGS:Fe³⁺ crystals, spatially distributed defects, luminescence studies 7-26770

luminescence of organic solids continued

- zinc phthalocyanine thin films, thermoelectroluminescence studies 7-7770
 $\text{Na}_3[\text{Sm}(\text{oxydiacetate})_2]\text{NaClO}_4\cdot 6\text{H}_2\text{O}$, circularly polarised luminesc. spectra 7-31091
 PrCl_3 organic complexes, spectral energies and oscillator strengths 7-3067
 Ru complex, $\text{Ru}(\text{bpy})_3^{2+}$, rigid solutions, luminescence, magnetic circular polarisation 7-64685

luminescence of solids

- see also *fluorescent screens; phosphors; scintillation counters*
 Auger recomb. of dislocation excitons 7-38578
 crystal phosphor, quantum yield, electron-hole pair hot escape effects 7-33433
 crystal struct. determ. by mechanoluminescence studies 7-59268
 disordered media, laser luminesc. spectroscopy, use of colour centre lasers 7-25822
 disordered systems, excitation diffusion and energy relax. 7-21792
 disordered systems, nonexponential relaxations 7-64566
 electron excitations, energy transport, luminesc. of impurity pairs, modelling 7-2508
 Fabry-Perot resonator, M-band cryst. luminesc., exciton-photon system, optical bistability phenomenon (Russian) 7-20323
 film, thin, cathodolum. spectrum in STEM 7-22355
 IR photoluminescence by Fourier transform spectroscopy 7-46134
 n-i-p-i heterostructures, luminesc. and nonlinear optical props. 7-7756
 organic cpds., in α -cyclodextrin-NaCl mixture, room-temp. luminesc. 7-36666
 polariton luminesc., anal. 7-27756
 quantum well structs., electric field effect for luminescence (Japanese) 7-13236
 rare earth R^{3+} ion systems, anti-Stokes luminescence 7-33426
 rhodamine dye intercalated smectite, fluorescence props. 7-22325
 secondary radiation in optically anisotropic infinite crystals, general theory 7-7709
 semiconductors, luminescence-Raman scattering transformation (Japanese) 7-59219
 semiconductors, nonequilibrium carrier recomb. processes, plasmon effects, luminesc. spectra calcs. 7-58818
 Wannier-Mott excitons, distrib. fn., secondary radiation of light 7-64090
 CdS/polymer composites, degenerate four-wave mixing 7-62795

luminescent devices

- see also *fluorescent screens; phosphors; scintillation counters*
 cryothermometer using molecular luminesc. 7-48740
 luminescent solar concentrator (Japanese) 7-23123
 MIM electroluminescent device structs., impurity centre electron impact-induced luminesc. mechanism 7-59260
 solar concentrators, glass and dye absorption and luminescence obs. (Finnish) 7-28390
 Z 7-57599
 Au/Cd stearate/n-GaP electroluminescent device struct., electron-hole recomb. luminesc., minority carrier injection mechanism 7-59260
 Au/i-ZnS/n-ZnS electroluminescent device struct., electron-hole recomb. luminesc., minority carrier injection mechanism 7-59260
 ZnSe-ZnS electroluminescent MIS structures, MOCVD growth and charactn. 7-59443

luminophors see *phosphors***luminors** see *phosphors***lunar atmosphere** see *Moon; planetary satellite atmospheres***lunar geology** see *lunar rocks and minerals***lunar rocks and minerals**

- agglutinate melting mechanics for shocked mixtures of Apollo 11 and 16 soils 7-55502
 Apollo 16 highland breccia, komatiite component, abundance characts. 7-60583
 Apollo 16 subregolith basement, comp., struct. and age 7-55500
 Apollo-16 impact melt splashes, petrography and major element comp. 7-55498
 breccias from North Ray crater, Apollo 16 site, precursor lithologies and metamorphic history 7-66482
 Cayley Formation, comp. determ., from Apollo 16 impact melt splashes 7-55499
 cosmogenic nuclide production in lunar samples, Monte Carlo simulation 7-23961
 crater ejecta blocks, size and distrib. 7-34903
 crust chemical and petrological model, implications for crust origin 7-55504
 highland breccias 60018, 67435 and 67455, single-stage exposure histories 7-55501
 highland crust composition from IR observations, review 7-24030
 Luna-16 soil samples, nuclear methods anal. (Rumanian) 7-18363
 regolith breccias from Apollo 15 site, petrology chemistry and origin 7-60584
 sample 76535, coarse-grained granulitic troctolite, crystal struct. refinement 7-55505
 solar cosmic ray inert gases in regolith minerals 7-14507
 volcanic ejecta and Cretaceous-Tertiary extinctions 7-8953

lunar seismology

- comet impacts responsible for UV dayglow holes, rel. to lunar seismicity 7-40727

lunar structure

- complex craters, terrace width var. 7-60585
 conducting core, precessional dynamo model rel. to lunar palaeomagnetism; 7-34892
 craters, morphology anal. 7-55503
 crust chemical and petrological model, implications for crust origin 7-55504
 earliest crust form. 7-60147

lung

- see also *pneumodynamics*
 3D computerised tomography and multinomial models for regional lung air content analysis 7-54801
 alveolar flooding: a computer simulation 7-23379
 asbestos workers autopsied lung tissue, Mossbauer effect study 7-65849
 attenuation and speed of ultrasound in lung: dependence upon frequency and inflation 7-28596
 blood flow, estimation by single-breath method, anal. 7-8622
 blood gases, effect of ventilation and blood flow in lung 7-34173
 breast cancer, late radiation injuries of the lungs after combined treatment (Russian) 7-28609

lung continued

- bronchial mucociliary clearance in unsedated dogs, meas. using radioaerosol technique 7-60137
 cancer after exposure to ^{222}Rn daughters in mines and homes (German) 7-65816
 cardiopulmonary rate monitor, microprocessor-based, using low-power Doppler microwaves 7-65828
 chest auscultation, reduction of heart sounds from lung sounds by adaptive filtering 7-54685
 chest radiography, ANDS-V1 computer detect. of lung nodule 7-47249
 clonogenic cells of Lewis lung carcinoma, survival after γ - and γ -neutron irradi. (Russian) 7-14055
 CT assessment of X-ray-induced damage in mice 7-65815
 dielectric polarisation of feline lung at radio freqs. 7-59968
 elastic stability and surface tension of lungs 7-54662
 foetal lungs, liq. flow to and from, influence of upper respiratory tract, sheep obs. 7-8617
 industrial workers, lung dust, inverse problem solution in magnetisation studies 7-54630
 intracellular motility and phagocytosis rate, mag. particle probe behaviour 7-47139
 macroscopic model, material to simulate properties at RF and microwave frequency 7-47155
 mechanic modeling with fixed tracheal stenosis 7-3818
 mechanical properties of human lung tissue (Chinese) 7-28549
 membrane lung performance during low blood flow CO_2 removal, model 7-8772
 microdistribution of α -active nuclides, CR-39 autoradiography study 7-54732
 mouse, long term radiation effects and combined modalities 7-28622
 nuclear techniques in diagnostic medicine, book 7-24312
 parenchymal and airways recoil hysteresis, time dependence 7-8625
 permeability of lung, measurement in nonsteady state using tracers 7-54802
 pleural liquid exchanges in anaesthetised rabbits, contrib. of Starling and lymphatic flows 7-8627
 positron emission tomography meas. of regional lung density 7-14116
 quaternary gas diffusion between alveolar and blood compartments, simulation 7-54508
 radiation-induced acute pulmonary changes, assessment by CRT 7-14117
 radiobiological effect of α -emitting nuclides incorporated in the lungs microdistrib. of radioactive substance and radiation protection (Russian) 7-47172
 radioisotope imaging, distrib. of an ultra-fine $^{99\text{m}}\text{Tc}$ aerosol and $^{81\text{m}}\text{Kr}$ gas, γ -camera obs. 7-40250
 radiotherapy, lung correction algorithms validity in treatment planning 7-40269
 rat tissue, mag. field effects, phase-contrast microscopy obs. 7-8645
 respiratory proprioceptor system in man, noninvasive technique for exam. 7-40374
 scanning equalisation radiography, beam geometry optimisation 7-65853
 tissue heterogeneity effect on operating regime selection of X-ray tube in radiodiagnostic investig. 7-40278
 tracheobronchial tree and pulmonary arteries, NMR imaging using electronic axial rot. 7-14102
 vascular compliance of canine lung, longit. distrib. 7-8624
 visceral pleura, excised canine, mech. behaviour obs. 7-54644
 volume of lung, effect on pulmonary mechs. in guinea pigs 7-8626
 ^{210}Pb concs. and states of equilib. with ^{218}U , ^{234}U and ^{230}Th in miners' lungs 7-28724
 ^{239}Pu , A=239,240, conc. in Japanese human tissues 7-18081
 ^{239}Pu and ^{244}Cm , lung clearance and translocation following inhalation, rat obs. 7-34290
 Rn daughter exposure and cigarette smoking, lung cancer in Navajo men, U mining relationship 7-8703
 ^{222}Rn , A=220, 222, progeny inhalation, lung cancer risk at low doses of α particles 7-28608

lutecium see *lutetium***lutetium**

- see also *nuclei with*
 adsorption with Ba on W, field emission characteristics 7-12466
 mean square amplitude of vibr. and Debye temp. 7-21368
 ^{147}Lu , A=173-6, resonance ionization mass spectrometry for high resolution optical spectra 7-19744
 ^{147}Lu , A=173,174, high resolution mass resolved spectra 7-15552

lutetium alloys

- AuLu, heat of form. and cryst. struct., linear augmented STO calcs. 7-51705
 Lu-Fe, superconducting transition temp. and lattice constants 7-64387
 LuAg, nonmag. cpds., transport props. and electronic struct. 7-2575
 $\text{Lu}_2\text{Co}_4\text{Si}_{14}$, monoclinic struct. type, rel. to $\text{Sc}_2\text{Co}_4\text{Si}_{10}$ and $\text{La}_2\text{Co}_2\text{Sn}_7$ 7-1944
 $\text{Lu}_2\text{Cu}_{0.37}\text{Y}_{0.63-x}$ metallic glasses, low temp. sp. ht. 7-64462
 α -Lu D_x single crystals, anisotropic ordering, resistivity and heat capacity studies 7-21894
 LuFe $_2$, electronic struct. and mag. props., tight-binding approx. calcs. 7-2475
 $\text{Lu}_2\text{Ir}_2\text{Si}_{10}$, superconducting, electronic phase transition and partially gapped Fermi surface 7-12902
 LuPd $_2$ Si $_2$ single crystal, Czochralski growth, charactn. 7-53557
 LuPd $_2$ Si $_2$ (RhSi $_2$) ternary compounds, superconductivity 7-12901
 Sn-Lu binary system, phase diagram and equilib. 7-7961

lutetium compounds**see also lutetium alloys**

- diphthalocyanine, γ -phase, cryst. and molecular struct. 7-21190
 existence and electrical props. (French) 7-17008
 laser material, spectroscopic props. 7-10957
 lutetium bisphthalocyanine, doped p- and n-type thin films, cond., visible spectra anal. 7-52865
 $(\text{LuYBiPb})_3(\text{FeGa})_5\text{O}_{12}$ crystn. from soln. melt, component distrib. 7-21149
 $(\text{YSmLuCa})_3(\text{FeGe})_5\text{O}_{12}$, bubble lattice, magnetisation curves 7-53094
 $(\text{BaLu})_2(\text{FeGa})_5\text{O}_{12}$, garnet films, pulsed magnetisation reversal, in-plane mag. field 7-45736
 $(\text{BiDySmLu})_3(\text{FeAl})_5\text{O}_{12}$ bubble garnet films, Bi-substituted, LPE growth rate reduction 7-45049
 $(\text{BiDySmLuGd})_3(\text{FeGa})_5\text{O}_{12}$ bubble garnet films, Bi-substituted, LPE growth rate reduction 7-45049
 $(\text{BiLu})_3(\text{FeGa})_5\text{O}_{12}$ epitaxial films, microdomain nucleation near moving domain walls 7-45778

lutetium compounds continued

- (BiLu)₃(FeGa)₂O₁₂ film, magnetic bubble motion, Rayleigh surface wave effects 7-33245
- (BiYLu)₃(FeGa)₂O₁₂, garnet films, pulsed magnetisation reversal, influence of temp. on integral characts. 7-45735
- (BiYLu)₃(FeGa)₂O₁₂ epitaxial films, microdomain nucleation near moving domain walls 7-45778
- CaLuAlO₄ crystals, growth by Czochralski method 7-22460
- Cs_{1-x}Lu_xF_{10-x} cryst. struct., space group, least-squares refinement 7-6604
- (Eu, Lu, La)₃Fe₂O₁₂ films, gyromagnetic ratio, damping parameter and mag. anisotropy 7-45777
- KLu(WO₄)₂:Ho³⁺, luminesc. kinetics, visible and UV spectra anal. 7-46144
- LiLuF₄ = Pr³⁺ (Nd³⁺) (Ho³⁺) (Er³⁺), stimulated emission spectroscopy 7-13179
- Lu₃Al₂O₁₂:Cr³⁺,Fm³⁺,Ho³⁺, 2 μm stimulated emission of Ho³⁺ ions, spectral composition and kinetics 7-46073
- LuBO₃, luminesc. of Sb³⁺ 7-33442
- LuCo_{1-x}Si_x cryst. struct., homogeneity range, X-ray diffr., electron probe anal. 7-37939
- Lu₂Os₄Si₁₃, existence and electrical props. (French) 7-17008
- LuPO₄:Gd³⁺, mag. hyperfine interactions, ³¹P and ⁵¹V ENDOR spectra 7-27630
- LuSi_{2-x}Si, silicide thin films, phase composition, conductance, surface morphology 7-7072
- Lu₂Si₂O₇:Nd³⁺, spontaneous and stimulated emission 7-39171
- LuVO₄:Gd³⁺, mag. hyperfine interactions, ³¹P and ⁵¹V ENDOR spectra 7-27630
- SmLu(FeGa)₂O₁₂ films, with submicron domain structures, mag. inhomogeneity 7-45782
- (SmLuGd)₃(FeGaSc)₂O₁₂ films, with submicron domain structures, mag. inhomogeneity 7-45782
- (Y, Lu)₃Al₂O₁₂:Er³⁺ single crystals, stimulated emission spectra 7-7716
- (YEuLuCa)₃(GeFe)₂O₁₂ films, mag. bubble motion in the presence of a modulated bias field 7-53098
- (YLuBi)₃(FeGa)₂O₁₂, Ne⁺ implanted, CEMS study (Chinese) 7-7620
- (YLuBi)₃(FeGa)₂O₁₂:Ne⁺ films, stripe domain stabilisation by ion implantation 7-53100
- (YLuSmCa)₃(FeGe)₂O₁₂ epitaxial films, transition layer 7-45779
- (YSmLuCa)₃(FeGe)₂O₁₂ epitaxial layer, conversion electron Mossbauer spectra 7-48926
- (YSmLuCa)₃(FeGe)₂O₁₂, epitaxial films, Faraday rot., Sm³⁺ conc. effect. 7-53070
- (YSmLuCa)₃(FeGe)₂O₁₂, film, stripe domain stabilisation for Bloch line memory 7-59087
- (YSmLuGd)₃(FeGa)₂O₁₂ garnet film struct. and mag. props., mag. bubble memory appls. (Japanese) 7-7575

Lyapunov methods

- Itô stochastic differential eqns., Lyapunov function method anal. (Russian) 7-35399
- solitary rotational water waves, Lyapunov stability, oceanic appl. 7-63164
- stationary probability distribts. and Lyapunov functions 7-24398
- V-function geometry and Lyapunov stability theory 7-55989

lymphocytes see blood; cellular biophysics

lyotropic liquid crystals see liquid crystals

lysozyme see proteins

	Abstract	Author	Source	Author
1986-88	20	30	7	-
1980-84	40	12	-	-
1985-88	60	20	-	-
1989-92	-	54	68	30
1973-78	600	150	76C	78
1977-80	770	250	250	120
1981-84	1000	350	344	188
1986-88	-	-	-	16

For US\$ and Yen prices please contact the agent or publisher below

ORDERING PROCEDURE

THE AMERICAS

North (including Canada), Central and South

Orders from the above areas, and orders from members of Institute of Electrical and Electronics Engineers Inc. anywhere in the world, should be sent to Fulfillment Manager, Institute of Electrical and Electronics Engineers Inc., 435 West 170th Street, New York, N.Y. 10024-1155, USA. Telephone (212) 512-2500

JAPAN

Orders from Japan should be sent to the Japanese Branch of the Institute of Electrical and Electronics Engineers Inc., 1-1-1 Higashi-Shinjyuku, Shinjyuku-ku, Tokyo 162, Japan. Telephone (03) 3356-1111

REMAINDER OF THE WORLD

Orders from the remainder of the world should be sent to the Fulfillment Manager, Institute of Electrical and Electronics Engineers Inc., 435 West 170th Street, New York, N.Y. 10024-1155, USA. Telephone (212) 512-2500

OTHER INSPEC SERVICES

INSPEC

INSPEC is a service individually tailored to the requirements and interests of the engineer or scientist. On file at Information Services is the primary source of information on the products, services and data being advertised for the INSPEC database. Information is distributed weekly on 160 mm x 110 mm (6 1/8 x 4 1/4 inch)

INSPEC

For a full INSPEC service based on standard 160 mm x 110 mm (6 1/8 x 4 1/4 inch) cards

INSPEC is a service individually tailored to the requirements and interests of the engineer or scientist. On file at Information Services is the primary source of information on the products, services and data being advertised for the INSPEC database. Information is distributed weekly on 160 mm x 110 mm (6 1/8 x 4 1/4 inch)

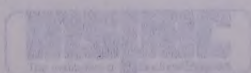
INTERNET

INSPEC is a service individually tailored to the requirements and interests of the engineer or scientist. On file at Information Services is the primary source of information on the products, services and data being advertised for the INSPEC database. Information is distributed weekly on 160 mm x 110 mm (6 1/8 x 4 1/4 inch)

INSPEC is a service individually tailored to the requirements and interests of the engineer or scientist. On file at Information Services is the primary source of information on the products, services and data being advertised for the INSPEC database. Information is distributed weekly on 160 mm x 110 mm (6 1/8 x 4 1/4 inch)

JAPAN UPDATE

INSPEC is a service individually tailored to the requirements and interests of the engineer or scientist. On file at Information Services is the primary source of information on the products, services and data being advertised for the INSPEC database. Information is distributed weekly on 160 mm x 110 mm (6 1/8 x 4 1/4 inch)



ABSTRACTS AND CURRENT PAPERS JOURNALS

SUBSCRIPTION PRICES 1987

	USA \$	UK £	ROW £	JAPAN ¥
PHYSICS ABSTRACTS (PA)	1765	725	935	327,250
2nd and subsequent copies	755	450	450	157,500
ELECTRICAL & ELECTRONICS ABSTRACTS (EEA)	1335	635	780	273,000
COMPUTER & CONTROL ABSTRACTS (CCA)	830	400	495	173,250
IT FOCUS (ITF)	100	75	82	28,700
PA/EEA/CCA/ITF COMBINED SUBSCRIPTION	3630	1605	2045	715,750
2nd and subsequent copies	2690	1335	1560	—
PA/EEA/CCA COMBINED SUBSCRIPTION	3550	1540	1980	693,000
2nd and subsequent copies	2615	1275	1500	525,000
EEA/CCA/ITF COMBINED SUBSCRIPTION	2040	965	1215	425,250
EEA/CCA COMBINED SUBSCRIPTION	1960	900	1150	402,500
CCA/ITF COMBINED SUBSCRIPTION	910	465	560	196,000
CURRENT PAPERS IN PHYSICS				
Member rate	103	53	53	—
Non-Member rate	230	137	140	49,000
CURRENT PAPERS IN ELECTRICAL & ELECTRONICS ENGINEERING				
Member rate	103	53	53	—
Non-Member rate	197	111	113	39,550
CURRENT PAPERS ON COMPUTERS & CONTROL				
Member rate	103	53	53	—
Non-Member rate	197	111	113	39,550
KEY ABSTRACTS				
Member rate*	53	27	27	—
Non-Member rate	110	50	52	18,200
All 14 Key Abstracts combined	1360	630	640	—

* The Key Abstracts Member rate is available to Members of IEE and IEEE only.

CUMULATIVE INDEXES

Cumulative indexes are available for *Physics Abstracts*, *Electrical & Electronics Abstracts* and *Computer & Control Abstracts*, for both authors and subjects. These cumulations generally cover a period of four years, with the exception of *Computer & Control Abstracts* where the initial volume covered the period 1966-68. The table below shows the prices and periods for the two types of cumulative index.

	PHYSICS ABSTRACTS		ELECTRICAL & ELECTRONICS ABSTRACTS		COMPUTER & CONTROL ABSTRACTS	
	Subject	Author	Subject	Author	Subject	Author
	£	£	£	£	£	£
1955-59	20	—	15	20	—	—
1960-64	40	17	20	12	—	—
1965-68	60	—	35	20	—	—
1969-72	—	—	72	64	48	30
1973-76	600	300	250	150	150	75
1977-80	770	450	380	250	250	120
1981-84	1000	600	500	350	345	165
1966-68	—	—	—	—	15	

For US\$ and Yen prices please contact the appropriate address below

ORDERING PROCEDURE

THE AMERICAS

North (including Canada), Central and South

All orders from the above areas, and orders from members of Institute of Electrical and Electronics Engineers Inc. anywhere in the world, should be sent to Fulfillment Manager, Institute of Electrical & Electronics Engineers Inc., 445 Hoes Lane, Piscataway, N.J. 08854-4150, USA. Telephone (201) 981 0060.

日本：

INSPEC 刊行物の購入価格は、すべて円建てとなっており、航空便(ASP扱)で送られます。詳細については、最寄りの洋書取扱店又は、総代理店ユサコ株式会社(昭和58年10月1日より社名変更)〒105東京都港区新橋1-13 12 電話(03)502-6471までお問合わせ下さい。

REMAINDER OF THE WORLD

All remaining subscriptions should be sent to INSPEC Marketing Department, P O Box 26, Hitchin, Herts SG5 1SA, England. Telephone Hitchin 53331, Telex 825962, Facsimile (0462) 59122 ©.

OTHER INSPEC SERVICES

SDI

(Selective Dissemination of Information.)

This is a service individually tailored to the requirements and interests of the engineer or research worker. Details of information relevant to the interest profile of the individual subscriber are selected from the data being processed for the INSPEC Database. Information is dispatched weekly on 150 mm x 100 mm (6" x 4") cards.

TOPICS

This is an SDI service based on standard pro-

files. There are over 90 subjects covering high-activity areas of research and development. This is an inexpensive card service designed to alert engineers and researchers to the availability of literature within their subject area.

MAGNETIC TAPES

Tapes containing all the information included in the INSPEC publications are issued twice monthly. They enable the larger research and development organisations to produce their

own internal information and current-awareness services.

JAPAN UPDATE

Six high-technology subjects are covered by Japan Update Services. Abstracts are provided for articles selected from about 300 Japanese journals and despatched weekly on conveniently-sized cards. This inexpensive service is designed to help engineers stay abreast of technological developments reported in the Japanese literature.

PROPERTIES OF Mercury Cadmium Telluride

This latest publication in the EMIS Datareviews series is the first authoritative work of reference on the properties of the Group II-VI ternary alloy Mercury Cadmium Telluride (HgCdTe). Current interest in this material centres on its unique infra-red detection properties and its resulting wide range of applications in the fields of meteorology, aerospace and defence.

To produce semiconductors to strict specifications, it is necessary to characterise them fully and consequently to have reliable materials data. This book will satisfy these requirements for MCT and so serve to advance research in the field.

Contents include:

- **Mechanical & Thermal Properties**
- **Diffusion**
- **Band Structure & Carrier Properties**
- **Segregation of Impurities**
- **Defect Etching**
- **Dielectric & Optical Properties**
- **Annealing & Doping**
- **Surfaces & Interfaces**
- **Precipitation**
- **Piezo-electric, Elasto- & Electro-Optic Properties**

Properties of Mercury Cadmium Telluride casebound 280 x 210mm is priced at £75 UK, \$170 USA, and £95 elsewhere.

To order your copy contact:

UK & ROW INSPEC Marketing Department
Institution of Electrical Engineers
Station House
Nightingale Road
Hitchin
Herts. SG5 1RJ
UNITED KINGDOM

Tel: 0462 53331
Fax: 0462 59122
Telex: 825962 IEE G

USA INSPEC
IEEE Service Center
445 Hoes Lane
P.O. Box 1331
Piscataway
NJ 08855-1331
USA

Tel: (201) 981 0060
Fax: (201) 981 0027
Telex: 833233 IEEE PWAY